Russian Chemical Reviews, Volume 63 (1994)

Contents of Volume

Number 1

Polymer monolayers and Langmuir-Blodgett films. The influence of the chemical structure of the polymer and of external conditions on the formation and properties of organised planar assemblies 1
V V Arslanov

Thermal, photolytic, and oxidative reactions of the homoligand carbonyls of metals in Groups VI-VIII 41
I V Spirina, V P Maslennikov

Clusters of IIA and IIIA groups metals: synthesis and reactivity 55
V V Smirnov, L A Tyurina

Derivatives of trivalent phosphorus in the synthesis of glycerophosphatides and related phospholipids 71
E E Nifantiev, D A Predvoditelev

Immunoassay of low-molecular-mass physiologically active substances of plant and microbial origin encountered in plants 91
S K Volkov

Number 2

Electron transport and electroluminescence in polymer layers 103
A V Vannikov, A D Grishina, S V Novikov

Reactions of hydrocarbons with electrophilic transition metal complexes in trifluoroacetic acid 125
N F Goldshleger, A P Moravsky

Photochemistry of 2-dialkylamino-1,4-naphthoquinones 139
R P Shishkina, V N Berezhnaya

Sulfides in organic synthesis. Application of sulfides 147
I V Koval'

New methods of synthesis of linear functionalised (*Z*)-isoprenoids and their 2,3-dihydro-derivatives 169
N Ya Grigorieva, O A Pinsker

The molecular weight distribution of the products of the Fischer-Tropsch synthesis 185
L S Glebov, G A Kliger

Number 3

Reactions of diazoalkanes with transition metal complexes 197
M Putala, D A Lemenovskii

Steric stabilisation of liquid films by adsorption layers of macromolecules 217
V G Babak

Aggregates of cyanine dyes: photographic problems 231
B I Shapiro

Reactions of aromatic diazonium salts with unsaturated compounds in the presence of nucleophiles 257
B D Grishchuk, P M Gorbovoi, N I Ganushchak, A V Dombrovskii

The synthesis and reactivity of organobromine compounds in homolytic addition and telomerisation processes 269
A B Terent'ev, T T Vasil'eva

Acid strength of proton donors in complexes of nontransition metal halides as a measure of the activity of electrophilic polymerisation catalysts 279
K S Minsker, V A Babkin, G E Zaikov

Number 4

Stereodynamics and degenerate ligand exchange in solutions of tetracoordinate chelate complexes of nontransition metals 289
V I Minkin, L E Nivorozhkin, M S Korobov

Thermal decomposition of aliphatic nitro-compounds 313
G M Nazin, G B Manelis

Sulfides: synthesis and properties 323
I V Koval'

The use of samarium diiodide in organic and polymer synthesis 345
N E Brandukova, Ya S Vygodskii, S V Vinogradova

Effect of additions of metals and their derivatives upon the thermal degradations of polymers 357
L V Ruban, G E Zaikov

The properties and applications of fluorine-containing polymer films with piezo- and pyro-activity 367
V V Kochervinskii

Number 5

Spin probes in micelles 373
A M Wasserman

Geminate electron-ion pairs generated by ionising radiation in nonpolar hydrocarbon glasses: recombination, polarisation, and separation 383
B S Yakovlev, G F Novikov

The vibrational spectra and characteristic features of the orthophosphates of Group I-III elements 399
M E Poloznikova, V V Fomichev

The synthesis and properties of nanocrystalline refractory compounds 411
R A Andrievskii

Proton conductivity of inorganic hydrates 429
A B Yaroslavtsev

Catalytic methods of synthesis of thiophenes from hydrocarbons and hydrogen sulfide 437
M A Ryashentseva

Number 6

Spiro[2.4]hepta-4,6-dienes: synthesis and chemical reactions 449
L G Menchikov, O M Nefedov

The mechanisms of antifoam action 471
P M Kruglyakov

Hydride forming metals and alloys as hydrogen acceptors in catalytic dehydrogenation 483
O V Chetina, V V Lunin

Cryopolymerisation 491
I M Barkalov, D P Kiryukhin

Characteristic features of the radical polymerisation of water-soluble monomers 507
V F Gromov, E V Bune, E N Teleshov

Marine prostanoids 519
M S Miftakhov, M E Adler, F A Akbutina, G A Tolstikov

Number 7

The structures of new germanates, gallates, borates, and silicates with laser, piezoelectric, ferroelectric, and ion-conducting properties 533
E L Belokoneva

The role of adsorbed hydrogen species in the dehydrogenation and hydrocracking of saturated hydrocarbons on supported metal catalysts 551
L V Babenkova, I N Naidina

Intermediates and mechanisms of the heterogeneous catalytic reactions. The simplest reactions of hydrocarbons, alcohols, and acids 559
O V Krylov, V A Matyshak

Trivalent phosphorus acids amides as phosphorylating agents for alcohols and amines 575
E E Nifantiev, M K Grachev

Immunochemical methods for the assays of herbicides of the 1,3,5-triazine group 611
S A Eremin, Zh V Samsonova, A M Egorov

Number 8

The chemistry of the compound semiconductor-intrinsic insulator interface 623
N N Berchenko, Yu V Medvedev

Trichloroethylene in organic synthesis 641
R V Kaberdin, V I Potkin

Organoelement derivatives of 2-pyrone and their applications in organic synthesis 661
V N Kalinin, O S Shilova

Kinetic nonuniformity in radical polymerisation processes 667
S S Ivanchev, V N Pavlyuchenko

Modification of chemical additives to elastomeric compositions 685
A A Mukhutdinov, B S Grishin

The synthesis and transformations of uronic acid nucleosides 695
V A Timoshchuk

Number 9

The chemical bonding and electronic properties of metal borides 711
G P Shveikin, A L Ivanovskii

The chemistry of disulfides 735
I V Koval'

Degradation of the carbon chain in the liquid-phase oxidation of saturated compounds 751
A L Perkel', S G Voronina, B G Freidin

The reactions of polycarboxylic acid *o*-dinitriles with aromatic diamines 767
S A Siling, S V Vinogradova

Tritium planigraphy of biological systems 781
A V Shishkov, L A Baratova

Number 10

Tetrazoles 797
G I Koldobskii, V A Ostrovskii

The chemistry of pyrroloindoles 815
Sh A Samsoniya, N L Targamadze, N N Suvorov

Polyarylates. Synthesis and properties 833
S V Vinogradova, V A Vasnev, P M Valetskii

Macrokinetic aspects of the biocompatibility and biodegradation of polymers 853
K Z Gumargalieva, G E Zaikov, Yu V Moiseev

Levoglucosenone: the properties, reactions, and use in fine organic synthesis 869
M S Miftakhov, F A Valeev, I N Gaisina

Number 11

Gradient lines on multidimensional potential energy surfaces and chemical reaction mechanisms 883
R M Minyaev

The application of luminescence-kinetic methods in the study of the formation of lanthanide ion complexes in solution 905
V L Ermolaev, E B Sveshnikova

Selective hydrogenation of unsaturated ketones and acetylene alcohols 923
E M Sul'man

Metal-complex catalysts in the hydrogenation of unsaturated glycerides of natural oils 937
S R Savel'ev, N F Noskova

The structural-functional organisation of natural peptides 945
E M Popov

Number 12

Problems in mechanochemistry and prospects for its development 965
P Yu Butyagin

Physical chemistry of the dissolution of metals 977
G V Khaldeev

The chemistry of isoindoles 997
V A Kovtunenko, Z V Voitenko

Heterophosphacyclanes in organic synthesis 1019
R A Cherkasov, M A Pudovik

Membrane distillation 1047
M T Bryk, R R Nigmatullin

© 2008 No Rights Reserved.

Russian Chemical Reviews **63** (1) 1–39 (1994)
©1994 Russian Academy of Sciences and Turpion Ltd

UDC 539.233; 241.183; 541.64

Polymer monolayers and Langmuir–Blodgett films. The influence of the chemical structure of the polymer and of external conditions on the formation and properties of organised planar assemblies

V V Arslanov

Contents

I.	Introduction	1
II.	The genuine existence of polymer monolayers on the surface of a liquid	3
III.	The stability of polymer monolayers	4
IV.	The influence of the molecular mass of the polymer on the properties of the monolayers	5
V.	The phase states of polymer monolayers	6
VI.	Polyacrylates and polymethacrylates	7
VII.	Poly(vinyl ethers) and poly(vinyl esters)	18
VIII.	Poly(vinyl acetals)	19
IX.	Polymers based on maleic and fumaric acid derivatives	21
X.	Synthetic polypeptides and polyorganosiloxanes. Monolayers consisting of helical molecules and thin films	23
XI.	Polysaccharides	31
XII.	Polyimides	33
XIII.	Conclusion	36

Abstract. The current state of the problem of the preparation from polymers of planar mono- and multi-layer organised structures on the surface of a liquid or a solid is analysed. The structure and physicochemical properties of the corresponding monolayers and Langmuir–Blodgett films are examined and the characteristic features of the packing of the macromolecules on the surface of the liquid, questions concerning the stability of their monomolecular films, the compatibility of high- and low-molecular-mass compounds in the monolayers, and the influence of the degree of polymerisation, size, and orientation of the side group on the phase state of the monolayers are discussed. Much attention is devoted to the methods of preparation of Langmuir–Blodgett polymer films with a specified architecture and to the study of the characteristics of these monolayer ensembles and the prospects for their practical employment in molecular devices. The bibliography includes 306 references.

I. Introduction

The perfection of the objects and processes in living nature has long attracted the attention of natural scientists, stimulating an endeavour to use the principles underlying the functioning of biological systems for the development of devices for different purposes operating at the molecular level. Evidently, this approach is applicable not only to the traditional objects in molecular engineering, namely functional (molecular) electronics, ionics, photonics, etc., but also to a wider range of systems. In particular, the idea of embodying in molecular constructions based on the biosimulation concept of a most important principle, namely the self-regulation of biological systems, appears extremely attractive. For example, in order to ensure the specified properties, it is at present necessary to introduce pigments, inhibitors, antioxidants, and plasticisers into polymer coatings and plastics at concentrations which are so high that they alter significantly (as a rule, impair) the entire set of the fundamental characteristics of the materials. The creation of systems capable of recognising external influences at the molecular level and of responding to them adequately is one of the urgent problems in modern science. The achievement of rapid, local, and selective recognition and response opens the way to a reduction of material and energy expenditure on the neutralisation of undesirable influences on the system.

In a broad sense, these problems constitute the subject of the rapidly developing supramolecular chemistry, i.e. the 'constructional chemistry of intermolecular linkages' according to the definition of Jean-Marie Lehn — the 1987 Nobel Laureate in chemistry.[1] The scheme presented in Fig. 1 (see over) demonstrates the transition from molecular chemistry to molecular and supramolecular devices.[1] Within the framework of the present review, the supra- and poly-molecular chemical characteristics of organised assemblies are examined in parallel (and not consecutively) because recognition, transformation, migration, etc. processes, assigned in Fig. 1 to the field of supramolecular chemistry, are discussed in relation to organised planar structures.

On the basis of the foregoing, the creation of molecular (supramolecular) devices must include at least three main stages.

1. The construction or synthesis of organic molecules carrying a specific function. This problem of molecular chemistry, in which questions concerning the organisation of individual atoms, their binding to one another, and their disposition in a specific manner relative to one another in order to impart to the molecule the required steric structure are considered.

V V **Arslanov** Laboratory of the Adhesion of Polymers,
Institute of Physical Chemistry, Russian Academy of Sciences,
Leninskii prosp. 31, 117915 Moscow, Russian Federation.
Fax (7-095) 952 75 14

Received 12 October 1993
Uspekhi Khimii **63** (1) 3–42 (1994); translated by A K Grzybowski

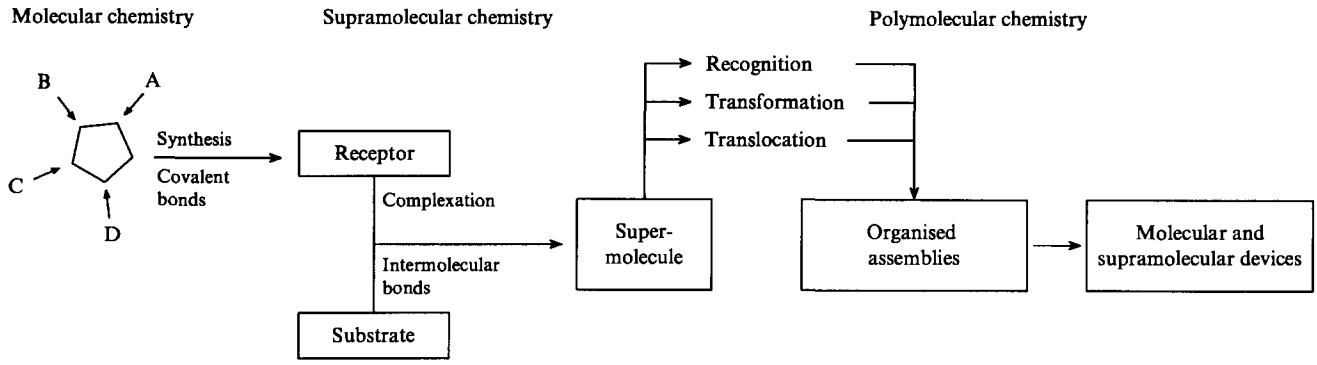


Figure 1. Transition from molecular to supramolecular chemistry.[1]

2. The creation of organised polymolecular assemblies. Evidently, the existing technological procedures for orienting materials, for example drawing, crystallisation, orientation in a flow, and epitaxial growth, are unsuitable for the preparation of assemblies of molecular dimensions. This problem is solved in two ways — primarily by self-assembly and forced organisation. The spontaneous formation of the nucleic acid double helix, which includes the recognition and selective pairing of bases, is a classical example of self-assembly. A second more recent example is the self-organisation of monolayers of alkylsiloxanes, aliphatic acids, dialkyl sulfides, dialkyl disulfides, and thiols on the surfaces of aluminium, silver, gold, silicon oxide, etc.[2-11] A higher level of this effect is illustrated in Fig. 2. A diphilic thiol and acid undergo selective adsorption and organisation on a mosaic surface consisting of sections of gold and aluminium oxide. Here too it is easy to identify two processes: the recognition of 'its own' support (Au for the thiol and Al_2O_3 for the acid) and self-organisation on the latter.

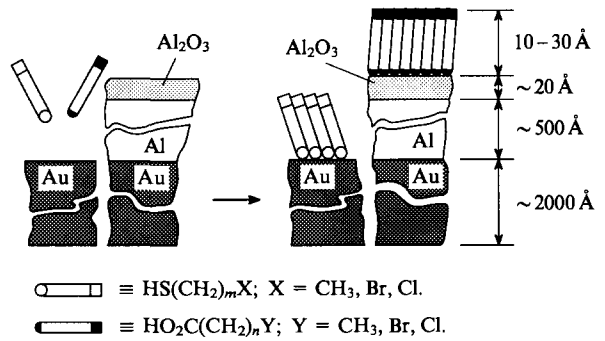


Figure 2. The formation of self-organised monolayers of diphilic molecules of an alkanethiol and a carboxylic acid on adsorption from solution on the surface of gold textured with aluminium oxide.[12]

The Langmuir–Blodgett method should be regarded as forced organisation, because the formation of a monolayer with a specified organisation on the surface of water and its transfer to a solid support require an energy expenditure.

Superlattices, i.e. nanometer layers of organic molecules with a specified alternation order with respect to their thickness, can be obtained only by the Langmuir–Blodgett method. It has been shown[13] that under these conditions the superlattices possess order also in the plane of the monolayers.

One may claim that the application of the Langmuir–Blodgett method always leads to the creation of molecular (supramolecular) constructions, the physical and chemical properties of which are largely determined by the cooperative nature of the behaviour of their constituent molecules.

3. The creation of molecular (supramolecular) devices. In order that a molecular construction should acquire the status of a device, it must be capable of performing a definite function. Solutions to this problem at a higher scale level are known — for example, in the existing devices for the storage and processing of information which employ only one physical effect and only one form of dynamic inhomogenity. The trend towards the miniaturisation of electronic instruments down to molecular devices entails the problem of the realisation and integration of various physical effects in one construction. However, being restricted solely by the 'safety tunnel', specifying the distances between molecular keys at 5–10 nm, such technology would make it possible to pack molecular electronic elements with a density of 10^{18} units per cm^3.[14]

Thus, in order to create molecular devices, it is necessary to seek molecular components capable of performing a specified function and suitable for incorporation into a system organised in a specific manner and formed by different types of polymolecular assemblies. The principal feature of these components and the devices formed from them consists in the fact that they perform their functions on the basis of the properties of molecules and supramolecules.[1] The nature of the components or functional groups introduced into the system determines the operations which can be performed by the molecular assemblies: energy, electron, and ion transfer, different types of chemical reactions, the recording, transmission, and storage of information, etc.

For low-molecular-mass diphilic compounds, studies involving all three stages indicated above are being actively prosecuted at the present time. One of the principal ways of carrying out the first of these (molecular chemistry) involves the grafting to the molecule carrying a definite physical functional group (tetracyanoquinodimethane, tetrathiafulvalene, thiophene, pyridine, dyes, etc.) of a hydrocarbon chain, which ensures the organisation of the monomolecular film on the surface of water.

In the case of polymer systems, this procedure is less appropriate in view of the limited set of macromolecules containing suitable functional groups. Therefore, in order to create monolayer-forming functional polymers, a different procedure is usually resorted to — side groups capable of responding to external influences are grafted onto the main hydrophobic chain. The polymerisation of functionalised monomers and their copolymerisation with inactive monomers, acting as spacer units in the polymer chain, are also employed.

The limited set of objects, the problem of the stability of the monolayers, and the complexity of the manipulations involved in the preparation of Langmuir–Blodgett films (LBF) are apparently the main causes of the appreciable lagging behind (especially in quantitative terms) of the research into high-molecular-mass mono- and multi-layer structures. On the other hand, the problem of the creation of molecular devices can hardly be solved without using high-molecular-mass compounds both in passive insulating layers and in active transforming and transmitting two-dimensional elements. However, the

studies on monolayers and LBF cannot be restricted to approaches traditional for low-molecular-mass compounds which have already been established as a result of attempts at the practical employment of the latter in molecular electronics, nonlinear optics, and other branches of engineering. The specific features of high-molecular-mass chemistry have given rise to a different range of fundamental questions and have influenced the applications of the corresponding monolayers and LBF.

A need has arisen for a more detailed consideration of the physical chemistry of the two-dimensional state of macromolecules and the establishment of a relation between the structure of polymers and their behaviour in a monolayer, the formation of multilayer, including alternating, high-molecular-mass assemblies, and for the study of the possibility of applying two-dimensional organised structures of high-molecular-mass compounds to traditional products of polymer chemistry—organic coatings, adhesives, and membranes (for example, for the preparation of materials with a specified gradient of a characteristic parameter). The theoretical interest in the phase behaviour of monolayers,[15] including high-molecular-mass monolayers, has arisen because certain approaches to the description of critical phenomena cannot be applied in the three-dimensional case but are fully applicable to a system with a smaller number of dimensions.[16]

In the first review, published in 1991,[17] two of the three known methods of preparation of polymeric LBF were examined: (1) the formation of monolayers from monomers on the surface of a liquid (water), their polymerisation in the monolayer, and their transfer to a solid support and (2) the formation of monolayers from monomers, their transfer to a solid support, and the polymerisation in the LBF of each layer or the multilayer film as a whole. A third method envisages the formation of monolayers on the surface of water from complete polymers with subsequent transfer to a solid support. The principal difference between these procedures (responsible for the differences between the approaches to the study of the corresponding systems) consists in the fact that in the first two cases the initial monolayers are formed from low-molecular-mass compounds (monomers), while in the last procedure they are formed from high-molecular-mass compounds. Although many of the problems associated with the transfer of polymer monolayers to solid supports are similar for the first and third procedures, this by no means applies to all of them. Thus the monomers forming the monolayer must be diphilic, insoluble in water, and involatile, but these requirements are not obligatory for monolayers of macromolecules. For example, poly(methyl methacrylate), which does not exhibit distinct diphilic properties, and cellulose derivatives or poly(vinyl alcohol), which are soluble in water, nevertheless form monolayers on the surface of water. These features of high-molecular-mass compounds, on the one hand, expand the number of objects of study and the possibility of using organised planar structures, and, on the other hand, create specific problems in the formation of LBF.

The study of the properties of macromolecules on the surface of water (a liquid) and their influence on the formation of multilayer structures on a solid support is essential for the preparation of high-quality LBF with a minimum number of defects and a homogeneous orientation, thickness, and surface density from polymer monolayers.

It is essential to note that the optimistic prediction in the first review[17] of an increase in the intensity of research into polymer monolayers and LBF expected in the immediate future has unfortunately not so far come true. Systematic studies on polymer monolayers, similar, for example, to the studies carried out on diacetylene monolayers and LBF, are not being prosecuted at the present time. Furthermore, the results of earlier investigations, many of which have not lost their current value, are inadequately taken into account in present day research.

The history of the research into macromolecules in monolayers began with the studies by Devaux in 1903.[18] Since then and up to the Second World War, mainly natural[19–21] and synthetic[22–24] polymers were investigated. However, most of these studies and systematic treatment of data on polymer monolayers date back to the 1940s–1950s.[25–27] In subsequent years, such investigations were performed quite vigorously and were marked by sudden surges due to the appearance of some new polymeric object or the discovery of interesting properties in an existing material. This refers, for example, to studies on polyorganosiloxanes (1960–1970) or to the current interest in conducting polymers (polythiophenes, polypyrroles), as well as fullerenes and their derivatives.[28,29]

Overall, two stages can be distinguished in the chronology of studies on thin polymer films. The early and longest stage involves mainly the investigation of monolayers of macromolecules on the surface of water. In the subsequent 15 years more attention was devoted to LBF in connection with the development of research into molecular architecture. Since LBF are formed by transferring monolayers from the surface of a liquid and reproduce to some extent the structure of these monolayers, the equivalence of both stages or aspects of the research into problems of molecular design becomes evident.

These considerations have determined the structure of the present review, in which the conditions governing the formation, equilibria, stability, and phase states of polymer monolayers and the influence on the latter by the molecular mass of the polymer, the length of the side chain, the composition and pH of the support, temperature, and other factors are analysed. Questions concerning the correspondence between the structural-morphological characteristics of monolayers of high-molecular-mass compounds on the surface of a liquid and in LBF also occupy an important place. The behaviour of monolayers in the collapse region as well as the specific features of the use of thin films of polymers for the formation of LBF are examined.

II. The genuine existence of polymer monolayers on the surface of a liquid

The short but rich in content review by Gaines in 1991[30] takes us back one hundred years to the period where the question of the genuine existence of monolayers of large molecules arose as a result of studies by Pokels.[31] Gaines believes that the 'either polymer or monolayer' dilemma still remains the order of the day, i.e. the question of the genuine existence of polymer monolayers remains of current interest. The genuineness of the monolayer or of the spreading process, i.e. of the existence of a state of the polymer layer in which each monomer unit is in contact with the surface of the subphase, has been tested in accordance with Crisp's recommendations.[26] According to the latter, genuine spreading occurs in the case where reproducible surface pressure (π)–area (A) relations are obtained when the concentration of the solution from which the monolayer is formed or the initial spreading area are altered, and also when the monolayer is deposited from different solvents. When the monolayer is formed by helical (polydimethylsiloxane on a low-energy liquid support[32]) or coiled (polystyrene[33]) macromolecules, it cannot formally be regarded as genuine. However, if its constituent molecules have several stable conformations and structural transformations (for example helix–coil) are possible on the surface of the liquid, then also the study of nongenuine monolayers of this kind may prove useful.

In the review mentioned above,[30] the author addresses the question whether it is possible that the macromolecular coils produced as a result of coiling up in the bulk of the solution could become uncoiled on reaching the surface of the liquid with formation of a true monolayer. There are apparently no fundamental objections to a positive answer to this question. Furthermore, an important argument in support of such an answer arises from the repeatedly established agreement

between the experimental limiting areas of the close-packed monolayer (A_0 at $\pi \to 0$) and the analogous parameters obtained from models.

Less unambiguous results were obtained in tests of the genuineness of the monolayers carried out in accordance with Crisp's criteria. In his studies on poly(vinyl acetate), poly(methyl methacrylate), and poly(methyl acrylate) monolayers, Crisp found that variation of the conditions in the preparation of the monolayers does not alter the compression isotherm. In these experiments, the concentration of the solutions was varied from 0.005% to 0.2% and the solvents were the 1 : 1 water–propyl alcohol mixture, acetone, and benzene for poly(vinyl acetate) and acetone, benzene, and toluene for the remaining two polymers.[25] However, in contrast to this, a dependence of the position of the compression isotherms on the concentration of the solution deposited on the surface of water has been observed in another study[27] for poly(methyl methacrylate) monolayers. Thus, when the concentration was varied from 0.018% to 0.2%, the limiting area per molecule (A_0) changed from 21 to 18 Å^2 (A_0 = 14.5 Å^2 according to Crisp). An even more marked influence of the concentration of the solution on A_0 has been observed[33] for polystyrene: an increase in the concentration of the solution from 0.033% to 0.2% lowered the area by a factor of 2.

The importance of these studies is evident, just as it is evident that they must be based on the ideas of the classical theory of polymer solutions and the modern views arising from the scaling method.

The deposition of monolayers from solutions in good, poor, and θ-solvents, where the macromolecular coils have different sizes and the nature of their interaction with the solvent and with one another is likewise different, can lead to the formation of various surface structures in the monolayers. The concentration of the polymer solution is also a fundamental parameter, which determines, for example, the degree of overlap of the coils. The transfer of the macromolecules from the bulk to the surface, occurring when the polymer solution spreads on the surface of a liquid, is accompanied by complex processes. The ratio of the rates of spreading and evaporation of the solvent, the replacement of the solvent by the liquid constituting the subphase (water), the influence of the field of surface forces, and the limitations as regards the possibility of a rearrangement in the conformation of the macromolecules imposed by the wall (surface) are factors which still have to be analysed.

The form of the macromolecules in the three- and two-dimensional states can be conveniently correlated by resorting to the scaling concept. We shall assume that the polymer is deposited from an effective solvent, the quality of which does not change on passing to the two-dimensional system, i.e. from the bulk-phase solution to the monolayer. In this case, the size of the macromolecules (R) is determined by a critical parameter in the form of a power exponent for different numbers of effective segments in the macromolecule (N) which are different for the three- and two-dimensional systems.[34,35]

Three-dimensional space: $R \sim N^{3/5}$
Two-dimensional space: $R \sim N^{3/4}$

This implies an increase in the size of the flattened macromolecular 'coils' when the molecules pass from the bulk of the solution to the surface and hence the existence of a threshold concentration

$$\frac{1}{A^*} = \frac{N}{S}$$

(where S is the area of the effective segment), for which there is a transition from a dilute two-dimensional solution to a semidilute solution where the flat coils begin to overlap on the surface of the solution. The possibility of a limited interpenetration of the planar coils in a two-dimensional system probably accounts for the stability of the polymer monolayers and the reversibility of the $\pi - A$ isotherms in compression–expansion cycles.

III. The stability of polymer monolayers

It is necessary to distinguish two approaches to the problem of the stability of monolayers. The first, commonest, reduces to the observation of the decrease in the area of the monolayer at a constant surface pressure and of the surface pressure when the mobile barrier is stopped (A = const) in the course of a definite arbitrarily selected time interval. As a rule, the purpose of such experiments is to establish the possibility of maintaining the necessary density of the monolayer in the course of the formation of the LBF.[36,37] Within the framework of this approach, the stability of the monolayers can be increased by altering the temperature and by introducing stabilising additives into the monolayer or the subphase and, in the case of ionogenic compounds, also by altering the pH of the support, by employing electrolyte solutions as the subphase, etc.

The second, more rigorous approach is associated with the establishment of thermodynamic equilibrium in the monolayers. It is based on a number of conditions, the main ones of which are the possibility of applying the techniques of thermodynamics and statistical physics to the calculation of the characteristics of the system, the determination of the phase state of the monolayers and of the transitions between them, and comparison of the results obtained by different workers. Within the framework of this approach, one has to solve the problem of the selection of a standard state of the system,[38] for which at least three versions have been proposed.

1. The state with an equilibrium spreading pressure,[39,40] i.e. with a surface pressure, established in the monolayer, which is in equilibrium with the volume of the substance.[41–44]

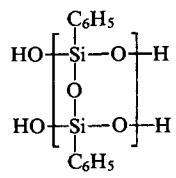
2. The state with a surface pressure corresponding to the phase transition between liquid-expanded and liquid-condensed states of the monolayer.[45,46]

3. The state with a surface pressure corresponding to the transition of the gaseous monolayer to a liquid one.[45,47]

Evidently the choice of the standard state is dictated by the behaviour of the monolayer. The rare data on the gaseous state of monolayers and the controversy concerning the phase transition between two liquid states do not engender optimism as regards the selection of the last two parameters as the standard ones even for the thoroughly investigated low-molecular-mass compounds. The only disadvantage of the equilibrium spreading pressure as a criterion of the thermodynamic stability of the monolayer is perhaps the fact that many compounds do not spread from the bulk phase under the usual experimental conditions (room temperature). The solution of this problem, i.e. the determination of the equilibrium spreading pressure (π_e) for such compounds, is seen by some workers[48] as a procedure involving the deposition on the surface of water of a concentrated solution of the test substance (for example, dipalmitoylphosphatidylcholine) until the maximum surface pressure is attained. This quantity is identified with π_e. It is believed[48] that this procedure is rapid, reliable, and reproducible and yields values of π_e which agree with the equilibrium spreading pressure determined by the traditional method involving spreading from the bulk phase. Another method for the determination of π_e has been proposed by Albrecht.[49] The pressure corresponding to the collapsed monolayer (palmitic acid), which is compressed under controlled conditions, is adopted as the equilibrium spreading pressure. Albrecht[49] notes the importance of this procedure for the determination of isotherms for polymers with long relaxation times. In principle, both procedures considered can be useful. However, one must understand that in either case the monolayer is in equilibrium not with its bulk phase (crystals) but with a hydrated form of the latter, which has an equilibrium spreading

pressure $\pi_e' > \pi_e$. For low-molecular-mass compounds, these questions have been examined in detail by Trapeznikov and coworkers.[50,51] For polymer monolayers, such studies have not yet been carried out.

Analysis of the temperature variations of the equilibrium spreading pressure has been carried out[52] in relation to ladder oligophenylsilsesquioxanes (M = 1 200) and polyphenylsilsesquioxanes (M = 60 000) on the surface of water.



1

As can be seen from Fig. 3, neither the oligomer nor the polymer spreads spontaneously from the bulk phase at 20 °C. The curve for the oligomer consists of the linear sections AB and BC with different slopes and of a high-temperature section parallel to the abscissa axis. The initial section (AB) has the highest slope; at T = 30 °C, the curve exhibits a break, the surface pressure at this point corresponding to the collapse pressure of the oligomer monolayer. This point may be associated with the onset of the formation of a new hydrated bulk phase of the oligomer, the properties of which differ from those of the bulk phase initially placed on the surface of water. The $\pi_e - T$ relation for the polymer is of a different type: as the temperature is raised from 20 to 35 °C, π_e changes insignificantly, after which its more rapid increase is observed. At T > 55 °C, the pressures π_e for the oligomer and polymer become similar and change only slightly on further increase in temperature. The appearance at the point C of yet another hydrated form of the oligomer is indicated by the following observations. At T = 60 °C, the white oligomer powder on the surface of water begins to undergo surface fusion and becomes transparent, assuming the form of lenses, which again become white at T = 70 °C. We may note that the melting points of the oligomer and the polymer are 150 and 400 °C respectively. Consequently, during spreading from the bulk phase on the surface of water, high-molecular-mass compounds can yield several hydrated forms, each of which has its own equilibrium spreading pressure π_e'. The existence of such forms with high values of $\pi_e' > \pi_e$ accounts for the possibility of obtaining reproducible and reversible monolayer compression isotherms for both low-molecular-mass compounds and for polymers. In this case, the metastable state of the monolayer of the initial (bulk phase) material proper becomes stable (corresponds to equilibrium) for hydrated derivatives of the latter. Therefore measurement of the temperature variations of the equilibrium spreading pressure or the determination of π_e' from data for the spreading of concentrated solutions may be recommended as procedures for the estimation of the degree of equilibrium in true monolayers.

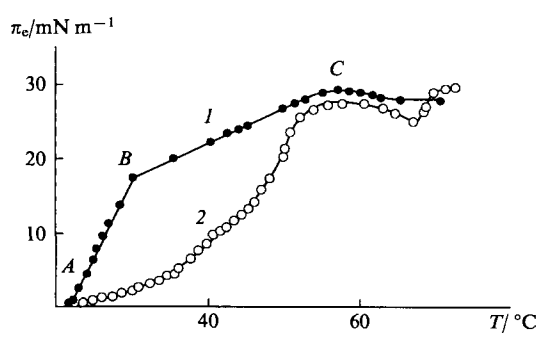


Figure 3. Temperature dependence of the equilibrium spreading pressure (π_e) for oligophenylsilsesquioxane (curve *1*) and polyphenylsilsesquioxane (curve *2*) on the surface of water.[52]

An important procedure for the determination of the stability of monolayers involves the analysis of their relaxation properties.[53–55] The critical parameters of the compression isotherms, obtained for surface pressures exceeding π_e or π_e', are determined by the relation between the relaxation times of the molecular processes occurring on compression of the monolayer and the time of the measurement, which is inversely proportional to the rate of deformation (but not compression) of the monolayer. It has been shown[56] for an arachidic acid monolayer that, with increase in the observation time from 600 to 3 × 10^5 s (the rate of deformation diminished correspondingly from 10% to 0.02% min^{-1}), the monolayer collapse pressure decreases from 60 to 20 mN m^{-1}. Unfortunately, such experiments are so far extremely rare for polymers having distinct viscoelastic properties and a large set of relaxation times.[57]

IV. The influence of the molecular mass of the polymer on the properties of the monolayers

The question of the influence of the molecular mass (or degree of polymerisation), a fundamental characteristic of macromolecules, on the behaviour of monolayers was actively discussed several decades ago. The outcome of these discussions is contained in the reviews already mentioned.[25,26,43,52] Here we present only a brief analysis of these problems, having supplemented it with the results of studies carried out in this field during the last twenty years. The commonest point of view is one according to which the $\pi - A$ isotherms are independent of the molecular mass in the range of surface pressures usually measured (π > 0.5 mN m^{-1}). This was first demonstrated[19] for cellulose derivatives. A similar result has been obtained[58] for hydroxypropyl- and hydroxyethyl-cellulose monolayers. A weak dependence of the compression isotherms on the degree of polymerisation has been established for poly(vinyl acetate),[25] poly(ethyl succinate),[23] and polyorganosiloxanes.[59–61] However, an increase in the limiting area per monomer residue from 18.7 to 26.8 Å^2 with increase in the molecular mass of the polymer from 2.5 × 10^4 to 10^6 has been observed[62] for poly(methyl methacrylate) monolayers. The ratio of the areas depends on the rate of compression of the monolayer, the monolayer of the high-molecular-mass specimen showing a more marked dependence. The dependence of A_0 on the molecular mass, found[63] for monolayers of oligoesters on the surface of water, vanishes when a 40% aluminium sulfate solution, which improves the spreading of the oligomers, is used as the subphase.

The differences in the behaviour of monolayers of polymers with low and high degrees of polymerisation are in many respects associated with the influence of the end groups of the molecules, which alter their polarity and the ability to spread or dissolve in the subphase. Naturally such influence is more significant in the case of short chains.

Whereas the question of the influence of molecular mass on surface pressure and surface potential remains controversial, the dependence of the mechanical properties of monolayers on the dimensions of macromolecules is not open to doubt. Despite this and also the large amount of information obtained from data on the viscoelastic properties of monolayers about the characteristics of the behaviour of macromolecules in a two-dimensional state (ranging from a dilute solution to the condensed phase), such studies are rarely carried out at the present time.

The final aim of the majority of studies designed to establish the dependence of the compression isotherms on the size of the macromolecules is the determination of the molecular masses of the polymers. Since this parameter is calculated on the basis of the two-dimensional analogue of the van't Hoff equation and its

modifications, the monolayer must be in the gaseous (vapour) state, although this state can be by no means always achieved for large molecules. Guastalla, who measured the surface pressure with a sensitivity to within 0.001 mN m^{-1}, may be regarded as the pioneer in this field of study.[64] Subsequently many attempts were undertaken to calculate the molecular masses of polymers in the region of isotherms with low surface pressures.[26,43,65] In particular, the molecular mass of a polymer obtained in the polymerisation of a double-stranded silane lipid in a monolayer has been determined recently.[66]

Numerous studies have been devoted to the determination of the molecular masses of polymers in the range of comparatively high surface pressures and hence high surface concentrations of the test substance. On the basis of such data, which have been reviewed,[52] one cannot reach a conclusion either about the possibility of using this region of compression isotherms to estimate the molecular mass of the polymer or whether the molecular mass found refers to the entire molecule or its segment.

V. The phase states of polymer monolayers

Much attention has been devoted in the past to the phase states of monolayers of low-molecular-mass compounds. There exist several classifications of these states,[67–69] which have been proposed by Adam,[42] Dervichian,[70] Harkins,[41] Stenhagen,[71] Lundquist,[72] and Lin.[73] Furthermore, the refinement of the structures of monolayers in different states is still being continued and communications are being published concerning the observation of new states of monolayers comprising small molecules.[67]

The phase states of monolayers of high-molecular-mass compounds have remained less investigated (and are being less investigated). Since Crisp's time, little attention has been paid to this question and the subdivision which he proposed for polymer monolayers into expanded and condensed can hardly be regarded as a classification of states. The causes of the situation which has arisen can be scarcely attributed to the poor 'distinctiveness', according to Gaines,[43] of the $\pi - A$ relations for polymer monolayers. It appears that, at the level attained in the study of polymer monolayers at the present time, it has not been possible to formulate an adequately rigorous classification of their phase states for a number of other reasons. Firstly, there have been virtually no systematic studies nowadays on the structure of polymer monolayers by modern methods, which are frequently employed for monolayers of low-molecular-mass compounds. The second reason is the complexity of polymeric objects and the consequent need to develop definite principles of study, which are applicable within the framework of a particular group of compounds. The latter consideration requires explanation. The classical objects for the study of the states of monolayers of low-molecular-mass substances are aliphatic acids and alcohols. By altering the length of the aliphatic chain in these compounds, it is possible to attain all the states of the monolayer ranging from gaseous to solid-condensed. From this it follows that the length of the hydrocarbon chain or its increment are fundamental characteristics, which determine the properties of the aliphatic alcohol and acid monolayers. In the previous section, it was shown that a fundamental characteristic of polymers—the molecular mass—hardly influences the state of the polymer monolayers and, if such influence does exist, it arises solely from the change in the fraction of the end groups on the surface. Therefore, comparison of the properties of monolayers of high-molecular-mass compounds is valid only within the framework of specially selected groups of polymers. Modern polymer chemistry provides interesting possibilities for the construction of homologous series of different types of large molecules. We shall attempt to designate such series.

1. Polymers without distinct diphilic properties, i.e. without side chains. Typical representatives are polyethers with different lengths of the polymethylene chain between the oxygen atoms. By increasing the complexity of the polar unit (ester, carbamate, and other groups) separating the polymethylene chains, it is possible to obtain other types of such systems. Copolymers and block copolymers of this series, with a variable ratio of the fragments in the main chain, are also interesting objects with controllable variation of the characteristics of the monolayers.

2. Polymers with weak diphilic properties, i.e. polymers having short side chains. In this case, the behaviour of the monolayer depends on the structure of not only the main chain but also of that of the side chain.

3. Polymers with long side chains. In the presence of long spacers in the main chain, the side chains behave to some extent independently of one another. The spacer can be inserted also between the main and side chains. The compatibility in the monolayer of incompatible monomers carrying specific functional groups can be achieved as a result of the spreading of the copolymer made up of the corresponding monomers.

4. Macrocyclic, ladder, and other polymers with a more complex chemical structure and behaviour.

The second possible method of combining different polymers may be based on a chemical principle where the variation of the properties of monolayers and LBF is considered within the framework of a single class of compounds, for example polyacrylates. This approach makes it possible to reduce to a minimum the differences in the chemical nature of the polymers and to trace in a fairly pure form the influence of the structure of the chains on the characteristics of the two-dimensional systems formed from them.

The latest reviews on polymer monolayers refer to the 1960s; during the period which has elapsed since then, many new studies, devoted to traditional and new polymers, including those specially synthesised for the formation of surface films, have been published. Bearing in mind the special interest in LBF, attention has been concentrated in these studies on functionalised monolayers.

It appears that analysis of the development of the field of surface chemistry should include a discussion of those properties of polymer monolayers which determine the possibility of the formation of high-quality LBF, functionalised films, and surfaces.

An essential condition for the preparation of LBF with a specified thickness and orientation is the formation of a genuine monolayer not containing nonspreading material. The question arises what should be the structure of the polymer chain and the ratio of the lengths and the compositions of the side chains and spacer groups. Should one in such cases graft the group with the required function to the polymer chain or should one produce a mixed monolayer with the matrix polymer? The use of binary mixtures (for the composition of side chains or copolymers) removes the problem of synthesis but the problem of compatibility then arises, especially if one is dealing with components having side chains of different lengths. Furthermore, it is essential to take into account the possibility of interlayer and intralayer diffusion in the LBF made up of mixed monolayers which disturbs the organisation of the monolayers established on the surface of the liquid. The immobilisation of the low-molecular-mass component can be achieved in at least four ways: (1) by the formation of a mixed monolayer from the chemically noninteracting polymer and an additive which are insoluble in the subphase; (2) by the introduction of a water-soluble polymer into the subphase under the monolayer of the second low-molecular-mass component; (3) by the introduction into the subphase of a functional additive under the polymer monolayer; (4) by the formation of a mixed monolayer of the polymer (oligomer, monomer) with an additive and subsequent immobilisation of the additive by cross-linking with a specified density.

The choice of the method for the formation of functionalised monolayers and LBF depends on the purpose of the two-dimensional system being formed. Modern macromolecular chemistry and molecular design have given rise to virtually unlimited possibilities for the construction of stable heteromolecular structures based on polymers.

Following the chosen chemical principle for the arrangement of polymers in groups, it is useful to begin the discussion with the traditional thoroughly investigated polymers of the acrylic and methacrylic series.

VI. Polyacrylates and polymethacrylates

1. Monolayers and Langmuir – Blodgett films based on homopolymers

The widely investigated acrylic and methacrylic polymers make it possible to follow the influence of the structure and composition of the main and side chains of the macromolecules on the properties of their monolayers. The base polymer is undoubtedly poly(methyl methacrylate) (PMMA). The increased interest in this polymer during recent years is due to its use as a positive electron-beam resist in the traditional technology for the deposition of a polymer solution onto a support.[74] The increase in the sensitivity and resolution of elements consisting of PMMA and its copolymers can be achieved by their deposition onto a solid support by the Langmuir – Blodgett method.[75]

The compression isotherms of monolayers of PMMA stereoisomers[76] are illustrated in Fig. 4, while Table 1 presents the molecular masses and limiting areas of the PMMA monolayers obtained by different workers. Evidently, in the formation of a true equilibrium monolayer, the differences between the polymer solution concentrations employed, the solvents, and the rates of compression should not have influenced quite so much the values of A_0. For monolayers of low-molecular-mass compounds (for example, aliphatic acids), it is difficult to imagine the existence of such discrepancies in the measurements of the limiting area. However, for small molecules the problems of stereoregularity, which are extremely important (as can be seen from Fig. 4) for the position of the compression isotherm, are manifested in a different way. Furthermore, the steric hindrance due to the chain structure of the polymers apparently precludes the complete assumption by the PMMA elementary units of the *cis*-conformation of the methoxycarbonyl groups most favourable for the formation of the monolayer (Fig. 5). It follows from the study of Labbauf and Zack[80] that the *cis*-form of the PMMA elementary unit gives rise to larger limiting areas than the *trans*-form. The experimental facts indicating the incomplete spreading of PMMA in a monolayer on the surface of water can apparently be explained[31]

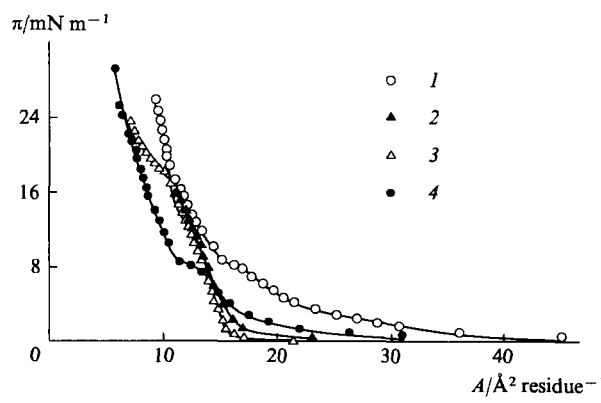


Figure 4. Surface pressure – area isotherms for monolayers of stereoisomers of poly(methyl methacrylate):[76] (*1*) isotactic; (*2*) atactic; (*3*) syndiotactic; (*4*) stereoblock (isotactic + syndiotactic).

Table 1. The limiting areas (A_0) of poly(methyl methacrylate) monolayers for different molecular masses of the polymer.

Molecular mass	A_0/Å² residue⁻¹	Ref.
–	14.5	25
25000	16.1	62
110000	16.1	62
640000	18.2	62
> 1000000	18.1	62
153000	17.6	77
90000	17.0	78
480000	16.4	79
76000	14.5[a]	33
32600	13.8[a]	33
30500	15.2[a]	33
200000	18.0	27
188000	15.6	75
139000	18.4	80
340000	15.8	81
71000	17.0	82
500000	17.0	82
265000	19.4	82
490000	17.7	83
56000	18.7	84
155000	18.7	84
–	16.0	30
–	20.0	85

[a] Calculated with the aid of $\pi - A$ relations quoted by Parker and Shereshefsky.[33]



Figure 5. Isomers of the ester groups of poly(methyl methacrylate): (*a*) *trans*-; (*b*) *cis*-.[80]

by the high cohesion between the main chains of the polymer. Naturally in this case it is extremely difficult to seek a relation between the molecular mass of the polymer and the limiting area of the monolayer. Such behaviour of the PMMA monolayers is not general: for other polymers forming true monolayers, there is good agreement between the experimental compression isotherms obtained by different workers.

The replacement of the methyl group in the main chain by a hydrogen atom, i.e. the transition from methacrylic to acrylic polymers, increases sharply the ability of the polymer to form a true monolayer.

More extensive possibilities for controlling the structure of the monolayer and for introducing into the latter functionally significant fragments are associated with the alteration of the side groups of the polymers under consideration. The simplest example is provided by the increase in the length of the chain of the ester alkyl group in poly(alkyl methacrylates). As can be seen from Fig. 6, the replacement of the methyl group by the ethyl group in the side chain of the polymer greatly diminishes the cohesion between the main chains of macromolecules and leads to the expansion of the monolayer. Further increase in chain length and temperature[86] steadily increases the limiting areas and intensifies

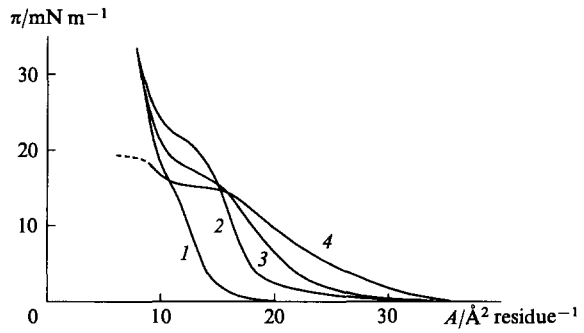


Figure 6. Surface pressure–area isotherms for monolayers of poly(alkyl methacrylates).[25] Alkyl: (*1*) methyl; (*2*) ethyl; (*3*) n-propyl; (*4*) n-butyl.

the tendency to form a plateau on the compression isotherms. Small side chains are incapable of interacting with adequate intensity and their role reduces to separating the main chains and lowering their cohesion. On the other hand, long hydrocarbon chains (C_{18}) impart a high rigidity to the condensed monolayer.[25]

The great interest in the study of poly(octadecyl acrylate) (PODA) and poly(octadecyl methacrylate) (PODMA) in monolayers[25,85–99] is caused, on the one hand, by the polymeric nature of these compounds and, on the other, by the presence of long hydrocarbon chains, which makes it possible to regard each elementary unit of the polymer as a classical diphilic surface-active low-molecular-mass substance. The discrepancies between the compression isotherms obtained by different workers for these polymers have been analysed.[90] It was postulated that these differences are caused by the type of solvent from which the monolayers were formed, the purity of the polymer, its molecular mass and/or its polydispersity, and the method used to obtain the compression isotherms. It has been shown that the discrepancies between the data of different workers are due mainly to methodological causes, i.e. the conditions under which the $\pi-A$ isotherms were obtained. It must be emphasised that the differences may be induced also by the crystallisation of the side chains of the polymer, which apparently begins from the hexadecyl members of this series.[86] An increase in temperature to 12 °C for poly(hexadecyl methacrylate) and to 29 °C for PODMA converts the solid polymer monolayers into liquid ones.[86]

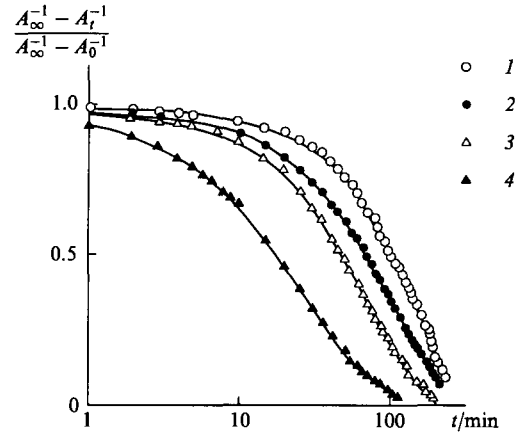
The crystallisation of PODMA in the monolayer at different temperatures and surface pressures has been investigated.[98] It has been shown that the crystallisation kinetics may be described with the aid of the Avrami equation:[100]

$$-\ln\frac{A_\infty^{-1}-A_t^{-1}}{A_\infty^{-1}-A_0^{-1}}=kt^n,$$

where A_0, A_t and A_∞ are the areas per monomer unit at times 0, t, and ∞, n is a constant characterising the mechanism of the formation of the nuclei and the type of the growing structures, and k is the rate constant of the process.

Using these constants as adjustable parameters, a good agreement was obtained between theory and experiment. Fig. 7 shows that the crystallisation process proceeds at low surface pressures and is completed in the course of 2 h. Crystallisation disturbs the equilibrium nature of the monolayer, which is manifested by the hysteresis of the compression isotherms.

The possibility of crystallisation must be taken into account in the study of the kinetics of two-dimensional polymerisation accompanied by the shrinking of the monolayer. This question has been examined[92] in the analysis of the polymerisation of octadecyl methacrylate (ODMA). The same communication contains interesting data concerning the compatibility of ODMA and PODMA monolayers. Fig. 8 presents the dependence of the



Symbols	π/mN m⁻¹	n	ln k (min⁻¹)
1	1.3	1.30	−6.40
2	1.9	1.20	−5.27
3	2.5	1.15	−5.01
4	3.2	1.00	−3.27

Figure 7. Dependence of $(A_\infty^{-1}-A_t^{-1})/(A_\infty^{-1}-A_0^{-1})$ on t for a PODMA monolayer at 30 °C.[98] Curves — theory; symbols — experiment.

average area of a mixed monomer and polymer monolayer on composition for different surface pressures. The shaded regions correspond to the crystallisation of the side chains, the upper contour of these regions corresponding to the area of the monolayer before crystallisation and the lower contour corresponding to the area after the completion of crystallisation. Crystallisation must be taken into account at low surface pressures and for degrees of conversion of the monomer exceeding 50%.

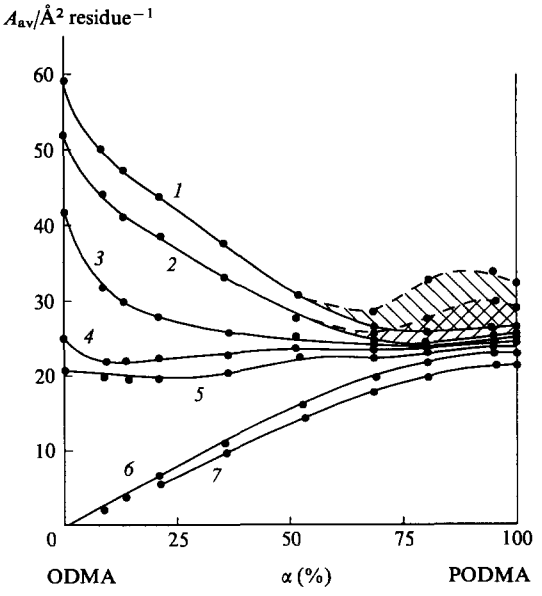


Figure 8. Dependence of the average area (A_{av}) per monomer residue on the polymer content (α = degree of conversion) in a mixed ODMA/PODMA monolayer at T = 27 °C and different surface pressures (mN m⁻¹): (*1*) 0.5; (*2*) 2.0; (*3*) 4.0; (*4*) 7.0; (*5*) 13.0; (*6*) 30.0; (*7*) 40.0. The cross-hatched regions correspond to the crystallisation of the side chains.[92]

Despite the major role of secondary cohesion, manifested for long-chain poly(alkyl methacrylate) in the crystallisation of side chains, the influence of the structure of the main chain of the polymer also persists. As can be seen from Fig. 9, the PODA monolayer is more condensed than the monolayer of its methacrylic analogue, i.e. the absence of methyl groups attached to the main chain in the first polymer diminishes the steric hindrance to its conformational rotation.[87]

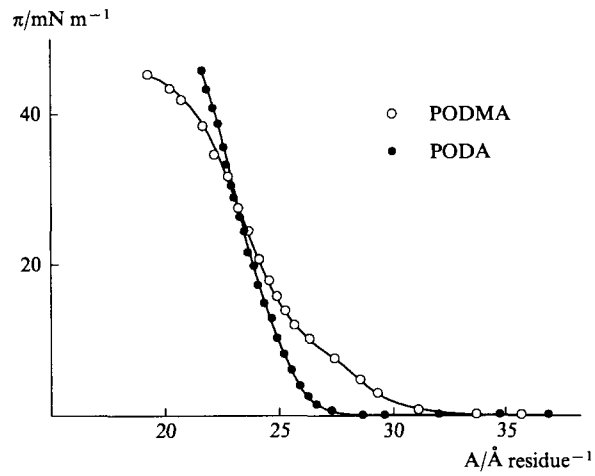


Figure 9. Surface pressure – area isotherms for PODA (M_w = 23 300, M_n = 13 000) and PODMA (M_w = 321 000, and M_n = 97 200) monolayers.[87]

These data agree with the results of the measurement of the resistance to the evaporation of water (r) through PODMA and PODA monolayers:[90] the values of r for the PODA monolayer are several times higher than for PODMA but are an order of magnitude lower than for octadecanol. Evidently, the high rigidity of the polymer chain prevents the close packing of the hydrocarbon chains in the monolayer. The introduction of a small amount of octadecanol into the polymer monolayer makes it possible to attain the level of r values characteristic of a pure octadecanol monolayer.[90]

The orientation of the side chains in LBF based on PODA and PODMA has been investigated[87,88] by polarisation IR spectroscopy in the transmission and glancing incidence versions. It has been shown[87] that an orientation of the hydro-carbon side chains almost perpendicular to the surface of the support occurs in mono- and multi-layer LBF of the Z type for both monomers. It has also been noted that their orientation depends on the type of the main polymer chain and the surface pressure at which the monolayers have been transferred. However, it has been found[88] that the orientation of the PODMA side chains in the monolayer LBF differs significantly from the perpendicular orientation of these groups in the multilayer LBF.

The introduction of aromatic substituents into the side chain of a methacrylic polymer [poly(phenyl methacrylate) and poly(benzyl methacrylate)],[101,102] leads to the formation of a condensed monolayer with small limiting areas. Although the authors themselves[101,102] have assigned the monolayers of these homopolymers to the expanded type, nevertheless the low values of A_0 and the temperature dependence of the surface pressure characteristic of a collapsed monolayer indicate the absence of true spreading.

Thus, among the investigated methacrylic homopolymers substituted most simply in the side chains, the most stable monolayers are formed by homopolymers which contain moderately and very long aliphatic side chains. We shall consider in greater detail the properties of one of them — poly(isobutyl methacrylate) (PIBMA), which forms true monolayers and high-quality LBF. It has been shown[103] that the compression isotherm for this polymer has a point of inflection at A = 19 Å^2 per monomer residue (the calculated A_0 is 20–21 Å^2 per residue), after which the monolayer collapses according to X-ray diffraction data. The linearity of the $\pi - A$ relation for $\pi < 0.5$ mN m^{-1} made it possible to determine the molecular mass of the polymer, which was found to be close to the value determined viscometrically for the PIBMA bulk-phase solution (1.7×10^5 and 2.3×10^5 respectively). There are interesting data, obtained by Naito,[103] concerning the influence of the hydrophobic properties of the surface of the solid support on the degree of transfer of the monolayer (ρ) onto the latter (the vertical method). Fig. 10 presents the dependence of ρ on the wetting angle (θ) for water on the surface of silicon. The degree of wetting was changed by varying the time of the preliminary treatment of the surface of silicon in hexamethyldisilazane. Fig. 10 shows that $\rho = 1$ for $0° < \theta < 90°$ as the support moves upwards from the aqueous subphase, while for the opposite direction of motion we have $\rho = 1$ for $\theta > 73°$. This angle corresponds to θ for water on both types of surfaces of the transferred polymer LBF. Fig. 11 illustrates the dependence of the degree of transfer on the number of LBF pairs for two silicon supports with $\theta = 65°$ and 100°. The first layer was deposited by immersing the support in the subphase. It is seen that ρ is close to 1 for a support with $\theta = 100°$. Supports with $\theta = 65°$ exhibit a considerable scatter in the values of ρ, i.e. the first monolayer exerts a significant influence on the formation of the subsequent layers. We may note two features of LBF made up PIBMA:[103] the absence of defects in the LBF (scanning electron microscopy, magnification 5×10^4) and the suppression of cadmium stearate recrystallisation processes in alternating LBF containing ten internal monolayers of the above low-molecular-mass surfactant and three outer PIBMA monolayers.

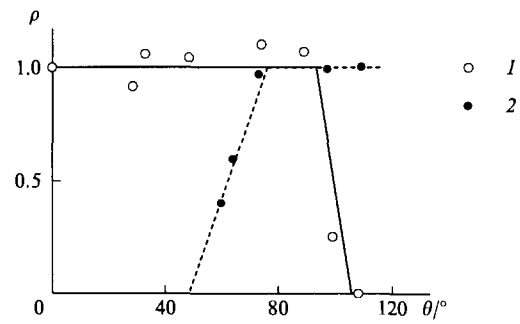


Figure 10. Dependence of the degree of transfer of the PIBMA monolayer on the wettability of the silicon surface which has been rendered hydrophobic.[103] Surface pressure in the transfer process 12.5 mN m^{-1}. Direction of motion of the support: (*1*) upwards; (*2*) downwards.

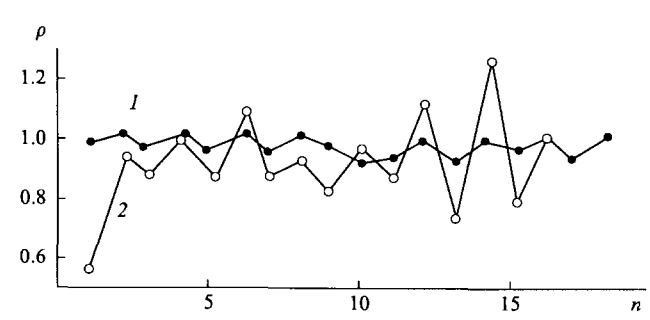


Figure 11. Dependence of the degree of transfer of the PIBMA monolayer onto silicon supports rendered hydrophobic to different extents on the number of layers.[103] Wetting angle for water: (*1*) 100°; (*2*) 65°.

Multilayer PIBMA LBF with a thickness up to 200 Å have also been investigated [104] and the extent of their defectiveness was analysed by the method involving electrolytic decoration with copper. In full agreement with Naito's data, [103] Matsuda et al. [104] showed that the LBF made up of four monolayers (42 Å) is homogeneous and has a lower density of defects (pin holes) than the analogous cadmium arachidate LBF.

More complex heterostructures containing PIBMA have been obtained: [105] (1) LBF made up of alternating PIBMA and heptacosa-10,12-diynoic or arachidic acid monolayers (altogether 20 heterolayers); (2) LBF made up of alternating units comprising one acid layer and three PIBMA layers (altogether 20 heterolayers); (3) LBF consisting of alternating PIBMA and acid bilayers (altogether 10 heterolayers). LBF of the Z type (relative to the acids) were formed in the first two cases, whilst in the third Y type LBF were produced. It was shown that, in the LBF of the first type, one polymer layer does not prevent its rearrangement and penetration by acid molecules. The diffusion of acid molecules is suppressed with increase in the number of PIBMA layers (the second type of the LBF structure). Nevertheless the authors [105] concluded that, in order to obtain more perfect heterostructures with a higher stability as a function of time, it is necessary to employ a polymer which is more rigid than PIBMA.

2. Monolayers and Langmuir – Blodgett films based on copolymers

The presence of substituents in each monomer unit of acrylic and methacrylic homopolymers creates definite difficulties in the formation of highly organised monolayers and LBF. [89] One of the ways of solving this problem involves the introduction of a hydrophilic spacer, which separates the side and main chains. It has been shown [106, 107] in relation to double-stranded methacrylic lipids that the introduction of a spacer leads to the formation of stable monolayers, the collapse pressure and the limiting area of which are close to the corresponding parameters for the monomeric lipid.

Another procedure, leading to an increase in the stability of polymer monolayers, involves the inclusion of a hydrophilic spacer in the main chain. A procedure such as hydrolysis of poly(n-butyl acrylate) to different extents has been used for this purpose. [108] Table 2 shows that, with increase in the degree of hydrolysis, the limiting area of the monolayer diminishes owing to the displacement of polar acid groups from the surface to the subphase. However, the presence of polar groups makes it possible to regulate the structure of the monolayer by varying the pH and by introducing an electrolyte into the subphase. According to the data in Table 2, an increase in the sodium chloride concentration in the aqueous subphase leads to the return of the acid groups to the surface and hence to an increase in the limiting areas, the theoretical and experimental values of A_0 being virtually identical for a 15% NaCl concentration.

Table 2. The limiting areas of poly(n-butyl acrylate) (PBA) monolayers for different degrees of hydrolysis of the polymer and different sodium chloride concentrations in the subphase. [108]

Degree of hydrolysis (%)	A_0/Å^2 residue^{-1}				
	Water	5% NaCl	10% NaCl	15% NaCl	Theoretical value
0	29.5	–	–	–	29.3
28	19.5	23.8	26.4	27.3	27.2
36	17.5	22.5	25.7	26.8	26.7
45	16.5	20.8	24.2	25.7	25.9
53	16.0	20.4	23.9	25.3	25.4

Studies of copolymer monolayers have just as long a history as those of homopolymer monolayers. As in the case of traditional investigations of copolymers in bulk and in solution, the main problem remains the elucidation of the influence of the ratio of the monomer residues constituting the copolymer on the characteristics of the systems considered — in the given instance two-dimensional systems. The properties of monolayers comprising copolymers and mixtures of the corresponding homopolymers have been compared in a number of studies. Attention was concentrated in these investigations (most of which were carried out during the period preceding the active study of LBF) on the phase behaviour of the systems. Recently much attention began to be devoted to the possibility of obtaining LBF from monolayers of copolymers (including block copolymers) and mixed monolayers. Mixed polymer monolayers and especially copolymer monolayers with low-molecular-mass surfactants are of great practical importance, since, compared with monolayers and LBF made up of copolymers and mixed polymer monolayers, they facilitate the introduction of functional additives and the regulation of the properties of the two-dimensional systems.

Hitherto these problems have been most fully investigated for methacrylic and acrylic copolymer monolayers containing side chains with different numbers of carbon atoms. Copolymers of methyl and hexadecyl acrylates, [109] butyl and dodecyl methacrylates, [110] octadecyl and dodecyl methacrylates, [111, 112] butyl and octadecyl methacrylates, [91] and methacrylic acid and methyl acrylate, [113] as well as diblock copolymers of PMMA and polyvinyl(4-pyridinium) bromide [114] have been investigated. Vigorous studies on monolayers have been carried out for copolymers containing double-stranded elementary units or spacers of different composition in the main chain. [106, 107, 115–117]

The properties of monolayers comprising copolymers and mixtures of the homopolymers of octadecyl methacrylate (PODMA) and butyl methacrylate (PBMA) examined above have been investigated. [91] Figs 12 and 13 illustrate the dependence of the surface pressure, corresponding to three characteristic points on the compression isotherms for the copolymers and mixtures, and of the limiting area of the monolayer on its composition. The PBMA monolayer of the liquid-condensed type has two singular points corresponding to a phase transition (14.3 mN m^{-1}) and collapse (16.7 mN m^{-1}), while the PODMA monolayer of the solid-condensed type has a single singular point at 52.6 mN m^{-1} corresponding to collapse. All three singular points are present on the isotherms for the mixed monolayers containing between 30 and 70 mol.% of PODMA. On the basis of Crisp's phase rule for mixed mono-layers (the two components are compatible in the monolayer if π at the singular point varies with composition and conversely), it was concluded [91] that, for a 70% PODMA content, the homopolymers are incompatible. The compression isotherms for copolymer monolayers have a single singular point (collapse) and, for PODMA contents in the copolymer molecule up to 60%, the monolayer remains in the liquid-condensed state. The transition of the copolymer monolayer from the liquid to the solid state can be detected also on the dependence of the limiting area of the monolayer on composition (Fig. 13), which exhibits a sharp jump towards lower values of A_0 for a 70% content of PODMA. It follows from Fig. 13 that three compatibility regions are characteristic of the mixed monolayers: for low contents of PODMA (low surface pressure) and PBMA (high surface pressure), the components are compatible, whereas in the middle range of compositions the polymers are incompatible in the monolayer.

The properties of monolayers of dodecyl methacrylate–octadecyl methacrylate copolymers and the corresponding mixed homopolymer monolayers have been compared. [111–113] As for other combinations of the monomers, (C_4 and C_{18}) [91] and (C_{14} and C_{16}), [109] an increase in the content of the long-chain fragment (C_{18}) in the copolymer leads to the formation of a more condensed monolayer: the collapse pressure increases, the singular points vanish, and the compressibility diminishes.

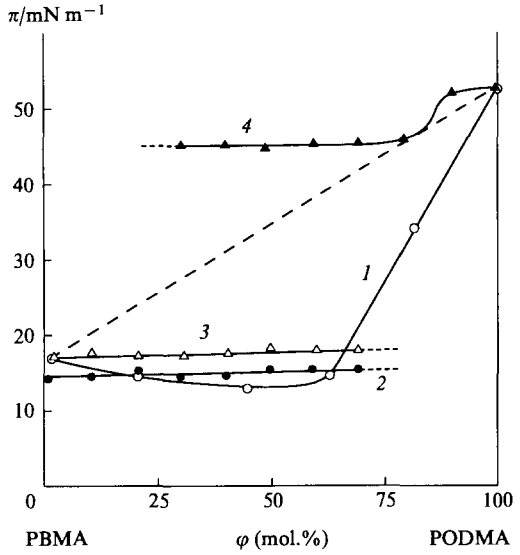


Figure 12. Dependence of the surface pressure at the characteristic points on the compression isotherms on the ratio of PODMA and PBMA in the copolymers (curve *1*) and the mixtures (curves *2*–*4*).[91]

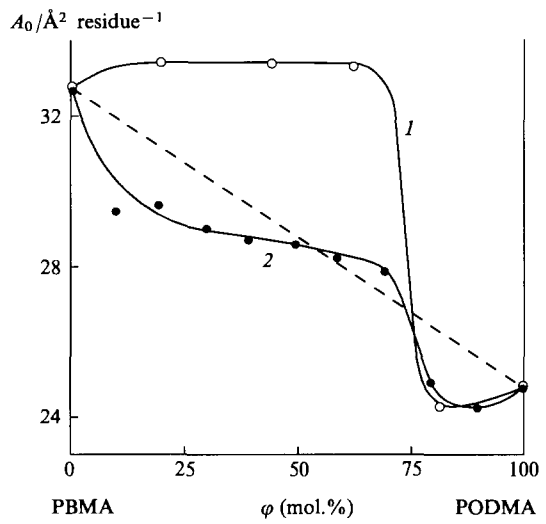


Figure 13. Dependence of the limiting areas (A_0) of the monolayers comprising the copolymers (curve *1*) and mixtures of the PODMA and PBMA homopolymers (curve *2*) on their ratio in the mixture.[91]

Consequently, by increasing the fraction of the long-chain fragment in the copolymer, it is possible to achieve a transition from the liquid to the solid state of the monolayer. The reverse transition, leading admittedly to disequilibrium in the monolayer, is achieved by increasing the temperature. For methacrylic copolymers containing C_{12} and C_{18} hydrocarbon groups in the side chain, such transitions occur in the temperature range 20–39 °C. Table 3 presents the conditions for the formation of liquid-condensed monolayers of poly(alkyl methacrylates) (homopolymers, copolymers, and mixtures). It is of interest to note that, on formation of the liquid state, the average length of the hydrocarbon side chain in the copolymer (copolymers *d*, C ⩽ 14.2) at 20 °C is the same as the number of carbon atoms in the side chain of the homopolymer (homopolymer *a*) at the same temperature. For a mixture of homopolymers, the transition to the liquid state occurs for a smaller average length of the side chain (mixture *f*, C ⩽ 12.6). Mixtures form more stable monolayers than the individual phases of the homopolymers, each of which may contain a small amount of another phase.[112]

Table 3. Conditions in the formation of liquid-condensed monolayers of poly(n-alkyl methacrylates).[112]

Monolayer	Average number of carbon atoms in alkyl group	Transition temperature/°C
Homopolymer		
a	⩽14	20
b	⩽16	35
c	⩽18	39
Copolymer (C_{12} + C_{18})		
d	⩽14.2 (⩽36% ODMA)	20
e	–[a]	35
Mixture of C_{12} and C_{18}		
f	⩽12.6 (⩽10% ODMA)	20
g	⩽13.2 (⩽20% ODMA)	35
h	–[a]	39

[a] Almost all the polymers form liquid-condensed monolayers.

The influence of the composition of the subphase on the properties of the monolayers and LBF of the 1 : 1 methacrylic acid – methyl acrylate copolymer has been investigated.[113] On the surface of pure water, this copolymer does not form a stable monolayer. The introduction of Cd^{2+} ions into the support improves its stability. The solid monolayer of the copolymer on the surface of an aqueous solution containing La^{3+} ions at pH 6.89 has the highest stability. When the copolymer monolayers are transferred to the hydrophilic surface of glass from the Langmuir trough by the usual vertical method, the dependence of the degree of transfer (ρ) on the number of cycles has the form illustrated in Fig. 14*a*. Evidently a Z type transfer takes place, the degree of transfer increasing with increase in the number of layers. In order to obtain higher-quality LBF from the copolymer, the authors[113] used a Langmuir trough with moving walls. This made

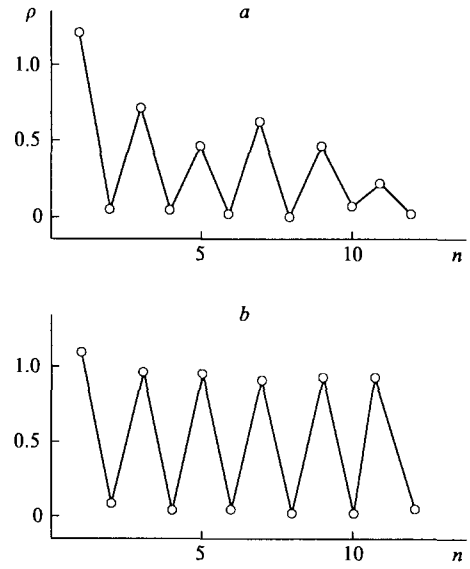


Figure 14. Dependence of the degree of transfer (ρ) on the number of cycles for the methacrylic acid – methyl acrylate copolymer LBF:[113] (*a*) usual Langmuir trough; (*b*) Langmuir trough with moving walls.

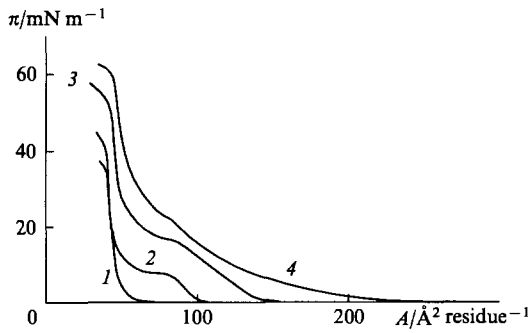
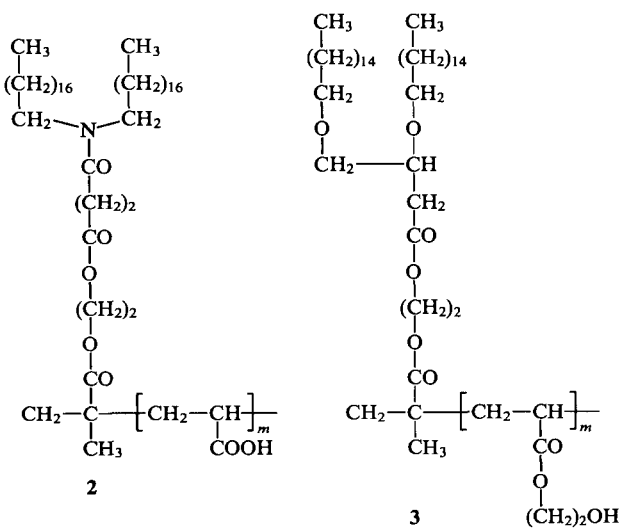


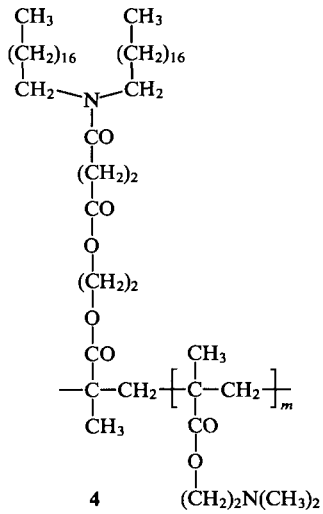
Figure 15. Surface pressure–area isotherms for the homopolymer (curve *1*, $m = 0$) and the copolymers **2** with different spacer: substituted residue ratios (m): (*2*) 1; (*3*) 5; (*4*) 10.[115]

it possible to improve significantly the quality of the LBF whilst retaining the Z type of transfer (Fig. 14*b*). This conclusion is confirmed by the measurements of the wetting angles (θ) for water after each passage of the support through the monolayer: θ for water does not change for two opposed directions of motion of the support. The values of $\cos\theta$ for LBF were lower than for coatings obtained from a solution on a rotating support. This indicates a definite preferred orientation of the elementary units of the copolymer in the LBF. It was shown by IR Fourier spectroscopy and X-ray diffraction that the La^{3+} ion-stabilised LBF comprising the copolymer, which does not possess long-chain side chains, has a layered structure with a monolayer thickness of 8.4 Å. The formation of LBF from cross-linked two-dimensional networks gives rise to hope for an improvement of their thermal and mechanical stabilities.

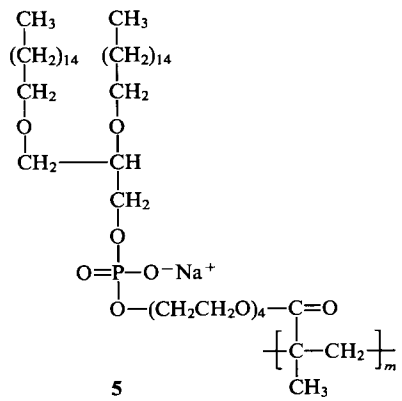
The influence of the hydrophilic spacer on the behaviour of monolayers of copolymers of double-stranded lipids with acrylic acid (**2**) and with hydroxyethyl acrylate (**3**) has been investigated.[106,107,115–117] Fig. 15 presents the $\pi-A$ relations for the 2-(3-dioctadecylcarbamoylpropionyloxy)ethyl methacrylate–acrylic acid copolymer **2** with different contents of a hydrophilic spacer in the main chain (m is the number of elementary units of the spacer per substituted monomer residue). Evidently, with increase in m, the monolayers expand and the pressure corresponding to the phase transition from the liquid to the solid state of the monolayer increases. With increase in the content of unsubstituted acrylic acid residues in the copolymer, the phase transition temperature falls. X-Ray diffraction analysis of 30-layer LBF made up of copolymer **2** showed[115] that the intensity of the diffraction peaks increases with increase in m, whilst their width diminishes. The repeat period increases from 40.8 Å for the homopolymer to 59.5 Å for the copolymer with $m = 5$ and then decreases to 55.9 Å for the copolymer with $m = 10$. When the fraction of acrylic acid in the copolymer is too high, it becomes impossible to obtain LBF. The thermal stability of LBF rises with increase in m: the multilayer structure of copolymer **2** breaks down at 40 °C for $m = 1$, at 70 °C for $m = 5$, and at temperatures exceeding 120 °C for $m = 10$. The acrylic acid residues in the copolymer play a dual role. Functioning as hydrophilic spacers, they increase the mobility and the degree of order in the long-chain components of the copolymer. At the same time, the thermal stability increases by virtue of the formation of hydrogen bonds. Evidently these characteristics may be controlled by introducing electrolytes into the support or by changing its pH. Similar results have been obtained[107] for copolymer **3**.



The possibility of the practical employment of LBF based on copolymer **4**, containing a double-stranded spacer and a double-stranded monomer in proportions of 5 : 1, as a selective gas membrane has been examined.[118–120] The LBF of this copolymer with a thickness up to 60 monolayers were formed on a porous polymer support and its permeability to CH_4, N_2, CO_2, and H_2S was investigated at different temperatures. It was established that the membrane is selective with respect to H_2S and CO_2 relative to N_2 and CH_4, the selectivity increasing on heating above 35 °C. The rise in selectivity with temperature was explained by the disordering of the hydrocarbon side chains of the copolymer, which was detected by reflection-adsorption IR spectroscopy. The possibility of the chemical interaction of gaseous H_2S and CO_2 with the copolymer constituting the LBF plays an important role in the variation of the selectivity of such membranes.

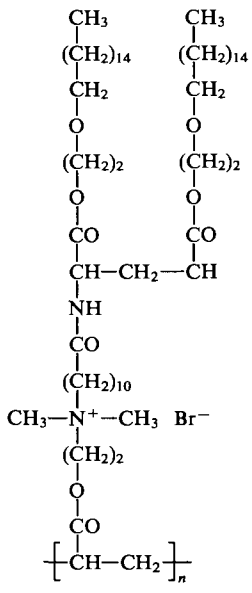


Asymmetric membranes have been formed[121] on the surfaces of porous polytetrafluoroethylene supports in the form of LBF of copolymer **2** ($m = 5$) and homopolymer **5**. The influence of heat treatment on the structure and properties of the membranes was investigated by IR Fourier spectroscopy, both in transmission and in reflection at glancing incidence, and also by high-resolution scanning electron microscopy. It was established that heat treatment of the LBF (20 and 30 monolayers) below the melting points of the block copolymers leads merely to an insignificant disordering of the alkyl chains ($2C_{18}$ and $2C_{16}$) and to the disappearance of a large number of macroscopic defects. The dependence of the permeability of the heat-treated membranes on the size of the penetrant molecules led Stroeve et al.[122] to the conclusion that microdefects are retained in the LBF after heat treatment. Heating of the LBF above the melting point of the block copolymers disturbs the order in the layers and leads to the appearance of cavities and to the flow of the polymer within the pores.



5

LBF based on double-stranded ammonium derivatives of the polyacrylic acid **6** have found an interesting application [123] in studies on surface forces, which had been carried out earlier [124–126] mainly using LBF made up of low-molecular-mass surfactants.



6

The monolayer of compound **6** was transferred onto a solid hydrophilic support (mica) the latter moving from the air into the aqueous phase. The relations between the reduced attractive force (F/R; R is the radius of curvature of the surface of mica) and the distance (D) between the two surfaces of mica coated by a monolayer of compound **6** are presented in Fig. 16 for three liquid media. It is seen from the figure that the attractive force between the surfaces and pure water extends over a distance up to 3000 Å and that the surfaces merge for $D \simeq 760$ Å. Their separation requires an adhesive (breaking away) force of 280 mN m^{-1}, which is characteristic of hydrophobic surfaces. [127] It has been noted [123] that these forces differ from the long-range electrostatic repulsive forces and van der Waals attractive forces ($D \leqslant 30$ Å; force required to break adhesion 55 mN m^{-1}), which arise between unmodified negatively charged mica surfaces. [128] The formation of a stable monolayer on the surface of mica, achieved by an unusual transfer procedure (downwards onto a hydrophilic support), is due to the electrostatic interaction between the cationic polymer and the negatively charged mica surface. The upward movement of the support through the air/water interface leads to the formation of a less stable monolayer.

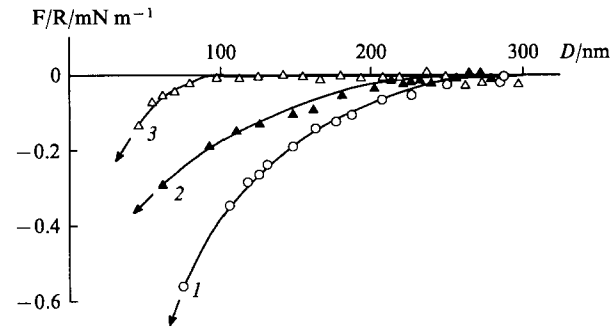


Figure 16. Dependence of the reduced attractive force on the distance between the surfaces of mica with monolayer LBF comprising polymer **6**. [123] Medium: (*1*) pure water; (*2*) 0.01 M NaBr solution; (*3*) 0.1 M NaBr solution.

Fig. 17 illustrates the influence of pH on the compression isotherms and on the $F/R-D$ relations for a monolayer of a derivative of the methacrylic acid oligomer **7**. The monolayer was deposited onto a mica surface which had been rendered hydrophobic. In a neutral aqueous medium, long-range repulsive forces are manifested ($D \sim 3000$ Å), increasing markedly with increase in pH (Fig. 17*b*). At low pH, repulsion occurs only over short distances $D \simeq 600$ Å, which is due to the influence of the degree of ionisation of the acid groups on the conformation of the macromolecules (at a high degree of ionisation, the extended conformation of macromolecules obtains). It is of interest to note that, when the mica surfaces coated by a monolayer of compound **7** approach one another, the repulsion increases gradually and not sharply, in contrast to pure mica. This has been explained by a change in the conformation of the chains and the recombination of charges. [128]

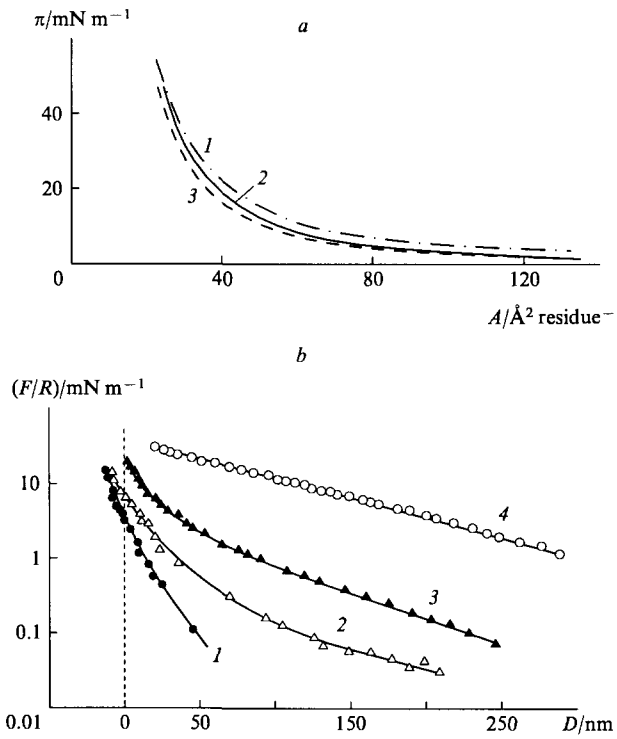
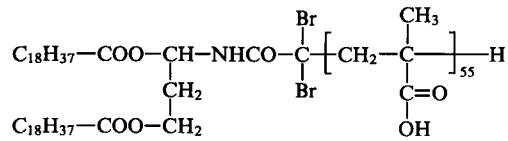


Figure 17. The influence of pH on the compression isotherms (*a*) and on the $F/R-D$ relations (*b*) for a monolayer comprising the oligomethacrylic acid derivative **7**: [123] (*a*) pH 3.1 (curve *1*), 5.6 (curve *2*), and 8.1 (curve *3*); (*b*) pH 3.5 (curve *1*), 4.6 (curve *2*), 5.6 (curve *3*), and 8.2 (curve *4*).



7

Thus the study of the surface forces acting between solid surfaces on which LBF have been deposited makes it possible to determine the quality of the LBF, the orientation of the molecule, and the interaction between them, i.e. to characterise quite fully the functionalised organic surfaces.

Gaines[30] formed homogeneous LBF from a homopolymer—syndiotactic PMMA—on the hydrophobic silicon surface. The dependence of the thickness of the LBF, measured ellipsometrically, on the number of transfer cycles is illustrated in Fig. 18. Evidently there is a linear relation between these parameters. The specific surface of a single monolayer, found ellipsometrically and on the basis of compression isotherms, was respectively 9.1 and 10.9 Å. Y type LBF have also been formed from PMMA on the surface of hydrophilic chromium films.[75] The thickness of 17-layer LBF, measured ellipsometrically, was 143 Å, i.e. 8.5 Å per monolayer. A test of this LBF as a positive electron-beam resist showed that the surface density of pin holes in the PMMA LBF was three orders of magnitude lower than in the film of the same thickness obtained from a solution of the polymer on a rotating support.

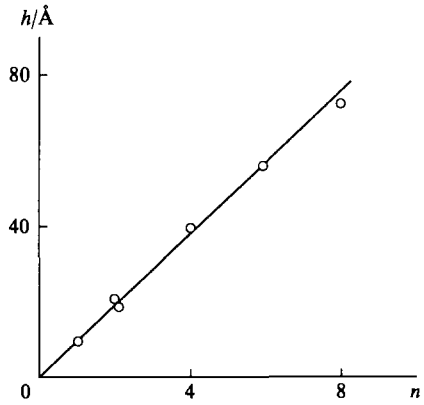


Figure 18. Dependence of the thickness of a syndiotactic PMMA film, deposited on a hydrophobic silicon surface at a surface pressure of 10 mN m^{-1}, on the number of transfer cycles.[30]

Acrylic and methacrylic polymers, into the side chains of which functional-group substituents have been introduced, have come to be widely used recently in the study of nonlinear optical (NLO) effects. A strategy for the creation of new NLO systems has been described.[129] It reduces, firstly, to the exclusive employment of monomeric objects and, secondly, to the introduction of perfluorocarbon groups, which ensure more marked hydrophobic properties for a shorter chain compared with hydrocarbon analogues. The influence of the number of bilayers formed by polymers **8** and **9** on the generation of the second optical harmonic was investigated.[129] Fig. 19 illustrates the dependence of the amplitude of the second harmonic (proportional to the square root of the intensity) on the number of bilayers (N) in the LBF comprising derivatives of acrylic (**8**) and oxazoline (**9**) polymers. Evidently the linearity of the relation is retained up to $N = 40$. The comparative decrease in the signal at $N > 40$ indicates the disturbance of the polar structure with increase in the number of layers. This effect may be associated with the fact that the LBF were obtained using two procedures: initially the first 40 layers and then, after several hours, the remaining layers.

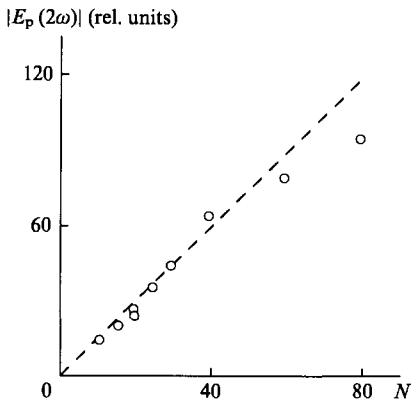
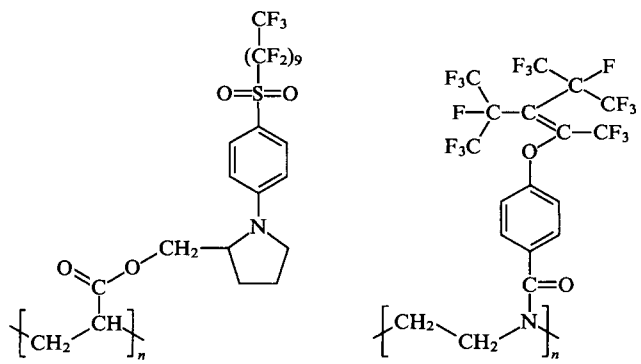


Figure 19. Dependence of the amplitude of the second harmonic on the number of LBF bilayers.[129] The dashed line represents the linear fit to the relaiton for $N \leqslant 40$.



8 9

Fig. 20 illustrates the high stability of the polymer LBF, confirming the usefulness of the strategy selected by the authors.

The synthesis of polymethacrylates containing NLO-active fragments in the side chains has been described[130] and the results of studies on second harmonic generation with the LBF of a polymethacrylate derivative have been presented.[131] It has been shown that the formation of LBF from mixed monolayers of polymer **10** and stearic acid hardly alters the orientation of the side chains: according to polarisation UV spectroscopic data, the angle of inclination of the side chains relative to the support in the LBF of polymer **10** is 30° and in that made up of a mixture of polymer **10** and the aliphatic acid is 25°.

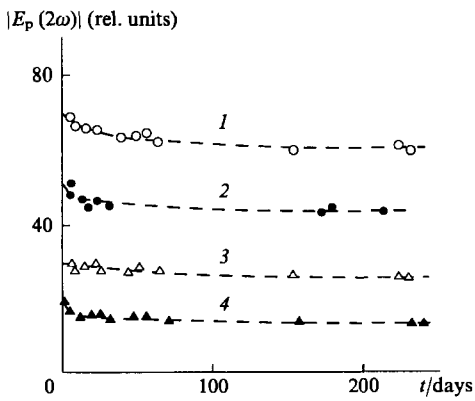
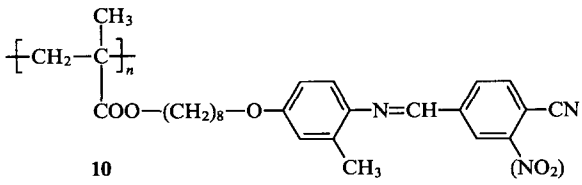
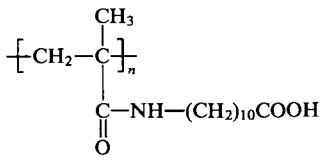


Figure 20. Dependence of the amplitude of the second harmonic on the LBF ageing time for specimens consisting of different numbers of bilayers:[129] (*1*) 40; (*2*) 30; (*3*) 20; (*4*) 10.



10

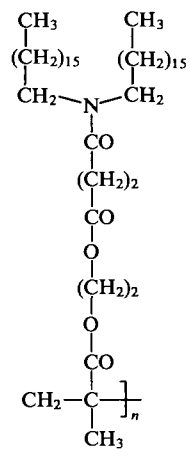
A similarity of the angles of chain inclination (36°) has been found [132] for the methacrylate derivatives **11** photopolymerised in the LBF. The authors note that this procedure is promising for the formation of LBF for NLO studies and applications.



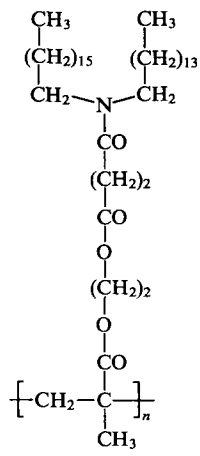
11

The employment of methacrylic polymers **12**–**15** with different configurations and compositions of the side chains for optical waveguides has been described. [133]

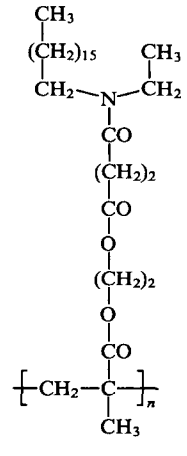
In the series of polymers presented above, the capacity for the formation of liquid monolayers increases from compound **12** to compound **15**. 500-Layer LBF (thickness 0.8 μm) have been obtained from polymer **14**. It was observed that the waveguides based on them suffer very low losses (2 dB cm^{-1} for wavelengths of 633 and 785 nm) by virtue of the low degree of order in the side chains, preventing the formation of light scattering domains.



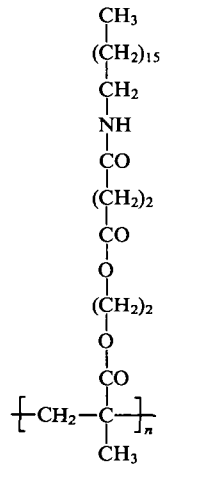
12



13



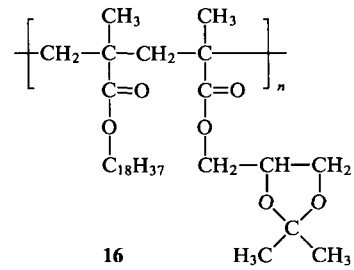
14



15

The low stability of LBF of low-molecular-mass compounds at elevated temperatures and *in vacuo*, the mutual diffusion of molecules belonging to different layers of the LBF, [134–137] and finally the possibility of the loss of the low-molecular-mass component from the monolayers (constituting the LBF) mixed with the polymer are all factors which have stimulated studies on high-molecular-mass multilayer, including alternating, structures.

The insulating properties and stability of LBF of stearic acid and the methacrylic copolymer **16**, deposited on the surface of silver, have been investigated [138] by the time-of-flight mass spectrometry of secondary ions.



16

Fig. 21 shows that the LBF of copolymer **16**, with a thickness equivalent to five monolayers, fully prevents the emission of secondary Ag^+ ions through the film. On the other hand, nine layers of stearic acid by no means fully suppress the diffusion of these ions.

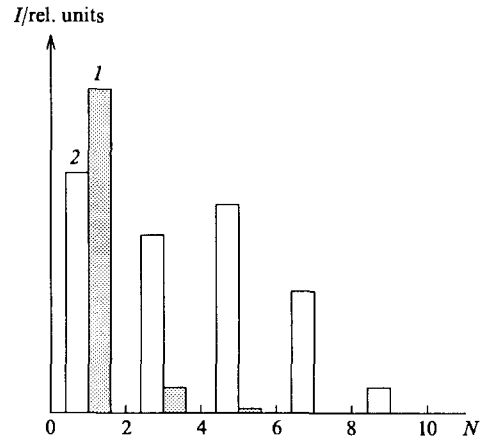
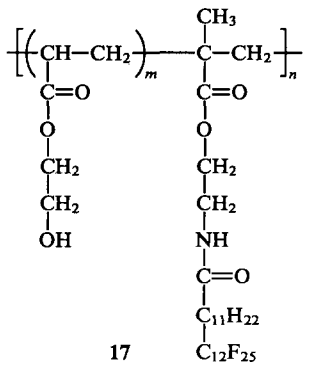


Figure 21. Dependence of the intensity of the signal due to secondary silver ions (normalised with respect to the $C_3H_5^+$ peak) on the number of layers: (*1*) for the methacrylic copolymer **16** LBF; (*2*) for the stearic acid LBF. [138]

In order to investigate the diffusion of the low-molecular-mass product from mixed monolayers involving the methacrylic polymer **16**, mixed 1 : 1 LBF with a fluorescent probe (a diphilic cyanine dye) were formed. Two mixed monolayers were deposited on the surface of silver on which a monolayer of copolymer **16** had already been deposited. Up to eight further monolayers of methacrylic copolymers were formed on the surface of the LBF obtained in this way. Fig. 22 illustrates the influence of the number of layers of copolymer **16** on the intensity of the mass spectrometric signal of the dye cation. Evidently two monolayers of the copolymer are sufficient to decrease significantly the signal intensity, but even eight layers do not fully suppress the diffusion of the dye ions through the copolymer LBF. The high stability of the LBF investigated is expressed by the retention of its properties on exposure to air at 10 °C for nine months and after boiling in water for 15 min. [138] Similar studies have been carried out [139] for copolymer **17**.



17

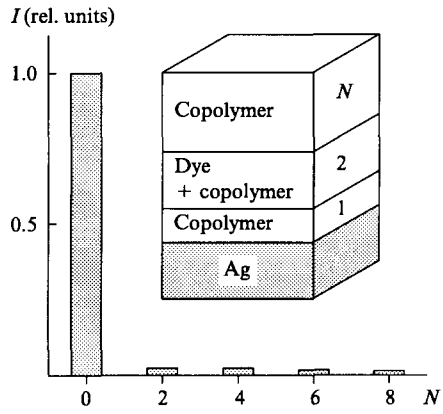


Figure 22. Dependence of the intensity of the signal due to secondary dye ions (normalised with respect to the $C_3H_5^+$ peak) on the number of outer layers of the methacrylic copolymer **16** for a mixed LBF.[138]

3. Mixed monolayers

In the analysis of the behaviour of monolayers of certain copolymers, the two-dimensional compatibility of mixtures of the corresponding homopolymers was examined. In this section we shall discuss in greater detail the behaviour of binary mixtures of polymers on the surface of a liquid. The principal questions which will be considered concern the compatibility of homopolymers in the two-dimensional state, the influence of the main and side chains on the compatibility of the polymers, including the case of markedly different lengths of the side chains in the components of the monolayer, and the determination of the thermodynamic parameters of the mixed monolayers.

The compatibility of the first and second members of the series of poly(alkyl acrylates)—PMMA and poly(ethyl methacrylate) (PEMA)—has been analysed.[81,140,141] On the basis of the compression isotherms for individual and mixed monolayers, calculations were made of the parameters characterising the excess free energy of mixing (ΔG_m) as described by Goodrich,[142] the coordination number of the two-dimensional quasi-lattice (Z') as described by Singer,[143] the partial immersion factor (f_m) as described by Frisch and Simha,[144] and the interaction energy (η^2/Z) between rigid segments lying on the surface†.[145] The dependence of ΔG_m on the mole fraction (φ) of PEMA in the PEMA–PMMA mixture is presented in Fig. 23. It is seen that the minimum negative value of ΔG_m corresponds to φ = 50%. The closeness of Z' to 2 for both the homopolymers themselves and for their mixtures (according to Davies and Rideal,[146] the flexibility is ~1%) indicates the rigidity of the acrylic macromolecules in the monolayers on the surface of water. The parameter f_m also does not change markedly for different component ratios, which indicates a similar degree of immersion of parts of the macromolecules in the aqueous subphase. The minima in the parameters η^2/Z and ΔG_m and also in the area of the monolayer at φ = 50% indicate the maximum cohesion between the segments of the macromolecules in this range of component ratios. As noted previously for other objects,[43,79,147] the maximum cohesion for the equimolar component content in the monolayer can be explained by the fact that the most rigorous alternation of the units of both polymers on the subphase can be attained for this component ratio. It has also been noted[81,140] that at 20–30 °C both components are compatible in the monolayer whatever the ratio.

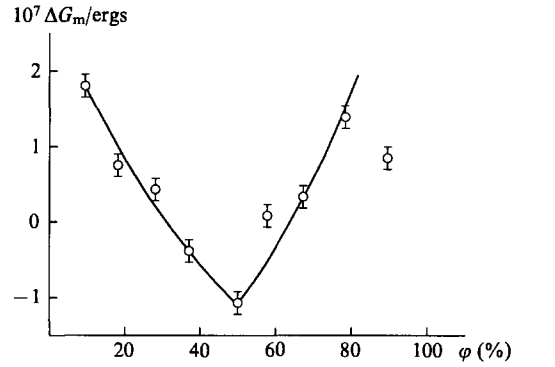


Figure 23. Dependence of the free energy of mixing on the composition of a monolayer comprising a PEMA–PMMA mixture.[140]

The compatibility with PMMA of the next member of the series—poly(propyl methacrylate) (PPMA)—has been investigated[148] for monolayers at the air/water and hexane/water interfaces. Using the parameters of the two-dimensional Huggins equation of state[149] and the ellipsometric method for the determination of the thickness of the monolayers, it has been shown that two-dimensional PMMA–PPMA mixtures are compatible on the surface of water and are thermodynamically more stable than monolayers of the pure polymers. The compatibility is due to the identical horizontal orientation of the side chains of both polymers on the surface of water, which is also promoted by the identical thickness (14 Å) of the PMMA and PPMA monolayers.[148,150]

The next member of the series—poly(n-butyl methacrylate) (PBMA)—is also compatible with PMMA in a monolayer on the surface of water.[79] The negative deviations of the surface area of the mixed monolayer from additivity and the minimum in the excess free energy for the equimolar component ratio (as for the mixed monolayers of PMMA and the lower homologues) indicate an increased stability of such a binary monolayer and the predominance of attractive forces between the molecules. The horizontal orientation of the side chains of the PBMA molecules for a low content of PMMA in the mixed monolayer changes to the vertical orientation and a strong interaction between the main chains of the polymers in the equimolar mixture.

Similar results, obtained for these binary mixtures, have been reported in another study.[140] The author analysed mixed monolayers of PEMA with PBMA. It is of interest that the behaviour of this system differs significantly from that of the mixed monolayers of PMMA with PEMA and PPMA: the monolayers of the individual components are thermodynamically more stable than the mixed PEMA–PBMA monolayers. It was shown that the maximum energy of mixing ΔG_m and the maximum parameter η^2/Z correspond to the 1:2 component ratio in the mixed monolayer. In this region, the positive deviations of the area of

† It is noteworthy that the thermodynamics, statistical physics, and molecular dynamics of monolayers of low-molecular-mass compounds and polymers are developing quite vigorously. However, analysis of the existing theories is outside the scope of the present review.

the monolayer from additivity reach maximum values. The results can be explained by the higher degree of hydration of the segments of the macromolecules in the mixture and the higher energies of repulsion between them for the component ratio indicated.

The vertical orientation of the long side chains of PODMA and the horizontal orientation of the short side chains of PMMA in their mixed monolayers on the surface of water prevent the formation of compatible monolayers.[148] This conclusion is based on data obtained with the aid of compression isotherms, according to which the area of the monolayer changes additively as its composition varies and the collapse pressure is independent of composition.

As mentioned above, mixed monolayers of PODMA and PBMA are compatible only in the range of compositions corresponding to a low content of the second component.[91] In mixed monolayers of poly(dodecyl methacrylate) and poly(octadecyl methacrylate), the inclined orientation of the dodecyl side chains and the vertical orientation of the octadecyl ones preclude the formation of a two-dimensional system with fully compatible components over the entire range of compositions,[112] although the mixtures can produce more stable films than the separate phases of the individual polymers.

A similar approach, based on the analysis of the dependence of the limiting areas and collapse pressures, for poly(phenyl methacrylate) – poly(hexyl methacrylate) systems permitted the conclusion[102] that the mixed binary monolayers are incompatible on the surface of water in all the two-dimensional phase states of the monolayer. These data can also be accounted for by the different orientations of the side groups. In the mixed monolayers of poly(phenyl methacrylate) and poly(benzyl methacrylate), the identical orientation of the aromatic groups leads to the formation of fully compatible two-dimensional systems whatever the component ratio.[102]

The study of the compatibility of high-molecular-mass and low-molecular-mass compounds in monolayers is important for the preparation of functionalised LBF. An increase in the compatibility of molecules belonging to different classes of compounds can be achieved by employing molecules with ionisable groups. This problem has been investigated in relation to binary mixtures of PMMA with stearic, arachidic, myristic, and oleic acids and with stearylamine, the degree of ionisation of which can be regulated by varying the pH of the aqueous subphase.[151–153] The compatibility of such components is determined by two factors: the orientation of the side groups and the intensity of the intermolecular interactions, which become more intense on ionisation of polar groups. Nonionisable saturated acids and PMMA are incompatible in the monolayer. The unsaturated oleic acid, the orientation of the chains of which is close to that of the ester groups of PMMA, is compatible with this polymer whatever the component ratio. The negative influence of the differences in the orientation of the side groups of the polymer and the chains of low-molecular-mass surfactants on the compatibility in the monolayers can be neutralised by intensifying the interactions between polar groups of the polymer and the ionised groups of the acid or the amine. Thermodynamic analysis of the PMMA – stearic acid and PMMA – stearylamine binary systems[151] demonstrated that the mixed layers are more stable than the monolayers of the individual compounds. With increase in temperature, the stability of the monolayers falls. The compatibility of the components in such monolayers is determined by the enthalpy term in the free energy and depends on the degree of ionisation of the molecules. Evidently, an improvement in compatibility can be achieved also for ionisable macromolecular systems.

* * *

The properties of the monolayers and LBF of acrylic and methacrylic homopolymers, their mixtures, and copolymers embrace virtually all the principal approaches to the analysis of the behaviour of macromolecules in monolayers and a considerable proportion of the existing ideas concerning the preparation and properties of polymeric LBF.

The properties of monolayers of nonionisable homopolymers can be regulated by altering the length of the ester side chains, by introducing a hydrophilic spacer uncoupling the main and side chains, or by the partial hydrolysis of the side chains, which leads to the formation of a copolymer incorporating ionisable groups. An increase in the length of the ester groups leads initially to the expansion of the monolayer and then to its condensation as a result of the secondary cohesion between the long side chains. Crystallisation of these chains explains, on the one hand, the discrepancies between the data of different workers who investigated poly(octadecyl methacrylate) monolayers under different experimental conditions and, on the other, can lead to the formation of poor quality LBF owing to the oscillations of the meniscus along the three-phase contact line. Crystallisation processes in the LBF itself can be suppressed by forming on the latter several monolayers of an amorphous polymer with a specified rigidity. The introduction of a hydrophilic spacer, separating the main and side chains of a double-stranded lipid, leads to the formation of stable monolayers, the collapse pressure and limiting area of which are close to the corresponding parameters of the low-molecular-mass lipid. The generation of ionisable acid groups on hydrolysis of an acrylic homopolymer extends the possibilities for the variation of the conformation and packing density of the units of the macromolecules on the surface of water by varying the concentration of the electrolyte in the aqueous support or its pH.

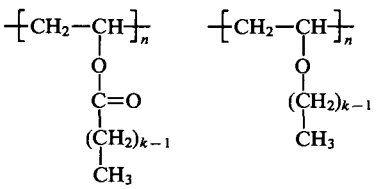
By varying the composition of the copolymer or the mixed monolayer, it is possible to achieve its transition from one state to another and to alter the phase composition and the structural organisation of the phases. These transformations are carried out by varying the length of the side chains of the comonomers, by the specific alteration of the length of the hydrophilic spacer in the main chain, and also by the copolymerisation of nonionogenic and ionogenic monomers.

Mixed monolayers of polymers and especially polymers and low-molecular-mass surfactants are of practical value, since, compared with monolayers and LBF based on copolymers, they facilitate the introduction of functional additives and the regulation of the properties of two-dimensional systems. Regulation of the states of these monolayers and phase separation processes makes it possible to create monolayers with definite molecular and phase compositions. This opens, in its turn, a path to the formation of, for example, skeletised LBF with a controllable size and disposition of cavities and to the formation of functionalised LBF with a specified structure and surface density of integrated special groups. The structures and properties of mixed monolayers have been scarcely analysed from these standpoints and the possibilities for the construction of a particular phase structure of the monolayers have still not been utilised.

Despite the rigidity of the PMMA monolayer, in many instances it is possible to create from this polymer fairly uniform LBF characterised by a low density of defects and to use them as a positive electron-beam resist. The formation of more ordered LBF is to be expected when acrylic and methacrylic polymers with moderate and considerable lengths of the hydrocarbon chains and their copolymers or mixed monolayers are employed. These polymers and their derivatives are already being used to create non-linear optical systems, thick (500 layers) wave guides with low losses, selective membranes, and insulating layers.

VII. Poly(vinyl ethers) and poly(vinyl esters)

Among the representatives of polymers of this type, the parent polymer of which is poly(vinyl alcohol), the poly(vinyl esters) **18** have been most thoroughly investigated in monolayers. The poly(vinyl ethers) **19** have not been attracting the attention of investigators recently.



18 **19**

The interest in poly(vinyl alcohol) (PVA) is associated with the possibility of obtaining monolayers of this water-soluble polymer on the surface of water. The stability of PVA monolayers on the surface of water is determined to a large extent by the acetate groups remaining after the hydrolysis of poly(vinyl acetate),[25] which is used to obtain PVA. PVA monolayers belong to the liquid-expanded type; their compressibility is high and they are disrupted at low surface pressures. The absence of appreciable dissolution of PVA in the support is indicated by the rapid restoration of the film following the expansion of a compressed monolayer, which could not have occurred for a simple equilibrium between the solution and the surface layer.

The characteristics of the variation of the compression isotherms for monolayers with increase in the length of the side (ester or ether) chain in poly(vinyl ethers)[154] and poly(vinyl esters)[155] are similar to those which were noted for acrylic and methacrylic polymers.

Poly(vinyl ester), especially poly(vinyl acetate) (PVAC) and poly(vinyl stearate) (PVST), monolayers have been investigated to a much lesser extent than poly(vinyl ether) monolayers.

The active study of PVAC monolayers on the surface of a liquid[25,26,77,79,85,155–172] has been undertaken in view of their highly equilibrium nature: there is no hysteresis on the compression–expansion isotherms obtained at high speed. The thermodynamic properties of PVAC monolayers have been investigated[156,158] and it has been shown that the macromolecules are arranged on the surface of water in the form of two-dimensional deformed coils. They are moderately flexible and the interaction (attractive) forces between them are weak. These properties of PVAC have led to prospects for the preparation of monolayers using nonspreading polymers, such as the ethylene–propene copolymer, by grafting vinyl acetate groups onto them.[145]

Interesting data concerning the inversion of the quality of solvents for PVAC on passing from three-dimensional to two-dimensional solutions have been published.[170] The surface θ temperatures have been calculated from the dependences of the second virial coefficient on the reciprocal of temperature, obtained from the compression isotherms, and it was shown that methanol (a poor solvent for the bulk phase solution) becomes a good solvent for PVAC in the monolayer. This result, confirmed by Huggins's theory and experimental data for supports containing NaCl or methanol, is associated with the competition of two processes in the formation of the monolayer: the spreading of the polymer and the solubilisation of the solvent by the subphase.

Poly(vinyl stearate) monolayers have been investigated in connection with the problem of their nonuniformity with respect to the area of the Langmuir trough.[173] A linear decrease in the surface pressure with increase in the distance from the mobile barrier has been established. Fig. 24 shows that the pressure gradient depends on the area of the monolayer and that the change in π may reach a considerable magnitude (> 10 mN m^{-1}). In the case of the monomer (vinyl stearate), a homogenous monolayer is formed. The effects due to the inhomogeneity of polymer monolayers must be taken into account in the study of LBF.[173,174] The inhomogeneity of polymer monolayers, associated with the low rate of relaxation, can be eliminated by introducing into the latter diphilic low-molecular-mass plasticisers. Problems concerning the compatibility of high- and low-molecular-mass components in monolayers become important under these conditions.

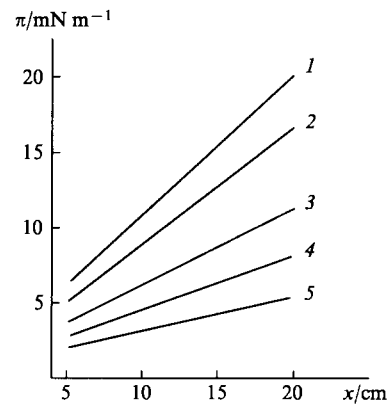


Figure 24. Dependence of the surface pressure in the poly(vinyl stearate) monolayer on the distance between the Wilhelmy plate and the fixed edge of the trough for different average areas (Å^2 per residue):[173] (*1*) 21.2; (*2*) 21.5; (*3*) 22.0; (*4*) 22.5; (*5*) 23.0.

The study of mixed monolayers of vinyl stearate and PVST showed[174] that the surface pressure, measured on collapse, depends in a complex manner on the composition of the surface film. These data permit the conclusion that the components are incompatible at least in this region of the compression isotherms. The surface potential of the monolayer and the absorption at 950 cm^{-1} (out-of-plane scissors vibrations of the hydrogen atoms of the vinyl group) of an 80-layer LBF comprising mixed monolayers deposited on a germanium plate varies linearly with composition under these conditions. These integral characteristics, which are insensitive (in the given version) to the phase composition, have been used[174] to analyse the kinetics of the two-dimensional polymerisation of vinyl stearate. The PVST monolayer, obtained by the polymerisation of the monomer on the surface of water, was transferred much less effectively onto the surface of the germanium film ($\rho = 0.1$) than the monolayer prepared from PVST polymerised in the bulk phase.

In the study of the properties of mixed PVAC monolayers with low-molecular-mass compounds, two interesting facts were noted:[157] the reversibility of the compression isotherms with a rigorous additivity of the areas for mixtures of equal weight and high collapse pressures of the mixed monolayers, exceeding in most cases the π_c for the individual compounds (Table 4).

Table 4. The monolayer collapse pressures (mN m^{-1}) for individual compounds and their equilibrium binary mixtures with PVAC.[157]

Component	Individual monolayer	Mixed monolayer
Poly(vinyl acetate)	23	23
Stearic acid	42	55
n-Hexacosanoic acid	58	68
n-Hexatriacontanoic acid	58	70
2-Hydroxyethylstearic acid	57	69
Methyl stearate	36	41
1-Octadecanol	42	39
Cholesterol	42	38

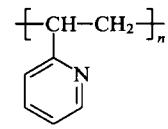
These results can be explained by the more intense interaction of the acetate groups with the carboxy-groups than their interaction with the hydroxy-groups or ester groups. Nevertheless, in view of the similarity of the collapse pressures for the monolayers of the pure polymer and its mixture, one can conclude, in conformity with Crisp's rule, that the compounds investigated are incompatible.

The identical orientation of the long hydrocarbon chains of PVST and stearic acid promotes their compatibility in mixed monolayers.[175] On the other hand, oleic acid, the hydrocarbon chain of which has the same length but is oriented horizontally along the surface of water owing to the presence of the double bond,[176] is incompatible with PVST in the monolayer but is compatible with PVAC.[177]

The decisive role of the orientation of the side chain is manifested also in the compatibility of polymer–polymer systems. Thus the similarity of the chemical structures of the PVAC and PMMA molecules promotes the complete compatibility of these polymers on the surface of water and the formation of ideal mixtures.[79,171] It must be emphasised that the dependences of the surface pressure on composition are monotonic for the uncollapsed and collapsed phases of this system and indicate the formation of true surface and bulk-phase solutions of the above polymer. A complete compatibility is also attained in mixed monolayers of PVAC and poly(ethyl acrylate) by virtue of the similar orientation of the units on the surface of water.[172] On the other hand, mixtures of PVAC with poly(vinyl butyrate) are compatible only in the region of equimolar ratios of the components. Such behaviour, similar to that examined above for PMMA–PBMA mixtures, can be explained in this instance not by the differences between the chain orientations but by the differences between the interactions of the units of these polymers with the molecules of the subphase.[171] All three isomeric poly(butyl methacrylates) (n-, *iso*-, and *tert*-butyl) are incompatible with PVAC in the monolayer.[79]

The PVST and PODMA polymers are compatible in mixed monolayers, which are more stable than the monolayers of the individual components. The incompatibility of PVAC and PVST in the monolayer is due to the different orientations of the ester side groups of these macromolecules on the surface of water.[148] Apparently a more homogeneous distribution of the monomer residues on the surface of water can be attained by forming the monolayers from copolymers of vinyl acetate and vinyl stearate.[155,178]

One of the few examples of compatibility in the monolayer of a polymer not containing a long hydrocarbon chain and classical surfactants is provided by binary mixtures of poly-2-vinylpyridine **20** with stearic acid, methyl stearate, or stearylamine.[179] In contrast to monolayers of the corresponding low-molecular-mass compound, neither temperature (15–35 °C) nor pH (6.2, 9.4) influence the compression isotherm. Thermodynamic analysis of the properties of monolayers of binary systems permitted the conclusion that the components are compatible in all three cases. For monolayers of compound **20** in a mixture with methyl stearate or stearylamine, the compatibility is determined by the enthalpy factor and is achieved through interactions between the polar groups of the components of the monolayer. The compatibility in the polymer **20**–stearic acid system is determined by the entropy factor and is apparently achieved by the immersion of the pyridylethylene units in the subphase. Owing to the high solubility of poly-2-vinylpyridine in the subphase, it has not been possible to obtain[30] a stable monolayer of poly-4-vinylpyridine with a reproducible surface pressure. Even the statistical copolymer of 4-vinylpyridine with 48 mol.% of acrylonitrile gives rise to monolayers which are stable only at a surface pressure $\leqslant 5$ mN m^{-1}.[30]

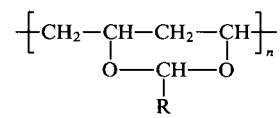


20

Thus the properties of the monolayers of poly(vinyl esters) have been investigated in fair detail. A distinctive feature of the first representative of this series—poly(vinyl acetate)—is the high stability of the monomers formed and high collapse pressures for mixed monolayers with low-molecular-mass compounds. These properties give rise to the hope for a wider employment of this polymer (and of its long-chain analogues) for the formation of stable monolayers and LBF. The ionisable polyvinyl derivatives of the type of polyvinylpyridine, which can be compatible with long-chain low-molecular-mass surfactants, merit a more vigorous investigation in monolayers. In the immediate future, one may expect an increase in the interest of investigators in the study of the structures and properties of LBF of these polymers and their mixtures with functionalised molecules.

VIII. Poly(vinyl acetals)

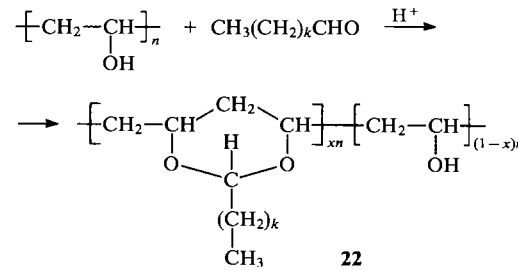
The polyalkylals **21** belong to the class of traditional polymers which have been used for a long time in practice. They are interesting objects for study in monolayers and LBF in view of the simplicity of their synthesis, which makes it possible to obtain macromolecules with different lengths of the side chains and with different degrees of acetal formation and also in view of the possibility of the cross-linking of the macromolecules.



21

Polymers containing electron-donating and electron-accepting groups have also been obtained recently, which has made it possible to investigate energy transfer processes in alternating LBF.

Polyacetals are obtained by the acetal formation reaction of poly(vinyl alcohol) in an acid medium. The degree of acetal formation x can vary within wide limits and can reach 80%.



22

Fig. 25 presents $\pi - A$ relations for five poly(vinyl acetals) with different lengths of the side chain ($k = 0-12$).[180] It can be seen that the collapse pressure of the monolayer increases and the compressibility diminishes with increase in k. The discrepancies between the limiting areas of the monolayers of poly(vinyl acetals) obtained by different workers[25,180,181] can be seen in Fig. 26. Evidently, the weak dependence of A_0 on n for long-chain homologues is due to the presence of the six-membered ring, which eliminates the influence of the hydrocarbon chain. The degree of polymerisation, which varies, for example for polyvinyloctal, from 300 to 2 600 ($x = 0.75-0.79$), also does not affect the limiting areas.[181] With decrease in x, the limiting areas diminish, which is associated with the hydrophilic nature of the

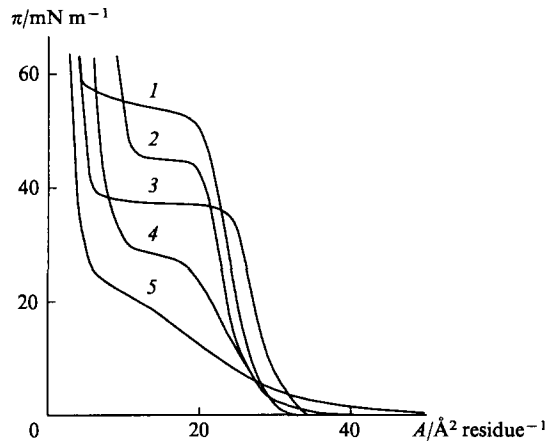


Figure 25. Compression isotherms for poly(vinyl acetals) **22** with different values of k: [180] (*1*) 12; (*2*) 10; (*3*) 6; (*4*) 2; (*5*) 0.

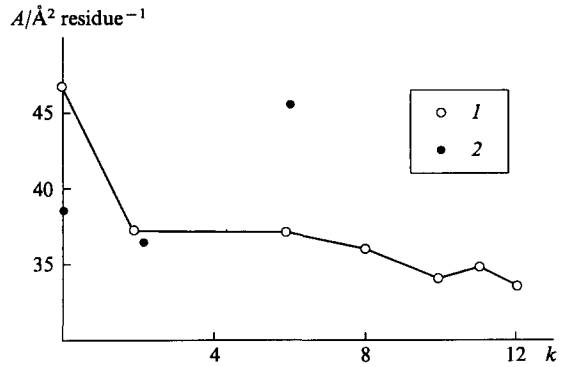


Figure 26. The influence of the length of the side chain (k) of poly(vinyl acetals) on the limiting areas of the monolayers according to the data of Oguchi et al. [180] (*1*) and Crisp [25] (*2*).

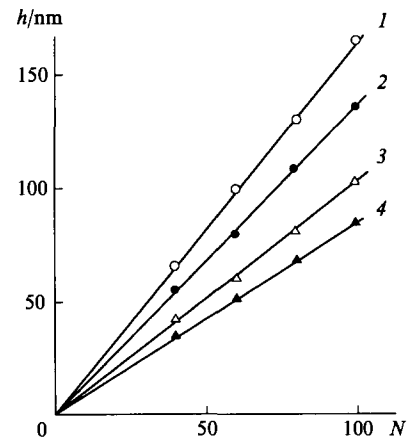


Figure 27. Dependence of the LBF thickness on the number of layers for four homologues of compound **22** with different values of k: [181] (*1*) 12; (*2*) 10; (*3*) 6; (*4*) 2.

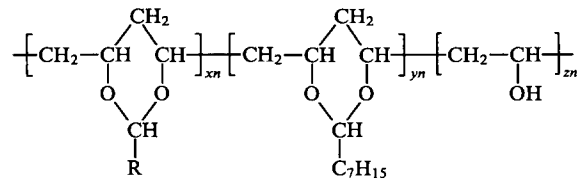
alcohol groups immersed in the subphase even at low surface pressures. The hysteresis of the isotherms for the polyvinyloctal monolayers compressed to $\pi \simeq 50$ mN m^{-1} [180,182] can be ruled out when the monolayers are obtained from mixed solutions of the polymer and iodine in chloroform. [182] The iodine atoms plasticise the monolayer and diminish its rigidity and the packing density of the side chains compared with the pure polyvinyloctal.

The fairly high homogeneity and stability of the poly(vinyl acetal) monolayers make it possible to obtain thick (up to 100 layers) Y type LBF. [180] Fig. 27 presents the dependence of the ellipsometrically determined thickness of the LBF on the number of layers for four homologues of compound **22** with k = 2, 6, 10, and 12. The linearity of the relations and their monotonic course in conformity with the size of the hydrocarbon chain as well as their slope, which yields the length of the hydrocarbon chain (~14 Å for k = 10 and 12), indicate the high quality of the LBF. [180,181]

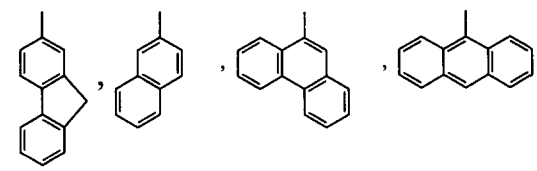
These LBF can be used as negative electron-beam resists. The sensitivity of such a resist depends on the chain length of the acetal groups through which cross-linking takes place. [183] Although the sensitivity of the resists was lower on deposition by the LBF method than in the case where they were prepared by the traditional centrifugal procedure, the resolution for the former is appreciably higher and is determined by the diameter of the electron beam.

It is of interest to carry out similar studies with Z type LBF, which can be obtained from monolayers of iodine-containing polyvinyloctal. The introduction of chromophoric electron-donating and electron-accepting groups into the molecules of poly(vinyl acetals) makes it possible to investigate the photophysical properties of polymeric LBF.

Chromophoric fluorene, naphthalene, phenanthrene, and anthracene groups have been introduced into polyvinyloctal **23** as a result of the reaction of PVA with the corresponding aldehydes. [184,185] The fraction of chromophoric groups in the chain (x) did not exceed 0.12.



23

R = 

Analysis of the fluorescence spectra of two-layer LBF of chromophoric polyvinyloctals showed that aggregation (formation of excimers) does not occur and that the chromophores are distributed in the amorphous film as isolated species.

The influence of the thickness of the inert spacer layer in polyvinyloctal on the effectiveness of the energy transfer from the donor (fluorenyl) to the acceptor (anthryl) is illustrated in Fig. 28. The alternating LBF consisted of two layers of fluorene and anthracene derivatives of polyvinyloctals, between which N layers of chromophore-free polyvinyloctal were distributed. It is seen from the fluorescence spectra that the effectiveness of the energy transfer is controlled by the number of layers N: for a system without a spacer layer (N = 0), the emission of fluorenyl (300–330 nm) is quenched by the acceptor and amounts to only 25% of the intensity for systems with N = 8 or 10. Under these conditions, the sensitised emission of anthryl is observed in the range 390–460 nm in the spectrum of the system with N = 0. [184]

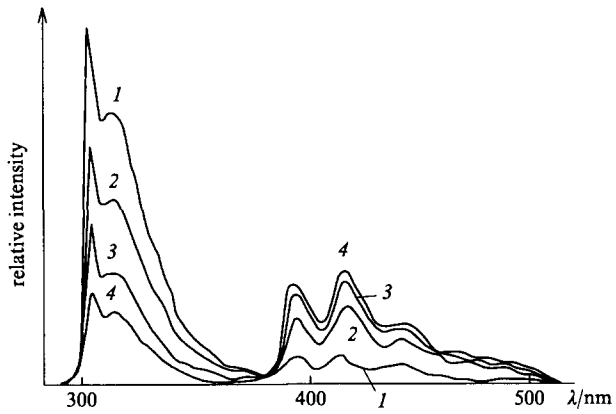


Figure 28. Fluorescence spectra of LBF containing layers of fluorenyl and anthryl derivatives of compound **23** separated by different numbers (N) of polyvinyloctal layers.[184] N = 10 (curve *1*), 8 (curve *1*), 4 (curve *2*), 2 (curve *3*), and 0 (curve *4*).

The effectiveness of the energy transfer can serve as a criterion for the determination of the thermal stability of LBF containing layers of chromophoric polyvinyloctals alternating with inert layers.[185] Fig. 29 presents the temperature variation of the ratio of the emission intensities of the acceptor at 438 nm (I_A) and the donor at 350 nm (I_P) for the 'phenanthryl/6/anthryl' system. Heating of this system (curve *1*) increases appreciably the ratio I_A/I_P starting from 40 °C. This is associated with the mutual approach of the chromophoric groups on heating. A further increase in temperature leads to the irreversible disordering of the system, which persists on its subsequent cooling (curve *1'*).

The thermal stability of poly(vinyl acetals) can be appreciably increased by cross-linking of the macromolecules with formaldehyde via the free alcohol groups.[185] The effectiveness of the cross-linking was determined from the change in the intensity of the fluorescence of the chromophoric poly(vinyl acetal) after it had been maintained in dichloromethane. As can be seen from Fig. 29, heating (curve *2*) and cooling (curve *2'*) of the cross-linked LBF have only a weak influence on the intensity ratio I_A/I_P, which indicates the constancy of the structure of the corresponding LBF.

Thus poly(vinyl acetals) provide a series of possibilities for the introduction of various functional groups into them. Based on them, it is possible to obtain cross-linked LBF with a high thermal stability. Evidently, these polymers will be investigated more vigorously in the immediate future.

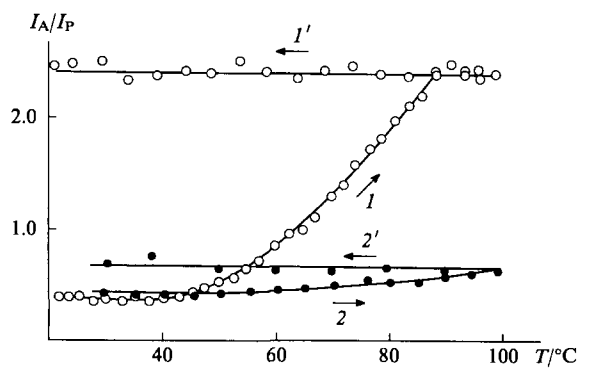


Figure 29. The influence of heating on the effectiveness of energy transfer (I_A/I_P) for noncross-linked (curves *1* and *1'*) and cross-linked (curves *2* and *2'*) 'phenanthryl/6/anthryl' systems.[185]

IX. Polymers based on maleic and fumaric acid derivatives

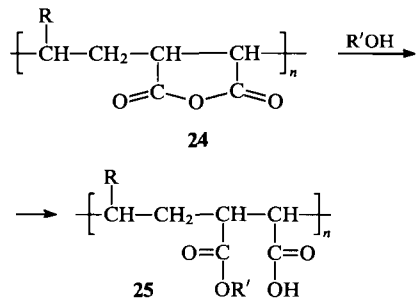
Two types of monomers and polymers derived from the isomeric maleic and fumaric acids and investigated in monolayers and LBF are known.

The first type includes the octadecyl monoesters of fumaric (ODF) and maleic (ODM) acids and the polymers based on them. The monolayer expands on photopolymerisation of ODF on the surface of water and contracts on photopolymerisation of ODM.[186,187] A 1:3 mixture of monomers polymerises without change in the area of the monolayer and can be used to form LBF with a low content of defects (cracks), the appearance of which is usually caused by the contraction of the monolayer on polymerisation.

The elastic properties of LBF of saturated ODF as well as the monomeric and polymerised ODF, 1:3 ODF–ODM mixtures, and ω-octadecenyl fumarate have been investigated by Brillouin spectroscopy.[188] The elastic constants of 30-layer LBF have been determined and it has been shown that they are low, decreasing still further on polymerisation for the majority of systems investigated owing to the formation of microcracks in the ODF on photopolymerisation. The polymerisation of mixed LBF comprising ODF and ODM leads to a slight increase in the elastic constants, which agrees with data obtained, showing the absence of contraction in this system on polymerisation.

Evidently the possibilities of these monomers for the creation of functionalised organic surfaces and organised films are far from having been exhausted.

Copolymers of vinylmaleic anhydride **24** belong to the second more widely investigated type. The reaction of compound **24** with water leads to the formation of poly(dicarboxylic acids) and that with alcohols affords the polyesters **25**.



24

25

Fig. 30 (see over) illustrates the influence of the ester side chain on the compression isotherms of the copolymers obtained by the esterification of poly(octadec-1-enyl-maleic anhydride). As can be seen from the figure, in contrast to the polymers examined previously in this instance the limiting areas of the monolayers increase linearly with increase in the length of the ester group, while the shape of the curves is retained. Hence it follows that the ester chains do not assume a vertical position on compression of the monolayer.[190]

Since the copolymers **25** contain unsubstituted carboxy-groups, the structure of their monolayer may be regulated by varying the pH of the subphase. For the copolymer with R' = CH_3, an increase in the pH of the subphase from 4.0 to 10.0 leads to an increase in the limiting area of the monolayer from 53 to 68 Å^2 per residue and to an increase in the collapse pressure from 22 to 40 mN m^{-1}.[189] Such behaviour can be explained by the ionisation of the carboxy-groups, which intensifies the repulsion between the molecules and the monolayer.

Recently these results were revised.[191] It was shown that at π = 30 mN m^{-1} the pH does not affect the area of the monolayer and that the collapse pressure does not increase with pH but either diminishes or passes through a minimum. The authors[191] note that the expansion of the monolayer as a result of the ionisation

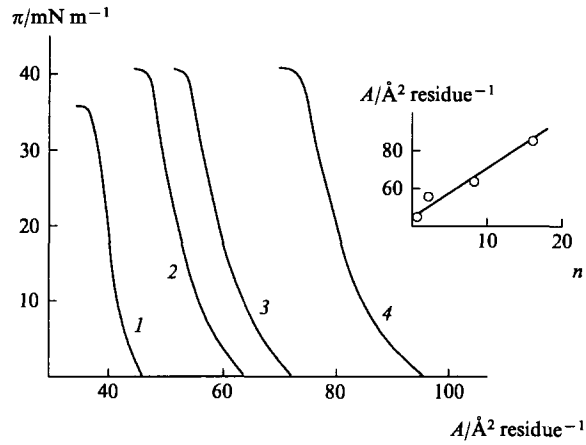


Figure 30. Compression isotherms for monolayers of copolymers of type **25** with R = $(CH_2)_{15}CH_3$ and different R′:[189] (*1*) H; (*2*) CH_3; (*3*) $(CH_2)_7CH_3$; (*4*) $(CH_2)_{15}CH_3$. The inset illustrates the dependence of the limiting area on the length of the group R′.

of the carboxy-groups can be compensated by the attraction due to the ion–dipole interactions or hydrogen bonding between the ionised carboxylate groups and the neutral acid residues.

High-quality Y type LBF have been obtained from compound **25** at pH 4.0–7.0 and 30 °C.[190,192,193] The introduction of Na^+ ions into the subphase significantly impairs the quality of the LBF, while in the presence of Cd^{2+} ions the LBF obtained are almost insoluble 'in all the solvents'.[189]

The influence of pH on the degree of transfer of copolymer monomers is illustrated in Fig. 31. The sharp decrease in ρ at pH > 8 can be explained by the development of repulsive forces between the surface of silicon and the ionised monolayer. The sharp increase in the viscosity of the monolayer at pH > 8.5 can also affect the quality of the LBF formed.[194] The degree of ionisation of the monolayers transferred onto a silicon prism has been determined[191] by distorted total internal reflection IR spectroscopy. The pK_a corresponding to the pH at which 50% ionisation takes place was found by monitoring the absorption bands of the unionised carboxy-groups. For the non-esterified and monoester derivatives of compound **25**, the pK_a were found to be in the range 8.0–8.5. This confirms the observed relation between the degree of transfer of the monolayer and the degree of ionisation of its constituent polymer.

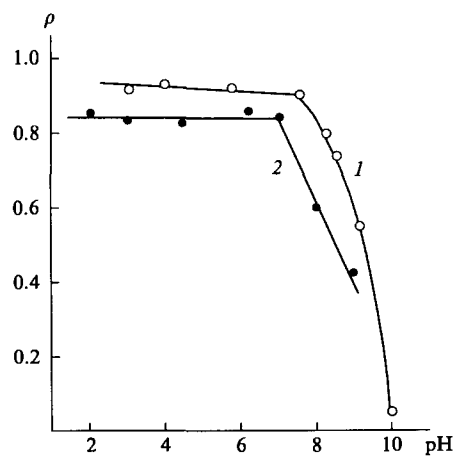


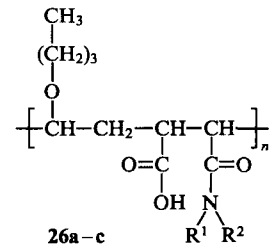
Figure 31. Dependence of the degree of transfer for the first ten LBF layers on pH for copolymer **25** with R = $(CH_2)_{15}CH_3$ and R′ = CH_3 (curve *1*) and H (curve *2*).[191]

The influence of pH, ionic strength, and the concentration of Ca^{2+} ions in the subphase on the properties of monolayers of the hexadecyl vinyl ether–maleic acid copolymer, which constitute models of biological membranes, has been investigated[195] in a study of processes involving the binding of Ca^{2+} ions by membranes during muscle and nerve activity, in membrane transport, in enzymic reactions, etc.

The height of the Schottky barrier in metal–dielectric–semiconductor heterostructures may be regulated with the aid of LBF of poly(octadec-1-enylmaleic anhydride).[193] A change in the degree of hydrolysis of the anhydride groups in the Au–LBF–GaP system alters the height of the Schottky barrier as a result of the accumulation of electrons (increase in the charge) on the oxygen atom of the anhydride group.

The copolymers obtained as a result of the modification by the corresponding amine of the butyl vinyl ether–maleic anhydride copolymer **25** have interesting properties.[196]

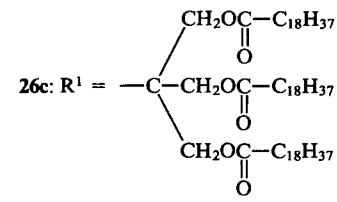
Y type LBF of compounds containing single-stranded (**26a**), double-stranded (**26b**), and triple-stranded (**26c**) side chains were formed in the above study on the surface of porous (0.2 μm) polycarbonate films (Nuclepore) and the influence of the structure of the monolayer and of the number of layers in the LBF on the permeability of such a membrane to the electrolyte (KCl) was analysed.



26a–c

26a: $R^1 = C_{18}H_{37}$, R^2 = H.

26b: $R^1 = R^2 = C_{18}H_{37}$.



R^2 = H.

In order to determine the KCl flux (0.5 M solution), the conductivity of the aqueous phase was measured, assuming that there is a linear relation between the conductivity and the KCl concentration. Fig. 32 presents the dependence of the KCl flux on the number of layers of compound **26b** in the LBF at 22 °C. It is seen from the figure that the electrolyte flux diminishes sharply on deposition of 6–8 monolayers and subsequently remains unchanged. The influence of the number of side chains in the elementary unit of the copolymer molecule on the electrolyte flux is illustrated in Fig. 33. The electrolyte flux is not arrested by the LBF of the single-stranded derivative **26a** and is weakly inhibited by the LBF of the triple-stranded derivative **26c**. The double-stranded copolymer **26b**, which gives rise to the closest packing in

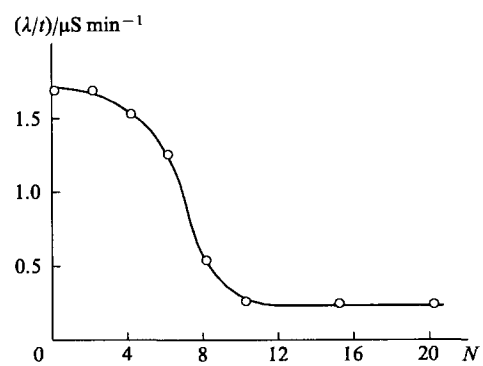


Figure 32. The influence of the number of layers of polymer **26b** (*N*) on the flux of KCl (λ/T) through a membrane at 22 °C.[196]

the monolayer (the limiting area of the **26b** monolayer is smaller than for the other two analogues), offers the greatest resistance to the electrolyte flux in the LBF. For membranes cast on a nuclear ultrafilter from solutions of compounds **26a–c**, the dependence of the flux on the number of side chains was not observed.[196] The stability of the LBF in aqueous solutions and the reproducibility of the results of the measurements of their permeability suggest the possibility of the practical employment of these selective membranes.

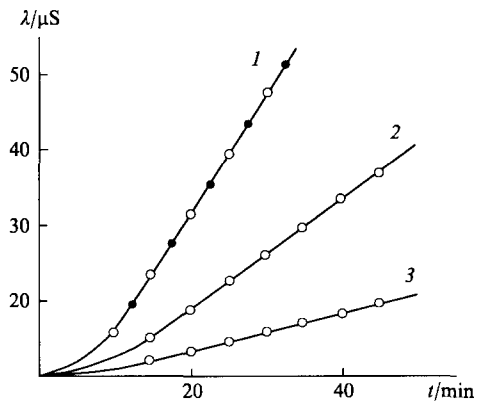


Figure 33. The permeability to KCl of LBF (20 layers) comprising polymers **26a** (curve *1*), **26c** (curve *2*), and **26b** (curve *3*) at 22 °C. Filled circles — data for the initial porous membrane (without LBF).[196]

X. Synthetic polypeptides and polyorganosiloxanes. Monolayers consisting of helical molecules and thin films

It was noted above that an essential condition for the preparation of LBF with a calibrated thickness and a definite orientation of molecules is the formation of a true equilibrium monolayer in which each monomer residue is in contact with the surface of the aqueous subphase. In contrast to monolayers of low-molecular-mass compounds, for which collapse with formation of the bulk phase almost always occurs for $A < A_0$, for polymeric objects with extensive conformational possibilities a decrease in the area can lead to the formation of monolayers made up of more complex molecular structures: helices and coils. We shall examine the properties of such monolayers in relation to synthetic polypeptides and polyorganosiloxanes. For the latter, we shall also analyse the possibility of the formation of stable thin polymer films on the surface of a liquid. Both these aspects are associated with the behaviour of the monolayers in the collapse region.

1. The behaviour of polymer monolayers on collapse

Many investigators[25,41–43,197–201] have been interested in the problem of the collapse of monolayers of low-molecular-mass compounds; polymer monolayers have been investigated to a much lesser extent in this respect. A brief analysis of this question can be usefully begun with the methods for the determination of the area of a close-packed polymer monolayer. Whereas the determination of the limiting areas of monolayers of low-molecular-mass substances by extrapolation to zero surface pressure is not open to disagreement, for polymer monolayers this parameter is determined in different ways. Two methods are normally employed for the determination of A_0: by extrapolation or from the beginning of the plateau on the compression isotherm. In this connection, it is essential to note that it is frequently difficult to determine the linear section for monolayers of the expanded type while for monolayers of the condensed type A_0 is frequently smaller than the area calculated on the basis of the model owing to the high interchain cohesion. Evidently, the uncertainty in the determination of the limiting area hinders the comparison and interpretation not only of experimental but also of theoretical results, since all the equations of state of monolayers include A_0 as a parameter.

There are differences in the behaviour of films of the liquid-expanded and condensed types compressed to small areas ($A < A_0$). The presence of a plateau over a wide range of areas is characteristic of the former, whereas for the latter the plateau is either absent or is weakly expressed. The first explanations, relating the existence of a plateau to the reorientation of the side chains, were criticised.[25] The concept of the 'upper film', based on the fact that the surface pressure increases on compression of the monolayer to a thickness equal approximately to $A_0/2$,[25] is poorly justified since the second rise in surface pressure (as will be seen from the data presented in the present section) depends on many factors. Nevertheless, data concerning the formation of two-layer or three-layer organic acid films have been presented for low-molecular-mass compounds.[202,203] However, there is no reliable evidence for the existence of such films.

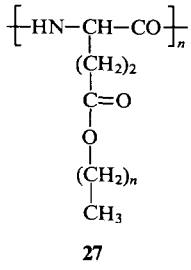
One of the ways of retaining the two-dimensional organisation after the collapse of the true monolayer involves the formation of single-layer films of helical molecules.

2. Polypeptides

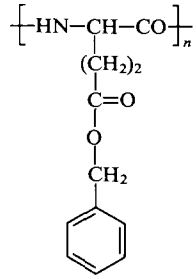
The properties of monolayers of natural proteins have been investigated very intensely and have been described in a series of monographs and review articles.[204–208]

Monolayers of synthetic polypeptides have been investigated in fair detail as models of biological membranes.[203,209–211] Since the biological aspects of the behaviour of monolayers of protein molecules are not the subject of the present review, we shall analyse the properties of synthetic polypeptide monolayers within the framework of the traditional approaches to polymeric objects. On this basis, we shall turn attention to the conformational transformations in the monolayers, the formation of multilayers on the surface of a liquid, the change in the structural homogeneity and rheological properties of monolayers on compression, and certain other questions.

Among synthetic polypeptides, poly-γ-alkyl-L-glutamates **27** and poly-γ-benzyl-L-glutamate **28** have been most thoroughly investigated. By altering the composition of the aqueous subphase and the type of solvent from which the monolayer is formed, it is possible to regulate the structure of the macromolecule on the surface of the liquid. The limiting area of the poly-γ-methyl-L-glutamate monolayer on the surface of a dilute solution of formic acid is greater by a factor of 1.5 than A_0 for the same monolayer on a pure aqueous subphase.[209] The authors' view[209] that a helical conformation of the macromolecules corresponds to the smaller areas has been frequently justly criticised.[212,213]



27



28

Fig. 34 presents the isotherms for poly-γ-methyl-L-glutamate monolayers deposited on the surface of water from a mixture of solvents.[212] It can be seen that the isotherms for the monolayers obtained from solution in pyridine with an admixture of chloroform have low values of A_0 and a high compressibility. On the other hand, the monolayer formed from solution in

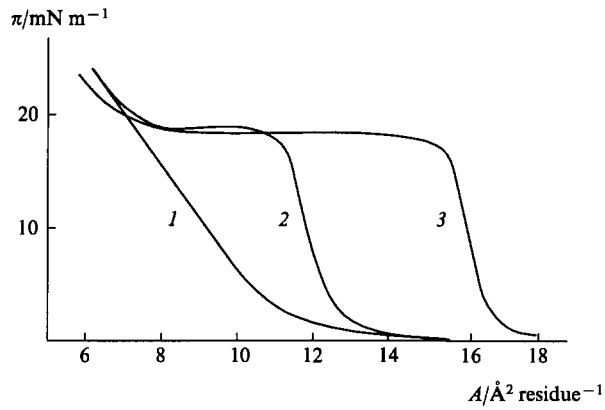


Figure 34. Compression isotherms for poly-γ-methyl-L-glutamate monolayers obtained on the surface of water from a mixed chloroform–pyridine solvent:[212] (*1*) 93% pyridine; (*2*) 77% pyridine; (*3*) 100% chloroform.

chloroform has a low compressibility, high limiting areas, and an extended plateau. Analysis of the IR spectra of monolayers of the polypeptides deposited at different surface pressures showed that the monolayers obtained from chloroform (higher A_0) consist of macromolecules in the form of α-helices, while in the monolayers formed from pyridine the macromolecules are in the extended β-conformations. It is of interest to note that, on compression of both types of monolayers, there is no transition from one type to another.[212]

Although doubts have been cast[211] on the possibility of the formation of β-structures in the monolayer, rheological studies[214] indicate significant differences in the behaviour of poly-γ-methyl-L-glutamate monolayers obtained from solutions in pyridine (β-structures) and in chloroform (α-helix). In contrast to the monolayer containing β-conformers, the surface viscosity (η_s) of which diminishes with increase in temperature, the η_s of the monolayer made up of α-helices increases. The $\eta_s - T$ relation for the poly-γ-methyl-L-glutamate monolayer, the molecules of which are in the form of α-helices, is illustrated in Fig. 35, which shows that an increase in temperature leads to irreversible changes in the monolayer: on subsequent decrease in temperature to 17 °C, the surface viscosity does not diminish. Such behaviour has been explained by the partial denaturation of the α-helices and the formation of hydrogen bonds between the molecules. The irreversibility of the temperature variation of the surface potential of the monolayer confirms this conclusion.[214]

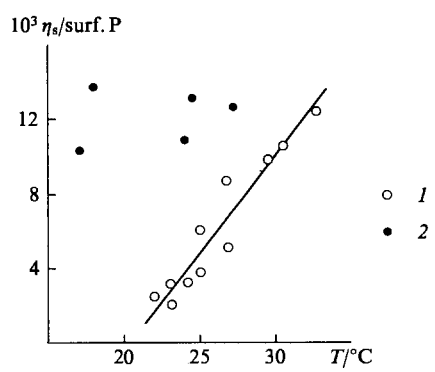


Figure 35. Temperature dependence of the surface viscosity (η_s) for a poly-γ-methyl-L-glutamate monolayer (initial structure—α-helices):[214] (*1*) data obtained with increase in temperature; (*2*) data obtained on subsequent reduction of temperature; A = 28.1 Å² per residue.

The novel results of Malcolm's studies[215,216] make it possible to examine the behaviour of polypeptide monolayers in the light of the important problem of the inhomogeneity of monolayers of viscoelastic systems, of which these polymers are typical representatives.

The form of the compression isotherms for poly-γ-ethyl-L-glutamate monolayers is influenced by the method of measurement of the surface pressure (Fig. 36).[216] For A > 12.5 Å² per residue, the isotherms obtained by the Wilhelmy and Langmuir (surface balance) methods are identical. However, the length of the plateau depends on the method of measurement, the position of the sensor (plate or strip) relative to the mobile barrier or the edge of the trough, and the orientation of the plate.

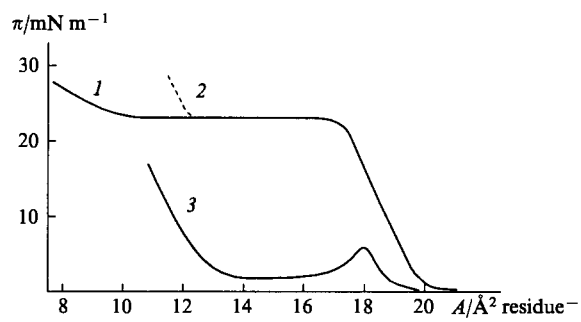


Figure 36. Compression isotherms for poly-γ-ethyl-L-glutamate monolayers:[216] (*1*) Langmuir balance with the sensor on the edge of the trough; (*2*) Wilhelmy method with the plate located 10 cm from the edge of the trough parallel to the barrier; (*3*) horizontal pressure applied to a glass plate 3 cm wide located in the same position as the Wilhelmy plate.

Thus in the measurement of the surface pressure by the Wilhelmy method, where the sensor is placed at a distance of 10 cm from the edge of the trough parallel to the mobile barrier, another increase in π (end of the plateau) is observed at A = 12.5 Å² per residue, while in the measurement by the Langmuir method, which is based on the measurement of the surface pressure at the edge of the trough, a new increase was observed at A = 9.5 Å² per residue. By placing the plate at different distances from the edge of the trough, Malcolm[216] showed that the length of the plateau decreases linearly with increase in this distance (Fig. 37).

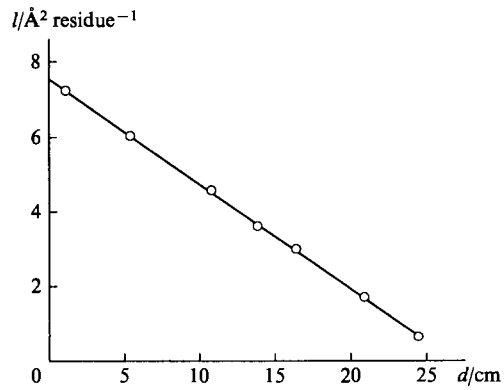


Figure 37. Dependence of the length of the plateau (*l*) on the compression isotherms for poly-γ-ethyl-L-glutamate monolayers on the distance (*d*) of the Wilhelmy plate from the edge of the trough.[216]

The deviation of the Wilhelmy plate from the vertical is characteristic of the measurement of π for viscoelastic polymer monolayers. Fig. 36 presents the dependence (curve *3*) of the horizontal force acting on the plate on the area of the monolayer.

Evidently the force increases in parallel with increase in the surface pressure before the beginning and at the end of the plateau. Together with this force, which is apparently thermodynamic in nature (the Marangoni effect), mechanical forces make a significant contribution to the displacement of the plate.

The effects described above are associated with the inhomogeneity of the poly-γ-ethyl-L-glutamate monolayers arising on compression. With the aid of thin strips of sulfur powder deposited through a template on the surface of the monolayer parallel to the barrier, the distribution of the inhomogeneities in the monolayer was visualised.[216] The displacement of the sulfur powder strips in the central part of the trough on compression of the monolayer is illustrated in Fig. 38.

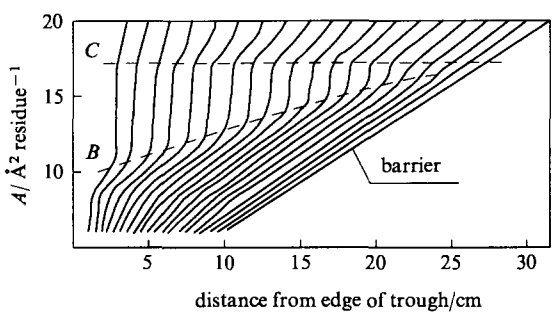


Figure 38. Displacement of sulfur powder strips along the central line of the trough from its edge on compression of a poly-γ-ethyl-L-glutamate monolayer.[216] Line *C* corresponds to the area for which the plateau begins; line *B* corresponds to transition to the bilayer film.

Up to the line *C*, corresponding to the onset of the increase in surface pressure and the formation of a bilayer film, the compression of the monolayer proceeds fairly uniformly. The region between the straight lines *C* and *B*, corresponding to the conversion of the monolayer film into a bilayer film, contains lines with slight displacements, and its size agrees well with the length of the plateau and the compression isotherms obtained by the Wilhelmy method. Finally, for $A < 9.5$ Å^2 per residue, the bilayer film collapses. The structure of the film is distorted most in the vicinity of the Wilhelmy plate and at the edges of the trough. The complex flow line distribution patterns arising on compression of the monolayers must be taken into account in the treatment of the results. In particular, viscometric data for polypeptide monolayers, which are interpreted in terms of denaturation processes,[214] can also be accounted for by experimental causes.[216] Similar problems arise in the analysis of the compatibility of the monolayers[217,218] and the kinetics of their collapse.[219]

In order to diminish or exclude the effects associated with the poor homogeneity of highly viscous monolayers, it is recommended[216] that symmetrical compression (the Wilhelmy method) or the surface balance method be employed. Naturally, these recommendations refer both to measurements of the surface potential and to viscometric studies on monolayers as well as the formation of homogeneous LBF. Different procedures for the compression of monolayers have been discussed[220,221] and the important role of rheological characteristics in the formation of homogeneous monolayers has been demonstrated[222] in relation to stearic acid and cadmium and aluminium stearates. By measuring the distribution of the surface pressure on the surface of the monolayer, it was shown[222] that the surface pressure is uniformly distributed over the entire surface for the acid and cadmium salt monolayers, the viscosity of which is low. In the case of the highly viscous aluminium stearate monolayer, the differences in π ($\Delta\pi$) can exceed 20 mN m^{-1}. Such behaviour has been explained from the standpoint of the dynamics of a liquid, which establishes direct proportionality between $\Delta\pi$ and η_s.

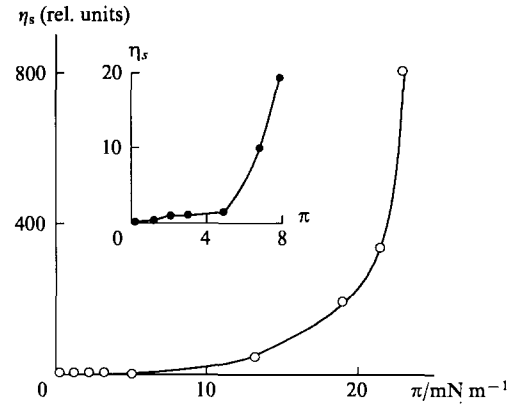


Figure 39. Dependence of the surface viscosity (η_s) on the surface pressure (π) for a poly-γ-methyl-L-glutamate monolayer at 17 °C.[218]

Fig. 39 presents the $\eta_s - \pi$ relation for a monolayer of poly-γ-methyl-L-glutamate α-helices.[218] Evidently the differences in the values of π on nonuniform compression of the monolayer can lead to abrupt changes in surface viscosity by factors of tens and hundreds.

In connection with the problem of the relationship between structure and the physicochemical properties of cell membranes, much attention has been devoted in the study of polypeptide films to their compatibility with lipids.[218,223–228] The compatibility was analysed for two conformations of the polymer molecules and also for monolayer and multilayer films.

The enantiomeric forms of poly-γ-methyl-L-glutamate are fully compatible in monolayers, like binary mixtures of other polypeptides.[211] The compatibility between polypeptides and lipids depends on the state of the monolayer of the latter (expanded or condensed).[223] The polypeptide in the β-form is incompatible with arachidic acid on the surface of 0.01 M HCl solution.[224] In the form of α-helices, poly-γ-benzyl-L-glutamate is compatible with palmitic and stearic acids in the monolayer for a polymer mole fraction in excess of 0.9.[227] In a multilayer film, these components are incompatible. On the other hand, poly-γ-methyl-L-glutamate is compatible with these acids both in the monolayer and in a multilayer film. The differences in the behaviour of the binary systems considered are determined by the different levels of aggregation of the polypeptide molecules in the films, by the different modes of interaction between the acids and polypeptides, and by the phase state of the acid monolayers. The properties of mixed monolayers of polypeptides and phospholipids can also be explained in the light of these ideas.[226] Analysis of the rheological properties of mixed monolayers of polypeptides with phospholipids and with cholesterol made it possible to establish a correlation between the surface viscosity of the monolayers and the stability of bilayer lipid membranes.[218]

Together with the use of polypeptide monolayers for the modelling of biological systems, multilayer (more than 500 monolayers) LBF of methyl glutamate–alkyl glutamate copolymers have attracted the attention of investigators recently as promising materials for optical wave guides with low losses[229,230] and also as photoresists and electron-beam resists.[231]

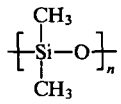
Thus the unusual feature of polypeptides consists in the fact that they form quasi-true monolayers of α-helices, the compression of which results in the formation of two- and three-layer films.[232–234] The breakdown of this conformation can be achieved by altering the temperature of the system and the composition of the support and of the solvent from which the monolayer is formed. The length of the plateau on the compression isotherms is determined by the method of measurement of the surface pressure and by the position of the sensor relative to the barrier and the walls of the trough. The inhomogeneity arising on compression of highly viscous monolayers, with long relaxation

times, leads to appreciable differences between the surface pressures for different sections of the trough. These effects can be reduced or eliminated in symmetrical compression or with the aid of special designs of the Langmuir trough. An increase in the homogeneity of polypeptide monolayers is essential for the construction of adequate models of biological membranes and also for the formation of high-quality LBF, which may find application in fibre optics.

3. Polyorganosiloxanes

a. Polydimethylsiloxane monolayers

Polyorganosiloxanes belong to the class of polymers which have been investigated in detail in monolayers. Most of the studies have been carried out on polydimethylsiloxane **29**.[235–245] The interest in this polymer is caused not only by its practical use as a surfactant in aqueous and nonaqueous media[246,247] but also by the possibility of forming stable monolayers from helical molecules.



29

Combined studies which have been carried out on polydimethylsiloxane (PDMS) monolayers and thin films made it possible to supplement the existing ideas concerning the structural transformations of this polymer on the surface of a liquid and also to consider the possibility of converting the monolayers into thin stable films.[52,239,240,245]

Fig. 40 presents the dependence of the surface pressure (determined by the Wilhelmy and Langmuir methods), the surface viscosity (determined using a rotating viscometer), and the surface potential (ΔV, determined by use of an ionising ^{210}Po electrode) on the area of the PDMS monolayer (M_η = 1.25 × 10^6). The sensitivity of the sensors (~0.01 mN m^{-1}) did not permit the measurement of surface pressures for areas in excess of 37 Å^2 per monomer residue. For A = 35–60 Å^2 per residue, the surface potential oscillates during scanning parallel to the surface, which indicates the inhomogeneity of the monolayer. In this range of areas, the macromolecules and their associated species lie on the surface of water in the form of discs—two-dimensional analogues of statistical coils; the siloxane dipoles adjoin the water molecules, while the methyl groups are directed towards the air phase. As a result, the *trans*-configuration of the PDMS molecules, which obtains in the bulk phase, is converted into the *cis*-configuration in the surface layer. In the range of areas from 37 to 20 Å^2 per residue, the isolated regions comprising the polymer approach one another and water is displaced from the gaps between them.[52,242] This process does not require much energy expenditure and π therefore increases only slightly. Starting from A = 20 Å^2 per residue, π increases sharply up to 7.6 mN m^{-1}; for A = 14 Å^2 per residue and in the range from 14 to 7.5 Å^2 per residue, π remains unchanged. The change in the hydration state of the monolayer when it is compressed has been examined in detail in a number of studies.[242–244] The constancy of the surface pressure for A < 14 Å^2 per residue indicates the formation of a helical conformation of the macromolecules: the energy expenditure in the displacement of the Si–O dipoles from the surface of the subphase is made good by the energy gain due to the internal compensation of the siloxane dipoles.

The exact determination of the region where macromolecules are converted into the helical form is of fundamental importance from the understanding of the processes involving the collapse of the true monolayer and the formation of transient films. Taking into account the ΔV–A relation as well as the temperature dependence of π (Fig. 40), one may conclude that the formation of helices in the monolayer begins for areas in the

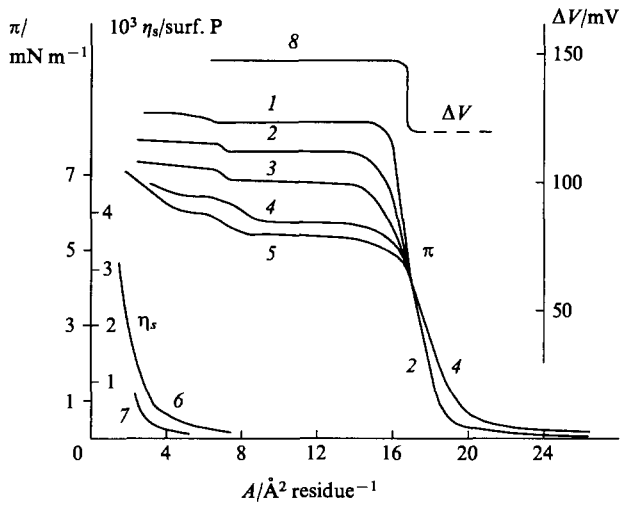


Figure 40. Dependence of the surface pressure (π), surface viscosity (η_s), and surface potential (ΔV) on the area of a PDMS monolayer on the surface of water at different temperatures (°C):[239] (*1*) 10; (*2*) 20; (*3*) 30; (*4*) 40; (*5*) 50; (*6*) 20; (*7*) 40; (*8*) 20.

range 16–17 Å^2 per residue, i.e. in the region of constant π. If a model comprising horizontally coaxial rings lying one on top of the other is used as an approximation to the helix, then in the case of PDMS containing 3, 6, and 8 monomer units corresponding to one turn of the helix, the following occupied areas are obtained: 10, 7.8, and 6.2 Å^2 per residue.[248] Thus the jump in surface pressure at A = 7.6 Å^2 per residue most probably corresponds to the formation of a close-packed monolayer of PDMS helices each containing six siloxane bonds per turn. The axes of the helices are arranged parallel to the surface of water.

In order to refine the mechanism of the conformational transformations in the PDMS monolayer, the temperature dependences of π and η_s were determined. Comparison of the dependences of the surface pressure on the area at different temperatures show that, for large values of A, the temperature coefficient of π is positive and small. With decrease in the area, the temperature coefficient changes sign and increases in absolute magnitude. The characteristic points for curves corresponding to different temperatures correspond to different areas. This permits the conclusion that the processes occurring in the monolayer at different temperatures during the compression process are identical.

In the region of the true monolayer, the surface viscosity is low (< 10^{-5} surf. P) (Fig. 40). An appreciable rise in η_s begins on formation of a close-packed monolayer made up of helices, the viscosity of the monolayer diminishing with increase in temperature.

The entropy (s_s) and enthalpy (h_s) of spreading were calculated with the aid of the temperature variations of the surface pressure.[41]

$$s_s = \left(\frac{\partial \pi}{\partial T}\right)_{A,a},$$

$$h_s = -\left[\frac{\partial(\pi/T)}{\partial(1/T)}\right]_{A,a} = T\left(\frac{\partial \pi}{\partial T}\right)_{A,a} - \pi,$$

where a is the overall area of the monolayer and of the free surface of water and T is the absolute temperature.

The calculation of the thermodynamic functions of spreading was preceded by the determination of the degree of equilibrium of the monolayer. By varying the concentration of the solutions, the number of drops, and the area provided for spreading and also by measuring the reversibility of the isotherms, it has been

shown that they are reproducible and hence the monolayer is in equilibrium.

The $s_s - A$ and $h_s - A$ relations for two temperatures are presented in Fig. 41. The thermodynamic functions and their relation with the structural transformations in the monolayer have been subjected to a detailed analysis.[52,239] Here we shall note that the change in the sign of the thermodynamic functions on compression of the monolayer in the region of $A \simeq 17$ Å^2 per residue indicates a transition of the system to a more ordered state. This transition may be associated with the formation of a monolayer of helical PDMS molecules, which is accompanied by the self-compensation of the Si–O dipoles.[236] The signs of s_s and h_s change for the same value of A as the one at which a jump ΔV was observed.

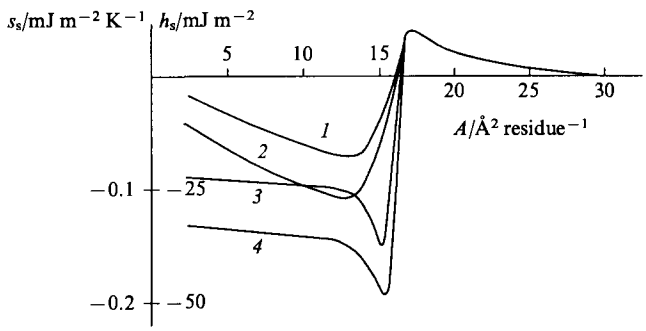


Figure 41. Dependence of the entropy (curves *1* and *3*) and enthalpy (curves *2* and *4*) of spreading on the area of a PDMS monolayer on the surface of water at 45 °C (curves *1* and *2*) and 15 °C (curves *3* and *4*).[239]

The experimental results obtained in the study of PDMS monolayers on the surface of water were subjected to a theoretical treatment using the familiar Singer,[143] Davies,[146] Motomura and Matuura,[249] and Frisch and Simha[144] equations of state for polymer monolayers. These equations and the parameters of the monolayers of high-molecular-mass compounds calculated with their aid have been subjected to a detailed analysis.[52] The calculations showed that the flexibility of the PDMS chains on the surface of water is extremely low despite the fact that in the bulk phase the polymer is extremely flexible. Evidently, the loss of one degree of freedom and also the retardation or complete absence of rotation, which are a consequence of the spreading of the polymer, render the chain conformationally rigid.

In order to refine the conclusions reached in the study of PDMS monolayers on the surface of water and also in order to elucidate the influence of the surface energy of the subphase on the properties of monolayers of this monomer, a study has been made of the behaviour of PDMS monolayers on the surface of aqueous 1,4-dioxane solutions at different concentrations.[52,250]

Dioxane concentration in solution (vol. %)	0	1	5	15	50	100
Surface tension of the solutions/nM m^{-1}	72.5	68.7	58.8	54.2	37.4	32.5

Fig. 42 presents the surface pressure (surface viscosity)–area isotherms at 20 °C for some of these subphases. The figure shows that, as the subphase becomes more hydrophobic, the shape of the $\pi - A$ isotherm changes: the surface pressure diminishes, the horizontal section vanishes, and the slope of the initial section decreases.

Evidently, replacement of the polar water molecules in the surface layer by the nonpolar dioxane molecules weakens the interaction of the subphase with the polar siloxane groups of the polymer. The change in the thermodynamic functions of spreading for polydimethylsiloxane monolayers on the surface

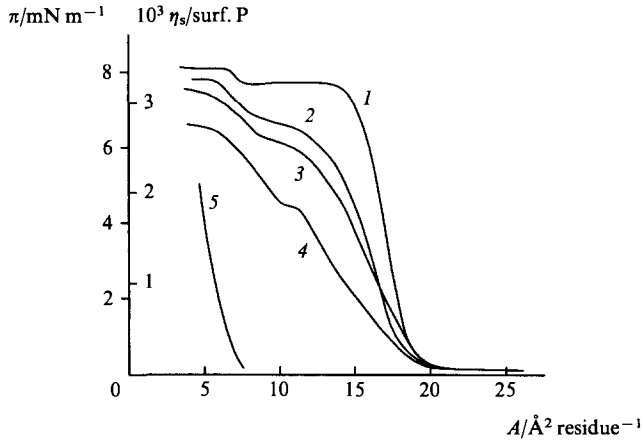


Figure 42. Dependence of the surface pressure (curves *1*–*4*) and surface viscosity (curve *5*) on the area of a PDMS monolayer on the surface of water (curve *1*) and solutions of dioxane in water (curves 2–5) at 20 °C.[250] Dioxane concentration (vol.%): (*2*) 5; (*3*) 15; (*4*) and (*5*) 50.

of a 50% aqueous solution of dioxane is illustrated in Fig. 43. Evidently, the entropy and enthalpy of spreading vary in the negative region for all the areas of the monolayer. The change in the sign of the thermodynamic functions on compression of the polymer monolayer on the surface of water (Fig. 41) was associated with the formation of the helical conformation of the macromolecules. On the other hand, in the case of the low-energy organic support, only the helical conformation is produced. The viscosity of this monolayer, like that of the monolayer on the surface of water, becomes appreciable only on formation of a close-packed film of helical molecules and when they are subsequently squeezed out from the surface of the support (Fig. 42).

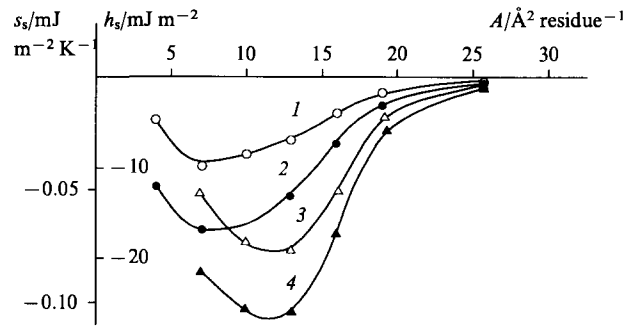


Figure 43. Dependence of the entropy (curves *1* and *3*) and enthalpy (curves *2* and *4*) of spreading on the area of a PDMS monolayer on the surface of a 50% solution of dioxane in water at 45 °C (curves *1* and *2*) and 15 °C (curves *3* and *4*).

In contrast to the PDMS monolayer on the surface of water, the compression of which up to the formation of a dense helical monolayer entails a change in ΔV by 150 mV which then remains constant, for the monolayer on the surface of 50% aqueous solution of dioxane $\Delta V = 0$ for all areas.

Important information about the influence of the surface energy of the subphase on the conformational transformations in the PDMS monolayer was obtained in a study of the spontaneous spreading of the polymer from the bulk phase on the surface of water, dioxane, and 5% and 50% solutions of dioxane in water. Fig. 44 presents the dependence of π and ΔV on the spreading time (t) of PDMS. Evidently the films are formed spontaneously on these supports. However, ΔV is nonzero only on

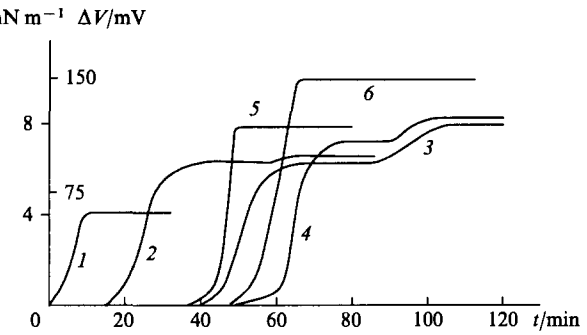


Figure 44. Kinetics of the spreading of PDMS on the surface of dioxane (curve *1*), solutions of dioxane in water [50% (curve *2*) and 5% (curves *3* and *5*)], and water (curves *4* and *6*): [250] (*2*)–(*4*) π; (*5*) and (*6*) ΔV.

dioxane solutions at concentrations ⩽5%. This result shows that the dipoles of the elementary units of PDMS are self-compensated in the helical macromolecule, while the zero dipole moment of the dioxane molecules ensures the constancy of ΔV whatever their orientation.

With increase in the concentration of dioxane in water, the rate of formation of the film from the bulk phase also increases and reaches a maximum on pure dioxane, despite the fact that PDMS hardly dissolves in dioxane and the surface tension of the latter is lower by a factor of 2 than that of water (Fig. 44). The macromolecules probably pass from the bulk phase to the film in the same helical conformation as that obtaining in the statistical coils of the bulk phase. The additional energy expenditure on the compression of two-dimensional discs and the new formation of helices on spontaneous compression of the monolayer, of the kind occurring at the air–water interface, is then ruled out.

Thus PDMS on a liquid hydrophobic surface forms a monolayer of helical molecules regardless of whether the polymer is deposited from solution or from the bulk phase.

b. Thin polydimethylsiloxane films on the surface of a liquid

The two-dimensional coil–helix conformational transition in the PDMS monolayer during its compression or spreading from the bulk phase must be regarded as a transition between a true monolayer and a thin polymer film. This film corresponds to equilibrium on the surface of the liquid. In this connection, a series of questions arise. What is the thickness which the films thus formed can have? Will they be stable? How will the stability be related to the surface energy of the subphase?

Hitherto the possibility of the formation of stable films thicker than single-layer films of both low-molecular-mass and high-molecular-mass substances on the surface of a liquid has been questioned. Whereas for low-molecular-mass compounds these ideas were based on numerous experimental studies,[41] such studies had not been made for high-molecular-mass compounds and in particular polymers.

In the studies of synthetic polypeptide monolayers on the surface of water examined above and in a recently published investigation [251] of monolayers of alkyl-trimethylammonium salts on the surface of mercury, the conclusion that multilayer films are formed was based on the presence of bends in the compression isotherms and on the analysis of the corresponding areas The stability of the films obtained in the above investigations is not discussed.

The possibility of the formation of a film as a result of the spreading of the substance from the bulk phase is regulated by the Young–Dupré relation

$$\sigma_A > \sigma_B + \sigma_{AB},$$

where σ_A, σ_B, and σ_{AB} are the interfacial tensions at the air–water, air–polymer, and polymer–water interfaces respectively.

The question of the thermodynamic stability of the film can be elucidated by comparing the free surface energies of the film and the close-packed monolayer. [52, 240, 245]

The specific free surface energy (F_s) for the phase state of the substance on a liquid surface is defined as $F_s = F_s^0 = \sigma_B + \sigma_{AB}$. With decrease in the film thickness (h), F_s becomes a function of h.

If the film is stable for all thicknesses up to and including the phase state, the following condition should hold:

$$\frac{dF_s}{dh} \leqslant 0.$$

The change in F_s can be calculated from the change in the surface pressure as a function of h. Fig. 45 (curve *2*) illustrates for cholanic acids [252] a typical F_s–h relation for films of low-molecular-mass crystalline compounds on the surface of water. Other traditional surfactants, for example cetyl alcohol and stearic acid, give rise to curves of similar shape. It is seen from Fig. 45 that, for a cholanic acid film, the stability condition holds only up to h = 20 Å. With further increase in thickness, the film collapses with formation of the bulk phase of the test substance in equilibrium with the monolayer. The difference between F_s corresponding to the plateau and the minimum value of F_s yields the energy expenditure in the transfer of the substance from the two-dimensional state (monolayer) to the three-dimensional state.

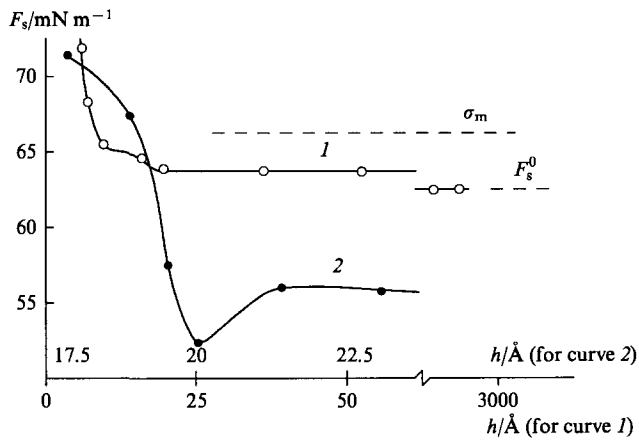


Figure 45. Dependence of the free surface energy (F_s) on the thickness (h) of PDMS (curve *1*) and cholanic acid (curve *2*) films on the surface of water. [240]

For a PDMS film on the surface of water (Fig. 45, curve *1*) we have for all values of h

$$\frac{dF_s}{dh} \leqslant 0.$$

However, if the F_s–h relation is plotted for liquid low-molecular-mass surfactants of the type of oleic acid, then the stability condition will also hold for them over a wide range of thicknesses but not for all thicknesses. When a layer of substance constituting a phase is formed on the surface of the support, i.e. $h \to \infty$, then

$$\frac{dF_s}{dh} > 0.$$

For such systems, it is convenient to consider the relation between the free surface energy of the film and the surface tension of the subphase coated by a close-packed monolayer (σ_m).

If the difference

$$\sigma_m - F_s^0 = S_f^0 ,$$

called by Harkins the finite spreading coefficient, is less than zero, then films thicker than the monomolecular film are unstable. In the opposite case ($\sigma_m - F_s^0 > 0$), the formation of a multimolecular film is energetically more favourable.

Evidently, the formulation

$$\sigma_m - F_s = S_f$$

is more general. In this case, the finite spreading coefficient is the limiting value of S_f, i.e. at $h \to \infty$, we have:

$$\lim_{F_s \to F_s^0} S_f = S_f^0$$

All the systems considered by Harkins[41] had $S_f^0 < 0$. In particular, $S_f^0 = -6$ mN m^{-1} for oleic acid on the surface of water. The results obtained for low-molecular-mass surfactants, the behaviour of which in monolayers differs from that of macromolecules, did not provide grounds for their formal transfer to surface layers of high-molecular-mass compounds.

We may also note that, according to the data of Joany and De Gennes,[253] the 'equilibrium thickness of the film deposited on a large area exceeds the monolayer thickness if the spreading coefficient (the initial spreading coefficient is considered) is sufficiently small'. This can be explained by the competition between the long-range forces, which endeavour to keep the film thicker, and spreading. A fairly low spreading coefficient is too weak a source of energy to transfer the molecules to the monolayer. Although these ideas of the above authors[253] refer to the initial spreading coefficient and not to the final one, the essence of the considerations which they express and which were described above does not change.

We now return to Fig. 45. The dashed line corresponds to the value of σ_m for a close-packed PDMS monolayer on the surface of water. The fact that the values of F_s for large thicknesses of the PDMS film (curve *1*) lie below the dashed line (the values of σ_m) indicates the stability of the film for all values of h. Fig. 45 also indicates the value of F_s^0 for PDMS on the surface of water.

We shall now consider the relation between the ability of PDMS to form thin stable films and the surface tension of the subphase.[240] Solutions of dioxane in water were used as the subphase. The values of σ_{AB} were calculated from the wetting angles (θ) for drops of these solutions on the surface of the polymer by the formula

$$\sigma_{AB} = \sigma_A - \sigma_B \cos\theta .$$

The results of the calculations (in mN m^{-1}) are compiled in Table 5, from which it is seen that the film stability condition ($S_f^0 > 0$) holds until the surface tension of the subphase is greater than 58.8 mN m^{-1} (5% solution of dioxane in water). The extremely interesting correlation between the stability of PDMS films and the two-dimensional discs – helices conformational transition is noteworthy: the PDMS films on the liquid surface are stable until there remains a possibility of the retention of the planar conformation, which occurs on subphases with $\sigma_A > 58.8$ mN m^{-1}.

In connection with the stable existence of PDMS films of different thickness on the surface of a liquid, the properties of the transitional region between the monolayer and the bulk state of the polymer were investigated. Fig. 46 illustrates the dependence of the surface pressure, the surface viscosity, and the resistance to the evaporation of water on the thickness of the PDMS film. Despite the high molecular mass of the polymer (1.25×10^6), the viscosity of its film for small thicknesses is low and varies only slightly with increase in thickness. The low values of η_s in the region of low h reflect the structure of the film, which consists of helical molecules, the cohesive interactions between which are weak, while the length of the sections of the chains displaced from

Table 5. The influence of the surface tension of the subphase on the finite spreading coefficient of PDMS.

Dioxane concentration in water (vol.%)	σ_A	σ_{AB}	F_s^0	σ_m	S_f^0
0	72.5	42.5	62.5	66.5	4.0
1	68.7	42.2	62.2	63.7	1.5
2	66.4	41.3	61.3	62.4	1.1
4	64.5	40.3	60.3	61.0	0.7
5	58.8	35.3	55.3	55.0	−0.3
10	55.5	33.0	53.0	52.0	−1.0

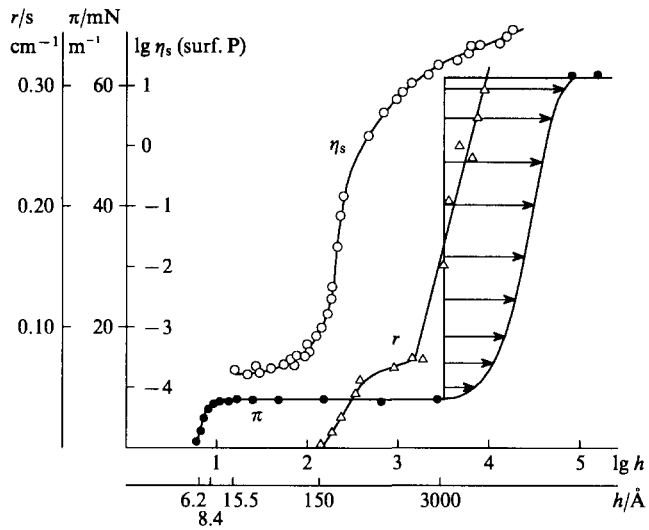


Figure 46. Dependence of the surface pressure (π), surface viscosity (η_s), and the resistance to the evaporation of water (r) on the thickness (h) of PDMS films on the surface of water.[240]

the surface is insufficient for intertwining. The absence of a measureable resistance of the film to the evaporation of water for small film thicknesses confirms this view. For h = 130 – 150 Å, the surface viscosity increases sharply and an appreciable increase in the protecting effect of the film against the evaporation of water is observed. This characteristic range of PDMS film thicknesses can be related to the formation of a monolayer from statistic coils. Calculation shows that the diameter of a dense statistical coil for a molecular mass of the polymer of the order of one million is 140 Å. The nature of the variation of lg η_s in the region where $h > 150$ Å shows that the increase in viscosity is caused by the intertwining of the chains of the macromolecules rather than by the increase in the number of layers in the film (in this case, the viscosity would have varied in proportion to the thickness). In the region where h = 3000 Å, the film viscosity becomes equal to the bulk viscosity: $\eta_0 = \eta_s/h$. The existence of a critical thickness of the transitional region in thin PDMS films has been confirmed in a study of the flow of the polymer into the pores of nuclear Lavsan ultrafilters.[254]

Starting with h = 3000 Å, the surface pressure rises sharply and π begins to depend on the rate of compression. If a load is applied instantaneously to the film perimeter, then π changes abruptly to 62 mN m^{-1} (the Langmuir method), remaining constant on further increase in thickness.[240] The increase in surface pressure in this region cannot be described by the equation

$$\pi = \sigma_A - (\sigma_B + \sigma_{AB}) .$$

Calculation of the correction term for this equation shows that its value (54 mN m^{-1}) is close to that of the thermodynamic work of adhesion of PDMS to water (52 mN m^{-1}). The equation presented above must be rewritten, adding to its right-hand side a correction term equal to the work of adhesion.

Thus there is a transitional region in stable films, the properties of which differ from those of the polymer in bulk, between the monolayer and the PDMS bulk phase on the surface of the liquid. These films, transferred by the Langmuir–Blodgett method onto the surface of mica, have a homogeneous structure according to data obtained by transmission electron microscopy.[52]

On the other hand, recent studies on PDMS monolayers by Brewster angle microscopy have shown[255] that the monolayers on the surface of water have a domain structure also for areas corresponding to the expanded state and to the collapsed film. The relaxation times for the deformation of the domains, agreeing with the extremely low linear tensions of the domain boundaries ($\sim 10^{-13}$ N), have been determined[255] and it has been noted that the relaxation times depend only slightly on the molecular mass of the polymer. This means that the polymer chains are not intertwined on the surface of water and that the interactions between them, determining the viscosity of the monolayer, take place via monomer units. The observed domain structure of the monolayer for large areas does not conflict with the ideas described above. However, the mechanism of the behaviour of the film after the collapse of the monolayer requires further refinement.

The possibility of the formation of stable thin films of polyphenylmethylsiloxane has been discussed[256] in connection with the unusual temperature variation of the surface pressure of its oligomers (Fig. 47). For the monolayer of a polymer with a molecular mass of 2240, π diminishes with increase in temperature and at 37 °C becomes zero. A similar trend has been observed for a polymer with a lower molecular mass and also for the temperature variation of the equilibrium spreading pressure. In the latter case, $\pi = 0$ at 55 °C. Such behaviour of the systems can be accounted for by the decrease in the initial spreading coefficient with increase in temperature, leading to the formation of stable thin films on the surface of a liquid.

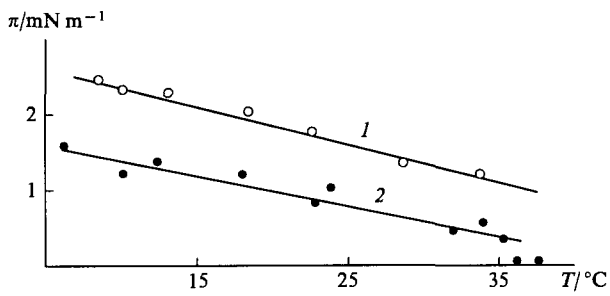


Figure 47. Temperature variation of the surface pressure of oligophenylmethylsiloxanes for a monolayer area of 11 Å^2 per residue.[256] Molecular mass: (*1*) 1470; (*2*) 2240.

c. Monolayers of certain other polyorganosiloxanes

The replacement of the methyl groups in PDMS by ethyl or phenyl groups weakens appreciably the ability of these polymers to form stable monolayers on the surface of water.[52] On the other hand, ladder polymers—polyphenylsilsesquioxane and polyethylsilsesquioxane—form stable viscous monolayers with high collapse pressures. For example, the collapse pressure for polyethylsilsesquioxane is higher by a factor of four than for PDMS.

The acid groups $(CH_2)_{10}COOH$ introduced into the side chains of polydimethylsiloxane and polyhydromethylsiloxane promote an increase in the surface activity of the polymers and in the collapse pressure (>30 mN m^{-1}). The monolayers are transferred quantitatively onto solid supports by the Langmuir–Blodgett method. Analysis of the electrical properties of alternating LBF of these polymers and eicosylamine showed that they are promising for use in pyroelectric devices.[257]

Monolayers of rod-shaped siloxane polymers—phthalocyaninatosiloxanes **30**—have been investigated.[258–261]

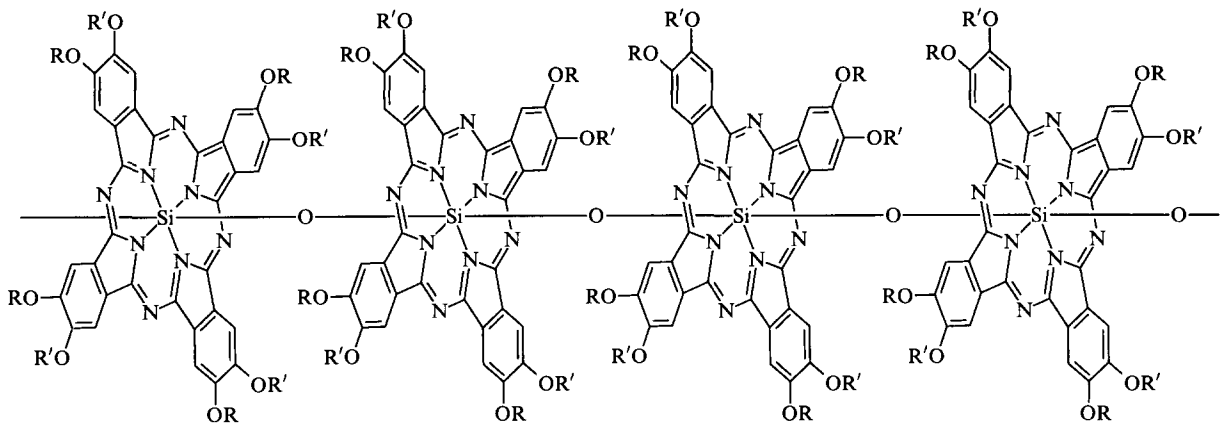
On compression of monolayers of polymer **30** with R = CH_3 and R′ = $(CH_2)_7CH_3$, the cylindrical molecules undergo a reorientation from the horizontal to the vertical position. The interactions between the polymer molecules and the aqueous subphase, which are responsible for the high stability of the monolayers, have been discussed resorting to ideas concerning the polarisation of the central aromatic nucleus, the proton exchange between the subphase and the monolayer, and the oxidation-reduction activity of the phthalocyanine group.[259] The way in which the molecules of compound **30**, containing unsaturated bonds in the peripheral chains, undergo reorientation changes on compression of the monolayer. In this case, the molecules creep onto one another, retaining the orientation parallel to the subphase. The process involving the aggregation of the molecules to microcrystallites has been investigated by transmission electron microscopy for monolayers having different areas transferred onto a carbon support by the Langmuir–Schaefer method.[261]

The diblock copolymers of dimethylsiloxane with methyl methacrylate and bisphenol A carbonate have been investigated in monolayers on the surface of water.[262,263] In both cases, blocks of the second type exert a condensing effect on the PDMS monolayers. It is of interest that the compression isotherms for the block copolymer and the mixed monolayer of the homopolymers (PDMS and PMMA) do not differ greatly from one another but do differ significantly in shape from the additive curve and deviate from the latter.[30] Analysis of the behaviour of binary mixed monolayers of PDMS and polymethylphenylsiloxane with oleic acid showed that the reconstruction of the surfactant monolayer in the presence of the polymer increases the collapse pressure.[264] For mixed monolayers of PDMS with palmitic acid and cetyl alcohol, this effect is manifested to a much lesser extent.[265]

Thus monolayers of polyorganosiloxanes possess a series of interesting features. Despite the low collapse pressure, the PDMS monolayers are stable on the surface of water. An increase in the length of the side chains in polyorganosiloxanes does not lead to the formation of more expanded monolayers and to an increase in the collapse pressure, in contrast to the acrylic and methacrylic polymers. The conversion of the PDMS macromolecules into the helical form, which can be regulated by varying the area of the monolayer or the surface energy of the subphase, is an important structural transition, the dynamics of which require detailed analysis. Polydimethylsiloxane forms stable thin films on the surface of a liquid. Questions concerning the transfer of these films onto solid supports and the study of their structure and properties have not so far been investigated.

Ladder polymers and functionalised polyorganosiloxanes form stable monolayers with high collapse pressures. The properties of the monolayers of these polymers depend to a large extent on the substituents in the side chain.

The nontoxicity and thermal stability of polyorganosiloxanes as well as the large set of functionalised polymers of this class[266] give rise to the hope that they will be investigated more vigorously in monolayers and LBF.

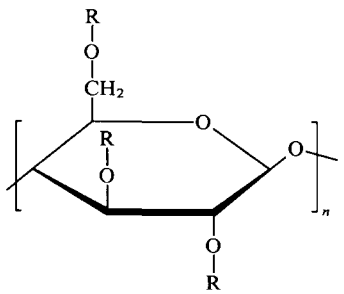


30

$R = CH_3, R' = (CH_2)_7CH3$; $R = CH_3, R' = (CH_2)_6CH=CH_2$.

XI. Polysaccharides

Cellulose ethers and esters are classical objects with which systematic studies on polymer monolayers began. It has been shown[267] that cellulose acetate **31a** (n = 0) does not form a stable monomolecular film on the surface of water but a monolayer is formed on the siloxane–water interface, its limiting area corresponding to the model in which the average plane of the glucose rings is arranged parallel to the surface. The influence of molecular mass on the compression isotherms for cellulose acetate has been studied.[33] Despite the fact that the limiting areas of the monolayers of three different fractions of cellulose triacetate were only $^1/_7-^1/_{10}$ of the values of A_0 specified by the high-molecular-mass model, the authors[33] calculated their molecular masses from the $\pi A-\pi$ relations. The molecular masses extrapolated from the region of low π were 3–6 times greater than the control values (57000, 45000, and 29000), while on extrapolation from the region π = 2–6 mN m^{-1} the molecular masses of the first two fractions proved to be close to the control values. The authors explained the better agreement in the latter case by the fact that, in contrast to a domain monolayer (for low values of π), in a dense monolayer account is taken of the contribution of the vibrational motions of the macromolecules to π.



31a: R = $-\overset{\overset{O}{\|}}{C}-(CH_2)_nCH_3$

31b: R = $-(CH_2)_3-OH$.

31c: R = $-(CH_2)_2-OH$.

31a–c

Recently this problem again attracted attention as a result of a study[268] in which monolayers and adsorption layers of hydroxypropylcellulose **31b** with molecular masses of 60000, 100000, 300000, and 1000000 and of hydroxyethylcellulose **31c** with molecular masses of 100000 and 900000 were investigated. Fig. 48 presents the dependence of the surface pressures of the monolayers of these polymers on the monolayer concentration. The molecular mass does not affect the compression isotherms for both polymers, while an increase in the length of the side chain by one CH_2 group increases the value of π corresponding to the plateau from 7 mN m^{-1} for compound **31c** to 28 mN m^{-1} for compound **31b**. It is of interest to note that this plateau is

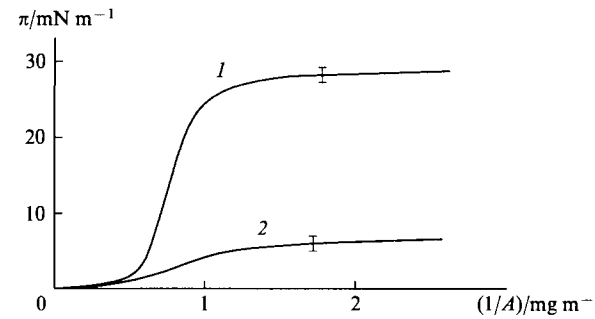


Figure 48. Dependence of the surface pressure (π) on the surface concentration ($1/A$) of monolayers of hydroxypropylcellulose (curve *1*) and hydroxyethylcellulose (curve *2*) specimens with different molecular masses, obtained by spreading from a solution at 25 °C.[268]

reproduced also for adsorption layers of polymers: after a change in concentration by a factor of 300–600, the surface pressure changes by not more than 5%. According to light scattering data, the viscoelastic properties of the monolayers and adsorption layers are also identical.

The importance of these results consist in the fact that they apparently demonstrated clearly for the first time the similarity of the structures and properties of polymers in monolayers obtained by a forced organisation procedure (compression) and in self-organised adsorption layers on the surface of water.

The compression isotherms for cellulose ethers (esters) with different lengths and numbers of side chains are presented in Fig. 49.[269,270] Cellulose triacetate **31a** (n = 0) and cellulose tripalmitate **31a** (n = 14) form condensed monolayers. The limiting area of cellulose triacetate (54 Å^2 per residue) is greater than the value 40–48 Å^2 per residue obtained by Zografi and coworkers[58,268] but is smaller than for compounds **31b** (119 Å^2 per residue) and **31c** (137 Å^2 per residue).[271] For ester groups of moderate length [in the trioctanoate **31a** (n = 6), tridecanoate **31a** (n = 8), and trilaurate **31a** (n = 10)], the liquid-expanded state obtains. The transition from this state to the condensed state is characterised by the constancy of the surface pressure. Monolayers of diesters (cellulose dilaurate) are more compressible and have smaller areas in the expanded and condensed states compared with the triester analogues (Fig. 49, curve *5*). The increase in secondary cohesion in the monolayer with increase in the length of the side chain to 16 carbon atoms (cellulose tripalmitate) leads to the formation of a condensed monolayer in which the glucose residues are arranged parallel to the surface of water, while the hydrocarbon chains are

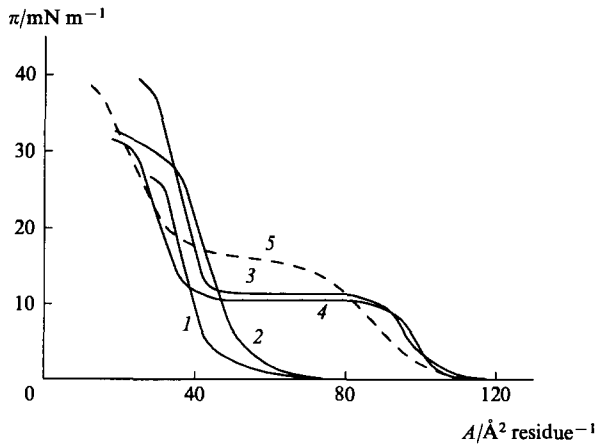


Figure 49. Compression isotherms for the triesters (curves *1*–*4*) and diester (curve *5*) of cellulose **31a**.[269] *n*: (*1*) 0; (*2*) 14; (*3*) and (*5*) 10; (*4*) 6 and 8.

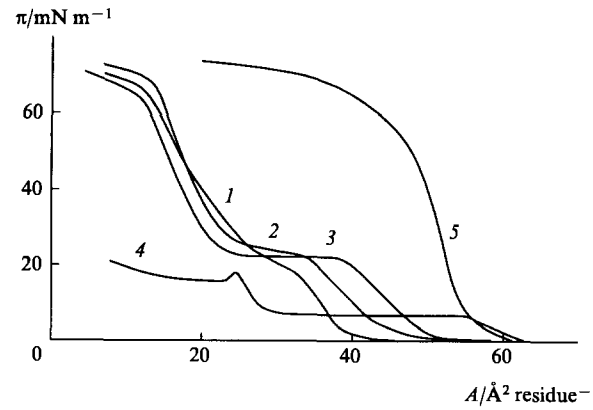


Figure 50. Compression isotherms for amylose esters at 24 °C:[273] (*1*) acetate; (*2*) propionate; (*3*) butyrate; (*4*) laurate; (*5*) palmitate.

arranged perpendicular to the surface of the subphase. Cellulose trioctadecanoate forms a condensed monolayer with a limiting area of 71 Å^2 per residue.[272]

The LBF films of cellulose esters are formed by the horizontal transfer method. X type cellulose trilaurate films with up to 60 layers have been obtained[269] from both expanded (9.5 mN m^{-1}) and condensed (20 mN m^{-1}) regions of the monolayer. Although the authors note that the cellulose trilaurate monolayers were too brittle to be transferred onto a solid support, in another study[272] it proved possible to obtain 10-layer Y type LBF from cellulose trioctadecanoate with even longer chains (horizontal transfer). For LBF of the same polymers into the side chains of which pyrene labels had been introduced, it was shown by fluorescence analysis that energy transfer or the formation of excimers within or between the layers are not observed in films containing up to 7% (percentage substitution of the side groups) of the label. This is associated with the fact that the thickness of the layers (24 Å) is smaller than the Forster radius between the pyrenyl groups localised in the middle part of the LBF layers. If the concentration of the pyrenyl fragments exceeds 7%, then the formation of two types of excimers with different structures and emission times can be detected by time-resolved fluorescence spectroscopy.

The change in the β-structure of the elementary unit of cellulose to the α-glucoside structure leads to amylose derivatives. Extensive studies on amylose esters have been carried out.[273] Monolayers and LBF of amylose acetate, propionate, butyrate, laurate, and palmitate were investigated. The compression isotherms for these polymers up to a degree of substitution in excess of 2.6 are presented in Fig. 50. It is seen that polymers with short, moderately long, and long side chains correspond to three types of isotherms. For short-chain derivatives, neither the temperature (10–37 °C) nor the rate of compression of the monolayer (1–10Å^2 per residue per minute) affect the compression isotherms in the region $\pi \leqslant 10$ mN m^{-1}. Comparison of model and experimental areas per elementary unit and also allowance for data[274] on the crystal structures of the homologous series of amylose esters led the authors[273] to the conclusion that mono-layers comprising helices are formed by short-chain amylose esters. In the region of the plateau, there is a transition from the helical monolayer to a bilayer. Unfortunately, the bilayers decompose on transfer of the film to a solid support and it was therefore not possible to determine their structural parameters.

An amylose ester with side chains of moderate length (laurate) also formed layers comprising helices on the surface of water. Finally, amylose palmitate, the long side chains of which are capable of crystallising, formed a true monolayer with a vertical disposition of the hydrocarbon chains.

Thus the properties of amylose ester monolayers with short side chains are determined by the conformation of the main chain, while those of the compounds with ester alkyl groups of moderate and great lengths are determined by the side chains. Comparison of the data in Figs 49 and 50 for monolayers of isotypical cellulose and amylose esters shows that both series of derivatives form expanded and condensed monolayers, but in the case of amylose esters the isotherms are displaced towards smaller areas.

Furthermore, in contrast to LBF of cellulose esters, those of amylose ester (up to 50 monolayers) can be obtained on solid hydrophobic surfaces by the vertical transfer method. In the case of amylose triacetate molecules, *Z*-layers are then formed whereas *Y*-layers are produced for other homologues. Amylose palmitate can be transferred only from the liquid state, the product being disubstituted derivatives. The arrangements of the LBF comprising monolayers of amylose esters with short and long side chains are compared in Fig. 51. These arrangements were obtained on the basis of polarisation IR spectroscopic, X-ray diffraction, and ellipsometric studies.[273]

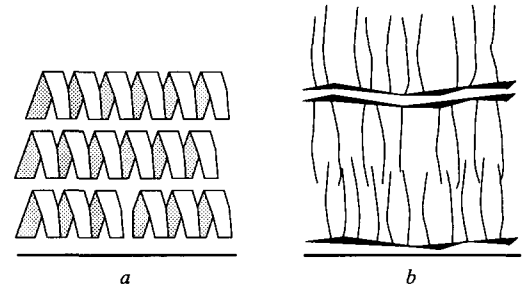


Figure 51. Schematic illustration of the arrangement of LBF of amylose esters with short (*a*) and long (*b*) side chains.[273]

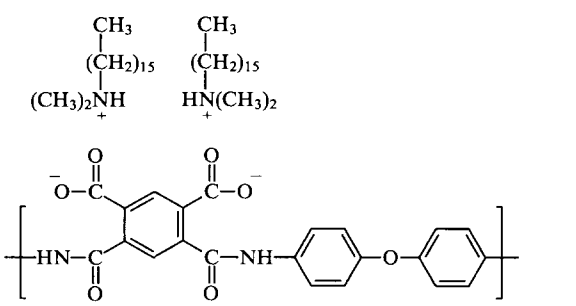
It has been suggested that amylose triacetate monolayers be used[275] as matrix layers for the immobilisation of a chromophore—the active element in a nonlinear optical system. A specially synthesised dye, the ester of palmitic acid and 4-nitro-4′(3R-hydroxypyrrolidino)-1,1′-azobisbenzene, does not afford at 23 °C stable monolayers on the surface of water suitable for use in LBF. Mixed monolayers of the dye and amylose triacetate are stable for a high dye content (up to 50%) and can be transferred onto solid supports by the horizontal and vertical methods. The mixed monolayers consist of amylose acetate domains and two-dimensional dye crystallites. The interfaces between the two types of structures play an appreciable role in increasing the stability of the monolayers. It is of interest that the

stabilisation of monolayers of the above dye by the formation of its mixed monolayers with other amylose esters cannot be achieved. On heating the LBF above the melting point of the dye (129 °C) and subsequent cooling to room temperature, the layered structure becomes more pronounced and virtually all the dye molecules are arranged in hydrogen-bonded aggregates.[276]

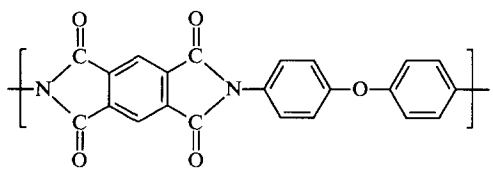
Thus, in relation to esters of cellulose and amylose, it is possible to follow the evolution of views on monolayers of these polymers and to demonstrate yet again the existence of discrepancies between data obtained by different workers in the study of identical polymers. The most interesting results presented in this section are the differences in the behaviour of monolayers of identical cellulose and amylose esters differing only in the configuration of the junctions between the glucose units and the similarity of the properties of monolayers of hydroxyalkyl derivatives of cellulose formed by spreading from solution and by adsorption from the subphase.

XII. Polyimides

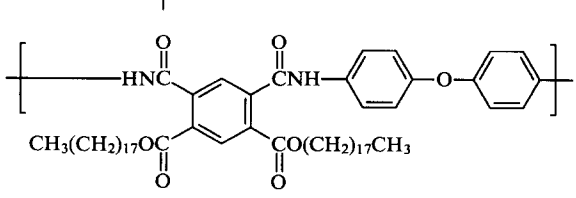
The effective dielectric and mechanical characteristics and the chemical and mechanical stabilities of polyimides have led to their extensive application in various branches of engineering and primarily in electronics.[277] The minimum thickness of films of polyimides obtained on a rotating support from solutions of a polyamidoacid with subsequent thermal or chemical conversion into the imide form is 25 Å.[278] Polymer films with a thickness from 4–6 to 1000 Å can be obtained with the aid of monolayers and LBF. Owing to the insolubility of polyimides in organic solvents, the LBF are formed in several stages. Monolayers of the alkylammonium salt of the polyamidoacid **32** or its long-chain ester **33** are obtained initially on the surface of water. After their transfer to a solid support, they are converted into the imide form by the thermal (~300 °C) or chemical (with a mixture of acetic anhydride and pyridine) methods. LBF of poly[*N,N'*-bis(phenoxyphenyl)pyromellitimide] **34** have been investigated most fully.[279–284]



32



34



33

The salt **32** forms stable monolayers of the liquid-expanded type on the surface of water. The limiting area of the monolayer (138 Å^2 per residue) agrees well with the area calculated from a model,[279] while the thickness of one layer, found ellipsometrically for a 50-layer LBF, is 16.5 Å.[285] The quantitative transfer of the polyamidoacid onto the solid support (Z type LBF) is indicated by the degree of transfer, which is unity, and also by the linearity of the dependences of the optical absorption and the reciprocal of the capacity on the LBF thickness. According to IR spectroscopic data for 200-layer LBF, the chemical imide formation process goes virtually to completion and aliphatic products are eliminated from the film. After this, the thickness of a single polyimide monolayer is 4 Å.[279]

The imide formation process depends on the type of the ammonium component of the salt, on the solvent in which the imide formation is carried out, and on the support on which it takes place. It has been shown with the aid of a piezoquartz microbalance that higher-quality Y type LBF are formed when *N,N*-dimethyloctadecylamine is used instead of *N*-octadecylpyrrolidine. The initial rate of imide formation, carried out using acetic anhydride and pyridine, is higher in hexane than in benzene, but the conversion is more complete in the latter.[286]

The structure and conformation of the main chain, the number of hydrophobic side chains, and the way in which they are attached to the main chain exert a significant influence on the arrangement of the molecules in the LBF. In particular, the presence of only one hydrocarbon chain in the unit does not allow the formation of an ordered LBF from the polyimide, while two hydrophobic chains attached to different parts of the polymer unit increase the capacity of the polymer for being ordered so much that the layered structure of the polyimide persists also on deposition of the polyamidoacid salt by casting from solution.[287] The influence of the chemical structure and of the flexibility of the main chain of the polyimide on the properties of the LBF has also been investigated by Nishikata et al.[288] LBF of the polyimide **34**, having a zigzag configuration, and also of a rigid linear polyimide containing the phenylenediamine group instead of the oxydianiline group have been investigated by scanning tunnelling microscopy (STM).[281–283,289] Individual polymer chains and their fragments were identified with the aid of STM. The LBF of both polyimides have an ordered structure. The geometrical parameters of the film structure on the surface of highly oriented pyrolytic graphite, evaluated with the aid of STM, agree with data on the orientation of the molecules and their fragments obtained by the molecular dynamics method[289] and EXAFS spectroscopy.[283]

Interesting data concerning the influence of the nature of the support and of the thickness of the LBF on the degree of imide formation have been published.[290] The authors established that the first monolayer of the octadecylammonium salt of the polyamidoacid interacts chemically with the surface of silicon and its molecules are not involved in the imide formation process. According to X-ray electron spectroscopy, the degree of conversion is fairly high in thicker three- and five-layer LBF, although alkyl chains still remain in the film up to 300 °C (annealing for 15 min *in vacuo*). The inhibition of imide formation in thin films of the polyamidoacid, obtained from solution on the surface of nickel and chromium, has been explained by the intense adhesion interactions between the carboxy-groups and the surface. The SiO_2 surface does not hinder the imide formation reaction.[278]

The disordered arrangement of the alkylammonium hydrocarbon chains of the polyamidoacid salt in the LBF and also the retention of these chains in the film at high annealing temperatures[290] are closely related to the question of the defectiveness of the polyimide films arising as a result of the removal of the initial hydrocarbon components. These problems are of key importance in the preparation of high-quality polyimide LBF and require further study.

The change in the orientation of the hydrocarbon chains in the monolayer of the dimethyloctadecylammonium salt of the polyamidoacid has been investigated[291] by the method based on the measurement of the displacement current generated on compression of the monolayer.[292,293] Fig. 52 presents the dependence of the surface pressure, the displacement current, and the dipole moment calculated[294] with its aid on the area of the polyamidoacid salt monolayer. Two peaks may be identified on the $I-A$ relation: one in the region of zero surface pressure and the other in the region of increasing π. With increase in the first peak in I, the dipole moment also increases. Both displacement current peaks can be accounted for by condensation of the polymer molecules in the monolayer.

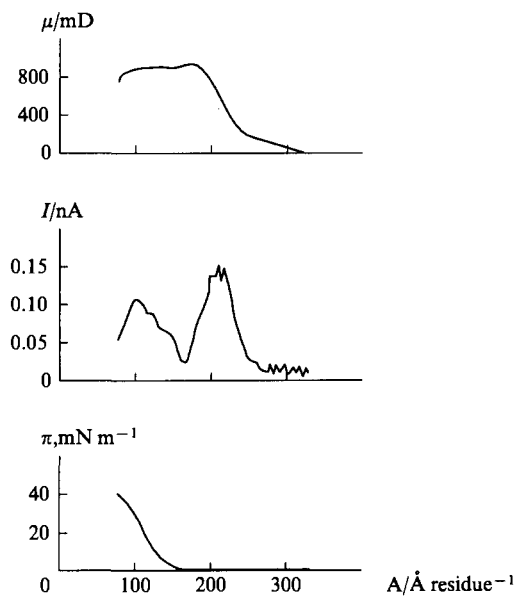


Figure 52. Dependence of the dipole moment (μ), the displacement current (I), and the surface pressure (π) on the area of a monolayer of an alkylammonium salt of a polyamidoacid on the surface of water.[291]

The photoinduced molecular 'switching' in monolayers of the polyamidoacid salt containing the azobenzene group instead of the phenoxyphenyl group has been detected from measurements of the displacement current.[259–297] It was established from molecular spectroscopic data that, on irradiation of the monolayer with UV light (λ_1 = 380 nm), the *trans–cis* isomerisation of the azobenzene group is observed, while on subsequent irradiation with visible light (λ_2 = 450 nm) the reverse *cis–trans* transition occurs. Fig. 53 presents the time variation of the displacement current and of the charge generated for the monolayer on the surface of water. It is seen that the photoisomerisation induces a sharp alteration of the displacement current. The absence of a displacement on irradiation of the monolayer with visible light alone shows that the current is generated precisely by the *trans–cis* isomerisation. Single-layer LBF of the same polyamidoacid salt deposited onto a mixed indium oxide–tin oxide electrode behave similarly.[298] Evidently these results are likely to find a practical application in molecular electronics.

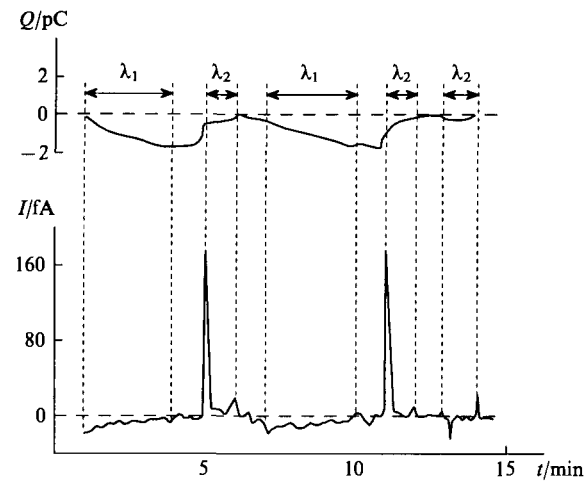


Figure 53. Time variation of the displacement current (I) and the charge (Q) for a monolayer of an alkylammonium salt of a polyamidoacid, containing azobenzene groups, on the surface of water.[295] The time intervals during which the specimen was irradiated with light at wavelengths of 380 nm (λ_1) and 450 nm (λ_2) are indicated.

A design has been proposed for a three-layer photodiode, each layer of which is a polyimide LBF.[299] The donor layer (D) consists of a polyimide containing triphenylamine groups. The sensitiser layer (S) incorporates tetraphenylporphyrin groups. The polyimide **34** LBF was used as the acceptor layer (A). Two types of photodiodes, differing in the position of the layers relative to a semitransparent gold electrode (E), were formed: E/D/S/A and E/A/S/D. The principle of the operation of such photodiodes is as follows: on irradiation with light, the excited electrons are transferred from the sensitiser layer S to the acceptor layer A; the electron deficiency in the S layer is made good from the donor D layer. Z Type LBF were formed in each layer in conformity with the procedure described above, i.e. from monolayers of polyamidoacid salts with subsequent chemical conversion into the imide form. The number of monolayers in each LBF was varied from 0 to 12. It was established that, on irradiation with monochromatic light at a wavelength of 430 nm, cathodic and anodic currents are generated in the photodiodes of the first and second types respectively. With increase in the number of monolayers in each LBF, the current also increases but that for the D layer reaches saturation while the current for the S and A layers passes through a maximum. On the basis of these data as well as the quantum yields, it was concluded that the D layer exhibits a high hole mobility and that the electron mobilities are low in the S and A layers.

LBF comprising the salt of a polyamidoacid based on pyromellitic dianhydride and bis(4-aminophenyl)tetramethyldisilane can be used as positive resists.[300] The quality of the LBF then depends significantly on the type of alkylamine used to obtain the polyamidoacid salt. Among the four dialkylamines selected for this purpose, a high-quality Y type LBF, containing 101 monolayers, could be formed only with *N*-eicosylpyrrolidine. With the aid of the three other alkylamines (*N,N*-dimethyloctadecylamine, *N*-octadecylpyrrolidine, and *N*-octadecylmorpholine), it is possible to obtain LBF the thickness of which does not exceed ten monolayers. After chemical or thermal conversion into the imide form, the LBF were irradiated with UV light through a photomask and were then treated in a mixture of organic solvents. The irradiated sections of the LBF were fully removed, whereas the polyimide on the covered sections of the LBF did not swell and did not dissolve. The use of such a LBF as a positive resist makes it possible to obtain a lithographic picture with a resolution of 0.25 μm.

The polyamidoacid ester **33** has also been used for photolithographic purposes.[301] A 31-layer LBF comprising mixed 1 : 1 monolayers of compound **33** and stearyl alcohol was formed on a silicon surface which had been rendered hydrophilic. The image was created by irradiating the LBF with UV light (254 nm) through a template followed by treatment in 2% KOH solution. The sensitivity, contrast, and resolution of the positive resist were 3.5 J cm^{-2}, 5.5, and 0.4 μm respectively. A characteristic feature of this resist is a low rate of etching in a CF_4/O_2 plasma and a high thermal stability (400 °C). The rates of etching of the LBF and of the silicon support were 1 and 350 nm min^{-1}. The high resistance of the polyamidoacid ester to etching can be accounted for by the presence of aromatic groups in the polymer and the perfection of the LBF structure. Unfortunately, Uekita et al.[301] do not consider the influence of stearyl alcohol, which may be washed out of the LBF on treatment in the liquid and may be desorbed during heat treatment. This should result in an increase in the effectiveness of the LBF and in the impairment of its structure.

Polyimide LBF are used as orienting layers in liquid crystal cells.[302, 303] In this case, the liquid crystals are oriented parallel to the direction of transfer of the monolayers from the surface of water onto the supporting surfaces of the cells; rubbing of the film is not then required.

A combination of conducting and orienting properties has been achieved recently on pyrolysed polyimide LBF based on biphenyl dianhydride [biphenyldicarboxylic acid dianhydride? (Translator)] and oxydianiline.[304, 305] The pyrolysis of the 31-layer Y type LBF was carried out under a nitrogen atmosphere for 60 min. Fig. 54 illustrates the dependence of the conductivity of the specimens obtained on the pyrolysis temperature. The sharpest increase in conductivity is observed for specimens obtained in the temperature range up to 800 °C. At 1000 °C, the conductivity of the LBF reaches 120 S cm^{-1}. The orienting properties of the films obtained were determined in a liquid crystal cell, arranging the supporting surfaces in such a way that the directions of transfer of the monolayers on them made an angle of 90° ('twist' structure). The cell was filled with a nematic liquid crystal and the optical and electrooptical properties of the system were analysed with the aid of a polarisation microscope. Fig. 55 presents the dependence of the transmittance on the angle between the analyser and the polariser for the twisted nematic structure in liquid crystal cells with supporting surfaces in the form of untreated quartz plates, a rubbed polyimide film, and a pyrolysed polyimide LBF. It is seen that the pyrolysed and rubbed polyimide films have similar orientation properties. However, the mechanism of the orienting effect of the pyrolysed LBF still remains obscure, since, according to polarisation optical spectroscopic data, the film has no planar anisotropy.[304]

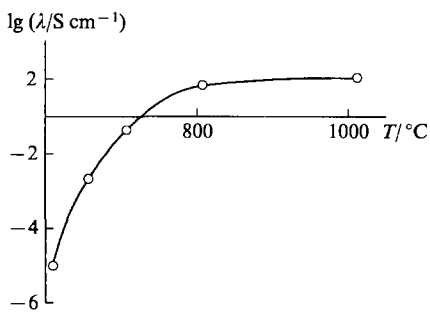


Figure 54. Dependence of the conductivity of specimens of pyrolysed polyimide LBF on the pyrolysis temperature.[305]

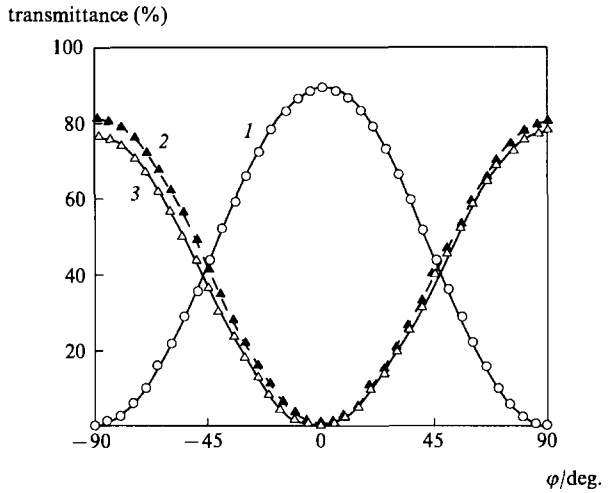


Figure 55. Dependence of the transmittance on the angle between the analyser and the polariser (φ) for a twisted nematic structure in liquid crystal cells with supporting surfaces in the form of untreated quartz plates (curve *1*), a rubbed polyimide film (curve *2*), and a pyrolysed polyimide LBF (curve *3*).[304]

The electrooptical properties of two liquid crystal cells with supporting surfaces comprising pyrolysed LBF and rubbed polyimide film are presented in Fig. 56. Both cells have similar characteristics. The response times to the switching on and switching off of an alternating potential are respectively 200 and 200 ms for the pyrolysed polyimide LBF and 100 and 200 ms for the rubbed film. Consequently, pyrolysed polyimide LBF can be used as more effective orienting layers and transparent electrodes in liquid crystal cells and also in ferroelectric liquid crystal cells.[304, 306]

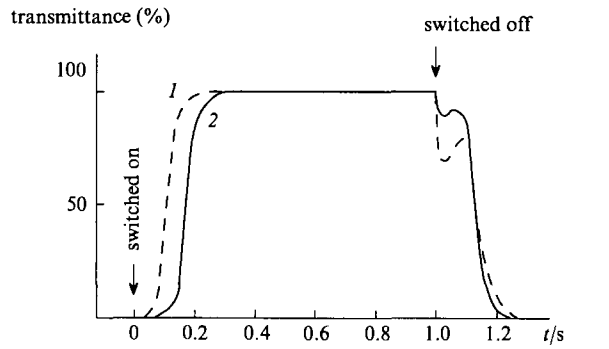


Figure 56. The electrooptical properties of a twisted nematic structure in liquid crystal cells with supporting surfaces comprising a rubbed polyimide film (curve *1*) and a pyrolysed polyimide LBF (curve *2*).[304]

Thus the possibility of obtaining insoluble polymer LBF has been demonstrated in relation to polyimides. In contrast to insoluble polymer LBF obtained by polymerising monomer and oligomer monolayers on a solid support, in the present instance the polymer retains the degree of polymerisation of the prepolymer — the polyamidoacid salt or ester. The imide formation process and the arrangement and quality of the LBF obtained depend on the type of amine component of the polymeric acid, on the solvent in which the chemical imide formation is carried out, and on the nature of the solid support.

The photoswitching effect, based on the *trans – cis* isomerisation of the chromophoric fragment of the main chain, can be achieved with the aid of LBF comprising polyimides containing the azobenzene group. There are also prospects for the application of polyimide LBF as positive photoresists, photodiodes, and orienting layers in liquid crystal cells.

XIII. Conclusion

On the basis of the above analysis of the behaviour of polymer monolayers and LBF, it is possible to arrive at general conclusions concerning the present state of this field of study and the trends in its development.

Among the theoretical aspects, questions concerning the two-dimensional state of macromolecules and the phase and structural transitions in systems with a reduced dimensionality are of greatest current interest. Unfortunately, it must be admitted that there has been no appreciable progress in the study of these fundamental problems of the two-dimensional state of macromolecules. The experimental studies on homopolymer and copolymer monolayers and mixed monolayers comprising polymers and low-molecular-mass compounds are developing more successfully. These involve the investigation of the packing of macromolecules on the surface of a liquid and the influence of the size and orientation of the side groups on the state of the monolayers, the elucidation of the structural correspondence between the components of the mixed monolayers, and the determination of the stability of monomolecular films. However, whereas previously these studies, traditional for monolayers, were of independent character and were sufficiently detailed, in recent years they have played an auxiliary role in most cases and reduce to the determination of the compression isotherms as an essential stage in the formation of LBF. Specific conclusions for each type of polymers considered, based on the results of these investigations, were presented in the appropriate sections of the review. These also contain information about the prospects for the practical employment of polymer LBF. The use of polymer LBF is based, as in the case of LBF comprising low-molecular-mass compounds, on the possibility of assembling multilayer planar structures with a controllable film thickness and orientation of the molecules in layers. Together with the independent role of functionalised polymer LBF in molecular devices, they can be used as matrices for the immobilisation of low-molecular-mass compounds (necessarily diphilic) carrying a specified physical function.

In order to realise these possibilities, it is essential to carry out extensive studies on polymer monomers and LBF, among which the following are of greatest current interest: the determination of the viscoelastic and relaxation properties of polymer monolayers, the establishment of criteria for the preparation of LBF of a specified type, the study of the structural-chemical correlations in the arrangement of monolayers on liquid and solid surfaces.

In conclusion we may note that the studies on monolayers and LBF are not restricted to the objects considered in the present review. Other polymers, the properties of the monolayers and LBF of which the author proposes to consider in subsequent publications, will include conducting high-molecular-mass compounds, water-soluble ionogenic polymers, and certain other functionalised polymers.

This review has been written with the financial support of the Russian Fundamental Research Fund (project code 93-03-5659).

References

1. J-M Lehn *Angew. Chem., Int. Ed. Engl.* **27** 89 (1988)
2. R Maoz, J Sagiv *J. Colloid Interface Sci.* **100** 465 (1984)
3. J Gun, J Sagiv *J. Colloid Interface Sci.* **102** 457 (1986)
4. D L Allara, R G Nuzzo *Langmuir* **1** 45 (1985)
5. D L Allara, S V Atre, C A Elliger, R G Snyder *J. Am. Chem. Soc.* **113** 1852 (1991)
6. R G Nuzzo, D L Allara, F A Fusco *J. Am. Chem. Soc.* **109** 2358 (1987)
7. E B Troughton, C D Bain, G M Whitesides, R G Nuzzo, D L Allara, M D Porter *Langmuir* **4** 365 (1988)
8. C D Bain, E B Troughton, Y T Tao, J Evall, G M Whitesides, R G Nuzzo *J. Am. Chem. Soc.* **111** 321 (1989)
9. M A Bryant, J E Pemberton *J. Am. Chem. Soc.* **113** 3629 (1991)
10. P Laibinis, G M Whitesides, A N Parikh, Y T Tao, D L Allara, R G Nuzzo *J. Am. Chem. Soc.* **113** 7152 (1991)
11. D M Collard, M A Fox *Langmuir* **7** 1192 (1991)
12. P E Laibinis, J J Hickman, M S Wrighton, G M Whitesides *Science* **245** 845 (1989)
13. M H Möhwald *Angew. Chem.* **100** 750 (1989)
14. M G Mneyan *Fizika Mashinnoi Pamyati* (The Physics of Machine Memory) (Moscow: Vysshaya Shkola, 1990)
15. J F Nagle, D A Pink *Can. J. Biochem. Cell. Biol.* **62** 760 (1984)
16. J F Nagle *Annu. Rev. Phys. Chem.* **31** 157 (1980)
17. V V Arslanov *Usp. Khim.* **60** 1155 (1991) [*Russ. Chem. Rev.* **60** 584 (1991)]
18. H Devaux *C. R. Hebd. Seances Acad. Sci.* **201** 109 (1935)
19. J R Katz, P J P Samwel *Liebigs Ann. Chem.* (472) 241; (474) 296 (1929)
20. N K Adam *Trans. Faraday Soc.* **29** 90 (1933)
21. S E Sheppard, R L Keeman *Nature (London)* **121** 938 (1928)
22. J R Katz, P J P Samwel *Naturwissenschaften* **16** 592 (1928)
23. S A Moss *J. Am. Chem. Soc.* **56** 41 (1934)
24. W D Harkins, E F Carman, H F Ries *J. Chem. Phys.* **3** 692 (1935)
25. D J Crisp *J. Colloid. Sci.* **1** 49 (1946)
26. D J Crisp *Surface Phenomena in Chemistry and Biology* (London: Pergamon Press, 1958)
27. H C Saraswat, A Kalyanasundaram *J. Polym. Sci.* **7** 325 (1951)
28. Y S Obeng, A J Bard *J. Am. Chem. Soc.* **113** 279 (1991)
29. T Nakamura, H Tachibana, M Yumura, M Matsumoto, R Azumi, M Tanaka, Y Kawabata *Langmuir* **8** 4 (1992)
30. G L Gaines, Jr *Langmuir* **7** 834 (1991)
31. A Pokels *Nature (London)* **46** 418 (1892); **48** 152 (1893)
32. V A Ogarev, V V Arslanov, A A Trapeznikov *Izv. Akad. Nauk SSSR, Ser. Khim.* **9** 1960 (1972)
33. J Parker, J L Shereshefsky *J. Phys. Chem.* **58** 850 (1954)
34. P G De Gennes *Scaling Concepts in Polymer Physics* (New York: Cornell Univ. Press, 1979)
35. T M Birshtein, O V Borisov, A A Mercurieva, E B Zhulina *Prog. Colloid Polym. Sci.* **85** 38 (1991)
36. R Aveyard, B P Binks, N Carr, A W Cross *Thin Solid Films* **188** 361 (1990)
37. R D Smith, J C Berg *J. Colloid Interface Sci.* **74** 273 (1980)
38. B A Pethica *Thin Solid Films* **152** 3 (1987)
39. W Retting, F Kuschel *J. Colloid Interface Sci.* **140** 169 (1990)
40. M Iwahashi, N Maehara, Y Kaneko, S R Middleton, N R Pallas, B A Pethica *J. Chem. Soc., Faraday Trans. 1* **81** 973 (1985)
41. W D Harkins *The Physical Chemistry of Surface Films* (New York: Reinhold, 1952)
42. N K Adam *Physics and Chemistry of Surfaces* (Translated into Russian; Moscow, Leningrad: Gostekhizdat, 1947)
43. G L Gaines, Jr *Insoluble Monolayers at Liquid-Gas Interfaces* (London: Interscience , 1966)
44. Y M Hifeda, G W Rayfield *J. Colloid Interface Sci.* **104** 209 (1985)
45. N R Pallas, B A Pethica *Langmuir* **1** 509 (1985)
46. S R Middleton, M Iwahashi, N R Pallas, B A Pethica *Proc. R. Soc. London, A. Math. Phys. Sci.* **396** 143 (1984)
47. N R Pallas, B A Pethica *J. Chem. Soc., Faraday Trans. 1* **83** 585 (1987)
48. Y M Hifeda, G W Rayfield *Langmuir* **8** 197 (1992)
49. O Albrecht *Thin Solid Films* **178** 93 (1989)
50. A A Trapeznikov *Zh. Fiz. Khim.* **20** 61 (1946)

51. A A Trapeznikov, Doctoral Thesis in Chemical Sciences, Institute of Chemical Physics, Academy of Sciences, Moscow, 1955
52. V V Arslanov, Candidate Thesis in Chemical Sciences, Institute of Physical Chemistry, Academy of Sciences of the USSR, Moscow, 1973
53. H Huehnerfuss *J. Colloid Interface Sci.* **107** 84 (1985)
54. K Helperin, J B Ketterson, P Dutta *Langmuir* **5** 161 (1989)
55. A G Bois *J. Colloid Interface Sci.* **105** 124 (1985)
56. T Kato *Langmuir* **6** 870 (1990)
57. K C O'Brien, J B Lando *Langmuir* **1** 433 (1985)
58. E J McNally, G Zografi *J. Colloid Interface Sci.* **138** 61 (1990)
59. H W Fox, P W Taylor, W A Zisman *Ind. Eng. Chem.* **39** 1401 (1947)
60. M J Newing *Trans. Faraday Soc.* **46** 755 (1950)
61. A A Trapeznikov, T N Zatsepina, T A Gracheva, R N Shcherbakova, V A Ogarev *Dokl. Akad. Nauk SSSR* **160** 174 (1965)
62. J E Sutherland, M L Miller *J. Colloid Interface Sci.* **32** 181 (1970)
63. A E Fainerman, Yu S Lipatov, V K Maistruk *Dokl. Akad. Nauk SSSR* **178** 1129 (1968)
64. J Guastalla *C. R. Hebd. Seances Acad. Sci.* **208** 1078 (1939)
65. V A Ogarev, Candidate Thesis in Chemical Sciences, Institute of Physical Chemistry, Academy of Sciences of the USSR, Moscow, 1963
66. K Ariga, Y Okahata *J. Am. Chem. Soc.* **111** 5618 (1989)
67. A M Bibo, C M Knobler, I R Peterson *J. Phys. Chem.* **95** 5591 (1991)
68. C M Knobler *J. Phys. Condens. Mater.* **3** 17 (1991)
69. M Engel, H J Merle, I R Peterson, H Riegler, R Steitz *Ber. Bunsenges. Phys. Chem.* **95** 1514 (1991)
70. D Dervichian *J. Chem. Phys.* **7** 931 (1939)
71. S Stillberg-Stenhagen, E Stenhagen *Nature (London)* **156** 239 (1945)
72. M Lundquist *Chem. Scr.* **1** 5 (1971)
73. B Lin, M C Shin, T M Bohanon, G E Ice, P Dutta *Phys. Rev. Lett.* **65** 191 (1990)
74. P Le Barny *Thin Solid Films* **152** 99 (1987)
75. S W J Kuan, C W Frank, C C Fu, D R Allee, P Maccagno, R F W Pease *J. Vac. Sci. Technol. B* **6** 2274 (1988)
76. N Beredjick, H E Rice, Jr *J. Polym. Sci.* **62** 64 (1962)
77. M J Schick *J. Polym. Sci.* **25** 465 (1957)
78. N Beredjick, R A Ahlbeck, T K Kwei, H E Ries *J. Polym. Sci.* **46** 268 (1960)
79. S Wu, J R Huntsberger *J. Colloid Interface Sci.* **29** 138 (1969)
80. A Labbauf, J R Zack *J. Colloid Interface Sci.* **35** 569 (1971)
81. G Gabrielli, M Puggelli, R Faccioli *J. Colloid Interface Sci.* **41** 63 (1972)
82. A Blumstein, H E Ries *J. Polym. Sci., Part B, Polym. Phys.* **3** 927 (1965)
83. M Puggelli, G Gabrielli *Colloid Polym. Sci.* **263** 879 (1985)
84. E Bringuier, R Vilanove, Y Gallot, J Selb, F Rondelez *J. Colloid Interface Sci.* **104** 95 (1985)
85. H Hotta *J. Colloid. Sci.* **9** 504 (1954)
86. T Nakahara, K Motomura, R Matuura *Bull. Chem. Soc. Jpn.* **40** 495 (1967)
87. S J Mumby, J D Swalen, J F Rabolt *Macromolecules* **19** 1054 (1986)
88. T Arndt, C Bubeck, A J Schouten, G Wegner *Microchim. Acta* 7 (1988)
89. J F Rabolt *J. Chim. Phys.* **85** 1027 (1988)
90. C J Drummond, P Elliott, D N Furlong, G T Barnes *Thin Solid Films* **210/211** 69 (1992)
91. S Yoshikawa, M Ueno, K Meguro *Bull. Chem. Soc. Jpn.* **51** 3136 (1978)
92. D Naegele, H Ringsdorf *J. Polym. Sci., Polym. Chem. Ed.* **15** 2821 (1977)
93. M Ueno, S Yoshikawa, K Meguro *J. Polym. Sci., Polym. Chem. Ed.* **17** 334 (1979)
94. N Beredjick, W J Burlant *J. Polym. Sci., Part A-1* **8** 2807 (1970)
95. G Gabrielli, M Puggelli, P Bagloni *J. Colloid Interface Sci.* **86** 485 (1982)
96. M Puggelli, G Gabrielli *Colloid Polym. Sci.* **261** 166 (1983)
97. M Hatada, M Nishii, K Hirota *J. Colloid Interface Sci.* **45** 502 (1973)
98. T Nakahara, K Motomura, R Matuura *J. Polym. Sci., Part A-2* **4** 649 (1966)
99. C S Winter, R H Tredgold, A J Vickers, E Khoshdel, P Hodge *Thin Solid Films* **134** 49 (1985)
100. M Avrami *J. Chem. Phys.* **8** 221 (1940)
101. G Caminati, G Gabrielli, M Puggelli, E Ferroni *Colloid Polym. Sci.* **266** 775 (1988)
102. G Caminati, G Gabrielli, M Puggelli, E Ferroni *Colloid Polym. Sci.* **267** 237 (1989)
103. K Naito *J. Colloid Interface Sci.* **131** 218 (1989)
104. H Matsuda, H Kawada, K Takimoto, Y Morikawa, K Eguchi, T Nakagiri *Thin Solid Films* **178** 505 (1989)
105. S Okada, H Nakanishi, H Matsuda, M Kato, T Abe, H Ito *Thin Solid Films* **178** 313 (1989)
106. R Elbert, A Laschewsky, H Ringsdorf *J. Am. Chem. Soc.* **107** 4134 (1985)
107. A Laschewsky, H Ringsdorf, J Schneider *Angew. Makromol. Chem.* **145/146** 1 (1986)
108. S Hironaka, K Meguro *J. Colloid Interface Sci.* **35** 367 (1971)
109. V A Kargin, Yu M Malinskii, S S Medvedev *Dokl. Akad. Nauk SSSR* **96** 307 (1954)
110. S Yoshikawa, M Ueno, K Meguro *Colloid Polym. Sci.* **256** 422 (1978)
111. S Yoshikawa, M Ueno, K Meguro *J. Colloid Interface Sci.* **69** 334 (1979)
112. S Yoshikawa, M Ueno, K Meguro *J. Polym. Sci., Polym. Chem. Ed.* **17** 2491 (1979)
113. H Kumehara, T Kasuga, T Watanabe, S Miyata *Thin Solid Films* **178** 182 (1989)
114. R Vilanove, F Rondelez *Phys. Rev. Lett.* **45** 1502 (1980)
115. M B Biddle, J B Lando, H Ringsdorf, G Schmidt, J Schneider *Colloid Polym. Sci.* **266** 806 (1988)
116. H Ringsdorf, G Schmidt, J Schneider *Thin Solid Films* **152** 207 (1987)
117. H Ringsdorf, B Schlarb, J Schneider *Polym. Prepr.* **27** 127 (1986)
118. P Stroeve, G J R Spooner, P J Bruinsma, L B Coleman, C H Erdelen, H Ringsdorf *ACS Symp. Ser.* **447** 177 (1991)
119. P J Bruinsma, C Sturesson, G J R Spooner, L B Coleman, P Stroeve *Polym. Prepr.* **32** 242 (1991)
120. P J Bruinsma, G J R Spooner, L B Coleman, R Koren, C Sturesson, P Stroeve *Thin Solid Films* **210/211** 440 (1992)
121. L B Coleman, T G Fiske, P Stroeve, M A N Coelho, S Dong, H Ringsdorf, J Schneider *Thin Solid Films* **178** 227 (1989)
122. P Stroeve, M A N Coelho, S Dong, P Lam, L B Coleman, T G Fiske, H Ringsdorf, J Schneider *Thin Solid Films* **180** 241 (1989)
123. K Kurihara, T Kunitake, N Higashi, M Niwa *Thin Solid Films* **210/211** 681 (1992)
124. J N Israelachvili *Intermolecular and Surface Forces* (London: Academic Press, 1985)
125. J N Israelachvili *Surf. Sci. Rep.* **14** 109 (1992)
126. R M Pashley, P M McGuiggan, B W Ninham, J Brady, D F Evans *J. Phys. Chem.* **90** 1637 (1986)
127. P Kekicheff, H K Chistenson, B W Ninham *Colloid Surf.* **40** 31 (1989)
128. K Kurihara, S Kato, T Kunitake *Chem. Lett.* 1555 (1990)
129. H Hsiung, J Rodriguez-Parada, R Bekerbauer *Chem. Phys. Lett.* **182** 88 (1991)
130. B K Mandal, T Takahashi, M Maeda, S Kumar, A Blumstein, S K Tripathy *Makromol. Chem.* **192** 1009 (1991)
131. T Takahashi, Y M Chen, A K Rahaman, J Kumar, S K Tripathy *Thin Solid Films* **210/211** 202 (1992)
132. P Tao, L Xu, G Chen, X Yang, G Wang, J Zheng, Z Zhang, W Wang *Thin Solid Films* **179** 381 (1989)
133. W Hickel, G Appel, D Lupo, W Prass, U Scheunemann *Thin Solid Films* **210/211** 182 (1992)
134. W Meisel, P Tippmann-Krayer, H Möhwald, P Gütlich, J Fresenius *Anal. Chem.* **341** 289 (1991)
135. K Kobayashi, K Takaoka, S Ochiai *Thin Solid Films* **178** 453 (1989)
136. P Tippmann-Krayer, H Möhwald *J. Phys. Chem.* **96** 5220 (1992)
137. B Hagenhoff, A Benninghoven, H-U Siegmund, D Holtkamp *Thin Solid Films* **210/211** 601 (1992)
138. B Hagenhoff, M Deimel, A Benninghoven, H-U Siegmund, D Holtkamp *J. Phys. D* **25** 818 (1992)
139. M Shimomura, K Song, J F Rabolt *Langmuir* **8** 887 (1992)

140. G Gabrielli, M Puggelli, R Faccioli *J. Colloid Interface Sci.* **37** 213 (1971)
141. G Gabrielli, M Puggelli, E Ferroni *J. Colloid Interface Sci.* **47** 145 (1974)
142. F C Goodrich, in *Proceedings of 2nd Int. Congr. Surface Activity, London, 1957* Vol. 1, p. 85
143. S J Singer *J. Chem. Phys.* **16** 872 (1948)
144. H L Frisch, R Simha *J. Chem. Phys.* **27** 702 (1957)
145. G Gabrielli, M Puggelli, E Ferroni *J. Colloid Interface Sci.* **32** 242; **33** 133 (1970)
146. J T Davies, E K Rideal *Interfacial Phenomena* (New York: Academic Press, 1963)
147. P Joos *Kolloid. Z.* **238** 499 (1970)
148. G Gabrielli, M Puggelli, P Baglioni *J. Colloid Interface Sci.* **86** 490 (1982)
149. M L Huggins *Kolloid. Z.* **251** 449 (1973)
150. G Gabrielli, G G T Guarini *J. Colloid Interface Sci.* **64** 185 (1978)
151. M Puggelli, G Gabrielli *Colloid Polym. Sci.* **263** 885 (1985)
152. G Gabrielli, A Maddii *J. Colloid Interface Sci.* **64** 19 (1978)
153. G Gabrielli, P Baglioni, A Fabbrini *Colloid Surf.* **3** 147 (1981)
154. E G Cocbain, K J Day, A J McMullen, in *Proceedings of 2nd Int. Congr. Surface Activity, London, 1957* Vol. 1, p. 56
155. T Isemura, H Hotta, T Miwa *Bull. Chem. Soc. Jpn.* **26** 380 (1953)
156. G Gabrielli, M Puggelli *J. Colloid Interface Sci.* **35** 460 (1971)
157. H E Ries, D C Walker *J. Colloid Sci.* **16** 361 (1961)
158. J Lopis, D V Rebollo *J. Colloid Sci.* **11** 543 (1956)
159. G Gabrielli, M Puggelli *J. Colloid Interface Sci.* **37** 503 (1971)
160. F H Müller *Z. Electrochem.* **59** 312 (1955)
161. D J Crisp *Research Suppl. Surf. Chem. (London)* **17** 23 (1947)
162. J Heller, D J Lyman *J. Polym. Sci., Polym. Phys. Ed.*, **1** 317 (1963)
163. H E Ries, Jr, R A Ahlbeck, J Gabor *J. Colloid Sci.* **14** 354 (1959)
164. G C Benson, R L McIntosh *J. Colloid Sci.* **3** 323 (1948)
165. F M Fowkes, M J Schick, A Bondi *J. Colloid Sci.* **15** 531 (1960)
166. J Gottlieb *J. Phys. Chem.* **64** 427 (1960)
167. H Schuller *Z. Elektrochem.* **60** 147 (1956)
168. K Huff, F H Müller *Kolloid. Z.* **120** 49 (1952)
169. R H Tredgold *Rep. Prog. Phys.* **50** 1609 (1987)
170. G Gabrielli, P Baglioni, E Ferroni *Colloid Polym. Sci.* **257** 121 (1979)
171. M Puggelli, G Gabrielli *J. Colloid Interface Sci.* **61** 420 (1977)
172. A Labbauf *J. Appl. Polym. Sci.* **10** 865 (1966)
173. J B Peng, G T Barnes *Langmuir* **6** 578 (1990)
174. S A Letts, T Fort, J B Lando *J. Colloid Interface Sci.* **56** 64 (1976)
175. K Fukuda, T Kato, S Machida, Y Shimizu *J. Colloid Interface Sci.* **68** 82 (1979)
176. G Gabrielli, C D'Aubert *Colloid Polym. Sci.* **56** 258 (1980)
177. G Gabrielli, P Baglioni, A Maddi *J. Colloid Interface Sci.* **79** 268 (1981)
178. N Beredjick *Newer Methods of Polymer Characterization* (Ed. K Bacon) (New York: Interscience, 1964)
179. M Puggelli, G Gabrielli *Colloid Polym. Sci.* **82** 261 (1983)
180. K Oguchi, T Yoden, Y Kosaka, M Watanabe, K Sanui, N Ogata *Thin Solid Films* **161** 305 (1988)
181. M Watanabe, Y Kosaka, K Oguchi, K Sanui, N Ogata *Macromolecules* **21** 2997 (1988)
182. T P Kenigsberg, N G Ariko, V E Agabekov, N I Mitskevich *Acta Chim. Hung.* **129** 545 (1992)
183. N Ogata, K Sanui, K Oguchi, T Nakada, Y Takahashi *J. Appl. Polym. Sci.* **28** 2433 (1983)
184. S Ito, H Okubo, S Ohmori, M Yamomoto *Thin Solid Films* **179** 445 (1989)
185. S Ito, T Ueno, M Yamomoto *Thin Solid Films* **210/211** 614 (1992)
186. J P Rabe, J F Rabolt, C A Brown, J D Swalen *J. Chem. Phys.* **84** 4096 (1986)
187. J P Rabe, J F Rabolt, C A Brown, J D Swalen *Thin Solid Films* **133** 153 (1985)
188. S Lee, B Hillebrands, G I Stegeman, L A Laxhuber, J D Swalen *J. Chem. Phys.* **91** 1882 (1989)
189. C S Winter, R H Tredgold, A J Vickers, E Khoshdel, P Honge *Thin Solid Films* **134** 49 (1985)
190. R H Tredgold, A J Vickers, P Hodge, A Hoorfar, E Khoshdel *J. Phys. D* **18** 1139 (1985)
191. B P Binks, P D I Fletcher, A Price, P Hodge *Thin Solid Films* **207** 273 (1992)
192. R H Tredgold, C S Winter *J. Phys. D* **15** 155 (1982)
193. R H Tredgold, C S Winter *Thin Solid Films* **99** 81 (1983)
194. M R Buhaenko, J W Goodwin, R M Richardson *Thin Solid Films* **159** 171 (1988)
195. L Ter-Minassian-Saraga, S J Abitboul *J. Colloid Interface Sci.* **48** 32, 42 (1974)
196. M Niwa, E Matsuyoshi, N Higashi *Langmuir* **5** 1256 (1989)
197. P DeKeyser, P Joos *J. Phys. Chem.* **88** 274 (1984)
198. E S Nikomarov *Langmuir* **6** 410 (1990)
199. H E Ries, Jr, H Swift *Langmuir* **3** 853 (1987)
200. A W Adamson *Physical Chemistry of Surfaces* (New York: Wiley, 1982)
201. B M Abraham, J B Ketterson *Langmuir* **1** 461 (1985)
202. P Ekwall, R Ekholm, A Norman *Acta Chem. Scand.* **11** 703 (1957)
203. H Sobotka, M Demeny, M Arnaki *J. Colloid Interface Sci.* **14** 281 (1959)
204. V N Izmailova, G P Yampol'skaya, B D Summ *Poverkhnostnye Yavleniya v Belkovykh Sistemakh* (Surface Phenomena in Protein Systems) (Moscow: Khimiya, 1988)
205. G P Yampol'skaya, P V Nuss, G Ts Raznikova, V N Izmailova, in *Uspekhi Kolloidnoi Khimii* (Advances in Colloid Chemistry) (Leningrad: Khimiya, 1991) p. 292
206. K S Birdi *Lipids and Biopolymers in Monolayers at Liquid Interfaces* (New York: Plenum, 1989)
207. S J Singer, G L Nicolson *Science* **175** 720 (1972)
208. V Erokhin, L A Feigin *Prog. Colloid Polym. Sci.* **85** 47 (1991)
209. T Isemura, K Hamaguchi *Bull. Chem. Soc. Jpn.* **25** 40 (1952)
210. B R Malcolm *Proc. R. Soc. London, A. Math. Phys. Sci.* **305** 363 (1968)
211. B R Malcolm *Prog. Surf. Membr. Sci.* **7** 183 (1973)
212. G I Loeb, R E Baier *J. Colloid Interface Sci.* **27** 38 (1968)
213. B R Malcolm *Polymer* **7** 595 (1966)
214. D W Goupil, F C Goodrich *J. Colloid Interface Sci.* **62** 142 (1977)
215. B R Malcolm *Thin Solid Films* **134** 201 (1985)
216. B R Malcolm *J. Colloid Interface Sci.* **104** 520 (1985)
217. G Gabrielli, E Ferroni, M L Huggins *Prog. Colloid Polym. Sci.* **58** 201 (1975)
218. P Baglioni, L Dei, E Ferroni, G Gabrielli *Colloid Surf.* **60** 399 (1991)
219. P Baglioni, L Dei, G Gabrielli *J. Colloid Interface Sci.* **93** 402 (1983)
220. B R Malcolm *Thin Solid Films* **178** 191 (1989)
221. B R Malcolm *Thin Solid Films* **178** 17 (1989)
222. S Egusa, T Nakayama, N Gemma, A Miura, M Azuma *Thin Solid Films* **178** 165 (1989)
223. T Yamashita, A Shibata, S Yamashita *Bull. Chem. Soc. Jpn.* **51** 2751 (1978)
224. G Gabrielli, P Baglioni, E Ferroni *J. Colloid Interface Sci.* **81** 139 (1981)
225. G Gabrielli, P Baglioni *J. Colloid Interface Sci.* **83** 221 (1981)
226. A Albert, J Corboda *Colloid Polym. Sci.* **262** 811 (1984)
227. F Kimura, S Uematsu, H Sakurai, Y Akahori, M Nakagaki. *J. Colloid Interface Sci.* **124** 290 (1988)
228. P Baglioni, L Dei, E Ferroni, G Gabrielli *J. Colloid Interface Sci.* **109** 109 (1986)
229. W Hickel, G Duda, M Jurich, T Kröhl, K Rochford, G I Stegeman, J D Swalen, G Wegner, W Knoll *Langmuir* **6** 1403 (1990)
230. H Motschmann, R Reiter, R Lawall, G Duda, M Stamm, G Wegner, W Knoll *Langmuir* **7** 2743 (1991)
231. K Mathauer, A Mathy, C Bubeck, G Wegner, W Hickel, U Scheunemann *Thin Solid Films* **210/211** 449 (1992)
232. T Takenaka, K Harada, M Matsumoto *J. Colloid Interface Sci.* **73** 569 (1980)
233. F Takeda, M Matsumoto, T Takenaka, Y Fujiyoshi *J. Colloid Interface Sci.* **84** 220 (1981)
234. F Takeda, M Matsumoto, T Takenaka, Y Fujiyoshi, N Uyeda *J. Colloid Interface Sci.* **91** 267 (1983)
235. H W Fox, P W Taylor, W A Zisman *Ind. Eng. Chem.* **39** 1401 (1947)
236. W Noll, H Steinbach, C Sucker *Ber. Bunsenges Phys. Chem.* **67** 407 (1963)
237. W H Banks *Nature (London)* **174** 365 (1954)
238. A H Ellison, W A Zisman *J. Phys. Chem.* **60** 416 (1956)
239. V A Ogarev, V V Arslanov, A A Trapeznikov *Kolloid. Zh.* **34** 372 (1972)

240. V V Arslanov, V A Ogarev *Dokl. Akad. Nauk SSSR* **196** 1105 (1971)
241. Y Kakihara, D M Himmelblau, R S Schechter *J. Colloid Interface Sci.* **30** 200 (1969)
242. W Noll *Pure Appl. Chem.* **13** 101 (1966)
243. W Noll, H Steinbach, C Sucker *J. Polym. Sci., Part C, Polym. Lett.* **34** 123 (1971)
244. H Steinbach, C Sucker *Adv. Colloid Interface Sci.* **14** 43 (1980)
245. V A Ogarev, V V Arslanov, A A Trapeznikov, in *Makromolekuly na Granitse Razdela Faz* (Macromolecules at a Phase Interface) (Kiev: Naukova Dumka, 1971) p. 155
246. G L Gaines *J. Polym. Sci., Part C* **34** 115 (1971)
247. M J Owen, T C Kendrick *J. Colloid Interface Sci.* **27** 46 (1968)
248. W Noll *Z. Elektrochem.* **67** 407 (1963)
249. K Motomura, R Matuura *J. Colloid Interface Sci.* **18** 52, 295 (1963)
250. V A Ogarev, V V Arslanov, A A Trapeznikov, in *Poverkhnostnye Yavleniya v Zhidkostyakh i Zhidkikh Rastvorakh* (Surface Phenomena in Liquids and Liquid Solutions) (Leningrad: Izd. Leningr. Univ., 1972) p. 79
251. M Matsumoto, H Yoshimura, V S Kulkarni, K Nagayama *Colloid Polym. Sci.* **268** 1174 (1990)
252. P Ekwall, R Ekholm, in *Proceedings of 2nd Int. Congr. Surface Activity London, 1957* Vol. 1, p. 23
253. J F Joany, P-G De Gennes *C. R. Acad. Sci., Ser. 2* **299** 279 (1984)
254. A A Vavkushevskii, V V Arslanov, V A Ogarev *Kolloid. Zh.* **50** 1180 (1988)
255. E K Mann, S Henon, D Langevin, J Meunier *J. Phys. France* **2** 1683 (1992)
256. S Granick, D J Kuzmenka, S J Clarson, J A Semlyen *Langmuir* **5** 144 (1989)
257. T Richardson, G G Roberts, S Holder, D Lacey *Thin Solid Films* **210/211** 299 (1992)
258. E Orthmann, G Wegner *Angew. Chem.* **98** 1114 (1986)
259. A A Kalachev, T Sauer, V Vogel, N A Plate, G Wegner *Thin Solid Films* **188** 341 (1990)
260. K S Schwieg, H Fisher, Y Xu, F Kremer, G Wegner *Macromol. Chem. Macromol. Symp.* **46** 211 (1991)
261. K Yase, K S Schwieg, G Lieser, G Wegner *Thin Solid Films* **213** 130 (1992)
262. G L Gaines, Jr *Adv. Chem.* **144** 338 (1975)
263. G L Gaines, Jr *J. Polym. Sci., Part C* **34** 115 (1971)
264. A A Trapeznikov, M A Kolobov *Kolloid. Zh.* **44** 277 (1982)
265. M A Kolobov, A A Trapeznikov *Kolloid. Zh.* **44** 690 (1982)
266. A Bachrach, A Zilkha *Eur. Polym. J.* **5** 493 (1984)
267. N K Adam *Trans. Faraday Soc.* **29** 108 (1933)
268. B A Johnson, J Kreuter, G Zografi *Colloid Surf.* **17** 325 (1986)
269. T Kawaguchi, H Nakahara, K Fukuda *J. Colloid Interface Sci.* **104** 290 (1985)
270. T Kawaguchi, H Nakahara, K Fukuda *Thin Solid Films* **133** 29 (1985)
271. M Hittmeier, L S Sandell, P Luner *J. Polym. Sci., Part C* **36** 267 (1971)
272. Y Tsujii, T Itoh, T Fukuda, T Miyamoto, S Ito, M Yamamoto *Langmuir* **8** 936 (1992)
273. M A Schoondorp, E J Vorenkamp, A J Schouten *Thin Solid Films* **196** 121 (1991)
274. P Zugenmaier, H Steinmeier *Polymer* **27** 1601 (1986)
275. M A Schoondorp, A J Schouten, B E Hulshof, B L Feringa, G T Ostergetel *Langmuir* **8** 1817 (1992)
276. M A Schoondorp, A J Schouten, B E Hulshof, B L Feringa *Langmuir* **8** 1825 (1992)
277. K L Mittal (Ed.) *Polyimides — Synthesis, Characterization and Application* (New York: Plenum, 1982) Vol. 1; (1984) Vol. 2
278. F Iacona, M Garilli, G Marletta, O Puglisi, G Pignatazo *J. Mater. Res.* **6** 861 (1991)
279. M Kakimoto, M Suzuki, T Konishi, Y Imai, M Iwamoto, T Hino *Chem. Lett.* 823 (1986)
280. M Suzuki, M Kakimoto, T Konishi, Y Imai, M Iwamoto, T Hino *Chem. Lett.* 395 (1986)
281. H Sotobayashi, T Schilling, B Tesche *Langmuir* **6** 1246 (1990)
282. T Schedel-Niedrig, H Sotobayashi, A Ortega-Villamil, A M Bradshaw *Surf. Sci.* **247** 83 (1991)
283. T Schedel-Niedrig, M Keil, H Sotobayashi, T Schilling, B Tesche, A M Bradshaw *J. Phys., Condens. Mater.* **3** 23 (1991)
284. M Sugi *Molecular Electronic Devices* (Ed. F Carter) (Amsterdam: Elsevier, 1988) p. 441
285. M Kakimoto, A Morikawa, Y Nishikata, M Suzuki, Y Imai *J. Colloid Interface Sci.* **121** 599 (1988)
286. Y Nishikata, K Kamatsu, M Kakimoto, Y Imai, K Ariga, Y Okahata *J. Chem. Soc. Jpn., Chem. Ind. Chem.* **10** 1150 (1990)
287. V P Kukhar', N I Mishchenko, V V Tsukruk, S Yu Petrash, E V Shelud'ko, A V Tolmachev, I P Krainov *Dokl. Akad. Nauk USSR* **13** 119 (1991)
288. Y Nishikata, T Konishi, A Morikawa, M Kakimoto, Y Imai *Polymer J.* **20** 269 (1988)
289. I Fujiwara, C Ishimoto, J Seto *J. Vac. Sci. Technol. B* **9** 1148 (1991)
290. A Killinger, C Thümmler, M Grunze, W Schrepp *J. Adhesion* **36** 229 (1992)
291. M Iwamoto, Y Majima, A Watanabe *Thin Solid Films* **210/211** 101 (1992)
292. M Iwamoto, Y Majima *Jpn. J. Appl. Phys.* **28** 721 (1988)
293. M Iwamoto, Y Majima *Thin Solid Films* **178** 67 (1989)
294. M Iwamoto, Y Majima *J. Chem. Phys.* **94** 5135 (1991)
295. Y Majima, H Naruse, M Iwamoto *Thin Solid Films* **210/211** 82 (1992)
296. Y Majima, M Iwamoto *Rev. Sci. Instrum.* **62** 2228 (1991)
297. M Iwamoto, T Kubota *Repts Asahi Glass Found.* **61** 195 (1992)
298. M Iwamoto, T Noguchi, H Fuwa, Y Majima *Jpn. J. Appl. Phys.* **30** 1020 (1991)
299. Y Nishikata, S Fukui, M Kakimoto, Y Imai, K Nishiyama, M Fujihira *Thin Solid Films* **210/211** 296 (1992)
300. M Iwamoto, S Kasahara, Y Yoneda, K Iriyama, Y Nishikata, M Kakimoto, Y Imai *Thin Solid Films* **210/211** 461 (1992)
301. M Uekita, H Awaji, M Murata, S Mizunuma *Thin Solid Films* **205** 109 (1991)
302. H Ikeno, A Oh-saki, M Nitta, N Ozaki, Y Yokoyama, K Nakaya, S Kobayashi *Jpn. J. Appl. Phys.* **27** L475 (1988)
303. S Baker, A Seki, J Seto *Thin Solid Films* **180** 263 (1989)
304. T Akatsuka, H Tanaka, J Toyama, T Nakamura, M Matsumoto, Y Kawabata *Chem. Lett.* 1351 (1991)
305. T Akatsuka, H Tanaka, J Toyama, T Nakamura, M Matsumoto, Y Kawabata *Thin Solid Films* **210/211** 458 (1992)
306. K Nakaya, B Y Zhang, M Yoshida, I Isa, S Sindoh, S Kobayashi *Jpn. J. Appl. Phys.* **28** L116 (1989)

Russian Chemical Reviews **63** (1) 41 – 53 (1994)
©1994 Russian Academy of Sciences and Turpion Ltd

UDC 543.87

Thermal, photolytic, and oxidative reactions of the homoligand carbonyls of metals in Groups VI – VIII

I V Spirina, V P Maslennikov

Contents

I. Introduction	41
II. Thermal decomposition of the carbonyl complexes of metals	41
III. Mechanisms of the photolytic breakdown of the carbonyls of the elements	44
IV. Oxidation of the metal carbonyls by oxygen, ozone, and peroxides	47
V. Conclusions	51

Abstract. The mechanisms of thermal, photolytic, and oxidative transformations of metal carbonyls into highly dispersed metallic and oxidic phases are discussed. The bibliography includes 142 references.

I. Introduction

The widespread use of the carbonyls of Group VI – VIII metals in the preparation of metal and oxide powders, films,[1,2] and catalysts for various chemical processes[3] has created a need for a detailed study of the mechanisms of the chemical transformations of the carbonyl complexes of the elements. The most recent reviews[3–5] which include a substantial volume of information on the synthesis and properties of metal carbonyls were published more than 10 years ago. However, during that period many new studies of the reactivity of the carbonyl complexes of Group VI – VIII metals towards thermal, photolytic, and oxidative transformations have been reported. They are discussed in the present review.

II. Thermal decomposition of the carbonyl complexes of metals

Most of the recent work on the thermal decomposition of the metal carbonyls is aimed at the preparation of metallic powders, films, and coatings.[1–3,6,7]

One method of preparing catalysts having a high activity and selectivity relies on the decomposition of metal carbonyls deposited on the surface of a solid support.[6,7] Depending on the properties of the surface and on the nature of the carbonyl we may observe the following processes: physisorption,[6–14] chemisorption with formation of various surface organometallic compounds,[6,10–18] and the decomposition of the starting compounds into polynuclear clusters.[13,19,20]

The interaction of pentacarbonyliron with the surface of silicon and of platinum monocrystals at 110 – 185 K results in the molecular adsorption of $Fe(CO)_5$.[8,9] It has been suggested that the adsorption is accompanied by a change in the molecular geometry of the pentacarbonyliron from a trigonal bipyramid to a square pyramidal form. Above 185 K we observe decarbonylation of the $Fe(CO)_5$, and a thin film of metallic iron is formed on the surface of the monocrystal. A similar process takes place during the photolysis of $Fe(CO)_5$ adsorbed on these supports[8,9] at 170 K, and during the thermal decomposition of pentacarbonyliron on the surface of graphite[6] and of dehydrated NaY zeolite.[14]

Highly dispersed metallic catalysts are prepared by thermal decomposition of the carbonyls $Fe_3(CO)_{12}$, $Ru_3(CO)_{12}$, and $Os_3(CO)_{12}$ supported on a clean carbon surface in a hydrogen or helium atmosphere.[21]

We know that when the surface of zeolites or of metal oxides is dehydroxylated by heat treatment under reduced pressure[7,14] the coordinatively unsaturated ions of the elements (Lewis acids) or the oxygen anions in the crystal lattice (Lewis bases) can act as adsorption centres. Depending on the reactivity of the carbonyl and on the nature of the surface, physisorption or chemisorption can be observed even at room temperature. A further increase in temperature results in the full decarbonylation of the initial compound.[6,7,10–15,22–27]

The decomposition of pentacarbonyliron in the micropores of NaY zeolite at 473 K and above produces the subcarbonyls $[Fe(CO)_{5-x}]_{ads}$, $[Fe(CO)_4]^{2-}$, and $[HFe_3(CO)_{11}]_x^-$.[6,14,23,24] The slowest step in the process is the removal of the last CO ligand from one of these species. The presence of small iron clusters in the pores makes possible the complete conversion of the pentacarbonyliron into metal-containing forms of zeolite.[24] The thermal dissociation of $Fe(CO)_5$ includes the disproportionation of CO to CO_2.

The decomposition of $Mo(CO)_6$ in the cavities of NaY zeolite takes place in two steps.[12,25,26] During the first step (at 373 K) we observe changes in the mass of the sample, corresponding to the loss of two carbonyl groups with formation of $Mo(CO)_4$. However, the IR spectrum of the reaction mixture in the 2000–1700 cm^{-1} region contains several ν_{CO} bands which suggest the presence[26] among the reaction products [in addition to $Mo(CO)_4$] of an unidentified molybdenum compound, possibly $[Mo_2(CO)_8Z_x]^{2-}$ (where Z_x is an adsorption centre). Heating the sample above 473 K results in the irreversible decarbonylation of the starting $MO(CO)_6$ with formation of metallic molybdenum within the zeolite lattice. Introducing H^+ ions into the NaY lowers the decomposition temperature of the molybdenum carbonyl to 333 K and produces more finely divided metal particles.[27] $Cr(CO)_6$ physisorbed on silicalite,[11] $Ru(CO)_{12}$ on V_2O_5, MgO, ZnO, and La_2O_3,[12,18] $Mn_2(CO)_{10}$ on NaY zeolite,[13] and $Mo(CO)_6$

I V Spirina, V P Maslennikov Chemistry Research Institute, Lobachevskii Nizhegorod State University, prosp. Gagarina 23, 603600 Nizhny Novgorod, Fax (7-831-2) 65 85 92

Received 27 May 1993
Uspekhi Khimii **63** (1) 43 – 56 (1994); translated by J I Carasso

on dehydroxylated Al_2O_3 [22] all undergo similar types of decomposition.

In the thermal decomposition of metal carbonyls on HY zeolite we observe the formation of hydridocarbonyl surface species, $[HM(CO)_m]^+$, which ultimately dissociate with formation of metallic clusters.[11,15,16,28]

On the surface of metal oxides containing hydroxyl groups the carbonyl complexes undergo nucleophilic attack from the side of the OH groups and are converted into compounds of the $[M_n(CO)_{m-x-y}(OH)_x(OZ)_y]\cdot n[HM_n(CO)_{m-1}]$ type, where Z is a metal ion in the corresponding oxide.[10,12,17,18,22] Further decarbonylation leads to the formation of oxidised forms of the metal with evolution of hydrogen.

Octacarbonylcobalt sublimed on to the surface of various zeolites is converted even at room temperature[13,19,20] into the polynuclear clusters $Co_4(CO)_{12}$ and $Co_6(CO)_{16}$. In this case the final product of the thermal decomposition are metal particles 10–15 Å in diameter.

Thus the nature of the surface of the solid phase plays an important role in determining the purity and the disperseness of the metallic powders prepared by the thermal decomposition of metal carbonyls. The reactivity of carbonyl compounds is unaffected by their physisorption on the clean surfaces of inert supports such as active carbon and monocrystalline silicon or platinum.[8,9,21] Metal oxides and zeolites of the NaY type interact with carbonyl complexes through coordinatively unsaturated ions of their elements or through the oxygen anions of the crystal lattice.[6,7,10–15,22–27] The HY zeolites and the oxides containing hydroxyl groups form surface compounds with the carbonyl complexes.[10–12,15–17,22,28] The detailed mechanism of the thermal decomposition of metal carbonyls on solid surfaces has not yet been investigated.

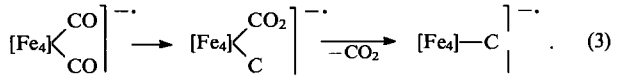
The synthesis of metallic powders and films by the thermal decomposition of metal carbonyls in the gas phase is widely used in industry.[1–3] A study of its mechanism by the fast IR spectroscopy method showed the presence of coordinatively unsaturated metal carbonyls in the reaction mixtures.[29] Depending on the experimental conditions the decomposition of the carbonyl complexes produces powders, films, or metal whiskers.[1–3,30–32] The solid products contain oxide and carbide impurities. Experiments with labelled atoms showed that the oxygen used to form oxides in the resulting solid phase is provided by the carbonyl ligand.[32]

A study by EPR of the thermal decomposition of pentacarbonyliron[33] established that the process takes place on the surface of the reaction vessel by a chain ion–radical clusterisation mechanism:

$$Fe(CO)_4^{-\cdot} + Fe(CO)_5 \longrightarrow Fe_2(CO)_8^{-\cdot} + CO, \quad (1)$$

$$Fe_2(CO)_8^{-\cdot} + Fe(CO)_5 \longrightarrow Fe_3(CO)_{12}^{-\cdot} + CO. \quad (2)$$

This mechanism describes the formation of anion-radical iron carbonyl clusters on the growing iron surface. When the number of nuclei in the cluster reaches four the carbon monoxide group in the coordination sphere of the anion radical undergoes disproportionation according to the Bell–Boudart scheme[33]



(3)

In the presence of an excess of $Fe(CO)_5$ vapour the $[Fe_4]-C^{-\cdot}$ clusters are further converted into clusters with 5 or 6 nuclei. Different ways of generating ion-radical centres on the growing surface by chemisorption, photo-ionisation, and other means have been suggested.[33]

In the thermal decomposition of pentacarbonyliron in the gas phase the formation of new metallic particles is observed mainly during the first stages. Thus, ~80% of all the particles have already been formed when 50% conversion of the $Fe(CO)_5$ is reached.[34]

Carlton and Oxley[35] have shown that the initial rate of decomposition of tetracarbonylnickel vapour at 373 K is proportional to its concentration, and that the resulting carbon monoxide limits the rate of the reaction. They proposed the following scheme for the reaction:

$$Ni(CO)_4 \rightleftharpoons Ni(CO)_3 + CO, \quad (4)$$

$$Ni(CO)_3 \xrightarrow{-CO} Ni(CO)_2 \xrightarrow{-CO} \quad (5)$$

$$\longrightarrow Ni(CO) \xrightarrow{-CO} Ni\ .$$

The activation energy for the thermal decomposition of nickel carbonyl in the gas phase[35] is 91.1 kJ mol^{-1}. The dissociation energy of the first Ni–CO bond in the $Ni(CO)_4$, calculated from quantum chemical[36] and from thermochemical data,[37] is 201.6 and 154.1 kJ mol^{-1} respectively. These values are substantially higher than the activation energy measured[35] for the decomposition of $Ni(CO)_4$: this is probably due to the catalytic effect of the resulting metal particles on the thermal decomposition of tetracarbonylnickel.

The decarbonylation of the tetranuclear clusters $Rh_4(CO)_{12}$, $Rh_2Co_2(CO)_{12}$, $RhCo_3(CO)_{12}$, and $Co_4(CO)_{12}$ has been studied[38] by the programmed decomposition temperature method in a hydrogen stream. The quantity of CO evolved during the complete conversion of $Rh_4(CO)_{12}$ suggests the formation of the $Rh_6(CO)_{16}$ complex, which is relatively stable under the chosen thermal decomposition conditions:

$$3\,Rh_4(CO)_{12} \longrightarrow 2\,Rh_6(CO)_{16} + 4\,CO. \quad (6)$$

The decarbonylation of $Co_4(CO)_{12}$ was completed by the formation of a mirror of metallic cobalt on the walls of the reaction vessel, whereas solid deposits of the powdered metal were obtained[38] from $RhCo_3(CO)_{12}$, $Rh_2Co_2(CO)_{12}$, and $Rh_4(CO)_{12}$.

A flow system with a differential reactor has been used[39–41] to study the kinetics of the gas-phase decomposition of the hexacarbonyls of metals in the chromium subgroup, and the effective activation energies of the processes have been determined: 45.8 and 54.6 kJ mol^{-1} for $Mo(CO)_6$ and $W(CO)_6$ respectively. The low values of the effective activation energy (as compared with the energy required to remove a single CO ligand[42]) suggest a complex process in the thermal decomposition of $M(CO)_6$, probably not involving catalytic stages.

By using pulsed laser photolysis, which suppresses heterogeneous reactions, Lewis et al.[43] studied the homogeneous gas-phase decomposition of mononuclear metal carbonyls (Fe, Cr, Mo, W). Dissociation energies of 171.4, 134.7, 167.2, and 191.5 kJ mol^{-1} for the first metal–ligand bond were obtained for $Fe(CO)_5$, $Cr(CO)_6$, $Mo(CO)_6$, and $W(CO)_6$ respectively. These values are close to those obtained in thermochemical experiments.[42] It was established[43] that additions of equimolar quantities of carbon monoxide do not affect the rate of the gas-phase decomposition of these metal carbonyls. For the iron, molybdenum, and tungsten carbonyls the rate-determining step of the process is the removal of the first CO ligand. In the thermal decomposition of $Cr(CO)_6$ the fast (equilibrium) elimination of the first CO ligand is followed[43] by the slower (but still at equilibrium) stage of the dissociation of $Cr(CO)_5$ to $Cr(CO)_4$.

Thus the thermal decomposition of the metal carbonyls in the gas phase involves the participation of coordinatively unsaturated species. The process is often retarded by the gaseous product (carbon monoxide),[29,33,35,43] and is catalysed by the resulting metallic phase used for the nucleation and growth of the carbonyl anion radicals.[33] The products of the reaction (metallic powders, whiskers, and films) contain oxide and carbide impurities.[32,33]

Particles of highly dispersed metals, having an average diameter of 63–110 Å, have been prepared[44,45,47] by the decomposition of metal carbonyls in liquid media. The thermal dissociation of $Fe(CO)_5$ and $Co_2(CO)_8$ in solutions of surface-active substances has yielded stable colloidal suspensions (ferromagnetic liquids).[45,46]

The decomposition of penta- and nonacarbonyliron in a closed system takes place by the reversible reaction

$$Fe_n(CO)_m \rightleftarrows Fe_n(CO)_{m-1} + CO, \quad (7)$$

and is rate-limited by the evolved carbon monoxide.[47] The coordinatively unsaturated carbonyl $Fe_n(CO)_{m-1}$ which is produced dissociates according to the scheme

$$Fe_n(CO)_{m-1} \rightleftarrows Fe_n(CO)_{m-x-1} + x\,CO; \quad (8)$$

$Fe_n(CO)_m = Fe(CO)_5$ or $Fe_2(CO)_9$.

The thermal decomposition of nonacarbonyliron produces $Fe(CO)_5$, which is relatively stable under the conditions of the experiment.[47] Dodecacarbonyliron decomposes in undecane at 353–383 K by the reaction

$$2\,Fe_3(CO)_{12} \longrightarrow 2\,Fe(CO)_5 + Fe_2(CO)_9 + 5\,CO + 2\,Fe. \quad (9)$$

The rate of the thermal decomposition of the iron carbonyls in paraffins is described by a kinetic equation of the first order with respect to the initial concentration of $Fe_n(CO)_m$. The dissociation of dodecacarbonyliron also obeys the first-order kinetic equation with respect to the time-dependent concentration of $Fe_3(CO)_{12}$ up to a 90% extent of reaction.[47]

The thermal stability of the carbonyl complexes of iron increases in the sequence $Fe_3(CO)_{12} < Fe_2(CO)_9 < Fe(CO)_5$. The rate constants for the dissociation of the iron carbonyl complexes in solution have been determined,[47] and in the case of $Fe(CO)_5$ the equilibrium constants and the rate constants of the recombination reaction are also known.

Octacarbonylcobalt is almost quantitatively converted into the dodecacarbonyl after 5 h at 363 K in toluene or in heptane.[48,49] The rate of the process is described by a second-order kinetic equation with respect to $Co_2(CO)_8$. At 363 K the rate constant is 5.27×10^{-6} dm^3 mol^{-1} s^{-1}:

$$\frac{d[Co_4(CO)_{12}]}{dt} = k\frac{[Co_2(CO)_8]^2}{[CO]^n} \quad (10)$$

The nature of the solvent has a powerful effect on the kinetics of the formation of dodecacarbonylcobalt. Thus, in heptane the parameter n in the expression for the rate of accumulation of $Co_4(CO)_{12}$ [Eqn (10)] is two, but when toluene is used $n = 4$. The following scheme has been proposed[48] to describe the process:

$$Co_2(CO)_8 \rightleftarrows Co_2(CO)_7 + CO, \quad (11)$$

$$Co_2(CO)_7 \rightleftarrows Co_2(CO)_6 + CO, \quad (12)$$

$$2\,Co_2(CO)_6 \longrightarrow Co_4(CO)_{12}, \quad (13)$$

$$Co_2(CO)_8 + Co_2(CO)_6 \longrightarrow Co_4(CO)_{12} + 2\,CO. \quad (14)$$

It is assumed that the main contribution to the formation of dodecacarbonyltetracobalt is provided by reaction (13) in heptane and by reaction (14) in toluene.

The thermal decomposition of tetracarbonylnickel in undecane at 323–353 K is slow, and yields the carbon oxides CO and CO_2.[50] After complete decomposition of the $Ni(CO)_4$ the yield of the two gaseous products is 3.2 and 0.4 mol per mole of converted carbonyl for CO and CO_2 respectively. Metallic nickel and nickel carbide can also be detected among the reaction products. Addition of CO to the reaction mixture before the start of the reaction suppresses the thermal decomposition of $Ni(CO)_4$. The rate of the thermal dissociation of tetracarbonylnickel in solutions is described by a first-order kinetic equation. The following scheme has been suggested:[5,50]

$$Ni(CO)_4 \rightleftarrows Ni(CO)_3 + CO, \quad (15)$$

$$Ni(CO)_3 \xrightarrow[-CO]{} Ni(CO)_2 \xrightarrow[-CO]{} NiCO \xrightarrow[-CO]{} Ni, \quad (16)$$

$$Ni(CO)_3 \longrightarrow Ni + (C) + CO + CO_2. \quad (17)$$

The rate constants for the removal of the first CO ligand (k_{15}) and those for the recombination of $Ni(CO)_3$ and CO(k_{-15}) have been determined.[50]

The thermal decomposition of pentacarbonylruthenium in a cyclohexane solution at 298–303 K leads to the formation of $Ru_3(CO)_{12}$. The conversion of $Ru(CO)_5$ into $Ru_3(CO)_{12}$ is the result[51] of the primary fission of a Ru–CO bond with formation of $Ru(CO)_4$:

$$Ru(CO)_5 \rightleftarrows Ru(CO)_4 + CO. \quad (18)$$

The tetracarbonylruthenium interacts with the $Ru(CO)_5$, ultimately giving $Ru_3(CO)_{12}$. The activation parameters of the process have been obtained, and the equilibrium constant of reaction (18) has been calculated: 3.0×10^6 mol dm^{-3} at 298 K.

Tunik et al.[52] have studied the kinetics and the mechanism of the conversion of dodecacarbonylrhodium into hexadeca-carbonylrhodium in heptane:

$$3\,Rh_4(CO)_{12} \longrightarrow 2\,Rh_6(CO)_{16} + 4\,CO. \quad (19)$$

The reaction takes place by two independent parallel paths—a dissociative and a nondissociative path—and it goes to completion even at pressures of carbon monoxide in the 360–420 bar range.

The dissociative path [process (20)–(23)] includes the reversible elimination of two molecules of carbon monoxide from the $Rh_4(CO)_{12}$, followed by the rate-limiting step, described[52] as the isomerisation of the cluster skeleton to give a cluster nucleus having a new and very different structure. A typical example of this stage is the conversion of the nucleus of the Rh_4 cluster from a tetrahedral configuration into a 'butterfly' configuration.[52] The nondissociative path [processes (24) and (25)] stipulates the activation of the initial cluster by a similar mechanism but without the preliminary dissociation of the CO ligands. The presence of carbon monoxide has no effect on the rate of this process.

$$Rh_4(CO)_{12} \rightleftarrows Rh_4(CO)_{11} + CO \quad (20)$$

$$Rh_4(CO)_{11} \rightleftarrows Rh_4(CO)_{10} + CO \quad (21)$$

$$Rh_4(CO)_{10} \longrightarrow [Rh_4(CO)_{10}]^* \quad (22)$$

$$[Rh_4(CO)_{10}]^* + 2\,Rh_4(CO)_{12} \xrightarrow{fast} 2\,Rh_6(CO)_{16} + 2\,CO \quad (23)$$

$$Rh_4(CO)_{12} \longrightarrow [Rh_4(CO)_{12}]^* \quad (24)$$

$$[Rh_4(CO)_{12}]^* + 2\,Rh_4(CO)_{12} \xrightarrow{fast} 2\,Rh_6(CO)_{16} + 4\,CO \quad (25)$$

Thus in most cases the first step in the decomposition of metal carbonyls in the liquid phase is the equilibrium elimination reaction of a CO ligand. The thermal stability of the carbonyl complexes is strongly influenced by the nature of the metal atom and by the structure of the resulting polynuclear clusters.[37]

III. Mechanisms of the photolytic breakdown of the carbonyls of the elements

The earliest information[1] on the decomposition of the metal carbonyls (in particular, pentacarbonyliron) under the influence of solar radiation appeared at the beginning of the 20th century, but the systematic study of the photolytic breakdown of pentacarbonyliron began in the late 1930s.[53-55]

It was established[53] that the quantum yield of the formation of CO during the decomposition of $Fe(CO)_5$ vapour (at an initial pressure of 5-15 Torr) under the influence of radiation (366, 405, and 465 nm) is 1.16. Additions of various gases (H_2, CO, CO_2, N_2, Ar) in amounts ranging from values close to the concentration of the pentacarbonyliron to a six-fold excess suppressed[35] the decomposition of the $Fe(CO)_5$ by up to ~50% and lowered the quantum yield of the formation of CO to 0.5. In the mechanism proposed to explain these effects the retardation by gaseous additives was ascribed to the deactivation of the excited $[Fe(CO)_5]^*$ molecules:

$$Fe(CO)_5 \xrightarrow{h\nu} [Fe(CO)_5]^*, \quad (26)$$

$$[Fe(CO)_5]^* + Fe(CO)_5 \longrightarrow Fe_2(CO)_9 + CO, \quad (27)$$

$$[Fe(CO)_5]^* + Q \longrightarrow Fe(CO)_5 + Q; \quad (28)$$

$Q = H_2, CO, CO_2, N_2, Ar.$

However, this mechanism was not confirmed by later work.

The absorption spectra of $Fe(CO)_5$ and $Ni(CO)_4$ vapour[55] consist of continuous curves at wavelengths below 410 nm for $Fe(CO)_5$ and 315 nm for $Ni(CO)_4$. This type of spectrum suggests that the potential energy curve of the excited state does not have a minimum, and therefore the excited $[Fe(CO)_5]^*$ and $[Ni(CO)_4]^*$ molecules are unstable and should dissociate. Thus the primary act of the photolysis is the dissociation of the activated $[Fe(CO)_5]^*$ or $[Ni(CO)_4]^*$ molecule to give $Fe(CO)_4$ or $Ni(CO)_3$.

The accumulation of $Fe(CO)_4$ or $Ni(CO)_3$ during the photolysis of $Fe(CO)_5$ or $Ni(CO)_4$ in inert gas matrices at 20 K and in hydrocarbon glasses at 70 K has been confirmed by IR spectroscopy.[56-60] The coordinatively unsaturated metal carbonyl can react reversibly with the matrix to give $[M(CO)_{n-1}]^*Q$ complexes (Q = H_2, Ne, Ar, Xe, CH_4; M = Fe, Ni; n = 5, 4).[57,60]

$$M(CO)_n \xrightarrow{h\nu} [M(CO)_n]^* \underset{-CO}{\rightleftharpoons} \quad (29)$$

$$\rightleftharpoons [M(CO)_{n-1}]^* \xrightarrow[\lambda > 357\ nm]{Q} [M(CO)_{(n-1)}]^*Q$$

By using the pulsed UV photolysis method with fast recording in the IR region it was shown[61,62] that processes like (29) can take place in gas and in liquid phases as well as in a solid matrix.

According to the above arguments the primary reactions taking place during the photolysis of pentacarbonyliron are described by the equations

$$Fe(CO)_5 \xrightarrow{h\nu} [Fe(CO)_5]^*, \quad (30)$$

$$[Fe(CO)_5]^* \longrightarrow Fe(CO)_4 + CO, \quad (31)$$

$$Fe(CO)_4 + Fe(CO)_5 \longrightarrow Fe_2(CO)_9. \ ^\circ C. \quad (32)$$

The photodissociation of pentacarbonyliron has been studied[63-65] in the gas phase with excitation by laser radiation of wavelength 193, 248, and 352 nm in the presence of PCl_3, PF_3, or SF_6, keeping the total pressure in the system below 200 Torr. Additions of PCl_3 and PF_3 or SF_6 were used to identify the carbonyl fragments produced by the reaction. The energy of the laser radiation and the irradiation time were chosen so as to exclude multiple absorption of photons, and the conversion of the $Fe(CO)_5$ was kept below 10%. It was shown that the absorption of one photon by a molecule of pentacarbonyliron in the gas phase leads to the formation of $Fe(CO)_{5-x}$ primary fragments, where x = 1-4, with an overall quantum yield close to unity. The degree of fragmentation of the pentacarbonyliron increases with the energy of the absorbed photon. The mechanism of the photodissociation is described by the scheme

$$[Fe(CO)_5]^* \longrightarrow [Fe(CO)_4]^{**} + CO, \quad (33)$$

$$[Fe(CO)_4]^{**} \longrightarrow [Fe(CO)_3]^{**} + CO, \quad (34)$$

$$[Fe(CO)_3]^{**} \longrightarrow [Fe(CO)_2]^{**} + CO, \quad (35)$$

$$[Fe(CO)_2]^{**} \longrightarrow [Fe(CO)]^{**} + CO. \quad (36)$$

The pentacarbonyliron molecule excited by the absorption of a photon, $[Fe(CO)_5]^*$, loses CO groups successively and forms coordinatively unsaturated intermediates which are in electronically and vibrationally excited $[Fe(CO)_{5-x}]^{**}$ states.[63,64]

In contrast to the photodissociation reaction induced by irradiation with a mercury lamp tetracarbonyliron formed under laser or flash photolysis from pentacarbonyliron retains up to 65% of the absorbed energy in the form of an electronic or a vibrational component, and is therefore very unstable.[64]

According to SCF MO LCAO calculations[66-68] the photochemical excitation of $Fe(CO)_5$ produces a spin-allowed transition to an excited singlet state. Spin-orbit interaction then populates the triplet state, from which the $[Fe(CO)_5]^*$ dissociates with formation of $Fe(CO)_4(T_i)$ and $CO(S_0)$. The calculated enthalpy of the reaction is 178.8 and the experimental value is 246.4 kJ mol^{-1}.[69]

A detailed study of the composition of the products and of the kinetic features of the photolytic decomposition of the iron carbonyls in solutions under the influence of radiation with wavelengths of 253.7 and 366 nm has been reported.[70] In hydrocarbon solutions pentacarbonyliron dissociates photolytically with formation of a mixture of carbon monoxide and of nona- and dodecacarbonyliron. The relative abundance of the polynuclear carbonyls shows that the dodecacarbonyl is produced by the photolytic decomposition of nonacarbonyliron. The photolysis of $Fe_2(CO)_9$ in solution leads to the formation of $Fe_3(CO)_{12}$, CO, and $Fe(CO)_5$. The decomposition of $Fe_3(CO)_{12}$ in octane under the influence of UV radiation is accompanied by the evolution of carbon monoxide, of penta- and of nonacarbonyliron, and also of metallic iron. The quantum yields for the conversion of the initial carbonyl complexes and for the accumulation of their decomposition products suggests that the processes are described by the following equations:

$$2\,Fe(CO)_5 \xrightarrow{h\nu} Fe_2(CO)_9 + CO, \quad (37)$$

$$2\,Fe_2(CO)_9 \xrightarrow{h\nu} Fe(CO)_5 + Fe_3(CO)_{12} + CO, \quad (38)$$

$$2\,Fe_3(CO)_{12} \xrightarrow{h\nu} 2\,Fe_2(CO)_9 + Fe(CO)_5 + Fe + CO. \quad (39)$$

The pentacarbonyliron formed by the decomposition of the nona- and dodecacarbonyls again undergoes photolysis by reaction (37). The nonacarbonyl formed by the photolysis of $Fe_3(CO)_{12}$ contributes to reaction (38). Thus the photolytic transformation of pentacarbonyliron in octane is a complex multistep process including the formation and decomposition stages of polynuclear iron carbonyls.

The synthesis of $Fe_2(CO)_9$ and $Fe_3(CO)_{12}$ takes place also during the photolysis of $Fe(CO)_5$ in inert gas matrices containing pentacarbonyliron in a proportion of 1:1000 relative to the inert matrix.[57,71] The photodissociation of $Fe(CO)_5$ adsorbed on Vycor porous glass or on zeolites produces polynuclear iron compounds.[72,73]

It has been shown [70] that the quantum yield of the formation of CO during the photolysis of the iron carbonyls in solution is unaffected by changes in the wavelength of the light between 253.7 and 366 nm. The rate of decomposition of the iron carbonyls in octane in concentrations below 5×10^{-4} mol dm^{-3} is described by a first-order kinetic equation. The mechanism of the photolysis of the iron carbonyls in solutions is consistent with the following scheme:

$$Fe_n(CO)_m \xrightarrow{h\nu} [Fe_n(CO)_m]^*, \quad (40)$$

$$[Fe_n(CO)_m]^* \longrightarrow Fe_n(CO)_m + h\nu, \quad (41)$$

$$[Fe_n(CO)_m]^* + RH \longrightarrow Fe_n(CO)_m + RH, \quad (42)$$

$$[Fe_n(CO)_m]^* \longrightarrow Fe_n(CO)_{m-1} + CO, \quad (43)$$

$$[Fe_n(CO)_m]^* + Fe_n(CO)_{m-1} \longrightarrow \text{products}; \quad (44)$$

RH is the solvent.

Several workers have reported [66, 69, 74] the formation of the $Fe_n(CO)_{m-1}$ fragment during the irradiation of penta- and nonacarbonyliron in inert gas matrices.

We know that the rates and the quantum yields of photochemical reactions are relatively insensitive to temperature, [75] which usually affects only the dark reactions. The activation energies reported [70] for the evolution of CO in the photolysis of octane solutions of iron carbonyls show that the formation of carbon monoxide by the scheme (40)–(44) during the decomposition of $Fe_n(CO)_m$ is accompanied by a process in which the photochemical act is the bimolecular interaction of an activated with a non-activated molecule of the carbonyl [Eqn (45)]. In this case the scheme of the photodissociation should include the steps (40)–(42), (45) and the deactivation of $[Fe_n(CO)_m]^*$ on other molecules of the carbonyl:

$$[Fe_n(CO)_m]^* + Fe_n(CO)_m \longrightarrow \text{products}, \quad (45)$$

$$[Fe_n(CO)_m]^* + Fe_n(CO)_m \longrightarrow 2\,Fe_n(CO)_m. \quad (46)$$

A kinetic analysis of the mechanism of photolysis of iron carbonyls in solutions shows [70] that the process can follow either of the suggested schemes. In the case of reactions (40)–(44) the quantum yield of the photodissociation of the iron carbonyls (φ_1) is independent of the initial concentration of $Fe_n(CO)_m$ [Eqn (47)]. If the photolysis of the carbonyl complexes takes place according to the scheme (40)–(42), (45), (46) the quantum yield of the reaction (φ_2) becomes a function of the concentration of the carbonyl:

$$\varphi_1 = \frac{2k_{43}}{k_{41}} + k_{42}[RH] + k_{43}, \quad (47)$$

$$\varphi_2 = \frac{2k_{45}[Fe_n(CO)_m]}{k_{41}} + k_{42}[RH] + k_{45}[Fe_n(CO)_m] + k_{46}[Fe_n(CO)_m]. \quad (48)$$

Since the quantum yield of the elimination of CO in the photolytic dissociation of $Fe(CO)_5$ at 293 K is not affected by changes in the initial concentration of the carbonyl we may conclude that under these conditions the photolysis of pentacarbonyliron takes place mainly by the mechanism described by Eqns (40)–(44). At 373 K the dependence of the reciprocal quantum yield on the concentration is described by the expression

$$\varphi_2^{-1} = \frac{k_{45} + k_{46}}{2k_{45}} + \frac{k_{42} + k_{45}[RH]}{2k_{45}[Fe_n(CO)_m]}. \quad (49)$$

A similar dependence is observed in the photolysis of $Fe_2(CO)_9$ in octane at 293 K. Therefore increasing the temperature of the reaction and changing from penta- to nonacarbonyliron increases the contribution of the path described by Eqns (40) to (46) to the photolytic breakdown of the carbonyl complexes of iron.

The photolysis of $Co_2(CO)_8$ and $Co_4(CO)_{12}$ is nonane under the influence of UV light produces a colour change in the solution, accompanied by the evolution of carbon monoxide. [76] An analysis of the spectra of the reaction mixtures obtained during the irradiation of $Co_2(CO)_8$ showed that octacarbonylcobalt is converted into $Co_4(CO)_{12}$ by the photolysis.

The initial rate of accumulation of CO in the photodissociation of the cobalt carbonyls is directly proportional to the number of quanta absorbed, and an increase in the wavelength of the light from 253.7 to 366 nm has almost no effect on the quantum yield of the formation of carbon monoxide. The quantum yield for the decomposition of octacarbonylcobalt (2.9×10^{-3}) and for the formation of the reaction products $Co_4(CO)_{12}$ (1.5×10^{-3}) and CO (6.0×10^{-3}) suggest that the photolysis of $Co_2(CO)_8$ is described by the equation

$$2Co_2(CO)_8 \xrightarrow{h\nu} Co_4(CO)_{12} + 4\,CO. \quad (50)$$

The kinetic order of the decomposition of $Co_2(CO)_8$ in nonane under the influence of UV radiation is close to unity; increasing the temperature from 293 to 313 K has no effect on the quantum yields of the photodissociation of the cobalt carbonyls.

The changes in the spectra recorded during the photolysis of $Co_4(CO)_{12}$ show that under the influence of radiation dodecacarbonylcobalt is converted into $Co_6(CO)_{16}$: [76]

$$2\,Co_4(CO)_{12} \xrightarrow{h\nu} Co_6(CO)_{16} + 8\,CO + 2\,Co. \quad (51)$$

The order of the reaction leading to the photolytic dissociation of $Co_4(CO)_{12}$ in nonane is close to unity.

The scheme of the photolytic dissociation of octacarbonylcobalt in solution is analogous to the photolysis mechanism of the iron carbonyls [Eqns (40)–(44)]. [76] A kinetic analysis of this scheme and the experimental dependence of the reciprocal quantum yield for the photolysis of $Co_2(CO)_8$ on its reciprocal concentration, described by Eqn (49), show that the elimination of a CO ligand from the excited carbonyl molecule plays only a minor role in this process. On the other hand, in the thermal dissociation of $Co_2(CO)_8$ in solutions it is the rate-determining step. [48] An electronically excited state relatively stable towards decarbonylation is probably created as a result of the absorption of a light quantum by octacarbonylcobalt. This effect can be attributed to the presence of a large number of bonds in $Co_2(CO)_8$, which allow the energy of the absorbed quantum to be redistributed. [76] As a result most of the activated carbonyl molecules are deactivated by processes such as (41), (42), and (46), leading to low values of the quantum yields in the photolysis of $Co_2(CO)_8$. A graphical analysis of the dependence of the reciprocal quantum yield on the reciprocal concentration of $Co_2(CO)_8$ suggests that the ratio of the rate constants of the bimolecular deactivation of the excited $Co_2(CO)_8$ molecule [Eqn (46)] and of the direct photochemical reaction [Eqn (45)] can be as high as 30. [76]

Early studies of the photolysis of tetracarbonylnickel in a CCl_4 solution [55] and in the gas phase [77] had established that this process results in the formation of four moles of CO. As in the case of pentacarbonyliron the primary act of the photolysis is the absorption of a light quantum and the conversion of the molecule into the excited $[Ni(CO)_4]^*$ state, from which it decomposes with the elimination of one CO group. The resulting $Ni(CO)_3$ is unstable and decomposes to the metal and carbon monoxide. Additions of CO suppress the decomposition of

$Ni(CO)_4$ in both the gas phase [77] and the liquid phase.[50] The observed[77] lifetime of the activated $[Ni(CO)_4]^*$ molecule was 7×10^{-9} s. The quantum yield of the photolytic decomposition of the tetracarbonyl in solution irradiated with 313 nm light was 1.8; the order of the photolysis reaction was close to unity.[50] According to a number of reports[50,55,77] the photolysis of nickel carbonyl takes place by an induced mechanism which includes reversible stages:

$$Ni(CO)_4 \xrightarrow{h\nu} [Ni(CO)_4]^*, \quad (52)$$

$$[Ni(CO)_4]^* \rightleftharpoons Ni(CO)_3 + CO, \quad (53)$$

$$[Ni(CO)_4]^* + M \longrightarrow Ni(CO)_4 + M, \quad (54)$$

$$Ni(CO)_3 \xrightarrow[-CO]{} Ni(CO)_2 \xrightarrow[-CO]{} \longrightarrow NiCO \xrightarrow[-CO]{} Ni, \quad (55)$$

$$Ni(CO)_4 + Ni(CO)_2 \longrightarrow 2\,Ni(CO)_3; \quad (56)$$

M = RH, CO.

The effective rate constant of the photolysis of tetracarbonylnickel in undecane was found to be[50] 1.47×10^{-5} s^{-1}.

Studies by IR spectroscopy of the photolysis of $Ru(CO)_5$ and $V(CO)_6$ in the gas phase revealed coordinatively unsaturated fragments, highly reactive towards the starting carbonyls with which they form binuclear complexes.[78,79] The mechanism of the process has not been studied in detail.

The photolysis of the carbonyls of the chromium subgroup in the gas phase, initiated by laser radiation with wavelengths of 351, 308, and 248 nm, takes place by the successive elimination of the CO ligands from the excited carbonyl molecule.[80–85] The number of particles into which the original carbonyl molecule becomes fragmented depends on the energy of the absorbed photon. Photolysis with light of 351 and 308 nm produces only $M(CO)_5$ molecules, whereas light of 248 nm wavelength generates mainly $M(CO)_4$.[80,83] $M(CO)_5$ and $M(CO)_4$ are both very reactive, and they readily attack the initial $M(CO)_6$ molecule or the CO in the gas phase.

The irradiation of metal hexacarbonyls isolated in a matrix (N_2, Ar, CH_4, petroleum jelly) at 12–293 K with UV or visible light leads to the reversible elimination of one carbonyl group with formation of a relatively unstable pentacarbonyl of the metal, which interacts with the material of the matrix:[85–87]

$$M(CO)_6 \xrightarrow{h\nu} [M(CO)_6]^* \xrightarrow[-CO]{} \longrightarrow [M(CO)_5]^* \xrightarrow{Q} [M(CO)_5]^*Q; \quad (57)$$

M = Cr, Mo, W; Q = N_2, Ar, CH_4, petroleum jelly.

Complexes with organic and with inorganic ligands are formed also during the photolysis of the carbonyls of the chromium subgroup in the gas phase in the presence of various gaseous additives[81,88] or in solutions.[89–92] The coordinatively unsaturated carbonyl $M(CO)_5$ is generated as two structures: square pyramidal (C_{4v}) and trigonal bipyramid (D_{3h}), with a lifetime not greater than 20 μs.[89–91] During this time the carbonyl forms complexes with the solvent or with the additive, the rate of interaction of the triplet (D_{3h}) form being 2.3 times greater than that of the reaction of $M(CO)_5$ in the square pyramidal (singlet) form.[91] In the solvated $[M(CO)_5]^*Q$ complexes (where Q is an alcohol or an alkane) coordination takes place at the alkyl group.[90]

Thus the primary stage in the photolysis of the hexacarbonyls of chromium, molybdenum, and tungsten, and of tetracarbonylnickel (in condensed and in gaseous media) is the reversible elimination of one CO ligand and the formation of a coordinatively unsaturated metal carbonyl. The photolytic decomposition of the iron and cobalt carbonyls includes, in addition to the unimolecular decomposition of $[M_n(CO)_m]^*$, the interaction of this species with a non-excited carbonyl molecule. The contribution from the bimolecular reaction increases with increasing temperature, and also on changing from $Fe(CO)_5$ to $Fe_2(CO)_9$, and it becomes predominant in the case of $Co_2(CO)_8$. The photolysis of polynuclear metal carbonyls has been studied most fully[93–99] for the decacarbonyls of manganese and of rhenium, and for their mixed derivatives.

The primary stages in the decomposition of the $M_2(CO)_{10}$ complexes (M = Mn, Re) have been studied[93–98] by pulsed laser photolysis in the gas phase, in an argon matrix, and in solutions in hydrocarbons. It has been established that the electronic excitation of the decacarbonyls of these metals induces two types of primary reaction: (1) the breaking of the metal–metal bond, with formation of $M(CO)_5$ species, and (2) the elimination of one CO group, with formation of an $M_2(CO)_9$ species containing a bridging carbonyl group:

$$M_2(CO)_{10} \xrightleftharpoons{h\nu} 2\,M(CO)_5, \quad (58)$$

$$M_2(CO)_{10} \xrightleftharpoons{h\nu} (CO)_4M(\mu\text{-}CO)M(CO)_4. \quad (59)$$

The relative yield of $M_2(CO)_9$ increases with the quantum energy of the chosen radiation. Thus, for $Mn_2(CO)_{10}$ in cyclohexane the ratio of the quantum yields of reactions (58) and (59) was found to be 0.21, 0.37, and 0.74 at wavelengths of 266, 337, and 355 nm respectively. For decacarbonylrhenium the ratio of the quantum yields for the photolytic decomposition by these two channels is 0.13 at 355 nm.[94,95] Particles of $M(CO)_5$ and $M_2(CO)_9$ are removed in the reverse reactions (58) and (59), with rate constants of 8.8×10^8 and 3.6×10^9 dm^3 mol^{-1} s^{-1} for $Mn(CO)_5$ and $Re(CO)_5$ respectively, and 1.2×10^5 and 4.4×10^4 dm^3 mol^{-1} s^{-1} for $Mn_2(CO)_9$ and $Re_2(CO)_9$ respectively.[94,95] The free-radical nature of the carbonyls $Re(CO)_5$ and $Re_2(CO)_9$ formed in the photolysis of $Re_2(CO)_{10}$ in CH_2Cl_2 has been demonstrated by the ESR method using spin traps.[99]

Information on the photochemical reactions of the binuclear carbonyls of metals of the iron subgroup [except $Co_2(CO)_8$] is scarce and fragmentary. Thus, it has been shown by the matrix isolation method[74,100] that the primary photochemical reaction of the iron and osmium nonacarbonyls is the dissociation of the excited molecule with formation of the $M_2(CO)_8$ fragment:

$$M_2(CO)_9 \xrightarrow{h\nu} [M_2(CO)_9]^* \longrightarrow M_2(CO)_8 + CO; \quad (60)$$

M = Fe, Os.

The coordinatively unsaturated iron carbonyl $Fe_2(CO)_8$ can exist in two forms: bridged and nonbridged.[74] Octacarbonylosmium does not contain bridging carbonyl ligands, probably because the Os–Os bond is much longer than the Fe–Fe bond and therefore hinders the bridging coordination of the carbonyl ligand.[100] Lengthy photolysis of nonacarbonylosmium isolated in an argon matrix results in cleavage of the metal–metal bond, with accumulation of the mononuclear carbonyl $Os(CO)_5$ among the final products.[100] Homolytic cleavage of the iron–iron bond has not been observed.[74]

Very little has been published on the photochemistry of clusters containing three or more metal atoms.[70,76,101–106] It has been shown[101–105] that after the absorption of a photon the $M_3(CO)_{12}$ carbonyl clusters of the iron subgroup can undergo two types of change. When the energy of the absorbed quanta is high we observe elimination of one of the carbonyl ligands from the initial complex, with formation of an intermediate which can add on another ligand or a solvent molecule. At low photon energies the excited $[M_3(CO)_{12}]^*$ molecule

undergoes isomerisation into a nonradical cluster, different from the initial structure, which then suffers fragmentation:

$$M_3(CO)_{12} \xrightarrow[\lambda > 420\ nm]{h\nu} [M_3(CO)_{12}]^* \longrightarrow \quad (61)$$

$$\longrightarrow [M_3(CO)_{12}] \xrightarrow{L} M(CO)_4L + M_2(CO)_8L;$$

L = CO, C_2H_4.

$$M_3(CO)_{12} \xrightarrow[\lambda > 420\ nm]{h\nu} [M_3(CO)_{12}]^* \xrightarrow{-CO} \quad (62)$$

$$\longrightarrow [M_3(CO)_{11}] \xrightarrow{Q} [M_3(CO)_{11}]^*Q;$$

Q is the solvent [PPh_3, $P(OM_3)_3$, etc.]

Cleavage of one of the metal–metal bonds and changes in the cluster skeleton were observed also in the photochemical initiation ($\lambda > 340$ nm) of the reaction of dodecacarbonylcobalt with alkynes.[106]

After irradiation with visible or UV light, metal carbonyl molecules are converted into an unstable electronically excited state. The next stage is the elimination of one CO ligand by a unimolecular or bimolecular reaction. The resulting coordinatively unsaturated fragment can recombine with CO or with the initial carbonyl molecule, or it can form a complex with a solvent molecule or with another ligand. Binuclear and polynuclear carbonyl compounds also undergo fragmentation with cleavage of the metal–metal bond: in polymetal carbonyls this stage is followed by isomerisation of the cluster skeleton.

IV. Oxidation of the metal carbonyls by oxygen, ozone, and peroxides

1. Oxidation of the metal carbonyls by oxygen

The earliest information on the oxidation reactions of metal carbonyls was published with the first reports of the synthesis of these compounds. The reaction of carbonyl complexes with oxygen is used at present to prepare various oxide materials, including ferromagnetics.[1-3]

The mechanism first put forward[35,53,107-110] to explain the decomposition of pentacarbonyliron in the presence of oxygen postulated the conversion of the primary photolysis product of the $Fe(CO)_5$ [the nonacarbonyl $Fe_2(CO)_9$] into iron oxide:

$$Fe(CO)_5 \xrightarrow{h\nu} [Fe(CO)_5]^* \longrightarrow Fe(CO)_4 + CO, \quad (63)$$

$$Fe(CO)_4 + Fe(CO)_5 \longrightarrow 2\,Fe_2(CO)_9, \quad (64)$$

$$Fe_2(CO)_9 + \left(3+\frac{x}{2}\right)O_2 \longrightarrow Fe_2O_3 + (9-x)CO + x\,CO_2. \quad (65)$$

A detailed study[76,111] of the photochemical interaction of $Fe_n(CO)_m$ (n = 1, 2, 3; m = 5, 9, 12) with oxygen in hydrocarbon solvents failed to confirm this scheme. The photooxidation of these iron carbonyls in solutions is accompanied by the evolution of the carbon oxides CO and CO_2 and by the formation of a highly dispersed, X-ray amorphous form of Fe_2O_3 containing iron compounds characterised by the Fe–CO bond.[76,111] Accumulation of gaseous products takes place at the same time as the disappearance of the initial iron carbonyl from the reaction mixture. The relative yields of CO and CO_2 remain constant up to a 70%–80% conversion of the initial carbonyl. The quantum yields of the formation of products and of the disappearance of the $Fe_n(CO)_m$, calculated from the initial rates of the appropriate reactions, have been reported.[76,111] The interaction of $Fe_n(CO)_m$ with oxygen, initiated by UV radiation, is described by the equations

$$2\,Fe(CO)_5 + \tfrac{5}{2}O_2 \xrightarrow{h\nu} Fe_2O_3 + 8\,CO + 2\,CO_2, \quad (66)$$

$$Fe_2(CO)_9 + 2\,O_2 \xrightarrow{h\nu} Fe_2O_3 + 8\,CO + CO_2, \quad (67)$$

$$2\,Fe_3(CO)_{12} + \tfrac{11}{2}O_2 \xrightarrow{h\nu} 3\,Fe_2O_3 + 22\,CO + 2\,CO_2. \quad (68)$$

The initial rate of the photo-oxidation of these iron carbonyls is directly proportional to the number of quanta absorbed, and is independent of temperature between 278 and 313 K. The photo-initiated oxidation of $Fe_n(CO)_m$ by molecular oxygen in nonane is kinetically of first-order with respect to the initial iron carbonyl. In the case of pentacarbonyliron the order of the reaction with respect to oxygen is zero. For the nona- and dodecacarbonyls the rate of the photooxidation decreases with increasing oxygen pressure.

A spectrophotometric analysis of the reaction mixtures carried out during the oxidation showed the absence of photolysis products of the initial iron carbonyls. This suggests that the initial rates of the photochemical interaction of $Fe_n(CO)_m$ with O_2 are approximately an order of magnitude greater than the initial rate of the photolysis.[76,111] Since the concentrations of the carbonyl solutions did not exceed 10^{-4} mol dm^{-3}, and since the quantum yields of the oxidation of $Fe_2(CO)_9$ and $Fe_3(CO)_{12}$ are much lower than unity, the presence of chain reactions in the oxidation process seems unlikely. In keeping with these results the following mechanism has been proposed[76] for the photochemical oxidation of $Fe(CO)_5$ by oxygen through the formation of oxo and peroxo complexes of iron:

$$Fe(CO)_5 \xrightarrow{h\nu} [Fe(CO)_5]^*, \quad (69)$$

$$[Fe(CO)_5]^* \longrightarrow Fe(CO)_5 + h\nu, \quad (70)$$

$$[Fe(CO)_5]^* \longrightarrow Fe(CO)_4 + CO, \quad (71)$$

$$[Fe(CO)_5]^* + M \longrightarrow Fe(CO)_5 + M, \quad (72)$$

where M = $Fe(CO)_5$, O_2, RH.

$$[Fe(CO)_5]^* + O_2 \longrightarrow (CO)_3Fe\begin{matrix}O\\|\\O\end{matrix} + 2\,CO, \quad (73)$$

$$[Fe(CO)_5]^* + O_2 \longrightarrow (CO)_3Fe{=}O + CO + CO_2, \quad (74)$$

$$Fe(CO)_4 + O_2 \longrightarrow (CO)_3Fe\begin{matrix}O\\|\\O\end{matrix} + CO, \quad (75)$$

$$Fe(CO)_4 + O_2 \longrightarrow (CO)_3Fe{=}O + CO_2, \quad (76)$$

$$(CO)_3Fe\begin{matrix}O\\|\\O\end{matrix} + (CO)_3Fe{=}O \longrightarrow Fe_2O_3 + 6\,CO. \quad (77)$$

A kinetic analysis produced a satisfactory correspondence between the proposed scheme and the experimental data. The formation of oxo and peroxo complexes of iron has been observed during the oxidation of the $Fe(CO)_5^-$ anions by oxygen in the gas phase and in the interaction of iron atoms with O_2 in argon matrices at 15 K.[113]

The experimentally observed negative kinetic order with respect to oxygen in the photooxidation of nona- and dodecacarbonyliron suggests that the mechanism of the process includes the reversible formation of a complex between an excited carbonyl molecule and oxygen, and the dissociation of this complex as a result of bimolecular reactions with O_2 and with the solvent.[111]

$$Fe_n(CO)_m \xrightarrow{h\nu} [Fe_n(CO)_m]^* \quad (78)$$

$$[Fe_n(CO)_m]^* \xrightarrow[\text{non-radiative deactivation}]{\text{radiative and}} Fe_n(CO)_m \quad (79)$$

$$[Fe_n(CO)_m]^* + O_2 \rightleftarrows [Fe_n(CO)_m^*O_2]^* \quad (80)$$

$$[Fe_n(CO)_m^*O_2]^* \longrightarrow \text{products} \quad (81)$$

$$[Fe_n(CO)_m^* O_2]^* + RH \longrightarrow Fe_n(CO)_m + O_2 + RH \quad (82)$$

$$[Fe_n(CO)_m^*O_2]^* + O_2 \longrightarrow Fe_n(CO)_m + 2O_2 \quad (83)$$

This mechanism provided a basis for the mathematical modelling of the kinetics of the oxidation of nona- and dodecacarbonyliron by oxygen.[111] The solution of the direct kinetic problem gave the time dependences of the concentrations of $Fe_2(CO)_9$ and $Fe_3(CO)_{12}$ during the photooxidation. Comparing the calculated concentrations with experimental values gave a satisfactory agreement.[111] The effect of the initial concentrations of the reactants on the rate of the photooxidation of the carbonyls was also satisfactorily consistent with experiment.

We have studied the possibility of complex formation between pentacarbonyliron and oxygen by measuring the specific heat and the IR spectra of a mixture of reactants at 150–273 K.[114] It was found that the structure of the absorption bands of the Fe–CO bending vibrations in the pure pentacarbonyliron and in its mixtures with oxygen is strongly affected by replacing the gas phase by a solid phase (or vice versa). No difference was detected between the spectra of the pure pentacarbonyliron and those of $Fe(CO)_5$ with additions of O_2. The temperature dependence of the specific heat of the carbonyl complex deviates from a monotonic curve at 153–175 K, both with and without oxygen additions. However, the $C_p = f(T)$ curves of mixtures of these reactants and those of pure $Fe(CO)_5$ are almost identical.

The observed changes in the IR spectra of $Fe(CO)_5$ and in the temperature dependence of its specific heat at 150–190 K suggest the occurrence of specific processes in the substance during heating. The enthalpy of the process observed in this work was 16.22 ± 0.02 kJ mol^{-1}. These effects could be due to changes in the symmetry of the molecular structure of the pentacarbonyliron (for example, a transition from a configuration with D_{3h} symmetry to one with C_{4v} symmetry). Calculations[114] suggest that the ground state of $Fe(CO)_5$ is a singlet with a configuration of D_{3h} symmetry. An assessment of the possibility of finding pentacarbonyliron in a tetragonal bipyramid form (C_{4v} symmetry) gave a difference in energy $E(C_{4v}) - E(D_{3h}) =$ 22.5 kJ mol^{-1}. The calculated value is substantially greater than the experimental enthalpy of the process. The discrepancy arises partly from the seriously overestimated energy of the transition of the $Fe(CO)_5$ molecule from a D_{3h} to a C_{4v} state, due to the chosen method of calculation, and partly from the possibility of a more radical change in the structure of the $Fe(CO)_5$ molecule while only a slight deformation is observed owing to the distortion of the Fe–C–O angles.

Thus the IR spectroscopic and calorimetric studies of the interaction of pentacarbonyliron with oxygen at 150–273 K have failed to establish unambiguously the formation of donor–acceptor complexes between the reactants. However, the possible existence of these complexes has been suggested by the quantum chemical method. Calculations of the potential energy curve for the interaction between pentacarbonyliron and oxygen[114] show that the $Fe(CO)_5 + O_2$ system can be stabilised by the formation of the $Fe(CO)_5O_2^*$ complex, whose energy of dissociation into separate molecules is 20–30 kJ mol^{-1}. This result indicates only a tendency towards complex formation betwen $Fe(CO)_5$ and O_2. The calculated dissociation energy of $Fe(CO)_5O_2^*$ is extremely high.

We know[5] that the crystalline cobalt carbonyls $Co_2(CO)_8$ and $Co_4(CO)_{12}$ are converted into the blue carbonates when stored in air. The oxidation of $Co_2(CO)_8$ by oxygen in toluene was shown[115] to be autocatalytic, leading to the formation of $CoCO_3$, CO, and CO_2:

$$5\,Co_2(CO)_8 + 13\,O_2 \longrightarrow 10\,CoCO_3 + 24\,CO + 6\,CO_2. \quad (84)$$

It was suggested[115] that the interaction of octacarbonylcobalt with oxygen is a chain reaction in which the active species are the $Co_2(CO)_7$ particles formed by the thermal dissociation of $Co_2(CO)_8$. A study of the interaction of $Co_2(CO)_8$ with oxygen in nonane[116] failed to confirm this hypothesis.

The oxidation of the octa- and the dodecacarbonyl of cobalt in solution was found to be accompanied by the formation of carbon oxides and by the deposition of a solid phase containing $CoCO_3$, Co_2O_3 and CoO. The composition of the solid phase depends on the nature of the carbonyl and on the ratio of the initial concentrations of the reactants.[116] The kinetic order of the reaction of octacarbonylcobalt with oxygen in nonane with respect to the initial concentration of the carbonyl is close to unity. Changes in the oxygen pressure over the solution from 300 to 500 Torr do not affect the rate of oxidation. The activation energy of this process is 56.9 ± 2.0 kJ mol^{-1} (in the range of 283–313 K). Additions of CO at the start of the reaction lower the rate of oxidation.

Irradiation of a solution of $Co_2(CO)_8$ with UV light having a wavelength of 366 nm accelerates the oxidation of the cobalt carbonyl. The quantum yield of this process is much higher than unity ($\varphi = 5$), which suggests a chain mechanism for the reaction. Since the formation of $Co_2(CO)_7$ by the photolysis of $Co_2(CO)_8$ in solution has a low probability[76] it has been suggested that the $^{\cdot}Co(CO)_4$ radicals behave as active intermediates in the oxidation of octacarbonylcobalt by oxygen.[116] The energy of the metal–metal bond has been reported by various workers to be in the range between 48 and 125 kJ mol^{-1}, which is much lower than the energy needed to break the Co–CO bond (134.9 kJ mol^{-1}).[37] The $^{\cdot}Co(CO)_4$ radicals were detected by EPR during the sublimation of $Co_2(CO)_8$ on to a surface cooled to 77 K. Carrying out this process in the presence of oxygen produces[117] $(CO)_4CoOO^{\cdot}$ peroxide radicals. The creation of active intermediates during the oxidation of $Co_2(CO)_8$ by oxygen in a polystyrene matrix is also indicated by the partial decomposition of the polymer.[118]

As reported,[116] peroxide radicals are formed during the oxidation of $Co_2(CO)_8$ in solutions. However, the application of various physicochemical methods of detecting free-radical species during the interaction of octacarbonylcobalt with oxygen in nonane (EPR, spectrophotometric analysis of the aqueous phase after hydrolysis of the reaction mixture in the presence of H_2O_2, effect of ionol additions on the rate of the process) produced ambiguous results. Nevertheless the accurately determined quantum yields of these reactions confirm that a chain mechanism is involved:[116]

$$Co_2(CO)_8 + h\nu\,(\Delta) \longrightarrow [Co_2(CO)_8]^*, \quad (85)$$

$$[Co_2(CO)_8]^* \longrightarrow 2\,^{\cdot}Co(CO)_4, \quad (86)$$

$$^{\cdot}Co(CO)_4 + O_2 \longrightarrow {}^{\cdot}OOCo(CO)_4, \quad (87)$$

$$^{\cdot}OOCo(CO)_4 \rightleftarrows [OOCo(CO)_{4-x}] + x\,CO, \quad (88)$$

$$[OOCo(CO)_{4-x}] + Co_2(CO)_8 \longrightarrow$$
$$\longrightarrow (CO)_{4-x}CoOOCo(CO)_4 + {}^{\cdot}Co(CO)_4, \quad (89)$$

$$[OOCo(CO)_{4-x}] \longrightarrow CoO + CO_2 + (3-x)CO, \quad (90)$$

$$(CO)_{4-x}CoOOCo(CO)_4 \xrightarrow{} 2\,CoO + (8-x)CO \quad (91)$$
$$\xrightarrow{O_2} 2\,CoCO_3 + (6-x)CO \quad (92)$$
$$\xrightarrow{O_2} Co_2O_3 + CO_2 + (7-x)CO. \quad (93)$$

In addition to reactions (85)–(93) the deactivation of the excited $[Co_2(CO)_8]^*$ also takes place (on the solvent molecules, and on the reactants) during the photooxidation of $Co_2(CO)_8$.

The dependence of the composition and yield of the oxidation products of octacarbonyldicobalt on the initial concentrations of $Co_2(CO)_8$ and O_2 is due to reactions (89) – (93). Thus, increasing the oxygen pressure increases the amount of Co_2O_3 and CO_2 in the product, whereas an increase in the concentration of the carbonyl increases the amount of carbonate in the deposit, owing to the increased contribution of reaction (92).[116]

The interaction of dodecacarbonylcobalt with oxygen in nonane is slower (by a factor of 10) than the oxidation of $Co_2(CO)_8$, but it is accelerated by the action of UV radiation. The order of the reaction with respect to the initial concentration of the carbonyl is close to unity. Increasing the oxygen pressure over the solution has no effect on the rate of the process. The activation energy of the oxidation of $Co_4(CO)_{12}$ in solution is 74.6 ± 3.0 kJ mol^{-1} (at temperatures between 278 and 313 K). Additions of carbon monoxide to the gas phase at the start of the reaction do not affect the reaction rate. The quantum yield of the oxidation of $Co_4(CO)_{12}$ by oxygen, initiated by UV light having a wavelength of 366 nm, is 0.3. These results led to the conclusion[116] that the reaction of dodecacarbonylcobalt with oxygen does not involve a chain mechanism.

The oxidation of tetracarbonylnickel by oxygen has a period of induction and critical pressure limits, depending on the pressure and on the diameter of the vessel.[35] These observations suggest that the $Ni(CO)_4$ is oxidised by oxygen in the gas phase by a chain mechanism with chain breaking on the walls of the vessel.[35] The initial stage of the process is the elimination of one CO ligand from the excited carbonyl molecule, and the final products of the reaction are the carbon oxides CO and CO_2 and nickel oxide containing unchanged carbonyl.[107]

The oxidation of tetracarbonylnickel by oxygen in solutions is relatively slow.[50] Thus, at 293 K only 10% of the initial carbonyl is oxidised in 5 h. Irradiation of the reaction mixture with 313 nm light increases the rate of interaction of the $Ni(CO)_4$ with oxygen. The quantum yield of the oxidation of the nickel carbonyl is 1.12. Each mole of converted $Ni(CO)_4$ produces 2.92 mol of CO and 0.96 mol of $NiCO_3$. The kinetic order of the reaction with respect to the carbonyl compound is 1.2. A change in the pressure of oxygen over the solution from 300 to 500 Torr has no effect on the initial rate of the process. Adding the solid products of the oxidation of carbonylnickel to the reaction mixture has no effect on the rate of the interaction with oxygen. However, adding carbon monoxide before the start of the reaction lowers the rate of oxidation of the carbonyl complex. The experimental results are consistent with the following mechanism for the oxidation:[50]

$$[Ni(CO)_4]^* \rightleftharpoons Ni(CO)_3 + CO, \quad (94)$$

$$Ni(CO)_3 \xrightarrow{-CO} Ni(CO)_2 \xrightarrow{-CO} \longrightarrow Ni(CO) \xrightarrow{-CO} Ni, \quad (95)$$

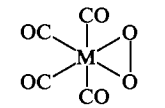
$$Ni(CO)_3 \longrightarrow Ni + (C) + CO + CO_2, \quad (96)$$

$$Ni(CO)_3 + O_2 \longrightarrow NiCO_3 + 2\,CO. \quad (97)$$

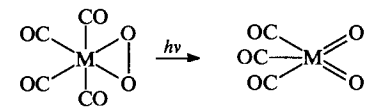
The interaction of the nonexcited $Ni(CO)_4$ molecule with O_2 can be ignored because the rate of the dark process is much lower than the rate of the photooxidation. A kinetic analysis of Eqns (94) – (97) showed that these reactions are consistent with experimental data. The effective rate constant for the oxidation of $Ni(CO)_4$ by oxygen at 293 K was 1.41×10^{-4} s^{-1}, which exceeds by an order of magnitude the rate of its photolytic decomposition.[50]

The oxidation of the carbonyls of the chromium subgroup in inert gas matrices has been studied by Almond et al.,[119–122] who showed that the primary stage of the process was the decomposition of an activated molecule of the carbonyl with formation of the pentacarbonyl of the metal and carbon monoxide. Further photolysis of the matrix leads to mixed carbonyl complexes which ultimately give the metal oxides MO_3 (or MO_2), CO, and CO_2.

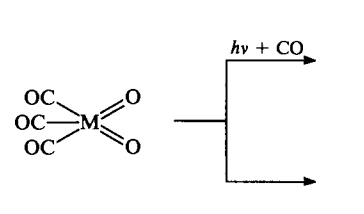
$$M(CO)_6 \xrightarrow[CH_4,\ Ar,\ 12\ K]{h\nu + O_2} M(CO)_5 + CO \xrightarrow{h\nu + O_2}$$



$$+ CO \quad (98)$$

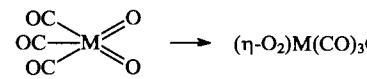


$$+ CO \quad (99)$$



$$(100)$$

$$(101)$$



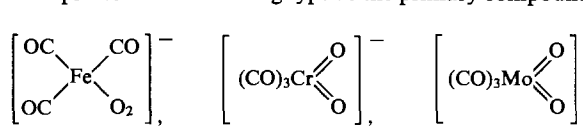
$$\longrightarrow (\eta\text{-}O_2)M(CO)_3O_2 \xrightarrow{h\nu} \quad (102)$$

$$\longrightarrow MO_3 + CO_2 + 2\,CO$$

The structure of the intermediate carbonyl–oxygen complexes was determined by IR spectroscopy, using the ^{18}O oxygen isotope.[120] It was shown by the isotope substitution method[122] that the MO_3 molecules (M = Mo, W) are formed from the peroxide $(\eta^2\text{-}O_2)M(CO)_3O_2$, which decomposes under the influence of the UV radiation to give MO_3 and oxygen atoms in the excited ^1D state. A sample of chromium dioxide having ferromagnetic properties and metallic conduction was obtained[121] by the photolysis of carbonylchromium in an argon matrix with O_2 additions.

It has been reported[123,124] that the arenetricarbonyls of metals (chromium, molybdenum, and tungsten) react with oxygen by previous coordination of the reactants.

The interaction with oxygen, in the gas phase and at room temperature, of the transition metal carbonyls $M(CO)_n^-$ (where M = Cr, Mo, W, Mn for $n = 5$; M = Fe, Co for $n = 4$), prepared by the electron impact method, leads to the formation of complexes of the following type as the primary compounds:



which are then converted into the metal oxides.[112,125]

Radicals of the peroxides $Re(CO)_5O_2^{\bullet}$ and $Mn(CO)_5O_2^{\bullet}$ were detected by EPR by using spin traps during the photolysis of $Re_2(CO)_{10}$ and $Mn_2(CO)_{10}$ in CH_2Cl_2 solutions in the presence of oxygen.[99,126] The active $Re(CO)_5O_2^{\bullet}$ species detach a hydrogen atom from a solvent molecule and form a hydroperoxide which dissociates further to give the radicals $Re(CO)_5^{\bullet}$ and $HOO^{\bullet}$.

Thus the oxidation of the carbonyl complexes of elements of Groups VI – VIII by oxygen in gaseous or liquid media is accompanied by the formation of the oxides and of the carbonate of the metal, and of carbon oxides. The composition and the yield of the reaction products are strongly dependent on the nature of the carbonyl complex and on the condition used for the oxidation. The process is accelerated under the influence of irradiation, and it can be hindered by additions of CO. The mechanism of the reaction includes the formation of intermediate carbonyl complexes of the metal in both radical and nonradical forms.

2. Oxidation of metal carbonyls by ozone

Data on the interaction of metal carbonyls with ozone are few. A study of the oxidation of pentacarbonyliron vapour by ozone–helium mixtures at room temperature and low pressure has been reported.[127] The product of the reaction was a highly dispersed diamagnetic aerosol of Fe_2O_3, formed according to the scheme

$$Fe(CO)_5 + O_3 \longrightarrow Fe(CO)_4 + CO_2 + O_2, \quad (103)$$

$$Fe(CO)_4 + O_3 \longrightarrow FeO + 4\,CO + O_2, \quad (104)$$

$$FeO + O_3 \longrightarrow Fe_2O_3 + O_2. \quad (105)$$

The oxidation of $Fe(CO)_5$ and $Ni(CO)_4$ vapours by ozone is accompanied by chemiluminescence in the 500–600 nm region,[128] due to the emission of light quanta by the excited FeO and NiO molecules formed in the exothermic reaction of the metal carbonyl with ozone. The oxidation of tetracarbonylnickel by ozone has been used in the purification of industrial effluents.[129]

Studies of the composition of the products and of the kinetics in the reaction of iron, cobalt, and nickel carbonyls with ozone in organic solvents have been reported.[50,130,131] The carbonyls of the iron subgroup were oxidised by an ozone–oxygen mixture by bubbling the gases through the liquid at 223–293 K. The final products of the reaction were the oxide and carbonate of the metal and the oxides of carbon; their composition and yield depended on the nature of the carbonyl complex.[50,130,131] The transformation of the metal carbonyl is accompanied by oxidation of the solvent. The rate of oxidation of pentacarbonyliron, octa- and dodecacarbonylcobalt, and tetracarbonylnickel in the liquid phase is determined by the rate of diffusion of ozone from the gas phase into the solution. The interaction of dodecacarbonyliron with ozone in nonane is activation-controlled, with an activation energy of 24.2 ± 5.3 kJ mol^{-1} at 255–293 K. The number of moles of ozone used to oxidise one mole of the carbonyl complex varies between 1 and 14, depending on the nature of the metal in $M_n(CO)_m$. In some cases (dodecacarbonyliron, tetracarbonylnickel) this number is smaller than the value calculated from the yield of oxygen-containing products. This is due to the contribution of oxygen to the oxidation of the metal carbonyl.[50,131]

The kinetic features of the interaction of metal carbonyls with O_3 in the liquid phase[132] and the increase in the reaction rate produced by increasing the polarity of the medium show that the rate-limiting step of the process is the attack of the metal–ligand bond by the ozone molecule.

Unlike the oxidation of metal carbonyls by oxygen, the interaction of $M_n(CO)_m$ with ozone is relatively fast and produces a large yield of CO_2 and of carbonate anions. The detailed mechanism of this process has not yet been established.

3. Oxidation of the metal carbonyls by peroxides

Pentacarbonyliron reacts violently with hydroperoxides to give iron(III) oxide and carbon monoxide.[133] Di(*tert*-butyl) peroxide oxidises the iron and cobalt carbonyls to $Fe(OBu^t)_3$ and $Co(OBu^t)_3$ (Schott and Wilke[134]). The kinetics and the mechanism of the interaction of $Co_2(CO)_8$, $Mn_2(CO)_{10}$, and $Fe(CO)_5$ with dibenzoyl peroxide in toluene at 293–333 K have been studied by volumetric and IR spectral methods.[135] The reaction is of the first order with respect to the cobalt and manganese carbonyls and to the peroxide. The interaction of $Fe(CO)_5$ with benzoyl peroxide is autocatalytic. Additions of styrene and of carbon monoxide suppress the oxidation of the manganese and iron carbonyls. The process is described by the reactions

$$Co_2(CO)_8 + 2\,PhC(O)OOC(O)Ph \longrightarrow 2\,Co(OOCPh)_2 + 8\,CO, \quad (106)$$

$$Mn_2(CO)_{10} + 2\,PhC(O)OOC(O)Ph \longrightarrow 2\,Co(OOCPh)_2 + 8CO, \quad (107)$$

$$Fe(CO)_5 + 1.5\,PhC(O)OOC(O)Ph \longrightarrow Fe(OOCPh)_3 + 5\,CO. \quad (108)$$

The formation of free-radical species during the oxidation of metal carbonyls by benzoyl peroxide has been suggested.[135] The rate-limiting step of the interaction of $Fe(CO)_5$ with PhC(O)OOC(O)Ph is the conversion of the carbonyl complex into iron(II) compounds, followed by their fast oxidation to $Fe(OOCPh)_3$.

Complexes of zero-valent nickel are oxidised by dibenzoyl peroxide and by di(*tert*-butyl) peroxide, giving nickel benzoate and *tert*-butoxide.[134] Studies[136] of the interaction of chromium, molybdenum, tungsten, and iron carbonyls with organosilicon peroxides suggest that the primary stage in the reaction of $Fe(CO)_5$ with $Me_2Si(OOBu^t)_2$ is the coordination of two molecules of the peroxide to the carbonyl ligands of the pentacarbonyliron. The interaction of $Mo(CO)_6$ with cyclohexyl and 1-methylcyclohexyl peroxides in heptane also leads to the formation of out-of-sphere complexes with an enthalpy of formation of 6.3 kJ mol^{-1}.[137]

Hexacarbonylmolybdenum is oxidised by *tert*-butyl and cumyl hydroperoxides in alkanes at temperatures above 373 K.[138] The use of an aromatic hydrocarbon as the solvent increases the rate of the oxidative degradation of the $Mo(CO)_6$ by hydroperoxides because of the conversion of the initial metal complex into an arenemolybdenumtricarbonyl complex. The latter species is readily oxidised to molybdenum oxides and peroxides. The hydroperoxides are catalytically decomposed on these products, and the resulting intermediates interact with the $Mo(CO)_6$.[138]

The EPR method with spin traps has been used[139] to study the free-radical dissociation of Bu^tOOBu^t in the presence of various metal carbonyls in hydrocarbon solutions. The formation of adducts of $Bu^t\dot{O}$ radicals with the spin traps was demonstrated, and a scheme which included an initial electron transfer from the carbonyl to the peroxide was proposed.

The writers have studied[140,141] the oxidation of the carbonyl complexes of the elements of the iron subgroup by *tert*-butyl and cumyl hydroperoxides and by *tert*-butyl peroxide in paraffin solutions, and by hydrogen peroxide in water. The reaction is very fast at room temperature, and is accompanied by the formation of solid deposits, carbon oxides, and transformation products of the peroxide fragments. The solid phase precipitated from the reaction mixture is an oxide or carbonate of the metal, or a mixture of the two compounds, containing adsorbed molecules of the solvent or of water. In the case of pentacarbonyliron the precipitate contains (in addition to iron oxide) iron compounds in which the metal atom is attached to CO groups.[141]

Complete conversion of $M_n(CO)_m$ (where M = Fe, CO) is achieved with an excess of hydroperoxide (6-fold and 30-fold for the iron and the cobalt carbonyl respectively). The excess of hydroperoxide in comparison with the stoichiometric amount is attributed to the catalytic decomposition of the peroxidic compound into products containing metal atoms in different states of oxidation. The interaction of $M_n(CO)_m$ with the organic hydroperoxides is accompanied by the oxidation of the paraffin used as solvent to a mixture of secondary alcohols in a yield of up to 10% relative to the ROOH consumed.[141]

The reactivity of the metal carbonyls towards organic hydroperoxides decreases as the nucleus of the cluster is increased in the sequence $Fe(CO)_5 > Fe_2(CO)_9 > Fe_3(CO)_{12}$ and $Co_2(CO)_8 > Co_4(CO)_{12}$. The reaction of $M_n(CO)_m$ with hydroperoxides is accompanied by oxidation of the central atom and of the ligands. Inner sphere changes in the ligands probably take place, as suggested by the presence of an oxalate ester among the reaction products.[141]

EPR studies of the oxidation of metal carbonyls by peroxidic compounds have shown that the spectra of a reaction mixture of pentacarbonyliron or its monotriphenylphosphine derivative with organic hydroperoxides in hexane or toluene at 203–293 K include signals from paramagnetic species, in particular from $Fe(CO)_5^{+\cdot}$ or $Fe(CO)_4PPh_3^{+\cdot}$. A signal from the $RO_2^{\cdot}$ radical has also been detected in the EPR spectrum of the products of the interaction of *tert*-butyl or cumyl hydroperoxide with the carbonyl derivatives of iron. This radical is generated by the catalytic decomposition of alkyl hydroperoxides. By using the 2- methyl-2-nitrosopropane spin trap in these measurements the writers established the presence of adducts with RO$^{\cdot}$ radicals.[141]

The oxidation of the carbonyls of metals in the iron subgroup by peroxidic compounds can be described by taking pentacarbonyliron as an example:

$$Fe(CO)_5 + ROOH \longrightarrow \{HO^-, Fe(CO)_5^{+\cdot}, RO^{\cdot}\} \longrightarrow \quad (109)$$

$$\longrightarrow RO^{\cdot} + [HO^-, Fe(CO)_5^{+\cdot}],$$

$$[HO^-, Fe(CO)_5^{+\cdot}] \longrightarrow [(CO)_4Fe{-}OH]^{\cdot} + CO, \quad (110)$$

$$[(CO)_4Fe{-}OH]^{\cdot} + ROOH \longrightarrow [(CO)_4Fe{-}OOR]^{\cdot} + H_2O, \quad (111)$$

$$[(CO)_4Fe{-}OOR]^{\cdot} \longrightarrow 4\,CO + FeO + RO^{\cdot}, \quad (112)$$

$$[(CO)_4Fe{-}OOR]^{\cdot} \longrightarrow CO_2 + [(CO)_3Fe{-}OR]^{\cdot}, \quad (113)$$

$$[(CO)_4Fe{-}OOR]^{\cdot} \longrightarrow [(CO)_3Fe{-}\underset{\underset{O}{\|}}{C}{-}\underset{\underset{O}{\|}}{C}{-}OR]^{\cdot}, \quad (114)$$

$$[(CO)_3Fe{-}\underset{\underset{O}{\|}}{C}{-}\underset{\underset{O}{\|}}{C}{-}OR]^{\cdot} + OR^{\cdot} \longrightarrow (CO)_2Fe\begin{array}{l}\diagup C(O)OR \\ \| \\ O \\ \diagdown C(O)OR\end{array} \longrightarrow$$

$$\longrightarrow \begin{array}{l}C(O)OR \\ | \\ C(O)OR\end{array} + FeO + 2\,CO, \quad (115)$$

$$[(CO)_nFe{-}OH\ (\text{or } OR)]^{\cdot} + {}^{\cdot}OR \longrightarrow$$

$$\longrightarrow n\,CO + FeO + ROH\ (\text{or } ROR), \quad (116)$$

$$2\,[(CO)_nFe{-}OH\ (\text{or } OR)]^{\cdot} \longrightarrow$$

$$\longrightarrow H_2O\ (\text{or } ROH) + CO + [(CO)_3FeOFe(CO)_3]; \quad (117)$$

$n = 3, 4.$

$$2\,[(CO)_4Fe{-}OOR]^{\cdot} \longrightarrow (CO)_2Fe\begin{array}{l}\diagup C(O)OR \\ \diagdown C(O)OR\end{array}{-}\underset{\underset{O}{\|}}{C}{-}OFe(CO)_4 \longrightarrow$$

$$\longrightarrow \begin{array}{l}C(O)OR \\ | \\ C(O)OR\end{array} + 4\,CO + [(CO)_2FeO\underset{\underset{O}{\|}}{Fe}], \quad (118)$$

$$Fe^{n+} + ROOH \longrightarrow RO^{\cdot} + Fe^{(n+1)+} + HO^-, \quad (119)$$

$$Fe^{(n+1)+} + ROOH \longrightarrow RO_2^{\cdot} + Fe^{n+} + H^+; \quad (120)$$

Fe^{n+} denotes any oxidised form of the carbonyl complex.

$$RO^{\cdot}(\text{or } RO_2^{\cdot}, [Fe]^{\cdot}) + SH \longrightarrow$$

$$\longrightarrow ROH\ (\text{or } ROOH, [Fe]H) + S^{\cdot}. \quad (121)$$

SH is the solvent.

The primary step in this process is the transfer of an electron from the carbonyl to the peroxide with formation of an ion–radical pair. This reaction may be preceded by complex formation between the reactants, as was shown for the hexacarbonyls of the Group VI metals.[136, 137] The subsequent transformation of the ion–radical pair and the interaction of the resulting species with a molecule of the peroxide cause the accumulation of oxygenated iron compounds, carbon oxides, and oxalate esters. The appearance of oxidised forms of iron in the system is responsible for the catalytic decomposition of the hydroperoxide.

The interaction of metal carbonyls with peroxidic compounds is a complicated process with a radical-chain mechanism. Its primary stage is the transfer of an electron from the carbonyl to the peroxide with formation of cation-radical carbonyls of the metals.

V. Conclusions

The thermal, photolytic, and oxidative degradation processes of the carbonyl complexes of metals are widely used in the preparation of highly dispersed powders and of films. The great diversity of the known metal carbonyls makes it impossible to describe their thermal, photolytic, and oxidative transformations in terms of a single mechanism.

However, in most cases of the thermal and the photodecomposition of metal carbonyls the primary stage consists in the elimination of one CO ligand from a thermally or photochemically activated $[M_n(CO)_m]^*$ molecule with formation of a coordinatively unsaturated fragment. During thermal decomposition this stage is at equilibrium, and the rate of the process is suppressed by additions of carbon monoxide for many typical compounds in this class. In contrast to the thermal processes, in the photolysis of the metal carbonyls the contribution of the recombination of the coordinatively unsaturated fragment with the carbon monoxide is insignificant, since for the majority of metal carbonyls this interaction is formally spin forbidden. The coordinatively unsaturated fragment dissociates by further elimination of CO radicals, or alternatively it can react with the initial molecule (producing a binuclear carbonyl) or form a solvato complex.

Instead of the removal of one CO ligand from the excited carbonyl complex of the metal the primary photochemical act leading to the observed products may consist in the bimolecular interaction of an activated $[M_n(CO)_m]^*$ molecule with a nonactivated molecule. In binuclear and polynuclear metal carbonyls another possibility is fragmentation with breaking of a metal–metal bond, preceded in some cases by the isomerisation of the skeleton of the complex.

The stability of the iron carbonyls towards thermal decomposition decreases in the order $Fe(CO)_5 > Fe_2(CO)_9 > Fe_3(CO)_{12}$. In the photolytic decomposition the same compounds are arranged in the opposite stability sequence. Evidently the photochemical excitation of the dodeca- and nonacarbonyliron to the triplet state (from which the initial compound can dissociate) requires a greater expenditure of energy than the activation of $Fe(CO)_5$. This difference is due to the presence (in the former compounds) of many bonds over which the energy of the absorbed photon has to be redistributed.

The thermal and the photolytic decomposition of the carbonyl complexes are complicated by catalytic reactions on the resulting metallic surface, which adsorbs pentacarbonyliron and assists the nucleation of anion radicals. The latter interact with the initial molecule of the carbonyl complex and are converted into polynuclear anion radicals which ultimately decompose and contaminate the metal with carbide and oxide impurities. In some cases CO molecules are incorporated into the metallic phase.

The interaction of metal carbonyls with oxygen, ozone, and peroxides is accompanied by the formation of oxides and carbonates of the metals and by the oxidation of CO to CO_2. The reaction of $M_n(CO)_m$ with O_2 is initiated by UV radiation. The rate of the photo-oxidation of the carbonyls of Group VIII metals is approximately an order of magnitude greater than the rate of their photochemical decomposition. This is probably because the reaction between the coordinatively unsaturated carbonyl $M_n(CO)_{m-1}$ (or the metal carbonyl radical) and oxygen is spin-allowed and fast.[142] The reverse recombination of $M_n(CO)_{m-1}$ and CO is forbidden. The photolysis of the carbonyls of Group VI metals takes place through the reversible elimination of one carbonyl group.

The competition between CO and O_2 for the reaction with $M(CO)_5$ is apparently responsible for the lower reactivity of the chromium, molybdenum, and tungsten carbonyls towards the oxidation by oxygen. The mechanism of the oxidation of the carbonyl complexes is strongly dependent on the nature of the resulting intermediate species, varying from a radical mechanism (peroxidic metal carbonyl radicals of cobalt, manganese, etc.) to a molecular mechanism (carbonyl–oxygen complexes of iron, chromium, molybdenum, tungsten, etc.).

The reaction of the carbonyls of Group VIII metals with peroxidic compounds is a free-radical chain process in which the primary stage is electron transfer from the metal carbonyl to the peroxide, with formation of cation radicals of the metal carbonyls. It may be assumed that a stage of complex formation between the reactants occurs before the electron transfer. In conclusion we should note that in spite of some useful advances in identifying the products of the oxidative reactions of the carbonyls of elements in Groups VI–VIII, their kinetic features, and the influence of the medium and of other factors, the detailed mechanisms of these processes have not yet been established.

References

1. K Masters *Homogeneous Catalysis by Transition Metals* (Translated into Russian; Moscow: Mir, 1983)
2. G A Razuvaev, B G Gribov, G A Domrachev *Metalloorganicheskie Soedineniya v Elektronike* (Organometallic Compounds in Electronics) (Moscow: Nauka, 1972)
3. A Nakamura, M Tsutsui *Principles and Applications of Homogeneous Catalysis* (Translated into Russian; Moscow: Mir, 1983)
4. A N Nesmeyanov (Ed.) *Organicheskie Sintezy Cherez Karbonily Metallov* (Organic Synthesises through Metal Carbonyls) (Moscow: Nauka, 1970)
5. A N Nesmeyanov, K A Kocheshkov (Eds) *Metody Elementoorganicheskoi Khimii. Tipy Metalloorganicheskikh Soedinenii Perekhodnykh Metallov* (Methods of Organoelemental Chemistry. Types of Organometallic Compounds of the Transition Metals) (Moscow: Nauka, 1975)
6. A L Lapidus, M M Savel'ev *Usp. Khim.* **54** 29 (1988) [*Russ. Chem. Rev.* **54** 17 (1988)]
7. B Walther *Z. Chem.* **29** 151 (1980)
8. R B Jackman, J S Food *Surf. Sci.* **209** 151 (1980)
9. F Zaera *J. Vac. Sci. Technol.* **7A** 640 (1989)
10. S Dobos, A Beck, L Guczi *J. Mol. Struct.* **174** 331 (1988)
11. A Zecchina, K M Rao, S Coluccia *J. Mol. Catal.* **53** 397 (1989)
12. K Asakura, K-K Bando, Y Iwasawa *J. Chem. Soc., Faraday Trans.* **86** 2645 (1990)
13. C Bremard, E Denneulin, C Depecker, in *Structure and Reactivity of Surfaces. Proceedings of European Conference, Amsterdam, 1989* p. 219; *Ref. Zh. Khim.* 20B4259 (1990)
14. C Bowers, P K Dutta *J. Phys. Chem.* **93** 2596 (1989)
15. S Ozkar, G A Ozin, K Moller *J. Am. Chem. Soc.* **112** 9575 (1990)
16. E P Giannellis, E G Rightor, T J Pinnavaia *J. Am. Chem. Soc.* **110** 3880 (1988)
17. P Dufour, L Huang, A Choplin *J. Organomet. Chem.* **354** 243 (1988)
18. L D'Orneals, A Theolier, A Choplin *Inorg. Chem.* **27** 1261 (1988)
19. A J Dabrowsky, M Solik-Dabrowska *React. Kinet. Catal. Lett.* **34** 367 (1987)
20. K M Rao, G Spoto, E Guglielminotti *J.Chem. Soc., Faraday Trans.* **84** 2195 (1988)
21. J J Venter, M A Vannice, in *Suppl. Thesis of 6th International Symposium Relating Homogeneous and Heterogeneous Catalysis, Pisa, 1989* p. 36; *Ref. Zh. Khim.* 10B4325 (1990)
22. J Goldwasser, S M Fang, M Houwalla *J. Catal.* **115** 34 (1989)
23. A N Zakharov, K Kh Vanegas, Fetekua, B A Romanovskii *Kinet. Katal.* **28** 1244 (1987)
24. H M Ziethen, A X Trautwein, in *Abstracts of the International Symposium on Zeolite Catalysts, Sorbents and Detergents ,Würtzburg, 1988* p. 140; *Ref. Zh. Chem.* 9B4239 (1989)
25. A Maezawa, H Kane, Y Okamoto *Chem. Express* **2** 531 (1988)
26. J You-Sing, R F Howe *J. Chem. Soc., Faraday Trans.* **82** 2887 (1986)
27. T Yashina, T Komatsu, S Namsa *Chem. Express* **1** 701 (1986)
28. C Dossi, J Schaefer, W M Sachtler *J. Mol. Catal.* **52** 193 (1989)
29. E Weitz *J. Phys. Chem.* **91** 3945 (1987)
30. N N Gonchakova, N A Kislov *IR-Spectroscopy and Rutherford Backscattering Studies of Films and Their Formation Processes during Laser-chemical Precipitation of Their Vapors* Preprint from Institute of Problems in the Technology of Microelectronic and Extra Pure Materials, Academy of Sciences of the USSR, Chernogolovka, 1988
31. T Majima, T Ishii, Y Matsumoto *J. Am. Chem. Soc.* **111** 2417 (1989)
32. I M Watson, J A Connor, R Whyman *Polyhedron* **8** 1794 (1989)
33. V G Syrkin, I V Dobryakova, V N Babin, in *Tezisy Dokladov Vsesoyuznoi Konferentsii po Metalloorganicheskoi Khimii, Kazan', 1988* (Abstracts of Reports at the All-Union Conference on Organometallic Chemistry, Kazan', 1988) Part 2, p. 70; *Ref. Zh. Khim.* 22B122 (1988)
34. V D Parkhomenko, A T Kolodyazhnyi, B I Mel'nikov *Poroshkovaya Metallurgiya (Kiev)* 10 (1991)
35. H Carlton, J Oxley *AIChE J.* **13** 86 (1967)
36. G R Pearson *J. Chem. Soc., Faraday Trans.* **80** 4678 (1984)
37. A K Baev *Struktura i Energetika Karbonilov Metallov* (Structure and Energetics of Metal Carbonyls) (Minsk: Vyssh. Shk., 1986)
38. R Pince, R Queau, D Labroue *J. Organomet. Chem.* **306** 251 (1986)
39. V I Podoprigora, A K Baev, in *Primenenie Metalloorganicheskikh Soedinenii dlya Polucheniya Neorganicheskikh Pokrytii i Materialov* (Application of Organometallic Compounds for the Preparation of Inorganic Coatings and Materials) (Moscow: Nauka, 1986) p. 76
40. V I Podoprigora, A K Baev *Zh. Obshch. Khim.* **57** 268 (1987)
41. V I Podoprigora, A K Baev *Zh. Fiz. Khim.* **65** 2910 (1991)
42. G P Smith *Polyhedron* **7** 1605 (1988)
43. K E Lewis, D M Golden, G O Smith *J. Am. Chem. Soc.* **106** 3905 (1984)
44. J Van Wonterghem, S Morup, S W Charles *Phys. Rev. Lett.* **55** 410 (1985)
45. J Van Wonterghem, S Morup, S W Charles *Hyperfine Interact.* **27** 333 (1986)
46. E Papirer, P Horny, H Balard *Bull. Soc. Chim. Fr.* 695 (1985)
47. I V Spirina, A V Kholodalova, V P Maslennikov *Metalloorg. Khim.* **5** 1028 (1992)
48. F Ungvary, L Marko *J. Organomet. Chem.* **71** 283 (1974)
49. R Tannenbaum, C L Flenniken, E P Goldberg *J. Polym. Sci., Part. B, Polym. Phys.* **25** 1341 (1987)
50. I V Spirina, A V Kholodalova, V P Maslennikov *Zh. Obshch. Khim.* **62** 981 (1992)
51. W R Hastings, M R Roussel, M C Baird *J. Chem. Soc., Dalton Trans.* 203 (1990)
52. S P Tunik, G S Voronina, L I Brezhneva *Izv. Sib. Otd. Akad. Nauk SSSR, Ser. Khim. Nauk* 70 (1986)
53. G Eiber *Z. Phys. Chem., Abt. B* **144** 1 (1929)
54. O Warburg, E Negelein *Biochem. Z.* **204B** 495 (1929)
55. H W Thompson, A P Garrat *J. Chem. Soc.* 524 (1934)
56. M Poliakoff, J J Turner *J. Chem. Soc., Dalton Trans.* 1351 (1973)
57. M Poliakoff, J J Turner *J. Chem. Soc., Dalton Trans.* 2276 (1974)
58. M Poliakoff *J. Chem. Soc., Dalton Trans.* 210 (1974)
59. M Poliakoff, J J Turner *J. Chem. Soc., Faraday Trans.* 93 (1974)
60. R L Sweany, M A Polito, in *Abstracts of Papers of the 194th ACS National Meeting, Washington, 1987* p. 643
61. A J Quoderkirk, P Wermer, N L Schultz *J. Am. Chem. Soc.* **105** 3354 (1983)
62. S P Curch, F-W Grevels, H Hermann *J. Chem. Soc., Chem. Commun.* (9) 594 (1985)
63. G Nathanson, B Giltin, A Rosan *J. Chem. Phys.* **71** 361 (1981)
64. J T Yardley, B Giltin, G Nathanson *J. Chem. Phys.* **71** 370 (1981)
65. T Majima, T Ishii, Y Matsumoto *J. Am. Chem. Soc.* **111** 2417 (1989)
66. C Daniel, M Bernard, A Dedieu *J. Phys. Chem.* **88** 4805 (1984)
67. C Daniel, A Veillard, in *Abstracts of the 40th International Meeting of the Society of Chemical Physics, Strasbourg, 1986* p. 363; *Ref. Zh. Khim.* 19B1053 (1988)
68. A Veillard, A Strich, C Daniel *Chem. Phys. Lett.* **141** 329 (1987)
69. G A Pearson *Inorg. Chem.* **23** 4675 (1984)
70. I V Spirina, A A Selyakov, V P Maslennikov *Zh. Obshch. Khim.* **59** 932 (1989)
71. Y Yamada, Y Minai, M Sato *J. Radioanal. Nucl. Chem.* **95** 503 (1985)

72. M S Darsillo, H D Gafney, M S Paquette *J. Am. Chem. Soc.* **109** 3275 (1987)
73. H D Gafney, in *Photochemistry of Solid Surfaces* (Amsterdam, 1989) p. 272
74. S C Fletcher, M Poliakoff, J J Turner *Inorg. Chem.* **25** 3597 (1986)
75. A V El'tsov (Ed.) *Vvedenie v Fotokhimiyu Organicheskikh Soedinenii* (Introduction to the Photochemistry of Organic Compounds) (Leningrad: Khimiya, 1976)
76. I V Spirina, A V Kholodalova, V P Maslennikov *Zh. Obshch. Khim.* **60** 1860 (1990)
77. A B Callear *Proc. R. Soc. London, Ser. A* **265** 77 (1961)
78. Y Ishikawa, P A Hackett, D M Rayner *J. Am. Chem. Soc.* **109** 6644 (1987)
79. P L Bogdan, E Weitz *J. Am. Chem. Soc.* **111** 3163 (1989)
80. T R Fletcher, R N Rosenfeld *J. Am. Chem. Soc.* **107** 2203 (1986)
81. W H Breckenridge, G M Steward *J. Am. Chem. Soc.* **108** 364 (1986)
82. J P Holland, R N Rosenfeld *J. Chem. Phys.* **89** 7217 (1988)
83. Y Ishikawa, P A Haskett, D M Rayner *J. Phys. Chem.* **89** 3863 (1988)
84. J A Ganske, R N Rosenfeld *J. Phys. Chem.* **93** 1959 (1989)
85. J Z Burdett, A G Downs, G R Gaskill *Inorg. Chem.* **17** 523 (1978)
86. J J Turner, M Poliakoff, M B Simpson *J. Mol. Struct.* **113** 359 (1984)
87. J Mascetti, A J Rest *J. Chem. Soc., Chem. Commun.* 221 (1987)
88. C E Brown, Y Ishikawa, P A Haskett *J. Am. Chem. Soc.* **112** 2530 (1990)
89. S P Church, F-W Grevels, H Hermann *J. Chem. Soc., Chem. Commun.* 30 (1985)
90. J D Simon, X Xie *J. Phys. Chem.* **91** 5538 (1987)
91. L Wang, X Zhu, K G Spears *J. Am. Chem. Soc.* **110** 8695 (1988)
92. A G Joly, K A Nelson *J. Phys. Chem.* **93** 2876 (1989)
93. T J Mayer *Chem. Rev.* **85** 187 (1985)
94. T Kobayashi, K Yasufuku, J Iwai *Coord. Chem. Rev.* **64** 1 (1985)
95. K Yasufuku, H Noda, J Iwai *Organometallics* **4** 2174 (1985)
96. T A Seder, S P Church, E Weitz *J. Am. Chem. Soc.* **108** 7518 (1986)
97. S Firth, P M Hodges, M Poliakoff *Inorg. Chem.* **25** 4608 (1986)
98. S Firth, P M Hodges, M Poliakoff *J. Organomet. Chem.* **331** 347 (1987)
99. D Rehorek, S Di Martino, T J Kemp *Z. Chem.* **29** 148 (1989)
100. A Haynes, M Poliakoff, J J Turner *J. Organomet. Chem.* **383** 497 (1990)
101. J G Bentsen, M S Wrighton *J. Am. Chem. Soc.* **109** 4518 (1987)
102. J G Bentsen, M S Wrighton *J. Am. Chem. Soc.* **109** 4530 (1987)
103. J-K Shen, J-C Gao, Q-Z Shi *J. Chem. Soc., Dalton Trans.* 1933 (1989)
104. J-K Shen, Y-C Gao, Q-Z Shi *Organometallics* **8** 2144 (1989)
105. P C Ford *J. Organomet. Chem.* **383** 339 (1990)
106. S P Tunik, V P Krym, A V Nikol'skii, in *Tezisy Dokladov VI Vsesoyuznogo Soveshchaniya po Fotokhimii, Novosibirsk, 1989* (Abstracts of Reports at the VIth All-Union Conference on Photochemistry, Novosibirsk, 1989) p. 85; *Ref. Zh. Khim.* 22B4352 (1989)
107. A B Callear *Proc. R. Soc. London, Ser. A* **265** 96 (1961)
108. A A Mazlovskii, N A Fuks *Kolloid. Zh.* **29** 120 (1967)
109. K-E Stumpf *Z. Anorg. Allg. Chem.* **270** 114 (1952)
110. Ya I Kogan *Dokl. Akad. Nauk SSSR* **161** 388 (1965)
111. I V Spirina, A A Selyakov, V P Maslennikov *Metalloorg. Khim.* **4** 618 (1991)
112. K Lane, L Sallens, R R Squires *J. Am. Chem. Soc.* **106** 2719 (1984)
113. U L Kettew, P H Barrett, R G Pearson, in *Physics and Chemistry of Small Clusters: Proceedings of the NATO Advanced Research Workshop and International Symposium, Richmond, 1986* p. 281; *Ref. Zh. Khim.* 24B1238 (1988)
114. I V Spirina, V A Alferov, V P Maslennikov *Zh. Obshch. Khim.* **62** 2115 (1992)
115. V Yu Topkin, V B Del'pin *Neftekhimiya* **13** 574 (1973)
116. I V Spirina, A V Kholodalova, V P Maslennikov *Zh. Obshch. Khim.* **62** 2411 (1992)
117. S A Fieldhouse, B W Fullam, G W Neilson *J. Chem. Soc., Dalton Trans.* 567 (1974)
118. R Tannenbaum, C L Flenniker, E P Goldberg *J. Polym. Phys.* **25B** 1341 (1987)
119. A J Crayston, M J Almond, A J Downs *Inorg. Chem.* **23** 3051 (1984)
120. M Almond, J J Turner, J A Crayston *Inorg. Chem.* **25** 19 (1984)
121. M Almond, N Hahne *J. Chem. Soc., Dalton Trans.* 2255 (1988)
122. M Almond, A J Downs *J. Chem. Soc., Dalton Trans.* 809 (1988)
123. B V Lokshin, I I Grinval'd *Metalloorg. Khim.* **2** 118 (1989)
124. V M Fomin *Koord. Khim.* **117** 214 (1991)
125. D L Bricker, D H Russel *J. Am. Chem. Soc.* **109** 3910 (1987)
126. W E Lindsell, P N Preston *J. Chem. Soc., Dalton Trans.* 1105 (1979)
127. W Grolt, U Schurat, K Weber *Z. Phys. Chem.* **93** 153 (1974)
128. E D Morris, H Niki *J. Am. Chem. Soc.* **92** 5741 (1970)
129. USSR P. 1 627 517; *Ref. Zh. Khim.* **18** 444i (1991)
130. I V Spirina, B I Tarunin, S A Sergeev *Zh. Prikl. Khim. (Leningrad)* **63** 888 (1990)
131. S A Sergeev, I V Spirina, B I Tarunin *Zh. Prikl. Khim. (Leningrad)* **64** 1971 (1991)
132. M L Perepletchikov, Yu A Aleksandrov *Zh. Obshch. Khim.* **61** 729 (1991)
133. A Mittasch *Z. Angew. Chem.* **41** 827 (1928)
134. H Schott, G Wilke *Angew. Chem.* **81** 896 (1969)
135. F Ungvary, A Sisak *Transition Met. Chem.* **9** 265 (1984)
136. Yu A Aleksandrov, N P Sluchevskaya, N V Yablokova *Zh. Obshch. Khim.* **51** 417 (1981)
137. R M Azhikova, A M Syroezhko, V A Proskuryakov *Kinet. Katal.* **29** 780 (1988)
138. V M Fomin, A V Lunin, Yu A Aleksandrov *Zh. Obshch. Khim.* **57** 2042 (1987)
139. D F Grishin, V A Dodonov, in *Radikal'nye Reaktsii Metalloorganicheskikh Soedinenii* (Radical Reactions of Organometallic Compounds) (Gorky: Gorky State Univ., 1986) p. 60
140. I V Spirina, V P Maslennikov, A A Selyakov, in *Khimiya Metalloorganicheskikh Soedinenii* (The Chemistry of Organometallic Compounds) (Gorky: Gorky State Univ., 1986) p. 88
141. I V Spirina, S A Sergeev, V P Maslennikov *Zh. Obshch. Khim.* **63** 153 (1993)
142. R J Ryther, E Weitz *J. Phys. Chem.* **95** 9841 (1991)

Russian Chemical Reviews **63** (1) 55–69 (1994)
©1994 Russian Academy of Sciences and Turpion Ltd

UDC 547.254.6

Clusters of IIA and IIIA group metals: synthesis and reactivity

V V Smirnov, L A Tyurina

Contents

I.	Introduction	55
II.	Preparation of clusters in solution	55
III.	Synthesis and properties of clusters in the gas phase	56
IV.	Structure and properties of clusters from quantum chemical calculations	57
V.	Semiempirical and empirical calculations on clusters	61
VI.	Reactions of clusters in the gas phase	61
VII.	Heteronuclear clusters	62
VIII.	Preparation of clusters and their reactions at low temperatures	64
IX.	Giant clusters prepared by cryosynthesis	66

Abstract. Experimental and theoretical data on the structure of clusters of Group IIA and IIIA metals are summarised. General trends in the properties of the clusters as a function of nuclearity are outlined, and special points on the dependences, corresponding to the so-called magic numbers, are identified. Data on the reactivity of clusters in the gas phase are used to establish the anomalies corresponding to these points. It is shown that the reactivity of mixed clusters obeys more complex relationships, determined by their electronic structure and geometry. A new type of organomagnesium cluster is described, and shown to be promising as a component of catalytic systems. The cryochemical synthesis of giant clusters of transition metals, which offer a high reactivity and catalytic activity, is described. The bibliography includes 176 references.

I. Introduction

Metal clusters occupy an intermediate position between metal atoms (which display the greatest possible dispersion) and bulk metals, and they constitute a new type of metallic state. According to the generally accepted terminology[1] clusters are species containing between 2 and 10^5 interconnected metal atoms, of size varying from 0.5 to several tens of nanometres. The boundary between the cluster and the metallic state is hard to define. Ultradispersed powders, and especially colloidal metals with a particle size of $10-10^3$ nm, show marked differences from bulk metals. They are often called giant or supergiant clusters. This terminology will be adopted here.

The special properties of the cluster state and the wide range of potential applications of clusters and colloidal metals in various areas of science and technology have stimulated an intense interest in this field of research. The results have been discussed in monographs[1-4] as well as in research papers. However, until recently most of the work had been aimed at clusters of the transition metals, and an interest in clusters of the typical (non-transition) elements has become evident only in the last few years. This new topic has come to the fore because of recent advances in experimental and (even more so) in computational methods, which have made the clusters of typical metals a promising field of study. Because of the great experimental difficulty met in the preparation and study of clusters we have witnessed an unusual state of affairs in which theoretical studies have outstripped the experimental work.

This review is aimed at clusters and colloidal solutions of metals from Groups IIA and IIIA. It does not attempt to provide comprehensive information on the physics and the physical chemistry of these materials: its object is to draw attention to the least fully investigated and yet the most interesting aspect of the problem: the chemical properties and the likely applications of clusters of typical metals.

V V Smirnov, L A Tyurina Chemistry Faculty, Lomonosov Moscow State University, 119899 Moscow, Vorob'evy gory, Fax (7-095) 932 88 46

Received 25 October 1993
Uspekhi Khimii **63** (1) 57–72 (1994); translated by J I Carasso

II. Preparation of clusters in solution

The characteristic properties of the metals in Group IIA are the presence of an occupied *s* shell and the absence of *p* electrons. In terms of the general propositions of the theory of valence the bond of the M_2 dimer is not likely to be strong: occupied bonding and antibonding σ MO are formed from the two *s* AO. Not surprisingly, therefore, no successful attempts to prepare homonuclear clusters of IIA group metals by 'classical' methods have so far been reported. Only one paper[5] describes the reduction of the tetramer of *o*-phenylmercury by magnesium in tetrahydrofuran (THF), which gave a crystalline complex of the tetramer of *o*-phenylmagnesium with THF. Each magnesium atom in the complex contributes to the formation of one σ bond and two bridging δ bonds with the phenyl radicals, and it is also coordinated with one molecule of THF. Under these conditions the distance between the magnesium atoms lies between 3.546 and 2.804 Å. The latter value formally justifies the assignment of this compound to the cluster type. However, the lack of data on the direct interaction between the magnesium atoms makes this assignment ambiguous.

A different state of affairs is found with the Group IIIA metals. The presence of a valence *p* electron allows the formation of a covalent metal–metal bond, and the preparation of cluster compounds by conventional chemical methods seems more likely. Significant differences are noted between aluminium, which has a stable (3+) and an unstable (1+) oxidation state,

and gallium and indium. The latter metals have, in addition, an even less stable state (2+). The synthesis of their cluster compounds by the dimerisation of derivatives of the bivalent metals immediately suggests itself:

$$2MX_2 \rightleftharpoons X_2M{-}MX_2.$$

In reality the dimers of the halides of bivalent indium and gallium are ionic species, $M^+[MX_4]^-$, and do not contain metal–metal bonds.[6] There are two methods of stabilising the cluster halides of indium and gallium. The first consists in complex formation with dioxan or other organic donors. In the resulting complexes of composition $M_2X_4 \cdot 2D$ (where D is a donor) the length of the Ga–Ga bond[7–9] is 2.40 ± 0.02 Å, and that of the In–In bond[10] is 2.775 Å. The cluster nature of these compounds was confirmed by X-ray diffraction and from their vibrational spectra. Complexes can also be prepared by the interaction of suitable donors with the metal dihalides in a hydrocarbon medium (for example, in benzene). Anion salts ($M_2X_6^-$) are another type of compound of these metals. Thus, in the ammonium salts $[R_4N]_2^+Ga_2Cl_6^{2-}$ the Ga–Ga distances are 2.39 Å (R = Me)[11] and 2.42 Å (R = Pr^i),[12] and in the triphenylphosphonium salts[13] they are 2.407–2.415 Å. In spite of the short interatomic distance the metal–metal bonds are weak, as shown by the low frequencies of the stretching vibrations (between 122 and 235 cm^{-1} in the case of gallium[14] and between 120 and 150 cm^{-1} for indium[15]). The dissociation energy of the metal–metal bond in these cluster halides was estimated[6] to be 25–35 kcal mol^{-1}. Another example of compounds containing a metal–metal bond are the gallium and indium chalcogenides, in which the Ga–Ga distance is 2.4–2.5 Å and the In–In distance is 2.75 Å. These compounds can be treated as salts of the simplest (M_2^{4+}) cluster cation.[16]

Only the simplest binuclear compounds have been obtained using classical methods of synthesis,[17] though the $In_6(C_5Me_5)_6$ hexamer (which is formally a cluster with an octahedral In_6 metal core) has been synthesised by the reaction between InCl and $Li(C_5Me_5)$. However, the In–In distances in this compound are so large (3.9 Å) that there is no justification for assuming the formation of metal–metal bonds. Even at 55 °C this product sublimes exclusively as a monomer.

Many attempts to prepare cluster compounds of aluminium in solutions have been reported. The formation of Al–Al bonds has been suggested, for example, in a mixed alkyl derivative of boron and aluminium synthesised by the reaction between Al_2Me_6 and $B_2(Me_4N)_4$, but no strict proof of this claim was advanced.[18,19] The same is true of the compound $[Bu^i_2Al]_2$, prepared[20] by treating Bu^i_2AlCl with potassium.

X-Ray confirmation of the structure of the cluster compounds of aluminium synthesised under normal conditions has only recently been obtained. The reduction (with potassium) of the compound $[(Me_3Si)_2CH]_2AlCl$ gives a binuclear product with an Al–Al bond.[21] The reaction of the tetrameric complex of aluminium(I) chloride with $Mg(C_5Me_5)_2$ at −78 °C in the absence of water vapour and oxygen gave[22] the product $[Al(C_5Me_5)]_4$, containing a tetrahedral metallic core with an Al–Al distance[22] of 2.773 Å. The synthesis of a salt of composition $K_2[Al_{12}Bu^i_{12}]$, stable up to 150 °C and containing a metal core consisting of the Al_{12} icosahedron (Al–Al distance 2.679 and 2.696 Å), has been reported.[23] This example offers the hope of a synthesis (in the near future) of cluster compounds of Al with metal cores in the form of regular polyhedra. One further example is provided by melts (prepared in a corundum crucible) of crystalline Al_7Te_{10}, in which the metal–metal distance (2.6 Å) is shorter than in the organic clusters.[24] However, the limitations of the classical approach cannot be ignored: there have been only two reports of the synthesis of cluster compounds with a substantial metal core, and there are no prospects to date of preparing ligand-free clusters by this method.

III. Synthesis and properties of clusters in the gas phase

Fully developed methods of preparing and studying metal clusters in the gas phase are now available. The key stage in these methods is the flash evaporation of a relatively large amount of the metal, achieved (for example) by ion or electron bombardment. More recently, powerful laser pulses have been used for the same purpose. The evaporated atoms and ions are entrained in a stream of inert gas in which the clusters are formed. The temperature of the particles can be rapidly lowered to room temperature by suddenly expanding the flow. If necessary the ions can be selected by means of a quadrupole mass spectrometer. The final stage consists in the mass spectrometric detection of the particles, either directly or after appropriate physical or chemical perturbations.

Clusters of the Group IIA metals have not been studied extensively. For Be the dissociation energy of the dimer (0.1 eV) has been determined.[25] For Mg_2 the absorption spectra have been measured,[26] and a dissociation energy of 0.05 eV has been reported.[27] It was also shown that the ionisation potential of Mg_2 is 6.7 eV, which is much lower than for atomic magnesium, and that the dissociation energy of the charged Mg_2^+ ion is close to 1 eV.[28] Thus the removal of one electron strengthens the magnesium–magnesium bond quite substantially.

Aluminium clusters have been studied in greater depth. Experiments with ionised clusters have yielded reliable data on their electron affinities (EA) and ionisation potentials (IP), shown in Table 1. It can be seen that the ionisation potential increases significantly on going from the atom (6.0 eV) to the small clusters, but then gradually decreases. For $N > 14$ it falls below the value for the atom. However, it is still far from the electronic work function for the compact metal (4.24 eV). Even for $N = 55$ the IP stays at 4.95 eV.[29]

Table 1. Electron affinity and ionisation potentials of Al_N clusters.

N	IP/eV	EA/eV	Ref.
2	5.9–6.3	–	29–31
3	6.4–7.2	–	29–31
3	–	1.4–1.9	32–34
4–6	6.0–6.5	–	29–31
4–6	–	1.74–2.7	32, 33
7	6.0	–	29
7	–	2.0–2.6	32, 33
8–12	6.2	–	29
8–12	–	2.2–3.2	29, 32–34
13	6.4	–	31
13	–	2.8–3.5	32–34
14–22	⩽ 5.5	–	29, 31
14–22	–	2.5–2.8	32, 33
23	–	2.86	32
24–25	–	2.75	32
26–32	–	2.8–2.85	32
55	4.95	–	29

The electron affinity, which is negative for the atom, increases rapidly for $N = 2–3$, but beyond this point the growth becomes slower. In clusters with 24–32 atoms the EA increases at the rate of 0.1 eV per 8–10 metal atoms in the cluster.

The most interesting observation is the presence of several special points in the dependence of these parameters on the size of the cluster. Thus the electron affinity of Al_6, Al_{23}, and especially Al_{13} is significantly higher than for their neighbours. The low ionisation potential of the Al_7 cluster is also noteworthy. This implies an abnormally high stability for the Al_6^-, Al_7^+, Al_{13}^-, and Al_{23}^- systems, which contain 19–20, 40, and 70 valence electrons. This is an example of the law of magic

numbers, well known in the chemistry of clusters, according to which systems having certain numbers of valence electrons have anomalously high stabilities.

Experimental tests of the magic numbers in terms of the dissociation energies of neutral clusters have not yet been carried out. We only know that the dissociation of Al_2 requires[35] an energy of 1.34 eV. More data are available for charged clusters. The high thermal stability of several Al_N^+ clusters, including easily identifiable clusters with 20 valence electrons (of composition Al_7^+),[36] has been demonstrated. A similar result has been reported[29,37] for cationic clusters of aluminium, which show a tendency for an increase in stability with nuclearity: anomalously high stabilities were found in the clusters with 7, 13, 14, and 23 aluminium atoms, containing 20, 38, 41, and 68 valence electrons respectively. This is consistent with data on clusters obtained[38] by bombarding an aluminium target with Xe^+ ions having an energy of 9 eV: in this case a stability maximum was again observed for the clusters with 7, 14, and 23 metal atoms. Less striking examples of the same effect were found in trinuclear clusters (8 electrons). Detailed studies of the photodissociation of Al_N^+ clusters revealed the existence of two main dissociation paths:

$$Al_N^+ \longrightarrow Al^+ + Al_{N-1}, \quad (1)$$

$$Al_N^+ \longrightarrow Al_{N-1}^+ + Al. \quad (2)$$

Path (1) is more typical of clusters with 5–7 and with 9 atoms; path (2) usually corresponds to 8 or 10–17 metal atoms.[39] The dissociation energies vary between wide limits (from 1.5 to 2.6 eV) and are anomalously high (3.1 eV) in cationic clusters with 7 and 13 aluminium atoms. Data[30] for small clusters ($N \leqslant 7$) differ quantitatively from other reports,[39] but they also point to a large increase in the strength of the bond on going from $N = 6$ ($E_{diss} = 1.55$ eV) to $N = 7$ (2.25 eV). Surprisingly, the elimination of Al^+ or Al from Al_3^+ ($E_{diss} = 1.3$ or 1.12 eV) is more difficult than the dissociation of Al_2^+ or Al_4^+.

The existence of magic numbers has been confirmed also for anionic clusters. In a mass spectrometric study of anionic clusters of aluminium containing up to 70 atoms the species Al_{13}^- (40 electrons) was found to have a very high stability, and a jump was noted also for Al_{13}^- (70 electrons).[40]

Gallium and indium clusters show the same magic numbers as the aluminium clusters, the effect being most marked for the M_7^+ clusters.[36]

The experimental determination of the electronic state of the clusters is a difficult problem. Measurements[41] of the magnetic moments of Al_N particles ($N = 2-25$) led to the conclusion that these clusters are in low-spin states: doublet for odd N and singlet or triplet for even N. In ESR studies of the Al_3 trimer (prepared by condensation of aluminium from the gas phase into an adamantane matrix[42]) it was found that the spectrum corresponds to a particle having the form of a regular triangle and in a quartet state. The state of the simplest (Al_2) particle is also not entirely clear. An analysis of the electronic spectra of the aluminium, indium, and gallium dimers, which have (when in a matrix) two groups of bands at $(1.3-1.5) \times 10^4$ and $(2.4-3.0) \times 10^4$ cm^{-1}, led to the assignment of both groups of bands to transitions from a $^1\Sigma_g^+$ state.[43] However, an analysis of the vibrational spectra and of the emission spectra suggests that the ground state is $^3\Sigma_g^-$.[44] We shall show in the next section that this ambiguity arises from the existence of several almost degenerate states.

IV. Structure and properties of clusters from quantum chemical calculations

Most of the currently available information on the clusters of typical metals has been obtained by quantum chemical methods. Let us examine the results in some detail.

Theoretical studies can be subdivided into two groups: quantitative calculations and calculation of a qualitative or semiquantitative character, based on the spherical shell model.

The spherical shell model[44,45] starts from the assumption that the metal core is most closely packed when in a spherical symmetry. The whole system is divided into two spheres: an inner (core) and an outer sphere (shell). The core includes the nucleus and all the electrons except the valence electrons, and the shell includes the valence electrons. It can easily be seen that in the case of a spherical symmetry this description is formally identical to the description of an atom in the one-electron approximation. Therefore the wave functions of the electrons in the shell can be split into a radial and an angular part. Like the spherical harmonics of the atom the angular functions will have s, p, d, f AO symmetry depending on the orbital angular momentum. The maximum numbers of electrons in the subgroups of this pseudoatom are the same as the typical numbers for atoms: 2, 6, 10, 14, etc. However, the greater diffuseness (as compared with the AO) of the cluster functions results in a number of differences. In particular, the normal sequence of increasing energies for the AO,

$$ns < np < (n+1)s \approx nd < (n+1)p < (n+1)d \approx nf$$

is replaced by

$$ns < np < nd < (n+1)s < nf < (n+1)p < ng < (n+1)d.$$

The following electron configurations are the most stable in this model: $1s^2p^6$, $1s^2p^6d^{10}2s^2$, $1s^2p^6d^{10}f^{14}2s^2p^6$, $1s^2p^6d^{10}f^{14}g^{18}2s^2p^6$, $1s^2p^6d^{10}f^{14}g^{18}2s^2p^6d^{10}3s^2$, containing 8, 20, 40, 58, and 70 electrons respectively. We can easily see that these are the same magic numbers as those which had been discovered experimentally. According to the model the species Al_3^+, Al_7^+, Al_{13}^-, Al_{19}^-, and Al_{23}^- should be the most stable. This is consistent with the IP and EA data quoted above, and with the corresponding cluster stabilities. The increased stability of Al_{14}^+, Al_{23}^+, etc. can be attributed to the fact that the occupancy of their electron shells is the closest to the stable configuration in the Al_N^+ series.

The simple and objective description of the clusters, and especially the possibility of predicting the magic numbers, are the strong points of the spherical shell model. Its limitations, however, are equally obvious. For small N values the real symmetry of the core is far from spherical. In general, as was pointed out by DeHeer et al.,[45] the predictions of the model are satisfactory for $N > 40$. The most serious limitation arises from the failure of the model to take account of the real geometry of the cluster. This limitation can be partially eliminated by adopting a variant of the theory which offers a compromise: the stipulation of a spherically symmetrical potential is retained, and departures of the geometry from the ideally spherical are treated as perturbations. Thus, the geometry of the sodium, magnesium, aluminium, and lead clusters has been optimised[46] by treating the ions of the core as exposed to a spherically averaged potential not identical to the potential of the simplest model.

Most of the cluster calculations were carried out by *ab initio* methods at various levels, or in the approximation of the local density functional (LDA). The electron correlation was allowed for by the Møller–Plesset theory at different levels (MP-2, MP-4, etc.) or by introducing the configurational interaction (CI) with allowance for singly and doubly perturbed states (CISD), as well as the CI for different initial configurations (MRCI, MRCI-SD).

1. Be clusters

The main result obtained at the SCF level was that the stability of the Be_2 dimer is very low and that the dissociation energy increases rapidly with N. Whereas the atomisation energy of one metal atom (D/N) at this level of calculation is only 0.05 eV for Be_2, in Be_3 it already has double that value and in Be_4 D/N is 0.43 eV.[47] This is explained by the rapid growth of the degree of sp hybridisation attributed to the relatively similar sizes of the $2s$

and $2p$ AO, which favour the formation of hybrid sp AO. SCF calculations also point to a large increase of the electron affinity with increase of N in the Be_N clusters. Even in the tetramer we find[48] EA $\approx$ 1 eV. For the neutral tetrahedral Be_4 molecule at the SCF (or a more precise) level a D/N value of 0.6 eV has been calculated,[47] with an interatomic distance of 2.08 Å.

Calculations allowing for electron correlation[49-54] have identified a series of important properties of the structure of Be clusters: a rapid increase in D/N with N (up to a value in excess of 0.9 eV for Be_{13}) with approximately constant values of Be–Be distance (2.0–2.2 Å) in the clusters, a similarity in the energies of different isomers (for example, the Be_{13} clusters of D_{3h} and D_{3d} symmetry differ by 5% in energy), and a singlet ground state. All the published papers have stressed the important role of the electron correlation, but according to Rubio et al.[51] in the case of large clusters ($N \geqslant 7$) good qualitative results can also be obtained without allowing for CI.

Small Be clusters ($N = 3-7$) have been studied[55-57] in great detail in recent years. The structures illustrated in Fig. 1 are available to these species. We can see that regular polyhedra of the highest possible symmetry are characteristic for Be. The bond length is 2.50 Å in the dimer, 2.23 Å in the trimer, and less than 2.10 Å in the Be_4 tetramer. The dissociation energies calculated per atom are 0.3, 0.8, and 0.9–1.0 eV for Be_3, Be_4, and Be_5 respectively. Thus even relatively small Be clusters can be treated as stable molecules.

Unlike other metals of interest in the present discussion Be has been the object of nonempirical calculations[58,59] for relatively large clusters (from Be_{51} to Be_{69}). However, in this case electron correlation effects were ignored. As we have already pointed out, in large clusters this omission is unimportant. The clusters are in a singlet ground state, with a bond energy (not allowing for correlation effects) of about 1.1 eV per atom for $N = 51$, 57, and 63 and about 1.2 eV per atom for $N = 69$. Allowing for correlation would bring these values to about 1.4–1.5 eV. A large decrease in the ionisation potential as compared with that of the atom and of the small clusters (IP = 3.62 eV) has been pointed out. As could have been expected, in large clusters a very effective sp hybridisation takes place: even in Be_{51} more than one electron of the central atom is transferred from a $2s$ AO to a $2p$ AO. Unlike the atoms of the outer layer, the central atoms of these clusters can be treated as indistinguishable from atoms in the bulk state.

2. Mg clusters

Magnesium clusters have a low bond energy. Calculations not allowing for correlation give a negative stabilisation energy for the dimer and the trimer, and a negligibly small stability (0.03 eV) for the tetramer.[48,60,61] The results of detailed calculations for neutral Mg clusters are summarised in Table 2.

All the Mg_N clusters with $N \leqslant 13$ are in a singlet state.[63-66] It can be seen from Table 2 that the tendency to form regular polyhedra is suppressed even for $N = 5$, and clusters with $N \geqslant 8$ have a low symmetry. Their geometry is determined by two opposing tendencies. Regular polyhedra are the best configuration for maximising the number of covalent bonds and for optimising the conditions leading to sp hybridisation. However, a high symmetry unavoidably produces degenerate electronic states which destabilise the molecule through the Jahn–Teller effect. In Mg_N clusters the stability of the M–Mg covalent bond is low, the role of this effect should be small, and the departures from the 'ideal' geometry are not very substantial.

We also see from Table 2 that the normal dependences of various properties on N are also displayed by Mg_N: an increase in the stability and in the electron affinity with N, and a decrease in the IP. Calculations can predict small peaks corresponding to the magic numbers on these otherwise monotonic curves. In particular, a marked increase in stability is found on passing from Mg_3 to Mg_4 (8 electrons). The magic number 20 is not so clearly recognisable, but nevertheless the stability of Mg_{10} ($D/N = 0.83$ eV) is higher than that of Mg_9 (0.78 eV) and of Mg_{11} (0.79 eV).[66] Calculations reveal a correlation between the stability and the population of the $3p$ level. For $N \leqslant 13$ the maximum p population corresponds to $N = 10$ (0.3); a second local maximum (0.2) corresponds to $N = 4$. It should also be noted that the stability of the clusters is relatively low for $N \leqslant 8$.

In spite of the small bond energy the excitation of Mg_N produces long-lived excited states. The thermal decomposition of Mg_N^* requires surmounting a high activation barrier[67] ($\geqslant 0.4$ eV in the case of Mg_2). Excitation can be induced by exposure to

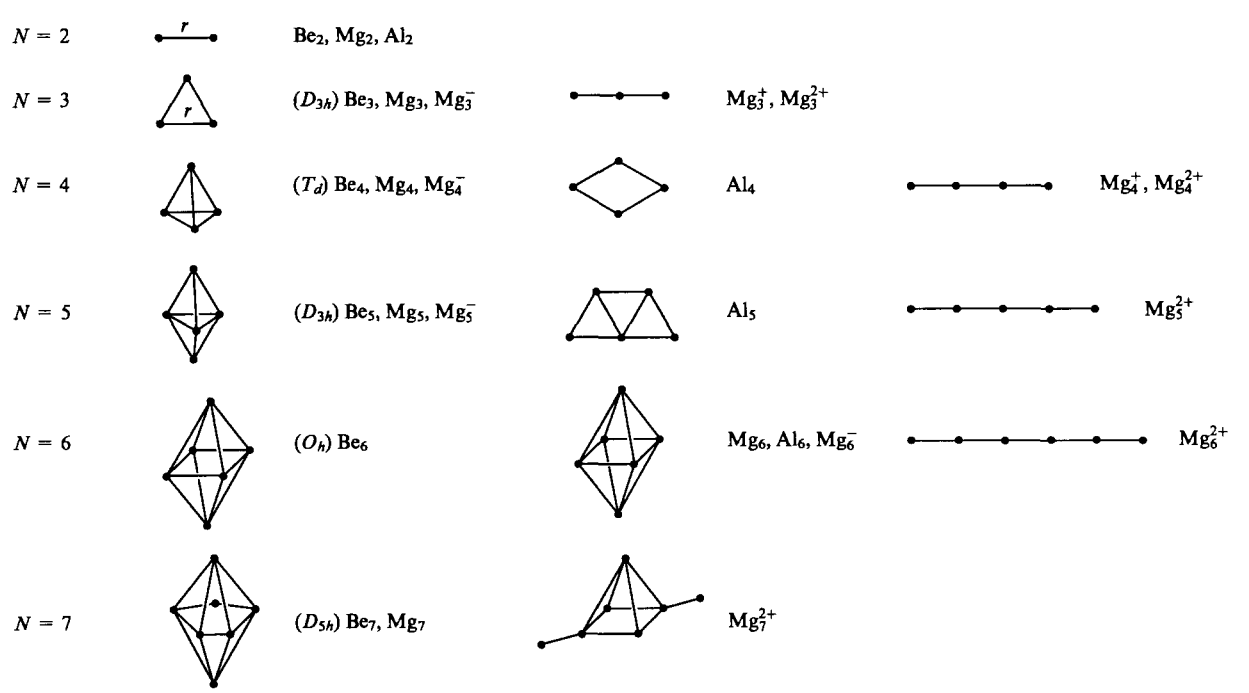


Figure 1. Typical geometric forms of small clusters of Group IIA and IIIA elements.

Table 2. Results of calculations on Mg_N clusters.

N	Method of calculation[a]	Geometry	r_{Mg-Mg}/Å	(D/N)/eV	IP/eV	EA/eV	Ref.
2	*Ab initio*, STO 6-31G, MR	$D_{\infty h}$	2.82	–	–	–	54
	VB	$D_{\infty h}$	–	0.026	6.2	–	62
	LDA (LSD approximation)	$D_{\infty h}$	3.6	0.11	6.42	0.39	63, 64
	LDA	$D_{\infty h}$	–	0.115	–	–	65
3	*Ab initio*, STO 6-31G, MR	D_{3h}	2.76	–	–	–	54
	VB	D_{3h}	–	0.05	5.6	–	62
	LSD	D_{3h}	3.15	0.26	6.43	0.93	63, 64
	Ab initio, CI	D_{3h}	3.38	0.13	–	–	56
	LDA	D_{3h}	–	0.284	–	–	65
4	*Ab initio*, STO 6-31G, MR	T_d	2.59	–	–	–	54
	VB	T_d	–	0.08	5.3	–	62
	LSD	T_d	2.97	0.5	6.61	1.0	63, 64
	Ab initio, CI	T_d	–	0.18	–	–	56
	LDA	T_d	–	0.53	–	–	65
5	LSD	Trigonal bipyramid	2.88 (3.20)[b]	–	5.71	1.14	63, 64
	LDA	"	2.88 (3.20)[b]	0.5	–	–	65
6	LSD	Rectangular bipyramid	3.08, 3.6 (3.13)[b]	–	–	–	63, 64
		"	3.08, 3.6 (3.13)[b]	0.53	5.76	1.46	63, 64
	LDA	"	3.08, 3.6 (3.13)[b]	0.566	–	–	65
7	LSD	Pentagonal bipyramid	3.21 (3.06)[b]	0.6	5.87	1.52	63, 64
		"	–	0.641	–	–	65
8	LDA	Pentagonal bipyramid with an additional apex	–	0.694	–	–	65
		Two-cornered trigonal prism	–	0.63	5.5	1.9	66
9	LDA	Three-cornered trigonal prism	–	0.809	–	–	65
		"	–	0.78	5.9	1.9	66
10	LDA	Four-cornered trigonal prism	–	0.83	5.6	1.4	66
13	LDA	Asymmetric structure based on two trigonal prisms	–	0.82	5.3	2.0	66

[a] VB, valence bond method; LSD, local spin density method.
[b] The Mg–Mg distance in the base is shown without parentheses; that in the edges is shown in parentheses.

light or by chemical action (for example, with sulfur atoms). As has been pointed out,[67] the stability of the excited states of Mg clusters suggests the possibility of developing a new type of laser based on this material.

Neutral and anionic magnesium clusters decompose by splitting off one metal atom:[64]

$$Mg_N \longrightarrow Mg_{N-1} + Mg,$$

$$Mg_N^- \longrightarrow Mg_{N-1}^- + Mg.$$

The geometry of the anionic clusters is similar to that of the neutral clusters. The interatomic distances in the anionic clusters are slightly smaller than in the neutral species, and the bond energy per single atom is approximately 0.2 eV higher.[63,64]

The highest singly occupied MO in Mg_N^- have a completely p character for $N = 2$, 3, 6, and 7, and an approximately 67% p character for $N = 4$ or 5.[64]

Removing one electron alters the geometry of the cluster. Thus, the structure of Mg_3 and Mg_3^- is an equilateral triangle, whereas that of Mg_3^+ is linear. The D_{3h} symmetry characterises a saddle point rather than a minimum on the potential energy surface (PES) of Mg_3^+.[62] Two structures have been proposed for Mg_4^+; an approximately square structure and an equilateral triangle with a central atom.[68] A calculation allowing for CI suggests that the energies of these molecules are equal: 0.51–0.53 eV per atom.[69] An analysis in the approximation of the valence bond method showed that the presence of many isomers with approximately equal energies is a distinguishing feature of the cationic Mg clusters.[62]

The geometry calculated for Mg_4^+–Mg_6^+ in the local spin density functional approximation[63,64] is different from the value calculated by Durand.[62] These results are compared in Table 3. They all suggest[62–64] that the singly charged clusters are much more stable than the neutral clusters, especially for small N. As for Mg_N^- and Mg_N their decomposition takes place by the detachment of one Mg atom. Small Mg_N^{2+} clusters are thermodynamically unstable, and undergo the so-called coulombic explosion: a decomposition induced by the coulombic repulsion of the nuclei.

Table 3. Cationic Mg_N^+ clusters.[63,64]

N	Geometry	(D/N)/eV	r_{Mg-Mg}/Å
2	$D_{\infty h}$ (linear)	0.76	2.98
3	"	0.85	2.99
4	"	0.83	2.96
5	D_{3h} (trigonal bipyramid)	0.93	3.04 (3.01)[a]
6	Rectangular bipyramid	0.84	3.54, 4.07 (3.06)[a]
7	Distorted pentagonal bipyramid	0.90	2.96 – 4.10[a]

[a] The Mg–Mg distance in the base is shown without parentheses; that in the edges is shown in parentheses.

A calculation in the LDA approximation[70] showed that Mg_N^{2+} clusters are stable only for $N > 14$. An alteration effect has been noted: the maxima in the curves of energy against number of atoms correspond to N values of 5, 10, 18, 21, 30, and 35 (with 8, 18, 34, 40, 58, and 68 electrons respectively), i.e. the number of electrons is equal or close to the magic numbers. The simplest decomposition scheme,

$$Mg_N^{2+} \longrightarrow Mg^+ + Mg_{N-1}^+.$$

takes place only in special cases. The general rule is that the preferred decomposition is the process in which both fragments have a number of electrons differing by unity from the magic number (an exact correspondence is impossible because the number of electrons in Mg_N^+ is odd).

Table 4. Decomposition of the Mg_N^{2+} clusters.[64]

N	Decomposition scheme	Energy barrier/eV
2	$Mg_2^{2+} \rightarrow 2Mg^+$	0.48
3	$Mg_3^{2+} \rightarrow Mg_2^+ + Mg^+$	0.77
4	$Mg_4^{2+} \rightarrow 2Mg_2^+$	0.90
5	$Mg_5^{2+} \rightarrow Mg_3^+ + Mg_2^+$	0.98
6	$Mg_6^{2+} \rightarrow 2Mg_3^+$	1.03

The coulombic repulsion favours the linear Mg_N^{2+} structure with positive charges located mainly at the chain ends.[63,64] Clusters with $N \leqslant 6$ are linear, but for $N = 7$ the structure becomes a pentagonal bipyramid. The linear molecule has an energy only 0.08 eV higher. The potential energy curves for the dissociation have also been calculated;[64] the results are summarised in Table 4. Because of their kinetic stability the unstable Mg_N^{2+} clusters can play an important role as intermediates in the reactions of neutral magnesium clusters.

3. Ca clusters

The energy gap between the 4*s* and 4*p* shells of Ca is smaller by a factor of 1.5 than the gap between the *s* and *p* valence shells of Be and Mg. This should favour *sp* hybridisation, but at the same time the more diffuse structure of the 4*p* AO suppresses the hybridisation. The compensation of these opposing factors should make the properties of the Ca clusters similar to those of the Mg clusters. Few calculations on the Ca clusters have been reported. At the SCF level a dissociation energy of about 0.2 eV per atom has been obtained for Ca_4. This is greater than for Mg_4 but smaller than for Be_4.[61] The Ca_3 trimer is even less stable ($\sim$0.11 eV per atom for an internuclear distance of $\sim$4 Å).[71]

No calculations have been reported for Ba or Sr.

4. Al clusters

The valence shell of Al contains an unpaired *p* electron which permits the formation of a σ bond with *sp* hybridisation. A relatively high stability can therefore be expected for the small Al clusters. This has been confirmed experimentally and by quantum chemical calculations.

The presence of isomers having similar energies and the small depth and large width of the minima in the PES make it difficult to obtain reliable calculated results. A recent analysis[72] has shown that in order to give an adequate description of Al_N clusters the chosen basis should include the *d* AO. Electron correlation effects account for up to one half of the stabilisation energy of the cluster, but their inclusion does not markedly affect the calculated geometry.[73] The main difficulty is the presence of several almost degenerate states having different geometries and multiplicities.

Specially meaningful results were obtained in calculations on the Al_2 dimer. Different ground states had been suggested for this species: $^1\Sigma_g^+$, $3\Pi_g$ (see Ref. 50) and $^3\Sigma_g^-$ (see Ref. 74), but more recently it was shown that this state is $^3\Pi_u$ (see Refs 75 and 76). This state is almost degenerate with $^3\Sigma_g^-$ ($\Delta E = 174$ cm^{-1}), and the $^1\Sigma_g^+$ energy is substantially higher (by 2000 cm^{-1}).[77] A similar state of affairs was noted for Al_3 (see Refs 78–81). The results of calculations for small Al clusters are shown in Table 5: we can see that Al_N clusters show a number of special features in addition to the more general properties such an increase in EA and in stability with increasing N. The most striking of the special features is a tendency to form planar structures (except in the case of Al_6). This is probably a consequence of the absence of *sp* hybridisation during cluster formation, which can destabilise the molecule. Therefore the three-dimensional structures most conducive to the formation of *sp* hybrid orbitals are difficult to produce. It should be noted that a planar structure is not consistent with the close packing postulated in the spherical shell model. Nevertheless, as was pointed out above, the model can successfully predict (at the qualitative level) many important properties of the clusters, and departures from the spherical symmetry can be treated as perturbations while retaining the model.[78]

The similarity in structure between the Al clusters and the crystalline metal have been analysed at the LDA level.[62] In the metal the cubo-octahedron can be chosen as the structural unit. In clusters, even when large, a packing based on the icosahedron as the structural unit is more stable. It is replaced by the cubo-octahedron only for $N > 2000$. The energy differences between the corresponding isomers calculated for $N = 13-55$ were found to be very small: not more than 2% of the total energy. Calculations of the IP[82] show that even for $N = 19$ the value obtained for the cluster (6.18 eV) is higher than for the Al atom (5.77 eV), and that it becomes significantly lower (5.04 eV) only for $N = 55$. Experimental results give a similar dependence of the IP on N, but the equality of the IP values for the atom and the cluster is seen at $N \approx 19$.

Table 5. Small aluminium clusters.

N	Method of calculation	Geometry	Ground state	(D/N)/eV	r_{Al-Al}/Å	IP/eV	EA/eV	Ref.
2	*Ab initio*, MRCI	$D_{\infty h}$	$^3\Pi_4$	0.7	2.76	–	–	77
	Ab initio, MRCI	$D_{\infty h}$	$^3\Pi_4$	0.62	2.70	–	–	73
	VB	$D_{\infty h}$	$^3\Pi_4$	0.77	2.62	6.02	0.09	78
	Ab initio, CI	$D_{\infty h}$	$^3\Pi_4$	0.60	2.76	–	–	75
3	*Ab initio*, MPY	$C_{2v} \sim D_{3h}$	$^2A_1{}^4A_2$	1.1	2.6	6.38	–	81
	Ab initio, CI	D_{3h}	$^4A_2$	0.92	2.64	–	–	75
	Ab initio, CI	D_{3h}	$^2A_1$	0.90	2.60	–	–	75
	VB	$C_{2v} \sim D_{3h}$	$^2A_1$	1.07	2.62	6.31	1.43	78
4	VB	D_{2h} (rhombus)	$^1A_1$	1.12	2.6	6.46	1.50	78
	Ab initio, CI	D_{2h} (rhombus)	$^1A_1$	1.09	2.67	–	–	75
5	VB	C_{2v} (rectangular pyramid)	$^2B_1$	1.06	2.72–2.92	5.57	1.91	78
	Ab initio, CI	C_{2v} (planar configuration)	$^2B_1$	1.15	–	–	–	75
6	VB	Distorted octahedron	$^3B_1$	1.22	2.78–2.81	6.55	2.16	78
	Ab initio, CI	Octahedron	$^3B_1$	1.42	–	–	–	75

5. Ga and In clusters

Experimental data on Ga and In clusters are adequately consistent with the predictions of the spherical shell model.[83] A strict calculation allowing for the CI has been reported only for the Ga dimer.[84] The ground state of the dimer is $^3\Pi_u$ (r_{Ga-Ga} = 2.762 Å), with a dissociation energy of 1.4 eV, and a $^3\Sigma_g^-$ state lying close to it (IP of the dimer 5.62 eV, EA = 1.04 eV). The anion of the dimer is more stable, with a dissociation energy of 2.2 eV, r_{Ga-Ga} = 2.562 Å, ground state $^4\Sigma_g^-$. The stability of the Ga_2^+ cation in the $^2\Sigma_g^+$ ground state is close to that of Ga_2 (1.5 eV, r_{Ga-Ga} = 3.24 Å).

V. Semiempirical and empirical calculations on clusters

Nonempirical calculations in wide basis sets which allow for electron correlation offer adequate descriptions of small clusters. However, in the case of large clusters their requirements of computer time are excessive. Therefore the search for promising methods of calculating the structure and the characteristics of these clusters by semiempirical approaches is now an urgent problem.

We are not aware of any successful attempts to describe clusters of Group IIA metals by these methods. Reported calculations of Mg_N clusters by the MNDO and CNDO/2 methods (*sp*, *spd*, and split *spd* basis sets) did not give satisfactory results: the bond energies were unacceptably high and the internuclear distances were too short.

Table 6. Calculation of Al clusters by semiempirical methods.

N	Method	Geometry	*s*	(*D*/*N*)/eV	IP/eV	Ref.
2	CNDO/2	$D_{\infty h}$	3	1.0	7.21	84
	MNDO	–	–	0.66	5.57	85
	INDO	$D_{\infty h}$	–	0.67	6.37	–
3	CNDO/2	$C_{2v} \sim D_{3h}$	2	2.04	7.18	84
	MNDO	–	–	0.8	6.15	–
	INDO	D_{3h}	–	1.12	6.13	85
4	CNDO/2	$C_{2v} \sim D_{4h}$	1	2.43	7.75	84
	MNDO	–	–	0.9	6.2	–
	INDO	Rhombus	–	1.37	6.44	85
5	CNDO/2	C_{4v}	2	2.60	7.12	84
6	CNDO/2	O_h	1	2.97	7.51	84

Better results were obtained for Al clusters. The results of a calculation[84] by the CNDO/2 method using corrected parameters are summarised in Table 6. As can be seen, the calculation gave reasonable values of the parameters *D*/*N* and IP, and it offers a correct description of the geometry of these clusters. However, a comparison with the data of Table 5 shows some quantitative discrepancies, less marked in the case of the MNDO calculations. Thus the shortcomings of these methods include a 10%–20% reduction of the internuclear distance as compared with the *ab initio* calculations.

Satisfactory results were obtained[85] by a special modification of the INDO method which gives internuclear distances and structures in good agreement with experiment.[82] It was used[85] in calculations for large clusters with $N \leqslant 49$. In clusters with $N \leqslant 43$ good results were obtained by the SINDOI method.[86] Thus the use of semiempirical methods in conjunction with special parametrisation provides an adequate description of Al clusters. Evidently, suitable alternative parametrisations can be produced also for other metals.

The low bond strength and the important role of the van der Waals interactions justify the use of empirical potentials for the intermolecular interactions when considering the structure and properties of the clusters. Thus, Halicioglu and Pamuk[87] have used a modified Lennard–Jones potential which gave stabilisation energies (1.226 and 1.274 eV per atom for Al_4 and Al_5 respectively) in good agreement with the results of nonempirical calculations. The same potential was used to calculate the activation energies of the regrouping of isomers. The activation barrier to the rearrangement of the tetrahedral Al_4 cluster into a rhombic cluster was 12.5 kJ mol^{-1}. In the case of Al_5 the conversion of a trigonal bipyramid into a square bipyramid requires surmounting a barrier of ~4 kJ mol^{-1}. These calculations[87] suggested the initial formation (in the gas phase) of the less stable Al_4 and Al_5 clusters, which are then transformed into the more stable planar structures. Thus the use of empirical potentials in calculations of the dynamics of the regrouping of small clusters can give satisfactory results. The conclusion that the barriers to isomeric regrouping are small has been shown[88] to apply also to magnesium.

VI. Reactions of clusters in the gas phase

The reactions of clusters have attracted great interest among research workers as models of the elementary stages of processes in heterogeneous catalysis. They are also of interest from the standpoint of the synthesis of unusual chemical compounds containing weak metal–metal bonds.

The interaction of Al_N^+ with oxygen destroys the cluster.[89] Most of the oxygen interacts with the uncharged core of the cluster to form particles of the Al_5O_2 and Al_4O_2 type. Products of the interaction of the charged core of the clusters with oxygen have also been detected: the Al_2O^+ and Al_3O^+ cluster oxides. The order of the changes in reactivity of neutral and cationic clusters of aluminium towards the reaction with oxygen has been established:[90] the reactivity decreases in the sequence dimer > atom > trimer. The rate of the process was slowest with Al_3^+, probably because of the stability of the 8-electron shell present in this species. Studies of the reactions of O_2 with neutral Al_N particles also revealed a high reactivity of the dimer, decreasing in the series $Al_2 > Al_3 > Al_4$ (Cox et al.[91]). Beyond this point the reactivity begins to increase again with the nuclearity. Notwithstanding the generally held view that the highest activity of a metal is found in the atomic state the reactivity of the clusters was found to be even higher.[92] Thus, the Al^+ and Al_N^+ ions (N = 2–8) require collision energies of 3.5 and 0–0.25 eV respectively to react with oxygen.[92]

The nonmonotonic dependence upon nuclearity of the activity of clusters towards the reaction with O_2 is clearly seen in the anionic Al_N^- clusters. In keeping with the spherical shells model the most stable and unreactive clusters are Al_7^-, Al_{23}^-, and Al_{43}^- (see Refs 93 and 94).

It is interesting to note that the reactivity of Al_N^- and Al_N^+ towards reactions with oxygen is weakly dependent on the sign of the charge, and that according to kinetic data[95] the effect of nuclearity in a series of clusters carrying the same charge is markedly stronger. For Al_N^+ with N between 1 and 33 the following oxygenated products have been obtained: AlO_x^+, $Al_2O_x^+$, $Al_3O_x^+$, $Al_3O_3^+$, and $Al_5O_2^+$. The rate constants k_2 of these reactions lie in the range of (1–2) × 10^{-12} cm^3 s^{-1} for N = 2, 3, 5, 9, 10, 17–33, and for N = 4, 8, and 14–17 they are 1.5–5.0 times lower. For Al^+, Al_6^+, and Al_7^+ the reaction is totally suppressed ($k_2 < 10^{-16}$ cm^3 s^{-1}).

Anionic clusters react by the scheme

$$Al_N^- + O_2 \longrightarrow \begin{cases} Al_{N-2}^- + Al_2O_2 \\ Al_{N-1}^- + AlO_2^- \\ Al_{N-1}O + AlO^- \end{cases}$$

The rate constants k_2 lie between 10^{-13} and 10^{-11} cm^3 s^{-1}. No interaction was detected for the magic clusters Al_{13}^- and Al_{23}^-.

The reactions of aluminium clusters with other molecules have been studied in less depth. The interaction with hydrogen (and deuterium) is hindered, and its rate is measurable only for

clusters with $N = 6-8$ ($Al_6 \gg Al_7 \gg Al_8$). The process probably takes place in two stages: [91]

$$Al_N + D_2 \longrightarrow Al_ND_2,$$

$$Al_ND_2 + Al \longrightarrow Al_ND + AlD.$$

The reactivity of the D_2 molecule towards the interaction with Al_6 is 1500 times lower than that of O_2.

The reactions of aluminium clusters with hydrogen have been analysed in terms of the modified spherical shells model.[96] Two factors play an important role: the stability of the cluster (magic numbers) and its structure (from the point of view of inserting a hydrogen atom into it). The icosahedral Al_{12} cluster has an internal cavity large enough to accept a hydrogen atom. On the other hand in the case of Al_{13}, in which the insertion of hydrogen seems even more favourable (since the total number of electrons in this case increases to the magic value), the cavity is absent and the hydrogen can be accommodated only with great difficulty.

The interaction of the lower Al clusters with molecular hydrogen has been examined theoretically in an *ab initio* study[97] of the heat of dissociative chemisorption of H_2 on Al_N. According to these calculations the process is endothermic for $N \leqslant 5$, and a small energy gain (approximately 5 kJ mol^{-1}) is observed only for $N = 6$. This effect can be treated in terms of the spherical shell model as a manifestation of the filling of the valence shell of the cluster superatom: in Al_6H_2 we reach the magic number of electrons (20). The results of the calculation agree satisfactorily with experimental data.[91]

Aluminium clusters (Al_N) can react with compounds containing a hydroxyl group. With methanol they give the adducts $Al_N(CH_3OH)_m$, where $m = 1-3$, the reactivity being a maximum for $N = 16$, 17, with a minima at $N = 7$, 14, 23. The rate of the reaction with methanol is only slightly lower than the rate of the reaction with oxygen.[91] It is interesting to note that water is approximately an order of magnitude less active than methanol. Adducts with the same composition as those formed with methanol are obtained with D_2O. The formation of oxides or hydroxides has not been observed.[91] The lower neutral clusters ($N = 2-7$) react with water to a negligible extent, whereas the cationic Al_N^+ clusters ($N = 1-3$) react with water, with formation of cluster hydroxides and evolution of hydrogen.[90]

In addition to the above, reactions of the Al_N clusters with carbon monoxide[91] and with acetone[98] have been observed. In the latter case particles of Al_NMeCO ($N = 1-15$) are formed as well as the Al_NMe_2CO adducts. The interaction of Al_N^+ ($N = 1-3$) with ethylene breaks down the hydrocarbon molecule:

$$Al_N^+ + C_2H_4 \longrightarrow Al_NCH_2^+ + \dot{C}H_2.$$

The Al^+ and Al_2^+ ions are much more active than Al_3^+.[90] With ammonia the Al_N clusters give the adducts $Al_N(NH_3)_m$, $m = 1-3$. Under the influence of radiation the ammonia is desorbed without dissociation of the cluster.[31] Aluminium clusters do not react with methanol in the gas phase.[91]

There have been effectively no studies of the gas-phase reactions of clusters of other metals of Groups IIA and IIIA. Only theoretical calculations have been carried out for some systems. The structures and energies of the Be_NH cluster hydrides have been calculated at the SCF level (without allowing for CI).[71] These molecules are much more stable than the corresponding Be clusters. The binding energy of the hydrogen increases rapidly with the nuclearity N: even for $N = 4$ it is close to the energy of sorption on the bulk metal. *Ab initio* calculations of the complexes of Be_2^{2+} with molecular hydrogen[99] identified two stable complexes formed by the reactions:

$$Be_2^{2+} + 2H_2 \longrightarrow \left[H_2\text{---}Be\text{—}Be\text{---}H_2\right]^{2+}, \quad (+2.45\ eV)$$

$$Be_2^{2+} + 4H_2 \longrightarrow \left[(H_2)_2\text{---}Be\text{—}Be\text{---}(H_2)_2\right]^{2+}. \quad (+3.27\ eV)$$

In these complexes the hydrogen is not dissociated: the H_2 molecules are located at right angles to the Be—Be bond. These complexes may be formed as intermediates in the interaction of charged Be clusters (and probably also Mg and Ca clusters) with molecular hydrogen.

Theoretical studies of the cluster compounds of magnesium[100-102] have shown that the addition of an Mg_2 dimer to F—F, Cl—Cl, H—H, and H—F bonds is more favourable than the addition of an Mg atom. The gain in energy is between 2 and 12 kJ mol^{-1}. For Ca the calculation also predicts the possibility of forming cluster compounds of the F—Ca—Ca—F type. As reported,[102] the interaction of the Mg_2 cluster with HF can take place through a four-atom transition state to give the cluster compound HMgMgF. However, in every case the calculated difference between the heats of reaction of Mg and Mg_2 is not large. It should not be forgotten that the calculation[100-102] can give erroneously low results for the clusters because of the failure to allow for electron correlation effects. The results of calculations on the magnesium—methyl halide system are discussed below, because this reaction has been observed in a condensed but not in a gaseous phase.

Only fragmentary information on the structure, properties, and reactivity of the clusters in the gas phase is available at present. Nevertheless we can formulate some general conclusions. The clusters of all metals in Groups IIA and IIIA are labile formations, with bonds having a strength intermediate between the weak van der Waals bonds and covalent bonds. The presence of numerous geometric isomers and of electronic states with similar energies leaves little doubt that clusters can easily become rearranged into a structure more favourable to the reaction. The low stability of the M—M bond allows us to observe both processes without decomposition of the cluster core (reactions with H_2, MeOH, CO) and reactions with dissociation (with O_2) under conditions of low activation energy. Two problems are still controversial. Firstly, it is not clear whether homogeneous gas-phase catalysis involving clusters is possible. The Be, Mg, and Al clusters can activate and split bonds with low reactivities such as H—H, C—C, etc. However, there is no evidence of the regeneration of the clusters from the resulting adducts. Secondly, the reaction mechanisms have not been made clear. In an attempt[91] to treat these reactions as one-electron processes the reactivity was correlated with the reciprocal energy difference between the HOMO of the donor and the LUMO of the acceptor. However, the arguments put forward are not entirely convincing. For example, in this approach methane could be said to be more active than hydrogen. Furthermore the low reactivity of the Al atoms as compared with their small clusters (which have a high IP) is difficult to understand. We believe that the high reactivity of the clusters arises from the possibility of simultaneous interaction of a cluster with several atoms of the substrate molecule. Under these conditions the activation may be associated with both an electron transfer and a synchronous bond breaking act in the substrate, with formation of substrate—metal bonds. The thermodynamic characteristics and the activation parameters are found (as could have been expected) to be sensitive to the electronic state of the cluster. The magic clusters have a low reactivity (at least, in reactions involving the breakdown of the metal core).

VII. Heteronuclear clusters

Metals of Groups IIA and IIIA can form heteronuclear as well as homonuclear clusters. The mixed clusters K_NMg were studied by Kappes et al.,[103] who found that these compounds did not satisfy the formal rules of the spherical shell model. In spite of

having eight valence electrons K_6Mg does not show an enhanced stability, as observed in the 10-electron K_8Mg cluster. The $MgLi^+$, $MgLi^{2+}$, Mg_2Li^+ clusters have been prepared by evaporation of the metals from the liquid phase using electron bombardment.[104] Experimental data on clusters of this type are few, and do not allow definite correlations to be identified. Theoretical studies have greatly outstripped the experimental work.

Mixed clusters containing Be and Mg are characterised by a moderately high symmetry and a tendency to form planar structures at low values of N. Typical geometric forms of Li_NBe clusters[105] are shown in Fig. 2. Three-dimensional structures are first encountered with Li_5Be in neutral clusters and with Li_6Be^+ in charged clusters. The bond is stronger in $LiBe_N$ clusters than in Be_N. The bond energies per atom are 0.25 eV in LiBe and 0.45 eV in Li_2Be. Similar effects were observed[106] for Li_NMg, the only difference being that Li_3Mg has the form of a centred triangle. The introduction of Mg or Al as adatoms into Li_N clusters produces a large increase in the stability of the cluster as a whole, with a corresponding decrease in the ionisation potential.[107]

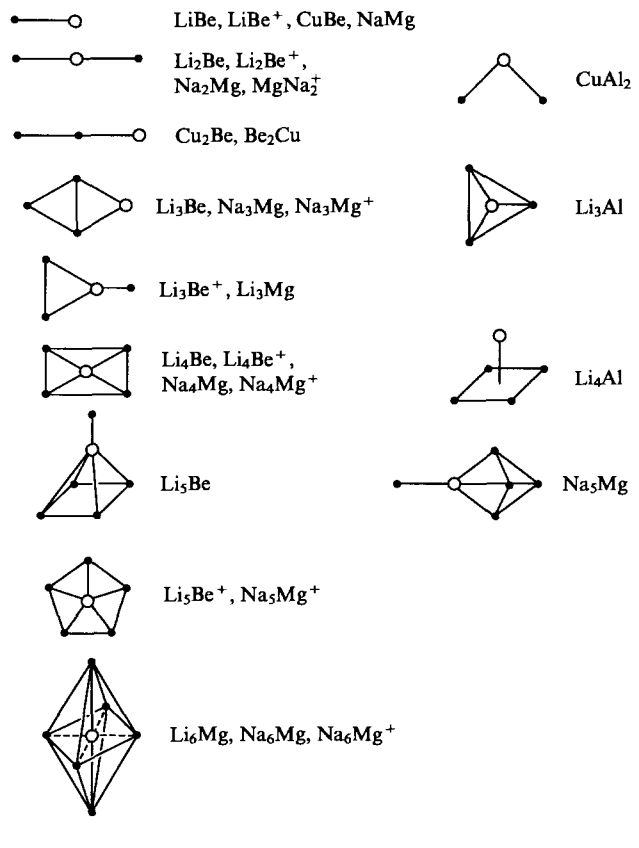


Figure 2. Typical forms of mixed clusters.

The Na_NMg and Li_NMg clusters were studied in great detail by Fantucci et al.,[108] who made *ab initio* calculations over a wide basis set allowing for CI. Though the geometry obtained for Li_NMg was similar (on the whole) to previous reports[106] the D/N and IP values were quite different. It was suggested[108] that the STO-6G basis used in the previous work[106] is inappropriate in this case and leads to unreal values of the energy. The MgNa and MgLi clusters are characterised by weak M – M′ bonds with $D/N < 0.1$ eV and internuclear distances of 3.59 and 3.2 Å. The stabilisation energy increases with N. The cations are much more stable. For example, the bond breaking energy is 0.87 eV in $MgNa_N^+$. The properties of the mixed clusters vary non-monotonically with N. In $MgLi_N^+$ and $MgNa_N^+$ even values of N correspond to a stabilisation energy greater than in the odd values. The ionisation potential of clusters with even N is also higher than that of their neighbours with odd N. The magic numbers expected on the basis of the spherical shell model are not clearly observed. In the neutral clusters an enhanced stability is found for 8, 9, and 10 electrons, and in the cationic clusters for 5, 7, and 9. This effect is probably due to the large departures of the geometry of the small MgM_N and MgM_N^+ clusters from the spherical form.

The theoretical model was modified as follows in order to provide a satisfactory explanation of the experimental data.[109,110] It is assumed that the additive atom is located at the centre and creates a region in which the charge density is different from the density in the remainder of the core. With a reasonable choice of parameters the resulting model of 'a sphere within a sphere' provides a sequence of energy levels different from that given by the simplest model: $1s < 1p < 2s < 1d$ etc. In this case even a configuration of 10 electrons produces a closed shell: $1s^2p^62s^2$. Under these conditions the stability of the 10-electron cluster K_8Mg is not surprising. The stipulation of a central location of the additive atom is clearly justified (see Fig. 2), as is also the assumption of a different charge density in the central region. For example, in the Li_NMg clusters the central Mg atom carries a greater positive charge (1.1 – 1.33), and in the Li_NAl clusters the charge on the Al atom is also greater than +1 (see Rao and Jene[107]). At the same time the departures from spherical symmetry become substantial.

The Al – B and Al – C mixed clusters are of interest from the standpoint of the spherical model. The clusters $Al_{12}B^-$, $Al_{22}B^-$, and $Al_{21}B_2^-$ have been shown (experimentally) to have a high stability.[111] Because B and Al are isoelectronic these clusters are analogues of the magic clusters Al_{13}^- and Al_{23}^-. The low stability of the $Al_{11}B_2^-$ cluster, which is isoelectronic with Al_{13}^-, seems inexplicable at first sight. Allowing for the geometric factor now becomes important. Thus, Al_{13}^- is an icosahedron with one central atom which can be replaced by B without substantial changes in geometry. On the other hand replacing a second atom in the outer sphere infringes the symmetry of the system and destabilises it. Two central atoms are present in Al_{23}^-, and both can be replaced without perturbing the structure: $Al_{21}B_2^-$ is therefore a very stable system.

The C atom differs little in size from the Al atom. Results analogous to those obtained[111] for the Al – B system could have been expected for Al_NC^-. However, a study of Al_NC^- clusters with $5 \leqslant N \leqslant 38$ gave unexpected results: a high stability was observed[40] for $Al_7C_4^-$ and $Al_{24}C^-$. These clusters contain a nonmagic number of electrons: 26 and 77. Their stability was ascribed[40] to the formation of tightly bound AlC subunits in the cluster, which do not contribute to the formation of a valence shell. These clusters should be treated as $Al_6^-(AlC)$ and $Al_{23}^-(AlC)$ respectively, with shells of 19 and 70 electrons, in complete agreement with the model. The absence of a stable $Al_{13}^-(AlC)$ cluster can be attributed to the same effects as the absence of $Al_{11}B_2^-$. The Al_{13}^- centred icosahedron simply does not have unoccupied sites for the interaction with an AlC subunit.

Mixed clusters containing transition and typical metals are of interest as models of new types of heterogeneous catalysts. They can be prepared in the gas phase or in solution. The reaction between diphenylmagnesium and CuBr in diethyl ether gave the $Cu_4Mg(C_6H_5)_6$ cluster, with a metal core consisting of a trigonal bipyramid having three Cu atoms at the base and Cu and Mg atoms at the apices.[112] The Mg – Cu distances are 2.75 Å, and the tetrahedral Mg configuration is produced by the coordination of ether molecules.

Ab initio calculations allowing for correlation[113] have been carried out for clusters containing Cu, Be, and Al. The CuBe cluster is much more stable than Be_2 ($D/N = 0.385$ eV), and CuAl has the same bond energy as Al_2. Both these clusters are almost nonpolar. It is interesting to note that asymmetric structure correspond to the more stable isomers of the linear

Cu_2Be and Be_2Cu clusters (see Fig. 2). The interaction of Be_2 with Cu greatly increases the stability of the Be–Be bond (dissociation energy 0.56 eV). The $CuAl_2$ cluster has a triangular structure; the energy needed to split off an atom is 2.28 eV for a Cu atom and 1.56 eV for an Al atom.

The reactivity of the mixed Al clusters has been studied for their interaction with hydrogen and oxygen. Hydrogen is not chemisorbed on solid Al, and does not react with Al atoms or clusters (except Al_6–Al_8). However, Co clusters are activated by introducing Al into them. Thus, the following activity series were obtained[114,115] for mixed Co–Al clusters with identical numbers of Co atoms:

$$Co_6 \approx Co_6Al \ll Co_6Al_2 > Co_6Al_3\,;$$

$$Co_8 \ll Co_8Al < Co_8Al_2 > Co_8Al_3\,.$$

Even one Co atom causes marked activation of the Al clusters. Thus, the $Al_{10}Co$ cluster has a high activity.

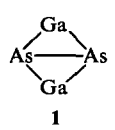
A different state of affairs is seen for Nb_N clusters. The activity of small Nb clusters with $N = 4-7$ falls off steeply when Al is introduced. For example, Nb_4Al_2 reacts with H_2 to a negligible extent, whereas Nb_4 is quite active. On the other hand the deactivation of Nb_N clusters with $N = 8-12$ by aluminium is relatively weak.

The effect of Al on the reactivity of Co_N clusters has been ascribed[114] to a decrease in the IP. However, direct measurements of the IP of mixed clusters failed to detect a decrease when the number of Al atoms was increased, or a correlation with the reactivity of the cluster.[116] The activation of the Co clusters by aluminium is probably caused by electron transfer within the metal core from the Al to the Co.

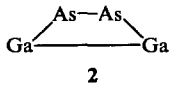
The reactivity of Nb clusters towards the reaction with H_2 is not correlated with the IP,[117] and the electronegativities of the Al and Nb atoms are not very different. The deactivation of small Nb_N clusters by aluminium has been attributed to the structural blocking of the most reactive atoms of the transition metal. At high N values the contribution from this effect is small.

A phenomenon analogous to the magic numbers effect has been observed for anionic Al clusters in the reactions of VAl_N^-, $NbAl_N^-$, and $VNbAl_N^-$ with oxygen.[94,118] It was found that $NbAl_4^-$ and VAl_6^- have an anomalously low reactivity. Any attempt to reconcile this result with the spherical shell model must take account of the number of electrons contributed by the transition metal. The valence shell of V and Nb have the $3d^34s^2$ and $4d^45s^1$ structure. It is not clear whether the d electrons are correlated in the cluster. In the case of $NbAl_4^-$ the participation of all the electrons produces a stable 18-electron shell. In this case we obtain a 24-electron configuration for VAl_6^-, which is far from the magic number. It may be assumed that only the s electrons are involved (or, more strictly, one s electron). The prospects of describing the reactions of mixed clusters containing transition and typical metals in terms of simple models are not favourable at present.

Before proceeding to other topics we should mention the mixed clusters of gallium and arsenic. Interest in these species was stimulated by their possible application in the production of gallium–arsenic semiconductor materials. Clusters of this type are prepared by the laser evaporation of gallium arsenide.[119] The ground state of GaAs is $^3\Sigma^-$, that of $GaAs^+$ is $^4\Sigma^-$ (see Knight and Petty[120]). The most stable of the binary clusters[121] is $GaAs^-$. The Ga_NAs_M clusters are characterised by the presence of several isomers with similar energies.[122] For example, in Ga_2As_2 we find the structures **1** and **2**, both unstable (though structure **1** is relatively more stable). The energy of the dissociation of cluster **1** into two GaAs molecules is greater than 3 eV (*ab initio* + MRCISD).[123]



1



2

These results exemplify the multiplicity of structures and of composition available to the mixed clusters. It is not unreasonable to suggest the possibility of preparing these compounds for any pair of metals and for many metal–nonmetal combinations.

VIII. Preparation of clusters and their reactions at low temperatures

So far we have dealt with clusters prepared and studied in the gas phase. Another, no less important approach to the problem relies on the cryochemical synthesis of cluster compounds.

Metal clusters can be prepared by the aggregation of atomic metal being condensed from the gas phase. Their stabilisation in a matrix or on a solid carrier surface allows their chemical properties to be studied. The nuclearity of the clusters is difficult to establish in solid-phase experiments because mass spectrometric detection is not available.

Studies in which the clusters are prepared by condensation from the gas phase can be divided into two groups: studies of small clusters and studies of giant clusters and of even larger species. The preparation and the chemical properties of moderately large clusters (tens of hundreds of atoms) have received little attention because of the difficulty of identifying these species in condensed phases. Let us examine the case of small clusters.

The spectra of small clusters of calcium and magnesium have been studied by Klabunde and coworkers.[124,125] For example, for Ca the following bands were observed: 374 (Ca_2, $^1\Pi_u \leftarrow {}^1\Sigma_g^+$), 415 (Ca, $^1P_1 \leftarrow {}^1S_0$), 448 (Ca, $^1D_2 \leftarrow {}^1S_0$), 470 (Ca_x, $x > 2$), 505 (Ca_2, Ca_x), 550 (Ca_x), 648 nm (Ca_2, $^1\Sigma_u^+ \leftarrow {}^1\Sigma_g^+$). Bands corresponding to clusters with N between 1 and 4 can be resolved for Mg; total absorption was observed for clusters with $N \geqslant 5$. The spectra of Al, Ca, and In dimers were reported by Douglas et al.[43]

The study of the reactivity of Al clusters is complicated by the very high activity of Al atoms towards the majority of reactants in the solid phase. At temperatures of about 77 K Al atoms react with ethylene,[126] propene,[127] butadiene,[128] tetrahydrofuran and halogen derivatives,[129] benzene,[130] and even methane.[131] Nevertheless the cluster halide Al_2Cl_4 was prepared by the simultaneous condensation of aluminium and chlorine in an inert matrix: the structure of its Al–Al bond was established by IR and ESR spectroscopy and by quantum chemical calculations.[132]

The cryochemical reactions of the elements of Group IIA, whose atoms are less reactive than those of aluminium, are of special interest. The formation of organomagnesium compounds (OMC) by the simultaneous condensation of Mg and organic halides was established 20 years ago.[133] More recently reactions between Mg clusters and relatively unreactive molecules such as C_6H_5F and CCl_4 (Refs 134 and 135) have been carried out. Similar reactions have been observed[136] also for Ca and Sr. In the course of this work it was shown that the formation of OMC is favoured by the same conditions as the aggregation of Mg atoms.[137] Furthermore, products of the Wurtz reaction can be obtained instead of the OMC under conditions conducive to the isolation of atoms.[138] This underlines the important role of the aggregation of metals in the synthesis of OMC. Strict proofs of these conclusions have been formulated[139,140]. It was shown that in an Ar matrix the Ca clusters (but not the Ca atoms) react with CH_3Br and CH_3I, and that only the Mg_N clusters with $N \geqslant 4$ react with CH_3F.

The low reactivity of Mg and Ca atoms can be understood by considering the mechanism of formation of the OMC. The direct addition of the atoms to the carbon–halogen bond is symmetry forbidden,[141] and the activation energy of the process should be at least 30–40 kJ mol^{-1} (see Davis[142]). Typically, in the gas phase the Mg atoms do not react with RCl molecules, irrespectively of the nature of R; radical detachment of Cl with formation of MgCl is observed only in the reaction with Cl_2.[143]

The formation of OMC requires an intermediate one-electron transfer whose possibility is determined by the ionisation potential of the metal-containing particles. As was pointed out above, the IP of Mg_N clusters decreases with increasing nuclearity, and the reaction becomes possible above a certain value of N. By starting from this simple scheme we can propose an alternative role for the aggregation in the case of Al. In the Al clusters the IP initially increases with increasing nuclearity, and small clusters can have a low activity towards reactions with RCl.

The addition of Mg_N to the bonds of organic halogen derivatives (RX) should lead to the formation of cluster compounds which we can call organopolymagnesium halides (OPMH). It has been suggested[140] that these compounds cannot be stable, and that they should decompose or react with the excess of RX when the matrix is allowed to warm up. Indeed, as reported,[101,102] the additional stabilisation energy of the OMC clusters (as compared with the Grignard reagent) is not more than 24.8 kJ mol^{-1}, and falls to zero as N increases to 5. We consider these conclusions[140] premature. Firstly, as can be seen from the calculated potential energy surfaces for Mg* and Mg^{2+}, these species should have a high kinetic stability. The activation energy for their decomposition could be quite large. Secondly, the published calculations[101,102] do not allow for electron correlation effects, which can predominate in the stabilisation of cluster compounds. For example, the *ab initio* calculation of the stable cluster tetramer $Al_4(C_5Me_5)_4$ isolated in a pure form[22] suggests that this species cannot be prepared.[144] This conclusion is quite correct, in spite of the neglect of correlation effects, but for Mg_N the correlation effects may be more important than for Al. Therefore the reported[101,102] stability of OMC clusters of the RMg_NX type appears to be too low.

The stability of OPMH under normal conditions has now been confirmed experimentally in the case of phenylpolymagnesium halides.[145,146] These compounds, of the general formula $PhMg_NX$ ($N = 2-4$; X = F, Cl, Br, I), can be prepared by cryochemical synthesis and are stable in solution for many weeks at 295 K: they can be isolated in a polycrystalline form and analysed. The effective state of oxidation of the Mg is less than 2. The action of water on OPMH causes hydrogen evolution according to the equation

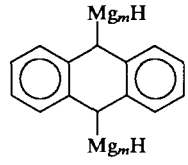
$$PhMg_NX + (2N-1)D_2O \longrightarrow$$

$$\longrightarrow PhD + MgX(OD) + (N-1)Mg(OD)_2 + (N-1)D_2.$$

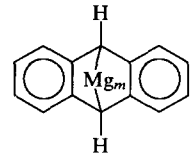
The decomposition of $PhMg_NX$ requires a temperature close to 100 °C. Compounds with alkyl substituents are less stable, and their structure is not entirely clear.[147]

The composition of RMg_NX is determined by the nature of the reagent X, and to a large extent by the stability of the C–X bond. Allyl bromides, which have the weakest bonds, give the classical Grignard reagents C_3H_5MgX ($N = 1$). With the stronger C–Br and C–I bonds, and also C–C, the parameter N takes the value 2 (on average). Lastly, from PhCl and PhF we obtain $PhMg_NX$ compounds in which the average value of N is 3–3.5 (X = Cl), and even 4 (X = F). The dependence of the nuclearity of the OPMH on the strength of the C–X bond is due to the competition between the metal aggregation process and the addition at the C–X bond. In C_3H_5X the bond is very weak, and the Mg atoms arriving from the gas phase react with the organic molecule faster than they can aggregate. The reaction probably takes place by a radical mechanism with intermediate removal of a halogen atom. Dimers and trimers react with the stronger C–Br and C–Cl bonds, whereas only the tetramers of larger particles can react with the strongest bonds (H–F). This explains the selectivity of the clusters in terms of activity as a function of the stability of the C–X bond.

The formation of cluster compounds of Group IIA is not confined to halogen derivatives. There is strong evidence for the existence of compounds of the RMg_NH type, formed by the simultaneous condensation of the metal and of aromatic hydrocarbons. Under these conditions, Al, Ca, and Mg form bright green condensates which become black when heated. It is assumed that complexes are formed in the first stage, and are then decomposed with formation of the dispersed metal.[129,148] However, in addition to this process we observe the activation of the C–H bonds of the aromatic with formation of hydride derivatives. The yield of hydrides during the interaction of alkylaromatic compounds with magnesium was thought to be a few per cent.[149] During the interaction of calcium with benzene a quantitative yield of hydrides is formed,[150] but their nature is not entirely clear. By analogy with the formation of organopolymagnesium halides we may suggest the addition of magnesium clusters to strong C–H bonds. More definite data are available for the magnesium–anthracene system. In this case a solid product of composition $C_{14}H_{10}Mg_N$ was obtained on removing the excess of ligand, with N varying between 4 and 8. Hydrolysis of these materials produces hydrogen, anthracene, and 9,10-dihydroanthracene, which suggests[151] the formation of the compounds **3** and **4**:



3



4

$m \approx 4$.

The cluster compounds of Mg are more reactive than their mononuclear analogues. For example, the cross-combination of the $PhMg_2X$ (X = I, Br) compounds with allyl bromide is faster by an order of magnitude[145] than the reaction of PhMgX. The course of the reaction is also different. The compounds $PhMg_3Cl$ and $PhMg_4F$ ($N = 3$ and 4) react with allyl bromide by exchanging organic radicals, and under these conditions cross-combination is almost never observed.

The high reactivity of organopolymagnesium halides can be attributed to a number of causes. These compounds contain the relatively weak Mg–Mg bonds, whose homolysis can lead to reactions which lower the nuclearity of the cluster. This could be the mechanism of the thermal breakdown of the cluster compounds at high temperatures. We should stress that the ionisation potential of the cluster OMC can be much lower than in RMgX, as shown by semiempirical calculations for model compounds.[146] One-electron transfer plays a fundamental role in many reactions of organomagnesium compounds.[152] Therefore a decrease in the IP should produce a strong activation of the molecule. Furthermore the coordination of the reacting molecules at several centres of the cluster simultaneously can be important, as it is in gas-phase reactions. For example, in the RMg_4X compounds all the magnesium atoms are coordinationally unsaturated, and the unsaturation persists even after dimerisation of these cluster molecules. In the absence of donor solvents these species will be reversibly coordinated to reagents which favour their interaction. From this point of view the exchange reaction discussed above can be represented by the scheme:

$$RMg_NX + R'Y \rightleftharpoons \begin{matrix} R & & Y \\ & Mg_N & \\ X & & R' \end{matrix} \rightleftharpoons R'Mg_NX + RY.$$

The high activity of cluster compounds offers new possibilities in organometallic synthesis. However, the use of these compounds in catalysis has attracted the greatest interest. The reversible coordination of the cluster core to various reagents creates the possibility of obtaining catalytic cycles. Thus, in the $C_6H_5F-n\text{-}C_8H_{17}Cl-C_6H_5Mg_4F$ system the yield of chloro-benzene and octyl fluoride exceeds the molar amount of magnesium by a substantial factor, suggesting a catalytic process.

Cluster organometallic hydrides are of special interest from the viewpoint of catalysis. The magnesium–anthracene system discussed above can be used as a hydrogen transfer system. In the presence of hydrogen donors such as alkylaromatic hydrocarbons the yield of $CHCl_3$ in reactions with CCl_4 exceeds the amount of magnesium by an order of magnitude or more.[151] Evidence of a high catalytic activity towards the polymerisation, alkylation, and isomerisation of olefins in the combined condensates of magnesium with aromatic hydrocarbons and $TiCl_4$ has recently been obtained.[153] In the absence of the aromatic hydrocarbon the activity of the catalyst is much lower, or completely absent.

The cluster compounds of nontransition metals are of considerable interest as the components of homogeneous catalytic systems. From the standpoint of heterogeneous catalysis the giant and supergiant clusters are the most promising. These are similar in size to the powders obtained by dispersing metals or by reducing their salts in solutions. However, the giant clusters prepared by the cryochemical method have a number of distinguishing features, not found in ordinary metals, which justify a separate discussion within the present review.

IX. Giant clusters prepared by cryosynthesis

In the previous section we discussed the interaction of small metal clusters with reactive matrices, leading to the formation of cluster compounds. The use of relatively inert matrices, and of compounds giving only low-stability metal adducts, offers a new pathway for the reaction: the aggregation of the metal with formation of giant clusters.

The most important methods of studying these systems include electron microscopy and UV and IR spectroscopy. Various theoretical models (Maxwell–Garnet, Drude, etc.[154, 155]) have now been developed to describe the spectra of highly dispersed metals. However, even by allowing for the cluster nature of the absorbing species these models fail to describe their IR spectra exactly.[156] A satisfactory quantitative description of the spectra is obtained by abandoning the use of all parameters relating to the bulk metal and allowing for the quantum effects associated with the small size of the absorbing species.[157] This model can be used to describe the spectra of large clusters of Al and other metals in the gas and the condensed phase.[158, 159]

Electron microscopic and spectral data show that ultradispersed particles of practically any size can be obtained by varying the condensation regime and the metal : inert matrix ratio. Under typical conditions (pressure of metal vapour ~ 0.1 Torr and metal : Ar matrix ratio ~ 10) almost all metals give particles having a diameter of the order of 1000 nm.[160] The particle size depends (among other factors) on the nature of the matrix and of the diluent gas. As a function of the latter factor it increases in the sequence: He < Ar < Xe (see Wada [161]). By varying the preparation regime of Mg clusters in the presence of tetrahydrofuran and of inert gases the size of the clusters can be varied between 2 and 100 nm or more (i.e. from 10^2 to 10^7 atoms).[162] Particles of about the same disperseness can be produced also without using inert matrices. Thus the condensation of Al vapour, both with and without hydrogen, gives crystalline particles of octahedral, cubo-octahedral, and trigonal bipyramid form having an average size of 40–200 nm.[163]

The giant clusters prepared by condensation in an inert gas matrix or on the surface of an inert carrier are similar in properties to the massive metals, the only difference being a very large specific surface area. The situation is entirely different for the products of the simultaneous condensation of the metal and of a formally inert organic compound. After removal of the excess of organic compound cocondensates of Mg with hexane and tetrahydrofuran are deeply coloured pyrophoric powders much more reactive than the Mg powders obtained by traditional methods.[164] The corresponding Ca condensates have been used [165] to prepare Ca analogues of the Grignard reagents.

Studies by electron microscopy of simultaneous condensates of Mg and tetrahydrofuran (after removing the excess of the latter) showed the formation of clusters approximately 35 nm in diameter. These condensates can absorb hydrogen at 200 °C, whereas dispersed magnesium prepared by any other method absorbs only at 350–450 °C. Treating the condensate with perylene increases the rate of sorption of hydrogen more than 10-fold.[166] This large increase in activity is due (at least in part) to an almost fourfold increase in specific surface area as compared with the most active samples of the compact metal. However, the main role is played by the specific structure of the clusters, resulting from the high proportion of organic substance. The condensate has the overall formula $Mg(C_xH_yO_z)_{0.0274}$, where $x:y = 3:1$.[167] The high catalytic activity of the condensate towards the H–D exchange reaction is observed even at 0 °C.[168] The sorption activity depends on the condensation conditions and on the shape and size of the clusters. Though in every case the arrangement of Mg atoms in the condensate corresponds to a hexagonal lattice, the morphology of the clusters is different: layered aggregations are formed in THF, whereas in a diethyl ether matrix the aggregates are columnar. A substantial activation of the condensate is achieved by adding 1%–2.5% of copper. Under these conditions the specific surface is increased by 1–2 orders. The copper is finely dispersed in the excess of magnesium and accelerates the sorption of hydrogen.[169] Similar results were obtained with cocondensates of magnesium and nickel. The nickel forms clusters 0.8–3.5 nm in diameter enclosed within larger aggregations containing an organic Mg species.[170]

The giant metal clusters obtained by cryochemical condensation have the size of colloidal particles. Therefore colloidal solutions are often produced by dissolving these condensates.[171] Giant clusters can also be synthesised by passing a flow of metal clusters or atoms in a stream of inert gas through a liquid solvent.[172] The possibility of formation and the stability of the colloidal metals obtained in this way are determined by the character of the interaction of the surface of the ultradispersed metal with the medium.

The colloidal solutions of aluminium have been studied in most detail. Thus, the dark blue solution in ethanol contains particles 30 nm in diameter. Bands at 215, 250, and 550 nm have been identified in its spectrum.[172] The solution is stable for one month: this has been attributed to the formation of a stabilising oxide film on the metal surface. The nature of the stability of the colloid is the same as in the Al colloid prepared by the aerosol method.[173]

The more active Ca metal also forms a light blue colloidal solution in ethanol. However, its lifetime is not more than 10–12 min, possibly because of the low strength of the oxide film. Stable colloids are not obtained even when the metal particles are combined with paraffins.

The mechanism of the stabilisation of colloids of typical metals prepared by cryochemical synthesis is not completely understood at present. Firm criteria defining their optimum formation conditions have not been formulated. It may be assumed that reactions on the surface of the initial clusters play a dominant role. Clearly, if the matrix is very active and reacts with atoms and small clusters in the solid phase a colloidal solution cannot be formed: for example, in calcium (or magnesium)–hydrocarbon halide systems. As in the case of the alkanes, inertness of the matrix does not stabilise particles of

colloidal dimensions because of coagulation and sintering effects. The best matrices have a moderately high reactivity: they are inactive during the preparation of the solid sample at low temperatures, and do not suppress the primary aggregation process in the solid phase, but they block the surface of the giant cluster by reacting with it near the melting point.

This simple criterion has been used in the synthesis of stable colloidal solutions of Mg in amines (triethylamine, dimethylamine, etc.[174,175] Heating the cocondensates of Mg and amines leads to the formation of coloured or colourless solutions containing (according to measurements by UV spectroscopy and electron microscopy) particles having dimensions between 30 and several hundred nanometers, depending on the amine. The interaction begins in the solid phase with formation of ion–radical particles, as shown by the characteristic ESR signal, which disappears upon heating the sample. Two competing processes apparently take place under these conditions: the aggregation of the small clusters formed during the condensation into larger formations and the conversion of the ion–radical species into compounds with stable chemical bonds. As a result we obtain relatively large metal particles with a surface coating of organometallic compounds. The formation of strong bonds is confirmed by the detection of up to several per cent of the organic component after pumping out the amine and lengthy vacuum heat treatment of the residue.

A slightly different stabilisation mechanism takes place in the magnesium–pyridine system. In this case very large aggregates (up to 2000 nm) are present in the solution. A strong ESR signal persists after the sample is melted. Pyridine has a high electron affinity, and therefore the ion radicals are reasonably stable on the metal surface. The resulting electric double layer stabilises the particles and prevents their coagulation. Oxygen additions cause the breakdown of this layer and destroy the colloidal solution.

Mg colloidal solutions have a high reactivity. They can be used in preparative work as a source of very active magnesium. However, their catalytic and initiating properties are the most interesting. They can activate various organic molecules, including hydrocarbons. In the presence of colloidal magnesium the catalytic migration of the double bond in olefins takes place effectively at room temperature. Normal alkanes are isomerised into isoalkanes, but the extent of reaction does not exceed 2%–4%. Colloidal magnesium is used as a powerful initiator of the radical addition of polyhalogenomethanes (CCl_4, $CHCl_3$, etc.) to the multiple bonds in olefins. The yield of product at 80 °C can be as high as 400 mol per mole of Mg per hour.[176] We note for comparison that the activity of one of the best initiators of this process (magnesium decacarbonyl) is several times lower at 120 °C and high pressure.

* * *

The study of the chemical reactions of clusters of the transition metal in the condensed phase and of the reactivity and catalytic properties of the resulting cluster compounds is only beginning. However, it is already evident that this work will generate new and very active homogeneous and heterogeneous catalysis systems. The stability of many cluster compounds of the transition metals in solutions opens new pathways to the realisation of unusual transformations and to the synthesis of new types of organometallic derivatives. Complex systems containing both clusters of the transition metals and compounds of these metals are of special interest. In this case we can expect the achievement of very high catalytic activities. The number of publications in this field will undoubtedly continue to increase.

References

1. S P Gubin *Khimiya Klasterov* (The Chemistry of Clusters) (Moscow: Nauka, 1987)
2. P Jena, B K Rao, S N Khanna *Physics and Chemistry of Small Clusters* (New York: Plenum, 1987)
3. M Moskovits (Ed.) *Metal Clusters* (New York, 1986)
4. M J Clarke (Ed.) *Clusters* (New York; Tokyo, 1985)
5. M A G Tinga, O S Akherman, F Bickelhaupt, E Horn, A L Spek *J. Am. Chem. Soc.* **113** 3604 (1991)
6. D G Tuck *Polyhedron* **9** 377 (1990)
7. J C Beamish, R W Small, I J Worrall *Inorg. Chem.* **18** 220 (1979)
8. R W Small, I J Worrall *Acta Crystallogr., Sect. B, Struct. Crystallogr.* **38** 250 (1982)
9. R W Small, I J Worrall *Acta Crystallogr., Sect. B, Struct. Crystallogr.* **38** 86 (1982)
10. M A Khan, C Peppe, D G Tuck *Can. J. Chem.* **62** 601 (1984)
11. K L Brown, D Hall *J. Chem. Soc., Dalton Trans.* 1843 (1973)
12. H J Cumming, D Hall *Acta Crystallogr., Sect. C* **3** 107 (1974)
13. M A Khan, M J Taylor, D G Tuck *J. Crystallogr. Spectrosc. Res.* **16** 895 (1986)
14. G A Evans, K H Tan, S P Tapper, M J Taylor *J. Chem. Soc., Dalton Trans.* 988 (1973)
15. B H Freeland, J L Hencher, D G Tuck *Inorg. Chem.* **15** 2144 (1976)
16. M J Taylor *Metal-to-metal Bonded States of the Main Group Elements* Ch. 3 (New York: Academic Press, 1975)
17. O T Beachley, M R Churchill, J C Fettinger *J. Am. Chem. Soc.* **106** 4666 (1986)
18. E P Schram *Inorg. Chem.* **5** 1291 (1966)
19. E P Schram, R E Hall, J D Glore *J. Am. Chem. Soc.* **91** 6643 (1969)
20. H Hoberg, S Krause *Angew. Chem.* **88** 760 (1976)
21. W Uhl *Z. Naturforsch., B Chem. Sci.* **43** 1113 (1988)
22. C Dohmerer, C Robi, M Touche, H Schnochel *Angew. Chem.* **103** 594 (1991)
23. W Hiller, K W Klinkhammer *Angew. Chem.* **103** 181 (1991)
24. R Nesper, J Curda *Z. Naturforsch.* **426** 557 (1987)
25. V E Bondybey *Chem. Phys. Lett.* **109** 436 (1984)
26. W J Balfour, A E Douglas *Can. J. Phys.* **48** 901 (1970)
27. K C Li, W C Stwalley *J. Chem. Phys.* **59** 4423 (1973)
28. P L Po, R E Porter *J. Phys. Chem.* **81** 2233 (1977)
29. M F Jarrold, J E Bower, J S Kraus *J. Chem. Phys.* **86** 3876 (1987)
30. L Hanley, S A Rudtta, S L Anderson *J. Chem. Phys.* **87** 260 (1987)
31. K Kaya, K Fuke, N Nonose, N Kikuchi *Z. Phys. D* **12** 571 (1989)
32. K J Taylor, C L Pettiette, M J Craycraft, O Chesnovsky, R E Smalley *Chem. Phys. Lett.* **152** 347 (1988)
33. G Gantefor, K H Meiwes-Broer, H O Lutz *Phys. Rev. A, Gen. Phys., Ser. 3* **37** 2716 (1988)
34. G Gantefor, M Gausa, K H Meiwes-Broer, H O Lutz *Z. Phys. D* **9** 253 (1988)
35. Z Fu, W Lemize, G Bishea, M D Morse *J. Chem. Phys.* **93** 8420 (1990)
36. F L King, M M Ross *Chem. Phys. Lett.* **164** 131 (1989)
37. W A Saunders, P Fayet, L Woste *Phys. Rev. A, Gen. Phys., Ser. 3* **39** 4400 (1989)
38. Y Saito, I Katahuse, H Ito *Chem. Phys. Lett.* **161** 332 (1989)
39. M F Jarrold, U Ray, E Bower, K M Greegan *J. Chem. Soc., Faraday Trans.* **86** 2537 (1990)
40. A Nakajuma, T Kishi, T Suqioha, Y Sono, K Haya *Chem. Phys. Lett.* **177** 297 (1991)
41. D M Cox, D J Trevor, R L Wetten, E A Rohlfing, A Kalder *J. Chem. Phys.* **84** 4651 (1986)
42. J A Howard, R Suteliffe, J S Tse, H Dahman, B M Le *J. Phys. Chem.* **89** 3595 (1985)
43. M A Douglas, R H Hauge, J L Margrave *J. Phys. Chem.* **87** 2945 (1983)
44. A J Stone *Inorg. Chem.* **20** 563 (1981)
45. W A DeHeer, P Milani, A Chatelain *Phys. Rev. Lett.* **63** 2834 (1989)
46. M P Iniguez, M J Lopez, J A Alonso, J M Soler *Z. Phys. D* **11** 163 (1989)
47. C W Bauschlicher, D S Liskow, C F Bender, H F Schaefer *J. Chem. Phys.* **62** 4815 (1975)
48. K D Jordan *J. Chem. Phys.* **72** 2889 (1980)

49. G Pacchioni, D Plavsic, J Koutecky *Ber. Bunsenges. Phys. Chem.* **87** 503 (1983)
50. L G Petterson, C W Bauschlicher *J. Chem. Phys.* **84** 2226 (1986)
51. J Rubio, F Illas, J M Ricart *J. Chem. Phys.* **84** 3311 (1986)
52. R J Harrison, N C Handy *Chem. Phys. Lett.* **123** 321 (1986)
53. C M Rohlfing, J S Binhley *Chem. Phys. Lett.* **139** 7771 (1987)
54. B K Rao, S N Khanna, P Jena *Physics and Chemistry of Small Clusters. NATO ASI, Ser. B, Physics* **158** 369 (1987)
55. M M Marino, W C Ermler *J. Chem. Phys.* **86** 6283 (1987)
56. T J Lee, A P Rendell *J. Chem. Phys.* **92** 489 (1990)
57. T J Lee, A P Rendell, P R Taylor *J. Chem. Phys.* **92** 7050 (1990)
58. R B Ross, W C Ermler, R M Pitzer, C W Kern *Chem. Phys. Lett.* **134** 115 (1987)
59. R B Ross, W C Ermler, R M Pitzer, N W Wintez *J. Chem. Phys.* **94** 7771 (1990)
60. R A Chiles, C T Duksta *J. Chem. Phys.* **75** 1044 (1981)
61. C W Bauschlicher, P S Bagus, B N Cox *J. Chem. Phys.* **77** 4032 (1982)
62. G Durand *J. Chem. Phys.* **91** 6225 (1989)
63. F Reuse, S N Khanna, V DeCoulon, T Buttet *Phys. Rev. B, Solid State, Ser. 3* **39** 12911 (1988)
64. F Reuse, S N Khanna, V DeCoulon, T Buttet *Phys. Rev. B, Solid State, Ser. 3* **41** 11743 (1990)
65. V Kumeir, R Car *Z. Phys. D* **19** 177 (1991)
66. P Delay, P Ballone, F Reuse, V DeCoulon, J Butter *Z. Phys. D* **19** 173 (1991)
67. P Jena, S N Khanna, B K Rao *Chem. Phys. Lett.* **171** 439 (1990)
68. G Durand, J P Daudey, J P Malrieu *J. Phys.* **47** 1335 (1986)
69. G Durand, J P Daudey, J P Malrieu *Theor. Chim. Acta* **74** 299 (1988)
70. M P Iniquez, J A Alonso, M A Aller, L C Balbas *Phys. Rev. B, Solid State, Ser. 3* **34** 2152 (1986)
71. S P Walsh, C W Bauschlicher *J. Chem. Phys.* **83** 5735 (1985)
72. S R Langhoff, C W Bauschlicher *J. Chem. Phys.* **92** 1879 (1990)
73. C W Bauschlicher, J L Ketterson *J. Chem. Phys.* **87** 2198 (1987)
74. J Koutecky, G Pacchioni, G H Jenng, E C Hass *Surf. Sci.* **156** 650 (1985)
75. L G Petterson, C W Bauschlicher *J. Chem. Phys.* **87** 2205 (1987)
76. L G Petterson, C W Bauschlicher *J. Chem. Phys.* **87** 2198 (1987)
77. P R Taylor, S P Walsh, J H Patrige, S R Langhoff, C W Bauschlicher *J. Chem. Phys.* **86** 7007 (1987)
78. T H Upton *J. Chem. Phys.* **86** 7054 (1987)
79. G Paechroni, J Koutecky *Ber. Bunsenges. Phys. Chem.* **88** 242 (1984)
80. P Fantucci, G Paechroni *Chem. Phys. Lett.* **142** 85 (1987)
81. J S Tse *J. Chem. Phys.* **92** 2488 (1990)
82. J Y Yi, D J Oh, J Berhole *Chem. Phys. Lett.* **174** 461 (1990)
83. M Seide, K H Meiwes-Broer, M Brack *J. Chem. Phys.* **95** 1295 (1991)
84. G V Gadnyak, Yu N Morozov *Zh. Strukt. Khim.* **30** 48 (1989)
85. P Fantucci, G Paechroni *Phys. Status Solidi B* **153** 193 (1989)
86. H J Nolte, K Jug *J. Chem. Phys.* **93** 2584 (1990)
87. T Halicioglu, H O Pamuk *Surf. Sci.* **215** 272 (1989)
88. J D Kress, M S Stare, A E DePristo *J. Phys. Chem.* **93** 1556 (1989)
89. M F Jarrold, J E Bower *J. Chem. Phys.* **85** 5373 (1986)
90. L Hanley, S L Anderson *Chem. Phys. Lett.* **129** 429 (1986)
91. D M Cox, D J Trevor, R L Wetten, A Kaldor *J. Phys. Chem.* **92** 421 (1988)
92. S A Ruatta, L Hanley, S L Anderson *Chem. Phys. Lett.* **137** 5 (1987)
93. A W Castleman, A C Harms, R E Leuchtner *J. Chem. Phys.* **91** 2753 (1989)
94. A W Castleman, A C Harms, R E Leuchtner *Z. Phys. D* **19** 343 (1991)
95. R E Leuchtner, A C Harms, A W Castleman *J. Chem. Phys.* **94** 1093 (1991)
96. J Robles, M P Iniquez, J A Alonso, A Mananes *Z. Phys. D* **13** 269 (1989)
97. T H Upton *Phys. Rev. Lett.* **56** 2168 (1986)
98. T G Dietz, M A Dunian, D E Powers, R E Smalkey *J. Chem. Phys.* **74** 6511 (1981)
99. C A Nicolaides, P Valtazanos *Chem. Phys. Lett.* **174** 489 (1990)
100. P Q Jasien, C E Dykstra *J. Am. Chem. Soc.* **105** 2089 (1983)
101. P Q Jasien, C E Dykstra *Chem. Phys. Lett.* **106** 276 (1984)
102. P Q Jasien, C E Dykstra *J. Am. Chem. Soc.* **107** 1891 (1985)
103. M M Kappes, P Kadi, M Schar, E Schumacher *Chem. Phys. Lett.* **119** 11 (1985)
104. Y Saito, T Noda *Z. Phys. D* **19** 129 (1991)
105. W Pewestorf, V Bonacic-Koutecky, J Koutecky *J. Chem. Phys.* **89** 5794 (1988)
106. B K Rao, S N Khanna, P Jene *Ultramicroscopy* **20** 51 (1986)
107. B K Rao, P Jene *Phys. Rev. B, Solid State, Ser. 3* **37** 2867 (1988)
108. P Fantucci, W Pewestorf, V Bonacic-Koutecky, J Koutecky *J. Chem. Phys.* **91** 4229 (1989)
109. C Balandron, J A Alonso, M P Iniquez *J. Phys. F* **17** 197 (1987)
110. C Balandron, J A Alonso *Phys. Lett. A* **140** 67 (1989)
111. A Nakajima, T Hishi, T Suqioha, K Haya *Chem. Phys. Lett.* **187** 239 (1991)
112. S E Khan, P G Edwards, H S Yuan, R Bosh *J. Am. Chem. Soc.* **107** 1682 (1985)
113. S P Walsh, J H Patrige, S R Langhoff, C W Bauschlicher *J. Chem. Phys.* **86** 5603 (1987)
114. S Nonose, Y Sone, K Onodera, S Sudo, K Kaya *Chem. Phys. Lett.* **164** 427 (1989)
115. S Nonose, Y Sone, K Kaya *Z. Phys. D* **19** 357 (1991)
116. W J Menezes, M B Knichelbein *Chem. Phys. Lett.* **183** 357 (1991)
117. A Kaldor, D M Cox, D J Trevor, M R Zahin *Z. Phys. D* **3** 195 (1986)
118. A C Harms, R E Leuchtner, S W Sigsworth, A W Castleman *J. Am. Chem. Soc.* **112** 5673 (1990)
119. B O'Brien, Y Lin, O L Zhang, J R Heuth, F K Titel, R F Curl *J. Chem. Phys.* **84** 4074 (1986)
120. L Knight, J L Petty *J. Chem. Phys.* **88** 481 (1988)
121. K Balasubramanian *J. Mol. Struct.* **139** 405 (1990)
122. K Balasubramanian *Chem. Phys. Lett.* **150** 71 (1988)
123. K Balasubramanian *Chem. Phys. Lett.* **171** 58 (1990)
124. K J Klabunde, A Whetten *J. Am. Chem. Soc.* **108** 6529 (1986)
125. Y Imizu, K J Klabunde *Inorg. Chem.* **23** 3602 (1984)
126. J H B Chenier, J A Howard, J S Fse, B Mile *J. Am. Chem. Soc.* **107** 7290 (1985)
127. M Histed, J A Howard, H Morris, B Mile *J. Am. Chem. Soc.* **110** 5290 (1988)
128. P H Kasai *J. Am. Chem. Soc.* **104** 1165 (1982)
129. K J Klabunde, T O Murdock *J. Org. Chem.* **44** 3901 (1979)
130. J A Howard, H A Joly, B Mile *J. Am. Chem. Soc.* **111** 8094 (1989)
131. K J Klabunde *J. Am. Chem. Soc.* **108** 7103 (1986)
132. G A Olah *J. Am. Chem. Soc.* **110** 3231 (1988)
133. P S Scell, J E Girard *J. Am. Chem. Soc.* **94** 5518 (1972)
134. G B Sergeev, V V Smirnov, F Z Badaev *J. Organomet. Chem.* **224** 129 (1982)
135. V V Zagorskii, V V Smirnov, G B Sergeev, A M Kosolapov *Dokl. Akad. Nauk SSSR* **256** 1169 (1981)
136. B S Ault *J. Am. Chem. Soc.* **102** 3480 (1980)
137. G B Sergeev, V V Smirnov, V V Zagorsky *J. Organomet. Chem.* **201** 9 (1980)
138. G B Sergeev, V V Smirnov, F Z Badaev, V V Zagorskii, in *Sovremennye Metody YaMR i EPR v Khimii Tverdogo Tela* (Modern Methods of NMR- and EPR-spectroscopy in the Chemistry of Solids) (Chernogolovka, 1982) Vol. 2, p. 159
139. K J Klabunde, in *Chemistry of Free Atoms and Particles* (New York: Academic Press, 1980) p. 380
140. K J Klabunde, A Whetten *J. Am. Chem. Soc.* **108** 6529 (1986)
141. G R Pearson, in *The Rules of Symmetry in Chemical Reactions* (Translated into Russian; Moscow: Mir, 1979) p. 80
142. S R Davis *J. Am. Chem. Soc.* **113** 4145 (1991)
143. N Shafizadeh, J Rostas, G Taieb, B Bourguignon, M Prisant *Chem. Phys.* **142** 111 (1990)
144. B Ahlrichs, M Ehrig, H Horn *Chem. Phys. Lett.* **183** 227 (1991)
145. L A Tyurina, S V Kambarova, N A Bumagin, I P Beletskaya *Metalloorg. Khim.* **3** 48 (1990)
146. V V Smirnov, L A Tyurina, in *V Vsesoyuznaya Konferentsiya po Khimii Nizkikh Temperatur* (Fifth All-Union Conference on Low Temperature Chemistry) (Moscow: Izd. Mosk. Gos. Univ., 1991) p. 120
147. S V Kambarova, L A Tyurina, V V Smirnov *Metalloorg. Khim.* **5** 1038 (1992)
148. K J Klabunde *Acc. Chem. Res.* **8** 393 (1975)

149. V V Smirnov, L A Tyurina, G B Barkovskii *Vestn. Mosk. Univ., Ser. 2: Khim. 3* **32** 464 (1991)
150. K Mochida, Y Hiraga, H Takeuchi, H Ogawa *Organometallics* **6** 2293 (1987)
151. L A Tyurina, G B Barkovskii, in *V Vsesoyuznaya Konferentsiya po Khimii Nizkikh Temperatur* (Fifth All-Union Conference on Low Temperature Chemistry) (Moscow: Izd. Mosk. Gos. Univ., 1991) p. 122
152. I P Beletskaya, G A Artamkina, O A Reutov *Usp. Khim.* **45** 661 (1976) [*Russ. Chem. Rev.* **45** 336 (1976)]
153. I G Tarkhanova, L A Tyurina, V V Smirnov, in *V Vsesoyuznaya Konferentsiya po Khimii Nizkikh Temperatur* (Fifth All-Union Conference on Low Temperature Chemistry) (Moscow: Izd. Mosk. Gos. Univ., 1991) p. 124
154. D M Wood, N V Ashcraft *Phys. Rev. B, Solid State, Ser. 3* **25** 6255 (1982)
155. F Cocchini, F Bassani, M Bourg *Surf. Sci.* **156** 851 (1985)
156. W Ekardt *Phys. Rev. B, Solid State, Ser. 3* **31** 6360 (1985)
157. Vo-Van Truong *P. Courteau* **62** 4863 (1987)
158. G L Carr, R L Henry, N E Russel, J C Garland, D B Tanner *Phys. Rev. B, Solid State, Ser. 3* **24** 777 (1981)
159. R P Devaty, A J Sievers *Phys. Rev. Lett.* **52** 1344 (1984)
160. H Abe, K P Charle, B Tesche, W Schulze *J. Chem. Phys.* **68** 137 (1982)
161. N Wada *Jpn. J. App. Phys.* **7** 1287 (1968)
162. K Kimura *Bull. Chem. Soc. Jpn.* **60** 3093 (1987)
163. S Yatsuya, K Yamauchi, T Hamakuna, Y Yanagida, H Wahayama, K Mihama *Surf. Sci.* **156** 1011 (1985)
164. K J Klabunde, H F Efner, L Satch, W Donley *J. Organomet. Chem.* **71** 309 (1974)
165. K Mochida, S Ogura, T Yamanishi *Bull. Chem. Soc. Jpn.* **59** 2633 (1986)
166. H Imamura, M Kawamiga, S Tsuchiya *J. Less-Common Met.* **95** 157 (1983)
167. H Imamura, T Nobunaga, M Kawamiga, S Tsuchiya *Inorg. Chem.* **23** 2509 (1984)
168. M Moskovits, G Ozin (Eds) *Cryochemistry* (New York: Wiley-Interscience, 1976)
169. H Imamura, Y Murata, S Tsuchiya *J. Less-Common Met.* **123** 59 (1986)
170. H Imamura, Y Murata, S Tsuchiya *J. Less-Common Met.* **135** 277 (1987)
171. N Satoh, K Kimura *Bull. Chem. Soc. Jpn.* **62** 1758 (1989)
172. K Kimura, S Bandow *Bull. Chem. Soc. Jpn.* **56** 3578 (1983)
173. K Kimura *Bull. Chem. Soc. Jpn.* **60** 3093 (1987)
174. S E Kondakov, V V Smirnov, in *V Vsesoyuznaya Konferentsiya po Khimii Nizkikh Temperatur* (Fifth All-Union Conference on Low Temperature Chemistry) (Moscow: Izd. Mosk. Gos. Univ., 1991) p. 126
175. S E Kondakov, V V Smirnov *Dokl. Akad. Nauk SSSR* **254** 320 (1991)
176. S E Kondakov, V V Smirnov, L A Tyurina *Dokl. Akad. Nauk SSSR* **325** 536 (1992)

Russian Chemical Reviews **63** (1) 71–89 (1994)
©1994 Russian Academy of Sciences and Turpion Ltd

UDC 547.953 + 547.915

Derivatives of trivalent phosphorus in the synthesis of glycerophosphatides and related phospholipids

E E Nifant'ev, D A Predvoditelev

Contents

I. Introduction	71
II. Phosphorylation of glycerol and related oligool derivatives by trivalent phosphorus reagents	71
III. Synthesis of phospholipids from glycerophosphorus acid esters and amides	75
IV. Conclusion	87

Abstract. The review is devoted to the analysis of one of the new trends in phospholipid synthesis. An attempt is made to demonstrate the likely usefulness of studies designed to establish an interdisciplinary field combining the interests and possibilities of the chemistry of lipids and the chemistry of trivalent phosphorus. The bibliography includes 218 references.

I. Introduction

Natural glycerophospholipids and their synthetic analogues, in the molecules of which phosphorus-containing functional groups have been modified, constitute a large group of compounds with a complex structure. Since many of these substances are very important for the development of physicochemical biology as well as certain modern branches of medicine and engineering, much attention is being devoted nowadays to their synthesis.[1–10]

Among other problems solved in the synthesis of glycerophospholipids and their analogues, the most difficult is that of the formation of the phosphorus-containing unit in these complex polyfunctional systems. For a long time, only pentavalent phosphorus reagents have been used in all the world research centres for the synthesis of phospholipids; we may note that a similar strategy was applied also in the synthesis of nucleic acids and certain other phosphorus-containing natural products. This situation can be accounted for by the relatively ready availability of pentavalent phosphorus-containing reagents, the knowledge of the compounds at the time, and the fact that their application in fine organic synthesis appeared evident. Nevertheless, these reagents frequently suffered from significant disadvantages. Thus they ensured only low rates of phosphorylation and exhibited a tendency to alkylate the electrolytes present in the reaction system and to undergo other side reactions. Furthermore, only a narrow range of synthetic possibilities is associated with pentavalent phosphorus-containing reagents.

In view of the foregoing, a trend has gradually arisen in the chemistry of phospholipids to change over to reagents containing trivalent phosphorus, which differ from the corresponding oxidised forms by a much higher phosphorylating capacity, better preparative results, and more extensive design possibilities. A very important factor is that specialists working actively in the chemistry of trivalent phosphorus have begun to be involved during the recent period in the study of problems in the chemistry of phospholipids of current interest. They were able to find a series of novel and fruitful solutions during a comparatively short period.

The first results of studies by methods from the chemistry of trivalent phosphorus in the synthesis of glycerophosphatides and their phosphorothioate, phosphoroselenoate, and other analogues were compiled and discussed by the authors of the present review at the beginning of the 1980s.[11,12] In the subsequent period, the interest in this problem increased sharply and a need therefore arose to return to this topic in order to survey the authors' own and literature data and to deduce the trends which have reliably arisen.

Analysis of the scientific facts published during recent years demonstrates not only quantitative but also qualitative changes in the overall series of studies being prosecuted. This factor necessitated a revision of the previous structure used in considering the available data. In the present review, we have differentiated two main problems. The first involves the phosphorylation of glycerol derivatives and related polyols using trivalent phosphorus-containing reagents. Here one may include also certain other reactions of trivalent phosphorus derivatives leading to the introduction of the phosphoryl functional group into the glycerol system. The second involves the conversion of the phosphites obtained into natural phospholipids or their analogues via reactions involving trivalent phosphorus atoms.

II. Phosphorylation of glycerol and related oligool derivatives by trivalent phosphorus reagents

The introduction of trivalent phosphorus reagents into the synthetic chemistry of lipids was initially problematical for several reasons. Thus reliable information concerning the use of phosphorous acid and other trivalent phosphorus acid derivatives for the phosphorylation of polyfunctional systems was lacking in the literature. There was also no experience in the identification and isolation of glycerophosphatides and related compounds with a complex structure. Finally, one had to be on one's guard against the ready disproportionation of asymmetric glycerophosphites similar to that occurring in studies with the simplest asymmetric phosphites.[13] In view of the foregoing, in the first stages of the investigation predominantly model systems were used, in which the necessary methodological problems were worked out. 1,2-*O*-Isopropylideneglycerol and other similar acetals were usually employed as models of this kind. A very

E E Nifant'ev, D A Predvoditelev Department of Organic Chemistry, Faculty of Chemistry, Lenin Moscow State Pedagogical University, Nesvizhskii per. 3, 119021 Moscow, Russian Federation, Tel. (7-095) 246 57 90, Fax (7-095) 248 01 62

Received 22 November 1993
Uspekhi Khimii **63** (1) 73–92 (1994); translated by A K Grzybowski

important factor is that subsequently a rational procedure was found for the conversion of these acetals,[14-16] as well as cyclic orthoesters[17] and oxazolidines,[18] into phospholipid systems.†

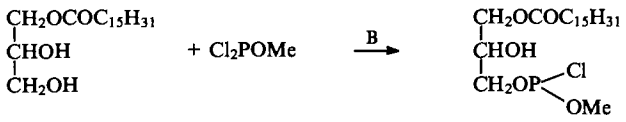
Various derivatives of tricoordinate phosphorus and hydrophosphoryl compounds were used as phosphorylating agents in the studies carried out.[21] Since each of the classes of these two types of reagents frequently exhibited significant chemical characteristic features, in the present review we have endeavoured to discuss topically the published data and to demonstrate the characteristics of the most important phosphorylating agents.

1. Phosphorylation by neutral derivatives of phosphorous acid

a. Phosphorylation by acid chlorides

In the synthesis of the simplest neutral esters of phosphorous acid, phosphorus trichloride and phosphorochloridites are usually employed as phosphorylating agents. These substances have been used also in the phospholipid synthesis. Thus diarylglycerols[22] and diacylglycerols[23-25] were treated with phosphorus trichloride to form glycerophosphorodichloridites. Unfortunately, the products of these reactions could not be isolated in a pure form and they were hydrolysed to the corresponding primary phosphites. Difficulties with isolation were noted also in the phosphorylation of diacylglycerols by 2,6-di-*tert*-butyl-4-methylphenyl phosphorodichloridite[26] and dimethyl and diphenyl phosphorochloridites.[27,28] In these cases, the primary reaction products were immediately converted by oxidation and subsequent hydrolysis (alcoholysis) into the corresponding phosphates. Unfortunately we must note that the use of phosphorochloridites for the synthesis of complex lipid systems has not always been carried out using well-founded schemes and in a number of instances was not accompanied by the demonstration of the structure. Thus the interaction of α-monopalmitoylglycerol with methyl phosphorodichloridite has been described.[27] The authors specify the mode of monophosphorylation, involving the formation of an alcohol-acid chloride (Scheme 1).

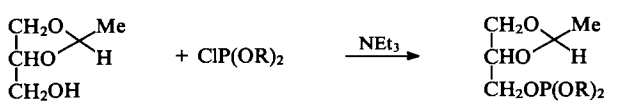
Scheme 1



It is most likely that such a product should either cyclise with formation of a 1,3,2-dioxaphosphorinane or should be converted into an oligophosphite. Therefore the probability that the above acid chloride exists for any [significant] period and then phosphorylates an extraneous nucleophile, as claimed by the authors,[27] is low.

More definite results were achieved using phosphoromonochloridites. The first investigation on these lines was carried out by Arbuzov and Yarmukhametova,[29] who synthesised dialkyl glycerophosphites from 1,2- and 1,3-*O*-ethyleneglycerols and dialkyl phosphorochloridites (Scheme 2).

Scheme 2



It was subsequently shown that phosphorylation yields better results when phosphoramidochloridites[30-37] as well as the readily available and experimentally more convenient cyclic acid chlorides—alkylene phosphorochloridites,[38-51] alkylene phosphoramidochloridites,[52-54] alkylene phosphorodiamidous chlorides,[54] and salicyl phosphorochloridites[55]—are employed. In this case, it was possible to obtain in satisfactory yields a series of neutral phosphites and phosphoramidites of the acetal and diacyl derivatives of glycerol[38-50,52-55] and thioglycerol.[51]

There are literature data concerning the analogous syntheses of phospholipids from etriol [2-hydroxymethyl-2-ethylpropane-1,3-diol (Translator)],[56] pentaerythritol,[57] ascorbic acid,[58] glycols,[59-61] higher aliphatic alcohols,[62-65] sphingophospholipids,[66-68] and fragments of lipid A.[69]

The use of phosphorus trichloride and phosphorochloridites in fine organic synthesis is not always justified. When complex lipid systems are synthesised, the application of reagents the use of which involves the evolution of hydrogen chloride is risky, because in this case there is a possibility of isomerisation, degradation of labile bonds, and other unfavourable processes. Furthermore, certain phosphorochloridites, for example those containing benzyl groups, exhibit a tendency to undergo rearrangements; the employment of such reagents may lead to explosions.[70] In view of the foregoing, a trend has recently arisen to employ mild phosphorylating agents in the synthesis of polyfunctional phosphorus-containing natural products, including phospholipids.

b. Phosphorylation by esters

The first experiments on this problem were carried out with model phosphorylating agents—phosphinous acid esters containing only one phosphorylating functional group. It was established that phosphinites are readily and effectively transesterified by 1,2- and 1,3-alkylideneglycerols.[71] Subsequently triphenyl[72] and triethyl phosphites[14-16,73,75] were transesterified.

Scheme 3



R = $C_{17}H_{35}$.

Phosphorylation by triethyl phosphite has been used for 1,2-diacylglycerols (Scheme 3).[74]

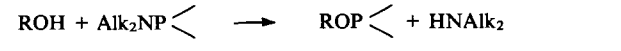
Transesterification has been used also for the synthesis of the phosphites of certain other polyols (see, for example, Petrov et al.[72]).

The transesterification method is also milder compared with the acid chloride method, but it too suffers from preparative disadvantages. Thus, in studies with partially acylated oligools, this procedure may be accompanied by side migrations, for example acyl migrations, owing to the high temperature of the main reaction. Investigators have therefore concentrated attention on the search for new phosphorylation procedures. The optimum procedure of this kind is examined below.

c. Phosphorylation by amides and amidoesters

Amides and amidoesters proved to be especially mild and convenient to use. Their employment ensured the maximum specificity and effectiveness of the phosphorylation reaction. We may also note that, when phosphoramides are used, amines are formed apart from the target esters. The amines can be readily evacuated from the reaction mixture and do not degrade the starting materials and reaction products (Scheme 4).[13]

Scheme 4

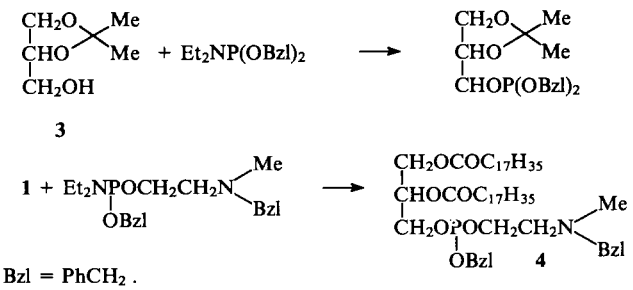


† In naming the phospholipids, we have employed, with some simplifications, the rules formulated by the IUPAC-IUB Commission on Chemical Nomenclature.[19,20]

We should draw attention to yet another factor. It has been shown that the rate of phosphorylation of nucleophiles by phosphorous acid amides can be regulated by catalysts. It has been proposed that amine hydrochlorides,[76,77] salts of dialkyldithiocarbamic acids,[78,79] and weak acids, for example tetrazole,[25,28,30–32,34–37,66–68,80–82] be used as catalysts of this kind. It has been stated that small amounts of added iodine have an activating effect in the phosphorylation reaction;[83–85] apparently hydrogen iodide and then its ammonium salts, which are in fact the catalysts, appear in the reaction mixture in such experiments.

Phosphoramides are used nowadays in syntheses of various lipid systems. Thus it has been suggested that phosphorous monoamides be used for the phosphorylation of glycerol acetals[26,74,86,87] and the corresponding esters[25,26,46,74,80,87] (Scheme 5).

Scheme 5

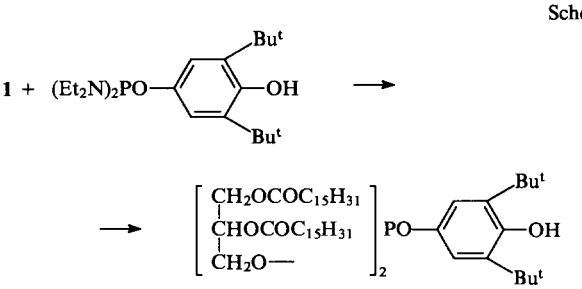


Bzl = $PhCH_2$.

The amides of cyclic phosphites and phosphoramidites are especially convenient to use and are promising for further reactions. A series of reactions with the amino-derivatives of phospholans,[88,89] phosphorinanes,[43,45,90] and phosphepans,[91,92] as well as oxazaphospholans[93–96] and oxazaphosphorinanes[52] have now been investigated.

Phosphorous diamides are even more widely used and it has been suggested that phosphomonoglycerides[26,74,86,87,97–102] and phosphodiglycerides[26,87] be obtained from them. We shall illustrate the latter possibility by the synthesis of a compound the structure of which includes a sterically hindered phenol fragment (Scheme 6).[26]

Scheme 6



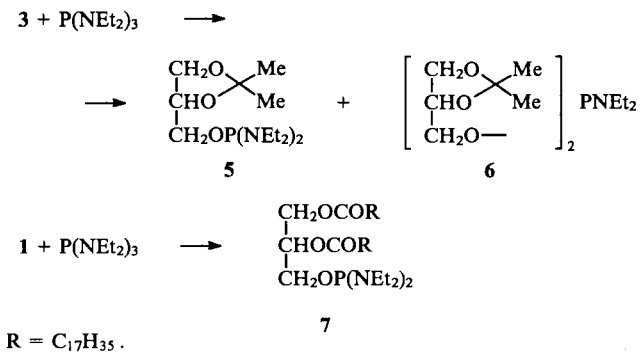
R = $C_{15}H_{31}$.

These and other similar compounds can be built into biological membranes and can protect the latter from homolytic oxidation.[103]

It has been suggested that phosphorous acid triamides be also employed as phosphorylating agents. Depending on the reactant ratio, it is possible to obtain in this case mono- or diglycerophosphoramidites (Scheme 7).[74,85,88,94,95,104,105]

In the course of the study of the phosphoramide method for the phosphorylation of diacylglycerols, fears arose concerning the possibility of acyl migrations. Indeed, as a strong nucleophile, the secondary amine produced should at least partially add to the carbonyl groups of the esters, which generally speaking can lead to rearrangements. Experimental data have confirmed the validity of such fears: in some

Scheme 7



R = $C_{17}H_{35}$.

experiments with 1,2- and 1,3-diacylglycerols isomerisations involving up to 10% of the starting materials were observed. Taking into account the foregoing considerations concerning the possible nature of the migrations, a study involving the search for optimum phosphorylation conditions was undertaken and it was observed that phosphorylation in a low vacuum (300 torr) makes it possible to achieve the timely evacuation of the amine produced and to protect the acylglycerol system against side reactions.[107]

Phosphorous acid amides have been used successfully in the synthesis of nonglycerol phospholipids—derivatives of ascorbic acid,[108] 1,1,1-tri(hydroxymethyl)alkanes,[18,56] pentaerythritol,[17,57,109] glycols,[78,79,83,110] fragments of lipid A,[69] and ceramide.[68,81,82]

The phosphoramidites and phosphorodiamidites of oligools have attracted attention not only in connection with their ready availability but also because they are convenient to use. They are optimum intermediates for the synthesis of a wide range of phospholipids, because they effectively phosphorylate the nucleophiles forming part of phospholipid systems—the choline, aminoalkyl, carbohydrate, acylglycerol, aminoacid, and other important synthons. This aspect of the problem will be considered below.

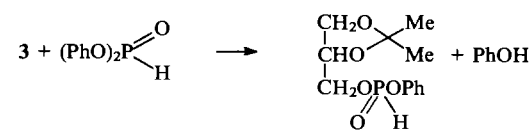
In conclusion of this section we shall deal with the problems of the stability of glycerophosphites and also with certain features of the experiments involving them. Depending on the molecular mass and nature of the glycerophosphites formed, the latter can be isolated by vacuum (high vacuum) distillation or chromatographically. However, in most cases this is superfluous. Bearing in mind the high phosphorylating capacities of trivalent phosphorus derivatives, the mild conditions, and hence the high effectiveness of the processes considered, it is useful to introduce glycerophosphites immediately into subsequent reactions without isolating them. An important preparative feature of glycerophosphites is noteworthy. In contrast to simple symmetric derivatives of phosphorous acid,[13] these compounds are thermally stable, i.e. are only poorly symmetrised on heating.

2. Phosphorylation by acid derivatives of phosphorous acid

a. Phosphorylation by diesters and diamides

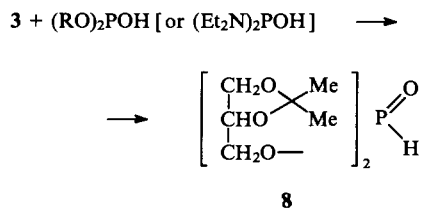
The possibility, in principle, of using the transesterification method for the synthesis of symmetrical and asymmetric disubstituted phosphites containing glycerol fragments in their structure has been demonstrated in the literature. Thus phenyl glycerophosphite has been synthesised from 1,2-*O*-isopropylideneglycerol **3** and diphenyl phosphite (Scheme 8).[72]

Scheme 8



Isopropylidenemetriol reacts similarly with diphenyl phosphite.[72] Subsequently the reaction was extended to aliphatic phosphites. The complete transesterification of dimethyl(ethyl) phosphite with 1,2-*O*-isopropylideneglycerol may serve as an example of the synthesis of symmetrical diglycerophosphites.[45,75,111,112] It was shown that the transesterification is accelerated by orthotitanic acid derivatives (Scheme 9).[112]

Scheme 9



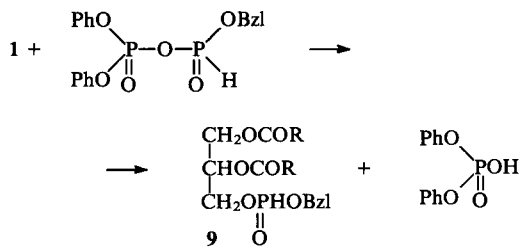
8

A similar result was obtained when phosphorus tetraethyldiamide was used.[111] Owing to the presence of two chiral centres and a pseudochiral centre in the molecule, the ^{31}P NMR spectra of diglycerophosphite **8** are relatively complex. It is noteworthy that the above compound was the first among hydrophosphoryl products in the molecules of which a pseudochiral phosphorus atom was detected.[75]

b. Phosphorylation by phosphorous acid monoesters

A promising method of synthesis of complex disubstituted phosphorous acid esters is based on the use of primary phosphites. The idea of this method is as follows. Primary phosphite salts, which are readily available and are convenient to use, are treated with strong electrophiles, usually the halides of organoelement and carboxylic acids. The alkyl phosphites are activated as phosphorylating agents as a result of the formation of mixed anhydrides. On contact with alcohols, the latter afford secondary phosphites. The practical application of the chlorides of organoelement acids was initiated by Corby et al. in relation to diphenyl phosphorochloridite.[113] This version of the phosphorylation method has been used in the chemistry of natural products, including lipids. As an illustration, we present the following example which resulted in the formation of benzyl 1,2-diacylglycerophosphite **9** (Scheme 10).[114–117]

Scheme 10



The application of carboxylic acid chlorides for the activation of monoalkyl phosphites has been proposed by Rogovin and the authors of the present review.[118,119] This version is apparently especially interesting for the chemistry of natural products.‡ It has already proved very useful in the synthesis of phosphorylated cellulose,[118,119] nucleic acids,[120–122] and sugar glycosyl phosphates.[123] At the present time, the above approach is one of the procedures in the chemistry of phospholipids for the phosphorylation of glycerols by primary phosphites of different nature and for the phosphorylation of the constituents of complex phospholipids by glycerophosphites (see Section III).

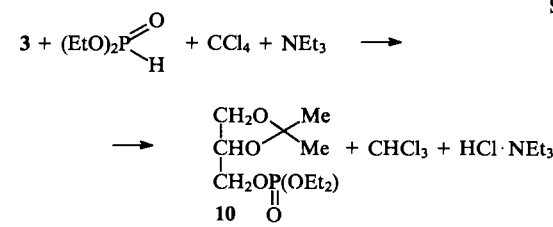
‡ This method is sometimes referred to in the literature, not entirely accurately, as the 'H-phosphonate' method. A more accurate term may be the 'hydrophosphoryl' method.

3. The use of trivalent phosphorus reagents for the oxidative introduction of phosphorus into the glycerol and related oligool systems

The direct phosphorylation reactions described above do not exhaust all the possibilities for the employment of trivalent phosphorus reagents in the synthesis of phosphoglycerol structures. Together with these reactions, studies have also been made on oxidation processes based on the use of phosphorous acid diesters and triesters, which made it possible to obtain glycerophosphates, glycerophosphorothiolates, and glycerophosphonates by a simple procedure.

The Todd–Atherton reaction is of great synthetic importance.[124] It has been studied in detail in relation to the phosphorylation of 1,2-*O*-isopropylideneglycerol **3** and 1,3-*O*-benzylideneglycerol by diethyl(methyl) phosphites in the presence of carbon tetrachloride.[14,15,74] As an example, we present the synthesis of diethyl 1,2-isopropylideneglycerophosphate **10** (Scheme 11).

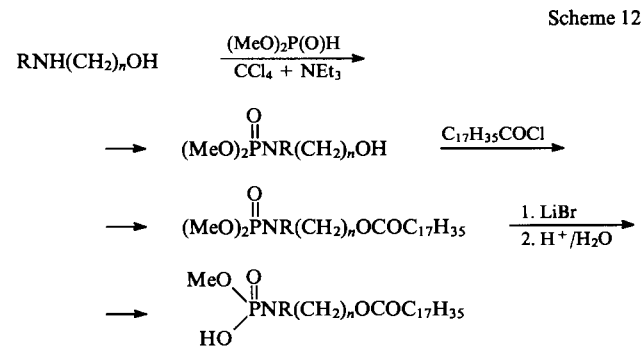
Scheme 11



The process is based on the use of readily available starting compounds, is carried out under mild conditions, and gives rise to high yields of the target products. In considering the Todd–Atherton reaction, one should bear in mind its extensive synthetic possibilities. We may point out that, in the oxidative phosphorylation of glyceroacetals and diacylglycerols, good results have been obtained not only with aliphatic but also with aromatic phosphites.[14] Furthermore, alkylene phosphites,[45] alkylene phosphorothioites,[40] and alkylene phosphoramidites[125] have been used in preparative practice. On the other hand, instead of glycerol derivatives it is possible to employ glycols and obtain diol phospholipids and their diphosphorus analogues.[56–61,126]

Important results have been achieved also in the phosphorylation of primary and secondary aminoalcohols.[127] This reaction made it possible to put forward a new strategy for the synthesis of the important, although nowadays little investigated, class of phospholipids (Scheme 12).

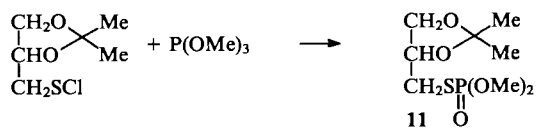
Scheme 12



n = 2, 3; R = H, Me.

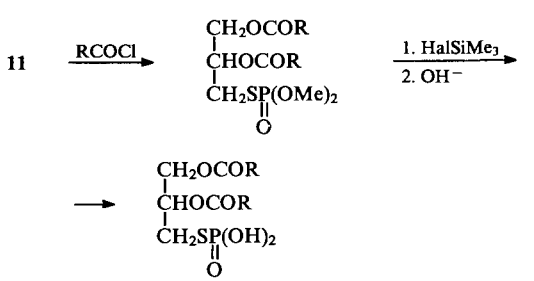
An elegant synthesis of lipids otherwise difficult to obtain, for example dimethyl 1,2-isopropylidenethioglycerophosphorothiolate **11**, has been described by Mlotkovska and Markovska,[128-130] who resorted to the reactions of sulfonyl chlorides derived from glycerol with neutral phosphites (Scheme 13).

Scheme 13



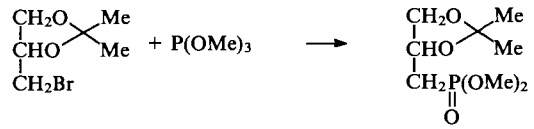
Analogues of natural phosphoglycerols can be readily obtained from such phosphoacetals.[14-16] In the molecules of phosphoglycerols, the glycerol residue is joined to the phosphorus atom via a labile thiol 'inset', which is of great interest for enzymological research for example (Scheme 14).[128]

Scheme 14



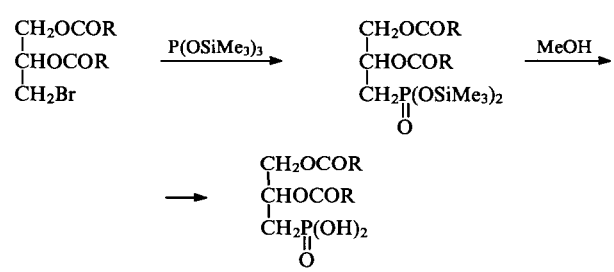
It has been suggested that the novel systems in the molecules of which the deoxyglycerol fragment is joined directly to the phosphorus atom be synthesised via the Arbuzov reaction (Scheme 15).

Scheme 15



Special reviews have been published on questions concerning the use of this reaction,[5,131,132] which makes it unnecessary to quote in detail the relevant studies in the present review. We shall only note the particularly good prospects for the use of trisilyl phosphites as the phosphorous component. This version of the reaction takes place particularly readily because of the high nucleophilicity of the silyl phosphites and makes it possible to obtain in the concluding stage the phosphono-analogues of phosphatidic acids by means of simple alcoholysis (Scheme 16).[133-135]

Scheme 16



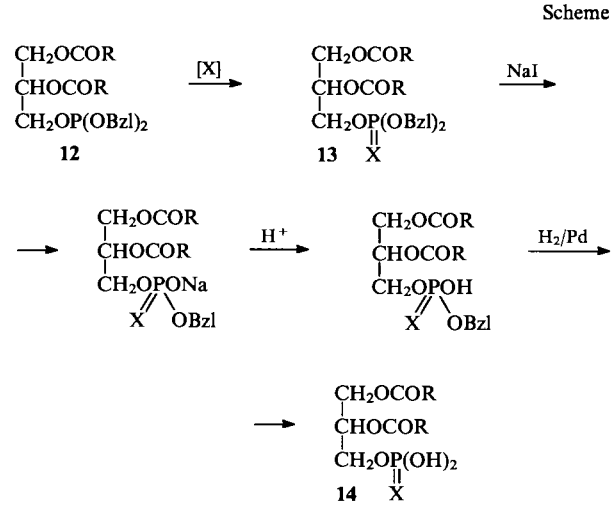
III. Synthesis of phospholipids from glycerophosphorous acid esters and amides

In this section, the literature data are discussed in three subsections. Each of them is devoted to the reactions of the most important classes of derivatives of glycerophosphorous acids which occur as key substances in lipid syntheses: neutral glycerophosphites, acid glycerophosphites, and glycerophosphoramidites. Sometimes the types of compounds considered are linked to one another by simple reactions which will be specially indicated.

1. Reactions of neutral glycerophosphites

In the first place, we shall consider the phospholipid syntheses based on neutral monoglycerophosphites.§ It has been suggested that the simplest of these compounds — acyclic esters — be used to synthesise phosphatidic acids.[74] Thus dibenzyl 1,2-diacylglycerophosphites **12** are oxidised¶ by nitrogen oxides or iodosobenzene with formation of the corresponding dibenzyl phosphates **13** (X = O), which were obtained previously via a much more complex scheme: by the reaction of the silver salts of dibenzylphosphoric acids with glycerol 1,2-diacylhalohydrins which are difficult to obtain and inconvenient to work with.[1,3,8,10] Dibenzyl phosphates **13** (X = O) are subsequently converted into the phosphatidic acids **14** (X = O). At the same time, it was shown that dibenzyl 1,2-diacylglycerophosphites **12** combine smoothly with sulfur and are converted into the phosphorothioates **13** (X = S), which are debenzylated to the thiophosphatidic acids **14** (X = S) (Scheme 17).

Scheme 17



R = $C_{15}H_{31}$, $C_{17}H_{35}$; X = O, S.

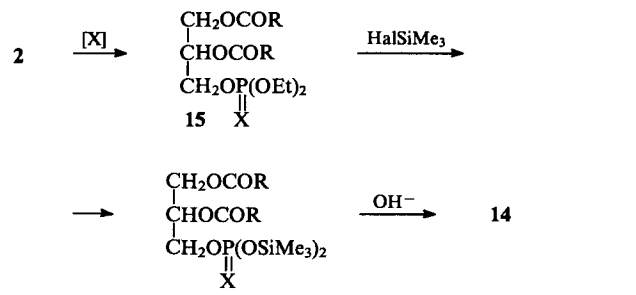
Another, apparently more promising version of the synthesis of phosphatidic acids **14** is based on the use of the glycerophosphates **2** with ethyl protecting groups in the phosphorus-containing functional group.[14-16,73] Diethyl 1,2-diacylglycerophosphites **2** are oxidised without complications to the phosphates **15** by a procedure similar to that used for the dibenzyl esters **12** already mentioned. Next the ethyl protecting groups are removed by silylation by a procedure similar to that used for the simplest phosphoric acid esters.[137-141]

§ Certain reactions of phosphoroamidites, in which only the valence state of the phosphorus atom changes, are also considered in this subsection. Subsection 3 is devoted to reactions involving the P–N bond.

¶ A method involving the selective development of trivalent phosphorus compounds in thin layer chromatography with the aid of a ninhydrin solution has been recommended for the monitoring of the oxidation reactions and also for the recognition of substances with similar R_f values.[136]

The scheme terminates with the hydrolysis of the trimethylsilyl derivatives of phosphatidic acids (Scheme 18).

Scheme 18



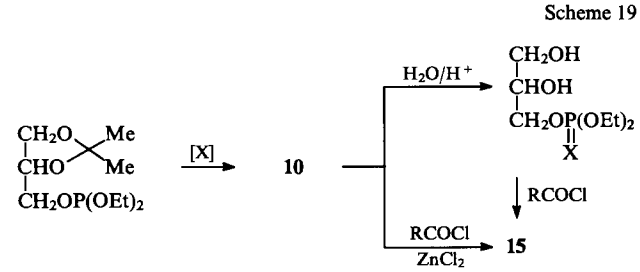
R = $C_{15}H_{31}$, $C_{17}H_{35}$; X = O, S.

The phosphatidic acids **14** have been obtained in a better yield (up to 56%) by using a solution of equimolar amounts of chlorotrimethylsilane and sodium iodide.

We may note that previously alkyl groups had already been considered for the temporary protection of acid hydroxyls in certain lipid syntheses. It was suggested that they be removed under severe conditions, for example by hydrolysis with lithium hydroxide, which involves considerable complications.[142,143] The new method—deethylation with the aid of halotrimethylsilanes—is carried out under mild conditions and ensures satisfactory yields of the lipids. It has therefore come to be widely used nowadays in many laboratories.[14-16,60,73,75,106,128,144-149]

The phosphatidic esters **15** can be obtained using diethyl (1,2-*O*-isopropylidene-3-glycero)phosphite by its oxidation or sulfurisation to phosphates (phosphorothioates) **10**, mild hydrolysis of the acetone protecting group, and acylation of the resulting phosphodiols.[14-16,73] Further progress on these lines was determined by the discovery of fundamentally new procedures for the acylation of the glycerophosphoacetals **10**, which markedly simplified the method of synthesis (Scheme 19).[14-16,73]

Scheme 19



The reaction presented in Scheme 19 (X = S) is an example of a convenient preparative method of synthesis of thiophosphatidic acids.

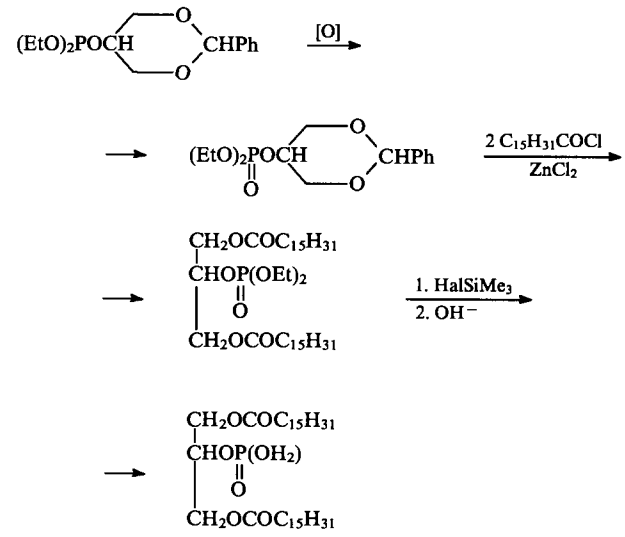
The version examined may be extended also to the synthesis of little investigated β-phosphatidic acids (Scheme 20).[14,15]

The series of studies on the acylation of 1,2- and 1,3-acetals with glycerols was completed by demonstrating the absence of acyl migrations in these decisive stages of the synthesis.[15]

The new method for the acylation of glyceroacetals probably merits extensive use. It has already been applied successfully in the synthesis of a series of ester phospholipids.[14-16,26,45,56,57,73,75,87,91,92,106,109,128,150-155]

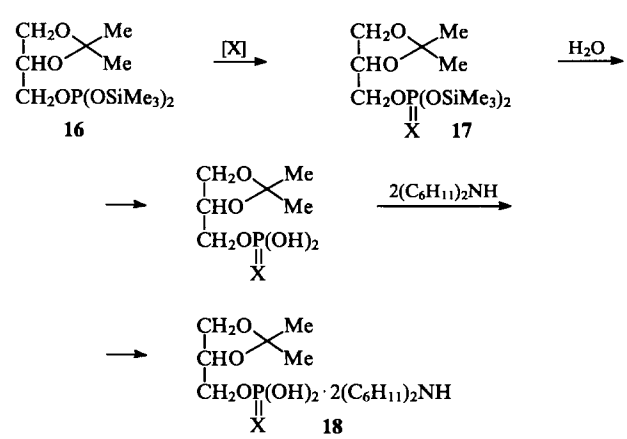
An even simpler version of the synthesis of phosphatidic acids, their thio-analogues, and also their previously unknown seleno-analogues is based on the use of the available bis(trimethylsilyl) 1,2-*O*-isopropylidene-3-glycerophosphite **16** (see below). This silyl phosphite was converted by oxidation (by the addition of oxygen, sulfur, and selenium) into the

Scheme 20



corresponding phosphates, phosphorothionates, and phosphoroselenonates **17**. Compounds **17** were isolated by high-vacuum distillation in yields up to 81%. Acid glycerophosphates and then their salts **18** were obtained by the hydrolysis of the neutral silyl esters **17** (Scheme 21).[106,156]

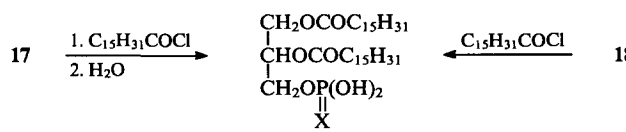
Scheme 21



X = O, S, Se.

The salts (or silyl phosphates) obtained are readily acylated and are converted ultimately into phosphatidic acids (Scheme 22).

Scheme 22



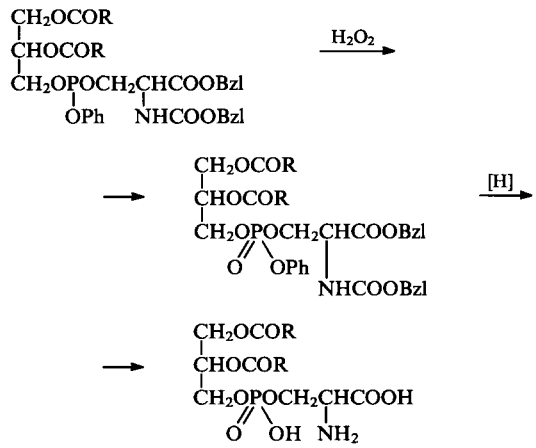
According to ^{31}P NMR data, thio- and seleno-phosphatidic acids exist in chloroform solutions in the thiono- and selenonophosphoryl forms. A similar conclusion concerning the structure of the seleno-acids was also reached from analysis of the direct $^{77}Se-^{31}P$ spin–spin coupling constants.

The method of synthesis of phosphatidic acids and their chalcogen analogues examined above was used to synthesise an optically active product—1,2-dipalmitoyl-*sn*-(3-glycero)-phosphate; in this case, the starting compound was 1,2-isopropylidene-*sn*-glycerol.[106]

The thionophosphatidic acids obtained in accordance with the schemes proposed immediately found applications in lipidology. Thus the use of a thionophosphatidic acid as a $^{31}P-\{^1H\}$ NMR probe (δ_P = 59 ppm) made it possible to investigate the polymorphic transformations of phosphatidic acids and of the phospholipid mixtures incorporating them.[157-161] Thionophosphatidic acids have also proved useful in the study of the permeability of bilayer lipid membranes in phase transitions and in the solution of other biophysical problems.[162-164] In connection with their spectroscopic characteristics, selenonophosphatidic acids (δ_P = 55 ppm) can also be used as ^{31}P NMR probes in the study of membranes. Additional information about the structure of the membranes can then be obtained by recording the satellites induced by the spin–spin splitting of the $^{31}P-^{77}Se$ signal. Selenonophosphatidic acids may be of interest as carriers which transfer selenium into biological membranes and also for the solution of other problems in physicochemical biology.[165,166]

The oxidative reactions of neutral glycerophosphites have been used in various laboratories also for the synthesis of diester phosphatides. Thus the oxidation of aminoalcohol and aminoacid glycerophosphites using hydrogen peroxide has been described (Scheme 23).[27,28]

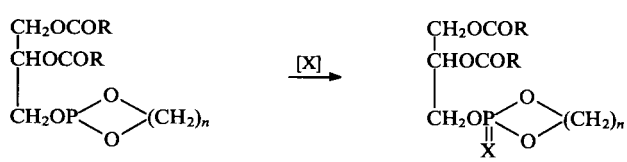
Scheme 23



As shown in the scheme presented above, the removal of the phenyl protecting group from the phosphate centre does not always yield satisfactory results. Therefore nowadays investigators usually select alternative solutions, including the formation of neutral glycerophosphites, the molecules of which contain β-cyanoethyl[60,69,167] or methyl[28,60,127] groups. After the oxidation of the phosphites to the corresponding neutral phosphates, these groups are readily and selectively removed by methods which have been thoroughly developed in the chemistry of nucleic acids.

The use of cyclic phosphites has proved particularly promising in oxidation reactions. They react smoothly and effectively with nitrogen oxide and dioxide, oxygen, ozone, iodosobenzene, sulfur, and selenium, forming cyclic phosphates, phosphorothionates, and phosphoroselenonates (Scheme 24).[41-46,47,49,51,88,150,168]

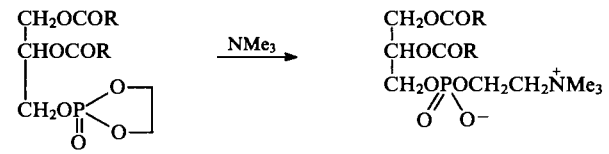
Scheme 24



n = 2, 3, 4; X = O, S, Se.

Owing to these processes, the attention of specialists in the chemistry of phospholipids has been fixed on cyclic phosphoglycerols. This trend proved to be extremely fruitful. It was established that the 1,3,2-dioxacyclanes synthesised are extremely useful alkyl donors, capable of novel reactions leading to conversion into most important classes of phospholipids. We shall illustrate the foregoing by a very simple synthesis of phosphatidylcholines (Scheme 25).[41,43,44,46,47,49,50,88,89,169,170]

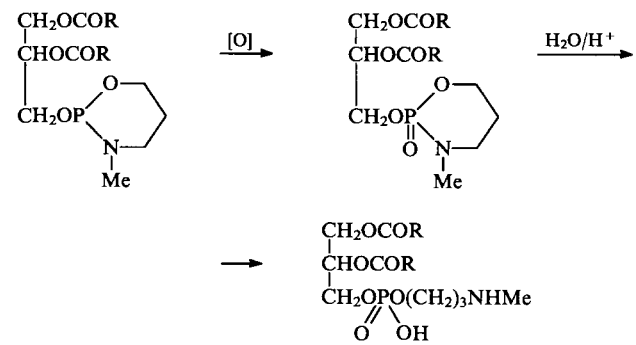
Scheme 25



Acetals can also be used in such reactions. They are converted into the required ester systems in the most convenient stages of the synthesis.[38-40,45,49,88,91,150,152-154,171,172] It is significant that alkylation has been used for the synthesis of nonglycerol phospholipids, for example diol,[59-61] etriol,[56,109] etc.[17,18,57,58,62,108,167] phospholipids.

The oxidation reactions of cyclic phosphoramidates[52,54,64,65,93,95,125,173-178] and cyclic phosphorodiamidates[54,63] have now been investigated. The phosphaza-derivatives of pentavalent phosphorus are also very promising for subsequent reactions. For example, they can be hydrolysed with formation of phosphatidylaminoalkanols, which are otherwise difficult to obtain and which are of great interest for lipidology (Scheme 26).[54,63]

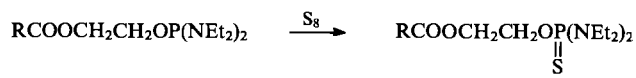
Scheme 26



The first studies on the use of cyclic phosphates and cyclic phosphoramidates in the synthesis of lipid systems were soon continued in various scientific centres and have been described in numerous publications which we shall not discuss in the present review.

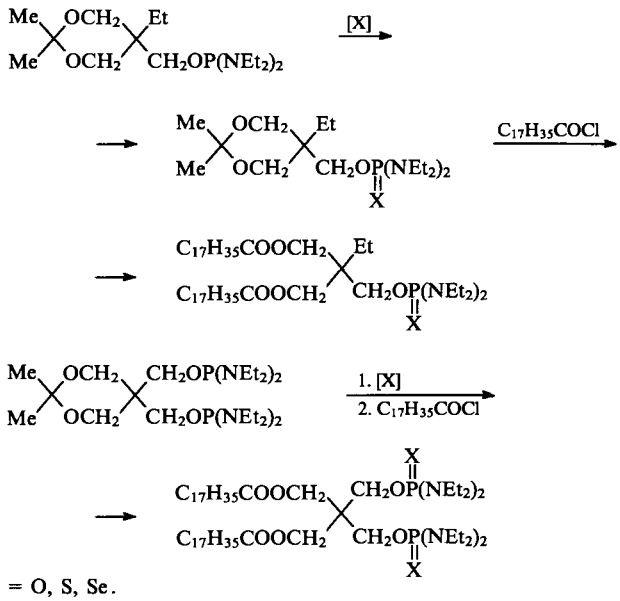
Oxidation reactions similar to those described above have been used also for the conversion of phosphites belonging to other classes of phosphorylated oligools. The phosphorodiamidites derived from monoacylglycols were sulfurised in this way (Scheme 27).[78,79,83,110]

Scheme 27



The possibilities in the use of etriol and pentaerylthritol phosphorodiamidites have been investigated in greater depth. Here is was possible to combine different new synthetic methods, for example those presented in Scheme 28.[56, 57, 109]

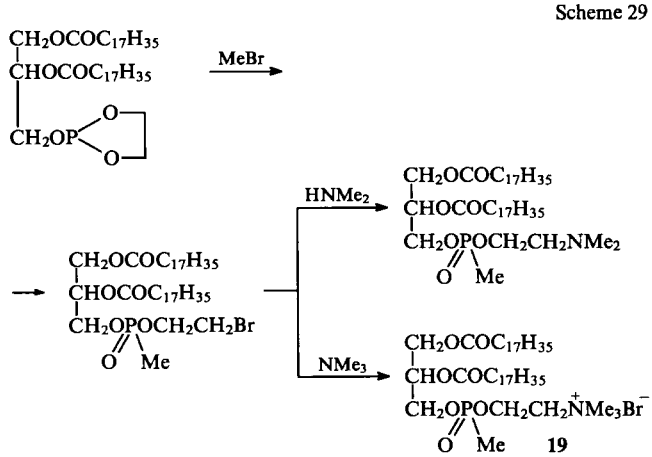
Scheme 28



X = O, S, Se.

A specific aspect of the use of cyclic glycerophosphatee is their involvement in the Arbuzov reaction. In this case, the main pathway in the process is the opening of the ring and the formation of the glycerophosphonate system. Attention should be drawn to the fact that phospholan glycerides react much more readily than phosphorinane glycerides, which can apparently be accounted for by the greater tendency of the five-membered ring to be opened in the second stage of the reaction. It has been suggested that the halo-derivatives formed initially be used for the preparation of the corresponding phosphonate analogues of phosphatidyldimethylethanolamine and phosphatidylcholine (Scheme 29).[39, 88]

Scheme 29



It is significant that, when the Arbuzov reaction is carried out, a second chiral centre—the phosphorus atom—is generated in the molecules of racemic glycerophosphonates. This results in the appearance of a mixture of two pairs of diastereoisomers, which are manifested separately in the $^{31}P-\{^{1}H\}$ NMR spectra.

It is noteworthy that a group of unique lipids **19**, having an electropositive molecular skeleton, have been obtained via the Arbuzov alkylation reaction. On the other hand, the natural products and synthetic compounds of this type obtained previously have an electronegative or neutral molecular skeleton. The lipids described are therefore of interest as carriers of biologically active compounds and also for the creation of selectively conducting membranes. For example, anion-selective channels were first detected in planar lipid bilayer membranes formed from compound **19**.[179]

For purposes of phospholipid chemistry, a study has been made of the interaction of the neutral phosphite of an important oligool (etriol) with carboxylic acid halides. Processes of this kind were investigated previously by Kabachnik, but he used trialkyl phosphites.[180] He showed that the phosphorus atom is subjected to electrophilic attack in the acylation reaction and that α-ketophosphonates are formed. It is very interesting that etriol phosphite behaves in an unusual way in the acylation reaction: electrophilic attack is directed not to the phosphorus atom but to an oxygen atom, which results in the formation of an ester with a phosphor(III)inane substituent (Scheme 30).[181]

Scheme 30

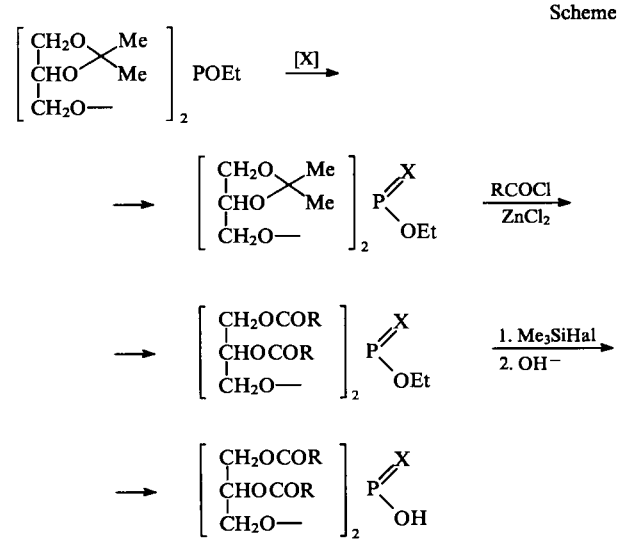


R = Me, $C_{17}H_{35}$.

Further reactions made it possible to obtain from this product unusual phospholipid compounds the molecules of which include a phosphorus-containing ring with a pentavalent phosphorus atom.

Neutral diglycerophosphites have also begun to be used for the synthesis of phospholipids. Thus a convenient method of synthesis of bisphosphatidic and previously unknown thiobisphosphatidic acids from ethyl diglycerophosphite has been developed with the aid of the fundamentally new synthetic solutions examined above [acylation of glycerol derivatives via the acetal bonds and the removal of the alkyl protecting groups by silylation and subsequent hydrolysis (Scheme 31)].[75]

Scheme 31



R = $C_{13}H_{27}$; $C_{17}H_{35}$; X = O, S; Hal = Br, Cl.

The influence of temperature and of the type of solvent on the effectiveness of the acylation of phosphobisglyceroketals and other stages of the synthesis was investigated in detail in the above study.

In the present review, we have already considered the acylation of phosphoglycerols the molecules of which contain only one glyceroketal fragment. The data illustrated by the last equation have significantly expanded the limits of the application of the new method of synthesis of ester derivatives of glycerol.

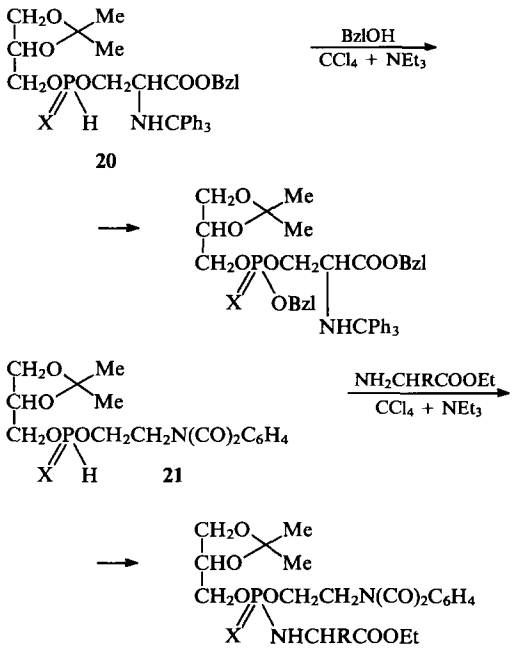
2. Reactions of acid glycerophosphites

The use of acid glycerophosphites has led to interesting prospects for phospholipid synthesis. Phosphorus as well as phosphorothious mono- and di-esters were usually assigned to this group of compounds.

Among these compounds, initially most attention was devoted to the diesters (secondary phosphites) which can be usefully subdivided into two groups—mono- and di-glyceroesters. We shall deal with these substances in the same sequence in considering their reactions.

Various types of secondary monoglycerophosphites are known at present: their molecules contain the residues of diacylglycerols, alkylglycerols, and the corresponding acetals. The structural characteristics of the systems listed above do not affect significantly their reactions, i.e. they all have the general properties of hydrophosphoryl compounds. Thus acetal systems enter widely into the Todd–Atherton oxidative phosphorylation.[124] As an example, one may quote the syntheses of lipids of different complexity: tri- and di-ester phosphoramidates based on isopropylideneglycerophosphites **20** and **21** (Scheme 32).[94,182–184]

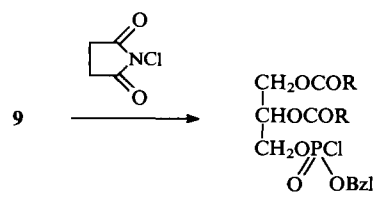
Scheme 32



R = H, Me; X = O, S.

When necessary, the Todd–Atherton reaction can be arrested in the intermediate stage involving the formation of phosphorochloridates.[104] It has been suggested that the phosphorochloridates be obtained also by chlorinating phosphites with *N*-chlorosuccinimide (Scheme 33).[114–117]

Scheme 33

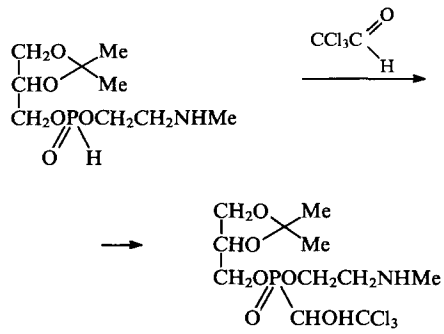


The phosphorochloridates obtained are usually employed without isolation to phosphorylate various nucleophiles, which affords, after debenzylation, phosphatidic acids, phosphatidylethanolamines, phosphatidylserines, phosphatide analogues of aminoacids phospholipids, and other important types of phospholipids.[114–117]

The oxidation reactions presented above began to be investigated also in relation to monoglycerophosphorothioites, which opens a simple path to the synthesis of neutral lipid phosphorothioates and phosphoramidothioates.[184,185]

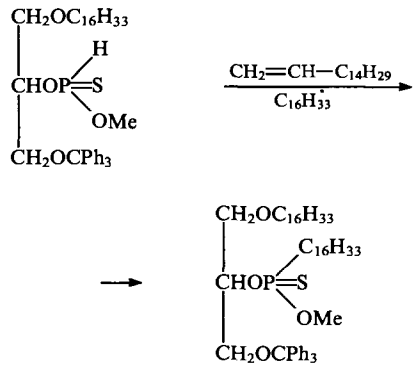
It has been suggested that α-hydroxyphosphonates be obtained from acid glycerophosphites by means of the Abramov reaction (Scheme 34).[174,186]

Scheme 34



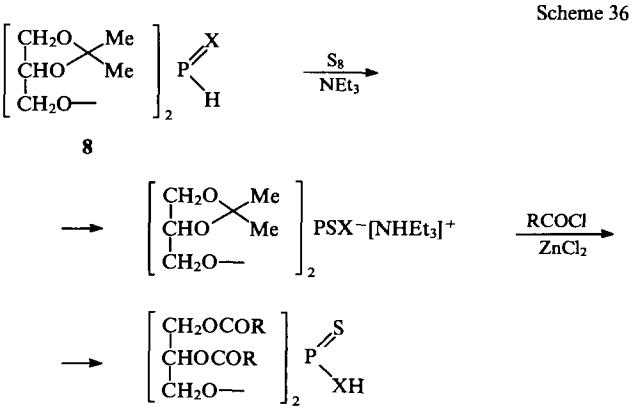
The phosphorus–carbon bond in the lipid systems can be formed also via the free-radical thiohydrophosphorylation of olefins for example (Scheme 35).[33]

Scheme 35



Secondary diglycerophosphites and their thio-analogues, represented by the 1,2-*O*-isopropylidene- and 1,3-*O*-benzylidene-derivatives, have been investigated in the Todd–Atherton oxidative phosphorylation reactions in greater detail than the monoglycerophosphites. A wide range of neutral ester diglycerophosphatides and thiophosphatides[104,111] and α- and β-bisphosphatidic acids[105] have been obtained from them. The thiophosphatides can also be obtained by direct sulfurisation (Scheme 36).[75]

Scheme 36

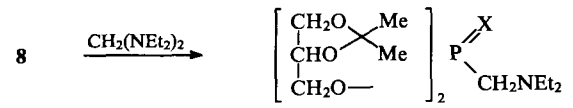


R = $C_{13}H_{27}$, $C_{17}H_{35}$; X = O, S.

Like the thio-analogues of other phospholipids, thiobisphosphatidic acids are promising substances in biochemical and biophysical research, since their resonance region in ^{31}P NMR spectroscopy is significantly different from that of natural phospholipids (δ_P = 65 and 97 ppm respectively).

The Kabachnik–Fields aminomethylation of diglycerophosphites, which makes it possible to obtain simply phospholipids belonging to the class of α-aminophosphonates and α-aminophosphonothioates, apparently merit much attention (Scheme 37).[48,104,185]

Scheme 37

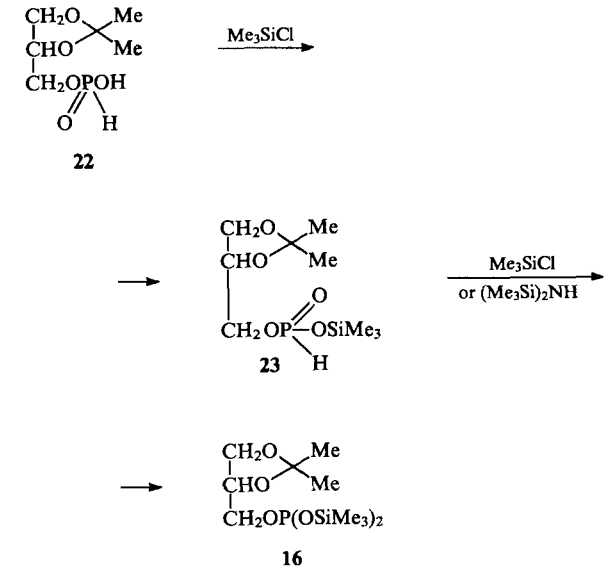


X = O, S.

The compounds obtained, which are effective chelating agents, can regulate the transport of certain metals in biological membranes. Furthermore, they can fix metals which are initiators of free-radical reactions in lipid compositions and thereby stimulate, when necessary, their oxidation and certain other reactions.

Studies on primary glycerophosphites from the standpoint of the interests of glycerophosphite chemistry are only just beginning. Nevertheless, here too important results have already been obtained and there are good prospects for the wide scale preparative application of these compounds. Thus it has been shown that 1,2-isopropylideneglycerophosphite **22** is readily converted into trimethylsilyl glycerophosphite **23** on treatment with chlorotrimethylsilane, while further silylation affords a satisfactory yield of bis(trimethylsilyl) glycerophosphites **16** (Scheme 38).[106,156]

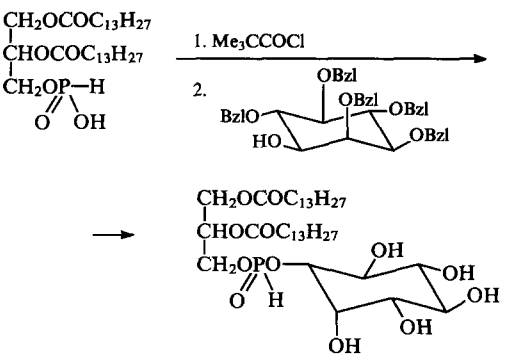
Scheme 38



As already stated in the discussion above, derivatives of tricoordinate phosphorus **16** are converted by means of simple reactions into phosphatidic acids and their thio- and seleno-analogues.

It has been suggested that primary glycerophosphites be made to react with pivaloyl chloride or other similar electrophiles to form highly reactive phosphorylating agents. The latter phosphorylate derivatives of aminoalcohols[23] and other biogenic nucleophiles,[23–25] which makes it possible to obtain rapidly valuable phosphite lipids (Scheme 39).

Scheme 39



This and similar phosphites were oxidised or were introduced into other oxidation reactions, which made it possible to obtain effectively a wide variety of phospholipids and their chalcogen analogues. We may note that similar syntheses also of other types of complex phospholipids have been achieved, for example the synthesis of sphingophospholipids — dihydrosphingomyelin and its *N,N*-dimethyl analogues from the primary phosphite of 3-benzoylceramide.[68,81]

3. Reactions of phosphoramidites

Recent years have been marked by the active employment of the phosphoramidites of glycerol (and other polyols) in phospholipid syntheses. Extensive data have accumulated in this field, their amount increasing steadily as a result of the appearance of new ones. We have already considered above certain reactions of glycerophosphoramidites, for example oxidation, the addition of sulfur, and alkylation, i.e. processes involving only the trivalent phosphorus atom and sometimes the P–O fragment. In the present subsection, attention will be concentrated on the reactions involving the dissociation of one or two P–N bonds, i.e. on the phosphorylation of nucleophiles (Scheme 40).

Scheme 40



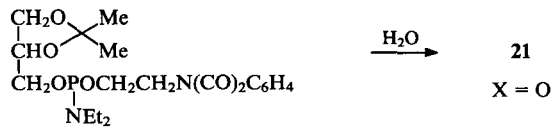
By virtue of the effectiveness and mildness of this reaction and its successful combination with the necessary 'routine' reactions (oxidation, removal of protecting groups, acylation, etc.), glycerophosphoramidites are readily converted into many complex substances, including those which are difficult to obtain by other popular methods of synthesis. We may note that the initial glycerophosphoramidites are readily available, are stable during storage, and are convenient to use. Thus they may prove to be valuable key products in the synthesis of phospholipids of different types.

The phospholipid syntheses from glycerophosphoramidites, described in the literature, have two aspects. The first of these concerns the phosphorylation of nucleophiles as a result of the selective removal of one amido-group or the successive removal of two amido-groups from the phosphorus atom. The second concerns the phosphorylation of bifunctional nucleophiles — glycols and aminoalcohols — with formation of cyclic phospha-compounds.

Natural diglycerophosphoramidites with different chemical structures can be selectively hydrolysed by cleaving only the P–N bond with the formation of the corresponding phosphites.[104,111,156]

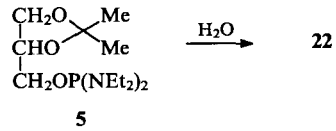
The hydrolysis of asymmetric phosphorus acid diesteramides is more complex (Scheme 41).[182–184]

Scheme 41



The diamides of glycerophosphorus acids are hydrolysed similarly. In this case, two phosphoramide bonds are cleaved and monosubstituted phosphites are formed, for example compound **11** (Scheme 42).[106, 156]

Scheme 42



5

The hydrolysis of phosphoramidites is accelerated by inorganic and organic acids and in this version is carried out without heating. This reaction is in fact the best method of synthesis of such acid phosphites.

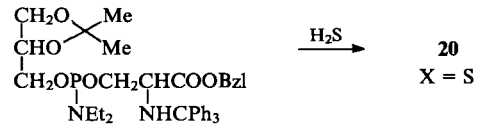
The sulfhydrolysis of glycerophosphoramides, which so far belongs to the class of little investigated reactions, also has considerable preparative prospects (Scheme 43).

Scheme 43



The cleavage of the P–N bond by treatment with hydrogen sulfide was discovered in the simplest of examples.[187, 188] Subsequently this reaction was investigated in more complex cases in our laboratory, where it was possible to introduce it into practical phospholipid syntheses.[40, 104, 184, 190] The possibilities of experiments with systems the structure of which includes acetal, ester, and trityl protecting groups were thus demonstrated (Scheme 44).[184]

Scheme 44



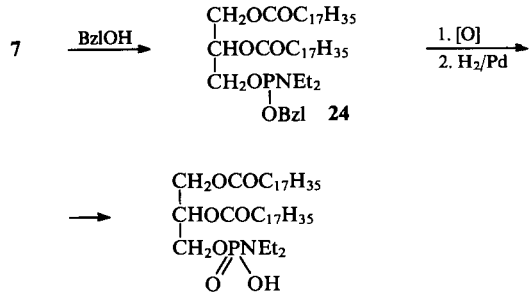
The thiohydrophosphoryl fragment in this and similar compounds exhibits a high chemical reactivity, for example in oxidative phosphorylation and in combining with sulfur.[40, 75, 104, 184, 185, 190]

Subsequently it was possible to achieve the sulfhydrolysis of phosphorous acid diamides accompanied by the cleavage of two P–N bonds, leading to the formation of phosphorodithioites which are difficult to obtain in other ways.[189] These compounds can be used to synthesise completely new types of phospholipids.

A special series of studies was devoted to the benzylolysis of glycerophosphoramidites and glycerophosphorodiamidites. These studies were mainly combined with those designed to obtain phosphatidic and other lipid acids. Thus it has been shown that the tetraethyldiamide derivative of 1,2-distearoylglycerol **7** is readily converted on treatment with two equivalents of benzyl alcohol into the neutral phosphite **12**, which is readily converted into the phosphatidic acid (see above).[74]

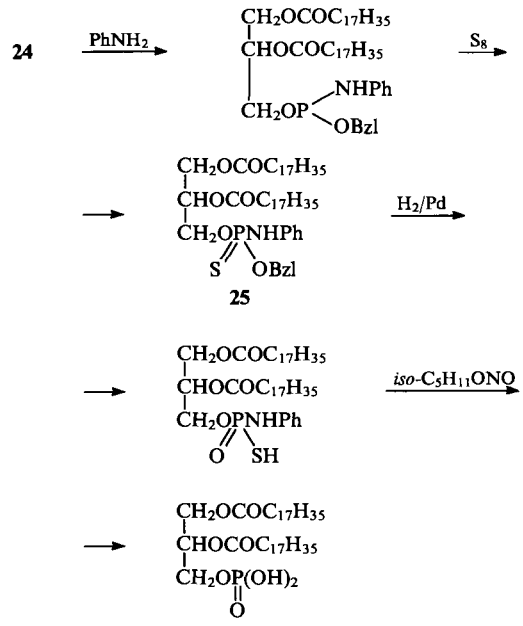
If the benzylolysis of the phosphorodiamidite **7** is carried out using an equivalent amount of alcohol, then selective monophosphorylation takes place. After oxidation and the removal of the protecting group, the product **24** was converted into an acid phosphoramidate—a representative of a rare class of phospholipids (Scheme 45).[74]

Scheme 45



Readily available and effective reagents—nitrogen(II) oxides and iodosobenzene—were used as oxidants in the schemes described above. Unfortunately they are not always convenient to use. A different way of converting glycerophosphoramidites into phosphatidic acids was therefore proposed. The idea of the synthesis consists in the fact that the benzyl glycerophosphorimidate, for example compound **24**, is transamidated with aniline† to form an anilide, which rapidly combines with sulfur, producing the neutral phosphoranilidothionate **25**. By means of a combined catalytic debenzylation and oxidative deamination, this compound is converted into a phosphatidic acid (Scheme 46).[99]

Scheme 46



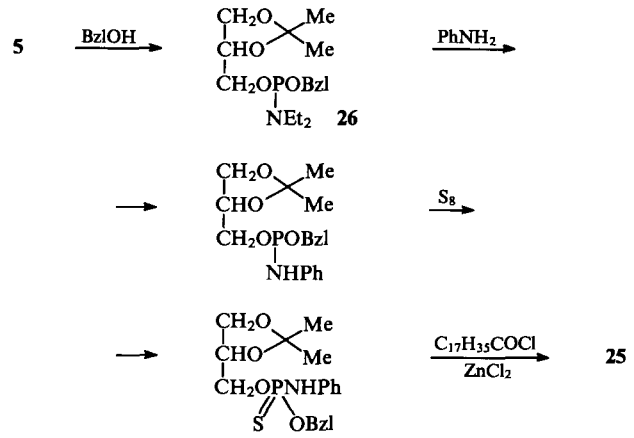
The somewhat longer synthesis in this case compared with the previous one is fully compensated by experimental convenient. It is also significant that the latter scheme affords good results when isopropylideneglycerophosphoramidites **5** are used as the starting materials (Scheme 47) (see over).[99]

Yet another factor is striking in the present instance: acylation of the acetals of the phosphorothioic derivative of glycerol is more effective than acylation of the corresponding phosphoryl product.[14, 16, 73] Thus yet another argument may be put forward in support of the second scheme.

Extremely varied and chemically significant syntheses of phospholipids consist in the stepwise interaction of glycerophosphorodiamidites with two different alcohols. The following strategy is often used in this case: instead of one of the amido-groups, an aminoalcohol, hydroxyaminoacid, substituted glycerol, carboyhydrate, or inositol residue, or one comprising

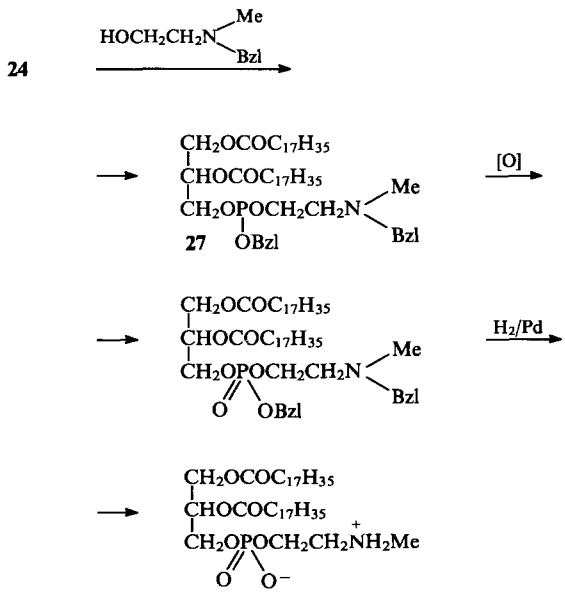
† The transamidation of the simplest phosphorous acid dialkylamides with aniline has been described.[191]

Scheme 47



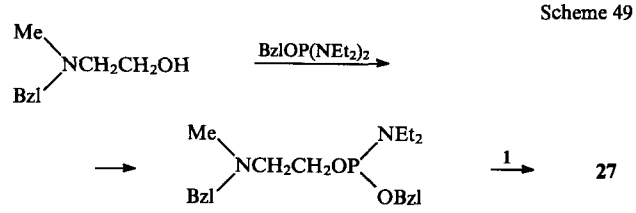
other important components of the complex natural lipids or related synthetic substances is introduced initially. Next, instead of the second amido-group, a new group protecting the hydroxyl is introduced. In many instances the opposite sequence of operations in the phosphorylation process is also employed. In some experiments primary phosphorylation of the alcohol component with subsequent condensation of the resulting phosphoromonoamidite and the glycerol derivative has been used too. All the syntheses listed above are terminated by oxidation processes, the removal of protecting groups, and, when necessary, a molecular reorganisation of the type involving the replacement of acetal fragments by ester fragments. We shall consider the most important data concerning these reactions. The use of glycerophosphoroamidites for the synthesis of phosphatidylaminoalcohols, for example phosphatidyl-*N*-methylethanolamine, has been described in detail in the literature,[46, 104, 175, 176, 182] For this purpose, the phosphatide **7** (a key compound) is converted by reaction with benzyl alcohol into the monoamide **24**, which is treated with benzylmethylethanolamine. After this the intermediate neutral phosphite **27** is oxidised and debenzylated twice (Scheme 48).[46]

Scheme 48



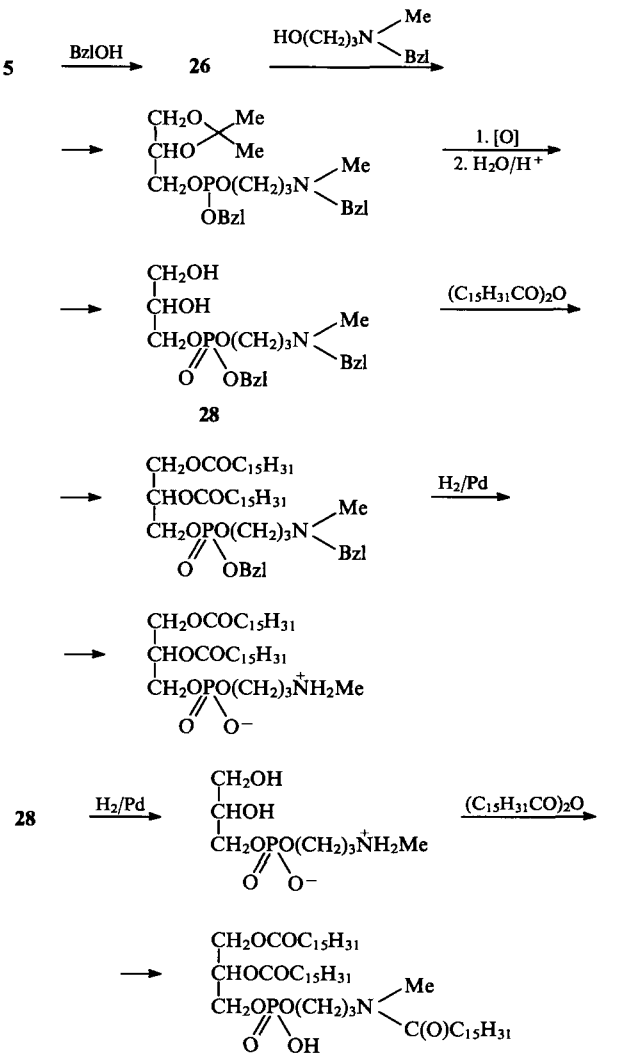
We may note that an alternative scheme, involving the initial phosphorylation of benzylmethylethanolamine with phosphorous acid diamine has certain preparative advantages (Scheme 49).[46]

Scheme 49



A fundamentally different method of synthesis of phosphatidylaminoalcohols presupposes the use of 1,2-*O*-isopropylideneglycerophosphorodiamidites **5** as the starting material. Experiments involving the hydrolysis of 1,2-isopropylideneglycerophosphate to the phosphate **28** unsubstituted in the glycerol residue and its subsequent acylation (Scheme 50) have been carried out for this purpose.[175, 176]

Scheme 50



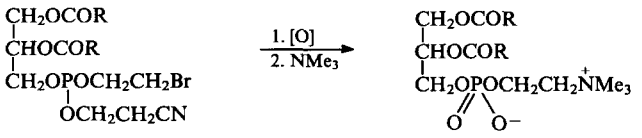
Unfortunately, nobody has investigated previously the possibility of using in this instance the acylation of a phosphorus-containing acetal with formation of ester systems, bypassing the diol stage.

In relation to the synthesis of the aminoalcohol lipids examined above, a number of workers have improved the classical scheme by a useful new feature—methyl phosphite derivatives were used as the reactants instead of benzyl phosphite derivatives. The former are readily oxidised to methyl phosphates, which exhibit an excellent methylating activity and readily lose the methyl group on treatment with, for example, ammonia in toluene or another nucleophile.[30–32]

Aminoalcohol derivatives of thiophosphatidic acids, including reactions where they were obtained as individual stereoisomers with chiral phosphorus atoms, have been obtained using this version of the synthesis.[32] These stereoindividual thiophospholipids are nowadays actively employed in biochemical research to elucidate the mechanism of the action of phospholipases.[32, 192–194]

There exists yet another version of the method described above. It differs by the use of neutral phosphites with a protecting β-cyanoethyl group. This protecting group is removed under milder conditions than the methyl group, which is the reason for the interest in the proposed modification. Phosphatidylcholine was obtained by this procedure. An additional advantage of the above scheme is the simultaneous occurrence of two reactions with trimethylamine: the removal of the cyanoethyl group and the formation of the ammonium group (Scheme 51).[60, 69, 80, 167]

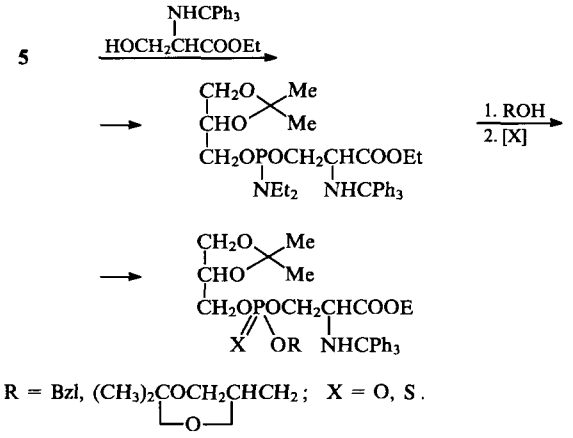
Scheme 51



The above schemes have also been used to synthesise sphingolipids.[66–68, 81, 82]

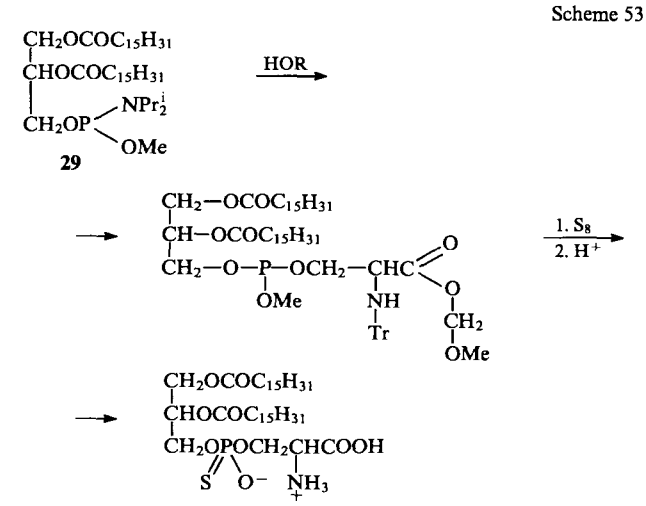
The phosphoroamidite method has been used to obtain models of lipids containing aminoacid, for example serine, residues (Scheme 52).[100, 183, 184]

Scheme 52



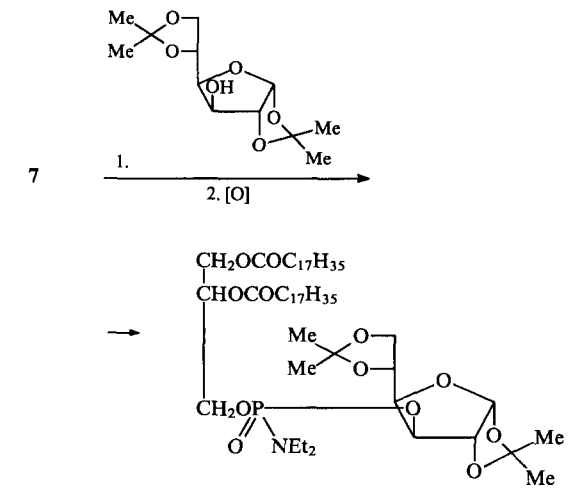
Similar reactions have been carried out also using *N,N*-diisopropyl-1,2-dipalmitoylglycerophosphoramidite **29** (Scheme 53).[35]

Scheme 53



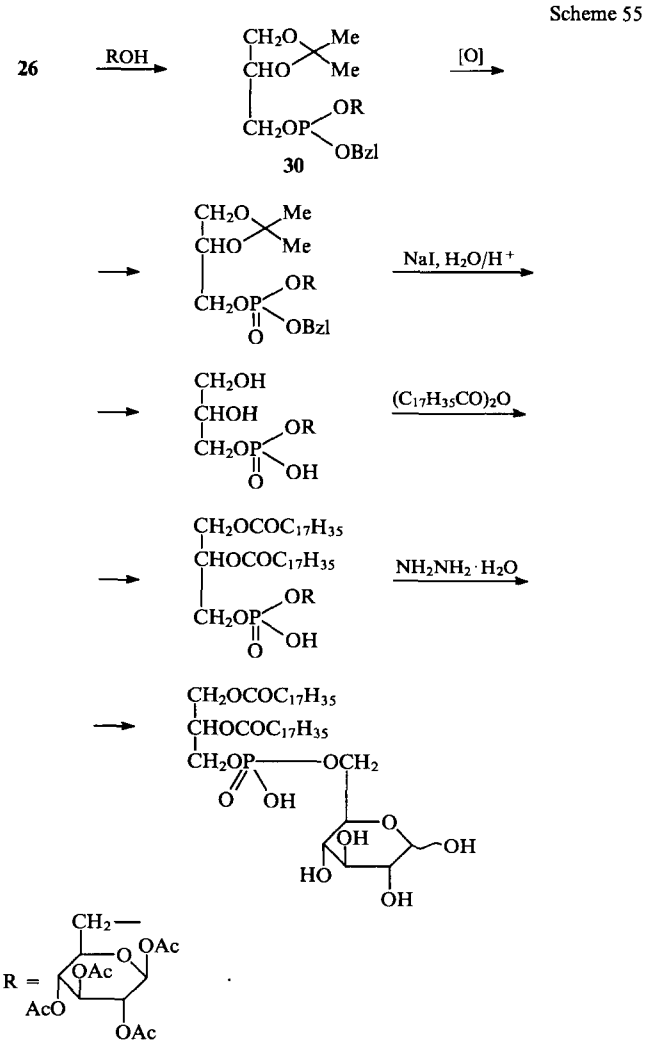
The use of glycerophosphoramidiates for the synthesis of carbohydrate-containing phospholipids, which have been recently attracting increasing attention, is especially valuable.[90, 195, 196] The reaction indicated in Scheme 54 indicates a simple path to these systems.[90, 96, 197, 198]

Scheme 54



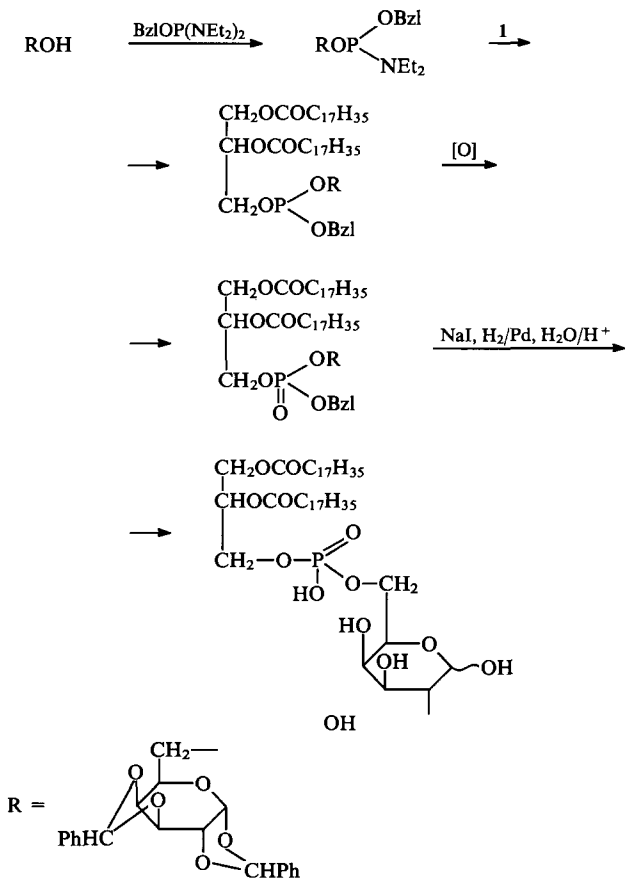
Another version of the synthesis of the complex lipid phosphatidyl-6-glucose is based on the employment of 1,2-*O*-isopropylideneglycerophosphoramidite **26** and 1,2,3,4-tetra-*O*-acetyl-β-D-glucopyranose as the starting compounds (Scheme 55).[86]

Scheme 55



The asymmetric benzyl glyceroglycophosphite **30**, used in the above study, can be obtained also by the initial phosphorylation of the sugar with benzyl *N,N,N',N'*-tetraethylphosphorodiamidite and subsequent incorporation of the 1,2-*O*-isopropylidene-glycerol residue in the phosphorus unit. When a sugar with acetate protecting groups is used, this phos-phorylation sequence is less preferable, since it involves prolonged heating of the reaction mixture and this leads to appreciable charring and hence to a decrease in the yield of the asymmetric phosphite. On the other hand, the above method can be usefully employed in the synthesis of glycophospholipids based on stable benzylidene derivatives of sugars, for example, 1,2,3,4-di-*O*-benzylidene-α-D-galactopyranose, because in this case the labile diglyceride fragment is phosphorylated last and is less subject to thermal and chemical influences. A similar solution is used in the total synthesis of phosphatidyl-6-galactose (Scheme 56).[97]

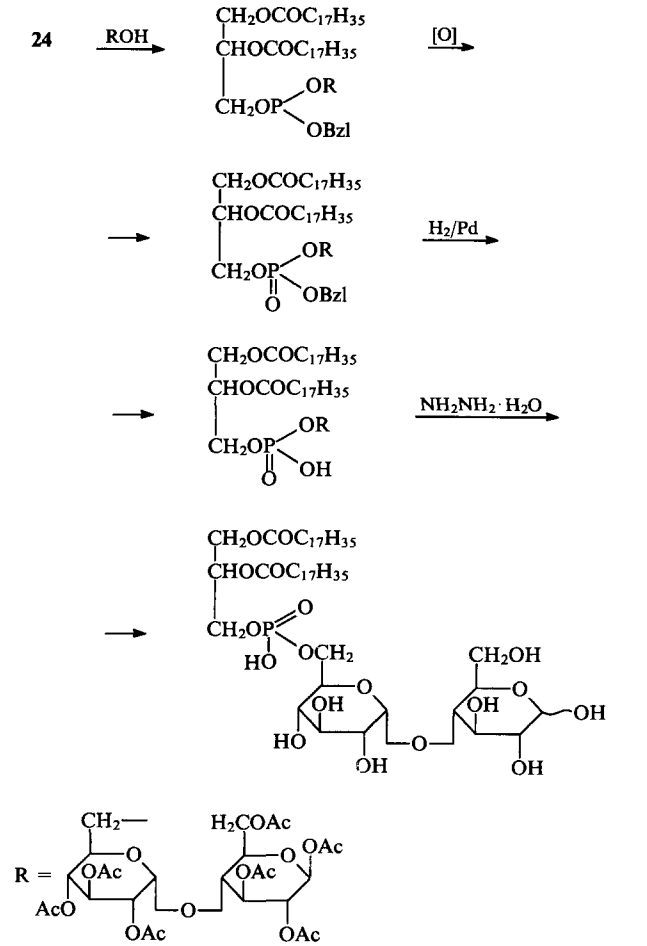
Scheme 56



The use of the synthetic ideas described above has led to the availability also of the very important disaccharide derivatives of glycerophospholipids.[199,200] We shall demonstrate this in relation to the synthesis of 6'-(1,2-distearoyl-3-glycerophospho)-maltose (Scheme 57).[198]

The methods of synthesis of glycophospholipids examined in the present subsection are distinguished by their simplicity. The main advantage of the 'phosphoramidite' method of synthesis of the phosphorus-containing unit compared with the commonest classical 'silver salt' method is the small number of stages. Thus, in order to phosphorylate a diglyceride or a partly protected carbohydrate with a free hydroxy-group by the 'silver salt' method, it is necessary to convert them in a preliminary step into halodeoxy-compounds. The yield of deoxy-derivatives usually does not exceed 50%. Furthermore, the alkyl dibenzyl phosphates used as phosphorylating agents must be converted by complex procedures into silver salts of monobenzyl phosphates.[1,195,196] The phosphoramidite method makes it

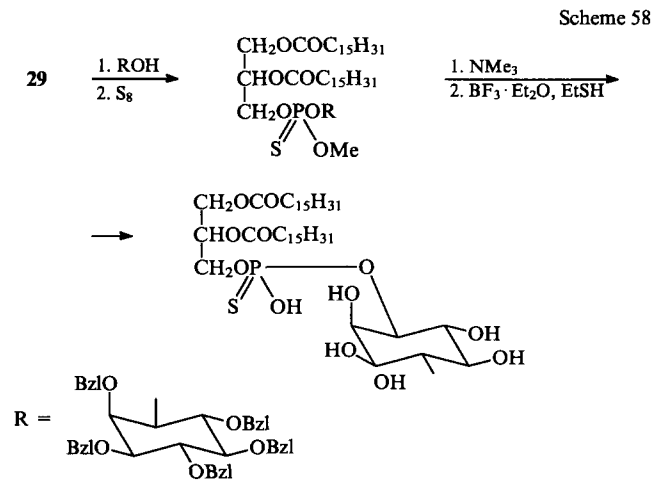
Scheme 57



possible to achieve directly the phosphorylation of diglycerides and of partly protected carbohydrates by phosphoramidites under mild conditions and with high yields in the decisive stages.

The phosphoramidite method has been recently used to synthesise inositylthiophosphatides. As in the synthesis of nitrogen- and carbohydrate-containing glycerophospholipids, in this case the synthesis is based both on the glycerophosphor-amidites **29** and myoinositol derivatives (Scheme 58).[34,36,37]

Scheme 58



The signals due to two diastereoisomers were detected in this instance in the $^{31}P-\{^{1}H\}$ NMR spectra for the optically active glycerol when a neutral phosphorothioate was used. These substances were resolved chromatographically. Their structure was demonstrated by enzyme analysis.

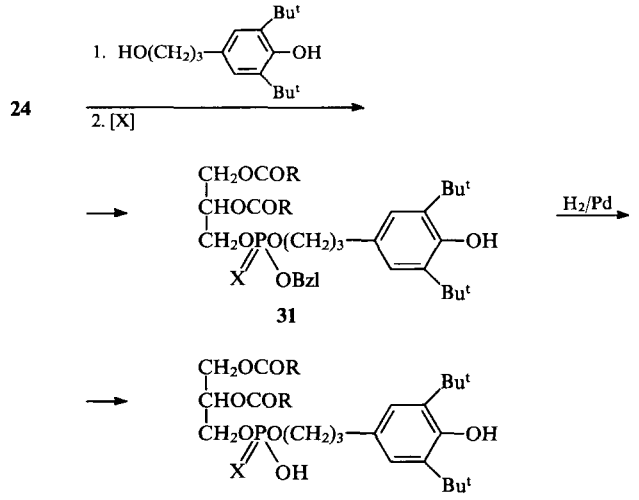
Neutral phosphoramidites with benzyl protecting groups, similar to those described above, have been used as the starting materials for the synthesis of the optically active natural phosphatidylinositol diphosphate and a fragment of a microbacterial phospholipid—phosphatidylmannomyo-inositol.[101,102]

The phosphoramidite method has been used also to synthesise other related complex lipids, for example ceramide phosphoinositol and its thio-analogue,[68,81,82] and in addition diolphospholipids containing cholesterol and certain other steroids.[78,84,110]

The following aspect of the use of phosphoramidites has been applied to the synthesis of lipid antioxidants. Such compounds can be obtained by the chemical combination of sterically hindered phenols and phosphatidic acids. We may note that previously a number of investigators demonstrated in studies on the peroxide oxidation of lipids that natural inhibitors of radical reactions play a significant role in the regulation of this process. These natural bioantioxidants initially contain the residues of sterically hindered phenols as protecting groups.[201-206] It was of interest to investigate the regulation of the peroxide oxidation of lipids in the presence of synthetic anitoxidants which are also derivatives of sterically hindered phenols. Such studies have been carried out in different laboratories and, in the case where ionol was used, led to positive results.[201-204,206-210] Unfortunately ionol and its analogues are not chemically related to lipids, which prevents the ready transport of the antioxidants into the membrane.[206,211] Taking into account the foregoing, the synthesis was undertaken of membrane-addressed antioxidants containing phosphatide groups and residues of sterically hindered phenols: 2,6-di-(*tert*-butyl)-4-(γ-hydroxypropyl)phenol, 2,6-di(*tert*-butyl)-hydroquinone, and ionol.

In the search for a convenient preparative method of synthesis of phosphatidyl(hydroxalkyl)phenols, various synthetic procedures were investigated. One of the schemes employed included the phosphorylation of γ-hydroxy-propylphenol by the phosphoramidites **24** (Scheme 59).[87]

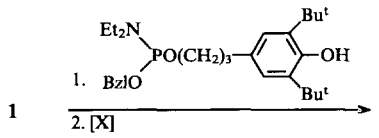
Scheme 59



R = $C_{15}H_{31}$, $C_{17}H_{35}$; X = O, S.

Of the two hydroxyls of the substituted phenols, the alcoholic hydroxyl reacts with the phosphoramidite.[212] In the second version, the key compounds **31** were obtained by phosphorylating 1,2-diacylglycerols **1** with benzyl γ-(di-*tert*-butylhydroxyphenyl)propyl *N,N*-diethylphosphoramidite (Scheme 60).

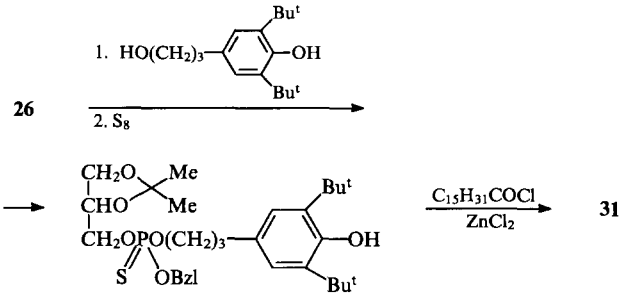
Scheme 60



R = $C_{15}H_{31}$, $C_{17}H_{35}$; X = O, S.

The lipid antioxidant has also been synthesised using the readily available 1,2-*O*-isopropylideneglycerophosphoramidite **26** instead of the phosphoramidite **24** as the starting compound (Scheme 61).

Scheme 61



The most important feature of the synthesis is the specificity of the acylation of the phenol-substituted phosphoacetal. It was shown that, on acylation with two moles of palmitoyl chloride, the phenolic hydroxyls are unaffected.

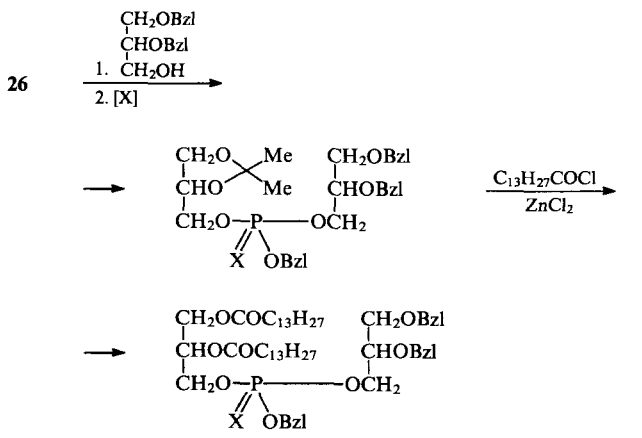
The synthesis of lipid antioxidants containing the 2,6-di-(*tert*-butyl)hydroquinone residue has also been investigated. The schemes presented above were used for this purpose.[26]

It was found that lipid antioxidants containing sterically hindered phenol residues have effective antioxidant properties.[103] There is therefore a prospect of formulating with the aid of these phospholipids (antioxidants) new problems in the study of the peroxide oxidation of membranes.

The phosphorylation of tocopherol, which is a carrier of antiradical properties, by *N,N,N',N'*-tetraalkylphosphorodiamidites is of definite interest for the synthesis of a new type of antioxidants.[78,83,110]

A very interesting fact was established in the search for lipid anitoxidants. It was found that certain glycerides containing phosphorothioic acid residues are also inhibitors of free-radical reactions.[103] Apparently, after a deeper investigation of such phosphorothioates, the procedures available in lipidology will be expanded by the inclusion of a new class of readily available antioxidants which are convenient to use.

Scheme 62



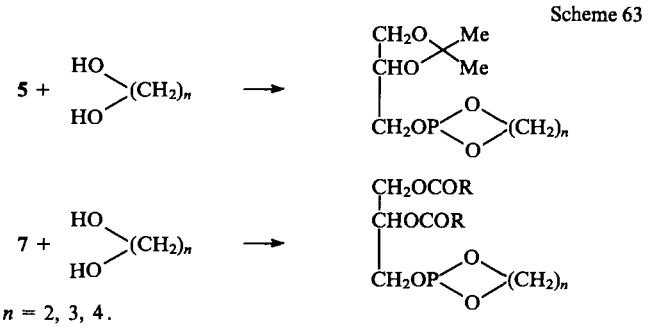
X = O, S.

We examined above the employment of monoglycerophosphoramidites for the synthesis of glycerophosphatides, the molecules of which contain one glycerol residue. We shall now proceed to the discussion of the syntheses of phospholipids containing two glycerol residues.[30,75,105] Thus phosphoramidites have been used to synthesis phosphatidylglycerols (Scheme 62) (see previous page).[75]

The neutral benzyl esters of phosphatide and thionophosphatide can be converted into phosphatidylglycerol (thiophosphatidylglycerol) by total debenzylation taking into account the results of other investigations.[1,3,8,10]

Another aspect of the synthetic application of glycerophosphoramidites concerns studies on the cyclophosphorylation of bifunctional nucleophiles, in the first place glycols (Scheme 63).

Scheme 63



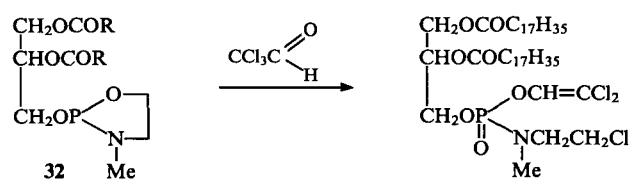
n = 2, 3, 4.

The choice of the diol has a considerable influence on the effectiveness of the cyclisation; 1,2- and 1,3-glycols react in accordance with the scheme presented and afford high yields of alkylene glycerophosphites (up to 70%).[46,88] Butane-1,4-diol is also converted into the expected glycero-1,3,2-dioxaphosphepan in 55% yield in the reaction with the diamine **5**. However, in this case a mixture of cyclic oligomers is formed simultaneously, but these can be readily separated from the target product.[91,92] It is of interest that the glycerophosphepan is a stable compound, while its analogues, containing chlorine, dialkylamino-groups, and other very simple substituents at the phosphorus atom, are very labile and readily oligomerise.[214-218] The last factor explains the low effectiveness of the synthesis of glycerophosphepans via an alternative scheme consisting in the phosphorylation of substituted glycerols by the chloro- and dialkylamino-phosphepans already mentioned.[91,92]

Glycerophospho(III)cyclanes are promising intermediates in the synthesis of different types of phospholipids. Data on this question have already been examined above in subsection 1 in the present section.

It has been suggested that cyclic glycerophosphoramidites — glycero-derivatives of oxazaphospholans[94,177,183] and oxazaphosphorinanes[52,175] — be synthesised via Scheme 63 but this time also using aminoalcohols.‡ These substances have already been used in oxidation reactions (see above) and in certain other syntheses. Thus treatment of glycerooxazaphospholans **32** with chloral in accorance with the Perkow procedure results in their conversion into unusual lipids belonging to the class of enol phosphates (Scheme 64).[95,186]

Scheme 64

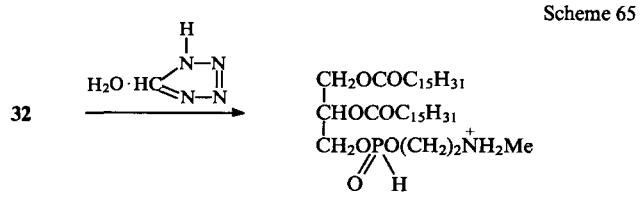


‡ The possibility of using also hydroxyaminoacid esters, for example serine, in such cyclisations has been demonstrated.[183]

The phosphorus centre in the molecules of enol glycerophosphates combines the structural features of the molecules of familiar alkylating ($\geq NCH_2CH_2Cl$) and phosphorylating [$\geq P(O)OCH=CCl_2$] preparations. Lipids, which contain such a functional group, can probably be regarded both as antitumour agents and as instruments for the study of the structures and functions of biological membranes. Phospholipids containing alkylating groups have also been obtained by the Arbuzov reaction between glycerophosphoramidites and methyl iodide.[186]

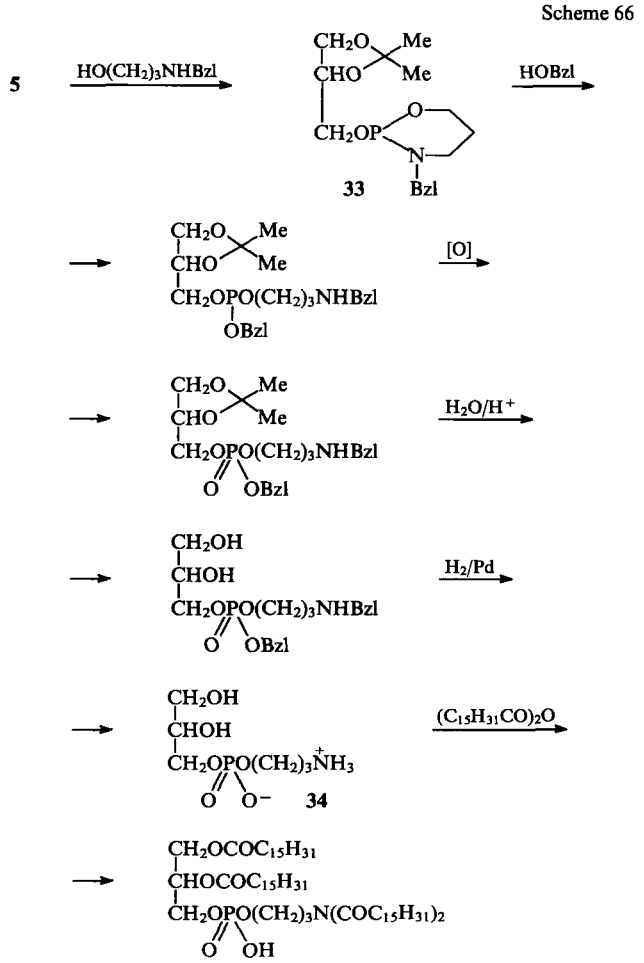
Another possible synthetic use of glycerophosphoramidites involves their reactions via the labile P—N bond. In this case, the fragment concealed by phosphorylation is immediately 'bared'. The simplest version of the cleavage of the P—N bond is acid hydrolysis, for example by monohydrates of sulfonic acids[52,173] or tetrazole,[53] and sulfhydrolysis,[185] which lead to hydrophosphoryl(thiohydrophosphoryl) analogues of phosphatidylaminoalcohols (Scheme 65).[53]

Scheme 65



The cyclic phosphoramidites examined above react satisfactorily also with alcohols of different chemical nature, which permits the solution of novel chemical problems. Thus the benzylolysis of glycerooxazaphosphorane **33** results in the formation of a neutral phosphite, the oxidation and deblocking of which lead to glycerophosphohomoethanolamine **34**. This

Scheme 66



polyfunctional product was acylated with palmitic acid anhydride, affording the tetrapalmitoyl derivative of a phospholipid which is difficult to obtain by other procedures (Scheme 66).[54, 176]

Alcoholysis can be used also to synthesise unusual neutral phosphites in the molecules of which the phosphorus atom is surrounded by residues of glycerol, aminoalcohols, and the reagent employed (carbohydrate, hydroxyaminoacid, glycerol derivative, etc.). The neutral phosphites obtained can be stabilised in either the phosphate or the phosphorothionate forms.[96, 184, 196] Such derivatives have been discussed in the literature in connection with the elucidation of the structures of natural complexes incorporating in their structure biopolymers and lipids.[8] Previously they were synthesised only by methods of classical phospholipid chemistry. The new suggestions based on the use of effective phosphorylation procedures apparently merit extensive use and can lead to progress in the study of such complex systems.

IV. Conclusion

The data presented have acquainted readers with the way in which the idea of replacing, in the intermediate stages of phospholipid syntheses, pentavalent phosphorus reagents by previously hardly used trivalent phosphorus reagents is applied. The application of this new synthetic strategy has entailed the vigorous utilisation of the possibilities of modern organophosphorus chemistry for the solution of problems in phospholipid chemistry of current interest and subsequently in membranology. On the other hand, further development of traditional studies on trivalent phosphorus derivatives has been greatly stimulated. All these factors suggest that a trend has arisen towards the establishment of a new interdisciplinary field of science.

Overall, the studies described demonstrate the necessity for their further expansion and deepening. Thus the absence of attempts to synthesis hypophosphite glycerolipids appears strange because all the previously investigated hypophosphites proved to be valuable key substances in the synthesis. Furthermore, hypophosphite glycerophospholipids as components of membranes can protect the latter against oxidation and other undesirable processes. The development of simple and effective methods of synthesis of glycerophosphites and similar compounds makes it necessary to undertake studies also on the corresponding metal complexes including transition metal complexes. Such coordination systems can play the role of a kind of carrier and can ensure the transport of metals into membranes. The distribution of metals in the lipid phases of membranes will clearly prove to be of fundamental importance since it will enable a series of important problems to be solved, for example that of the regulation of homolytic reactions in membranes or the binding to one another of individual lipid molecules as a result of the oxidative addition of C–H bonds to the metal.

References

1. R P Evstigneeva, E N Zvonkova, G A Serebrennikova, V I Shvets *Khimiya Lipidov* (The Chemistry of Lipids) (Moscow: Khimiya, 1983)
2. L D Bergel'son *Biolog. Membr.* **1** 794 (1984)
3. H Eibl *Angew. Chem.* **96** 247 (1984)
4. K Yu Gordeev, G A Serebrennikova, R P Evstigneeva *Bioorg. Khim.* **10** 1589 (1984)
5. M C Moschides *Prog. Lipid Res.* **23** 223 (1984)
6. F Ramirez, J F Marecek *Synthesis* 449 (1985)
7. O V Ostapenko, G A Serebrennikova, R P Evstigneeva *Bioorg. Khim.* **12** 1145 (1986)
8. A E Stepanov, V I Shvets *Chem. Phys. Lipids* **41** 1 (1986)
9. H K Mangold, in *Progress in Biochemical Pharmacology* (Ed. R Paoletti) *Biologically Active Ether Lipids* (Eds P Braquete, H K Mangold, B B Vargattig) (Basel: Karger, 1988) Vol. 22, p. 1
10. O V Bogomolov, A P Kaplun, V I Shvets *Usp. Khim.* **57** 684 (1988) [*Russ. Chem. Rev.* **57** 382 (1988)]
11. E E Nifant'ev, D A Predvoditelev *Bioorg. Khim.* **7** 1285 (1981)
12. R P Evstigneeva, E N Zvonkova, G A Serebrennikova, V I Shvets, in *Khimiya Lipidov* (The Chemistry of Lipids) (Moscow: Khimiya, 1983) p. 78
13. E E Nifant'ev *Khimiya Fosfororganicheskikh Soedinenii* (The Chemistry of Organophosphorus Compounds) (Moscow: Izd. Mosk. Gos. Univ., 1971)
14. E E Nifant'ev, D A Predvoditelev, L I Smirnova, I V Fursenko *Bioorg. Khim.* **6** 1346 (1980)
15. D A Predvoditelev, L I Smirnova, M B Smirnov, E E Nifant'ev *Dokl. Akad. Nauk SSSR* **256** 402 (1981)
16. E E Nifantyev, D A Predvoditelev, I V Fursenko, L I Smirnova *Synthesis* 132 (1982)
17. D A Predvoditelev, G A Savin, E E Nifant'ev *Zh. Obshch. Khim.* **62** 2008 (1992)
18. D A Predvoditelev, G A Savin, E E Nifant'ev *Zh. Org. Khim.* **30** (in the press) (1994)
19. IUPAC-IUB Commission of Biochemical Nomenclature (CBN) *Eur. J. Biochem.* **79** 1 (1977)
20. *The Nomenclature of Lipids* **21** 141 (1978)
21. E E Nifant'ev *Khimiya Gidrofosforil'nykh Soedinenii* (The Chemistry of Hydrophosphoryl Compounds) (Moscow: Nauka, 1983)
22. D R Royd *J. Chem. Soc.* **79** 122 (1901)
23. I Lindh, J Stavinski *J. Org. Chem.* **54** 1338 (1989)
24. C Murakata, O Tomoya *Tetrahedron Lett.* **32** 101 (1991)
25. C Murakata, T Ogawa *Tetrahedron Lett.* **32** 671 (1991)
26. E E Nifant'ev, D A Predvoditelev, M A Zolotov *Bioorg. Khim.* **8** 1263 (1982)
27. S F Martin, J A Josey *Tetrahedron Lett.* **29** 3631 (1988)
28. K Inami, T Teshima, J Emura, T Shiba *Tetrahedron Lett.* **31** 4033 (1990)
29. B A Arbuzov, D Kh Yarmukhametova *Izv. Akad. Nauk SSSR, Otd. Khim. Nauk* 292 (1957)
30. K S Bruzik, G M Salamonczyk *J. Org. Chem.* **51** 2368 (1986)
31. V Zamant, H Chap, A Klaébe, J J Perie, M Willson *J. Chem. Soc., Chem. Commun.* 1608 (1987)
32. T Rosario-Jansen, R-T Jiang, M-D Tsai, D J Hanahan *Biochemistry* **27** 4619 (1988)
33. W Yuan, K Fearon, M H Gelb *J. Org. Chem.* **54** 906 (1989)
34. G Lin, M-D Tsai *J. Am. Chem. Soc.* **111** 3099 (1989)
35. W M Loffredo, M-D Tsai *Bioorg. Chem.* **18** 78 (1990)
36. G Lin, C F Bennett, M-D Tsai *Biochemistry* **29** 2747 (1990)
37. G M Salamonczyk, K S Bruzik *Tetrahedron Lett.* **31** 2015 (1990)
38. N H Phuong, N T Thuong, P Chabrier *Bull. Soc. Chem. Fr.* 2326 (1975)
39. E E Nifant'ev, D A Predvoditelev, Kh Kh Alarkon *Zh. Obshch. Khim.* **46** 912 (1976)
40. D A Predvoditelev, D N Afanasyeva, E E Nifant'ev *Zh. Obshch. Khim.* **46** 40 (1976)
41. N H Phuong, N T Thuong, P Chabrier *C. R. Hebd. Seances Acad. Sci., Ser. C* **283** 229 (1976)
42. N H Phuong, N T Thoung, P Chabrier *C. R. Hebd. Seances Acad. Sci., Ser. C* **283** 323 (1976)
43. E E Nifant'ev, D A Predvoditelev, Kh Kh Alarkon *Zh. Org. Khim.* **14** 63 (1978)
44. D A Predvoditelev, Kh Kh Alarkon, E E Nifant'ev *Zh. Org. Khim.* **16** 1549 (1980)
45. D A Predvoditelev, T G Chukbar, T P Zeleneva, E E Nifant'ev *Zh. Org. Khim.* **17** 1305 (1981)
46. D A Predvoditelev, E N Rasadkina, M K Grachev, E E Nifant'ev *Zh. Org. Khim.* **18** 1115 (1982)
47. K Bruzik, S M Gupte, M-D Tsai *J. Am. Chem. Soc.* **104** 4682 (1982)
48. L I Mizrakh, L Yu Polonskaya, E D Vorontsov *Zh. Obshch. Khim.* **53** 426 (1983)
49. K Bruzik, R-T Jiang, M-D Tsai *Biochemistry* 2478 (1983)
50. R Garrigues *Helv. Chim. Acta* **71** 274 (1988)
51. B Molotkowska, A Markowska *Liebigs Ann. Chem.* 833 (1991)
52. M K Grachev, D A Predvoditelev, E E Nifant'ev *Zh. Obshch. Khim.* **46** 1677 (1976)
53. R Stumpf, P Lemmen *Z. Naturforsch., B Chem. Sci.* **45** 1729 (1990)

54. C McGuigan, M S Anson, B Swords *J. Chem. Soc., Perkin Trans. 1* 2075 (1992)
55. R-T Jiang, Y J Shya, M-D Tsai *Biochemistry* **23** 1661 (1989)
56. E E Nifant'ev, D A Predvoditelev, G A Savin *Bioorg. Khim.* **17** 126 (1991)
57. D A Predvoditelev, G A Savin, E E Nifant'ev *Zh. Obshch. Khim.* **62** 2445 (1992)
58. D A Predvoditelev, M A Malenkovskaya, A R Bekker, L K Vasyanina, E E Nifant'ev *Zh. Org. Khim.* **27** 1655 (1991)
59. E E Nifant'ev, D A Predvoditelev, E N Rasadkina, G G Kozlova *Bioorg. Khim.* **16** 407 (1990)
60. E N Rasadkina, D A Predvoditelev, G G Kozlova, E E Nifant'ev *Zh. Org. Khim.* **27** 498 (1991)
61. D A Predvoditelev, E N Rasadkina, G G Kozlova, E E Nifant'ev *Zh. Obshch. Khim.* **61** 2497 (1991)
62. C McGuigan *J. Chem. Soc., Chem. Commun.* 533 (1986)
63. S A Anson, C McGuigan *J. Chem. Soc., Perkin Trans 1* 715 (1989)
64. C McGuigan, B Swords *J. Chem. Soc., Perkin Trans 1* 783 (1990)
65. C McGuigan, B Swords *J. Chem. Soc., Perkin Trans 1* 51 (1992)
66. K S Bruzik *J. Chem. Soc., Chem. Commun.* 329 (1986)
67. K S Bruzik *J. Chem. Soc., Perkin Trans. 1* 423 (1988)
68. A Yu Frantova, A S Bushnev, E N Zvonkova *Biorg. Khim.* **17** 1562 (1991)
69. P Werterduin, G H Veereman, J H Van Boom *Recl. Trav. Chim. Pays-Bas* **106** 601 (1987)
70. A I Razumov *Zh. Obshch. Khim.* **14** 464 (1944)
71. K A Petrov, E E Nifant'ev, L V Khorkhoyants *Zh. Obshch. Khim.* **31** 2889 (1961)
72. K A Petrov, E E Nifant'ev, L V Khorkhoyants, I G Shcherba *Zh. Obshch. Khim.* **34** 70 (1964)
73. D A Predvoditelev, L I Smirnova, E E Nifant'ev *Zh. Org. Khim.* **15** 2223 (1979)
74. M I Smirnova, M A Malenkovskaya, D A Predvoditelev, E E Nifant'ev *Zh. Org. Khim.* **16** 1170 (1980)
75. D A Predvoditelev, T G Chukbar, M A Malenkovskaya, E N Rasadkina, E E Nifant'ev *Zh. Org. Khim.* **17** 2524 (1981)
76. E E Nifant'ev, N L Ivanova, N K Bliznyuk *Zh. Obshch. Khim.* **36** 765 (1966)
77. E E Nifant'ev, M K Gratchev, S Yu Burmistrov, L K Vasyanina, M Yu Antipin, Yu T Struchkov *Tetrahedron* **47** 9839 (1991)
78. S D Stamatov, S A Ivanov *Phosphorus Sulfur Relat. Elem.* **37** 213 (1988)
79. S D Stamatov, S A Ivanov *Phosphorus Sulfur Silicon Relat. Elem.* **45** 73 (1989)
80. N Hebert, G Just *J. Chem. Soc., Chem. Commun.* 1497 (1990)
81. F Yu Frantova, A E Stepanov, A S Bushnev, E N Zvonkova, V I Shvets *Tetrahedron Lett.* **33** 3539 (1992)
82. A Yu Zamyatina, A E Stepanov, A S Bushnev, E N Zvonkova, V I Shvets *Bioorg. Khim.* **19** 347 (1993)
83. S D Stamatov, S A Ivanov *Phosphorus Sulfur Relat. Elem.* **40** 167 (1988)
84. S D Stamatov *Chem. Phys. Lipids* **50** 79 (1989)
85. S D Stamatov, S Gronovitz *Lipids* **25** 149 (1990)
86. E E Nifant'ev, D A Predvoditelev, M K Grachev, V A Shin *Bioorg. Khim.* **4** 1213 (1978)
87. E E Nifant'ev, D A Predvoditelev, M A Zolotov *Bioorg. Khim.* **7** 1100 (1981)
88. Kh Kh Alarkon, D A Predvoditelev, E E Nifant'ev *Bioorg. Khim.* **4** 1513 (1978)
89. V A Vaver, T A Simonova, G V Titeeva *Bioorg. Khim.* **6** 146 (1980)
90. D A Predvoditelev, M K Grachev, M V Galakhov, E E Nifant'ev *Zh. Obshch. Khim.* **49** 285 (1979)
91. D A Predvoditelev, M A Malenkovskaya, E E Nifant'ev *Bioorg. Khim.* **17** 1149 (1991)
92. E E Nifant'ev, D A Predvoditelev, M A Malenkovskaya *Zh. Obshch. Khim.* **62** 1985 (1992)
93. Y Kodira, T Makaiyama *J. Org. Chem.* **31** 2903 (1966)
94. D A Predvoditelev, G A Podzhunas, E E Nifant'ev *Zh. Obshch. Khim.* **41** 2195 (1971)
95. D A Predvoditelev, G A Urvantseva, E E Nifant'ev *Zh. Obshch. Khim.* **43** 948 (1973)
96. E E Nifant'ev, D A Predvoditelev, V A Shin *Zh. Obshch. Khim.* **46** 2369 (1976)
97. E E Nifant'ev, D A Predvoditelev, V A Shin *Zh. Vses. Khim. O-va im D. I. Mendeleeva* **23** 220 (1978)
98. D A Predvoditelev, M K Grachev, M B Smirnov, E E Nifant'ev *Biorg. Khim.* **5** 1509 (1979)
99. D A Predvoditelev, M K Grachev, E E Nifant'ev *Bioorg. Khim.* **7** 601 (1981)
100. L K Nikonorova, N P Grechkin, L A Zhelonkina *Zh. Obshch. Khim.* **51** 1975 (1981)
101. C E Dreef, C J J Elie, P Hoogerhout, G A Van der Marel, J H Van Boom *Tetrahedron Lett.* **29** 6513 (1988)
102. C J J Elie, C E Dreef, R Verduin, G A Van der Marel, J H Van Boom *Tetrahedron* **45** 3477 (1989)
103. T V Sotnichenko, I A Vasilenko, R P Evstigneeva, D A Predvoditelev *Khim.-farm. Zh.* 561 (1983)
104. D A Predvoditelev, T G Chukbar, E E Nifant'ev *Zh. Org. Khim.* **46** 291 (1976)
105. D A Predvoditelev, T G Chukbar, E E Nifant'ev *Bioorg. Khim.* **3** 76 (1977)
106. D A Predvoditelev, I V Fursenko, E E Nifant'ev *Bioorg. Khim.* **7** 1426 (1981)
107. D A Predvoditelev, M K Grachev, M B Smirnov, E E Nifant'ev *Zh. Obshch. Khim.* **18** 1326 (1982)
108. M A Malenkovskaya, D A Predvoditelev, E E Nifant'ev *Zh. Obshch. Khim.* **27** 1668 (1991)
109. G A Savin, D A Predvoditelev, E E Nifant'ev *Bioorg. Khim.* **17** 280 (1991)
110. S D Stamatov, V K Staneva, S A Ivanov *Chem. Phys. Lipids* **46** 199 (1988)
111. D A Predvoditelev, T G Chukbar, G A Urvantseva, E E Nifant'ev *Zh. Obshch. Khim.* **44** 1203 (1974)
112. M Froneman, T A Modro *Tetrahedron Lett.* **30** 5469 (1989)
113. N S Corby, G W Kenner, A R Todd *J. Chem. Soc.* 3669 (1952)
114. D M Brown, P R Hammond *J. Chem. Soc.* 4232 (1960)
115. M A Grum-Grzhimailo, L V Volkova, M I Komakhina, N A Preobrazhenskii *Zh. Org. Khim.* **4** 1157 (1968)
116. M K Petrova, V I Shvets, V A Dachkovskaya, N I Preobrazhenskii *Zh. Obshch. Khim.* **5** 1198 (1969)
117. S P Kozlova, N B Tarusova, N A Preobrazhenskii *Zh. Obshch. Khim.* **39** 2463 (1969)
118. D A Predvoditelev, E E Nifant'ev, Z A Rogovin *Vysokomol. Soedin.* **8** 76 (1966)
119. D A Predvoditelev, E E Nifant'ev, Z A Rogovin *Cellul. Chem. Technol.* **1** 179 (1967)
120. P J Garegg, T Regberg, J Stavinski, R Stromberg *Chem. Scr.* **25** 280 (1985)
121. B C Frochler, M D Mattencci *Tetrahedron Lett.* **27** 469 (1986)
122. V A Efimov, I Ya Dubei *Bioorg. Khim.* **16** 211 (1990)
123. A V Nikolaev, I A Ivanova, V N Shibaev, A V Ingat'enko *Bioorg. Khim.* **17** 1550 (1991)
124. F R Atherton, Y T Openshaw, A R Todd *J. Chem. Soc.* 660 (1945)
125. E E Nifant'ev, D A Predvoditelev, M K Grachev *Zh. Obshch. Khim.* **44** 2779 (1974)
126. E E Nifant'ev, D A Predvoditelev, E N Rasadkina, G G Kozlova *Zh. Obshch. Khim.* **63** 602 (1993)
127. E N Rasadkina, D A Predvoditelev, E E Nifant'ev *Bioorg. Khim.* **18** 302 (1992)
128. B Mlotkovska, A Markovska *Liebigs Ann. Chem.* 1 (1984)
129. B Mlotkovska, A Markovska *Liebigs Ann. Chem.* 191 (1988)
130. B Mlotkovska *Liebigs Ann. Chem.* 1361 (1991)
131. A F Rosenthal *Methods Enzymol., Part B* **35** 429 (1975)
132. R Engel *Chem. Rev.* **77** 349 (1977)
133. Y-C Tang, B F Tropp, R Engel, A F Rosenthal *Chem. Phys. Lipids* **17** 169 (1976)
134. P W Deroo, A F Rosenthal, L A Isiason, L A Vargus, R Bittman *Chem. Phys. Lipids* **16** 60 (1976)
135. P W Schwartz, B E Tropp, R Engel *Chem. Phys. Lipids* **49** 131 (1988)
136. D A Predvoditelev, V I Ivanov, Kh Kh Alarkon, E E Nifant'ev *Zh. Obshch. Khim.* **48** 1273 (1978)
137. M E Jung, M A Lysta *J. Am. Chem. Soc.* **99** 968 (1977)
138. T Marita, Y Okamoto, H Sakurai *Tetrahedron Lett.* **19** 2523 (1978)
139. B Boreska, J Chojnowski, M Cypryk, J Michalski *J. Organometal. Chem.* **171** 17 (1979)

140. K Issleib, A Balszuveit, B Stiebitz *Z. Anorg. Allg. Chem.* **546** 147 (1987)
141. L Wozniak, J Chojnowski *Tetrahedron* **45** 2465 (1989)
142. A F Rosenthal, S V Chodsky, S C H Han *Biochim. Biophys. Acta* **187** 385 (1969)
143. A F Rosenthal, L A Vargas *J. Chem. Soc., Chem. Commun.* 976 (1981)
144. K C Tang, E Tropp, R Engel *Tetrahedron* **34** 2873 (1978)
145. A S Bushnev, N T Tazabekova, I V Nikolaevskaya, E N Zvonkova, R P Evstigneeva *Bioorg. Khim.* **9** 553 (1983)
146. R Bittman, A F Rosenthal, L A Vargas *Chem. Phys. Lipids* **34** 201 (1984)
147. L A Vargas, L Z Miao, A F Rosenthal *Biochim. Biophys. Acta* **796** 123 (1984)
148. K L Mayer, J Marasco Canio, S L Morris-Matsche, K S Ishag, C Piantadosi *J. Med. Chem.* **34** 1377 (1991)
149. A N Chuvilin, V G Trusov, G A Serebrennikova *Bioorg. Khim.* **18** 862 (1992)
150. D A Predvoditelev, Kh Kh Alarkon, E E Nifant'ev *Bioorg. Khim.* **6** 1087 (1980)
151. E V Malina, G A Serebrennikova, R P Evstigneeva *Zh. Org. Khim.* **18** 967 (1982)
152. E N Rasadkina, D A Predvoditelev, M B Smirnov, E E Nifant'ev *Zh. Org. Khim.* **20** 38 (1984)
153. D A Predvoditelev, E N Rasadkina, E E Nifant'ev *Bioorg. Khim.* **13** 710 (1987)
154. D A Predvoditelev, E N Rasadkina, A R Bekker, E E Nifant'ev *Zh. Obshch. Khim.* **58** 1504 (1988)
155. M A Malenkovskaya, A R Bekker, S V Meshkov, D A Predvoditelev, E E Nifant'ev *Zh. Obshch. Khim.* **63** (11) (1993)
156. E E Nifant'ev, D A Predvoditelev, I V Fursenko *Zh. Obshch. Khim.* **51** 2435 (1981)
157. V V Chupin, I A Vasilenko, D A Predvoditelev, G A Serebrennikova, R P Evstigneeva *Dokl. Akad. Nauk SSSR* **248** 235 (1979)
158. V F Eckstein *Angew. Chem., Int. Ed. Engl.* **22** 423 (1983)
159. V F Eckstein *Angew. Chem.* **95** 431 (1983)
160. I A Vasilenko, R P Evstigneeva *Izv. Akad. Nauk SSSR, Ser. Biol.* 550 (1986)
161. I A Vasilenko, V L Borovyagin *Biol. Membr.* 7 677 (1990)
162. V F Antonov, E T Kozhomkulov, E V Shevchenko, A N Vasserman, E Yu Smirnova, S A Voznesenskii, Yu V Morozov *Biofizika* **31** 252 (1986)
163. E Yu Smirnova, E T Kozhomkulov, A N Vasserman, S A Vosnesensky, E V Shevchenko, Yu V Morosov, V F Antonov *Chem. Phys. Lipids* **41** 173 (1986)
164. V F Antonov, E Yu Smirnova, E V Shevchenko *Chem. Phys. Lipids* **52** 251 (1990)
165. F Ursini, A Bindoli *Chem. Phys. Lipids* **44** 255 (1987)
166. F I Abdulaev *Usp. Sovrem. Biol.* **108** 279 (1989)
167. E N Rasadkina, D A Predvoditelev, E E Nifant'ev *Bioorg. Khim.* **18** 1559 (1992)
168. D A Predvoditelev, T G Chukbar, E E Nifant'ev *Zh. Obshch. Khim.* **17** 1547 (1981)
169. E E Nifant'ev, D A Predvoditelev, Kh Kh Alarkon USSR P. 577 211 (1975); *Byull. Izobret.* **39** (1977)
170. E E Nifant'ev, D A Predvoditelev, Kh Kh Alarkon USSR P. 586 643 (1975); *Byull. Izobret.* **38** (1978)
171. E E Nifant'ev, D A Predvoditelev, E N Rasadkina, A R Bekker *Zh. Obshch. Khim.* **57** 213 (1987)
172. E E Nifantyev, D A Predvoditelev, E N Rasadkina, A R Bekker *Phosphorus Sulfur Relat. Elem.* **34** 109 (1987)
173. E E Nifant'ev, G A Podzhunas, D A Predvoditelev, Yu B Filippovich *Zh. Obshch. Khim.* **42** 1842 (1972)
174. G A Urvantseva, D A Predvoditelev, E E Nifant'ev *Zh. Obshch. Khim.* **43** 2187 (1973)
175. E E Nifant'ev, D A Predvoditelev, M K Grachev *Bioorg. Khim.* **3** 68 (1977)
176. M K Grachev, V A Sukhanov, D A Predvoditelev, V I Shvets, E E Nifant'ev *Zh. Org. Khim.* **13** 1830 (1977)
177. D A Predvoditelev, M A Malenkovskaya, E E Nifant'ev *Zh. Org. Khim.* **21** 498 (1985)
178. D A Predvoditelev, M A Malenkovskaya, E E Nifant'ev *Zh. Org. Khim.* **23** 588 (1987)
179. V F Antonov, V V Petrov, A A Molnar, D A Predvoditelev, A C Ivanov *Nature (London)* **283** 585 (1980)
180. M I Kabachnik, P A Rossiiskaya *Izv. Akad. Nauk SSSR, Otd. Khim. Nauk* 364 (1945)
181. E E Nifant'ev, D A Predvoditelev, G A Savin *Dokl. Akad. Nauk SSSR* **320** 905 (1991)
182. D A Predvoditelev, V B Kvantrishvili, E E Nifant'ev *Zh. Org. Khim.* **11** 1190 (1975)
183. D A Predvoditelev, V B Kvantrishvili, E E Nifant'ev *Zh. Org. Khim.* **12** 38 (1976)
184. D A Predvoditelev, V B Kvantrishvili, E E Nifant'ev *Zh. Org. Khim.* **13** 1392 (1977)
185. D A Predvoditelev, G A Urvantseva, Yu B Filippovich, E E Nifant'ev *Zh. Obshch. Khim.* **43** 1799 (1973)
186. D A Predvoditelev, G A Urvantseva, E E Nifant'ev *Zh. Obshch. Khim.* **43** 1801 (1973)
187. K A Petrov, V P Evdakov, M I Mizrakh, V P Romodin *Zh. Obshch. Khim.* **32** 3062 (1962)
188. L Maier *Helv. Chim. Acta* **49** 1249 (1966)
189. G Porritt, C Reese *Tetrahedron Lett.* **30** 4713 (1989)
190. D A Predvoditelev, D N Afanas'eva, Yu B Filippovich, E E Nifant'ev *Zh. Obshch. Khim.* **43** 73 (1973)
191. Yu G Grishin, V N Chistokletov, V V Kosovtsev, A A Petrov *Zh. Obshch. Khim.* **11** 1752 (1975)
192. M-D Tsai, R-T Jiang, K Bruzik *J. Am. Chem. Soc.* **105** 2478 (1983)
193. T-C Tsai, J Hart, R-T Jing, K Bruzik, M-D Tsai *Biochemistry* **24** 3180 (1985)
194. T Rosario-Jansen, H Pownal, R-T Jiang, M-D Tsai *Bioorg. Chem.* **18** 179 (1990)
195. R Gigg *Chem. Phys. Lipids* **26** 287 (1980)
196. J Gigg, R Gigg *Top. Curr. Chem.* **154** 77 (1990)
197. E E Nifant'ev, D A Predvoditelev, M K Grachev, V A Shin *Dokl. Akad. Nauk SSSR* **235** 595 (1977)
198. V A Shin, D A Predvoditelev, E E Nifant'ev *Zh. Org. Khim.* **14** 948 (1978)
199. J J Oltvoort, C A A Van Boeckel, J H Koning, J H Van Boom *Recl. Trav. Chim. Pays-Bas* **101** 87 (1982)
200. C E Dreef, A R P M Valentijn, E de Vroom, G A Van de Marel, J H Van Boom *Tetrahedron Lett.* **29** 1199 (1988)
201. E B Burlakova. *Usp. Khim.* **44** 1871 (1975) [*Russ. Chem. Rev.* **44** 871 (1975)]
202. V V Ershov, G A Nikiforov, A A Volod'kin, in *Prostranstvenno-zatrudnennye Fenoly* (Sterically Hindered Phenols) (Moscow: Khimiya, 1972) p. 321
203. N A Zakharova, G N Bogdanov, M N Zaprometov, N A Tyukavkina, K E Kruglyakova, N M Emanuel' *Zh. Obshch. Khim.* **42** 1414 (1972)
204. R M Arneson *Lipids* **15** 203 (1980)
205. S G Batrakov, N N Pridachina, E B Kruglyak, E D Novogrudskaya, E V Chekasina *Izv. Akad. Nauk SSSR, Ser. Biol.* 177 (1984)
206. E B Burlakova, N E Khrapova *Usp. Khim.* **54** 1540 (1985) [*Russ. Chem. Rev.* **54** 907 (1985)]
207. V A Belyakov, V A Roginskii, N M Emanuel' *Dokl. Akad. Nauk SSSR* **257** 628 (1981)
208. N M Emanuel' *Usp. Khim.* **50** 1721 (1981) [*Russ. Chem. Rev.* **50** 901 (1981)]
209. V H Sies *Angew. Chem.* **98** 1061 (1986)
210. A P Khokhlov, K N Yarygin, E B Burlakova *Biol. Membr.* **6** 133 (1989)
211. J A Rogers, S S Davis *Biochim. Biophys. Acta* **598** 392 (1980)
212. E E Nifant'ev, D A Predvoditelev, A P Tuseev, M K Grachev, M A Zolotov *Zh. Obshch. Khim.* **50** 1702 (1980)
213. M A Zolotov, D A Predvoditelev, E E Nifant'ev *Zh. Obshch. Khim.* **50** 2380 (1980)
214. A E Arbuzov, V M Zoroastrova *Izv. Akad. Nauk SSSR, Otd. Khim. Nauk* 208 (1948)
215. A E Arbuzov, V M Zoroastrova *Izv. Akad. Nauk SSSR, Otd. Khim. Nauk* 770 (1952)
216. D C Ayres, S Rydon *J. Chem. Soc.* 1109 (1957)
217. O N Nuretdinova *Izv. Akad. Nauk SSSR, Ser. Khim.* 1808 (1979)
218. B A Arbuzov, R A Kadyrov, R P Arshinova, I Kh Shakirov, R R Shagidullin *Zh. Obshch. Khim.* **55** 1975 (1985)

Russian Chemical Reviews **63** (1) 91 — 101 (1994)
©1994 Russian Academy of Sciences and Turpion Ltd

UDC 615.37 + 543.06 + 543.8 : 581.19

Immunoassay of low-molecular-mass physiologically active substances of plant and microbial origin encountered in plants

S K Volkov

Contents

I. Introduction 91
II. Immunoassay 91
III. Conclusion 99

Abstract. The application of immune methods for the assay of both endogenic and exogenic low-molecular-mass physiologically active substances encountered in plants is considered. The bibliography includes 161 references.

I. Introduction

The determination of the content of biologically active substances in plant tissue constitutes one of the most important parts of the science of medicinal plants. The content of physiologically active substances in plant raw material determines not only the economic parameters of the manufacture of a number of medicinal preparations but also their quality.

Selection of the most productive types of plants is based on the quantitative assay of biologically active substances in various parts of plants. The development of biotechnological methods for the cultivation of plant cells and tissues likewise cannot take place without the quantitative assay of biologically active substances. Since many biologically active compounds of plant origin are narcotics, their quantitative determination is important from the criminological point of view.

The most important groups of biologically active substances of plant origin are alkaloids, including a series of narcotic substances, terpenoids, flavonoids, anthrones, steroids, plant growth and development regulators, and certain others. Certain substances which are not endogenic but enter the plant material from outside frequently have to be determined in plant tissues, particularly those used as food by man and as cattle feed. These include antibiotics and mycotoxins.

This review constitutes a continuation of the previously published article on the immunoassay of alkaloids [1] and for this reason alkaloids will not be considered here except for those groups of alkaloids which were not dealt with in the previous review. For the same reason, narcotic alkaloids (opiates and cocaine group alkaloids) will not be considered here either.

The principal advantages and disadvantages of the immune methods for quantitative assay, the approaches to the immunoassay of low-molecular-mass compounds, and the commonest methods of immunoassay were also examined in fair detail in the previous review.

S K Volkov The Standardisation Division, 'All-Russia Institute of Medicinal and Aromatic Plants' Scientific-Industrial Association, ul. Grina 7, 113628 Moscow, Russian Federation, Tel. (7-095) 388 45 22

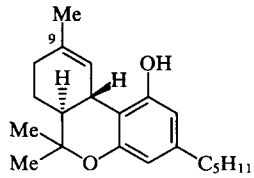
Received 28 November 1993
Uspekhi Khimii **63** (1) 93 – 103 (1994); translated by A K Grzybowski

II. Immunoassay

1. Narcotic substances

Narcotics of plant origin include not only many alkaloids but also a series of nonalkaloid compounds with biological activity. Biologically active substances of hemp (cannabinoids) occupy a by no means unimportant place among them.

Cannabinoids constitute a group of powerful narcotics — hallucinogens. Among cannabinoids, tetrahydrocannabinols are particularly dangerous. Thus Δ^9-tetrahydrocannabinol **1** (or Δ^1-tetrahydrocannabinol when a different system for the numbering of atoms is used) is the principal component of hashish and marijuana, which are prepared from Indian hemp (*Cannabis sativa*). When it acts on the organism in doses of the order of 10^{-5}–10^{-6} g (kg body weight)$^{-1}$, compound **1** induces a psychiatric disorder, a decrease in blood pressure, and a decrease in sensitivity to pain.



1

Several methods exist at present for the immunoassay of compound **1**. The fluorescence polarisation method is simple and convenient in the assay of a large number of specimens, but its sensitivity (5×10^{-5} g L^{-1}) is not always adequate. [2] The immunofluorescence method using antibodies bound covalently to magnetic particles, which makes it possible to carry out easily the stage involving the separation of the bound and free antigens, is more sensitive; as a result of the above features of this method, its sensitivity reaches 5×10^{-6} g L^{-1}. [2]

There exist also a homogeneous immunoenzyme method for the determination of cannabinoids, [3] the sensitivity of which is $(1.5-2.5) \times 10^{-2}$ g L^{-1}, and a solid-phase heterogeneous immunoenzyme method. [4] In the latter case, the immunogenic conjugate was obtained by oxidising compound **1** with potassium hexacyanoferrate(III) and conjugating the derivative obtained with the protein. The sensitivity of the solid-phase immunoenzyme method reaches 10^{-4} g L^{-1}.

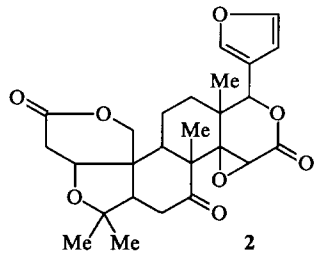
Diagnostic sets produced by the Abbot Company (UK) enable detection of **1** at a concentration of 9×10^{-6} g L^{-1}.

The immunoassay methods have been used hitherto only in the determination of cannabinoids and their metabolites in human biological liquids [6,7] but not for the quantitative assay of cannabinoids in plants.

2. Terpenoids

The class of terpenoids or isoprenoids, the first representatives of which were isolated from turpentine, constitute a large group of biologically active compounds of plant and animal origin. Terpenoids include certain natural glycosides (saponins), yellow and orange plant pigments (carotenoids, xanthophylls), natural rubber, products derived from pine resin, and a number of other substances.

Limonin 2. This triterpene is concentrated in the seeds of many types of plants of the genus *Citrus* (*Rutaceae*) and when it contaminates lemon juice it imparts an excessively bitter flavour to the latter. Since the amount of compound **2** in the plant can differ greatly from batch to batch, its content must be monitored, since the bitterness of the juice increases sharply in the range of concentrations of compound **2** from 10^{-7} to 10^{-6} g L^{-1}. This requirement has led to the development of a series of methods for the immunoassay of compound **2**.



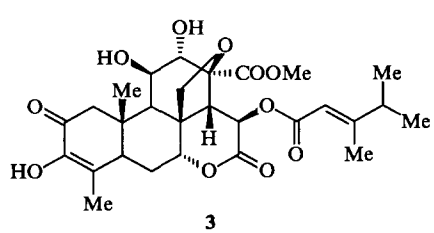
2

In order to obtain an immunogenic conjugate, compound **2** was attached to bovine serum albumin (BSA) with the aid of aminooxoacetic acid. The antiserum to this conjugate was used to develop radioimmunoassay methods using the conjugate of the methyl ester of 7-(*O*-carboxymethyl)limonin with the ^{125}I-labelled aminooxo-derivative of tyrosine[8] and also ^{3}H-labelled limonol.[9] The same antiserum has been used for the development of an immunoenzyme assay method using the 7-(*O*-carboxymethyl)oxime of compound **2** conjugated with alkaline phosphatase by the carbodiimide method.[10] Radioimmune methods using ^{125}I- and ^{3}H-labelled compounds make it possible to determine compound **2** in the ranges $10^{-10}-10^{-7}$ and $5 \times 10^{-10}-10^{-7}$ g respectively. Although the immunoenzyme method is somewhat less sensitive (the range of the determination is $10^{-9}-10^{-7}$ g), nevertheless it makes it possible to work with more stable substances and to carry out the assay in 1 h.

The radioimmune method has been used to investigate the distribution of compound **2** in the tissues of *Citrus paradisi*.[8] The immunoenzyme method has been applied to the assay of specimens of lemon juice and a satisfactory agreement has been observed with the results of assay by the HPLC method, but the immunoenzyme method does not require special preparation of the specimen and takes less time.[10]

A set for the immunoenzyme assay of compound **2** is manufactured by the Idetek Company (USA).[11]

Bruceantin 3. This secotriterpenoid, isolated from *Brucea antidisenterica* (*Simaroubaceae*), exhibits an appreciable antitumour activity. As for other medicinal drugs, immunoassay methods greatly facilitate the study of the pharmacological properties of compound **3**.

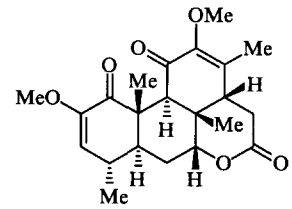


3

In the development of the radioimmunoassay method, compound **3** was conjugated with BSA with the aid of succinic anhydride, and an antiserum to this conjugate was obtained.[12] Radioimmunoassay with the use of [^{3}H]acetylbruceantin, obtained by treating compound **3** with [^{3}H]acetic anhydride, makes it possible to determine compound **3** in the range 5×10^{-10} to 5×10^{-8} g.[12]

The method has been used to study the distribution of compound **3** in mouse body tissues and for its removal from the dog; immune methods have not been applied to the assay of compound **3** in plants.

Quassin 4. This secotriterpenoid, which has an extremely bitter taste, has been isolated from *Quassia amara*. It is used to impart a bitter flavour in the food industry. Methods for the immunoassay of compound **4** have been developed in order to monitor the manufacture of products and also for the analysis of plant cell clones.



4

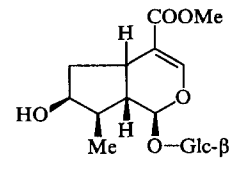
In devising an immunoenzyme method, the δ-lactone of quassin was converted into a derivative with a free carboxy-group, which was stabilised by epimerisation to form isoquassinic acid.[13] Isoquassinic acid was conjugated with BSA by the mixed anhydride method and a rabbit was immunised with the conjugate. The competing conjugate of compound **4** with the haemocyanine of the edible snail (KLH) was obtained by the carbodiimide method. The immunoenzyme method using goat antibodies to rabbit immunoglobulins G (Ig G), conjugated to alkaline phosphatase, makes it possible to determine the concentration of compound **4** in the range $2 \times 10^{-9}-2 \times 10^{-7}$ g. Appreciable cross-reactions were noted for methyl isoquassinate, α- and β-neoquassin, 14,15-dehydroquassin, 12- and 18-hydroxyquassin, and also nigakilactones and picrasin A from *Picrasma excelsa*.

Another method is based on the application of the antiserum to 18-hydroxyquassin conjugated with BSA by means of succinic anhydride. In other respects, the method is similar to the previous one and makes it possible to determine quassin in the range $5 \times 10^{-9}-10^{-7}$ g.[14] The method has been used to investigate the distribution of immunoresponsive substances in the tissues of *Q. amara*, *Q. indica*, and *P. excelsa*.[14]

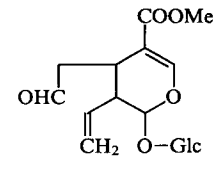
The immunoenzyme method for the determination of quassinoids has been used in the study of the tissues and cell cultures of *Ailanthus altissima*.[15]

3. Iridoid glycosides

The monoterpene glycosides loganin **5** and secologanin **6** are intermediates in the biosynthesis of many alkaloids.



5



6

Radioimmunoassay methods have been developed for the investigation of the biogenetic transformations of compounds **5** and **6**.[16] Loganin was converted into the 6′-carboxy-derivative involving the glucose residue and was conjugated with BSA by the carbodiimide method. The radioimmune method using the ^3H-labelled derivative, obtained by the periodate cleavage of compound **5** and subsequent reduction by NaB^3H_4, makes it possible to determine compound **5** in the range 5×10^{-10} to 10^{-7} g. Cross reactions with compound **6** (0.07%) and the aglycone of compound **5** (30%) have been noted.

The method was used to determine compound **5** and to investigate its conversion into compound **6** in *Weigela gigantiflora* and *Lonicera tatarica* cell cultures.[16]

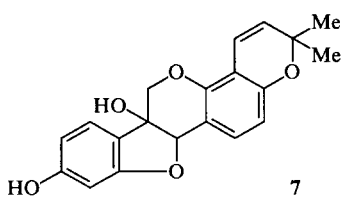
4. Sesquiterpenes

Sesquiterpenoid compounds are contained in various plant essential oils and resins (balsams). The group of sesquiterpenes includes substances such as juvenile hormones, perfumes, sesquiterpene lactones and phytoalexins, as well as ichthyotoxins.

5. Phytoalexins

The group of phytoalexins includes highly reactive compounds which protect plants against disease. They are synthesised by plants only in response to tissue trauma and for this reason they are also referred to as stress metabolites. The system for the production of phytoalexins by plants is sometimes referred to as the immune system of plants. Phytoalexins possess antimicrobial properties.

Glyceollin I (compound 7) is the main phytoalexin accumulating at the sites of tissue trauma or infection of soya bean (*Glycine max L. Merrill*).



7

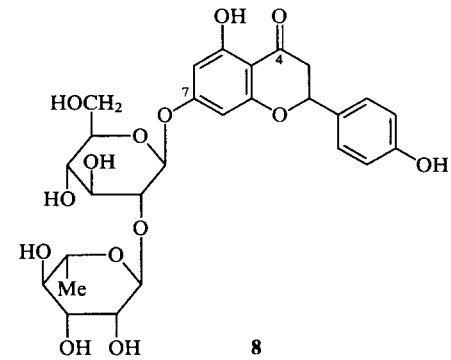
In the synthesis of the immunogenic conjugate of compound **7**, the BSA derivative of *p*-aminohippuric acid was obtained initially. For this purpose, a mixture of *p*-aminohippuric acid and BSA at pH 6.4 was treated with the hydrochloride of 1-ethyl-3-(3-dimethylaminopropyl)carbodiimide.[17] The derivative obtained was treated with $NaNO_2$ at pH 1.5 at 0 °C (the excess $NaNO_2$ was decomposed with ammonium sulfamate) and was then conjugated with compound **7** at pH 9.0 at 0 °C.[18]

The antiserum to the resulting conjugate is highly specific to compound **7**. Structural isomers of compound **7** — glyceollin II and glyceollin III — are fairly poorly recognised by the antiserum: 5.7% and 1.0% respectively. The radioimmunoassay method using [^{125}I]glyceollin I makes it possible to determine compound **7** at a concentration of 1×10^{-5} M.[19] The method has been used to determine compound **7** in soya bean tissues.

6. Flavonoids

The group of flavonoids combines the hydroxy-derivatives of flavanone, flavanonol, catechins, flavone, flavonol, and anthocyanins. These substances are present in many plants and exhibit vitamin P activity.

A series of bitter flavonoid 7-*O*-neohesperidosides have been detected in *Citrus* (*Rutaceae*) fruits. The main one is **naringin 8**. The content of compound **8** in the grapefruit (*C. paradisi*) can reach a level such that both the fruits themselves and the juice obtained from them acquire an excessively bitter flavour. Two radioimmunoassay methods for compound **8** have been developed for the rapid monitoring of the quality of the produce. In the synthesis of the immunogenic conjugate, the amino-groups of BSA were modified with *p*-aminohippuric acid and were then attached to compound **8** by diazotisation. The radioimmunoassay method using a ^{125}I-labelled competing conjugate makes it possible to determine compound **8** in the range $5 \times 10^{-9} - 2 \times 10^{-7}$ g. The method is very sensitive to the nature of the sugar residue in the 7-position, but is insensitive to changes in the aromatic ring. All the flavonoid 7-*O*-neohesperidosides are recognised by the antiserum to the same extent.[20]



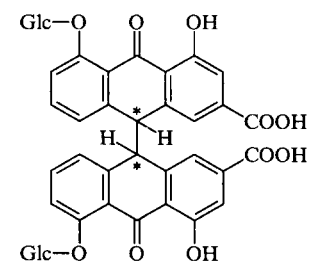
8

In another instance, the immunogenic conjugate was synthesised by activating the 4-oxo-group in compound **8** with aminooxoacetic acid and was attached to BSA by the mixed anhydride method. The ^3H-labelled conjugate was obtained by condensing the (4-*O*-carboxymethyl)oxime of compound **8** with 5-aminolevulinic acid by the mixed anhydride method and by the reduction of the side chain with NaB^3H_4. The radioimmunoassay method permits the determination of compound **8** in the range $5 \times 10^{-10} - 5 \times 10^{-8}$ g.[21]

Both these methods have been used to determine the content of flavonoid 7-*O*-neohesperidosides in grapefruit juice and in the study of the distribution of immunoresponsive substances in grapefruit tissues.[21] It was shown that the data obtained by the radioimmune method agree well with the results of the assay by the HPLC method. The second method has been used also to analyse grapefruit juice under the conditions of large scale production.

7. Anthrones

Isomeric dianthrone glucosides — **sennosides A (compound 9)** and **B (compound 10)** isolated from a series of *Cassia* (*Caesalpinaceae*) species — are highly active laxatives and constitute one of the classes of substances of plant origin most widely used in pharmaceutical practice. This stimulated the development of a method for the radioimmunoassay of dimeric glucosides.[22]



9, 10

In order to obtain the immunogenic conjugate, compound **10** was attached to BSA by the carbodiimide method. The radioimmune method using [^{3}H]-8-glucosidorheinanthrone, obtained by reducing compound **10** with NaB^3H_4, makes it possible to determine compound **10** in the range $4 \times 10^{-10} - 8 \times 10^{-9}$ g. Cross reactions have been noted for compound **9** (75%), sennoside C (100%), 8-glucosidorheinanthrone (55%), and sennidins A (25%) and B (10%).

The method has been used to investigate the distribution of compounds **9** and **10** in various parts of *Cassia augustifolia*.

8. Steroids

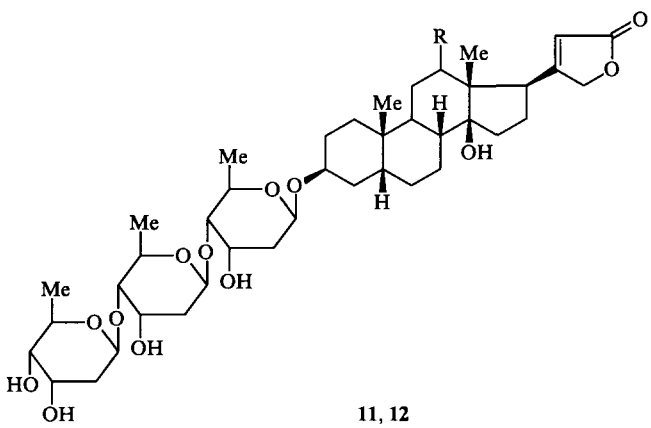
A large group of steroid glycosides of plant and animal origin is combined under the general name cardioactive or cardiotonic substances. At low concentrations, they normalise the working of the heart muscle, whilst in large doses they induce cardiac arrest in the systolic period. In contrast to their aglycones, cardiac glycosides are concentrated in heart muscle and their content in the latter is 10–40 times greater than in other tissues of the organism.

a. Digitalis cardenolides

The myocardium-stimulating digoxin and digitoxin are isolated from the leaves of *Digitalis lanata* (*Scrophulariaceae*), where they accumulate together with related glucosides.

Digoxin 11 (R = OH) is one of the substances of plant origin for the assay of which immune methods are used very widely.

The first attempts to devise an immunoassay method for compound **11** date back to 1967 when antibodies specific to compound **11** were obtained.[23] A method for the radioimmunoassay of compound **11** for use under clinical conditions was developed in 1970[24,25] and subsequently methods suitable for the determination of compound **11** in plant tissues were developed.[26–28] All these methods employ the rabbit antiserum to the conjugate of compound **11** with BSA or human serum albumin (HSA) obtained by the periodate oxidation method. The range of the determination of compound **11** is 8×10^{-10} to 4×10^{-8} g when [^{3}H]digoxin is used[25] and 5×10^{-10} to 5×10^{-9} g when the methyl ester of digoxin-[^{125}I]tyrosine is employed.[26] The study of cross-reactions with a large number of related structures showed that the serum obtained makes it possible to determine the sum of the digitoxigenin glycosides in extracts from *D. lanata*.



11, 12

Immune methods have been used to determine the level of compound **11** in the serum of blood from patients[25] and also for the investigation of the distribution of compound **11** in the tissues of *D. lanata*.[26,27] It was established that the main bulk of compound **11** accumulates in leaves after 8–12 weeks. The radioimmune method makes it possible to determine the optimum period for the harvesting of leaves. The same method has been applied in the selection of plants most productive as regards compound **11**.[28] The content of compound **11** in the tissues of *D. lanata* and *D. purpurea* was determined with its aid during the growth of these plants.[29]

In subsequent years, many immunoassay methods for compound **11** were developed: radioimmune,[30–32] immunoenzyme,[29,32–34] immunoluminescence,[29,35] and fluoroimmune[36] methods, a combined liquid chromatographic-immune method,[37] immune methods involving the measurement of the degree of polarisation of fluorescence,[32,38–43] an immune method using particles of polystyrene latex,[44] a chemiluminescence immunoenzyme method,[45] a heterogeneous competitive immunoenzyme method with electrochemical detection,[46] a fluorescence method with transfer of excitation energy,[32,47–49] and a number of others.[42,50] The methods developed have been used to assay compound **11** in the serum,[32,33,42,47–49,51–58] plasma,[30,39,42,49,59] urine,[30] saliva,[31] and blood of patients[60] and also for the investigation of the pharmacokinetics of compound **11**.[61] Only one of these methods has been applied to its determination in the cell culture of *D. lanata* roots.[33]

Comparison of the immune methods with one another and also with methods based on high performance liquid chromatography showed that many substances related to digoxin, frequently present in the specimen, as well as certain metabolites of compound **11** affect appreciably the results of the determination of compound **11** by immune methods.[30,32,38–40,51–57,62,63] The attempts to eliminate this influence led to the appearance of immune methods based on monoclonal antibodies[58] and to the introduction of stages involving additional purification of the specimens analysed.[37,43,44,64]

Many Companies manufacture sets for the immunoassay of compound **11**. The sets produced by Companies such as Syva Corporation, E.I. du Pont de Nemours, New England Nuclear, Amersham Corporation (USA), and a number of others have come to be most widely used. These sets are widely employed in clinical and laboratory practice for the determination of compound **11** in blood plasma and serum, in urine, and in other physiological liquids. A method for the radioimmunoassay of the total digoxigenin glycosides in the *D. lanata* plant has been developed on the basis of one of such sets — the 'Digoxin RIA kit' produced by the Farmos Diagnostica Company (Finland).[64]

Digitoxin 12 (R = H). An antiserum to the conjugate of digitoxigenin (aglycone) with BSA, obtained by 3-*O*-succinylation and carbodiimide condensation, was isolated in 1968 from rabbit.[65] The radioimmune method using the conjugate of the methyl ether of 3-*O*-succinyldigitoxigenin with [^{125}I]tyrosine makes it possible to determine compound **12** in the range 2×10^{-10}–2×10^{-8} g. The contribution of the cross-reaction with compound **11** is 10%. The method has been used to determine the content of compound **12** in the serum of blood from patients.

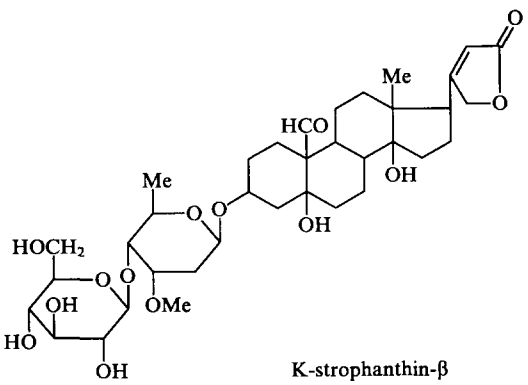
The method developed subsequently for the analysis of patients' blood, involving the measurement of the degree of polarisation of fluorescence, yielded the same results as the radioimmune method.[66]

The radioimmune method using [^{125}I]digitoxigenin has been applied to the assay of compound **12** in urine specimens after preliminary purification of the extract by reverse-phase HPLC.[67] Immune methods have not so far been applied to the assay of compound **12** in plants.

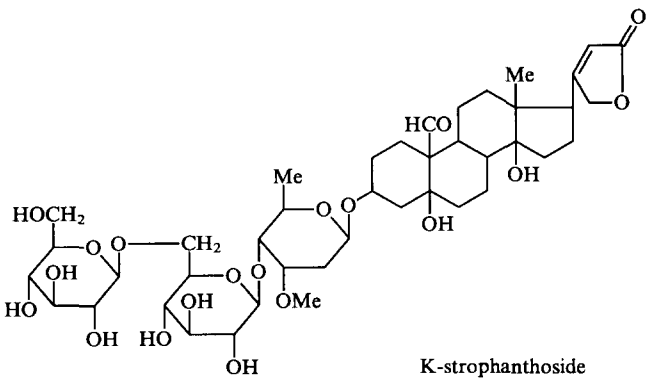
b. K-Strophanthin

K-Strophanthin **13** is a typical representative of cardiac glycosides with a cardenolide aglycone. It is a mixture of the cardiac glycosides K-strophanthin-β and K-strophanthoside. Strophanthin is present in various *Strophanthus* species.

The immunogenic conjugate with BSA was obtained by the periodate oxidation of compound **13**.[68] The use of this conjugate made it possible to obtain antibodies specific to compound **13** and to devise an immunoenzyme assay method whereby it is possible to determine compound **13** in the concentration range 10^{-9}–10^{-3} M.[69] Subsequently immunoenzyme methods were developed for the assay of compound **13** using the antigen immobilised on AH-agarose,[70] on nitrocellulose membranes,[71] and also on activated polystyrene pellets.[72] The latter methods make it possible to determine compound **13** in the concentration range 10^{-8}–10^{-3} M; the sensitivity of the method reaches 10^{-10} M.[71,72] These methods were developed to assay compound **13** in the blood and other biological liquids of patients; immune methods have not so far been applied to the assay of compound **13** in plant tissues.



K-strophanthin-β



K-strophanthoside

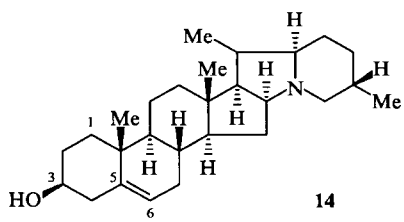
9. Steroid glycoalkaloids in *Solanaceae*

Plants of the genus *Solanum* (*Solanaceae*) produce a series of steroid glycoalkaloids. Certain representatives of *Solanaceae* are of greatest interest from this standpoint.

1. The potato (*S. tuberosum*) contains a number of bitter toxic derivatives of solanidine, mainly α-solanine and α-chaconine. The assay of these compounds is important for work involving selection. Furthermore, during incorrect storage of the tubers or when the potato is grown under unfavourable climatic conditions, the content of these glycoalkaloids can increase greatly, impairing the flavour of the potato.

2. The alkaloid solasodine, which serves as the starting material for the synthesis of a series of steroid preparations (progesterone and corticosteroids), accumulates in the leaves of a series of *Solanaceae* species (*S. laciniatum* and *S. aviculare*).

Glycoalkaloids — glycosidic derivatives of solanidine 14. A radioimmunoassay method for compound **14**, based on the use of the antiserum to compound **14** conjugated with BSA via the 3-hydroxy-group, was developed in 1979.[73] This method makes it possible to determine compound **14** in the range 2×10^{-10} to 5×10^{-8} g. The contribution of the cross-reaction with α-solanine is 28%.

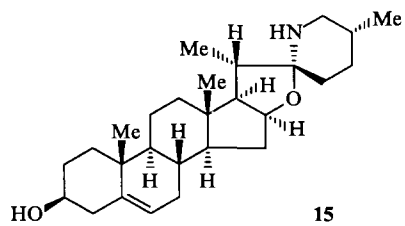


14

The conjugate of α-solanine with BSA was synthesised in 1983 by the periodate cleavage method.[74,75] The rabbit antiserum to this conjugate is equally sensitive to compound **14**, α-solanine, α-chaconine, and demissidine, which is very convenient for the determination of the overall content of glycoalkaloids in potato tubers. The radioimmune method using ^{3}H-labelled compound **14** makes it possible to determine these glycoalkaloids in the range $2 \times 10^{-10}-8 \times 10^{-9}$ g,[76] while the immunoenzyme method permits their determination in the range $10^{-11}-10^{-9}$ g.[75]

The radioimmune method has been used to determine compound **14** in human blood serum.[76,77] The results of assays obtained by the immunoenzyme and chemical methods have been compared. It was established that they agree well, but the immunoenzyme method is simpler, rapid, and less subject to technical errors.[78,79]

Glycoalkaloids — glycosidic derivatives of solasodine 15. The immunogenic conjugate was obtained by subjecting a 2:3 mixture of solasonine and solamargine to periodate cleavage followed by attachment to HSA.[75] The radioimmune method using ^{3}H-labelled glycoalkaloids, based on the application of the rabbit antiserum, makes it possible to determine derivatives of compound **15** in the range $10^{-9}-10^{-7}$ g. Reactions with solasonine (100%), solamargine (110%), and tomatine (104%), as well as the aglycones of tomatidine (21%), soladulcine (5%), and compound **15** (7%) have been noted.



15

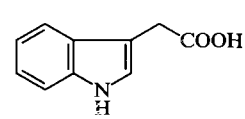
This method has been applied in the study of the content of compound **15** in the tissues of *S. laciniatum* and *S. aviculare*.[75]

10. Plant growth and development regulators

Plant bioregulators are low-molecular-mass products of the secondary metabolism of plants. Phytohormones, natural stimulators, and inhibitors are distinguished among them.

Phytohormones include auxins, gibberellins, abscisic acid, cytokinins, and ethylene. In contrast to other physiologically active compounds, phytohormones are bioregulators common to all plants. They are synthesised in actively dividing cells, after which they are transported to other organs and tissues where they initiate chemically physiological programs. The molecular mechanisms of the action of plant hormones are apparently associated with the regulation of protein synthesis, the activity of enzymes, and transport through a biological membrane.

Auxins constitute a group of natural compounds which stimulate cell division (mitosis), root formation, respiration, and the synthesis of protein in plants. The main representative of auxins is indolylacetic acid **16**.

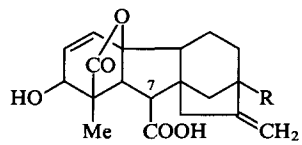


16

The Mannich reaction was used to synthesise the immunogenic conjugate of compound **16** with BSA; compound **16** is linked to the protein via the nitrogen atom.[76]

The formation of the bond via the carboxy-group (the mixed anhydride method) affords more stable conjugates, which induce a somewhat greater immune response both in rabbits[77] and in mice.[78]

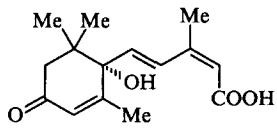
Gibberellins are diterpenoid tetracyclic mono-, di-, and tricarboxylic acids. The mechanism of the biological action of gibberellins has been inadequately investigated. It is known that they alter the properties of membranes and induce the synthesis of α-amylase in barley grains, while in the tissues of other plants they alter the systems comprising RNA and functioning enzymes. About 70 gibberellins have now been found in nature and antisera have been obtained and immunoassay methods have been developed for some of them [including the gibberellins A_3 **17** (R = OH) and A_7 **18** (R = H)].[79–83]



17, 18

The immunogenic conjugates are obtained by forming an amide linkage between the C(7)-carboxy-group of gibberellin and the amino-groups of the protein.[79] Alternatively, the mixed anhydride method is used, but in this case conjugates with a fairly low hapten density are obtained owing to steric hindrance. A spacer is introduced between the hapten and the protein in order to increase the hapten density.[82,83]

Abscisic acid 19 is a highly specific inhibitor of the growth of higher plants. It causes a transition of the plant to the resting state and induces wilting and shedding of leaves and fruit.

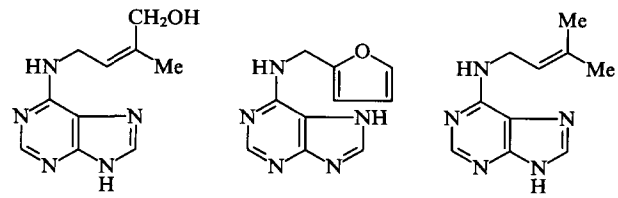


19

The conjugates of compound **19** may be synthesised using both the carboxy-group[84,85] and the carbonyl[85] group. In order to obtain a conjugate of compound **19** with a protein via the carboxy-group, a solution of the hapten and the protein in a mixture of dimethylformamide and water at pH 8 is treated with the hydrochloride of 1-ethyl-3-(3-dimethylaminopropyl)-carbodiimide.[85] The antiserum to this conjugate interacts with the protonated form of compound **19** and its esters but hardly interacts with the deprotonated compound **19**, which is the main one actually present under the conditions of the immunoassay (pH 7–8).

The conjugate via the carbonyl group is synthesised by carrying out initially the reaction between compound **19** and tyrosine hydrazide in the presence of acetic acid in order to obtain the tyrosylhydrazone of compound **19**. BSA *p*-aminohippurate is obtained simultaneously by the reaction of *p*-aminohippuric acid with BSA in the presence of 1-ethyl-3-(3-dimethylaminopropyl)-carbodiimide. The modified protein is treated with $NaNO_2$ at pH 1.5 and ammonium sulfamate and is condensed with the tyrosylhydrazone of compound **19** at pH 9.[85] The antibodies to this conjugate are preferable in those cases where it is proposed to assay compound **19** in the form of the anion. Such antibodies interact very weakly or not at all with the protonated form of compound **19**.

Cytokinins constitute a special group of plant growth and development regulators which stimulate cell division (cytokinesis). This group includes the *N*(6)-derivatives of adenine—zeatin **20**, kinetin **21**, and isopentenyladenine **22**. In plants, they are frequently encountered in the form of the less active ribosides and ribotides and are one of the constituents in the structures of certain transport RNA of plants.



20 **21** **22**

The mechanism of the biological action of cytokinins is apparently associated with the intensification of the biosynthesis of DNA, RNA, and protein and also with their influence on the functioning of biological membranes.

Cytokinins have been traditionally assayed by biological methods, but the sensitivity and selectivity of these is low.[86,88] The physicochemical and immunochemical assay methods are superior to the biological methods as regards sensitivity, specificity, and reproducibility and take less time.[89,90]

The preparation of the immunogenic conjugates of cytokinins is based on the periodate oxidation of the riboside to the corresponding aldehyde, which can interact with the amino-groups of the carrier protein. For this purpose, the cytokinin riboside in methanol was treated with sodium periodate, the excess of which was decomposed with ethylene glycol. A solution of the carrier protein at pH 9.3 was treated with the dialdehyde obtained from the cytokinin riboside; the complex thus produced was stabilised by reduction with tetrahydroborate.[91]

The first radioimmunoassay methods permitting the determination of compound **22** in an amount of about 10^{-8} g were used in the study of plant transport RNA.[92–94] Analysis of the cross-reactions showed that the antiserum obtained to the conjugate of compound **22** with the protein interacts with the phosphate of compound **22** (100%) and with isopentenyladenine (10%).[94] The interaction of the antiserum with compound **21** is weaker by a factor of 100 and that with adenosine is weaker by a factor of 300 000 than the interaction with compound **22**.[94]

The use of the immune method for the assay of cytokinins in plants was described in 1979, but the antibodies to compound **22** interacted strongly with *trans*-zeatin riboside and dihydrozeatin riboside.[95]

A sensitive and specific radioimmune method for the determination of *trans*-**20** was developed in 1980.[96] The limit of the determination of *trans*-**20** amounted to several femtomoles. The antibodies did not interact with *cis*-**20**.

The antisera to compound **22** made it possible to attain a limit in the determination of compound **22** of 5×10^{-11} to 10^{-9} g.[89,97–99] These antisera interact only weakly with cytokinins of the zeatin group, but they do interact appreciably with 6-benzylaminopurine cytokinins.

It was established that the interaction of cytokinin molecules with the corresponding antibodies depends mainly on the nature of the substituent at the N(6) atom. Owing to the appreciable cross-interactions, the accurate assay of cytokinins by the immune methods requires the introduction of a stage involving preliminary chromatographic purification.[100] Column chromatography on cellulose phosphate and Sephadex LH-20 is used for this purpose.[100,101] However, these procedures require a fairly long time, so that simpler purification procedures with the aid of thin-layer chromatography (TLC)[99] and HPLC[102] have been proposed. The choice of a suitable sorbent for HPLC makes it possible to attain the complete separation of the cytokinins assayed. As a rule, reversed-phase sorbents are used for this purpose—Bondapak C 18,[102–104] Lichrosorb RP-8,[105] Hipersil ODS,[106,107] and Sep-Pak C 18.[97,108] The preliminary purification of the specimen can be carried out with the aid of an immunoaffine column.[109]

11. Other compounds

Immunoassay methods for compounds which are not endogenic in plants but which it is sometimes necessary to determine in plant material will be examined in this part of the review. In the first place, these are undesirable substances in plants designed for use as food. Such substances are formed on microbial infection of the plant material.

a. Antibiotics

In a number of instances, as a result of the infection of the plant raw material by microorganisms, such material may be contaminated with the antibiotics produced by such microorganisms.

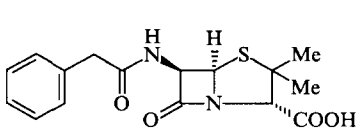
Natural substances and the products of their chemical modification, capable of suppressing at low concentrations ($10^{-6}-10^{-5}$ g L^{-1}) the development of bacteria, lower fungi, protozoa, viruses, and malignant tumour cells, are classified nowadays as antibiotics.

The group of β-lactam antibiotics includes penicillins, cephalosporins, cephamycins, and certain other antibiotics. The mechanism of the action of β-lactam antibiotics involves the suppression of the synthesis of the bacterial cell wall.

Penicillins possess a broad spectrum of antibacterial activity, exhibiting both bacteriostatic and bactericidal activities in relation to many gram-positive microorganisms (staphylococci, pneumococci, and streptococci), certain gram-negative cocci (gonococci, meningococci), Siberian ulcer bacilli, clostridia, spirochaetes, and certain fungi.

In the immunoassay of penicillins, serious problems, associated with their instability, arise: penicillins readily hydrolyse in aqueous solutions, the hydrolysis products being capable of binding to proteins. Because of this, the sensitivity, the degree of cross-interaction, and the parameters of the binding of antibodies to antigens vary as a function of the degree of hydrolysis of penicillins and the composition of the buffer solution. Hydrolysis of the β-lactam ring of penicillins in 0.1 M NaOH solution or on treatment with β-lactamase also affects these parameters. An additional source of error is the nonspecific binding of penicillins to the proteins present in the specimen assayed.[110]

Despite the complexities in the development and application of immunoassay methods for penicillins, their description is appearing with increasing frequency in the scientific literature. Thus an immunoenzyme method has been developed for the determination of penicillin G **23** and its derivatives in cow's milk and in bovine blood serum.[111]

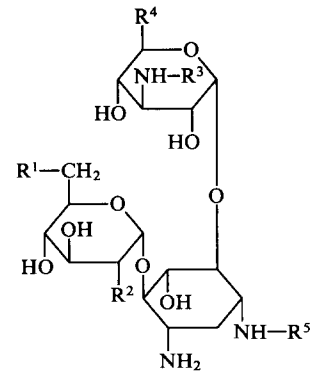


23

Aminoglycoside antibiotics represent a large family of antibiotics numbering more than 100 natural compounds produced by microorganisms of the genera *Streptomyces, Micromonospora,* and *Bacillus* as well as a large number of semisynthetic analogues. The mechanism of the action of these antibiotics has not been finally established.

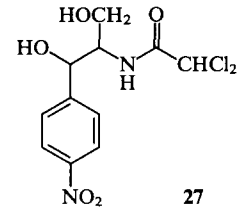
A wide range of immunoassay methods are used for the assay of aminoglycoside antibiotics.[112–114] Thus immunoassay methods have been used in the assay of gentamicin **24** (R^1 = OH, R^2 = NH_2, R^3 = Me, R^4 = R^5 = H),[115,117] amikacin **25** [R^1 = NH_2, R^2 = OH, R^3 = H, R^4 = CH_2OH, R^5 = C(O)CH(OH)Pr],[117,118] and tobramycin **26** (R^1 = R^2 = NH_2, R^3 = R^5 = H, R^4 = CH_2OH).[117,119–121] Immunofluorescence methods are also widely used in the assay of these antibiotics.[118,121,122]

The 'Optimate' automatic system, based on the immunofluorescence assay method, is used for the assay of compounds **24** and **25**.



24–26

Chloramphenicol 27 occupies a special place among antibiotics. It proved to be the first preparation active against rickets and intracellular parasites which give rise to diseases such as typhus and spotted fever. Chloramphenicol suppresses also many gram-negative and certain gram-positive bacteria and is effective in the treatment of typhoid fever and infections induced by *Haemophilus influenzae, Klebsiella pneumoniae,* spirochaetes, and especially salmonellas, which are resistant to other antibiotics. The therapeutic use of compound **27** is restricted by allergic reactions and the rare instances where the erythropoiesis in the bone marrow is affected, but it is widely used for the inhibition of the biosynthesis of protein in plant chloroplasts.



27

Antibodies to the conjugate of compound **27** with bovine γ-globulin, synthesised by the diazotisation method, were obtained in 1966.[123] An immunoenzyme method for the assay of compound **27**, based on the use of the rabbit antiserum to the conjugate of compound **27** with KLH, obtained with the aid of succinic anhydride and carbodiimide, was developed in 1984.[124] The use of goat antibodies to rabbit Ig G conjugated with peroxidase permits the determination of compound **27** in the range $4 \times 10^{-10}-4 \times 10^{-8}$ g.

A radioimmunoassay method has been developed for residues of compound **27** in food products.[125,126] A review on the immunoenzyme and liquid-chromatographic methods for the determination of residues of compound **27** in milk and pig tissues has been published recently.[127] A set for the immunoenzyme assay of compound **27** in human blood serum is manufactured by the Aesculaap BV Company (Holland).[128]

Immune methods have not so far been used to determine antibiotics in plant raw material.

b. Mycotoxins

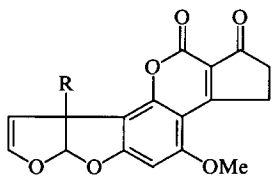
Certain mould species (*Aspergillus, Penicillium*) produce under certain conditions mycotoxins—highly toxic, sometimes carcinogenic secondary metabolites. A special effort has been made to develop methods for the immunoassay of mycotoxins. There are several reasons for this. Firstly, contaminated batches of products are frequently inhomogeneous, which requires the analysis of a large number of specimens. Secondly, in view of their high toxicity, the toxins must be assayed at a level of 10^{-12} g. Thirdly, owing to the presence of large amounts of chemically related compounds, the methods must be highly specific.

Although several tens of studies on the immunoassay of mycotoxins have already appeared in 1976, very often only a few of the proposed methods have found practical application. This is associated as a rule either with the low quality of the antiserum obtained (small amount, low avidity, poor specificity) or with the unsatisfactory reproducibility of the method.

However, the interest in the development of immunoassay methods for mycotoxins has not weakened owing to the large losses of food products due to their contamination by myxotoxins. According to data produced by Biotech Research Company (USA), about 50 million dollars were spent in 1985 on tests for the presence of aflatoxins in food products alone. [129]

There are at present a series of methods for the immunoassay of mycotoxins. [130, 131]

Among the large number of mycotoxins, aflatoxins, which are secondary metabolites produced by *A.flavus* and *A.parasiticus* species, constitute a special danger. [132] Several immunoassay methods for aflatoxins have been developed. [132–136]



28, 29

Aflatoxin B_1 28 (R = H). This mycotoxin is one of the most carcinogenic among substances known at the present time. It is produced by several *Aspergillus* species. It has been shown that compound **28** causes cirrhosis and cancer of the liver in children. When it enters the organism, aflatoxin B_1 is epoxidised by cytochrome P-450 and binds to RNA, which leads to the inhibition of protein synthesis. LD_{50} for compound **28** is $3 \times 10^{-4} - 1.02 \times 10^{-2}$ g (kg bodyweight)$^{-1}$.

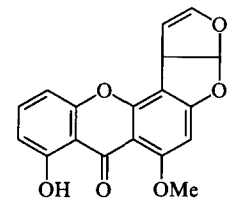
In order to obtain an antiserum aminooxoacetic acid was attached to the keto-group in compound **28** and the resulting derivative was conjugated with BSA by the mixed anhydride method. Polyclonal [138] and monoclonal [139] antisera were obtained on the basis of this conjugate. When used in the immunoenzyme method, both antisera make it possible to attain a limit of determination of 10^{-13} g. They are used to monitor the content of compound **28** in grain and in other food products, for example in groundnut oil. [138, 139]

In another method, the hemiacetal of compound **28** was conjugated by the Mannich reaction with methylalbumin either indirectly or via ε-aminocaproic acid. [140] An immunoenzyme method was developed on the basis of antisera to these conjugates. It makes it possible to determine compound **28** and aflatoxin M_1 **29** (R = OH) in the range $10^{-12} - 2 \times 10^{-10}$ g, aflatoxins P_1 in the range $10^{-11} - 2 \times 10^{-10}$ g, and aflatoxins G_1 in the range $(1-2) \times 10^{-10}$ g.

Sets for the immunoenzyme assay of compound **28** are manufactured by Neogen Corporation, Agritech Systems, Immuno Systems, Biotech Research Laboratories, Biokits (USA), and May and Baker Diagnostics (Great Britain). The URVJT Company (Czechoslovakia) manufactures a set for the radioimmunoassay of compound **28**. [11, 141]

Aflatoxin M_1 29 (R = OH). This aflatoxin is a product of the metabolic oxidation of compound **28** in the cow. On passing with cow's milk into humans, it can be the cause of cancer or cirrhosis of the liver. For this reason, almost all the methods developed for the immunoassay of compound **29** are designed particularly for the analysis of cow's milk. [142–145]

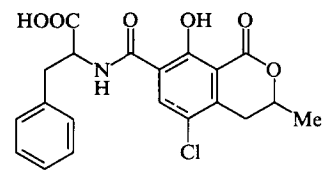
Sterigmatocystin 30. This substance, which is a toxic metabolite of the *Aspergillus* species, exhibits powerful hepatocarcinogenic properties. In view of the sparing solubility of compound **30** in water, a method has been developed for the assay of its hydrolysed derivative.



30

For this purpose, the conjugate of compound **30** with BSA was converted into a hemiacetal with which rabbits were immunised. [146, 147] The immunoenzyme method, developed on the basis of the resulting antiserum, makes it possible to determine compound **30** in the range $10^{-12} - 10^{-9}$ g.

Ochratoxin A 31 is a powerful liver poison, frequently formed during the storage of grain in temperate climatic zones. In order to develop an immunoenzyme assay method, compound **31** was attached to protein via the carboxy-group and an antiserum was obtained, which makes it possible to detect compound **31** in amounts down to 10^{-11} g. A cross-reaction has been noted only for the non-toxic ochratoxin B (0.5%). [148, 149]



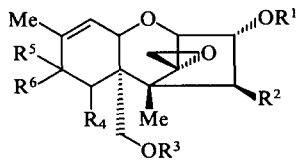
31

The method developed has been used in the study of specimens of the kidneys [150] and livers [151] of pigs fed with grain subjected to prolonged storage and also in the assay of compound **31** in the grain itself. [152]

The application of monoclonal antibodies made it possible to devise an immunoenzyme method for the determination of ochratoxin A in the range $5 \times 10^{-13} - 2.5 \times 10^{-10}$ g. [153, 154] Cross-reactions with the ethyl ester of compound **31** and with ochratoxin C have been noted.

Sets for the immunoenzyme assay of compound **31** are manufactured by the AFRC Food Research Institute (Great Britain) and Biokits. The URVJT Company manufactures a set for the radioimmunoassay of compound **31**. [11]

Tricothecene mycotoxins constitute a dangerous group of mycotoxins. They are produced mainly by the toxic fungi of the genus *Fusarium*. The most poisonous are diacetoxyscirpenol **32** ($R^1 = R^4 = R^5 = R^6 = H$, $R^2 = OAc$, $R^3 = Ac$) and the toxin T-2 **33** ($R^1 = R^4 = R^5 = H$, $R^2 = OAc$, $R^3 = Ac$, $R^6 = OCOCH_2C_4H_7$-*cyclo*). The producers of tricothecenes contaminate mainly grain, while in the animals consuming this grain the toxins induce damage to the skin, sepsis and necrosis of the mucous membranes of the intestine, kidneys, lymphatic glands, and bone marrow. In humans, the effect of tricothecenes is believed to be associated with flare-ups of the alimentary-toxic aleukia, the main symptoms of which are necrosis of the tissues of the alimentary tract and leukopenia. The reason for these infections is apparently suppression of protein biosynthesis.



32–34

Immune methods are used fairly widely for the assay of tricothecene mycotoxins. In the preparation of the immunogenic conjugate, compound **32** was converted into the hemiglutarate which was conjugated with BSA. The antibodies formed on immunisation of animals with this conjugate were used to develop radioimmune [155] and immunoenzyme [156,157] methods for the assay of compound **32**.

Using similar procedures, antibodies were obtained and immunoenzyme methods were developed for the assay of compound **33** [158,159] and 3-acetyldeoxynivalenol **34** (R^1 = Ac, R^2 = R^3 = H, R^4 = OH, R^5 + R^6 = O).[160]

III. Conclusion

Immune methods make it possible to assay virtually any low-molecular-mass biologically active substances encountered in plants.[161] These methods are superior to the chromatographic procedures as regards sensitivity and speed of preparation of the assay sample and are hardly inferior to them as regards accuracy and reproducibility.

However, an individual approach to each specific substance is necessary for the development of immunoassay methods and in each case this requires a fairly considerable amount of preparatory work, which depends on the objects of the analysis. From this standpoint, the greatest difficulties are associated with the development of immunoassay methods for objects in which the biosynthesis or biodegradation of the substances assayed takes place, since the specimen then contains a large amount of structurally very similar compounds. Physiologically active substances of plant origin are in fact objects of this kind.

Despite the difficulties associated with the development of immunoassay methods (the main ones of which are the synthesis of the immunogenic conjugate and the preparation of highly specific antibodies), such methods are already widely used in clinical practice for the monitoring of the course of therapy and in studies on the metabolism of physiologically active substances of plant origin.

The use of immune methods in the assay of low-molecular-mass physiologically active compounds in plant cells and tissues is hindered by the presence of a large number of closely related compounds (biogenetic precursors and metabolites), which participate in intense cross-interactions with the antibodies used in the assay. However, the application of immunoassay methods is expanding to an increasing extent in biotechnology in connection with the preparation of plant cell and tissue cultures producing physiologically active substances. Immunoassay methods are also applied on an increasing scale in the cultivation of plants — in the study of the biosynthesis of physiologically active substances and in their assay in plant tissues. Methods developed for use in clinical practice, supplemented by stages involving the preliminary purification of the specimen, are frequently employed.

In recent years, the most vigorously developing field of application of immunoassay methods is the monitoring of the content of substances contaminating plant material (mycotoxins, etc.).

The appearance of automated systems for immunoassays and laboratory work suggests that the application of immune methods will expand.

References

1. S K Volkov *Usp. Khim.* **62** 831 (1993) [*Russ. Chem. Rev.* **62** 787(1993)]
2. D L Colbert, A M Sidki, G Gallacher, J Landon *Analyst* **112** 1483 (1987)
3. R Rodgers, C P Crowl, W M Eimstad, M W Hu, J K Kam, R C Ronald, G L Rowley, E F Ullman *Clin. Chem.* **24** 95 (1978)
4. M A Myagkova, E B Zapol'skaya, M V Lushnikova, O Yu Polevaya *Khim. Farm. Zh.* **26** 101 (1992)
5. C R Hamlin *Clin. Chem.* **34** 158 (1988)
6. T J Silber, P Getson, S Ridley, M Iosefsohn, J M Hicks *J. Pediatr.* **111** 299 (1987)
7. G M Ellis, M A Mann, B A Judson, N T Schramm, A Tashchian *Clin. Pharmacol. Ther.* **38** 572 (1985)
8. R L Mansell, E W Weiler *Phytochemistry* **19** 1403 (1980)
9. E W Weiler, R L Mansell *J. Agric. Food Chem.* **28** 543 (1980)
10. P S Jourdan, R L Mansell, D G Oliver, E W Weiler *Anal. Biochem.* **138** 19 (1984)
11. L Fukal, J Kas *Trends Anal. Chem.* **8** 112 (1989)
12. K-L L Fong, D H W Ho, C J K Carter, N S Brown, R S Benjamin, E J Freireich, G P Bodey *Anal. Biochem.* **105** 281 (1980)
13. R J Robins, M R A Morgan, M J C Rhodes, J M Furze *Anal. Biochem.* **136** 145 (1984)
14. R J Robins, M R A Morgan, M J C Rhodes, J M Furze *Phytochemistry* **23** 1119 (1984)
15. M Jaziri *Phytochemistry* **29** 829 (1990)
16. T Tanahashi, N Nagakura, H Inouye, M H Zenk *Phytochemistry* **23** 1917 (1984)
17. E W Weiler *Planta* **148** 262 (1980)
18. P Moesta, M G Hahn, H Grisebach *Plant Physiol.* **73** 233 (1983)
19. H Grisebach, P Moesta, M G Hahn, in *Immunology in Plant Sciences* (Eds H F Linskens, J F Jackson) (Berlin: Springer, 1986) p. 77
20. P S Jourdan, R L Mansell, E W Weiler *Planta Med.* **44** 82 (1982)
21. P S Jourdan, E W Weiler, R L Mansell *J. Agric. Food Chem.* **31** 1249 (1983)
22. R Atzorn, E W Weiler, M H Zenk *Planta Med.* **41** 1 (1981)
23. V P Butler Jr, J P Chen *Proc. Natl. Acad. Sci. USA* **57** 71 (1967)
24. T W Smith, V P Butler Jr, E Haber *New Engl. J. Med.* **281** 1212 (1969)
25. T W Smith, V P Butler Jr, E Haber *Biochemistry* **9** 331 (1970)
26. E W Weiler, M H Zenk *Phytochemistry* **15** 1537 (1976)
27. E W Weiler, in *Plant Tissue Culture and Its Biotechnological Application* (Eds W Barz, E Reinhard, M H Zenk) (Berlin: Springer, 1977) p. 266
28. E W Weiler, P Westekemper *Planta Med.* **35** 316 (1979)
29. S Nickel, E J Staba, in *Plant Tissue Culture and Its Biotechnological Application* (Eds W Barz, E Renhard, M H Zenk) (Berlin: Springer, 1977) p. 278
30. P H Hinderling, J O Magnusson, L Molin *J. Pharm. Sci.* **75** 517 (1986)
31. S Mahmod, D S Smith, J Landon *Ther. Drug Monit.* **9** 91 (1987)
32. B J Mora, C J M Queralto, L R Arcelus, R M Cortes *Farm. Clin.* **2** 44 (1985)
33. K Yoshimatsu, M Satake, K Shimomura, J Sawada, T Terao *J. Nat. Prod.* **53** 1498 (1990)
34. J J Chang, C P Crowl, R S Schneider *Clin. Chem.* **21** 967 (1975)
35. W Hubl, G Daxenbichler, D Meissner, H J Thiele *Clin. Chem.* **34** 2521 (1988)
36. N C Paterson, M J Stewart *Ann. Clin. Biochem.* **24** 205 (1987)
37. J A Stone, S J Soldin *Clin. Chem.* **34** 2547 (1988)
38. M Pupp *G. Ital. Chim. Clin.* **10** 143 (1985)
39. J C Carrelts, D E Sweet *Drug Intell. Clin. Pharm.* **21** 381 (1987)
40. H Nekashima, K Tsutsumi, M Hashiguchi, Y Kumagai, A Ebihara *J. Chromatogr.* **489** 425 (1989)
41. M Bohbot, N Chouvalidze, J-L Durand, A-C Steinmetz, C Divine, G Fredj, A Thuillier *Feuill. Biol.* **28** 71 (1987)
42. P K Ng, D LeGatt, J Coates, R L Collins-Nakai *Am. J. Pharm.* **42** 1977 (1985)
43. A M Al-Fares, S A Mira, Y M El-Sayed *Ther. Drug Monit.* **6** 454 (1984)
44. B B Lentrichia, S J Sciotto-Brown, M F Turanchik, I K Ropiak, K K Yeung *Clin. Chem.* **33** 1548 (1987)
45. S Takayasu, M Maeda, A Tsuji *J. Immunol. Methods* **83** 317 (1985)
46. K R Wehmeyer, H B Halsall, W R Heineman, C P Volle, I-W Chen *Anal. Chem.* **58** 135 (1986)

47. D B Frewin, H Marmanidis, D R Lehmann, R G Morris *Aust. N. Z. J. Med.* **16** 241 (1986)
48. M Plebani, A Burlina *Clin. Chem.* **31** 1879 (1985)
49. D R Lehmann *Clin. Biochem.*, **18** 300 (1985)
50. J Masse *Ann. Biochem. Clin. Que.* **26** 1 (1987)
51. R L Smith *Clin. Chem.* **33** 1679 (1987)
52. W F Skogen, M R Rea, R Valdes Jr *Clin. Chem.* **33** 837 (1987)
53. E Evrard, M Lesne *J. Pharm. Belg.* **41** 380 (1986)
54. J Frisolone, L M Sylvia, J Gelwan, S Pal, C Pellechia *Clin. Pharm.* 7 444 (1988)
55. D C Greenway, A A Nanji *Clin. Chem.* **31** 1078 (1985)
56. T J Hoon, M B Bottorf, J L Baumann *Hosp. Ther.* **12** 80 (1987)
57. I A Kulaots, M R Pudek, D W Seccombe *Clin. Chem.* **33** 1490 (1987)
58. D Wahyono, M Piechaczyk, J M Scherrmann, J C Mani, B Pau *Ther. Drug Monit.* **13** 113 (1991)
59. A A Sanchez, G G Sangrador, V B Quintana *Farm. Hosp.* **15** 307 (1991)
60. T Suzuki, H Nagaoka, Y Nakagawa, K Sugawara *J. Jpn. Soc. Hosp. Pharm.* **23** 469 (1987)
61. R A Blum, J M DeVito, R A Pleasants, R E Crass, R H Gadsden, R B Leman *Ther. Drug Monit.* **9** 416 (1987)
62. J Stone, Y Bentur, E Zalstein, S Soldin, E Giesbrecht, G Kogen. *J. Pediatr.* **177** 321 (1990)
63. T Lehtola, A Huhtikangas, R Hiltunen, M V Schantz *Planta Med.* **42** 250 (1981)
64. G C Oliver, B M Parker, D L Brasfield, C W Parker *J. Clin. Invest.* **47** 1035 (1968)
65. H I Bussey, W A Watson, D W Hawkins, P Wang *Ther. Drug Monit.* **8** 90 (1986)
66. S R C J Santos, W Kirch, E E Ohnhaus *J. Chromatogr. Biomed. Appl.* **63** 155 (1987)
67. R P Vallejo, C D Ercegovich, in *Trace Organic Analysis: a New Frontier in Analytical Chemistry. Proceedings 9th Materials Res. Symp.* Natl. Bureau Standards (USA) Spec. publ. 519, 1979, p. 333
68. P K Nakane, F Kawaoi *J. Histochem. Cytochem.* **22** 1084 (1974)
69. E I Plyugacheva, M I Savenkova D I Metelitsa *Khim. Farm. Zh.* **22** 1392 (1988)
70. M I Savenkova *Khim. Farm. Zh.* **23** 195 (1989)
71. M I Savenkova, D I Metelitsa *Khim. Farm. Zh.* **24** 82 (1990)
72. E I Tarun, M I Savenkova, D I Metelitsa *Zh. Anal. Khim.* **48** 145 (1993)
73. M R A Morgan, R McNerney, J A Matthew, D T Coxon, H W-S Chan *J. Sci. Food Agric.* **34** 593 (1983)
74. E W Weiler, H Kruger, M H Zenk *Planta Med.* **39** 112 (1980)
75. J A Matthew, M R A Morgan, R McNerney, H W-S Chan *Food Chem. Toxicol.* **21** 637 (1983)
76. W L Pengelly, F Meins, Jr *Planta* **136** 173 (1977)
77. E W Weiler *Planta* **153** 319 (1981)
78. R Mertens, J Eberle, A Arnscheidt, F Ledebur, E W Weiler *Planta* **166** 389 (1985)
79. E W Weiler, U Wieczorek *Planta* **152** 159 (1981)
80. R Atzorn, E W Weiler *Planta* **159** 1 (1983)
81. R Atzorn, E W Weiler *Planta* **159** 7 (1983)
82. P C Oden, E W Weiler, L Schwenen, J E Graebe *Physiol. Plant.* **64** 21A (1985)
83. J Bianco, B Ferrua *Plant Physiol. Biochem.* **28** 799 (1990)
84. E W Weiler *Planta* **144** 255 (1979)
85. E W Weiler *Planta* **148** 262 (1980)
86. L M Brenner *Ann. Rew. Plant Physiol.*, **32** 511 (1981)
87. E W Weiler *Physiol. Plant.* **54** 230 (1982)
88. D Ernst, W Schafer, D Oesterhelt *Planta* **159** 216 (1983)
89. D R Reeve, A Crozier, in *Hormonal Regulation of Development. I. Molecular Aspects of Plant Hormones* (Ed. J McMillan) (Berlin: Springer, 1980) p. 203
90. B F Erlanger, S M Beiser *Proc. Natl. Acad. Sci. USA* **52** 68 (1964)
91. B Hacker, H VanVunakis, L Levine *J. Immunol.* **6** 1726 (1972)
92. M Z Humayun, T M Jacob *Biochem. J.* **141** 313 (1974)
93. S A Khan, M Z Humayun, T M Jacob *Anal. Biochem.* **83** 632 (1977)
94. D S Milstone, D S Vold, D C Glitz, N Shutt *Nucl. Acid Res.* **5** 3439 (1978)
95. D L Brandon, J W Corse, L L Layton *Plant Physiol.* **63(S)** 82 (1979)
96. E W Weiler *Planta* **149** 155 (1980)
97. E M S McDonald, D E Akiyoshi, R O Morris *J. Chromatogr.* **214** 101 (1981)
98. E W Weiler, K Spanier *Planta* **153** 326 (1981)
99. J Badenoch-Jones, D S Letham, C W Parker, B G Rolfe *Plant Physiol.* **75** 1117 (1984)
100. R Horgan, in *Isolation of Plant Growth Substances* (Ed. J R Hillman) (Cambridge: Cambridge University Press, 1978) p. 97
101. D Ernst, D Oesterhelt *Plant Cell Rep.* **4** 140 (1985)
102. M G Carnes, M L Brenner, C R Andersen *J. Chromatogr.* **108** 95 (1975)
103. R A Andersen, T R Kemp *J. Chromatogr.* **172** 509 (1979)
104. J M Hardin, C A Stutte *J. Chromatogr.* **208** 124 (1981)
105. J A Holland, E H McKerrell, K J Fuell, W J Burrows *J. Chromatogr.* **166** 545 (1978)
106. R Horgan, M R Kramers *J. Chromatogr.* **173** 263 (1979)
107. I M Scott, R Horgan *J. Chromatogr.* **237** 311 (1982)
108. R O Morris, J B Zaerr, R W Chapman *Planta* **131** 271 (1976)
109. C Jayabaskaran, T M Jacob *Plant Physiol.* **70** 1396 (1982)
110. T H Elsasser, R K Munns, W Shimoda *J. Immunoassay* **8** 73 (1987)
111. P Rohner, M Schallibaum, J Nicolet *J. Food Protection* **48** 59 (1985)
112. E G Boyce, L A Lawson, G A Gibson, I Nachamkin *Ther. Drug Monit.* **11** 97 (1989)
113. E Evrard, F Clerckx-Braun, M Lesne, P Pellegrin *J. Pharm. Belg.* **42** 177 (1987)
114. L O White *Trends Anal. Chem.* **5** 29 (1986)
115. K P Pavel, W Hubl *Z. Med. Laboratoriumsdiagn*, **28** 301 (1987)
116. W M Cai, J Chen, G Chen *Clin. J. Hosp. Pharm.* **11** 485 (1991)
117. T Kitaura, H Fukuchi, S Tsukiai, Y Wada *Jpn. J. Hosp. Pharm.* **12** 345 (1986)
118. B E Bleske, T A Larson, J C Rotschafer *Ther. Drug Monit.* **9** 48 (1987)
119. A S Lewis, G Tailor, H N Rowe, H O Williams, M H Lewis *Am. J. Pharm.* **44** 568 (1987)
120. R J Anders, A Lau, Sharifi, M Lee. *Ther. Drug Monit.* **9** 472 (1987)
121. R A Plasants, R E Dupuis, W T Sawyer, C Howlett *ASHP Midyear Clin. Meet.* **23** 237 (1988)
122. M A Wilkerson, S M Toler, T L Golsmith, W H Porter, M H Chandler *Clin. Pharm.* **8** 867 (1989)
123. R N Hamburger *Science* **152** 203 (1966)
124. G S Campbell, R P Mageau, B Schwab, R W Johnston *Antimicrob. Agents Chemother.* **25** 205 (1984)
125. D Arnold, D Von Berg, A K Boertz, U Mallik, A Somogyi *Arch. Lebensmittelhygiene* **35** 131 (1984)
126. D Arnold, A Somogyi *J. Assoc. Off. Anal. Chem.* **68** 984 (1985)
127. C Van De Water, N Haagsma *J. Chromatogr.* **566** 173 (1991)
128. L Fukal, J Kas *Trends Anal. Chem.* **8** 112 (1989)
129. T Li *Biotech Research Announces First Aflatoxin Detection Kit Using Enzyme Immunoassay Technology* Press release, April 9, 1985 (New York: Robert Marston and Assoc., 1985)
130. J J Pestka, F S Chu *J. Food Protection* **47** 305 (1984)
131. M R A Morgan *Tetrahedron* **45** 2237 (1989)
132. A P Wilkinson, A S Kang, H W-S Chan, M R A Morgan, in *Immunoassays for Veterinary and Food Analysis* Vol. 1 (Eds B A Morgan, M N Clifford, R Jackman) (London: Elsevier, 1988) p. 343
133. J D Groopman, L J Trudel, P R Donahue, A Marshak-Rothstein, G N Wogan *Proc. Natl. Acad. Sci. USA.* **81** 7728 (1984)
134. C P Wild, B Chapot, E Scherer, L DenEngelse, R Montesano, in *Methods for Detecting DNA Damaging Agents in Humans: Application in Cancer Epidemiology and Prevention* (Eds H Bartsch, K Hemminki, I K O'Neil) (Lyon: International Agency for Research on Cancer, 1988) p. 67
135. C P Wild, F A Pionneau, R Montesano, C F Mutiro, C J Chetsanga *Int. J. Cancer* **40** 328 (1987)
136. P Sizaret, C Malaveille, R Montesano, C Frayssinet *J. Natl. Cancer Inst.* **69** 1375 (1982)
137. J E Smith *World's Poultry Science Journal* **38** 201 (1982)
138. M R A Morgan, A S Kang, H W-S Chan *J. Sci. Food Agric.* **37** 908 (1986)
139. A A G Candlish, W H Stimson, J E Smith *Lett. Appl. Microbiol.* **1** 57 (1985)
140. T S L Fan, F S Chu *J. Food Protection* **47** 263 (1984)
141. J Marrero *J. Med. Technol.* **1** 47 (1984)
142. J M Fremy, F S Chu *J. Assoc. Off Anal. Chem.* **67** 1098 (1984)
143. W J Hu, N Woychik, F S Chu *J. Food Protection* **47** 126 (1984)
144. E Martlbauer, G Terplan *Arch. Lebensmittelhygiene* **36** 58 (1985)
145. R Jackman *J. Sci. Food Agric.* **36** 685 (1985)

146. M R A Morgan, A S Kang, H W-S Chan *J. Sci. Food Agric.* **37** 873 (1986)
147. A S Kang, M R A Morgan, H W-S Chan, in *Proceedings 5th Meeting on Mycotoxins in Animal and Human Health* (Eds M O Moss, M Frank) (Guildford: Surrey University Press, 1984) p. 80
148. M R A Morgan, R McNerney, H W-S Chan *J. Assoc. Off. Anal. Chem.* **66** 1481 (1983)
149. M R A Morgan, R McNerney, H W-S Chan, in *Immunoassays in Food Analysis* (Eds B A Morris, M N Clifford) (London: Elsevier, 1985) p. 159
150. M R A Morgan, R McNerney, H W-S Chan, P H Anderson *J. Sci. Food Agric.* **37** 475 (1986)
151. P H Anderson, G A H Wells, R Jackman, M R A Morgan *Proceedings 5th Meeting on Mycotoxins in Animal and Human Health* (Eds M O Moss, M Frank) (Guildford: Surrey University Press, 1984) p. 23
152. S C Lee, F S Chu *J. Assoc. Off. Anal. Chem.* **67** 45 (1984)
153. A A G Candlish, W H Stimson, J E Smith *J. Assoc. Off. Anal. Chem.* **77** 961 (1988)
154. A A G Candlish, W H Stimson, J E Smith in *Immunoassays for Veterinary and Food Analysis* (Eds B A Morris, M N Clifford, R Jackman) (London: Elsevier, 1988), p. 351
155. F S Chu, M Y Chen-Liang, G S Zhang *Appl. Environ. Microbiol.* **48** 777 (1984)
156. J U Pauly, D Bitter-Suermann, K Dose, in *Proceedings of the 2nd World Congress on Food-borne Infections and Intoxications* Institute of Veterinary Medicine, Robert von Ostertag Institute, Berlin, 1986, p. 1212
157. E N C Mills, J M Johnston, H A Kemp, M R A Morgan *J. Sci. Food Agric.* **42** 225 (1988)
158. K W Hunter, A A Brimfield, M Miller, F D Finkelman, F S Chu *Appl. Environ. Microbiol.* **49** 168 (1985)
159. E H Gendloff, J J Pestka, S P Swanson, L P Hart *Appl. Environ. Microbiol.* **47** 1161 (1984)
160. H A Kemp, E N C Mills, M R A Morgan *J. Sci. Food Agric.* **37** 888 (1986)
161. R J Robins, in *Immunology in Plant Sciences* (Eds H F Linskens, J F Jackson) (Berlin: Springer, 1986) p. 86

Russian Chemical Reviews **63** (2) 103 – 123 (1994)
©1994 Russian Academy of Sciences and Turpion Ltd

UDC 541.64:537.31

Electron transport and electroluminescence in polymer layers

A V Vannikov, A D Grishina, S V Novikov

Contents

I.	Introduction	103
II.	Main characteristics of the transport of charge carriers	104
III.	Models of the transport of charge carriers in disordered organic matrices	106
IV.	Electroluminescent polymer layers	112
V.	Injection of charges into polymer transport layers	120

Abstract. We shall discuss the transport of charge carriers (electrons and holes) in disordered polymeric dielectric matrices and electroluminescence phenomena in transport layers of various structures, and also the injection of charges into transport layers through a boundary bearing a solid layer of a different type. The temperature, field, and concentration dependences of the mobility of the carriers will be considered, as well as the effect of the structure of the polymer matrix and of the transport centres on the mobility. The most reliable theoretical models of charge transport in these media will be examined. The bibliography includes 150 references.

I. Introduction

Significant advances in the study of the electronic properties of organic materials have been made in recent years. Attention has been focussed mainly on the electric conductance and on the electron transport properties of these materials. Some of the studies were aimed at developing organic materials having electronic properties close to those of inorganic semiconductors. Since organic materials (and, principally, polymeric) display a great variety of chemical structures and physico-mechanical characteristics, and since they can be prepared by a variety of methods, an improvement of their parameters to the level achieved in inorganic semiconductors would reveal a new world in microelectronics. The use of organic polymeric photoconductors in electrophotography is the first (and, so far, the only) example of the wide-scale industrial application of these materials in order to exploit their unique electric properties.[1] We need only to note that at present most of the photocopying ('Xerox') devices, laser printers, and other electrophotographic (EP) equipment use organic polymeric photoreceptors as the main active element. These photoreceptors usually consist of two polymer layers: a photogeneration layer and a transport layer. The photogeneration layer, deposited on an electrically conducting substrate, is a dispersion of a pigment in a polymer binder, and the transport layer is an amorphous (polymeric) dielectric containing electron transport centres.[2]

A V Vannikov, A D Grishina, S V Novikov A N Frumkin Institute of Electrochemistry of the Russian Academy of Sciences, Leninskii prosp. 31, 117071 Moscow. Fax (7-095) 952 08 46.

Received 12 October 1993
Uspekhi Khimii **63** (2) 107 – 129 (1994); translated by J I Carasso

The principle of the operation of these receptors is the following. The surface of the transport layer is negatively charged by a corona discharge. When the sample is exposed through a mask photons are absorbed in the generation layer of the illuminated parts of the photoreceptor, with formation of electron – hole pairs. Free holes are injected into the transport layer and drift through it under the influence of the electric field, discharging the surface of the transport layer. As a result, a potential contour (latent image) is formed on the surface of the transport layer: this is a replica of the spatial distribution of optical density in the original mask.

We should stress that the charges must cross the whole thickness of the layer until they reach the surface, and therefore we are dealing with electron transport not accompanied by mass transport. The quantitative characteristic of this process is the time of flight of the charge carriers t_τ through the transport layer. The time of flight is a critical parameter which determines the operating speed of the whole apparatus, since it must be shorter than the time interval between exposure and development, which is usually a fraction of a second. The fundamental technological problem is to develop organic polymer layers with the smallest possible t_τ.

We should stress that the transfer of a charge between adjacent transport centres during its drift through the film is an elementary redox reaction between a neutral molecule and its cation radical (for hole transport) or its anion radical (for electron transport).[3] Surprisingly, electron transfer can take place between particles not in direct contact (at distances up to 20 Å, determined by the concentration of transport centres in the sample).

However, interest in thin polymer layers showing electronic transport phenomena has been stimulated not only by their transport properties but also by their electroluminescence (EL) properties, which allow them to be used as the elements of flat, flexible colour displays, luminescent and television screens, electrically pumped lasers, etc.[4] Again, the transport of the charge carriers is the factor which determines the effectiveness of the conversion of electric into light energy.

The distinguishing feature of EL layers (as compared with EP layers) is that their transport centres act also as luminescence centres. The essential component of an EL diode is a polymer layer sandwiched between two electrodes, one of which injects holes while the other injects electrons. The injection of charges into the transport layer through a phase boundary is an operating stage common to EP and EL systems.

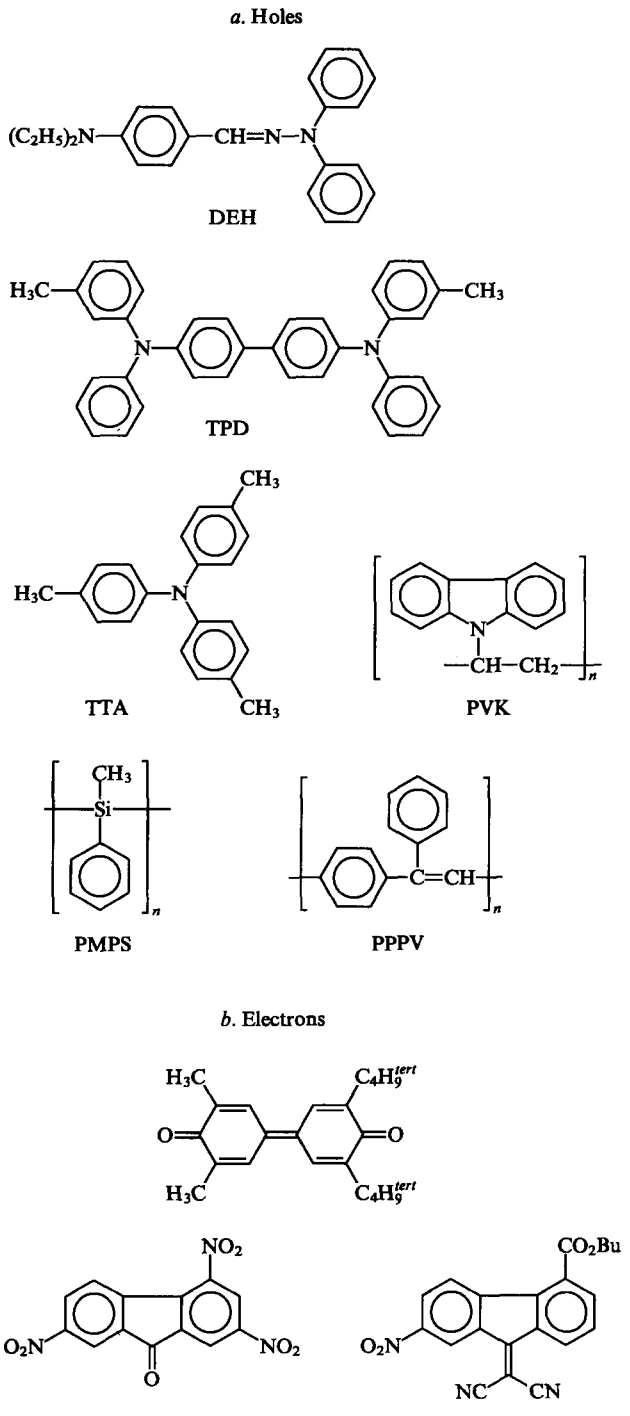


Figure 1. Typical compounds used as transport centres in polymer matrices containing mobile holes or electrons.

Electron transport phenomena in dielectric polymers are also responsible for the photorefractive effect (recently discovered in nonlinear optical polymers doped with molecules having electron transport properties[5-7]). Thus, holograms can be phase recorded by irradiating photorefractive polymer layers in a strong electric field. This four-step process includes: (1) the photogeneration of mobile charge carriers, (2) the transport and separation of charges of opposite sign, (3) the trapping of mobile charges and the generation of a nonuniform electric field by the space charge, (4) the modulation of the refractive index by the nonuniform electric field through the electro-optical effect. Uniform irradiation of the layer with a strong light erases the hologram and makes the recording process reversible.

In the present review we shall discuss only the special features and the mechanisms of charge transfer processes in polymeric transport layers, and also their electroluminescence. Photorefractive polymers lie beyond the scope of this article because their study is only beginning.

In spite of the many recent experimental and theoretical publications on electron transport in dielectric polymers a generally accepted theoretical model able to explain the basic experimental findings is still awaited. We shall examine the most significant experimental results on the temperature, field, and concentration dependence of the carrier mobility, and the effects on the mobility resulting from the structure of the polymer matrix and of the dopants introduced into the polymer and not contributing directly to the carrier transport, from the electroluminescence of transport layers of different structures, from the injection of charges into the transport layer through a boundary with a different solid layer, and also the most reliable theoretical models of charge transport in polymeric dielectric layers, i.e. models able to explain the total fund of experimental results.

II. Main characteristics of the transport of charge carriers

The polymers in which the mobility of the charge carriers can be measured by the direct time of flight method can be classified into the following groups: (1) molecularly doped polymers such as aromatic amines [triphenylamine (TPA), tritolylamine (TTA), etc.] and polyesters; (2) carbon chain polymers with chromophoric aromatic side substituents such as polyvinylcarbazole (PVK) and polyepoxypropylcarbazole (PEPK); (3) polymers with transport centres in the main chain such as polyhydroxyaminoethers (PHAE); (4) σ- and π-conjugated polymers [polysilylenes, polyphenylenevinylenes (PPV), etc.]

Some members of the different classes of transport centre are shown in Fig. 1. In groups 1–3 the localised transport centres are nitrogen atoms conjugated with phenyl groups, whereas in polymers of group 4 the transport centres are ordered parts of the polymer chains or the so-called effectively conjugated segments.[8]

Our discussion of the experimental data will invariably assume (unless accompanied by a statement to the contrary) that the transport of charge carriers is nondispersive, i.e. the injected charges are in thermal equilibrium with the medium, since this hypothesis makes the characteristics of the transport process of interest much easier to extract from the experimental results without complications from complementary factors. Detailed descriptions of dispersive (stochastic) transport can be found in existing reviews and monographs.[9-11]

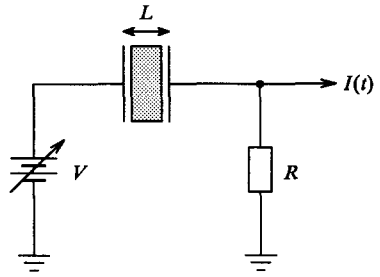


Figure 2. Scheme of the time of flight experiment.

Let us examine the basic information on transport discovered experimentally. The great majority of the data was obtained by the so-called time of flight experiment, shown schematically in Fig. 2. Charge carriers, injected (by a laser pulse or electric discharge) on one side of a flat sample of the dielectric

polymer exposed to a transverse electric field corresponding to a potential difference V, drift towards the opposite electrode. The dependence of the current I of carriers on the time t is determined experimentally. In the ideal case, when all the carriers move at the same speed, the $I(t)$ dependence is stepped: for $t < t_\tau$ the current is independent of time, but for $t > t_\tau$ it decreases rapidly with time. The transport properties of the carriers are usually defined through their mobility μ, where

$$\mu = \frac{L^2}{Vt_\tau}, \tag{1}$$

which in the ideal case is independent of the sample thickness L. The real $I(t)$ dependence has a more complex form: the sharp step is replaced by a shoulder, followed by a more gradual decrease. The latter feature shows that carrier transport in disordered systems is always to some extent dispersive. Nevertheless, when the position of the shoulder (identified with the time t_τ) is linearly dependent on L, we can confidently assume that the transport is mainly nondispersive and can be described in terms of a mobility independent of L.

The most important of the parameters which influence the transport of charge carriers are the temperature T, the electric field strength F, the concentration of transport centres c, and also the structure of the transport centres and of the polymer matrix. Many papers have been published on these topics, and we shall discuss only the most important. For a more detailed description the reader is referred to recent reviews[12-14] and to Borsenberger and Weiss's exhaustive monograph.[1] All the systems listed above have more or less similar dependences of μ on T and F.

Let us first consider the temperature dependence. The great majority of workers conclude that the temperature dependence of the mobility denotes activation control:

$$\ln\mu \propto -\frac{E_a}{T}, \tag{2}$$

where E_a is the activation energy (which we shall express in units for which the Boltzmann constant k_B is unity). However, the problem has not yet been finally solved. Recent publications by Borsenberger and coworkers[15-19] argue that the temperature dependence of the mobility is better described by an equation of the form

$$\ln\mu \propto -\left(\frac{T_0}{T}\right)^2. \tag{3}$$

(The physical significance of T_0 is examined in detail below.) A similar dependence had been proposed earlier,[20] but later work showed[12] that this observation was due to the erroneous inclusion of temperatures above the glass transition temperature, where the activation energy usually decreases steeply without a corresponding decrease in the mobility, thus stimulating a dependence such as Eqn (3). The experimentally accessible temperature range is not usually wide enough to allow an unambiguous distinction between the dependences (2) and (3). Therefore the choice of one of these functional $\mu(T)$ dependences is usually based on other considerations.[15]

In the vast majority of cases the dependence of the carrier mobility on the strength F of the electric field takes the form

$$\ln\mu \sim \text{const} + bF^{1/2}, \tag{4}$$

where b is a temperature-dependent coefficient. This is known as the Poole–Frenkel relationship because it was first proposed by Poole[21] and by Frenkel[22] in an attempt to describe the effect of an external field on the rate of escape of charge carriers from a Coulomb trap. The Poole–Frenkel model ascribes the dependence (4) to a lowering of the activation energy by the external field (Fig. 3), which gives

$$\ln\left(\frac{\mu}{\mu_0}\right) = -\frac{E_0 - \beta_{PF}F^{1/2}}{T},$$

$$\beta_{PF} = 2\left(\frac{e^3}{\varepsilon}\right)^{1/2}, \tag{5}$$

where E_0 is the depth of the potential well (trap) in a zero external field, e is the elementary charge, and ε is the permittivity of the medium. It is now generally thought that the Poole–Frenkel mechanism cannot be realised in disordered organic matrices because of the absence of significant numbers of transport centres in the great majority of organic materials.[13,23-25] Surprisingly, however, the Poole–Frenkel model gives a correct estimate of the proportionality coefficient in Eqn (4) though the experimental values of β are usually 2–3 times lower than those calculated by Eqn (5). Many experimental results show that in the majority of systems with nondispersive charge transport the overall dependence of μ on T and F is satisfactorily described by the equation

$$\mu = \mu_0 \exp\left[-\left(E_0 - \beta F^{1/2}\right)\left(T^{-1} - T_0^{-1}\right)\right], \tag{6}$$

proposed by Gill[26] and (in a slightly different form) by Pfister[27]. According to this equation the temperature dependences of the mobility measured in various electric fields should intersect at the temperature T_0, while the field dependences of μ for different temperatures have the common point $F_0 = (E_0/\beta)^2$. This behaviour has been observed in many systems of the first and second group,[1] in polyhydroxyaminoethers (third group),[28] and also in various polymers with a system of conjugated bonds in the main chain.[29,30]

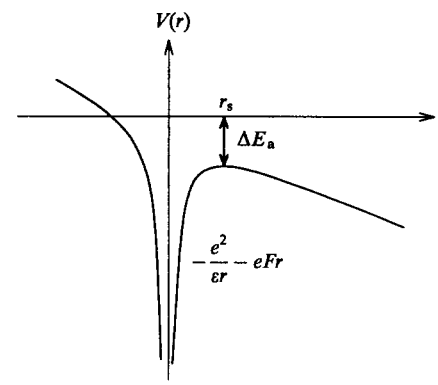


Figure 3. Lowering of the activation energy (ΔE_a) for the emission of a charge from a charged trap in an external electric field (Poole–Frenkel effect). r_s is the position of the saddle point in the potential energy.

An interesting property of Eqn (6) is the presence of the parameter T_0, which usually lies between 400 and 500 K. Formally it follows from Eqn (6) that for $T > T_0$ the mobility should decrease as the field is increased. This behaviour has been observed in recent experiments.[15,31-33] Furthermore, it was found that the mobility can be a nonmonotonic function of the field: it decreases with increasing F in weak fields and begins to increase in stronger fields.[13,34] An atypical variation of the mobility (increasing in moderately strong fields, and decreasing above $F = 10^6$ V cm^{-1}) has been reported.[35] We believe this to be an artefact, arising from the determination of the time of flight by different methods in experimental data for $F > 10^6$ and $F < 10^6$ V cm^{-1}, since the nondispersive component [the

plateau in the $I(t)$ dependence] could not be detected at high fields in those measurements. On the whole, individual instances of unusual field dependences of the mobility have been reported [with a sign inversion of b, or not consistent with Eqn (6)], but according to the Gaussian model (see below) the sign inversion of b at high temperatures and the decrease of μ in weak fields should be a common occurrence. Whether this is the case can be established only when additional experimental information becomes available.

The study of the transport properties of systems of the first group offers a unique opportunity to establish the dependence of the mobility carriers on the concentration of the transport centres, i.e. (effectively) on the average distance between the transport centres centres. It has been established that mobility decreases rapidly as the concentration of transport centres decreases.[36-38] The concentration dependence of the mobility will be discussed in more detail in the description of the various transport models given below.

The completely analogous dependence of the mobility of the two types of carrier (electrons and holes) on the temperature, field, and concentration is a fundamental experimental fact. Since the oxidation products of organic compounds have a relatively high electron affinity and act as deep traps it is easier to obtain polymer systems with hole conduction; nevertheless many systems with electron conduction have been studied in depth. Data on the transport of electrons in matrices with transport centres of the acceptor type (for example, quinone or nitrile derivatives) suggest that Eqn (6) is usually obeyed in these systems.[16,26,39] We can therefore assume that the same mechanism applies to transport by electrons and by holes.

Aromatic molecules containing nitrogen, which have low ionisation potentials (IP), have been used as transport centres for holes (see Fig. 1). A low IP is needed because fortuitous impurities with an even lower IP would act as traps for the holes. Correspondingly, molecules with the highest possible electron affinity are chosen to optimise the electron transport. It can be seen from Fig. 1 that the hole centres usually contain several nitrogen-containing $>N-C_6H_5$ groups. This facilitates the transport of positive charge within the relatively large transport centre. Kitamura and Yokoyama[40] have proposed the concepts of intramolecular and intermolecular charge mobility. The large linear size of the $>N-C_6H_5$ groups increases the intermolecular mobility, because under these conditions the length of the intermolecular jumps for a given concentration of molecules is decreased.[3] The intramolecular 'mobility' is a maximum when the density of positive charge is the same on the two functional groups of the cation radical, i.e. in symmetrical molecules.

Layers with bipolar carrier transport can sometimes be obtained, though the formation of charge transfer complexes (CTC) between donor and acceptor components strongly lowers the mobility. A well known example is PVK doped with trinitrofluorenone (THF).[26] Bipolar conduction has been observed[41] in polycarbonate (PC) doped with an alkyl derivative of diphenoquinone and tetra(*m*-tolyl)-1,3-diaminobenzene. Because of their bulky alkyl substituents the acceptor molecules cannot interact strongly with the donor molecules, and a CTC is not formed. Bipolar transport was observed also[42,43] in poly-[phenylenedi(phenoxyphenol)vinylene] (DPOP–PPV), one of the systems of the fourth group, without the addition of low-molecular-mass dopants. As will be shown below, bipolar transport is responsible for the very efficient electroluminescence of DPOP–PPV layers.

Important information is provided by data on the effect of the polarity of the matrix on the transport characteristics of the charge carriers. The existence of this effect, which shows that the role of the polymer matrix is not confined to providing sites for the transport centres, was first established in our laboratory.[44,45] The polarity of the medium can be varied either by adding chemically inert polar molecules (usually various isomers of dinitrobenzene or dinitrotoluene),[43-49] or be replacing the polymer matrix itself (for example, polystyrene by polycarbonate).[19,49] An increase in the dipole moment (or in the concentration) of the polar dopant usually lowers μ and increases β,[45,47,49] though other situations have also been observed[43,46,48] (usually in cases of strongly dispersive transport of the carriers).

In recent years the effect of the dipole moment of the transport centre on the transport characteristics of the charge carriers has been intensively studied. The most detailed contributions were made by Borsenberger and Fitzgerald[50] and by Sugiuchi and Nishizawa,[51] who studied the properties of fifteen different transport centres with dipole moments between 1.5 and 5.5 D. It was shown that an increase in the dipole moment of the centre lowers the absolute value of the mobility and increases the coefficient β.

III. Models of the transport of charge carriers in disordered organic matrices

Three main models of charge transport in disordered organic matrices have been proposed so far: the model of hopping transport over centres with a Gaussian distribution of energy levels, the polaron model, and the dipolar traps (transport centres) model. The situation is far from clear, and even the nature of the charge carriers in these matrices is still controversial.

1. Hopping transport over centres with a Gaussian distribution of energy levels

Bässler and coworkers[52-57] developed in greath depth the following model for the motion of the charge carriers. The organic matrix with the added transport centres is modelled by a cubic lattice with edge a with a transport centre located at each lattice point. The position of the energy level E involved in the charge transport is an independent, random quantity in each centre because of the random and noncorrelated effect of the surroundings. The corresponding density of states is described by the Gaussian distribution

$$\rho(E) = (2\pi\sigma^2)^{-1/2} \exp\left(-\frac{E^2}{2\sigma^2}\right). \tag{7}$$

Additional grounds for this choice of $\rho(E)$ are provided by the experimentally observed Gaussian form of the absorption and fluorescence bands of many polymers[58,59] and by the assumption that the central limit theorem must apply to some extent: the physical meaning of this model is that the overall energy of the interaction of the centre with the surroundings is the sum of many independent terms having not very different probability densities. The frequency of the jumps between the centres i and j is expressed in the form proposed by Miller and Abrahams:[60]

$$\nu_{ij} = \nu_0 \exp\left(-2\gamma a \frac{\Delta R_{ij}}{a}\right) \begin{cases} \exp\left(-\dfrac{E_j - E_i}{T}\right), & E_j > E_i \\ 1, & E_j < E_i \end{cases}. \tag{8}$$

Here ν_0 is the pre-exponential frequency factor, γ is the decrement of the wave function, and ΔR_{ij} is the distance between the centres. In the case of a nonzero external electric field an electrostatic contribution is included in the energy E_i:

$$E_i = E_i^0 - e\boldsymbol{F}\boldsymbol{R}_i. \tag{9}$$

The function $\rho(E)$ describes the effect of the energy disorder. The geometric disorder can be described phenomenologically by introducing the arbitrary parameter γa. It was assumed that

$$2\gamma a = \Gamma_{ij} = \Gamma_i + \Gamma_j, \tag{10}$$

where Γ_i and Γ_j are independent Gaussian arbitrary quantities having a dispersion σ_Γ, and the dispersion of Γ_{ij} is $\Sigma = 2\sqrt{\sigma_\Gamma}$.

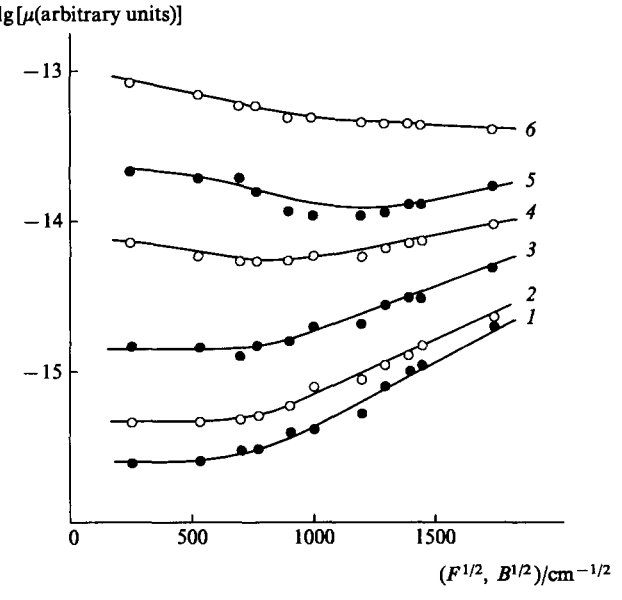


Figure 4. Field dependence of the carrier mobility in the Gaussian model (Monte Carlo calculation).[56] $\sigma/T = 3.0$; Σ: 0.00 (*1*), 1.41 (*2*), 2.12 (*3*), 2.54 (*4*), 2.80 (*5*), 3.26 (*6*).

Specific calculations by this model were possible only by the numerical modelling (Monte Carlo) method. The field dependence of the mobility is S-shaped (Fig. 4), and its middle part corresponds approximately to a linear dependence of $\ln \mu$ on $F^{1/2}$. However, this region is much narrower than the region covered by the experiment. The explanation proposed[61] for this discrepancy in terms of the difference in the definition of the mobility (through the average time of flight in the numerical experiment and through the time for the signal to fall to one half of its value at the plateau, or through the intersection of the corresponding asymptotics in the real experiment) is incompatible with the experimental results, according to which all these times have the same field dependence.[12] The calculation of the geometric disorder ($\Sigma > 0$) in terms of this model produces an interesting corollary: the mobility becomes a nonmonotonic function of the field, decreasing at first and then increasing as the field is increased.[56] This behaviour corresponds to the experimental observations of Borsenberger[34] and of Abkowitz[13].

The temperature dependence of the mobility in a zero field is not of the Arrhenius type, and is described by Eqn (3), with

$$T_0 = \tfrac{2}{3}\sigma . \tag{11}$$

In sufficiently strong fields the overall dependence of μ on T and F for $\Sigma \geqslant 1.5$ can be written[17]

$$\mu = \mu_0 \exp\left[-\left(\frac{2\sigma}{3T}\right)^2\right] \exp\left(-C\left[\left(\frac{\sigma}{T}\right)^2 - \Sigma^2\right]F^{1/2}\right), \tag{12a}$$

and for $\Sigma \leqslant 1.5$

$$\mu = \mu_0 \exp\left[-\left(\frac{2\sigma}{3T}\right)^2\right] \exp\left(-C\left[\left(\frac{\sigma}{T}\right)^2 - 2.25\right]F^{1/2}\right), \tag{12b}$$

where C is a universal constant equal to 2.9×10^{-4} cm$^{1/2}$ V$^{-1/2}$. However, the universality of this constant seems doubtful. In particular, Bässler's most recent paper[14] stresses that the field F should be interpreted as the dimensionless effective field

$$F_{\text{eff}} = \frac{eF\rho}{2T}, \tag{13}$$

where ρ is the average distance between the transport centres of the matrix. This replacement produces a change in the temperature dependence of μ. It is stated[14] that this change is unimportant in relation to the experimentally accessible temperature range. Nevertheless when using formula (12) we must treat the parameter C as a function of temperature rather than as a constant. Since in previous papers[16,34] the satisfactory consistency of the experimental 'constant' C with the calculated value had been repeatedly stressed in the comparisons with experiment the whole of the comparison procedure becomes open to doubt. This is a serious shortcoming, especially because of the recent tendency to treat the model of hopping transport over a system of levels normally distributed in density of states as the most promising candidate for the correct description of the transport of charge carriers in disordered organic matrices. Therefore the following list of the main weaknesses of the model could be useful.

1. The range of fields in which the mobility is linearly dependent on $F^{1/2}$ is much narrower than the experimental range. The suggested explanation[61] of this discrepancy is not consistent with experiment.

2. Nondispersive transport of the carriers is observed experimentally under conditions for which the model predicts dispersive transport (i.e. for $\sigma/T > 4.4$).[12]

3. The temperature independence of the parameter σ at temperatures below the glass transition temperature T_g of the matrix is difficult to understand, especially when σ and T have similar values: for example, $\sigma \approx (6-7) \times 10^{-2}$ eV and $T \approx 300$ K.[48] As expected, for $T > T_g$ the parameter σ begins to increase with T (see Abkowitz et al.[62]).

4. The following is probably the most serious deficiency of the model. The results (temperature and field dependence of the mobility) are to a large extent based on a specific (Gaussian) form of the density of states function. However, if $\sigma/T \gg 1$ (for example, if $\sigma/T \approx 4-6$) the main contribution to the carrier transport is provided by the decrease in the density of states in the region of $E/\sigma \gg 1$. The functional form of the density of states in this region does not have to be Gaussian. Whereas in the neighbourhood of the maximum a Gaussian distribution function can be produced by the central limit theorem, an additional decrease in the density of the distribution usually arises from infrequent fluctuations in the surroundings,[63-66] and the central limit theorem does not apply under these conditions.

Many specific problems of this type are met during familiarisation with the above model. For example, to what extent can the Miller–Abrahams model [Eqn (8)] be justified, and in particular the stipulated temperature independence of the probability of a jump giving a decrease in energy? How valid is the modelling of an organic matrix as a regular cubic lattice with transport centres at the corners? How are the results affected by the specific choice of an expression such as Eqn (10) to describe the geometric disorder?

Nevertheless at present the Gaussian model offers the most correct description of the transport of charge carriers, because it allows an integrated description of all its characteristics, including the transition from nondispersive to dispersive transport induced by a decrease in temperature, and it also allows the direct modelling of the current curve in the time of flight experiment.[34,67] It is interesting to note that the Gaussian model describes the time dependence of the stochastic transition current in a form different from that of the standard Scher–Lax–Montroll theory[68-71] of stochastic transport:

$$I(t) \sim \begin{cases} t^{-(1-\alpha)}, & t < t_\tau \\ t^{-(1+\alpha)}, & t < t_\tau \end{cases} . \tag{14}$$

This difference makes possible, in principle, an additional test of the model, though the experimental precision which has been achieved so far is not yet adequate for such a test.

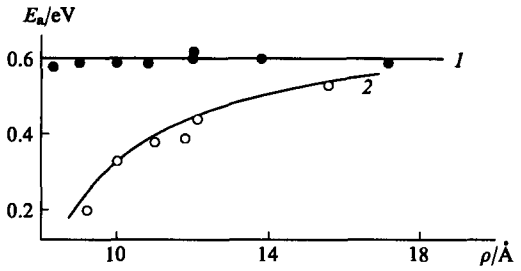


Figure 5. Dependence of the activation energy on the average distance between the transport centres in the DEH/PC (*1*) and TPD/PC (*2*) systems.[72]

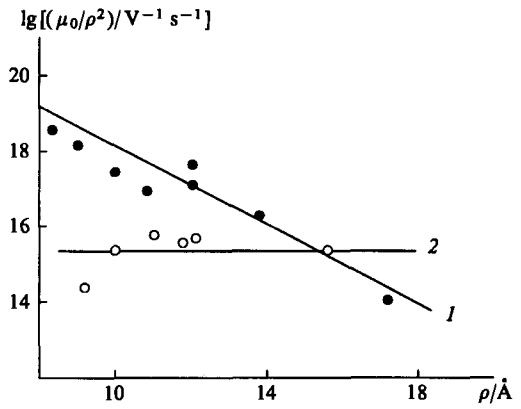


Figure 6. Dependence of the pre-exponential factor in Eqn (15) on the average distance between the transport centres in the DEH–PC (*1*) and TPD–PC (*2*) systems.[72]

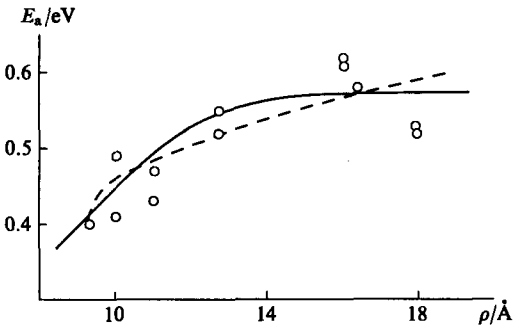


Figure 7. Dependence of the activation energy on the average distance between the transport centres in the TTA–PC system.[74]

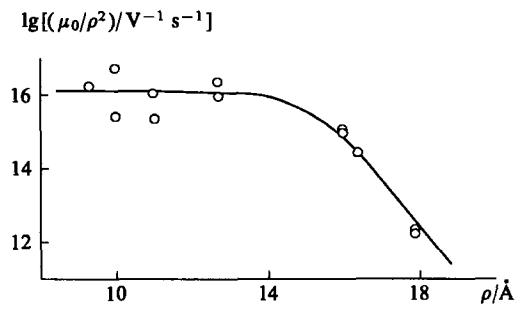


Figure 8. Dependence of the pre-exponential factor in Eqn (15) on the average distance between the transport centres in the TTA–PC system.[74]

2. The polaron model

Schein and coworkers[72–74] have actively developed the concept that the current carriers in disordered organic matrices are small polarons. As we know, the polaron is a bound state of a charge carrier and a vibrational mode (intramolecular, or involving phonons) which can move in a solid as a single entity. Those workers consider that a polaron is formed by the interaction of a carrier with an intramolecular vibrational mode.

A very large number of publications have dealt with the development of a theory of polarons as current carriers in solids of various types, such as semiconductors and organic crystals (see recent reviews, including a monograph[75–78]). In the limit of a weak external field the mobility of a polaron can be expressed as:[79]

$$\mu = \frac{e\rho^2}{T} P \frac{\omega}{2\pi} \exp\left(-\frac{\frac{1}{2}E_p - J}{T}\right), \tag{15}$$

where P is the probability of the transfer of a charge carrier from site to site in the lattice for identical energy levels in the two sites, ω is the frequency of the vibrational mode, E_p is the binding energy of the polaron, and J is the two-centre resonance integral. The function P has a complex form,[76] but a much simpler description can be used in the two limits of large and of small J. In the former (adiabatic regime) we have

$$P = 1, \tag{16}$$

and in the latter (nonadiabatic regime)

$$P \propto J^2 \propto \exp(-2\gamma\rho). \tag{17}$$

As has been pointed out[73] it follows from Eqn (15) that in the former case the activation energy increases with the average distance between centres (since J decreases), and in the latter it is almost independent of the distance (since J is small). An attempt was made to confirm this behaviour experimentally by studying the change in the mobility of the charge carriers in molecularly doped polymeric matrices as a function of the concentration of the dopant. Polycarbonate was used as the matrix, and the dopants included diphenylhydrazone-*p*-diethylaminobenzaldehyde (DEH)[72] and tri-*p*-tolylamine (TTA).[74] Results obtained in earlier work[38] with *N*,*N*′-bis(*m*-tolyl)-*N*,*N*′-diphenyl-1,1′-biphenyl-4,4′-diamine (TPD, see Fig. 1) were also discussed. It was found that in the DEH–PC system the activation energy is independent of the average distance between the transport centres, whereas the parameter P decreases exponentially as ρ increases, whereas in the TPD–PC system the activation energy increases with ρ but (conversely) P is independent of ρ (Figs 5 and 6). This difference was interpreted as a manifestation of nonadiabatic and of adiabatic polaron transport respectively. Since the resonance integral decreases exponentially with increase in ρ it follows that decreasing the concentration of transport centres in any system must sooner or later induce a transition to nonadiabatic transport. Schein et al.[74] claim to have detected this transition experimentally in the TTA–PC system (Figs 7 and 8). The different response observed in DEH, TPD, and TTA to a change in ρ (covering the same range) was ascribed to differences in geometry of the dopant molecules, leading to different packing in the polymer matrix and therefore to differences in the overlap of the π electron systems of the molecules.

Thus the experimental data are formally consistent, as a whole, with a polaron transport scheme. However, there are also some discrepancies. Firstly, the values obtained for J, E_p, and ω [0.25 (or more), 0.5, and 1 eV respectively] are unacceptably high in the case of J and ω. One obvious reason is the failure to allow for the disorder of the system. It was particularly stressed[74] that the concentration dependence of the activation energy and of the pre-exponential in Eqn (15) is explained by the polaron model without explicitly allowing for disorder effects.

The suggested explanation was that the activation energy in Eqn (15) is much greater than typical fluctuations in the position of the levels, i.e. the parameter σ as defined in the language of the Gaussian model. In this sense the suggested approach and the Gaussian model are totally incompatible. Furthermore Eqn (15) is not an exact formula but is essentially an interpolation (qualitative) expression. Kenkre and Dunlap[80,81] looked for a stricter expression for μ which also allowed for disorder effects through fluctuations in the energy levels (but not through fluctuations in the transition probability arising from geometric factors). This gives a slightly different functional dependence of the carrier mobility on the concentration for the TTA–PC system, but still as consistent with experiment as the earlier results[74] (see Fig. 7, broken curve). It was also suggested[80,81] that nonadiabatic polaron transport takes place in all the molecularly doped organic systems examined, since no transition to adiabatic transport was observed in the TTA–PC system. The same workers described[80,81] experimental data for the TPD–PC system by using their model. However, their model fails to describe satisfactorily the DEN–PC system, for which the activation energy is independent of ρ.

The proposed[80,81] modification of the polaron model did not eliminate its initial shortcoming: unacceptably high values of J were still obtained (of the same order as in the previous work[74]). Kenkre and Dunlap[81] stressed the fact that even in organic crystals, where the distance between the molecules is smaller than in molecularly doped polymers, the parameter J is at least an order of magnitude smaller than the values given by the model. Furthermore Bässler[14] correctly points out that the conclusions of Schein et al.[74] on the transitions between adiabatic and nonadiabatic transport regimes are based on the hypothesis of a temperature dependence of the mobility, undoubtedly of the Arrhenius type [see Eqn (2)], though this hypothesis now seems unjustified. For example, it yields (from the experimental data[74]) values of the pre-exponential factor in Eqn (15) of 100 $cm^2 V^{-1} s^{-1}$ and higher, which are unacceptably high for the hopping mechanism of mobility.

A recent paper[82] describes another attempt to choose between the polaron and the Gaussian model on the basis of the effect of small additions of diethylaminobenzaldehyde methylphenylhydrazone (DEMPH) on the transport of holes in the DEH–PC system. The transport level in DEMPH is located just below the corresponding level in DEH, and therefore it was suggested[82] that according to the Gaussian model a small addition of DEMPH should produce only a small widening of the distribution (7), whereas according to the polaron model the DEMPH molecules should act as shallow traps. As reported,[82] the observed increase in the activation energy can be explained only by adopting the polaron model. We do not agree that such an equivocal conclusion is justified, since the appearance of impurity levels in the low-energy region is essential to the transport of carriers in the Gaussian model for $\sigma/T \gg 1$ (see above). We suggest that the assumption of an effective widening of the distribution (7) as the only result of small additions of DEMPH is incompatible with the Gaussian model.

Thus it is impossible at present to produce unambiguous arguments for the occurrence of a transition from adiabatic to nonadiabatic polaron transport upon increasing ρ. The same must be said of the possibility of realising the polaron mechanism in general. The reason is that the main shortcoming of the polaron model (at least, in its present form) is its inability to account for the observed field dependence of the mobility. In the polaron model[79]

$$\mu \propto F^{-1} \sinh\left(\frac{e\rho F}{2T}\right), \tag{18}$$

which is totally incompatible with the experimental dependence (4). We believe that the ability to reproduce the field dependence of the mobility is the decisive test of the validity of any model of charge transport. Indeed, the temperature dependence of the mobility has an Arrhenius or similar form in the majority of the models which have been used, but the narrowness of the experimentally accessible temperature range makes it impossible to distinguish even between dependences of types (2) and (3). Different concentration dependences give an impression of artificiality, and often need to be combined with various extrapolation procedures.[14] Furthermore the extraction of unambiguous information from the concentration dependences is complicated by the frequent presence of large concentrations of dopant (10% or more), which make the separation of the system into transport centres and an inert medium an arbitrary decision. In fact a different effective medium corresponds to each concentration of dopant. Under these conditions the field dependence of the mobility offers a unique opportunity to test various models by a relatively simple experiment, using ranges of field strength covering two orders of magnitude in recent experiments.[23] This is why we believe that the strongest argument against the polaron model of charge transport is its failure to offer a correct description of the field dependence of the mobility.

Vannikov and coworkers[44,45,47] have tried to use the theory of Marcus[83] to describe the transport of charge carriers in polymers. In practice this meant allowing for the interaction of the charge carrier both with the intramolecular vibrations and with the vibrational modes of the medium in the polaron model. This approach allowed the activation energy of the carrier transport process to be related to parameters of the medium, such as the static relative permittivity, and thus to explain the influence of added inert polar molecules of the *o*-dinitrobenzene type on various characteristics of the transport. Unfortunately this variant of the polaron model suffers from the same serious shortcoming: as before, it gives Eqn (18) for the field dependence of the mobility.

3. The dipolar traps (transport centres) method

The dipolar traps method[84–88] is still only in the initial stage of its development. Nevertheless the results so far achieved show considerable promise. The model was first proposed in order to account for the field dependence of the mobility, which neither the Gaussian nor the polaron model could explain. However, it was later found that the new model offers interesting information as well on the temperature dependence of the mobility.

The model is based on the following considerations. Let the mobility be determined by the rate of emission of charge carriers from the traps (the transport centres). This state of affairs can be realised if the transport occurs (for example) by jumps of the carriers in a system of relatively shallow traps, and the rate of emission of the carriers from the transport centres determines their concentration in the mobile 'transport' state. Basically this idea underlies the Poole–Frenkel model,[21,22] but in addition that model also stipulates that the transport centres are charged even in the absence of charge carriers. Unfortunately, in the vast majority of matrices so far examined charged traps cannot exist in significant concentrations. Furthermore, as has been pointed out,[23] the distance from which the carrier is emitted from the charged trap according to the Poole–Frenkel model (i.e. the position of the saddle point in the potential energy surface, which determines the decrease in the activation energy, see Fig. 3) takes values of 50–400 Å in typical fields of 10^4–10^6 V cm^{-1}, i.e. it is unrealistically large. Since the transport traps are usually aromatic compounds or groups containing nitrogen they often possess sizeable dipole moments. Therefore it was suggested[84,85] that the effect of the field on the rate of emission of the charge carriers from a dipolar trap can explain the experimentally observed dependence of the mobility on the field strength. In the simplest case this effect can be evaluated through the lowering of the activation energy barrier to the emission of a carrier caused by an external electric field.

We assume that the carrier emerges from the trap in a region close to the saddle point, where the activation energy is a minimum, so that averaging over the different emergence directions becomes unnecessary, and quantum effects can be ignored. The interaction of a charge with a point dipole is described by the well known expression

$$V(r) = \frac{edr}{\varepsilon r^3} - eFr\,, \tag{19}$$

where d is the dipole moment of the trap. This leads to a dependence of the type

$$\Delta E_0 \propto F^{2/3}\,, \tag{20}$$

and therefore to $\ln\mu \propto F^{2/3}$, which is not consistent with experimental data. However, the decrease in the activation energy ΔE_0 depends also on the mutual orientation of the dipole and the field. By assuming that the orienting influence of the field on the dipolar transport centre is similar to its influence for a free dipole, we obtain the following expression for the mobility after averaging over the orientations of the dipole:

$$\mu = \mu_0 \int_0^{\pi} \sin\alpha \exp\left(-\frac{E_0 + \Delta E_0(\alpha, F) - dF\cos\alpha}{T}\right) d\alpha\,,$$

where

$$\Delta E_0(\alpha, F) = -e\left(\frac{dF^2}{\varepsilon}\right)^{1/3} G(\alpha)\,, \tag{21}$$

$$\begin{cases} G(\alpha) \approx \alpha, & \alpha \to 0 \\ G(\alpha) \approx \dfrac{3}{2^{2/3}}\left[1 - (\pi - \alpha)^2/9\right], & \alpha \to \pi \end{cases},$$

and α is the angle between the vectors d and F. In a weak field this expression gives

$$\ln\mu = \ln\mu_0 - \frac{E_0 - \beta_1 F^{2/3}}{T}\,,$$

$$\beta_1 = \frac{3}{2} e\left(\frac{2d}{\varepsilon}\right)^{1/3}\,, \tag{22}$$

whereas in a strong field

$$\ln\mu = \ln\mu_0 - \frac{E_0 - \beta_2 F^{1/3}}{T}\,,$$

$$\beta_2 = \frac{1}{2} e^2 \left(\frac{1}{d\varepsilon^2}\right)^{1/3}\,. \tag{23}$$

The change from Eqn (22) to (23) is brought about by the orientation of the dipoles in the external field, and takes place in fields of magnitude $F_t \approx 0.01 e^3/\varepsilon d^2$. Thus an increase in the field strength produces a change from the $\ln\mu \propto F^{2/3}$ to the $\ln\mu \propto F^{1/3}$ dependence. In the relatively wide intermediate range of field strength the change in mobility is satisfactorily described by Eqn (5) with

$$\beta = 0.36\beta_{PF}\,. \tag{24}$$

Furthermore the distance between the dipole and the saddle point of the potential surface (19) is 10–40 Å, which is a reasonable value. An attempt[85] to describe the experimental data[23] by means of Eqn (21) gave good agreement between experiment and theory, though the adjustable parameters had to be given unreasonably high values (d_{opt} = 18 D and ε_{opt} = 7.5). In order to resolve this discrepancy an attempt was made[86,87] to allow for the dynamics of the motion of charge carriers in the trap by assuming that the motion is stochastic and can be described by a Markov controlling equation of the form

$$\frac{\partial P}{\partial t} = \int_{E_{min}}^{\infty} \left[K(E, E')P(E', t) - K(E', E)P(E, t)\right] dE' - k_d(E)P(E, t)\,, \tag{25}$$

where $K(E, E')$ is the probability of the transition from a state of energy E' to a state of energy E in unit time, $P(E, t)$ is the distribution function over the energies of a charge bound in a trap, $k_d(E)$ is the rate constant of the dissociation of the bound state of the charge in the trap, and E_{min} is the position of the bottom of the potential well. The nucleus $K(E, E')$ was chosen as a phenomenological Bhatnagar–Gross–Krook (BGK)[89] nucleus, for which in $\Gamma = (\mathbf{r}, \mathbf{p})$ phase space the function $K(\Gamma, \Gamma')$ takes the form

$$K(\Gamma, \Gamma') = \nu\delta(r - r')P_{eq}(p)\,, \tag{26}$$

where ν is the characteristic frequency of the interaction with the external medium, r is the coordinate and p is the momentum of the charged particle, and $P_{eq}(p)$ is the equilibrium distribution function over the momentum. The use of the BGK nucleus implies that every collision leads to a completely stochastic momentum distribution without change in the spatial coordinates. Intuitively this stipulation seems correct in the case of effective collisions of short durations, and therefore the BGK nucleus is often used to analyse and to model the dynamics of various systems.

A solution of Eqn (25) has been obtained[86–88] by two numerical methods: direct modelling of the random walk over energies of a charge carrier in the trap, by using the Monte Carlo method to calculate the rate constant for the dissociation of the bound state through the reciprocal mean time to reach the dissociation threshold, and by the direct calculation of the quasistationary solution of Eqn (25), whose decrement defines the rate of dissociation of the bound state. The latter method can be used for the low-temperature region, which is not accessible to the Monte Carlo method because of its unreasonable requirements of computer time. The two methods gave satisfactorily consistent results. The mobility of the carriers was also calculated by averaging the rate constant $k_e(\alpha)$ over the angle α, using both a chaotic distribution and the distribution corresponding to Eqn (21).

Calculations showed[86–88] that in moderately weak fields the field dependences of the mobility have the typical Poole–Frenkel form (Fig. 9), irrespectively of the assumed distribution of the dipoles over the orientations. This effect is attributed to the fact that the parameter $\ln k_e(\alpha)$ is linearly dependent on $F^{1/2}$ for strong enough fields (Fig. 10). The suppression of the $\ln k_e(\alpha) \propto F^{2/3}$ dependence, indicated by the calculation of the rate constant, can be explained through a decrease in the activation energy. This is because the field F has a double influence on the motion of the charge carrier in the potential well. The strongest effect is a lowering of the activation energy. However, there is also a second effect which limits the space available for the motion of the particle, and therefore the application of a nonzero electric field converts the long-range potential of the dipole into a short-range potential. This ensures that at energies just below the threshold value the particle spends much less time in a state of low kinetic energy (a typical situation for a long-range potential), i.e. the average kinetic energy of the particle (the charge carrier) increases. In our mechanism, which assumes interaction of the particle with the thermal fluctuations of the surroundings, this leads to an increased rate of dissipation

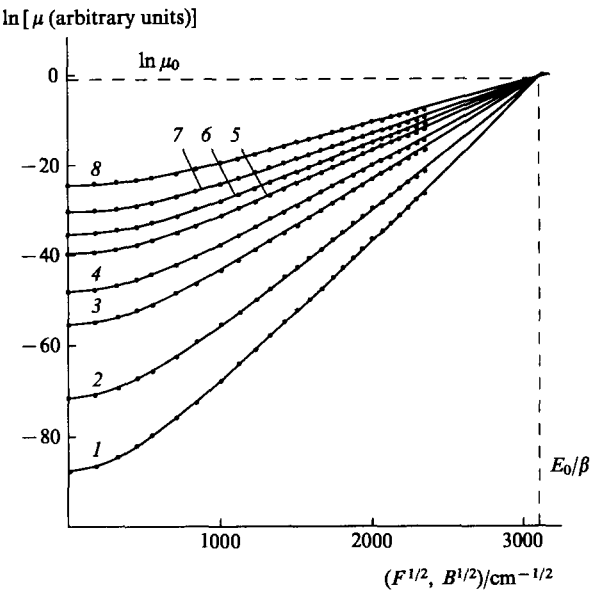


Figure 9. Field dependences of the mobility for different temperatures.[88] T/E_0: 0.01 (*1*), 0.012 (*2*), 0.015 (*3*), 0.017 (*4*), 0.02 (*5*), 0.022 (*6*), 0.025 (*7*), 0.03 (*8*). Calculated for $E_0 = 0.8$ eV, $T = 0.01E_0$, $d = 5$ D, and $\varepsilon = 1$.

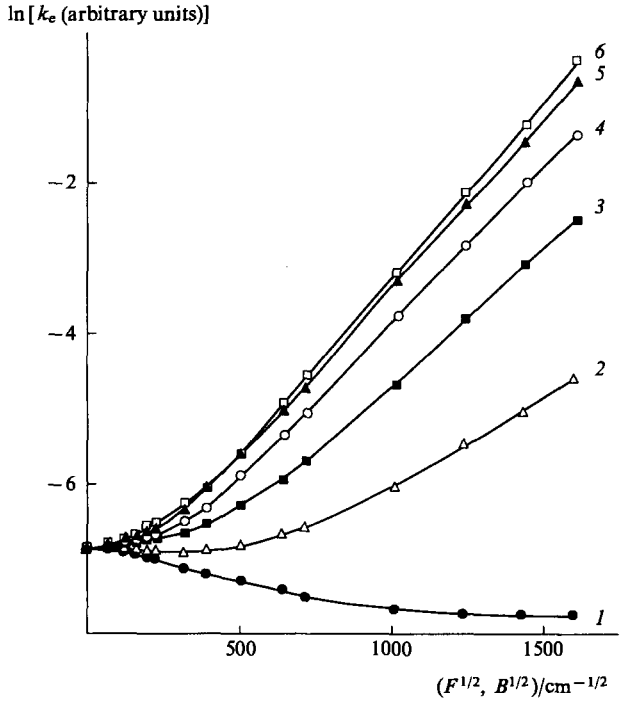


Figure 10. Field dependences of the rate constant k_e for different values of the angle α.[86] α/rad: 0 (*1*), $\pi/5$ (*2*), $2\pi/5$ (*3*), $3\pi/5$ (*4*), $4\pi/5$ (*5*), π (*6*). Calculated for $E_0 = 0.4$ eV and $T = 300$ K, other parameters as in Fig. 9.

of energy for a particular close to the threshold, and therefore to a decrease of $k_e(\alpha)$. This effect is most clearly seen for $\alpha = 0$, when there is no lowering of the activation energy and therefore $k_e(0)$ decreases as F increases.

The temperature dependence of the mobility was shown to be a complex phenomenon of the Arrhenius type at low temperatures and approaching the dependence described by Eqn (3) at high temperatures (where high temperatures are defined by the condition $T/E_0 > 0.03$, Fig. 11). Additional

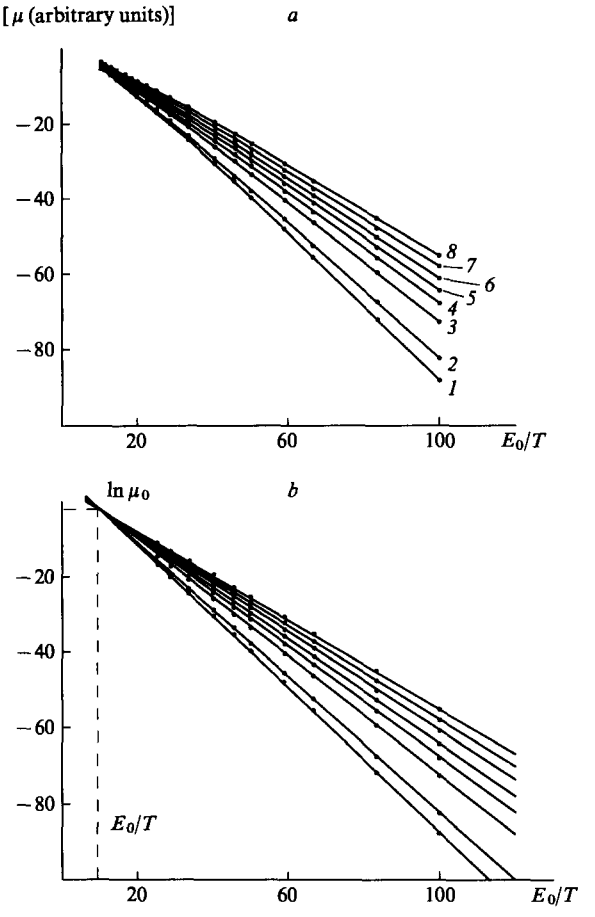


Figure 11. Temperature dependences of the mobility (*a*) for different values of the electric field,[88] and temperature dependences averaged by least squares (*b*) for temperatures not exceeding $0.05E_0$. $(10^{-5}E)$/V cm^{-1}: 0 (*1*), 2 (*2*), 7 (*3*), 10 (*4*), 12.5 (*5*), 15 (*6*), 17.5 (*7*) 20 (*8*). All the other parameters as in Fig. 9.

confirmation of the Arrhenius form of the $\mu(T)$ dependence is provided by the equality of the activation energy and of the depth of the trap (which depends on F).

The overall dependence of μ on F and T in not very weak fields is accurately described by the Gill–Pfister Eqn (5) (see Figs 9 and 11). It follows from Fig. 11 that a crude estimate of the temperature T_0 can be obtained by the formula

$$T_0 \approx 0.1\,E_0\,. \tag{27}$$

Evidence that the temperature T_0 is determined only by the parameter E_0 has been obtained.[88] The estimate (27) agrees reasonably well with experimental data,[24,39,40,90,91] especially if its approximate nature is not forgotten. Another interesting conclusion follows from the calculations: the constant μ_0 of the Gill–Pfister Eqn (5) corresponds approximately to the limit value of the mobility at $T \to \infty$, which is independent of F, whereas it follows formally from Eqn. (5) that

$$\mu(T \to \infty) = \mu_0 \exp\left(\frac{E_0 - \beta F^{1/2}}{T_0}\right). \tag{28}$$

For $F = 0$ we find from Eqns (27) and (28) that Eqn (5) gives a value of the limiting mobility too high by a factor of 2×10^4. Of course, the approximation (27) is quite arbitrary and has a low precision, and it is clear that it overestimates the limiting mobility by several orders of magnitude. Therefore the choice of the dependence (3) [rather than (2)] on the grounds that (2) gives an unreal value of the mobility as $T \to \infty$ is not justified.[15,92]

At the same time, in the light of the dipolar traps model, the relative advantages of the expression (2) or (3) are arguable. Depending on the temperature interval chosen the mobility can be better described by Eqn (2) or by Eqn (3).

To conclude this section we shall discuss the sign inversion at high temperatures[15,31-33] of the coefficient b in the field dependence of the mobility [Eqn (4)], which was mentioned above. This behaviour follows formally from Eqn (5) for $T > T_0$. The dipolar traps model in its most recent variant cannot account for this behaviour, and this is, in fact, its most serious shortcoming. Nevertheless we should stress that the Gill–Pfister formula applies with satisfactory precision to almost all the systems so far examined, whereas in practice the sign inversion has been established experimentally only in a few cases. For the great majority of compounds the temperature T_0 is found to lie well above the glass transition temperature of the matrix, and is therefore not experimentally accessible. Therefore we believe that the temperature T_0 is not directly related to the sign inversion of the coefficient b of Eqn (4), and is only a parameter which describes the deviation of the temperature dependence of the mobility from the Arrhenius form. From our point of view the sign inversion of b must be explained by the action of some specific and (obviously) rarely met mechanism. The same is true of the nonmonotonic field dependence of the mobility.[13,34] This dependence is a very rare exception. Only future work can show whether this is really the case, or whether these effects are unavoidable characteristics of charge transport in disordered organic matrices.

The dipolar traps model also offers a natural explanation of the effect of inert polar additives on the transport of charge carriers. It is reasonable to assume that the dipoles can form aggregates of various compositions and geometries with the transport centres, and that the effective dipole moment of these aggregates can vary within defined limits. Clearly, the dipole moment of the aggregates is directly correlated with the bond energy of the carrier, since the electrostatic interaction of the charge with the dipole adds a substantial contribution to the total energy of the bond. Since the number of carriers is usually small in comparison with the number of traps, the charge transport is dominated by the deepest traps, i.e. by the traps with the largest dipole moment. This decreases the absolute value of the mobility as a result of the increase in E_0, but it also increases β since an increase in d strengthens the long-range interaction of the charge with the dipole, which is responsible for the emission of the charge from the trap.[88] Similar arguments apply to the changes in dipole moment of the transport centre itself.

We note that an increase in d without a change in the depth of the trap results in an increase in μ as a result of the accompanying strengthening of the long-range interaction. This effect can be used to explain an interesting experimental observation:[45] the carrier mobility in the polystyrene–triphenylamine system is decreased by a factor of 320 after doping with *o*-dinitrobenzene, whereas allowing only for the change in the activation energy should lower the mobility by a factor of 5×10^4.

The most characteristic difference between the dipolar traps model and the Gaussian or the polaron models is the substantial role played by the medium (the polymer matrix). The latter two models treat the polymer matrix as a nontransport medium whose function is to accommodate the transport centres at a well defined mutual distance and which affects the transport only indirectly by acting on the parameters of the centres. Transport directly through the polymer matrix is excluded.

In the dipolar traps model the controlling step is the emission of the charge carrier from an isolated transport centre. In this case the transition to a neighbouring centre requires a stage of transport along the polymer matrix. Data on the radiation-induced electric conduction in polymers show that this mode of transport can easily account for the transport of the charge carrier for the required distance. We know that the radiation-induced electric conduction in polymers, which has undoubtedly an electronic nature, includes an instantaneous and a delayed component,[93,94] and that the instantaneous component γ_m (defined by the drift of the charge carrier between its generation and its capture by a trap) bears a direct relationship to the motion of the carriers in the polymer matrix between neighbouring transport centres. The instantaneous component is characterised by the constant K_m. Under these conditions $\gamma_m = K_m R_0$, where R_0 is the dose rate. If γ_m is expressed in C m^{-1}, and R_0 in Gy s^{-1} we can write

$$G\mu_0\tau_0 = 0.1\,\frac{K_m}{g}, \tag{29}$$

where G is the radiation-chemical yield of charge carriers per 100 eV of absorbed energy; μ_0 and τ_0 are the mobility of the carrier in the free state and the time elapsing before its capture by a deep trap; $\mu_0\tau_0$ is the specific path, m^2 V^{-1}; g is the density of the polymer, g cm^{-3}. In organic substances, including polymers, $G = 1$. In polycarbonate, the polymer matrix most often used in electron transport layers, $K_m = 1.6 \times 10^{-15}$ F m^{-1} Gy^{-1}, whence $\mu_0\tau_0 = 1.6 \times 10^{-12}$ cm^2 V^{-1}. The interval usually obtained for the change in F is 10^5–10^6 V cm^{-1}, i.e. the charge carrier travels a distance of 16–160 Å before being captured by a deep trap, whereas the average distance between the transport centres is usually 10–20 Å.

The dipolar traps model in its current form is only a model of a single trap, not a model of the transport process as a whole. Therefore it cannot claim to describe characteristics of the transport such as the various concentration dependences and dispersion phenomena. Nevertheless it can be used to give descriptions of field and temperature dependences in good agreement with experiment.

IV. Electroluminescent polymer layers

In recent years studies of radiative recombination and the preparation of flat, flexible polymer diodes which emit light upon the application of an electric potential difference have become one of the leading new areas in applied science.[4,95,96] The main part of these electroluminescent diodes is a polymer layer located between two electrodes: the cathode injects electrons and the anode injects p-type carriers. Metals having a low work function (ϕ) are used for the cathode (Al, In, Ca, or Mg), whereas the hole-injecting anode is a compound having a high electron affinity: In_2O_3/SnO_2 (ITO), or a polyaniline (PAn) film in the form of the conducting (acid-doped)[97,98] emaraldin salt, or oligothiophen.[99] When a voltage is applied the injected electrons and holes move into the layer from opposite directions and recombine (when they meet) with emission of light:

$$p^{+\cdot} + e^{-\cdot} \longrightarrow {}^{1,3}(p^{+\cdot}\cdots e^{-\cdot}) \longrightarrow$$

$$\xrightarrow{25\%} S_1 \longrightarrow h\nu^{fl} + S_0 + \text{phonons} \tag{30a}$$

$$\xrightarrow{75\%} T_1 \longrightarrow S_0 + \text{phonons}. \tag{30b}$$

In keeping with the multiplicity of the states S_1 and T_1 25% of the charges which collide in reaction (30) recombine through a singlet excited state, and 75% through a triplet state.[100] Electrophosphorescence was not observed in these diodes. As will be shown below, the triplet excitons T_1 contribute to the electroluminescence by virtue of the reaction (30c) in competing processes:

$$T_1 + T_1 \longrightarrow S_1 \longrightarrow h\nu^{fl} + S_0 + \text{phonons} \tag{30c}$$

$$T_1 + T_1 \longrightarrow S_0 + \text{phonons}. \tag{30d}$$

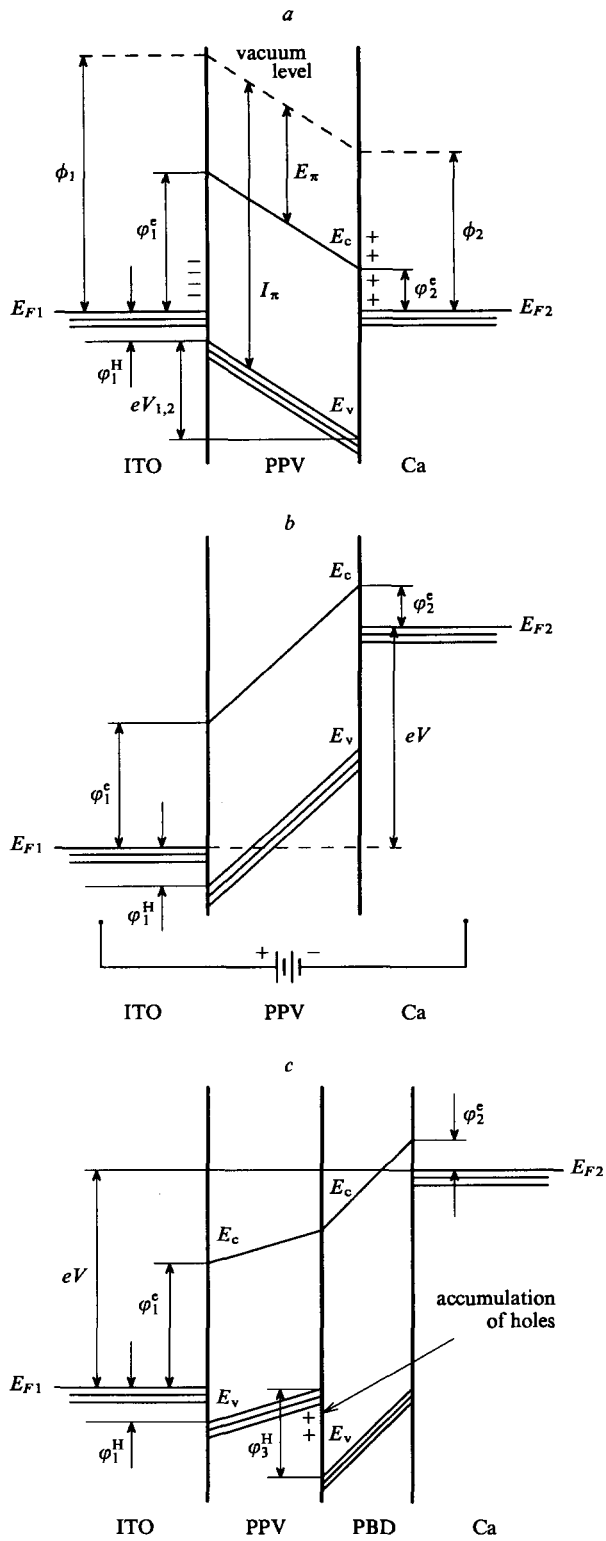


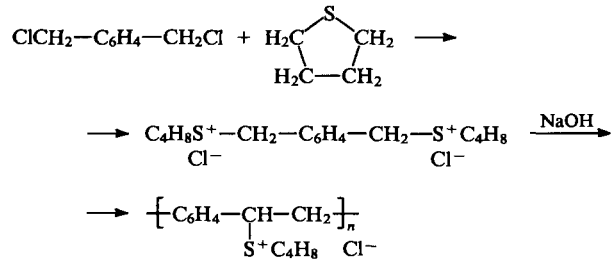
Figure 12. Energy diagram of the processes in single-layer (*a*, *b*) and in bilayer (*c*) electroluminescent diodes (symbols defined in text). Applied potential difference $V = 0$ (*a*), V (*b*, *c*).

Two types of system have been examined so far. The first type includes single-layer systems with one or more components. The one-component systems rely on polymers with conjugated bonds, in which charge transport and light emission can take place simultaneously (PPV and its derivatives,[4,95,97,98,101-107] poly-3-alkylthiophens,[100,108,109] poly-*p*-phenylene,[110] etc.). A typical example of a single-layer multicomponent system is a composition consisting of PMMA with a dissolved triphenyldiamine additive (TPD, see Fig. 1) responsible for the transport of holes, and the organoaluminium complex (Alq_3), responsible for the transport of electrons and for the emission of light.[112] An energy diagram of the processes in single-layer systems is shown in Figs. 12*a* and 12*b*, where ϕ_1 and ϕ_2 are the work functions of the anode and of the cathode respectively; I_π and E_π are the ionisation potential and the electron affinity of the polymer layer in the solid phase [respectively, the distance from the vacuum level to the upper edge of the valence band (E_v) and to the lower edge of the conduction band (E_c)]. Under these conditions $h\nu^{fl} \approx I_\pi - E_\pi$. In PPV I_π is equal to 6.2 eV and E_π to 2.5 eV.[113] The strength of the EL is determined by the effectiveness of the radiative recombination channel, by the energy barriers which the electrons and holes must overcome before recombining, and also by the transport of electrons and/or holes, all of which contribute to the encounter of electrons and holes in the polymer.

Systems of the second type include structures consisting of two (or more) polymer layers (see Fig. 12*c*), one of which (PPV) is responsible for the transport of holes while the other [PPMA containing 2-(4-biphenyl)-5-(4-*tert*-butylphenyl)-1,3,4-oxadiazole (PBD)] is responsible for the transport of electrons.[104,114-117] In these systems the emission of light takes place from the contact region of the two layers.[104,114-117] Structures in which the polymeric transport layer is in contact with a sputtered layer of a low-molecular-mass compound have also been prepared. The transmission of electrons through interlayer boundaries is discussed in detail in Section V.

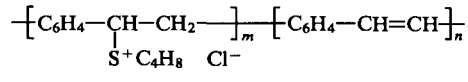
1. Electroluminescence of PPV derivatives

In the method widely used to synthesise PPV its precursor is first obtained from α,α′-dichloro-*p*-xylene in the form of the polyelectrolyte **1**, for example by reaction with tetrahydrothiophen (THT).[118]



1

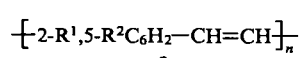
The polymer **1** is unstable, and conjugated phenylenevinylene portions of the chain are formed in the molecule during lengthy storage at elevated temperatures (160–300 °C).



2

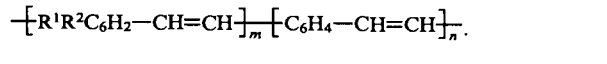
The polymer **2** is completely converted into PPV when stored in vacuum at 300 °C for several hours.[118]

If substituted α,α′-dichloro-*p*-xylenes [$ClCH_2-2\text{-}R^1,5\text{-}R^2.C_6H_2-CH_2Cl$ (R^1 and R^2 = CH_3O, NO_2, or other groups)] are used in the synthesis derivatives of PPV are obtained,



3

or copolymers of the structure



As will be shown below, PPV has a weak EL, and polymer **2** is most often used in the preparation of diodes. Since the conversion of polymer **2** into PPV continues in the prepared diode it is difficult to control the degree of development of the unsaturated chains in PPV. This may be the reason for the large scatter of the characteristics of the EL obtained in different laboratories. Changes in the region of the Schottky barrier caused by the interaction of the cation material (for example, Ca) with the sulfur-containing impurity produced during the conversion of the polymer **2** into PPV also contribute to the scatter of the results.[119]

The position of the EL band is determined mainly by the size of the system of conjugated bonds, and also by the structure of the side substituents in the polymer chain and by other factors which control the position of the energy levels contributing to reaction (30). The optical absorption of the PPV film lies in the energy range above 2.4 eV and has a maximum at ~3.0–3.2 eV (410–390 nm).[118–120] The long-wave threshold of the optical absorption of the polymers **3** is bathochromically shifted by the introduction of donor substituents from ~2.4 eV in PPV ($R^1 = R^2 = H$) to 2.18 eV for R^1 and $R^2 = OCH_3$ and to ~2.1 eV for R^1 and $R^2 = O-(CH_2)_7-CH_3$, or $R^1 = O-CH_2-CH(CH_2CH_3)-C_4H_9$, $R^2 = O-CH_3$; or for $R^1 = R^2 = O-(CH_2)_5-CH_3$.[121] A hypsochromic shift of the spectrum has been observed for the oligomeric analogues of PPV ($n = 3$) with $R^2 = NO_2$.

The EL spectra are usually similar to the photoluminescence (PL) spectra of the polymers. The similarity is due to the fact that in both cases the formation of an exciton is an intermediate stage, and the same excited states take part in the radiative transitions. As an example we show in Fig. 13 the photoluminescence spectra of poly[1,4-phenylene-1,2-di-(4-phenoxy-phenyl)vinylene], DPOP–PPV, measured at room temperature,

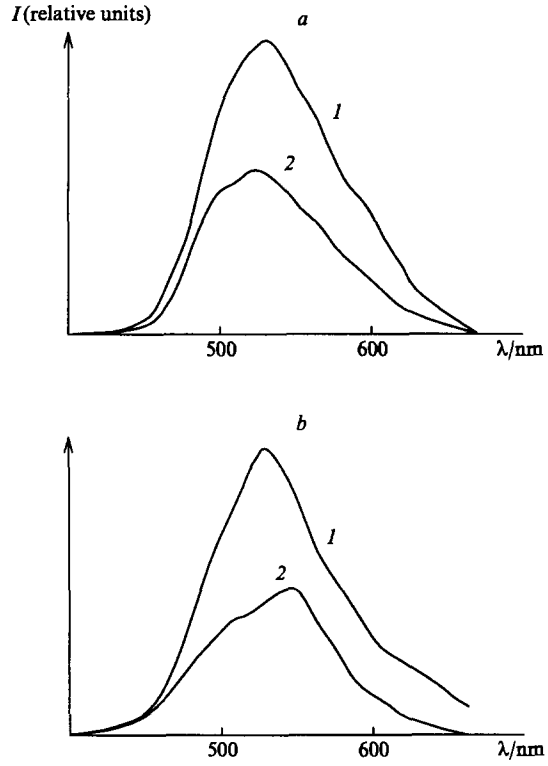
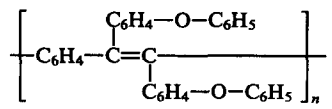


Figure 13. Photoluminescence spectra (*a*) of a layer of DPOP–PPV ($\lambda^{exc} = 370$ nm) and electroluminescence spectra (*b*) of a layer of DPOP–PPV in an ITO/PAn/DPOP–PPV/Al cell ($V = 12$ V) without (*1*) and with 10 wt.% of *o*-DNB (*2*).



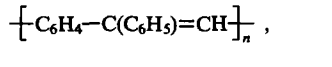
and their electroluminescence spectra, measured in an ITO/PAn/DPOP–PPV/Al cell with an applied voltage of 10–20 V. It can be seen that the EL and PL spectra lie in the same region (450–650 nm) and have a maximum at ~530 nm (2.34 eV) in the absence of additives.[98] The spectral changes produced by the addition of *o*-DNB are discussed below. In cells of this type the brightness of the EL is proportional to the density of the current flowing through the sample when the voltage is applied. The heating of the sample at high current densities shifts the EL spectrum towards shorter wavelengths.[105]

2. Photoluminescence of PPV derivatives

The fluorescence excitation and emission spectra of PPV are similar in form to those of *trans,trans*-1,4-distyryl benzene $C_6H_4(CH=CHC_6H_5)_2$,[123,124] bispropylstilbene[124] $C_3H_7-(C_6H_4-CH=CH)_2-C_6H_4-C_3H_7$ or oligomeric analogues having the structure $H-(C_6H_4-CH=CH)_n-C_6H_5$, $n = 3-7$.[125,126] In all these compounds the PL spectrum has a well resolved fine structure. The energy of the $S_1 \rightarrow S_0$ 0–0 transition (ΔE), measured from the fluorescence spectra in frozen (6 K) solutions of the oligomeric analogues of PPV, depends on the size of the π conjugation system (n) and corresponds to the Kohn potential box model[122,125–127]

$$\Delta E = \Delta E_\infty + \frac{\text{const}}{n}. \qquad (31)$$

An analysis of the optical absorption spectra of polyphenylphenylenevinylene (PPPV),



during the oxidation of the polymer (in contact with $SbCl_5$) showed[127] that, as the polymer was consumed by being converted into the oxidised form, the optical absorption maximum was hypsochromically shifted from 25×10^3 to 30×10^3 cm^{-1}. These changes, which suggest a nonuniform broadening of the spectra, were ascribed[126] to a nondegenerate energy ground state, i.e. to a weak exchange interaction of the overall collection of segments of the polymer with different effective lengths of conjugated bond systems. In this case the nonuniform broadening of the spectrum is due to the contribution of the optical transitions from conjugated segments having different n values [see Eqn (31)]. The longest conjugated segments are oxidised first, because they have the lowest ionisation potential. This results in a lowering of the optical density at the low-energy absorption edge of the initial polymer and in the appearance of three optical absorption bands belonging to the oxidised form. As the oxidation proceeds, increasingly short conjugated chains begin to contribute to the reaction (i.e. n decreases), and this produces a gradual hypsochromic shift of the spectra of both the initial polymer and its oxidation products.

By comparing the ΔE energies in the polymers and the oligomer analogues with the known values of n we can calculate by Eqn (31) the maximum length of the system of conjugated bonds in the polymers: it is found to be $n \simeq 5-7$ in PPPV and ~10 in PPV.[122,126,127] The value $n \simeq 4$ was obtained for the average length of the conjugation chain in PPPV,[127,128] and in other derivatives of PPV,[128] and this was ascribed to a nonplanar structure of the polymer chain. It was suggested[127] that because of the weak exchange interaction the photoexcitation generates a Frenkel exciton, delocalised within one particular conjugated region. During its random motion (spectral diffusion) the exciton

gradually loses energy and migrates towards more extensive regions of effective conjugation: thus, radiative transitions take place with a higher probability from the regions with the highest n value.

These concepts are consistent with the lack of dependence of the maximum in the fluorescence emission spectra on the energy of the exciting light $h\nu^{ex}$, which has been established experimentally for PPV and PPPV, if $h\nu^{ex} \geqslant h\nu^{loc}$, where $h\nu^{loc}$ depends on the morphology of the polymer and lies in the region of 2.5–2.36 eV [$\nu^{loc} \sim (20.2-19) \times 10^3$ cm^{-1}].[126,129] Lowering ν^{ex} into the region below ν^{loc} at 6 K produces uniformly broadened radiative transitions, resulting from the local excitation of the largest π conjugated segments.[126,129] Since the diffusion of low-energy excitons is hindered, the absorption and the emission of light take place in the same fragment. A dependence of the displacement between the maxima of the excitation and radiation PL spectra (Stokes shift) upon the degree of order in the polymer chains has been established for this case. This effect justifies the conclusion that the Stokes shift is determined by a change in conformation of the polymer chain in the photoexcited state[129] rather than by the electron–photon interaction, as had been suggested previously.[126] The Stokes shift is 500 cm^{-1} (0.062 eV) in PPPV, but it depends on the extent of conversion of the polymer **2** into the conjugated PPV, decreasing from ~100 cm^{-1} for $n \simeq 10$ (see Mahrt et al.[125]) to zero for $n \simeq 20$ (see Heun et al.[129]). In the highly oriented PPV crystals the Stokes shift is close to zero,[130] and singlet excitation extends over more than seven monomer units of the chain. These observations led to the conclusion that the electronic excitation in ordered crystalline PPV corresponds to the Wannier type of exciton.[130]

The PL quantum yield in 1,4-distyrylbenzene at room temperature[120,124] is ~94%. It is substantially lowered by changing to polymer analogues, and in PPV it is variously reported to be $\leqslant 0.1\%$ at room temperature[120,123] and ~4%–0.4% in the 10–293 K region.[124] Separating the basic π conjugated chains by introducing bulky side substituents in the change to PPPV increases the quantum yield at 10–293 K to 20%–10%, and if the PPPV is additionally diluted with polycarbonate the yield increases to 32%–25%. On these grounds it was concluded that a competition between radiative and nonradiative recombination is occurring. The nonradiative disappearance of the excitons is due to their capture by randomly distributed traps, formed by the interaction of the π conjugated chains of the polymer. The effectiveness of the capture of excitons by these traps is increased by the increase in their rate of migration at higher temperatures.

The EL and PL spectra of polyphenylenevinylene lie at ~2.6–1.8 eV, with a maximum at ~2.1–2.4 eV,[105,108] and they have similar fine structures with a resolution of ~0.16 eV.[120] However, in the partially conjugated polymer **2**, with segments containing the saturated precursor PPV, the PL and EL emssion spectra were found[118] not to be exactly identical: in particular, differences were noted in the relative intensities of the fine structure bands. These differences were tentatively ascribed to contributions to the PL and EL from different parts of the polymer chain.[118] The main contribution to the PL is provided by portions of the chain with a high content of nonconjugated segments, since on the conjugated segments the emission is preferentially quenched by nonradiative recombination processes. On the other hand, in EL the oppositely charged species can approach each other to within a distance which allows recombination within the conjugated regions, where the charge carriers have their highest mobility.[118]

Measurements of the EL and PL in DPOP–PPV are consistent with these arguments. As is shown in Fig. 13, the addition of *o*-DNB to the polymer (which increases the hole mobility[42]) lowers the intensity of both the EL and the PL, and therefore the *o*-DNB is acting as a quencher of the singlet excitation of the polymer. The suppression of the intensities is accompanied by a hypsochromic shift of the maximum of the PL spectrum and by a bathochromic shift of the maximum of the EL spectrum (see Fig. 13). These changes can be explained in terms of nonuniform broadening of the spectrum. Evidently, the displacement of the PL towards higher energies is associated with preferred interactions giving a CTC of the quencher with the most extensive π conjugation regions, which have the lowest I_π. The bathochromic shift in the maximum of the EL spectrum may be due to a simultaneous increase in the mobility of the charge carriers upon the addition of *o*-DNB, which increases their time of residence in regions with a more developed system of conjugated bonds.

According to published results EL and PL have different characteristic times. Thus, the application of nanosecond voltage pulses to a PPV film produces a decrease in the EL intensity which can be described by two exponentials with time constants of <11 and 60 ns respectively.[105] The slow component is determined by the distortion of the electric pulse by the *RC* constant of the sample, and the fast component by the EL process itself, which suggests the possibility of fabricating fast EL devices by optimising their geometry. Another important result of the pulse measurements was the observation of a proportionality between the current density and the brightness of the EL, up to current densities of the order of 10 A cm^{-2}. In the absence of limitations associated with the geometry of the sample the PL can be measured in the picosecond range. The decay of the PL also involves two components. Initially the PL intensity decreases 2.7-fold in PPV and PPPV at 10 K in ~135 and 430 ns respectively, and at room temperature in ~70 and 120 ns. Diluting the PPPV with polycarbonate increases this time to 780 ns and eliminates the temperature dependence. The slow component has a time constant of 1.1–1.4 ns,[124] which coincides with the 1.3 ns time constant measured in 1,4-distyrylbenzene.

3. Role of the spin constants in electroluminescence

Data on the electronic processes which accompany reaction (30) in EL diodes based on PPV and its derivatives were obtained by measuring the electric conductivity (σ) and the EL,[131] and also the PL [131,132] under conditions of paramagnetic resonance of the species which contribute to the process (electrons, holes, triplet excited states). These characteristics were measured at 20 K in diodes placed in the resonator of an ESR spectrometer, in which the magnetic field was scanned in the region of spin allowed ($\Delta m_s = 1$, $g \approx 2$) and of spin forbidden transitions ($\Delta m_s = 2$, $g \approx 4$). The increase in the PL intensity is accompanied by the appearance of a narrow signal ($\Delta H_{1/2} = 13$ *G*) with a g factor of 2.0023. Under paramagnetic resonance conditions the Boltzmann distribution of the population of Zeeman levels is perturbed as a result of the reorientation of the spins, and the fractional number of charged particles for which the charge recombination process (30a) becomes spin allowed is increased:

$$^3(p^{+\cdot}\uparrow \cdots e^{-\cdot}\uparrow) \xrightarrow{PMR} {}^1(p^{+\cdot}\uparrow \cdots e^{-\cdot}\downarrow) \quad p^{+\cdot} + e^{-\cdot} \qquad (32a)$$

Swanson et al.[131] assume that the increase in the PL under conditions of resonant change in spin orientation is due to the participation in reaction (30a) of the triplet pairs $^3(p^{+\cdot} \cdots e^{-\cdot})$, and that [as shown in the scheme (32a)] under spin forbidden conditions and in the absence of resonance these pairs dissociate into the free current carriers which are responsible for the photoconduction.[133] A broad spectrum (from 2600 to 4200 G) due to the increased fluorescence intensity produced by the reactions of the triplet excitons T_1 is superimposed on the narrow signal. The appearance of this spectrum shows that the probability of reaction (30c) in the competing processes

(30c) and (30d) is increased under paramagnetic resonance conditions.[131,132] For this reason the PL increases also in the region of forbidden transitions with $\Delta m_s = 2$, $g = 4.07$.

In contrast to the PL, a decrease in the electric conductivity σ and in the EL brightness was observed in the region of resonance spin transitions with $\Delta m_s = 1$. This effect is due to the possible existence, in equilibrium with the singly charged particles, of doubly charged particles with zero spin (depending on the chosen model, they have been called PPV^{2-} and PPV^{2+})[122,125-127] or bipolarons[121,131,132] bp^{++} and bp^{--}. As a result of the reorientation of the spins at resonance by the schemes (32b) and (32c) the probability of formation of doubly charged particles by scheme (32d) should increase:

$$p^{+\cdot}\uparrow + p^{+\cdot}\uparrow \xrightarrow{PMR} p^{+\cdot}\uparrow + p^{+\cdot}\downarrow \qquad (32b)$$

$$e^{-\cdot}\uparrow + e^{-\cdot}\uparrow \xrightarrow{PMR} e^{-\cdot}\uparrow + e^{-\cdot}\downarrow \qquad (32c)$$

$$p^{+\cdot}\uparrow + p^{+\cdot}\downarrow \rightleftharpoons bp^{++}$$
$$e^{-\cdot}\uparrow + e^{-\cdot}\downarrow \rightleftharpoons bp^{--} \qquad (32d)$$

According to Swanson et al.[131] the bipolarons have a much lower mobility than the singly charged current carriers, and therefore the decrease in σ and in EL under paramagnetic resonance conditions is interpreted as a confirmation that the reaction (32d) is taking place in the forward direction. In the region of forbidden transitions ($\Delta m_s = 2$) we find marked differences in the dependence of the EL and of σ on the magnetic field. Both these dependences demonstrate the two resonant transitions of the triplet excitons (low-field at 1.61 kG and high-field at 1.63 kG). Whereas σ is increased as a result of the two transitions the EL signal falls in the 1.61 kG region and rises at 1.63 kG. In agreement with reaction (30a) 75% of the charged particles form triplet excited states in their interaction. As in the case of the PL the increase in the EL is due to the increased probability of reaction (30c) under PMR conditions. It is assumed that the low-field triplet excitons with a resonance at 1.61 kG are more localised than the high-field excitons, and therefore that the process (30c) to which they contribute takes place in the immediate vicinity of the cathode surface. The S_1 singlet formed in the interaction with the electrode surface either undergoes nonradiative deactivation or rapidly decomposes into p^+ and e^-, the p^+ being discharged on the electrode. These changes lower the EL and increase σ under resonance conditions at 1.61 kG.[131]

Thus we conclude from the above discussion that the derivatives of PFV are usually characterised by a greater hole mobility, and that the reaction (30a) takes place in the space adjacent to the negatively charged electrode. The most serious problems are the decreased rate of the forward hole discharge reaction on this electrode, the equalisation of the concentrations of electrons and holes injected into the layer, and the limitation by the deactivation of excited S_1 states as a result of interaction with the electrode.

4. Quantum efficiency of the electroluminescence

The quantum efficiency η of the electroluminescence, defined as the ratio of the number of photons $h\nu$[f1] produced by the reactions (30) to the number of injected charges, depends on the mechanism of the motion of the charged particles, and also (as in the case of the PL) on the factors which affect the deactivation of the excited states.

It has been established[118] that the brightness of the EL in the ITO/polymer **2**/calcium cell depends on the degree of conversion of the saturated sulfur-containing precusor **1** into the π conjugated PPV, i.e. it is determined by the temperature and duration of the heat treatment of the precursor during the synthesis of the PPV. The quantum efficiency is 0.08% if the polymer **1** is heated for 2 h at 140 °C. If the temperature of the two-hour heat treatment is increased the efficiency η initially increases to a maximum of 0.75% at 160 °C and then falls again to ~0.05% at 300 °C. Increasing the time of heating at 300° C to 20 h lowers η further to $\leqslant 0.003\%$. The PL intensity shows similar dependences on the temperature and time of the heat treatment. A substantial lowering of the PL and EL intensities upon increasing the length of the conjugated bond system has been ascribed[118,120] to an increase in the rate of diffusion of the excitons and in the mobility of the charge carriers, which increases the probability of their migration to sites responsible for the nonradiative recombination.

An analysis of the dependence of the mobility of holes on the degree of thermal conversion of the polymer **1** into the π conjugated PPV, or of other precursors in which the $S^+(C_4H_8)Cl^-$ group is replaced by chlorine, dimethyl-, or diethyl sulfide, or by the methoxy or butoxy group, has been reported.[134] In all the polymers prepared by this method, and whatever their degree of conversion, the hole mobility exceeds the mobility of electrons by more than two orders of magnitude. In spite of a marked lack of reproducibility of the results, increasing the number of conjugated segments in the polymer **2** produces an unmistakable increase in the mobility of holes, but this increase is suppressed by lengthy storage of the sample at room temperature or by heat treatment of the precursor above 150 °C.

Antoniadis et al.[134] were unable to detect the motion of charge carriers through a film of polymer having a high level of conjugation prepared by heat treating **2** for 2 h at 250° C. They showed that increasing the heat treatment temperature increases the dispersion of the time of flight of the charge carriers through the sample. These results were ascribed to the formation (after heat treatment at 150 °C) of polymer **2**, in which the regions of π conjugation include 2–3 phenylene-vinylene units. As was pointed out in Section II, the hopping model of transport, characteristic of many amorphous polymers, is applicable to this polymer containing isolated transport centres. As the extent of conversion of polymer **2** into PPV is increased, the size of the system of conjugated bonds also increases, and so does the dispersion of the times of flight through the transport layer, since the longest π conjugated segments (which have the lowest ionisation potentials) are hole traps. Furthermore, segments with a large n tend to form crystalline domains whose inclusion into an amorphous polymer produces an additional increase in the dispersion of the time of flight of the holes.[134]

In the copolymer of phenylenevinylene (PV) and 2,5-dimethoxy-*p*-phenylenevinylene (CH_3O-PV)[102] the EL spectrum is the same as in PPV, but the quantum efficiency increases more than 30-fold, reaching 0.3% for $m:n = 1:9$ in the ITO/copolymer/Al structure. Burn et al. point out[102] that the quantum efficiency can be increased to $\eta > 1\%$ by controlling the $m:n$ ratio during the synthesis through an appropriate choice of components:

$$-\left[C_6H_4-CH=CH\right]_n-\left[C_6H_2(OCH_3)_2-CH=CH\right]_m-$$

(CH_3O-PV)

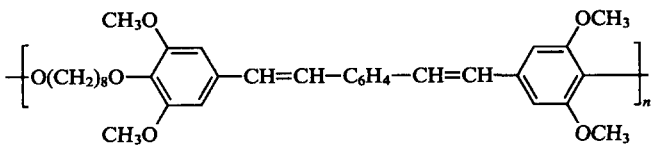
The PL radiation from this copolymer is characterised by two spectra with maxima at 555 and 608 nm, resulting from the different emissions of the PV regions in CH_3O-PV. In contrast to the EL, the PL intensity decreases on passing from PPV to the copolymer. As the $m/(m+n)$ ratio is increased from 0 to 0.33 the PL intensity decreases by about a factor of 8 and takes a constant value, characteristic of CH_3O-PV ($n = 0$).[135] It is suggested that the PL quenching in a copolymer is due to the photodissociation of excitons as a result of the transfer of an electron between parts of the chain of different nature.[135]

In the copolymer

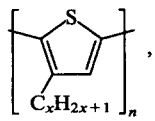
$$-\left[C_6H_4-CH(OCH_3)-CH_2\right]_m-\left[C_6H_4-CH=CH\right]_n-$$

the conjugated structures are also separated by segments containing different bonds. The maximum of the emission spectrum corresponds to 508 nm (2.44 eV). At this light energy the quantum efficiency of the EL is 0.02% in the ITO/polymer (1000 Å)/Al structure.[103]

The electroluminescence lies in the blue region, and has a maximum near 470 nm (2.64 eV), in a polymer whose chain is divided into short segments of conjugated bonds by longer chains of single bonds:[107]

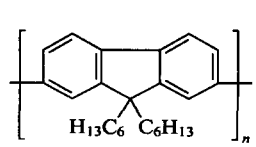


Attempts to prepare EL diodes on the basis of poly-(3-alkylthiophens) (PAT) have been reported: [100, 108, 109]



where $x = 8$ (see Ref. 100), 12, 18, and 22 (see Refs 108, 109). The electroluminescence is characterised by a broad spectrum with a maximum at 620–640 nm (1.9–2.0 eV). The position of the maximum in this spectrum is unaffected by the size of the neutral C_xH_{2x+1} side groups.[100, 108, 109] In the system based on poly(3-octylthiophen), replacing a Ca cathode by an In cathode increases the voltage needed to generate EL, but this does not affect the quantum efficiency of the reaction (30a) to a significant extent: in the diode based on Ca the parameter η lies in the range $10^{-4}\% - 10^{-3}\%$ [for working strengths of the electric field of $(0.2-0.7) \times 10^6$ V cm^{-1}], whereas in an In diode it lies in the range $(1-3) \times 10^{-3}\%$ [for fields of $(1-3) \times 10^6$ V cm^{-1}].[100] These low values of η were explained in terms of the presence in the final polymer of an impurity of $FeCl_3$, which is used in the synthesis and generates defects leading to the nonradiative recombination of the current carriers. A 4-fold increase of η upon increasing the length of the alkyl side chain x from 12 to 22 has been demonstrated.[108, 109] This observation led to the conclusion that the intermolecular interaction of the main chains containing the conjugated structures, which is weakened by an increase in x, is responsible for the nonradiative recombination of the charge carriers in these polymers as in the case of PPV. In PAT an increase in the applied voltage and in the current flow produce an anomalous superlinear increase in the EL.[108, 109] This effect is attributed to the increase in temperature and to the corresponding (temperature-induced) twist rotations of the main chains, leading to a shortening of the effective conjugation chain. The final result is a weakening of the intermolecular interaction of the main chains and a decrease in the rate of the nonradiative processes.

An electroluminescence with $\lambda_{max} = 470$ nm (2.5 eV) has been measured in a cell based on poly(9,9-dihexylfluorene):[111]



5. Effect of the material of the injecting layer

The efficiency of the EL can be improved by lowering the energy barriers which the electrons and holes have to surmount during injection. The quantum efficiency in single-layer diodes based on the derivatives of polyphenylenevinylene with p-type mobile carriers increases when cathodes such as Al (($\phi_2 = 3.8$ eV, see Fig. 12*a*)[136] or In ($\phi_2 = 4.2$ eV) are replaced by an electrode with a much lower work function, for example Ca ($\phi_2 = 3$ eV).[101] In a diode based on unsubstituted PPV [ITO/PPV (1000Å)/Al] the quantum efficiency (photons per electron) has been variously reported to be 0.01% (Refs 102, 103) or 0.05% (Ref. 100). When the aluminium cathode is replaced by a calcium cathode in this structure the quantum efficiency increases to 0.1%.[104]

In a diode based on poly[2-methoxy, 5-(2-ethylhexoxy)-1,4-phenylenevinylene], MEG–PPV [structural formula **3**, where $R^1 = O-CH_3$, $R^2 = O-CH_2-CH(CH_2CH_3)-C_4H_9$], ITO/MEG–PPV/In(or Ca), an electroluminescence in the spectral region between ~1.6 and 2.3 eV with a maximum at ~2.15 eV (at 300 K) or two maxima at 2.03 and 1.88 eV (at 90 K) is produced at voltages above 1.8 V.[97, 101] For a constant diode current density of 2 mA cm^{-2} the quantum efficiency is 0.05% and 1% (photons per electron) in the case of an In or a Ca cathode respectively.[101] In both diodes the increase in η is due to the fact that lowering the electronic work function strengthens the injection of electrons into the polymer for a constant hole current. It should also not be forgotten that in polymers with mobile carriers of a single sign (holes) the injected electrons are captured in traps directly on the metallic electrode, and recombination with formation of excited states by reaction (30) also takes place on the cathode. Under these conditions the nonradiative dissipation of the exciton energy on the metallic surface can compete effectively with the radiative $S_1 \rightarrow S_0$ transition (30).

Attempts to solve these problems have been made by synthesising derivatives of polyphenylenevinylene in which charge carriers of both signs are mobile,[42, 43, 98, 137, 138] and their recombination by reaction (30a) takes place not only in the immediate vicinity of the electrode but also throughout the polymer layer. For example, charges of both signs are mobile in the polymer DPOP–PPV. At 20 °C the quantum efficiency of reaction (30), measured at the emission maximum (530 nm, see Fig. 13) in ITO (or PAn)/DPOP–PPV (3000 Å)/Al cells for a constant voltage of 20–40 V, was 0.13% in the case of the ITO anode ($\phi_1 = 4.1$ eV,[97] see Fig. 12), and was increased to 0.38% by changing to a PAn anode ($\phi_1 = 4.3$ eV,[97]).[98] In the latter case the energy efficiency of the transformation of electric into light energy is 0.32%. As can be seen, when polymers with mobile carriers of both signs are used the anode material also has a marked effect on the quantum efficiency of the EL. In contrast, in a cell based on the MEG/PPV polymer, in which only the holes are mobile, the quantum efficiency of the EL is unaffected by replacing ITO by PAn: the current through the cell is increased by a factor of 10^3-10^4 for applied voltages below 1.5 V, but it ceases to be a function of the anode material at voltages above 1.8 V, where the EL is produced in the bulk of the polymer.[97] In this case, as was pointed out above, the controlling processes are those taking place directly on the cathode and involving its material.

6. Molecularly doped polymers

Molecularly doped polymers, in which compounds with both donor and acceptor properties are introduced into the polymer matrix to generate transport at both holes and electrons,[112] are a special class of electroluminescent layer. Poly(methyl methacrylate) (PMMA) is often used as the polymer matrix. Direct measurements of the mobility of the excess charge carriers in PMMA in the absence of additives or in the presence of a donor (triphenylamine, TPA) and an acceptor (chloranil, CA) showed[139] that the polymer matrix itself is reactive towards the excess electrons. Dissociative electron capture by the polymer

matrix competes effectively with all electron transport processes, and no electron drift from the generation region can be observed. No motion of holes is detected in the undoped PMMA because of the presence of structural traps (T), which capture holes according to the scheme

$$T + p^{+\cdot} \longrightarrow T^{+\cdot}.$$

The drift of holes begins at temperatures above 50 °C and 80 °C in the presence of TPA and CA respectively, but it is observed at room temperature in the simultaneous presence of TPA and CA. The formation of donor–acceptor complexes was not detected even at the maximum concentration of the dopants, which corresponded to an average intermolecular distance of ~20 Å. It was therefore concluded that the effect of the dopants on the drift of the holes was additive. It was suggested[139] that the drift of holes takes place by a hopping mechanism (between TPA molecules):

$$TPA^{+\cdot} + TPA \longrightarrow TPA + TPA^{+\cdot}.$$

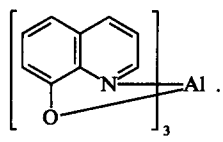
Under these conditions the structural traps terminate the transfer by the scheme

$$TPA^{+\cdot} + T \longrightarrow TPA + T^{+\cdot}.$$

Chloranil interacts with defects of the hole trap type, lowering their concentration and thus increasing the drift mobility of the holes:

$$CA + T \longrightarrow CA^{-\cdot} + T^{+\cdot}.$$

The donor *N,N'*-bis(*m*-tolyl)-*N,N'*-diphenyl-1,1'-biphenyl-4,4'-diamine (TPD, see Fig. 1) was used to provide transport centres for p-type carriers in a single-layer EL diode based on PMMA, and the aluminium complex of tris(8-hydroxyquinoline) (Alq_3) was used as the acceptor:[112]



In systems based on two evaporated layers (a donor and an acceptor) the EL spectrum is shifted towards lower energies with respect to the PL spectrum of the individual component as a result of the formation of a charge transfer complex (responsible for the emission) or of an exciplex.[140] In a system consisting of a PMMA matrix containing TPD and Alq_3 the EL spectrum coincides with the PL spectrum of the complex of Alq_3 in PMMA and has a maximum at 510 nm (2.44 eV). Steric hindrance to the formation of an exciplex with the donor (TPD)[112] may be created by the octahedral configuration of the metal in the Alq_3.

The following jump model of the bipolar transport of charge carriers in this composition, involving the oxidation–reduction reaction

$$TPD^{+\cdot} + TPD \longrightarrow TPD + TPD^{+\cdot}$$
$$Alq_3^{-\cdot} + Alq_3 \longrightarrow Alq_3 + Alq_3^{-\cdot},$$

has been proposed, followed by the recombination

$$TPD^{+\cdot} + Alq_3^{-\cdot} \longrightarrow Alq_3^{*} + TPD$$
$$Alq_3^{*} \longrightarrow Alq_3 + h\nu^{fl}.$$

The luminescence of Alq_3 has been detected in the photoexcitation of the TPD in this composition, and therefore the possibility of the following reaction cannot be excluded:

$$TPD^{+\cdot} + Alq_3^{-\cdot} \longrightarrow Alq_3 + TPD^{*}$$
$$Alq_3 + TPD^{*} \longrightarrow TPD + Alq_3^{*}.$$

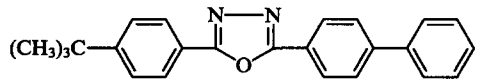
The diode current and the EL brightness are shown below for different TPD : Alq_3 ratios (by weight) in a diode based on ITO/TPD : Alq_3 : PMMA (1000 Å)/Mg with an applied voltage of 17 V and a ratio by weight of (TPD + Alq_3) : PMMA = 0.5.

TPD : Alq_3	0.43	0.67	1.0
i/mA cm^{-2}	60	170	90
EL/cd m^{-2}	180	920	430

7. Systems with separate transport layers

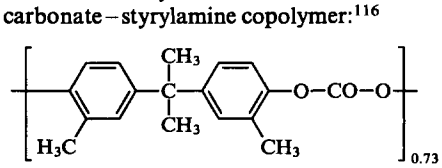
In order to minimise the direct discharge of the mobile current carriers on the electrodes, diodes consisting of two polymer layers (one providing electron transport, the other, hole transport) have been fabricated. We shall discuss them below, together with the characteristics of structures consisting of a polymer layer and an evaporated layer of a low-molecular compound. In these diodes the radiative recombination of injected charges is shifted from the cathode region to the region close to the boundary of the two polymer layers[96,103–105,107] (see Fig. 12*c*).

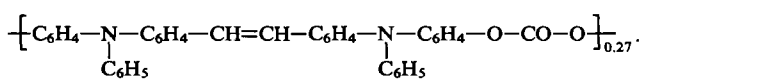
Brown et al.[104] have described the main characteristics of an EL diode consisting of PPV in contact with an electron transporting layer: 2-(4-biphenyl)-5-(4-*tert*-butylphenyl)-1,3,4-oxadiazole (PBD)



molecularly dispersed in PMMA. The EL spectrum of the structure ITO/PPV (3500 Å)/PBD in PMMA (300 Å)/Ca is identical to the EL spectrum of the PPV polymer. Hence the PPV layer is responsible for the emission of light in this two-layer system. The upper edge of the filled band in PPV lies ~1.5 eV above the highest occupied level of PBD, and the injected holes accumulate and contribute to reaction (30a) in the PPV layer near the PPV/PBD boundary (Fig. 12*c*). The accumulated holes create a large space charge which strengthens the electric field in the electron transport layer. This effect produces an increase in the number of injected electrons, and consequently an increased EL brightness. The quantum efficiencies of the two-layer and the single-layer structures (in the absence of PMMA containing PBD) for a current density of 1 mA cm^{-2} are, respectively, 1.1% and 0.07%, and at a current density of 15 mA cm^{-2} they are 0.8% and 0.1%. In the two-layer structure the ratio of luminescence brightness to current density is 0.85–0.6 cd A^{-1} over a wide range of current densities. In the one-layer structure this ratio is 0.017 cd A^{-1}, increasing to 0.034 cd A^{-1} when the current density is increased to 15 mA cm^{-2}.

The two-layer structures include a system based on a carbonate–styrylamine copolymer:[116]





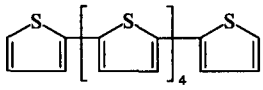
The self-repeating styrylamine segment is responsible for the transport of holes and the emission of light. An electron-transport layer of PBD was evaporated onto the polymer.[116] ITO and Mg were used as electron and hole injecting electrodes respectively. The electroluminescence was characterised by λ_{max} = 460 nm (2.7 eV), the brightness was 130 cd m^{-2} for a current of 80 mA cm^{-2} and an applied voltage of 11 V. The conversion of electric energy into light energy was 0.05 lm W^{-1} at 11 V.[116]

The evaporated electron-transport layer of PBD was studied[115] in conjunction with polymethylphenylsilane (PMPS, see Fig. 1) doped with a europium complex, tris(phenyltrifluoroacetonato)europium, responsible for the transport of holes and the electroluminescence. ITO and Mg were used as the anode and the cathode respectively. A weak EL was observed in the red region, the luminescence being brightest (0.3 cd m^{-2}) at 18 V: it was attributed to the fact that effective nonradiative recombination of charge carriers can take place in europium complexes.

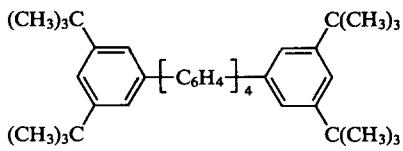
In the absence of additives the polymer PMPS is a p-type organic semiconductor, with a drift mobility of holes of 10^{-4} cm^2 V^{-1} s^{-1} at 20 °C. The ITO/PMPS (350 Å)/Alq_3 (1000 Å)/Mg system, in which a layer of Alq_3 had been evaporated onto the PMPS layer, produced EL with a maximum at 520 nm:[114] an applied voltage of 18 V produces a diode current density of 150 mA cm^{-2}, and the brightness of the electroluminescence rises to 1500 cd m^{-2}. Decreasing the thickness of the Alq_3 film to 600 Å lowered the brightness to 400 cd m^{-2}. Increasing the thickness of the PMPS layer from 350 to 460 Å did not affect the brightness, but decreasing it from 350 to 220 Å lowered the brightness approximately five-fold.

Studies of systems prepared from PMPS (350 Å) and Alq_3 (1000 Å) revealed a serious shortcoming of two-layer structures: the heating produced by high current densities through the device induces crystallisation of the evaporated film, which rapidly degrades the diode by disrupting the contact between the layers. It was established that at high enough voltages (20 V) the EL is irreversibly quenched in a period of a few seconds.

Alq_3 emission was observed[99] in cells having the structure ITO/T6 (200 Å)/TBP/Alq_3 (600 Å)/Mg, where T6 is the oligothiophen



(I_π = 5.2 eV, E_π = 2.9 eV), TBP is the tetrabutyl derivative of the six-ring polyphenyl



(I_π = 5.7 eV, E_π = 2.9 eV); EL was observed in the region of 450–700 nm with a maximum at 510 nm, due to the emission from Alq_3.[99] A linear dependence of the EL brightness on the device current density (i) and a superlinear increase of the current density with the applied voltage V were discovered: for $V > 4$ V, $i \propto V^n$, where $n > 9$. At voltages of 9 and 13 V the following characteristics were obtained for the EL cell with and without a TBP layer (300 Å thick).

	Without TBP	With TBP	
V/V	9	9	13
i/mA cm^{-2}	93	93	313
EL/cd m^{-2}	290	700	2300

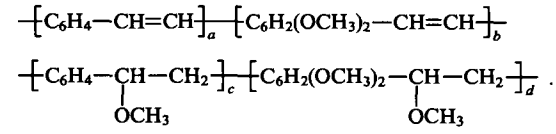
At V = 9 V the conversion of electric energy into light energy is 0.1 lm W^{-1} in the cell without a TBP layer and 0.32 lm W^{-1} when the TBP has been included. The large increase in brightness of the EL as a result of the insertion of a TBP interlayer is ascribed[99] to the suppression by the TBP of the penetration of electrons, which inhibits the transfer of energy from the emitter to the semiconductor polymer.

The brightest EL was obtained in a two-layer system, in which a film of Alq_3 was deposited by vacuum evaporation on a polymer layer of PMMA or polycarbonate (PC) doped with TPD (see Kido et al.[117]). An increase in EL brightness upon increasing the dopant concentration was observed in the diode based on ITO/TPD:PMMA (400 Å)/Alq_3 (500 Å)/Mg. At an applied voltage of 16 V the following dependences of the diode current density and of the EL brightness on the ratio by weight of TPD:PMMA were obtained:

TPD:PMMA	0.3	0.5	0.8
i/mA cm^{-2}	100	180	420
EL/cd m^{-2}	1400	2300	7400.

Comparing these characteristics with those given above for the ITO/TPD:Alq_3:PMMA/Mg system shows that the change from a one-layer to a two-layer structure increases the brightness of the EL by almost an order of magnitude. A further increase in brightness was obtained by using a matrix of PC: for a component ratio of TPD:PC of 0.5 and an applied voltage of 14 V the diode current density reaches 420 mA cm^{-2}, and the EL brightness reaches 7700 cd m^{-2} (see Kido et al.[117]). It has been suggested that the improvement in the EL characteristics on replacing PMMA by PC is associated with the corresponding increase in the rate of hopping transport, resulting from the higher glass transition temperature and greater aromaticity of the PC. In the light of the results obtained with evaporated layers of low-molecular-mass compounds,[141] we can expect further improvements in the EL brightness by replacing the Alq_3 by other metal complexes, for example bis(10-hydroxybenzo-[h]quinoline)beryllium.

Electroluminescent diodes containing several mutually insoluble polymer layers are of considerable interest:[106] for example, MEG–PPV, or PPV and a copolymer having the structure



Structures of four types were studied:

A. ITO/copolymer/PPV (2300 Å)/MEG–PPV/Ca;
B. ITO/MEG–PPV/PPV (500 Å)/copolymer/Ca;
C. ITO/copolymer/MEG–PPV/PPV (1500 Å)/copolymer/Ca;
D. ITO/copolymer/PPV (300 Å)/copolymer/Ca.

In all the structures the thicknesses of the copolymer and of the MEG–PPV layers were 200 and 500 Å respectively. The quantum efficiency of reaction (30) was measured for light intensities of 5 cd m^{-2}: it was found to be η = 0.3%, 0.22%, 0.26%, and 0.16% (photons per injected electron) for the structures A, B, C, and D respectively. It was found that the structure A is the sole one for which only the (MEG–PPV) layer contributes to the EL spectrum (the characteristics of this spectrum are quoted above). Polyphenylenevinylene and the copolymer are responsible only for the transport of holes. Neither the electrons nor the excited states formed by reaction (30) extend beyond the (MEG–PPV) layer. The structure B is characterised by a broad emission spectrum, lying at 1.62–2.5 eV with a maximum at 2.13 eV. The intensity of the

radiation of light quanta with an energy of 1.75 eV is 15% of the maximum value (I_{max}). In this spectral region the MEG–PPV is the only luminescent component, and neither the copolymer nor the PPV emit radiation. At the same time the intensity of the emission of light quanta with an energy of 2.35 eV reaches 30% of I_{max}. This emission lies beyond the limits of the emission spectrum of MEG–PPV, and is due to the formation of excited states in the PPV or in the copolymer. The emission spectrum of the structure C is identical to that obtained for the structure B, confirming that both the intermediate MEG–PPV layer and the PPV (or the copolymer) layer are contributing to the process. The emission spectrum of the cell D also contains contributions from the radiation of the PPV and of the copolymer. Thus by allowing for the thickness of the individual layers we may conclude that the emission zone of the structures B–D extends over more than 500 Å. According to calculations the distance travelled by the charge carriers before their encounter is 2600 Å. The distance to which a neutral excitation can diffuse is $(Dt)^{1/2} \approx 50$ Å [D is the diffusion coefficient ($D \simeq 10^{-3}$ cm^2 s^{-1})], t is the lifetime of the excited state ($t \simeq 0.25$ ns)]. It can be seen that this distance is 10 times smaller than the emission zone. Thus the mobile species responsible for the fairly extensive emission zone are the charge carriers and not the excited states. The preparation of structures from layers emitting light in different spectral regions may provide a path to the development of EL sources of white light.

We may conclude from the above arguments that the best characteristics obtained from different structures are the following: quantum efficiency of the conversion, 1%;[118] brightness, $\sim 10^4$ cd m^{-2} (see Kido et al.[117]); stability of the parameters of the light-emitting polymer diode, 16 h.[118] The wide practical exploitation of EL layers now depends on the prospects of combining all these favourable characteristics into a single layer and of greatly increasing its operating and storage life.

V. Injection of charges into polymer transport layers

Our discussion has shown that in EP and EL systems the charge carriers can surmount various phase separation barriers: metal–polymer, inorganic semiconductor–polymer, and molecularly doped polymer–polymer with conjugated bonds.

In the EP layers light absorption in the generation layer produces charge carriers which are then injected into the transport layer. The properties of the contact (layer of molecules with developed regions of conjugated bonds)/(molecularly doped polymer layer), often used in EP and EL systems, have been extensively reviewed by Kanemitsu and Imamura[142] in the specific case of a polyester (PC), and of doped DEH/phthalocyanine. Like PPV, polythiophen (PT), and PAn, phthalocyanine contains a system of conjugated bonds which produces photosensitivity. This allows a given concentration of charge carriers to be generated in the material, providing quantitative data on the injection coefficient.[142] The sensitivity of the photoreceptor is defined as the ratio of the number of charges passing through the transport layer to the number of photons absorbed in the generation layer; for a given value of the electric field the injection coefficient of the carriers $\eta(F)$ is calculated as the ratio of the number of charge carriers (determined by electrophotographic or time of flight methods) passing through the molecularly doped transport layer to the number of photogenerated carriers which abandon the generation layer through its interface with the transport layer (photoacoustic method); the photoinjection coefficient η_f is the ratio of the number of carriers crossing the transport layer to the number of photogenerated free charge carriers.

Clearly, $\eta(F)$ is determined by the competition between the transport of charge carriers and their capture by deep traps at the interface, and it can be measured only by using pulse kinetic methods, whereas η_f depends on the rate of recombination of the photogenerated charges in the generation layer and on the rate of injection through the boundary. Since the ionisation potentials of DEH and phthalocyanine are almost identical (5.5 and 5.4 eV respectively) an interfacial barrier is not formed at the contact between the layers.

The parameter $\eta(F)$ increases markedly when F is increased: in a field of 10^5 V cm^{-1} $\eta(F)$ is 0.1, but it increases to 0.7 in a field of 10^6 V cm^{-1}. This effect is associated with the fact that the mobility of holes increases exponentially with F, as was shown in Section II, and their time of flight through the boundary and of capture by traps decreases correspondingly. It is interesting to note that increasing the concentration of the hydrazone DEH in the transport layer lowers $\eta(F)$ slightly. This effect is determined by the capture of holes at the interface by traps of an unspecified type, associated with the method of establishing the interface, of forming the charge transfer complexes between the hydrazone and the phthalocyanine, etc. Similar results were obtained in studies of the injection of positive charges from PPV into a transport layer consisting of polycarbonate molecularly doped with diaryldiamine (TPD).[134] In this case the injection coefficient in a field of 4×10^5 V cm^{-1} is equal to or greater than 0.25, and only a small trapping of carriers is observed at the interface of the two polymer layers at large F values.

These results suggest that in relatively high fields the interface between two polymer layers of different nature is permeable to the transfer of positive charge. However, in lower fields we must allow for the trapping of holes at the layer interface, leading to the formation of a barrier as a result of the passage of a sufficiently high electric current. Under stationary conditions $\eta(F) = 1$, and the barrier affects the value of η_f and the electric characteristics of the EP and EL devices. The interface between SeTeAs and a transport layer consisting of PVK or PC doped with pyrazoline derivatives has been examined in depth.[143–145] Under stationary conditions the following relationship is obeyed:[145]

$$\eta_f = a\left[(1 + 2\eta_c/a)^{1/2} - 1\right], \tag{33}$$

where $a = [k_i(F)]^2/2J_0k_r$ (k_i is the injection rate constant, k_r is the rate constant of the recombination in the bulk of the generation layer), η_c is the quantum yield of the photogeneration of free charge carriers. In large fields with $(2\eta_c/a) \ll 1$ it follows from Eqn (33) that $\eta_f \simeq \eta_c$, i.e. that all the generated charges are injected into the transport layer, and η_f is determined exclusively by η_c and is independent of the nature of the transport layer. In moderately large fields, when $(2\eta_c/a) \gg 1$, $\eta_f = (2a\eta_c)^{1/2}$ and η_f is determined, among other factors, by the function k_i, which depends on the height of the barrier formed at the interface as a result of the capture of holes by deep traps. It was found[145] that for a constant generation layer, and with a transport layer consisting of pyrazoline with $N(C_2H_5)$, OCH_3, and H as substituents, and also PVK, η_f decreases: for example an η_f value of 0.15 is reached in this series of compounds for $F = 1.7 \times 10^4$, 4×10^4, 1.2×10^5, and 2.5×10^5 V cm^{-1} respectively. In very strong fields ($F > 5 \times 10^5$) the differences between the field dependences for different layers disappear, and η_f becomes equal to 1. Thus in strong fields all the photogenerated charge carriers are injected into the transport layer, but in weak fields η_f depends on the nature of the transport layer, and in particular on the ionisation potential of the transport centres.

In multilayer EL systems the application of a potential difference introduces dark charge carriers into the luminescent layer, unlike the EP systems, in which photogenerated carriers are introduced into the transport layer. In EL diodes the energy efficiency of the conversion of electric current into light is strongly dependent (as it is in EP photoreceptors) on the

injection mechanism of charge carriers into the EL layer, but it should be noted that in this case dark charges are injected and the injecting layer should be transparent to the emitted light. In practice this means that ITO is used as a hole-injecting transparent and conducting layer. Let us examine in detail a typical ITO/PPV/Ca structure,[106] whose energy diagram is shown in Figs 12*a* and 12*b* . To make the discussion simpler and more meaningful we shall assume that the contacts between layers are neutral, i.e. that the PPV region, in direct contact with the interfaces, does not contain space charges.[146] In this case a potential difference $V_{1,2} = \phi_1 - \phi_2 = \varphi_1^e - \varphi_2^e$ is generated in the semiconductor: this impedes the access of electrons from the Ca and of holes from the ITO to the PPV layer, and the electric field is uniform in this layer ($F = V_{1,2}/L$). The barriers for electrons are given by the expression $\varphi_i = \phi_i - E_\pi$, and for $E_\pi = 2.5$ eV they take the values $\varphi_1^e = 1.6$ and $\varphi_2^e = 0.5$ eV (Fig. 12*a*). The application of a large external potential V (with its negative polarity on the electrode with the lower work function) produces a relative shift of the Fermi levels: ($E_{F1} - E_{F2} = eV$), and as can be seen from Fig. 12*b* the electrons and holes can easily overcome the barriers φ_2^e and φ_1^H. Since in PPV the holes are mobile but the electrons are captured by traps in the polymer near the metallic electrode, recombination takes place at the surface of the metal layer in parallel with the discharge of holes at the cathode.

The inclusion of an additional PBD electron transport layer between the Ca and the PPV (see Fig. 12*c*) creates a barrier to the motion of holes at the PPV/PBD boundary (φ_3^H), where the holes accumulate and recombine with the electrons drifting towards this barrier, with emission of luminescence. As was shown in the previous section, the PBD layer greatly improves the efficiency of the EL. Additional layers are added not only to create barriers opposing the escape of charges from the EL layer but also, conversely, to lower the barrier at the boundary of the EL layer. Thus, as was shown above, the insertion of oligothiophen[99] or PAn[97] between the EL layer and the metallic anode greatly increases the hole current because the edge of the valence band of the conjugated polymers lies only slightly above the Fermi level in the ITO. Evidently, neutral contacts are actually formed, in most cases, at the interface between polymer layers. A more complex state of affairs is found at the metal/polymer interface. The simple model of neutral contacts, though qualitatively consistent (in general) with experimental results, fails to explain many important observations. Since the work functions of Ca and Al differ by almost 1 eV we would not expect significant current flows at the PPV/Al interface because of the height of the φ_2^e barrier. Nevertheless, replacing the Ca by Al lowers the current (for the same bias) by only 1–2 orders of magnitude. Furthermore the neutral contact gives a linear current–voltage characteristic for both positive and negative bias.[145] In reality a rectification effect is observed at the metal/polymer boundary, and with forward bias the current is exponentially dependent on the potential, which is characteristic of a Schottky barrier.[147, 148] In this case a space charge is formed near the electrode in the polymer, and the applied potential is dropped mainly in the space charge region.

A Schottky barrier or an ohmic injecting contact can be formed at the contact between the metal and the polymer (doped with conjugated molecules or containing conjugated double bonds in the main chain), depending on the work function ratio of the metal and of the polymer. Metals with the lowest possible work function are chosen to inject electrons into an EL layer. A Schottky barrier is formed at the contact with In or Al, because these metals have a relatively high work function: $\phi = 4.2$ and 3.8 eV respectively. Changing to Ca ($\phi = 3$ eV) increases the EL by more than an order of magnitude. Nevertheless even in this case a barrier to electrons is formed. This is an important feature. A study of the metal/PPV interface by X-ray emission spectroscopy showed[119] that the bending of the bands in the PPV gradually increases, starting with an Al layer approximately 1 Å thick (monolayer), and reaching a constant value for an evaporated thickness of about 5 Å. No chemical interaction between the Al and the PPV is observed under these conditions. Conversely, when calcium is evaporated as an electrode the bands in the PPV begin to bend only when the thickness of the Ca layer reaches 8 Å, and at 15 Å the process goes to completion and the energy of the bond falls by 0.4 eV. As in the case of Al no interaction takes place between the Ca and the PPV. The behaviour can be explained by the presence on the surface of oxygen as hydroxyl groups and of sulfur as sulfide groups, formed during the synthesis of the polymer. These impurities protect the PPV macromolecules from attack by the calcium. Thus the real metal/polymer contact is a multilayer structure including metal oxides and other compounds.

Studies of polyacetylene, PAn, and other polymers with p-type conductivity have shown that a Schottky barrier is formed at the contact with metals having a work function $\varphi_M < 4.5$ eV. Because of the low charge mobility in polymers the electrons are transmitted through the barrier by a diffusion mechanism rather than by thermionic emission (as in extrinsic inorganic semiconductors).[147, 148]

For a sufficiently high potential difference the current is exponentially dependent on the temperature:

$$J_d = J_{0d}\left[\exp\left(\frac{eV}{nkT}\right) - 1\right], \tag{34}$$

where

$$J_{0d} = e\mu N_c F_g \exp\left(-\frac{e\varphi}{kT}\right),$$

and n is the ideality factor (in our case, close to 1), N_c is the effective density of states in the polymer, F_g is the electric field at the barrier, and φ is the height of the barrier at the metal/polymer contact, equal to the difference between the corresponding work functions.[147] The upper limit of the injection current is set by the resistance of the polymer layer, and therefore the smaller the thickness of the EL layer, the greater is the injected current, and the greater the energy efficiency of the transformation. The temperature dependence of the current through the aluminium/poly(3-octylthiophen) interface was used to establish[149] that an over-barrier transition takes place at temperatures above 340 K. At low temperatures the injected currents are greater than the values expected for a diffusion mechanism: this suggests a tunnel effect.

At the boundary between a metal with a high work function and a p-type semiconductor polymer, such as Au ($\phi = 5.2$ eV)/PPV, we find an ohmic contact[150] which efficiently injects holes into the transport layer. We should note that studies of the mechanisms of carrier injection from solid electrodes into polymer layers are much less widespread than the studies of transport and of electroluminescence: this state of affairs is inconsistent with the important role of injection in the processes which we have considered.

* * *

Our discussion has shown that the problems of electron transport in disordered dielectric layers are closely associated with a number of fundamental questions: the mechanism of electron transfer between identical centres in an organic medium, the effect of the physicochemical characteristics of the medium on the transfer, the formation of excited light-emitting recombination states, and the need to optimise the electric and the light-emission parameters of the organic layers used in newly developed and widely used optoelectronic devices. Studies in these directions should help the achievement of interesting new results and should assist the further progress of the problem as a whole.

This study was carried out with financial support from the Russian fund for fundamental research (project 93-03-5703) and from the American Physical Society (Sloan Foundation Grant).

References

1. P M Borsenberger, D S Weiss *Organic Photoreceptors for Imaging Systems* (New York: Marcel Dekker, 1993)
2. A V Vannikov, A D Grishina *Vysokomol. Soedin., Ser. A* **32** 1811 (1990)
3. A V Vannikov, A D Grishina *Usp. Khim.* **58** 2056 (1989) [*Russ. Chem. Rev.* **58** 1169 (1989)]
4. J H Burroughes, D D C Bradley, A R Brown, R N Marks, K Mackay, R H Friend, P L Burn, A B Holmes *Nature (London)* **347** 539 (1990)
5. S Ducharme, J C Scott, R J Twieg, W E Moerner *Phys. Rev. Lett.* **66** 1846 (1991)
6. J C Scott, S Ducharme, R J Twieg, W E Moerner *ACS Polym. Preprints* **32** 107 (1991)
7. J C Scott, L T Pautmeier, W E Moerner *J. Opt. Soc. Am. B* **9** 2059 (1992)
8. M Stolka, M A Abkowitz *Synth. Metals* **41-43** 3385 (1991)
9. G Pfister, H Scher *Adv. Phys.* **27** 747 (1978)
10. J M Marshall *Rep. Prog. Phys.* **46** 1235 (1983)
11. V I Gol'danskii, L I Trakhtenberg, V N Flerov *Tunnel'nye Yavleniya v Khimicheskoi Fizike* (Tunnel Effects in Chemical Physics) (Moscow: Nauka, 1986)
12. L B Schein *Philos. Mag. B* **65** 795 (1992)
13. M A Abkowitz *Philos. Mag. B* **65** 817 (1992)
14. H Bässler *Phys. Status Solidi (B)* **175** 15 (1993)
15. P M Borsenberger *J. Appl. Phys.* **68** 5682 (1990)
16. P M Borsenberger, H Bässler *J. Imag. Sci.* **35** 79 (1991)
17. P M Borsenberger, L Pautmeier, H Bässler *J. Chem. Phys.* **95** 1258 (1991)
18. P M Borsenberger *ACS Polym. Preprints* **33** 806 (1992)
19. P M Borsenberger, L J Rossi *J. Chem. Phys.* **96** 2390 (1992)
20. L B Schein, A Rosenberg, S L Rice *J. Appl. Phys.* **60** 4287 (1986)
21. H H Poole *Philos. Mag.* **32** 112 (1916)
22. J Frenkel *Phys. Rev.* **54** 647 (1938)
23. L B Schein, A Peled, D Glatz *J. Appl. Phys.* **66** 686 (1989)
24. M Stolka, M A Abkowitz, F E Knier, R J Weagley, K M McGrane *Synth. Metals* **37** 295 (1990)
25. M A Abkowitz, M J Rice, M Stolka *Philos. Mag. B* **61** 25 (1990)
26. W G Gill *J. Appl. Phys.* **43** 5033 (1972)
27. G Pfister *Phys. Rev. B* **16** 3676 (1977)
28. A A Pakhratdinov, Candidate's Thesis in Chemical Sciences, Institute of Electrochemistry of RAS, Moscow, 1993
29. A V Vannikov, A Yu Kryukov, H H Horhold *Synth. Metals* **41-43** 331 (1991)
30. A V Vannikov, A C Saidov *Mol. Cryst. Liq. Cryst.* **228** 87 (1993)
31. A Peled, L B Schein *Chem. Phys. Lett.* **153** 422 (1988)
32. M A Abkowitz, K M McGrane, F E Knier, M Stolka *Mol. Cryst. Liq. Cryst.* **183** 2157 (1990)
33. M A Abkowitz, M Stolka *Solid State Commun.* **78** 269 (1991)
34. P M Borsenberger, L Pautmeier, H Bässler *J. Chem. Phys.* **94** 5447 (1991)
35. G Verbeek, M Van der Auweraer, F C DeSchryver, C Geelen, D Terrell, S DeMeuter *Chem. Phys. Lett.* **188** 85 (1992)
36. M A Abkowitz, M Stolka, M Morgan *J. Appl. Phys.* **52** 3453 (1981)
37. S J Santos Lemus, J Hirsch *Philos. Mag. B* **53** 25 (1986)
38. M Stolka, J F Yanus, D M Pai *J. Phys. Chem.* **88** 4707 (1984)
39. Y Yamaguchi, M Yokoyama *J. Appl. Phys.* **70** 3726 (1991)
40. T Kitamura, M Yokoyama *J. Appl. Phys.* **69** 821 (1991)
41. Y Yamaguchi, T Fujiama, M Yokoyama *J. Appl. Phys.* **70** 855 (1991)
42. A Yu Kryukov, A Saidov, A V Vannikov *Mendeleev Commun.* 15 (1991)
43. A Yu Kryukov, A Saidov, A V Vannikov *Thin Solid Films* **209** 84 (1992)
44. A G Tyurin, A Yu Kryukov, T S Zhuravleva, A V Vannikov *Vysokomol. Soedin., Ser. B* **30** 793 (1988)
45. A V Vannikov, A Yu Kryukov, A G Tyurin, T S Zhuravleva *Phys. Status Solidi (A)* **115** K47 (1989)
46. A V Vannikov, A Yu Kryukov *J. Inf. Rec. Mat.* **18** 341 (1990)
47. A Yu Kryukov, A Ch Saidov, A V Vannikov *Khim. Fiz.* **10** 567 (1991)
48. P M Borsenberger, H Bässler *Phys. Status Solidi (B)* **170** 291 (1992)
49. H-Y Yuh, D M Pai *J. Imag. Sci. Tech.* **36** 477 (1992)
50. P M Borsenberger, J J Fitzgerald *J. Phys. Chem.* **97** 4815 (1993)
51. M Sugiuchi, H Nishizawa *J. Imag. Sci. Tech.* **37** 245 (1993)
52. H Bässler *Phys. Status Solidi (B)* **107** 9 (1981)
53. H Bässler *Philos. Mag. B* **50** 347 (1984)
54. R Richert, L Pautmeier, H Bässler *Phys. Rev. Lett.* **63** 547 (1989)
55. L Pautmeier, R Richert, H Bässler *Philos. Mag. Lett.* **59** 325 (1989)
56. L Pautmeier, R Richert, H Bässler *Synth. Metals* **37** 271 (1990)
57. L Pautmeier, R Richert, H Bässler *Philos. Mag. B* **63** 587 (1991)
58. R Jankowiak, K D Rockwitz, H Bässler *J. Phys. Chem.* **87** 552 (1983)
59. U Rauscher, H Bässler *Macromolecules* **23** 398 (1990)
60. A Miller, E Abrahams *Phys. Rev.* **120** 745 (1960)
61. L Pautmeier, PhD thesis Philipps-Universität, Marburg, 1991
62. M A Abkowitz, H Bässler, M Stolka *Philos. Mag. B* **63** 201 (1991)
63. B I Shklovskii, A L Efros, in *Elektronnye Svoistva Legirovannykh Poluprovodnikov* (Electronic Properties of Doped Semiconductors) (Moscow: Nauka, 1979) Ch. 12
64. I M Lifshits, S A Gredeskul, L A Pastur, in *Vvedenie v Teoriyu Neuporyadochennykh Sistem* (Introduction to the Theory of Disordered Systems) (Moscow: Nauka, 1982) Ch. 4
65. J M Ziman, in *Models of Disorder* (Translated into Russian; Moscow: Mir, 1982) Ch. 9
66. V L Bonch-Bruevich, I P Zvyagin, R Kaiper, A G Mironov, R Enderlain, B Esser, in *Elektronnaya Teoriya Neuporyadochennykh Poluprovodnikov* (Electronic Theory of Disordered Semiconductors) (Moscow: Nauka, 1981) Ch. 3
67. P M Borsenberger, L Pautmeier, H Bässler *Phys. Rev. B* **46** 12145 (1992)
68. H Scher, M Lax *Phys. Rev. B, Solid State, Ser. 3* **7** 4491 (1973)
69. H Scher, M Lax *Phys. Rev. B, Solid State, Ser. 3* **7** 4502 (1973)
70. H Scher, E W Montroll *Phys. Rev. B, Solid State, Ser. 3* **12** 2455 (1975)
71. M F Shlesinger *J. Stat. Phys.* **10** 421 (1974)
72. L B Schein, J X Mack *Chem. Phys. Lett.* **149** 109 (1988)
73. J X Mack, L B Schein, A Peled *Phys. Rev B, Solid State, Ser. 3* **39** 7500 (1989)
74. L B Schein, D Glatz, J C Scott *Phys. Rev. Lett.* **65** 472 (1990)
75. S I Pekar *Issledovaniya po Elektronnoi Teorii Kristallov* (Investigations on the Electronic Theory of Crystals) (Moscow: Gostekhizdat, 1951)
76. Yu A Firsov (Ed.) *Polyarony* (Polarons) (Moscow: Nauka, 1975)
77. P S Zyryanov, M I Klinger *Kvantovaya Teoriya Yavlenii Elektronnogo Perenosa v Kristallicheskikh Poluprovodnikakh* (Quantum Theory of Electron Transfer Phenomena in Crystalline Semiconductors) (Moskow: Nauka, 1976)
78. M I Klinger *Usp. Fiz. Nauk* **146** 105 (1985)
79. D Emin, in *Electronic and Structural Properties of Amorphous Semiconductors.* (Eds P G LeComber, J Mort) (New York: Academic Press, 1973) Ch. 7
80. D H Dunlap, V M Kenkre *University of New Mexico Preprint* 1991
81. V M Kenkre, D H Dunlap *Philos. Mag. B* **65** 831 (1992)
82. L T Pautmeier, J C Scott, L B Schein *Chem. Phys. Lett.* **197** 568 (1992)
83. R A Marcus *Ann. Rev. Phys. Chem.* **15** 155 (1964)
84. S V Novikov, A V Vannikov *Khim. Fiz.* **10** 1692 (1991)
85. S V Novikov, A V Vannikov *Chem. Phys. Lett.* **182** 598 (1991)
86. S V Novikov, A V Vannikov *Khim. Fiz.* **12** 90 (1993)
87. S V Novikov, A V Vannikov *Chem. Phys.* **169** 21 (1993)
88. S V Novikov, A V Vannikov *Philos. Mag. B* (1994) (in the press)
89. P L Bhatnagar, E P Gross, M Krook *Phys. Rev.* **94** 511 (1954)
90. T Sasakawa, T Ikeda, S Tazuke *Macromolecules* **22** 4253 (1989)
91. J Ulanski, J Sielski, D T Glatzhofer, M Kryszewski *J. Phys. D* **23** 75 (1990)

92. P M Borsenberger, L Pautmeier, R Richert, H Bässler *J. Chem. Phys.* **94** 8276 (1991)
93. A V Vannikov, V K Matveev, V P Sichkar', A P Tyutnev *Radiatsionnye Effekty v Polimerakh. Elektricheskie Svoistva* (Radiation Effects in Polymers. Electrical Properties) (Moscow: Nauka, 1982)
94. A P Tyutnev, A V Vannikov, G S Mingaleev *Radiatsionnaya Elektrofizika Organicheskikh Dielektrikov* (Radiation Electrophysics of Organic Dielectrics) (Moscow: Energoatomizdat, 1989)
95. D D C Bradley *Chem. Brit.* **27** 719 (1991)
96. M Hiramoto, J Tani, M Yokoyama *Appl. Phys. Lett.* **62** 666 (1993)
97. G Gustafsson, Y Cao, G M Treacy, F Klaveretter, N Colaneri, A J Heeger *Nature (London)* **357** 477 (1992)
98. A V Vannikov, A Ch Saidov *Mendeleev Commun.* 54 (1993)
99. C Hosokawa, H Higashi, T Kusumoto *Appl. Phys. Lett.* **62** 3238 (1993)
100. D Braun, G Gustafsson, D McBranch, A J Heeger *J. Appl. Phys.* **72** 564 (1992)
101. D Braun, A J Heeger *Appl. Phys. Lett.* **58** 1982 (1991)
102. P L Burn, A B Holmes, A Kraft, D D C Bradley, A R Brown, R H Friend, R W Gymes *Nature (London)* **356** 47 (1992)
103. P L Burn, A B Holmes, A Kraft, D D C Bradley, A R Brown, R H Friend *J. Chem. Soc., Chem. Commun.* 32 (1992)
104. A R Brown, D D C Bradley, J H Burroughes, R H Friend, N C Greenham, P L Burn, A B Holmes, A Kraft *Appl. Phys. Lett.* **61** 2793 (1992)
105. D Braun, D Moses, C Zhang, A J Heeger *Appl. Phys. Lett.* **61** 3092 (1992)
106. A R Brown, N C Greenham, J H Burroughes, D D C Bradley, R H Friend, P L Burn, A Kraft, A B Holmes *Chem. Phys. Lett.* **200** 46 (1992)
107. Z Yang, I Sokolik, F E Karasz *Macromolecules* **26** 1188 (1993)
108. Y Ohmori, M Uchida, K Muro, K Yoshino *Solid State Commun.* **80** 605 (1991)
109. Y Ohmori, M Uchida, K Muro, K Yoshino *Jpn. J. Appl. Phys.* **30** L1938 (1991)
110. G Grem, G Leditzky, B Ulrich, G Leising *Adv. Mater.* **4** 36 (1992)
111. Y Ohmori, M Uchida, K Muro, K Yoshino *Jpn. J. Appl. Phys.* **30** L1941 (1991)
112. J Kido, M Kohda, K Okuyama, K Nagai *Appl. Phys. Lett.* **61** 761 (1992)
113. N Sato, M Lodlund, R Lazzaroni, W R Salaneck, J-L Bredas, D D C Bradley, R H Friend, K E Ziemelis *Chem. Phys.* **160** 299 (1992)
114. J Kido, K Nagai, Y Okamoto, T Skotheim *Appl. Phys. Lett.* **59** 2760 (1991)
115. J Kido, K Nagai, Y Okamoto, T Skotheim *Chem. Lett.* 1267 (1991)
116. C Hosokawa, N Kawasaki, S Sakamoto, T Kusumoto *Appl. Phys. Lett.* **61** 2503 (1992)
117. J Kido, K Hongawa, M Kohda, K Nagai, K Okuyama *Jpn. J. Appl. Phys.* **31** L960 (1992)
118. C Zhang, D Braun, A J Heeger *Appl. Phys. Lett.* **62** 5177 (1993)
119. Y Gao, K T Park *J. Appl. Phys.* **73** 7894 (1993)
120. D D C Bradley, R H Friend, K S Wong, W Hayer, M Linderberger, S Roth, in *Electronic Properties of Conjugated Polymers* (Eds H Kuzmany, M Mehring, S Roth) (Berlin: Springer, 1987) p. 107
121. K F Voss, C M Foster, L Smilowitz, D Mihailovic, S Askari, G Srdanov, Z Ni, S Shi, A J Heeger, F Wudl *Phys. Rev. B* **43** 5109 (1991)
122. J M Oberski, A Greiner, H Bässler *Chem. Phys. Lett.* **184** 391 (1991)
123. N F Colaneri, D D C Bradley, R H Friend, P L Burn, A B Holmes, C W Spangler *Phys. Rev. B* **42** 11670 (1990)
124. U Lemmer, R F Mahrt, Y Wada, A Greiner, H Bässler, E O Gobel *Appl. Phys. Lett.* **62** 2827 (1993)
125. R Mahrt, J Yang, A Greiner, H Bässler, D D C Bradley *Makromol. Chem., Rapid Commun.* **11** 415 (1990)
126. U Rausher, H Bässler, D D C Bradley, M Hennecke *Phys. Rev. B* **42** 9830 (1990)
127. M Deussen, H Bässler *Chem. Phys.* **164** 247 (1992)
128. A Yu Kryukov, A V Vannikov, A A Pakhratdinov, H-H Horhold, I Opfermann *Vysokomol. Soedin., Ser. A* **32** 348 (1990)
129. S Heun, R F Mahrt, A Greiner, U Lemmer, Y Wada, H Bässler, D A Holliday, D D C Bradley, P L Burn, A B Holmes *J. Phys.: Condens. Matter* **5** 247 (1993)
130. P Gomes de Costa, E M Conwell *Phys. Rev. B* **48** 1993 (1993)
131. L S Swanson, J Shinar, A R Brown, D D C Bradley, R H Friend, P L Burn, A Kraft, A B Holms *Phys. Rev. B* **46** 15072 (1992)
132. L S Swanson, P A Lane, J Shinar, F Wudl *Phys. Rev. B* **44** 10617 (1991)
133. E L Frankevich, A A Lymarev, I Sokolik, F E Karasz, S Blumstengel, R H Baughman, H-H Horhold *Phys. Rev. B* **46** 9320 (1992)
134. H Antoniadis, B R Hsieh, M A Abkowitz, M Stolka *Appl. Phys. Lett.* **62** 3167 (1993)
135. M Onoda, S Morita, H Nakayama, K Yoshino *Jpn. J. Appl. Phys.* **32** L82 (1993)
136. V S Fomenko *Emissionnye Svoistva Materialov (Spravochnik)* [Emission Properties of Materials (Handbook)] (Kiev: Naukova Dumka, 1981)
137. H-H Horhold, M Helbig *Makromol. Chem., Makromol. Symp.* **12** 229 (1987)
138. H-H Horhold, M Helbig, D Weiss, D Raabe *Mater. Sci. Forum* **62–64** 411 (1990)
139. A V Vannikov, A D Grishina, E I Merkulov *Vysokomol. Soedin., Ser. A* **18** 183 (1976)
140. C Adachi, T Tsutsui, S Saito *Appl. Phys. Lett.* **56** 799 (1990)
141. Y Hamada, T Sano, M Fujita, T Fuji, Y Nishio, K Shibata *Chem. Lett.* 905 (1993)
142. Y Kanemitsu, S Imamura *J. Appl. Phys.* **67** 3728 (1990)
143. D M Pai, in *Progress in Basic Principles of Imaging Systems* (Eds T Grancer, E Moizar) (Braunschweig, 1987) p. 585
144. D M Pai, B E Springlett *Rev. Mod. Phys.* **65** 163 (1993)
145. P J Melz, R B Champ, C Chiou, C S Keller, L C Liclican, P R Nieman, M D Shattuck, W J Weiche *Photogr. Sci. Eng.* **21** 73 (1975)
146. K Kao, W Huang *Electron Transport in Solids with Reference to Organic Semiconductors* (Translated into Russian; Moscow: Mir, 1984)
147. A V Vannikov, T S Zhuravleva *Mol. Electron.* **5** 63 (1989)
148. T S Zhuravleva, A V Vannikov, in *Khimiya i Tekhnologiya Vysokomolekulyarnykh Soedinenii, Vyp. 28 (Itogi Nauki i Tekhniki)* [Chemistry and Technology of High-Molecular-Mass Compounds, Vol. 28 (Advances in Science and Engineering)] (Moscow: VINITI, 1991) p. 99
149. A Assadi, Y Fu, M Willander, C Swensson *Jpn. J. Appl. Phys.* **32** 1696 (1993)
150. I D Parker, R W Gymer, M G Harrison, R H Friend, H Ahmed *Appl. Phys. Lett.* **62** 1519 (1993)

Russian Chemical Reviews **63** (2) 125 – 138 (1994)
©1994 Russian Academy of Sciences and Turpion Ltd

UDC 541.127

Reactions of hydrocarbons with electrophilic transition metal complexes in trifluoroacetic acid

N F Gol'dshleger, A P Moravskii

Contents

I. Introduction 125
II. Trifluoroacetic acid and transition metal carboxylates as components of catalytic systems 125
III. Reactions of hydrocarbons with participation of electrophilic metal complexes in trifluoroacetic acid 126

Abstract. The results of studies on the catalytic and stoichiometric activation of C–H and C=C bonds in hydrocarbons by electrophilic metal complexes in trifluoroacetic acid are surveyed. Reactions involving the dehydrogenation of cycloalkanes, carboxylation and oxidative carbonylation of alkanes and aromatic compounds, oxidative coupling of aromatic hydrocarbons, oligomerisation of norbornadiene with participation of transition metal trifluoroacetates, and certain others are examined. Much attention is devoted to the conditions for the generation of active species and their nature. The bibliography includes 185 references.

I. Introduction

The reactions of alkanes with participation of transition metal complexes have aroused much interest in connection with the possibility of devising new selective catalytic procedures for the processing of hydrocarbons. Metal complex activation of alkanes was discovered in relation to platinum(II) complexes in 1969.[1] The wide scale study of this process made it possible to elucidate the factors affecting the reactivity of C–H bonds in alkanes and the mechanism of the activation of saturated hydrocarbons by transition metal complexes,[2–5] to extend the range of metal complexes capable of activating alkanes,[6–11] and to discover new reactions of alkanes, including methane.[12–16]

The role of electrophilic metal-containing centres in the catalytic and stoichiometric activation of C=C and C–H bonds in hydrocarbons is discussed in the present review and other reactions, the occurrence of which is favoured by an increase in the electron-accepting capacity of the metal centre, are considered. Data on the functionalisation of alkanes, alkenes, and aromatic compounds in the presence of transition metal complexes in trifluoroacetic acid are summarised. Questions concerning the oxidation of alkyl-substituted aromatic compounds by variable valence metal ions and thallium(III) trifluoroacetate have been dealt with in other reviews,[17,18] the oxidation of other substrates has been examined in a book,[19] and studies on the selective substitution of hydrogen attached to a saturated carbon atom, mainly a tertiary carbon atom, have been surveyed by Boguslavskaya et al.[20]

N F Gol'dshleger, A P Moravskii ¶ Laboratory for the Synthesis of Electrically Conducting and Catalytically Active Compounds (¶ Laboratory for Metal Complex Catalysts), Institute of Chemical Physics in Chernogolovka, Russian Academy of Sciences, 142432 Chernogolovka, Moscow Region, Russian Federation, Fax (7-096) 515 35 88

Received 9 December 1993
Uspekhi Khimii **63** (2) 130 – 143 (1994); translated by A K Grzybowski

II. Trifluoroacetic acid and transition metal carboxylates as components of catalytic systems

Trifluoroacetic acid (TFA) is usually obtained by the electrolytic fluorination of acetyl chloride or fluoride; the acidity of its aqueous solutions is comparable to that of aqueous solutions of inorganic acids. It is a mild dehydrating but not oxidising agent.

Acid	pK_a	ε
CF_3COOH	0.2	8.4
CH_3COOH	4.76	9.55
HCOOH	3.7	62.0

The low dielectric constant shows that TFA is a poor ionising solvent—ions are solvated in CF_3COOH much less effectively than in water. However, TFA is a convenient solvent for the nitration of aromatic compounds with nitric acid,[21] the bromination of toluene,[22] the synthesis of adamantanol,[23] the hydroxylation of alkanes,[24] and a number of other reactions, and also for the investigation of the kinetics of electrophilic substitution processes. Solutions of mixtures of alkali metal nitrates and chlorides in aqueous TFA can be used for the selective halogenation of aromatic compounds.[25] A series of new oxidation reactions involving H_2O_2 in trifluoroacetic acid,[26,27] including perfluorinated aromatic and olefin compounds, have been discovered.

Metal trifluoroacetates are obtained by the reactions of the corresponding oxides, hydroxides, carbonates, sulfates, and amalgamated metals (in the case of aluminium and magnesium) with TFA,[28] via the oxidative addition of TFA to low-valence complexes,[29] and also by the reactions of metal chlorides (or organometallic compounds) with a solution of CF_3COOAg in organic solvents (nitromethane, acetone).[28,30] A widely used method of synthesis of metal trifluoroacetate complexes involves carboxylate exchange.[28,31,32]

$$Rh_2(O_2CCH_3)_4 + 4\,CF_3COOH \xrightarrow{k_i} \longrightarrow Rh_2(O_2CCF_3)_i(O_2CCH_3)_{4-i} + i\,CH_3COOH\ .$$

It has been shown for this reaction that the substitution of the acetate anion by the trifluoroacetate anion is a stepwise process, the ratios of the rate constants for the successive reactions being $k_1 : k_2 : k_3 : k_4 = 1 : 2.0 : 0.1 : 0.025$.

It is known from the totality of the physicochemical properties of carboxylates that the stability of the RCOO–M bond as a rule decreases as the electron-accepting properties of the group R become more marked.[33]

$CH_3 > CH_2Cl > CH_2F$,

$CH_3 > CH_2F > CHF_2 > CF_3$,

$CH_3 >$ Nic > *iso*-Nic,

where Nic = nicotine.

The principal feature of the carboxy-group is the multiplicity of its structural functions; it can play the role of a monodentate, cyclic bidentate, bridging bidentate, tridentate, and even tetradentate ligand with different (*syn* or *anti*) orientations of the bonds with the metal.[33] Monodentate and bridged coordinations are most characteristic of the trifluoroacetate group.[28] Comparatively numerous structural investigations of the carboxylates of 3*d* elements have been carried out hitherto and have made it possible to discover an extremely wide and varied spectrum of structures of these substances and the functional possibilities of the carboxylate ligands.[33,34]

The crystal and molecular structures of palladium acetate, the interest in which is due to its catalytic properties, have been investigated.[35] This substance is a symmetrical trimer $Pd_3(O_2CCH_3)_6$ with double *syn, syn*-bridges between each pair of palladium atoms, which was demonstrated by X-ray diffraction study of its solvates.[35–37] The oxygen atoms surrounding each palladium atom in this compound are arranged approximately in the same plane and give rise to the square configurations usual for d^8 metals. The compound differs sharply from the trimeric carboxylates of d^3-d^6 elements,[33] which must be stabilised by a μ_3-ligand (usually a μ_3-O atom located at the centre of an isosceles triangle comprising three M atoms), and also from platinum acetate, which is a tetramer[38] with strong covalent metal–metal bonds. X-Ray diffraction study of volatile trinuclear palladium(II) carboxylates—$Pd_3(O_2CBu^t)_6$ and $Pd_3(O_2CCF_3)_6$—showed[39] that both complexes are trimers like palladium acetate, but palladium trifluoroacetate has this structure in solution in benzene only at temperatures below 37 °C. The molecular geometries of the complexes are also extremely similar. The observed Pd...Pd distances (3.1–3.2 Å) exceed greatly the usual lengths of palladium–palladium bonds and indicate the absence of valence interactions. The replacement of an electron-donating substituent (CH_3) in the carboxylate ligand by an electron-accepting substituent (CF_3) leads to an increase in the Pd...Pd distance.

Monodentate coordination of the CF_3COO^- anion has been demonstrated by X-ray diffraction for different complexes, including $Pd_2(dppm)_2(O_2CCF_3)_2$[40] and $Pd(dppm)(O_2CCF_3)_2$,[41] where dppm = bis(diphenylphosphinomethane), $M(O_2CCF_3)_2 \cdot (NO)(PPh_3)_2$, where M = Rh or Ir,[42] and $Rh(CO)(O_2CCF_3) \cdot (PPh_3)_2$.[43] Both the monodentate and bridged coordinations of the trifluoroacetate groups have been found in the complex $Pr(O_2CCF_3)_3(H_2O)_3$,[44] which is a centrosymmetrical dimer in the solid state, and in the dimer $[Ru(C_6H_9)P(C_6H_{11})_2]_2 \cdot (\mu\text{-}CF_3CO_2)_2(CF_3CO_2)_2(\mu\text{-}OH_2)_2$.[45]

Vibrational spectroscopic data, determinations of the molecular mass, and the ready oxidisability of the complexes led to the hypothesis of the η^2-coordination of the trifluoroacetate group in complexes of the type $H_2IrL_2(O_2CCF_3)$ (L = PAr_3)[46] and $[Rh(PPh_3)_2(O_2CCF_3)]_2$.[47] The electrical conductivity found for the complex $Ir(NO)(O_2CCF_3)_2(PPh_3)_2$ permitted the conclusion that it is partly ionised in polar solvents, which confirmed the lability of the M–$OCOCF_3$ bond. Its treatment with sodium tetraphenylborate leads to the complex $[Ir(O_2CCF_3)(NO) \cdot (PPh_3)_2]^+BPh_4^-$ with an anomalously low ν_{OCO}^{as} frequency at 1572 cm^{-1}, which may indicate a bidentate cyclic coordination of the CF_3COO group in this compound.[34,42]

Since TFA is a strong acid, its conjugate base CF_3COO^- is relatively weak and the M–$OCOCF_3$ bond is labile, which, together with the thermal stability of the complexes and the ability of the trifluoroacetate anion to behave as a η^1- and η^2-ligand as well as the chemical resistance of the trifluoroacetate anion to oxidation, makes it attractive to employ TFA in catalytic metal complex systems. The introduction of CF_3COO^- groups into the coordination environment of the central metal atom enhances the electrophilic properties of the complexes, which as a rule ensures the possibility of the occurrence of the reaction at a lower temperature.

III. Reactions of hydrocarbons with participation of electrophilic metal complexes in trifluoroacetic acid

1. Activation of the C–H bond by metal complexes

Analysis of the literature data on the reactions of alkanes in solutions of metal complexes shows that a whole series of possible mechanisms of the primary interaction between the components exist.[2,3] The complexity of the problem of the activation of alkanes arises from their chemical inertness. In most of the known reactions leading to the formation of stable molecular products, one of the strong covalent C–H or C–C bonds in alkanes must be ultimately broken. In this respect, the problem of the activation of a C–H σ-bond of a paraffin is similar to that of the activation of the hydrogen molecule.[2,48]

Alkanes are very weak electron donors and poor electron acceptors.[2] However, the occurrence of intramolecular interactions between a nonactivated C–H sp^3-bond of the ligand and the transition metal atom surrounded by ligands has been noted in a series of structural studies.[49,50] The term 'agostic' bond has been proposed for this interaction;[51] data on complexes with such bonds have been summarised in two communications.[52,53] It has been shown that the electron deficiency of the metal is a necessary but not sufficient condition for the formation of the agostic bond. The metal must also possess fairly strong acid properties. Thus the replacement of π-acceptor ligands in the complex by π-donor ligands weakens the agostic bond.[54]

The low reactivity of saturated hydrocarbons is associated with the absence of low-lying unoccupied orbitals in the latter (the first band in the electronic absorption spectra of alkanes is located in the region above 10 eV). The transition state in reactions of such compounds frequently involves the excitation of electrons to antibonding orbitals. The reactivity of alkanes should accordingly be highest relative to species having low-lying unoccupied orbitals, i.e. electrophiles. The reactions of methane in superacids[55] and of its homologues in organic superacids[15] are well known. A high oxidation state of the central transition metal ion also favours the formation of its complexes with alkanes, which follows, in particular, from the similarity between these reactions and those of alkanes in superacids, which proceed with formation of carbenium ions.[55]

$$RH + H^+ \rightleftharpoons RH_2^+$$

Analysis[56] carried out for different types of interaction of C–H bonds with transition metals permits the following conclusions:

1. One-electron transfer reactions on treatment with oxidants which are stable in aqueous solutions are thermodynamically impossible for alkanes (the equilibrium oxidation–reduction potentials of the RH^+/RH pairs are 3.4–4.1 V).

$$L_nM + RH \longrightarrow L_n\bar{M} + RH^+$$

On the other hand, strong oxidants can abstract an electron from aromatic compounds (the corresponding oxidation–reduction potentials are in the range 1.6–2.0 V).

2. The mechanism of the reactions of alkanes with metal complexes involving the formation of free radicals with the simultaneous abstraction and solvation of a proton can be regarded as probable in the case of strong oxidants such as Co(III), Cr(VI), and Mn(VII), particularly in solutions of strong acids in which the oxidation-reduction potential of the $M^{(n+1)+}/M^{n+}$ pairs is a maximum.

$$L_nM + RH \longrightarrow L_n\bar{M} + \dot{R} + H^+$$

3. The formation of a M–R bond, coupled with the liberation and formation of H^+, diminishes the requirements as regards the strength of the oxidant. For the electrophilic substitution reaction

$$L_nM + RH \longrightarrow L + L_{n-1}\bar{M}R + H^+,$$

the energy expenditure on the creation of a coordination vacancy (E) is given by [56]

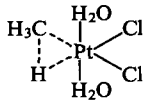
$$E = E(M-L) - Q_s(L) - Q_s(ML_{n-1}) + Q_s(ML_n),$$

where Q_s are the heats of formation of the system components.

Thus substitution is promoted by a low bond energy E(M–L) and high enthalpy of solvation of the ligand Q_s(L).

The substitution of H^+ by a metal ion M^+ as a result of the interaction of hydrocarbons with metal complexes is characteristic of aromatic compounds (mercuration and thallation reactions). For a high strength of the M–C bond, such a step becomes possible also for alkanes, but it differs from classical electrophilic substitution. For example, the interaction of platinum(II) complexes with alkanes [1] apparently begins with the oxidative addition of a C–H bond, which leads to the formation of an alkylplatinum(IV) hydride complex and terminates with the synchronous formation of a Pt(II)–C bond and the elimination of a proton. The proton may be bound by a water molecule, which is a stronger base than the Pt centre. [2, 56]

The results of a quantum-chemical study [57] of the model reaction of methane with the complex *trans*-$PtCl_2(H_2O)_2$ have shown that, in the initial stage of the interaction before the attainment of the transition state, the C–H bond is polarised with a significant intensification of the acidity of the hydrogen atom without change of the charge on the platinum.



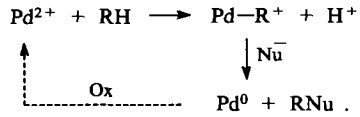
In the presence of a base stronger than the platinum(II) complex, the transfer of H^+ to a molecule of the base is easier than the continuation of the oxidative addition process after the loosening and polarisation of the C–H bond [as a result of the initial stage of the interaction of CH_4 with Pt(II)]. The binding of the leaving group to the base is the driving force of the electrophilic substitution reaction. [48] The addition of methane with participation of zirconium complexes, [58] for example $(RNH)_2Zr$ = NR, where R = $SiBu^t_3$, may serve as an example of such interaction.

The study of the cyclometallation reactions has shown that cyclopalladation is predominantly electrophilic in character, whilst the interaction of a C–H bond of a coordinated ligand with platinum(II) is more likely to proceed via an oxidative addition mechanism. [59] The type of mechanism depends on the nature of the metal and the substrate or, which appears more likely, the balance between the steric and electronic factors determines the final product in each case. For example, the rate of the cyclometallation reaction increases in the sequence Cl < Br < I for PdX_2L_2 (L = hindered phosphine; X = Cl, Br, I), whilst the reverse sequence obtains for phosphite complexes. [59]

2. Reactions of hydrocarbons with participation of palladium complexes

Palladium occupies a special place in the series of oxidants. It is a good electrophile, [60] a typical two-electron oxidant, and can be reoxidised by fairly mild oxidants, which permits its use in catalysis. [61–63]

Scheme 1



a. Palladium(II) trifluoroacetate

Palladium(II) trifluoroacetate and acetate are trimeric in the crystalline state, but in benzene at 37 °C the trifluoroacetate is monomeric, in contrast to the acetate. [32, 35, 39] According to X-ray photoelectron studies, the influence of the ligands in palladium(II) compounds affects strongly the position of the Pd($3d_{5/2}$) level, the range of variation of the binding energy E_b amounting to 2 eV depending on the ligands. The binding energies of the internal electrons of the palladium atoms in complexes with ligands having pronounced π-acceptor properties are especially high (Table 1); the closest approximation to E_b [Pd($3d_{5/2}$)] for palladium(IV) is observed in the case of $Pd(O_2CCF_3)_2$, which agrees with the pronounced electron-accepting properties of palladium in this compound.

Table 1. The Pd($3d_{5/2}$) binding energies in palladium complexes.

Complex	E/eV	Ref.
Pd (metal)	335.8	64
$PdCl_2$	338.0	65
K_2PdCl_4	338.4	65
$Pd(O_2CCH_3)_2$	338.8	64
$Pd(CH_3CN)_4(PF_6)_2$	339.5	66
$Pd(CN)_2$	339.6	65
$Pd(O_2CCF_3)_2$	339.7	67
K_2PdCl_6	340.3	65

b. Alkanes and cycloalkanes

Palladium differs from platinum by the lower stability of the d^6 state of palladium(IV) and the smaller strength of the Pd–C bond. Oxidative addition via the C–H bonds of alkanes is therefore less probable for palladium(II) complexes than for platinum(II) complexes. On the other hand, it has been found that electrophilic substitution reactions at a carbon atom with participation of the palladium(II) centre proceed extremely effectively. The absorption of alkanes and benzenes, accompanied by the formation of metallic palladium, was observed in 1973–1974 in the $PdSO_4$–H_2SO_4 and $Pd(O_2CCF_3)_2$–anhydrous CF_3COOH systems. [68, 69]

Hydrocarbons (hexane, cyclohexane, benzene) reduced $Pd(O_2CCH_3)_2$ or $Pd(O_2CCF_3)_2$ in CF_3COOH at 92 °C. [69] For the ratio $Pd(O_2CCF_3)_2 : CF_3COOH$ = 1 : 10, palladium trifluoroacetate forms a stable homogeneous solution and dehydrogenates cyclohexane in accordance with the stoichiometric equation

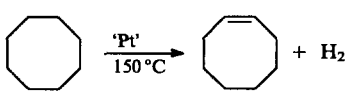
$$3\,Pd(O_2CCF_3)_2 + C_6H_{12} \longrightarrow 3\,Pd^0 + C_6H_6 + 6\,CF_3COOH.$$

Together with benzene, the products of its further reaction—biphenyl and phenyl trifluoroacetate—were detected. The absence of an induction period and autoacceleration as well as direct control experiments ruled out the possibility that the reaction takes place on the surface of precipitated metallic palladium. The reactivity of the hydrocarbons in the reaction with palladium trifluoroacetate decreases in the sequence benzene > cyclohexane > hexane.

Cyclohexane and methylcyclohexane are also dehydrogenated in the presence of the so called platinum(III) complexes [mixed-valence platinum(II) and platinum(IV) dimers] to benzene and toluene respectively.[70] It is noteworthy that palladium and platinum acetates are inert in CH_3COOH to hydrocarbons. The dehydrogenation of cycloalkanes apparently proceeds stepwise like the dehydrogenation of hydrocarbons in the presence of palladium(II) in solution in H_2SO_4.[71] This is confirmed by the detection of small amounts of cyclohexene in the dehydrogenation of cyclohexene with participation of platinum(III) complexes and by the rapid disproportionation of cyclohexene[72] to cyclohexane and benzene in the presence of palladium trifluoroacetate.

In contrast to platinum complexes, deuterium exchange is not observed in saturated hydrocarbons in solution in CF_3COOD following the addition of $Pd(O_2CCF_3)_2$, which is caused by the lower stability of palladium alkyls (see Scheme 1) compared with platinum alkyls. Indeed the reactions of the organomercury compounds RHgBr (R = CH_3, C_2H_5) with $Pd(O_2CCF_3)_2$ in CF_3COOD lead to ethane in the first case and to ethylene in the second, neither compound containing deuterium.[68] The decrease in the multiple exchange parameter M (the average number of deuterium atoms incorporated in the product molecule during one step of the interaction) to 1.34 in the H–D exchange in cyclohexane in the presence of $Pt(O_2CCF_3)_2$ in CF_3COOD compared with platinum(II) chloride complexes (M = 1.8) also indicates a decrease in the stability of the Pt–C bond with enhancement of the electron-accepting capacity of the ligand.[73] It is noteworthy that, on alkylation of $Pt(O_2CCF_3)_2$ with ethylmercury bromide in the gas phase, a significant increase in the fraction of ethylene, formed as a result of the β-elimination of hydrogen (ethylene : ethane = 9 : 1), is observed compared with the alkylation of $PtCl_2(H_2O)_2$ (ethylene : ethane = 1 : 3).

It has been shown[74,75] that the replacement of a chloride ion in platinum(II) complexes by the strong π-acceptor ligand $SnCl_3^-$ makes it possible to carry out reactions in organic media and favours dehydrogenation and hydrogen transfer for cyclohexene and cyclohexa-1,3-diene but not cyclohexane. Metallic platinum separated in the course of the reaction, but, as in the case of the H–D exchange in the presence of $PtCl_4^{2-}$,[1] it did not exhibit a catalytic effect. It was later found that a neutral complex of the pentacoordinated platinum(II) with π-acceptor ligands, namely $Pt(SnCl_3)_2[P(OR)_3]_3$ (R = CH_3, C_2H_5), which possesses electrophilic properties, dehydrogenates cycloalkanes with liberation of molecular hydrogen.[76] The authors believe that the active species is the coordinatively unsaturated d^8-ML_4 (a 16-electron complex).



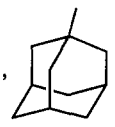
Thus the π-acceptor properties of the ligands are decisive in preventing the reduction of Pt(II) to Pt(0) during the reaction. The strong σ-donor properties of $SnCl_3^-$, which should promote the transition Pt(II) → Pt(0), are evidently of secondary importance. This is the first example of a reaction of this type for platinum complexes. It had been shown earlier that linear cyclic alkanes are dehydrogenated both thermally and photochemically to the corresponding alkenes in the presence of the complex $IrH_2(OCOCF_3)[P(FC_6H_4)_3]_2$.[46] *tert*-Butylethylene is used as a hydrogen acceptor in the thermal dehydrogenation reaction, but in the photochemical process it is not required. The activity of the above iridium complex is determined by the ability of the CF_3COO^- group to behave both as a η^1- and η^2-ligand, which ensures the occurrence of β-elimination in the intermediate alkyliridium hydride complex $Ir(H)(R)(\eta^2\text{-}OCOCF_3)(PR_3)_2$. The iridium complex with the acetate anion is inactive in the dehydrogenation of alkanes. The thermocatalytic formation of molecular hydrogen and cyclooctene from cyclooctane in the presence of rhodium complexes has also been described.[77] A negative test with metallic mercury showed that the colloidal metal, formed apparently at temperatures in the range 150–180 °C, does not participate in the reaction of the substrate.

As already noted,[72] rapid disproportionation of cyclic olefins is observed in the presence of palladium trifluoroacetate at room temperature. When maleic acid is introduced as a hydrogen acceptor, they are dehydrogenated to substituted benzenes, the rate of formation of the aromatic compound in the presence of $Pd(O_2CCF_3)_2$ being appreciably higher than the rate of reaction with participation of $Pd(O_2CCH_3)_2$.

Later studies extended the range of hydrocarbons which can react with palladium(II) in TFA. The reaction of adamantane or methane with palladium acetate in TFA at 80 °C affords adamantyl trifluoroacetate and methyl trifluoroacetate respectively in 60% yield.

$$RH + Pd(O_2CCH_3)_2 \xrightarrow{CF_3COOH} CF_3CO_2R + Pd^0 + H^+;$$

R = CH_3,



.

The significant role of the quality of palladium acetate, especially in the oxidation of methane, was indicated. When the reaction was carried out with $Pd(O_2CCD_3)_2$, deuterium was not detected in the reaction product, which indicates, in the authors' view, the stability of the acetate group under the reaction conditions. Oxygen does not affect the reaction, which demonstrates the absence of radical stages. The test with metallic mercury for the heterogeneity of the reaction gave a negative result.[79] Since it has been stated in a number of investigations[80,81] that the high yields of the methane oxidation products are not reproducible in the presence of $Pd(O_2CCH_3)_2$ in TFA, the source of the differences is probably the acetate ion present in the study of Gretz and coworkers.[78,79]

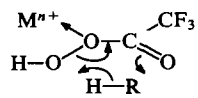
Pronounced electrophilic properties are retained even in the palladium(II) centre surrounded by phosphine ligands when aromatic C–H bonds are attacked. The alkylation of aromatic compounds by alkylpalladium complexes, in particular $(PhCH_2)ClPd(PPh_3)_2$, has been investigated. Experiments using a 1 : 1 C_6H_6–$CH_3OC_6H_5$ mixture showed[82] that the rate of alkylation of anisole is three times higher than that of benzene, which confirms the electrophilic character of the RPd^+ species.

Platinum and rhodium trifluoroacetates also interact with ethane at 80–150 °C and a pressure of 10–15 MPa with formation of methyl trifluoroacetate (0.5%–5.0%), the metal black, CO_2, and fluoroform.[81] The presence of CF_3H among the products indicates the instability of TFA under the reaction conditions and the possible involvement of the trifluoromethyl radical or cation in the C–H bond dissociation processes in methane. The presence of the acetate ion, which is even less stable in relation to decarboxylation, may lead, with a high degree of probability, to the formation of analogous intermediates in systems based on palladium acetate.[78,79] These intermediates can be the cause of the high yield of methyl trifluoroacetate, which is not reproduced in systems based on $Pd(O_2CCF_3)_2$.

Hydrogen peroxide has been used as the oxidant in the reactions of methane with $Pd(O_2CR)_2$ (R = CH_3, C_2H_5) in trifluoroacetic anhydride [90 °C, $p(CH_4)$ = 9 MPa].[83] It has been shown that the yield of $CF_3CO_2CH_3$ passes through a maximum as a function of time. In view of the hydrolysis of $CF_3CO_2CH_3$, the methane oxidation reaction can be represented by the equation

$$CH_4 + H_2O_2 \xrightarrow[(CF_3CO)_2O]{Pd(O_2CR)_2,\ 90\,^\circ C} CH_3OH + H_2O\,.$$

Excess of trifluoroacetic anhydride (TFAN) binds the water evolved during the reaction, preventing hydrolysis of the esters. In this system, palladium(II) can either oxidise ethane, being converted into a zerovalent palladium compound which is then oxidised by CF_3COOOH completing the catalytic cycle, or it can provide electrophilic cooperation in the reaction of the CF_3COOOH molecule with CH_4 by coordination to the oxygen of the peroxy-group in a transition state of the type [84]



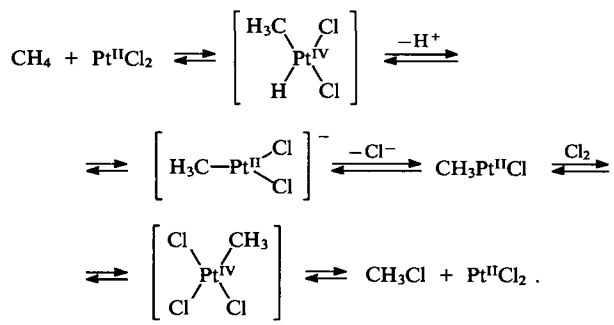
It has been stated that, under the reaction conditions, the acetate group is oxidised with formation of methyl trifluoroacetate. Similar data on the oxidation of CH_3COO^- in the presence of MnO_4^- with formation of $CF_3CO_2CH_3$ have been published. [81]

It has been observed that one of the methane oxidation products is methyl trifluoroacetate in the $V^V-H_2O_2-RCOOH$ system, where R is CH_3 or CF_3, under mild conditions [$p(CH_4)$ = 3–3.5 MPa, 20 °C]. [85]

Irradiation with light of a solution of adamantane and $Pd(O_2CCF_3)_2$ or $Cu(O_2CCF_3)_2$ in CH_3CN leads to the oxidation of the hydrocarbon mainly at the tertiary C–H bond. [86] Alkyl(aryl) trifluoroacetates are formed on irradiation with light of solutions of alkanes(arenes) in TFA in the presence of vanadate ions. [87]

In the presence of a deposited highly electrophilic rhodium(III) complex, methane is chlorinated with formation mainly of methyl chloride. [88] The authors of the above study postulated that the coordinatively unsaturated rhodium(III) attacks a C–H bond of the hydrocarbon. A proton then migrates to the ligand in the coordination sphere of rhodium. A more detailed study of the possible formation in this system of the catalytically active [SiO]–Rh(η^3-C_3H_5)(H) showed [89] that the activation of the C–H bond is apparently a result of the classical mechanism of the dissociation of a C–H bond in an alkane on the surface of a metal and is not caused by the electrophilic cleavage in the presence of rhodium(III).

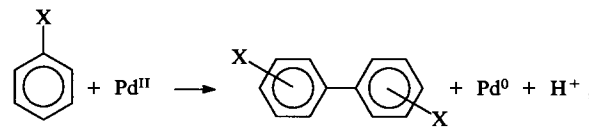
A platinum(II)-modified heterogeneous catalyst for the oxidative chlorination of methane, namely $CuCl_2$ + Pt^{II}/Al_2O_3, has been obtained. [90] It is more active as a result of the appearance of a new reaction pathway involving the formation of methylplatinum(II) complexes. Methylplatinum(II) is subsequently oxidised by molecular chlorine with liberation of CH_3Cl. On the basis of earlier data, [2,90] Olah [55] demonstrated that the heterogeneous-catalytic technology for the synthesis of methanol and olefins via methyl halides is promising.



A new selective low-temperature (200–400 °C) catalyst, namely [$PdCl_2-H_9(PV_6Mo_6O_{40})$]/$SiO_2$, for the oxidative chlorination of methane with formation of methyl chloride has been discovered. [91] The absence of polychloromethanes and molecular chlorine from the reaction products may indicate the electrophilic properties of the system, which agrees with the behaviour of palladium in other reactions. It has been noted [92,93] that the selectivity of the oxidation of hydrocarbons in the presence of the heterogeneous analogue ($PdSO_4-H_2SO_4$)/SiO_2 (220 °C) is lower than for the homogeneous system. [3] One of the functions of H_2SO_4 as a strong Brønsted acid is to increase the oxidising capacity of palladium(II) and to enhance its electrophilicity.

c. Aromatic compounds

The oxidative coupling of arenes on treatment with palladium(II) compounds was discovered in 1965. [94] These reactions take place in organic and, more rarely, in aqueous solutions at a temperature not exceeding 120 °C.



X = H, Alk, Hal, Ar, OR, O_2CR, OH, etc.

In the general case, a mixture of all possible isomers of biaryls is formed, their ratios being determined by the nature of the substituent X.

When $Pd(O_2CCH_3)_2$ is used instead of the complex $PdCl_2$–CH_3COONa, acetoxylation in the ring and, in the case of methylbenzenes, in the alkyl group takes place together with oxidative dimerisation. Perchloric acid inhibits the acetoxylation reaction, while the introduction of sodium acetate increases the yield of the product acetoxylated in the methyl group. [61,62,95,96]

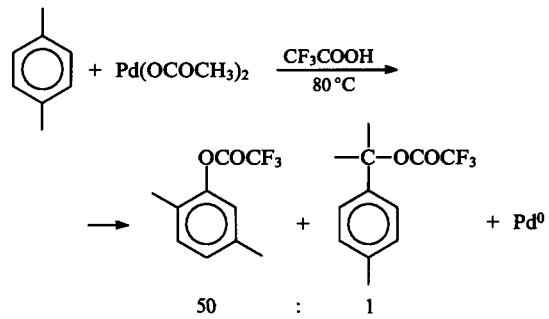
The reactions of palladium with aromatic compounds in TFA occupy a special place. Benzene and its derivatives containing electron-accepting groups reduce palladium trifluoroacetate mainly with formation of oxidative dimerisation products [67] and also of small amounts of trifluoroacetoxylated derivatives under conditions where palladium acetate is inert to aromatic compounds. The preferential formation of oxidative coupling products has been attributed to the decrease in the basicity of the ligand on passing from acetate to trifluoroacetate.

Organopalladium compounds have been isolated in the reaction of benzene and naphthalene with palladium trifluoroacetate in TFA. On the basis of chemical reactions and IR and NMR spectra, Azzoumanidis and Rauch [97] considered these compounds as π-arene complexes in which there is a Pd–C bond. Palladium(II) acetate reacts with benzene in the presence of dialkyl sulfides at 70 °C with formation of a new diphenyltripalladium(II) complex, $(R^1SR^2)PhPd(\mu\text{-}CH_3CO_2)_2Pd(\mu\text{-}CH_3CO_2)_2$. .$PdPh(R^1SR^2)$, where $R^1 = R^2$ = Bu^t, Bu^i, Pr^i, Et, or CH_2Bu^t. [98] The study of these complexes demonstrated the presence in their structures of two phenyl groups and four bridging acetate groups.

As already mentioned above, [67] benzene and mono-, di-, and poly-substituted benzenes reduce palladium(II) in TFA. Benzene, *m*-xylene, and 1,2,3-trimethylbenzene then form mainly biaryls. The reactions of toluene and *p*-xylene involve the appearance of a new pathway, which leads to diarylmethanes. It becomes the main pathway for aromatic compounds with a low ionisation potential. [99]

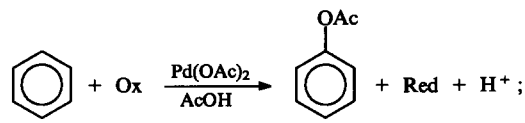
Studies on the interaction of palladium trifluoroacetate with benzene, *p*-dimethoxybenzene, *p*-xylene, and toluene confirmed the electrophilic nature of the process, [79] because the C–H benzyl bonds were hardly attacked by palladium, as in Henry's study. [100] The increase in the rates of oxidation of benzenes containing electron-donating groups in the sequence *p*-dimethoxybenzene (1), *p*-xylene (0.1), toluene (0.02), benzene (0) (the rates are indicated in brackets) is consistent with the electrophilic attack by palladium on the C–H bond, while the primary kinetic isotope effect (k_H/k_D) for the oxidation of toluene and toluene-d_8 is 5.0, which is characteristic of analogous electrophilic systems. [61,62]

It is noteworthy that, in their analysis of the reactivity of aromatic compounds, Sen et al. [79] take into account only the acetoxylation reaction and ignore the oxidative coupling reaction.



d. The effect of the oxidant

The reactions of aromatic compounds with participation of palladium can be carried out under catalytic conditions using fairly mild oxidants. However, the oxidant not only participates in the reoxidation of palladium but is also capable of altering the mode of reaction. [100] In the absence of the oxidant, only oxidative coupling is observed, while in its presence the acetoxylation reaction occurs.



Ox = Cr(IV), $Pb(OAc)_4$, $NaClO_3$, $KMnO_4$, $NaNO_3$, $NaNO_2$.

In addition, there is a possibility of substitution in the aromatic ring by an external nucleophile Nu = N_3^-, Cl^-, NO_2^-, Br^-, CN^-, or SCN^-. Eberson and Jönsson [101] investigated in detail the ring acetoxylation reaction. They showed that the use of a bipyridylpalladium complex and $K_2S_2O_8$ as the oxidant makes it possible to carry out the acetoxylation reaction with formation of a smaller proportion of the *m*-isomer. [101] Potassium persulfate has also been used to oxidise the palladium formed as a result of the interaction of naphthalene with $Pd(O_2CCH_3)_2$ in solution in TFA. [78] The use of oxygen as the oxidant for zerovalent palladium [102] in reactions of aromatic compounds with palladium(II) leads, in contrast to other oxidants, to the formation of oxidative coupling products. [100] Biaryls are formed in high yields in the presence of oxygen also in systems based on palladium salts and heteropolyacids. [103] The oxidation of toluene by oxygen in the $Pd(OAc)_2-Sn(OAc)_2-KOAc-AcOH$ system takes place with formation of benzyl acetate, which indicates the influence of the components of the system on the nature of the processes occurring in it. [104] In particular, the oxidation of divalent tin salts involves the formation of active intermediates (for example, the OH radical), [105] which can in fact be responsible for the attack on the methyl group in the system mentioned above.

Attempts have been made to dehydrogenate cyclohexane with palladium trifluoroacetate in TFA under palladium reoxidation conditions. It was found that TFA attacks oxidants such as chromium(VI) and manganese(VII), enhancing their electron-accepting properties such that they are able to oxidise hydrocarbons rapidly without the participation of palladium. [70,81] However, aromatic compounds are formed only in the presence of palladium(II). Analogous results have been obtained by Sen and coworkers [106] for a wide range of cyclohexane derivatives.

e. The mechanism of the interaction of hydrocarbons with palladium

The mechanism adopted for the oxidation of arenes by palladium(II) includes the formation of an organopalladium intermediate and its reactions without the participation of free radicals. [61,62]

$$ArH + Pd^{2+} \longrightarrow ArPd^+ + H^+$$
$$2\,ArPd^+ \longrightarrow Ar_2Pd + Pd^{2+}$$
$$Ar_2Pd \longrightarrow Ar_2 + Pd^0$$

It has been shown by Kozhevnikov et al. [107] in a study of the oxidation of *o*- and *p*-xylenes by palladium(II) trifluoroacetate in TFA that the formation of diarylmethanes in a strongly acid medium can be explained by one-electron transfer with participation of aromatic radical-cations as intermediates, similar to the oxidation by cobalt(III) and lead(IV) salts. [17] The mechanism of the oxidation of methylbenzenes by palladium(II) (palladation or electron transfer) depends on the type of arene and the acidity of the medium.

$$Pd^{II} + ArH \longrightarrow (\pi\text{-}ArH)Pd^{II} \begin{cases} \longrightarrow ArPd^{II} + H^+ \\ \longrightarrow ArH^{+\cdot} + Pd^{I} \end{cases}$$

In relation to the reactions of toluene, palladation has been compared [108] with other aromatic substitution reactions in terms of the ratio of Brown's selectivities $\lg f_n = a \lg (f_n/f_m)$ (for toluene, $a = 1.31$), which characterises the relation between the substrate

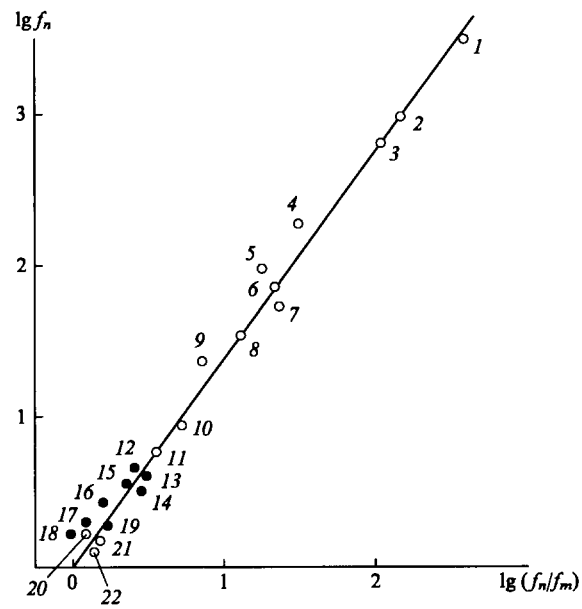


Figure 1. The ratios of selectivities for substitution in the toluene ring. [108] Filled circles — reactions with palladium(II). Bromination: (*1*) Br_2, 85% AcOH, 25 °C; chlorination: (*2*) Cl_2, AcOH, 25 °C; benzoylation: (*3*) PhCOCl in $PhNO_2$, 25 °C; thallation: (*4*) $Tl(O_2CCF_3)_3$, CF_3COOH, 10 °C; (*5*) 73 °C; nitration: (*6*) HNO_3, 90% AcOH, 45 °C; thallation: (*7*) $Tl(OAc)_3 + H_2SO_4$, AcOH, 70 °C; mercuration: (*8*) $Hg(OAc)_2 + HClO_4$, AcOH, 50 °C; (*9*) $Hg(OAc)_2$, AcOH, 50 °C; sulfonation: (*10*) $MeSO_2Cl + AlCl_3$, 100 °C; isopropylation: (*11*) *iso*-$C_3H_7Br + Ga_2Br_2$, 25 °C; palladation: (*12*) $Pd(OAc)_2 + H_2SO_4$, AcOH, 95 °C; (*13*) $Pd(OAc)_2 + HClO_4$, AcOH, 55 °C; (*14*) 95 °C; (*15*) $PdCl_2 +$ NaOAc, AcOH, 90 °C; (*16*) $Pd(OAc)_2 + CF_3COOH$, AcOH, 95 °C; (*17*) $Pd(OAc)_2$ + NaOAc, AcOH, 95 °C; (*18*) $Pd(OAc)_2$ in AcOH, 95 °C; catalytic coupling: (*19*) $Pd(OAc)_2$ in ArH, $p(O_2)$ = 2.5 MPa, 150 °C; radical arylation: (*20*) attacking radical *p*-$NO_2C_6H_4$, 20 °C; (*21*) *p*-$MeC_6H_4^{\cdot}$; (*22*) $\dot{P}h$.

(f_n) and positional (f_n/f_m) selectivities (the positional selectivity characterises the selectivity of the attack on different positions in the ring) of the substitution in the ArH ring. Fig. 1 shows that palladation is the least selective reaction in the series of electrophilic substitution processes, its selectivity approaching that of radical substitution, which is similar to the statistical selectivity with respect to the *meta*- and *para*-isomers.

Table 2 presents the electron affinities and electron excitation energies for a series of electrophiles—transition metals and traditional Lewis acids.[60] Evidently the electron affinity of palladium(II) is comparable to those of zinc(II) and mercury(II). However, palladium(II) has a much lower excitation energy. This leads to a strong donor–acceptor interaction with alkenes and aromatic compounds in the case of palladium (palladium is a soft acid in terms of Pearson's theory of hard and soft acids and bases), which results in the compensation of the influence of the polar (electronic) effects of the substituents in the ArH ring on the reaction centre. A similar result was obtained in a study of the H–D exchange and the oxidation of substituted benzenes in the presence of 'soft' acids—platinum(II) complexes.[109] With increase in the 'hardness' of the ligand environment of palladium(II) (transition from CH_3COO^- to the electron-accepting CF_3COO^- and ClO_4^-), the effectiveness of the compensation falls as a consequence of the weakening of the dative bond. Both the selectivity of the palladation reaction and its rate increase under these conditions. The electrophilic character of the metallation of arenes increases in the sequence Pd(II) < Hg(II) < Tl(III) and the values of ρ are –2.2,[110] –5.3,[111] and –7.5[108] respectively.

Table 2. The excitation energies [$nd^x \rightarrow nd^{x-1}(n+1)p^1$] and electron affinities for a series of metal ions.

Ion	Excitation energy/eV	Electron affinity/eV
Rh(I)	1.6[a]	7.31
Ir(I)	2.4[a]	7.95
Pt(II)	3.05[a]	18.56
Pd(II)	3.39[a]	19.42
Cu(I)	8.25	7.72
Ag(I)	9.94	7.59
Zn(II)	17.1	17.96
Cd(II)	16.6	16.90
Hg(II)	12.8	18.75
Tl(III)	18.3	29.80

[a] The values for Rh^0, Ir^0, Pd^I and Pt^I are presented.

By analogy with the existence of a common intermediate in the H–D exchange and oxidative chlorination of alkanes in the presence of platinum(II) and platinum(IV) complexes, which was postulated and demonstrated by kinetic methods,[2,112,113] in the case of palladation reactions there should also be a common intermediate, which affords the oxidative coupling products in the absence of an added oxidant and ring acetoxylation products in its presence. The primary isotope effect and the dependence of the rate of reaction on the concentration of the acid oxidant have been interpreted within the framework of ideas postulating that arylpalladium(II) and arylpalladium(IV) are intermediates leading to biaryls and aryl acetates respectively.[19,114]

$$Ph_2Pd^{II} \xleftarrow{C_6H_6} PhPd^{II}(OAc) \xrightarrow{Ox} PhPd^{IV}(OAc)_3$$

$$\downarrow \qquad\qquad\qquad\qquad \downarrow$$

$$Pd^0 + Ph_2 \qquad\qquad PhOAc + Pd^{II}(OAc)_2 .$$

3. Carboxylation and oxidation of hydrocarbons with participation of palladium(II)

The formation of reactive organopalladium compounds in the reaction of hydrocarbons with palladium(II) made it possible to achieve the acetoxylation and oxidative coupling of arenes, the arylation of olefins, and also the direct oxidation and carboxylation of aromatic compounds and alkanes.

The stoichiometric carboxylation of arenes with carbon monoxide in the presence of palladium acetate has been carried out.[115] It was found that the reactivity of monosubstituted benzenes diminishes in accordance with the electrophilic character of the reaction in the following series of substituents: $OCH_3 > CH_3 > H > Cl$. The achievement of a single-stage synthesis of aromatic acid anhydrides from compounds such as benzene, toluene, anisole, chlorobenzene, thiophene, and furan, which are carbonylated in the β-position, has been reported.[116] A significant difference between the reaction conditions and those described by Fujiwara et al.[115] is the presence of 1,2-dibromoethane, the role of which is believed by the authors[116] to be the reoxidation of the metallic palladium formed in the reaction. Other polyhalo-compounds diminished the yield of the anhydrides.

$$ArH \xrightarrow[p(CO) = 1.5\ MPa]{Pd^{II}} (ArCO)_2O .$$

In the presence of *tert*-butyl hydroperoxide, the synthesis of aromatic acids with participation of palladium(II) in solution in acetic acid, which permits the use of a low carbon monoxide pressure, becomes catalytic.[117,118]

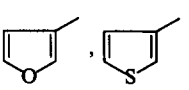
$$ArH \xrightarrow[Ox]{Cat} ArCOOH ;$$

Cat = $Pd(OAc)_2$;
Ox = Bu^nOOH, $CH_2{=}CHCl$, AcOH; $p(CO)$ = 0.1 MPa.

It is of interest to note that certain oxidants—H_2O_2, *m*-ClC_6H_4COOOH, $O{=}C_6H_4{=}O$, $CuCl_2$, $Pb(OAc)_4$, $FeCl_3$, and $K_2S_2O_8$—lower the yield of the oxidative carbonylation products.

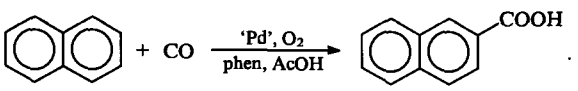
The insertion of CO_2 in the Pd–C bond of an organopalladium compound leads to the formation of acids, but the reaction selectivity is low,[119] the reactivity of CO_2 amounting to approximately 0.01 of the reactivity of CO. The joint employment of palladium(II) and Bu^tOOH increases the yield of aromatic acids in this case too.

$$ArH + CO_2 \xrightarrow{Pd(OAc)_2,\ Pd(NO_3)_2} ArCOOH ;$$

Ar = Ph, ClC_6H_4, $CH_3OC_6H_4$,  .

The proportions of the isomers of substituted benzenes are consistent with their proportions obtained on electrophilic substitution in an aromatic compound.

β-Naphthoic acid can be obtained with a selectivity in excess of 80% by the single-stage carboxylation of naphthalene with carbon monoxide in the presence of palladium(II) under mild conditions.[120]

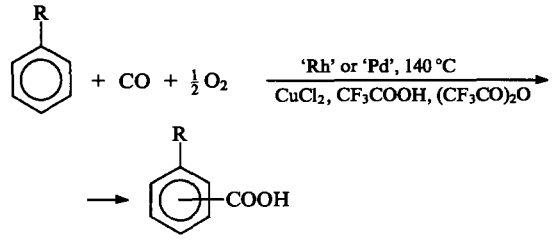


It is significant that the maximum yield of β-naphthoic acid is attained in the simultaneous presence of acetic acid, oxygen, and *o*-phenanthroline (phen), the last compound regulating the reaction selectivity. Palladium on charcoal or palladium black catalyse, like palladium(II) acetate, the carboxylation of naphthalene. The reaction apparently proceeds via a stage involving the formation of a σ-arylpalladium(II) complex via the electrophilic substitution of hydrogen in the aromatic compound in the case of palladium(II) or the oxidative addition of naphthalene in the case of zero-valent palladium. It may be that large palladium clusters, which are in fact the carboxylation catalysts, are formed during the reaction. [121]

The palladium-catalysed carboxylation of aromatic C–H bonds by carbon monoxide takes place with high yields and under mild conditions [p(CO) = 0.1 MPa, 20–50 °C] in TFA in the presence of sodium acetate as the cocatalyst. [122] The yield of the products corresponds to the stoichiometric consumption of palladium, but the reaction can be carried out under catalytic conditions with participation of $NaNO_3$, $Tl(O_2CCF_3)_3$, and $Hg(O_2CCF_3)_2$ like the carboxylation phenylmercury chloride in the presence of palladium(II). [123] The reaction with substituted aromatic compounds, such as anisole and toluene, is a typical electrophilic substitution process. The electrophilic character of the reaction agrees with the positive effect exerted by the addition of strong acids (CF_3COOH). Since in the presence of an oxidant the regioselectivity of the process increases compared with the stoichiometric reaction, thallium(III) and mercury(II) compounds probably not only oxidise the zerovalent palladium formed but also play the role of *ortho*- and *para*-directing agents. The role of sodium acetate is less clear. On the one hand, its presence can weaken the electrophilic properties of palladium (compared with trifluoroacetate) and, on the other, it should stabilise the catalytic system in relation to the reduction of palladium by carbon monoxide. These postulates require the existence of an optimum Pd : NaOAc ratio.

The palladium-catalysed carboxylation of the C–H bonds of thiophene and furan by carbon monoxide proceeds in acetic acid (both compounds are unstable in TFA) with participation of mercury(II) and thallium(III) carboxylates under mild conditions [p(CO) = 0.1 MPa, 20–50 °C]. [124]

The oxidative carbonylation of benzene and its derivatives in the presence of rhodium(III) trifluoroacetate as well as palladium and copper compounds has been investigated. [125]

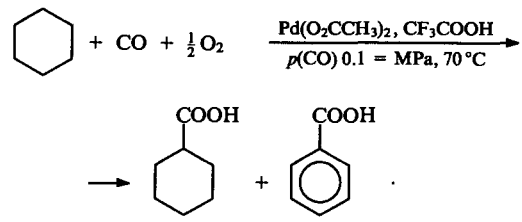


R = H, CH_3, CH_3O, Cl.

We may note that the replacement of rhodium in the form of $Rh(O_2CCF_3)_3$ by $Pd(O_2CCF_3)_2$ leads to a significant increase in the overall yield of toluic acids. It has been shown that, in conformity with the data of Gol'dshleger et al., [126] rhodium(III) trifluoroacetate is an electrophile which directs the carboxy-group predominantly to the *para*-position. We may also note that the system components—the copper(II) compounds CuX_2 (X = CH_3COO, CF_3COO, ClO_4)—themselves effectively catalyse the carboxylation of aromatic compounds.

The Rh^{3+}/nafion catalyst reacts as a strong electrophile: [127] *p*-toluic acid is formed under these conditions with a selectivity of 94%.

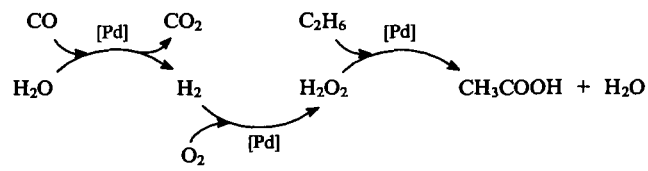
The first study on the carboxylation of cycloalkanes by carbon monoxide without irradiation in the presence of palladium(II) was carried out by Japanese investigators. [128]



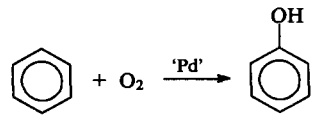
Cyclohexanecarboxylic and benzoic acids are obtained in molar proportions of 1 : 3. Potassium peroxydisulfate proved to be a convenient oxidant in this case also. [129–131] The introduction of methanol and the increase in the reaction time and temperature appreciably increased the yield of cyclohexanecarboxylic acid. [129] The reactivity of the C–H bonds of cycloalkanes diminishes on passing from tertiary to primary bonds. [130] In the case of hexane, the 1-, 2-, and 3-carboxylic acids are obtained in molar proportions of 2 : 29 : 20, [129] which differ appreciably from the photochemical alkane carbonylation reactions in the presence of $RhCl(CO)[P(CH_3)_3]_2$. [9] In this connection, the results obtained in the oxidation and oxidative carbonylation of methane in the presence of potassium persulfate in aqueous solution are of interest. [132] It was shown that the $SO_4^{-\bullet}$ radical-anion, generated from $S_2O_8^{2-}$, abstracts a hydrogen atom from methane and ethane at 105–115 °C with formation of an alkyl radical, which can subsequently effectively interact with carbon monoxide, affording an acyl radical, the latter being converted in the final stages into carboxylic acids, CH_3COOH and C_2H_5COOH respectively, in high yields. It may be that this reaction makes an appreciable contribution to the oxidative carbonylation of cycloalkanes in the presence of the Pd(II)–$K_2S_2O_8$ system [the yield of carboxylic acid relative to the palladium(II) taken for the reaction reached 19 000%]. [131]

The carbonylation of methane by carbon monoxide in solution in TFA in the presence of $K_2S_2O_8$ as the oxidant is possible with participation of copper complexes, which presupposes a reaction mechanism different from the mechanism of the carboxylation of cyclohexane with participation of a σ-organopalladium compound. [133]

A highly effective system for the direct oxidation of lower alkanes by oxygen in aqueous solution has been proposed. [134] Pd/C serves as the catalyst of the low-temperature synthesis of carboxylic acids.



The direct hydroxylation of benzene by molecular oxygen or H_2O with formation of phenol, which proceeds via a stage with C–H bond activation by palladium(II) compounds, has been achieved. The reaction temperature is appreciably higher than the temperature necessary for the carboxylation of aromatic compounds by CO or for the oxidative coupling reaction. The selective synthesis of phenol requires the presence of carbon monoxide, phenanthroline, and oxygen. [135]



The effect of CO on the selectivity of the hydroxylation of aromatic compounds in the presence of palladium(II) is associated with the possibility of the acceptance of one oxygen atom with formation of CO_2, while the other is inserted in the Pd–C bond. A decrease in the concentration of palladium increases the yield of phenol. In the absence of CO, biphenyl is formed in addition to phenol. [136]

4. Reactions of aromatic compounds with participation of platinum(IV)

The interaction of platinum(II) and platinum(IV) complexes with aromatic hydrocarbons has been investigated. [137] The degree of reduction of platinum(IV) in the oxidative coupling of toluene in the $Hg(OAc)_2-H_2PtCl_6-AcOH$ system depends on the acidity of the medium: in a weakly acid medium, the reduction proceeds as far as platinum(II), while in a strongly acid medium it continues to zerovalent platinum with formation in the latter case of two moles of bitolyl per mole of platinum(IV). As in the case of palladium(II), the introduction of perchloric acid apparently increases the electrophilicity of platinum(II), which has been confirmed by data [138] indicating a greater activity of platinum(II) complexes with a low chlorine content — $PtCl(H_2O)_3^+$ and $Pt(H_2O)_4^{2+}$ — in the oxidation of benzene.

Evidence for the formation of relatively stable intermediate acyl and phenyl derivatives of platinum(IV) in the oxidation of methane and benzene in the platinum(II)–platinum(IV) system has been obtained by ^1H and ^{13}C NMR spectroscopy. [12,139]

Further studies demonstrated that σ-arylplatinum(IV) complexes can be obtained in yields up to 95% on heating the aromatic compound ArH with H_2PtCl_6 in CH_3COOH or a $CF_3COOH-H_2O$ mixture. [140,141]

$$ArH + H_2PtCl_6 \xrightarrow[2.\ SiO_2,\ NH_3]{1.\ CF_3COOH-H_2O} NH_4^+\left[(\sigma\text{-}Ar)PtCl_4NH_3\right]^-$$

Naphthalene and *o*-nitrotoluene complexes have been characterised by X-ray diffraction. [140,142] It has been established by the method of competing reactions [143,144] that the relative rates of reaction involving PhX, indicated below in brackets, decrease in the following sequence of X: OH (16), OCH_3 (8.5), CH_3 (3.0), C_2H_5 (2.7), OC_2H_5 (2.0), $CH(CH_3)_2$ (1.9), H (1.0), Ph (0.9), F (0.9), $COCH_3$ (0.1), COOH (0.09), Cl (0.08), NO_2 (0.04). The logarithms of the rates are correlated with Hammett's σ constant and Brown's σ^+ constants (the parameters ρ and ρ^+ are –3.0 and –1.5 respectively). On the basis of the data obtained, a mechanism is proposed for electrophilic substitution in the aromatic ring with participation of platinum(IV) complexes. [145] The behaviour of platinum(IV) in arene metallation reactions resembles that of palladium(II) complexes (ρ ad ρ^+ are –3.0 and –2.2 respectively). [110,144]

It is of interest that the interaction of mesitylene with $PtCl_6^{2-}$ in TFA with formation of (2,4,6,3′,5′-pentamethyl)diphenylmethane in the first stage apparently includes electron transfer from the arene to the platinum(IV) complex. Thus the behaviour of platinum(IV) is similar to that of palladium(II) in TFA. [146]

5. Oxidation of hydrocarbons by cobalt(III), manganese(III), lead(IV), and silver(II) carboxylates

Cobalt(III), manganese(III), and lead(IV) carboxylates are used to oxidise alkyl-substituted aromatic hydrocarbons. [17,19] Whereas cobalt(III) acetate is stable in acetic acid even at a high temperature, manganese(III) acetate decomposes even on slight heating with formation of radicals, which participate in further reactions.

$$\dot{C}H_2COOH \longrightarrow \dot{C}H_3 + CO_2.$$

This mechanism is characteristic of aromatic compounds with an ionisation potential above 8 eV. In the presence of more readily oxidised compounds, $Mn(O_2CCH_3)_3$ reacts via an electron-transfer mechanism with formation of the radical-cation of the aromatic compound. After the addition of a strong acid, this pathway becomes the only one. [147] The introduction of a strong acid such as CF_3COOH plays a decisive role in the interaction of these oxidants with benzene, toluene, and unsaturated hydrocarbons. [148–152] The effect of TFA may be attributed to the formation of a cationic species which renders cobalt(III) a stronger electrophile. [147]

$$Co(O_2CCF_3)_3 \longrightarrow Co(O_2CCF_3)_2^+(CF_3COO)^- \xrightarrow{H^+} \longrightarrow Co(O_2CCF_3)_2^+ + CF_3COOH$$

As a result, the oxidation of alkanes by cobalt(III) acetate in TFA becomes possible at low temperatures. Under an inert atmosphere, the reaction products are esters while in the presence of oxygen ketones are formed. When CCl_3COOH was used as the activator, alkyl chlorides, primarily secondary alkyl chlorides, were obtained under an inert atmosphere. Cobalt(III) trifluoroacetate was quantitatively reduced in TFA by cyclooctane and 2,3-dimethylbutane in 2 and 3 h respectively, but the esters were formed in a low yield. Cyclohexyl trifluoroacetate was obtained in a yield of 35% under similar conditions, which indicates its subsequent transformation under the reaction conditions (for example, the splitting off of TFA and subsequent reactions of cyclohexene). However, benzene was oxidised quantitatively to phenyl acetate with participation of $Co(O_2CCF_3)_3$ at room temperature. [151]

The interaction of manganese(III), iron(III), cobalt(III), copper(II), and lead(IV) trifluoroacetates with methane in solution in TFA at 100–200 °C and a methane pressure of 1–4 MPa has been investigated. The activity of the metal trifluoroacetates diminishes in the sequence Co(III) > Mn(III) > Pb(IV) ≫ Cu(II) > Pd(II); $Fe(O_2CCF_3)_3$ was inactive. The degree of formation of methyl trifluoroacetate reaches 90% in the case of cobalt(III) and takes place in conformity with the following equation: [80,153]

$$CH_4 + 2Co(O_2CCF_3)_3 \longrightarrow \longrightarrow CF_3CO_2CH_3 + 2Co(O_2CCF_3)_2 + CF_3COOH.$$

Further study of this system showed that the addition of oxygen (0.1–0.5 MPa) to methane leads to the catalytic synthesis of $CF_3CO_2CH_3$ from methane. The same yields of methyl trifluoroacetate were attained in the $Co(III)-O_2-CH_4$ and $Co(II)-O_2-CH_4$ systems. [80]

$$CH_4 + \tfrac{1}{2}O_2 + CF_3COOH \xrightarrow{\text{'Co'}} CF_3CO_2CH_3$$

It has been found [154] that ethane and propane also react with $Co(O_2CCF_3)_3$ under similar conditions in solution in TFA with formation of alkyl trifluoroacetates as the main products.

$$C_2H_6 + 2Co(O_2CCF_3)_3 \longrightarrow \longrightarrow CF_3CO_2C_2H_5 + 2Co(O_2CCF_3)_2 + CF_3COOH$$

$$C_3H_8 + 2Co(O_2OCF_3)_3 \longrightarrow \longrightarrow \textit{iso}\text{-}C_3H_7O_2CCF_3 + 2Co(O_2CCF_3)_2 + CF_3COOH$$

As in the case of methane, this interaction is accompanied by the decarboxylation of TFA, catalysed by cobalt salts, with formation of CO_2 and CF_3H. The oxidation of ethane and propane is a less selective process than the oxidation of methane. A reaction mechanism has been proposed. It involves direct electron transfer from the alkane RH molecule to Co(III) with formation of the radical-cation $RH^{+\bullet}$ in the first stage, as in the oxidation of alkanes in the presence of $Co(O_2CCH_3)_3$.

It has been found that bis(bipyridyl)silver(II) peroxydisulfate oxidises aromatic compounds in acetic acid at room temperature. The system becomes catalytic with respect to silver when an excess of potassium persulfate is used. [155]

Adamantane and other cyclic compounds are oxidised with a satisfactory yield to adamantyl and cycloalkyl trifluoroacetates [156] by the silver 'peroxide' $Ag(I)Ag(III)O_2$, which generates an active Ag(III) complex in the TFA–TFAN mixture.

6. Oxidation of hydrocarbons by manganese(VII), chromium(VI), and ruthenium(IV) in acetic acid

The oxidation of alkanes, cycloalkanes, and aromatic compounds by potassium permanganate $KMnO_4$ in aqueous trifluoroacetic acid has been investigated. It was found that the oxidising capacity of manganese(VII) increases with increasing acid concentration. The rate of oxidation of alkanes by manganese(VII) is sensitive to the structural differences in the substrate, in particular to the branching of the chain. A series of specific rates have been observed in terms of the selectivity of the oxidation of primary, secondary, and tertiary C–H bonds: 1, 60, and 2100 respectively. The rate of oxidation increases with increase in chain length; the methylene group is more reactive than the methyl group. After the introduction of electron-accepting substituents in the carbon chain, the rate of reaction falls. The primary isotope effect, determined for $C_6H_{12}-C_6D_{12}$ as 4.3, confirms that the rate-determining stage of the reaction is the cleavage of a C–H bond. It has been suggested [157] that the active species is the permanganyl cation MnO_3^+ in the free form or as the ester $MnO_3(O_2CCF_3)$.

The rate constants and the substrate selectivities for the first stage of the oxidation of RH (C_2-C_8 alkanes, benzene, toluene) by permanganate in TFA–H_2O solutions have been determined from the consumption of the substrate. [158] These data differ significantly from the results of the study of Stewart and Spitzer [157] obtained by a standard method from the consumption of the oxidant. Arguments have been put forward in support of the hypothesis that the reactants in solutions in TFA are MnO_4^-, $HMnO_4$, and $MnO_3(O_2CCF_3)$, the contribution of the last species becoming significant at a TFA concentration in excess of 50 mass%.

In the presence of manganese(VII), toluene in TFA is oxidised to CO_2, but, with increase in the concentration of water, the yield of benzoic acid increases; [159] rapid degradation of the aromatic compound, which follows the electrophilic attack by MnO_3^+, was also noted. [157]

Solutions of $KMnO_4$ in the TFA–TFAN mixture are capable of oxidising selectively methane to the product of its two-electron oxidation — methyl trifluoroacetate. [160–161] Methyl trifluoroacetate and methyl formate are formed in solution in the course of several hours at 60 °C and $p(CH_4)$ = 20 MPa, their overall yield reaching 90% relative to the unused oxidation equivalents of manganese(VII), converted during the reaction into manganese(IV) and manganese(III), in proportions of 3 : 1, which are inactive with respect to methane and sparingly soluble. Dimethyl formal $(CH_3O)_2CH_2$ is also formed (2%–4%). Fluoroform and carbon dioxide were detected in the reaction products, their amount corresponding to the consumption of ~10% of the oxidation equivalents of manganese(VII) on decarboxylation of TFA. The addition of small amounts of water reduces sharply the yield of the partial oxidation products as a result of the hydrolysis of the esters to methanol, which is relatively rapidly oxidised by potassium permanganate to CO_2. The use of methane enriched in $^{13}CH_4$ affords products containing the corresponding amount of the ^{13}C isotope. Manganese(VII) participates in the primary interaction with a methane molecule in the form of the cation MnO_3^+ or the ester $MnO_3(O_2CCF_3)$, the rate constants for this interaction amounting to 4×10^{-5} litre mol^{-1} s^{-1} at 70 °C and 1.5×10^{-5} litre mol^{-1} s^{-1} at 60 °C, which is higher than the corresponding constant for the $HMnO_4$ species determined in sulfuric acid solutions (10^{-5} litre mol^{-1} s^{-1} at 70 °C) and exceeds by three orders of magnitude the rate constant for the MnO_4^- species determined in neutral aqueous solutions. [160] Thus the rate constant for the reaction of methane with the manganese(VII) species increases sharply with increase in their electrophilicity.

In the presence of a large excess of sodium periodate, capable of oxidising in acid media the final product of the stoichiometric reaction [manganese(IV) and manganese(III) compounds] to permanganate, the process becomes catalytic with respect to the initial manganese both in aqueous acid media (10 cycles) and in TFA (2–3 cycles). [161] A simplified mechanism of the interaction for the TFA solutions is as follows:

$$\tfrac{2}{3}Mn^{VII} + CH_4 \xrightarrow[70\,^\circ C]{CF_3COOH} CF_3CO_2CH_3 + \tfrac{2}{3}Mn^{IV} + H_2O\,.$$

$$\tfrac{2}{3}Mn^{IV} \xrightarrow{NaIO_4} \tfrac{2}{3}Mn^{VII}$$

We may note that, in the absence of permanganate, the periodate exhibits an intrinsic activity in the oxidation of methane, which, however, is 20–30 times lower than the activity of permanganate. This apparently indicates unusual properties of oxo-complexes of metals in the C–H bond activation reaction and the fact that a higher standard two-electron redox potential of the periodate/iodate couple is insufficient for a more effective oxidation of the C–H bond.

A similar set of products [$CF_3CO_2CH_3$, CH_3CO_2H, $(CH_3O)_2CH_2$, CO_2, and CF_3H] was also found in the oxidation of methane in TFA by chromium(VI) compounds. [161]

A solution of potassium dichromate in TFA at room temperature oxidises n-pentane to the trifluoroacetic acid esters of 2-pentanol and 3-pentanol in molar proportions of 2 : 1 respectively. [162] Apart from these esters, the formation of small amounts of acetic and propionic acid was observed. Kinetic and spectrophotometric study of the reaction showed that the mononuclear chromium(VI) complexes are inactive and that the two-electron oxidation of a C–H bond of the methylene group of the alkane is effected by the dimeric complexes [$Cr^{VI}\cdots Cr^{VI}$]. The role of the second chromium ion in the complex apparently reduces to the enhancement of the electron-accepting properties of the oxo-groups of the first ion, [3] which serve as the active centre for the electrophilic interaction with a C–H bond of the alkane.

Extremely pronounced oxidising properties are characteristic of chromyl trifluoroacetate: in its presence, hydrocarbons reacted at temperatures in the range –20 to 25 °C in solvents without a C–H bond such as CCl_4 and $F_2ClC-CF_2Cl$. [163]

$$RH + CrO_2(OCOCF_3)_2 \longrightarrow$$

$$\longrightarrow \left[CF_3CO_2\overset{\displaystyle HO\quad R}{\overset{|\quad /}{Cr}}O_2CCF_3\right] \longrightarrow ROH\ (RO_2CCF_3)\,.$$

Ruthenium(IV) trifluoroacetate was used for the first time in the study of Lardais et al. [164] for the oxidative coupling reaction. The yield of the products of the oxidative dimerisation of phenylalkylisoquinolines in its presence was higher than in the case where $Tl(OCOCF_3)_3$ had been used.

7. Reactions of olefinic hydrocarbons with transition metal carboxylates

The oxidation, dehydrogenation, oxidative coupling, acetoxylation, and carboxylation reactions of saturated and aromatic hydrocarbons, which take place effectively when acted upon by metal complexes with electron-accepting ligands, were examined above. Reactions such as the oxidation of olefins, conversion into cyclopropane derivatives, and cyclodimerisation of strained hydrocarbons are also sensitive to the electron-accepting properties of the carboxylate ligand. Several examples are presented below.

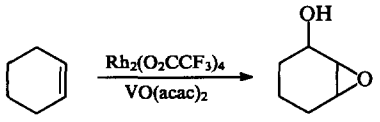
tert-Butyl peroxide complexes of palladium(II) ($RCO_2PdOO.Bu^t)_4$ have been synthesised. They are highly effective reagents for the selective stoichiometric oxidation of terminal olefins at the usual temperatures.[165] In the presence of an excess of *tert*-butyl peroxide, the oxidation reaction is catalytic.

$$Bu^tOOH + R'CH{=}CH_2 \xrightarrow{Pd(OCOR)_2} \longrightarrow Bu^tOH + R'{-}\overset{O}{\overset{\|}{C}}{-}CH_3$$

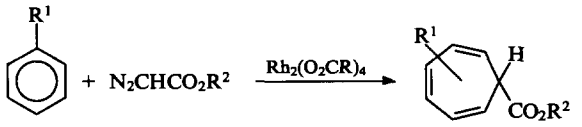
It was found that the rate of formation (indicated in brackets below) of, for example, 2-hexanone increases by two orders of magnitude on passing from the acetate to the trifluoroacetate in the following series of R: CF_3 (130), C_5H_{11} (80), CCl_3 (60), CH_3 (1).

The interaction of palladium complexes such as $Pd(OAc)_2$, $Pd(OPr)_2$, $Pd(O_2CCF_3)_2$, and $Pd(PPh_3)_4$ with H_2O_2 or K_2O_4 leads to the formation of superoxo-complexes of two types differing in the mode of coordination of the molecular oxygen radical-anion to the metal (η^1- or η^2-type of coordination) and hence in the reactivity with respect to olefins and carbon monoxide.[166]

Dirhodium(II) tetracarboxylate exhibits a catalytic activity in olefin oxidation reactions and in the conversion of the latter into cyclopropane derivatives.[167] The presence of the trifluoroacetate group ensures a high selectivity in the formation of epoxycyclohexanol in the oxidation of cyclohexene.



The addition of a carbenoid species to an aromatic compound is controlled by electronic factors. The effectiveness of the catalyst depends greatly on the electron-accepting capacity of the carboxylate ligand.[168]

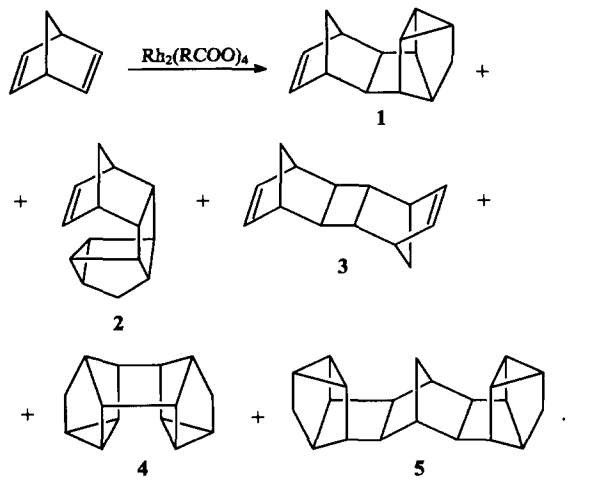


For example, the data for benzene are as follows:

Acid	pK_a	Yield (%)
CF_3COOH	0.23	100
C_6H_5COOH	1.48	89
CH_3OCH_2COOH	3.57	30
CH_3COOH	4.76	7
HCOOH	5.03	5

Dirhodium(II) tetracarboxylates $Rh_2(CO_2R)_4$ (R = CH_3, CCl_3, CF_3) have been investigated as catalysts for the cyclodimerisation of norbornadiene. It was found that in their presence the reaction proceeds with the preferential formation of *exo,endo*- and *endo,endo*-hexacyclo[9.2.1.$0^{2,10}$.$0^{3,7}$.$0^{4,9}$.$0^{6,8}$]-tetradec-12-enes (compounds **1** and **2**), but, depending on the reaction conditions, the pentacyclic dimers **3**, binor S **4**, and the norbornadiene trimer *endo,exo,endo*-decacyclo-[9.9.1.$0^{2,10}$.$0^{3,8}$.$0^{4,6}$.$0^{5,9}$.$0^{12,20}$.$0^{13,19}$.$0^{14,16}$.$0^{15,19}$]heneicosane **5** may be formed (Scheme 2).[30] The catalytic activity of the complexes increases with enhancement of the electron-accepting properties of the ligand in the sequence $Rh_2(O_2CCH_3)_4$ < $Rh_2(O_2CCCl_3)_4$ < $Rh_2(O_2CCF_3)_4$.

Scheme 2



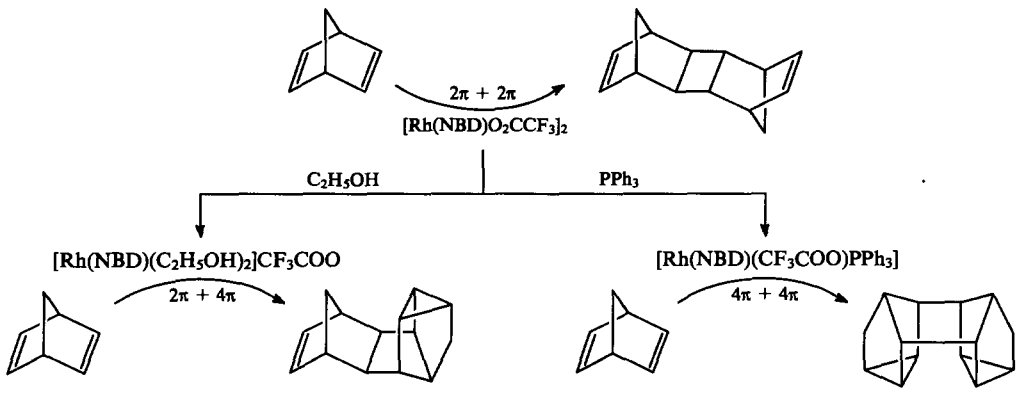
The cyclodimerisation reaction was investigated in detail in the presence of $Rh_2(O_2CCF_3)_4$. It was shown that di(μ-trifluoroacetato)bis(norbornadiene)dirhodium(I), formed on reduction of $Rh_2(O_2CCF_3)_4$ by norbornadiene, is catalytically active.[169] A similar reaction was not observed for other olefins and dienes. The interaction of $Rh_2(O_2CCF_3)_4$ with olefins and dienes[170,171] also leads, like the interaction with norbornene,[172] to the rapid and reversible formation of axial monoadducts, the structure of one of which has been investigated.[173]

The interaction of rhodium(II) with norbornadiene (NBD) has been investigated spectrophotometrically and it has been shown that the reduction of $Rh_2(O_2CCF_3)_4$ proceeds via the intermediate formation of rhodium complexes of norbornadiene of the type $Rh_2(O_2CCF_3)_4$.NBD differing in the coordination of norbornadiene.[169] For the ratio $Rh_2(O_2CCF_3)_4$: NBD = 1 : 1, an adduct is formed in which the Rh—Rh bond is retained, which was demonstrated by the formation of the familiar complex $Rh_2(O_2CCF_3)_4.2PPh_3$ via the reaction of the adduct with PPh_3. On treatment with an excess of norbornadiene or polar agents such as alcohol and acetone, rhodium(II) is reduced in the adduct to rhodium(I) with formation of $[Rh(O_2CCF_3)NBD]_2$. The observed rate constants for the reduction of $Rh_2(O_2CCF_3)_4$ and $Rh_2(O_2CCH_3)_4$ by norbornadiene, measured at 90 °C, amounted to 9.26×10^{-3} and 0.31×10^{-3} litre $mol^{-1}s^{-1}$ respectively, which agrees with the results of the electrochemical reduction of rhodium(II) carboxylates.[174] The selectivity in the formation of cyclic norbornadiene dimers in the presence of $[Rh(O_2CCF_3)NBD]_2$ is determined by the ligand environment of the rhodium atom (Scheme 3).[175]

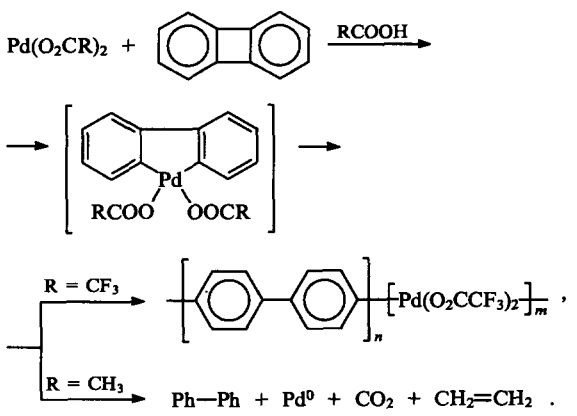
It may be that the rhodium(II) dimer disproportionates when acted upon by norbornadiene with formation of the intermediate $(NBD)Rh^I\cdots Rh^{III}$. The reduction of rhodium(III) by norbornadiene to a rhodium(I) complex, namely $[Rh(O_2CCF_3).NBD]$, confirms this pathway in the reaction of rhodium(II) on treatment with norbornadiene.[176] Rhodium(III) trifluoroacetate interacts in alcohol with $PRPh_2$ (R = Ph, *m*-$C_6H_4SO_3Na$) to form $Rh(O_2CCF_3)(PRPh_2)_3$ and $Rh(O_2CCF_3)(CO)(PPh_3)_2$.[43]

The study of the reactions of biphenylene, a tricyclic aromatic hydrocarbon, is of interest in view of the possibility of obtaining highly conducting polymers from it.[177] It has been found that the interaction of biphenylene in solutions in carboxylic acids with palladium(II) carboxylates takes place in accordance with Scheme 4.[178]

Scheme 3



Scheme 4



This reaction pathway differs significantly from the familiar reactions of biphenylene with mercury(II) carboxylates.[179,180]

* * *

The possibility of the selective functionalisation of alkanes and aromatic compounds with participation of electrophilic metal-containing centres in trifluoroacetic acid has been demonstrated in the present review in relation to dehydrogenation, carbonylation, carboxylation, and a number of other reactions. The problem of the activation of a C—H bond in alkanes still continues to engage the attention of investigators. For example, problems of the mechanism of the electrophilic activation of hydrocarbons in solutions in protic superacids have been discussed.[181] A new effective $CBr_4 \cdot n AlBr_3$ system has been proposed for the low-temperature reactions of alkanes and cycloalkanes.[182] Alkanes and cycloalkanes have been dehydrogenated with participation of low-valence rhodium complexes.[183,184] New evidence has been presented for the intermediate formation of alkylplatinum(IV) hydride in the activation of alkanes by platinum(II) complexes.[185]

References

1. N F Gol'dshleger, M B Tyabin, A E Shilov, A A Shteinman *Zh. Fiz. Khim.* **43** 2174 (1969)
2. A E Shilov *Activation of Saturated Hydrocarbons by Transition Metal Complexes* (Dordrecht: Reidel, 1984)
3. E S Rudakov *Reaktsii Alkanov s Okislitelyami, Metallokompleksami i Radikalami v Rastvorakh* (Reactions of Alkanes with Oxidants, Metal Complexes, and Radicals in Solution) (Kiev: Naukova Dumka, 1985)
4. A E Shilov, G B Shul'pin *Usp. Khim.* **56** 754 (1987) [*Russ. Chem. Rev.* **56** 442 (1987)]
5. A E Shilov, G B Shul'pin *Usp. Khim.* **59** 1468 (1990) [*Russ. Chem. Rev.* **59** 853(1990)]
6. R H Crabtree *Chem. Rev.* **85** 245 (1985)
7. R G Bergman *Science* **223** 902 (1984)
8. D Baudry, M Ephritikhine, H Felkin, R Holmes-Smith *J. Chem. Soc., Chem. Commun.* 788 (1983)
9. T Sakakura, T Sodeyama, M Tanaka *New J. Chem.* **13** 737 (1989)
10. W D Jones, F J Feher *Acc. Chem. Res.* **22** 91 (1989)
11. M E Thompson, S M Baxter, A R Bulls, B J Burger, M C Nolan, B D Santarsiero, W P Schaefer, J E Bercaw *J. Am. Chem. Soc.* **109** 203 (1987)
12. L A Kushch, V V Lavrushko, Yu S Misharin, A P Moravskii, A E Shilov *Nouv. J. Chim.* **7** 729 (1983)
13. E A Grigoryan *Usp. Khim.* **53** 347 (1984) [*Russ. Chem. Rev.* **53** 210 (1984)]
14. C K Ghosh, W A G Graham *J. Am. Chem. Soc.* **111** 375 (1989)
15. M Vol'pin, I Akhrem, A Orlinkov *New. J. Chem.* **13** 771 (1989)
16. T B Rubtsova, N V Kiryakov, G L Soloveichik, A E Shilov *Mendeleev Commun.* 89 (1993)
17. I P Beletskaya, D N Makhon'kov *Usp. Khim.* **50** 1007 (1981) [*Russ. Chem. Rev.* **50** 534 (1981)]
18. A Ya Usyatinskii, V I Bregadze *Usp. Khim.* **57** 1840 (1988) [*Russ. Chem. Rev.* **57** 1054 (1988)]
19. W J Mijs, C R H J DeLonge (Eds) *Organic Synthesis by Oxidation with Metal Compounds* (New York: Plenum, 1986)
20. L S Boguslavskaya, A V Kartashov, N N Chuvatkin *Usp. Khim.* **59** 865 (1990) [*Russ. Chem. Rev.* **59** 501 (1990)]
21. R O C Norman, W J E Parr, C B Thomas *J. Chem. Soc., Perkin Trans. 1* 369 (1974)
22. S Fukuzumi, J K Kochi *J. Org. Chem.* **46** 4116 (1981)
23. E A Shokova, V V Kovalev, Yu N Luzikov, P A Sharbatyan *Neftekhimiya* **21** 271 (1981)
24. U Frommer, V Ulrich *Z. Naturforsch. B, Chem. Sci.* **26** 322 (1974)
25. D I Makhon'kov, A V Cheprakov, M A Rodkin, I P Beletskaya *Zh. Org. Khim.* **24** 241 (1988)
26. A E Gekhman, N I Moiseeva, I I Moiseev, in *The XXVIIIth International Conference on Coordination Chemistry (Abstracts of Reports) 1990* Vol. 3, p. 20
27. I I Moiseev, A E Gekhman, D I Shishkin *New J. Chem.* **13** 683 (1989)
28. C D Garner, B Hughes *Adv. Inorg. Chem. Radiochem.* **17** 2 (1975)
29. H C Clark, A B Goel, S Goel *Inorg. Chem.* **18** 2803 (1979)
30. N F Gol'dshleger, B I Azbel', A A Grigor'ev, I P Sirotina, M L Khidekel' *Izv. Akad. Nauk SSSR, Ser. Khim.* 635 (1982)
31. J L Bear, J Kitchens, M R Willcott III *J. Inorg. Nucl. Chem.* **33** 3479 (1971)
32. T A Stephenson, S M Morehouse, A R Powell, J P Heffer, G Wilkinson *J. Chem. Soc.* 3632 (1965)
33. M A Porai-Koshits *Kristallokhimiya T. 15 (Itogi Nauki i Tekhniki)* [Crystal Chemistry, Vol. 15 (Advances in Science and Engineering)] (Moscow: Izd. VINITI, 1981)
34. G B Deacon, R J Phillips *Coord. Chem. Rev.* **33** 227 (1980)
35. A C Skapski, M L Smart *J. Chem. Soc., Chem. Commun.* 658 (1970)
36. F A Cotton, S Han *Rev. Chim. Miner.* **20** 496 (1983)
37. F A Cotton, S Han *Rev. Chim. Miner.* **22** 277 (1985)
38. M A A F de C T Carrondo, A C Skapski *Acta Crystallogr., Sect. B, Struct. Crystallogr.* **34** 1857 (1978)

39. A S Batsanov, G A Timko, Yu T Struchkov, N V Gerbeleu, K M Indrichan, G A Popovich *Koord. Khim.* **15** 858 (1989)
40. T E Kraft, C I Hejna, J S Smith *Inorg. Chem.* **29** 2682 (1990)
41. D J Wink *Acta Crystallogr., Sect. C, Cryst. Struct. Commun.* **46** 56 (1990)
42. A Dobson, S D Moore, D S Robinson, A M R Galas, M B Hursthouse *J. Chem. Soc., Dalton Trans.* 611 (1985)
43. V I Sokol, N F Gol'dshleger, M A Porai-Koshits *Koord. Khim.* **19** 47 (1993)
44. S P Bone, D B Sowerby, R D Verma *J. Chem. Soc., Dalton Trans.* 1544 (1978)
45. T Arliguie, B Chaudret, G Chung, F Dahan *Organometallics* **10** 2973 (1990)
46. M J Burk, R H Crabtree *J. Am. Chem. Soc.* **109** 8025 (1987)
47. D Commereuc, I Douek, G Wilkinson *J. Chem. Soc., A* 1771 (1970)
48. J Halpern *Inorg. Chim. Acta* **100** 41 (1985)
49. F A Cotton, T La Cour, A G Stanislowski *J. Am. Chem. Soc.* **96** 754 (1974)
50. P B Hitcock, M F Lappert, P L Rye, S Thomas *J. Chem. Soc., Dalton Trans.* 1929 (1979)
51. M Brookhart, M L H Green *J. Organomet. Chem.* **250** 395 (1983)
52. G L Soloveichik *Metalloorg. Khim.* **1** 277 (1988)
53. A G Ginzburg *Usp. Khim.* **57** 2046 (1988) [*Russ. Chem. Rev.* **57** 1175 (1988)]
54. N J Fitzpatrick, M A McGinn *J. Chem. Soc., Dalton Trans.* 1637 (1985)
55. G Olah *Acc. Chem. Res.* **20** 422 (1987)
56. A F Shestakov, A E Shilov *Khim. Fiz.* 1591 (1984)
57. S M Vinogradova, A F Shestakov *Khim. Fiz.* 371 (1984)
58. C C Cummins, S M Baxter, P M Wolczanski *J. Am. Chem. Soc.* **110** 8731 (1988)
59. M J Bruce *Angew. Chem., Int. Ed. Engl.* **16** 73 (1977)
60. R S Nyholm *Proc. Chem. Soc. London,* 273 (1961)
61. P M Henry *Palladium Catalyzed Oxidation of Hydrocarbons* (Boston: Reidel, 1980)
62. R F Heck *Palladium Reagents in Organic Synthesis* (New York: Academic Press, 1985)
63. A K Yatsimirsky, A D Ryabov, I V Berezin *J. Mol. Catal.* **5** 399 (1979)
64. V I Nefedov, Ya V Salyn, I I Moiseev, A P Sadovsky, A S Berenbljum, A G Knizhnik, S L Mund *Inorg. Chim. Acta* **35** L343 (1979)
65. G Kumar, J R Blackburn, R G Albridge, W E Madderman, M M Jones *Inorg. Chem.* **11** 296 (1972)
66. P Brant, L S Benner, A L Balch *Inorg. Chem.* **18** 3422 (1979)
67. M K Starchevskii, M N Vargaftik, I I Moiseev *Izv. Akad. Nauk SSSR, Ser. Khim.* 242 (1979)
68. E S Rudakov, V V Zamashchikov, N P Belyaeva, R I Rudakova *Zh. Fiz. Khim.* **47** 2732 (1973)
69. N F Gol'dshleger, M L Khidekel', A E Shilov, A A Shteinman *Kinet. Katal.* **15** 261 (1974)
70. N F Goldshleger, A P Moravsky, B I Azbel, in *The International Symposium Homog. Catal. (Abstracts of Reports) 1990* p. 163
71. E S Rudakov, R I Rudakova *Dokl. Akad. Nauk SSSR* **218** 1377 (1974)
72. B M Trost, P J Metzner *J. Am. Chem. Soc.* **102** 3572 (1980)
73. N F Goldshleger, A A Shteiman *React. Kinet. Catal. Lett.* **6** 43 (1977)
74. T Yamakawa, T Fujita, S Shinoda *J. Mol. Catal.* **52** L41 (1989)
75. T Yamakawa, T Fujita, S Shinoda *J. Mol. Catal.* **66** 321 (1991)
76. T Yamakawa, T Fujita, S Shinoda *Chem. Lett.* 905 (1992)
77. T Fujii, Y Saito *J. Chem. Soc., Chem. Commun.* 757 (1990)
78. E Gretz, T F Oliver, A Sen *J. Am. Chem. Soc.* **109** 8109 (1987)
79. A Sen, E Gretz, T F Oliver, Z Jiang *Nouv. J. Chem.* **13** 755 (1989)
80. M N Vargaftik, I P Stolyarov, I I Moiseev *J. Chem. Soc., Chem. Commun.* 1049 (1990)
81. N F Gol'dshleger, E I Kresova, A P Moravskii *Kinet. Katal.* **32** 1023 (1991)
82. E Gretz, A Sen *J. Am. Chem. Soc.* **108** 6038 (1986)
83. L C Kao, A C Hutson, A Sen *J. Am. Chem. Soc.* **113** 700 (1991)
84. A Sen *Plat. Met. Rev.* **35** 126 (1991)
85. D I Shishkin, A E Gekhman, I I Moiseev *Kinet. Katal.* **30** 1513 (1989)
86. J Muzart, F Hemin *C. R. Acad. Sci., Ser. 2* **307** 479 (1988)
87. M M Kats, G B Shul'pin *Izv. Akad. Nauk SSSR, Ser. Khim.* 2461 (1990)
88. N Kitajima, J Schwarz *J. Am. Chem. Soc.* **106** 2220 (1984)
89. P Dufour, C C Santini, C Houtman, J M Basset *J. Mol. Catal.* **66** L23 (1991)
90. V P Tret'yakov, A N Osetskii *Kinet. Katal.* **23** 1126 (1982)
91. V P Tret'yakov, L K Volkova, G P Zimtseva, E S Rudakov *Kinet. Katal.* **34** 183 (1993)
92. V P Tret'yakov, L K Volkova, E S Rudakov *Kinet. Katal.* **34** 90 (1993)
93. V P Tret'yakov, G P Zimtseva, E S Rudakov *Kinet. Katal.* **32** 1022 (1991)
94. R Van Helden, G Verberg *Recl. Trav. Chim. Pays-Bas* **84** 1263 (1965)
95. J M Davidson, C Triggs *J. Chem. Soc., A* 1324 (1968)
96. J M Davidson, C Triggs *J. Chem. Soc., A* 1331 (1968)
97. G G Azzoumanidis, F C Rauch *Chem. Tech.* 700 (1973)
98. Y Fuchita, K Hiraki, Y Kamogawa, M Suenaga, K Tohgoh, Y Fujiwara *Bull. Chem. Soc. Jpn.* **62** 1081 (1989)
99. F R S Clark, R O C Norman, C B Thomas, J S Wilson *J. Chem. Soc., Perkin Trans. 1,* 1289 (1974)
100. P M Henry *J. Org. Chem.* **36** 1886 (1971)
101. L Eberson, L Jöhnsson *Acta Chem. Scand., Ser. B* **30** 361 (1976)
102. H Iataaki, H Yoshimoto *J. Org. Chem.* **38** 76 (1973)
103. G U Mennenga, A I Rudenkov, K I Matveev, I V Kozhevnikov *React. Kinet. Catal. Lett.* **5** 401 (1976)
104. S K Ivanov, S K Tanielyan *Oxid. Commun.* **7** 69 (1984)
105. Yu V Geletii, E I Karasevich, A P Moravskii, A E Shilov, A A Shteinman *Kinet. Katal.* **22** 349 (1981)
106. L C Kao, A Sen *New J. Chem.* **15** 575 (1991)
107. I V Kozhevnikov, V I Kim, E P Talzi *Izv. Akad. Nauk SSSR, Ser. Khim.* 2167 (1985)
108. I V Kozhevnikov *Usp. Khim.* **52** 244 (1983) [*Russ. Chem. Rev.* **52** 138 (1983)]
109. J L Garnett, R J Hodges *J. Am. Chem. Soc.* **89** 4546 (1967)
110. I V Kozhevnikov *React. Kinet. Catal. Lett.* **17** 233 (1981)
111. A J Kresge, H C Brown *J. Org. Chem.* **32** 756 (1967)
112. N F Gol'dshleger, I I Moiseev, M L Khidekel', A A Shteinman *Dokl. Akad. Nauk SSSR* **206** 106 (1972)
113. V P Tret'yakov, E S Rudakov, A A Galenin, R I Rudakova *Dokl. Akad. Nauk SSSR* **225** 583 (1975)
114. L M Stock, K-Tuen Tse, L J Vorvick, S A Walstrum *J. Org. Chem.* **46** 1757 (1981)
115. Y Fujiwara, T Kawauchi, H Taniguchi *J. Chem. Soc., Chem. Commun.* 220 (1980)
116. Y Fujiwara, I Kawata, T Kawauchi, H Taniguchi *J. Chem. Soc., Chem. Commun.* 132 (1982)
117. Y Fujiwara, I Kawata, H Sugimoto, H Taniguchi *J. Organomet. Chem.* **266** 35 (1983)
118. Jpn. P. 63 115 847; *Chem. Abstr.* **109** 171 071 (1988)
119. H Sugimoto, I Kawata, H Taniguchi, Y Fujiwara *J. Organomet. Chem.* **266** C44 (1984)
120. T Jintoku, H Taniguchi, Y Fujiwara *Chem. Lett.* 1159 (1987)
121. M N Vargaftik, V P Zagorodnikov, I P Stolyarov, I I Moiseev, D I Kochubey, V A Likholobov, A L Chuvilin, K I Zamaraev *J. Mol. Catal.* **53** 315 (1989)
122. R Ugo, A Chiesa *J. Chem. Soc., Perkin Trans. 1* 2625 (1987)
123. A Chiesa, R Ugo *J. Organomet. Chem.* **279** 215 (1985)
124. R Ugo, A Chiesa, P Nardi *J. Mol. Catal.* **59** 23 (1990)
125. I O Kalinovskii, A A Leshcheva, M M Kuteinikov, A I Gel'bshtein *Zh. Obshch. Khim.* **60** 123 (1990)
126. N F Gol'dshleger, A P Moravskii, Yu M Shul'ga *Izv. Akad. Nauk SSSR, Ser. Khim.* 258 (1991)
127. F J Waller *Catal. Rev. Sci. Eng.* **28** 1 (1986)
128. Y Fujiwara, T Jintoku, Y Uchida *New J. Chem.* **13** 649 (1989)
129. Y Fujiwara, K Takaki, J Watanabe, Y Uchida, H Taniguchi *Chem. Lett.* 1687 (1989)
130. Ko-Ichi Satoh, J Watanabe, K Takaki, Y Fujiwara *Chem. Lett.* 1433 (1991)
131. K Nakata, J Watanabe, K Takaki, Y Fujiwara *Chem. Lett.* 1437 (1991)
132. M Lin, A Sen *J. Chem. Soc., Chem. Commun.* 892 (1992)
133. T Nishiguchi, N Nakata, T Takaki, Y Fujiwara *Chem. Lett.* 1141 (1992)

134. M Lin, A Sen *J. Am. Chem. Soc.* **114** 7307 (1992)
135. T Jintoku, H Taniguchi, Y Fujiwara *Chem. Lett.* 1865 (1987)
136. T Jintoku, K Nishimura, K Takaki, Y Fujiwara *Chem. Lett.* 1687 (1990)
137. M O Unger, R A Fonty *J. Org. Chem.* **34** 18 (1969)
138. E S Rudakov *Zh. Fiz. Khim.* **61** 289 (1987)
139. N F Gol'dshleger, V M Nekipelov, A T Nikitaev, K I Zamaraev, A E Shilov, A A Shteinman *Kinet. Katal.* **20** 538 (1979)
140. G B Shul'pin, V P Rozenberg, R P Shibaeva, A E Shilov *Kinet. Katal.* **20** 1570 (1979)
141. G B Shulpin, A E Shilov, A N Kitaigorodskii, J V Z Krevor *J. Organomet. Chem.* **201** 319 (1980)
142. R P Shibaeva, L P Rozenberg, R M Lobkovskaya, A E Shilov, G B Shulpin *J. Organomet. Chem.* **202** 271 (1981)
143. G B Shul'pin *Zh. Obshch. Khim.* **51** 2100 (1981)
144. G B Shul'pin, A N Kitaigorodskii *Zh. Fiz. Khim.* **55** 266 (1981)
145. G B Shulpin, G V Nizova, A T Nikitaev *J. Organomet. Chem.* **276** 115 (1984)
146. G B Nizova, G B Shul'pin *Izv. Akad. Nauk SSSR, Ser. Khim.* 935 (1987)
147. K Nyberg, L G Wistrand *Chem. Scr.* **6** 234 (1974)
148. J Hanotier, P Camerman, M Hanotier-Bridoux, P De Radzitzky *J. Chem. Soc., Perkin Trans. 2* 2247 (1972)
149. J Hanotier, M Hanotier-Bridoux *J. Chem. Soc., Perkin Trans. 2* 1035 (1973)
150. J Hanotier, M Hanotier-Bridoux, P De Radzitzky *J. Chem. Soc., Perkin Trans. 2* 381 (1973)
151. R Tang, J K Kochi *J. Inorg. Nucl. Chem.* **35** 3845 (1973)
152. S R Jones, J M Mellor *J. Chem. Soc., Perkin Trans. 2* 511 (1977)
153. I P Stolyarov, M N Vargaftik, I I Moiseev *Kinet. Katal.* **30** 1513 (1989)
154. I P Stolyarov, M N Vargaftik, D I Shishkin, I I Moiseev *J. Chem. Soc., Chem. Commun.* 938 (1991)
155. K Nyberg, L G Wistrand *Acta Chem. Scand., Ser. B* **29** 629 (1975)
156. J V Grivillo *Synth. Commun.* **6** 543 (1976)
157. R Stewart, U A Spitzer *Can. J. Chem.* **56** 1273 (1978)
158. E S Rudakov, N A Tishchenko, L K Volkova *Kinet. Katal.* **27** 1101 (1986)
159. D Lee *The Oxidation of Organic Compounds by Permanganate Ions and Hexavalent Chromium* (Open Court, 1980)
160. B V Belavin, E I Kresova, A P Moravskii, A E Shilov *Kinet. Katal.* **31** 764 (1990)
161. B V Belavin, E I Kresova, A P Moravskii, A M Uskov, A E Shilov, in *V Vsesoyuznaya Konferentsiya po Mekhanizmam Kataliticheskikh Reaktsii, 1990 Tez. Dokl.* (Abstracts of Reports at the Vth All-Union Conference on Mechanisms of Catalytic Reactions, 1990) p. 50
162. M S Ioffe, V S Sharivker *Oxid. Commun.* (1994) (in the press)
163. J W Siggs, L Ytuarte *Tetrahedron Lett.* **27** 437 (1986)
164. Y Lardais, D Rambault, J P Robin *Tetrahedron Lett.* **28** 543 (1987)
165. H Mimoun, R Charpentier, A Mitschler, J Fischer, R Weiss *J. Am. Chem. Soc.* **102** 1047 (1980)
166. E P Talsi, V P Babenko, A A Shubin, V D Chinakov, V M Nekipelov, K I Zamaraev *Inorg. Chem.* **26** 3871 (1987)
167. A F Noels, A J Hubert, P Teyssie *J. Organomet. Chem.* **166** 79 (1979)
168. A J Anciaux, A Demonceau, A J Hubert, A F Noels, N Petiniot, P Teyssie *J. Chem. Soc., Chem. Commun.* 765 (1980)
169. B I Azbel, N F Goldshleger, M L Khidekel, V I Sokol, M A Porai-Koshits *J. Mol. Catal.* **40** 57 (1987)
170. M P Doyle, M R Colsman, M S Chinn *Inorg. Chem.* **23** 3684 (1984)
171. V Shurig *Inorg. Chem.* **25** 945 (1986)
172. N F Gol'dshleger, B I Azbel', Ya I Isakov, E S Shpiro, Kh M Minachev *Dokl. Akad. Nauk SSSR* **314** 378 (1990)
173. F A Cotton, L R Falvello *J. Am. Chem. Soc.* **112** 8979 (1990)
174. K Das, K M Kadish, J L Bear *Inorg. Chem.* **17** 930 (1978)
175. N F Gol'dshleger, B I Azbel', M L Khidekel' *Izv. Akad. Nauk SSSR, Ser. Khim.* 1342 (1983)
176. N F Gol'dshleger, S Z Makova, Yu M Shul'ga *Izv. Akad. Nauk, Ser. Khim.* 1438 (1992)
177. J L Bredas, R H Baughman *J. Polym. Sci., Polym. Lett.* **21** 475 (1983)
178. N F Goldshleger *Oxid. Commun.* **13** 129 (1990)
179. W Baker, J W Barton, J F W McOnie *J. Chem. Soc.* 2666 (1957)
180. J L Courtneidge, A G Davis, D C McGuchan, S N Yazdi *J. Organomet. Chem.* **341** 63 (1988)
181. J Sommer, J Bukala *Acc. Chem. Res.* **26** 370 (1993)
182. I Akhrem, A Orlinkov, M Vol'pin *J. Chem. Soc., Chem. Commun.* 671 (1993)
183. T Fujii, Y Higashino, Y Saito *J. Chem. Soc., Dalton Trans.* 557 (1993)
184. K Shin, A S Goldman *Organometallics* **12** 3390 (1993)
185. V V Zhamashchikov, V G Popov, E S Rudakov, S A Mitchenko *Dokl. Akad. Nauk* **333** 34 (1993)

Russian Chemical Reviews 63 (2) 139 – 146 (1994)
©1994 Russian Academy of Sciences and Turpion Ltd

UDC 541.124 + 541.141.7 + 547.655.6

Photochemistry of 2-dialkylamino-1,4-naphthoquinones

R P Shishkina, V N Berezhnaya

Contents

I. Introduction	139
II. Photochemical reactions of 2-dialkyl (1, ω-alkylene) amino-1,4-naphthoquinones	139
III. *ortho*-Substituted 2-dialkyl (1, ω-alkylene) amino-1, 4-naphthoquinones	143
IV. Conclusion	146

Abstract. The review surveys the results of studies on the photolysis of 1,4-naphthoquinones with 2-dialkylamino- and heterocyclic amino-groups. New data on the structures of the primary photolysis products and the mechanisms of their subsequent dark reactions are presented in relation to the reaction conditions and structure. The bibliography includes 53 references.

I. Introduction

Derivatives of 1,4-naphthoquinone are highly reactive and have a wide variety of valuable properties. Among naphthoquinones, dyes, vitamins, antibiotics, and pesticides are known. The ease of their excitation by light has led to the use of naphthoquinone derivatives as sensitisers and photoreducing agents in photographic materials of various types. Quinones with an internal source of hydrogen are most favoured. 2-Dialkylamino-1,4-naphthoquinones occupy a special place among them. They have found applications as photosensitive components in nonsilver photographic materials,[1–5] in particular in materials with physical development[1,2] and also in photoresist compositions.[4] Furthermore, the photochemical reactions of 2-dialkyl (1, ω-alkylene) amino-1, 4-naphthoquinones make it possible to obtain relatively easily derivatives of heterocyclic compounds which are either difficult or impossible to obtain by other procedures.[6–8] Much attention has therefore been devoted in recent years to the development of methods for the synthesis and study of the properties of 2-dialkylaminonaphthoquinones with various physicochemical characteristics.[9–21]

The wide variety of photochemical reactions of quinones has been most fully presented in the reviews by El'tsov et al.[22] and Maruyama and Osuka,[23] which cover the studies up to 1984. The present review is devoted to the photolysis of only 2-dialkyl (1, ω-alkylene) amino-1, 4-naphthoquinones, a characteristic feature of which is the intramolecular photochemical reduction reaction involving the abstraction of a hydrogen atom from the 2-position in the side chain via a readily formed six-membered transition state.[24] This determines the structure of the radicals formed — the primary photolysis products — and also the nature of the products formed when they are stabilised in secondary processes. The stabilisation can become, in the first place both intramolecular and intermolecular, i.e. with participation of the solvent.[22] The secondary intramolecular photochemical reduction reactions of 2-dialkylamino-1,4-naphthoquinones are primarily considered in the present review. In speaking of the primary photolysis products, we have in mind the primary products formed as a result of the stabilisation of the radicals.

The knowledge of the structure of the primary products and of the mechanism of the photolysis of photosensitive quinones makes it possible to determine the influence of various factors both on the process itself and on the stability of the primary photolysis products, which makes it possible to control the photochemical behaviour of the photosensitive component and the subsequent reactions of its photoinduced form in solutions and in polymer films.

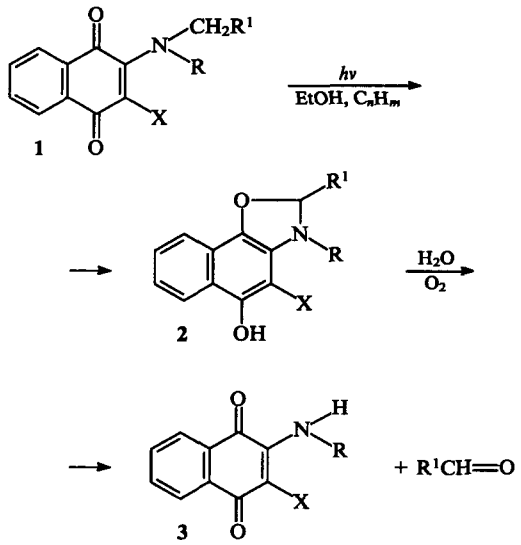
Recently published studies on the photolysis of 2-dialkyl-(1, ω-alkylene) amino-1, 4-naphthoquinones, using NMR spectroscopy as the main research method, made it possible not only to establish the structures of the primary photolysis products but also to distinguish the photochemical and thermal processes, which enables one to explain the formation of a wide variety of photolysis products. The data dealt with in the present review have been divided into two parts: studies concerning mainly the results of the photolysis of 2-dialkylamino-1, 4-naphthoquinones, without a substituent in the quinone ring or having a substituent not involved in the photolysis, and subsequent reactions are discussed in the first part; the second part deals with studies on the photolysis of 2-dialkylamino-1, 4-naphthoquinones with a substituent in the 3-position which participates in the formation of the photolysis product.

II. Photochemical reactions of 2-dialkyl (1, ω-alkylene) amino-1, 4-naphthoquinones

1, 4-Naphthoquinones **1**, having a dialkyl- or an alkylarylamino-group in the 2-position, enter into an intramolecular photochemical reduction reaction on exposure to light with formation of relatively unstable naphtho [2, 1-*d*]-2, 3-dihydrooxazoles **2**,[25] which afford on decomposition the products **3** of the dealkylation of the initial quinones.[25–28]

R P Shishkina, V N Berezhnaya Laboratory of Organic Photosensitive Materials, Novosibirsk Institute of Organic Chemistry, Siberian Division of the Russian Academy of Sciences, prosp. Akad. Lavrent'eva 9, 630090 Novosibirsk, Russian Federation
Tel. (7-383) 352 65 33, Fax (7-383) 235 47 52

Received 29 December 1993
Uspekhi Khimii 63 (2) 145 – 153 (1994); translated by A K Grzybowski

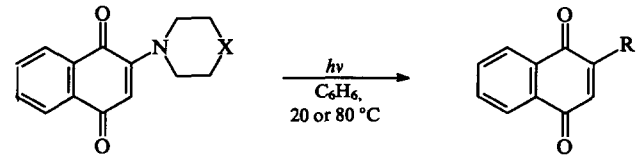


R = Me, Et, Ph; R^1 = H, Me; X = H, Cl.

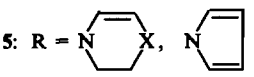
In contrast to 2-dialkylaminonaphthoquinones **1**, 1,4-naphthoquinones **4**, having a heterocyclic amino-group in the 2-position, give rise to dehydrogenation products **5**[29–31] and the products of the degradation of the heterocyclic ring **6**[30,31] on photolysis.

The study of the photolysis of 2-dialkylamino-1,4-naphthoquinones **1** (R = Me; R^1 = H, Me; X = H, Cl) and 2-morpholino-1,4-naphthoquinone **4** by measuring the optical spectra[32] showed that the primary photochemical stages of their photolysis are the same, so that also in the presence of a heterocyclic amino-group the primary photolysis products have the structure of naphthodihydrooxazole **7**, which was subsequently demonstrated by ^{1}H and ^{13}C NMR spectroscopy.[33,34]

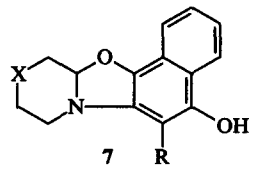
The conjunction of the amino-group with the π-system of the quinone is highly characteristic of 2-dialkylamino-1,4-naphthoquinones, which makes it possible to transfer the charge from the nitrogen atom to the oxygen atom directly during the



X = bond, CH_2, O.



6: R = $NH(CH_2)_3CHO$, $NH(CH_2)_4CHO$, $NH(CH_2)_2OCH_2CHO$, $NHCO(CH_2)_3CHO$, $NH(CH_2)_2OCHO$, $NH(CH_2)_2OH$, NH_2.

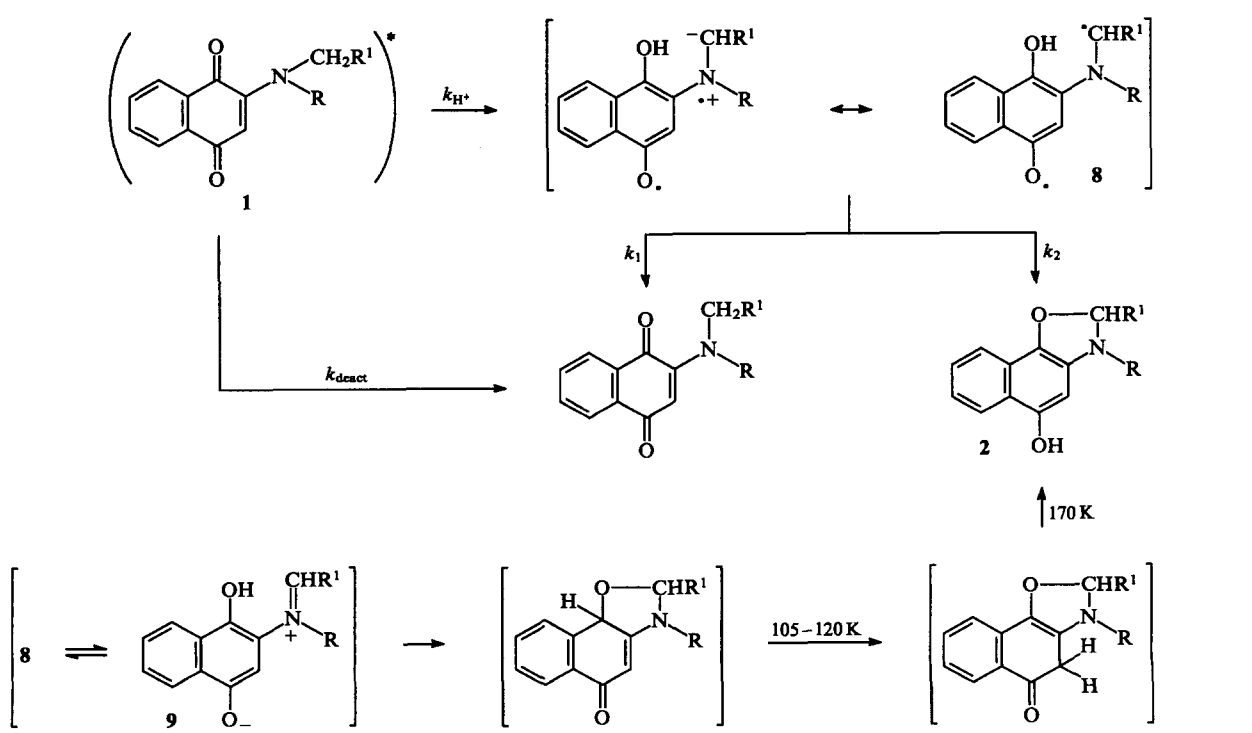


7: R = H, Me, OAlk; X = CH_2, O.

excitation process.[35] Quantum-chemical calculations of the electronic structures of 2-dialkylamino-1,4-naphthoquinones in the ground and excited triplet and singlet states showed that, on excitation of 2-aminonaphthoquinones, the electron density on the nitrogen atom falls appreciably[36,37] and increases on virtually all the atoms of the quinone ring, the increase being most significant not on the oxygen atom O(1) of the nearest carbonyl group but on the O(4) atom, which may be responsible for the subsequent migration of a hydrogen atom to the latter and this leads to cyclic structures of types **2** and **7**.[36]

The study of the influence of various factors on the quantum yields of the formation reaction of naphthodihydrooxazoles **2** is of interest both from the standpoint of the elucidation of the details of the mechanism and of the selection of the optimum

Scheme 1

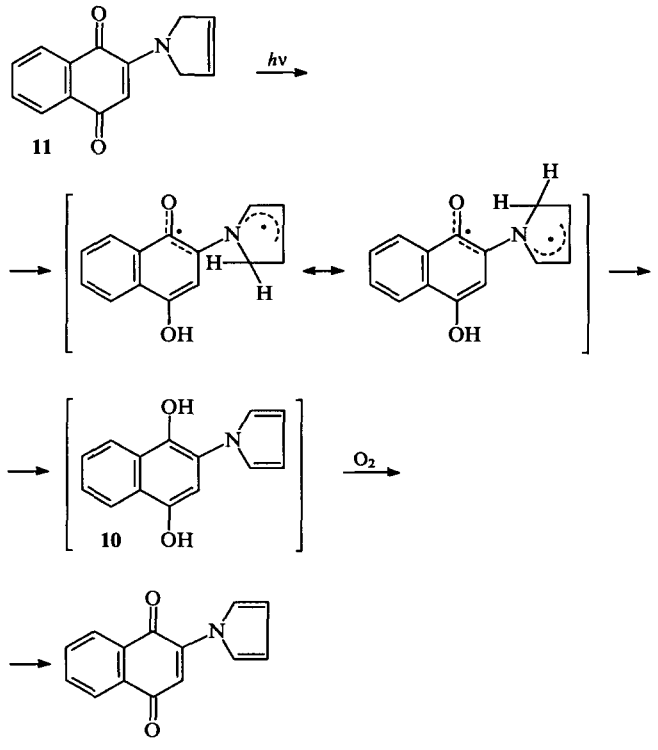


photolysis conditions. The nature of the solvent exerts a significant influence on the photolytic process. The photochemical reaction proceeds most effectively in nonpolar media such as hexane, benzene, and carbon tetrachloride; in alcohols, the effectiveness of the photolysis is appreciably lower owing to the formation of a hydrogen bond, which indicates the intramolecular abstraction of a hydrogen atom.[37] It has been established that this is a one-quantum and unimolecular process. A state of the $r_a\pi^*$ type is reactive, but the multiplet nature of the reactive state could not be established experimentally.[32,37] It has been shown that the nature of the photolysis product is independent of the irradiation wavelength (250–500 nm), the light intensity, and the concentration of the solutions ($0-2 \times 10^{-3}$ M). This permitted the assumption that the primary stage of the process is proton phototransfer and made it possible to put forward a hypothetical mechanism of the photolysis of 2-dialkylamino-1,4-naphthoquinones (Scheme 1).[32,35]

The multistage mechanism of the conversion of the photolysis products at 77 K into the product **2**, detected at room temperature, was put forward on the basis of low-temperature photolysis data. However, a biradical structure of type **8** could not be detected and its isomerisation to the zwitterion **9** was postulated.[35]

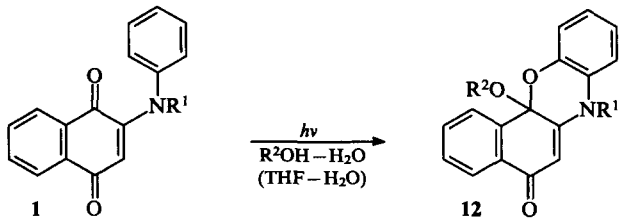
A somewhat different mechanism for the photolytic reaction—via the unstable 1,4-dihydroxy-2-(1-pyrrolyl)naphthalene **10**, which was detected as the diacetate—was proposed for the naphthoquinone **11** (Scheme 2).[30] The study of the photolysis of 2-(1-indolyl)-1,4-naphthoquinone in the presence of dienophiles may serve as its confirmation.[38]

Scheme 2

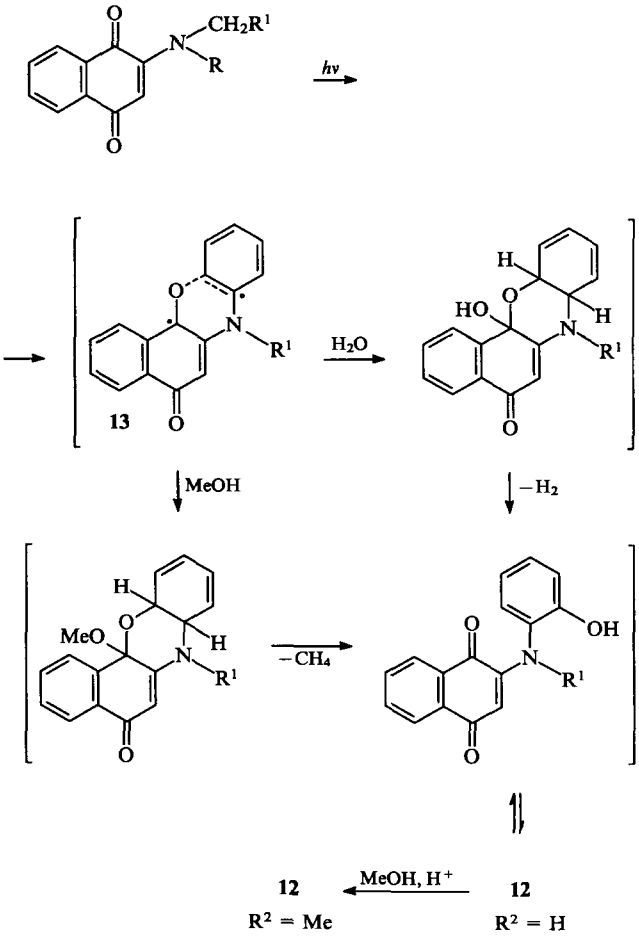


There are contradictory data as regards the products of the photolysis of 2-alkylphenylamino-1,4-naphthoquinones **1** (X = H, R = Ph). As already stated above, according to some data[25] irradiation results in the formation of naphthodihydrooxazoles **2**, whilst according to others[28] the products are benzophenoxazone derivatives **12**. It is noteworthy that the conditions of the photolysis in the above studies,[25,28] were different (water was present in the latter study[28]), which may partly alter the course of the reaction. It has been suggested[28] that the nonbonding orbital on the oxygen atom of the carbonyl group interacts in the excited state with the π electrons of the aromatic ring. There is then insufficient time for the occurrence of the intra- and intermolecular abstraction of a hydrogen atom by the biradical **13** formed and the latter is stabilised by combining with the solvent and cyclising (Scheme 3). Nevertheless, together with benzo[*c*]phenoxazone derivatives, dealkylation products (in some cases a product of this kind was the main one) were obtained with the preferential elimination of the alkyl residue compared with the aryl residue. This type of dealkylation is the result of the hydrolysis of the relatively unstable naphthodihydrooxazoles of type **2**.[25]

Scheme 3

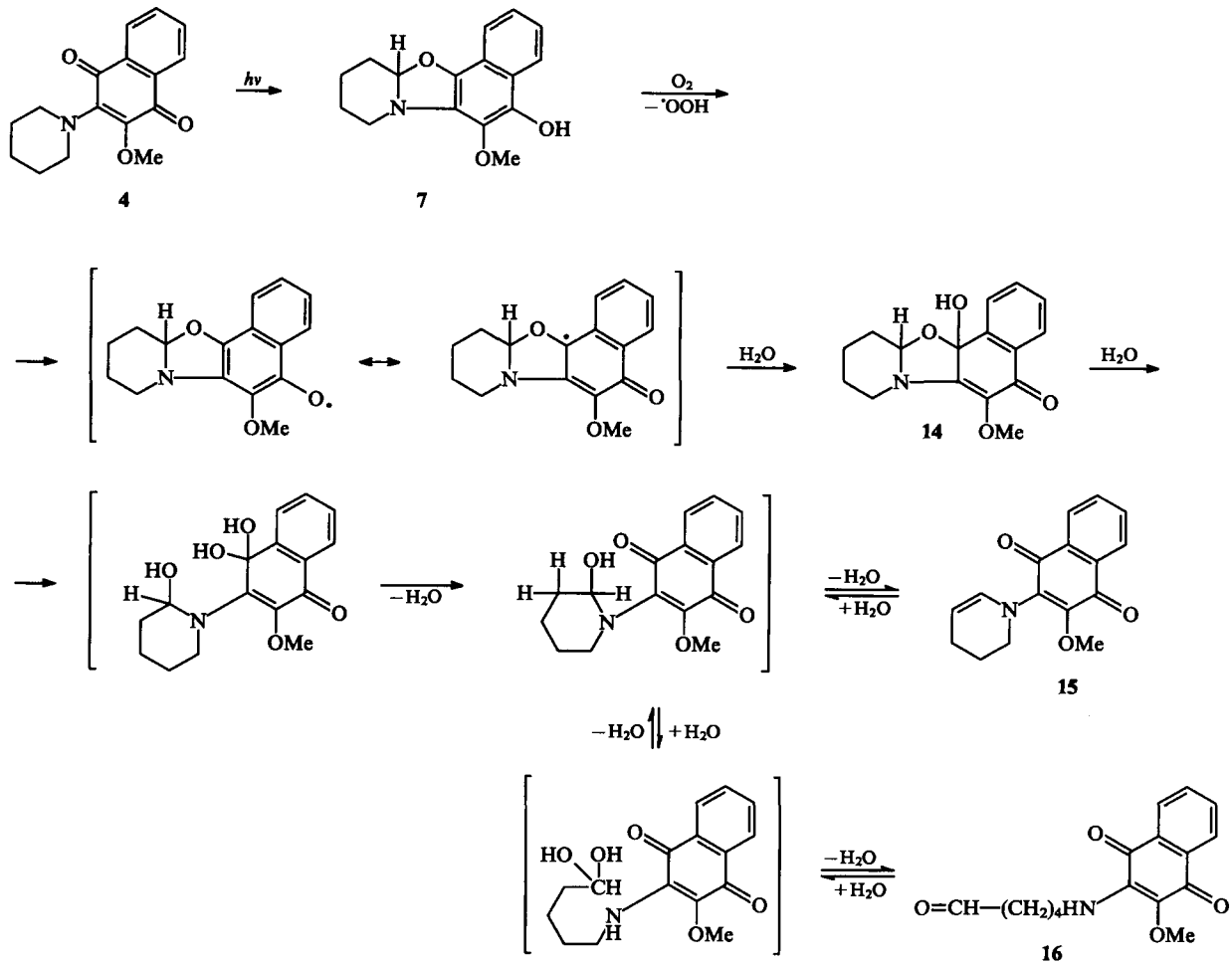


R^1 = H, Me, Et, CH_2CH_2OH.
R^2 = H, Me.



According to the results of Gritsan and Bazhin,[32] the primary stage in the dark reactions of the naphthodihydrooxazoles **2** and **7** is the hydrolysis of the C–O bond, while according to Maruyama et al.[30] oxygen exerts the primary effect. The study of the properties of compounds **7** (R = Me, OMe, OPr^i; X = CH_2) showed that they are stable

Scheme 4

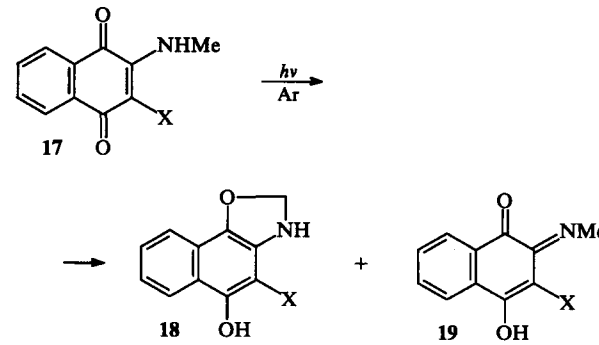


in the absence of oxygen for a long time at temperatures in the range from −70 to +23 °C.[33,39] The smallest traces of oxygen lead to the decomposition of the photolysis products; 6-methoxy-9,10,11,11*a*-tetrahydro-8*H*-naphtho[2′,1′:4,5]oxazolo-[3,2-*a*]pyridin-5-ol **7** gives rise to a mixture of compounds — the enaminoquinone **15**, the aminoaldehyde **16**, and compounds in which the oxazole ring is retained, namely 12*a*-hydroxy-6-methoxytetrahydroxazolopyridin-5-one **14**. The formation of compound **14** and the study of its properties enabled Shishkina et al.[33] to propose a mechanism of the dark reactions of the primary products of the photolysis of naphthodihydrooxazoles **7** including oxidation as the first stage (Scheme 4).

The methoxy-group as well as the more bulky isopropoxy-group[39] in the 3-position of 2-dialkylamino-1,4-naphthoquinones do not participate in photolysis on irradiation with light at $\lambda > 400$ nm,[33] although there are data showing that 2-alkoxy-1,4-naphthoquinones unsubstituted in the 3-position undergo photochemical reactions under more severe conditions.[40]

The methyl group is retained on irradiation of 2-dialkyl-(1,ω-alkylene)amino-3-methyl-1,4-naphthoquinones,[34] but its presence exerts a significant influence on the effectiveness of the photolysis: the quantum yields are 2–6 times higher than for 2-dialkylaminonaphthoquinones without a methyl group in the 3-position.[34,41,42] The greater effectiveness of the photochemical reaction of 2-dialkylamino-3-methyl-1,4-naphthoquinones made it possible to observe photochemical dealkylation also in the case of 2-monoalkylamino-1,4-naphthoquinones — a reaction which had not been known previously.

It has been found[45] that, on irradiation ($\lambda > 400$ nm) in organic solvents and under an inert atmosphere, compounds **17** are converted into naphthodihydrooxazoles **18** and 1,2-naphthoquinone 2-imines **19**. In the series of 1,4-benzoquinones, the stability of monoalkylamino-derivatives on irradiation has been explained by the presence of an intramolecular hydrogen bond between the NH and CO groups of the quinone.[43,44]



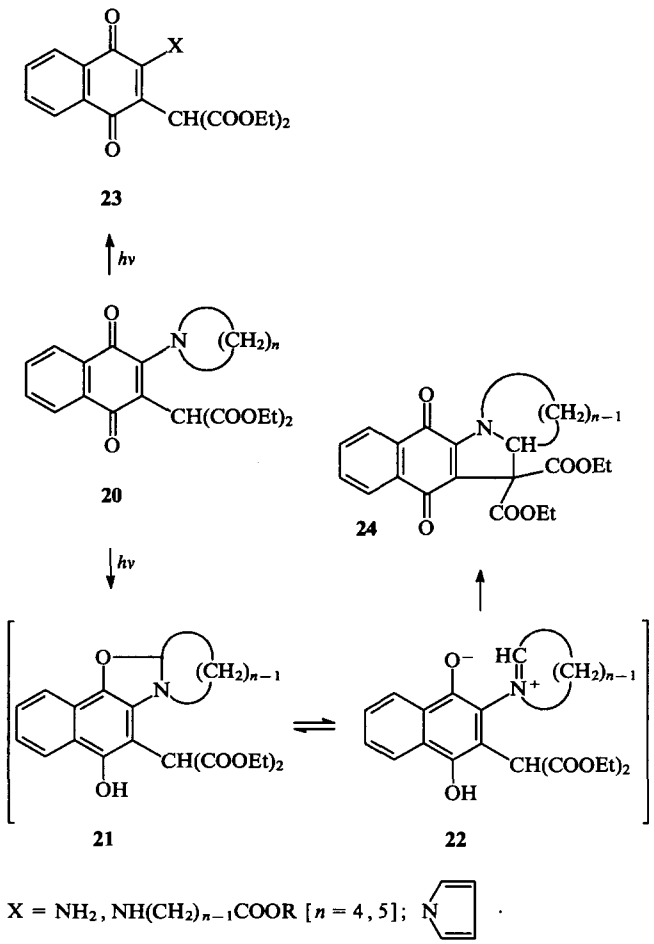
X = Me, OMe.

Since the methyl group gives rise to approximately the same bathochromic shift as the chlorine atom and the methoxy-group in the electronic absorption spectra of the corresponding 2-dialkylamino-1,4-naphthoquinones,[34] its activating effect is apparently not determined solely by the electronic effect of the substituent. It may be that the enhanced effectiveness of the photolysis of 2-dialkylamino-3-methyl-1,4-naphthoquinones is associated with their ability to form the quinone methide structure similar to that described by Serdobov.[46] However, one cannot rule out the additional involvement of the methyl group in the stabilisation of biradicals of type **8** as a result of the delocalisation of one of the unpaired electrons.[42]

III. *ortho*-Substituted 2-dialkyl(1,ω-alkylene)-amino-1,4-naphthoquinones

The results of the photochemical reactions of 2-dialkyl-(1,ω-alkylene)amino-1,4-naphthoquinones without substituents in the *ortho*-position or with substituents such as a halogen, an alkoxy-group, or a methyl group, which do not affect the nature of the photolysis products, were discussed in the previous section. At the same time, there have been studies indicating the possible involvement of the *ortho*-substituent in the overall photolytic process.

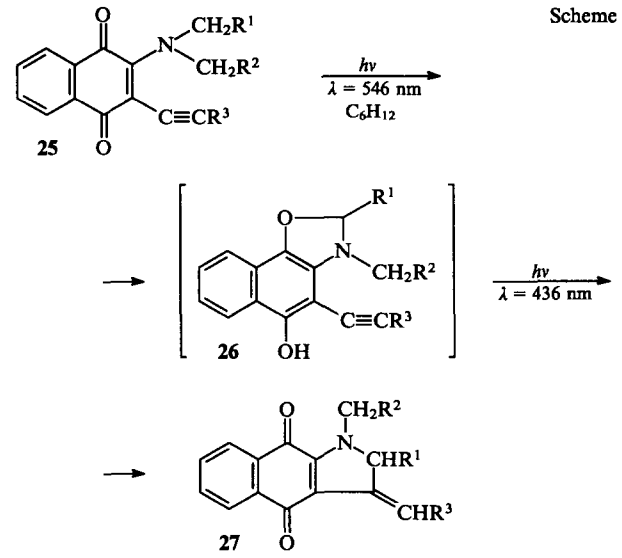
Thus irradiation of 2-piperidino- and 2-pyrrolidino-1,4-naphthoquinones **20**, having an active methylene group in the 3-position, leads both to the products **23** of the dehydrogenation and degradation of the heterocyclic ring (a situation similar to that indicated by the results of Fokin and Detsina[29] and Maruyama et al.[30]) and to the indoloquinones **24**, the yield of the latter increasing in polar solvents.[7] It has been suggested that the intermediate oxazole **21** is converted into the indoloquinone **24** via the zwitterionic intermediate **22** in a polar medium.



There exists an example of the photochemical activity of the naphthodihydrooxazoles **26** formed on photolysis of 2-dialkylamino-3-alkynyl-1,4-naphthoquinones **25**, but the mechanism of the formation of the indole derivatives **27** has not been discussed.[47] This fact merits special attention, since it had been shown earlier[38] that naphthodihydrooxazoles without a substituent in the 3-position are stable on irradiation with light at $\lambda > 300$ nm (Scheme 5).

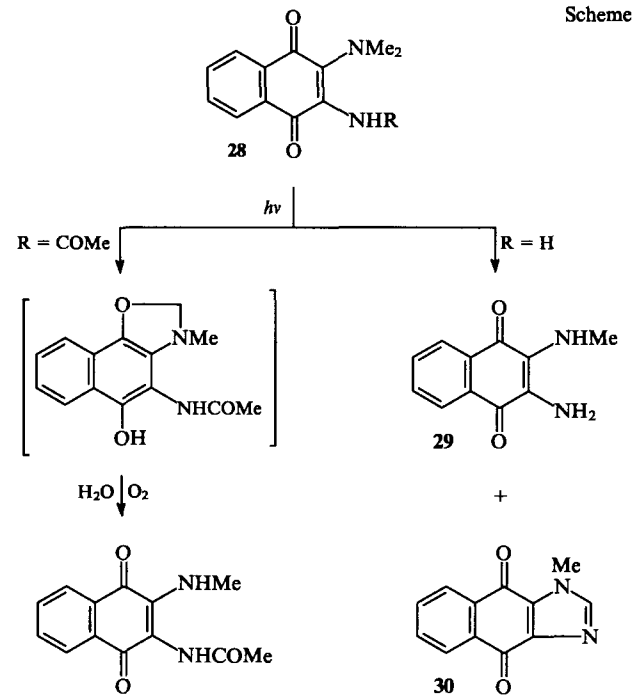
The products of the photolysis of 3-amino-2-dialkylamino-1,4-naphthoquinones are distinguished by the greatest variety. Thus irradiation of 3-amino-2-dimethylamino-1,4-naphthoquinone **28** (R = H) afforded, together with the dealkylation

Scheme 5



R¹ = H, Me; R² = Me, Et; R³ = H, Ph, CH_2OPh, CH_2OCOMe.

Scheme 6

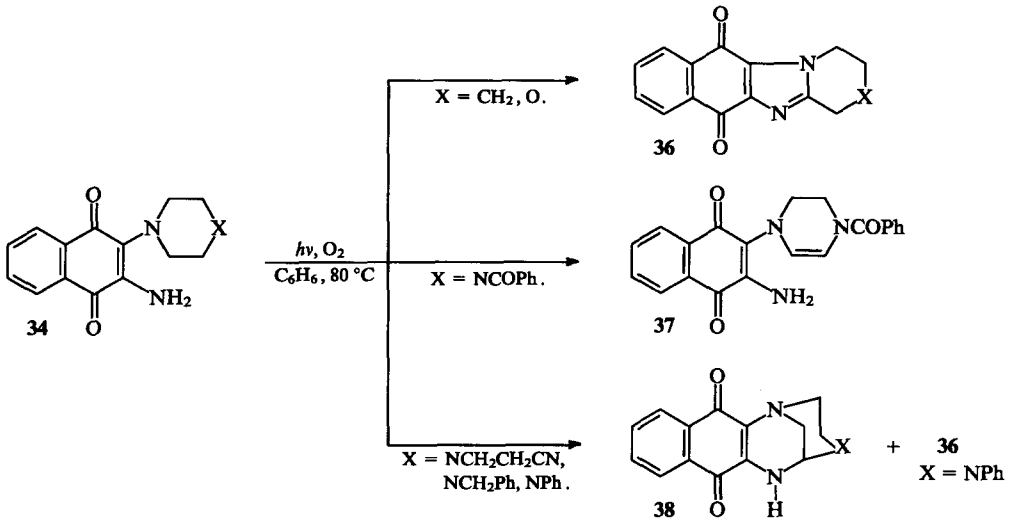


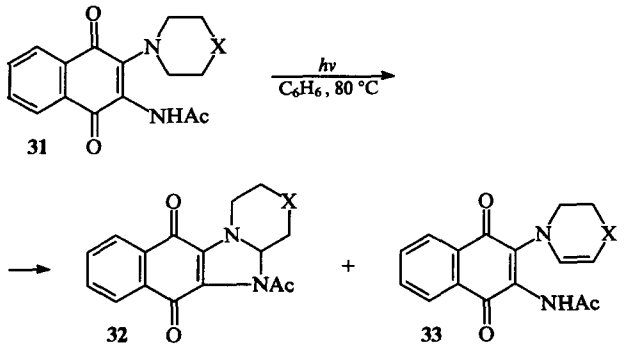
product **29**, 1-methylnaphtho[2,3-*d*]imidazole-4,9-dione **30**, whereas only the dealkylation product is formed on photolysis of the 3-acetamido-derivatives **28** (R = COMe) (Scheme 6).[48]

When the 2-dialkylamino-group is replaced by a heterocyclic group, 3-acetamidonaphthoquinones **31** form on irradiation the dihydroimidazole derivatives **32** as well as the ring dehydrogenation products **33**.[49]

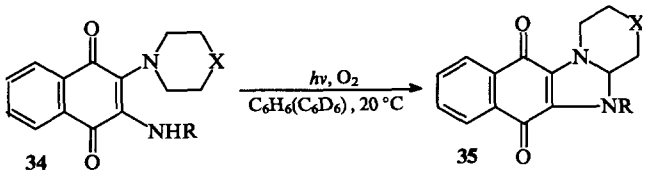
For the 3-aminonaphthoquinones with a cyclic alkylamino-group in the 2-position, the nature of the photolysis product is determined not only by the structure of the initial quinone but also by the reaction temperature. Thus the products of the photolysis of 2-cycloalkylamino-1,4-naphthoquinones with both primary[48,49] and secondary (alkyl,[39,50] and aryl[50,51]) amino-groups in the 3-position in the quinone at 20 °C are exclusively the unstable naphthodihydroimidazolediones **35**. Compounds **35** (R = Et) can be detected only spectroscopically,[39,51] since they are dealkylated with formation of naphthoimidazolediones **36** and, according to the data of Rubashko et al.,[50] the process takes place only under the influence of light. Depending on the

Scheme 7

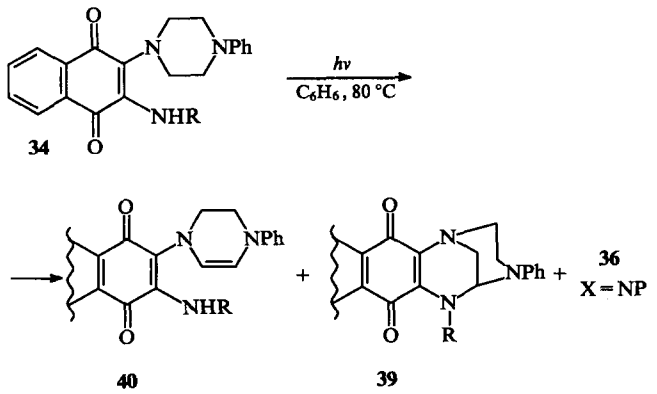




X = CH_2, O, NCOPh.



R = H, Et, C_6H_4Me-*p*, C_6H_4COMe-*p*;
X = CH_2, O, NCH_2CH_2CN, NPh, NCOPh.



R = Et, C_6H_4Me-*p*.

nature of the cyclic alkylamino-group, naphthoimidazole derivatives **36**,[49] enaminoquinones **33**,[49,51] as well as 1,2,3,4-tetrahydro-13-alkylphenyl)-3,1-(iminoethano)benzo[*g*]quinoxaline-5,10-diones **38** [51–53] are formed at 80 °C (Scheme 7).

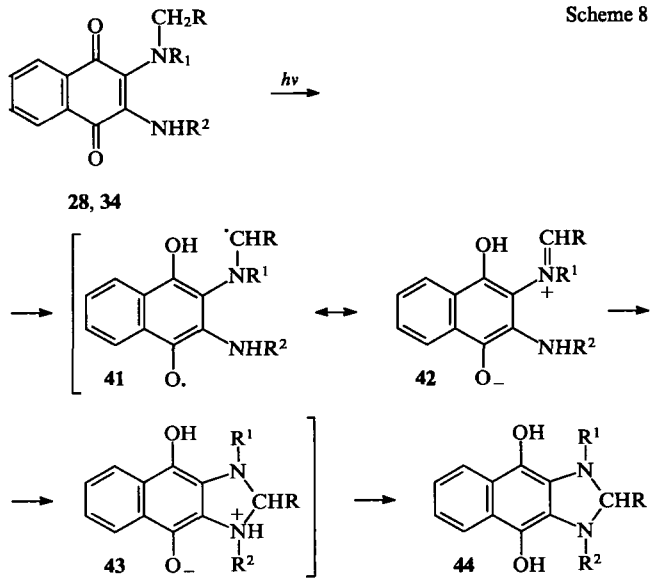
Tetrahydrobenzo[*g*]quinoxalinediones of type **38** are also the main products of the photolysis of 2-(4-alkylpiperazino)-1,4-naphthoquinones with a secondary amino-group in the 3-position; compound **34** (R^1 = C_6H_4Me-*p*), having a phenyl group in the 4-position in the piperazine ring, gives rise to the enaminoquinone **40** and the corresponding naphthoimidazoledione **36** (X = NPh) in addition to benzoquinoxalinedione **39**.[51–53]

The wide variety of the data obtained is due to the increased sensitivity of the primary photolysis product to atmospheric oxygen and heating. It has been established by NMR spectroscopy that this product has the structure of naphthodihydroimidazolediol **44**. In contrast to a polar medium where the spectrum is recorded directly, in a nonpolar medium the spectrum of the photolysis product cannot be recorded; it has been suggested that the photolysis stops at the stage involving the formation of the zwitterion **43**. This enabled the authors[39] to conclude that the *ortho*-amino-group participates in the reactions of the biradicals **41** arising in the intramolecular photochemical reduction process (Scheme 8).

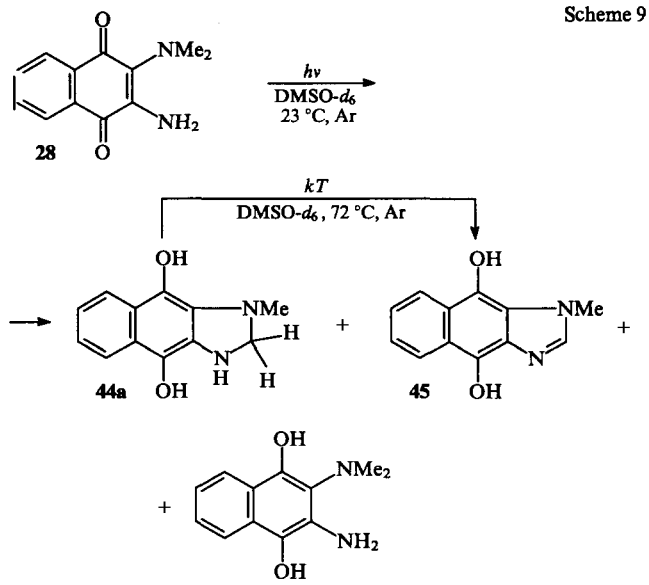
The naphthodihydroimidazolediols **44** are relatively unstable. In order to elucidate the pathway leading to the formation of a wide variety of final photolysis products from them (of the type of compounds **30** and **35**–**38**), a study was made of the influence of various factors (temperature, atmospheric oxygen, and the structure of the compounds) on their further reactions.[39,51,52] It was shown that naphthodihydroimidazolediols **44a**, which are unsubstituted in the 2-position, are oxidised under an inert atmosphere at a temperature in excess of 20 °C to the corresponding naphthoimidazolediols **45**, with the initial quinone or the solvent serving as the hydrogen acceptor.[39] In contrast to dihydroimidazolediol **44a**, which has no substituent in the 2-position in the imidazoline ring (Scheme 9), solutions of the products of the photolysis of 3-amino-2-piperidino-1,4-naphthoquinones **44** [R, R^1 = $(CH_2)_4$, R^2 = H, Et, *p*-MeC_6H_4] are stable at ~20 °C under an inert atmosphere. On exposure to atmospheric oxygen, they give rise to the products of the oxidation of the imidazoline and naphthalene rings of type **35** and **36**.[39,51]

A significant influence of the structure of naphthodihydroimidazolediols on their subsequent thermal reactions has been observed for compounds **44b**, c in which the imidazoline ring has a [2-*a*]-junction with a piperidine or 4-substituted piperazine ring. It was found that heating of compound **44b** — the product

Scheme 8

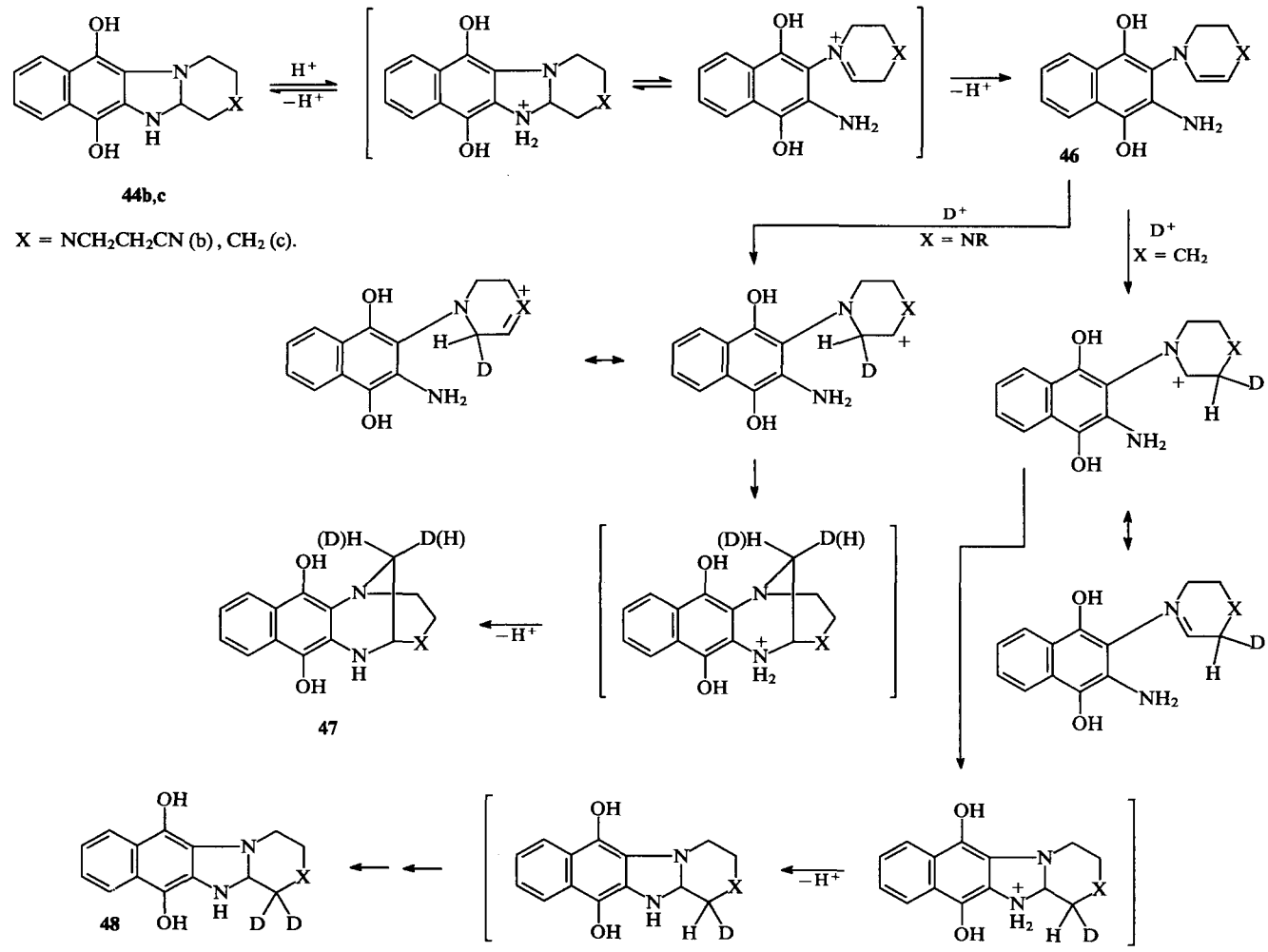


Scheme 9



of the photolysis of 2-[4-(2-cyanoethyl)piperazino]-1,4-naphthoquinone — leads to recylisation with formation of 1,2,3,4-tetrahydro-13-(2-cyanoethyl)-3,1-(iminoethano)benzo[*g*]quinoxaline-5,10-diol **47**, which is oxidised to the corresponding dione **38**. In the case of the [1,2-*a*]-junction between the imidazoline ring of naphthodihydroimidazolediol and a piperidine (compound **44c**) or piperazine ring having an electron-accepting substituent in the 4-position (compound **44b**), the thermolysis product has the structure of naphthodihydroimidazolediol **48**, i.e. the rearrangement is degenerate in character. On the basis of deuterium exchange data, a mechanism was proposed for the recyclisation of naphthodihydroimidazolediols, including the intermediate formation of the reduced form **46** of the enaminoquinone (Scheme 10).[51,52]

Scheme 10



Thus it has been shown[39,51,52] that, in the photolysis of 3-amino-2-dialkylamino-1,4-naphthoquinones, the *ortho*-substituent participates in the formation of the structure of the primary stable photolysis product—naphthodihydroimidazolediol, the subsequent reactions of which are determined by its structure and the photolysis conditions.

IV. Conclusion

It follows from the few available data on the mechanism of the photolysis of 2-dialkyl(1,ω-alkylene)amino-1,4-naphthoquinones that, regardless of the presence of other substituents in the naphthoquinone, the primary stage of the process is the phototransfer of a proton from the carbon atom in the α-position in the dialkylamino-group to the oxygen atom of the carbonyl group. The postulate that biradical structures of type **8** are formed and isomerise to the zwitterions **9**,[37] the subsequent cyclisation of which proceeds, depending on the structure, either with participation of the oxygen atom (formation of naphthodihydrooxazoles)[25, 33,34] or with participation of the *ortho*-substituent,[7,39,47–52] is entirely logical. The structure of the final photolysis product depends both on the irradiation conditions (temperature, the presence of atmospheric oxygen and water) and on the structure of the initial quinone.

NMR spectroscopy proved to be useful for the establishment of the mechanism of the photolysis of various 2-dialkylamino-1,4-naphthoquinones. It makes it possible to determine reliably the structure of the primary photolysis products and the structure of the compounds formed as a result of further dark reactions.

The questions concerning the structure of the primary photolysis products when 2-dialkyl(cycloalkyl)amino-1,4-naphthoquinones contain in the 3-position substituents other than a hydrogen or halogen atom and alkyl, alkoxy- and amino-groups and their influence on the subsequent reactions remain obscure. The problem of the behaviour of the primary photolysis products on further irradiation requires resolution.

References

1. US P. 4 171 221; *Ref. Zh. Khim.*, 6R 306P (1980)
2. USSR P. 679 925; *Byull. Izobret.* **30** 171 (1979)
3. Russian P. 1 584 606 (1993)
4. US P. 4 684 599; *Chem. Abstr.* **108** 85 322c (1988)
5. Jpn. P. 80 153 935; *Chem. Abstr.* **94** 217 627k (1981)
6. USSR P. 362 834; *Byull. Izobret.* **3** 50 (1973)
7. M Akiba, Y Kosugi, M Okuyama, T Takada *Heterocycles* **6** 1113 (1977)
8. M Akiba, S Ikuta, T Takada *Heterocycles* **9** 813 (1978)
9. USSR P. 480 705; *Byull. Izobret.* **30** 72 (1975)
10. R P Shishkina, L V Ektova, K I Matoshina, E P Fokin *Izv. Sib. Otd. Akad. Nauk SSSR, Ser. Khim. Nauk* **5** 136 (1982)
11. USSR P. 1 181 267; *Byull. Izobret.* **38** 284 (1987)
12. R P Shishkina, V N Berezhnaya, A M Detsina, E P Fokin *Interaction of 2,3-epoxy-2,3-dihydro-2-methyl-1,4-naphthoquinone with Secondary Aliphatic Amines* (Novosibirsk, 1989) Article deposited at the All-Union Institute of Scientific and Technical Information (VINITI), No 4277 (1989) (in Russian)
13. R P Shishkina, V I Mamatyuk, L V Ektova, E P Fokin *Izv. Akad. Nauk SSSR, Ser. Khim.* 2524 (1985)
14. R P Shishkina, V N Berezhnaya, E P Fokin *Izv. Akad. Nauk SSSR, Ser. Khim.* 2332 (1985)
15. V N Berezhnaya, R P Shishkina, E P Fokin *Izv. Akad. Nauk SSSR, Ser. Khim.* 2822 (1988)
16. V N Berezhnaya, R P Shishkina *Izv. Akad. Nauk SSSR, Ser. Khim.* 2103 (1990)
17. V N Berezhnaya, R P Shishkina, E P Fokin *Izv. Sib. Otd. Akad. Nauk SSSR, Ser. Khim. Nauk* **2** 101 (1987)
18. R P Shishkina, I K Korobeinicheva, L V Ektova *Sib. Khim. Zh.* **4** 102 (1991)
19. S V Rubashko, T V Mikhalina, E P Fokin *Izv. Sib. Otd. Akad. Nauk SSSR, Ser. Khim. Nauk* **3** 46 (1990)
20. S V Rubashko, T V Mikhalina, E P Fokin *Izv. Sib. Otd. Akad. Nauk SSSR, Ser. Khim. Nauk* **6** 121 (1990)
21. T V Mikhalina, V N Krasheninina, E P Fokin, S V Rubashko *Izv. Sib. Otd. Akad. Nauk SSSR, Ser. Khim. Nauk* **6** 115 (1990)
22. A V El'tsov, O P Studzinskii, V M Grebenkina *Usp. Khim.* **46** 185 (1977) [*Russ. Chem. Rev.* **46** 93 (1977)]
23. K Maruyama, A Osuka *The Chemistry of the Quinonoid Compounds, Vol. 2, Pt 1* (Eds S Patai, Z Rappoport) (Chichester: Wiley, 1988) Ch.13
24. J M Bruce *The Chemistry of the Quinonoid Compounds: Photochemistry of Quinones. Pt. 1* (Ed. S Patai) (London: Wiley, 1974) Ch. 9
25. E P Fokin, E P Prudchenko *Izv. Sib. Otd. Akad. Nauk SSSR, Ser. Khim. Nauk* **3** 98 (1966)
26. I Ya Postovskii, I F Vladimirtsev *Dokl. Akad. Nauk SSSR* **84** 73 (1952)
27. I Ya Postovskii, I F Vladimirtsev, L F Trefilova *Zh. Obshch. Khim.* **24** 181 (1954)
28. M Agata, H Kano *Tetrahedron* **24** 3725 (1968)
29. E P Fokin, A M Detsina *Izv. Sib. Otd. Akad. Nauk SSSR, Ser. Khim. Nauk* **3** 95 (1969)
30. K Maruyama, T Kozuka, T Otsuki *Bull. Chem. Soc. Jpn.* **50** 2170 (1977)
31. M Akiba, M Okuyama, Y Kosugi, T Takada *Heterocycles* **6** 1773 (1977)
32. N P Gritsan, N M Bazhin *Izv. Sib. Otd. Akad. Nauk SSSR, Ser. Khim. Nauk* **4** 118 (1981)
33. R P Shishkina, V N Berezhnaya, V I Mamatyuk *Izv. Akad. Nauk SSSR, Ser. Khim.* 709 (1991)
34. A D Bukhtoyarova, V N Berezhnaya, R P Shishkina, V P Vetchinov, V I Eroshkin, T A Stavitskaya *Izv. Akad. Nauk SSSR, Ser. Khim.* 2387 (1991)
35. N P Gritsan, N M Bazhin *Izv. Akad. Nauk SSSR, Ser. Khim.* 280 (1981)
36. T A Stavitskaya, A D Bukhtoyarova, R P Shishkina, V N Berezhnaya, L N Shchegoleva, V I Eroshkin *Khim. Vys. Energ.* **25** 265 (1991)
37. N P Gritsan, N M Bazhin *Izv. Akad. Nauk SSSR, Ser. Khim.* 1275 (1980)
38. K Maruyama, T Kozuka, T Otsuki, Y Naruta *Chem. Lett.* 1125 (1977)
39. V N Berezhnaya, V P Vetchinov, R P Shishkina, V I Mamatyuk *Izv. Akad. Nauk, Ser. Khim.* 358 (1993)
40. J V Ellis, J E Jones *J. Org. Chem.* **40** 485 (1975)
41. V N Berezhnaya, R P Shishkina, N V Pavlova, A S Trofimov, V I Eroshkin *Izv. Akad. Nauk SSSR, Ser. Khim.* 657 (1990)
42. V V Russkikh *Izv. Akad. Nauk, Ser. Khim.* 707 (1992)
43. R G F Giles *Tetrahedron Lett.* **23** 2253 (1972)
44. A M Yuodvirshes, E P Fokin *Izv. Sib. Otd. Akad. Nauk SSSR, Ser. Khim. Nauk* **2** 124 (1970)
45. V N Berezhnaya, V P Vetchinov, V I Mamatyuk, R P Shishkina, in *Tez. Dokl. Vsesoyuznoi Konferentsii po Khimii Khinonov i Khinoidnykh Soedinenii, Krasnoyarsk, 1991* (Abstracts of Reports at the All-Union Conference on the Chemistry of Quinones and Quinonoid Compounds, Krasnoyarsk, 1991) p. 220
46. M V Serdobov *Izv. Akad. Nauk SSSR, Ser. Khim.* 2004 (1982)
47. N P Gritsan, V M Shvartsberg, V S Romanov, M S Shvartsberg *Izv. Akad. Nauk SSSR, Ser. Khim.* 469 (1984)
48. E P Fokin, A M Detsina *Izv. Sib. Otd. Akad. Nauk SSSR, Ser. Khim. Nauk* **3** 106 (1972)
49. V N Berezhnaya, R P Shishkina, E P Fokin *Izv. Akad. Nauk SSSR, Ser. Khim.* 694 (1989)
50. S V Rubashko, T V Mikhalina, E P Fokin *Sib. Khim. Zh.* **3** 67 (1992)
51. V N Berezhnaya, Candidate's Thesis in Chemical Sciences, Novosibirsk Institute of Organic Chemistry of RAS, Novosibirsk, 1993
52. V N Berezhnaya, V P Vetchinov, V I Mamatyuk, R P Shishkina *Izv. Akad. Nauk, Ser. Khim.* 944 (1993)
53. V N Berezhnaya, R P Shishkina, in *Tez. Dokl. VI Vsesoyuznogo Soveshchaniya po Fotokhimii, Novosibirsk, 1989* (Abstracts of Reports at the VIth All-Union Conference on Photochemistry, Novosibirsk, 1989) p. 146

Russian Chemical Reviews **63** (2) 147 – 168 (1994)
©1994 Russian Academy of Sciences and Turpion Ltd

UDC 547.425.5

Sulfides in organic synthesis. Applications of sulfides

I V Koval'

Contents

I.	Introduction	147
II.	Cleavage of the C–S bond	147
III.	Generation of α-sulfenylcarbanions	153
IV.	Generation of α-sulfenylcarbonium ions	156
V.	Reactions involving the rearrangement of sulfides	156
VI.	Syntheses based on the primary products of the reactions of sulfides	158
VII.	Practical applications of sulfides	164

Abstract. The results of studies on the use of sulfides as synthons in organic synthesis are treated systematically and surveyed. The practical applications of sulfides are examined. The bibliography includes 187 references.

I. Introduction

The application of sulfides as synthons in fine organic synthesis is based on the characteristics of their reactivity manifested in the polarisation and low strength of the C–S bond, as a result of which it is relatively easily cleaved by both nucleophiles and electrophiles. The high lability of this bond makes it possible to eliminate, when required, the sulfide functional group, which thus fulfills its purpose. The use of sulfides for the protection of various functional groups and also as synthons for alkyl halides, acid chlorides, etc. is based on this fact. For example, methyl methylthiomethyl sulfide is a synthon for the non-existent formyl nucleophile,[1] because the conversion of RX into RCHO can be achieved with its aid.

$$(MeS)_2CH_2 \xrightarrow{BuLi} (MeS)_2CHLi \xrightarrow{RX} (MeS)_2CHR \xrightarrow{HgCl_2(H_2O)} RCHO$$

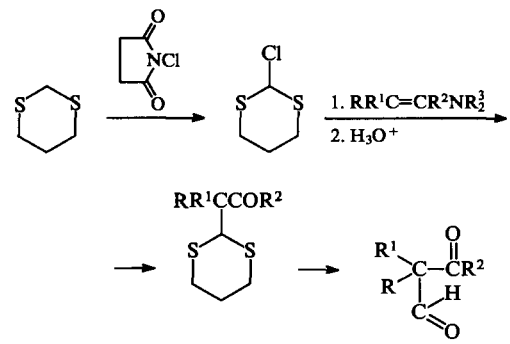
Bearing in mind the final results of the use of 2-chloro-1,3-dithiane in the synthesis (Scheme 1), it can be regarded as a synthon for the formyl cation.[2]

It is noteworthy that the strength of the C–S bond in sulfides is greatly influenced by the presence in the α-position of other heteroatoms (Cl, Br, N, O) and functional groups (C=O, C=C, C≡C, OH, SR, SO_2R, etc.). Therefore the introduction of heteroatoms and groups in the α-position relative to the sulfur atom makes it possible to regulate the lability of the C–S bond in sulfides.

I V Koval' Department of the Chemical Engineering of High-Molecular-Weight Compounds, Ukrainian Chemical Engineering University, prosp. Gagarina 8, 320005 Dnepropetrovsk, Ukraine.
Fax (7-056) 247 33 16

Received 1 October 1993
Usdpekhi Khimii **63** (2) 154 – 176 (1994); translated by A K Grzybowski

Scheme 1



Yet another feature of sulfides used in organic synthesis is the high susceptibility of the sulfur atom to attack by nucleophiles with formation of relatively stable and at the same time highly reactive intermediates (sulfonium salts, ylides, carbenes, etc.) participating in the transfer of alkylidene and other groups and also in a wide variety of rearrangements with formation of various products.

The ability of the sulfur atom in sulfides to pass fairly readily from one valence state to another and also to stabilise the α-carbanionic centre is frequently used in organic synthesis, for example, for the formation of saturated and unsaturated carbon–carbon bonds.

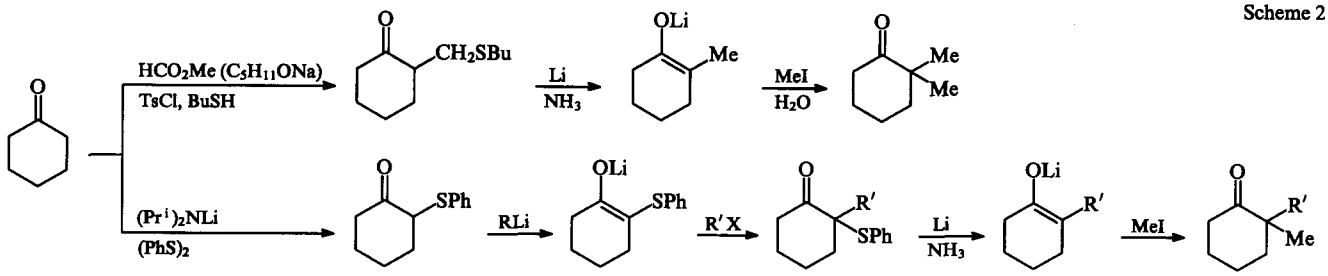
The primary products of the reactions of sulfides such as sulfoxides, sulfonium salts, sulfur ylides, sulfilimines, etc. have found extensive application in organic synthesis. Therefore a whole series of syntheses based on sulfides involve the conversion of the sulfide group into these products with subsequent transformation of the latter without their isolation from the reaction mixture.

Apart from fine organic synthesis, sulfides are widely used in agriculture, in the industrial manufacture of polymers, in the pharmaceutical industry, and in other fields of human activity. This is also reflected in the present review.

II. Cleavage of the C–S bond

The application of sulfides in organic synthesis, based on the cleavage of the C–S bond, has been known for a relatively long time.[1] For example, chlorolysis of the C–S bond in sulfides serves as a basis of a series of preparative methods of synthesis of sulfenyl chlorides. The reductive cleavage of the C–S bond is

Scheme 2

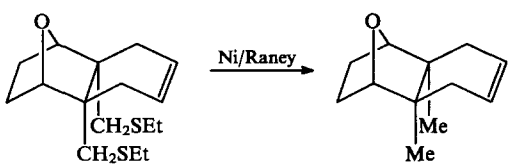


used in the synthesis of certain thiols and, in particular, toluenethiol and 2-propene-1-thiol. The thermal disproportionation of dialkyl sulfides and carboxylic acid esters is a useful alternative esterification procedure. By virtue of the high lability of the C–S bond, benzyl methyl sulfide $PhCH_2SMe$ is used as a source of the benzylcarbonium ion $PhCH_2^+$, the interaction of which with activated arenes in the presence of $ZnCl_2$ or $CuCl_2$ results in the formation of *ortho*- and *para*-substituted derivatives. The use of sulfides for the interconversion of functional groups in complex multistage organic syntheses began to be used only in the last 10–15 years, which can be explained by the lack of effective methods for the generation and removal of the sulfide functional group. Some of these reactions can be achieved also by other procedures, but the reactions using sulfides are as a rule distinguished by a higher selectivity.[1] A series of effective methods based on the use of thiols,[1,3] sulfenyl chlorides,[4–10] α-chlorosulfides,[1,11–13] unsaturated sulfides,[14,15] α-chlorocarbonyl sulfides,[16] α-chloroimide sulfides,[17] and organometallic compounds[18] have been developed in recent years for the introduction of the sulfide functional group into the molecules of organic substances. Depending on the nature of the reaction, a whole series of chemical, electrochemical, thermal, photolytic, and other methods have been developed for the removal or transformation of the sulfide functional group.

1. Hydrogenolysis of the C–S bond

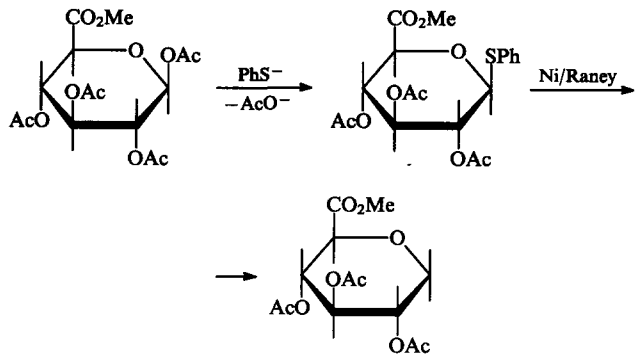
The hydrogenolysis and reductive cleavage of the C–S bond take place in the presence of reagents such as lithium in ethylamine, sodium in liquid ammonia, lithium tetrahydroaluminate, Raney nickel in boiling ethanol, and sodium tetrahydroborate in isopropyl alcohol. The electrochemical reductive cleavage of the C–S bond has come to be used increasingly in recent years.[1]

One of the first examples which demonstrated the advantage of the generation of the sulfide functional group with its subsequent removal by reductive cleavage has been Stork's synthesis of cantharidin, in the last stages of which the reductive cleavage of the C–S bond with the aid of Raney nickel was used to convert the ethylthiomethyl group into the methyl group.

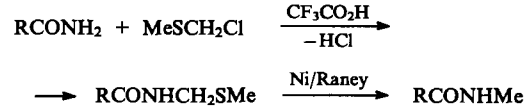


The replacement of the acetoxy-group by the phenylthio-group with subsequent reductive cleavage of the C–S bond is used for the selective elimination of the acetoxy-group and the conversion of a D-glucuronic acid derivative into the deoxy-analogue.[19]

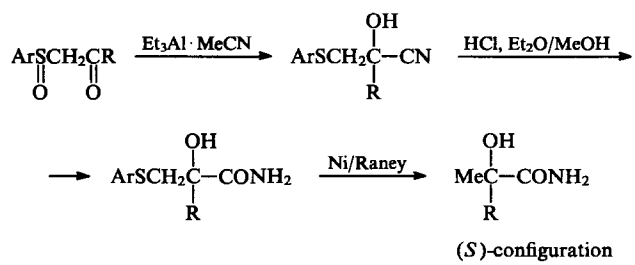
The introduction of the sulfide functional group with subsequent hydrogenolysis of the C–S bond (Scheme 2) has found extensive applications for the synthesis of alkyl-substituted cyclic ketones.[1]



The application of chloromethyl methyl sulfide in the synthesis of *N*-methyl-substituted carboxylic acid amides has been described.[20] The reductive cleavage of the C–S bond is used to eliminate the methylthio-group in the last stage of this synthesis.



The hydrogenolysis of the C–S bond has been used increasingly in recent years in stereospecific syntheses.[21–23] For example, the asymmetric synthesis of α-hydroxyacid amides from chiral β-oxosulfoxides[23] includes stages involving the reduction of the sulfoxide group to the sulfide group and the hydrogenolysis of the C–S bond with the aid of Raney nickel.



(*S*)-configuration

2. Hydrolysis of the C–S bond

Aqueous solutions of mercury acetate and inorganic acids, hydrogen chloride and bromide in acetic acid, divalent mercury salts in an acid medium, etc. are used for the hydrolytic cleavage of the C–S bond.[1]

In contrast to unsaturated sulfides, the hydrolysis of which proceeds under severe conditions, unsaturated sulfides are relatively easily hydrolysed with formation of unsaturated alcohols which rearrange to carbonyl compounds. This is frequently used to synthesise aldehydes and ketones. For example,

the conversion of phosphorus ylides into ketones[24,25] includes stages where the sulfide functional group is introduced and the C–S bond is subjected to hydrolytic cleavage.

$$Ph_3P{=}CHR \xrightarrow[-HCl]{R^1SCl} Ph_3P{=}C(R)SR^1 \xrightarrow[-Ph_3PO]{R^2CHO} R^2CH{=}C(R)SR^1 \xrightarrow[-R^1SH]{H_2O} R^2CH_2COR$$

R = H, Me, COOEt, CN, COPh, 2-$NO_2C_6H_4$;
$R^1 = R^2$ = Alk, Ar.

A similar synthetic procedure has been used in the preparative synthesis of α-alkylthioketones.[26]

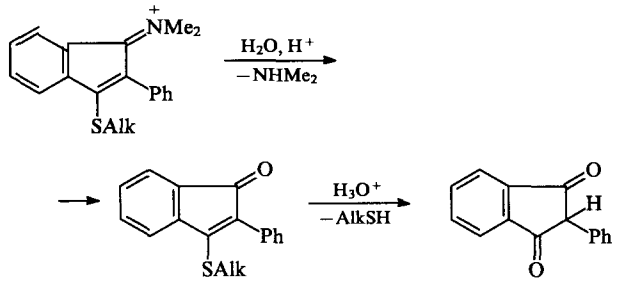
$$(EtO)_2P(O)CH{=}CH_2 \xrightarrow{MeSCl} (EtO)_2P(O)CH(SMe)CH_2Cl \xrightarrow{Et_3N} (EtO)_2P(O)C(SMe){=}CH_2 \xrightarrow[EtONa]{RSH} (EtO)_2P(O)CH(SMe)CH_2SR \xrightarrow{ArCHO} ArCH{=}C(SMe)CH_2SR \xrightarrow{H_3O^+} ArCH_2C(=O)CH_2SR$$

A new method of synthesis of ketones from organotin compounds[27] also includes a stage involving the hydrolytic cleavage of the C–S bond.

$$RCH{=}C(SPh)SnBu_3 \xrightarrow[CH_2Cl_2]{SnCl_4} RCH{=}C(SPh)SnCl_3 \xrightarrow{ArH\ (AlCl_3)} RCH{=}C(SPh)Ar \xrightarrow{HCl\ (AcOH)} RCH_2C(=O)Ar$$

R = Pr, Pr^i, Bu^i; Ar = Ph, *p*-MeC_6H_4.

In the synthesis of cyclic 1,3-diketones from 3-alkylthio-2-phenyl-1-indenyl-*N*,*N*-dimethyliminium salts,[28] one of the keto-groups is formed as a result of the hydrolytic cleavage of the C–S bond.



A new method of synthesis of conjugated dienals, consisting of the stepwise introduction of the aldehyde group as a result of hydrolytic cleavage of the C–S bond and the introduction of a double bond as a result of the elimination of the tosyl group, has been described.[29]

$$TsCH_2CH{=}CH{-}CH{=}CHSMe \xrightarrow[2.\ RBr]{1.\ BuLi,\ THF} TsCH(R)CH{=}CH{-}CH{=}CHSMe \xrightarrow{HCl\ (H_2O,\ MeCN)} TsCH(R)CH_2CH{=}CH{-}C(=O)H \xrightarrow[80\ ^\circ C]{MeCN} RCH{=}CH{-}CH{=}CH{-}C(=O)H$$

$$TsCH_2CH{=}CH{-}CH{=}CHSMe \xrightarrow[2.\ 2\,RBr]{1.\ NaH,\ THF} TsC(R)_2{-}CH{=}CH{-}CH{=}CHSMe \xrightarrow[MeCN,\ 80\ ^\circ C]{HCl} R_2C{=}CH{-}CH{=}CH{-}C(=O)H$$

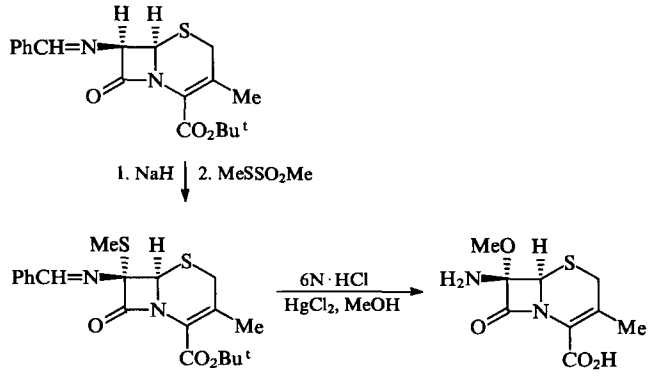
R = $PhCH_2$.

$$TsCH_2CH{=}CH{-}CH{=}CHSMe \xrightarrow[2.\ KH\ (THF,\ TMDA)]{1.\ Br(CH_2)_4CH(Br)Et} \text{Ts-substituted cyclohexene} \xrightarrow{HCl\ (MeCN)} \text{cyclohexene-CH=CH-CH=CH-C(=O)H}$$

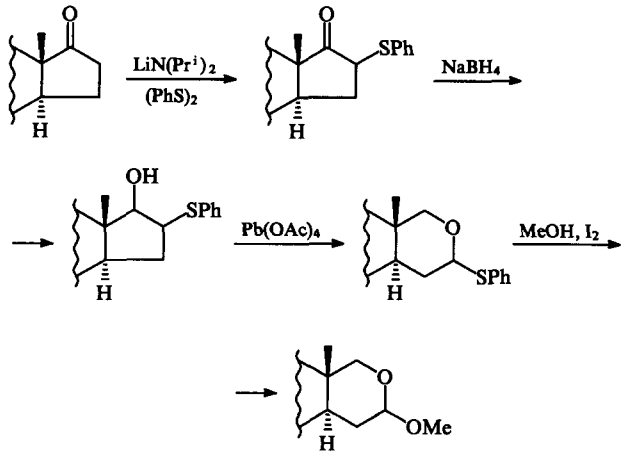
TMDA = tetramethylenediamine.

3. Alcoholysis of the C–S bond

The reaction involving the substitution of the sulfide group by an alkoxy group is used in rare instances, which is evidently due to the lack of effective methods for carrying out this process. As a rule, the alcoholysis of the C–S bond proceeds on treatment with alcohols in the presence of mercury dichloride, iodine, and other inorganic reagents. For example, methanol in the presence of mercury dichloride is used to substitute the methylthio-group by the methoxy-group in the synthesis of a derivative of cephalosporin.[1]

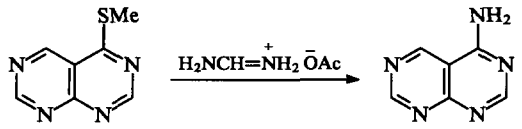


In the synthesis of acetals from cyclic ketones,[30] methanol in the presence of iodine is used to substitute the phenylthio-group by the methoxy-group.

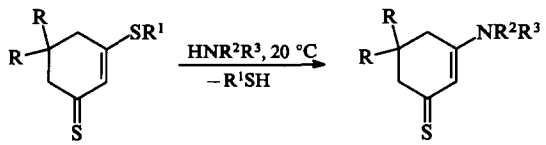


4. Aminolysis of the C–S bond

The replacement of an alkylthio-group with a saturated carbon atom by the amino-group or a substituted amino-group takes place when sulfides are treated with ammonia, amines, amidines, and other nitrogen-containing compounds. For example, azaheterocyclic sulfides undergo aminolysis fairly readily on treatment with formamidine [formamidinium? (Translator)] acetate—a process which is used in subsequent reactions of these heterocyclic compounds. [1]

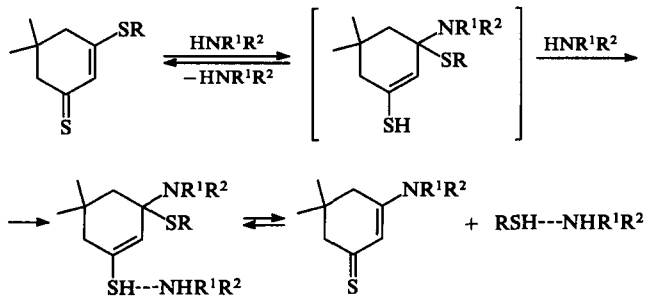


As a synthetic procedure, the aminolysis of the C–S bond has been used in recent years to modify groups such as $RSC=CR^1-CR^2=S$ and $RSC=CH-CH=NR^1$ in thiones and enamines. It has been noted, [31] for example, that 3-alkylthiocyclohex-2-ene-1-thiones react readily with ammonia and primary and secondary amines at 20 °C in benzene, chloroform, and alcohols, and dimethylformamide (DMF), affording 3-aminocyclohex-2-ene-1-thiones:

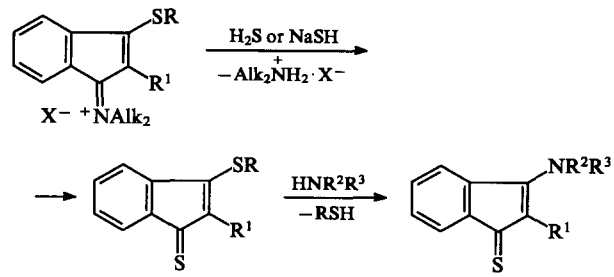


R = Me; R^1 = Me, Et; R^2 = Me; R^3 = Alk.

Detailed study of this reaction showed [32] that the aminolysis proceeds via a stage involving the formation of a stable intermediate in mobile equilibrium with the final product and that the aminolysis process itself can be described as 1,4-addition–elimination.

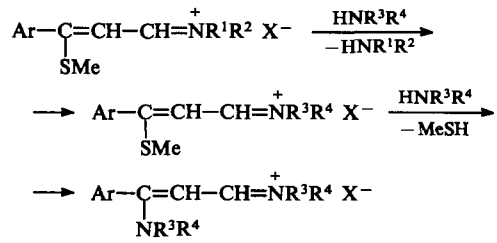


N,N-Disubstituted indenyliminium salts are converted into 3-amino-2-arylindene-1-thiones via a stage in which the intermediate 3-alkylthio-2-arylindene-1-thiones are subjected to aminolysis. [32]



R = Me, Et; R^1 = Ph; R^2 = Ph, Me; R^3 = Me; X = BF_4, I.

It has been noted [33] that, in the reaction of 3-alkylthiopropenyliminium salts with alkyl- and aryl-amines, transamination is accompanied by the aminolysis of the C–S bond, which results in the formation of salts of enaminoimines containing identical substituents at the nitrogen atom.

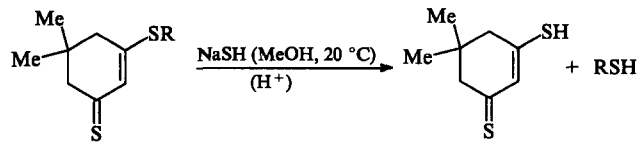


Ar = Ph, 4-$MeOC_6H_4$;
R^1 = R^2 = Alk; R^3 = Alk, H; R^4 = Alk, Ar;
X = ClO_4, I.

The exchange of the alkylthio-group for the amino-group proceeds in an acid medium. In the case of X = ClO_4, the yield of the final product is 80%, while for X = I it is only 38%.

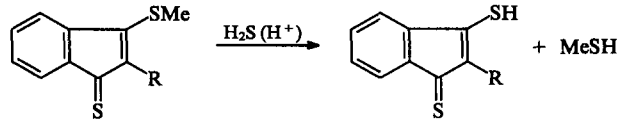
5. Hydrothiolysis of the C–S bond

The replacement of the alkylthio-group by the mercapto-group at an unsaturated carbon atom takes place in the reaction of unsaturated sulfides with sodium hydrogen sulfide in methanol, which is used in the synthesis of 5,5-dialkyl-3-mercaptocyclohex-2-ene-1-thiones. [34]



R = Me, Et.

A similar replacement occurs in the reaction of unsaturated sulfides with hydrogen sulfide in an acid medium. This property is used in the synthesis of 3-mercaptoindene-1-thiones. [32,36]

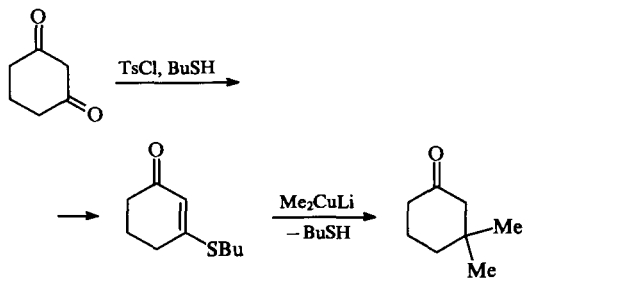


R = H, Et, Ph, 4-$MeOC_6H_4$, 4-ClC_6H_4.

6. Cleavage of the C–S bond by organometallic compounds

When sulfides are acted upon by organometallic compounds, the sulfide group may be replaced by an alkyl group. The presence in the α-position in sulfides of groups such as C=O, C=C, C≡C, etc. promotes this reaction. For example, ketones are formed in high yields in the reactions of α-oxoalkyl sulfides with R_2CuLi; the formation of tertiary alcohols due to the competing attack on the carbonyl group is not observed under these conditions.[1,36] One of the stages of the synthesis of the pheromone of the German cockroach [3,11-dimethyl-2-nonacosanone (Translator)] involves the cleavage of the C–S bond by treat-ment with similar reagents.[37]

The replacement of the sulfide group by alkyl groups with the aid of organometallic compounds is used also in the synthesis of cyclic ketones[38,39] and acetylenes.[40]



$$MeSC{\equiv}C{-}C{\equiv}CEt + PrLi \xrightarrow[-MeSLi]{} PrC{\equiv}C{-}C{\equiv}CEt$$

7. Desulfurisation of sulfides

Sulfides containing other heteroatoms and functional groups in the α-position tend as a rule to undergo sulfur displacement reactions. The desulfurisation of such sulfides proceeds in the presence of alkali metal hydrides or trivalent phosphorus compounds. Thiirans are then formed at an intermediate stage.[1]

$$ArCH_2SCH(Cl)Ar \xrightarrow{Ph_3P,\ Bu^tOK} \left[\begin{array}{c} ArCH-CHAr \\ \quad\ \backslash / \\ \quad\ S \end{array}\right] \xrightarrow[-H_2S]{} ArCH{=}CHAr$$

The desulfurisation of sulfides is used as a synthetic procedure in the synthesis of sterically hindered alkenes[41] and also in the synthesis of corrins in order to form a C=C bond.[1]

$$RN{=}CR^1SCH_2COAr \xrightarrow{(EtO)_3P} RNHC(R^1){=}CHCOAr$$

8. Thermolysis of the C–S bond

The cleavage of the C–S bond in sulfides at high temperatures leads to the formation of thiyl and alkyl (or aryl) radicals.[42–45] The radicals undergo further reactions under the thermolysis conditions with formation of the final products, the composition of which is determined both by the structure of the initial sulfide and by the thermolysis conditions. For example, the thermolysis of diethyl sulfide results in the formation in the gas phase of a mixture, the main components of which are hydrogen sulfide and ethylene.[42,45]

$$(C_2H_5)_2S \xrightarrow{\Delta} C_2H_5\dot{S} + \dot{C}_2H_5 \longrightarrow C_2H_5SH + CH_2{=}CH_2$$

$$C_2H_5SH \longrightarrow C_2\dot{H}_5 + S\dot{H}$$

$$C_2H_5SH + \dot{S}H \longrightarrow Me\dot{C}HSH + H_2S$$

$$C_2H_5SH + \dot{C}_2H_5 \longrightarrow Me\dot{C}HSH + C_2H_5H$$

The thermolysis of dimethyl sulfide at 600–650 °C leads to the formation of thiophene.[46,47]

$$Me_2S \xrightarrow[-H_2]{600-650\ ^\circ C} \left[\begin{array}{c} CH_2-CH_2 \\ \quad\ \backslash / \\ \quad\ S \end{array}\right] \longrightarrow \left[CH_2{=}CHSH\right] \longrightarrow \text{thiophene}$$

At 450–500 °C in the presence of phenylacetylene, the same sulfide gives rise to 3-phenylthiophene and benzo[*b*]thiophene.[48]

$$Me_2S \xrightarrow{450-500\ ^\circ C} \left[CH_2{=}CH\dot{S}\right] \xrightarrow{PhC{\equiv}CH} \left[\begin{array}{c} C{=}C\dot{H} \\ \quad\ | \\ \quad\ S \\ \quad\ | \\ H_2C{=}CH \end{array}\right] \xrightarrow[-[\dot{H}]]{-[CH_2{=}\dot{C}H]} \text{benzo[b]thiophene},\ \text{3-phenylthiophene}$$

The thermolysis of certain disulfides results in the formation of extremely rare and synthetically valuable intermediates. For example, the vacuum thermolysis of dipropargyl sulfide has been used as a selective path to the synthesis of the unstable thiopropynal.[49]

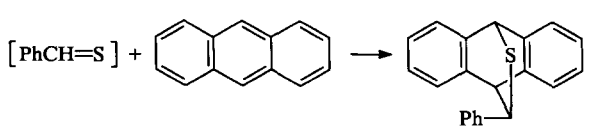
$$(CH{\equiv}CCH_2)_2S \xrightarrow[-MeC{\equiv}CH]{750-850\ ^\circ C,\ 10^{-3}\ Torr} \left[CH{\equiv}C{-}CH{=}S\right]$$

The flash thermolysis of diallyl sulfide and allyl benzyl sulfide leads to the formation of thioacrolein and thiobenzaldehyde respectively.[50–53]

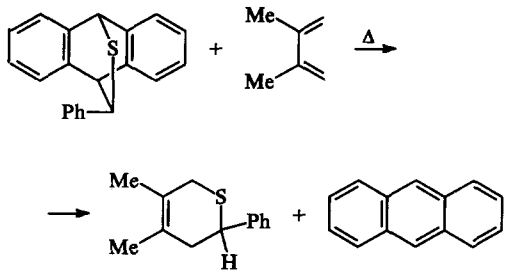
$$(H_2C{=}CH{-}CH_2)_2S \xrightarrow[-MeCH{=}CH_2]{550\ ^\circ C,\ 10-50\ Torr} \left[CH_2{=}CH{-}CH{=}S\right]$$

$$PhCH_2SCH_2CH{=}CH_2 \xrightarrow[-MeCH{=}CH_2]{500-600\ ^\circ C,\ 10-50\ Torr} \left[PhCH{=}S\right]$$

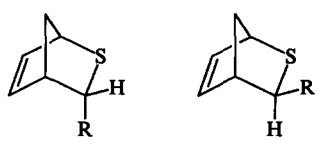
The thermolysis of these sulfides is usually carried out in the presence of dienes or anthracene, which serve as 'trapping agents' for the thioaldehyde formed. For example, anthracene reacts with thiobenzaldehyde to form an adduct which is itself a source of thiobenzaldehyde.[54,55]



When this adduct is heated with 2,3-dimethylbutadiene in a sealed tube, the corresponding 2*H*-dihydrothiane and anthracene are formed.

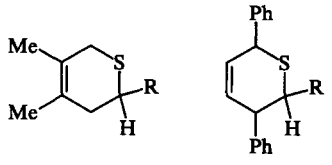


The α-sulfonyldisulfides $RCH_2SSCH(Ts)R$ (R = EtOCO) are excellent substrates for the synthesis of alkoxycarbonylthioformaldehydes.[56] The interaction of these disulfides with triethylamine in the presence of cyclopentadiene affords a mixture of *endo*- and *exo*-adducts, which are extremely valuable for preparative purposes.



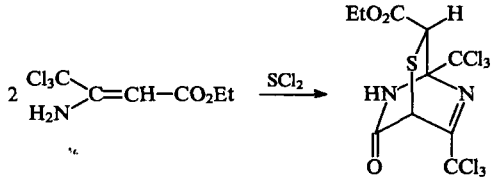
R = EtOCO.

Ethoxycarbonylthioformaldehyde may be generated from these adducts and made to react with other conjugated dienes. For example, when it is heated with 2,3-dimethylbuta-1,3-diene and 1,4-diphenylbuta-1,3-diene, the following adducts are formed:

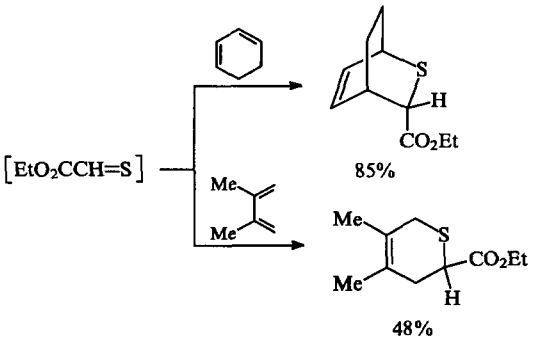


R = EtOCO.

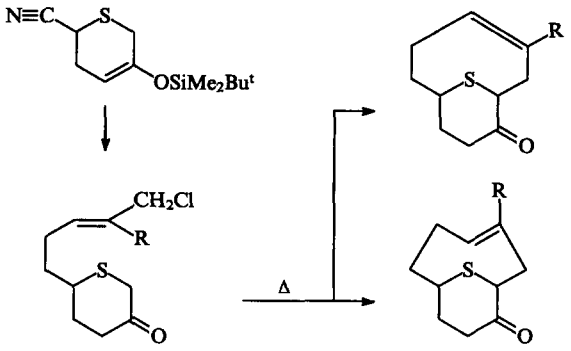
It has been suggested also that a derivative of diazathiabicyclooctane, formed in 34% yield in the reaction of ethyl 3-amino-4,4,4-trichlorocrotonate with sulfur dichloride, be used as a source of alkoxycarbonylthioformaldehydes.[57]



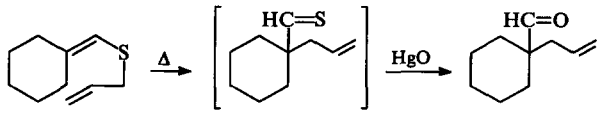
Heating of a solution of this compound in chlorobenzene at 80 °C induces the Diels-Alder retro-reaction and the formation, together with other products, of ethoxycarbonylthioformaldehyde, which reacts with cyclohexa-1,3-diene and also with 2,3-dimethylbuta-1,3-diene.[58]



The synthesis of 11-thiabicyclo[5.3.1]undecenes, which are otherwise difficult to obtain, from the adduct of cyanothioformaldehyde with 2-(*tert*-butyldimethylsiloxy)-buta-1,3-diene has been developed.[59,60]

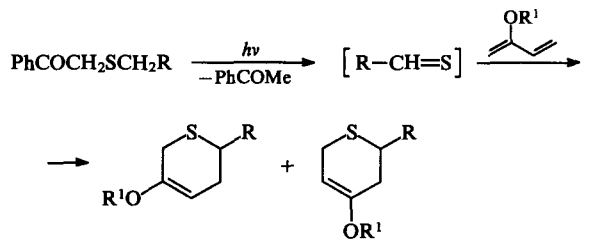


The thermolysis of certain sulfides in the presence of oxidants is of interest for preparative synthesis. For example, whereas the thermolysis of a cyclic sulfide at 160–180 °C leads to polymeric products, in the presence of mercury(II) oxide an aldehyde is formed in 82% yield.[58]



9. Photolysis of the C–S bond

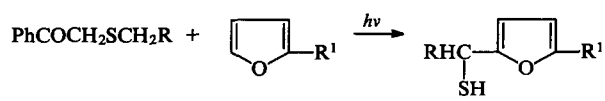
There are so far few examples of the photolytic cleavage of the C–S bond in sulfides and it has not found extensive application as a synthetic procedure for the transformation of the sulfide group. A simple method for the generation of dienophile thioaldehydes by the irradiation of a mixture of organyl phenacyl sulfides with a diene at 0 °C has been described.[58,61]



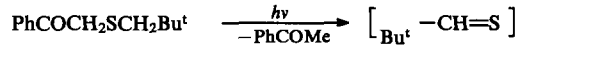
R = H, Ph, MeCO, PhCO, CN, AlkOCO, Ph_2PO, $PhSO_2$;
R^1 = $SiMe_2Bu^t$.

The use of the most reactive dienes in this process makes it possible to 'trap' even thioformyl sulfone $PhSO_2CH=S$ and thioformylphosphine oxide $Ph_2P(O)CH=S$, the oxygen analogues of which are unknown.

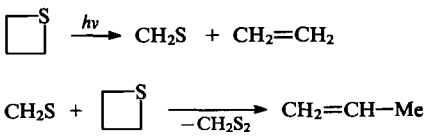
The photolysis of organyl phenacyl sulfides in the presence of furan proved to be a convenient and effective method of synthesis of mercaptoalkylfurans.[62]



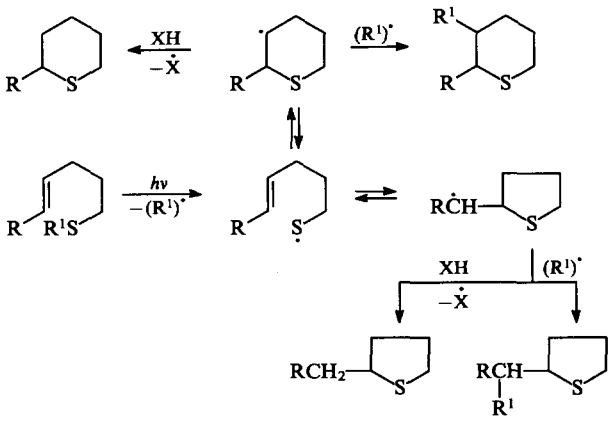
The photochemical decomposition of neopentyl phenacylsulfide is one of the most important methods of synthesis of the relatively stable 2,2-dimethylpropanethial.[63]



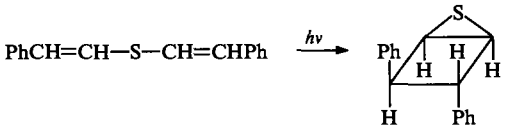
When thietane is irradiated with UV light at wavelengths of 254 and 313 nm in the temperature range 20–200 °C, ethylene and thioformaldehyde are formed. The latter reacts with a molecule of thietane to form an intermediate biradical, the subsequent decomposition of which leads to propene. [64]



The primary stage of the photolysis of alkenyl sulfides is again the cleavage of the C–S bond. The thiyl radicals produced in this process undergo subsequent intramolecular cyclisation with formation of cyclic products. [64]



UV irradiation of bis(2-phenylvinyl) sulfide leads to *trans*-2,3-diphenyl-5-thiabicyclo[2.1.0]pentane. [64]

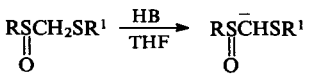


III. Generation of α-sulfenylcarbanions

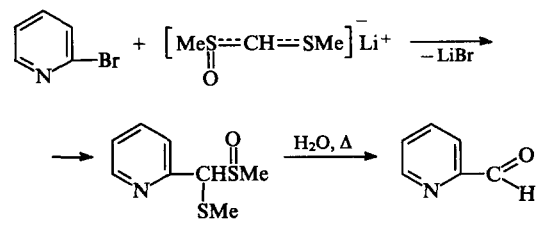
The stabilisation of the α-carbanionic centre by a divalent sulfur atom is used to generate α-sulfenylcarbanions, which are widely used in organic synthesis to produce both single and double carbon–carbon bonds. Together with alkyl(aryl)thio-groups, other functional groups such as C=O, [6,66] CN, [7,66] EtOCO, [8,66] RSO, [67] NO_2, [68,69] $SiMe_3$, [70,71] RSO_2, [72] etc. can participate in the stabilisation of the carbanionic centre. Carbon–carbon bonds are formed as a result of the alkylation or acylation of α-sulfenylcarbanions and also as a result of the addition of the carbanionic centre to the sp^2-hybridised carbon atom in the C=O and C=C bonds. These synthetic procedures are widely used in the preparation of various compounds together with the elimination of the sulfide group.

1. Synthesis of carbonyl compounds

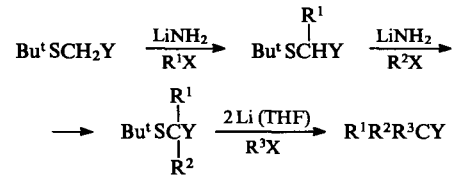
Carbanions containing functional groups other than the alkylthio- or arylthio-groups are frequently employed in the syntheses of carbonyl compounds. For example, the carbanions generated from ethyl methylthiomethyl or ethylthiomethyl methyl sulfoxide by treatment with NaH, BuLi, or Pr^i_2NLi in tetrahydrofuran are used successfully as synthons for acyl anions.



In the form of sodium or lithium salts, these carbanions react readily with primary alkyl halides or tosylates, affording aldehydes after hydrolysis. The interaction of the carbanion MeS(O)$\bar{C}$HSMe with 2-bromopyridine leads to an intermediate, which affords pyridine-2-aldehyde on distillation. [67]



α-(*tert*-Butyl)thio-derivatives of carboxylic acid esters, nitriles, and ketones undergo stepwise alkylation via α-carbanions. The subsequent removal of the *tert*-butylthio-group by lithium in tetrahydrofuran with added naphthalene or trimesitylborane at 20 °C leads to alkyl-substituted carbonyl compounds. [64]

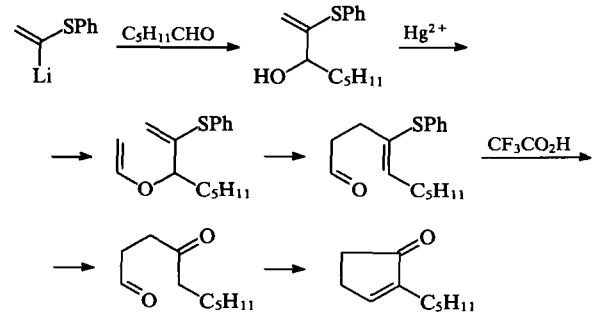


Y = CO_2Me, CO_2Bu^t, CN, COMe.

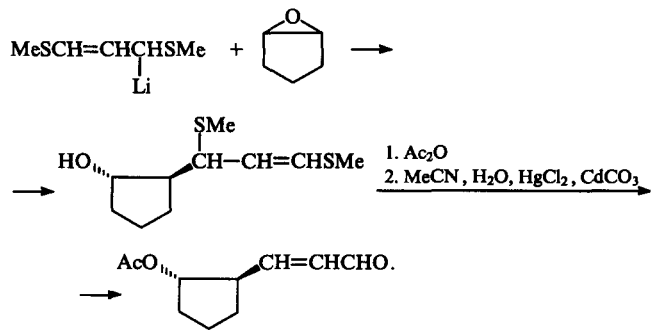
Phenylthiotrimethylsilylcarbanions are used to convert alkyl halides into aldehydes via alkylation, oxidation of the alkylation products to the sulfoxide, and rearrangement of the sulfoxide to α-trimethylsiloxysulfide, the hydrolysis of which leads to an aldehyde. [73]



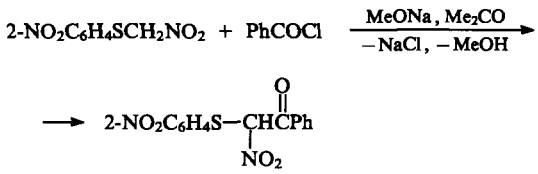
The α-carbanions obtained from vinyl sulfides can be regarded as acyl-anionic synthons, since they are capable of hydrolysing with formation of a carbonyl group, which in fact determines their use in organic synthesis. The synthesis of an unsaturated cyclic ketone by the addition of the carbanion of phenyl vinyl sulfide to hexanal has been described. [64] The alcohol formed is converted by transacetalisation with vinyl ether in the presence of divalent mercury salts into [a substituted?, Translator] vinyl ether, which is converted at 120 °C into an aldehyde. The hydrolysis of the aldehyde in the presence of trifluoroacetic acid leads to a ketoaldehyde, which cyclises to 2-pentylcyclo-penten-2-one.



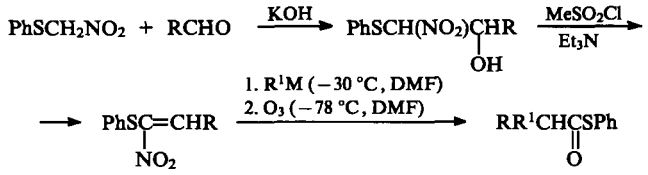
1,3-Bis(methylthio)allyllithium, which is a synthetic equivalent of the anion $\bar{C}H=CH-CH=O$, has found extensive application in the synthesis of *trans*-α,β-unsaturated aldehydes. One of the examples of such synthesis is presented in the scheme below: [64]



It has been shown in relation to the carbanion of 2-nitrophenylthionitromethane [68,69] that α-sulfenylcarbanions are relatively easily acylated by carboxylic acid chlorides with formation of α-arylthioketones.



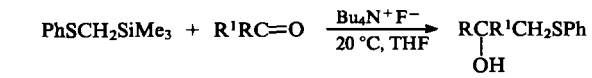
In view of the possibility of the subsequent removal of the sulfide group, one can regard this method as one of the alternative procedures for the synthesis of ketones.



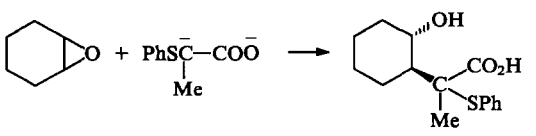
The addition of the anion of phenylthionitromethane to the carbonyl group of aldehydes with subsequent dehydration and ozonisation is used in the synthesis of thioloesters of carboxylic acids. [74]

2. Synthesis of alcohols

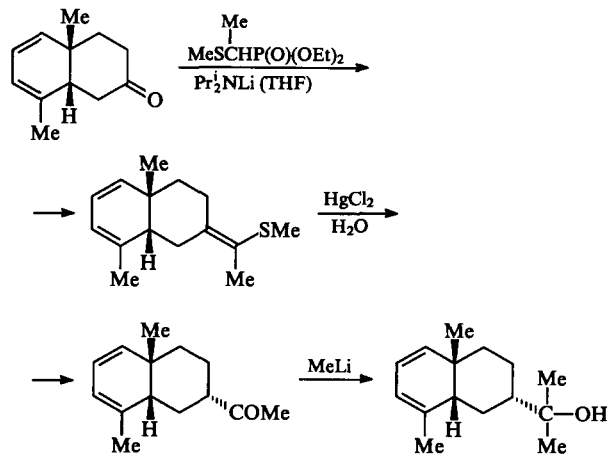
A hydroxy-group may be formed either as a result of the addition of α-sulfenylcarbanions to the sp^2-hybridised carbon atom of the carbonyl group or as a result of the opening of the oxirane ring. For example, the synthesis of secondary alcohols containing the phenylthio-group in the α-position from phenylthio(trimethylsilyl)methane and ketones with subsequent elimination of the trimethylsilyl group has been described. [75]



The opening of the oxirane ring by treatment with the dianion of 1-carboxyethyl phenyl sulfide is used in the synthesis of α-derivatives of cyclohexanol. [65]

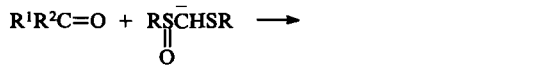


A multistage synthesis of tertiary alcohols has been described in the literature. [76] It is based on the addition of methyl α-diethoxyphosphonoethyl sulfide to the carbonyl group of a cyclic ketone, the subsequent stepwise elimination of the diethyl phosphonate and of the methylthio-group, and the addition of methyllithium to the carbonyl group.

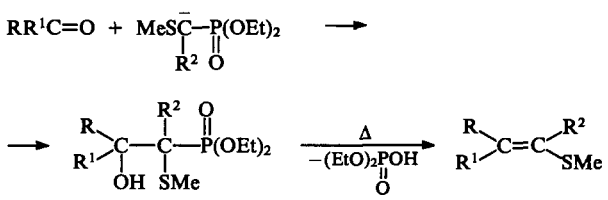


3. Synthesis of unsaturated compounds

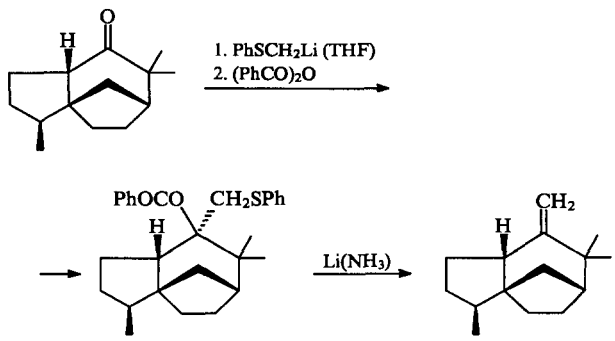
The use of α-sulfenylcarbanions for the formation of new C=C bonds under mild conditions is very important. The addition of α-sulfenylcarbanions to the carbonyl group of ketones leads to β-hydroxysulfides, which are converted into unsaturated sulfides after the elimination of the hydroxy-group. [1]



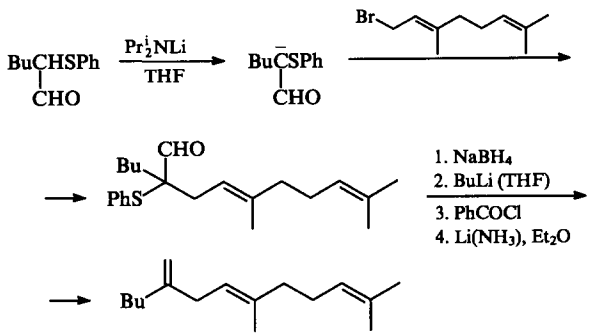
R = Me, Et; $R^1 = R^2 = Me$.



Several methods for the methylenation of ketones involving the use of α-sulfenylcarbanions have been developed. [64] One of them consists in the addition of α-sulfenylcarbanions to ketones with formation of β-hydroxysulfides, which are converted into methylene derivatives after acylation and reductive elimination of the phenylthio-group. The sesquiterpene zizaene has been obtained in this way.

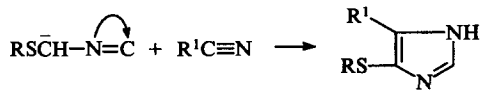


Alkylation of the carbanion $Bu\bar{C}(CHO)-SPh$ followed by the reductive cleavage of the C–S bond is used in the synthesis of 2-butyl-5,9-dimethyldeca-1,4,8-triene. [1]

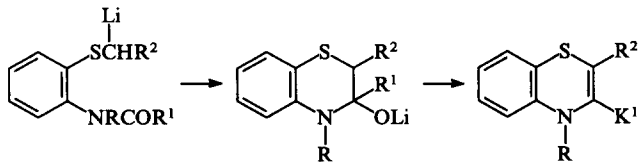


4. Synthesis of heterocyclic compounds

α-Sulfenylcarbanions with functional group substituents are frequently used in the synthesis of heterocyclic compounds. For example, the interaction of the α-isocyano-α-sulfenylcarbanion with nitriles leads to the formation of imidazoles. [64]

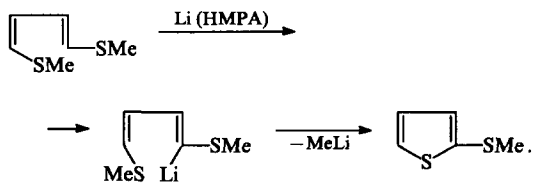


The synthesis of 4*H*-1,4-benzothiazines in accordance with the scheme

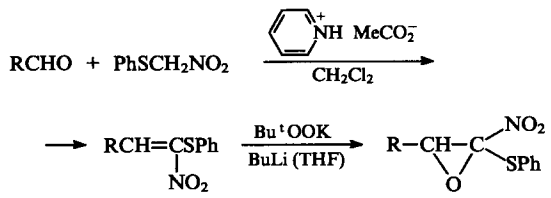


has also been described. [71]

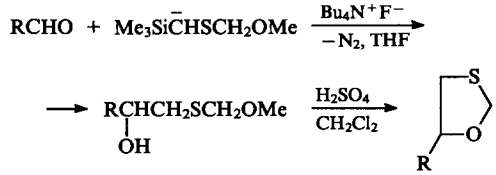
It has been noted [64] that the metallation of a 1,4-bis(alkylthio)alkadiene with lithium in the presence of hexamethylphosphoramide (HMPA) is accompanied by cyclisation with formation of alkylthio-derivatives of thiophene, for example:



The addition of the phenylthionitromethane anion to the carbonyl group in aldehydes with subsequent dehydration and selective oxidation of the ethylene bond constitutes the basis of the synthesis of oxiranes containing the phenylthio-group. [78, 79]



Functionalised β-hydroxysulfides, formed as a result of the addition of α-sulfenylcarbanions to the carbonyl group of aldehydes, can cyclise with participation of the hydroxy-group and other functional groups, which is used in the synthesis of 1,3-oxathiolanes. [80]



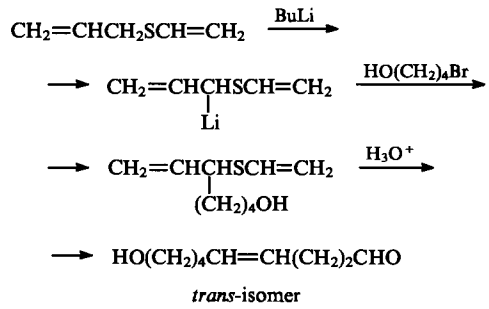
R = Ph, 4-MeOC$_6$H$_4$, 4-ClC$_6$H$_4$.

The synthesis of thiiranes [80] and other heterocyclic compounds [81] from α-sulfenylcarbanions has also been described.

5. Synthesis of natural products

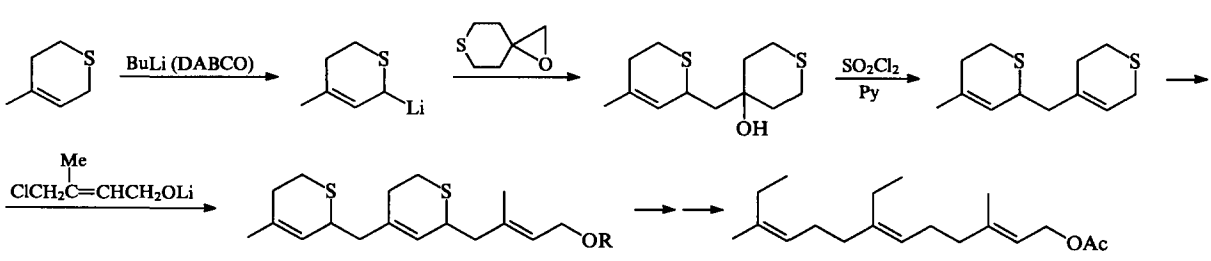
Apart from the synthesis of the sesquiterpene zizaene described above, α-sulfenyl carbanions with functional group substituents have found extensive application also in the syntheses of other natural products. For example, allyl carbanions are most important intermediates in the synthesis of juvenile hormones — cembranolides (Scheme 3). [64]

The hydroxyaldehyde which is a key compound in the synthesis of the pheromone propylure has been obtained by metallating allyl vinyl sulfide and subsequent alkylation and thio-Claisen rearrangement. [64]

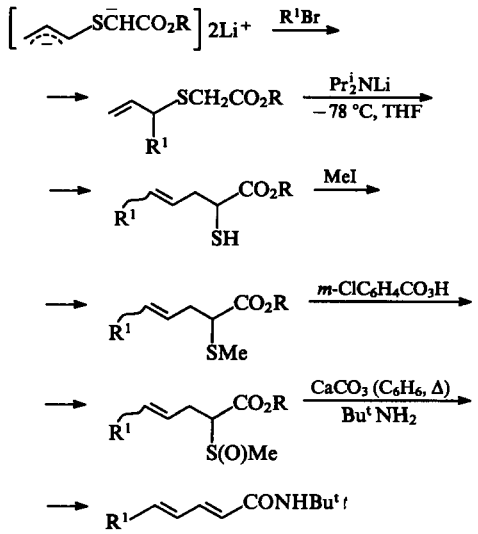


The dianion of allylthioacetic ester is a convenient reagent for the stereoselective synthesis of derivatives of (2*E*,4*E*)-dienoic acids, for example the precursor of the insecticide pellitorine. [82, 83]

Scheme 3

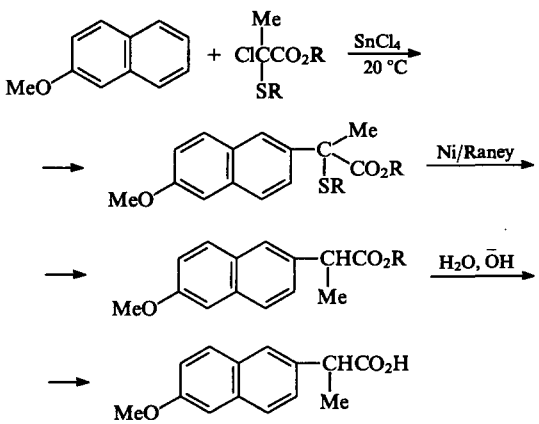


DABCO = diazabicyclo[2.2.2]octane

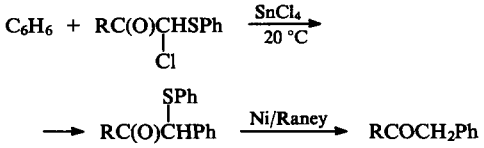


IV. Generation of α-sulfenylcarbonium ions

The sources of α-sulfenylcarbonium ions are as a rule α-chlorosulfides, on the basis of which a series of methods have been developed for the introduction of the sulfide group into aromatic compounds. This synthetic procedure is used in multistage organic syntheses, in particular in the syntheses of various carbonyl compounds. For example, the synthesis of α-(6-methoxy-2-naphthyl) propionic acid includes stages in which β-methoxynaphthalene is alkylated by the α-alkylthio-α-chloropropionic acid ester with subsequent elimination of the alkyl group and hydrolysis of the ester group.[84]

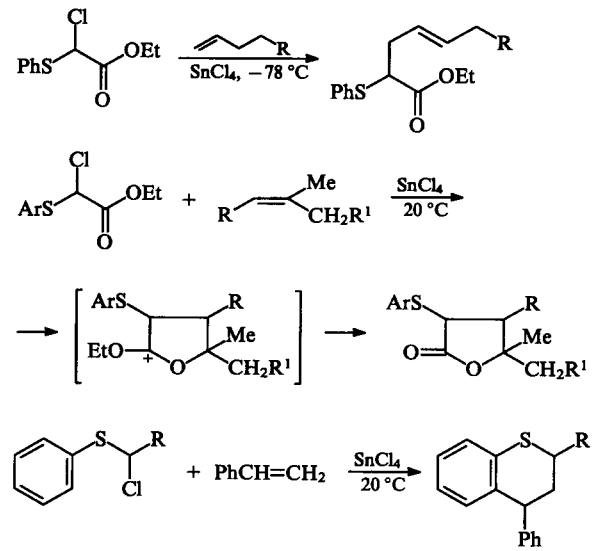


A series of alkyl(aryl) benzyl ketones have been obtained by alkylating benzene with acylchloromethyl phenyl sulfide in the presence of tin tetrachloride and subsequent reductive elimination of the phenylthio-group.[85]



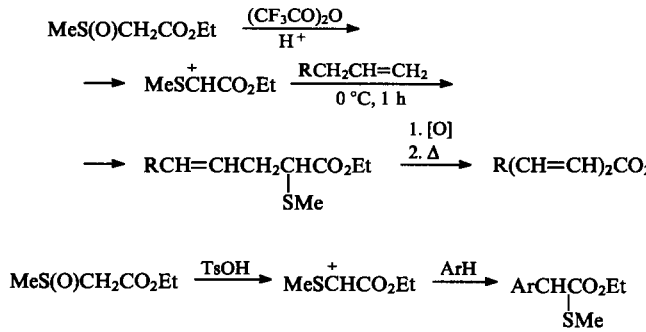
R = Me, Ph, CH_2Ph, $(CH_2)_2Ph$.

Another aspect of the use of α-sulfenylcarbonium ions in multistage organic syntheses involves their ene-type interaction with terminal alkenes,[86] which is sometimes used to obtain certain heterocyclic compounds.



R = CO_2Et, $CONMe_2$; R^1 = Alk.

Certain sulfoxides are also used as sources of α-sulfenylcarbonium ions. They generate α-sulfenylcarbonium ions under the conditions of the Pummerer rearrangement. For example, it has been noted[64] that the carbonium ion $MeS\overset{+}{C}HCO_2Et$, obtained by the Pummerer rearrangement from the sulfoxide $MeS(O)CH2CO_2Et$, reacts with terminal alkenes via the ene pathway (it is used in the synthesis of dienoic acids) and also enters into alkylation reactions of aromatic hydrocarbons.[87]

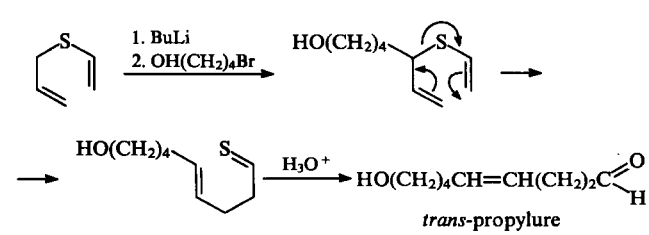


Ar = Ph, C_6H_4Me, C_6H_4Cl.

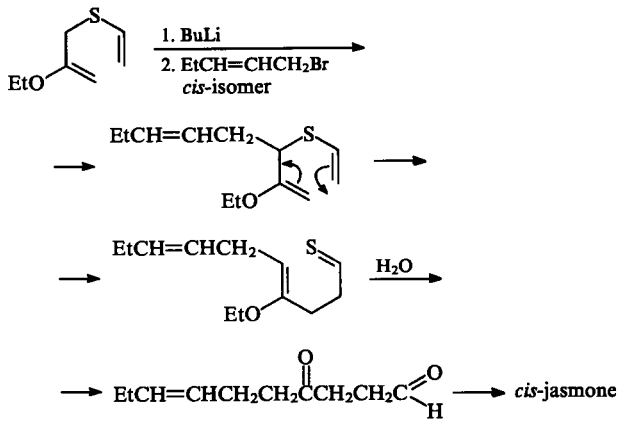
V. Reactions involving the rearrangement of sulfides

Among the known rearrangements of sulfides, the thio-Claisen rearrangement and also various sigmatropic migrations of alkylthio- and arylthio-groups have found most extensive application. Rearrangements involving the migration of other functional groups and hydrogen atoms are also used.

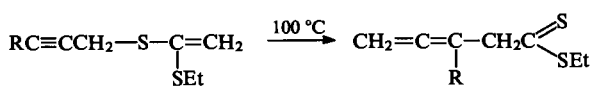
The thio-Claisen rearrangement of carbanions derived from allyl sulfides with subsequent alkylation and cleavage of the $C_{All}-S$ bond (or its hydrolysis) constitutes a convenient method of synthesis of certain aliphatic natural products.[1]



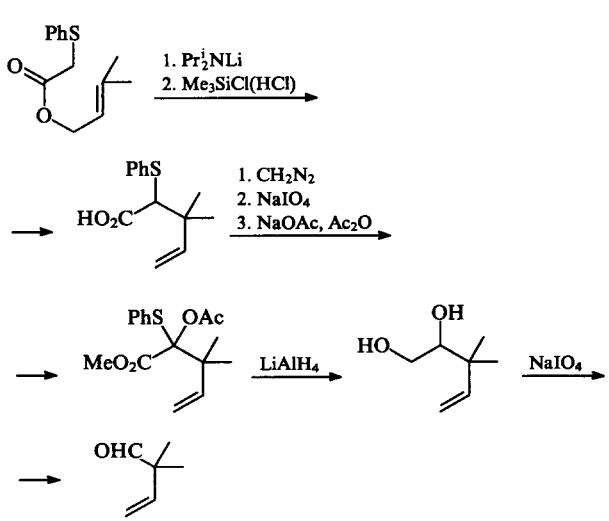
trans-propylure



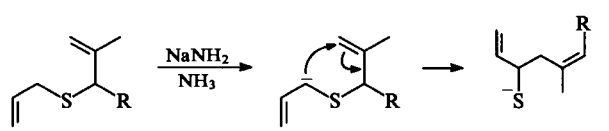
The thio-Claisen rearrangement of 1-alkylthio-1-propargylthioalkenes[1] to the alkyl esters of dienedithiocarboxylic acids, which are otherwise difficult to obtain and for which other methods of synthesis have not yet been developed, is of special interest.



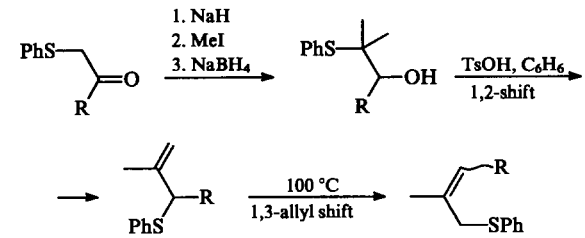
The Claisen rearrangement of allyl α-phenylthioacetates leads to α-phenyl-substituted thiocarboxylic acids, which can be converted further into β,γ-unsaturated aldehydes and the relatively difficult to obtain (*Z*)-diene-2-carboxylic acids.[88]



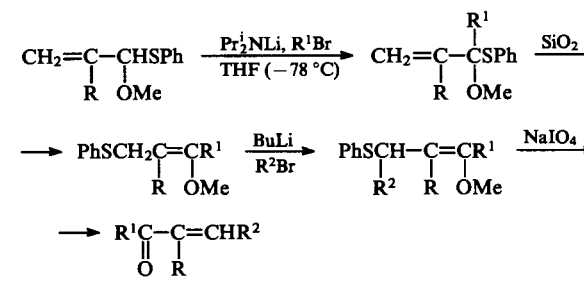
In the synthesis of unsaturated thiolates from allyl sulfides, the [2,3]-sigmatropic rearrangement of the carbanion derived from the allyl sulfide takes place.[89]



A large number of the rearrangements of sulfides involve the migration of the alkylthio- or arylthio-groups.[90–95] For example, the synthesis of unsaturated sulfides from β-oxoalkyl sulfides includes rearrangements involving 1,2- and 1,3-shifts, which make it possible to move the phenylthio-group by one carbon atom along the chain.[90]

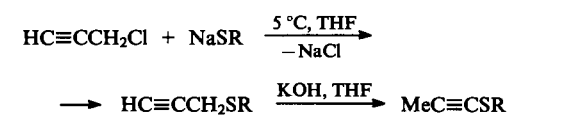


The synthesis of unsaturated ketones from β-methoxysulfides[91] includes a stage involving a rearrangement with migration of the phenylthio-group of the 1,3-shift type.



R = H, Me; $R^1 = R^2$ = Me, Et.

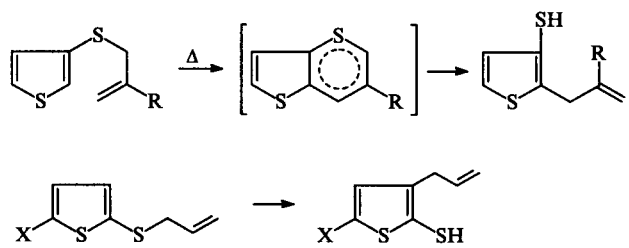
The rearrangement of alkyl propargyl sulfides with the 1,3-shift of the alkylthio-group constitutes the basis of the synthesis of alkylthiopropynes, which are used to obtain polymers.[93]



R = Me, Et, Bu, C_6H_{13}, C_8H_{17}, $C_{10}H_{21}$.

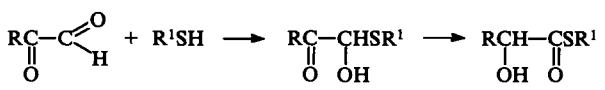
The migration of the alkylthio-group in indole from the 3-position to the 2-position, occurring under the influence of trifluoroacetic acid,[95] is extremely important for the synthesis of alkyl 2-indolyl sulfides, since the sulfenylation of indole by sulfenyl chlorides takes place as a rule in the 3-position.[96,97]

The [3,3]-sigmatropic rearrangement of allyl 2-thienyl and allyl 3-thienyl sulfides, which proceeds via a six-membered transition state, is very important from the standpoint of the synthesis of 2- and 3-allylthiophenethiols.[89]



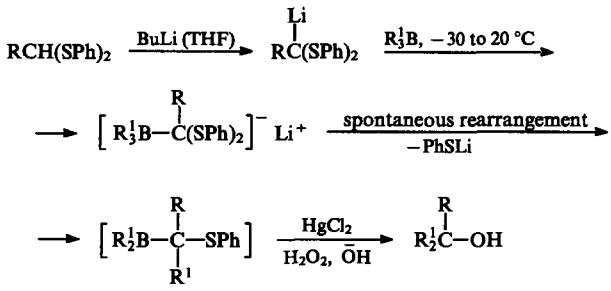
X = H, Me, MeO, MeS, Cl, Br.

Together with the syntheses presented above, a whole series of syntheses based on rearrangements involving the migration of hydrogen atoms and alkyl, arenesulfonyl, and other functional groups have been developed. For example, the synthesis of α-hydroxy-substituted thiocarboxylic acids from α-oxoaldehydes and thiols is based on the rearrangement of the intemediate α-hydroxy-β-oxoalkyl sulfides, which proceeds with migration of a hydrogen atom.

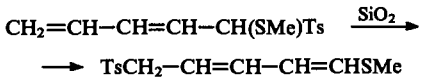


R = Me, Et, Pr; R^1 = Et, Bu.

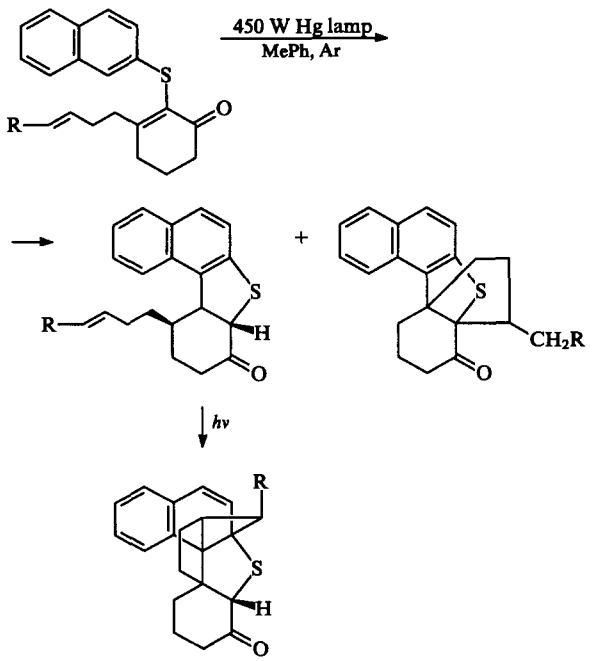
The migration of an alkyl group is especially characteristic of sulfides containing boralkyl groups, which are used in the synthesis of tertiary alcohols from thioacetals. [98]



The rearrangement with migration of the arenesulfonyl group is characteristic of sulfides containing arenesulfonyl and alkyl(aryl)thio-groups at the allylic carbon atom. [99,100] For example, the synthesis of 1-methylthio-5-tosylpenta-1,3-diene is based on the rearrangement of 1-methylthio-1-tosylpenta-2,4-diene.



The synthesis of cyclic sulfides based on the photoinduced intramolecular cycloaddition reactions of arylthiocyclohexenones [101] and phenylthiocyclohexanones has been described. [102]

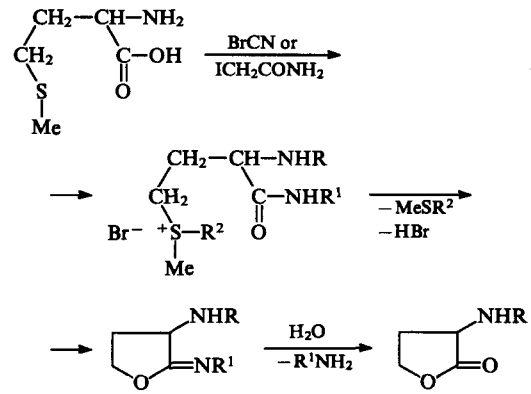


VI. Syntheses based on the primary products of the reactions of sulfides

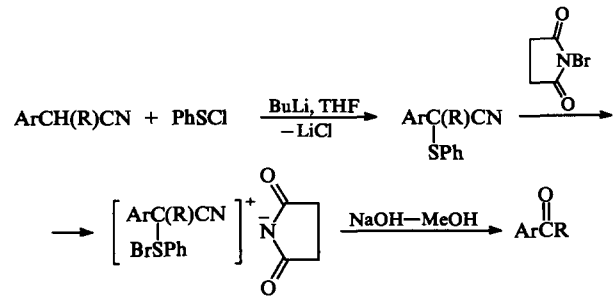
The conversion of the sulfide group into the sulfonium, ylide, sulfoxide, sulfilimine, and other groups with their subsequent transformation is widely used in multistage organic syntheses. The products of the primary reactions of sulfides are then formed as a rule in high yields and are frequently employed without isolation from the reaction mixture.

1. Syntheses via sulfonium salts

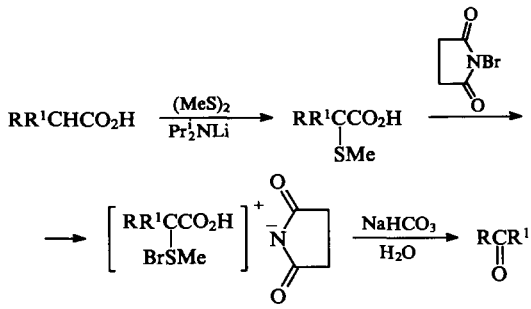
The conversion of the sulfide group into the sulfonium group is one of the most important synthetic procedures widely used in multistage organic syntheses. For example, the protection of the carboxy-group by means of the formation of alkylthiomethyl esters $RCO_2CH_2SR^1$ affords derivatives resistant to the action of alkalis and reductants, which has found applications in the peptide and phosphatide syntheses. [1] In order to remove the alkylthiomethyl group by treatment with methyl iodide, the former is converted into the sulfonium group, which is then cleaved by a solution of alkali, i.e. the conversion of the sulfide group into the sulfonium group with subsequent cleavage is one of the methods for the elimination of the former. A method for the specific cleavage of peptides at the methionine linkages with intramolecular substitution of the oxygen atom of a neighbouring amide group has been developed on the basis of the formation reaction of sulfonium salts. [1]



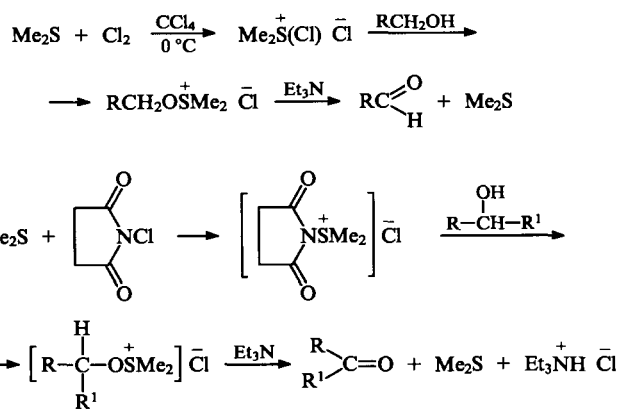
The synthesis of ketones from nitriles ArCHRCN (R = alkyl, aryl) consists in the phenylsulfenylation of the nitrile, the conversion of the sulfide group into the sulfonium group, and the cleavage of the latter with the aqueous NaOH solution–MeCN system.



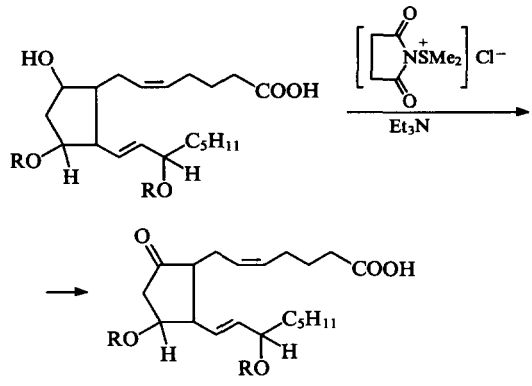
A similar synthetic procedure has been used in the oxidative decarboxylation of carboxylic acids, where *N*-bromosuccinimide served as the oxidant. [1]



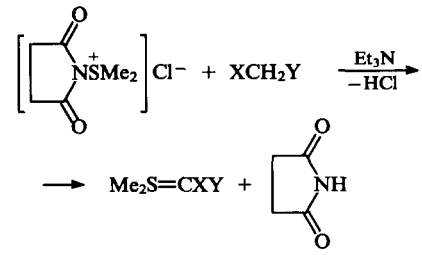
The complexes of dimethyl sulfide with chlorine and *N*-chlorosuccinimide (the Corey–Kim reagent) are widely used in the oxidation of primary and secondary alcohols to carbonyl compounds in synthetic organic chemistry. The carbonyl compound is formed in this case as a result of the cleavage of the intermediate alkoxysulfonium salt. [103]



In the improved synthesis of prostaglandins described by Fieser and Fieser,[103] the Corey–Kim reagent is used to convert the hydroxy-group into the keto-group.

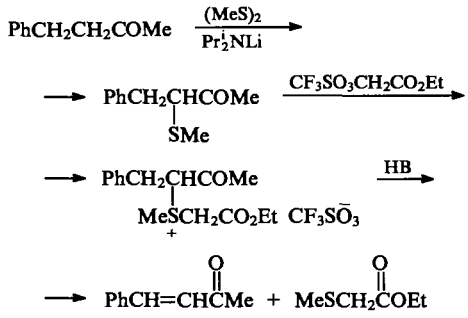


It has been shown [104] that the interaction of the above reagent with CH acids in the presence of triethylamine leads to the formation of sulfur ylides.



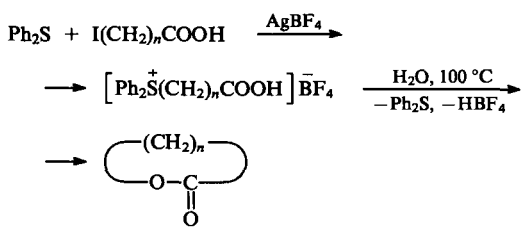
X = Br, Ac, CN; Y = Br, Ac, CO_2Et, CO_2Me, Ph.

The sulfonium centre attacks the β-hydrogen atoms, while the eliminated sulfonium group can function as the leaving nucleophile in E_2 reactions. The conversion of the sulfide group into a sulfonium group with subsequent removal of the latter is used as a method for the introduction of a carbon–carbon double bond, for example in the synthesis of unsaturated ketones from saturated ones. [105]



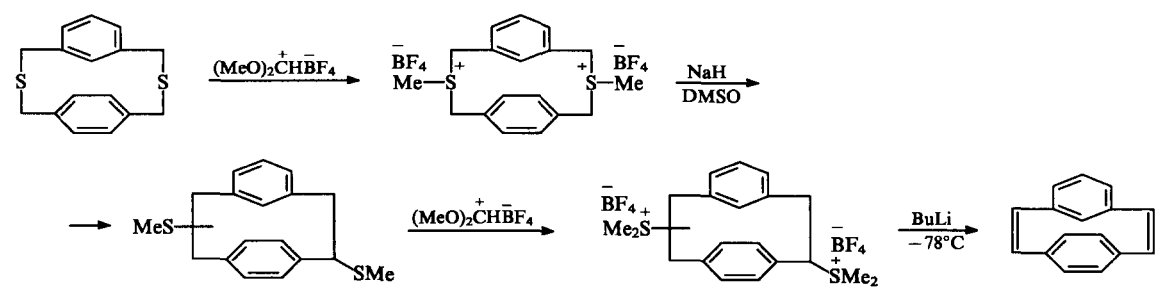
A similar synthetic procedure has been used to convert macrocyclic sulfides into unsaturated hydrocarbons. [103] For example, the key stage in the synthesis of *m,p*-[2,2]cyclophane-1,9-diene is the replacement of the sulfide group by a carbon–carbon double bond, which is achieved as a result of the Stevens rearrangement of the intermediate ylide with subsequent elimination of the sulfonium group (Scheme 4).

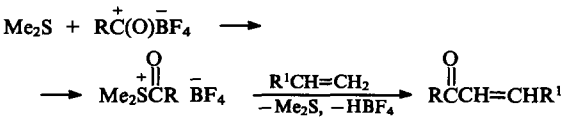
The high lability of the C–S bond in sulfonium salts makes it possible to employ them as alkyl and acyl group transferring agents, which has found applications in biological methylation reactions [106] and also in the syntheses of alkanecarboxylic acid lactones [107] and unsaturated ketones. [108, 109]



n = 3–7

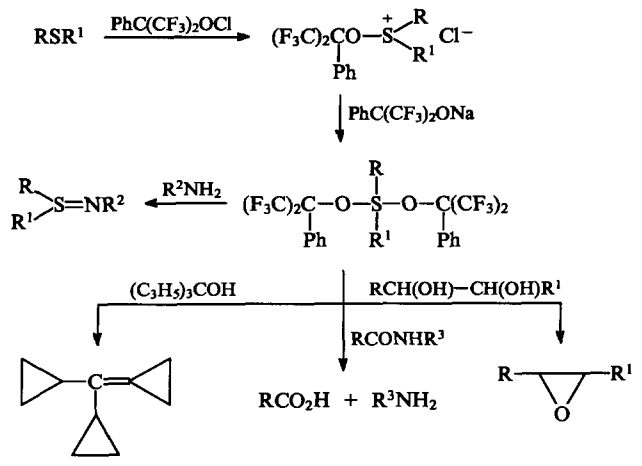
Scheme 4





R = Me, Bu^t; R^1 = Ph.

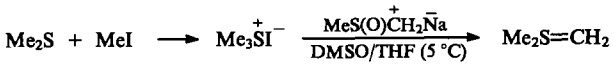
Alkyl sulfonium salts, formed in the reactions of sulfides with alkyl hypochlorites, are readily converted in the presence of alkoxides into highly reactive and relatively stable dialkoxysulfuranes, on the basis of which a whole series of syntheses of sulfilimines, oxiranes, carboxylic acids, and unsaturated hydrocarbons have been developed. [110]



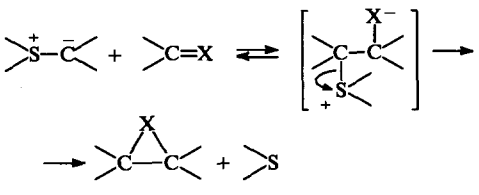
2. Formation of sulfur ylides

a. Transfer of alkylidene groups

The conversion of sulfides into sulfur ylides in multistage organic syntheses is determined primarily by the fact that the latter, being nucleophiles, can participate in the transfer of alkylidene groups to the electrophilic double bond with formation of a three-membered ring, which is frequently used in the syntheses of cyclopropanes, oxiranes, and other cyclic compounds. In view of the ready availability of aldehydes and ketones, the conversion of sulfides into sulfur ylides followed by their condensation with aldehydes and ketones is an important synthetic method for the preparation of oxiranes with a wide variety of structures. [1, 103, 111, 112] Dimethylsulfonium methylide, formed as a result of the reaction of dimethyl sulfide with methyl iodide and subsequent dehydrogenation of the resulting sulfonium salt, is widely used in preparative organic chemistry as a methylene group transferring agent. [1, 66]

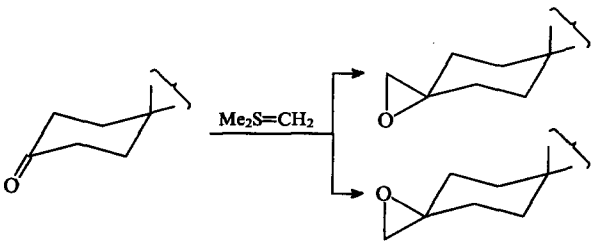


The overall mechanism of the transfer of the alkylidene group with the aid of ylides is presented below. [1] The inter-mediate betaine cyclises via direct substitution at a carbon atom.



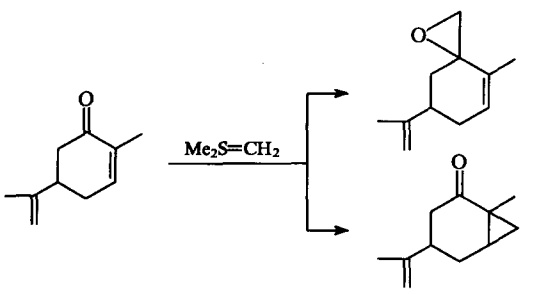
X = O, C.

Depending on the structure of the ylide and the substrate, their addition to one another can lead to the formation of diastereoisomeric or structurally isomeric betaines. The decomposition of such betaines affords various products. For example, the addition of dimethylsulfonium methylide to cholestan-3-one leads to the formation of two structurally isomeric products with oxirane rings.

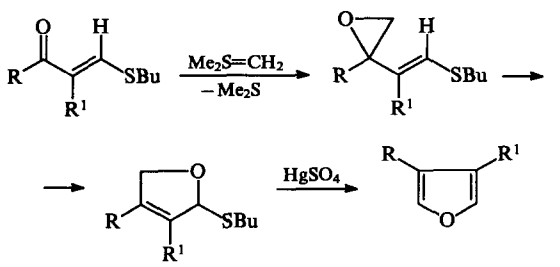


main product

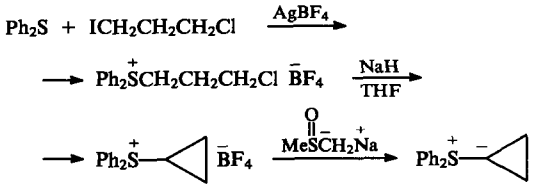
The addition of the same ylide to carvone leads to two different products containing the oxirane and cyclopropane rings with the former predominating.



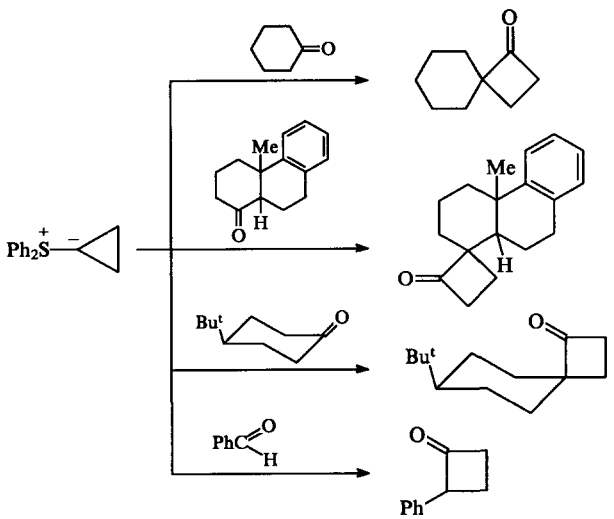
When the substrate molecule contains a mobile hydrogen atom, the oxirane ring formed may be opened with subsequent formation of a five-membered ring, which is used in the synthesis of furans from dimethylsulfonium methylide and unsaturated ketones. [103]



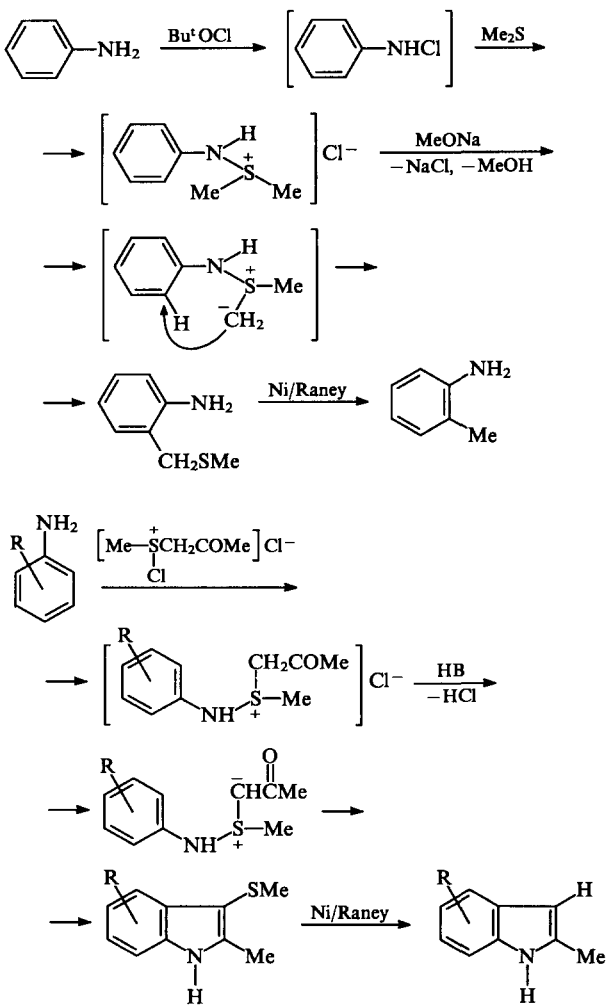
Diphenylsulfonium cyclopropylide, formed in the reaction of diphenyl sulfide with 3-chloro-1-iodopropane in the presence of silver tetrafluoroborate, is used in preparative organic chemistry for the transfer of the trimethylene fragment. [103]



The transfer of the trimethylene fragment to the electrophilic double bond with the aid of diphenylsulfonium cyclopropylide is one of the alternative methods of synthesis of spirocycloalkanones and cyclic ketones. [103]

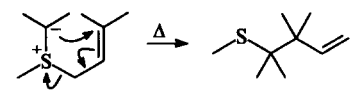


The intramolecular transfer of alkylthiomethylene groups in sulfur ylides is used for the *ortho*-methylation of anilines [113] and in the synthesis of indoles. [114]

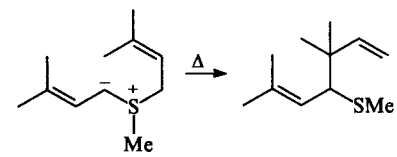


b. Rearrangements of ylides

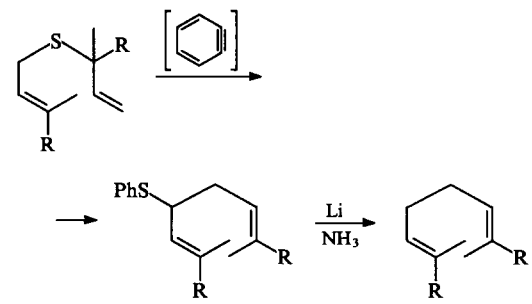
A second aspect of the use of sulfur ylides in organic synthesis is the formation of products as a result of their rearrangement. These rearrangements usually occur fairly readily with formation of a new carbon–carbon bond. For example, the [2,3]-sigmatropic rearrangement of allylsulfonium alkylides leads to but-3-enyl sulfides. [1]



As a rule, this rearrangement takes place with inversion of the allyl group and can be used for the transfer of chirality from the sulfur to a carbon atom. [115]

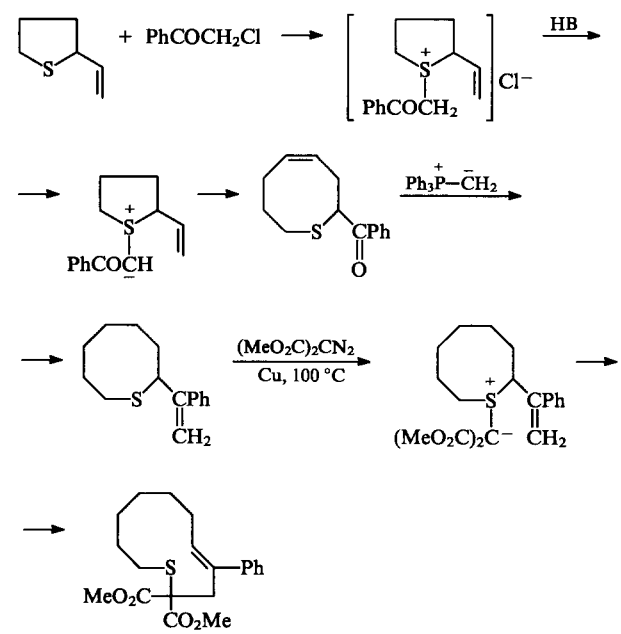


The [2,3]-sigmatropic rearrangement of allylsulfonium alkylides has been used in the synthesis of squalene. [116]

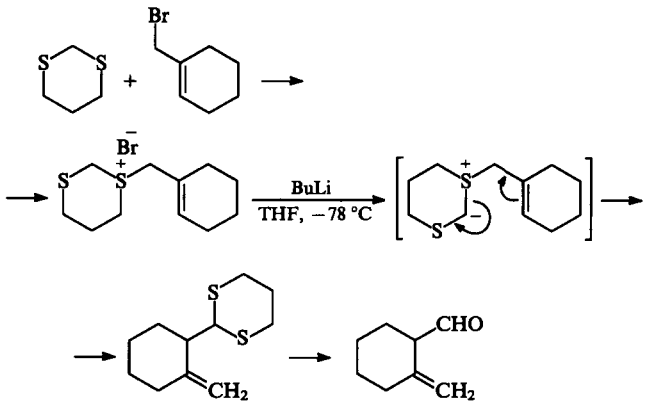


R = $Me_2C{=}CH(CH_2)_2C(Me){=}CH(CH_2)_2$.

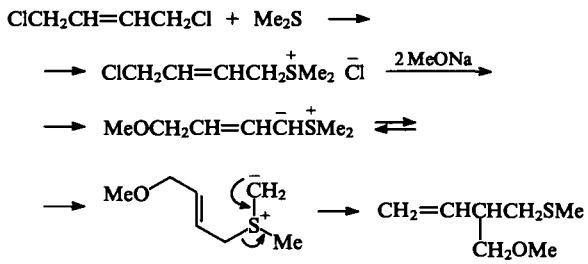
A similar rearrangement is used in the method involving successive ring expansion in cyclic sulfides described by Vedejs and Hagen. [117].

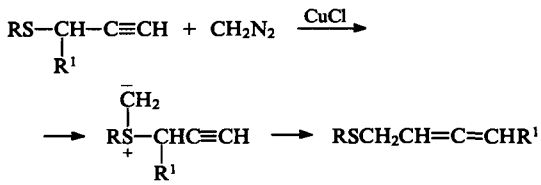


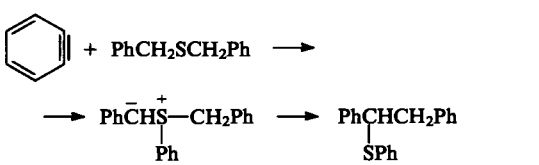
One of the stages in the synthesis of β,γ-unsaturated aldehydes from 1,3-dithiane [103] involves the [2,3]-sigmatropic rearrangement of an intermediate ylide.



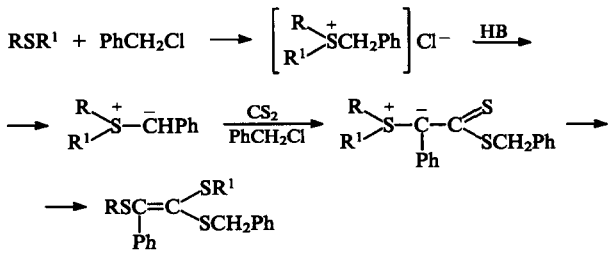
A series of methods of synthesis of polyfunctional sulfides have been developed on the basis of the rearrangement of the corresponding sulfur ylides via a 1,2-shift.[1,118]





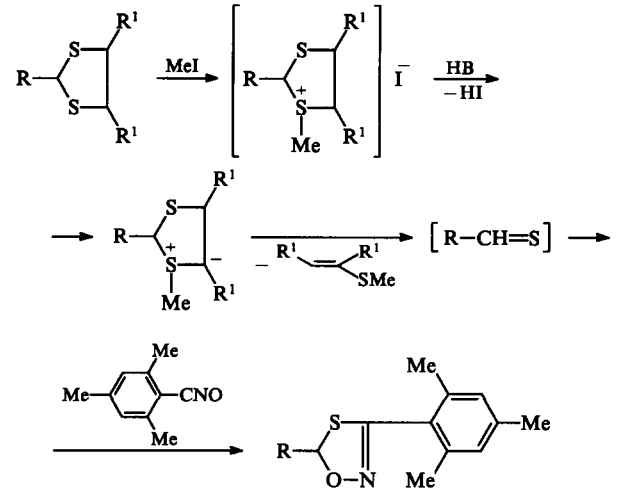


Examples of the use of other rearrangements of sulfur ylides in syntheses of sulfides have been described. For example, the synthesis of 1,1,2-tris(alkylthio)alkenes from dialkyl sulfides includes the rearrangement of ylides stabilised by the introduction of the thiocarbonyl group.[118]



c. Fragmentation of sulfur ylides

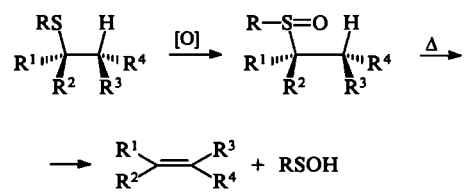
The conversion of 1,3-dithiolanes into thioaldehydes is based on the fragmentation of the intermediate ylide.[119] Mesitonitrile *N*-oxide is used to trap the thioaldehyde. It reacts with the thioaldehyde to form stable 1,4,2-oxathiazoles. In the absence of a 'trapping agent', polymers or trimers are formed.



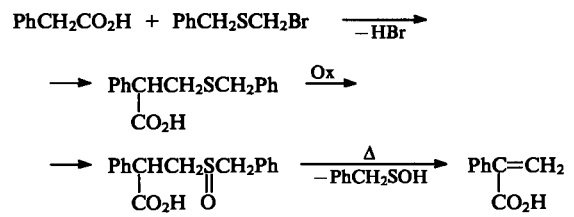
By virtue of the fragmentation reaction of sulfur ylides, 1,3-dithiolanes are convenient reagents for the synthesis of various thioaldehydes.

3. Syntheses of sulfoxides

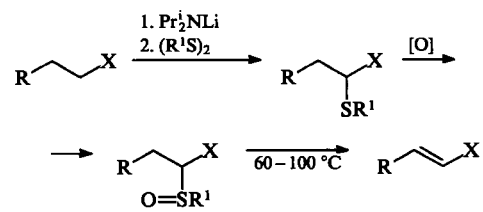
Another approach to the problem of the cleavage of the C–S bond in sulfides is based on the tendency of sulfoxides to undergo thermal *cis*-elimination, which results in the formation of a carbon–carbon double bond.[1]



An important factor for this reaction is the availability of effective selective methods for the oxidation of sulfides, the search for which has been prosecuted vigorously in recent years.[120–126] The presence of powerful electron-accepting groups in the sulfoxide molecule promotes the thermal *cis*-elimination. A clear example of this is provided by the synthesis of α-phenylacrylic acid.[127]

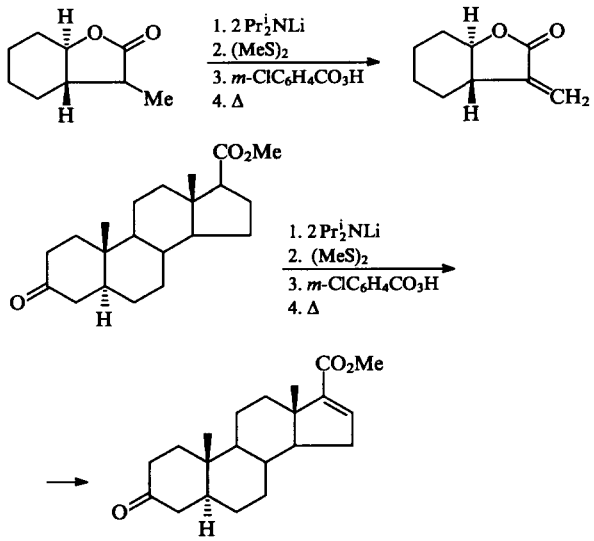


The method for the introduction of a carbon–carbon double bond with the (*E*)-configuration has been investigated in greater detail by Trost et al.[128] The essential feature of the method is the introduction of the phenylthio- or methylthio-group into the α-position relative to the electron-accepting group, the oxidation of the sulfide group to the sulfoxide group, and thermal elimination of the latter.

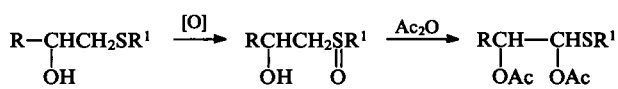


X = COR, CO_2R, CN; R = Alk, Ar; R^1 = Ph, Me.

The elimination of benzenesulfenic acid takes place very readily on refluxing in benzene or carbon tetrachloride, whereas heating in toluene is necessary to split off methanesulfenic acid. A similar chain of reactions is used in the synthesis of α-methylene-3-lactones and also for the selective introduction of a double bond in the α,β-position relative to the ester group in steroids. [129]



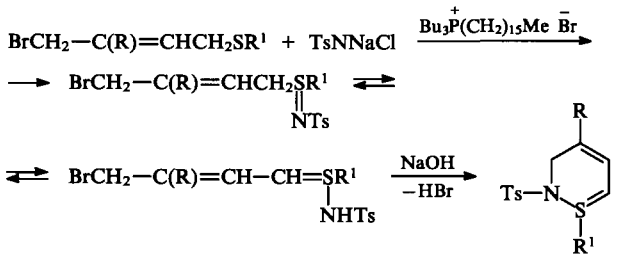
Another aspect of the use of sulfoxides in organic synthesis is their rearrangement in the presence of acetic anhydride (the Pummerer rearrangement). This rearrangement is used widely to convert one sulfide into another. [1,130]



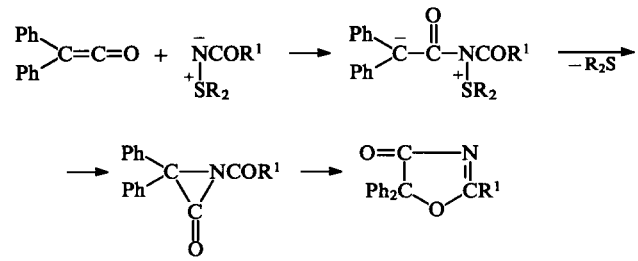
4. Reactions accompanied by the formation of sulfilimines

a. Cyclisation and cycloaddition reactions

The conversion of sulfides into sulfilimines with their subsequent cyclisation or cycloaddition to compounds containing double or triple bonds is used in syntheses of heterocyclic compounds. For example, the preparation of nitrogen-containing heterocyclic compounds from alkyl allyl sulfides, involving a stage with oxidative imination of the sulfide by the sodium salt of the chloramide of toluene-*p*-sulfonic acid and subsequent cyclisation of the resulting sulfilimine, has been described. [131]

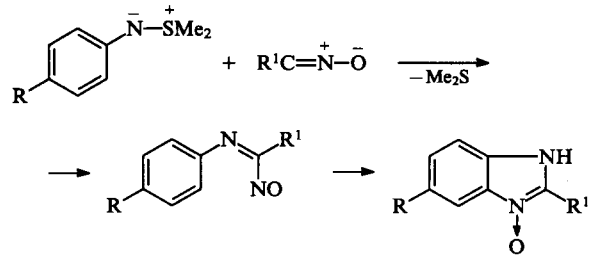


N-Acylsulfilimines, formed as a result of the reaction of sulfides with the *N*-chloramides of carboxylic acids, enter relatively readily into a cycloaddition reaction with diphenylketene, which is used in the synthesis of 1,3-oxazol-4-ones. [132]

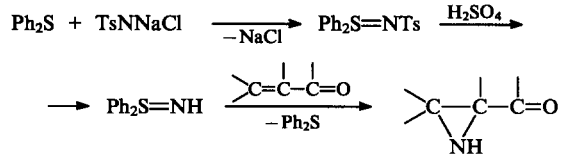


In essence, the reaction represents the transfer of the acylamino-group to the electrophilic double bond.

The cycloaddition of *N*-arylsulfilimines to nitrile oxides is used to obtain benzimidazole *N*-oxides. [133]

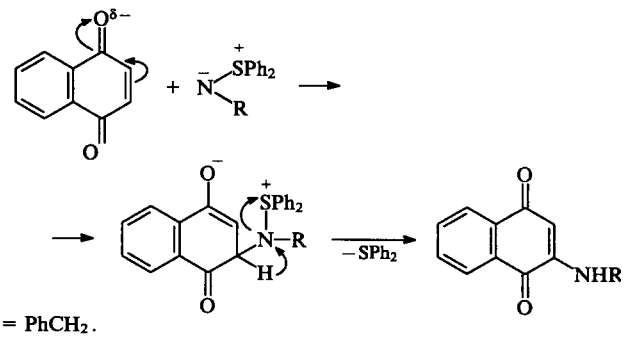


The synthesis of aziridines from sulfides is based on the cycloaddition of diphenylsulfilimines to the double bond in α,β-unsaturated ketones. [134,135]

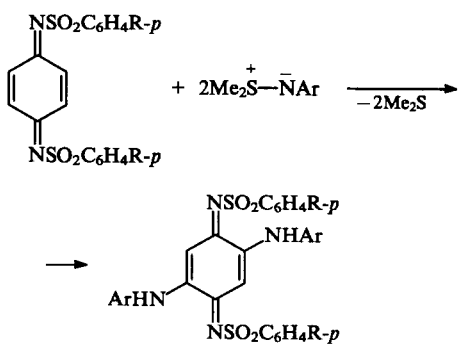


b. Transfer of arylamino-groups

Apart from the cycloaddition reactions, the transfer of the imine fragment of sulfilimines to the electrophilic double bond is used also to introduce arylamino-groups into the quinonoid rings of quinones [136] and quinone imines. [137]



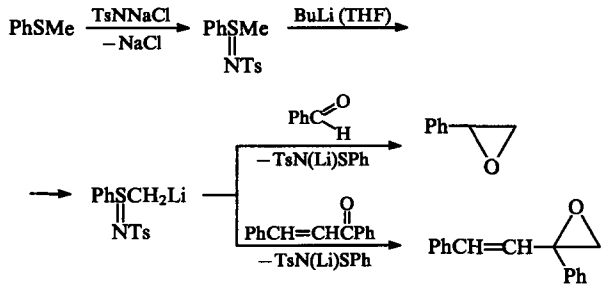
R = PhCH$_2$.



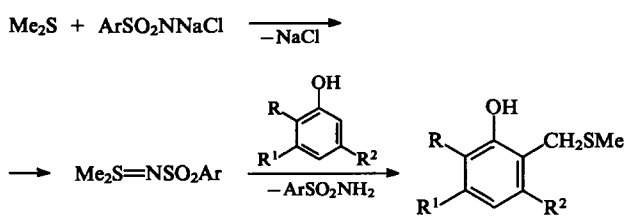
R = H, Me; Ar = Ph, *p*-MeC$_6$H$_4$, *p*-ClC$_6$H$_4$, *p*-NO$_2$C$_6$H$_4$.

c. Transfer of alkylidene groups

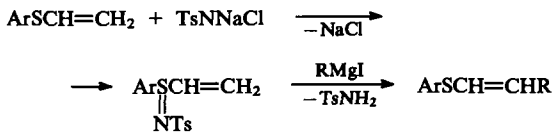
The strong electron-accepting influence of the arenesulfonylimino-group in *N*-arenesulfonylsulfilimines increases the acidity of the α-hydrogen atoms in the *S*-alkyl groups, which promotes their substitution by an alkali metal atom. Such organo-metallic compounds are used as nucleophiles which transfer alkylidene groups to an electrophilic double bond (for example, C=O) with formation of a three-membered ring.[138,139] The stable anion of *N*-arenesulfonylsulfenamide is the leaving group, the elimination of which leads to the formation of a three-membered ring, which also promotes the occurrence of this process.



The introduction of the methylthiomethyl group into the ring of phenols with the aid of *N*-arenesulfonyl-*S*,*S*-dimethylsulfilimines is used in the synthesis of benzylmethyl sulfides.[139,140]

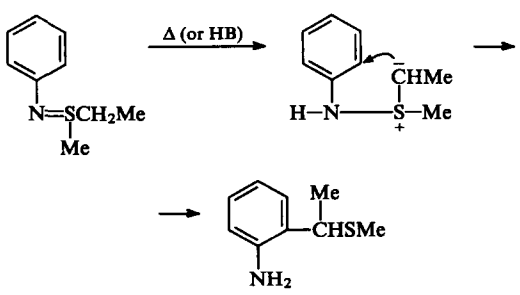


The conversion of the vinyl sulfide $ArSCH=CH_2$ into $ArSCH=CHR$ via the corresponding sulfilimine by means of a Michael type reaction using organomagnesium compounds has been described.[141]

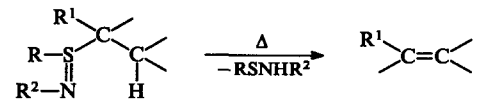


d. Rearrangements of sulfilimines

On heating and also on treatment with bases, certain *N*-arylsulfilimines undergo a Sommelet type rearrangement, which is used to introduce alkylthiomethyl groups into the *ortho*-position in anilines.[139]

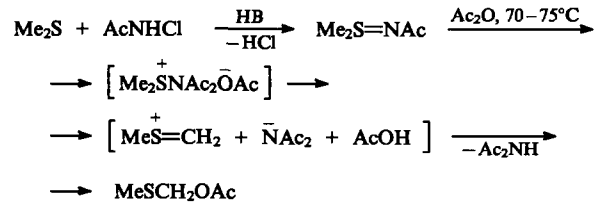


S-Alkylsulfilimines containing β-hydrogen atoms undergo on heating a rearrangement with formation of alkenes,[142] which can serve as one of the methods for the elimination of the sulfide group.



R^1 = H, Me; R^2 = Ar, MeCO.

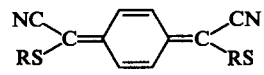
The Pummerer rearrangement of *N*-acylsulfilimines is used to convert dimethyl sulfide into acetoxymethyl methyl sulfide.[1]



VII. Practical applications of sulfides

1. Sulfides in macromolecular chemistry

Sulfides are used in macromolecular chemistry in several ways. One of these involves the employment of sulfides as monomers. As a rule, in this case sulfides contain, apart from the sulfide group, unsaturated bonds or other functional groups which participate directly in the formation of the polymer chain as a result of polymerisation or polycondensation reactions.[143] Thus a series of homopolymers and copolymers containing sulfur atoms in the main chain have been obtained from divinyl sulfide.[144] The synthesis of 7,8-bis[alkyl(aryl)thio]-7,8-dicyanoquinodimethanes having the general formula



R = Et, Bu^t, Ph,

has been described and their reactions have been investigated.[145] For R = Et, the polymerisation proceeds via radical, anionic, and cationic mechanisms with formation of a polymer having an ethylthio-group in the side chain, for R = Ph it proceeds via radical and anionic mechanisms, and for R = Bu^t the monomer does not polymerise, which the authors believe[145] to be due to a steric effect.

The synthesis of poly(phenylene sulfide) via the polycondensation of *o*- and *m*-di(chlorophenyl) sulfides with sodium sulfide in an organic solvent has been described in the patent literature.[146,147] Aromatic polythioesteramideimides with effective mechanical properties, a high heat resistance, and a high plasticity have been obtained by the polycondensation of the disulfide $NH_2C_6H_4SC_6H_4SC_6H_4NH_2$ with the monochloride of trimellitic acid and subsequent cyclisation of the polyamido-acid.[148] The synthesis of aromatic polyketones containing sulfur atoms in the main chain is based on the polycondensation of diphenyl sulfide and phosgene.[149] A new type of sulfide-formaldehyde polymer, capable of being cross-linked, has been obtained by the polycondensation of di(2-hydroxyphenyl) sulfide and formaldehyde.[150]

A second application of sulfides in macromolecular chemistry involves their participation in the regulation of polymer formation processes. It has been noted,[151] for example, that the sulfides $PhCH_2SR$ and $C_6H_4(CH_2SR)_2$ are inifers of the radical polymerisation of styrene. The principle of the action of such

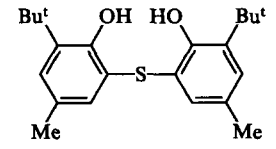
inifers consists in the initiation of the radical polymerisation and transfer of the polymer chain in the concluding stage of the polymerisation reaction, which leads ultimately to a linear dependence of the number-average molecular weight of the polymer on the polymerisation time. The influence of sulfides on the cationic polymerisation of vinyl ethers initiated by UV light and sulfonium salts,[152] the rate of which diminishes with increase in the nucleophilicity of the sulfide, has also been noted.

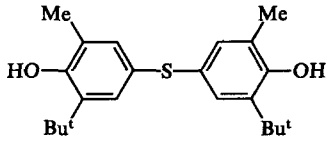
2-Benzothiazolyl 2,4-dinitrophenyl sulfide has found extensive application in the manufacture of white and light-coloured rubbers as a vulcanisation accelerator which does not induce additional vulcanisation.[153]

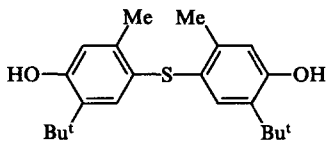
The third application of sulfides in macromolecular chemistry is the stabilisation and protection of polymeric materials against the negative influence of various factors (light, heat, oxygen, etc.) For example, dialkyl sulfides decompose the peroxides formed in the oxidative degradation of polymers without the formation of free radicals, which is very important for the arrest of oxidative degradation.[154,155] These compounds are very effective in mixtures with other stabilisers, in particular stabilisers of the phenolic or amine types.

The mutual intensification of the protecting effect can be explained by the fact that one of the stabilisers terminates the degradation process, giving up hydrogen to the peroxyl radicals, while the other decomposes hydroperoxides. Dialkyl and diaryl sulfides mixed with other substances are effective stabilisers of vinyl polymers, polyolefins, and poly(vinyl acetals).

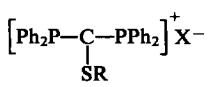
Diaryl sulfides containing hydroxy- and alkyl groups in the aromatic rings have found an application as stabilisers of rubber, protecting it against the effects of oxygen and heat.[156]







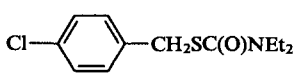
Phosphorus-containing sulfides are effective antipyrenes, which protect polymeric materials against combustion.[25]



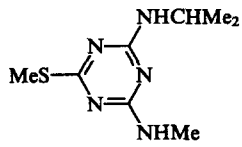
X = SO_4, BF_4, $AlCl_4$.

2. Biological activity of sulfides

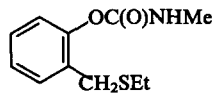
A whole series of compounds containing the sulfide group are used in agriculture as effective pesticidal preparations.[157] For example, 2-chlorobenzyl-2-chlorophenyl sulfide, known under the commercial name chlorbenzid or chlorocid, is used as an effective acaricidal preparation against plant ticks on fruit. Benthiocarb



and desmetryn



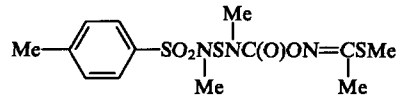
are used as herbicidal preparations to combat oat-like weeds. Ethiofencarb



is used as an insecticide against aphids. 2-Benzothiazolyl butyl sulfide is employed as a defoliant of the thin-fibre cotton plant.

Studies on the biological activity of sulfides have been directed in recent years both to the search for new and the modification of already known pesticides in order to reduce their toxicity to warm-blooded animals. For example, methomyl MeNHCOON=C(Me)–SMe and aldicarb MeNHCOON=CH–$(CH_2)_2$–SMe possess outstanding insecticidal and acaricidal properties, but are toxic to warm-blooded animals.[158]

It has been established for carbamates[159] that the substitution of a hydrogen atom at the nitrogen atom by an amino- or amidosulfenyl group lowers sharply their toxicity to warm-blooded animals whilst retaining and in certain cases actually intensifying their pesticidal activity. Several groups of investigators therefore undertook studies on the synthesis of aminosulfenylated derivatives of methomyl, aldicarb, and ethiofencarb.[159–167] Apart from *N*-amino(amido)sulfenylated derivatives of methomyl,[168–173] aldicarb,[174] ethiofencarb,[25] and their analogues, these studies led to the synthesis also of a whole series of *N*,*N*′-dicarbamoyl sulfides[175–178] and *N*-sulfenylated 2-(alkylthiomethyl)phenyl-*N*-alkylcarbamates[179] with insecticidal activity. The above studies also made it possible to obtain an insectoacaricidal preparation with systemic activity, a better phytotoxicity than methomyl, and an effectively long duration of activity.[180]



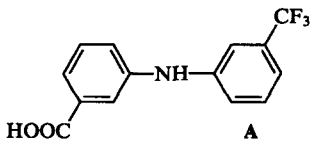
A series of biologically active sulfides which are potential pesticides have been synthesised in recent years. For example, it has been noted[69] that the sulfides 2-$NO_2C_6H_4SCH_2NO_2$ and (2-$NO_2C_6H_4S)_2CHNO_2$ exhibit a relatively high nematocidal activity and an insectoacaricidal activity against the beetroot aphid. The sulfides 4-$NO_2C_6H_4SCH(CN)_2$, 2,4-$(NO_2)_2C_6H_3SCH(CN)_2$, and 2-$NO_2C_6H_4SCH(COMe)_2$ possess a relatively high insectoacaricidal activity in relation to the rice snout-beetle and the arachnoid tick.[68]

3. Sulfides as pharmaceutical preparations

One of the important properties of medicinal preparations is solubility in lipids, its increase enhancing their effectiveness (by facilitating their transport in the organism and their permeation through membranes and by increasing their concentration in lipid regions).[181,182] The solubility of medicinal preparations can be increased by introducing into their molecules lipophilic groups, the relative lipophilicity of which is characterised by Hantzch's π constants. According to literature data,[183,184] these constants for certain groups have the following values: 1.44 (SCF_3), 1.28 (SCF_2Br), 1.23 (C_2F_5), 1.04 (OCF_3), 1.01 (OCF_2Br), 0.88 (CF_3), 0.68 (SCF_2H), 0.61 (SMe), 0.58 (OCF_2H), 0.56 (Me), 0.55 (SO_2CF_3).

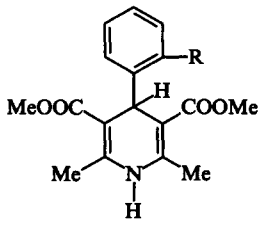
As can be seen from these data, the trifluoromethylthio-group exhibits a fairly high lipophilicity and its introduction into the molecules of medicinal preparations should evidently increase their effectiveness.

This hypothesis has been to some extent confirmed by the introduction of the trifluoromethylthio-group and other lipophilic groups in various positions in the benzene ring A of flufenamic acid.[182]



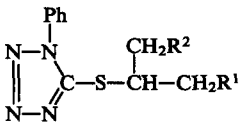
A

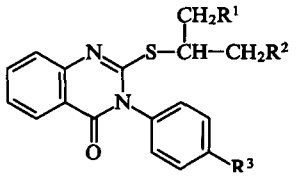
It was found that the sulfide formed as a result of the introduction of the trifluoromethylthio-group has a lower anti-inflammatory activity than flufenamic acid, but is superior to the latter in its antiproteinase activity. The antiproteinase activity of derivatives of flufenamic acid increases in the following sequence of substituents $HF_2CO < CHF_2SO_2 < CF_3 < SCF_3$, which corresponds approximately to the increase in their lipophilicity. Especially interesting results have been obtained following the introduction of the above substituents in the *ortho*-position in the benzene ring of 4-phenyl-1,4-dihydropyridine.



Such preparations exert a powerful effect on the cardiovascular system and are antagonists of calcium ions.[182]

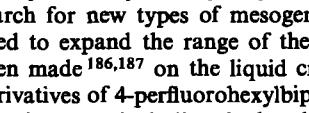
Certain sulfides, in particular those containing the tetrazole and pyrimidine rings, have radioprotecting properties.[185]





4. The liquid crystal properties of sulfides

Organic compounds forming liquid crystals have found extensive applications in the reproduction and recording of information in various branches of science and engineering. Such compounds have the ability to generate, on heating and cooling in the range between the liquid crystal state and the isotropic liquid melt, intermediate smectic and nematic mesophases which differ in the degree of molecular order.[182] Derivatives of various classes of organic compounds, the molecules of which have a linear shape and have largely a structure of the same type, possess the properties of liquid crystals. These compounds (mesogens) contain a central rigid fragment, consisting of a conjugated aromatic or bridged system, and also end groups of different nature (alkyl, alkoxy-, alkoxycarbonyl, cyano-, nitro-groups, etc.). In the search for new types of mesogens and in connection with the need to expand the range of their characteristics, studies have been made[186,187] on the liquid crystal properties of a series of derivatives of 4-perfluorohexylbiphenyl containing various functional groups, including the butylthio-group in the *para*-position in the second benzene ring.



X = H, CN, NHBu, SBu.

It has been established that the introduction of the strong electron-donating butylamino-group ($\sigma_n = -0.60$) leads to the appearance of a liquid crystal phase of the more ordered smectic type with an increased thermal stability. When the butylamino-group is replaced by the less electron-donating butoxy-group ($\sigma_n = -0.32$), the formation of a liquid crystal phase of the smectic type is nevertheless still ensured. On further weakening of the electron-donating properties of the substituents and, in particular, following the introduction of the butyl group ($\sigma_n = -0.16$) and the butylthio-group ($\sigma_n = 0.03$), the mesogenic property vanishes.

* * *

It is seen from the present review that the use of sulfides as synthons in fine organic synthesis has undergone in recent years considerable expansion based on the characteristic features of the reactivity of sulfides — the high lability of the C–S bond. The sulfide group can be replaced by a hydrogen atom and hydroxy-, alkyl, alkoxy-, thiyl, and other functional groups. The thermal and photolytic cleavage of the C–S bond leads to the formation of highly reactive intermediates, which are used in the synthesis of various cyclic adducts. A characteristic feature of the reactivity of sulfides, which is of great synthetic importance, is their tendency to form α-sulfenylcarbanions, which are used widely in multistage organic syntheses for the formation of carbon–carbon bonds. The ease of the conversion of sulfides into sulfonium, ylide, sulfoxide, and sulfilimine intermediates is also used widely in multistage organic syntheses for the transfer of various groups to an electrophilic double bond, for the formation of a carbon–carbon double bond, and for other transformations.

The practical applications of sulfides in macromolecular chemistry, in agriculture, in pharmaceutical industry, and in other fields of human activity are no less important and this too has been reflected in the present review.

References

1. D K Barret, in *Comprehensive Organic Chemistry* (Eds D H R Barton, W D Ollis) (Translated into Russian; Moscow: Khimiya, 1983) Vol. 5, p. 163
2. E C Taylor, J L LaMattina *Tetrahedron Lett.* **18** 2077 (1977)
3. A Toshimitsu, C Hirosawa, S Tanimoto *Tetrahedron Lett.* **32** 4317 (1991)
4. I V Koval', V V Andrushchenko, M M Kremlev *Zh. Org. Khim.* **18** 841 (1982)
5. I V Koval', V V Andrushchenko, M M Kremlev, A I Tarasenko *Zh. Org. Khim.* **21** 1286 (1985)
6. I V Koval', T G Panasenko, R M Minyaev, I S Panchenko *Zh. Org. Khim.* **23** 325 (1987)
7. I V Koval', T G Panasenko, A I Tarasenko, N R Molchanova *Zh. Org. Khim.* **25** 835 (1989)
8. I V Koval', T G Panasenko *Zh. Org. Khim.* **25** 1677 (1989)
9. I V Koval', T G Panasenko *Zh. Org. Khim.* **26** 1728 (1990)
10. I V Koval' *Usp. Khim.* **59** 681 (1990) [*Russ. Chem. Rev.* **59** 396 (1990)]
11. A Hosomi, V Matsuyama, H Sakurai *J. Chem. Soc., Chem. Commun.* **14** 1073 (1986)
12. B M Dilworth, M A McKervey *Tetrahedron* **42** 3731 (1986)
13. C C Fortes, E A Okino *Synth. Commun.* **20** 1943 (1990)
14. P A Magriotis, T J Doyle, K O Kim *Tetrahedron Lett.* **31** 2541 (1990)
15. S Konesama, H Kobayashi, J Tanaka, O Tsuge *Bull. Chem. Soc. Jpn.* **61** 3957 (1988)
16. H Ishibashi, I Takamuro, Y Mizukami, M Irie, M Ikeda *Synth. Commun.* **19** 443 (1989)
17. M Hans, H Dehne, R Harfwig *Z. Chem.* **26** 204 (1986)
18. T Takeda, F Kanamori, H Matsusita, T Fujiwara *Tetrahedron Lett.* **32** 6563 (1991)

19. R J Ferrier, R H Furneaux *J. Chem. Soc., Chem. Commun.* 332 (1977)
20. L Bernardi, R DeCastiglione, U Scarponi *J. Chem. Soc., Chem. Commun.* 320 (1975)
21. T Cohen, in *The XVth International Symposium of Organic Chemistry of Sulfur, Caen, 1992 (Abstracts of Reports)* p. 2
22. K Chibale, S Warren *Tetrahedron Lett.* **32** 6615 (1991)
23. J L R Garda, A M M Castro, J H Rodriguez *Tetrahedron Lett.* **32** 3195 (1991)
24. I N Zhmurova, V G Yurchenko, A M Pinchuk *Zh. Obshch. Khim.* **55** 321 (1985)
25. Yu G Gololobov, N I Gusar *Sul'fenkhloridy* (Sulfene Chlorides) (Moscow: Nauka, 1989)
26. M Mikolajczuk, P Kielbasinski, S Grzejszak *Synthesis* 332 (1983)
27. T Taheda, F Kanamori, M Masuda, T Fujiwara *Tetrahedron Lett.* **32** 5567 (1991)
28. N A Korchevin, V A Usov, L A Oparina, I A Dorofeev, Ya S Tsetlin, M G Voronkov *Zh. Org. Khim.* **16** 1842 (1980)
29. N Yahate, M Fujima, K Ogura *Bull. Chem. Soc. Jpn.* **63** 3601 (1990)
30. B M Trost, K Hiroi *J. Am. Chem. Soc.* **97** 6911 (1975)
31. L V Timokhina, V A Usov, M G Voronkov *Zh. Org. Khim.* **14** 2226 (1978)
32. V A Usov *Izv. Akad. Nauk Latv. SSR* **1** 94 (1986)
33. V A Usov, L V Timokhina, M G Voronkov *Usp. Khim.* **15** 1761 (1986) [*Russ. Chem. Rev.* **15** 1003 (1986)]
34. V A Usov, L V Timokhina, L I Lavlinskaya, M G Voronkov *Zh. Org. Khim.* **15** 2598 (1979)
35. I A Dorofeev, N A Korchevin, V A Usov, M G Voronkov *Zh. Org. Khim.* **20** 1727 (1984)
36. R J Anderson, C A Henrick, L D Rosenblum *J. Am. Chem. Soc.* **96** 3654 (1974)
37. L D Rosenblum, R J Anderson, C A Henrick *Tetrahedron Lett.* **17** 419 (1976)
38. G H Posner, D J Brunell *J. Chem. Soc., Chem. Commun.* 907 (1973)
39. R B Gamill, T A Bryson *Tetrahedron Lett.* **16** 3793 (1975)
40. S I Radchenko *Zh. Org. Khim.* **12** 229 (1976)
41. A I Meyers, M E Ford *Tetrahedron Lett.* **16** 2861 (1975)
42. M G Voronkov, E N Deryagina *Usp. Khim.* **59** 1338 (1990) [*Russ. Chem. Rev.* **59** 778 (1990)]
43. A R Katritzky, A R Lapucha, J V Greenhill, M Siskin *Energy Fuels* **4** 562 (1990)
44. A M Gaber, M S Abbady *Phosphorus Sulfur Silicon Relat. Elem.* **69** 7 (1992)
45. H Bock, S Mohmand *Angew. Chem.* **89** 105 (1977)
46. E N Sukhomazova, E N Deryagina, M G Voronkov *Zh. Org. Khim.* **16** 405 (1980)
47. M G Voronkov, E N Deryagina, E N Sukhomazova *Zh. Org. Khim.* **18** 1736 (1982)
48. L A Ostroukhova, N A Korchevin, E N Deryagina, M G Voronkov *Zh. Org. Khim.* **23** 2016 (1987)
49. V A Korolev, J Tamash, K Uisasi, A K Mal'tsev, O M Nefedov *Izv. Akad Nauk SSSR, Ser. Khim.* 2398 (1987)
50. H G Giles, R A Marty *Can. J. Chem.* **54** 537 (1976)
51. K Georgiou, H W Kroto *J. Mol. Spectrosc.* **83** 94 (1980)
52. H Bock, S Mohmand, T Hirabayashi, A Semkow *J. Am. Chem. Soc.* **104** 312 (1982)
53. H Bock, S Mohmand, T Hirabayashi, A Semkow *Chem. Ber.* **115** 1339 (1982)
54. J E Baldwin, R C G Lopez *J. Chem. Soc., Chem. Commun.* 1029 (1982)
55. J E Baldwin, R C G Lopez *Tetrahedron* **39** 1487 (1983)
56. G W Kirby, A W Lochead, G N Sheldrake *J. Chem. Soc., Chem. Commun.* 1469 (1984)
57. L F Lee, M G Dolson, R K Howe, B R Stults *J. Org. Chem.* **50** 3216 (1985)
58. V A Usov, L V Timokhina, M G Voronkov *Usp. Khim.* **59** 649 (1990) [*Russ. Chem. Rev.* **59** 378 (1990)]
59. E Vedejs, C L Fedde, C E Schwarts *J. Org. Chem.* **52** 4269 (1987)
60. E Vedejs, J S Stults *J. Org. Chem.* **53** 2226 (1988)
61. E Vedejs, T H Eberlein, D L Varie *J. Am. Chem. Soc.* **104** 1445 (1982)
62. G A Krafft, P T Meinke *Tetrahedron Lett.* **26** 135 (1985)
63. E Vedejs, D A Perry *J. Am. Chem. Soc.* **105** 1683 (1983)
64. L I Belen'kii (Ed.), in *Khimiya Organicheskikh Soedinenii Sery* (Chemistry of Organic Compounds of Sulfur) (Moscow: Khimiya, 1989) p. 319
65. K Iwai, M Kawai, H Kasugi, H Uda *Chem. Lett.* 385 (1974)
66. I V Koval' *Usp. Khim.* **59** 1409 (1990) [*Russ. Chem. Rev.* **59** 819 (1990)]
67. G R Newkome, J M Robinson, J D Sauer *J. Chem. Soc., Chem. Commun.* 410 (1974)
68. I V Koval', T G Panasenko *Ukr. Khim. Zh.* **56** 638 (1990)
69. I V Koval', T G Panasenko *Zh. Org. Khim.* **28** 325 (1992)
70. A Hosomi, Y Matsuyama, H Sahurai *J. Chem. Soc., Chem. Commun.* 1073 (1986)
71. S Kanemasa, H Kobayashi, J Tanaka, O Tsuge *Bull. Chem. Soc. Jpn.* **61** 3957 (1988)
72. I V Koval', T G Panasenko *Zh. Org. Khim.* **27** 217 (1991)
73. D J Ager *J. Chem. Soc., Perkin Trans. 1* 1131 (1983)
74. B J Banks, A G M Barrett, M A Russell *J. Chem. Soc., Chem. Commun.* 670 (1984)
75. A Hosomi, K Ogata, K Hoashi, S Kohra, Y Taminaga *Chem. Pharm. Bull.* **36** 3736 (1988)
76. D S Watt, E J Corey *Tetrahedron Lett.* **16** 4531 (1975)
77. F Babudri, S Florio, A M Vitrani, L DiNunno *J. Chem. Soc., Perkin Trans. 1* 1899 (1984)
78. M Aswell, R F W Jackson *J. Chem. Soc., Chem. Commun.* 282 (1988)
79. M Aswell, R F W Jackson, J M Kirk *Tetrahedron* **46** 7429 (1990)
80. C R Johnson, A Nakanishi, N Nakanishi, K Tanaka *Tetrahedron Lett.* **16** 2865 (1975)
81. G M A Barrett, A J Flygare, D C Spilling *J. Org. Chem.* **54** 4723 (1989)
82. K Tanaka, M Tarauchi, A Kaji *Chem. Lett.* 315 (1981)
83. K Tanaka, M Tarauchi, A Kaji *Chem. Lett.* 351 (1982)
84. K Arai, Y Ohara, T Iizumi, Y Takakawa *Tetrahedron Lett.* **24** 1531 (1983)
85. M A McKervey, P Pananukuc *Tetrahedron Lett.* **24** 117 (1983)
86. K Akiba, Y Takasu, M Wada *Tetrahedron Lett.* **26** 2463 (1985)
87. M Wada, T Shigehisa, H Kitami, K Akiba *Tetrahedron Lett.* **24** 1715 (1983)
88. B Lythgoe, J R Milner, J Tideswell *Tetrahedron Lett.* **16** 2593 (1975)
89. A V Anisimov, E A Viktorova, T A Danilova *Molekulyarnye Peregruppirovki Seroorganicheskikh Soedinenii* (Molecular Rearrangements of Organic Compounds of Sulfur) (Moscow: Izd. Moscovsk. Gos. Univ., 1989)
90. P Brownbridge, S Warren *J. Chem. Soc., Chem. Commun.* 820 (1975)
91. T Mandai, T Moriyama, Y Nakayama, K Sugino, M Kawada, J Otera *Tetrahedron Lett.* **25** 5913 (1984)
92. I E Mikhailov, V I Minkin, A A Klenkin, G A Dushenko, O E Kompan, A I Yanovskii, Yu T Struchkov *Zh. Org. Khim.* **36** 28 (1990)
93. T Masuda, T Matsumoto, T Yoshimura, T Higashimura *Macromolecules* **23** 4902 (1990)
94. K Chibale, S Warren *Tetrahedron Lett.* **32** 6645 (1991)
95. P Hamel, Y Girard, G J Atkinson *J. Org. Chem.* **57** 2694 (1992)
96. M Raban, L J Chern *J. Org. Chem.* **45** 1688 (1980)
97. I V Koval' *Usp. Khim.* **60** 1645 (1991) [*Russ. Chem. Rev.* **60** 830 (1991)]
98. R G Haghes, S Naube, A Pelter, K Smith, E Negishi, T Yoshida *J. Chem. Soc. Perkin Trans. 1* 1172 (1977)
99. N Yahata, M Fujita, K Ogura *Bull. Chem. Soc. Jpn.* **63** 3601 (1990)
100. K Ogura, N Yahata, T Fujimori, M Fujita *Tetrahedron Lett.* **31** 4621 (1990)
101. J P Dittami, X Y Nie, C J Buntel, S Rigatti *Tetrahedron Lett.* **31** 3821 (1990)
102. J P Dittami, X Y Nie, H Nie, H Ramanathan, C Buntel, S Rigatti, J Bordner, D L Decosta, P Williard *J. Org. Chem.* **57** 1151 (1992)
103. L Fieser, M Fieser, in *Reagents for Organic Synthesis* (Translated into Russian; Moscow: Mir, 1978) Vol. 7, p. 461
104. S Katayama, T Watanabe, M Yamauchi *Chem. Lett.* 973 (1989)
105. E Vedejs, D A Engler *Tetrahedron Lett.* **17** 3487 (1976)
106. G Grue-Sorensen, A Kjaer, E Wieczorkowska *J. Chem. Soc., Chem. Commun.* 355 (1977)

107. T Nakamura, H Matsuyama, M Takahashi, N Kamigata *Phosphorus Sulfur Silicon Relat. Elem.* **66** 59 (1992)
108. P V Verteletskii, E S Belenkova *Zh. Org. Khim.* **26** 2446 (1990)
109. V G Nenaidenko, P V Verteletskii, E S Belenkova, in *XVIII Konf. po Khimii i Tekhnologii Organicheskikh Soedinenii Sery, Kazan' 1992. (Tez. Dokl.)* [The XVIIIth Conference on the Chemistry and Technology of Organic Compounds of Sulfur (Abstracts of Reports)] p. 168
110. J C Martin, E F Perozzi *Science* **191** 154 (1976)
111. L Breau, W W Ogilvie, T Durst *Tetrahedron Lett.* **31** 35 (1990)
112. T Durst *The XVth International Symposium of Organic Chemistry of Sulfur, Caen, 1992 (Abstracts of Reports)* p. 16
113. P G Gassman, G D Gruetzmacher *J. Am. Chem. Soc.* **95** 588 (1973)
114. P G Gassman, G D Gruetzmacher, T J Van Bergen *J. Am. Chem. Soc.* **96** 5512 (1974)
115. B M Trost, R F Hammen *J. Am. Chem. Soc.* **95** 962 (1973)
116. G M Blackburn, W D Ollis, C Smith, I O Sutherland *Chem. Commun.* 99 (1969)
117. E Vedejs, J P Hagen *J. Am. Chem. Soc.* **97** 6878 (1975)
118. G Pourcelot, L Veniard, P Cadiot *Bull. Soc. Chim. Fr.* 1281 (1975)
119. E Schaumann, G Rühter *Tetrahedron Lett.* **26** 5265 (1985)
120. K Wojciechowski *Org. Prep. Proceed. Int.* **20** 493 (1988)
121. J J Eisch, M Behrooz *Org. Synth.* **4** 494 (1988)
122. N Sakurava, K Natori, Y Tanaka *J. Org. Chem.* **56** 4126 (1991)
123. H L Holland, C G Rand, P Viski, F M Brown *Can. J. Chem.* **69** 1989 (1991)
124. S W Kaldor, M Hammond *Tetrahedron Lett.* **32** 5043 (1991)
125. V Farina, S I Hauck *J. Org. Chem.* **56** 4317 (1991)
126. E H Folsam *Synth. Commun.* **22** 1799 (1992)
127. H J Reich, J M Renga *J. Chem. Soc., Chem. Commun.* 135 (1974)
128. B M Trost, T N Salzmann, K Hiroi *J. Am. Chem. Soc.* **98** 4887 (1976)
129. P A Grieco, J J Reap *Tetrahedron Lett.* **15** 1097 (1974)
130. H Ishibashi, M Ikeda *J. Synth. Org. Chem. Jpn.* **47** 386 (1989)
131. R E Dolle, Li Chung-Sing, A N Shaw *Tetrahedron Lett.* **30** 4723 (1989)
132. M Abou-Charbia, D M Ketcha, D E Zacharius, D E Swern *J. Org. Chem.* **50** 2224 (1985)
133. S Shinsaki, S Tagashi, O Shafiro *Bull. Chem. Soc. Jpn.* **51** 563 (1978)
134. N Furukawa, S Oae, T Yashimura *Synthesis* **30** (1976)
135. K Buggie, B Fallon *J. Chem. Res. (S)* **11** 349 (1988)
136. Y Tamura, H Matsushima, M Ikeda, K Sumoto *Tetrahedron* **32** 431 (1976)
137. N P Bezverkhii, S I Protashchuk *Zh. Org. Khim.* **22** 461 (1986)
138. Y Tamura, H Matsushima, M Ikeda, K Sumoto *Synthesis* (1976)
139. I V Koval' *Usp. Khim.* **62** 813 (1993) [*Russ. Chem. Rev.* **62** 769 (1993)]
140. T Yamamoto, M Okawara *Bull. Chem. Soc. Jpn.* **51** 2443 (1978)
141. T Yamamoto, M Kakimoto, M Okawara *Tetrahedron Lett.* **18** 1659 (1977)
142. P K Claus, W F Silbernagel, W Franck, W Rieder *Monatsh. Chem.* **116** 841 (1985)
143. V V Korshak, N M Kozyreva, A I Kirilin, N I Bekasova, L G Komarova, E S Krongauz, V A Sergeev, V I Nedel'kin, A A Zhdanov, M M Levitskii, V P Alekseeva, in *Uspekhi v Oblasti Sinteza Elementoorganicheskikh Polimerov* (Advances in the Synthesis of Organoelement Polymers) (Moscow: Nauka, 1988) p. 113
144. O G Vokina, L Ya Tsarik, S N Istomina, G B Kazantseva, E D Solov'eva, S V Amosova, A V Kalabina *Izv. Sib. Otd. Akad. Nauk SSSR, Ser. Khim. Nauk* **19** 107 (1988)
145. S Iwatsuki, T Itoh, I Miyashita *Macromolecules* **21** 557 (1988)
146. Jpn. P. 1 275 634; *Ref. Zh. Khim.* 20S 730 (1990)
147. Jpn. P. 1 306 425; *Ref. Zh. Khim.* 22S 641P (1990)
148. US P. 4 724 257; *Ref. Zh. Khim.* 3S 634P (1989)
149. US P. 4 707 536; *Ref. Zh. Khim.* 16S 512P (1988)
150. N Al-Jabri, A Adam Georgius, M N Khalaf *Polym. Plast. Technol. Eng.* **27** 351 (1988)
151. T Otsu *Kagakv Kogakv* **54** 670 (1990); *Ref. Zh. Khim.* 10S 536 (1991)
152. O Skolling, J Hilborn, S Jönsson, in *The Xth Symposium Cationic Polym. Relat. Ionic Process. Debrecen 1991, (Abstracts of Reports)* p. 82
153. G N Shalygina, G F Shalygin, Z N Nudel'man, in *Spravochnik Rezinshchika* (Rubber Specialist's Handbook) (Moscow: Khimiya, 1971) p. 279
154. J von Voigt *Die Stabilisierung der Kunststoffe Gegen Licht und Wärme* (Translated into Russian; Leningrad: Khimiya, 1972)
155. V G Plotnikov, A A Efimov *Usp. Khim.* **59** 1362 (1990) [*Russ. Chem. Rev.* **59** 792 (1990)]
156. L G Angert, in *Spravochnik Rezinshchika* (Rubber Specialist's Handbook) (Moscow: Khimiya, 1971) p. 324
157. N N Mel'nikov, K V Novozhilov, T N Pylova *Khimicheskie Sredstva Zashchity Rastenii* (Chemical Plant Protecting Agents) (Moscow: Khimiya, 1980)
158. A A Shamshurin, M Z Krimer *Fiziko-Khimicheskie Svoistva Pestitsidov* (Physicochemical Properties of Pesticides) (Moscow: Khimiya, 1976)
159. T A Mastryukova, M I Kabachnik *Agrokhimiya* **6** 76 (1983)
160. BRD P. 3 215 256; *Ref. Zh. Khim.* 16O 320P (1984)
161. BRD P. 2 434 184; *Ref. Zh. Khim.* 23O 334P (1976)
162. BRD P. 2 254 359; *Ref. Zh. Khim.* 8O 341P (1976)
163. BRD P. 2 600 981; *Ref. Zh. Khim.* 13O 373P (1978)
164. BRD P. 2 609 830; *Ref. Zh. Khim.* 15O 429P (1978)
165. Europ. P. 49 684; *Chem. Abstr.* **97** 91 977 (1982)
166. US P. 4 315 928; *Ref. Zh. Khim.* 22O 331P (1982)
167. US P. 4 413 008; *Ref. Zh. Khim.* 16O 329 (1984)
168. E G Gemrich, B L Lee, S J Nelson, V L Rizzo *J. Agric. Food Chem.* **26** 391 (1978)
169. Swiss P. 608 692; *Ref. Zh. Khim.* 14O 364P (1983)
170. BRD P. 2 655 212; *Chem. Abstr.* **88** 6344 (1978)
171. US P. 4 364 959; *Ref. Zh. Khim.* 15O 325P (1983)
172. French P. 2 337 128; *Chem. Abstr.* **88** 136 153 (1978)
173. M A H Fahmy, N M Mallipudi, T R Fukuto *J. Agric. Food Chem.* **26** 550 (1978)
174. US P. 4 108 991; *Ref. Zh. Khim.* 11O 444P (1979)
175. BRD P. 2 344 175; *Ref. Zh. Khim.* 22O 302P (1975)
176. US P. 3 812 174; *Ref. Zh. Khim.* 10O 378P (1975)
177. US P. 3 920 830; *Ref. Zh. Khim.* 3O 352P (1977)
178. BRD P. 2 824 394; *Ref. Zh. Khim.* 16O 305P (1980)
179. BRD P. 2 737 606; *Ref. Zh. Khim.* 10O 314P (1975)
180. E Kühle, E Klauke *Angew. Chem.* **89** 797 (1977)
181. Yu A Fialkov, L M Yagupol'skii *Fiziol. Aktivn. Veshchestva* **14** 3 (1982)
182. L M Yagupol'skii *Aromaticheskie i Geterotsiklicheskie Soedineniya s Ftorsoderzhashchimi Zamestitelyami* (Aromatic and Heterocyclic Compounds with Fluorine-containing Substituents) (Kiev: Naukova Dumka, 1988)
183. C Hansch, A Leo *Substituent Constants for Correlation Analysis in Chemistry and Biology* (New York: Wiley, 1979)
184. I Rico, C Wakselman *Tetrahedron Lett.* **22** 323 (1981)
185. B V Golomolzin, E A Tarakhtii, I P Tregubenko, G A Ryazanova, F P Sidel'kovskaya, V A Ponomarenko, M M Vlasova *Khim.-farm. Zh.* **22** 839 (1988)
186. Yu A Fialkov, S V Shelyazhenko, L M Yagupol'skii *Zh. Org. Khim.* **19** 1048 (1983)
187. S V Shelyazhenko, M I Dronkina, Yu A Fialkov, L M Yagupol'skii *Zh. Org. Khim.* **24** 619 (1988)

Russian Chemical Reviews **62** (2) 169—183 (1994)
©1994 Russian Academy of Sciences and Turpion Ltd

UDC 541.63 : 542.91 : 541.64 : 547.366

New methods of synthesis of linear functionalised (*Z*)-isoprenoids and their 2,3-dihydro-derivatives

N Ya Grigor'eva, O A Pinsker

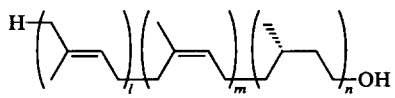
Contents

I. Introduction	169
II. Construction of the (*Z*)-isoprenoid chain with formation of a C—C bond	169
III. Construction of the isoprenoid chain with formation of a new (*Z*)-trisubstituted C=C bond	174
IV. Synthesis of (*Z*)-isoprenoids with formation of new C—C and (*Z*)-trisubstituted C=C bonds	180
V. Regioselective and enantioselective hydrogenation of the Δ^2-bond in α-functionalised isoprenoids	181

Abstract. The chemical and microbiological methods developed for the synthesis of polyprenols and dolichols are examined. These methods involve the construction of regular functionalised (*Z*)-isoprenoids accompanied by the creation of new C—C and/or (*Z*)-trisubstituted C=C bonds. Also considered are the highly regioselective and enantioselective procedures for the conversion of α-functionalised isoprenoids into their 2,3-dihydro-derivatives. The bibliography includes 87 references.

I. Introduction

Polyprenols **1** and dolichols **2** occupy an important place in the series of biologically active isoprenoids.



1, 2

1: $l = 3, 4$; $m > 3$; $n = 0$.
2: $l = 3$; $m = 8 \div 20$; $n = 1$.

It has now been reliably established that these regular polyisoprenoid alcohols are low-molecular-mass bioregulators of the coenzyme type, ensuring the transport of monosaccharides through cell membranes and their subsequent inclusion in the biosynthesis of carbohydrate-containing biopolymers of the cell wall in prokaryotes and eukaryotes.[1—3] The problem of the total synthesis of the individual polyprenols, dolichols, and their modified analogues, which arose in connection with the study of the mechanism of this process, required for its solution the development of methods for the stereoselective construction of a fairly long (*Z*)-isoprenoid chain—the principal structural element of the molecules of compounds **1** and **2**. In the course of studies carried out on these lines during the last twenty years, general methods have been devised for the construction of (*Z*)-disubstituted methylolefins, a special case of which is the construction of the (*Z*)-isoprene unit, and procedures have been developed for the regioselective and enantioselective transformation of compounds **1** into compounds **2**. These methods have expanded the range of procedures available in synthetic chemistry and can be used for the construction of new natural and biologically active products. The Laboratory of Polyunsaturated Compounds of the Institute of Organic Chemistry of Russian Academy of Sciences, headed by A M Moiseenkov, a Corresponding Member of the Russian Academy of Sciences, has made an appreciable contribution to the development of the above methods. This review has been written in honour of the memory of A M Moiseenkov.

II. Construction of the (*Z*)-isoprenoid chain with formation of a C—C bond

1. Biogenetic-like conversion of isoprenoids into higher (*Z*)-C_5-homologues

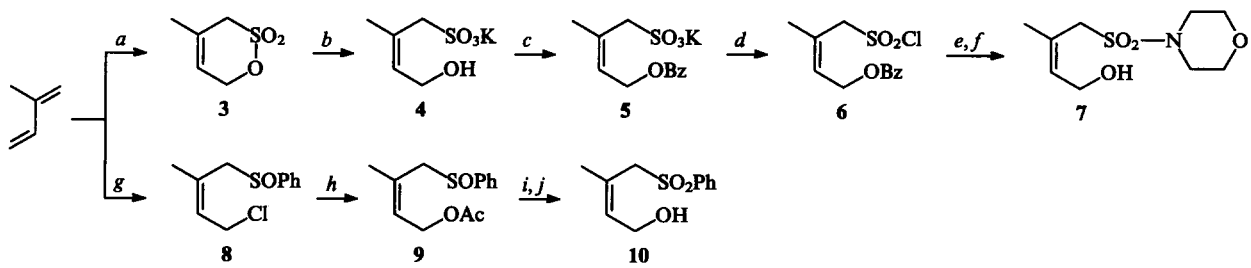
Moiseenkov and coworkers[4—7] showed that the δ-sultone **3**, which can be readily obtained from isoprene, dissociates at the S—O bond during controlled hydrolysis with the exclusive formation of the (*Z*)-sulfonate **4**, which affords the hydroxysulfonamide **7** via the benzoate **5** and sulfonyl chloride **6** stages with complete retention of the configuration (Scheme 1). The hydroxysulfonamide was used as the key block-synthon for the biogenetic-like (*Z*)-C_5 growth of the isoprenoid chain in the construction of the polyprenyl molecule. As shown in Scheme 2, this operation is carried out in three stages. Thus the conversion of (*E,E*)-farnesol **11** into the corresponding bromide **12**, alkylation by the latter of the dilithio-derivative **13** of the hydroxysulfonamide **7**, and finally the reductive desulfurisation of the resulting hydroxysulfonamide **14** to (*Z,E,E*)-geranylgeraniol **15** illustrate the conversion of the sesquiterpenoid skeleton into a diterpenoid skeleton. The repetition of the above transformations starting with compound **15** leads, via the hydroxysulfonamide **16** stage, to the (*Z,Z,E,E*)-sesterterpenol **17**, which is similarly converted, via the hydroxysulfonamide **18**, to a (*Z,Z,Z,E,E*)-triterpenol—the hexaprenol WT_2C_3OH† **19**.

N Ya Grigor'eva, O A Pinsker Laboratory of Polyunsaturated Compounds, Zelinskii Institute of Organic Chemistry, Russian Academy of Sciences, Leninskii prosp. 47, 117913 Moscow. Fax (7-095)135 53 28

Received 1 December 1993
Uspekhi Khimii **63** (2) 177—191 (1994); translated by A K Grzybowski

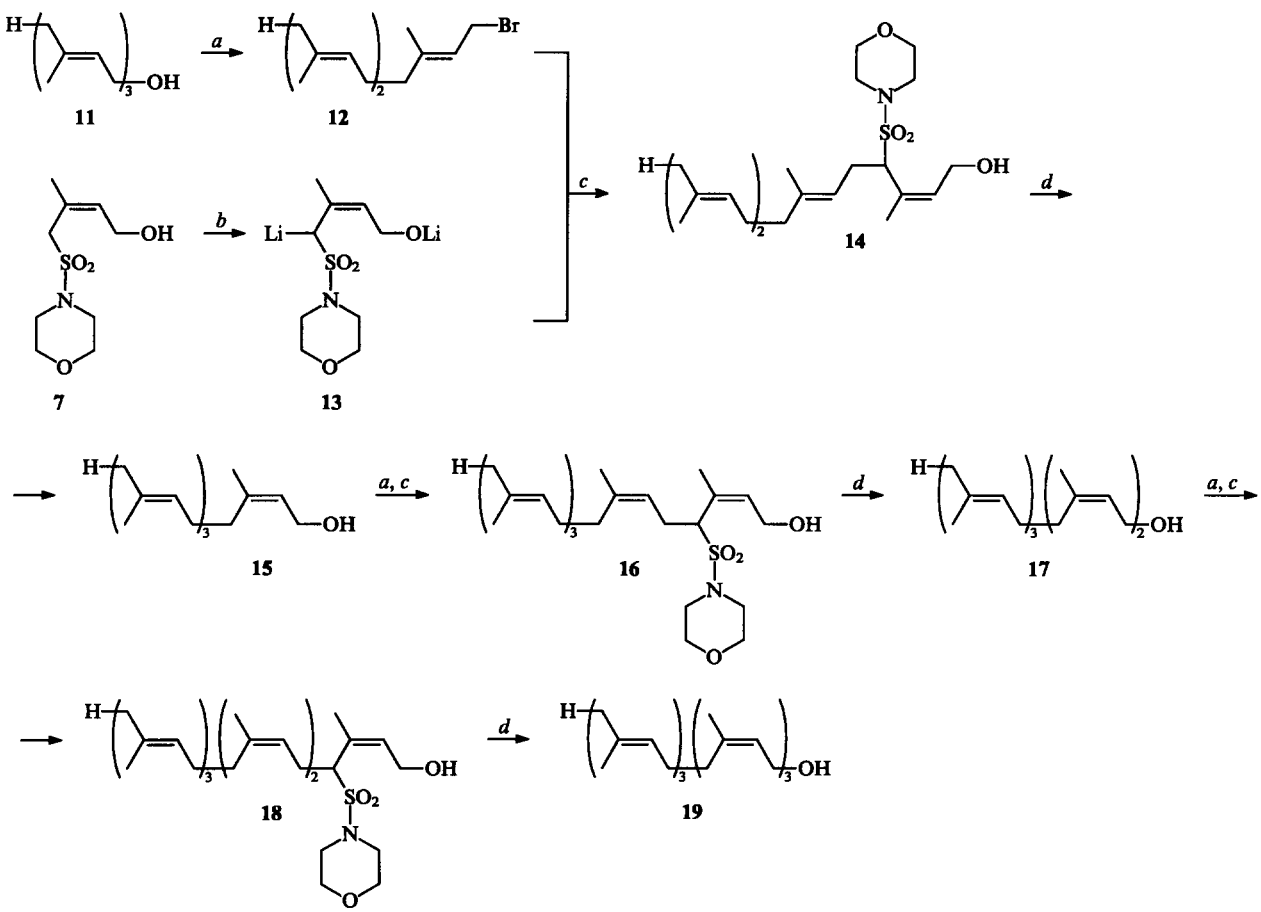
† Here and henceforth the following abbreviations recommended by IUPAC[9] are used to designate the configurations of polyprenols: W is the terminal unit, T and C are the inner (*E*)- and (*Z*)-isoprene units, and S is the 2,3-dihydroisoprene unit.

Scheme 1



Bz = benzoyl;
(*a*) SO_3; (*b*) aq. KOH (pH 7 – 8); (*c*) BzCl/Py; (*d*) $POCl_3$; (*e*) HN⟨O⟩; (*f*) $LiAlH_4$;
(*g*) PhSOCl, 5 kbar; (*h*) AcOK/AcOH; (*i*) *m*-$ClC_6H_4CO_3H/CH_2Cl_2$; (*j*) H_3O^+.

Scheme 2

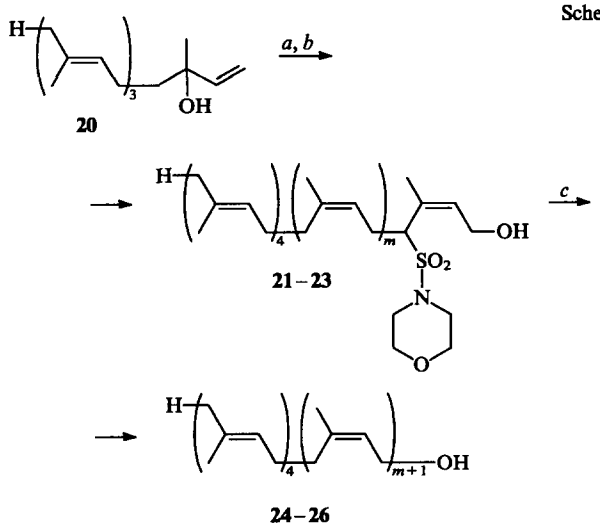


(*a*) PBr_3/Py; (*b*) Bu^nLi; (*c*) **13**/THF, −70 °C; (*d*) $Na/NH_3-C_6H_{14}-Et_2O$, DB18C6
(DB18C6 = dibenzo-18-crown-6).

The reactions presented in Scheme 2 constituted the first reliably documented total synthesis of polyprenols.[8]

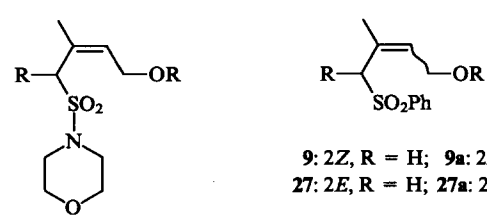
The pentaprenol WT_3COH **24**, hexaprenol WT_3C_2OH **25**, and heptaprenol WT_3C_3OH **26** were obtained similarly in succession from geranyllinalool **20** (Scheme 3) via stages involving the sulfonamides **21**–**23** respectively.[10] Compounds **25** and **26** were subsequently isolated from the leaves of the palm *Serenoa repans*.[11]

Scheme 3



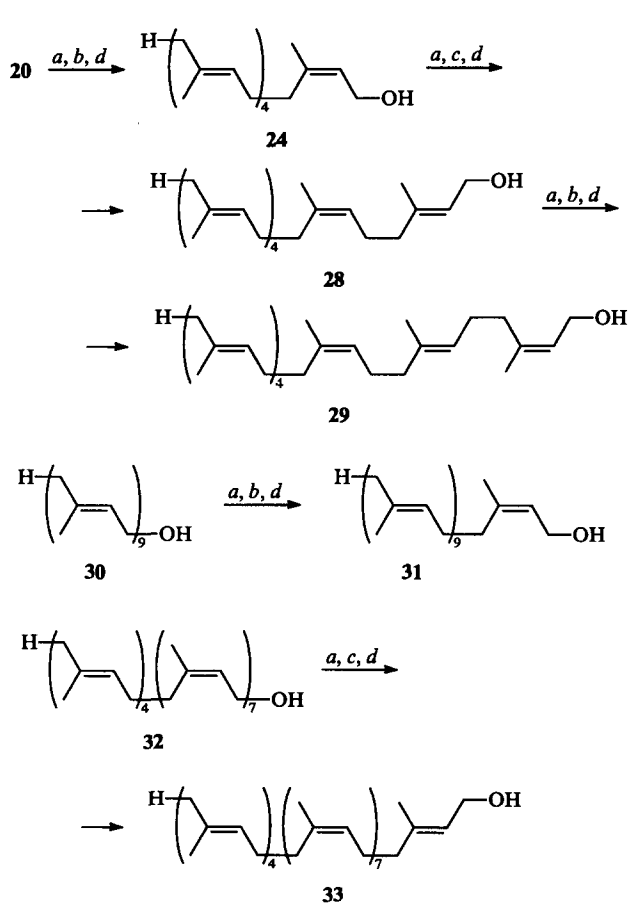
21, 24: $m = 0$; **22, 25**: $m = 1$; **23, 26**: $m = 2$.
(*a*) PBr_3/Py; (*b*) **13**/THF, −50 °C; (*c*) $Na/NH_3-C_6H_{14}-Et_2O$, DB18C6.

Scheme 4



9: 2*Z*, R = H; **9a**: 2*Z*, R = Li.
27: 2*E*, R = H; **27a**: 2*E*, R = Li.

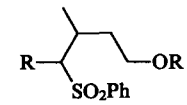
7: R = H.
13: R = Li.



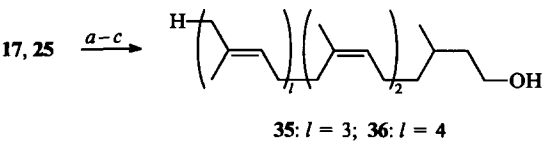
(*a*) PBr_3/Py; (*b*) **13**; (*c*) **27a**; (*d*) $Na/NH_3-C_6H_{14}-Et_2O$, DB18C6.

The approach considered proved to be extremely fruitful in the synthesis of modified polyprenols with a specified nonnatural sequence of the (*Z*)- and (*E*)-isoprene units in the molecule as well as dolichol-like structures. A more readily available block-synthon — the hydroxysulfone **10** — was used successfully together with compound **7** for the formation of (*Z*)-C_5-homologues. Compound **10** was obtained from the acetate **9** via the (*Z*)-chlorosulfoxide **8** (Scheme 1), which is formed smoothly in its turn from isoprene and benzenesulfinyl chloride at a high pressure.[12,13] Accordingly, the (*E*)-hydroxysulfone **27** in the form of its dilithio-derivative **27a** was used as the (*E*)-C_5-block.[14] The heptaprenol WT_3CTCOH **29** was synthesised by the (*Z*)/(*E*)-C_5-homologue formation method from geranylinalool **20** via the pentaprenol **24** and hexaprenol WT_3CTOH **28** stages using the block-synthons **7** and **27**, while the decaprenol WT_8COH **31**[16] and the dodecaprenol WT_3C_7TOH **33**[16] were obtained from the readily available natural products solanesol **30** and moraprenol **32**[15] respectively (Scheme 4).

The use of the saturated block-synthon **34** in the form of its dilithio-derivative **34a** in the concluding stage of the C_5-homologue formation reaction made it possible to obtain the racemates of the dolichol-like hexaprenol WT_2C_2SOH **35**[18] and the heptaprenol WT_3C_2SOH **36**[17] from the pentaprenol **17** and hexaprenol **25** respectively, while the use of the chiral (3*R*)-form of the block-synthon **34** led to the above compounds with the natural (*S*)-configuration of the α-isoprene unit.[19]



34: R = H; **34a**: R = Li.

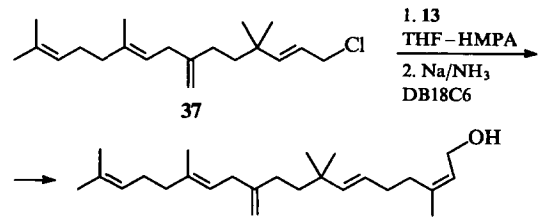


35: $l = 3$; **36**: $l = 4$

(*a*) PBr_3/Py; (*b*) **34a**; (*c*) $Na/NH_3-C_6H_{14}-Et_2O$, DB18C6.

A partial synthesis of a combined preparation of (*S*)-dolichols **2** ($l = 2$, $m = 11-19$, $n = 1$) and their (*R*)-analogues from a mixture of the polyprenols **1** ($l = 2$, $m = 11-19$, $n = 0$), isolated from the leaves of *Ginkgo biloba*, has also been achieved with the aid of the (*R*)- and (*S*)-forms of compound **34**.[20]

The C_5 isoprene chain C_5-homologue formation method, developed for the synthesis of polyprenyl structures, was used successfully subsequently in the synthesis of the (*Z*)-isoprene section of the non-regular sesterterpenol moenocinol **38** from the chloride **37**.[21]



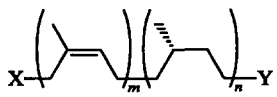
37

38

THF = tetrahydrofuran, HMPA = hexamethylphosphoramide.

2. A block method for the construction of the isoprenoid chain

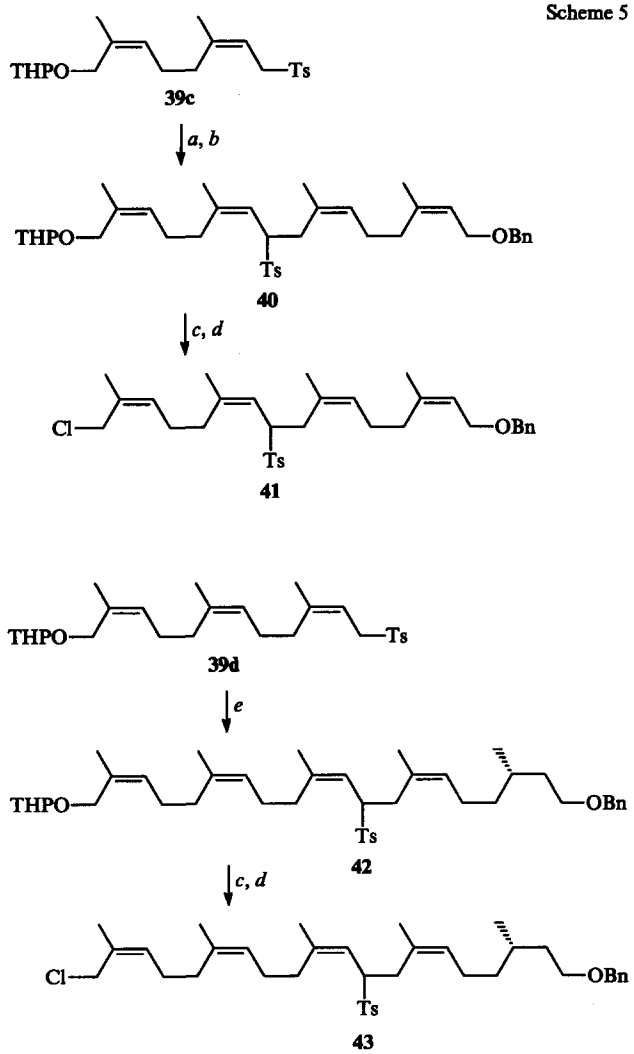
During approximately the same years, Sato et al.[22] proposed that the (*Z*)-isoprenoid chain be constructed by 'cross-linking', via the C–C bonds, block-synthons of type **39** containing two or more (*Z*)-isoprenoid units. Such compounds became available after the observation by the authors of the high (*Z*)-stereoselectivity of the Wittig reaction with participation of hydroxyacetone derivatives.[23] This question is considered in detail in Section III.1. Here one should only note that the key (*Z*)-C_{10} and (*Z*)-C_{15}-bifunctional building blocks of type **39** were obtained precisely from the benzyl ethers of nerol, (*Z,Z*)-farnesol, and (*S*)-citronellol.[22,24,25]



39a–e

39a: $m = 2$, $n = 0$, X = Cl, Y = OBn.
39b: $m = 3$, $n = 0$, X = Cl, Y = OBn.
39c: $m = 2$, $n = 0$, X = OTHP, Y = Ts.
39d: $m = 3$, $n = 0$, X = OTHP, Y = Ts.
39e: $m = 1$, $n = 1$, X = Cl, Y = OBn.
(Bn = benzyl, THP = Tetrahydropyranyl, Ts = toluene-*p*-sulfonyl).

Scheme 5

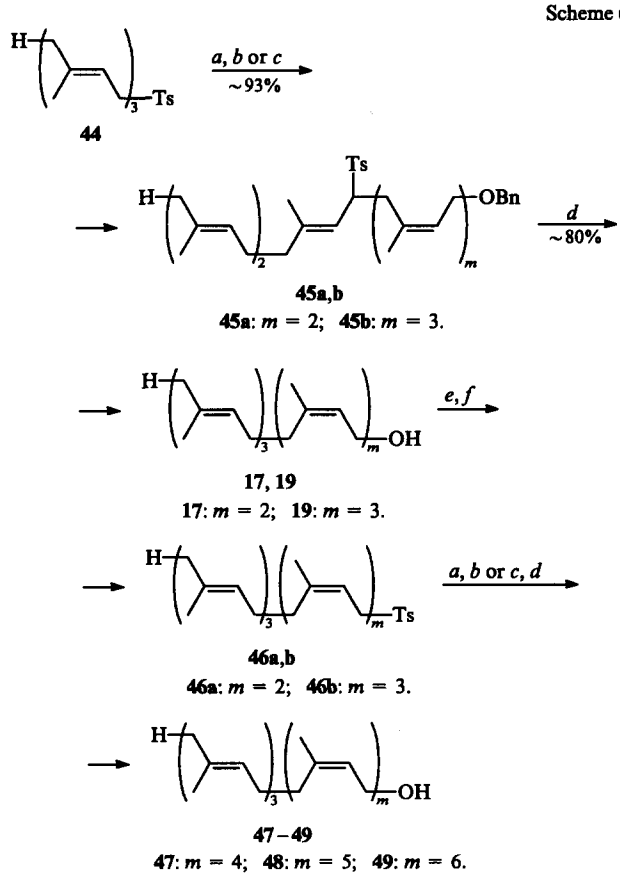


(*a*) Bu^nLi/THF–HMPA, –78 °C; (*b*) **39a**; (*c*) H_3O^+; (*d*) MsCl, LiCl, *sym*-collidine, DMF; (*e*) **39e**, Bu^n_4NBr/50% NaOH, 20 °C (Ms = methanesulfonyl).

In order to construct the (*Z*)-isoprenoid chain with the aid of these blocks, Sato's group[25] used one of the modern versions of the Wurtz reaction, first proposed by Biellmann[26] and then developed in detail by Altman[27] and Masaki[28] for the construction of the regular (*E*)-polyisoprenoid chain. This method includes the alkylation of the carbanions (stabilised by sulfur-containing functional groups) with the aid of allyl halides and the subsequent Birch reductive cleavage of the C–S bond in the reaction products. Thus the alkylation of the tolyl sulfone **39c** with the aid of the chloride **39a** affords the tolyl sulfone **40** containing four (*Z*)-isoprene units. The latter is converted by a standard method into the chloride **41**, used for the subsequent increase in the length of the (*Z*)-isoprenoid chain (Scheme 5). The tolyl sulfone **42** with a (3*S*)-α-isopentane unit, which is smoothly converted into the chloride **43**, was obtained similarly from the block-synthons **39d** and **39e**.

Having at their disposal (*Z*)-C_{10}-, (*Z*)-C_{15}-, and (*Z*)-C_{20}-block-synthons (compounds **39a**, **39b**, and **41** respectively), Sato's group[24,29] achieved the effective syntheses of pentaprenol (WT_2C_2OH, **17**), hexaprenol (WT_2C_3OH, **19**), heptaprenol (WT_2C_4OH, **47**), octaprenol (WT_2C_5OH, **48**), nonaprenol (WT_2C_6OH, **49**) (Scheme 6), and undecaprenol (WT_2C_8OH, **52**) (Scheme 7). (*E,E*)-Farnesyl tolyl sulfone **44** was used to introduce the transoid fragment into the target compound.

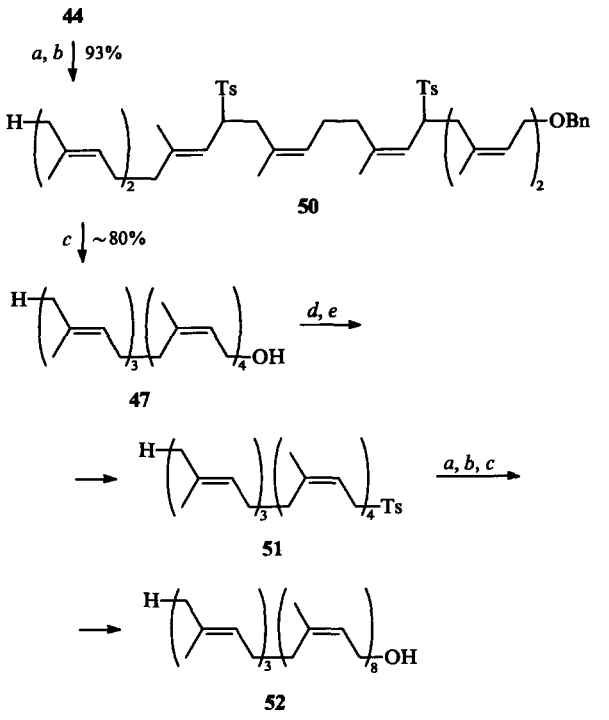
Scheme 6



(*a*) Bu^nLi/THF–HMPA, –78 °C; (*b*) **39a**; (*c*) **39b**; (*d*) Li/$EtNH_2$; (*e*) MsCl, LiCl, *sym*-collidine/DMF; (*f*) TsNa/DMF.

As shown in Scheme 6, the alkenylation by the chlorides **39a, b** of the (*E*)-tolyl sulfone **44** deprotonated by treatment with Bu^nLi affords the tolyl sulfones **45a, b**, the reductive desulfurisation of which is accompanied by the removal of the benzyl protecting groups and leads to pentaprenol **17** and hexaprenol **19** respectively. The latter are smoothly converted by a standard method into the tolyl sulfones **46a, b**, the introduction of which into the sequence of reactions described above gives rise to heptaprenol **47**, octaprenol **48**, and nonaprenol **49** respectively.

Scheme 7



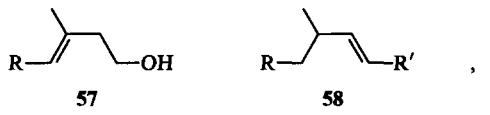
(*a*) Bu^nLi/THF–HMPA, −78 °C; (*b*) **41**; (*c*) $Li/EtNH_2$; (*d*) MsCl, LiCl, *sym*-collidine/DMF; (*e*) TsNa/DMF.

The use of the block-synthon **41** proved to be extremely convenient for the synthesis of higher polyprenols. Thus alkylation of the deprotonated tolyl sulfone **44** by the chloride **41** leads to the tolyl sulfone **50** in 93% yield. The latter loses simultaneously the tosyl and benzyl groups on treatment with lithium in $EtNH_2$ and is converted into heptaprenol **47**. The tolyl sulfone **51** obtained from heptaprenol **47** was transformed similarly into undecaprenol **52**.[29]

Undecaprenol **52** served in its turn as the starting material for the total synthesis of (*S*)-dolichol (20-eicosaprenol, WT_2C_{16}. .SOH, **56**), achieved with record speed in the chemistry of prenols by Sato and coworkers[25] via a stage involving the synthesis of pentadecaprenol **54** (Scheme 8) by using the C_{20}-block **41** and the (3*S*)-C_{25}-block **43** to increase the length of the (*Z*)-isoprenoid chain.

It is noteworthy that, as in the synthesis of the C_{25}-block **43**, in this synthesis the authors use successfully the effective and technologically convenient method for the alkylation of the toluene sulfones **39d**, **53**, and **55** under phase transfer catalytic conditions.

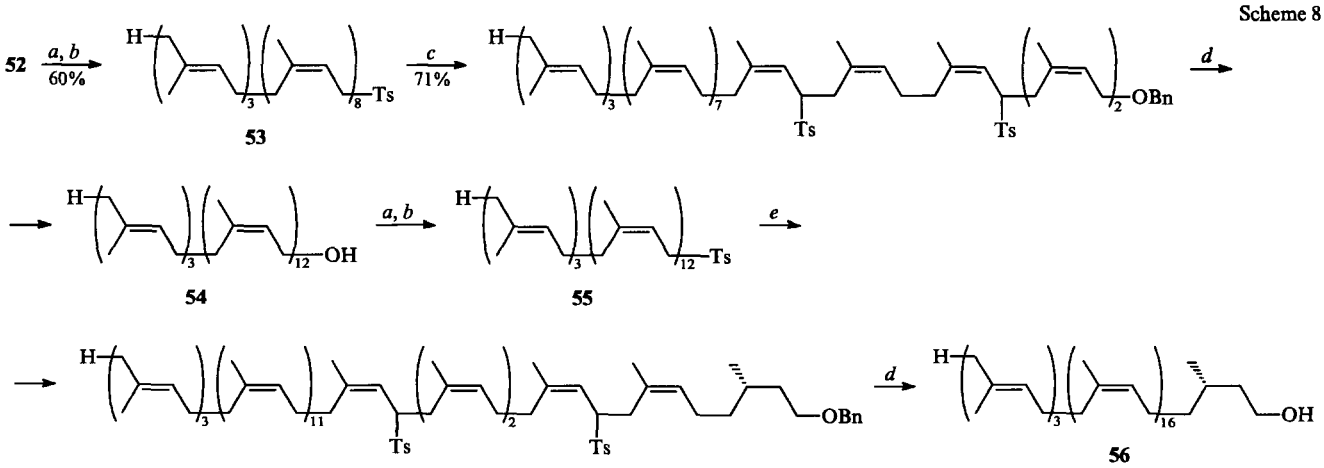
The version of the Wurtz reaction examined in Section II can be used successfully for the construction of the (*Z*)-isoprenoid chain. However, despite all its advantages, the method suffers from a significant disadvantage, which was noted by the authors of the studies quoted above. In the reductive cleavage of the C–S bond in sulfones of type **21**–**23** and in tolyl sulfones of type **45a, b**, the formation of the target products is accompanied by the formation of their regioisomers, which can be explained by the migration of the C=C bond in the carbanionic intermediate: in the case of the C_5-homologue formation reaction, these are the homoallyl alcohols **57**, while in Sato's block syntheses they are products of type **58**:



where R and R′ are the corresponding polyprenyl groups.

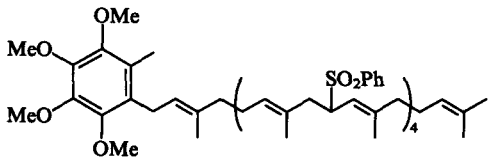
Systematic study of the desulfurisation conditions in relation to the tolyl sulfones **21**–**23**, undertaken to overcome this disadvantage, showed[10,18,30] that, when the reaction is carried out with the aid of sodium in the 4:4:1 ammonia–hexane–ether emulsion in the presence of 10 mol.% of DB18C6 at −50 °C, it is possible to reduce to 5%–10% the admixture of the isomer **57** and also to suppress completely the hydrogenolysis of the allylic C–O bond. The residual homoallyl alcohol **57** either decomposes in the conversion of the corresponding isoprenols (for example, compounds **15** and **17**) into the corresponding bromides[10,31] or can be removed (as well as an admixture of type **58**) with the aid of precision chromatography on silica gel impregnated with $AgNO_3$.[22,24,29]

Scheme 8



(*a*) MsCl, LiCl, *sym*-collidine/DMF; (*b*) TsNa/DMF; (*c*) **41**, Bu^n_4NBr/50% NaOH, 20 °C; (*d*) $Li/EtNH_2$; (*e*) **43**, Bu^n_4NBr/50% NaOH, 20 °C.

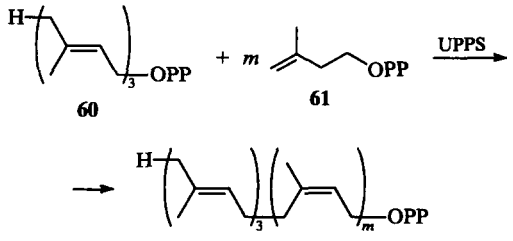
In this connection, one should note an interesting procedure for the selective reduction of allyl sulfones,[32] which was used by the authors of one of the specific syntheses of ubiquinone (10),[33] who showed that all four $PhSO_2$ groups can be removed from the sulfone **59** (without shift of the C=C bond) by means of $LiBHEt_3$ in the presence of catalytic amounts of 1,3-bis-(diphenylphosphino)propanopalladium dichloride.



59

3. Construction of the chain with the aid of enzyme catalysis

Studies in recent years on the biosynthesis of polyprenols have led to the isolation and characterisation of the enzyme responsible for the construction of the (*Z*)-isoprenoid section of the molecule of compound **1**, which has been called undecaprenyl pyrophosphate synthetase (UPPS).[34] Preparations of this enzyme, obtained from various bacterial sources,[34–37] exhibited *in vitro* a high and virtually identical activity in the successive (*Z*)-C_5-homologue formation reactions of the phosphates of isoprenols[38] using isopentenyl pyrophosphate **61** as the source of the (*Z*)-C_5-unit. Thus pyrophosphates of decaprenol (WT_2C_7OH, **62**) and undecaprenol (WT_2C_8OH, **63**) have been synthesised from (*E,E*)-farnesyl pyrophosphate **60**, which is the primary substrate of UPPS *in vivo*.



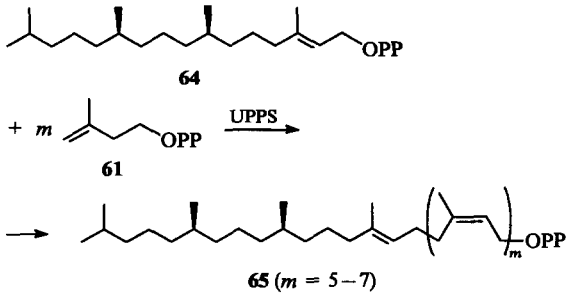
60 **61**

62, 63

62: m = 7; **63**: m = 8.

OPP = pyrophosphate.

The enzyme UPPS does not exhibit a high substrate specificity in relation to the primary substrate and can 'work' with allyl alcohols having different structures.[34–36] For example, the C_{45}–C_{55} glycinoprenols **65**, detected recently in the leaves of the soya bean *Glycine max Merrill*,[40] have been obtained from phytyl pyrophosphate **64** with the aid of the UPPS preparation isolated from *Escherichia coli*.[39]



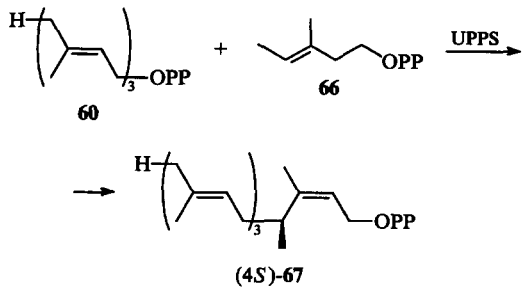
64

61

65 (m = 5–7)

The requirements of UPPS as regards the structure of the homoallyl substrate are more definite. The enzyme exhibits an adequate activity in relation to only one non-natural homoallyl substrate—the pyrophosphate **66**. The presence of the methyl group at the C(4) atom in compound **66** completely alters the nature of the reaction: regardless of the chain length of the allyl substrate, the enzyme catalyses only its conversion into the C_6-homologue, forming 4-methylpolyprenol with the (*S*)-configuration of the C_4 centre, which is illustrated by the conversion of farnesyl pyrophosphate **60** into the phosphate (4*S*)-**67** (Scheme 9).[41]

Scheme 9



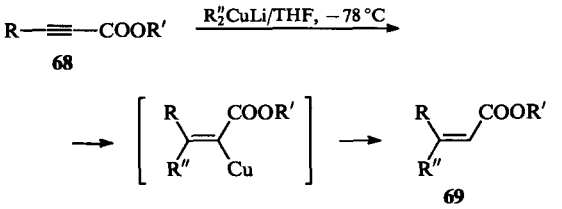
60

(4*S*)-**67**

It may be hoped that the high stereo- and enantio-selectivity of this reaction will find further practical application, as has been shown in relation to farnesyl pyrophosphate synthetase, with the aid of which, the syntheses of faranal and 4-methyl-substituted juvenile hormones have been achieved.[42–44] Thus studies on the biosynthesis of polyprenols provided chemists engaged in organic synthesis with a new valuable reagent for the construction of the (*Z*)-isoprenoid chain.

III. Construction of the isoprenoid chain with formation of a new (*Z*)-trisubstituted C=C bond

The elucidation of the biological functions of (*E*)-isoprenoids, in the first place the acyclic steroid precursor squalene, and insect juvenile hormones aroused at the end of the 1960s and the beginning of the 1970s an explosion of interest by chemists concerned with organic synthesis in the development of stereoselective methods for the construction of the (*E*)-trisubstituted C=C bond.[45,46] On the other hand, the methods for the synthesis of (*Z*)-trisubstituted olefins in general and (*Z*)-isoprenoids in particular did not develop adequately before the start of systematic studies on the synthesis of polyprenols. Nevertheless, towards the beginning of the 1970s several methods were described in the literature for the stereoselective construction of (*Z*)-trisubstituted olefin systems. Thus Corey and Katzenellenbogen[47] showed that the addition of dialkyl cuprates to α,β-acetylenic acids and their esters in THF at low temperatures proceeds exclusively as a *cis*-process[47] and they suggested that it be used, in particular, for the conversion of esters of β-alkyl- and β-alkenyl-propiolic acids **68** into esters of type **69**.



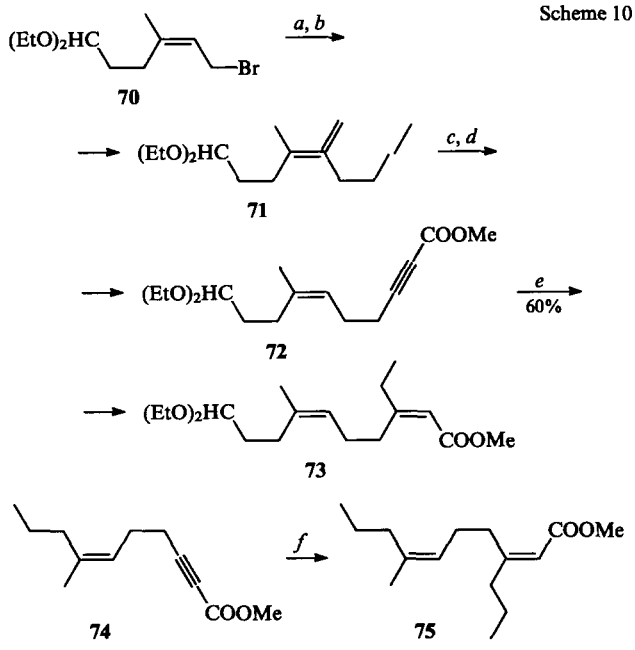
68

69

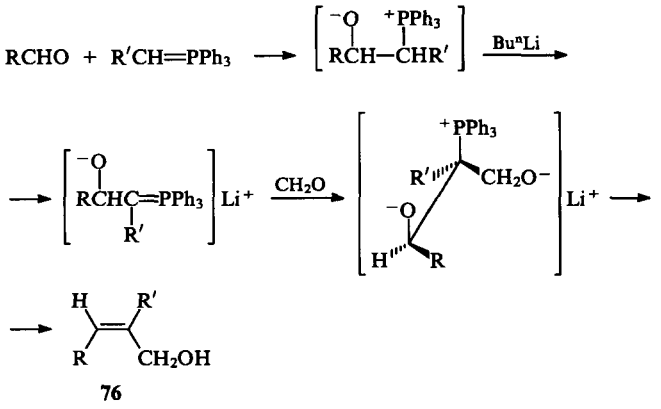
R = Me, Et, Bu^n, Ph; R′ = Me, Et, Bu^s; R″ = Me, Et.

The application of the method is illustrated in Scheme 10. The allyl bromide **70** is synthesised and converted via the enyne **71** and ester **72** stages into the ester **73**—the key block-synthon in the synthesis of the natural ionophore monensin,[48] while the ester **74** is converted into the pheromone of the lesser apple-worm *Laspeyresia pomonella L.* **75**.[49]

Scheme 10

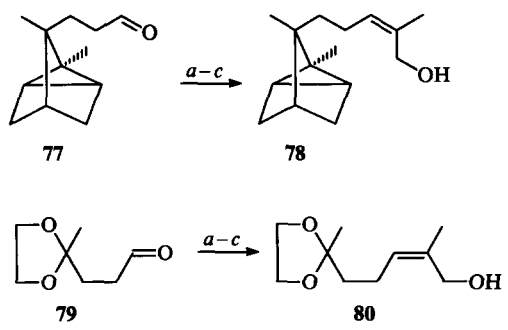


(*a*) $LiCH_2C{\equiv}CSiMe_3$; (*b*) $AgNO_3$, NaCN; (*c*) Bu^nLi; (*d*) $ClCO_2Me$; (*e*) Et_2CuLi/THF, −70 °C; (*f*) Pr^n_2CuLi/THF, −70 °C.



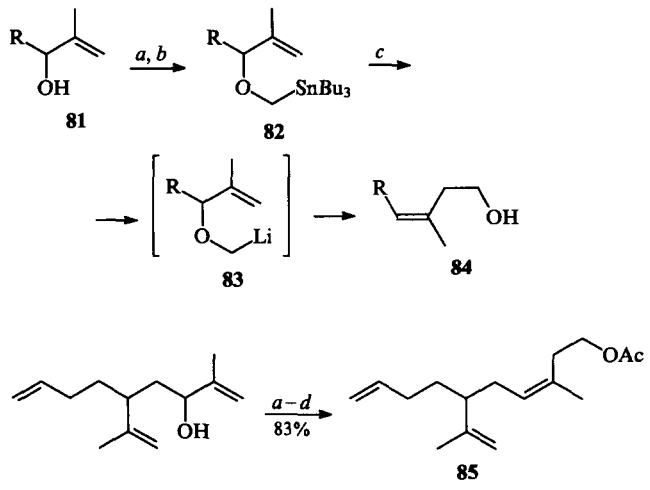
A highly stereoselective method for the construction of allyl alcohols **76** with the aid of two consecutive Wittig reactions achieved in one reactor (using formaldehyde as the carbonyl component in the second reaction) was developed simultaneously in Corey's laboratory.[50]

For R′ = Me, this sequence of reactions makes it possible to construct the terminal (*Z*)-isoprene unit, as shown for the conversion of the aldehyde **77** into α-santalol **78**[50] and of the aldehyde **79** into the ketal alcohol **80**. The latter is a key block-synthon for the synthesis of (±)-trisporal B and (±)-trisporic acid.[51]



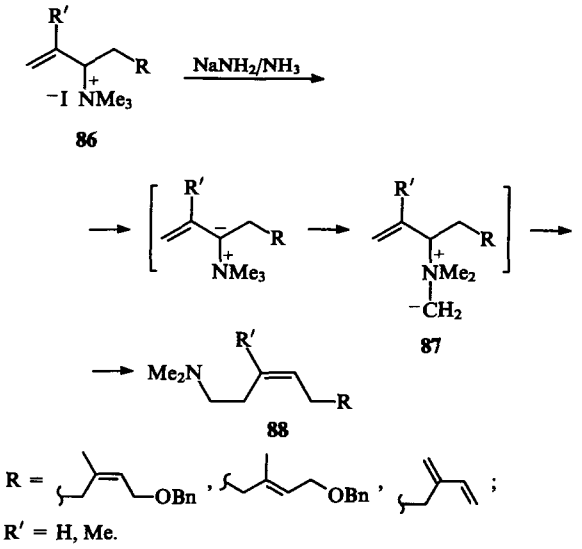
(*a*) $MeCH{=}PPh_3$; (*b*) Bu^nLi; (*c*) CH_2O.

An effective method of synthesis of (*Z*)-homoallyl alcohols **84** is also noteworthy. It was developed by Still and Mitra[54] on the basis of the stereochemically unusual [2,3]-sigmatropic rearrangement (cf. Masaki et al.[52] and Inoue et al.[53]) of the methylallyloxymethyllithio-derivatives of compound **83**, which they observed. The rearrangement takes place *in situ* on treatment of the tributylstannylmethyl ethers of the methylallyl alcohols **82** with Bu^nLi.[54] The method has been used successfully in the synthesis of the component **85** of the pheromone of the red San Jose scale.[54]



(*a*) KH; (*b*) Bu_3SnCH_2I; (*c*) Bu^nLi; (*d*) Ac_2O–Py.

Yet another example of the [2,3]-sigmatropic rearrangement, leading to the highly stereoselective synthesis of di- and tri-substituted (*Z*)-olefins, appeared later in the literature. It was discovered by Sato's group[55] in relation to the ylides **87**, which are converted into the amines **88** on treatment with $NaNH_2$ in NH_3 at the instant of formation from the quaternary ammonium salts **86**.[55] The amines **88** can be readily transformed by standard methods into the corresponding (*Z*)-homoallylic aldehydes or alcohols.

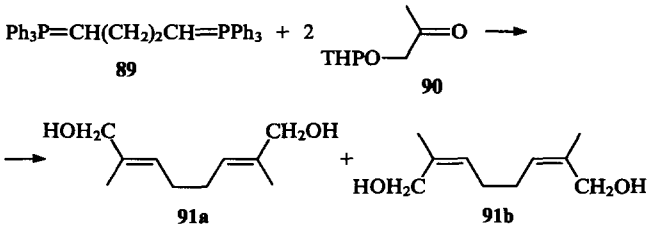


All the methods considered above yield satisfactory results in the synthesis of the terminal (*Z*)-isoprene unit (for example, in the alcohol **76** for R' = Me or in compound **84**), but they are fundamentally unsuitable for the synthesis of the disubstituted (*Z*)-methylalkene fragment in the middle of the chain. The attempt to construct a fairly long (*Z*)-isoprenoid chain from them by the multistage growth of the (*Z*)-C_5-units was also relatively ineffective because the construction of each succeeding unit requires a multistage preparatory step involving the preparation of the necessary starting materials. These disadvantages were overcome in the method of synthesis of (*Z*)-trisubstituted olefins examined below, which were developed for the synthesis of polyprenols.

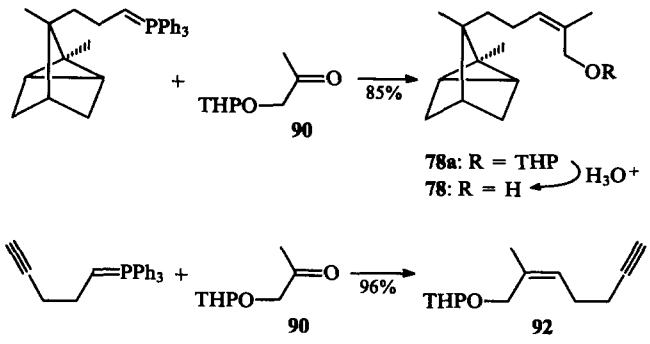
1. Conversion of derivatives of hydroxyacetone into olefins by the Wittig reaction

As already mentioned in Section II. 2, Sato and coworkers [22, 24, 25] suggested that fairly large (*Z*)-(C_{20}–C_{25})-isoprenoid blocks, obtained by alkylating (*Z*)-tolyl sulfones **39c, d** by the chlorides **39a, b, e** be used for the synthesis of polyprenols and dolichols. On the other hand, the authors used the Wittig reaction between unstabilised phosphonium ylides and derivatives of hydroxyacetone, for example its THP-derivative **90**, in order to synthesise the ω-functionalised (*Z*)-block-synthons of type **39**, which are otherwise difficult to obtain.

The considerable predominance of the (*Z*)-isomer in products of this reaction was first noted by Bhalerao and Rapoport [56] in the conversion of the ketone **90** into an olefin by treatment with the bisylide **89**, which led to a mixture of the diols **91a** and **91b** in proportions of 1 : 4.

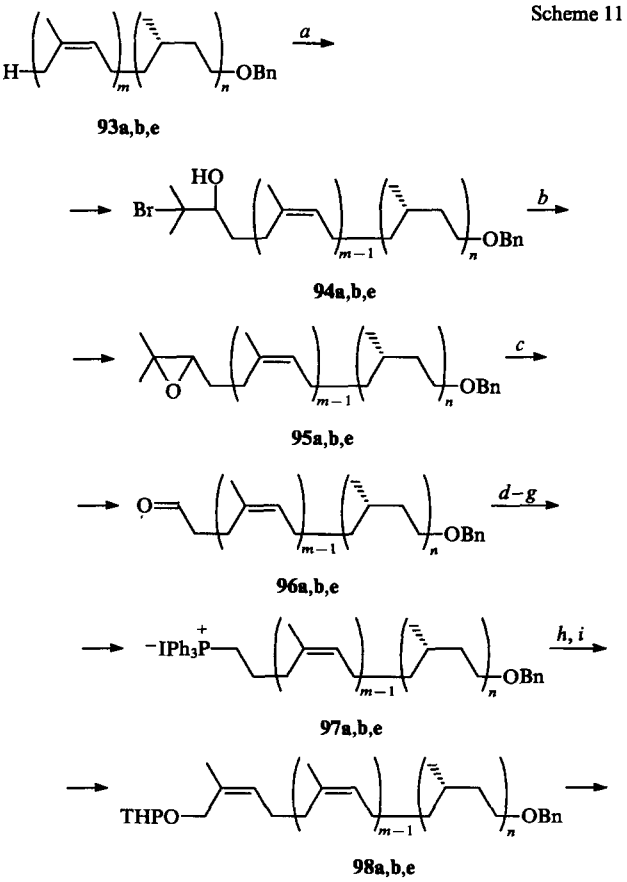


Systematic study of the influence of the reaction conditions on reaction stereochemistry, carried out simultaneously by Sato's [57] and Still's [58] groups, made it possible to increase the (*Z*)-stereoselectivity of the process to 95%–99% with virtually quantitative yields of the product. Still's group synthesised α-santalol **78** with precisely such stereochemical purity, [58] while Sato's group obtained the enyne **92** — a key block-synthon in the total synthesis of (*Z*,*Z*)-farnesylacetone — with the same stereochemical purity. [57]

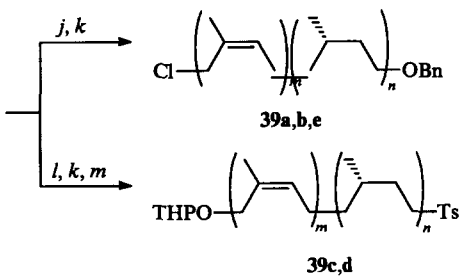


On the basis of the above results, Sato's group [22, 24, 25] achieved the stereoselective synthesis of the block-synthons **39**, having obtained by a standard procedure the phosphonium salts **97a, b, e** required for this purpose from the aldehydes **96a, b, e**, which were prepared in their turn by transforming, by means of the van Tammelen method, the benzyl ethers of nerol (**93a**), (*Z*,*Z*)-farnesol (**93b**), and (3*S*)-citronellol (**93e**) via stages involving the formation of the bromohydrins **94a, b, e** and the epoxides **95a, b, e** (Scheme 11). The condensation of the ylides generated from the phosphonium salts **97** with the THP-derivatives of hydroxyacetone **90** affords the (*Z*)-isoprenoids **98** containing hydroxy-groups in different positions — the α- and ω-positions. As a result of this, the blocks **98a, b, e** can be selectively converted by standard methods both into the chlorides **39a, b, e**, modelling the 'tail' (OH-containing) fragment of polyprenols of types **1** and **2**, and into the tolyl sulfones **39c, d** containing the central (*Z*)-fragment of these compounds.

Scheme 11



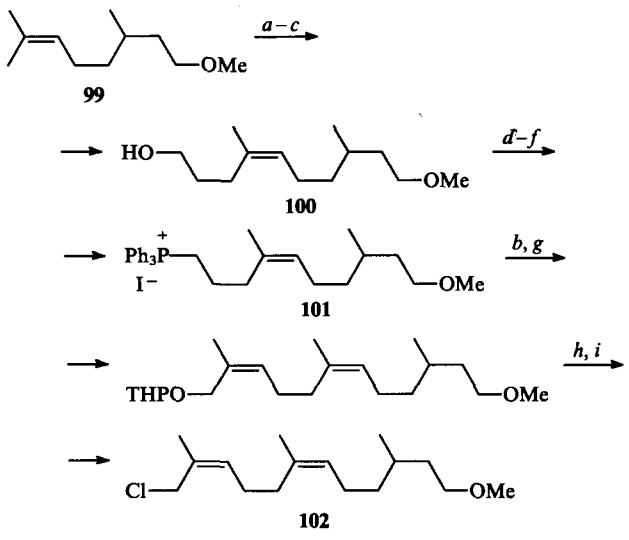
Scheme 11 (continued)



a,**c**: $m = 2, n = 0$; **b**,**d**: $m = 3, n = 0$; **e**: $m = n = 1$.
(*a*) NBS; (*b*) K_2CO_3/NaOH; (*c*) H_5IO_6; (*d*) $NaBH_4$; (*e*) TsCl; (*f*) NaI; (*g*) PPh_3; (*h*) Bu^nLi; (*i*) **90**; (*j*) H_3O^+; (*k*) MsCl, LiCl; (*l*) Na/NH_3; (*m*) TsNa.

The same authors[59] recently patented yet another method for the (*Z*)-functionalisation of isoprenol ethers. It consists in the successive treatment of the methyl ether of the corresponding isoprenol, for example citronellol **99**, with strong bases and epoxyethane. This affords the (*Z*)-bishomoallyl alcohol **100**, which can be readily converted into the phosphonium salt **101** and the latter is subsequently transformed, as shown above for the phosphonium salt **97**, into the chloride **102** (Scheme 12).

Scheme 12

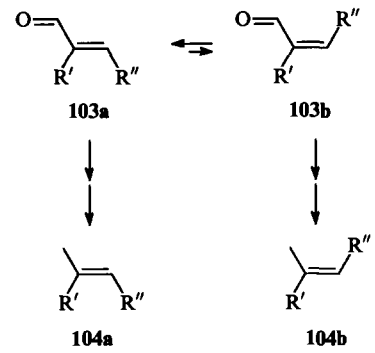


(*a*) Bu^tOK; (*b*) Bu^nLi; (*c*)  ; (*d*) TsCl; (*e*) NaI; (*f*) Ph_3P; (*g*) **90**; (*h*) H_3O^+; (*i*) MsCl, LiCl.

It was demonstrated in Section II, 2 how polyprenols **1** and **2**, containing up to 16 (*Z*)-isoprene units, were synthesised with the aid of the sulfones **39c**,**d** and the chlorides **39a**,**b**,**e**, **41**, and **43**.

2. A general method for the construction of the (*Z*)-trisubstituted C=C bond by specific aldol condensation

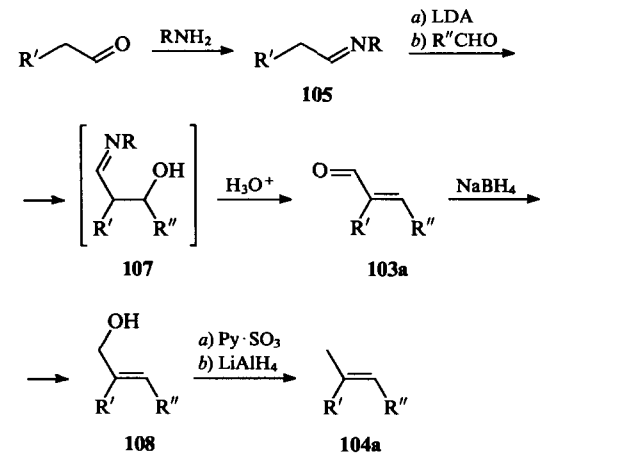
Another approach to the construction of (*Z*)-trisubstituted olefins has been developed in the Laboratory of the Chemistry of Polyunsaturated Compounds of the Institute of Organic Chemistry of Russian Academy of Sciences. It is based on the fact, observed by Grigor'eva et al.,[60] that α,β-disubstituted (*E*)-acroleins **103a** are thermodynamically preferable to their (*Z*)-isomers **103b**, which ensures the presence of more than 95% of the (*E*)-isomer **103a** in the equilibrium mixture (^1H NMR data).[61] This rule is general in the case of acroleins **103** without a branched chain at the allylic carbon atom.[60]



Since the acroleins **103** can be converted by Corey's method[62] into the methylalkenes **104** with complete retention of the configuration, the observed ability of the CHO group to fix the configuration of compound **103a** opened a highly stereoselective path to the construction of the disubstituted (*Z*)-methylalkenes **104a** (involving the synthesis of compound **103a**) and their subsequent stereospecific reductive transformation.

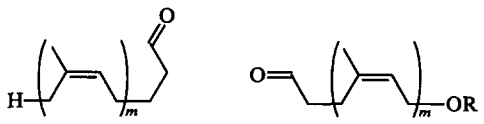
In order to obtain the key (*E*)-acroleins **103a**, the authors applied a version of the cross-condensation of aldehydes, one of which is in the form of the aldimine **105** (Scheme 13). In the literature, this reaction is known as the specific Wittig condensation.[63] The interaction of aldimines **105** deprotonated by means of lithium diisopropylamide (LDA) with the aldehyde **106** leads, after mild acid hydrolysis of the intermediate β-hydroxyimines **107**, to the (*E*)-acroleins **103a**, the stereochemical purity of which in all the cases investigated exceeds 95%.[64] The subsequent reductive transformation of compound **103a** via the stage of the allyl alcohols **108** and the corresponding sulfoesters by the method of Corey and Ahiwa[62] affords the (*Z*)-methylalkenes **104a**.

Scheme 13



R = *tert*-C_4H_9, *cyclo*-C_6H_{11}; R′ = C_2H_5, n-C_4H_9, n-C_6H_{13}, n-C_7H_{15}; R″ = n-C_5H_{11}, n-C_6H_{13}, n-C_7H_{15}, $(CH_2)_nOTHP$ (n = 5, 8), $(CH_2)_nOAc$ (n = 8).

α-Trishomoisoprenals of type **109** and ω-bisnorisoprenals of type **110** are necessary for the construction of the (*Z*)-isoprenoid chain with the aid of this method.

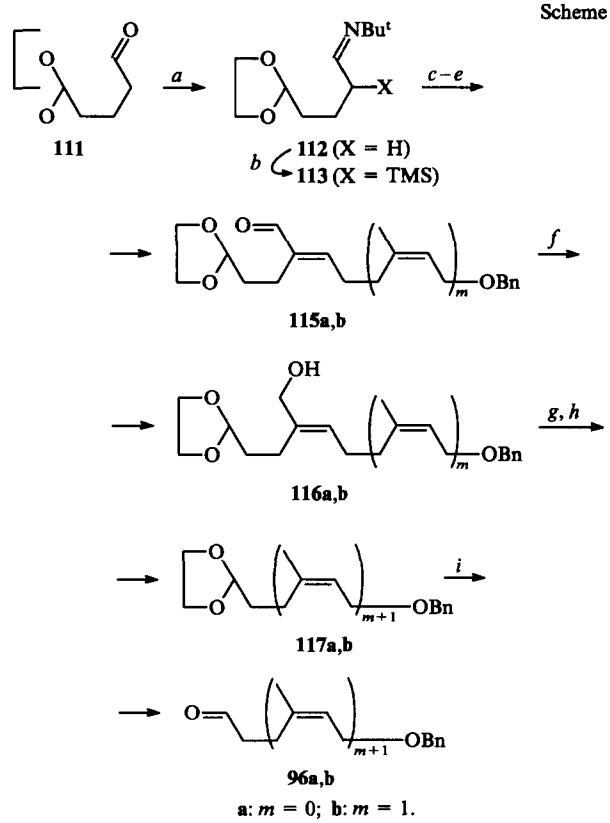


109 **110**

Compounds **109** and **110** can be obtained by the transformation of natural (*Z*)-isoprenoids, as shown above for the aldehydes **96a, b, e** (Scheme 11) or aldehydes which can be readily obtained by oxidising the alcohols **100** (Scheme 12). The method of synthesis of disubstituted (*Z*)-methylalkenes considered leads to the possibility of synthesising aldehydes of types **109** and **110** from non-isoprenoid compounds. The monoacetal of glutaraldehyde **111** and the corresponding *tert*-butylimine **112** are convenient starting materials for this purpose. Block synthons of both types indicated have been synthesised from them.[65]

Thus the synthesis of the aldehyde **96b** from the α-TMS-derivative of *tert*-butylimine **113** is illustrated in Scheme 14.[66] The process includes the condensation of the TMS-derivative of compound **113**, deprotonated by means of LDA, with benzyloxyacetaldehyde **114**, which leads to the (*E*)-acrolein **115a** in a preparative yield and with a stereoselectivity in excess of 95%. On reductive transformation via stages involving the formation of the allyl alcohol **116a** and the corresponding sulfoester, the acrolein **115a** is converted into the acetal **117a** in an overall yield of 25%. When the aldehyde **96a**, formed on hydrolysis of the acetal **117a** via the (*E*)-acrolein **115b** ($E \geqslant 95\%$), the alcohol **116b**, and the acetal **117b** stages, was introduced into the sequence of reactions described, the target aldehyde **96b** was obtained. By repeating the above chain of reactions, it is possible, in principle, to continue the growth of the (*Z*)-isoprenoid chain still further from its α-unit to its ω-unit.

Scheme 14



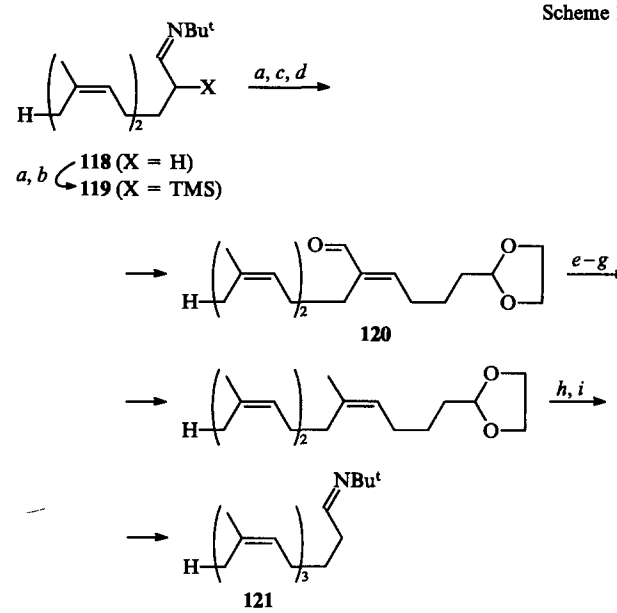
111 **112** (X = H), **113** (X = TMS) **115a,b** **116a,b** **117a,b** **96a,b**

a: $m = 0$; **b**: $m = 1$.

(*a*) Bu^tNH_2; (*b*) LDA, Me_3SiCl; (*c*) LDA; (*d*) O=⟨ OBn (**114**); (*e*) H_3O^+ (pH 4); (*f*) $NaBH_4$; (*g*) Py·SO_3; (*f*) $LiAlH_4$; (*i*) H_3O^+.

The conversion of the aldehydes **96a, b** into olefins by the Wittig method[67] affords the stereochemically pure nerol and (*Z,Z*)-farnesol. The latter were used to synthesise with the aid of the monoacetal **111** the imines of trishomoprenals of type **109**, which is illustrated (Scheme 15) by the conversion of the α-TMS-derivative of the aldimine **119**, prepared in six stages from nerol,[68] into the aldimine **121** via the key (*E*)-acrolein **120** stage in an overall yield of ~10%.

Scheme 15

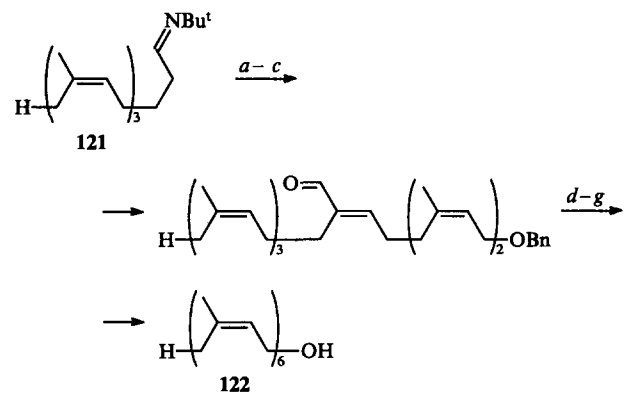


118 (X = H), **119** (X = TMS) **120** **121**

(*a*) LDA; (*b*) Me_3SiCl; (*c*) **111**; (*d*) H_3O^+ (pH 4); (*e*) $NaBH_4$; (*f*) Py·SO_3; (*g*) $LiAlH_4$; (*h*) H_3O^+; (*i*) Bu^tNH_2.

The aldimine **121** and the aldehyde **96b** obtained in this way were used to construct the (*Z*)-isoprenoid chain in the synthesis of the fully cisoid hexaprenol WC_5OH **122** with a nonnatural configuration of the ω-section of the chain (Scheme 16).[66]

Scheme 16

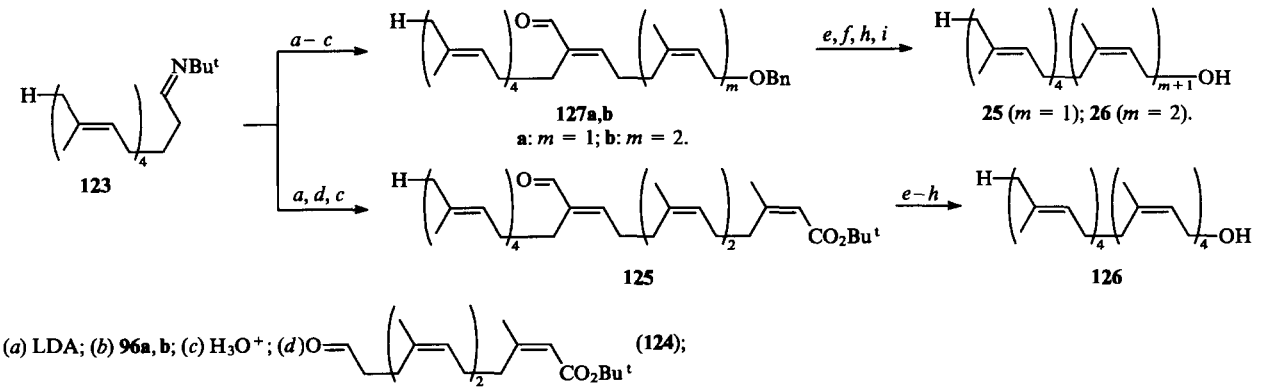


121 **122**

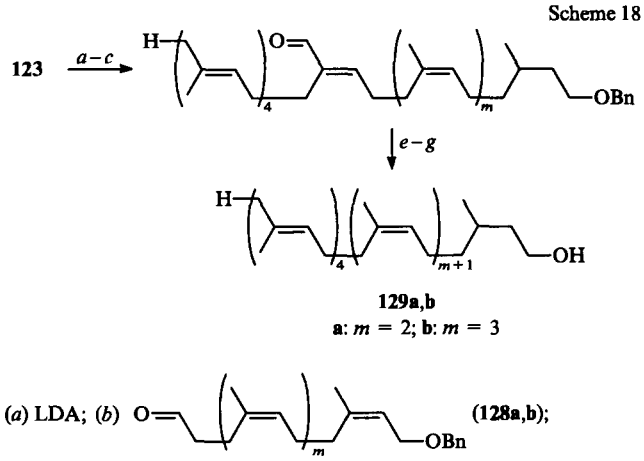
(*a*) LDA; (*b*) **96b**; (*c*) H_3O^+; (*d*) $NaBH_4$; (*e*) Py·SO_3; (*f*) $LiAlH_4$; (*g*) Li/NH_3.

The approach considered proved to be extremely effective also in the construction of natural polyprenols, as shown in relation to hexaprenol (WT_3C_2OH, **25**),[69] heptaprenol (WT_3C_3.OH, **26**),[10] and octaprenol (WT_3C_4OH, **126**)[70] isolated from the juice of the palm *Serenoa repens* (Scheme 17).[11] They were synthesised with participation of the aldimine **123**, containing a ω-transoid fragment of the above polyprenols and prepared from geranyllinalool,[71] and the aldehydes **96a, b** and **124** respectively[70] via key stages involving the formation of the (*E*)-acroleins **127a, b** and **125**.

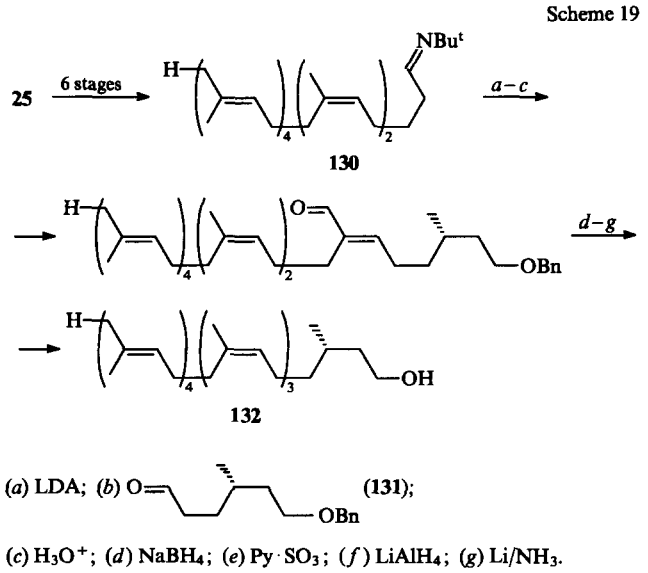
Scheme 17



Scheme 18



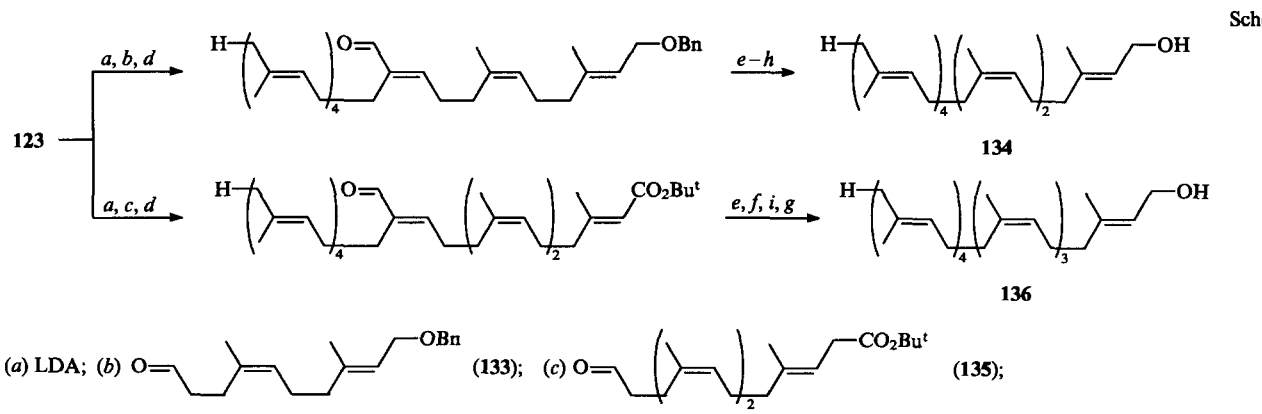
Scheme 19



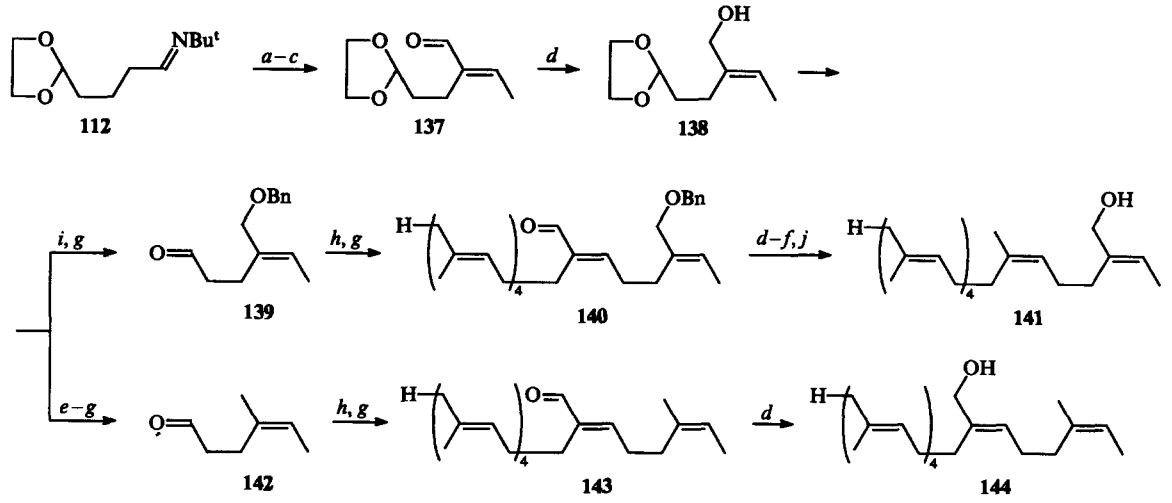
By means of the same methodology,[72] the racemic octaprenol (WT_3C_3SOH, **129a**) and nonaprenol (WT_3C_4SOH, **129b**), related to dolichols, were obtained from the aldimine **123** and the aldehydes **128a, b** (Scheme 18), while the dolichol-like octaprenol WT_3C_3SOH **132**,[69] with the natural (*S*)-configuration of the α-unit, was synthesised from the aldimine **130** prepared from the hexaprenol **25** described above and the chiral aldehyde **131** (Scheme 19).

The method has also found a successful application in the synthesis of modified polyprenols necessary for biochemical research. Thus the polyprenols **134**[71] and **136**,[70] with the non-natural (*E*)-configuration of the α-unit, have been obtained with its aid using the aldimine **123** block and the aldehyde **133** and **135** blocks (Scheme 20).

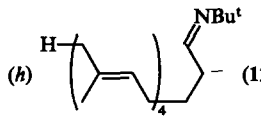
Scheme 20



Scheme 21



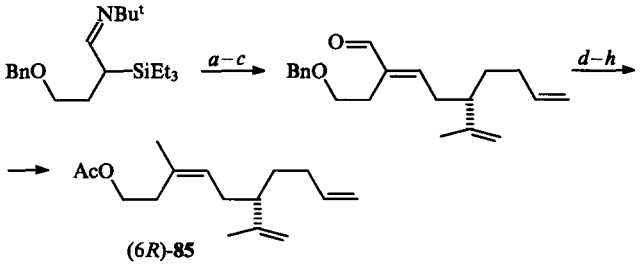
(*a*) LDA; (*b*) CH_3CHO; (*c*) H_3O^+ (pH 4); (*d*) $NaBH_4$; (*e*) Py·SO_3; (*f*) $LiAlH_4$; (*g*) H_3O^+;



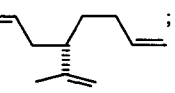
(*h*) (**123a**); (*i*) BnCl/NaH; (*j*) Li/NH_3.

The modified hexaprenols **141** and **144**,[73] with a nonnatural disposition of the OH group, were synthesised similarly from the same aldimine **123** and the aldehydes **139** and **142**. We may note that the block-synthons **139** and **142** were also obtained with the aid of the method, considered here, for the construction of (*Z*)-isoprenoids from the common precursors **137** and **138** (Scheme 21).

French chemists showed recently[74] that the method under discussion is optimal for the synthesis of the (6*R*)-**85** component of the pheromone of red San Jose scale and that its stereoselectivity is superior to that of other procedures[54,75] proposed for the synthesis of this compound.



(6*R*)-**85**

(*a*) LDA; (*b*)  ; (*c*) H_3O^+; (*d*) $LiAlH_4/Et_2O$;

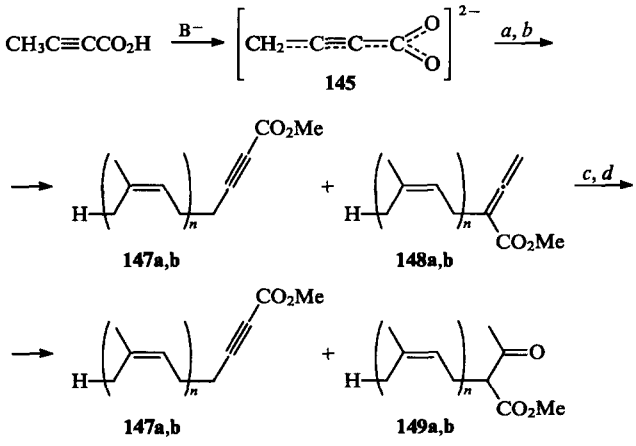
(*e*) Py SO_3; (*f*) $LiAlH_4$/THF; (*g*) Li/NH_3; (*h*) Ac_2O–Py.

Thus the method for the construction of (*Z*)-trisubstituted olefins, based on the thermodynamic preference for α,β-disubstituted (*E*)-acroleins, leads to extensive possibilities for the synthesis of biologically active (*Z*)-isoprenoids.

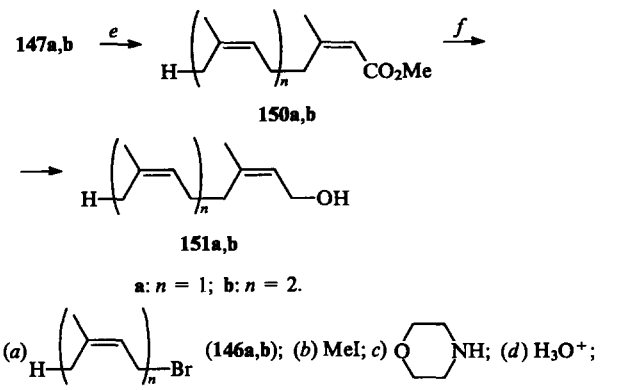
IV. Synthesis of (*Z*)-isoprenoids with formation of new C–C and (*Z*)-trisubstituted C=C bonds

In 1975, Baran and coworkers[76,77] investigated the possibility of the specific γ-alkylation of α,β-unsaturated acids in order to use the above reaction in the synthesis of polyprenols. They showed that the alkylation of the dianion of 2-butynoic acid **145** by prenyl bromide **146a** or neryl bromide **146b** leads to mixtures of products of γ- and α-alkylation stabilised in the form of the methyl esters **147a, b** and **148a, b**, which can be readily separated chromatographically after the conversion of the allene esters **148a, b** into the ketoesters **149a, b** (Scheme 22). The regioisomers ratio **147** : **148** is to a large extent determined by the nature of the base used to generate the dianion **145** and amounts to 2 : 1 in the case of lithium tetramethylpiperidide[76] and 3 : 1 in the case of LDA.[77] The use of the Bu^nLi–TMEDA (TMEDA = tetramethylethylenediamine) system made it possible to obtain the target ester **147** virtually free of compound **148**.[78]

Scheme 22

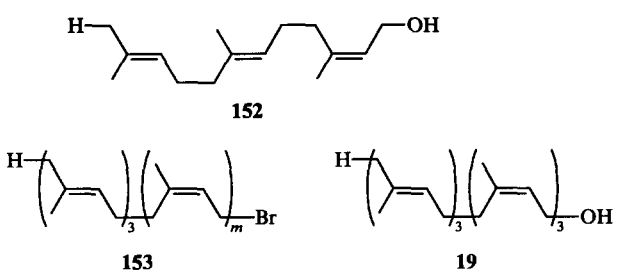


Scheme 22 (continued)



The stereoselective addition of dimethyl cuprate to the acetylenic fragment **147** by Corey's method[47] completes the formation of the new (*Z*)-isoprene unit and affords the esters **150** with an isomeric purity of about 98%, which can be smoothly reduced to the target (*Z*)-isoprenols **151**.

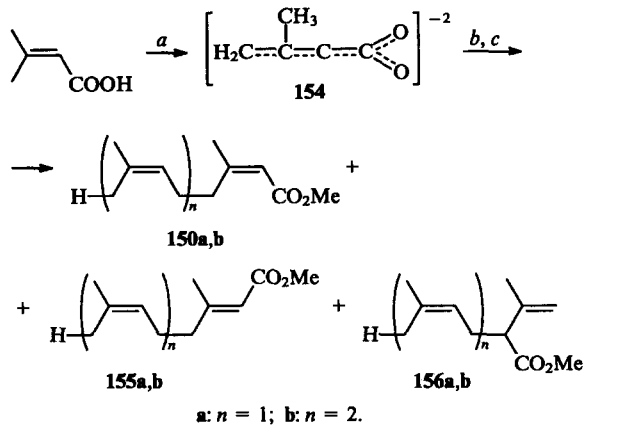
The involvement of geranyl bromide in the reaction chain presented in Scheme 22 led to (*Z,E*)-farnesol **152**[77] and the successive employment in these reactions of the isoprenoid bromides **153** (m = 0–2) enabled Baran et al.[79] to achieve the total synthesis of the hexaprenol WT_2C_3OH **19**, which they published without experimental details.



The version, investigated by the same authors,[77] of the synthesis of (*Z*)-isoprenols **151a,b** by alkylating the dianion of 3-methylcrotonic acid **154**, which is *a priori* more attractive than the γ-alkylation of 2-butynoic acid examined above since it makes it possible to construct in one stage the required isoprenoid skeleton (Scheme 23), proved to be less successful. Experimental tests showed that the interaction of the dianion of the acid **154** with prenyl bromide **146a** or neryl bromide **146b** affords, after methylation of the carboxy-group, a mixture of the products of γ-(*Z*)-alkylation (compound **150**), γ-(*E*)-alkylation (compound **155**), and α-alkylation (compound **156**) in proportions of 1 : 4 : 11. The γ : α product ratio can be increased[77] to ~4 : 1 and even to ~13 : 1 by using the cuprate complex.[154] This procedure has little effect on the stereochemistry of the reaction. The isomer ratio **150** : **155** in this reaction does not exceed ~5 : 3 and the isolation of the target product **150** requires repeated chromatography.

The data described in Section IV make it possible to conclude that, although the method involving the regioselective γ-alkylation of 2-butynoic acid developed for the synthesis of polyprenols is less effective than the alternative methods for the construction of the (*Z*)-isoprenoid systems examined in Sections II and III, nevertheless it can be used successfully for the synthesis of acetylenic esters of type **147**, which are convenient block-synthons in organic synthesis.

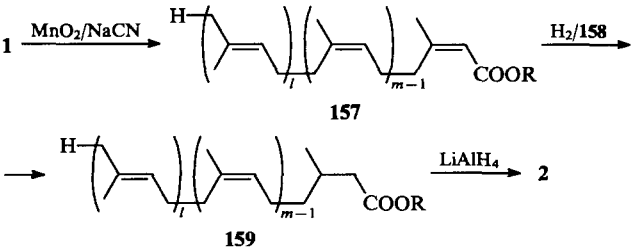
Scheme 23



V. Regioselective and enantioselective hydrogenation of the Δ^2-bond in α-functionalised isoprenoids

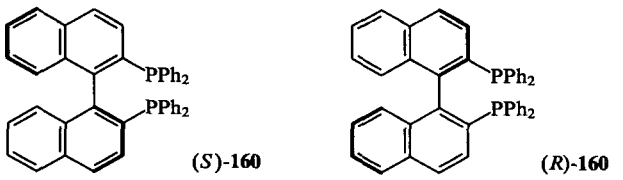
The methods for the construction of the (*Z*)-isoprenoid chain examined above made it possible to achieve the total syntheses of polyprenols **1**, dolichols **2**, and their modified analogues. At the same time, the possibility of the regioselective and enantioselective hydrogenation of the Δ^2-bond of polyprenols **1** is of significant interest for the partial synthesis of dolichols (which are a characteristic type of polyprenols in mammals) from much more readily available polyprenols of plant origin. The first attempt on these lines was by Polish biochemists[80] but did not yield the required results. Hydrogenation of the undecaprenol WT_2C_8OH **52** in alcohol over a platinum catalyst in the presence of $NaBH_4$, which they investigated, led to a mixture of the undecaprenols WT_2C_7SOH, WT_2C_6SCOH, $WT_2C_5SC_2OH$, and $WT_2C_4SC_3OH$.

The regioselective reduction of the α,β-unsaturated esters **157**, described in a patent,[81] proved more successful. The esters were obtained by standard methods from polyprenols **1** of plant origin with the aid of lithium in NH_3 or hydrogen in the presence of a metal complex catalyst — μ,μ'-dichlorobis-(cycloocta-1,5-diene)-rhodium/neopentyldiphenylphosphine **158**. The racemic esters **159** formed in this reaction are reduced smoothly by $LiAlH_4$ to the target dolichols **2**.

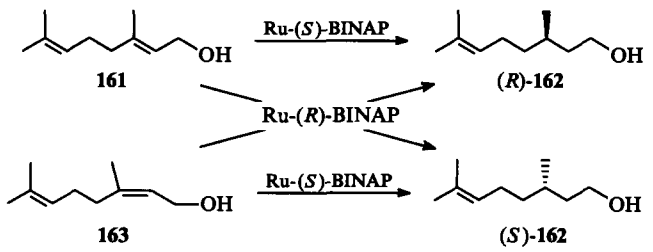


R = H, Alk; l = 2, m = 15.

The introduction of metal complex catalysts with optically active ligands into practical organic synthesis made possible the single-stage conversion of polyprenols **1** into (*S*)- or (*R*)-dolichols. Ruthenium complexes of the (*S*)- or (*R*)-form of 2,2'-bis(diphenylphosphino)-1,1'-binaphthyl (BINAP) **160** proved to be optimal for this process.[82]



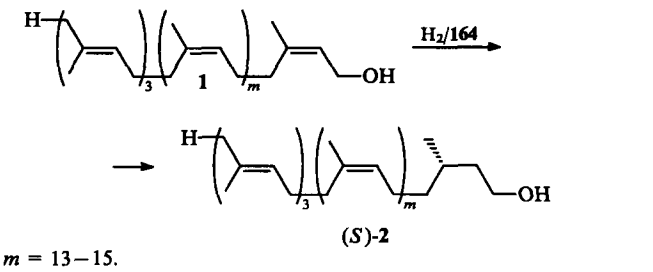
It was shown in relation to the simplest isoprenols—geraniol **161** and nerol **163**—that there is a rigorous correlation between the olefinic geometry of the substrate, the configuration of the chiral ligand in the catalyst, and the configuration of the chiral centre in the reaction product. Thus hydrogenation of the alcohol **161** in the presence of a ruthenium dicarboxylate complex with (*S*)-BINAP ligands affords (*R*)-citronellol **162**, whilst in the presence of the analogous complex with (*R*)-BINAP ligands the product is (*S*)-citronellol **162**. On the other hand, hydrogenation of compound **163** in the presence of the complexes with (*S*)-BINAP and (*R*)-BINAP ligands leads to (*S*)-**162** and (*R*)-**162** respectively.[83]



The method involving hydrogenation using the above catalysts has all the qualities necessary to achieve total asymmetric synthesis: high yields and enantiomeric purity in excess of 96%, a high regioselectivity of the reaction, the absence of the migration of the C=C bond and of the *E*/*Z* isomerisation, a high substrate/catalyst molar ratio, and, ease of recovery and regeneration of the catalyst without loss of its activity and selectivity.

The asymmetric hydrogenation of the mixture of polyprenols **1** isolated from *Ginkgo biloba*, catalysed by Ru-(*S*)-BINAP bistrifluoroacetate **164** and carried out taking into account the above features, led to a mixture of the corresponding dolichols **2** in a high yield and with an enantiomeric purity in excess of 95%. The mixture contained less than 2% of the products involving the reduction of other C=C bonds (Scheme 24).[84]

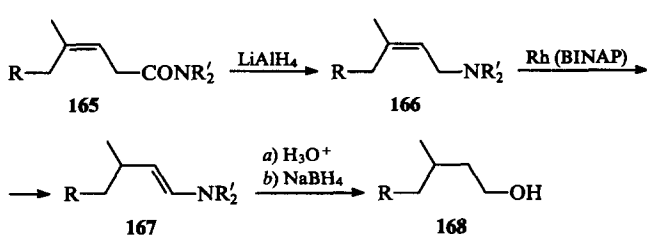
Scheme 24



m = 13–15.

The synthesis of dolichols **2** with the aid of metal complex catalysis can also be achieved starting with derivatives of polyprenylcarboxylic acids isolated, together with polyprenols **1**, from plant raw material. Thus it has been found[85] that BINAP-containing rhodium catalysts exhibit a high activity in the isomerisation of tertiary allylamines **166**, formed smoothly on hydride reduction of the amides **165** (Scheme 25).

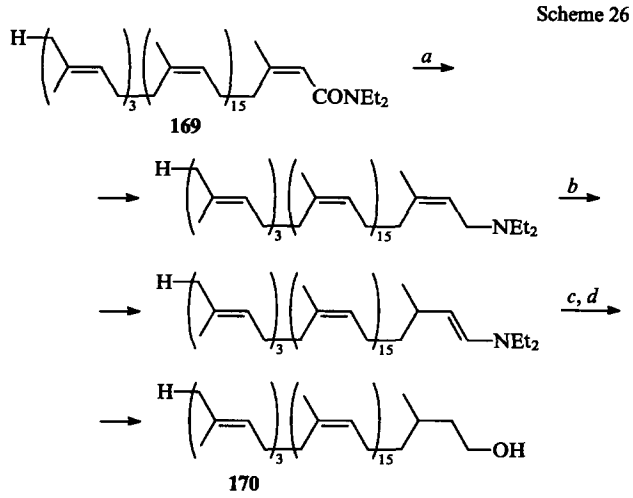
Scheme 25



R = Alk, ; R' = Alk, cycloalk, Ar.

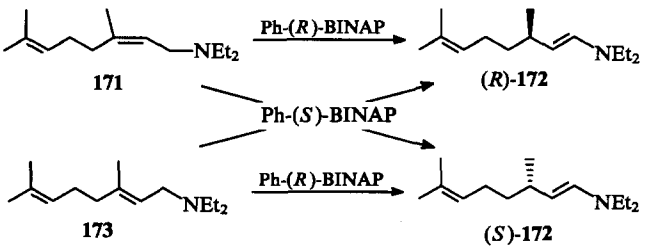
The enamines **167** thus obtained can be readily converted by standard methods into the correpsonding 4-C-substituted isopentanols **168**. The method has been applied successfully in the synthesis of the racemic dolichol $WT_2C_{15}SOH$ **170** from the amide **169** (Scheme 26).[86]

Scheme 26



(*a*) $LiAlH_4$; (*b*) Rh[BINAP(COD)]ClO_4; (*c*) H_3O^+; (*d*) $NaBH_4$
COD = cycloocta-1,5-diene.

The successful use of the Rh-(*R*)- and Rh-(*S*)-BINAP catalysts for the conversion of *N*,*N*-diethylnerylamine **171** and *N*,*N*-diethylgeranylamine **173** respectively into the enamines (*R*)- and (*S*)-**172**, which are intermediates in the synthesis of (*R*)- and (*S*)-citronellol, permits the hope that it will be possible also to achieve the synthesis of chiral dolichols with the aid of these catalysts.



By virtue of its high effectiveness and enantioselectivity, the method for the asymmetric hydrogenation of polyprenols **1** examined above appears to be the best of the known procedures for the conversion of (*Z*)-isoprenols into their (*S*)- or (*R*)-2,3-dihydro-derivatives.[18,87]

* * *

The data described show that the synthetic studies on polyprenols and dolichols provided organic chemistry with a series of effective and highly stereoselective methods for the construction of disubstituted (*Z*)-methylalkene systems, as well as regioselective and enantioselective procedures for the conversion of α-functionalised isoprenoids into their 2,3-dihydro-derivatives, which have already found interesting applications in the synthesis of other biologically active compounds.

References

1. F W Hemming, in *Biochemistry* Vol. 4 (MTP Int. Rev. Sci. Ser. 1) (Ed. T W Goodwin) (London: Butterworths, 1974) p. 39
2. F W Hemming *Biosynthesis of Isoprenoid Compounds* Vol. 2 (New York: Wiley, 1983) p. 303
3. J W Rip, C A Rupar, K Ravi, K K Carrol *Prog. Lipid Res.* **24** 269 (1985)
4. A M Moiseenkov, E V Polunin, I M Zaks, A V Semenovskii *Dokl. Akad. Nauk SSSR* **236** 124 (1977)
5. A V Semenovskii, E V Polunin, I M Zaks, A M Moiseenkov *Izv. Akad. Nauk SSSR, Ser. Khim.* 1327 (1979)
6. E V Polunin, A M Moiseenkov, A V Semenovskii *Izv. Akad. Nauk SSSR, Ser. Khim.* 1354 (1981)
7. A M Moiseenkov, E V Polunin, A V Semenovsky *Tetrahedron Lett.* **20** 4759 (1979)
8. A M Moiseenkov, E V Polunin, A V Semenovsky *Tetrahedron Lett.* **22** 3309 (1981)
9. V N Shibaev *Usp. Biol. Khim.* **17** 187 (1976)
10. A V Semenovskii, N Ya Grigor'eva, I M Avrutov, V V Veselovskii, M A Novikova, A M Moiseenkov *Izv. Akad. Nauk SSSR, Ser. Khim.* 152 (1984)
11. G Jommi, L Verotta, P Gariboldi, P Gabetta *Gazz. Chim. Ital.* **118** 823 (1988)
12. V V Veselovskii, Z G Makarova, A I Lutsenko, V A Smit, A M Moiseenkov, V M Zhulin *Izv. Akad. Nauk SSSR, Ser. Khim.* 811 (1987)
13. A M Moiseenkov, V V Veselovsky, Z G Makarova, V M Zhulin, W A Smit *Tetrahedron Lett.* **25** 5929 (1984)
14. W E Truce, C T Goralski, L W Christensen, R H Bavry *J. Org. Chem.* **35** 4217 (1970)
15. G I Vergunova, I S Glukhoded, L L Danilov, G I Eliseeva, N K Kochetkov, M F Troitskii, A I Usov, A S Shashkov, V N Shibaev *Bioorg. Khim.* **3** 1484 (1977)
16. M A Novikova, A V Lozanova, V V Veselovskii, V A Dragan, A M Moiseenkov *Izv. Akad. Nauk SSSR, Ser. Khim.* 356 (1987)
17. H Julia, D Uguen, A Callipolitis *Bull. Soc. Chim. Fr.* 519 (1976)
18. V A Koptenkova, V V Veselovskii, M A Novikova, A M Moiseenkov *Izv. Akad. Nauk SSSR, Ser. Khim.* 817 (1987)
19. V V Veselovskii, V A Koptenkova, M A Novikova, A M Moiseenkov *Izv. Akad. Nauk SSSR, Ser. Khim.* 2052 (1989)
20. Eur. P. 87 638; *Chem. Abstr.* **100** 68 570z (1983)
21. D Bottger, P Welzel *Tetrahedron Lett.* **24** 5201 (1983)
22. K Sato, O Miyamoto, S Inoue, F Furusawa, Y Matsuhashi *Chem. Lett.* 725 (1983)
23. K Sato, A Onishi, K Watanabe, in *The 35th National Meeting of the Chem. Soc. of Japan, Saporo, 1976 (Abstracts of Reports)* p. 3128
24. K Sato, O Miyamoto, S Inoue, F Furusawa, Y Matsuhashi *Chem. Lett.* 1105 (1984)
25. S Inoue, T Kaneko, Y Takahashi, O Miyamoto, K Sato *J. Chem. Soc., Chem. Commun.* 1036 (1987)
26. J E Biellmann, J B Ducep *Tetrahedron* **27** 5861 (1971)
27. L J Altman, L Ash, S Marson *Synthesis* 129 (1974)
28. Y Masaki, K Hashimoto, T Kaji *Tetrahedron Lett.* **19** 5123 (1978)
29. K Sato, O Miyamoto, S Inoue, Y Matsuhashi, S Koyama, T Koneko *J. Chem. Soc., Chem. Commun.* 1761 (1986)
30. A M Moiseenkov, M A Novikova, E V Polunin, S I Torgova *Izv. Akad. Nauk SSSR, Ser. Khim.* 1558 (1983)
31. N Ya Grigor'eva, I M Avrutov, A V Semenovskii, V N Odinokov, V R Akhunova, G A Tolstikov *Izv. AN SSSR, Ser. Khim.* 382 (1979)
32. M Mohri, H Kinoshita, K Inomata, H Kotake *Chem. Lett.* 451 (1985)
33. D Eren, E Keinan *J. Am. Chem. Soc.* **110** 4356 (1988)
34. I Takahashi, K Ogura *J. Biochem. (Tokyo)* **92** 1527 (1982)
35. S Fujisaki, T Nishino, H Kattsuki *J. Biochem. (Tokyo)* **99** 1327 (1986)
36. C M Allen, M V Keenan, J Sack *Arch. Biochem. Biophys.* **175** 236 (1976)
37. T Baba, C M Allen *Arch. Biochem. Biophys.* **200** 474 (1980)
38. L L Danilov, V N Shibaev, N K Kochetkov *Synthesis* 404 (1985)
39. S Ohnuma, T Koyama, K Ogyra *Tetrahedron Lett.* **32** 241 (1991)
40. T Suga, S Ohta, A Nakai, K Munesada *J. Org. Chem.* **54** 3390 (1989)
41. S Ohnuma, M Ito, T Koyama, K Ogyra *Tetrahedron* **45** 6145 (1989)
42. T Nishino, K Ogyra, S Seto *J. Am. Chem. Soc.* **94** 6849 (1972)
43. M Kobayashi, T Koyama, K Ogyra, S Seto, F J Pitter, I E M Bruggeman-Rotgaus *J. Am. Chem. Soc.* **102** 6602 (1980)
44. T Koyama, K Ogyra *J. Am. Chem. Soc.* **109** 2853 (1987)
45. J Reucroft, P G Sammer *Quart. Rev. Chem. Soc.* **25** 135 (1971)
46. D J Foulkner *Synthesis* 175 (1971)
47. E J Corey, J A Katzenellenbogen *J. Am. Chem. Soc.* **91** 1851 (1969)
48. D M Walba, P D Edwards *Tetrahedron Lett.* **21** 3531 (1980)
49. S B Bowlus, J A Katzenellenbogen *J. Org. Chem.* **38** 2733 (1973)
50. E J Corey, H Yamamoto *J. Am. Chem. Soc.* **92** 229 (1970)
51. H P Prisbylla, K Takanabe, J D White *J. Am. Chem. Soc.* **101** 762 (1979)
52. Y Masaki, K Hashimoto, K Kaji *Tetrahedron Lett.* **21** 5123 (1980)
53. S Inoue, N Iwase, O Miyamoto, K Sato *Chem. Lett.* 2035 (1986)
54. W C Still, A Mitra *J. Am. Chem. Soc.* **100** 1927 (1978)
55. K Honda, S Inoue, K Sato *J. Am. Chem. Soc.* **112** 1999 (1990)
56. U T Bhalerao, H Rapoport *J. Am. Chem. Soc.* **93** 5311 (1971)
57. K Sato, O Miyamoto, S Inoue, T Kobayashi, F Furusawa *Chem. Lett.* 1711 (1981)
58. C Sreekumar, K P Darst, W C Still *J. Org. Chem.* **45** 4260 (1980)
59. Jpn. P. 62-59 237; *Chem. Abstr.* **107** 217 882b (1987)
60. N Ya Grigor'eva, E P Prokof'ev, A V Semenovskii *Dokl. Akad. Nauk SSSR* **245** 366 (1979)
61. E P Prokof'ev, N Ya Grigor'eva, A V Semenovskii *Izv. Akad. Nauk SSSR, Ser. Khim.* 834 (1980)
62. E J Corey, K Ahiwa *J. Org. Chem.* **34** 3667 (1969)
63. G Wittig, H D Flommeld *Chem. Ber.* **97** 3548 (1964)
64. N Ya Grigor'eva, I M Avrutov, O A Pinsker, O N Yudina, A I Lutsenko, A M Moiseenkov *Izv. Akad. Nauk SSSR, Ser. Khim.* 1824 (1985)
65. N Ya Grigorieva, O N Yudina, A M Moiseenkov *Synthesis* 591 (1989)
66. N Ya Grigor'eva, O N Yudina, E D Daeva, A M Moiseenkov *Izv. Akad. Nauk SSSR, Ser. Khim.* 89 (1990)
67. G Wittig, U Schollkopf *Chem. Ber.* **87** 1318 (1954)
68. N Ya Grigor'eva, O N Yudina, O A Pinsker, E D Daeva, A M Moiseenkov *Izv. Akad. Nauk SSSR, Ser. Khim.* 97 (1990)
69. N Ya Grigor'eva, O A Pinsker, E D Daeva, A M Moiseenkov *Izv. Akad. Nauk SSSR, Ser. Khim.* 2325 (1991)
70. N Ya Grigor'eva, O A Pinsker, A M Moiseenkov *Izv. Akad. Nauk SSSR, Ser. Khim.* 2333 (1991)
71. N Y Grigorieva, I M Avrutov, A V Semenovsky *Tetrahedron Lett.* **24** 5531 (1983)
72. N Ya Grigor'eva, O A Pinsker, V N Odinokov, G A Tolstikov, A M Moiseenkov *Izv. Akad. Nauk SSSR, Ser. Khim.* 1546 (1987)
73. N Ya Grigor'eva, O N Yudina, A M Moiseenkov *Izv. Akad. Nauk SSSR, Ser. Khim.* 2036 (1986)
74. R Baudouy, P Prince *Tetrahedron* **45** 2067 (1989)
75. D Caine, E Crews *Tetrahedron Lett.* **25** 5359 (1984)
76. B S Pitzele, J S Baran, D H Steinman *J. Org. Chem.* **40** 269 (1975)
77. B S Pitzele, J S Baran, D H Steinman *Tetrahedron* **32** 1347 (1976)
78. S S Shen, C Ainsworth *Tetrahedron Lett.* **20** 82 (1979)
79. J S Baran, B S Pitzele, D D Langford, D H Steinman, L Hansen, T Kosobud, J Mueller, in *The 174th National Meeting, Chicago, 1979 (Abstracts of Reports)* p. 1076
80. T Mankowski, W Jankowski, T Chojnacki, P Franke. *Biochemistry* **15** 2125 (1976)
81. Jpn. P. 60-41 628; *Chem. Abstr.* **103** 160 733q (1985)
82. R Noyori, H Takaya *Acc. Chem. Res.* **23** 345 (1990)
83. H Takaya, T Ohta, N Sayo, H Kumoboyashi, S Akutagawa, S Inoue, I Kasahara, R Noyori *J. Am. Chem. Soc.* **109** 1596 (1987)
84. B Imperiali, J W Zimmerman *Tetrahedron Lett.* **29** 5342 (1988)
85. K Tani, T Yamagata, S Akutagawa *J. Am. Chem. Soc.* **106** 5208 (1984)
86. Jpn. P. 69-42 343; *Chem. Abstr.* **103** 142 217v (1985)
87. S Suzuki, F Mori, T Takigawa, K Ibata, J Ninagawa, T Nishida, M Mizuno, J Tanaka *Tetrahedron Lett.* **24** 5103 (1983))

Russian Chemical Reviews **63** (2) 185–195 (1994)
©1994 Russian Academy of Sciences and Turpion Ltd

UDC 541.128.13 : 542.01 : 546.72–44 : [546.11 + 546.262.3–31] : 542.952.6

The molecular weight distribution of the products of the Fischer–Tropsch synthesis

L S Glebov, G A Kliger

Contents

I. Introduction 185
II. Models of the molecular weight distribution 185
III. Experimental molecular weight distributions 189
IV. The influence of the conditions in the Fischer–Tropsch synthesis on the molecular weight distribution 192

Abstract. The literature data on the principal types of experimental molecular-weight distributions in the products of the Fischer–Tropsch synthesis are examined and classified. The influence of the catalyst composition and the experimental conditions in the Fischer–Tropsch synthesis on the type of molecular weight distribution is considered. The possible mechanisms of the propagation and termination of the hydrocarbon chain in the Fischer–Tropsch synthesis are discussed using the available data on the molecular-weight distribution. The bibliography includes 94 references.

I. Introduction

The study of the molecular weight distribution (MWD) in the products obtained in the Fischer–Tropsch (FT) synthesis constitutes a rapidly developing field of research. Data on the MWD of the products obtained are quoted in virtually every study published after 1980 and devoted to the FT synthesis. These data are of great interest in understanding the mechanism of the FT synthesis and can serve as a basis for the regulation of the process selectivity — an important and complex problem. The increase in the number of publications on this aspect of research has been caused to some extent by the advances in the development of methods for the determination of the quantitative and qualitative compositions of multicomponent mixtures of organic compounds — in the first place high prerformance gas–liquid capillary chromatography and chromatograph-linked mass spectrometry.

Insufficient attention has been devoted to the molecular weight distribution in the monographs and reviews on the FT synthesis.[1–9] For example, the eighth chapter of the book 'Chemical Substances from Coal'[1] is wholly devoted to the FT synthesis but there are no MWD data. In the monographs,[10,11] the examination of the MWD is restricted to data obtained up to 1980 inclusive. It has therefore become necessary to survey theoretical and experimental studies on the MWD which have appeared in the literature during the last 15 years.

L S Glebov Department of Industrial Ecology, Gubkin State Academy of Petroleum and Gas, Leninskii prosp. 65, 117 917 Moscow, Russian Federation, Fax (7-095)135 88 95.
G A Kliger Topchiev Institute of Petrochemical Synthesis, Russian Academy of Sciences, Leninskii prosp. 29, 117 912 Moscow, Russian Federation, Fax (7-095)230 22 24

Received 26 October 1993
Uspekhi Khimii **63** (2) 192–202 (1994); translated by A K Grzybowski

II. Models of the molecular weight distribution

The experimental molar distribution of the n-alkanes obtained in the FT synthesis as a function of the number of carbon atoms in the molecule was first formulated by Herington[12] [Table 1, Eqn (1)]. It follows from Eqn (1) that the ratio β_n of the mole fraction m_n of an n-alkane with n carbon atoms in the molecule to the sum of the mole fractions of n-alkanes containing between $n + 1$ and ∞ carbon atoms is constant.

On the basis of experimental MWD data for hydrocarbons produced by the FT synthesis, Anderson et al.[13] obtained Eqn (2), from which it follows that the ratio α of the mole fractions of n-alkanes containing $n + 1$ (m_{n+1}) and n (m_n) carbon atoms in the molecule is independent of n within the limits of experimental error. The parameter α of the distribution of the FT synthesis products is in the range $0 < \alpha < 1$. It is easy to show that, when β_n is independent of n, the parameters α and β are linked by the following relation:

$$\alpha = \frac{1}{1+\beta}.$$

Eqns (1) and (2) were obtained by analysing multicomponent† products which consisted mainly of a mixture of n-alkanes. An attempt has been made[14] to derive an equation for the distribution of the FT synthesis products, incorporating, apart from hydrocarbons, an appreciable amount of oxygen-containing compounds (mainly alcohols). Eqn (3), describing the MWD for alcohols, was obtained by combining the familiar formulae for the m_n term, i. e.

$$m_n = m_1^{n-1},$$

and the sum of n terms, i. e.

$$\sum_{n=1}^{\infty} m_n = \frac{m_1}{1-\alpha},$$

of an infinitely diminishing geometrical progression, where α is the denominator of the progression. Shuikin et al.[14] understood by $\sum m_n$ the sum of the numbers of moles (or quantities proportional to them) of the oxygen-containing compounds formed in the FT synthesis. The experimental data on the composition of the oxygen-containing compounds were treated in terms of Eqn (3′) — the logarithmic form of Eqn (3). The dependence of MWD on n for n-alkanols, expressed by a plot of $\lg m_n$ against n,

† The components of the FT synthesis products are understood as organic compounds of one class (n-alkanes, n-alkanols, etc.).

Table 1. Equations describing the molecular weight distribution for the FT synthesis products.

Equation	Number of equation	Author(s) of equation	FT synthesis products to which the equation was first applied	Ref.
$m_n = \beta_n \sum_{n=1}^{\infty} m_{ni}$	(1)	Herington	n-Alkanes	12
$m_n = m_{ni}\alpha^{n-1}$	(2)	Anderson, Friedel, and Storch	"	13
$m_n = (1-\alpha)\sum_{n=1}^{\infty} m_{ni}\alpha^{n-1}$	(3)	Shuikin, Kryukov, and Bashkirov	n-Alkanols	14
$\lg m_n = \lg\left[(1-\alpha)\sum_{n=1}^{\infty} m_{ni}\right] + (n-1)\lg\alpha$	(3′)	"	"	
$g_n = (\ln^2\alpha)\, n\alpha^n$	(4)	Schulz	n-Alkane, n-alkanols, and n-alkylamines	15, 18
$\lg(g_n/n) = \lg(\ln^2\alpha) + n\lg\alpha$	(4′)	"	"	
$m_n = (1\alpha)\alpha^{n-1}$	(5)	Flory	n-Alkanes, alkenes, and alkanols	19
$\lg m_n = \lg[(1\alpha)/\alpha] + n\lg\alpha$	(5′)	"	"	
$\lg m_n = \lg(1\alpha) + (n-1)\lg\alpha$	(5″)	"	"	
$g_n = (1\alpha)^2 n\alpha^{n-1}$	(5‴)	Madon	n-Alkanes	20

Note. m_n and g_n are respectively the mole and weight fractions of the components of the FT synthesis products with n carbon atoms in the molecule.

has the form of a straight line, which shows that this equation is applicable to the description of the MWD for the oxygen-containing FT synthesis products.

1. The Anderson–Schulz–Flory distribution

Until the publication of the study of Henrici-Olive and Olive,[15] the analysis of the MWD for the FT synthesis products was not systematic. The authors of this and a series of subsequent studies, surveyed in a monograph,[11] applied to the description of the MWD for the FT synthesis products the Schulz[16] [Eqn (4)] and Flory[17] [Eqn (5)] equations familiar in polymer chemistry. These equations were derived for the analysis of the MWD for polymers obtained respectively by radical polymerisation and linear polycondensation. The MWD calculated by Eqns (4) and (5) are similar for $\alpha > 0.5$,[11,15] so that both equations can be applied with equal success. The logarithmic forms of the Schulz equation [Eqn (4′)] and the Flory equation [Eqns (5′) and (5″)] are more convenient for analysis. As an illustration, Fig. 1 presents the theoretical MWD for a monofunctional product calculated by Eqn (5‴) for $\alpha = 0.9$. Here one may note that there exists an internal check of the agreement between the distribution and Eqns (4′) and (5′) or (5″) based on the equality of the values of α calculated by two independent methods — from the slope of the straight line (α_{sl}) and from the intercept on the ordinate axis (α_{int}). The possibility of describing the MWD for the products with the aid of the Schulz and Flory equations confirms the idea that the polycondensation and polymerisation processes and the mechanism of the formation of C–C bonds in the FT synthesis are all related. By analogy with the polycondensation and polymerisation processes, the parameter α for the FT synthesis occurring under stationary conditions can then be defined by the relation

$$\alpha = \frac{r_p}{r_p + r_t},$$

where r_p and r_t are the rates of propagation and termination of the carbon chain respectively. Here it is assumed that α is independent of chain length.

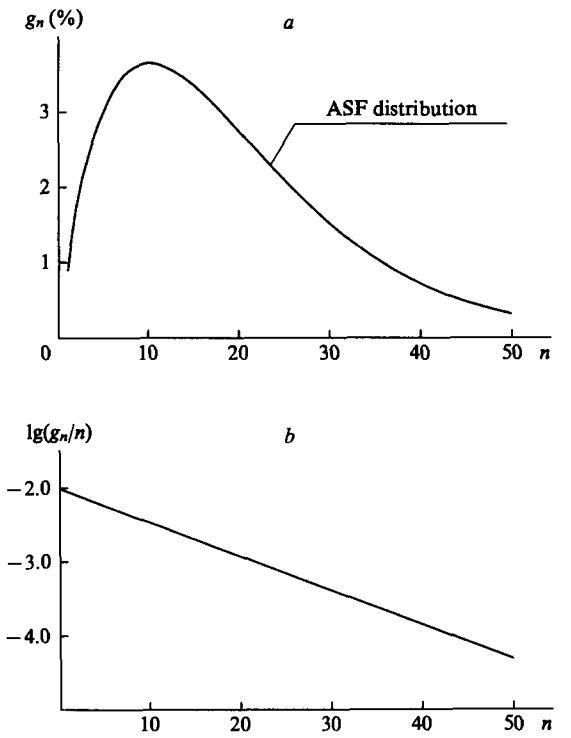


Figure 1. The Anderson–Schulz–Flory normal distribution for the FT synthesis product with $\alpha = 0.9$.[25] (*a*) $g_n - n$ plot; (*b*) semilogarithmic $\lg(g_n/n) - n$ plot.

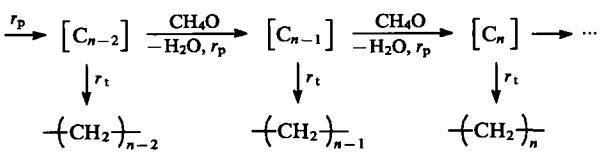
Evidently, the Schulz and Flory equations are applicable to the MWD for the products of the FT synthesis proceeding in accordance with Scheme 1 and the formal Scheme 2 when a polymer having the composition C_nH_{2n} is formed from n hypothetical monomers having the empirical formula CH_4O. Strictly speaking, only alkenes correspond to the polymer in the product.

Scheme 1

$$n(CO+2H_2) \longrightarrow \text{-}(CH_2)_n\text{-} + nH_2O$$

monomer polymer

Scheme 2



Here C_{n-2}, C_{n-1}, and C_n are intermediates with $n-2$, $n-1$, and n carbon atoms respectively.

In the general case, a multicomponent product is formed in the FT synthesis. It consists mainly of alkanes, alkenes, alkanols, and alkanals with a normal structure and contains from 1 to 100 or more carbon atoms.[21,22] The attempts to apply Eqns (4′) and (5′) or (5″) to the description of the MWD for the real products were unsuccessful because of the failure of the internal check of the MWD in terms of α. This difficulty can be partially obviated by applying Eqns (4′) and (5′) or (5″) separately to each component of the FT synthesis product (alkanes, alkanols, etc.). It is noteworthy that Eqn (3′) is transformed into Eqn (5″) if the sum of the moles of the components is unity:

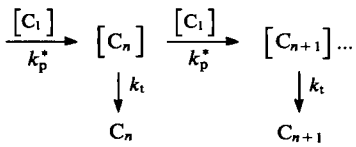
$$\sum_{n=1}^{\infty} m_n = 1.$$

Following Henrici-Olive and Olive,[15] other investigators also began to refer to the molecular weight distributions obeying Eqns (4′) and (5″) as the Schulz–Flory (SF) distributions. At the present time the term Anderson–Schulz–Flory (ASF) distribution is more often employed in the literature.

2. Special problems of the Anderson–Schulz–Flory distribution

A number of problems arise when the ASF distribution is applied to the analysis of real multicomponent FT synthesis products obtained under stationary and nonstationary conditions complicated by the occurrence of secondary reactions, various types of termination of the hydrocarbon chain, and other factors. Before proceeding to their discussion, it is appropriate to return yet again to the consideration of the classical model on the basis of which Eqns (4) and (5) may be obtained. Consider Scheme 3.

Scheme 3

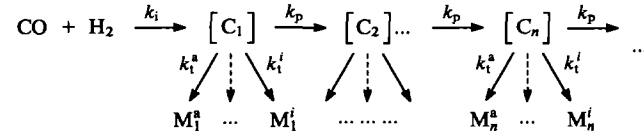


Here $[C_1]$, $[C_n]$, and $[C_{n+1}]$ are the concentrations of intermediates with 1, n, and $n+1$ carbon atoms on the surface of the catalyst, and k_p^* and k_t are the hydrocarbon chain propagation and termination constants respectively.

By use of Scheme 3, the above equations can be derived on the basis of the following postulates: the propagation of the carbon chain takes place as a result of the addition of the C_1 intermediate; chain termination is the result of simple desorption; k_p^* and k_t are independent of the length of the carbon chain. It is then evident that for stationary FT synthesis we have $[\dot{C}_n] = 0$ and, when $k_p = k_p^*[C_1]$ and $\alpha = k_p/(k_p = k_t)$, it is easy to obtain, for example, Eqn (5). In this case, the state involving the formation of the $[C_1]$- intermediate from CO and H_2 (the initiation stage) is unimportant for the derivation of the equation.

Multicomponent products of the FT synthesis. The attempts to apply Eqns (4) and (5) to the analysis of the MWD for real multicomponent FT products, which were unsuccessful because of the failure of the internal check of the MWD in terms of α, were already mentioned above. Eqn (5″) has been derived[23] for the multicomponent FT synthesis products on the basis of the following model (Scheme 4):

Scheme 4



Here $[C_1]$, $[C_2]$, and $[C_n]$ are the concentrations of the intermediates with 1, 2, and n carbon atoms on the catalyst surface, k_i and k_p are the initiation and carbon chain propagation rate constants, k_t^a and k_t^i are the carbon chain termination rate constants for the formation of an alkanol and the ith component of the FT synthesis product, and M_1^a, M_n^a, M_1^i, and M_n^i are the alkanols and the ith components of the product with 1, ..., n carbon atoms respectively.

The derivation of the MWD equation for a multicomponent FT synthesis product involves an increase in the number of postulates from three to five. A further two postulates are added to those described above for the classical model of the ASF distribution: the product components with the same number of carbon atoms n are formed from the C_n intermediate via parallel pathways; the constants for the termination of the carbon chain of the alkanol and the ith components are independent of chain length.

In the stationary state, the rate of initiation r_i is equal to the sum of the rates of termination, i. e.

$$r_i = \sum^{i} r_t^i = \sum^{i} k_t^i \sum_{n=1}^{\infty}[C_n], \tag{6}$$

$$[\dot{C}_1] = \sum^{i} k_t^i \left(\sum_{n=1}^{\infty}[C_n] - k_p[C_1] - \sum^{i} k_t^i[C_1] \right) = 0,$$

$$[\dot{C}_2] = k_p[C_1] - k_p[C_2] - \sum^{i} k_t^i[C_2] = 0, \tag{7}$$

.....

$$[\dot{C}_n] = k_p[C_{n-1}] - k_p[C_n] - \sum^{i} k_t^i[C_n] = 0.$$

Simultaneous solution of Eqn (6) and Eqns (7), taking into account

$$k_p \Big/ \left(k_p + \sum^{i} k_t^i \right) = \alpha,$$

makes it possible to obtain the Flory equation for the intermediates:

$$[C_n] \Big/ \sum_{n=1}^{\infty}[C_n] = (1-\alpha)\alpha^{n-1}. \tag{8}$$

It is seen that $[C_n]/[C_{n-1}] = \alpha$ and, since $[M_n^i] = k_t^i[C_n]$ and $[M_{n-1}^i] = k_t^i[C_{n-1}]$, we have

$$\frac{[M_n]}{[M_{n-1}]} = \alpha . \tag{9}$$

It follows from Eqn (9) that, when the propagation of the carbon chains of the components of the FT synthesis products takes place in accordance with Scheme 4, then the data for the composition of such products, expressed in terms of the semilogarithmic variables of the Flory equation, should fit on straight lines with the same slope. Having solved the equations

$$\begin{aligned} \sum^i [\dot{M}_1^i] &= \sum^i k_t^i[C_1] , \\ \sum^i [\dot{M}_2^i] &= \sum^i k_t^i[C_2] , \\ &\cdots\cdots\cdots\cdots \\ \sum^i [\dot{M}_n^i] &= \sum^i k_t^i[C_n] , \end{aligned} \tag{10}$$

we obtain, after integrating the expression for the mole fraction of the ith components of the products,

$$\sum^i m_n^i = \sum^i [M_n^i] \Big/ \sum_{n=1}^{\infty} \left(\sum^i [M_n^i] \right) = (1-\alpha)\alpha^{n-1} , \tag{11}$$

$$\sum^i g_n^i = n(\ln^2 \alpha)\alpha^n . \tag{11'}$$

Eqns (11) and (11') represent the Flory [Eqn (5)] and Schulz [Eqn (4)] equations for a multicomponent product. The differences between Eqns (11) and (5) and between Eqn (11') and Eqn (4) consists in the fact that the left-hand side of Eqn (11) contains the sum of the mole fractions, while in Eqn (11') it contains the sum of the mass fractions of the ith components of the product with the same number of carbon atoms. An equation analogous to Eqn (11) for the special case of the formation of n-alkanes and n-alkanols has also been obtained by O'Young and Buchwalter.[24]

Chain propagation with two intermediates. In contrast to the classical model of the ASF distribution, the propagation of the carbon chain of a multicomponent product with participation of two intermediates, C_1 and C_2, has been examined.[25] In this case, the rate of formation of the C_n intermediate in the stationary state with $n \geqslant 3$ is described by the equation

$$\begin{aligned} [\dot{C}_n] &= k_p[C_{n-1}] - k_p[C_n] - k_t[C_n] + k_p^*[C_{n-2}] - k_p^*[C_n] \\ &= 0 \end{aligned} \tag{12}$$

Here the MWD parameter α^* is defined by the relation

$$\alpha^* = \frac{k_p}{k_p + k_t + k_p^*} = \frac{\alpha}{1 + y\alpha} , \tag{13}$$

where $y = k_p^*/k_p$.

An analytical solution of Eqn (12) has been described.[25] Fig. 2 presents the calculated MWD curves for two values of y. Evidently, the curves have an oscillatory form.

The dual nature of chain termination. A more involved version of the termination of the carbon chain, determined by the possibility that part of the monocomponent product with n carbon atoms is formed as a result of the interaction of the intermediates with $n - m$ and m carbon atoms in the molecule,

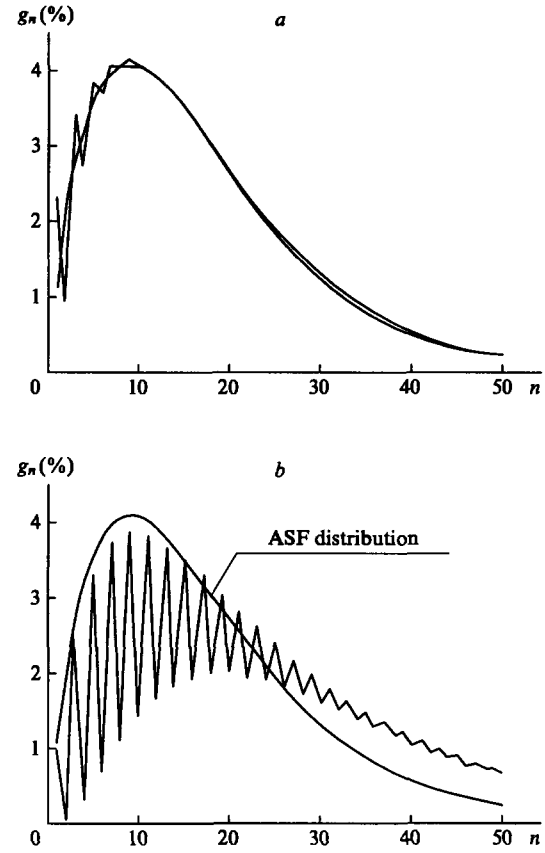


Figure 2. Molecular weight distribution for the FT synthesis products in the case where the carbon chain is propagated with participation of C_1 and C_2 intermediates for different values of y: (*a*) 1; (*b*) 10.[25]

has been analysed.[25] In this case, the rate of formation of the C_n intermediate in the stationary state is described by Eqn (14), such termination being taken into account by the term $k_t'[C_n]$:

$$[\dot{C}_n] = k_p[C_{n-1}] - (k_p + k_t + k_t')[C_n] = 0 . \tag{14}$$

The MWD parameter α' for this case is defined by the relation

$$\alpha' = \frac{k_p}{k_p + k_t + k_t'} = \frac{\alpha}{1 + \mu(1-\alpha)} , \tag{15}$$

where $\mu = k_t'/k_t$.

The exact solution of Eqn (14) has been published.[25] Fig. 3 presents as an illustration the calculated MWD curve for $\mu = 2.7$. It is seen that the selectivity with respect to C_{10} under the conditions of the dual type of termination of the carbon chain is higher than the selectivity for the ASF distribution.

MWD taking into account the propagation of the carbon chain with participation of the products formed as well as the possibility of the cracking of these products have also been examined.[25,26] However, such MWD are so far of purely theoretical importance because under real conditions the contribution by such reactions of the FT synthesis products is extremely low.[27]

Molecular weight distribution for branched FT synthesis products. Depending on the conditions of the FT synthesis, its products may contain different (sometimes appreciable—up to 10%) amounts of alkanes with a branched carbon skeleton—mainly 2- and 3-monomethyl-substituted isomers. The MWD for such hydrocarbons were first examined by Anderson and

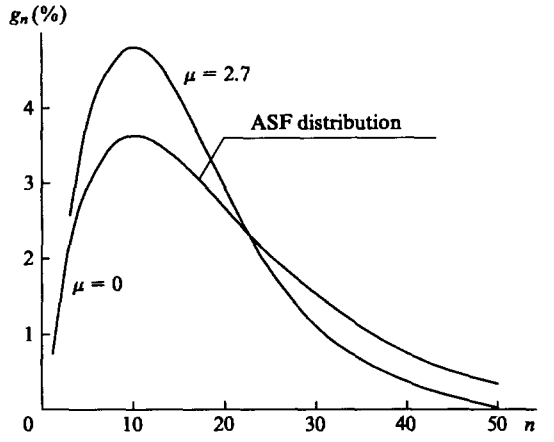
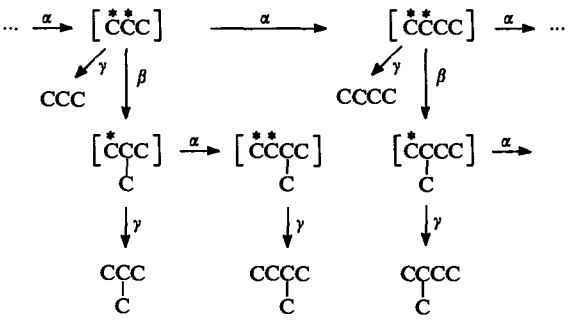


Figure 3. Molecular weight distribution for the FT synthesis product under the conditions of mutual termination of the carbon chain.[25]

coworkers.[28–31] There exist several models of the propagation of the carbon chain of isoalkanes differing from one another by the number of limitations and the extent to which the isomeric composition of the alkanes is taken into account.[10,28–35] In the most complete form, these models have been described by Wojciechowski.[35] We shall confine ourselves to the consideration of Anderson's model.[10]

Evidently the problem associated with the estimation of the proportions of isoalkanes arises in the case of a carbon chain containing four carbon atoms in the molecule. It is then postulated that there is no isomerisation of the normal carbon chain. In this connection, we shall consider a fragment of the model of the propagation of an isomeric alkyl chain (Scheme 5).

Scheme 5



Here $[\overset{**}{C}CC]$, $[\overset{**}{C}CCC]$, $[\overset{*}{C}(C)C]$, $[\overset{*}{C}(C)CC]$ are the concentrations of the intermediates with the normal and isomeric carbon chains on the surface of the catalyst; the asterisks denote the carbon atoms to which the addition of the intermediate $[C_1]$ is postulated, α and β are the propagation rate constants for the normal and isomeric carbon iso-chains respectively, and γ is the rate constant for the termination of the carbon chain in the n-alkanes and isoalkanes.

In the stationary state two equations can be written for the intermediate containing four carbon atoms: for the isomers with the normal $[C_4]$ and branched [*iso*-C_4] chains:

$$\dot{[C_4]} = \alpha[C_3] - \alpha[C_4] - \gamma[C_4] - \beta[C_4] = 0, \quad (16)$$

$$\dot{[iso\text{-}C_4]} = \beta[C_3] - \gamma[iso\text{-}C_4] - \alpha[iso\text{-}C_4] = 0. \quad (17)$$

The following relations can be obtained readily from Eqns (16) and (17):

$$\frac{[C_4]}{[C_3]} = \frac{\alpha}{\alpha + \gamma + \beta} = a,$$

$$\frac{[iso\text{-}C_4]}{[C_3]} = \frac{\beta}{\alpha + \gamma} = b.$$

If the notation $b/a = f$ is used, then the concentration of isobutane relative to that of n-butane depends only on f.

Anderson[10] obtained the following MWD equation for isomeric alkanes — the products of FT synthesis:

$$g_n = \frac{g_3 n F_{(n)} a^{n-3}}{3} \quad \text{for } n \geqslant 4, \quad (18)$$

where

$$F_{(n)} = 1 + (n-3)f + \frac{(n-4)(n-5)f^2}{2} + \ldots .$$

Data on the compositions of the isomeric and normal alkanes are usually expressed in a tabular form.

The special problems of the ASF distribution are not exhausted by the examples examined. Thus the kinetic parameters of the FT synthesis have been determined from MWD data.[35,36] A method has been proposed for the calculation of α as a function of the ratio H_2/CO.[37,38] Using the method of chemical potentials, an equation has been derived for the description of the ASF distribution.[39]

III. Experimental molecular weight distributions

Very many publications have been devoted to the experimental study of the MWD for monocomponent and multicomponent FT synthesis products. In most cases, the experimental MWD obey satisfactorily the ASF distribution (Fig. 1*b*), i.e. are assumed to be normal MWD.[11,15,19,40–47] At the same time, there is a large number of MWD characterised by deviations from the normal ASF distribution. In terms of the semilogarithmic variables of the Schulz and Flory equations, these deviations are manifested either by the curvature of the MWD or are associated with the appearance of different kinds of breaks on the linear MWD plots. However, in such cases the possibility, in principle, of describing part of the experimental MWD by the Flory and Schulz equations remains.

We shall examine the types of experimental MWD most frequently encountered (Fig. 4).

1. The molecular weight distribution characteristic of hydrocarbon FT synthesis products with an enhanced content of methane.[11,15,48,49] The composition of the hydrocarbons, with the exception of the C_1 product, corresponds to the ASF distribution. The maximum of the distribution, corresponding to the C_1 product is probably associated with the existence of an additional path to its formation, either via the $[C_1^*]$ intermediate, different from the $[C_1]$ intermediate, with the participation of which other hydrocarbons are obtained, or via the $[C_1]$ intermediate, which is converted into the C_1 product on other active centres of the catalyst, or, finally, via the intermediate $[C_1^*]$, which is in addition transformed on other active centres of the catalyst.

2. The molecular weight distribution characteristic of hydrocarbon FT synthesis products with a reduced content of C_2 products.[11,15,50–56] The reduced content of ethane and ethylene compared with the normal ASF distribution can be due to several causes in such cases: the propagation and termination of the carbon chain with participation not only of the $[C_1]$ intermediate but also the $[C_2]$ intermediate and secondary reactions involving C_2 products, for example the hydroformylation of ethylene.[57] Sometimes the breaks on the

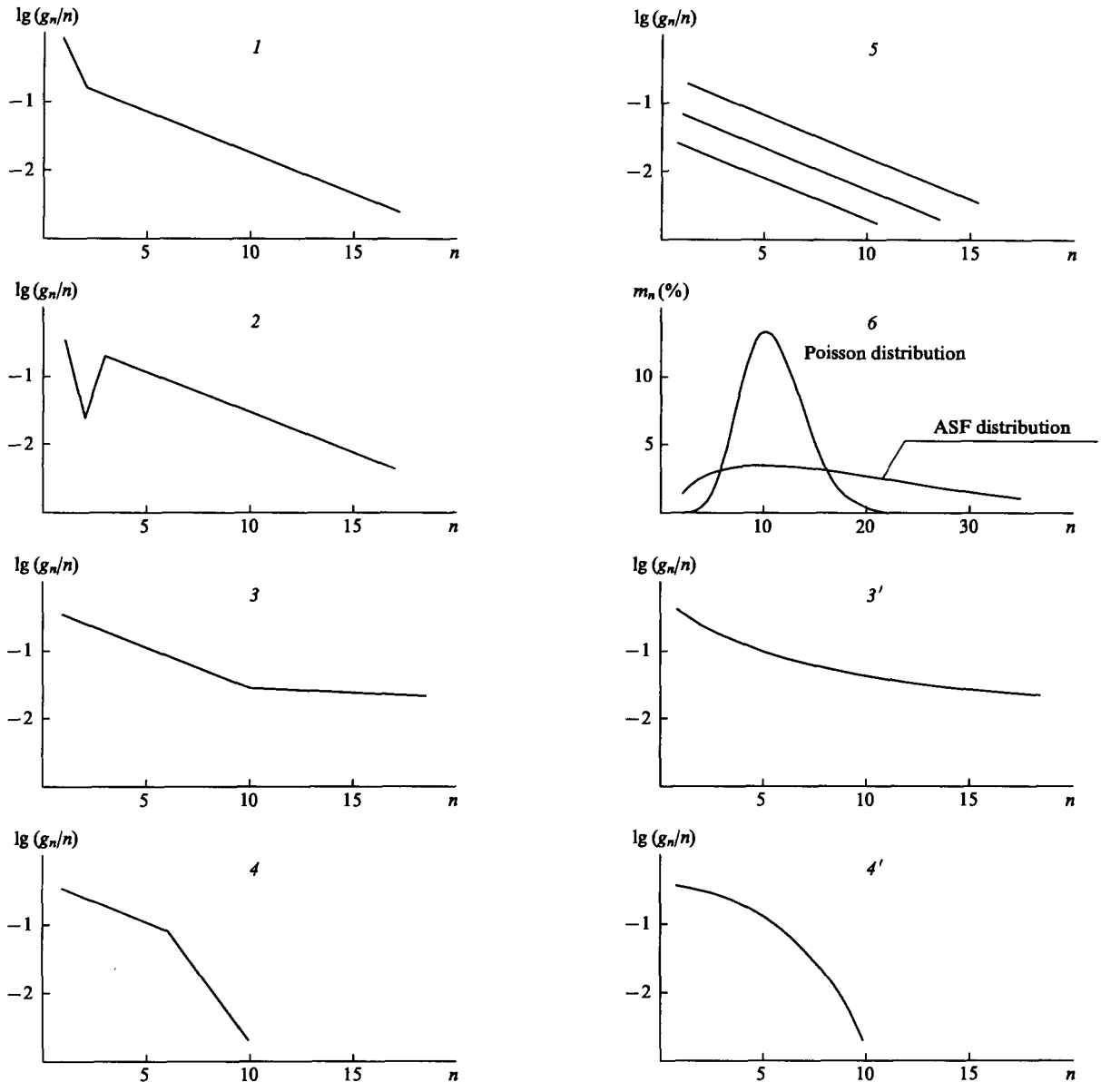
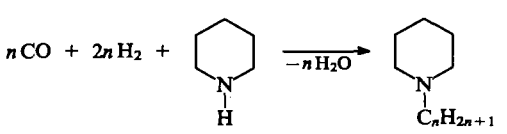


Figure 4. Different types of experimental MWD for the FT synthesis products: (*1*)–(*6*) see text.

linear distribution plots correspond to the C_3-C_4 products[11] which is probably due to the same causes as for the C_2 products. More complex cases, representing a combination of versions *1* and *2*, are encountered.[11,58,59]

3. The molecular weight distribution characteristic of the case where α increases with increase in n. This type of MWD is encountered for alkanes,[34,53,58–73] alkanols,[74] and alkylamines.[75,76] The last can be obtained, for example, in the piperidine-modified FT synthesis in accordance with Scheme 6.

Scheme 6



The break on the MWD curves for alkanes, alkanols, and alkylamines is usually observed at $n = 5-13$, the parameter α for low-molecular-weight products (α_1) being smaller than for high-molecular-weight products (α_2). If the degree of nonlinearity of the MWD is determined in terms of $\Delta\alpha = \alpha_2 - \alpha_1$, then it amounts to 0.12–0.20 for alkanes,[60,66] 0.26 for alkanols,[74] and 0.20 for alkylamines.[75,76] In some cases, there is no break on the MWD curves. Such MWD constitutes type *3'*. The appearance of MWD of types *3* and *3'* can arise from the following causes: the nonstationary nature of the FT synthesis, as a result of which α increases significantly during the period necessary for the collection of the FT synthesis products for analysis; the presence on the catalyst surface of two or more types of active centres on which products with different values of α are obtained;[7,60] the increase in the probability of the propagation of the carbon chain, which is proportional to the number of carbon atoms in the molecule. Several equations have been proposed for the description of MWD of types *3* and *3'*.[60,76,77] The simplest of these is based on the Flory equation [Eqn (5)] and has the following form:

$$m_n = x(1-\alpha_1)\alpha_1^{n-1} + (1-x)(1-\alpha_2)\alpha_2^{n-1}, \qquad (19)$$

where x and $1-x$ are the fractions of the products having the molecular weight distribution parameters α_1 and α_2 respectively.

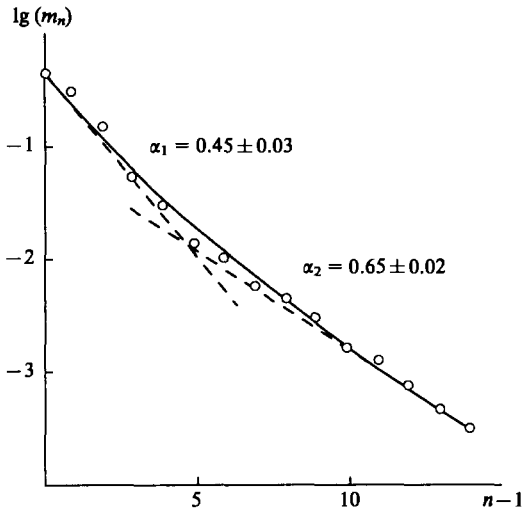


Figure 5. Molecular weight distribution for *N*-(n-alkyl)piperidines obtained in synthesis from CO, H_2, and piperidine on a reduced fused iron catalyst promoted with 5% V_2O_5:[75] circles—experimental data; curve—calculation by Eqn (19) for $x = 0.36$.

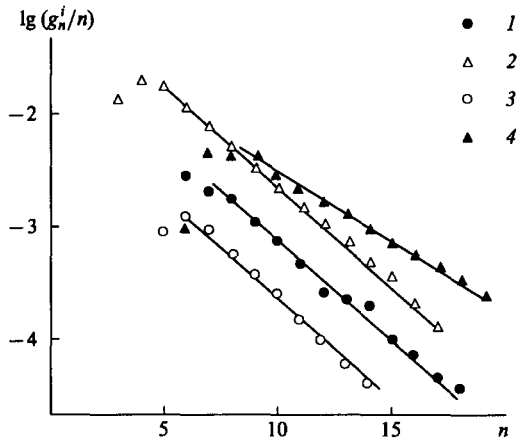


Figure 6. Molecular weight distribution for the liquid fraction of the multicomponent product of synthesis from CO and H_2 (for the conditions of the synthesis, see Table 4):[82] (*1*) α-alkenes; (*2*) n-alkanols; (*3*) n-alkyl methyl ketones; (*4*) n-alkanes; $\alpha = 0.66 \pm 0.02$ (*1–3*) and 0.77 ± 0.02 (*4*).

Evidently the change in the MWD parameters from α_1 to α_2 with increase in n from 1 to ∞ takes place continuously. The chemical significance of such continuity is associated with the simultaneous formation of the FT product independent of n, part of which is characterised by α_1 and is obtained on centres of one type, while another part is characterised by α_2 and is formed on other active centres. Eqn (19) describes MWD of type *3'* with a smaller error. As an illustration, Fig. 5 presents the MWD for *N*-n-alkylpiperidines obtained in accordance with Scheme 6 on a reduced fused iron catalyst containing 5% V_2O_5 as the promoting agent.[75] The experimental molecular weight distribution can be fitted either by two straight lines intersecting at $n = 6$, each of which is described by the Flory equation [Eqn (5)] with $\alpha_1 = 0.45 \pm 0.03$ or $\alpha_2 = 0.65 \pm 0.02$ ($\Delta = 0.20$), or by a curve corresponding to the equation

$$\lg m_n = \lg [0.36\,(0.45)^{n-1} + 0.64\,(0.65)^{n-1}].$$

The maximum standard deviation when the above equation is used for $n = 6$ is 55%, while in the range $1 < n < 15$ it is only 14%. The large error of the description of the experimental MWD by Eqn (19) in the vicinity of the break point may indicate the lack of validity of the approach used by Huff and Satterfield[60] and the inadequacy of Eqn (19) for such sections of the MWD. It is entirely likely that the type of the FT synthesis products obtained depends on n: FT products with only α_1 or α_2 are formed for $1 < n < 6$ and $n > 6$ respectively. The appearance of a break can then be associated with, for example, the steric control of the FT synthesis occurring with participation of two types of active centres of the catalyst.

4. The molecular weight distribution characteristic of cases where the parameter α diminishes with increase in n. Such MWD are also encountered in the study of hydrocarbon FT synthesis products.[21,48,51,78–80] Sometimes there is no break and the MWD reduces to type *4'*. The MWD of types *4* and *4'* arise under nonstationary conditions of the FT synthesis (in the presence of temperature and concentration gradients)[78] or for large losses in the stages involving the collection and/or analysis of low- and high-molecular-weight products.[79]

5. The molecular weight distribution in the form of several, often parallel, straight lines occurs in the study of real multicomponent FT products containing (a) only hydrocarbon components (n-alkanes, isoalkanes, α-alkenes, *cis*- and *trans*-alkenes),[53,63,64] (b) hydrocarbons and oxygen-containing compounds (n-alkanes, alkenes, alkanols, alkanals),[61,65,81] and (c) hydrocarbons and oxygen- and nitrogen-containing compounds in the case of the FT synthesis products modified by the addition of ammonia or dimethylamine (Fig. 6).[82–84] Different equations are used to describe the MWD. Some of them were examined above. Fig. 6 presents the MWD for the part of the product obtained from CO, H_2, and Me_2NH on a reduced, promoted, and fused iron catalyst (RPFIC).[82,84] It is seen from these data that Eqn (11') describes satisfactorily the experimental results.

6. The molecular weight distribution differing from the ASF distribution and not described by the Schulz or Flory equation.[2,11,20,85–89] Successful attempts to consider such MWD with the aid of the Poisson equation[90] are described in the literature:[11,88]

$$m_n = \frac{e^{-v} v^{n-1}}{(n-1)!}, \tag{20}$$

$$g_n = \frac{e^{-v} v^{n-1} n}{(n-1)!\,\bar{n}}, \tag{21}$$

where m_n and g_n are the mole and weight fractions of the FT synthesis product with n carbon atoms, v is the average number of chain propagation stages, and $\bar{n} = v + 1$ is the average degree of polymerisation.

Products obtained from CO and H_2 on Ru, Co, or Fe catalysts deposited on carriers with a high specific surface (of the order of 100 $m^2\,g^{-1}$ and above) have a type *6* distribution. The position of the maximum on the distribution curve depends on the carrier surface,[85] the maximum shifting towards low-molecular-weight synthesis products with its increase. The most probable causes of the MWD of this type are a high degree of dispersion of the catalyst particles,[87] the internal diffusion control of the chain propagation by the carrier ('the cage effect'),[87] and the nonstationary nature of the FT synthesis.

IV. The influence of the conditions in the Fischer–Tropsch synthesis on the molecular weight distribution

The catalyst as well as the conditions in the Fischer–Tropsch synthesis are known to influence the composition of the products, in particular the ratio of the hydrocarbon and oxygen-containing components.[10,11] In this section, attention is concentrated on studies which consider the influence of the conditions in the FT synthesis on the MWD. Only those investigations are analysed in which there were no effects due to the nonstationary nature of the FT synthesis, as well as those in which the parameter α was determined taking into account the experimental error, including cases where the data presented in the original papers made it possible to estimate the accuracy of the calculation of α. The temperature, pressure, the composition of the synthesis of gas and its space velocity, the type of reactor and the catalyst, the duration of the synthesis, and the addition of a third component to the mixture of CO and H_2 (modified FT synthesis) represent a list of factors (regime parameters), the effect of which on the MWD for the products will be examined below.

Temperature. The influence of temperature on the MWD has been investigated for products obtained on iron-containing heterogeneous catalysts in the gas phase in a reactor with a stationary catalyst bed[19,23] and in the liquid phase in a reactor with a stirrer and a suspended catalyst.[65,66,73] The temperature was varied from 159 to 285 °C. In all cases, α remained constant regardless of the temperature of the FT synthesis within the limits of the error of the determination. For example, in the study of Glebov et al.[23] the 'productivity' of the FT synthesis with respect to the products (hydrocarbons + oxygen-containing compounds) increased by a factor of 3.1 with increase in temperature from 159 to 180 °C, whereas the parameter α remained constant at 0.5 ± 0.1.

Table 2 presents the values of the MWD parameter α for the FT synthesis product obtained at different temperatures on iron catalysts of different composition. It is seen from the tabulated data that, when the temperature is varied in the range of ~ 50 °C, the MWD parameter hardly changes.

Space velocity. The influence of the space velocity of the synthesis gas on the MWD for the FT synthesis products has been frequently investigated.[19,60,65,74] It has been noted that the degree of conversion of CO changes significantly (by tens of percentage points) but the parameter α hardly varies. For example, when the space velocity of the synthesis gas ($H_2/CO = 1.3$) changes from 88 to 424 h^{-1} in FT synthesis at 269 °C in the liquid phase on a RPFIC, the degree of conversion of CO diminishes from 96% to 76%, while the MWD parameter α remains at the level of 0.67 ± 0.02.[73]

Table 2. The molecular weight distribution parameters α for the FT synthesis products at different temperatures.[65,66]

Catalyst[a]	T/°C	α	$\bar{\alpha}$
100% Fe_3O_4	285	0.61	
+ (2–3)% Al_2O_3	273	0.59	
+ (0.7–1.2)% CaO	262	0.61	0.60 ± 0.01
+ (0.5–0.8)% K_2O	251	0.60	
+ 0.4% SiO_2	239	0.60	
	231	0.62	
100% Fe_2O_3	241	0.59	
	223	0.63	
	214	0.60	0.63 ± 0.04
	199	0.64	
	188	0.68	
100% Fe_2O_3	261	0.66	
+ 0.6% K_2O	251	0.66	0.67 ± 0.01
	224	0.69	
	211	0.68	

[a] The composition of the catalyst is quoted for a nonreduced specimen.

Pressure and the H_2/CO ratio. Data concerning the influence of pressure on the MWD for the FT synthesis products have been published[8,51,67] and are contradictory. Thus, on a cobalt catalyst at 250 °C and for $H_2/CO = 3$, an increase in pressure from 1 to 7.8 atm led to a slight increase in α. However a further increase in the overall pressure to 14 atm no longer affected the MWD parameter.[51]

Ambiguous data are available also for the influence of the composition of the synthesis gas on the MWD for the FT synthesis products.[40,65,66,71] For example, when polycrystalline iron foil was used as the catalyst at 287 °C and an overall pressure of 1 atm for the ratio $H_2/O = 100$, $\alpha = 0.13$ was obtained while in the case where $H_2/CO = 4$ it amounted to 0.30.[40]

Table 3 presents the MWD parameters α for different H_2/CO ratios, different catalysts, and a degree of conversion of CO of 5%.[65,66] It is seen from the data presented that the simultaneous change in the H_2/CO ratio from 0.5 to 5 and in the overall pressure from 3 to 13 atm hardly affects the parameter α. However, we may note that the simultaneous alteration of two inde-pendent factors (H_2/CO and P_{tot}) does not permit the estimation of the influence of the H_2/CO ratio on the MWD in a pure form.

Duration of the FT synthesis. Data concerning the influence of the duration of the FT synthesis on the MWD for the products obtained have also been published.[8,23,79] It has been shown that the parameter α increases by 0.1–0.2 with increase in the synthesis time. For example, in the study of Glebov et al.[23] α

Table 3. The molecular weight distribution parameters α for the FT synthesis products corresponding to different H_2/CO ratios.

Catalyst	T/°C	P_{tot}/atm	H_2/CO	α	$\bar{\alpha}$
Fe_2O_3	212	5	4	0.58	
	212	6	2	0.64	0.64 ± 0.04
	212	8	1	0.66	
	212	12	0.5	0.67	
100% Fe_2O_3 + 6% K_2O	240	6	5	0.68	
	240	7	2.5	0.68	0.69 ± 0.01
	240	9	1.2	0.69	
	240	13	0.6	0.70	
100% Fe_3O_4 + (2–3)% Al_2O_3	248	3	0.5	0.67	
+ (0.7–1.2)% CaO + (0.5–0.8)% K_2O	248	4	1	0.66	0.64 ± 0.03
+ 0.4% SiO_2	248	6	2	0.63	
	248	10	4	0.61	

reached 0.5 ± 0.1 in the gas-phase FT synthesis in a flow reactor with a stationary RPFIC bed after 100 h, whereas after 1000 h it amounted to 0.7 ± 0.1.

Type of reactor. The results of studies on FT synthesis by different groups of investigators using a flow reactor (stationary RPFIC bed)[14,23] and a reactor with a stirrer (a suspension of RPFIC in a solvent)[19,60,65,66] demonstrated with acceptable accuracy that the type of reactor hardly affects the parameter α, which varies in the range 0.6 ± 0.1. There has been one study,[91] specially devoted to this question, in which it was shown that the values of α for the FT synthesis products obtained on the same RPFIC and under the same conditions but in reactors of two different types are similar.

Reduction of the catalyst. Reduced heterogeneous catalysts are usually employed in FT synthesis because the reduction (or activation) operation is accompanied by an increase in the rate of the FT synthesis and ultimately leads to an increase in its productivity. The influence of the RPFIC reduction time on the MWD for the FT synthesis product has been investigated.[65] As expected, the rate of the FT synthesis increases by a factor of 20 with increase in the reduction time from 0 to 92 h, while the molecular weight distribution parameter α hardly changes.

Composition of the catalysts for the FT synthesis. Heterogeneous catalysts exhibit the greatest effectiveness in the FT synthesis. Their composition exerts the greatest influence on the MWD for the FT synthesis products.[42,43,45,47,49,55,66] It is sometimes sufficient to introduce a small amount (several per cent only) of promoting additives in order to observe a change in the MWD. We shall consider such additives in greater detail.

The addition of alkali metal compounds in the form of carbonates or oxides to the prepared catalysts or in the course of their preparation frequently increases the average molecular weight of the product.[8,40,51] However, when FeB is used as the catalyst (250–270 °C), its promotion with 1%–2% of Na_2O does not affect α.[45]

Promotion of the Ru/SiO_2 catalyst with copper diminishes α. For example, the addition of 15% of copper reduces the MWD parameter from 0.55 to 0.44.[55]

The results of the study of the influence of lanthanide metals on the MWD for the FT synthesis products have been published.[43,49] When nickel catalysts are used, the addition of 1%–1.5% of lanthanum or cerium expands the range of hydrocarbon fractions obtained from C_1–C_4 to C_1–C_8, its alteration being accompanied by a significant increase in α.[49]

FT synthesis on the (5%Fe + 2%Cu)/SiO_2 catalyst at 350 °C, at a pressure of 100 atm, and for the H_2/CO = 1 ratio results in the formation of hydrocarbons and alkanols, characterised by the same value of α = 0.37. The promotion of this catalyst with 10% La under the same conditions leads to the retention of α = 0.37 in the case of alcohols, whereas in the case of hydrocarbons α increases to 0.52.[43]

So far only one instance of the influence on α of the addition of MoS_2 to catalysts based on molybdenum carbide is known.[47] For alkanols, the addition of molybdenum sulfide diminishes α from 0.31 to 0.14.

Carriers. The carrier can also affect the MWD for the FT synthesis products. A study has been made[42] of the catalyst 5%Ru + 5%Mo + 1.25%Na_2O deposited on different carriers: activated charcoal (AC), SiO_2, and Al_2O_3. It was found that the parameters α for the products obtained at 255 °C, at a pressure of 86 atm, and for the H_2/CO = 2 ratio are different on the above carriers and increase from 0.26 to 0.39 in the sequence AC < SiO_2 < Al_2O_3.

The influence of the regime parameters and the catalyst on the break on the MWD curves. As already mentioned, breaks may appear on the MWD curves for the FT synthesis products plotted in terms of the semilogarithmic variables of the Schulz or Flory equation. The question of the stability of the breaks as a function of time and of the influence on the latter of the regime parameters (temperature, pressure, etc.) arises in this connection. There are literature data concerning exclusively the type *3* MWD characterised by two values of the distribution parameter: α_1 and α_2 with $\alpha_1 < \alpha_2$ (Fig. 4).

The stability as a function of time of the break on the MWD curves obtained on a commercial (produced by the Ruhrchemie Company) deposited catalyst having the composition 100Fe : 4.3Cu : 4.1K : 25SiO_2 at 250–265 °C, at a pressure of 15 atm, and for H_2/CO = 1 over a period of 700 h has been investigated.[73] The results of tests in both a flow reactor with a stationary catalyst bed and in a stirred reactor proved to be similar. Thus, in the flow reactor, α_1 and α_2 were respectively 0.58 and 0.94 after 71 h and 0.60 and 0.88 after 427 h. In the stirred reactor, α_1 and α_2 were found to be respectively 0.57 and 0.92 after 95 h and 0.60 and 0.85 after 619 h.

Data on the MWD for the FT synthesis products, obtained using commercial catalysts produced by various companies, have been analysed[69] and in all the instances investigated the break on the MWD curve persisted throughout the period of the tests. Similar results have been published in another communication.[70]

The influence of the composition of iron-containing catalysts on the breaks on the MWD curves has been examined.[62,68]

The following catalysts were investigated: RPFIC having the composition Fe(30%–37%) + Fe_2O_3 (59%–65%) + Al_2O_3 (3%–4%) + CaO (1%–1.3%) + K_2O (0.7%–0.9%), a 10% Fe/SiO_2 deposited catalyst (the specific surface of SiO_2 was about 700 $m^2 g^{-1}$), and a 6% ThO_2/Fe_2O_3 deposited catalyst.[68] It was established that the initial value of the distribution parameter was α = 0.61 ± 0.02 for all the products. However, after a certain time had elapsed (after 56, 30, and 14 days for the first, second, and third catalysts respectively), breaks appeared on the MWD curve at n = 11. In the range n = 1–11, we have $\alpha_1 = \alpha$, while under conditions where $n > 11$ the parameter α_2 is different for all the catalysts, reaching, for example, 0.8 for the first catalyst.

The pressure and space velocity influence the MWD with break points.[60,67] Without altering the position of the break point, their increase leads to some increase in α_2.

Modification of FT syntheses with ammonia and amines. The MWD for the FT synthesis products under conditions where a third component was added to CO and H_2 has been investigated.[44,75,76,82–84] The third component employed was NH_3,[83] Me_2NH,[82] Et_2NH,[44] and piperidine.[75,76,84] All the results were obtained on iron-containing catalysts under the conditions of gas-phase synthesis in a reactor with a stationary catalyst bed.

Thus, in the presence of the 20.4% Fe_2O_3/SiO_2 catalyst at 220 °C at a pressure of 1–10 atm and for the H_2/CO = 2–3.6 ratios, the addition of Et_2NH to the synthesis gas hardly resulted in the formation of the corresponding alkyl(diethyl)amines, the synthesis products being the usual mixture of hydrocarbons and alcohols. The molecular weight distribution parameter α for the products remained virtually constant and amounted to 0.72 for n-alkanes (0.70 in the absence of the additive) and 0.32 for n-alkanols (0.25 without the additive).[44]

Results different from those presented above were obtained in the presence of the RPFIC.[75,76,82–84] As an illustration, we shall consider in greater detail the MWD and the overall composition for the products obtained via the CO + H_2 + Me_2NH reaction (Table 4, Fig. 7).

Table 4. Composition of the products of the synthesis on a reduced, promoted, and fused iron catalyst (RPFIC).[84]

Composition of products (%)	$CO + H_2$	$CO + H_2 + Me_2NH$
n-Alkanes	26	29
α-Alkenes	9	8
n-Alkyl methyl ketones	3	3
n-Alkanols	51	18
n-Alkyl(dimethyl)amines	–	26
Unidentified components	12	16

Note. The composition of the RPFIC was 100% Fe_3O_4 + 1% V_2O_5 + 0.75% BaO for a nonreduced specimen; the Me_2NH concentration in the synthesis gas was 7 vol.%; the content of n-alkanals was less than 1%; conditions of synthesis: T = 172 °C, P_{tot} = 120 atm, H_2/CO = 4, space velocity 10^3 h^{-1}.

The data presented in Table 4 show that the addition of Me_2NH to a mixture of CO and H_2 induces the formation of n-alkyl(dimethyl)amines having the general formula $C_nH_{2n+1}Me_2N$, where $n \leqslant 17$. On the other hand, it is seen from Fig. 6 that, in terms of the semilogarithmic variables of the Schulz equation [Eqn (4′)], the linear MWD plots for alkenes, n-alkanols, and n-alkyl methyl ketones are parallel, while the distribution parameter α, calculated from the slope of the straight line, is the same for these components, amounting to 0.66 ± 0.02. However, the n-alkanes synthesised from CO and H_2 have the parameter $\alpha = 0.77 \pm 0.02$.

After the addition of Me_2NH to the synthesis gas (Fig. 7), the MWD parameters for alkenes, n-alkanols, and n-alkyl methyl ketones remain the same. Furthermore, the n-alkyl(dimethyl)amines formed in the presence of the above components have the same $\alpha = 0.66 \pm 0.02$. The MWD parameter α for n-alkanes (0.73 ± 0.02) is again different from those for the other components. The reader is referred to other communications[82–84] for a detailed analysis of the MWD for the products of the modified FT synthesis and the mechanism of their formation and here we shall only note that the introduction of Me_2NH does not affect the nature of the MWD for all the components of the product with the exception of a slight influence on the MWD for n-alkanes (α diminished from 0.77 to 0.73).

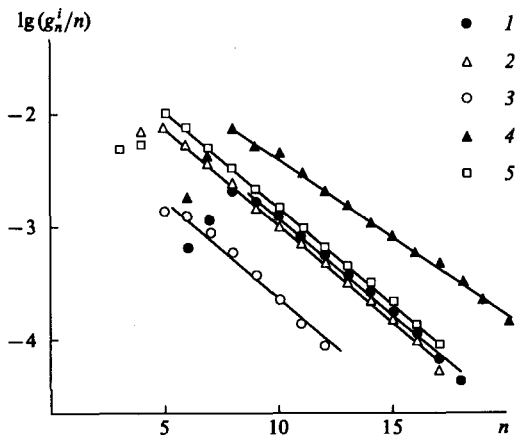


Figure 7. Molecular weight distribution for the liquid fraction of the multicomponent product of synthesis from CO, H_2, and dimethylamine (for the conditions of the synthesis, see Table 4):[82] (*1*)–(*4*) see Fig. 6; (*5*) n-alkyl(dimethyl)amines.

Zeolite-containing catalysts. New data on the MWD for the synthesis products have been obtained as a result of the study of zeolite-containing catalysts.[92,93]

Thus the catalyst having the composition 10% Fe_2O_3 + 15% MnO + 39% HY was used in the synthesis from CO and H_2 at 300–370 °C and P_{tot} = 21 atm, for a space velocity of 230 h^{-1}, and for the ratio H_2/CO = 3. The synthesis products contained C_6–C_{11} aromatic hydrocarbons which did not obey the ASF distribution. The introduction of the HY zeolite into the catalyst induced (apart from the appearance of aromatic hydrocarbons among the synthesis products) a change in the MWD for the alkanes, expressed by a shift of the break point on the MWD curve for the alkanes from n = 12 to n = 10 and was accompanied by a decrease $\Delta\alpha$ in the distribution parameter.[92] Failure of the aromatic hydrocarbons obtained in the synthesis from CO and H_2 to obey the ASF distribution was noted also in another study,[93] where the 14.7% Co/SiO_2 + ZSM-5 catalyst was used.

The deviation of the MWD for aromatic hydrocarbons from the ASF distribution has been observed also by Savel'ev et al.[94] The synthesis from CO and H_2 on an iron-containing catalyst having the composition (8.3% Fe + 4.5% K)/Al_2O_3 at 380–420 °C and P_{tot} = 1 atm, for a space velocity of 75–150 h^{-1}, and for H_2/CO = 2 yielded a product containing up to 20% of C_6–C_9 aromatic hydrocarbons apart from C_1–C_6 aliphatic hydrocarbons. On the basis of data for the MWD for the synthesis products, the authors[94] concluded that the paths leading to the formation of aliphatic and aromatic hydrocarbons are independent.

* * *

Thus the study of the MWD for the real synthetic products obtained in the FT synthesis or its modifications constitutes a vigorously developing field of research. Answers to a number of questions associated with the mechanisms of these syntheses and with the occurrence of side reactions have been obtained with the aid of the MWD. Attention has been turned to the possible hydrocondensation and hydropolymerisation character of the FT syntheses. For example, it has been possible to demonstrate that the paths leading to the formation of the main components of the product from the common intermediate in FT synthesis on the RPFIC are parallel and it has been established that the paths leading to the formation of aliphatic and aromatic hydrocarbons are independent. There is also no doubt that further improvement of highly effective analytical methods will promote the development and progress in the studies on the MWD for the products. One may claim that the study of the MWD for the FT synthesis products occupies a special place among modern methods for the investigation of the FT synthesis, such as the kinetic and isotopic methods under stationary and non-stationary conditions, spectroscopic methods applied in situ, and methods involving the organometallic analogues of the reactions of CO and H_2. The MWD method helps to obtain more complete experimental data in this interesting and promising and hitherto not fully investigated field of the synthesis of organic compounds.

References

1. *Khimicheskie Veshchestva iz Uglya* (Chemical Substances from Coal) (Moscow: Khimiya, 1980)
2. *Hydrocarbon Synthesis from Carbon Monoxide and Hydrogen (Advances in Chemistry, Ser. 178)* (Washington: Am. Chem. Soc., 1979)
3. *Kataliz v C_1-Khimii* (Catalysis in C_1-Chemistry) (Leningrad: Khimiya, 1987)
4. R A Sheldon, in *Chemicals from Synthetic Gas. Catalytic Reactions of CO and H_2* (Translated into Russian; Moscow: Khimiya, 1987) p. 247
5. Yu B Yan, B K Nefedov *Sintezy na Osnove Oksidov Ugleroda* (Syntheses from Oxides of Carbon) (Moscow: Khimiya, 1987)

6. P Biloen, W M H Sachtler *Adv. Catal.* **30** 165 (1981)
7. L Konig, J Gaube *Chem. -Ing. -Tech.* **55** 14 (1983)
8. H Schulz *C_1 Mol. Chem.* **1** 231 (1985)
9. M Dry, in *Applied Industrial Catalysis* (Ed. B E Leach) Vol. 2 (Translated into Russian; Moscow: Mir, 1986) p. 161
10. R B Anderson *The Fischer-Tropsch Synthesis* (Orlando: Academic Press, 1984)
11. G Henrici-Olive, S Olive *The Chemistry of Catalyzed Hydrogenation of Carbon Monoxide* (Translated into Russian; Moscow: Mir, 1987)
12. E F G Herington *Chem. Ind.* **65** 246 (1946)
13. R B Anderson, R A Friedel, H H Storch *J. Chem. Phys.* **19** 313 (1951)
14. A N Shuikin, Yu B Kryukov, A N Bashkirov *Neftekhimiya* **8** 741 (1968)
15. G Henrici-Olive, S Olive *Angew. Chem.* **88** 144 (1976)
16. G V Schulz *Z. Phys. Chem.* **30** 379 (1935)
17. P J Flory *J. Am. Chem. Soc.* **58** 1877 (1936)
18. G Henrici-Olive, S Olive *J. Mol. Catal.* **4** 379 (1978)
19. C N Satterfield, G A Huff *J. Catal.* **73** 187 (1982)
20. R J Madon *J. Catal.* **57** 183 (1979)
21. H G Stenger, H E Johnson, C N Satterfield *J. Catal.* **86** 477 (1984)
22. R Shel, J Zwart *Appl. Catal.* **22** 337 (1986)
23. L S Glebov, A N Shuikin, G A Kliger, V M Vorontsov, C M Loktev *Kinet. Katal.* **29** 1110 (1988)
24. C L O'Young, S L Buchwalter *C_1 Mol. Chem.* **2** 1 (1987)
25. S Novak, R J Madon, H Suhl *J. Chem. Phys.* **74** 6083 (1981)
26. S Novak, R J Madon, H Suhl *J. Catal.* **77** 141 (1982)
27. L S Glebov, G A Kliger *Usp. Khim.* **58** 1721 (1989) [*Russ. Chem. Rev.* **58** 977 (1989)]
28. R A Fridel, R B Anderson *J. Am. Chem. Soc.* **72** 1212 (1950)
29. R A Fridel, R B Anderson *J. Am. Chem. Soc.* **72** 2307 (1950)
30. H Storch, N Golumbic, R Anderson, in *The Fischer-Tropsch and Related Syntheses* (Translated into Russian; Moscow: Inostr. Lit., 1954) p. 516
31. R B Anderson *J. Catal.* **55** 114 (1978)
32. L E McCandlish *J. Catal.* **83** 362 (1983)
33. C B Lee, E M Carverley, R B Anderson *J. Catal.* **92** 180 (1985)
34. N O Egibor, W C Cooper *C_1 Mol. Chem.* **1** 411 (1986)
35. B W Wojciechowski *Catal. Rev. Sci. Eng.* **30** 629 (1988)
36. L Fu, J L Rankin, C H Bartholomew *C_1 Mol. Chem.* **1** 369 (1986)
37. A A Adesina *J. Catal.* **124** 297 (1990)
38. A A Adesina *J. Mol. Catal.* **62** 23 (1990)
39. C W Norval, M J Phillips *J. Catal.* **126** 87 (1990)
40. H J Krebs, H P Bonzel *Surf. Sci.* **88** 269 (1979)
41. G Henrici-Olive, S Olive *J. Mol. Catal.* **16** 111 (1982)
42. M Inoue, T Miyake, Y Takegami, T Inui *Appl. Catal.* **11** 103 (1984)
43. A Razzaghi, J P Hindermann, A Kiennemann *Appl. Catal.* **13** 193 (1984)
44. K G Anderson, J G Ekerdt *J. Catal.* **95** 602 (1985)
45. C Wang, C H Bartholomew *Appl. Catal.* **62** 221 (1990)
46. E G Rightor, M S Tzou, T J Pinnavaia *J. Catal.* **130** 29 (1991)
47. H C Woo, K V Park, Y G Kim, I S Nam, J S Chang, J S Lee *Appl. Catal.* **75** 267 (1991)
48. L Fu, C H Bartholomew *J. Catal.* **92** 376 (1985)
49. J Barrault, A Chafi, P Gallezot *Appl. Catal.* **67** 257 (1991)
50. P Biloen, J N Helle, W M H Sachtler *J. Catal.* **58** 95 (1979)
51. K B Arcuri, L H Schwartz, R D Piotrowski, J B Butt *J. Catal.* **85** 349 (1984)
52. A K Datye, J Schwank *J. Catal.* **93** 256 (1985)
53. N O Egiebor *C_1 Mol. Chem.* **1** 253 (1985)
54. A F H Wielers, G W Koebrugge, J W Geus *J. Catal.* **121** 375 (1990)
55. J C Kelzenberg, T S King *J. Catal.* **126** 421 (1990)
56. K R Krishna, A T Bell *J. Catal.* **130** 597 (1991)
57. A N Bashkirov, Yu B Kryukov, E G Simon'yants, L G Liberov *Dokl. Akad. Nauk SSSR* **171** 609 (1966)
58. R J Madon, W F Taylor *J. Catal.* **69** 32 (1981)
59. A A Adesina, R R Hudgins, P L Silveston *Appl. Catal.* **62** 295 (1990)
60. G A Huff, C N Satterfield *J. Catal.* **85** 370 (1984)
61. C N Satterfield, H G Stenger *Ind. Eng. Chem., Process Res. Dev.* **23** 849 (1984)
62. N O Egibor, W C Cooper *Appl. Catal.* **14** 323 (1985)
63. N O Egibor, W C Cooper, B W Wojciechowski *Can. J. Chem. Eng.* **63** 826 (1985)
64. H Schulz, E Erich, H Gorre, E Van Steen *Catal. Lett.* **7** 157 (1990)
65. R A Dictor, A T Bell *Appl. Catal.* **20** 145 (1986)
66. R A Dictor, A T Bell *J. Catal.* **97** 121 (1986)
67. H A Dabbagh, L M Tau, S Bao *Stud. Surf. Sci. Catal.* **38** 61 (1988)
68. L M Tau, H A Dabbagh, T P Wilson, B H Davis *Appl. Catal.* **56** 95 (1989)
69. L M Tau, H A Dabbagh, S Bao, B H Davis *Catal. Lett.* **7** 127 (1990)
70. C S Huang, H A Dabbagh, B H Davis *Appl. Catal.* **73** 237 (1991)
71. T J Donnelly, C N Satterfield *Appl. Catal.* **52** 93 (1989)
72. T J Donnelly, C N Satterfield *Appl. Catal.* **56** 231 (1989)
73. D B Bukur, S A Patel, X Lang *Appl. Catal.* **61** 329 (1990)
74. M Inoue, T Miyake, T Inui *J. Catal.* **105** 266 (1987)
75. L S Glebov, G A Kliger, S M Loktev *Neftekhimiya* **30** 626 (1990)
76. G A Kliger, O A Lesik, A I Mikaya, E V Marchevskaya, V G Zaikin, L S Glebov, S M Loktev *Izv. Akad. Nauk SSSR, Ser. Khim.* 503 (1991)
77. H G Stenger *J. Catal.* **92** 426 (1985)
78. F M Dautzenberg, J N Helle, R A Van Santen, H Verbeek *J. Catal.* **50** 8 (1977)
79. R A Dictor, A T Bell *Ind. Eng. Chem., Process Res. Dev.* **22** 678 (1983)
80. R Shel *Catal. Lett.* **1** 327 (1988)
81. W M H Sachtler, in *Proceedings of the 8th International Congress on Catalysis* (Berlin: Verlag Chemie, 1984) Vol. 1, p. 151
82. L S Glebov, G A Kliger, T P Popova, V E Shiryaeva, V P Ryzhikov, E V Marchevskaya, O A Lesik, S M Loktev, V G Beryezkin *J. Mol. Catal.* **35** 335 (1986)
83. G A Kliger, L S Glebov, T P Popova, E V Marchevskaya, V G Beryezkin, S M Loktev *J. Catal.* **111** 418 (1988)
84. L S Glebov, G A Kliger *Khim. Tverdogo Topliva* **6** 49 (1992)
85. D Vanhove, P Makambo, M Blanchard *J. Chem. Soc., Chem. Commun.* **14** 605 (1979)
86. H H Nijs, P A Jacobs, J B Uytterhoeven *J. Chem. Soc., Chem. Commun.* **23** 1095 (1979)
87. H H Nijs, P A Jacobs *J. Catal.* **65** 328 (1980)
88. G Henrici-Olive, S Olive *J. Mol. Catal.* **24** 7 (1984)
89. T Mitsudo, H Boku, S Murachi *Chem. Lett.* **10** 1463 (1985)
90. P J Flory *J. Am. Chem. Soc.* **62** 1561 (1940)
91. C N Satterfield, G A Huff, G H Stenger *Ind. Eng. Chem., Fundam.* **24** 450 (1985)
92. N O Egibor, W C Cooper, B W Wojciechowski *Appl. Catal.* **55** 47 (1989)
93. V Udaya, S Rao, R J Gormley *Catal. Today* **6** 207 (1990)
94. M M Savel'ev, M V Tsapkina, Yu D Koreshkov, A L Lapidus *Izv. Akad. Nauk SSSR, Ser. Khim.* 40 (1991)

Russian Chemical Reviews **63** (3) 197–216 (1994)
©1994 Russian Academy of Sciences and Turpion Ltd

UDC 546.821 : 546.852

Reactions of diazoalkanes with transition metal complexes

M Putala, D A Lemenovskii

Contents

I. Introduction	197
II. Complexes with the ligand coordinated through a nitrogen atom	198
III. Complexes with the ligand coordinated through a carbon atom	206
IV. Reactions of diazoalkane complexes	210
V. Conclusion	215

Abstract. The results of studies on the interaction of diazoalkanes with transition metal complexes are presented and the successive transformations of the diazoalkane complexes formed are traced. The reactions have been classified in terms of the proposed mechanism and the structure of the products. The principal structural parameters of the diazo-ligands are presented. The bibliography includes 145 references.

I. Introduction

The reactions of diazoalkanes with transition metal complexes have become the subject of intensive study during the last 20 years. The products of these reactions are important both theoretically (for example, diazoalkanes coordinated to a metal are possible intermediates in the insertion of molecular nitrogen into organic compounds[1,2]) and synthetically (the reactions with diazoalkanes constitute the most convenient method of synthesis of bridged carbene complexes of transition metals[3,4]).

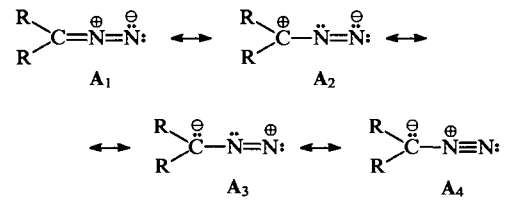
Generally speaking, several review articles have been devoted to the reactions of diazoalkanes with transition metal complexes.[5–8] In the present review, an attempt has been made to classify the available data in terms of the type of reactions or the structure of the complexes formed, mainly the interactions of diazoalkanes with mono- and bi-metallic complexes of transition metals being considered. On the other hand, the reactions of polynuclear (trinuclear and more highly condensed species) complexes are presented only in those cases where they strongly resemble the reactions of the mono- and di-nuclear complexes in terms of the mechanism or the structure of the complexes formed.

It is essential to note that a systematic approach to the consideration of the mechanisms of the processes occurring is difficult since the available literature data about them are usually restricted to the description of the structures of the complexes obtained. One should also recall that the information about the structure of the complexes can be frequently unreliable if it is based solely on data obtained by individual spectroscopic methods and not the results of X-ray diffraction studies.

M Putala Department of Organic Chemistry, Comenius University, Mlynska dolina, 84215, Bratislava, Slovakia.
D A Lemenovskii Laboratory of Physical Organic Chemistry, Lomonosov Moscow State University, Vorob'evy Gory, 119899 Moscow, Russian Federation. Fax (7-095) 939 55 46

Received 15 February 1994
Uspekhi Khimii **63** (3) 207–227 (1994); translated by A K Grzybowski

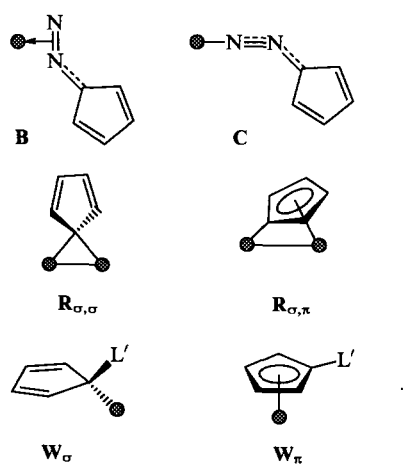
The electronic structure of diazoalkanes may be represented by the following canonical structures:[3,6]



On the basis of these structures, one can postulate that diazoalkanes enter into reactions (including those with transition metal complexes) as 1,3-dipoles (A_2, A_3), N-nucleophiles (A_1, A_2), or C-nucleophiles (A_3, A_4). Furthermore, bearing in mind the unsaturated nature of the diazoalkanes, one may also expect the formation of complexes of the π-type.

Naturally the result of the interaction of transition metal complexes with diazoalkanes depends on the nature and reactivity of the complexes. Fig. 1 presents the principal structural types of the products obtained as a result of such interaction.

It is essential to note that the simultaneous formation of several complexes of different types has been repeatedly observed in one reaction. Furthermore, the same initial complex can afford different products in reactions with different diazoalkanes and, conversely, the same diazoalkane can lead to the formation of products of a completely different type in reactions with different complexes. For example, the interaction of diazocyclopentadienes substituted in different ways with transition metal compounds afforded six types of complexes:



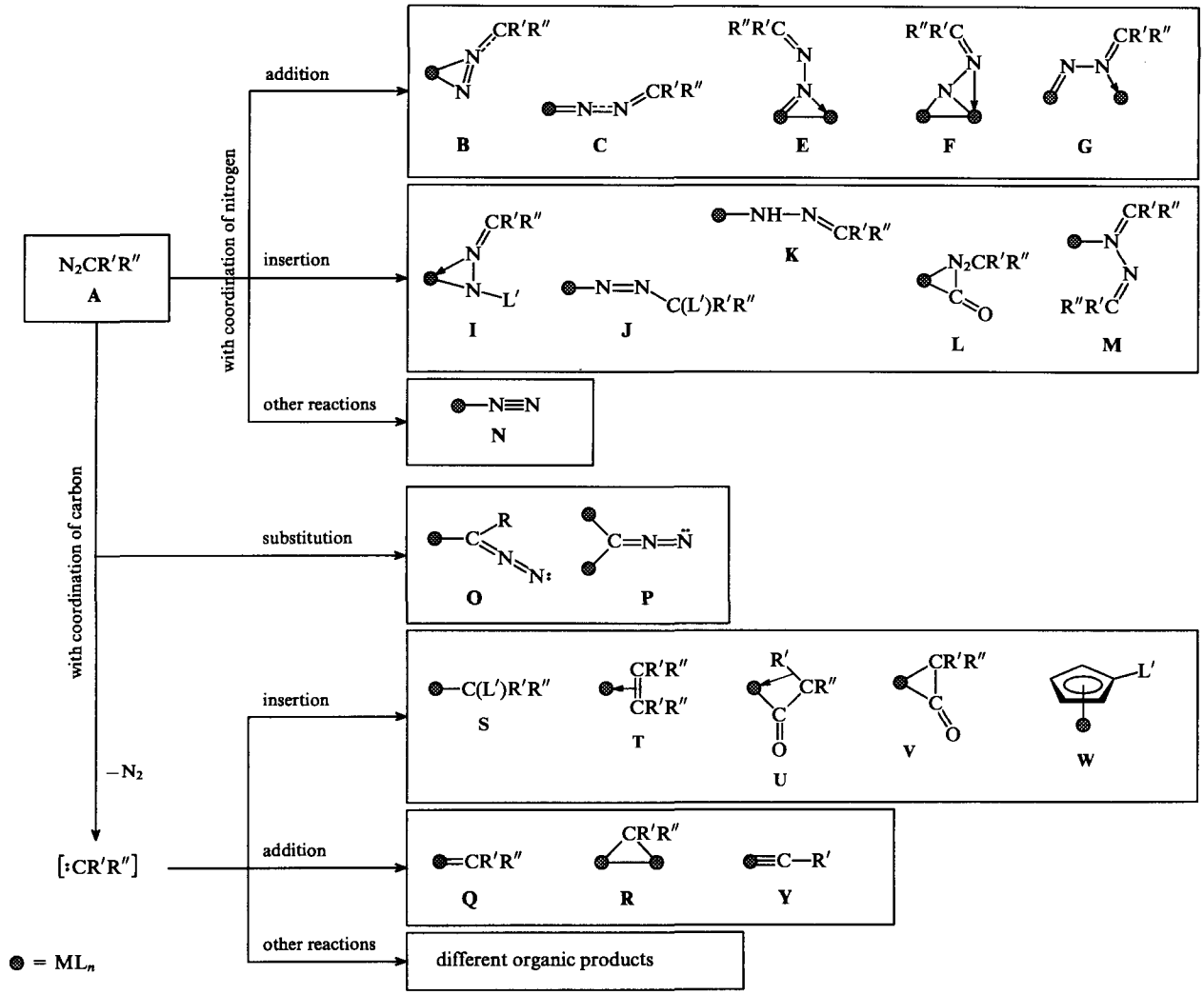


Figure 1. The principal structural types of the products of the interaction of transition metal complexes with diazoalkanes.

It follows from the wide variety of the products that the classification of reactions of diazoalkanes with transition metal complexes is by no means a trivial task. We have classified these reactions in terms of the structure of the products taking into account as far as possible the proposed reaction mechanism and the type of complex entering into the reaction.

II. Complexes with the ligand coordinated through a nitrogen atom

1. Addition reactions with formation of η^1-*N*- and η^2-*N*, *N'*-diazoalkane complexes

Coordinatively unsaturated transition metal complexes (ML_n)[9–19] or their precursors (ML_nY), containing only readily eliminated ligands Y such as hydrogen,[20–23] nitrogen,[24–29] carbon monoxide,[30–32] phosphine,[31–33] tetrahydrofuran,[34–36] or an alkene,[9,10,29,32,37] can enter into oxidative addition (or ligand exchange) reactions, which lead to the formation of η^2-*N*, *N'*-diazoalkane complexes (**B**) or η^1-*N*-diazoalkane complexes (**C**).

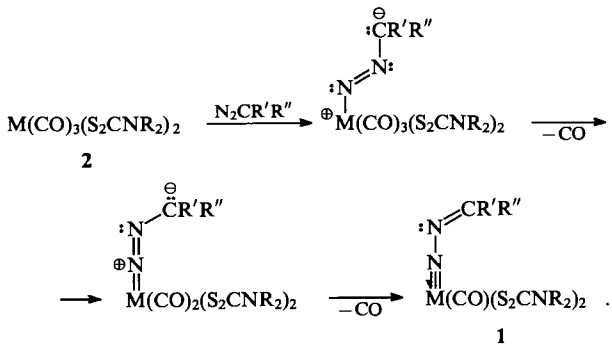
$$N_2CR'R'' \xrightarrow[(\text{or } ML_nY)]{ML_n} \longrightarrow L_nM\langle N{=}N{=}CR'R'' \quad \text{or} \quad L_nM{=}N{=}N{=}CR'R''$$

B **C**

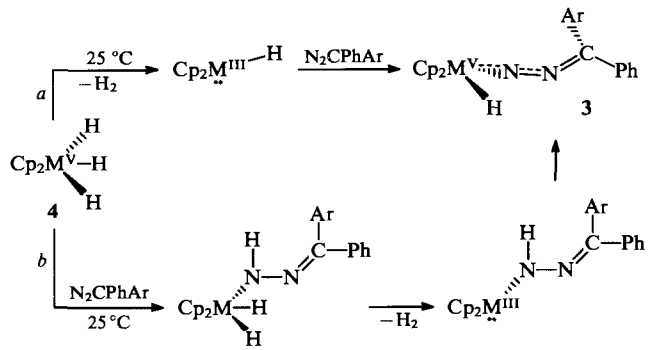
Y = H_2, N_2, CO, PR_3, THF, alkene.

In the presence of an excess of the diazoalkane, the elimination of the phosphine ligand may be accompanied by the formation of the phosphazine $R_3PN_2CR'R''$.[32]

The mechanism of the replacement of the ligand Y can be both associative and dissociative—depending on the coordination capacity of the metal atoms and the ability of the other ligands to undergo a change in their electron-donating properties. Thus it has been suggested[17] that molybdenum and tungsten complexes of the type $M(CO)(S_2CNR_2)_2(\eta^1\text{-}N_2CR'R'')$ (M = Mo, W) **1** are formed from $M(CO)_2(S_2CNR_2)_2$ **2** and $N_2CR'R''$ in several stages, in which the diazoalkane $N_2CR'R''$ is consecutively a 0-, 2-, and 4-electron-donating ligand (the process is accompanied by the elimination of two CO molecules in successive stages:

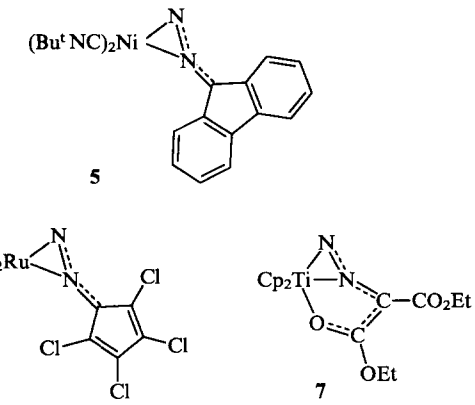


A mechanism differing from the usual one for the formation of η^1-*N*-diazoalkane complexes has been proposed for the formation of diaryldiazomethane complexes of niobocene and tantalocene $Cp_2M(H)(N_2CPh_2)$ (M = Nb, Ta) **3** [21,22] by the reaction of the corresponding metallocene trihydride **4** with the diazoalkane. Since the rate of elimination of hydrogen from Cp_2MH_3 (pathway *a*) is appreciably lower than the rate of formation of compound **3**, pathway *b*, involving the insertion of the diazoalkane in a M – H bond and only then the elimination of hydrogen, is more likely.



In the first communications [9,10,24] (up to 1975) in which the synthesis of stable monometallic diazoalkane complexes was reported, the question of the type of coordination of the diazoalkane usually remained open. The hypothesis, put forward in 1966,[38] that diphenyldiazomethane is coordinated to cyclododeca-1,5,9-trienenickel exclusively via the carbon atom can hardly be regarded as realistic in the light of present day knowledge.

The results of X-ray diffraction studies on the complexes $Ni(CNBu^t)_2(N_2Fld)$ (N_2Fld = 9-diazofluorene) **5** [14] and $Ru(CO)_2(PPh_3)_2(N_2C_5Cl_4)$ **6** [11] indicate that diazoalkanes are involved in η^2-*N,N'*-coordination (type **B**) in both complexes. The above complexes with the η^2-*N,N'*-coordination of the diazoalkane are regarded as π-type complexes. A similar type of coordination has been demonstrated by X-ray diffraction for the complex $Cp_2Ti[\eta^3$-*N,N',O*-$N_2C(CO_2Et)_2]$ **7**, [12] in which the metal atom is additionally coordinated to an oxygen atom of the carboxy-group. The displacement of the ν_{CNN} vibration band from 2050–2150 cm^{-1} for the free diazoalkanes to 1400–1600 cm^{-1} for the complexes has been observed in the spectra of the complexes. On this basis, it has been suggested that this type of coordination of the diazoalkane occurs also in many other complexes, in particular in $Cp_2V(N_2CR_2)$ (R = Ph, CO_2Et),[12,13] $Cp_2M(H)(N_2CPh_2)$ (M = Nb, Ta) **3**,[20] and $Cp_2Mo(N_2Fld)$,[23] and in certain complexes of the type $L_2M(N_2CR_2)$ (L = $CNBu^t$, PR_3; M = Ni, Pd; CR_2 = CPh_2, $C(CN)_2$, Fld, C_5X_4; X = H, Cl, Br).[9–11,14]



Complexes with the η^1-*N*-coordination of the diazoalkane ligand were obtained later — for example, $IrCl(N_2C_5Cl_4)(PPh_3)_2$ **8a**.[33] It was then also suggested [11] that the η^2-*N,N'*-coordination of the diazoalkane is more probable in those cases where the electron-accepting nature of the nonterminal nitrogen atom becomes enhanced under the influence of the electron-deficient CR_2 of the diazoalkane and when the *d* orbitals of the transition metal are filled to a greater extent.

Numerous data are already available on complexes for which the η^1-*N*-coordination of the diazoalkane has been postulated with a high degree of probability or reliably established:

$MClL_2(N_2CR'R'')$ — $Cp_2Ti(PMe_3)(N_2CPh_2)$ [31]

8 — **9**

$Cp_2M(X)(N_2CPhAr)$ [21,22,39] — M = Nb, Ta; X = H, Cl, Br.

3, 10

$M(CO)(S_2CNR_2)_2(N_2CR'R'')$ [15,30] — M = Mo, W.

1

$MX_2(N_2CR'R'')L(PMe_2Ph)_2$ [40,41] — M = Mo, W; X = Hal, OR; L = PMe_2Ph, π-ligands.

11

$[MX(N_2CR'R'')(dppe)_2]^+Y^-$ [42–48]

12

M = Mo, W; X = Hal; dppe = $PPh_2(CH_2)_2PPh_2$; Y = Br, BF_4, PF_6.

$X_2W(\mu\text{-}CSiMe_3)_2WX_2(N_2CPh_2)$ [16] — X = CH_2SiMe_3, OPr^i.

13

$Mo(OBu^t)_4(N_2CAr_2)$ [18]

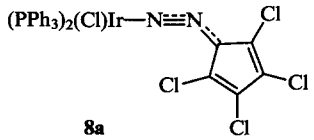
14

$Cp'Mn(CO)_2[N_2C(CO_2R')_2]$ [34,35] — Cp' = C_5H_5, C_5H_4Me.

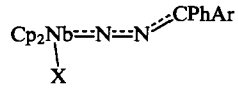
15

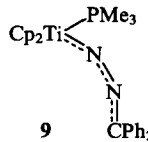
$MCl_{3-x}H_xL_2(N_2CR'R'')$ [26,27,29,37] — M = Ir, Rh; x = 1, 2; L = CO, PR_3.

It was observed that the absorption band for the ν_{CNN} vibration in the spectra of these complexes is in the same range as for the complexes with η^2-*N,N'*-coordination of the diazoalkane, i.e. in the region 1400–1600 cm^{-1}.



8a

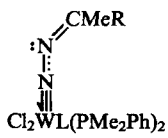




9

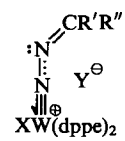
3a,10a,b

3a: X = H; Ar = Ph.
10a: X = Cl; Ar = *o*-C_6H_4Br.
10b: X = Br; Ar = *o*-C_6H_4Br.



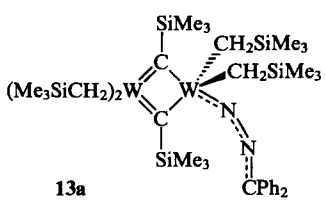
11a,b

11a: L = *p*-MeC_6H_4CHO; R = Ph.
11b: L = C_2H_4; R = Me.

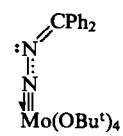


12a–c

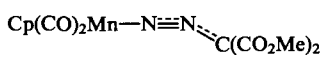
12a: X = Y = Br; R′ = R″ = Me.
12b: X = Br; Y = PF_6; R′ = H; R″ = $(CH_2)_3OH$.
12c: X = F; Y = BF_4; R′ = Me; R″ = CH_2COMe.



13a

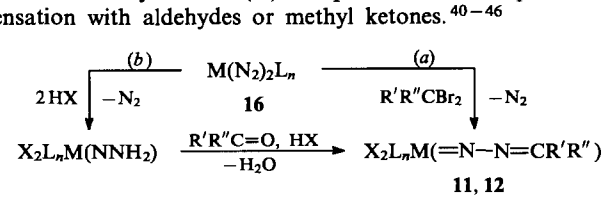


14a



15a

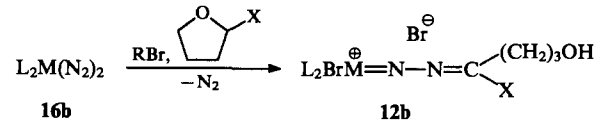
Apart from the reactions involving the addition of diazoalkanes to the coordinatively unsaturated complex or the substitution of another ligand by the diazoalkane, other methods of synthesis of η^1-*N*-diazoalkane complexes have also been discovered. Among the molybdenum and tungsten complexes $M(N_2)_2L_n$ **16** containing coordinated molecular nitrogen, the diazoalkane complexes **11** and **12** have been obtained in two ways: (*a*) by reaction with geminal dibromocompounds;[46–48] (*b*) by the protonation of the nitrogen with formation of hydrazinate(2-) complexes and subsequent condensation with aldehydes or methyl ketones.[40–46]



11, 12

M = Mo, W;
X = F, Cl, Br, I, BF_4, PF_6;
L = PMe_2Ph, dppe;
R′ = H, Me; R″ = H, R, COR, Ar.

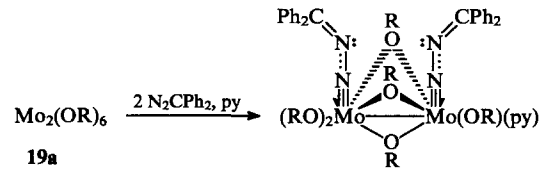
The tungsten complex of diazobutanol **12b** and the related complexes $[MBr(N_2C(X)CH_2CH_2CH_2OH)(dppe)_2]^+$ (M = Mo, W; X = H, Me)[48–50] have been obtained by the reaction of $M(N_2)_2(dppe)_2$ **16b** with 2-X-substituted tetrahydrofuran (THF) in the presence of alkyl bromides.



16b **12b**

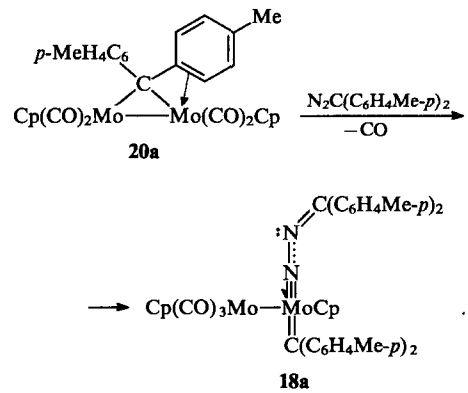
M = Mo, W; L = dppe; R = Alk; X = H, Me.

The molybdenum complexes $Mo(OBu^t)_4(N_2CAr_2)$ **14**,[18] $(RO)_2(N_2CAr_2)Mo(\mu\text{-}OR)_3Mo(OR)(N_2CAr_2)(py)$ **17**, where R = Pr^i or CH_2Bu^t,[18,51] and $Cp(CO)_3MoMoCp(CAr_2)\cdot(N_2CAr_2)$ **18**[52,53] with η^1-*N*-coordination of the diazoalkanes have been obtained from the complexes $Mo_2(OR)_6$ **19** and $Cp(CO)_2Mo(\mu\text{-}CAr_2)Mo(CO)_2Cp$ **20**. The addition of the diazoalkane molecule takes place as a result of the transformation of the coordination sphere in the initial complexes, for example:



19a **17a**

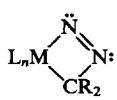
R = Pr^i.



20a **18a**

The diazoalkanes in complexes with η^1-*N*-coordination can be formally regarded as neutral diazoalkane or nitrene ligands or as hydroazonate(2-) ligands. However, the nature of the bonds in them, particularly that of the N–N bonds, differs from those in hydrazones. The N–N bond length in these complexes is close to that in a double bond, while the M–N–N angle tends to 180°. The principal structural parameters of diazoalkane and related complexes are presented in Table 1 and the average C–C and C–N bond lengths in organic molecules are shown for comparison in Table 2. On the basis of the structural data for the diazoalkane complexes, one can postulate the *sp* hybridisation of the terminal nitrogen atom. The M–N bond length is also close to that of a double bond, so that the diazoalkane ligand can be regarded as a 2-electron donor (in complexes **3**, **8**, **9**, **10**, and **15**) and a 4-electron donor (in complexes **11**–**14**, **17**, **18**) depending on the coordination capacity of the metal atom.

The formation of metallocyclobutane complexes of type **D** with 1,3-*N*,*C*-coordination of the diazoalkane has been postulated only as intermediates in the catalytic decomposition of diazoalkanes, leading to carbenes and hence to the products of the reactions of carbenes.



D

Table 1. Structural parameters of η^1-*N*- and η^2-*N,N'*-diazoalkane and related complexes.

No.	Complex	Bond lengths/Å		Bond angles/deg		Ref.
		N–N'	N'–C	M–N–N'	N–N'–C	
	Free N_2CH_2	1.12	1.32	–	180	54
	B. Complexes with η^2-*N,N'*-coordination					
5	$Ni(CNBu^t)_2(N_2Fld)$	1.25	1.34	69	134	14
6	$Ru(CO)_2(N_2C_5Cl_4)(PPh_3)_2$	1.22	1.37	70	132	11
7	$Cp_2Ti[N_2C(CO_2Et)_2]$	1.21	1.37	84	147	12
–	$CpTiCl_2(N_2Ph)$	1.22	–	71	126	55
	C. Complexes with η^1-*N*-coordination					
9	$Cp_2Ti(PMe_3)(N_2CPh_2)$	1.26	1.31	157	126	31
3a	$Cp_2Nb(H)(N_2CPh_2)$	1.29	1.31	171	124	21
10a	$Cp_2Nb(Cl)[N_2(C(Ph)(o\text{-}C_6H_4Br)]$	1.29	1.30	169	126	22
10b	$Cp_2Nb(Br)[N_2C(Ph)(o\text{-}C_6H_4Br)]$ [a]	1.20	1.31	159	126	39
		1.35	1.34	171	121	
11a	$WCl_2(N_2CMePh)(p\text{-}MeC_6H_4CHO)(PMe_2Ph)_2$	1.29	1.27	166	121	56
11b	$WCl_2(N_2CMe_2)(C_2H_4)(PMe_2Ph)_2$	1.34	1.29	167	117	56
12a	$[WBr(N_2CMe_2)(dppe)_2]Br$	1.34	1.28	171	124	57
12b	$[WBr(N_2CH(CH_2)_3OH)(dppe)_2]PF_6$	1.31	1.29	172	116	49
12c	$[WF(N_2C(Me)CH_2COMe)(dppe)_2]BF_4$	1.32	1.30	174	125	44
13a	$(RCH_2)_2W(\mu\text{-}CR)_2W(CH_2R)_2(N_2CPh_2)$ R = $SiMe_3$	1.36	1.29	158	123	16
14a	$Mo(OBu^t)_4(N_2CPh_2)$	1.31	1.31	168	122	18
17a	$(RO)_2(N_2CPh)_2Mo(\mu\text{-}OR)_3Mo(OR)(N_2CPh_2)(py)$ R = Pr^i	1.32	1.28	164	124	18
		1.30	1.31	153	122	
17a	$(RO)_2(N_2CPh)_2Mo(\mu\text{-}OR)_3Mo(OR)(N_2CPh_2)(py)$ R = Pr^i	1.30	1.30	164	124	51
		1.30	1.31	155	122	
18a	$Cp(CO)_3Mo-MoCp(CAr_2)(N_2CAr_2)$ Ar = C_6H_4Me-*p*	1.32	1.32	175	121	52, 53
15a	$CpMn(CO)_2[N_2C(CO_2Me)_2]$	1.17	1.35	177	151	34
8a	$IrCl(N_2C_5Cl_4)(PPh_3)_2$	1.17	1.35	175	141	33
–	*trans*-$WI(NNSiMe_3)(PMe_2Ph)_4$	1.24	–	168	152	58
–	*mer*-$WI_2(NNHSiMe_3)(PMe_2Ph)_3$	1.32	–	171	127	58
–	*mer*-$WI_2(NNSiMe_2CH_2CH_2SiMe_2)(PMe_2Ph)_3$	1.36	–	173	120	59
					126	

[a] Two independent molecules in the unit cell of the complex.

Table 2. Average N–N and N–C bond lengths (Å) in organic compounds.[60–62]

Bond	Single	Single [a]	Double	Triple
N–N	1.40–1.45	1.37	1.22–1.25	1.12
C–N	1.47–1.49	1.33–1.35	1.28–1.33	1.14

[a] The length of a single bond conjugated with a double bond.

2. Addition (insertion) reactions with formation of bridged diazoalkane complexes

Bridged diazoalkane complexes have been obtained in several ways: (a) by addition (insertion) to multiple (Mo≡Mo, W≡W[63–69] and Os=Os[70]) or single (Zr–Zr[71] and Ru–Ru[72]) metal–metal bonds; (b) by the dimerisation of coordinatively unsaturated metal complexes (Ti,[19,36] Zr,[17] Nb,[73,74] Mn, Co[75]); (c) by the substitution of other bridging ligands (Rh[76]):

(a) $L_nM{\equiv}ML_n + N_2CR_2 \longrightarrow (L_nM)_2(\mu\text{-}N_2CR_2)$ (M–M)

$L_nM{=}ML_n + N_2CR_2 \longrightarrow (L_nM)_2(\mu\text{-}N_2CR_2)$ (M–M)

$L_nM{-}ML_n + N_2CR_2 \longrightarrow (L_nM)_2(\mu\text{-}N_2CR_2)$

(b) $2\left[L_nM{=}\ddot{N}{-}\ddot{N}{=}CR_2\right] \longrightarrow (L_nM)_2(\mu\text{-}N_2CR_2)_2$

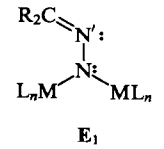
$2\,L_nM + N_2CR_2 \longrightarrow (L_nM)_2(\mu\text{-}N_2CR_2)$

(c) $(L_nM)_2(\mu\text{-}Y)_2 + N_2CR_2 \xrightarrow[-Y_2]{} (L_nM)_2(\mu\text{-}N_2CR_2)$

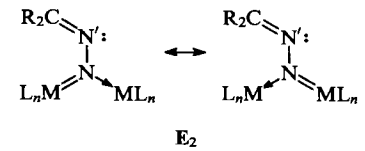
Y = H.

One can postulate at least four types of coordination of bridging diazoalkanes to a bimetallic centre (regardless of whether the direct valence metal–metal interaction is then retained):[7]

(a) A symmetrical bridge with the coordination of only the terminal nitrogen atom — with $\mu\text{-}\eta^1:\eta^1$-*N*-coordination of the diazoalkane, the diazoalkane being capable of functioning both as a 2-electron donating (E_1) or a 4-electron-donating (E_2) ligand.

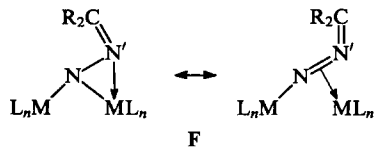


E_1



E_2

(b) An asymmetric bridge with additional coordination of the nonterminal N' atom to one metal atom (type **F**) — with μ-η^1 : η^2-*N,N,N'*- or μ-σ,π-coordination of the diazoalkane.



F

(c) A bridge where each nitrogen atom is coordinated to only one specific metal atom — with μ-η^1 : η^1-*N,N'*-coordination of the diazoalkane (type **G**).

(d) A bridge the terminal nitrogen atom of which is coordinated to one metal atom while the carbon atom is coordinated to the second metal atom — with μ-η^1 : η^1-*N,C*-coordination of the diazoalkane (type **H**).



G **H**

In bimetallic complexes, the asymmetric type **F** coordination of the diazoalkane is most often encountered. Such coordination has been established (or postulated) for the following complexes:

$CpClTi(N_2CPh_2)_2TiClCp$ [19,36]

21

$CpClZr(\mu\text{-}\eta^5\text{:}\eta^5\text{-}C_{10}H_8)(N_2CPh_2)ZrClCp$ [71]

22

$Cp'(CO)_2Mo(\mu\text{-}CO)(N_2CR'R'')Mo(CO)Cp'$ [63-65]

23

$Cp' = C_5H_5, C_5H_4Me, C_5Me_5$; $R' = R'' = Me$; $R' = H$, $R'' = CO_2Et$

$C_5Me_5(CO)_2Mo(\mu\text{-}CH_2)(N_2CH_2)Mo(CO)_2C_5Me_5$. [66]

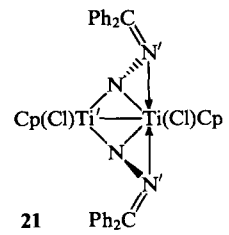
24

It has been observed (Table 3) that the N–N' bond in these complexes is intermediate between a double and single bond, while N'–C is very close to a double bond.

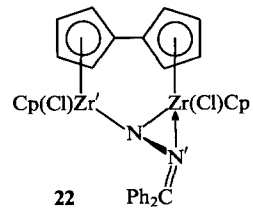
Table 3. Selected structural parameters of diazoalkane and related complexes.

No.	Complex	Bond lengths/Å		Bond angles/deg			Ref.
		N–N'	N'–C	M–N–M'	M–N–N' (M'–N–N')	N–N'–C	
	Complexes with μ-η^1 : η^1-*N*-coordination						
25a	$Cp'_2Zr(N_2CHPh)(N_2CHPh)ZrCp'_2$ $Cp' = C_5H_4Me$	1.36	1.29	100	121 (140)	120	17
26	$[CpNb(\eta^5\text{-}C_5H_4C(CO_2Et)=N_2)]_2$	1.34	1.31	93	127 (140)	118	73
27a	$(Bu^tO)_3W(N_2CAr_2)_2W(OBu^t)_3$ $Ar = p\text{-}C_6H_4Me$	1.41	1.26	[a]	[a]	137	18
28a	$Cp(CO)_2Mo(\mu\text{-}CO)(N_2CPh_2)Mo(CO)Cp$	1.35	1.28	97	130 (128)	122	65
	$CpClTi(N_2Ph_2)(N_2Ph_2)TiClCp$	1.39	1.47 1.47	95	81	[a]	78
	Complex with μ_3-*N*-coordination						
	$Fe_3(CO)_9(N_2CPh_2)$	1.40	1.26	[a]	[a]	[a]	80
	Complex with μ_4-*N*-coordination						
	$Ru_5(CO)_{12}(\mu_4\text{-}C{\equiv}CPh)(N_2CPh_2)(\mu\text{-}PPh_2)$	1.40	1.30	[a]	[a]	[a]	72
	Complexes with μ-η^1 : η^2-*N,N,N'*-coordination						
21	$CpClTi(N_2CPh_2)_2TiClCp$	1.33	1.30	94	78 (154)	[a]	19
		1.34	1.31	95	78 (157)		
22	$CpClZr(\mu\text{-}C_{10}H_8)(N_2CPh_2)ZrClCp$	1.34	1.31	131	74 (152)	129	71
23a	$Cp^*(CO)_2Mo'(\mu\text{-}CO)(N_2CMe_2)Mo(CO)Cp^*$ $Cp^* = C_5Me_5$	1.37	1.30	92	71 (113)	133	63
23b	$Cp^*(CO)_2Mo'(N_2CHCO_2Et)Mo(CO)Cp^*$ $Cp^* = C_5Me_5$	1.34	1.29	97	128 (130)	122	65
25a	$Cp'_2Zr(N_2CHPh)(N_2CHPh)ZrCp'_2$ $Cp' = C_5H_4Me$	1.32	1.29	101	74 (174)	124	17
–	$CpClTi(N_2CPh_2)(N_2Ph_2)TiClCp$	1.38	1.43 1.43	94	128 (138)	[a]	78
	Complexes μ-η^1 : η^2-*N,N',O*-coordination						
29a	$Cp(CO)_2Mo[(N_2CPh)C(O)Ph]Mo'(CO)_2Cp$	1.26	1.44	[a]	174	[a]	64
29b	$Cp(CO)_2Mo[N_2C(CO_2Et)_2]Mo'(CO)_2Cp$	1.24	1.42	[a]	[a]	122	65

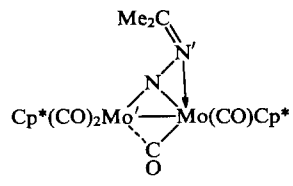
[a] The value of the given parameter is not quoted.



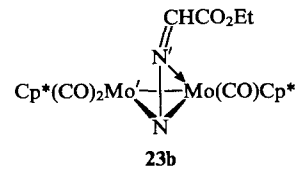
21



22



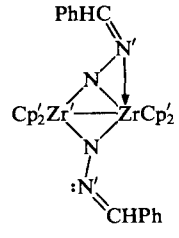
23a



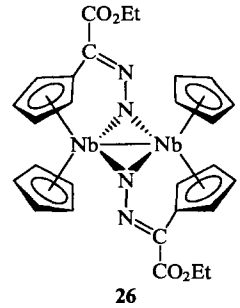
23b

Cp* = C_5Me_5.

Dimerisation of the coordinatively unsaturated complexes [$Cp'_2Zr{=}NN{=}CHAr$] generated afforded the interesting complexes $Cp'_2Zr(\mu\text{-}\eta^1:\eta^1\text{-}N\text{-}N_2CHAr)(\mu\text{-}\eta^1:\eta^2\text{-}N,N,N'\text{-}N_2CHAr).ZrCp'_2$ **25** (Cp′ = C_5H_5, C_5H_4Me),[17,76] in which the symmetrical (**E**) and asymmetric (**F**) coordination of the diazoalkane has been established. The titanium and zirconium diphenylhydrazinate(2-) complexes $CpXM(\mu\text{-}\eta^1:\eta^1\text{-}N\text{-}N_2Ph_2)(\mu\text{-}\eta^1:\eta^2\text{-}N,N,N'\text{-}N_2Ph_2).MXCp$ (M = Ti; X = Cl; M = Zr; X = Cp), similar to complexes **25**, have also been synthesised.[76,77]



25a

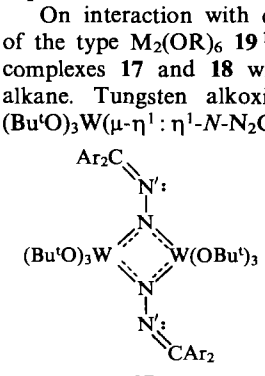


Cp′ = C_5H_4Me. 26

The interaction of the complex Cp_2NbH_3 **4a** with diazoacetate afforded the unique bimetallic complex [$CpNb\text{-}\eta^5\text{-}C_5H_4C.(CO_2Et){=}N\text{-}\mu\text{-}\eta^1:\eta^1\text{-}N]_2$ **26** containing a diazoalkane ligand coordinated to the metal atom and simultaneously bound to one of the ligands.[73] The substitution of the Cp ligand in the metallocene complexes of the early transition metals is encountered extremely rarely. It has been suggested that the formation of complex **26** also includes a stage in which coordinatively unsaturated monometallic intermediates dimerise (see Section IV.1).

A bridged diazoalkane complex $[Cp_2Nb(\mu\text{-}N_2CPh_2)]_2$ [74] has been obtained from $Cp_2(Br)Nb(\eta^1\text{-}N\text{-}N_2CPh_2)$ **10c** and sodium naphthalide.

On interaction with diazoalkanes, molybdenum alkoxides of the type $M_2(OR)_6$ **19** [18] give rise to mono- and bi-metallic complexes **17** and **18** with η^1-*N*-coordination of the diazoalkane. Tungsten alkoxides afford the bridged complexes $(Bu^tO)_3W(\mu\text{-}\eta^1:\eta^1\text{-}N\text{-}N_2CAr_2)_2W(OBu^t)_3$ **27** in this reaction.



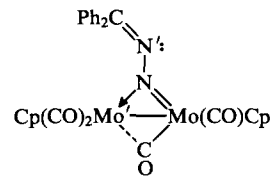
27a

Ar = C_6H_4Me-*p*.

The complexes $Rh_2(\mu\text{-}N_2CRCO_2Et)(CO)_2(dppm)_2$, where R = H or CO_2Et and dppm = $PPh_2CH_2PPh_2$,[76] have been obtained by replacing the bridging hydride atoms in $Rh_2(\mu\text{-}H)_2.(CO)_2(dppm)_2$ by the diazoalkane.

Coordination to the terminal nitrogen atom of the diazoalkane (related to type **E**) has been observed in the clusters $Os_3(CO)_9(\mu_3\text{-}PhC{=}CPh)(\mu_2\text{-}N\text{-}N_2CH_2)$,[70] $Fe_3(CO)_9(\mu_3\text{-}N\text{-}N_2.CPh_2)$,[80] $Co_4(CO)Cp_4(\mu_3\text{-}N\text{-}N_2CPh_2)$,[75] and $Ru_5(CO)_{12}(\mu_4\text{-}C{\equiv}CPh)(\mu_4\text{-}N\text{-}N_2CPh_2)(\mu\text{-}PPh_2)$,[72] the N—N′ bond being somewhat lengthened compared with that in the type **E** bimetallic complexes (Table 3).

The $\mu\text{-}\eta^1:\eta^1$-N-coordination of the diazoalkane (type **E**) has been observed in bimetallic molybdenum complexes in those cases where the groups R′ and R″ in this diazoalkane molecule are bulky and can prevent the additional coordination of the N′ atom as a consequence of steric hindrance. A coordination of this type has been observed in the complexes $Cp(CO)_2Mo(\mu\text{-}CO)(N_2CAr_2).Mo(CO)_2Cp$ **28** (Ar = Ph, C_6H_4Me-*p*).[65,66] According to spectroscopic data, at room temperature the diazoalkane bridge in complex **28** is fully symmetrical, but X-ray diffraction study of complex **28a** demonstrated some deviation from total symmetry.

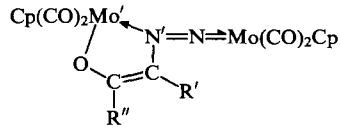


28a

It was shown later[64,65] that the ^1H NMR spectra of the complexes $Cp'(CO)_2Mo(\mu\text{-}CO)(N_2CR'R'')Mo(CO)Cp'$ **23** (Cp′ = C_5H_5, C_5H_4Me, C_5Me_5; R′ = R″ = Me; R′ = H, R″ = CO_2Et)[63,65] are only partly consistent with the structure established. In the case of the diazopropane derivative (R′ = R″ = Me), a slow isomerisation of two structures, **F** ⇄ **E**, was observed at room temperature on the basis of NMR spectroscopic data.[64] It has been suggested for the diazoacetic acid ester derivative **23b** (R′ = H, R″ = CO_2Et) [65] that thermodynamic equilibrium is established at room temperature between the complexes in which the N′ nitrogen atom is involved in type **F** coordination to one or several metal atoms.

It has been postulated that bridged type **E** and **F** complexes are formed as intermediates also in the reaction of diazoalkanes with other bimetallic complexes containing a multiple metal—metal bond. For example, in the interaction of complexes of the type $[Cp'(CO)_2W]_2$ with diazoalkanes at negative [below 0 °C (Ed.)] temperatures, the formation of type **E** and **F** complexes was observed, but only the products of the subsequent interactions, analogous to those obtained on heating the corresponding molybdenum analogues (see Section IV.1), were isolated.[81]

In the interaction of α-diazoketones with the molybdenum complex $Cp'(CO)_2Mo{\equiv}Mo(CO)_2Cp'$ **30** (Cp′ = C_5H_5, C_5Me_5), the Mo≡Mo bond is fully cleaved and type **G** complexes are formed with additional coordination of the oxygen atom of the oxo-group to one metal atom. The complexes $Cp'(CO)_2Mo(\mu\text{-}\eta^1:\eta^2\text{-}N,N',O\text{-}N_2C(R'){=}C(R'')OMo'(CO)_2Cp'$ **29** [Cp′ = C_5H_5, C_5Me_5; R′ = R″ = Ph; R′ = CO_2Et, R″ = OEt; R′—R″ = $C(O)CH_2CMe_2CH_2$] have been obtained in the same way.[64,65,69]



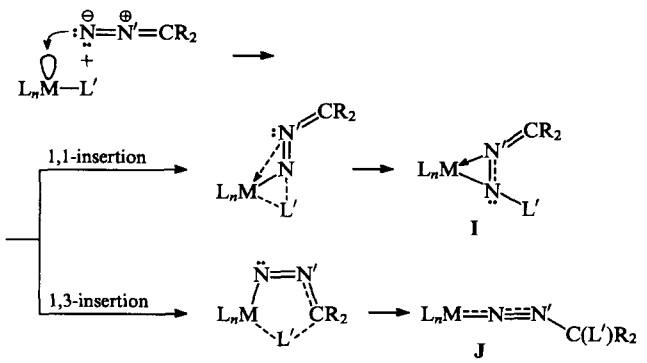
29a,b

29a: R′ = R″ = Ph.
29b: R′ = CO_2Et; R″ = OEt.

Type **H** complexes have not been isolated but it has been suggested that they are intermediates in the formation of carbenes from diazoalkanes [3,4,7] catalysed by bimetallic transition metal complexes.

3. Reactions involving insertion in the M–L bond with formation of hydrazonate, alkyldiazene, and ketazine complexes

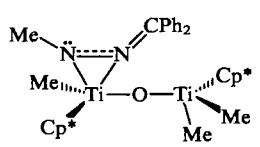
Diazoalkanes are capable of being inserted in highly reactive metal–ligand bonds (in the first place in M–H and M–C bonds) and the reaction can proceed as 1,1- or 1,3-insertion of the diazoalkanes. The η^2-*N,N'*-hydrazonate complexes **I** and alkyldiazene complexes **J** have been obtained in this way.



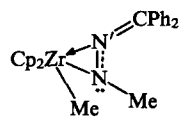
I **J**

The 1,1-insertion reactions proceed as a rule more readily in those cases where the initial metal complex is coordinatively unsaturated and preliminary coordination of the diazoalkane promotes its subsequent insertion. However, the insertion product must be coordinatively unsaturated and stabilised as a result of the additional coordination of the nonterminal nitrogen atom (type **I** complex). The nonterminal nitrogen atom is not coordinated in insertion reactions with bridged complexes **K**.

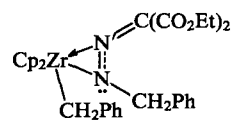
The reaction involving the insertion of N_2CPh_2 in the Ti–CH_3 bonds of the dinuclear and trinuclear titanium oxides $[Cp^*Me_2Ti]_2(\mu\text{-}O)$ and $[Cp^*MeTi(\mu\text{-}O)]_3$ ($Cp^* = C_5Me_5$) leads to the formation of hydrazonate complexes with η^2-*N,N'*-coordination (type **I**).[82] The reaction products are the following titanium complexes: $Cp^*Me_2Ti(\mu\text{-}O)TiMe(\eta^2\text{-}N,N'\text{-}NMe\text{–}N'=CPh_2)Cp^*$ **31** and $(Cp^*MeTi)_2(\mu\text{-}O)_3Ti(\eta^2\text{-}N,N'\text{-}NMe\text{–}N'=CPh_2)Cp^*$. Complex **31** can interact with another N_2CPh_2 molecule to form $(\mu\text{-}O)[TiMe(\eta^2\text{-}N,N'\text{-}NMe-N'=CPh_2)Cp^*]_2$. It has also been observed that diazoalkanes are inserted in the Zr–H, Zr–C, and Zr–P bonds of the corresponding zirconocene derivatives. The complexes $Cp_2ZrR(\eta^2\text{-}N,N'\text{-}NRN'=CR'_2)$ **32** (R = Me, CH_2Ph; R' = Ph, CO_2Et),[83,84] $Cp_2ZrCl(\eta^2\text{-}N,N'\text{-}NHN'=CPhAr)$ **33** (Ar = Ph, *o*-C_6H_4Br),[83–85] and $Cp_2Zr.[(\eta^2\text{-}N,N'\text{-}NR'N'PPh)_2PPh]$ **34** (R' = $CHCO_2Et$)[86] have been obtained similarly. Complex **33** has been synthesised also by the reaction of Cp_2ZrCl_2 with $LiHNN=CPh_2$, although the authors[17,77] assumed that only the η^1-*N*-coordination of the hydrazonate ligand takes place in it. It has been shown for complexes **32** and **33**[83–85] that only the *exo*-isomers are formed. An azametallocyclobutene derivative—the complex $Cp_2^*Zr.(\eta^2\text{-}N,C\text{-}CPh=CPh-NN'=CPh_2)$—has been obtained by inserting N_2CPh_2 in the acetylene complex $Cp_2^*Zr(C_2Ph_2)$.[87]



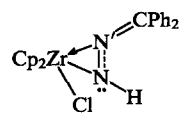
31



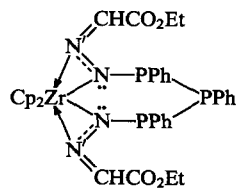
32a



32b

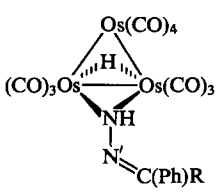


33a



34

Although the bridging hydride atoms in the rhodium complex $[Rh_2(\mu\text{-}H)_2(CO)_2(dppm)_2]$ are substituted in the reaction with diazoalkanes,[76] in the osmium cluster $(\mu\text{-}H)_2.Os_3(CO)_{10}$ the diazoalkane is inserted with formation of the complex $(\mu\text{-}H)Os_3(CO)_{10}(\mu\text{-}NH-N=CR'R'')$ **35** (R', R'' = H, Me, Ph).[88,89] The analogous ruthenium complexes $(\mu\text{-}H)Ru_3.(CO)_{10}(\mu_2\text{-}N\text{-}NH-N=CR'R'')$ have been obtained in the reaction of hydrazones with $Ru_3(CO)_{12}$;[90,91] when yet another CO molecule is lost, the complex $(\mu\text{-}H)Ru_3(CO)_9(\mu_3\text{-}N,N,N'\text{-}NH-N=CR'R'')$, with the μ_3-*N,N,N'*-coordination of the hydrazonate ligand, is formed.

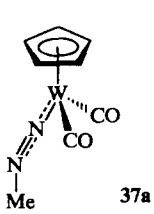


35a,b

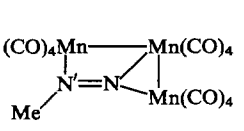
35a: R = Ph.
35b: R = Me.

1,3-Insertion has been observed only for metal hydride complexes. This is probably due to the great mobility of the H atom. The 1,3-insertion products are derivatives of alkyldiazenes $HN=N-CHR_2$, which are tautomeric forms of diazoalkanes (hydrazones) $H_2N-N=CR_2$. According to quantum-chemical calculations,[92] either one or other tautomeric form is more convenient (depending on R) for the simplest alkyl substituents R; the energy difference between them does not exceed 5 kcal mol^{-1}.

It has been found that the alkyldiazene complexes $CpM.(CO)_2(\eta^1\text{-}N\text{-}N=N-CHR'R'')$ **37** are formed as the main products in the reactions of $CpM(CO)_3H$ **36** (M = Mo, W) with the diazo-compounds $N_2CR'R''$ (R', R'' = H, Me, CO_2Et).[93–96] Under analogous conditions, the reaction of the manganese hydride $(CO)_5MnH$ with N_2CH_2 gives rise to a mixture of products,[54,97,98] from which the product of the insertion of diazomethane in the Mn–H bond, namely $(\mu_3\text{-}N,N,N'\text{-}N_2CH_3)[Mn(CO)_4]_3$ **38**, was obtained in ~10% yield.



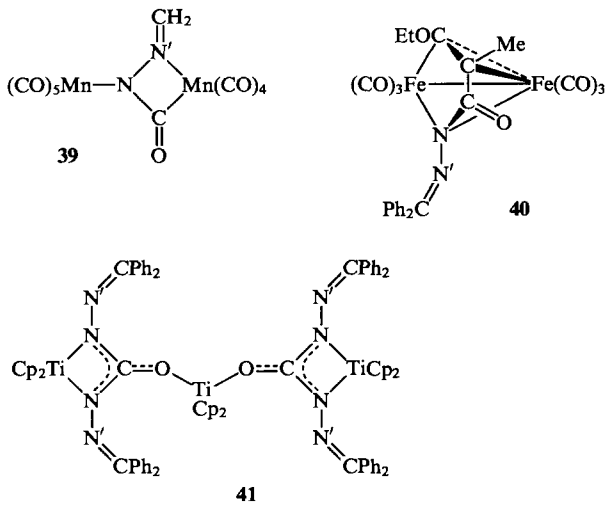
37a



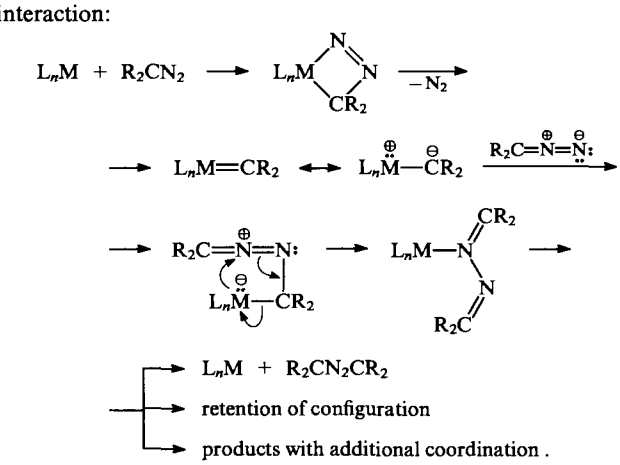
38

The products of the insertion of N_2CH_2 in the M–CO multiple bond, i.e. the manganese carbohydrazonate complex $(CO)_5Mn(\mu\text{-}N,N',C\text{-}C(O)-NN'=CH_2)Mn(CO)_4$ **39**, is formed in the same reaction in 25%–30% yield.[54,98,99] The dinuclear

complex $Fe_2(CO)_6[Ph_2C=N'NC(O)C(Me)C(OEt)]$ **40**, also containing the carbohydrazonate fragment, has been obtained in the reaction of the cluster $Fe_3(CO)_9(\mu_3\text{-CMe})(\mu_3\text{-COEt})$ with N_2CPh_2.[100] The double insertion of a diazoalkane in a M—CO bond has been observed in the interaction of $Cp_2Ti(CO)_2$ with N_2CPh_2. The product also contains a ligand of the carbohydrazonate type $(Cp_2Ti)_3[Ph_2CN_2C(O)N_2CPh_2]_2$ **41**.[9] On the other hand, the reaction of $Cp_2Ti(PMe_3)_{2-x}(CO)_x$ ($x = 0.1$) with N_2CPh_2 afforded a product with the η^1-*N*-coordination of the diazoalkane ligand—$Cp_2Ti(PMe_3)(N_2CPh_2)$ **9**.[31]



Diazoalkanes are capable of being inserted not only in a multiple M—CO bond in carbonyl complexes but also in a M=C double bond in carbene complexes. The products are then either ketazine complexes or a free ketazine (depending on the coordination capacity of the metal atom). The products of the interaction of diazoalkanes with transition metal complexes can also be carbene complexes (see Section III, 2). Generalising these results, a number of workers,[101—104] who observed the formation of ketazine complexes and the decomposition of diazoalkanes into a ketazine and nitrogen in the interaction of the diazoalkanes with transition metal complexes, proposed the following mechanism of this interaction:



Ketazine complexes have also been obtained by the direct interaction of ketazines with transition metal complexes, usually at elevated temperatures.[105]

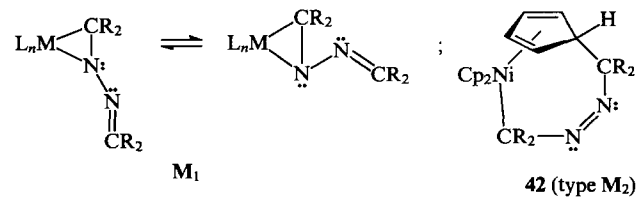
$[(\mu\text{-OAc})_2\overline{Pd(\eta^2\text{-}N,C\text{-}Ar'_2CN'NC(Ar')\text{-}2\text{-}C_6H_3(4\text{-}OR))}]_2$

Ar′ = *p*-C_6H_4OR; R = Alk.

The decomposition reactions of diazoalkanes, catalysed by transition metal complexes [for example, $Pd(OAc)_4$ [106] and $Ni(C_{12}H_{18})$ [38]] and proceeding with evolution of nitrogen, are encountered fairly often and correspond to the very simple mechanism

$$2\,N_2CR_2 \xrightarrow{ML_n} N_2 + R_2CN_2CR_2.$$

There are several ways in which ketazines may be coordinated in transition metal complexes. The π-(η^2-*N*,*C*)-coordination (type M_1) of one of the C=N bonds of the ketazine has been proposed in studies at the beginning of the 1970s [24,101] for the complexes $L_2M(R'_2C=NN=CR'_2)$ (M = Pt, Pd, Ni; L = RNC, PR_3; R′ = CF_3). The interaction of nickelocene with $N_2C(CF_3)_2$ afforded the compound $Cp_2Ni(C_6F_{12}N_2)$ **42**.[102] It is suggested that complex **42** has the structure M_2. It is essential to note that the structures M_1 and M_2 presented have not been elucidated by objective methods.



It has been established that in ketazine complexes whose structure has been determined [these are in all cases the derivatives $N_2C(C_6H_4R\text{-}p)_2$, where R = H or Me] the transition metal atom is always coordinated solely to one nitrogen atom of the ketazine ligand. Three types of structures have been found:

(a) with η^1-*N*-coordination (type M_3)

$Ar_2Pt(CO)(\eta^1\text{-}N\text{-}Ph_2CN_2CPh_2)$ (Ar = C_6F_5)[103];

(b) with η^2-*N*,*C*-coordination (type M_4)

$(CO)_2(PPh_3)\overline{OsH[\eta^2\text{-}N,C\text{-}Ar'_2CN'NC(Ar')\text{-}2\text{-}C_6H_3(4\text{-}Me)]}$

Ar′ = C_6H_4Me-*p*[104]

$Ar\overline{Pt(CO)(\eta^2\text{-}N,C\text{-}Ph_2CN'NC(Ph)-C_6H_4\text{-}o)}$

Ar = C_6F_5[103]

$[(\mu\text{-OAc})_2\overline{Pd(\eta^2\text{-}N,C\text{-}Ar'_2CN'NC(Ar')\text{-}2\text{-}C_6H_3(4\text{-}OR))}]_2$

Ar′ = C_6H_4OR-*p*; R = Alk.[105]

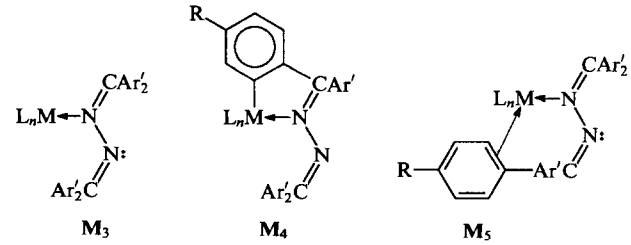
A case has also been described where the ketazine *ortho*-metallated at the benzene ring behaves as a bridging ligand, i.e. $(\mu\text{-}OAc_2)_4.Pd_3[\mu\text{-}\eta^2:\eta^2\text{-}(\text{-}NC(Ph)\text{-}C_6H_4\text{-}o)_2]$:[106]

(c) with η^2-π-coordination (type M_5)

$Ar_2Pt(Ph_2C\text{-}\eta^1\text{-}NNC(Ph)\text{-}\eta^2\text{-}C_6H_5)$

Ar = C_6F_5.[103]

Thermolysis of the latter afforded the platinum complex $Ar_2Pt.[\eta^1\text{-}(C_6H_4\text{-}o)\text{-}C(Ph)\text{-}\eta^1\text{-}NNC(Ph)\text{-}\eta^2\text{-}C_6H_5)$,[103] for which both types of coordination were found simultaneously—M_4 and M_5.



The structural parameters of a series of hydrazonate, alkyldiazene, carbohydrazonate, and ketazine complexes are presented in Table 4.

Table 4. Selected structural parameters of the hydrazonate, alkyldiazene, and ketazine complexes.

No.	Complex	Bond lengths/Å		Bond angles/deg		Ref.
		N–N′	N′–C	M–N–N′	N–N′–C	
	η^2-*N,N′*-Hydrazonate complexes					
31	$Cp^*Me_2Ti(\mu\text{-}O)TiMe(NMeN'{=}CPh_2)Cp^*$	1.33	1.30	78	126	82
	$Cp^* = C_5Me_5$		1.44[a]			
32a	$Cp_2ZrMe(NMe-N'{=}CPh_2)$	1.34	1.31	80	132	83, 84
			1.45[a]			
32b	$Cp_2ZrR(NR-N'{=}C(CO_2Et)_2)$	1.30	1.31	75	132	84
	$R = CH_2Ph$		1.47[a]			
33a	$Cp_2ZrCl(NH-N'{=}CPh_2)$	1.30	1.32	78	127	84
33a	$Cp_2ZrCl(NH-N'{=}CPh_2)$	1.35	1.30	78	126	85
34	$Cp_2Zr[(NR'-N'-PPh-)_2PPh]$	1.34	1.28[a]	83	126	86
	$R' = CHCO_2Et$	1.34	1.31[a]	80	125	
	η^3-*N,N,N′*-Hydrazonate complexes					
35a	$(\mu\text{-}H)Os_3(CO)_{10}(\mu\text{-}NH-N'{=}CPh_2)$	1.43	1.29	[b]	116	88
35a	$(\mu\text{-}H)Os_3(CO)_{10}(\mu\text{-}NH-N'{=}CPh_2)$	1.39	1.27	117	117	89
				116		
35b	$(\mu\text{-}H)Os_3(CO)_{10}(\mu\text{-}NH-N'{=}CPhMe)$	1.42	1.28	117	118	89
				114		
	Alkyldiazene complexes					
37a	$CpW(CO)_2(\eta^1\text{-}N\text{-}N_2CH_3)$	1.22	1.48	173	117	96
38	$[Mn(CO)_4]_3(\mu_3\text{-}N,N,N'\text{-}N_2CH_3)$	1.22	1.57	146	112	54, 97
				120		
				107		
	Carbohydrazonate complexes					
39	$(CO)_5Mn(\mu\text{-}N,N',C\text{-}OCNN'CH_2)Mn(CO)_4$	1.39	1.28		124	54
40	$Fe_2(CO)_6[Ph_2CNNC(O)C(Me)C(OEt)]$	1.44	1.27	126	[b]	100
			1.41[a]	120		
41	$(Cp_2Ti)_3(Ph_2CN_2C(O)N_2CPh_2)_2$	1.38	1.31	119	114	12
		1.39	1.27	119	114	
	Ketazine complexes					
M4	$(CO)_2(PPh_3)OsH[\eta^2\text{-}N,C\text{-}Ar'_2CN'NC(Ar')\text{-}2\text{-}C_6H_3(4\text{-}Me)]$	1.41	1.27	118	120	104
	$Ar' = C_6H_4Me\text{-}p$		1.30[a]			

[a] The N–C bond length is indicated. [b] The value of the angle is not quoted.

4. Reactions with formation of other complexes

It was shown above that the diazoalkane complexes can be obtained from complexes containing coordinated molecular nitrogen.[40–50] However, there have also been cases where the opposite process — the cleavage of the diazoalkane in the coordination sphere of the metal and the coordination of the nitrogen thus produced (type **N**) — was observed in the interaction of diazoalkanes with transition metal complexes.[107,108]

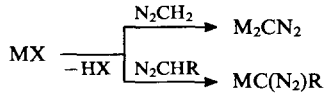
$$(ON^*)Os(Cl)(PPh_3)_3 + IC(N_2)CO_2Et \longrightarrow$$

$$\longrightarrow EtO_2CCH{=}N^*{-}Os(N_2)(Cl)_2(PPh_3)_2$$
$$\quad\quad\quad

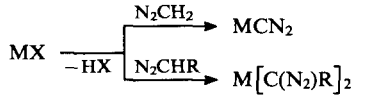
Table 5. Structural parameters of α-metallated diazoalkane complexes and free diazoalkanes.

Complex	Bond lengths/Å		Bond angles/deg		Ref.
	N–N′	N′–C	M–N–N′	N–N′–C	
Free diazoalkanes	1.12–1.13	1.28–1.32	–	–	61, 62
$(PMe_3)_3MeIRh[C(N_2)SiMe_3]$	1.09	1.30	119	175	114
$(PPh_3)_2ClPd[C(N_2)CO_2Et]$	1.16	1.28	122	177	112, 113
$(PBu_3)_2Pd[C(N_2)CO_2Et]_2$	1.13	1.28	120	176	113

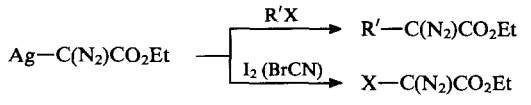
α-*C*-metallated diazoalkane derivatives of Group IB and IIB elements—silver,[109] mercury,[110,111] zinc, and cadmium[111]—have been fairly widely investigated. They have been synthesised directly from the corresponding inorganic compounds of the above metals and diazoalkanes. The compounds obtained can be used in the synthesis of substituted diazoalkanes.



M = Ag; X = $\frac{1}{2}$O.
M = RHg; X = NR_2, OR.

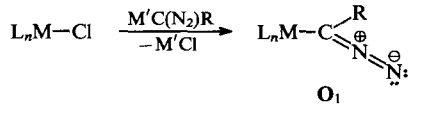


M = Hg; X = NR_2, $\frac{1}{2}$O, OR.
M = Zn, Cd; X = NR_2.



X = I, Br.

α-Metallated diazoalkane complexes of palladium,[112,113] rhodium,[114,115] yttrium, lutetium, and ytterbium[116] (type $\mathbf{O_1}$) are also known. They were obtained via a transmetallation reaction:



$\mathbf{O_1}$

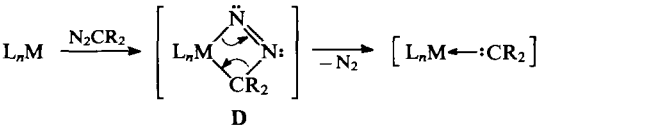
L_nM = Pd(Hal)$(PR'_3)_2$; M′ = Li, $\frac{1}{2}$Hg; R = CO_2Et, COMe, Ph.
L_nM = $Rh(PMe_3)_4$; M′ = Li; R = $SiMe_3$, $P(NR_2)S$, $P(NR_2)_2$.
L_nM = YCp^*_2, $LuCp^*_2$, $YbCp^*_2$; M′ = Li; R = $SiMe_3$.

Type $\mathbf{O_2}$ palladium complexes $(PR'_3)_2Pd[C(N_2)R]_2$ have been synthesised in a similar way.[113] Owing to the hindered rotation about the Pd–C bond in this complex, the conformational *anti*- and *syn*-isomers $\mathbf{O'_2}$ and $\mathbf{O''_2}$ were found to be present.

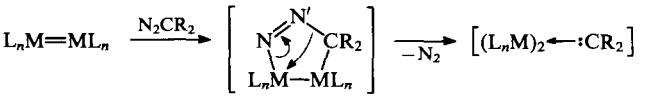
The IR spectra of the α-metallated diazoalkane complexes show a bathochromic shift of the absorption band due to the ν_{CNN} vibrations by 0–100 cm^{-1} relative to its position in the spectra of the free diazoalkanes. This finding is consistent with the observed lengthening of the N–N bond (Table 5). On the other hand, the C–N bond in α-metallated diazoalkane complexes is shorter than in the free diazoalkanes.

2. Reactions with evolution of nitrogen and the formation of carbene complexes

Apart from the coordination of the diazoalkane, the mono- and bi-metallic transition metal complexes can promote the cleavage of the diazoalkane with evolution of nitrogen and the formation of a carbene as an intermediate. It has been suggested that this stage of the interaction of the diazoalkane with the transition metal complex proceeds via a four-membered (type **D**) metallocycle in the case of monometallic complexes and a five-membered (type **H**) metallocycle in the case of bimetallic complexes.



D



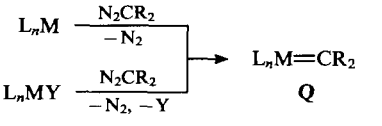
H

The intermediate coordinated carbene enters into subsequent reactions. The structure of the final product depends both on the nature of the diazoalkane itself and on the coordination capacities of the 'carbene' complexes mentioned above, on the presence in the latter of other highly reactive bonds, and also on the presence of other reactive substrates in the reaction mixture.

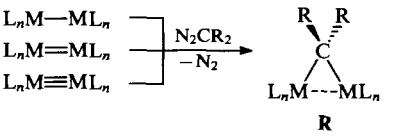
The reactions of transition metal complexes with the carbenes formed as a result of the interaction of the complexes with diazoalkanes will be examined here only to an extent sufficient to emphasise the principal features of these reactions. Since there are excellent reviews on this topic,[3,4,7] embracing the literature up to 1983, only specific studies carried out mainly since 1983 will be referred to.

a. The addition of the carbene to transition metal complexes

The simplest version of the reaction between transition metal complexes and the carbenes generated involves the addition of the latter either to a coordinatively unsaturated monometallic complex [or the substitution of another readily eliminated ligand Y with formation of carbene complexes (type **Q**)] or its addition to the metal–metal bond of a dinuclear complex with formation of methylene or other bridged complexes (Type **R**).



Q

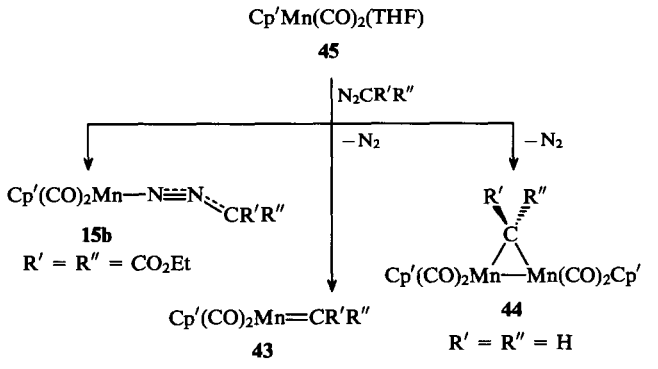


R

For example, the complex $(PPh_3)_3(NO)ClOs(=CH_2)$ has been obtained by the reaction of $(PPh_3)_3(NO)ClOs$ with N_2CH_2,[117] while the interaction of the molybdenum and tungsten complexes $M(N_2)_2(dppe)_2$ **16b** with N_2CH_2[25] leads to

the formation of $M(CH_2)_2(dppe)_2$. The products **15b**, **43**, and **44** have been synthesised by the reaction of $Cp'Mn(CO)_2(THF)$ **45** ($Cp' = C_5H_5$, C_5H_4Me) with diazoalkanes (Scheme 1).[3, 34, 118]

Scheme 1

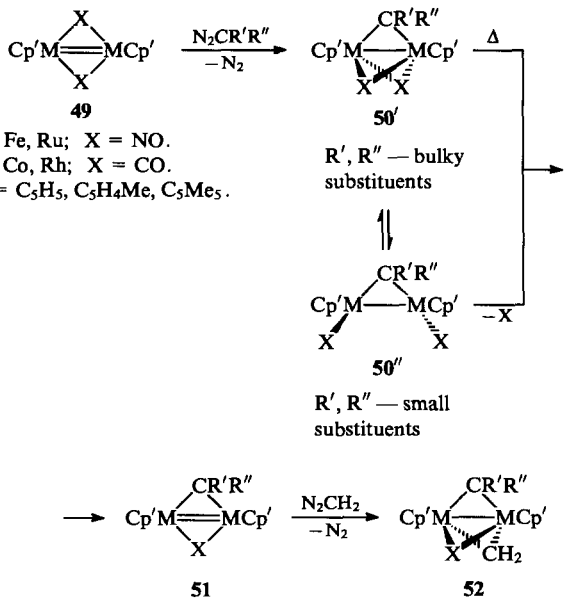


R′ = Ar; R″ = various groups.

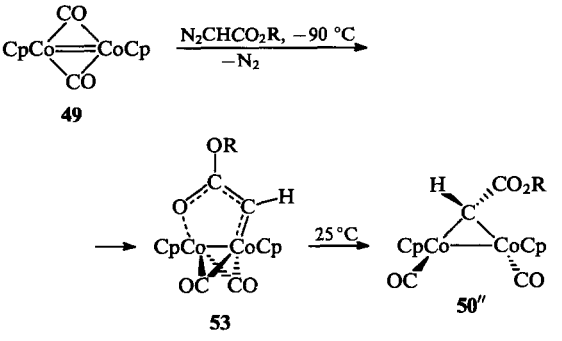
A multiplicity of various compounds have been obtained by the reaction of $Cp'_2Mo_2(CO)_4$ **46** ($Cp' = C_5H_5$, C_5H_4Me, C_5Me_5) with diazoalkanes.[65] The carbene complex **18**, the methylene-bridged complexes **24** and **47**, and the σ,π-bridged complexes **20** and **48** have been synthesised apart from the μ-η¹ : η¹-*N,N*-bridged diazoalkane complexes **18**, **24**, and **28**, the μ-η¹ : η²-*N,N,N'*-bridged diazoalkane complex **23**, and the μ-η¹ : η²-*N,N',O*-bridged diazoalkane complex **30** [Sic. Ed. possibly **29** is intended] (Scheme 2).

It is seen from Schemes 1 and 2 that the cleavage of the diazoalkane into nitrogen and a carbene is more likely when the carbon atom of the diazoalkane is more accessible (N_2CH_2) or when the substituents R′ and R″ in $N_2CR'R''$ are capable of stabilising the intermediate carbene.

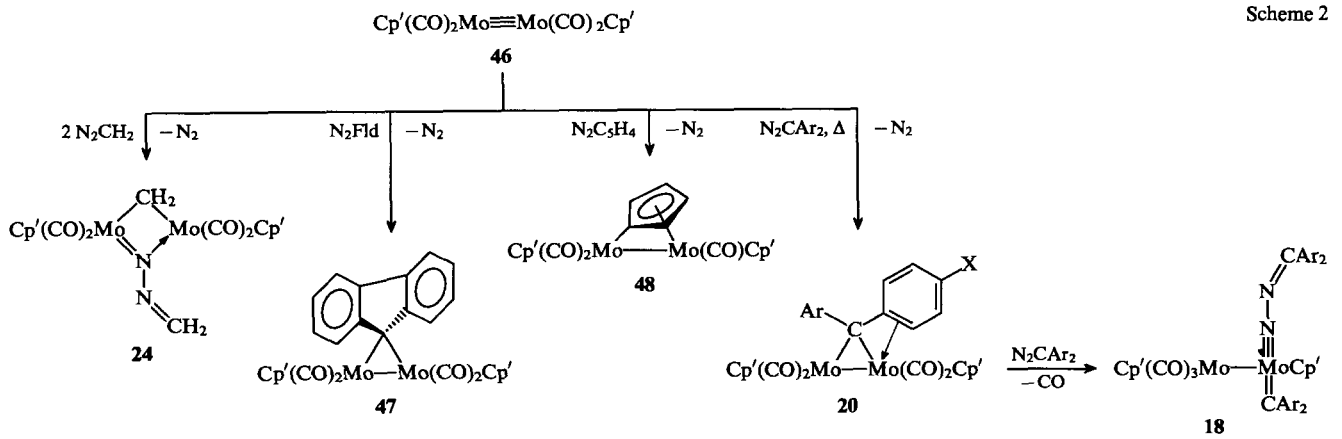
The cleavage of the diazoalkane and the formation of new bridging ligands are almost always observed in the interaction of diazoalkanes with dinuclear complexes of Group VIII transition metals ($Cp'MX)_2$ **49** (M = Fe, Ru, Co, Rh, Ni)[3, 4, 7, 66, 119–125] containing a metal–metal double bond. If the substituents R′ and R″ are relatively bulky (for example Ar), then complex **50′** with three bridging ligands obtained initially is usually the final product. If the groups R′ and R″ are small (H, n-alkyl), then the isomer **50″**, in which the ligands X (NO, CO) are terminal, is more stable. Thermodynamic equilibrium is observed between the two isomers. On heating they can both lose one molecule of X, affording complex **51**, which can react with yet another equivalent of N_2CH_2, forming thereby complex **52** with two methylene bridging ligands.

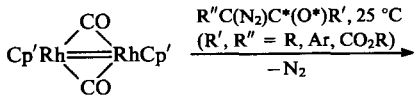


If the diazoacetic acid esters are used in the given reaction with cobalt complexes,[3] then at a reduced temperature it is possible to obtain complexes **53** with the bridging μ-η¹ : η¹-*C,O*-coordination of the carbene and, when α-diazoketones are introduced into the reaction with rhodium complexes, then more complex products **54** are formed at an elevated temperature.[3, 121]

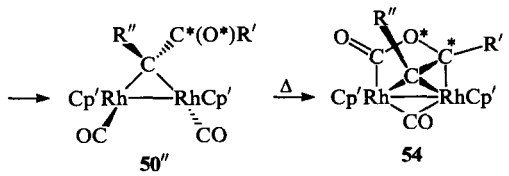


Scheme 2



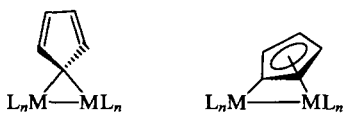


49



50″ 54

Certain carbene ligands may be coordinated in different ways in bimetallic complexes. For example, both μ-η¹: η¹- coordination (type $\mathbf{R}_{\sigma,\sigma}$) in $[CpFe(\mu\text{-}NO)]_2(\mu\text{-}C_5H_4)$, $[Cp^*Co(\mu\text{-}CO)]_2 \cdot (\mu\text{-}C_5Cl_4)$ and in all the fluorene complexes and μ-η¹: η⁵-coordination (type $\mathbf{R}_{\sigma,\pi}$) in the dimeric complexes $Cp_2(CO)_3Mo_2(\mu\text{-}C_5H_4)$ and $[Cp^*Co(\mu\text{-}CO)]_2(\mu\text{-}C_5H_4)$ have been found for the cyclopentadienylidene ligand.[3,126,127]



$\mathbf{R}_{\sigma,\sigma}$ $\mathbf{R}_{\sigma,\pi}$

It has been found that certain carbene complexes obtained from α-diazoketones may rearrange with formation of π-ketene complexes.[3]

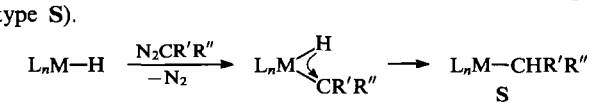
Instead of diazoalkanes, their precursors — hydrazones (in the presence of MnO_2) or *N*-alkyl-*N*-nitrosoureas — have been used successfully in the synthesis of carbene and related complexes.[3,124]

Bridged methylene complexes have also been synthesised by inserting diazoalkanes in the Pt–Pt bond in a platinum complex[128] or by substituting the bridging groups NCMe in an osmium complex[129] and CO in a palladium complex.[130]

b. Insertion of the carbene in the metal–ligand bond

Another version of the interaction of transition metal complexes with carbenes generated from diazoalkanes involves the insertion of the carbenes in metal–ligand bonds. These reactions usually take place at reduced temperatures — under conditions where the diazoalkanes themselves are stable. However, certain reactions require either elevated temperatures or UV irradiation, i.e. conditions under which the diazoalkanes themselves decompose, forming carbenes initially.[131] It is at present impossible to draw a clear-cut boundary between the thermal or photolytic decomposition of diazoalkanes and their decomposition on interaction with transition metal complexes.

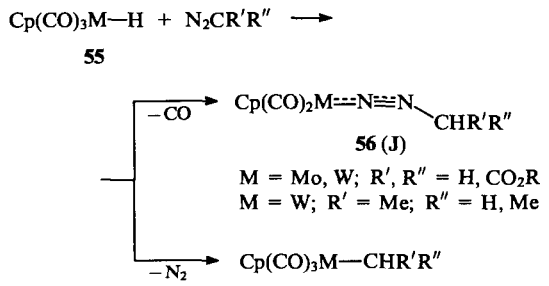
Since the M – H bond belongs to the class of the most reactive M – L bonds, it is to be expected that the carbene may be inserted in this bond too. This results in the formation of alkyl complexes (type S).



S

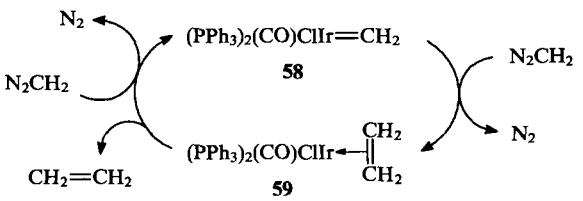
Thus the reactions of $Cp_2Zr(H)Cl$ with N_2CH_2[73] and of $(CO)_5MnH$ and $Cl(PEt_3)_2PtH$ with $N_2C(CF_3)_2$[132,133] afforded the corresponding alkyl complexes. One of the complexes of this type, namely $Fp-CH(CF_3)_2$, where Fp = $Cp(CO)_2Fe$, has been synthesised quite unexpectedly in the reaction of Fp_2 with $N_2C(CF_3)_2$ in THF.[34] The solvent served as the source of hydrogen in this process.

The interaction of molybdenum and tungsten hydride complexes $Cp(CO)_3MH$ **55** with diazoalkanes[95] leads to a mixture of products of the insertion of the diazoalkanes (compounds **56**) and carbenes (compounds **57**) in M–H bonds. The ratio of the alkyldiazene complex **56** (type **J**) and the alkyl complex **57** (type **S**) depends on the nature of the substituents R′ and R″ in the diazoalkane.



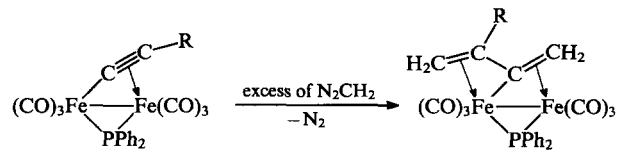
M = Mo, W; R′ = H; R″ = H, Ar.
M = W; R′ = Me; R″ = H, Me.

The insertion of the carbene has been observed also in metal–carbon multiple bonds. For example, the carbene complex of iridium **58** gives rise to the ethylene complex **59** (type **T**) on interaction with diazomethane.[134] When an excess of N_2CH_2 is used, the process proceeds as catalytic decomposition of the latter into nitrogen and ethylene.



Diazomethane diluted with an inert gas decomposes similarly on the surfaces of transition metals (Ni, Pd, Fe, Co, Ru, Cu),[136] which results in the formation of ethylene and nitrogen, while its reaction in a mixture with hydrogen affords a mixture of alkanes. A reaction mechanism involving the formation of carbenes coordinated on the surfaces of metals has been proposed[135] and the reaction has been compared with the Fischer–Tropsch reaction.

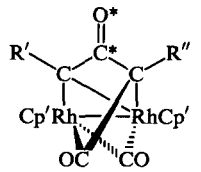
The interaction of the dinuclear iron complex **60**,[136] containing a π-bound alkyne, with diazomethane leads to the butadiene complex **61**.



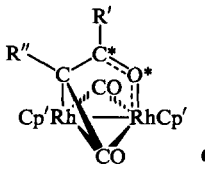
60 **61**

A similar reaction has been described also for a trinuclear ruthenium complex.[137]

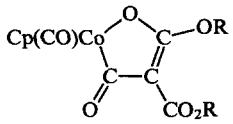
If the reaction of the rhodium complex $[Cp'Rh(\mu\text{-}CO)]_2$ (Rh = Rh) **49** (Cp′ = C_5Me_5) described above is carried out with diazodimedone $(R'C^*(O^*)C(N_2)R''$, where R′ = R″ = Ph or R′–R″ = $-CH_2CMe_2CH_2CO-$)[3,121] or benzoylphenyldiazomethane, it is possible to obtain more involved complexes **62** and **63**, which are the products of the insertion of the carbene in the Rh–CO bond. The insertion of the carbene formed from diazomalonate in the Co–CO bond of the monomeric analogue of complex **49**,[3,7] leading to complex **64** (type **U**) with additional coordination of the oxygen atom of the carboxy-group, has also been described.



62 R′ = R″ = Ph.



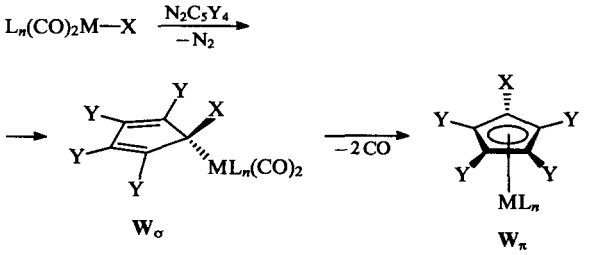
63 R′–R″ = $C(O)CH_2CMe_2CH_2$.



64 R = Me, Et.

The synthesis of the η^2-*C*,*C*-ketene complex $Cp'Mn(CO)_2.[C(O)-CR_2]$ (CR_2 = 9-anthron-10-ylidene) (type **V**) from $Cp'Mn(CO)_3$ and N_2CR_2 catalysed by the complex $CpMn.(CO)_3(THF)$ can serve as the next example of the reaction involving the insertion of the carbene in the M–CO bond.[3]

The insertion of the carbene generated from $N_2C(CF_3)_2$ in metal–halogen bonds has been described[24] for the platinum and palladium complexes $(PhCN)_2MCl_2$. The complex $(PhCN)_2.M[C(CF_3)_2Cl]_2$ (type **W**) is then formed. The carbenes obtained from substituted diazocyclopentadienes are readily inserted in metal–halogen bonds. The reaction leads to the formation of halo-substituted 5-cyclopentadienyl complexes ($\mathbf{W}_\sigma$).[3] The reactions proceed tentatively via the formation of η^1-cyclopentadienyl complexes ($\mathbf{W}_\pi$), which were successfully detected in some cases [ML_n = $Mn(CO)_3$; X = Cl, Br; Y = Cl].



ML_n = $Mn(CO)_3$, $Re(CO)_3$, $Fe(CO)_2X$, RhL_2;
X = Cl, Br, I; C_5Y_4 = C_5H_4, C_5X_4, indenyl.

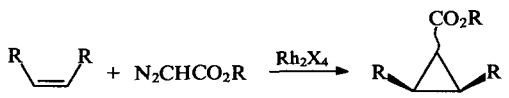
The insertion of carbenes obtained from various diazoalkanes in the Co–S and Rh–S bonds has also been observed.[138]

c. Reactions of the carbenes with other reactive substrates

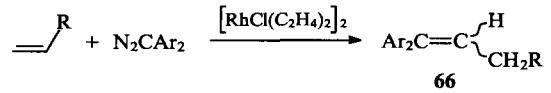
The carbenes generated from diazoalkanes can react with other reactive substrates in the reaction mixture. In such cases, the transition metal complexes behave as catalysts of the reactions.

There is in fact a large amount of information in the literature about reactions of this kind and reviews on this topic have appeared regularly (for example those of Hegedus[139] and Shapiro et al.[140]) and they will therefore not be described in this review.

We shall only note that among these processes the greatest importance attaches to the reactions of diazoalkanes with alkenes catalysed by transition metal complexes, which lead to the formation of cyclopropanes **65**[139] or substituted alkenes **66**.[29,37]



65



66

IV. Reactions of diazoalkane complexes

Diazoalkane complexes, i.e. complexes with coordinated diazoalkanes of types **B**, **C**, **E**, **F**, and **O**, are of undoubted theoretical interest as an individual class of compounds. In this sense, they have been thoroughly characterised structurally: their parameters differ from those of the free diazoalkanes. However, in order to obtain exhaustive information about such complexes, it is essential to know to what extent the coordination to the transition metal atom promotes a change in the electron density and polarity of the bonds and hence a change in the reactivity of the coordinated diazoalkane ligands compared with the free diazoalkanes.

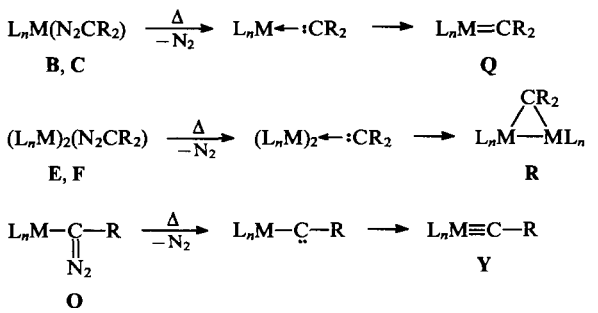
There have been few studies on the reactions of diazoalkane complexes of transition metals and they have almost all been carried out during the last decade. The diazoalkane complexes obtained were usually introduced into other reactions. Hitherto there have been no systematic studies on the reactions of diazoalkane complexes.

The available information about the reactions of diazoalkane complexes can be divided into two groups: studies involving the investigation of the products of the thermolysis of diazoalkane complexes and studies on the interaction of diazoalkane complexes with different classes of reagents.

1. Thermolysis of diazoalkane complexes

The majority of diazoalkane complexes have a limited thermal stability. When they are heated, nitrogen is usually evolved and it has been assumed tentatively that a carbene is formed and interacts with the initial complex. In principle, these are the products which have been obtained by the reaction of diazoalkanes with transition metal complexes (see Section III.2). The difference is insignificant and in essence consists only in the fact that some diazoalkane complexes decompose even below room temperature, whilst others are stable under these conditions. When the product of the reaction of the carbene with the initial complex is formed directly (sometimes at reduced temperatures), it is possible to detect diazo-complexes, which are converted into more stable products on slight heating.[6]

The thermolysis of diazoalkane complexes proceeds mainly in three ways. In the first, simplest version of the thermolysis, the evolution of nitrogen and the formation of carbene (type **Q**) or bridged methylene (type **R**) complexes is observed, while in the case of α-metallated diazoalkane complexes (type **O**) carbyne complexes are obtained (type **Y**).



For example, the carbene complex $[Cp(CO)_2Mo]_2(\mu\text{-}CPh_2)$ **20** has been synthesised from $[Cp(CO)_2Mo]_2(\mu\text{-}N_2CPh_2)$ **28a**,[65] while the complex $(PEt_3)_2Pd(CCO_2Et)_2$ has been obtained from $(PEt_3)_2Pd[C(N_2)CO_2Et]_2$.[113]

Together with the hydrazone $H_2NN=CPh_2$, the complex $Cp_2(Cl)Zr(\eta^2\text{-}NH-N=CPh_2)$ **33a**[73] gave rise to its disproportionation products—molecular nitrogen, Cp_2ZrCl_2, and the carbene complex $[Cp_2Zr(\mu\text{-}CPh_2)]_2$.

The second type of thermolysis occurs when the initial transition metal complex is insufficiently reactive in relation to the carbene or it does not form a sufficiently strong bond with the lattice. The formation of the corresponding ketazine is then observed. Ketazines are the main products of the thermolysis[104]

and photolysis[131] of the diazoalkanes themselves. In the case of α-metallated diazoalkane type **O** complexes, quantitative evolution of nitrogen is observed and the corresponding acetylenes are formed. Alkenes and alkanes may be obtained as side products in the first reaction and alkenes in the second.

$$L_nM(N_2CR_2) \xrightarrow[-N_2]{\Delta} L_nM{\leftarrow}{:}CR_2 \xrightarrow{L_nM(N_2CR_2)}$$

B, C

$$\longrightarrow L_nM + R_2C{=}N{-}N{=}CR_2$$

$$(+ R_2C{=}CR_2 + R_2HC{-}CHR_2)$$

$$L_nM{-}\underset{\underset{N_2}{\|}}{C}{-}R \xrightarrow[-N_2]{\Delta} L_nM{-}\ddot{C}{-}R \xrightarrow[-N_2]{L_nM[C(N_2)R]}$$

O

$$\longrightarrow L_nM + R{-}C{\equiv}C{-}R \ (+RHC{=}CHR)$$

For example, diphenylacetylene with an admixture of stilbene has been synthesised from the complex $(PEt_3)_2Pd[C(N_2)Ph]_2$,[113] while thermolysis of $(Bu^tNC)_2Ni(N_2Fld)$ **2** in the presence of phosphine[10] afforded fluorenone azine and $(Bu^tNC)_2Ni(PPh_3)_2$ as the main products. The formation of the products of the coupling of the carbenes to other reactive ligands is possible. For example, thermolysis of the nickel complexes $(Bu^tNC)_2.Ni(N_2CR_2)$ [CR_2 = Fld, CPh_2, $C(CN)_2$] without phosphine afforded a mixture of the corresponding azine and the ketene imine $(R_2C{=}C{=}N{-}Bu^t)$.[9,10] For CR_2 = CPh_2 or $C(CN)_2$, the latter gives rise to the complex $(Bu^tNC)_2Ni(\eta^2\text{-}N,C\text{-}(Bu^t).N{=}C{=}CR_2)$.

Ketazines have been obtained in the reaction of diazoalkane complexes **3**[21,22] and **33**[85] of the oxophilic early transition metals (Nb and Zr) with atmospheric oxygen. Oxidation of the niobium complexes **3** results in the formation also of the free diazoalkanes.

$$Cp_2Zr(Cl)(HNNCPhAr) \xrightarrow{O_2}$$

33

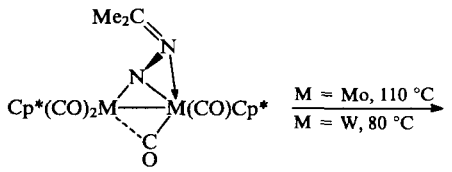
$$\longrightarrow [Cp_2ZrCl]_2O + N_2 + ArPhC{=}N{-}N{=}CPhAr$$

$$Cp_2Nb(H)(N_2CPhAr) \xrightarrow{O_2}$$

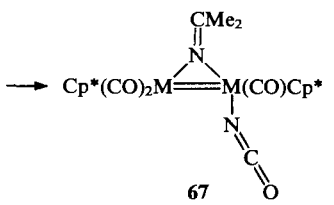
3

$$\longrightarrow (Cp_2NbO)_n + N_2 + ArPhC{=}N{-}N{=}CPhAr + N_2CPhAr$$

The third type of thermolysis comprises special cases where moderate heating can result in rearrangements or other structural changes in the molecules of the diazoalkane complexes. Thus the N–N bond is ruptured in the bridged diazopropane complexes **23a** of molybdenum[67] and tungsten[81] and in the μ-alkylideneaminometal isocyanate complex **67**.



23a

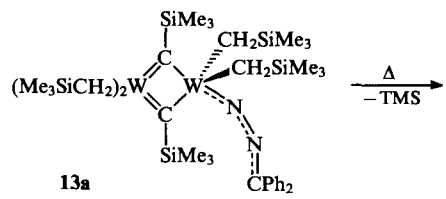


67

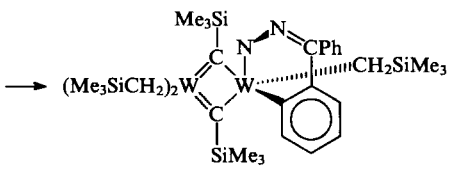
Cp* = C_5Me_5.

The same process has been described also for a tungsten complex of diazocyclopentadiene,[81] but it occurs already at −10 °C. The molybdenum bimetallic complex **67** $Cp^*(CO)_2Mo.(\mu\text{-}\eta^1:\eta^2\text{-}N_2CH_2)(\mu\text{-}CH_2)Mo(CO)_2Cp^*$ of a similar type loses one CO molecule on heating and isomerises to the complex $Cp^*(CO)_2Mo(\mu\text{-}\eta^1:\eta^1\text{-}N{=}CH_2)Mo(\eta^1\text{-}N{=}CH_2)(CO)_2Cp^*$ containing two different alkylideneamino-groups.

In a crystal the M–N–N fragments of the η^1-*N*-diazoalkane ligands (Table 1) are usually almost linear (the M–N–N and N–N–C angles are 153°–177° and 117°–151° respectively). However, reactions have been discovered in which the M–N–N–C fragment is distorted, which promotes the intramolecular interaction of the reactive bonds of the CR_2 group with metallic or other reaction centres in the molecule of the complex. For example, when the diphenyldiazomethane complex of tungsten **13a** is heated, the metal is inserted in a C–H bond of the benzene ring of the diazoalkane.[17] This reaction results in the formation of the product **68** containing a metalpyridazine ring.



13a



68

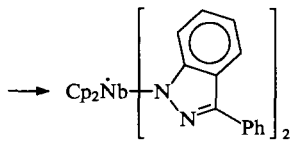
Whereas the interaction of Cp_2NbH_3 **4a** with $N_2C(Ph).(C_6H_4Br\text{-}o)$ at room temperature results in the formation of the η^1-*N*-diazoalkane complex **3b**, moderate heating of complex **4a** with an excess of the same diazoalkane afforded the bisindazole complex **69**.[22]

$$Cp_2NbH_3 \xrightarrow[25\,^\circ C]{N_2C(Ph)(o\text{-}C_6H_4Br)}$$

4a

$$\longrightarrow Cp_2Nb(H)NNC(Ph)(o\text{-}C_6H_4Br) \xrightarrow[50-60\,^\circ C]{N_2C(Ph)(o\text{-}C_6H_4Br)}$$

3b



69

In the interaction of compound **4a** with ethyl diazoacetate, the unstable η^1-*N*-diazoalkane complex **3c** is formed initially and is then slowly converted into complex **26** substituted in the Cp ring.[22,73]

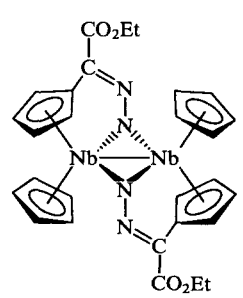
Cp_2NbH_3

4a

$\downarrow N_2CHCO_2Et$

$Cp_2Nb(H)NNCHCO_2Et$ →

3c



26

Thermolysis of the complex $(PPh_3)_2ClIr[N_2C(COPh)_2]$ afforded[140] the products of the *ortho*-metallation of the benzene ring of both the dibenzoyldiazomethane ligand and the triphenylphosphine ligand.

It has been found that, when the iridium complex $(PPr^i_3)_2.ClH_2Ir(N_2CPh_2)$ is heated,[29] a reaction which is the opposite of its formation reaction takes place—diphenyldiazomethane and the coordinatively unsaturated complex $IrH_2Cl(PPr^i_3)_2$ are formed.

When the hydrazonate complex $Os_3(\mu\text{-}H)(CO)_{10}(\mu\text{-}\eta^2\text{-}NH\text{-}N=CMe_2)$ obtained from $Os_3(\mu\text{-}H)_2(CO)_{10}$ and diazopropane is heated, it loses nitrogen and the 'carbene', reforming the cluster $Os_3(\mu\text{-}H)_2(CO)_{10}$.[89]

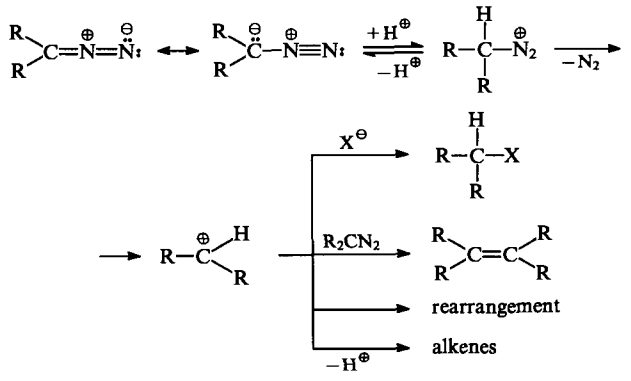
Photolytic reactions can sometimes lead to products related to the thermolysis product. As already stated above, diazoalkanes themselves usually afford ketazines in both these reactions. Unfortunately, special studies of the effect of UV radiation have been scarcely performed.

So far as we are aware, only one case of photolytic decomposition has been described in the literature, namely that of the diazoalkane complex[30] $(PPr^i_3)_2MeIr(N_2CPh_2)$, the product of which is the complex $(PPr^i_3)_2MeIr(N_2)$ with coordinated molecular nitrogen (structural type **N**).

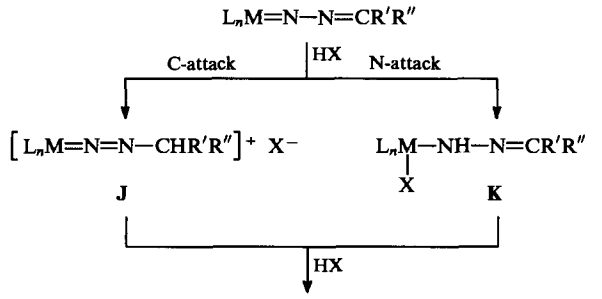
2. Interaction of diazoalkane complexes with electrophiles

In order to account for the reactions of diazoalkanes coordinated to transition metal atoms with other reagents, it is necessary to analyse the distribution of electron density in this diazo-ligand. Schwartz and coworkers,[17,77,142] claim, on the basis of reactions with the 'metalloazine' complexes of zirconium, that these compounds are exceptionally easily subjected to electrophilic attack on the carbon atom, i.e. a characteristic feature of the diazoalkane fragment in relation to this carbon atom is the repolarisation ('umpolung') of the quasi-carbonyl group of which it is a derivative.

As a consequence of the attack by a proton on the carbon atom of the diazo-group, the diazoalkanes themselves lose nitrogen in the reaction with protic acids[143] and give rise to a carbonium ion, which may be stabilised as a result of reactions with a nucleophile X and a diazoalkane, rearrangement, or deprotonation. Thus the decomposition of diazoalkanes in an acid medium can afford different products depending on the nature of the substituents R in the diazoalkane and the nucleophile present.



The protonation of the coordinated diazoalkanes can be directed both to the carbon atom and to the terminal nitrogen atom, while on treatment with a stoichiometric amount of acid the protonation products obtained initially (products of type **J** and **K**) are usually stable. Only on interaction with an excess of acid does the diazoalkane ligand decompose with formation of organic compounds.



products of the dissociation of the M – N(N – C) bonds

The above hypothesis concerning the direction of electrophilic attack on a carbon atom of the coordinated diazoalkane in the reaction with acids was confirmed directly in only one case—in the reaction of $[Rh_2(\mu\text{-}N_2CHCO_2Et)(CO)_2(dppm)_2]$ with HBF_4,[76] which leads to the formation of the cationic alkyldiazene complex $[Rh_2(\mu\text{-}N_2CH_2CO_2Et)(CO)_2(dppm)_2]BF_4$. The reaction is reversible—the initial diazoacetate complex was obtained on interaction with EtONa.

The interaction with HBF_4 resulted in the conversion of the related diazomalonate complex $[Rh_2(\mu\text{-}N_2C(CO_2Et)_2)(CO)_2.(dppm)_2]$ into $[Rh_2(\mu\text{-}H)(CO)_2(dppm)_2]BF_4$.[76]

In the remaining cases described, the site of attack by the proton is not a carbon atom but the terminal nitrogen atom of the diazo-group. The diazoalkane then undergoes a formal transformation from a hydrazonato(2-)-ligand (type **C**) into a hydroazonato(1-)-ligand (type **K**). Overall, the reaction with one equivalent of hydrogen halide proceeds as addition of HX to the metal–nitrogen bond. For example, the diazoalkanetungsten complex **11c** reacts with one equivalent of HBr via this mechanism.[42]

$$[(PMe_2Ph)_3Br_2W{=}N{-}N{=}CMe_2] \xrightarrow{1\ \text{equiv. HBr}}$$

11c

$$\longrightarrow [(PMe_2Ph)_3Br_3W{-}NH{-}N{=}CMe_2]$$

A mixture of products containing $WBr_4(PMe_2Ph)_2$ (65%), hydrazine, and acetone ketazine (25%–30%) was obtained by reaction with HBr. The cationic complex $[WBr(N_2CH_2).(dppe)_2]^+Br^-$ does not react with HBr at all.[47] The interaction of another tungsten complex **1a** with an excess of HBr afforded[30] the product of the addition of two HBr molecules (compound **70**), which slowly decomposed with formation of a hydrazone.

$$(Me_2NCS_2)_2(CO)W(=N{-}N{=}CHAr) \xrightarrow[-CO]{\text{excess of HBr}}$$

1a

$$\longrightarrow (Me_2NCS)_2Br_2W(N_2H_2CHAr) \longrightarrow$$

70

$$\longrightarrow (Me_2NCS)_2WBr_2 + ArCH{=}NNH_2$$

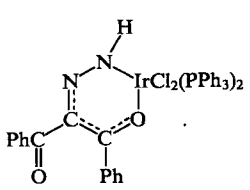
Ar = C_6H_4Me-*p*.

In the interaction of the iridium complex **8b** with HCl, the oxidative addition of hydrogen chloride takes place initially and is followed by a shift of the proton with a rearrangement of the coordination sphere.[26]

$$(PPh_3)_2ClIr[N_2C(COPh)_2] \xrightarrow{HCl}$$

8b

$$\longrightarrow (PPh_3)_2Cl_2HIr[N_2C(COPh)_2] \longrightarrow$$



The complete decomposition of the diazoalkane coordinated to a transition metal atom has been described[13] for diazoalkane complexes **71** of vanadocene.

$$Cp_2V(N_2CR'R'') \xrightarrow[-N_2]{\text{excess of HCl}} Cp_2VCl_2 + R''R'CHCl + R''R'CH{-}CHR'R''$$

71

The interaction of the dinuclear diazoalkane complex **25b** with $Et_3O^+BF_4^-$ (or EtI),[77] which resulted in the formation of a *N*-alkylated hydrazone **72** and a *N*- and *C*-alkylated hydrazone **73** (in approximately equal amounts), is an example of the reactions of diazoalkane complexes with aprotic electrophiles.

$$[Cp_2Zr(\mu\text{-}N_2CHPh)]_2 \xrightarrow[or\ EtI]{Et_3O^+BF_4^-} \underset{\mathbf{72}}{Ph(H)C{=}N{-}N(H)Et} + \underset{\mathbf{73}}{Ph(Et)C{=}N{-}N(H)Et}$$

25b

Free diazoalkanes are known to decompose on treatment with the halogens,[143] producing nitrogen and geminal dihaloalkanes. On the other hand, the interaction of the molybdenum and tungsten complexes $(R_2NCS_2)_2(CO)M(N_2CHAr)$ (**1a**) (Ar = C_6H_4Me-*p*) with an equimolar amount of chlorine or bromine[30] entails the exchange of CO for halogen atoms and the formation of the complex $(R_2NCS_2)_2X_2M(N_2CHAr)$.

Among other electrophiles, carbonyl compounds have been investigated in the reactions with diazoalkane complexes. Their interaction with the free diazoalkanes usually leads to the formation of the product of the insertion of the carbene,[140] obtained from the diazoalkane, in the C–CO bond or the products of the addition of the carbene to the C=O bond. The diazoalkane fragment in the zirconium complex **25b** behaves as both a N- and a C-nucleophile in reactions with various aldehydes and ketones,[17,77,142] which results in the formation of a mixture of the alkene **74** and the ketazine **75** in a nearly equimolar ratio.

$$[Cp_2Zr(\mu\text{-}N_2CHPh)]_2 \xrightarrow{R'(R)C{=}O} \underset{\mathbf{74}}{Ph(H)C{=}C(R)R'} + N_2 + \underset{\mathbf{75}}{Ph(H)C{=}N{-}N{=}C(R)R'} + \text{'}Cp_2ZrO\text{'}$$

25b

It has been observed that the enhanced electron-accepting nature of the carbonyl compounds promotes the formation of alkenes, whilst the use of substituted derivatives (steric factor) promotes the formation of ketazines. If the benzene ring in the diazoalkane fragment in complex **25b** is substituted, the rate of the second-order reaction increases with enhancement of the electron-donating nature of the substituent in the *para*-position in the benzene ring. Two mechanisms have been proposed[17,77,142] for the formation of alkenes and ketazines. They both involve the formation of an intermediate as a result of the coordination of the oxygen atom of the carbonyl compound to the oxophilic zirconium atom and the formation of a bond between the carbonyl carbon atom and the diazoalkane (with either a C- or N-nucleophile). This reaction is an analogue of the Wittig reaction and is synthetically valuable because the diazoalkane complex has also been obtained from a carbonyl compound.

In contrast to the free diazoalkanes, the diazo-ligands are resistant to the action of mild electrophiles such as alkyl halides. For example, the interaction of the niobium complex $Cp_2Nb(H).(N_2CPhAr)$ **3** with various alkyl and aryl halides involves only the substitution of the hydride atom by the halogen, which leads to the formation of the complexes $Cp_2Nb(X)(N_2CPhAr)$ **10** (X = Cl, Br, I).

3. Interaction of diazoalkane complexes with nucleophiles

Although free diazoalkanes are relatively stable in a neutral or alkaline medium, the diazoalkane complexes are appreciably more sensitive to the action of bases and nucleophiles. The attack by the nucleophile in such a reaction is usually directed to a carbon atom of the coordinated diazoalkane and leads to the formation of alkyldiazene complexes (type **J**).[46]

$$L_nM{\equiv}N{=}N{=}CR'R'' + \ddot{X} \longrightarrow \underset{\mathbf{J}}{L_nM{\equiv}N{\equiv}N{-}CXR'R''}$$

Reactions of this type have been observed for 4-electron-donating diazoalkane complexes of tungsten and molybdenum.[2,40,42,46,47,49,144] The polarisation of the carbon atom of the diazoalkane fragment in such a reaction must be the opposite to that observed in reactions with electrophiles. On this basis, one may postulate that either the reactivities of 2- and 4-electron-donating diazoalkane ligands differ very greatly or that the diazoalkane fragment in the diazo-complexes is not markedly polar and is capable of becoming adjusted to the reagent introduced.

The neutral methyldiazene complex **76a**, the ethyldiazene complex **76b**, and the benzyldiazene complex **76c** have been obtained from the cationic diazomethanetungsten complex **12d** by its reaction with the corresponding nucleophiles.[47,49]

$$\underset{\mathbf{12d}}{[(dppe)_2BrW(N_2CH_2)]^+} \xrightarrow{LiAlH_4} \underset{\mathbf{76a}}{[(dppe)_2BrW(N_2CH_3)]}$$

$$\xrightarrow{MeLi} \underset{\mathbf{76b}}{[(dppe)_2BrW(N_2CH_2CH_3)]}$$

$$\xrightarrow{PhLi} \underset{\mathbf{76c}}{[(dppe)_2BrW(N_2CH_2Ph)]}$$

The analogous diazopropanetungsten complex **12a**[46] and diazobutanoltungsten complex **12b**[49] $[(dppe)_2BrW(N_2CR'R'')]^+$ [R' = R'' = Me; R' = H, R'' = $(CH_2)_3OH$] react with $LiAlH_4$ to form the alkyldiazene complexes $[(dppe)_2BrW(N_2CHR'R'')]$.

On treatment with $LiAlH_4$, the neutral diazoalkane complexes $[(PMe_2Ph)_3Br_2W(N_2CR'R'')]$ **11c,d** [R' = R'' = Me; R'–R'' = $(CH_2)_5$] decompose quantitatively to the corresponding amine R'R''CHNH$_2$ and ammonia.[42]

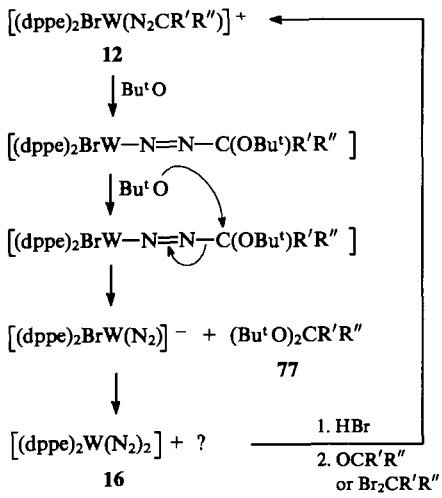
The interaction of the dinuclear rhodium complex $[Rh_2.(\mu\text{-}N_2CHCO_2Et)(CO)_2(dppm)_2]$ with $NaBH_4$ involves the substitution of the bridging dialkyl ligand by hydride atoms with formation of $[Rh_2(\mu\text{-}H)_2(CO)_2(dppm)_2]$.[76]

The attack by the nucleophile can be directed also to other highly reactive bonds of the diazoalkane complex. Thus the reaction of $Cp_2Nb(Br)(N_2CPh_2)$ **10c** with MeLi leads to the formation of the complex $Cp_2Nb(Me)(N_2CPh_2)$, while the reaction of $Cp_2Nb(H)(N_2CPh_2)$ **3a** with BuLi affords the salt $[Cp_2Nb(N_2CPh_2)]^-Li^+$.[39]

The reactions of diazoalkane complexes with oxygen-containing nucleophiles usually proceed with dissociation of metal–nitrogen or nitrogen–carbon bonds. Thus the interaction of complexes of the type $(RO)_2W(N_2CR'R'')$ with alcohols[40] led to the formation of the corresponding hydrazones $H_2NN{=}CR'R''$. On hydrolysis in air,[30] the diazoalkane complexes of molybdenum and tungsten $(Me_2NCS_2)_2(CO)M.(N_2CHC_6H_4Me\text{-}p)$ **1a** decompose, forming the hydrazone

($H_2NN=CHC_6H_4Me$-*p*), CO, and $(Me_2NCS_2)_2MO$. The complexes $Cp_2Nb(H)(N_2CPhAr)$ **3** [39] and $Cp_2Zr(Cl)(N_2CPhAr)$ **33** [85] also hydrolyse readily to the corresponding hydrazone and oxo-complex (especially in an alkaline medium).

The interaction of the cationic tungsten complexes **12** with an excess of Bu^tOK leads to the formation [46] of the initial nitrogen complex **16** (from which complex **15** was obtained) and the geminal diether **77**. It is of interest that the analogous reaction proceeds differently with MeONa.

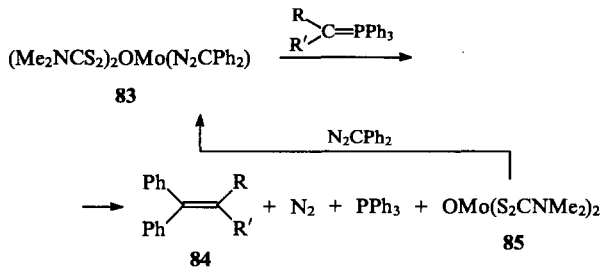


R′, R″ = H, Me.

The interaction of cationic diazoalkane complexes of molybdenum and tungsten **12** with strong bases [145] entails the deprotonation of the diazoalkane ligand, leading to the alkenyldiazenide complexes **78**. Certain reactions of the alkenyldiazenide complexes, resulting in the formation of the coupling product **79** and the alkylation product **80** and in the nucleophilic addition of the α-carbon atom of the diazo-group and of H^+ to the C=N bond (compound **81**) and the C=O bond (compound **82**) (Scheme 3), have been investigated.

Schwartz and coworkers [15,17] have described another reaction of the diazoalkane complexes that is analogous to the Wittig reaction. The diazoalkanes coordinated to a molybdenum atom behave in this process as C-electrophiles, which is the opposite of the behaviour found for the diazoalkanezirconium complexes.

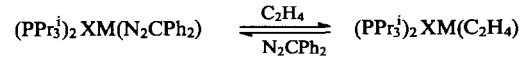
The interaction of the diazoalkane complex **83** with various alkylidenephosphines afforded the corresponding alkenes **84**. Nitrogen and the free phosphine are then evolved and the molybdenum complex **85** is formed. The initial diazoalkane complex **83** can be synthesised from it.



The olefins obtained are identical with those formed in the reaction of benzophenone with alkylidenephosphines. In the case of the analogous complex of phenylmethyldiazomethane with asymmetrically substituted alkylidenephosphines, the (*Z*)- and (*E*)-alkenes are formed in approximately the same proportions as in the classical Wittig reaction [the (*Z*)-isomer predominates]. However, in contrast to the classical Wittig reaction, the authors suggest that this reaction be regarded as an oxidation-reduction process.

The reactions of diazoalkane complexes with alkenes are in principle similar to the reactions of the carbenes (obtained from the diazoalkanes) with alkenes (Section III.2.b). The difference consists solely in the thermal stability of the diazoalkane complexes. On heating, diazoalkane complexes usually lose nitrogen and the carbene (the electrophile) formed thereby adds to the C=C double bond; the main reaction product is then a substituted cyclopropane. For example, the diazofluorene complexes $(Bu^tNC)_2M(N_2Fld)$ **5** (M = Ni, Pd) react in this way. The reactions of these complexes with dialkyl maleate afforded a mixture of the *cis*- and *trans*-isomers of the cyclopropane derivative produced thereby.[14]

Another type of reaction involves the interaction of the diphenyldiazomethane complexes of iridium and rhodium **8**, in which the diazoalkane ligand is displaced.[29,37]

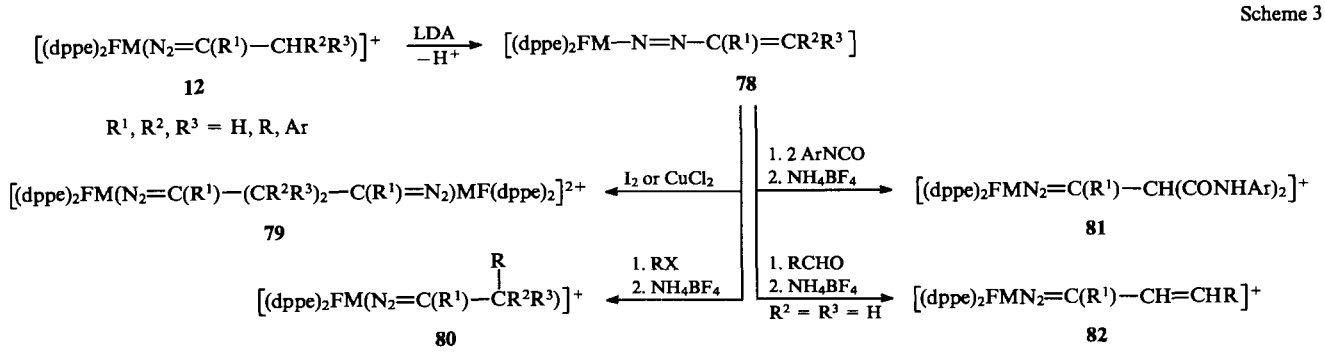


M = Ir; X = Me.
M = Ph; X = Cl.

The replacement of the diazoalkane ligand by another one has been described also in the reaction of $[Rh_2(\mu\text{-}N_2CRCO_2Et).(CO)_2(dppm)_2]$ (R = H, CO_2Et) with CO.[76]

Numerous exchange reactions of other ligands (not diazoalkanes) in the diazoalkane complexes of transition metals have also been described in the literature. However, the description of these reactions is outside the scope of the present review.

Scheme 3



V. Conclusion

The review presents and surveys the results of studies of the interaction of diazoalkanes with transition metal complexes and the reactions of the diazoalkane complexes obtained.

The results of these reactions are varied — both as regards the class of ligands formed from the diazoalkanes and as regards the type of coordination of the latter. The structure of the product depends both on the nature of the transition metal and its valence state and on the nature of the diazoalkane itself.

The interaction of a diazoalkane with a transition metal complex is usually accompanied either by the addition or insertion of the diazoalkane itself or of the carbene formed from it.

Apart from the principal structural parameters of the MN_2C fragment, the diazo-complexes have been characterised by their chemical behaviour — thermal reactions and interaction with various reagents. The principal differences between the structures and properties of the diazo-ligands and the free diazoalkanes have been elucidated.

However, it is essential to note that, as a consequence of the complexity and great variety of the reactions of diazoalkanes with transition metal complexes and the reactions of the products obtained, the studies in this field have been unsystematic and the results presented are not always sufficiently reliable.

The above reactions can serve as convenient methods of synthesis of valuable classes of complexes, in the first place hydrazonate, alkyldiazene, carbene, and alkyl complexes.

References

1. J Chatt, J R Dilworth, R L Richards *Chem. Rev.* **78** 589 (1978)
2. J Chatt, R L Richards *J. Organomet. Chem.* **239** 65 (1982)
3. W A Herrmann *Adv. Organomet. Chem.* **20** 159 (1982)
4. W A Herrmann *Pure Appl. Chem.* **54** 65 (1982)
5. A Albini, H Kisch *Top. Curr. Chem.* **65** 105 (1976)
6. H M Niemeyer, in *The Chemistry of the Diazonium and Diazo Groups, Pt 1* (Ed. S Patai) (New York: Wiley, 1978) p. 231
7. W A Herrmann *J. Organomet. Chem.* **250** 319 (1983)
8. D Sutton *Chem. Rev.* **93** 995 (1993)
9. S Otsuka, A Nakamura, T Koyama, Y Tatsuno *J. Chem. Soc., Chem. Commun.* 1105 (1972)
10. S Otsuka, A Nakamura, T Koyama, Y Tatsuno *Liebigs Ann. Chem.* 626 (1975)
11. K D Schramm, J A Ibers *Inorg. Chem.* **19** 2441 (1980)
12. S Gambarotta, C Floriani, A Chiesi-Villa, C Guastini *J. Am. Chem. Soc.* **104** 1918 (1982)
13. J Martin, C Moise *J. Organomet. Chem.* **193** C57 (1980)
14. A Nakamura, T Yoshida, M Cowie, S Otsuka, J A Ibers *J. Am. Chem. Soc.* **99** 2108 (1977)
15. J A Smegal, I K Meier, J Schwartz *J. Am. Chem. Soc.* **108** 1322 (1986)
16. M H Chisholm, J A Heppert, J C Huffman, C D Ontiveros *Organometallics* **8** 976 (1989)
17. G M Arvanitis, J Smegal, I Meier, A C C Wong, J Schwartz, D Van Engen *Organometallics* **8** 2717 (1989)
18. M H Chisholm, K Folting, J C Huffman, A L Ratermann *Inorg. Chem.* **23** 2303 (1984)
19. S Gambarotta, C Floriani, A Chiesi-Villa, C Guastini *J. Chem. Soc., Chem. Commun.* 1015 (1982)
20. J F Lebouf, J C Leblanc, C Moise *J. Organomet. Chem.* **364** C22 (1989)
21. G I Nikonov, M Putala, A I Zinin, N B Kazennova, D A Lemenovskii, A S Batsanov, Yu T Struchkov *J. Organomet. Chem.* **452** 87 (1993)
22. D A Lemenovskii, M Putala, G I Nikonov, N B Kazennova, D S Yufit, Yu T Struchkov *J. Organomet. Chem.* **454** 123 (1993)
23. A Nakamura, M Aotake, S Otsuka *J. Am. Chem. Soc.* **96** 3456 (1974)
24. J Clemens, M Green, F G A Stone *J. Chem. Soc., Dalton Trans.* 1620 (1973)
25. A J L Pombeiro, R L Richards *Monatsh. Chem.* **123** 749 (1992)
26. M Cowie, S J Loeb, I R McKeer *Organometallics* **5** 854 (1986)
27. K D Schramm, J A Ibers *Inorg. Chem.* **19** 1231 (1980)
28. K D Schramm, J A Ibers *Inorg. Chem.* **19** 2435 (1980)
29. L Brandt, J Wolf, H Werner *J. Organomet. Chem.* **444** 235 (1993)
30. G L Hillhouse, B L Haymore *J. Am. Chem. Soc.* **104** 1537 (1982)
31. B L Kool, M D Rausch, H G Alt, M Herberhold, A F Hill, U Thewalt, B Wolf *J. Chem. Soc., Chem. Commun.* 408 (1986)
32. H F Klein, H F Ellrich, B Hammerschmitt, U Koch, G Cordier *Z. Naturforsch., B Chem. Sci.* **45** 1291 (1990)
33. K D Schramm, J A Ibers *J. Am. Chem. Soc.* **100** 2932 (1978)
34. W A Herrmann, G Kriechbaum, M L Ziegler, P Wulknitz *Chem. Ber.* **114** 276 (1981)
35. W A Herrmann *J. Organomet. Chem.* **84** C25 (1977)
36. S Gambarotta, C Floriani, A Chiesi-Villa, C Guastini *J. Am. Chem. Soc.* **105** 7295 (1983)
37. J Wolf, L Brandt, A Fries, H Werner *Angew. Chem.* **102** 584 (1990); *Angew. Chem., Int. Ed. Engl.* **29** 590 (1990)
38. B Bogdanovic', M Kröner, W Günther *Liebigs Ann. Chem.* **699** 1 (1966)
39. E Stankovich, M Putala, G I Nikonov, D A Lemenovskii, E V Avtomonov *J. Organomet. Chem.* (1994) (in the press)
40. A Watakabe, T Takahashi, D-M Jin, I Yokotake, Y Uchida, M Hidai *J. Organomet. Chem.* **254** 75 (1983)
41. Y Mizobe, Y Uchida, M Hidai *Bull. Chem. Soc. Jpn.* **53** 1781 (1980)
42. P C Bevan, J Chatt, M Hidai, G J Leigh *J. Organomet. Chem.* **160** 165 (1978)
43. M Hidai, Y Mizobe, Y Uchida *J. Am. Chem. Soc.* **98** 7824 (1976)
44. M Hidai, Y Mizobe, M Sato, T Kodama, Y Uchida *J. Am. Chem. Soc.* **100** 5740 (1978)
45. Y Mizobe, R Ono, Y Uchida, M Hidai, M Tezuka, S Mone, A Tsuchiya *J. Organomet. Chem.* **204** 377 (1981)
46. R Ben-Shoshan, J Chatt, G J Leigh, W Hussain *J. Chem. Soc., Dalton Trans.* 771 (1980)
47. R Ben-Shoshan, J Chatt, W Hussain, G J Leigh *J. Organomet. Chem.* **112** C9 (1976)
48. R A Head, P B Hitchcock *J. Chem. Soc., Dalton Trans.* 1150 (1980)
49. J Chatt, P C Bevan, R A Head, P B Hitchcock, G J Leigh *J. Chem. Soc., Chem. Commun.* 509 (1976)
50. P C Bevan, J Chatt, A A Diamantis, R A Head, G A Heath, G J Leigh *J. Chem. Soc., Dalton Trans.* 1711 (1977)
51. M H Chisholm, K Folting, J C Huffman, A L Ratermann *J. Chem. Soc., Chem. Commun.* 1229 (1981)
52. M D Curtis, L Messerle *Organometallics* **6** 1713 (1987)
53. L Messerle, M D Curtis *J. Am. Chem. Soc.* **104** 889 (1982)
54. K Weidenhammer, M L Ziegler *Z. Anorg. Allg. Chem.* **457** 174 (1979)
55. I A Latham, G J Leigh, G Huttner, I Jibril *J. Chem. Soc., Dalton Trans.* 385 (1986)
56. T Aoshima, A Tamura, Y Mizobe, M Hidai *J. Organomet. Chem.* **435** 85 (1992)
57. J Chatt, R A Head, P B Hitchcock, W Hussain, G J Leigh *J. Organomet. Chem.* **133** C1 (1977)
58. M Hidai, K Komori, T Kodoma, D-M Jin, T Takahashi, S Sugiura, Y Uchida, Y Mizobe *J. Organomet. Chem.* **272** 155 (1984)
59. H Oshita, Y Mizobe, M Hidai *Organometallics* **11** 4116 (1992)
60. F H Allen, O Kennard, D G Watson, L Brammer, A G Orpen, R Taylor *J. Chem. Soc., Perkin Trans. 2* S1 (1987)
61. J B Moffat, in *The Chemistry of the Diazonium and Diazo Groups, Pt 1* (Ed. S Patai) (New York: Wiley, 1978) p. 1
62. S Sorriso, in *The Chemistry of the Diazonium and Diazo Groups, Pt 1* (Ed. S Patai) (New York: Wiley, 1978) p. 95
63. L K Bell, W A Herrmann, G W Kriechbaum, H Pfisterer, M L Ziegler *J. Organomet. Chem.* **240** 381 (1982)
64. J J D'Errico, L Messerle, M D Curtis *Inorg. Chem.* **22** 849 (1983)
65. M D Curtis, L Messerle, J J D'Errico, W D Butler, M S Hay *Organometallics* **5** 2283 (1986)
66. W A Herrmann, L K Bell *J. Organomet. Chem.* **239** C4 (1982)
67. W A Herrmann, L K Bell, M L Ziegler, H Pfisterer, C Pahl. *J. Organomet. Chem.* **247** 39 (1983)
68. L Messerle, M D Curtis *J. Am. Chem. Soc.* **102** 7789 (1980)
69. W A Herrmann, G W Kriechbaum, M L Ziegler, H Pfisterer *Angew. Chem.* **94** 713 (1982)
70. A D Clauss, J R Shapley, S R Wilson *J. Am. Chem. Soc.* **103** 7387 (1981)
71. W A Herrmann, B Menjón, E Herdtweck *Organometallics* **10** 2134 (1991)

72. D Nucciarone, N J Taylor, A J Carty *Organometallics* **5** 2565 (1986)
73. G I Nikonov, M Putala, G P Brusova, N B Kazennova, D A Lemenovskii *Izv. Akad. Nauk, Ser. Khim.* (1994) (in the press)
74. M Putala, D A Lemenovskii, unpublished results
75. W A Herrmann, I Schweizer *Z. Naturforsch., B Chem. Sci.* **33** 911 (1978)
76. C Woodcock, R Eisenberg *Organometallics* **4** 4 (1985)
77. G M Arvanitis, J Schwartz, D Van Engen *Organometallics* **5** 2157 (1986)
78. D L Hughes, I A Latham, G J Leigh *J. Chem. Soc., Dalton Trans.* 393 (1986)
79. P J Walsh, M J Carney, R G Bergman *J. Am. Chem. Soc.* **113** 6343 (1991)
80. M M Bagga, P E Baikie, O S Mills, P L Pauson *J. Chem. Soc., Chem. Commun.* 1106 (1967)
81. W A Herrmann, G Ihl *J. Organomet. Chem.* **251** C1 (1983)
82. R Serrano, J C Flores, P Royo, M Mena, M A Pellinghelli, A Tiripicchio *Organometallics* **8** 1404 (1989)
83. S Gambarotta, M Basso-Bert, A Chiesi-Villa, C Guastini *J. Chem. Soc., Chem. Commun.* 374 (1982)
84. S Gambarotta, C Floriani, A Chiesi-Villa, C Guastini *Inorg. Chem.* **22** 2029 (1983)
85. E V Avtomonov, D A Lemenovskii, unpublished results
86. E Hey, F Weller *Chem. Ber.* **121** 1207 (1988)
87. G A Vaughan, G L Hillhouse, A L Rheingold *J. Am. Chem. Soc.* **112** 7994 (1990)
88. M R Churchill, H J Wasserman *Inorg. Chem.* **20** 2905 (1981)
89. K Burgess, B F G Johnson, J Lewis, P R Raithby *J. Chem. Soc., Dalton Trans.* 263 (1982)
90. T Jenke, H Stoeckli-Evans, G Süs-Fink *J. Organomet. Chem.* **391** 395 (1990)
91. T Jenke, U Bodensieck, H Stoeckli-Evans, G Süs-Fink *J. Organomet. Chem.* **414** C28 (1991)
92. M L McKee *J. Am. Chem. Soc.* **112** 7957 (1990)
93. M L Lappert, J S Poland *J. Chem. Soc., Chem. Commun.* 1061 (1969)
94. W A Herrmann *Angew. Chem.* **87** 358 (1975); *Angew. Chem., Int. Ed. Engl.* **14** 355 (1975)
95. W A Herrmann, H Biersack *Chem. Ber.* **110** 896 (1977)
96. G L Hillhouse, B L Haymore, W A Herrmann *Inorg. Chem.* **18** 2423 (1979)
97. W A Herrmann, M L Ziegler, K Weidenhammer *Angew. Chem.* **88** 379 (1976)
98. W A Herrmann, H Biersack, K K Mayer, B Reiter *Chem. Ber.* **113** 2655 (1980)
99. W A Herrmann, M L Ziegler, K Weidenhammer, H Biersack, K K Mayer, R D Minard *Angew. Chem.* **88** 191 (1976); *Angew. Chem., Int. Ed. Engl.* **15** 164 (1976)
100. D Nuel, F Dahan, R Mathieu *Organometallics* **5** 1278 (1986)
101. J Clemens, R E Davis, M Green, J D Oliver, F G A Stone *J. Chem. Soc., Chem. Commun.* 1095 (1971)
102. J Clemens, M Green, F G A Stone *J. Chem. Soc., Dalton Trans.* 93 (1974)
103. J Formiés, B Menjón, N Gómez, M Tomás *Organometallics* **11** 1187 (1992)
104. M A Gallop, C E F Rickard, W R Roper *J. Organomet. Chem.* **395** 333 (1990)
105. P Espinet, E Lalinde, M Marcos, J Perez, J L Serrano *Organometallics* **9** 555 (1990)
106. I N Busygina, T A Stromnova, S B Katser, A S Antsyshkina, M A Porai-Koshits, S G Sakharov, I I Moiseev *Metalloorg. Khim.* **3** 312 (1990)
107. M A Gallop, C E F Rickard, W R Roper *J. Organomet. Chem.* **269** C21 (1984)
108. I A Tikhonova, V B Shur, M E Vol'pin *Izv. Akad. Nauk SSSR, Ser. Khim.* **25** 229 (1976)
109. M Schöllkopf, N Rieber *Chem. Ber.* **102** 488 (1969)
110. J Lorberth *J. Organomet. Chem.* **27** 303 (1971)
111. J Lorberth, F Schmock, G Lange *J. Organomet. Chem.* **54** 23 (1973)
112. S-I Murahashi, Y Kitani, T Hosokawa *J. Chem. Soc., Chem. Commun.* 450 (1979)
113. S I Murahashi, Y Kitani, T Uno, T Hosokawa, K Miki, T Yonezava, N Kasai *Organometallics* **5** 356 (1986)
114. M J Menu, P Desrosiers, M Dartiguenave, Y Dartiguenave *Organometallics* **6** 1822 (1987)
115. M J Menu, G Crocco, M Dartiguenave, Y Dartiguenave *Organometallics* **7** 2231 (1988)
116. H Siebald, M Dartiguenave, Y Dartiguenave *J. Organomet. Chem.* **438** 83 (1992)
117. A F Hill, W R Roper, J Waters, A H Wright *J. Am. Chem. Soc.* **105** 5939 (1983)
118. W A Herrmann, J Plank, G W Kriechbaum, M L Ziegler, H Pfisterer, J L Atwood, R D Rogers *J. Organomet. Chem.* **264** 327 (1984)
119. W Kalcher, W A Herrmann, C Pahl, M L Ziegler *Chem. Ber.* **117** 69 (1984)
120. W A Herrmann, C Weber, M L Ziegler, C Pahl *Chem. Ber.* **117** 875 (1984)
121. W A Herrmann, G W Kriechbaum, C Bauer, B Konmbours, H Pfisterer, E Guggolz, M L Ziegler *J. Organomet. Chem.* **262** 89 (1984)
122. W A Herrmann, C Bauer, J M Huggins, H Pfisterer, M L Ziegler *J. Organomet. Chem.* **258** 81 (1983)
123. W A Herrmann, M Flöel, C Weber, J L Hubbard, A Schäfer. *J. Organomet. Chem.* **286** 369 (1985)
124. W A Herrmann, C Weber, M L Ziegler, O Serhadli *J. Organomet. Chem.* **297** 245 (1985)
125. M J Chetcutti, B E Grant, P E Fanwick *Organometallics* **9** 1345 (1990)
126. W A Herrmann, G W Kriechbaum, C Bauer, E Guggolz *Angew. Chem.* **93** 838 (1975); *Angew. Chem., Int. Ed. Engl.* **20** 815 (1975)
127. W A Herrmann, J M Huggins, B Reiter, C Bauer *J. Organomet. Chem.* **214** C19 (1981)
128. A A Kazi, A A Frew, B R Lloyd, L Manojlovic'-Muir, K W Muir, R J Puddephatt *J. Chem. Soc., Chem. Commun.* 614 (1982)
129. J R Shapley, A C Sievert *J. Am. Chem. Soc.* **103** 6975 (1981)
130. I N Busygina, T Stromova, D I Kochubei, M Ya Botnikov, I I Moiseev *Metalloorg. Khim.* **4** 69 (1991)
131. W Ando, in *The Chemistry of the Diazonium and Diazo Groups, Pt 1* (Ed. S Patai) (New York: Wiley, 1978) p. 366
132. J Cooke, W R Cullen, M Green, F G A Stone *J. Chem. Soc., Chem. Commun.* 170 (1968)
133. J Cooke, W R Cullen, M Green, F G A Stone *J. Chem. Soc., A* 1872 (1969)
134. F D Mango, I Dvoretzky *J. Am. Chem. Soc.* **88** 1654 (1966)
135. R C Brady, R Pettit *J. Am. Chem. Soc.* **102** 6181 (1980)
136. S M Breckenridge, S A McLaughlin, N J Taylor, A J Carty *J. Chem. Soc., Chem. Commun.* 1718 (1991)
137. D Nucciarone, N J Taylor, A J Carty *Organometallics* **3** 177 (1984)
138. M Sakurada, M Kajitani, K Dokhi, T Akiyama, A Sugimori *J. Organomet. Chem.* **423** 141 (1992)
139. L S Hegedus *J. Organomet. Chem.* **422** 301 (1992)
140. E A Shapiro, A B Dyatkin, O M Nefedov *Usp. Khim.* **62** 485 (1993) [*Russ. Chem. Rev.* **62** 447 (1993)]
141. M Cowie, I R McKeer, S J Loeb, M D Gauthier *Organometallics* **5** 860 (1986)
142. J M Arvanitis, J Schwartz *Organometallics* **6** 421 (1987)
143. A F Hegarty, in *The Chemistry of the Diazonium and Diazo Groups, Pt 1* (Ed. S Patai) (New York: Wiley, 1978) p. 571
144. F N N Carvalho, A J L Pombeiro, O Orama, U Schubert, C J Pickett, R L Richards *J. Organomet. Chem.* **240** C18 (1982)
145. Y Ishii, H Miyagi, S Jitsukuni, H Seino, B S Harkness, M J Hidai *J. Am. Chem. Soc.* **114** 9890 (1992)

Russian Chemical Reviews **63** (3) 217–230 (1994)
©1994 Russian Academy of Sciences and Turpion Ltd

UDC 541.182+541.18.046+539.196.3

Steric stabilisation of liquid films by adsorption layers of macromolecules

V G Babak

Contents

I. Introduction	228
II. Theories of the steric stabilisation of liquid films	228
III. Experimental study of the interaction between adsorption layers of polymers	235
IV. Conclusions	240

Abstract. Modern theories of the steric stabilisation of dispersions containing polymers and experimental results of studies of the interaction between adsorption layers of polymers in microscopic liquid films are critically reviewed. The bibliography includes 109 references.

I. Introduction

Polymeric adsorption layers (AL) formed on the surface of particles of a dispersed phase in disperse systems containing polymers control the stability and the structural and mechanical properties of these systems.

Adsorption layers have thicknesses of the order of the size of the macromolecules in the bulk of the solution (a few nanometres). They hinder the approach to the surfaces of particles, and they limit it to the distances at which the forces of intermolecular attraction (van der Waals) lead to an irreversible thinning of the microscopic liquid films (MLF) formed in the contact region between the particles, i.e. to the coagulation or coalescence of the particles.

Thus, since the energy of molecular interaction of the interfaces in disperse systems containing a polymer becomes negligibly small owing to the relatively large thickness of the MLF, and furthermore since the ionic–electrostatic interaction between the electric double layers vanishes at high enough electrolyte concentrations in the system, the main contribution to the energetics of the contact interactions in these systems is provided by the interaction between the AL of macromolecules and by the energy properties of these AL.

The interaction between polymeric AL takes place when the segments of macromolecules are in direct ('steric') contact, and is determined by short-range forces such as hydrogen bonds, hydrophobic interaction, and Born repulsion, and also by the Coulomb interaction between the ionised functional groups in the case of polyelectrolytes and (to a smaller extent) by the molecular forces between the macromolecules themselves in the adsorption layers.

If the energy of the steric interaction between two AL in a liquid film is small (for example, a few kT, where k is Boltzmann's constant and T is the absolute temperature) the disperse system becomes stable by aggregation. In this case the stabilisation of the disperse system is said to be steric.[1,2] Detailed reviews of the theory and of the experimental foundations of the steric stabilisation in these systems have been published.[3–7]

The aim of the present review is to analyse theoretical and experimental studies of the interaction between adsorption layers of macromolecules in microscopic liquid films whilst allowing for nonequilibrium effects in the thermodynamic description of the steric stabilisation of dispersions.

II. Theories of the steric stabilisation of liquid films

Some procedural difficulties are met in the thermodynamic description of the steric interaction between adsorption layers of macromolecules in microscopic liquid films.

One of the problems is the lack of an unambiguous definition of the specific interfacial free energy (interfacial tension) of the phase boundary in the presence of a polymeric adsorption layer whose thickness usually exceeds the radius of action of the molecular forces. In the modern theories of the adsorption of polymers and of interacting adsorption layers of polymers in liquid films[11–23] the interfacial tension σ is expressed as the sum of two components,

$$\sigma = \sigma_s(\varphi_s) + I(\varphi_s, \varphi_b), \quad (1)$$

where φ_b and φ_s are the densities of the polymer in the bulk of the solution and at the contact with the interfacial surface respectively.

The $\sigma_s(\varphi_s)$ component allows for the interfacial tension at distances of the order of the molecular size, and is often expressed as[18,24]

$$\sigma_s(\varphi_s) = \sigma_{s0} + \sigma_1\varphi_s + \sigma_2\varphi_s^2 + \ldots, \quad (2)$$

where σ_1 and σ_2 are the virial coefficients of the expansion, which allow for the interaction between the monomers and the surface, and also between the segments of the macromolecules in the adsorption layer closest to the surface.

The component $I(\varphi_s, \varphi_b)$ describes the contribution to the surface tension of effects associated with a change in the density profile $\varphi(z)$ of the segments close to the interfacial surface. Thus, in order to describe the thermodynamic properties of interfaces (and, even more, their interactions in liquid films) we require information on the density profile of the segments $[\varphi(z)]$ in the adsorption layer, which is a new element, not previously

V G Babak Department of Physical and Colloid Chemistry, Moscow State Correspondence Institute of the Food Industry, 109803 Moscow, Zemlyanoi val 73, Fax (7-095) 292 65 11

Received 21 December 1993
Uspekhi Khimii **63** (3) 228–242 (1994); translated by J I Carasso

considered in the thermodynamics of interfaces and films stabilised by low-molecular surface-active substances (SAS).[25,26]

Hence we should expect the properties of interfaces in liquid films stabilised by polymers to depend on factors such as the molecular mass, the degree of ionisation of the macroions, the hydrophilic–lipophilic balance (HLB) of the molecules, the rigidity of the macromolecular network, and also on the physicochemical factors (pH and ionic strength of the solution, bulk concentration of the polymers, temperature, nature of the solvent, etc.) which affect both the energy of the intermolecular interactions and the conformation of the macromolecules in the adsorption layer.

We should note that tensometry (the main experimental method of determining the energy properties of interfaces stabilised by low-molecular SAS) can no longer characterise unambiguously the energy properties of interfaces when these are stabilised by polymeric AL. Indeed, the measured values of the interfacial tension do not allow for or include the interaction between the segments of the macromolecules in the AL separated from the physical interface by a distance greater than the action radius of the molecular forces. This problem is not found in the measurements of interfacial tension of surfaces stabilised by low-molecular SAS, because the molecules of these SAS are localised within the force field of the interface.

Another problem in the thermodynamic description of liquid films stabilised by polymeric adsorbed layers arises from the indefiniteness of the concept of thermodynamic equilibrium in a system of interacting adsorption layers of macromolecules when interfacial surfaces are brought closer together in a solution of the polymer.

Whereas in the adsorption of low-molecular SAS the equilibrium between the bulk concentration and the concentration in the film is established rapidly, at the contact of adsorption layers of high-molecular SAS the 'true' equilibrium may never be reached (at least, under the conditions of the experiment). de Gennes[19] understood the problem, and suggested that the steric interaction should be calculated for two extreme cases: (1) ideal equilibrium, corresponding to the possibility of reversible adsorption of the macromolecules during the interaction of polymeric adsorption layers, and (2) a limited equilibrium, corresponding to a condition of constant adsorption, reached when the two AL are placed in contact and unchanged thereafter.

However, as will be shown below, the conclusions of the theory of the aggregation stability of a disperse system are strongly influenced by the subjective choice of a hypothesis concerning the type of equilibrium. As was pointed out by de Gennes,[19] with a thermodynamically good solvent, and assuming ideal equilbrium, we must conclude that an attraction exists between polymeric AL, whereas under conditions of limited equilibrium, mutual repulsion between the layers becomes possible. Thus we are faced with the problem of defining and assigning the type of equilibrium in the interaction of AL of macromolecules.

This problem is closely associated with that of determining the extent of the mutual penetration of the AL, when the film thickness is increased, in order to calculate the relative contribution of the entropic and the osmotic effect to the total free energy of interaction of the polymeric AL. This problem could not be solved by using the 'early' theories of the interaction of adsorption layers of macromolecules, such as the Hesselink–Vrij–Overbeek (HVO) theory,[27] because the solution requires a knowledge of the exact form of the density distribution function of the segments of the macromolecule with respect to the distance to the interfacial surface.

At present the most widely used approaches to the construction of a thermodynamic theory of adsorption and of the interaction between adsorption layers of polymers are those developed by Scheutjens and Fleer,[11–17] de Gennes,[18,19] and Klein and coworkers.[20–23]

1. The Scheutjens–Fleer theory

The statistical theory of the adsorption of polymer proposed by Scheutjens and Fleer allows for the effect on the structure of the polymeric AL of interactions between the segments of polymeric molecules and also for those of the interactions between the macromolecules, the solvent molecules, and the interfacial surface. The physical basis of this theory is the postulate that under equilibrium conditions (assuming that the adsorption of polymers is reversible under equilibrium conditions) [17] the conformation of the adsorbed macromolecule is unambiguously determined by the energy of the interaction between the segments of the macromolecules χ and between a macromolecule and the surface χ_s, and also by the length (degree of polymerisation) of the molecule N.

The special feature of this approach is that its authors exploit the concept of the conformational probability of the macromolecule p_c, which is determined in the framework of the quasi-crystalline lattice model by the distribution of segments over the layers of the lattice, by the orientation in space of the bonds between the segments, and by the parameters χ and χ_s (Fig. 1).

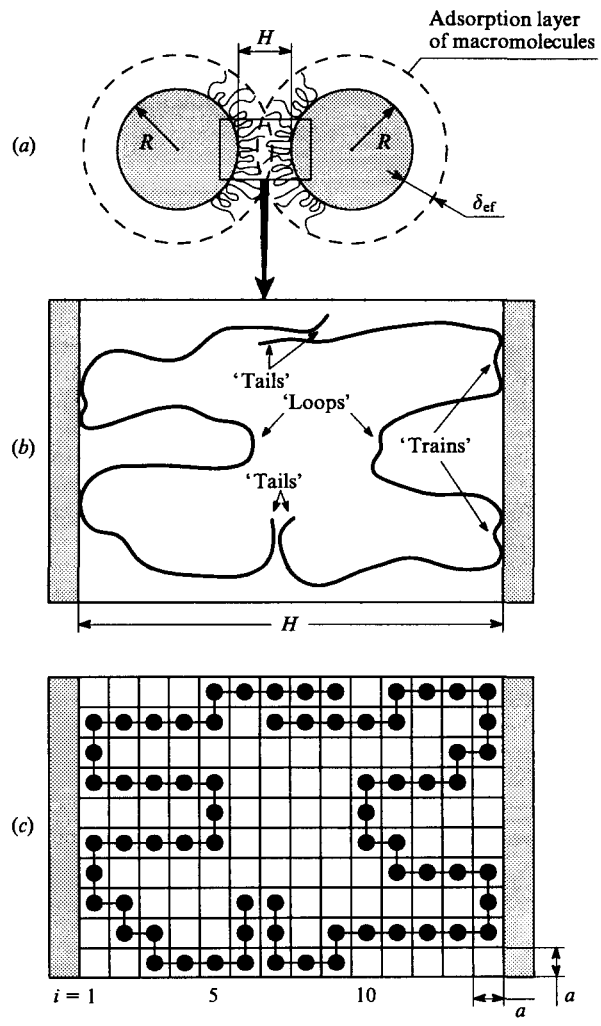


Figure 1. Calculation of the energy of the interaction between adsorption layers of macromolecules in a liquid film. (*a*) Contact of two particles of the disperse phase, of radius R, coated with adsorption layers of the polymer having an effective thickness δ_{ef}; direct steric contact between the two AL takes place in the gap thickness H within the liquid microscopic film; (*b*) the conformation of the interacting adsorbed macromolecules is characterised by 'tails', 'loops', and 'trains'; (*c*) schematic representation of interacting macromolecular chains between two planes in the lattice model used by Scheutjens and Fleer.[13,14]

Assuming that all the states of a segment in a layer of the lattice parallel to the surface are energetically equivalent the authors determined the density profile $\varphi_i = \varphi(z)$ of the segments of the AL in the ith layer of the lattice ($i \approx z/a$, where a is the lattice constant) as the mean probability (weighted over all the conformational states of the macromolecule) of finding the segment in the ith layer of the lattice, i.e.

$$\varphi_i = \varphi_b \sum_c r_{i,c} p_c , \tag{3}$$

where φ_b is the density of the segments in the bulk of the solution and $r_{i,c}$ is the number of segments in the ith layer of the lattice for the given conformation c. The conformational probability p_c of the macromolecule, characterised by the number of segments r_i in the ith lattice layer ($\Sigma r_i = r$), is expressed as

$$p_c = \lambda_0^q \lambda_1^{r-1-q} \sum_{i=1} p_i^{r_i} , \tag{4}$$

where λ_0 is the relative coordination number of the cell in a layer parallel to the surface ($\lambda_0 = 2/3$ for a cubic lattice), λ_1 is the relative coordination number of the cell in contact with the neighbouring layers ($\lambda_1 = 1/6$ for a cubic lattice), q and $(r - 1 - q)$ are the numbers of steps parallel and perpendicular to the surface, and p_i is a weighting factor determined by the configurational entropy and by the parameters χ and χ_s (expressed in units of kT), so that

$$p_i = \frac{\varphi_i^0}{\varphi_b^0} \left\{ \exp\left[-2\chi \left(\langle \varphi_i^0 \rangle - \langle \varphi_b^0 \rangle \right) \right] \right\} \exp(\chi_s - \lambda_1 \chi) \delta_{i,1} , \tag{5}$$

where

$$\langle \varphi_i^0 \rangle = \lambda_i \varphi_{i-1}^0 + \lambda_0 \varphi_i^0 + \lambda_1 \varphi_{i+1}^0 , \tag{6}$$

φ_i^0 is the density of solvent molecules in the ith layer, φ_b^0 is the same density in the equilibrium solution, and $\delta_{i,1}$ is the Kronecker delta function ($\delta_{i,1} = 1$, if $i = 1$; $\delta_{i,1} = 0$, if $i \neq 1$).

A matrix formalism was developed[28] to solve the system of equations (3) and (4): it was based on a calculation of the density profile $\varphi(z)$ of the segments in the vicinity of the surface for noninteracting segments, i.e. when $p_i = 1$ for $i > 1$ and $p_1 = \exp \chi$. In Scheutjens and Fleer's modified matrix formalism[13,14] allowance is made for the effect of interactions between the polymer and the solvent by including in p_i the parameter χ [see Eqn (5)], thus allowing the density profile $\varphi(z)$ of the segments to be calculated as a function of the thermodynamic quality of the solvent.

The new theory offers an additional advantage: it allows the individual contributions to the overall density of the layers of polymer near the interface from its various components to be calculated, i.e. it expresses the density of segments in the form

$$\varphi(z) = \varphi_f + \varphi_t + \varphi_l + \varphi_{tr} ,$$

where φ_f, φ_t, φ_l, and φ_{tr} are the densities of free (nonadsorbed) macromolecules, and the densities of 'tails', 'loops', and 'trains' respectively. This is achieved by introducing a formal calculation procedure which involves using a new method of calculating the probability p_c in Eqn (3):[29-31]

$$\sum_c r_{i,c} p_c = \frac{1}{r p_i} \sum_{s=1}^{r} p(i,s)\, p(i, r - s + 1) , \tag{7}$$

where p_i is given by Eqn (5); $p(i,s)$ and $p(i, r-s+1)$ are the probabilities of finding the sth segment in the ith layer, and the first and subsequent segments of the macrochain occupy all the positions allowed for the given conformation of the macromolecule. Then all the conformations for which neither both chain ends nor one of the intermediate segments are found (even once) in the first layer will correspond to a 'free' (not adsorbed) macromolecule. The corresponding contribution φ_f to the density of the segments can be allowed for by using Eqn (3). The contribution from 'tails' and 'loops' is determined by allowing for the conformations having only one or two contacts with the surface respectively.

The authors carried out numerical calculations of the density profile $\varphi(z)$ and of its components for different values of r (up to 10^4), for several values of the parameter χ (0 for an athermal solvent, 0.5 for a θ-solvent, and 0.7 for a poor solvent), and also for different values of the bulk density of the segments in solution φ_b (Fig. 2). The authors also considered the case of adsorbed ($\chi_s = 1$) and nonadsorbed ($\chi_s = 0$) polymers.

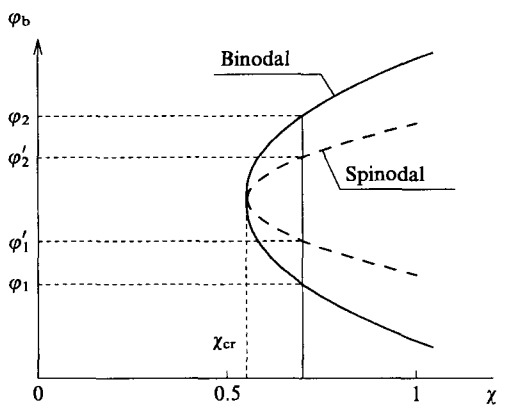


Figure 2. Phase diagram $\varphi_b(\chi)$ for the polymer solution.

For an adsorbable polymer at low coverages φ_s of the surface by adsorbate in a good solvent the proposed theory predicts a 'prone' conformation of the macromolecules on the surfaces, and a density profile $\varphi(z)$ decreasing exponentially with increasing distance from the surface, as expected from the early theories of adsorption known as the 'isolated chain' theories.[32-37] For finite values of φ_b (even quite small, of the order of 10^{-6}) the density profile $\varphi(z)$ takes a specific form, characterised by the presence of a fairly extensive region where the density φ_b is low (Fig. 3). In the layer nearest to the surface the density profile $\varphi(z)$ is determined mainly by the energy of

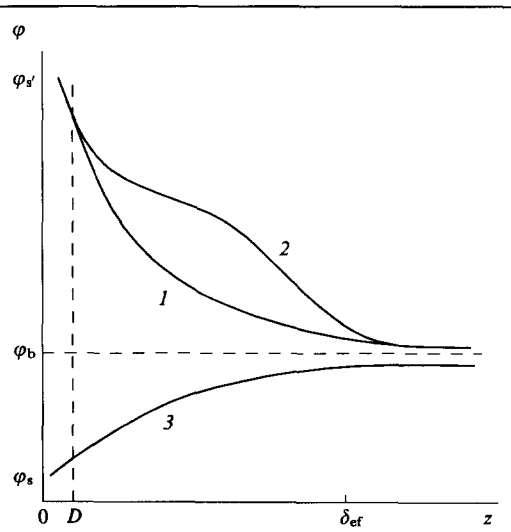


Figure 3. Density profiles of the polymer segments $\varphi(z)$ as a function of the distance to the interfacial surface in a thermodynamically good (*1*, *3*) or bad solvent (*2*) for adsorbed (*1*, *2*) and for nonadsorbed polymers (*3*).

adhesion χ_s, and as the chain length r of the macromolecule is increased the dependence on φ_b is effectively suppressed and replaced by an exponential decrease with increasing distance from the surface. In the more remote layers the density profile is determined essentially by the 'tails'. This is a new element, not considered in the 'isolated chain' theories. It was shown that the root-mean-square thickness δ_{ef} of the adsorption layer in a good solvent is proportional to $M^{0.5}$ (where M is the molecular mass of the polymer). At high adsorptions of the polymer the thickness δ_{ef} becomes comparable with the size of the macromolecular cluster in the bulk of the solution.

A calculation of the density profile of the segments for a thermodynamically poor solvent[16] is of special relevance to the attempt to reconcile the Scheutjens–Fleer theory with other theories (in particular, that of de Gennes[18]). The authors considered the cases of $\chi = 0.7$ ($r = 100$) and $\chi = 0.56$ ($r = 1000$) for $\varphi_b = 10^{-6}$. The problem was that in the transition region of the AL (i.e. in the region between the first layer, with a relatively high density, and the solution, with a relatively low density) the density corresponds to the liquid–liquid phase separation region in the Flory–Huggins diagram (see Fig. 2), i.e. $\varphi_1 < \varphi < \varphi_2$, if the parameter χ exceeds the critical χ_{cr}. For example, for the case of $\chi = 0.7$ ($\varphi_b = 10^{-4}$ and $r = 100$) the binodal concentrations are $\varphi_1 = 1.5 \times 10^{-4}$ and $\varphi_2 = 0.37$; under these conditions the spinodal concentrations are $\varphi_1' = 2.7 \times 10^{-2}$ and $\varphi_2' = 0.27$ respectively, and $\chi_{cr} = 0.605$, i.e. in the transition region of the adsorption layer the condition mentioned above ($\varphi_1 < \varphi < \varphi_2$) is realised. The authors did not observe any anomalous deviations of the density profile $\varphi(z)$ from the corresponding density profile for a thermodynamically good solvent [but we note that for the latter type of solvent the de Gennes theory predicts[20–22] the formation of a plateau in the $\varphi(z)$ profile].

In the case of a nonadsorbable polymer Scheutjens and Fleer[14] determined the density profile $\varphi(z)$ and used it to calculate the energy of the interaction between the surfaces (see Fig. 3).

The interaction energy Δg (referred to one cell of area a^2) is defined as follows in the lattice models for an 'ideal'[19] (or 'full'[13]) equilibrium:

$$\Delta g = kT\left[\left(1-\frac{1}{r}\right)\Gamma + \sum_i \ln\frac{\varphi_i^0}{\varphi_b^0} + \chi\sum_i(\varphi\langle\varphi_i\rangle - \varphi_b^2)\right], \quad (8)$$

where

$$\Gamma = \sum_i(\varphi_i - \varphi_b)$$

is the adsorption of the polymer.

In the case of a 'limited' equilibrium the expression for Δg becomes[13,19]

$$\Delta g = kT\left(\frac{\Gamma_t}{r}\ln\frac{\Gamma_t}{\sum p_c} + \sum_i \ln\varphi_i^0 + \chi\sum_i \varphi_i\langle\varphi_i\rangle\right), \quad (9)$$

where $\Gamma_t = \Sigma\,\varphi_i$.

In the present quasicrystalline lattice model the term containing the parameter χ in the expressions (8) and (9) allows for the interaction between the ith segment and its nearest neighbours. An exact determination of the density profile of the polymer and of the solvent, involving the solution of Eqns (3)–(7), allows for the entropy factor associated with the volume limitation effects.

Most of the calculations were carried out for thermodynamically 'good' solvents under conditions of 'limited' equilibrium, i.e. on the assumption that in the case of adsorbable polymers the macromolecules are not desorbed when the two surfaces come close together. In this case the energy of adsorption associated with one segment is fairly large (1 kT, which corresponds to $\chi_s = 1$). The above results lead to the following conclusions.

In an 'ideal' equilibrium we find attraction between the adsorbed layers for both good and poor solvents, and at all coverages of the surface by polymeric molecules. The authors assume[14,16] that this case is a bad representation of the real state of affairs, and they confine all further discussions to the case of a 'limited' equilibrium.

In a limited equilibrium in poor solvents the close approach of the AL produces attraction, which is replaced by repulsion as the film is additionally thinned. In good solvents attraction occurs at low coverages, but at high coverages only repulsion can be observed. It is pointed out that in the case of a good solvent the attraction is created by 'bridge formation', in which the macromolecule is adsorbed at its end segments on the surfaces of different particles. In a poor solvent a negative osmotic pressure is induced in addition to bridge formation, and leads to attraction between the particles (whereas positive osmotic pressure causes repulsion of the particles stabilised by polymeric adsorption layers).

In the theory of Scheutjens and Fleer great importance is attached to the formation of long 'tails' on the outer side of the adsorption layer at high coverages of the surface by adsorbed molecules. This feature distinguishes the theory from the early theories of steric stabilisation. In spite of the depletion of the outer part of the AL the concentration of the 'tails' is sufficient to produce repulsion when the interfacial layers in the film are brought closer together. The frequently observed film thicknesses substantially greater than double the diameter of the average cluster of macromolecules in solution are attributed to this effect.

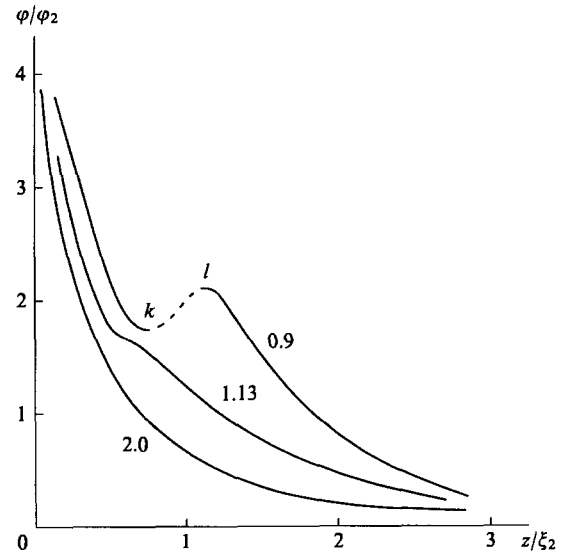


Figure 4. Density profiles of adsorbed layers of polymer in a thermodynamically poor solvent calculated by Eqn (19) for several fixed values of the parameter β^2.

As was pointed out above, in the case of nonadsorbable polymers the local concentration $\varphi(z)$ of segments close to the surface is much lower than the bulk concentration φ_b (Fig. 4). In dilute solutions this 'depletion zone' leads to the development of attraction between the surfaces. However, with a large bulk concentration of the polymer in solution the dislodgment of the macromolecules from the gap between the plates can be hindered, because when the plates are brought closer together the dislodgment should be accompanied by an increase in the free energy of the system (since the macromolecule is being transferred from a region of low bulk concentration of polymer

to a region of high concentration). This produces a coagulation barrier at distances of the order of the size of the macromolecule in solution, similar in shape to the coagulation barrier produced by the electrostatic interaction between electric double layers in the Deryagin–Landau–Overbeek theory. However, in this case the development of a barrier is associated with a decrease in the entropy of the system upon the mutual approach of the surfaces, i.e. the coagulation barrier has an entropic nature.

2. The de Gennes theory

In the theory of the adsorption of polymers proposed[18] by de Gennes the density profile $\varphi(z)$ of segments in the AL is described in terms of the average field approximation in conjunction with the ideas on the theory of polymer solutions developed by Flory and Huggins.[38] For a monodispersed polymer solution having a degree of polymerisation N, described by the Flory–Huggins model with a constant a and a coordination number λ, the free energy of the solution F_0 referred to the volume of one cell of the lattice model can be written as

$$F_0 = kT\left[\frac{\varphi}{N}\ln\varphi - \frac{1}{2}\upsilon\varphi^2 + \frac{1}{6}w\varphi^3 + \ldots\right], \tag{10}$$

where υ and w are the second and the third virial coefficient of the expansion respectively, the first term of the expansion corresponding to the usual Flory–Huggins combinatorial entropy, whereas the second and the third term characterise the interaction between the monomers in solution. The free energy of the system is expressed[39] as

$$F = F_0 + \frac{kT}{24\varphi(z)}\left[a\nabla\varphi(z)\right]^2. \tag{11}$$

The specific interfacial free energy σ is written[18]

$$\sigma = \sigma_s(\varphi_s) + \int_0^\infty \left(\frac{F}{a^3} - \mu_0\varphi + \pi_0\right)dz, \tag{12}$$

where $\sigma_s(\varphi_s)$ is the specific energy of the contact (the energy of adhesion of the first layer of the lattice to the interface), and μ_0 and π_0 are the standard values of the chemical potential and of the osmotic pressure respectively. The integrand expression is the excess of the free energy [referred to unit volume of a solution of density $\varphi(z)$] over a solution having the parameters μ_0 and π_0.

According to Cahn[24] the expression $\sigma_s(\varphi_s)$ in a dilute solution at low coverage of the interfacial surface can be written in the form of Eqn (2) with $\sigma_2 \approx 0$ (since $\varphi_s \ll 1$). Furthermore a weak link between the monomer and the surface is postulated, i.e. it is assumed that $\sigma_1 < kT/a^2$. According to de Gennes[18] this postulate is not inconsistent with the condition of positive adsorption if allowance is made for the multitude of contacts between the polymer and the surface. Thus, in spite of the smallness of the ratio $|\sigma_1|a^2/kT$ in the expression

$$p = A\exp\left[-\theta N\frac{|\sigma_1|a^2}{kT}\right] \tag{13}$$

for the distribution coefficient of the macromolecule units, the large value of N in Eqn (13) ensures a substantial adsorption. (θ is the coverage and A is the preexponential factor introduced by allowing for the increase in entropy produced by the desorption of the macromolecules).

These relationships can be analysed further by determining the density profile of the segments $\varphi(z)$ in the AL [by minimising the interfacial energy σ given by Eqn (12)].[18] The main postulate of the theory is the assumption that the profile $\varphi(z)$ is fully determined by the term $(d\varphi/dz)^2$ in the expression (11). By combining the equality $\varphi(z) = \psi^2(z)$ with expressions (2) and (11), Eqn (12) can be rewritten

$$\sigma - \sigma_{s0} = \sigma_1|\psi_s|^2 + \int_0^\infty \left[\frac{1}{2}L\left(\frac{\psi}{z}\right)^2 + G(\psi^2)\right]dz, \tag{14}$$

where ψ_s is the density of segments in contact with the surface, $L = kT/3a$, $G(\psi^2)$ is a function of the parameter ψ^2, and $\psi_s = \varphi_s^{0.5}$.

Cahn[24] published a detailed analysis of the problem of minimising the functional (14). He showed that the function of state ψ obeys a linear second-order differential equation whose first integral is

$$\frac{1}{2}L\left(\frac{d\psi}{dz}\right)^2 = G(|\psi|^2) - G(|\psi_b|^2), \tag{15}$$

where $\psi_b = \varphi_b^{0.5}$ corresponds to the density of segments in the solution.

The boundary condition on the surface is found by minimising the functional (14), with $\psi = \psi_s$ for $z \to 0$ (see Cahn[24]):

$$2\sigma_s|\psi_s| - L\frac{d\psi}{dz}\bigg|_0 = 0. \tag{16}$$

Expressing (16) as

$$\frac{1}{\psi}\frac{d\psi}{dz}\bigg|_0 = 2\frac{\sigma_1}{L} = \frac{1}{D},$$

we obtain (allowing for $L = kT/3a$)

$$D = \frac{kT}{6a\sigma_1}. \tag{17}$$

Here D is the characteristic thickness of the AL near the surface, where the interaction between the monomer and the wall is substantial.

According to de Gennes's theory of adsorption[18] the structure of the adsorption layer is defined by three regions (see Fig. 3): (1) a near region of thickness D [see Eqn (17)] inversely proportional to the energy of the monomer–surface interaction σ_1; (2) an intermediate region $D < z < \zeta_b$, where the upper limit is the correlation length for the polymer solution; (3) a far region $z > \zeta_b$, in which the density of segments $\varphi(z)$ tends exponentially towards φ_b.

It has been shown[39] that $\zeta_b = a\varphi^{-3/4}$, $\mu_b \sim kT\varphi^{5/4}$, and $\pi_b \sim kTa^{-3}\varphi^{3/4}$. Furthermore, for good solvents in the intermediate region we can write[18]

$$\varphi(z) = \left(\frac{a}{z}\right)^{4/3}.$$

Since the main contribution to $\varphi(z)$ is provided by the 'loops' the effective thickness δ_{ef} of the adsorption layer can be significantly greater than D, and it can approach the thermodynamic radius R_F of the statistical macromolecular cluster. This latter feature is of special interest because it can be checked experimentally. Equally interesting is the expression obtained[18] for the adsorption of the polymer:

$$\Gamma \sim a^{-2}\left(\frac{a}{D}\right)^{1/3},$$

according to which Γ is independent of the degree of polymerisation, i.e. of the molecular mass of the polymer.

The concepts of the de Gennes theory, which had been developed for a good solvent, were extended to thermodynamically poor solvents by Klein et al.[20,22] On the assumption of monomolecular adsorption they determined the profile $\varphi(z)$ of

the adsorption layer of macromolecules by minimising the functional (14) while allowing for the negative sign of the second virial coefficient in Eqn (10).

These authors postulated a small ($\sigma_1 a^2/kT \ll 1$) and irreversible adsorption [$N \gg 1$, see Eqn (13)]. As a result of the adsorption the local concentration of the polymer in the AL exceeds its bulk value in the solution, and it can also exceed the value φ_1 corresponding to the metastable concentration of the polymer on the Flory–Huggins phase diagram (see Fig. 2), and therefore the profile $\varphi(z)$ in the transition region should differ from the profile obtained by de Gennes [18] for a good solvent. In their calculations the authors assumed that the binodal curves (determined from the condition of equality of the chemical potentials in the different phases) and the spinodal curves [determined from the condition of zero osmotic compressibility $a^{-3}\varphi(\partial^2 F/\partial\varphi^2) = 0$] are indistinguishable, and they used the phase curve (spinodal) equation

$$\upsilon(\varphi) = \frac{1}{N\varphi} + w\varphi \,. \tag{18}$$

The region $\varphi_1 < \varphi < \varphi_2$, which includes dilute and semidilute states of the solution, corresponds to phase separation of the system (see Fig. 2). From this standpoint the critical concentration φ_{cr} is given (in terms of N and w) by the expression

$$\varphi_{cr} = (Nw)^{-0.5} \,,$$

where the critical temperature T_{cr} exceeds the temperature of the given state of the system. By using the correlation length $\zeta = a(3\upsilon\varphi/2)^{-0.5}$ (see Klein and coworkers [21,23]), or $\zeta = a\varphi^{0.75}$ (see Babak [7]), and also the new coordinates $y = (\varphi/\varphi_2)^{0.5}$ and $x = z/\zeta_2$, we can minimise the functional σ in Eqn (14) and obtain the expression

$$\left(\frac{dy}{dx}\right)^2 = \alpha y^6 - \gamma y^4 + \beta^2 y^2 + b \,. \tag{19}$$

Here $\alpha = 1$ (Refs 18 and 20) or $\alpha = w\varphi_2^{0.5}$ (Ref. 7), $\gamma = 2$ (Refs 21 and 23) or $\gamma = 3\upsilon/\varphi_2^{0.5}$ (Ref. 7), $\beta^2 \simeq 2\gamma(\ln\varphi_b)/(\ln\varphi_1)$, b is a constant adjustable parameter [chosen by using the condition $y \to y_s \gg 1$ for $x \to 0$, where $y_s = (\varphi_s/\varphi_2)^{0.5}$].

By using the numerical values $\varphi_1 \simeq 2 \times 10^{-4}$ and $\varphi_2 \simeq 0.2$, reported by Klein,[40–42] and also $w \simeq 0.2$ and $\upsilon = w\varphi_2 \simeq 0.04$, and $\gamma \simeq 0.3$, it is easy to prove [7] the existence of a critical value of the parameter β_{cr}^2 [$\beta_{cr}^2 = 1.125$ for the numerical values used above, below which Eqn (19) has no real solution]. For $\beta_{cr} > \beta$ the calculated density profiles tend to become S-shaped when β decreases (Fig. 4). For $\beta = \beta_{cr}$ the $\varphi(z)$ curve has a point where $d\varphi/dz = 0$. For $\beta < \beta_{cr}$ we find a region (the part of the curve between the points k and l) for which Eqn (19) has no real solution. This region can be interpreted as a region of 'condensation' of the polymeric molecules,[7] where the molecules are spontaneously densified from a thickness z_l to z_k. If this interpretation is legitimate we may conclude that in a poor solvent a bulk concentration $\varphi_{cr\,b}$ can be defined above which direct 'condensation' of the macromolecules can take place, producing a continuous increase in the adsorption of the polymer with time.

The critical value of the bulk concentration of the polymer $\varphi_{cr\,b}$, corresponding to the instability region of the AL, is related to the concentrations φ_1 by the expression [40]

$$\varphi_{cr\,b} \simeq \varphi_1^{\upsilon} \,,$$

where $\upsilon \simeq \beta_{cr}^2/2\gamma$. It follows that at polymer concentrations above $\varphi_{cr\,b} \approx 10^{-7}$ multimolecular adsorption can be expected. Thus, in real system there is no equilibrium between the AL and the solution in the case of poor solvents, though phase separation in the bulk may not take place if $\varphi_b < \varphi_1$.

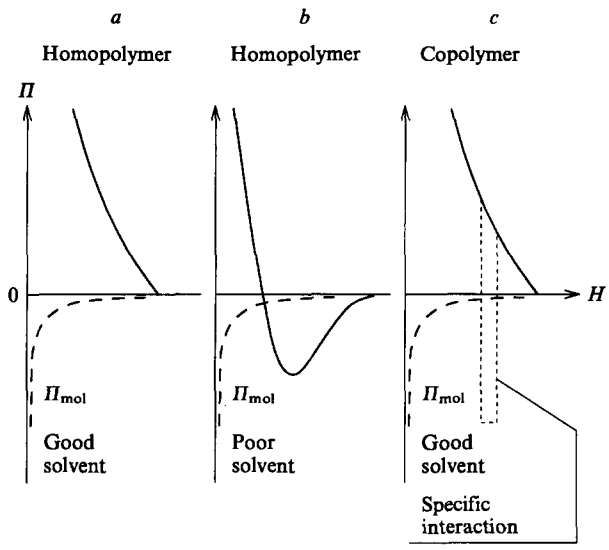


Figure 5. $\Pi(H)$ disjoining pressure isotherms for a plane-parallel liquid film stabilised by adsorption layers of a homopolymer in a good (*a*) and in a poor solvent (*b*), and for a copolymer in a good solvent (*c*).

de Gennes [19] studied the contact between two parallel surfaces in a solution of a polymer in a good solvent and determined the dependence of the disjoining pressure $\Pi(H)$ on the width of the gap (H) between the plates. To this end he used Eqn (14), and expressed its first integral as

$$\frac{1}{2}L\left(\frac{\partial\psi}{\partial z}\right) = G(|\psi|^2) - \tilde{G}(|\psi_{H/2}|^2) \,, \tag{20}$$

where $\tilde{G}(|\psi_{H/2}|^2)$ is an integration constant chosen from the condition $d\psi/dz|_{H/2} = 0$. By using the boundary condition (16) he determined unambiguously the distribution function of the equilibrium profile $\varphi(z)$, and also the function $\sigma(z)$, from which the disjoining pressure was calculated;

$$\Pi = -\frac{\partial\sigma}{\partial z} \,.$$

The main conclusions of the theory of de Gennes [19] relating to thermodynamically good solvents can be formulated as follows: (1) in the case of an 'ideal' equilibrium (i.e. when the adsorption is reversible) a force of attraction is observed beween the surfaces; (2) in the case of a 'limited' equilibrium (i.e. for a constant adsorption of the polymer) a force of repulsion between the surfaces is observed for all values of the distance H. Thus, in relation to these topics the conclusions of the theories of de Gennes [19] and of Scheutjens and Fleer [13,14] are fully consistent.

When applying the results of theoretical studies of adsorption and of the interaction between adsorbed layers of polymers to real dispersions containing polymers the difference in interacting conditions between parallel platelets and spherical particles should not be forgotten.[19] Whereas in the approach of infinite parallel surfaces the desorption of macromolecules from the surfaces is hindered, leading to mutual repulsion of the surfaces, at the contact between spherical particles the macromolecules can migrate away from the region of increased pressure at the centre of the contact and move towards the periphery of the contact region. In the latter case the local adsorption Γ at the centre of the contact zone can decrease, thus inducing mutual attraction between the particles. Similarly, at the contact between liquid interfaces, for which the lateral mobility of the macromolecules is greater than on solid surfaces, we may find that other conditions being equal emulsion particles experience attraction whereas the solid particles of sols experience repulsion.

Furthermore, the brief contacts of particles in Brownian motion may generate mutual repulsion, whereas in the deposits from suspensions or emulsions the desorption of the macromolecules is more likely, leading to mutual attraction of the particles.

Thus the problem of the aggregation stability of dispersions stabilised by polymeric AL in thermodynamically good solvents in still unsolved. It is directly related to a more complex problem: how can the degree of equilibration (or the reversibility of the adsorption) be estimated under actual experimental or technological conditions?

The interaction between platelets in a solution of a polymer in a thermodynamically poor solvent was studied by Klein and coworkers,[20-22] who used the computation schemes proposed by de Gennes[19] supplemented by an additional condition: a negative value of the second virial coefficient v in the expansion (10). In particular, it was shown[22] that the type of interaction between AL of macromolecules is determined by parameters which characterise the bulk properties of the polymer solution, for example by parameters of its phase separation diagram (see Fig. 2), and also by the unperturbed radius of the polymer cluster in solution and by the third virial coefficient w of the expansion (10). One of the consequences of this conclusion is that, in the range of parameters corresponding to mutual attraction between two AL in contact, the adsorption of macromolecules at the boundary with the bulk solution should increase indefinitely with time, and the thicknesses of the AL should also increase indefinitely.[7] We note that Scheutjens and Fleer[14-16] criticised the suggestion[22] that the phase separation diagram of polymers can be used to describe the interaction between AL of macromolecules in a polymer solution.

3. Interaction between adsorption layers of polyelectrolytes

Lyklema et al.[17] have pointed out that the adsorption theories developed to explain the steric stabilisation of dispersions by nonionic macromolecules with flexible chains can be extended (in principle) to copolymers and polyelectrolytes by adding to Eqn (5) the term: $\exp(y_i - y)$ (where $y = e\phi/kT$, and ϕ is the electrostatic potential in the solution), in order to allow for the specific (electrostatic) interaction. However, a statistical theory of the adsorption of polyelectrolytes has not yet been developed.

Hesselink's theory of the adsorption of polyelectrolytes[43,44] is often quoted in the discussion of experimental results. It is an approximate theory, because the exponential dependence of the density of segments upon distance from the surface $\varphi(z)$ is postulated rather than established. Furthermore the theory makes the following assumptions: low concentration of polyelectrolytes in solution (which allows the intermolecular interactions in solution to be neglected), and high ionic strength of the solution [which allows the effect of ionic electrostatic forces between charged functional groups upon the distribution $\varphi(z)$ to be neglected]. This theory establishes the interrelation between the parameters of the adsorption layer of polyelectrolyte (layer thickness, extent of adsorption, density of charges on the interfacial surface) and the physicochemical parameters (degree of dissociation of the macroion, ionic strength of the solution, concentration of the polyelectrolyte, molecular mass, surface charge density, etc.).

The conclusion of Hesselink's theory, that the adsorption of a polyelectrolyte decreases as the degree of dissociation of the macroion is increased, is attributed to a decrease in the electrostatic component of the energy of adsorption. The effect is also explained by an increase in the hydrodynamic radius of the polymer cluster with increasing charge. According to Hesselink's theory a lowering of the Debye screening length (for example, by increasing the ionic strength of the solution) should result in an increased adsorption of the polyelectrolytes (PE): this prediction is confirmed experimentally by a study[46,47] of the effect of pH and of the concentration of sodium chloride on the surface activity of poly(acrylic acid) (PAA) at the solution–air interface. In particular it has been shown that for ionisation levels of the macroion $\alpha \geqslant 0.2$ (i.e. at pH $\geqslant 4$) the PAA becomes surface-inactive because of the increase in solubility of the polyacid with increase in α.

Hydrophobic interactions play an important role in the conformation of polyelectrolytes and in their adsorption at the oil–water inteface.[2,48-52] Hydrophobic binding favours the formation of a more convoluted and rigid conformation of the macroion. The interaction between the hydrophobic (residual acetate) functional groups of poly(vinyl alcohol) and the water–oil interface increases the surface activity of the macromolecule by lowering the free energy in response to the accumulation of hydrophobic groups in the oil phase.[50,51] Increasing the content of acetate groups in the copolymers of acrylic acid and vinyl acetate leads to the formation of gel-like layers at the interface, and therefore also to an increase in the stability of the emulsion films towards rupture (coalescence).[8,9,52-57] The effect of hydrophobic and of electrostatic interactions on the conformation of natural PE (proteins, polysaccharides, etc.) under given physicochemical conditions can be used to explain (at least, qualitatively) the special aspects of their adsorption at phase boundaries.[58-60]

A working theory of the steric stabilisation of dispersions of polyelectrolytes has not yet been developed, in spite of the wide technological use of these materials as stabilisers (especially in mixtures with nonionic polymers).[56,61,62] The difficulty of describing the specific interactions in terms of statistical theories is responsible for this state of affairs, as well as the long-standing interest of researchers in this area in the opposite effect of PE on disperse systems (i.e. in aggregative destabilisation effects such as flocculation and coagulation). However, studies of stabilisation based on the work of La Mer[63,64] and Gregory[65,66], now form a substantial part of the work of Baran,[67] Audebert and coworkers,[68-71] and others.

III. Experimental study of the interaction between adsorption layers of polymers

The most serious problem in the interpretation of experimental results on the properties of AL of polymers and on the interaction between AL is the lack of a criterion for recognising and controlling the thermodynamic equilibrium in disperse systems containing polymers. Because of the finite diffusion time of the macromolecules from the solution to the surface, and of the slowness of the conformational rearrangements of an adsorbed molecule (in particular, at relatively high bulk concentrations of the polymer in solution) we can define a time beyond which the rate of the transition processes falls to zero (i.e. ceases to be an experimentally determinable quantity). This time is of the order of hours or days. The probability of reaching what has been called the 'equilibrium' state of these systems decreases still further if structure formation processes can take place in the AL as a result of the specific interactions between the macromolecules.

Another difficulty met in the experimental study of the properties of AL is the correct choice of a model substance (both for the polymer and for the surface) for difference studies of the effect of physicochemical factors on the adsorption of polymers. In particular, uncontrolled polydisperseness of the polymer samples is reported[67,72] to introduce serious distortions into the results of adsorption measurements, because of the difference in surface activity between macromolecules with small and with large molecular masses. Most probably the adsorption of macromolecules on immobile surfaces (vessel walls, mica laminae, or quartz surfaces in the modelling of contact interactions)[20-23,41,42,52,73-85] or on colloidal deposits[67] is markedly different from their adsorption on the particles of sols undergoing Brownian motion, partly because of the difference in the accessibility of the surface to the molecules and partly because of the hydrodynamic effects produced by the motion of the particles. The effect of the method of measuring adsorption on the result of the measurement has been examined in depth.[67]

1. Measurement of the thickness and of the density profile of adsorption layers of polymers

As was pointed out above, modern theories of the steric stabilisation of disperse systems by polymer layers[11-13] attach great importance to the structure of the AL of macromolecules in their outer side (oriented towards the solution). The layer, formed by 'tails' (and to a smaller extent by 'loops'), makes a relatively minor contribution to the density profile $\varphi(z)$ of the adsorption layer, but its role in the stabilisation of the disperse phase is dominant. The stabilising power of this layer is associated with the mutual repulsion of 'tails' and 'loops' at their steric contact (see Fig. 1*a*).

Unfortunately, only a small number of experimental methods of determining the density profile or the thickness of the outer part of the AL is available at present. Among the methods most recently reported we should include the low-angle neutron diffraction method,[86] and also the measurement of contact interactions between molecularly smooth mica surfaces[20,74,83] or between liquid interfacial surfaces (air bubbles or oil drops approximately 1 mm in diameter) in aqueous solutions of polymers.[84] However, other indirect methods have also been a valuable source of information on the structure of AL. Detailed analyses of all these methods have been published.[5,7,67]

Many systematic studies of the effect of various physico-chemical factors on the thickness of AL of polymers have been reported.[41,42,52,53,74,79-84,87-95] All these works concluded that the effective thickness of the AL is substantially greater than the root-mean-square distance between the ends of the statistical macromolecular cluster ($2R_F$), or than double the hydrodynamic radius R_h of the macromolecule, in keeping with the ideas proposed in the steric stabilisation theories[11-23] on the structure of the AL (i.e. on the mutual repulsion between 'tails' and 'loops' of the macromolecular chains in the liquid film).

The experimental determination of the dependence of the effective thickness of the AL on the molecular mass of the polymer is of great importance because its results can be compared with calculations based on the steric stabilisation theories.

In particular, the following dependence was obtained[88] for AL of poly(vinyl alcohol) (PVA) on particles of polystyrene latex:

$$\delta_{ef} = M^{\beta},$$

where $\beta = 1.14$ in the range $8000 < M < 67000$. On the other hand, a study of aqueous emulsion layers stabilised by PVA gave[93] $\beta \simeq 0.2$. This suggests a weak dependence of δ_{ef} on M. It was also stated[93] that the thickness of an adsorption layer of poly(ethylene oxide) on a solid surface, measured ellipsometrically, corresponds to a value of the β coefficient of 0.4, which differs from the value (0.5) predicted by the theories of Hoeve[29] and of Scheutjens and Fleer.[11,14] Kawaguchi et al.[93] interpret this result on the basis of the de Gennes theory,[18] developed for thermodynamically good solvents, by assuming that the size of the 'tails' is comparable with the size of the macromolecule R_F in the bulk of the solution, and that the density profile is described by the function $\varphi(z) \sim z^{-4/3}$, which is valid for the bulk of the solution. By determining δ_{ef} by the expression

$$\delta_{ef} = \int_0^{R_F} z\varphi(z)\mathrm{d}z$$

and putting $R_F \sim M^{0.6}$ (see de Gennes[18]) they obtained the value of 0.4 for β quoted above.

It should be noted that according to de Gennes[18] the adsorption Γ should be independent of the molecular mass M of the polymer. In this respect the reported[93] $\delta_{ef}(M)$ dependence [which is effectively a $\Gamma(M)$ dependence, having been measured ellipsometrically] is incompatible with the de Gennes theory for good solvents.[18] Therefore it is relevant to note the comment[18] that an increase in the adsorption Γ with M can be expected if the adsorbent surface has a mosaic structure with extended 'active' centres (such as dislocations) which can bond to the segments of the macromolecule with a relatively large energy.

The effective thickness of AL of poly(ethylene oxide) on a mica surface in a thermodynamically good solvent (an aqueous 0.1 mol dm^{-3} KNO_3 solution and toluene) was measured by Klein and Luckham[23] by the contact interactions method. The result ($\beta = 0.43 \pm 0.02$) differed from de Gennes' prediction of $\beta = 0.6$, but allowing for the experimental error it is consistent with the theory of Scheutjens and Fleer.[11,14] It has been reported[23] that the agreement with the de Gennes theory[18] is improved by making a correction for the rigidity of the dynamometer used to detect the instant of contact between the two AL. Klein et al.[22] showed that in a thermodynamically poor solvent (polystyrene in cyclohexane) $\beta \leqslant 0.5$. In particular, when calculating the dependence of the thickness δ_{ef} of the adsorption layer on the molecular mass of the polymer in the limit of $f_a^* \to 0$ (where f_a^* is the maximum force, leading to the dislodgment of a particle) these workers obtained the relationship $\delta_{ef} \sim M^{0.5}$ whereas for a finite value of the adhesion force the relationship was $\delta_{ef} \sim M^{0.3}$, which is not inconsistent with any of the adsorption theories.

As regards the effect of the quality of the solvent on the adsorption and on the thickness of the adsorption layer it is usually found that worsening the solvent increases the adsorption of nonionic polymers from aqueous solutions on hydrophobic surfaces.[70] This is attributed to the decrease in size of the macromolecules, to their aggregation, and to the increase in the adsorption energy. In particular, an increase in the adsorption of polymers on hydrophobic surfaces (PVA on polystyrene, and polyvinylpyrrolidone on silica) has been observed upon worsening the quality of the solvent.[90,92,97] The same workers noted a decrease in the thickness of AL of the polymers δ_{ef} when a worse solvent was used, which contradicted Klein's experimental data[22] on the adsorption of poly(ethylene oxide).

In a study[52] of the contact interactions between mica sheets and drops of heptane ($\sim$1 mm in diameter) in aqueous solutions of polymers it was found that although the thickness of the undeformed AL of macromolecules [poly(acrylic acid) (PAA) and copolymers of acrylic acid and vinyl acetate with different contents of acetate groups] exceeded the size of the average macromolecular cluster in the bulk of the solution it increased monotonically with R_F (for example, upon increasing the pH or decreasing the ionic strength of the solution).

A special study[83] by the contact interactions method of the effect of the time of formation of adsorption layers of PVA on a molecularly smooth mica surface in aqueous solutions upon the thickness δ_{ef} of undeformed AL showed that this thickness increases with time at a rate of $\sim 10^{-4}$ nm s^{-1} (the δ_{ef} value doubling in approximately 48 h). Under these conditions structuring effects (gel formation processes) develop within the AL, as shown by the increase in the effective viscosity of the layers (a decrease in their rate of thinning).[8]

Structural changes in the adsorption layers of PVA, dependent on time and leading to an increase in the refractive index of the thin liquid layers, were observed[97] at the contact of a silicone sphere and a solid surface in a solution of PVA, but the authors were unable to draw any firm conclusions as to the nature of this phenomenon. In the experiments of Sonntag and coworkers,[76,85] and of Rabinovich et al.,[73,98] who studied the contact interactions between crossed filaments in solutions of PVA, the change in thickness of the AL could not be determined because the method can measure the absolute deformation of the AL but not their thickness.[47] A study[2,91,99] of foam and emulsion films stabilised by adsorption layers of PVA, and in particular of the dependence of their thickness on the difference in hydrostatic pressure ΔP, allowed the disjoining pressure (or its

steric component) to be expressed as a function of the film thickness, thus making it possible to calculate the thickness of the undeformed adsorption layers of PVA in the limit of $\Delta P \to 0$. The time-changes in the properties of the films observed in these experiments were interpreted as a consequence of the failure of the transition processes to go to completion, which complicated the experiment and compelled the hold time of the interfaces prior to film formation (i.e. the time of formation of the adsorption layers of polymer) to be fixed arbitrarily between 0.5 and 2 h. Thus in these experiments no attempt was made to study the effect of the formation time of the adsorption layers of PVA on their thickness or on the adsorption. Estimates of the thickness of AL of polymers formed on the surface of particles in sols and suspensions have a much lower precision than the direct measurements.[5,67] In particular, even an integral characteristic such as the adsorption of the polymer depends on the chosen measurement method (rate of displacement, method of precipitation of the dispersion, etc.).[67]

Thus our analysis of experimental studies aimed at measuring the thickness of the adsorption layers of polymers or their density profile has shown that the conclusions of the steric stabilisation theories of Scheutjens and Fleer[11-17] and of de Gennes[18,19] on the structure of AL of polymers (the presence of 'tails' and 'loops' in the outer part of the AL, oriented towards the solution, and making an important contribution to the steric stabilisation of the dispersions) is essentially confirmed both for nonionic polymers and for polyelectrolytes. However, we should stress the fact that experimental tests of the dependences predicted by these theories (for example, of the dependence of the thickness of the AL on the molecular mass of the polymer) have given contradictory results. There is very little information on the properties of AL of polymers in thermodynamically poor solvents, and no experimental approaches towards solving this problem have so far been developed. In particular it has been shown[83] that the thickness of adsorption layers of PVA on a molecularly smooth mica surface increases monotonically with time, in spite of the fact that aqueous solutions of electrolytes are moderately good for this polymer ($\chi = 0.45-0.48$).[5] Evidently, in polymers with thermodynamically poor solvents the increase in the thickness of the AL should be even more marked. Therefore experimental methods of studying the properties of AL of polymers should allow for possible time-changes of the parameters of the AL (thickness, rheological properties, etc.), and they should be designed to measure these changes.[52]

2. Steric repulsion between adsorption layers of polymers

According to the thermodynamic theories of steric stabilisation[11-23] an increase in the thickness of liquid films stabilised by AL of polymers produces an increase in the free energy of the repulsion between these AL (Fig. 6). The direct determination of this energy as a function of the film thickness H is a difficult problem. This accounts for the small number of publications on this topic. We shall consider only the experimental methods which allow the pressure P to be measured as a function of the contact pressure force (in the case of a contact between solid surfaces), or of the difference in hydrostatic pressure ΔP (in the case of liquid films).

The first measurements of the repulsive force f_p between bent mica plates in a polymer solution [an aqueous solution of poly(ethylene oxide), PEO, with a molecular mass of the order of 150 000] as a function of the width of the gap between the plates (H) were reported by Israelachvili et al.[74] These workers found that after a 2 h exposure to the solution the thickness of the film (double the thickness of the undeformed AL) reached 300 nm, and that in this region the force of repulsion increased exponentially as H was decreased. In the 10–150 nm region the force f_p depended on the rate of compression of the plates, and showed hysteresis phenomena (the thickness of the AL after loading was not restored to its initial value). Lastly, in the region < 5 nm a steep increase in the repulsive force was observed: it was accompanied by removal of the polymer from the gap and the appearance of a cohesive force as a result of 'bridge formation'.

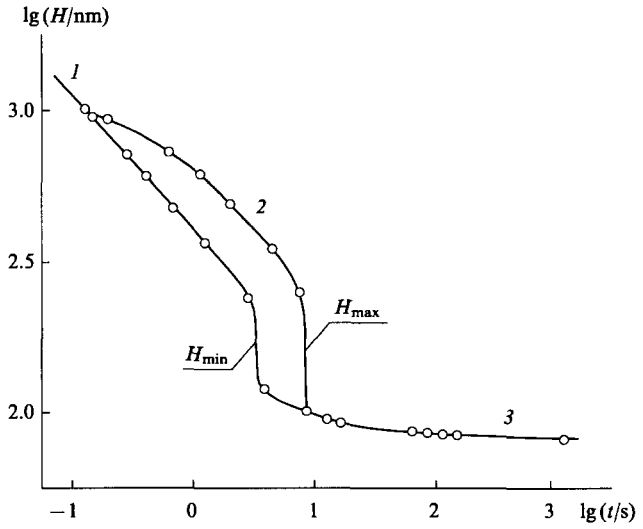


Figure 6. Kinetic curve for the thinning of a water film stabilised by a copolymer of acrylic acid and vinyl acetate containing 74% of acetate groups.[53]

The main conclusions from the work of Israelachvili et al.[74] can be formulated as follows: (1) the adsorption of PEO in a moderately good solvent (Flory–Huggins parameter $\chi = 0.45-0.48$)[100] is multimolecular, since a continuous increase in the thickness of the AL was observed; (2) a gel-like structure is formed in adsorption layers of PEO, with an elastic deformation time (after compression) exceeding the characteristic relaxation time of the sample, thus leading to hysteresis effects; (3) the achievement of film thicknesses $H < 5$ nm in the experiments indicates the absence of contaminants such as dust and microgel particles in the PEO solution.

Klein and Luckham,[41] using a similar apparatus, repeated the measurements of the deformation properties of AL of PEO in an aqueous solution of KNO_3 (0.1 mol dm^{-3}). The PEO samples had molecular masses of 4×10^4 and 1.6×10^5, and the formation time of the AL of polymers was 16 h (as opposed to 2 h, used by Israelachvili et al.[74]). Their main conclusions[41] were: (1) the adsorption of PEO on a mica surface is monomolecular; (2) the adsorption of PEO is irreversible, i.e. the so-called 'limited' equilibrium is established between the polymer solution and the AL (whereas Israelachvili[74] stipulated a 'full' equilibrium since macromolecules are removed from the gap when its thickness is reduced to < 5 nm); (3) the possibility of forming a gel-like structure in the AL is denied; (4) though mica plates were compressed as far as $H \simeq 6$ nm no adhesion between the AL of the polymer was detected (in contrast to the report[74] of the development of a cohesive force between the adsorbed layers of PEO at gap thicknesses < 5 nm).

Klein and Luckham[41] noted the good agreement between the results of measurements of the interaction energy of AL of polymers and those given by the steric stabilisation theory developed by de Gennes[19] for thermodynamically good solvents. The specific free energy of repulsion as a function of the film thickness $\Delta F(H)$ was found by the expression $\Delta F(H) \sim f_p/R$, where R is the radius of curvature of the surface. On the assumption that in the region of weak overlapping of the AL ($H \approx 80$ nm) the mutual repulsion effect between the AL is associated with an increase in the osmotic pressure in the contact region, with $\Delta F(H) \sim V\pi$, where $V = 2\delta - H$ (δ is the thickness of the undeformed AL, π is the excess osmotic pressure), the authors expressed π in terms of the density profile

$\varphi(H)$ of the segments in the contact region [stated[19] to obey the expression $\varphi(H) \sim \exp(-H/2\zeta)$, where ζ is the correlation length], and

$$\pi \sim v\varphi^2(H) \sim \exp\left(\frac{-H}{\xi}\right).$$

Then,

$$\Delta F(H) \sim (2\delta - H)\exp\left(\frac{-H}{\xi}\right),$$

and the parameter $\Delta = \partial[\lg \Delta F(H)]/\partial(\lg H) = -H/(2\delta - H) - H/\zeta$. In the region of slight overlapping of the AL the inequality $H \leqslant 2\delta$ applies, and the parameter Δ is negative, with $\Delta \to -\infty$ for $H \to 2\delta$. Exactly this law for the changes in Δ was observed[41] for a good solvent in the region of slight overlapping of the adsorption layers of PEO.

Conversely, in the region of strong overlapping of the AL, i.e. for $H < 10$ nm, the following dependence is observed (on the assumption of a constant adsorption of the polymer):[19]

$$\varphi(H) \sim H^{-1},$$

whence we find

$$\pi \sim \varphi^2 \sim H^{-2},$$

which leads to the expression

$$\Delta F(H) \sim H^{-1},$$

which was formulated experimentally.

Klein and Luckham[41] also discovered a hysteresis on the $\Delta F(H)$ curve during a heating–cooling cycle, the parameter $\Delta F(H)$ being smaller during unloading than during loading and remaining always positive (i.e. adhesion between the AL was not observed).

The present writer has reported[83] measurements of the time-dependence curves $H(t)$ of films of aqueous soutions of PVA while compressing mica sheets with gradually increasing forces (f_p). A sudden increase in f_p produces a thinning of the film at a measurable rate even after 10^3 s of observation, though the deformation is mostly completed in 100–200 s after the application of the constant force f_p. After a sudden decrease in the force f_p to a new constant value the thickness of the film relaxes to the previous value in a period of $\sim 10^3$ s in the case of adsorption layers of PVA formed over a time $t_f > 10^5$ s. No relaxation was seen for $t_f < 10^3$ s. As has been pointed out,[52] the experimental $\Delta F(H)$ dependences are not well correlated with the theoretical dependences $\Delta F(H) \sim (2\delta - H)\exp(-H/\zeta)$ and $\Delta F(H) \sim H^{-1}$ for a weak and a strong overlapping of the adsorption layers respectively in a thermodynamically good solvent.[19] The best concurrence is found for AL formed in times $t_f > 10^4$ s, with weak overlapping of the AL, by formally choosing the parameters $\delta = 80$ nm and $\zeta = 7$ nm. We note that the value $\delta = 80$ nm greatly exceeds the value $\delta = 35$ nm, which corresponds to the contact interaction force $f_p \simeq 10^{-8}$ N, i.e. to the precision of the measurement of force in these experiments.

It was also pointed out[52,83] that for an extent of overlapping corresponding to a film thickness $H > 40$ nm (and $t_f \sim 10^4$ s) the $\Delta F(H)$ curves are satisfactorily described on the basis of the HVO theory † (see Ref. 27). Those papers also discuss an attempt to describe the deformation of adsorption layers of PVA by rheological methods based on a simplified solution of the Hertz contact problem[101,102]

$$\frac{f_p}{R} = 0.75E\left(\delta - \frac{H}{2}\right)^{5/2}(R+\delta)^{1/2}, \qquad (21)$$

† More exactly, on the basis of a variant of the HVO theory which assumes an exponential distribution of the density of segments with increasing distance from the surface.

where E is the effective elastic compression modulus of the AL of polymer.

It has been shown that none of the theoretical curves drawn by using Eqn (21) describes the experimental dependence over the whole region of overlap of the adsorption layers. However, by formally assuming that the layer is not uniformly thick the appropriate elastic modulus can be calculated by Eqn (21) for each value of the thickness δ. The following values of E/Pa were obtained for adsorption layers of PVA having $c_{PVA} = 0.1\%$, $c_{KCl} = 10^{-2}$ mol dm^{-3}, and $t_f \geqslant 2.2 \times 10^4$ s: 4.2×10^3, 2.0×10^5, 2.5×10^6 for δ values of 50, 30, and 20 nm respectively.

Thus we have to consider a gradient of the elastic properties of AL of polymers, probably generated by the density gradient of the the polymer segments near the surface or by the gradient in the bulk density of the number of contacts between the segments, responsible for the formation of a gel-like structure within the AL.

The studies by Klein and Luckham,[20,41] of the polystyrene–cyclohexane system were aimed at the interactions between AL of polymers in thermodynamically poor solvents. They stress the presence of an equilibrium minimum on the $\Delta F(H)$ curve [or the $\Pi(H)$ curve, see Fig. 5*b*], having a depth of 10^{-3} J m^{-2}. A strong repulsion arises between the AL when mica sheets are squeezed together.

A group of experimental papers[89,91,99] describes studies of the steric interaction between AL of polymers in free emulsion and foam films. In this work the thickness of the films H was determined interferometrically as a function of the difference in hydrostatic pressure ΔP (which is equal, under equilibrium conditions, to the disjoining pressure in the film). In particular, it was found[91] that the dependence of the disjoining pressure Π on the deformation is linear up to values of $\Delta H/H \simeq 0.3$ when the film is compressed under hydrostatic presure, which is markedly different from the dependence $\Pi \sim \exp(-H/\zeta)$ predicted for good solvents at low coverages by the AL.[19]

The steric interaction between adsorption layers of polymers in microscopic foam or emulsion films (about 100 μm in size) located between air bubbles or liquid droplets in a solution of the polymer has been widely discussed[52,53,96,103]. In particular, it has been shown that when a load is suddenly applied as a constant compressive force f_p between two liquid or gaseous particles with a radius of ~ 1 mm three characteristic regions can be distinguished on the curve which describes the thinning of the liquid film [$H(t)$] between the particles (see Fig. 6). In the first region ($H \sim 1$ μm) the form of the approaching surfaces remains spherical (as shown by the interference image of the film in reflected light), and the thinning of the film can be described by Taylor's equation for the flow of a medium of constant velocity η out of the gap between two undeformed spheres of radius R (see Ref. 52).

$$-\frac{dH}{dt} = \frac{4f_p H}{3\pi R^2 \eta}. \qquad (22)$$

The parameter η calculated by formula (22) is satisfactorily consistent with the bulk viscosity of the polymer solutions.[52,53]

In the second region ($H < 1$ μm) we observe a compression of the spherical surface of the drops and the formation of lenticular thickenings ('dimples') at the centre of the circular films, from which the polymer solution flows through a gap of thickness H_{min} towards the periphery of the film.

Lastly, when the compression of the 'dimple' is almost complete we come to the third stage of thinning of the film, taking place against a background of steric interactions between AL of macromolecules with a variable effective viscosity and a velocity of the order of 10^{-2}–10^{-1} nm s^{-1} (see Refs 52 and 53). The deformation of the element of the flat film has been described by using the rheological model of Kelvin, consisting of elastic (E_K) and viscous elements (η_K) connected in parallel,

according to which

$$\Delta P = E_K \varepsilon + \eta_K \frac{d\varepsilon}{dt}, \quad (23)$$

where $\varepsilon = (H_0 - H)/H_0$ is the relative deformation of the film, H is its thickness, and H_0 is the effective thickness of the undeformed film, i.e. the thickness of the film for $\Delta P = 0$. By solving Eqn (23) we obtain the expression

$$H(t) = H_0\left[1 - \frac{\Delta P}{\eta_K}\tau\left(1 - \exp\frac{-t}{\tau}\right)\right], \quad (24)$$

in which $\tau = \eta_K/E_K$. In spite of the fact that Eqn (24) does not describe the experimental curves for the third stage of thinning of the film $H(t)$ a formal application of this equation to the separate parts of the $H(t)$ curve can determine the rheological parameters E_K and η_K as a function of the film thickness.

It has been shown[52,53] that the elastic modulus of the adsorption layers of PVA can vary between 100 and 500 Pa, suggesting a relatively low value of the density of segments for film thicknesses between 90 and 75 nm. According to the steric stabilisation theories[11-23] relatively low values of the elastic modulus (and therefore also of the free energy of mutual repulsion between the AL of macromolecules) are typical of a bulk density of segments not much greater than the bulk density of the polymer in solution, and may be attributed to the entropic component of the disjoining pressure associated with the limitation imposed on the volume of the macromolecules (in terms of the HVO theory[27]).

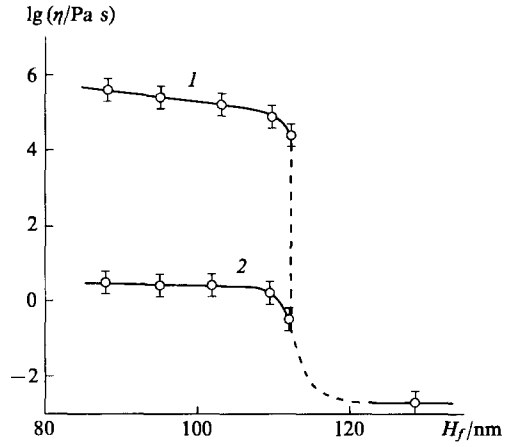


Figure 7. Dependences of η_K (*1*) and η_0 (*2*) for a water film stabilised by PVA upon its thickness H_f.

A characteristic feature of the dependence of the viscosity η_K upon the thickness H of the film is the sudden increase in η_K over a relatively narrow range of film thickness (Fig. 7). The H_0 value can be interpreted as the thickness of the film formed by almost undeformed adsorption layers of the polymer. The effective value of the viscosity η_0 calculated by the expresssion

$$\eta_K = \frac{3}{2}\frac{r_0^2 H_0}{H^3}\eta_0,$$

which corresponds to the plane-parallel disc model, also increases in this range of film thickness but only by 2-3 orders of magnitude (see Fig. 7). Unfortunately, the estimated value of η_0 thus obtained does not justify any unambiguous conclusions on the structure of the steric contact region between AL of macromolecules. For example, the above estimate of η_0 can be obtained by assuming the presence in the central region of the film of a layer of dispersion medium ~ 10 nm thick flowing almost freely.[52] By assuming 'tails' and 'loops' of the macromolecules (which impart a positive disjoining pressure to the film) can penetrate into this layer we are compelled to allow for the hydrodynamic resistance of the segments to the outflow of the liquid medium, i.e. to postulate that the thickness of the layer in which the flow of the liquid is fast can be much greater than 10 nm.

Babak and Monissova[53,96] reported the first attempt to determine the specific free energy of the interaction $\Delta F(H_f)$ in a film of thickness H_f stabilised by polymers. They used the expression

$$\Delta F(H_f) \simeq \Delta P(H_{\min} - H_f), \quad (25)$$

where H_{min} is the minimum thickness of the idealised profile, which can be obtained by extrapolating the profile of the surface of constant average curvature to the region of the bulk meniscus on the intermediate region of the film.[26] It was shown that the positive quantity $\Delta H_{\min} - H_f$ is not greater than 4-6 nm, which sets the following upper limits for $\Delta F(H_f)$: 4×10^{-7} J m^{-2} for PVA [96] and 1.5×10^{-7} J m^{-2} for PAA.[53] The values thus obtained for $\Delta F(H_f)$ are consistent with those predicted by the steric stabilisation theory for the interaction between AL of polymers in liquid films.

3. Adhesion between adsorption layers of polymers in liquid films

The development of adhesion between AL of macromolecules in thermodynamically poor solvents is predicted by all the steric stabilisation theories[11-19] and is confirmed by direct measurements of the cohesive forces between the mica plates in polymer solutions.[20-23]

In the case of thermodynamically good solvents the steric stabilisation theories predict mutual repulsion between AL of polymers at high coverages and on the assumption of a limited thermodynamic equilibrium (constant adsorption of the polymer in the region of steric contact between the two AL in the film, i.e. no desorption of macromolecules upon compressing two AL). Under full thermodynamic equilibrium these theories predict mutual attraction between AL in good solvents.

Direct measurements of the attachment forces between AL of polymers in good solvents are inconsistent. As was pointed out above, Klein and Luckham[41] failed to detect any cohesive forces between adsorption layers of PEO. On the other hand Israelachvili et al.[74] observed large adhesion forces for AL of the same polymer upon bringing mica surfaces within 5 nm of each other. Rabinovich and coworkers[73,85,98] reported the absence of adhesion between adsorption layers of PVA formed on the molecularly smooth surfaces of quartz fibres. Large adhesion forces were detected between adsorption layers of PVA on a mica surface,[8,52,78,83] and also on other solid or liquid interfaces.[104,105] Some of these studies[8,52,57,106] included a systematic examination of the effect of different physicochemical factors on the force of adhesion between two air bubbles or heptane drops in aqueous solutions of PVA.

Concentrated emulsions of oil (heptane) in water, stabilised by PVA, acquire a finite plastic shear strength P_s (see Refs 8, 9, 52, 57) after sedimentation in a centrifuge. We shall assume that the plastic strength can be calculated from the expression

$$P_s \simeq n\bar{f}_a^*. \quad (26)$$

Here n is the surface density of broken contacts in the shear plane, equal to $\approx 1/\bar{R}^2$ ($\bar{R}$ is the average radius of the emulsion drops), $\bar{f}_a^*$ is the average adhesion force between drops of emulsion, given (according to the theory of adhesion of liquid particles[107]) by the expression

$$\bar{f}_a^* = \pi v_a R \Delta F_a, \quad (27)$$

where ν_a is a parameter dependent on the capillary pressure and on the shape of the profile of the disjoining pressure, varying between 0.5 and 1, and $\Delta F_a = \Delta F(H_f)$ is the specific free energy of adhesion in a liquid emulsion film of thickness H_f, formed between emulsion drops. Using Eqns (26) and (27) gives the expression [8,9]

$$P_s \simeq \frac{\Delta F_a}{\bar{R}}. \tag{28}$$

Calculations of ΔF_a by means of Eqn (27) from measured values of the plastic strength of concentrated emulsions give values of the order of (-10^{-5}) to (-10^{-4}) J m^{-2} (see Refs 8–10, 52, 57).

It should be noted that the plastic strength of very concentrated emulsions is measured at a small but finite relative shear velocity. Under these conditions the breaking of the adhesion contacts between the emulsion drops and the formation of new contacts take place in a finite time. Thus the adhesion force f_a^* calculated by Eqn (26) cannot be assumed to be an equilibrium adhesion force, just as the ΔF_a value calculated by Eqn (28) is not an equilibrium value of the specific free energy of adhesion. We can expect (as is found in practice) [52,78,83] a decrease in the cohesive force between emulsion drops on lowering the shear rate, i.e. on lowering the velocity of the breaking load applied to the drops

$$f_a = \frac{df_a}{dt}.$$

On the rheological curve this region corresponds to creep. The creep phenomenon itself is characteristic not only of disperse systems stabilised by AL of polymers (interacting through short-range forces, including hydrophobic interactions produced by hydrogen bonds), but also of very concentrated dispersions with contacts of the coagulation type between particles, interacting through molecular and electric forces.

When the size of the particles is decreased, i.e. when the potential energy of the interaction between particles is lowered to a level comparable with kT, the breaking of the adhesion force between particles is caused by thermal fluctuations and becomes controlled by probability laws.[108] The same is true of the breaking of the adhesion contact between two AL of macromolecules, when the discrete bonds between 'active' functional groups are not broken simultaneously upon the application of a disjoining pressure. Under these conditions we can expect the force of adhesion between particles coated with AL of polymers to depend on the rate of application of the disjoining pressure P_a, decreasing as dP_a/dt is decreased.

The effect was discovered in measurements of the cohesive force between two mica sheets in a solution of PVA while increasing the disjoining load at a controlled rate to the value

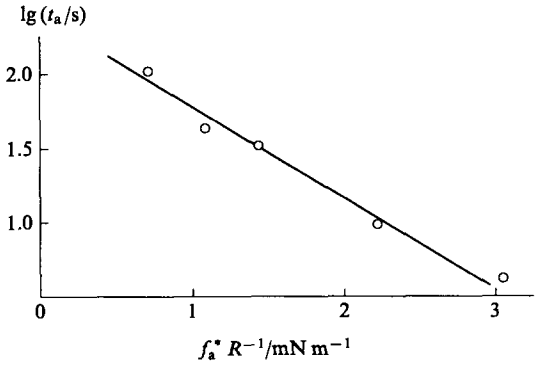


Figure 8. Dependence of the breaking time t_a of the contact between mica sheets in an aqueous solution of PVA upon the pull force f_a^*/R (see Babak [83]).

$f_a^* \leqslant 10^{-5}$ N s^{-1} (see Refs 52, 78, 83). Furthermore, in these experiments the authors measured the time t_a needed to break down the adhesion contact after the application of a constant pulling force to the particles, and they noted that t_a decreases as f_a^* increases (Fig. 8). The following expression was used [108,109] to describe the dependence $t_a(f_a)$ on the assumption that a thermal fluctuation mechanism is applicable to the breaking of the adhesion contact between the surfaces:

$$t_a = t_0 \exp\left[\frac{E_a - \gamma P_a}{kT}\right], \tag{29}$$

where t_0 is a constant parameter, E_a is the activation energy for bond breaking, γ is the activation volume of the bond breaking, and $P_a = f_a/A$ is the detachment pressure (A is the area of contact).

The value thus obtained ($\gamma \simeq 500$ nm^3) has been interpreted [52,78,83] as the volume assigned to one acetate group in the macromolecule of PVA (the content of residual acetate groups in the sample of PVA used in this work was $\sim 1\%$).

It has been pointed out that the volume γ is smaller by a factor of 100 than the volume of one molecule, and approximately 100 times greater than the volume assigned to one hydroxyl group. We also note that the activation energy E_a obtained from the temperature dependence of the force of adhesion f_a^* between adsorption layers of PVA is $(0.1-0.4) \times 10^{-20}$ J (see Refs 8, 52), i.e. it is a quantity of the order of kT, which is in keeping with the suggested thermal fluctuation character of the breaking of the adhesion bond between AL of the polymer.

There have been repeated references [9,52,57] to the practical problems met in the measurement and in the determination of the specific free energy of the interaction $\Delta F(H_f)$ between the AL of polymers resulting from the short-range forces between the bonds which are not broken simultaneously, and also from the long-range elastic compression forces between the AL during compression. In particular, during the compression of two AL in the film the corresponding work of elastic compression of the macromolecules can be arbitrarily assigned to the dividing surface of the liquid film, and it can be assumed that the interfacial tension σ_0 is increased by an amount $\Delta F(H_f)$, which can be found for the profile of the film by using Eqn (25). A positive sign of $\Delta F(H_f)$ corresponds to long-range forces of mutual repulsion between the phase boundary surfaces in the film, containing elastically compressed AL. Under these conditions if specific interactions between the AL of macromolecules (hydrophobic interactions, hydrogen bond formation, electrostatic interaction between oppositely charged functional groups) are taking place in the region of steric contact, leading to a decrease in the free energy, the shape of the film profile can be almost unaffected by this decrease in the free energy because of the short-range influence of these interactions. In experiments aimed at the direct measurement of the contact interaction forces in the compression cycle of mica plates [41,74,83] or of quartz fibres [73,85,98] the decrease in free energy could not be detected against the background of long-range repulsive forces between the elastically compressed AL of macromolecules.

However, dilution of the samples produces an elastic expansion of the macromolecules in the AL as a result of the short-range specific interactions, which formally converts these interactions into 'long-range' interactions since the deformed macromolecules in the AL produce a deformation of the interfacial surface and give the characteristic 'neck' shape to the film profile: in other words, a finite contact angle is created. The formal application of formula (25) in this case leads to negative values of $\Delta F(H_f)$. However, the magnitude of this effect, i.e. the value of the negative energy $\Delta F(H_f)$, will depend on the relationship between the rate of change of the external interaction and the rate of the relaxation processes in the AL of polymers. Since the specific interactions are short-range forces

and cannot be assigned to the dividing surfaces of the film their contribution is arbitrarily shown as a broken line[8,9,52] on the disjoining pressure isotherm (Fig. 5*c*).

IV. Conclusions

The new ideas[8-10,52,57] on the mechanism of the interaction between AL of macromolecules clearly point to the need to devote proper attention to the kinetic factors in experimental studies of the steric interaction between the AL of polymers: these factors include the ageing time of the AL (i.e. the time of formation of the AL), the time of formation of the steric contact between two AL, the rate of application of the pull force when breaking the adhesion contact between the AL, etc. This state of affairs arises because in the stabilisation theories[11-19] the problem of choosing between a 'limited' and a 'full' equilibrium in a system of two interacting AL (see Introduction) is solved arbitrarily, since there are no rational criteria for choosing the type of equilibrium which best describes the steric interaction between AL of polymers. However, the conclusions suggested by the theory as to the stability of sterically stabilised dispersions are strongly affected by the type of equilibrium, since (as was pointed out above) in the case of thermodynamically good solvents these theories predict the formation of adhesive forces between AL of polymers on the assumption of a 'full' equilibrium but not on the assumption of a 'limited' equilibrium.

Evidently the best approach in these circumstances is to assume that, when the time of formation or of steric contact between AL of polymers is increased, a 'limited' equilibrium will tend towards a 'full' equilibrium, thus creating adhesion forces between the particles coated with AL and suppressing the aggregative stability of the dispersions. Similarly, lowering the rate of application of the pull force creates conditions favouring a 'full' equilibrium between the interacting AL of macromolecules, and the adhesive force between particles will be lowest when the equilibrium is most evident. In the limit of a 'full' equilibrium the force of adhesion between polymer particles coated with AL in a thermodynamically good solvent will vanish, as predicted by the steric stabilisation theories.[11-19]

The above concepts were used as a foundation for the interpretation of the results of measurements of the rheological properties of very concentrated emulsions stabilised by adsorption layers of PVA. The development of plastic strength in the emulsions stabilised by this polymer, for which aqueous solutions of electrolytes are thermodynamically good solvents, and also the increase of this strength with time of centrifuging,[9,57] can only be explained by allowing for the finite time needed for the transition of the system from a 'limited' to a 'full' equilibrium. Allowing (in terms of the steric stabilisation theories) for the kinetic factor which characterises the achievement of a 'full' equilibrium by a system of two interacting AL of macromolecules, which can be determined experimentally, should bring the steric stabilisation theories closer to the description of actual nonequilibrium processes in disperse systems containing polymers.

References

1. W Heller, Th Pugh *J. Polym. Sci.* **47** 203 (1960)
2. T Van Vliet, Ph D Thesis, Landbouwhogeschool, Wageningen, Netherlands **77-1** 1977
3. B Vincent *Adv. Colloid Interface Sci.* **4** 193 (1974)
4. B Vincent, S Whittington, in *Surface and Colloid Science* Vol. 12 (London: Academic Press, 1982) p. 1
5. Th F Tadros, in *The Effect of Polymers on Dispersion Properties* (Ed. Th F Tadros) (London: Academic Press, 1982) p. 38
6. Th F Tadros, in *Thin Liquid Films. Fundamentals and Applications* (Ed. I B Ivanov) (New York: Marcel Dekker, 1988) p. 331
7. V G Babak *Physicochemistry of Microscopic Liquid Films Stabilized by Polymers. Thermodynamics of Contact Interaction in Liquid Media* (Sverdlovsk: Ural University Press, 1988)
8. V G Babak *Langmuir* **3** 612 (1988)
9. V G Babak *Colloid. Surf.* **30** 307 (1988)
10. V G Babak *J. Chem. Soc., Faraday Trans.* **89** (22) 4059 (1993)
11. J M H M Scheutjens, G J Fleer *J. Phys. Chem.* **83** 1619 (1979)
12. J M H M Scheutjens, G J Fleer *J. Phys. Chem.* **84** 178 (1980)
13. G J Fleer, J M H M Scheutjens *Adv. Colloid Interface Sci.* **16** 341 (1982)
14. J M H M Scheutjens, G J Fleer *Adv. Colloid Interface Sci.* **16** 361 (1982)
15. J M H M Scheutjens, G J Fleer *Macromolecules* **18** 1882 (1985)
16. G J Fleer, J M H M Scheutjens *J. Colloid Interface Sci.* **111** 504 (1986)
17. J Liklema, G J Flir, J M G M Skheutjens *Kolloid. Zh.* **49** 211 (1987)
18. P-G de Gennes *Macromolecules* **14** 1637 (1981)
19. P-G de Gennes *Macromolecules* **15** 492 (1982)
20. J Klein *Adv. Colloid Interface Sci.* **16** 101 (1982)
21. J Klein, P Pincus *Macromolecules* **15** 1129 (1982)
22. K Ingersent, J Klein, P Pincus *Macromolecules* **19** 1374 (1986)
23. J Klein, P F Luckham *Macromolecules* **19** 2007 (1986)
24. J W Cahn *J. Chem. Phys.* **66** 3667 (1977)
25. V G Babak *Usp. Khim.* **62** 14 (1993) [*Russ. Chem. Rev.* **62** 11 (1993)]
26. V G Babak *Usp. Khim.* **62** 747 (1993) [*Russ. Chem. Rev.* **62** 703 (1993)]
27. F Th Hesselink, A Vrij, J Ph G Overbeek *J. Chem. Phys.* **75** 2094 (1971)
28. E A Di Marzio, R J Rubin *J. Chem. Phys.* **55** 4318 (1971)
29. C A J Hoeve *J. Polym. Sci.* **30** 361 (1970)
30. E Helfand, Y Pagami *J. Chem. Phys.* **56** 3592 (1972)
31. S Levine, M M Tomlinson, K Robinson *Faraday Discuss. Chem. Soc.* **65** 202 (1978)
32. E A Di Marzio *J. Chem. Phys.* **42** 2101 (1965)
33. E A Di Marzio, F L McCracken *J. Chem. Phys.* **43** 539 (1965)
34. R J Roe *J. Chem. Phys.* **43** 1591 (1965)
35. R J Roe *J. Chem. Phys.* **44** 4264 (1966)
36. C A J Hoeve, E A Di Marzio, P Peyser *J. Chem. Phys.* **42** 2558 (1965)
37. C A J Hoeve *J. Chem. Phys.* **46** 3007 (1965)
38. P J Flory *Statistical Mechanics of Chain Molecules* (Translated into Russian; Moscow: Mir, 1971)
39. P-G de Gennes *Scaling Concepts in Polymer Physics* (Ithaca: Cornell University Press, 1979)
40. J Klein *J. Colloid Interface Sci.* **111** 305 (1986)
41. J Klein, P F Luckham *Macromolecules* **17** 1041 (1984)
42. J Klein *J. Chem. Soc., Faraday Trans. 1* **79** 99 (1983)
43. F Th Hesselink *J. Electroanal. Chem. Interfacial Electrochem.* **37** 317 (1972)
44. F Th Hesselink *J. Colloid Interface Sci.* **60** 448 (1977)
45. N M Soboleva, A A Baran *Ukr. Khim. Zh.* **49** 1160 (1983)
46. Y Ishimuro, K Ueberreiter *Colloid Polym. Sci.* **258** 928 (1980)
47. Y Ishimuro, K Ueberreiter *Colloid Polym. Sci.* **258** 1052 (1980)
48. M Yacobi, A Ben-Naim *J. Solution Chem.* **2** 425 (1973)
49. V A Pchelin *Gidrofobnye Vzaimodeistviya v Dispersnykh Sistemakh* (Hydrophobic Interactions in Dispersed Systems) (Moscow: Znanie, 1976)
50. J M G Lankveld, J Lyklema *J. Colloid Interface Sci.* **41** 454 (1972)
51. R A Kul'man *Makromolekuly na Granitse Razdela Faz* (Macromolecules on Phase Boundaries) (Kiev: Nauk. Dumka, 1976)
52. V G Babak *Physicochemistry of Microscopic Liquid Films Stabilized by Polymers. Modelling of Contact Interaction in Polymer-Containing Disperse Systems* (Sverdlovsk: Ural University Press, 1988)
53. V G Babak, R A Monissova *J. Dispersion Sci. Technol.* **6** 539 (1985)
54. V G Babak *Kolloid. Zh.* **48** 124 (1986)
55. V G Babak, R A Monisova, V I Nesterova, N V Meiya, N A Kruglova *Vysokomol. Soedin. Ser. A* **28** 1151 (1986)
56. V G Babak *Kolloidnaya Khimiya v Tekhnologii Mikrokapsulirovaniya* (Colloid Chemistry in the Technology of Microencapsulation) (Sverdlovsk: Ural University Press, 1991)
57. V G Babak *Food Hydrocolloids* **6** 45 (1992)
58. D E Graham, M C Phillips *J. Colloid Interface Sci.* **70** 403 (1979)

59. E Dickinson, B S Murray, G Stainsby, in *Advances in Food Emulsions and Foams* (Eds E Dickinson, G Stainsby) (London: Elsevier, 1988) p. 123
60. E Tornberg, A Olsson, K Persson, in *Food Emulsions* (Eds K Larsson, S E Friberg) (New York: Marcel Dekker, 1990) p. 247
61. M H Gutcho, in *Microcapsules and Microencapsulation Technique* (New Jersey: Noyes Data Corp., 1976) p. 350
62. *Biomedical Applications of Microencapsulation* (Ed. F Lim) (Boca Raton: CRC Press, 1984)
63. V K LaMer, T W Healy *Pure Appl. Chem.* **13** 112 (1963)
64. V K LaMer *Discuss. Faraday Soc.* **42** 248 (1966)
65. J Gregory *Trans. Faraday Soc.* **65** 2260 (1969)
66. J Gregory *J. Colloid Interface Sci.* **42** 448 (1973)
67. A A Baran *Polimersoderzhashchie Dispersnye Sistemy* (Polymer-Containing Dispersed Systems) (Kiev: Nauk. Dumka, 1986)
68. R Audebert, T K Wang *J. Colloid Interface Sci.* **119** 459 (1987)
69. G Durand-Piana, F Lafuma, R Audebert *J. Colloid Interface Sci.* **119** 474 (1987)
70. S Vaslin-Reinmann, F Lafuma, R Audebert *J. Colloid Interface Sci.* **268** 476 (1990)
71. A Guyot, R Audebert, R Bodet, B Cabane, F Lafuma, R Jullien, E Pefferkorn, C Pichot, A Revillon, R Varoqui *J. Chem. Phys.* **87** 1859 (1990)
72. M A Cohen Stuart, J M H M Scheutjens, G J Fleer *J. Polym. Sci.* **18** 559 (1980)
73. Ya I Rabinovich, B V Deryagin, N V Churaev *Dokl. Akad. Nauk SSSR* **233** 349 (1977)
74. J N Israelachvili, R K Tandon, L R White *J. Colloid Interface Sci.* **78** 430 (1980)
75. K Mühle, H Domasch *Colloid Polym. Sci.* **258** 1391 (1980)
76. H Sonntag, B Ehmke, R Miller, in *The Effect of Polymers on Dispersion Properties* (Ed. Th F Tadros) (New York: Academic Press, 1982) p. 423
77. H Domasch, K Mühle *CHEMTECH* **34** 360 (1982)
78. V G Babak, V N Sokolov, E V Sveshnikova, V I Osipov *Inzh. Geol.* **4** 57 (1984)
79. J Klein, P F Luckham *Nature (London)* **308** 836 (1984)
80. J Klein, P F Luckham *Colloid Surf.* **10** 65 (1984)
81. J N Israelachvili, M Tirell, J Klein, Y Almog *Macromolecules* **18** 204 (1984)
82. P F Luckham, J Klein *Macromolecules* **18** 721 (1985)
83. V G Babak *Kolloid. Zh.* **48** 641 (1986)
84. J Klein *Macromol. Chem. Macromol. Symp.* **1** 125 (1986)
85. Th Götze, H Sonntag, Y Rabinovitch *Colloid Polym. Sci.* **265** 134 (1987)
86. K G Barnett, T Cosgrove, B Vincent, A N Burgess, T L Crowley, T A King, J D Turner, Th F Tadros *Polymer* **22** 283 (1981)
87. M J Garvey, Th F Tadros, B Vincent *J. Colloid Interface Sci.* **49** 57 (1974)
88. M J Garvey, Th F Tadros, B Vincent *J. Colloid Interface Sci.* **55** 440 (1976)
89. J Lyklema, T Van Vliet *Faraday Discuss. Chem. Soc.* **65** 25 (1978)
90. Th Van den Boomgaard, T A King, Th F Tadros, H Tang, B Vincent *J. Colloid Interface Sci.* **66** 68 (1978)
91. H Sonntag, B Unterberger, S Zimontovski *Colloid Polym. Sci.* **257** 286 (1979)
92. Th F Tadros, B Vincent *J. Colloid Interface Sci.* **72** 505 (1979)
93. M Kawaguchi, K Hayakawa, A Takahashi *Macromolecules* **16** 631 (1983)
94. M Kawaguchi, M Mikura, A Takahashi *Macromolecules* **17** 2063 (1984)
95. A T Clark, I D Robb, R Smith *J. Chem. Soc., Faraday Trans. 1* **72** 1489 (1976)
96. V G Babak *Kolloid. Zh.* **47** 582 (1985)
97. F W Cain, R H Ottewill, J R Smitham *Faraday Discuss. Chem. Soc.* **65** 33 (1978)
98. Y I Rabinovich, B V Derjaguin, N V Churaev *Adv. Colloid Interface Sci.* **16** 63 (1982)
99. A A Baran *Teor. Eksp. Khim.* **15** 534 (1979)
100. B Vincent, P F Luckham, F A Waite *J. Colloid Interface Sci.* **73** 508 (1980)
101. L D Landau, E M Lifshits *Teoriya Uprugosti* (Theory of Elasticity) (Moscow: Nauka, 1965)
102. K Jückel *Kolloid. Z—Z. Polym.* **197** 143 (1964)
103. V G Babak, V A Babaitsev *Izv. Vyssh. Uchebn. Zaved., Khim. Khim. Tekhnol.* **29** 64 (1986)
104. F V Vader, H Dekker, in *Trudy 7-go Mezhdunar. Kongressa po PAV* (Proceedings of the 7th International Congress on Surface-Active Substances) (Moscow: Vneshtorgizdat, 1978) p. 691
105. F V Vader, H Dekker *J. Colloid Interface Sci.* **83** 377 (1981)
106. V G Babak, V A Chlenov *J. Dispersion Sci. Technol.* **4** 221 (1983)
107. V G Babak *Colloid Surf.* **28** 123 (1987)
108. I N Vlodavets, G V Stratulat, V M Serb-Serbina *Dokl. Akad. Nauk SSSR* **189** 1035 (1969)
109. V R Regel', A I Slutsker, E V Tomashevskii *Kineticheskaya Priroda Prochnosti Tverdykh Tel* (Kinetic Nature of the Strength of Solids) (Moscow: Nauka, 1974)

Russian Chemical Reviews **63**(3) 231–255 (1994) ©1994 Russian Academy of Sciences and Turpion Ltd

UDC 771.534.21.01

Aggregates of cyanine dyes: photographic problems

B I Shapiro

Contents

I. Introduction	231
II. Desensitising effect of *J*-aggregates	233
III. Selective desensitisation and self-desensitisation of *J*-aggregates	236
IV. Supersensitisation of *J*-aggregating dyes as inhibition of their self-desensitisation	239
V. Conclusion	252

Abstract. The aggregation of cyanine dyes on the surfaces of AgHal microcrystals is examined. It is shown that the photochemical activity of the aggregates in processes involving the spectral sensitisation of photographic materials is determined to a large extent by the occurrence of secondary dark reactions in which photoelectrons recombine with dye holes—the so called type II dye self-desensitisation processes. The inhibition of the self-desensitisation of dyes increases the effectiveness of the spectral sensitisation, i.e. leads to supersensitisation. The principal mechanisms of the supersensitisation of photographic emulsions are discussed. The bibliography includes 149 references.

I. Introduction

The history of more than a century of the development of the spectral sensitisation of silver halides (AgHal) has led to a definite selection of the cyanine dyes used to sensitise AgHal in the visible and infrared ranges of the spectrum. *J*-Aggregating dyes, which make it possible to attain the highest level of additional photosensitivity, are nowadays as a rule generally used for the spectral sensitisation of colour and black and white photographic materials. The phenomenon of the aggregation of cyanine dyes is a striking example of the self-organisation of matter. It was discovered by Jelley[1] and Scheiber,[2] although the first observations apparently date back to an earlier period.[3] They showed that an increase in the concentration of solutions of the dyes displaces the absorption maximum towards shorter wavelengths (*H*-aggregation) or shifts it sharply towards longer wavelengths (*J*-aggregation). The anomalously large (up to 90–100 nm) bathochromic shift of the absorption and sensitisation of certain dyes adsorbed on silver halides, which are characteristic of thiacarbocyanines with substituents in the *meso*-position in the chain, were classified in 1939 by Schwarz as sensitisation of the second kind.[4] Numerous communications and reviews (see, for example, Refs 3–7) have been devoted to the phenomenon of the aggregation of dyes and the influence on the latter by the substrate, by the structure of the dyes, and by a series of emulsion factors and also to problems of the structure and properties of the aggregates themselves.

The *J*-aggregation of dyes on the surface of microcrystals of silver halides is by itself a necessary but not a sufficient condition for their high photographic effectiveness. Many satisfactory *J*-aggregating dyes are relatively ineffective under certain emulsion conditions. Here a characteristic feature is that there is no unambiguous relation between the energy levels of the dyes forming part of the aggregate and the sensitising effect of the *J*-states. This is illustrated in Fig. 1 (see over), which presents the absorption and spectral sensitivity distribution curves for photolayers sensitised by four cyanine dyes forming *J*-aggregates with close absorption maxima of the *J*-bands. The convention adopted in the literature[7] is that the energy levels of the dyes (Dy) are characterised by the polarographic half-wave oxidation and reduction potentials. The potential $E_{1/2}^{Ox}$ represents the energy of the highest occupied electronic level of the dye (ε_{ho}), while $E_{1/2}^{Red}$ reflects the energy of the lowest unoccupied (ε_{lu}) level from which the photoelectron is transferred to AgHal. It is assumed that for effective spectral sensitisers the ε_{lu} level of the dye should be higher than or close to the bottom of the conductivity band of AgHal.[7] On the electrochemical scale, the potential at the bottom of the conductivity band (E_{cb}^{0}) of silver bromide is -1.1 V [relative to the normal hydrogen electrode (rel. n.h.e.)] or -1.34 V [relative to the normal calomel electrode (rel. n.c.e.)].[8] The potential of the top of the valence band (E_{vb}^{0}) = 1.5 V (rel. n.h.e.) or 1.26 V (rel. n.c.e.).[8]

It follows from Fig. 1 (curves *2* and *3*, Fig. 1*b*) that the photographic effectiveness, characterised by the logarithm of the spectral sensitivity (lg S_λ) is significantly different for the two imidacarbocyanines of similar structure. Whereas 2-[3-(5-chloro-1,3-diethyl-2,3-dihydrobenzimidazol-2-ylidene)prop-1-enyl]-5-chloro-1,3-diethylbenzimidazolium iodide **1** ($E_{1/2}^{Ox}$ = 0.55 V and $E_{1/2}^{Red}$ = -1.73 V rel. n.c.e. in methanol) is relatively ineffective, 2-[3-(5,6-dichloro-1,3-diethyl-2,3-dihydrobenzimidazol-2-ylidene)prop-1-enyl]-5,6-dichloro-1,3-diethylbenzimidazolium iodide **2** ($E_{1/2}^{Ox}$ = 0.60 V, $E_{1/2}^{Red}$ = -1.58 V) is highly effective, although the difference between the potentials is comparatively small ($\Delta E_{1/2}^{Ox}$ = 0.05 V, $\Delta E_{1/2}^{Red}$ = 0.15 V). The ε_{lu} levels lie above the bottom of the conductivity band (-1.34 V) for both dyes. The sharply reduced activity of the *J*-aggregate of 2-(1-ethyl-1,2-dihydroquinolin-2-ylidenemethyl)-1-ethylquinolinium iodide **3** (curve *1*, Fig. 1*b*) might seemingly be attributed to the deeper location of the ε_{ho} and ε_{lu} levels ($E_{1/2}^{Ox}$ = 0.99 V, $E_{1/2}^{Red}$ = -1.04 V) relative to the levels of compound **2** and primarily to the higher value of $E_{1/2}^{Ox}$ ($\Delta E_{1/2}^{Ox}$ = 0.39 V). However, 2-[3-(3-ethyl-5-phenyl-2,3-dihydrobenzoxazol-2-ylidene)-2-ethylprop-1-enyl]-3-ethyl-5-

B I Shapiro Laboratory of Physicochemical and Photographic Research, Research and Design Institute of the Chemical-Photographic Industry, Leningradskii prosp. 47, 125167 Moscow, Russian Federation
Fax (7-095) 157 66 90

Received 29 December 1993
Uspekhi Khimii **63** (3) 243–268 (1994); translated by A K Grzybowski

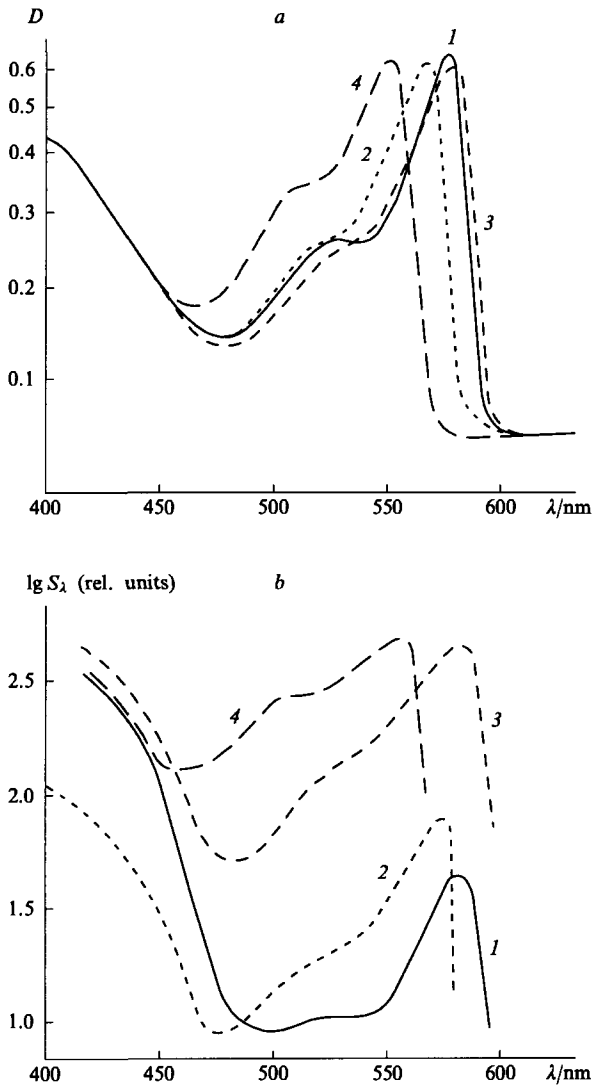
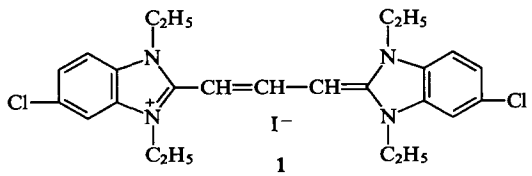
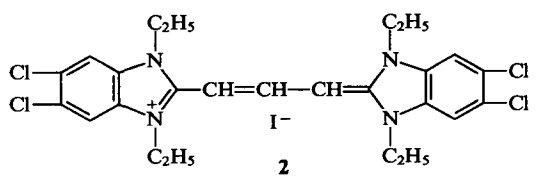
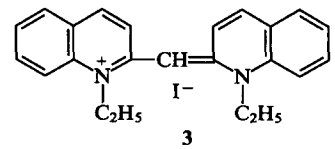


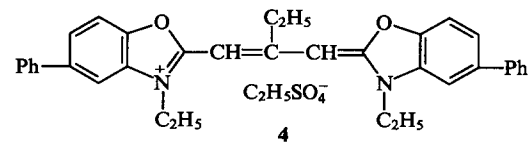
Figure 1. Reflection spectra (*a*) and spectral sensitivity curves (*b*) for the AgBr emulsion [cubic crystals, l = 0.17 μm, (S + Au)-sensitisation] sensitised by dyes **3** (curve *1*), **1** (curve *2*), **2** (curve *3*), and **4** (curve *4*); concentration of dyes — 2 × 10^{-4} mol (mol AgBr)$^{-1}$.

phenylbenzoxazolium ethyl sulfate **4** with $E_{1/2}^{Ox}$ = 0.93 V, which is close to the potential of compound **3**, and with $E_{1/2}^{Red}$ = −1.33 V, which is less negative than for compound **2**, is just as highly effective as compound **2** (curve *4*, Fig. 1*b*). On these grounds, one may conclude that the energetics of the molecules forming part of the *J*-aggregate is not the principal limiting factor.









The absence of a correlation between the photographic activity of cyanine dyes and the positions of their energy levels is apparently due to the following cause. The spectral sensitisation process takes place on the surface of the AgHal microcrystal where the dye is adsorbed. Impurity centres (IC), formed during the chemical sensitisation of the photographic emulsion, are located on the same surface. They play an extremely important role in the separation of the photogenerated charges — photoelectrons and photoholes. The capture of photoelectrons by the impurity centres is in essence the first stage of the formation of the latent photographic image. However, when problems of spectral sensitisation are discussed, as a rule processes in the dye–AgHal binary systems are considered. On the other hand, the real processes include a third important component of the system — the impurity centres which can accept both photoelectrons and holes. The interaction of dyes with impurity centres may be the cause of the secondary reactions which diminish the photographic sensitivity — the so called AgHal desensitisation processes. Methods for the supersensitisation of photographic materials are used to suppress these processes.

The influence of additionally introduced organic compounds — the supersensitisers (S) — on the photographic process in the region where the dye *J*-aggregates absorb is well known (see the relevant reviews [7–13]). The use of supersensitisers has made it possible to increase sharply the photographic activity of a series of *J*-aggregating dyes, frequently without change in the absorption bands of the sensitisers. As will be shown below, because of this the effectiveness of dyes **1**–**4** considered may be made virtually identical. The first publications on supersensitisation date back to 1920 when Bloch and Renwick [14] demonstrated the appreciable supersensitising effect of auramine on layers sensitised by different cyanines. More detailed studies, which led to the formulation of a series of supersensitisation mechanisms, were carried out by West and Carroll, [15] Scheibe and coworkers, [16,17] Bird, Rosenoff, Zuckerman, et al., [18–21] Riester, [22,23] Gilman, [10,24] and other investigators. [10–13] West and Carroll [15] noted that the role of the supersensitiser consists in creating a trap for the exciton formed on photoexcitation of the *J*-aggregate and moving towards the latter at a high rate. The capture of the exciton results in an increase in the probability of its decomposition and of the transfer of a photoelectron to AgHal. According to the ideas of Brunner and coworkers, [16,17] in the supersensitisation step the excitation energy is transferred from the dye to the supersensitiser, the longer lifetime of the excited (triplet) state of which is in fact responsible for the greater probability of the energy transfer to AgHal. Zuckerman and coworkers [18–21] examined the hypothesis that the dye aggregates are broken up with the aid of the supersensitiser molecules, as a result of which the antisensitiser, incorporated in the *J*-aggregate and diminishing the effectiveness of the dye, is localised in small regions of the aggregate and its deactivating effect on the photoexcited state of the entire dye *J*-aggregate (Dy_J^*) is reduced thereby. The separation of the dye from AgHal with the aid of the supersensitiser constitutes the basis of Riester's adsorption model. [22,23] The formation of a layer of supersensitiser (potentiator) molecules between the dye and AgHal promotes, according to Riester, [22,23]

a more effective energy or electron transfer from the photoexcited dye Dy* to AgHal, particularly as a result of the decrease in the contribution by recombination processes.

According to Gilman,[10,24] the supersensitiser, which is a more readily oxidisable compound, captures from the dye a hole formed on photoexcitation of the *J*-aggregate and on photo-transfer of an electron from Dy* to AgHal. There is then a possibility of electron transfer from the supersensitiser to the Dy* molecule (to the ε_{ho} level of the dye liberated on photoexcitation), with formation of the radical-anion $Dy^{-\cdot}$, or to the radical-cation $Dy^{+\cdot}$ (arising after the transfer of an electron to AgHal) with regeneration of the dye. In the first case, the effectiveness of the spectral sensitisation increases by virtue of the higher level of the electron in $Dy^{-\cdot}$ compared with Dy* and in the second it increases as a result of the decrease in the probability of the recombination of electrons with the holes of the dye ($Dy^{+\cdot}$). The above mechanisms have been examined in greater detail in other reviews.[7-13]

It is striking that in the world literature there is no single approach to the supersensitisation processes and the mechanisms discussed are specific to the given case and sometimes contradictory and they are not always justified experimentally. Gilman's hole capture mechanism is most justified for *J*-aggregating dyes, but it is subject to a series of exceptions which will be discussed below. It is essential to note that studies involving the supersensitisation and desensitisation of silver halides by dyes were largely uncoordinated for a long time.

A generalised chemical concept concerning the spectral sensitisation processes has been described in a series of studies by the present author.[8,25,26] According to this concept, the effectiveness of the sensitisation is determined by secondary dark dye desensitisation reactions, whilst the supersensitisation of photographic materials inhibits these processes. The kinetics of the desensitisation processes, which depend on supersensitisers to a greater extent than the energetics of the sensitiser levels, limit the photographic activity of the dye. The main task of the present review is therefore to examine systematically the relation between the processes involving the desensitisation of silver halide emulsions by *J*-aggregates of dyes and the inhibition of these processes by organic compounds of different nature. New approaches to the problem of the effectiveness of spectral sensitisation are also considered.

II. Desensitising effect of *J*-aggregates

Desensitisation is understood as a decrease in the intrinsic (blue) photosensitivity of silver halides under the influence of the adsorbed dye. The desensitisation of AgHal is known to be induced by dyes with a low electron affinity ($E_{1/2}^{Red} < -1.0$ V).[7,27] The desensitisation by such dyes (type II desensitisation) takes place via a mechanism involving the capture of a hole from AgHal.[7,28-36] The dye radical-cations thus produced can serve as centres for recombination with photoelectrons, which are thereby prevented from creating a latent image. This process was first examined by Carroll[37] and Saunders et al.[38] The degree of desensitisation increases as a rule with increase in the dye concentration and is particularly characteristic of dyes adsorbed as polymolecular *J*-aggregates.[7] A hole from the dye moving through the aggregate can reach the electron capture centre and can recombine with a captured electron or even oxidise the silver in the latent image. The type II desensitisation may be represented schematically in the form of the following sequence of reactions:[27]

$$AgHal + h\nu_b \longrightarrow [AgHal]^* \quad (1)$$

$$[AgHal]^* + Dy \longrightarrow [AgHal]^- + Dy^{+\cdot} \quad (2)$$

$$[AgHal]^- + Ag^+ \longrightarrow [AgHal/Ag^0] \quad (3)$$

$$[AgHal]^- + Dy^{+\cdot} \longrightarrow [AgHal] + Dy \quad (4)$$

$$[AgHal/Ag^0] + Dy^{+\cdot} \longrightarrow [AgHal/Ag^+] + Dy. \quad (5)$$

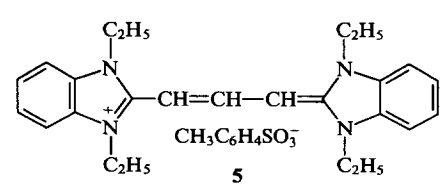
According to the above scheme, the silver halide photoexcited by a 'blue' light quantum ($h\nu_b$) oxidises the dye to the radical-cation $Dy^{+\cdot}$ (the convention that this is referred to as the dye hole may be adopted), which competes with silver ions for the capture of a photoelectron [stages (3) and (4)] or oxidises [stage (5)] the silver of the latent image formed in stage (3).

The desensitisation via the hole mechanism requires that the highest occupied electronic level of the dye ε_{ho} should lie above the top of the valence band (VB) of AgHal. Since the ε_{ho} level may be characterised by the polarographic potential $E_{1/2}^{Ox}$, it would seem that a relationship should be observed between the type II desensitisation and $E_{1/2}^{Ox}$ for dyes. Unfortunately, the dependence of the degree of desensitisation on $E_{1/2}^{Ox}$ for dyes has been investigated to a much lesser extent than its dependence on the reduction potentials $E_{1/2}^{Red}$. This is due to the fact that, for the *J*-aggregating dyes, which desensitise emulsions to the maximum extent (particularly monodisperse emulsions with sulfur sensitisation), the measured potentials $E_{1/2}^{Ox}$ (in solution in the molecular state) do not always characterise adequately the ε_{ho} level of the aggregate.

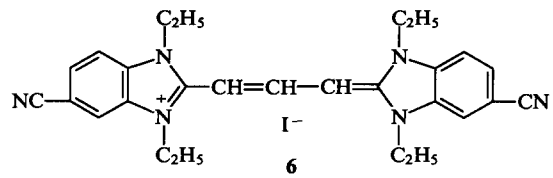
Leubner[39,40] showed that dyes having $E_{1/2}^{Ox} < 0.95$ V actually increase the intrinsic sensitivity of emulsions at low concentrations by accepting holes from AgHal. Only on raising the concentration of the dyes is desensitisation observed.[40] The increase in the sensitivity of fine-grain emulsions under the influence of dyes in the molecular state with $E_{1/2}^{Ox} \leqslant 0.76$ V (rel. n.c.e.) has also been demonstrated in other studies.[41,42] Tani[43] investigated the dependence of the desensitisation on the calculated value of ε_{ho} for a series of dyes. It was found that, with increase in the ε_{ho} level, the degree of desensitisation increases. It is striking that for dyes in which ε_{ho} lies 0.3 eV above the top of the valence band of AgHal not only is desensitisation observed but an EPR signal appears, which the author attributes to the dye radical-cation formed on excitation of AgHal [stage (2)]. These conclusions concerning the position of ε_{ho} relative to the AgHal valence band are not unambiguous because the dyes investigated were adsorbed in different states (in the molecular state *M* and in the aggregated states *H* and *J*), while the calculations of ε_{ho} were performed for molecular forms of the dyes. Another study by Tani was devoted to the exchange of holes between the dye and the valence band of AgHal.[44]

It is essential to note that the hole desensitisation is determined to a large extent by the topography of the centres formed on chemical sensitisation. For example, emulsions with bulk-phase chemical sensitisation[45,46] or emulsions containing Ir^{3+} ions in the bulk of the microcrystals[40] are desensitised by *J*-aggregating dyes to a lesser extent than by the surface sensitivity centres. The influence of oxygen on the type II desensitisation is not quite so unambiguous as for electron-accepting dyes.[7]

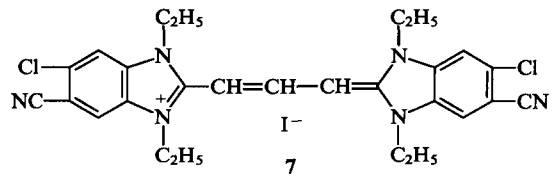
In order to determine the dependence of the type II desensitisation on the structure of the dyes and on their oxidation-reduction potentials (in the first place $E_{1/2}^{Ox}$), a systematic study has been made[47-49] of the influence on photosensitivity by four types of dyes with a low electron affinity ($E_{1/2}^{Red} < -1.0$ V): imidacarbocyanines, thiacarbocyanines, oxacarbocyanines, and quino-2-monomethinecyanines. Dyes **1**–**4** and **5**–**17**, the structures of which are presented below, were investigated.



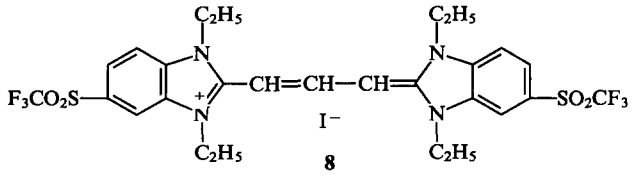
5



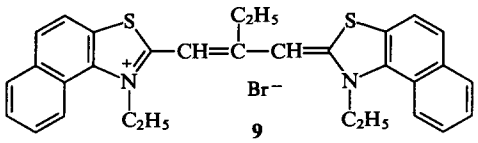
6



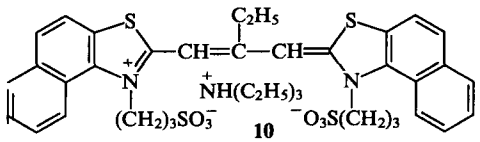
7



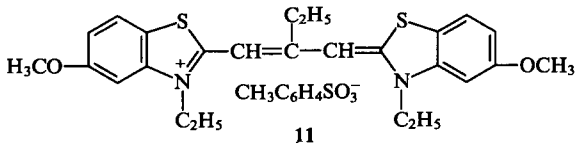
8



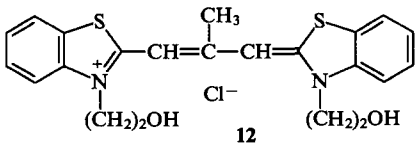
9



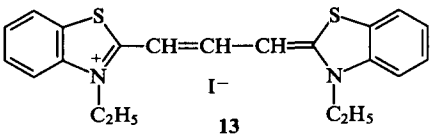
10



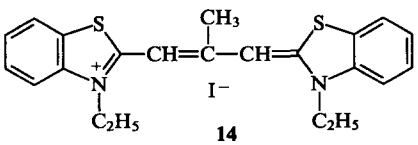
11



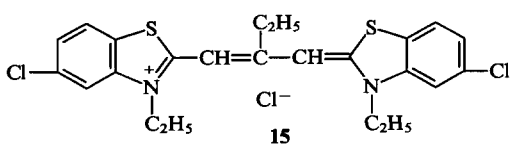
12



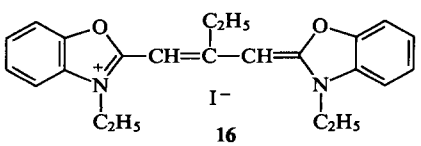
13



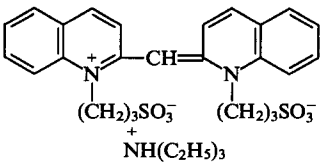
14



15



16



17

The photographic effect of the dyes was studied on a monodisperse AgBr emulsion with cubic microcrystals subjected to sulfur–gold (S + Au) sensitisation.

Table 1 presents certain characteristics of the dyes investigated. Depending on their structure, the dyes have been divided into the following groups: imidacarbocyanines **1**, **2**, and **5**–**8**, thiacarbocyanines **9**–**15**, oxacarbocyanines **4** and **16**, and quino-2-monomethinecyanines **3** and **17**. The influence of sensitisers on the intrinsic sensitivity of AgBr emulsions (behind a UFS-1 light filter with a transmittance range of 240–400 nm) has been characterised by the degree of desensitisation (DD).

It follows from the data in Table 1 that all the dyes investigated desensitise the AgBr emulsion. The degree of desensitisation (DD) varies from 1.2 to 3.6. In the series of dyes, a lower degree of desensitisation is induced by dyes in the *M* state (compounds **8** and **13**). The *J*-aggregating dyes **1**, **5**, **6**, and **11** give rise to

Table 1. Desensitising activity of cyanine dyes and some of their characteristics.[49]

Dye	DD	$E_{1/2}^{Ox}$/V	$E_{1/2}^{Red}$/V	$\lambda_{C_2H_5OH}^{max}$/nm	λ_{AgBr}^{max}/nm	State
5	3.0	0.49	−1.83	500	507	*M*
					528	J_1
					555	J_2
1	3.5	0.55	−1.73	507	568	*J*
2	1.6	0.60	−1.58	515	577	*J*
6	3.3	0.67	−1.53	513	581	*J*
7	1.7	0.70	−1.44	523	598	*J*
8	1.5	0.79	−1.37	522	555	*M* (*H*)
9	1.9	0.67	−1.27	578	606	*M*
					662	*J*
10	2.1	0.67	−1.34	581	668	*J* (*H*)
11	3.1	0.68	−1.31	562	590	*M*
					630	*J*
12	1.6	0.76	−1.28	549	523	*J*
					595[a]	
13	1.7	0.76	−1.04	562	592	*M* (*H*) (*J*)
14	2.1	0.77	−1.16	544	518	*J*
					590[a]	
15	2.8	0.94	−1.05	553	643	*J*
16	1.4	0.93	−1.36	492	500	*M*
					524	*J*
4	2.1	0.93	−1.33	504	545	*J*
3	1.3	0.99	−1.04	523	575	*J*
17	1.2	0.99	−1.14	530	575	*J*

Note. The concentration of the dyes was 2×10^{-4} mol mol^{-1} AgHal and the polarographic potentials in CH_3OH are expressed relative to the normal calomel electrode. The absorption maxima of the dye solutions refer to solutions in ethanol and in the AgBr emulsion; if the state of the dye adsorbed on AgBr is insufficiently clear-cut to determine the absorption band maximum, the latter is indicated in brackets. The degree of desensitisation (DD) was calculated on the basis of the criterion $D = 0.85 + D_0$; the colour temperature of the light source was 5000 K; developer — UP-2; development time — 8 min; layer contrast coefficient $\gamma \geqslant 4.0$.

[a] Two transitions.

the maximum desensitisation (DD $\geqslant 3.0$). However, an unambiguous relation between the tendency of the dyes to undergo *J*-aggregation and their desensitising activity has not been discovered. For example, dyes **1** and **2**, which have similar structures and absorptions and form aggregates, differ significantly as regards desensitisation. A similar behaviour has been observed also for dyes **6** and **7**. The quino-2-monomethinecyanines **3** and **17**, which give rise to *J*-aggregates, have a weak desensitising effect. Thus *J*-aggregation itself is not a necessary and sufficient condition for desensitisation.

It is noteworthy that the desensitisation is not associated in a definite manner with the charge on the dyes, since cationic and ionic dyes with the same chromophoric component of the molecule desensitise to approximately the same extent (cf. compounds **11** and **12** and compounds **3** and **17**). There is also no unambiguous relation between the degree of desensitisation and the potentials $E_{1/2}^{Ox}$ of the dyes. For example, dyes **1** and **2** as well as **6** and **7** with similar potentials $E_{1/2}^{Ox}$ differ by a factor of approximately two in terms of their desensitising activity. This is partly associated with the fact that, on aggregation of the dyes, their energetics may change and it is not altogether legitimate to characterise the aggregates by their polarographic potentials. It has been shown by luminescence and photographic methods in relation to quino-2,2′-monomethinecyanine **3**[48] that the energies of the levels of the dye do indeed change on *J*-aggregation. A change in the positions of the energy levels of a series of carbocyanines on *J*-aggregation has also been demonstrated by photoelectrochemical methods.[50,51] However, the main cause is different, namely the probability of desensitisation is determined not only by energy factors but also to a considerable extent by kinetic factors.[8,26]

A kinetic model of the electron transfer reactions in a photographic emulsion has been developed in the present author's studies[8,25–27,52,53] on the basis of the electrochemical potentials of the dyes and other components of the emulsion. Since the processes examined are typical oxidation-reduction reactions, the ideas of Marcus's theory, which describes electron transfer reactions in polar media, are applicable to them.[54–56] According to this theory, there is a linear relation between the change in the free energy of the transition state and the thermodynamic characteristics of the elementary oxidation-reduction step:

$$\Delta G^{\neq} = -RT \ln k \approx a\Delta G^0 + b \approx anF\Delta E^0 + b \ , \qquad (6)$$

where k is the reaction rate constant, ΔG^0 the change in the standard free energy of the reaction, a and b are constants for a particular class of reactions, n is the number of electrons involved in the reaction, F the Faraday, and ΔE^0 the difference between the standard potentials in volts.

In this case, the rates of electron transfer reactions between the components of the photographic layer — the Dy*, Dy, [AgHal]*, and AgHal molecules as well as those of other compounds — can be expressed in kinetic equations in which the activation energy is a function of the difference between the normal oxidation-reduction potentials of the systems participating in the electron transfers. The kinetics of the hole processes are determined by the rate of exchange of the hole between [AgHal]* and Dy, between Dy* and AgHal, and between $Dy^{+\cdot}$ and other components of the layer. The rate of capture of holes from the valence band of AgHal by the components of the emulsion and in the first place by the dye can be represented by the sum of the reaction rates:

$$\sum_i -\frac{dn_i(p)}{dt} = \sum_i k_i c_i n(p)$$

$$= \sum_i A_i \exp(-\alpha_i \Delta E_i^0/T) c_i n(p) \ , \qquad (7)$$

where $n_i(p)$ is the number of holes, c_i the concentration of the hole-acceptor form of the ith system, and ΔE_i^0 the difference between the normal potential of the ith system and the potential of the top of the valence band (E_{vb}^0). When a hole is captured by the dye, $\Delta E_i^0 = E_{1/2}^{Ox} - E_{vb}^0$. According to the data of Mikheeva et al.,[57] $E_{vb}^0 = 1.5$ V (or 1.26 V rel. n.c.e.) for AgBr. Thus the capture of holes from AgHal by the dye is in principle possible for dyes with $E_{1/2}^{Ox} < 1.26$ V, i.e. for all the dyes presented in Table 1.

However, the capture of holes from AgHal by the dye is only the beginning of the type II desensitisation process, which ultimately represents the recombination of the dye hole with the photoelectrons present in the traps, including the impurity centres (IC_e). Such impurity centres may be chemical sensitisation products (in the first place, the products of the sulfur or sulfur-gold sensitisation).[7] According to the kinetic model, the rate of recombination can be defined by an equation of type (7) in which ΔE_i^0 is the difference between the electrochemical potentials of the electron in the trap and the dye hole ($\Delta E_D^0 = E^0(IC_e) - E_{1/2}^{Ox}(Dy)$]. Consequently the desensitisation rate constant can be formulated as follows:[53]

$$k_D = A_D \exp(-\alpha_D \Delta E_D^0/T) \ . \qquad (8)$$

Since ΔE_D^0 is a function of $E_{1/2}^{Ox}$ (Dy), one would have to expect the existence of a relation between the degree of desensitisation, determined by k_D, and $E_{1/2}^{Ox}$(Dy). However, as mentioned above, such a relation does not exist. The question arises of the cause of such behaviour of the dyes.

According to Eqn. (8), the rate of desensitisation is determined not only by the exponential term but also by the pre-exponential term A_D. One may assume that in type II desensitisation processes the pre-exponential term plays an appreciable role. As a rule, for simple electron transfer processes, the rate of the oxidation-reduction reactions in nonorganised (stochastic) systems, particularly in solutions, depends significantly on the exponential term, i.e. on the activation energy, or, according to the Marcus theory, on ΔE^0. It is noteworthy that such a dependence on ΔE^0 has indeed been observed for type I desensitisation reactions proceeding via a mechanism involving electron capture by electron-accepting dyes in the ground state.[7,27,46,57–61] This is manifested by the steady increase in the degree of desensitisation with increase in the electron affinity of the dyes. However, in the case of organised systems, such as the *J*-aggregates of dyes on the surface of AgHal, the characteristic features of the rates of oxidation-reduction processes are different. Here the frequency factor A_D assumes a special importance. Type II desensitisation processes should depend significantly on the position in space of the *J*-aggregate (in which the hole is located) relative to the impurity centre (in which a photoelectron is captured), i.e. on the distance r between Dy and IC_e.[53,62] This is illustrated schematically in Fig. 2 (see over). On photoexcitation of AgHal, an electron (e) – hole (p) pair is formed. The electron is captured by the electron-acceptor centre IC_e, while the hole is captured either by the hole-acceptor centre IC_p or by the dye aggregate.

If the self-organisation of the dye molecules in the form of a *J*-aggregate is difficult, it begins on the surface defects of AgHal, which diminish the activation energy for the initiation of the aggregates.[63] Surface defects have in addition centres for the localisation of the impurity centres, including the photosensitivity centres formed during sulfur sensitisation.[7,64,65] As a result of the contact between the *J*-aggregate and the electron-acceptor impurity centre $IC_e(r \to 0)$, the frequency factor A_D and the rate of recombination increase, which is manifested by the appreciable desensitisation of the dye. The probability of contact between the *J*-aggregates and IC_e is high, since according to estimates[64] the number of Ag_2S centres is several thousand per μm^2, i.e. approximately per single AgHal microcrystal. On the other hand, the number of dye molecules on such a microcrystal reaches $10^5 - 10^6$, so that there are between several tens and several hundreds of dye molecules per Ag_2S centre.

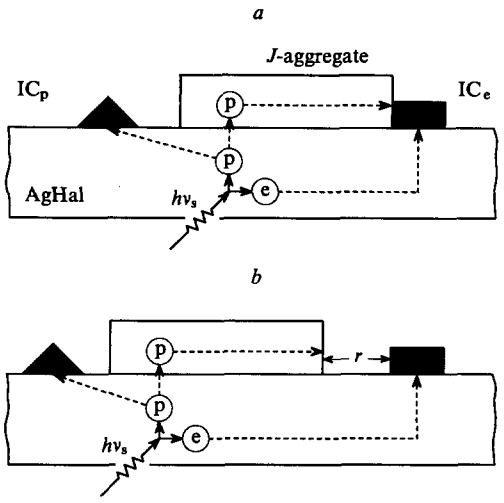


Figure 2. Schematic representation of the type (II) desensitisation processes via the hole mechanism: (*a*) *J*-aggregate in contact with the electron acceptor impurity centre (IC_e); (*b*) *J*-aggregate separated from the IC_e by a distance *r*; IC_p—hole acceptor impurity centre; $h\nu_s$—light quantum absorbed by AgHal; e = photoelectron; p = photohole.

On the other hand, if *J*-aggregation is achieved readily aggregates may be formed not only on AgHal defects but also at other sites, the probability of contact between the aggregate of IC_e falls, *r* increases (Fig. 2*b*), and hence the frequency factor A_D and the rate of recombination diminish.

If a hole is transferred from $Dy^{+\cdot}$ to IC_e via a tunnel mechanism, then the probability *W* of the transfer of the particle under the potential barrier per unit time is expressed by Gamow's classical formula, the simple version of which is

$$W = \nu \exp(-2r/a) , \qquad (9)$$

where ν is the frequency factor, *r* the distance corresponding to the width of the barrier, $a = \gamma h/[2m(U_{max}-E)]^{1/2}$ is the parameter characterising the attenuation of the wave function of the particle under the barrier, $\gamma \approx 1$ is a numerical coefficient which depends on the form of the barrier, *m* is the mass of the particle, U_{max} is the height of the barrier, and *E* is the energy of the particle. It follows from Eqn. (9) that the probability of the tunnel transition diminishes exponentially with the distance *r*. Thus $A_D = f[\exp(-2r/a)]$ and the type II desensitisation rate constant should therefore depend very greatly on *r*. This approach may serve as one of the explanations of the complex dependence of the hole desensitisation on the structure of the dyes.

The oxidising capacity of holes derived from all the dyes presented in Table 1 is apparently sufficient to accept electrons located on the impurity centres. According to the data of Berriman and Gilman,[59] the electrochemical potential corresponding to the oxidation of the silver film on the AgHal surface is 0.4 V (rel. Ag/AgCl electrode). Thus, even if account is taken of the possibility of a change in $E_{1/2}^{Ox}$ on aggregation of the dyes, all the sensitisers investigated are capable of oxidising the silver particles formed on the impurity centres. The observed difference between the desensitising properties [of the dyes] can be attributed to their different capacities for *J*-aggregation or the consequent different distances *r* between the *J*-aggregate and the IC_e.

Apart from the distance *r*, the frequency factor A_D can be determined by the velocity of the hole within the *J*-aggregate or by the mobility of the dye hole μ. The latter quantity must be related to the structure of the *J*-aggregate and in the first place to the interplanar distance between the dye molecules, their packing angle, and the molecular structure. For a low hole velocity in the aggregate, the probability of the decomposition of the latent image centre is naturally lower than for a high hole velocity. Therefore in a general form we have $A_D = f(r, \mu)$.[53]

III. Selective desensitisation and self-desensitisation of *J*-aggregates

The desensitisation processes should occur also on photoexcitation of dyes. In this case, one is dealing with selective desensitisation in the region of spectral sensitisation, the presence of which has been discussed.[35,66,67] Unfortunately the selective desensitisation of the spectral sensitiser itself, or, in terms of the nomenclature used by James[7] and Shapiro,[25] the self-desensitisation of the dye, cannot be measured directly, since it is impossible to achieve a controlled exposure of the photographic material at the same wavelength without the spectral sensitiser. At the present time, the degree of selective desensitisation is estimated by an indirect method from the influence of compounds introduced additionally on the intrinsic and spectral sensitivities of photographic emulsions. This method has been used to investigate selective type I desensitisation; electron-accepting compounds with a variable electron affinity were introduced into spectrally sensitised layers. It has been shown[57] that selective desensitisation can greatly exceed the intrinsic desensitisation.

One may postulate that experiments on the selective desensitisation of photographic emulsions via additionally introduced *J*-aggregating dyes, in which there is a possibility of the translation of a hole from the main spectral sensitiser, may serve as a definite test for type II self-desensitisation processes. Such a method has been used by the present author and his coworkers.[68]

Compositions comprising highly effective and weakly desensitising dyes combined with dyes which are weakly effective and induce an appreciable desensitisation via the hole mechanism were investigated. The highly effective dyes were compounds **4** and **14**, while the desensitising dyes were compounds **1** and **6** (Table 1). The dyes were introduced at equal concentrations and in a series of experiments the order of their introduction into the composition was varied. Fig. 3 presents spectral sensitivity and absorption curves for layers sensitised by dyes **4** and **1** individually and also by the **1** + **4** composition. According to the absorption spectrum (Fig. 3*a*), the use of a sensitiser composition has little effect on the positions of the absorption bands of the individual dyes (of curves *1*, *2*, and *3*). However, the introduction of the desensitising dye **1** leads to an appreciable suppression of the effectiveness of the spectral sensitisation at the sensitisation maximum of compound **4** (cf. curves *1* and *3*, Fig. 3*b*). The degree of desensitisation in the region of the AgHal absorption also increases under these conditions.

Fig. 4 illustrates the results for the **14** + **1** composition. Two absorption bands with λ_{max} = 518 and 590 nm are characteristic of 9-methylthiacarbocyanine **14**. Different assignments of these bands exist. They have been attributed either to the *H*- or *J*-aggregates respectively or to two spectral transitions in a single *J*-aggregate with a 'parquet' type of structure. According to Reich,[69] the splitting of excited dye levels into two components (S_1^1 and S_1^2) is observed for such molecular packing, where the structure cell contains two dye molecules at an angle close to 90°. Two spectral transitions, $S_0 \rightarrow S_1^1$ and $S_0 \rightarrow S_1^2$, of equal intensity then take place. The addition of dye **1** does not alter the positions of the absorption bands of dye **14** (cf. curves *1* and *3*, Fig. 4*a*), but it suppresses sharply the effectiveness of the sensitisation in bands with λ_{max} = 518 and 590 nm and approximately to the same extent for both bands (cf. curves *1* and *3*, Fig. 4*b*). It is noteworthy that similar results have been obtained for the reverse order of introduction of the dyes into the composition, i.e. **14** + **1** and **4** + **1**. The replacement of the desensitising dye **1** by compound **6** did not alter fundamentally the results—its introduction together with dye **14** diminished the photographic activity of the *J*-aggregates of dye **14**. Thus selective type II desensitisation does indeed take place.

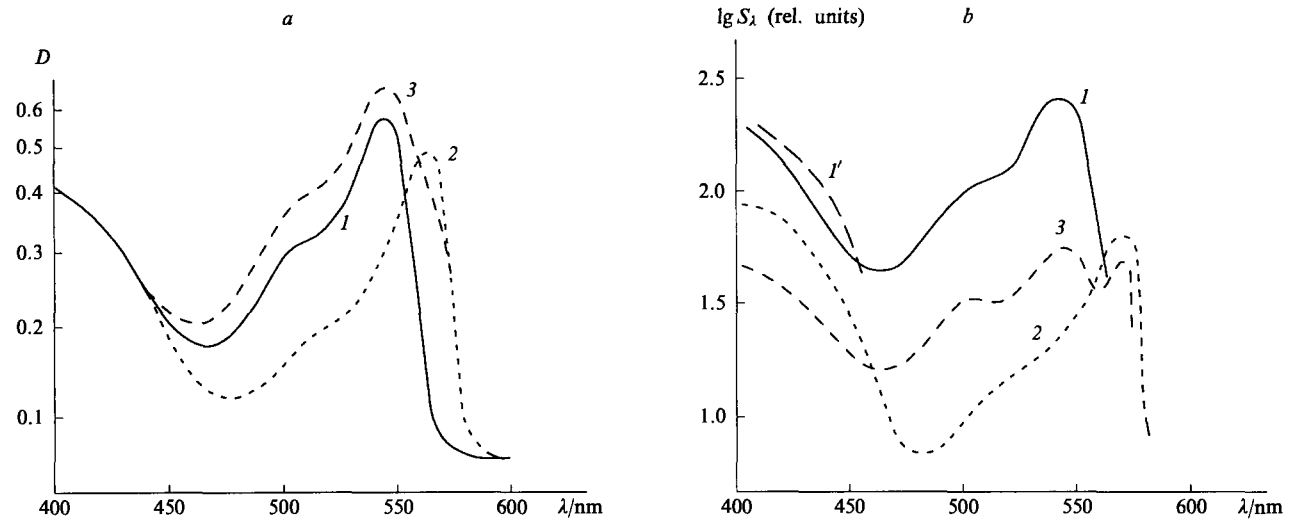


Figure 3. Reflection spectra (*a*) and spectral sensitivity curves (*b*) for AgBr emulsion layers sensitised by dyes **4** (curve *1*) and **1** (curve *2*) and by the **1** + **4** dye composition (curve *3*); (*1'*) layer without dye. AgBr emulsion—cubic crystals, $\bar{l} = 0.17$ μm, (S + Au)-sensitisation; concentration of dyes—2×10^{-4} mol (mol AgBr)$^{-1}$.

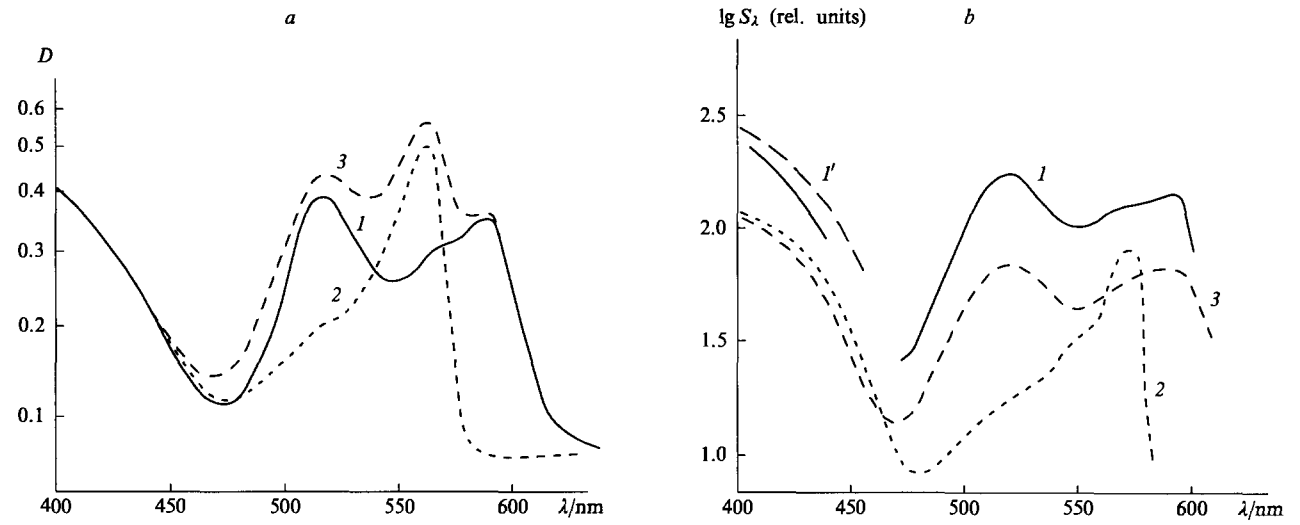


Figure 4. Reflection spectra (*a*) and spectral sensitivity curves (*b*) for AgBr emulsion layers sensitised by dyes **14** (curve *1*) and **1** (curve *2*) and by the **1** + **14** dye composition (curve *3*); (*1'*) layer without dye. Concentration of dyes—2×10^{-4} mol (mol AgBr)$^{-1}$.

The desensitising effect of dyes **1** and **6**, i.e. the decrease in the intrinsic sensitivity of AgHal, is apparently due to the capture of a hole from AgHal, its translation in the *J*-aggregate to the photoelectron capture centre (IC_e), and the recombination of the dye hole with the captured electron (Fig. 2*a*). The large desensitisation effects produced by these dyes (Table 1) may be due to two causes. Firstly, we have the energy-based cause. According to the data in Table 1, $E^{Ox}_{1/2}(\mathbf{1}) = 0.55$ V and $E^{Ox}_{1/2}(\mathbf{6}) = 0.67$ V, i.e. is appreciably lower than the potential corresponding to the upper limit of the AgBr valence band [estimated as 1.26 V on the same electrochemical potential scale (rel. n.c.e.)].[57] Thus the capture of a hole from AgBr by the dye is extremely likely (even when account is taken of the possible change in the energy levels on *J*-aggregation[48,50]). Secondly there is the kinetic cause. The probability of desensitisation may increase owing to contact between the *J*-aggregates of dyes **1** and **6** and the impurity centres—electron acceptors.[49] In the case of the effective dyes **4** and **14**, the lower desensitising effect is to some extent due to energy dependent causes [$E^{Ox}_{1/2}(\mathbf{4}) = 0.93$ V, $E^{Ox}_{1/2}(\mathbf{14}) = 0.77$ V (Table 1)], but it is determined to a large extent by kinetic causes—due to the lower probability of contact between the *J*-aggregates and the impurity centres.

We shall consider the effect of dye compositions. The decrease in the effectiveness of the spectral sensitisation by dyes **4** and **14** following the additional introduction of the desensitiser **1** or **6**, observed by Shapiro et al.,[68] may be a consequence of the decrease in the probability of processes involving the recombination of dye photoelectrons and holes. The use of the second dye is equivalent to a decrease in the distance *r* between the *J*-aggregate and the IC_e, which is illustrated schematically in Figs. 5*a* and 5*b* (see over). According to this scheme, the hole of the first dye (for example, compound **4**) is translocated to the second dye (compound **1**), as a result of which there is a sharp increase in the pre-exponential term A_D in Eqn. (8) and hence in the rate of desensitisation. The translocation of the holes of dyes **4** and **14** to dyes **1** and **6** is possible, since $E^{Ox}_{1/2}(\mathbf{4}, \mathbf{14}) > E^{Ox}_{1/2}(\mathbf{1}, \mathbf{6})$.

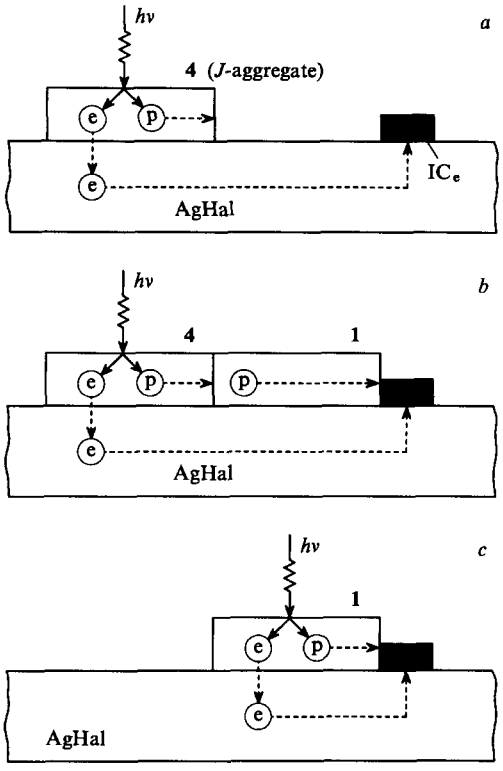


Figure 5. Schematic representation of the selective type (II) desensitisation (*a*, *b*) and self-desensitisation (*c*) of dyes.

According to Fig. 4*b*, the additional introduction of compound **1** has the same influence on the effectiveness of sensitisation in both absorption bands of dye **14** (cf. curves *1* and *3*, Fig. 4*b*), so that one can assume that they indeed belong to the same *J*-aggregate and, according to Reich,[69] both spectral transitions take place from the same ground level S_0. As a result of this, the holes generated under the conditions of both bands have the same energy. In essence, it is the same hole and its transfer through the *J*-aggregate of the second dye is equally probable regardless of the band used for its excitation.

It is essential to bear in mind that the translocation of a hole from one aggregate to another should not always be manifested as desensitisation. One can imagine a situation where, on photoexcitation of a desensitising dye in contact with the impurity centre, on the one hand, and with the *J*-aggregate of another dye, on the other, the hole of the first *J*-aggregate may be captured by the second. For this, it is necessary that Gilman's condition[10] $E_{1/2}^{Ox}(Dy'') < E_{1/2}^{Ox}(Dy')$ should hold. On the other hand, on photoexcitation of the second dye, the *J*-aggregate of the first as it were insulates the hole from IC_e. Thus there is a possibility of the mutual supersensitisation of the dyes. This case is apparently characteristic of the so called cation-anionic dyes containing in their structure two dyes one of which (cationic) has alkyl groups attached to the nitrogen atom of the heterocycle, while the other (anionic) has acid groups. As a rule individual sensitisers have different values of $E_{1/2}^{Ox}(Dy)$. Furthermore, the composition comprising such dyes frequently incorporates the desensitising quinomonomethinecyanine **3** as the orthochromatic sensitiser and one of the effective thiacarbocyanines as the panchromatic sensitiser. The cation-anionic dyes are known[70,71] to be highly effective and photochemically more active than a mixture of individual sensitisers. The explanation of this may be as follows. Since the charge on the individual cyanines is compensated by the counterion, on aggregation the *J*-aggregates of two different dyes need not necessarily be in contact. On the other hand, in the case of cation-anionic dyes contact between oppositely charged *J*-aggregates of the two dyes is more probable and hence there is also a greater probability of the supersensitising transfer of a hole from one aggregate to the other.

It is noteworthy that the processes involving the translocation of a hole from one dye to another should be manifested particularly clearly in direct positive materials. In such materials, the holes oxidise the silver fogging centres generated beforehand and the translation of holes between different dyes should lead not to the desensitisation of the photographic layers but actually to their supersensitisation. Indeed the supersensitisation of the photobleaching of the fogging centres by cyanine dye compositions has been observed.[72] The possibility of the translocation of holes from one dye to another with a lower value of $E_{1/2}^{Ox}$, leading to an increase in the effectiveness of the direct positive process, has been discussed.[73]

Thus the reality of selective type II desensitisation processes has been demonstrated.[68] This can be regarded as an argument in support of the existence of type II dye self-desensitisation processes via a hole mechanism. The probability of this process as well as the type II desensitisation process is determined by the distance *r* between the *J*-aggregate and the IC_e impurity centre of the electron-acceptor type. The self-sensitisation on photoexcitation of the dye (the spectral sensitiser) is particularly probable on contact between the *J*-aggregate and the IC_e (Fig. 5*c*).

It is essential to note that the type II desensitisation process consists of a greater number of stages than the self-desensitisation of the dyes. This condition is illustrated conventionally in Fig. 2 *a*. On photoexcitation of AgHal, some of the holes may be captured by the dye on the surface of the microcrystal with formation of dye holes, whilst others are captured by impurity centres—hole acceptors (IC_p). On the other hand, the type II self-desensitisation process is simpler, since a dye hole inevitably arises on spectral sensitisation, i.e. on transfer of electrons from the photoexcited dye to AgHal (Fig. 5*c*). Thus the number of dye holes may be larger. The probability of self-desensitisation can therefore be also greater than the probability of desensitisation and hence its influence on the spectral sensitivity may exceed that of desensitisation on the intrinsic photosensitivity of the emulsion. This apparently leads to the very pronounced difference between the effectiveness of the spectral sensitisation by dyes **1**—**4** illustrated in Fig. 1 despite the similar maxima and intensities of the absorption bands of the *J*-aggregates. Table 2 presents certain photographic characteristics of the layers sensitised by individual *J*-aggregating dyes.[68] The relative quantum yield of the spectral sensitisation was determined by means of the equation[74]

$$\varphi_r = \frac{A_{410}\, S_\lambda\, 410}{A_\lambda\, S_{410}\lambda}, \qquad (10)$$

where A_{410} and A_λ are the absorption coefficients of the emulsion layer at 410 nm and at the wavelength λ corresponding to the absorption maximum of the dye, while S_{410} and S_λ ($cm^2\,erg^{-1}$) are the photosensitivities of the layer at the corresponding wavelengths. The coefficient φ_r is the ratio of the number of quanta in the regions corresponding to absorption by AgHal (410 nm) and the dye (λ, nm) leading to the same photographic effect—in the given instance to the blackening density $D = 0.5$ over the fogging level.

According to the data in Table 2, dye **1**, which exhibits a desensitising effect, tends to decrease the intrinsic sensitivity of the emulsion (S_{410}). In contrast to dye **1**, dye **3** has little effect on S_{410}, which may be due to the difference between the potentials $E_{1/2}^{Ox}$ (Table 1). The highly effective dyes **2**, **4**, and **14** have virtually no desensitising effect [cf. the degrees of desensitisation (DD) in Table 2]. The quantum yields φ_r for the dyes are comparatively high—0.70 to 0.85, i.e. in order to induce the same effect as that of the 'blue' quantum 1.2—1.4 quanta absorbed by the dye are required. In the case of self-desensitising dyes **1** and **3**, the quantum yields φ_r are significantly smaller (0.40—0.08), i.e. 2.5—12 quanta are now required per 'blue' quantum.

Table 2. Photographic characteristics of layers based on the AgBr emulsion sensitised by individual *J*-aggregating dyes.[68]

Dye	λ_{max}^{sens}/nm	S_{410}^{a}/cm² erg⁻¹	S_{λ}/cm² erg⁻¹	DD	φ_r[a]
Without dye	–	1.2	–	–	–
1	568	0.5	0.4	2.4	0.40
2	577	1.1	1.6	1.1	0.85
3	575	1.1	0.2	1.1	0.08
4	545	1.1	1.6	1.1	0.85
14	518	1.1	0.9	1.1	0.70
	590		0.7		0.70

[a] Calculated on the basis of the criterion $D = 0.5 + D_0$.

Thus the effectiveness of the light quanta absorbed by the sensitiser is much smaller than that of the photons absorbed by the AgHal lattice, the latter being suppressed by desensitisation in the case of dye **1**.

The well known experimentally observed decrease in spectral sensitisation with increase in the concentration of *J*-aggregating dyes above the optimum value can also be accounted for within the framework of ideas concerning the self-desensitisation of dyes. By virtue of the increase in the coating of the surface of the AgHal microcrystals by the *J*-aggregates, the distance *r* between them and the IC_e should decrease and hence the rate of recombination process should increase.

On the basis of the foregoing, one may conclude that the self-desensitisation processes can in essence determine the effectiveness of the spectral sensitisation itself. As a result of the examination of the role of the self-desensitisation processes in the spectral sensitivity of silver halide photographic materials, it has been concluded[25] that the spectral sensitisation of negative silver halide emulsions is determined not by the primary photoreaction but by the kinetics of secondary reactions, i.e. self-desensitisation reactions. The theory of the spectral sensitisation of such materials must therefore be in the first place a theory of the self-desensitisation of dyes. It is noteworthy that this postulate is valid only if desensitisation (and self-desensitisation) via the hole mechanism is included in the concept of desensitisation. Subsequent studies[8,26,47–49,57,68] only increased the author's certainty about the validity of this postulate.

IV. Supersensitisation of *J*-aggregating dyes as inhibition of their self-desensitisation

Within the framework of the mechanism of the spectral sensitisation of *J*-aggregating dyes under discussion, it is possible to consider at least three methods for increasing the effectiveness of the sensitisation, i.e. three supersensitisation methods. They all reduce to the inhibition of the self-desensitisation via the hole mechanism and hence to the inhibition of recombination processes. One of the supersensitisation methods mentioned in the introduction consists, according to Gilman's 'reductive' mechanism,[10,24] in the capture (reduction) of the dye holes by the more readily oxidised organic compound. Thus the supersensitisation conditions already mentioned may be expressed in the form[10]

$$E_{1/2}^{Ox}(S) < E_{1/2}^{Ox}(Dy) .$$

A hole of the *J*-aggregate is then translocated to the supersensitiser (S), loses its mobility, and no longer participates in the recombination processes. Since Gilman's supersensitisation mechanism has already become in essence classical and has been discussed in detail in a number of reviews,[7–13] it will not be considered separately in the present article.

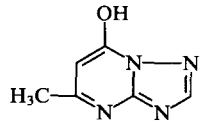
The second supersensitisation method reduces to the insulation of the *J*-aggregates of the impurity centres, which prevents the recombination of the dye holes with the electrons captured by these centres. This 'insulation' mechanism of supersensitisation will be examined in detail below.

The generally acknowledged factors influencing the aggregation of dyes are their structure, the halide composition of the photographic emulsion, the type of faces of the AgHal microcrystals, the concentration of silver ions, the acidity of the medium, and the nature of various substances introduced into the emulsion.[7] Since the self-association of dyes is a process which takes place over a period of time, it is logical to postulate that some of the factors enumerated influence the kinetics of the formation of the ordered structures of the aggregates. On the other hand, the aggregation kinetics can undoubtedly determine the structure of the aggregate — primarily the packing angle of the dye molecules in the aggregate and their number and hence the topography on the surface of AgHal and in particular the distance *r* from the IC_e. The third supersensitisation method consists in the regulation of the *J*-aggregation of the dyes with the aid of organic substances, introduced additionally into the emulsion, which are either adsorbed or not adsorbed on AgHal.

1. The 'insulation' mechanism of supersensitisation

Towards the end of the 1970's, a considerable number of experimental data accumulated according to which the supersensitisation of photographic layers with *J*-aggregating dyes was induced by organic compounds oxidised with greater difficulty than the dyes. Since the principal condition for supersensitisation via Gilman's 'reductive' mechanism was infringed in such cases, it followed naturally that one could deal only with some other supersensitisation mechanisms.

The supersensitising effect of a familiar stabiliser — 4-hydroxy-6-methyl-1,3,3*a*,7-tetraazaindene **18** (the sta-salt) — has been described in greatest detail. It is manifested on emulsions with sulfur sensitisation.[3,9,75–79]



18

The increase in the additional sensitivity induced by certain *J*-aggregating dibenzothiacarbocyanines and unaccompanied by a change in the nature of the absorption centres has been explained[78,79] by the facilitation of the transfer of the energy absorbed by the dye to the AgHal lattice. The effect of various 2- and 5-alkyl derivatives of compound **18** has been investigated.[80] An increase in the intrinsic sensitivity and the preferential growth of the spectral sensitivity of the emulsion were noted. The influence of the compounds on the additional sensitivity is regarded by the authors as the sum of two effects: (1) the influence on the intrinsic sensitivity of the microcrystals because of the deactivation of a number of sensitivity centres following the chemisorption of compound **18** and its derivatives on the impurity centres as a result of which the latter cease to serve as the sites for the capture of electrons;[81] (2) the influence on the state of aggregation of the dye adsorbed on AgHal.

The photographic effect of compound **18** and other tetra- and penta-azaindenes has been investigated in a series of studies by Tani and coworkers.[82–86] It was shown[82] that compound **18** is primarily a chemical sensitiser of monodisperse emulsions with sulfur sensitisation. Various sulfur-containing anti-fogging substances exhibit an influence similar to that of compound **18**.[83] The mechanism of the action of the stabiliser **18** on the intrinsic sensitivity of AgHal is treated as an increase in the depth of the electron traps formed on sulfur sensitisation and a decrease in the number of fine traps on the surface of microcrystals acted upon by the adsorbed tetraazaindene.[85] It is not difficult to see in this interpretation a definite similarity with the concept proposed previously.[80,81] The preferential influence of compound **18** and other supersensitisers on the spectral sensitivity of emulsions with

sulfur sensitisation has been explained[84] by a decrease in the desensitising effect of dyes both due to the increase in the fraction of electrons captured by the sulfide-silver centres at greater depth and due to the decrease in the mobility of the dye holes in the aggregates. In addition, the increase in the rate of electron transfer on fragmentation of the *J*-aggregates by the supersensitiser,[87] similar to that described by West and Carroll,[15] has been considered.

The influence of compound **18** on various *J*-aggregating dyes has been considered in a series of studies by the present author.[8,26,47–49,68] In the first place, the influence of the sta-salt was considered in relation to the repeatedly investigated quino-2,2′-monomethinecyanine **3**. For a monodisperse AgBr emulsion (cubic crystals, $\bar{l} = 0.17$ μm) with sulfur-gold sensitisation it has been shown that a transformation of the *J*-band ($\lambda^{J}_{max} = 575$ nm) is observed under the influence of the sta-salt, namely its hypsochromic shift at low concentrations of compound **18** amounting to $(1-2) \times 10^{-3}$ mol (mol AgBr)$^{-1}$, the appearance of two absorption bands ($\lambda^{J_1}_{max} = 570$ nm, $\lambda^{J_2}_{max} = 581$ nm) with increase in the concentration of compound **18** to $(2-5) \times 10^{-3}$ mol (mol AgBr)$^{-1}$, and finally the appearance of one long-wavelength J_2 band at a concentration equal to or greater than $(8-10) \times 10^{-3}$ mol (mol AgBr)$^{-1}$ (Fig. 6). According to Fig. 6*b*, the content of compound **18** does not induce the growth of the photographic activity of the J_1-aggregates (cf. curves *1* and *2*, Fig. 6*b*) but it does supersensitise the J_2-aggregates. It is noteworthy that the nature of the aggregation and the effectiveness of the supersensitisation depend to a large extent on the order in which the supersensitiser and the dye are introduced. When compound **18** is introduced before the dye, the maximum supersensitisation effect and subsequent formation of the J_1- and J_2- aggregates are observed; when compound **18** is introduced after the dye, the effectiveness of the supersensitisation is reduced sharply and is accompanied by a slight transformation of the *J*-band.[47] The influence of the order in which compound **18** is introduced on the aggregation has been noted also in another study.[76]

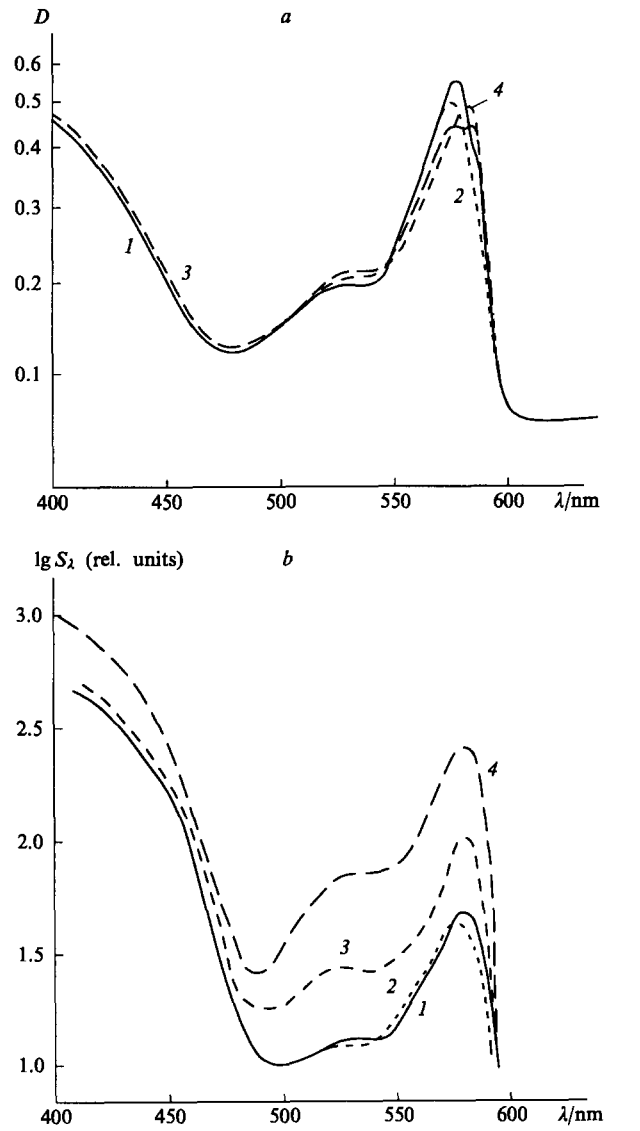
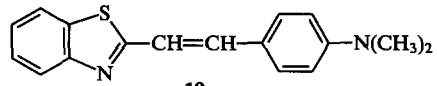


Figure 6. Reflection spectra (*a*) and spectral sensitivity curves (*b*) for AgBr emulsion layers sensitised by dye **3** [2×10^{-4} mol (mol AgBr)$^{-1}$] without a supersensitiser (curve *1*) and with the supersensitiser **18** at different concentrations [10^{-3} mol (mol AgBr)$^{-1}$]: (*2*) 1.0; (*3*) 4.0; (*4*) 8.0; emulsion with (S + Au)-sensitisation.

It has been shown[47] that the introduction of the supersensitiser 2-(*p*-dimethylaminostyryl)benzothiazole **19**, which is traditional for dye **3** and which operates via Gilman's 'reductive' mechanism, into spectrally sensitised layers containing various amounts of compound **18** does not alter the nature of the absorption spectra.



19

It is striking that the supersensitising effect of compound **19** on layers with J_1-aggregates is significantly smaller than the effect on the *J*-aggregates of dye **3** without compound **18** (cf. curves *5* and *6*, Fig. 7), while on layers with J_2-aggregates an additional supersensitisation effect was observed (cf. curves *3* and *7* and curves *4* and *8* in Fig. 7).

Table 3 presents the calculated relative quantum yields of the spectral sensitisation of the photographic layers investigated.[47] It follows from the data in Table 3 that, at low concentrations of compound **18**, whereupon J_1-aggregates are formed preferentially, there is virtually no supersensitising effect of compound **19**. On the other hand, at higher concentrations of compound **18**, in the region where J_2-aggregates are formed, a superadditive effect of compounds **18** and **19** is observed. In this case, $\Delta\lg S_\lambda^{18+19} \approx \Delta\lg S_\lambda^{18} + \Delta\lg S_\lambda^{19}$, and $\varphi_r^{18+19} > \varphi_r^{18} + \varphi_r^{19}$. These data led to the conclusion[47] that the superadditive effect may serve as definite evidence for the different mechanisms of the supersensitisation of the layers by compounds **18** and **19**.

Table 3. The influence of the supersensitisers **18** and **19** on the relative quantum yield of the spectral sensitisation of the photolayers sensitised by quino-2-monomethinecyanine **3** [2×10^{-4} mol (mol AgBr)$^{-1}$].[47]

Supersensitiser	$10^3 c$/mol (mol AgBr)$^{-1}$ [a]	φ_r [b]			Nature of *J*-aggregation[c]
		λ_{570}	λ_{575}	λ_{581}	
–	–	0.02	0.02	0.02	*J*
18	2.0	0.03	0.02	0.03	J_1
18	5.0	0.09	0.11	0.16	J_1+J_2
18	20.0	0.19	0.21	0.19	J_2
19	0.02	0.23	0.22	0.20	*J*
18+19	2.0+0.02	0.04	0.04	0.04	J_1
18+19	5.0+0.02	0.36	0.44	0.53	J_1+J_2
18+19	20.0+0.02	0.49	0.69	0.55	J_2

[a] *c* = supersensitiser concentration.
[b] Calculated on the basis of the criterion $D = 0.2 + D_0$.
[c] AgBr emulsion with (S + Au)-sensitisation.

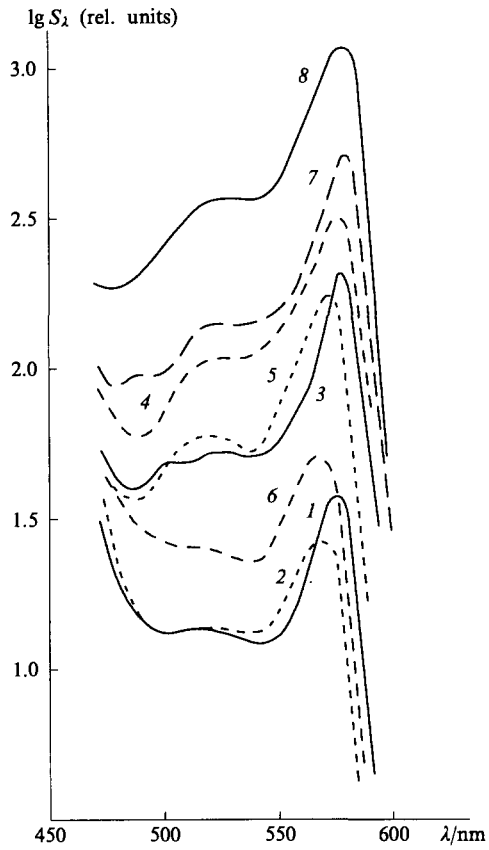


Figure 7. Spectral sensitivity distribution curves for AgBr emulsion layers sensitised by dye **3** [2 × 10^{-4} mol (mol AgBr)$^{-1}$] without a supersensitiser (curve *1*) and with the supersensitiser **18** at different concentrations [10^{-3} mol (mol AgBr)$^{-1}$]: (*2*) 2.0; (*3*) 5.0; (*4*) 20.0; emulsions sensitised by dye **19** at a concentration of 2 × 10^{-5} mol (mol AgBr)$^{-1}$ (curve *5*); emulsion sensitised by the **18** + **19** composition at different concentrations [mol (mol AgBr)$^{-1}$]: (*6*) 2 × 10^{-3} and 2 × 10^{-5}; (*7*) 5 × 10^{-3} and 2 × 10^{-5}; (*8*) 20 × 10^{-3} and 2 × 10^{-5}; emulsion with (S + Au)-sensitisation.

It is striking that the photographic effect of compound **18** on the same AgBr emulsion but without chemical sensitisation is completely different despite the similar influence of compound **18** on the transformation of the *J*-bands of aggregates of dye **3**. At low concentrations of compound **18** [$\leqslant$ 2 × 10^{-3} mol (mol AgBr)$^{-1}$], a slight increase in the photographic sensitivity of the layer is observed in the region of absorption by the J_1-aggregates, but, as the content of compound **18** rises and J_2-aggregates are formed, a decrease in the effectiveness of the dye is observed. This is illustrated in Fig. 8, from which it also follows that aminostyrylbenzothiazole **19** supersensitises the *J*-aggregates of dye **3** regardless of its chemical sensitisation (cf. curves *1* and *5*, Fig. 8*b*). Thus the photographic effect of compound **18** is due to at least three causes: (a) the adsorption of compound **18** on the AgBr surface before the adsorption of the dye, (b) the presence of the products of the sulfur-gold sensitisation, and (c) the type of the *J*-aggregate.

The effect of the sensitiser **18** has been investigated[49] for a series of *J*-aggregating dyes of different structure: imidacarbocyanines **1**, **2**, **6**, and **7**, thiacarbocyanines **9**, **11**, **12**, **14**, and **15**, and oxacarbocyanine **4**. It is striking that the greatest photographic effect of compound **18** is observed on photographic emulsions sensitised by aggregating dyes, which gives rise to appreciable desensitisation (compounds **1**, **6**, **9**, and **15**). For dyes similar to quinomonomethinecyanine **3**, after the introduction of compound **18** a hypsochromic shift of the absorption *J*-bands is observed initially, then their bathochromic shift, and finally, at concentrations [**18**] $\geqslant$ 10^{-2} mol (mol AgHal)$^{-1}$ (except for compound **15**) there is again a hypsochromic shift of the *J*-band. On formation of long-wavelength J_2-aggregates under the influence of compound **18**, there is an appreciable decrease in the degree of desensitisation and there is a sharp jump in the additional photosensitivity. For example, for dye **6**, the supersensitisation coefficient is K_s = 20. Under these conditions, K_s significantly exceeds the change in the degree of desensitisation. For the highly effective and less desensitising dyes **2**, **7**, **12**, **14**, and **4**, for which only a slight hypsochromic shift of the *J*-band under the influence of the stabiliser **18** is observed, the decrease in the degree of desensitisation leads to an increase in the additional sensitivity of similar magnitude. The significantly greater value of K_s relative to the change in the degree of desensitisation for dyes **1**, **6**, **9**, and **15** has

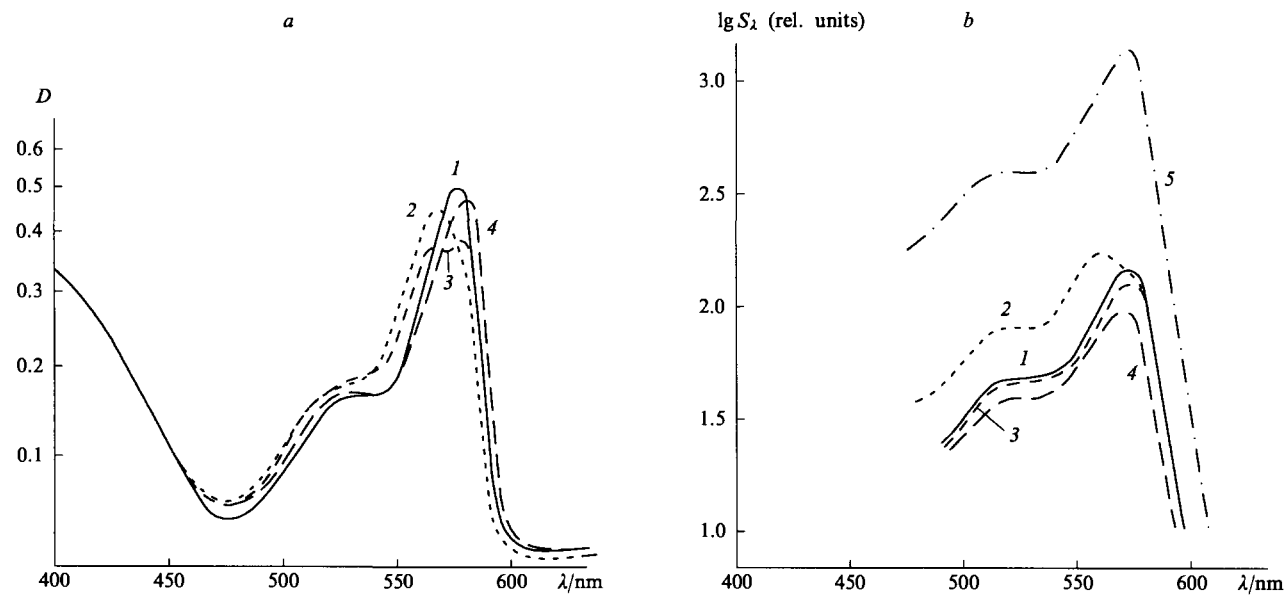


Figure 8. Reflection spectra (*a*) and spectral sensitivity curves (*b*) for AgBr emulsion layers sensitised by dye **3** [2 × 10^{-4} mol (mol AgBr)$^{-1}$] without a supersensitiser (curve *1*) and with the supersensitiser **18** at different concentrations [10^{-3} mol (mol AgBr)$^{-1}$]; (*2*) 1.0; (*3*) 5.0; (*4*) 20.0; with the supersensitiser **19** at a concentration of 2 × 10^{-5} mol (mol AgBr)$^{-1}$ (curve *5*); emulsion without chemical sensitisation.

been considered[49] as additional evidence for the difference between the processes involving the desensitisation of AgHal by dyes and the self-desensitisation of the dyes. If this is so, then the inhibition of the self-desensitisation by compound **18** should affect the spectral sensitivity of the emulsion to a greater extent than its intrinsic sensitivity.

The effect of the stabiliser **18**, manifested on AgHal emulsions with chemical sensitisation, has been explained by the formation of an 'insulating' layer between the *J*-aggregates and the impurity centres (IC_e) — the products of the sulfur-gold sensitisation. This layer, comprising molecules of the supersensitiser (S), should prevent the recombination of the dye holes with the electrons captured by the IC_e, which is illustrated schematically in Fig. 9*a*. The formation of the layer between the products of the sulfur sensitisation and the dye should be promoted by the known preferential adsorption of compound **18** on Ag_2S compared with AgHal.[88] The formation of such a layer between the dye *J*-aggregates and the silver sulfide clusters has been demonstrated by the luminescence method.[89,90] It has been established[91–93] that the sulfur sensitisation of silver halide emulsions is accompanied by the appearance of a low-temperature luminescence in the near infrared. The sulfide-silver clusters of the type $(Ag_2S)_n$ or $(Ag_2S)_n.Ag_m$ generated during chemical sensitisation, are responsible for the above luminescence, the position of the luminescence band in the spectrum depending on the value of n.[93,94] Belous and Tolstobrov[95] observed that the absorption of light by the dye *J*-aggregate adsorbed on silver sulfide in the dye–Ag_2S cluster system diminishes the intensity of the luminescence of the Ag_2S cluster in the IR region of the spectrum.

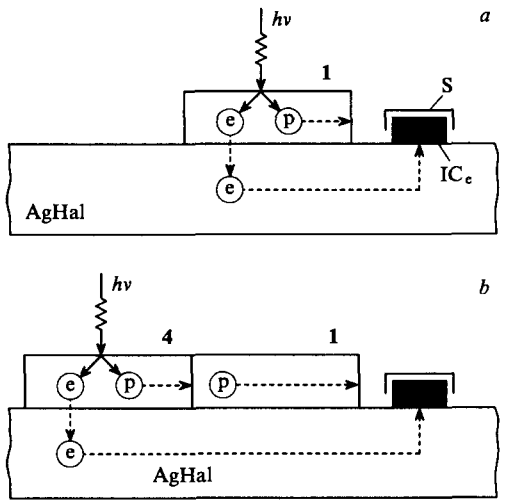
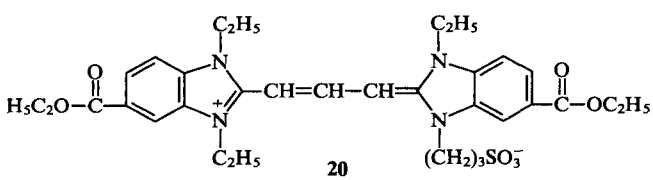


Figure 9. Schematic representation of the 'insulation' supersensitisation mechanism involving the inhibition of the type (II) self-desensitisation (*a*) and the selective desensitisation by compositions comprising *J*-aggregating dyes (*b*).

Fig. 10 presents the dependence of the luminescence intensity I of the silver sulfide clusters on the exciting light wavelengths λ_e.[90] The Ag_2S clusters were spectrally sensitised by dye **3** and 3-{2-[3-(5-ethoxycarbonyl-1,3-diethyl-2,3-dihydrobenzimidazol-2-ylidene)prop-1-enyl]-5-ethoxycarbonyl-1-ethylbenzimidazol-3-yl}propanesulfonate **20**.



20

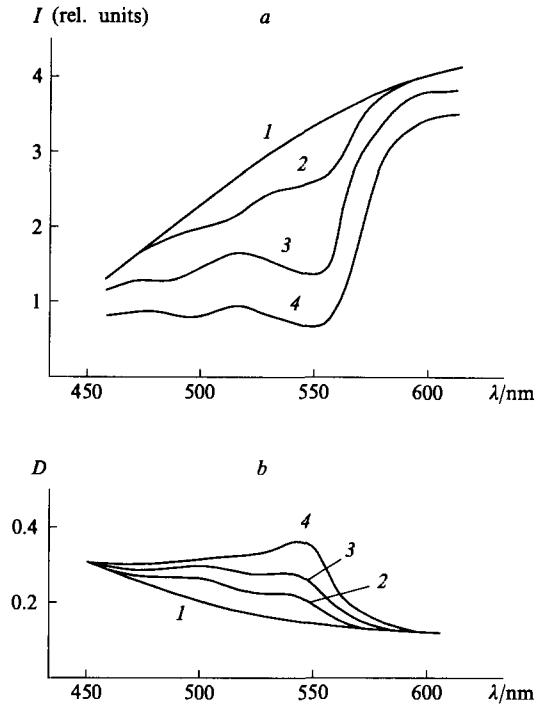


Figure 10. Dependence of the intensity of IR luminescence on the incident light wavelength (*a*) and the spectral distribution of the absorbances (*b*) of gelatine layers containing Ag_2S clusters and compound **18**. Dye concentration (10^{-4} M): (*1*) 0; (*2*) 0.1; (*3*) 0.25; (*4*) 0.5.

According to Fig. 10, as the *J*-aggregates of the dyes are formed, a decrease in I is observed. The decrease was explained by the Fano antiresonance effect[96] due to the interference of the excited state of the dye and Ag_2S, which may lead to the observation of a sharp decrease in the absorption coefficient within narrow spectral regions. A similar decrease in the luminescence intensity of the Ag_2S clusters (with λ_{max} = 800 nm), formed on sulfur sensitisation of monodisperse AgBr emulsions with cubic microcrystals, occurred on excitation by light corresponding to the absorption band of the *J*-aggregates of different dyes.[89,90] Fig. 11*a* illustrates the decrease in the intensity of the IR luminescence of Ag_2S clusters at the wavelength of the band due to the *J*-aggregate of dye **20**. A similar pattern has been observed also for other *J*-aggregating dyes.[90]

A necessary condition for the manifestation of the antiresonance, apart from the energy correspondence between the excited levels of the dye and the Ag_2S clusters, is also direct contact of the sensitiser with the impurity centre. The luminescence method therefore makes it possible to establish unambiguously the occurrence of the direct interaction of the dyes with the chemical sensitisation products. An increase in the distance between the cluster and the dye should entail a sharp decrease in the antiresonance and hence an increase in the intensity of the sensitised luminescence of the Ag_2S cluster. Experiments[89,90] have shown that the introduction of compound **18** weakens the decrease in I caused by the antiresonance (Fig. 11*b*) and, at concentrations exceeding 0.1 g per litre of the emulsion, a typical case of sensitised luminescence can be recorded. A similar pattern has been observed when the Ag_2S and dye aggregates were separated by AgBr shells grown on the AgBr microcrystal after sulfur sensitisation and before the introduction of the dye (Fig. 11*c*). Thus comparison of the data presented permits the conclusion that compound **18** does indeed ensure the spatial insulation of the dye from the Ag_2S clusters and the explanation of the photographic effect of this compound may be the inhibition by the above 'insulating' layer of the secondary reactions involving the oxidation of the photographically active centres by the dye

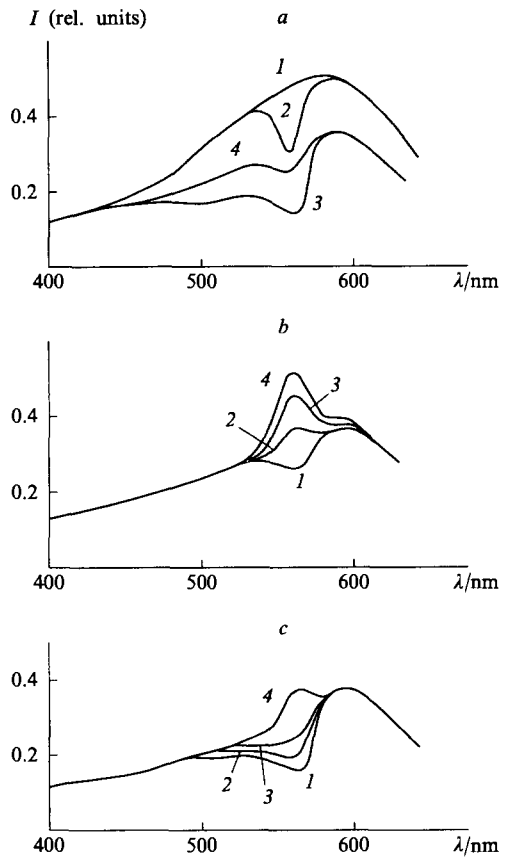


Figure 11. Dependence of the luminescence intensity of the sulfur-sensitised AgBr emulsion with λ_{max} = 800 nm on the wavelength of the light incident on layers sensitised by dye **20** [10^{-4} mol (mol AgBr)$^{-1}$]: (*a*) without a dye (curve *1*); with the dye at concentrations of 0.1 (curve *2*), 0.6 (curve *3*), and 1.0 mol (mol AgBr)$^{-1}$ (curve *4*): (*b*) with the dye and the supersensitiser **18** at concentrations of 0 (curve *1*), 0.1 (curve *2*), 0.3 (curve *3*), and 0.8 g litre^{-1} (curve *4*); (*c*) with the dye at a concentration of 6 × 10^{-5} mol (mol AgBr)$^{-1}$; thickness of the AgBr shell on the microcrystals (Å): (*1*) 0; (*2*) 10; (*3*) 15; (*4*) 30. The $I = f(\lambda)$ relations have been normalised for λ = 400 nm.

holes (Fig. 9*a*). Evidence for the insulation of the dye from the impurity centres is provided by the experiments, mentioned above, designed to elucidate the influence of the order of the introduction of compound **18** into the emulsion on the photographic and spectral characteristics of the photolayers. When compound **18** is introduced before the dye, the adsorption of the supersensitiser on the Ag_2S centres and hence their insulation from the dye *J*-aggregates are more likely. When the dye is introduced first, the *J*-aggregates apparently come into contact with the Ag_2S centres and the subsequent addition of compound **18** now has little influence on the state of the dye and its photographic effect.

The question arises of the cause of the different photographic effects of compound **18** on the dye J_1- and J_2-aggregates and in particular on the *J*-aggregates of quinomonomethinecyanine **3**. When the light quanta absorbed by the *J*-aggregates of dye **3** are of similar magnitude ($\Delta h\nu$ = 0.04 eV), this difference may be a consequence of the different oxidising capacities of the holes, which are determined both by the positions of the highest occupied electronic levels of the aggregates ε_{ho} (the energy factor) and by the length of the associated dye species and their proximity to the impurity centres (the frequency factor). An attempt to determine the position of the energy levels of the *J*-aggregates of dye **3** has been undertaken [48] using photographic and luminescence methods for the purpose. The difference between the oxidising capacities of the J_1- and J_2-aggregates has been demonstrated in a study of the photochemical oxidation of the latent image centres generated by the preliminary exposure to light of the AgBr emulsion with sulfur-gold sensitisation. *N,N'*-Dimethyl-4,4'-bipyridylium dichloride (methylviologen) was used as the photoelectron acceptor. The J_1- and J_2-aggregates were formed by the procedures described above with the aid of the stabiliser **18**. Fig. 12 presents the corresponding spectrograms. The photochemical oxidation of the latent image is most effective in layers which do not contain or contain only small amounts of compound **18**, i.e. in the presence of J_1-aggregates (Figs 12*b* and 12*c*). Photobleaching is then most pronounced in the region of the absorption maximum of the J_1-aggregates at 570 nm. On raising the concentration of compound **18**, i.e. with increase in the amount of J_2-aggregates, the effectiveness of the photobleaching falls (Figs 12*d*, 12*e*, and 12*f*). It is striking that in the region of the absorption by the J_2-aggregate (λ = 581 nm) the extent of photobleaching diminishes sharply and then is not observed at all. Furthermore, a negative image is produced (Figs 12*d* and 12*e*). The formation of the J_2-aggregate is accompanied by a decrease in the extent of photobleaching by the light corresponding to the intrinsic absorption band of AgBr (λ < 400 nm, cf. Figs 12*a* and 12*c* and Figs 12*d*, 12*e*, and 12*f*). At concentrations of compound **18** greater than 10^{-2} mol mol^{-1} AgBr, at which new J_2'-aggregates are formed (λ = 578 nm), the effectiveness of the bleaching again increases (Figs 12*g* and 12*h*). Thus the oxidising capacity of the holes of the J_1-aggregate is greater than that of the holes of the J_2-aggregate; the J_2'-aggregate apparently occupies an intermediate position.

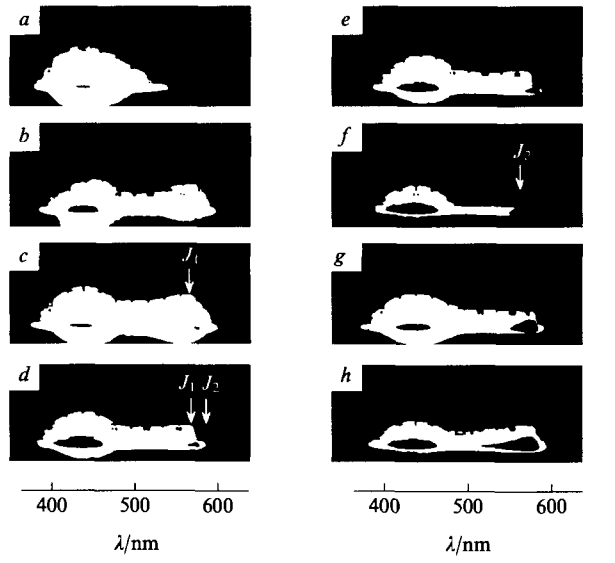


Figure 12. Photobleaching sensitisation spectra for AgBr emulsion layers without a dye (*a*), spectrally sensitised by dye **3** [2 × 10^{-4} mol (mol AgBr)$^{-1}$] without a supersensitiser (*b*), and with the supersensitiser **18** introduced before the dye at different concentrations [10^{-3} mol (mol AgBr)$^{-1}$]: (*c*) 2; (*d*) 4; (*e*) 5; (*f*) 9; (*g*) 10; (*h*) 20; emulsion with (S + Au)-sensitisation exposed beforehand to light until the attainment of a fogging level D_0 = 2.0; methylviologen concentration 7.5 × 10^{-4} mol (mol AgBr)$^{-1}$.

The question arises why the stabiliser **18** layer does not protect the latent image centres from the holes of the J_1- and J_2'-aggregates but prevents their oxidation by the holes of the J_2-aggregates. One of the explanations may be that the position of the ε_{ho} level of the J_1-aggregate is adequate for the injection of the hole directly into the silver halide, as a result of which the insulation of the J_1-aggregates from the impurity centres cannot significantly inhibit the recombination of the electrons captured by the traps in AgBr with the holes which have also been injected into AgBr. Experiments, using Gilman's method, [10] on the supersensitisation of these aggregates by the additionally introduced

carbocyanine dyes with different polarographic potentials $E_{1/2}^{Ox}$ varied in the range 0.54–0.98 V (in methanol, rel. n.c.e.) were carried out in order to characterise the disposition of the ε_{ho} levels of the J_1- and J_2-aggregates of dye **3** relative to one another and relative to the AgBr valence band. It was shown[48] that, in the case of the J_1-aggregates of dye **3**, the supersensitising dyes do not affect the spectral sensitivity over the entire range of $E_{1/2}^{Ox}$. For layers containing J_2-aggregates, a distinct supersensitisation effect is observed (Fig. 13). This is consistent with data[47] indicating the different supersensitising effects of the traditional supersensitiser 2-(*p*-dimethylaminostyryl)-benzothiazole **19** on the J_1- and J_2-aggregates of compound **3** (Table 3). For layers with J_2-aggregates over a certain range of $E_{1/2}^{Ox}(S)$, a nearly linear dependence of the logarithm of the supersensitisation coefficients lg K_s on $E_{1/2}^{Ox}(S)$ is observed (Fig. 13). For a potential $E_{1/2}^{Ox}(S) \geqslant 0.82$ V, there is no supersensitisation effect and this value was therefore chosen as a characteristic of the position of the ε_{ho} level of the J_2-aggregate. The conclusion that the ε_{ho} level of the J_1-aggregate is deeper (by 0.10–0.15 eV) than the ε_{ho} level of the J_2-aggregate was reached on the basis of experiments on the quenching of the fluorescence of the aggregates by the same supersensitising dyes.[48] The ε_{vb} level of the J_1-aggregates was estimated in terms of the potential $E_{1/2}^{Ox}(J_1) \approx 0.9-0.95$ V. If one assumes, in conformity with the data of Mikheeva et al.,[57] that the potential of the top of the valence band of AgBr is $E_{vb} = 1.26$ V (rel. n.c.e.), then, in conformity with the data of Shapiro et al.,[48] the time required for the injection of a hole from the J_1-aggregate into the valence band of AgBr is $\tau = 10^{-7}$ s. For the J_2-aggregate, this time is much longer ($\sim 10^{-4}$ s). Thus the injection of a hole from the J_1-aggregate of dye **3** into AgBr is entirely probable.

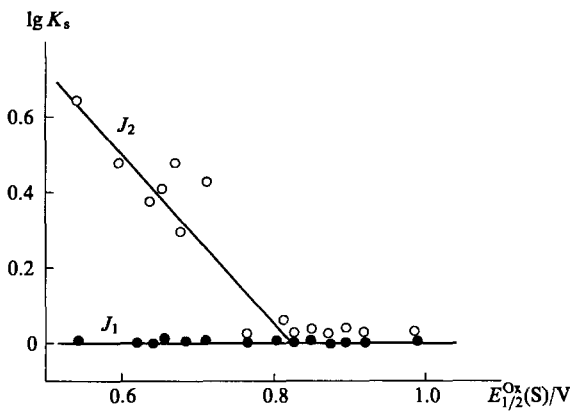


Figure 13. Dependence of the logarithm of the supersensitisation coefficient (lg K_s) for AgBr emulsion layers spectrally sensitised by dye **3** [2×10^{-4} mol (mol AgBr)$^{-1}$] in the J_1- and J_2-states on the potential $E_{1/2}^{Ox}$ of the supersensitiser dyes [4×10^{-6} mol (mol AgBr)$^{-1}$].

In view of the foregoing, it is important to revise the conditions for the supersensitisation via Gilman's 'reductive' mechanism. When rapid injection of holes from the *J*-aggregate into AgHal is possible, supersensitisers satisfying Gilman's condition $E_{1/2}^{Ox}(S) < E_{1/2}^{Ox}(Dy)$ may have insufficient time to capture a dye hole owing to kinetic limitations. The conditions for supersensitisation via the 'reductive' mechanism have been expressed[48] in the form 0.8 V $> E_{1/2}^{Ox}(S) < E_{1/2}^{Ox}(Dy)$.

Thus a dual influence on the spectral sensitisation processes is characteristic of the hydroxy-derivative of tetraazaindene **18**. This compound promotes the formation of *J*-aggregates of certain types. It has been noted[63] that the formation of the dye *J*-aggregates begins on defects and primarily on AgHal surface steps. The rate of formation of aggregates is then higher and their size is smaller (absorption at shorter wavelengths) on the more defective (111) surface than on the (100) surface. The influence of surface defects on the formation of *J*-aggregates has been fully accounted for from the standpoint of the initiation of a regular structure such as the *J*-aggregate.[7] Apparently the stage involving the initiation of aggregates, requiring a definite activation energy, determines to a large extent the aggregation process itself. Surface defects diminish its energy.

One should recall that surface defects are the sites at which impurity centres are located, including photosensitivity centres formed in the sulfur sensitisation process.[7] One may assume that the introduction of compound **18** at low concentrations leads to the insulation of a comparatively small number of 'deep' defects by the molecules of compound **18** adsorbed on them and that *J*-aggregates are formed on a large number of 'fine' surface defects, which leads to the formation of the smaller J_1-aggregates. We may note that without compound **18** *J*-aggregates are formed on both 'deep' and 'fine' defects, which is the reason for the appearance of a single band with $\lambda_{max} = 575$ nm, arising as a consequence of the superposition of the absorption bands due to at least two *J*-aggregates.

On further increase in the concentration of compound **18**, the tetraazaindene molecules are adsorbed also on finer defects as a result of which the number of these defects diminishes, which promotes the formation of the larger J_2-aggregates. Finally, for a still higher content of compound **18**, the defectiveness of the surface diminishes so much that new J_2'-aggregates are formed on a larger number of surface sites—defects of another type. Thus the stabiliser **18** is a regulator of the defectiveness of the AgHal surface and hence a regulator of the aggregation of the dye.

As a consequence of the causes discussed above, the stabiliser **18** influences the energy levels of the *J*-aggregates. The observed changes in the energy levels of the *J*-aggregates of the same dye either depend on the different numbers of molecules combined in the aggregate or may be determined by the angle of inclination of the molecules in the aggregate.[7] As a rule, an increase in the number of molecules and a decrease in the angle of inclination lead to a bathochromic shift of the absorption owing to the increased length of the delocalised π-system. If the main cause of the difference between the properties of the *J*-aggregates is the number of molecules in the aggregate, then this can be regarded as evidence for a small number of structural elements entering into the polymer, since only in this case should one expect a significant difference between the energetics of the aggregates on increase in their size. This agrees, in particular, with the conclusions reached in studies[97,98] in which *J*-aggregates comprising four dye molecules were considered. *J*-Aggregates consisting of tens or several tens of molecules have been considered in the literature.[7,99]

Fig. 14 presents a photomicrograph of luminescing *J*-aggregates of oxacarbocyanine on a real cubic 1 μm AgBr crystal.[100] It follows from the figure that, at the dye concentrations employed in practice, the *J*-aggregates are preferentially extended in one direction and their size is small.

The lower photographic effectiveness of the J_1-aggregates in the negative process compared with the J_2-aggregates[47] is determined by the deeper disposition of both the highest occupied level ε_{ho} and the lowest unoccupied level ε_{lu} (since the J_1- and J_2-aggregates absorb approximately the same energy). A consequence of the deepening of the ε_{ho} level is the injection of holes into the valence band of AgHal and an increase in the probability of secondary recombination processes, including, as shown by Shapiro and his coworkers,[48] the oxidation of the latent image centres. Owing to the high rate of injection of holes into AgHal, under these conditions the supersensitisers operating in accordance with Gilman's mechanism are apparently unable to capture a dye hole. According to luminescence data,[48,101] the ε_{lu} levels of the *J*-aggregates of dye **3** are located under the conduction band of AgBr. A decrease in the ε_{lu} level in the J_1-aggregate therefore reduces also the probability of the photochemical reduction of AgHal via electron transfer either to the conduction band or to the surface capture levels. Despite the absence of the direct injection of holes from the J_2-aggregate into

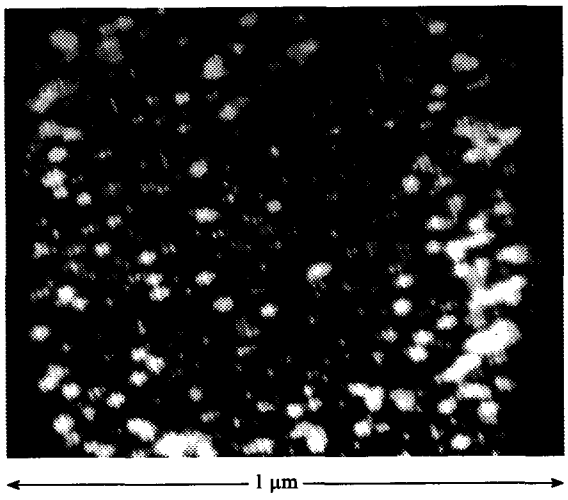
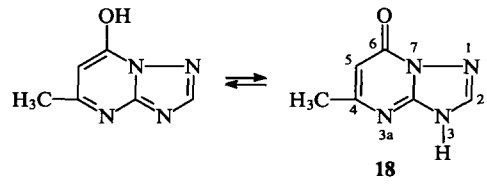


Figure 14. Photomicrograph of luminescing *J*-aggregates of oxacarbocyanine on a 1 μm cubic AgBr microcrystal.

the valence band of AgBr and the higher location of ε_{lu}, the photographic effectiveness of these aggregates is also low in the absence of compound **18**.[47] This indicates the occurrence of secondary reactions involving the recombination of photoelectrons and holes without the participation of the valence band of AgBr. As already noted, the recombination reactions or dye self-desensitisation processes proceeding via a hole mechanism[8,25,26] are apparently determined to a large extent by the presence of direct contact between the *J*-aggregates and the impurity of sulfide-silver centres (Fig. 5*c*). This contact may be a consequence of the localisation of the impurity centres on the surface defects, i.e. the sites where *J*-aggregation begins. Another possible cause is increased adsorption of the dyes on the Ag_2S centres themselves.

Owing to the specific adsorption on Ag_2S, the stabiliser **18** insulates the J_2-aggregates from the impurity centres and hence inhibits the self-desensitisation reactions of the dyes in accordance with the scheme in Fig. 9*a*. Additional evidence in support of the 'insulation' mechanism has been obtained in experiments on the inhibition by compound **18** of the type II selective desensitisation caused by the use of compositions comprising two *J*-aggregating dyes,[68] which was considered in Section III (see Figs. 3 and 4). If the selective desensitisation is associated, in conformity with Fig. 5*b*, with the translation of a hole of the highly effective dye **4** through the *J*-aggregate of dye **1** in contact with the IC_e and hence with the increase in the probability of the recombination processes at the IC_e, then the insulation of the impurity centres in the *J*-aggregates should sharply diminish the selective desensitisation. Indeed it has been shown[68] that the introduction of the sta-salt before the introduction of the **1** + **4** and **1** + **14** dye compositions suppressed the selective desensitisation to a large extent at wavelengths corresponding to the absorption bands of dyes **4** and **14** (Fig. 15). It follows from a comparison of Figs. 4 and 15 that, in the presence of compound **18**, a sharp increase in sensitivity is observed at the wavelengths corresponding to both absorption bands of dye **14** (λ_{max} = 518 and 590 nm) despite the presence of dye **1** in the photographic layer (cf. curves *3* in Figs. 4*b* and 15*b*). This constitutes another piece of evidence indicating that these bands belong to the same dye *J*-aggregate. A similar picture has been observed for the **6** + **14** dye composition. It is striking that the supersensitisation effect at the wavelengths corresponding to the bands of dyes **14** and **4**, estimated in terms of K_s, is close to the selective desensitisations (SD_λ),[68] on the basis of which one may conclude that the supersensitisation is definitely associated with the inhibition of the selective desensitisation and in the general case with the self-desensitisation of the dye. Thus the translation of a hole of one dye through the *J*-aggregate of another becomes ineffective probably owing to the insulation of the *J*-aggregates from the impurity centres, which is illustrated schematically in Fig. 9*b*.

The question arises what determines the specific adsorption of compound **18** on the sulfide-silver centres which imparts unique properties to this stabiliser and supersensitiser. In order to discover the structural element in the molecule of compound **18** promoting the 'insulating' effect, model experiments were performed with heterocyclic compounds having structural elements in common with the sta-salt.[102] The structural formulae of some of them are presented below.



18

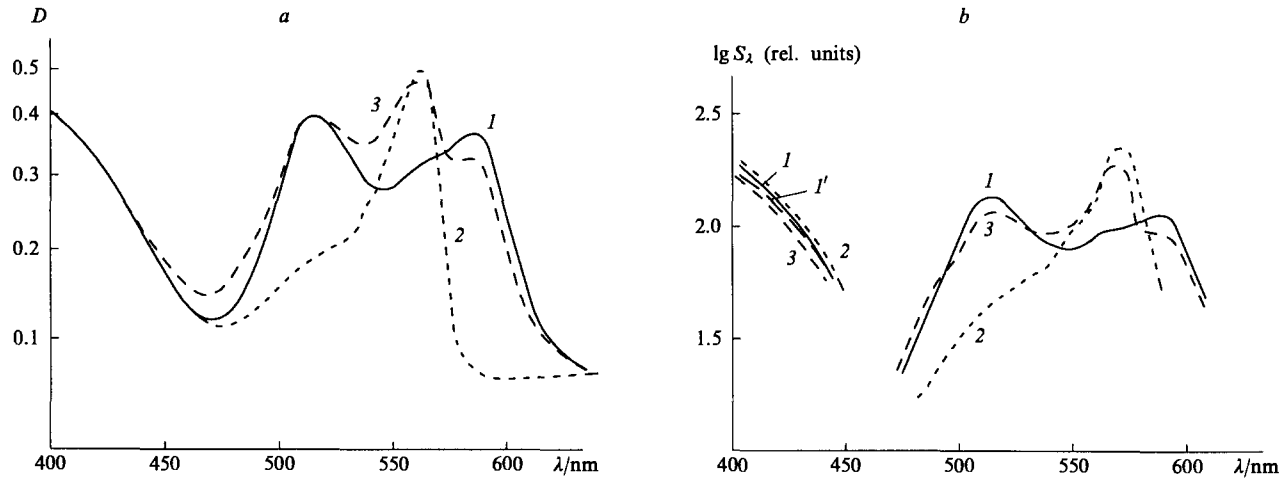
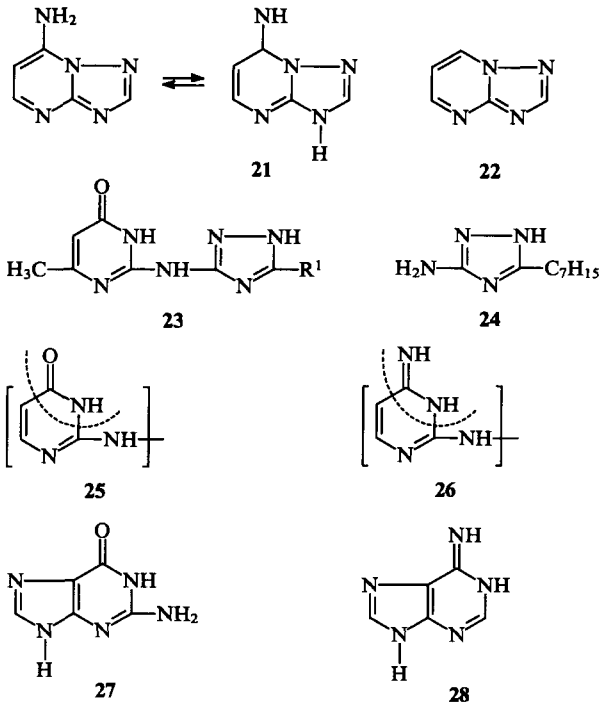


Figure 15. Reflection spectra (*a*) and spectral sensitivity distribution curves (*b*) for AgBr emulsion layers containing the supersensitiser **18** and sensitised by dyes **14** (curve *1*) and **1** (curve *2*) and the **1** + **14** dye composition (curve *3*); (*1'*) layer without dye. Concentration of compound **18**—8 × 10^{-3} mol (mol AgBr)$^{-1}$; concentration of dyes—2 × 10^{-4} mol (mol AgBr)$^{-1}$.



The structural formula with a carbonyl oxygen atom is best justified for compound **18**.[103,104] The study was carried out on fine-grain monodisperse AgBr emulsion [cubic crystals, $\bar{l}$ = 0.17 μm, (S + Au)-sensitisation spectrally sensitised by dye **1**; dye concentration 2 × 10^{-4} mol (mol AgBr)$^{-1}$]. According to the results presented above, the *J*-aggregates of this dye are appreciably supersensitised by compound **18**. The concentration of the substances introduced into the emulsion before the dye was varied over a wide range [from 10^{-4} to 10^{-2} mol (mol AgBr)$^{-1}$].

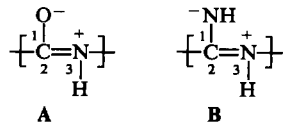
It has been shown that the replacement of the CH_3 group in the 6-position in compound **18** by hydrogen and also the introduction of alkyl groups (up to n-C_7H_{15}) in the 2- and 5-positions do not affect fundamentally the supersensitisation effect. The replacement of the hydroxy-group in the 4-position in compound **18** by an amino-group (compound **21**) also did not change significantly the results, which is illustrated by the supersensitisation coefficients presented in Table 4. On the other hand, compound **22** (without a hydroxy-group) was photographically inactive. Experiments with compound **23** (R^1 = H, CH_3, n-C_7H_{15}, C_6H_5) in which the triazole ring is not condensed with the rest of the molecule, demonstrated their photographic activity, although these compounds were in fact inferior to compound **18** as regards the supersensitising effect. 5-Amino-1,2,4-triazole **24**, which is a fragment of compound **23** (R^1 = C_7H_{15}), by itself had little effect in the concentration range investigated.

Table 4. Photographic effect of compounds **18**, **21**–**24**, **27**, and **28** on layers sensitised by imidacarbocyanine **1**.[102]

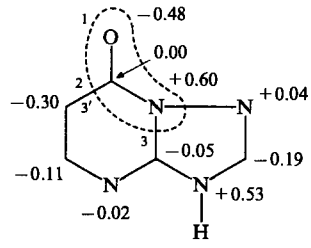
Compound	10^4c/mol (mol AgBr)$^{-1}$	K_s	D_0	λ_{max}^{sens}/nm
Control	–	1.0	0.10	568
18	60	8.0	0.20	571
21	60	7.0	0.26	571
22	60	0.8	0.16	568
23 (R^1 = n-C_7H_{15})	60	3.5	0.11	569
24	60	1.4	0.12	567
27	30	4.8	0.30	569
28	30	6.0	0.20	569

On the basis of the experiments presented, it proved possible to locate extremely approximately the photographically active group within the limits of fragments **25** and **26**. The results obtained with purine bases (guanine **27** and adenine **28**), the structure of which contains the fragments **25** and **26** mentioned above, served as indirect confirmation of this finding. According to the data presented in Table 4, these compounds also have a supersensitising effect on layers with dye **1**.

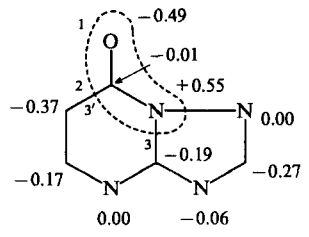
It has been postulated, with a certain amount of caution,[62] that the photographic activity of compounds containing the fragments **25** and **26** is associated with the presence of amide (**A**) or amidinium (**B**) 1,3-dipolar structures.



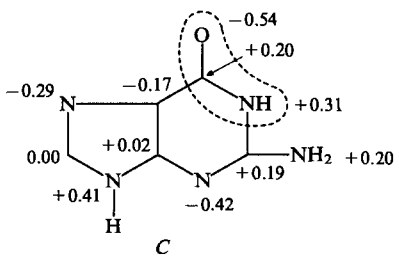
Molecular diagrams of the distribution of π-electron density in the molecule of compound **18** (*A*) and in its anion (*B*), calculated by the molecular orbital method in terms of the Hückel approximation (MOH), are presented below.[62] The parameters taken from Streitwieser[105] were adopted for the Coulombic and exchange integrals. The calculations for the anion of compound **18** were carried out because the anion has in fact been considered in the literature[104] as the photographically active form of compound **18**.



A



B



C

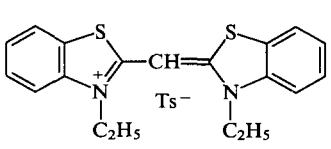
According to molecular diagrams, structures *A* and *B* both contain distinct 1,3-dipoles with a marked localisation of the charges on the oxygen and nitrogen. A characteristic feature of the structures examined is also the presence of a large negative charge on the C(3′) atom of the pyrimidine ring, i.e. a second 1,3-dipole incorporating N(3) and C(3′). A similar pattern in the distribution of π-electron density in guanine has been presented by Pullman and Pullman.[106] The diagram of the π-charges (*C*), calculated by the MOH method, also contains a 1,3-dipole.

The presence of 1,3-dipolar structures is apparently an essential but not a sufficient condition for the photographic activity of the compound. The inclusion of such groups (one or several) in the cyclic system probably promotes the manifestation of supersensitising properties associated with the specific adsorption on the Ag_2S centres.

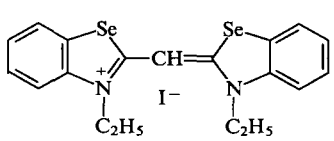
The stabiliser **18** is not the only compound oxidised with difficulty which exerts a supersensitising effect on the dye *J*-aggregates. For example, the application for supersensitisation of compounds, which are clearly oxidised with greater difficulty than the dyes which they supersensitise, has been described in a series of patents mentioned in Mudrovčič's review.[9] It was shown in the early studies by Scheibe and coworkers[17,107] that, together with the readily oxidisable bases of styryl dyes, thiamonomethinecyanine, the polarographic oxidation potential of which ($E_{1/2}^{Ox}$ = 1.20 V) exceeds significantly the potential of quinomonomethinecyanine **3** ($E_{1/2}^{Ox}$ = 0.99 V in CH_3OH rel. Ag/AgCl electrode), has a supersensitising effect on quinomonomethinecyanine **3** *J*-aggregates.[108] We confirmed that certain monomethinecyanines supersensitise the *J*-aggregates of dye **3**; under these conditions, a bathochromic shift of the absorption band maximum of the *J*-aggregate is observed, as for compound **18**.[109] It has been suggested that in this case the 'insulation' supersensitisation mechanism operates.[62,109] It is essential to note that the application of monomethinecyanines as well as quaternary salts of heterocyclic bases as substances increasing the spectral sensitivity of AgHal emulsions sensitised by cyanine dyes has been claimed in a series of patents in the 1970s–1980s (see, for example, Refs 110–113).

The photographic effect of such compounds has been studied in detail.[114] The experiments were performed on a monodisperse AgBr emulsion with cubic microcrystals ($\bar{l}$ = 0.17 μm) with sulfur-gold sensitisation. The principal studies were carried out on two *J*-aggregating dyes—quinomonomethinecyanine **3** and imidacarbocyanine **1**. The choice of these two particular dyes was determined by the following factors. Firstly, following adsorption on AgBr microcrystals, both dyes form *J*-aggregates with similar absorption maxima—λ_{max}(**3**) = 575 nm and λ_{max}(**1**) = 568 nm. Secondly, they have significantly different potentials $E_{1/2}^{Ox}$ ($\Delta E_{1/2}^{Ox}$ = 0.44 V), which should affect the type (II) hole self-desensitisation processes.

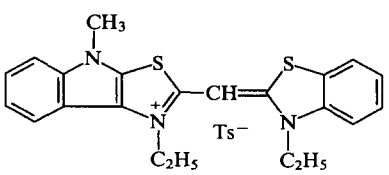
Numerous monomethinecyanines, merocyanines, and styryl dyes have been investigated as supersensitisers. However, the most detailed study has been made of the photographic effect of the four supersensitiser dyes (Dy-S) **29**–**32**. The polarographic potentials of these supersensitiser dyes are presented in Table 5.



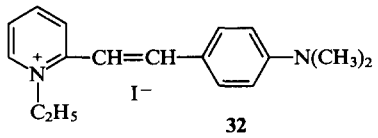
29



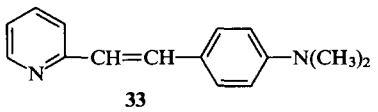
30



31



32



33

Table 5. Characteristics of the dyes investigated[144] (potentials in acetonitrile rel. n.c.e.).

Compound	$E_{1/2}^{Ox}$/V	$-E_{1/2}^{Red}$/V
3	0.94	1.15
1	0.50	1.77
29	1.21	1.52
30	1.21	1.53
31	0.75	1.84
32	0.73	1.24
33	0.60	1.50
19	0.60	1.62

It follows from Table 5 that the supersensitiser dyes **29** and **30** are oxidised with greater difficulty than dye **3** and in addition all the supersensitisers **29**–**32** investigated are oxidised less effectively than dye **1**. The supersensitiser dyes were introduced into the emulsion over a wide range of concentrations [(0.5–8) × 10^{-4} mol (mol AgBr)$^{-1}$] before the *J*-aggregating dyes. Their effect was compared with that of compound **18** and also with the effect of readily oxidisable bases of the styryl dyes **19** and **33** (Table 5) acting on the layers containing dye **3** via Gilman's 'reductive' mechanism.[10]

The main result of the investigation[114] was that the supersensitiser dyes, also oxidised with greater difficulty than dyes **3** and **1**, gave rise to the supersensitisation effect in photographic layers with *J*-aggregates of both spectral sensitisers. It is striking that a definite analogy was observed between the spectral and photographic effects of these supersensitiser dyes and compound **18**. When thiamonomethinecyanine **29** is introduced into the emulsion, the same transformation of the spectra as that occurring after the addition of compound **18** is observed, namely at comparatively low concentrations of compound **29** the maximum of the main absorption band initially undergoes a hypsochromic shift, then, as the concentration is increased, two absorption bands due to two *J*-aggregates (J_1 and J_2) are observed simultaneously, and finally, after further rise in concentration, the longer-wavelength band of the J_2-aggregate is established. The appearance of J_2-aggregates is accompanied by an increase in the effectiveness of the spectral sensitisation by dye **3**. A similar pattern in the changes in the spectra of dye **3** has been observed on treatment with supersensitisers **30**–**32**.

The supersensitising effect is also characteristic of other short-wavelength dyes **30**–**32** investigated (Fig. 16), the maximum effect being obtained for compounds **31** and **32** (by a factor of 5–6). The observed effect of the monomethinecyanines **29** and **30** (in conformity with the potentials $E_{1/2}^{Ox}$), which are difficult to oxidise, cannot be accounted for within the framework of Gilman's 'reductive' mechanism. On the other hand, the capture of a hole from dye **3** is possible for the supersensitiser dyes **31** and **32** in conformity with the potentials $E_{1/2}^{Ox}$ listed in Table 5. However, one should note that, in contrast to the typical supersensitiser **19** (according to Gilman), these dyes induce a significant transformation of the *J*-bands already noted above.

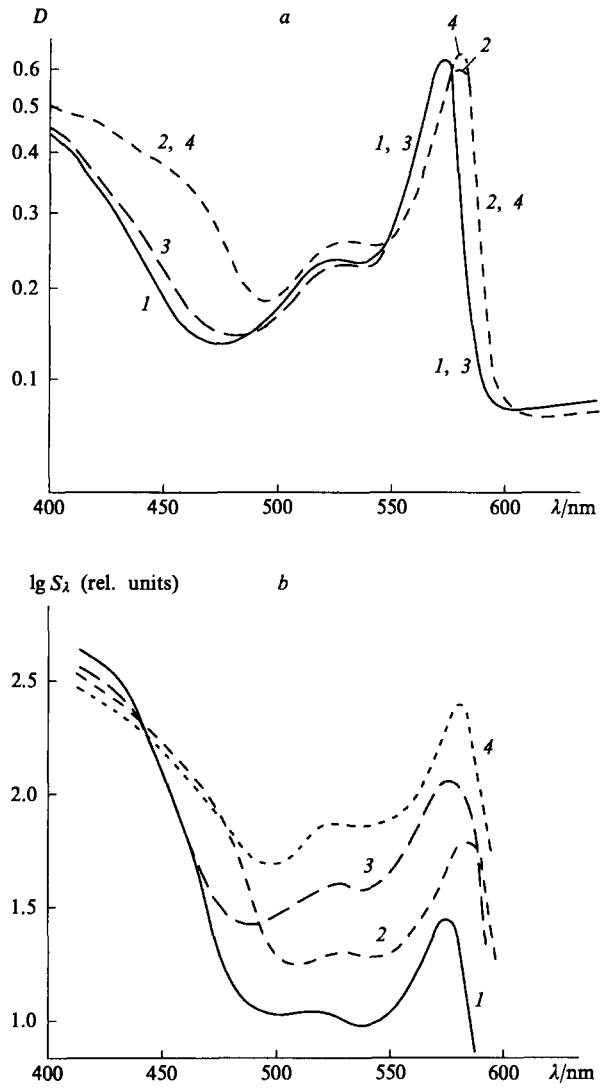


Figure 16. Reflection spectra (*a*) and spectral sensitivity curves (*b*) for AgBr emulsion layers spectrally sensitised by dye **3** [2 × 10^{-4} mol (mol AgBr)$^{-1}$] without a sensitiser (curve *1*) and in the presence of other dyes: (*2*) dye **30** at a concentration of 4 × 10^{-4} mol (mol AgBr)$^{-1}$; (*3*) dye **19** at a concentration of 0.5 × 10^{-4} mol (mol AgBr)$^{-1}$; (*4*) the **30** + **19** composition at concentrations of 4 × 10^{-4} and 0.5 × 10^{-4} mol (mol AgBr)$^{-1}$.

The results of experiments in which compositions of difficult to oxidise supersensitiser dyes with styryl bases **19** and **33** ($E_{1/2}^{Ox}$ = 0.60 V) were used to provide evidence for another mechanism of the influence of compounds **29** and **30** (a non-Gilman mechanism). As with compositions comprising compounds **18** and **19** in earlier studies[47] (Fig. 7 and Table 3), a supersensitisation effect greatly exceeding the effect of the individual substances was observed for the supersensitiser compositions under these conditions. One of the examples of such superadditive effect of compounds **30** and **19** is presented in Fig. 16 (cf. curves *1*–*4*, Fig. 16*b*). It is striking that, in contrast to selenamonomethinecyanine **30**, the styryl base **19** does not alter the position of the *J*-band of the dye (cf. curves *1*, *2*, and *3*, Figs 16*a* and 16*b*). A similar effect has been observed also for the styryl dye **32** and the corresponding base **33**.

The study of the photographic effect of compositions comprising the stabiliser **18** and the supersensitiser dyes **29** and **30** which are difficult to oxidise demonstrated the absence of an additive supersensitisation effect by the compositions, which can be regarded as evidence that the components of the compositions exert an influence of the same type.

The supersensitisation by compounds which are difficult to oxidise is manifested even more clearly on layers with imidacarbocyanine **1**. In this case, all the supersensitisers **29**–**33** were oxidised with greater difficulty than the *J*-aggregating dye **1** (cf. $E_{1/2}^{Ox}$ in Table 5). When compounds **29**–**32** as well as compound **18**[49] are introduced into the emulsion, a characteristic transformation of the *J*-band, analogous to that occurring under the influence of compound **18**, and an increase in the effectiveness of the spectral sensitisation (by a factor up to 5) are observed. Fig. 17 presents examples of the supersensitising effect of the monomethinecyanines **29** and **30**. The introduction of these dyes before the *J*-aggregating dye **1** leads to a bathochromic shift of the absorption bands and to an increase in the spectral sensitivity of the layers (cf. curves *1*–*3*, Figs 17*a* and 17*b*).

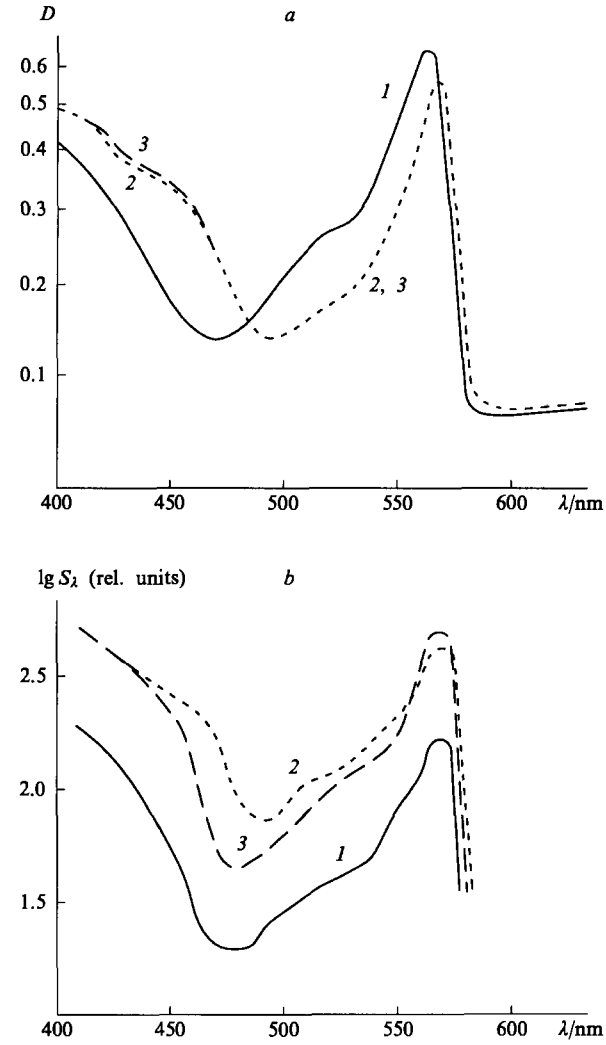


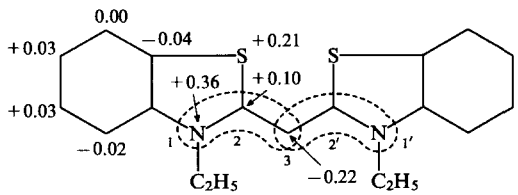
Figure 17. Reflection spectra (*a*) and spectral sensitivity curves (*b*) for AgBr emulsion layers spectrally sensitised by dye **1** [2 × 10^{-4} mol (mol AgBr)$^{-1}$] without a sensitiser (curve *1*) and in the presence of selenamonomethinecyanine **30** (curve *2*) and thiamonomethinecyanine **29** (curve *3*); concentration of the supersensitiser — 4 × 10^{-4} mol (mol AgBr)$^{-1}$.

Since dye **1** is itself a readily oxidised compound ($E_{1/2}^{Ox}$ = 0.50 V), it is hardly subjected to a supersensitising influence by the typical supersensitiser **19** ($E_{1/2}^{Ox}$ = 0.60 V) described in the literature;[10] on the other hand, all the dyes investigated belonging to the classes of monomethinecyanines, merocyanines, and styryl dyes, which are known to be oxidised with greater difficulty than dye **1**, lead to an appreciable increase in the effectiveness of the sensitisation at the wavelength corresponding to the *J*-band of

imidacarbocyanine. It is quite natural that there is also no additive increase in the sensitivity for compositions of the supersensitiser dyes **29** and **30** with the styryl base **19**.

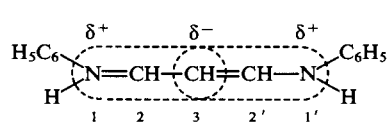
The change in the spectra and in the photographic effect of the difficult to oxidise dyes investigated, similar to the influence of compound **18**, permits the conclusion that the nature of their photographic effect is the same, namely that it entails a single 'insulation' supersensitisation mechanism. This is probably due to the preferential adsorption of dyes belonging to the classes of thia(selena)monomethinecyanines, styryl dyes, and merocyanines on the Ag_2S centres. The selective adsorption of dyes and of the sta-salt on the Ag_2S lattice may be associated with the significant difference between the parameters of this lattice and those of the AgHal lattice and also with the specific properties of the Ag_2S centres having a high concentration of mobile silver ions according to Van Doorselaer's hypothesis.[115] The superionic properties of Ag_2S were examined by Kartuzhalskii et al.[116]

It had been postulated earlier in relation to the sta-salt and its analogues[102] that the selective adsorption of the supersensitiser on the Ag_2S centre may be due to the presence of 1,3-dipolar structures. It is striking that distinct 1,3-dipolar fragments are present in the molecules of cyanines and in the first place monomethinecyanines. According to the molecular diagram for the distribution of π-electron density in thiamonomethinecyanine **29**,[62] calculated by the PPP method, there are several 1,3-dipoles in the supersensitiser dye, including the nitrogen and sulfur atoms of the heterocyclic nuclei and the methine carbon atom.

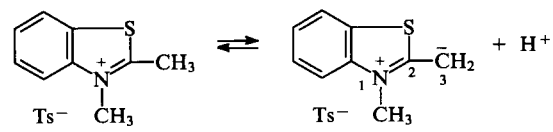


It is striking that the distance between the sulfur atom and the methine carbon atom (~2.6 Å) is close to the distance between the Ag^+ and S^{2-} ions in the Ag_2S clusters (2.58 Å on the AgBr surface).[117] It is significantly smaller than the distance between the Ag^+ and Br^- ions in the AgBr lattice (~2.9 Å). Thus the selective adsorption of organic compounds containing 1,3-dipoles may be due to the correspondence of the distance between the charge centres in the 1,3-dipoles and the distance between the Ag^+ and S^{2-} ions in the Ag_2S clusters.

Experiments with the simplest streptocarbocyanines, also containing 1,3-dipoles in their structure, showed that their introduction into an emulsion sensitised by dye **1** leads to a fourfold increase in additional sensitivity. The increase in sensitivity is accompanied by a bathochromic shift of the *J*-band. The alternation of the π-electron density in the most effective of these dyes is illustrated below.



The supersensitising effect of a quaternary benzothiazole salt (2-methylbenzothiazolium toluene-*p*-sulfonate **34**) has been noted,[114] although it is significantly lower than that of the supersensitiser dyes **29**—**32**. It is well known that the quaternary salts of thiazoles, exhibit, like compound **18**, antifogging and stabilising effects on photographic emulsions.[118] The supersensitisation by the quaternary salt of 2-methylbenzothiazole may be a consequence of the acid properties of the salt, in which a 1,3-dipole may arise after dissociation in accordance with the scheme below.



34

It was noted at the beginning of this review that the first publication by Bloch and Renwick on supersensitisation described the appreciable photographic effect of auramine on layers sensitised in the panchromatic region of the spectrum.[14] We confirmed the sensitising effect of auramine G on layers with the *J*-aggregating dye **1**. Like compound **18**, auramine induces a bathochromic shift of the band of the aggregate. According to the molecular π-electron distribution diagram, calculated by the MHO method, the molecule of auramine G contains 1,3-dipolar fragments and supersensitisation by this dye can therefore also be considered within the framework of the 'insulation' mechanism.

The special role of surface defects in the 'insulation' supersensitisation mechanism necessitated the development, as the next task, of a method which would make it possible to infer the interaction of spectral sensitisers and supersensitisers with the impurity centres formed on chemical sensitisation. The fogging effect of a phenothiazine dye—Methylene Blue (MB)—has been described.[119–121] Eggert and Reitstötter[119] as well as Steigman[120] attribute the fogging to the catalysis of electron transfer from the developer to AgHal involving the adsorbed MB^+ cation. Dähne[121] explains the fogging as a result of the formation of MB^+ dimers following their adsorption on AgHal. It has been noted[119,120] that other sulfur-containing dyes as well as the sulfur-free dye Janus Green also exhibit a fogging capacity.

Preliminary experiments carried out on a monodisperse AgBr emulsion containing cubic microcrystals with sulfur-gold sensitisation showed that the introduction of MB in an amount of $(1-5) \times 10^{-5}$ mol (mol AgBr)$^{-1}$ induces an intense increase in the fog density D_0, from 0.12 to 2.0—4.0, when unexposed emulsions are treated in UP-2 developer (development time 8 min). Naturally, an appreciable desensitisation is also observed under these conditions. It is striking that there was virtually no fogging at the same MB^+ concentrations on the same emulsion not subjected to the (S + Au)-sensitisation. However, in the course of chemical sensitisation, the fogging due to the MB steadily increased[122] with increase in sensitivity, the latter being attributed to the formation of electron-accepting Ag_2S sensitivity centres.[59]

Thus fogging is undoubtedly associated with the presence of Ag_2S centres, formed on sulfur and sulfur-gold sensitisation. One can therefore assume that the fogging effect of MB^+ is caused by its adsorption not on silver halides, as claimed by Eggert and Reitstötter,[119] but on impurity Ag_2S centres (IC_e). The adsorption of MB^+ can be associated with the presence of 1,3-dipoles in the structure of the phenothiazine dye. As a result of the specific adsorption of the electron-accepting MB^+ on the IC_e, there is a possibility of catalysis of the electron transfer from the developer to the Ag_2S centre and further to AgHal. This is illustrated schematically in Fig. 18 (see over), according to which direct electron transfer from the developer (Red) to the Ag_2S centre is kinetically hindered owing to the high energy barrier corresponding to the activation energy E_{act} (Fig. 18*a*). As a result of the specific adsorption of MB^+ on the Ag_2S centre, the electron transfer reaction is divided into two stages, the first of which is electron transfer from Red to MB^+. Owing to the lower activation energies for the two stages (E'_{act} and E''_{act}) compared with E_{act}, catalysis of the oxidation-reduction reaction, expressed by the fogging of the photolayers, is observed (Fig. 18*b*). According to the data of Eggert and Reitstötter,[119] the dye Janus Green also exhibits a fogging capacity. It has likewise been demonstrated that electron-accepting pyrylo- and thiapyrylo-monomethinecyanines are effective fogging agents.

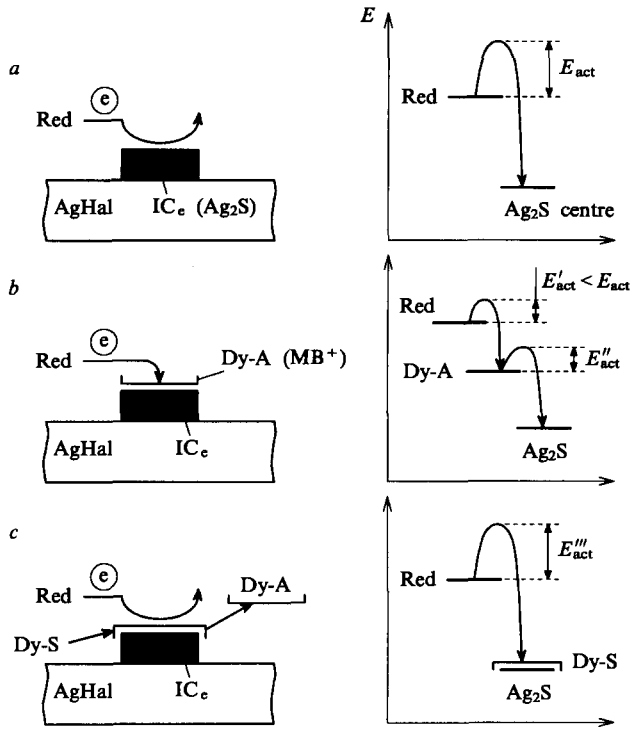


Figure 18. Schematic representation of the catalysis of electron transfer from the developer (Red) to the Ag_2S centre (IC_e) with the aid of an electron acceptor dye (Dy-A) and of the inhibition of the transport process by the supersensitiser dye (Dy-S).

By use of the specific adsorption of MB^+ and other electron-accepting dyes on the Ag_2S centres, manifested by the fogging of the AgBr and AgBr(I) photographic emulsions, experiments designed to investigate the influence of a series of supersensitisers, operating, in conformity with our ideas, via the 'insulation' mechanism, on the fog within the photolayers, have been carried out.[62,122] For the selective adsorption of the supersensitisers on the Ag_2S centres, one should expect the desorption of the fogging dyes from these centres and hence a decrease in fogging. Experimental methods involved the initial introduction of supersensitisers into the AgBr emulsion in amounts inducing the supersensitisation of the *J*-aggregating dyes, with subsequent addition of MB or another fogging dye at concentrations leading to a fog level $D_0 = 2.0-3.0$ within the layers. Supersensitiser dyes **29** and **30** have been studied in greatest detail.

Indeed the introduction of thia- and selena-monomethinecyanines **29** and **30** suppresses sharply the fogging in the photolayers due to MB. It is striking that it is not associated with the desorption of MB from AgBr because the desensitisation of the emulsion not only does not diminish under these conditions but sometimes actually increases. The influence of the stabiliser **18** on fogging is weaker than that of monomethinecyanines. Like monomethinecyanines, auramine G also suppresses the fogging induced by MB, i.e. its effect is similar to that of cyanines.

The explanation of the antifogging effect of supersensitisers can also be associated with the displacement of MB^+ from the impurity centres, with the increase in the activation energy for the redox reaction E''_{act}, and with the inhibition of the catalysis. This is illustrated schematically in Fig. 18*c*. Thus, on the basis of the experimental data obtained one may conclude that the supersensitisers are adsorbed selectively on the Ag_2S centres and hence that the 'insulation' supersensitisation mechanism really operates.

It is essential to note that, in the course of the development of methods designed to demonstrate the existence of the 'insulation' supersensitisation mechanism, the present author [122] observed in essence a new phenomenon—catalysis by dyes and reactions involving electron transfer from reductants to Ag_2S impurity centres. Whereas in the classical photographic negative process, the catalysis is effected by the Ag_n^+ silver species, formed on the Ag_2S centres following exposure, in the present instance the catalyst is the electron-accepting dye molecule having a specific affinity for the impurity centre. The possibility of the inhibition of the catalysis (negative catalysis) with the aid of substances competing with the acceptors for specific adsorption sites is no less important.

It must be emphasised that monomethinecyanines and other dyes can function not only as supersensitisers but also as stabilisers as well as antifogging agents in photographic emulsions as a consequence of their specific adsorption on the Ag_2S centres. The results obtained lead to the expectation that the stabilising capacity of cyanine dyes is higher than that of the traditional stabiliser **18**. According to modern ideas,[104] the stabilisation of emulsions is associated with the interaction of compound **18** with the Ag_2S centres. Thus the method developed may be useful for a rational selection of not only supersensitisers but also of stabilisers and antifogging agents.

The results obtained indicate the existence of at least two mechanisms of the supersensitisation of the *J*-aggregating dyes: the 'insulation' and Gilman's 'reductive' mechanisms. The difference between these two mechanisms is shown particularly clearly in the experiments, already examined, with compositions comprising readily oxidisable bases of the styryl dyes (compounds **19** and **33**) together with the supersensitisers **18**, **29**, and **30** which are difficult to oxidise. The observed superadditive supersensitisation effect (Figs 7 and 16, Table 3) can be explained by the hypothesis that supersensitisers of two types act on two consecutive stages in the inhibition of the hole-type self-desensitisation reactions. In this case, there is either initial hole capture from the dye by the readily oxidisable supersensitiser **19** (in accordance with Gilman's mechanism) and subsequent insulation of the remaining holes from the photographically active centres by compound **18**, which is difficult to oxidise, or the supersensitisers act in the opposite sequence. When the supersensitisers act consecutively, the probability of the entire recombination process is in fact determined by the product of the probabilities of the processes involving each of the individual substances, as a result of which the supersensitisation coefficient may approach the product of the coefficients for the individual supersensitisers, i.e. may be superadditive.[8,52]

The requirements which must be met by supersensitisers working in accordance with the above mechanisms are different: $0.8\ V > E_{1/2}^{Ox}(S) < E_{1/2}^{Ox}(Dy)$ for supersensitisers of the first kind working in accordance with the 'reductive' mechanism; $E_{1/2}^{Ox}(S) > E_{1/2}^{Ox}(Dy)$ for supersensitisers of the second kind working in accordance with the 'insulation' mechanism.[8,48] There is also a possibility of a variant where the supersensitiser dyes exhibiting a specific affinity for the Ag_2S centres and at the same time meeting the requirements of the 'reductive' mechanism may operate simultaneously via the two mechanisms. This case is in principle applicable to the supersensitiser dyes **31** and **32**, which were examined above and which are oxidised more readily than the quinomonomethinecyanine **3** supersensitised by them.

It is essential to note that the 'insulation' mechanism of the supersensitisation of the *J*-aggregating dyes differs significantly from Riester's mechanism.[23,24] Whereas the insulation of dye molecules from the AgHal surface and from one another is considered in Riester's model, the essence of the 'insulation' mechanism consists in the insulation of the sensitiser from the impurity centres alone. Furthermore, the introduction of Riester's potentiators leads to the decomposition of the dye *J*-aggregates and hence to the suppression of the spectral sensitivity.

The model involving the 'insulation' of the dye *J*-aggregates from the photographically active centres is apparently realised in emulsions with deep electron capture centres—in emulsions of the 'core–shell' type and in emulsions with Ir^{3+}.[45,123–127] As a consequence of the capture of photoelectrons, electron-hole

recombination processes are hindered in the bulk of the AgHal microcrystals, which makes it possible to diminish significantly type (II) self-desensitisation and hence to increase the effectiveness of the sensitiser.

2. Regulation of the *J*-aggregation of dyes

The self-association of dyes into *J*-aggregates should apparently have a series of analogies with crystallisation processes and should therefore involve at least two stages — the nucleation stage and the stage involving the growth of the ordered structure. Cyanine dyes aggregate on the real, and hence defective surface of AgHal microcrystals. The nucleation stage should therefore be determined by, apart from the structure of the dye molecule, the number and type of surface defects as well as the degree of supersaturation of the dye solution. On the other hand the *J*-aggregate growth stage is determined mainly by the degree of supersaturation of the sensitiser solution. The defectiveness of the surface of microcrystals is linked directly to the type of faces of the microcrystals and to the type of chemical sensitisation during which new defects (impurity centres) are formed. An analysis of the factors influencing the *J*-aggregation may be found in a number of reviews.[3,7,66]

The organic or inorganic substances introduced into a photographic emulsion during the growth of microcrystals and chemical and spectral sensitisation are capable of influencing the *J*-aggregation either in the aggregate nucleation stage, by altering the defectiveness of the surface, or in the aggregate growth stage. The influence of the stabiliser **18**, some of its analogues, and cyanines on the *J*-aggregation as regulators of the defectiveness of the surface was examined in Section I. In the present section, we shall consider the effect of a number of other organic compounds on the *J*-aggregate growth stage.

It has already been noted that the influence of a series of photographically relatively inactive compounds (for example, ketones, nitriles, quinoline derivatives, etc.) on the *J*-aggregation of dyes has been described in the literature.[9] The photographic effect of phenol added to the emulsion together with dyes has been investigated.[128] Its strong influence on the position of the absorption *J*-bands and on the effectiveness of the spectral sensitisation was observed. At a phenol concentration of 0.5–1.0 mol (mol AgHal)$^{-1}$, a bathochromic shift of the *J*-band up to 20 nm occurs. This is illustrated in Fig. 19 for the cation-anionic dye **35** and the anionic dye **36** adsorbed on a monodisperse AgBr(I) emulsion (cubic crystals, $\bar{l} = 0.25$ μm).

According to Fig. 19, phenol induces a bathochromic shift of the bands of orthochromatic and panchromatic sensitisers incorporated in compound **35** (cf. curves *1* and *2*) and of the *J*-band of the panchromatic dye **36** (cf. curves *3* and *4*). The changes in the *J*-bands are accompanied by an increase in the effectiveness of the spectral sensitisation. The influence of phenol was observed also for a series of other cationic, anionic, and cation-anionic dyes.

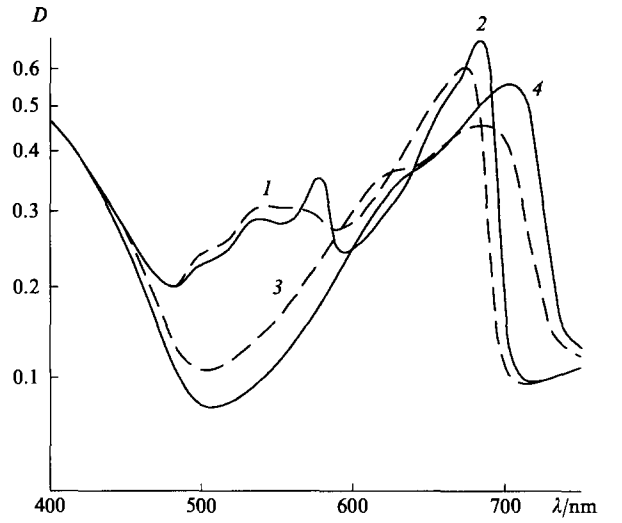
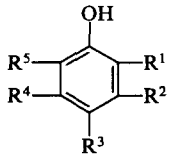


Figure 19. Reflection spectra of AgBr emulsion layers spectrally sensitised by dyes **35** (curves *1* and *2*) and **36** (curves *3* and *4*) individually (curves *1* and *3*) and in the presence of phenol (curves *2* and *4*). Concentration of dyes — 2 × 10^{-4} mol (mol AgBr)$^{-1}$; concentration of phenol — 0.5 mol (mol AgBr)$^{-1}$.

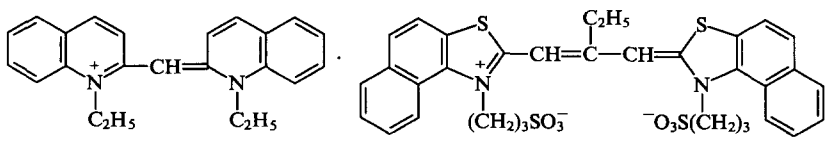


37

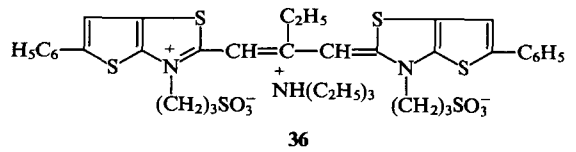
R^1–R^5 = H, Alk;

The influence of phenols having the general formula **37** has been investigated.[128] It was shown that cresol (R^3 = CH_3; R^1, R^2, R^4, R^5 = H) acts similarly to phenol. The introduction of longer alkyl groups in the *para*-position suppresses the *J*-aggregation. Dimethylphenols (1,2,4-, 1,3,4-, 1,3,5-, and 1,4,5-xylenols) have an effective influence on the *J*-aggregation at significantly lower concentrations [0.1–0.25 mol (mol AgHal)$^{-1}$] than phenol.

The bathochromic shift of the *J*-bands is usually attributed either to a decrease in the packing angle of the dyes or to an increase in the number of sensitiser molecules in the aggregate.[3,7] Both parameters should depend on the rate of aggregation. For fast aggregation, the random formation of many aggregates of different sizes should occur on the AgHal surface defects. It has



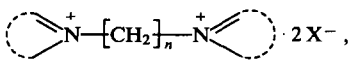
35



36

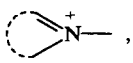
been shown[120] that the influence of the phenol persisted also when it was introduced into the emulsion after the formation of the *J*-aggregates. It was postulated that the 'recrystallisation' of the *J*-aggregates or, in the usual photographic terminology, the 'first ripening of the *J*-aggregates' takes place under the influence of phenols.[62,120] Phenols play the role of the medium (solvent) promoting the recrystallisation. One of the results of this may be the formation of more ordered structures of the *J*-aggregates (having bands which have undergone a bathochromic shift) remote from the impurity centres ($r > 0$, Fig. 2). The second result is the increase in the photographic activity of the *J*-aggregates. It is noteworthy that this may not in fact be a general rule because, for a sufficiently long ordered *J*-aggregate, contact between the latter and the IC_e can arise again with the consequent self-desensitisation of the dye. In this case the insulation of the *J*-aggregates from the IC_e with the aid of supersensitisers should be the main method for increasing the photographic activity of the long-wavelength *J*-aggregates.

Bisquaternary salts of heterocyclic bases having the general formula **38**,



38

exert an appreciable influence on the *J*-aggregation. Here



represents the quaternary salt of the nitrogen-containing base ($n > 2$).

Bisquaternary salts of a hydrogen-containing heterocycle have been used for a comparatively long time.[129–132] The influence of bisquaternary salts of benzimidazole has been studied in detail by Lifshits and coworkers,[133–135] while that of α-picoline has been investigated by the present author and Schelkina.[62,136] The introduction of bisquaternary salts into a photographic emulsion at concentrations comparable to that of the *J*-aggregating dye intensifies the tendency of the dye towards *J*-aggregation, gives rise to a bathochromic shift of the absorption band maximum, and increases the effectiveness of the spectral sensitisation. The effect of the bis-salts is manifested not only on AgHal but also on other semiconductors, in particular on WO_3.[50,51,137,138]

The influence of bisquaternary salts has been treated[62,136] from the standpoint of the facilitation of the *J*-aggregation of the dyes. This phenomenon has been designated as aggregation catalysis. Additional experiments using MB as a test for specific adsorption of the Ag_2S centres demonstrated that the bisquaternary salts do not exhibit an affinity for these centres and hence do not operate via the 'insulation' mechanism. Owing to the correspondence between the paired positive charges localised on the nitrogen atoms and the paired negative charges of the halide ions on the AgHal centre, a potential surface relief of a kind which facilitates the formation of *J*-aggregates not only on the defects but also on other surface sites and which favours the growth of the ordered structures of the aggregates is probably created in the adsorption of the bis-salts on the AgHal microcrystals. A consequence of this may be the absence of contact between the *J*-aggregate and the impurity centre IC_e, which is in its turn manifested by an increase in the photographic effectiveness of the dye. The formation of the ordered structures of the *J*-aggregates may influence the effectiveness of the spectral sensitisation as a consequence of the decrease in the probability of the dissipation of the excitation energy among different *J*-aggregates differing from one another by their sets of energy levels.

It has already been mentioned that the tendency of dyes towards *J*-aggregation is determined to a large extent by the molecular structure. The familiar fact that the replacement of alkyl groups at nitrogen atoms by sulfoalkyl groups, while the chromophoric part of the molecule of the cyanine dye remains unaltered, intensifies the tendency towards *J*-aggregation merits special attention.[7,137] The presence of dipolar betaine structures in anionic dyes can probably facilitate both the nucleation stage on the dipolar surface of the AgHal microcrystals (Ag^+ and Hal^- ions) and the growth of the aggregates themselves. According to Meyer's hypothesis,[140] the molecules of betaine dyes form more stable *J*-aggregates than the cations of the alkylates of carbocyanines.

The creation on the surface of AgHal microcrystals, before the introduction of the spectral sensitiser, of a multiplicity of new defects stimulating the growth of *J*-aggregates at sites not bound to the impurity centres should promote *J*-aggregation. Such numerous defects arise, for example, in the synthesis of AgHal microcrystals with a variable halide composition, particularly in the synthesis of AgBr(I) emulsions. *J*-Aggregation therefore is as a rule facilitated with increase, up to a certain limit, in the content of iodide ions in AgBr(I) emulsions. It has been shown[141] that the addition of iodide ions to a AgBr emulsion with cubic microcrystals leads to the formation on the vertices and edges of the microcrystals of silver iodide, on which *J*-aggregation is facilitated. The influence of thiocyanate and cyanide ions, forming sparingly soluble compounds with Ag^+ ions,[142] can be explained in the same way. There is apparently a possibility also of other methods of regulating the defectiveness of the surface of AgHal microcrystals.[136] In addition, mention should be made of the control of the *J*-aggregation by reducing the rate of introduction of the dye into the solution. This is achieved by introducing into the emulsion dyes sparingly soluble in water in the form of aqueous sols or, for example, by the readsorption of dyes from the surface of an inert substrate (SiO_2 etc.) on AgHal.[7,143] The three principal supersensitisation procedures, examined above, are summarised in Fig. 20.

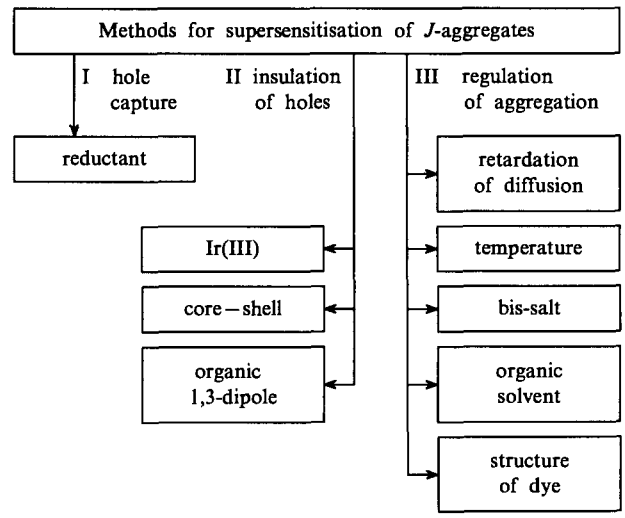


Figure 20. Principal methods for the supersensitisation of *J*-aggregating dyes.

V. Conclusion

The characteristics of the spectral sensitisation of silver halide photographic materials by *J*-aggregating dyes are determined primarily by the unusual structure of the aggregates, which consist of organised structures with delocalised π-electrons. This is reflected both in the spectra (λ_{max}, line widths, absorption coefficient, and the lifetime of the excited state) and in the photographic behaviour of cyanines. The system of delocalised π-electrons of the *J*-aggregate creates conditions for the transfer of

the photogenerated charge carriers (electrons and holes) over distances larger than the molecular size. The delocalisation of holes within the limits of the *J*-aggregates constitutes the basis of the desensitisation and the type (II) self-desensitisation examined above. The hole desensitisation is a typical example of the catalysis of recombination processes in which the *J*-aggregate plays the role of an intermediate species promoting the reaction.

The processes involving the transfer of holes and photoelectrons between aggregates of various dyes not only play a major role in the spectral sensitisation of photographic materials but are also of considerable interest for the future developments in molecular microelectronics.[144–148] Artificially organised systems on the basis of *J*-aggregates serve as electronic elements of molecular dimensions (switches, triodes, memory cells, etc.). Thus one is dealing with the organisation of photoinitiated electronic processes in the microsystems of the *J*-aggregates.

The uniqueness of the *J*-aggregates of cyanine dyes as spectral sensitisers, which has been responsible for their general application in the black and white and colour photographic materials is apparently determined by the effective primary separation of the photogenerated charges between the molecules in the system of the *J*-aggregate. Here one can trace a definite analogy between the spectral sensitisation process created artifically by man and the natural spectral sensitisation processes in photosynthesis, which in the course of many millions of years of evolution have been brought to perfection. The primary step of the spectral sensitisation in the photosynthesising reaction centre involves the separation of charges in the dimeric molecules of bacteriochlorophyll.[149] The effectiveness of the primary charge separation creates favourable conditions for the subsequent multistage processes involving the separation of the charges from one another. The primary charge separation in the *J*-aggregates promotes in exactly the same way the subsequent effective separation of electrons and holes in the dark stages with participation of silver halides. Nature has devoted much effort to the creation of a perfect mechanism of the 'dark' separation of charges in photosynthesis. This has been achieved exclusively by an exact spatial organisation of a transport system for electrons and holes in which electron and hole acceptors are located at rigorously defined distances from the reaction centre.[149] According to the results obtained, the disposition of the *J*-aggregates relative to electron and hole acceptors on the AgHal surface also determines to a significant extent the effectiveness of the charge separation in the photographic process and the spectral sensitivity associated with this. Consequently the topography of the *J*-aggregates on the real surface of AgHal microcrystals is extremely important and the specific regulation of the *J*-aggregation therefore in fact constitutes, in our view, the essential feature of the future developments in the spectral sensitisation of new photographic materials.

It is essential to note that the difficulties which many investigators encountered in their attempts to find a relation between the effectiveness of the spectral sensitisation of specific photographic emulsions and the structure of the *J*-aggregating dyes, which were mentioned in the Introduction, arose in the first place from the one-sided nature of the approach to the problem of spectral sensitisation. This was either a consequence of a one-sided study of the structure and energetics of the energy levels of the dyes incorporated in the *J*-aggregate without reference to the emulsion system (in the first place its impurity levels) or, conversely, a result of overestimating the role of the substrate without taking into account the structural characteristics of the dye. The hopes of the investigators are therefore frequently associated either with the search for a kind of 'golden' dye or with the preparation of a 'special' photographic emulsion showing a tendency towards supereffective spectral sensitisation. Naturally, because of its limitations, neither approach is able to solve this problem. Only the study of processes in a single system incorporating the dye, the AgHal surface, its defects, and, in the first place, the products of the sulfur sensitisation can help to find an answer to the question why a particular cyanine dye in one or other emulsion is either highly effective or, conversely, is photochemically inactive. This review represents an attempt at an integrated consideration of the problem of the effectiveness of the spectral sensitisation of *J*-aggregating dyes.

Attention should be drawn also to one, largely ideological, limitation of the approach adopted to the problem of the effectiveness of spectral sensitisation. Hitherto processes involving the supersensitisation of photographic layers with *J*-aggregating dyes have been considered from the standpoint of the prohibitive principle of the 'fight against holes'. Both the 'reductive' and 'insulation' supersensitisation mechanisms correspond to precisely this principle. However, practice has shown that another principle is more promising — the 'collaboration' principle, in the present instance the principle of collaboration with holes. This means that a desirable organisation of the spectral sensitisation process is one in which it would be useful to employ the energy of the holes, namely their oxidising capacity, which leads to the liberation of the chemical energy stored in the photographic system. One is dealing with the oxidation of certain organic substances — supersensitisers of a new type — as a result of which the oxidised molecule, depleted in bonding electrons, would react with decomposition of the initial cyclic skeleton. Ultimately another molecule would arise with a new cyclic skeleton, possessing reducing properties in relation to AgHal. This means that the chemical reactions of the oxidised form of the supersensitiser would result in the injection into the AgHal microcrystal of one (or more) electron capable of intensifying the latent photographic image. Consequently one is dealing with a latent image intensification process in which the relative quantum yield of the spectral sensitisation can be formally greater than unity. In fact, one would inject not one but several electrons into AgHal per quantum adsorbed by the *J*-aggregate — one electron from the photoexcited dye and the others from the products $Dy^{+\cdot}$ of the oxidation by the hole. The ability of the *J*-aggregate to effect the translation of the hole should in principle increase the probability of such a process. The process probability should increase to an even greater extent following the specific adsorption of a supersensitiser of the type considered on the impurity centre functioning as the electron acceptor. In this case, on capture of a hole by the supersensitiser and after the chemical reaction of the

$$Dy + h\nu \longrightarrow Dy^{*}; \quad (12)$$

$$Dy^{*} + AgHal \longrightarrow Dy^{+\cdot} + [AgHal]^{-}; \quad (13)$$

$$[AgHal]^{-} + Ag^{+} \longrightarrow [AgHal/Ag^{0}]; \quad (14)$$

$$Dy^{+\cdot} + BH \longrightarrow Dy + BH^{+\cdot}; \quad (15)$$

$$BH^{+\cdot} + R^{-} \longrightarrow B^{\cdot} + HR; \quad (16)$$

$$B^{\cdot} + [AgHal/Ag^{0}] \longrightarrow B^{+\cdot} + [AgHal/Ag^{0}]^{-}; \quad (17)$$

$$[AgHal/Ag^{0}]^{-} + Ag^{+} \longrightarrow [AgHal/Ag_{2}^{0}]; \quad (18)$$

$$B^{+\cdot} + \text{medium} \longrightarrow \text{products}; \quad (19)$$

oxidised supersensitiser molecule, a second electron would enter directly the IC_e. A hypothetical mechanism of the 2-electron process could be represented, for example, in the following form: where BH is the supersensitiser and R^- the base. According to this scheme, the supersensitiser BH is oxidised by a dye hole to the radical-cation $BH^{+\cdot}$, which interacts with the base R^- as a consequence of its acid properties, affording the radical $B^{\cdot}$. The latter can serve as a reductant in relation to the silver halide, i.e. it can inject a second electron into AgHal and intensify thereby the latent photographic image centre.

References

1. E Jelley *Nature (London)* **138** 1009 (1936)
2. G Scheibe *Angew. Chem.* **49** 563 (1936)
3. F Dietz *J. Signal AM* **1** 157, 237 (1973)
4. G Schwarz *Sci. Ind. Photogr.* **10** 233 (1939)
5. S E Sheppard *Phot. J.* **32** 300 (1908); *Proc. R. Soc. A* **82** 256 (1909)
6. I Levkojev, S Natanson *Acta Physicochemica URSS* **21** 437 (1946)
7. T James *The Theory of the Photographic Process* (Translated into Russian; Leningrad: Khimiya, 1980)
8. B I Shapiro *Usp. Nauchn. Fotogr.* **24** 69 (1986)
9. R M Mudrovčič *Sci. Ind. Photogr.* **24** 47 (1953)
10. P B Gilman *Photogr. Sci. Eng.* **18** 418 (1974)
11. F Dietz *J. Signal AM* **6** 245, 337 (1978)
12. B H Carroll *Photogr. Sci. Eng.* **21** 151 (1977)
13. B I Shapiro *Zh. Nauchn. Prikl. Fotogr. Kinematogr.* **25** 64 (1980)
14. O Bloch, F F Renwick *Photogr. J.* **60** 145 (1920)
15. W West, B H Carroll *J. Chem. Phys.* **15** 529 (1947); **19** 417 (1951)
16. R Brünner, A Graf, G Scheibe *Z. Wiss. Photogr., Photophys. Photochem.* **53** 214 (1959)
17. R Brünner, A Oberth, G Pick, G Scheibe *Z. Electrochem.* **62** 132, 146 (1958)
18. A E Rosenoff, K S Norland, A E Ames, V K Walworth, G R Bird *Photogr. Sci. Eng.* **12** 185 (1968)
19. G R Bird, B Zuckerman, A E Ames *Photochem. Photobiol.* **8** 393 (1968)
20. B Zuckerman, H Mingace *J. Chem. Phys.* **50** 3432 (1969)
21. B Zuckerman *Photogr. Sci. Eng.* **14** 336 (1970)
22. O Riester *Photogr. Sci. Eng.* **13** 13 (1969)
23. O Riester *Photogr. Sci. Eng.* **18** 295 (1974)
24. P B Gilman *Photogr. Sci. Eng.* **12** 230 (1968)
25. B I Shapiro *Zh. Nauchn. Prikl. Fotogr. Kinematogr.* **26** 208 (1981)
26. B I Shapiro *Zh. Nauchn. Prikl. Fotogr. Kinematogr.* **31** 68 (1986)
27. B I Shapiro *Zh. Nauchn. Prikl. Fotogr. Kinematogr.* **22** 143 (1977)
28. T Tani *Photogr. Sci. Eng.* **14** 63 (1970)
29. T Tani *Photogr. Sci. Eng.* **14** 237 (1970)
30. T Tani *Photogr. Sci. Eng.* **15** 384 (1971)
31. T Tani *Photogr. Sci. Eng.* **18** 215 (1974)
32. T Tani *Photogr. Sci. Eng.* **18** 569 (1974)
33. T Tani *Photogr. Sci. Eng.* **18** 576 (1974)
34. A S Kheinman, V P Donatova *Zh. Nauchn. Prikl. Fotogr. Kinematogr.* **15** 374 (1970)
35. K Meyer, W Nesawibatko *Z. Wiss. Photogr., Photophys. Photochem.* **56** 196 (1962)
36. Yu N Gorokhovskii *Spektral'nye Issledovaniya Fotograficheskogo Protsessa* (Spectral Investigation of the Photographic Process) (Moscow: Fizmatgiz, 1960)
37. B H Carroll *Photogr. Sci. Eng.* **5** 65 (1961)
38. Y I Saunders, R W Tyler, W West, in *Photographic Science: Symposium. Torino* (London: Focal Press, 1963) p. 73
39. I H Leubner *Photogr. Sci. Eng.* **20** 61 (1976)
40. I H Leubner *J. Photogr. Sci.* **31** 93 (1983)
41. L Ya Kaplun. B I Shapiro, K S Bogomolov *Zh. Nauchn. Prikl. Fotogr. Kinematogr.* **25** 142 (1980)
42. B I Shapiro, L Ya Kaplun, L G Kurkina *Usp. Nauchn. Fotogr.* **22** 142 (1984)
43. T Tani *Photogr. Sci. Eng.* **19** 356 (1975)
44. T Tani *J. Imag. Sci.* **31** 263 (1987)
45. F J Evans, P B Gilman *Photogr. Sci. Eng.* **19** 333 (1975)
46. D M Sturmer, W S Gaugh *Photogr. Sci. Eng.* **19** 344 (1975)
47. B I Shapiro *Zh. Nauchn. Prikl. Fotogr. Kinematogr.* **29** 31 (1984)
48. B I Shapiro, L L Mkrtchyan, A F Peshkin, L G Kurkina *Zh. Nauchn. Prikl. Fotogr. Kinematogr.* **32** 358 (1987)
49. B I Shapiro, L L Mkrtchyan, Z I Moskalenko, G P Shumelyak *Zh. Nauchn. Prikl. Fotogr. Kinematogr.* **32** 444 (1987)
50. D V Sviridov, A I Kulak, B I Shapiro *Khim. Vys. Energ.* **24** 151 (1990)
51. D V Sviridov, B I Shapiro, A I Kulak *J. Photochem. Photobiol. A: Chem.* **67** 377 (1992)
52. B I Shapiro *J. Inf. Rec. Mater.* **19** 105 (1991)
53. B I Shapiro *J. Soc. Photogr. Sci. Technol. Jpn.* **55** 55 (1992)
54. R A Marcus *Annu. Rev. Phys. Chem.* **15** 155 (1964)
55. F Basolo, R Pearson *Mechanisms of Inorganic Reactions. A Study of Metal Complexes in Solution* (Translated into Russian; Moscow: Mir, 1971)
56. R R Dogonadze, A M Kuznetsova, in *Elektrokhimiya (Itogi Nauki i Tekhniki)* [Electrochemistry (Advances in Science and Engineering)] (Moscow: Izd. VINITI, 1969) Vol. 9, p. 5
57. L I Mikheeva, A I Tolmachev, B I Shapiro *Zh. Nauchn. Prikl. Fotogr. Kinematogr.* **30** 426 (1985)
58. S Dähne *Z. Wiss. Photogr., Photophys. Photochem.* **59** 113 (1965)
59. R W Berriman, P B Gilman *Photogr. Sci. Eng.* **17** 235 (1973)
60. P B Gilman *Photogr. Sci. Eng.* **18** 475 (1974)
61. D M Sturmer, W S Gaugh, B J Bruschi *Photogr. Sci. Eng.* **18** 49, 56 (1974)
62. B I Shapiro *Zh. Nauchn. Prikl. Fotogr. Kinematogr.* **37** 139 (1992)
63. Y I Saunders, S P Lovell *Photogr. Sci. Eng.* **24** 171, 176 (1980)
64. T H James *Adv. Photochem.* **13** 329 (1986)
65. V M Belous *Usp. Nauchn. Fotogr.* **25** 5 (1989)
66. K Meese, T James *The Theory of the Photographic Process*, 3rd Ed. (Translated into Russian; Leningrad: Khimiya, 1973)
67. T H James *Photogr. Sci. Eng.* **18** 100 (1974)
68. B I Shapiro, E N Sergeeva, A V Butuzova *Zh. Nauchn. Prikl. Fotogr. Kinematogr.* **33** 256 (1988)
69. C Reich *Photogr. Sci. Eng.* **18** 335 (1974)
70. USSR P 286 691; *Byull. Izobret.* **39** (1976)
71. E B Lifshits, I I Levkoev, in *Aktual'nye Voprosy Khimii i Tekhnologii Fotograficheskikh Materialov* (Actual Problems in the Chemistry and Technology of Photographic Materials) (Moscow: NIIKhIMFOTOProekt, 1986) p. 67
72. V M Belous, V I Tolstobrov, O I Sviridova, B I Shapiro *Dokl. Akad. Nauk SSSR* **251** 1152 (1980)
73. R Steiger, J F Reber *Photogr. Sci. Eng.* **25** 127 (1981)
74. J Spence, B H Carroll *J. Phys. Chem.* **52** 1090 (1948)
75. Z I Gratsianskaya, Candidate's Thesis in Technical Sciences, Leningrad Inst. of Motion Picture Engineer., Leningrad, 1956
76. K Meyer, H Polenz *Z. Wiss. Photogr., Photophys. Photochem.* **54** 81 (1960)
77. A V Borin, P I Logak, V Sh Telyakova *Zh. Nauchn. Prikl. Fotogr. Kinematogr.* 7 245 (1962)
78. M K Grechko, S V Natanson, M A Al'perovich *Kinotekhnika* **4** 92 (1963)
79. M K Grechko, Candidate's Thesis in Technical Sciences, NIIKhIMFOTOProekt, Moscow, 1966
80. M V Mishakova, A V Borin, N A Shvink *Usp. Nauchn. Fotogr.* **14** 112 (1970)
81. M V Mishakova, A V Borin, L R Shaimardanova *Zh. Nauchn. Prikl. Fotogr. Kinematogr.* **12** 245 (1967)
82. T Tani *Photogr. Sci. Eng.* **21** 37 (1977)
83. T Tani *Photogr. Sci. Eng.* **22** 179 (1978)
84. T Tani *Photogr. Sci. Eng.* **23** 55 (1979)
85. T Tani, M Saito *Photogr. Sci. Eng.* **23** 323 (1979)
86. T Tani, Y Sano, S Takada, M Saito *J. Photogr. Sci.* **28** 28 (1980)
87. T Tani *J. Imag. Sci.* **34** 143 (1990)
88. H W Wood *J. Photogr. Sci.* **14** 72 (1966)
89. V M Belous, V I Tolstobrov, B I Shapiro *Zh. Nauchn. Prikl. Fotogr. Kinematogr.* **26** 140 (1981)
90. V M Belous, V I Tolstobrov, B I Shapiro *Usp. Nauchn. Fotogr.* **22** 125 (1984)
91. V M Belous, N A Orlovskaya, V I Tolstobrov, K V Chibisov *Dokl. Akad. Nauk SSSR* **235** 1339 (1977)
92. V M Belous, Yu A Breslav, V I Tolstobrov, V P Churashov *Zh. Nauchn. Prikl. Fotogr. Kinematogr.* **22** 452 (1977)
93. V M Belous, V I Tolstobrov *Dokl. Akad. Nauk SSSR* **245** 593 (1979)
94. V M Belous, V I Tolstobrov, K V Chibisov *Dokl. Akad. Nauk SSSR* **246** 632 (1979)
95. V M Belous, V I Tolstobrov *Opt. Spektrosk.* **50** 682 (1981)
96. U Fano *Phys. Rev.* **124** 1866 (1961)
97. A H Herz *Photogr. Sci. Eng.* **18** 323 (1974)
98. K Stil, U Veker, U Freier, K Teger, Z Dene, in *Aktual'nye Voprosy Fiziki i Khimii Fotograficheskikh Protsessov (Tez. Dokl. Mezhdunarodnogo Simpoziuma)* [Actual Problems in the Physics and Chemistry of Photographic Processes (Abstracts of Reports at the International Symposium)] (Tbilisi, 1984) p. 158
99. T Tani, Y Sano *J. Appl. Phys.* **69** 4341 (1991)

100. H Saijo, T Isshiki, M Shiojiri, H Ohtani, G Ning, K Ogawa, in *Thesis International East – West Symposium III* (Hawaii, 1992) p. B-37
101. V M Belous, V I Tolstobrov, B I Shapiro *Opt. Spektrosk.* **49** 532 (1980)
102. B I Shapiro, A V Butuzova, N A Shvink, in *V Simpozium po Fizike i Khimii Polimetinovykh Krasitelei (Tez. Dokl.)* [The Vth Symposium on the Physics and Chemistry of Polymethine Dyes (Abstracts of Reports)] (Chernogolovka: Inst. of Chemical Physics, 1989) p. 218
103. Ya A Levin, V M Gorokhovskii, I P Sotnikova, A P Fedotova, N F Rakova, V V Karunina *Usp. Nauchn. Fotogr.* **14** 30 (1970)
104. G Fischer *J. Inf. Rec. Mater.* **16** 91 (1988)
105. A Streitwieser *Molecular Orbital Theory for Organic Chemists* (Translated into Russian; Moscow: Mir, 1965)
106. B Pullman, A Pullman *Quantum Biochemistry* (Translated into Russian; Moscow: Mir, 1965)
107. G Scheibe, R Brünner, A Oberth, G Pick, in *Thes. Wissenschaft Photogr. Intern. Konferenz, Köln, 1956* (Darmstadt: Othmar Nelwick, 1958) p. 102
108. R F Large, in *Photographic Sensitivity* (Ed. R J Cox) (London: Academic Press, 1973) p. 241
109. B I Shapiro, L L Mkrtchyan, in *International Congress of Photogr. Sci.* (Köln, 1986) p. 255
110. Jpn. Appl. 61-14503 (1976)
111. Jpn. Appl. 59-9900 (1984)
112. Jpn. Appl. 59-9901 (1984)
113. US P. 5 596 767 (1984)
114. B I Shapiro, A V Butuzova, E F Klimzo *Zh. Nauchn. Prikl. Fotogr. Kinematogr.* **34** 443 (1989)
115. M K Van Doorselaer *J. Photogr. Sci.* **35** 42 (1987)
116. A L Kartuzhanskii, L K Kudryashova, V A Reznikov *Zh. Nauchn. Prikl. Fotogr. Kinematogr.* **33** 295 (1988)
117. T Shiozawa, T Kobayashi *J. Soc. Photogr. Sci. Technol. Jpn.* **53** 135 (1990)
118. E J Birr *Stabilization of Photographic Silver Halide Emulsion* (London: Focal Press, 1974)
119. J Eggert, J Reitstötter *Kolloid Z.* **36** 298 (1925)
120. A Steigman *Z. Wiss. Photogr., Photophys. Photochem.* **30** 69 (1931)
121. S Dähne *Z. Wiss. Photogr., Photophys. Photochem.* **56** 71 (1962)
122. B I Shapiro *Zh. Nauchn. Prikl. Fotogr. Kinematogr.* **34** 468 (1990)
123. J M Simson, W S Gaugh *Photogr. Sci. Eng.* **19** 339 (1975)
124. US P. 3 347 717 (1967)
125. US P. 3 688 676 (1972)
126. US P. 3 690 891 (1972)
127. P B Gilman *J. Photogr. Sci.* **31** 185 (1983)
128. B I Shapiro, A V Butuzova, in *V Simpozium po Fizike i Khimii Polimetinovykh Krasitelei (Tez. Dokl.)* [The Vth Symposium on the Physics and Chemistry of Polymethine Dyes (Abstracts of Reports)] (Chernogolovka: Inst. of Chemical Physics, 1989) p. 203
129. US P. 2 276 622 (1942)
130. US P. 2 276 623 (1942)
131. US P. 2 288 226 (1942)
132. US P. 2 448 858 (1948)
133. E B Lifshits. L I Kirenskaya, D Ya Shagalova, N V Kudryavskaya, G G Ushanov, L N Yashunova, L G Kurnina, Yu M Varlypina, in *Organicheskie Veshchestva i Ikh Primenenie v Khimiko-fotograficheskoi Promyshlennosti* (Organic Substances and Their Application in the Photographic Chemical Industry) (Moscow: NIIKhIMFOTOProekt, 1984) p. 166
134. E B Lifshits, D Ya Shagalova, N V Kudryavskaya, G P Pyl'eva, in *Vsesoyuzn. Konf. po Problemam Sozdaniya Sovremennykh Tsvetnykh Kinofotomaterialov (Tez. Dokl.)* [The All-Union Conference on Problems in the Production of Modern Colour Film Photographic Materials (Abstracts of Reports)] (Chernogolovka: Inst. of Chemical Physics, 1987) p. 43
135. E B Lifshits, R D Raikhina, L I Kirenskaya, D Ya Shagalova, L G Kurkina, N N Eventova, in *V Simpozium po Fizike i Khimii Polimetinovykh Krasitelei (Tez. Dokl.)* [The Vth Symposium on the Physics and Chemistry of Polymethine Dyes (Abstracts of Reports)] (Chernogolovka: Inst. of Chemical Physics, 1989) p. 215
136. B I Shapiro, in *Vsesoyuzn. Konf. po Problemam Sozdaniya Sovremennykh Tsvetnykh Kinofotomaterialov (Tez. Dokl.)* [The All-Union Conference on Problems in the Production of Modern Color Film Photographic Materials (Abstracts of Reports)] (Chernogolovka: Inst. of Chemical Physics, 1987) p. 45
137. D V Sviridov, A I Kulak, B I Shapiro *J. Inf. Rec. Mater.* **15** 243 (1987)
138. D V Sviridov, B I Shapiro, in *V Simpozium po Fizike i Khimii Polimetinovykh Krasitelei (Tez. Dokl.)* [The Vth Symposium on the Physics and Chemistry of Polymethine Dyes (Abstracts of Reports)] (Chernogolovka: Inst. of Chemical Physics, 1989) p. 206
139. E B Lifshits, D Ya Shagalova, E F Klimzo *Usp. Nauchn. Fotogr.* **22** 103 (1984)
140. K Meyer *Z. Wiss. Photogr., Photophys. Photochem.* **52** 170 (1958)
141. R Steiger, J N Albischer, E Haselbach *J. Imag. Sci.* **35** 1 (1991)
142. S V Natanson, E B Lifshits *Usp. Nauchn. Fotogr.* **17** 23 (1976)
143. I M Zul', G D Kovshulya, M N Ushomirskii, in *V Simpozium po Fizike i Khimii Polimetinovykh Krasitelei (Tez. Dokl.)* [The Vth Symposium on the Physics and Chemistry of Polymethine Dyes (Abstracts of Reports)] (Chernogolovka: Inst. of Chemical Physics, 1989) p. 210
144. F L Carter *Molecular Electronic Devices* (New York: Marcel Dekker, 1982)
145. F L Carter *J. Vac. Sci. Technol.* 1 939 (1984)
146. *Proceedings of the International Symposium on Future Electronic Devices* (Takyo: Press Central Hall, 1985)
147. N G Rambidi, V M Zamalin *Molekulyarnaya Mikroelektronika: Istoki i Nadezhdy* (Molecular Microelectronics: Issues and Hopes) (Moscow: Znanie, 1985)
148. M F Alfimov, R F Khairutdinov *Usp. Nauchn. Fotogr.* **25** 154 (1989)
149. *Zh. Vses. Khim. O-va im. D I Mendeleeva* **31** 482, 489, 495, 502, 508, 514, 525 (1986)

Russian Chemical Reviews **63**(3) 257–267 (1994) ©1994 Russian Academy of Sciences and Turpion Ltd

UDC 547.638+547.556.7

Reactions of aromatic diazonium salts with unsaturated compounds in the presence of nucleophiles

B D Grishchuk, P M Gorbovoi, N I Ganushchak, A V Dombrovskii (deceased)

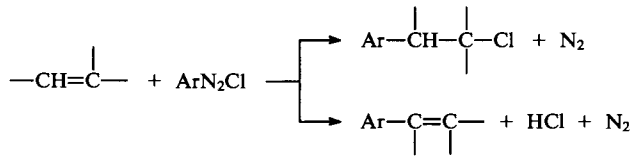
Contents

I. Introduction	257
II. Factors determining the effectiveness of the reaction	257
III. Anionarylation of 1,3-dienes	258
IV. Anionarylation of monounsaturated compounds	261
V. The mechanism of the anionarylation reaction	265

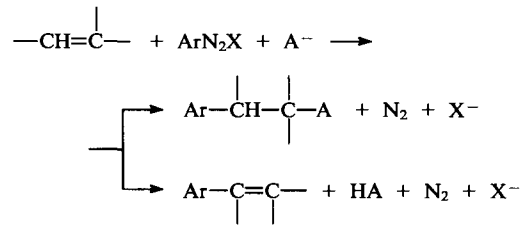
Abstract. The review surveys the reactions of aromatic diazonium salts with diene and monounsaturated compounds in the presence of nucleophiles. Certain further reactions of the reaction products and their applications are considered. The bibliography includes 63 references.

I. Introduction

The reaction of arenediazonium chloride with unsaturated compounds in the presence of copper salts (the Meerwein or Meerwein–Schuster reaction) was described in 1939[1] and immediately found extensive applications in synthetic organic chemistry for the preparation of aryl- and chloroaryl-substituted derivatives.[2–19]



The view that the reaction is catalysed solely by copper halides while diazonium sulfates and nitrates as well as other diazonium salts do not interact with unsaturated compounds was held for a long time. The explanation is that acid and not neutral diazonium salts plus divalent copper salts were used in the reaction, whereas it is univalent copper salts that are the catalysts of the decomposition of diazonium salts. Ethylene derivatives are known to be able to reduce divalent copper halides to the univalent state under certain conditions. However, divalent copper sulfates and nitrates are apparently difficult to reduce in an acid medium, since acids inhibit the reduction of divalent copper salts.[19] It was not until the beginning of the 1980s that conditions were found under which arenediazonium sulfates, nitrates, and tetrafluoroborates react with unsaturated compounds in the presence of external nucleophiles to form products of the addition of the aryl group and the anion to the double bond.[10–15] We suggested that this type of reaction be called anionarylation.[10,16] If sodium chloride is used as the anionoid reagent, then the Meerwein reaction becomes a special case of the anionarylation reaction.[14]



II. Factors determining the effectiveness of the reaction

The possibility of the anionarylation of dienes by diazonium sulfates and nitrates as well as other diazonium salts was discovered by Ganushchak et al.[10] The factors determining the effectiveness of the anionarylation reaction were elucidated later.

Diazonium salts. Among arenediazonium sulfates, nitrates, acetates, and tetrafluoroborates, arenediazonium tetrafluoroborates proved to be the most convenient in the anionarylation reaction. They are extremely stable compounds which can be stored for a long time.

It was noted that the highest yields of the products of the anionarylation reaction are obtained if there are no substituents at all in the aromatic ring or the substituents are in the *para*- or *ortho*-position regardless of their nature. *Meta*-substituted compounds afford significantly lower yields.[20]

Unsaturated compounds. Both monounsaturated and diene derivatives have been investigated in the anionarylation reaction. If the reaction system contains the same anionoid reagent, the yields of the anionarylation products (buta-1,3-diene, isoprene, and chloroprene) are comparable.[11–13]

The vinyl monomers $CH_2=CH-X$ and $CH_2=CX_2$, in which the double bond is activated by one or two electron-accepting groups (X = Cl, CN, Ar, COR, COOH, COOAlk, $P^V=O$, etc.) enter most readily into the anionarylation reaction.[20–22] Owing to the high capacity of copper or iron salts for the transfer of radical chains, such monomers do not produce high-molecular-mass compounds under the reaction conditions.

Catalysts. Various compounds, in particular copper acetate, thiocyanate, hydroxycarbonate [bicarbonate?], tetrafluoroborate, *O,O*-diethyl phosphorodithioate, and ethylxanthate as

B D Grishchuk, P M Gorbovoi Department of Chemistry, Ternopol Pedagogic Institute, ul. M. Krivonosa 2, 282009 Ternopol, Ukraine
Tel. (7-035 22) 34 910
N I Ganushchak Department of Organic Chemistry, Lvov State University, Universitetskaya ul. 1, 290000 Lvov, Ukraine

Received 8 September 1993
Uspekhi Khimii **63**(3) 269–279 (1994); translated by A K Grzybowski

well as the $CuSO_4 + FeSO_4$, $Cu(NO_3)_2 + Cu$, and $Cu(NO_3)_2 + Fe$ systems have been tested as catalysts of the anionarylation reaction. The optimum molar ratio of the diazo-salt to the catalyst is in the range from 0.1 to 0.01–0.025. It is essential to note that the anion of the copper salt hardly affects the reaction. Furthermore, under these conditions as exchange reaction takes place between the copper salts and the anionoid reagents with formation of CuA_2. In most cases, the presence of the catalyst—copper or iron salts—is an obligatory condition, but sometimes the anionarylation reaction can occur also in the absence of the catalyst.[17,18,20,22]

Anionoid reagents. Alkali metal or ammonium salts have been most often used as anionoid reagents. Anionoid reagents such as chlorides, bromides, iodides, fluorides, sulfides, nitrites, thiocyanates, *O,O*-diethyl phosphorodithioates, xanthates, *N,N*-diethyldithiocarbamates, and carboxylates have been investigated in the reaction. Apart from the salts, water, methyl, ethyl, isopropyl, n-butyl, isobutyl, *sec*-butyl, *tert*-butyl, and benzyl alcohols, ethylene glycol, and formic acid have been used successfully as the anionoid reagents.

Solvents. The anionarylation reaction has been carried out in various solvents: water, acetone, acetonitrile, diethyl ether, dimethyl sulfoxide, dimethylformamide, and alcohol. If the unsaturated compound dissolves in water, the reaction can be carried out in an aqueous medium,[23] but, in view of the fact that the majority of unsaturated compounds are insoluble in water, the reaction is usually carried out in an aqueous organic medium. The optimum reaction media are water–acetone or water–acetonitrile mixtures in 1:(1–4) proportions.[14,20–22] In many instances, the reaction takes place only in an organic solvent. When water–acetone or alcohol–acetone systems are used as the organic medium in the absence of other anionoid reagents, the alcohol or water functions as an external nucleophile, whereupon hydroxyarylation and alkoxyarylation reactions occur.

Acidity of the medium. The optimum pH of the reaction medium is in the range from 4 to 6; in order to maintain and regulate the necessary pH, the following additives are introduced: CH_3COONa, CaO, $Ca(OH)_2$, $NaHCO_3$.

Temperature conditions. The anionarylation reaction takes place at temperatures from −65 to +25 °C depending on the nucleophilicity of the anion introduced and the order in which the reagents are added. If the temperature is not regulated, the reaction becomes uncontrolled, the temperature rises rapidly, and nitrogen is evolved abundantly; in such cases, the process involving the substitution of the diazo-group by the anions present in the mixture predominates.

Reaction procedure. The following order of the introduction of reagents into the reaction mixture is optimal: catalyst, solvent, unsaturated compound, diazonium salt. If the anionoid reagent is introduced last, the reaction proceeds as a rule very rapidly, which is indicated by the vigorous evolution of nitrogen. When the last reagent is the diazonium salt, the reaction proceeds quietly even at a higher temperature. The most successful diazonium salt: unsaturated compound: anionoid reagent reactant ratios are 1:(1–1.5):(1.25–2).

III. Anionarylation of 1,3-dienes

The influence of the nature of the aromatic diazonium salt, the catalyst and its amount, and the pH of the medium on the yields of the final products of the hydroxyarylation of buta-1,3-diene (hydroxyarylbutenes) and on the ratio of the 1,2- and 1,4-adducts have been studied.[24] A more detailed investigation established[11] that arenediazonium sulfates and nitrates react with buta-1,3-diene in the presence of a catalyst in a water–acetone medium at pH 5–7 with vigorous evolution of nitrogen and the formation of hydroxyphenylbutenes.[11] The best yields of the products of the hydroxyphenylation of buta-1,3-diene are obtained when mixtures of copper and iron(II) sulfates and of copper nitrate and copper powder or iron filings are used as the catalyst. The hydroxyphenylation of buta-1,3-diene proceeds in both the 1,2- and 1,4-positions with the preferential formation of the 1,4-adduct. 4-Hydroxy-1-phenylbut-2-ene (28%) and 2-hydroxy-1-phenylbut-3-ene (7%) were isolated and their structures were confirmed by chemical reactions.

$$ArN_2X + CH_2{=}CH{-}CH{=}CH_2 + HOH \xrightarrow[Cu(NO_3)_2 + Cu(Fe)]{CuSO_4 + FeSO_4}$$
$$\rightarrow ArCH_2{-}CH{=}CH{-}CH_2OH$$
$$\rightarrow ArCH_2{-}\underset{OH}{CH}{-}CH{=}CH_2$$

Ar = C_6H_5, *p*-$CH_3C_6H_4$, *p*-$CH_3OC_6H_4$, *p*-$NO_2C_6H_4$.
X = HSO_4, NO_3.

Under analogous conditions, arenediazonium tetrafluoroborates interact with buta-1,3-diene in the presence of copper acetate or bicarbonate to form hydroxyarylbutenes.

In the anionarylation of isoprene, the aryl group adds to the isoprene molecule in the 1-position while the hydroxy-group adds in the 2- and 4-positions of the diene chain (the yield of the corresponding products is 30%–42%).[13]

$$ArN_2X + CH_2{=}C(CH_3){-}CH{=}CH_2 + HOH \xrightarrow{Cat.}$$
$$\rightarrow ArCH_2{-}C(CH_3){=}CH{-}CH_2OH$$
$$\rightarrow ArCH_2{-}\underset{OH}{C}(CH_3){-}CH{=}CH_2$$

Treatment of 4-hydroxy-2-methyl-1-phenylbut-2-ene and 2-hydroxy-2-methyl-1-phenylbut-3-ene with thionyl chloride afforded in both cases only 4-chloro-2-methyl-1-phenylbut-2-ene.[25] γ-Benzyl-β-methylacrolein, identified by the melting point of the semicarbazone, was obtained by the reaction of 4-hydroxy-2-methyl-1-phenylbut-2-ene with oxygen in dimethyl sulfoxide (DMSO) and also by the reaction of 4-chloro-2-methyl-1-phenylbut-2-ene, obtained from 4-hydroxy-2-methyl-1-phenylbut-2-ene, with a secondary nitropropane in an alkaline medium.[26] Furthermore, treatment of 4-chloro-2-methyl-1-phenylbut-2-ene with potassium hydroxide in dioxane led to the synthesis of 2-methyl-1-phenylbuta-1,3-diene.[25]

$$C_6H_5CH_2{-}C(CH_3){=}CH{-}CH_2OH \xrightarrow{SO_2Cl} C_6H_5CH_2{-}C(CH_3){=}CH{-}CH_2Cl$$
$$C_6H_5CH_2{-}C(CH_3){=}CH{-}CH_2OH \xrightarrow[DMSO]{O_2} C_6H_5CH_2{-}C(CH_3){=}CH{-}CHO$$
$$C_6H_5CH_2{-}C(CH_3){=}CH{-}CHO \xleftarrow{CH_3CH(NO_2)CH_3} C_6H_5CH_2{-}C(CH_3){=}CH{-}CH_2Cl$$
$$C_6H_5CH_2{-}C(CH_3){=}CH{-}CH_2Cl \xrightarrow{KOH} C_6H_5CH{=}C(CH_3){-}CH{=}CH_2$$

The reactions of arenediazonium tetrafluoroborates with buta-1,3-diene and isoprene both in acetone and in a water–acetone mixture in the presence of copper fluoride or acetate and various added alcohols take place with evolution of nitrogen and the formation of 4-alkoxy-1-arylbut-2-enes.[27]

$$ArN_2X + CH_2{=}CR{-}CH{=}CH_2 + AlkOH \xrightarrow{-N_2}$$
$$\rightarrow ArCH_2{-}CR{=}CH{-}CH_2{-}OAlk$$

Ar = C_6H_5, *p*-$CH_3C_6H_4$, *p*-ClC_6H_4.
X = BF_4, HSO_4, NO_3.
R = H, CH_3.

Similar products have been obtained by the interaction of arenediazonium sulfates and nitrates with dienes in the anionarylation reaction with the corresponding alcohols. Methyl, ethyl, isopropyl, n-butyl, isobutyl, *tert*-butyl, and benzyl alcohols as well

as ethylene glycol were used. In the presence of ethylene glycol, the alkoxyarylation takes place with participation of both hydroxy-groups.

$$2\,CH_2{=}CR{-}CH{=}CH_2 + 2\,ArN_2BF_4 \xrightarrow[-N_2]{HOCH_2CH_2OH} \longrightarrow [ArCH_2CR{=}CHCH_2OCH_2]_2$$

15%–20%

The best yields of the alkoxyarylation products are attained when primary alcohols are used (31%–57%). In the presence of secondary alcohols, the yields of the products fall (14%–23%), whilst tertiary alcohols do not react, which can probably be accounted for by steric factors.

Grishchuk showed for the first time[28] that the anionarylation and arylation reactions can take place simultaneously. Thus the interaction of arenediazonium tetrafluoroborates with buta-1,3-diene in the 1 : 2 water–acetone mixture in the presence of formic acid or its salts proceeds with formation of a mixture of compounds via the following mechanism:

$$C_6H_5N_2BF_4 + CH_2{=}CH{-}CH{=}CH_2 + X{-}O{-}\overset{\overset{O}{\|}}{C}{-}H \longrightarrow$$

X = H, Na.

$$\longrightarrow C_6H_6 + C_6H_5OH + C_6H_5CH_2{-}CH{=}CH{-}CH_2O{-}\overset{\overset{O}{\|}}{C}{-}H$$

1.8% 11.2% 4.3%

$$+ C_6H_5CH_2{-}CH{=}CH{-}CH_2OH + C_6H_5CH_2{-}\underset{\underset{OC(O)H}{|}}{CH}{-}CH{=}CH_2$$

26.3% 7.8%

$$+ C_6H_5CH_2{-}\underset{\underset{OH}{|}}{CH}{-}CH{=}CH_2 .$$

48.6%

Gas–liquid chromatography is used to separate and identify the reaction products.

It has been found that arenediazonium tetrafluoroborates interact vigorously with buta-1,3-diene and isoprene under the conditions of oxidation-reduction catalysis in the presence of added sodium nitrite, chloride, bromide, fluoride, propionate, butyrate, and acetate with formation of anionarylation products (in 32%–47% yield).[14] The aryl group and the anionic residue add regioselectively in the 1,4-positions in the diene fragment.

$$ArN_2X + CH_2{=}CR{-}CH{=}CH_2 \xrightarrow[-MX,\,-N_2]{MA} \longrightarrow ArCH_2{-}CR{=}CH{-}CH_2{-}A$$

X = BF_4, HSO_4, NO_3.
R = H, CH_3.
A = NO_2, F, Cl, Br, Ac.

Nitro-, fluoro-, chloro-, bromo-, and carboxy-arylbutenes have been obtained in this way.

Ganushchak et al.[14] were the first to find that arenediazonium tetrafluoroborates interact with isoprene in the presence of an excess of sodium sulfide in anhydrous acetone to form sulfidearylation products [arylalkenyl sulfides] in 25% yield.

$$2\,ArN_2BF_4 + 2\,CH_2{=}C(CH_3){-}CH{=}CH_2 + Na_2S \xrightarrow[-N_2]{} \longrightarrow [ArCH_2{-}C(CH_3){=}CH{-}CH_2]_2S$$

Ar = C_6H_5, p-$CH_3C_6H_4$.

Arenediazonium tetrafluoroborates were introduced into the reaction in the form of dry salts in acetone, whilst the sulfates and nitrates were introduced in solution in aqueous acetone (pH 5–7). The catalysts employed were copper acetate in the case of the tetrafluoroborates and copper and iron(II) sulfates or copper nitrate and iron and copper powders respectively in the case of the sulfates and nitrates.

In order to investigate the influence of the nature of the anion of the diazonium salts further, a study has been made[12] of the interaction of buta-1,3-diene, isoprene, and chloroprene with arenediazonium acetates in aqueous acetone in the presence of copper acetate. It was established that arenediazonium acetates react under the above conditions with dienes, the process involving the evolution of nitrogen and the addition of the aryl residue and of the acetoxy-group preferentially in the 1,4-positions in the diene chain respectively. Only in a few individual instances were the products of 1,2-acetoxyarylation isolated in small amounts. The corresponding aromatic hydrocarbons (10% to 15%) and esters $ArOCOCX_3$ (5%–7%) are formed as side products.

The familiar 1-acetoxy-4-phenylbut-2-ene and the isomeric 2-acetoxy-1-phenylbut-3-ene were synthesised in proportions of 6 : 1 by the interaction of benzenediazonium acetate with buta-1,3-diene. The reactions of benzene- and toluene-p-diazonium acetates with isoprene afforded the 2-acetoxy-1-phenyl and 4-acetoxy-1-phenyl derivatives. After the reaction of ring-substituted benzenediazonium acetates with buta-1,3-diene and isoprene, only the products of 1,4-acetoxyarylation were isolated.

$$ArN_2O\overset{\overset{O}{\|}}{C}CX_3 + CH_2{=}CR{-}CH{=}CH_2 \xrightarrow[-N_2]{Cu(CH_3COO)_2}$$

$$\longrightarrow ArCH_2CR{=}CHCH_2O\overset{\overset{O}{\|}}{C}CX_3$$

$$\longrightarrow ArCH_2{-}\underset{\underset{OC(O)CX_3}{|}}{CR}{-}CH{=}CH_2$$

Ar = C_6H_5, p-$CH_3C_6H_4$, p-$CH_3OC_6H_4$, p-ClC_6H_4.
X = H, Cl, F.
R = H, CH_3.

Arenediazonium trichloroacetates and trifluoroacetates were also tested in the anionarylation reactions of 1,3-dienes, which led to the corresponding acetoxy(aryl)butenes. The yields of 1-acetoxy-4-arylbutenes were 25%–40%.

A number of studies have been devoted to the interaction of diazonium salts with dienes under both catalytic and non-catalytic conditions with participation of thiocyanates.[29–31] It was established that arenediazonium tetrafluoroborates interact vigorously with buta-1,3-diene and isoprene in the presence of catalytic amounts of copper salts and alkali metal thiocyanates. This entails the coupled addition of the aryl group in the 1-position and of the isothiocyanate group predominantly in the 2-position in the diene chain. The reaction was carried out in acetone or aqueous acetone at temperatures between –30 and –15 °C.

$$ArN_2BF_4 + CH_2{=}CR{-}CH{=}CH_2 + MSCN \longrightarrow$$

$$\longrightarrow ArCH_2{-}\underset{\underset{N{=}C{=}S}{|}}{CR}{-}CH{=}CH_2 + N_2 + MBF_4$$

Ar = C_6H_5, p-$CH_3C_6H_4$, p-$CH_3OC_6H_4$.
R = H, CH_3.

Table 1. Conditions in the reactions of aromatic diazonium salts with 1,3-dienes in the presence of nucleophiles.

Anionarylation reaction	Diazonium salt	Diene	Anionoid reagent	Catalyst	Diazonium salt : diene : catalyst	Reaction medium	Yield[a] (%)	Ref.
Hydroxyarylation	ArN_2HSO_4	Buta-1,3-diene	HOH	$CuSO_4 + FeSO_4$	1 : 1.25 : (0.2 + 0.4)	Acetone – water (2 : 1)	30 – 40[b]	11
	ArN_2NO_3	"	HOH	$Cu(NO_3)_2 + Cu(Fe)$	1 : 1.25 : [0.125 + + 0.125 (0.125)]	"	30 – 40[b]	11
	ArN_2BF_4	"	HOH	$Cu(CH_3COO)_2$	1 : 1.25 : 0.05	"	40[b]	11
	ArN_2BF_4	Isoprene	HOH	$Cu(CH_3COO)_2$	1 : 1.25 : 0.05	"	30 – 42[b]	13
Alkoxyarylation	ArN_2BF_4	Buta-1,3-diene, isoprene	CH_3OH, C_2H_5OH, C_3H_7OH	$Cu(CH_3COO)_2$	1 : 2 : 0.1	Acetone – alcohol (4 : 1)	30 – 57	15
	ArN_2BF_4	Isoprene	$C_6H_5CH_2OH$	$Cu(CH_3COO)_2$	1 : 2 : 0.1	"	30	15
	ArN_2BF_4	"	$HOCH_2CH_2OH$	$Cu(CH_3COO)_2$	1 : 2 : 0.1	"	15 – 20	15
Nitroarylation	ArN_2BF_4	Buta-1,3-diene, isoprene	$NaNO_2$	$Cu(CH_3COO)_2$	1 : 1.5 : 0.1	Acetone	32 – 42	14
Carboxyarylation	ArN_2BF_4	"	CH_3COONa, C_2H_5COONa, C_3H_7COONa	$Cu(CH_3COO)_2$	1 : 1.5 : 0.1	"	30 – 47	14
Sulfidoarylation	ArN_2BF_4	"	Na_2S	$Cu(CH_3COO)_2$	1 : 1.5 : 0.1	"	25	14
Acetoxyarylation	$ArN_2OC(O)CH_3$	Buta-1,3-diene, isoprene, chloroprene	–	$Cu(CH_3COO)_2$	1 : 1.5 : 0.1	Acetone – water (1 : 1)	25 – 42[b]	12
Trifluoroacetoxyarylation	$ArN_2OC(O)CF_3$	Isoprene	–	$Cu(CH_3COO)_2$	1 : 1.5 : 0.1	"	25 – 32	12
Trichloroacetoxyarylation	$ArN_2OC(O)CCl_3$	"	–	$Cu(CH_3COO)_2$	1 : 1.5 : 0.1	"	8	12
Isothiocyanatoarylation	ArN_2BF_4	Buta-1,3-diene, isoprene	NaSCN	$Cu(BF_4)_2$	1 : 1.5 : 0.05	"	47 – 63[c]	30, 31
Thiocyanatosulfoarylation	ArN_2HSO_4	Buta-1,3-diene, isoprene, 2,3-dimethylbutadiene	NaSCN	$Cu(SCN)_2$	0.5 : 1 : 0.1	Acetone – acetic acid (1 : 1)	60 – 72	32
(*O,O*-Diethyl phosphoro-dithioato)sulfonylarylation	ArN_2HSO_4	Buta-1,3-diene, isoprene	$NaSP(S)(OC_2H_5)_2$	$Cu[SP(S)(OC_2H_5)_2]_2$	0.5 : 1 : 0.1	"	40 – 42	32
(*O*-Ethyl dithiocarbonato)-sulfoarylation	ArN_2HSO_4	Isoprene	$NaSC(S)OC_2H_5$	$Cu[SC(S)OC_2H_5]_2$	0.5 : 1 : 0.1	"	53	32
Iodoarylation	ArN_2Cl, ArN_2Br, ArN_2HSO_4	"	NaI	–	1 : 2	Water – alcohol (1 : 4)	29 – 44	33

[a] The yield of 1,4-adducts is quoted.
[b] The overall yield of 1,2- and 1,4-adducts.
[c] The yield of the 1,2-adducts is quoted.

It was established that, together with copper acetate and bicarbonate, copper(II) tetrafluoroborate is an effective catalyst of the isothiocyanatoarylation of dienes. The yields of 1-aryl-2-isothiocyanatobut-3-enes are almost the same when the above catalysts are employed and amount to 45% – 63%. It was shown that the reaction can occur also in the absence of copper(II) salts, but the yields of 1-aryl-2-isothiocyanatobut-3-enes are then lower by 17% – 24%. Small amounts of side products (~ 10%) resulting from the reduction of the diazonium salts and substituted isothiocyanatobenzenes were isolated.

1-Aryl-2-isothiocyanatobut-3-enes proved to be fairly convenient starting reagents for the synthesis of previously unknown mono-1,3-di- and 1,1,3-tri-substituted thioureas, namely *N*-(1-arylbut-3-en-2-yl)thioureas, by reaction with ammonia and aliphatic amines.[31]

$$ArCH_2-\underset{\underset{N=C=S}{|}}{CR^1}-CH=CH_2 + HNR^2R^3 \longrightarrow$$

$$\longrightarrow ArCH_2-\underset{\underset{\underset{\underset{NR^2R^3}{|}}{C=S}}{|}}{\overset{\overset{HN}{|}}{CR^1}}-CH=CH_2$$

80% – 90%

Ar = C_6H_5, *p*-$CH_3C_6H_4$, *p*-$CH_3OC_6H_4$.
R^1 = H, CH_3; R^2, R^3 = H, CH_3, C_2H_5.

The antibacterial and antifungal properties of 1-aryl-2-isothiocyanatobut-3-enes have been described.[30]

The interaction of aromatic diazonium salts with butadiene, 2,3-dimethylbutadiene, and isoprene in solution in a sulfur dioxide-saturated acetic acid – acetone mixture in the presence of sodium chloride, bromide, thiocyanate, *O,O*-diethyl phosphorodithioate, and xanthate in such a way that the arenesulfonyl group adds to the diene chain in the 1-position while the anion adds in the 4-position with formation of 4-anion-1-arenesulfonylbut-2-enes has been demonstrated.[32]

$$ArN_2X + CH_2=CR^1-CR^2=CH_2 + MA \xrightarrow[SO_2]{CuA_2}$$

$$\longrightarrow ArSO_2CH_2CR^1=CR^2-CH_2A + N_2 + MX$$

41% – 80%

The absence, until recently, of data on the iodoarylation of unsaturated compounds can be explained, in our view by the fact that copper salts and arenediazonium iodides were used as the catalyst by analogy with the Meerwein reaction. Arenediazonium iodides are known to be extremely unstable and, in addition, the iodide anion is readily oxidised to molecular iodine under the experimental conditions.

$$ArN_2X + CH_2=C(CH_3)-CH=CH_2 + MI \longrightarrow$$

$$\longrightarrow ArCH_2C(CH_3)=CHCH_2I$$

29% – 44%

Ar = C_6H_5, *p*(*m*)-$CH_3C_6H_4$.
X = Cl, BF_4, HSO_4.

Ganushchak et al.[33] achieved for the first time the iodoarylation of isoprene. They used ethyl alcohol, acetone, DMSO, dimethylformamide (DMF), and water as the solvents. The best yields of the iodo-derivatives are obtained when DMF and arenediazonium tetrafluoroborates are used. The conditions in the reactions of aromatic diazonium salts with 1,3-dienes in the presence of nucleophiles are presented in Table 1.

IV. Anionarylation of monounsaturated compounds

The possibility of the anionarylation of monounsaturated compounds was first described by Grishchuk.[34] It was shown that arenediazonium tetrafluoroborates interact with acrylonitrile, methyl methacrylate, vinyl chloride, and vinylidene chloride in the presence of sodium nitrite, chloride, and bromide and catalytic amounts of copper salts in such a way that coupled addition of the aryl group and the anion takes place at the point of rupture of the double bond and arylchloro(bromo)ethanes are formed in 25% – 75% yield.

$$ArN_2BF_4 + CH_2=CX^1X^2 + NaA \xrightarrow[-N_2]{}$$

$$\longrightarrow ArCH_2CX^1X^2A + NaBF_4$$

Ar = C_6H_5, *p*-$CH_3C_6H_4$.
X^1 = H, CH_3; X^2 = Cl, Br, CH_3COO, CN, C_6H_5.

The reaction of benzenediazonium tetrafluoroborate with styrene in the presence of sodium nitrite leads to the formation of 1-nitro-1,2-diphenylethane and *trans*-stilbene,[34] while the reaction of acrylonitrile, methyl methacrylate, and vinylidene chloride in the presence of an excess of sodium sulfide affords the corresponding sulfide in 25% yield under catalytic conditions.[34]

$$C_6H_5N_2BF_4 + CH_2=CX^1X^2 + Na_2S \xrightarrow[-N_2]{}$$

$$\longrightarrow [C_6H_5CH_2CX^1X^2]_2S$$

X^1 = H, CH_3, Cl; X^2 = CN, CH_3COO, Cl.

It has been established[35] that *p*-nitrobenzenediazonium sulfates react vigorously with acrylonitrile at 5 – 10 °C in aqueous acetone in the presence of copper and potassium thiocyanate to form β-(*p*-nitrophenyl)-α-thiocyanatopropionitrile in 50% yield.

It was later established[21] that, regardless of the anion of the diazonium salt, arenediazonium sulfates, nitrates, and tetrafluoroborates form the same anionarylethanes on interaction with acrylonitrile, methyl methacrylate, vinyl acetate, styrene, and vinylidene chloride in the presence of sodium chloride, bromide, thiocyanate, and nitrite as well as the catalyst (copper acetate).

$$p\text{-}NO_2C_6H_4N_2HSO_4 + CH_2=CHCN + KSCN \longrightarrow$$

$$\longrightarrow p\text{-}NO_2C_6H_4CH_2-\underset{\underset{SCN}{|}}{CHCN} + N_2 + KHSO_4$$

Under the same conditions, the corresponding sulfides are formed in the presence of sodium sulfide.[21]

$$ArN_2X + CH_2=C\begin{matrix}R^1\\R^2\end{matrix} \xrightarrow{NaA} ArCH_2-\underset{\underset{A}{|}}{\overset{\overset{R^1}{|}}{C}}-R^2 + N_2 + NaX$$

30% – 35%

Naidan et al.[36] investigated the thiocyanatoarylation of acrylonitrile, methyl methacrylate, and styrene. They showed that benzenediazonium sulfates interact with the above monounsaturated compounds in aqueous acetone in the presence of thiocyanate ions.

$$CH_2=CR^1R^2 + ArN_2HSO_4 + NH_4SCN \longrightarrow$$

$$\longrightarrow ArCH_2C(SCN)R^1R^2 + N_2 + (NH_4)_2SO_4$$

R^1 = H, CH_3; R^2 = CN, $COOCH_3$, C_6H_5.

The thiocyanatoarylation reaction in a sulfur dioxide-saturated acetic acid–acetone mixture at temperatures between −16 and −20 °C results in the addition of the thiocyanato- and arenesulfonyl groups to the unsaturated compound. For example, the thiocyanato-group adds in the α-position of styrene, while the arenesulfonyl group adds in the β-position. The yield of 2-arene-sulfonyl-1-phenyl-1-thiocyanatoethane is 53%–58%.

$$ArN_2HSO_4 + SO_2 + C_6H_5CH{=}CH_2 + NH_4SCN \xrightarrow{Cu(SCN)_2} C_6H_5CH(SCN)CH_2SO_2Ar + N_2 + (NH_4)_2SO_4$$

It has also been noted[36] that the earlier hypothesis[35] that copper(II) thiocyanate is the reaction catalyst is incorrect; in fact the catalyst is copper(I) thiocyanate, which is formed readily under the reaction conditions.

In aqueous acetone at 5–10 °C in the presence of copper(I) ethylxanthate and potassium xanthate, acrylonitrile reacts with benzene- and *p*-nitrobenzene-diazonium sulfates.[37] The reaction proceeds with evolution of nitrogen and leads to α-(ethoxythiocarbonylthio)-β-phenylpropionitrile (51%) and α-(ethoxythiocarbonylthio)-β-(*p*-nitrophenyl)propionitrile (40%).

$$CH_2{=}CHCN + ArN_2HSO_4 + C_2H_5OC(S)SK \longrightarrow ArCH_2CH(SC(S)OC_2H_5)CN + N_2 + KHSO_4$$

Ar = C_6H_5, *p*-$NO_2C_6H_4$.

It has been established[38] that in the anionarylation reaction *p*-nitrobenzene-diazonium sulfate interacts with acrylonitrile in the presence of sodium diethyl phosphorodithioate to form α-(diethoxythiophosphorylthio)-β-(*p*-nitrophenyl)-propionitrile in 72% yield.

$$p\text{-}NO_2C_6H_4N_2HSO_4 + CH_2{=}CHCN + (C_2H_5O)_2P(S)SNa \longrightarrow p\text{-}NO_2C_6H_4CH_2CH(CN)SP(S)(OC_2H_5)_2 + N_2 + NaHSO_4$$

The reaction takes place at room temperature and the catalyst is copper *O,O*-diethyl phosphorodithioate.

Interesting data have been published on the anionarylation of acrylic and methacrylic acid esters.[20,39] It was shown that arenediazonium tetrafluoroborates react with acrylic and methacrylic acid esters in acetone or the 1 : 2 water–acetone mixture in the presence of potassium thiocyanate with evolution of nitrogen and the addition of the aryl and thiocyanato-groups at the site of rupture of the double bond in the monounsaturated compound to form 1-alkoxycarbonyl-2-aryl-1-thiocyanatoethanes.

$$R^1C_6H_4N_2BF_4 + CH_2{=}CR^2COOR^3 + KSCN \longrightarrow R^1C_6H_4CH_2{-}\underset{SCN}{CR^2}COOR^3 + KBF_4 + N_2$$

R^1 = H, *m*(*p*)-CH_3, *p*-CH_3O.
R^2 = H, CH_3; R^3 = CH_3, C_2H_5, C_4H_9, *iso*-C_4H_9.

Thiocyanatoarylation takes place at temperatures from −30 to −15 °C. The structure of the diazonium salt and of the monounsaturated compound as well as the nature of the reaction medium (acetone or aqueous acetone) hardly affect the yields of 1-alkoxycarbonyl-2-aryl-1-thiocyanatoethanes, which are ~50%–70%. When toluene-*m*-diazonium tetrafluoroborate is introduced into the reaction, the yields of 1-alkoxycarbonyl-1-thiocyanato-2-(*m*-tolyl)ethanes are somewhat lower (~40%). Isothiocyanatobenzenes are formed in ~20% yield together with the thiocyanatoarylation reaction.

Copper(II) salts were tested as the catalysts: the acetate, bicarbonate, and tetrafluoroborate. It was established that the catalysts ensure comparable yields of 1-alkoxycarbonyl-2-aryl-1-thiocyanatoethanes, i.e. the anion of the copper salt does not affect the anionarylation process.

The study of the thiocyanatoarylation of acrylic and methacrylic acid esters in the absence of copper salts is of definite interest. In this case, the yield of isothiocyanatobenzenes predominates over that of thiocyanatobenzenes [the yield of the corresponding 1-alkoxycarbonyl-2-aryl-1-thiocyanatoethanes in the absence of copper(II) salts is lower by 40%–50%].

It has been shown[40] that arenediazonium tetrafluoroborates interact with α,β,β′-trifluorostyrene and potassium thiocyanate in acetone, forming the thiocyanatoarylation products—2-aryl-1,2,2-trifluoro-1-phenyl-1-thiocyanatoethanes (yield 36% to 46%).

$$ArN_2BF_4 + C_6H_5CF{=}CF_2 + KSCN \longrightarrow ArCF_2CF(SCN)C_6H_5 + KBF_4 + N_2$$

Ar = C_6H_5, *p*-$CH_3C_6H_4$, *p*-$CH_3OC_6H_4$.

This reaction proceeds also in the absence of catalysts—copper or iron salts. Apparently, depending on the degree of electron saturation of the double bond and the nature of the anion, the reaction proceeds via different mechanisms.

$$C_6H_5CHal{=}CH_2 + ArN_2BF_4 + KSCN \xrightarrow{(CH_3)_2CO} \begin{cases} C_6H_5C(SCN){=}CHAr \\ 19\% \\ C_6H_5CH{=}CHAr \\ 22\% \end{cases}$$

The interaction of α-bromo- and α-chloro-styrenes[41] with potassium thiocyanate and arenediazonium salts in acetone in the presence of copper(II) salts leads to *trans*-α-thiocyanatostilbenes and *trans*-stilbenes. The ratio of the reaction products depends on the nature of the solvent: both compounds are formed in acetone whereas *trans*-stilbenes are formed predominantly in aqueous acetone.

It has been established that[22,42] arenediazonium tetrafluoroborates actively interact with vinyl chloride and vinylidene chloride in acetone or the 1 : 4 water–acetone mixture in the presence of copper or iron thiocyanate and potassium (sodium or ammonium) thiocyanate at temperatures between −15 and −5 °C with evolution of nitrogen, affording the products of the addition of the aryl and thiocyanato-groups at the site of the dissociation of the double bond of the monounsaturated compound—2-aryl-1-chloro-1-thiocyanatoethanes and 2-aryl-1,1-dichloro-1-thiocyanatoethanes (yield 73%–82%).

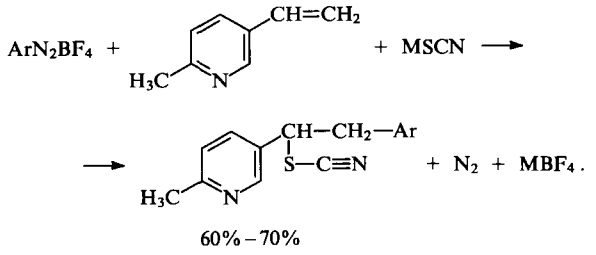
$$ArN_2BF_4 + CH_2{=}CR^1Cl + MSCN \longrightarrow ArCH_2{-}\underset{SCN}{CR^1Cl} + N_2 + MBF_4$$

Ar = C_6H_5, *p*-$CH_3C_6H_4$, *p*-$CH_3OC_6H_4$.
R^1 = H, Cl; M = K, Na, NH_4.

The optimum diazonium salt : unsaturated compound : thiocyanate reactant ratios are 1 : 2 : 1.5. Isothiocyanatobenzenes are formed as side products (10%–15%). The excess of the olefin in the reaction system promotes the main reaction and is also necessary to compensate for the amount of the olefin carried away by the evolved nitrogen.[22]

Arenediazonium tetrafluoroborates interact with allyl chloride and bromide between −15 and −5 °C in the presence of alkali metal thiocyanates to form 1-aryl-3-chloro(bromo)-2-thiocyanatopropanes.[43] The reaction takes place only with participation of copper or iron salts. The yields of the thiocyanatoarylation products are 35%−40%.

2-Methyl-5-vinylpyridine reacts with arenediazonium tetrafluoroborates in the 1:4 water−acetone mixture in the presence of thiocyanates[44] to form 5-(2-aryl-1-thiocyanatoethyl)-2-methylpyridines in accordance with the following mechanism:



60%−70%

The reaction proceeds at a temperature between −65 and −50 °C both in the presence and absence of the catalyst−copper or iron salts. Isothiocyanatobenzenes are formed as side products in a yield of ~7%−10%.

It has been shown[45] that a sulfur-dioxide-saturated solution of benzenediazonium chloride containing copper chloride reacts with styrene at room temperature. The chlorine atom and the benzenesulfonyl group then add at the site of the dissociation of the carbon−carbon double bond, forming 2-benzenesulfonyl-1-chloro-1-phenylethane in 42% yield. Apparently, when benzenediazonium chloride is saturated with sulfur dioxide, benzenesulfonyldiazonium chloride is formed and subsequently reacts with styrene after splitting off nitrogen.

$$C_6H_5N_2Cl + SO_2 + C_6H_5CH{=}CH_2 \xrightarrow{CuCl_2}$$
$$\longrightarrow C_6H_5CHClCH_2SO_2C_6H_5 + N_2$$

In a sulfur-dioxide-saturated mixture of acetic acid and acetone, styrene reacts with aromatic diazonium salts in the presence of chloride and bromide anions, *O,O*-diethyl phosphorodithioates, xanthates, and catalytic amounts of copper ions, affording respectively 1-chloro-, 1-bromo-, 1-(diethoxythiophosphorylthio)-, and 1-(ethoxythiocarbonylthio)-derivatives of 2-arenesulfonyl-1-phenylethanes in 28%−83% yields.[46]

$$ArN_2X + SO_2 + C_6H_5CH{=}CH_2 + MA \xrightarrow{CuA_2}$$
$$\longrightarrow C_6H_5CH(A)CH_2SO_2Ar + N_2 + MX$$

X = Cl, Br, HSO_4.

It has been suggested[41] that an important factor promoting the anionarylation reaction in the absence of a catalyst is an increase in the nucleophilicity of the anion in the added anionoid reagent. In order to confirm this hypothesis, a study has been made[47,48] of the interaction of diazonium salts with acrylic and methacrylic acid esters in the presence of the *N,N*-diethyldithiocarbamate anion, which is more nucleophilic than the thiocyanate anion.

Arenediazonium tetrafluoroborates, sulfates, and nitrates react vigorously with acrylic and methacrylic acid esters, evolving nitrogen and forming 2-aryl-1-(*N,N*-diethylthiocarbamoylthio)-1-methoxycarbonylethanes. The reaction takes place at a temperature between −50 and −20 °C in acetone or aqueous acetone for a 1:1.5 molar ratio of the diazonium salt and the salts of *N,N*-diethyldithiocarbamic acid. The presence of a catalyst — copper(II) or iron(II) salts — hardly affects the *N,N*-diethyldithiocarbamatoarylation of acrylates. The yields of the products are 51%−62%. Those of the target products are independent of the order in which the reagents are introduced into the reaction medium. When arenediazonium sulfates and nitrates are used, the yields of aryl(*N,N*-diethylthiocarbamoylthio)ethanes are lower by 25%−30% than in the case where tetrafluoroborates are used. This can be explained by the fact that aqueous solutions of diazonium salts have pH 3−4 and *N,N*-diethyldithiocarbamic acid is formed under these conditions. The acid is unstable and immediately decomposes.

$$ArN_2X + CH_2{=}CR^1C(O)OCH_3 + MS(S)CN(C_2H_5)_2 \longrightarrow$$
$$\longrightarrow ArCH_2CR^1(COCH_3)SCN(C_2H_5)_2 + N_2 + MX$$

Ar = C_6H_5, *p*-$CH_3C_6H_4$, *p*-$CH_3OC_6H_4$.
X = BF_4, HSO_4, NO_3; R^1 = H, CH_3; M = Na, K, NH_4.

The considerable difference between the nucleophilicities of the thiocyanate and *N,N*-diethyldithiocarbamate groups as well as the presence in the second case of unshared electrons at the second sulfur atom (α-atom) joined to the nucleophilic centre can apparently explain why the dithiocarbamatoarylation process proceeds also in the absence of a catalyst.

It has been shown[47,48] that diazonium salts interact with salts of *N,N*-diethyldithiocarbamic acid in acetone or aqueous acetone at temperatures between −50 and −10 °C, forming *N,N*-diethylthiocarbamoylthiobenzenes in 60%−70% yields.

The iodoarylation of methyl acrylate and methacrylate was described for the first time by Ganushchak et al.[49]

$$ArN_2X + CH_2{=}CR^1R^2 \xrightarrow{MI} ArCH_2{-}\overset{I}{C}R^1R^2$$

X = Cl, BF_4, HSO_4; R^1 = H, CH_3; R^2 = $COOCH_3$.

Alcohol, acetone, dimethyl sulfoxide, dimethylformamide, and water were used as solvents.

The iodoarylation of acrylic ar ylic acid esters and acrylonitrile has been investiga· ·ie fully.[50] It has been established that these compounds interact with aromatic diazonium salts and iodide ions, the aryl group and the iodide ion being added to the double bond. The aryl group adds to the extreme methylene group.

$$ArN_2X + CH_2{=}CR^1R^2 + MI \longrightarrow$$
$$\longrightarrow ArCH_2{-}\overset{I}{C}R^1R^2 + MX + N_2$$
22%−60%

R^1 = H, CH_3, C_3H_7; R^2 = $COOC_4H_9$, CN; X = Cl, BF_4, HSO_4.
R^2 = $C(O)OCH_3$; M = K, Na, NH_4.

The optimum diazonium salt:monomer:iodide reactant ratios are 5:3:5. The reaction takes place in an aqueous medium and in various organic solvents (alcohol, benzene, dioxane, dimethyl sulfoxide, dimethylformamide). The yields of aryliodoethanes are influenced by the structure of the substrate and also by the nature and position of the substituent in the aromatic ring of the diazonium salt. The iodoarylation of acrylonitrile proceeds more vigorously than that of the acrylic acid esters. The yields of the aryliodo-derivatives increase on passing from methyl esters of acrylic acids to the butyl esters and following the introduction of alkyl substituents in the α-position, which may be accounted for by the stability of the intermediate $Ar{-}CH_2\dot{C}(R^1)C(O)OAlk$. Arenediazonium salts containing electron-donating substituents in the *para*-position afford higher yields of the target products compared with the *ortho*- and *meta*-isomers.

Table 2. Conditions in the reactions of aromatic diazonium salts with alkenes in the presence of nucleophiles.

Anionarylation reaction	Diazonium salt	Alkene	Anionoid reagent	Catalyst	Diazonium salt : diene : catalyst	Reaction medium	Yield (%)	Ref.
Nitroarylation	ArN_2BF_4	Acrylonitrile, styrene, methyl methacrylate	$NaNO_2$	$Cu(CH_3COO)_2$	1 : 1 : 0.1	Acetone – water (4 : 1)	20 – 30	21
Sulfidoarylation	ArN_2BF_4	"	Na_2S	$Cu(CH_3COO)_2$	1 : 1 : 0.1	"	20 – 32	21
Thiocyanatoarylation	ArN_2HSO_4	Acrylonitrile, styrene	NaSCN	$Cu(SCN)_2$	1 : 1 : 0.25	Acetone – water (2 : 1)	41 – 72	36
	ArN_2BF_4	Acrylic and methacrylic acid esters	NaSCN	$Cu(CH_3COO)_2$, $(CuOH)_2CO_3$, $Cu(BF_4)_2$	1 : 1.12 : 0.05	"	41 – 72	20
	ArN_2BF_4	Vinyl chloride, vinylidene chloride	NaSCN	$Cu(SCN)_2$	1 : 2 : 0.05	Acetone or acetone – water (4 : 1)	79 – 82	22
	ArN_2BF_4	Allyl chloride, allyl bromide	NaSCN	$Cu(SCN)_2$	1 : 1.25 : 0.1	Acetone – water (3 : 1)	34 – 54	43
(*O*-Ethyl dithiocarbonato)arylation	ArN_2HSO_4	Acrylonitrile	$KS(S)COC_2H_5$	$Cu[S(S)COC_2H_5]_2$	1 : 1 : 0.25	"	40 – 51	37
(Diethyl phosphorodithioato)arylation	ArN_2HSO_4	"	$KS(S)P(OC_2H_5)_2$	$[(C_2H_5O)_2P(S)S]_2Cu$	1 : 1 : 0.25	"	72	38
Chloroarylation	ArN_2BF_4	Allyl chloride	NaCl	$CuCl_2$	1 : 1.25 : 0.1	"	51 – 60	43
Chlorosulfoarylation	ArN_2Cl	Styrene	–	$CuCl_2$	1 : 3 : 0.3	Acetic acid	42	45
Thiocyanatosulfoarylation	ArN_2HSO_4	"	SO_2, NH_4SCN	$Cu(SCN)_2$	1 : 3 : 0.3	Acetone – acetic acid (4 : 3)	40 – 69	36
Bromosulfoarylation	ArN_2HSO_4	"	SO_2, KBr	$CuBr_2$	1 : 3 : 0.3	"	59 – 83	46
(*O,O*-Diethyl phosphorodithioato)arylation	ArN_2HSO_4	"	SO_2, $KS(S)P(OC_2H_5)_2$	$Cu[S(S)P(OC_2H_5)_2]_2$	1 : 3 : 0.3	"	44 – 58	46
(*O*-Ethyl dithiocarbonato)arylation	ArN_2HSO_4	"	SO_2, $KS(S)OC_2H_5$	$Cu[S(S)OC_2H_5]_2$	1 : 3 : 0.3	"	45 – 81	46
N,N-Diethyldithiocarbamatoarylation	ArN_2BF_4	Acrylic and methacrylic acid esters	$NaS(S)CN(C_2H_5)_2$	–	1 : 1.5	Acetone – water (2 : 1)	51 – 62	18
Iodoarylation	ArN_2BF_4	"	NaI	–	5 : 3	Acetone or DMSO	22 – 60	50
(*O,O*-Diethyl phosphorodithioato)arylation	$(BF_4N_2-C_6H_4-)_2X$	"	$KS(S)P(O)_2R^1$	$Cu(CH_3COO)_2$, Cu	2.5 : 5 : 0.75	Acetone	14, 15, 5	52

Together with the iodoarylation products, the products of the iodination of the aromatic ring are formed in all cases. Both reactions apparently begin with the reduction of the diazonium cation by the iodide anion to give the aryl group, which forms an iodoarene or an aliphatic-aromatic radical. The radical reaction mechanism has been confirmed by the formation of aryliodo-derivatives in the presence of other anions.

When 2-aryl-1-iodo-1-methoxycarbonyl(cyano)alkanes are treated with alcoholic alkali, the compound is dehydroiodinated and the ester group is hydrolysed; derivatives of cinnamic acid, containing substituents in the α-position and in the aromatic ring, are then formed in high yields (48%–90%).[50]

In order to extend the limits of the iodoarylation reaction, a study has been made[51] of the interaction of arenediazonium tetrafluoroborates with phenyl-acetylene and lithium iodide in aqueous dimethyl sulfoxide at pH 5–7 and at a temperature of 20–37 °C.

$$ArN_2X + HC{\equiv}C{-}C_6H_5 + LiI \longrightarrow \underset{H\ \ I}{\overset{Ar\ \ C_6H_5}{C{=}C}} + LiBF_4 + N_2$$

Ar = C_6H_5, *o*(*m*,*p*)-$CH_3C_6H_4$, *p*-$CH_3OC_6H_4$.

The yields of *cis*-(*E*)-α-iodostilbenes are 36%–48%.

The influence of heteroatomic substituents on the possibility of the involvement of the double bond in the iodoarylation reaction has also been investigated[51] in relation to vinyl derivatives of phosphorus containing the $\geq P(O)-CR{=}CH_2$ fragment. The ethyl esters of vinylphosphonic and 2-propenylphosphonic acids were chosen as the objects of study.

It was established that arenediazonium tetrafluoroborates react with the above phosphorus-containing olefins in the presence of lithium fluoride in the same way as with acrylic acid esters and acrylonitrile.

$$ArN_2BF_4 + CH_2{=}C(R^1)P(O)(OC_2H_5)_2 + LiI \longrightarrow$$

$$\longrightarrow ArCH_2{-}\underset{I}{C}(R^1)P(O)(OC_2H_5)_2 + LiBF_4 + N_2$$

21%–49%

Ar = C_6H_5, *o*(*m*,*p*)-$CH_3C_6H_4$; R^1 = H, CH_3.

The direct iodoarylation of unsaturated compounds has not so far been achieved because arenediazonium iodides have not been obtained and, furthermore, Cu_2I_2 is sparingly soluble under the reaction conditions.

Ganushchak et al.[52] investigated anionarylation reactions with the aid of diazonium salts synthesised from benzidine and di(4-aminophenyl) ether. It was shown that the tetrafluoroborates of the diazonium salts derived from benzidine and di(4-aminophenyl) ether react with acrylic and methacrylic acid esters and potassium *O*,*O*-dialkyl phosphorodithioates in the presence of copper acetate and copper powder, forming 4,4′-bis[2-(dialkoxythiophosphorylthio)-2-methoxycarbonylethyl(propyl)]-biphenyls and 4,4-bis[2-(dialkoxythiophosphorylthio)-2-methoxycarbonylethyl(propyl)]-diphenyl ethers.

$$2\,CH_2{=}C(R)COOCH_3 + BF_4N_2{-}C_6H_4{-}X{-}C_6H_4{-}N_2BF_4$$

$$+\ 2\,(R^1O)_2P(S)SK \xrightarrow[-N_2,\ -KBF_4]{Cu(CH_3COO)_2/Cu}$$

$$\longrightarrow H_3COOC(R)CH_2{-}C_6H_4{-}X{-}C_6H_4{-}CH_2C(R)COOCH_3$$

$SP(S)(OR^1)_2$ $SP(S)(OR^1)_2$

14%–15%

X = bond, O; R^1 = n-C_3H_7, *iso*-C_3H_7.

The majority of the olefin anionarylation products, for example, 1-chloro-1-thiocyanato-, 1,1-dichloro-1-thiocyanato-, and 1-alkoxycarbonyl-1-thiocyanato-derivatives of 2-arylethanes exhibit antifungal and antibacterial properties.[39,42]

The conditions in the reactions of aromatic diazonium salts with alkenes in the presence of nucleophiles are presented in Table 2.

V. The mechanism of the anionarylation reaction

A necessary condition for the occurrence of the anionarylation reaction is in many cases the presence of a catalyst — copper or iron salts — in the reaction mixture. The reaction occurs in the absence of a catalyst only occasionally. This depends on the structure of the unsaturated compound and the nucleophilicity of the anion introduced.

The data available at present concerning different aspects of the reaction of diazonium salts with unsaturated compounds suggest that it proceeds via a radical-anion mechanism in the presence of a catalyst and via a radical mechanism in its absence.

We shall now consider the mechanism of the anionarylation reaction catalysed by copper and iron compounds, which is presented in Scheme 1. The principal stages of this reaction have been described in detail.[8] In stage (1), arenediazonium tetrafluoroborates interact with anionoid reagents to form the anion-arenediazonium. Under the reaction conditions, copper(II) is readily reduced to copper(I).[3,4,22] Next, the copper(I) salt formed in stage (2) forms a double bond with the anionarenediazonium in which the diazo-group is coordinated to the complex anion $(CuA_2)^-$. In individual instances, such salts have been isolated in a pure form[53] or their existence has been demonstrated conductometrically.[4,55] Next, the double salt forms with the unsaturated compounds a ternary reaction complex A [stage (3)] in which the diazo-group and the olefin are bound to the copper ion.[3,34,54]

Scheme 1

$$ArN_2X + MA \longrightarrow ArN_2A + MX \quad (1)$$

$$ArN_2A + CuA \longrightarrow ArN_2^+(CuA_2)^- \quad (2)$$

$$ArN_2^+(CuA_2)^- + CH_2{=}CR^1R^2 \rightleftharpoons$$

$$\rightleftharpoons \underset{(A)}{\left[ArN_2^+(CuA_2)^- \overset{CH_2}{\underset{CR^1R^2}{\|}}\right]} \quad (3)$$

$$\left[ArN_2^+(CuA_2)^- \overset{CH_2}{\underset{CR^1R^2}{\|}}\right] \xrightarrow[-N_2]{} \left[Ar{-}CH_2{-}\dot{C}R^1R^2{\cdots}CuA_2\right] \quad (4)$$

$$\left[Ar{-}CH_2{-}\dot{C}R^1R^2{\cdots}CuA_2\right] \xrightarrow[-CuA]{} Ar{-}CH_2{-}CR^1R^2A \quad (5)$$

The formation of transition metal, including copper and iron, complexes with arenediazonium salts has been demonstrated.[34,53–55] Such complexes are relatively stable in aqueous organic, organic, and aqueous solutions in the cold and at room temperature, but begin to decompose after the addition of the unsaturated compound.

It has long been known that copper(I) salts form π-complexes with diene and monounsaturated compounds in organic and aqueous media[54,56] (this factor constitutes the basis of the industrial chemisorption separation of hydrocarbons[57]). The evolution of nitrogen, which occurs only after the addition of the unsaturated compound, is a sign of the onset of the reaction.

Electron transfer from copper(I) to the diazonium cation in complex A (see Scheme 1) leads to the evolution of nitrogen from the diazo-group and the formation of the radical Ar$^\cdot$ and copper(II). It has been shown[58] that, on exposure to the polarising action of the copper ion, the arenediazonium cation is reduced to the radical Ar$^\cdot$ via a one-electron mechanism.

$$C_6H_5N_2^+ + e \longrightarrow C_6H_5N_2^{\cdot} \longrightarrow C_6H_5^{\cdot} + N_2$$

Next, the radical Ar$^{\cdot}$ forms an aliphatic–aromatic radical with the unsaturated compound without passing to the bulk of the solution [stage (4)]. On interaction with CuA_2, the aliphatic–aromatic radical then affords anionarylation products as a result of the transfer of the radical-anion [stage (5)]. The formation of such radicals has been detected by EPR with the aid of spin-trapping agents.[59]

When iron(II) salts are used, the reaction proceeds in accordance with the following scheme in our view.

Scheme 2

$$ArN_2A \longrightarrow A\dot{r} + N_2 + A^{\cdot} \quad (6)$$

$$A\dot{r} + CH_2{=}CR^1R^2 \longrightarrow \underset{\textbf{(B)}}{Ar{-}CH_2{-}\dot{C}R^1R^2} \quad (7)$$

$$Ar{-}CH_2{-}\dot{C}R^1R^2 + A^{\cdot} \longrightarrow Ar{-}CH_2{-}\underset{\displaystyle A}{\underset{|}{C}}R^1R^2 \quad (8)$$

$$A\dot{r} + A^{\cdot} \longrightarrow ArA \quad (9)$$

$$Ar{-}CH_2{-}\dot{C}R^1R^2 + CH_2{=}CR^1R^2 \longrightarrow Ar{-}CH_2{-}CR^1R^2{-}CH_2{-}\dot{C}R^1R^2 \longrightarrow \text{tarry polymeric substances.} \quad (10)$$

Apart from copper and iron salts, the salts of other variable-valence metals with similar oxidation–reduction potentials can also play the role of catalysts.

We shall now proceed to the consideration of the anionarylation of olefins in the absence of a catalyst (Scheme 2). In this case, the diazonium salts interact in the first stage with the anionoid reagents to form the anionarenediazonium, which then readily decomposes via reaction (6).[60,61] The aryl radical formed interacts with the olefin, affording the aliphatic–aromatic radical **B** [stage (7)].[58,62] The subsequent mode of reaction is determined by the stability of this radical. If radical **B** is sufficiently stable, the anionarylation of unsaturated compounds [stage (8)] takes place, but if radical **B** is unstable, reaction (10), leading mainly to tarry polymeric substances, occurs.

The presence of anionoid reagents in systems containing a diazonium salt is known to lead to its decomposition via a radical mechanism. The aryl radicals formed have been detected by EPR.[63]

* * *

In conclusion we may note that the expansion of the range of unsaturated compounds and aromatic diazonium salts used in the anionarylation reaction in order to obtain aliphatic-aromatic synthons containing several reaction centres, which are otherwise difficult to obtain, is of undoubted interest for organic synthesis. The improvement of methods used in anionarylation reactions is an important aspect. It will make it possible to reduce competing reactions to a minimum.

References

1. H Meerwein, E Büchner, K Emster *J. Prakt. Chem.* **152** 237 (1939)
2. E Müller *Angew. Chem.* **61** 179 (1949)
3. S C Dickerman, D J DeSouza, N Jacobson *J. Org. Chem.* **34** 710 (1969)
4. M Allard *Bull. Soc. Chim. Fr.* **5** 1921 (1972)
5. A Krutosikova *Collect. Czech. Chem. Commun.* **39** 1892 (1974)
6. A V Dombrovskii *Usp. Khim.* **26** 695 (1957)
7. A V Dombrovskii, in *Reaktsii i Metody Issledovaniya Organicheskikh Soedinenii* (Reactions and Methods of Investigation of Organic Compounds) (Moscow: GNTIKhL, 1962) p. 285
8. A V Dombrovskii *Usp. Khim.* **53** 1625 (1984) [*Russ. Chem. Rev.* **53** 956 (1984)]
9. C S Rondestvedt, in *Organic Reactions* Vol. 2 (Translated into Russian: Moscow: Mir, 1965) p. 199
10. N I Ganushchak, N F Stadniichuk, B D Grishchuk, A V Dombrovskii, in *II Ukrainskaya Respublikanskaya Konferentsiya po Organicheskoi Khimii (Tezisy Dokladov)* [The 2nd Ukrainian Republic Conference on Organic Chemistry (Abstracts of Reports)] (Dnepropetrovsk: Dnepropetrov. Univ., 1971) p. 85
11. N I Ganushchak, B D Grishchuk, A V Dombrovskii *Zh. Org. Khim.* **9** 1004 (1973)
12. N I Ganushchak, B D Grishchuk, V A Baranov, A V Dombrovskii *Zh. Org. Khim.* **9** 2142 (1973)
13. N I Ganushchak, B D Grishchuk *Zh. Vses. Khim. Ova im D I Mendeleeva* **18** 357 (1973)
14. N I Ganushchak, B D Grishchuk, V A Baranov, A V Dombrovskii *Izv. Vyssh. Uchebn. Zaved., Khim. Khim. Tekhnol.* **18** 1381 (1975)
15. N I Ganushchak, B D Grishchuk, A V Dombrovskii *Ukr. Khim. Zh.* **41** 499 (1975)
16. B D Grishchuk, P M Gorbovoi, N I Ganushchak, in *16 Ukrainskaya Konferentsiya po Organicheskoi Khimii (Tezisy Dokladov)* [The 16th Ukrainian Conference on Organic Chemistry (Abstracts of Reports)] (Ternopol': Pedagogicheskii Inst., 1992) p. 244
17. E E Bilaya, N I Ganushchak, N D Obushak, B D Grishchuk, Yu A Pozderskii, A L Bel'ferman *Zh. Obshch. Khim.* **56** 1916 (1986)
18. B D Grishchuk, P M Gorbovoi, L P Sviderskaya, A A Dyachuk, V P Tikhonov, N I Ganushchak *Zh. Obshch. Khim.* **60** 432 (1990)
19. J K Kochi *J. Am. Chem. Soc.* **78** 4815 (1956)
20. B D Grishchuk, P M Gorbovoi, N I Ganushchak *Zh. Obshch. Khim.* **59** 1868 (1989)
21. N I Ganushchak, B D Grishchuk, V A Baranov, T A Shilo, V G Nemesh *Ukr. Khim. Zh.* **43** 130 (1977)
22. B D Grishchuk, P M Gorbovoi, E Ya Kudrik, N I Ganushchak *Zh. Obshch. Khim.* **61** 2583 (1991)
23. B D Grishchuk, P M Gorbovoi *Tiotsianato-, Brom- i Khlorarilirovanie Akrilamida* (Thiocyanato-, Bromo- and Chloroarylation of Acrylamide) (Kiev, 1993) article deposited at the GNTB of Ukraine No 1057-Uk 93
24. N I Ganushchak, B D Grishchuk, V S Buryak, V I Mogil'nikov, N F Stadniichuk, A V Dombrovskii, in *12 Ukrainskaya Respublikanskaya Konferentsiya po Organicheskoi Khimii (Tezisy Dokladov)* [The 12th Ukrainian Republic Conference on Organic Chemistry) (Abstracts of Reports)] (Uzhgorod: Uzhgorod. Univ., 1974) p. 63
25. A V Dombrovskii, N I Ganushchak *Ukr. Khim. Zh.* **24** 217 (1958)
26. M M Yukhomenko, A V Dombrovskii *Ukr. Khim. Zh.* **33** 76 (1967)
27. N I Ganushchak, B D Grishchuk, A V Dombrovskii *Ukr. Khim. Zh.* **41** 499 (1975)
28. B D Grishchuk, P M Gorbovoi, N I Ganushchak, E Ya Kudrik, V B Grishchuk, O G Tikhonchuk, O V Mikhal'chuk, in *16 Ukrainskaya Konferentsiya po Organicheskoi Khimii (Tezisy Dokladov)* [The 16th Ukrainian Conference on Organic Chemistry (Abstracts of Reports)] (Ternopol': Pedagogicheskii Inst., 1992) p. 242
29. B D Grishchuk, P M Gorbovoi, N I Ganushchak *Zh. Obshch. Khim.* **58** 616 (1988)
30. B D Grishchuk, N G Prodanchuk, P M Gorbovoi *Khim.-Farm. Zh.* **11** 25 (1990)
31. B D Grishchuk, P M Gorbovoi, M V Vovk, A A Dyachuk, I A Martynyak, N I Ganushchak *Ukr. Khim. Zh.* **57** 89 (1991)
32. V M Naidan, G D Naidan, S G Drozdova, V M Musienko *Zh. Obshch. Khim.* **55** 391 (1985)
33. N I Ganushchak, N D Obushak, O P Polishchuk *Zh. Org. Khim.* **20** 654 (1984)
34. B D Grishchuk, Author's abstract of Candidate's Thesis in Chemical Sciences, Chernov. Univ., Chernovtsy, 1974
35. V M Naidan, G D Naidan *Zh. Org. Khim.* **10** 664 (1974)
36. V M Naidan, G D Naidan, A V Dombrovskii *Zh. Obshch. Khim.* **49** 1829 (1979)
37. V M Naidan, G D Naidan, G V Litvin *Zh. Org. Khim.* **14** 2010 (1978)
38. V M Naidan, G D Naidan *Zh. Obshch. Khim.* **48** 2787 (1978)

39. B D Grishchuk, N G Prodanchuk, P M Gorbovoi, V N Nivalov, V G Sinchenko *Khim.-Farm. Zh.* **2** 139 (1990)
40. E E Bilaya, N I Ganushchak, N D Obushak, B D Grishchuk, Yu A Pozderskii, A L Bel'ferman *Zh. Obshch. Khim.* **56** 1916 (1986)
41. N D Obushak, N I Ganushchak, E E Bilaya, B D Grishchuk, in *15 Ukrainskaya Respublikanskaya Konferentsiya po Organicheskoi Khimii (Tezisy Dokladov)* [The 15th Ukrainian Republic Conference on Organic Chemistry) (Abstracts of Reports)] (Uzhgorod: Uzhgorod. Univ., 1986) p. 270
42. B D Grishchuk, N G Prodanchuk, V G Sinchenko, P M Gorbovoi, E Ya Kudrik *Khim.-Farm. Zh.* **12** 47 (1991)
43. B D Grishchuk, P M Gorbovoi, N I Ganushchak, D M Brush, E Ya Kudrik *Zh. Obshch. Khim.* **63** 1655 (1993)
44. B D Grishchuk, P M Gorbovoi, E Ya Kudrik, V B Grishchuk, M V Volk, L P Sviderskaya, in *16 Ukrainskaya Konferentsiya po Organicheskoi Khimii (Tezisy Dokladov)* [The 16th Ukrainian Conference on Organic Chemistry (Abstracts of Reports)] (Ternopol': Pedagogicheskii Inst., 1992) p. 243
45. V M Naidan, G D Naidan, G V Litvin *Zh. Org. Khim.* **14** 2622 (1978)
46. V M Naidan, G D Naidan *Zh. Obshch. Khim.* **50** 2611 (1980)
47. B D Grishchuk, P M Gorbovoi, L P Sviderskaya, A A Dyachuk, V P Tikhonov, N I Ganushchak *Zh. Obshch. Khim.* **60** 432 (1990)
48. P M Gorbovoi, B D Grishchuk, Yu P Filinov *Neftepererabotka i Neftekhim.* **40** 63 (1991)
49. N I Ganushchak, N D Obushak, O P Polishchuk *Zh. Org. Khim.* **20** 654 (1984)
50. N I Ganushchak, N D Obushak, O P Polishchuk *Zh. Org. Khim.* 2554 (1986)
51. O P Polishchuk, Author's abstract of Candidate's Thesis in Chemical Sciences, L'vov, Polytechnical Inst., 1987
52. N I Ganushchak, N D Obushak, N S Fedorovich *Ukr. Khim. Zh.* **53** 970 (1987)
53. N D Obushak, N I Ganushchak, M B Lyakhovich *Zh. Org. Khim.* **27** 1757 (1991)
54. N I Ganushchak, V D Golik, I V Migaichuk *Zh. Org. Khim.* **8** 2356 (1972)
55. O Sulton *Chem. Rev.* **3** 443 (1975)
56. A Wells, in *Structural Inorganic Chemistry* Vol. 3 (Translated into Russian; Moscow: Mir, 1988) p. 239
57. S Yu Pavlov, in *Vydelenie i Ochistka Monomerov dlya Sinteticheskogo Kauchuka* (Isolation and Purification of Monomers for Synthetic Rubber) (Leningrad: Khimiya, 1987) p. 115
58. E P Koval'chuk, N I Ganushchak, N D Obushak, I N Krupak *Ukr. Khim. Zh.* **49** 161 (1983)
59. M B Lyakhovich, R G Gasanov, N D Obushak, N I Ganushchak, Z V Todres *Izv. Akad. Nauk SSSR, Ser. Khim.* **5** 1214 (1991)
60. D C Nonhebel, J C Walton, in *Free Radical Chemistry* (Translated into Russian; Moscow: Mir, 1977) p. 445
61. G Tsolinger *Khimiya Azokrasitelei* (Chemistry of Azo Dyes) (Leningrad: GNTIKhL, 1960)
62. N I Ganushchak, N D Obushak, E P Koval'chuk, G V Trifonova *Zh. Obshch. Khim.* **54** 2334 (1984)
63. L A Kiprianova, A F Levit, I P Gragerov *Teor. Eksp. Khim.* **12** 219 (1976)

Russian Chemical Reviews **63**(3) 269–277 (1994)
©1994 Russian Academy of Sciences and Turpion Ltd

UDC 547.539:66.095.21:541.127:541.515

The synthesis and reactivity of organobromine compounds in homolytic addition and telomerisation processes

A B Terent'ev, T T Vasil'eva

Contents

I. Introduction 269
II. Reactions of bromine-containing addends 270
III. Charge-transfer complexes as possible intermediates in radical processes 274
IV. Application of ^{13}C NMR spectroscopy in the establishment of the structures of organobromine compounds 276

Abstract. Studies carried out in recent years on the radical chemistry of organobromine compounds, primarily on their application as addends in addition and telomerisation reactions, are surveyed. The use of metal complex initiating systems based on iron pentacarbonyl, together with traditional peroxide initiators, is described. This made it possible to expand significantly the synthetic possibilities of these reactions in view of their highly selective course involving the C–Br bond, and the involvement in the reaction of organic monobromo- and dibromo-compounds which hardly react under the conditions of peroxide initiation. The first examples of the stereocontrolled occurrence of the radical addition of organobromine addends to chiral monomers, leading to one of the stereoisomers, are presented. The bibliography includes 36 references.

I. Introduction

The radical reactions occurring with dissociation of the C–Br bond have been investigated to a lesser extent than the analogous processes with organochlorine compounds, but the greater ease of the dissociation of the C–Br bond as well as the high reactivity of even single bromine atoms activated by neighbouring groups lead to extensive possibilities for the synthesis of a wide variety of polyfunctional organic compounds. Organic bromo-derivatives readily enter into radical addition and telomerisation reactions; in the initiation stage, they actively generate radicals as a consequence of the dissociation of the C–Br bond, while in the chain-transfer stage their reactivity is caused by the greater ease (than for the chloro-derivatives) of electron transfer in the transition state as a consequence of the ready polarisability of the C–Br bond. This determines also the wide range of initiators and initiating influences which may be used—peroxides, azo-compounds, irradiation, oxidation–reduction systems, and, in certain cases, also ordinary illumination.

The significant difference in the chemical behaviour of chloro- and bromo-derivatives as telogens (addends) can be clearly seen on comparing the reactions of chloro- and bromoacetic acid esters: the esters of monochloroacetic acid react under radical conditions exclusively via a C–H bond, while monobromoacetic acid esters react via the C–Br bond. Experimental results have shown that the greater the number of halogen atoms at the carbon atom to which bromine is attached, the greater the reactivity of such a compound in addition and telomerisation reactions both in the initiation and chain-transfer stages. The C–Br bond is also activated by electron-accepting substituents in the α-position, for example by ester groups.

Among the bromine-containing compounds investigated, CBr_4 and CCl_3Br are the most reactive. When suitable initiators are used, the reactions involving them proceed at 50–70 °C, which is close to the optimum temperatures.

Dibromodichloromethane is fairly reactive in radical reactions. Among hydrogen-containing polybromomethanes, bromoform is outstanding. In contrast to chloroform, it reacts exclusively with dissociation of the C–Br bond regardless of the initiation conditions. However, the nature of the secondary and side reactions occurring is determined primarily by the nature of the initiating system (see below). Methylene bromide, which also reacts predominantly via the C–Br bond although isolated instances of reactions proceeding via the dissociation of a C–H bond are known,[1] is less effective.

Nonactivated α-alkyl bromides react nonselectively under radical conditions because the radicals formed in the chain propagation stage actively abstract hydrogen atoms from the alkyl chain of the bromoalkane. On the other hand, organic monobromo-compounds with functional group substituents enter readily into addition and telomerisation reactions exclusively via the C–Br bond.

The high effectiveness of bromine-containing compounds in homolytic processes makes it possible to involve readily polymerising monomers—vinyl chloride, acrylic esters, and styrene—in reactions with them. This affords individual adducts or, in isolated instances, mixtures of lower telomers. The first examples of stereocontrolled radical reactions with participation of chiral monomers, which make it possible to drive the process towards the formation of only one of the stereoisomers, have been described. The reaction of bromomethanes with vinyl carbonate provides a simple path to the synthesis of carbohydrates.[2]

The use of monomers with functional group substituents in addition and telomerisation reactions with organobromine compounds, taking into account the possibility of the successive replacement of bromine atoms by other groups, leads to polyfunctional compounds with different lengths of the main chain.

Acetylenes are not very promising in these reactions because they require fairly severe conditions which are incompatible with their explosive nature. The reactions with dienes frequently

A B Terent'ev, T T Vasil'eva Laboratory of Homolytic Reactions of Organoelement Compounds, Nesmeyanov Institute of Organoelement Compounds, Russian Academy of Sciences, ul. Vavilova 28, 117 813 Moscow, Russian Federation, Fax (7-095) 135 50 85

Received 14 December 1993
Uspekhi Khimii **63**(3) 280–288 (1994); translated by A K Grzybowski

proceed in different ways (1,2- and 1,4-addition), which hinders the isolation of individual compounds.

The comparatively high reactivity of even a single bromine atom in the adduct and telomers determines the possibility of the occurrence of secondary processes. The adducts formed may react with a new monomer molecule, affording stepwise telomerisation products. The presence of a bromine atom next to the radical centre leads to the probability of fragmentation with ejection of a bromine atom, which initiates a new reaction chain. Finally, under the conditions of metal complex initiation in the presence of a hydrogen donor, there is a possibility of the reduction of the tri- and di-halomethyl groups in the adduct and also of chain transfer via a C–H bond.

In the present review, we shall consider the literature data obtained during the last 6–7 years; earlier studies have been surveyed fairly completely in a monograph[3] (in the chapter devoted to organobromine compounds). The earlier data will be included when necessary.

II. Reactions of bromine-containing addends

1. Polybromomethanes

a. Reactions of carbon tetrabromide

A series of interesting features have appeared in recent years in reactions involving CBr_4. They are associated with the use of initiators, which are new for reactions of the given type, and also with the expansion of the range of monomers employed.

The addition of CBr_4 to a series of monomers, including monomers with functional group substituents (hept-1-ene, oct-1-ene, styrene, methyl acrylate) has been achieved in the presence of divalent samarium iodide under mild conditions; the yield of the adducts reaches 80% under these conditions.[4] The reaction is carried out in the presence of 5%–10% SmI_2 in solution in acetonitrile at 60 °C. The overall reaction mechanism described by the authors[4] includes the formation of an intermediate initiating complex **A** and subsequent chain transfer by the radical-adduct **B** to the initial polyhalomethane.

$$YCX_3 + SmI_2 \longrightarrow \underset{\mathbf{A}}{(YCX_3)^{-\cdot}SmI_2^{+}}$$

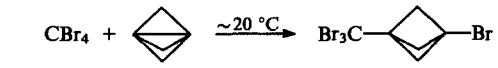
$$\mathbf{A} \longrightarrow SmI_2Y + \dot{C}X_3$$

$$\dot{C}X_3 + CH_2{=}CHR \longrightarrow \underset{\mathbf{B}}{CX_3CH_2\dot{C}HR}$$

$$\mathbf{B} + YCX_3 \longrightarrow CX_3CH_2CHYR$$

Trivalent samarium compounds do not participate in the chain transfer; the reconversion of Sm^{3+} into Sm^{2+} apparently requires a fairly powerful reductant. This constitutes a significant difference between the given reaction and the analogous processes initiated by systems based on $Fe(CO)_5$, where the halogen-containing iron carbonyl complex formed as an intermediate participates in the chain-transfer stage (the halogen passes from the complex to the radical-adduct), after which a zerovalent iron species, capable of propagating the reaction, is regenerated.[3]

The reaction of carbon tetrabromide with 1,1,1-propellane proceeds almost instantaneously, affording the corresponding adduct in a high yield.[5]



The process does not require illumination and proceeds at room temperature. The radical nature of the process has been confirmed by the presence of the corresponding signals in the EPR spectrum.

The ready homolysis of the C–Br bond in CBr_4 made it possible to carry out under the usual conditions (with benzoyl peroxide as the initiator) a radical chain reaction between carbon tetrabromide and 3,3,3-trifluoropropene, although in this instance highly electrophilic compounds function as the reactants (the addend and the monomer), i.e. a combination of polar factors highly unfavourable for the reaction is present.[6]

$$CBr_4 \xrightarrow{(C_6H_5CO)_2O_2} \dot{C}Br_3$$

$$\dot{C}Br_3 + CH_2{=}CHCF_3 \longrightarrow CBr_3CH_2\dot{C}HCF_3$$

The presence of the CF_3 group next to the radical centre imparts to the radical a highly electrophilic character and only the low dissociation energy of the C–Br bond makes it possible to achieve the subsequent process as a chain reaction.

$$CBr_3CH_2\dot{C}HCF_3 + CBr_4 \longrightarrow \underset{\mathbf{T_1}}{CBr_3CH_2CHBrCF_3} + \dot{C}Br_3$$

However, the unfavourable combination of polar factors renders this stage less effective, as a result of which the radical-adduct also participates in the competing chain propagation reaction with formation of the telomer $\mathbf{T_2}$, which is in principle atypical for reactions with carbon tetrabromide.

$$CBr_3CH_2\dot{C}HCF_3 + CH_2{=}CHCF_3 \xrightarrow{CBr_4} \underset{\mathbf{T_2}}{CBr_3CH_2CH(CF_3)CH_2CHBrCF_3}$$

The partial chain transfer constants $C_n = k_{tr}/k_p$ (k_{tr} is the transfer rate constant and k_p the chain propagation rate constants) have been estimated for this reaction involving the first three growing radicals ($C_1 = 15$, $C_2 = 64$, $C_3 = 60$), their values indicating in this case that chain transfer by the growing radicals is appreciably more effective than chain propagation. Similar values of the constants were obtained earlier also for the reaction with vinyl chloride,[7] although the properties of this monomer differ significantly from those of trifluoropropene (vinyl chloride readily polymerises, whereas this is not a characteristic feature of trifluoropropene).

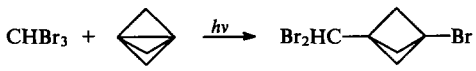
From the subsequent exposition, it will be clear that a less effective addend (for example, $CHBr_3$) reacts differently with these monomers. This applies to both chemical and kinetic results. The reaction of CBr_4 with vinyl chloride proceeds under the usual conditions as telomerisation mainly with formation of the first two telomers having the structure $CBr_3(CH_2CHCl)_nBr$, an appreciable amount (up to 10%) of the third telomer being formed only for high monomer : telogen ratios.[7]

Asahara and Chou[8] estimated the quantitative composition of the mixture of telomers by thin-layer chromatography and obtained values of C_n significantly less than unity (0.33), which is unlikely bearing in mind the high effectiveness of the telogen. The results were subsequently checked using gas–liquid chromatography.[7] In this case $C_1 = 14.6$ and $C_2 = 73.5$ were obtained, these values being in better agreement with the real reactivities of the reactants.

b. Reactions of bromoform

The C–Br bond in bromoform undergoes homolysis with greater difficulty than in CBr_4, which is the reason for a number of characteristic features of the reactions involving it: the use of effective initiation methods (up to the metal complex method) and comparatively severe reaction conditions. Relatively small differences in the nature of the reactants have a more marked effect on the results. Thus, in contrast to CBr_4, the reactions with $CH_2{=}CHCl$ and $CH_2{=}CHCF_3$ proceed differently; in certain cases, nonselective processes are observed under the conditions of peroxide initiation.

The reaction of bromoform with 1,1,1-propellane requires irradiation.[5]



The adduct is formed in a high yield (88%) and the process is not accompanied by the formation of telomers. The presence of a bromine atom at a tertiary carbon atom in the adduct molecule makes these compounds promising synthons for further chemical reactions.

As mentioned above, because of the smaller effectiveness of bromoform, compared with CBr_4, as a reaction chain-transfer agent, the intermediate radicals begin to participate also in competing reactions.

The interaction of bromoform with 3,3,3-trifluoropropene, in which the nature of the products and the composition of the reaction mixtures depend significantly on the method of initiation, is instructive in this respect.[9] Investigation showed that, in the presence of benzoyl peroxide, the reaction proceeds in a complex manner with formation of a mixture of compounds containing from two to four bromine atoms in the molecule. Together with telomers with the normal structure, the reaction mixture contains substances formed as a result of the involvement of the intermediate radical in rearrangements, hydrogen-transfer reactions, successive addition of a new monomer molecule, etc. This reaction was carried out selectively[9] using the $Fe(CO)_5$+DMF system. In this case, the reaction proceeds exclusively via the C–Br bond with formation of only one series of telomers containing three bromine atoms in the molecule.

$$CHBr_3 \xrightarrow{Fe(CO)_5+DMF} \dot{C}HBr_2$$

$$\dot{C}HBr_2 + CH_2{=}CHCF_3 \longrightarrow CHBr_2(CH_2CHCF_3)_n^{\cdot}$$

$$CHBr_2(CH_2CHCF_3)_n^{\cdot} \xrightarrow{DBr} CHBr_2(CH_2CHCF_3)_nBr$$

(DBr = bromine donor)

Telomers with $n = 1-3$ have been isolated in a pure form. The nature of the activity of metal complex initiating systems in radical reactions of polyhalomethanes with unsaturated compounds has been examined in detail in a monograph.[3] Their employment proved particularly promising when the reactions were carried out with readily polymerising acrylic monomers when initiation by peroxides is ruled out. The $Fe(CO)_5$+DMF system made it possible to achieve selective homolytic addition of bromoform to acrylic monomers at the C–Br bond without significant polymerisation.[10]

$$CHBr_3 + CH_2{=}CRX \xrightarrow{Fe(CO)_5+DMF} CHBr_2CH_2CRBrX$$

R = H; X = CN, CO_2CH_3;
R = CH_3; X = CO_2CH_3.

The radical nature of the process is confirmed in this instance by the structure of the adducts obtained (addition as a result of the dissociation of the C–Br bond). Haloforms are known to undergo ionic addition to a C–H bond, which leads to adducts with a CX_3 group at the end of the chain.[11] The best yield of the adduct with bromoform has been noted for methyl acrylate (78% relative to the unreacted $CHBr_3$); for acrylonitrile and methyl methacrylate, the yields are significantly lower (25% and 15% respectively).

The radical addition of bromoform to ketene silyl acetals, initiated by azobisisobutyronitrile (AIBN) or $B(C_2H_5)_3$, has been described.[12] Polyfunctional silicon-containing complexes of the type $CHBr_2CR^1R^2CBr(OR^3)OSiR^4_3$ or the products of their chemical reactions (hydrolysis, fragmentation, etc.) have been obtained as a result of such addition.

c. Reactions of methylene bromide

Methylene bromide is much less effective as a chain-transfer agent for the reaction via the C–Br bond than other polybromomethanes and the reaction with this compound is therefore as a rule nonselective and involves a low conversion of the addend. The reaction requires more severe conditions in this case. Thus the telomerisation of methylene bromide with 3,3,3-trifluoropropene has been carried out at 140–145 °C using the $Fe(CO)_5$+DMF initiating system. Telomers having the general formula $CH_2Br(CH_2CHCF_3)_nBr$ are the main but by no means the only reaction products.[9] The first two telomers (n = 1, 2) were isolated in a pure form. The reactions of methylene bromide with other monomers had been investigated earlier.[3]

2. Bromochloromethanes

The reactivity of polyhalomethanes in the reactions with the same monomer depends mainly on the number of halogen atoms in the polyhalomethane, while the nature of the halogen (chlorine or bromine) has much less influence. Comparison of relative kinetic data for the reactions of a series of polyhalomethanes with vinyl chloride makes it possible to arrange the addends investigated in the following series:[7] $CBr_4 > CCl_2Br_2 > CCl_3Br \gg CHBr_3$. Evidently, bromochloromethanes with two C–Br bonds and even one such bond in the molecule are more effective as reaction chain-transfer agents than bromoform.

a. Reactions of bromotrichloromethane

Among the mixed bromochloromethanes reacting via the C–Br bond, bromotrichloromethane has been most widely investigated. Monomers of different nature have been involved in the reaction with this compound and a wide variety of initiation procedures have been used.[3]

The employment of divalent samarium salts, which actively initiated these reactions under mild conditions, is fundamentally new, as for CBr_4.[4]

$$CCl_3Br + CH_2{=}CHR \xrightarrow[60\ ^\circ C,\ 10\ h]{SmI_2,\ CH_3CN} CCl_3CH_2CHBrR$$

R = C_4H_9, C_6H_{13}, C_6H_5, CO_2CH_3.

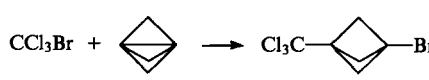
The authors suggest that one-electron transfer takes place with participation of the $(BrCCl_3)^{-\cdot}/SmI_2^+$ species (possibly a charge-transfer complex), which generates the chain-propagating $\dot{C}Cl_3$ radical.

Despite the high effectiveness of bromotrichloromethane as a chain-transfer agent, its reactions with the readily polymerising methacrylic acid esters are accompanied by the formation of telomers with two and three monomer units in an expectedly large amount.[13]

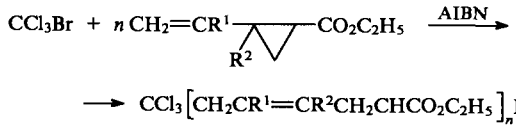
$$CCl_3Br + CH_2{=}C(CH_3)CO_2R \longrightarrow CCl_3\left[CH_2C(CH_3)CO_2R\right]_nBr$$

n = 1–3; R = *iso*-C_3H_7, *tert*-C_4H_9.

On the other hand, the reaction with propellane leads to the formation mainly of an adduct even in an excess of propellane.[14]



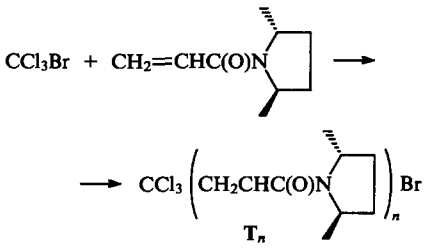
From the standpoint of the synthesis of polyfunctional compounds, the reaction of bromotrichloromethane with alkenylcyclopropanes is of interest.[15]



R^1, R^2 = H, CH_3; n = 1–7.

Telomers are formed mainly in the (*E*)-form and the partial chain transfer constants C_n for the growing radicals are close to unity and hardly change with increase in the chain length of the radical. This is quite reasonable because, even in the first growing radical ($n = 1$) the CCl_3 group is fairly remote from the radical centre and hardly affects its reactivity, which is determined for all the growing radicals mainly by the presence of ethoxycarbonyl groups in the neighbouring positions. The closeness to unity of the partial constants reflects the equal probability of the involvement of the growing radical in the chain-transfer and propagation stages.

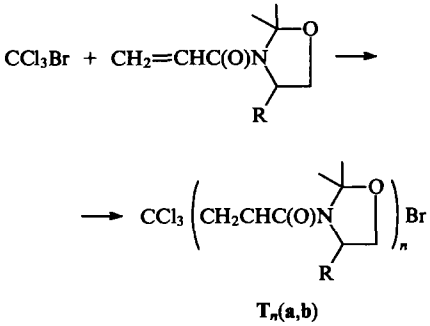
Several studies demonstrating the possibility, in principle, of stereocontrol in radical addition and telomerisation processes have been published recently.[16-18] In particular, the photochemical telomerisation of bromotrichloromethane with the chiral *N*-acryloyl-2,5-dimethylpyrrolidine has been described.[16]



T_n

The first five members of the series ($n = 1-5$) have been isolated and identified. It has been shown that the telomers T_2 and T_3 are formed predominantly in one stereoisomeric form (in the presence of small amounts of other possible stereoisomers), i.e. the radical addition reaction permits asymmetric control in the addition and chain transfer stages. The partial constants C_n are also given in the above communication, their values lying in the range 0.3–0.5. These quantities are not very reliable because, judging from the chromatograms presented in the communication (liquid and gel chromatography), the telomer ratio can be estimated quantitatively only very approximately.

The addition of bromotrichloromethane to substituted *N*-acryloyloxazolidines also proceeds with stereochemical selectivity.[17]

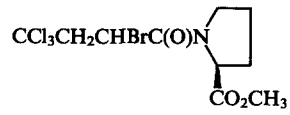


T_n(a,b)

R = C_6H_5 (a), *iso*-C_3H_7 (b).

The stereospecificity of this reaction for the telomer T_3^a reaches 15:1. The telomer T_3^a proved to be crystalline; this made it possible to use X-ray diffraction to investigate its stereochemistry. The stereoselectivity of the formation of T_3^a demonstrates that stereochemical control is achieved both in the addition stage and in the stage involving the transfer of the halogen to the growing radical.

Yet another example of this type of reaction is the addition of CCl_3Br to (*S*)-1-acryloyl-2-methoxycarbonylpyrrolidine catalysed by the $Fe(CO)_5 + P(C_6H_5)_3$ system.[18] In this case, it proved possible to achieve the virtually complete exclusion of the formation of telomers and to obtain the adduct



in 80% yield. It is one of the two possible diastereoisomers. This first example of the stereoselective occurrence of radical reactions initiated by $Fe(CO)_5$-based metal carbonyl complexes demonstrates the possibility and likely usefulness of metal complex initiators in the synthesis of stereoisomerically pure adducts.

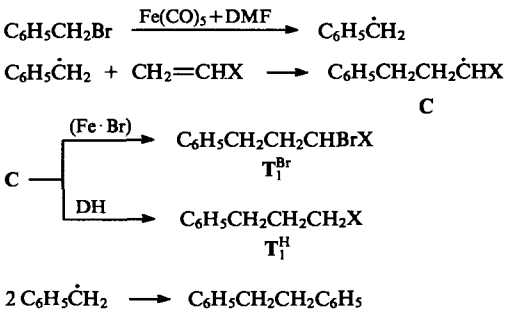
b. Reactions of dibromodichloromethane

The reaction of dibromodichloromethane with vinyl chloride under the usual conditions proceeds as telomerisation[7] and, when the monomer:telogen ratio is varied from 1.5 to 15, the content of the adduct in the reaction mixture falls from 80% to 30%. The first three telomers $CCl_2Br(CH_2CHCl)_nBr$ ($n = 1-3$) were isolated in a pure form. The values of C_n obtained ($C_1 = 7.7$; $C_2 = 54.3$) indicate a high effectiveness of dibromodichloromethane as a chain-transfer agent, comparable with the effectiveness of CBr_4 ($C_2 = 74.2$) in the analogous process with vinyl chloride.[7]

3. Benzyl bromide

Organic monobromo-compounds which have not been activated by functional groups do not enter as a rule into radical reactions under the conditions of peroxide initiation. The selective homolysis of the C–Br bond with a satisfactory yield of the adducts can be achieved under these conditions only when metal complex initiators are employed. Benzyl bromide has been most widely investigated among the monobromo-derivatives. Studies have shown that $Fe(CO)_5$-based initiating systems are most promising for its reactions with unsaturated compounds. Thus, in the presence of the $Fe(CO)_5$ + DMF(HMPA) (HMPA = hexamethylphosphoramide) system, the reactions of benzyl bromide with a wide range of monomers, differing significantly from one another by the polar characteristics of their substituents and by their capacity for polymerisation, have been achieved.[19,20] The addition of $C_6H_5CH_2Br$ to monomers with functional group substituents constitutes a promising method of synthesis of polyfunctional aliphatic–aromatic compounds. This reaction is a model for the study of the reactivity of benzyl radicals.

The addition of $C_6H_5CH_2Br$ to the $CH_2=CHX$ [X = H, C_4H_9, $Si(CH_3)_3$, Cl, CF_3, CO_2CH_3, CN] monomers using $Fe(CO)_5$ (up to 10%) combined with DMF or HMPA as the reaction initiator has been investigated under comparable conditions.[19,20] The reactions proceed in accordance with the general mechanism



The authors suggest that the radical-adduct **C** transfers the chain as a result of the abstraction of a bromine atom from the bromine-containing iron carbonyl complex whereupon the adduct T_1^{Br} is formed. The stabilisation of the radical **C** by the abstraction of hydrogen leads to the formation of the adduct T_1^H.

The identification of bibenzyl in the reaction mixture constitutes, according to the authors, one of the pieces of evidence in support of the radical nature of the reaction. It was noted that the amount of bibenzyl in the reaction mixture decreases with increase in the monomer concentration. For all the monomers, the main reaction product is T_1^{Br}. From the standpoint of the reactivity of the monomers, it was noted that the best results have been obtained with trimethylvinylsilane and somewhat worse ones with hex-1-ene. In the reaction with hex-1-ene using DMF and HMPA as initiators, an appreciable difference was observed between the yields of the adducts—in the case of HMPA the yield of the adduct increases by a factor of 2.5 for virtually the same degree of conversion of the telogen, i.e. the $Fe(CO)_5$+HMPA system is more effective as a complex initiator of the reaction. When the reaction is carried out with CH_2=CHX monomers containing electron-accepting groups (Cl, CF_3, CO_2CH_3, CN), the yield of the adducts is lower while the degree of conversion of benzyl bromide is high. 3,3,3-Trifluoropropene is of special interest in the above series of monomers. A multiplicity of reactions of the intermediate telomeric radicals have been noted for this compound, which stimulated a more detailed study of this process. Together with telomers having the structure $C_6H_5CH_2(CH_2CHCF_3)_nBr$ (n = 1, 2), the compound $C_6H_5CH{=}CHCH(CF_3)CH_2CH_2CF_3$ was detected in the reaction mixture. The authors explain its formation by a rearrangement of the radical with two monomer units and its subsequent ready dehydrobromination:

$$C_6H_5CH_2CH_2CH(CF_3)CH_2\dot{C}HCF_3 \xrightarrow[k_{re}]{1.5\text{-H}} \longrightarrow C_6H_5\dot{C}HCH_2CH(CF_3)CH_2CH_2CF_3,$$

where k_{re} is the rearrangement rate constant.

The intramolecular mechanism of the rearrangement was demonstrated and the rearrangement rate constant was determined [$k_{re} = (5.0 \pm 0.3) \times 10^4 s^{-1}$] at 22 °C on model radicals, generated by abstracting a bromine atom from T_2^{Br}, in a special EPR investigation.[21,22] In addition, the fragmentation of the radical $C_6H_5CH_2CH_2\dot{C}HCF_3$ was observed for the first time by the EPR method, i.e. a third process—fragmentation which introduces certain corrections to the kinetic process parameters—is added to the two competing processes with participation of the radical (chain transfer and propagation).[23]

$$C_6H_5CH_2CH_2\dot{C}HCF_3 \longrightarrow C_6H_5\dot{C}H_2 + CH_2{=}CHCF_3$$

A similar process has been detected by the EPR method also for the $C_6H_5CH_2CH_2\dot{C}H_2$ radical (the reaction of benzyl bromide with ethylene), whereas fragmentation is not observed under similar conditions for the radicals $C_6H_5CH_2CH_2\dot{C}HX$ [X = Cl, $Si(CH_3)_3$]. Concerning the kinetics of the addition reactions, the rate constants $k_{add}(X)$ for the addition of the radical $C_6H_5\dot{C}H_2$ to the unsaturated compounds listed above were estimated under the conditions of metal complex initiation using the method of competitive kinetics;[24] the addition of the benzyl radical to trimethylvinylsilane was adopted as the standard: $k_{add}[Si(CH_3)_3]$.

X	$k_{add}(X)/k_{add}[Si(CH_3)_3]$
C_4H_9	0.29
CF_3	0.22
$Si(CH_3)_3$	1
Cl	1.02
CO_2CH_3	11.9
CN	24.0

It is seen from these data that the benzyl radical adds much more readily to the electrophilic methyl acrylate and acrylonitrile than to the relatively nucleophilic hex-1-ene. This is one of the pieces of evidence for the nucleophilic nature of the benzyl radical. Judging from the ratios $k_{add}(CN)/k_{add}(C_4H_9)$ = 83 and $k_{add}(CO_2CH_3)/k_{add}(C_4H_9)$ = 41, the polar effect influences significantly the kinetic parameters of the processes. In the study of the kinetics of the addition of the nucleophilic cyclohexyl radical to the monomers $CH_2=CXC_6H_5$, for which the decisive influence of the polar factor on the rate of addition has been established,[25] the ratio $k_{add}(CO_2C_2H_5)/k_{add}(CH_3)$ = 46, i.e. of the same order of magnitude as that obtained for $C_6H_5\dot{C}H_2$, was found.

The authors also drew attention to a fairly unexpected result—the ratio $k_{add}(CF_3)/k_{add}[Si(CH_3)_3]$ is close to that for hex-1-ene but not for methyl acrylate. One of the possible explanations is the fragmentation of the radical-adduct mentioned above, which ultimately decreases the content in the reaction mixture of the adduct whose concentration is used in the calculation. The same feature has been noted also for the reaction of benzyl bromide with vinyl chloride: $k_{add}(Cl)/k_{add}[Si(CH_3)_3]$ = 1. Although fragmentation was not observed in the EPR study of the $C_6H_5CH_2CH_2\dot{C}HCl$ radical, under real conditions (140 °C) it may play a decisive role. This appears particularly likely, since calculation of the activation energy[20] for the stage involving the addition of $C_6H_5\dot{C}H_2$ to vinyl chloride yielded a significantly lower value (by 7 kcal mol^{-1}) than that for the reaction of trimethylvinylsilane, i.e. there are no anomalies whatever in the addition stage. For vinyl chloride, this stage is more favourable in energy terms than for trimethylvinylsilane.

The reaction of benzyl bromide with trimethylvinylsilane has been used to investigate the overall kinetics of the addition reaction under the conditions of metal complex initiation.[26] One of the fundamental problems in this case is the mechanism of the chain transfer stage:

(a) 'purely' homolytic mechanism—via benzyl bromide:

$$C_6H_5CH_2(CH_2\dot{C}HX)_m + C_6H_5CH_2Br \longrightarrow C_6H_5CH_2(CH_2CHX)_mBr + C_6H_5\dot{C}H_2,$$

(b) redox-catalytic mechanism:

$$C_6H_5CH_2(CH_2\dot{C}HX)_m + [Fe(CO)_nL_{4-n}Br] \longrightarrow C_6H_5CH_2(CH_2CHX)_mBr + \left[Fe(CO)_nL_{4-n}\right].$$

Naturally, the overall kinetic equation is different in each case. For a radical process, we have

$$V(T_1^{Br}) = k_{rad}[Fe \cdot L]_0^{1/2}[S]_0^{1/2}[M]_0^{1/2},$$

where V is the rate, T_1^{Br} is the adduct, L is the ligand, S benzyl bromide, and M the monomer. For a redox process, we have

$$V(T_1^{Br}) = k_{red}[Fe \cdot L]_0[S]_0.$$

The study of the reaction order with respect to each reactant [for the 1 : 3 $Fe(CO)_5$+DMF initiator] showed that in the given competitive case the radical mechanism of chain transfer is more likely. The authors believe that the mechanism may change in other reactions depending on the nature of the reactants and their capacity to form more or less stable complexes with $Fe(CO)_5$.

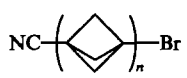
In the study of the competitive kinetics in the reaction of benzyl bromide with acrylonitrile and trimethylvinylsilane, modelling the cotelomerisation reaction of one telogen with two monomers,[27] an interesting feature was observed—the virtually complete alternation (rigorous alternation) of the monomer units under the conditions of the decisive influence of the polar factor. This reaction results in the formation of only one of the possible cotelomers

$$C_6H_5CH_2CH_2CH(CN)CH_2CHBrSi(CH_3)_3,$$

in which the nucleophilic benzyl radical adds effectively to acrylonitrile and the electrophilic radical $C_6H_5(CH_2)_2\dot{C}HCN$ formed adds to the relatively nucleophilic trimethylvinylsilane.

4. Reactions of functional bromine-containing compounds

The reaction of bromocyanogen with 1,1,1-propellane differs significantly from the reaction with bromotrichloromethane. In the case of BrCN, the telomers



are mainly formed,[14] but their proportions are unusual for telomerisation — the main reaction products are the second ($n = 2$) and third ($n = 3$) telomers in proportions of 4 : 1. It may be that their formation is a consequence of the secondary reaction of the adduct via the third bromine atom, i.e. stepwise telomerisation takes place.[3] Furthermore, bromocyanogen behaves in this reaction also as a brominating agent — the corresponding dibromo-derivative was detected among the products.

The photochemically initiated reaction of 1,2-dibromo-1-chlorotrifluoroethane with chlorotrifluoroethylene results in the formation of mainly the first two telomers.[28]

$$BrCFClCF_2Br + CClF{=}CF_2 \longrightarrow Br(CF_2CFCl)_n(CClFCF_2)_mBr$$

$n = 1$; $m = 1, 2$.

The general formula of the telomers adopted by the authors implies the possibility of the involvement of several molecules of not only the monomers but also of the telogen in the same molecular chain, although the corresponding compounds were not identified in the above investigation.

On irradiation or heating, *N*-bromodifluoromethyleneimine readily reacts with the fluoroolefins $CF_2{=}CFX$ (X = F, Br), affording the adducts $CF_2{=}NCF_2CFBrX$ in satisfactory yields (the yield is 82% for X = F and 67% for X = Br).[29]

The examples considered are summarised in Table 1.

III. Charge-transfer complexes as possible intermediates in radical processes

Complex systems based on $Fe(CO)_5$ combined with nucleophilic coinitiators (DMF, HMPA) are extremely effective as initiators of radical processes with participation of organic polybromo-compounds. Extensive experimental data indicate the existence of a relation between the effectiveness of the systems, the nature of the reactants, and the polar character of the intermediate radicals. Using UV spectroscopy, the nature of the transition state was discovered and the quantitative parameters correlated with the effectiveness of the system were found.[30,31] It was shown that charge-transfer complexes (CTC) are formed in many reactions with participation of organic bromo-compounds and that the quantitative characteristics of the charge-transfer band (CTB) (the intensity and the shift of the band in the spectrum compared with its position for the initial systems) are correlated with the effectiveness of the given metal complex system as the reaction initiator.

Selected data for the charge-transfer complexes of various metal carbonyls (MC) are presented in Table 2.[30-32] In the first place, one should note that a charge-transfer band whose position (λ_{max}) and intensity (I) differ significantly from the parameters for the initial compounds is observed in the metal carbonyl + CBr_4 system, i.e. a charge-transfer complex is indeed formed. In this connection, metal carbonyls can be clearly divided into two groups: for $Fe(CO)_5$ and $Mn_2(CO)_{10}$, there is a bathochromic shift of the charge-transfer band, whereas for the chromium, molybdenum, and tungsten carbonyls there is a hypsochromic shift. The same significant difference has been observed also between the initiating capacities of the systems based on the carbonyls: $Fe(CO)_5$ and $Mn_2(CO)_{10}$ are highly effective initiators of the reactions involving the dissociation of the C–halogen bond, while the remaining carbonyls are relatively ineffective as initiators.

Table 1. Radical reactions of organobromine addends with unsaturated compounds.

Addend	Monomer	Reaction conditions	Compounds identified [yield (%); C_n]	Ref.
CBr_4	$CH_2{=}CHCl$	$C_6H_5CO)_2O_2$	$CBr_3(CH_2CHCl)_nBr$; $n = 1-3$; $C_1 = 14.6$, $C_2 = 73.5$.	7
	$CH_2{=}CHCF_3$	$(C_6H_5CO)_2O_2$	$CBr_3(CH_2CHCF_3)_nBr$; $n = 1-3$; $C_1 = 15$, $C_2 = 64$, $C_3 = 60$.	6
	$CH_2{=}CHR$ R = C_4H_9, C_6H_{13}, C_6H_5, CO_2CH_3	SmI_2, 60°C	$CBr_3CH_2CH(R)Br$ (30–75)	4
		T_{room}	Br_3C–  –Br (high yield)	3
$CHBr_3$	$CH_2{=}CHCN$	$Fe(CO)_5$ + DMF, 95–100 °C, 2 h	$CHBr_2CH_2CHBrCN$ (25)	10
	$CH_2{=}CHCO_2CH_3$	"	$CHBr_2CH_2CHBrCO_2CH_3$ (78)	10
	$CH_2{=}C(CH_3)CO_2CH_3$	"	$CHBr_2CH_2C(CH_3)BrCO_2CH_3$ (15)	10
	$CH_2{=}CHCF_3$	$(C_6H_5CO)_2O_2$	$CHBr_2[CH_2CH(CF_3)]_nBr$; $n = 1, 2$. $CBr_3CH_2CHBrCF_3$, $CBr_3CH_2CH(CF_3)CH_2CHBrCF_3$, $CHBr_2CH_2CH(CF_3)CH_2CH_2CF_3$, $CBr_3CH_2CH(CF_3)CH_2CH_2CF_3$	9
		$Fe(CO)_5$ + DMF, 100 °C	$CHBr_2[CH_2CH(CF_3)]_nBr$; $n = 1-3$.	9
		20–30 °C, 1.5 h	Br_2HC–  –Br (88)	5

Table 1 (continued)

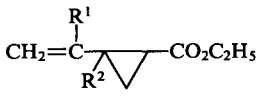
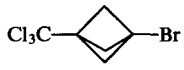
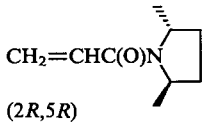
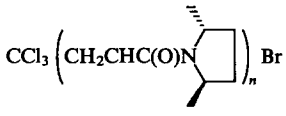
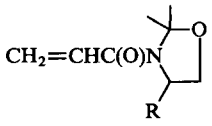
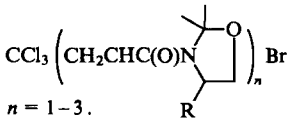
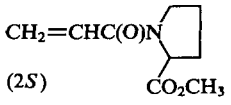
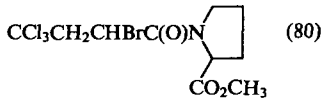
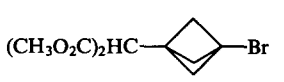
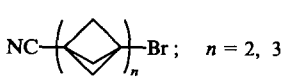
Addend	Monomer	Reaction conditions	Compounds identified [yield (%); C_n]	Ref.
CH_2Br_2	$CH_2{=}CHCF_3$	$Fe(CO)_5$ + DMF, 145 °C	$CH_2Br[CH_2CH(CF_3)]_nBr$; $n = 1, 2$.	9
CCl_2Br_2	$CH_2{=}CHCl$	$(C_6H_5CO)_2O_2$, 60 °C	$CCl_2Br(CH_2CHCl)_nBr$; $n = 1-3$; $C_1 = 7.7$, $C_2 = 54.3$.	7
CCl_3Br	$CH_2{=}C(CH_3)CO_2R$ R = *iso*-C_3H_7, *tert*-C_4H_9	50–90 °C	$CCl_3[CH_2C(CH_3)CO_2R]_nBr$; $n = 1-3$.	13
	$CH_2{=}CHR$ R = C_4H_9, C_6H_{13}, C_6H_5, CO_2CH_3	SmI_2, 60 °C	$CCl_3CH_2CH(R)Br$ (30–70)	4
	 $R^1 = R^2 = H, CH_3$	AIBN	$CCl_3(CH_2CR^1{=}CR^2CH_2CHCO_2C_2H_5)_nBr$; $n = 1-3$; $C_n \cong 1$.	15
		20 °C		14
	 (2*R*,5*R*)	*hν*	 $n = 1-5$; $C_2-C_5 \approx 0.3-0.5$.	16
	 R = C_6H_5, *iso*-C_3H_7	*hν*	 $n = 1-3$.	17
	 (2*S*)	$Fe(CO)_5 + P(C_6H_5)_3$, 75 °C, 2 h	 (80)	18
$C_6H_5CH_2Br$	$CH_2{=}CH_2$	$Fe(CO)_5$ + DMF(HMPA), 140 °C	$C_6H_5CH_2CH_2CH_2Br$	19
	$CH_2{=}CHC_4H_9$	"	$C_6H_5CH_2CH_2CHBrC_4H_9$	19
	$CH_2{=}CHSi(CH_3)_3$	"	$C_6H_5CH_2CH_2CHBrSi(CH_3)_3$	19
	$CH_2{=}CHCF_3$	"	$C_6H_5CH_2(CH_2CHCF_3)_nBr$; $n = 1, 2$.	19, 21, 22
	$CH_2{=}CHCO_2CH_3$	"	$C_6H_5CH_2CH_2CHBrCO_2CH_3$	19
	$CH_2{=}CHCN$	"	$C_6H_5CH_2CH_2CHBrCN$	19, 27
	$CH_2{=}CHCN$ + + $CH_2{=}CHSi(CH_3)_3$	"	$C_6H_5CH_2CH_2CHBrCN$, $C_6H_5CH_2CH_2CHBrSi(CH_3)_3$, $C_6H_5CH_2CH_2CH(CN)CH_2CHBrSi(CH_3)_3$	27
	$CH_2{=}CHCl$	"	$C_6H_5CH_2(CH_2CHCl)_nBr$; $n = 1, 2$.	20
$BrCH(CO_2CH_3)_2$		*hν*	 (69)	5
$BrCF_2CFClBr$	$CClF{=}CF_2$	UV	$Br(CF_2CClF)_n(CClFCF_2)_mBr$; $n = m = 1$; $n = 1$, $m = 2$; $n = m = 2$.	28
BrCN		*hν*	 $n = 2, 3$.	14
$CF_2{=}NBr$	$CF_2{=}CFX$, X = F, Br	*hν*	$CF_2{=}NCF_2CFBrX$ (82, 67)	29

Table 2. Charge-transfer complex formation data for various metal carbonyls.[30-32]

Compound	λ_{max}/nm	CTB for reaction with CBr_4	
		λ_{max}/nm	I
$Fe(CO)_5$	202.0	218.0	10200
DMF	204.0	221.0	3030
$Fe(CO)_5$+DMF	224.0	221.0	11000
$Mn_2(CO)_{10}$	202.4	227.0	14390
$Cr(CO)_6$	227.0	217.0	4545
$Mo(CO)_6$	229.6	219.0	3800
$W(CO)_6$	226.0	218.4	3800

I is the relative intensity.[32]

The shift of the charge-transfer band in the reaction with CBr_4 is much smaller for $Fe(CO)_5$ than for $Mn_2(CO)_{10}$ and reaches approximately the same level only in the system containing DMF. There is a distinct correlation in this instance with chemical data—$Mn_2(CO)_{10}$ actively initiates the reactions without any additives, whereas $Fe(CO)_5$ initiates the reactions virtually only in the presence of additives (DMF, HMPA). Furthermore, $Mn_2(CO)_{10}$ is a much more effective initiator in the reaction with methyl bromoacetate than $Fe(CO)_5$ and the systems based on it.[33]

Analysis of data obtained when the reactants are added in succession suggests that the initial stage of the reactions with participation of organic bromo-compounds is the formation of an involved charge-transfer complex incorporating all the reactants. On the other hand, the study of the complexes formed in the case of simpler systems—binary, ternary, and finally quaternary [reaction components: $Fe(CO)_5$, DMF or HMPA, CBr_nH_{4-n}, CH_2=CHX]—enabled the authors to estimate fairly objectively the initiating activity of each complex system and its likely usefulness for initiation precisely for the given combination of reactants.[30]

In practice, this can facilitate significantly the choice of the initiating systems without carrying out a complex chemical experiment.

A similar study was later carried out also using chromium, molybdenum, and tungsten carbonyls.[32] Satisfactory quantitative correlations were obtained for these systems between the characteristics of the charge-transfer band and the effectiveness of the initiation of the homolytic addition and telomerisation proceeding with dissociation of the C–Br bond.

IV. Application of ^{13}C NMR spectroscopy in the establishment of the structures of organobromine compounds

Extensive and systematic study of radical reactions with participation of organobromine compounds led, as regards synthesis, to the formation of bromine-containing compounds with a fairly complex structure, sometimes including several different bromine-containing groups and functional groups. The ^{13}C NMR method proved to be one of the most promising for the study of their structures. The accumulated experimental data have been surveyed.[34] The tables in the above communication, in which the chemical shifts of carbon atoms involved in a C–Br bond and having different environments are compiled, are significantly helpful in the study of the structures of new compounds and in the determination of certain characteristics of the variation of the chemical shifts of the signals due to carbon atoms in particular groups as a function of the presence and nature of neighbouring substituents. Thus analysis of the spectra of 48 bromopolychloroalkanes showed that, in contrast to chlorine-containing groups for which the ^{13}C chemical shifts are usually in the range 38–105 ppm, the chemical shifts of the bromine-containing fragments (with the exception of $-CBr_2-$) are mainly in the range 25–50 ppm and are as a rule displaced upfield compared with the analogous organochlorine groups. These investigations showed[35] that the additivity of the influence of the α-, β-, and γ-halogen atoms on the ^{13}C chemical shifts frequently breaks down. Therefore the application of the usual additive schemes for calculations based on structural increments to organobromine compounds involves large discrepancies between the calculated ^{13}C chemical shifts and the experimental values.

The specific values of the α-, β-, and γ-effects have been obtained, taking into account the influence of the binary and ternary interactions of the halogen atoms, on the basis of ^{13}C NMR data for the most frequently encountered bromine-containing groups in 60 bromopolychloroalkanes. The increments reflecting the overall influence of the halogen atoms in *gem*-halogen-containing groups and also groups with a halogen atom attached to a secondary carbon atom on the ^{13}C shift in polyhaloalkanes were calculated. The increments obtained for the calculation of the chemical shifts of polyhaloalkanes make it possible to assign the ^{13}C signals of the isomers, their mixtures, and structurally similar compounds, when the differences between the chemical shifts of isotypical carbon atoms are small. A fairly detailed topological scheme for the empirical estimation of the ^{13}C NMR chemical shifts of polybromoalkanes, having definite predictive possibilities, was developed subsequently on the basis of these data.[35,36] An attempt was made in the above investigations to find an equation relating the topological image of the molecule to the experimental ^{13}C chemical shifts of polybromoalkanes taking into account the possibilities of interaction both through the chain and through space.

References

1. T Kunieda, T Takizawa *Heterocycles* **8** 662 (1977)
2. K Hosoda, T Kunieda, T Takizawa *Chem. Pharm. Bull.* **24** 2927 (1976)
3. R Kh Freidlina, F K Velichko, S S Zlotskii, D L Rakhmankulov, A B Terent'ev, in *Radikal'naya Telomerizatsiya* (Radical Telomerization) (Moscow: Khimiya, 1988) p. 78
4. Sh Ma, Xi Lu *J. Chem. Soc., Perkin Trans. 1* 2031 (1990)
5. N S Zefirov, L S Surmina, N K Sadovaya, A V Blokhin, N A Tyurekhodzhaeva, Yu N Bubnov, L I Lavrinovich, A V Ignatenko, Yu K Grishin, O A Zelenkina, N T Kolotyrkina, S V Kudrovich, A S Koz'min *Zh. Org. Khim.* **26** 2317 (1990)
6. T T Vasil'eva, V A Kochetkova, B V Nelyubin, V I Dostovalova, R Kh Freidlina *Izv. Akad. Nauk SSSR, Ser. Khim.* 808 (1987)
7. T T Vasil'eva, V A Kochetkova, V I Dostovalova, B V Nelyubin *Izv. Akad. Nauk SSSR, Ser. Khim.* 109 (1989)
8. T Asahara, M C Chou *Bull. Chem. Soc. Jpn.* **42** 1373 (1969)
9. T T Vasil'eva, V A Kochetkova, V I Dostovalova, B V Nelyubin, R Kh Freidlina *Izv. Akad. Nauk SSSR, Ser. Khim.* 2558 (1989)
10. T T Vasil'eva, F K Velichko, V A Kochetkova, O P Bondarenko *Izv. Akad. Nauk SSSR, Ser. Khim.* 1904 (1987)
11. L H Chance, J D Timpa *J. Chem. Eng. Data* **22** 116 (1977)
12. M Katsukiya *Bull. Chem. Soc. Jpn.* **65** 1513 (1992)
13. T Kimura, H Tasaka, M Hamashima *Polym. J. (Tokyo)* **19** 305 (1987)
14. K B Wiberg, S T Waddell *J. Am. Chem. Soc.* **112** 2194 (1990)
15. A M Guliev, S P Kasimova, A N Lemeshev, O M Nefedov *Zh. Org. Khim.* **26** 1261 (1990)
16. N A Porter, R A Breyer, E Swaan, J Nally, J Pradhan, T Allen, A T McPhail *J. Am. Chem. Soc.* **113** 7002 (1991)
17. N A Porter, J D Bruhnke, Wen-Xue Wu, I J Rosenstein, R A Breyer *J. Am. Chem. Soc.* **113** 7788 (1991)
18. R G Gasanov, S O Videnskaya, L V Il'inskaya, Yu N Belokon' *Izv. Akad. Nauk, Ser. Khim.* 2007 (1993)
19. T T Vasil'eva, S I Gapusenko, S V Vitt, A B Terent'ev *Izv. Akad. Nauk, Ser. Khim.* 2347 (1992)
20. T T Vasil'eva, S I Gapusenko, A B Terent'ev, V V Pinyaskin, I V Stankevich, A L Chistyakov, E I Mysov *Izv. Akad. Nauk, Ser. Khim.* 886 (1993)

21. R G Gasanov, T T Vasil'eva, S I Gapusenko *Kinet. Katal.* **32** 1466 (1991)
22. R G Gasanov, T T Vasilieva, S I Gapusenko *Mendeleev Commun.* 70 (1991)
23. R G Gasanov, T T Vasilieva, S I Gapusenko, Yu A Borisov *Mendeleev Commun.* 111 (1991)
24. A B Terent'ev, S I Gapusenko, T T Vasil'eva, S V Vitt *Izv. Akad. Nauk, Ser. Khim.* 2017 (1992)
25. B Giese, J He, W Mehl *Chem. Ber.* **121** 2063 (1988)
26. A B Terent'ev, S I Gapusenko, T T Vasil'eva *Izv. Akad. Nauk, Ser. Khim.* 1418 (1993)
27. A B Terent'ev, S I Gapusenko, T T Vasil'eva, V I Dostovalova *Zh. Org. Khim.* **28** 1579 (1992)
28. W Dedek, Z Chvatal *J. Fluorine Chem.* **31** 363 (1986)
29. C W Bauknight, Jr., D D DesMarten *J. Org. Chem.* **53** 4443 (1988)
30. L V Balabanova, T T Vasil'eva, A B Terent'ev, F K Velichko *Izv. Akad. Nauk SSSR, Ser. Khim.* 1457 (1991)
31. F K Velichko, T T Vasil'eva, L V Balabanova, G A Shvekheimer *Izv. Akad Nauk SSSR, Ser. Khim.* 1446 (1988)
32. F K Velichko, L V Balabanova, T T Vasil'eva, A B Terent'ev *Izv. Akad Nauk SSSR, Ser. Khim.* 454 (1990)
33. A B Terent'ev, M A Moskalenko, R K Freidlina *Izv. Akad. Nauk SSSR, Ser. Khim.* 1800 (1985)
34. V I Dostovalova, F K Velichko, T T Vasilieva, N V Kruglova, R Kh Freidlina *Org. Magn. Reson.* **16** 251 (1981)
35. V I Dostovalova, T T Vasil'eva, F K Velichko *Izv. Akad. Nauk SSSR, Ser. Khim.* 2770 (1988)
36. V I Dostovalova, T T Vasil'eva, F K Velichko, A V Goncharov, D S Yufit, Yu T Struchkov, M G Ezernitskaya, B V Lokshin *Izv. Akad. Nauk SSSR, Ser. Khim.* 2228 (1989)

Russian Chemical Reviews **63** (3) 279–288 (1994)
©1994 Russian Academy of Sciences and Turpion Ltd

UDC 541.128 : 541.49 : 547.256.2'131 : 541.64

Acid strength of proton donors in complexes of nontransition metal halides as a measure of the activity of electrophilic polymerisation catalysts

K S Minsker, V A Babkin, G E Zaikov

Contents

I. Introduction	279
II. Complexes based on aluminium chlorides	279
III. Complexes based on magnesium chlorides	283
IV. Complexes based on boron fluorides	284
V. Conclusions	286

Abstract. Data on one of the most urgent problems in modern theoretical chemistry are reviewed: the calculation of the acid strength of the complexes formed by the interaction of Lewis acids with proton donors, and the correlation of the acid strength with the activity and selectivity of these complexes as catalysts of electrophilic processes. Complexes based on aluminium and magnesium chlorides and on boron fluorides are discussed. It is shown that increasing the acid strength of these complexes as catalysts of electrophilic polymerisation reactions increases their activity but lowers their selectivity. The bibliography includes 43 references.

I. Introduction

Complex catalysts based on non-transition metal halides (R_nAlCl_{3-n}, R_nMgCl_{2-n}, R_nBF_{3-n}, where $n = 0 - 3$, R = OH, CH_3, C_2H_5, *iso*-C_3H_7, *tert*-C_4H_9) and on proton donors (H_2O, HCl, HF, ROH) are the classical initiators of electrophilic processes. The donor–acceptor interaction of the components leads to the formation of complexes having an acid strength greater than that of the initial compounds.[1,2] The strengthening of the acidic properties of the systems during complex formation is accompanied by a marked increase in their catalytic activity.[3] The formation of complexes between individually inactive protogenic compounds such as alcohols (or water) and the appropriate Lewis acids offers an enhanced selectivity in the cationic polymerisation of olefins.[3,4] However, in spite of significant progress in the study of the behaviour of complexes of this type in various electrophilic reactions, the role of the acid strength is still unclear.[1,5] Therefore the current interest in the theoretical calculation of the acid strength of complex catalysts of different chemical nature is not surprising. A reasonably precise estimate can be obtained by calculating the charges on the hydrogen atoms in the proton donors (q_{H^+}). These values are well correlated with the universal acidity indicator of chemical compounds δpK_a.

K S Minsker, V A Babkin Department of High-molecular-mass Compounds, Bashkir State University, 450076 Ufa, ul. Frunze 32. Tel. (7-347-2) 26 24 05
G E Zaikov Semenov Institute of Chemical Physics of the Russian Academy of Sciences, 117977 Moscow, ul. Kosygina 4, Fax (7-095) 938 21 56

Received 7 September 1993
Uspekhi Khimii **63** (3) 289–298 (1994); translated by J I Carasso

The characteristics of the acid strength (q_{H^+}, Δq_{H^+}) of the adducts of R_nAlCl_{3-n}, R_nMgCl_{2-n}, and R_nBF_{3-n} with proton donors are determined by calculating the models of the complexes with a 1 : 1 stoichiometric composition by the semiempirical CNDO/2 quantum-mechanical method specially parametrised to give the best description of the charge characteristics.[7] This approach has been used successfully in calculations of the acidic catalyst properties of complex electrophilic catalysts.[6]

The structures of the model complexes (usually in the form of tetrahedra, or distorted tetrahedra) are close to the structures recently discussed by various workers.[8–11] The calculations were carried out without allowing for the effect of the solvent, i.e. in the isolated molecule approximation. This approach does not detract from the value of the chosen method of modelling the complex catalyst, since these catalysts are extremely active in hydrocarbon (indifferent) media.

The aim of the present review is to generalise data on the acid strength of the complexes R_nAlCl_{3-n}, R_nMgCl_{2-n}, and R_nBF_{3-n} with proton donors (HCl, H_2O, HF, ROH), and on the relationship between the acid strength of these compounds and their activity and selectivity as catalysts of electrophilic processes (in particular, of the cationic polymerisation of olefins). Establishing correlations between these parameters is important from the standpoint of rationalising the choice of the most effective catalysts for chemical processes, and also as an approach to establishing fundamental concepts on the effect of the acid strength on the behaviour of complex catalysts in electrophilic reactions.

II. Complexes based on aluminium chlorides

The formation of complexes based on aluminium chlorides R_nAlCl_{3-n} and on proton donors (HCl, H_2O, ROH) has been demonstrated both experimentally and theoretically.[12–15]

1. Complexes based on aluminium chlorides and hydrogen chloride

The formation of complexes between R_nAlCl_{3-n} and HCl has to compete with processes involving the substrate and the relatively stable counterion in the reaction with a proton.[15,16] Depending on the nature of the Lewis acid and on some other factors, the complexes formed with HCl have H–Cl bonds with different levels of looseness. In proton complexes, or in the Gustavson complexes (GC), ionisation of the $H^{\delta+}...Cl^{\delta-}$ bond is responsible for the high acid strength.[2,17] This gives the GC an enhanced activity towards the electrophilic polymerisation of olefins and of some other monomers, which is seen, in particular, as the

formation of polymeric products with a higher molecular mass (isobutene, styrene, vinyl butyl ether), as the ability to initiate the oligomerisation of propene, etc. These effects are associated both with a greater stability of the complex counterion towards dissociation into its components under the influence of the carbenium ion and with the acid strength of the GC. The characteristic features of the cationic fragment (positive charge delocalised over the aromatic system) explain the unique properties of these complexes as electrophilic agents. For example, the proton-donor activity of the GC decreases in the sequence

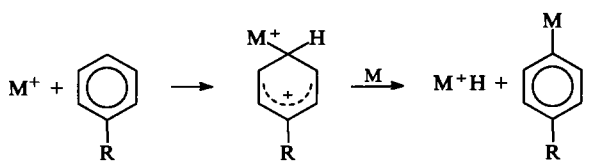
$$3\,C_6H_5CH_3\cdot HCl\cdot Al_2Cl_6 > 4\,(CH_3)_3C_6H_3\cdot HCl\cdot Al_2Cl_6 > > 3\,(CH_3)_6C_6\cdot HCl\cdot AlCl_3\,.$$

This series is the opposite of the basicity series of aromatic hydrocarbons

$$(CH_3)_6C_6 > (CH_3)_3C_6H_3 > CH_3C_6H_5\,.$$

The role of the basicity of the aromatic component of the GC in the initiation of the polymerisation is ambiguous: increasing the basicity increases the stability of the arenonium ion, but it weakens the bond between the carbenium ion and the counterion. [18]

Polymeric GC are formed in a similar way from their low-molecular analogues. However, the presence in the GC of a solvation shell of aromatic nuclei bound to the polymer chain (polystyrene, styrene–divinylbenzene copolymer) affects the stoichiometric composition and other properties of the resulting complexes. [19] Irrespective of the composition of the GC, initiating the polymerisation of olefins reduces to accepting a proton from the arenonium ions. The free aromatic hydrocarbon formed from the arenonium ions by H-initiation can be alkylated by a growing carbenium ion. The reaction which terminates the polymeric chain leads to the formation of new (polymeric) σ complexes, more stable than the initial GC and able (under appropriate conditions) to reinitiate the polymerisation of the olefin:



The mechanism of the catalytic action of the $R_nAlCl_{3-n}\cdot HCl$ complexes (where R = CH_3, C_2H_5, etc.) is simple and self-evident. [10] Therefore a confirmation of the experimentally observed behaviour of the HCl complexes by calculation can be used as a test of the validity of the CNDO/2 method in calculations for other complexes. A calculation of the parameters of the known complexes of hydrogen chloride with aluminium chloride was therefore carried out first.

Some quantum chemical characteristics of the complexes $R_nAlCl_{3-n}\cdot HCl$ [the charges on the hydrogen atom in the HCl (q_{H^+}), the increase in the charge on the hydrogen atom in HCl upon forming the complexes with R_nAlCl_{3-n} (Δq_{H^+}) and the acidity indicator (δpK_a) are shown in Table 1].

Table 1. Acid strength of the $R_nAlCl_{3-n}\cdot HCl$ complexes. [10]

Complex	q_{H^+}	Δq_{H^+}	δpK_a
HCl	+0.09	–	−7
$HCl\cdot(CH_3)_3Al$	+0.18	0.09	−16.3
$HCl\cdot(CH_3)_2AlCl$	+0.18	0.09	−16.3
$HCl\cdot CH_3AlCl_2$	+0.18	0.09	−16.0
$HCl\cdot C_2H_5AlCl_2$	+0.18	0.10	−16.0
$HCl\cdot AlCl_3$	+0.19	0.10	−16.0
$HCl\cdot HOAlCl_2$	+0.20	0.11	−18.0

When the complexes of R_nAlCl_{3-n} with HCl are formed the charge on the hydrogen atom increases from +0.09 in the free HCl to +0.18 to +0.20 in the complexes. The removal of H^+ is accompanied by an evolution of energy of 260–340 kJ mol^{-1}, i.e. it is energetically favourable. [10] The acidity indicators of the complexes are only very slightly dependent on the nature of the Lewis acid (R_nAlCl_{3-n}, $HOAlCl_2$) varying from −16 to −18.

Thus the quantum chemical calculations of the $R_nAlCl_{3-n}\cdot HCl$ complexes are consistent with the experimental data on their high acidity and thus confirm the validity of the CNDO/2 method for calculations of other models based on the aluminium chlorides. The lack of dependence of the acid strength of the complexes on the nature of the Lewis acid shows that all the complexes of R_nAlCl_{3-n} with HCl have a propensity towards self-ionisation. This conclusion is consistent with experimental data on the high activity of the complexes of HCl with Lewis acids (from $AlCl_3$ to AlR_2Cl) in the cationic polymerisation of olefins. [1] At the same time the data obtained in these calculations show that the preferred scheme for the direct initiation of the electrophilic polymerisation reaction is

$$HCl + R_nAlCl_{3-n} \rightleftharpoons H^{\delta+}, [R_nAlCl_{4-n}]^{\delta-} \xrightarrow[-M]{} \longrightarrow M_1^{\delta+}, [R_nAlCl_{4-n}]^{\delta-}$$

However, it should be noted that the increase in the acidity of the $R_nAlCl_{3-n}\cdot HCl$ catalysts in the electrophilic polymerisation of the olefins is accompanied by a large decrease in the selectivity of their action (Table 2).

Table 2. Polymerisation of isobutene from the C_4 hydrocarbon fraction under the influence of $R_nAlCl_{3-n}\cdot HCl$.

Catalyst	Selectivity for *iso*-C_4H_8/ vol.%
$HCl\cdot 3\,C_6H_5CH_3\cdot 2\,AlCl_3$	36 ± 2
$HCl\cdot C_6H_5CH_3\cdot C_2H_5AlCl_2$	43 ± 2
$HCl\cdot C_6H_5CH_3\cdot (C_2H_5)_2AlCl$	53 ± 3

Notes. Composition of fraction, wt.%: C_3H_6, 0.6; C_4H_{10}, 55.1; *iso*-C_4H_8, 14.9; α,β-C_4H_8, 29.5; $[R_nAlCl_{3-n}] = 7.3 \times 10^{-3}$ mol dm^{-3}, $[C_4] = 1.3$ mol dm^{-3}, solvent CH_2Cl_2, 253 K, reaction time 10 min.

2. Complexes based on aluminium chlorides and water

The formation of 1:1 complexes (aqua complexes) by the interaction of R_nAlCl_{3-n} with water has been established. [4,12] Like other electron donors, water easily undergoes donor–acceptor interaction with aluminium compounds.

In inert solvents the aqua complexes of aluminium ($R_nAlCl_{3-n}\cdot H_2O$) have a reasonably high thermal stability and stability towards hydrolysis of the Al–Cl bond, and a low electric conductivity ($\sigma \approx 10^{-10}$ S cm^{-1}). As shown by a qualitative reaction with xanthone they are not H-acids. [12]

The H-activity of the complexes, established for model systems of the type of $CH_3CH(CH_3)=CH_2-C_2H_5AlCl_2\cdot D_2O$ and resulting from the low Brønsted acidity, is not obvious, [16,20] and therefore it does not look as if the ionisation of the aqua complex in the absence of a monomer can take place by the scheme

$$C_2H_5AlCl_2 + H_2O \longrightarrow H^+, [C_2H_5AlCl_2\cdot OH]^-$$

When the cationic polymerisation of olefins is initiated by aqua complexes of the aluminium chlorides the latter undergo various transformations, in particular into aqua complexes of alumoxane or ternary complexes of the $HCl\cdot R_nAlCl_{3-n}\cdot H_2O$

Table 3. Acid strength of the aqua complexes of some aluminium chlorides. [10,20,23]

Aqua complex	q_{H^+} (±0.02)	δpK_a
Group I		
$H_2O \cdot AlCl_3$	+0.20	+7.1
$H_2O \cdot HOAlCl_2$	+0.18	+8.5
$H_2O \cdot (HO)_2AlCl$	+0.17	+12
$H_2O \cdot (HO)_3Al$	+0.17	+12
Group II		
$H_2O \cdot CH_3AlCl_2$	+0.19	+7.7
$H_2O \cdot (CH_3)_2AlCl$	+0.16	+14.4
$H_2O \cdot (CH_3)_3Al$	+0.16	+14.4
Group III		
$H_2O \cdot C_2H_5AlCl_2$	+0.20	+7.5
$H_2O \cdot (C_2H_5)_2AlCl$	+0.18	+8.5
$H_2O \cdot (C_2H_5)_3Al$	+0.17	+12
Group IV		
$H_2O \cdot (C_3H_7)_nAlCl_{3-n}$	+0.19±0.17	+7.7 to +12
Group V		
$H_2O \cdot (C_4H_9)_nAlCl_{3-n}$	+0.19±0.17	+7.7 to +12
Group VI		
$H_2O \cdot Al_2Cl_4O$	+0.21	+4.4
$H_2O \cdot CH_3Al_2Cl_3O$	+0.20	+7.1
$H_2O \cdot (CH_3)_2Al_2Cl_2O$	+0.20	+7.1
$H_2O \cdot (CH_3)_3Al_2ClO$	+0.18	+8.5
$H_2O \cdot (CH_3)_4Al_2O$	+0.18	+8.5
GroupVII		
$HCl \cdot H_2O \cdot AlCl_3$	–	+1.5
$HCl \cdot H_2O \cdot CH_3AlCl_2$	–	+1.3

type.[20] Therefore other models, appropriate to these transformations, were calculated together with the models of the initial complexes (Table 3). The tendency to form aqua complexes between R_nAlCl_{3-n} and H_2O increases as the strength of the Lewis acid is increased: $(HO)_3Al < (CH_3)_3Al < (C_2H_5)_3Al < (C_3H_7)_3Al < (C_4H_9)_3Al < AlCl_3$. This is suggested by the nature of the changes in q_{H^+} and in δpK_a and by other experimental results.[22] For example, acidic catalysts are universally found in the composition of various complexes of $AlCl_3$ or $RAlCl_2$, and the $R_3Al(R_2AlCl) \cdot H_2O$ system (whose acidic properties are weaker) catalyses preferentially the low-temperature polymerisation of strongly basic monomers (styrene, isobutene).[23]

The aqua complexes $R_nAlCl_{3-n} \cdot H_2O$ have a relatively low acid strength (see Table 3). The extraction of a proton from complexes of this type is not energetically favourable, requiring an expenditure of energy of between 70 and 790 kJ mol^{-1} (see Sangalov et al.[10]). Nevertheless these complexes have a relatively high activity in electrophilic polymerisation processes (isobutene), with a selectivity of almost 100% (Table 4), suggesting either the formation (during initiation) of active centres with an enhanced acid strength, susceptible to protonation, or a more complex initiation mechanism for the process.[20]

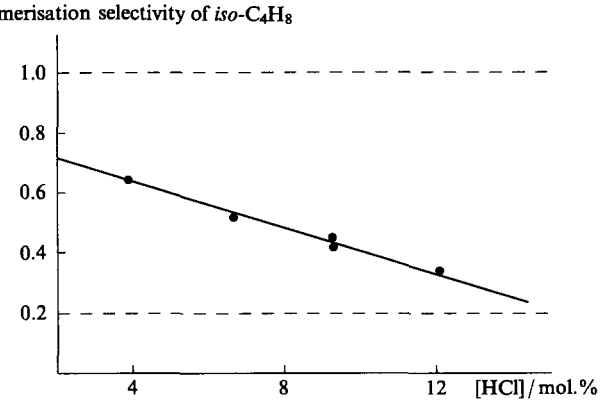


Figure 1. Dependence of the selectivity of the polymerisation of isobutene on the concentration of HCl added to $H_2O \cdot C_2H_5AlCl_2$. The upper broken line shows the selectivity of the process in the presence of $H_2O \cdot C_2H_5AlCl_2$ (without additives); the lower broken line is the selectivity in the presence of $HCl \cdot C_2H_5AlCl_2$. Polymerisation conditions: $[C_4] = 3 \times 10^{-6}$ mol g^{-1}, $[C_2H_5AlCl_2] = 8 \times 10^{-6}$ mol dm^{-3}, 250 K.

The ternary aluminium complexes listed in group VII of Table 3 have a high acid strength. However, in a comparative study of the selectivity of catalysts for the polymerisation of isobutene ($H_2O \cdot C_2H_5AlCl_2$, $HCl \cdot C_2H_5AlCl_2$, and $HCl \cdot H_2O \cdot C_2H_5AlCl_2$) it was shown experimentally that the activity of the starting aqua complex $R_nAlCl_{3-n} \cdot H_2O$ is independent of the intermediate formation of HCl (Fig. 1). The addition of HCl to $C_2H_5AlCl_2 \cdot H_2O$ markedly lowers the selectivity, which approaches that of the process initiated by $HCl \cdot C_2H_5AlCl_2$.

The lowest Brønsted acidity among the catalysts of the first six groups (see Table 3) is found in the aqua complexes $Al_2Cl_4O \cdot H_2O$ ($\delta pK_a = +4.4$), $Al_2Cl_3O \cdot H_2O$ ($\delta pK_a = +7.1$), and $C_2H_5AlCl_2 \cdot H_2O$ ($\delta pK_a = +7.5$). These same aqua complexes are universal acidic catalysts for a large number of electrophilic reactions, including the polymerisation of olefins. The aluminium complexes $Al_2Cl_4O \cdot H_2O$ and $C_2H_5AlCl_2 \cdot H_2O$ have similar acidic catalyst properties. Theoretical calculations are consistent with experimental data on the equality of the first alkylation rate constants of benzene by propene in the presence of $C_2H_5AlCl_2 \cdot H_2O$ [$k = (21.5 \pm 0.6) \times 10^{-4}$ s^{-1}] and

Table 4. Oligomerisation of isobutene from mixtures of hydrocarbons in the presence of the complexes of aluminium chlorides with proton donors.

Catalyst	Composition of the hydrocarbon mixture before the reaction/vol.%				Conversion of *iso*-C_4H_8/ mass%	Selectivity for *iso*-C_4H_8/ mass%
	C_3H_8	C_4H_{10}	*iso*-C_4H_8	α,β-C_4H_8		
$H_2O \cdot C_2H_5AlCl_2$	3.0	55.5	37.9	3.5	96	100
$H_2O \cdot C_2H_5AlCl_2$	3.9	67.5	11.3	17.3	98	100
$H_2O \cdot C_2H_5AlCl_2$	0.9	45.1	31.1	23.0	99	100
$H_2O \cdot C_2H_5AlCl_2$ [a]	4.9	63.2	8.5	23.5	100	57
$C_2H_5AlCl_2$	3.0	55.5	37.9	3.5	95	60
$(C_6H_5)_3COH \cdot C_2H_5AlCl_2$	0.6	55.1	14.9	29.5	90	79
$CH_3OH \cdot C_2H_5AlCl_2$	0.6	55.1	14.9	29.5	95	74

Notes. Polymerisation conditions: volume of the mixture of C_4 hydrocarbons 30 cm^3; concentration of catalyst 5.6×10^{-2} mol dm^{-3}; solvent, heptane (20 cm^3); 293 K; reaction time 10 min.
[a]Solvent CH_2Cl_2.

of $Al_2Cl_4O \cdot H_2O[k = (19.8 \pm 1.2) \times 10^{-4}\ s^{-1}]$ at 297 K. However, the low acid strength of the aqua complexes based on aluminium chlorides and on some of their transformation products (alumoxanes, aluminium alkoxides) implies that the electron donors (olefins, arenes) play an active role in the development of acidic catalyst properties in these materials.

3. Complexes based on aluminium chlorides and alcohols

The ability of alcohols to display both proton-donor (H^+) and carbo-cation activity (R^+) is the most distinguishing feature of the behaviour of the $R_nAlCl_{3-n} \cdot ROH$ aluminium complexes as electrophilic catalysts for the polymerisation of olefins. In particular, in the $AlCl_3 \cdot ROH$ complexes we observe the classical H-initiation scheme for the cationic polymerisation of olefins: [21]

$$ROH + AlCl_3 \rightleftharpoons ROH \cdot AlCl_3 \rightleftharpoons H^+, [AlCl_3 \cdot OR]^-$$

In this process the catalytic acitivity of $AlCl_3 \cdot ROH$ increases with the acidity of the alcohol. [23,24]

The carbo-cation activity of $C_2H_5AlCl_2 \cdot ROH$ has also been demonstrated and shown to vary in the following sequence with the coordination of ROH to $RAlCl_3$: *tert*-C_4H_9OH < < C_6H_5OH < $(C_6H_5)_3COH$. This order is confirmed by quantum chemical calculations on the aluminium complexes $R_nAlCl_{3-n} \cdot ROH$ or similar compounds. [10,15,25]

The parameters of the acid strength, the bond orders, and the predominant type of activity in complexes of alcohols with various reagents are shown in Table 5. About 70 model compounds were studied, including the individual alcohols ROH (CH_3OH, C_2H_5OH, C_3H_7OH, *tert*-C_4H_9OH), and also the compounds $H^+ \cdot ROH$, $R_nAlCl_{3-n} \cdot ROH$, $H_3C^+ \cdot ROH$, and $(CH_3)_3C^+ \cdot ROH$, i.e. complexes with Brønsted and with Lewis acids.

As can be seen, the bond orders P_{OH} and the charges on a hydrogen atom q_{H^+} are almost the same for all the alcohols. This is consistent with the experimental values [26] δpK_a = (+16) to (+19). The bond order P_{OC} tends to decrease with increasing branching of the radical R in the alcohol molecule; a minimum value of P_{OC} is found for *tert*-C_4H_9OH.

In protonated alcohols (models 5–8 in Table 5) the bond order P_{OC} and the charge on a hydrogen atom (of the same order of magnitude as the charge on a hydrogen atom in a hydroxonium ion) [5] remain almost unchanged. At the same time P_{OC} decreases as the extent of replacement of the carbon atom attached to the OH group in the alcohol molecule increases. The charge per hydrogen atom q_{H^+} is thereby increased by a factor of 2–3, which corresponds to a substantial increase in the acid strength of the complex to δpK_a = −29 to −20. When the alcohols are coordinated to acids stronger than H^+ [the carbocations H_3C^+ and $(CH_3)_3C^+$] this behaviour persists, but the

Table 5. Quantum-chemical parameters of the complexes of alcohols with some reagents. [10,25]

No. of model	Model	Group	q_{H^+}	δpK_a	P_{OH}	P_{OC}	Activity type
1–4	ROH	I	+0.14, +0.13, +0.13, +0.12	+16, +18, +18, +19	0.96, 0.96, 0.96, 0.96	1.0, 0.99, 0.97, 0.94	H^+, H^+, H^+-R^+, R^+
5–8	$H^+ \cdot ROH$	II	+0.36, +0.34, +0.33, +0.32	−29, −24, −22, −20	0.85, 0.85, 0.87, 0.87	0.87, 0.81, 0.74, 0.71	H^+-R^+, R^+, R^+, R^+
9–12	$H_3C^+ \cdot ROH$	III	+0.34, +0.32, +0.32, +0.32	−24, −20, −20, −20	0.86, 0.88 0.87, 0.87	0.87, 0.78, 0.73, 0.70	H^+-R^+, R^+, R^+, R^+
13–16	*tert*-$C_4H_9 \cdot ROH$	IV	+0.30, +0.27, +0.28, +0.27	−17, −11, −13, −11	0.87, 0.87, 0.88, 0.88	0.89, 0.81, 0.78, 0.70	H^+-R^+, R^+, R^+, R^+
17–20	$Cl_3Al \cdot ROH$	V	+0.20, +0.19, +0.18, +0.17	+7.5, +7.7, +8.5, +12	0.93, 0.94, 0.94, 0.94	0.99, 0.93, 0.90, 0.88	H^+, H^+-R^+, R^+, R^+
21–24	$CH_3AlCl_2 \cdot ROH$	VI	+0.20, +0.18, +0.19, +0.17	+7.5, +8.5, +7.7, +12	0.93, 0.93, 0.94, 0.94	0.99, 0.94, 0.91, 0.90	H^+, H^+-R^+, R^+, R^+
25–28	$(CH_3)_2AlCl \cdot ROH$	VII	+0.18, +0.17, +0.16, +0.15	+8.5, +12, +14.4, +15.1	0.92, 0.92, 0.92, 0.93	0.98, 0.93, 0.90, 0.89	H^+, H^+-R^+, R^+, R^+
29–32	$(CH_3)_3Al \cdot ROH$	VIII	+0.17, +0.16, +0.16, +0.15	+12, +14.4, +14.4, +15.1	0.95, 0.94, 0.93, 0.93	0.97, 0.93, 0.91, 0.90	$H^+-R^+, H^+-R^+, R^+, R^+$
33–36	$C_2H_5AlCl_2 \cdot ROH$	IX	+0.20, +0.19, +0.18, +0.18	+7.5, +7.7, +8.5, +8.5	0.94, 0.94, 0.95, 0.94	0.99, 0.94, 0.90, 0.90	H^+, H^+-R^+, R^+, R^+
37–40	$(C_2H_5)_2AlCl \cdot ROH$	X	+0.17, +0.17, +0.17, +0.15	+12, +12, +12, +15.1	0.93, 0.95, 0.94, 0.92	0.98, 0.94, 0.91, 0.89	H^+, H^+-R^+, R^+, R^+
41–44	$(C_2H_5)_3Al \cdot ROH$	XI	+0.17, +0.16, +0.16, +0.15	+12, +14.4, +14.4, +15.1	0.93, 0.92, 0.93, 0.92	0.97, 0.93, 0.90, 0.99	H^+, H^+-R^+, R^+, R^+
45–48	$C_3H_7AlCl_2 \cdot ROH$	XII	+0.20, +0.19, +0.19, +0.18	+7.5, +7.7, +7.7, +8.5	0.94, 0.94, 0.93, 0.94	0.99, 0.93, 0.90, 0.89	H^+, H^+-R^+, R^+, R^+
49–52	$(C_3H_7)_2AlCl \cdot ROH$	XIII	+0.17, +0.16, +0.16, +0.15	+12, +14.4, +14.4, +15.1	0.93, 0.92, 0.94, 0.94	0.99, 0.93, 0.91, 0.90	H^+, H^+-R^+, R^+, R^+
53–56	$(C_3H_7)_3Al \cdot ROH$	XIV	+0.17, +0.17, +0.16, +0.15	+12, +12, +14.4, +15.1	0.93, 0.93, 0.94, 0.93	0.98, 0.94, 0.94, 0.90	$H^+, H^+-R^+, H^+-R^+, R^+$
57–60	$C_4H_9AlCl_2 \cdot ROH$	XV	+0.20, +0.20, +0.18, +0.17	+7.5, +7.5, +8.5, +12	0.94, 0.94, 0.94, 0.93	0.98, 0.94, 0.90, 0.88	H^+, H^+-R^+, R^+, R^+
61–64	$(C_4H_9)_2AlCl \cdot ROH$	XVI	+0.17, +0.16, +0.15, +0.15	+12, +14.4, +14.4, +15.1	0.93, 0.93, 0.92, 0.93	0.99, 0.93, 0.90, 0.89	$H^+, H^+-R^+, H^+-R^+, R^+$
65–68	$(C_4H_9)_3Al \cdot ROH$	XVII	+0.17, +0.16, +0.15, +0.15	+12, +14.4, +15.1, +15.1	0.93, 0.93, 0.92, 0.93	0.99, 0.94, 0.90, 0.92	H^+, H^+-R^+, H^+-R^+

Notes. The sequence of numbers and symbols in the columns corresponds to the alcohol series with R = CH_3, C_2H_5, *iso*-C_3H_7, *tert*-C_4H_9; the following symbols are used: H^+ denotes a dominant proton-donor activity; R^+ denotes a dominant carbo-cation activity; H^+-R^+ states that the two activities have equal probabilities.

acidity of the resulting complexes is lower (δpK_a = −24 to −11). On the whole the complexes $H^+ \cdot ROH$, $H_3C^+ \cdot ROH$, and $(H_3C)_3C^+ \cdot ROH$ (models 5–16) have a high acid strength and usually display a carbo-cation activity.

In the $R_nAlCl_{3-n} \cdot ROH$ complexes (models 17–68) we find a levelling of the differences in the bond orders P_{OH} and P_{OC} for each alcohol and of the bond orders P_{OC} for different alcohols. Therefore there is no overall dominant path for the fragmentation of the alcohols in these complexes, and depending on the nature of R in the alcohol molecule they can display either proton-donor or carbo-cation activity. Like the $R_nAlCl_{3-n} \cdot H_2O$ complexes the $R_nAlCl_{3-n} \cdot ROH$ complexes are characterised by a low acid strength, with δpK_a in the range of −15.1 to −7.1. In the light of the negative values[27] of the energy of proton removal (−590 to −390 kJ mol^{-1}) the removal is energetically unfavourable in the complexes of alcohols with aluminium chlorides. Therefore their activity can manifest itself only in the presence of direct participation of electron donors (olefins, arenes, etc.).[28] As regards selectivity the complexes of this type occupy an intermediate place between $R_nAlCl_{3-n} \cdot H_2O$ and $R_nAlCl_{3-n} \cdot HCl$ (see Tables 2 and 4).

Thus increasing the strength of the Lewis acid coordinated to the alcohol increases the probability of forming a carbo-cation. This trend is quite easily observed, for example in the case of *tert*-C_4H_9OH, i. e. of an alcohol with a strongly branched hydrocarbon radical. Obviously, we can expect to find the same trend in other alcohols containing branched R radicals. A calculation of the complexes of alcohols with different Lewis acids based on aluminium chlorides (not allowing for the effect of the anion, the solvent, and other factors) confirms the dependence of the fragmentation path followed by the alcohol (H^+ or R^+ activity) on the nature of its radical and on the type of the acid.

Published experimental data on the cationic properties of systems consisting of an alcohol and an acidic agent can also be classified according to the behaviour of the alcohol during the formation of the active centres, i. e. according to whether proton or carbo-cation activity (or both simultaneously) predominates. By comparing calculated with experimental data we can test the validity of the fragmentation paths suggested for the alcohols in the complexes.

The stability of the resulting ionic fragments is one of the fundamental factors determining the fragmentation path chosen by the alcohols. The presence of substituents on the α carbon atom and the possibility of binding an hydroxyl group as a stable anion produce reliably identified carbonium ions: for example, in the $(C_6H_5)_3COH - H_2SO_4$ system.[29] The presence of stable carbo-cations, owing to the high stability (low nucleophilicity) of the counterions, has been observed[1] also by NMR during the formation of complexes of the alcohols with 'superacids':

$$(CH_3)_3COH \xrightarrow{SbF_5,\ FSO_3H} (CH_3)_3C^+, SbF_5 \cdot FSO_3^- + H_2O$$

The formation of $(CH_3)_3C^+ \cdot BF_4^-$ was observed also[1] in the interaction of *tert*-butanol with another strongly acid system: $BF_3 \cdot HF$. Thus, *tert*-substituted alcohols in the presence of strong acids are easily dissociated at the C–O bond.

If the experimental conditions do not adequately stabilise the carbonium ions, the fragmentation path adopted by the alcohol bound in a complex with a Lewis acid is determined by other factors, and in particular by the chemical bonding of the detached groups to form stable compounds. For example, according to a calculation[30] the interaction of *tert*-butyl cations with ROH in the presence of a proton acceptor (ammonia) takes place through the breaking of the O–H bond (not the C–O bond). When phenols are used the fragmentation along the O–H bond in the cationic polymerisation of isobutene[30] is favoured by the H-acidity, which is higher than in aliphatic alcohols, and by the p_π-p_π conjugation of the oxygen atoms with the aromatic nucleus, which suppresses the breaking of the bond between the aromatic carbon and the oxygen.

It follows from the calculations on the complexes of Lewis acids (R_nAlCl_{3-n}) with alcohols that the fragmentation of the alcohols by either of the possible directions (H^+ or R^+) has comparable probabilities. This conclusion is confirmed by experimental results. For example, when diisobutene (which is polymerised with difficulty) is used as a nucleophilic acceptor the protonation of the olefin is accompanied by a parallel reaction with the carbo-cation of the alcohol.[31]

Therefore according to both experimental and calculated data the fragmentation of alcohols substituted at the α carbon atom in complexes with strong acids takes place along the C–O bond, with formation of carbonium ions (i.e. R^+ activity is displayed). Conversely, decreasing the acid strength of the complex former, and especially using alcohols with unbranched radicals, strengthens the H^+ activity.

III. Complexes based on magnesium chlorides

The complexes of the magnesium chlorides with proton donors $R_nMgCl_{2-n} \cdot n_1 H_2O$ (n = 0–2; n_1 = 1, 2, 4, 6, 8, 12; R = OH, CH_3, C_2H_5, *iso*-C_3H_7, *tert*-C_4H_9) have a low activity towards the polymerisation of olefins, but nevertheless they allow us to prepare (under comparable conditions) a polymer having a molecular mass higher than would be obtained with other electrophilic initiating systems.[22]

1. Complexes based on magnesium chlorides and water

The values of the universal acidity indicator δpK_a and the charges on the hydrogen atom of the proton donor in the compounds of magnesium with H_2O are shown in Table 6.

Table 6. Acid strength of the aqua complexes $R_nMgCl_{2-n} \cdot n_1 H_2O$ (R = CH_3, C_2H_5, *iso*-C_3H_7, *tert*-C_4H_9).[10,32]

Aqua complex	q_{H^+}	δpK_a
H_2O	+0.140	+15.7
$H_2O \cdot MgCl_2$	+0.194	+7.1
$2\,H_2O \cdot MgCl_2$	+0.185	+7.7
$4\,H_2O \cdot MgCl_2$	+0.165	+10
$6\,H_2O \cdot MgCl_2$	+0.160	+14.4
$8\,H_2O \cdot MgCl_2$	+0.160	+14.4
$12\,H_2O \cdot MgCl_2$	+0.150	+15.1
$H_2O \cdot RMgCl$	+0.175 ± 0.005	+8.1 to +10
$2\,H_2O \cdot RMgCl$	+0.175 ± 0.005	+8.5 to +10
$H_2O \cdot R_2Mg$	+0.175 ± 0.005	+8.5 to +10
$2\,H_2O \cdot R_2Mg$	+0.175 ± 0.005	+8.5 to +10

The aqua complexes of the magnesium chlorides are characterised by high negative values of the overall energy of the system. These features are responsible for their stability and for the high energy of complex formation [E = −265 to −167 kJ mol^{-1}].

Irrespective of the nature of the ligands surrounding the magnesium the aqua complexes $R_nMgCl_{2-n} \cdot H_2O$ have a low Brønsted acidity (δpK_a = +7.1 to +15.1). The highest acid strength is found in the complexes $MgCl_2 \cdot H_2O$ (δpK_a = +7.1) and $MgCl_2 \cdot 2\,H_2O$ (δpK_a = +7.7), which suggests a high activity as catalysts for the polymerisation of isobutene.[22] However, the acid strength alone cannot account for the electrophilic properties of these complexes. It should not be forgotten that the geometry and the electronic structure of the $MgCl_2 \cdot H_2O$ aqua complexes are determined by the unusual type of coordination[10] of the H_2O to the $MgCl_2$. Under these conditions the size of the $MgCl_2 \cdot H_2O$ aqua complex (0.7–0.8 nm) increases in comparison with the $(CH_3)_2Mg \cdot H_2O$ aqua complex (0.3–0.4 nm).[9] Kennedy[22] came to the same conclusion. The polymerisation of isobutene under the influence of $MgCl_2$ takes place only in the presence of water and is associated with the complex nature of

Table 7. Characteristics of the $MgCl_2 \cdot n_1 H_2O$ complexes and some kinetic parameters of the thermocatalytic selective degradation of polyisobutene ($\overline{M}_n^0 = 5.75 \times 10^5$) and of butyl rubber ($\overline{M}_n^0 = 3.2 \times 10^5$) for $[MgCl_2 \cdot n_1 H_2O] = 1$ mol dm^{-3} (see Ref. 32).

Temperature/K	Conversion/mass %		Yield of isobutene/vol. %		$z \pm 10\%$		$10\,\upsilon\,(\pm 5\%)$/mol IB dm^{-3}		$10\,\upsilon_i\,(\pm 12\%)$/mol IB dm^{-3}	
	PIB	BR	PIB	BR	PIB	BR	PIB	BR	PIB	BR
Catalyst $MgCl_2 \cdot n H_2O$ ($n = 1, 2$)										
583	1.1	15.4	–	95.5	4.0	6.0	0.8	2.4	0.2	0.4
603	8.5	25.0	78.3	96.8	2.5	5.5	3.6	9.0	1.4	1.6
623	36.2	48.2	84.5	97.0	2.5	3.8	10.0	15.3	4.0	4.0
583	12.4	27.4	96.2	96.0	9.9	88.3	6.5	14.0	0.7	0.2
603	81.9	92.0	99.5	96.4	8.1	68.0	13.4	25.0	1.7	0.4
623	100.0	100.0	99.5	97.0	7.1	48.0	29.8	35.0	4.2	0.8
Catalyst $MgCl_2 \cdot 4 H_2O$										
583	11.4	19.7	90.1	93.1	9.4	72.0	6.5	7.7	0.7	0.1
603	36.2	31.6	92.4	92.0	6.8	70.0	12.4	14.5	1.8	0.2
623	62.0	35.9	98.6	97.0	–	56.0	–	20.4	–	0.4

Notes. υ is the rate of the reaction; υ_i is the rate of initiation.

the catalyst. The polymerisation requires the participation of growing carbonium ions, and the electric conductivity of the system is due to the presence of large complex counterions which may be incorporated in the solid phase. In the $MgCl_2 \cdot n_1 H_2O$ series of aqua complexes, with $n_1 = 4$, 6, 8 and 12, the energy of complex formation decreases, the charge on the hydrogen atom q_{H^+} decreases from 0.20 to 0.15, and δpK_a increases from +7.3 to +15.1. The charges on the hydrogen atoms in the water molecule, the energies of complex formation, and the δpK_a values in $RMgCl \cdot H_2O$ and $R_2Mg \cdot H_2O$ are effectively independent of the nature of the ligand surroundings of the magnesium. Similar results were obtained for the $R_2Mg \cdot 2H_2O$ and $R_2MgCl \cdot 2H_2O$ complexes.

Because of the low acid strength of the aqua complexes based on the magnesium chlorides (see Table 6), for example when used as catalysts for the electrophilic polymerisation of olefins, it is reasonable to suggest that the initiation stage of the process can be affected by the reacting bases (in particular, by the monomer molecules). An experimental confirmation of the views outlined above is provided by data obtained in studies of the electrophilic depolymerisation of isobutene polymers (PIB) and of butyl rubber (BR), containing ~1.6% of isoprene units, in the presence of $MgCl_2 \cdot n_1 H_2O$ (Table 7). We find a substantial (7-fold) decrease in the total yield of degradation products of PIB in the hydrogenation of the C=C end bonds. Because of the predominance of reactions proceeding by the 'laws of chance' over reactions proceeding by the 'law of end groups' (depolymerisation) in the degradation of polymers, the length of the kinetic chain z in the selective degradation of PIB and BR is much less than the length of the material chain $\overline{P}_n^0$. The lengths of the kinetic chain and the rates of initiation in the depolymerisation of PIB are commensurate with the values of these parameters in the purely thermal polymer degradation process. The presence of a second water molecule in $MgCl_2 \cdot 2H_2O$ (in contrast to $MgCl_2 \cdot H_2O$) has no effect on the rate of depolymerisation of PIB and BR, since the temperature of the transition of the dihydrate $MgCl_2 \cdot 2H_2O$ to the monohydrate $MgCl_2 \cdot H_2O$ (515 K) lies below the reaction temperature (523–623 K). The decrease in the positive charge in the series of magnesium aqua complexes ($MgCl_2 \cdot n_1 H_2O$) results in a marked decrease in the conversion of PIB into BR.[31,32]

These results show that the activity of the $MgCl_2 \cdot n_1 H_2O$ complexes in electrophilic processes, and in particular in the thermocatalytic selective degradation of PIB and BR, is due to their low acid strength.

2. Complexes based on magnesium chlorides and alcohols

The quantum chemical characteristics of the magnesium complexes $R_nMgCl_{2-n} \cdot ROH$ are shown in Table 8. Models of the complexes of alcohols with the magnesium haldies have been proposed by Sangalov et al.[10] To simplify the analysis all the models are divided into nine groups, depending on the nature of the ligand surroundings of the magnesium and on the extent of branching of the radical in the alcohol molecule. Aqua complexes of this type are characterised by high negative values of the total energy, which ensures the stability of catalysts based on complexes of alcohols with magnesium halides. The energy of formation of these complexes is quite high. The possibility of forming $R'_nMgCl_{2-n} \cdot ROH$ donor-acceptor complexes has been confirmed by quantum-chemical calculations (see Table 8).[10] Irrespectively of the nature of the substituents on the magnesium atom the complexes of magnesium halides with alcohols are characterised by a low Brønsted acidity ($\delta pK_a = +7.1$ to +12.0). The increase in δpK_a in the series CH_3OH, C_2H_5OH, C_3H_7OH, C_4H_9OH is dictated by the chemical structure of the compounds.

In the case of methanol the values of P_{OH} and P_{OC} for the R'_nMgCl_{2-n} complexes suggest a predominantly proton-donor activity, but with isopropanol (and, especially, *tert*-butanol) a carbo-cation activity is found. The $R'_nMgCl_{2-n} \cdot C_2H_5OH$ complexes can show H^+ and R^+ activities with equal probability.

To conclude this section we should note that irrespective of the ligand surroundings the acid strength of the complexes based on the magnesium chlorides and alcohols is relatively small (as it is with the $R'_nMgCl_{2-n} \cdot n_1 H_2O$ complexes). It follows that H^+ or R^+ activity can be displayed only through the direct participation of the reacting bases (olefins, arenes) in the initiation stage of the electrophilic polymerisation process.

IV. Complexes based on boron fluorides

Published reports of quantum-chemical calculations on complex cation-active centres of the type H^+, $[BF_4]^-$; H^+, $[BF_3 \cdot OH]^-$; R^+, $[BF_3 \cdot OH]^-$, and R^+, $[BF_3 \cdot OR]^-$ are not very abundant.[9,22,33–36] H^+ activity of the alcohols has been observed in compositions of the $BF_3 \cdot ROH$ complexes with R = CH_3, C_2H_5, n-C_3H_7, *iso*-C_3H_7, and others during the oligomerisation and polymerisation of propene, isobutene, and but-2-ene, and also in the alkylation of phenols by olefins.[37–39] However, the arguments put forward in support of H^+ initiation, such as the tenfold increase in the rate of polymerisation of styrene under the influence of $BF_3 \cdot C_2H_5OH$ as compared with the rate of the same reaction in the presence of $BF_3 \cdot O(C_2H_5)_2$ (see Refs 39 and 40) are not fully convincing. For this reason the formulae given to the electrophilic complex catalysts of the R^+, $[BF_3 \cdot OR]^-$ and H^+, $[BF_3 \cdot OH]^-$ type, widely used for the initiation of electrophilic reactions by the hydrates and etherates of boron trifluoride, are only hypothetical (though apparently reasonable).

Table 8. Quantum chemical parameters of the $ROH \cdot R_nMgCl_{2-n}$ models ($n = 0-2$; R = CH_3, C_2H_5, *iso*-C_3H_7, *tert*-C_4H_9).

Model No.	Model	Group	q_{H^+}	δpK_a	P_{OH}	P_{OC}	Activity type
1–4	$ROH \cdot MgCl_2$	I	0.20, 0.20, 0.19, 0.17	7.5, 7.5, 7.7, 12.0	0.93, 0.93, 0.93, 0.94	0.99, 0.93, 0.90, 0.89	H^+, H^+-R^+, R^+, R^+
5–8	$ROH \cdot CH_3MgCl$	II	0.20, 0.19, 0.19, 0.17	7.5, 7.7, 7.7, 12.0	0.94, 0.94, 0.94, 0.93	0.98, 0.94, 0.91, 0.91	H^+, H^+-R^+, R^+, R^+
9–12	$ROH \cdot (CH_3)_2Mg$	III	0.20, 0.19, 0.18, 0.18	7.5, 7.7, 8.5, 8.5	0.96, 0.94, 0.94, 0.93	0.97, 0.95, 0.91, 0.90	H^+-R^+, H^+-R^+, R^+, R^+
13–16	$ROH \cdot C_2H_5MgCl$	IV	0.20, 0.19, 0.18, 0.17	7.5, 7.7, 8.5, 12.0	0.93, 0.94, 0.93, 0.93	0.99, 0.93, 0.90, 0.89	H^+, H^+-R^+, R^+, R^+
17–20	$ROH \cdot (C_2H_5)_2Mg$	V	0.20, 0.19, 0.18, 0.17	7.5, 7.7, 8.5, 12.0	0.93, 0.93, 0.94, 0.93	1.0, 0.93, 0.91, 0.90	H^+, H^+-R^+, R^+, R^+
21–24	$ROH \cdot C_3H_7MgCl$	VI	0.19, 0.18, 0.18, 0.17	7.7, 8.5, 8.5, 12.0	0.92, 0.93, 0.93, 0.93	0.98, 0.94, 0.90, 0.90	H^+, H^+-R^+, R^+, R^+
25–28	$ROH \cdot (C_3H_7)_2Mg$	VII	0.20, 0.19, 0.17, 0.17	7.5, 7.7, 12.0, 12.0	0.93, 0.94, 0.93, 0.94	0.99, 0.94, 0.92, 0.89	H^+, H^+-R^+, H^+-R^+, R^+
29–32	$ROH \cdot C_4H_9MgCl$	VIII	0.20, 0.20, 0.19, 0.18	7.5, 7.5, 7.7, 8.5	0.94, 0.94, 0.94, 0.94	0.99, 0.93, 0.90, 0.89	H^+, H^+-R^+, R^+, R^+
33–36	$ROH \cdot (C_4H_9)_2Mg$	IX	0.20, 0.20, 0.18, 0.17	7.5, 7.5, 8.5, 12.0	0.92, 0.94, 0.94, 0.93	0.98, 0.95, 0.91, 0.90	H^+, H^+-R^+, R^+, R^+

Notes. Here and in Table 10 the sequence of numbers and symbols in the columns corresponds to the alcohols series with R = CH_3, C_2H_5, *iso*-C_3H_7, *tert*-C_4H_9; the following symbols are used: H^+ denotes a dominant proton-donor activity, R^+ denotes a dominant carbo-cation activity, H^+-R^+ states that the activities have equal probabilities.

1. Complexes based on boron fluorides and hydrogen fluoride

The quantum-chemical characteristics of the acid strength of the $R_nBF_{3-n} \cdot HF$ complexes are shown in Table 9. The structures calculated for the complexes based on the boron fluorides and hydrogen fluoride are distorted tetrahedra, similar to the structures of HBF_4 and $H_3O \cdot BF_4$ (see Eizner and Erusalimskii[9]). The very high positive charge concentrated on the hydrogen atoms (the proton donors) is surprising. The numerical values of the charges on the hydrogen atoms, $q_{H^+} = +0.48$ to $+0.50$, correspond to very low values of δpK_a. Therefore, according to Olah,[1] the complexes based on R_nBF_{3-n} and HF have 'superacid' properties. As in the case of the complexes based on the aluminium chlorides with strong proton donors ($R_nAlCl_{3-n} \cdot HCl$) the acidity of $RBF_{4-n} \cdot HF$ is independent of the nature of the ligand surroundings of the heteroatom.

Table 9. Acid strength of the complexes based on boron fluorides $R_nBF_{3-n} \cdot HF$ and $R_nBF_{3-n} \cdot H_2O$.

Complex	q_{H^+}	δpK_a
$HF \cdot BF_3$	+0.50	−60
$HF \cdot CH_3BF_2$	+0.49	−59
$HF \cdot (CH_3)_2BF$	+0.49	−59
$HF \cdot (CH_3)_3B$	+0.48	−58
$HF \cdot C_2H_5BF_2$	+0.49	−59
$HF \cdot (C_2H_5)_2BF$	+0.48	−58
$HF \cdot (C_2H_5)_3B$	+0.48	−58
$H_2O \cdot BF_3$	+0.23	+1.5
$H_2O \cdot CH_3BF_2$	+0.22	+4.4
$H_2O \cdot (CH_3)_2BF$	+0.22	+4.4
$H_2O \cdot (CH_3)_3B$	+0.21	+7.1
$H_2O \cdot F_4B_2O$	+0.24	+1.0

The removal of a proton H^+ is energetically favourable and offers a gain in energy of more than 350 kJ mol^{-1}. These electron-energy characteristics do not indicate the preliminary formation of a complex between HF and R_nBF_{3-n}, leading to the formation of stronger Lewis acids: rather, they suggest a preferential direct initiation of the cationic polymerisation of olefins by the scheme

$$HF + R_nBF_{3-n} \rightleftharpoons H^{\delta+}, [R_nBF_{4-n}]^{\delta-} \xrightarrow{M} HM^+, [R_nBF_{3-n}]^-.$$

Therefore the consensus of the quantum-chemical calculations and of the experimental data points to an ordinary, classical H^+ initiation mechanism for the electrophilic polymerisation process in the presence of complexes of boron fluoride with proton donors.

2. Complexes based on boron fluorides and water

The aqua complexes $R_nBF_{3-n} \cdot H_2O$ are characterised by high negative values of the total energy and of the overall energy of the bonds, which ensure the stability of the complexes. Additional evidence of the donor–acceptor nature of the complexes based the boron fluorides and water has been provided by data[10] on their geometry and on their electron-energy characteristics. The parameters of the acid strength of $R_nBF_{3-n} \cdot H_2O$ (q_{H^+} and δpK_a) show that these complexes have a low acidity irrespective of the chemical nature of the ligand surroundings of the heteroatom. However, the aqua complexes of the $R_nBF_{3-n} \cdot H_2O$ type have a slightly greater acid strength than the aqua complexes based on the chlorides of magnesium and aluminium. This corresponds to well known experimental data on the greater activity and slightly lower selectivity of the $R_nBF_{3-n} \cdot H_2O$ as compared with $R_nAlCl_{3-n} \cdot H_2O$ complexes in the cationic polymerisation of olefins.[13,23] The spontaneous protonation of the compound $R_nBF_{3-n} \cdot H_2O$ is effectively impossible because the removal of a proton requires an expenditure of energy of more than 150 kJ mol^{-1}. Therefore even in the aqua complexes of the boron fluorides the appearance of proton-donor activity is determined by the acceptor function of the base (olefin, arene, etc.).

3. Complexes based on boron fluorides and alcohols

Quantum-chemical calculations for the complexes $R'_nBF_{3-n} \cdot ROH$, analogous to the calculations for $R'_nAlCl_{3-n} \cdot ROH$ and $R'_nMgCl_{2-n} \cdot ROH$, have established the mutual dependence of their electrophilicity and of the appearance of proton-donor (as opposed to carbo-cation) activity.

Table 10. Quantum chemical parameters of the ROH · R_nBF_{3-n} · ROH complexes (n = 0–3; R = CH_3, C_2H_5, *iso*-C_3H_7, *tert*-C_4H_9).

Model No.	Complex	Group	q_{H^+}	δpK_a	P_{OH}	P_{OC}	Activity type
1–4	ROH · BF_3	I	0.24, 0.23, 0.21, 0.21	1.0, 1.5, 7.1, 7.1	0.92, 0.92, 0.92, 0.92	0.98, 0.97, 0.94, 0.94	H^+, H^+, H^+-R^+, R^+
5–8	ROH · CH_3BF_2	II	0.23, 0.22, 0.20, 0.19	1.5, 4.4, 7.3, 7.7	0.92, 0.92, 0.93, 0.93	1.01, 0.96, 0.90, 0.89	H^+, H^+, R^+, R^+
9–12	ROH · $(CH_3)_2BF$	III	0.23, 0.21, 0.20, 0.20	1.5, 7.1, 7.3, 7.3	0.92, 0.94, 0.92, 0.93	1.0, 0.97, 0.94, 0.90	H^+, H^+, H^+-R^+, R^+
13–16	ROH · $(CH_3)_3B$	IV	0.24, 0.23, 0.22, 0.20	1.0, 1.5, 4.4, 7.3	0.94, 0.92, 0.94, 0.92	0.96, 0.95, 0.91, 0.89	H^+-R^+, H^+, R^+, R^+
17–20	ROH · $C_2H_5BF_2$	V	0.23, 0.22, 0.22, 0.20	1.5, 4.4, 4.4, 7.1	0.93, 0.92, 0.94, 0.93	0.98, 0.96, 0.93, 0.89	H^+, H^+, H^+-R^+, R^+
21–24	ROH · $(C_2H_5)_2BF$	VI	0.24, 0.23, 0.21, 0.20	1.0, 1.5, 7.1, 7.3	0.92, 0.92, 0.92, 0.93	0.97, 0.95, 0.93, 0.90	H^+, H^+, H^+-R^+, R^+
25–28	ROH · $(C_2H_5)_3B$	VII	0.22, 0.21, 0.21, 0.20	4.4, 7.1, 7.1, 7.3	0.92, 0.93, 0.92, 0.93	0.90, 0.95, 0.93, 0.90	H^+, H^+-R^+, H^+-R^+, R^+
29–32	ROH · $C_3H_7BF_2$	VIII	0.23, 0.22, 0.20, 0.20	1.5, 4.4, 7.3, 7.3	0.92, 0.93, 0.92, 0.92	0.98, 0.97, 0.93, 0.89	H^+, H^+, H^+-R^+, R^+
33–36	ROH · $(C_3H_7)_2BF$	IX	0.24, 0.24, 0.21, 0.20	1.0, 1.0, 7.1, 7.3	0.92, 0.93, 0.93, 0.92	0.99, 0.96, 0.94, 0.89	H^+, H^+, H^+-R^+, R^+
37–40	ROH · $(C_3H_7)_3B$	X	0.22, 0.22, 0.21, 0.19	4.4, 4.4, 7.1, 7.7	0.92, 0.92, 0.92, 0.92	0.99, 0.96, 0.93, 0.89	H^+, H^+, H^+-R^+, R^+
41–44	ROH · $C_4H_9BF_2$	XI	0.23, 0.21, 0.21, 0.20	1.5, 7.1, 7.1, 7.3	0.92, 0.93, 0.92, 0.92	0.99, 0.96, 0.93, 0.89	H^+, H^+, H^+-R^+, R^+
45–48	ROH · $(C_4H_9)_2BF$	XII	0.23, 0.22,	1.5, 4.4,	0.92, 0.93,	1.0, 0.97,	H^+, H^+,

A detailed collection of the quantum-mechanical evidence for the existence of the R'_nBF_{3-n} · ROH (electronic structure, geometry) has been published.[10] The charges on the hydrogen atoms of the alcohol, which are well correlated with the values of the universal acidity indicator, and the predominant type of activity of the alcohol are listed in Table 10. In all 13 groups the positive charge on the hydrogen atom in the complexes based on boron fluorides and alcohols decreases as the branching of the radical in the molecule is increased. Therefore the q_{H^+} values are independent of the ligand surroundings of the heteroatom, and are determined by the chemical structure of the radical in the ROH molecule. The acid strength of the R'_nBF_{3-n} · ROH complexes decreases in the alcohol series methanol > ethanol > > isopropanol > *tert*-butanol, but the P_{OH} bond orders remain practically unchanged for all 52 models of the alcohol–boron fluoride complexes. The P_{OC} bond order tends to decrease when the acidity indicator of the complexes δpK_a is lowered. The complexes of CH_3OH and C_2H_5OH with the boron fluorides show preferentially H^+ activity. When isopropanol is used the proton-donor and the carbo-cation activity appear with equal probabilities. Alternative possibilities for the fragmentation of the alcohol molecules in the complexes with boron fluorides have been identified experimentally[25,37–40] is a function of the chemical structure of the alcohol residue R.

Thus the R'_nBF_{3-n} · ROH complexes are characterised by a low Brønsted acidity irrespective of the nature of the ligands. The development of proton-donor or of carbo-cation activity in the alcohols is determined by the chemical structure of the radical in the alcohol molecule, and is associated with the direct participation of bases in the polymerisation reactions of the olefins (in particular, molecules of the monomer, of the aromatic solvent, etc.).

V. Conclusions

The accumulated fund of experimental data on the acid strength and catalytic activity of adequately stable complexes consisting of the halides, alkyls, and alkyl halides of the nontransition metals (Al, B, Mg) and of proton donors (H_2O, ROH, HCl, HF) in electrophilic polymerisation processes, in conjunction with corresponding quantum-chemical calculations, justify the conclusion that the acid strength of the proton donors in these complexes is a measure of the activity and selectivity of their action as catalysts in electrophilic reactions. Important new information has been acquired, offering a deeper understanding of the role of the acid strength of these complexes in electrophilic polymerisation processes.

1. Complexes of the R_nAlCl_{3-n} · HCl and R_nBF_{3-n} · HF type have a high acid strength, independent of the ligand surroundings of the heteroatom (Al, B) ($\delta pK_a = -16$ to -60). The removal of a proton is energetically favourable. The complexes undergo spontaneous ionisation and can initiate electrophilic polymerisation.

2. Complexes of the R_nAlCl_{3-n} · H_2O, R_nMgCl_{2-n} · H_2O, and R_nBF_{3-n} · H_2O type, and products of their transformation ($HOAlCl_2$ · H_2O, Al_2Cl_4O · H_2O, R_nAlCl_{3-n} · H_2O · HCl, etc.), have a low acid strength ($\delta pK_a = +1.3$ to $+14.4$). The removal of a proton is energetically unfavourable. Complexes of this type are not prone to spontaneous ionisation, and they can initiate electrophilic polymerisation in the presence of weak bases.

3. Complexes of the R'_nAlCl_{3-n} · ROH, R'_nMgCl_{2-n} · ROH, and R'_nBF_{3-n} · ROH type are characterised (like the corresponding aqua complexes) by a small acid strength ($\delta pK_a = +1.0$ to $+15.1$). The removal of a proton is energetically unfavourable. Complexes of this type do not undergo spontaneous ionisation. Depending on the chemical structure of the radical R in the alcohol molecule, on the acid strength of the complex former, and (if the acid strength is low) on the specific interactions of the reactants, and also depending on the special features of the coordination of the proton donors (H_2O, ROH) with the Lewis acids (mainly, magnesium compounds), the alcohol molecules bound in complexes can display either a proton activity or a carbo-cation activity. In the electrophilic polymerisation of olefins this effect influences the initiation stage, and therefore also the character of the end groups in the resulting macromolecules. Increasing the size of the ligand in the Lewis acid (see Table 2) or the volume of the

radical R in the alcohol molecules (see Table 4) included in the composition of complexes of nontransition metal halides with proton donors increases the selectivity of the polymerisation.

Thus the complexes of the halides of nontransition metals with weak proton donors (H_2O, ROH) have a low acid strength, which casts doubts on the ability of these materials to show a catalytic activity in electrophilic processes, and a weak dependence of the acid strength on the chemical nature of the initial Lewis acid. In this case the role of the monomer as an electron donor and its direct participation in the formation of active centres become the dominant factors.[41]

The method of calculating the acid strength of the complex catalysts in the R_nAlCl_{3-n}–proton-donor system[41–43] can be extended to a wider class of complexes based on the halides of nontransition metals (B, Mg, etc.) and on proton donors (H_2O, ROH, HCl, HF, etc.). The method is convenient and promising for calculating the acid strength of newly synthesised H complexes in order to predict their catalytic activity and selectivity in electrophilic processes. The acidity parameters q_{H^+} obtained in this way by calculations on appropriate models of the complex catalysts are expressed in the form of δpK_a by using a well known correlation expression.[6] An analysis of the acidity of more than 300 compounds and complexes thought to be potential catalysts for electrophilic polymerisation processes in olefins identified the following ranges of δpK_a values (see Fig. 2):

from +50 to +12 (very low values); complexes having these acidities show no catalytic activity towards electrophilic polymerisation processes (the individual compounds ROH and H_2O, and also $AlR_3 \cdot H_2O$, $AlR_3 \cdot ROH$, etc., see Tables 3, 5, and 6);

from +12 to +1 (optimum values); catalysts having these acidities have a high activity and selectivity ($C_2H_5Cl_2Al \cdot H_2O$, $AlCl_3 \cdot H_2O$, $MgCl_2 \cdot H_2O$, $C_2H_5AlCl_2 \cdot ROH$ etc., see Tables 3, 5, 6);

from +1 to −60 (high values); at these acidities the H complexes are much more active, but very much less selective ($R_nAlCl_{3-n} \cdot HCl$, $R_nBF_{3-n} \cdot HF$, protonated alcohols, see Tables 1 and 2).

We may conclude from the above that increasing the acid strength of electrophilic polymerisation catalysts increases the activity of the catalysts but lowers the selectivity of the process.

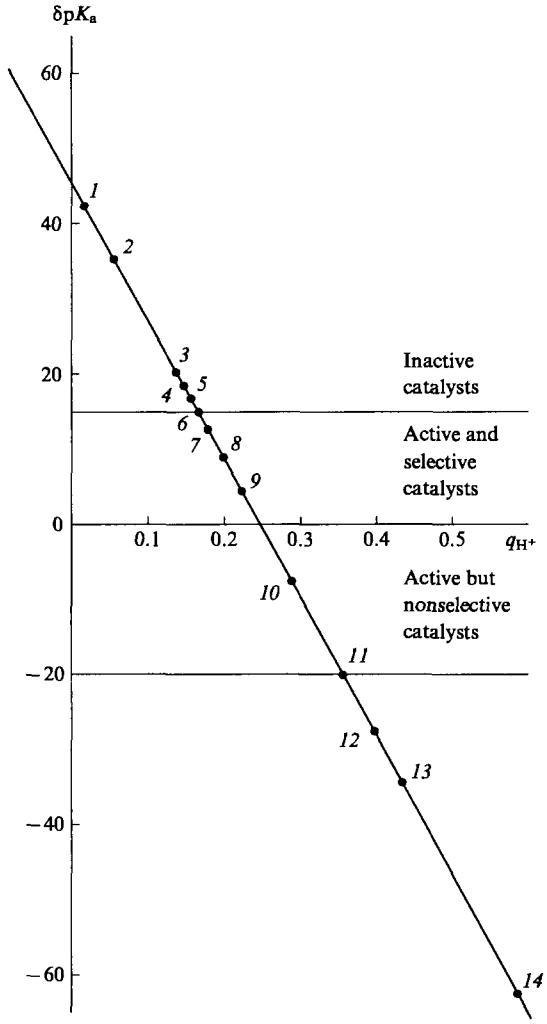


Figure 2. Relationship between the universal acidity indicator and the charge on the hydrogen atom.[6,41]

(*1*) CH_4; (*2*) NH_4^+;
(*3*) $(CH_3)_3COH$; (*4*) CH_3OH;
(*5*) $H_2O \cdot R_2AlCl$, $H_2O \cdot R_3Al$; (*6*) H_2O;
(*7*) $Si(OH)_4$; (*8*) $H_2O(ROH) \cdot AlRCl_2 \cdot (R_nMgCl_{2-n})$;
(*9*) $H_2O \cdot Al_2Cl_4OH$; (*10*) $(CH_3)_3C^+ \cdot HOC_2H_5$;
(*11*) $H_3C^+ \cdot HOC_2H_5$; (*12*) $H_3C^+ \cdot CH_3OH$;
(*13*) $H^+ \cdot CH_3OH$; (*14*) $HF \cdot R_nBF_{3-n}$.

References

1. G A Olah *Friedel–Crafts Chemistry* (New York, 1973)
2. V A Koptyug *Sovremennye Problemy Khimii Karbonievykh Ionov* (Modern Problems in the Chemistry of Carbonium Ions) (Novosibirsk: Nauka, 1975)
3. K Tanabe *Solid Acids and Bases. Their Catalytic Properties* (Translated into Russian; Moscow: Mir, 1973)
4. V D Petrova, N N Rzhevskaya, N V Shcherbakova, Yu A Sangalov, K S Minsker *Dokl. Akad. Nauk SSSR* **233** 602 (1977)
5. M Imal, T Saegusa, J Furukawa *Macromol. Chem.* **81** 92 (1965)
6. W Grabowski, M Misono, Y I Yoneda *J. Catal.* **61** 103 (1980)
7. J A Pople, D Beveridge, in *Approximate Molecular Orbital Theory* (New York: McGraw-Hill, 1970) p. 214
8. E A Chernova, R P Tiger, O G Tarakanov *Zh. Strukt. Khim.* **27** 19 (1986)
9. Yu E Eizner, B L Erusalimskii *Elektronnyi Aspekt Reaktsii Polimerizatsii* (Electronic Aspects of Polymerization Reactions) (Leningrad: Nauka, 1976)
10. Yu A Sangalov, V A Babkin, E M Nel'kenbaum *Kvantovokhimicheskii Raschet Kislotnykh Katalizatorov. Kislotnost' i Kataliticheskie Svoistva Kompleksov Soedinenii Metallov s Protonodonorami* (Quantum-chemical Calculations of Acid Catalysts. Acidity and Catalytic Properties of Complexes of Metal Compounds with Donors of Protons) (Bashkir Scientific Centre, Ural Division of the Academy of Sciences of the USSR, Ufa, 1989)
11. N V Kozak, Yu N Nizal'skii *Teor. Eksp. Khim.* **26** 345 (1990)
12. V D Petrova, N N Rzhevskaya, N V Shcherbakova, Yu A Sangalov, K S Minsker *Izv. Akad. Nauk SSSR, Ser. Khim.* 1373 (1978)
13. K S Minsker, Yu A Sangalov *Izobutilen i Ego Polimery* (Isobutene and Its Polymers) (Moscow: Khimiya, 1986)
14. Yu A Sangalov, Yu B Yasman, E M Nel'kenbaum, V Ya Badretdinova, K S Minsker *Vysokomol. Soedin., Ser. A* **22** 1588 (1980)
15. Yu A Sangalov, O A Ponomarev, V G Romanko, K S Minsker *Teor. Eksp. Khim.* **13** 623 (1977)
16. I M Alpatova, V V Gavrilenko, Yu M Kessler, O R Osipov, D N Maslin *Kompleksy Metalloorganicheskikh Gidridnykh i Galoidnykh Soedinenii Alyuminiya* (Complexes of Organometallic Hydrated and Halogen Compounds of Aluminum) (Moscow: Nauka, 1970)
17. Yu A Sangalov, Yu B Yasman, F A Valeev, K S Minsker *Vysokomol. Soedin., Ser. A* **20** 1339 (1978)
18. G G Perkampus, in *New Problems of Physical and Organic Chemistry* (Translated into Russian; Moscow: Mir, 1969) p. 257
19. Yu A Sangalov, Yu B Yasman, I F Gladkikh, K S Minsker *Dokl. Akad. Nauk SSSR* **265** 671 (1982)

20. Yu A Sangalov, K S Minsker, V A Babkin, O A Ponomarev *Teor. Eksp. Khim.* **18** 535 (1982)
21. N I Ermakova, E N Kropacheva, A I Kol'tsov, B A Dolgoplosk *Vysokomol. Soedin., Ser. A* **11** 1639 (1969)
22. J P Kennedy *Cationic Polymerization of Olefins: a Critical Inventory* (Translated into Russian; Moscow: Mir, 1978)
23. T Aoyali, T Araki, H Tani *Macromol. Chem.* **163** 45 (1973)
24. S Aoki, M Imoto *Macromol. Chem.* **65** 243 (1963)
25. Z Zlamal, A Kazda *J. Polym. Sci. Part A* 3199 (1963)
26. Yu A Sangalov, V A Babkin, Yu Ya Nel'kenbaum, K S Minsker *Teor. Eksp. Khim.* **19** 615 (1983)
27. A J Gordon, R A Ford *The Chemist's Companion. A Handbook of Practical Data Techniques and References* (Translated into Russian; Moscow: Mir, 1976)
28. Yu A Sangalov, Yu B Yasman, Yu Ya Nel'kenbaum, V A Babkin *Izv. Akad. Nauk SSSR, Ser. Khim.* 2661 (1986)
29. K S Minsker, Yu A Sangalov, V A Babkin, O A Ponomarev *Teor. Eksp. Khim.* **20** 669 (1984)
30. P Plesch *The Chemistry of Cationic Polymerization* (Translated into Russian; Moscow: Mir, 1966)
31. M Attina, F Cacace, G Ciranni, P Giacomello *J. Chem. Soc., Chem. Commun.* 938 (1978)
32. Yu A Sangalov, O A Ponomarev, Yu Ya Nel'kenbaum, V G Romanko, V D Petrova, K S Minsker *Vysokomol. Soedin. Ser.A* **20** 1331 (1978)
33. A A Berlin, E F Gumerova, S R Ivanova, K S Minsker, M M Karpasas *Vysokomol. Soedin., Ser. B* **29** 604 (1987)
34. E Silla, E Scrocco, I Tamasi *Theor. Chim. Acta* **44** 8 (1975)
35. P Hallpap, G Heublein *Z. Chem.* **17** 446 (1977)
36. P Hallpap, G Heublein, V Ya Bogomolni, Yu Ya Eizner, B L Erusalimski, S S Skorokhodov *Eur. Polym. J.* **14** 1027 (1978)
37. G Alogona, E Scrocco, E Silla *Theor. Chim. Acta* **45** 127 (1977)
38. G E Zaikov *Int. J. Polym. Mat.* **24** 3 (1994)
39. I Deroualt, T Driembovska, M T Forel *J. Mol. Struct.* **47** 59 (1978)
40. M Imoto, S Aoki *Macromol. Chem.* **48** 72 (1961)
41. Yu A Sangalov, Yu B Jasman, Yu Ya Nelkenbaum, V A Babkin *Acta Polym.* **38** 134 (1987)
42. K S Minsker, V A Babkin, G E Zaikov *Polym. Plast. Technolog. Eng.* **29** 43 (1990)
43. K S Minsker, V A Babkin, G E Zaikov *Plastmassy* **9** 6 (1988)

Russian Chemical Reviews **63** (4) 289–311 1994
© 1994 Russian Academy of Sciences and Turpion Ltd

UDC 541.49+541.632

Stereodynamics and degenerate ligand exchange in solutions of tetracoordinate chelate complexes of nontransition metals

V I Minkin, L E Nivorozhkin, M S Korobov

Contents

I.	Introduction	289
II.	Stereochemically nonrigid structures with tetracoordinate centres	290
III.	The mechanisms of the stereochemical nonrigidity of tetracoordinate structures	292
IV.	Beryllium complexes	294
V.	Complexes of boron, gallium, and indium	295
VI.	Zinc complexes	298
VII.	Cadmium complexes	301
VIII.	Complexes of mercury and lead	304
IX.	Complexes of copper, silver, and gold	305
X.	Complexes of nickel and other transition metals	307
XI.	Conclusion	309

Abstract. Nontransition metal (d^0, d^{10}) chelate complexes possessing a tetrahedral configuration at the metal centre undergo fast intramolecular stereoisomerisation and intermolecular ligand exchange reactions in solution. Inversion of the stereochemical configuration is governed by two types of intramolecular reaction: (1) polytopal rearrangement (digonal twist) and (2) dissociation-recombination reaction due to the cleavage-formation of one of the metal–ligand bonds. The energetically preferred mechanism for the inversion is chiefly determined by the nature of the metal, but it also depends on the type of ligating atoms and their environment. The energy barriers to the inversion of the tetrahedral configuration vary in the range of 10–30 kcal mol^{-1}. The bibliography includes 175 references.

I. Introduction

As long as two or three decades ago, the structure of a molecule was regarded as fully described by its three-dimensional geometrical representation. Currently, such a description may be considered as inadequate if it is not complemented by data on the degree of stereochemical nonrigidity of the molecule. Stereochemical nonrigidity implies the ability of the molecule to undergo fast and reversible intramolecular isomerisation. The energy barrier to this is lower than that allowing for the preparative isolation of individual isomers at room temperature. Owing chiefly to the remarkable progress in the development of NMR spectroscopic technique and its wide application to the study of dynamic processses, the tendency of virtually all types of molecular structures to display stereochemical nonrigidity has been established. The degree of such nonrigidity is regulated by electronic and steric factors. It is the rigidity of the molecular structure (i.e. its association with a very deep minimum on the potential energy surface) that is to be regarded as a characteristic molecular property, whereas stereochemical nonrigidity—the ability of the molecule to fluctuate between several isomeric or topomeric forms separated by an energy barrier lower[1,2] than 20–25 kcal mol^{-1}—is a general property of the molecular structure. Thus the full structural description of a molecule must also include, in addition to three spatial dimensions, a fourth, time (or energy) dimension—the lifetime of the molecule in the given geometrical coordination.

The mechanisms of stereochemical nonrigidity are extremely varied. For metal coordination compounds, these may be categorised, in principle, into two main types: (1) rearrangements of compounds with multicentre bonds (π-complexes, organometallic clusters, polyhedral boranes and carbaboranes); (2) isomerisations and topomerisations (i.e. degenerate rearrangements) of the coordination poly-hedra formed by the central atom by means of two-centre two-electron bonds. In the terminology of the topological and graph-theoretical descriptions of the isomerisations of metal clusters and polyhedral structures, the two types are classified as globally delocalised and edge delocalised mechanisms respectively.[3]

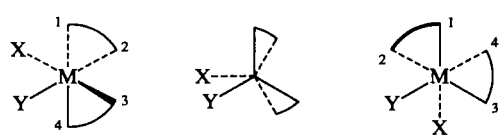
Formally, the rearrangements of coordination polyhedra may be thought of as permutations of the ligands in the central atom environment. The character of such a permutation defines the so called permutation mechanism[4,5] of the rearrangement. Nuclear magnetic resonance (NMR) spectroscopy serves as the most powerful tool for the differentiation of various permutational rearrangements including those of the degenerate type. It should be borne in mind, however, that in some cases certain types of permutation mechanisms are not NMR-distinguishable. In recent years, the potential of NMR spectroscopy in the study of the kinetics and selection of the mechanisms of chemical reactions has been substantially enhanced by the development of two-dimensional (2D) NMR spectroscopic methods.[6] The applications of 2D NMR in studies of chemical exchange reactions occurring in solutions of organometallic and metal coordination compounds have been reviewed.[7,8] Examples of the successful use of three-, four-, and even five-dimensional NMR spectroscopy in characterising the dynamics of organic and metal coordination compounds are known.[9]

V I Minkin Institute of Physical and Organic Chemistry,
L E Nivorozhkin, M S Korobov NMR Laboratory,
Rostov State University, prosp. Stachki 194/3, 344104 Rostov-on-Don,
Russian Federation. Fax (7-863-2) 28 56 67

Received 14 February 1994
Uspekhi Khimii **63** (4) 303–326 (1994); translated by A K Grzybowski

The determination of the permutation mechanism of the rearrangement is the initial stage of the investigation into the real (physical) mechanism of the processes determining the stereochemical nonrigidity. After the permutation mechanism has been elucidated, it must be assigned to a specific physical process involving the displacement of atoms and atomic groups within one or several interacting molecules, i.e. attributed to definite isomerisation or topomerisation reactions. Several different physical mechanisms can correspond to the same permutation mechanism. This general approach to the analysis of the mechanisms of stereochemical nonrigidity has been currently employed in the study of a wide range of metal complexes with central atom coordination numbers varying from 2 to 9.[10] As the number of ligands attached to the central atom grows, the number of possible permutation mechanisms increases rapidly and the types of the corresponding metal-centred intramolecular rearrangements become more diverse. Nevertheless, regardless of the complexity of the initial structure, the intramolecular rearrangements can be divided into two main classes in terms of the type of isomerisation: isomerisation (topomerisation) of the coordination centre without intermediate breakage of individual bonds (polytopal rearrangements[11]), and isomerisation via a dissociation-recombination mechanism. In the latter case, an intermediate with a reduced coordination number of the central atom usually arises in the course of the rearrangement.

The above mechanisms of the stereochemical nonrigidity have been most fully characterised in the case of pentacoordinate[1,12,13] and hexacoordinate[14–18] metal complexes. Depending on the structure of the complex and to a lesser extent on the nature of the medium, a particular mechanism predominates. Thus in the case of bischelate hexacoordinate complexes *cis*-$M(AB)_2XY$, a polytopal rearrangement of the trigonal twist type constitutes the only low energy barrier mechanism of the inversion of the octahedron for titanium(IV) dialkoxybis(β-diketonates)[17] and phenylchlorobis(benzoylacetonato)tin(IV).[16] One of the four rearrangement mechanisms, determined by the rotation relative to one of the four C_3 axes of the octahedron, is presented below.



1a **1c** **1b**

However, in the case of the (2,6-diisopropylphenoxy)titanium bischelate complexes based on 8-hydroxyquinoline or 8-hydroxyquinaldine[19] the rate-limiting stage of the configurational rearrangement involves the dissociation of one of the Ti–N bonds of the chelate ring, while in the case of dialkoxy(dimethyl phosophorodithioate)titanium(IV), the dissociation of the Ti–S bond assumes this role.[20] Pentacoordinate trigonal-bipyramidal structures arise as intermediates. Their importance for the mechanism of the stereoisomerisation of octahedral complexes was already predicted by Werner.[21]

Intermolecular associative mechanisms, involving the formation of intermediates with an increased coordination number of the central atom, are an alternative to the intramolecular stereoisomerisation mechanisms.[22–24] In those cases where nucleophilic catalysis of the stereoisomerisation is ruled out and a noncoordinating solvent is employed, the role of the nucleophilic species may be assumed by a second molecule of the complex, one (or two) donor atoms of which are coordinated to the central metal atom of the first molecule. The addition process is usually followed by a polytopal rearrangement in the intermediate with an increased coordination and then by a stage involving the splitting off of the leaving group (dissociation of one of the initial bonds). If the leaving ligand passes to the coordination environment of the metal in the second complex molecule (Scheme 1), such autosubstitution or degenerate ligand exchange reaction can be regarded as a manifestation of the stereochemical nonrigidity of the dimeric associated species.

Scheme 1

$$ML_n + M^*L_n^* \rightleftharpoons [MM^*L_nL_n^*] \rightleftharpoons \rightleftharpoons ML_{n-1}L^* + M^*L_{n-1}^*L$$

The present review deals with processes in which the stereochemical nonrigidity of tetracoordinate chelate complexes of nontransition metals (i.e. having unfilled d^0 or filled d^{10} electron shells according to IUPAC rules[25]) with a tetrahedral configuration in the ground electronic state is manifested. For comparison, data on intramolecular stereoisomerisation processes in solutions of tetrahedral chelate nickel complexes, occurring on the NMR time scale, are also considered. The identification and kinetic characteristics of the three fundamental types of rearrangement mechanisms (polytopal rearrangement, dissociation-recombination mechanism, and associative degenerate ligand exchange mechanism) are emphasised.

The stereoisomerisation of compounds of dicoordinate and tricoordinate nontransition elements (planar, pyramidal, and edge forms of inversion) are usually considered in the context of ideas concerning the stereochemistry of organic compounds (see, for example, Refs 26–28). The permutation and physical mechanisms of the stereochemical nonrigidity of pentacoordinate[12,13,29,30] and hexacoordinate[4,12–14,18,29] structures have been analysed in fair detail. Theoretical[29,31–33] and experimental[34,35] data on fluctuating hepta- and octa-coordinate metal complexes as well as complexes with higher (up to 12) coordination numbers[3,36,37] are rapidly accumulating. On the other hand, only short sections in an early review by Holm[1] and in a recent review[38] have been devoted, apart from the original communications, to the molecular dynamics of tetracoordinate metal complexes. The aim of the present review is to fill this gap.

II. Stereochemically nonrigid structures with tetracoordinate centres

The main type of dynamic rearrangements of stereochemically nonrigid structures of tetracoordinate transition and nontransition metal complexes is the interconversions of the tetrahedral and planar forms. The case of bischelate complexes based on asymmetric bidentate ligands (AB), which includes the interconversion of enantiomeric tetrahedral structures and the geometrical isomerisation of *cis*- and *trans*-planar structures, is fairly general. The scheme presented in Fig. 1 reflects two possible cases:† (1) the tetrahedral form corresponds to the most stable structure of the ground state (Fig. 1*a*) and (2) the planar (square) form is energetically more favourable (Fig. 1*b*). The latter version is more characteristic of transition metal complexes.

Not only the relative energies of the tetrahedral and planar structures but also the type of the stationary point on the potential energy surface corresponding to them depend critically on the nature of the central atom and the ligand structure. In the case of nontransition metal complexes of the type $M(AB)_2$, it has not been possible hitherto to detect reliably planar forms in equilibrium with tetrahedral forms‡ and, as follows from the results of

† The true symmetry of the coordination unit in the $M(AB)_2$ complexes (Fig. 1) is lower than the symmetry of the tetrahedron or square. However, it has become usual in the literature to designate these complexes as tetrahedral or square planar, emphasising the topological and not the geometrical characteristics.

‡ Individual communications concerning the existence in solution of equilibrium between the tetrahedral and planar tetracoordinate nontransition metal structures can be encountered in the literature. Thus, according to ^{1}H NMR data, magnesium(II) bisacetylacetonate exists[34] in solutions as two forms: tetrahedral (D_{2d}) and planar (D_{2h}).

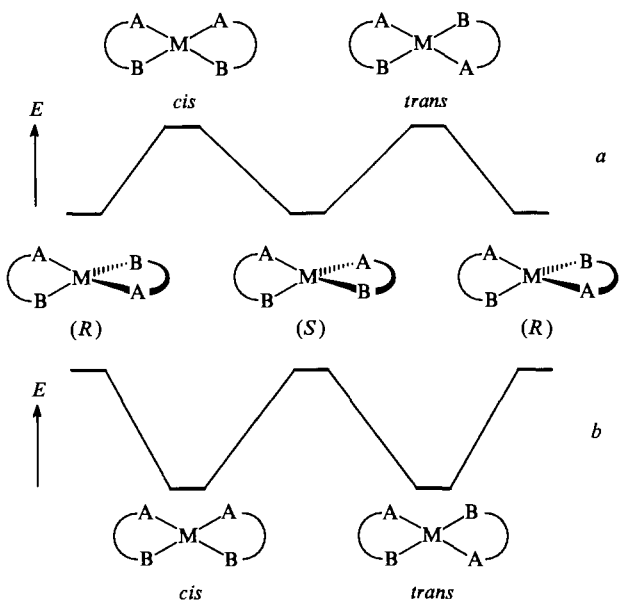


Figure 1. Schematic illustration of the configurational isomerisation of the tetrahedral structures of bischelate metal complexes: (*a*) M = non-transition metal; (*b*) M = transition metal.

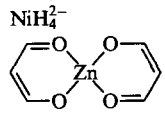
quantum-chemical calculations discussed below, they represent not metastable forms but the structures of transition states or even correspond to higher-order saddle points[39] in the interconversions of tetrahedral structures.§ The reverse situation, where tetrahedral structures correspond to transition states in the *cis–trans* isomerisation reactions of planar forms, is characteristic of Pt(II) and Pd(II) complexes.[35] The *trans*-planar and tetrahedral[41,42] or *cis*-planar and tetrahedral[43,44] forms of Ni(II) complexes may be stable and may coexist in solution. In the crystalline state, complexes of tetracoordinate Cu(II) and Ni(II) can assume configurations over a wide range, intermediate between planar and tetrahedral, depending on the structure of the ligands.[38,45]

The rate of the interconversions of the tetrahedral and planar structures of nickel(II) complexes in solution reaches 10^6-10^{13} s^{-1}.[1,46] In contrast to this, the tetrahedral structures formed by Group IVA elements possess a high degree of stereochemical rigidity. As can be seen from the data in Table 1, which presents the energy differences between the stable tetrahedral and square planar structures of the hydrides AH_4 calculated by nonempirical quantum-chemical methods, these quantities exceed the A–H bond dissociation energies, which implies that polytopal rearrangements of the type square ⇆ tetrahedron cannot be achieved.

Direct calculations and analysis based on allowance for the second-order Jahn–Teller effect[47-49] indicate the principal ways in which tetracoordinate structures can undergo a structural modification leading to a decrease in the energy gap between the tetrahedral and planar configurations. For the MX_4 structures with d^0 or d^{10} electronic configurations of the central atom, which is less electronegative than the carbon atom, the highest occupied molecular orbital of the square planar form has the b_{1g} symmetry, while the electronic ground state is $^1A_1(\delta)$. The lower the electronegativity of the central atom M and the higher the electronegativity of the ligand atoms X, the smaller the energy

§ A communication based on STO-3G calculations[40] concerning the possibility of the existence of a local minimum for the $C_{21}H_{28}$ (octaplane) structure, containing a planar tetracoordinate carbon atom between two chair-shaped cyclooctane rings, has appeared recently. However, the strain energy is ~15 kcal mol^{-1} per carbon atom for this hydrocarbon.

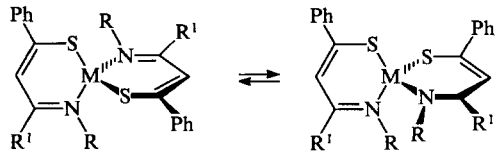
Table 1. The energy barriers to the planar inversion of the tetrahedral hydrides and fluorides MX_4 according to the results of nonempirical quantum-chemical calculations.

MX_4	Method of calculation	$\Delta(E_{D_{4h}}-E_{T_d})$ /kcal mol^{-1}	Ref.
CH_4	MP2/6-311+G**	141 [a]	47
SiH_4	3-21G*	95	47
SiH_3Cl	3-21G*	77 [b]	47
SiH_3NH_2	3-21G*	64 [b]	47
$Si(NH_2)_4$	3-21G*	53	47
BH_4^-	MP2/6-31G*	140	50
AlH_4^-	STO-3G*	76	50
CF_4	MP2/DZ+P	127	28, 51
SiF_4	MP2/DZ+P	63	28, 51
GeF_4	MP2/DZ+P	48	28, 51
SnF_4	MP2/DZ+P	37	28, 51
ScH_4^-	DZDH+P	28	48
TiH_4	DZDH+P	46	48
NiH_4^{2-}	8*S* 6*P* 3*d* (8*s*,6*p*,3*d*)	−26 [c]	52
	MINI	12	53

[a] The most rigorous of the currently available estimates[39] [MCSCF-6-31G(*d*,*p*), all the singly and doubly excited configurations are taken into account] is 159.5 kcal mol^{-1}.
[b] The energy difference between the C_{2v} and C_{3v} forms is presented.
[c] The planar D_{4h} form is stable.

difference between the planar and tetrahedral forms. Indeed, in the case of SnF_4 the energy difference expected on the basis of calculated data is close to the range of energy barriers for stereochemically nonrigid structures, while in the case of the bischelate Zn(II) complex with the ZnO_4 coordination unit it falls within this range.

The structure of the first stereochemically nonrigid transition metal complexes **2**, investigated in the pioneer study by Eaton and Holm,[54] corresponds fully to the criteria considered. These investigators observed for the first time that the tetrahedral bischelate Zn(II) and Cd(II) complexes of type **2**, containing electronegative nitrogen and sulfur atoms coordinated to the metal atom, undergo in solution the reversible enantiomerisation (*R*) ⇄ (*S*) associated with the inversion of the configuration of the tetrahedral metal atom occurring on the ^1H NMR time scale.

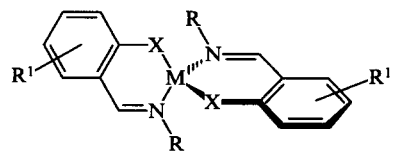


2(*R*) **2**(*S*)

M = Zn, Cd; R = Pr^i, CH_2Ph; R^1 = H, Me

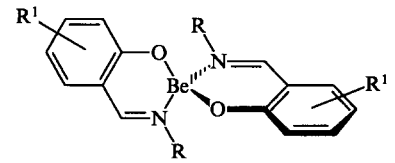
The presence of prochiral substituents R in dissymmetric chelate structures **2** makes it possible to detect the enantiomerisation process by NMR without resorting to the preliminary separation of the (*R*)- and (*S*)-enantiomers. The energy barriers to the enantiomerisation process, found from data for the temperature dependence of the diastereotopic averaging of the signals due to the methyl protons of the isopropyl group or the methylene protons of the benzyl group, amounted to ~21 kcal mol^{-1} for Zn(II) complexes and 12–15 kcal mol^{-1} for Cd(II) complexes.

It was soon shown that the tetrahedral bischelate Zn(II) and Cd(II) type **3** complexes[55] and Be(II) type **4** complexes[56,57] also exhibit stereochemical nonrigidity, whereas the kinetic and activation parameters of the enantiomerisation process $(R) \rightleftarrows (S)$ depend greatly on the nature of the donor atom X and the substituents R^1.



3

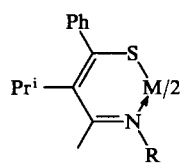
M = Zn, Cd; X = O, S, Se;
R = Pr^i, CH_2Ph
$\Delta G_{25}^{\neq}$ = 9.8–22.3 kcal mol^{-1}.



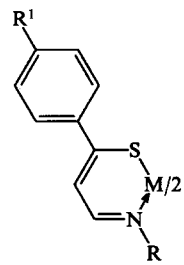
4

R = Pr^i, CH_2Ph
$\Delta G_{25}^{\neq}$ = 22–24.5 kcal mol^{-1}.

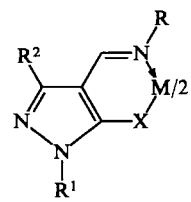
A fairly wide range of chelate complexes of nontransition (as well as transition) metals exhibiting stereochemical nonrigidity in solutions has now also been investigated. The principal structural types of such complexes are represented below by formulae **5**–**15**.



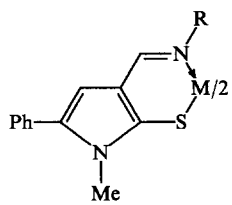
5



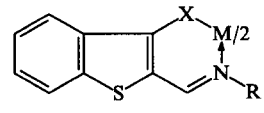
6



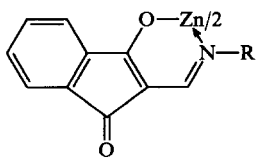
7



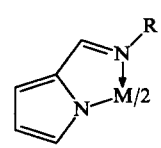
8



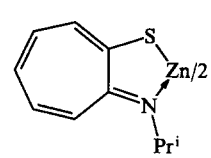
9



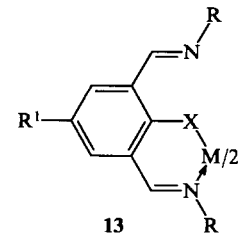
10



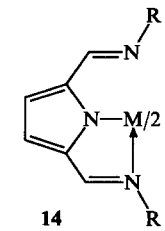
11



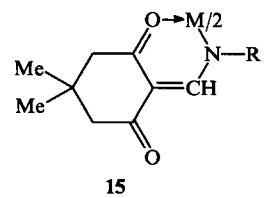
12



13



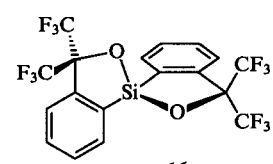
14



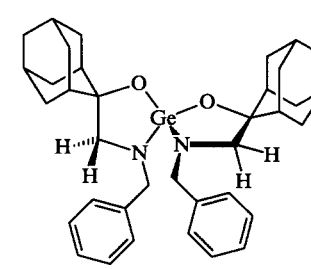
15

M = Be, Zn, Cd, Hg, Pb; M/2 = BAr(Y);
Y = Ar′, OAlk, $GaMe_2$, $InMe_2$;
X = O, S, Se; R = Pr^i, CH_2Ph, Ar, Alk;
R^1 = H, Cl, Br, OMe, Me, NO_2, Alk, Ar;
R^2 = Me, Pr^i.

The tetrahedral configuration inversion processes have been studied in much less detail for compounds of Group IVA elements. Early communications stating that the bicyclic orthosilicic acid esters can have a preferred planar structure[58] or a low barrier to the conversion of the tetrahedral (D_{2d}) form into the planar form[59] were not subsequently confirmed. However, for another tetracoordinate silicon derivative (compound **16**), the energy barrier to the intramolecular inversion with transition through a planar structure, estimated as 28 kcal mol^{-1} from the data quoted by Martin et al.,[60] is close to the upper limit of the energy scale for stereochemically nonrigid structures.



16



17

Apparently the first true stereochemically nonrigid structure with a tetrahedral centre (a tetracoordinate Group IVA element) was the germanium spirane **17**.[61] The inversion barrier determined from data derived from the temperature dependence of the ^1H NMR spectrum in the region of the signals of the diastereotopic methylene protons (toluene-d_8) amounted to 22.2 ± 2.5 kcal mol^{-1}.

III. The mechanisms of the stereochemical nonrigidity of tetracoordinate structures

An important question arising in the study of inversion processes is that of the choice of the energetically preferred reaction pathway. Three principal mechanisms, capable of leading to the inversion of the configuration of the central atom of the coordination polyhedron, were indicated above. They are presented in Fig. 2 for a specific case—the inversion of the configuration of the central atom in the tetrahedral bischelate complexes of Group IIA–IVA elements, to which all the compounds of types **2**–**17** belong.

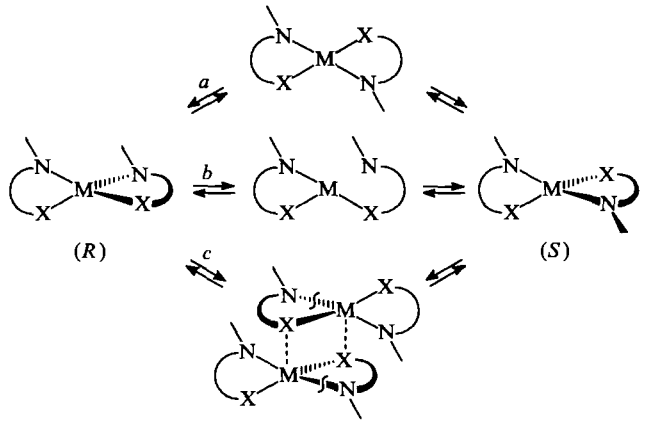


Figure 2. General scheme of the inversion mechanisms for tetrahedral bischelate complexes **2**–**17**: (*a*) polytopal rearrangement of the digonal twist type involving passage through a planar *trans*-structure; (*b*) intramolecular process determined by the dissociation-formation of one of the M–N bonds; (*c*) intermolecular degenerate ligand exchange process.

The intramolecular processes include, apart from the polytopal rearrangement occurring via the digonal twist mechanisms without the dissociation of the metal–ligand bonds (see, for example, Muetterties[11]) with formation in the transition state (or as intermediates) of *trans*- or *cis*-structures (the latter are not shown in Fig. 2) (pathway *a*), also a mechanism involving the dissociation of one of the metal–ligand bonds. The dissociation of this bond leads to the formation of an intermediate tricoordinate achiral structure, which then rapidly recyclises (pathway *b*). The third mechanism leading to the inversion of the configuration of the tetrahedral metal atom is associated with intermolecular ligand exchange proceeding via the formation of a dimeric structure via pathway *c* or *b*+*c*.

Studies have shown that all three types of mechanisms considered operate in thermal reactions involving the inversion of the configuration of the tetrahedral centre in metal chelate complexes. The choice of the preferred pathway in the inversion process is dictated mainly by the nature of the metal, but it depends significantly also on other structural features of the complex.[38] The general methodology, widely applied in various studies, is based on the following four effective approaches: (1) the introduction into the structures of the stereochemically nonrigid complexes **2**–**15** of prochiral groups R as substituents at the nitrogen atoms as well as into other parts of the molecules of the complexes; (2) the introduction of 'spin labels', usually magnetic ($S = ½$) isotopes of the metal atoms and the ligating atoms; (3) structural modelling of the dissociation-recombination mechanism in complexes of types **13**–**15** based on alterdentate ligands, i.e. ligands in which the number of structurally equivalent donor centres exceeds the coordination capacity of the metal;[62] (4) the determination of the kinetic orders (n) of the observed degenerate transformations by investigating the dependence of the lifetime (τ) of the exchanging states on the solute concentration and using the relation

$$\tau^{-1} = kc^{n-1} , \qquad (1)$$

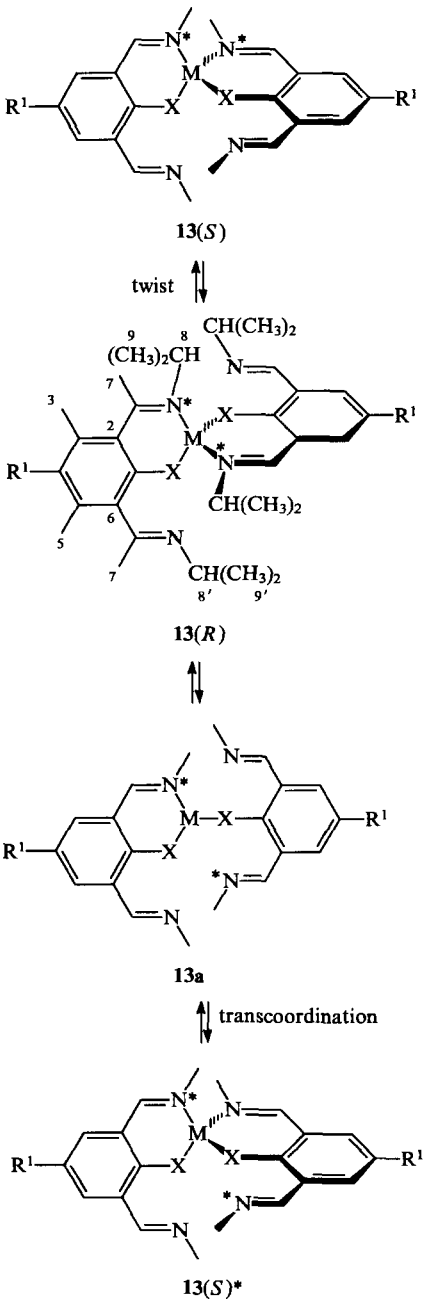
where k is the rate constant for the reaction of kinetic order n and c is the concentration of the solute.

We shall consider briefly what information about the mechanism of the inversion process can be extracted when each of the above approaches is employed.

1. The standard procedure for the introduction of prochiral groups such as Pr^i or CH_2Ph into an asymmetric or dissymmetric structure and analysis of the temperature-dependent diastereotopic averaging[24,63–65] makes it possible to detect the interconversion of enantiomers, by-passing the operation involving their preliminary separation, under conditions of unrestricted monitoring of the reversibility and reproducibility of the experiment. The dynamic process recorded in this way does not, however, permit the differentiation of the possible ways in which the molecule can undergo a structural reorganisation, leading to the inversion of the tetrahedral configuration of the central metal atom.

2. The introduction into the molecular structure of a 'spin' label — a metal isotope with a half-integral spin ($^{111,113}Cd$, ^{199}Hg, ^{207}Pb) linked by spin–spin coupling to the ligand nuclei — makes it possible to observe directly the metal–ligand bond dissociation-formation processes via pathways *b*, *c*, or *b* + *c* (Fig. 2). These processes can be detected both by investigating the temperature dependence of the line forms of the corresponding spectral multiplets (the disappearance of the metal–ligand nucleus spin–spin coupling constant on dissociation of the bond) and with the aid of two-dimensional NMR spectroscopic methods.

Scheme 2



If, however, the lifetime of the intermediate structure [the tricoordinate intermediate on pathway *b* (Fig. 2)] is shorter than the relaxation time of the metal and ligand nuclei linked by spin–spin coupling, the correlation of the spins of these nuclei is retained, while the spin–spin coupling is manifested in the spectrum despite the occurrence of an intense intramolecular dissociative process.[66] In this admittedly rare case, the observation of a temperature dependence of the spin–spin coupling constant is not diagnostic in the study of the inversion process mechanism.

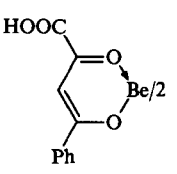
3. The dissociative type *b* inversion mechanism (Fig. 2) has been detected, for example, in the study of the structural nonrigidity of complexes **13** with bischelate rings based on alterdentate ligands, i.e. ligands providing the metal with two equivalent imine donor centres. In view of the steric hindrance, the alternative donor centres in complex **13** cannot participate simultaneously in intramolecular coordination. However, in the presence of dissociative processes (modelling pathway *b* in Fig. 2), the recombinations of the metal–nitrogen bond on recyclisation of the intermediate tricoordinate structure **13a** with participation of each of the unoccupied donor centres are equally probable. The intramolecular transcoordination (bond switching) process occurring under these conditions, illustrated in Scheme 2, has been reliably detected by the NMR method from the averaging of the signals due to the nuclei, separated by the effective plane of symmetry, under the conditions of rapid exchange.

4. The observation of a concentration dependence for the exchange processes detected by NMR spectroscopy is a clear indication of the intermolecular nature of the reaction and of the inclusion of degenerate ligand exchange processes in the overall stereochemical result of the reaction. The importance of taking this process into account (pathway *c* in Fig. 2) had been already indicated in the pioneer study of Eaton and Holm,[54] who noted that, in the case of Cd(II) chelates (complex **2**), the rate of associative processes involving the inversion of the tetrahedral configuration of the metal atom is very close to the rate of the intramolecular reaction. Careful allowance for the associative reactions proceeding via the ligand exchange mechanism (Scheme 1) is essential, particularly in the light of data[67] indicating the appreciable association of the chelate complexes in solutions in noncoordinating solvents.

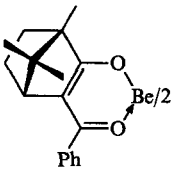
The combination of the above approaches to the study of the kinetics of processes involving the inversion of the tetrahedral configuration of metal chelate complexes, with specific structural modelling of the latter, has made it possible to penetrate to a considerable extent details of the mechanisms of structural nonrigidity in solution and also to establish the principal characteristics of the influence of the nature of the metal atom, the donor atoms, and substituents in the ligands on the kinetics of the inversion process $(R) \rightleftarrows (S)$ and the possible ways of achieving it. The data obtained are presented and discussed in the present review in conformity with the type of metal, starting with beryllium and boron complexes and ending with heavy metal (lead and mercury) complexes. The review also contains a section on the dynamic tetrahedral configuration inversion processes in bischelate Ni(II) complexes. Reactions whose rates permit their direct observation on the NMR time scale are discussed. Although nickel in its usual oxidation state Ni(II) is a typical transition metal, the nature of the stereodynamic processes in solutions of its complexes is extremely close to that of the processes determining the inversion of the configuration of the central nontransition metal atom in complexes **2**–**15**.

IV. Beryllium complexes

In the early experiments on the preparative separation of optical isomers of bischelate Be(II) complexes — bis(benzoylpyruvato)-beryllium **18** and bis(benzoylcamphorato)beryllium **19** — based on the crystallisation of the diastereoisomeric salts with brucine, an enrichment of the racemic mixture in one of the enantiomers was already achieved and mutarotation was observed in solution at the usual temperature.[68,69] The energy barriers to the racemisation reaction, calculated later[56] from the polarimetric data presented in the above studies,[68,69] are 21–25 kcal mol^{-1} depending on the solvent.



18



19

Energy barriers to the $(R) \rightleftarrows (S)$ enantiomerisation of beryllium bis(*N*-alkyl-5-R^1-salicylaldiminates) **4** close to the above values were found from the temperature dependence of the change of line shape of the signals due to the diastereotopic methyl and methylene groups of the Pr^i and CH_2Ph substituents at the nitrogen atom.[56,57,70]

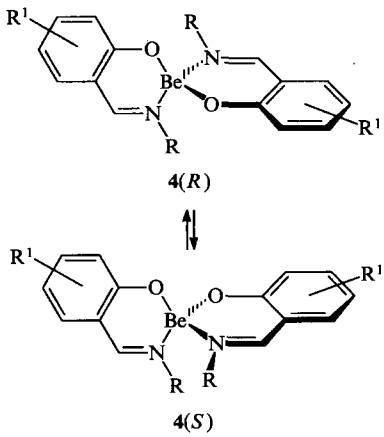
Table 2 presents the results of the kinetic studies on processes involving the inversion of the tetrahedral configuration of beryllium in complexes **4** (Scheme 3), obtained with the aid of the dynamic ^{1}H NMR method.

Table 2. Kinetic and activation parameters of the enantiomerisation of type **4** Be(II) bischelate complexes (solvent — nitrobenzene).[56,57,70]

R	R^1	$10^4 k_{25}$/s^{-1}	$\Delta H^{\neq}$/kcal mol^{-1}	$\Delta S^{\neq}$/cal mol^{-1} K^{-1}	$\Delta G^{\neq}_{25}$ [a]/kcal mol^{-1}
Pr^i	H	3.6	24.0	6.4	22.1 (22.2/143 °C)
CH_2Ph	H	5.8	22.0	−3.9	23.2
Pr^i	5-Br	3.6	24.9	6.4	22.1 (22.4/147 °C)
Pr^i	5-NO_2	7.9	30.0	18.8	24.4 (23.4/167 °C)
Pr^i	5,6-C_6H_4	1.4	26.8	13.8	22.7
Pr^i	3-NO_2	2.2	21.2	−3.2	22.4
Pr^i	5-OMe				(22.4/131 °C)
Pr^i	5-Me				(21.7/139 °C)
Pr^i	5-Cl				(22.1/144 °C)

[a] The free energies of activation estimated[56,70] at the temperature corresponding to the coalescence of the signals of the diastereotopic groups are presented in brackets.

Scheme 3



The energy barriers increase with increase in the electron-accepting capacity of the substituent R^1 and are satisfactorily correlated with Hammett's σ constants.[70]

$$\Delta G^{\neq}_{T_c} = 1.81\sigma + 21.96 \text{ (kcal mol}^{-1}\text{)} \quad (2)$$

The variation of the concentrations of solutions of complexes **4**, listed in Table 2, in the range $10^{-3}-10^{-1}$ M is not reflected in the rate of isomerisation. This indicates the absence of a contribution by degenerate ligand exchange intermolecular processes (pathway *c* in Fig. 2) to the observed kinetics of the inversion of the configuration of the tetrahedral beryllium atom: $4(R) \rightleftarrows 4(S)$.

In order to choose between the alternative intramolecular pathways *a* and *b* (Fig. 2), a study was made of the thermal enantiomerisation of the bischelate type **13** (X = O) beryllium complexes obtained from alterdentate ligands (Scheme 2).[71,72]

The ^{1}H NMR spectra of beryllium complexes **13** at room temperature include two sets of signals due to nonequivalent protons of the chelated and nonchelated aldimine fragments [(7,7′), (8,8′), and (9,9′)] and the benzene ring (3,5) (for the numbering of the atoms, see Scheme 2). The protons of the diastereotopic methyl groups 9 and 9′ are anisochronic and are represented by doublets of doublets in the spectra. If the stereoisomerisation occurred solely via the digonal twist mechanism *a*, the chemical exchange process would reduce to the temperature-dependent exchange-induced broadening and coalescence of the signals due to the diastereotopic groups of the prochiral substituents. In contrast to this, the dissociative mechanism *b*, which involves the formation and recyclisation of the tri-coordinate intermediate **13a** (M = Be), should lead not only to diastereotopic averaging but also to averaging of the signals due to the ^{1}H and ^{13}C nuclei in the 3,5-, 2,6-, 7,7′-, 8,8′-, and 9,9′-positions.

The observed temperature-dependent evolution of the line shapes of the indicator signals of all the type **13** beryllium complexes corresponds to the transcoordination of the metal atom with dissociation of the M–N bonds and enantiomerisation involving both possible types of reactions: $\mathbf{13}(R) \rightleftarrows \mathbf{13}(S)$ and $\mathbf{13}(R) \rightleftarrows \mathbf{13a} \rightleftarrows \mathbf{13}(S)'$.

It has been found[71,72] that, within the limits of the usual experimental errors, the energy barriers to the dynamic processes detected from exchange averaging of the (7,7′) and (3,5) pairs of indicator signals and the signals due to the diastereotopic 9,9′-groups, calculated using the full analysis of the line shape, are the same. Variation of the concentrations of the solutions hardly affects the kinetics of the observed reactions, which agrees with the first-order kinetics of the reaction (n = 1) in Eqn (1). The rate constants and activation parameters for the enantiomerisation of complexes **13** (M = Be) in solution in nitrobenzene-d_5 are presented in Table 3.

Table 3. Kinetic and activation parameters of the enantiomerisation of type **13** (X = O, R = Pr^i) Be(II) bischelate complexes (solvent—nitrobenzene-d_5).[71,72]

R	$10^5 k_{25}$/ s^{-1}	$\Delta H^{\neq}$/ kcal mol^{-1}	$\Delta S^{\neq}$/ cal mol^{-1} K^{-1}	$\Delta G^{\neq}_{25}$/ kcal mol^{-1}
H	7.2	23.7	2.3	23.1
Me	4.2	27.3	13.3	23.4
Br	46	23.8	5.5	22.2
OMe	52	23.8	6.3	21.9
NO_2	0.16	28.8	11.8	26.3

Comparison with the data on the kinetics of the enantiomerisation of complexes **4** (Table 2) shows that the free energies of activation for the dynamic processes involving both types of complexes with analogous substitution are very similar. This serves as a basis for the hypothesis that the enantiomerisation $4(R) \rightleftarrows 4(S)$ (Scheme 3) also takes place via a dissociative mechanism (pathway *b*, Fig. 2) and not via the alternative pathway *a* involving a polytopal rearrangement.

The results of theoretical modelling with the aid of the MNDO method of the mechanism of the inversion of the tetrahedral configuration of the Be atom in the bis(*N*-methylaminopropenoato)beryllium complex, differing from complex **4** by the absence of condensed benzene rings, fully agrees with this conclusion. The energy barrier calculated for the dissociation-recombination inversion mechanism is lower by 8–10 kcal mol^{-1} for the stereoisomerisation involving transition through planar *trans*- or *cis*-tetracoordinate structures.[73]

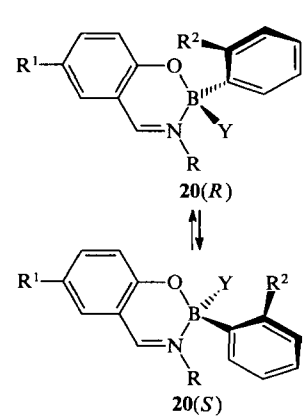
An attempt[74] to investigate by dynamic ^{1}H NMR the inversion process in Be(II) and Zn(II) β-diketonates containing a prochiral isopropyl group in the 2-position was unsuccessful. The diastereotopic methyl groups in these complexes remained isochronic up to −80 °C.

Since, as mentioned above, the bischelate Be(II) complexes with the analogous type of chelate unit BeO_4 can be separated into optical isomers by a preparative procedure (see also Ferroni and Cini[75]), Ronsisvalle et al.[74] attribute this fact to the extremely small diastereotopic splitting in the prochiral substituent which is more remote from the stereogenic centre in these complexes than in complexes **4**.

V. Complexes of boron, gallium, and indium

The thermal inversion of the configuration of the tetrahedral boron atom was first investigated quantitatively in 2,2-diaryl-5,6-benzo-1,3,2-oxazaborines **20**—chiral monochelates formed by the imine derivatives of aromatic *o*-hydroxyaldehydes and asymmetric diarylborinic acids incorporating an asymmetric boron atom (Scheme 4). The tetrahedral configuration of the bonds at the boron atom was characterised by X-ray diffraction of

Scheme 4



R = Pr^i, CH_2Ph; Y = Ar, OAlk.

Table 4. Kinetic and activation parameters of the enantiomerisation of type **20** boron chelates.[78,79]

R	R^1	R^2	Y	Indicator group	k_{25}/s^{-1}	$\Delta H^{\neq}$/ kcal mol^{-1}	$\Delta S^{\neq}$/ cal mol^{-1} K^{-1}	$\Delta G^{\neq}_{25}$/ kcal mol^{-1}
Pr^i	H	H	*o*-$MeOC_6H_4$	Pr^i	9.3×10^{-3}	20.6	1.1	20.2
Pr^i	Br	H	*o*-$MeOC_6H_4$	Pr^i	1.3×10^{-2}	21.6	5.5	20.0
Pr^i	H	H	1-$C_{10}H_7$	Pr^i	1.1×10^{-2}	22.5	6.3	20.1
Pr^i	Br	H	1-$C_{10}H_7$	Pr^i	7.9×10^{-3}	22.3	6.6	20.2
Pr^i	NO_2	H	1-$C_{10}H_7$	Pr^i	1.5×10^{-3}	23.8	8.6	21.3
Pr^i	H	MeO	1-$C_{10}H_7$	Pr^i	1.1×10^{-2}	22.4	7.6	20.1
Pr^i	Br	MeO	1-$C_{10}H_7$	Pr^i	3.0×10^{-2}	21.0	4.8	19.5
Pr^i	NO_2	MeO	1-$C_{10}H_7$	Pr^i	3.8×10^{-3}	23.9	10.5	20.8
CH_2Ph	H	MeO	1-$C_{10}H_7$	Pr^i	8.6×10^{-4}	23.6	6.8	21.6
Me	H	H	OPr^i	Pr^i	4.2×10^{-1}			17.9
CH_2Ph	H	H	OPr^i	Pr^i	6.7×10^{-2}			19.0
				CH_2Ph	6.9×10^{-1}			17.7
Pr^i	H	H	OMe	Pr^i	5.0×10^{-1}			17.8
Pr^i	NO_2	Me	OCH_2Ph	Pr^i	7.1×10^{-1}			17.5
				CH_2Ph	2.5			16.9
Pr^i	H	Me	OCH_2Ph	Pr^i	6.2×10^{-1}			17.8
				CH_2Ph	3.0			16.8
Me	5,6-C_6H_4	Me	OCH_2Ph	CH_2Ph	7.7×10^{-2}			19.0
Pr^i	5,6-C_6H_4	Me	OCH_2Ph	Pr^i	7.2×10^{-2}			19.0
				CH_2Ph	1.1			17.4
CH_2Ph	5,6-C_6H_4	Me	OMe	CH_2Ph	8.8×10^{-1}			17.6

Note. *o*-Dichlorobenzene was the solvent in the first nine cases and bromobenzene in the remaining cases.

certain compounds of this type.[76,77] The presence of prochiral isopropyl and benzyl groups in compound **20** (Y = Ar) makes it possible to investigate the dynamics of the enantiomerisation in accor-dance with Scheme 4 by means of dynamic ^1H and ^{13}C NMR without enriching the racemate in one of the enantiomers. The energy barriers to the inversion process (Table 4) are in the range 19.6–21.5 kcal mol^{-1} [78–80] which is lower by 1–2 kcal mol^{-1} than the barriers observed in the enantiomerisation (Scheme 3) of beryllium complexes **4** based on the analogous salicylaldimines.

The energy barriers listed in Table 4 depend only slightly on the nature of the substituents R, R^1, R^2, and Y. However, as in the series of type **4** beryllium compounds, in complexes **20** the maximum barrier is attained when the electron-accepting NO_2 group is present in the *para*-position relative to the oxygen of the salicylaldiminate fragment.

Change in solvent polarity and increase in solute concentration from 0.1 to 3 M do not exert an appreciable influence on the stereoisomerisation kinetics. The intermolecular degenerate ligand exchange processes were modelled by mixing in solution various pairs of boron chelates **20** containing different substituents. The reaction proceeds at an appreciable rate only at temperatures above 90–100 °C. Thus, in the above temperature range the contribution of the intermolecular degenerate ligand exchange process to the inversion mechanism is insignificant, which makes it possible to make a choice between the intramolecular variants *a* and *b* (Fig. 2).

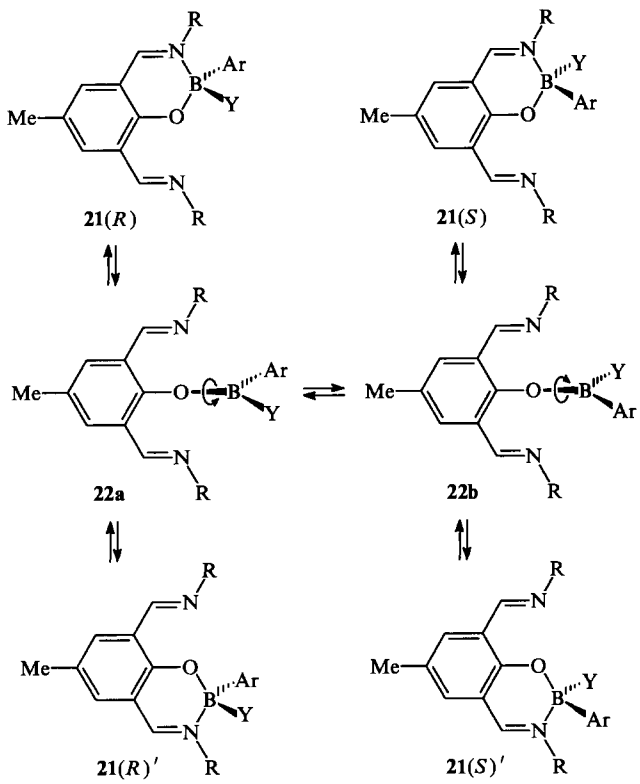
The hypothesis was put forward initially[80] that the digonal twist type polytopal rearrangement mechanism is more probable. This mechanism is favoured, in conformity with predictions,[59,81] by the presence at the boron atom of π-donor (O) and σ-acceptor (O, N) ligating centres, which stabilise the planar structure with a tetracoordinate boron atom. However, MNDO calculations carried out by Schleyer and Würthwein[82] for the model 1,3,2-oxazaborine led to the conclusion that structures with a tetracoordinate planar or pyramidal boron atom are in general unstable and cannot correspond to the transition states in the tetrahedral inversion reaction. The calculations[82] revealed another structure of the transition state, incorporating a tricoordinate boron atom with a single ruptured B–N bond. The calculated activation energy for the inversion of the configuration of the boron atom via this mechanism proved to be extremely close to the experimental values obtained for compound **20** (Table 4). Subsequent calculations[83] carried out with a higher degree of approximation (*ab initio*, 4-31G) yielded a different structure of the transition state in the tetrahedral inversion process, corresponding to the digonal twist type with a planar tetracoordinate boron atom, but its energy relative to the structure of the ground state (95 kcal mol^{-1}) was found to be much higher than the experimental inversion barriers.

Boulton and Prado[84] were the first to draw attention to the possibility of using the specific features of the spectroscopic behaviour of chiral chelate boron complexes of type **13**, based on alterdentate ligands, as a test which makes it possible to separate the intramolecular stereoisomerisation processes $(R) \rightleftarrows (S)$ via pathways *a* and *b* (Fig. 2). By analysing the temperature-dependence of the ^1H NMR spectra of a series of type **13** monochelates of diarylboron (M/2 = BArAr′, X = O, R = CH_2Ph, R^1 = Me), obtained from 2,6-bis(*N*-benzylideneamino)-4-methylphenol, the above investigators estimated the energy barriers to the B–N bond dissociation-formation reaction in these compounds at the temperatures corresponding to the coalescence of the signals due to the methylene protons of the benzyl groups in solutions in $CD_3OC_6H_4Cl$-*p* (~20 kcal mol^{-1}), which proved to be comparable with the energy barriers to the enantiomerisation of the boron chelates **20**. On this basis, it was concluded that the inversion of the tetrahedral configuration of the boron atom in compound **20** also proceeds via a dissociative mechanism involving the dissociation of the B–N bond.

However, a direct comparison of the dissociative reaction and the polytopal twist rearrangement (which should have been reflected by the diastereotopic averaging of the signals due to the methylene protons of the benzyl group) proved to be impossible for the type **13** compounds investigated in the above study.[84] As a result of the considerable temperature drift, the AB multiplet of the methylene protons of the benzyl group is transformed on raising the temperature into an average singlet virtually without intermediate broadening. For the same reasons, it proved impossible to characterise quantitatively the inversion processes for some of the compounds **20** with substituents R = CH_2Ph described by Korobov et al.[78]

A better justified identification of the mechanisms of the inversion of the configuration of the tetrahedral boron atom in chelate complexes was achieved in the study of compounds **13** (M/2 = BArAr′, R = Pr^i) and 2-alkoxy-5,6-benzo-1,3,2-azaborines of types **20** and **21**, containing a second prochiral substituent Y at the boron atom.[79]

Scheme 5



The tetrahedral inversion of the chelates **21** (Y = OPr^i, OCH_2Ph) is independent of concentration. It was characterised quantitatively on the basis of the diastereotopic averaging of the signals of the *N*- and/or *O*-isopropyl and the corresponding benzyl substituents. The energy barriers to the inversion reaction (Table 4) were found to be slightly lower (by 1–2 kcal mol^{-1}) than those found for the diarylboron chelates **20**.

The dynamic ^{1}H NMR spectra of compounds **21** (Nos. *1–3* in Table 5) reveal separately the occurrence of two dynamic processes. The inversion of the enantiomers (*R*) ⇄ (*S*), which reflects overall both possible reaction pathways, *a* and *b* (Fig. 2), is detected from the diastereotopic averaging of the signals due to the Pr^i and $PhCH_2$ groups in the substituent Y. The dissociative reaction involving the dissociation-formation of the B–N coordinate bonds is detected from the dynamic averaging of the chemical shifts of the signals due to the protons of the chelated and non-chelated aldimine fragments and also from the averaging of the ^{1}H and ^{13}C signals from the benzene ring linked to the aldehyde fragments.

The overall mechanism of the stereodynamic processes in compounds **21** (Nos. *4–7* in Table 5) is reflected by the reactions presented in Scheme 5. Two parallel reaction pathways, which rule out the inconversion of the intermediates (**22a** ⇄ **22b**), correspond to the interconversion–transcoordination processes in the temperature range below 110 °C detected in the dynamic ^{1}H NMR spectra of compounds of this type. The stereoisomerisation mechanism presented in Scheme 5 is clearly visualised by 2D exchange ^{1}H NMR spectra. The dissociation of the B–N bond and the formation of intermediates are detected from the appearance of four multiplet cross-peaks for compound **21**, (R = Y = OCH_2Ph, Ar = Ph), with which the frequencies of the downfield and upfield components of the doublets of doublets due to the methyls of the isopropyl groups at different nitrogen centres are correlated.

Rotation about the B–O bond in complexes **22a–b** requires an additional energy expenditure and takes place at a higher temperature. The energy barriers to the interconversion (*R*) ⇄ (*S*) and transcoordination in compounds **21** (Table 5) as well as the inversion processes in complexes **20** (Table 4) are extremely similar, which shows that the dissociative mechanism of the inversion of the tetrahedral configuration of the boron atom in the types of complexes indicated is preferred.

The dissociation of the B–N bond is the rate-limiting stage also in a number of other stereoisomerisation reactions of tetracoordinate boron compounds. It has been shown by dynamic ^{1}H and ^{13}C NMR methods that the inversion of the configuration of the tetracoordinate nitrogen atom in the chelate boron complex **23** involves the opening of the 1,3,2-oxazaborolidine ring and its subsequent closure at the hydroxyethyl group accompanied by proton transfers (Scheme 6).[85]

Scheme 6

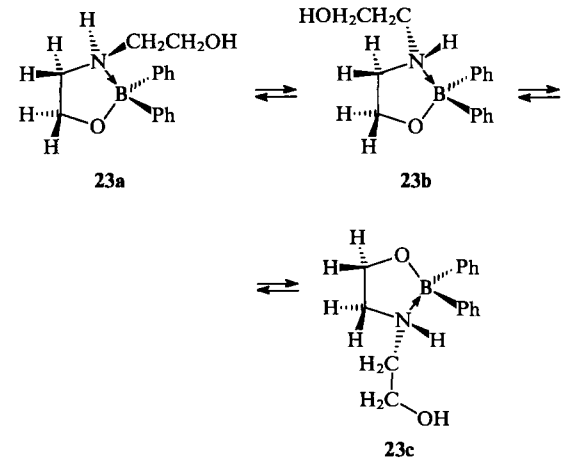


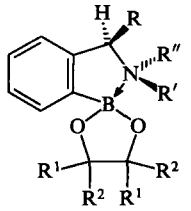
Table 5. Kinetic and activation parameters of the B–N bond dissociation and of the rotation of the boron-containing B(Ar)Y fragment about the B–O bond in type **21** compounds (solvent—nitrobenzene-d_5).[79]

No. of compound	R	Ar	Y	Indicator group	k_{25}/s^{-1} for:		$\Delta G^{\neq}_{25}$/kcal mol^{-1} for:	
					B–N bond dissociation	rotation about B–O bond	B–N bond dissociation	rotation about B–O bond
1	Me	*o*-$MeOC_6H_4$	OPr^i	Pr^i	1.4×10^{-1}		18.8	
2	Me	*o*-$MeOC_6H_4$	OCH_2Ph	CH_2Ph	2.7×10^{-1}		18.2	
3	cyclo-C_6H_{11}	*o*-$MeOC_6H_4$	OCH_2Ph	CH_2Ph	1.1		17.4	
4	Pr^i	*o*-$MeOC_6H_4$	OMe	Pr^i	7.9×10^{-2}	4.6×10^{-4}	18.9	22.0
5	Pr^i	*o*-$MeOC_6H_4$	OCH_2Ph	Pr^i	4.9×10^{-1}	5.4×10^{-3}	17.9	21.4
6	Pr^i	Ph	OCH_2Ph	Pr^i	1.5	4.5×10^{-6}	16.9	24.5
7	Pr^i	Ph	*o*-$MeOC_6H_4$	Pr^i	3.0×10^{-2}	–	19.6	>30

The energy barrier in the reaction (in solution in CD_2Cl_2) is 14.7 ± 0.3 kcal mol^{-1}, which is close to 12.9 kcal mol^{-1} found for the barrier in the dissociation of the B–N bond in the trimethylamine–trimethylboron complex.[86]

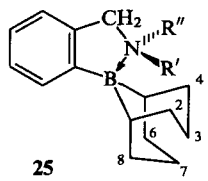
The asymmetric transformation, which makes it possible to obtain individual diastereoisomers of optically pure tetracoordinate boron complexes (oxazaborolidinones) by crystallisation from a suitable solvent, also includes a slow stage—the dissociation of the B–N bond, similar to that presented in Scheme 6.[87]

The intramolecular stereotransformations of [2-(dialkylaminomethyl)phenyl]boronates **24**,[88,89] 9-[2-(dialkylaminomethyl)phenyl]-9-borabicyclo[3.3.1]nonanes **25**,[90] and 9-[2-(ethylthiomethyl)phenyl]-9-borabicyclo[3.3.1]nonanes **(26)**[91] have been investigated in fair detail.



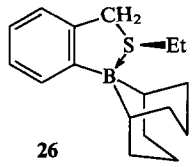
24

R = H, Me;
R′ = R″ = Me, Et;
$\Delta G_{25}^{\neq}$ = 11.5–11.6 kcal mol^{-1}.



25

R′ = R″ = Me, Et;
$\Delta G_{25}^{\neq}$ = 14.1–18.3 kcal mol^{-1}.



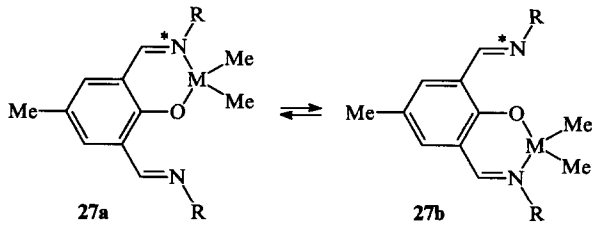
26

$\Delta G_{25}^{\neq}$ = 11.6 kcal mol^{-1}.

Depending on the type of substitution at the stereogenic centre—nitrogen, sulfur, and boron, the thermal dissociation of the B–N bonds in complexes **24** and **25** and of the B–S bond in compound **26** leads to the stereoisomerisation or topomerisation of the above centres. It has been found[89] that the energy barriers corresponding to the averaging of the signals due to the ^{13}C 3(7)-, 2(4)-, and 6(8)-atoms in compounds **25** are lower by 1.2 kcal mol^{-1} than those corresponding to the averaging of the signals due to the diastereotopic protons of the methylene group. This is because the first process reflects the dissociation of the B–N bond, whereas the averaging of the signals due to the methylene protons is attained after the inversion of the nitrogen atom following dissociation of this bond.

Particular attention has been devoted[89,90] to the quantitative determination of the contribution of the entropy of activation to the free energy of activation for the stereoisomerisation. The value of $\Delta S^{\neq}$ is regarded as an important diagnostic test of the mechanism and of the structure of the transition state of the reaction. The large positive values of $\Delta S^{\neq}$ found in the stereoisomerisation reactions of the intrachelate complexes **24–26** (15–20 e.u.) indicate[89–91] a significantly lower polarity of the transition state in the B–N bond dissociation reaction compared with the structure of the ground state. It follows from the kinetic data in Table 4 that positive activation entropies are likewise characteristic of the inversion of the configuration of the boron atom in the chelates **20**, which takes place via the dissociation of the B–N bond.

There are so far few quantitative data on the configurational lability of tetrahedral chelate Ga(III) and In(III) complexes. The enantiotopomerisation reactions of dimethylgallium and dimethylindium derivatives **27** have been investigated[92] on the basis of the temperature-dependent evolution of the line shape of the signals due to the nonequivalent protons of the phenyl and azomethine fragments in the dynamic ^1H NMR spectra.

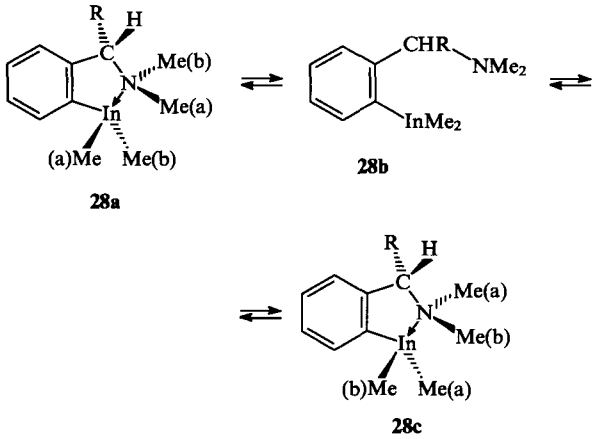


27a **27b**

R = Pr^i; M = Ga; k_{25} = 0.44 s^{-1}; $\Delta G_{25}^{\neq}$ = 17.9 kcal mol^{-1}.
M = In; k_{25} = 7.3 × 10^3 s^{-1}; $\Delta G_{25}^{\neq}$ = 12.2 kcal mol^{-1}.

Another known example of the enantiotopomerisation of a tetracoordinate indium atom is provided by the configurational dynamics of *o*-dimethylaminomethylphenyl(dimethyl)indium **28** (Scheme 7).[93]

Scheme 7



28a **28b** **28c**

R = H, Me.

The prochiral tetrahedral centres—nitrogen and indium atoms—in the chelated inner complex **28a** are responsible for the diastereotopic splitting of the methyl group signals (R = Me), which vanishes at room temperature owing to the dissociation of the In–N bond.

With increase in the atomic number of the central atom, the strength of the M–N bond diminishes and the energy barriers in the transcoordination reaction (Schemes 5 and 7), associated with the thermal dissociation of these bonds, diminish in the sequence B > Ga > In.

VI. Zinc complexes

The Zn(II) ion in complexes is known to be able to adapt its configuration and coordination capacity readily to the structural features of the ligands linked to it.[94–96] As a result of this ability, induced to a large extent by the absence of stabilising crystal field effects, the zinc atom is incorporated in the macromolecules of many enzymes functioning as active catalysts of biological processes.[97,98] It is not surprising that the stereochemical nonrigidity of the coordination compounds of tetracoordinate Zn(II) is determined (depending on the ligand environment) by all the types of mechanisms presented in Table 2 and also by certain others which will be considered in this section.

The most complete data concerning the influence of various structural factors on the kinetics and mechanisms of the processes determining the stereochemical nonrigidity of the tetrahedral configuration of the tetracoordinate nontransition metal atom have been obtained for the bischelate Zn(II) complexes of types **2**, **3**, and **5**–**15**.[54,55,70,99–110] The influence of the following structural factors has been studied: (1) the nature of the chelating centre X = O, S, or Se; (2) the nature of the substituents R and R^1 in complexes **6** and **7** and also of the condensed arene and heteroarene rings in complexes **3** and **5**–**15**; (3) the steric and electronic characteristics of the substituents R attached to the coordinated nitrogen atoms in complexes **5** and **7**.

Some of the results of such investigations are compiled in Table 6. The observed energy barriers are in the range from 10 to 24 kcal mol^{-1}, while the rate constants are from 10^3 to 10^{-5} s^{-1} (at the usual temperature). Analysis of the data in Table 6 makes it possible to differentiate the following principal trends in the changes in the energy barriers to enantiomerisation as a function of the characteristics of the ligand structure:

1. When the nature of the donor centre X in isotypical series of compounds **3** and **7**–**9** is varied, the activation energies increase in the sequence O < Se < S.

2. The condensation of the benzene, benzothiophene, and benzocyclopentene rings with the chelate ring in type **2** complexes and their oxygen analogues (X = O) (complexes **3**, **9**, and **10**) diminishes $\Delta G_{25}^{\neq}$ [for complex **6** (R = Pr^i, R^1 = H), it amounts to 20.6 kcal mol^{-1} [54]], whereas the condensation of five-membered nitrogen-containing heterocycles — the pyrrole (compound **8**) and pyrazole (compound **7**) rings — increases the energy barrier to the inversion of the tetrahedral Zn(II) atom.

3. The differences between the electronic and steric characteristics of the substituents at the coordinated nitrogen atom in the series of compounds **5** have little effect on the inversion barriers.

4. In contrast to the beryllium complexes **4**, the introduction of electron-accepting substituents into the benzene rings of the analogous zinc complexes **3** (X = O) reduces the inversion barrier. The negative sign of the reaction constant in the correlation equation obtained by Bottino and Finocchiaro[70] is consistent with this [cf. Eqn. (2)].

$$\Delta G_{T_c}^{\neq} = -2.48\sigma + 15.44 \text{ (kcal mol}^{-1}\text{)}$$

This difference reflects in all probability the inversion mechanism of enantiomerisation in Zn(II) complexes for which the reaction pathway associated with the type *a* polytopal rearrangement (Fig. 2), proceeding without the preliminary dissociation of the Zn–N coordinate bond, becomes energetically preferred. This hypothesis is supported also by the negative entropies of activation for the inversion of the tetrahedral configuration of Zn(II) with the N_2O_2 ligand environment (Table 6).

Clear-cut evidence indicating that the digonal twist mechanism (a) (Fig. 2), not involving the dissociation-formation of coordinate bonds, is energetically preferred has been obtained in a study of the dynamic ^1H NMR spectra of bischelate zinc complexes **13** (X = O) with alterdentate ligands.[107]

Table 6. Kinetic parameters of the inversion of the configuration of the tetrahedral Zn(II) in bischelate complexes with a ZnN_2X_2 coordination unit.

Type of complex	R^1, R^2	X	R	Solvent	k_{25}/s^{-1}	$\Delta H^{\neq}$/ kcal mol^{-1}	$\Delta S^{\neq}$/ cal mol^{-1} K^{-1}	$\Delta G_{25}^{\neq}$/ kcal mol^{-1}	Ref.
3	5-OMe	O	Pr^i	$CDCl_3$	–	–	–	16.0/33 °C[a]	70
	H	O	Pr^i	CD_2Cl_2 ($CDCl_3$)	51	9.3	−19.6	15.1 (15.5/19 °C)[a]	55, 70
	5-Br	O	Pr^i	$CDCl_3$	–	–	–	14.9/12 °C[a]	70
	5-NO_2	O	Pr^i	$CDCl_3$	–	–	–	13.3/−21 °C[a]	70
	3,4-C_6H_4	O	Pr^i	Bromobenzene-d_5	2.8	15.3	−5.2	16.8	108
	4,5-C_6H_4	O	Pr^i	"	14.9	13.0	−9.7	16.0	108
	5,6-C_6H_4	O	Pr^i	"	3.1×10^3	9.0	−12.5	12.7	108
	5-OMe		Pr^i	"	7.3	15.1	−3.8	15.3	72
	H		Pr^i	"	2.3	17.7	2.7	16.9	72
	5-Br		Pr^i	"	2.1	18.0	3.3	17.0	72
	5-NO_2		Pr^i	"	0.5	17.7	−0.5	17.8	72
	3,4-C_6H_4		Pr^i	"	1.3	23.8	21.8	17.4	108
	4,5-C_6H_4		Pr^i	"	3.8	22.0	18.0	16.6	108
	5,6-C_6H_4		Pr^i	"	43.9	13.1	−7.1	15.2	108
5	–	–	CH_2Ph	Chlorobenzene	0.6	20.1	8.1	17.7	99
	–	–	Pr^i	"	1.5	17.1	−0.2	17.2	99
	–	–	Bu^t	"	4.1	14.7	−6.3	16.6	99
	–	–	Ph	"	4.7	13.3	−10.9	16.5	99
	–	–	2,4,6-$C_6H_2Me_3$	"	0.1	25.6	22.5	18.8	99
7	Ph/Pr^i	O	Pr^i	*o*-Dichlorobenzene	2.3×10^{-2}	20.0	1.2	19.7	100
	Ph/Pr^i		CH_2Ph	"	5.1×10^{-5}	26.2	9.7	23.3	100
	Ph/Pr^i		CH_2Ph	"	4.0×10^{-3}	19.7	−3.3	20.7	100
	Ph/Me		Pr^i	"	1.3×10^{-3}	23.3	6.4	21.4	100
9	–	O	Pr^i	"	8.2	11.4	−15.8	15.9	109
10	–	O	CH_2Ph	CH_2Cl_2	5.1×10^3	8.2	−14.2	12.4	109
12	–	–	Pr^i	Nitrobenzene	2.7×10^{-1}	15.7	−8.4	18.2	109

[a] The quantity $\Delta G^{\neq}$ was determined from the coalescence of the signals due to the diastereotopic methyl groups at the temperature indicated.

Table 7. Kinetic and activation parameters of the enantiomerisation reactions of the zinc complexes **13** (R = Pr^i, X = O, S) (solvent—bromobenzene-d_5).[71,107]

X	R^1	Digonal twist				Transcoordination			
		k_{25}/ s^{-1}	$\Delta H^{\neq}$/ kcal mol^{-1}	$\Delta S^{\neq}$/ cal mol^{-1} K^{-1}	$\Delta G^{\neq}_{25}$ [a]/ kcal mol^{-1}	k_{25}/ s^{-1}	$\Delta H^{\neq}$/ kcal mol^{-1}	$\Delta S^{\neq}$/ cal mol^{-1} K^{-1}	$\Delta G^{\neq}_{25}$/ kcal mol^{-1}
O	OMe	110	13.3 ± 1.1	−4.6 ± 4.1	14.6	0.15	18.0 ± 0.2	−1.9 ± 0.6	18.4
O	Me	100	9.1 ± 0.5	−18.1 ± 1.2	14.7	0.18	14.9 ± 0.4	−11.9 ± 1.7	18.4
O	H	83	9.0 ± 0.6	−22.8 ± 3.8	14.8	0.18	14.8 ± 1.9	−12.2 ± 6.2	18.4
O	Br	130	13.4 ± 0.5	−9.9 ± 1.6	14.6	0.14	16.7 ± 1.1	−6.3 ± 3.0	18.5
O	NO_2	470	4.2 ± 0.5	−32.3 ± 1.9	13.8	0.48	16.6 ± 0.9	−4.4 ± 2.6	17.8
S	OMe	–	–	–	–	14.4	15.3 ± 0.8	−2.0 ± 0.3	15.8
S	Me	–	–	–	–	9.0	13.6 ± 0.7	−8.6 ± 0.8	16.1
S	Br	–	–	–	–	9.1	12.0 ± 0.5	−14.0 ± 1.7	16.1
S	NO_2	–	–	–	–	3.5	13.0 ± 0.4	12.4 ± 1.6	16.7

[a] For sulfur-containing compounds, $\Delta G^{\neq}_{twist} > \Delta G^{\neq}_{transcoord}$

In contrast to beryllium complexes, both types of dynamic transformations have been detected in the dynamic ^{1}H and ^{13}C NMR spectra of zinc complexes **13** (X = O) (Scheme 2): the digonal twist and the transcoordination process occurring at a higher solution temperature and detected from the complete averaging of the spectrum relative to the X–C(R^1) axes. The kinetic sequence of the above transformations is retained for all the complexes **13** (M = Zn, X = O) investigated regardless of the nature of the substituents R^1. The rate of the polytopal rearrangement is three orders of magnitude higher than the rate of the simultaneous dissociation-recombination reaction.

Variation of the solvent polarity and of the concentrations of the solutions hardly affects the kinetics of the observed dynamic reactions, which indicates their intramolecular nature. The kinetic parameters of the processes investigated are presented in Table 7.

The energy barriers to inversion via the digonal twist mechanism for zinc complexes **13**, presented in Table 7, are close to the values characterising the enantiomerisation of zinc bis-salicylaldiminates **3** (M = Zn) with identical substituents R^1 (Table 6), which confirms that this stereoisomerisation pathway is likewise preferred for complexes **3** (X = O).

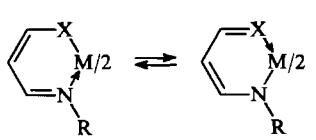
The modification of the structure of the alterdentate ligand in zinc complexes **13** by replacing the donor oxygen atom by a sulfur atom alters radically the energy sequence of the enantiomerisation mechanisms. The dissociative mechanism of the inversion of configuration of the tetrahedral centre becomes preferred, as for the beryllium and boron chelates **13** considered previously. The barriers in the dissociation-recombination mechanism found in zinc complexes **13** (X = S) are significantly lower than those detected for the similar process in the analogous complexes with (X = O) (Table 7).

The difference between the mechanisms of the enantiomerisation of the Zn(II) complexes with the N_2O_2 and N_2S_2 chelate environments is reflected in the difference between the activation entropies for the enantiomerisation of complexes **3** of this type and also in the nature of the effect of the substituents R^1 on the free energies of activation. For the majority of complexes **3** (M = Zn, X = S), the activation entropies are positive or have low negative values (Table 6), which is characteristic of reactions proceeding with dissociation of metal–ligand bonds[91] (in this case, the reactions of complexes **13** in accordance with Scheme 2 are not quite so characteristic in view of the superposition of a number of secondary processes involving rotation about the M–N and M–X bonds). The correlation equation,[72] linking the inversion barriers in zinc complexes **3** (X = S) to the parameters of the 5-R^1 substituents, has a form similar to that of Eqn. (2) for the analogous Be(II) complexes.

$$\Delta G^{\neq}_{25} = 1.41\sigma + 16.74 \text{ (kcal mol}^{-1}\text{)}; \quad r = 0.984.$$

Such changes in the mechanisms of the inversion processes can be attributed to the lengthening of the Zn–N bonds (2.036–2.112 Å for three compounds of this type) and hence to their weakening in the six-membered chelate ring ZnN_2S_2 com-pared with the ZnN_2O_2 analogues (1.981–2.017 Å for the eight examples described in the literature).[38,110–114]

In type **3** complexes and their analogues, there is, in principle, a possibility of the dissociation-recombination mechanism involving the rupture of the M–X (X = O, S) and not M–N bonds, since the structure of the chelate ring is evidently reflected by the resonance of canonical structures of type **29**,[115] the relative contribution of which may vary greatly depending on the type of metal and of the substitution in the ligand.



29a **29b**

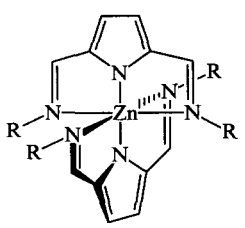
However, hitherto all attempts to observe the enantiomerisation of bischelate complexes with the MN_2X_2 coordination unit, where M is a main subgroup metal, proceeding via the M–X bond dissociation mechanism have been unsuccessful. The resultsof the study of the stereodynamics of chelate complexes **15** (M = Zn, R = Pr^i) with alterdentate ligands, the structure of which was selected in such a way that the transcoordination process involving the dissociation of the Zn–O bond can be modelled, are instructive. The tetrahedral configuration of Zn(II) is inverted via the intramolecular digonal twist mechanism ($\Delta G^{\neq}_{T_c} = 11.8$ kcal mol^{-1} in CD_2Cl_2, $T_c = -55$ °C). Transcoordination with dissociation of the Zn–O bond is not observed in solution in nitrobenzene-d_5 on heating to 150 °C ($\Delta G^{\neq}_{150} > 22$ kcal mol^{-1}), above which the decomposition of the complex begins.

The wide variety, characteristic of the Zn(II) central ion, of coordination types—ranging from planar tricoordinate in anionic complexes, for example in $Zn(SR)_3^-$,[116,117] to hexacoordinate, which occurs preferentially in cationic complexes[118]—in reactions of tetracoordinate zinc should be manifested respectively by tendencies to undergo dissociative or associative reactions. Examples of the stereoisomerisation of complexes of the first type were examined above.

At high concentrations of the solutions, the degenerate ligand exchange mechanism (pathway c in Fig. 2), involving the formation of dimeric association complexes with pentacoordinate zinc atoms [characteristic of many tetrahedral Zn(II) complexes in the

crystalline state[96]], actually begins to compete with mechanisms *a* and *b*. For the pyrrole complexes **11**, the degenerate ligand exchange mechanism is energetically preferred for the inversion of the configuration of tetrahedral Zn(II) even at very low concentrations (when the dynamic NMR method is used).

The associative mechanism of the enantiomerisation of tetrahedral Zn(II) complexes can be made also to operate intramolecularly by means of an appropriate design of the alterdentate ligands. Whereas the steric structure of the ligand in type **13** complexes rules out the possibility of an increase in the coordination number of the central metal atom as a result of the intramolecular interaction with the excess donor centres in the ligand with 6,6′-aldimine groups, in type **14** complexes, based on 2,5-diformylpyrrole bisimines, the formation of both pentacoordinate **30** and hexacoordinate **31** structures of the complexes is sterically unhindered.



31

The dynamic ^1H and ^{13}C NMR spectra of complexes **14** (R = Pr^i, cyclo-C_6H_{11}) are fully averaged in solution in CD_2Cl_2 even at −80 °C (f_0 = 300 MHz), which corresponds to an effective D_{2d} symmetry. Of the two possibilities — the stable octahedral structure **31** or the very rapid dynamic inversion of the configuration of the tetrahedral Zn(II) centre (Fig. 3) — the latter is actually realised.[106] This conclusion is supported by the following evidence: (a) nonzero dipole moments of complexes **14** (3.17 D for R = cyclo-C_6H_{11} in benzene), (b) X-ray diffraction data for this complex [pentacoordinate trigonal-bipyramidal structure with the central Zn(II) atom delocalised over two unequally populated positions], and (c) the deaveraging of the ^{15}N NMR spectrum of the $^{15}N{=}CH$ isotopomer occurring in solution in CD_2Cl_2–Et_2O at −110 °C. The energy barrier to the tetrahedral inversion estimated from the ^{15}N NMR spectroscopic data is 8.6 kcal mol^{-1} at −70 °C.

VII. Cadmium complexes

In solutions of cadmium(II) complexes **3**,[53] **5**,[119,120] **2**,[121] **7**,[100] **8** and **9**,[122] and **13**,[123] it is possible to follow separately and characterise quantitatively the kinetics of both intramolecular and intermolecular stereoisomerisation processes. The study of the dynamic behaviour of the ^{111}Cd ($S = \frac{1}{2}$) isotopomers of the above complexes has been widely used in the above investigations. The manifestation of the spin–spin coupling of the ^{111}Cd nuclei with ^{13}C nuclei and protons enriches significantly the spectroscopic information. Thus the dynamics of metal–ligand bond dissociation processes can be followed directly from the temperature dependence of the constants $^nJ_{^{111}Cd-H}$ and $^nJ_{^{111}Cd-^{13}C}$ as well as $^nJ_{^{111}Cd-X}$ (X = other nuclei). The dynamic pattern in the ^1H NMR spectrum of complex **5** (R = Pr^i), for example, is extremely characteristic.[119] Below −30 °C (CD_2Cl_2), all the exchange processes are 'frozen' — the methyl groups in both prochiral isopropyl substituents are anisochronic and we have the constant $^3J_{^{111}Cd-N=CH}$ = 30 Hz.[119] An increase in the solution temperature leads initially merely to a concentration-independent diastereotopic averaging of the signals due to the methyls of the isopropyl groups, which reflects the intramolecular inversion of the configuration of the tetrahedral Cd(II) (at T_c = −1 °C, the inversion rate constant is k = 115 s^{-1}).

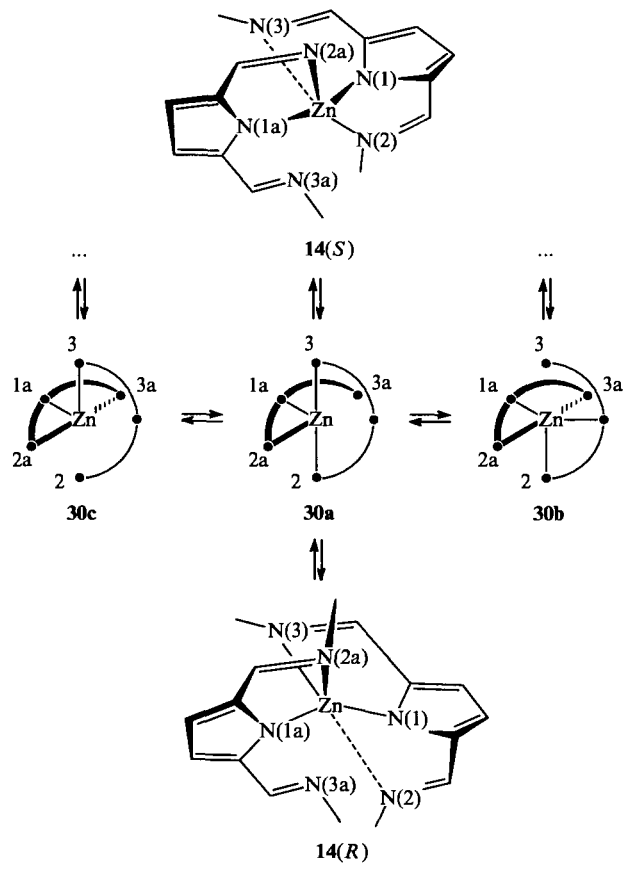
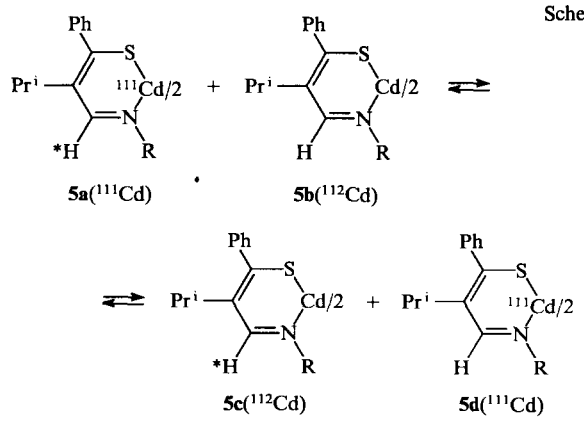


Figure 3. The associative (S_N2 type) mechanism of the intramolecular inversion of the tetrahedral configuration of Zn(II) in complexes **14** according to NMR and X-ray diffraction data.[106]

Above T_c, exchange processes, leading ultimately to the disappearance of the constant for the spin–spin coupling of the proton in the azomethine fragment of the ligand with the ^{111}Cd nuclei, begin to be manifested in the spectra. In contrast to the higher-temperature dynamic transformation observed for the first process, a linear relation has been established between τ and c^{-1}, showing that the process is kinetically second order and indicating the occurrence of a bimolecular degenerate ligand exchange reaction [n = 2 in Eqn. (1)] in the type **2** complex (pathway *c* in Fig. 2).

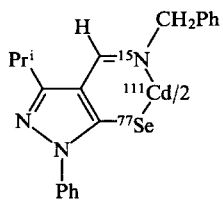
The intermolecular character of the degenerate ligand exchange processes is illustrated particularly clearly by the temperature-dependent two-dimensional ^1H NMR spectra of a mixture of the ^{111}Cd ($S = \frac{1}{2}$) and ^{112}Cd (S = 0) isotopomers of the type **5** complex (R = cyclo-C_6H_{11}) in the resonance region

Scheme 8

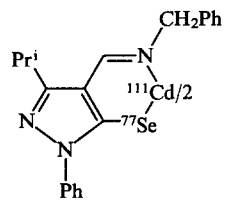


of the CH=N protons.[124,125] At temperatures below 10 °C, only diagonal (auto) peaks are present in the ^{1}H NMR spectra (f_0 = 100 MHz). The two extreme peaks among them correspond to the azomethine protons of the ^{111}Cd ($^3J_{^{111}Cd-N=CH}$ = 30 Hz) isotopomer, while the central peak corresponds to the ^{112}Cd isotopomer. An increase in the solution temperature to 33 °C leads to the appearance of six cross-peaks, two of which induce, at the resonance frequencies of the extreme auto-peaks, chemical exchange in the ^{111}Cd isotopomer, while the remaining four induce the intermolecular ligand exchange of the ^{111}Cd and ^{112}Cd isotopomers. This form of the spectra corresponds directly to the form of the exchange matrix for the reaction (Scheme 8). At a temperature above 53 °C, the coalescence of all the diagonal peaks and cross-peaks is observed in the ^{1}H NMR spectrum as a consequence of the intense ligand exchange.

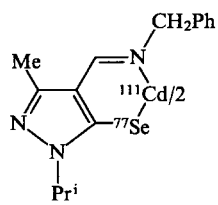
It has been suggested that observation of the temperature dependence of the spin–spin coupling constants for the ^{111}Cd atom in the isotopomeric type **7** complexes, incorporating the ^{15}N and ^{77}Se magnetic nuclei in the coordination unit, would make it possible to answer the question which of the bonds (Cd–Se or Cd–N) in these and structurally similar complexes is the most labile in the ligand exchange reaction (Scheme 1).



7a



7b



7c

However, analysis of the dynamic ^{111}Cd, ^{77}Se, and ^{1}H NMR spectra of the series of complexes **7a–c** showed that the rate constants and activation barriers for the dissociation of these bonds, indicated by the dynamics of the disappearance of the spin–spin coupling constants $^3J_{^{111}Cd-N=CH}$ in the ^{1}H NMR spectra and $J_{^{111}Cd-^{77}Se}$ in the ^{77}Se{H} NMR spectra, are identical within the limits of the usual experimental errors.[126] The synchronous nature of the Cd–N and Cd–X (X = S, Se) bond dissociation-formation steps in the ligand-exchange reactions is also demonstrated by data indicating the thermoinduced disappearance of the spin-spin coupling constants for the ^{111}Cd nucleus of the ligand: $^4J_{^{111}Cd-N=C-CH}$ = 3.5 Hz and $^3J_{^{111}Cd-N=CH}$ = 22 Hz in the spectra of complex **6** (R = Pr^i, R^1 = Br), $^nJ_{^{111}Cd-^{13}C}$ for the α,β-carbon atoms and the carbon atoms of the benzene ring in the ^{13}C{H} spectra of the bischelates **5** (R = Pr^i) and **6** (R = Pr^i, R^1 = H), as well as $J_{^{111}Cd-^{77}Se}$ and $J_{^{111}Cd-^{15}N}$) in the dynamic ^{111}Cd NMR spectra of the triply labelled compound **7a**.

Selected kinetic parameters of the observed dynamic reactions of the bischelate cadmium [^{111}Cd(II)] complexes are presented in Tables 8 and 9. Analysis of these and other data obtained in the study of type **6** complexes shows that, at solution concentrations in the range 10^{-1}–10^{-2} M, the intramolecular enantiomerisation reaction proceeds in all cases at a rate 1–2 orders of magnitude higher and the energy barriers are then lower by 2.5–4 kcal mol^{-1} than the values characteristic of the degenerate ligand exchange process.[100,119,120]

Comparison of the data in Tables 6 and 8 shows that the energy barriers to the intramolecular enantiomerisation of the bischelate cadmium(II) complexes are lower by 4–7 kcal mol^{-1} than that observed for a series of isoligand zinc(II) complexes. The calculated entropies of activation have higher negative values both for the intramolecular inversion process and for the bimolecular association reaction. The influence of structural factors on the barriers in the intramolecular inversion of the tetrahedral configurations of Cd(II) and Zn(II) in isoligand complexes is largely of the same type. The significantly more marked dependence of the configuration inversion barrier in the intermolecular reaction (the energy barriers increase approximately in parallel with increase in the bulk of the

Table 8. Kinetic parameters of the intramolecular inversion of the configuration of the tetrahedral Cd(II) in bischelate complexes with a CdN_2X_2 coordination unit (solvents—$CDCl_3$, *o*-$Cl_2C_6H_4$).

Type of complex	R^1, R^2	X	R	k_{25}/s^{-1}	$\Delta H^{\neq}$/kcal mol^{-1}	$\Delta S^{\neq}$/cal mol^{-1} K^{-1}	$\Delta G^{\neq}_{25}$/kcal mol^{-1}	Ref.
3	H	O	Pr^i	8.1×10^3	5.5	−22.1	12.1	55
	H	S	Pr^i	1.2×10^4	5.4	−21.7	11.9	55
5		S	CH_2Ph	2.1×10^4	8.2	−10.7	11.5	120
		S	Pr^i	5.5×10^2	9.9	−12.7	13.7	120
		S	Bu^t	9.7×10^2	12.8	−1.8	13.4	120
		S	Ph	8.2×10^3	6.5	−18.9	12.1	120
		S	C_6H_4OMe-*p*	1.3×10^4	6.5	−17.6	11.8	120
		S	C_6H_4Cl-*p*	1.0×10^4	6.6	−17.9	11.9	120
7	Ph, Pr^i	S	CH_2Ph	4.7×10^2	5.8	−26.8	13.8	100
	Pr^i	S	cyclo-C_6H_{11}	1.6×10^1	13.6	−26.6	15.9	100
	Ph, Pr^i	Se	cyclo-C_6H_{11}	4.7×10^2	5.8	−26.8	13.8	–
	Pr^i	S	CH_2Ph	7.5×10^2	9.5	−13.5	13.6	100
	Pr^i, Me	Se	CH_2Ph	2.1×10^2	6.0	−22.9	12.9	100
	CH_2Ph, Pr^i	S	Pr^i	1.6×10^1	14.4	−4.8	15.8	100
		Se	Pr^i	3.8×10^2	10.0	−13.3	13.9	100
9		S	Pr^i	3.0×10^3	5.9	−23.0	12.7	122

Table 9. Kinetic parameters of the degenerate ligand exchange reaction (Scheme 8) in solutions (in $CDCl_3$ or CD_2Cl_2) of Cd(II) bischelate complexes obtained from the temperature variation of the $^3J_{^{111}Cd-N=CH}$ for the isotopomeric complexes **5** and **7** (95% enrichment in ^{111}Cd).

R	X	k_{25} [a]/s^{-1}	$\Delta H^{\neq}$/kcal mol^{-1}	$\Delta S^{\neq}$/cal mol^{-1} K^{-1}	$\Delta G^{\neq}_{25}$/kcal mol^{-1}	Ref.
Complex **5**						
CH_2Ph		4.1×10^2	10.6	−11.2	14.0	120
Pr^i		5.7	19.6	−10.7	16.4	120
Bu^t		6.7	12.3	−13.5	16.3	120
Ph		1.6×10^3	8.5	−15.3	13.1	120
C_6H_4OMe-*p*		5.5×10^2	9.8	−13.1	13.7	120
C_6H_4Cl-*p*		4.1×10^3	8.5	−15.3	13.1	120
Complex **7** ($R^1 = Pr^i$, $R^2 = Me$)						
Et	S	1.0×10^2	8.9	−9.6	14.7	126
CH_2Ph	S	4.2	15.5	−3.8	16.6	–
cyclo-C_6H_{11}	S	6.7×10^{-3}	19.3	−3.6	20.4	126
Bu^t	S	2.7×10^{-2}	17.2	−7.9	19.6	126
Me	Se	7.6×10^3	9.9	−7.5	13.6	126
Ph	S	1.7×10^2	6.1	−27.8	14.3	126
C_6H_4Me-*p*	S	8.2	10.8	−18.0	16.0	126
CH_2Ph	Se	2.7	7.4	−3.2	16.8	126

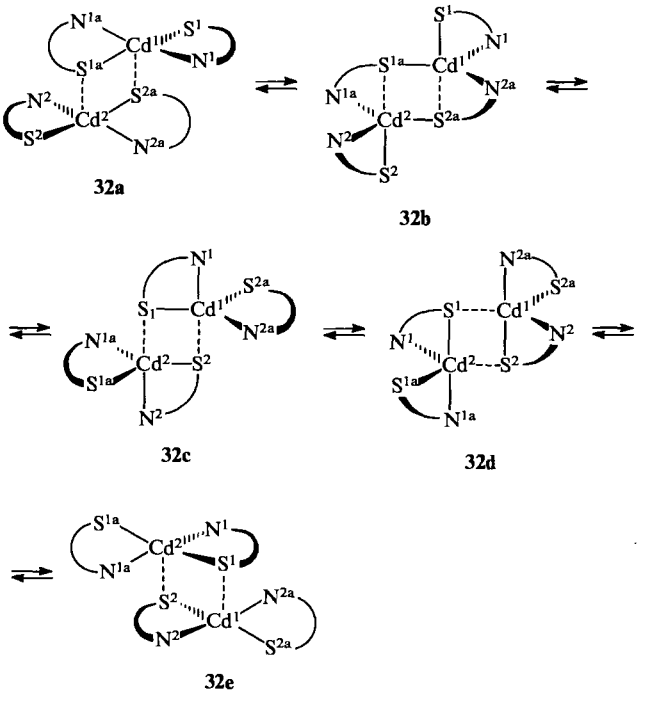
[a] All the reactions investigated are kinetically second order. For comparison with the kinetic parameters of the intramolecular inversion of configuration of Cd(II) (Table 8), the rate constants were assumed to be pseudofirst order, i.e. $k = k_2 c$ for $c = 3 \times 10^{-2}$ M.
[The second entry of the table appears to be in error (Ed. of Translation)]

substituent: Et < Ar < CH_2Ph < Bu^t < cyclo-C_6H_{11}) compared with the intramolecular process constitutes an exception. The ligand exchange reaction mechanism (Scheme 8), which makes it possible to account for the synchronisation of the Cd–N and Cd–S bond dissociation-formation processes, is presented in Scheme 9, which presupposes the formation in solution of fairly stable dimeric intermediates with four-membered Cd_2S_2 rings.[119,121,124]

The formation of dimeric structures with planar M_2X_2 (X = O, S, Se, Te) metallocycles is extremely characteristic of zinc[117,127] and cadmium[128,129] phenoxides, thiophenoxides, selenoxides, and telluroxides. The configuration of the bonds at the metal atom in the dimeric intermediates **32a** is then close to the trigonal-bipyramidal configuration for the Zn(II)[95] and Cd(II)[130,131] complexes according to X-ray diffraction data. Intermolecular coordination leads to partial loosening of one of the metal–ligand bonds and promotes its dissociation with subsequent binding to the cadmium atom of another chelate complex. The series of concerted metal–ligand bond dissociation-formation processes, including the rearrangements of pentacoordinate structures of the Berry pseudorotation type, in the stages **32b** ⇄ **32c** ⇄ **32d** ensures the exchange of cadmium atoms between the two units of the dimer, i.e. degenerate ligand exchange. It has been shown[117,129] that a ligand exchange of this type does indeed occur in solutions of zinc and cadmium thiophenoxides via the dissociation and formation of M–S bonds in the dissociation and formation of the dimers respectively.

The energetically preferred mechanism of the intramolecular enantiomerisation of the bischelate complexes with the CdN_2X_2 coordination unit most probably involves the dissociation-formation of Cd–N bonds (pathway *b* in Fig. 2) and not a digonal twist (pathway *a*). This has been confirmed by the results of a study of the temperature dependence of the ^1H and ^{13}C NMR spectra of the bischelate cadmium complex **13** (M = ^{111}Cd, X = S, R = Pr^i, R^1 = Me) based on 2,6-diformyl-4-methylthiophenol bisalkylimine.[123] Fig. 4 shows that the ^{13}C {H} NMR spectrum of this compound at −90 °C does not reveal the occurrence of the chemical exchange reaction but does indicate $^{111}Cd-^{13}C$ spin–spin coupling for certain carbon nuclei of the ligand. An increase in solution temperature leads to the dynamic averaging of the signals due to the carbon atoms of the diastereotopic methyl groups in each of the isopropyl substituents and at the same time to the averaging of the ^{13}C chemical shifts of

Scheme 9



both groups as well as the ^{13}C nuclei in the 3,5-, 7,7′-, and 8,8′-positions. Examination of the dynamic ^1H NMR and two-dimensional exchange (2D EXSY) spectra of this complex leads to the similar conclusion that the intramolecular processes involving the inversion of configuration and the switching of coordination (Scheme 2) are synchronous. The observed disappearance of the constants for the spin–spin coupling of the ^{111}Cd nucleus with the C(1), C(2), and C(6) atoms of the ligand, observed in the temperature-dependent ^{13}C spectra (Fig. 4), is caused by the activation of the intermolecular degenerate ligand exchange process with a relatively higher barrier. Thus the inversion of the configuration of the tetrahedral Cd(II) atom in the given compound is determined by the intramolecular bond dissociation-formation process leading to the (*R*) ⇄ (*S*) inversion (the transcoordination pathway is indicated in Scheme 2).

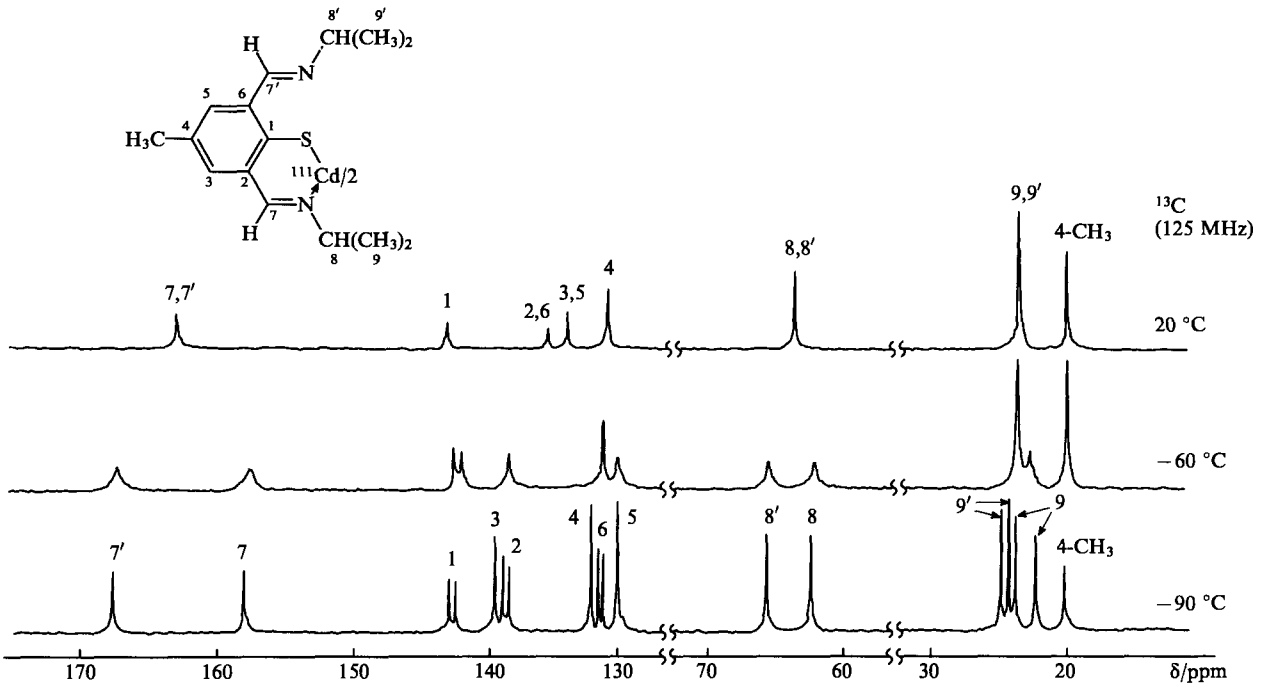


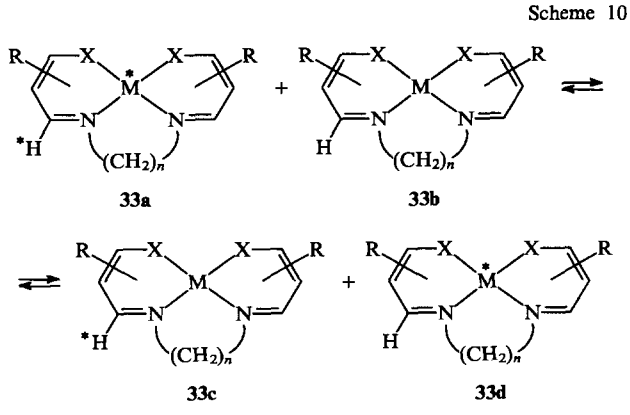
Figure 4. Temperature variation of the ^{13}C NMR spectra (125 MHz, CD_2Cl_2) of the type **13** (X = S, R^1 = CH_3) ^{111}Cd (95%) complex[123]. $J_{^{111}Cd-^{13}C}$ (Hz): 13.3 for C(1), 28.5 for C(2), and 15.6 for C(6); $\Delta G_{25}^{\neq}$ = 12.8 kcal mol^{-1}.

The free energy of activation for the process (12.8 kcal mol^{-1}) is very close to the corresponding value for the intramolecular inversion process in cadmium bis(*N*-isopropylthiosalicylaldiminate) **3**. This is evidence in support of the operation of a similar dissociative mechanism of the enantiomerisation $(R) \rightleftarrows (S)$ in Cd(II) complexes of types **5**, **7**, and **9** (Table 8).

The retention of the spin–spin coupling constants for the ^{111}Cd nucleus of the ligand in the temperature range in which the intramolecular dissociative process is detected in the cadmium complex **13** (M = ^{111}Cd, X = S, R = Pr^i, R^1 = Me) and in the cadmium complexes of types **3**, **5**, **7**, and **9** (Table 8), based on the usual bidentate ligands, may be justified by the argument that the lifetimes of the intermediate tricoordinate structures linked by spin–spin coupling of the ^{111}Cd and ligand nuclei are shorter than the relaxation time (Fig. 1 and Scheme 2).

Evidently, this is the reason why it is impossible to detect the operation of the intramolecular metal–ligand bond dissociation-formation mechanism in solutions of the sterically strained bischelate ^{111}Cd (and ^{207}Pb) complexes **33** with an enforced (*n* = 2) *cis*-planar configuration at the metal centre (Scheme 10).[103,124]

Scheme 10



X = S, Se; M = Cd, Pb; *n* = 2, 4, 6.

Only the degenerate ligand exchange process, occurring at unexpectedly high rates and having energy barriers only 2.5–4.0 kcal mol^{-1} higher than in the analogous complexes with a tetrahedral configuration based on bidentate ligands, could be detected in the dynamic ^1H NMR spectra of these compounds.

With increase in the length and mobility of the polymethylene bridge in the tricyclic complexes **33**, the cadmium ion assumes (starting with *n* = 4) a tetrahedral configuration and these complexes exhibit, like their analogues **5** and **6**, two types of reactions in solutions: intramolecular inversion of the configuration of the tetrahedral centre and intermolecular degenerate ligand exchange also accompanied by the inversion of the configuration at the metal atom (Scheme 10).

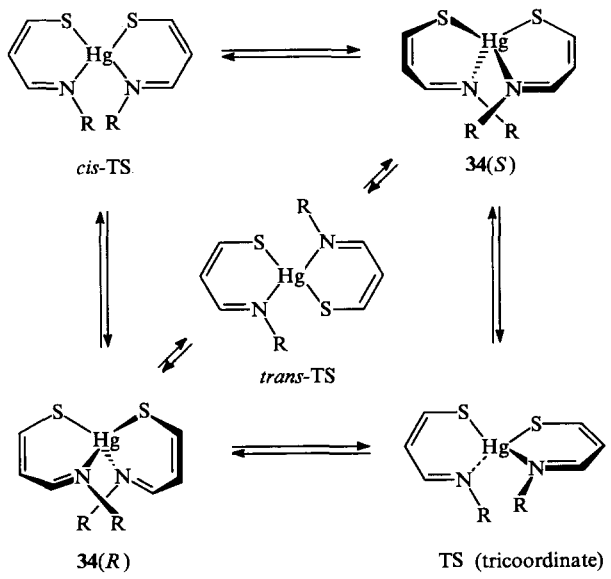
VIII. Complexes of mercury and lead

Both the intramolecular and intermolecular exchange processes occurring in solutions of Hg(II) bischelate complexes are much faster than for the zinc and cadmium analogues and the determination of quantitative data is difficult in view of the small separations between the diastereotopic indicator signals. For these reasons, there are fairly limited data on the stereochemical lability of Hg(II) complexes. For complex **7** (M = Hg, X = S, R = cyclo-C_6H_{11}, R^1 = Pr^i, R^2 = Me), the rate of the inversion process, detected from the diastereotopic averaging of the signals due to the methyls of the isopropyl substituent R^1 ($\Delta\delta$ = 0.01 ppm in CD_2Cl_2) is independent of the solution concentration and the type of solvent employed, which indicates its intramolecular nature (k_{-80} = 4 s^{-1}, k_{25} = 1.9×10^3 s^{-1}, $\Delta G_{25}^{\neq}$ = 12.9 kcal mol^{-1}).[132]

A theoretical modelling of the possible mechanisms of the intramolecular enantiomerisation has been carried out[133] using the MNDO method for the tetrahedral bischelate complex **34** (Scheme 11), which serves as a model of complexes **7** (M = Hg).

The MNDO method reproduces satisfactorily the highly distorted tetrahedral configuration of the bonds at the mercury atom in complex **34**, which agrees with the X-ray diffraction data[132] for the pyrazole complex **7** (R = cyclo-C_6H_{11}, R^1 = Pr^i, R^2 = Me) having the identical chelate unit (the SHgS and NHgN bond angles are 141° and 103.2°, and the Hg–S bond length is

Scheme 11



2.39 Å). The greater SHgS bond angle indicates that the Hg–S bonds are highly covalent, while the Hg–N bonds in this complex are predominantly dative.[115]

Calculations revealed three structures of the transition state (TS), which are presented in Scheme 11.

As can be seen from the calculated data (Table 10), one may expect the energy barriers to depend fairly strongly on the steric bulk of the substituent R. For R = H, the digonal twist (*trans*-TS) is energetically preferred, while the replacement of hydrogen by the more bulky methyl group (R = Me) results, as expected, in the dissociative mechanism of the inversion of the configuration with dissociation of the Hg–N bond being preferred. For the type **7** complex, the calculated activation energies are fairly close to the experimental inversion barrier for mercury. They also illustrate clearly the extremely fine balance between the principal mechanisms of the intramolecular inversion of the configuration of the pseudotetrahedral mercury atom, providing evidence on the whole in support of the dissociation-recombination pathway *b* in the enantiomerisation of the type **7** Hg(II) chelates (Fig. 2).

Table 10. Modelling of the mechanisms of the intramolecular enantiomerisation of Hg(II) bischelate complexes by means of the MNDO method (with parameters taken from Minkin et al.[133]).

Parameter	**34**	Transition state		
		cis	*trans*	tricoordinate
R = H				
$\Delta\Delta H^{\neq}$/kcal mol^{-1}	0	12.5	8.2	16.0
Hg–N/Å	2.16	2.19	2.18	3.30
$\upsilon_{im}^{\neq}$ /cm^{-1}	–	61	52	64
R = Me				
$\Delta\Delta H^{\neq}$/kcal mol^{-1}	0	24.4	16.1	9.2
Hg–N/Å	2.23	2.27	2.40	3.01
$\upsilon_{im}^{\neq}$/cm^{-1}	–	141	129	94

The gradual decrease in the energy barriers in the dissociative configuration inversion reaction involving the dissociation of the M–N bonds in the type **13** and **7** chelate complexes in the sequence Zn > Cd > Hg correlates with the decrease in the energies of these bonds in the same sequence. According to calorimetric measurements[136] of the heats of hydrolysis of zinc, cadmium, and mercury bis(trimethylsilyl)amides M[N(SiMe$_3$)]$_2$, the M–N bond energies are (kcal mol^{-1}) 50.0 (Zn–N), 34.4 (Cd–N), and 25.8 (Hg–N).

The rate of the degenerate ligand exchange for the type **7** bischelate complexes of mercury is 2–3 orders of magnitude lower than the rates of the intramolecular inversion processes. The intermolecular ligand exchange processes, which are kinetically second order, have been detected in solution from the temperature dependent changes in $^3J_{CH=N-^{199}Hg}$ in the ^{1}H NMR spectra and in $J_{^{199}Hg-^{15}N}$ the ^{199}Hg NMR spectra. The corresponding kinetic data are presented in Table 11.

In the series of the bischelate lead complexes **7** (X = Se), the protons of the diastereotopic grounds remain isochronic (^{1}H NMR) when the solutions in CD_2Cl_2 are cooled to −80 °C, which may be associated with the extremely high rates of the inversion process ($\Delta G_{25}^{\neq} < 7$ kcal mol^{-1}). However, for a series of compounds of this type (Table 11) enriched in ^{207}Pb, it is possible to detect an intermolecular degenerate ligand exchange process, which is indicated by the disappearance of the spin–spin coupling constant $J_{^{207}Pb-^{77}Se}$ in the ^{77}Se{H} NMR and $^3J_{^{207}Pb-N=CH}$ in the ^{1}H NMR spectra. This is also found with the aid of two-dimensional ^{1}H NMR spectroscopy.[135] As in the case of the isoligand cadmium complexes, the reaction is kinetically second order and the Pb–N and Pb–Se bond dissociation-formation processes are synchronous. The rate of reaction diminishes with increase in the bulk of the substituent at the coordinated nitrogen atom.

IX. Complexes of copper, silver, and gold

In the +1 oxidation state, copper, silver, and gold have the d^{10} valence electron shell, like the zinc, cadmium, mercury, and lead complexes in the +2 oxidation state examined above. For this reason, their bonds at the metal centre have a tetrahedral configuration in the tetracoordinate structures.

The Cu(I), Ag(I),[137] and Au(I)[138] bischelate complexes with neutral bidentate ligands of type **35** and having the general formula $[ML_2]^+PF_6^-$ (**36**), where L represents bis(tertiary arsines) and bis(tertiary phosphines), have been investigated in fair detail.

Table 11. Kinetic and activation parameters of the degenerate ligand exchange in type **7** Hg(II) and Pb(II) complexes [solvents—$CDCl_3$, $(CHCl_2)_2$, toluene-d_8].[132,135]

M	R	$^3J_{M-N=CH}(S=\frac{1}{2})$/Hz	k_{25}/s^{-1}	$\Delta H^{\neq}$/kcal mol^{-1}	$\Delta S^{\neq}$/cal mol^{-1} K^{-1}	$\Delta G_{25}^{\neq}$/kcal mol^{-1}
Hg	cyclo-C_6H_{11}	33.0	5.75	7.3	−30.7	16.4
	Bu^t	45.0	17.7	3.4	−41.3	15.8
	Pr^i	12.0	22.8	5.1	−35.1	15.6
	C_6H_4Me-*p*	13.0	13.5	6.2	−32.3	15.9
Pb	cyclo-C_6H_{11}	14.0	7.1×10^2	8.2	−17.9	13.6
	CH_2Ph	16.5	2.7×10^3	10.3	−8.3	12.8
	C_6H_4Me-*p*	16.0	4.3×10^3	5.76	−16.2	10.6

Note. In the mercury complexes, X = S, R^1 = Pr^i, R^2 = Me; in the lead complexes X = Se, R^1 = Pr^i, R^2 = Me.

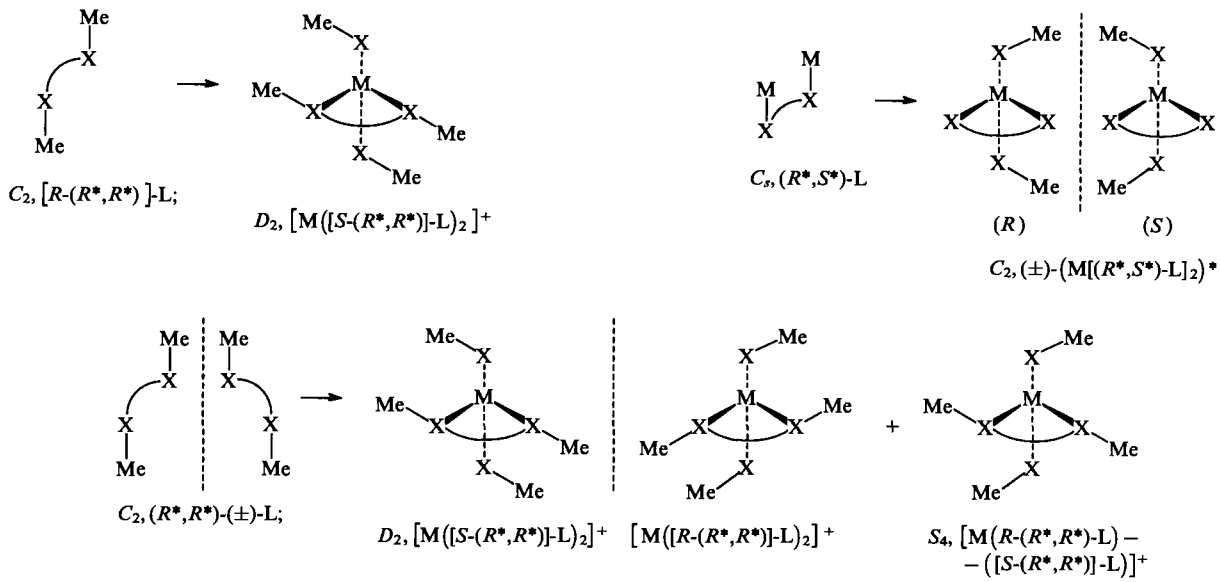
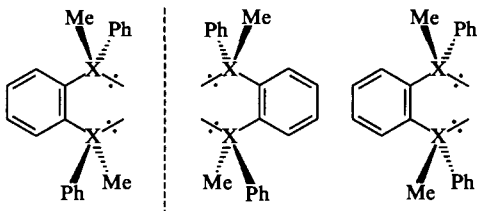
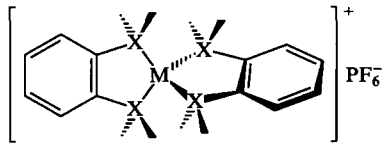


Figure 5. Stereochemical representation, according to the data of Salem et al.,[137] of the tetrahedral complexes **36** using the nomenclature of Cahn et al.[140] for the stereochemical descriptors.

When the donor centres in these ligands are chiral, as in 1,2-phenylenebis(methylphenylphosphines) and the corresponding arsines,[139] the complexes formed by them constitute a complex mixture of diastereoisomers (Fig. 5).





36

X = PMePh, AsMePh;
M = Cu, Ag, Au

The optically active forms of the dissymmetric ligands **35** (C_2-symmetry) give rise to discrete enantiomers of the complexes with D_2 symmetry, in which the PMe or AsMe groups are equivalent. The (*R**,*R**)-forms afford a mixture of chiral (D_2 symmetry) and achiral (S_4 symmetry) chelate complexes. Evidently, the interconversion of these diastereoisomeric forms is possible only as a result of the intermolecular ligand exchange. The achiral (*R**,*S**)-diastereoisomers of the ligand **35** form complex cations with C_2 symmetry in which the PMe or AsMe groups are diastereotopic. The possibility of detecting the intramolecular inversion of configuration in complexes **36** appears in those cases where the tetrahedral metal complex, produced by the (*R**,*R**)-(±)-form of the ligand, is stable in relation to the ligand redistribution reaction between different metal centres.

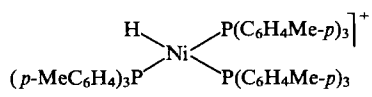
Both types of processes involving the inversion of the configuration of the metal centre have been observed in solutions of the bischelate complexes **36**. For example, when the mirror enantiomers of the phosphinecopper complex **36** are mixed in solution in CH_2Cl_2, the signals due to the PMe groups of the achiral diastereoisomer (S_4-symmetry) gradually appear in the ^{1}H NMR spectrum. The equilibrium ratio is $D_2 : S_4 = 1 : 6$ (at 20 °C). The time of attainment of equilibrium between the above diastereoisomers, induced by the intermolecular liquid exchange reactions in solution in CD_2Cl_2, is between 1 and 20 min for the copper complexes **36** at the usual temperature and between 1 min and 1 month for the gold(I) complexes.[137,138] Since the ligand exchange reactions are fairly slow under these conditions for all the complexes investigated, there is a possibility of the independent detection of the intramolecular inversion of the tetrahedral configuration of the metal centre in complexes **36** from the diastereotopic averaging of the signals due to the XMe (X = P, As) groups. Table 12 presents the free energies of activation for the inversion process determined at the coalescence temperatures. The observed values are very close to those listed in Tables 7, 8, and 11 for the Zn(II), Cd(II), Hg(II), and Pb(II) bischelate complexes. Although Salem et al.[137] were unable to obtain definite evidence in support of one of the two possible intramolecular inversion mechanisms, they suggest that the reaction follows the digonal twist mechanism without involving the intramolecular dissociation of the bonds between the central atom and ligating atoms.

Table 12. Free energies of activation at the coalescence temperatures (f_0 = 200 MHz) for the intramolecular inversion of the tetrahedral configuration of the metal centre in type **36** complexes (±)-(M[(*R**,*S**)–L]$_2$)PF_6 (L = compound **35**).[137,138]

M	X	Solvent	T_c/°C	$\Delta G^{\neq}_{T_c}$/kcal mol^{-1}
Cu	P	$C_6D_5NO_2$	> 120	20.5
Cu	As	CH_2Cl_2	5	13.1
Ag	P	CH_2Cl_2	5	11.9
Ag	As	CH_2Cl_2	−55	10.4
Au	P	$C_6D_5NO_2$	120	18.7
Au	As	CH_2Cl_2	−29	11.7

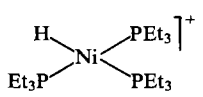
X. Complexes of nickel and other transition metals

The principal cause of the instability of the planar configuration of the complexes of d^{10} metals — the filling of the antibonding b_{1g} molecular orbital with electrons — is eliminated for the complexes of d^8 metals.[141-143] The planar configuration is therefore energetically preferred for the 16-electron valence shell of the Ni(II), Pd(II), Pt(II), Au(III), etc. complexes. In a number of instances, the stable configuration in the crystalline state for Cu(II) and especially Ni(II) complexes is intermediate between the planar and tetrahedral configurations and the dihedral angle, which determines the transition from planar (θ = 0°) to tetrahedral (θ = 90°) coordination, can vary within very wide limits (see the references in the review of Garnovskii et al.[38]). The situation where tetrahedral structures play the role of the reaction transition states in the isomerisation or topomerisation of the planar forms is more general (Fig. 1).[35,144] In a number of instances, the relative energies of these structures — transition states in the isomerisation reaction — are fairly low and the planar complexes of the tetracoordinate metals are then fluctuating molecules and the isomerisation itself is recorded on the timescale of NMR spectra. Certain examples of such complexes (compounds **37-39**) are given below (the free energies $\Delta G_{25}^{\neq}$ for the *cis-trans* isomerisation are indicated).



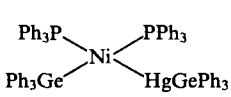
37

$\Delta G_{25}^{\neq}$ = 14.6 kcal mol^{-1}
(Eaton et al.[145])



38

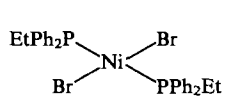
$\Delta G_{25}^{\neq}$ = 12.0 kcal mol^{-1}
(English et al.[146])



39

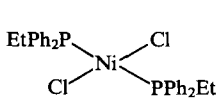
$\Delta G_{25}^{\neq}$ = 12.3 kcal mol^{-1}
(Grishin et al.[147])

In some cases, the tetrahedral structures are isomeric in relation to the planar forms and exist in solution in equilibrium with them. The barriers to the interconversion of the planar and tetrahedral structures are usually very low (see the Introduction), but for certain complexes (compounds **40-42**) the barriers reach values which can be determined with the aid of the dynamic NMR method.



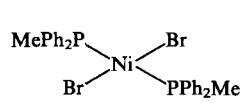
40

$\Delta G_{25}^{\neq}$ = 10.4 kcal mol^{-1}
(LaMar and Sherman[148])



41

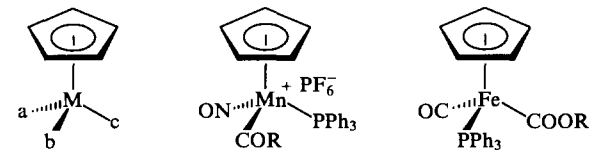
$\Delta G_{25}^{\neq}$ = 9.3 kcal mol^{-1}
(LaMar and Sherman[148])



42

$\Delta G_{25}^{\neq}$ = 9.2 kcal mol^{-1}
(Pignolet et al.[149])

Within the framework of the present review, transition metal complexes for which the tetrahedral forms correspond to the structures of the ground states and the tetracoordinate metal centre is itself chiral are of special interest. A wide range of such complexes of the general type **43** are now known.



43 **43a** **43b**

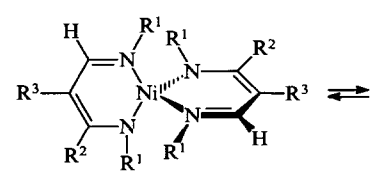
M = Mn, Fe, Ru, Cr, Mo, W, Co.

Some of them, for example, complexes **43a** and **43b**, are configurationally stable compounds which can be resolved into their optical isomers on a preparative scale.[150,151] The mechanisms of the inversion of the tetrahedral configuration of the metal atom in type **43** complexes have been subjected to a careful kinetic analysis and have also been investigated by a computational method.[152] The most probable is the dissociative mechanism involving, for example in complex **43a**, the splitting off of the phosphine ligand and the formation of a chiral intermediate with a tricoordinate pyramidal metal atom undergoing rapid inversion.

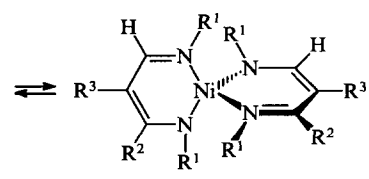
Knorr and coworkers[153-156] obtained the bischelate and configurationally stable nickel complexes **44** and **45** with high barriers to tetrahedral inversion.

The inversion process in complex **44** (Scheme 12) has been investigated from the temperature-dependent diastereotopic averaging of the signals due to the methylene groups of the ethyl substituent (R^3) or the methyl group of the *o*-tolyl substituent (R^3). The energy barriers to the inversion process at the temperatures of the coalescence of the indicator signals (at 95-180 °C in cyclohexane or tetralin) are in the range 17.2-23.8 kcal mol^{-1}.[153,155]

Scheme 12



44(*R*)



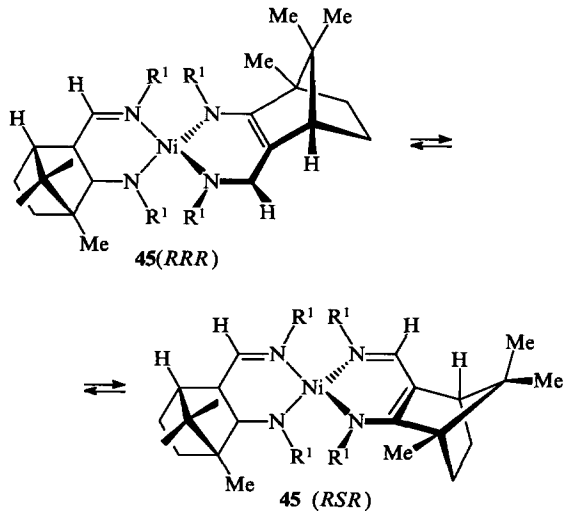
44(*S*)

R^1 = Me, Ph; R^2 = Me, Pr; R^3 = Et, C_6H_4Me-*o*.

The bischelate complexes **45** contain an additional chiral unit — the (*R*)-camphor fragment, so that the inversion of the tetrahedral Ni(II) (Scheme 13) (see over) represents not enantiomerisation but diastereoisomerisation, both diastereoisomers being chiral. It has been established[154] that this process is purely intramolecular. The kinetics have been investigated both by integrating the signals due to the pairs of hydrogen atoms involved in the exchange (in view of the paramagnetism of complexes **44** and **45**, the chemical shifts of their protons were very large) and polarimetrically (slow mutarotation). The values of $\Delta H^{\neq}$ and $\Delta S^{\neq}$ ($\Delta H^{\neq}$ = 22.5 ± 0.8 kcal mol^{-1} and $\Delta S^{\neq}$ = −15 ± 3 cal mol^{-1} K^{-1} in tetralin) found for complex **45** (R^1 = Ph) indiate the possibility of the preparative separation of the enantiomers of tetrahedral paramagnetic bischelate Ni(II) complexes. For complex **45** (R = Me), the height of the barrier corresponds to $\Delta G^{\neq}$ = 17 ± 1 kcal mol^{-1}.

The possibility of the operation of the dissociative intramolecular mechanism of the enantiomerisation of the bischelate complexes of type **44** with the NiN_4 chelate unit and involving the

Scheme 13

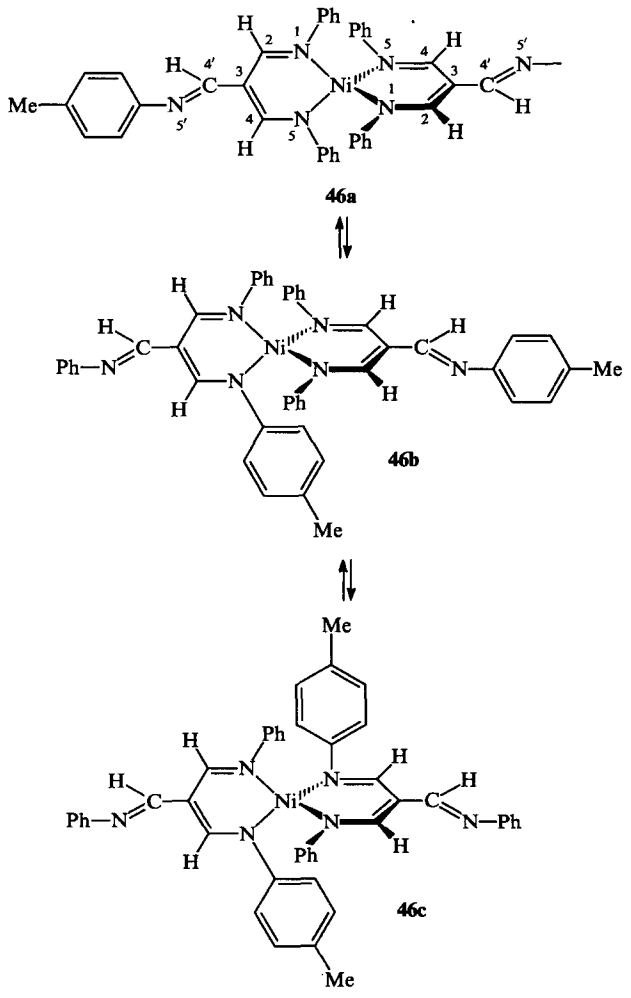


45(*RRR*)

45 (*RSR*)

dissociation of the Ni–N bond has been demonstrated in a study of the transcoordination of the metal atom in complex **46** (Scheme 14).[156] It was established that the transcoordination reaction is very slow [$k = (38 \pm 5) \times 10^{-8}$ s^{-1} at 24.5 °C in solution in the 3 : 1 $CCl_4/CDCl_3$ mixture] and cannot therefore make an appreciable contribution to the observed inversion transformations.

Scheme 14



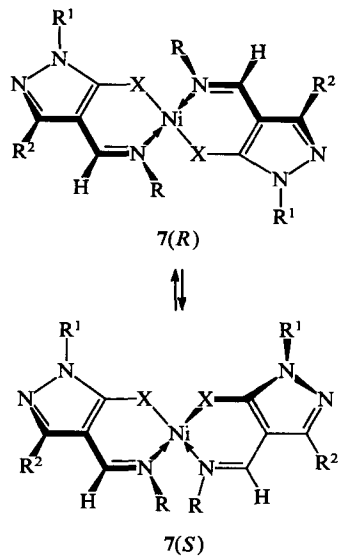
46a

46b

46c

The possibility of the intramolecular tetrahedral inversion of Ni(II) with a fairly high barrier in the series of metal chelates with a NiN_2X_2 (X = O, S, Se) coordination unit, the rate of which corresponds to the characteristic time scale of dynamic ^{1}H NMR, was first demonstrated for type **7** complexes of the pyrazole series (Scheme 15).[157–160]

Scheme 15



7(*R*)

7(*S*)

The condensation of the pyrazole ring with the chelate ring in complexes **7** stabilises sharply the tetrahedral configuration relative to the planar structure,[43,157,161–163] which can be explained by the steric strain in the chelate ring induced by the condensation of the five-membered heterocycle with it.[164] The pseudotetrahedral structure of complexes **7** in the solid state has been confirmed by X-ray diffraction studies.[38,111,165]

The inversion of the tetrahedral configuration (Scheme 15) has been investigated from the temperature-dependent diastereotopic averaging of the signals due to the corresponding groups of prochiral substituents (Pr^i, CH_2Ph) at the coordinated nitrogen atom and in the 1- and 3-positions in the pyrazole ring. Although the multiplet structure of the signals due to the protons of the diastereotopic groups is not resolved in the spectra owing to the broadening of the signals ($\Delta\nu_{1/2}$ = 12 Hz) typical for paramagnetic complexes, the difference between their chemical shifts at low rates of the exchange processes is 25–500 Hz (f_0 = 100 MHz), which explains the adequate accuracy of the determination of the rate constants and energy barriers for the inversion process at temperatures corresponding to coalescence of the indicator signals.

The energy barriers to the inversion of the tetrahedral configuration of Ni(II) in the bischelate complexes **7** are presented in Table 13. It is seen that the barriers increase with increase in the steric bulk of the substituent R, the increase being particularly notable for R = Bu^t. This effect is fully consistent with a feature well known for complexes of tetracoordinate Ni(II) with NiN_2X_2 chelate units (complexes of types **2**, **3**, **5**, **9**, and **11**)—the shift of the square–tetrahedron equilibrium to the right in the series of substituents R: n-alkyl < *sec*-alkyl < *tert*-alkyl.[1,27,28]

It follows from data of Nivorozhin and coworkers[158,159] that the observed inversion process proceeds via the digonal twist mechanism (pathway *a* in Fig. 2) with formation in the transition state of the planar achiral *cis*-structure typical for the complexes NiN_2S_2 and NiN_2Se_2.[157,160,167–169] It may be expected that, in connection with the rapid development of the NMR methods for the investigation of the kinetics of reactions of paramagnetic compounds,[170] the available information on the dynamics of the stereoisomerisation of tetrahedral Ni(II) complexes will soon expand significantly.

Table 13. Energy barriers to the inversion of the tetrahedral configuration of Ni(II) in type **7** bischelate complexes (solvent—$CDCl_3$).[158,159]

X	R	R^1	R^2	T_c/°C	$\Delta G^{\neq}_{T_c}$/kcal mol^{-1}
S	Me	Pr^i	Me	−50	10.2
S	Pr^i	Pr^i	Me	−20	12.1
S	Bu^t	Pr^i	Me	100	17.6[a]
Se	Me	Pr^i	Me	−25	11.5
Se	Pr^i	Pr^i	Me	−10	12.5
S	$C_6H_4NMe_2$-*p*	Pr^i	Me	−20	12.3
S	C_6H_4Me-*p*	Pr^i	Me	−40	11.4
S	$C_6H_4NO_2$-*p*	Pr^i	Me	−50	11.0
Se	C_6H_4Me-*p*	Pr^i	Me	−20	12.3
S	Pr^i	CH_2Ph	Me	−20	11.6
Se	Pr^i	Ph	Me	−5	12.4
S	Pr^i	Ph	Pr^i	−43	11.1
S	Bu^t	Ph	Pr^i	60	16.9
Se	Pr^i	Ph	Pr^i	−48	11.1

[a] Solvent—DMSO-d_6.

XI. Conclusion

The data presented in this review show that all the theoretically possible types of mechanisms of the inversion of the tetrahedral configuration operate in the enantiomerisation reactions of dissymmetric chelate complexes of transition metals. The majority of these compounds have stereochemically nonrigid structures and the energy barriers to the tetrahedral inversion fit within the characteristic time scale of NMR spectroscopy. In the presence of suitable prochiral substituents in the complexes, the stereoisomerisation processes can be investigated and characterised quantitatively by means of the dynamic NMR method without the preliminary separation of the enantiomeric forms, while with the aid of structural modelling of the ligand, especially when alterdentate ligands are used, it is possible to differentiate reliably the different intramolecular stereoisomerisation mechanisms.

Table 14 summarises the principal results of the studies carried out in this field. For comparison, it also includes the energy barriers to the intramolecular inversion of the tetrahedral configuration of the sp^3-carbon centres. The preferred enantiomerisation pathway is determined mainly by the nature of the centre undergoing inversion.

The data available hitherto on the kinetics and mechanisms of the processes involving the inversion of the tetrahedral configuration in nontransition metal complexes, examined in this review, are still far from complete. Nevertheless, they are already sufficient to reveal certain general trends in the behaviour of the stereochemically nonrigid complexes of this type and to compare them with the much more detailed results obtained in the study of the stereodynamics and ligand exchange reactions for transition metal complexes.

This review has been written with financial support from the Russian Fundamental Research Fund (project 93-03-18692).

Table 14. Energy barriers (kcal mol^{-1}) to the inversion of the tetrahedral configurations of the tetracoordinate d^0 and d^{10} metals and Ni(II).

M(R^1,R^2,R^3,R^4)	Digonal twist	Dissociation-formation of M−R bonds	Intermolecular associative mechanism
C(IV)	Not found[a]	18–28[b]	$(RR^1CHLi)_4$[c]
Be(II)	"	18–25	20–27
B(III)	"	20–22	22–25
Ga(III)	Not investigated	18	$(RR^1R^2Ga)_n$[d]
In(III)	"	12	$(RR^1R^2In)_n$[d]
Zn(II)	9–20	>15	17–22
Cd(II)	9–14[e]	>11	11–17
Hg(II)	11–13[e]	13	14–17
Pb(II)	Not investigated	10	9–14
Cu(I)	13–20	No data	[f]
Ni(II)	3–18	>26	14–20

[a] See Table 1.
[b] The energy barriers were determined by dynamic NMR for the intramolecular isomerisations of indolinospirobenzopyrans and 2-oxaindanospirobenzopyrans involving the thermal dissociation of the C_{sp^3}—O bonds.[170–173]
[c] This mechanism operates readily at the usual temperature in solutions of associated organolithium[174] and other organometallic compounds.
[d] This mechanism operates readily in solutions of dimers and polymeric associated species of organogallium and organoindium compounds.[175]
[e] The choice between the digonal twist intramolecular mechanism and the intramolecular mechanism involving the dissociation-formation of the M–N bond is not unambiguous.
[f] When enantiomers of Cu(I) complexes are mixed with type **35** ligands, racemisation takes place with a half-life $\tau_{1/2}$ = 1–20 min in solution in CH_2Cl_2 at 25 °C.[137,138]

References

1. R H Holm, in *Dynamic Nuclear Magnetic Resonance Spectroscopy* (Eds L M Jackman, F A Cotton) (New York: Academic Press, 1975) p. 319
2. V I Minkin, L P Olekhnovich, Yu A Zhdanov *Molecular Design of Tautomeric Compounds* (Dordrecht: Reidel, 1988)
3. R B King *Coord. Chem. Rev.* **122** 91 (1993)
4. J Brocas, M Gielen, R Willem *The Permutational Approach to Dynamic Stereochemistry* (New York: McGraw-Hill, 1983)
5. V I Sokolov *Introduction to Theoretical Stereochemistry* (New York: Gordon and Breach, 1991)
6. J Jeener, B H Meier, P Bachmann, R R Ernst *J. Chem. Phys.* **71** 4546 (1979)
7. K G Orrell, V Sik, D Stephenson *Prog. Nucl. Magn. Reson. Spectrosc.* **22** 141 (1990)
8. C L Perrin, T J Dwyer *Chem. Rev.* **90** 935 (1990)
9. L E Kay, G M Clore, A Bax, A M Gronenborn *Science* **249** 411 (1990)
10. S L Hawthorne, A H Bruder, R C Fay *Inorg. Chem.* **22** 3368 (1983)
11. E L Muetterties *Acc. Chem. Res.* **3** 266 (1970)
12. R R Holmes *Prog. Inorg. Chem.* **32** 119 (1984)
13. R Luckenbach *Dynamical Stereochemistry of Pentacoordinated Phosphorus and Related Elements* (Stuttgart: Georg Thieme, 1973)
14. N Serpone, D G Bickley *Prog. Inorg. Chem.* **17** 391 (1972)
15. R Willem, M Gielen, H Pepermans, J Brocas, D Fastenakel, P Finocchiaro *J. Am. Chem. Soc.* **107** 1146 (1985)
16. R Willem, M Gielen, H Pepermans, K Hallenga, A Recca, P Finocchiaro *J. Am. Chem. Soc.* **107** 1153 (1985)
17. R C Fay, A F Lindmark *J. Am. Chem. Soc.* **105** 2118 (1983)
18. K G Orrell *Coord. Chem. Rev.* **96** 1 (1989)
19. D G Bickley, N Serpone *Inorg. Chem.* **18** 2200 (1979)
20. H-M Gau, R C Fay *Inorg. Chem.* **29** 4974 (1990)
21. A Werner *Chem. Ber.* **45** 3061 (1912)
22. F Basolo, R G Pearson, in *Mechanisms of Inorganic Reactions* (New York: Wiley, 1958) p. 284
23. A J Deeming, in *Mechanisms of Inorganic and Organometallic Reactions* Vol. 2 (Ed. M V Twigg) (New York: Plenum, 1984) p. 319
24. E W Abel, S K Bhargava, K G Orrell *Prog. Inorg. Chem.* **32** 1 (1984)
25. *Nomenclature of Inorganic Compounds* (London: Butterworths, 1977); *Pure Appl. Chem.* **28** 1 (1971)
26. L M Jackman, in *Dynamic Nuclear Magnetic Resonance Spectroscopy* (Eds L M Jackman, F A Cotton) (New York: Academic Press, 1975) p. 203
27. M Nógrádi *Stereochemistry. Basic Concepts and Applications* (Budapest: Akadèmiai Kiadù, 1981)
28. D A Dixon, A J Arduengo *J. Phys. Chem.* **91** 3195 (1987)

29. D L Kepert *Inorganic Stereochemistry* (Berlin: Springer, 1982)
30. E L Muetterties *Tetrahedron* **30** 1595 (1974)
31. R Hoffmann, B F Beier, E L Muetterties, A R Rossi *Inorg. Chem.* **16** 511 (1977)
32. J K Burdett, R Hoffmann, R C Fay *Inorg. Chem.* **17** 2553 (1978)
33. P J McDougall *Inorg. Chem.* **25** 4400 (1986)
34. H G Brittain *Inorg. Chem.* **14** 2858 (1975)
35. G K Anderson, R J Cross *Chem. Soc. Rev.* **9** 185 (1980)
36. M C Favas, D L Kepert *Prog. Inorg. Chem.* **28** 310 (1981)
37. B F G Johnson, R Mallocs, E Parisini, Y V Roberts *Polyhedron* **12** 897 (1993)
38. A D Garnovskii, A L Nivorozhkin, V I Minkin *Coord. Chem. Rev.* **126** 1 (1993)
39. M S Gordon, M W Schmidt *J. Am. Chem. Soc.* **115** 7486 (1993)
40. M P McGrath, L Radom *J. Am. Chem. Soc.* **115** 3320 (1993)
41. S Yamada, A Takeuchi *Coord. Chem. Rev.* **43** 187 (1982)
42. R H Holm, C J Hawkins *NMR of Paramagnetic Molecules* (Eds G H LaMar, W D Horrocks, R H Holm) (New York: Academic Press, 1973)
43. L S Minkina, V P Kurbatov, O A Osipov, V I Minkin, L E Nivorozhkin *Zh. Neorg. Khim.* **16** 1075 (1971)
44. V P Kurbatov, O A Osipov, V I Minkin, L E Nivorozhkin *Zh. Neorg. Khim.* **19** 2191 (1974)
45. R Knoch, A Wilk, K J Wannowius, D Reinen, H Alias *Inorg. Chem.* **29** 3799 (1990)
46. L L Lohr *J. Am. Chem. Soc.* **100** 1093 (1978)
47. W J Hehre, L Radom, P V R Schleyer, J A Pople, in *Ab initio Molecular Orbital Theory* (New York: Academic Press, 1986) p. 428
48. A I Boldyrev, O P Charkin *Zh. Strukt. Khim.* **26** 158 (1985)
49. V I Minkin, R M Minyaev, Yu A Zhdanov *Nonclassical Structures of Organic Compounds* (Moscow: Mir, 1987)
50. M-B Krogh-Jespersen, J Chandrasekhar, E U Würthwein, J B Collins, P V R Schleyer *J. Am. Chem. Soc.* **102** 2263 (1980)
51. D A Dixon, A J Arduengo *J. Chem. Soc., Chem. Commun.* 498 (1987)
52. O Gropen, U Wahlgren, L Peterson *Chem. Phys. Lett.* **66** 453 (1982)
53. F Hirota, S Shibata *J. Mol. Struct. (Theochem)* **137** 373 (1986)
54. S S Eaton, R H Holm *Inorg. Chem.* **10** 1446 (1971)
55. V I Minkin, L E Nivorozhkin, L E Konstantinovskii, M S Korobov *Koord. Khim.* **3** 174 (1977)
56. F A Bottino, A Recca, P Finocchiaro *J. Organomet. Chem.* **160** 373 (1978)
57. L E Nivorozhkin, L E Konstantinovskii, M S Korobov, V I Minkin *Koord. Khim.* **5** 508 (1979)
58. H Meyer, G Nagorsen *Angew. Chem.* **91** 587 (1979)
59. E Würthwein, P V R Schleyer *Angew. Chem.* **91** 588 (1979)
60. J C Martin, W H Stevenson, D Y Lee, in *Organosilicon and Bioorganosilicon Chemistry* (Ed. H Sakurai) (Chichester: Ellis Horwood, 1985) p. 141
61. A J Arduengo, D A Dixon, D C Roe, M Kline *J. Am. Chem. Soc.* **110** 4437 (1988)
62. A Von Zelewsky *Inorg. Chem.* **20** 4448 (1981)
63. K Mislow, M Raban *Top. Stereochem.* **1** 3 (1967)
64. G Binsh, E Eliel, H Kessler *Angew. Chem.* **83** 618 (1971)
65. W B Jennings *Chem. Rev.* **75** 307 (1981)
66. J P Jesson, E L Muetterties, in *Dynamic Nuclear Magnetic Resonance Spectroscopy* (Eds L M Jackman, F A Cotton) (New York: Academic Press, 1975) p. 253
67. J C Lockart *Redistribution Reactions* (New York: Academic Press, 1970)
68. W H Mills, R A Gotts *J. Chem. Soc.* 3121 (1926)
69. H Burgess, T M Lowry *J. Chem. Soc.* 2081 (1924)
70. F A Bottino, P Finocchiaro *Polyhedron* **8** 1507 (1985)
71. L E Nivorozhkin, M S Korobov, N I Borisenko, G S Borodkin, Yu E Chernysh, V I Minkin *Zh. Obshch. Khim.* **55** 2149 (1985)
72. G S Borodkin, Candidate's Thesis in Chemical Sciences, Rostov Univ., Rostov-on-Don, 1990
73. V I Minkin, V A Pichko, I A Abubikerova, B Ya Simkin *Zh. Obshch. Khim.* **62** 481 (1992)
74. G Ronsisvalle, F A Bottino, E Libertini, O Puglisi, A Recca *J. Inorg. Nucl. Chem.* **42** 1 (1980)
75. E Ferroni, R Cini *J. Am. Chem. Soc.* **82** 2427 (1960)
76. O E Kompan, N G Furmanova, L M Sitkina, V A Bren', V I Minkin *Zh. Strukt. Khim.* **21** 90 (1980)
77. V I Bregadze, N G Furmanova, L M Golubinskaya, O E Kompan, Yu T Struchkov, V A Bren, A E Lyubarskaya, V I Minkin, L M Sitkina *J. Organomet. Chem.* **192** 1 (1980)
78. M S Korobov, L E Nivorozhkin, L V Belen'kaya, L E Konstantinovskii *Zh. Obshch. Khim.* **52** 860 (1982)
79. M S Korobov, G S Borodkin, N I Borisenko, T A Ryskina, L E Nivorozhkin, V I Minkin *J. Mol. Struct. (Theochem)* **200** 61 (1989)
80. M S Korobov, L E Nivorozhkin, L E Konstantinovsky, V I Minkin *J. Chem. Soc., Chem. Commun.* 169 (1982)
81. K Krogh-Jespersen, D Cremer, D Poppinger, J A Pople, P V R Schleyer, J Chandrasekhar *J. Am. Chem. Soc.* **101** 4843 (1979)
82. P V R Schleyer, E-U Würthwein *J. Chem. Soc., Chem. Commun.* 542 (1982)
83. R M Minyaev, G V Orlova, V I Minkin, in *III Vsesoyuznaya Konferentsiya "Uspekhi Khimii Azotistykh Geterotsiklov"* (Tezisy Dokladov) [The IIIrd All-Union Conference "Advances in the Chemistry of Nitrogen-containing Heterocycles" (Abstracts of Reports)] (Rostov-on-Don: Rostov Univ., 1983) p. 192
84. A J Boulton, G S Prado *J. Chem. Soc., Chem. Commun.* 1008 (1982)
85. H Kessler, G Zimmermann, H Fietze, H Mhrle *Chem. Ber.* **111** 2606 (1978)
86. A H Cowley, J L Mills *J. Am. Chem. Soc.* **91** 2911 (1969)
87. E Vedejs, S C Fields, M R Schrimpf *Pure Appl. Chem.* **65** 723 (1993)
88. T Burgameister, R Grobe-Einsler, R Grotstollen, A Mannschreck, G Wulff *Chem. Ber.* **114** 3403 (1981)
89. S Toyota, M Oki *Bull. Chem. Soc. Jpn.* **63** 1168 (1990)
90. S Toyota, M Oki *Bull. Chem. Soc. Jpn.* **64** 1554 (1991)
91. M Oki *Pure Appl. Chem.* **61** 699 (1989)
92. M S Korobov, G S Borodkin, L E Nivorozhkin, V I Minkin, V I Bregadze, L M Golubinskaya, in *IV Vsesoyuznaya Konferentsiya po Metalloorganicheskoi Khimii, Kazan', 1988* (Tezisy Dokladov) [The IVth Conference on Organometallic Chemistry, Kazan', 1988 (Abstracts of Reports)] p. 396
93. J T B Jastzebski, G Van Koten, D Tuck, H Meinema, J G Noltes *Organometallics* **1** 1492 (1982)
94. R J P Williams *Polyhedron* **6** 6 (1987)
95. T P E Auf der Heyde, R L Nassimbeni *Acta Crystallogr.* **1340** 582 (1984)
96. C Zhang, R Chanda, H K Reddy, G N Schrauzer *Inorg. Chem.* **30** 3865 (1991)
97. J Bartini, C Luchiat, W Muret, M Zeppezaner (Eds) *Zinc Enzymes* Vol. 1 (Boston: Birkhauser, 1986)
98. E Kimura *Pure Appl. Chem.* **65** 355 (1993)
99. L E Nivorozhkin, M S Korobov, R Ya Olekhnovich, L E Konstantinovskii, V I Minkin *Koord. Khim.* **8** 1080 (1982)
100. L E Nivorozhkin, M S Korobov, A L Nivorozhkin, L E Konstantinovskii, V I Minkin *Zh. Obshch. Khim.* **55** 1125 (1985)
101. Z N Budarina, L S Minkina, L P Olekhnovich, O A Osipov *Koord. Khim.* **3** 409 (1981)
102. A Recca, F A Bottino, P Finocchiaro *J. Inorg. Nucl. Chem.* **42** 479 (1980)
103. M S Korobov, R Ya Olekhnovich, L E Konstantinovskii, N I Borisenko, L E Nivorozhkin, V I Minkin *Koord. Khim.* **15** 1622 (1989)
104. L E Konstantinovskii, R Ya Olekhnovich, M S Korobov, L E Nivorozhkin, V I Minkin *Zh. Obshch. Khim.* **60** 1930 (1990)
105. L E Konstantinovsky, R Ya Olekhnovich, M S Korobov, L E Nivorozhkin, V I Minkin *Polyhedron* **10** 77 (1991)
106. V I Minkin, M S Korobov, L E Nivorozhkin, O E Kompan, R Ya Olekhnovich, G S Borodkin, Yu T Struchkov *Mendeleev Commun.* **2** (1993)
107. M S Korobov, G S Borodkin, L E Nivorozhkin, V I Minkin *Zh. Obshch. Khim.* **61** 929 (1991)

108. M S Korobov, R Ya Olekhnovich, E V Sukholenko, G S Borodkin, L E Nivorozhkin, V I Minkin, in *XVII Vsesoyuznoe Chugaevskoe Soveshchanie po Khimii Kompleksnykh Soedinenii, Minsk, 1990* (Tezisy Dokladov) [The XVIIth All-Union Chugaev Conference on the Chemistry of Coordination Compounds Minsk, 1990 (Abstracts of Reports)] p. 429
109. L E Nivorozhkin, Doctoral Thesis in Chemical Sciences, Rostov Univ., Rostov-on-Don, 1987
110. V I Usacheva, V A Bren', L O Atovmyan, V V Tkachev, V I Minkin *Koord. Khim.* **2** 1514 (1976)
111. T G Takhirov, O A D'yachenko, D B Tagiev, A L Nivorozhkin, L E Nivorozhkin, V I Minkin *Koord. Khim.* **14** 237 (1988)
112. P Orioli, L Sacconi *Inorg. Chem.* **5** 400 (1966)
113. J Mocksen *Acta Crystallogr., Sect. B, Struct. Crystallogr.* **34** 429 (1978)
114. V V Litvinov, V V Sergeenko, M I Knyazhansky, M A Porai-Koshits, A D Garnovskii, A E Mistryukov *Koord. Khim.* **16** 1360 (1990)
115. A Haaland *Angew. Chem., Int. Ed. Engl.* **28** 992 (1990)
116. E S Gruff, S A Koch *J. Am. Chem. Soc.* **111** 8762 (1989)
117. M Bochmann, G Bwembya, R Grinter, J Lu, K J Webb, D J Williamson, M B Hursthouse, M Mazid *Inorg. Chem.* **32** 537 (1993)
118. H J Kneppers, K Wieghardt, B Nuber, J Weiss *Z. Anorg. Allg. Chem.* **577** 155 (1989)
119. L E Nivorozhkin, V I Minkin, N I Borisenko, L E Konstantinovskii, M S Korobov, R Ya Olekhnovich *Dokl. Akad. Nauk SSSR* **260** 1176 (1981)
120. L E Nivorozhkin, R Ya Olekhnovich, M S Korobov, L E Konstantinovskii *Koord. Khim.* **12** 899 (1986)
121. L E Nivorozhkin, R Ya Olekhnovich, M S Korobov, N I Borisenko, L E Konstantinovskii, V I Minkin *Koord. Khim.* **13** 466 (1987)
122. V A Bren', O A Osipov, V I Minkin, Zh V Bren', L S Minkina, L O Atovmyan, S M Aldoshin, O A D'yachenko *Koord. Khim.* **5** 1058 (1979)
123. M S Korobov, G S Borodkin, L E Nivorozhkin, V I Minkin *Dokl. Akad. Nauk SSSR* **309** 367 (1989)
124. L E Nivorozhkin, Yu E Chernysh, G S Borodkin, R Ya Olekhnovich, Yu A Zhdanov, V I Minkin *Dokl. Akad. Nauk SSSR* **273** 144 (1983)
125. L E Konstantinovskii, Yu E Chernysh, G S Borodkin *Zh. Vses. Khim. O-va im. D. I. Mendeleeva* **30** 197 (1985)
126. L E Nivorozhkin, G A Kalabin, A L Nivorozhkin, R B Valeev, V I Minkin *Koord. Khim.* **12** 608 (1986)
127. D M Knotter, M D Janssen, D M Grove, W J J Smeets, E Horn, A L Spek, G Van Koten *Inorg. Chem.* **30** 4361 (1991)
128. M Bochmann, K Webb, K Harman, M B Hursthouse *Angew. Chem.* **102** 703 (1990)
129. M Bochmann, K Webb, M B Hursthouse, M Mazid *J. Chem. Soc., Dalton Trans.* 2317 (1991)
130. H B Bürgi *Angew. Chem., Int. Ed. Engl.* **14** 460 (1975)
131. A Domeniciano, L Torelli, A Vaciado, L Lambonelli *J. Chem. Soc. A* 1351 (1968)
132. A L Nivorozhkin, E V Sukholenko, L E Nivorozhkin, N I Borisenko, V I Minkin, Yu K Grishin, O A Diachenko, T G Takhirov, D B Tagiev *Polyhedron* **8** 569 (1988)
133. V I Minkin, V A Pichko, B Ya Simkin, I A Abubikerova *J. Mol. Struct. (Theochem)* **227** 481 (1992)
134. M J S Dewar, G L Grady, K M Merz, J J P Stewart *Organometallics* **4** 1964 (1985)
135. L E Nivorozhkin, Yu E Chernysh, A L Nivorozhkin, G S Borodkin, N I Borisenko, V I Minkin *Dokl. Akad. Nauk SSSR* **296** 358 (1987)
136. J E Gümrükcuoglu, J Jeffrey, M F Lappert, J B Pedley, A K Rai *J. Organomet. Chem.* **341** 53 (1988)
137. G Salem, A Shier, S B Wild *Inorg. Chem.* **27** 3029 (1988)
138. S A Palmer, S B Wild *Inorg. Chem.* **22** 4054 (1983)
139. N K Roberts, S B Wild *J. Am. Chem. Soc.* **101** 6254 (1979)
140. R S Cahn, C K Ingold, V Prelog *Angew. Chem., Int. Ed. Engl.* **5** 385 (1966)
141. T A Albright, J K Burdett, M-H Whangbo, in *Orbital Interactions in Chemistry* (New York: Wiley, 1985) p. 304
142. E A Halevi, R Knorr *Angew. Chem.* **94** 307 (1982)
143. T Ziegler *Inorg. Chem.* **24** 1547 (1985)
144. R H Cayton, M H Chisholm, D L Clark, C E Hammond *J. Am. Chem. Soc.* **111** 2751 (1989)
145. D R Eaton, M J McGlinchey, K A Moffat, R J Buist *J. Am. Chem. Soc.* **106** 8110 (1984)
146. A D English, P Meakin, J P Jesson *J. Am. Chem. Soc.* **98** 422 (1976)
147. Yu K Grishin, V A Domrachev, Yu A Ustynyuk, S N Titova, G A Domrachev, G A Rasuvaev *Polyhedron* **2** 895 (1983)
148. G N LaMar, E O Sherman *J. Am. Chem. Soc.* **92** 2691 (1970)
149. L H Pignolet, W De, W Horrocks, R H Holm *J. Am. Chem. Soc.* **92** 1855 (1970)
150. H Brunner *Adv. Organomet. Chem.* **18** 152 (1980)
151. W G Jackson, in *Stereochemistry of Organometallic and Inorganic Compounds* Vol. 1 (New York: Academic Press, 1986) p. 255
152. P Hofman *Angew. Chem., Int. Ed. Engl.* **16** 536 (1977)
153. R Knorr, A Weiss, H Polzer, E Rüppe *J. Am. Chem. Soc.* **99** 650 (1977)
154. R Knorr, F Ruf *J. Am. Chem. Soc.* **101** 5424 (1979)
155. R Knorr, A Weiss *Chem. Ber.* **114** 2104 (1981)
156. R Knorr, F Ruf *Angew. Chem.* **96** 350 (1984)
157. O A Osipov, A D Garnovskii, V I Minkin, V A Kogan, V P Kurbatov, L E Nivorozhkin, L S Minkina, I Ya Kvitko *Izv. Severo-Kavkazsk. Nauch. Tsentra Vyssh. Shkoly, Estestv. Nauki* **2** 11 (1975)
158. L E Nivorozhkin, L E Konstantinovskii, M S Korobov, A L Nivorozhkin, V I Minkin *Zh. Obshch. Khim.* **52** 205 (1982)
159. L E Nivorozhkin, A L Nivorozhkin, M S Korobov, L E Konstantinovskii, V I Minkin *Polyhedron* **4** 1701 (1985)
160. A L Nivorozhkin, M S Korobov, L E Konstantinovskii, L E Nivorozhkin, V I Minkin *Zh. Obshch. Khim.* **55** 849 (1985)
161. L E Nivorozhkin, L E Konstantinovskii, M A Voronov, V I Minkin, O A Osipov, V P Kurbatov, L S Minkina. *Zh. Neorg. Khim.* **18** 2456 (1973)
162. L E Nivorozhkin, L E Konstantinovskii, V I Minkin, O A Osipov, A D Garnovskii, V P Kurbatov, I Ya Kvitko *Zh. Neorg. Khim.* **20** 3012 (1975)
163. L E Nivorozhkin, L E Konstantinovskii, V I Minkin, M S Korobov, I Ya Kvitko *Koord. Khim.* **6** 568 (1980)
164. N N Kharabaev, V A Kogan *Dokl. Akad. Nauk SSSR* **282** 396 (1985)
165. A I Uraev, A L Nivorozhkin, A S Frenkel, A S Antsishkina, M A Porai-Koshits, L E Konstantinovsky, G K-I Magomedov, A D Garnovsky *J. Organomet. Chem.* **308** 303 (1989)
166. T G Takhirov, Candidate's Thesis in Chemical Science, Rostov Univ., Rostov-on-Don, 1988
167. A Cour, D Adhikhari, H Toftlund, A Hazell *Inorg. Chem. Acta* **202** 145 (1992)
168. O A D'yachenko, L O Atovmyan, S M Aldoshin, V V Tkachev *Zh. Strukt. Khim.* **19** 829 (1978)
169. V A Kogan, N N Kharabaev, O A Osipov, S G Kochin *Zh. Strukt. Khim.* **22** 126 (1981)
170. L Banci, M Piccioli, A Scozzafava *Coord. Chem. Rev.* **120** 1 (1992)
171. W D Ollis, K L Ormand, I O Sutherland *J. Chem. Soc., Chem. Commun.* 1697 (1968)
172. S P Makarov, B Ya Simkin, V I Minkin *Khim. Geterotsikl. Soedin.* 171 (1988)
173. S M Aldoshin, V A Lokshin, A I Rezonov, N V Volbushko, N E Shelepin, M I Knyazhanskiĭ, L O Atovmyan, V I Minkin *Khim. Geterotsikl. Soedin.* 744 (1987)
174. B J Wakefield *The Chemistry of Organolithium Compounds* (Oxford: Pergamon Press, 1974)
175. D G Tuck *Comprehensive Organometallic Chemistry* (Oxford: Pergamon Press, 1982), Vol. 1, p. 683

Russian Chemical Reviews **63** (4) 313 – 322 (1994)
©1994 Russian Academy of Sciences and Turpion Ltd

UDC 547.465 : 541.127

Thermal decomposition of aliphatic nitro-compounds

G M Nazin, G B Manelis

Contents

I.	Introduction	313
II.	Gas-phase decomposition via the molecular mechanism	313
III.	Gas-phase decomposition via the radical mechanism	316
IV.	Reactions in the condensed state	320

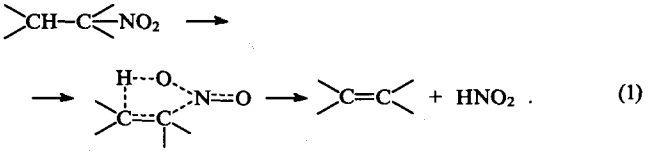
Abstract. Literature data on the thermal decomposition reactions of aliphatic nitro-compounds are surveyed and described systematically. Information concerning the influence of molecular structure on the rates and mechanisms of the gas-phase reactions is presented and the structures of the transition states in the C–N dissociation and HNO_2 elimination processes are examined. The characteristic features of the decomposition of nitro-compounds in the condensed phase are described. Data are presented on the C–N bond dissociation energy and the influence on the latter of electronic, steric, and conformational effects. The bibliography includes 86 references.

I. Introduction

The high rates of development of the chemistry of aliphatic nitro-compounds observed during recent decades were associated mainly with the search for new explosives and rocket fuel oxidants. The predominance of this aspect was responsible for the vigorous investigation of the thermal decomposition reactions of both the high-energy compounds themselves and of their numerous analogues and models. Thermal decomposition of virtually all the structural types of nitro-compounds has been studied: mononitroalkanes, *gem*-dinitroalkanes, 1,1,1-trinitroalkanes, pentane derivatives containing between 4 and 8 nitro-groups, unsaturated nitro-compounds, aliphatic-aromatic nitro-compounds, and α-halonitro-compounds, as well as numerous compounds with linked mixed functional groups in which the C–NO_2 fragments are the most reactive parts of the molecules. Whereas only 8 compounds were examined in the first (and hitherto the only) review on this topic published in 1968,[1] at the present time the number of systems investigated has exceeded 100 and in almost all cases the studies have reached the stage in which the decomposition mechanism has been established. This makes it possible to classify the available data not only in terms of the types of substances but also in terms of the reaction mechanisms. In the classification based on the mechanisms, large reaction series arise within the framework of which it is easy to trace the relation between structure and reactivity and to predict the stability of new compounds. It is also useful to consider separately the gas phase and the condensed state in which the decomposition reactions have a number of characteristic features.

On the basis of all the available data, one may conclude that the following principal decomposition mechanisms operate in the gas phase:

1. The molecular mechanism involving the elimination of HNO_2 via a five-membered transition state:



(1)

2. The radical mechanism, where the reaction proceeds via the dissociation of the C–N bond with formation of free radicals:

$$RNO_2 \longrightarrow \dot{R} + NO_2^{\cdot} . \qquad (2)$$

Mononitroalkanes having a hydrogen atom in the α-position, α-halonitro-compounds of the type RCH_2CHXNO_2 (X = halogen), and many α-nitroolefins decompose via the first mechanism at moderate temperatures (up to 300 °C). Owing to the reduced strength of the C–N bond, the decomposition of *gem*-dinitroalkanes, 1,1,1-trinitroalkanes, α,α-dihalo-derivatives RCX_2NO_2, and other compounds with a large number of nitro-groups proceeds via the second mechanism. At fairly high temperatures, reaction (2) becomes dominant in all cases because it has a higher pre-exponential factor in the expression for its rate constant than reaction (1).

II. Gas-phase decomposition via the molecular mechanism

1. Mononitroalkanes

The gas-phase decomposition of mononitroalkanes is complicated by a heterogeneous reaction on the surface.[2,3] The dependence of the rate of reaction on the ratio of the surface area to the volume of the vessel (S/V) is significant in the case of primary [2] nitroalkanes and is virtually absent for tertiary nitroalkanes.[3] Accordingly, an appreciable scatter of the literature data, due to failure to take into account heterogeneous reactions, is observed only in the case of primary nitroalkanes.[1] The 'elimination' of the heterogeneous reaction is achieved by calculating the dependence of the observed rate constants k_o on the parameter S/V.

G M Nazin Laboratory for Reactions in Condensed Systems,
G B Manelis Division of Combustion and Explosions,
Institute of Chemical Physics, Russian Academy of Sciences,
142432 Chernogolovka, Moscow region. Fax (7-096) 515 35 88

Received 8 February 1994
Uspekhi Khimii **63** (4) 327 – 337 (1994); translated by A K Grzybowski

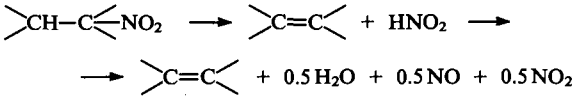
Table 1. Characteristics of the molecular decomposition of nitroalkanes.[4]

Compound	T/ °C	E/kJ mol^{-1}	lg(A/s^{-1})	ω_{rel} at 570 K	D(C–N)/kJ mol^{-1}	Q/kJ mol^{-1}	ε_0/kJ mol^{-1}
Nitroethane	320–380	188.5	12.24	1.00	237.1	70.3	118.2
1-Nitropropane	320–380	188.1	12.15	1.09	247.2	64.3	123.8
1-Nitrobutane	320–380	181.8	11.79	1.47	227.9	67.4	114.4
1-Nitropentane	320–380	181.8	11.82	1.66	–	–	–
1-Nitrohexane	320–380	181.4	11.81	1.79	–	–	–
2-Methyl-1-nitropropane	320–380	182.7	11.65	0.93	–	–	–
3-Methyl-1-nitrobutane	320–380	183.9	11.99	1.59	–	–	–
2-Nitropropane	280–340	182.3	12.72	11.7	246.4	81.5	100.8
2-Nitrobutane	280–340	181.4	12.70	13.5	251.8	–	–
2-Nitrohexane	280–340	183.1	12.93	15.7	–	–	–
3-Methyl-2-nitrobutane	280–320	179.3	12.68	–	–	–	–
3,3-Dimethyl-2-nitrobutane	280–320	177.2	12.74	36.2	–	–	–
2-Methyl-2-nitropropane	250–320	179.3	13.63	170.0	242.2	84.8	94.5
2-Methyl-2-nitrobutane	250–300	173.0	13.30	312.3	–	–	–
3-Methyl-2-nitropropane	250–280	170.5	13.33	363.0	–	–	–
2,3-Dimethyl-2-nitrobutane	230–280	170.5	13.43	721.0	–	–	–

Note. The thermochemical data for the calculation of D and Q were taken from Lebedev et al.[12]

The characteristics of the homogeneous gas-phase reactions are presented in Table 1.

The decomposition of nitroalkanes results in the formation of the corresponding olefins.[4–6] During the reaction, they are oxidised, but these processes do not proceed to an appreciable extent[3] and in all cases the final gas pressure is close to $2.5p_0$ (p_0 is the initial pressure), i.e. is the same as for the expected initial process.



In the decomposition of secondary and tertiary nitroalkanes, the yield of alk-1-enes and alk-2-enes is close to the statistical value and is almost independent of temperature (Table 2). Only in the case of 2,3-dimethyl-2-nitrobutane is steric hindrance to the formation of alk-2-ene observed.

a. The importance of the pre-exponential factor

The increase in rate on passing from primary to tertiary nitroalkanes is caused to a significant extent by the increase in the pre-exponential factor A. If account is taken of the change in the statistical reaction factor σ, which is equal to twice the number of hydrogen atoms in the β-positions, then, within the limits of the series of primary, secondary, and tertiary nitroalkanes, the values of lg(A/σ) are approximately constant and equal on average to 11.34, 11.80, and 12.35 respectively. These differences between the values can be explained by the stepwise increase in the barrier to the internal rotation V_{int} about the C–N bond on α-alkylation (from <4 kJ mol^{-1} for primary nitroalkanes to >40 kJ mol^{-1} for tertiary nitroalkanes). The increase in the barrier to the internal rotation about the C–C bond also exerts some influence on the change in A. The loss of this partly hindered rotation is responsible for the reduced value of A/σ in *tert*-nitroalkanes (compared with the 'normal' value $A = 10^{13.5}$ s^{-1}). The details of the calculation of A for reactions involving elimination from primary nitroalkanes have been published.[7]

Table 2. The relative yields (γ) of alk-1-enes on decomposition of nitrocompounds.[4]

Compound	T/ °C	γ(%)	
		experiment	calculation
2-Nitrobutane	250	55	60
	330	56	60
2-Nitrohexane	300	58	60
3-Methyl-2-nitrobutane	300	78	75
2-Methyl-2-nitrobutane	190	77	75
	250	77	75
3-Methyl-3-nitropentane	250	43	42.8
2,3-Dimethyl-2-nitrobutane	250	95	85.7

b. The polar nature of the HNO_2 elimination reaction

Reaction (1) is endothermic and its activation energy is

$$E = Q + \varepsilon_0,$$

where Q is the heat of reaction and ε_0 the activation energy for the reverse process involving the addition of HNO_2 to the olefin.

It is seen from Table 1 that under the influence of alkyl substituents Q and ε_0 change in opposite directions and the energy E therefore remains almost constant.

α-Methylation has comparatively little influence on the rate of reaction (1) (Table 3) and, in terms of this feature, the elimination of HNO_2 can be assigned (in Maccoll's terminology[9]) to weak quasi-heterolytic processes. However, in terms of another feature of these reactions, according to which the rate of elimination depends directly on the degree of charge separation in the transition state, reaction (1) can be assigned to highly polar reactions, since its rate exceeds those of any other reactions of this type. There is no doubt that the high electronegativity of the NO_2 group and the high dipole moment of the nitroalkane molecule (~3.5 D), which is almost twice as high as for haloalkanes (~2.0 D), facilitate the formation of a highly polar transition state. As a result of the low polarisability of the C–N bond and the simultaneously high electronegativity of the NO_2 group, the bond is polarised to the maximum extent already in nitroethane and, on further alteration of the structure of the alkyl residue, the state of this bond and the charge on the nitro-group hardly vary and hence the rate of the decomposition reaction varies only little. The extent of the change in the polarisation of the C–N bond on α-methylation may be estimated from the relative increase in the dipole moment $\Delta\mu$ on passing from CH_3X to *tert*-C_4H_9X. For example, $\Delta\mu$ is 20% for X = Cl and only 5% for X = NO_2. Similarly, $\Delta\mu$ is small in the series of alcohols, amines, esters, and isocyanates[8] and hence there is only a slight variation of the rate of α-methylation of these compounds.

Table 3. The influence of α-methylation on the relative rate of elimination of HX from the alkyl derivatives RX.[8]

X	R = *iso*-C_3H_7	R = *tert*-C_4H_9
Cl	223	41000
Br	280	78000
I	100	35000
CH_3COO	26	1600
HCOO	20	720
SCN	38	800
NO_2	12	172
$H_2C=CHO$	13	126
OH	10	38

Note. The relative rate is unity for R = C_2H_5.

In terms of the change in ε_0 ($\Delta\varepsilon_0$) for the reaction involving addition to olefins of different structure, HNO_2 does not differ from other acids HX (Table 4) and the above process is quantitatively consistent with the theoretical calculations for four-centre reactions based on the polar transition state model made up of two semi-ionic pairs in proximity.[10]

Using ε_0 for nitroethane, the $\Delta\varepsilon_0$ data for olefins,[11] and additive schemes for the calculation of the enthalpies of formation of nitro-compounds,[12] it is possible to estimate Q and E for the elimination reactions involving many nitroalkanes. Absence of a preferential elimination from *sec*-nitroalkanes has been explained by the mutual compensation of Q and ε_0 (Table 1).

2. α-Halonitroalkanes

The α-halogenation of nitroalkanes lowers the activation energy and increases the rate of reaction (Tables 1 and 5). However, this decrease is small (4–12 kJ mol^{-1}) and reaches 20 kJ mol^{-1} in only one case ($C_2H_5CHClNO_2$). However, on the whole the activation energy for the molecular decomposition of α-halonitroalkanes is in the range 166–184 kJ mol^{-1}, as for nitroalkanes.

In terms of their influence on the rate of the decomposition reaction, the halogens can be arranged in the sequence Cl > Br > F. This sequence in the influence of the halogens may be accounted for within the framework of the concept of the polar nature of the transition state. The inductive effect of the halogen atoms, which diminishes the electron density of the NO_2 group, should increase the rate of decomposition of halonitroalkanes in the sequence Br < Cl < F. On the other hand, the ability of the halogens to exhibit a positive mesomeric effect decreases the rate of decomposition in this series. The mesomeric effect may be expressed by the stabilisation of the transition state or by the supply of electrons to the NO_2 group in the ground state.

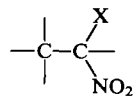


Table 5. Characteristics of the reactions involving the elimination of HNO_2 from halonitroalkanes.[13]

Compound	T/ °C	E/kJ mol^{-1}	$\lg(A/s^{-1})$	ω_{rel} [a]
CH_3CHFNO_2	300–340	184.3	12.62	5.4
$C_2H_5CHClNO_2$	250–300	165.9	12.55	174.0
$C_2H_5CHBrNO_2$	280–320	173.9	12.48	31.6
$(CH_3)_2CClNO_2$	240–300	176.8	13.62	24.5
$(CH_3)(C_2H_5)CClNO_2$	250–280	171.8	13.37	36.3
$(CH_3)_2CBrNO_2$	250–290	176.8	13.40	14.8
$(CH_3)_2CHCCl(NO_2)CH_3$	230–270	167.6	13.20	40.0
$(CH_3)_2CHCBr(NO_2)CH_3$	230–270	165.9	13.19	40.0

[a] ω_{rel} is the ratio of the rate of decomposition of the halonitroalkane to the rate of decomposition of the analogous unsubstituted nitroalkane at the temperature corresponding to $k = 10^{-4}\ s^{-1}$ for the nitroalkane.

The sequence in the influence of the halogens is in fact a consequence of the superposition of these two effects. The same sequence has been observed in the decomposition of α-polyhaloalkanes.[8,9,14]

3. α-Nitroolefins

In terms of the rate and kinetic parameters of their decomposition reactions, α-nitroolefins are close to their saturated analogues (Table 6). β-Alkylation influences the rate and activation energy more than does α-alkylation. The quantity $\lg(A/\sigma)$ for the decomposition of nitroalkenes is actually equal to that for the decomposition of *sec*-nitroalkanes. In the case of nitroalkenes, the internal rotation about the C–N bond is lost on formation of a cyclic transition state, while in the case of nitroalkenes the internal rotation about the C–N and C–C bonds is lost. Consequently the potential barrier to the internal rotation of the nitro-group in nitroalkenes is higher than in *sec*-nitroalkanes.

The decomposition of unsaturated nitro-compounds can also proceed via other mechanisms, but these too are of the molecular type. It has been shown for 2-methyl-3-nitroprop-2-ene that,[15] when the NO_2 and CH_3 groups are forced to

Table 6. Characteristics of the molecular decomposition of nitroalkenes.[13]

Compound	T/ °C	E/kJ mol^{-1}	$\lg(A/s^{-1})$	ω_1	ω_2
$CH_2=CHNO_2$	340–400	191.9	12.10	1.0	1.3
$CH_3CH=CHNO_2$	307–360	176.8	11.82	9.2	8.1
$C_2H_5CH=CHNO_2$	290–340	176.0	11.92	13.8	8.3
$C_6H_5CH=CHNO_2$	290–350	176.0	12.04	18.2	–
$C_2H_5C(NO_2)=CH_2$	323–380	187.3	12.16	2.6	0.25

Note. The following notation has been adopted: ω_2 is the relative rate at 350 °C and ω_2 is the ratio of the rates of decomposition of the nitroalkene and of its saturated analogue at the temperature corresponding to $k = 10^{-4}\ s^{-1}$ for the nitroalkene.

Table 4. The absolute change $\Delta\varepsilon_0$ (kJ mol^{-1}) in reactions involving the addition of HX to olefins.[8]

Olefin	Orientation [a]	Calculation	Experiment for HX					
			HCl	HBr	HI	H_2O	CH_3OH	HNO_2
C_2H_4	–	0	0	0	0	0	0	0
C_3H_6	M	−17.6	−23.1	−17.2	−19.7	−26.0	–	−17.6
	AM	+1.7	−3.3	−0.8	–	−0.8	–	+5.7
C_4H_8	M	−24.7	−35.2	−31.4	–	–	–	−23.9
	AM	−2.1	−3.3	−3.3	–	–	–	−3.7
iso-C_4H_8	M	−50.3	−62.0	−49.4	−42.7	−43.1	−44.0	−23.6

[a] The following notation has been adopted: M — addition in accordance with the Markovnikov rule, AM — addition contrary to the Markovnikov rule.

assume the *cis*-disposition, decomposition via isomerisation takes place readily.

$$(CH_3)_2C{=}CHNO_2 \longrightarrow H_2C{=}\underset{\displaystyle CH_3}{\overset{\displaystyle |}{C}}{-}CHNOOH \longrightarrow \text{products}$$

For this compound, we have

$$k = 10^{11.8} \exp\left(-\frac{151680}{RT}\right).$$

The composition of the products of the decomposition of $PhCH=C(CH_3)NO_2$ at 600 °C and a pressure of 10^{-3} torr has been determined.[16] Since the main products are PhCHO and CH_3CN, one may conclude that the reaction proceeds via an intramolecular oxidation mechanism.

$$PhCH{=}C(CH_3)NO_2 \longrightarrow Ph{-}\overset{\displaystyle H}{\overset{\displaystyle |}{C}}{:::}\overset{\displaystyle CH_3}{\overset{\displaystyle |}{C}} \longrightarrow$$

$$\longrightarrow PhCHO + CH_3CN + O$$

However, in order to confirm this mechanism, it is essential to carry out further studies on this reaction and in the first place to determine its kinetic parameters, to elucidate the influence of p_0 on the composition of the products and on the rate, and to investigate nitrostyrene analogues.

It has been shown[17] that on hot (650 °C) iron and nickel surfaces nitroethylene loses an oxygen atom and is converted into nitrosoethylene. The reaction was carried out at low pressures with activation by collisions with the surface. Nitrosoethylene was in fact obtained for the first time by this method and its reactions on the surface were elucidated.

$$H_2C{=}CH{-}NO \longrightarrow CH_2{=}CH{-}N{:} \longrightarrow H_3CCN$$

III. Gas-phase decomposition via the radical mechanism

1. The chemical mechanism

The decomposition reactions the first stage of which is the dissociation of the C–N bond are complicated by chain processes only in the case of mononitro-compounds such as nitromethane[18–21] and chloropicrin.[22] For nitromethane, heterogeneous decomposition on the surface is also important.[18] The mechanism of the decomposition of nitromethane at all temperatures up to the inflammation temperature[23–25] includes at least 26 reactions. Some of the reactions presented in Scheme 1 are kinetically important and explain the formation of the principal intermediates (CH_2O, NO, NO_2) and final products (CH_4, CH_3OH, HCN, H_2O) at moderate temperatures.

Scheme 1

$$CH_3NO_2 \longrightarrow \dot{C}H_3 + NO_2$$

$$CH_3NO_2 + \dot{C}H_3 \longrightarrow CH_4 + \dot{C}H_2NO_2$$

$$\dot{C}H_3 + NO_2 \longrightarrow CH_3\dot{O} + NO$$

$$CH_3NO_2 + CH_3\dot{O} \longrightarrow CH_3OH + \dot{C}H_2NO_2$$

$$\dot{C}H_2NO_2 \longrightarrow CH_2O + NO$$

$$\dot{C}H_3 + NO \longrightarrow CH_3NO$$

$$CH_3NO \longrightarrow HCN + H_2O$$

Starting with *gem*-dinitroalkanes, the polynitro-compounds decompose unimolecularly. The surface, pressure, and impurities do not as a rule affect the rate. Nitrogen oxide and dioxide, formed in the decomposition, inhibit all the free-radical processes. Processes on the surface are characteristic only of substances of the type of di- and tri-nitromethane having a hydrogen atom in the α-position.[26] Typical decomposition reactions of polynitro-compounds are presented in Scheme 2. The scheme is based on the composition of the products of the decomposition of 1,1,1-trinitroethane (Table 7).[27] All the stages in this scheme, except the fourth, correspond to the generally accepted ideas concerning the reactions of free radicals in NO_2 and NO. The fourth reaction is new and is observed only for compounds having at least two nitro-groups at one carbon atom. The yield of nitriles increases following the addition of NO. RCN and ClCN are formed from $RCCl(NO_2)_2$.[14] When iodine is added to $C(NO_2)_4$ and $ClC(NO_2)_3$, ICN is formed in the first case, while in the second only ClCN is produced.[28]

Scheme 2

$$CH_3C(NO_2)_3 \longrightarrow CH_3\dot{C}(NO_2)_2 + NO_2$$

$$CH_3\dot{C}(NO_2)_2 \longrightarrow CH_3\dot{C}O + NO + NO_2$$

$$CH_3\dot{C}(NO_2)_2 + NO_2 \longrightarrow CH_3\dot{C}O + NO + 2\,NO_2$$

$$CH_3\dot{C}(NO_2)_2 + NO \longrightarrow CH_3C(NO)(NO_2)_2 \longrightarrow$$

$$\longrightarrow CH_3CN + NO_2 + NO_3$$

$$CH_3\dot{C}O \longrightarrow \dot{C}H_3 + CO$$

$$CH_3\dot{C}O + NO_2 \longrightarrow CH_3CO\dot{O} + NO$$

$$CH_3CO\dot{O} \longrightarrow \dot{C}H_3 + CO_2$$

$$CH_3CO\dot{O} + RH \longrightarrow CH_3COOH + \dot{R}$$

$$CH_3CO\dot{O} + \dot{C}H_3 \longrightarrow CH_3COOCH_3$$

$$\dot{C}H_3 + NO_2 \longrightarrow CH_3NO_2$$

$$\dot{C}H_3 + NO_2 \longrightarrow CH_3\dot{O} + NO$$

$$\dot{C}H_3 + NO \longrightarrow CH_3NO \longrightarrow HCN + H_2O$$

$$CH_3NO + 2\,NO \longrightarrow \dot{C}H_3 + N_2 + NO_3$$

$$CH_3NO + NO_2 \longrightarrow CH_3NO_2 + NO$$

$$\dot{C}H_3 + RH \longrightarrow CH_3OH + \dot{R}$$

$$CH_3\dot{O} + NO_2 \longrightarrow CH_3ONO_2$$

$$CH_3\dot{O} + NO_2 \longrightarrow CH_2O + HNO_2$$

$$CH_3\dot{O} + NO \longrightarrow CH_3ONO$$

$$CH_3\dot{O} + NO \longrightarrow CH_2O + HNO$$

$$2\,HNO \longrightarrow H_2O + N_2O$$

$$NO_2 + CH_2O \longrightarrow NO + CO_2 + H_2O$$

Table 7. Dependence of the yield of the products of the decomposition of 1,1,1-trinitroethane on the degree of reaction at 170 °C.[27]

Product	Degree of reaction (%)						
	2	10	20	37	48	86	100[a]
CH_3NO_2	0.09	0.10	0.13	0.15	0.09	0.16	0.11
CH_3CN	0.01	0.02	0.02	0.03	0.05	0.02	–
CH_3OH	0.02	0.04	0.02	0.05	0.04	0.04	0.01
CH_3ONO_2	0.34	0.24	0.22	0.13	0.12	0.12	0.47
CH_3COOCH_3	–	0.001	0.004	0.008	0.005	0.005	–
CH_3COOH	–	0.10	0.13	0.34	0.42	0.52	–
CH_3NO	0.20	0.04	0.02	–	–	–	–
CH_3ONO	–	traces	traces	–	–	–	0.01

[a] In an excess of NO_2.

The decomposition of compounds of the type of hexanitroethane with a vicinal disposition of the nitro-groups results in the formation of olefins. Thus it has been shown[29] that the vacuum pulse pyrolysis of hexanitroethane affords a high yield of tetranitroethylene. Since the kinetic parameters of the decomposition of this compound correspond to the abstraction of NO_2 and not the elimination of N_2O_4, it must be recognised that the olefin is formed as a result of a secondary reaction involving the ejection of NO_2 from the radical $(NO_2)_3CC(NO_2)_2$. The splitting off of two NO_2 molecules on decomposition of 1,2-difluorotetranitroethane in the gas phase at low pressures[30] and other instances of the decomposition of vicinal dinitroalkanes can be explained similarly.

The reactions of the 1-adamantyl radical, formed on radical decomposition of 1-nitroadamantane (600 °C), have been traced.[31]

2. Activation energies for the decomposition reactions and the strength of the C–N bonds in polynitro-compounds

Data on the radical decomposition of nitro-compounds are presented in Table 8. The activation energy for the decomposition reaction is determined by the strength of the C–N bond, $D(C-N) = E - RT_{av}$, and varies within wide limits. There is no doubt that D(C–N) is influenced by the inductive, steric, and resonance effects of the substituents. The resonance effect stabilises the transition state with a planar radical, remaining after the abstraction of the nitro-group. The mesomeric effect explains the sharp decrease in D(C–N) on passing from CH_3NO_2 to $PhCH_2NO_2$. It may be that the very strong influence of the sulfur atom in the α-position on D(C–N) (compounds **43–50**, Table 8) is associated with this effect. The steric effect of bulky α-substituents is reflected by the increase in the rate in the sequence H < Cl < Br < I for methane derivatives (compounds **6–10**, **14–16**, and **24–26**, Table 8 — see over).

The influence of all α-substituents on D(C–N) has been attributed[7] solely to the steric effect, which appears unlikely. The nitro-groups in polynitro-compounds are known to undergo mutual polarisation. Furthermore, the Cl, Br, and NO_2 substituents influence equally the strength of the C–H and C–F bonds, which are not subject to steric hindrance.[44] It has been shown[45] that the rate of reaction is influenced primarily by the electronic charges on the reaction centre. In a series of isotypical compounds without α-steric effects (compounds, **1**, **2**, **17**, and **27–32**, Table 8), the inductive effect is manifested in a pure form and is expressed by the relation

$$D(C-N) = 220 - 15.2\sigma^*. \quad (3)$$

The values of σ^* for substituents containing nitro-groups may be calculated from literature data.[46,47] Thus the constants σ^* are respectively 4.65, 4.54, and 2.93 for $C(NO_2)_3C(NO_2)_2$, $C(NO_2)_3$, and $CH_3C(NO_2)_2$.

We may also note that a method has been proposed[48] for the estimation of the activation energies for the radical decomposition of *C*-nitro-compounds based on the empirical correlation

$$E = 46.73 + 2.52(\Delta H_{CN} - 70) + 0.22(\Delta H_{CN} - 70)^2,$$

where ΔH_{CN} is a simplified energy characteristic of the C–N bond,[49] which is calculated by the MINDO/3 method and requires little computer time.

The study of the influence of molecular structure on D(C–N) has shown that there are two rules. The first is that a fluorine atom in the α-position acts on the bond not like an electronegative substituent but like a neutral hydrogen atom or alkyl group. Whereas D(C–N) decreases successively by 2–4 kJ mol^{-1} on replacement of the NO_2 group by Cl, Br, or I, its replacement by F increases D(C–N) by 20 kJ mol^{-1}. This increased stability of α-fluoronitro-compounds is associated with this fact. The unusual behaviour of fluorine as a α-substituent is characteristic not only of the C–N bond but also of the C–H and C–Hal bonds. The equivalence of hydrogen and fluorine as α-substituents was first noted by Vedeneev and Purmal'[50] and may be traced on the basis of data published in a handbook.[44]

The second rule concerns the manifestation of the field effect (the *F*-effect, anchimeric participation) in pentane derivatives with a large number of nitro-groups (compounds **33–36** and **38–42**, Table 8). In the main conformation of these compounds,[51] which is fixed under the influence of steric strain, one of the oxygen atoms of the γ-nitro-group approaches the terminal carbon atom to a distance corresponding to the van der Waals radius. This weakens the C–NO_2 bond as a result of the stabilisation of the radical, formed following the abstraction of NO_2, by the electron density on the oxygen of the γ-nitro-group. The effect intensifies with increase in the bulk of the second γ-substituents (H < F < Cl < Br).

The enthalpies of formation of the nitroalkyl free radicals (Table 9) and then D(C–H), D(C–C), or D(C–Hal) (Table 10) in nitro-compounds may be determined from the values of D(C–N) found by the kinetic method. The dissociation energies D calculated in this way differ somewhat from those found by a thermochemical method[12] from the variation of the enthalpies of formation of the compounds and supplement them. We may note that, with increase in the number of nitro-groups, D(C–H) also increases (owing to the polarisation of the C–H bond). Following a one-sided introduction of electronegative substituents, D(C–C) increases, whilst for a symmetrical disposition of the substituents it falls sharply.

Table 9. Enthalpies of formation of nitroalkyl radicals.

Radical R	D(R–NO_2)/ kJ mol^{-1}	$\Delta H_f^\circ(\dot{R})$/ kJ mol^{-1}	
		from D(C–N)	data of Lebedev et al.[12]
CH_2NO_2	230.5	103.5	132.4
$CH(NO_2)_2$	173.9	139.1	157.1
CH_3CHNO_2	193.6	62.0	76.3
$C_2H_5CHNO_2$	197.3	21.4	24.7
$(CH_3)_2CNO_2$	199.0	90.9	91.3
$CH_3C(NO_2)_2$	177.2	65.8	62.4
$C_2H_5C(NO_2)_2$	173.5	44.4	36.7
$(NO_2)_3CC(NO_2)_2$	147.1	276.5	271.1
$FC(NO_2)_2$	174.3	−42.7	–
F_2CNO_2	194.4	−243.0	–
$FC(NO_2)_2C(NO_2)_2$	150.0	30.2	–
$ClC(NO_2)_2$	153.3	160.0	–
$BrC(NO_2)_2$	148.3	120.7	–
$C(NO_2)_3$	140.7	10.9	–

Note. The values of ΔH_f° for the compounds RNO_2 necessary for the calculation of $\Delta H_f^\circ(\dot{R})$ were taken from Lebedev and coworkers and Carpenter et al.[12,52,53]

3. Characteristics of the variation of the pre-exponential factor

The pre-exponential factor in the expression for the rate constant for the dissociation of the R_3C-NO_2 bond reaches high values for several reasons.[54] The principal of these are as follows:

1. The decrease in the frequencies of the deformation vibrations associated with the C–N bond. Judging from the secondary kinetic deuterium isotope effect,[55] the frequency of the deformation vibration, which becomes the out-of-plane vibration of the R_3C radical, diminishes by a factor of 2. The frequencies of the two rocking vibrations of the R_3C group and of the analogous vibrations of the NO_2 group also decrease by this factor.

Table 8. Kinetic characteristics of the radical decomposition of aliphatic nitro-compounds.

No.	Compound	T/ °C	E/kJ mol^{-1}	lg[(A/σ)/s^{-1}]	$\Delta S^{\#}$/e.u.	Ref.
1	CH_3NO_2	360–390	227.5	14.34	4.2	18
		620–1200	245.1	16.21	12.72	21
2	$C_2H_5NO_2$	490–555	233.1	15.90	15.9	32
3	n-$C_3H_7NO_2$	600–900	245.1	15.36	8.8	33
4	iso-$C_3H_7NO_2$	600–900	226.3	15.38	8.9	33
5	$PhCH_2NO_2$	380–430	176.4	13.75	1.4	ü.[a]
6	Cl_3CNO_2	140–170	156.7	15.35	8.8	22
7	$Cl_2C(NO_2)_2$	110–150	143.7	14.96	7.0	34
8	$ClC(NO_2)_3$	120–165	152.5	15.27	8.4	34
9	$BrC(NO_2)_3$	110–160	151.7	15.58	10.0	34
10	$IC(NO_2)_3$	113–150	144.1	14.77	6.1	34
11	$FC(NO_2)_3$	178–236	175.6	14.92	6.8	35
		–	(178.0)	(15.20)	(8.8)	–
12	$HFC(NO_2)_2$	244–264	203.2	16.38	13.5	26
		–	(199.0)	(15.98)	(11.4)	–
13	$F_2C(NO_2)_2$	235–270	198.6	15.88	9.8	35
14	$FClC(NO_2)_2$	170–214	173.9	15.44	9.0	36
15	$FBrC(NO_2)_2$	170–210	165.5	15.00	7.2	36
16	$FIC(NO_2)_2$	160–197	166.3	15.40	9.0	36
17	$HC(NO_2)_3$	180–200	177.6	15.46	9.3	26
18	$C(NO_2)_4$	86–177	160.1	15.70	10.4	37
19	$CH_3CH(NO_2)_2$	197–260	197.4	16.44	13.8	38
20	$C_2H_5CH(NO_2)_2$	215–265	201.1	16.60	14.5	38
21	$C_3H_7CH(NO_2)_2$	220–265	201.7	16.70	15.0	38
22	$CH_3C(NO_2)_2CH_3$	175–210	211.6	18.20	21.8	39
		–	(199.0)	(16.81)	(15.5)	–
23	$CH_3CF(NO_2)_2$	214–262	199.9	16.70	15.0	35
24	$CH_3CBr(NO_2)_2$	160–190	169.9	15.84	11.0	14
25	$CH_3CCl_2NO_2$	190–235	178.5	15.22	8.2	14
26	$C_2H_5CCl_2NO_2$	200–258	178.9	15.15	7.9	14
27	$CH_3C(NO_2)_3$	160–210	181.0	16.70	15.0	40
28	$C_2H_5C(NO_2)_3$	160–200	177.2	16.32	13.5	40
29	$C_3H_7C(NO_2)_3$	160–200	182.7	17.22	17.3	40
		–	(178.1)	(16.72)	(15.00)	–
30	$FC(NO_2)_2C(NO_2)_2F$	107–180	176.8	17.4	18.2	35
31	$FC(NO_2)_2C(NO_2)_3$	88–140	152.9	16.60	14.5	35
32	$(NO_2)_3CC(NO_2)_3$	90–135	150.0	16.52	14.1	37
33	$[(NO_2)_3CCH_2]_2CHNO_2$	120–140	148.5	15.08	7.5	41
34	$[(NO_2)_3CCH_2]_2CFNO_2$	120–140	147.2	15.42	9.1	41
35	$[(NO_2)_3CCH_2]_2CClNO_2$	120–140	146.2	15.43	9.1	41
36	$[(NO_2)_3CCH_2]_2CBrNO_2$	120–140	143.3	15.15	7.7	41
37	$[F(NO_2)_2CCH_2]_2$	150–200	192.7	15.84	11.0	41
38	$[F(NO_2)_2CCH_2]_2CHNO_2$	180–220	172.6	15.00	7.1	41
39	$[F(NO_2)_2CCH_2]_2CFNO_2$	160–200	165.5	14.77	6.1	41
40	$[F(NO_2)_2CCH_2]_2CClNO_2$	160–200	165.5	15.48	9.4	41
41	$[F(NO_2)_2CCH_2]_2CBrNO_2$	160–200	162.1	15.12	7.7	41
42	$[F(NO_2)_2CCH_2]_2C(NO_2)_2$	130–160	152.1	15.22	8.2	41
43	$CH_3SC(NO_2)_3$	50–80	129.0	15.72	10.5	42
44	$PhSC(NO_2)_3$	80–100	194.0	15.52	9.6	42
45	2,4-$(NO_2)_2C_6H_3SC(NO_2)_3$	75–90	133.2	15.72	10.5	42
46	$CH_3SC(NO_2)_2CH_3$	120–150	161.3	17.45	18.4	42
47	$PhSC(NO_2)_2CH_3$	120–150	160.0	17.70	19.5	42
48	2,4-$(NO_2)_2C_6H_3SC(NO_2)_2CH_3$	120–135	157.1	17.25	18.2	42
49	$CH_3SO_2C(NO_2)_2CH_3$	160–190	164.7	14.85	6.5	42
50	$PhSO_2C(NO_2)_2CH_3$	170–195	163.0	14.70	5.8	42
51	$ClCH_2OCH_2C(NO_2)_2F$	210–256	196.3	16.50	14.0	43
52	$O_2NCH_2CH_2C(NO_2)_2F$	200–235	194.0	16.55	14.3	43

Note. σ is the statistical factor for the reaction equal to the number of equivalent nitro-groups. The entropies $\Delta S^{\#}$ were calculated for 200 °C from the relation $A = \sigma(ekT/h)\exp(\Delta S^{\#}/R)$. Data corrected by means of Eqn. (3) are indicated in brackets.

[a] The authors' unpublished data.

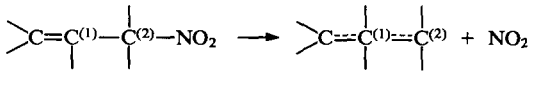
Table 10. Bond dissociation energies in nitro-compounds (kJ mol^{-1}).

Bond	From data in Table 8	From data of Lebedev et al.[12]
$H-CH_2NO_2$	375.8	–
$H-CH(NO_2)CH_3$	380.4	395.1
$H-CH(NO_2)C_2H_5$	394.7	397.6
$H-CH(NO_2)C_3H_7$	383.4	387.2
$H-C(NO_2)(CH_3)_2$	393.4	396.4
$H-CH(NO_2)_2$	416.9	434.9
$H-C(NO_2)_2CH_3$	410.2	411.9
$H-C(NO_2)_2C_2H_5$	393.9	400.6
$H-C(NO_2)_2C_3H_7$	405.2	398.0
$H-C(NO_2)_3$	419.4	427.4
$F-C(NO_2)_3$	426.1	–
$F-C(NO_2)_2F$	474.7	–
$F-C(NO_2)_2CH_3$	442.4	–
$F-C(NO_2)_2C(NO_2)_3$	486.9	–
$F-C(NO_2)FC(NO_2)_2F$	495.2	–
$F-C(NO_2)_2C(NO_2)F$	447.5	–
$Cl-C(NO_2)_3$	306.3	–
$Br-C(NO_2)_3$	221.2	–
$I-C(NO_2)_3$	145.0	–
$H_3C-CH_2NO_2$	348.2	371.2
$C_2H_5-CH_2NO_2$	333.5	362.4
$C_3H_7-CH_2NO_2$	323.0	352.0
$CH_3-CH(NO_2)CH_3$	344.4	354.5
$C_2H_5-CH(NO_2)CH_3$	329.7	357.4
$CH_3-CH(NO_2)C_2H_5$	357.0	355.3
$CH_3-C(NO_2)(CH_3)_2$	356.1	357.4
$CH_3-CH(NO_2)_2$	384.2	397.6
$C_2H_5-CH(NO_2)_2$	356.1	381.3
$C_3H_7-CH(NO_2)_2$	357.4	375.4
$C_4H_9-CH(NO_2)_2$	348.6	365.5
$CH_3-C(NO_2)_2CH_3$	363.3	359.5
$CH_3-C(NO_2)_3$	395.9	399.7
$C_2H_5-C(NO_2)_3$	382.1	390.5
$C_4H_9-C(NO_2)_3$	372.5	380.5
$O_2NCH_2-CH_2NO_2$	302.9	360.8
$(CH_3)_2(NO_2)C-C(NO_2)(CH_3)_2$	294.1	306.3
$CH_3(NO_2)_2C-C(NO_2)_2CH_3$	266.5	267.3
$CH_3(NO_2)_2C-C(NO_2)_3$	257.7	266.0
$(NO_2)_3C(NO_2)_2C-CH_3$	385.1	375.4
$(NO_2)_3C-C(NO_2)_3$	246.8	262.7
$F(NO_2)_2C-C(NO_2)_2F$	267.3	–
$F(NO_2)_2C-C(NO_2)_3$	244.3	–

2. The liberation of the internal rotation about the C–N bond. The maximum contribution by this factor to the activation entropy $\Delta S^{\#}$ is 3 e. u. (0.6 lg A).

3. The decrease in the frequencies of the torsional vibrations (up to free rotation) of the groups R adjoining the reaction centre. In the case of nitro-compounds, R may be alkyl groups and NO_2. The effect of the neighbouring groups can be very large but it was never observed previously.

4. In unsaturated and aliphatic-aromatic compounds, there is a possibility of a negative effect of the neighbouring groups owing to the conjugation of the double bond with a free valence on the reaction centre. Thus the order of the $C^{(1)}-C^{(2)}$ bond in the transition state of the reaction



is 1.5, as a result of which the torsional vibration frequency increases and $\Delta S^{\#}$ diminishes.

In the case of nitromethane, for which the barrier to the internal rotation V_{int} is low,[56] the factors 2–4 do not play any role and the slight increase in $\Delta S^{\#}$ compared with the normal value $\Delta S^{\#} = 0$ is due solely to the first cause. The decrease in the frequencies of the one asymmetric deformation vibration (1482 cm^{-1}) and the four rocking vibrations (1087, 1100, 605, and 477 cm^{-1})[57] by a factor of 2–2.5 increases $\Delta S^{\#}$ by 6 e. u., which is consistent with the experimental value.[18]

A detailed calculation of the pre-exponential factors for the decomposition reactions of $CH_3(NO_2)$, $HC(NO_2)_3$, $F_2C(NO_2)_2$, $HFC(NO_2)_2$, and $CH_3CF(NO_2)_2$ has been carried out by the MINDO/3 quantum-chemical method on the basis of the Rice–Ramsperger–Kassel–Marcus theory.[58] The best agreement with experiment was achieved within the framework of the semirigid activated complex model with a critical C–N bond length of 2.45 Å. The introduction of halogen atoms or of the NO_2 group into the nitromethane molecule leads to an increase in V_{int} and of $\Delta S^{\#}$ by a further 2 e. u.

The positive effect of the neighbouring groups is manifested only slightly for the NO_2 group (compounds **11–13**, **17**, and **18**, Table 8) and very markedly for alkyl substituents (compounds **19–23** and **27–29**, Table 8). NMR data indicate a marked hindrance of the rotation about the C–C bond in 1,1,1-trinitroethane.[59] A β-deuterium isotope effect is observed on decomposition of this compound,[55] which indicates a change in the vibration frequencies of the CH_3 group in the transition state.

There is no positive effect of the neighbouring NO_2 and alkyl groups in compounds having the large chlorine, bromine, and iodine atoms in the α-position (compounds **24–26**, Table 8), which hinder the rotation of the groups not only in the initial tetrahedral form but also in the planar form of the R_3C group. As already mentioned, steric factors influence also D(C–N) in these compounds.

$\Delta S^{\#}$ is smaller for $PhCH_2NO_2$ than for CH_3NO_2 owing to the negative effect of the Ph group.

4. Competition between the radical and molecular mechanisms

The quantitative characteristics described above make it possible to predict the characteristics of different decomposition pathways and to find the temperature T_{eq} at which the rates of elimination of HNO_2 and of the dissociation of the C–N bond are equal. The radical decomposition predominates above this temperature. The data for typical compounds are presented in Table 11. Approximate estimates of T_{eq} for certain mono- and di-nitro-compounds have also been carried out by Shaw.[60]

5. The nitro-nitrite rearrangement

Apart from the processes described above, which occur in the gas-phase reactions of nitroalkanes[15,16] the possibility of the nitro–nitrite rearrangement (NNR) as an alternative to the radical decomposition has been considered for several years. Thus the formation of CH_2O, which might have been a product of the NNR, has been observed in a study[61] of the decomposition of nitromethane in a molecular beam during laser heating (1078 cm^{-1}). The rate of rearrangement was 60% of the rate of dissociation of the C–N bond and its activation energy (233 kJ mol^{-1}) proved to be close to the C–N bond dissociation energy. The first theoretical calculation by the MINDO/3 method[62] yielded an activation energy of 188 kJ mol^{-1} for the NNR. However, later and more rigorous calculations[63] failed to confirm this result and indicate that the activation energy for the NNR is higher by 40 kJ mol^{-1} than the C–N bond dissociation energy.

In principle, the NNR can actually occur as a reaction accompanying the dissociation of the C–N bond and not as a kinetically independent process. This is possible when the decomposition proceeds via a loose transition state[64] in which there is a considerable distance between the fragments R and NO_2 being separated and when they execute three-dimensional rotation. The recombination of R with NO_2 can also occur in this state through an oxygen atom with the simultaneous elimination of NO. The loose transition state arising under these conditions is similar to that formed on decomposition of nitrobenzene and its

Table 11. Competition between the radical and molecular mechanisms of the decomposition reaction.

Compound	Radical decomposition				Molecular decomposition				T_{eq}/ °C
	I	II	III	IV	I	II	III	IV	
$CH_3CH_2NO_2$	–	–	233	15.9	–	–	189	12.2	340
$(CH_3)_2CHNO_2$	238	15.0	–	–	–	–	182	12.7	1000
$(CH_3)_3CNO_2$	234	15.2	–	–	–	–	179	13.6	1500
$CH_3CH(NO_2)_2$	–	–	197	16.7	176	13.0	–	–	80
$C_2H_5CH(NO_2)_2$	–	–	201	16.9	176	12.8	–	–	50
$C_2H_5CHClNO_2$	200	15.0	–	–	–	–	165	12.5	550
CH_3CHFNO_2	239	14.8	–	–	–	–	184	12.6	960
$CH_3CF(NO_2)_2$	–	–	200	17.0	172	13.0	–	–	100
$C_2H_5C(NO_2)_3$	–	–	177	16.8	168	13.5	–	–	−130
$CH_3CCl_2NO_2$	–	–	179	15.1	163	13.2	–	–	160
$CH_3CBr_2NO_2$	178	15.2	–	–	167	13.2	–	–	10
$CH_3CF_2NO_2$	239	14.8	–	–	176	12.2	–	–	1000
$CH_2{=}CHNO_2$	272	14.5	–	–	–	–	191	12.1	1600

Note. The following notation has been adopted: I, III — E/kJ mol^{-1}; II, IV — lg (A/s^{-1}); I, II — calculated values; III, IV — experimental values.

derivatives [D(C–N) > 288 kJ mol^{-1}], for which the NNR is, incidentally, observed.[65] The decomposition of aliphatic nitro-compounds always proceeds via a semirigid transition state (this is indicated by the constants for the recombination of alkyl radicals with NO_2)[66] and the rearrangement of such compounds is unlikely to be a secondary process accompanying the dissociation of the C–N bond. An experimental solution of the problem of the occurrence of the NNR can be achieved by studying the decomposition of CH_3NO_2 in the presence of $N^{18}O_2$ (in a medium comprising RH hydrogen donors) from the dependence of the ratio $CH_3OH/CH_3{}^{18}OH$ on the $N^{18}O_2$ concentration.

IV. Reactions in the condensed state

Mononitro- and halonitro-alkanes having a hydrogen atom in the α-position, dinitro-compounds with terminal $CH(NO_2)_2$ groups, and nitroform decompose in the liquid state much faster than in the vapour phase apparently as a result of isomerisation to nitronic acids or ionisation and autoprotolysis. For example, liquid nitroform decomposes at an appreciable rate at 80 °C whereas in the vapour phase the reaction does not begin until 180 °C. The liquid-phase reactions are subjected to fairly pronounced autocatalysis with the aid of NO and NO_2. They may be stabilised on acidification, which prevents the formation of the aci-form and ionisation.

The influence of the aci-form on the decomposition of liquid nitro-compounds and their capacity for detonation has been demonstrated convincingly in relation to nitromethane and nitroethane.[67] A characteristic feature of these compounds is the decrease in the critical detonation diameter under the influence of small amounts of added bases (dimethylenetriamine, pyridine), high pressure, which shifts the equilibrium towards the formation of the aci-form (the molar volume of which is smaller by 15% than that of the keto-form), and UV irradiation, under the influence of which isomerisation also occurs. A marked isotope effect in the decomposition of CD_3NO_2 is observed at a pressure of 10 kbar.[68]

The formal kinetic characteristics have been determined for liquid nitromethane and an expression has been obtained for its rate of decomposition with the maximum filling of the vessel by the test substance:

$$\frac{d\eta}{dt} = 10^{12.42}\exp\left(-\frac{173900}{RT}\right)(1-\eta) + 10^{3.64}\exp\left(-\frac{62850}{RT}\right)(1-\eta)\eta^2.$$

An even lower activation energy (136 kJ mol^{-1}) has been observed for the first-order decomposition reaction of nitromethane in the liquid phase at pressures of 40–50 kbar and temperatures of the order of 140 °C.[70] It was noted in the above study that the decomposition of nitromethane obeys a second-order equation at low pressures and temperatures below 120 °C.

In order to explain the decrease in the activation energy for the decomposition of nitromethane in the liquid state compared with the gas phase, a bimolecular decomposition mechanism, justified by quantum-chemical calculations, has been proposed.[69,70]

$$2\,CH_3NO_2 \longrightarrow (CH_3NO_2)_2 \longrightarrow TS \longrightarrow CH_3NO + HOCH_2NO_2$$

The enthalpies of formation of the dimer and the transition state (TS) proved to be −88.4 and 89.7 kJ mol^{-1} respectively.[69] Thus the calculated activation energy (178 kJ mol^{-1}) agreed with the experimental value. However, it is possible that this is merely fortuitous. The decrease in the activation energy in the liquid phase can be explained also by the decomposition of nitromethane via the aci-form and autoprotolysis and not via the transfer of oxygen. We may note that the calculation carried out by Khrapkovskii et al.[69] refers to free molecules and in no way takes into account the specific features of the condensed state. On the other hand, in the gas phase there is no bimolecular interaction. The question of the mechanism of the decomposition of nitromethane can apparently be elucidated, as pointed out by Khrapkovskii et al.,[69] by a detailed study of the kinetics of the decomposition of nitromethane in solutions. In order to identify the reactions involving the isomerisation of nitroalkanes, it is desirable to have information about the reactions of nitronic acids. Unfortunately, the kinetics and mechanisms of these reactions have not so far been investigated. These substances are known to be unstable.[71,72] On the basis of quantum-chemical estimates, the elimination of water has been suggested[7] for nitroalkanes having two hydrogen atoms in the α-position.

$$H_2C(NO_2)_2 \longrightarrow H(NO_2)C{=}NOOH \longrightarrow H_2O + O_2NC{\equiv}N^{+}{\rightarrow}O^{-}$$

$$CH_3NO_2 \longrightarrow H_2C{=}NOOH \longrightarrow H_2O + HC{\equiv}N^{+}{\rightarrow}O^{-}$$

The conversion of nitronic acids of the type $ArCH=NOOH$ into ArCHO and $ArCH=NOH$ has been postulated.[73]

The decomposition of nitromethane in the gas phase at high pressures and temperatures in the range 400–860 °C,[74] i.e. under supercritical conditions, apparently proceeds via the aci-form. For a vapour density of 0.6 g cm^{-3}, the activation volume is between −25 and −15 cm^3 mol^{-3}, i.e. has the same value as for the isomerisation reaction.

An ionic decomposition mechanism has been observed[75,76] for compounds containing the trinitromethyl group in structures of the type $ROCH_2C(NO_2)_3$. Analysis of the volumes of the evolved gas (cm^3 g^{-1}) over a period of 48 h at 100 °C, carried out by Khrapkovskii et al.,[7] showed that the stability of such compounds differs markedly from that of their $RCH_2C(NO_2)_3$ analogues.

$(NO_2)_3CCH_2CH_3$	0.5
$(NO_2)_3CCH_2OCH_2CH_3$	>25
$(CN)(NO_2)_2CCH_2OCH_3$	≫ 25
$(CN)(NO_2)_2CCH_2CH_2OAc$	>25
$(CN)(NO_2)_2CCH_2CH(OAc)_2$	≫ 25
$[(NO_2)_3CCH_2NH]_2C=O$	0.8
$[(NO_2)_3CCH(CH_3)NH]_2C=O$	>25 (5 h, 90 °C)
$(NO_2)_3CCH(OAc)CH_3$	19 (20 min, 100 °C)

The following reaction has been proposed for them:

$$(NO_2)_3CCH_2OCH_2CH_3 \longrightarrow (NO_2)_3C^- + {}^+CH_2OCH_2CH_3.$$

Branching at the β-carbon atom also stabilises the positive charge and promotes the heterolytic cleavage of the C–C bond.

It may be expected that the decomposition of polynitro-compounds having substituents separated by a large distance and not containing a α-hydrogen atom proceeds at the same rates in the liquid phase as in the vapour. Direct measurements have been made for $C(NO_2)_4$, $IC(NO_2)_3$, and $MeC(NO_2)_3$.[77] The activation energies for the decomposition reactions and their rates in the liquid and gas phases are virtually identical with the gas-phase parameters. Table 12 presents data on the decomposition of certain nitro-compounds in solutions.[78,79] The decomposition of all the compounds listed in the table with the exception of hexanitroethane hardly differs from their decomposition in the gas phase and is independent of the nature of the solvent. In the case of hexanitroethane, such a dependence is manifested. Presumably, being a strong acceptor, hexanitroethane is capable of being influenced by even weak donors owing to the formation of charge-transfer complexes.

An attempt has been made[80,81] at a direct determination by IR spectroscopy of the influence of solvation and other intermolecular interactions on the activation energies for unimolecular bond dissociation reactions. The method is based on the use of the relation

$$E = \frac{c\hbar\omega_0^2}{4(\chi_{11})},$$

where ω_0 is the bond vibration frequency and χ_{11} is the anharmonicity of the vibration in which the involvement of the bond is fairly considerable (the C–N bond stretching vibration with ω_0 = 920 cm^{-1} in nitromethane). An experiment with nitromethane yielded the following values of E: 211 kJ mol^{-1} for the liquid state, 193 kJ mol^{-1} for a solution in CCl_4, and 377 kJ mol^{-1} for the solid phase (experiments at −173 °C). This apparently requires a more rigorous justification and tests.

The influence of complex formation, the mechanism of the decomposition of nitronic acids, and kinetic study of the proposed heterolytic reactions are apparently not the only problems which must be investigated in order to understand the essential features of the liquid-phase decomposition of nitrocompounds. New aspects may appear in the study of compounds with mixed functional groups in which the di- and trinitromethyl groups are the most reactive components of the molecules. Such studies are already being carried out.[82–85] Thus processes involving the evolution of gaseous products on rapid (up to 200 K s^{-1}) heating of the compounds $(NO_2)_3CCH_2N(NO_2)CH_2C(NO_2)_3$, $[(NO_2)_3CCH_2N(NO_2)CH_2]_2$, and $Cl(NO_2)_2CCH_2N(NO_2)CH_2C(NO_2)_2Cl$ have been described.[82] There is no doubt that the decomposition of the trinitromethyl group is the primary process for the first two substances.

The introduction of nitroamino-, azide, or nitrate groups into nitroalkane molecules increases the melting points and intensifies the explosive properties of the compounds. Comparison of the kinetic characteristics of the decomposition of monofunctional compounds permits the conclusion that, in the absence of mutual influence, the trinitromethyl group always decomposes at a higher rate than reactive groups such as $-CH_2N(NO_2)CH_2-$, $-CH_2ONO_2$ and $-CH_2N_3$. On the other hand, the fluorodinitromethyl group is more stable than the above fragments. Intramolecular interactions and the solid phase may introduce significant corrections to the above prediction. In the series of nitroalkanes, the decomposition in the solid state has been investigated for only one compound — hexanitroethane,[79] which has a melting point of 135 °C and the rates of its decomposition in the solid state can be easily measured. Crystals of this substance exist in a plastic state and the crystal lattice inhibits the decomposition only slightly: the rate in the solid state is lower by a factor of 5–7 than in the vapour phase.[79] In compounds with high melting points and strong intermolecular interactions, the effect of the solid phase may be much greater[86] and the crystal lattice may exert different influences on the decomposition of different groups. In this case, polynitro-compounds of the mixed type can serve as convenient models for experimental studies.

Table 12. Characteristics of the decomposition reactions of polynitro-compounds in solutions.[78,79]

Compound	Solvent	T/ °C	E/kJ mol^{-1}	$\lg(A/s^{-1})$	ω_{rel} at 85 °C
$C(NO_2)_4$	Carbon tetrachloride	85–150	166.3	16.7	1
	Freon-114B	120–135	173.0	17.7	–
	Freon-113	100–135	166.7	16.8	–
$ClC(NO_2)_3$	Carbon tetrachloride	85–146	159.9	16.5	8.5
$BrC(NO_2)_3$	"	85–131	155.9	16.6	17
$ClC(NO_2)_2C(NO_2)_2Cl$	Freon-113	45–85	129.9	16.6	1.8×10^6
$C(NO_2)_3C(NO_2)_3$	Carbon tetrachloride	70–120	158.3	18.6	860
	Heptane	70–120	119.3	13.0	3296
	Cyclohexane	70–120	88.0	9.1	6593

References

1. G M Nazin, G B Manelis, F I Dubovitskii *Usp. Khim.* **37** 1443 (1968) [*Russ. Chem. Rev.* **37** 603 (1968)]
2. V V Dubikhin, G M Nazin, G B Manelis *Izv. Akad. Nauk SSSR, Ser. Khim.* 1412 (1971)
3. V V Dubikhin, D N Sokolov, G M Nazin, G B Manelis *Izv. Akad. Nauk SSSR, Ser. Khim.* 1416 (1971)
4. V V Dubikhin, G M Nazin, G B Manelis *Izv. Akad. Nauk SSSR, Ser. Khim.* 1554 (1971)
5. D J Waddington, M A Warriss *J. Phys. Chem.* **75** 2427 (1971)
6. C D Weis, G R Newkome *J. Org. Chem.* **55** 5801 (1990)
7. G M Khrapkovskii, Yu I Rubtsov, V A Rafeev, G N Marchenko, G B Manelis, in *Proceedings of the 17th International Pyrotechnics Seminar* Vol. 1 (Beijing: Beijing Inst. of Technology Press, 1991) p. 424
8. V V Dubikhin, G M Nazin *Izv. Akad. Nauk SSSR, Ser. Khim.* 1345 (1974)
9. A McKaul, in *Theoretical Organic Chemistry* (Ed. R Kh Freidlina) (Translated into Russian; Moscow: Izd. Inostr. Lit., 1963) p. 289
10. S W Benson, G R Haugen *J. Phys. Chem.* **70** 3336 (1966)
11. G R Haugen, S W Benson *Int. J. Chem. Kinet.* 235 (1970)
12. Yu A Lebedev, E A Miroshnichenko, Yu K Knobel' *Termokhimiya Nitrosoedinenii* (Thermochemistry of Nitro Compounds) (Moscow: Nauka, 1970)
13. V V Dubikhin, G M Nazin, G B Manelis *Izv. Akad. Nauk SSSR, Ser. Khim.* 923 (1974)
14. G M Nazin, G B Manelis, F I Dubovitskii *Izv. Akad. Nauk SSSR, Ser. Khim.* 1239 (1971)
15. V G Matveev, V V Dubikhin, G M Nazin *Kinet. Katal.* **17** 280 (1976)
16. T H Kinstle, J G Stam *J. Org. Chem.* **35** 1771 (1970)
17. H Egsgaard, L Carisen *J. Chem. Res. (S)* 18 (1987)
18. V V Dubikhin, G M Nazin *Izv. Akad. Nauk SSSR, Ser. Khim.* 1339 (1971)
19. G G Crawforth, D J Waddington *Trans. Faraday Soc.* **65** 1334 (1969)
20. A A Borisov, S M Kogarko, G I Skachkov *Kinet. Katal.* 589 (1966)
21. K Glenzer, J Troe *Helv. Chim. Acta* **55** 2884 (1972)
22. V V Dubikhin, G M Nazin, G B Manelis *Izv. Akad. Nauk SSSR, Ser. Khim.* 1338 (1971)
23. A R Perche, J C Tricot, M Lucquim *J. Chem. Res. (S)* 116 (1979)
24. A R Perche, J C Tricot, M Lucquim *J. Chem. Res. (S)* 304 (1979)
25. A R Perche, M Lucquim *J. Chem. Res. (S)* 306 (1979)
26. G M Nazin, G B Manelis, F I Dubovitskii *Izv. Akad. Nauk SSSR, Ser. Khim.* 1035 (1969)
27. G M Nazin, G N Nechiporenko, D N Sokolov, G B Manelis *Izv. Akad. Nauk SSSR, Ser. Khim.* 315 (1968)
28. G M Nazin, G B Manelis, G N Nechiporenko, F I Dubovitsky *Combust. Flame* **12** 102 (1968)
29. K Baum, D Tzeng *J. Org. Chem.* **50** 2736 (1985)
30. K Baum, T G Archibald, D Tzeng, R Gilardi, J L Flippen-Anderson, C George *J. Org. Chem.* **56** 537 (1991)
31. A I Feinstein, E K Fields *J. Org. Chem.* **36** 996 (1971)
32. K Glanzer, J Troe *Helv. Chim. Acta* **56** 577 (1973)
33. K Glanzer, J Troe *Helv. Chim. Acta* **56** 1691 (1973)
34. G M Nazin, G B Manelis, F I Dubovitskii *Dokl. Akad. Nauk SSSR* **177** 1387 (1967)
35. G M Nazin, G B Manelis, F I Dubovitskii *Izv. Akad. Nauk SSSR, Ser. Khim.* 2631 (1968)
36. G M Nazin, G B Manelis, F I Dubovitskii *Izv. Akad. Nauk SSSR, Ser. Khim.* 2801 (1968)
37. G M Nazin, G B Manelis, F I Dubovitskii *Dokl. Akad. Nauk SSSR* **177** 1128 (1967)
38. G M Nazin, G B Manelis, F I Dubovitskii *Izv. Akad. Nauk SSSR, Ser. Khim.* 2629 (1968)
39. J M Flournoy *J. Chem. Phys.* **36** 1107 (1962)
40. G M Nazin, G B Manelis, F I Dubovitskii *Izv. Akad. Nauk SSSR, Ser. Khim.* 389 (1968)
41. V N Grebennikov, V V Prokudin, G M Nazin *Izv. Akad. Nauk SSSR, Ser. Khim.* 2822 (1984)
42. V N Grebennikov, V I Erashko, G M Nazin, A V Sultanov, S A Shevelev *Izv. Akad. Nauk SSSR, Ser. Khim.* 310 (1977)
43. V N Grebennikov, G M Nazin *Izv. Akad. Nauk SSSR, Ser. Khim.* 1635 (1978)
44. L V Gurvich, G V Karachevtsev, V N Kondrat'ev, Yu A Lebedev, V A Medvedev, V K Potapov, Yu S Khodeev, in *Energii Razryva Khimicheskikh Svyazei. Potentsialy Ionizatsii i Srodstvo k Elektronu. Spravochnik* (Energies of Rupture of Chemical Bonds. Ionization Potentials and Electron Affinities. Handbook) (Moscow: Nauka, 1974) p. 64
45. Yu Yu Nikishev, I Sh Saifullin, I F Falyakhov *Kinet. Katal.* **32** 749 (1991)
46. V I Slovetskii, S A Shevelev, A A Fainzil'berg *Izv. Akad. Nauk SSSR, Ser. Khim.* 989 (1962)
47. V A Pal'm *Usp. Khim.* **30** 1069 (1961) [*Russ. Chem. Rev.* **30** 471 (1961)]
48. V A Shlyapochnikov, K I Rezchikova, V N Solkan, S V Zakharkinskaya *Izv. Akad. Nauk SSSR, Ser. Khim.* 1420 (1983)
49. V A Shlyapochnikov, K I Rezchikova, V N Solkan, S V Zakharkinskaya *Izv. Akad. Nauk SSSR, Ser. Khim.* 2399 (1982)
50. V I Vedeneev, A P Purmal' *Zh. Fiz. Khim.* **32** 1472 (1958)
51. N G Yunda, I Yu Kozyreva, G V Lagodzinskaya, G B Manelis *Izv. Akad. Nauk SSSR, Ser. Khim.* 1772 (1983)
52. V I Pepekin, Yu A Lebedev, A Ya Apin *Dokl. Akad. Nauk SSSR* **208** 153 (1973)
53. G A Carpenter, M F Zimmer, E E Boroody, R A Robb *J. Chem. Eng. Data* **15** 553 (1970)
54. G M Nazin, G B Manelis *Izv. Akad. Nauk SSSR, Ser. Khim.* 811 (1972)
55. G M Nazin, G B Manelis, F I Dubovitskii *Izv. Akad. Nauk SSSR, Ser. Khim.* 2627 (1969)
56. D Stall, E Vestram, G Zinke *The Chemical Thermodynamics of Organic Compounds* (Translated into Russian; Moscow: Mir, 1971)
57. D C Smith, G Y Ran, J R Nielsen *J. Chem. Phys.* **18** 706 (1950)
58. K I Rezchikova, V N Solkan, S L Kuznetsov *Izv. Akad. Nauk SSSR, Ser. Khim.* 339 (1990)
59. A V Kissenikh, S A Shevelev, A A Fainzil'berg, in *Radiospektroskopicheskie i Kvantovomekhanicheskie Metody v Strukturnykh Issledovaniyakh* (Radiospectroscopic and Quantum-mechanical Methods in Structural Investigations) (Ed. L A Blyumenfel'd) (Moscow: Nauka, 1967) p. 194
60. R Shaw *Int. J. Chem. Kinet.* **5** 261 (1973)
61. A M Wodtke, E J Hintsa, Y T Lee *J. Phys. Chem.* **90** 3549 (1986)
62. M J S Dewar, P Pitchie, J Alster *J. Org. Chem.* **50** 1031 (1985)
63. M L McKee *J. Phys. Chem.* **93** 7365 (1989)
64. B M Rice, D L Thompson *J. Chem. Phys.* **93** 7986 (1990)
65. B L Korsunskii, G M Nazin, V R Stepanov, A A Fedotov *Kinet. Katal.* **34** 775 (1993)
66. G M Nazin *Usp. Khim.* **41** 1537 (1972) [*Russ. Chem. Rev.* **41** 471 (1972)]
67. R Engelke, W L Earl, C M Rohlfing *Int. J. Chim. Kinet.* **18** 1205 (1986)
68. R Shaw, P S Decarli, D S Ross, E L Lee, S D Stromberg *Combust. Flame* **50** 123 (1983)
69. G M Khrapkovskii, P N Stolyarov, V P Dorozhkin, E A Ermakov, A M Rozin, G M Marchenko *Khim. Fiz.* **9** 648 (1990)
70. G J Piermarini, S Block, P J Miller *J. Phys. Chem.* **93** 457 (1989)
71. E B Hadge *J. Am. Chem. Soc.* **73** 2341 (1951)
72. A T Nielson, in *The Chemistry of Nitro and Nitroso Groups* Vol. 1 (Eds G Foier, S S Novikov) (Translated into Russian; Moscow: Mir, 1972) p. 284
73. C F Allen, G P Happ *Can. J. Chem.* **42** 650 (1964)
74. K R Brower *J. Org. Chem.* **53** 3776 (1988)
75. H G Adolph *Combust. Flame* **70** 343 (1987)
76. T B Brill, R Subramanian *Combust. Flame* **80** 150 (1990)
77. G M Nazin, G B Manelis, F I Dubovitskii *Izv. Akad. Nauk SSSR, Ser. Khim.* 2628 (1968)
78. H P Marshall, F G Borgardt, P Noble, Jr *J. Phys. Chem.* **69** 25 (1965)
79. H P Marshall, F G Borgardt, P Noble, Jr *J. Phys. Chem.* **72** 1513 (1968)
80. N V Chukanov, B L Korsunskii, F I Dubovitskii, O V Anan'ina *Dokl. Akad. Nauk SSSR* **265** 1445 (1982)
81. N V Chukanov, B L Korsunskii, F I Dubovitskii, O V Anan'ina *Dokl. Akad. Nauk SSSR* **277** 1181 (1984)
82. R Subramanian, T B Brill *Propellants, Explos.* **15** 187 (1990)
83. Y Oyumi, T B Brill, A L Rheingold *J. Phys. Chem.* **89** 4824 (1985)
84. Y Oyumi, T B Brill *Combust. Flame* **62** 225 (1985)
85. Y Oyumi, T B Brill *Combust. Flame* **68** 209 (1987)
86. Yu M Burov, G B Manelis, G M Nazin *Dokl. Akad. Nauk SSSR* **275** 1142 (1984)

Russian Chemical Reviews **63** (4) 323 – 344 (1994)
©1994 Russian Academy of Sciences and Turpion Ltd

UDC 547.425.5

Sulfides: synthesis and properties

I V Koval'

Contents

I. Introduction	323
II. The structure and physicochemical properties of sulfides	323
III. Methods of synthesis of sulfides	324
IV. Reactions of sulfides	332

Abstract. The review gives a systematic account and surveys the results of recent studies of the chemistry of sulfides. The structure and physicochemical properties of sulfides, the methods for their synthesis, as well as their reactions are considered. The bibliography includes 211 references.

I. Introduction

Sulfides constitute one of the simplest classes of organosulfur compounds, which play an extremely important role in organic synthesis. This is due primarily to the presence of the sulfur atom — an active reaction centre with variable valence, the relatively high lability of the C–S bond which may be cleaved by nucleophiles and electrophiles, and also the tendency of sulfur to stabilise the α-carbanionic centre. Together with extensive synthetic possibilities, certain sulfides possess valuable practical properties, which has also aroused an increased interest in the chemistry of sulfides. They have found extensive applications as polymer stabilisers,[1,2] vulcanising agents,[3] pharmaceutical preparations,[4] and biologically active substances.[5] The importance of sulfides in biochemical processes, especially in the metabolism of lipids, is great.[6] In the conversion of the aliphatic acids of lipids into 2-carbon fragments, a key role is assumed by coenzyme A (Co-A), which forms a thioester bond with the aliphatic acid molecule.

Two excellent reviews,[7,8] covering the literature up to 1978, have been devoted to the chemistry of sulfides. However, many new data, which need to be surveyed, have accumulated since the time of their publication. This is in fact the topic of the present review.

II. The structure and physicochemical properties of sulfides

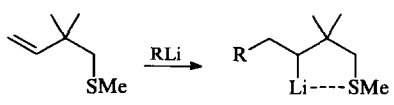
The structure of the groups attached to the sulfur atom exerts a strong influence on the C–S–C bond angle, the C–S bond length, and the dissociation energy of the latter (E_d), which varies over a relatively wide range:[9]

Sulfide	E_d/kcal mol^{-1}
MeS–Me	77.0 ± 1.5
MeS–Et	74.0 ± 1.5
MeS–CH_2Ph	59.4 ± 2.0
PhS–Me	67.4 ± 1.5
AlkS–Bu	71.0 ± 1.5
MeS–Ph	89.2 ± 2.0
MeS–CN	97.0 ± 1.5

The length of the C–S bond in sulfides varies in the range 175–180 pm depending on the structure of the group attached to the sulfur atom, while the C–S–C bond angle is 98.9° for dimethyl sulfide and 105.6° for hexafluorodimethyl sulfide.[7] The enthalpy of the C–S bond is 69 kcal mol^{-1}.[9]

Sulfides are 10^{14}–10^{17} times weaker bases than thiolate anions.[7] In contrast to their oxygen analogues, sulfides show a considerable tendency to generate α-carbanions and α-radicals, which has been explained by the increased stabilisation of these species by $p_\pi - d_\pi$ conjugation[7] or by the greater polarisability of sulfur compared with oxygen.[10,11] α-Carbonium ions based on sulfides are less stable than those based on the oxygen analogues. It has been suggested[10,11] that the stabilisation of the carbonium ions is due to the p,π conjugation and, since this stabilisation is directly proportional to the distance separating the two nuclei, the alkoxycarbonium ion is stabilised to a greater extent than the alkylthiocarbonium ion.

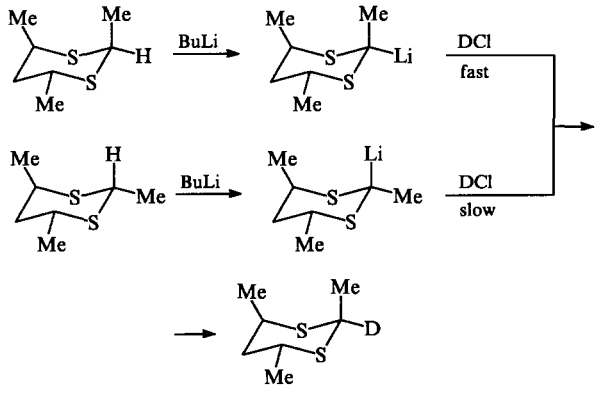
Aliphatic sulfides are very active photoexcitation 'quenching agents'. For example, 1 mol of dibutyl sulfide can prevent the photochemical reduction of 23 mol of benzophenone by alcohols, which has been explained[8] by the formation of the complex $Ph_2CO^{\bullet-}\cdots{}^{+}SBu_2$. According to ^{1}H NMR spectroscopic data obtained using shift reagents,[12] sulfides form unstable complexes with Eu(fod)$_3$. Macrocyclic sulfides are much stronger complex-forming agents for silver ions than macrocyclic ethers but are weaker for alkali metal ions, which is apparently associated with the greater size and lower electronegativity of the sulfur atom compared with oxygen. It has been noted that the addition of organolithium compounds to a nonconjugated carbon–carbon bond becomes possible by virtue of the formation of an alkali metal complex with participation of the sulfur atom.[12]



I V Koval' Department of the Chemical Technology of Macromolecular Compounds, Ukrainian Chemical-Technological University, Prosp. Gagarina 8, 320005 Dnepropetrovsk, Ukraine, Fax (7-056) 247 33 16

Received 20 July 1994
Uspekhi Khimii **63** (4) 338 – 360; translated by A K Grzybowski

1,3-Dithianes assume the twisted boat (twist) conformation more readily than the corresponding O- or C-analogues because nonbonding interactions are weakened in the larger 1,3-dithiane ring, while the torsional barriers are reduced for the C–S bonds compared with those for the C–O and C–C bonds. The twist-form of 3,3,6,6-tetramethyl-1,2,4,5-tetrathiane is actually more stable by 2.1–2.5 kJ mol^{-1} than the chair form. The equilibrium isomerisation of 2-substituted 1,3-dithianes on treatment with butyllithium leads to the formation mainly of isomers with an axial disposition of the substituents. Although such disposition is sterically unfavourable, it occurs even for 2-butyl-1,3-dithiane because lithium tends to occupy the equatorial position.[8] As a consequence of the above feature, there is a possibility of the stereospecific deuteriation of 2,4,6-trimethyl-1,3-dithiane.

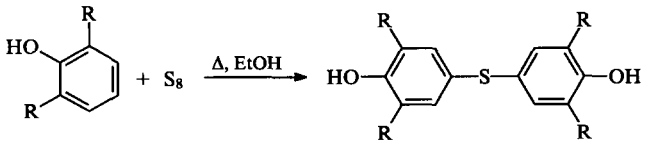


The absorption bands in the UV spectra of alkyl sulfides lie in the region of 200, 220, and 240 nm,[13] while those in the spectra of alkyl aryl sulfides are in the region of 205–230, 235–270, and 275–300 nm.[14] The positions of the absorption bands depend significantly on the structure of the substituents at the sulfur atom and on the nature of the solvent. The long-wavelength absorption is usually very weak and is not characteristic of sulfides. The chemical shift (δ) of the protons in the CH_3S group is in the region of 2 ppm.[15] The mass spectra of alkyl sulfides[16] are characterised by fairly intense peaks due to molecular ions, the intensity of which diminishes with increase in the number of carbon atoms in the molecule and as the sulfur atom moves to one of the ends of the chain. Two types of fragment ions are mainly present: the sulfur-containing ions $[C_nH_{2n+1}S]^+$, $[C_nH_{2n}S]^{\cdot+}$, and $[C_nH_{2n-1}S]^+$ and the hydrocarbon ions $[C_nH_{2n+1}]^+$, $[C_nH_{2n}]^{\cdot+}$, and $[C_nH_{2n-1}]^+$. The main components of the chemical ionisation mass spectra of sulfides[17,18] are the quasi-molecular ions $[M-1]^-$. According to Tokarev et al.,[19] the relative ionisation cross-section of diethyl sulfide is 0.23 (reagent gas—isobutane, 14 Pa, 150 °C).

III. Methods of synthesis of sulfides

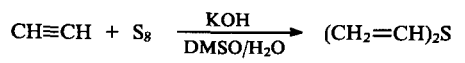
1. Syntheses based on elemental sulfur and its inorganic derivatives

Elemental sulfur is fairly rarely used in the synthesis of sulfides, which is due to the need for its activation or the application of highly reactive aromatic compounds, for example compounds such as dialkylphenols.[16]



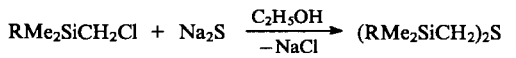
R = Me, Et, Bu^t.

Under chemical activation conditions (a superbasic medium), sulfur reacts with acetylene and its derivatives to form divinyl sulfide.[20]



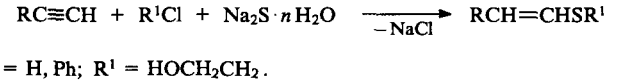
Unsaturated sulfides are also formed on interaction of unsaturated ethers with organomagnesium compounds and sulfur in the presence of palladium complexes.[21] Under electrochemical activation conditions (decomposing sulfur electrode), elemental sulfur reacts with aromatic ethers, amines, and phenols as well as certain heterocyclic compounds to form the corresponding sulfides.[22,23]

Inorganic sulfur derivatives, for example sodium sulfide, are used much more frequently in the synthesis of sulfides. A whole series of preparative methods for the synthesis of symmetrical sulfides have been developed on the basis of the reaction involving the alkylation and arylation of sodium sulfide by alkyl halides and activated aryl halides. As a rule, these reactions proceed in homophase systems. In the case of heterophase systems, phase transfer catalysts are employed.[24] These methods are applicable also in the synthesis of silicon-containing sulfides.[25]



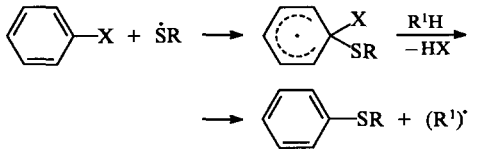
R = Me, Ph.

Another aspect of the use of sodium sulfide in the synthesis of organic sulfides involves its interaction with acetylenic hydrocarbons in the presence of halogen derivatives.[26]



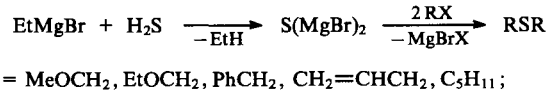
R = H, Ph; $R^1 = HOCH_2CH_2$.

Hydrogen sulfide is much more rarely used in the synthesis of sulfides because its reactions with chloro- and bromo-substituted aromatic and heteroaromatic compounds proceed as a rule at high temperatures to form thiols and other products together with sulfides.[27–30] These reactions proceed via a radical mechanism with the formation of intermediate adduct-radicals stabilised by the π-system of the aromatic ring.[16]



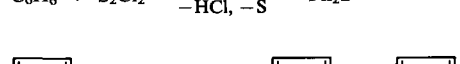
R = H, Ar; X = Cl, Br.

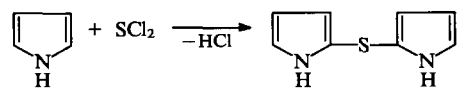
The reaction of hydrogen sulfide with ethylmagnesium bromide, affording bis(bromomagnesium) sulfide, which readily interacts with electrophiles to form organic sulfides, is of preparative interest.[31]



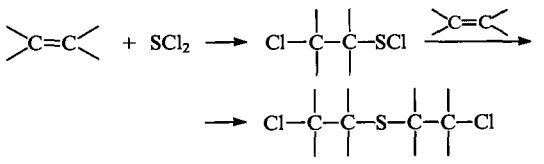
R = $MeOCH_2$, $EtOCH_2$, $PhCH_2$, $CH_2=CHCH_2$, C_5H_{11};
X = Cl, Br.

Among inorganic sulfur derivatives, sulfur monochloride and dichloride are also used in the synthesis of sulfides. The sulfenylation of aromatic and heterocyclic hydrocarbons by these reagents constitutes the basis of a preparative method for the synthesis of symmetrical sulfides.[8]





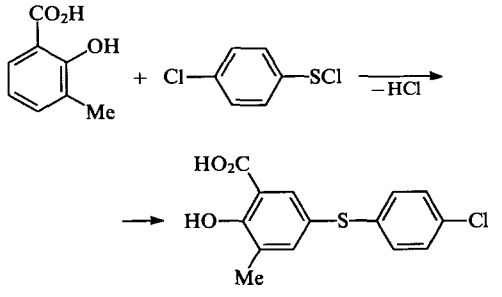
The addition of sulfur dichloride to ethylenic hydrocarbons leads to bis(β-chloroalkyl) sulfides.[16]



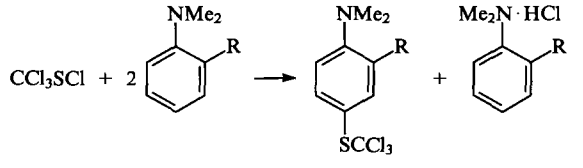
2. Syntheses based on sulfenyl halides

a. Sulfenylation of aromatic and heterocyclic compounds by sulfenyl chlorides

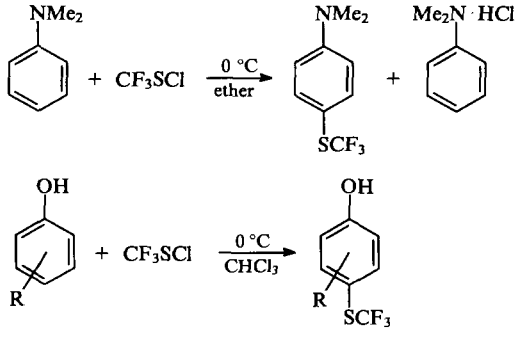
Sulfenyl chlorides react with aromatic hydrocarbons via the S_E2 electrophilic substitution mechanism to form both symmetrical and asymmetric sulfides. Aromatic sulfenyl chlorides react with benzene and its homologues only in the presence of catalysts ($AlCl_3$, $FeCl_3$, Fe, etc.). Sulfenyl chlorides react relatively easily with benzene and naphthalene derivatives containing strong electron-donating substituents (NMe_2, OH, OMe etc.). For example, *p*-chlorobenzenesulfenyl chloride reacts with 6-methylsalicylic acid in the absence of a catalyst to form the corresponding sulfide.[32]



Trichloromethanesulfenyl chloride reacts relatively easily with dimethylaniline and its derivatives, forming the corresponding aryl trichloromethyl sulfides.[33]

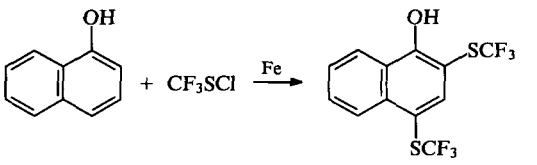


Trifluoromethanesulfenyl chloride reacts with dimethylaniline[4] and with phenol and its homologues[34] even at 0 °C. Under these conditions, the trifluoromethylthio-group adds in the *ortho*- and *para*-positions relative to the substituent.

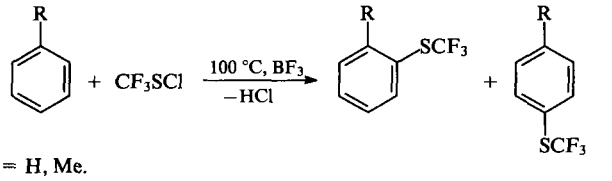


R = H, 2-Me, 3-Me, 2-OH.

The reaction of trifluoromethanesulfenyl chloride with α-naphthol affords 2,4-bis(trifluoromethylthio)naphthol.[35]

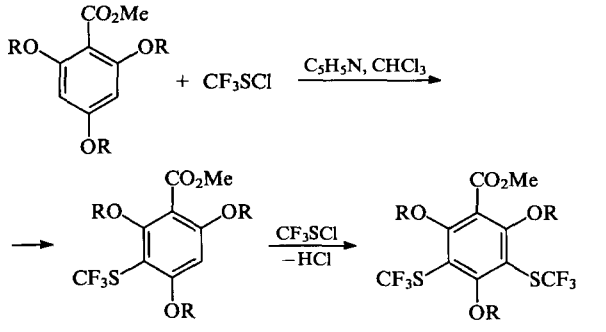


Trifluoromethanesulfenyl chloride reacts with benzene and toluene in the presence of BF_3 at 100 °C in an autoclave, forming phenyl trifluoromethyl sulfide or a mixture of 2- and 4-tolyl trifluoromethyl sulfides.[4,33]

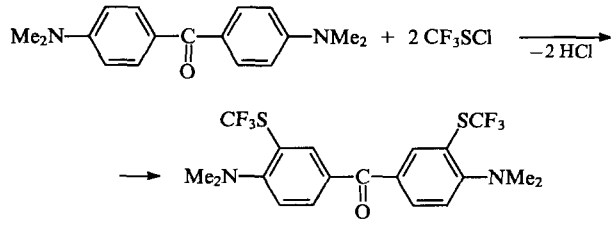


R = H, Me.

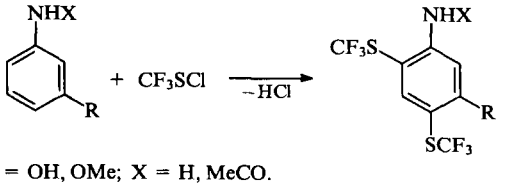
Trifluoromethanesulfonic acid is a more effective catalyst of the trifluoromethanesulfenylation of benzene. Its employment makes it possible to reduce the temperature of the above reaction to 20 °C.[36] The introduction of a second trifluoromethylthio-group into the benzene ring is difficult even in the presence of trifluoromethanesulfonic acid. Trifluoromethanesulfenyl chloride reacts with chlorobenzene under severe conditions in the presence of HF, forming two isomers—*p*- and *o*-chlorophenyl trifluoromethyl sulfides.[36] If there are electron-donating groups (OH, OMe, NMe_2) in the aromatic ring together with electron-accepting groups (MeCO, PhCO, MeOCO, CHO), then one, two, and even three trifluoromethylthio-groups enter into the reaction depending on the conditions.[4,37]



R = H, Me.

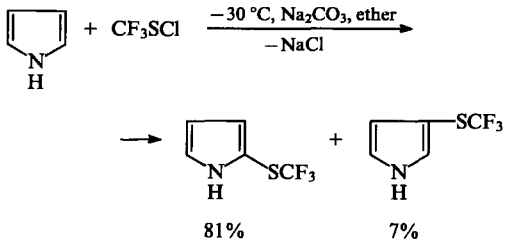


Derivatives of aniline and acetanilide containing the electron-donating OH or OMe groups in the *meta*-position also react readily with trifluoromethanesulfenyl chloride to form bis(trifluoromethylthio)-derivatives.[34]



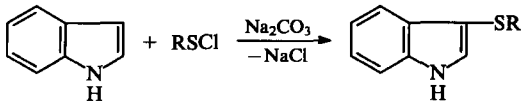
R = OH, OMe; X = H, MeCO.

Similar rules have been established for the interaction of sulfenyl chlorides with cyclic compounds.[4] The presence in the latter of a high π-electron density promotes this reaction. For example, pyrrole reacts with trifluoromethanesulfenyl chloride even at −30 °C, forming 2-trifluoromethylthiopyrrole and a small amount of 3-trifluoromethylthiopyrrole.[37–39]



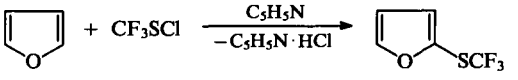
81% 7%

In the presence of catalytic amounts of a perfluoroalkanesulfonic acid, two, three, and even four trifluoromethylthio-groups may be introduced into the pyrrole ring.[38] In indole, the substitution of a hydrogen atom by the sulfenyl group takes place in the 3-position.[37, 40]

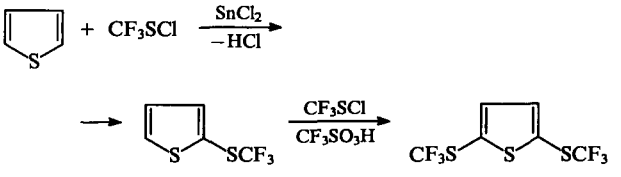


R = CF_3, 2(3,4)-$NO_2C_6H_4$, 2,4-$(NO_2)_2C_6H_3$.

2-Trifluoromethylthiofuran is the product of the reaction of furan with trifluoromethanesulfenyl chloride in the presence of pyridine.[39]



Trifluoromethanesulfenyl chloride reacts with thiophene, giving rise to 2-(trifluoromethylthio)thiophene or 2,5-bis(trifluoromethylthio)thiophene depending upon which catalyst is employed.[36, 39, 41]



b. Sulfenylation of C-nucleophiles

Sulfenyl chlorides react vigorously with organomagnesium compounds via the nucleophilic substitution mechanism, forming sulfides.[33]

$$RSCl + R^1MgX \longrightarrow RSR^1 + MgXCl$$

R = CCl_3, CF_3; R^1 = Et, Ph, 3(4)-MeC_6H_4;
X = Cl, Br.

Under these conditions, a small amount (up to 15%) of halohydrocarbons is formed as a rule, which hinders the isolation of the sulfides obtained. Organomercury compounds react with sulfenyl chlorides similarly to organomagnesium compounds.[42] The substitution of the chlorine atom at the sulfur atom by a hydrocarbon group is then accompanied by the simultaneous replacement of the HgCl fragment by chlorine and also by demercuration.

$$RSCl + p\text{-}R^1C_6H_4HgCl \longrightarrow RSC_6H_4R^1\text{-}p + p\text{-}R^1C_6H_4Cl + PhR^1$$

R = CF_3; R^1 = H, Me, MeO, Cl, NO_2.

Electron-accepting groups promote the formation of sulfides, whereas electron-donating groups promote the formation of halo-derivatives. A method of synthesis of sulfides involving the interaction of arenesulfenyl chlorides with perfluoro-*tert*-butylcaesium in acetonitrile or diglyme,[43, 44] and also its interaction with perfluoromethyl(trimethyl)silane in tetrahydrofuran,[45] has been described in the literature. The yield of the sulfides is 75%–85%.

$$RC_6H_4SCl + (CF_3)_3CCs \xrightarrow[-CsCl]{} RC_6H_4SC(CF_3)_3$$

R = H, 3(4)-F, 4-Cl, 2(3,4)-NO_2, 3(4)-COOMe.

$$RC_6H_4SCl + Me_3SiCF_3 \longrightarrow RC_6H_4SCF_3 + Me_3SiCl$$

R = 4-Cl, 4-NO_2.

Treatment of copper acetylide with arenesulfenyl chlorides leads to the formation of alkynyl aryl sulfides.[8]

$$RC{\equiv}CCu + ArSCl \longrightarrow RC{\equiv}CSAr$$

R = H, Me; Ar = Ph, *p*-MeC_6H_4.

A whole series of methods of synthesis of sulfides are based on the sulfenylation of CH acids by sulfenyl chlorides and other sulfenylating agents. The choice of the reaction conditions is dictated both by the nature of the CH acid and that of the sulfenyl chloride. For example, the sulfenylation of nitromethane by trichloromethanesulfenyl chloride is carried out at 0 °C in an aqueous alkaline medium.[33]

$$CCl_3SCl + CH_3NO_2 \xrightarrow[-NaCl]{0\ ^\circ C,\ NaOH} CCl_3SCH_2NO_2$$

Nitromethane reacts with benzenesulfenyl chloride[46] in absolute alcohol in the presence of sodium ethoxide, while its reaction with *o*-nitrobenzenesulfenyl chloride takes place in anhydrous benzene in the presence of triethylamine and affords the corresponding sulfides. Diacetyl- and dibenzoyl-methanes and acetoacetic and malonic acid esters interact with arenesulfenyl chloride in anhydrous benzene in the absence of bases,[47–49] whereas diphenylmethane[50] and dicyanomethane[51] require the use of triethylamine.

$$ArSCl + CH_2XY \xrightarrow[-HCl]{} ArSCH(X)Y$$

Ar = Ph, 4-MeC_6H_4, 2(4)-$NO_2C_6H_4$, 2,4-$(NO_2)_2C_6H_3$;
X = Y = Ph, MeCO, PhCO, EtOCO, CN;
X = MeCO, Y = EtOCO;
X = H, Y = NO_2;
X = NO_2, Y = 2-$NO_2C_6H_4$.

The sulfenylation of tris(trifluoromethyl)methane by benzenesulfenyl chloride also takes place in the presence of triethylamine.[52]

$$PhSCl + HC(CF_3)_3 \xrightarrow[-Et_3N\cdot HCl]{Et_3N} PhSC(CF_3)_3$$

The trifluoromethanesulfenylation of the CH acids RCX.CH_2R^1 (X = O, NH; R = Ph, Me; R^1 = $CONH_2$, CN, C(S)NH.C_6H_4Br-*p*) is carried out in anhydrous chloroform at 0–20 °C with the use of bases.[53]

Numerous studies have been devoted to the sulfenylation of phosphorus-containing CH acids and their anions, studies that are associated with the search for new biologically active preparations.[54] For example, a study has been made[55] of the interaction of perhalomethanesulfenyl chlorides with the anions of tetraalkyl methylphosphonates, generated by treating tetraalkyl methylphosphonates with butyllithium, sodium hydride, or metallic sodium. The formation of sulfenylation and chlorination products was established. In the case of dichlorofluoro- and chlorodifluoromethanesulfenyl chlorides, sulfenylation products were obtained under these conditions, in which the trihalomethanesulfenyl groups are enriched in fluorine compared with those in the initial sulfenyl chlorides.

$$[(RO)_2P(O)]_2CHM + CCl_{3-n}F_nSCl \xrightarrow{AlCl_3}$$
$$\longrightarrow [(RO)_2P(O)]_2CHSCCl_{3-n}F_n + [(RO)_2P(O)]_2CHCl +$$
$$+ [(RO)_2P(O)]_2CHSCCl_{2-n}F_{n+1} + [(RO)_2P(O)]_2CHSCF_3$$

R = Pr^i; M = Li, Na.

It is believed[55] that the products with a fluorine-enriched trihalomethanesulfenyl group are formed as a result of the substitution of chlorine atoms by fluorine in the initial sulfenyl chloride and not in the sulfenylation products. The fluoride anion, appearing on decomposition of the trihalomethylthio-anion, which is a side product in the chlorination of tetraalkyl methylenediphosphonate, acts as the fluorinating agent under these conditions.

$$[(RO)_2P(O)]_2CHM + CCl_{3-n}F_nSCl \longrightarrow$$
$$\longrightarrow [(RO)_2P(O)]_2CHCl + CCl_{3-n}F_nS^-$$
$$CCl_{3-n}F_nS^- \longrightarrow Cl_{3-n}F_{n-1}C{=}S + F^- + M^+$$
$$CCl_{3-n}F_nSCl + F^- \longrightarrow CCl_{2-n}F_{n+1}SCl + Cl^-$$

The fraction of the chlorination products increases in the following sequence: $CF_3SCl < CF_2ClSCl < CFCl_2SCl$. This has been explained[54,55] by the increase in the same sequence in the steric hindrance to nucleophilic attack on the sulfur atom by the carbanion. It has been noted[56] that, when benzenesulfenyl chloride is added to an excess of sodium diethyl cyanomethylphosphonate, the corresponding sulfide is formed almost exclusively.

$$(EtO)_2P(O)\underset{CN}{\underset{|}{C}}HNa + ClSPh \xrightarrow{-NaCl} (EtO)_2P(O)\underset{CN}{\underset{|}{C}}H{-}SPh$$

The similar interaction of α-substituted ethylphosphonic acid esters with benzenesulfenyl chloride leads to the corresponding sulfides in an almost quantitative yield.[57]

$$(EtO)_2P(O)\underset{R}{\underset{|}{C}}HMe + ClSPh \xrightarrow[-NaCl]{NaH} (EtO)_2P(O)\underset{R}{\overset{Me}{\overset{|}{\underset{|}{C}}}}{-}SPh$$

R = CN, COOEt.

The reaction of triisopropyl phosphonoacetate with benzenesulfenyl chloride in the presence of aluminium isopropoxide[58] leads to the substitution of one or two hydrogen atoms by the phenylthio-group depending on the reactant ratio.

$$(Pr^iO)_2P(O)CH_2COOPr^i \xrightarrow{Al(OPr^i)_3}$$
$$\xrightarrow{PhSCl} (Pr^iO)_2P(O)CH(SPh)COOPr^i$$
$$\xrightarrow{2\,PhSCl} (Pr^iO)_2P(O)C(SPh)_2COOPr^i$$

The reaction of the chloride of diethoxyphosphorylacetic acid with benzenesulfenyl chloride takes place without a solvent. After treatment with water or methanol, the product is converted into α-diethoxyphosphoryl-α-phenylthioacetic acid or its ethyl ester (in 50% yield).[59]

$$(EtO)_2P(O)CH_2COCl + PhSCl \xrightarrow{H_2O} (EtO)_2P(O)\underset{COOH}{\underset{|}{C}}HSPh$$
$$\xrightarrow{MeOH} (EtO)_2P(O)\underset{COOMe}{\underset{|}{C}}HSPh$$

Phosphorus ylides readily exchange the hydrogen atom of the methylene group for an alkylthio- or arylthio-group.[60]

$$Ph_3P{=}CHR + R^1SCl \xrightarrow[-HCl]{} Ph_3P{=}\underset{R}{\underset{|}{C}}{-}SR^1$$

R = Me, EtOCO, CN, PhCO; R^1 = Alk, Ar.

Depending on the reactant ratio, it is possible to substitute one or two hydrogen atoms by the phenylthio-group in methylenetriphenylphosphorane.[60]

$$Ph_3P{=}CH_2 \xrightarrow{PhSCl} Ph_3P{=}CHSPh + HCl$$
$$\xrightarrow{2\,PhSCl} Ph_3P{=}C(SPh)_2 + 2\,HCl$$

Together with sulfenyl chlorides, other sulfenylating agents are also used in the reactions with C-nucleophiles. For example, aryl thiocyanates have been employed successfully for the sulfenylation of perfluorocarbanions[61] and organomagnesium compounds.[61,62] The yields of sulfides are then 50%–55%.

$$XC_6H_4SCN \xrightarrow[-KCN]{(CF_3)_2CFK} XC_6H_4SCF(CF_3)_2$$
$$\xrightarrow[-Mg(CN)I]{BuMgI} XC_6H_4SBu$$

X = H, 4-NO_2, 4-Cl.

Two versions of the synthesis of alkyl trichloromethyl sulfides from alkyl thiocyanates have been developed. The first involves the interaction of alkyl thiocyanates with chloroform under the conditions of phase transfer catalysis.[63]

$$RSCN + CHCl_3 \xrightarrow[-HCN]{} RSCCl_3$$

R = Me, Et.

The second version involves the interaction of alkyl thiocyanates with perchlorocarbanions obtained from perhalomethanes by treatment with KOH in the presence of phase transfer catalysts such as, for example, tetrabutylammonium bromide.[64]

$$CCl_3X + OH^- \underset{}{\overset{Bu_4NBr}{\rightleftharpoons}} \bar{C}Cl_3 \xrightarrow{MeSCN} MeSCCl_3$$

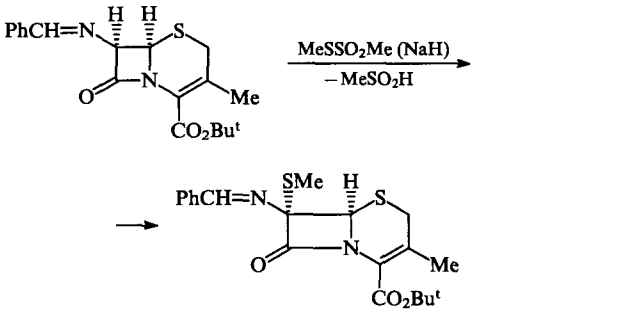
X = Cl, Br.

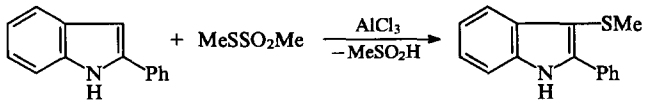
It has been noted[65] that in the presence of bases certain CH acids are sulfenylated by the RSH–CCl_4 system.

$$RSH + Na\underset{Y}{\underset{|}{\overset{X}{\overset{|}{C}}}}R^1 \xrightarrow[-CHCl_3]{CCl_4} RS\underset{Y}{\underset{|}{\overset{X}{\overset{|}{C}}}}R^1 + NaCl$$

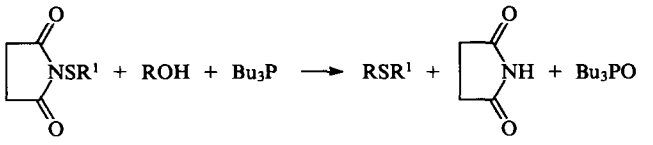
R = Alk, Ar; R^1 = H, Alk, Ar; X = Y = COMe, COOEt.

The use of thiolo-esters of sulfonic acids [66] and sulfenamides [67] as sulfenylating agents for CH acids has not come to be widely employed in the synthesis of sulfides owing to the formation of side products which hinder the isolation of the sulfides. However, in rare instances these compounds are nevertheless used as mild sulfenylating agents. For example, the methyl thiolo-ester of methanethiosulfonic acid is used to introduce the methylthio-group into certain derivatives of cephalosporin and indole. [8]



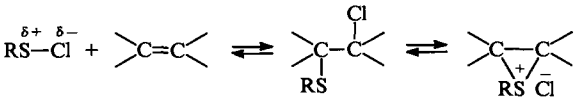


Certain sulfenamides form sulfides on interaction with alcohols in the presence of trialkylphosphines. [8]

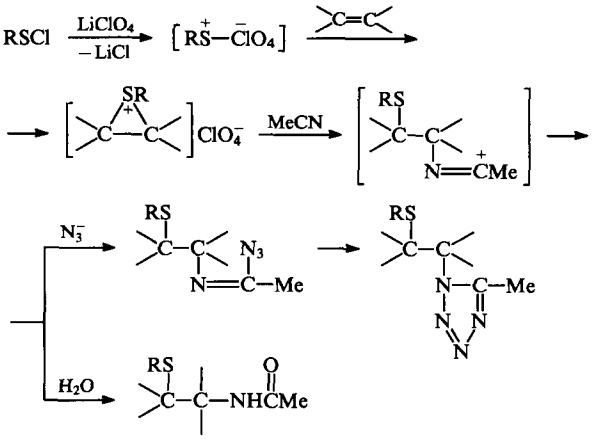


c. Addition of sulfenyl chlorides to the C = C bond

Sulfenyl chloride adds smoothly to alkenes with formation of β-chlorosulfides, [7,68,69] which are the starting materials for the synthesis of saturated and unsaturated sulfides. [69] It has been suggested that this reaction proceeds via an Ad_E2 mechanism, in which the cationic intermediate is an episulfonium ion, and leads as a rule to stereospecific *trans*-addition.

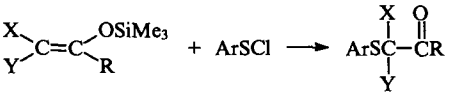


Sulfenyl chlorides are relatively weak electrophiles and the intermediate episulfonium cation has a small positive charge, which does not allow it to react with weak nucleophiles. A method developed by Zefirov and coworkers, [70,71] involving the coupled addition of sulfenyl chlorides to a double bond in the presence of a strong electrophile, for example lithium perchlorate, which increases the effective electrophilicity of sulfenyl chlorides ('doping process'), is therefore of interest. The episulfonium cation formed in this process reacts even with a weak nucleophile such as acetonitrile, affording an immonium ion, which is converted into the final products on treatment with various reagents.

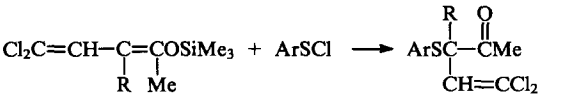


This reaction has been investigated for cyclohexene, norbornene, hept-1-ene and other olefins.

A novel method has been developed for the synthesis of aryl β-oxoalkyl sulfides involving the interaction of vinyloxysilanes [72–74] and divinyloxysilanes [75] with arenesulfenyl chlorides. The reaction proceeds via stages involving the 1,2-addition of ArSCl and the elimination of chlorotrimethylsilane. [74]

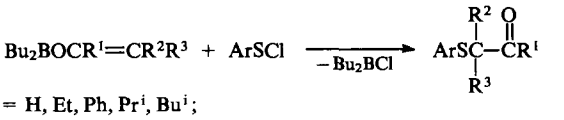


X = H, Cl, Br; Y = Cl; R = H, Bu^t, Ph, 4-ClC$_6$H$_4$, 4-BrC$_6$H$_4$;
Ar = 4-MeC$_6$H$_4$, 4-ClC$_6$H$_4$, 4-NO$_2$C$_6$H$_4$.



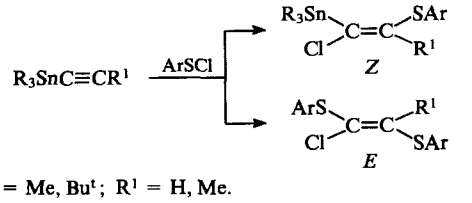
R = H, Ac, COOEt;
Ar = 4-MeC$_6$H$_4$, 4-ClC$_6$H$_4$.

Arenesulfenyl chlorides react similarly with the enols of dibutyl borinates. [76]



R^1 = H, Et, Ph, Pr^i, Bu^i;
R^2 = H, Me, Et, Pr; R^3 = H, Me, Ph;
R^3 = H, Me, Ph; Ar = Ph.

Arenesulfenyl chlorides react with trialkylstannylacetylenes to form either the products of addition to the triple bond or the products of their subsequent arylthiodestannylation—(*E*)-1,2-bis(arylthio)chloroethylenes. [77] The addition reaction takes place stereospecifically and regioselectively regardless of the structure of the alkyl groups at the tin atom.



R = Me, Bu^t; R^1 = H, Me.

3. Syntheses of sulfides from thiols

The syntheses of sulfides from thiols have been described in detail in a previously published review by the author [78] and in the literature quoted therein and they will not therefore be considered here.

4. Syntheses from disulfides

a. Cleavage of disulfides

The cleavage of disulfides by nucleophiles has not so far been used widely in the syntheses of sulfides owing to the formation of a series of side products. Nevertheless, some of these methods can be recommended for preparative purposes. For example, disulfides are frequently cleaved in the presence of NaCN in order to synthesise cyanoaryl sulfides.[7]

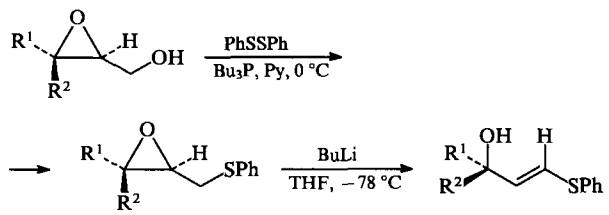
$$ArSSAr + NaCN \xrightarrow{\Delta} ArSCN + ArSNa$$

In the presence of alcohols, such cleavage is accompanied by the formation of sulfides containing alkoxy- and imino-groups.[8]

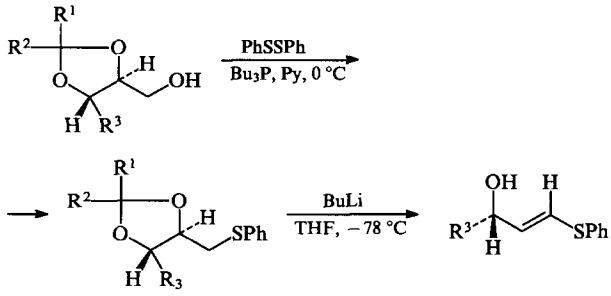
$$ArSSAr + ROH + \bar{C}N \longrightarrow ArSC(=NH)OR$$

Ar = Ph, *p*-MeC_6H_4; R = Me, Et.

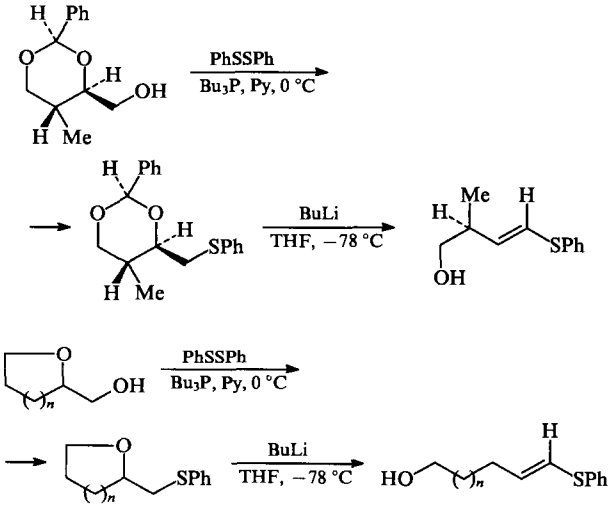
The cleavage of diphenyl disulfide by tributylphosphine and the addition of the PhS radical to oxacyclic alcohols are used in the synthesis of ω-hydroxyalk-1-enyl phenyl sulfides.[79]



$R^1 = CH_2{=}CH(CH_2)_3$; R^2 = H;
R^1 = Ph, R^2 = H.



$R^1 = R^2$ = Me, R^3 = $BuOCH_2$;
$R^1 = R^2$ = Ph, R^3 = $BuOCH_2$;
$R^1 = R^2$ = Me, R^3 = $Me(CH_2)_4$.



n = 1, 2.

An oxidative decarboxylation method has been developed in recent years on the basis of the cleavage of dialkyl disulfides in the presence of sodium hydride in dimethyl sulfoxide (DMSO) or tetrahydrofuran (THF). It involves the replacement of a carboxy- or ester-group by an alkylthio-group.[80,81]

$$XCH_2COOR \xrightarrow[NaH,\ DMSO\ (THF)]{MeSSMe} XCH_2SMe$$

X = $(EtO)_2PO$, $PhSO_2$;
R = H, Et.

b. Interaction of disulfides with organometallic compounds

The interaction of disulfides with organomagnesium compounds leads to the formation of mixtures of sulfides and thiols, which is sometimes used in the synthesis of sulfides.[7]

$$RSSR + R^1MgX \longrightarrow RSMgX + R^1SR$$

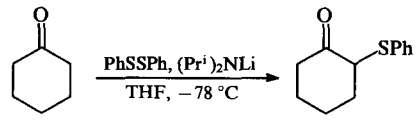
R = R^1 = Et, Ph.

Disulfides react similarly with organolithium compounds.[7,82]

$$RSSR + R^1Li \longrightarrow RSR^1 + RSLi$$

R = Me, Et, C_6H_{11}, $PhCH_2$;
R^1 = HC ≡C, $(EtO)_2CHC{\equiv}C$, $ClC{\equiv}C$, 2-$(Me_2NCHMe)C_6H_4$.

The reaction of disulfides with organolithium compounds constitutes the basis of one of the methods for the introduction of the sulfide group, which is used widely in multistep organic syntheses. For example, in order to introduce the phenylthio-group in the α-position in cyclic ketones, the latter are treated with lithium diisopropylamide in the presence of diphenyl disulfide in THF.[16]



c. Alkylation and arylation of disulfides

The alkylation of diphenyl disulfides with triethyloxonium tetrafluoroborate leads to a sulfonium salt, the hydrolysis of which affords a mixture of two sulfides—PhSEt (51%) and *p*-$PhSC_6H_4SEt$ (30%).[8] Disulfides are also alkylated by alkyl fluorides in the presence of SbF_5 and trifluoroiodomethane in liquid ammonia on exposure to UV light.[83]

$$XC_6H_4SSC_6H_4X + CF_3I \xrightarrow{NH_3,\ h\nu} XC_6H_4SCF_3$$

X = H, 4-Cl, 2-NO_2, 4-NO_2.

The yields of sulfides are 12% – 36% for X = H or 4-Cl and 58% and 72% respectively for X = 2-NO_2 and 4-NO_2.

Disulfides are arylated by aryl iodides in diphenyl ether at 230–270 °C.[84]

$$PhSSPh + ArI \xrightarrow{Ph_2O,\ 230-270\ ^\circ C} PhSAr$$

Ar = Ph, *p*-MeC_6H_4.

c. Desulfurisation of disulfides

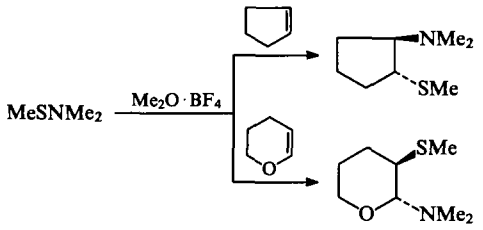
The desulfurisation of certain disulfides usually proceeds on heating,[85] whereas the conversion of other disulfides into sulfides requires the use of desulfurisation reagents, for example $(Et_2N)_3P$ or $Et_4N^+F^-$.[86] In the presence of phosphines, thiolocarbonates and xanthates are also converted into sulfides.[8]

$$ArSSAr \xrightarrow[-S]{\Delta} ArSAr$$

Ar = 2,4-$(NO_2)_2C_6H_3$.

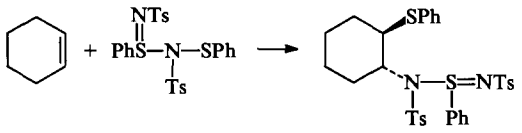
5. The syntheses from sulfenamides

The heterolytic cleavage of the S–N bond in sulfenamides in the presence of olefins is accompanied by the addition of the resulting fragments to the double bonds of the olefins with formation of aminosulfides.[87] Thus the heterolytic cleavage of the S–N bond in *N*-(dimethyl)methylsulfenamide in nitromethane in the presence of cyclopentene or 3,4-dihydro-2*H*-pyran leads to the formation of *trans*-1-dimethylamino-2-methylthiocyclopentane or *trans*-2-dimethylamino-3-methylthiotetrahydropyran.[88,89]



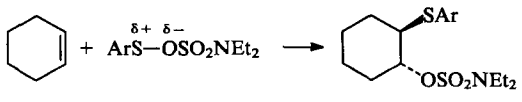
The addition of the sulfenamides $PhSNR^1R^2$ [R^1 = H, R^2 = Bu^t, $R^1+R^2 = (CH_2)_4$, $(CH_2)_2O(CH_2)_2$] to the C=C bond of cyclohexene, octene, and indene[90,91] also takes place preferentially in the *trans*-position. Strong proton-donating acids or Lewis acids are catalysts of the aminosulfenylation of olefins.

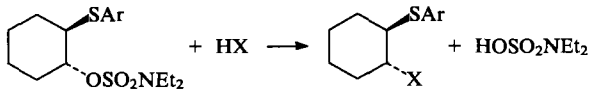
Under the conditions of acid catalysis, *N*-arenesulfenylamidines of sulfinic acids add to the C=C bonds of cyclohexene with formation of aminosulfides.[92]



The reactivity of sulfenamides in relation to olefins in the heterolytic addition reaction increases with increased electrophilicity of the sulfur atom, which can be achieved by inserting sulfur dioxide in the S–N bond of sulfenamides.[93] Using this procedure, Zefirov et al.[94] achieved for the first time the sulfamatosulfenylation of olefins, which involves the interaction of sulfenamides with sulfur dioxide in an inert solvent at a reduced temperature (–85 °C) with subsequent addition of the insertion products to the C=C bond of olefins. The reaction involving the sulfamatosulfenylation of cyclohexene is stereospecific and leads to the *trans*-1,2-adduct, which is converted into the corresponding sulfides on treatment with inorganic and organic acids.[94]

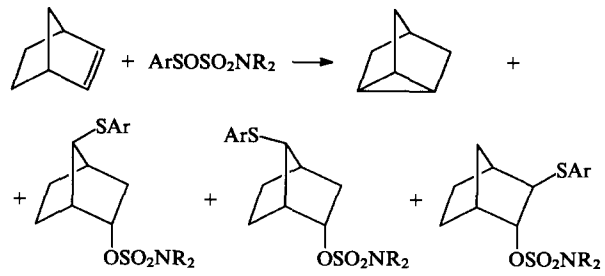
$$ArSNEt_2 + SO_3 \xrightarrow{-85\ ^\circ C,\ CH_2Cl_2} ArSOSO_2NEt_2$$

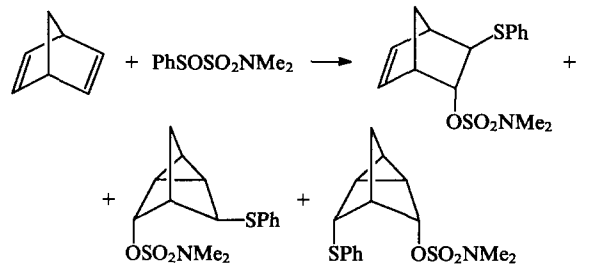




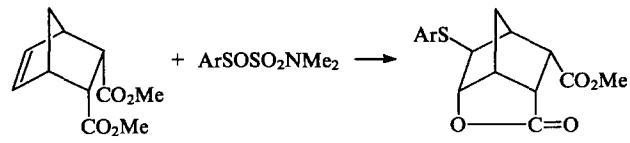
X = Br, MeCOO, CF_3COO, HCOO.

The sulfamatosulfenylation of norbornene and norbornadiene[95] is accompanied by a rearrangement of the carbon skeleton, which ultimately leads to a mixture of several products.

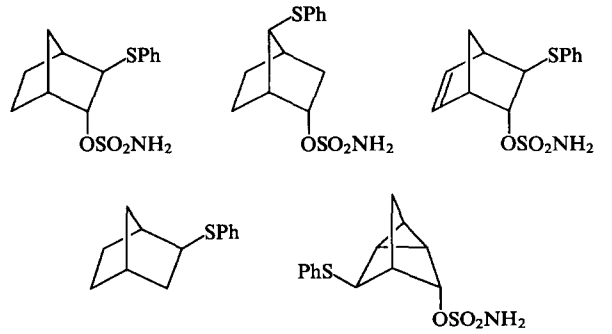




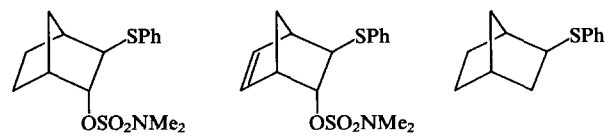
In the sulfamatosulfenylation of dimethyl *endo-cis*-bicyclo[2.2.1]hept-2-ene-5,6-dicarboxylate, the adducts cyclise with formation of arylthiolactones.[95]



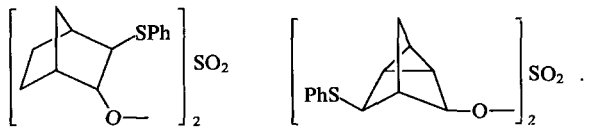
The addition of *N,N*-dimethylbenzenesulfinamide to the olefins RCH = CH_2 (R = H, C_5H_{11}, Ph) in chloroform in the presence of the sulfur trioxide–pyridine complex at 20–25 °C leads to a mixture of two aminosulfides: $RCH(SPh)CH_2NMe_2$ and $RCH(NMe_2)CH_2SPh$.[96,97] It has been suggested[97] that these compounds are formed as a result of the rearrangement of the esters of *N,N*-dimethylsulfamic acid formed in the first stage of the addition reaction. The reaction of the sulfenamide $PhSNEt_2$ with cyclohexene and sulfamic acid in acetonitrile at 90–100 °C affords an adduct, the treatment of which with 10% HCl leads to the hydrochloride of *trans*-2-phenylthiocyclohexylamine.[98] In the case of norbornene and norbornadiene,[99] a mixture of the following products is formed:



Together with the expected products



the interaction of norbornene and norbornadiene with *N,N*-dimethylbenzenesulfenamide in the presence of $K_2S_2O_7$ affords also[100]

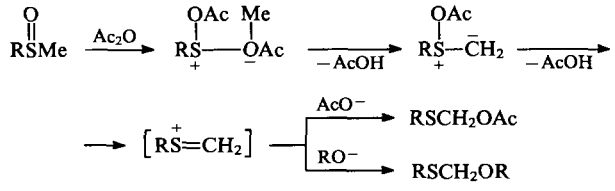


Consequently in the reaction of sulfenamides with SO_3 liberated from the pyrosulfate anion, the generation of the sulfenyl species PhS^+ is accompanied by the simultaneous formation of two counterions — the sulfate and sulfamate anions.

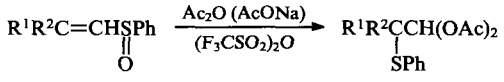
Ethyl benzenesulfenate also reacts with SO_3 in chloroform at −60 °C to form the highly reactive electrophile $PhSOSO_2OEt$, the reaction of which with norbornene and camphene affords a mixture of stereoisomeric sulfides.[101]

6. Syntheses from sulfoxides

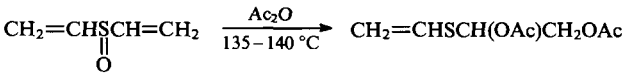
Sulfoxides are usually obtained from sulfides and the reduction of these compounds is therefore not used as a rule to synthesise simple sulfides. Other reactions of sulfoxides, which lead to the formation of sulfides whose structure differs from those of the sulfides used to synthesise the initial sulfoxide, are of preparative importance. For example, the Pummerer rearrangement of sulfoxides on treatment with acetic anhydride in the presence of alcohol leads to α-alkoxyalkyl sulfides, whereas in the absence of alcohol the formation of α-acetoxyalkyl sulfides is observed.[80]



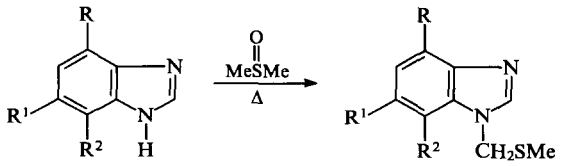
The rearrangement of vinyl sulfoxide[102] and divinyl sulfoxide[103] in acetic anhydride leads to diacetoxyalkyl sulfides.



R^1 = Me, Et, 4-MeC_6H_4, 4-ClC_6H_4, 3(4)-$MeOC_6H_4$;
R^2 = H, Me.



A convenient preparative method of synthesis of methyl sulfides has been developed. It involves the interaction of dimethyl sulfoxide with benzimidazole derivatives.[104]



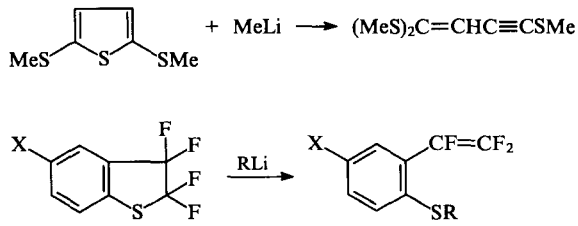
R = H, Me; R^1 = H, NO_2; R^2 = H, NO_2.

Dimethyl sulfoxide reacts similarly with phthalimide, isatin, saccharin, and pyridopyrimidines.[105]

7. Other methods of synthesis of sulfides

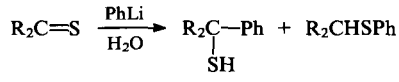
A preparative method of synthesis of bis(*o*-arylthiophenyl) sulfides by the reaction of 5-(4-R-phenyl)thianthrenium perchlorates (R = OMe) with thiophenols RC_6H_4SH (R = 4-Me, 4-MeO, 2-Cl, 2-NH_2) in THF in the presence of sodium hydride has been described.[106]

Polyfunctional sulfides are sometimes synthesised by opening the rings of sulfur-containing heterocyclic compounds on treatment with organolithium compounds.[8,107]



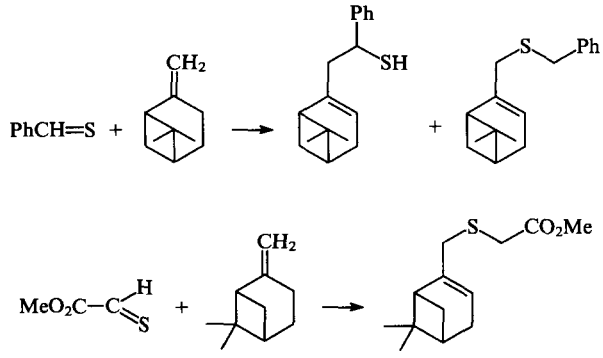
R = Alk, Ar; X = H, Br, Alk.

In the reactions of thiones with organometallic compounds,[78] there is a possibility of addition both to the carbon atom and to the sulfur atom, which results in the formation of a mixture of tertiary thiols and isomeric sulfides.

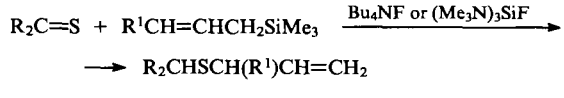


R = Bu^t.

The addition of thiones to the double bond of pinenes also leads to the corresponding sulfides.[9]

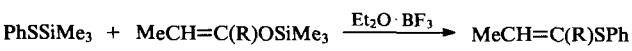


The interaction of thiones with silylated olefins, induced by the fluoride ion, is accompanied by the elimination of the silyl fragment and the formation of allyl sulfides.[108,109]



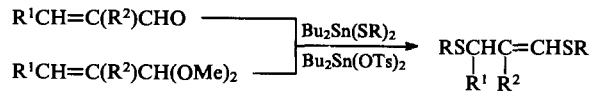
R = 2-MeC_6H_4; R^1 = H, Ph, PhMeCH.

In the presence of the complex $Et_2O.BF_3$, phenylthiosilanes react with alkenyl silyl ethers to form vinyl sulfides.[110,111]



R = Alk, *cyclo*-Alk.

It has been noted[112] that the interaction of alkyl(aryl)-thiostannanes with α,β-unsaturated aldehydes or unsaturated acetals leads to the formation of 1,3-di-alkyl(aryl)thiopropenes in the form of a mixture of (*Z*)- and (*E*)-isomers.



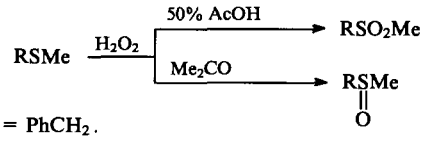
R = Me, Ph, C_6H_{11}; R^1 = H, Me, Pr; R^2 = H, Me, Et.

IV. Reactions of sulfides

1. Reactions involving an increase in the valence of sulfur

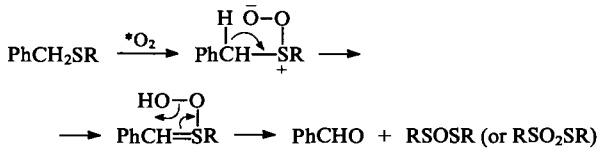
a. Oxidation of sulfides to sulfoxides

Mainly reagents of two types are used to convert sulfides into sulfoxides:[7,113] derivatives of peroxyacids [*m*-chloroperbenzoic and peroxydodecanoic acids activated by manganese(IV) peroxide and sodium periodate] and compounds which serve as sources of a halogen (*tert*-butyl hypochlorite, *N*-bromo- and *N*-chloro-succinimides, 1-chlorobenzotriazole, chlorine, etc.). Individual examples of the use of other reagents are also known, for example nitric acid,[4] cerium ammonium nitrate,[7] hydrogen peroxide in the presence of tellurium dioxide,[114] urea and phthalic anhydride,[115] *o*-iodosylbenzoic acid,[116] tetranitromethane,[117] the ozonides of phosphites,[118] and peroxides.[119] The use of hydrogen peroxide as the oxidant can lead to sulfoxides or sulfones depending on the conditions.[7]

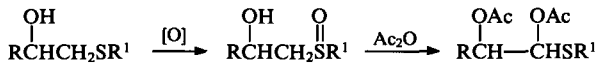


R = $PhCH_2$.

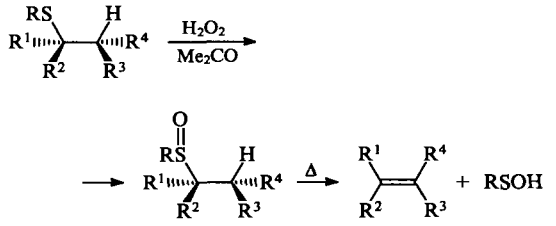
The photochemical oxidation of alkyl benzyl sulfides leads to the formation of a mixture of products, one of which is benzaldehyde.[120]



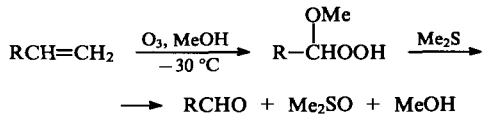
The oxidation of β-hydroxyalkyl sulfides leads to the formation of sulfoxides capable of undergoing the Pummerer rearrangement on heating in acetic anhydride.[8]



Taking into account the tendency of sulfoxides to undergo thermal *cis*-elimination, the oxidation of sulfides to sulfoxides is used in organic synthesis to convert sulfides into alkenes.[16]

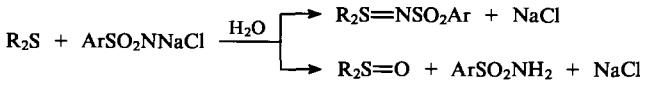


Dimethyl sulfide is used to reduce hydroperoxides.[8]



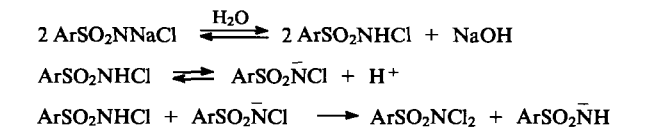
b. Oxidative imination of sulfides

The reactions accompanied by the oxidation of an element and the formation of the imino-group have come to be called oxidative imination.[121] The oxidative imination of sulfides by sodiochloroamides of sulfonic acids proceeds as a rule in aqueous media. Together with sulfilimines, sulfoxides are also formed in this reaction.

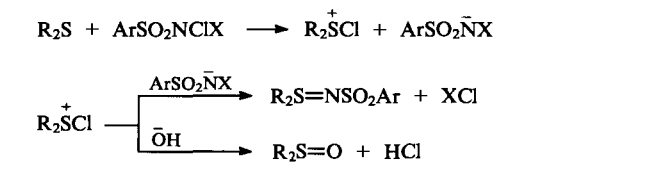


R = Alk, Ar, Het.

The ratio of sulfilimines and sulfoxides depends on the nature of the groups at the sulfur atom in the initial sulfide, the pH of the medium, and the nature of the solvent employed. It has been suggested[122] that the sulfonic acid sodiochloroamide is converted in an aqueous alcoholic medium via a reversible reaction into *N*-chlorosulfonamide (rapidly) and *N,N*-dichlorosulfonamide (slowly), which are fairly reactive electrophiles.



The reaction of a sulfide with *N*-chlorosulfonamide or *N,N*-dichlorosulfonamide[123–126] affords the chlorosulfonium cation R_2S^+Cl, which interacts with the sulfonamide anion $ArSO_2N^-X$ (X = H, Cl) to form a sulfilimine, whereas the hydrolysis of the chlorosulfonium cation leads to sulfoxides.[127]



R = H, Cl.

A low acidity of the medium promotes the conversion of the sulfonic acid sodiochloroamide into the more reactive *N*-chloro- and *N,N*-dichlorosulfonamides, but it reduces the probability of the existence of the sulfonamide anion. According to Tsujihara et al.,[128] pH 6 is optimum in the imination of dialkyl and alkyl aryl sulfides by the sodiochloroamide of toluene-*p*-sulfonic acid. Since aqueous solutions of sulfonic acid sodiochloroamides are alkaline, the addition of a small amount of acetic acid to the reaction medium increases the yield of sulfilimines.[128] In view of the sparing solubility of sulfides in water, aqueous solutions of methanol, acetone, and dioxan as well as two-phase systems, for example water–methylene chloride, are used for their imination, which naturally reduces the yield of sulfilimines and promotes the formation of sulfoxides. The use of anhydrous organic solvents, for example methylene chloride, as the reaction medium and of *N*-chloro-*N*-(tetraalkylamino)arenesulfonamides, readily soluble in these solvents, instead of sulfonic acid sodiochloroamides, leads to the formation of sulfilimines in a quantitative yield.[129]



R = Ph, *p*-MeC_6H_4, *p*-ClC_6H_4, $PhCH_2$;
R^1 = Me, Bu; R^2 = Bu, $C_{12}H_{25}$, $C_{14}H_{29}$, $C_{18}H_{37}$.

An increase in the yield of sulfilimines in the case where two-phase reaction media are employed is also promoted by phase transfer catalysts.[130]

The susceptibility of the sulfur atom in the sulfide to electrophilic attack by the chlorine cation is directly related to the electron density on the sulfur atom, which depends on the nature

of the substituents. Electron-accepting groups at the sulfur atom hinder the imination reaction or preclude it altogether. Because of this, the search for and development of procedures designed to increase the electron density on the sulfur atom in sulfides is important from both theoretical and synthetic points of view. Analysis of the effective charges in the molecule of methanethiol and its carbanion, obtained as a result of quantum-mechanical calculations by the CNDO/2 method, showed[121,131] that one of these procedures involves the creation of an α-C-anionic centre in the sulfide molecule. The possibility, in principle, of arenesulfonylimination of aryl diacylmethyl sulfides containing a mobile α-H atom together with electron-accepting groups has been demonstrated,[139] but the sulfilimines formed in this case undergo further reactions as a result of the imino-ylide tautomerism.

$$X_2CH{-}\underset{\underset{NR}{\|}}{S}Ar \rightleftharpoons X_2C{=}\underset{\underset{NHR}{|}}{S}Ar \longrightarrow X_2\underset{\underset{NHR}{|}}{C}{-}SAr$$

X = PhCO, MeCO; Ar = 2(4)-$NO_2C_6H_4$, 2,4-$(NO_2)_2C_6H_3$;
R = $PhSO_2$, 4-$MeC_6H_4SO_2$.

The use of sodium salts of sulfides instead of the sulfides themselves promotes the arenesulfonylimination of these compounds in an anionic form and also the stabilisation of the resulting *N*-arenesulfonylsulfilimino-anions.[47,121,131,133–136]

$$\left[\begin{matrix}X\\ Y\end{matrix}\!\!>\!C{=}{=}SR\right]^{-}Na^{+} + ArSO_2NNaCl \xrightarrow[-NaCl]{} \left[\begin{matrix}X\\ Y\end{matrix}\!\!>\!C{=}{=}\underset{\underset{NSO_2Ar}{\|}}{S}R\right]^{-}Na^{+}$$

R = 2(4)-$NO_2C_6H_4$, 2,4-$(NO_2)_2C_6H_3$;
X = Y = PhCO, MeCO, CN, EtOCO; X = MeCO, Y = EtOCO;
X = NO_2; Y = H, $PhCH_2$, PhCO, 2-$NO_2C_6H_4$.

Other *N*-chloro-compounds such as chloroamine, carboxylic acids *N*-chloroamides, *N*-chlorourethanes, *N*-chloroamidines, and *N*-chlorourea and its derivatives react with dialkyl and alkyl aryl sulfides to form aminosulfonium salts, which are converted into the corresponding sulfilimines on treatment with bases.[121]

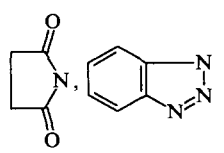
$$R_2S + XNHZ \longrightarrow R_2\overset{+}{S}NHZ\ X^{-} \xrightarrow[-HX]{HB} R_2S{=}NZ$$

R = Alk, Ar; X = Cl, Br;
Z = H, Alk, Ar, Het, AlkCO, ArCO, EtOCO,
RN=CR, NH_2—N=CH, NH_2CO.

Chlorine,[137] *tert*-butyl hypochlorite,[138–140] sulfuryl chloride,[121] *N*-chlorosuccinimide,[141–143] and other *N*-chloro-compounds,[137] the reactions of which with sulfides at low temperatures afford chlorosulfonium intermediates which are converted into sulfilimines by treatment with *N*-nucleophiles, are also used as sources of the chlorine cation.

$$R_2S + ZCl \longrightarrow [R_2\overset{+}{S}{-}Z]\overset{-}{Cl} \xrightarrow{R^1NH_2}$$

$$\longrightarrow R_2\overset{+}{S}NHR^1\overset{-}{Cl} \xrightarrow[-HCl]{HB} R_2S{=}NR^1$$

R = Alk, Ar;
Z = Cl, Bu^tO, SO_2Cl_2, 

Aliphatic, aromatic, and heterocyclic amines, *N*-aminophthalimide, cyanamide, and the sodioamides of sulfonic and carboxylic acids are used as the *N*-nucleophiles.[121]

The oxidative imination of sulfides by hydroxyaminosulfonic acid[121] is a special case of the general reaction involving the imination of sulfides by derivatives of hydroxylamine, in particular by *N*-arenesulfonyl-*O*-*p* nitrobenzenesulfonylhydroxylamine, *N*-ethoxycarbonyl-*O*-*p*-nitrobenzenesulfonylhydroxylamine, and *O*-mesitylenesulfonylhydroxylamine.

$$R_2S + XYNOY \longrightarrow R_2\overset{+}{S}NH(X)\overset{-}{O}Y \xrightarrow[-HOY]{HB} R_2S{=}NX$$

R = Alk, Ar;
X = H, $ArSO_2$, EtOCO;
Y = HSO_3, 2,4,6-$Me_3C_6H_2SO_2$, 4-$NO_2C_6H_4SO_2$.

Sulfilimines are also formed in the reaction of sulfides with nitrenes generated by photochemical, thermal, and chemical methods. The procedure involving the photolysis of various organic azides in the presence of an excess of the sulfide has come to be most widely used.

$$XN_3 \xrightarrow{h\nu} :NX \xrightarrow{R_2S} R_2S{=}NX$$

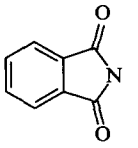
X = $ArSO_2$, PhCO, EtOCO, R_2PO;
R = Alk, Ar.

The reaction has been studied for a series of arenesulfonyl,[144] acyl,[121] alkoxycarbonyl,[121,144] diphenylphosphonyl, and dialkylphosphonyl azides.[145] It has been noted[121] that sulfides react with singlet nitrenes faster than with triplet nitrenes, since the presence in the reaction mixture of substances inducing the formation of triplet nitrenes inhibits the formation of sulfilimines. The low yields of the latter may be caused by their chemical instability. Under the conditions of photolysis, the sulfilimines are themselves sources of nitrenes, which has been noted[121] in the case of the photolysis of *N*-ethoxycarbonyl-*S*-*S*-dimethylsulfilimine. Certain unstable heterocyclic compounds, the photolysis of which in the presence of sulfides leads to the formation of sulfilimines, also function as sources of nitrenes.

$$Ph{-}\underset{\underset{O}{\|}}{\overset{N{-}O}{C}}{-}\underset{\underset{O}{|}}{C}{=}O + Me_2S \xrightarrow{h\nu} Me_2S{=}NCOPh + CO_2$$

The main disadvantage of the methods of synthesis of sulfilimines by the reaction of sulfides with thermally generated nitrenes is the thermal instability of the sulfilimines formed, for example, in the thermolysis of acyl azides,[146] alkoxycarbonyl azides, and arenesulfonyl azides in the presence of sulfides.[146,147] In the presence of copper, the thermolysis of the azides and hence the interaction of nitrenes with sulfides proceed at a lower temperature, which promotes a higher yield of sulfilimines.[148] The chemical synthesis of nitrenes with the aim of obtaining sulfilimines is more rarely employed. The synthesis of certain sulfilimines by the reaction of sulfides with arenesulfonamides and *N*-aminophthalimide in the presence of lead tetraacetate has been described.[121]

$$R_2S + NH_2X \xrightarrow{Pb(OAc)_4} R_2S{=}NX$$

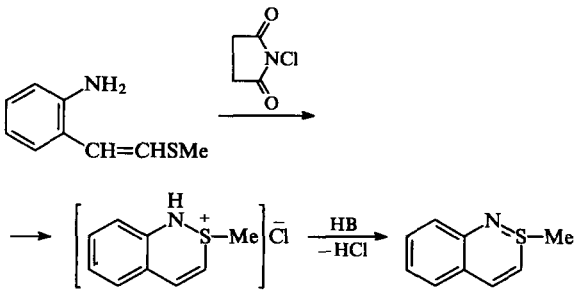
X = $ArSO_2$, 

One cannot rule out the possibility that the formation of sulfilimines in the reactions of sulfides with compounds having an E=N bond (E = S, I), which has been described in the literature,[149,150] also proceeds via a nitrene generation stage.

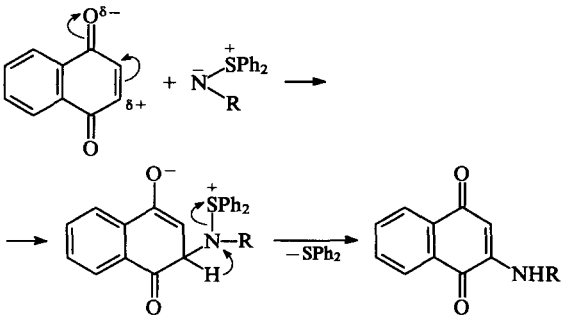
$$R_2S + X{=}NTs \longrightarrow R_2S{=}NTs$$

X = TsN =S, ArI.

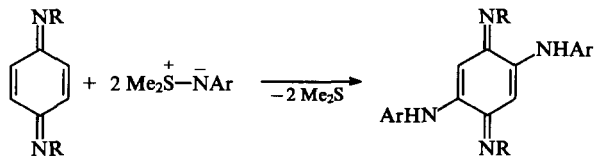
It has been shown[151] that, on treatment with *N*-chlorosuccinimide, aromatic amines containing an alkylthio-group in the *ortho*-position give rise to cyclic aminosulfonium salts, which are converted into cyclic sulfilimines in the presence of bases.



The conversion of sulfides into sulfilimines is of great synthetic importance, since the latter possess a series of valuable properties used in organic syntheses. Some of these syntheses are accompanied by the regeneration of the initial sulfides. For example, the high nucleophilicity of the nitrogen in *N*-arenesulfilimines makes it possible to use them for the introduction of aryl amino-groups into the quinonoid ring of quinone imines with regeneration of the initial sulfide.[121,152]

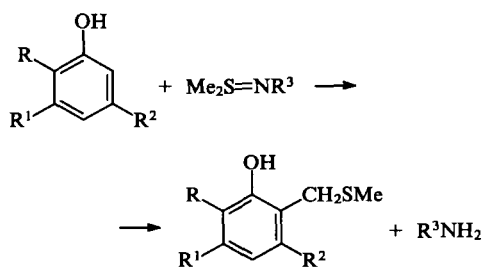


R = $PhCH_2$.



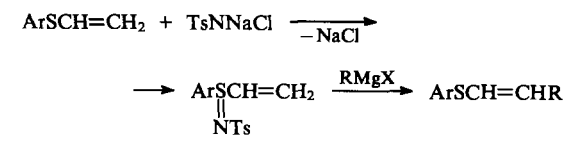
R = $PhSO_2$, *p*-$MeC_6H_4SO_2$;
Ar = Ph, *p*-MeC_6H_4, *p*-ClC_6H_4, *p*-$NO_2C_6H_4$.

S,*S*-Dimethylsulfilimines are used to introduce the methylthiomethylene group into the aromatic ring of phenols.[121]



R = Me, OMe; R^1 = H, Me; R^2 = $ArSO_2$; 2,4-$(NO_2)_2C_6H_3$.

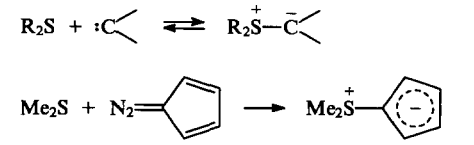
Substituents can also be introduced into vinyl sulfides $ArSCH=CH_2$ via the sulfilimine formation stage, whereupon the compounds ArSCH=CHR are formed.[8]



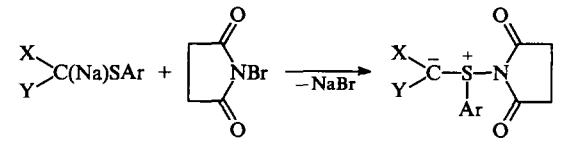
S-Alkyl-*S*-allyl-*N*-tosylsulfilimines cyclise intramolecularly on treatment with NaOH, affording 2-vinyl-substituted cyclic amines.[153]

c. The formation of sulfur ylides

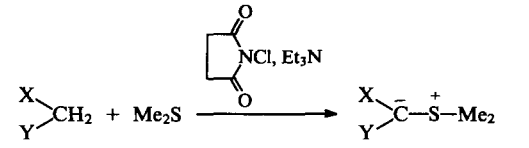
The interaction of sulfides with carbenes leads to sulfur ylides, which are not always stable and can undergo various rearrangements.[7]



The formation of relatively stable sulfur ylides on interaction of the sodium salts of α-arylthio-derivatives of CH acids with *N*-bromosuccinimide in acetone[154] and also on interaction of dimethyl sulfide and *N*-chlorosuccinimide with CH acids in the presence of triethylamine[155] has been noted.

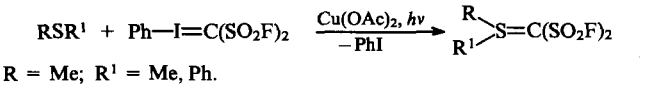


X = MeCO, Y = EtOCO; X = $PhSO_2$, Y = Ph;
Ar = 2-$NO_2C_6H_4$, 4-$NO_2C_6H_4$.



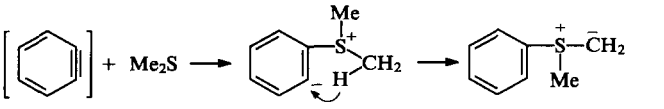
X = Br, Ac, CN, $PhCH_2$; Y = Br, $EtCO_2$, $MeCO_2$, Ph.

The thermal and photochemical decomposition of phenyliodonium bis(fluorosulfonyl)methylides in the presence of sulfides leads to the formation of relatively stable sulfur ylides.[156]

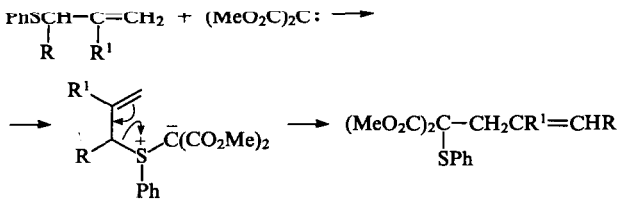


R = Me; R^1 = Me, Ph.

The addition of sulfides to dehydrobenzene also affords relatively stable sulfur ylides.[8]

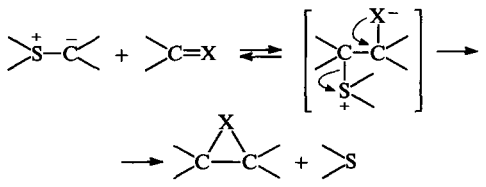


The insertion of carbenes in the allylic C–S bond[8,157] proceeds via the formation of ylides.



R = H, Me; R^1 = H, Me.

Sulfur ylides are used widely in organic synthesis for the transfer of the alkylidene group to an electrophilic double bond with formation of a three-membered ring.[121]

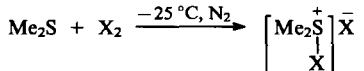


X = O, C.

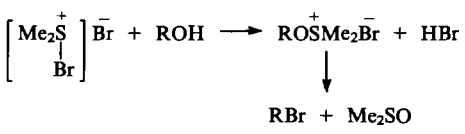
It has been suggested[8] that the biosynthesis of the cyclopropane ring in a number of natural products proceeds via the copper-catalysed transfer of the methylene group of the ylide formed from *S*-adenosylmethionine.

d. The formation of halosulfonium halides and other sulfonium salts

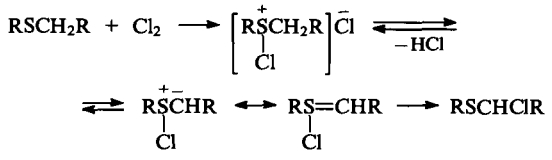
Dimethyl sulfide reacts with Cl_2 or Br_2 at −25 °C in $CHCl_3$ to form charge-transfer complexes or halodimethylsulfonium halides and is used in organic synthesis to convert alcohols into alkyl halides.[7]



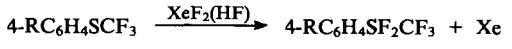
X = Cl, Br.



Chlorosulfonium chlorides are intermediates in the α-chlorination of sulfides.[7]

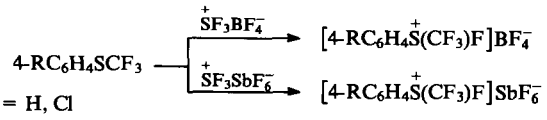


Aryl trifluoromethyl sulfides do not react with chlorine or bromine, but, on treatment with xenon fluoride, they combine with two fluorine atoms, affording readily hydrolysable aryldifluoro(trifluoromethyl)sulfuranes in a quantitative yield.[4]



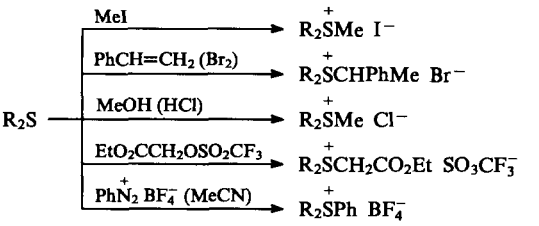
R = H, Cl, NO_2.

Treatment of aryl trifluoromethyl sulfides with the complexes $SF_3^+BF_4^-$ and $SF_3^+SbF_6^-$ yields arylfluoro(trifluoromethyl)-sulfonium salts,[158] which are used in the synthesis of *N*-arenesulfonyl-*S*-aryl-*S*-trifluoromethylsulfilimines.[4]

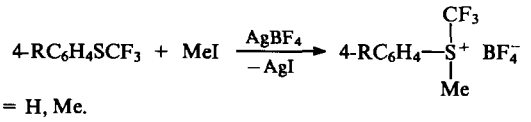


R = H, Me.

The interaction of sulfides with electrophiles or reagents capable of forming cationoid species results in the formation of sulfonium salts, which remain unchanged under the reaction conditions only in rare cases. The reaction involving the alkylation (arylation) of sulfides by alkyl halides, alkenes, alcohols, trifluoromethanesulfonates, and diazonium salts is usually employed to obtain sulfonium salts in a pure form.

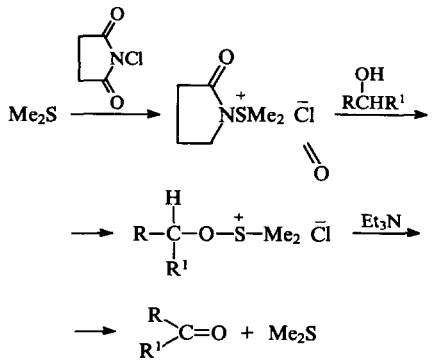


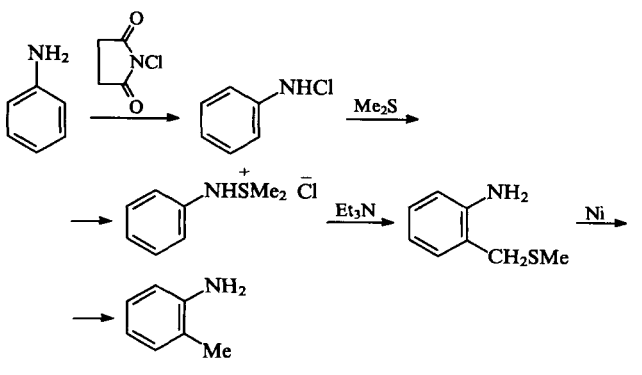
Despite the low nucleophilicity of the sulfur atom, aryl trifluoromethyl sulfides are alkylated by methyl iodide in the presence of $AgBF_4$.[4]



R = H, Me.

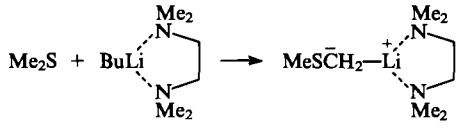
Aminosulfonium salts, used to oxidise alcohols and to *ortho*-methylate anilines, are formed on interaction of sulfides with *N*-chlorosuccinimide and also with amines in the presence of *N*-chlorosuccinimide.[121]





2. Generation of α-sulfenylcarbanions

Sulfides containing a mobile α-H atom relatively easily form carbanions in the stabilisation of which the sulfur atom is directly involved.[159] Depending on the acidity of such sulfides, sodium methoxide,[131–136] potassium *tert*-butoxide,[160] alkali metal hydroxides,[161–163] sodium hydride,[167] and *tert*-butyllithium in THF[16] are used to synthesise carbanions. For example, dimethyl sulfide forms a carbanion on reaction with the butyllithium–tetramethylethylenediamine (TMEDA) complex.[16]



Methyl phenyl sulfide is converted into phenylthiomethyllithium on treatment with butyllithium in the presence of diazabicyclo[2.2.2]octane (DABCO).[16]

Reactions involving the substitution by a metal of atoms and groups such as Br, $SnBu_3$ and SePh as well as reactions involving the addition of organometallic reagents to the C=C bond of vinyl sulfides and to the C=S bonds of thioketones are much more rarely used in the synthesis of α-sulfenylcarbanions.[16,165]

The stability of the α-C-anionic centre increases following the enhancement of the *s* character of the carbon atom and also with increase in the number of sulfenyl groups linked directly to this atom, which is clearly confirmed by the comparison of the pK_a of the following compounds: PhSMe (49), $(PhS)_2CH_2$ (30.8), and $(PhS)_3CH$ (22.8).[166] The stability of the α-C-anionic centre is also influenced by other factors, in particular by the presence of neighbouring electron-accepting groups and atoms participating in the delocalisation of the negative charge,[47–51,167] the possibility of the transfer of the negative charge to other atoms as a result of tautomerism or isomerisation,[131,135] and also the possibility of the stabilisation of the counterion as a result of chelate formation.[16]

The question of the mechanism of the stabilisation of the α-C-anionic centre by a divalent sulfur atom has not so far been ultimately elucidated and still remains controversial. There are several concepts which explain the ability of sulfur to stabilise the α-C-anionic centre. According to one of them,[7] the α-C-anionic centre is stabilised by the sulfur atom as a result of the transfer of electrons from the carbanionic centre to the *d* orbitals of the sulfur atom. Despite the fact that doubts have been repeatedly cast on this concept, nevertheless investigators still prefer to resort to it even in recent years.[47,131–135]

According to another concept, the α-C-anionic centre is stabilised by the sulfur atom as a result of the dispersion of the negative charge owing to the more ready polarisability of the electron cloud of the sulfur atom compared with the carbon atom.[16] The polarisabilities of the sulfur and carbon atoms are 3.8×10^{40} and 1.9×10^{40} C m^2 V^{-1}, while the values for the C–S and C–C bonds are 2.1×10^{40} and 1.1×10^{40} C m^2 V^{-1} respectively.[16]

The concept of η,σ^*-delocalisation (hyperconjugation) has also been proposed, in satisfactory agreement with X-ray diffraction data for the lithio-derivatives of dimethyl sulfide, methyl phenyl sulfide, 1,3-dithiane, and 2-phenyl-1,3-dithiane as well as ^{13}C and ^6Li NMR spectrometric data.[16]

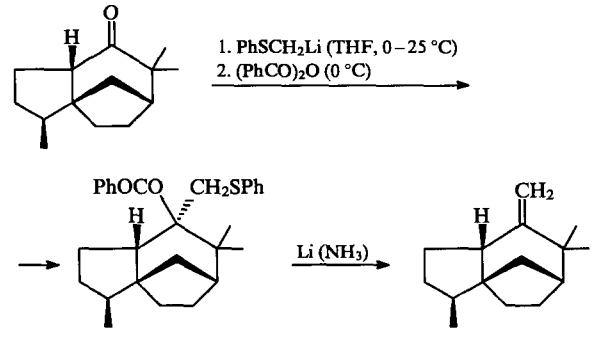
In studying the reactivity of α-sulfenylcarbanions and the reactions involving them, it is necessary to begin with the fact that α-sulfenylcarbanions are in essence ambident anions and their reactions with electrophiles proceed either via the carbon atom or the sulfur atom depending on the nature of the electrophile. By exerting its stabilising influence on the α-C-anionic centre, the divalent sulfur atom undergoes an increase in its electron density owing to the displacement of the latter from the anionic centre, which has been confirmed by quantum-mechanical calculations.[131] As a result of such increase in electron density, the sulfur atom becomes more susceptible to attack by the electrophile.

Examples of the reactions of α-sulfenylcarbanions with electrophiles involving the participation of the carbon atom are provided by the *C*-alkylation[16,47] and *C*-acylation[47] reactions and also by the reactions involving the addition of the α-C-anionic centre to the electron-deficient carbon atom of the carbonyl group.[161–163] In view of the possibility of the subsequent elimination of the sulfenyl group, these reactions play a major role in fine organic synthesis and, in particular, in the formation of the C–C and C=C bonds in the synthesis of various natural products. The formation of higher homologues of alkyl iodides[168] and the synthesis of the sesquiterpene zizaene may be quoted as clear-cut examples.[169]

The formation of higher homologues of alkyl iodides involves the alkylation of phenylthiomethyllithium by an alkyl iodide and subsequent replacement of the phenylthio-group by iodine on treatment with methyl iodide in the presence of sodium iodide. Ultimately one obtains an alkyl iodide containing one or several carbon atoms more than the initial compound.

$$PhSCH_2Li + RCH_2I \xrightarrow[-LiI]{} RCH_2CH_2SPh \xrightarrow[NaI]{MeI} RCH_2CH_2I$$

The synthesis of the sesquiterpene zizaene consists in the addition of phenylthiomethyllithium to the carbonyl group of a cyclic ketone and subsequent benzoylation of the resulting β-hydroxysulfide and the reductive elimination of the phenylthio-group with the aid of lithium in liquid ammonia.



The reactions of α-sulfenylcarbanions with electrophiles involving the sulfur atom were discovered comparatively recently. They include the reactions of the sodium salts of sulfides with *N*-halo-derivatives and in particular the oxidative imination[47,131,134,135] and oxidative imidation[154] of the sodium salts of sulfides, which were considered in the previous Section. The primary step in these reactions is attack on the positively charged halogen atom of the *N*-halo-compound by the sulfur atom with formation of a halosulfonium intermediate,[121] which reacts with the *N*-anion to form the reaction product. The sodium salts of *N*-arenesulfonylsulfilimines, synthesised by the arenesulfonylimination of the sodium salts of sulfides, readily undergo *C*-alkylation,[131,135] which is very important for the synthesis of new *N*-arenesulfonylsulfilimines.

$$RSC(Na)X_2 \,\|\, NSO_2Ar + MeI \xrightarrow[-NaI]{} RSC(Me)X_2 \,\|\, NSO_2Ar$$

R = 2(4)-$NO_2C_6H_4$; X = MeCO, EtOCO; Ar = 4-MeC_6H_4.

3. Reactions involving the cleavage of the C–S bond

The C–S bond is cleaved comparatively readily compared with the C–C bond or a nonactivated C–H bond under the influence of heat or chemical reagents. For example, the pyrolysis of benzyl phenyl sulfide in cyclohexane begins already at 200 °C with the homolytic cleavage of the C–S bond.[170] The composition of the products of the pyrolysis of sulfides is then determined both by the structure of the initial sulfide and by the pyrolysis conditions.

For example, in the gas phase at 400–800 °C diethyl sulfide decomposes to hydrogen sulfide and ethylene, which are formed as a result of the following reactions.[171]

$$CH_3CH_2SCH_2CH_3 \xrightarrow{\Delta} CH_3CH_2\dot{S} + CH_3\dot{C}H_2$$

$$CH_3\dot{C}H_2 + CH_3CH_2SCH_2CH_3 \longrightarrow$$

$$\longrightarrow CH_3CH_3 + CH_3CH_2S\dot{C}HCH_3$$

$$CH_3CH_2S\dot{C}HCH_3 \longrightarrow CH_3CH_2\dot{S} + CH_2{=}CH_2$$

$$CH_3CH_2\dot{S} + CH_3\dot{C}H_2 \longrightarrow CH_3CH_2SH + CH_2{=}CH_2$$

$$CH_3CH_2SH \longrightarrow H_2S + CH_2{=}CH_2$$

The formation of hydrogen sulfide and the corresponding alkenes has been observed[172] also in the thermolysis of other dialkyl sulfides. Under these conditions, dialkyl sulfides with the iso-structure and asymmetric dialkyl sulfides are thermally less stable than symmetrical sulfides with the normal structure. The pyrolysis of allyl methyl sulfide at 427 °C leads to thioformaldehyde and propene.[173] Other alkyl allyl sulfides are converted into the corresponding thiocarbonyl compounds and alkenes under the conditions of vacuum pulse pyrolysis at 615–650 °C.

$$>CH{-}S{-}CH_2{-}CH{=}CH_2 \longrightarrow >C{=}S + MeCH{=}CH_2$$

Diallyl and allyl benzyl sulfides form thioacrolein and thiobenzaldehyde respectively under these conditions.[174] The vacuum pulse pyrolysis of allyl phenyl sulfide proceeds with formation of phenylthiyl and allyl radicals, which dimerise under the pyrolysis conditions.[172] The vacuum pyrolysis of alkyl ethynyl sulfides at 500 °C leads to the formation of thioketene.[16]

$$CH{\equiv}CSCMe_3 \xrightarrow{500\ ^\circ C} [CH{\equiv}C\dot{S} + \dot{C}Me_3] \longrightarrow$$

$$\longrightarrow CH{\equiv}CSH + CH_2{=}CMe_2$$

$$CH{\equiv}CSH \longrightarrow CH_2{=}C{=}S$$

The products of the pyrolysis of the sulfide $PhCH_2CH(Ph)SPh$ at 250 °C are H_2S, PhMe, $PhCH_2CH_2Ph$, PhCH = CHPh, PhSH, Ph_2S, thianthrene, and 2,3,4,5-tetraphenylthiophene.[175]

The thermal disproportionation of alkyl sulfides in the presence of carboxylic acid esters is one of the transesterification methods.[8]

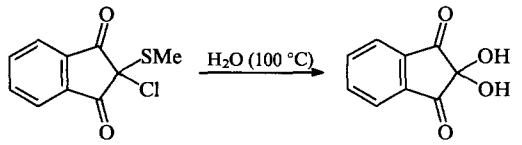
$$RCO_2Me + R^1SR^1 \xrightarrow{\Delta} RCO_2R^1 + R^1SMe$$

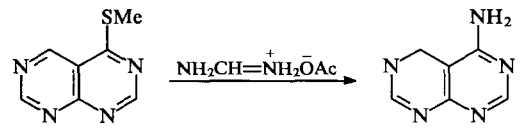
The dealkylation of butyl methyl sulfide in the presence of alkanechalcogenolate anions, which proceeds with formation of butanethiolate and methanethiolate anions in 40% and 35% yields respectively, has been described.[176] The thiolate anions react with propyl iodide, affording the corresponding sulfides.

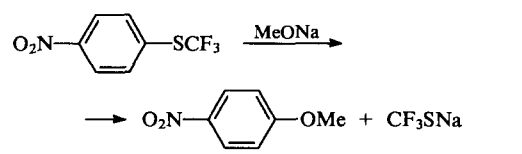
The reductive cleavage of sulfides, in which there is a clear tendency towards the preferential cleavage of one of the two C–S bonds, is used in the synthesis of thiols. The ease of the cleavage of the C–S bond diminishes in the sequence alkynyl > vinyl > allyl > alkyl.[78] Sodium in liquid ammonia or lithium in ethylamine are used for the reductive cleavage of allyl and benzyl sulfides. The reductive cleavage of 3-alkylthioindolenine to indole proceeds on treatment with $LiAlH_4$, Raney nickel in ethanol, or $NaBH_4$ in isopropyl alcohol. The reductive cleavage on treatment with CF_3COOH in the presence of a suitable nucleophilic trapping agent is also used.[177] One of the methods for the protection of the SH group involves its conversion into the sulfide group, which is as a rule achieved as a result of alkylation, acylation, or addition reactions. The protecting groups are removed by means of various methods for the cleavage of the C–S bond, using bases, acids, mercury acetate and sulfate, silver nitrate in pyridine, and trifluoromethanesulfonic acid, as well as electrolytic cleavage.[78]

The anodic[178] and oxidative[179] desulfurisation of cyclic dithioacetals by *N*-halo-compounds in the presence of sources of fluoride ions ($Bu_4N^+H_2F_3^-$, $Et_3N \cdot HF$) may be used as preparative methods of synthesis of geminal difluoroalkanes.

Certain sulfides undergo relatively easily hydrolysis, aminolysis, and alcoholysis with cleavage of the C–S bond.[4,8]







The sulfides in which the sulfur atom is linked to the benzyl or an acyl[180] group undergo chlorinolysis comparatively readily, which is frequently used in the synthesis of sulfenyl chlorides.

$$ArSCH_2Ph + Cl_2 \xrightarrow{CH_2Cl_2} ArSCl + PhCH_2Cl$$

$$RSAc + SO_2Cl_2 \xrightarrow{CCl_4} RSCl + AcCl + SO_2$$

R = Me, Bu, Bu^t, Ph, 2-MeC_6H_4, 4-$NO_2C_6H_4$.

Asymmetric sulfides are obtained by the cleavage of the C–S bond in symmetrical sulfides in the presence of iodonium[181] or sulfonium[182] salts.

$$Me_2S + [\overset{+}{I}C_6F_{13}]BF_4^- \longrightarrow$$

$$\longrightarrow [Me_2\overset{+}{S}C_6F_{13}]BF_4^- \xrightarrow{Me_2S} MeSC_6F_{13} + \overset{+}{S}Me_3\ BF_4^-$$

$$R_2CHBr + R^1_2S \longrightarrow$$

$$\longrightarrow \left[\begin{array}{l} R^1_2\overset{+}{S} \\ \quad | \\ \quad CHR_2 \end{array}\right] \bar{B}r \xrightarrow{R^1_2S} R_2CHSR^1 + R^1_3\overset{+}{S}\ \bar{B}r$$

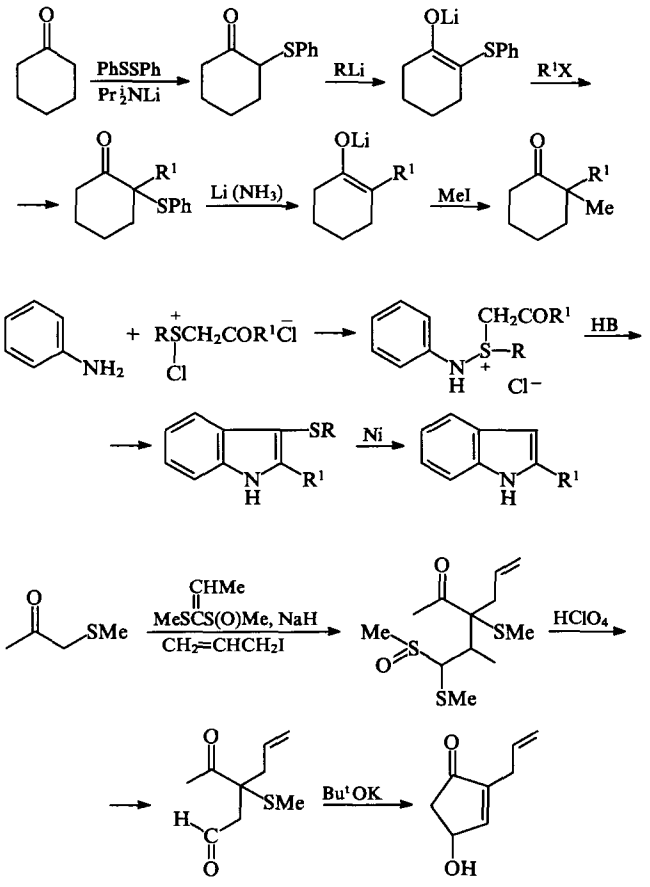
On treatment with bromocyanogen, the C–S bond in aliphatic sulfides is cleaved with formation of thiocyanates and alkyl bromides.[8] Asymmetric sulfides are then cleaved in such a way that the thiocyanate group is bound to the alkyl group.

$$BuSPr + BrCN \longrightarrow BuSCN + PrBr$$

The sulfides in which the sulfur atom is linked to the carbon atom in the β-position relative to unsaturated groups, for example to a carbonyl group or a benzene ring, very easily undergo elimination with cleavage of the C–S bond, which is catalysed by bases;[15] the driving factor in this case is the formation of a system of conjugated bonds.

$$O{=}C{-}CH{-}C{-}SR \xrightarrow{\bar{O}H} O{=}C{-}C{=}C + H_2O + RS^-$$

The elimination of alkylthio- and arylthio-groups has found extensive application in recent years in the syntheses of various cyclic compounds.[8]

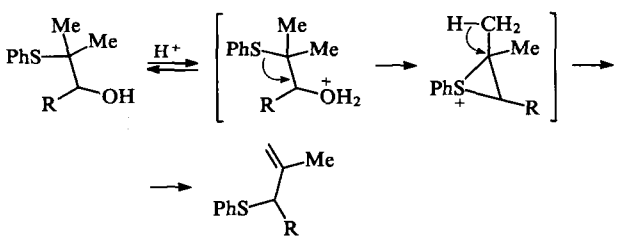


4. Rearrangements of sulfides

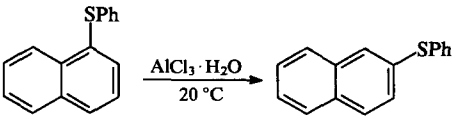
Among all the divalent sulfur compounds, sulfides show perhaps the greatest tendency towards various rearrangements in which the sulfur atom participates directly in the formation of transition states.[183] Sigmatropic rearrangements, which proceed with migration of σ-bonds via a transition state in which the sulfur atom is frequently involved, are characteristic of sulfides under these conditions. The theoretical possibility of the occurrence of a particular rearrangement in the series of sulfides is regulated by the selection rules for pericyclic reactions. In practice 1,2-, 2,3-, and 3,3-sigmatropic rearrangements are observed in the series of sulfides.

a. 1,2-Sigmatropic rearrangements

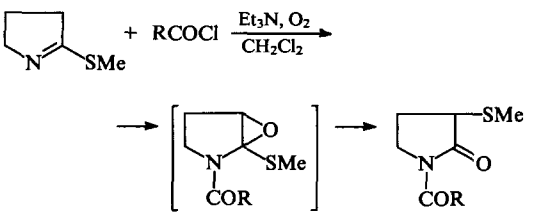
According to the correlation rules, the 1,2-migration of arylthio- and alkylthio-groups in the neutral molecules of sulfides is prohibited. It can occur either in a cation or on radical initiation.[183] Indeed, the 1,2-shift of the phenylthio-group, which occurs in aryl β-hydroxyalkyl sulfides on treatment with toluene-*p*-sulfonic acid, is due to the formation of a cationoid intermediate.[184]



The intramolecular 1,2-migration of the arylthio-group in the molecule of 1-naphthyl phenyl sulfide in the presence of aluminium chloride also evidently proceeds via the stage involving the formation of a cationoid intermediate.[183]

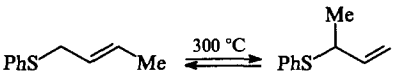


The *N*-acylation of 2-methylthiodihydropyrroline, in which the initial compound is epoxidised by atmospheric oxygen with subsequent opening of the epoxide ring and the migration of the methylthio-group to the 3-position, may be quoted as an example of the 1,2-migration of the methylthio-group.[185]

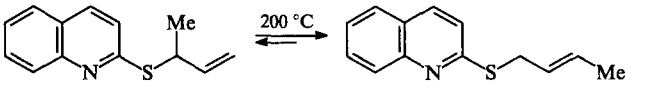


b. 1,3-Sigmatropic rearrangements

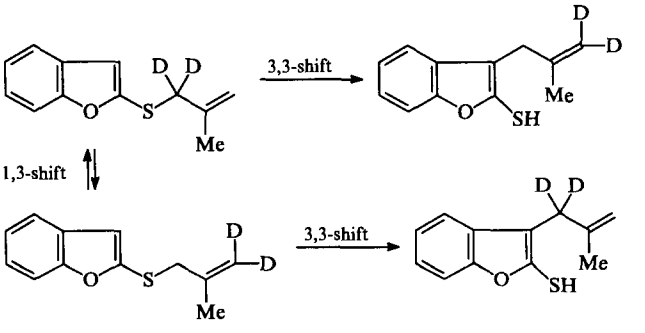
1,3-Sigmatropic rearrangements are characteristic primarily of allyl sulfides. For example, 2-butenyl phenyl sulfide is converted into 1-methylallyl phenyl sulfide at 300 °C as a result of the 1,3-migration of the phenylthio-group.[183]



The 1,3-sigmatropic rearrangement of 1-methylallyl 2-quinolinyl sulfide is a reversible reaction the equilibrium in which at 200 °C is appreciably displaced towards the formation of 2-butenyl 2-quinolinyl sulfide.[183]



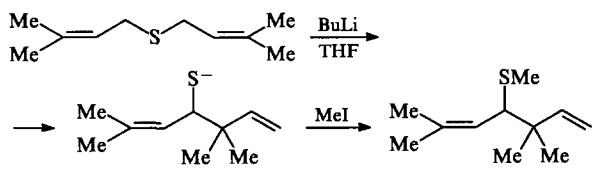
In a number of instances, the 1,3-sigmatropic rearrangement of sulfides is accompanied by their subsequent 3,3-sigmatropic rearrangement. Thus, the 1,3-sigmatropic rearrangement of the deuterium-labelled 2-benzofuryl 2-methylallyl sulfide is accompanied by the 3,3-sigmatropic rearrangement, which occurs at a higher temperature.[186–188]

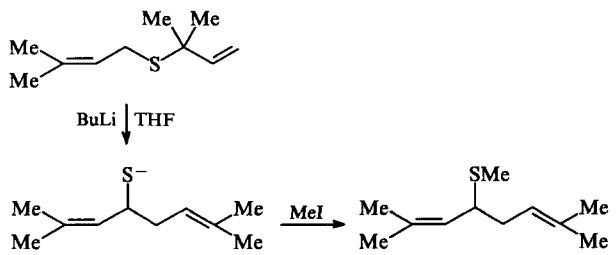


This behaviour is observed most frequently in the 1,3-sigmatropic rearrangement of allyl phenyl sulfide and allyl 2-thienyl sulfide.[187,188] The 1,3-sigmatropic rearrangement of allyl aryl sulfides is accelerated by singlet oxygen obtained photochemically or on decomposition of peroxides.[189] Diaryl sulfides also exhibit an accelerating effect on the 1,3-sigmatropic rearrangement of allyl aryl sulfides.[190]

c. 2,3-Sigmatropic rearrangement

The 2,3-sigmatropic rearrangements of sulfides proceed as a rule under the influence of basic catalysts with formation of α-sulfenylcarbanions as intermediates. The possibility of the 2,3-sigmatropic rearrangement is then determined by the structure of the initial sulfide and the nature of the catalyst and the solvent. For example, on treatment with butyllithium in THF, diallyl sulfides undergo the 2,3-sigmatropic rearrangement with formation of the corresponding thiolates, which react with methyl iodide, affording dienyl methyl sulfides.[183–191]





In the DMSO – KOH system, diallyl sulfide merely isomerises to di(1-propenyl) sulfide.[192]

$$CH_2{=}CH{-}CH_2SCH_2{-}CH{=}CH_2 \xrightarrow{DMSO/KOH} CH_3{-}CH{=}CHSCH{=}CH{-}CH_3$$

Treatment of allyl benzyl sulfide with butyllithium in the presence of diaza-1,4-bicyclo[2.2.2]octane and methyl iodide at −15 °C leads to the formation of a mixture of three sulfides.[193]

$$PhCH_2SCH_2CH{=}CH_2 \xrightarrow[MeI]{BuLi,\ DABCO} \begin{cases} PhCH(SMe)CH_2CH{=}CH_2 & 23\% \\ PhCH_2SCH(Me){=}CH_2 & 76\% \\ PhCH_2SCH{=}CHCH_2Me & 1\% \end{cases}$$

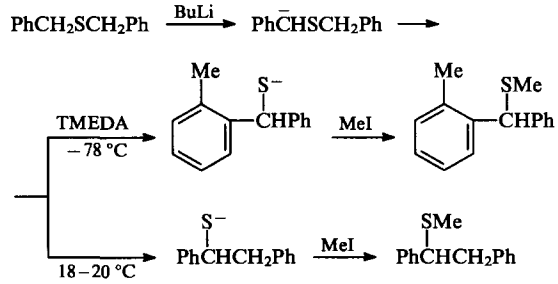
These results indicate the formation of two intermediate carbanions — with the negative charge on the benzyl and allyl carbon atoms. The carbanion with the negative charge on the benzyl carbon atom undergoes a 2,3-sigmatropic rearrangement whereas the carbanion with the negative charge on the allyl carbon atom is stable; it is merely methylated by methyl iodide and isomerises with migration of the double bond.

The 2,3-sigmatropic rearrangement of benzyl γ,γ-dimethylallyl sulfide under similar conditions leads to only one product.

$$PhCH_2SCH_2{-}CH{=}C(Me)_2 \xrightarrow[2.\ MeI]{1.\ BuLi,\ DABCO} Ph{-}CH(SMe){-}C(Me){=}CH_2$$

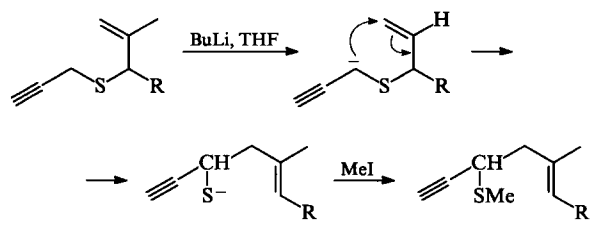
It has been suggested[183] that in this case only the carbanion with the negative charge on the benzyl carbon atom is involved in the 2,3-sigmatropic rearrangement, whereas the carbanion with the negative charge on the allyl carbon atom does not participate in the rearrangement and other reactions.

Depending on the conditions, the carbanion of dibenzyl sulfide can undergo the Stevens rearrangement or the 2,3-sigmatropic rearrangement.[193]

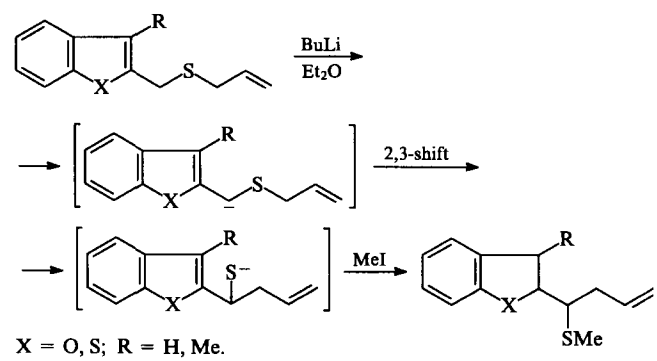


Since the Stevens rearrangement proceeds in the presence of *N,N,N′,N′*-tetramethylethylenediamine (TMEDA), it has been suggested[193] that the 2,3-sigmatropic rearrangement occurs in the presence of free anions. On the other hand, if the anion is solvated, the Stevens rearrangement takes place.

Sulfides containing the propargyl group also undergo the 2,3-sigmatropic rearrangement on treatment with butyllithium in THF.[183]

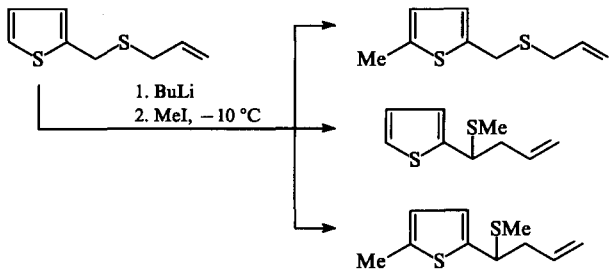


The possibility of the 2,3-sigmatropic rearrangement in the series of allyl heteroaryl sulfides is determined by the nature of the heteroaryl group.[194] For example, on treatment with butyllithium in diethyl ether at −70 °C, 2-(allylthiomethyl)benzofuran and 2-(allylthiomethyl)-3-methylbenzothiophene undergo the 2,3-sigmatropic rearrangement, affording the corresponding thiols, which give rise to sulfides on interaction with methyl iodide.

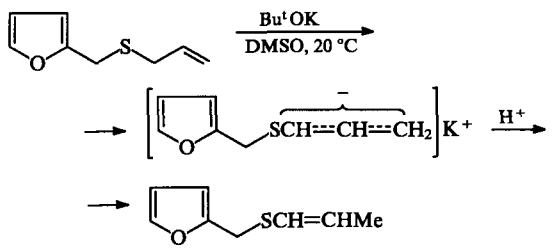


X = O, S; R = H, Me.

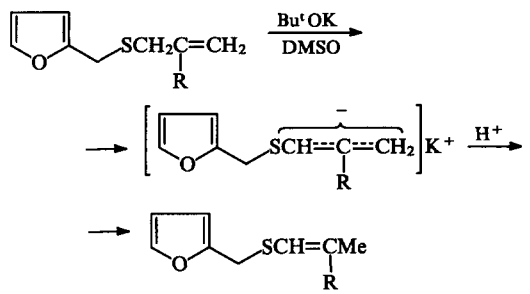
Under the same conditions, 2-(allylthiomethyl)thiophene remains unchanged and produces a mixture of sulfides only at −10 °C. Among these, the last two are the products of the 2,3-sigmatropic rearrangement of the initial sulfide.



The interaction of 2-(allylthiomethyl)furan with butyllithium leads to the metallation of the free α-position of the heterocycle. The replacement of butyllithium by potassium *tert*-butoxide leads to the selective formation of 2-(propenylthiomethyl)furan.

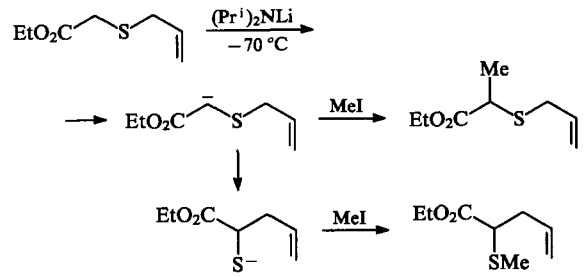


Other allyl furylmethyl sulfides undergo a similar isomerisation.[286]

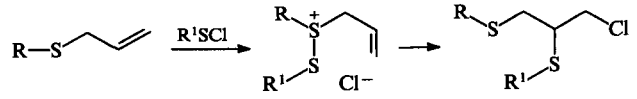


R = H, Me.

The 2,3-sigmatropic rearrangement of allyl ethoxycarbonylmethyl sulfide takes place in the presence of lithium diisopropylamide.[195]



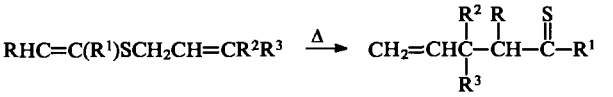
It has been suggested[196] that the products of the reactions of allyl sulfides with sulfenyl chlorides are formed not as a result of the addition of the sulfenyl chlorides to the allyl fragment but as a result of the 2,3-sigmatropic rearrangement of the sulfonium cation produced due to the attack by the sulfenyl chloride on the sulfur atom.



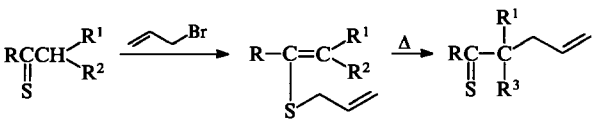
R = R¹ = Me.

d. The 3,3-sigmatropic rearrangement

The 3,3-sigmatropic rearrangement is characteristic primarily of allyl sulfides. The structure of the initial sulfide exerts a significant influence in this instance both on the rate of the rearrangement and on the nature of the product formed. The sulfides $RCH=C(R^1)SCH_2CH=CR^2R^3$ (R = H, Alk, Ph; $R^1 = NMe_2$, NEt_2, OEt, SEt; $R^2 = R^3$ = H, Me), for example, rearrange to the corresponding thiones even on slight heating.[183]



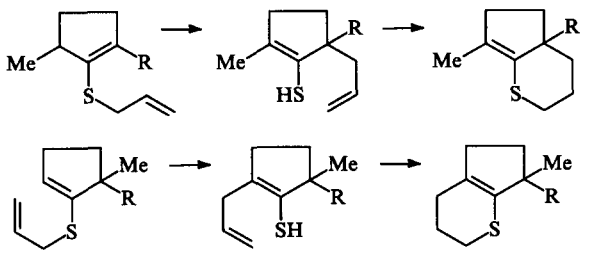
Substituted allyl vinyl sulfides, formed in the reactions of aliphatic thioketones with allyl bromides, undergo the 3,3-sigmatropic rearrangement even on distillation, affording thioketones.[183,197]



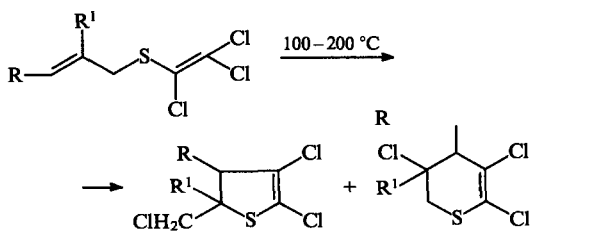
R = R¹ = R² = H, Me, Pr^i, Bu^t.

The presence of electron-accepting groups such as the nitrile group in the molecules of allyl vinyl sulfides hinders the 3,3-sigmatropic rearrangement. For example, dicyano-substituted allyl vinyl sulfides are converted into the isomeric ketones only after prolonged heating.

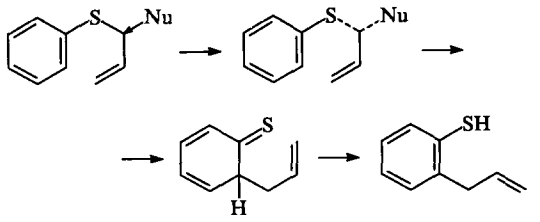
If one of the double bonds in allyl vinyl sulfides is part of an alicyclic system, the rearrangement results in the formation of enethiols, which slowly cyclise even at room temperature to the corresponding bicyclic sulfur-containing compounds.[183]



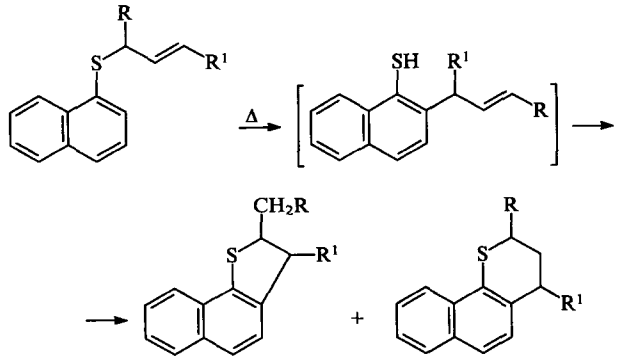
The thermal rearrangement of trichloro-substituted allyl vinyl sulfides involves the migration of the chlorine atoms, which results in the formation of chloro-substituted dihydrothiophenes and dihydrothiopyrans.[198]



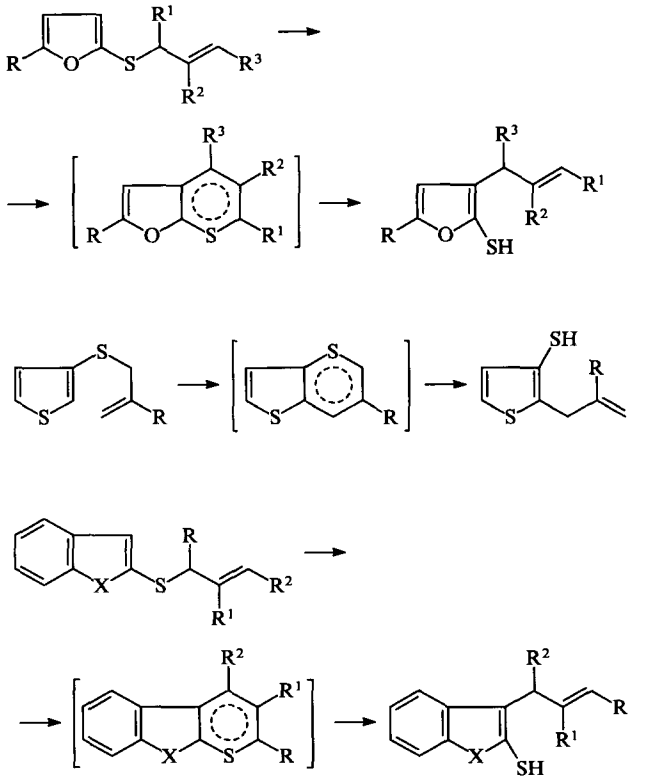
On distillation in the presence of quinoline and *N*,*N*-dimethylaniline, allyl phenyl sulfide rearranges to 2-allylthiophenol, which is converted under the reaction conditions into 2-methyl-2,3-dihydrobenzothiophene and other products. The study of this reaction provided Kwart et al.[199] with a basis which they used to put forward a mechanism of the nucleophilic catalysis with participation of solvent molecules.



Allyl 1-naphthyl sulfides rearrange similarly to allylnaphthalenethiols, which cyclise under the reaction conditions to 2,3-dihydronaphtho[1,2-*b*]thiophenes and 2,3-dihydronaphtho[1,2-*b*]thiopyrans.[188,200]

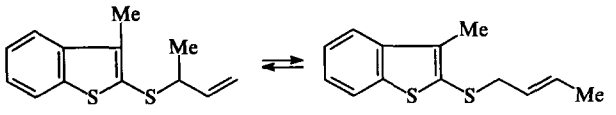


On heating in the absence of a solvent, substituted allyl furyl and allyl thienyl sulfides and their benzo-derivatives undergo a 3,3-sigmatropic rearrangement with formation of allyl-substituted heterocyclic thiols.[201–208]



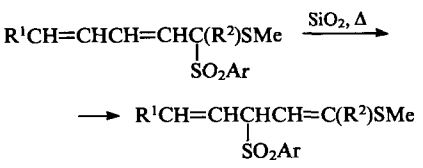
X = O, S; R = R¹ = R² = R³ = H, Me, MeO, MeS, Cl, Br.

It has been noted[187,204] that the 3,3-sigmatropic rearrangement of alkenyl heteroaryl sulfides is as a rule accompanied by the 1,3-sigmatropic shift and this course of the reaction is virtually the only one for allyl benzothienyl sulfides containing a substituent in the 3-position in the thiophene ring.[206]



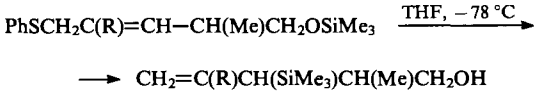
The replacement of the double bond in the allyl or vinyl fragments of allyl vinyl sulfide by a triple bond hardly affects the mode of the 3,3-sigmatropic rearrangement. The products of the 3,3-sigmatropic rearrangements of sulfides with a triple bond are also thiols, thiones, and cyclic compounds with the sulfur atom in the heterocycle.[183]

Among other rearrangements of unsaturated sulfides, mention should be made of the rearrangements of phenylthioacetylene, which is converted into 1,2-di(phenylthio)ethylene in the DMSO–KOH system[209] and also the rearrangement of allyl sulfides containing an arenesulfonyl group at the allylic carbon atom, which proceeds with migration of the arenesulfonyl group.[210]



R^1 = H, Et; R^2 = Et, $PhCH_2$; Ar = Ph, 4-MeC_6H_4.

The rearrangement of allyl sulfides containing the trimethylsiloxane group has been described.[211] The rearrangement takes place in the presence of di-*tert*-butylbiphenylyllithium with migration of the trimethylsilyl group, which results in the formation of allylsilanes with a high regioselectivity and stereoselectivity.



R = H, Me.

* * *

It is seen from the present review that studies in the field of the chemistry of sulfides during the last ten years have been directed mainly to the further development of the methods of synthesis of sulfides already available such as the sulfenylation of hydrocarbons, the alkylation of thiols, and the thiylation of unsaturated compounds, as well as to the search for new methods of synthesis (aminosulfenylation and sulfamatosulfenylation of olefins, etc.). Much attention has been devoted to further study of the reactivity of sulfides and in particular of the reactions occurring with formation of halosulfonium intermediates, α-sulfenylcarbanions, and sulfur ylides, as well as rearrangements. Many investigations have been devoted to syntheses based on sulfides.

References

1. J Voigt *Stabilisation of Plastics against Light and Heat* Monographs on the Chemistry, Physics, and Technology of Plastics, No. 10 (Berlin: Springer, 1966) (Translated into Russian; Leningrad: Khimiya, 1972)
2. V G Plotnikov, A A Efimov *Usp. Khim.* **59** 1362 (1990) [*Russ. Chem. Rev.* **59** 792 (1990)]
3. G A Blokh, in *Organicheskie Uskoriteli Vulkanizatsii i Vulkaniziruyushchie Sistemy dlya Elastomerov* (Organic Accelerants of Vulcanisation and Vulcanising Systems of Elastomers) (Leningrad: Khimiya, 1973) p. 25

4. L M Yagupol'skii *Aromaticheskie i Geterotsiklicheskie Soedineniya s Ftorsoderzhashchimi Zamestitelyami* (Aromatic and Heterocyclic Compounds with Fluorine-containing Substituents) (Kiev: Naukova Dumka, 1988)
5. N N Mel'nikov, K V Novozhilov, T N Pylova *Khimicheskie Sredstva Zashchity Rastenii* (Chemical Agents for the Protection of Plants) (Moscow: Khimiya, 1980)
6. D Applequist, C H DePuy, K L Rinehart *Introduction to Organic Chemistry* (Third Ed.) (New York: Wiley, 1982) (Translated into Russian; Moscow: 1985)
7. S Oae *Organic Chemistry of Sulfur* (New York: Plenum) (Translated into Russian; Moscow: Khimiya, 1975)
8. D Barton, W D Ollis (Eds), in *Comprehensive Organic Chemistry* Vol. 5 (Translated into Russian; Moscow: Khimiya, 1983) p. 163
9. M G Voronkov, E N Deryagina *Usp. Khim.* **59** 1338 (1990) [*Russ. Chem. Rev.* **59** 778 (1990)]
10. A Streitweiser, J E Williams *J. Am. Chem. Soc.* **97** 191 (1975)
11. F Bernardi, I G Csizmadia, A Mangini, H B Schlegel, M H Whangho, S Wolfe *J. Am. Chem. Soc.* **97** 2209 (1975)
12. T C Morrill, R A Clark, D Bilobran, D S Young *Tetrahedron Lett.* **16** 397 (1975)
13. G L Bendazzoli, G Gottarelli, P Palmieri *J. Am. Chem. Soc.* **96** 11 (1974)
14. I W Jones, J C Tebby *J. Chem. Soc., Perkin Trans. 1* 1125 (1973)
15. K Reid *Course of Physical Organic Chemistry* (Translated into Russian; Moscow: Mir, 1972)
16. L I Belen'kii (Ed.) *Khimiya Organicheskikh Soedinenii Sery* (Chemistry of Organic Sulfur Compounds) (Moscow: Khimiya, 1988)
17. V I Khvostenko *Mass-spektrometriya Otritsatel'nykh Ionov* (Mass Spectrometry of Negative Ions) (Moscow: Nauka, 1981)
18. A A Polyakova *Molekulyarnyi Mass-spektral'nyi Analiz Organicheskikh Soedinenii* (Molecular Mass-spectrum Analysis of Organic Compounds) (Moscow: Khimiya, 1983)
19. M I Tokarev, A A Polyakova, L O Kogan *Zh. Anal. Khim.* **40** 1703 (1985)
20. B A Trofimov, S V Amosova *Divinilsul'fid i Ego Proizvodnye* (Divinylsulfide and Its Derivatives) (Novosibirsk: Nauka, 1983)
21. A G Ibragimov, E V Gribanova, A B Morozov, U M Dzhemilev, in *XVIII Konferentsiya po Khimii i Tekhnologii Organicheskikh Soedinenii Sery, Kazan', 1992 (Tezisy Dokladov)* (Abstracts of Reports at the XVIIIth Conference on the Chemistry and Technology of Organic Sulfur Compounds, Kazan', 1992) p. 210
22. H Viola *Z. Chem.* **27** 15 (1987)
23. G LeGuillanton, D T Elofmani, J Simanet, in *Abstracts of Reports at the XVth International Symposium on Organic Chemistry of Sulfur, Caen, 1992* p. 31
24. S I Gevus', M A Dikii, S K Makovskii, S A Voronov, in *XVI Ukrainskaya Konferentsiya po Organicheskoi Khimii, Ternopol', 1992 (Tezisy Dokladov)* (Abstracts of Reports at the XVIth Ukrainian Conference on Organic Chemistry, Ternopol', 1992) p. 166
25. A Hosomi, K Ogata, M Ohkuma, M Hojo *Synlett.* 557 (1991)
26. V V Nasyreva, S V Amosova, B A Trofimov *Zh. Org. Khim.* **19** 2044 (1983)
27. M G Voronkov, E N Deryagina *Phosphorus Sulfur Relat. Elem.* **7** 123 (1979)
28. M G Voronkov, E N Deryagina, E N Sukhomazova, G M Panova, N A Korchevin *Kinet. Katal.* **25** 266 (1984)
29. M G Voronkov, E N Deryagina, G M Ivanova *Zh. Prikl. Khim.* **55** 2625 (1982)
30. M G Voronkov, E N Deryagina, L K Papernaya, V Yu Vitkovskii *Zh. Org. Khim.* **19** 134 (1983)
31. A N Nedugov, N N Pavlova *Zh. Org. Khim.* **28** 1401 (1992)
32. J K Landquist, D R Summers, in *Collected Lectures at the VIIth International Symposium on the Organic Chemistry of Sulfur, Hamburg, 1976* p. 146
33. I V Koval' *Usp. Khim.* **60** 1645 (1991) [*Russ. Chem. Rev.* **60** 830 (1991)]
34. T S Croft *Phosphorus Sulfur Relat. Elem.* **2** 133 (1976)
35. A Haas, U Niemann *Adv. Inorg. Chem. Radiochem.* **18** 143 (1976)
36. A Haas, V Hellwig *J. Fluorine Chem.* **6** 521 (1976)
37. A Haas, U Niemann *Chem. Ber.* **101** 67 (1977)
38. M R C Gerstenberger, A Haas *J. Fluorine Chem.* **19** 461 (1982)
39. M R C Gerstenberger, A Haas *J. Fluorine Chem.* **23** 525 (1983)
40. M Raban, Chern Lin-Ju *J. Chem. Soc.* **45** 1688 (1980)
41. A Haas, V Hellwig *Chem. Ber.* **100** 2475 (1976)
42. V I Popov, N V Kondratenko, A Khaas *Ukr. Khim. Zh. (Russ. Ed.)* **49** 861 (1983)
43. N V Kondratenko, V I Popov, L G Yurchenko, A A Kolomiitsev, L M Yagupol'skii *Zh. Org. Khim.* **14** 1914 (1978)
44. Yu V Zeifman, L T Lantseva, I L Knunyants *Izv. Akad. Nauk SSSR, Ser. Khim.* 2640 (1978)
45. V N Movchun, A A Kolomiitsev, N V Kondratenko, Yu L Yagupol'skii, in *XVI Ukrainskaya Konferentsiya po Organicheskoi Khimii, Ternopol', 1992 (Tezisy Dokladov)* (Abstracts of Reports at the XVIth Ukrainian Conference on Organic Chemistry, Ternopol', 1992) p. 39
46. A G M Barrett, G G Grabovski, M Sabat, S J Taylor *J. Org. Chem.* **52** 4693 (1987)
47. I V Koval', T G Panasenko *Zh. Org. Khim.* **28** 325 (1992)
48. T N Dubinina, E S Levchenko *Zh. Org. Khim.* **15** 743 (1979)
49. I V Koval', T G Panasenko, V A Martyushenko, in *III Regional'noe Soveshchanie Respublik Srednei Azii i Kazakhstana po Khimicheskim Reaktivam, Tashkent, 1990 (Tezisy Dokladov)* (Abstracts of Reports at the IIIrd Regional Conference of Central Asian Republics and Kazakhstan on Chemical Reagents, Tashkent, 1990) Vol. 1 p. 148
50. I V Koval', V V Andrushchenko, M M Kremlev, I A Tarasenko *Zh. Org. Khim.* **21** 1286 (1985)
51. I V Koval', T G Panasenko *Ukr. Khim. Zh. (Russ. Ed.)* **56** 638 (1990)
52. Yu V Zeifman, L T Lantseva *Izv. Akad. Nauk SSSR, Ser. Khim.* 1102 (1980)
53. W Zankowska-Jasinska *J. Fluorine Chem.* **38** 85 (1988)
54. Yu G Gololobov, N I Gusar' *Sul'fenilkhloridy* (Sulfenylchlorides) (Moscow: Nauka, 1989)
55. G M Blackburn, T Macojej *J. Chem. Soc., Perkin Trans. 1* 1935 (1985)
56. S E Dinizo, R W Freerksen, W E Pabst, D S Walt *J. Org. Chem.* **41** 2846 (1976)
57. T Minami, H Suganyma, T Agawa *Chem. Lett.* **3** 285 (1978)
58. B A Kashemirov, V N Osipov, A M Emel'yanovich, P S Khokhlov *Zh. Obshch. Khim.* **62** 1195 (1992)
59. B A Kashemirov, Yu A Strepikheev, B Ya Chvertkin, P S Khokhlov *Zh. Vses. Khim. O-va im. D. I. Mendeleeva* **32** 596 (1987)
60. I N Zhmurova, V G Yurchenko, A M Pinchuk *Zh. Obshch. Khim.* **55** 321 (1985)
61. T Nguyen, M Rubinstein, C Wakselman *J. Org. Chem.* **46** 1938 (1981)
62. Yu N Polivin, R A Karakhanov, A I Mikaya, F S Sheveleva, in *XVIII Konferentsiya po Khimii i Tekhnologii Organicheskikh Soedinenii Sery, Kazan', 1992 (Tezisy Dokladov)* (Abstracts of Reports at the XVIIIth Conference on the Chemistry and Technology of Organic Sulfur Compounds, Kazan', 1992) p. 194
63. M Makosza, M Fedorynski *Synthesis* 274 (1974)
64. M Fedorynski, A Dzikinska, A Jonozyk, in *Collected Lectures at the VIth International Conference on Organic Synthesis, Moscow, 1986* p. 160
65. M Heydenreich, I Kühn, R Runge, E Wenschun *Sulfur Lett.* **9** 65 (1989)
66. B G Boldyrev, L N Aristarkhova, Ya I Stoyanovskii, T K Bilozor *Zh. Org. Khim.* **20** 1276 (1984)
67. E Busi, G Capozzi, S Menichetti, C Nativi *Synthesis* **7** 643 (1992)
68. R R Khaliullin, E I Grishchenko, V V Plemenkov, I G Bolesov, in *V Mezhdunarodnaya Konferentsiya po Khimii Karbenov, Moscow, 1992 (Tezisy Dokladov)* (Abstracts of Reports at the Vth International Conference on the Chemistry of Carbenes, Moscow, 1922) p. 108
69. T V Morar', Yu B Kal'yan, M Z Krimer, V A Smit, in *XVIII Konferentsiya po Khimii i Tekhnologii Organicheskikh Soedinenii Sery, Kazan', 1992 (Tezisy Dokladov)* (Abstracts of Reports at the XVIIIth Conference on the Chemistry and Technology of Organic Sulfur Compounds, Kazan', 1992) p. 75
70. N S Zefirov, N K Sadovaya, A M Magarramov, I V Bodrikov *Zh. Org. Khim.* **13** 245 (1977)
71. N S Zefirov, T N Velikokhat'ko, N K Sadovaya *Zh. Org. Khim.* **19** 1593 (1983)
72. V V Shchepin, I Yu Petukhova, A N Nedugov *Zh. Org. Khim.* **26** 679 (1990)

73. V V Shchepin, I Yu Petukhova, N Yu Russkikh, in *XVIII Konferentsiya po Khimii i Tekhnologii Organicheskikh Soedinenii Sery, Kazan', 1992 (Tezisy Dokladov)* (Abstracts of Reports at the XVIIIth Conference on the Chemistry and Technology of Organic Sulfur Compounds, Kazan', 1992) p. 112
74. V V Shchepin, I Yu Petukhova, A N Nedugov, M I Vakhrin *Zh. Obshch. Khim.* **62** 1838 (1992)
75. V V Shchepin, I Yu Petukhova, N Yu Russkikh *Zh. Obshch. Khim.* **62** 1303 (1992)
76. I Paterson, S Osborne *Synlett.* **7** 145 (1991)
77. A M Khabibov, V S Zavgorodnii, A A Petrov *Metalloorg. Khim.* **5** 1113 (1992)
78. I V Koval' *Usp. Khim.* **62** 813 (1993) [*Russ. Chem. Rev.* **62** 769 (1993)]
79. S Takano, V Sugihara, K Ogasawara *Synlett.* **8** 668 (1992)
80. B Wladislaw, L Marzorati, C Vitta, in *Abstracts of Reports at the XVth International Symposium on Organic Chemistry of Sulfur, Caen, 1992* p. 45
81. M Mikolajczyk, H W Midura *Synlett.* **7** 245 (1991)
82. M Shimazaki, M Takahashi, H Komatsu, A Ohta, K Kenzo, Y Kodawa *Synthesis* 555 (1992)
83. L Z Gandel'sman, V N Boiko *Ukr. Khim. Zh. (Russ. Ed.)* **43** 1224 (1977)
84. Wang Zhi Yuan, Hay Allan S *Tetrahedron Lett.* **31** 5658 (1990)
85. V I Stepanov, V Yu Rodionov, T A Chibisov *Zh. Org. Khim.* **10** 79 (1974)
86. J T B Ferreira, F Simonelli, J V Comosseto, E S Lang, V P Correia, in *Collected Lectures at the VIth International Conference on Organic Synthesis, Moscow, 1986* p. 72
87. I V Koval' *Usp. Khim.* **59** 681 (1990) [*Russ. Chem. Rev.* **59** 396 (1990)]
88. R A Abramovitch, J Pilski *J. Chem. Soc., Chem. Commun.* 704 (1981)
89. M C Caserio, J K Kim *J. Am. Chem. Soc.* **104** 3231 (1982)
90. P Brownbridge *Tetrahedron Lett.* **25** 3759 (1984)
91. I Benati, P C Montevecchi, P Spagnolo *Tetrahedron Lett.* **25** 2039 (1984)
92. D H R Barton, M R Britten-Kelly, D Ferreira *J. Chem. Soc., Perkin Trans. 1* 1682 (1978)
93. N S Zefirov, N V Zyk, A G Kutateladze, S I Kolbasenko, Yu A Lapin *Zh. Org. Khim.* **22** 214 (1986)
94. N S Zefirov, N V Zyk, A G Kutateladze, Yu A Lapin, A O Chizhov *Zh. Org. Khim.* **22** 2462 (1986)
95. N S Zefirov, N V Zyk, A G Kutateladze, Yu A Lapin. *Zh. Org. Khim.* **23** 392 (1987)
96. N S Zefirov, N V Zyk, A G Kutateladze, Yu A Lapin. *Zh. Org. Khim.* **23** 229 (1987)
97. N S Zefirov, N V Zyk, A G Kutateladze, B I Ugrek, Yu T Struchkov, K A Potekhin, A V Maleev *Dokl. Akad. Nauk SSSR* **301** 1385 (1988)
98. N S Zefirov, N V Zyk, A G Kutateladze, E K Butina, S Z Vatsadze *Izv. Akad. Nauk SSSR, Ser. Khim.* 2870 (1989)
99. N S Zefirov, N V Zyk, A G Kutateladze, E K Butina. *Zh. Org. Khim.* **26** 671 (1990)
100. N S Zefirov, N V Zyk, A G Kutateladze, E S Ignatenko *Zh. Org. Khim.* **26** 670 (1990)
101. N V Zyk, Yu A Lapin, A G Kutateladze, N S Zefirov *Zh. Org. Khim.* **25** 198 (1989)
102. D Craig, K Daniels, R A McKenzie *Tetrahedron Lett.* **32** 6973 (1991)
103. B A Trofimov, N A Chernysheva, N K Gusarova *Zh. Org. Khim.* **28** 602 (1992)
104. K Nowak, H Poradowska, in *Collected Lectures at the VIth International Conference on Organic Synthesis, Moscow, 1986* p. 115
105. T Kowalska, in *Collected Lectures VIth International Conference on Organic Synthesis, Moscow, 1986* p. 116
106. Kim Kyongtae, Rim Han Jo *Tetrahedron Lett.* **31** 5631 (1990)
107. A M Maksimov, V E Platonov, P P Rodionov, in *IV Mezhdunarodnaya Konferentsiya po Organicheskomu Sintezu, Moscow, 1986 (Tezisy Dokladov)* (Abstracts of Reports at the IVth International Conference on Organic Synthesis, Moscow, 1986) p. 56
108. A Capperucci, G M Ferrara, A Degl'innocenti, F B Bonini, G Mazzanti, P Zani, A Ricci *Synlett.* **8** 880 (1992)
109. A Degl'innocenti, B Bonini, G Mazzanti, A Capperucci, G M Ferrara, A Ricci, P Zani, in *Abstracts of Reports at the XVth International Symposium on Organic Chemistry of Sulfur, Caen, 1992* p. 26
110. A Degl'innocenti, P Ulivi, A Capperucci, A Mordini, G Reginato, A Ricci *Synlett.* **8** 499 (1992)
111. A Degl'innocenti, A Capperucci, P Ulivi, A Mordini, G Reginato, A Ricci, in *Abstracts of Reports at the XVth International Symposium on the Organic Chemistry of Sulfur, Caen, 1992* p. 36
112. T Sata, J Otara, H Nozaki *Synlett.* **7** 903 (1991)
113. M Madesclaire *Tetrahedron* **42** 5459 (1986)
114. Kim Kwan Soo, Hwang Hye Jung, Cheomy Chan Seong, Hahn Chi Sun *Tetrahedron Lett.* **31** 2893 (1990)
115. R Balicki, L Kaczmarek, P Nantka-Namirski *Liebigs Ann. Chem.* **8** 883 (1992)
116. E H Folson, J Castrillon *Synth. Commun.* 1799 (1992)
117. W Adam, E N Gonzalez *Tetrahedron* **47** 3773 (1991)
118. V V Sheremovets, N M Korotaeva, V D Komissarov, G A Tolstikov *Izv. Akad. Nauk SSSR, Ser. Khim.* 2133 (1990)
119. Kim Yong Hae, Yoon Dae Chul *Tetrahedron Lett.* **29** 6453 (1988)
120. E J Corey, C Ouannes *Tetrahedron Lett.* **17** 4263 (1976)
121. I V Koval' *Usp. Khim.* **59** 1409 (1990) [*Russ. Chem. Rev.* **59** 819 (1990)]
122. F Ruff, A Kucsmann *Phosphorus Sulfur Relat. Elem.* **6** 261 (1979)
123. N V Kondratenko, R Yu Gavrilova, L M Yagupol'skii *Zh. Org. Khim.* **24** 456 (1988)
124. R Yu Gavrilova, N V Kondratenko, V I Popov, L M Yagupol'skii *Zh. Org. Khim.* **25** 1118 (1989)
125. T I Drozdova, A N Mirskova, G G Levkovskaya, I D Kalikhman, V Yu Vitkovskaya, M G Voronkov *Zh. Org. Khim.* **25** 1466 (1989)
126. L M Yagupolski, R Yu Garlyauskaite, N V Kondratenko *Synthesis* **8** 749 (1992)
127. F Ruff, A Kucsmann *J. Chem. Soc., Perkin Trans. 2* 503 (1975)
128. K Tsujihara, N Furukawa, K Oae, S Oae *Bull. Chem. Soc. Jpn.* **42** 2631 (1969)
129. T Yamamoto, D Yoshida, J Hojio, H Terauchi *Bull. Chem. Soc. Jpn.* **57** 3341 (1984)
130. T Yamamoto, D Yoshida *Org. Prep. Proced. Int.* **20** 271 (1988)
131. I V Koval', T G Panasenko, R M Minyaev, I S Panchenko *Zh. Org. Khim.* **23** 325 (1987)
132. I V Koval', V V Andrushchenko, M M Kremlev *Zh. Org. Khim.* **18** 841 (1982)
133. I V Koval', A I Tarasenko, T G Panasenko, M M Kremlev, A Yu Romanenko, in *IV Mezhdunarodnaya Konferentsiya po Organicheskomu Sintezu, Moscow, 1986 (Tezisy Dokladov)* (Abstracts of Reports at the IVth International Conference on Organic Synthesis, Moscow, 1986) p. 87
134. I V Koval', T G Panasenko, A I Tarasenko, N R Molchanova *Zh. Org. Khim.* **25** 835 (1989)
135. I V Koval', T G Panasenko *Zh. Org. Khim.* **25** 1677 (1989)
136. I V Koval', T G Panasenko *Zh. Org. Khim.* **26** 1728 (1990)
137. A D Davson, D Swern *J. Org. Chem.* **42** 592 (1977)
138. S Oae, K Kikuchi, M Moriyama, N Furukawa *Chem. Lett.* **11** 1723 (1982)
139. P K Claus, W F Silbernagel, W Franck, W Rieder *Monatsh. Chem.* **116** 841 (1985)
140. C M Marson, U Grabowska, T Walsgrove, D S Eggleston, P W Baures *J. Org. Chem.* **56** 2603 (1991)
141. D T Hurst *Aust. J. Chem.* **36** 2119 (1983)
142. H Shimizu, K Matsuo, T Kataoka, M Hori *Chem. Pharm. Bull.* **32** 4360 (1984)
143. O A Rakitin, O G Vlasova, L I Khmel'nitskii, I V Filyakov, T N Sobachkina *Khim. Geterotsikl. Soedin.* 1536 (1990)
144. W O Moss, R H Bradbury, N J Hales, T Gallagher *Tetrahedron Lett.* **29** 6475 (1988)
145. M J P O Harger, S Westlake *J. Chem. Soc., Perkin Trans. 1* 2357 (1984)
146. O Meth-Cohn, G Van Vuuren *J. Chem. Soc., Chem. Commun.* 190 (1984)
147. O Meth-Cohn, G Van Vuuren *J. Chem. Soc., Perkin Trans. 1* 233 (1986)
148. S P Horak *Synthesis* 596 (1979)
149. G Kresze, N Schonberger *Liebigs Ann. Chem.* 1721 (1975)

150. Y Yorinibu, Y Tamotsu, O Makoto *Chem. Lett.* **4** 361 (1975)
151. H Shimizu, K Matsuo, T Kataoka, M Hori *Chem. Pharm. Bull.* **32** 4360 (1984)
152. N P Bezverkhii, S I Protashchuk *Zh. Org. Khim.* **22** 461 (1986)
153. R E Dolle, Li Chun-Sing, A N Shaw *Tetrahedron Lett.* **30** 4723 (1989)
154. I V Koval', T G Panasenko *Zh. Org. Khim.* **27** 217 (1991)
155. S Katayama, T Watanabe, M Yamaguchi *Chem. Lett.* **6** 973 (1989)
156. I I Maletina, S V Iksanova, V V Orda, Yu L Yagupol'skii *Zh. Org. Khim.* **28** 987 (1992)
157. A M Al'-Shura, A A Bratkov, A V Anisimov *Vestn. Mosk. Univ., Ser. 2: Khim.* **31** 392 (1990)
158. L M Yagupol'skii, N V Kondratenko, G N Timofeeva *Zh. Org. Khim.* **20** 115 (1984)
159. P C Page, M B Bulman van Niel, J C Prodger *Tetrahedron* **45** 7643 (1989)
160. M Somei, V Saida *Heterocycles* **23** 3173 (1985)
161. B J Banks, A G M Barette, M A Rusell *J. Chem. Soc., Chem. Commun.* 670 (1984)
162. A G M Barette, G G Grabovski, M Sabat, S S Taylor *J. Org. Chem.* **52** 4693 (1987)
163. M Aswell, R F W Jackson *J. Chem. Soc., Chem. Commun.* 282 (1988)
164. K Ogura *J. Synth. Org. Chem. Jpn.* **12** 1152 (1984)
165. V Farina, I S Hauck *J. Org. Chem.* **56** 4317 (1991)
166. F G Bordwell *Pure Appl. Chem.* **49** 963 (1977)
167. E Block, M Aslam *Tetrahedron* **44** 281 (1988)
168. J C Stowell *Carbanions in Organic Synthesis* (New York: Wiley, 1979)
169. R L Sowerby, M Coates *J. Am. Chem. Soc.* **94** 4758 (1972)
170. A R Katritsky, A R Lapucha, J V Greenhill, M Siskin *Energy Fuels* **4** 562 (1990)
171. H Bock, S Mohmand *Angew. Chem.* **89** 105 (1977)
172. T Hirobayashi, S Mohmand, H Bock *Chem. Ber.* **115** 483 (1982)
173. H Bock *Chem. Ber.* **115** 492 (1982)
174. S Mohmand, H Bock *Phosphorus Sulfur Relat. Elem.* **14** 185 (1983)
175. A M Gabor, M S Abbady *Phosphorus Sulfur Silicon Relat. Elem.* **69** 7 (1992)
176. V A Potapov, S V Amosova, P A Petrov *Izv. Akad. Nauk, Ser. Khim.* 2456 (1992)
177. P Hamel, N Zajac, Y Girard, J G Atkinson, in *Abstracts of Reports at the XVth International Symposium on the Organic Chemistry of Sulfur, Caen, 1992* p. 39
178. T Yoshigama, T Fuchigami *Chem. Lett.* **10** 1995 (1992)
179. K Manabu, H Tamejiro *Synlett.* **7** 909 (1991)
180. S Thea, G Cevascko *Tetrahedron Lett.* **29** 2865 (1988)
181. A A Mironova, I I Maletina, V V Orda, L M Yagupol'skii *Zh. Org. Khim.* **26** 549 (1990)
182. A J H Lobuschangue, J S Malherbe, C J Meyer, D F Schneider *Tetrahedron Lett.* 3571 (1976)
183. A V Anisimov, E A Viktorova, T A Danilova *Molekulyarnye Peregruppirovki Seraorganicheskikh Soedinenii: Organicheskie Sul'fidy* (Molecular Rearrangements of Organic Compounds of Sulfur: Organic Sulfides) (Moscow: Izd. Mosk. Univ., 1989)
184. P Brownbridge, S Warren *J. Chem. Soc., Chem. Commun.* 820 (1975)
185. H Takahata, T Yamazaki, K Aoc *J. Org. Chem.* **50** 4648 (1985)
186. A V Anisimov, V S Babaitsev, E A Viktorova *Zh. Org. Khim.* **17** 1316 (1981)
187. A V Anisimov, V F Ionova, E A Viktorova *Khim. Geterotsikl. Soedin.* 186 (1978)
188. R G Aukharieva, V S Babaitsev, E A Viktorova *Vestn. Mosk. Univ., Ser. 2: Khim.* **23** 50 (1982)
189. H Kwart, N A Johnson, T Eggerichs, T J George *J. Org. Chem.* **42** 172 (1977)
190. H Kwart, N A Johnson *J. Org. Chem.* **42** 2855 (1977)
191. J F Biellman, J B Ducep, D Schirlin *Tetrahedron* **36** 1249 (1980)
192. S V Amosova, G K Musorin *Abstracts of Reports at the XVth International Symposium on the Organic Chemistry of Sulfur, Caen, 1992* p. 124
193. J F Biellmann, J L Schmitt *Tetrahedron Lett.* **14** 4615 (1973)
194. A V Anisimov, G N Murin, L V Mozhaeva, N B Kazenkova, E A Viktorova *Khim. Geterotsikl. Soedin.* 744 (1984)
195. E Vedejs, M J Arnost, J R Hagen *J. Org. Chem.* **44** 3230 (1979)
196. J K Kim, M L Kline, M C Caserio *J. Am. Chem. Soc.* **100** 6243 (1978)
197. D Bariller, L Morin, D Paguer, P Rioult, M Vazeux, C G Andrieu *Bull. Soc. Chim. Fr.* 688 (1977)
198. E Nagaschima, K Suzuki, M Sekuja *Tetrahedron Lett.* **22** 2587 (1981)
199. H Kwart, W H Miles, A G Horgan, H D Kwart *J. Am. Chem. Soc.* **103** 1757 (1981)
200. R G Aukharieva, T A Danilova, A V Anisimov, E A Viktorova *Khim. Geterotsikl. Soedin.* 611 (1981)
201. A V Anisimov, V F Ionova, E A Viktorova *Zh. Org. Khim.* **13** 2624 (1977)
202. S M Panova, A V Anisimov, E A Viktorova *Khim. Geterotsikl. Soedin.* 181 (1982)
203. A V Anisimov, V S Babaitsev, S Ya Grobovenko, T A Danilova, E A Viktorova *Khim. Geterotsikl. Soedin.* 615 (1981)
204. A V Anisimov, V F Ionova, V K Govorek, V S Babaitsev, E A Viktorova *Dokl. Akad. Nauk SSSR* **244** 106 (1979)
205. A V Anisimov, S M Panov, E A Viktorova *Khim. Geterotsikl. Soedin.* 1195 (1982)
206. A V Anisimov, V S Babaitsev, T A Kolosova, E A Viktorova *Khim. Geterotsikl. Soedin.* 1138 (1982)
207. A V Anisimov, S M Panov, E A Viktorova *Dokl. Akad. Nauk SSSR* **267** 97 (1982)
208. A V Anisimov, S M Panov, V F Sizoi, S A Nepogod'ev, E A Viktorova *Khim. Geterotsikl. Soedin.* 1348 (1983)
209. A M Vasil'tsov, A I Mikhaleva, R N Nesterenko, G A Kalabin *Izv. Akad. Nauk SSSR, Ser. Khim.* 1702 (1980)
210. K Ogura, N Yahera, T Fugimori, M Fujita *Tetrahedron Lett.* **31** 4621 (1990)
211. S Marumoto, I Kuwajima *Chem. Lett.* **8** 1421 (1992)

Russian Chemical Reviews **63** (4) 345–355 (1994)
© 1994 Russian Academy of Sciences and Turpion Ltd

UDC 546.659:547.1

The use of samarium diiodide in organic and polymer synthesis

N E Brandukova, Ya S Vygodskii, S V Vinogradova

Contents

I. Introduction 345
II. The synthesis and properties of divalent lanthanide salts 345
III. Reactions involving samarium diiodide 346

Abstract. The methods of synthesis and properties of samarium diiodide are examined and the results of its employment for the synthesis of a wide variety of compounds are surveyed. New reactions involving samarium diiodide are described and the prospects for its application in polymer chemistry are indicated. The bibliography includes 87 references.

I. Introduction

There has been considerable progress in recent years in the use of the unique properties of divalent lanthanide (Eu, Yb, Sm, etc.) halides in the synthesis of a wide variety of organic compounds.[1–3] Comparison of the oxidation–reduction potentials of lanthanide salts and various transition metal salts has shown that the former, in particular samarium and ytterbium diiodides, belong to the class of the strongest reductants soluble in organic media.

The standard oxidation–reduction potentials of the lanthanides in aqueous solutions are as follows:[2]

$$Eu^{2+}/Eu^{3+} = -0.35\ eV;\ Yb^{2+}/Yb^{3+} = -1.15\ eV;$$

$$Sm^{2+}/Sm^{3+} = -1.55\ eV;\ Tm^{2+}/Tm^{3+} = -2.10\ eV.$$

It is seen from the data presented that Tm^{2+} has the most pronounced reducing properties, but, because of this, it is much less stable than Sm^{2+} and Yb^{2+}. It has been shown[4] that, in the absence of O_2, solutions of Eu^{2+}, Yb^{2+}, and Sm^{2+} in THF are stable for a long time (several days),[5] in contrast to Tm^{2+} solutions. Furthermore, thulium is a naturally scarce element.

Bearing these data in mind, it becomes understandable why divalent lanthanide compounds have been isolated only for europium, samarium, and ytterbium.[5] At the same time Eu^{2+} is a very weak electron donor[1] and its reactivity in organic reactions is low. For the same reason, the reactivity of Yb^{2+} is relatively low, which limits significantly the range of reactions in which it is used, such reactions requiring as a rule comparatively severe conditions.

Among all the elements examined, samarium is most preferable because of its high oxidation–reduction potential, which gives rise to its pronounced reducing properties.

N E Brandukova, Ya S Vygodskii Laboratory of Condensation Polymers, **S V Vinogradova** Laboratory for Heterochain Polymers, Nesmeyanov Institute of Organoelement Compounds, Russian Academy of Sciences, ul. Vavilova 28, 117813 Moscow, Russian Federation. Fax (7-095) 135 50 85, Tel. (7-095) 135 92 44

Received 10 March 1994
Uspekhi Khimii **63** (4) 361–372 (1994); translated by A K Grzybowski

Until recently divalent lanthanide halides have been obtained by complex procedures requiring the reduction of lanthanide trihalides with hydrogen or the corresponding metal at very high temperatures (700–900 °C), their thermal dissociation in a high vacuum, etc.[6,7]

A new comparatively simple method of synthesis of divalent lanthanide diiodides from diiodoethane and the corresponding metal was proposed in 1977,[8] which initiated their wide scale employment in organic and polymer chemistry. Thus the use of YbI_2 and especially SmI_2 promotes many organic reactions at high rates and with a high yield of the target product even at low temperatures (−78 to 20 °C) and also makes it possible to carry out reactions which could not be performed using other reductants (iodomethylation of carbonyl compounds, synthesis of large lactone rings, selective reduction of the aldehyde group in the presence of the keto-group, etc.[9]).

Using samarium diiodide as the reagent in the chemistry of high-molecular-mass compounds, we obtained a series of new functional polymers and demonstrated for the first time the formation of the Si–Si bond on treatment with SmI_2.[10]

In contrast to previously published reviews,[11,12] we shall consider here for the first time the possibility of using samarium diiodide in the chemistry of high-molecular-mass compounds as well as new reactions in organic chemistry.

II. The synthesis and properties of divalent lanthanide salts

Lanthanide diiodides are obtained nowadays by the reaction of the corresponding metal with 1,2-diiodoethane (DIE) in anhydrous tetrahydrofuran (THF) under an inert atmosphere at room temperature.[5] The LnI_2 synthesised in this way are used, without being isolated from solution, in reactions with various compounds.

In contrast to other procedures, an interesting feature of this method is the possibility of obtaining exclusively a Ln^{2+} compound and not a mixture of the Ln^{2+} and Ln^{3+} salts. This is

$$Ln + ICH_2CH_2I \longrightarrow LnI_2 + CH_2{=}CH_2$$

Ln = Sm, Yb.

indicated by the colour of the solutions obtained (blue-green for SmI_2 and yellow-green for YbI_2) and the results of various analytical methods: iodometric titration, complexometric titration with ethylenediaminetetraacetic acid (EDTA), absorption spectroscopy, NMR, etc.[13,14]

Since the most stable oxidation state of the lanthanides is +3, Ln^{2+} salts should behave as powerful reductants. The stability of solutions of divalent lanthanides is therefore determined primarily by the stability of the solvent employed under the conditions of high reduction potentials.

As mentioned above, THF is one such stable solvent, but the necessity for the thorough removal of the accumulated peroxides from the initial THF and for its preparation in an anhydrous form give rise to certain difficulties.

Apart from THF, certain other aprotic solvents are resistant to powerful reductants.[15] Kamenskaya et al.[16] showed that lanthanide diiodides do in fact react with, for example, hexamethylphosphoramide (HMPA), whereas in common aprotic solvents such as diethyl ether, dioxane, methylal, and 1,2-dimethoxyethane samarium diiodide does not react with DIE at all; in pyrrolidinone the reaction takes place but solutions containing divalent and trivalent lanthanide compounds are then obtained.[17]

The study of the physicochemical properties of divalent Nd, Sm, Yb, Eu, etc. salts showed that these compounds are in fact most stable in THF.[18] Thus THF is nowadays the most suitable solvent for experiments with divalent lanthanide salts, especially SmI_2. Unfortunately the solubility of these compounds in THF is limited, amounting to 0.1 mol litre^{-1} for SmI_2 and 0.04 mol litre^{-1} for YbI_2 at 20 °C.[1]

An improvement in the solubility of SmI_2 can be achieved by employing organic complexones such as crown-ethers and sodium tetraphenylborate.[18] Thus the Yb^{2+} and Sm^{2+} ions form complexes readily with crown-ethers, which are 3–4 orders of magnitude more stable than the Yb^{3+} and Sm^{3+} complexes. This is associated with the greater size and smaller charge on the Ln^{2+} ions.[19,20] These complexes are readily soluble in the majority of organic solvents, including even nonpolar or weakly polar solvents such as benzene, hexane, halohydrocarbons, etc. (by virtue of the hydrophobic properties of the aliphatic groups of crown-ethers).[21]

The use of crown-ethers also makes it possible to increase greatly the stability of Ln^{2+} solutions in many solvents, which can be accounted for by the shielding effect of the complexone molecule.[18]

Various diiodoalkanes such as diiodomethane and 2,2-diiodobutane can be used for the preparation of SmI_2 instead of DIE.[17] Other haloalkanes react much less effectively. Thus the reaction with 1,2-dibromoethane in THF is very slow and leads to sparingly soluble samarium dibromide,[17] and the reaction with 1,2-dichloroethane does not occur at all.[9]

In contrast to the dichloride and dibromide, samarium diiodide is readily soluble not only in THF but also in HMPA, acetonitrile, and ethanol.[22]

Thus samarium iodide is best among all the salts because of its high reactivity, higher solubility in organic solvents, and the comparative ease of its formation and storage.†

III. Reactions involving samarium diiodide

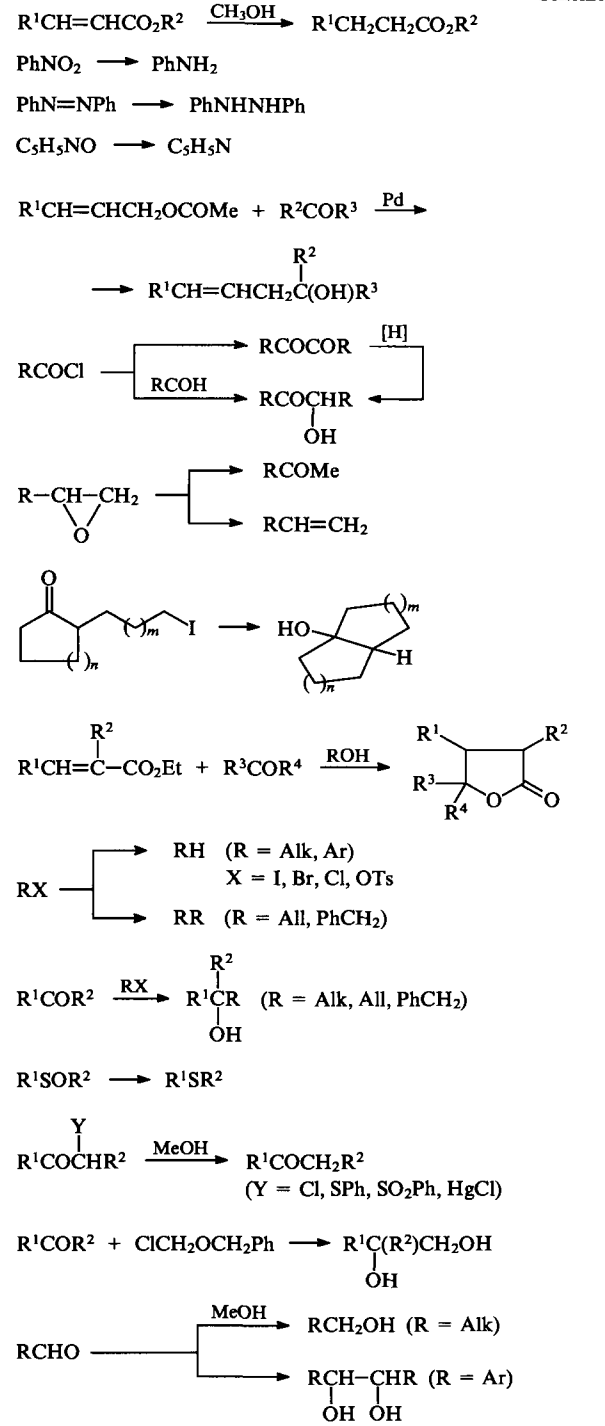
Samarium diiodide is a powerful reductant, soluble in organic solvents, which behaves under the conditions of organic synthesis as an electron donor and is therefore a reagent capable of promoting reactions involving electron transfer.[24]

In a general form, the known reactions that are carried out successfully in the presence of samarium iodide are presented in Scheme 1. The mechanism of organic reactions involving SmI_2 can be represented by Scheme 2 in the most general form.

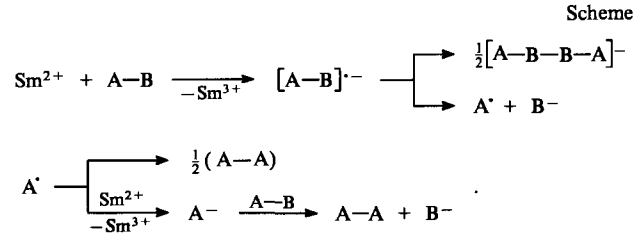
It is noteworthy that the reactions involving electron transfer from SmI_2 to the organic substrate A–B with formation of a radical-anion, which subsequently dimerises or is cleaved into an anion and a radical, the latter being capable of reacting subsequently in different ways, have a stepwise radical-ion mechanism.

† SmI_2 is distributed by Aldrich in the form of a 0.1 M solution in THF.[23]

Scheme 1



Scheme 2



The ability of Sm^{2+} and Sm^{3+} ions to form highly coordinated compounds also exerts a specific effect on the reaction. This probably accelerates electron transfer and can affect the mode of reactions with participation of a free radical (see below).

It is seen from Scheme 2 that processes with participation of reactive species of three different types can take place in the system: free radicals, radical-anions, and carbanions, which lead to extensive possibilities for a wide variety of chemical reactions — reduction, condensation, addition, and nucleophilic substitution. It is very significant that reactions of this type take place effectively in the given instance in a virtually neutral medium.

Various types of reactions carried out with the aid of SmI_2 and their mechanisms are examined below.

1. Reduction of halogen-containing hydrocarbons and tosylates

On refluxing for several hours in 0.1 M solution of SmI_2 in THF, primary and secondary alkyl bromides and iodides RHal produce the corresponding alkanes RH in a high yield (80%–95%).[5] Hydrocarbons are obtained similarly from the corresponding tosylates ROTs.[5]

$$RX \xrightarrow[65\ ^\circ C,\ 2\ h]{SmI_2,\ THF} RH$$

X = Hal, OTs.

For X = OTs, the reaction is accelerated in the presence of small amounts of NaI. This gives grounds for the hypothesis that the tosylates are initially converted into the iodides and then into the alkanes (small amounts of alkyl iodides have been detected among products of the reation even when the latter was carried out in the absence of NaI).[25]

Inanaga et al.[26] observed that the redution potential of SmI_2 increases abruptly after the addition of HMPA to a THF solution of SmI_2. Thus phenyl and vinyl halides react with SmI_2 only in the presence of 5% HMPA as the catalyst. Tertiary alkyl halides also react under similar conditions and in both cases even chlorides, which do not usually enter into a reaction of this kind, are reduced. It has been shown that the use of the SmI_2–THF–HMPA system makes it possible not only to expand significantly the range of halogen-containing hydrocarbons reduced with the aid of SmI_2 but also to eliminate the need for prolonged treatment by refluxing. In this case the thermal conditions are milder and the process proceeds at a higher rate and with a quantitative yield of the product.[27]

The addition of HMPA proved to be effective also in a series of other reactions involving samarium diiodide (see below).[28]

In contrast to alkyl halides, benzyl or allyl halides are not reduced by SmI_2 but dimerise in several minutes at room temperature.

$$2\ PhCH_2Br + 2\ SmI_2 \xrightarrow[20\ min]{20\ ^\circ C} PhCH_2CH_2Ph + 2\ SmBrI_2$$

The following mechanism has been proposed for the reactions of halogen-containing hydrocarbons with SmI_2 in THF:[24]

$$RX + Sm^{2+} \longrightarrow RX^{\cdot -} + Sm^{3+},$$

$$RX^{\cdot -} \longrightarrow \dot{R} + X^-,$$

$$\dot{R} + Sm^{2+} \longrightarrow R^- + Sm^{3+},$$

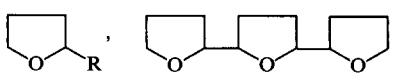
$$\dot{R} + THF \longrightarrow RH + (THF)^{\cdot},$$

$$R^- + THF \longrightarrow RH + (THF)^-,$$

$$\dot{R} + \dot{R} \longrightarrow R{-}R,$$

R = All, $PhCH_2$.

The presence of THF radicals or carbanions in the reaction medium has been confirmed by the formation of small amounts of different 2-substituted THF derivatives, for example:



Under these conditions, the reaction $R^{\cdot} + SmI_2 \rightarrow R^-SmI_2^+$ apparently does not occur because $RSmI_2$ is absent from the reaction products, although in principle such compounds are known and are entirely stable in an organic medium.[1]

It has been suggested[1] that alkyl halides are hydrogenated in the coordination sphere of the samarium(II) ion bound to several THF molecules (like all lanthanide derivatives, samarium diiodide has the high coordination number 8). This can account for the absence of dimerisation products in the reaction of samarium diiodide with aliphatic halides, while benzyl and allyl halides afford only dimerisation products because the radicals formed are too stable to attack THF molecules and can diffuse into the bulk of the solution and recombine there with another radical.

It is of interest to note that benzyl and allyl halides in many instances form under the influence of samarium diiodide dimeric hydrocarbons in higher yields than in the presence of other reagents, for example Cr^{3+} salts.[29]

A similar recombination of silyl radicals with formation of the Si–Si bond was first observed by the present authors in a study of the effect of SmI_2 on organochlorosilanes.[30] The common method of synthesis of polysilanes used previously, namely from organodichlorosilanes by the Wurtz–Fittig reaction using alkali metals, suffers from a series of disadvantages: severe reaction conditions, low process selectivity, and difficulty in the regulation of the molecular weight characteristics of the polymers formed and in the synthesis of polysilanes with functional group substituents.[31] The methods proposed in recent years are complex, comprise many stages, and are characterised by low yields of the target products.[32]

At the same time, polysilanes, which have specific optical properties, have attracted increased attention.[33] We have developed a single-stage method of synthesis of hexaorganodisilanes from triorganochlorosilanes and SmI_2.

$$2\ R^1R^2R^3SiCl + 2\ SmI_2 \longrightarrow (R^1R^2R^3Si)_2 + 2\ SmI_2Cl.$$

Radicals	Yield (%)
$R^1 = R^2 = R^3 = Me$	< 5
$R^1 = R^2 = Me$, $R^3 = CH_2{=}CH{-}$	75
$R^1 = R^2 = Me$, $R^3 = Ph$	85
$R^1 = R^2 = R^3 = Ph$	90

It was established that, as in the case of the carbo-analogues, the mode and rate of the reaction and the yield of the target product depend on the structure of the organochlorosilane employed (compounds with benzyl and allyl substituents dimerise most effectively). It was also shown that the reaction of diorganodichlorosilanes with SmI_2 affords oligosilanes.

$$n\ R^1R^2SiCl_2 \xrightarrow{SmI_2} Cl{-}\left(R^1R^2Si\right)_n{-}Cl;$$

$R^1 = R^2 = Me$; $R^1 = CH_3$, $R^2 = Ph$.

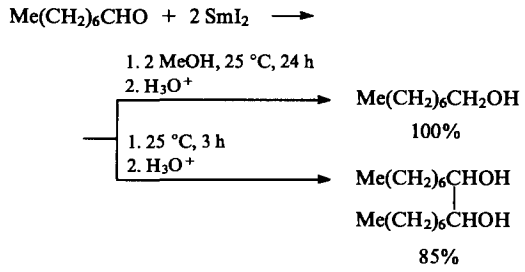
Thus the reduction method based on the use of SmI_2 may be assigned to the class of the most progressive and effective methods of synthesis of hydrocarbons and organosilanes from organic and organosilicon halides.

2. Reactions with carbonyl compounds

Aldehydes and ketones are reduced by SmI_2, the mode of the reaction depends on its conditions and on the structure of the initial compounds. One of the most interesting features of SmI_2 is its ability to promote the formation of a C–C bond between ketones and aldehydes, on the one hand, and various organic compounds having the general formula RX (X = Hal, OTs, OSO_2Me, OAc), on the other.[24]

a. Reduction of aldehydes and ketones

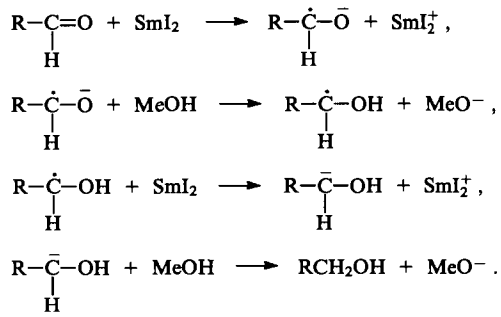
The interaction of aliphatic aldehydes with SmI_2 in THF in the presence of a proton donor (for example, 1% methanol solution) affords alcohols, whilst in aprotic media the products are pinacols.[2]



Aliphatic ketones are also reduced under analogous conditions but much more slowly. For example, the yield of 2-octanol in the reaction of 2-octanone with SmI_2 is only 12%.[5]

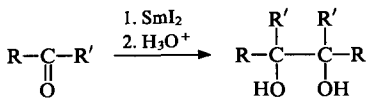
The nature of the proton donor exerts a strong influence on the reaction. Thus, when water is used instead of methanol, 2-octanone is reduced in a satisfactory yield, whereas phenol suppresses the formation of the ketone [alcohol ?].[5]

The selective reduction of the aldehyde group in the presence of a keto-group, which constituted previously a complex problem, is based on the significant difference between the reactivities of the above compounds. Suitable reagents, including modified hydroborates and hydroaluminates, have been proposed for this reaction only recently,[34] but SmI_2 is the most selective. It has been suggested[1] that the reaction proceeds via the following mechanism:



This mechanism is confirmed by the fact that, when MeOD is used instead of MeOH, 90% of RCHDOH and 10% of RCH_2OH is formed. The formation of a small fraction of the protonated rather than deuteriated product can apparently be accounted for by the possibility that hydrogen may be abstracted from THF by the hyroxyalkyl radical.

Table 1. The synthesis of pinacols from aldehydes and ketones by treatment with SmI_2.



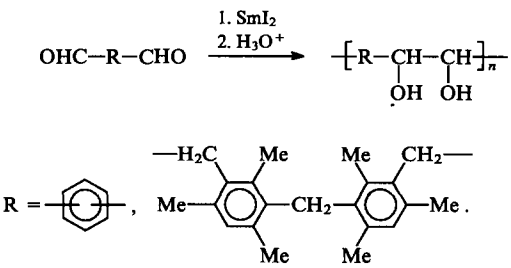
R	R′	Reaction time/min	Yield (%)
H	Ph	0.5	95
H	*p*-CNC_6H_4	0.5	95
H	*p*-$NO_2C_6H_4$	0.5	95
H	*p*-$HOOCC_6H_4$	0.5	66
H	*p*-$MeOC_6H_4$	1.0	90
Me	Ph	0.5	95
Me	n-C_6H_{13}	1440	80

In the absence of a suitable proton donor (methanol), recombination of the intermediate radical-anions leads to a pinacol. Pinacols are formed almost exclusively from aromatic aldehydes and ketones, the reaction involving aldehydes being very fast (taking only 30–60 s at room temperature) with an almost quantitative yield, while the degree of reaction with aliphatic ketones after 24 h is 80%.[35]

The possibility of obtaining pinacols in high yields from aromatic aldehydes containing various substituents in the *para*-position is especially attractive (Table 1). The above method has significant advantages over other procedures for the synthesis of pinacols because of the attainment of high yields of the target product and the exceptionally high reaction rate.

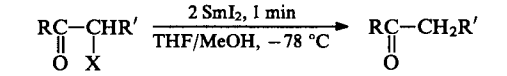
For example, when CeI_2 in THF is used, 12 h is required to synthesise a pinacol from benzaldehyde in 94% yield,[36] while in the presence of aqueous $TiCl_3$ in an alkaline medium the reaction with benzaldehyde is rapid, mainly an alcohol being formed as a side product.[37]

By treating dialdehydes with SmI_2, we synthesised polypinacols with a molecuar mass of the order of $(12-15) \times 10^3$.[38]



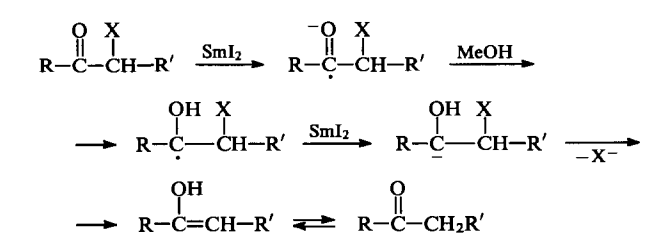
Previously only oligomeric pinacols with a molecular mass not exceeding 2×10^3 were obtained by treating terephthalic aldehyde with a zinc complex of $TiCl_4$.[39]

Although ketones are reduced via a mechanism similar to that described for aldehydes, α-substituted ketones require special consideration.[40] Analysis of literature data shows that the α-substituent can be abstracted from such compounds only under extremely severe conditions at an elevated temperature.[41,42] The use of SmI_2 for this purpose in the presence of a proton donor makes it possible to obtain unsubstituted ketones from a wide range of α-substituted ketones in high yields at low temperatures.



X = OAc, $OSiMe_3$, OTs, Cl, SPh, SO_2Ph, OCO_2CH_2Ph, HgCl.

It has been suggested[40] that the reaction proceeds via the formation of a ketyl, which is rapidly protonated by methanol. Treatment with a second equivalent of SmI_2 leads to the formation of a carbanion from which X is then split off. The unsubstituted ketone is obtained as a result of the tautomerisation of the enol produced.



b. Reactions of aldehydes and ketones via the CO group

One of the remarkable properties of samarium diiodide is its ability to promote the formation of a C–C bond between ketones or aldehydes and compounds of different types. It has

been shown that halogen-containing hydrocarbons and tosylates undergo reductive addition to ketones under the influence of SmI_2.[5] Formally this reaction is analogous to the reactions of ketones with a Grignard reagent.

$$n\text{-}C_6H_{13}COMe + MeI \xrightarrow[2.\ H_3O^+]{1.\ SmI_2,\ 65\ ^\circ C,\ 1\ h} n\text{-}C_6H_{13}C(OH)Me_2;\quad 75\%$$

$$n\text{-}C_6H_{13}COMe + Bu^nOTs \xrightarrow[2.\ H_3O^+]{1.\ SmI_2,\ THF} n\text{-}C_6H_{13}C(Me)(OH)\text{—}Bu^n.\quad 95\%$$

Various ketones, both alicyclic and aromatic, interact with the SmI_2–RX system and their reactivities hardly differ from that of 2-octanone described above. The reactivity of the halides diminishes in the sequence RI > RBr ≫ RCl. It is of interest to note that allyl and benzyl halides, which usually tend to dimerise rapidly on treatment with SmI_2, in the presence of a ketone react readily with the latter, forming tertiary alcohols.

$$n\text{-}C_6H_{13}COMe + ICH_2CH{=}CH_2 \xrightarrow[25\ ^\circ C,\ 25\ min]{2\ SmI_2} n\text{-}C_6H_{13}C(Me)(OH)CH_2CH{=}CH_2.\quad 72\%$$

On the other hand, vinyl halides and aromatic halo-compounds do not react with ketones in the presence of SmI_2; in such cases, only the conversion of the ketones into pinacols to the extent of 10%–20% is observed.[5]

The following mechanism has been proposed for the alkylation of ketones, involving the formation of intermediate radical compounds:[24]

$$RX + SmI_2 \longrightarrow RX^{\bullet-}SmI_2^+ \longrightarrow \dot{R} + SmI_2X, \quad (1)$$

$$\dot{R} + SmI_2 \longrightarrow R^-SmI_2^+, \quad (2)$$

$$R^1R^2C{=}O + SmI_2 \longrightarrow R^1R^2\dot{C}O^-SmI_2^+, \quad (3)$$

$$R^1R^2\dot{C}O^-SmI_2^+ + \dot{R} \longrightarrow RR^1R^2CO^-SmI2^+ \xrightarrow{H_3O^+} RR^1R^2COH, \quad (4)$$

$$R^1R^2C{=}O + R^-SmI_2^+ \longrightarrow RR^1R^2CO^-SmI_2^+ \xrightarrow{H_3O^+} RR^1R^2COH. \quad (5)$$

The mechanism of the reactions of the radical R$^\bullet$ has not been elucidated in detail: it may be that it is reduced by SmI_2 to R^- [reaction (2)] or recombines with the ketyl radical arising as a result of electron transfer from SmI_2 to the ketone [reaction (4)]. At any rate, the radical mechanism explains the presence in the reaction product of small amounts of compounds such as the α-R-alkylated THF.

The reaction is much faster when small amounts of $FeCl_3$ (1 mass % of SmI_2) are added. The catalytic effect of $FeCl_3$ may be due to its ability to promote the formation of ketyl radicals (this was demonstrated for the Grignard reaction) or the conversion of Sm^{2+} into Sm^{3+}.[43] In one way or another, $FeCl_3$ behaves as a compound facilitating electron transfer in reactions with SmI_2. HMPA also functions as a catalyst of the reaction.[44]

The reduction of aliphatic aldehydes, leading to a mixture of products, proceeds in a more complex manner.[45]

$$n\text{-}C_7H_{15}CHO + MeI \xrightarrow[2.\ H_3O^+]{1.\ SmI_2,\ 25\ ^\circ C} n\text{-}C_7H_{15}CH(OH)Me\ (16\%) + n\text{-}C_7H_{15}COMe\ (6\%) + n\text{-}C_7H_{15}CH_2OH\ (38\%) + n\text{-}C_7H_{15}C(OH)Me_2\ (32\%).$$

The observed reactions may be based on the Meerwein–Ponndorf reaction, which proceeds very rapidly with participation of secondary samarium alkoxides: $n\text{-}C_{17}H_{15}CH(Me)OSmI_2$ is formed initially and then reacts rapidly with the aldehyde, forming $n\text{-}C_7H_{15}COMe$ and $n\text{-}C_7H_{15}CH_2OSmI_2$; a tertiary alcohol is obtained from the ketone and CH_3I in the presence of SmI_2.

It has been shown recently[43] that dicyclopentadienylsamarium, readily and rapidly obtained by the exchange reaction between SmI_2 and cyclopentadienylsodium, is significantly more effective in the reaction of aliphatic aldehydes with halogen-containing hydrocarbons. In contrast to SmI_2, it does not catalyse the Meerwein–Ponndorf or Tishchenko side reaction.

It has also been found that secondary alcohols are formed from aldehydes in a satisfactory yield when the more reactive benzyl or allyl halides are employed.[45]

$$n\text{-}C_7H_{15}CHO + ICH_2CH{=}CH_2 \xrightarrow[25\ ^\circ C,\ 5\ min]{2\ SmI_2,\ THF} n\text{-}C_7H_{15}CH(OH)CH_2CH{=}CH_2\quad 75\%$$

A mechanism similar to that discussed above for the reduction of ketones has been proposed for this reaction.

$$RX + SmI_2 \longrightarrow RX^{\bullet-}SmI_2^+ \longrightarrow \dot{R} + SmI_2X$$

$$R'CHO + SmI_2 \longrightarrow R'CHO^{\bullet-}SmI_2^+$$

$$R'CHO^{\bullet-}SmI_2^+ + \dot{R} \longrightarrow RR'CHO^-SmI_2^+ \xrightarrow{H_3O^+} RR'CHOH$$

It is interesting to note that the CN, NO_2, CO_2R, and other groups are not then involved.[35]

$$n\text{-}C_6H_{13}COMe + TsO(CH_2)_9CO_2Me \xrightarrow[2.\ H_3O^+]{1.\ 2\ SmI_2,\ 65\ ^\circ C,\ 2\ h} n\text{-}C_6H_{13}C(OH)(CH_2)_9CO_2Me\ (CH)\quad 63\%$$

γ-Hydroxynitriles have been obtained in a low yield in the reaction of ketones with acrylonitrile.[47]

$$R^1COR^2 + CH_2{=}CH\text{—}CN \xrightarrow[THF,\ KOH]{2\ SmI_2} R^1R^2C(OH)\text{—}CH_2CH_2CN\quad 17\%\text{–}20\%$$

It has been observed recently that, on treatment with samarium diiodide, allyl acetates also interact with carbonyl compounds in the presence of catalytic amounts of a palladium complex [$Pd(OAc)_2$ + PPh_3 or $Pd(PPh_3)_4$] to form homoallyl alcohols in a good yield.[46]

$$R^1CH{=}CHCH_2OCOCH_3 + R^2COR^3 \xrightarrow[SmI_2,\ 0\ ^\circ C,\ 2\ h]{Pd(PPh_3)_4} R^1CH{=}CHCH_2C(OH)R^2R^3.$$

Aromatic and α,β-unsaturated carbonyl compounds react differently, affording mainly dimerisation products — pinacols.[46] The use of readily available allyl acetates in the aldehyde and ketone reduction reactions makes it possible to replace allyl halides, which are difficult to obtain, unstable, and toxic.

In the presence of SmI_2, aldehydes and ketones also react with chloromethyl sulfides $ClCH_2SR$ to form hydroxythioethers.[48]

$$ClCH_2SR + R^1R^2CO \xrightarrow{SmI_2,\ THF} R^1R^2C(OH)CH_2SR$$

R = Me, Ph.

A reaction involving the coupling of carbonyl compounds $R^1C(O)R^2$ [$R^1 = PhCH_2$, $R^2 = Me$; $R^1 + R^2 = (CH_2)_{11}$; $R^1 = cyclo\text{-}C_6H_{11}$, $R^2 = H$] with alkynes $R^3C{\equiv}CX$ (X = Ph, CH_2OAc, Bu^t) has also been described. The reaction is promoted by the SmI_2–HMPA–THF system (Bu^tOH, 20 °C, 5 min); it results in the formation of the allyl alcohols $R^1R^2C(OH)CH=CHX$.[49]

Thus the use of samarium diiodide in reactions involving reductive addition to the carbonyl group makes it possible to obtain alcohols with a wide variety of structures in satisfactory yields.

c. Hydroxymethylation of carbonyl compounds

The interesting reaction involving the hydroxymethylation of carbonyl compounds on treatment with samarium diiodide has been recently achieved by Imamoto et al.[50] Ketones readily interact in this reaction with benzyl chloromethyl ether at room temperature, forming alcohols, which afford diols on subsequent hydrogenation.

$$R'\underset{\underset{O}{\|}}{C}R + ClCH_2OCH_2Ph \xrightarrow{2\ SmI_2,\ 20\ °C}$$

$$\longrightarrow RR'\underset{\underset{OH}{|}}{C}CH_2OCH_2Ph \xrightarrow[Pd/C]{H_2} RR'\underset{\underset{OH}{|}}{C}CH_2OH$$

Aldehydes are not reduced to alcohols but are converted into pinacols in 80%–90% yield. However, in the presence of equimolar amounts of the dimethyl or dibenzyl ether of tetraethylene glycol, which form a complex with SmI_2, it is possible to obtain alcohols in 50%–70% yield.

$$PhCH_2CH_2CHO + ClCH_2OCH_2Ph \xrightarrow{2\ SmI_2,\ 20\ °C}$$

$$\longrightarrow PhCH_2CH_2CH(OH)CH_2OCH_2Ph \xrightarrow[Pd/C]{H_2}$$

66%

$$\longrightarrow PhCH_2CH_2\underset{\underset{OH}{|}}{C}HCH_2OH$$

90%

In the interaction of carbonyl compounds with diiodomethane in the presence of metallic samarium or SmI_2, an iodohydrin is formed as an intermediate, its hydrolysis subsequently affording the corresponding diol.[51, 52]

$$R^1\underset{\underset{O}{\|}}{C}R^2 + CH_2I_2 \xrightarrow{SmI_2\ or\ Sm} R^1R^2\underset{\underset{OH}{|}}{C}CH_2I$$

Thus the hydroxymethylation of carbonyl compounds may be an effective reaction in the synthesis of 1,2-diols.

d. Reactions with carboxylic acids and their derivatives

Carboxylic acids and their derivatives (esters, amides, and anhydrides) are as a rule resistant to the action of SmI_2.[5] However, it has been shown recently that, in the presence of bases and a proton donor, they are readily reduced by SmI_2 to the corresponding alcohols at room temperature.[53]

$$PhCOOR^1 \xrightarrow[THF,\ R^1OH,\ 20\ °C]{SmI_2,\ HB} PhCH_2OH$$

$$+ \left\{[PhCH(OH)]_2 + PhCH_2CH(OH)Ph + PhCH_2COPh\right\}$$

R^1 = Me, PhCO; HB = $LiNH_2$, LiOMe, KOH.

$$PhCONHR^2 \xrightarrow[THF,\ R^2OH,\ 20\ °C]{SmI_2,\ HB} PhCH_2OH + PhCH_2NHR^2$$

R^2 = H, Ph.

Carboxylic acid chlorides do not form the expected reduction products, such as aldehydes or primary alcohols, on reaction with SmI_2. On the other hand, they enter very rapidly into an addition reaction. The main product obtained is then an α-diketone RCOCOR in a yield ranging from 40% (R = Alk) to 80% (R = Ar), an α-ketol RCOCH(OH)R being formed as a side product.[55]

$$2\ RCOCl + 2\ SmI_2 \xrightarrow{25\ °C,\ 2-4\ min} R\underset{\underset{O}{\|}}{C}\text{–}\underset{\underset{O}{\|}}{C}R + 2\ SmI_2Cl$$

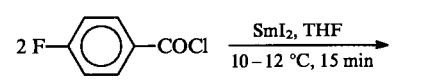
R = Ph (78%), *p*-ClC_6H_4 (72%), *p*-$MeOC_6H_4$ (69%), $Cl(CH_2)_4$ (54%).

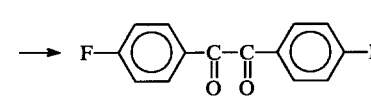
The product yields vary depending on R.

The asymmetric reduction of benzil to benzoin takes place in the presence of optically active compounds such as quinine or quinidine. This reaction proceeds even more effectively in the presence of HMPA.[54]

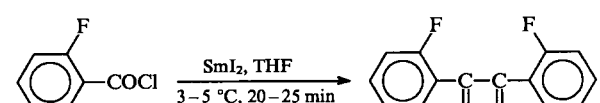
$$Ph\underset{\underset{O}{\|}}{C}\text{–}\underset{\underset{O}{\|}}{C}Ph \xrightarrow[[H]]{SmI_2} Ph\underset{\underset{OH}{|}}{\overset{\overset{H}{|}}{C}}\text{–}\underset{\underset{O}{\|}}{C}Ph$$

We have obtained difluorobenzils by condensing under mild conditions the chlorides of *p*- and *o*-fluorobenzoic acids by treatment with SmI_2 in THF.[10]





50%



65%

These products were then used to synthesise high-molecular-mass aromatic ethers by the nucleophilic substitution of the fluorine atom by alkali metal bisphenoxides and subsequent conversion of the α-diketone groups into quinoxaline groups.[10]

A paraffin-like admixture of C_{23-25} alkanes was also detected in the unpurified product of the reactions of acid chlorides or fluorides.[56] They can be produced in the oligomerisation

of ethylene, formed at an early stage in the interaction of metallic samarium with diiodoethane. SmI_2 or SmI_2Cl might have served as the oligomerisation initiator both in the samarium diiodide formation stage and in the stage involving the synthesis of the diketones.

According to ideas put forward in the literature,[57] the acid chloride condensation reaction proceeds via the formation of radical-ions, which are cleaved to acyl radicals and these are reduced to acyl anions. The latter react in their turn with a second molecule of the acid chloride, affording an α-diketone (the direct recombination of the acyl radicals is insignificant).

$$RCOCl + SmI_2 \longrightarrow [RCOCl]^{\cdot -}\ SmI_2^+$$

$$[RCOCl]^{\cdot -} \longrightarrow RC\dot{O} + Cl^-$$

$$RC\dot{O} + SmI_2 \longrightarrow$$

$$\longrightarrow RCO^-SmI_2^+ \xrightarrow{RCOCl} ROC{-}COR + SmI_2Cl$$

$$2\,RC\dot{O} \longrightarrow ROC{-}COR$$

The last process takes place to a very insignificant extent. The proposed mechanism explains the satisfactory yield (75%) of the α-diketone from $PhCH_2COCl$. It is known that the acyl radical $PhCH_2CO^{\cdot}$ is rapidly decarbonylated ($k_c = 5.2 \times 10^7\ s^{-1}$) to $PhCH_2^{\cdot}$. The absence of toluene and 1,2-diphenylethane from the reaction products is evidence that the acyl radical is reduced to the acyl anion at a rate greatly exceeding $5.2 \times 10^7\ s^{-1}$. The anion is then acylated by the acid chloride, affording the α-diketone. The presence of the intermediate acyl anion $RCO^-SmI_2^+$ in the reaction is also confirmed by its interaction with electrophiles other than RCOCl, for example aldehydes and ketones, which results in the formation of α-hydroxyketones after hydrolysis: their formation can be accounted for by nucleophilic acylation.[57]

$$Bu^tCOCl + EtC(=O)H \xrightarrow[20\ ^\circ C,\ 4\ min]{2\ SmI_2} Bu^t{-}C(=O){-}CH(OH){-}Et$$

64%

The direct synthesis of α-diketones from carboxylic acid chlorides by treatment with SmI_2 has undoubted advantages over other methods of synthesis of these compounds based on multistage procedures such as the oxidation of monocarbonyl compounds or their α-substituted derivatives (for example acyloins, derivatives of enediols, glycols, etc.) or their synthesis from aromatic compounds and oxalyl chloride by the Friedel–Crafts reaction.[58]

A new strategy for the synthesis of α-hydroxyketones by the reaction of an alkyl halide, isonitrile, and a carbonyl compound with SmI_2 has also been proposed.[59]

$$R^1Hal + ZNC \xrightarrow[-15\ ^\circ C,\ 3\ h]{2\ SmI_2,\ THF/HMPA} R^1C(=NZ){-}SmI_2 \xrightarrow[0\ ^\circ C,\ 14\ h]{R^2R^3C=O}$$

$$\longrightarrow R^1C(=NZ){-}CR^2R^3(OH) \xrightarrow{H_3O^+} R^1C(=O){-}CR^2R^3(OH)$$

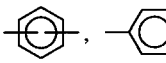
Z = 2,6-dimethylphenyl (Me, Me)

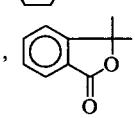
The mild conditions make it possible to employ this method for the synthesis of compounds with various functional groups, including, for example, terminal acetylenic and trimethylsilyl ether groups, and also for the synthesis of α-hydroxyaldehydes.

The formation of α-diketones in the reaction of carboxylic acid chlorides with SmI_2 may serve as a basis for the formation of the corresponding polymers. The available information about the synthesis of such polymers by other methods is extremely scant. The possibility of obtaining polyhydroxyketones and polybenzoins by the acyloin or benzoin condensation of terephthalic acid chloride and terephthalic anhydride respectively, which were oxidised to poly-α-diketones by prolonged refluxing in nitric acid, has been described.[60,61] Only insoluble high-molecular-mass oligomers were obtained in 50%–70% yield.[62]

We synthesised for the first time α-diketone homopolymers and copolymers in a quantitative yield[63] by the reaction of aromatic dicarboxylic acid chlorides with SmI_2 in THF at room temperature for 10–15 min. It was found that the acid fluorides are also reactive in this process.

$$XOCRCOX + SmI_2 \longrightarrow -\left[R{-}CO{-}CO\right]_n-$$

R =  ,

R′ = —O—, —C(CF₃)₂—,  ;

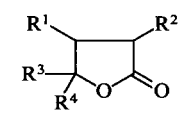
X = Cl, F.

The polymers synthesised have an amorphous structure, a molecular mass of the order of 25×10^3, and a softening temperature of 250–290 °C. They are readily soluble in various organic solvents.

e. The cyclisation reactions of carbonyl compounds

Intermolecular cyclisation. In the presence of samarium diiodide and a proton donor, aldehydes and ketones interact with alkenes containing electron-accepting substituents.[47]

$$R^1CH{=}CR^2CO_2Et + R^3COR^4 \xrightarrow[ROH,\ 3\ h]{2\ SmI_2}$$



Methyl, ethyl, and especially butyl alcohols can be used as the proton donor. In order to suppress the reduction of the ketone, the dimethyl ether of tetraethylene glycol, which forms a complex with SmI_2, is added to the reaction mixture.[64]

Whereas in the routinely used method of the electrochemical synthesis of γ-lactones from activated olefins and ketones or aldehydes in the presence of chlorotrimethylsilane only aliphatic compounds are reactive, when samarium diiodide is used the reaction can be extended to aromatic aldehydes and ketones.[64] The reaction apparently proceeds via a radical mechanism.[47]

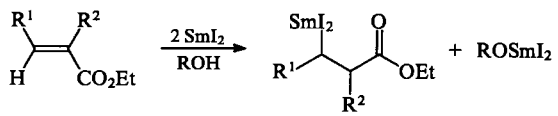
$$R^3R^4C{=}O \xrightarrow{SmI_2} R^3R^4\dot{C}{-}OSmI_2 \xrightarrow{H\ =\ CR^1R^2CO_2Et}$$

$$\longrightarrow R^3R^4C(OSmI_2){-}HCR^1{-}\dot{C}R^2{-}CO_2Et \longrightarrow$$

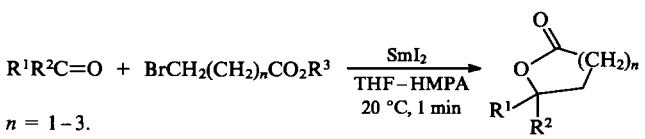
$$\xrightarrow{ROH,\ SmI_2} R^3R^4C{-}HCR^1{-}HCR^2{-}CO_2Et$$

$$\xrightarrow{-EtOSmI_2}$$

However, another mechanism involving the formation of samarium homoenolate is not ruled out either.



The use of small amounts of HMPA in this reaction makes it possible to achieve the direct synthesis of γ-, δ-, or ε-lactones from the corresponding bromoesters, in particular from the readily available industrially produced β-bromopropionate, γ-bromobutyrate, or δ-bromovalerate, in satisfactory yields. [52,65]



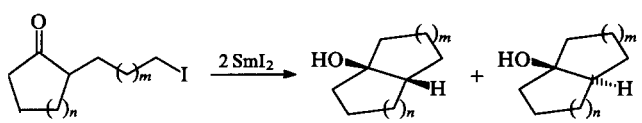
$n = 1-3$.

75%–82%

Thus the use of SmI_2 has made it possible to develop a new single-stage method of synthesis of lactones, the distinctive features of which are simplicity, technological convenience, and effectiveness.

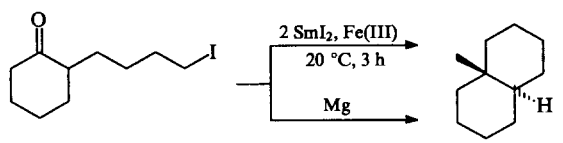
Intramolecular cyclisation. Molander and coworkers [66–68] have shown that, when SmI_2 is used as the reagent, the Barbier as well as Reformatsky reactions take place readily and smoothly. [69]

The intramolecular cyclisation reaction (the Barbier reaction) plays an important role in organic synthesis. A series of methods for carrying out a reaction of this type have been developed. [70] The most common include the cyclisation of 2-(ω-iodoalkyl)cycloalkanones with formation of the corresponding mixture of diastereoisomeric bicyclic alcohols.



By regulating the length of the iodoalkyl side chain and the ring size in the initial cycloalkanone, it is possible to obtain a wide variety of bicyclic compounds. However, the use of traditional reductants, in particular alkali [71] and alkaline earth metals, [72] in this process led to the formation of bicyclic alcohols with only three-, four-, and five-membered rings.

The use of SmI_2 makes it possible to achieve the intramolecular cyclisation of haloketones accompanied by the formation of bicyclic alcohols with six-membered and in certain cases also with seven-membered rings in a high yield. [66]

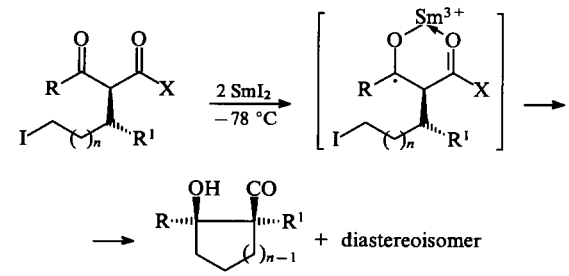


95%

In addition, the stereocontrolled cyclisation of 2-(ω-iodoalkyl)β-ketoesters and 2-(ω-iodoalkyl)-β-ketoamides‡ takes place on treatment with SmI_2, affording high yields of the esters and amides respectively of *cis*-2-hydroxycycloalkanecarboxylic acids with five-, six-, and even seven-membered rings. [67]

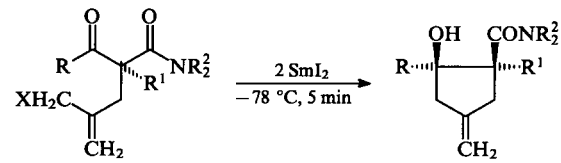
‡ When activated magnesium is used at room temperature, cyclisation does not occur and the initial reagent is isolated. [73]

In view of the very strong affinity of the samarium ion for the oxygen atom in the reactions of carbonyl compounds with SmI_2, a stable chelate is formed fairly readily and the process proceeds via an intermediate stage involving the formation of a samarium-containing metallocycle. The stereoselectivity of all the processes is exceptionally high under these conditions.



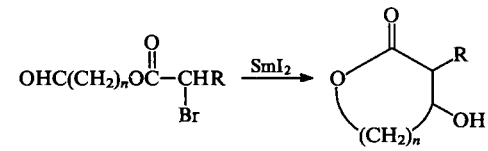
$X = NR^2_2, OR^2$.

2-(ω-Haloallyl)-β-ketoamides also cyclise readily.



In the presence of SmI_2, the reaction proceeds under mild conditions, which makes it possible to obtain cyclic systems with various functional groups which remain unaffected. Thus SmI_2 proved to be an extremely effective reagent in the stereocontrolled intramolecular Barbier reactions.

Tabuchi et al. [74] established that the use of SmI_2 proved to be most effective in the synthesis of medium and large lactone rings. In particular, eight- and nine-membered rings, the synthesis of which by the traditional method has been extremely difficult, can now be obtained fairly readily. Inanaga and coworkers have also been working on these lines. [12]

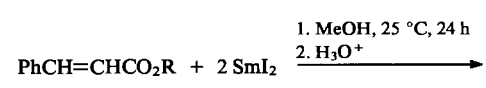


76%–96%

$n = 4-10$.

3. Reduction of C=C double bonds

On treatment with SmI_2 solutions, the conjugated double bond is reduced even at room temperature in contrast to an isolated double bond. [5] Thus α,β-unsaturated acids and esters are reduced in a high yield by samarium diiodide in THF in the presence of methanol. [1]



R = H, Et.

However, for conjugated esters, this reaction is not the only one possible. For example, when an unsaturated ester having a more complex structure is acted upon by SmI_2, the following reaction takes place with 90% conversion: [2]

$$MeCH(OH)CH{=}C(Me)CO_2Et + 2\,SmI_2 \xrightarrow[2.\,2\,H_2O^+]{1.\,THF} MeCH{=}CHCH(Me)CO_2Et\,.$$

The carbonyl groups in α,β-unsaturated ketones and aldehydes are also partially reduced, so that competing reactions involving the reduction of the C=O and C=C groups are possible.

4. Reactions with nitrogen-containing compounds

The effect of SmI_2 on various nitrogen-containing functional groups has been investigated. Aromatic and aliphatic nitriles do not undergo any changes in its presence.[75] Aromatic nitro- and azo-compounds are readily reduced by SmI_2 in THF at room temperature.[76]

$$PhNO_2 \xrightarrow[20\ ^\circ C,\ 5\ min]{8\,SmI_2} PhNH_2 \quad 85\%$$

$$NO_2C_6H_4NH_2 \xrightarrow[20\ ^\circ C,\ 5\ min]{8\,SmI_2} NH_2C_6H_4NH_2 \quad 89\%$$

$$Ph{-}N{=}N{-}Ph \xrightarrow[2\%\ MeOH,\ 20\ ^\circ C]{2\,SmI_2} PhNHNHPh \quad 95\%$$

Picoline and pyridine *N*-oxides are converted into the corresponding bases.[75]

$$MeC_5H_4NO \xrightarrow[20\ ^\circ C,\ 5\ min]{2\,SmI_2} MeC_5H_4N \quad 83\%$$

$$C_5H_5NO \xrightarrow[65\ ^\circ C,\ 10\ min]{2\,SmI_2} C_5H_5N \quad 80\%$$

Arsenic oxides are reduced similarly.[76]

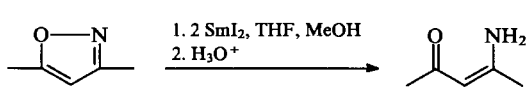
The rapid and selective reduction of *m*- and *p*-nitrobenzonitriles to the corresponding cyanoanilines is particularly remarkable.[75]

$$m\text{-}NCC_6H_4NO_2 + 8\,SmI_2 \xrightarrow[MeOH,\ 25\ ^\circ C]{THF} m\text{-}NCC_6H_4NH_2\,.$$

It may be that the reactivity of the nitro-group in these compounds is enhanced by the electron-accepting effect of the CN group.[75]

Schiff bases, for example benzylideneaniline, are reduced to the amines by samarium diiodide in the presence of methanol. Oximes form complex mixtures; isomeric amines have been isolated for benzaldehyde oxime.

It has been observed recently that the N–O bond in isoxazoles is cleaved selectively by SmI_2.[77]



96%

5. Reactions with epoxides and sulfoxides

On treatment with samarium diiodide, epoxides are converted into olefins even at room temperature.[5]

$$PhCH_2CH{-}CH_2 \xrightarrow[25\ ^\circ C,\ 24\ h]{2\,SmI_2} PhCH_2CH{=}CH_2\,.$$

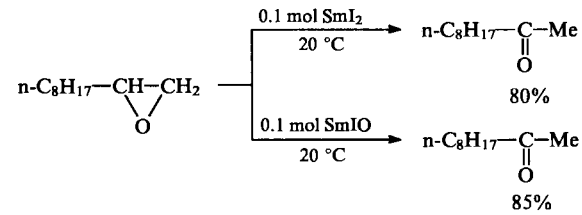
82%

Sulfoxides are similarly reduced to sulfides.

$$R{-}\overset{\overset{O}{\|}}{S}{-}R^1 \xrightarrow[65\ ^\circ C,\ 2\ h]{2\,SmI_2} R{-}S{-}R^1 \quad 90\%$$

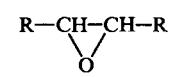
The deoxidation of organic heteroatomic oxides takes place almost instantaneously in the presence of HMPA in a quantitative yield; even triphenylphosphine oxide is reduced under these conditions.[23]

$RCOCH_3$ is obtained as a side product in the reactions of SmI_2 with terminal epoxides. Its formation is apparently associated with the effect of Sm^{3+}, which accumulates during the reduction process.[78] During the reaction, SmI_2 is converted into $I_2SmOSmI_2$, which decomposes slowly, affording a mixture of SmI_3 and SmIO. The authors suggest that it is in fact the latter compound which acts as the catalyst of the rearrangement of the terminal epoxide to the corresponding methyl ketone. The following reactions indicate this:

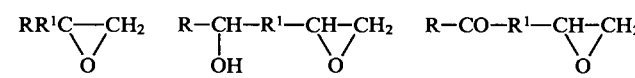


Consequently small amounts of samarium diiodide catalyse the isomerisation of terminal epoxides RCOMe, in contrast to other catalysts which lead to the exclusive formation of an aldehyde.[74]

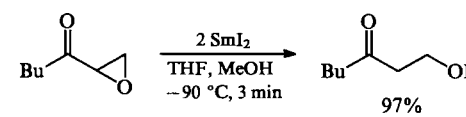
The rearrangement of 1,2-disubstituted epoxides to the corresponding methyl ketones proceeds with greater difficulty. Internal epoxides



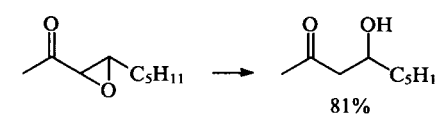
are also converted into ketones very slowly. The reaction is altogether uncharacteristic of epoxides of other types.



It has been shown recently that α,β-epoxyketones are converted into β-hydroxyketones (aldols) on treatment with SmI_2.[79]



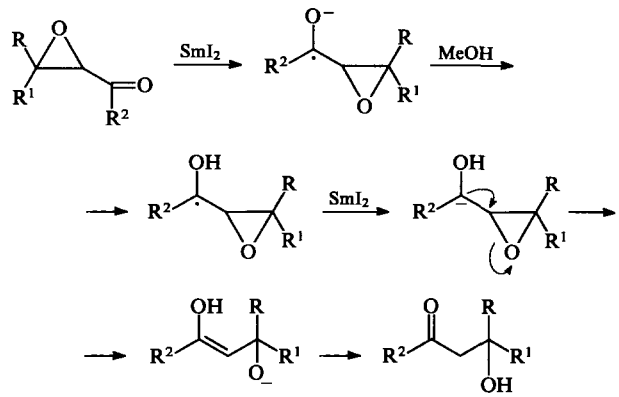
97%



81%

Primary, secondary, and tertiary cyclic and alicyclic aldols can be obtained in high yields by this procedure.

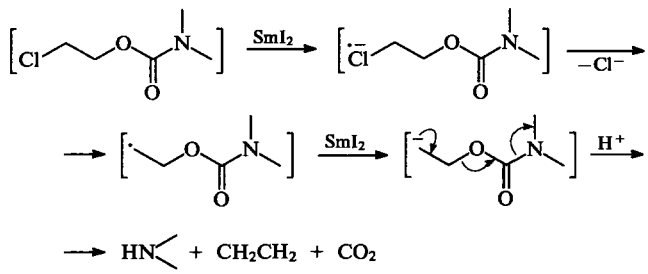
It has been suggested[79] that the reaction proceeds via the formation of a ketyl, which is rapidly protonated by methanol. On treatment with a second equivalent of samarium diiodide, a carbanion, which induces the opening of the epoxide ring, is obtained. Tautomerisation of the enol formed leads to the formation of a ketone.



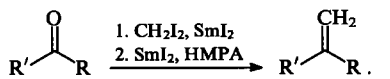
Thus a wide variety of aldols, including chiral aldols which are not obtainable by traditional methods, can be synthesised by treatment with samarium diiodide.[80–82]

6. Other reactions

The use of SmI_2 as a very powerful reducing agent frequently makes it possible to solve problems in organic chemistry of the kind which it has not so far been possible to solve using other reductants. Thus it has been impossible for a long time to obtain an amine from 2-chloroethyl carbamate; the use of all the reagents known for reactions of this kind led to the formation of hydroxyethyl carbamate as the main product.[83] On the other hand, samarium diiodide cleaves 2-chloroethyl carbamate effectively, forming an amine.[84] The rapid and selective course of the reaction can be accounted for by the ability of samarium diiodide to reduce rapidly the intermediate radical to the anion.



It has also been possible to achieve the monoiodomethylation of carbonyl groups at room temperature (with subsequent reductive elimination), i.e. to achieve a reaction which had been regarded hitherto as impossible.[27,85] The process is completed after 3 min and the product yield is extremely high (73%–80%).



Thus, by virtue of the very high reduction potential of divalent samarium, it has become possible to carry out various kinds of substitutions for functional groups which cannot be achieved by traditional methods.

* * *

The range of organic reactions with participation of SmI_2 has been expanding continuously. Thus it has been possible to achieve recently the reduction of triple bonds (in combination with a catalyst based on transition metals),[12] the cyclisation of aromatic radicals,[86] dimerisation reactions with reduction of derivatives of conjugated unsaturated carboxylic acids,[12] intramolecular cyclisation of nonactivated unsaturated ketones,[87] etc.

Samarium diiodide is used in the synthesis of new functional polymers and oligomers. It is of interest to employ the reactions with SmI_2 not only for the synthesis of new polymers but also for the modification of known polymers by incorporating reactive groups in their main chain. This leads to extensive prospects for subsequent chemical reactions of the polymers, including the formation of heat-resistant and thermostable linear, branched, and network heterochain high-molecular-mass compounds, including organometallic compounds.

This review has been written with the financial support of the Russian Fundamental Research Fund [grant 94-03-08082a (320)].

References

1. H B Kagan, J L Namy, in *Handbook on the Physics and Chemistry of the Rare Earth* (Eds K A Gschneider, L Eyring) (Amsterdam: Elsevier, 1984) p. 525
2. H B Kagan, in *Fundamental and Technological Aspects of Organo-f-element Chemistry* (Eds T J Marks, I L Fragala) (Boston: Reidel, 1985) p. 49
3. J R Long *Aldrichimica Acta* **18** 87 (1985)
4. A N Kamenskaya, N B Mikheev, N P Kholmogorova *Zh. Neorg. Khim.* **28** 2499 (1983)
5. P Girard, J L Namy, H B Kagan *J. Am. Chem. Soc.* **102** 2693 (1980)
6. A N Kamenskaya, N B Mikheev, N P Kholmogorova, V I Spitsyn *Dokl. Akad. Nauk SSSR* **266** 393 (1982)
7. G Jantsh, N Skalla, H Jawurek *Z. Anorg. Allg. Chem.* **201** 207 (1931)
8. J L Namy, P Girard, H B Kagan *Nouv. J. Chim.* **1** 5 (1977)
9. J E Hyneey, in *Inorganic Chemistry* (New York: Harper and Row, 1975) p. 275
10. N E Brandukova, Ya S Vygodskii, S V Vinogradova *Metalloorg. Khim.* **5** 1251 (1992)
11. H B Kagan, J L Namy *Tetrahedron* **42** 6573 (1986)
12. J Inanaga *Yuki Gosei Kagaku Kyokai Shi* **47** 200 (1989)
13. D F Evans *J. Chem. Soc.* **191** 2003 (1959)
14. D F Evans, G V Fazakerley, R F Phillips *J. Chem. Soc., A* 1931 (1971)
15. A N Kamenskaya, N B Mikheev, S A Kulyukhin, S V Kondrashova *Zh. Neorg. Khim.* **30** 615 (1985)
16. A N Kamenskaya, N B Mikheev, N A Konovalova *Zh. Neorg. Khim.* **22** 2130 (1977)
17. J L Namy, P Girard, H B Kagan *Nouv. J. Chim.* **5** 479 (1981)
18. A N Kamenskaya, N B Mikheev, A I Strekalov *Zh. Neorg. Khim.* **28** 1711 (1983)
19. P I Borin, A I Karelin *Termodinamika Okislitel'no-vosstanovitel'nykh Protsessov v Tekhnologii Aktinoidov* (Thermodynamics of Redox Processes in the Technology of Actinides) (Moscow: Energoatomizdat, 1977) p. 37
20. J Massayex, J F Desreux, C Delchambre, Y Duyckaerts *J. Inorg. Chem.* **19** 1893 (1980)
21. M Khiraoka, in *Crown Compounds* (Amsterdam: Elsevier, 1982) (Translated into Russian; Moscow: Mir, 1984) p. 151
22. A N Kamenskaya, N B Mikheev, K Buketynska, V I Spitsyn, B Gzhebyatovska *Zh. Neorg. Khim.* **24** 1139 (1979)
23. H B Kagan *New J. Chem.* **14** 453 (1990)
24. H B Kagan, J L Namy, P Girard *Tetrahedron, Suppl. 1* 175 (1981)
25. P Place, M L Roumestant, J Gore *Bull. Soc. Chim. Fr.* 169 (1976)
26. J Inanaga, M Ishikawa, M Yamaguchi *Chem. Lett.* 1485 (1987)
27. T Imamoto *Yuki Gosei Kagaku Kyokai Shi* **46** 540 (1988)
28. X Handa, J Inanaga, M Yamaguchi *J. Chem. Soc., Chem. Commun.* 298 (1989)
29. Y Okuda, T Hiyama, H Nozaki *Tetrahedron Lett.* **18** 3829 (1977)
30. B G Zavin, A I Chernyavskii, Ya S Vygodskii, N E Brandukova, in *Proceedings of the Xth International Symposium on Organo-Silicon Chemistry, Poznan, Poland, 1993* p. 293
31. R D Miller, J Michl *Chem. Rev.* **89** 1359 (1989)
32. J Chrusciel, E Fossum, K Matyjaszewski *Polymer Preprints* **34** 221 (1993)
33. T Sakakura, H-J Lautenschlager, M Makajima, M Tanaka *Chem. Lett.* 913 (1991)
34. G H Posner, A W Runquist, M J Chapdelaine *J. Org. Chem.* **42** 1202 (1977)
35. J L Namy, J Souppe, H B Kagan *Tetrahedron Lett.* **24** 765 (1983)

36. T Imamoto, T Kusumoto, J Hatanaka, M Yokoyama *Tetrahedron Lett.* **23** 1353 (1982)
37. A Clerici, O Porta *Tetrahedron Lett.* **23** 3517 (1982)
38. N E Brandukova, Ya S Vygodskii, S V Vinogradova *Vysokomol. Soedin., Ser. A* **36** 10 (1994)
39. A W Cooke, K B Wagener *Synth. Met.* **29** 525 (1989)
40. G A Molander, G Hahn *J. Org. Chem.* **51** 1135 (1986)
41. L Paquette, J S Ward, R A Boggs, W B Farnham *J. Am. Chem. Soc.* **97** 1101 (1975)
42. B M Trost, S A Godleski, J Ippen *J. Org. Chem.* **43** 4559 (1978)
43. E C Ashby, T L Wiesemann *J. Am. Chem. Soc.* **100** 189 (1978)
44. J L Namy, J Collin, J Zhang, H B Kagan *J. Organomet. Chem.* **328** 81 (1987)
45. J Souppe, J L Namy, H B Kagan *Tetrahedron Lett.* **23** 3497 (1982)
46. T Tabuchi, J Inanaga, M Yamaguchi *Tetrahedron Lett.* **27** 1195 (1986)
47. S Fukuzawa, A Nakanishi, T Fujinami, S Sakai *J. Chem. Soc., Chem. Commun.* 624 (1986)
48. Y Masayuki, K Kazuhiro, O Takashi, I Yashiko, M Akiho, K Ikuo, O Shunsaku *Chem. Lett.* 653 (1993)
49. J Inanaga, J Katsuki, O Ujukawa, M Yamaguchi *Tetrahedron Lett.* **32** 4921 (1991)
50. T Imamoto, T Takeyama, M Yokoyama *Tetrahedron Lett.* **25** 3225 (1984)
51. K Otsubo, K Kawamura, J Inanaga, M Yamaguchi *Chem. Lett.* 1487 (1987)
52. G A Molander, B E LaBelle, G Hahn *J. Org. Chem.* **51** 5259 (1986)
53. Ya Kamochi, T Kudo *Tetrahedron Lett.* **32** 3511 (1991)
54. S Takeuchi, I Ohgo *Chem. Lett.* 403 (1988)
55. P Girard, R Couffignal, H B Kagan *Tetrahedron Lett.* **22** 3959 (1981)
56. V V Korshak, S V Vinogradova, Ya S Vygodskii, N A Churochkina, N E Brandukova *Vysokomol. Soedin., Ser. A* **29** 1480 (1987)
57. J Souppe, J L Namy, H B Kagan *Tetrahedron Lett.* **25** 2869 (1984)
58. E S Krongauz *Usp. Khim.* **46** 112 (1977) [*Russ. Chem. Rev.* **46** 69 (1977)]
59. M Masahiro, K Teiji, I Hajime, I Yoshihiko *J. Org. Chem.* **58** 1458 (1993)
60. C Nallaiah *J. Polym. Sci.* **22** 3107 (1984)
61. C Nallaiah *J. Polym. Mat. Int. J.* **3** 11 (1986)
62. S N Kaul, J E Fernandez *Macromolecules* **20** 2320 (1987)
63. N E Brandukova, Ya S Vygodskii, S V Vinogradova, H Raubach *Acta Polym.* **42** 82 (1991)
64. T Shono, H Ohmizu, S Kawakami, H Sugiyama *Tetrahedron Lett.* **21** 5029 (1980)
65. S Fukuzawa, S Sakai *J. Chem. Soc. Jpn., Chem. Ind. Chem.* 513 (1993)
66. G A Molander, J B Etter *Tetrahedron Lett.* **25** 3281 (1984)
67. G A Molander, J B Etter, P W Zinke *J. Am. Chem. Soc.* **109** 453 (1987)
68. G A Molander, J B Etter *J. Org. Chem.* **51** 1778 (1986)
69. G A Molander, J B Etter *J. Am. Chem. Soc.* **109** 6556 (1987)
70. M E Jang *Tetrahedron* **32** 3 (1976)
71. H O House, J J Riehl, C G Pitt *J. Org. Chem.* **30** 650 (1965)
72. J K Crandall, H S Magaha *J. Org. Chem.* **47** 5368 (1982)
73. R D Rieke, P T-J Li, T P Burns, S T Uhm *J. Org. Chem.* **46** 4324 (1981)
74. T Tabuchi, K Kawamura, J Inanaga, M Yamaguchi *Tetrahedron Lett.* **27** 3889 (1986)
75. J Souppe, L Danon, J L Namy, H B Kagan *J. Organomet. Chem.* **250** 227 (1983)
76. Y Zhang, R Lin *Synth. Commun.* **17** 329 (1987)
77. N R Natale *Tetrahedron Lett.* **23** 5009 (1982)
78. J Prandi, J L Namy, G Menoret, H B Kagan *J. Organomet. Chem.* **285** 449 (1985)
79. G A Molander, G Hahn *J. Org. Chem.* **51** 2596 (1986)
80. T Mukaiyama *Org. React.* **28** 203 (1982)
81. L F Fieser *J. Am. Chem. Soc.* **25** 4395 (1953)
82. E L Shapiro, M J Gentles *J. Org. Chem.* **46** 5017 (1981)
83. R Scheffold, E Amble *Angew. Chem., Int. Ed. Engl.* **19** 629 (1980)
84. T P Ananthanarayan, T Gallagher, P Magnus *J. Chem. Soc., Chem. Commun.* 709 (1982)
85. T Imamoto, T Takeyama, H Koto *Tetrahedron Lett.* **27** 3243 (1986)
86. J P Dittami, H Ramanathan *Tetrahedron Lett.* **29** 45 (1988)
87. G A Molander, J A McKie *J. Org. Chem.* **57** 3132 (1992)

Russian Chemical Reviews **63** (4) 357–365 (1994)
©1994 Russian Academy of Sciences and Turpion Ltd

UDC 541.64

Effect of additions of metals and their derivatives upon the thermal degradation of polymers

L V Ruban, G E Zaikov

Contents

I. Introduction 357
II. Effect of metals on the thermal degradation of polymers 357
III. Thermal degradation of polymers in the presence of metal halides 358
IV. Effect of metal acetylacetonates on the thermal degradation of polymers 362

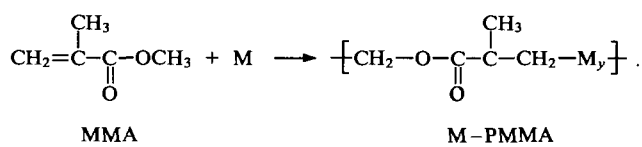
Abstract. The effect of additions of metals and of their halides and acetylacetonates on the thermal degradation of polymers [mainly, poly(methyl methacrylate)] has been studied by various physicochemical methods (thermogravimetry, NMR, IR, and UV spectroscopy, X-ray structural analysis, DSC, etc.). The results are analysed in terms of the use of these additives in polymers as ecologically clean retardants. The bibliography includes 40 references.

I. Introduction

The study of the pyrolysis of polymers with formation of gaseous combustible thermal degradation products is important from the point of view of the protection of polymer materials from contact with flames. Nonmetallic compounds containing chlorine, bromine, phosphorus, boron, and sulphur have previously been used[1,2] as additives in order to protect the polymers from combustion. The study of the effect of metals and their compounds on the thermal degradation of polymers was stimulated by the current search for retardants in which the currently used toxic additives[3,4] are replaced by other materials.

II. Effect of metals on the thermal degradation of polymers

Cardenas and Retamal[5] studied the effects of the metals Au, Cu, Ga, In, Ge, Sn, Sb, and Bi (when dispersed in methyl methacrylate MMA) on the polymers (PMMA) produced by the polymerisation of MMA in the presence of azo-isobutyronitrile. The following reaction was proposed[5–8] for the synthesis of polymers containing a metal previously dispersed in the monomer:



MMA M–PMMA

L V Ruban, G E Zaikov Chemical Stability of Polymers Laboratory, Semenov Institute of Chemical Physics of the Russian Academy of Sciences, ul. Kosygina 4, 117977 Moscow, Fax (7-095) 938 21 56

Received 2 March 1994
Uspekhi Khimii **63** (4) 373–382 (1994); translated by J I Carasso

The polymer samples contained only 2% of the metal; the molecular mass of the polymers was $(2.7-5) \times 10^5$ (see Ref. 8).

The thermogravimetric curves obtained in the study of the polymer samples are shown in Fig. 1. The temperatures of the onset of decomposition (T_d) of these polymers are given in Table 1. The highest T_d values are found for Au–PMMA and Bi–PMMA.

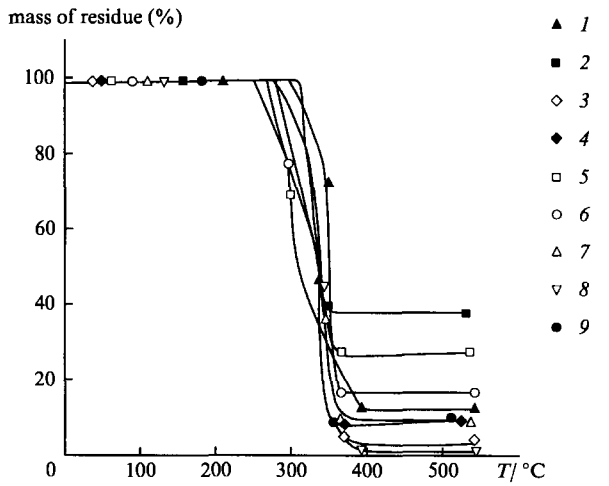


Figure 1. Thermogravimetric curves for the dissociation of M–PMMA compositions containing Bi (*1*), Sn (*2*), Au (*3*), Pd (*4*), Cu (*5*), Ge (*6*), Ga (*7*), In (*8*), and Sb (*9*) at a heating rate of 10 °C min^{-1}.

Table 1. Kinetic parameters for metal polymethacrylates.

Polymer	Z/s^{-1}	E_a/kJ mol^{-1}	T_d/°C
Au–PMMA	2.6×10^4	99.3	300
Bi–PÛÛÀ	2.3×10^2	78.9	325
In–PÛÛÀ	1.4×10^2	74.2	275
Cu–PÛÛÀ	2.4×10^2	70.6	240
Ge–PÛÛÀ	4.8×10^1	64.1	225
Sb–PÛÛÀ	2.5×10^1	63.9	275
Pd–PÛÛÀ	1.5×10^1	61.5	250
Sn–PÛÛÀ	1.4×10^1	61.0	250
Ga–PÛÛÀ	4.3	51.5	200

By analysis of the kinetic data on the loss of mass of the samples in an inert medium it was found that the metal polymers dissociate by a zero-order reaction whose activation energies (E_a) and pre-exponential factors (Z) are given in Table 1. It follows from these results that the activation energy depends on the nature of the metal. In particular, Au–PMMA is a very stable system, just as gold is stable towards oxidation. On the other hand gallium is an easily oxidised metal, and in the Ga–PMMA system we observe the lowest values of the activation energy and of the incipient decomposition temperature.

Systems containing rhodium and cobalt were studied in detail by Wilkie and coworkers,[9–12] who reported a continuing study of the effect of metals on the thermal degradation of polymers aimed at the possibility of using these compounds as retardants of the combustion of polymers.

The aim of this review is to discuss some other recently reported studies of the mechanism of the effect of metal compounds on the thermal degradation of polymers in the case of the halides of chromium and magnesium.

III. Thermal degradation of polymers in the presence of metal halides

Beer et al.[12] studied the effects of Cr(III) in anhydrous salts and crystal hydrates on the oxidation of PMMA. The prepared compositions of these materials were placed in glass tubes which were evacuated and sealed. The tubes were then heated for 2 h at predetermined temperatures. The IR spectra of the uncondensed reaction products detected 6% of methane and carbon monoxide from the starting material. The condensed gases amounted to 44% of the sample (mainly the monomer, CO_2, HCl, and water). The fraction soluble in chloroform was 13%. The IR spectra of this fraction showed the presence of carbonyl and carboxyl products.

In the pyrolysis of pure PMMA the products contain many oligomers, but if the reaction is carried out in the presence of $CrCl_3$ no oligomers are detected.

The fraction insoluble in chloroform contained 36% of the initial sample. The IR spectrum in this case suggests the presence of anhydrides with absorption bands at 1800, 1760, and 1150 cm^{-1}. An X-ray analysis of the solid residue showed the presence of CrOCl and CrO_3.

The chromium crystal hydrate $CrCl_3 \cdot 6H_2O$ is a mixture of the three isomers $[Cr(H_2O)_6]Cl_3$, $[Cr(H_2O)_5Cl]Cl_2 \cdot H_2O$ and $[Cr(H_2O)_4Cl_2]Cl \cdot 2H_2O$, which behave in different ways during thermolysis.[13] At temperatures below 100 °C the first and the third isomer evolve only water, whereas the second isomer evolves only HCl. Since the sample of chromium chloride used in this work evolved both HCl and H_2O at temperatures below 100 °C it must have been a mixture of hydrated isomers. Between 200 and 300 °C all these isomers form chromium hydroxide chloride $Cr(OH)Cl_2$. At higher temperatures chromium oxide chloride CrOCl is formed. At these high temperatures the anhydrous chromium chloride $CrCl_3$ can lose a chlorine atom and give the chloride $CrCl_2$ (see Gmelin's Handbook[14]). It follows that the system contains several chemical compounds of chromium, and it is difficult to establish which of these actively influences the degradation of the polymer.

The results of a thermogravimetric analysis[12] of a mixture of PMMA and $CrCl_3 \cdot 6H_2O$ (taken in a mass ratio of 1 : 1) are shown in Fig. 2. As can be seen, the decomposition of the polymer becomes marked at ~250 °C, above which the rate of the reaction increases rapidly, though 22% of the sample is lost below it. The reaction products include water, HCl, and the monomer. Water and HCl are formed by the thermolysis of aqueous $CrCl_3$: anhydrous $CrCl_3$ produces only HCl, and the monomer is formed by the depolymerisation of the PMMA.

Most of the mass (62%) is lost between 250 and 500 °C. In this case the volatile products include the monomer, carbon oxides, an unidentified organic acid, and traces of methane. The monomer is

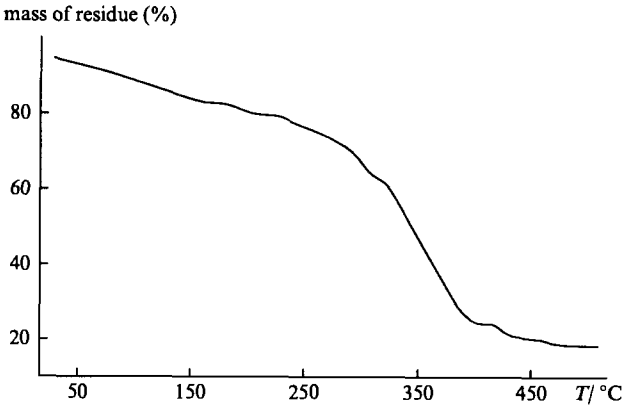


Figure 2. Thermogravimetric curve for a 1 : 1 mixture of aqueous $CrCl_3$: PMMA at a heating rate of 20 °C min^{-1}.

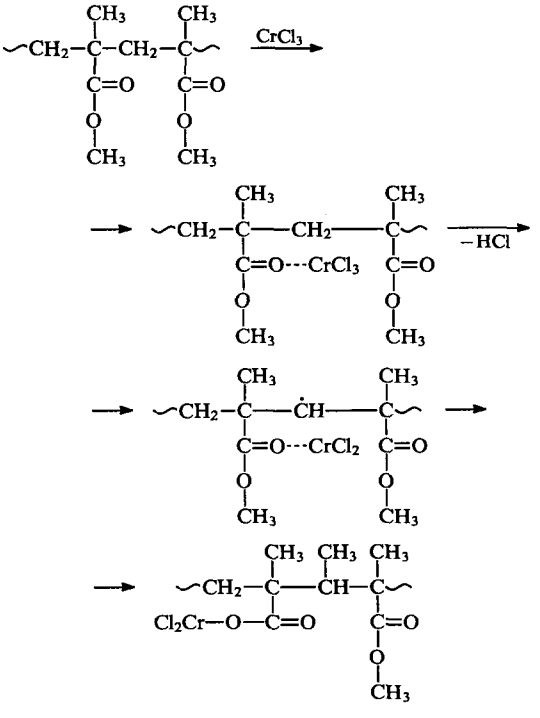
the main product of the decomposition at 430 °C. Above this temperature the relative amount of monomer decreases, and the amount of carbon oxides and of the organic acid increases.

In the decomposition of mixtures containing aqueous chromium salts evolution of HCl takes place at 150 °C as a result of the decomposition of aqueous $CrCl_3$, and again at temperatures above 450 °C. In compositions containing anhydrous chromium chloride HCl begins to be evolved at 430 °C and continues to be formed up to 500 °C.

The solid residue beyond 500 °C contains 16% of the initial mass of the sample. However, if the whole of the water had been evolved from the hydrated $CrCl_3$ and the whole of the PMMA had depolymerised the fraction of $CrCl_3$ in the solid residue would have been 30% of the initial mass of the sample, and if $CrCl_2$ and CrOCl had been formed the solid residue would have been 23% and 20% respectively. The finding that, in reality, the solid residue amounts to 16% shows that none of these compounds can be (in the pure form) the final product of the reaction.

These results have been explained[12] in terms of Scheme 1. Most probably the $CrCl_3$ is coordinated at the carbonyl group of PMMA. This postulate has been confirmed independently.[15–17]

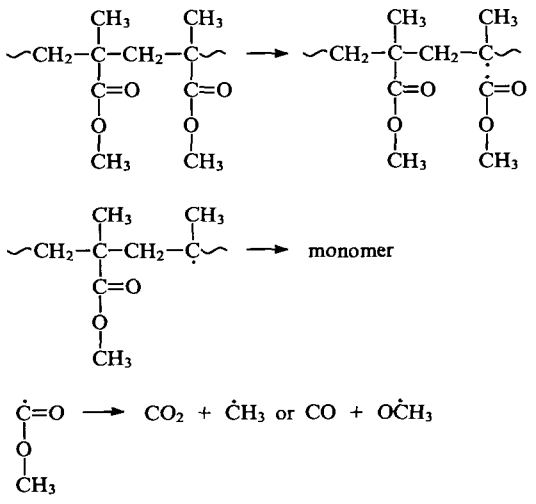
Scheme 1



We know that $CrCl_3$, when heated, splits off a chlorine atom [14] which then removes a hydrogen from the main chain of the PMMA, forming a polymeric radical. This scheme is confirmed by the presence of HCl among the reaction products.

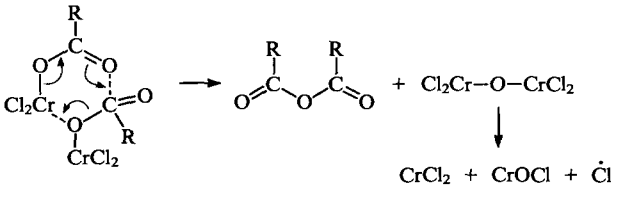
Manring and coworkers [18–21] have attributed the presence of CO, CO_2, and CH_4 among the decomposition products of PMMA to the removal of carbomethoxy groups from the main chain of the polymer, accompanied by the formation of an unstable carbomethoxy radical which then decomposes, giving CO and $CH_3\dot{O}$ or CO_2 and $\dot{C}H_3$ (Scheme 2).

Scheme 2



Scheme 2 is confirmed by the detection by NMR of unsaturated oligomers among the reaction products. All the gaseous products are also formed by Scheme 2. The presence among the solid products of chromium anhydride and chromium oxides is ascribed to processes described by Scheme 3. The atomic chlorine removes a hydrogen atom from the PMMA chain, generating polymeric radicals which can decompose or become cross-linked.

Scheme 3



Thus in the pyrolysis of compositions consisting of chromium chloride and PMMA the most important reactions are: (1) the coordination of the chromium chloride at the carbonyl group of PMMA with subsequent elimination of a chlorine atom; (2) the removal by the chlorine atom of a hydrogen atom from the PMMA; (3) the corresponding migration of the methyl ether to the main chain of the PMMA, leading to the formation of a chromium carboxylate salt; (4) the dissociation of this salt to the anhydrides; (5) the stabilisation of the polymer by the chromium carboxylate or through the cross-linking of the polymeric radicals formed in the preceding stage. The interaction of the chromium chloride with the PMMA does not affect the formation of the monomer, and therefore it seems unlikely that $CrCl_3$ may act as an inflammation retarder.

Wilkie et al. [22] studied the thermal degradation of PMMA–$MnCl_2$ (anhydrous) mixtures by standard methods. The more volatile reaction products contained carbon monoxide and traces of methane. The condensable gas consisted of carbon dioxide, the monomer, and traces of methyl chloride and methanol. The IR spectrum of the fraction soluble in chloroform [23] showed the presence of ether and an anhydride. The insoluble products were washed free from $MnCl_2$ with methanol, which left a fraction consisting of MnO_2 and an organic salt. It should be noted that the proportion of the monomer in the thermal degradation products of PMMA in the presence of anhydrous $MnCl_2$ decreases as compared with pure PMMA, and depends on the method of preparation of the system. [24] Thus, in samples prepared by simple mixing of PMMA and $MnCl_2$ the yield of monomer after vacuum heat treatment (400 °C, 2 h) was 30%–35%, whereas pure PMMA under the same conditions produced 50%–70% of the monomer. With compositions prepared from solutions of $MnCl_2$ and PMMA in an acetone–methanol mixture, followed by removal of the solvents, thermal decomposition does not usually produce any monomer.

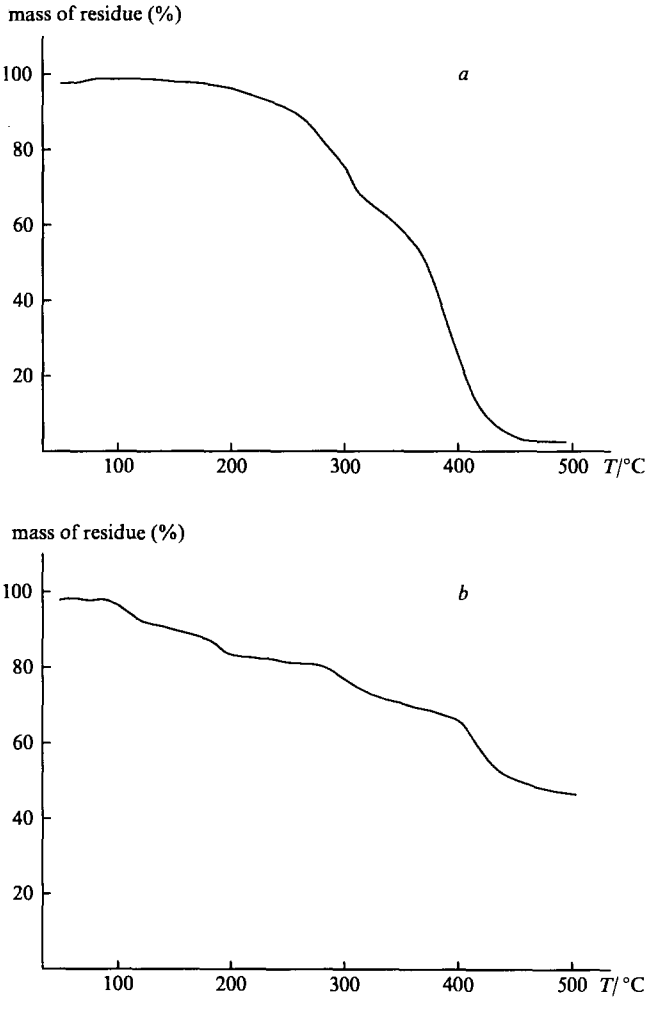


Figure 3. Thermogravimetric curves: (*a*) PMMA, (*b*) PMMA : $MnCl_2$ (1 : 1); heating rate 20 °C min^{-1}.

The molecular mass of the fraction dissolved in chloroform was 10% of that of the initial polymer. [25] It follows that the greater part of the polymer decomposes to the monomer, and the latter repolymerises with formation of a low-molecular oligomer; this reoligomerisation is probably catalysed by $MnCl_2$. By using thermogravimetric analysis methods it was confirmed that the monomer is formed and then slowly consumed. The TGA curves of $MnCl_2$–PMMA mixtures prepared from solutions are shown in Fig. 3. It can be seen from Fig. 3*b* that the breakdown of this composition is characterised by five temperature regions.

Between 100 and 145 °C 7.5% of the composition is gasified. The Fourier transform IR spectra of the gaseous products show that this loss is mainly water introduced into the system with the salt and easily removed. A further 9.5% of the composition is gasified between 145 and 215 °C: the IR spectra show that in this regime the monomer is evolved. In the case of pure PMMA the evolution of the monomer begins at higher temperatures.

The third plateau of the weight-loss curve is found at 215 to 345 °C. It is characterised by the evolution of the monomer and by the formation of methyl chloride and methanol. The formation of methyl chloride is evidence of the interaction between $MnCl_2$ and PMMA, involving the ester group of the latter.

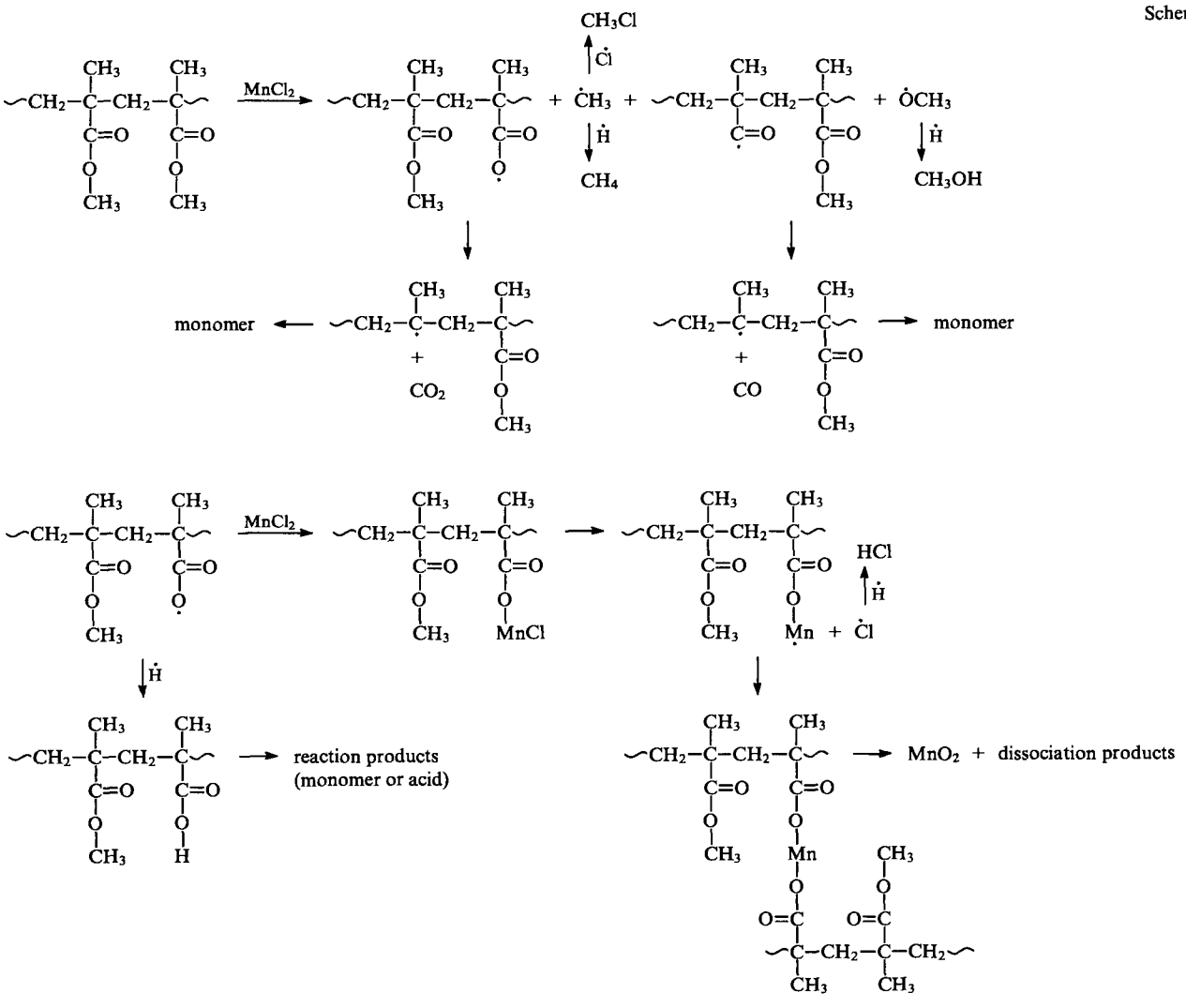
A further 19% of the composition is dissociated between 345 and 455 °C. CO_2, CO, CH_4, HCl, and an aliphatic acid were identified among the gaseous products.

A further 5% of the composition is decomposed in the region of 455–600 °C with formation of HCl.

The overall result is that up to 600 °C 51.5% of the composition is gasified, leaving a 48.5% residue of involatile products. Since the ratio of PMMA to $MnCl_2$ in the initial composition is 1 : 1 it might be thought that the whole of the PMMA is gasified and the residue consists of $MnCl_2$. However, an analysis of the thermal degradation products does not confirm this assumption: firstly, because the IR spectrum of the solid residue shows the presence of organic substances (hydrocarbon and carbonyl groups), and secondly because the solid residue is found to contain a new, insoluble organomanganese compound in addition to $MnCl_2$.

Wilkie et al.[22] proposed the following scheme to account for the degradation of the PMMA–$MnCl_2$ compositions (Scheme 4). The manganese chloride initiates the breaking of the carbonyl bonds in PMMA, giving methoxy and methyl radicals. These radicals can abstract a proton, giving methanol and methane respectively. The methyl radical can also recombine with a chlorine radical, forming methyl chloride. The carbonyl radical can be further converted into carbon monoxide and a tertiary radical, and the carboxyl radical can produce carbon dioxide and the same tertiary radical. These tertiary radicals initiate the decomposition of PMMA with preferential formation of the monomer and other low-molecular products. Since the decomposition products contain more CO_2 than CO it follows that the methyl radicals are consumed faster than the methoxy radicals. The carboxyl radical can react in various directions. Firstly it can interact with $MnCl_2$, giving MnCl and Cl˙. The latter can recombine with any other radical, giving different products. Methyl chloride mentioned above is one of these products; the manganese chloride salt of PMMA can split off a chlorine radical and form a manganese radical attached to the PMMA chain. The recombination of this radical with the carboxyl radical gives the manganese monomer of PMMA. This monomer can dissociate thermally, giving MnO_2 and other products. This reaction also produces an aliphatic acid, which can also be formed during the abstraction of hydrogen by a carboxylic radical, followed by depolymerisation, to give monomeric methacrylic acid and other dissociation products.

Scheme 4



The limiting oxygen index (OI) for the PMMA – $MnCl_2$ system shows that manganese chloride has some flame-retardant properties.[26] Thus, as compared with pure PMMA, whose OI is 14, the OI of a PMMA – $MnCl_2$ composition (1 : 1 ratio) increases to 25. This increase in the OI is convincing evidence of the effectiveness of $MnCl_2$ as an additive.

These results differ from those reported by McNeill and McGuiness[15,16] for the $ZnBr_2$ – PMMA system. The gaseous products are the same for the two systems, but different reaction paths were proposed in the two cases. Whereas in the presence of $ZnBr_2$, methyl bromide appears at 160 °C, in the $MnCl_2$ system methyl chloride is formed at temperatures above 220 °C; furthermore, in the $MnCl_2$ system the monomer appears at temperatures well below those observed in pure PMMA. In both cases the reaction product is the metal salt of methacrylic acid.

When the common features of these two reactions are examined it seems very likely that all the main processes are the same in the two cases. Wilkie et al.[22] conclude that $MnCl_2$ plays a dual role in the system. On the one hand it accelerates the initial depolymerisation of PMMA, and thus assists its combustion, but on the other hand it also markedly increases the amount of incombustible reaction products.

Kochneva et al.[27] studied the effect of $ZnCl_2$ on the thermal stability of polymethacrylates and polyacrylates. These polymers were found to decompose by different mechanisms. The polymethacrylates are almost completely depolymerised, whereas the polyacrylates are degraded by breakdown of the ester groups.

The loss of mass of PMMA and polymethacrylate (PMA) after 2 h at 300 °C in a vacuum is shown in Fig. 4 as a function of the concentration of $ZnCl_2$. Increasing the concentration of $ZnCl_2$ lowers the degree of decomposition for PMMA (curve *1*) and increases it for PMA (curve *2*). The decomposition products of these polymers in the presence of $ZnCl_2$ are listed in Tables 2 – 5.[27]

In the decomposition of PMMA in the presence of $ZnCl_2$ the yield of monomer decreases, which suggests a depolymerisation process, whereas the yields of alcohol, of chain breakdown products, and of CO_2 increase (Table 2). Similar effects have been observed in poly(n-butyl methacrylate) (PBMA) (Table 3).

In the thermal degradation of PMA (Table 4) the yields of alcohol and CO_2 rapidly increase after even small additions of $ZnCl_2$. A similar effect is found in poly(n-butyl acrylate) (PBA) (Table 5).

Alkyl chlorides were determined qualitatively in the thermal degradation products of the polymethacrylic and the polyacrylic ester in the presence of $ZnCl_2$. On the basis of these results Kochneva et al.[27] suggested that CH_3Cl is formed mainly by the reaction of $ZnCl_2$ with the carbonyl group of the ester.

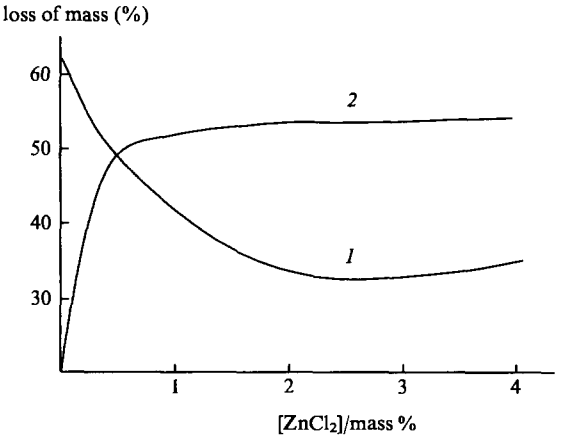


Figure 4. Mass loss curves for PMMA and PMA as a function of concentration of $ZnCl_2$. (*1*) PMMA, (*2*) PMA.

Table 2. Main products of the thermal degradation of PMMA in the presence of $ZnCl_2$ (mass % of the initial mass of polymer).

Products and degree of thermal degradation	[$ZnCl_2$] / mass %				
	0	0.05	0.5	2	10
Degree of degradation	60.7	55.6	44.8	30.0	25.0
Solid residue	39.3	44.4	55.2	70.0	75.0
MMA	60.2	54.0	43.0	25.3	11.5
CH_3OH	0.40	0.34	0.40	0.90	2.60
H_2O	0	0	0	0	3.10
CH_3Cl	0	0.03	0.28	1.29	2.64
CO_2	0	0.12	0.15	0.25	0.20
Other products (CO, CH_4, C_3H_6)	0	0.020	0.03	0.11	1.14

Table 3. Main products of the thermal degradation of PBMA in the presence of $ZnCl_2$ (mass % of the initial mass of polymer).

Products and degree of thermal degradation	[$ZnCl_2$] / mass %		
	0	0.5	2
Degree of degradation	56.5	58.0	33.0
Solid residue	43.5	42.0	67.0
BMA	49.0	43.5	23.0
n-C_4H_9OH	4.0	7.5	6.4
H_2O	0.25	0.39	0.60
CO_2	0.17	0.24	0.20
C_4H_9Cl	0	0.14	0.35
C_4H_8	1.0	0.9	0.6
Other products (H_2, CH_4, C_3H_6, CO)	0.1	0.9	0.6

Table 4. Main products of the thermal degradation of PMA in the presence of $ZnCl_2$ (mass % of initial mass of polymer).

Products and degree of thermal degradation	[$ZnCl_2$] / mass %				
	0	0.05	0.5	2	10
Degree of degradation	15.6	32.0	47.0	43.5	49.0
Solid residue	84.4	68.0	53.0	56.5	51.0
CH_3OH	2.6	13.6	20.4	16.6	17.6
MMA	Trace	0.2	0.3	0.3	0.4
H_2O	0.1	0.2	0.3	0.35	1.0
CO_2	0.3	1.1	5.0	7.0	7.7
CH_3Cl	0	0.04	0.3	1.1	5.1
Other products (H_2, CH_4, CO)	0	Trace	0.3	0.4	1.1

Table 5. Main products of the thermal degradation of PBA in the presence of $ZnCl_2$ (mass % of the initial mass of polymer).

Products and degree of thermal degradation	[$ZnCl_2$] / mass %			
	0	0.05	0.5	2
Degree of degradation	21.8	14.3	20.6	20.2
Solid residue	78.2	85.7	79.4	79.8
n-C_4H_9OH	9.0	10.0	16.0	15.5
H_2O 0.4	0.2	0.3	0.5	
BMA	Trace	Trace	Trace	Trace
CO_2	0.8	0.8	0.8	1.2
C_4H_8	1.4	1.3	1.0	1.5
C_4H_9Cl	0	Trace	0.1	0.3
Other products (H_2, CH_4, CO)	0.1	0.1	0.1	0.2

Table 6. Formation of alkyl chlorides (mass %) as a function of the concentration of $ZnCl_2$ during the thermal degradation of polymethacrylates and polyacrylates (300 °C, vacuum, 2 h).

$[ZnCl_2]$/ mass %	CH_3Cl		C_4H_9Cl	
	PMMA	PMA	PBMA	PBA
0.05	0.03	0.04	0.03	0.03
0.5	0.3	0.4	0.1	0.1
2	1.3	1.2	0.4	0.3
10	2.6	5.1	–	–

Table 6 shows the effect of the concentration of $ZnCl_2$ on the yield of alkyl chlorides during the thermal breakdown of polymethacrylates and polyacrylates after 2 h at 300 °C *in vacuo*.

It follows from the data in Table 6 that the rate of formation of alkyl chlorides decreases with increasing length of the hydrocarbon radical in the ester group. Zinc chloride has similar effects on the formation of the insoluble fraction in the thermal degradation of PMMA and PMA, and therefore the authors suggest that reticular cross-linking of the polymer takes place mainly through the interaction of the ester groups with $ZnCl_2$. The contribution of this reaction is not large, but it is neverthe-less significant in compositions including large quantities of zinc chloride.

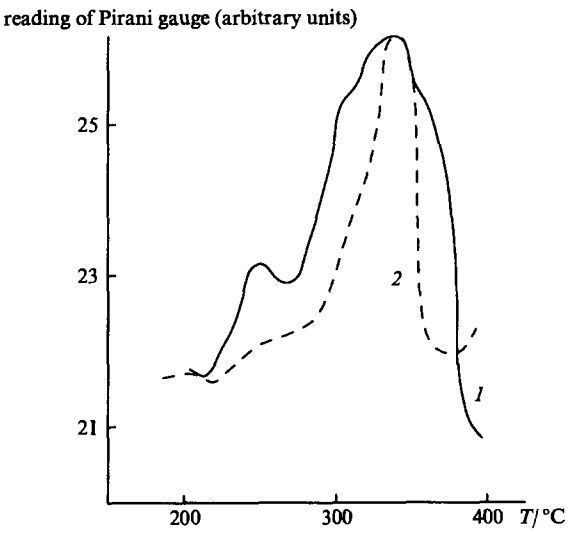
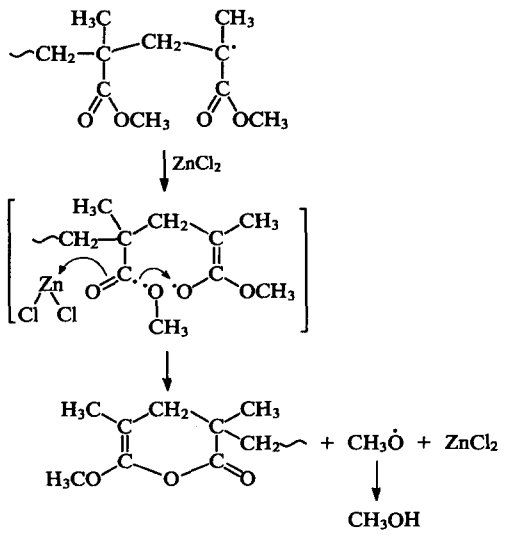


Figure 5. Thermovolumetric curves: (*1*) PMMA; (*2*) PMMA + 2 mass % $ZnCl_2$.

Scheme 5



A thermovolumetric analysis [28] of the thermal degradation of PMMA showed that $ZnCl_2$ when present in the system suppresses the formation of the monomer by removing the unsaturated end groups (note the disappearance of the characteristic monomer peak at 250 °C in Fig. 5).

The formation of a complex between $ZnCl_2$ and the end groups of the macroradicals leads to the evolution of alcohol and inhibits the depolymerisation. This process is described [27] by Scheme 5.

The IR spectrum of samples of PMMA dissociating in the presence of $ZnCl_2$ includes an absorption band at 1760 cm^{-1} corresponding to γ,δ-unsaturated lactones.

IV. Effect of metal acetylacetonates on the thermal degradation of polymers

Metal acetylacetonates are of interest because they are used as polymerisation indicators, accelerators, and antioxidants for polyolefins. As a result it has been suggested [29–33] that these compounds could act as flame retardants and suppress the formation of smoke in various polymers.

McNeill and Liggat [34] studied the effect of cobalt(III) acetylacetonate on the thermal degradation of PMMA, and concluded that this effect is responsible for the formation of an acetylacetonato complex of cobalt with the ester groups of PMMA.

Very different compositions were studied: from 1 part of $Co(acac)_3$ per 400 monomer units to 1 part per 10 monomer units.

The thermal degradation was studied by the thermovolumetric analysis method, [35,36] which allows four fractions of products to be studied: (1) uncondensable gases, (2) condensable gases and volatile liquids, (3) solid fractions (resins, waxes, etc.), (4) the residue at any stage in the decomposition.

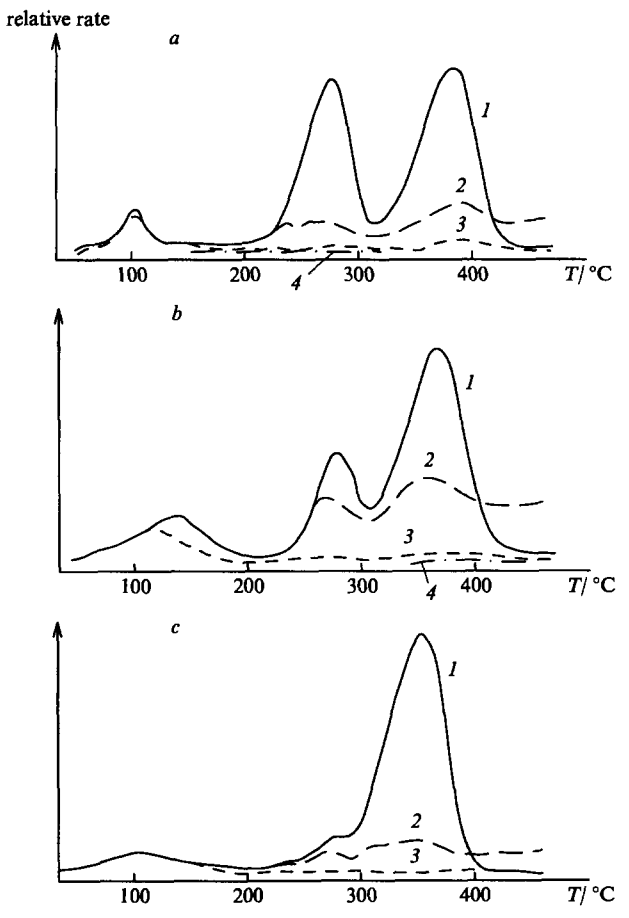
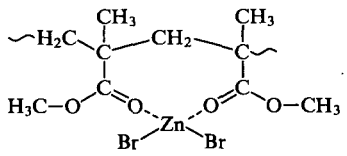


Figure 6. Thermovolumetric curves (vacuum, 10 °C min^{-1}). $\bar{M}_n$ = 2 × 10^4 (*a*), 1.5 × 10^5 (*b*), 10^6 (*c*); *T*/°C = 0 (*1*), 75 (*2*), 100 (*3*), 196 (*4*).

Fig. 6 shows the thermovolumetric curves for PMMA samples of different molecular mass: we observe two peaks, corresponding to two stages in the decomposition (initiation at the end groups and random initiation respectively).

The rate of degradation of PMMA is strongly influenced by the presence of complexing agents such as metal halides or acetylacetonates. For example, in the presence of $ZnBr_2$ the main decomposition products are methyl bromide and methanol, and the yield of monomer is negligibly small.[37,38] This is due to the formation of a complex having the following structure:



It could be expected that stable metal acetates will interact with the ester groups of PMMA, and that this process will be reflected in the stability and dissociation mechanism of the polymer.

The thermal degradation of $Co(acac)_3$ at 210 °C takes place by the scheme

$$Co(acac)_3 \longrightarrow Co(acac)_2 + acac^{\cdot};$$

$$acac^{\cdot} \xrightarrow{H^+} Hacac.$$

The UV spectra of PMMA films with additions of $Co(acac)_3$ show that in this case the $Co(acac)_3$ does not contribute to complex formation with the PMMA at the ester groups, whereas the UV spectra of PMMA films with additions of $Co(acac)_2$ indicate the formation of these complexes.

It follows that during the degradation of the composition $Co(acac)_3$–PMMA the $Co(acac)_3$ first changes into $Co(acac)_2$, which then forms a complex with the PMMA.

The four stages in the breakdown of the composition $Co(acac)_3$–PMMA are shown diagrammatically in Fig. 7.[34]

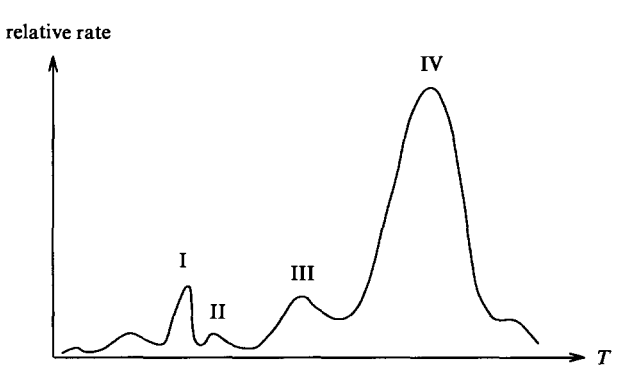


Figure 7. Schematic diagram of the decomposition of a $Co(acac)_3$–PMMA mixture, based on an analysis of the thermovolumetric curves.

Stage I: $T_{max} \approx 135$ °C. The height of the peak is inversely proportional to the molecular mass of the polymer, and is independent of the concentration of $Co(acac)_3$. The main decomposition product in this stage is the monomer. It is assumed that depolymerisation initiated at the ends of the molecule takes place in stage I, so that the $Co(acac)_3$ forms a complex with the unsaturated end groups (on average, one unsaturated end group per 400 monomer units in a sample of low molecular mass).

Stage II: $T_{max} \approx 190$ °C. The height of the peak is proportional to the molecular mass of the polymer and to the concentration of $Co(acac)_3$. The only exceptions to this rule are samples with a high molecular mass of the polymer and a high concentration of $Co(acac)_3$. The main decomposition product in this stage (as in the previous stage) is the monomer. In addition, gaseous acetylacetone and methanol are formed towards the end of stage II (above 200 °C). At high concentrations of $Co(acac)_3$ traces of an uncondensable gas are formed. The authors note that in this stage the chain length for the reaction is greater.

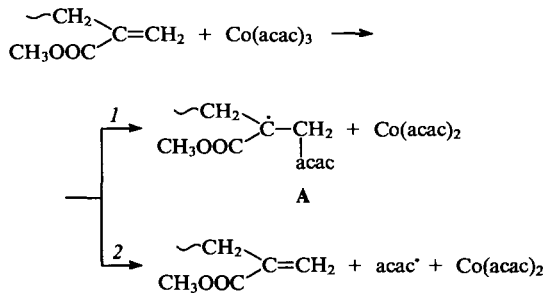
Stage III: $T_{max} \approx 270$ °C. The height of the peak decreases in all the compositions with respect to the peak height for pure PMMA, irrespective of the concentration of $Co(acac)_3$. As a rule the monomer is formed in this stage. The main process is depolymerisation, initiated at the end groups. Unsaturated end groups are nevertheless present, or can be formed in stage I. The chain length of the reaction decreases.

Stage IV: $T_{max} = 360-380$ °C. This peak is characterised by the formation of uncondensable gases. The authors attribute this to a decrease in the length of the reaction chain and to the development of new reactions accompanying the depolymerisation reaction. In addition to the monomer the following gaseous products are formed towards the end of this stage: acetylacetone, methanol, carbon oxides, keten, methyl acetate, acyclic anhydride, isobutene (traces), and dimethyl ether (traces).

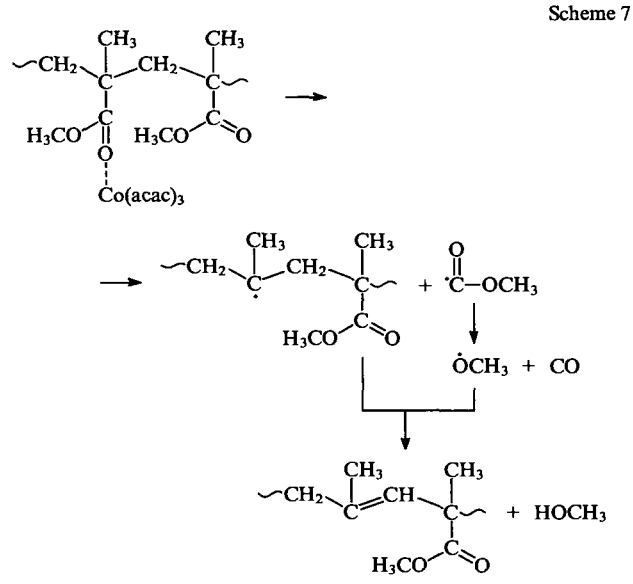
The IR and UV spectra of films of PMMA compositions containing $Co(acac)_3$, heat treated at temperatures up to 500 °C, have also been studied. The results were used to produce the following interpretation of the dissociation mechanism of these compositions.

1. At low temperatures (100 °C) the monomer is thought to be formed by the dissociation of the complex between $Co(acac)_3$ and the unsaturated end groups in the polymer (Scheme 6).

Scheme 6



Scheme 7



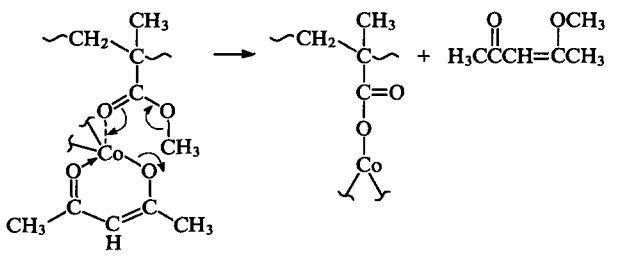
In the depolymerisation of the radical A by path *1* not all the unsaturated end groups can be removed when the part of the chain being broken down in the polymer molecule is shorter than the same molecule (a short length of the part being broken down probably corresponds to temperatures close to the glass transition temperature of the polymer).

During depolymerisation by path *2* the unsaturated end groups are not used, and the depolymerisation is initiated by attack on the chain by the acac radical.

2. The thermal degradation of $Co(acac)_3$ produces $Co(acac)_2$ and acac radicals. Complex formation of $Co(acac)_2$ with the ester groups accelerates the reactions of these groups and the formation of CH_3OH, CO, and double bonds in the main chain of the polymer (Scheme 7).

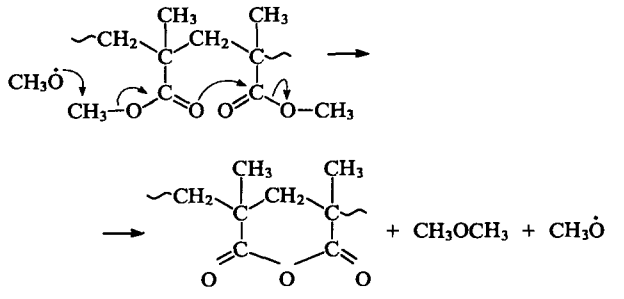
The complex can also decompose to a cobalt carboxylate structure (Scheme 8).

Scheme 8



3. The CH_3O radicals can also attack some ester groups, forming anhydride rings (Scheme 9).

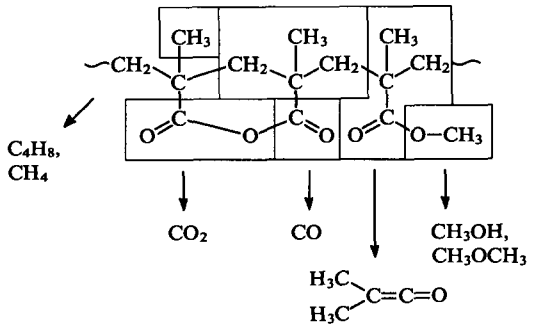
Scheme 9



4. The presence of these rings in the chain decreases the chain length and stabilises the polymer in the high-temperature region.

5. The fragmentation of the modified polymer structures gives mainly monomers, and small quantities of other products characteristic of these structures (Scheme 10).

Scheme 10



McNeill and Liggat[39] carried out a similar study for the PMMA–$Mn(acac)_3$ system, using the procedure of Wilkie et al.[22] The DSC curve for $Mn(acac)_3$ (Fig. 8) shows a characteristic combination of endothermic and exothermic peaks at 170, 175, and 257, 260 °C. The peaks at 170 and 175 °C are assigned to the homolytic breaking of the single bond between the ligand and Mn in $Mn(acac)_3$, with formation of acetylacetone and the bischelate,[40] whereas the peaks at 257 and 260 °C (and at higher temperatures) correspond to the breakdown of the bischelate.

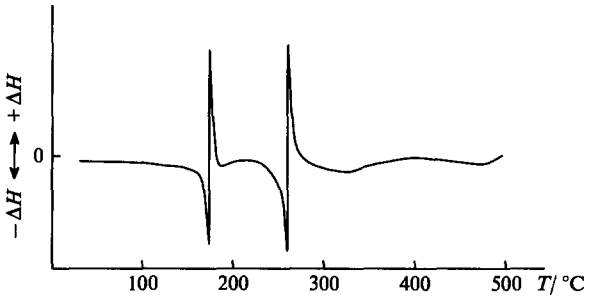


Figure 8. DSC curve for $Mn(acac)_3$ (nitrogen, 10 K min^{-1}).

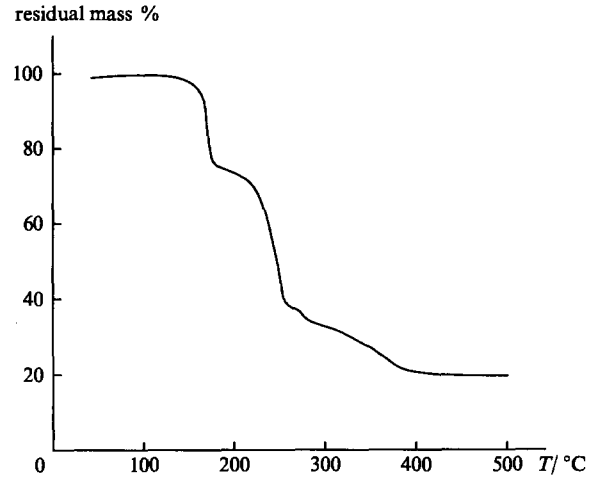
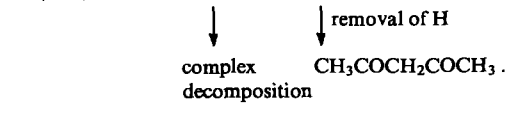


Figure 9. Thermogravimetric curve for $Mn(acac)_3$ (rate of decomposition 10 K min^{-1}).

The data from the thermogravimetric curve (Fig. 9) are fully consistent with the above conclusions, since the initial weight loss (24%) corresponds to the removal of one acac group. The next loss of mass has a more complex explanation: it is assumed that radicals can be formed in this stage, and that the final reaction product is the metal oxide. Hence the thermal degradation of $Mn(acac)_3$ can be represented as follows:



This mechanism is similar to the mechanism of the dissociation of $Co(acac)_3$, and therefore it was assumed that the thermal degradation of the PMMA system with a Mn(III) salt has a similar nature.

Table 7. Comparison of the thermal stability of PMMA and of its compositions with $Mn(acac)_3$.

	PMMA of high molecular mass			PMMA of intermediate molecular mass		
	PMMA	50:1 [a]	10:1 [a]	PMMA	50:1 [a]	10:1 [a]
T_d/ °C	210	130	125	220	130	130
T_{max} of the main decomposition / °C	350	365	400	360	365	400

[a] Number of monomer units per molecule of $Mn(acac)_3$.

In Table 7 we show results on the thermal stability of PMMA – $Mn(acac)_3$ compositions. It can be seen that pure PMMA is not gasified at temperatures up to 210 °C when heated at 10 °C min^{-1}. In the compositions with $Mn(acac)_3$ the decomposition of PMMA begins at 125 °C. The data in Table 7 show that although under these conditions the temperature of the onset of degradation in PMMA is lowered, the onset of the main process is moved to higher temperatures. From this point of view $Mn(acac)_3$ behaves like $Co(acac)_3$ in compositions with PMMA.

The dissociation diagram as a function of temperature for the composition PMMA – $Mn(acac)_3$ is shown schematically in Fig. 10. Three main dissociation stages can be identified. In stage I two overlapping processes at 150–160 °C are associated with the formation of acetylacetone and a small quantity of the monomer. These products are formed through the dissociation of $Mn(acac)_3$, initiated by the depolymerisation of the polymer produced by attack from the acac radicals and by the corresponding rupture of the chain with formation of a macroradical which can disproportionate as far as the monomer.

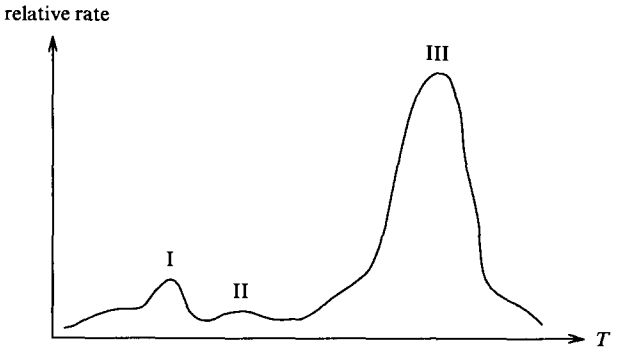


Figure 10. Schematic decomposition diagram for a $Mn(acac)_3$ – PMMA mixture.

In stage II acetone and carbon dioxide are formed. This process is ascribed to the breakdown of the $Mn(acac)_2$ produced in the preceding phase. The breakdown of the complex at the bond between $Mn(acac)_2$ and the ester side groups is accompanied by the formation of carboxylate structures which suppress the breaking of the PMMA chain in stage III.

The mechanism of the processes taking place during the thermal degradation of the PMMA – $Mn(acac)_3$ system has been treated like the corresponding mechanism for the PMMA – $Co(acac)_3$ system, discussed in detail in this review. It is stressed that the ability of $Mn(acac)_3$ to form complexes at the ester groups is not reflected, in general, by the mechanism of the thermal degradation processes of the system. This conclusion is again confirmed by the important role played by $Co(acac)_2$ and $Mn(acac)_2$ in the thermal degradation of PMMA compositions containing these salts.

References

1. C F Cullis, M M Hirschler *The Combustion of Organic Polymers* (Oxford: Oxford University Press, 1981)
2. M M Hirschler, in *Developments in Polymer Stabilisation* Vol. 5 (Ed. G Scott) (London: Applied Science Publishers, 1981) p. 107
3. R M Aseeva, G E Zaikov *Makromol. Chem. Makromol. Symp.* **74** 335 (1993)
4. R M Aseeva, G E Zaikov *Combustion of Polymer Materials* (New York: Hanser, 1981)
5. G-T Cardenas, C-C Retamal *Thermochim. Acta* **176** 233 (1991)
6. G-T Cardenas, K Klabunde, E Dale *Langmuir* **3** 986 (1987)
7. G-T Cardenas, K Klabunde, E Dale *Proc. Opt. Eng., SPEI* **821** 206 (1987)
8. G-T Cardenas, C-C Retamal *XVIII Jornadas Chilenas de Quimica, Nov. 1989.* Santiago (Chile) p. 350
9. S J Sirdesai, C A Wilkie *J. Appl. Polym. Sci.* **37** 863 (1989)
10. S J Sirdesai, C A Wilkie *J. Appl. Polym. Sci.* **37** 1595 (1989)
11. C A Wilkie, S J Sirdesai, T Suebsaeng, P Chang *Fire Safety J.* **15** 297 (1989)
12. R S Beer, C A Wilkie, M L Mittleman *J. Appl. Polym. Sci.* **46** 1095 (1992)
13. D Kiraly, K Zalatnai, M T Beck *J. Inorg. Nucl. Chem.* **11** 1 (1959)
14. L Gmelin, in *Gmelins Handbuch der Anorganischen Chemie* (Berlin: Verlag Chemie, 1962) p. 208
15. I C McNeill, R C McGuiness *Polym. Degrad. Stabil.* **9** 1 (1984)
16. I C McNeill, R C McGuiness *Polym. Degrad. Stabil.* **9** 2 (1984)
17. C A Wilkie, J W Pettigrew, C E Brown *J. Polym. Sci., Polym. Lett.* **19** 409 (1981)
18. L E Manring *Macromolecules* **21** 528 (1988)
19. L E Manring *Macromolecules* **22** 2673 (1989)
20. L E Manring, D Y Sogah, G M Cohen *Macromolecules* **22** 4652 (1989)
21. L E Manring *Macromolecules* **24** 3304 (1991)
22. C A Wilkie, J T Leone, M L Mittleman *J. Appl. Polym. Sci.* **42** 1133 (1991)
23. R H Pierson, A N Fletcher, E S Gantz *Anal. Chem.* **28** 1218 (1956)
24. T Kashiwagi, A Inaba, J E Brown, K Hatada, T Kitayama, E Masuda *Macromolecules* **19** 2160 (1986)
25. H R Allcock, F W Lampe, in *Contemporary Polymer Science* (Englewood Cliffs, NJ: Prentice-Hall, 1981) p. 378
26. D E Stuetz, A H Diedwardo, F Zitomer, B P Barnes *J. Polym. Sci., Polym. Chem. Ed.* **13** 585 (1975)
27. L S Kochneva, N A Kopylova, L M Terman, Yu D Semchikov *Eur. Polym. J.* **15** 575 (1979)
28. S L Madorsky *Thermal Degradation of Organic Polymers* (New York: Wiley, 1964)
29. E M Arnett, M A Mendelsohn *J. Am. Chem. Soc.* **84** 3821, 3824 (1962)
30. T Otsu, N Minimii, Y Nishikawa *J. Macromol. Sci., Chem.* **A2** 983 (1968)
31. H S Laver, in *Developments in Polymer Stabilisation* Vol. 1 (Ed. G Scott) (London: Applied Science Publishers, 1977) p. 167
32. M U Amin, G Scott *Eur. Polym. J.* **10** 1019 (1974)
33. N J Kroenke *J. Appl. Polym. Sci.* **26** 1167 (1981)
34. I C McNeill, J J Liggat *Polym. Degrad. Stabil.* **29** 93 (1990)
35. I C McNeill *Eur. Polym. J.* **3** 409 (1967)
36. I C McNeill *Eur. Polym. J.* **6** 373 (1970)
37. I C McNeill, R C McGuiness *Polym. Degrad. Stabil.* **9** 167 (1984)
38. I C McNeill, R C McGuiness *Polym. Degrad. Stabil.* **9** 209 (1984)
39. I C McNeill, J J Liggat *Polym. Degrad. Stabil.* **37** 25 (1992)
40. I Yoshida, H Kobayashi, K Ueno *Bull. Chem. Soc. Jpn.* **47** 2203 (1974)

Russian Chemical Reviews **63**(4) 367–371 (1994)
©1994 Russian Academy of Sciences and Turpion Ltd

UDC 541(15+64):537.5

The properties and applications of fluorine-containing polymer films with piezo- and pyro-activity

V V Kochervinskii

Contents

I. Introduction 367
II. Technical applications of poly(vinylidene fluoride) and its copolymers 368
III. The use of piezopolymer films in medicine 369
IV. Thermal radiation sensors based on piezofilms 370

Abstract. Polymer films based on poly(vinylidene fluoride) and its copolymers, which exhibit piezo- and pyro-electric properties after appropriate treatment, are described. The principal advantages of materials of this class include high values of the piezomoduli, which permit their practical use. Another valuable property, which is difficult to achieve in inorganic materials, is the wide range of frequencies over which the given active element can operate. The possibility of achieving large areas and fairly simple methods of preparation of thin films also leads to the assignment of the above polymers to the category of promising materials for the creation of new classes of recording devices. The trends in the development of new instruments based on these materials, where use is made of the phenomenon of photopyroelectric activity, are demonstrated. The advantages of using these materials for medical techniques are noted. The flexibility of the film and its acoustic impedance, which is close to that of a biological tissue, as well as the properties noted above place it beyond competition with other materials. Furthermore, the ferroelectric nature of the above polymers makes them promising for use in nonlinear optics. The bibliography includes 89 references.

I. Introduction

In the search for new materials to be used in energy converters, Kawai[1] observed in 1969 intense piezoelectricity in poly(vinylidene fluoride) (PVDF). Vigorous investigation of this phenomenon began afterwards. There have been numerous individual communications and fairly detailed reviews (see, for example, Refs. 2–5), where certain current established ideas concerning the mechanisms of piezo- and pyro-activity of the given class of polymers are described. The principal results reduce to the fact that the nature of the piezo-effect is not unique. It has come to be assumed that three phenomena contribute to the magnitude of the piezoelectric response: (1) the piezo-effect in the classical sense, which requires the presence of noncentrosymmetric crystals, (2) electrostriction (which has been very little investigated in polymers), and (3) the dimensional effect, which takes into account the change in volume on deformation resulting in a change in polarisation. The contributions of these effects to the macroscopic response may vary according to the results of different workers. Poly(vinylidene fluoride) and its copolymers belong to the class of flexible chain crystallisable polymers characterised by a low glass point (−40 °C). In the initial (isotropic) state, the material has the texture of a polycrystalline substance in which the crystallites (with a volume fraction of 0.4–0.5) have a random orientation. After averaging over a fairly large volume, this is equivalent to the presence of an effective centre of symmetry in this system, and the material does not exhibit piezo- and pyro-activity. Such activities are induced by treating the film with a high-frequency field.

It has been established[6] that the above polymers are ferroelectric and that the principal coefficients of piezo- and pyro-activity are linear functions of the residual polarisation P_r. The relation between the ferroelectric characteristics of the crystallisable polymers and their structure has been poorly elucidated and much that is obscure still remains to be solved. In particular, the role of the amorphous or mesomorphic phases in ferroelectric phenomena is not understood. Such phases are frequently represented by an inert matrix in which the crystals of the polar (β) and nonpolar (α) phases are immersed. There is no doubt that the contributions of these liquid-like phases (their fraction may reach 0.7) is by no means trivial. The influence of the characteristics of the nonordered region both on the quantity[7] P_r and on other piezoelectric constants[8] may serve as evidence for this. Data[9,10] concerning the influence of small irradiation doses (whereupon the changes refer mainly to the nonordered phase) and the ferroelectric properties of PVDF also confirm the above idea. Films of PVDF and its copolymers, obtained for practical purposes, are usually uniaxially extended. The role of the extension cannot be reduced solely to the method for the conversion of the polymorphic α-form into the β-form, although a decrease in coercive fields and an increase of P_r on polarisation have in fact been noted under these conditions.[11]

Experiments involving stretching the films crystallising immediately in the piezoactive β-phase[8–12] indicate that the piezoresponse and the ferroelectric characteristics in textured films are more pronounced and that the ultimate procedure for the latter is the creation of the 'ideal single crystal' texture. The above series of studies[8–12] indicate that the piezo- and pyro-effects in these compounds are dipolar in nature, although there is no doubt that here one should take into account the contribution of the space charge generated by the injected carriers in high polarisation fields. Under the usual conditions (at room temperature, normal pressure), the nonordered phase in the above polymers is in the highly elastic state and its pliability is an order of

V V Kochervinskii Division of Pulse Energetics, Troitsk Institute for Innovations and Thermonuclear Research, 142 092 Troitsk, Moscow Region, Fax (7-095) 334 57 76

Received 29 March 1994
Uspekhi Khimii **63**(4) 383–388 (1994); translated by A K Grzybowski

magnitude higher than that of the crystal. Thus, when such polymers are acted upon by a mechanical (acoustic) perturbation, the phase exhibits a local response (while the specimen as a whole exhibits a macroscopic response). The high mobility of the chains in the amorphous phase ensures their response to the thermal perturbation in the observation of the pyroeffect.

The difficulty of creating a rigorous molecular model of the above noted phenomena in such polymers is partly associated with the absence of ideas, worked out in all their details, concerning the structure of textured crystallising polymers. One may, for example, take the view that simplified ideas concerning the two-phase nature of the crystallising polymers do not help to elucidate the true mechanisms of the piezo- and pyro-response in PVDF and its copolymers. The lack of true (in the thermodynamic sense) interfaces between the ordered and amorphous phase can create a qualitatively new situation in the description of the mechanisms of the piezo- and pyro-responses in such polymers. In particular, attention has been drawn recently to the fact that the strained chains, passing through the amorphous phase and connecting neighbouring crystallites, play a special role in the response of textured crystallising polymers to the electric field.[7] In the vicinity of the interface between the above phases, which exists in a partially ordered (mesomorphic) state, the chains also behave in an unusual manner on exposure to an acoustic or thermal perturbation. This hypothesis is supported indirectly by data demonstrating an increase in the acoustic modulus and in the double refraction on deformation of textured films of the copolymer of vinylidene fluoride and tetrafluoroethylene.[8] Direct evidence for this was obtained by the X-ray diffraction method.[13] A change in the form of the azimuthal distribution of the 110 and 200 reflections after the immersion of the film was noted and was treated from the standpoint of reversible paraelectric $\rightleftarrows$ ferroelectric transitions when these phases coexist. The VDF homopolymer, a characteristic feature of which is reversible changes in crystallinity during the observation of the pyroeffect, behaves similarly.[14]

As stated in the Introduction, the mechanisms of the piezo- and pyro-effects in the compounds of the class considered are insufficiently clear. The very extensive experimental data available on this question need to be surveyed separately. Despite this, compounds of the given class have been most thoroughly investigated as regards their practical application. The aim of the present review is therefore to draw the readers' attention to branches of engineering where the given polymers are already used as the active element in the finished primary energy converters. The discovery of specific properties of the polymeric materials which make it possible to devise instruments with novel characteristics is emphasised.

Piezo- and pyro-coefficients which enable the above compounds to compete seriously with traditional piezoceramic materials have been reported in the latest communications. Thus PVDF films with the piezocoefficient $d_{31} = 60$ pC N^{-1} and the pyrocoefficient $p = 6$ nC cm^{-1} K^{-1} have been obtained by a modification of the polarisation method.[15] Table 1 presents a comparison of a series of characteristics of films of PVDF and of its copolymer with trifluoroethylene (TrFE) with the analogous characteristics of quartz and the PZT-4A ceramic.[16,17]

The choice in favour of the above materials may be dictated by a series of their specific properties and advantages. These include the following: (1) the existence of an effective technology (here one can use the equipment already available for the manufacture of polymeric film materials); (2) the possibility of achieving high areas of the active elements, which permits the construction of second generation sensors;[18] (3) a wide transmittance band (a realistic specification is 0–500 MHz), which is required in diagnostic systems;[19,20] (4) the closeness of the acoustic impedance of PVDF to that in human tissue and water, which is used in the construction of sensors for medical diagnostics; (5) the high impact strength of polymer films (this quality of PVDF is used in shock wave sensors); (6) the high corrosion stability of PVDF (this property becomes essential for work involving reactive media); (7) the low relative permittivities of the materials ($\varepsilon' = 10-14$) and the correspondingly higher values (almost by an order of magnitude and above) of the piezoconstant g and the pyrosignal (p/ε') sensitivity; (8) the lower thermal conductivity of PVDF compared with the piezoceramic and the possibility of obtaining thin films (one micrometer and less), which ensures a higher transverse resolution in the analysis of the spatial separation of the incoming electromagnetic radiation; (9) the possibility of imparting to the material an arbitrary form (cone, self-supporting dome, etc.), which makes it possible to produce elements with unusual forms of directional emission.

Table 1. Comparative characteristics of piezo- and pyro-electric materials.[16–19]

Characteristic	Material			
	PVDF	PVDF/TrFE	Quartz	PZT-4A
Density, ρ/g cm^{-3}	1.78	1.88	2.65	7.5
Velocity of sound, v/km s^{-1}	2.25	2.40	5.7	4.63
Acoustic impedance, $Z = \rho v/10^6$ kg m^{-2} s^{-1}	4.02	4.51	15.1	34.8
Modulus of elasticity, C_{33}/GPa	9.1	11.3	86	159
Electromechanical coupling coefficient, k_t	0.2	0.3	0.1	0.51
Piezoconstants:				
d_{31}/pC N^{-1}	60	25	–	–
g_{31}/V m N^{-1}	0.18	0.16	–	–
e_{33}/C m^{-2}	0.16	0.23	0.17	15.1
g_{33}/V m N^{-1}	0.32	0.38	0.05	0.017
Relative permittivity, ε'	12	20	4.6	625
Pyroelectric coefficient, p/nC cm^{-2} K^{-1}	6	–	–	38
Pyroelectric Q factor (p/ε')/nC cm^{-2} K^{-1}	0.5	–	–	0.061

II. Technical applications of poly(vinylidene fluoride) and its copolymers

A number of devices are described below in which the above qualities of the materials under considerations are actually employed. One of the most important properties is the presence in films of PVDF and its copolymers of longitudinal and transverse piezoeffects, which is used in the construction of headphones and high-frequency speakers. The possibility of using such films in piezoelectric piano-key switches and in the receptor sensors of electric pianos has been demonstrated.[17]

Piezoelectric polymer films are most widely used as bimorphic elements consisting of two combined films. By virtue of the elasticity of the polymeric materials, high vibration amplitudes are achieved in the bimorphic elements. As early as 1981, the Kodak company reported the development on the basis of PVDF of bimorphic elements operating under the conditions of the reverse piezoeffect and generating high-amplitude low-frequency vibrations.[21] Bearing in mind the low density and high pliability of the PVDF piezofilm, it was possible to achieve on the latter, under the conditions of the same fixing geometry, parameters of the excited bending vibrations approximately twice as high as on traditional materials such as $BaTiO_3$ and PZT.[21] An attempt has been made recently to use this property in displays, small pumps, light switching devices, etc.[22]

Because of the flexibility of the polymer films, completely new aspects of their application arise under these conditions. For example, it has become possible for the first time to focus sound waves. Thus standing concentric ultrasonic waves have been

achieved in water (with a frequency of 10 MHz) with the aid of PVDF [23] and have been recorded from the diffraction of light. Piezoelectric speakers, the operation of which is based on the transverse piezoeffect, have already become commercially available. Sound waves arise in them as a result of the bending movements of the polymer membrane.[24] A spherical emitter with a unique directional diaphragm has been constructed from PVDF.[25] PVDF is a suitable material for use in pressure measuring devices, for example, in presses operating in the quasi-static region, and also as a pressure switch in various switching devices.[24]

Bearing in mind that polymeric piezoelectric elements have a low Q factor, it is possible to generate short pulses with a low reverberation. This property ensures the wide-band characteristics of these materials, noted above, which has been used to construct an ultrasonic spectrometer for the simultaneous measurement of the absorption and velocity of ultrasound over a wide frequency range. For example, it has been possible to obtain with its aid information about the mechanisms of the phase transition in liquid crystals from the nematic state to the isotropic phase.[26,27] The changes in strongly frequency-dependent properties can be inferred from the analysis of the form of a single pulse. The principle of this measurement was proposed a long time ago, but its practical realisation became possible only after the appearance of polymeric piezoelectric converters with wide-band characteristics. Yet another advantage of materials based on PVDF is the possibility of creating very small sensors, which are used, for example, in the study of the elastic characteristics of certain superconductors and their anomalies in the region of transitions.

Taking into account the wide-band property of the converters considered, it has been suggested [28] that they be used to estimate all the components of the elasticity tensor in an anisotropic body. The possibilities of the methods were tested on quartz crystals. A satisfactory agreement was found between the elastic constants obtained by this method and those measured by other procedures.

Among the new applications of piezoelectric polymers, mention should be made of their use in the stereospecific vision sensors in robots,[27] in field sensors where the optical fibres are coated by the piezoelectric polymer,[29] and also in sonic pressure sensors of a hybrid type consisting of layers of the piezopolymer and semiconductor in direct contact.[30] Digital signals can be converted directly into sound signals in digital speakers based on piezoelectric polymers.[31]

The possibility of creating sensors (in the form of an elastic body), one of the elements of which is a piezoelectric PVDF film, has been discussed.[32] The mechanical stresses developing as the sensor moves along the object generate a charge on PVDF. The available mathematical procedure makes it then possible to estimate the rate of sliding of the sensor along the object and its coefficient of friction respectively from the real and imaginary components of the signal arising on PVDF. PVDF piezofilms can be used to create a gas sensor, the resonance parameters of which in the torsional and bending modes depend on the composition of the binary gas (SF_6 + air) and on its pressure. It has been found that, although such a sensor is less sensitive than the sensor based on silicon resonators, it can compete with other sensors. The possible region of application is in the monitoring of binary gas mixtures with known components.[33]

PVDF-based piezofilms are also used to combat deposits arising from microorganisms on the bottoms of ships. The film operates under the conditions of the reverse piezoeffect where the supplied electrical energy is transformed into the vibrational energy of the surface. The film adheres to the surface in contact with the aqueous medium. Here it has been noted that the control panel (without the piezofilm) becomes fully covered by microorganisms after only 2 months, whereas the panel with PVDF, on which vibrations developed (at a frequency of 5 kHz for a 0.05 g level), remained completely clean even after 5.5 months.[34]

Because of the ability of PVDF to be moulded into any shape, one can use it to construct ultrasonic converters and hydrophones with a spherical or needle-shaped receiving surface.[35] The high flexibility of the PVDF films makes it possible to construct sensors that can be used to estimate the nature of the air stream in aerodynamics. It has been shown that such sensors are fairly simple to construct and make it possible to record the transition from the laminar flow of air to a turbulent flow around the relevant body.[36] The piezoactive PVDF is used in sensors for the recording of shock waves, where the maximum pressure reaches 100 MPa. It is emphasised that sensors of this kind can find an application in underwater studies and in medicine, where one has to deal with focussed waves.[37]

The possibility of achieving high working areas and the high flexibility of the PVDF films provide a basis for the conversion of the energy of sea waves into electrical energy. According to the data of Hausler and Stein,[38] this idea may be not only ecologically attractive but also economically promising.

III. The use of piezopolymer films in medicine

Studies concerning the use of such materials in medicine need a separate consideration. Their advantages are associated with their low acoustic impedance Z and its closeness to the value for water and biological objects ($Z = 1.4 \times 10^6$ kg m^{-2} s^{-1}). Since the amplitude coefficient of the transmittance T_{12} for an ultrasonic element having an acoustic impedance Z_1 into a medium having an impedance Z_2 is given by the relation

$$T_{12} = \frac{2Z_1}{Z_1 + Z_2},$$

it follows that an important factor is that the impedances should be matched. This makes it possible to transmit 50% of the energy generated in the film into water, whereas in the case where a piezoceramic is used this amount is an order of magnitude smaller.[19] The above quality of the PVDF films permits their employment for the recording of electrocardiograms or for the monitoring of respiration.[19] By virtue of the large area of the sensor, the signal arising under these conditions is fairly high, so that it is possible to record it immediately on the pen recorder without preliminary amplification. The possibility of observing the difference between the incoming blood flow pulses at two different points on the human body may be of interest for physicians.[19] The copolymer of VDF and TrFE, for which the electromechanical coupling coefficients k is higher than for PVDF (see Table 1), is used widely in ultrasonic probes for medical diagnostics where bulky resonators are normally employed (see Yagi [17] and contained references). Owing to the similarity of the acoustic impedances of the probe and the living tissue, in this case the presence of an adjusting layer is no longer required. By virtue of the ability of the polymer film to assume the shape of the given body, there is also no need to employ an acoustic lens. All these factors lead to a better focussing of the ultrasonic waves and make it possible to record defects with a satisfactory resolution even for deep regions. Therefore, such probes are employed for the diagnostic investigation of internal organs — mammary glands, vocal chords, and the liver (see Yagi [17] and contained references).

The use of PVDF-sensors make it possible to obtain a series of characteristics of the pulse (frequency and rhythm), the pulse rate (in the two sensors version), and also a property which may be characterised by the form of the pressure wave.[39] The high flexibility of the piezofilm and its low acoustic impedance serve as a basis for transducers used to monitor the parameters of the contractions of the heart and of intrauterine contractions.[40]

The low Q factor of PVDF films makes it possible to generate short pulses with a low reverberation, while the high degree of resolution as regards position in space permits their application in elements for ultrasonic diagnostics in medicine.[41-43] Using piezoelectric bimorphic polymer films, it is possible to monitor the movement of the lips and to recognise vocal sounds and words (see Yagi [17] and contained references). Piezoelectric polymers can be used in medical diagnostics to monitor the blood flow pressure

and heart beat.[44] There have been reports of the use of PVDF films for the treatment of osteopathic affections, which is based on the influence of piezoelectricity on the human organism.[44,45]

IV. Thermal radiation sensors based on piezofilms

Films based on PVDF have found application as pyroelectric materials in local IR radiation sensors. They are used in fire detectors, in security signalling devices,[46] in contact-free instruments for the measurement of temperature, and in radar calorimeters. The employment of these materials in two-dimensional sensors, in particular in pyrovidicons, is expected in the future. An IR detector has been described[47] in which a small thickness (several micrometers) of the active element is achieved by spinning a solution of the vinylidene fluoride–trifluoroethylene copolymer immediately onto a silicon support. The use of this polymer arises from the fact that it crystallises as the polar ferroelectric β-phase, which renders the material pyroactive after polarisation. As a comparative detector, the pyrosensor based on PVDF can operate over a wide spectral range: from visible light to $\lambda = 12$ μm.[48] When an active layer of the VDF/TrFE copolymer is deposited onto an optical fibre, phase modulation is achieved.[49] Comparison of the characteristics of pyrovidicons based on triglycine sulfate crystals and PVDF films have shown that the sensitivity of the former is only 30% higher, while PVDF has a significant advantage as regards resolving power.[50]

The Siemens company has reported that PVDF is likely to be useful as a material for passive IR detectors.[51] The latter may be used to record the presence of a heat source, the directions and distances between the detector and the heat source, and also the rate of movement of the latter.[51,52] According to the ideas being developed and experiments on the recording of a moving object, it has been concluded that the response times of the above sensors are an order of magnitude shorter than those of traditional pyroelectric materials.

In discussing the question of the use of a pyroelectric PVDF-based calorimeter for the measurement of thermal diffusion, it was shown that the material has a number of undoubted advantages. In the first place, there is the possibility of making measurements under the conditions of minimal heating of the specimen and with a very low temperature gradient in the latter. This may be useful in studies on materials with a low thermal conductivity or materials extremely sensitive to temperature. On pulsed excitation, thermal diffusion may be recorded in a time interval of several milliseconds.[53] The possibility of using this type of calorimeter for the investigation of transient thermal processes with a time resolution of several nanoseconds and a sensitivity to within several nanocalories has been demonstrated.[54] A study has been devoted to technical problems associated with the improvement of the characteristics (including resolution) of such calorimeters.[55] Problems concerning the conditions in the preparation of the active element of such pyrodetectors have been touched upon.[56] PVDF-based pyrodetectors have proved successful in the estimation in a single experiment of a series of properties: specific heat, thermal diffusion, etc.[57]

The wide-band nature of photopyroelectric PVDF-based receivers has been used to estimate the distribution of the absorption coefficient in depth in specially formulated multilayer thin-film structures.[58] The form of the response curve, transformed into an optical absorption profile as a function of depth, has been analysed. The improvement of contrast in such spectra in the case of a discrete multilayer structure, combined with other procedures, makes it possible to minimise the thickness of the PVDF detector.

One of the latest reviews by Lang[59] surveys the possible applications of pyrodetectors based on ferroelectric polymers. Detectors for the monitoring of laser power in the range from 1 mW to 50 W,[60] for the determination of the energy of microwave radiation,[61,62] for the investigation of the change in temperature on nerve excitation,[63] for the recording of phase transitions in solids,[64] for the detection of defects in CdS crystals,[65] for the recording of changes in the surface of copper following the desorption of xenon from the latter by a laser pulse,[66] for the detection of thermal waves by measuring radiative emission,[67] for the investigation of adsorption phenomena,[68] for the detection of ultraheavy nuclei,[69] and for the detection of cosmic radiation[70–72] have been noted among them (in addition to those listed above). Such detectors are used in medicine,[73] in the optical fibre technology,[74,75] in photopyroelectric spectroscopy[76–78] (including the pulse response version[79]), and in photopyroelectric scanning microscopy.[80]

Reports on the potential possibility of using PVDF in vibrodiagnostics[81] and in calibration measurements of the rate of deformation[82] also merit attention.

There are definite prospects of using PVDF as a material with nonlinear optical properties. This is based on the conclusion, reached by Tsutsumi et al.,[83] according to which the internal field in the PVDF—poly(methyl methacrylate) polymer mixture can reach values of the order of 1 MV cm^{-1}. Combined with a high optical transparency of the above mixture, this makes it possible to obtain the optical nonlinearity coefficient $d_{33} = 9 \times 10^{-9}$ esu. Compared with other organic materials used in nonlinear optics, the stability of the characteristics of which is as a rule low, in the case of PVDF there is a definite possibility of increasing it by modifying the technological film preparation process. It has been shown, for example, that, on vacuum sputtering of PVDF in an electric field onto a support at a specified temperature, the stability of the resulting optical nonlinearity was increased significantly.[84] At the present time, attempts have been made to achieve these properties of PVDF films in memory elements. One of the latest reports[85] concerns advances in the use of the vinylidene fluoride–trifluoroethylene copolymer in optical memory elements. Bearing in mind that these polymers are characterised by high coercive fields and that control is usually achieved by a potential of several volts, it proved possible to obtain by a spinning method films with thicknesses less than 1 μm. It was then shown that a decrease in film thickness to ~0.2 μm is not accompanied by any significant changes in the ferroelectric characteristics. An increase in the coercive field and a decrease in the residual polarisation have been noted in films with $d < 0.2$ μm. When recording is carried out with the aid of a focussed laser beam, the minimum area employed for the recording is ~50 μm^2. Information can also be recorded and read over a period of about 1 μs and the signal-to-noise ratio has been estimated as 50 dB.[86] It appears that the presence of large internal fields in such ferroelectric materials makes them promising for use as elements in electrooptical light modulators operating in the mode involving the reflection of the light beam from a polarised polar polymer films with a dye.[87,88] On the basis of the foregoing considerations, a device has been constructed for the recording of an image in which use is made of a thin (2 μm) film of a vinylidene fluoride–trifluoroethylene copolymer. It has been shown that there are good prospects for the employment of such devices in electrophotography.[89]

References

1. H Kawai *Jpn. J. Appl. Phys.* **8** 975 (1969)
2. R G Kepler, R A Andersen *Adv. Phys.* **41** 1 (1992)
3. R P Singh *SETE Techn. Rev.* **9** 140 (1992)
4. H S Nalwa *Rev. Macromol. Chem. Phys.* **31** 341 (1991)
5. G M Sessler *IEEE Trans. Elec. Insul.* **24** 395 (1989)
6. T Furukawa *IEEE Trans. Elec. Insul.* **24** 375 (1989)
7. V V Kochervinskii, V G Sokolov *Vysokomol. Soedin., Ser. A* **33** 1625 (1991)
8. V V Kochervinskii, V F Romadin, V A Glukhov, V G Sokolov, M A Sandakhmetov *Vysokomol. Soedin. Ser. A* **31** 1382 (1989)
9. K A Verkhovskaya, V V Kochervinskii *Vysokomol. Soedin., Ser. A* **32** 1669 (1990)
10. V V Kochervinskii *Vysokomol. Soedin., Ser. A* **35** 1978 (1993)

11. V V Kochervinskii *Vysokomol. Soedin., Ser. A* **33** 2106 (1991)
12. V V Kochervinskii, V G Sokolov, V M Zubkov *Vysokomol. Soedin., Ser. A* **33** 530 (1991)
13. V V Kochervinskii, V A Glukhov, V G Sokolov, Yu K Ovchinnikov, N A Trofimov, B V Lokshin *Vysokomol. Soedin., Ser. A* **31** 1829 (1989)
14. R G Kepler, R A Andersen, R R Lagasse *Ferroelectrics* **57** 151 (1984)
15. T Kaura, R Nath, M M Perlmann *J. Phys. D, Appl. Phys.* **24** 1848 (1991)
16. K Matsushige *Kino Dzaire* **6** 30 (1986)
17. T Yagi *Kindzoku Khemen Gidzyutsu* **37** 640 (1986)
18. Kh Aoki *Kobunshi Kagaku* **38** 14 (1988)
19. H Sussner, K Dransfeld *Colloid Polym. Sci.* **257** 591 (1979)
20. H Sussner, D Micbas, A Assfalg, S Hunklinger, K Dransfeld *Phys. Lett. A* **45** 475 (1973)
21. J K Lee, M A Marcus *Ferroelectrics* **32** 93 (1981)
22. M Toda *Ferroelectrics* **32** 127 (1981)
23. H Sussner, Doctoral Thesis, Universität Konstanz, 1976
24. N Murayama, K Nakamura, H Obara, M Segawa *Ultrasonics* **14** 15 (1976)
25. M V Schickfus, H Sussner, DDR P. 241 796
26. K Matsushige, H Okabe, S Shichijyo, T Takemura *Jpn. J. Appl. Phys. Suppl.* **24** 30 (1985)
27. K Matsushige, T Takemura *Oe Butsuri* **54** 940 (1985)
28. S D Maynard *J. Acoust. Soc. Am.* **91** 1754 (1992)
29. P D Dario, D DeRossi *Preprint of the 13th ISIR, 1983* p. 13; see Ref. 17
30. R G Swartz, J D Plummer *IEEE Trans. Elec. Dev.* **26** 1921 (1979)
31. J L Flanagan *Bell Syst. Tech. J.* **59** 1693 (1980)
32. H Shinoda, T Kinoshita, S Ando *Ann. Report Eng. Res. Institute Faculty Eng. University Tokyo* **51** 191 (1992)
33. R Block, G Fickler, G Lindner, H Muller, M Wohnas *Sensors and Actuators* **7** 596 (1992)
34. M Latour, P V Murphy *Ferroelectrics* **32** 33 (1981)
35. M Platte *Ferroelectrics* **75** 327 (1987)
36. W Nitsche, N Weiser *Ferroelectrics* **75** 339 (1987)
37. G Heine *Ferroelectrics* **75** 357 (1987)
38. E Hausler, L Stein *Ferroelectrics* **75** 363 (1987)
39. W Nitsche, R Thunker *Ferroelectrics* **75** 381 (1987)
40. K Kobayashi, T Yasuda *Ferroelectrics* **32** 181 (1981)
41. N Murayama, H Obara *Jpn. J. Appl. Phys. Suppl.* **22** 3 (1983)
42. Kh Okhigashi *Seidenki Gakkaisi* **7** 92 (1983)
43. E Sanko *Seidenki Gakkaisi* **7** 85 (1983)
44. P Dario, D DeRossi, R Bedini, F Francesconi, M G Trivella *Preprint of INPBBD, 1983,* p. 38; see Ref. 17
45. J J Ficat, P Durroux, M J Fanzan, G Escourrou, P Ficat, C Lacabanne *Polymer Preprints* **24** 30 (1983)
46. K Okhara *Dzaire Kagaku* **20** 164 (1983)
47. E Yawaka *Ferroelectrics* **57** 327 (1984)
48. G W Day, C A Hamilton, K W Pyatt *Appl. Opt.* **15** 1865 (1976)
49. A Odajima, M Imai, in *Abstracts of Reports at the 1st European Conference and International Symposium on the Application of Polar Dielectrics and Ferroelectrics, E-8, Zurich, 1986* p. 35
50. J E Jacobs, S A Remily *Infrared Phys.* **19** 1 (1979)
51. H Meizner *Ferroelectrics* **75** 345 (1987)
52. R Freitag, H Meixner *IEEE Trans. Elec. Insul.* **24** 469 (1989)
53. H Coufal, P Hefferle *Appl. Phys. A* **38** 213 (1985)
54. H Coufal *IEEE Trans. Elec. Insul.* **21** 495 (1986)
55. W Mieszkowski, K F Leung, A Mandelis *Rev. Sci. Instrum.* **60** 306 (1989)
56. A H Franzan, N F Leite, L C M Miranda *Appl. Phys. A* **450** 431 (1990)
57. S Bauer, B Ploss *J. Appl. Phys.* **60** 6361 (1990)
58. J F Power *Appl. Spectrosc.* **45** 1240, 1252 (1991)
59. Y Dang Quan, S B Lang *IEEE Trans. Elec. Insul.* **23** 503 (1988)
60. M Hammer, A Olafson *J. Phys. E* **21** 80 (1988)
61. T Iwasaki, T Inoue, T Nimoto *IEEE Trans. Inst. Meas.* **28** 88 (1979)
62. T M Lee, A P Andersen, F A Bensen *Elec. Lett.* **22** 200 (1986)
63. I Tasci, K Iwaga *Biochem. Biophys. Res. Commun.* **101** 172 (1981)
64. A Mandelis, F Care, K K Chan, L C M Miranda *Appl. Phys. A* **38** 117 (1985)
65. A Mandelis, W Lo, R E Wagner *Appl. Phys. A* **44** 123 (1987)
66. I Hussla, H Coufal, F Trager, T J Chuang *Can. J. Phys.* **64** 1070 (1986)
67. H Coufal *IEEE Trans. Ultrason. Ferroelectrics Freq. Contr.* **33** 507 (1986)
68. H J Coufal, R Crygier, D E Horue, J E Fromm *J. Vac. Sci. Technol. A* **5** 2875 (1987)
69. J A Simpson, A J Tuzzolino *Phys. Rev. Lett.* **52** 601 (1984)
70. J A Simpson, A J Tuzzolino *Nucl. Instrum. Methods Phys. Res. A* **236** 187 (1985)
71. M A Perkins, J A Simpson, A J Tuzzolino *Nucl. Instrum. Methods Phys. Res. A* **236** 310 (1985)
72. J A Simpson, R Z Sagdeev, A J Tuzzolino, M A Perkins, L V Ksanfomality, D Rabinowitz, G A Lentz, V V Afonin, J Ero, E Keppler, J Kosozokov, E Petrova, L Szabó, G Umlauft *Nature (London)* **321** 278 (1986)
73. D DeRossi, P Dario *Ferroelectrics* **49** 49 (1983)
74. R Kashyap, P Pantelis *J. Phys. D* **18** 1709 (1985)
75. N Iwasaki, I Yokoshima, K Nokamura *Electron. Lett.* **18** 385 (1982)
76. A Mandelis *Chem. Phys. Lett.* **108** 388 (1984)
77. H Coufal *Appl. Phys. Lett.* **44** 59 (1984)
78. A Mandelis, M M Zver *J. Appl. Phys.* **57** 4021 (1985)
79. J F Power, A Mandelis *Rev. Sci. Inst.* **58** 2018, 2024, 2033 (1987)
80. I F Faria, C C Chizzoni, L C M Miranda *Appl. Phys. Lett.* **47** 1154 (1985)
81. J Irens, W Kennedy *Proc. Inst. Mech. Eng.* **204** 43 (1990)
82. K-C Lee, T C Sillivan *J. Acoust. Soc. Am.* **90** 945 (1991)
83. N Tsutsumi, Y Veda, T Kiyotsukuri *Polymer* **33** 3305 (1992)
84. A Kubono, T Kitoh, K Kajikawa, S Umemoto, H Takezoe, A Fukada, N Okui *Jpn. J. Appl. Phys.* **31** 1195 (1992)
85. K Tashiro, S Watanabe, T Furukawa *Polymer Preprints Jpn.* **34** 2977 (1985)
86. T Furukawa *Polymer Preprints* **33** 381 (1992)
87. G H Cross, Y Karalcus, D Bloor *IEEE Trans. Elec. Insul.* **29** 136 (1993)
88. C C Teng, H T Man *Appl. Phys. Lett.* **56** 1734 (1990)
89. Y Guo, K Hoshino, S-I Hanna, H Kokado *Jpn. J. Appl. Phys.* **31** 1432 (1992)

Russian Chemical Reviews **63** (5) 373–382 1994
© 1994 Russian Academy of Sciences and Turpion Ltd

UDC 541.18; 541.6

Spin probes in micelles

A M Wasserman

Contents

I.	Introduction	373
II.	Determination of the shape and size of micelles by ESR spectroscopy	373
III.	Direct micelles	374
IV.	Polymeric micellar systems	378
V.	Reverse micelles	379
VI.	Conclusion	381

Abstract. The results of studies of the molecular dynamics and structure of direct, polymeric and reverse micelles by the spin probe method using stationary ESR spectroscopy and electron spin echo spectroscopy are considered. The spin probes permit the determination of the characteristic rotation times, shapes and sizes of micelles and the local molecular mobility and polarity of different micelle regions. They also make it possible to record the processes involving the formation of micelles and premicellar aggregates and to determine the state of water in the cores of reverse micelles. Electron spin echo spectroscopy provides information about the detergent conformation and the permeability of the hydrocarbon regions of micelles. The bibliography includes 78 references.

I. Introduction

Spin probes are fine instruments for the study of complex heterogeneous systems.[1–4] Ordered micellar systems (direct and reverse micelles, microemulsions, vesicles, etc.) are important in solving many fundamental and applied problems (see, for example, Refs 6 and 7) and are convenient objects for investigations using the spin probe method. For these reasons, micellar systems have been of great interest for many years.[5] The continuing development of the ESR spectroscopic methods and the synthesis of new spin labels make it possible to solve many problems at a new level.

The present work discusses the recent results of studies on direct, reverse, and polymeric micelles by the spin probe technique.

II. Determination of the shape and size of micelles by ESR spectroscopy

The shape of a direct micelle formed by an ionic detergent in water near the critical micelle concentration (CMC) differs only slightly from spherical symmetry. The micelle consists of a hydrocarbon core, a water–hydrocarbon layer whose thickness is determined by the depth of penetration of water molecules into the hydrocarbon part of the micelle, hydrated polar groups, and a layer of aqueous solution adjacent to the micelle.[7] The charged polar groups form a compact zone several ångstroms thick on the surface of the micelle (the Stern layer), where the majority of the counterions compensating the total micelle charge are localised. The remaining counterions are located in the Gouy–Chapman layer (with a thickness up to several hundred ångstroms). They are totally dissociated and can be exchanged with other ions present in the solution.[8]

The micelle is a dynamic formation: the lifetime of a detergent molecule in the micelle is normally $10^{-7}-10^{-6}$ s, whereas the half-life of the micelle is $10^{-3}-1$ s.[7,9]

Different physicochemical experiments reveal different effective sizes of the micelle. For example, the rotational and translational dynamics of the micelle as a whole are determined by its outward size (R), evidently including the Stern layer, whereas the kinetics and recombination mechanism of hydrophobic active radicals[10] are governed by the size of the hydrocarbon core, where these radicals are dissolved.

Table 1 presents some parameters of alkyl sulfate micelles in water: the critical micelle concentration, the aggregation number, i.e. the average number of detergent molecules localised in the micelle, the micelle radius (R), and the rotational correlation time of the micelle as a whole calculated by the Stokes–Einstein equation using the values of R reported in Ref. 13.

$$\tau = \frac{4\pi\eta R^3}{3kT} \qquad (1)$$

Here η is the viscosity of water.

The rotational correlation time can be easily determined from the ESR spectrum of the spin probe,[1–4] and the radius of the rotating particle can be calculated by Eqn (1). Furthermore, the anisotropy of the rotation of the probe, i.e. the ratio of the rotation frequencies around different molecular axes,[2,14] can be determined from the ESR spectrum of the spin probe. If the rotating species is represented by an ellipsoid of rotation whose rotational anisotropy is determined by the shape of the particle, then the degree of nonsphericity of the particle, i.e. the ratio of the main axes of the ellipsoid, can be determined from the rotational diffusion data.

In order to find the rotational correlation time of the micelle and its nonsphericity from the ESR spectra of the spin probe, one important condition must be fulfilled: the spin probe should rotate only together with the micelle. In other words, rotation of the probe relative to the micelle is inadmissible.

A M Wasserman Semenov Institute of Chemical Physics, Russian Academy of Sciences, ul. Kosygina 4, 117334 Moscow, Russian Federation. Fax (7–095) 938 21 56

Received 25 March 1994
Uspekhi Khimii **63** (5) 391–401 (1994); translated by S S Veselyi

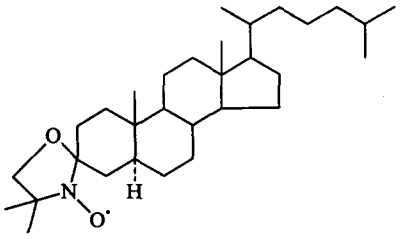
Table 1. Critical micelle concentrations, aggregation numbers, and rotational correlation times of micelles of sodium alkyl sulfates in water at 25 °C.

Detergent	CMC/M	n	R/Å		τ/ns
			I	II	
C-6	4.2×10^{-1}	17			
C-7	2.2×10^{-1}	22		16.0	0.40
C-8	1.3×10^{-1}	27	15.5	17.1	0.45
C-9	6.0×10^{-2}	33	18.0[a]	19.2	0.65
C-10	3.3×10^{-2}	41	19.8	21.3	0.90
C-11	1.6×10^{-2}	52	22.2	23.5	1.20
C-12	8.2×10^{-2}	64	25.2	25.6	1.50
C-14	2.05×10^{-3}	80			
C-16	4.5×10^{-4}	100			

Note. The first column indicates the number of carbon atoms in the detergent alkyl chain; the values of n are based on data reported in Ref. 12; (I) determined by the light scattering method[11] at [NaCl] = 0.1 M; (II) estimated from the sizes of detergent molecules.[13]
[a] [NaCl] = 0.2 M.

An attempt to determine the shape of a sodium dodecyl sulfate micelle (concentration 0.1 M) in water by the spin probe method has been undertaken.[15] This attempt is undoubtedly interesting since the spherical micelles adopt a cylindrical shape as the detergent and electrolyte concentrations are increased;[16] this process can be monitored by the spin probe method.

3-Doxylcholestane, with a molecular size comparable to the size of the micelle, was chosen[15] as the probe:



It was assumed that the probe rotates only together with the micelle and the nonsphericity of the micelle, i.e. the ratio of the main axes of the ellipsoid of rotation (d), was determined from the data on the anisotropy of the rotation. It turned out that the shape of the micelle at 22 °C is not spherically symmetrical but can be approximated by an ellipsoid of rotation whose long axis is 7.4 times longer than the short axis. The value of d increases as the temperature is increased, but even at 59 °C $d = 5.7$, i.e. the micelle is not spherical.

Unfortunately, in this case, the rotation of the probe itself relative to the micelle cannot be excluded. Also, one cannot rule out the fact that the rotational anisotropy is due not only to the nonsphericity of the micelle but also to the nonsphericity of the spin probe molecule. Therefore, it is difficult to agree with the authors above[15] that the sodium dodecyl sulfate micelles are nonspherical. However, further investigations with probes of various sizes differing in the shape and structure of the molecule might allow the separation of the two factors — rotation of the micelle and rotation of the spin probe itself — and provide a technique for the determination of the shapes and sizes of micelles using spin probes.

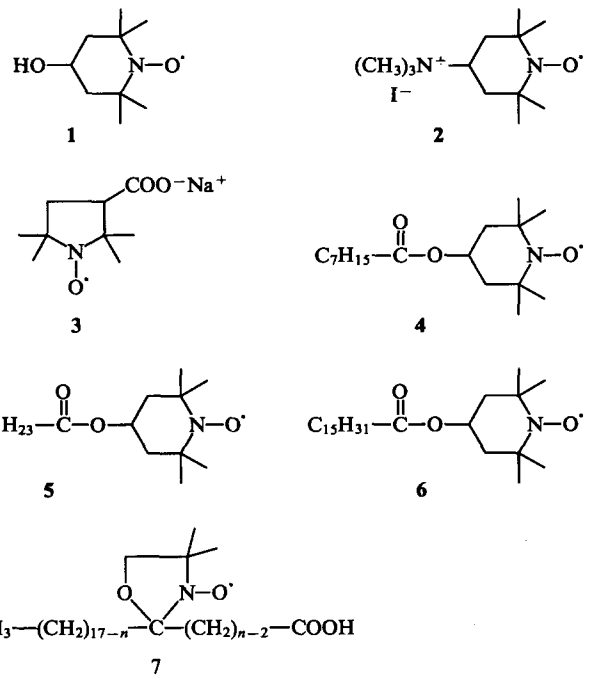
III. Direct micelles

Direct micelles are constructed in such a way that the molecules of a surface-active compound (surfactant) are combined via their hydrophobic hydrocarbon (or fluorocarbon) chains, whereas the polar groups are directed towards water.[7] Let us consider the results of studies on the local molecular dynamics and structure of such micelles by the traditional ESR spectroscopic and spin echo methods.

1. ESR spectroscopy of spin probes

A micelle is a complex heterogeneous system. Therefore, the question of the location of the probe in micelles is of fundamental importance. In essence, it concerns the region (hydrocarbon core, interface, the Stern layer, etc.) about which the spin probe provides information.

The formulae of several nitroxyl radicals used as spin probes in the study of the molecular dynamics and structure of direct micelles[17–21] are given below.



The solubility of radical **1** in water is 100 times higher than in heptane.[2] It is believed[17] that this radical is located in the aqueous solvate layer surrounding the micelles of anionic detergents such as sodium octyl sulfate $C_8H_{17}SO_4Na$ (SOS), sodium dodecyl sulfate $C_{12}H_{25}SO_4Na$ (SDS), and sodium hexadecyl sulfate $C_{16}H_{33}SO_4Na$ (SHS). This radical is located mainly outside the micelle; it has not found wide use as a spin probe for studying micellar systems.

The positively charged radical **2** and the negatively charged radical **3** interact electrostatically with the negatively charged surfaces of anionic detergents (radical **2**) and the positively charged surfaces of anionic detergents (radical **3**). Radical **2** is located closer to the surface of the sodium dodecyl sulfate micelle than radical **3** is to that of the dodecyltrimethylammonium bromide micelle. This explains the fact that the ESR spectra of radical **2** are more sensitive to the structure and dynamics of the micelle than those of radical **3**.[20]

The hydrocarbon regions of radicals **4**, **5**, and **6** are located in the hydrocarbon core of the direct micelle, but the nitroxy-group is located near the micelle surface.[18,20] When using probes **5** and **6**, one should keep in mind that these probes can themselves form micellar solutions.[18]

Doxylstearic acids **7** (n-DSA, n = 5, 7, 10, 12, 16) are located in direct micelles in such a way that the carboxy-group is in the polar layer of the interface, whereas the nitroxy-group resides in the hydrocarbon core of the micelle.[21]

Spin probes make it possible to find the critical micelle concentration, determine the polarity and local molecular mobility of micelle regions where the probe is located, and detect the formation of premicellar aggregates.

At the critical micelle concentration redistribution of the probe in solution occurs which results in an abrupt change in its ESR spectrum. At concentrations below the CMC, the probe is dissolved in water. If the concentration is above the CMC, the probe is located in the micelle or on its surface. At a detergent concentration equal to CMC, a sharp change in the polarity of the probe environment and in its rotational mobility occurs. As a rule, the values of CMC determined by the spin probe method differ insignificantly from the corresponding values determined by other methods. For example, CMC values of 0.14, 8.3×10^{-3}, and 5.5×10^{-4} M were found for sodium octyl, dodecyl, and hexadecyl sulfates, respectively using probe **2**.[17] These values differ only slightly from the CMC values presented in Table 1.

The determination of the polarity of the probe environment and of its location in the molecule is based on the fact that the isotropic hyperfine coupling constant of the unpaired electron of the radical with the nitrogen nucleus (a_N) and its g-factor depend on the polarity of the medium where the spin probe is sited.[1] For example, a_N = 17.16 G for the di(*tert*-butyl)nitroxyl radical in water, whereas in heptane[3] a_N = 15.10 G. For many nitroxyl radicals, the difference between the a_N values in water and heptane is ~2 G. The value of a_N changes monotonically as the polarity of the environment changes. Hence, measurement of a_N makes it possible to determine the polarity of the probe environment and to draw a conclusion as to where the probe is located in the micelle. For example, the formation of micelles by sodium hexadecyl, dodecyl, or octyl sulfates results in a 1.0, 0.62, or 0.32 G decrease in a_N for probe **2** (in water, a_N = 16.85 G for this radical) respectively. In the opinion of the authors[17,20] such changes may be due to two reasons. First, the longer the hydrocarbon chain of the radical, the closer is the spin probe to the micelle core. Second, the arrangement and polarity of the aqueous layer in the vicinity of the micelle surface can depend on the length of the hydrocarbon group of the detergent. In our opinion, the first reason is more probable.

The determination of the local molecular mobility is based on the measurement of the rotational correlation time[1-4] of the radical. This value is linked to the viscosity of the system by the Einstein–Stokes relation [see Eqn (1)] and characterises the microviscosity and the local molecular mobility of the micelle at the location of the probe. However, it is important to be sure that the rotation of the probe is governed by the local mobility rather than the rotation of the whole micelle. This condition is fulfilled if the rotational mobility of the probe is much greater than that of the micelle.

The rotational correlation times of probe **2** on the surfaces of micelles of sodium octyl, dodecyl, and hexadecyl sulfates (which amount to 5.8×10^{-11}, 2.2×10^{-10} and 1.6×10^{-10} s) are much lower than the rotational correlation times of the micelle as a whole (see Table 1) and 5–20 times greater than the rotational correlation time of the probe in water.[17] This is explained by the fact that the local microviscosity of the surface layer of the micelle, where the spin probe is located, is markedly greater than the microviscosity of water. However, it is important to emphasise that the mobility of the surface layer is rather high.

The conclusion about the high local mobility of the surface layer of the micelle is also confirmed by results obtained using spin probes with long hydrocarbon radicals. The rotational correlation times of radical **4** in a micelle of sodium octyl sulfate, radical **5** in a micelle of sodium dodecyl sulfate, and radical **6** in a micelle of sodium hexadecyl sulfate are 1.2×10^{-10}, 2.4×10^{-10}, and 1.6×10^{-10} s, respectively; they differ insignificantly from the rotational correlation times of radical **2**. The hydrocarbon regions of these radicals are dissolved in the micelle hydrocarbon core, whereas the nitroxy-group is located in the surface layer, and its mobility is determined predominantly by the local molecular mobility of the micelle in the vicinity of the surface layer.[18,19]

Of particular interest are the results in Ref. 21 obtained using doxylstearic acids (*n*-DSA), in which the nitroxy-group is bound to different atoms of the alkyl chain, as spin probes. These probes are located in the micelle in such a way that the carboxy-group is in the polar layer of the micelle, whereas the nitroxy-group is in the hydrocarbon core. The correlation times of these probes in micelles are fairly high (Table 2) and are comparable with the rotational correlation times of the micelle as a whole (cf. the data in Table 1).

Table 2. Rotational correlation times of doxylstearic acids in sodium dodecyl sulfate and dodecyltrimethylammonium bromide micelles at 25 °C (concentration 0.1 M) (cf. Ref. 21).

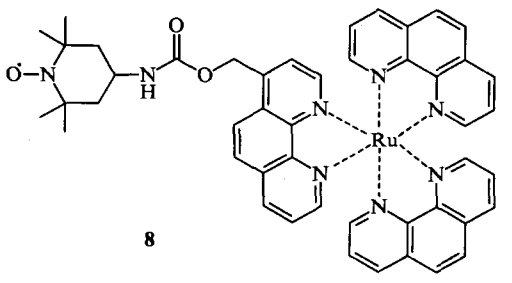
Detergent	τ/ns		
	5-DSA	12-DSA	16-DSA
Sodium dodecyl sulfate	1.1	0.82	0.43
Dodecyltrimethylammonium bromide	1.0	0.82	0.43

Apparently, the times observed are mainly determined by the intramolecular mobility rather than the rotation of the micelle as a whole. In the latter case, the values of τ for the three doxylstearic acids should not differ.

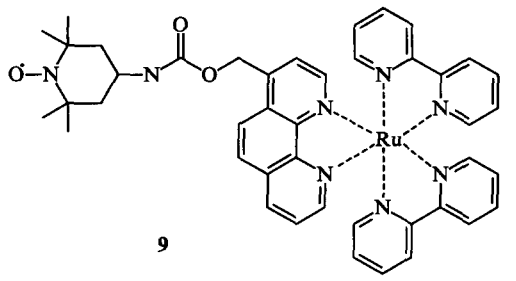
The local motions in the hydrocarbon core of the micelle occur at frequencies of $\sim 10^{-9}$ s^{-1}; the mobilities in the core of anionic (sodium dodecyl sulfate) and cationic (dodecyltrimethylammonium bromide) micelles are practically equal. The mobility of the hydrocarbon chains near the polar shell is lower than in the micelle centre. This explains the fact that the rotational correlation times of spin probes decrease as the nitroxy-groups move further away from the micelle surface.

Let us consider the results obtained using spin-labelled ruthenium complexes, whose formulae are shown below, as spin probes.[22] These complexes without spin probes are often used in the studies of photophysical processes in micelles.[23]

The sizes of the complexes are fairly large and comparable to the sizes of micelles (e.g. the diameter of complex **8** is ~18 Å). The rotational correlation times increase monotonically for micelles of sodium alkyl sulfates with hydrocarbon chains of different sizes (the number of carbon atoms varied from 7 to 14), while a_N decreases as the alkyl chain length increases. This is explained by the fact that the ruthenium complex is submerged deeper into the micelle the longer the hydrocarbon chain of the detergent. However, the difference between the a_N values for the complex in water and in the micelle is not high; for example, it does not exceed 0.4 G for $C_{14}H_{27}SO_4Na$. This implies that even for the largest micelles, the spin-labelled complex is located near the micelle surface and its mobility is determined by the molecular dynamics of the surface layers of the micelle. The rotational mobility of the complex is well correlated with the translational mobility determined from photophysical experiments.[24] The rotational and translational dynamics of large species, such as ruthenium complexes, on the micelle surface are probably correlated and the local molecular mobility of the micelle affects these motions similarly.



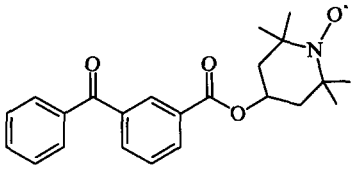
8



9

The rotational mobility of the complex depends not only on the length of the hydrocarbon group of the detergent but also on the nature of the polar group: the rotational correlation times of the ruthenium complex in the sodium dodecyl sulfate micelle are greater than in the sodium laurate micelle. This difference arises from the fact that a micelle containing sulfate groups interacts with the complex more strongly than a micelle containing carboxy-groups (in both cases, the hydrocarbon group of the detergent contains 12 carbon atoms).

The rotational correlation time of the spin probe



in the micelle increases by a factor of ~2.5 [10] when the number of carbon atoms in a sodium alkyl sulfate molecule increases from 7 to 14. Unfortunately, the value of a_N has not been reported in Ref. 10. Therefore, it is difficult to reach a conclusion as to why its rotational mobility changes, i.e. due to a change in the microviscosity of the micelle or due to a change in the site of the latter in the micelle. In our opinion, the second reason is more important.

It is interesting to note that an attempt has been made to determine the lifetime of radical **2** on the micelle surface by analysing the widths of the ESR spectral lines. [17,24] This value characterises the rate of transfer of the spin probe from the micelle into the aqueous solution. The values of $> 5.7 \times 10^{-7}$, $\sim 0.93 \times 10^{-7}$, and $\ll 1.8 \times 10^{-7}$ s were obtained for micelles of sodium hexadecyl, dodecyl, and octyl sulfates respectively. These values differ only slightly from those characterising the lifetime of molecules of the respective detergents in micelles determined by other methods. [25]

Recently, [26] the results of measuring the rotational mobility of a spin probe (doxylstearic acid) were used to establish the compatibility of hydrocarbon and fluorocarbon ionic detergents in a micelle; [26] earlier, the spin probe method was used extensively to diagnose the compatibility of polymers in mixtures. [4]

The formation of premicellar aggregates has been detected in solutions of alkyl sulfate detergents by using spin-labelled ruthenium complexes as spin probes. [22] The ESR spectrum of a spin probe at concentrations of the detergent far below the CMC (for example 1.5×10^{-3} M for sodium dodecyl sulfate at CMC $\simeq 8.3 \times 10^{-3}$ M) represents a superposition of a narrow triplet (the spectrum of the probe in water) and a broad triplet arising from the molecules of the probe located on premicellar aggregates. These aggregates are small and their sizes are much smaller than those of a micelle. Several spin probe molecules are adsorbed on one premicellar aggregate. The spin probes are spaced so closely that their dipole interaction results in a noticeable broadening of the ESR spectrum. The formation of premicellar aggregates has been observed for sodium alkyl sulfates with 7 – 14 carbon atoms in the hydrocarbon chain.

Naturally, one cannot rule out the possibility that the formation of the premicellar aggregates can be initiated in this case by the spin probe molecules. However, it is important to emphasise that the conclusion that premicellar aggregates exist in detergent solutions [22] is in good agreement with the results of thermodynamic calculations, [7] photophysical measurements, [27] and data obtained by other methods. [28,29]

2. Electron spin echo modulation spectroscopy

The idea of applying the electron spin echo modulation method to determine the structure of the micelle consists in the following. The electron spin echo signal of the probes can be modulated by the weak dipole hyperfine interaction of the unpaired electron of the probe with the magnetic moments of the surrounding nuclei. The modulation depth depends on the number of surrounding atoms and their distance from the unpaired electron, provided that this distance does not exceed ~6 Å. [30] Usually, the depth of modulation by deuterium atoms is determined. Once the modulation depth has been determined, one can conclude which magnetic nuclei surround the spin label and how far away they are located.

Experiments on the determination of the micelle structure by the electron spin echo modulation method are normally performed in quickly frozen solid solutions at 4.2 K (the dipole interaction in the liquid is averaged to zero due to molecular motion). [31–41]

Much effort has been devoted to ensuring that the structure of the micelles does not change upon rapid freezing. For example, the radical-cation of *N, N, N′, N′*-tetramethylbenzidine (TMB) is readily formed when TMB is illuminated. This radical-cation is stable in micellar systems, but is quickly destroyed in homogeneous media. [42] It turned out that if this radical-cation is obtained in a micellar system which is then quickly frozen and allowed to thaw, then the ESR spectrum of the radical-cation is observed for a long time at room temperature. [34] A similar result is observed when the radical-cation is generated in a frozen micellar system, and the ESR spectrum is observed at room temperature. [33] According to the authors [31–41], these results imply that the micellar structure of the system is retained upon freezing.

There is also other evidence that the micellar structure is retained upon rapid freezing. In particular, the aggregation numbers of sodium dodecyl sulfate micelles in water at room temperature and in a frozen system differ only slightly. [43] The conclusion that the micellar structure is retained upon rapid freezing is also confirmed by electron microscopy. [44]

The most interesting data were obtained by the electron spin echo modulation method; doxylstearic acids, in which the nitroxy-group is linked to different carbon atoms of the alkyl chain, were used as spin probes. [31–41]

Let us now consider the results obtained for ionic and nonionic detergents.

a. Ionic micelles

Studies of the micelles formed by sodium, lithium, and tetramethylammonium dodecyl sulfates showed [31–34,41] that the structures of these micelles differ strongly, although the lengths of the alkyl parts of the detergent molecules are the same (12 carbon atoms). The differences in the structure and permeability of these micelles are governed by the nature of the counterion. Detergent molecules deuteriated at the terminal methyl groups, deuteriated water, and the deuteriated tetramethylammonium cation were used in these studies.

The modulation depth of the spin echo of sodium dodecyl sulfate micelles, which characterises the dipole interaction of the lone pair belonging to the spin label with the deuteriated terminal methyl groups of the detergent, increases monotonically as the nitroxy-group moves further away from the carboxy-group of the doxylstearic acid (i.e., as *n* in the formula of compound **7**, *n*-DSA, increases). This implies that the distance between the spin label and the terminal methyl groups increases.

The depth of modulation due to dipole interaction with the magnetic moments of the deuterium in D_2O decreases as the spin label moves further away from the carboxy-group, since this results in an increase in the distance between the spin label and the micelle surface. According to the authors,[32,33] the doxylstearic acids in a sodium dodecyl sulfate micelle have an extended conformation and the detergent molecules are ordered in such a way that the terminal methyl groups are located near the micelle centre. Water hardly penetrates into the hydrocarbon micelle core.

Quite different behaviour is observed in the case of micelles of tetramethylammonium and lithium dodecyl sulfates. They are characterised by a nonmonotonic variation of the spin echo modulation depth due to interactions with the terminal methyl groups of the detergent and with D_2O as the spin label in *n*-DSA moves away from the carboxy-group. Furthermore, the depth of modulation due to the interaction with D_2O is much greater for these micelles than the corresponding value for the sodium dodecyl sulfate micelles.

The features observed can be explained by the fact that the doxylstearic acid in micelles of tetramethylammonium and lithium dodecyl sulfates, in contrast to that in micelles of sodium dodecyl sulfate, has the bent conformation[32] drawn schematically in Fig. 1. Moreover, the structures of the micelles of lithium and tetramethylammonium dodecyl sulfates differ significantly from that of sodium dodecyl sulfate (Fig. 2). In the former case, the detergent molecules in the micelle are bent and the micelle has an open structure, where the counterion can be located between the anionic 'heads' of the micelle. As a result, water penetrates much deeper into the hydrocarbon core of these micelles than into the core of the sodium dodecyl sulfate micelle.

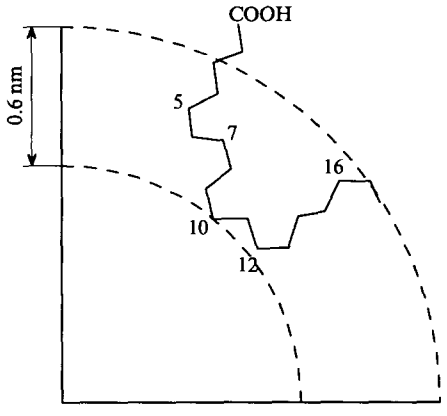


Figure 1. Conformation of *n*-DSA in a tetramethylammonium dodecyl sulfate micelle.[32] The numbers specify the carbon atoms to which the nitroxy-group is attached.

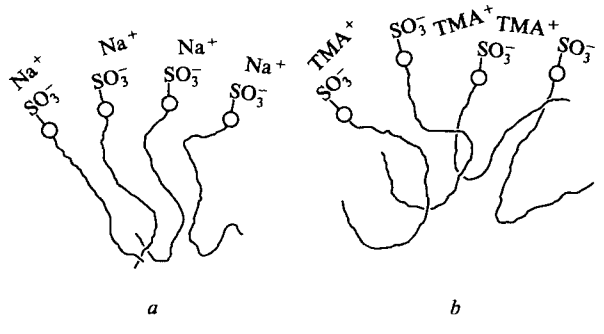


Figure 2. Fragments of a sodium dodecyl sulfate micelle (*a*) and a tetramethylammonium dodecyl sulfate micelle (*b*).[32] TMA^+ is the tetramethylammonium cation.

The results obtained[31–34,41] demonstrated that minor changes in the detergent structure, i.e. replacement of the Na^+ cation by Li^+ or the tetramethylammonium cation, result in significant changes in the micelle structure and in the permeability of the hydrocarbon core.

A study of the effect of urea on the structure of micelles of anionic (sodium dodecyl sulfate) and cationic (dodecyltrimethylammonium bromide) detergents has shown[35] that in both cases urea interacts with the polar groups of the micelle surface. Since this interaction is stronger for dodecyltrimethylammonium bromide, more urea molecules are solubilised on the micelle surface. This explains the fact that urea changes the CMC of dodecyltrimethylammonium bromide more strongly than that of sodium dodecyl sulfate.

The results obtained by the spin echo method are in good agreement with the results of studies on the effect of urea on the structure of the micelles of sodium dodecyl sulfate and dodecyltrimethylammonium bromide by ESR spin probe spectroscopy.[21] The latter show that urea is solubilised on the micelle surface and partially penetrates into the hydrocarbon core near the surface. Urea partially substitutes water in the micelle hydrate shell; this has a weak effect on the polarity but increases markedly the microviscosity of the micelle surface layer.

Crown ethers are also localised on the surfaces of sodium and lithium dodecyl sulfate micelles, giving rise to complexes of the crown ether with the counterion.[36,37] The complex is localised on the micelle surface; as a result, the hydration of the surface decreases.

The addition of an alcohol results in an increase in the penetration of water into the sodium dodecyl sulfate micelle core; at high concentrations of alcohol, destruction of the micelle can occur. The effect of the alcohol depends on the length and degree of branching of the alkyl chain of the aliphatic alcohol in the series 1-propanol < 2-propanol < 1-pentanol < 1-octanol.[38,39]

The spherical micelles of ammonium perfluoroctanoate $[CF_3(CF_2)_6COONH_4]$ were studied by the electron spin echo method[45] using doxylstearic acids **7** whose nitroxy-groups were linked to the hydrocarbon chain at the 5-, 12-, or 16-positions (5-DSA, 12-DSA or 16-DSA). The study of the structures of the micelles of perfluorinated detergents is undoubtedly of interest, since the properties of these micelles differ significantly from those of similar hydrogen-containing detergents. For example, the aggregation number (*n*) for the $CF_3(CF_2)_6COONH_4$ micelles is about twice that for the $CH_3(CH_2)_6COONH_4$ micelles.

It has been found that doxylstearic acids in ammonium perfluoroctanoate micelles are arranged in such a way that the carboxy-group is located in the polar layer of the interface and is surrounded by the polar groups of the detergent. The hydrocarbon chain of the spin probe is not directed to the micelle centre (along the fluorocarbon chains) but is located in the micelle core close to the interface. It turned out that the distances from different carbon atoms of the alkyl chain in *n*-DSA to the interface differ insignificantly. The nitroxy-groups of all *n*-DSA are accessible to water molecules, but the nitroxy-group of 12-DSA is slightly closer to the interface (it is surrounded by four water molecules) than the nitroxy-groups of 5-DSA or 16-DSA (each of them is surrounded by two water molecules). It is noteworthy that the local environment of the nitroxy-groups of 5-DSA in an ammonium perfluoroctanoate micelle is apparently not the same as that of 16-DSA. This follows from the fact[46] that the rotational correlation time of the probe determined by ESR is much lower for 5-DSA (2.3×10^{-10} s) than for 16-DSA (1.1×10^{-9} s).

b. Nonionic micelles

The micelles formed by nonionic detergents in water can solubilise organic compounds. These detergents have a low toxicity and are extensively used in the food and pharmaceutical industries.[47]

Typical representatives of nonionic detergents are polyoxyethylene compounds with the general formula[48] $n\text{-}C_nH_{2n+1}.(OCH_2CH_2)_mOH$. They consist of an alkyl chain comprising 8–12 carbon atoms and the more polar oxyethylene groups. The structure of the micelles formed by these detergents has been studied in detail by the spin echo method.[40,41]

Detergents containing a different number of carbon atoms in the alkyl chains (C_n) and a different number of oxyethylene groups (E_m) were used: $C_{12}E_6$, $C_{12}E_8$, C_6E_8, and C_8E_8. The detergent molecules were selectively deuteriated, either at the alkyl chain or at the oxyethylene groups. The same doxylstearic acids (7, *n*-DSA) with the spin labels at different carbon atoms of the alkyl chain were used as spin probes. D_2O was used to elucidate whether water can penetrate deeply into the micelle.

The following results were obtained.

1. The doxylstearic acid introduced as the spin probe into a micelle is predominantly localised in the polyoxyethylene part of the micelle and has a bent conformation (Fig. 3). The spin label does not penetrate deeply into the hydrocarbon core (for example, not more than by ~1 Å for the $C_{12}E_6$ micelle). The hydrocarbon and polyoxyethylene parts do not mix with each other and are separated by a distinct boundary.

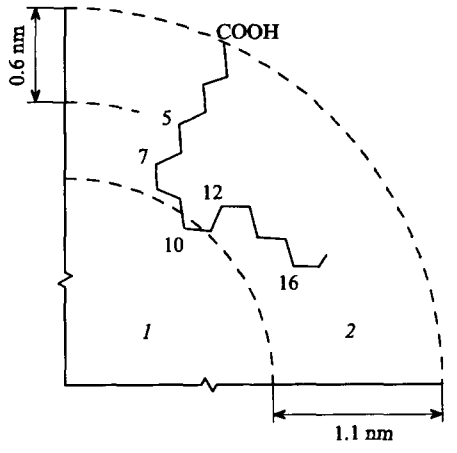


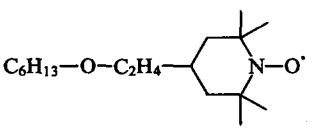
Figure 3. Conformation of *n*-DSA in a polyoxyethylene $C_{12}E_6$ micelle. The numbers specify the carbon atoms to which the nitroxy-group is attached:[40] (*1*) hydrocarbon core; (*2*), polyoxyethylene shell.

2. Water virtually does not penetrate into the micelle hydrocarbon core and penetrates only slightly into the outer polyoxyethylene shell. The polyoxyethylene layer is a reliable protection against the penetration of water into the hydrocarbon core. Only 1–2 oxyethylene moieties, located in the immediate vicinity of the micelle boundary are in contact with water. The longer the hydrocarbon and polyoxyethylene groups, the greater the difficulty with which water penetrates into the micelle. The surfaces of nonionic micelles are hydrated much more weakly than those of ionic micelles.

IV. Polymeric micellar systems

Polymer chains can be involved in the formation of ordered micellar structures in water. Polyelectrolyte complexes, i.e. the products formed by polyelectrolytes and surfactants,[49] are an example of these structures. The electrostatic interaction of the oppositely charged groups of the polyelectrolyte and the detergent and the hydrophobic interaction of the hydrocarbon regions of the detergent molecules play the major role in the formation of polyelectrolyte complexes. When a polyelectrolyte complex is formed, the detergent molecules form an internal macromolecular hydrophobic region (the micellar phase) reinforced by a polymer chain. Either water-soluble or insoluble polyelectrolyte complexes can be formed, depending on the polymer/detergent ratio in the aqueous solution. For example, the polyacrylic acid—dodecyltrimethylammonium bromide system at pH 6 with the concentration ratio of the surfactant and the polyacrylic acid monomer units $\varphi \leqslant 0.3$ yields a water-soluble complex whose composition (φ) is the same as that of the reaction mixture. The solubility of this complex is determined by the length of the polymer regions not bonded with detergent molecules. If the molar fraction of the detergent is increased, a complex is formed whose composition corresponds to $\varphi = 1$. Not all polyelectrolyte molecules dissolved in water participate in the formation of these complexes. However, all the units of the polymer chain participating in the complex formation interact with the detergent molecules. These complexes are insoluble in water and form precipitates.

A spin probe, whose structure is shown below, has been used to study the structure and molecular dynamics of both water-soluble and insoluble polyacrylic acid — dodecyltrimethylammonium bromide complexes.



The structure of this complex and the assumed location of the probe are presented in Fig. 4.

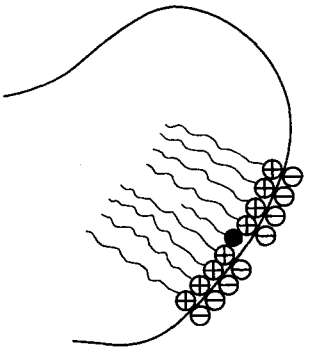


Figure 4. Structure of a polyelectrolyte–detergent complex.[50] The filled circle represents a spin probe.

The following results were obtained:[50]

1. The a_N constant for a polymeric micellar system (16.2 G) is lower than that for an aqueous solution of the polymer (16.9 G). Evidently, the nitroxy-group of the probe is located near the polymer chain of the complex and not in water (see Fig. 4).

2. The rotational correlation time of the probe in the polymer complex (7.2×10^{-10} s) is almost twice as long as that in a dodecyltrimethylammonium bromide micelle. This implies that the local mobility in polymeric micelles is much smaller than in spherical micelles of the same detergent. It cannot be ruled out that detergent molecules are more densely packed in a polymeric micelle than in a spherical micelle.

The rotational correlation time of a spin probe at $\varphi \leqslant 0.3$ does not depend on the composition of the complex. Moreover, the rotational correlation time of the probe in a water-soluble complex is almost equal to that in an insoluble complex. These results are consistent with the hypothesis of the block structure of polyelectrolyte–detergent complexes[49] and permit the conclusion that the phase separation accompanied by the formation of insoluble complexes does not result in an appreciable change in the molecular mobility and hence in the packing density of the detergent molecules in ordered polymeric micellar systems.

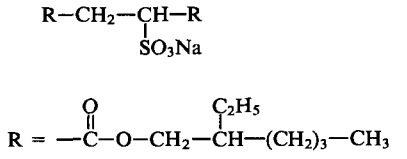
V. Reverse micelles

Many ionic and nonionic detergents form reverse micelles in nonpolar solvents.[51] These micelles consist of a polar core and a nonpolar shell. The main feature of these micelles is their ability to solubilise the polar molecules localised in the micelle core; for example, water molecules. When the water content is high, thermodynamically stable microemulsions are formed. Their use as microreactors opens up new prospects for conducting photochemical, catalytic, polymerisation, oxidation, and other processes. Reverse micelles are also of interest as models of biological membranes.[52–55]

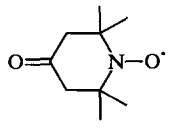
The conditions for the appearance of reverse micelles, their structure and properties, and the characteristics of the kinetics and mechanisms of the reactions occurring in them have been thoroughly studied by various physicochemical methods.[51–55] We shall discuss certain results obtained by the spin probe method.[56–65]

1. Ionic reverse micelles

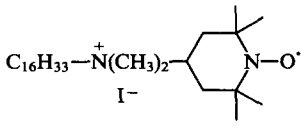
In the studies by the spin probe method particular attention has been devoted to reverse micelles of sodium bis(2-ethylhexyl)-sulfosuccinate or Aerosol OT (AOT).[56–59, 61, 62, 64]



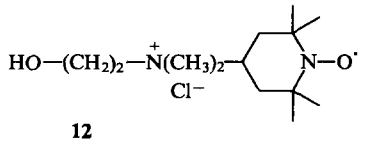
Various probes, soluble either in the aqueous core or in the hydrocarbon shell of the micelle, were used.



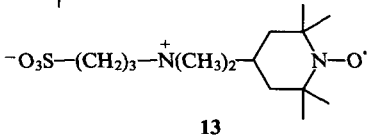
10



11



12



13

n-DSA (where n = 5, 6, 7, 9, 10, or 16) were also used as probes.

It was shown by use of the light scattering technique[66] that the aggregation number of micelles formed by AOT molecules in nonaqueous media is ~23 in the absence of water. The micelle is almost spherical with a diameter of ~24 Å. The addition of water results in an increase in the micelle size and an improvement in its sphericity. Moreover, a cavity consisting of water molecules and surrounded by a monolayer of AOT molecules is formed inside the micelle. The monolayer thickness is ~11 Å and the radius of the aqueous cavity can be calculated (in ångstroms) according to the formula [58, 62, 67]

$$r \sim 1.5\, W_0,$$

where W_0 is the ratio of the concentrations of water and AOT in the system.

It is interesting to note that the length of the hydrocarbon part of the AOT molecule calculated on the basis of the standard interatomic distances in organic molecules[68] is 12.57 Å, whereas the length of the hydrophilic head ($Na^+O_3S^-$) is 5 Å.

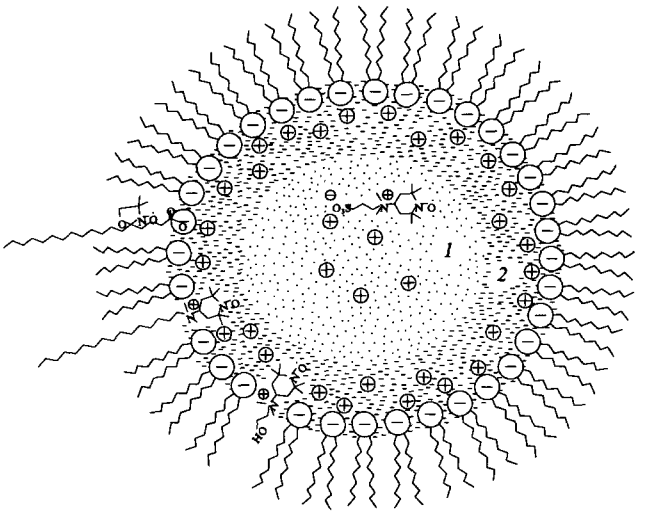


Figure 5. Schematic illustration of an AOT reverse micelle with spin probes:[62] (*1*) 'free' water; (*2*) hydrate layer.

Fig. 5 illustrates schematically an AOT reverse micelle in isooctane and shows the assumed locations of the probes.

The following questions are of interest when the results of studies on the molecular dynamics and structure of reverse micelles by the spin probe method are discussed.

1. What is the state of the water in the centre of a reverse micelle? Is the water 'free', i.e. with the properties of bulk-phase water, or does it participate in the formation of the hydrate layer?

2. Does water penetrate into the micelle hydrocarbon shell and is this penetration sufficiently deep?

3. What is the mobility of the micelle hydrocarbon shell, and how does this depend on the distance from the polar group and on the water content in the micelle?

The conclusion was reached on the basis of analyses of the isotropic hyperfine coupling constants and the rotational mobility of spin probes located in different micelle regions [52–59, 62, 64] that, for a high water content ($W_0 > 20$), the central region of the micelle contains 'free' water whose properties do not differ from those of the usual water. Not all the water solubilised in the micelle is free, a proportion of its molecules participating in the formation of the hydrate layer. For a low water content ($W_0 < 10$), all the water participates in the formation of the hydrate layer. For $10 < W_0 < 20$, the formation of free water begins.

Specimens with $W_0 = 30$ studied at low temperatures display a superposition of the ESR spectra for radicals **10** localised in water and in the micelle hydrocarbon shell.[58] The activation energy for probe transfer from the hydrocarbon shell to water was determined (~30 kJ mol^{-1}) from the temperature dependence of the line widths. The conclusion was reached[59] on the basis of detailed modelling of the spectra that fast probe exchange between the hydrocarbon shell and the hydrate layer and slow exchange between the hydrate layer and free water occur. However, the question why the frequency of probe exchange between the two aqueous phases is lower than between the aqueous phase and the hydrocarbon shell remains open.

Fig. 6 presents the dependence of the hyperfine coupling constant for doxylstearic acid in an AOT reverse micelle on the number of the carbon atom linked to the nitroxy-group. The value of a_N is a maximum for 5-DSA and decreases as n increases, i.e. as the nitroxy-group moves away from the micelle core. An analysis of the a_N constants for doxylstearic acids incorporated into the shells of micelles with different water contents led to the conclusion[62] that water penetrates into the hydrocarbon shell and that the accessibility of the shell to water is greater the closer the given shell region to the micelle centre and the higher the water content in the micelle core.

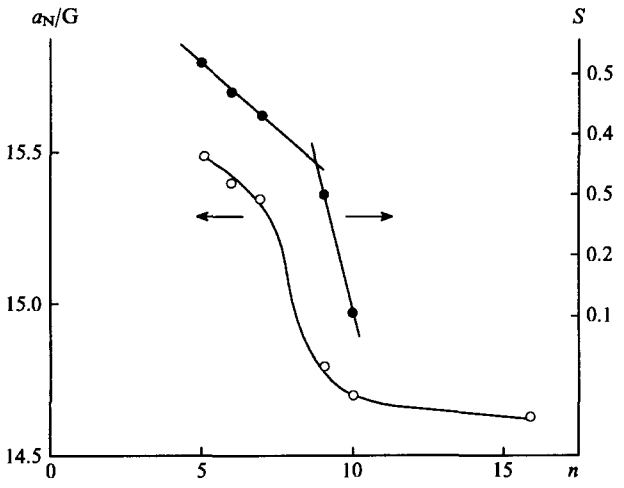


Figure 6. Dependence of the isotropic hyperfine coupling constant (a_N) and the order parameter (S) of the spin probe on the number of the carbon atom (n) to which the nitroxy-group in the n-DSA incorporated in the micelle is attached.[62]

The molecular mobility of doxylstearic acids in the shell of the AOT micelles was characterised[62] by the order parameter S calculated by the equation[69,70]

$$S = \frac{A_{\parallel} - A_{\perp}}{A_{zz} - \frac{1}{2}(A_{xx} + A_{yy})} \frac{a_0}{a_N}. \quad (2)$$

Here A_{xx} = 6.3, A_{yy} = 5.8, and A_{zz} = 33.6 G are the main values of the hyperfine coupling tensor for doxylstearic acids, $A_{\parallel}$ and $A_{\perp}$ are the corresponding parameters determined from the experimental ESR spectra,[69,70] and a_0/a_N is a correction for the polarity of the probe environment: $a_0 = (1/3)(A_{xx} + A_{yy} + A_{zz})$, $a_N = \frac{1}{3}(A_{\parallel} + 2A_{\perp})$. The S parameter is frequently used to characterise the strongly anisotropic rotation of spin labels, for example, the rotation of lipid spin labels in biomembranes.[69]

The S parameter depends on the frequency and amplitude of the motion of the spin label. In particular, the model of the rapid oscillation of the long axis of a lipid spin label (at frequencies above 10^8 s^{-1}) assumes that $S = 0$ if the oscillation half-amplitude is 90° and $S = 1$ if the oscillation half-amplitude is zero.[70] The S parameter is normally used to characterise the relative variation of the molecular mobility, for example, for constructing the flexibility profiles of biomembranes.[70]

The S parameter determined for doxylstearic acid in AOT reverse micelles decreases almost linearly as the spin label moves further away from the carboxy-group (Fig. 6).[62] Simultaneously, the rotation of the label becomes increasingly more isotropic. This implies that the amplitude of the movement of the hydrocarbon chain segment of the AOT molecule in the micelle increases as it moves further away from the micelle centre. In other words, the mobility of the micelle hydrocarbon shell increases as it approaches the terminal methyl groups. The conclusion that the molecular mobility of the micelle shell depends on the distance from its centre is consistent with the results[71] obtained by the ^{13}C NMR method.

The S parameter depends not only on the distance of the spin label from the micelle centre but also on the water content in the micelle: it increases with the diameter of the aqueous core of the micelle. An increase in the water content in the micelle is accompanied by a decrease in the intensity of the molecular motion in the hydrocarbon shell.

It is important to emphasise that the S value could be determined reliably only for micelles with $W_0 > 10$ whose radii were above 25 Å.[62] The rotation of small micelles (for $W_0 < 10$) as a whole and the lateral diffusion of the spin probe along the micelle surface to a large extent average out the hyperfine coupling anisotropy, thus preventing the correct determination of the S parameter.

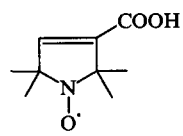
The structure and permeability of the AOT reverse micelle in isooctane were determined by the electron spin echo modulation method,[64] using the same doxylstearic acids as in the ESR studies of the structure of this micelle.

Analysis of the dipole interaction of the spin label with the magnetic moments of deuterium in D_2O and deuteriated isooctane led to the conclusion that the doxylstearic acid is incorporated into the micelle in such a way that the carboxy-group is located near the hydrophilic SO_3^- group of the detergent. The doxylstearic acid in the AOT micelle has an extended conformation similar to that in direct micelles of sodium alkyl sulfates. Isooctane virtually does not penetrate into the bulk of the micelle but readily enters the outer regions of the hydrocarbon shell. An increase in the volume of the aqueous cavity results in a decrease in the hydrocarbon shell permeability to isooctane. For a low water content ($W_0 < 10$) the area of the hydrocarbon shell–water interface is too small to accommodate all the polar 'heads' of the molecules at this boundary. An increase in the water content leads to a structural rearrangement. As a result, all the polar 'heads' are located at the interface. The results obtained[64] confirm the existing idea that the shell almost completely prevents the penetration of the hydrocarbon into the micelle core.

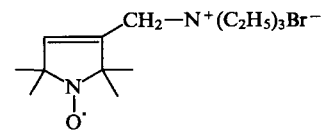
2. Nonionic reverse micelles

The compound $CH_3(CH_2)_8C_6H_4(OCH_2CH_2)_4OH$ readily forms reverse micelles in cyclohexane in the presence of a small amount of water.[72]

The following nitroxyl radicals were used in the study of the molecular dynamics and structure of these micelles by spin probe ESR spectroscopy.[65]



14

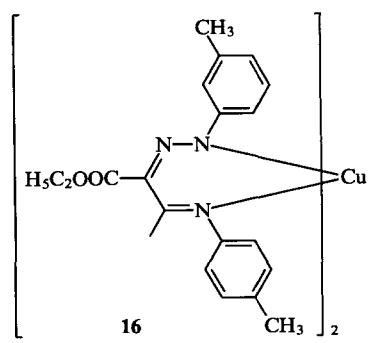


15

5-DSA was also used as the probe.

Radical **14** is soluble in water and cyclohexane, but its solubility in water is 10^3 times greater than in cyclohexane.[2] Radical **15** is only soluble in water and practically insoluble in cyclohexane and other nonpolar solvents. The 5-DSA radical is readily soluble in the micelle hydrocarbon shell and also in cyclohexane.

Apart from nitroxyl radicals, paramagnetic copper compounds were also used: $CuCl_2$ (water-soluble) and complex **16** (soluble in cyclohexane and other nonpolar solvents).



16

Specimens with $W_0 = [H_2O]/[\text{surfactant}] = 0.1-6.9$ were used (nonionic reverse micelles solubilise less water than ionic micelles).

For probe **14** in all the specimens with $W_0 > 0.3$, a superposition of the ESR spectra of the radicals in the aqueous core (a_N = 16.1 G in water) and in cyclohexane (a_N = 14.1 G) was

observed. The solubility of the radical in water is much higher than in cyclohexane, but the amount of cyclohexane in the specimen is much greater than that of water. As a result, the number of radicals dissolved in water is comparable to that in cyclohexane and a superposition of the spectra is therefore observed.

If $CuCl_2$ is added to the water involved in the formation of the micelle core, then the spectrum of radical **14** is observed only in cyclohexane. If paramagnetic complex **16** is added to cyclohexane, the ESR spectrum of the radical is observed only in the aqueous core of the micelle. In both cases, the disappearance of one of the spectra is caused by its broadening due to the exchange interaction with the paramagnetic copper ion. This method for the separation of complex spectra [2,73] is extensively used in the study of complex microheterogeneous systems. Not only paramagnetic copper compounds, but also iron compounds such as $K_3Fe(CN)_6$, are used as broadening agents that penetrate differently into different regions of a complex system.

Radical **15** is insoluble in cyclohexane or in the micelle hydrocarbon shell and is localised in the aqueous core. The results obtained using radicals **14** (with the addition of complex **16** to cyclohexane) and **15** are in good agreement.

The aqueous core of the micelle has a minimal local mobility for $W_0 = 0.6$ (for radical **15** $\tau = 5.4 \times 10^{-10}$ s and $a_N = 15.1$ G). An increase in the water content in the micelle results in a decrease in the rotational correlation time of the radical, while τ and a_N approach the corresponding values for this radical in water ($\tau = 0.5 \times 10^{-10}$ s, $a_N = 15.9$ G).

Comparison of the values of τ and a_N and of the temperature dependences of the rotational correlation times for radical **15** in the aqueous core of the micelle and in a model system — polyoxyethylene swollen in water — shows [65] that an aqueous cavity, whose formation involves free water molecules, appears in the micelle centre. The micelle core is inhomogeneous and water is not distributed uniformly along the oxyethylene chains, at least a fraction of the water being segregated as a separate phase in the centre of the micelle.

When complex **16** is added to cyclohexane, the intensity of the ESR spectrum of radical **15** localised in the aqueous core of the micelle decreases. This is explained by the dipole interaction of the complex with the radical depending on their distance of closest approach. [74–76] The distance of closest approach is the minimum distance that can be reached between the complex and the radical as they approach each other. When the water content in the micelle increases (W_0 increases from 0.6 to 6.9), the distance of closest approach of the complex (in cyclohexane) and the radical (in the micelle core) increases approximately by a factor of two. This is explained by the fact that an increase in the water content results in a decrease in the permeability of the micelle hydrocarbon shell to the molecules of cyclohexane and the organic compounds dissolved in it. The decrease in the shell permeability can be due to a decrease in the intensity of the molecular motion of the hydrocarbon chains.

The conclusion that the intensity of the molecular motions of the hydrocarbon chains of the micelle shell decreases with increase in the water content has been confirmed by studying the ESR spectra of the 5-DSA radical. This radical is almost totally solubilised in the micelle hydrocarbon shell. The ESR spectrum of the radicals dissolved in cyclohexane is fully broadened [is broadened until its complete disappearance? (Translator)] when complex **16** is added to cyclohexane. The radical is localised in the micelle shell so that the nitroxy-group is located in the region consisting of the polyoxyethylene groups. In the $1.8 < W_0 < 6.9$ range, ESR spectra indicate a highly anisotropic rotation of the probe. An increase in the water content in the micelle leads to a monotonic growth of the S parameter calculated according to Eqn (2) ($S = 0.35$ and 0.44, respectively for $W_0 = 1.8$ and 6.9). The reason is that an increase in the volume of the micelle aqueous phase results in a decrease in the intensity of the molecular motion of the micelle shell.

Thus the molecular structure, dynamics, and permeability of the hydrocarbon shells of nonionic reverse micelles depend markedly on the amount of water solubilised by the micelle core. [65]

It is interesting to note that the ESR spectra of spin probes **14** and 5-DSA for low water contents ($W_0 < 0.3$) indicate that a fast exchange (at frequencies above 10^8 s^{-1}) of the radicals localised in the micelle shell and in cyclohexane occurs. Evidently, a fast exchange between detergent molecules localised in the micelle shell and dissolved in cyclohexane also takes place under these conditions. If the content of water increases, the rate of exchange decreases, and the process becomes slow (on the ESR time scale).

VI. Conclusion

Spin probes are a unique instrument for studying the molecular dynamics and structure of ordered micellar systems. They make it possible to determine the characteristic rotational times and the shape of the micelles, to record the micelle formation process and the formation of premicellar aggregates, and to determine the local molecular mobility and polarity of different micelle regions. The use of electron spin echo spectroscopy provides interesting information about the conformational state and permeability of the micelle hydrocarbon regions. It has been found unexpectedly that small changes in the structure of the detergent molecule, for example, the replacement of the Na^+ cation by Li^+ or the tetramethylammonium cation, result in substantial changes in the packing, conformation, and permeability of the hydrocarbon core of an alkyl sulfate micelle. Water hardly penetrates into the hydrocarbon cores of nonionic direct micelles of polyoxyethylene detergents and penetrates into the outer polyoxyethylene shell only to a very slight extent.

Polymeric membrane systems, whose detailed investigation has recently begun, are of particular interest. It has been shown by the spin probe method that the local mobility of detergent molecules in a polymeric micelle is much lower than in micelles of the same detergent containing no polymer.

The studies on reverse micelles have revealed the state of water in the micelle core (bound water participating in the formation of the hydrate layer or free water possessing the properties of the usual water). It was found how the local mobility and permeability of the hydrocarbon shell of the micelle depend on its water content and on the distance from the shell to the micelle centre.

It is important to stress that the above principles and approaches, developed during the study of the molecular dynamics and structure of direct, reverse, and polymer micelles, are used successfully to study more complex ordered molecular systems, such as multicomponent emulsions and vesicles (see, for example, Refs 77, 78).

This review has been written within the scope of works supported by the Russian Fund for Fundamental Research (grant 94-03-08572).

References

1. A L Buchachenko, A M Wasserman *Stabil'nye Radikaly* (Stable Radicals) (Moscow: Khimiya, 1973)
2. A N Kuznetsov *Metod Spinovogo Zonda* (The Spin Probe Method) (Moscow: Nauka, 1976)
3. L J Berliner (Ed.) *Spin Labeling. Theory and Applications* (New York: Academic Press, 1976) (Translated into Russian; Moscow: Mir, 1979)
4. A M Wasserman, A L Kovarskii *Spinovye Metki i Zondy v Fizikokhimii Polimerov* (Spin Labels and Probes in the Physical Chemistry of Polymers) (Moscow: Nauka, 1985)
5. A S Waggoner, O H Griffith, C R Christensen *Proc. Natl. Acad. Sci. USA* **57** 1198 (1967)
6. K L Mittal, B Lindeman (Eds) *Surfactants in Solutions* (New York: Plenum, 1984), Vols 1–3; K L Mittal, P Botherel (Eds) *Surfactants in Solutions* (New York: Plenum, 1986) Vols 4–6

7. A I Rusanov *Mitselloobrazovanie v Rastvorakh Poverkhnostno-aktivnykh Veshchestv* (The Formation of Micelles in Solutions of Surfactants) (St Petersburg: Khimiya, 1992)
8. E J Fendler, J H Fendler *Advances in Physical Organic Chemistry* (Ed. V Gold) (London: Academic Press, 1970) Vol. 8; *Progress in Physical Organic Chemistry* (Eds A Streitwieser Jr, R W Taft) (New York: Interscience, 1970) Vol. 7 (Translated into Russian; Moscow: Mir, 1979) p. 119
9. M G Kuz'min, N K Zaitsev, in *Elektrokhimiya (Itogi Nauki i Tekhniki)* Vol. 28 [Electrochemistry (Advances in Science and Engineering)] (Moscow: Izd. VINITI, 1988) p. 248
10. V F Tarasov, N D Ghatlia, A L Buchachenko, N J Turro *J. Am. Chem. Soc.* **114** 9517 (1992)
11. P J Missel, N A Mazer, G B Benedek, M C Carey *J. Phys. Chem.* **87** 1264 (1983)
12. E A Anianson, S N Wall, S N Almgen, H Hoffman, I Killman, W Ulbricht, R Zana, J Lang, C Toudre *J. Phys. Chem.* **80** 905 (1976)
13. K R Capidas, A R Leheny, G Caminati, N J Turro, D A Tomalia *J. Am. Chem. Soc.* **113** 7335 (1991)
14. J Frid, in *Spin Labeling. Theory and Applications* (Ed. L J Berliner) (New York: Academic Press, 1976) (Translated into Russian; Moscow: Mir, 1979) p. 64
15. A Panata, V M Coiro, F Massa *Chem. Phys. Lett.* **200** 130 (1992)
16. P J Missel, N A Mazer, G B Benedek, C Y Young, M C Carey *J. Phys. Chem.* **84** 1044 (1980)
17. M F Ottaviani, P Baglioni, G Martini *J. Phys. Chem.* **87** 3146 (1983)
18. P Baglioni, E Ferroni, G Martini, M F Ottaviani *J. Phys. Chem.* **88** 5107 (1984)
19. P Baglioni, M F Ottaviani, G Martini *J. Phys. Chem.* **90** 5878 (1986)
20. P Baglioni, in *Surfactants in Solutions* Vol. 4 (Eds K L Mittal, P Botherel) (New York: Plenum, 1986) p. 393
21. P Baglioni, E Rivara-Minten, L Dey, E Ferroni *J. Phys. Chem.* **94** 8218 (1990)
22. M F Ottaviani, N D Ghatlia, N J Turro *J. Phys. Chem.* **96** 6075 (1992)
23. K R Gopidas, A R Leheny, G Caminati, N J Turro, D A Tomalia *J. Am. Chem. Soc.* **113** 7335 (1991)
24. P Baglioni, M F Ottaviani, G Martini, E Ferroni, in *Surfactants in Solutions* Vol. 1 (Eds K L Mittal, B Lindeman) (New York: Plenum, 1984) p. 541
25. A G Anianson, S N Wall, M Almgren, H Hoffman, I Kielmann, W Ulbricht, R Zana, J Long, C Tondre *J. Phys. Chem.* **80** 905 (1976)
26. K Kamagava, K Tajima *J. Phys. Chem.* **97** 9506 (1993)
27. J H Baxendale, M A Rodgers *J. Phys. Chem.* **86** 4906 (1982)
28. T Tominage, S Matsumoto, T Koshiba, Y Yamamoto *Chem. Lett.* 1427 (1988)
29. D Kuhn, C A Craus *J. Phys. Chem.* **72** 3676 (1950)
30. L Kevan *Time Domain Electron Spin Resonance* (Eds L Kevan, R N Schwartz) (New York: Wiley, 1979) Ch. 8
31. E Szajdzinska-Pietek, R Maldonado, L Kevan, R R M Jones *J. Am. Chem. Soc.* **106** 4675 (1984)
32. E Szajdzinska-Pietek, R Maldonado, L Kevan, R R M Jones, M J Coleman *J. Am. Chem. Soc.* **107** 784 (1985)
33. R R M Jones, R Maldonado, E Szajdzinska-Pietek, L Kevan *J. Phys. Chem.* **90** 1126 (1986)
34. R Maldonado, E Szajdzinska-Pietek, L Kevan, R R M Jones, in *Surfactants in Solutions* Vol. 4 (Eds K L Mittal, P Botherel) (New York: Plenum, 1986) p. 253
35. P Baglioni, E Ferroni, L Kevan *J. Phys. Chem.* **94** 4296 (1990)
36. P Baglioni, L Kevan *J. Chem. Soc., Faraday Trans. 1* **84** 467 (1988)
37. P Baglioni, R Rivara-Minten, L Kevan *J. Phys. Chem.* **92** 4726 (1988)
38. E Szajdzinska-Pietek, R Maldonado, L Kevan, R R M Jones *J. Colloid Interface Sci.* **110** 514 (1986)
39. P Baglioni, L Kevan *J. Phys. Chem.* **91** 1516 (1987)
40. P Baglioni, P Bongiovanni, R Rivara-Minten, L Kevan *J. Phys. Chem.* **93** 5574 (1989)
41. L Kevan, P Baglioni *Pure Appl. Chem.* **62** 275 (1990)
42. P Narayana, A S W Li, L Kevan *J. Am. Chem. Soc.* **103** 3603 (1981)
43. S Nahimoto, J K Thomas *J. Am. Chem. Soc.* **105** 5230 (1983)
44. W John, R Strey *J. Phys. Chem.* **92** 2294 (1988)
45. M Romanelli, S Ristory, G Martini, Y-S Kang, L Kevan *J. Phys. Chem.* **98** 2125 (1994)
46. S Ristory, G Martini *Langmuir* **8** 1937 (1992)
47. V Degiorgio, in *Physics of Amphiphiles: Micelles, Vesicles and Microemulsions* (Eds V Degiorgio, M Corty) (Amsterdam: North-Holland, 1985) p. 303
48. D J Mitchel, G J T Tiddy, L Waring, T Bostock, M P McDonald *J. Chem. Soc., Faraday Trans. 1* **79** 975 (1983)
49. Z Kh Ibragimova, V A Kasaikin, A B Zezin, V A Kabanov *Vysokomol. Soedin., Ser. A* **28** 1640 (1986)
50. Yu A Zakharova, A D Kolbanovskii, L A Krinitskaya, V G Sergeev, V A Kasaikin, A M Wasserman *Vysokomol. Soedin.* (in the press, 1994)
51. H F Eicke, in *Topics in Current Chemistry* (Ed. F L Boschke) (Berlin: Springer, 1980) p. 86
52. P L Luisi, B E Straub (Eds) *Reverse Micelles* (New York: Plenum, 1984)
53. *Structure and Reactivity in Reverse Micelles* (Amsterdam: Elsevier, 1989)
54. W J Rosen *Surfactants and Interfacial Phenomena* (New York: Wiley, 1989)
55. J H Fendler, E J Fendler *Catalysis in Micellar and Macromolecular Systems* (New York: Academic Press, 1975)
56. F M Menger, G Sato, G V Sanzero, J R Dodd *J. Am. Chem. Soc.* **97** 909 (1975)
57. H Yoshioka *J. Colloid Interface Sci.* **83** 214 (1981)
58. H Yoshioka *J. Colloid Interface Sci.* **95** 81 (1983)
59. H Yoshioka, S Kazama *J. Colloid Interface Sci.* **95** 240 (1983)
60. Y Y Lim, J H Fendler *J. Am. Chem. Soc.* **100** 7490 (1978)
61. A Barelli, H F Eicke *Langmuir* **2** 780 (1986)
62. G Haering, P L Luigi, H Hausser *J. Phys. Chem.* **92** 3574 (1988)
63. C Kumur, C Balasubramanian *J. Phys. Chem.* **84** 1895 (1980)
64. P Baglioni, N Makamura, L Kevan *J. Phys. Chem.* **95** 3856 (1991)
65. H Caldaruri, A Caragheorgheopol, M Dimonil, D Donescu, I Dragutan, N Marinescu *J. Phys. Chem.* **96** 7109 (1992)
66. P Ekwall, K Fontell *J. Colloid Interface Sci.* **33** 215 (1970)
67. W Wong, J K Thomas, T Nowak *J. Am. Chem. Soc.* **99** 4730 (1977)
68. E Y Sheu, S H Chen, J S Huang *J. Phys. Chem.* **91** 3306 (1987)
69. O H Griffith, P Jost, in *Spin Labeling. Theory and Applications* (Ed. L J Berliner) (New York: Academic Press, 1976) (Translated into Russian; Moscow: Mir, 1979) p. 489
70. G McConnell, in *Spin Labeling. Theory and Applications* (Ed. L J Berliner) (New York: Academic Press, 1976) (Translated into Russian; Moscow: Mir, 1979) p. 570
71. J Carneli, O Sodeman, H Walderhaug *Langmuir* **2** 51 (1986)
72. A Kitahara *J. Phys. Chem.* **69** 2788 (1965)
73. G I Likhtenshtein *Metod Spinovykh Metok v Molekulyarnoi Biologii* [The Spin Labeling Method in Molecular Biology) (Moscow: Nauka, 1974)
74. J S Leigh, Jr *J. Phys. Chem.* **52** 2608 (1970)
75. J Hyde, H M Swartz, W E Antholine, in *Spin Labeling II* (Ed. L J Berliner) (New York: Academic Press, 1979) p. 71
76. R S Sealy, C C Felix, J S Hyde, H M Swartz, in *Free Radicals in Biology* (Ed. W A Pryor) (New York: Academic Press, 1980) p. 209
77. P Baglioni, C M C Camby, D Goldfarb *J. Phys. Chem.* **95** 2577 (1991)
78. P J Bratt, L Kevan *J. Phys. Chem.* **97** 7371 (1993)

Russian Chemical Reviews **63**(5) 383–398 (1994) ©1994 Russian Academy of Sciences and Turpion Ltd

UDC 541.15

Geminate electron–ion pairs generated by ionising radiation in nonpolar hydrocarbon glasses: recombination, polarisation, and separation

B S Yakovlev (deceased), G F Novikov

Contents

I. Introduction	383
II. Trapped electrons in solid nonpolar hydrocarbons	384
III. Photo- and thermo-stimulated electron–ion recombination	387
IV. Electric polarisation of electron–ion pairs	390
V. Thermo- and photo-stimulated separation of electron–ion pairs	394

Abstract. Nonpolar hydrocarbons which vitrify at a low temperature constitute a 'classical' model system for the investigation of the characteristic features of the radiolysis of nonpolar organic compounds. Considerable experimental data have now accumulated for hydrocarbon glasses, which permit in many instances quantitative assessments of the applicability of various theories. 3-Methylpentane occupies a special place among these substances. Attention is concentrated mainly in this review on the recombination, polarisation, and separation of the electron–ion pairs generated by ionising radiation. The bibliography includes 163 references.

I. Introduction

The greatest advances in the study of reactions involving excess electrons have been achieved previously for liquid media (see the relevant reviews[1–4]). However, free electrons were first detected in weakly polar glasses. The results of many investigations of liquid and solid hydrocarbons have shown that most of the electrons generated by ionising radiation are thermalised during the interaction with the molecules of the given substance over distances at which the Coulombic potential of the attraction of 'own' positive ions is greater than the thermal energy.[1,5] The charge separation in space depends on the type of ionising radiation. For example, radiation with a low linear density of energy losses (high energy electrons, ^{60}Co γ-radiation, etc.) leads, according to Mozumder,[5,6] to the formation of mainly isolated pairs of charges, in a proportion of 60%–70%. The fraction of pairs forming part of groups containing between 4 and 30 pairs is ~14% while that of pairs in groups with more than 30 pairs is <10%.

The behaviour of 'geminate' pairs of charges (or groups forming a track) is not described by the equations of 'usual' homogeneous kinetics.[7] The unusual feature involving the generation of charged particles on exposure to ionising radiation was noted long ago.[8] At the present time, it has been established that this determines the nature of the kinetics of the ionic processes in the liquid-phase radiolysis of hydrocarbons. Again, this feature must not be disregarded in considering the kinetics of the various phenomena induced by ionising radiation in solid hydrocarbons: isothermal and thermostimulated luminescence, optical absorption, electric conductivity, and photoconductivity.

Extensive experimental data have now accumulated from studies on the behaviour of electrons in solid and liquid nonpolar hydrocarbons. These data indicate the similarity of such systems. The appreciable difference between the time scales of the processes led in the beginning to more active studies on solid hydrocarbons. Certain details of the processes were then elucidated, but these became available to experimenters studying liquid systems only during the last decade. In particular, this applies to the electric polarisation of electron–ion pairs. Many questions concerning the behaviour of electrons in various solid nonpolar media have been answered in a series of review publications (see, for example, Refs 9–12). However, the 'classical' system—vitrifying nonpolar hydro-carbons—still remains under consideration by investigators. This review is devoted to the behaviour of electrons in such a system during processes involving the ionisation, recombination, and separation of electron–ion pairs.

1. Yield of separated pairs of charges

Two very important processes control the kinetics of the reactions involved in the generation of charges by ionising radiation in nonpolar glasses: separation and recombination of electron–ion pairs. The diffusion-drift ideas, based on the consideration of the motion of classical particles with a mean free path much shorter than the characteristic dimension of the problem, are usually employed to describe these processes in an amorphous nonpolar substance.[13,14] The simplest case is that of isolated pairs.

Having applied the Smoluchowski equation to this case, Onsager[15] obtained the exact expression for the probability $\phi(\boldsymbol{r},\boldsymbol{E})$ of the separation of charged particles, the position of which is specified by the vector $\boldsymbol{r}$ directed at an angle θ relative to the external field $\boldsymbol{E}$ with a strength E (Fig. 1).

$$\phi(\boldsymbol{r},\boldsymbol{E}) = \exp\left[-\frac{r_c}{r} - \beta r(1+\cos\theta)\right] \times \sum_{m,n=0}^{\infty} \frac{\beta^{n+m}(1+\cos\theta)^{n+m} r_c^m r^n}{m!(m+n)!} \quad (1)$$

B S Yakovlev (deceased) Branch of the Institute of Energy Problems in Chemical Physics, Russian Academy of Sciences, 142432 Chernogolovka, Moscow Region, Russian Federation
G F Novikov Institute of Chemical Physics Chernogolovka, Russian Academy of Sciences, 142432 Chernogolovka, Moscow Region, Russian Federation. Tel. (7-096) 524 50 06 Fax (7-096) 515 35 88
E-mail: novikov@icph 24.sherna.msk.su

Received 12 March 1994
Uspekhi Khimii **63**(5) 402–418 (1994); translated by A K Grzybowski

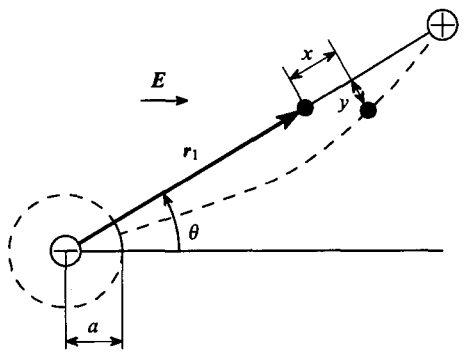


Figure 1. Schematic explanation of the notation. The radius vector of the electron in the absence of an external field is r_1; the trajectory in the mutual approach of ions without allowance for diffusion in the presence of an external field E is shown dashed; x and y are respectively the radial and tangential deviations of the position of the electron from r_1 in the presence of an external field.

After averaging with respect to the angle θ, we have[16]

$$\phi(r,E) = 1 - (2\beta r)^{-1} \sum_{m=1}^{\infty} P(m,2\beta r) P\left(m,\frac{r_c}{r}\right) , \qquad (2)$$

where

$$\beta = \frac{eE}{2k_B T}, \quad P(m,x) = [(m-1)!]^{-1} \int_0^x \exp(-t) t^{m-1} dr .$$

For $E = 0$, Eqn (1), known as the Onsager formula, reduces to

$$\phi_0 = \exp\left(-\frac{r_c}{r}\right) , \qquad (3)$$

where r_c, given by

$$r_c = \frac{e^2}{\varepsilon k_B T} ,$$

is the so called Onsager radius, ε is the relative permittivity, k_B is the Boltzmann constant, and e is the charge on the electron. According to Mozumder,[17] the Onsager model can be used also for electron–ion pairs generated by ionising radiation.

On this hypothesis, it is possible to relate the initial distribution function of thermalised electrons $F(r)$ to the yield $G_{fi}(E)$ of the separated pairs of charges (or the number of separated pairs per unit ionising radiation energy absorbed by the substance):

$$G_{fi}(E) = G_0 \int_0^{\infty} F(r)\,\phi(r,E) dr , \qquad (4)$$

where G_0 is the overall initial yield of the pairs of charges. Eqn (4) makes it possible to infer from the experimental data for G_{fi} the distribution function of the thermalised electrons. This approach has been hitherto one of the important sources of information about $F(r)$.[18,19]

For many liquids, the experimental $G_{fi}(E)$ data were obtained as early as the 1970s, mainly with the aid of electrical methods based on the measurement of the number of charges drawn by the electric field onto the electrodes under conditions preventing the influence of bulk-phase recombination (see, for example, Freeman[20] and Schiller and Vass[21]). The yield in a zero field $G_{fi}(0)$ may be found by extrapolating the $G_{fi}(E)$ relation to $E = 0$. Another, more reliable method for the estimation of $G_{fi}(0)$ involves the use of the cleaning field method.[22] In this method, the electric field withdrawing charges onto electrodes is applied after a short electron–ion pair generation pulse for a period sufficient to complete pair recombination.

Until recently, experimental G_{fi} data referred almost exclusively to liquid dielectric materials. For solid amorphous substances, the determination of G_{fi} by the method involving the withdrawal of charged species is handicapped by the fact that the mobility of such species is as a rule very low. G_{fi} data for solid organic glasses were obtained much later.

2. The spatial distribution function of thermalised electrons

The form of $F(r)$ is difficult to determine from experimental $G_{fi}(E)$ data and Eqn (4). For practical purposes, some kind of simple form of the $F(r)$ relation is normally employed.[1,13] In the analysis of experimental data for liquids, most attention has been devoted to the following types of distribution:

simple exponential:[23]

$$F(r) = C\exp\left(-\frac{r}{b}\right) , \qquad (5)$$

Gaussian:[24]

$$F(r) = Cr^2 \exp\left(-\frac{r^2}{b^2}\right) , \qquad (6)$$

amplified Gaussian:[25]

$$F(r) = \begin{cases} Cr^2 \exp\left(-\dfrac{r^2}{b^2}\right) & r < 2.4b , \\ Cr^2 \exp\left(-\dfrac{r^2}{b^2}\right) + 0.5\left(\dfrac{b^2}{r^2}\right) & r > 2.4b . \end{cases} \qquad (7)$$

Here C is the normalising multiplier and b the parameter of the distribution function.

Apart from Eqns (5)–(7), others have also been tested: the delta-function, the Gaussian relation with a displaced maximum, etc. Among these relations, functions (5) and (7) yielded the most satisfactory agreement with experimental data for $G_{fi}(E)$.[13,18,19,26]

Estimates based on Eqn (4) and G_{fi} data for different liquids yield approximately identical values of b for functions (5) and (7). In the case of unbranched hydrocarbons, the values of parameter b are in the range 50–70 Å,[20–26] which indicates a fairly narrow (compared with the Onsager radius) distribution of the thermalised electrons.

In order to compare the paths traversed by superthermal electrons in various substances, it is convenient to employ the values of b normalised with respect to density (or the product $b\rho$, where ρ is the density of the substance). The values of $b\rho$ in liquid hydrocarbons (in contrast to gases) are independent of ρ and depend only slightly on the temperature of the substance.[18,19]

II. Trapped electrons in solid nonpolar hydrocarbons

1. Detection of a trapped electron

The study of trapped (stabilised) electrons e_{tr}^- in solid hydrocarbons was initiated long ago. The first attempts to detect e_{tr}^-, undertaken in 1962,[27] did not lead to positive results. Subsequently, using an improved technique for the measurement of the optical absorption spectra in frozen hydrocarbons γ-irradiated at 77 K, it was possible to observe an absorption band in 3-methylpentane,[28] extremely sensitive to 'bleaching' by IR light, the maximum of which was at a much higher wavelength than the absorption band of a trapped electron in alcohols with a relatively low IR sensitivity.

Later a broad ($\Delta E_{1/2} \approx 0.5$ eV) structureless optical absorption band with a maximum in the range 1500 to 2000 nm was observed in the spectra of other substances: on radiolysis of alkane

and olefin glasses and also on UV irradiation of substances with a low ionisation potential or containing the anions of aromatic hydrocarbons in alkane glasses as additives. This absorption, attributed in all cases to trapped electrons, is readily bleached by visible and by near IR irradiation within the limits of the absorption band, disappearing gradually in the dark even at 77 K.[12]

The use of electron-accepting additives is of decisive importance for the identification of the optical absorption bands in the near infrared in irradiated hydrocarbons at a low temperature. In their presence, the intensity of the optical absorption diminishes with the simultaneous formation of the radical-anions of the additive, which have been reliably identified from the known optical absorption or EPR spectra.

The concentration of electrons stabilised in hydrocarbons decreases also in the presence of substances reacting with slow electrons via a dissociative capture mechanism (alkyl halides, esters, etc.). On the other hand, the addition of positive charge acceptors (olefins, alcohols, ethers, aromatic amines) increases the radiation yield of the stabilised charges. All these data as well as the presence of a narrow signal in the EPR spectra[29] permitted the conclusion that the optical absorption band in the near infrared in the irradiated hydrocarbons is due to trapped electrons.[12]

On exposure to light or with increase in the temperature of the specimen, the electrons stabilised in the irradiated specimens are liberated. In the presence of an acceptor, this entails an increase in the concentration of the radical-anions, since the electrons leaving the traps are captured by the additive.[30] After successive illumination of the specimens, Gallivan and Hamill[31] observed reversible electron transfer between the 3-methylpentane and added biphenyl from the absorption spectra at wavelengths corresponding to the absorption bands of e_{tr}^- and the biphenyl radical-anion. The molar absorption coefficient of the trapped electron (λ = 1600 nm) $\epsilon(e_{tr}^-) = 3 \times 10^4$ litre mol^{-1} cm^{-1} was first determined from these data. From this value, the radiation yield G_{tr} of the trapped electrons in 3-methylpentane was found.[31,32] Immediately after γ-irradiation at 77 K, G_{tr} was ~0.8, but this value diminishes rapidly with increase in the dose. The estimated $\epsilon(e_{tr}^-)$ agrees to within 25% with the estimate of 4×10^4 litre mol^{-1} cm^{-1} (for λ = 1600 nm) based on the EPR spectrum.[29] The values of $\epsilon(e_{tr}^-)$ for the majority of saturated hydrocarbons are similar.[31,33–35]

2. The nature of the optical absorption of the trapped electron

In the first studies[32] on γ-irradiated alkanes at 77 K, it was found that the quantum yield φ of the photobleaching of e_{tr}^- is ~0.8 for λ = 950 nm, ~0.4 for λ = 1300–1600 nm, and 10^{-2} for $\lambda >$ 1700 nm. The low quantum yield for the long-wavelength absorption edge of e_{tr}^- is caused, according to Hamill,[36] by the transition to the bound state at $\lambda >$ 1700 nm, while $\varphi \approx 1$ for the short-wavelength edge is due to the transition to a continuum with formation of a mobile electron e_m^-:

$$e_{tr}^- + h\nu \rightarrow e_m^- \ . \qquad (8)$$

A more detailed study of this relation for the range 1300 < λ < 2150 nm in 3-methylpentane was undertaken by Miller and Willard,[37] who observed that φ(1800 nm) = 0.7 φ(1600 nm) and φ(2000 nm) = 0.2 φ(1600 nm). Some photobleaching at $\lambda \approx$ 2150 nm was also noted, while at $\lambda >$ 2300 nm photobleaching was not observed. The decrease in φ with increase in λ in the region $\lambda > \lambda_{max}$ could not be induced by the transition to a bound state in the trap but might be caused by the recapture of electrons[37] or the absorption of light by the hydrocarbon molecules.[38]

The dependence of the induced photoconductivity current on the wavelength $I_{ph}(\lambda)$ was later used to obtain the similar dependence of the number of photoionisation steps per absorbed photon $\beta'(\lambda)$†.[39] This is a more direct method for the study of the photoionisation of e_{tr}^- than photobleaching and recombination luminescence. It was found by this procedure[39] that $\beta'(\lambda) \approx$ const for $\lambda <$ 1150 nm in 3-methylhexanes; the decrease in the photocurrent in the region $\lambda >$ 1150 nm was attributed to[39] the decrease in $\beta'(\lambda)$. Narrow 'dips' in the induced photoconductivity spectra of γ-irradiated isooctane, cyclohexane, methylcyclohexane, and 3-methylpentane have been observed;[39,40] a correspondence between the dips in the spectra and the overtone absorption of the hydrocarbon matrices was established.

The slight 'temperature-induced' changes in the form of the absorption spectra of e_{tr}^- in the long-wavelength region (a hypsochromic shift) have been observed for 3-methylpentane at a constant temperature (T = 76 K) at time intervals from milliseconds to minutes[41] and also on varying the irradiation temperature of 3-methylpentane (in the range from 4 to 73 K[35] and from 77 to 110 K[42,43]) and on annealing the specimen before irradiation.[44]

The available literature data, based mainly on spectroscopic measurements, permit the following conclusions:

1. The decrease in the intensity of the absorption of light by e_{tr}^- observed following the introduction of acceptor additives, on isothermal decay, on photobleaching, and after annealing the specimens before irradiation, accompanied by significant changes in the form of the optical absorption band of e_{tr}^-, indicates the stabilisation of electrons in traps of the same nature.

2. Integration of the absorption band of e_{tr}^- yields the oscillator strength $f \approx 1$. This quantity is characteristic of the 'initial' absorption spectra of e_{tr}^- in alkane glasses.[31,34,35,45]

3. The broad structureless absorption band of e_{tr}^- cannot be fully caused by optical transitions to the bound state. At least its short-wavelength edge is due to the transition to a continuous spectrum with a quantum yield close to unity.[30,32,37,40,41,46–54]

The problem of the nature of the optical absorption of e_{tr}^- in nonpolar hydrocarbons — transition to a bound state in a trap or transition to a continuum — has still not been solved.[53] Both views have been maintained in numerous publications. In particular, it has been suggested that detailed comparison of the spectra of the induced photoconductivity and the induced optical absorption in optical glasses would make it possible to separate these transitions for trapped electrons.[30,40,50–52,54] For example, it is assumed that, for transitions to a continuous spectrum, the photoconductivity spectra should be superimposed on the optical absorption spectra.[49] However, this conclusion is evident only for free electrons.[53] The characteristic features of the contributions to the photoconductivity by bound and free electrons are discussed below.

a. The nature of electron traps

The molecules of saturated hydrocarbons have no electron affinity in the ground state. It is natural to expect that in the solid phase for low irradiation doses the physical inhomogeneities in the matrix serve as electron traps.[55,56] This is indicated by the following facts: (1) the dependence of the recombination luminescence and the electrical conductivity induced by the ionising radiation on the degree of crystallinity of the specimen; (2) the influence of preliminary annealing of the 3-methylpentane glass at 77 K on the yield of stabilised electrons; (3) the continuous variation of the optical spectra of stabilised electrons in irradiated glasses following the addition of another glass-forming component.

For large irradiation doses, free radicals, which may serve as electron traps, accumulate in low-molecular-mass hydrocarbons.[57,58] An estimate of the radius of the reaction involving electron capture by a radical from measurements of the induced photoconductivity[59] and of the thermostimulated current in γ-irradiated 3-methylpentane yielded the following value:[60]

$$R_r = \frac{k_R}{4\pi D} = 15 \pm 3 \text{ Å} \ ,$$

where k_R is the constant for the trapping of the electron by the radical, and D is the diffusion coefficient.

† It is necessary to distinguish the quantities $\beta'(\lambda)$ and $\varphi(\lambda)$. The latter decreases, according to Skelly and Hamill,[32] during the bleaching of e_{tr}^-.

Data for the concentrations of traps in hydrocarbons have been obtained largely by the method of competing electron-accepting additives. The concentrations of the traps estimated in studies by different workers vary within wide limits—from 10^{16} to 10^{20} cm^{-3}. Reversible electron transfer between the traps in methylcyclohexane and 3-methylpentane matrices (specially freed from electron acceptors) and the added pyrene and also between traps in isooctane and isooctane free radicals has been observed on the basis of induced photoconductivity spectra.[30] These investigations led to the following concentrations of traps (in cm^{-3}): 1×10^{18} for 3-methylpentane, 3×10^{17} for methylcyclohexane, and 1×10^{15} for isooctane.

The first estimate of the depth of electron traps was probably made for 3-methylpentane and amounted to 0.09 eV.[31] The same depth of traps was found in early studies on recombination luminescence at 77 K; traps with energies of 0.1 and 0.25 eV have been detected in 3-methylpentane[61,62] and traps with energies of 0.18 and 0.21 eV have been found in n-heptane.[63] Relatively small depths of electron traps in hydrocarbon glasses are characteristic of the early investigations. In later studies, the authors of which used many fewer substances and applied better founded theoretical models, greater depths were found. For example, an activation energy of 0.65 ± 0.05 eV has been obtained from the analysis of the form of the radiothermoluminescence peak of specially pure γ-irradiated 3-methylpentane.[64] This result agrees with data obtained in other investigations[65,66] (the temperature jump method). In order to account for the great depth found for the traps, the authors of these studies suggested that the molecular rearrangement of the hydrocarbon matrix plays a significant role in the thermal liberation of an electron.

Fig. 2 presents the temperature dependence of the drift mobility μ_d of an electron in 3-methylpentane.[67] Evidently, in the temperature range 94–296 K, the value of μ_d changes by more than eight orders of magnitude when account is taken solely of data obtained by the direct method. When account is taken of the estimate for 77 K (the lifetime of the electron in the trap is $\tau_{77} \approx 1.5 \times 10^3$ s[68]), the changes in μ_d are by more than fourteen orders of magnitude. On the $\mu_d(1/T)$ relation, it is possible to distinguish two temperature ranges to which activation energies of ~0.14 and ~0.4 eV correspond; the boundary between them corresponds approximately to the melting point of 3-methylpentane. The form of the $G_{fi}(1/T)$ relation changes sharply in the same temperature range.

The activation energies for nondeuteriated and deuteriated amorphous methylcyclohexane have been found from the initial sections of the low-temperature radiothermoluminescence and thermostimulated current peaks. At 92 K, they amounted to 0.32 ± 0.05 and 0.37 ± 0.08 eV in the former case and 0.34 ± 0.05 and 0.38 ± 0.08 eV in the latter.[69]

Estimates of the minimum depth of traps from the threshold of the photoabstraction of an electron from the e_{tr}^- state lead to somewhat higher energies than in the thermal liberation of electrons from traps. Thus the following estimates have been obtained for the minimum energy of the light quantum necessary to liberate an electron in 3-methylpentane (eV): 0.7,[32,36] 0.53,[37] 0.37,[46] and 0.62.[51] Data concerning the influence of IR irradiation on the yield of free charges and 3-methylpentane are best explained for a photoabstraction threshold of 0.5 eV.[70] For methylcyclohexane, the results of experiments designed to investigate the influence of photobleaching on the initial induced photoconductivity spectra have shown that 80% of the traps have an electron photoabstraction energy in the range 0.44–0.62 eV.[40] It may be that the smaller photo- and thermal-abstraction energies correspond to the e_{tr}^- in 'closer' pairs. The observed higher electron photoabstraction energies compared with the thermal abstraction are usually attributed, in most investigations, to the fact that the photoabstraction of an electron takes place in conformity with the Franck–Condon principle.

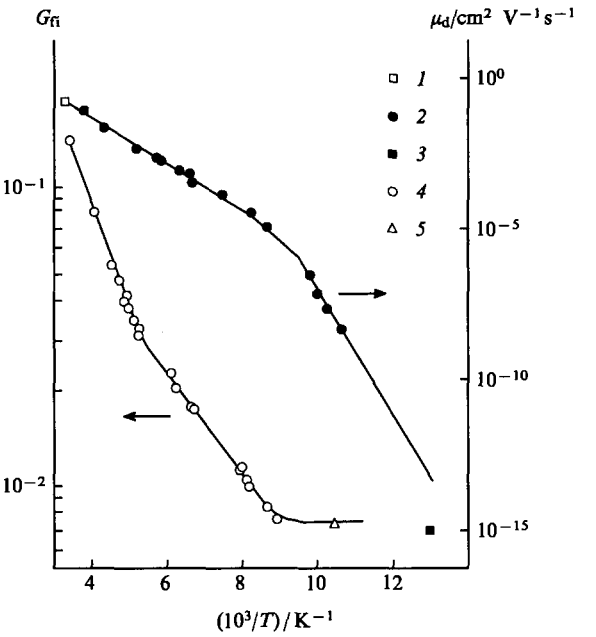


Figure 2. Temperature dependence of the radiation yield G_{fi} (1/100 eV) and of the drift mobility μ_d of electrons in 3-methylpentane.[67] The results were obtained by different methods: (*1*) from the time of flight and the conductivity amplitude; (*2*) from the conductivity amplitude; (*3*) calculation of the mobility based on the quantity $G\mu_0\tau_0$ for ^{60}Co γ-irradiation and of the lifetime of the electron in the trap τ_{77}; (*4*) from the range of conductivity currents; (*5*) from the integration of the thermostimulated current peak.

b. 'Polaron' and 'nonpolaron' models of a trapped electron

Theoretical models of trapped electrons in hydrocarbon glasses have been discussed frequently (see, for example, the relevant reviews[12,56]), but so far there is no reliable model. Despite the fact that this topic is not the main one under consideration in the present review, we shall make several comments.

One might postulate that, when a thermalised electron enters the stabilisation region, a potential well arises as a result of the polarisation of the surrounding molecules and one should consider a model analogous to the polarised cavity model for polar substances.[71] However, soon after the detection of e_{tr}^- it was noted[72] that the polaron model is not applicable to the description of the localised state of an electron in nonpolar substances; the total energy of the electron in the polaron model can be formulated as follows:

$$E' \propto \frac{h^2}{8mr^2} - \frac{e^2}{r}\left(\frac{1}{\varepsilon_\infty} - \frac{1}{\varepsilon_0}\right), \qquad (9)$$

where the first term on the right-hand side is the kinetic energy of an electron bounded by a sphere with a radius r and an infinite potential barrier and m is the mass of the electron; the second term represents the attraction energy, while ε_∞ and ε_0 are the optical and static relative permittivities. In polar media, the difference between ε_∞ and ε_0 is fairly large, so that the second term in Eqn (9) is greater than the first. In nonpolar media, ε_∞ and ε_0 differ only by the contribution of the atomic polarisation, which does not exceed 5%–10% of ε_∞.

The experimental band of e_{tr}^- is narrower than the band for the dependence of the cross-section for the photoabstraction of an electron from H^- on the energy[73] when the latter is recalculated for $\lambda_{max} = 1600$ nm.[46] For a theoretical description of the form of the e_{tr}^- spectrum, the form of the potential of the trap has been varied[45] using the hydrogen-like atom model. Best agreement with experiment was achieved in a calculation on the assumption that the absorption spectrum of e_{tr}^- is due to the

transition to a continuum. The required form of the potential of the trap proved to be more 'rectangular' than in the case of a Coulombic well. The first attempt to relate the absorption spectrum of e_{tr}^- to the structure of the frozen hydrocarbon was apparently made in the paper of Funabashi and Maruyama.[74] These workers indicated the possibility, in principle, of describing the form of the e_{tr}^- spectrum in both visible and IR regions on the assumption that the traps in solid hydrocarbons consist of regions with a nonordered arrangement of the molecules.

The results of the majority of studies indicate that regions with a low density (cavities) serve as traps in alkanes.[56] This agrees with the 'bubble' model, which has been used successfully to describe the properties of the localised state of an electron in liquefied and solid noble gases,[75] which also have no electron affinity in the gas phase. The stability criterion obtained when this model is extended to solid hydrocarbons[72] differs from that found in the case of the polaron model:

$$\frac{h^2}{8mr^2} - \frac{n'e^2\alpha_0 4}{2r} \leq V_0 \ , \qquad (10)$$

where the second term on the left-hand side takes into account the energy of electronic polarisation (n' is the density of the substance for r greater than the radius of the cavity, and α_0 is the polarisability), while V_0 is the energy level of the quasi-free state of an electron in the given substance relative to the level in vacuo. In contrast to Eqn (9), the criterion specified by Eqn (10) satisfied reasonable values of V_0, α_0, and r.[72]

According to the results[76] for deuteriated 3-methylpentane (77 K, spin echo), the contribution to the stabilisation of the electron comes not only from the dipoles of the C–H bonds of the neighbouring molecules, as postulated previously, but also from the polarisability of the C–C bonds. A satisfactory agreement between the calculation within the framework of the 'bubble' model (potential well with vertical walls) and the initial experimental photoionisation spectrum of e_{tr}^- in methylcyclohexane has been achieved for a cavity radius of 3.73–3.85 Å and a photoionisation threshold of 0.40–0.44 eV.[40]

III. Photo- and thermo-stimulated electron–ion recombination

Studies on the radiation-induced luminescence should apparently be regarded as the initial experimental data which determine the direction adopted in the investigation of the recombination of geminal electron–ion pairs in nonpolar glasses. This method made it possible to observe the changes in the rate of recombination over a wide dynamic range.

1. Studies on recombination luminescence

A prolonged afterglow (half-life $\tau_{1/2}$ = 5–20 min at 77 K)—isothermal luminescence (IL)—has been noted in solid saturated,[77] unsaturated,[78] and aromatic[79] hydrocarbons subjected to the action of ionising radiation. After its decay, a new flash of luminescence may be induced by a rise in temperature—radiothermoluminescence (RTL)—or by illumination by light at wavelengths corresponding to the region in which e_{tr}^- absorbs—radiophotoluminescence (RPL).

It had already been established in early studies that the kinetics of the decay of the isothermal luminescence $L^*(t)$[46,80] and of the optical density of the trapped electron $D(t)$[31,32,80] are inconsistent with either first- or second-order kinetics for the process and cannot be expressed in terms of their combination. Joint studies on the decay of $D(t)$ and $L^*(t)$ showed[32,80] that the optical density and the intensity of isothermal luminescence are linked by the relation

$$\int_0^t L^*(t)\mathrm{d}t \propto D^0 - D(t) \ , \qquad (11)$$

where D^0 is the initial optical density of e_{tr}^- at $t = 0$.

The decay of $D(t)$ and $L^*(t)$ in solid nonpolar hydrocarbons is independent of the irradiation dose. In many cases the decay of $L^*(t)$ can be described by the relation[78]

$$\frac{L_0^*}{L^*(t)} = 1 + \varrho(t - t_0) \ , \qquad (12)$$

(ϱ is a constant and t_0 the time at the start of the observation), formally corresponding to a second-order reaction. However, since ϱ is independent of the irradiation dose, it follows that $L^*(t)$ is not determined by the average concentration of charges in the bulk of the substance and in this sense the decay law (12) corresponds to a pseudo first-order reaction.[81]

Pure hydrocarbons give rise to a weak RTL. Typical RTL curves consist of several peaks (for example, two peaks at $T_1 \approx 81$ K and $T_2 \approx 85$ K for 3-methylpentane[32,82–86]). The luminescence intensifies after the addition of electron acceptors[85,86] and both monomeric and dimeric luminescence due to the added acceptor is then observed (in conformity with studies on the luminescence arising on excitation of liquid solutions by ionising radiation[87]).

If the γ-irradiated specimens are bleached by IR light before heating, the low-temperature peaks are suppressed. This fact has been attributed to the recombination of the electrons e_{tr}^- liberated by light from the traps.[32,82] Together with this effect, a sharp increase in the RTL intensity was observed at higher temperatures and for low irradiation doses in specially pure substances, which was manifested by the appearance of new peaks.[84–86] The new RTL peaks are not associated with geminate recombination but are due to the recombination of free ions, the irradiation yield of which increases on photostimulated (in contrast to thermostimulated) separation of the geminate pairs.

With increase in the γ-irradiation dose (for example, from 5×10^2 to 3×10^4 rad for 3-methylpentane),[64] the form of the RTL peaks does not change and their intensity remains proportional to the dose. Such a dose dependence is usual for RTL in organic dielectric materials[88–90] and has been attributed to the pair recombination mechanism.

The difference between the RTL curves for the specimens unbleached and bleached by IR light initially increases sharply during bleaching and then reaches saturation (for 3-methylpentane in the range from 10^2 to 10^3 in units of $\sigma_{ph}Lt$, where σ_{ph} is the photoionisation cross-section and L is the light intensity). The decay of the RPL by a factor greater than 10^3 has been observed in 3-methylpentane at 77 K.[64,91] The integral RTL_{bl} intensity agrees with the integral RPL intensity during IR illumination (this has been tested for 3-methylpentane as far as the decrease in the RPL by a factor of 400).[64]

2. The problem of the kinetics of the thermo- and photo-stimulated electron–ion recombination

In the analysis of experimental data on the kinetics of inhomogeneous processes in liquid hydrocarbons (geminate recombination, the trapping of an electron from a geminate pair by an acceptor, separation of the pair), both deterministic and stochastic approaches are used nowadays to equal extents (see, for example, the relevant review publications[7,13,92,93]). No examples of the analysis of data within the framework of the stochastic approach are known for solid hydrocarbons (including numerical calculations by the Monte Carlo methods).

Two types of processes differing appreciably in time have been differentiated in solid hydrocarbons: (1) recombination of quasi-free electrons which had never been captured by traps before recombination; (2) comparatively slow recombination of electrons which had been captured by a trap at least once. The recombination of the first type proceeds with a characteristic time $t \approx \varepsilon b^3/3\mu_0 e \approx 10^{-13}$–$10^{-9}$ s, where b is the thermalisation length and μ_0 the mobility of the quasi-free electrons.[94] The characteristic time of the recombination of the second type is determined by the lifetime of the electron in the localised state and

for systems at a low temperature can attain considerable durations (minutes and hours). Almost all the experimental studies on the kinetics of recombination in solid amorphous substances have been devoted to this particular type of recombination.

A general approach to the description of the kinetics of the pair recombination of e_{tr}^- and a positive ion M^+ must take into account three factors: firstly, the distribution with respect to distances in the pair $\{e_{tr}^-, M^+\}$; secondly, the distribution of e_{tr}^- with respect to the depth of the traps; thirdly, the possibility of transcapture, i.e. of the transfer of an electron from one trap to another. The case of recombination where it is possible to disregard the last factor is easiest for the description of the kinetics. In such recombination, the electron passes from the localised state e_{tr}^- to M^+ without being captured by another trap. The transition can occur either as a result of a tunnelling process or via the photo- or thermo-abstraction of an electron from the trap. Regardless of the mechanism of the transition, the problem reduces to the summation of the rates of unimolecular reactions occurring with different characteristic times.[95,96]

We shall consider the proportion of e_{tr}^- recombining without transcapture. For photostimulated recombinations, an answer to this question is provided by measurement of the quantum yield φ of the bleaching of e_{tr}^-. According to the data of Skelly and Hamill[32] and Oka et al.,[97] φ for irradiated 3-methylpentane glass diminishes in the course of bleaching from 0.4–0.8 to zero. These data show that a considerable proportion (40%–80%) but by no means all the captured electrons recombine without transcapture. This fraction includes mainly electrons located at short distances from M^+.

Allowance for the other part of the e_{tr}^-, recombining as a result of one or several transitions between traps, appears important for the analysis of the kinetics of various phenomena.[98] This part is in fact mainly responsible for the trapping of electrons by acceptor molecules at relatively low concentrations and also for the postradiative change in the electrical and optical properties of dielectric substances.

The solution of Smŏjuchowski's equation in the form proposed by Ichikawa et al.[99] has been used to describe the kinetics of the recombination of such pairs in studies[83] of the isothermal luminescence of 3-methylpentane at 77 K:

$$\frac{1}{D_0}\frac{\partial W(r,\tau)}{\partial \tau} = \frac{\partial^2 W(r,\tau)}{\partial r^2} + \left(\frac{2}{r}+\frac{r_c}{r^2}\right)\frac{\partial W(r,\tau)}{\partial r}\ , \qquad (13)$$

where $\tau = t/t_{1/2}$ is dimensionless time, $t_{1/2}$ the half-life of the luminescence, $D_0 = Dt_{1/2}$ the temperature-independent diffusion coefficient, and $W(r,\tau)$ the probability of observing the electron at time τ at a distance r from the cation. Having expressed the time variation of the luminescence intensity $L^*(t)$ as the sum of the exponential functions,

$$L^* = \sum a_i \exp(-k_i\tau) \qquad (14)$$

(a_i and k_i are coefficients), with the aid of the substitution $W(r,\tau) = \sum R_i \exp(-k_i\tau)$, Eqn (13) can be reduced to a system of ordinary differential equations:

$$\frac{d^2R_i(r)}{dr^2} + \left(\frac{2}{r}+\frac{r_c}{r^2}\right)\frac{dR_i(r)}{dr} + \frac{k_i}{D_0}R_i(r) = 0\ , \qquad (15)$$

subject to the conditions $[R_i(r)]_{r=r_0} = 0$ and $[dR_i(r)/dr]_{r=r_0} = k_i a_i/4\pi r_0^2 D_0$. After adjusting the calculated experimental data for consistency, a half-life of 140 s and an electron diffusion coefficient of $\sim 10^{-13}$ cm^2 s^{-1} were obtained[83] at 77 K.

The use of the concept of the diffusion of classical species for the description of the pair recombination in solid amorphous substances cannot be justified in the general case, since the diffusion of the species is strongly hindered in this case: an appreciable proportion of the electrons are stabilised in traps, forming a comparatively long-lived e_{tr}^- state. Discrepancies between the diffusion theory and experiment may be expected in the early stages of the electron–ion recombination.[100]

The tunnelling mechanism of the recombination has been reliably established for glasses at $T \sim 4$ K and also for hard hydrocarbon glasses (of the type of methylcyclohexane) at higher temperatures (see, for example, the relevant reviews[95,96]). The conclusion that such a mechanism operates has been based on the weak temperature dependence of the rate of decay of the isothermal recombination luminescence or on the concentration of the radical-ions detected by optical or EPR methods. The concentration dependence, which can be expressed in a linear form by plotting the concentration against lg t, is characteristic of the tunnelling mechanism.[101] Such a dependence corresponds to a decrease in the intensity of the recombination luminescence in accordance with the law defined by Eqn (12).

As in the case of the reactions of heavy particles,[102] the dominant role of the tunnelling mechanism of recombination is to be expected at low temperatures and for short distances between the reacting particles. With increase in the temperature of the medium or in the distance between the reacting particles, the role of transitions over the barrier should increase. The temperature at which the effectiveness of these processes becomes equal can be estimated from the relation[103]

$$\tilde{T} = \frac{\hbar}{\pi k_B l}\sqrt{\frac{\Delta E}{2m}}\ , \qquad (16)$$

where l is the distance between the reacting species, and ΔE is the height of the tunnelling barrier or the difference between the energies of the ground states of the quasi-free and trapped electrons.

According to Eqns (16), the predominance of the activation mechanism in the electron–ion recombination may be expected in nonpolar hydrocarbons at $\tilde{T} \geqslant 100$ K. This agrees with the estimate[101] of the typical average distance (40–50 Å) between the anion and the cation in a nonpolar medium, whereupon the tunnelling mechanism of the reactions begins to predominate. One of the examples of the thermoactivated recombination is provided by the electron–ion recombination in the 3-methylpentane glass at $\tilde{T} \geqslant 70$ K.[66,83,104]

3. The distribution function of the pairs with respect to the number of electron transitions between traps before recombination

It is frequently convenient to divide charges arbitrarily into two groups—bound or geminate and free—depending on whether they recombine with positive ions in their own or another track respectively, and the rate of recombination can be written in the form[64,68,91,105]

$$W_r(t) = W_g(t) + W_{fi}(t)\ . \qquad (17)$$

The term $W_g(t)$—the rate of recombination of bound charges—should correspond to a pseudo first order of the reaction according to numerous experimental data.

The recombination of free charges can be described by the equations of normal homogeneous kinetics, whereupon

$$W_{fi} = k_r \bar{n}_+ \bar{n}_-\ , \qquad (18)$$

where $\bar{n}_+$ and $\bar{n}_-$ are the average concentrations of the positive and negative charges and k_r is the recombination reaction rate constant.

We shall consider a simple model taking into account the electron recapture.[68,105] In the analysis of the kinetics of the recombination, we shall take into account only that part of $W_r(t)$ which is associated with the recombination of electrons which have been captured by traps. We shall assume that only one current carrier (an electron) is mobile and that the contribution of the tunnelling transitions to the rate of the recombination reaction is negligible compared with the thermal liberation of the electrons from traps.

One can then write for the rate of the recombination reaction

$$W_r(t) \propto \sum_{N=1}^{\infty} Y(N)\, \omega_N(t)\left(\frac{1}{\tau}\right) , \qquad (19)$$

where $Y(N)$ is the initial distribution function for electrons with respect to the number of captures N by traps before recombination, ω_N is the probability that the electron executes $N-1$ transitions between traps at time t, τ is the lifetime of the electron in the trap equal, for example, to $(\sigma_{ph}L)^{-1}$ on photoliberation, σ_{ph} is the photoionisation cross-section, and L is the light intensity.

The functions $\omega_N(t)$ satisfy the equations

$$\frac{d\omega_1}{dt} = -\frac{1}{\tau}\omega_1 , \qquad \frac{d\omega_{i>1}}{dt} = \frac{1}{\tau}(-\omega_i + \omega_{i-1}) , \qquad (20)$$

and the initial conditions

$$\omega_{i=1}(t=0) = 1 , \qquad \omega_{i>1}(t=0) = 0 .$$

The Poisson function

$$\omega_N(x) = \frac{(x)^{N-1}}{(N-1)!}e^{-x} , \qquad (21)$$

where

$$x = \int_0^t \frac{dt}{\tau} ,$$

is a solution of Eqn (20). The type (21) functions $\omega_N(x)$ are normalised with respect to unity and have a maximum at $x = N-1$ with a width at half the height $\Delta_{1/2} \approx \sqrt{N}$ for $N \gg 1$.

When account is taken of the number of light quanta corresponding to one recombination step, Eqns (19) and (21) make it possible to find the relation $L^*(t) \propto W(t)$ for the recombination luminescence when the functions $Y(N)$ and $\tau(t)$ are known.

a. The lifetime of the electron in the trap.
Data on the distribution $Y(N)$

Since the optical absorption of e_{tr}^- at $\lambda = 1000$ nm leads to the liberation of the electron from the trap with a quantum yield $\beta \approx 1$ (see Section II.2), the characteristic lifetime of the electron in the trap during bleaching can be expressed as follows:

$$\tau_b^{-1} = \sigma_{ph}L + \tau_{77}^{-1} ,$$

where τ_{77} is the 'dark' lifetime ($L = 0$, $T = 77$ K). It follows from Eqn (19) that, for example, for RPL,

$$\frac{L^*}{L} \propto \sum_{N=1}^{\infty} Y(N)\omega_N(x) , \qquad x = \int_0^t \sigma_{ph}L\, dt . \qquad (22)$$

Using Eqn (22) and the data for the decay of RPL, one can obtain information about the distribution $Y(N)$ when account is taken of the thermal liberation of the electron from the trap during the period from the instant of generation to the beginning of the IR illumination:

$$x_0 = \frac{0.5\Delta t_\gamma + \Delta t_{77}}{\tau_{77}} ,$$

where Δt_γ is the duration of the γ-irradiation and Δt_{77} the time after the cessation of irradiation and before the start of illumination. Such an estimate yielded $\tau_{77} = 20-35$ min.[64] Analysis of literature data,[31,32,46,80] carried out by the present authors,[68] also led to a similar value of τ_{77} ($\approx 26.5 \pm 3$ min). A satisfactory agreement with experiment has been achieved[64,91] for the distribution function

$$Y(N) = \begin{cases} 2.5 & N = 1 ; \\ N^{-3/2} & N > 1 . \end{cases} \qquad (23)$$

Naturally, this is one of the possible distributions. The version involving a similar distribution $Y(N) \propto N^{-3/2} + 6N^{-6}$ has been described.[68] However, one should note that this distribution is based on experimental data up to $N \approx 90$ because $x \leqslant 90$ in the experiment and the functions $\omega_N(x)$ have a sharp maximum at $x \approx N$ for $N \gg 1$. Under such conditions, the derivation of the function $Y(N)$ for $x \gg 1$ from the decay of $L^*(x)$ at $x \gg 1$ reduces in essence to the use of the relation $Y(x) \propto L^*(x)$.

The marked difference between the forms of the relations $\omega_N(x)$ for different values of N when N and x are approximately unity justifies fairly reliable conclusions concerning the nature of the $Y(N)$ relation also when $N \approx 1$. For example, the change in the quantity $Y(1)$ by 30% from 2.5 [for the same values of $Y(N)$ with $N > 1$ as in Eqn (23) and for $\tau_{77} = 26$ min] already gives rise to a discrepancy with experiment greater than 15% in the region where $x \approx 1$ for any $Y(N)$ with $N \geqslant 1$. When account is taken of the accuracy of the determination of τ_{77} (20–35 min.) for the same values of $Y(N > 3)$ as in Eqn (23), a satisfactory agreement with experimental relations can be obtained for $Y(1) = 1.5-3.5$.

Numerical calculation has shown[64] that the theoretical form of the RTL_{bl} curve, including the maximum, agrees satisfactorily with the experimental curve for $\tau(T) = \tau_0 \exp(E/k_BT)$, where the activation energy $E = 0.65 \pm 0.05$ eV and $\tau_0 = \tau_{77} = 26$ min. An important feature is that only data on $Y(N)$ for $N \leqslant 10$, which corresponds to the range of values of x in which the RPL curve can be satisfactorily recorded, were needed to describe the initial section of the RTL_{bl} curve, including the maximum.

b. The quantum yield in the bleaching of e_{tr}^-.
Isothermal decay of the optical density

The available information about the $Y(N)$ relation makes it possible to calculate the rate of change of the bleaching quantum yield or of the number of trapped electrons recombining on absorption of a single light quantum:

$$\varphi = \frac{1}{D}\frac{dD}{dx} , \qquad x = \sigma_{ph}Lt , \qquad (24)$$

where $D(t)$ is the concentration of e_{tr}^- at time t given by the following equation in the model with a single depth of traps:

$$D(t) = \sum_{N=1}^{\infty} Y(N) \sum_{i=1}^{N} \omega_i(t) . \qquad (25)$$

Numerical calculation of the $\varphi(D/D_0)$ relation from Eqns (21), (24), and (25) agrees satisfactorily with experimental data[32,97] according to the result of a number of studies.[64,68,91]

Eqns (19)–(21), (23), and (25) can be used to describe the kinetics of the isothermal decay of the optical density of e_{tr}^-. The experimental relations $\varphi(t)$ and $D(t)$ then make it possible to determine τ from the relation

$$\tau = \varphi\left(\frac{dD}{dt}\frac{1}{D}\right)^{-1} . \qquad (26)$$

The use of data[32] for φ and D in the time interval 0.3–30 h leads to $\tau = 26 \pm 3$ min.[68] The data for the isothermal decay of $D(t)$ in 3-methylpentane at 77 K, quoted in the literature,[31,32,80] are also described satisfactorily under these conditions.

Thus the approach based on the use of the distribution function for electrons with respect to the number of captures by traps before recombination makes it possible to consider from a single standpoint the kinetics of the electron–ion recombination luminescence arising both on thermo- and photo-liberation of electrons from traps in an amorphous nonpolar dielectric material.

c. Comparison of $Y(N)$ with data on the radiolysis of liquid hydrocarbons

The significance of the distribution $Y(N)$ can be readily understood by comparing data for the kinetics of the recombination of electron–ion pairs in hydrocarbon glasses with the results of the study of the radiolysis of liquid hydrocarbons. According to Rzad et al.,[106] the yield of the electron–ion pairs which avoided recombination at time t in liquid hydrocarbons is given by the relation

$$G(t) = G_0 \exp\{\lambda' t\} \operatorname{erfc}\{\lambda' t\}^{1/2} , \quad (27)$$

where $G_0 \approx 4$ is the overall initial yield of the electron–ion pairs and λ' is a constant characterising the rate of recombination. For long times ($\lambda' t \gg 1$), Eqn (27) can be expressed approximately as

$$-\frac{d}{dt}G(t) \approx \frac{\lambda' G_0}{2\sqrt{\pi}}(\lambda' t)^{-3/2} . \quad (28)$$

Eqn (28) describes satisfactorily the decay of the optical density of excess electrons in a number of liquid hydrocarbons with a relatively low mobility.[107] If it is assumed that in both liquid and solid hydrocarbons the motion of the electron can be represented as a sequence of jumps from one trap to another,[94] so that the electron spends the same time τ in each trap, then one can write the following expression for the electron–ion recombination in a liquid:

$$G(t) = G_{tr}^0[1 - \zeta(t)] , \quad (29)$$

where $\zeta(t)$ is the probability of the neutralisation of the pair at time t. Since we have

$$d\zeta_N = \frac{1}{\tau}\omega_N(t)\,dt , \quad (30)$$

for pairs executing N transitions between traps before recombination, we obtain from Eqns (21), (29), and (30)

$$\frac{d\zeta}{dt} = \sum_{N=1}^{\infty} Y'(N)\frac{d\zeta_N}{dt} = \frac{1}{\tau}\sum_{N=1}^{\infty} Y'(N)\omega_N\frac{t}{\tau} , \quad (31)$$

where

$$Y'(N) = \frac{Y(N)}{\sum_{N=1}^{\infty} Y(N)}$$

is a function normalised with respect to unity. We have from Eqns (29) and (31)

$$-\frac{dG(t)}{dt} = G_{tr}^0\frac{1}{\tau}\frac{\sum_{N=1}^{\infty} Y(N)\omega_N\frac{t}{\tau}}{\sum_{N=1}^{\infty} Y(N)} . \quad (32)$$

For $N \gg 1$, the functions $\omega_N(t)$ have a single sharp maximum at $t_{max} \approx N\tau$. Therefore we obtain from Eqns (28) and (32) for $t \gg \tau$ and $t \gg (\lambda')^{-1}$

$$\frac{\lambda' G_0}{2\sqrt{\pi}}(\lambda' t)^{-3/2} \approx G_{tr}^0\frac{1}{\tau}\frac{Y(t/\tau)}{\sum_{N=1}^{\infty} Y(N)} . \quad (33)$$

It follows from Eqn (33) that $Y(N) \approx N^{-3/2}$ for $N \gg 1$. This result agrees with Eqn (23) obtained for solid hydrocarbons. In other words, for the same spatial distribution of thermalised electrons and positive ions in the liquid and solid phases, the photostimulated recombination time for an electron executing N jumps is proportional to the number of these jumps: $t_r \propto N$.

IV. Electric polarisation of electron–ion pairs

The conductimetric method, involving the recording of changes in the electric conductivity of the specimen on exposure to a short ionising radiation pulse, is the most direct procedure for the investigation of the kinetics and mechanisms of chemical reactions of charged species in a condensed phase. If only free ions participate in conduction, the conditions governing the application of this method are evident. However, such a relatively simple situation arises in nonpolar substances when most of the generated charges, having an initial inhomogeneous distribution in space, have already reacted. The contribution to the electric conduction by 'bound' charges (for example, the electrons of geminate pairs recombining in the absence of acceptors over short periods) requires special consideration.

1. Characteristic features of the relaxation of the electrical conductivity induced by ionising radiation in low-molecular-mass hydrocarbons

Polarisation by an external electric field may result in the participation of electron–ion pairs in nonstationary electrical conduction. The kinetics of the polarisation current of such pairs differ significantly from the kinetics of the polarisation current for the usual mechanisms of the polarisation of dielectric substances associated with the inhomogeneity of the specimens, the nonuniformity of the generation of current carriers, etc. Indeed the recombination of the electron with its 'own' positive ion implies zero integral charge transfer:

$$\int_0^{\infty} I_r dt = 0 , \quad (34)$$

which should lead to an unusual involvement of this electron in conduction. The unusual feature consists in the fact that, for example, in a constant electric field, the electron initially contributes to the conduction and then 'takes back' this contribution, moving against the external electric field.

This feature of the electrical conduction by electrons participating in pair recombination was apparently first noted by Frankevich and coworkers.[108,109] Later, similar considerations were used in the interpretation of the results of the study of quasi-stationary electrical conductivity,[10,11,110–112] thermostimulated current,[60,70] and photoconductivity[10,59,68,112–116] induced by ionising radiation in an organic dielectric substance.

For a sufficiently high intensity of light with a wavelength in the region corresponding to the absorption by e_{tr}^-, a decrease in the photocurrent as a function of time is observed after an initial increase. This can be explained by the decrease in the concentration of the trapped electrons.[10,113]

For isooctane at 77 K, the decrease in photoconductivity is described by a hyperbolic relation.[68] For 3-methylpentane and methylcyclohexane, the form of the initial section of the curve describing the decrease in photoconductivity $\tilde{\omega}_{ph}(t)$ is independent of the dose up to 10^5 rad,[68] while the rate of decrease corresponding to longer times rises with increase in dose.[59] The form of the photocurrent decrement curves for $x = \sigma_{ph}Lt < 30$ in 3-methylpentane ($L \approx 10^{14}$ photons cm^{-2} s^{-1}) remained unchanged, within the limits of experimental error, for a tenfold alteration in the γ-irradiation dose, whereas for $x > 30$ the form of the curves depended significantly on the dose.

Direct measurements of the polarisation current of electron–ion pairs in the 3-methylpentane glass at 77 K have been undertaken.[113] An increase in the electrical conductivity (radiation conductivity) of solid 3-methylpentane at 77 K was observed directly on exposure to γ-radiation. The time required to establish a quasi-stationary value of the current I_γ was shorter than the time taken to measure the current, whilst I_γ was independent of the duration of γ-irradiation up to doses of $\sim$0.1 Mrad.

The characteristic time variations of the photocurrent induced by IR light in a solid dielectric material (for example, in 3-methylpentane) for different combinations of the electric potential on the electrodes during (V_γ) and after (V_{ph}) exposure to radiation are presented in Fig. 3.

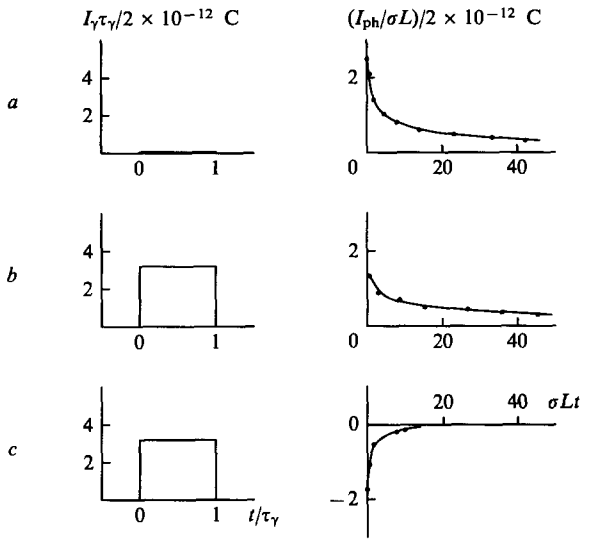


Figure 3. Time variation of the current due to the γ-induced conductivity and of the photocurrent for different combinations of the potential on the electrodes of a 3-methylpentane specimen at 77 K during γ-irradiation and IR illumination.[113] Dose 0.01 Mrad, λ = 1600 nm, $L = 3 \times 10^{14}$ photons cm^{-2}: (*a*) $V_\gamma = 0$, $V_{ph} = 1$ kV; (*b*) $V_\gamma = 1$ kV, $V_{ph} = 1$ kV; (*c*) $V_\gamma = 1$ kV, $V_{ph} = 0$.

In the case where $V_\gamma = 0$ and $V_{ph} = 1$ kV, the $I_{ph}(x)$ relation (Fig. 3*a*) is similar to that obtained by Yakovlev and coworkers.[59,68] Fig. 3 shows that the application of an electric field ($V_\gamma = 1$ kV, $V_{ph} = 1$ kV) during γ-irradiation (Fig. 3*b*) is accompanied by a decrease in the initial value and in the rate of decrease in the photocurrent (λ = 1600 nm) compared with the $I_{ph}(x)$ relation for the first case. For $V_\gamma = 1$ kV and $V_{ph} = 0$ (Fig. 3*c*), a reverse photocurrent or depolarisation current, comparable in absolute magnitude with the photocurrent in the case illustrated in Fig. 3*a*, is observed. Comparison of the normalised current amplitudes $\tilde{I}_\gamma = I_\gamma\tau_\gamma$ and $\tilde{I}_{ph} = I_{ph}/L$ shows that $\tilde{I}_\gamma : \tilde{I}^a_{ph} : \tilde{I}^b_{ph} : \tilde{I}^c_{ph} = 1 : 0.7 : 0.4 : 0.5$. Under these conditions, $\int_0^{\tau_\gamma} \tilde{I}_\gamma dt = \int_0^\infty \tilde{I}_\gamma dt$ with an accuracy to within 50%.

2. Kinetics of conduction in the presence of transcapture

a. Dependence of the current kinetics on the number of electron capture steps

If the photoconductivity is due to the involvement of free electrons, in the absence of recombination (which corresponds to the linear section of the $I_{ph} \propto D_r$ relation) the decrease in photoconductivity as a function of illumination time at the wavelength corresponding to the e^-_{tr} absorption band can be represented as follows:[68]

$$\tilde{\omega} = \frac{\tilde{\omega}_0}{1 + k_r\tau_0 n_0 L\sigma_{ph} t}, \qquad (35)$$

where $\tilde{\omega}_0 = en_0\mu_0\tau_0 L\sigma_{ph}$, $n_0 = GD_r$ is the initial concentration of free electrons, and k_r, μ_0 and τ_0 are respectively the recombination reaction rate constant, the mobility, and the lifetime of an electron liberated by light from a trap to the conducting state.

Since the photoconductivity decrement curves in isooctane are described satisfactorily by Eqn (35), the present authors assume[68] that the free charges are responsible for the main component of the photocurrent, i.e. $I_{ph} \approx I_{fi}$. Furthermore, the ratio $k_r/\mu_0 \approx 10^{-6}$ cm V, calculated using Eqn (35) and the measured quantity $(d\tilde{\omega}/dt)|_{t=0}$, proved to be $\sim 4\pi e/\varepsilon$, which is characteristic of free charges for the Langevin recombination law. The $\tilde{\omega}(t, D_r)$ relation for 3-methylpentane is not described by Eqn (35); the quantity k_r/μ_0, calculated formally using Eqn (35), proved to be much greater than $4\pi e/\varepsilon$, which indicates that the photocurrent in 3-methylpentane is associated with charges recombining in pairs,[68] i.e. $I_{ph} \approx I_{gi}$.

The difference between the kinetics of the photocurrent in isooctane and 3-methylpentane can be understood if one takes into account the difference between the values of $\mu_0\tau_0$ for these substances. The product $\mu_0\tau_0$ determines the number of steps N in which an electron is captured during its motion towards the positive ion. For an isolated pair of charges (e^-_{tr} and a positive ion), we have

$$N \approx \frac{t_r}{\tau_0}, \qquad (36)$$

where $t_r \approx r_0^3\varepsilon/3e\mu_0$ is the recombination time for a pair with an initial distance r_0 without allowance for the lifetime in the localised state. For $N \approx 0$ and a constant duration of the recording of the current $\tau_d \gg \tau_0$, there is no photocurrent due to bound charges. The occurrence of even one transcapture of an electron by a trap and hence a contribution by the bound pair of charges to the photoconductivity should be expected when

$$\mu_0\tau_0 < \frac{r_c^3}{3e} \approx 5 \times 10^{-9} \text{ cm}^2\text{V}^{-1}. \qquad (37)$$

For isooctane, $\mu_0\tau_0 \gg 10^{-8}$ cm^2V^{-1} and, on the photoabstraction of an electron from a trap, the bound charges recombine without repeated capture. On the other hand, for 3-methylpentane $\mu_0\tau_0 \ll 10^{-9}$ cm^2V^{-1} and, in the case where $r_0 \approx r_c$ and $G \approx 0.1$, the number $N \sim 10^3$.

By postulating the involvement of only free electrons in conduction, it is difficult to explain the independence of the form of the photocurrent decrement curve of the irradiation dose observed for $x < 30$[59] and the linear dependence of the amplitude of the reverse current I^c_{ph} on the γ-irradiation dose D_γ. On this hypothesis, the appearance of the reverse current could be attributed to the formation of a space charge in the regions near the electrodes, but in this case one would have to expect that $I^c_{ph} \propto D^2_\gamma$.

On the other hand, the form of the $I_{ph}(x)$ and $I_{ph}(D_\gamma)$ relations, the ratios of the amplitudes of the photocurrents in the cases presented in Fig. 3 and of the radiation conductivity current can be described satisfactorily if it is assumed that the observed current is determined largely by the polarisation of the electron pairs.[113]

Taking into account the differences between the characteristics of the changes in the induced electrical conductivity in different hydrocarbons, it is frequently possible to divide the photocurrent induced by the ionising radiation into two components:[10,68]

$$I_{ph} = I_{gi} + I_{fi}, \qquad (38)$$

where I_{fi} and I_{gi} are the parts due to the free and bound electrons respectively.

b. Polarisation of electron–ion pairs

Numerous studies have been devoted to the analysis of the behaviour of an isolated pair of ions initially located in a dielectric medium at short distances from one another. The use of the Onsager model[15] is apparently most justified for thermalised pairs in a nonpolar liquid.[2] The influence of an external electric field on the behaviour of the pair has been considered in a number of investigations,[17,117,118] but the effect of the external field on the electric dipole moment of the pair has been little investigated within the framework of this model.

If the pairs are isolated and only thermalised electrons‡ in a conducting state, with a constant mobility μ_0 ($\approx 1\ cm^2\ V^{-1}\ s^{-1}$ for 3-methylpentane at 77 K [119]) and having an initial spherically symmetrical distribution with respect to radii, participate in the polarisation, then the radiation and photoconductivity currents can be expressed in the form [113]

$$I_\gamma = \frac{1}{\tau_\gamma}\sum_{N=1}^{\infty} Y(N) q_0^N \ , \tag{39}$$

$$I_{ph} = \sum_{N=1}^{\infty} Y(N) I_q^N(t) \ . \tag{40}$$

Under these conditions, we have for the photocurrent $I_q^N(t)$, determined by electrons executing N jumps before recombination,

$$I_q^N(t) = \sum_{i=1}^{N} q_i^N \omega_i(t) \frac{1}{\tau} \ , \quad \frac{1}{\tau} = \sigma L \ , \tag{41}$$

where q_i^N is the charge, averaged for pairs with different initial orientations, transferred to an external circuit either during the period from the instant of the generation of the electron to its capture by the trap (q_0) or during the time taken for the transfer of the electron from the ith to the $(i+1)$th localised state($q_{i\neq 0}$).

According to the present authors, [68, 113] the hypothesis that the dependence of the distance r between the positive ion and an electron on the residence time of the electron in the conducting state t_0 is determined mainly by the drift of the ion in the electric field is justified for the estimation of q_i in weak external electric fields. The average number of captures of an electron with an initial distance r_0 from the positive ion before recombination is defined by Eqn (36). This leads to a value of q_0^N approximately equal to the charge transferred along the direction of the external field by the free electron during its lifetime before capture by the trap: [68, 70]

$$q_0^N \approx q_0 = \frac{e\mu_0\tau_0 E}{d} \ , \tag{42}$$

where d is the distance between the electrons.

The model considered describes satisfactorily the characteristics of the variation of the radiation conductivity current in a nonpolar dielectric substance [111] and the ratio of the currents for different combinations of the electric potential on the electrodes of the specimen during exposure to ionising radiation and photoexcitation of e_{tr}^-. [59, 68, 113]

If the pairs interact with one another, then, in view of the possibility of the recombination of the electron with a foreign ion, one cannot generally speaking neglect the contribution to the conductivity by electrons recombining after preliminary capture by a trap and Eqn (34) cannot be regarded as valid, as in the case of isolated pairs. However, in view of the fact that the Coulombic field (generated by all the charges at the location of the given electron), averaged with respect to all the electrons at the site of their thermalisation, is zero ($E_k' = 0$), Eqn (42) remains in force for the polarisation current also in the case of interacting pairs. [68, 113]

3. The diffusion-drift model

In the early investigations, [68, 113, 120] the polarisation of the pairs was considered without taking into account the diffusion of the species. This approximate approach did not allow, in principle, the study of significant features such as the appearance of a negative current and the change in the current at long times. The kinetics of the electric polarisation of an isolated pair of ions have been studied [112, 116, 121–123] on the hypothesis that the ions execute Brownian motion in the Coulombic field of their partners and in the weak external electric field (see also the review of Tyutnev et al. [11]).

If the current of free electrons I_{fi} is adopted as the unit current and the mobility is assumed equal to the overall mobility of the positive and negative ions, then the polarisation current of N isolated pairs can be expressed in the form [112]

$$I(t) = \frac{1}{e\mu NE}\frac{d}{dt}P_E(t) \ , \tag{43}$$

where P_E is the projection of the overall electric moment of all the pairs on to the direction of the electric field $\boldsymbol{E}$ generated by the charges at the electrodes. In view of the axial symmetry of the problem, we have

$$P_E(t) = N\int_0^\infty \int_{-1}^{1} 2\pi e r^3 n(r, \tilde{\mu}, t)\, d\mu\, dr \ , \tag{44}$$

where r is the distance between the ions of the pair, $n(r, \tilde{\mu}, t)$ is the density of the probability of finding a pair of ions with the parameters r and $\tilde{\mu}$, and $\tilde{\mu} = \cos\theta$.

We shall assume that the charged species execute Brownian motion in the Coulombic field of their partners $\boldsymbol{E}_c$ and in the external field $\boldsymbol{E}$ and recombine when they approach an oppositely charged species to a distance a approximately equal to the molecular size. The calculation of the current then reduces to the solution of the Smŏjuchowski equation

$$\begin{cases} \dfrac{\partial n}{\partial t} = -\operatorname{div} \boldsymbol{J} \\ \boldsymbol{J} = -D\vec{\nabla} n + \mu(\boldsymbol{E}_c + \boldsymbol{E})n \end{cases} \tag{45}$$

with the initial and boundary conditions

$$n(r, \tilde{\mu}, 0) = f(r) \ , \tag{46}$$

$$n(a, \tilde{\mu}, t) = 0 \ , \tag{47}$$

where D is the overall diffusion coefficient of the positive and negative ions. The case where it is possible to neglect the diffusion of the species and to consider only their drift in the electric field is simplest to analyse. Since the ratio of the rates of diffusion and drift diminishes with decrease in temperature, this case corresponds to low temperatures.

a. Low temperatures

If one neglects the diffusion of the species, the problem reduces to finding the time variation of the radius vector $\boldsymbol{r}(r_0, \tilde{\mu}, t)$ for a pair of ions the relative positions of which are described by the equation

$$\frac{d\boldsymbol{r}}{dt} = \mu(\boldsymbol{E}_c + \boldsymbol{E}) \ . \tag{48}$$

The significance of the notation is clear from Fig. 1.

The polarisation current has been examined [112] for four types of spherically symmetrical initial distributions, usually postulated in order to interpret the kinetics of ionic processes in photochemistry and radiation chemistry: [124, 125] the δ-function and the exponential Gaussian, and displaced Gaussian $\{f(r) \propto \exp[-16(r-b')^2/(b')^2]\}$ distributions (b' is a constant). For the $f(r) \propto \delta(r - r_0)$ distribution and short times, the polarisation current is approximately equal to the current of the same number of free ions; with increase in t, the current initially increases and then, following the onset of recombination, falls and becomes negative.

It is not difficult to understand such variation of the current. Taking into account Eqns (43) and (48), we have

$$I \propto \bar{E} = \bar{E}_c + E \ , \tag{49}$$

‡Only those electrons which during their lifetime before recombination t_r have been captured by a trap at least once are of interest; the electrons recombining without being captured by a trap do not contribute to the measured current in view of Eqn (34) and the relation $t_r \approx \tau_0 \ll \tau_d$.

where $\bar{E}$ and $\bar{E}_c$ are respectively the projections of the $\boldsymbol{E}_c + \boldsymbol{E}$ field averaged for all the pairs and of the field $\boldsymbol{E}_c$ on to the direction of the external field. $\bar{E}_c \approx 0$ for $t \approx 0$, so that the initially $I \propto E$, as for free ions. As a result of the motion of the ions, the pairs for which the vectors $\boldsymbol{E}_c$ and $\boldsymbol{E}$ are pointed in the same direction fall within the regions of a stronger Coulombic field sooner than the pairs with the opposite orientation. This leads to an increase in $\bar{E}$ and hence to an increase in I. The monotonic increase in the current occurs before the onset of recombination. The pairs for which the directions of the fields $\boldsymbol{E}_c$ and $\boldsymbol{E}$ are identical are the first to begin recombining. The dipole moment of such a pair is $p < 0$, so that the onset of their destruction leads to an abrupt increase in the current. A similar variation of the current (from negative values to zero) occurs when recombination is completed. The maximum absolute negative and positive currents are approximately equal to $5aE_c^0/r_0E$, where $E_c^0 = e/\varepsilon r_0^2$.

In contrast to the distribution $f(r) \propto \delta(r - r_0)$, in the case of other distributions the current initially diminishes monotonically with increase in t, becomes negative, and then increases, tending to zero. For sufficiently wide distributions ($b' \gg a$), the maximum negative current is almost independent of b'. Under these conditions, the values of I_{max}^-/I_{fi} for these distributions are respectively 6×10^{-3}, 0.09, and 0.6.[112]

b. Allowance for the diffusion of ions

Various approaches have been used for the numerical solution of Eqn (45).[17,117,118] The most rigorous and general method of solution, proposed by Noolandi and Hong,[117,118] is based on the calculation of the Green's function for Eqn (45). Since solutions for smooth initial distribution $f(r)$ are usually of interest, in analysing the experimental data it is more convenient to use a simpler approach to the numerical solution of Eqn (45)—the method of finite differences. The difficulties which arise in the solution of Smoluchowski's equation, subject to the boundary condition (47), by this method were associated with the high gradient $n(r, \tilde{\mu}, t)$ at the boundary, which requires the application of small steps. However, we may note that, for the attraction potential between the ions and $a \leqslant 1$ nm, the rate of destruction of the species near the boundary is mainly determined not by diffusion but by the drift of the species in the Coulombic field. Therefore in many cases the numerical calculation can be significantly simplified[112] by dividing the region corresponding to the solution into two parts: the narrow boundary region in which it is possible to neglect diffusion, i.e. one can put $D = 0$ in Eqn (45), and the main region where Eqn (45) is solved without neglecting the diffusion of the species subject to the following condition at the inner boundary:

$$\left.\frac{\partial n}{\partial r}\right|_{r=a'} = 0 \ . \qquad (50)$$

Fig. 4 presents the results of the calculation of the pair polarisation current for the initial exponential and displaced Gaussian distribution functions.[112] The same figure also illustrates the time variation of the 'survival' function $\Omega(t)$ for the overall number of pairs of ions at time t. For $t \geqslant 0.2r_c^2/D$, the values of $\Omega(t)$ obtained correspond to the asymptotic formula[17]

$$\Omega(t) = \Omega_\infty\left(1 + \sqrt{\frac{r_c^2}{\pi D t}}\right) .$$

The time variation of the average field $\bar{E} = I(t)/\Omega(t)$ has a minimum at $tD/r_c^2 \approx 10^{-4} - 10^{-3}$, which is associated with the polarisation of the spatial distribution of the geminal electrons in the external field.[123]

The characteristic features of the polarisation current arising after the formation of ion pairs at $t = 0$ in a permanent electric field can be summarised as follows:

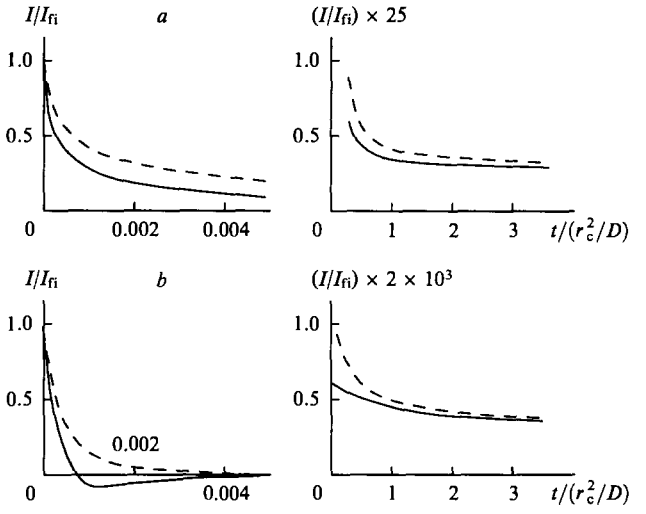


Figure 4. Time variation of the current calculated from the numerical solution of the Smoluchowski equation for the exponential initial distribution (*a*) and a displaced Gaussian distribution (*b*) of the pairs.[112] $a = 0.05r_c$, $b' = 0.1r_c$; the time variation of the probability of the survival of the pairs $\Omega(t)$ is shown dashed.

1. For the exponential and Gaussian distribution functions of the pairs with respect to the initial distances between the ions, the polarisation current is initially [for $\Omega(t)/\Omega(0) \geqslant 0.5$] approximately equal to the current due to the same number of free ions.

2. The maximum negative current I_{max}^- depends significantly on the form of the initial distribution.

3. Allowance for the diffusion of the species (or transition to high temperatures) leads to the appearance, at long times, of a direct current associated with the separation of ion pairs into free charges (Fig. 4). The maximum negative current I_{fi} diminishes with increase in temperature and the time when the current changes sign increases. Whether or not this current is negative depends on the form of the distribution.

c. Induced photoconductivity in the 'two states of the electron model'

The kinetics of the current due to the geminate ions have been frequently discussed by many investigators.[68,112–116] However, all these studies were concerned solely with thermalised charged species. On the other hand, the observed influence of the wavelength of the IR illumination on the yield of free charges (see below) shows that the characteristic features of the stage involving the thermalisation of the electrons liberated from traps by light are important for the description of the kinetics of the processes with their participation.

In order to take this factor into account, a model has been proposed[53,126,127] postulating that the photoexcitation of e_{tr}^- creates nonthermalised 'hot' electrons e_{hot}^-, which undergo a transition to a new trapped state having passed through the stage involving the thermalised state e_0^-. This hypothesis does not conflict with the idea that the electron is trapped in a molecular medium, which was put forward by Mozumder.[128] Furthermore, if one assumes that the drift displacement Δ_{hot} of e_{hot}^- in a single electric field is negligibly small § compared with the displacement Δ of a thermalised electron e_0^- during the period before its solvation, i.e. $\Delta_{hot} \ll \Delta$, then an additional term must be included in the Smoluchowski equation in such a 'two-step' model for the description of the diffusion and drift of charged species.

§ The hypothesis is based on the estimate $\Delta_{hot} = 4 \times 10^{-13}$ cm^2 V^{-1} for hydrocarbon liquids similar to 3-methylpentane with a low mobility of the excess electrons[129] and on the estimate $\Delta \approx 5 \times 10^{-12}$ cm^2 V^{-1} for the photoliberated electron in the 3-methylpentane glass at 77 K.[126]

The calculation of the photocurrent $I(t)$ can be reduced to the calculation of a new distribution function $f_i(r,\theta)$ for the pairs $\{e_{tr}^-, M^+\}$ after the ith e_{tr}^- photoionisation step:

$$I(t) = \frac{1}{d}\frac{dP_E}{dt}, \tag{51}$$

where P_E is the projection of all dipoles on to the direction of E:

$$P_E(t) = \sum_{i=0}^{N} p_i \omega_i(\sigma_{ph} L t), \tag{52}$$

$$p_i = eN \int 2\pi r_i^2 \sin\theta \cos\theta f_i(r,\theta)\, d\theta\, dr. \tag{53}$$

Here p_i is the projection of the dipole moment of the pairs for which the trapped electrons have been photoionised i times onto the direction of E and $\omega_i(x) = x_i \exp(-x)/(i!)$ is the Poisson function. The function $f_i(r,\theta)$ is given by

$$f_i(r,\theta) = \int n(r,\theta,t)\,\tau_0^{-1}\, dt, \tag{54}$$

where τ_0^{-1} is the rate constant for the reaction $e_0^- \rightarrow e_{tr}^-$, and $n(r,\theta,t)$ is the density of e_0^- defined by the Smołuchowski's equation

$$\frac{\partial n}{\partial t} = -D_0 \Delta n + \mu_0 (E_c + E)\,\mathrm{grad}\, n - \tau_0^{-1} n, \tag{55}$$

subject to the initial condition

$$n(r,\theta,t=0) = n_i(r,\theta) = \int b(|r - r'|) f_{i-1}(r,\theta)\, d(r')^3. \tag{56}$$

Here E_c is the Coulombic field, $b(a)$ is the distribution of e_{hot}^- with respect to the thermalisation lengths, and $D_0 = \mu_0 k_B T/e$ and μ_0 are respectively the average diffusion coefficient and the mobility of e_0^-. Thus in this model $\Delta = \mu_0 \tau_0$. If the form of the distributions $b(a)$ and $f_0(r,\theta)$ is known, then in this approach one can estimate $I(t)$ from the experimental values of $\mu_0\tau_0$ and σ_{ph}.

It has been shown[53] that the two states model predicts a marked dependence of the photocurrent, induced by the excitation of the geminate electrons, on the thermalisation length for the liberated electron. In this case, the spectral dependence of the photocurrent, normalised with respect to the optical absorption of e_{tr}^-, may depend on the wavelength of the exciting light even when the ionisation quantum yield is unity throughout the absorption band of e_{tr}^-. Therefore the conclusion concerning the nature of the optical absorption of e_{tr}^-, postulating that it is due to the transition to a bound state and based on the difference between the photocurrent and optical absorption spectra for geminate electrons, as well as the use of the equations of the usual homogeneous kinetics for the photocurrent cannot be regarded as sufficiently justified.

V. Thermo- and photo-stimulated separation of electron–ion pairs

Despite the fact that a large number of publications have been devoted to the localisation of excess electrons in nonordered molecular media, the mechanism of this process remains unelucidated.[128,130–137] Three cases have been differentiated in the formation of thermodynamically stable localised electrons: thermalisation, localisation, and solvation:

$$e_{hot}^- \rightarrow e_{qf}^- \rightarrow e_{loc}^- \rightarrow e_{sol}^-. \tag{57}$$

These describe the degradation of the energy of the 'hot' electrons e_{hot}^- with formation of a quasi-free electron e_{qf}^- and the solvation of the electron e_{loc}^- localised beforehand (for nonpolar media—the 'trapped' electron e_{tr}^-). By virtue of the effective application of the optical absorption method, most data have been accumulated on e_{tr}^-. However, very little is known about the precursors of e_{tr}^- and, in particular, about the spatial evolution of the low-energy electrons during their transformation into e_{sol}^- or e_{tr}^-. On the other hand, this process involves the migration of e_{hot}^- before thermalisation, the migration of the thermalised electron e_{qf}^- before thermalisation, and also the possible displacement of e_{loc}^- during solvation.

In discussing the processes involving the thermalisation of low-energy electrons in hydrocarbon glasses, three stages are also differentiated:[138,139] (1) excitation of the electronic states of molecules with a threshold energy of ~6 eV; (2) intramolecular excitations for electron energies in the range $6 \geqslant E_e \geqslant 0.4$ eV; (3) excitation of the rotational and intermolecular vibrations for $E_e < 0.4$ eV. For solid amorphous dielectric substances, the available information about the spatial distributions of thermalised $[F(r)]$ and trapped $[F_{tr}(r)]$ electrons is extremely limited and is based mainly on the analysis of the few existing data concerning the radiation yield of free ions.

1. The influence of the external electric field on the radiation yield of free ions

The method based on the integration of the thermostimulated current, arising on heating specimens γ-irradiated at low doses at 77 K, has been applied[67,70] to the determination of G_{fi} in 3-methylpentane and methylcyclohexane. The integral Q of the difference between the currents I_{TCT} for γ-irradiated and non-irradiated specimens in 3-methylpentane is proportional to the irradiation dose D_γ for $D_\gamma < 10$ rad. A similar $Q(D_\gamma)$ relation for methylcyclohexane has been obtained in the dose range < 3 rad. The quantity Q and the linear relation $Q(D_\gamma)$ indicated that most of the charged species generated by the ionising radiation in the space between the electrodes were drawn on to the electrodes and did not recombine in the bulk of the specimen.[140] The radiation yield of the separated pairs of charges in 3-methylpentane has been estimated from the linear section of the $Q(D_\gamma)$ relation.[67,70]

$$G_{fi}(E = 6 \times 10^3 \text{ V cm}^{-1}) = \frac{Q}{\rho v D_\gamma} = 1.2 \times 10^{-2} \text{ (1 pair per 100 eV)}, \tag{58}$$

where v is the volume between the electrodes.

In order to determine G_{fi} in a zero field, a method similar to the cleaning field method[22] applied to liquid dielectric substances has been used.[70] According to the results of a study of thermostimulated recombination luminescence of γ-irradiated 3-methylpentane, on heating 3-methylpentane above 77 K the electron–ion recombination is largely complete at ~90 K. Therefore, if after γ-irradiation of 3-methylpentane the specimen is initially heated at $E = 0$ to ~90 K and then recooled and again heated at $E \neq 0$, then most of the electron–ion pairs will be separated in a zero field. The number of electron–ion pairs separated on heating in a zero field has been determined[70] by integrating I_{TCT} on reheating the specimen in the field $E_{TCT} = 6 \times 10^3$ V cm^{-1}. $G_{fi}(0) = (6 \pm 1) \times 10^{-3}$ pairs of free ions per 100 eV of the absorbed radiation energy has been obtained for the 3-methylpentane glass. The observed value of $G_{fi}(0)$, like that of G_{fi} for $E_\gamma = E_{TCT} \neq 0$, was referred to the temperature 85 ± 5 K.

The same method has been applied[70] to the determination of $G_{fi}(0)$ in methylcyclohexane with the sole difference that the specimen γ-irradiated at 77 K was subjected to preliminary heating to ~100 K. This temperature corresponds to the region in which the methylcyclohexane RTL peak is observed.[141,142] The yield of the separated pairs of charges in methylcyclohexane is $(2.0 \pm 0.03) \times 10^{-2}$ per 100 eV; it was referred to the temperature $T \approx 100 \pm 10$ K at which most of the electron-ion pairs are separated.[70] As was to be expected from Eqn (1), in the low field limit the $G_{fi}(E)$ relations in 3-methylpentane and methylcyclohexane were found to be linear.

2. The influence of IR illumination on G_{fi}, the rate of recombination, and trapping

It has been observed [143] that the IR illumination of a γ-irradiated 3-methylpentane specimen before heating increased I_{TCT} appreciably. Since the optical absorption in the range 600–2000 nm of 3-methylpentane γ-irradiated at 77 K is mainly due to the trapped electrons, the increase in G_{fi} on IR illumination was attributed [143] to the fact that electron–ion pairs are separated more effectively on photoliberation of e^-_{tr} than during the thermoactivated motion of the charged species.

According to Onsager, [15] the probability of the separation of charged species (within the framework of diffusion-drift ideas concerning the separation of ion pairs in thermal equilibrium with the medium) is independent of their diffusion coefficients and is defined by Eqn (3). Assuming that Eqn (3) is valid for the electron–ion pairs in γ-irradiated 3-methylpentane, the increase in G_{fi} on IR illumination has been attributed [70, 143] to the formation of hot electrons [having an average kinetic energy greater than $\frac{3}{2}k_BT$] on IR illumination. This hypothesis agrees with the interpretation of the optical absorption of e^-_{tr} in 3-methylpentane in the range 600–2000 nm as being due to the direct transition to a continuum, [30, 40, 132] since a photoliberated electron e^-_{hot} is then formed in the initial stage of reaction (8):

$$e^-_{tr} + h\nu \rightarrow e^-_{hot} \quad . \tag{59}$$

It has an initial kinetic energy $E_0 = h\nu - E_t$, where $h\nu$ is the energy of the light quantum and $E_t = 0.5$ eV [38, 40] is the threshold energy of the photoabstraction of e^-_{tr}.

a. Dependence of G_{fi} on the energy of the bleaching light quantum

It has been observed [70, 143] that, on IR illumination, G_{fi} increases with the duration of bleaching and with increase in $h\nu$ (Fig. 5), reaching the limiting values $G^{h\nu}_{fi}$. This can be understood if the estimated distance $l \approx 80$ Å which the mobile electron e^-_m traverses in 3-methylpentane at 77 K before localisation [144] is adopted and if account is taken of the fact that the distance from the positive ion to most of the e^-_{tr} ($\sim 10^2$ Å) [25] is much smaller than $r_c \approx 10^3$ Å, i.e. the electron must execute several transitions from one localised state to another before it escapes from its positive ion. The number of such transitions can be estimated from the relation

$$N \approx \frac{r_c^2}{l^2} \approx 200 \ .$$

As for the separation of pairs in the dark, the $G^{h\nu}_{fi}$ relations proved to be linear.

Analysis showed [70] that the increase in the yields $G^{h\nu}_{fi}$ limiting in terms of the bleaching time, with decrease in the wavelength of the bleaching light cannot be related to the distribution of traps with respect to the electron photoabstraction threshold E_t: if after bleaching by light with a wavelength of 2000 or 1800 nm the specimen is also bleached by light with $\lambda = 1000$ nm, the effect is smaller than for light with $\lambda = 1000$ nm alone (Fig. 5).

The observed increase in G_{fi} following the additional bleaching of the specimen by light with $\lambda \approx 1000$ nm [70, 143] can be associated with the fact that, after prolonged bleaching by light (for example with $\lambda \approx 2000$ or 1800 nm), a proportion α of the total number of e^-_{tr} before the start of bleaching still remains in the vicinity of their 'own' positive ions. An estimate [70] yielded the following values of α: 0.18 ($\lambda \approx 2000$ nm) and 0.13 ($\lambda \approx 1800$ nm). Hence it follows that the structural traps with a photoabstraction threshold $E_t > 0.65$ eV constitute only a small proportion $\delta \approx 10^{-3}$ in 3-methylpentane.

b. Participation of hot electrons in reactions

The influence of IR illumination on the yield of free electrons and also on the recombination luminescence [84–86] caused by free electrons confirms the participation of hot electrons in photostimulated electron–ion recombination processes. It may be expected that the hot electron is appreciably involved also in other reactions initiated by the photoionisation of the trapped electron. This is apparently indicated by data [44, 145–147] which permit the hypothesis that the effectiveness of the trapping of an electron by an alkyl radical [44] and certain halogen-containing acceptors [147] in solid hydrocarbons is different in the photo- and thermostimulated liberation of electrons from traps.

The involvement of hot electrons in the formation reaction of pyrene dimers in 3-methylpentane at 77 K has been demonstrated. [85, 86] An increase by a factor greater than 20 in the intensity of the RTL peaks associated with the dimer luminescence of pyrene, arising as a result of the reaction of free ions on photobleaching of e^-_{tr}, was observed in these investigations.

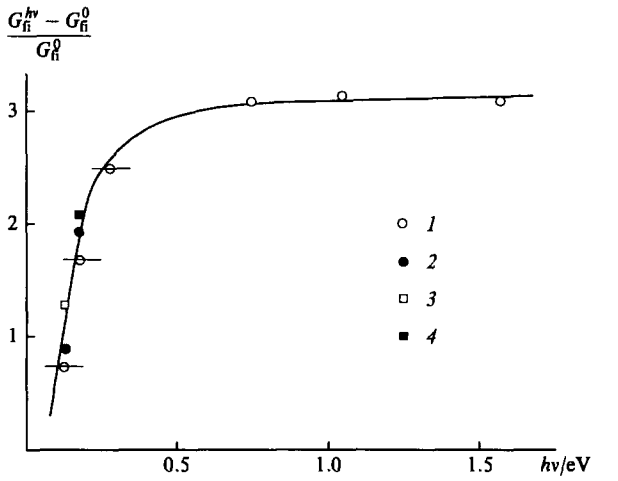


Figure 5. Dependence of the yield of free ions in 3-methylpentane on the energy of the bleaching light quantum: [70] (*1*) bleaching by light at a single wavelength; (*2*) allowance for ions remaining after bleaching; (*3*) point obtained after illuminating the specimen initially by light with $h\nu = 0.62$ eV and then by light with $h\nu = 1.2$ eV; (*4*) point obtained after illumination initially by light with $h\nu = 0.69$ eV and then by light with $h\nu = 1.2$ eV.

3. Drift displacement of the photoliberated electron in a unit electric field

Measurements of the radiation conductivity and the induced photoconductivity have proved hitherto the most reliable method for securing data on the drift displacement of electrons in a unit field $\mu_0\tau_0$. These data are usually quoted as the product $G\mu_0\tau_0$, where G is understood as the radiation yield of the charges participating in the conduction and μ_0 and τ_0 are the mobility and the lifetime in the conducting state. According to Ametov et al., [113] the dependence of the specific radiation electrical conductance on the power of the radiation J for γ-irradiated 3-methylpentane can be expressed as $\tilde{\omega} = 10^{-19} J\,\Omega^{-1}\,\mathrm{cm}^{-1}\,\mathrm{rad}^{-1}\,\mathrm{s}$. For the electronic mechanism of the radiation conduction in solid saturated hydrocarbons, this relation yields the product [10]

$$G\mu_0\tau_0 = \frac{10^2\tilde{\omega}}{eJ} = 1 \times 10^{-12}\ \mathrm{cm^2\,V^{-1}}. \tag{60}$$

In order to determine $G\mu_0\tau_0$ on UV- and γ-excitation, many workers [10, 30, 40, 50, 51, 54, 148] investigated the induced photoconductivity in hydrocarbons. The initial slope of the dependence of the conductivity on the dose $\tilde{\omega}(D_r)$ makes it possible to estimate the quantity

$$G\mu_0\tau_0 = \frac{1}{e\sigma_{ph}L}\frac{d\tilde{\omega}}{dD_r} \ . \tag{61}$$

This quantity is different in crystalline and amorphous hydrocarbons. For example, for isooctane, methylcyclohexane, and 3-methylpentane which have been specially freed from electron

acceptors, its values are[68] 1.2×10^{-7}, 2.3×10^{-10}, and 0.8×10^{-12} $cm^2 V^{-1} eV^{-1}$ respectively (the radiation yield G was calculated per 100 eV of the energy absorbed in 1 cm^3). The value of $G\mu_0\tau_0$ obtained in 3-methylpentane at 77 K agrees to within 30% with the estimate[113] based on measurements of the radiation conductivity. When account was taken of the quantities G and β', the photoconductivity data led to a drift displacement of the electron in 3-methylpentane at 77 K $\mu_0\tau_0 = 1.6 \times 10^{-12}$ $cm^2 V^{-1}$,[68] which is close to the value 1.5×10^{-12} $cm^2 V^{-1}$.[51]

Nevertheless one should note (despite such agreement between the experimental data of different workers) that the majority of the estimates were made under the conditions of the photoexcitation of the electrons of geminate pairs.[126] The estimation of $\mu_0\tau_0$ requires in this case a detailed analysis of the contributions of the free and bound charges to the photoconductivity, which is not a simple task.[53,112]

Apparently there has been only one study[59] in which the photocurrent in γ-irradiated 3-methylpentane at 77 K was measured over sufficiently long times such that almost complete separation of the pairs $\{e_{tr}^-, M^+\}$ occurred. Together with the yield of free ions, $G_{fi}^{h\nu} = 0.05$, measured during the photobleaching of a γ-irradiated specimen under the same conditions ($h\nu = 1.2$ eV and $E = 6 \times 10^3$ V cm^{-1}), and the photoionisation quantum yield $\beta' \approx 1$,[70] these data lead to $\mu_0\tau_0 = (5 \pm 1) \times 10^{-12}$ $cm^2 V^{-1}$.[59,126]

4. Spatial distribution of thermalised and trapped electrons

The G_{fi} data for solid dielectric materials make it possible to obtain information about the initial spatial distribution of the thermalised electrons $F(r)$ using Eqn (4), as for liquid systems. Furthermore, the yields G_{fi} obtained make it possible to infer the initial spatial distribution of trapped electrons $F_{tr}(r)$ from the radiation yields of such electrons G_{tr}^0:

$$G_{fi}(0) = G_{tr}^0 \int_0^\infty F_{tr}(r) \exp\left(-\frac{r_c}{r}\right) dr \,, \tag{62}$$

where $F_{tr}(r)$ is a function normalised with respect to unity.

The numerical calculation of $G_{fi}(0)$ by Eqn (4) using simple distributions $F(r)$ [functions (5)–(7)] has been carried out.[70] For $G_0 = 4$,[23,149] agreement of both function (5) and (7) with experimental yields $G_{fi}(0)$ was obtained (with $b \approx 60$ Å for 3-methylpentane and $b = 70$ Å for methylcyclohexane). The values of b found are close to the analogous quantities known for the same hydrocarbons in the liquid phase. Such a result might have been expected on the hypothesis of approximately the same electron thermalisation processes in liquid and solid amorphous hydrocarbons. However, if an exponential distribution [Eqn (5)] is postulated also for $F_{tr}(r)$, then Eqn (62) with $G_{tr}^0 = 0.8$ for 3-methylpentane[32] and $G_{tr}(0) = 6 \times 10^{-3}$ yields $b = 105$ Å,[70] which is significantly greater than the analogous distribution parameter for thermalised electrons. When the characteristic features of the electron thermalisation process are taken into account within the framework of the two states model (see Section VI), other results are obtained.

If the increase in G_{fi} on IR illumination is attributed to the fact that the kinetic energy of the electron e_m^- is higher than the thermal energy, then it is natural to assign to such an electron an effective temperature T_{ef}. T_{ef} may be estimated from the quantity $G_{fi}^{h\nu}(0)$ in a zero field from a relation similar to Eqn (62):

$$G_{fi}^{h\nu}(0) = G_{tr}^0 \int_0^\infty F_{tr}(r) \exp\left(\frac{-e^2}{\varepsilon k_B T_{ef} r}\right) dr \,. \tag{63}$$

Calculation of the dependence of T_{ef} on the energy of the bleaching light quantum[70] by means of Eqn (63) from G_{fi} data,[143] based on the hypothesis that the function $F_{tr}(r)$ is exponential with the parameters $b = 105$ Å and $G_{tr}^0 = 0.8$,[32] shows that, for $h\nu < 0.6$ eV, the temperature T_{ef} differs little from the temperature of the medium. But, after an increase in $h\nu$, the temperature T_{ef} initially rises rapidly and then, for $1.0 < h\nu < 2.5$ eV, hardly changes and amounts to ~140 K. A satisfactory agreement between the calculated and experimental temperatures T_{ef} for $h\nu < 0.8$ eV was achieved with $E_t = 0.5 \pm 0.1$ eV. The small change in T_{ef} with increase in $h\nu$, for $h\nu > 0.1$ eV, may be associated with the postulated[138] sharp increase in the rate of consumption of the electron energy on excitation of intramolecular vibrations in the region of the kinetic energy of the electron ~0.4 eV.[150]

The use of the Onsager formula might be justified by the fact that the photoliberated electron is captured many times (~200) by traps before it escapes from the 'Coulombic well' of its ion. Indeed, within the framework of the Onsager model, ϕ is independent of the mechanism of the migration of species. In essence, the probability of the separation of the pair is determined by the competition between two processes: the diffusional motion of the species during the transition between localised states, leading on average to the 'escape' of the species from the centre, and its displacement to the centre as a result of the drift in the Coulombic field of the ion during the same period. The first process may be characterised by the mean square of the distance between the successive localised states (l_s^2) and the second by the mean displacement Δ between the localised states in a unit field. For a thermalised species, the ratio of these quantities,

$$\frac{l_s^2}{\Delta} = 6\frac{k_B T}{e} \,, \tag{64}$$

corresponds to the Einstein relation

$$\frac{D}{\mu} = \frac{k_B T}{e} \,,$$

because the diffusion coefficient $D = l_s^2/6\tau$ and the drift mobility $\mu = \Delta/\tau$, where τ is the time of the transition between localised states.

However, the participation of nonthermalised species in the migration process would seem to infringe Eqn (64). In order to avoid this contradiction, it has been suggested[53,126,127,151] that the effective temperature be defined by the relation

$$T_{ef} = \frac{e}{6k_B}\frac{l_s^2}{\Delta} \,. \tag{65}$$

This approach makes it possible to determine the ratio l_s^2/Δ from the values of $G_{fi}^{h\nu}$ obtained after prolonged bleaching of the irradiated specimens and to find l_s^2 from the known value of Δ. Estimation of the lower limit yields $l_s \approx 20$ Å[151] on the basis of the results of Yakovlev et al.[70]

A more detailed approach to the description of the separation process, based on the application of the two states model, has been used.[126] The following estimates were made: the mean square thermalisation distance in 3-methylpentane $l_{hot} \approx 49$ Å, the mean square distance traversed by the thermalised precursor of the electron $l_0 \approx 45$ Å, the mean square solvation distance $l_s = (l_{hot}^2 + l_0^2)^{1/2} \approx 66$ Å, and the effective temperature $T_{ef} \approx 169$ K. The following feature may be noted: if it is assumed that the estimates[144,152] refer not to l_{hot} (as claimed by the authors) but to l_s, then the values of l_s quoted by Yakovlev[126] agree also with the estimated values of ~80 Å for 3-methylpentane (injection of electrons at 77 K)[144] and of ~65 Å for methylcyclohexane (thermoluminescence).[152]

The mean square electron thermalisation length in 3-methylpentane estimated by Yakovlev[126] agrees also with the experimental data for the thermalisation of low-energy electrons (20–60 Å) in liquid hydrocarbons with a low electron mobility. Various methods were used to obtain these data: photoemission from metals into a liquid,[153] electron transport across thin films,[154] and photoionisation of liquid solutions.[155–159]

The above value is also close to the analogous value for liquid solutions,[160,161] although its monotonic increase with increase in the energy of the electrons, observed in a later study,[162] is outside the calculated limits of the error[126] in the range of electron energies 0.5–2 eV.

If it is assumed that the electrons generated by the ionising radiation are localised like the photoliberated electrons, then, in order to determine $f_0(r)$ by Eqns (54) and (55), it is necessary to have data only on the initial distribution of the thermalised electron–ion pairs and the product $\mu_0\tau_0$. Best agreement with experimental results has been achieved[53] using in the calculation the distribution of the trapped electrons $f_0(r)$ corresponding to the initial distribution of the thermalised pairs and consisting of two parts: a Gaussian function with a maximum of 20 Å and a half-width of 35 Å and an exponential function which begins at 240 Å with a parameter of 70 Å (the overall density of the second part is ~5% under these conditions). Similar distributions of pairs with respect to thermalisation lengths and with a high initial density and a long 'tail' had been postulated also in previous studies in order to interpret data on the yield of free ions in liquid hydrocarbons[19,163] and for the description of the kinetics of recombination luminescence in glasses.[83]

References

1. A Hummel *Can. J. Phys.* **68** 858 (1990)
2. A Hummel, in *Advances in Radiation Chemistry* Vol. 4 (Eds M Burton, J L Magee) (New York: Wiley, 1974) p. 1
3. B S Yakovlev *Usp. Khim.* **48** 1153 (1979) [*Russ. Chem. Rev.* **48** 615 (1979)]
4. B S Yakovlev, L V Lukin *Adv. Chem. Phys.* **60** 99 (1985)
5. A Mozumder, in *Advances in Radiation Chemistry* Vol. 1 (Eds M Burton, J L Magee) (New York: Wiley, 1969) p. 1
6. A Mozumder *J. Chem. Phys.* **55** 3020 (1970)
7. G R Freeman *Can. J. Phys.* **68** 655 (1990)
8. J L Magee *Can. J. Phys.* **68** 853 (1990)
9. V A Andreev, M V Kurik, S Neshpurek, E A Silinsh, V I Sugakov, L F Taure, E L Frankevich, V Chapek, in *Elektronnye Protsessy v Organicheskikh Molekulyarnykh Kristallakh. Perenos, Zakhvat, Spinovye Effekty* (Electronic Processes in Organic Molecular Crystals. Transport, Trapping, and Spin Effects) (Ed. E A Silinsh) (Riga: Zinatne, 1992) p. 363
10. E L Frankevich, B S Yakovlev *Int. J. Radiat. Phys. Chem.* **6** 281 (1974)
11. A P Tyutnev, A V Vannikov, G S Mingaleev *Radiatsionnaya Elektrofizika Organicheskikh Dielektrikov* (Radiation Electrophysics of Organic Dielectrics) (Moscow: Energoatomizdat, 1989)
12. L Kevan, in *Advances in Radiation Chemistry* Vol. 4 (Eds M.Burton, J L Magee) (New York: Wiley, 1974) p. 181
13. T Goulet, I Mattel, J-P Jay-Gerin *Can. J. Phys.* **68** 912 (1990)
14. Yu A Berlin *Int. J. Radiat. Phys. Chem.* **8** 305 (1976)
15. L Onsager *Phys. Rev.* **54** 554 (1938)
16. J Terlecki, J Fiutak *Int. J. Radiat. Phys. Chem.* **4** 469 (1972)
17. A Mozumder *J. Chem. Phys.* **55** 3026 (1971)
18. G Ramanan, N Gee, G R Freeman *Can. J. Phys.* **68** 925 (1990)
19. N Gee, G R Freeman *Can. J. Phys.* **68** 930 (1990)
20. G R Freeman *Kinetics of Nonhomogeneous Processes* (Ed. G R Freeman) (New York: Wiley-Interscience, 1987)
21. R Schiller, S Vass *Int. J. Radiat. Phys. Chem.* **7** 193 (1975)
22. W F Schmidt, A O Allen *J. Phys. Chem.* **72** 3730 (1968)
23. K Fueki *Bull. Chem. Soc. Jpn.* **48** 2236 (1975)
24. J P Dodelet, P G Fuochi, G R Freeman *Can. J. Chem.* **50** 1617 (1972)
25. J P Dodelet, K Schinsaka, U Korsch, G R Freeman *J. Chem. Phys.* **59** 2376 (1973)
26. A Hummel, in *Kinetics of Nonhomogeneous Processes* (Ed. G R Freeman) (New York: Wiley-Interscience, 1987) p. 215
27. M R Ronayne, J P Guarino, W H Hamill *J. Am. Chem. Soc.* **84** 4230 (1962)
28. J P Guarino, W H Hamill *J. Am. Chem. Soc.* **86** 777 (1964)
29. D R Smith, J J Pieroni *Can. J. Chem.* **43** 2141 (1965)
30. G F Novikov, B S Yakovlev *Opt. Spektrosk.* **39** 93 (1975)
31. J B Gallivan, W H Hamill *J. Chem. Phys.* **44** 1279 (1966); **44** 2378 (1966)
32. D W Skelly, W H Hamill *J. Chem. Phys.* **44** 2891 (1966)
33. J Lin, K Tsuji, F Williams *J. Am. Chem. Soc.* **90** 2766 (1968)
34. N V Klassen, H A Gillis, D C Walker *J. Chem. Phys.* **55** 1979 (1971)
35. H Hase, T Higashimura, M Ogasawara *Chem. Phys. Lett.* **16** 214 (1972)
36. W H Hamill *J. Chem. Phys.* **53** 473 (1970)
37. J R Miller, J E Willard *J. Phys. Chem.* **76** 2341 (1972)
38. M Magat, in *International Discussion on Progress and Problems in Contemporary Radiation Chemistry* (Prague, 1971) Vol. 2, p. 423
39. L Kevan *J. Phys. Chem.* **76** 3830 (1972)
40. G F Novikov, B S Yakovlev *Int. J. Radiat. Phys. Chem.* **7** 479 (1975)
41. N V Klassen, H A Gillis, G G Teather *J. Phys. Chem.* **76** 3847 (1972)
42. G V Buxton, G A Salmon, J L Gebicki *Radiat. Phys. Chem.* **6** 397 (1981)
43. G V Buxton, in *Radiation Chemistry, Principles and Application* (Eds Farahataziz, M A J Rodgers) (New York: VHC Publishers, 1987) p. 321
44. T B Truong, A Bernas *J. Phys. Chem.* **76** 3894 (1972)
45. T Shida, S Iwata, T Watanabe *J. Phys. Chem.* **76** 3683 (1972)
46. M Burton, K Funabashi *Mol. Cryst. Liq. Cryst.* **9** 153 (1969)
47. R Lugo, P Delahay *J. Chem. Phys.* **57** 2122 (1972)
48. A Bernas, D Grand, T B Truong *J. Chem. Soc., Chem. Commun.* 759 (1972)
49. S A Rice, L Kevan *J. Phys. Chem.* **81** 847 (1977)
50. K Funabashi, N Okabe, T Kimura, K Fueki *J. Chem. Phys.* **75** 1576 (1981)
51. N Okabe, T Kimura, K Fueki *Can. J. Chem.* **61** 2789 (1983)
52. T Kimura, K Hirao, N Okabe, K Fueki *Can. J. Chem.* **62** 64 (1984)
53. B S Yakovlev *Radiat. Phys. Chem.* (In the press 1994)
54. T Huang, L Kevan *J. Am. Chem. Soc.* **95** 3122 (1973)
55. E L Frankevich *Usp. Khim.* **35** 1161 (1966) [*Russ. Chem. Rev.* **35** 487 (1966)]
56. K Funabashi, in *Advances in Radiation Chemistry* Vol. 4 (Eds M Burton, J L Magee) (New York: Wiley, 1974) p. 103
57. V L Tal'roze *Izv. Akad. Nauk SSSR, Ser. Khim.* 369 (1959)
58. B S Yakovlev, E L Frankevich *Izv. Akad. Nauk SSSR, Ser. Khim.* 402 (1966)
59. G F Novikov, K K Ametov, B S Yakovlev *Khim. Vys. Energ.* **16** 555 (1982)
60. K K Ametov, G F Novikov, B S Yakovlev *Khim. Vys. Energ.* **12** 377 (1978)
61. K Funabashi, D Herley, M Burton *J. Chem. Phys.* **43** 3939 (1965)
62. M Burton, M Dillon, R Rein *J. Chem. Phys.* **41** 2228 (1964)
63. J Boustead *Proc. R. Soc. London A, Math. Phys. Sci.* **319** 237 (1970)
64. B S Yakovlev, K K Ametov, G F Novikov *Int. J. Radiat. Phys. Chem.* **11** 219 (1978)
65. J Bullot, D Ceccaldi, H Szwarc *Chem. Phys. Lett.* **34** 528 (1975)
66. D Ceccaldi *Int. J. Radiat. Phys. Chem.* **8** 539 (1976)
67. G F Novikov, B S Yakovlev *Int. J. Radiat. Phys. Chem.* **8** 517 (1976)
68. B S Yakovlev, G F Novikov *Int. J. Radiat. Phys. Chem.* **7** 679 (1975)
69. G Dolivo, T Gaumann *Radiat. Phys. Chem.* **10** 207 (1977)
70. B S Yakovlev, K K Ametov, G F Novikov *Radiat. Phys. Chem.* **11** 77 (1978)
71. A K Pikaev, in *Sovremennaya Radiatsionnaya Khimiya. Radioliz Gazov i Zhidkostei* (Modern Radiation Chemistry. Radiolysis of Gases and Liquids) (Moscow: Nauka, 1986) p. 330
72. M Magat *Ber. Bunsenges. Phys. Chem.* **75** 666 (1971)
73. T Ohmura, H Ohmura *Phys. Rev.* **118** 154 (1960)
74. K Funabashi, Y Maruyama *J. Chem. Phys.* **55** 4494 (1971)
75. J Jortner *Ber. Bunsenges. Phys. Chem.* **75** 696 (1971)
76. P A Narayana, L Kevan *J. Chem. Phys.* **65** 3379 (1976)
77. V G Nikol'skii, N Ya Buben *Dokl. Akad. Nauk SSSR* **134** 134 (1960)
78. Kh S Bagdasar'yan, R N Milyutinskaya, Yu V Kovalev *Khim. Vys. Energ.* **1** 127 (1967)
79. M V Alfimov, V G Nikol'skii, N Ya Buben *Kinet. Katal.* **5** 268 (1964)

80. K Funabashi, G Hebert, J L Magee *J. Chem. Phys.* **75** 3221 (1971)
81. L Kevan *Act. Chim. Biol. Radiat.* **15** 81 (1971)
82. J A Leone, W H Hamill *J. Chem. Phys.* **49** 2544 (1968)
83. U Bruhlmann, J R Huber *J. Phys. Chem.* **81** 386 (1977)
84. K K Ametov, B S Yakovlev *Khim. Vys. Energ.* **12** 471 (1978)
85. G F Novikov, L I Novikova, B S Yakovlev *Khim. Vys. Energ.* **14** 8 (1980)
86. B S Yakovlev, L I Novikova, G F Novikov *Radiat. Phys. Chem.* **15** 355 (1980)
87. L I Novikova, K K Ametov, B S Yakovlev *Int. J. Radiat. Phys. Chem.* **6** 15 (1974)
88. B Brocklehurst *Int. J. Radiat. Phys. Chem.* **6** 483 (1974)
89. A Mozumder, M Tachia *J. Chem. Phys.* **62** 979 (1975)
90. O A Anisumov, A M Raitsimiring, Yu N Molin, in *The Fourth International Conference on Positron Annihilation* (Helsingør, Denmark, 1975) p. 32
91. K K Ametov, E L Frankevich, G F Novikov, B S Yakovlev *Can. J. Chem.* **11** 2063 (1977)
92. G R Freeman, in *Kinetics of Nonhomogeneous Processes* (Ed. G R Freeman) (New York: Wiley-Interscience, 1987)
93. J L Magee, A Chattergee, in *Kinetics of Nonhomogeneous Processes* (Ed. G R Freeman) (New York: Wiley-Interscience, 1987)
94. H T Davis, R G Brown *Adv. Chem. Phys.* **31** 329 (1975)
95. J R Miller *Science* **189** 221 (1975)
96. K I Zamaraev, R F Khairutdinov *Chem. Phys.* **4** 181 (1974)
97. K Oka, H Yamazaki, Y Hatano *Bull. Chem. Soc. Jpn.* **48** 1107 (1975)
98. A A Belyi, A A Ovchinnikov *Khim. Vys. Energ.* **4** 346 (1967); **5** 331 (1971)
99. T Ichikawa, H Yoshida, K Hayashi *Bull. Chem. Soc. Jpn.* **48** 2685 (1975)
100. V I Goldanskii, L I Trakhtenberg, V N Flerov *Tunnelling Phenomena in Chemical Physics* (New York: Gordon and Breach, 1989)
101. A I Mikhailov *Dokl. Akad. Nauk SSSR* **197** 186 (1971)
102. V A Benderskii, V I Goldanskii *Int. Rev. Phys. Chem.* **11** 1 (1992)
103. V I Gol'danskii *Dokl. Akad. Nauk SSSR* **124** 1261; **127** 1037 (1959)
104. F Kieffer, C Laporsonne-Meyer, J Rigaut *Int. J. Radiat. Phys. Chem.* **6** 79 (1974)
105. G F Novikov, K K Ametov, B S Yakovlev *Khim. Vys. Energ.* **7** 136 (1973)
106. S J Rzad, P P Infelta, J Warman, R H Schuller *J. Chem. Phys.* **52** 3971 (1970)
107. J H Baxendale, G Bell, P Wardman *Chem. Phys. Lett.* **12** 347 (1971)
108. E L Frankevich, E I Balabanov *Fiz. Tverd. Tela* **7** 1667 (1965)
109. E L Frankevich, B S Yakovlev *Zh. Fiz. Khim.* **40** 1617 (1966)
110. E L Frankevich *Khim. Vys. Energ.* **1** 572 (1967)
111. B S Yakovlev, G F Novikov *Fiz. Tverd. Tela* **174** 3070 (1975)
112. G F Novikov, B S Yakovlev *Khim. Vys. Energ.* **19** 282 (1985)
113. K K Ametov, G F Novikov, B S Yakovlev *Radiat. Phys. Chem.* **10** 43 (1977)
114. M C Sauer, Jr, A D Trifunac, R Cooper, L D Meise *Chem. Phys. Lett.* **92** 178 (1982)
115. K H Schmidt *Chem. Phys. Lett.* **103** 129 (1983)
116. A V Tolmachev, B S Yakovlev *Chem. Phys. Lett.* **113** 99 (1985)
117. J Noolandi, K M Hong *Chem. Phys. Lett.* **58** 575 (1978)
118. K M Hong, J Noolandi *J. Chem. Phys.* **68** 5172 (1978)
119. A C Albrecht, in *International Discussion on Progress and Problems in Contemporary Radiation Chemistry* (Prague, 1971) Vol. 2, p. 331
120. A V Shelenin, A P Tyutnev, in *Trudy VNIIIEM* (Transactions of the VNIIIEM) (Moscow, 1982) Vol. 69, p. 88
121. L V Lukin, A V Tolmachev, B S Yakovlev *Khim. Fiz.* **4** 367 (1985)
122. A V Tolmachev, W M Bartczak, J Kroh, in *The Xth International Conference on Dielectric Liquids* (Grenoble, France, 1990) p. 80
123. L V Lukin, A P Chalov, B S Yakovlev *Khim. Fiz.* **12** 1242 (1993)
124. G C Abell, K Funabashi *J. Chem. Phys.* **58** 1079 (1973)
125. H Sano, A Mozumder *J. Chem. Phys.* **66** 689 (1977)
126. B S Yakovlev *Radiat. Phys. Chem.* **40** 37 (1992)
127. B S Yakovlev *Chem. Phys. Lett.* (In the press 1994)
128. A Mozumder *Radiat. Phys. Chem.* **32** 287 (1988)
129. A A Balakin, B S Yakovlev *Chem. Phys. Lett.* **66** 299 (1979)
130. J Jortner, N R Kestner, in *Electrons in Fluids* (Eds J Jortner, N R Kestner) (Berlin: Springer, 1973) p. 1
131. R Schiller, S Vass *Int. J. Radiat. Phys. Chem.* **6** 223 (1974)
132. J E Willard *J. Phys. Chem.* **79** 2966 (1975)
133. K Fueki, D-F Feng, L Kevan *J. Phys. Chem.* **80** 1381 (1976)
134. G A Kenney-Wallace *Can. J. Chem.* **55** 2009 (1977)
135. L Kevan *J. Phys. Chem.* **84** 1232 (1980)
136. D C Walker *J. Phys. Chem.* **84** 1140 (1980)
137. J Rips, R J Silbey *J. Chem. Phys.* **94** 4495 (1991)
138. A Mozumder, J L Magee *J. Chem. Phys.* **47** 939 (1967)
139. B S Yakovlev *Izv. Akad. Nauk Latv. SSR, Ser. Fiz. Tekh. Nauk* 31 (1981)
140. P Langevin *C. R. Acad. Sci.* **134** 533 (1902)
141. J Kroh, R Leszczynski, J Mayer *Int. J. Radiat. Phys. Chem.* **8** 247 (1976)
142. J Kroh, E Hankiewer, J Piekarska *Int. J. Radiat. Phys. Chem.* **8** 289 (1976)
143. K K Ametov, G F Novikov, B S Yakovlev *Fiz. Tverd. Tela* **18** 3720 (1976)
144. J Bullot *Chem. Phys. Lett.* **29** 216 (1974)
145. A Bernas, J Blais, M Gauthier, D Grand, T B Truong *Int. J. Radiat. Phys. Chem.* **6** 401 (1974)
146. M Kongshoug, J Moan, B Bockmann, H Hovik *Chem. Phys. Lett.* **47** 225 (1977)
147. K Harada, M Irie, H Yoshida *Int. J. Radiat. Phys. Chem.* **8** 331 (1976)
148. K D Cadogan, A C Albrecht *J. Chem. Phys.* **51** 2710 (1969)
149. M Tanaka, K Fueki *J. Phys. Chem.* **77** 2524 (1973)
150. A A Balakin, I A Boriev, E L Frankevich, L V Lukin, B S Yakovlev *Can. J. Chem.* **55** 2156 (1977)
151. B S Yakovlev *Khim. Vys. Energ.* **15** 435 (1981)
152. M Gauthier-Bodard, J Bullot *Ber. Bunsenges. Phys. Chem.* **72** 348 (1968)
153. R A Holroyd, B K Dietrich, H A Schwarz *J. Phys. Chem.* **76** 3794 (1972)
154. Y C Chang, J Berry *J. Chem. Phys.* **61** 2727 (1974)
155. H T Choi, D C Sethi, C L Braun *J. Chem. Phys.* **77** 6027 (1982)
156. I Gyorgy, G R Freeman *J. Chem. Phys.* **86** 681 (1987)
157. A M Brealy, D D McDonald *Chem. Phys. Lett.* **155** 83 (1989)
158. W F Schmidt, M C Sauer, Jr, Y Lu, A Lin *J. Phys. Chem.* **94** 244 (1990)
159. Y Hirato, N Mataga *J. Phys. Chem.* **95** 1640 (1991)
160. A M Raitsimiring, S D Babenko, G I Velichko, A G Krivenko, V A Benderskii, A A Ovchinnikov, Yu D Tsvetkov *Dokl. Akad. Nauk SSSR* **247** 627 (1979)
161. C D Jonah, A C Chernovitz *Can. J. Phys.* **68** 935 (1990)
162. V V Konovalov, A M Raitsimiring, Yu D Tsvetkov *Rad. Phys. Chem.* **32** 623 (1988)
163. J P Dodelet, K Schinsaka, G R Freeman *Can. J. Chem.* **54** 744 (1976)

Russian Chemical Reviews **63** (5) 399 – 409 (1994)
© 1994 Russian Academy of Sciences and Turpion Ltd

UDC 547.424:546.185

The vibrational spectra and characteristic features of the orthophosphates of Group I – III elements

M E Poloznikova, V V Fomichev

Contents

I. Introduction	399
II. Alkali metal orthophosphates	399
III. Alkaline earth metal orthophosphates	400
IV. Lanthanide orthophosphates	401
V. Double orthophosphates	405

Abstract. The results of the spectroscopic studies (IR absorption, spontaneous Raman scattering) on orthophosphates of Group I–III elements are presented. The characteristic features of the vibrational spectra and the influence of the characteristics of the crystal structure on such features are discussed. The bibliography includes 58 references.

I. Introduction

The orthophosphates of various elements and the materials based on them have found extensive application in many branches of modern engineering and technology. This constitutes a natural stimulus to the search for new compounds and to the investigation of their physicochemical properties. It is not surprising that a number of monographs and reviews containing extensive information concerning the crystal structure of orthophosphates have appeared in recent years. Thus the nomenclature and certain characteristic features of the structure of the phosphates of Group I and II elements have been described in a review,[1] numerous data on the phosphates of divalent elements have been compiled in a monograph,[2] and a classification of the phosphates and X-ray diffraction data for the latter are presented in a book.[3] A review has been devoted to the X-ray diffraction and spectroscopic methods for the investigation of materials based on inorganic phosphates.[4] The IR absorption spectra of many phosphates are presented in the atlas of Mel'nikova et al.,[5] while those of double phosphates are in the atlas of Pechkovskii et al.[6]

However, despite the fact that vibrational spectroscopy (IR absorption and spontaneous Raman scattering) constitutes a powerful method for the investigation of the details of the structure and of the nature of the chemical bonds in compounds, while orthophosphates are convenient objects for study by this method by virtue of the characteristic features of their structure (the presence of discrete tetrahedral PO_4 groups in the structure) and the ratio between the atomic masses and bond energies, the known spectroscopic studies have not been far-reaching and systematic. Qualitative approaches have been used as a rule for the interpretation of the experimental data obtained.

M E Poloznikova, V V Fomichev Spectroscopic Analysis Sector, Lomonosov Moscow State Academy of Fine Chemical Technology, pr. Vernadskogo 86, 117571 Moscow, Russian Federation.
Fax (7-095) 430 79 83; Tel. (7-095) 247 16 00

Received 1 April 1994
Uspekhi Khimii **63** (5) 419 – 430 (1994); translated by A K Grzybowski

In all the known investigations, the vibrational spectra have been described, quite justifiably, on the assumption that the vibrations can be divided into internal vibrations (stretching and deformation vibrations of the PO_4 groups) and external vibrations (translational vibrations of the cations and the librations of the PO_4 groups). The assignment of the internal vibration frequencies is in its turn based, as has become customary in the case for compounds with tetrahedral anions such as $[SO_4]^{2-}$, $[CrO_4]^{2-}$, $[MoO_4]^{2-}$, $[ReO_4]^-$, etc., on the vibration frequencies of the 'free' ion. Group-theoretic analysis yields the following distribution of the vibrations of the free ion in terms of irreducible representations of the T_d symmetry point group and their activities in the IR absorption and Raman spectra:

$$\Gamma_{vib} = A_1(R) + E(R) + 2F_2(IR, R).$$

(R = Raman).

Frequencies of 980 cm^{-1} and 1082 cm^{-1} have been found[7] respectively for the fully symmetrical $\nu_1(A_1)$ stretching vibration of the free $[PO_4]^{3-}$ ion and the triple degenerate $\nu_3(F_2)$ stretching vibration. The deformation vibrations are characterised by lower frequencies: 363 cm^{-1} for the doubly degenerate $\nu_2(E)$ vibration and 515 cm^{-1} for the triply degenerate $\nu_4(F_2)$ vibration.

Naturally, in the vibrational spectra of crystalline substances containing phosphate anions, the frequencies of the corresponding vibrations vary as a function of the nature of the cations and the crystal structure. The latter determines the symmetry of the PO_4 groups in the crystal lattice and the possibility of the splitting of the degenerate modes and of the resonance interaction of the vibrations, which increases the number of bands in the spectra and gives rise to appreciable difficulties in their interpretation. Unfortunately, the occurrence of such interaction, leading to the factor-group (Davydov) splitting is by no means always taken into account by investigators. A correct analysis of the manifestations of this effect is possible only when studies are performed on single crystal specimens in polarised light.

In the present review, the authors' aim was to survey as fully as possible the results of studies on the orthophosphates of Group I–III elements by vibrational spectroscopic methods, promoting thereby further researches on these lines.

II. Alkali metal orthophosphates

The vibrational spectra of alkali metal orthophosphates have been investigated for solutions,[8] melts,[9] and the crystalline state.[9,10] The tetrahedral symmetry of the $[PO_4]^{3-}$ anions is retained in aqueous K_3PO_4 and Na_3PO_4 solutions. This follows from the maintenance of the selection rules determined for the free ion.

The intense absorption band at 1004 cm^{-1} has been recorded in the IR absorption spectra. It corresponds to the triply degenerate F_2 stretching vibration to which corresponds a line at a frequency of 1014–1026 cm^{-1} in the Raman spectrum. The fully symmetrical stretching vibration is manifested only in the Raman spectrum by a line at 936 cm^{-1}.

Despite the fact that the phosphate anion does not include hydrogen atoms, in aqueous solutions there is a possibility of the formation of hydrogen bonds as a result of the interaction of the oxygen atoms of the anions with the protons of the water molecules. These fairly strong bonds influence the nature of the spectrum of the $[PO_4]^{3-}$ anions and are manifested significantly in the region of the stretching vibration frequencies of water molecules. In particular, an intense broad shoulder is observed[8] on the low-frequency slope of the IR absorption band due to the ν(OH) stretching vibration at 2900–3000 cm^{-1} (at 2200–2300 cm^{-1} in solutions in D_2O).

It has been noted that the hydrogen bonds involving phosphate anions are much stronger than those between water molecules. On partial deuteriation of water, the fully symmetrical stretching vibration becomes active in the IR absorption spectrum at a frequency of 936 cm^{-1} as a consequence of the decrease in the symmetry of the hydrogen-bonded phosphate ion. The strength of the phosphorus–oxygen covalent bonds in the $[PO_4]^{3-}$ tetrahedra ensures the stability of the latter as structural assemblies also in alkali metal phosphate melts.[9] Whereas the vibrational spectra of lithium and sodium phosphates in the condensed state[5] are fairly complex and differ appreciably owing to the differences between their crystal structures, in the Raman spectra of their melts only four lines corresponding to the internal vibrations of the free phosphate anion remain: at 1012, 930, 587, and 442 cm^{-1} for Li_3PO_4; at 1017, 907, 571, and 412 cm^{-1} for Na_3PO_4.

The observed frequencies differ somewhat from those obtained for solutions of orthophosphates,[8] which is explained by the influence of the solvent already mentioned. On the other hand, the Raman spectra of $M^{I}_3PO_4$ phosphate melts differ as regards the positions of the lines, which is a consequence of the influence of the alkali metal cation on the vibrations of the anions. The existence of a prefusion region at 100–200 °C for alkali metal orthophosphates is characterised by a smooth decrease in the intensities of certain Raman lines corresponding to the external vibrations of the anions up to their complete disappearance and has been attributed by the investigators to the orientational disordering of the PO_4 tetrahedra. Unfortunately, the vibrational spectra of alkali metal phosphates have been studied at an insufficiently high level of sophistication[11] and cannot be discussed in the present review. Recently the crystal structures of these salts have attracted the attention of investigators.[12,14]

III. Alkaline earth metal orthophosphates

A more detailed analysis of the vibrational spectra has been carried out for the alkaline earth metal orthophosphates $M^{II}_3(PO_4)_2$, in particular for barium and strontium orthophosphates, on the basis of experimental IR absorption spectra[14] in the region up to 50 cm^{-1} and the Raman spectra for polycrystalline specimens, resorting to the results of the calculation of the frequencies and modes of the normal vibrations of the crystals.[15]

For the crystal lattices of the isostructural $Sr_3(PO_4)_2$ and $Ba_3(PO_4)_2$ (space group $R3m = D^5_{3d}$), the representation of the vibration of the crystals is

$$\Gamma_{vib} = 5A_{1g} + A_{2g} + 6E_g + A_{1u} + 5A_{2u} + 6E_u,$$

among which the $A_{2g} + E_g + E_u + A_{1u}$ librational modes and the $2A_{1g} + 2E_g + 2E_u + 2A_{2u}$ translational modes correspond to the lattice vibration.

The two translationally nonequivalent PO_4 groups in the unit cell occupy positions with the C_{3v} local symmetry. Table 1 presents a scheme for the correlations between the irreducible representations of the vibrations of the free ion and the PO_4 groups in the $Sr_3(PO_4)_2$ or $Ba_3(PO_4)_2$ structure. According to the results of group-theoretic analysis, the alternative prohibition rule holds in these spectra and, out of the twelve internal vibrations of the PO_4 group in each set, six should be active in IR absorption and six in the Raman spectrum.

Table 1. A scheme of correlations between the irreducible representations of the vibrations of the PO_4 group in $Ba_3(PO_4)_2$.

Vibration	'Free' ion (T_d point group)	C_{3v} symmetry of the position	Factor-group of the D_{3d} space group of the crystal
ν_1	A_1	A_1	A_{1g}(R) + A_{2u}(IR)
ν_2	E	E	E_g(R) + E_u(IR)
ν_3	F_2	$A_1 + E$	A_{1g}(R) + E_g(R) + A_{2u}(IR) + E_u(IR)
ν_4	F_2	$A_1 + E$	A_{1g}(R) + E_g(R) + A_{2u}(IR) + E_u(IR)

R = Raman (Ed. of Translation).

All the predicted modes have been recorded in the experimental Raman spectra of $Sr_3(PO_4)_2$ and $Ba_3(PO_4)_2$ crystals.[15] The frequencies and the assignments are presented in Table 2. The most intense lines correspond to the fully symmetrical $\nu_1(A_{1g})$ vibration and their frequencies, 955 cm^{-1} for $Sr_3(PO_4)_2$ and 931 cm^{-1} for $Ba_3(PO_4)_2$, agree well with the values obtained for the $[PO_4]^{3-}$ ion in solution. By analogy with data for the free ion, the next lines in terms of intensity were assigned to the $\nu_2(E)$ vibration. The high vibration frequencies (together with ν_1) and the relatively low intensity of the Raman lines served as the criteria for the assignment of the $\nu_3(A_{1g} + E_g)$ components. However, the lack of data for single crystal specimens precludes a correct assignment of the components of both stretching and deformation triply degenerate vibrations. As in the case of the alkali metal phosphates in the crystalline state, a relation between the internal vibration frequencies and the nature of the cation cannot be traced. Apart from those listed above, three lines due to the external vibrations of the crystal lattice were recorded in the Raman spectra[14] and these proved to be fairly sensitive to the replacement of the cation.

Table 2. The vibration frequencies (cm^{-1}) in the spectra of $Sr_3(PO_4)_2$ and $Ba_3(PO_4)_2$ and their assignments.[14]

Raman		Assignment	IR absorption		Assignment
$Sr_3(PO_4)_2$	$Ba_3(PO_4)_2$		$Sr_3(PO_4)_2$	$Ba_3(PO_4)_2$	
142	108	External			
163	163	modes	166	146	External
242	203	(E_g)	232	220	modes
416	412				
			450	450	$\nu_2(E_u)$
572	564	$\nu_4^1(E_g)$	570	561	$\nu_4^1(E_u)$
621	602	$\nu(A_{1g})$		580	$\nu_4(A_{2u})$
998	982	$\nu_3^1(E_g)$	951	928	$\nu_1(A_{2u})$
1072	1046	$\nu_3(A_{1g})$	1029	1007	$\nu_3^1(E_u)$
955	931	$\nu_1(A_{1g})$	1099	1053	$\nu_3(A_{2u})$

It has been suggested that the IR absorption bands be assigned similarly. The two intense absorption bands in the high-frequency part of the spectra have been assigned to the A_{2u} and E_u components of the ν_3 mode. It is assumed that the higher-frequency moderately intense band corresponds to a vibration of the A_{2u} type of symmetry, while the most intense band corresponds to E_u. The low-intensity IR band in the spectra of the phosphates considered has been assigned to $\nu_1(A_{2u})$. The lack of evidence for this mode in studies on the spectra of other phosphates is probably

due to its unduly low intensity and its being masked by the two much more intense ν_3 components. However, this assignment is based on general considerations and is not sufficiently well founded.

The assignment of the $\nu_4(A_{2u} + E_u)$ and $\nu_2(E_u)$ deformation vibration bands has been extremely arbitrary. In each of the regions of the manifestation of these modes, two bands are recorded instead of the three predicted by the group-theoretical study of the vibrations of the crystals. Such a situation is actually observed for $Sr_3(PO_4)_2$: the absorption band at 570 cm^{-1} has been assigned to ν_4 (without resolution into components), while the band at 450 cm^{-1} has been assigned to $\nu_2(E_u)$. A fuller experimental picture has been obtained for $Ba_3(PO_4)_2$. The components of the ν_4 mode are manifested by two IR bands with different intensities at 580 and 561 cm^{-1}, whilst the ν_2 mode is manifested by a weak band at 450 cm^{-1}.

As a rule, the deformation vibration frequencies of the EO_4 oxo-anions depend on the nature of both the central atom and the external cation. The measured frequencies change slightly on passing from strontium to barium, demonstrating that the deformation vibrations of the PO_4 group are characteristic.

In the absence of polarisation measurements, the applicability of the alternative prohibition rule to the vibrations of the centrosymmetrical $Sr_3(PO_4)_2$ and $Ba_3(PO_4)_2$ crystals is an extremely significant factor, ensuring that the assignments of the frequencies are to some extent well founded. Since the inversion operation converts one of the PO_4 groups, within the framework of the unit cell, into another both components are not observed simultaneously in either IR or Raman spectra for any of the resonance doublets. This factor was taken into account by the authors of the proposed assignment.

The conclusions described above have been confirmed by calculations of the frequencies and modes of the normal vibrations [16] of these typical representatives of orthophosphates.

The zeroth approximation for the force constants of the PO_4 group was devised by resorting to the corresponding quantities obtained in the study of aqueous solutions of phosphoric acid.[7] The results of the calculation demonstrate that the interaction of the internal vibrations of the PO_4 groups and the crystal lattice vibrations is insignificant. This makes it possible to regard the complex anions as rigid fragments participating in the lattice vibrations and characterised by their mass, moments of inertia, and the forces linking the terminal oxygen atoms to the cations.

Analysis of the calculated lattice vibrational modes confirmed the legitimacy of a clear-cut separation of the orientational and translational modes not only in those cases where their symmetries differ but also within the framework of the same irreducible representations. The authors were able to subdivide comparatively reliably the translational lattice vibrations into those induced predominantly by the displacements of the PO_4^{3-} anions and the alkaline earth metal cations.

The double orthophosphates $Ca_{3-x}M^{II}_x(PO_4)_2$, where M = Sr or Ba, have been described.[17] At normal pressure, usually two phases of these substances coexist, undergoing a transition to a new phase with orthorhombic symmetry at 50 kbar. The double phosphate $BaZn_2(PO_4)_2$, crystallising in the monoclinic system (space group $P2_1/c$, $Z = 4$) is also known. The ZnO_4 and PO_4 tetrahedra are linked into a three-dimensional framework via their common vertices. The crystal structure of β-$Cd_3(PO_4)_2$ has been described.[17] In the monoclinic crystal lattice (space group $P2_1/c$, $Z = 12$), the cadmium atoms, distributed among nine nonequivalent positions, are surrounded by five oxygen atoms of the PO_4 groups arranged in a trigonal bipyramidal arrangement. We are not aware of any spectroscopic studies on these compounds.

IV. Lanthanide orthophosphates

The vibrational spectra of lanthanide orthophosphates have been investigated in fair detail.[18–21] It has been suggested that the spectroscopic data for $LnPO_4$ be interpreted [22] in accordance with their subdivision into the following three groups: La–Tb orthophosphates with the monazite structure, Sc, Y, Er, Tm, Yb, and Lu orthophosphates crystallising with the xenotime structure, and Dy and Ho orthophosphates, the symmetry of the crystal lattices of which is reduced compared with the second group of compounds.

Lanthanide phosphates crystallising with a monazite type of structure are characterised by a monoclinic system (space group $P2_1n = C_{2h}^5$) with four formula units in the unit cell.[19–21] The model of the crystal structure is made up of the coordination nonagons of the lanthanide cations linked to one another via distorted phosphate groups.

The crystal lattice of the orthophosphates with the xenotime structure has a tetragonal symmetry[18] [space group $I4_1/amd = D_{4h}^{18}$ ($Z = 4$)]. The lanthanide cations in crystals of this type are coordinated to eight oxygen atoms with two sets of interatomic spacings. The phosphate groups in compounds of this type have a distorted tetrahedral structure. The study of the EPR spectra of the impurity ions [23] in YPO_4 single crystals made it possible to obtain information about the crystal field parameters for the cations in this structure.

In crystals with the monazite structure, the anions can occupy only general positions, since the symmetry group of the possible specific positions of the C_i space group $P2_1/c$ is not a subgroup of the intrinsic symmetry group of the tetrahedral ion. This factor implies the complete removal of the degeneracy of the internal vibrations of the PO_4 group and the activity of all the modes in the IR absorption and Raman spectra. A detailed analysis of the IR absorption spectra of compounds of this type [24,25] confirmed the latter hypothesis. Nevertheless, all three components of the triply degenerate ν_3 stretching vibration of the tetrahedron of the orthophosphate anion could be resolved only in the spectrum of $EuPO_4$. The magnitude of the splitting of these components and the intensity of the fully symmetrical ν_1 vibrational band, which is not active in the spectrum of the free ion, constitutes quantitative characteristics of the distortion of the tetrahedron of the orthophosphate ion in the inner field of the crystal. The strength and anisotropy of the crystal field are determined by the interaction between the cations and anions. In the series of lanthanide elements from La to Eu, the intensity of the ν_1 band and the splitting of ν_3 into components increase, these increases being attributed to an increase in the strength of the inner field with decrease in the size of the lanthanide cation. An increase in the frequencies of the vibrations under consideration is observed at the same time.

A greater number of IR absorption bands have been recorded [22] in the spectra of phosphates of the first group than has been postulated on the basis of the results of a group-theoretic analysis (Table 3). In particular, in the range of ν_3 stretching vibration frequencies, five bands were observed in each case, while in the range of the ν_4 deformation frequencies four bands were observed for each compound. The authors believe that the reason for the appearance of the additional band is the manifestation of fairly intense overtones and compound vibrations. In the region of the ν_3 vibration, these bands can correspond to the $2\nu_4$ overtone or the $\nu_4 + \nu_2$ combination. Considerable difficulties arise when an attempt is made to explain the nature of the spectrum in the region of the ν_4 deformation vibration frequencies.

For the orthophosphates of the second group with the tetragonal xenotime symmetry,[18] the distribution of the PO_4 groups among positions with the D_{2d} symmetry leads to the splitting of the $\nu_3(F_2)$ vibration into two components with the E and B_2 symmetries. Both modes should be active in the IR absorption spectra. According to the scheme of correlations between the irreducible representations of the vibrations (Table 4), the $\nu_1(A_1)$ mode should retain its type A_1 symmetry and its activity in the IR absorption spectrum. Doublets corresponding to the ν_3 stretching vibration of the phosphate anion have been recorded in the experimental [25] IR spectra of

Table 3. The vibration frequencies (cm^{-1}) in the IR absorption spectra of lanthanide orthophosphates.[23]

Compound	Vibration frequencies											
$LaPO_4$	1087	1075	1053	1025	1010	980	946	621	575	559	532	487
$CePO_4$	1107	1092	1058	1014	994		953	623	576	564	538	490–460
$PrPO_4$	1111	1093	1058	1015	995		955	625	578	565	538	486
$NdPO_4$	1111	1095	1055	1017	999		958	626	578	567	539	493
$SmPO_4$	1099	1062	1040	1018	1000		962	635	580	568	539	488
$EuPO_4$	1104	1050	1031	1015	1000		963	629	581	570	542	485
$GdPO_4$	1105	1070	1042	1028	1007		967	629	583	575	545	488
$TbPO_4$	1124	1105	1070	1044	1026	1010	969	635	583	575	542	490
YPO_4		1058	990					641	521			
$LuPO_4$		1068	1010					644	518			
$YbPO_4$		1081	1020					649	521			
$TmPO_4$		1075	1020					646	519			
$ErPO_4$		1058	995					645	521			
$DyPO_4$		1053	1020					635	524			
$HoPO_4$		1058	1020					639	523			

Table 4. A scheme of the correlations of the irreducible representations of the vibrations of the PO_4 group in the xenotime structure.

Vibration	'Free' ion (T_d point group)	Symmetry of the D_{3d} position	Factor-group of the D_{4d} space group of the crystal
ν_1	A_1	A_1	$A_{1g}(R) + B_{2u}(in)^a$
ν_2	E	$A_1 + B_1$	$A_{1g}(R) + B_{2g}(R) + A_{1u}(in)^a + B_{2u}(in)^a$
ν_3	F_2	$B_2 + E$	$B_{1g}(R) + E_g(R) + A_{2u}(IR) + E_u(IR)$
ν_4	F_2	$B_2 + E$	$B_{1g}(R) + E_g(R) + A_{2u}(IR) + E_u(IR)$

[a] in = the given vibration is inactive in the spectra.
R = Raman (Ed. of Translation)

YPO_4, $GdPO_4$, and $YbPO_4$ (Table 3), but no absorption bands were observed in the range of frequencies where the ν_1 vibration might be manifested. The frequencies of the triply degenerate vibration of the PO_4 groups increase with decrease in the ionic radius of the lanthanide, similarly to the frequencies of the orthophosphates of the monazite group.

The presence of two PO_4 groups in the unit cells of compounds with the xenotime structure and the possibility of the resonance interaction of their vibrations have led to the hypothesis that the number of the corresponding IR absorption bands should be doubled. However, the authors[25] were unable to detect this effect apparently because of the small splitting of the vibration frequencies.

The decrease in the symmetry of the phosphate anions from T_d to D_{2d} also leads to the partial removal of the degeneracy of the ν_2 and ν_4 modes. The $\nu_2(E)$ mode is split into two components with the A_1 and B_1 symmetries, while the $\nu_4(F_2)$ mode is split, similarly to ν_3, into B_2 and E. All these vibrations are active in the Raman spectrum, whereas in the IR absorption spectrum the appearance of only components of the B_2 and E types is possible.

According to the results of group-theoretic analysis,[26] carried out taking into account the overall symmetry of the xenotime crystal lattice, the normal vibrations are distributed among the following irreducible representations of the factor-group D_{4h} of the space group

$$\Gamma_{mech} = 2A_{1g} + A_{2g} + 4B_{1g} + B_{2g} + 5E_g + A_{1u} + 4A_{2u} + B_{1u} + 2B_{2u} + 5E_u,$$

including the $A_{2u} + E_u$ acoustic modes, the $2B_{1g} + B_{2g} + 2E_u + 2E_g + A_{1u} + 2A_{1g} + 2A_{2u} + 2B_{2u}$ internal modes of the PO_4 groups, the $A_{2g} + E_g + B_{1u} + E_u$ librational modes, and the $2B_{1g} + 2E_g + A2_u + E_u$ translational modes.

In the case of $DyPO_4$, it was possible to record[26,27] virtually all the vibrations with even symmetry active in the Raman spectrum. The absence of two modes (B_{1g} and E_g) from the spectrum is apparently caused by their low intensity or masking by the more intense lines. The results of the IR spectroscopic study of $LnPO_4$ (Ln = Y, Er, Tm, Yb, Lu) [22] agree fully with the theoretical ideas. However, $DyPO_4$ and $HoPO_4$ have been segregated as a separate subgroup of the xenotime group, because their absorption spectra demonstrate the presence in each case of three ν_3 components and four components in the ν_4 region, ν_1 remaining inactive as before.

The X-ray diffraction patterns of these compounds also shows certain differences. On the basis of the analysis of the entire set of experimental data, Hesel and Ross[22] suggested that $DyPO_4$ and $HoPO_4$ have a structure with a symmetry higher than that of monazite but lower than that of xenotime.

Apart from the dependence of the nature of the spectrum on the symmetry in the arrangement of the PO_4 groups and the crystal lattice as a whole, the above investigators[22] considered the influence of the coordination of cations on the P–O bond. It has been suggested that the polarising effect of the cation be estimated in terms of the ratio e/r^2, where e is the formal charge of the cation and r is the ionic radius, and also from the decrease in the frequencies of the symmetrical stretching vibrations of the phosphate anion. It has been postulated that the Ln–OPO_3 bond is strongest for the polarised Tb^{3+}, which agrees with the minimal frequency of the symmetrical stretching vibration of the PO_4 groups. The steady tendency towards an increase in frequency with decrease in the polarising power of the cation was discovered in this connection.

The authors were unable to estimate the polarising power of the cations in the spectra of the phosphates of the second group owing to the absence of the ν_1 vibration bands from the IR spectrum.

A small number of absorption bands, compared with the number recorded in the IR spectra of phosphates with the monazite structure, are characteristic of these compounds,[22] again due to characteristic features of the symmetry. Thus in the region corresponding to the manifestation of the ν_3 and ν_4 vibrations, only two modes were measured in each case. As in the interpretation of the spectra of phosphates with the monazite structure, the authors attempted to explain the appearance of additional bands by the activity of harmonics or combined vibrations. However, selection rules prohibit the activity of harmonics and compound frequencies of the ν_4 components in

the IR spectra, although they become allowed on decrease to the overall C_1 symmetry. The authors were also unable to explain the appearance of additional bands in the region of the ν_4 frequencies.

In the spectra of the orthophosphates of the monazite group, two doublets are recorded in each case in the region of the ν_4 frequencies. The splitting for the high-frequency doublet is ~ 45 cm^{-1}, while that for the low-frequency doublet is ~ 25 cm^{-1}. The corresponding frequencies increase along the series of lanthanides. The latter factor does not permit the assignment of the measured bands to combinations with lattice modes because the frequencies of all of them should decrease in the La – Tb series.

The ratio of the ν_4 and ν_2 band intensities renders improbable, in its turn, the hypothesis that the additional band in the ν_4 frequency region is due to combinations with participation of the ν_2 component.

Somewhat different results were obtained by Elliott et al.[27] In particular, the orthophosphate $TbPO_4$ was assigned to compounds of the xenotime series and doubts were cast on the justification of the segregation of $DyPO_4$ and $HoPO_4$ in a separate group. Detailed analysis of experimental data (Table 3) revealed a series of spectroscopic features of lanthanide orthophosphates of the xenotime type. The theoretically predicted splitting of the ν_3 mode of the PO_4 tetrahedron into two components in conformity with D_{2d} symmetry of its position in the crystal lattice was manifested in the Raman spectra. A line at 1020 – 1040 cm^{-1} has been observed, together with the line at 1000 – 1030 cm^{-1}, for a series of compounds in the range of frequencies assigned to ν_3, while in the spectra of $TbPO_4$, $DyPO_4$, and $LuPO_4$ there is a distinct asymmetry of the lines at 990 – 1015 cm^{-1}. The $\nu_3(B_2)$ bands at 1040 – 1075 cm^{-1} correspond to them in the IR spectrum. The Raman lines corresponding to the high-frequency $\nu_3(E)$ shoulder at 1135 – 1140 cm^{-1} in the IR spectrum were not detected. The most intense Raman line at 986 – 1015 cm^{-1} was assigned to $\nu_1(A_1)$ with a high degree of probability.

Major difficulties arose in the analysis of the region corresponding to the deformation vibrations of the PO_4 groups. The bands referring to the ν_4 vibration have been measured in the IR spectra in the range 500 – 600 cm^{-1} and in the Raman spectra of $TbPO_4$ (525 cm^{-1}), $HoPO_4$ (580 cm^{-1}), and $YbPO_4$ (578 cm^{-1}). The ν_2 modes have been detected in the form of Raman lines (A_{1g}, B_{1g}) in the range 360 – 500 cm^{-1} but are absent from the IR absorption spectra. Although the frequencies below 350 cm^{-1} have in fact been assigned to ν(Ln – O), no well founded analysis of the vibrations in this part of the spectrum have been carried out.

The dependence of the positions of the Raman lines of $HoPO_4$ on the exciting light wavelength and the appearance of a series of additional narrow fluorescence lines create additional difficulties in the interpretation of the experimental data.[26]

The Raman spectra of xenotime type YPO_4 and $YbPO_4$ crystals have also been investigated by Richman.[28] The vibrational frequencies were assigned on the basis of semiempirical data, by using the results of factor-group analysis of the vibrations of the crystals.

A precision study of the Raman spectra of the isostructural YPO_4, $HoPO_4$, and $ErPO_4$ single crystals in polarised light, supplemented by calculation of the frequencies and modes of normal vibrations, has been carried out at a higher level.[29] It was shown that in the previous studies[28] it was not possible to detect all the resolved Raman lines for YPO_4 and $YbPO_4$.

The frequencies of the symmetrical and the antisymmetrical stretching vibrations of the orthophosphate ions in the compounds investigated increase somewhat with decrease in the ionic radius of the cation, i.e. with increase in the packing density in the isostructural crystal cells of the xenotime type, which corresponds to the known tendency for other lanthanide salts. Analysis of the behaviour of the deformation vibration frequencies demonstrated their parallel variation, apparently caused by the significant interaction of these vibrations with external lattice vibrations, which are strongly influenced by a change in the mass of the cation in the series of lanthanides.

The complex problem of the separation of the external lattice vibrations into librations and translational vibrations in the case where it is impossible to distinguish them in terms of symmetry in polarisation spectra has been solved[29] on the hypothesis of a significant dependence of the translational vibrations, in contrast to the librations, on the mass of the cations. Such a dependence has been noted for two E_u vibrations and a single type A_{2u} vibration. However, the assignment of the E_g (translational vibrations and librations) and B_{1g} (translational vibrations) frequencies on the basis of these postulates did not prove to be quite so unambiguous. Some increase in frequencies on moving along the series of cations Y – Ho and Er has actually been noted for one of the B_{1g} vibrations. These data indicate the limited nature of the quasi-isotopic approximation used in the study of the influence of the geometrical characteristics of the crystal lattice on its dynamic parameters.

In contrast to lanthanide orthophosphates of the monazite series, representatives of the xenotime series are characterised by an appreciable resonance interaction of the vibrations. Thus the factor-group splitting for the doubly degenerate component of the ν_3 mode of the free ion is of the order of 30 cm^{-1}, while for the ν_4 vibration it reaches 60 cm^{-1}.

The study of the IR reflection spectra[29] of YPO_4, $HoPO_4$, and $ErPO_4$ single crystals demonstrated a decrease in the band intensities in the series of lanthanides. Since the band intensities in the IR reflection spectra are determined, in particular, by the effective atomic charges, the authors suggested that the decrease in the deformation vibration frequencies of the PO_4 groups in the spectra of the orthophosphates of the series considered is determined by the weakening of the electrostatic oxygen – oxygen interaction within the framework of the phosphate tetrahedron.

In the same study,[29] an attempt was undertaken to estimate the contribution of the dipole – dipole mechanism to the splitting of the bands due to the internal vibrations of the PO_4 groups in xenotime type crystals. In this case where it exerts a dominant influence on the nature of the spectrum, one would observe a decrease in the splitting of the bands in the series of orthophosphates YPO_4, $ErPO_4$, and $LuPO_4$. However, this was not confirmed experimentally. Furthermore, the large splittings ($\sim 60 - 80$ cm^{-1} for ν_1) are also difficult to account for because, according to the symmetry conditions, this vibration in the given crystal lattice does not alter the dipole moment. The influence of the quadrupole moment, determined merely by the slight distortion of the phosphate anion, for which the fully symmetrical vibration is not accompanied by a change in the quadrupole moment in the case of an ideal tetrahedral symmetry, should also be small. Thus the above considerations led the authors to the conclusion that the dipole – dipole interactions model is inapplicable to the description of the splittings of the internal vibrations of the PO_4 groups in crystals with a xenotime type of structure observed experimentally in both Raman spectra and IR reflection spectra.

The normal vibrations of the crystal have been calculated for YPO_4.[29] The valence force field zeroth approximation was devised by resorting to the force constants obtained for the free ion $[PO_4]^{3-}$ in solution and the force constants of the Y – O bonds for the first coordination sphere of the cation. In the calculation, account was taken of the interaction between the oxygen atoms of the neighbouring PO_4 tetrahedra and between the yttrium and phosphorus atoms (Y – Y, P – P, Y – P). The results of the calculation of the frequencies and modes of the normal vibrations and of the distribution of the potential energy made it possible to specify in detail and refine the assignment of the vibration frequencies. A significant correction to the assignment of the vibration frequencies was made on the basis of theoretical data for the E_g and E_u modes of the translational vibrations and librations. It was found that in these representations it is impossible to separate fully the two types of external lattice vibrations and that the change in the mass of the cation exerts a definite influence on

the frequencies of predominantly those translational vibrations for which significant amplitudes of the displacements of atoms have been established. The distribution of the potential energy obtained demonstrates a slight mixing of the modes of the internal vibrations of the phosphate ions with those of the lattice vibrations. The latter confirms the legitimacy of the approach used to interpret the vibrational spectra of all the phosphates and based on the separation of the internal and external vibrations. Among the stretching vibrations, the symmetrical pulsating vibration of the PO_4 groups proved to be mixed to the greatest extent, in terms of mode, with the vibrations of the cationic sublattice.

Comparison of the partial derivatives of the frequencies with respect to the force constants led to the conclusion that the Davydov resonance splitting of modes with identical symmetries in the IR spectra may be predicted in the case where it is determined by the dipole–dipole interactions. Analysis of the data obtained led the authors to the conclusion that the force field model employed is of limited applicability because it cannot be used to describe the elastic forces arising in the reorientation of complex phosphate anions.

Agreement with the results described above was achieved in the study of the Raman spectra of the single crystals of the orthophosphates of all the lanthanides (with the exception of promethium), yttrium, and scandium,[30] the Raman spectra being recorded for the first time for the orthophosphates of the lanthanides of the monazite group. The polarisation measurements permitted a correct assignment of the fundamental frequencies in terms of the symmetry types (Table 5). The data presented agree well with those of Lazarev et al.[29] for YPO_4, $HoPO_4$, and $ErPO_4$, and of Elliott et al.[27] for $DyPO_4$, but there is some discrepancy between the frequencies and those found earlier[26] for other compounds with the xenotime structure.

Table 5. The vibration frequencies (cm^{-1}) in the Raman spectra of the tetragonal orthophosphates $LnPO_4$ (Ln = Y, Tb–Lu).[31]

Y	Tb	Dy	Ho	Er	Tm	Yb	Lu	Assignment
96							98	
121	130	132	132	132	132	132	138	$B_{1g}(T)$
157	141	141	141	132	132	138	144	$E_g(T)$
185	183	185	184	185	185	186	191	$B_{1g}(T)$
210								
267	267				266	268		$E_g(T)$
299	293	295	297	300	303	302	302	$E_g(R)$
332	331	331	336	330	330	330	334	B_{2g}
484	484	485	486	477	488	491	493	A_{1g}
581	576	578	578	580	580	582	587	E_g
660	649	654	656	659	660	663	670	B_{1g}
10011	995	998	1001	1004	1006	1009	1014	A_{1g}
1027	1014	1019	1021	1024	1027	1030	1032	E_g
1048	1043					1048		
1058	1049	1054	1055	1061	1064	1068	1069	B_{1g}

The complete set of twelve allowed Raman vibrations has been recorded for orthophosphates with the xenotime structure. The interpretation of the spectra became possible only when account was taken of the resonance interaction of the vibrations within the framework of the unit cell in terms of the factor-group representations of the space group of the crystals.

The crystals of the phosphates with the monazite structure have much more complex spectra as a consequence of the low symmetry. The spectra were analysed resorting to IR absorption data.[22] The group-theoretic analysis of the vibrations of the orthophosphates with the monazite structure presupposes that 36 modes are active in the Raman spectrum and that 33 modes, obeying the alternative prohibition rule, are active in the IR spectra, but only 23 modes were recorded experimentally in the Raman spectra. Swanson et al.[31] suggest, on the basis of these data, that the vibration frequencies be assigned in terms of the representations of the local symmetry group C_1 for PO_4. In this case, it is assumed that all the internal vibrations of the PO_4 groups are active in both IR absorption and Raman spectra (Table 6).

Table 6. The vibration frequencies (cm^{-1}) in the Raman spectra of the monoclinic orthophosphates $LnPO_4$ (Ln = La–Gd).[31]

La	Ce	Pr	Nd	Sm	Eu	Gd	Assignment
90	88	90	89	88	87	87	B_g
100	100	105	106	107	108	108	A_g
120	118	122	123	123	124	123	A_g, B_g
131	129	133	133	132	132	130	B_g
151	152	158	155	156	158	158	B_g, A_g
170	172	177	164	170	175	178	B_g, A_g
183	188	188	180	185	189	192	B_g, A_g
220	219	224	227	232	233	236	B_g
227	227	230	230	242	244	247	B_g
255	254	251	263	265	265	270	A_g
271	270	282	286	294	310	308	B_g
414	414	417	420	423	423	429	A_g
465	467	469	470	473	471	480	A_g
537	536	538	539	538	538	540	A_g
572	571	572	574	575	576	579	A_g
589	589	592	595	595	597	599	B_g
619	618	623	625	627	629	632	A_g, B_g
					945		
967	970	974	977	982	989	987	A_g
991	990	994	997	999		1004	A_g
1025	1024	1028	1032	1035		1043	B_g
1055	1054	1058	1062	1065	1069	0172	A_g
1065							
1073	1070	1075	1079	1083	1082	1092	B_g
					1093		

However, this approach does not appear to be well founded. Firstly, the occurrence of a fairly strong resonance interaction of the vibrations has been established experimentally. Only five of the recorded Raman lines have the same frequencies as those measured in the IR spectra. In particular, the frequency of the $\nu_1(PO_4)$ symmetrical stretching vibration in the Raman spectra proved to be higher by 20 cm^{-1} than in the IR absorption spectra. Secondly, in the experiment on a single crystal in polarised light, the identity of certain frequencies of the A_g and B_g components cannot be an obstacle to their assignment regardless of whether this is due to the inadequate resolving power of the instrument or to the small factor-group splitting.

The frequencies of the internal vibrations of the PO_4 groups in the spectra of lanthanide orthophosphates increase linearly with the atomic number and ionic radius of the lanthanide. Thus the symmetrical stretching vibration frequencies vary from 967 cm^{-1} ($LaPO_4$) to 1011 cm^{-1} ($LuPO_4$). On the other hand, the frequencies of the lattice vibrations demonstrate a very slight dependence on the atomic number of the lanthanide.

Such tendencies in the variation of the vibration frequencies in the series of lanthanide orthophosphates conflict with those established previously[29] but do agree with those presented for lanthanide hydroxides.[31] The decrease in ionic radius from lanthanum to lutitium ensures a closer packing of the PO_4 groups. The contraction of the latter is accompanied by the deformation of the anion, a decrease in the interatomic phosphorus–oxygen distances, and an increase in the stretching and deformation vibration frequencies.

V. Double orthophosphates

Much attention has been devoted in recent years to the investigation of the structures and properties of double orthophosphates.[1,6,32] The existence of structural information for representatives of this class facilitates the interpretation of their vibrational spectra, which have been investigated in fair detail. A number of studies[33–35] have been devoted to the analysis of the vibrational spectra of the double phosphates $M^{I}M^{II}PO_4$ (M^{I} = Li, Na; M^{II} = Mg, Sr, Ba, Pb, Cd, Mn, Fe, Co, Ni).

X-ray diffraction data[36] have shown that the double phosphates $NaM^{II}PO_4$ (M^{II} = Mn, Fe, Co, Cd) are isostructural with Na_2SO_4-III and have the $Cmcm = D_{2h}^{17}$ symmetry space group. The internal vibrations of the PO_4 groups lie in the same frequency ranges within the spectrum as in the case of the individual phosphates.[33] The lattice vibration frequencies at 100–350 cm^{-1} depend, as expected, on the nature of the divalent cation. In order to refine the assignments in this part of the spectrum, the cadmium isotope ($^{106}Cd-^{116}Cd$)-substituted $NaCdPO_4$ specimens were investigated. However, the data obtained did not permit a reliable differentiation of the librational and translational modes. The authors believe that one of the probable causes of this is the interaction of lattice modes of identical symmetry. Certain features observed in the spectrum led the authors to the idea that the Na_2SO_4-III structural type has been modified for the series of compounds considered despite the similarity of the ionic radii. The lower symmetry of the unit cell in the phosphates considered (factor-group C_{2v}) was postulated. Under these conditions, agreement is achieved between the number and activity in the spectra of the vibrations predicted by the group-theoretic analysis and observed experimentally. In this connection, it is useful to recall the X-ray and neutron diffraction studies on $LiCaPO_4$,[37] isostructural with $LiNaSO_4$, which showed that this compound crystallises in the trigonal system with the space group $P31c = C_{3v}^{4}$.

The interpretation of the IR absorption and Raman spectra of the orthophosphates $LiM^{II}PO_4$ (M^{II} = Mg, Cd, Mn, Fe, Co, Ni) with the olivine structure by Paques-Ledent and Tarte[34] was based on a comparative analysis of data for the individual compounds, their solid solutions, and specimens with isotope substitution of the cations. The crystal structure of olivine is described by the space group $Pnma = D_{2h}^{16}$ ($Z = 4$). In the unit cell, there are two types of positions with a distorted octahedral environment: the divalent M^{II} cations occupy positions with the C_s symmetry, while the alkali metal cations M^{I} occupy C_i positions. There is also a possibility of a statistical distribution of the cations among these positions. Phosphate groups occupy positions with the C_s symmetry. The frequency assignment was carried out in terms of the approximation involving the subdivision of the vibrations into internal and external. The IR absorption spectra of the isotope-substituted $LiMgPO_4$ ($^{6}Li-^{7}Li$, $^{24}Mg-^{26}Mg$) and $LiNiPO_4$ ($^{6}Li-^{7}Li$, $^{62}Ni-^{68}Ni$) specimens as well as the Raman spectra of $LiMnPO_4$ and $LiCdPO_4$ specimens have been studied in greatest detail. The spectra of the isostructural series of compounds $LiM^{II}PO_4$, differing significantly only in the low-frequency region, which is associated with the manifestation of the vibration of the cations of different chemical nature, have been recorded.[34] In the remaining regions (stretching and deformation vibrations of the PO_4 groups), they are similar.

The four intense fairly broad IR bands at 960–1200 cm^{-1} were assigned to the components of the antisymmetrical ν_3 stretching vibration of the phosphate anion, while the weak, narrow, and lower-frequency bands were assigned to the ν_1 symmetrical vibration. The argument used in support of this conclusion was the agreement between the observed frequencies ν_1 and those of the most intense Raman lines and the ν_1 frequency in the IR absorption spectrum of a solution of the orthophosphate. However, the proposed assignment is not entirely correct in view of the possibility of the complete removal of the degeneracy of the vibrations and of the interaction of components with identical symmetries. The factor-group, resonance interaction is not manifested in the spectra of dilute $LiM^{II}(P_{0.02}As_{0.98})O_4$ solid solutions, while the site-group splitting of the ν_3 mode of the anion is observed in the form of three components, which agree with the C_s symmetry of its position.

Table 7. The vibration frequencies (cm^{-1}) for the isotope-substituted specimens[35] in the IR spectrum of $LiMgPO_4$.

$^{6}Li^{24}MgPO_4$	$^{7}Li^{24}MgPO_4$	$^{7}Li^{26}MgPO_4$	Assignment
158	157.5		Predominantly translations of Mg cations
230	229	226	
245	241.5	240.5	
290	280		
296	294	289	Predominantly translations of Li cations
235	322	318	
374	372	371	
416	407	399	
495	479	479	Translations of Li and Mg cations
518	517	515	
	535	534	
559	558	558	
594	593	592	Predominantly $\nu_4(PO)_4$
659	655	655	
673	669	688.5	

Analysis of the changes in the spectra of the isotope-substituted $LiM^{II}PO_4$ specimens (Tables 7–9) made it possible to differentiate three types of absorption bands:

the IR absorption bands at 550–700 cm^{-1}, for which isotopic shifts have not been detected or are insignificant, were assigned to the deformation vibrations of the anions;

several bands in the low-frequency part of the spectrum, which are also insensitive to the mass of the cation (the band at 372 cm^{-1} is the most characteristic in this respect), were assigned to librations bearing in mind that the frequencies are too low for deformation vibrations;

bands with appreciable isotopic shifts were assigned to external translational vibrations.

On the basis of the selective sensitivity to a particular isotope, it was possible in a number of instances to assign bands of the last type to the translational vibrations of various sublattices of the cations (Tables 7–9). Here one should note the fairly high (350–550 cm^{-1}) frequencies of the translational vibrations of

Table 8. The vibration frequencies (cm^{-1}) for the isotope-substituted specimens[34] in the IR spectrum of $LiNiPO_4$.

$^{7}LiNiPO_4$	$^{6}LiNiPO_4$	$^{7}Li^{62}NiPO_4$	$^{7}Li^{58}NiPO_4$	Assignment
163	163	163	163	Librations
192	192	187		
	203	194	192	Translations of Li cations
226	226	224	226	
246.5	250	246	246	
256	257	254.5	256	
304	306	303	304	Predominantly translations of Ni cations
313	313	312.5	313	
327	339	326	328	
360	357	359	361	
396	412	395	395	Predominantly translations of Li cations
477	509	477.5	477	
510				
529		528	528	Predominantly $\nu_4(PO)_4$
550	553	551	551	
650	650	650	650	
661	661	660.5	661	

Table 9. The frequencies (cm^{-1}) in the Raman spectrum of $LiM^{II}PO_4$ and their assignments.[35]

$LiMnPO_4$	$LiCdPO_4$	Assignment
148	94	Translations and librations of M^{II}
203	217	
237	217	
305	297	
410	410	$\nu_2(PO)_4$
442	438	
580	570	$\nu_4(PO)_4$
590	580	
626	622	
948.5	944	$\nu_1(PO)_4$
999		$\nu_3(PO)_4$
1006	988	
1018	1005	
1067	1064	
1080	1073	

the cations in the lithium sublattices, demonstrating the isotopic effect in the $^6Li-^7Li$ replacement. These vibrations may be mixed with the deformation vibrations of the anions, hindering the assignment of the latter.

The most intense line at 950 cm^{-1} in the Raman spectra of $LiM^{II}PO_4$ was assigned to the symmetrical ν_1 stretching vibration of the anion. The lower-intensity lines at higher frequencies (1000–1100 cm^{-1}) were attributed to the components of the triply degenerate ν_3 vibration (Table 9). Raman lines sensitive to lithium isotope substitution were not detected. This situation agrees fully with the theoretical postulates. The lithium cations occupying positions with the C_i symmetry cannot participate in the vibrations active in the Raman spectra. This permitted a more reliable assignment of the deformation vibration frequencies of the PO_4 groups. The ν_2 and ν_4 deformation frequencies were assigned on the basis of the relative intensities of the corresponding Raman lines and the vibration frequencies of the free anion in solution. The Raman lines at frequencies below 350 cm^{-1} were assigned to librations and translation vibrations without further specification. On the basis of the results, the authors[34] suggest that the approximation involving the subdivision of the vibrations into internal and external is justified. However, allowance for the factor-group splitting of the vibrations and for the subsequent interaction of their components with identical symmetries may introduce corrections to the results.

The available data for dilute solid solutions of a series of compounds $LiM^{II}PO_4$ showed that the observed splittings of the degenerate stretching vibration are not associated with geometrical distortions. The study of the crystal structure of $LiMnPO_4$ demonstrated the similarity of the four phosphorus–oxygen interatomic distances in the PO_4 groups (the differences between them do not exceed the experimental error). The deformation of the tetrahedral anions, expressed by changes in the bond angles from 106° to 112°, should most probably affect the behaviour of the deformation modes but cannot induce a significant splitting of ν_3.

Since appreciable splittings of ν_3 have been observed for compounds of different composition with the olivine structure ($M^{II}_2SiO_4$, $M^{II}_2GeO_4$, $M^{I}M^{II}AsO_4$, $M^{I}M^{III}SiO_4$, and $M^{I}M^{III}GeO_4$) as well as the orthophosphates considered, the authors[34] concluded that this effect is determined not only by the chemical nature of the cations or the anions but also by the crystal structure. Even when the cations in two different octahedral positions in the olivine structure are chemically identical, two sets of nonequivalent cation–oxygen distances are postulated in the compounds $M^{II}_2SiO_4$. Each oxygen atom of the tetrahedral anion is linked to three cations located in different positions, namely $2\,M^{II}(C_i) + 1\,M^{II}(C_s)$ or $1\,M^{II}(C_i) + 2\,M^{II}(C_s)$. The difference between the energies of the cation–oxygen bonds leads in this case to the appearance of two types of bonds in the tetrahedral anions and is responsible for the splitting of the ν_3 mode. This is naturally also responsible for the dependence of the splitting on the nature of the cations in the octahedral positions. Indeed, there is a quantitative dependence of the splitting on the second ionisation potential of the divalent cation, which demonstrates the validity of the proposed explanation of the observed effect.[34]

The structures of the double phosphates $LiSrPO_4$, $LiBaPO_4$, and $LiPbPO_4$ have not been investigated, although it is known that they are not isomorphous. The crystal structure of $LiBaPO_4$ resembles[35] the orthorhombic structure of $LiKSO_4$ with the symmetry space group $Pna2_1 = C^9_{2v}$ ($Z = 4$). Despite the similarity of the ionic radii of strontium and lead, their double orthophosphates with lithium salts crystallise differently. The $LiPbPO_4$ crystals have the $Pna2_1 = C^9_{2v}$ symmetry with eight formula units in the unit cell, while the space group $P2_1/b = C^5_{2h}$ has been proposed for $LiSrPO_4$. Using vibrational spectroscopic methods, the investigators[35] attempted to establish certain details of the structures of these compounds. The measured IR absorption spectrum of $LiBaPO_4$ proved to be similar to those obtained for $LiKSO_4$ and $LiCsSO_4$ over the entire range (up to 50 cm^{-1}). The vibration frequencies and their assignments for $LiBaPO_4$ are compiled in Table 10. Apart from the stretching and deformation vibration frequencies of the PO_4 groups, the IR absorption spectra contain bands at 400–500 cm^{-1}, undergoing an appreciable isotopic shift following the $^6Li-^7Li$ substitution which permitted their assignment to the vibrations of the lithium sublattice cations. The relatively high corresponding frequencies suggest a tetrahedral coordination of the lithium cations and agree with X-ray diffraction data. The three IR absorption bands recorded in the low-frequency region were assigned to lattice vibrations with participation of the heavy barium atoms.

Analysis of the isotopic shifts enabled the authors[36] to conclude that there are no appreciable interactions between the internal and external vibrations of the crystals having the structure investigated. It was possible to detect experimentally only some of the theoretically predicted vibration frequencies. In many cases, it was noted that the frequencies in the Raman and IR absorption spectra do not agree, which is consistent with the centrosymmetrical space group proposed for $LiBaPO_4$.

The observed isotopic effect assisted significantly also in the assignment of the Raman spectroscopic frequencies. The 954 and 930 cm^{-1} lines were assigned to the components of the symmetrical stretching vibration of the PO_4 groups, while the three lines in the range 1000–1150 cm^{-1} were assigned to the components of the triply degenerate vibration. The intense line at 424 cm^{-1} as well as the 580 and 570 cm^{-1} lines, which do not shift following lithium isotope substitution, have been assigned to the components of the ν_2 deformation vibration. Lines assigned to the vibrations of the cations of the lithium sublattice have been detected in the same range (390–500 cm^{-1}). A more complex vibrational spectrum has been obtained[35] for $LiSrPO_4$, which is due to the lower symmetry of the crystals. However, the range of the stretching vibration frequencies of the PO_4 groups proved to be similar to that for $LiBaPO_4$. The most significant shifts following lithium isotope substitution ($^7Li-^6Li$) have been recorded for the 618 (639), 516 (555), and 343 (393) cm^{-1} bands in the frequency range corresponding to the tetrahedral coordination of lithium in the crystal lattice. The components of the ν_4 vibrations of the PO_4 group are manifested at 590 and 576 cm^{-1}, while those of the ν_2 vibrations are manifested at 428 cm^{-1}. The authors note an appreciable, compared with $LiBaPO_4$, interaction of the deformation vibrations of the PO_4 groups with the vibrations of the lithium cations.

The presence of two bands, at 964 and 919 cm^{-1}, in the range of the stretching vibration frequencies of the anions in the IR spectrum of $LiPbPO_4$, has been attributed[35] to the presence in the

Table 10. Frequencies of the vibrations (cm^{-1}) of $LiM^{II}PO_4$ (M = Ba, Pb).[35]

$LiBaPO_4$				$LiPbPO_4$				Assignment
IR		Raman		IR		Raman		
^7Li	^6Li	^7Li	^6Li	^7Li	^6Li	^7Li	^6Li	
64	64	107		71	71			Lattice modes
82	83	168		75	75	37	37	including
154	160	295		93	93	57	57	predominantly
		398	405	115	116	71	71	M–O vibrations
				135	135	94.5	94.5	
				169	169	137	137	
				202	202	247	247	
				246	246			
				257	257			
				380	385			
	426	424	426	405	410	395	393.5	$\nu_2(PO)_4$
420	445			443	459		408	
						422	433	
463	487	455	473	482	508	433	455	
482	510					482.5	495.5	
572	573	570	576			560	560	$\nu_4(PO)_4$
587	592	580	585	580	584	582	582	
		600	600					
958	958	930.5		919	919	926		$\nu_1(PO)_4$
		954		964	926			
1037	1039	1021.5		1000	1000	1015		$\nu_3(PO)_4$
		1033.4		1034	1034	1058		
		1108		1062	1062	1078		

crystal lattice of two sets of nonequivalent PO_4 groups. The Raman lines sensitive to lithium isotope substitution have been detected in the frequency range 500–600 cm^{-1}. Identical absorption frequencies have been noted for many vibrations of $LiPbPO_4$, which agrees with the absence of a centre of symmetry in the crystal lattice (space group $Pna2_1 = C_{2v}^9$). The authors[35] do not propose any approaches to a detailed interpretation of the long-wavelength (below 300 cm^{-1}) part of the spectra of the group of compounds considered, postulating the manifestation in this region of vibrations involving the heavy cations. Nevertheless, comparison of the spectra of compounds differing appreciably in the mass of the cations permits the analysis also of this spectral region, thus differentiating also the librations of the PO_4 groups.

The IR absorption spectra of polycrystalline specimens (mulls in liquid paraffin) of $RbMgPO_4$ and $CsMgPO_4$ have been measured[37] in the restricted range 400–1800 cm^{-1}. The very great similarity of the spectra enabled the authors to conclude that the compounds have the same structure. The splitting of the bands due to the stretching and deformation vibrations of the PO_4 groups as well as the activity in the IR spectrum of the fully symmetrical ν_1 stretching vibration suggest a decrease in the symmetry of the anion in the crystal lattice. The lack of sufficient experimental data made it impossible to secure more complete information about the structure of these phosphates.

Apart from the compounds considered here, the crystal structures have been described for a further two orthophosphates $M^IM^{II}PO_4$. X-Ray diffraction analysis of $RbZnPO_4$ led to the conclusion[38] that this compound crystallises in the monoclinic system [space group $P2_1 = C_2^2$ ($Z = 4$)]. It was shown that the structure is based on a three-dimensional skeleton made up of ZnO_4 and PO_4 tetrahedra related to the tridymite skeleton. The heptacoordinated rubidium cations are located in the channels of the skeleton. The crystal structure of $KBaPO_4$[23] with the $Pnma = D_{2h}^{16}$ ($Z = 4$) symmetry belongs[39] to the β-K_2SO_4 (arcanite) type in which some of the potassium cations have been replaced by barium. Unfortunately, we do not possess spectroscopic data on these compounds.

The crystal structures and vibrational spectra of double orthophosphates of Group I and III elements have been most fully investigated. Extensive information about these substances has been surveyed in a series of reviews.[32,40–42] X-Ray and physicochemical studies on phases of the type of nasicon $Na_3M_2^{III}(PO_4)_3$, where M is Sc, Cr, or Fe, demonstrated[40,42] the possibility of the occurrence in the latter of a high-temperature orthorhombic γ-phase with superionic conductivity, an intermediate phase (β-phase), and a low temperature α-phase. A detailed analysis of the structure, ion transport, and phase transitions in compounds of the type of nasicon has been carried out.[43] On the basis of X-ray diffraction and spectro-scopic studies,[44,45] the structure of nasicon $M_3^IM_2^{III}(PO_4)_3$ has been described as a superposition of the sublattices of PO_4 tetra-hedra and the M^I and M^{III} cations which fill the existing cavities. For compounds with a wide range of cations (M^I = Li, Na, K, Cu, Ag; M^{III} = Fe, Sc), the distortion of the structure relative to the initial prototype[40] $NaZr(PO_4)_3$ with the space group $R3c = C_{3v}^6$ as the cavities in the skeleton are filled has been studied.[44] In the course of the investigation of the vibrational spectra, both the range of symmetrical and antisymmetrical stretching vibration frequencies of the PO_4 groups, sensitive to the distortions of the tetrahedral anion, and the long-wavelength range (50–300 cm^{-1}), analysis of the bands in which makes it possible to estimate the degree of ordering of the cations, were examined. The minimum activation energy for conduction was found for compounds with most local disorder in the distribution of the cation. The conductivity diminishes as the cavities are filled.

An interpretation of the temperature-induced changes in the IR absorption and Raman spectra of orthophosphates of the type of nasicon $M_3^ISc_2(PO_4)_3$, where M = Li, Na, K, or Ag, in the range 100–300 K has been proposed.[45] In particular, the frequencies of the internal vibrations of the PO_4 groups and the vibrations of the scandium sublattice and of the conducting M^I cations as well as the librations of the tetrahedral anions were assigned. A correlation was established between the local disorder, the phase transitions, and the changes in the activation energy for conduction. Studies of the Raman spectrum of

$Li_3Fe_2(PO_4)_3$ as a function of temperature were continued.[46] Investigation of the $\alpha-\beta$ and $\beta-\gamma$ phase transitions demonstrated that the disordering of the cationic sublattice of the orthorhombic γ-phase leads to the broadening of the lines due to both the internal stretching vibrations of the PO_4 groups and the lattice modes. Analysis of the calculated and experimental frequencies of the relaxation modes led the authors[28] to the assumption that low-frequency phonons are involved in the activation process.

The crystals of alkali metal lanthanide double phosphates can be divided into several types.[32] The parent of this structural family is glaserite $K_3Na(SO_4)_2$ [48] having a layered structure. The layers are formed by the tetrahedral sulfate anions and sodium cations, the potassium cations occupying the interatomic space.

Among compounds of this series, lithium compounds have been least investigated. The structure of the monoclinic $Li_3Sc_2(PO_4)_3$, corresponding to the space group $P2_1/n = C_{2h}^2$ ($Z = 4$), is known.[48] The crystal lattice is made up of the scandium coordination octahedra linked via the common vertices to the PO_4 tetrahedra. The lithium cations occupy the tetrahedral and trigonal-bipyramidal (two types) positions. The lithium polyhedra linked via common vertices form infinite chains. The results of a neutron diffraction study of $Li_3Sc_2(PO_4)_3$ [49] revealed insignificant differences between the parameters of the monoclinic cell and those obtained by X-ray diffraction.

A study of the structural features of the double sodium lanthanide orthophosphates $Na_3Ln(PO_4)_2$ showed[47] that the nature of the ordering of the cations in the glaserite-like lattice depends on the size of the lanthanide. Most of them have the orthorhombic symmetry and form a group of the $Na_3La(VO_4)_2$ structural type.[32] However, the available literature data are contradictory.[32,47]

Double potassium lanthanide orthophosphates have been investigated in greater detail[32,50] and, in conformity with their crystal structure, they can be divided into three groups:

Ln = La, or Sc—compounds with the triple glaserite unit cell;

Ln = Gd–Yb—compounds with a monoclinic distortion of the $K_3Lu(PO_4)_2$ lattice and the lattice volume increased by a factor of eight;

Ln = Nd—the intrinsic $K_3Nd(PO_4)_2$ structural type.

Among recent studies on the double orthophosphates, mention should be made of the investigation[51] devoted particularly to the phase relations in the $K_2O-Y_2O_3-P_2O_5$ system, where the existence of the $K_3Y(PO_4)_2$ phase was confirmed by the results of physicochemical and X-ray diffraction analysis and by IR spectra.

The more symmetrical trigonal structure occurs in the rubidium compounds of similar composition. This is ensured, firstly, by the 'moving apart' of the layers of the PO_4 tetrahedra and the lanthanide octahedra by the larger rubidium cations and their smoothing and, secondly, by the displacement of electron density and the increase in the covalent component of the Ln–O bond when potassium is replaced by rubidium, which also increases the symmetry of the layers. The intrinsic structural type occurs for $Rb_3Sc(PO_4)_2$.[32] According to the available data,[32] the double orthophosphate $Ag_3Sc(PO_4)_2$ has no structural analogues among the compounds described above. Silver compounds with lanthanides having this composition are unknown.

The vibrational spectra of $M_3^IM_2^{III}(PO_4)_3$, where M^I = Li or Na and M^{III} = Sc, Cr, Fe, or In, have been investigated.[52] Attention was concentrated on the temperature-induced changes in the Raman and IR absorption spectra of $Na_3Fe_2(PO_4)_3$. The two crystalline modifications of this phosphate differ by the distribution of the sodium cations—it is fully ordered for the monoclinic α-phase but is only partly ordered for the hexagonal β-phase. The authors[52] were able to discover certain significant differences between the vibrational spectra of these two modifications of $Na_3Fe_2(PO_4)_3$.

Analysis of the temperature dependence of the behaviour of the IR absorption bands of $Na_3Fe_2(PO_4)_3$ made it possible to divide the spectrum arbitrarily into two regions:

the 300–650 cm^{-1} frequency range, assigned to the deformation vibrations of the PO_4 groups and the translational vibrations of the iron cations, this part of the spectrum hardly changing in the given temperature range;

the higher frequency range 900–1250 cm^{-1}, corresponding to the stretching vibrations of the PO_4 groups, in which the fine structure of the absorption bands undergoes changes (a slight bathochromic shift and a broadening of the bands) at 84 °C.

More significant changes in the spectrum were recorded in the temperature range of the $\alpha-\beta$ polymorphic transition at 95–102 °C. The spectrum of β-$Na_3Fe_2(PO_4)_3$ obtained resembles that of $NaZr_2(PO_4)_3$ with a structure having hexagonal symmetry. However, solely on the basis of symmetry consideration without allowance for the disordering of the cations, the authors were unable to interpret all the recorded temperature-induced changes.

The results of the studies on the IR spectrum agree satisfactorily with the results of Raman measurements as a function of temperature. The fine structure of the Raman lines in the range 400–1250 cm^{-1} is almost completely smeared on raising the temperature to 110 °C, whilst in the region of moderate and low frequencies no significant changes take place. The 238 cm^{-1} line, which completely disappears with increase in temperature, is an exception.

The synthesis and study[53] of the double orthophosphates $Na_3Ln(PO_4)_2$ and $Na_3Ln_2(PO_4)_3$, where Ln = Tb–Lu, have been described. The formation of several polymorphic modifications with different symmetries is characteristic of each of the compounds investigated. The authors obtained the γ-phase for the first time. The phosphates of the series considered can be divided into four structural types. The X-ray diffraction pattern and the Raman spectrum of the γ-phase isolated differ from those known for any other phosphates. The temperature-induced changes in the Raman spectrum of the double phosphate $Na_3Ho(PO_4)_2$ are of considerable interest. At 465 °C, the three most intense lines of the Raman spectrum in the range of the stretching vibration frequencies of the PO_4 groups were broadened and exhibited two absorption shoulders on their slopes. The frequencies of the maxima increased and then remained unchanged up to 940 °C. A roughly similar behaviour has been demonstrated by the Raman lines of $Na_3Dy(PO_4)_2$. The single line generated when the three components merge in the region of the stretching vibration frequencies of the PO_4 groups at 750 °C has a frequency 16 cm^{-1} lower than that of the most intense initial line. The authors explained the observed effect by the occurrence of a phase transition. Manifestations of a phase transition have been noted[53] also in the Raman spectra of $Na_3Yb_2(PO_4)_2$. On the basis of the spectroscopic data obtained, the authors established the temperature limits of the stability of different polymorphic modifications of the phases studied.

The double orthophosphates $M_3^{II}M^{III}(PO_4)_3$ have been examined.[54,55] The formation of cubic crystals with the space group $I43d = T_d^6$ is characteristic of compounds of the series with M^{II} = Sr, Ba, or Pb and M^{III} = Y, Sc, Ln, or Bi. $Ca_3Bi(PO_4)_3$ and $Ca_3Eu(PO_4)_3$ have also been obtained. The results of the X-ray diffraction and IR spectroscopic study of the double calcium europium orthophosphate indicate[55] that its structure is the same as that of β-$Ca_3(PO_4)_2$.

Double lanthanide orthophosphates have been vigorously investigated in recent years.[56–58] They are isostructural with monazite or zircon and with the lanthanide orthophosphates. It may be expected that the distribution of lanthanides of different masses at the cationic sites would lead to changes in the longer-wavelength part of the vibrational spectra.

* * *

The foregoing demonstrates the possibility of securing extensive information, which is also predictive in character, in those cases where systematic spectroscopic studies have been carried out using all the possibilities of the method. Unfortunately, such investigations have been carried out fully for a very limited number of phosphates. The existing frequently controversial results have not been confirmed by theoretical calculations of the vibrations of the crystals. The vibrational spectra of alkali metal orthophosphates have not been investigated. On the other hand, vigorous studies are being prosecuted on the synthesis and X-ray diffraction of new complex orthophosphates and also compounds with systems of condensed phosphate anions. Reliable information can be secured from the analysis of the vibrational spectra of the latter only on the basis of a detailed knowledge of the nature of the vibrations of simpler orthophosphates.

References

1. A A Fakeev *Vysokochist. Veshchestva* (4) 38 (1991)
2. L N Shchegrov *Fosfaty Dvukhvalentnykh Metallov* (Phosphates of Divalent Metals) (Kiev: Naukova Dumka, 1987)
3. I Kostov, V Breskovska *Phosphate, Arsenate and Vanadate Minerals. Crystal Chemistry and Classification* (Sofia: Kliment Ohridski Univ. Press, 1989)
4. Umegaki Takao *Mater. Technol.* **9** 135 (1991)
5. R Ya Mel'nikova, V V Pechkovskii, E D Dzyuba, I E Malashonok *Atlas Infrakrasnykh Spektrov Fosfatov. Kondensirovannye Fosfaty* (Atlas of Infrared Spectra of Phosphates. Condensed Phosphates) (Moscow: Nauka, 1985)
6. V V Pechkovskii, N I Chudinova, R Ya Mel'nikova, E D Dzyuba, I E Malashonok, T I Barannikova, V A Lyutsko (Eds) *Atlas Infrakrasnykh Spektrov Fosfatov. Dvoinye Mono- i Difosfaty* (Atlas of Infrared Spectra of Phosphates. Double Mono- and Diphosphates) (Moscow: Nauka, 1990)
7. E Steger, K Herzog Z. *Anorg. Allg. Chem.* **331** 169 (1964)
8. A C Chapman, L E Thirlwell *Spectrochim. Acta* **20** 937 (1964)
9. A F Banishev, Yu K Voron'ko, V V Osiko, A A Sobol' *Dokl. Akad. Nauk SSSR* **274** 559 (1984)
10. M Smaihi, D Petit, F Gourbilleau, F Chaput, J P Boilot *Solid State Ionics* **48** 213 (1991)
11. F A Miller, G L Carlson, F F Bentley, W H Jones *Spectrochim. Acta* **16** 135 (1960)
12. Landolt-Bornstein *Phys.-Chem. Tabellen* **2** (1951)
13. J T S Irvine, A R West *J. Solid State Chem.***74** 385 (1988)
14. P Tarte, J Thelen *Spectrochim. Acta, Part A* **28** 5 (1972)
15. A N Lazarev, A P Mirgorodskii, I S Ignat'ev *Kolebatel'nye Spektry Slozhnykh Okislov* (Vibrational Spectra of Complex Oxides) (Leningrad: Nauka, 1975)
16. W H Zachariasen *Acta Crystallogr.* **1** 263 (1948)
17. P Rouxm, G Bonel *Rev. Chim. Miner.* **22** 767 (1985)
18. W O Milligan, D F Mullica, G W Beall, L A Boatner *Inorg. Chim. Acta* **60** 39 (1982)
19. G W Beall, L A Boatner, D F Mullica, W O Milligan *J. Inorg. Chem.* **43** 101 (1981)
20. F Weigel, V Scherer, H Henschel *J. Am. Chem. Soc.* **48** 383 (1965)
21. M A Aia *J. Electrochem. Soc.* **114** 367 (1967)
22. A Hesel, S R Ross *Spectrochim. Acta* **22** 1949 (1966)
23. Hinatsu Yukio, Edelstein Norman *J. At. Energy Soc. Jpn.* **33** 80 (1991)
24. A N Lazarev *Kolebatel'nye Spektry i Stroenie Silikatov* (Vibrational Spectra and Structure of Silicates) (Leningrad: Nauka, 1968)
25. T F Tenisheva, T M Pavlyukevich, A N Lazarev *Izv. Akad. Nauk SSSR, Ser. Khim.* 1771 (1965)
26. E N Yurchenko, E B Burgina, V I Bugakov, E N Murav'ev, V P Orlovskii, T V Belyaevskaya *Izv. Akad. Nauk SSSR, Neorg. Mater.* **14** 2038 (1978)
27. R J Elliott, R T Harley, W Hayes, S R P Smith *Proc. R. Soc. London A* **328** 217 (1972)
28. I Richman *J. Opt. Soc. Am.* **56** 1589 (1966)
29. A N Lazarev, N A Makhinov, A P Mirgorodskii *Izv. Akad. Nauk SSSR, Neorg. Mater.* **14** 2107 (1978)
30. G M Begun, G W Beall, L A Boatner, W J Gregor *J. Raman Spectrosc.* **11** 273 (1981)
31. B I Swanson, C Machell, G W Beall, W O Milligan *J. Inorg. Nucl. Chem.* **40** 694 (1978)
32. P P Mel'nikov, L N Komissarova *Koord. Khim.* **12** 1299 (1986)
33. M-Th Paques-Ledent *Rev. Chim. Miner.* **10** 785 (1973)
34. M-Th Paques-Ledent, P Tarte *Spectrochim. Acta, Part A* **30** 673 (1974)
35. M-Th Paques-Ledent *J. Solid State Chem.* **23** 147 (1978)
36. M-Th Paques-Ledent *C. R. Acad. Sci.* **274** 1998 (1972)
37. V M Yakunina, T V Smurova, I F Poletaev, V E Plyushchev *Zh. Neorg. Khim.* **20** 3198 (1975)
38. L Elammari, B Elouadi *J. Chim. Phys. Phys.-Chim. Biol.* **88** 1969 (1991)
39. R Masse, A Durif *J. Solid State Chem.* **71** 574 (1987)
40. V B Kalinin *Izv. Akad. Nauk SSSR, Neorg. Mater.* **26** 2229 (1990)
41. W A Dollase, L H Merwin, A Sebald *J. Solid State Chem.* **83** 140 (1989)
42. M de la Rochere, F d'Yvoire, G Collin, R Comes, J P Boilot *Solid State Ionics* **9 – 10** 825 (1983)
43. F d'Yvoire, M Pintard-Scripel, E Bretly, M de la Rochere *Solid State Ionics* **9 – 10** 851 (1983)
44. M Barj, H Perthuis, Ph Colomban *Solid State Ionics* **9 – 10** 845 (1983)
45. M Barj, H Perthuis, Ph Colomban *Solid State Ionics* **11** 157 (1983)
46. A Orliukas, R Taitkus, A Kezionis, S Aukselis *Solid State Ionics* **40 – 41** 158 (1990)
47. M Vlasse, C Parent, R Salmon, G le Flem, P Hagenmuller *J. Solid State Chem.* **35** 318 (1980)
48. E A Genkina, L A Muradyan, B A Maksimov *Kristallografiya* **31** 595 (1986)
49. B A Maksimov, L A Muradyan, N N Bydanov, V A Sarin, A B Bykov, V A Timofeeva, V I Simonov *Kristallografiya* **36** 1431 (1991)
50. V A Efremov, P P Melnikov, L N Komissarova *Rev. Chim. Miner.* **22** 666 (1985)
51. G Czupinska *Pr. Nauk. AE Wroclaw.* (589) 1 (1991)
52. P Tarte, J-M Winand, A Rulmont *C. R. Acad. Sci., Ser. 2* **302** 553 (1986)
53. C E Bamberger, W R Busing, G M Begun, R G Haire, L C Ellingbol *J. Solid State Chem.* **57** 248 (1985)
54. G von Engel *Z. Anorg. Allg. Chem.* **387** 22 (1972)
55. B I Lazoryak, B N Viting, P B Fabrichnyi, L Furnes, R Salmon, P Khagenmyuller *Kristallografiya* **35** 1403 (1990)
56. D F Mullica, E L Sappenfield, L A Boatner *Inorg. Chim. Acta* **174** 155 (1990)
57. D F Mullica, E L Sappenfield, L A Boatner *J. Solid State Chem.* **99** 313 (1992)
58. D F Mullica, D A Grossie, L A Boatner *Inorg. Chim. Acta* **118** 173 (1986)

Russian Chemical Reviews **63** (5) 411 – 427 (1994)
©1994 Russian Academy of Sciences and Turpion Ltd

UDC 546.07 + 661.5/.6 + 669.018.2/.4/.6

The synthesis and properties of nanocrystalline refractory compounds

R A Andrievskii

Contents

I. Introduction	411
II. Ultradisperse powders and their properties	411
III. Consolidated powdered nanocrystalline materials	419
IV. Nanocrystalline films	421
V. Conclusion	424

Abstract. The methods of synthesis of refractory carbides, borides, nitrides, and oxides in the form of ultradisperse powders, consolidated materials, and films with a grain size less then 100 nm are examined. Information about the properties of nanocrystalline refractory compounds is described systematically and discussed. The bibliography includes 233 references.

I. Introduction

It is believed that one of the most important roles of chemical synthesis is in the establishment and improvement of the properties of modern ceramic, polymeric, and other materials (see, for example, Refs 1 – 5). The dimensional, phase, impurity, morphological, structural, and other features, which to a significant extent determine the physicochemical, physicomechanical, and operational properties of the materials, are in fact established at this stage of the synthesis. The important role of chemical synthesis is also indicated by the following facts: since 1984, the American Materials Science Society has held regular symposia, twice a year, on 'Chemical Methods for the Improvement of Ceramics'; the journals Chemistry of Materials and Journal of Materials Chemistry have been published by the American Chemical Society and the British Royal Society since 1989 and 1991 respectively.

Interest in the methods of synthesis used to create a new class of substances — nanocrystalline materials (NM) the characteristic structural size (grain or subgrain size) of which is less than 100 nm — is understandable. It has been shown for many nanocrystalline materials based on metals and intermetallic compounds (Ni, Pd, Ag, Cu, TiAl, $NbAl_3$, etc.) that a significant change in properties, the nature of which is frequently nonmonotonic, is observed for this grain size.[6-8]

The available review publications mainly describe the properties of the above nanocrystalline materials but are hardly concerned with the problems of refractory compounds (RC). The latter usually include carbides, nitrides, borides, oxides, and other phases with a melting point above 2000 °C.[9] The remarkable properties of these compounds (high hardness and high modulus of elasticity and strength; chemical inertness and low rate of evaporation; a wide range of electrical properties, including superconductivity, etc.) have long attracted to them the attention of a wide range of specialists in the field of the physical chemistry and technology of materials. Recently this interest has intensified in connection with the creation of nanocrystalline materials. The available information about the synthesis and properties of nanocrystalline materials based on refractory compounds is scattered and needs to be surveyed and treated systematically.

The problems of the synthesis of nanocrystalline materials from refractory compounds have several aspects. These are, firstly, the preparation and consolidation of ultradisperse powders and, secondly, the preparation of nanocrystalline films. Apart from these, there are also the characteristic features of the synthesis of amorphous substances which are converted into nanocrystalline materials after crystallisation. Our review is devoted predominantly to nanocrystalline materials in the powder and film form, in both consolidated and discrete states. For this reason, certain questions concerning the complex problem of the consolidation of nanocrystalline materials are also dealt with. So far as we are aware, such an approach had not been used previously although individual data are available in some communications.[10-13]

Clearly, the temperature limit of refractory compounds indicated above is extremely arbitrary and is largely dictated by convenience. According to estimates,[14] there are about 240 two-component refractory compounds for which T_f† > 2000 °C. On the other hand, the number of thoroughly investigated refractory compounds which are used in practice is much smaller. Therefore the subject of our review concerns nanocrystalline refractory compounds such as Si_3N_4, SiC, TiN, TiC, TiB_2, NbC, NbN, WC, Al_2O_3, AlN, ZrO_2, Y_2O_3, MgO, BN, and certain others. It is easily seen that they virtually all form part of the promising group of ceramics popular at present (Advanced Ceramics).

II. Ultradisperse powders and their properties

1. Preparation

The problem of the preparation of ultradisperse powders has long been discussed in publications devoted to ceramics, powder metallurgy, catalysis, and other fields. Various methods for the chemical synthesis of ultradisperse powders of oxygen-free refractory materials, used in ceramics and catalysis, have been

R A Andrievskii Laboratory for Special Inorganic Synthesis, Institute of New Chemical Problems, Russian Academy of Sciences, 142432 Chernogolovka, Moscow Region, Russian Federation. Fax (7-095) 292 65 11.

Received 12 April 1994
Uspekhi Khimii **63** (5) 431 – 448 (1994); translated by A K Grzybowski

† Melting point (Ed. of Translation).

Table 1. Methods of preparation of ultradisperse powders of refractory compounds.

Method	Compound	Ref.
Physical methods		
Vaporisation and condensation		
In an inert gas or a vacuum	MgO, Al_2O_3, SiC;	17, 18
	Al_2O_3, Y_2O_3	19
	ZrO_2	20
in a reactive gas	TiN, ZrN, NbN, AlN, VN, HfN;	21
	ZrO_2, Y_2O_3	20, 22
	Al_2O_3, AlN	23
High energy disruption		
grinding	ZrC, NbC;	24, 25
	Si_3N_4	26, 27
mechanosynthesis	TiC, ZrC, HfC, VC, TaC, WC, SiC, MoC;	28–31
	TiB_2;	32, 33
	TiN, BN, Si_3N_4, AlN, NbN	34–36
detonation treatment	BN;	37, 38
	Al_2O_3, MgO;	39
	SiC, TiC, Al_2O_3	40, 41
Chemical methods		
Synthesis		
plasmochemical	TiN, ZrN, HfN, NbN, Ti(C,N), VN;	10, 42
	AlN, BN, Si_3N_4, TiC, SiC, Si_3N_4 + SiC;	43–51
	Al_2O_3;	52
	TiN + TiB_2	53
laser	Si_3N_4, SiC;	54–56
	TiB_2;	57
	Si_3N_4 + SiC	58
thermal	BN, SiC;	59–61
	SiC;	62
	HfB_2, ZrC;	63
	WC + Co;	64
	$(Mo,W)_2C$;	65
	TiN, ZrN;	66
	ZrO_2;	67
	TiN + TiB_2	68
electrochemical	WC;	69
	ZrO_2;	70
	WB_4, MoB_4	71
in solutions	Mo_2C, W_2C;	72
	TiB_2, SiC	15, 73
Thermal decomposition		
condensed precursors	Si_3N_4, SiC, BN, AlN;	15, 74–76
	ZrO_2, Y_2O_3;	74, 77, 78
	NbN;	79
	Si_3N_4 + SiC	80, 81
gaseous precursors	TiB_2, ZrB_2;	16, 82, 83
	BN	84

analysed in a review.[15] Its authors reduced arbitrarily the wide variety of synthetic methods to four types of reactions — solid-phase, gas-phase, liquid-phase, and reactions of the gas–solid type. Nontraditional methods of synthesis of oxygen-containing and oxygen-free powders such as the sol-gel process, hydrothermal synthesis, pyrolysis of polymers, reactions in nonaqueous solutions, and different versions of the gas-phase synthesis (plasmochemical, laser, etc.) have come to be widely used in recent times.[1,16] One can add to these mechanosynthesis, electrochemical synthesis, self-propagating high-temperature synthesis (SHS), and synthesis in shock waves. The methods of preparation of solid powders of refractory compounds can be divided into two groups — physical and chemical (Table 1). This subdivision is naturally arbitrary because, for example, virtually all the physical methods include an appreciable chemical component and it is indeed frequently difficult to draw a clear-cut boundary between different procedures. Table 1 includes by no means all the examples of the preparation of ultradisperse powders of refractory materials, only the most characteristic being listed. We shall examine certain characteristic features of the methods of preparation of such powders.

a. Vaporisation and condensation

The condensation methods of preparation of clusters and ultradisperse powders have long been known and their theory has been described in many publications (see, for example, Uyeda[18] and Morokhov et al.[85]). There are at least two necessary and sufficient conditions for the condensation of ultradisperse powders — a high supersaturation and the presence in the condensed vapour of the molecules of a neutral gas. An interpretation of the phenomena in the gas-phase condensation, including homogeneous and heterogeneous nucleation, the mechanism of the growth of particles, the influence of impurities, etc., may be found in the sources mentioned above.[18,85]

In relation to nanocrystalline materials, condensation methods have developed after the publication of the communications of Birringer et al.[86] and Siegel and Hahn.[87] They describe the apparatus which makes it possible to combine the condensation process leading to the formation of ultradisperse powders with the vacuum pressing of small specimens (with a diameter up to 10–15 mm and thickens up to 0.2–0.5 mm) at high pressures (up to 3–5 GPa). This made it possible to avoid contamination to a large extent, by excluding contact between the ultradisperse powder and the surrounding medium, which is particularly important in the case of metallic and intermetallic substances. Ultradisperse aluminium, zirconium, yttrium, etc. oxide powders can be obtained in such apparatus by vaporising the oxide targets in a helium vacuum,[19] by the magnetron atomisation of zirconium cathodes in an argon–oxygen medium,[20] and also by forming an ultradisperse yttrium powder with subsequent controlled oxidation.[22] The reactive laser ablation synthesis, designed to obtain spherical Al_2O_3 and AlN particles on evaporation of aluminium, has been described.[23]

Mention should be made of the work of Japanese investigators on the vaporisation of transition metals in a nitrogen or ammonia vacuum (130 Pa) using electron-beam heating[21] and also on the application of the plasma, laser, and arc methods of heating in order to obtain ultradisperse MgO, Al_2O_3, and SiC powders.[17,18]

An advantage of the condensation method is the possibility of obtaining fairly pure ultradisperse powders with an extremely small particle size (with a particle diameter d down to 5–10 nm and less) over a comparatively narrow range of the latter. However, their productivity is low and the energy consumption is considerable. Naturally one has to bear in mind also the possible complications associated with the maintenance of the specific composition, which applies particularly to compounds with a wide range of homogeneity (for example, transition metal carbides and nitrides).

b. High-energy disruption

The usual grinding process is employed comparatively rarely to obtain ultradisperse powders because a grindability limit exists corresponding to the attainment of a kind of equilibrium between the disruption of the particles and their agglomeration.[4] Even when brittle materials are ground, the diameter d is usually not less than 50–100 nm. Furthermore, during grinding the product is contaminated by the material of the spheres and of the lining and also by oxygen. Admittedly, this can be avoided to a large extent by employing special spheres and lining prepared from the same material as the product being ground but the contamination with oxygen of oxygen-free refractory compounds

cannot be prevented. This can be illustrated by the example of the grinding of silicon nitride in a specially lined attrition mill:[26]

	Initial characteristics	4-h grinding	12-h grinding
d/nm	220	95	60
O_2 (mass %)	0.9	2.1	3.9

The characteristics of the preparation of ultradisperse powders of refractory materials by mechanosynthesis have been vigorously investigated recently. This was preceded, starting in the 1970s, by the study of the characteristic features of the so called mechanical alloying — the formation of alloys and intermetallic compounds under the conditions of high-energy grinding. One of the first mentions of the possibility of the synthesis of titanium (TiB_2), molybdenum (MoB), and niobium (NbB_2) borides when the corresponding metallic powder and boron are ground together in a planetary mill can be found in a monograph.[88] The mechanism and characteristics of the mechanosynthesis of refractory materials have been the subject of a lively discussion in the literature.[89-91]. The formation of refractory compounds during grinding is attributed both to the vigorous generation of new active surfaces and intense mixing (which intensifies diffusion processes) and to the exothermic nature of the reactions of the metals with the nonmetallic components (carbon, boron, and nitrogen). Mechanical activation as it were initiates the subsequent development of the self-propagating high-temperature synthesis. In some cases (systems of the Ti–C, Zr–B, and Nb–C type) explosive mechanosynthesis has been noted. This was detected thermographically from the abrupt increase in temperature.[92]

Fig. 1 illustrates the dependence of the nitrogen content in Group IV–VI transition metal nitrides on the duration of mechanosynthesis.[93] The relative disposition of the saturation curves, corresponding to the known differences between the exothermicities of the formation reactions of the nitrides of the test metals, is a characterisic feature. In experiments described by Atsumi et al.,[93] a vibromill of the YAMP-2SND type with a working volume of 1300 cm^3 and a ball charge of 90 : 1 was used; nitrogen was supplied continuously to the reaction space from a 34 litre reservoir. When a mill of the SPEX 8000 type (working volume 90 cm^3, ball charge 13 : 1) was employed, the duration of grinding was reduced severalfold (for example, it was approximately 30 h for TiN with a nearly stoichiometric composition.[35] Electron microscope and X-ray diffraction studies have shown that the particle size of such powders amounts to several nanometers.

Investigators working in the field of mechanosynthesis suggest that this method of preparation of ultradisperse powders can be used on a fairly large scale and is one of the promising procedures for the preparation of nanocrystalline materials.[31] Its advantage consists also in the possibility of obtaining alloyed and composite powders and in the use of nonconditioned raw material. However, the purity and technological properties of the powders obtained in this way have so far been inadequately investigated.

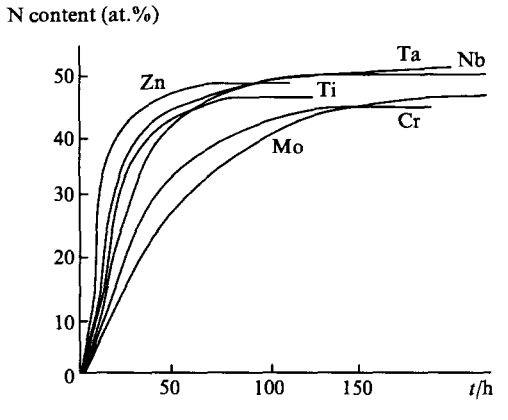


Figure 1. The influence of the duration of grinding on the nitrogen content in the nitrides.[93]

Detonation treatment (synthesis in shock waves and fragmentation) has long been known,[37-41] but, so far as we are aware, there have been few studies of such treatment in relation to nanocrystalline materials. The preparation of ultradisperse powders by the electrical explosion of wires belongs to the class of high-energy disruption methods, but this procedure has not so far been applied to brittle refractory compounds.

c. Synthesis

The chemical methods of the preparation of ultradisperse powders are more universal than the physical methods. Plasmo-chemical synthesis is one of the most popular. Extensive studies on these lines have been carried out in Russia,[10,42] Latvia,[43,44] Ukraine,[45,46] Japan,[18] and other countries.[15,94] The synthesis in a low temperature plasma is carried out at high temperatures, up to $(6-8) \times 10^3$ K, which ensures a high level of supersaturation and high rates of reaction and condensation processes. Examples of the modelling of the thermodynamic equilibrium, the vaporisation and condensation processes, as well as the coagulation of particles in the plasmochemical synthesis of ultradisperse powders of refractory compounds have been described in detail in the literature (see, for example, Refs. 10, 42–46, 95, and 96) and we shall not dwell on them here.

There is, in principle, the possibility of plasmochemical synthesis of virtually all ultradisperse refractory compound powders. Table 1 presents only a proportion of them. In addition, one may point to tungsten, tantalum, niobium, and boron carbide powders.[15,97,98] In order to obtain ultradisperse powders of refractory compounds, both arc plasmatrons[43-47,49,51-53,98] and high-frequency (including UHF) plasma generators[10,42,48] are employed; hybrid apparatus has also been described.[50] Arc plasmatrons are more productive and more readily available, but high- and ultrahigh-frequency devices ensure a higher purity of the products synthesised. Thus an ultradisperse β-SiC powder with a particle size of 5–20 nm and a high purity as regards cationic impurities (99.999%) has been obtained from silane and ethylene in an argon high-frequency plasma.[48] The oxygen content in these powders was ~1%.

It is also significant that plasmochemical technology ensures the preparation of multicomponent ultradisperse refractory compound powders: Si_3N_4+SiC, Ti(N, C), Nb(N, C), $TiN+TiB_2$, Si_3N_4+TiN (MgO, Al_2O_3, Y_2O_3), etc.[10,11,50,53] The manufacture of such powders on a semi-industrial scale has been introduced in a number of countries.

Electric spark dispersion, which combines the discharge-induced metal and alloy fragmentation process in reactive media with the synthesis of carbides and oxides (for example, TiC, SiC, WC, Al_2O_3), is closely related both to plasmochemical synthesis and to high-energy fragmentation.[99,100]

An effective procedure for the stimulation of the gas-phase synthesis involves the use of laser radiation. The optical heating source initiates and maintains the chemical reaction, promoting thereby the uniform 'self-heating' of the molecule, which ensures controlled homogeneous nucleation and rules out the possibility of contamination and of the influence of surfaces. Different versions of the thermochemical effect of laser radiation and the kinetics of these processses have been analysed.[101,102] Detailed studies of the characteristics of the laser synthesis of ultradisperse Si_3N_4, SiC, and TiB_2 powders have been carried out.[54,57] Study of the influence of the radiation intensity, pressure, and flow rate of the gas and its dilution on the dispersity of Si_3N_4 powders, obtained by the reaction

$$3\,SiH_4 + 4\,NH_3 \longrightarrow Si_3N_4\downarrow + 12\,H_2, \qquad (1)$$

showed that an increase in radiation intensity makes the greatest contribution to the decrease in the particle size and to the content of free silicon:

CO_2 laser radiation intensity/W cm^{-2}	760	2×10^4	1×10^5
d/nm	17.6	11.4	9.8
Free silicon (mass %)	35	2	traces

The influence of the intensity is attributed to the increase in the reaction temperature (from ~870 °C to > 1020 °C) and to the higher degree of saturation due to the increase in heating [rate] (from 10^6 to 10^8 K s^{-1}), which promotes an increase in the rate of nucleation, a high degree of completion of reaction (1), and a decrease in grain size. In order to improve the process efficiency, two laser sources, arranged opposite one another in such a way that the radiation axes coincide minimising losses thereby, are used; the stream of gas mixture is usually introduced at right angles to the beam. However, so far as we are aware, the laser synthesis of ultradisperse refractory compound powders has not so far gone beyond the limits of laboratory research or the preparation of small experimental batches.

In the concept 'thermal synthesis', we included various processes such as carbothermal reduction of oxides,[59-61,103] carbothermal and borothermal reduction combined with magnesiothermal reduction of oxides,[62,63] including reduction under SHS conditions,[62] direct solid-phase synthesis,[65] thermolysis of zirconium chloride under a NO_2 atmosphere,[67] etc. Whereas in some of the studies [59-61,65,103] comparatively low-temperature conditions were employed and the starting material was highly disperse, which in fact ensured the formation of ultradisperse powders, in others [62,63] the magnesium oxide formed played the role of a coalescence preventing agent. The synthesis of ultradisperse TiN powders in accordance with the scheme

$$\mathrm{Ti} \xrightarrow[400\ ^\circ\mathrm{C}]{\mathrm{NH_4Cl}} \mathrm{TiH_{1.924}} \xrightarrow[>500\ ^\circ\mathrm{C}]{\mathrm{NH_4Cl,\ NH_3}\ (p = 1\ \mathrm{MPa})} \mathrm{TiN}, \qquad (2)$$

has been described.[66]

It has been suggested that ultradisperse TiN and ZrN powders ($d \approx 10$ nm) are formed as a result of the dispersion of the initial metal powders (their particle size is much greater than 150 nm) and their hydrides at a low nitrogenation temperature under pressure; ammonium chloride plays the role of the hydrogen source and activator of the transfer process through the gas phase and to some extent prevents recrystallisation.

The development of a technology for the preparation of nanophase solid-alloy WC + Co compositions using as precursors triethylenediaminecobalt tungstate and tungstic acid or ammonium metatungstate and cobalt chloride $\{Co(en)_3WO_4 + H_2WO_4$ or $[(NH_4)_6(H_2W_{12}O_{40}) \cdot 4H_2O] + CoCl_2 \cdot nH_2O$ respectively$\}$ has been reported.[64] These carefully prepared solutions are spray-dried and subjected to low-temperature reduction and carbidisation in a fluidised bed in special reactors, which ensures, on the one hand, a high dispersity, and, on the other, a strict constancy of composition and hence satisfactory physicomechanical properties.

It has been suggested that boron-containing polymers of the type of polyborazole $[B_3N_3H_4]_x$ be used as additives to a titanium powder in order to synthesise nanophase TiN + TiB_2 compositions.[68] Finely disperse Group IV and V transition metal diborides are also synthesised from the oxides with the aid of boron- and carbon-containing precursors of the type decaborane-dicyanopentane, $[-B_{10}H_{12}NC-(CH_2)_5-CN-]_n$.[104]

The familiar sol-gel technology and different versions of the coprecipitation procedure play an appreciable role in the preparation of ultradisperse oxide powders; the synthesis and thermolysis are closely intertwined in this technology.[105,106] The preparation of monodisperse β-SiC powders with spherical particles by the hydrolysis of a mixture of triethoxyphenylsilane and tetraethyl orthosilicate $[C_6H_5Si(OC_2H_5)_3 + Si(OC_2H_5)_4]$ followed by heat treatment under argon at 1500 °C may serve as an example of the synthesis of oxygen-free compounds.[107] Fig. 2 presents the structure of such ~0.6 μm spherical particles. Each particle consists of primary ~40 nm β-SiC nanoparticles. Such agglomeration of particles is undoubtedly useful for the improvement of the technological characteristics, but the properties of the nanocrystalline materials obtained from the conglomerates have to be investigated.

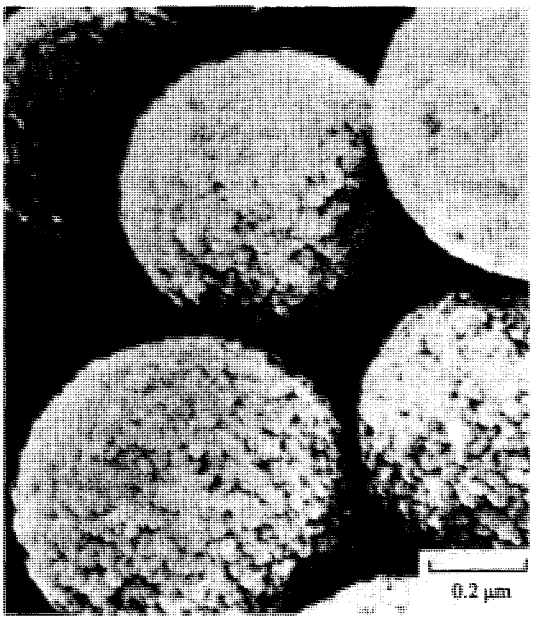


Figure 2. The microstructure of monodisperse β-SiC powders with spherical particles obtained in the sol-gel process [107]

Methods for the hydrothermal synthesis of ultradisperse oxide powders are less common, although some examples of the preparation of such ZrO_2 and Al_2O_3 powders may be found in the literature, for example in Refs. 74, 108, and 109.

An interesting method for the comparatively low-temperature gas-phase synthesis of titanium borides has been described.[73] Vaporising liquid sodium mixed with argon as the carrier gas reduces gaseous titanium boron chloride; the exothermic nature of the reactions ensures the maintenance of combustion conditions and the formation of ultradisperse powders.

The electrochemical synthesis of ultradisperse tungsten carbide and tungsten and molybdenum boride powders in melts and of zirconium oxide powder in aqueous solution has been investigated.[69-71] There is a communication [110] concerning the preparation of ultradisperse AlN powders ($d \sim 25$ nm) by the anodic dissolution of aluminium in a NH_4Br-NH_3 solution at −70 °C without subsequent annealing of the electrolysis products at 1100 °C. The electrochemical method has also been used to synthesise the polymeric precursor $[Al(NH_2)_3NH]_n$, which was subsequently subjected to annealing in ammonia at 600 °C with formation of an ultradisperse AlN powder (particle size ~8 nm).[111]

The liquid-phase synthesis of certain carbides and borides is likewise carried out under low-temperature conditions. Thus an ultradisperse TiB_2 powder may be synthesised by the following reactions:[15,73]

$$\mathrm{TiCl_4(l) + 2\,BCl_3(l) + 10\,Na(s)} \xrightarrow[100-160\ ^\circ\mathrm{C}]{\text{heptane}} \mathrm{TiB_2(s) + 10\,NaCl(s)}, \qquad (3)$$

$$TiCl_4(l) + 4\,NaBH_4(l) \longrightarrow \quad (4)$$
$$\longrightarrow Ti(BH_4)_3 \cdot n\,Solv + 4\,NaCl + \tfrac{1}{2}B_2H_6 + \tfrac{1}{2}H_2,$$

$$Ti(BH_4)_3 \cdot n\,Solv \xrightarrow[\sim 215\ ^\circ C]{} \quad (5)$$
$$\longrightarrow TiB_2(s) + \tfrac{1}{2}B_2H_6 + \tfrac{1}{2}H_2 + n\,Solv.$$

l = liquid; s = solid.

The powder thus obtained is amorphous to X-rays but after annealing at 900–1000 °C, which is also necessary to distill away sodium chloride, it crystallises. The size of the particles obtained by reaction (3) is ~50 nm,[15] while reactions (4) and (5) afford also larger particles of different morphology.[73] In the last investigation, triglyme was used as the solvent.

d. Thermal decomposition

Many ultradisperse refractory compound powders are prepared by the thermal decomposition (thermolysis) of solid, liquid, and gaseous precursors. We differentiated arbitrarily two varieties, although it is evident that the gas phase plays a role in virtually all cases. It is important to emphasise that, together with traditional precursors of oxide powders such as nitrates, oxalates, sulfates, hydroxides, and other compounds, recently the expansion of research into the refractory compounds of silicon, boron, titanium, and aluminium entailed appreciable use of organometallic polymers of these elements. A new term — preceramic polymers — has come to be widely used. Compounds of this type, used in synthetic procedures, were mentioned above.

Some of these polymers, used for the pyrolysis, are presented in Table 2. For example, polycarbosilane has an average molecular mass of 1200–2000 with a molecular mass distribution of 300–10 000; its softening temperature is in the range 130–180 °C, while fusion begins at 250–330 °C.[115] The pyrolysis temperature is usually ~1300 °C. As shown for ultradisperse Si–C powders, plasma heating (for example, with the aid of a nitrogen arc plasmotron) is preferable to the usual thermal heating.[115] The application of an industrial CO_2 laser for the pyrolysis of liquid silazane $[CH_3SiHNH]_n$, supplied to the reaction zone via a special ultrasonic nozzle in the form of an aerosol, has also been described. The pyrolysis results in the formation of an ultradisperse Si_3N_4 + SiC powder.[81]

Table 2. Organometallic polymers and monomers used as precursors in the preparation of refractory compounds.[112–114]

Precursor		Product
name	formula	
Polycarbosilanes	$\{Si(CH_3)(C_6H_5)-Si(CH_3)_2\}_n$,	SiC
	$\{SiH(CH_3)-CH_2\}_n$	SiC
Polycarbosiloxane	$\{Si(R_2)-O\}_n$, (R = H, alkyl, siloxyl)	SiC
Polysilazanes	$\{Si(R_2)-N(R)\}_n$,	Si_3N_4;
	$\{Si(R_2)-Si(R_2)-N(R)\}_n$, (R = H, alkyl)	Si_3N_4 + SiC
Aluminium amides and polyimides	$[AlR_2(NR_2)]_2$, (R = H, alkyl), $\{Al-NR\}_n$, (R = alkyl)	AlN
Polyborazole	$[B_3N_3H_4]_n$	BN
Polyvinylborazole	$\{C_2H_3(B_3N_3H_5)\}_n$,	BN
Polyvinylpentaborane	$\{C_2H_3(B_5H_8)\}_n$,	B_4C
Poly(titanium imide)	$\{Ti(NR)_2\}_n$, (R = alkyl)	TiN
Titanium tetrakis-(dimethylamide)	$[(CH_3)_2N]_4Ti$	Ti(C,N,O)

Certain features of the reactions occurring in the pyrolysis of preceramic polymers have been studied.[114,116] One should bear in mind that, after the laser or plasma treatment, the products of pyrolysis of preceramic polymers must be subjected to additional annealing for the final stabilisation of the structure and composition. The temperature of such treatment of the SiC, Si_3N_4, and SiC + Si_3N_4 powders is usually 1100–1200 °C, but it sometimes reaches as much as 1400–1600 °C.[81,114,115]

Heat treatment (calcining) invariably forms part of the technological cycles in the technologies of the sol-gel and coprecipitation processes mentioned above. Certain schemes for processes combining hydrolysis, synthesis, and decomposition are presented below.[74]

$$ZrOCl_2 + 2\,H_2O \longrightarrow \underline{ZrO(OH)_2} + 2\,HCl \quad (6)$$
$$\xrightarrow{\text{heat treatment}} ZrO_2$$

$$Zr(C_3H_7O)_4 + Y(C_3H_7O)_3 + 7\,H_2O \longrightarrow \quad (7)$$
$$\longrightarrow \underline{Zr(OH)_4 + Y(OH)_3} + 7\,C_3H_7OH$$
$$\xrightarrow{\text{heat treatment}} (Zr, Y)O_x$$

$$Zr(C_2H_5O)_4 + C_2H_5OH \quad (8)$$
$$\downarrow +\,H_2O$$
$$Zr(OH)_x(C_2H_5O)_{4-x}$$
$$\downarrow +\,H_2O$$
$$\underline{Zr(OH)_4}$$
$$\xrightarrow{\text{heat treatment}} ZrO_2$$

The first two schemes [reactions (6) and (7)] refer to the technologies for hydrolytic coprecipitation, while the last refers to the sol-gel process, where zirconium alkoxide in alcoholic solution is subjected to slow hydrolysis under controlled conditions. The conditions in the hydrolysis, coprecipitation, and heat treatment determine the composition, structure, morphology, and particle size of the ultradisperse powders. Preparation with the aid of oxalate precipitation of the monoclinic and tetragonal forms of the particles of ultradisperse ZrO_2 powders, including Y_2O_3-modified powders, has been described[117].

Fig. 3 presents a thermogravimetric curve for the heat treatment of yttrium hydroxide chloride prepared by sol-gel technology from yttrium trichloride.[77] The temperature of the final heat treatment, attained after 2 h, is 950 °C. A powder with a specific surface at ~20 $m^2\,g^{-1}$ is formed at this temperature.

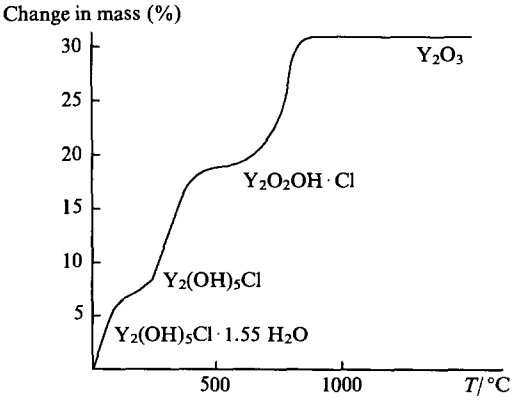


Figure 3. Variation of mass during the heating of an yttrium hydroxide chloride powder.[77]

In recent years, interest has been shown in ultradisperse transition metal boride powders. In this connection, we shall consider the possibility of obtaining them by the thermolysis of highly volatile hydroborates. The latter can dissociate in the range 300–400 °C, which is much lower than the usual temperatures for the preparation of borides. The thermolysis of zirconium tetrakis(tetrahydroborate) $Zr(BH_4)_4$ by a pulse type CO_2 laser has been described;[82] the preparation of powders having the overall composition $ZrB_{3.3-3.7}$, i.e. apparently containing an appreciable amount of free boron, with a specific surface of 40–125 $m^2\ g^{-1}$ has been reported. The thermal decomposition of $Zr(BH_4)_4$ at 300 °C results in the formation of an amorphous $ZrB_{2.76}$ powder, while at 350 °C the product is $ZrB_{3.74}$.[83] Experiments also showed that the excess content of free boron in the borides can be accounted for by the decomposition of the diborane formed.

$$Zr(BH_4)_4 \longrightarrow ZrB_2 + B_2H_6 + 5\,H_2\,. \qquad (9)$$

Indeed analysis of the gas phase showed that the ratio $[H_2]/[B_2H_6]$ is 9 and 12 at 300 and 400 °C respectively. This is appreciably higher than the theoretical value of 5 corresponding to reaction (9). During the annealing of the amorphous powders formed, crystallisation begins at 350 °C and terminates at 1000 °C. Work with transition metal tetrahydroborates requires much caution because they are explosive on contact with air and moisture.

2. Properties

a. Particle size. Morphology and structure

Particle size is one of the most important characteristics of an ultradisperse powder. In order to determine the size and shape of the particles, transmission and scanning electron microscopy (TEM and SEM respectively) is usually employed. Measurement of the specific surface (S) by the method involving the low-temperature adsorption of nitrogen and other gases with subsequent estimation of the so called average particle diameter or the equivalent diameter (d_s) by the familiar formula

$$d_s = \frac{6}{\gamma_t S}, \qquad (10)$$

where γ_t is the theoretical density, is likewise extremely common. Table 3 presents the values of S for certain ultradisperse refractory compound powders as a function of d_s and γ_t. Evidently the range of specific surfaces S extends from several to several hundreds of square metres per gram.

Some information about the particle size (more correctly about the regions corresponding to coherent scattering — blocks) can also be obtained by analysing the broadening of the reflections on the X-ray and neutron diffraction patterns for ultradisperse powders taking into account the possible contribution of lattice deformation. Agreement of the values of d obtained by measuring S and from the X-ray diffraction data for the TiN ultradisperse powder has been observed only for $S > 30$ $m^2\ g^{-1}$ ($d < 30$ nm).[118] In the study of ultradisperse ZrN powder, a satisfactory agreement of the results of the determination of d by different methods (TEM, low-temperature adsorption of nitrogen, and neutron diffraction) was noted for particles with $d \approx 20$ nm.[119] For the ZrO_2 ultradisperse powder with a particle size of 8–20 nm, a satisfactory agreement between the values of d measured by different methods has likewise been observed.[120] In the vast majority of cases, it is necessary to resort to several methods of measurement in order to increase the reliability of the information about the particle size of ultradisperse powders because factors such as particle shape, the capacity of the particles for agglomeration, and the presence of lattice distortions cannot be always unambiguously taken into account.

The morphology of ultradisperse powders has been studied in many investigations (see, for example Refs 10, 18, 21, and 121–125). The results of the investigation of Al_2O_3 and SiC powders by high-resolution TEM methods have been reported in a review.[18] Polyhedral (in many cases cubic) forms of particles of carbides and nitrides obtained by plasmochemical synthesis have been frequently noted. Fig. 4 presents electron photomicrographs of TiN particles illustrating the characteristic crystal form of the plasmochemical titanium nitride. A cubic crystal form has also been noted for γ-Al_2O_3 and $TiC_{0.95}$ ultradisperse powders; titanium diboride has a hexagonal form.[123] The nitride powders obtained by the reactive atomisation method has a less distinct crystal habit.[21] NbN particles synthesised by the plasmochemical method had a spherical form.[122] The change in the ammonia concentration in the plasma promoted a transformation of the AlN particles from the spherical to the polygonal form.[45] The ZrB_n particles formed in the thermolysis of zirconium tetrakis-(tetrahydroborate) also have a nearly spherical form.[83] Various morphologies are characteristic of ultradisperse powders synthesised by the electrochemical method.[127] The majority of the particles formed on exposure to high energy influences have an irregular form.

Since the conditions in the preparation of ultradisperse powders are in most cases far from equilibrium, the particle form cannot always be predicted on the basis of any kind of *a priori* postulates. The latter can be based on the crystallographic analysis of Wulf polyhedra taking into account the contribution of the surface energy (see, for example, Refs 5, 85, and 128). Since close-packed structures are known to possess the minimum surface energy, crystal shapes characteristic of face-centred cubic and hexagonal close-packed lattices therefore frequently occur in small particles. Various complicating factors associated with the crystal form of the clusters have been discussed in a review.[128] Processes involving the possible interaction with impurities (for example, oxidation), capable of distorting particular estimates, are also important in relation to ultradisperse powders.

It has been noted in a monograph[85] that the nature of the size distribution of the particles may indicate the condensation mechanism. A logarithmic normal distribution may be a consequence of the coagulation crystallisation of the vapour–liquid–crystal type; on deviation from this relation, the vapour–crystal mechanism (a normal type of distribution) is more probable. Experiments have shown that[124] in the case of ultradisperse tungsten powders, the first version applies, while in the case of titanium there is an appreciable deviation from the logarithmic normal distribution. The coagulation mechanism of the growth of ultradisperse tungsten powders has been confirmed by the

Table 3. The specific surfaces of certain ultradisperse powders of refractory compounds ($m^2\ g^{-1}$).

d_s/nm	B_4C, BN	Si_3N_4, SiC, MgO, AlN	Al_2O_3, TiB_2, TiC	TiN, Y_2O_3	NbN	WC
	(2.3–2.5)	(3.3–3.5)	(4–4.9)	(5.0–5.4)	(8.3)	(15.8)
100	24–26	18–19	12–25	11–12	7	4
50	48–52	36–38	24–25	22–24	14	8
10	240–260	180–190	120–125	110–120	70	40

Note. The theoretical density (g cm^{-3}) is indicated in brackets.

spherical shape of the particles; the noncoagulation crystallisation of TiN is indicated in its turn by the shape of these particles (Fig. 4). However, the logarithmic normal distribution is sometimes accompanied also by a crystalline form of the particles (TiC, TaC, and NbC ultradisperse powders).[121]

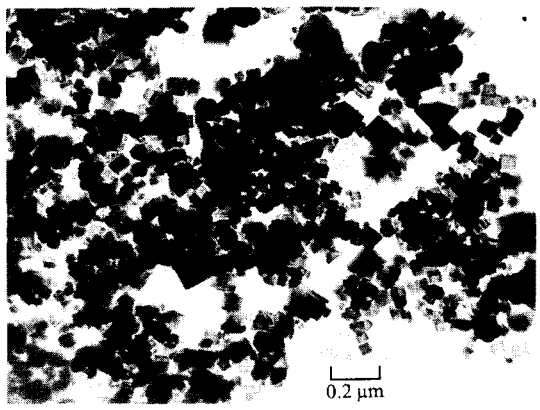


Figure 4. Electron photomicrograph of a plasmochemical ultradisperse TiN powder.[126]

Much attention has been devoted in the literature to the study of the structures of ultradisperse powders by X-ray, neutron, and electron diffraction methods. A detailed description of these results is outside the framework of the present review and we shall therefore quote only the most important of them.

1. Many compounds (Si_3N_4, Al_2O_3, SiC, TiB_2, etc.) may exist in the amorphous state.[19,49,56,76,83]

2. In certain cases (Al_2O_3, ZrO_2), anomalous structures are observed.[85,120]

3.Particle size influences the lattice period and microdeformation (distortions) of the lattice and also the mean square displacement of the atoms.[118,119,125,129,130]

4. The absence of dislocations has been noted in small particles.[118]

The influence of the excess surface free energy on the thermodynamic conditions in phase equilibria has been analysed in a general form in a monograph[85] and in a review.[5] It is evident from general considerations that the phase transition temperatures and the limits of the existence regions of the phases may be different in ultradisperse powders from those in large particles. It has been shown for aluminium oxide that mainly the γ-phase is present in ~30 nm particles, whereas coarser ultradisperse powders ($d \approx 110$ nm) contain also other modifications (ε, β, and θ).[85] Certain structural-morphological features of AlN, Si_3N_4, and Al_2O_3 ultradisperse powders have been analysed in a review.[131]

Table 4 presents data demonstrating the influence of the particle size on the lattice period and the mean square displacements of the atoms in TiN particles.[130] With decrease in d_s, the lattice period diminishes appreciably, while the evolution of the mean square displacements can be less clearly traced. A decrease in the lattice period has been observed also for many small metallic particles[85] and for ZrN particles.[119] This has been attributed to the manifestation of capillary compression. The capillary forces in ultradisperse powders may be appreciable: thus the capillary pressure for ~10 nm particles with a surface tension of ~2 N m^{-1} may be ~1 GPa and this can induce in its turn a deformation of ~10^{-3} nm, which is comparable with the data presented in Table 4.

Two remarks must be made here. Firstly, the capillary compression effect is not always accompanied by a decrease in the lattice constant.[128] Secondly, it has been noted in a review[125] that many results of the investigation of the phase composition and the lattice period of particles of ultradisperse refractory compound powders are to a large extent vitiated by the lack of a detailed specification of the oxygen content in the substances and their nonuniform composition in the region of homogeneity. An attempt has been made to take into account the latter factor to some extent,[130] but the oxygen content in the substances listed in Table 4 was not indicated. Furthermore, both the deviation from stoichiometry and the presence of oxygen affect significantly the lattice period in transition metal carbides and nitrides.[9] Many results of diffraction studies on these ultradisperse powders are distorted by various factors which have not been taken into account. The question of the influence of the refractory compound particle size on the lattice period requires additional study.

Table 4. Certain characteristics of ultradisperse TiN powders.[130]

Composition	$S/m^2\ g^{-1}$	d_s/nm	Lattice period, 10^5 a/nm	Overall square atomic displacements 10^4 a/nm
$TiN_{0.96\pm0.02}$	39	27	42402 ± 8	98 ± 7
$TiN_{1\pm0.05}$	50.3	22	42381 ± 8	100 ± 20
$TiN_{0.98\pm0.03}$	53.2	21	42384 ± 9	80 ± 20
$TiN_{0.87\pm0.08}$	76.4	14	42371 ± 10	100 ± 10
$TiN_{0.98\pm0.04}$	83.5	13	42367 ± 11	101 ± 5
$TiN_{0.96\pm0.04}$	95.4	11	42354 ± 14	131 ± 2

In conclusion, we emphasise that, although according to TEM and diffraction data the absence of dislocations and microdistortions has been noted in 20–40 nm TiN particles,[118] the question of the defectiveness of ultradisperse refractory compound powder particles requires a more wide-ranging study.

b. The content of impurities and gases. Chemical properties

In terms of the level of impurities and gas content, ultradisperse powders are in most cases inferior to the usual powders let alone single crystals and other highly pure substances. This is associated with, on the one hand, the characteristics of their preparation and, on the other, with their extremely high surface area and the conditions in their storage. Nevertheless, as mentioned previously, it has been possible to synthesise β-SiC which was extremely pure as regards cationic impurities.[48] However, only the use of a special condensation technique[19,20,86,87] creates conditions for the preparation of refractory compound powders with a high purity, including purity as regards oxygen admixtures. However, this method, like, incidentally, others, is not universal.

We shall analyse data on the content of impurities in ultradisperse powders with different dispersities in relation to silicon nitride powders, which have been studied in detail.[132] Analysis of the data in Table 5 permits the following conclusions.

1. There is no correlation whatsoever between the overall chemical composition and the particle size of the powders in the experimental range of values of d_s.

2. The surface of the particles is greatly enriched in oxygen and especially carbon, which is indicated by X-ray photoelectron spectroscopic (XPS) data for a layer 2.3–4.6 nm thick. With the exception of the powder in the R2 batch, the difference between the nitrogen contents on the surface and in the bulk of the particles is not very great—the ratio [N]/[Si] = 0.665 for the stoichiometric Si_3N_4. We may note that the enrichment in carbon of the plasmochemical Si_3N_4 ultradisperse powder (S = 42 $m^2\ g^{-1}$) has been noted also in another study.[133] It is attributed to the formation of carbonate and carboxy-compounds.

The independence of the composition of the particles on their size (Table 5) can be due to the different methods of preparation and storage of the powders. The enrichment of the surface layers in oxygen and carbon is likewise weakly correlated with the overall content of these impurities. Whereas the increased content of oxygen on the surface can be naturally attributed to oxidation, in order to elucidate the causes of the enrichment of the surface in

Table 5. Chemical composition of Si_3N_4 powders of different origin in the bulk phase (I) and on the surface (II) of the particles.[132]

Type of powder	Method of preparation	Composition (mass %)				d_s/nm	[O]/[Si]		[C]/[Si]		[N]/[Si]	
		N	Si	O	C		I	II	I	II	I	II
SNE 10	Decomposition of the diimide	38	60.8	1.0	0.08	125	0.016	0.34	0.001	0.1	0.63	0.54
A 2	Carbothermal synthesis	36.3	60.2	2.5	0.86	110	0.042	0.1	0.014	0.22	0.6	0.64
LC 12	Furnace nitrogenation of silicon	38.5	59.7	1.5	0.17	90	0.025	0.1	0.003	0.3	0.65	0.64
R 2	Nitrogenation of silicon in high-frequency plasma	38.0	58.5	3.1	0.18	60	0.053	0.59	0.003	0.29	0.65	0.41
P 1[a]	Interaction of $SiCl_4$ with NH_3 in high-frequency plasma	38.5	59.6	1.6	0.07	40	0.027	0.26	0.001	0.11	0.65	0.60

[a] Contains 1 (mass %) of chlorine.

carbon it is useful to turn to the results of the study of gas evolution during the vacuum heat treatment of ultradisperse powders.[4,126,134]

Fig. 5 illustrates the influence of the heat treatment temperature on the rate of gas evolution from TiN powders with the usual grain size ($d_s \approx 8$ μm) and from the ultradisperse powders ($d_s \approx 0.07$ μm).[126] There are two gas evolution peaks ($T_1 = 250-300$ and $600-700$ °C), carbon monoxide predominating appreciably in the evolving gases. The overall content of the gases correlates with the particle size: the values of S for the usual ultradisperse powder were 0.15 and 16 $m^2\ g^{-1}$, while the total amounts of gases were 1 and 7 $cm^3\ g^{-1}$ respectively under normal conditions. X-Ray photoelectron and Auger spectroscopic studies on these powders showed that the surface layers of the particles contain oxide nitride phases and carbon-containing components, the amount of the latter being appreciably reduced after vacuum annealing. The enrichment of the surface of nitride powders (Si_3N_4 [132,133] and TiN [126]) in carbon-containing components is associated with the selective adsorption of CO_2 from the ambient medium, but the mechanism of the subsequent formation of CO under these conditions requires additional detailed study. The predominance of carbon monoxide in the gases evolved during vacuum annealing has been noted also in the study of Si_3N_4 powders with different dispersities.[135] Naturally, mainly components with mass numbers of 28 (CO) and 44 (CO_2) are evolved into the gas phase from ultradisperse powders of boron, silicon, and titanium carbides.[134] The possible chemical reactions during the heat treatment of ultradisperse powders of β-sialon ($Si_{6-z}Al_zO_zN_{8-z}$) and, in particular, the formation of ammonia as a result of hydrolysis and its subsequent catalytic decomposition have been discussed.[136]

Thus the distribution of impurities in the particles of ultradisperse powders is usually nonuniform. Different fine effects, associated with the possibility of estimating the surface segregation of atoms in small two-component particles, have been analysed.[85,137] XPS and Auger spectroscopic methods have proved to be very useful experimentally in this connection. Ultradisperse powders of refractory compounds began to be investigated by XPS methods about twenty years ago. It is necessary to differentiate between the studies[138-141] devoted to these methods. In an early investigation,[139] attention had already been drawn to the different forms in which oxygen exists in an ultradisperse TiN powder (dissolution in the nitride, the formation of individual oxide nitride phases, and adsorption in the form of CO, CO_2, and H_2O on the surface of the particles) and an attempt was made to estimate their amounts. Niobium nitrides and carbide nitrides, silicon nitride and carbide, and other ultradisperse refractory compound powders were also investigated. It was discovered that the F, Cl, Fe, Al, Ca, and Na impurities are present on the surfaces of the SiC and Si_3N_4 powders.[142] The chlorine and sodium impurities may influence significantly the stability of the cubic and tetragonal phases during the annealing of the ultradisperse ZrO_2 powders.[143]

The chemical properties of ultradisperse powders (interaction with acids and alkalis, thermo-oxidative stability, etc.) have also been the subject of study in many investigations (see, for example, the relevant reviews[44,122,125]). Comparative study of the decomposition of an ultradisperse TiN powder ($S = 12.4\ m^2\ g^{-1}$) as well as coarser TiN powders, obtained by self-propagating high-temperature synthesis ($S = 0.1\ m^2\ g^{-1}$) in solutions in sulfuric and nitric acids, showed that the absence of an induction period is characteristic of substances with a larger surface area. Their entire surface is involved simultaneously in the reaction, which occurs in dilute acids and at lower temperatures than in the case of coarse-grained powders.[144] The specific rate of decomposition of the ultradisperse TiN powder in sulfuric acid in the concentration range 9.5–12.6 M and in the temperature range 130–150 °C is $(0.4-3.3) \times 10^{-6}$ mol $min^{-1}\ m^{-2}$. The kinetics of the decomposition of the powder in solutions in the $H_2SO_4-H_2O_2$ system have been investigated.[145]

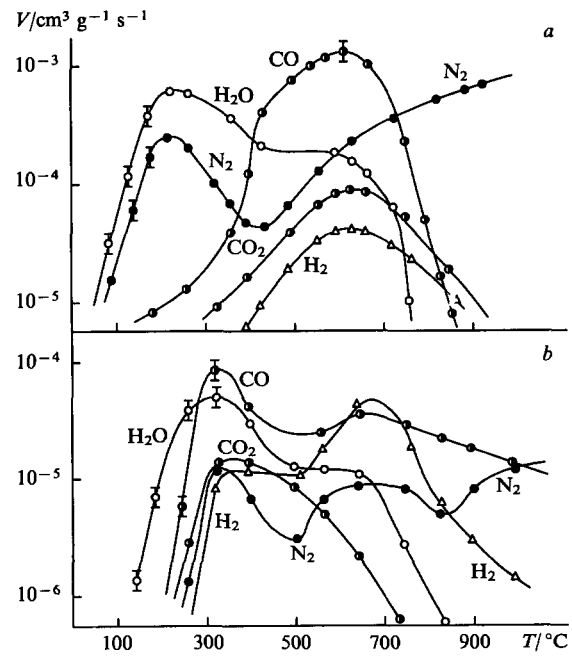


Figure 5. Temperature dependence of the rate of gas evolution from an ultradisperse (*a*) and an ordinary (*b*) TiN powder.[126]

For the temperature of the onset of oxidation of TiN powders, differing in S by five orders of magnitude, the following empirical equation has been proposed:

$$\frac{T}{T_m} = \left(\frac{S}{S_m}\right)^{-n}, \quad (11)$$

where the subscript m refers to the massive material (T_m = 1120 K; S_m = specific surface of ~1 mm particles); n = 0.064.[122]

Many investigators have noted that, when ultradisperse powders are stored in air, hydrolysis takes place. The acid–base properties of the surfaces of ultradisperse powders have been investigated in greatest detail for titanium and silicon nitrides.[146] The position of the zero-charge point in these substances corresponds to a highly acid medium, while the zero electrokinetic potential corresponds to an acid or weakly acid medium. This means that there are uncompensated positive centres. It has been suggested that these comprise coordinated ammonia molecules capable of combining with protons:

$$-NH_3 + H^+ \longrightarrow -NH_4^+. \quad (12)$$

Contact with water leads to the creation of a weakly alkaline medium and to the appearance of uncompensated negative groups.

The high sensitivity of ultradisperse powders to the ambient medium has given rise to an increased interest in methods for their storage; a hermetically sealed container filled with dry argon is usually employed in practice. Thermochemical methods for the treatment of ultradisperse powders with different reagents, which form a protectic shell on the surface of the particles and prevent both oxidation in air and hydration in water and can be removed on heating, have been analysed.[147] It has been suggested that solutions of organofluorine compounds (epilemmas) in Freon-113 be employed as reagents of this kind.

c. Physicochemical and physical properties

The fraction of surface atoms in particles of ultradisperse powders may reach several tens per cent and this exerts a significant influence on the lattice and electronic properties of the substance. The characteristic correlation size (or the characteristic length of the transfer process) for a particular phenomenon in solids may range from several tenths of a nanometer to several tens of nanometers.[148] Two factors which are largely responsible for the differences between the properties of small particles (d < 10 nm) and massive bodies have been noted. The characteristics of the spectral density of vibrations, anomalies in the heat capacity, and the specific features of electronic states and electrical, thermophysical, optical, and magnetic properties of small particles, mainly metallic particles, have been analysed.[5,85,128,148–150] Questions concerning the thermodynamics of small particles have been discussed in the same studies: the minimum size to which the concepts of 'phase' and 'surface energy' are applicable; the possible transformation in relation to small particles of the familiar Thompson formula for the vapour pressure as a function of the radius of curvature, fusion and other phase transitions in small particles, etc. (see also Refs 151–154). Without dwelling on these topics in detail, we shall only note that there exists little reliable experimental information on the dimensional effect for ultradisperse powders of refractory compounds.

The critical magnetic field (H_{C_2}) increases with decrease in the particle size of transition metal nitrides (NbN, VN, TiN, NbNC).[155,156] The increase in H_{C_2} was ~200% when d changed from ~75 to ~15 nm. Comparative study by XPS and the spectroscopy of characteristic energy losses of a well crystallised hexagonal BN and an ultradisperse BN powder showed that a lower atomic ratio [N]/[B] and a lower concentration of valence electrons per unit volume are characteristic of the latter.[140] A study of the IR spectra of an ultradisperse BN powder with different dispersities (d_s = 5–66 nm), which were regulated by annealing at 800–1800 °C, revealed an appreciable deformation of the basal planes of the lattice of the unannealed small particles, which was also confirmed by X-ray diffraction data.[157]

The band structure of ultradisperse powders of superconducting niobium carbide nitrides (NbC_xN_{1-x}, x = 0.06 to 0.09) was investigated by Auger spectroscopy.[141] It was shown that the effective energies of the hole interaction in the valence band for the metallic and nonmetallic positions are significantly different. Analysis of the IR and fluorescence emission spectra in the ultraviolet region for an ultradisperse powder of amorphous Si_3N_4 led to the conclusion that the width of the forbidden gap is greater for nanoparticles than for massive objects.[158]

III. Consolidated powdered nanocrystalline materials

1. Principal characteristic features of the consolidation of ultradisperse powders

Virtually all the consolidation methods known in powder technology—pressing and sintering, different versions of hot pressing, etc.[4]—are applicable also to ultradisperse powders. However, if one is dealing with the preparation of compact materials with a nanocrystalline structure, i.e. largely with retention of the grain size characteristic of ultradisperse powders, then the usual sintering and hot pressing temperatures are inapplicable because vigorous recrystallisation processes occur. In essence, in the vast majority of cases only high-energy consolidation methods, involving the use of static and dynamic high pressures, electric pulse influences, etc. are suitable for the maintenance of the above conditions.

Certain features of the pressing, sintering, and hot pressing of ultradisperse powders of refractory compounds, including such procedures at high pressures, were described in our earlier communication[13] and here we shall confine ourselves to stating the most important factors. Figs 6 and 7 illustrate the variation of the relative densities of ultradisperse powders of Si_3N_4 and TiN over a wide pressure range.[4,159] Data referring to coarser Si_3N_4 powders are also presented (the experiments were performed under different conditions). It is clearly seen from these results that the susceptibility to compaction on pressing diminishes significantly with decrease in dispersity and that it is impossible to attain or even approach the theoretical density at pressures up to 7–9 GPa. The low susceptibility to compaction of ultradisperse BN, SiC, and Si_3N_4 powders has also been noted in other investigations.[48,160,161]

The low susceptibility to compaction of such powders is associated with a high level of the interparticle friction characteristic of powders with a high surface area.[4] Hence it is understandable why it has not been possible to prepare compact

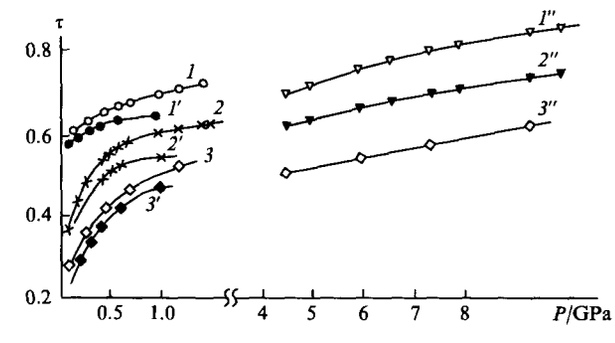


Figure 6. The influence of the pressing pressure on the relative densities (τ) of silicon nitride powders:[4] (*1*)–(*3*) pressing in a hydrostat; (*1'*)–(*3'*) pressing in the usual press-moulds; (*1''*)–(*3''*) pressing in high-pressure apparatus; (*1*), (*1'*), and (*1''*) $d_s \approx 1$ μm; (*2*), (*2'*), and (*2''*) $d_s \approx 0.05$ μm; (*3*), (*3'*), and (*3''*) $d_s \approx 0.017$ μm.

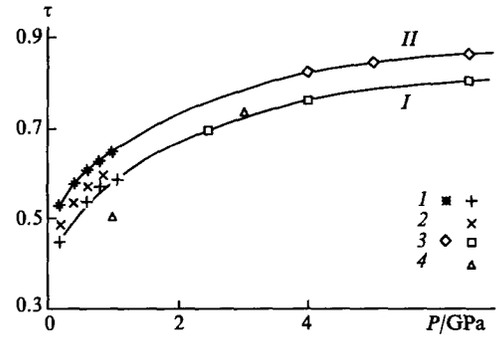


Figure 7. The influence of the pressing pressure on the relative density of an ultradisperse TiN powder:[159] (*I*) $d_s \approx 0.07$ μm; (*II*) $d_s \approx 0.08$ μm; (*1*) usual pressing, specimen diameter 10 mm, height 5 mm; (*2*) ditto, specimen dimensions 15 × 15 × 15 mm; (*3*) pressing at high pressure, specimen diameter 8 mm, height 5 mm; (*4*) magnetopulse pressing, specimen diameter 7 mm, height 15 mm.

specimens from ultradisperse powders obtained by the condensation method:[86,87] the porosity of even metallic pellets in such experiments has rarely been less than 10%. High pressures combined with heating to temperatures not inducing intense crystallisation can lead to appreciable compaction with retention of the nanocrystalline structure.

Unfortunately insufficient data have been accumulated hitherto concerning the preparation of such specimens. As an illustration of the possibilities of hot pressing, we shall quote the results of a study[162] for ultradisperse $ZrO_2-3\%\ Y_2O_3$ powders ($d_s = 40-60$ nm) (Table 6). The sintering and hot pressing temperatures for ultradisperse zirconium oxide powders are low as a consequence of the increased reactivity of these powders, but, despite the short duration of the process, it is impossible to achieve a sufficient compaction and to prevent the growth in grain size at a pressure of 1.6 GPa. By reducing the temperature and by increasing the duration of the sintering ($T = 1050$ °C, $t = 5$ h), it is possible to obtain partially stabilised zirconium dioxide with a relative density of ~99.9% and a grain size of ~85 nm at low heating rates (5 K min^{-1}).[163] Similar data have been obtained in another study.[164] The deagglomeration of ultradisperse powders is also important for active compaction during sintering.[165]

Table 6. Variation of the relative density (τ) and grain size (L) during the sintering and hot pressing of ultradisperse ZrO_2-3 mol % Y_2O_3 powders.

T/°C	Sintering		Hot pressing	
	τ	L/nm	τ	L/nm
1100	0.72	120	0.87	130
1200	0.83	150	0.93	170
1300	0.94	170	0.97	250

Note. In all cases, the pressure was 1.6 GPa and the duration of treatment at the temperatures indicated was 10 s.

Attention should be drawn to possible methods of preparation of nanocrystalline materials from refractory compounds such as dynamic recrystallisation at high pressures[166] and crystallisation from the amorphous state.[167] The temperature conditions, which again should not lead to vigorous growth in grain size, are fundamentally important in both cases. Studies on these lines are only just beginning.[168]

An interesting combination of the pyrolysis of a precursor—polysilazane (Table 2)—with pressing and sintering methods at comparatively low temperatures (1100–1600 °C) made it possible to obtain a Si_3N_4+SiC nanocrystalline composition (overall composition $Si_{1.73}N_{1.56}C_1$) with a relative density of 92%–93%.[169]

2. Properties

Hardness is one of the most thoroughly investigated characteristics of nanocrystalline materials based on refractory compounds. Table 7 shows that the main information about hardness refers to specimens prepared using high dynamic and static pressures. However, even under these conditions it is in many cases impossible to suppress recrystallisation and the grain size increases. An appreciable scatter of the results is characteristic of specimens obtained by explosive methods, which is manifested particularly clearly in the case of ultrahard materials (for comparison, the table includes data for diamond), although other methods also lead to some nonuniformity of the results.

The data[64] obtained for the WC + 10 mass % CO solid alloy, which has been thoroughly investigated, are of great interest. As a result of the application of the thoroughly developed technology for the preparation of ultradisperse powders and their low-temperature consolidation, it has been possible to attain hardness parameters exceeding the corresponding characteristics of standard solid alloys by a factor of 1.5–2.

The overall level of hardness is also affected by the residual porosity, which amounted to several per cent for the majority of the specimens presented in Table 7. According to data of Averback et al.[179] a decrease in τ from 0.94 to 0.89 (i.e. an increase in porosity by 5%) for nanocrystalline titanium oxide leads to a decrease in hardness by more than 30%.

However, even if this fact is taken into account, the hardness of Al_2O_3, SiC, MgO, TiN, ZrO_2, and Si_3N_4 specimens is nevertheless low and does not exceed greatly the hardness of the usual polycrystalline and single crystal refractory compounds or is actually approximately the same.[9] This finding appears strange from at least two points of view. Firstly, measurements have shown that the hardness of nanocrystalline metals and intermetallic compounds (Cu, Ni, Ag, Fe, Pb, TiAl, $NbAl_3$; see, for example, Refs 6–8, 12, and 180–185) can exceed the hardness of the usual polycrystalline materials by a factor of 3–6. Secondly, as will be seen from the consideration below of the refractory compound-based films, the hardness of these substances is appreciably greater than that of the usual massive refractory compounds.

The familiar Hall–Petch relation between hardness (critical splitting shear stress) and grain size:

$$H = H_0 + kL^{-1/2}, \qquad (13)$$

where k and H_0 are constants [L is average grain diameter (Ed. of Translation)], holds for the majority of the nano-crystalline metals and intermetallic compounds mentioned above. Admittedly inversion relations of type (13) (for example, for TiAl [182]) and nonmonotonic relations $H = f(L)$ (for example, for Cu [181] and $NbAl_3$ [183]) are observed fairly frequently. This can be explained by the influence of impurities, residual stresses, sliding along boundaries, etc. One cannot rule out the possibility that the low level of hardness of the materials presented in Table 7 is due to the limited amount of available information: none of the existing publications contain data obtained for a wide range of values of L. It may be that the results in Table 7 were found for an unfavourable range of values of L and that the determination of the purities of the test specimens left something to be desired.

The physicomechanical properties of two-phase nanocrystalline materials based on refractory compounds have been studied.[186–192]. Certain characteristics of percolation effects have been investigated in ultradisperse TiN + AlN, Si_3N_4 + SiC, and ZrO_2 + Ni compositions.[186–189] The critical point for the last system, corresponding to a sharp increase in electrical conductivity of the compositions, is in the range 25 vol.% – 30 vol % Ni,[186] while for the Si_3N_4 + SiC composition it is at the level predicted by percolation theory (~17 vol.% SiC).[187] Special interfaces with a reduced resistance to phonon scattering have been discovered in the TiN + AlN system.[189]

A nonmonotonic variation of the high-temperature and decomposition strengths in the SiC + Si_3N_4 system has been noted.[190] A higher temperature of the degradation of hardness and

Table 7. The hardness (H_v) of nanocrystalline refractory compounds.[13,170]

Compound	Method of consolidation	Characteristics of specimen		H_v/GPa	Ref.
		τ	L/nm		
SiC	Explosive pressing	0.97	60–100	26.4	171
BN	"	0.96	25	43–80	172
Al_2O_3	"	0.94	70	14	173
Si_3N_4	Hot pressing at high pressures	0.99	500	32.4	174
TiN	"	0.95–0.96	200–300	12–18	175
TiN + 30% TiB_2	"	0.95	100–1000	19.1	176
WC + Co	Hot isostatic pressure in the solid phase	1.0	200	19.5	64
ZrO_2	Rapid hot pressing	0.97	250	14	162
MgO	Hot forging	0.99	100–200	8–10	177
Diamond	Explosive pressing	0.91		63–68	178
		0.94		56–65	

of the modulus of elasticity as well as a greater strength compared with aluminium oxide without additives have been observed in the $Al_2O_3 + SiC$ nanocomposites.[191,192] Nanocrystalline ZrO_2–Al_2O_3 specimens are also distinguished by a high decomposition strength and ordinary strength.[193]

The present authors have shown[194] that the use of a plasmochemical ultradisperse Si_3N_4 powder in the $TiB_2 + Si_3N_4$ composition hot-pressed at high pressures is accompanied by a sharp increase in the rate of creep, which may be attributed to the manifestation of superplasticity (Fig. 8). The values of L for these specimens were ~0.5 μm for Si_3N_4 and ~2–4 μm for TiB_2 (the grain size in the usual Si_3N_4 powders was 2–4 μm).

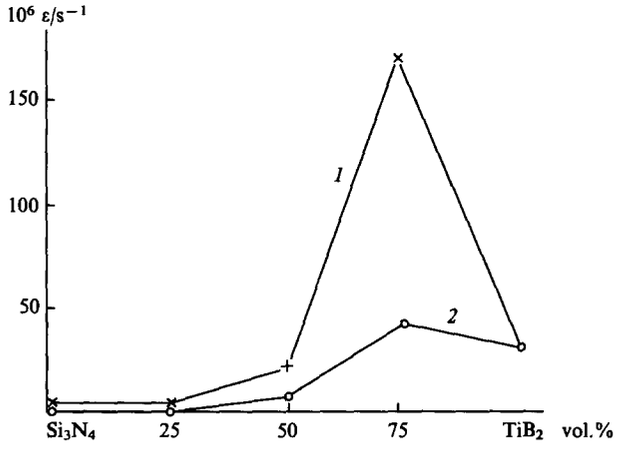


Figure 8. Variation of the rate of creep with the composition of the TiB_2–Si_3N_4 system (T = 1600 °C, tension 20 MPa, t = 30 min):[194] (*1*) Si_3N_4 ($L \approx 0.5$ μm); (*2*) Si_3N_4 ($L \approx 2-4$ μm). The TiB_2 grain size was ~2 μm in both cases.

The superplasticity in the deformation of nanocrystalline sialon at 1500–1600 °C (L = 100–200 nm) has been described.[195] High rates of creep at 1100 °C are also characteristic of zirconium dioxide (L = 100–140 nm), specimens of which (τ = 0.93–0.97) were obtained by the hot forging method.[196]

The optical properties of nanocrystalline silicon nitride obtained by pressing ultradisperse powders at high pressures (up to 5 GPa) and at the temperature of liquid nitrogen with subsequent low-temperature sintering (T = 1400 °C), have been described.[161]

The role of dimensional effects in the establishment of ferromagnetic, ferroelectric, and elastic characteristics on transition from multidomain to single-domain and nanodomain structures has been discussed in a review.[197]

Owing to the presence of an excess surface free energy, specific phase equilibria may be observed in multiphase systems containing ultradisperse particles. Several computational studies, in which the influence of dispersity on the equilibrium in the Zr + C,[198] TiC(TiN) + TiB_2,[12] and TiN + AlN [199] systems was estimated, have been carried out hitherto. Table 8 presents estimates of the influence of dispersity on the eutectic temperature in the TiC + TiB_2 and TiN + TiB_2 systems. These calculations were performed in the simplest regular solution approximations and their results may be regarded as estimates. Nevertheless, they indicate the necessity to take into account the displacement of phase equilibria on passing to multiphase nanocrystalline materials. The desirability of setting up the corresponding experimental studies is likewise quite evident.

Table 8. The influence of the particle size of one of the components in the TiC + TiB_2 and TiN + TiB_2 systems on the eutectic temperature (T_e = 2790 K in the $TiC_{0.9}$ + TiB_2 system, and T_e = 2870 K in the $TiN_{0.9}$ + TiB_2 system).[9,12]

Particle radius/nm	$-\Delta T_e$/K	
	TiC(TiN) + TiB_2	TiB_2 + TiC(TiN)
100	~45	~35
50	~90	~70
10	~450	~350
5	~900	~700

To conclude the description of the properties of consolidated powdered nanocrystalline materials, one should note that the available data are limited, which has a lot to do with the difficulties in the preparation of representative thoroughly authenticated nanocrystalline specimens. As noted in our earlier publications,[13,70] studies concerning titanium dioxide, carried out mainly by American and German investigators, contain somewhat more information (see, for example, Refs 6, 7, 86, 87, and 179). These workers used the condensation method in combination with the preparation of the specimens at high pressures. However, as a consequence of the porosity of the specimens, these data are not always sufficiently representative. Therefore progress in nanocrystalline materials science depends in many respects on the level of the technology for the preparation of test specimens.

IV. Nanocrystalline films

1. Characteristics of the preparation

Available information about films and coatings based on refractory compounds is extremely extensive (see, for example, Refs 200–205) and we shall therefore confine ourselves merely to a description of information on multilayer films as well as films with a specified grain size.

The principal methods for the preparation of refractory compound-based films are presented in Table 9. It is easy to see the similarity between Tables 1 and 9: with a few exceptions, the methods of preparation of ultradisperse powders and films are virtually identical and in many instances differ only in the conditions determining the formation and growth of nuclei in the bulk phase or on the surface. The arbitrary nature of the subdivision of preparative methods into chemical and physical, noted above, applies to an even greater extent to the preparation of films. The existing terms Chemical Vapour Deposition (CVD) and Physical Vapour Deposition (PVD) are mainly of historical significance. In many instances, chemical refractory compound formation reactions are decisive factors in the formation of the structure and properties of films on thermal vaporisation, in atomisation processes, and in the plasma methods. Methods for the modification of the surface such as ion implantation should be added to this list. Plasma (the so called plasma-accelerated or plasma-accompanied processes) and lasers are being used increasingly to activate, for example, processes involving the reduction of halides and the pyrolysis of silazanes and hydroborates.[202,206]

Table 9. The principal methods of preparation of films based on refractory compounds[a].

Method	Compound
Physical	
Thermal vaporisation	
electron beam	Oxides, borides, nitrides
laser	Oxides, nitrides
Ionic atomisation	
ionic-plasma	Nitrides, carbides
magnetron	Nitrides, carbides, borides, oxides
Chemical	
Synthesis	
deposition from gas phase	Nitrides, carbides, borides oxides
Sol–gel technology	Oxides
Thermal decomposition	
condensed precursors	Carbides, oxides, nitrides
gaseous precursors	Borides, oxides

[a] See also Table 1, monographs,[202,204] and a review[203].

The thermal vaporisation methods, used to obtain nanocrystalline films based on refractory compounds, are less universal compared with the plasma and magnetron methods, although they have come to be used to some extent in the formation of oxide films. For example, the preparation of ZrO_2–10 mol.% Y_2O_3 films by the laser pulse vaporisation of metals in a beam of oxygen ions has been described.[207] In the range of deposition temperatures 100–400 °C, the size of crystallites was 10–30 nm.

In the course of the study of wear-resistant instrumental coatings, extensive experimental data have accumulated on the ionic-plasma and magnetron films based on titanium and other transition metal nitrides and carbides (see, for example, Refs 202–204 and 208). Mainly metallic targets, atomised in nitrogen- and carbon-containing media, are used for the preparation, although the magnetron technique in fact makes it unnecessary to resort to reactive methods involving directly refractory compound targets. Such a procedure has been used successfully, for example, in the synthesis of borides. The employment of a relatively low temperature of the support (approximately 200–500 °C) makes it possible to avoid appreciable recrystallisation when physical deposition methods are resorted to, and in many cases a nanocrystalline structure can be formed. Multilayer and two-phase films as well as films with complex alloying are preferable in this respect.[209–212]

The rate of deposition of magnetron films under direct current conditions usually amounts to several tenths of a micrometer per minute; high-frequency devices, which make it possible to atomise dielectric targets, ensure rates approximately an order of magnitude lower. In ionic-plasma devices (of the 'Bulat' type), the rates of deposition are also high, but it is not always possible to avoid the appearance in the films of the so called drop phase as a consequence of the incorporation in the plasma of drops from the fused cathodic crater.

The size of the crystallites in the films obtained by the traditional deposition methods from the gas phase (CVD) is usually several micrometers and a temperature not less than 850–900 °C is then usually developed. Only in the case of multilayer or multiphase films is it possible to achieve nanostructures. In particular, this applies to the TiB_2+TiC composition obtained by deposition at 1000 °C from a $TiCl_4+n\text{-}C_7H_{16}+BCl_3+H_2$ mixture at atmospheric pressure ($L < 100$ nm).[213] The use of the laser technique also makes it possible in many instances to reduce the temperature and to synthesise nanocrystalline films. Thus the formation of silicon carbide films ($L < 50$ nm), deposited from a $Si_2H_8+C_2H_2+Ar$ mixture with exposure to the excimer ArF laser ($T = 518$ K), has been reported; this is the so called photo-CVD process.[214]

Sol-gel technology, involving the preparation of a solution, immersion, drying, and annealing and requiring simple apparatus, is becoming an increasingly popular method of preparation of oxide films (in particular, lead titanates and zirconates as ferroelectric materials). According to Tohye et al.,[215] the physical properties of these films are not inferior to those of magnetron films. The preparation of zirconium oxide films by the sol-gel method has been described.[216]

Thermolysis of organometallic compounds in order to obtain thin films has long attracted the attention of a wide range of investigators (see, for example, Refs 200 and 201). The characteristics of formation of the structure and the properties of thin Al_2O_3 films (~100 nm), arising in the oxidative pyrolysis of aluminium tris(acetylacetonate) $Al(Acac)_3$, have been described.[217] The authors suggest that the molecules of the initial compound in the adsorption layer do not decompose fully and that organic fragments are removed from the upper layers of the film formed. The reason for the instability of the charge in these films is the migration of OH^- and H^+ ions produced by the electrolysis of the water of crystallisation present in the film. Thin ZrO_2 films with Y_2O_3 as the stabilising additive (3–8 mol. %) are obtained by pyrolysing the acetates.[218] The preparation of an ultradisperse Si_3N_4+SiC powder by the thermal decomposition of organosilicon precursors on exposure to a CO_2 laser as well as the formation of films of similar composition have been described.[81] In exactly the same way, the decomposition of Group IV transition metal hydroborates leads to the formation of not only ultradisperse powders but also of films.[82,83]

Comparative results of the analysis of zirconium diboride powders and films, formed in the pyrolysis of the hydroborate $Zr(BH_4)_4$, are presented in Table 10. The characteristic features of the films are evidently crystallinity (the parameters of the structure are close to the tabulated data) and slight deviation from stoichiometry. The powdered deposits are amorphous and contain an appreciable excess of free boron, the origin of which has already been considered in connection with the discussion of reaction (9).

The superstoichiometric content of the nonmetallic component in films is characteristic also of other refractory compounds, for example the nitrides obtained by the ionic-plasma, magnetron, and other methods. Thus zirconium nitride films acquire a superstoichiometric composition at a nitrogen pressure in excess of ~10^{-3} Torr under the conditions of high-frequency magnetron atomisation.[219] The appearance of superstoichiometric zirconium

Table 10. Characteristics of films prepared from zirconium diboride powders obtained by the decomposition of zirconium hydroborate.[83]

T/°C	Deposit	[B]/[Zr]	Lattice period/nm		S/m^2 g^{-1}	$[H_2]/[B_2H_6]$ in gas phase
			a	c		
250		No decomposition				
300	Amorphous powder	2.76			27.7	9
	Film	2.03	0.3167	0.3528	–	9
350	Amorphous powder	3.74			26.2	12
	Film	2.15	0.3165	0.3534	–	12

Note. The duration of treatment at the temperatures indicated was 5 h in all cases.

nitride has also been detected in the electron beam vaporisation of zirconium accompanied by bombardment with nitrogen ions having energies in the range 400–700 eV.[220] The mechanism of their formation (the appearance of vacancies in the metallic sublattice, the presence of phases of the Zr_3N_4 type, etc.) is still not entirely clear and is the subject of lively discussion in the literature.

2. Properties

Although the number of publications on the properties of thin films is fairly large, only some of them refer to nanocrystalline refractory compound-based films. Furthermore, not all these data are accompanied by a more or less detailed specification of the size of crystallites in the film. It appears that the study of the characteristic features of the formation and growth of refractory compound films, obtained by many and varied methods (Table 9), is in the initial stage. The overall scheme describing the crystallisation of coatings and films, proposed in the familiar study of Movchan and Demchishin[221] and then amplified by Thornton,[222] should be made significantly more specific in relation to refractory compounds.

For example, there is an interesting approach to the estimation of the stability of polycrystalline thin films obtained by the pyrolysis of zirconium acetate and yttrium nitrate solutions.[218] Heat treatment at 1200 °C is accompanied by the formation of ~25 nm crystallites, but, after annealing at 1400 °C, the continuous film is disrupted and converted into isolated fragments. The latter phenomenon can be described in terms of the hypothesis of the etching of grain boundaries using the energy approach and estimating the critical dihedral angle between the grains. Certain problems of the recrystallisation of thin films, including those based on nitrides, have been examined.[212,223]

Among the properties of films, their hardness has been studied to the greatest extent (as for powdered nanocrystalline materials). It has been demonstrated convincingly in a review[203] that the increased hardness of TiN films can be explained mainly by the small grain size (20–70 nm). Measurement of the hardness of thin films has its characteristic features. It is preferable to use small and even ultrasmall loads (the so called nanoindentation) in order to avoid the influence of the support. Fig. 9 illustrates the influence of the load applied to the indentor on the hardness of Ti–B, Ti–B–N, Ti–B–C, and Ti–B–N–C films obtained by magnetron atomisation (film thickness 3–5 μm; support—solid alloy).[210] Evidently, the hardness remains most stable for loads up to ~0.5 N. The Ti–B–N system has the best parameter. The presence of a phase of the $TiB_{1.6}N_{0.6}$ type has been discovered with the aid of X-ray powder diffraction and Auguer spectroscopy. The hardness of boride films alone is also fairly high, surpassing that of TiB_2 (in the form of the usual polycrystalline material or single crystals) by a factor of approximately 1.5–2. This has also been noted in other investigations.[211,224]

Particularly interesting results have been obtained in the study of multilayer refractory compound-based films.[209,212,225] Fig. 10 illustrates the influence of the number of layers on the hardness of TiN + ZrN, TiN + NbN, and TiN + CrN films (the film thickness was 2 μm in all cases). An appreciable increase in the hardness of

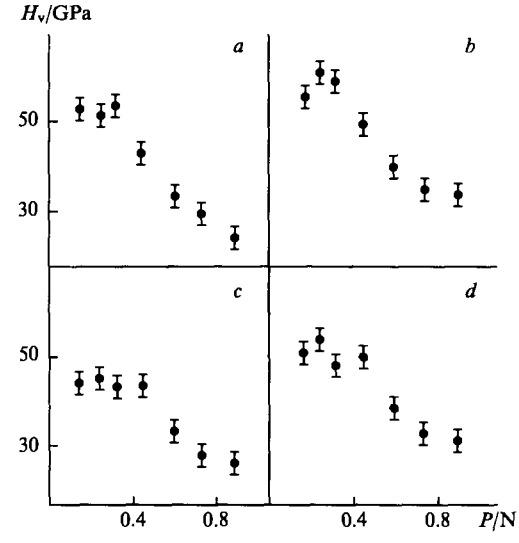


Figure 9. The influence of the load on the hardness of different films: (*a*) Ti–B; (*b*) Ti–B–N; (*c*) Ti–B–C; (*d*) Ti–B–C–N.[210]

the films of the first two systems and its nonmonotonic variation in the TiN–CrN system have been observed. X-Ray powder diffraction revealed the formation of a (Ti,Cr)N solid solution in the latter case, which had not been observed (or had been detected only in the initial stage) for multilayer films of the first two types. Thus the appearance of the solid solution and hence the disappearance of the interfaces with increase in grain size is accompanied by a decrease in the hardness parameters. The strengthening effect due to formation of the solid solution is less significant than the influence of the interfaces on the recrystallisation and the retention of the nanocrystalline structure.

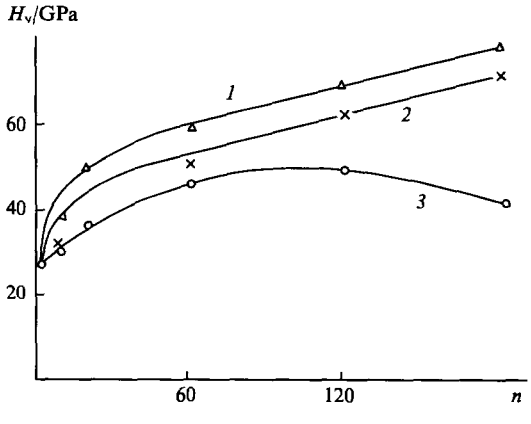


Figure 10. The influence of the number of layers (n) on the hardness of the films:[225] (*1*) TiN–NbN; (*2*) TiN–ZrN; (*3*) TiN–CrN.

Available information about other properties of films based on nanocrystalline refractory compounds is limited to data on the electrical resistance[203] and elastic characteristics[226] of mainly nitride films. In particular, the considerable influence of oxygen on the electrical resistance of TiN, which may vary in the range from 10^4 to ~ 20 $\mu\Omega$ cm, has been noted. In this connection, the precise identification of the role of grain boundaries as one of the factors governing the scattering of carriers (together with structural vacancies, lattice distortions, etc.) is by no means a trivial problem. The deviations from stoichiometry also greatly influence the modulus of elasticity.[226] Several studies using scanning and transmission electron miscroscopy combined with microdiffraction have been devoted to the morphological features and the dislocational structure of W–C–(Co),[227] Ti–N and Ti–B–N,[228] TiN, NbN, VN, and (Ti, Nb)N,[229] TiC + TiB_2,[230] etc. films. However, it is thought that this is only the beginning and systematic studies are still a matter for the future.

V. Conclusion

It is seen from the foregoing that only the first steps have been taken in the study of the properties of nanocrystalline refractory compounds in powder and film form. The amount of information obtained is much smaller than that on nanocrystalline metals.[6–8] It is also smaller than the amount of information available on ultradisperse powders.

The possible applications of nanocrystalline refractory compounds, apart from the materials of the hexanit type based on boron nitride and ultradisperse powders added to the usual powders (see, for example, Refs 231–233), include the technology of the preparation of nanocrystalline WC + Co solid alloys[64] with a high hardness and wear resistance (Table 7) for the manufacture of microtomes and other suitable devices. On the one hand, bearing in mind the high hardness parameters of nanocrystalline metals and intermetallic compounds as well as films, one may hope for the creation of new ultrahard materials based on nanocrystalline refractory compounds. On the other hand, the small grain size of these materials increases significantly their capacity for deformation and the development of ultraplastic compositions based on brittle refractory compounds becomes entirely realistic. The possible temperature of the hot pressing of such materials (1200–1400 °C) is technically entirely acceptable.

Promising applications of nanocrystalline refractory compounds such as preparation of highly selective filters (with fine 5–20 nm filtration apertures) and ion-conducting membranes (in fuel cells and oxygen sensors), the formation of solid-phase junctions between ceramic components, and finally their use for a significant reduction of the sintering temperature have been noted in a review.[165] New possible applications of nanocrystalline refractory compounds in catalysis must be added to the above list.

There is no doubt that the effectiveness of the above materials for particular applied purposes depends significantly on further progress in the study of the methods of preparation of nanocrystalline materials and of the establishment of their properties.

This review has been written with financial support by the International Scientific Fund (ISF, grant No. MTF 000) and the Russian State Scientific-Technical Program 'New Principles and Methods of Preparation of Chemical Substances and Materials' (project No. 3.5.15.93).

References

1. D Segal *Chemical Synthesis of Advanced Ceramic Materials* (Cambridge: Cambridge University Press, 1989)
2. *Inorganic and Metal-Containing Polymeric Materials* (Eds J E Sheats, C Carraher, C Pittman, M Zedlin, B Currell) (New York: Plenum, 1990)
3. V Ya Shevchenko, S M Barinov *Tekhnicheskaya Keramika* (Technical Ceramics) (Moscow: Nauka, 1993)
4. R A Andrievskii *Poroshkovoe Materialovedenie* (Powder Materials Technology) (Moscow: Metallurgiya, 1991)
5. I V Tananaev, V B Fedorov, E G Kalashnikov *Usp. Khim.* **56** 193 (1987) [*Russ. Chem. Rev.* **56** 107 (1987)]
6. H Gleiter *Nanostruct. Mater.* **1** 1 (1992)
7. R W Siegel *Nanostruct. Mater.* **3** 1 (1993)
8. L N Larikov *Metallofizika* **14** 3 (1992)
9. R A Andrievskii, I I Spivak *Prochnost' Tugoplavkikh Soedinenii i Materialov na Ikh Osnove* (Strength of Refractory Compounds and Materials Based upon Them) (Chelyabinsk: Metallurgiya, 1989)
10. V M Batenin, I I Klimovskii, G V Lysov, V N Troitskii *SVCh-Generatory Plazmy: Fizika, Tekhnika, Primenenie* (Ultra-High Frequency Plasma Generators: Physics, Engineering and Application) (Moscow: Energoatomizdat, 1988)
11. T Millers *Mater. Sci. Eng.* **168A** 171 (1993)
12. R A Andrievskii *Zh. Vses. Khim. O-va im. D. I. Mendeleeva* **36** 11 (1991)
13. R A Andrievskii *J. Mater. Sci.* **29** 614 (1994)
14. R A Andrievskii, in *Tugoplavkie Soedineniya* (Refractory Compounds) (Ed. T Ya Kosolapova) (Kiev: Naukova Dumka, 1991) p. 54
15. R W Chorley, P W Lednor *Adv. Mater.* **3** 474 (1991)
16. D L Segal, in *The Physics and Chemistry of Carbides, Nitrides, and Borides* (Ed. R Freer) (Dordrecht: Kluwer, 1990) p. 3
17. M Kato *Jpn. J. Appl. Phys.* **14** 181 (1975); **15** 757 (1976)
18. R Uyeda *Prog. Mater. Sci.* **35** 1 (1991)
19. B Gunther, A Kumpmann *Nanostruct. Mater.* **1** 27 (1992)
20. H Hahn, R S Averback *J. Appl. Phys.* **67** 1113 (1990)
21. S Iwama, K Hayakama, T Arizumi *J. Cryst. Growth* **56** 265 (1982); **66** 189 (1984)
22. G Skandan, H Hahn, J C Parker *Scr. Metall. Mater.* **25** 2389 (1989)
23. G Johnston, R Muenchausen, D M Smith, W Fahrenholtz, S Foltyn *J. Am. Ceram. Soc.* **75** 3293, 3465 (1992)
24. A E Kravchik, V S Neshpor *Poroshk. Metall.* (4) 14 (1976)
25. A E Kravchik, G A Savel'ev, V S Neshpor, S S Ordan'yan *Poroshk. Metall.* (3) 7 (1977)
26. W G Schmidt *Interceram* **40** 15 (1991)
27. S Malghan, D Minor, L Lum *Powder Technol.* **67** 201 (1991)
28. V Yu Davydkin, L I Trusov, P Yu Butyagin, I V Kolbanev, V F Petrunin, V I Novikov, A V Burkhanov, in *Fizikokhimiya Ul'tradispersnykh Sred* (Physical Chemistry of Ultradispersed Mediums) (Ed. Ya K Vaivads) (Riga: Izd. Akad. Nauk Latv. SSR, 1989) p. 187
29. G Le Caer, E Bauer-Grosse, A Pianelli, E Bouzy *J. Mater. Sci.* **25** 4726 (1990)
30. P Matteazzi, G Le Caer *J. Am. Ceram. Soc.* **74** 1382 (1991)
31. P Matteazzi, D Basset, F Miani, G Le Caer *Nanostruct. Mater.* **2** 217 (1993)
32. A Calka, A Radinski *J. Less-Common Met.* **161** L23 (1990)
33. Y-H Park, H Hashimoto, M Nakamura, T Abe, R Watanabe *J. Jpn. Inst. Met.* **57** 952 (1993)
34. A Calka, J Williams *Mater. Sci. Forum* **88/90** 787 (1992)
35. Y Ogino, M Miki, T Yamasaki, T Inuma *Mater. Sci. Forum* **88/90** 795 (1992)
36. M Miki, T Yamasaki, Y Ogino *Mater. Trans. Jpn. Ins. Met.* **33** 839 (1992)
37. A V Kurdyumov, A N Pilyankevich *Fazovye Perekhody v Uglerode i Nitride Bora* (Phase Transitions in Carbon and Boron Nitride) (Kiev: Naukova Dumka, 1979)
38. N Frantsevich (Ed.) *Sverkhtverdye Materialy* (Ultrahard Materials) (Kiev: Naukova Dumka, 1980)
39. S Eidelman, A Altshuler *Nanostruct. Mater.* **3** 31 (1993)
40. B Bergman, J Barrington *J. Am. Ceram. Soc.* **49** 502 (1966)
41. V V Skorokhod, G I Savvakin, S M Solonin, L L Kolomiets *Poroshk. Metall.* (8) 80 (1974)

42. V N Troitskii, S V Gurov, V I Berestenko *Khim. Vys. Energ.* **13** 267 (1979)
43. T N Miller *Izv. Akad. Nauk SSSR, Neorg. Mater.* **15** 557, 595 (1979)
44. T N Miller (Ed.) *Vysokotemperaturnyi Sintez i Svoistva Tugoplavkikh Soedinenii* (The High-Temperature Synthesis and Properties of Refractory Compounds) (Riga: Zinatne, 1979)
45. T Ya Kosolapova, G N Makarenko, D P Zyatkevich *Zh. Vses. Khim. Ov-a im. D. I. Mendeleeva* **24** 30 (1979)
46. V D Parkhomenko, P I Soroka, Yu I Krasokutskii, V I Vereshchak *Zh. Vses. Khim. Ov-a im. D. I. Mendeleeva* **36** 62 (1991)
47. K Tshizaki, T Egashira, K Tanaka, P Cells *J. Mater. Sci.* **24** 3553 (1989)
48. K Kijima, H Noguchi, M Konishi *J. Mater. Sci.* **24** 2929 (1989)
49. F Allaire, S Kallaire *J. Mater. Sci.* **26** 6736 (1991)
50. H Lee, K Eguchi, T Yoshida *J. Am. Ceram. Soc.* **73** 3356 (1990)
51. I V Blinkov, A V Ivanov, I E Orekhov *Fiz. Khim. Obrab. Mater.* (2) 73 (1992)
52. G P Vissokov, K D Manolova, L B Brakalov *J. Mater. Sci. Lett.* **16** 1716 (1981)
53. J Krastins, U Cielens, L Cera, T Millers *Izv. Akad. Nauk Latv. SSR, Ser. Khim.* 651 (1978)
54. J Huggerty, W R Cannon, in *Laser-Induced Chemical Reactions* (Ed. J I Steinfeld) (Translated into Russian; Moscow: Mir, 1984) p.183
55. R Fantoni, E Borsella, S Piccirillo, R Ceccato, S Enzo *J. Mater. Res.* **5** 143 (1990)
56. R A Bauer, J G M Becht, F E Kruis, B Scarlett, J Schoonman *J. Am. Ceram. Soc.* **74** 2759 (1991)
57. L D Casey, J S Hallerty *J. Mater. Sci.* **22** 737 (1987)
58. M Suzuki, Y Maniette, Y Nakata, T Okutani *J. Am. Ceram. Soc.* **76** 1195 (1993)
59. E V Prilutskii, L T Domashevich, A V Neshpor, T Ya Kosolapova, in *Karbidy i Materialy na Ikh Osnove* (Carbides and Materials Based upon Them) (Ed. T Ya Kosolapova) (Kiev: Naukova Dumka, 1983) p. 123
60. P T B Shatter, K A Blakely, M A Janney *Adv. Ceram.* **21** 257 (1987)
61. E S Bartnitskaya, L A Ivanchenko, T Ya Kosolapova *Poroshk. Metall.* (6) 52 (1988)
62. K Rigtrup, R A Cutler *Int. J. Self-Prop. High-Temp. Synthesis* **1** 96 (1992)
63. H Kobayashi, K Shimosaka, T Mitomura *J. Ceram. Soc. Jpn.* **101** 456 (1993); *J. Am. Ceram. Soc.* **76** 2389 (1993)
64. L E McCandlish, B H Kear, B K Kim *Nanostruct. Mater.* **1** 119 (1992)
65. L I Trusov, Yu A Voskresenskii, I A Repin, V I Novikov, V N Lapovok, V N Troitskii, S S Plotkin *Poroshk. Metall.* (7) 117 (1989)
66. S Somiya, K Suzuki, M Yoshimura, in *Horizons of Powder Metallurgy* Part I (Eds W A Kayser, W J Huppmann) (Freiburg: Verlag Schmid, 1986) p. 179
67. A N Zelikman, O B Bystrova, L N Leonova, in *Metallurgiya Redkikh Metallov. Poroshk. Metall.* (Metallurgy of Rare Metals. Powder Metallurgy) (Moscow: Metallurgiya, 1987) p. 39
68. K Su, M Novakowski, D Bonnel, L G Sneddon *Chem. Mater.* **4** 1139 (1992)
69. V I Shapoval, Kh B Kushkhov, I A Novoselova *Zh. Prikl. Khim.* **58** 1027 (1985)
70. J Switzer, R Phillips, in *Better Ceramics through Chemistry III* (Eds C J Brinker, D E Clark, D R Ulrich) (Pittsburgh, 1988) p. 111
71. Kh B Kushkhov, V V Malyshev, A A Tishchenko, V I Shapoval *Poroshk. Metall.* (1) 8 (1993)
72. D Zeng, M J Hampden-Smith *Chem. Mater.* **4** 968 (1992)
73. R L Axelbaum, S E Bates, W E Buhro, C Frey, K Kelton, S Lawton, S Sastry *Nanostruct. Mater.* **2** 139 (1993)
74. G Franz, G Schwier, in *Raw Materials for New Technologies* (Ed. M Kursten) (Stuttgart: Nagele & Obermuller, 1990) p. 1
75. G Schwier, G Nietteld, G Franz *Mater. Sci. Forum* **47** 1 (1989)
76. H Kodama, T Miyoshi *Adv. Ceram. Mater.* **3** 177 (1988)
77. T Hours, P Bergez, J Charpin, A Larbot, C Guizard, L Cot *Am. Ceram. Soc. Bull.* **71** 200 (1992)
78. M Adachi, K Okuyama, S Moon, N Tohge, Y Kousaka *J. Mater. Sci.* **24** 2275 (1989)
79. O M Grebtsova, V N Troitskii, Yu M Shul'ga *Zh. Prikl. Khim.* **58** 2181 (1985)
80. R Riedel, R Strecker, G Petzow *J. Am. Ceram. Soc.* **71** 2071 (1988)
81. K E Gonsalves, P R Strutt, T D Xiaao, P G Klemens *J. Mater. Sci.* **27** 3231 (1992)
82. G W Rice, R L Woodin *J. Am. Ceram. Soc.* **71** 181 (1988)
83. R A Andrievski, S E Kravchenko, S P Shilkin *Jpn. J. Appl. Phys.* (in the press, 1994)
84. R Kalyoncu *Ceram. Eng. Proc.* **6** 1356 (1985)
85. I D Morokhov, L I Trusov, V N Lapovok *Fizicheskie Yavleniya v Ul'tradispersnykh Sredakh* (Physical Phenomena in Ultradisperse Media) (Moscow: Energoatomizdat, 1984)
86. R Birringer, U Herr, H Gleiter *Trans. Jpn. Inst. Met. Suppl.* **27** 43 (1986)
87. R W Siegel, H Hahn, in *Current Trends in Physics of Materials* (Ed. M Yussouff) (Singapore: World Scientific, 1987) p. 403
88. E G Avvakumov *Mekhanicheskie Metody Aktivatsii Khimicheskikh Protsessov* (Mechanical Methods for the Activation of Chemical Processes) (Novosibirsk: Nauka, 1979)
89. P H Shingu (Ed.) *Mechanical Alloying* (Switzerland: Trans. Tech. Publ., 1992)
90. *Mekhanokhimicheskii Sintez* (Report at the All-Union Scientific-Technical Conference on Mechanochemical Synthesis) (Vladivostok: Izd. Dal'nevost. Gos. Univ., 1990)
91. *Mekhanokhimicheskii Sintez v Neorganicheskoi Khimii* (Mechanochemical Synthesis in Inorganic Chemistry (Ed. E G Avvakumov) (Novosibirsk: Nauka, 1991)
92. A A Popovich, V P Reva, V N Vasilenko *Izv. Akad. Nauk SSSR, Neorg. Mater.* **28** 1871 (1992)
93. N Atsumi, K Yoshioka, T Yamasaki, Y Ogino *J. Jpn. Soc. Powder and Powder Metall.* **40** 261 (1993)
94. R A Andrievskii, A A Nuzhdin, in *Itogi Nauki i Tekhniki. Poroshk. Metall.* Vol. 2 (Advances in Science and Engineering. Powder Metallurgy) (Ed. L I Trusov) (Moscow: Izd. VINITI, 1986) p. 3
95. L I Krasovskaya *Khim. Vys. Energ.* **24** 346 (1990)
96. S V Gurov, A O Larionov, A A Levitskii, V Yu Pustil'nikov, V I Torbov *Khim. Vys. Energ.* **26** 163 (1992)
97. F Thevenot, in *The Physics and Chemistry of Carbides, Nitrides and Borides* (Ed. R Freer) (Dordrecht: Kluwer, 1990) p. 87
98. N V Alekseev, Yu V Blagoveshchenskii, G N Zviadadze, I K Tagirov *Poroshk. Metall.* (8) 1 (1980)
99. U A Asanov, B Ya Petrenko, I E Sakavov *Fiz. Khim. Obrab. Mater.* (2) 47 (1978)
100. R Roy *Solid State Ionics* **32/33** 23 (1989)
101. N V Karlov, N A Kirichenko, B S Luk'yanchuk *Lazernaya Termokhimiya* (Laser Thermochemistry) (Moscow: Nauka, 1992)
102. N V Karlov, N A Kirichenko, B S Luk'yanchuk *Usp. Khim.* **62** 223 (1993) [*Russ. Chem. Rev.* **62** 203 (1993)]
103. V Kevorkijan, M Komac, D Kolar *J. Mater. Sci.* **27** 2705 (1992)
104. K Su, L S Sneddon *Chem. Mater.* **5** 1659 (1993)
105. L Hench, J West *Chem. Rev.* **90** 33 (1990)
106. G Wilson, A Patel *Mater. Sci. Techn.* **9** 937 (1993)
107. F Hatakeyama, S Kanzaki *J. Am. Ceram. Soc.* **73** 2107 (1990)
108. A Bleier, R Cannon, in *Better Ceramics Through Chemistry II* (Eds. C J Brinker, D E Clark, D R Ulrich) (Pittsburgh, 1986) p. 71
109. V M Chertov, V I Litvin, I F Mironyuk, V V Tsyrina *Neorg. Mater.* **29** 1019 (1993)
110. C B Ross, T Wade, R M Crooks, D M Smith *Chem. Mater.* **3** 768 (1991)
111. T Wade, J Park, E G Gazza, C B Ross, D M Smith, R M Crooks *J. Am. Chem. Soc.* **114** 9457 (1992)
112. M G L Mirabelli, A T Lynch, L G Sneddon *Solid State Ionics* **32/33** 655 (1989)
113. K E Gonsalves, K T Kembaiyan *Solid State Ionics* **32/33** 661 (1989)
114. M Peuckert, T Vaahs, M Bruck *Adv. Mater.* **2** 398 (1990)
115. A M Tsirlin, E K Florina, G Ya Khodov, N A Popova, A V Obolenskii, B I Shemaev, S I Malashin, in *Karbidy i Materialy na Ikh Osnove* (Carbides and Materials Based upon Them) (Ed. T Ya Kosolapova) (Kiev: Inst. Polym. Mater. Akad. Nauk Ukr. SSR, 1991) p. 4
116. Y D Blum, K B Schwartz, R M Laine *J. Mater. Sci.* **24** 1707 (1989)

117. J L Shi, Z X Lin *Solid State Ionics* **32/33** 544 (1989)
118. A E Kravchik, V S Neshpor *Poroshk. Metall.* (1) 31 (1990)
119. V F Petrunin, Yu G Andreev, T Millers, J Grabis *Poroshk. Metall.* (9) 90 (1987)
120. V F Petrunin, A G Ermolaev, A V Burkhanov, E V Knyazev, L I Trusov, A N Zelikman, S A Vasil'ev *Poroshk. Metall.* (3) 46 (1989)
121. E Neuenschwander *J. Less-Common Met.* **11** 365 (1966)
122. S V Gurov, V N Troitskii, in *Plazmokhimiya-89* (Plasmochemistry-89) (Ed. L S Polak) (Moscow: Nauka, 1989) p. 114
123. M I Aivazov, V V Volod'ko, B A Evseev, Yu N Nikulin *Poroshk. Metall.* (1) 1 (1981)
124. L I Trusov,V N Lapovok, V N Troitskii, E E Vlasov, S B Terekhov, T V Rezchikova *Kristallografiya* **27** 571 (1982)
125. T N Millers, A A Kuzjukevics, in *Progress in Crystal Growth and Characterization* (London: Pergamon Press, 1988) Vol. 16, p. 367
126. R A Andrievskii, R A Lyutikov, O D Torbova, V I Torbov, V G Vil'chinskii, O M Grebtsova, E P Domashneva, A A Eremenko, A Z Rakhmatullina *Neorg. Mater.* **29** 1641 (1993)
127. O N Grigor'ev, Kh B Kushkhov, A M Shatokhin, V I Shapoval *Poroshk. Metall.* (8) 1 (1991)
128. E L Nagaev *Usp. Fiz. Nauk* **162** 50 (1992)
129. S V Gurov, V N Troitskii, A L Dorosinskii *Izv. Akad. Nauk SSSR, Neorg. Mater.* **17** 431 (1981)
130. V F Petrunin, Yu G Andreev, T C Millers, J Grabis, A G Ermolaev, F M Zelenyuk *Poroshk. Metall.* (8) 12 (1984)
131. G P Vissokov *J. Mater. Sci.* **27** 5561 (1992)
132. J Szepvolgyi, I Bertoti, I Mohai-Toth, E Gilbari, F Riley, M Patel *J. Mater. Chem.* **3** 279 (1993)
133. J Vaivads, T Millers, A A Kuzyukevich, I Bertoti, T Sekei, M Lukach *Poroshk. Metall.* (3) 80 (1990)
134. I V Blinkov, V N Vas'kin, I E Orekhov, A A Telegin *Fiz. Khim. Obrab. Mater.* (4) 147 (1993)
135. R A Andrievskii, Yu F Khromov, R A Lyutikov, S A Zhmurov, E A Galkin, R S Yurkova *Zh. Fiz. Khim.* **68** 5 (1994)
136. G M Voloshko, M Lokenbaha, Ya K Vaivads, in *Fizikokhimiya Ul'tradispersnykh Sistem* (Physical Chemistry of Ultradisperse Systems) (Ed. Ya K Vaivads) (Riga: Izd. Akad. Nauk Latv. SSR, 1989) p. 164
137. A S Ivanov, G K Dvoryadkina, S A Borisov *Zh. Fiz. Khim.* **57** 444 (1983)
138. Yu M Shul'ga, V N Troitskii, M I Aivazov, Yu G Borod'ko *Zh. Neorg. Khim.* **21** 2621 (1976)
139. Yu M Shul'ga, V N Troitskii *Poroshk. Metall.* (10) 1 (1979)
140. Yu M Shul'ga, T M Moravskaya, S V Gurov, V I Chukalin, Yu G Borod'ko *Poverkhnost'* (10) 155 (1990)
141. V I Rubtsov, Yu M Shul'ga *J. Electr. Spectr. Relat. Phen.* **58** 247 (1992)
142. M N Rahaman, Y Boiteux, L C De Jonghe *Am. Ceram. Soc. Bull.* **65** 1171 (1986)
143. E Bernstein, M G Blanchin, R Ravelle-Chapuis, J Rodriguez-Carvajal *J. Mater. Sci.* **27** 6519 (1992)
144. M Valeskalne, V E Dombrovskaya, T Millers, M Cheral *Izv. Akad. Nauk SSSR, Neorg. Mater.* **15** 630 (1979)
145. I D Chausskaya, G N Komratov *Neorg. Mater.* **29** 873 (1993)
146. L Cera, M E Salgrave, R Vilsone, in *Fizikokhimiya Ul'tradispersnykh Sistem* (Physical Chemistry of Ultradisperse Systems) (Ed. Ya K Vaivads) (Riga: Izd. Akad. Nauk Latv. SSR, 1989) p. 141
147. B N Sharupin, S A Shevchenko, E V Tupitsyna, in *Fizikokhimiya Ul'tradispersnykh Sistem* (Physical Chemistry of Ultradisperse Systems) (Ed. Ya K Vaivads) (Riga: Izd. Akad. Nauk Latv. SSR, 1989) p. 143
148. S A Nepiiko *Fizicheskie Svoistva Malykh Metallicheskikh Chastits* (Physical Properties of Small Metallic Particles) (Kiev: Naukova Dumka, 1985)
149. I V Tananaeva (Ed.) *Fizikokhimiya Ul'tradispersnykh Sistem* (Physical Chemistry of Ultradisperse Systems) (Moscow: Nauka, 1987)
150. Yu I Petrov *Klastery i Malye Chastitsy* (Clusters and Small Particles) (Moscow: Nauka, 1986)
151. M V Astakhov, B S Bokshtein, T L Lepkova *Poverkhnost'* (4) 108 (1992)
152. E I Asinovskii, L S Polak *Khim. Vys. Energ.* **26** 276 (1992)
153. E L Nagaev *Poverkhnost'* (2) 14 (1993)
154. D I Zhukhovitskii *Zh. Fiz. Khim.* **67** 1962 (1993)
155. I A Domashnev, in *Dispersnye Poroshki i Materialy na Ikh Osnove* (Dispersed Powders and Materials Based upon Them) (Ed. V V Skorokhod) (Kiev: Naukova Dumka, 1982) p. 167
156. V N Troitskii, I A Domashnev, E N Kurkin, O M Grebtsova, A A Budanov, S V Gurov *Neorg. Mater.* **30** 59 (1994)
157. N V Chukanov, V I Chukalin, S V Gurov, F I Dubovitskii *Dokl. Akad. Nauk SSSR* **307** 1376 (1989)
158. C Mo, L Chang, C Xie, T Wang *J. Appl. Phys.* **73** 5185 (1993)
159. R A Andrievskii, O M Grebtsova, E P Domashneva, I A Kiyanskii, E N Kurkin, V E Perel'man, V I Sinitsyn, O D Torbova, V I Torbov *Dokl. Akad. Nauk* **331** 306 (1993)
160. S S Dzhamarov, N P Pavlenko, A V Bozhko, P A Kornienko *Poroshk. Metall.* (10) 6 (1982)
161. A Pechenik, G Piermarini, S C Dantorth *J. Am. Ceram. Soc.* **75** 3283 (1992)
162. M D Matthews, A Pechenik *J. Am. Ceram. Soc.* **74** 1547 (1991)
163. D -J Chen, M J Mayo *Nanostruct. Mater.* **2** 469 (1993)
164. G S Theunissen, A J Winnubst, A J Burggraaf *J. Eur. Ceram. Soc.* **10** 315 (1993)
165. M J Mayo *Mater. Des.* **14** 323 (1993)
166. A N Pilyankevich, G S Oleinik, in *Vliyanie Vysokikh Davlenii na Veshchestvo* (Influence of High Pressure on Matter) (Ed. A N Pilyankevich) (Kiev: Naukova Dumka, 1987) p. 77
167. K Lu, J T Wang, W D Wei *J. Appl. Phys.* **69** 522 (1991)
168. R Chaim *Nanostruct. Mater.* **1** 479 (1992)
169. R Riedel, G Passing, H Schontelder, R Brook *Nature (London)* **355** 714 (1992)
170. R A Andrievskii *Poroshk. Metall.* (11/12) 85 (1994)
171. K Kondo, S Soga, A Sawaoka, A Araki *J. Mater. Sci.* **20** 1033 (1985)
172. V I Kovtun, A V Kurdyumov, V B Zelyavskii, N F Ostrovskaya, V I Trefilov *Poroshk. Metall.* (12) 38 (1992)
173. T Taniguchi, K Kondo *Adv. Ceram. Mater.* **3** 399 (1988)
174. M A Leont'ev, Candidate Thesis in Chemical Sciences, Lomonosov Inst. of Fine Chem. Technol., Moscow, 1990
175. R A Andrievski, V I Torbov, E I Kurkin, in *Plansee Proceedings of the 13th International Plansee Seminar '93* Vol. 3 (Eds H Bildstein, R Eck) (Reutte: Plansee Metall, 1993) p. 649
176. J Krastins, I Zalite, T Millers *Poroshk. Metall.* (3) 47 (1990)
177. T Nishida, H Fujioka, K Adachi, K Urabe *J. Soc. Mater. Sci. Jpn.* **41** 855 (1992)
178. K Kondo, S Sawai *J. Am. Ceram. Soc.* **73** 1983 (1990)
179. R S Averback, H J Hofler, H Hahn, J C Logas *Nanostruct. Mater.* **1** 173 (1992)
180. R A Andrievskii, in *Advances in Powder Metallurgy and Particulate Materials-1992* Vol. 7 (Comps J M Capus, R M German) (Princeton, MPIF, 1992) p. 41
181. A H Chokshi, A Rosen, J Karch, H Gleiter *Scr. Metall. Mater.* **23** 1679 (1989)
182. H Chang, H J Hofler, C J Altstetter, R S Averback *Scr. Metall. Mater.* **25** 1161 (1991)
183. D K Kim, K Okazaki *Mater. Sci. Forum* **88/90** 553 (1992)
184. G W Nieman, J R Weertman, R W Siegel, S Kim *Scr. Metall. Mater.* **26** 1879 (1992)
185. N P Kolobov, J M Soifer, R A Andrievski, B Gunther *Nanostruct. Mater.* **2** 537 (1993)
186. N G Askuntovich, R P Borovikova, L I Trusov, V N Lapovok, R G Mikeladze *Fiz. Tverd. Tela* **27** 3152 (1985)
187. A Savaguchi, K Toda, K Niihara *J. Am. Ceram. Soc.* **74** 1142 (1991)
188. L I Trusov, N G Askuntovich, R P Borovikova, M A Baklastov, V P Fedotov *Phys. Lett.* **167A** 306 (1992)
189. O L Dozhdikova, Yu P Zarichnyak, A V Zuev, S O Krylov, S S Ordan'yan, E K Stepanenko *Poroshk. Metall.* (5) 70 (1992)
190. K Niihara, K Izaki, T Kawakami *J. Mater. Sci. Lett.* **10** 112 (1990)
191. A Nakamura, T Sekino, Y Suzuki, K Niihara *Ann. Chim. Fr.* **18** 403 (1993)
192. A Kerber, R Wagner, in *Third Euro-Ceramics* Vol. 3 (Eds P Duran, J F Fernandez) (San Vincente: Faenza Editrice Iberica, 1993) p. 595
193. S Inamura, M Miyamoto, Y Imaida, M Takagawa, K Hirota, O Yamaguchi *J. Mater. Sci. Lett.* **12** 1368 (1993)

194. R A Andrievski, V T Ivannikov, V S Urbanovich, in *Silicon Nitride '93* (Eds M J Hoffmann, P F Becher, G Petzow) (Switzerland: Trans. Tech. Publ., 1993) p. 369
195. I-W Chen, Sh-L Hwang *J. Am. Ceram. Soc.* **75** 1073 (1992)
196. A J Burggraaf, A J A Winnubust, H Verweij, in *Third Euro-Ceramics* Vol. 3 (Eds P Duran, J F Fernandez) (San Vincente: Faenza Editrice Iberica, 1993) p. 561
197. R E Newnham, in *Third Euro-Ceramics* Vol. 2 (Eds P Duran, J F Fernandez) (San Vincente: Faenza Editrice Iberica, 1993) p. 1
198. V B Fedorov, M A Gurskii, E G Kalashnikov, V N Lapovok, M Kh Shorshorov, L I Trusov *Poroshk. Metall.* (3) 56 (1981)
199. R A Andrievskii, I A Anisimova *Izv. Akad. Nauk SSR, Neorg. Mater.* **27** 1450 (1991)
200. B G Gribov, G A Domrachev, B V Zhuk, B S Kaverin, B I Kozyrkin, V V Mel'nikov, O N Suvorova *Osazhdenie Plenok i Pokrytii Razlozheniem Metalloorganicheskikh Soedinenii* (Deposition of Films and Coatings by Decomposition of Organometallic Compounds) (Moscow: Nauka, 1981)
201. G.A.Razuvaev (Ed.) *Primenenie Metalloorganicheskikh Soedinenii dlya Polucheniya Neorganicheskikh Pokrytii i Materialov* (The Use of Organometallic Compounds for the Preparation of Inorganic Coatings and Materials) (Moscow: Nauka, 1986)
202. M G Hocking, V Vasantasree, P S Sidky *Metallic and Ceramic Coatings: Production, High-Temperature Properties and Applications* (Harlow: Longman Scientific & Technical, 1989)
203. D S Rickerby, A Matthews *Reviews on Powder Metallurgy and Physical Ceramics* **4** 155 (1991)
204. M Konuma *Film Deposition by Plasma Techniques* (Berlin: Springer, 1992)
205. V P Tolstoi *Usp. Khim.* **62** 260 (1993) [*Russ. Chem. Rev.* **62** 237 (1993)]
206. T Noda, H Suzuki, H Araki, F Abe, M Okada *J. Mater. Sci. Lett.* **11** 477 (1992)
207. Yu A Bykovskii, V P Kozlenkov, Yu B Krasil'nikov, I N Nikolaev *Poverkhnost'* (12) 69 (1992)
208. S Chatterjee, S Chandrashekhar, T S Sudarshan *J. Mater. Sci.* **27** 3409 (1992)
209. H Holleck, H Shulz *Surf. Coat. Technol.* **36** 707 (1988)
210. C Mitterer, M Rauter, P Rodhammer *Surf. Coat. Technol.* **41** 351 (1990)
211. O Knotek, F Loffler *J. Hard Mater.* **3** 29 (1992)
212. R A Andrievski, I A Anisimova, V P Anisimov *Thin Solid Films* **205** 171 (1991)
213. K Bartsch, B Arnold, A Leonhardt, in *Proceedings of the Third International Conference on Advanced Materials. Symposium on Nanophase and Nanocomposite Materials* (Eds K Niihara, R W Siegel, C Allen, K Wakino, I A Aksay) (Tokyo: Hoikusha, 1993) Paper BB1-2
214. T Noda, H Suzuki, H Araki, F Abe, M Okada *J. Mater. Sci. Lett.* **11** 477 (1992)
215. N Tohye, S Takahashi, T Minami *J. Am. Ceram. Soc.***74** 67 (1991)
216. K Yamada, T Y Chow, T Horihata, M Nagata *J. Non-Cryst. Solids* **100** 316 (1988)
217. O N Mittov, B I Sysoev, M N Bezryadin, V D Linnik *Poverkhnost'* (10 – 11) 50 (1992)
218. K T Miller, F F Lange, D B Marshall, in *Better Ceramics through Chemistry III* (Eds C J Brinker, D E Clark, D R Ulrich) (Pittsburgh, 1988) p. 823
219. M Yoshitake, T Yotsuya, S Ogawa *Jpn. J. Appl. Phys.* **31** 4002 (1992)
220. S Horita, T Tujikawa, H Akahori, M Kobayashi, T Hata *J. Vac. Sci. Technol.* **11A** 2452 (1993)
221. B A Movchan, A V Demchishin *Fiz. Met. Metalloved.* **28** 653 (1969)
222. J A Thornton *Ann. Rev. Mater. Sci.* **7** 239 (1977)
223. C V Thompson *Mat. Sci. Forum* **94/96** 246 (1992)
224. W Herr, B Matthews, E Broszeit, K H Kloos *Mater. Sci. Eng.* **140A** 616 (1991)
225. R A Andrievskii, I A Anisimova, V P Anisimov *Fiz. Khim. Obrab. Mater.* (2) 99 (1992)
226. S Chatterjee, T S Subarshan, S Chandrashekhar *J. Mater. Sci.* **28** 1989 (1993)
227. A Cavaleiro, M T Vieira, G Lemperiere *Thin Solid Films* **213** 6 (1992)
228. D G Rickerby *Philos. Mag.* **68B** 939 (1993)
229. L Hultman, M Shinn, P B Mirkarimi, S A Barnett *J. Crystal Growth* **135** 309 (1994)
230. H Holleck, M Lahres *Mater. Sci. Eng.* **140A** 609 (1991)
231. I N Frantsevich, A N Gromyko, A V Kurdyumov, in *Sverkhtverdye Materialy: Sintez, Svoistva i Primenenie* (Ultrahard Materials: Synthesis, Properties and Applications) (Ed. N V Novikov) (Kiev: Naukova Dumka, 1983) p. 24
232. O N Grigor'ev, V I Trefilov, A M Shatokhin *Poroshk. Metall.* (12) 75 (1983)
233. I I Osipova, E L Shvedkov *Poroshk. Metall.* (9) 31 (1992)

Russian Chemical Reviews **63** (5) 429–435 (1994)
© 1994 Russian Academy of Sciences and Turpion Ltd

UDC 541.135.4

Proton conductivity of inorganic hydrates

A B Yaroslavtsev

Contents

I. Introduction	429
II. Formation of charge carriers	430
III. Proton transfer	430
IV. Proton transfer on the surface of particles	433
V. Some features of solid proton-conducting electrolytes	434

Abstract. A wide range of inorganic crystal hydrates possessing proton conductivity is analysed. The possible mechanisms of defect formation and proton transfer are considered, including those for a series of specific compounds. The main directions in the search of compounds having high proton conductivity at room temperature are outlined. The bibliography includes 65 references.

I. Introduction

One of the priority aspects of the development of modern chemistry is the elaboration of materials possessing special electrical properties; in particular, the search for solid electrolytes having proton conductivity. The prospects for their application are exceedingly wide. For example, they have been used to create high-performance fuel cells (with an efficiency approaching 100%) based on the oxidation of hydrogen,[1,2] water vapour electrolysers, devices for the extraction of hydrogen from water gas,[3] and highly sensitive sensors for hydrogen, carbon monoxide, and several other gases.[4,5] Recently a new field of application of proton-conducting materials was discovered: their use for the non-faradaic electrochemical modification of the catalytic activity (EMCA) of metal catalysts, resulting in a manifold increase in their activity and selectivity, e.g., in the 'catalytic cross-linking' of methane.[6] It should also be noted that the same requirements must be met for a compound to possess proton conductivity as those for the existence of acid–base catalytic activity in organic syntheses.[7] These properties are therefore directly correlated for many compounds,[8] and proton conductivity is used in several scientific centres as the primary test for screening proposed catalysts. The above factors led to a broad development of the search for and study of new solid proton-conducting electrolytes. Not only electrical conductivity but also other properties of the material, such as thermal stability, solubility, dispersity, etc., appear to be of primary importance.

If one considers the list of compounds possessing a high proton conductivity at the usual, relatively low temperatures, it is easy to see that virtually all of them, including all 'record holders', are hydrates of bases, acids, acid salts, or oxides with distinct acidic properties. For example, the highest proton conductivity at room temperature (0.17 S cm^{-1}) is exhibited by highly hydrated heteropolyacids.[9,10] The following compounds have conductivities lower by two orders of magnitude: uranyl phosphate,[11] some hydrated acid sulfates,[12] hydrates of sulfonic acids,[13] hydrated tetramethylammonium,[14] and certain finely dispersed materials, such as acid phosphates of zirconium, tin, antimony,[15–17] polyantimonic acid,[18] etc. Taking this into consideration, we shall devote most attention in this review to the proton conductivity of inorganic hydrates of acids, acid salts, and bases.

We shall present here several known general relations for ionic conductivity which will be used below. In the general case, electrical conductivity is defined by the following equation:

$$\sigma = \sum n_i q_i \mu_i, \quad (1)$$

where n_i is the number of the charge carriers, q_i is their charge, and μ_i is their mobility.

Temperature dependence of the number of carriers is expressed by the equation:

$$n_d = N\exp(-\Delta G_d/2kT), \quad (2)$$

where N is the overall number of possible sites for the formation of the carriers (most frequently proton defects in the case under consideration), ΔG_d is the free energy for defect formation, and k is the Boltzmann constant.

In its turn, the mobility of the charge carriers also depends on temperature:

$$\mu = (a^2 q/kT)\, v_0 \exp(-E_m/kT), \quad (3)$$

where a is the distance between the neighbouring positions in the structure, q is the proton charge, v_0 is the frequency of proton vibrations near the equilibrium position ($\sim 10^{14}$ s^{-1}), and E_m is the energy barrier to migration.

Thus the temperature dependence of the overall conductivity is defined by the equation

$$\sigma = (a^2 q/kT)\exp[-(\Delta G_d/2 + E_m)/kT]. \quad (4)$$

In practice, this equation is used in an abbreviated form adjusted to molar values and is known as the Frenkel equation:

$$\sigma T = A\exp(-E/RT). \quad (5)$$

To understand the essential nature of the proton conduction process, it is important to formulate the mechanisms for the formation of defects and their transfer in the structure of the substance.

A B Yaroslavtsev Higher Chemical College of the Russian Academy of Sciences, 9 Miusskaya pl., 125 820 Moscow, Russian Federation. Fax (7-095) 200 42 04, Tel. (7-095) 258 85 27

Received 22 April 1994
Uspekhi Khimii **63** (5) 449–455 (1994); translated by S S Veselyi

II. Formation of charge carriers

As a rule, the formation of charge carriers reduces to proton transfer from the ground state to an excited state characterised by a higher energy. Most often, this can be described by reactions of the following types:[19,21]

$$2HSO_4^- \rightleftharpoons H_2SO_4 + SO_4^{2-}, \quad (6)$$

or

$$O_3SO^{2-} - HOH_2^+ \rightleftharpoons O_3SOH^- - OH_2 . \quad (7)$$

The concentration of charge carriers for reaction (6) at room temperature can be estimated easily from the equilibrium constant, which is equal to the ratio of the successive dissociation constants of the corresponding acids in solution. This concentration is normally of the order $10^{-10}-10^{-6}$, although, strictly speaking, the corresponding values for a solid can differ significantly. The concentration for reaction (7) is determined by the difference between the proton-accepting capacities of water molecules and the anion. It can vary within very wide limits, reaching values close to 1 when the above capacities are equal. The proton transfer can occur along a chain of successively linked water molecules and oxonium ions, as in the case of highly hydrated molybdo- and tungsto-phosphoric acids. Since for the latter even the identification of the H_3O^+ ions in the structure is problematical, it can be assumed that all the acid protons act as charge carriers. Their absolute concentration, calculated from the unit cell volume, is 1.9×10^{21} cm^{-3} (or 3.2×10^{-3} mol cm^{-3}). If one takes the above considerations into account, the concentration of carriers in the hydrates of weaker acids is usually lower and can reach 10^{11} cm^{-3} or even less. For example, Chandra[20] suggests that the boundary between compounds with low and high concentrations of carriers lies at 10^{18} cm^{-3}. If the proton mobility is high, the former are assigned to the class of the so-called superionic conductors. However, the boundary between these and the usual ionic electrolytes is very arbitrary. Furthermore, proton defects can be formed due to the interaction of the compound with the molecules of water of hydration. A characteristic example is given by salts of heteropolyacids, in which the processes described by the reactions

$$PW_{12}O_{40}^{3-} + 7H_2O \rightleftharpoons PW_{11}O_{39}^{7-} + H_2WO_4 + 4H_3O^+, \quad (8a)$$

or

$$-W-O-W- + 3H_2O \rightleftharpoons 2-W-O^- + 2H_3O^+, \quad (8b)$$

result in a high effective concentration of the carriers even in the case of neutral salts.[21] Evidently, the same processes result in the existence of excess protons in the highly hydrated heteropolyacids, found by Ukshe et al.[22]

In addition, the concentration of defects is affected very strongly by various admixtures that can be present in solid proton-conducting electrolytes owing to various reasons. On the one hand, these materials normally exhibit ion-exchange properties. As a result, a portion of the protons can be replaced by various cations with a much lower mobility, which decreases the concentration of the carriers. This results in a decrease in the electrical conductivity of these compounds, as in the case of acid zirconium phosphate, even though the degree of hydration can increase.[23-27] On the other hand, doping the solid electrolytes with heterovalent cations can 'force' the generation of an excess concentration of the carriers correlated with the concentration of the admixture. A typical example of such doping is presented by oxygen-conducting materials based on the cubic modification of zirconium dioxide, stabilised with yttrium or calcium, as well as by halides. In this case Eqn (4) transforms into

$$\sigma = [N_0 + N \exp(-\Delta G_d/2kT)](a^2 q \nu_0/kT) \exp(-E_m/kT), \quad (9)$$

where N_0 is the number of admixture-generated defects. In contrast to individual compounds, the logarithmic conductivity plot for such a material consists of two straight lines intersecting at the point where the concentrations of the admixture- and thermally-generated charge carriers are equal. The effective activation energy is higher for the high-temperature branch. Unfortunately, the specific procedures used for the preparation of hydrates of inorganic acids and acid salts and their specific structure make it difficult to introduce doping ions into some materials and result in a high surface defectiveness of other materials. This makes it very difficult to investigate correctly the effect of doping with various admixtures on the electrical conductivity of these compounds.

III. Proton transfer

Like many other cations that can act as carriers in solid electrolytes, the proton is singly charged. However, it is distinguished by an exceedingly small radius, mass, small coordination number, and the absence of an electronic shell. It follows from these facts that the presence of large channels in the structure is not obligatory for the existence of proton conductivity. On the other hand, the activation energy for the transfer of charged species in structures with ionic conductivity passes through a minimum for cations with a radius of about 1 Å, as in β-alumina. The transfer of large cations encounters steric hindrance, whereas small cations 'stick' to the channel 'walls' forming fairly strong bonds. Therefore, proton transport is characterised by several specific features:

over a reasonable temperature range, the proton is always bound covalently to one of the electronegative atoms;

the hydrogen bond is always directed;

the proton can be effectively 'delocalised' between two electronegative atoms, and its oscillation along the H-bond, $O-H\cdots O \leftrightharpoons O\cdots H-O$, is an important step in the transfer reaction and can proceed by the tunnelling mechanism.

1. The 'carriage' mechanism

At present, the most common view is that a proton in a solid can move either by the 'relay' mechanism, i.e. by transfer from one electronegative atom to another, or by the so-called 'carriage' mechanism. The latter was suggested on the basis of the fact that the maximum proton conductivity at low temperatures is shown by compounds containing water or ammonia molecules together with protons. In this case, the formation of H_3O^+, NH_4^+, and other ions becomes possible. The authors of this theory suggest that these ions can migrate through the structure as a single whole structure, thus ensuring proton transfer.[28]

This view is fairly common and is supported by a number of facts. For example, the 'carriage' mechanism has been ascribed to uranyl phosphate tetrahydrate on the basis of the similarity of the activation energies for electrical conduction and the migration of oxygen atoms.[29] Although this view is popular, the existence of solid proton-conducting electrolytes with the 'carriage' transfer mechanism seems questionable, primarily because the actual time for a proton jump in uranyl phosphate is no more than 10^{-9} s,[30-32] whereas the lifetime of the oxonium ion is 10^{-12} s.[33] Furthermore, the environment of the H_3O^+ and $H_5O_2^+$ ions in the crystals is not restricted to oxygen atoms forming hydrogen bonds directly with these ions, but also includes at least one additional atom. The law governing this phenomenon can be readily understood from the fact that the energy of the dipole–charge interaction is inversely proportional to the cube of the distance between them, whereas that of the charge–charge interaction is inversely proportional to the distance. Hence, if the O^{2-} ion moves farther from the oxonium ion oriented towards it with its oxygen atom, then, starting from a certain distance, the attraction between them as oppositely charged species becomes the dominant effect. Moreover, in terms of the close-packed spheres structure, the oxonium ions are often located in tetrahedral cavities and more rarely in octahedral cavities with a somewhat distorted environment. This also implies that these ions are surrounded by more than three electronegative atoms.

The existence of such additional bonds in several real hydrates of acid salts has been demonstrated.[34] Assuming that the lengths of the three main H-bonds are 2.6, 2.8, and 2.8 Å (which is most typical for the hydrated oxonium ions) and that the mean statistical angles between them are 114°, one can find that the radius of an inscribed circle for the cross-sections formed by three oxygen atoms, through which the oxonium ion should pass, is 2.63–2.69 Å (less than the sum of two ionic radii of oxygen). Clearly, the diffusion process will involve substantial steric hindrance. When calculating the channel radius in real compounds, one has to take more atoms into account; hence this value can become even less. For example, the radii are 2.52 and 2.12 Å for the tetra- and monohydrates of indium bisulfate respectively.

Finally, there is also a direct method permitting an experimental choice between the 'carriage' and 'relay' proton transfer mechanisms. The replacement of oxonium ions or H_2O-H^+ fragments by NH_4^+ should result, in the case of the 'carriage' mechanism, in an increase in the concentration of carriers owing to the higher stability of the latter cation, and in an increase in their mobility owing to lower strength of the hydrogen bonds. On the other hand, in the case of the 'relay' mechanism, this change complicates the proton transfer owing to the high activation energy for its transfer from the ammonium cation to the anion. It has been shown, using this method, that the transfer in $D_3OZr_2(PO_4)_3$,[35] $Sn(HPO_4)_2.2H_2O$,[16] $H_3OM(SO_4)_2$[12] (where M = Al, Ga, In, Tl, Ti, V, Mn, or Fe), and some other compounds occurs by proton jumps. A degree of probability of the carriage transfer mechanism can perhaps be retained only for the ammonium salts formed by acids in which the proton-accepting capacity of the anion is exceedingly low. This assumption is based on the fact that the electrical conductivities of ammonium, rubidium, and caesium perchlorates are similar. However, it is noteworthy that the analogous value for oxonium perchlorate is nine orders of magnitude higher.

2. The 'relay' mechanism

Unlike the situation with other ions, the transfer of the proton never occurs in one step, but normally consists of a series of jumps along the hydrogen bond and of rotations of proton-containing groups. It should be noted that a prerequisite condition for the transfer is an excess of potential hydrogen bonds in comparison with the number of protons present in the system. As was shown above, this condition should almost always be fulfilled for hydrates of inorganic salts and acid salts. 'Hydrogen bonds' of this type involving no proton are called the Bjerrum L-defects. In its turn, a Bjerrum D-defect is a hydrogen bond involving two protons. Their formation can be easily imagined if one rotates a water molecule in the structure of ice by 120° relative to any of the hydrogen bonds. The D-defects should have extraordinarily high energies. For this reason, some authors consider that their existence is, in principle, impossible. However, a hydrogen bond with a length of 1.91 Å has been found in $H_{3.33}Fe(CN)_6.2.7H_2O$.[36] The exceedingly short length of this bond is thought to be due to the fact that it incorporates two protons. Note that this ambiguous finding has not been supported by any other evidence.

Consider a hypothetical system containing oxonium ions and XO_4^{n-}, and assume that it already contains defects consisting of water molecules formed by the dissociation of oxonium. The transfer process in such a system can be represented by the scheme

$$\begin{aligned} &H_2O-H^+\cdots O_a\cdots OH_2 \overset{a}{\rightleftharpoons} \\ &\rightleftharpoons H_2O\cdots H^+-O_a\cdots OH_2 \overset{b}{\rightleftharpoons} \\ &\rightleftharpoons H_2O\cdots O_a-H^+\cdots OH_2 \overset{c}{\rightleftharpoons} \\ &\rightleftharpoons H_2O\cdots O_a\cdots H^+-OH_2. \end{aligned} \qquad (10)$$

The process with the maximum activation energy should be the rate-determining step. The activation energy for proton transfer along the hydrogen bond (steps *a* and *c*) increases abruptly with increasing bond length,[33] whereas the activation energy for the rotation of the $X-O\diagup H$ moiety relative to the X–O bond (step *b*) actually decreases.[34] It follows that there exists an optimum length for hydrogen bonds, which should maximise the proton mobility. Using the data in Refs 33 and 34, one can conclude that, provided that the proton-accepting capacities of the oxygen atoms participating in the transfer are close, the systems with ~2.8 Å hydrogen bonds should have the lowest activation energies (of the order of 15–20 kJ mol^{-1}).

An example of proton transfer by this mechanism is provided by acid indium and thallium sulfate monohydrates $H_3OM(SO_4)_2$ (Fig. 1) described by us previously.[12] The *a*, *b*, *c*, and *d* indices refer to the states which the system adopts successively. The arrows indicate the directions of the movement of hydrogen ions resulting in these transformations (proton jumps and rotation of proton-containing groups). The environment of each oxonium ion incorporates six equivalent oxygen atoms of the anion, but only three of these can form hydrogen bonds with the oxonium ion simultaneously.[37] Thus the system initially contains three Bjerrum L-defects for three actually existing hydrogen bonds. The proton defects are formed by reaction (7). Judging from the equilibrium constant of this reaction, which can be easily estimated from NMR spectra at 77 K, ΔG for this process is close to 1.5 kJ mol^{-1}. The activation energy for the oxonium ion rotation in these compounds is only 18 kJ mol^{-1}; an excess of hydrogen bond acceptors plays an important role in decreasing this activation energy.[34] The rotation of the S–O–H moiety proceeds even more readily, since it requires the breaking of only one hydrogen bond and rotation around a S–O single bond. On the other hand, the proton transfer along hydrogen bonds with a length of 2.87 Å, formed by oxygen atoms possessing similar proton-accepting capacities, should be characterised[33] by an activation energy of ~ 33 kJ mol^{-1}, which determines the overall proton mobility in this case. Thus, the activation energy $E \sim 33 + 0.7 = 33.7$ kJ mol^{-1} can be obtained from Eqns (4) and (5) (cf. the experimental values of 30–34 kJ mol^{-1}).

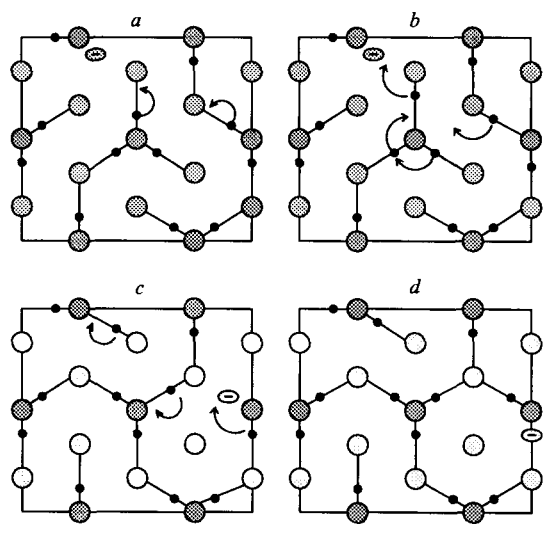


Figure 1. Schematic illustration of proton transfer in $H_3OM(SO_4)_2$: (*a*)–(*d*), consecutive conformations of the system; ◎ – oxonium oxygen; ○ – anion oxygen.

The proton transfer in a number of other hydrates of acids and acid salts, including oxonium perchlorate, occurs similarly.[38,39] The electrical conductivity of the latter compound increases abruptly in the first-order phase transition at 250 K,[33,38] after which the oxonium ions pass to the isotropic rotation state[40] and are surrounded by seven oxygen atoms at a distance of 2.86–3.40 Å.[41] It should be noted that the occurrence of phase

transitions resulting in an increase in proton conductivity is quite typical for these compounds.[19,39]

Usually, as in the above examples, the mobility of the proton is limited by the step involving its transfer along the hydrogen bond. However, the rotation of the proton-containing moieties is strictly necessary for the existence of proton conductivity. A typical example of a compound having an exceedingly low proton conductivity due to the hindered rotation of the proton-containing groups is provided by sulfuric acid octahydrate. The infinite planar networks $(H_9O_4)_n^{n+}$ in this compound are built up on the basis of the $H_5O_2^+$ ions with R(O—O) = 2.447 Å and with equivalent oxygen atoms. Each OH_2 moiety in these ions is a donor in hydrogen bonds with the anion and with a water molecule characterised by equal lengths of 2.654 Å. In turn, the water molecules form H-bonds with the anion (2.735 Å) and with similar molecules (2.762 and 2.765 Å). In the latter two bonds, each participant can act with equal probability as a proton donor or acceptor.[42] The proximity of a further two H_2O molecules not bonded directly is noteworthy. Thus the structure of $H_2SO_4.8H_2O$ seems to be ideal for proton conductors. However, the formation of numerous strong hydrogen bonds hinders the rotation of the proton-containing moieties. This inhibits in its turn the transfer of protons, which, according to our data,[43] do not pass to the mobile state below the melting point.

A number of solid proton-conducting electrolytes, whose conductivity is limited by different proton transfer steps, have been reported in the literature. Unfortunately, this assignment was not sufficiently well founded in most of the studies and was based merely on the activation energies for proton transfer (which is not always unreasonable). Some typical frequencies and activation energies for the elementary proton transfer steps reported in the literature are given in Table 1.

Table 1. Some typical frequencies and activation energies for the elementary proton transfer steps.

Process	Frequency/Hz	E_a/kJ mol^{-1}	Ref.
Reorientation of polyatomic ions	$10^{11}-10^{12}$	< 10	44
Reorientation of interlayer water molecules or 'zeolite'-type water	$10^{7}-10^{12}$	20–30	30, 32, 44
Reorientation of coordinated water	10^{9}	20–30	44
Proton jumps	$10^{8}-10^{10}$	20	30, 32, 44
Oxygen diffusion	10^{9}	80	30

In our opinion, these data can be used for a preliminary comparison of the energetic and frequency parameters of conductivity-determining processes. For example, it follows from these data that the transfer process can normally be limited by the rotation of polyatomic ions such as HPO_4^{2-}, $HSeO_4^-$, etc. On the other hand, the parameters of these tabulated processes may be outside these limits for some compounds.[16]

In real structures, the proton should be transferred by ~3 Å in one step. By substituting this value, together with the previously estimated minimum activation energy of 15 kJ mol^{-1}, in Eqn (3), it is possible to obtain a proton mobility of 8×10^{-3} cm^{2}V^{-1}s^{-1}. On combining this with the maximum concentration of carriers, we obtain from the Frenkel equation (5) $A_{max} = 3.3$ S cm^{-1} and $\sigma = 2.5 \times 10^{-5}$ S cm^{-1} for the 'relay' mechanism.

3. The Grotthus mechanism

The structures of many solid proton-conducting electrolytes are characterised by a large number of virtually equivalent oxygen atoms, which nevertheless form different proton-containing groups (H_3O^+ and H_2O, OH^- and H_2O). The conditions for proton transfer are most favourable in such systems—ice might be an ideal proton conductor. However, the main obstacles to this are the low concentration of charge carriers (10^{-7}) and the low rotational mobility of water molecules in ice. The situation changes completely if oxonium ions or hydroxide ions are introduced into an ice-like structure. This results in the concentration of carriers and the proton mobility increasing abruptly; the rotational mobility of the proton-containing moieties is stimulated very strongly.[45,46] However, the combination of the above factors does not explain the anomalously high proton mobility, which is at least an order of magnitude higher than that of other ions in aqueous solutions and in a number of other compounds. It is also difficult to explain the difference between the maximum electrical conductivity for the 'relay' mechanism quoted in the previous section (2.5×10^{-5} S cm^{-1}) and the electrical conductivity of highly hydrated heteropolyacids (0.17 S cm^{-1}). One explanation for these facts is the equivalence of protons in H_3O^+ and H_2O. According to Haggins[47] and Zundel,[48] the transfer in these systems can be represented as structural migration of $H_5O_2^+$ ions (Fig. 2). This model is reminiscent of the familiar fairy tale about a race between a hedgehog and a hare, where a twin hedgehog awaited the exhausted hare at the finish. Zundel remarks that the proton jump occurs against the background of the vibration of the system of oxygen atoms, which leads to a shift of the shortest bond (the change from Fig. 2*b* to Fig. 2*c*). Undoubtedly, this condition favours proton migration,[48,49] although it is not essential.

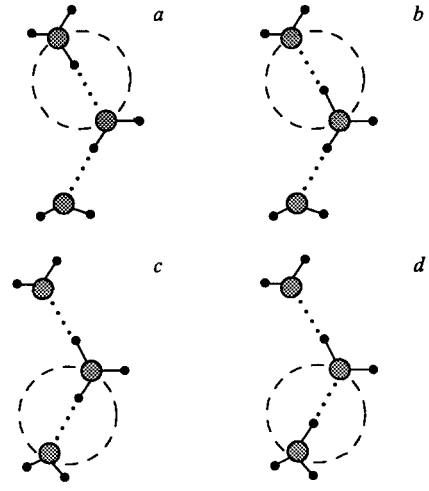


Figure 2. Schematic illustration of proton transfer by the Grotthus mechanism (the circles indicate the short hydrogen bond);[48] (*a*)–(*d*), consecutive conformations of the system.

Strictly speaking, the above scheme describes only the polarisation of the system, whereas proton conductivity requires, in addition, reorientation of the newly-formed proton-containing groups. It is easily seen that the rotation of any of these groups would result in a Bjerrum D-defect. Therefore, the view exists that such rotations occur in a concerted manner, i.e. the rotation of one water molecule initiates the rotation of a second molecule, then a third, etc., with a small phase lag. As a result, the D-defect migrates cooperatively in a wave-like manner (this is also called the soliton mechanism). The rapid overall proton transfer consisting of jumps between equivalent proton-containing groups alternating with their rotations was called the Grotthus mechanism. Combination of the above factors results in a

cooperative proton jump over an enormous distance, which in this case should be called more appropriately 'the length of the free path'. For example, this length for heteropolyacids estimated by Eqn (4) is 100 Å.

This mechanism is quite common not only for hydrates of acid salts[50,51] but also for bases.[14,52] The proton transfer in $CsOH.H_2O$ takes place in this way. This process is quite instructive and has been studied thoroughly, and so it seems reasonable to discuss it although formally this is beyond the scope of this review. Below 229 K, the compound crystallises in the monoclinic system with the structurally nonequivalent OH^- groups and H_2O forming a planar network (Fig. 3). This conclusion is also confirmed by ^2D NMR data.[52] However, above this temperature a phase transition occurs, which is accompanied by the transformation of the monoclinic crystal lattice into the hexagonal form with structurally equivalent oxygen atoms. The symmetrical hydrogen bond with $R(O-O) = 2.64$ Å is characterised by two possible positions of the proton 1 Å apart. The transfer between these positions is characterised by a frequency of 8×10^{10} Hz. When combined with the rotation of the proton-containing groups at a frequency of 2.8×10^9 Hz, this leads to the occurrence of two-dimensional proton diffusion in $CsOH.H_2O$, via the Grotthus mechanism.[52] Similar disordering is observed in $RbOH.2H_2O$, in which the hydroxyl groups participate in the formation of four hydrogen bonds with water molecules.[53]

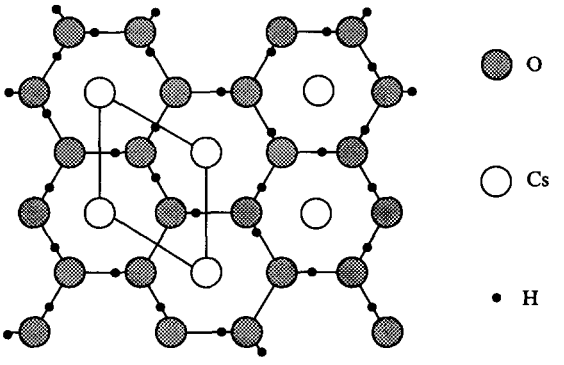


Figure 3. The structure of $CsOH.H_2O$.

A proton hydrate sublattice having the composition $H(H_2O)_n^+$ with a three-dimensional framework of hydrogen bonds is also formed in highly hydrated heteropolyacids. The existence of several variants of proton transfer ensures the extremely high electrical conductivity of these compounds, which decreases as the degree of hydration decreases.[9-11]

IV. Proton transfer on the surface of particles

Since in most cases the surface layer of particles of a compound constitutes a small proportion of the bulk, its contribution to the electrical conductivity is low. However, the situation changes completely when compounds such as hydrated oxides of polyvalent elements are considered. X-Ray microanalysis often indicates the presence of lines resembling those of the corresponding lines of oxides but differing mainly in having larger widths. This allows the assumption that the compounds have the globular structures[54,55] shown in Fig. 4 for tin hydroxide.

The composition inside the globules is close to that of the corresponding metal oxide. However, the surface of the globules incorporates fairly numerous OH groups, water molecules, and, possibly, anions trapped from the solution. The charged species located on the surface are highly reactive and can be readily exchanged when in contact with the solution.[54,55] A fraction of the water molecules are located in the intergranular space and,

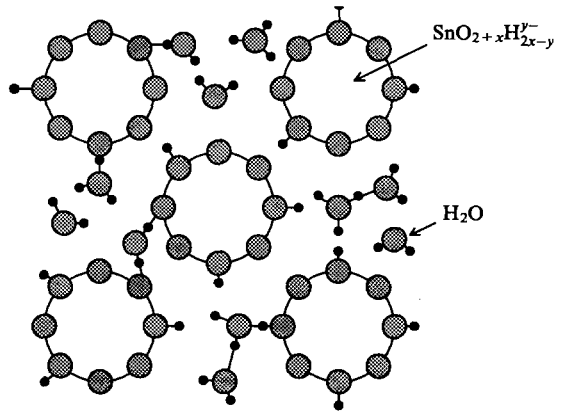


Figure 4. The structure of $SnO_2 . nH_2O$.

being retained only by hydrogen bonds, are highly mobile.[55,56] The overall composition of tin hydroxide may be represented by the formula $SnO_{2-x}(OH)_{2x}.nH_2O$. In this composition there are $2+x$ oxygen atoms per tin atom. For 25 Å particles, $x = 0.6$, while for 100 Å particles $x = 0.15$.[54] There is a special term for these compounds in the English language literature, namely, 'particle hydrates'; in the Russian-language literature they are sometimes called 'globular hydrates', although this name is not generally accepted. The acidic nature of the hydroxyl groups in $SnO_2.nH_2O$ brings about their partial dissociation via the mechanism:

$$SnO_{2+x}H_{2x} + yH_2O \rightleftharpoons SnO_{2+x}H^{y-}_{2x-y} + yH_3O^+. \quad (11)$$

Thus the intergranular space contains a highly mobile solution with the composition $yH^+ . nH_2O$ ensuring the high electrical conductivity of this compound, which reaches 3×10^{-4} S cm^{-1} at room temperature. Obviously the transfer itself occurs via the Grotthus mechanism.

The highly hydrated heteropolyacids are a prominent example of compounds with this type of proton transfer mechanism. In these, the heteropolyanions, in which all three OH groups are completely dissociated, act as globules whose radii are about 12 Å. Evidently this is why these compounds have the highest electrical conductivities.[9] Insoluble alkali metal tungsto-phosphates possessing cation-exchanging properties and a proton conductivity up to 10^{-2} S cm^{-1} form larger particles.[57] Ice doped with strong acids can be regarded as a system of this kind with a minimal core of particles (these are anions).

Hydrated acid zirconium phosphate is one of the best known proton conductors. Depending on the degree of crystallinity and atmospheric humidity, its electrical conductivity varies over five orders of magnitude, which indicates that the intercrystallite component plays the major role. The mobility of surface protons is four orders of magnitude higher than that of the bulk-phase protons.[58,59] The replacement of the OH groups by the $-C_xH_ySO_3H$ or $-C_xH_yCOOH$ fragments, or the sorption of bulky amines on some of them, significantly increases the interplanar distance in lamellar phosphates such as $Zr(HPO_4)_2 . nH_2O$. In the opinion of some authors,[60-64] this might lead to the properties of the surface being acquired by almost the whole material. Unfortunately, this idea has not found practical confirmation. The maximum electrical conductivity of such compounds, which reaches 10^{-2} S cm^{-1} at room temperature and 90% humidity, is apparently also due to the surface component.[60-64] Furthermore, the authors postulated that proton transfer in compounds containing acid groups at the end of a flexible hydrocarbon moiety ($-C_xH_{2x}COOH$) can occur when the latter come closest together during their vibrations.

V. Some features of solid proton-containing electrolytes

Undoubtedly the presence and magnitude of proton conductivity in a compound depend primarily on its structural features. For example, the existence of a continuous network of hydrogen bonds, or the possibility of one being formed due to the rotation of hydrogen-containing groups, is a prerequisite. Furthermore, as shown above and by Potier,[39] the hydrogen bonds should have an optimum length, etc.

Despite these requirements, one can outline fairly confidently the range of hydrates and acid salts among which materials with a high proton conductivity should be sought at comparatively low temperatures. It is convenient to use the classification proposed by us,[65] based on the proton-accepting capacity of the acid residue and its spatial structure in the compound. For example, both the formation of carriers and their transfer are hindered in the salts of weak acids (class I, $pK_a > 3$).

The class II compounds ($-3 \leqslant pK_a \leqslant 3$) are much more suitable for this purpose, since the proton transfer from the anion to water molecules and vice versa occurs comparatively easily. The behaviour of the class IIa compounds (where the proton is localised on the oxygen atom of the anion in the ground state) is often restricted by the low degree of hydration. Therefore, these compounds usually exhibit a high electrical conductivity only in a finely dispersed state [$Zr(HPO_4)_2 . nH_2O$]. In the class IIc compounds with isolated anions, the latter form fairly strong hydrogen bonds with the hydrated proton, which significantly restricts its mobility. The class IIb compounds with a bulky anion forming skeletal structures are good proton electrolytes. The majority of these compounds have layered structures ($MH(SO_4)_2 . nH_2O$, $MH(PO_4)_2 . nH_2O$, $UO_2HPO_4 . 4H_2O$).

The hydrates of strong acids ($pK_a < -3$) tend to form hydrogen bonds between the H_3O^+ or $H_5O_2^+$ ions and water molecules and hence to exhibit a high degree of hydration.[65] Consequently, despite some hindrance to proton transfer from the proton-hydrate sublattice to the anion (which, incidentally occurs comparatively easily, for example, in oxonium perchlorate), proton transfer by the Grotthus mechanism is most probable in this case ($H_3PW_{12}O_{40} . nH_2O$). This is why compounds possessing the maximum proton conductivity have been found among these compounds. The search for proton-conducting electrolytes among highly hydrated class III compounds is especially advisable. However, their tendency to change their hydrate composition (dehydration in air or absorption of moisture) can be a limiting factor in their employment.[65]

References

1. S Kamasaki *Mem. Fac. Technol., Tokio Metrop. Univ.* **35** 3621 (1985)
2. A Sawata, K Tsuneyoshi, J Mizuscki *Solid State Ionics* **40–41** 415 (1990)
3. M Iwahara, T Esaka, H Uchida, T Yamauchi, K Ogaki *Solid State Ionics* **18–19** 1003 (1985)
4. H Kawase, S Ito, S Nariki, N Koura, N Yoneda *Solid State Ionics* **40–41** 448 (1990)
5. N Miura, K Kanamaru, Y Shimizu, N Yamazoe *Solid State Ionics* **40–41** 452 (1990)
6. C G Vagenas, S Bebelis, I V Yenetekakis, P Isiakaras, H Karasali, C Karavasilis *ISSI Lett.* **2** (2) 5 (1991)
7. K Tanabe *Catalysts and Catalytic Processes* (Translated into Russian; Moscow: Mir, 1993) p. 455
8. M Akimoto, M Okamoto, H Niiyamo *Chem. Lett. Jpn.* 501 (1985)
9. O Nakamura, J Kodama, I Ogino, J Miyakeet *Chem. Lett.* 17 (1979)
10. L O Atovmyan, L I Erofeev, A I Korosteleva, L S Leonova, V P Tarasov, E A Ukshe, V G Shteinberg *Khim. Fiz.* **3** 1518 (1984)
11. A T Howe, M G Shilton *J. Solid State Chem.* **34** 149 (1980)
12. A B Yaroslavtsev, E K Chernova, Z N Prozorovskaya, V F Chuvaev *Elektrokhimiya* **26** 1456 (1990)
13. E A Ukshe, L S Leonova, A M Mikhailova *Elektrokhimiya* **24** 110 (1988)
14. N Kuriyama, T Sakay, H Miyamura, G Mariotto *Solid State Ionics* **40–41** 906 (1990)
15. G Alberti *Inorganic Ion Exchange Membranes* **7** 1 (1976)
16. A B Yaroslavtsev, Z N Prozorovskaya, V F Chuvaev, V I Spitsyn *Dokl. Akad. Nauk SSSR* **301** 153 (1988)
17. A B Yaroslavtsev, Z N Prozorovskaya, V F Chuvaev *Zh. Neorg. Khim.* **35** 1100 (1990)
18. A P Martsenyuk-Kukharuk, Candidate's Thesis in Chemical Sciences, Kiev, 1988; V V Pototskaya, T A Karaseva, A P Martsenyuk-Kukharuk *Teor. Eksp. Khim.* **24** 111 (1988)
19. N G Khainovskii, E F Khairetdinov *Izv. Sib. Otd. Akad. Nauk SSSR, Ser. Khim. Nauk* 84 (1986)
20. S Chandra, N Singh, A Hashmi *Proc. Indian Acad. Sci., Sect. A* **52** 338 (1986)
21. A B Yaroslavtsev, E M Yaroslavtseva, V F Chuvaev *Zh. Neorg. Khim.* **35** 2769 (1990)
22. E A Ukshe, L S Leonova, L O Atovmyan, A I Korosteleva, L I Erofeev, V P Tarasov, V G Shteinberg *Dokl. Akad. Nauk SSSR* **285** 1157 (1985)
23. T A Karaseva, T M Lityuga, A V Gorodynskii *Dokl. Akad. Nauk SSSR* **265** 123 (1982)
24. E Skou, I G Krogh Andersen, E Krogh Andersen, M Casciola, F Guerrini *Solid State Ionics* **35** 59 (1989)
25. E Skou, R Palombari, F Guerrini, M Casciola *Solid State Ionics* **46** 129 (1991)
26. M Casciola, R Palombari *Solid State Ionics* **47** 155 (1991)
27. A B Yaroslavtsev, Z N Prozorovskaya, V F Chuvaev *Zh. Neorg. Khim.* **35** 1379 (1990)
28. K D Kreuer, W Weppner, A Rabenau *Mat. Res. Bull.* **17** 501 (1982)
29. A T Home, M G Shilton *J. Solid State Chem.* **34** 149 (1980)
30. K D Kreuer *J. Mol. Struct.* **177** 265 (1988)
31. L V Kobets, V L Filimonov *Izv. Akad. Nauk SSSR, Neorg. Mater.* **24** 1327 (1988)
32. S B Luksyanis, G E Boyars, K S Pitre, A R Luske, R A Vaitkus, A S Orlyukas, R A Mizeris *Litov. Fiz. Sb.* **28** 257 (1988)
33. J M Janik, M Rashawalsku, J A Janic *Physics* **72** 168 (1974)
34. A B Yaroslavtsev *Zh. Neorg. Khim.* **39** 585 (1994)
35. N J Clyden *Solid State Ionics* **29** 117 (1987)
36. R Haser, C Pennel, M Pierrot *Acta Crystallogr., Sect. B* **28** 2548 (1972)
37. A B Yaroslavtsev, Z N Prozorovskaya, V F Chuvaev *Zh. Neorg. Khim.* **33** 1144 (1988)
38. A Potier, D Rousselet *J. Chim. Phys., Phys.-Chim. Biol.* **70** 873 (1973)
39. A Potier *Optica Pura Apl.* **21** 7 (1988)
40. M A Herzog-Cance, G Potier, A Potier *Adv. Mol. Relax. Interact. Process.* **14** 245 (1979)
41. F S Lee, G B Carpenter *J. Phys. Chem.* **63** 279 (1959)
42. D Mootz, A Merschenz-Quarck *Z. Naturforsch. B, Chem. Sci.* **42** 1231 (1987)
43. A B Yaroslavtsev, V F Chuvaev, Z N Prozorovskaya, E M Yaroslavtseva *Zh. Neorg. Khim.* **28** 2979 (1983)
44. Ph Colomban, J C Badot *Solid State Ionics* **61** 55 (1993)
45. R Mourer *Suche nach Schneller Proton Bewegung in Mineralsäuren: eine Kernresonanzstudie* Vorgelegte Dissertation, Berlin, 1986
46. Y F Zaretskii, V A Petrenko, V A Chesnakov *Phys. Status Solidi A* **109** 373 (1988)
47. M L Huggins *J. Phys. Chem.* **40** 723 (1936)
48. E G Weidemann, G Zundel *Z. Naturforsch. A, Phys. Sci.* **25** 627 (1970)
49. J Esquivel, J F Mota-Segreda *Int. J. Quantum Chem.* **38** 522 (1990)
50. M Catti, C M Mari, E Cazzanelli, G Mariotto *Solid State Ionics* **40–41** 900 (1990)
51. C M Mari, F Bonino, M Catti, R Pasinetti, S Pizzini *Solid State Ionics* **18–19** 1013 (1986)
52. J Gallier, B Toudic, M Stahn, R E Lechner, H Dachs *J. Phys. (Paris)* **49** 949 (1988)
53. H Jacobs, A Schardey *Z. Anorg. Allg. Chem.* **565** 34 (1988)
54. A Clearfield *Chem. Rev.* 125 (1988)
55. A V Erin, Z N Prozorovskaya, A B Yaroslavtsev *Zh. Neorg. Khim.* **38** 200 (1993)

56. Z N Prozorovskaya, V V Parshutkin, A B Yaroslavtsev, A I Mun *Zh. Neorg. Khim.* **30** 67 (1985)
57. A B Yaroslavtsev, V F Chuvaev, E M Yaroslavtseva *Zh. Neorg. Khim.* **39** 955 (1994)
58. M Casciola, D Bianchi *Solid State Ionics* **17** 287 (1985)
59. V Sadaoka, M Matsugushi, V Sakai, S Mitsui *J. Mater. Sci.* **23** 2666 (1988)
60. G Alberti, U Costantino, M Casciola, R Vivani, A Peraio *Solid State Ionics* **46** 61 (1991)
61. G Alberti, U Costantino, M Casciola, A Peraio, E Montoneri *Solid State Ionics* **50** 315 (1992)
62. G Alberti, M Casciola, R Palombari, A Peraio *Solid State Ionics* **58** 339 (1992)
63. M Casciola, S Chieli, U Costantino, A Peraio *Solid State Ionics* **46** 53 (1991)
64. M Casciola, U Costantino, A Colevi, A Peraio *Solid State Ionics* **61** 245 (1993)
65. A B Yaroslavtsev, Z N Prozorovskaya, V F Chuvaev *Zh. Neorg. Khim.* **35** 1645 (1990)

Russian Chemical Reviews **63**(5) 437–447 (1994)
©1994 Russian Academy of Sciences and Turpion Ltd

UDC 547.73; 547.732; 542.971.3; 542.97; 547.53

Catalytic methods of synthesis of thiophenes from hydrocarbons and hydrogen sulfide

M A Ryashentseva

Contents

I.	Introduction	437
II.	Interaction of acetylene with hydrogen sulfide	437
III.	Interaction of C_4 hydrocarbons with hydrogen sulfide	438
IV.	Interaction of C_5 hydrocarbons with hydrogen sulfide	440
V.	The mechanism of the formation of thiophenes from C_4-C_5 hydrocarbons and hydrogen sulfide	441
VI.	Interaction of C_6-C_8 hydrocarbons with hydrogen sulfide	441
VII.	Physicochemical properties of chromium-containing oxide catalysts	443
VIII.	Industrial methods of synthesis of thiophenes	446

Abstract. The synthesis of thiophene and alkylthiophenes by the reaction of acetylene, C_4-C_8 alkanes, and C_4-C_6 alkenes and alkadienes with hydrogen sulfide in the presence of metal oxides and sulfides as well as their mixtures is examined. The conditions for the testing of catalysts in flow type apparatus in stationary and fluidised catalyst beds are presented. The calculated equilibrium yields of thiophenes from C_4-C_6 hydrocarbons and hydrogen sulfide are compared with experimental data. Together with the heterocyclisation reaction, the interaction of C_6-C_8 hydrocarbons with hydrogen sulfide involves dehydrocyclisation with formation of aromatic hydrocarbons. The mechanism of the interaction of C_4-C_5 hydrocarbons with hydrogen sulfide, investigated by the isotope-kinetic method, is discussed. Certain physicochemical properties of active chromium-containing oxide heterocyclisation catalysts and industrial methods of synthesis of thiophene are described. The bibliography includes 63 references.

I. Introduction

During the 1960s, information concerning the selection of effective catalysts for the synthesis of thiophene and alkylthiophenes by the heterocyclisation reaction was available, with some exceptions, only in the patent literature. Transition metal oxides and sulfides were used as the catalysts.

A review of catalytic methods of synthesis of thiophene and alkylthiophenes from petroleum processing products and organic sulfur-containing compounds was published in 1971.[1] Analysis of the review data leads to the conclusion that it is most useful to obtain thiophenes from readily available starting materials — hydrocarbons and hydrogen sulfide. The selection of an effective catalyst capable of being regenerated would make such a process promising. The use of sulfur-containing organic compounds is difficult in practice because dialkyl sulfides, mercaptans, and thiophane are not yet produced on an industrial scale.

M A Ryashentseva Laboratory for Catalysis by Rare and Dispersed Elements, Zelinskii Institute of Organic Chemistry, Russian Academy of Sciences, Leninskii prosp. 47, 117913 Moscow, Russian Federation. Fax (7-095) 135 53 28. Tel (7-095) 137 65 18.

Received 29 March 1994
Uspekhi Khimii **63** (5) 456–466 (1994); translated by A K Grzybowski

By virtue of their high reactivity, thiophene and its homologues are a potential starting material for the synthesis of a wide variety of both aliphatic and alicyclic compounds. Methods of synthesis of certain polyorganosiloxanes, herbicides, physiologically active substances, and perfumes from thiophene have been developed. The successful development of thiophene chemistry, especially during the last ten years, has made it possible to develop a series of valuable medicinal preparations, including antibiotics. Like benzene, thiophene is known to possess biological activity but it is less toxic. Compounds containing thiophene and its derivatives can be used in the treatment of diseases of the central nervous system and also as anti-inflammatory, cardiovascular, antihistamine, and other agents.

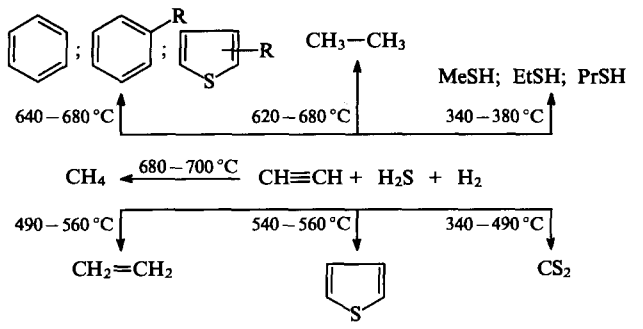
The literature data on thiophene and its derivatives published up to 1982 have been surveyed in a monograph[2] which was published in 1985. The methods of synthesis of thiophene by a cyclisation reaction and from other cyclic systems are described in the monograph and the pharmacological activity of thiophene and its derivatives have also been considered.[3,4]

II. Interaction of acetylene with hydrogen sulfide

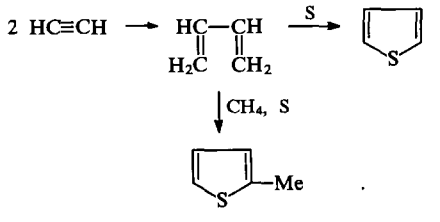
Thiophene was first obtained from acetylene and hydrogen sulfide by Chichibabin in 1915.[5] The reaction was carried out in the presence of aluminium oxide at 425–450 °C. The studies on the catalytic synthesis of thiophene from hydrogen sulfide and acetylene up to 1952 have been surveyed in a monograph.[6]

Interesting results have been obtained[7,8] in experiments on γ-Al_2O_3 in the study of the interaction of hydrogen sulfide and an acetylene-containing gas from the electrocracking of petroleum products, the gas having the following composition (vol.%): 29.0 C_2H_2, 7.8 C_2H_4, 0.6 C_2H_6, 5.6 CH_4, and 57.0 H_2. The yield of thiophene proved to be higher than in the case where pure acetylene was used and amounted to 50%–52% relative to the acetylene passed through the system instead of 38%. The high activity at γ-Al_2O_3 is probably associated with the presence of hydrogen in the initial mixture, which promotes hydrogenation and the removal of carbonaceous deposits — the condensation products on the surface of alumina.

Depending on the temperature, the following products are obtained in the interaction of the acetylene-containing electrocracking gas with hydrogen sulfide on γ-Al_2O_3:



The introduction of transition metal (Cr, La) oxides as well as K_2O intensifies the hydrogenating function of the catalyst — the yield of ethylene and ethane increases by a factor of 1.5, but the yield of thiophene does not increase. These data, as well as the results of experiments in which a mixture of 30% of ethylene with H_2S was used, show that thiophene is not formed via hydrogenation products. It is most likely that the formation of thiophenes and alkylthiophenes involves the intermediate formation of dimerisation and alkylation products in accordance with the mechanism[9]



The yield of thiophene on γ-Al_2O_3 did not change with increase in the rate of supply of acetylene.[10] The size of the catalyst grains also did not affect the yield of thiophene. The concentration of the helium-diluted hydrogen sulfide was varied from 0 to 87.5 mass% at an acetylene concentration of 12.5 mass%. The activation energy for the synthesis of thiophene from hydrogen sulfide and acetylene at 300–400 °C was 153 kJ mol^{-1}.[10] The reaction is influenced by the surface acidity of γ-Al_2O_3. The presence on the catalyst surface of weak acid centres, probably electron-accepting, is necessary for the formation of thiophene. Strong proton centres promote appreciable coke formation, which results in a rapid loss of activity by the catalyst.[11]

In the search for a possible increase in the activity of γ-Al_2O_3 in the temperature range 350–450 °C, a study was made of the influence of La, Ti, V, Cr, Mn, Fe, Co, Ni, Cu, and Zn oxides.[12] Catalysts containing 0.5–2.5 mass% of Cr, Co, and Ni oxides showed the highest activity. In terms of their activity in the formation of thiophene from acetylene and hydrogen sulfide, the catalysts can be arranged in the sequence Cr_2O_3, Al_2O_3 > Co_3O_4, Al_2O_3 > NiO, Al_2O_3 > Al_2O_3. An increase in the content of the additives leads to an increase in the rate of formation of side products, in particular of the condensation of acetylene. The introduction of promoting oxides increases the activity of γ-Al_2O_3 in reactions involving the elimination of hydrogen from ethanethiol and the redistribution of hydrogen, the catalyst with added Cr_2O_3 showing the highest activity.

The dependence of the activity of a two-component catalyst on the structure of the *d* electron shell of the constituent ions has two peaks.[12] The Al, Cr and Al, Co catalysts show the maximum activity, their ions having the d^3, d^6, and d^7 electronic configurations. The introduction of ions with the d^8, d^9, and d^{10} electron shells probably hinders the activation of hydrogen sulfide molecules, which do not tend to form a dative bond, and enhances the activation of acetylene molecules, which increases the rate of formation of high-molecular-mass products on the catalyst surface. The low activity of the catalyst containing Ti^{4+} and Fe^{3+} has been explained[12] in terms of the zero stabilisation energy of ions with d^0 and d^5 configurations.

When the acetylene–hydrogen mixture containing 30 vol.% of acetylene was used (490–500 °C, space velocity v_{sp} = 300 to 320 h^{-1} with respect to acetylene, and H_2S : C_2H_2 = 1), thiophene was obtained on γ-Al_2O_3 in 16.4% yield.[13] The introduction of chromium oxide into aluminium oxide increased the rate of heterocyclisation: the yield of thiophene increased by a factor of 1.6. At the same time, the content of acetylene rose by a factor of 10 and that of ethane by a factor of 2. Under these conditions, the amount of coke diminished by a factor of 2. The dimerising effect of the aluminium oxide–chromium oxide catalyst was manifested by an increase in the yield of C_4 hydrocarbons by a factor of almost 2. The addition of lanthanum and potassium oxides to the aluminium oxide–chromium oxide catalyst increased the hydrogenating activity and diminished coke formation. The highest yield (26.3%) of thiophene from the acetylene–hydrogen mixture was obtained in the presence of the 5% Cr_2O_3–95% γ-Al_2O_3 catalyst.[13]

III. Interaction of C_4 hydrocarbons with hydrogen sulfide

Thiophene has been obtained mainly from C_4 olefins and hydrogen sulfide over various catalysts containing chromium or molybdenum oxides on aluminium oxide, bauxite, or silica gel.[1] The reaction is slightly endothermic and can be carried out in a flow system. However, the catalyst requires periodic regeneration with air. Since this entails a large exothermic effect and an increase in temperature, it is more convenient to employ a catalyst in a fluidised bed. This diminishes the temperature rise during regeneration.

Thiophene has been obtained in a high yield from hydrogen sulfide and n-C_4 hydrocarbons.[14] The yield of thiophene from butenes is higher than from n-butane. Thus the yields of thiophene were 31.2%, 52.9%, and 55.4% from butane, but-1-ene, and but-2-ene respectively in the presence of the 5% SiO_2–10% MoO_3–85% Al_2O_3 catalyst (590 °C, H_2S : hydrocarbon = 1.6:1.8, v_{sp} = 1.5–1.7 h^{-1}).

An effective aluminium oxide–chromium oxide catalyst with oxide additives was selected for the reaction of butane, butene, or butadiene with hydrogen sulfide.[16] It was shown[15,16] that the γ-Al_2O_3 carrier exhibits mainly a cracking activity and a weak heterocyclising activity, whereas chromium oxide exhibits dehydrogenating, hydrogenating, heterocyclising, and cracking properties. The following reactions take place on the aluminium oxide–chromium oxide catalyst when butane interacts with hydrogen sulfide: heterocyclisation with formation of thiophene, dehydrogenation with formation of alkenes and alkadienes, cracking with formation of C_1–C_3 hydrocarbons, and coke formation. By introducing the lanthanum oxide[15] and potassium oxide[16] additives into the aluminium oxide–chromium oxide catalyst, it is possible to increase its heterocyclising and dehydrogenating activities and to weaken its cracking and coke forming functions. Potassium oxide also increases the stability of the catalyst. By selecting the concentrations of the components, the optimum composition of the polyfunctional catalyst (mass%) was found: 5 Cr_2O_3, 5 La_2O_3, 1 K_2O, and 89 γ-Al_2O_3.[16] The introduction of lanthanum and potassium oxides into the aluminium oxide–chromium oxide catalyst increased the yield of thiophene by a factor of 1.4–1.75 and diminished the formation of C_1–C_3 hydrocarbons by a factor of 1.2–1.5 and the deposition of coke by a factor of 1.5–2.8 (Table 1).

It has been shown that the heterocyclisation, dehydrogenation, and cracking reactions proceed on the same catalyst active centres. The cracking functions can be suppressed to a slight extent by introducing alkaline additives.[17] Under optimum conditions in the interaction of C_4 hydrocarbons with hydrogen sulfide in the presence of the catalyst comprising chromium, lanthanum, potassium, and aluminium oxides, thiophene was formed in

Table 1. The interaction of hydrogen sulfide with C_4 hydrocarbons in the presence of chromium-containing catalysts (according to the data of Ryashentseva et al.[18]).

Initial hydrocarbon	Catalyst mass%	T/°C	Yield relative to C_4 passed through system (%)				
			of thiophene (rel to theoretical)	C_1-C_3	C_4H_8	C_4H_{10}	coke
Butane	5 Cr_2O_3, 95 Al_2O_3	580	12.5	45.7	8.3	–	3.3
	5 Cr_2O_3, 5 La_2O_3, 1 K_2O, 89 Al_2O_3	580	21.8	39.7	11.0	–	1.3
But-1-ene	5 Cr_2O_3, 95 Al_2O_3	500	21.7	31.2	–	6.0	6.5
	5 Cr_2O_3, 5 La_2O_3, 1 K_2O, 89 Al_2O_3	500	37.9	20.4	–	8.0	2.3
Butadiene	5 Cr_2O_3, 95 Al_2O_3	500	21.9	13.9	27.1	9.2	6.4
	5 Cr_2O_3, 5 La_2O_3, 1 K_2O, 89 Al_2O_3	500	30.6	9.2	27.1	8.9	4.2

40%–55% yield relative to the hydrocarbon passed through the system. Under conditions where this catalyst was used continuously, the yield of thiophene from butane and hydrogen sulfide fell from 37%–40% in the first 2–3 h to 23% in the next 7 h. The conditions for the regeneration of the catalyst after its use for 1, 2, and 3 h were found; the regeneration time is equal to the contact time.[17,18]

Thermodynamic calculations for the reactions involving the formation of thiophene from n-butane, but-1-ene, *cis*- and *trans*-but-2-enes, buta-1,3-diene, and hydrogen sulfide, taking into account the extent of side reactions,[19] made it possible to determine the equilibrium constants for these reactions in the temperature range 300–1000 K and also to calculate the equilibrium yields of thiophene for the stoichiometric and excess amounts of hydrogen sulfide relative to the hydrocarbon at 700–900 K. In order to compare the experimental and calculated equilibrium yields of thiophene in the presence of the Cr, La, K, Al catalyst, experiments were performed with [the determination] of the material balance of the products of the interaction of C_4 hydrocarbons and hydrogen sulfide. The experimental yields of thiophene obtained by the reaction of butane, but-1-ene, and buta-1,3-diene with hydrogen sulfide were 60%, 70%, and 90% respectively relative to the calculated equilibrium yield (taking into account side reactions).[19]

Certain data concerning the synthesis of thiophene from alkenes and alkadienes have been published in Japanese patents.[20,21] In the presence of the 12 Cr_2O_3–5 K_2O–83 Al_2O_3 catalyst (compositions in mass%) at 500 °C and for a contact time of 8.8 s, 26% of thiophene was formed from but-1-ene and hydrogen sulfide in the presence of nitrogen (molar ratios 1 : 2 : 4).[20] In the presence of the V_2O_5–Al_2O_3 catalyst at 410 °C, 49.7% of thiophene was obtained from buta-1,3-diene and hydrogen sulfide.[21]

The interaction of hydrogen sulfide with a butane–butene fraction (BBF) having the composition (mass%) 0.9 C_2-C_3, 11.3 iso-C_4H_8, 22.9 n-C_4H_8, 40.5 iso-C_4H_{10}, 23.2 n-C_4H_{10}, and 1.2 C_5 hydrocarbons has been investigated.[22] The reaction was carried out in a reactor with a vibrofluidised bed of a catalyst comprising Cr, La, K, and Al oxides (Cr, La, K, Al catalyst) at temperatures in the range 400–600 °C, with v_{sp} = 100–700 h^{-1}, and for the component ratio H_2S : BBF = (0.5–5.0) : 1. The yield of thiophene was higher than in the reactor with a stationary catalyst bed. The use of a gradient-free reactor with forced fluidisation facilitates the measurement of the rate of reaction in the initial instants of the employment of the catalyst, which is particularly important when catalysts with a variable activity are used.[22]

The synthesis of thiophene in the presence of a catalyst in which lanthanum oxide has been replaced by a mixture of lanthanide oxides may be of interest from the practical point of view. In the presence of the catalyst having the composition (mass%) 5 Cr_2O_3, 1 K_2O, 5 Ln (2.7 CeO_2, 1.3 La_2O_3, 0.75 Nd_2O_3, and 0.25 Pr_6O_{11}), and 89 Al_2O_3, the interaction of hydrogen sulfide with BBF was investigated and it was shown that the effectiveness of the reaction in a vibrofluidised bed is higher than in a stationary bed.[23,24] The corresponding data are presented in Table 2.

Table 2. The interaction of hydrogen sulfide with the butane–butene fraction (BBF) over the Cr, Ln, K, Al catalyst (according to the data of Abramovich et al.[24]).

T/°C	v_{sp}/h^{-1}	H_2S : BBF (mol.%)	Yield of thiophene[a] relative to			
			n-butane		BBF	
			A	B	A	B
520	200	1.4	–	41.6	32.5	55.4
545	243	2.2	27.7[b]	75.0	–	–
562	128	1.7	–	84.1	44.8	71.7
565	123	2.7	–	88.1	–	–
580	153	2.7	66.8	–	46.2	76.8
595	216	2.2	49.7[b]	91.2	57.7	89.1
610	152	1.7	38.0	–	46.2	76.8
614	145	3.0	–	83.7	–	–

[a] A—in a stationary bed, B—in a vibrofluidised bed.
[b] For v_{sp} = 229 h^{-1}.

The best yield of thiophene (66.8% relative to the hydrocarbon passed through the system) in a stationary catalyst bed was achieved at 580 °C for v_{sp} = 153 h^{-1} and H_2S : BBF = 2.7. The yield of thiophene falls with increase in temperature. In a reactor with a vibrofluidised bed under similar conditions (595 °C, v_{sp} = 216–228 h^{-1}, H_2S : BBF = 2–2.2), the yield of thiophene reached 91.2% relative to n-butane passed through the system or 89.1% relative to BBF. Above 600 °C, the yield of thiophene in both stationary and vibrofluidised beds diminishes, which is apparently associated with the decomposition of the initial hydrocarbon. Gradient-free conditions with respect to temperature are achieved in a reactor with a vibrofluidised bed; the reaction takes place under isothermal conditions, where a higher equilibrium degree of conversion and lower equilibrium concentrations of the initial hydrocarbons than under adiabatic conditions are attained.[24]

The influence of modifying additives on the heterocyclising activity of the aluminium oxide–chromium oxide catalyst has been investigated in the reaction of BBF with hydrogen sulfide. Li, K, Rb, Cs, Sr, Cd, Be, Se, Ti, and Mo oxides were used as additives.[25] The content of butane and butene in the industrial BBF was 40%–50%. The reaction was carried out at 570–590 °C, at a space velocity of 100–500 h^{-1}, for a molar ratio H_2S : BBF = (1.5–3.0) : 1, and with a duration of the experiment of 60 min. The replacement of potassium oxide by lithium, rubidium and caesium oxides proved ineffective: the yield

of thiophene was appreciably lower than in the presence of the Cr, K, Al catalyst. The yield of thiophene relative to the n-C_4 hydrocarbon passed through the system in the presence of the Cr, K, Al catalyst promoted with selenium dioxide was 85.4%. Among lanthanide oxides, those of scandium, praseodymium, and gadolinium as well as that of indium proved to be the most effective promoting agents. Catalysts with added samarium and cerium oxides are of special interest, the yield of thiophene in the presence of the latter attaining 85%–90%. In order to carry out the reaction in a fluidised catalyst bed, the mechanically strong γ-Al_2O_3 in the form of spherical pellets was employed. In the presence of the catalysts (the compositions are in mass%), $15.5\,Cr_2O_3-1.9\,K_2O-4.5\,In_2O_3-78.1\,\gamma$-$Al_2O_3$ and $14.8\,Cr_2O_3-2.0\,K_2O-4.9\,Sm_2O_3-78.3\,Al_2O_3$, the yields of thiophene (relative to the n-C_4 hydrocarbon passed through the system) were 71.6% and 66.0% respectively. However, the activity of these catalysts was not higher than that of the Cr, K, Ln, Al catalyst.[24]

When a zeolite was used as a carrier, the chromium catalysts had a low activity in the reaction of BBF with H_2S.[25] Catalysts based on type A zeolites in both the sodium- and calcium-forms proved to be completely inactive. The low activity of the chromium oxide–zeolite catalyst can be accounted for by the discrepancy between the dimensions of the window-channels and the dimensions of the molecules of the initial compounds and products.

Thiophene has also been obtained on sulfide catalysts. The properties of the aluminorhenium sulfide [aluminium sulfide–rhenium sulfide?] catalysts have been investigated in relation to the reaction of n-butane with hydrogen sulfide.[26] Rhenium sulfide Re_2S_7 has a high catalytic activity, for example in the hydrogenation of sulfur- and nitrogen-containing heterocyclic compounds.[27] In contrast to the chromium-containing Cr, La, K, Al and Cr, Ln, K, Al catalysts, carbon disulfide (12%) was obtained together with thiophene (14%) in the presence of a H_2S-treated catalyst comprising 11% Re and 89% γ-Al_2O_3 [580 °C, $v_{sp} = 250\ h^{-1}$, H_2S : n-C_4 = (3–5) : 1]. The formation of carbon disulfide can be explained by the interaction of sulfur with the carbon produced as a result of the cracking of the hydrocarbons on the catalyst. The source of sulfur may be both the surface of the sulfided catalyst and the decomposition of hydrogen sulfide under the catalytic conditions. This is confirmed by the increase to 24% of the yield of carbon disulfide with increase in the molar ratio of H_2S and n-butane to 9. The yield of thiophene also increases under these conditions (to 21%). These data indicate indirectly the formation of thiophene and carbon disulfide on the same catalyst active centres.

A multistage mechanism has been proposed for the formation of thiophene from butadiene and hydrogen sulfide in the presence of sulfide catalysts.[28] It is postulated that butadiene interacts with the surface sulfur in the slow stage. This is followed by the resulfidation of the catalyst by the sulfur from the reaction medium and the restoration of the stationary composition of the surface. Sulfided Cr and Mo oxides as well as Re_2S_7 were used as the catalyst. The activity of the catalyst was determined by a pulse method at 400–500 °C for a contact time of 1.2–3 s using helium as the diluent gas. It was postulated that the surface becomes coated with sulfur as a result of the treatment of the catalyst with hydrogen sulfide before the start of the experiment. The resulfidation stage is not rate-limiting, the removal of sulfur from the surface by butadiene with formation of thiophene occurring most slowly. The most active catalysts contain sulfur weakly bound to the surface.[28]

IV. Interaction of C_5 hydrocarbons with hydrogen sulfide

There exist patent data concerning the synthesis of alkylthiophenes by the reaction of C_5 alkadienes with hydrogen sulfide in the presence of aluminium oxide–chromium oxide catalysts.[5] Various multicomponent catalysts have been compared in the synthesis of 2-methylthiophene by the reaction of piperylene with hydrogen sulfide.[29] Under optimum conditions [480–500 °C, $v_{sp} = 0.5-0.7\ h^{-1}$, $H_2S:C_5 = (2-4):1$], the yield of 2-methylthiophene in the presence of the Cr, K, Al catalyst was 35 to 40 mass%. The catalyst was regenerated with a 1 : 1 air–nitrogen mixture in order to remove coke, after which it was exposed to a stream of hydrogen.[30] The catalytic activity increases with increase in the temperature of the preliminary treatment of the catalyst with hydrogen up to 600 °C and at a space velocity up to 200 h^{-1}. The effect obtained has been explained by the enhancement of the desorption of water formed as a result of the reduction of Cr^{6+} by hydrogen.[31]

Preliminary treatment of the Cr, K, Al catalyst with hydrogen sulfide increases its activity and selectivity as a consequence of the interaction of sulfur with the surface.[32] In order to elucidate the nature of the bond between sulfur and the catalyst [Cat(S)], the latter was treated with hydrogen sulfide for 5–90 min at 200–500 °C and a space velocity of 600–700 h^{-1}. The influence of this treatment on the activity of the catalyst was estimated from the yield of 2-methylthiophene from H_2S and piperylene at 500 °C, $v_{sp} = 2.7\ h^{-1}$, and $H_2S:C_5 = 2.1-2.2$.[33] The kinetic model of the process can be described by the equations presented in Scheme 1.

Scheme 1

$$H_2S \rightleftharpoons H_2 + S \quad (1)$$

$$Cat(S)S + C_5H_8 \longrightarrow C_5H_6S + H_2 + CatS \quad (2)$$

$$C_5H_8 \longrightarrow \text{coke} \quad (3)$$

$$C_5H_6S \longrightarrow \text{coke} \quad (4)$$

$$C_5H_8 \longrightarrow \text{gas} \quad (5)$$

Hydrogen sulfide dissociates in the first stage at a temperature above 400 °C. This is confirmed by the fact that treatment of the catalyst surface with hydrogen sulfide at lower temperatures does not increase the activity of the catalyst. Thiophene is formed mainly as a result of the interaction of piperylene with the sulfur chemisorbed on the sulfided catalyst.[33]

In the presence of an effective catalyst having the composition (mass%)[34] 18 Cr_2O_3, 4 K_2O, and 78 Al_2O_3 under optimum conditions [470–500 °C, $v_{sp} = 0.5-0.7\ h^{-1}$, $H_2S:C_5 = (2-1):1$], 2-methylthiophene was obtained from hydrogen sulfide and piperylene in 62% yield, while 3-methylthiophene was obtained from 2-methylbut-2-ene and hydrogen sulfide in 75% yield.[29–33] 3-Methylthiophene was obtained in 53% yield from isoprene and hydrogen sulfide at 500 °C and a gas flow rate $v_{mass} = 0.34\ h^{-1}$ [$H_2S:C_5 = (4-5):1$] in the presence of a catalyst having the composition (mass%) 5 Cr_2O_3, 5 La_2O_3, 1 K_2O, and 89 Al_2O_3.[16] 2-Methylthiophene was obtained in 43.2% yield from piperylene and hydrogen sulfide under the same conditions.[17] It has been stated that aluminium oxide (77.5 mass%–78.5 mass%) with a specific surface of 150 to 170 $m^2\ g^{-1}$ is used to increase the activity and mechanical strength of the catalyst the composition of which includes Cr_2O_3 (14.5 mass%–15.5 mass%), K_2O (2 mass%–2.5 mass%), and lanthanides (4.5 mass%–5 mass%).[35]

The principal disadvantage of the synthesis of 2-methylthiophene from piperylene and hydrogen sulfide is the comparatively short operating lifetime of chromium-containing catalysts. For example, the catalysts (compositions in mass%) $18\,Cr_2O_3-4\,K_2O-78\,Al_2O_3$ (Cr, K, Al) and $5\,Cr_2O_3-1\,K_2O-5\,La_2O_3-89\,Al_2O_3$ (Cr, K, La, Al) have a high initial activity: the yields of 2-methylthiophene in their presence are respectively 60 mass% and 40 mass% relative to the piperylene passed through the system.[36] However, after they have been used for only 3–4 h, their activity begins to fall and after 6–7 h the yields diminish to 12 mass% and 22 mass% respectively. The less marked decrease in the activity of the Cr, K, La, Al catalyst is apparently associated with the presence of lanthanum oxide in

the latter. The experiments were performed at 500 °C, v_{sp} = 0.3 to 0.5 h^{-1}, and $H_2S:C_5$ = (2–4):1. These catalysts have a running-in period of 1.5–2 h. Their activity is fully restored after regeneration with an air–nitrogen mixture containing 10 vol.%–11 vol.% of oxygen at 550–580 °C for 5–7 h. After 8–10 regeneration cycles, the activity of the catalyst diminishes somewhat and then stabilises. Preliminary treatment of the catalyst with hydrogen makes it possible to increase its operating lifetime to 150 cycles at a constant activity and to increase the yield of 2-methylthiophene by a factor of 1.5–2 (35%–50%).[36]

The formation of thiophenes from diene hydrocarbons (butadiene, isoprene, and piperylene) and hydrogen sulfide has been investigated in the presence of the sulfided oxides and sulfides of metals in Periods 3–6 in the absence of a carrier. The experiments were performed at 200–550 °C, for a contact time of 1.2–6 s, and for a 1:1 molar ratio of the diene and hydrogen sulfide in the presence of sulfided Fe, V, Mo, Co, Cr, Mn, Ni, Cu, Ti, Zr, Mg, Si, and Al oxides as well as Re, Pd, Pt, and W sulfides. Catalysts containing reactive sulfur weakly bound to the catalyst surface were the most active. It has been suggested that thiophenes are formed by a multistage mechanism. This is confirmed by the fact that thiophene can be obtained both from a diene–hydrogen mixture and when only the diene is passed over the sulfided catalyst surface. In the latter case, thiophene cannot be formed without the participation of the sulfur in the catalyst. The rates of interaction of the diene with the catalyst sulfur and of the synthesis of thiophene from the diene–hydrogen sulfide mixture are similar. Consequently hydrogen sulfide does not participate directly in the formation of thiophene and is required to maintain a stationary state of the sulfide catalyst surface. The yields of 2- and 3-methylthiophenes from piperylene and isoprene were respectively 55.0 mol% and 45.0 mol% (relative to the C_5 hydrocarbon passed through the system) in the presence of sulfided vanadium oxide at 420 °C and for a contact time of 3 s. The activity of the catalyst was estimated from the specific rate of formation of thiophenes, which was calculated in accordance with a first order equation and was referred to the unit catalyst surface. The most active catalysts are Re, V, Fe, Mo, and platinum metal sulfides. The activation energies for the formation of thiophenes from various dienes are similar.[37,38]

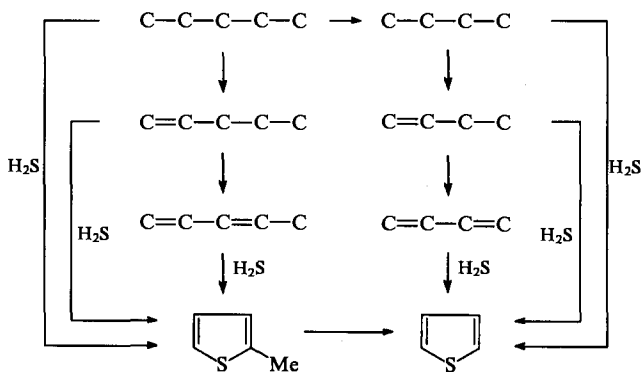
In order to estimate the activity of C_5 hydrocarbons of different structure in heterocyclisation processes, the interaction of n-pentane, pent-1-yne, isopentane, 2-methylbut-2-ene, and isopentenes with hydrogen sulfide in the presence of a Cr, K, Ln, Al catalyst was investigated.[39–42] The comparison was carried out at 550 °C, v_{sp} = 0.3–0.9 h^{-1}, and $H_2S:C_5$ = 2. The presence of CO_2 and N_2 in the reaction medium influences the selectivity of the catalyst. Under a CO_2 atmosphere, the yield of the heterocyclisation products increases and the cracking function of the catalyst is weakened. Under these conditions, the yield of liquid products increases from 60% to 98%. In terms of their capacity to undergo heterocyclisation in the presence of the Cr, K, Ln, Al catalyst, C_5 hydrocarbons can be arranged in the sequence n-pentane < pent-1-yne < isopentenes < isopentane < 2-methylbut-2-ene. Hydrocarbons with the iso-structure exhibit a higher reactivity in the formation of methylthiophenes than hydrocarbons with the normal structure. The yield of 2-methylthiophene from n-pentane and hydrogen sulfide is 55.3%, while the yields of 3-methylthiophene from isopentane and 2-methylbut-2-ene are 74.9 mass% and 79.5 mass% (relative to the hydrocarbon passed through the system) respectively. The heterocyclising properties of rhenium oxides and sulfides deposited on aluminium oxide are manifested in the interaction of n-pentane with hydrogen sulfide.[41–43] The yield of 2-methylthiophene at 550 °C, v_{sp} = 0.8–0.9 h^{-1}, and H_2S: n-C_5 = 2 in the presence of 5% of rhenium in the catalyst did not exceed 8%.

Under the same conditions, thiophene and 3-methylthiophene are formed respectively in yields of 19.2% and 12.1% (relative to the n-pentane passed through the system) together with 18.8% of 2-methylthiophene in the presence of the catalyst (composition in mass%) 2 Re_2O_7–2 Cr_2O_3–5 Ln–81 Al_2O_3. The catalytic reaction mixture contains also up to 10% of CS_2. Carbon dioxide and nitrogen have different effects on the selectivity of the reaction. In nitrogen, 2–3 times more of methylthiophene is formed than under a CO_2 atmosphere. 3-Methylthiophene can be produced as a result of the interaction of carbon disulfide with isopentane, which is obtained as a result of the isomerisation of n-pentane.[41]

V. The mechanism of the formation of thiophenes from C_4–C_5 hydrocarbons and hydrogen sulfide

The mechanism of the formation of 2-methylthiophene and thiophene in the presence of the Cr, La, K, Al catalyst has been investigated by the isotope-kinetic method using ^{14}C-labelled molecules.[44,45] Measurement of the concentration and of the molar radioactivity of the reaction products when n-pentane is supplied together with a small amount of added n-pentane labelled with ^{14}C makes it possible to determine the rates of individual stages of the reaction in which both pentane and pentene participate. As a rule, these rates are calculated from the dependence of the molar radioactivity on the contact time. The proposed mechanism is presented in Scheme 2.

Scheme 2



2-Methylthiophene is mainly formed consecutively from hydrogen sulfide and n-pentane via dehydrogenation products—pentenes and pentadiene. Thiophene is also formed via the hydrogenation products—butene and butadiene, with subsequent ring closure at the sulfur atom. Butane is obtained by the cleavage of a C–C bond in n-pentane. A small proportion of 2-methylthiophene is a product of the interaction of n-pentane and pentene with hydrogen sulfide, while thiophene is also partly formed by the reaction of hydrogen sulfide with n-butane or butene and by the demethylation of 2-methylthiophene.

VI. Interaction of C_6–C_8 hydrocarbons with hydrogen sulfide

In the interaction of C_6 hydrocarbons with hydrogen sulfide in the presence of chromium oxide catalysts, the heterocyclisation is accompanied by the dehydrocyclisation reaction with formation of benzene.[46] The dehydrocyclisation of n-hexane to benzene in the presence of chromium oxide catalysts has been investigated very widely. The reaction proceeds via the intermediate formation of hexenes, hexadienes, and trienes.[47] However, one cannot rule out the possibility that the dehydrocyclisation is suppressed by the hydrogen sulfide present in the system. Thus the interaction of 2,3-dimethylbuta-1,3-diene with hydrogen sulfide in the presence of the Cr, K, Al catalyst leads to the formation of only 3,4-dimethylthiophene, while dehydrocyclisation hardly occurs.[34] At 500 °C, v_{mass} = 0.2–0.3 h^{-1} and $H_2S:C_6$ = 2–1 for a reaction time of 1.25 h, the yield of 3,4-dimethylthiophene is 56%–60%.[48] The interaction of n-hexane, 2-methylpentane, hex-1-ene, hex-2-ene, hex-1-yne,

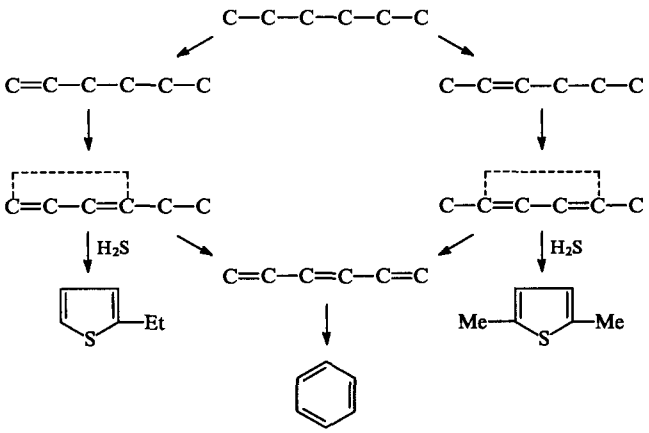
2-methylpent-1-ene, 2-methylpent-2-ene, 4-methylpent-1-ene, 4-methylpent-2-ene, and 2,3-dimethyl butane with hydrogen sulfide has been investigated in the presence of a Cr, Ln, K, Al catalyst under comparable conditions (550 °C, v_{mass} = 0.8 h^{-1}, and $H_2S:C_6$ = 4:1).[43,46] The heterocyclisation of normal C_6 hydrocarbons proceeds with formation of 2-ethylthiophene and 2,5-dimethylthiophene. In terms of their reactivity, C_6 alkanes, alkenes, and alkynes can be rearranged in the following sequence:

$$C-C-C-C-C-C \leqslant C-C=C-C-C-C$$
$$\simeq C=C-C-C-C-C < C\equiv C-C-C-C-C\ .$$

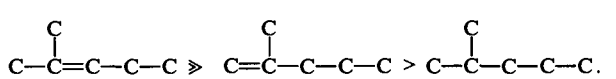
Alkynes show the highest reactivity in the heterocyclisation reaction and are followed by alkenes and alkanes. With increase in the reactivity of the hydrocarbon, the fraction of 2,5-dimethylthiophene in the reaction products increases compared with 2-ethylthiophene, i.e. ring closure at the sulfur atom involves the 2–5 carbon atoms to a greater extent than the 1–4 carbon atoms. It is noteworthy that, on raising the reaction temperature to 475 °C, n-hexane undergoes dehydrocyclisation with formation of benzene, together with heterocyclisation.

On the basis of data concerning the mechanism of the formation of 2-methylthiophene from hydrogen sulfide and n-pentane, according to which the reaction proceeds via alkenes and alkadienes,[44,45] one can postulate that 2,5-dimethylthiophene and 2-ethylthiophene are formed by a similar mechanism (Scheme 3).

Scheme 3



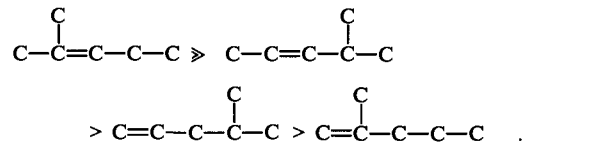
In the synthesis of dialkylthiophenes by the reaction of C_6 hydrocarbons having the iso-structure with hydrogen sulfide, there is virtually no dehydrocyclisation. In terms of their tendency to undergo heterocyclisation, the C_6 iso-hydrocarbons investigated can be arranged in the sequence



The yields of 2,4-dimethylthiophene from the above compounds are 40.2%, 23.4%, and 11.8% respectively (relative to the hydrocarbon passed through the system).

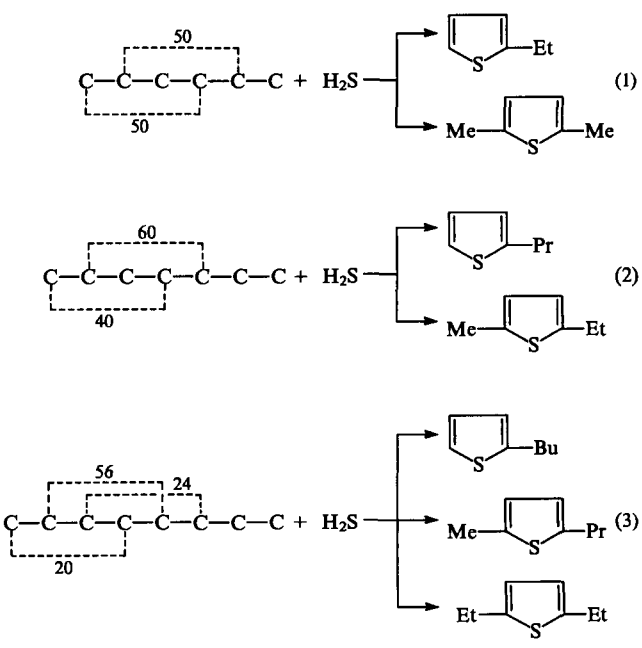
The position of the methyl group in α-alkenes hardly affects the yield of 2,4-dimethylthiophene and influences only the yield of 2-methylthiophene. The latter is a product of the interaction of hydrogen sulfide with pentane, which is formed owing to the dissociation of a C–C bond in the alkene. Thus the yield of 2-methylthiophene in the interaction of hydrogen sulfide with 4-methylpent-1-ene is twice as great as in the interaction with 2-methylpent-1-ene. The presence of a methyl group in β-alkenes promotes heterocyclisation. The yield of 2,4-dimethylthiophene is 40.2% from 2-methyl-pent-2-ene and 26.4% from 4-methylpent-2-ene.[43,46]

Thus, C_6 α- and β-isoalkenes with a methyl group in different positions in the hydrocarbon chain can be arranged in the following sequence in terms of their tendency to undergo the heterocyclisation reaction (the yields of 2,4-dimethylthiophene are 40.2%, 26.4%, 23.4%, and 22.4% respectively):



Thermodynamic analysis showed that experimental yields of the products of the heterocyclisation and dehydrocyclisation of n-hexane at 820 K are 82.8% (alkylthiophenes) and 81% (benzene), while at 750 K the corresponding yields are 24.4% and 10% respectively relative to the equilibrium yields.[49] In the interaction of C_6 normal alkenes and isoalkenes with hydrogen sulfide at 820 K, the heterocyclisation reaction virtually reaches equilibrium and the yields of ethyl- and dimethylthiophenes are 81.7%–97.8% of the equilibrium values (taking into account side reactions). The reactivity of n-alkanes, which give rise to alkylthiophenes and aromatic hydrocarbons on interaction with hydrogen sulfide, depends on their chain length.[50] In the presence of a Cr, Ln, K, Al catalyst at 450 °C, v_{mass} = 0.8 h^{-1}, and H_2S : n-C_6(n-C_7, n-C_8) = 2 under a nitrogen atmosphere, mainly 2-ethylthiophene and 2,5-dimethylthiophene are obtained from n-hexane, 2-propylthiophene and 2-methyl-5-propylthiophene are obtained from n-heptane and 2-butylthiophene, 2,5-diethylthiophene, and 2-methyl-5-propylthiophene are obtained from n-octane [reactions (1)–(3), Scheme 4]. Dehydrocyclisation results in the formation of benzene and toluene respectively from normal hexane and heptane, while ethylbenzene and *o*-xylene are formed from n-octane. The numerals in Eqns (1)–(3) (Scheme 4) represent the percentage contributions of the ring closure reactions at the sulfur atom involving the 1–4, 2–5, and 3–6 carbon atoms. Heterocyclisation with formation of the thiophene ring, proceeds as shown in relation to n-hexane, with ring closure at the sulfur atom involving the carbon atoms in the 1- and 4-positions or the 2- and 5-positions. With increase in the chain length of the alkane from C_6 to C_7, the fraction of alkylthiophenes formed via ring closure at the sulfur atom involving the carbon atoms in the 2- and 5-positions increases. In the case of n-octane, the 1–4 and 2–5 heterocyclisations are accompanied also by ring closure at the sulfur atom involving the carbon atoms in the 3- and

Scheme 4



6-positions. With increase in the chain length of the n-alkane, the yield of the heterocyclisation product diminishes, while the yield of the dehydrocyclisation product increases. The molar ratios of alkylthiophenes and aromatic hydrocarbons formed in the interaction of hydrogen sulfide with n-hexane, n-heptane, and n-octane are respectively 5.5, 1.25, and 0.7.

As shown for the interaction of hydrogen sulfide with n-hexane, the alkylthiophene and benzene formation reactions probably include a common stage involving the dehydrogenation of alkanes to unsaturated hydrocarbons. The longer the n-alkane chain, the more readily the unsaturated hydrocarbons obtained undergo closure to an aromatic ring compared with ring closure at the sulfur atom with formation of the thiophene ring.[50] The different abilities of n-alkanes (depending on the chain length) to enter into heterocyclisation or dehydrocyclisation reactions in the presence of chromium oxide catalysts may have to be taken into account in considering the genesis of petroleum containing both aromatic and thiophene oxide compounds.

VII. Physicochemical properties of chromium-containing oxide catalysts

The active chromium-containing heterocyclisation catalysts have been investigated by various physicochemical methods.[51–53] X-Ray diffraction analysis of the Cr, La, K, Al catalyst after the heterocyclisation reaction has been carried out in its presence (560 °C, v_{mass} = 225 h^{-1}, $H_2S:C_n$ = 2.0, yield of thiophene 33.2% after 3 h) demonstrated the presence of the crystalline γ-Al_2O_3 phase. The addition of potassium and lanthanum oxides does not affect the phase composition of the aluminium oxide–chromium oxide catalyst.[51] The formation during the heterocyclisation process of a solid solution of Cr_2O_3 in Al_2O_3, accompanied by an increase in the unit cell parameter from 7.90 to 7.95 Å, is influenced by the Cr_2O_3 content and the reaction conditions.

In order to account for the effect of added potassium and lanthanum oxides on the heterocyclising properties of the aluminium oxide–chromium oxide catalyst, the optical and EPR spectra of the oxidised and reduced specimens were analysed.[53–55] The catalysts were reduced at a pressure of 200–300 Torr and a temperature of 580 °C for 1 h. The optical and EPR spectra were obtained for the same specimens. After the catalysts had been treated at 500–700 °C in air or under a helium atmosphere, Cr^{6+}, Cr^{5+}, and Cr^{3+} ions were detected in them. The optical spectra of the reduced catalyst contain three absorption maxima: at 22 300, 16 200, and 10 200 cm^{-1}. The absorption maxima at 22 300 and 16 200 cm^{-1} are typical for aluminium oxide–chromium oxide catalysts. Octahedrally coordinated Cr^{3+} ions are responsible for them. The 10 200 cm^{-1} maximum is due to square-pyramidal Cr^{3+} ions. This maximum vanishes after the adsorption of water and hydrogen sulfide molecules. Hence it follows that these ions are in fact the centres for the adsorption of H_2O and H_2S. The adsorbed molecules enter the first coordination spheres of the above ions, increasing their coordination to octahedral.

It follows from analysis of the optical spectra of the reduced specimens that the nature of the spectra is independent of the lanthanum and potassium oxides added to the aluminium oxide–chromium oxide catalyst. On the other hand, the EPR spectra of the reduced catalysts do depend on these additives. They contain in all cases a broad asymmetric band, which results from superposition of signals due to the magnetically concentrated phase (β-phase) and the magnetically dilute phase (δ-phase) of the Cr^{3+} ions. In the spectra of the specimens containing added lanthanum and potassium oxides, the width of the band due to the β-phase (ΔH = 900 Oe) is much smaller than in the spectrum of the aluminium oxide–chromium oxide catalyst (ΔH = 1150 Oe). The additives influence the state of the Cr^{3+} ions in the catalyst.

Preliminary heat treatment of the specimens at 700 °C (the last stage of the preparation of the catalyst) increases the amount of chromium ions responsible for the appearance of the absorption maximum at 10 200 cm^{-1}, i.e. the surface square-pyramidal coordinated Cr^{3+} ions.

The above spectroscopic data for the Cr, La, K, Al catalysts agree with the results obtained for the aluminium oxide–chromium oxide catalyst for the dehydrogenation of alkanes.[53–55] The Cr, Ln, K, Al catalyst is active both in the heterocyclisation of hexane in the reaction with hydrogen sulfide and in the dehydrocyclisation of n-hexane to benzene. Both reactions proceed via common stages involving the dehydrogenation of alkanes to alkenes and alkadienes.[46]

The content of the lowest-valence chromium and lanthanide ions in the above catalyst was determined from the chemisorption of oxygen at 20 °C.[56] The Cr^{2+} ions are formed in the aluminium oxide–chromium oxide catalyst only on reduction above 300 °C, while at 500 °C their amount reaches a maximum.[57] The compositions of the dehydrogenating centres of the aluminium oxide–chromium oxide dehydrogenation and dehydrocyclisation catalysts include Cr^{2+} ions.[58] After the reduced catalysts have come into contact with O_2 at 20 °C, oxygen is first chemisorbed on the Cr^{2+} ions, but there is also a possibility of its chemisorption on the coordinatively unsaturated Cr^{3+} ions. In a reducing medium, under the conditions of the synthesis of 2-methylthiophene at 550 °C, the aluminium oxide–chromium oxide catalyst, without additives and with added potassium and lanthanum oxides, contains Cr^{2+} ions on which the dehydrogenation stages, common to heterocyclisation and dehydrocyclisation, most probably occur. Indeed, we find that (a) in the absence of Cr^{2+} ions the above reactions do not occur on the catalyst, (b) the number of active dehydrogenation centres, found from the curves for the poisoning of the catalyst with oxygen during the dehydrogenation of isopentane, agrees with the number of Cr^{2+} ions determined by titration with iron ammonium alum, and (c) the dehydrogenating and dehydrocyclising activities of the aluminium oxide–chromium oxide, aluminium oxide–chromium oxide–potassium oxide, and aluminium oxide–chromium oxide–calcium oxide catalysts increase in proportion to their Cr^{2+} content.

As in the dehydrocyclisation catalysts, in the heterocyclisation catalysts potassium oxide influences the productivity of the active centres because it alters the environment of the Cr^{2+} ion and its energetic characteristics. The lanthanum oxides in the aluminium oxide–chromium oxide catalyst also play the role of a promoting agent and not of the main active dehydrogenation component, although their amount is the same (5 mass%) as that of chromium oxide. Lanthanide ions in a low-valence state, with very powerful electron-donating properties and capable of functioning as dehydrogenation active centres, have been detected in the Cr, Ln, K, Al catalyst.[56]

It has been shown by X-ray photoelectron spectroscopy that the surface concentration of chromium on the 5% Cr_2O_3–95% Al_2O_3 catalyst decreases by a factor of two after the heterocyclisation reaction, whereas no change in the chromium concentration was observed after the addition of potassium and lanthanide oxides.[43] During the reaction, Cr^{6+} and Cr^{5+} are reduced mainly to Cr^{3+}.

It follows from the data obtained that the aluminium oxide–chromium oxide heterocyclisation catalysts promoted by potassium and lanthanide oxides contain low-valence chromium and lanthanide cations, which may form part of the composition of the catalyst active centres.[56] A study of the properties of the chromium ions in different oxidation states on the surfaces of chromium-containing catalysts by optical and EPR spectroscopy has been described in a review.[59]

Table 3. Catalytic synthesis of thiophenes by the reaction of C_2 and C_4-C_6 hydrocarbons with hydrogen sulfide in the presence of oxide catalysts.

Hydrocarbon	Catalyst composition (mass%)	T/°C	v_{sp}/h^{-1}	$H_2S:C_n$	Yield relative to hydrocarbon passed through system (mass%)	Thiophenes	Ref.
Acetylene	Al_2O_3	425–450	392[a]	1.5	38.4	Thiophene	7
Acetylene, electrocracking gas (29 vol.% C_2H_2, 57 vol.% H_2)	Al_2O_3	540–560	392[a]	1.5	50.2	"	7, 8
Butane	5 Cr_2O_3, 5 La_2O_3, 90 Al_2O_3	580	1.2–1.3	2–2.2	38–40	"	15
	5 Cr_2O_3, 5 La_2O_3, 1 K_2O, 89 Al_2O_3	580	1–1.2	2–2.5	40.0	"	16
Butene	5 SiO_2, 10 MoO_3, 85 Al_2O_3	590	1.7	1.6	52.9	"	14
But-2-ene	5 SiO_2, 10 MoO_3, 85 Al_2O_3[b]	590	1.7	1.5	55.4	"	14
	5 SiO_2, 10 Cr_2O_3, 85 Al_2O_3	590	1.4	2–2.4	53.3	"	14
	5 Cr_2O_3, 5 La_2O_3, 1 K_2O, 85 Al_2O_3	580	0.9	2.1	52.0	"	16–18
Buta-1,3-diene	5 Cr_2O_3, 1 K_2O, 94 Al_2O_3	500	1.0	2.1	49.0	"	16–18
	5 Cr_2O_3, 5 La_2O_3, 1 K_2O, 89 Al_2O_3	500	1.0	4.2	51.0	"	16–18
		580	0.9–1.2	2.1–2.6	55.0	"	16–18
Butane–butene fraction	5 Cr_2O_3, 5 BBF,[c] 1 K_2O, 89 Al_2O_3	580	130–140[a]	2.2	90.9		22–24
Pentane	5 Cr_2O_3, 5 BBF,[c] 1 K_2O, 89 Al_2O_3	550	0.3–0.4	2.0	45	Methylthiophene	39, 41
Pent-1-ene	15 SiO_2, 10 MoO_3, 85 Al_2O_3	570	1.6	1.8	33.3	"	14
Pent-1-yne	15 Cr_2O_3, 5 BBF,[c] 1 K_2O, 89 Al_2O_3	550	0.5	2.0	68.3	"	39, 41
Piperylene	18 Cr_2O_3, 4 K_2O, 78 Al_2O_3	500	0.3	2.6	69.9	"	31, 34
	5 Cr_2O_3, 5 BBF,[c] 1 K_2O, 89 Al_2O_3	500	0.3	2.0 (N_2)	71.4	"	41

Isopentane	5 SiO_2, 10 MoO_3, 85 Al_2O_3	530	1.6	1.9	22.8	3-Methylthiophene	14
2-Methylbutane	12 Cr_2O_3, 5 K_2O, 83 Al_2O_3	500	0.32	2.0 (N_2)	70.1	"	20
2-Methylbut-2-ene	5 Cr_2O_3, BBF[c] 1 K_2O, 89 Al_2O_3	550	0.3	2.0	79.5	"	41
	12 Cr_2O_3, 5 K_2O, 83 Al_2O_3	500	0.22	22.0 (N_2)	84.7	"	20
	12 Cr_2O_3, 5 Li_2O, 83 Al_2O_3	500	0.17	2.0 (N_2)	58.8	"	20
	12 Cr_2O_3, 5 Na_2O, 83 Al_2O_3	500	0.22	2.0 (N_2)	63.2	"	20
	12 Cr_2O_3, 5 MgO, 83 Al_2O_3	500	0.17	2.0 (N_2)	43.0	"	20
	12 Cr_2O_3, 5 CaO, 83 Al_2O_3	500	0.18	2.0 (N_2)	51.4	"	20
	18 V_2O_5, 2 ThO_2, 2 K_2O, 78 Al_2O_3	410	0.4	2.0	56.6	"	21
3-Methylbut-1-ene	12 Cr_2O_3, 5 K_2O, 83 Al_2O_3	500	0.22	2.0 (N_2)	81.2	"	20
Isopentenes	5 Cr_2O_3, 5 BBF,[c] 1 K_2O, 89 Al_2O_3	550	0.5	2.0	61.6	"	46
2-Methylpent-2-ene	5 Cr_2O_3, 5 BBF,[c] 1 K_2O, 89 Al_2O_3	550	0.8	4.0	40.2	2,3-Dimethylthiophene	46
2,3-Dimethylbutane	5 Cr_2O_3, 5 BBF,[c] 1 K_2O, 89 Al_2O_3	480	0.4	5.0	56.9	3,4-Dimethylthiophene	46
2,3-Dimethylbutadiene	18 Cr_2O_3, 4 K_2O, 78 Al_2O_3	500	0.2	2.0	60.0	"	48

[a] The ratio of the volume of gaseous hydrocarbons to the volume of the catalyst in 1 h; in the remaining cases—the ratio of the volume of liquid hydrocarbons to the volume of the catalyst.
[b] In a fluidised catalyst bed.
[c] Composition of lanthanide oxides (%): 2.7 CeO_2, 1.3 La_2O_3, 0.75 Nd_2O_3, 0.25 Pr_2O_3.

VIII. Industrial methods of synthesis of thiophenes

The Pennwalt Corporation in the USA and the Croda Synthetic Chemicals, Ltd and Pennwalts Holland B.V in Europe are known to produce various thiophenes.[60] The requirement by the world market for thiophene in 1982 amounted to 1000–1400 tonnes.

The synthesis is based on the interaction of butene and butadiene with carbon disulfide (as a source of sulfur) in contact with methane or CO_2 at 500 °C in the presence of an 11% chromium oxide catalyst promoted by alkali metals (6% K_2CO_3). The catalyst is regenerated periodically to remove the coke deposit. This process can also be used to obtain 2- and 3-alkyl-thiophenes from C_6 hydrocarbons.[61]

A plant in which thiophene was produced from C_4 hydrocarbons and fused sulfur — the Socony-Vacuum process — began operating in the USA in the 1950s.[6] The process is carried out at temperatures up to 700 °C and atmospheric pressure. Apart from the high temperature, a disadvantage of this procedure is appreciable tar formation, etc.

Thiophene is obtained also from a mixture of butane, gaseous sulfur, and hydrogen sulfide in the presence of 19% Cr_2O_3–81% Al_2O_3 catalyst at 500 °C (yield: 49% after 168 h). The maximum conversion into thiophene is attained for a ratio H_2S : n-C_4H_{10} = 15 : 1. The temperature in the reactor is maintained by the reaction between sulfur and side products. The hydrogen evolved on dehydrogenation of n-butane reacts with sulfur to form hydrogen sulfide; this highly exothermic reaction compensates for lack of external heating. Corrosion of the reactor is thereby greatly reduced. The catalyst is regenerated periodically. The method makes it possible to increase the yield of thiophene compared with the Socony-Vacuum process, to reduce corrosion, and to diminish tar formation. By this procedure, one can obtain 2- and 3-methylthiophenes from the corresponding hydrocarbons.

There is a possibility of synthesising thiophenes from the gases generated in the semicoking of shale.[63] Apart from C_1–C_5 hydrocarbons, the semicoking gases contain also CO, CO_2, and hydrogen sulfide, the content of which can reach 5%–12%. At 650 °C in the presence of the hydrogen sulfide-treated Cr, La, K, Al catalyst, the yield of the liquid catalytic reaction mixture containing 71.3% of thiophene is 85%. This method of synthesis may prove promising in countries possessing deposits of shale raw material containing sulfur compounds.

* * *

One of the main tasks in modern petroleum processing is rational use of the hydrocarbon raw material and hydrogen sulfide. The employment of oxide catalysts makes it possible to obtain thiophene and alkylthiophenes by the heterocyclisation of C_2 and C_4–C_8 hydrocarbons with participation of hydrogen sulfide. Table 3 indicates the optimum conditions and compositions of the active heterocyclisation catalysts. The reaction of hydrogen sulfide with the acetylene-containing gas generated in electrocracking on γ-Al_2O_3 may be of practical interest. Thiophenes can be obtained in appreciable yields by the reaction of C_4–C_6 hydrocarbons with hydrogen sulfide in the presence of chromium-containing oxide catalysts. In order to increase the yield of thiophenes, it is useful to employ the butane–butene fraction and hydrogen sulfide and to carry out the reaction in a vibrofluidised bed. 2-Methylthiophene may be obtained (in a yield up to 68%) from hydrogen sulfide and piperylene, while 3-methylthiophene may be obtained (in 75% yield) from hydrogen sulfide and isopentane. The results obtained in the study of the interaction of hydrogen sulfide with C_6 hydrocarbons having the iso-structure also merit attention: 3,4- and 2,4-dimethylthiophenes have been synthesised in this way from 2,3-dimethylbutane and 2-methylpent-2-ene respectively. Thus processes involving the catalytic synthesis of thiophenes from a petrochemical raw material — hydrocarbons and hydrogen sulfide — can be used successfully to satisfy the increasing need for these heterocycles.

References

1. M A Ryashentseva, Yu A Afanas'eva, Kh M Minachev *Khim. Geterotsikl. Soed.* 1299 (1971)
2. S Gronowitz (Ed.) *Thiophene and Its Derivatives* (New York: Interscience, 1985)
3. S Gronowitz, in *Thiophene and Its Derivatives* (Ed. S Gronowitz) (New York: Interscience, 1985) p. 1
4. J B Press, in *Thiophene and Its Derivatives* (Ed. S Gronowitz) (New York: Interscience 1985) p. 353
5. A E Chichibabin *Zh. Russ. Fiz.-Khim. Ova* **47** 703 (1915)
6. H D Hartough *Thiophene and Its Derivatives* (New York: Interscience, 1952)
7. USSR P. 257 460; *Byull. Izobret.* **36** 21 (1963)
8. D A Sibarov, M A Ryashentseva, V G Barinov, A D Kokurin, Kh M Minachev *Zh. Prikl. Khim.* **12** 1767 (1970)
9. W Steinkopf *Annalen* **428** 123 (1922)
10. V F Timofeev, D A Sibarov, V A Proskuryakov, in *Issledovaniya v Oblasti Khimii i Tekhnologii Produktov Pererabotki Goryuchikh Iskopaemykh* (Studies in the Chemistry and Technology of the Products of the Processing of Fossil Fuels) (Leningrad, 1974) p. 58; *Chem. Abstr.* **85** 62 389x (1976)
11. V F Timofeev, D A Sibarov, in *Issledovaniya v Oblasti Khimii i Tekhnologii Produktov Pererabotki Goryuchikh Iskopaemykh* (Studies in the Chemistry and Technology of the Products of the Processing of Fossil Fuels) (Leningrad, 1975) p. 29; *Chem. Abstr.* **85** 192 474d (1976)
12. V F Timofeev, D A Sibarov, in *Issledovaniya v Oblasti Khimii i Tekhnologii Produktov Pererabotki Goryuchikh Iskopaemykh* (Studies in the Chemistry and Technology of the Products of the Processing of Fossil Fuels) (Leningrad, 1975) p. 26; *Chem. Abstr.* **85** 192 473d (1976)
13. D A Sibarov, V F Timofeev, A F Timofeev, M A Ryashentseva, V A Proskuryakov, in *Organicheskie Soedineniya Sery* Vol. 2 (Organic Sulfur Compounds) (Riga: Zinatne, 1980) p. 369
14. R F McCleary, L E Ruidish, J T Clarke, L V Devaney, C H Culnane, R E Conary, in *Proceedings of the Third World Petroleum Congress, The Hague, 1951* p. 49
15. USSR P. 186 393: *Byull. Izobret.* **19** 18 (1965)
16. USSR P. 199 103; *Byull. Izobret.* **15** 21 (1967)
17. M A Ryashentseva, Yu A Afanas'eva, Kh M Minachev, in *Geterogennyi Kataliz v Reaktsiyakh Polucheniya i Prevrashcheniya Geterotsiklicheskikh Soedinenii* (Heterogeneous Catalysis in the Syntheses and Reactions of Heterocyclic Compounds) (Riga: Zinatne, 1971) p. 221
18. M A Ryashentseva, Yu A Afanas'eva, Kh M Minachev *Izv. Akad. Nauk SSSR, Ser. Khim.* 1538 (1972)
19. Yu A Afanas'eva, M A Ryashentseva, Kh M Minachev, I I Levitskii *Izv. Akad. Nauk SSSR, Ser. Khim.* 2012 (1970)
20. Jpn. P. 75 123 661; *Chem. Abstr.* **85** 5 486c (1976)
21. Jpn. P. 76 122 061; *Chem. Abstr.* **86** 189 703w (1977)
22. V B Abramovich, B I Baglai, K M Vaisberg, M F Pankratova, M A Ryashentseva, in *Geterogennyii Kataliz v Sinteze i Prevrashcheniya Geterotsiklicheskikh Soedinenii, Vsesoyuznyi Simpozium, Riga, 1972* (Heterogeneous Catalysis in the Syntheses and Reactions of Heterocyclic Compounds, All-Union Symposium) (Riga: Zinatne, 1972) p. 57
23. USSR P. 380 658; *Byull. Izobret.* **21** 88 (1973)
24. V B Abramovich, K M Vaisberg, M F Pankratova, B I Baglai, R M Masagutov, M A Ryashentseva, D A Khisaeva *Neftekhimiya* **14** 289 (1974)
25. V B Abramovich, K A Pavlova, M F Pankratova, V F Morozov, E V Semenova *Neftekhimiya* **17** 309 (1977)
26. M A Ryashentseva, A G Pogorelov, E P Belanova, R F Merzhanova *Neftekhimiya* **13** 840 (1973)
27. M A Ryashentseva, Kh M Minachev *Renii i Ego Soedineniya v Geterogennom Katalize* (Rhenium and Its Compounds in Heterogeneous Catalysis) (Moscow: Nauka 1983)
28. T S Sukhareva, L V Shepel', A V Mashkina, L S Zabrodova, in *Katalizatory Protsessov Polucheniya i Prevrashcheniya Sernistykh Soedinenii* (Catalysts for the Syntheses and Reactions of Sulfur Compounds) (Novosibirsk, 1979) p. 92

29. V B Abramovich, V N Kulakov, M F Pankratova, in *Sbornik Trudov Ufimskogo Neftyanogo Instituta, Ufa, 1971* (Collected Reports from the Ufa Oil Institute) p. 154
30. V B Abramovich, Ya S Amirov, I Ya Isyanov, M F Pankratova, V P Zemtsov, A A Shiryaeva *Neftepererabotka. Neftekhimiya* 27 (1971)
31. V B Abramovich, V N Kulakov, M F Pankratova, V P Zemtsov *Kinet. Katal.* **10** 209 (1969)
32. V B Abramovich, A A Kaluzhskii, K M Vaisberg, V S Bogdanov, M F Pankratova, in *Neftekhimicheskii Sintez. Tekhnicheskii Progress* (Ed. R V Nusenkis) (Petrochemical Synthesis. Technical Progress) (Ufa: Vses. Khim. Ovo im. D I Mendeleeva, 1976) p. 74
33. V B Abramovich, M F Pankratova, R M Masagutov, in *Katalizatory Protsessov Polucheniya i Prevrashcheniya Sernistykh Soedinenii* (Catalysts for the Syntheses and Reactions of Sulfur Compounds) (Novosibirsk, 1979) p. 96
34. USSR P. 171 004; *Byull. Izobret.* **10** 34 (1965)
35. USSR P. 448 882; *Byull. Izobret.* **51** 13 (1974)
36. V B Abramovich, M A Ryashentseva, Kh M Minachev, Yu A Afanas'eva, M F Pankratova, in *Geterogennyi Kataliz v Reaktsiyakh Polucheniya i Prevrashcheniya Geterotsiklicheskikh Soedinenii* (Heterogeneous Catalysis in the Syntheses and Reactions of Heterocyclic Compounds) (Riga: Zinatne, 1971) p. 229
37. L V Shepel', T S Sukhareva, A V Mashkina, L S Zabrodova, in *Katalizatory Protsessov Polucheniya i Prevrashcheniya Sernistykh Soedinenii* (Catalysts for the Syntheses and Reactions of Sulfur Compounds) (Novosibirsk, 1979) p. 88
38. T S Sukhareva, L V Shepel', A V Mashkina *Kinet. Katal.* **20** 1179 (1979)
39. USSR P. 527430; *Byull. Izobret.* **44** 75 (1977)
40. M A Ryashentseva, Kh M Minachev, E P Belanova, in *The VIIth International Symposium on Organic Sulphur Chemistry, Hamburg 1976* p.154
41. M A Ryashentseva, E P Belanova, Kh M Minachev *Izv. Akad. Nauk SSSR, Ser. Khim.* 2756 (1978)
42. M A Ryashentseva, in *Kataliticheskii Sintez Organicheskikh Soedinenii Sery, Novosibirsk, 1979. Sbornik Nauchnykh Trudov* (Catalytic Synthesis of Organo-Sulfur Compounds. Novosibirsk, 1979. Collected Reports) p. 129
43. E P Belanova, Candidate's Thesis in Chemical Sciences, Zelinskii Institute of Organic Chemistry, Moscow, 1987
44. M A Ryashentseva, Kh M Minachev, A A Greish, G V Isagulyants, Ju A Afanas'eva *Int. J. Sulfur Chem.* 415 (1973)
45. G V Isagulyants, A A Greish, M A Ryashentseva, Kh M Minachev, E P Belanova, L I Kovalenko *Izv. Akad. Nauk SSSR, Ser. Khim.* 2562 (1978)
46. M A Ryashentseva, E P Belanova, Kh M Minachev *Neftekhimiya* **22** 231 (1982)
47. M I Rozengart, B A Kazanskii *Usp. Khim.* **40** 1537 (1971) [*Russ. Chem. Rev.* **40** 715 (1971)]
48. V B Abramovich, V N Kulakov, I I Tokarevskaya *Khim. Geterotsikl. Soedin. N 3, Serusoderzhashchie Geterotsikly* 25 (1971)
49. M A Ryashentseva, E P Belanova *Neftekhimiya* **24** 799 (1984)
50. M A Ryashentseva, Kh M Minachev, E P Belanova, V S Bogdanov *Izv. Akad. Nauk SSSR, Ser. Khim.* 2690 (1985)
51. M A Ryashentseva, D P Shashkin *Izv. Akad. Nauk SSSR, Ser. Khim.* 588 (1969)
52. M A Ryashentseva, Yu A Afanas'eva, Kh M Minachev, V A Shvets, in *Organicheskie Soedineniya Sery* Vol. 2 (Organic Sulfur Compounds) (Riga: Zinatne, 1980) p. 274
53. V A Shvets, V B Kazanskii *Kinet. Katal.* 7 712 (1966)
54. V A Shvets, V B Kazanskii, in *Kompleksoobrazovanie v Katalize. Problemy Kinetiki i Kataliza* (Complex Formation in Catalysis. Problems of Kinetics and Catalysis) (Moscow: Nauka, 1968) p. 217
55. D E O'Reilly, D S MacIver *J. Phys. Chem.* 276 (1962)
56. M A Ryashentseva, E P Belanova, K I Slovetskaya, E G Aleshin *Izv. Akad. Nauk SSSR, Ser. Khim.* 782 (1986)
57. K I Slovetskaya, E G Aleshin, A M Rubinshtein *Izv. Akad. Nauk SSSR, Ser. Khim.* 749 (1973)
58. O D Sterligov, K M Gitis, K I Slovetskaya, E S Shpiro, A M Rubinstein, Kh M Minachev, in *Proceedings of the International Symposium on Catalyst Deactivation, Belgium, 1980*; *Stud. Surf. Sci. Catal.* 363 (1980)
59. V A Shvets *Usp. Khim.* **55** 427 (1986) [*Russ. Chem. Rev.* **55** 200 (1986)]
60. B Buchholz (Ed.), in *Encyclopedia of Chemical Technology* (3rd Ed.) Vol. 22 (New York: Kirk-Othmer, 1983) p. 965
61. BRD P. 2 225 443; *Chem. Abstr.* **78** 111 110z (1973)
62. BRD P. 2 441 414; *Chem. Abstr.* **83** 28 089y (1973)
63. D Yu Zhogin, A M Myasoedov, G E Voropanov, M A Ryashentseva *Neftekhimiya* **30** 819 (1990)

Russian Chemical Reviews **63** (6) 449 – 469 (1994)
©1994 Russian Academy of Sciences and Turpion Ltd

UDC 542.97 : 547.514.721 : 547.412.2

Spiro[2.4]hepta-4,6-dienes: synthesis and chemical reactions

L G Menchikov, O M Nefedov

Contents

I. Introduction	449
II. Methods of synthesis of spiro[2.4]hepta-4,6-dienes	449
III. Chemical reactions of spiro[2.4]hepta-4,6-dienes	458
IV. Conclusion	467

Abstract. Data on the chemistry of compounds of the spiro[2.4]hepta-4,6-diene series are surveyed and described systematically. The methods of their synthesis, the characteristic features of their reactivity, and their principal chemical reactions are examined. The applications of spiro[2.4]hepta-4,6-dienes in specific organic synthesis are noted. The bibliography includes 230 references.

I. Introduction

Compounds of the spiro[2.4]hepta-4,6-diene (SHD) series, the first representatives of which were synthesised only 40 years ago, have now become a class of chemical substances the interest in which is manifested from a wide variety of directions. Highly effective insecticides of the pyrethroid series[1–10] and new medicinal preparations[11,12] have been synthesised from these compounds. Methods have been proposed for the synthesis of a series of natural and biologically active compounds, in particular prostaglandins,[13] and polymeric materials of practical value have been obtained.[14–24] Furthermore, SHDs are interesting objects for the study of important problems in model organic chemistry such as that of spiroconjugation and complex formation.

SHD has a high degree of symmetry which, together with spiroconjugation, is responsible for a series of unusual chemical and physical properties. These have been investigated by means of a wide variety of instrumental[25–32] and quantum-chemical methods.[33–36]

Extensive data have now accumulated in the literature both on the synthesis of SHDs and on their chemical reactions and use in specific organic synthesis. However, there are no reviews in this field. The principal methods of synthesis of SHD and its derivatives and some of their chemical reactions of greatest synthetic interest are described systematically and examined below.

L G **Menchikov, O M Nefedov** Laboratory of the Chemistry of Carbenes and Small Rings, Zelinskii Institute of Organic Chemistry, Russian Academy of Sciences, Leninskii prosp. 47, 117913 Moscow, Russian Federation, Tel. (7-095) 137 70 71, Fax (7-095) 135 53 28

Received 5 May 1994
Uspekhi Khimii **63** (6) 471 – 492 (1994); translated by A K Grzybowski

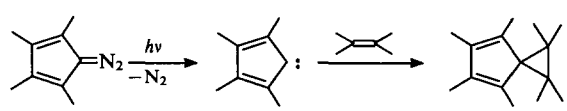
II. Methods of synthesis of spiro[2.4]hepta-4,6-dienes

Spiro[2.4]hepta-4,6-diene was synthesised by Levina et al.[37] as early as 1955 by the reaction of cyclopentadiene with 1,2-dibromoethane on treatment with sodium in liquid ammonia, but its first derivatives were obtained only later in 1965 by Moss,[38] who developed the first method of synthesis of compounds of the SHD series. Moss's method, which is based on the reaction of diazocyclopentadiene (DACPD) with unsaturated compounds, led to the possibility of synthesising a wide variety of SHD derivatives, and initiated the vigorous study of these compounds. Since then, numerous SHD derivatives have been obtained and new methods of their synthesis have been developed.

The methods of synthesis of compounds of the SHD series described in the literature hitherto can be divided arbitrarily into two groups. The first includes methods for the construction of the SHD skeleton by the cyclomethylenation of double bonds (reaction of DACPD and its derivatives with olefins) and also the cyclomethylenation of the exocyclic double bond in fulvenes. The second group includes methods based on nucleophilic substitution (in particular alkylation and cyclialkylation†) and nucleophilic addition (addition of carbanions to Michael acceptors) reactions of the cyclopentadienyl anion generated as an intermediate. In addition, the formation of compounds of the SHD series, usually in the form of minor products, has been observed in certain photochemical and carbene reactions.

1. Interaction of diazocyclopentadienes with unsaturated compounds

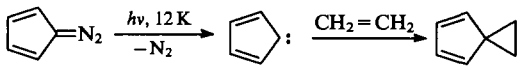
DACPD and its derivatives are highly reactive compounds, which decompose photochemically with formation of free cyclopentadienylidene (CPDI).[39–41]



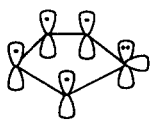
†Cyclialkylation is alkylation with formation of a new ring [see G L Mishchenko, K V Vatsuro *Sinteticheskie Metody Organicheskoi Khimii* (Synthetic Methods in Organic Chemistry) (Moscow: Khimiya, 1982) pp 400, 404].

An example of the catalytic decomposition of a substituted DACPD is also known.[42] The CPDI formed and its derivatives enter into reactions characteristic of carbenes, in particular they add to the C=C double bonds of unsaturated compounds, affording compounds of the SHD series in 10%–60% yields.

The reaction of free CPDI with ethylene, leading to SHD, has been detected in an $Ar-N_2O$ matrix at low temperatures (between 12 and 45 K).[43,44]



Since CPDI is an electrophilic carbene,[40,41,45–47] the rate of its addition, like that of other electrophilic carbenes,[40,41] to multiple bonds is retarded by electron-withdrawing substituents at the multiple bonds and is facilitated by electron-releasing substituents.[45,46] It is also noteworthy that, although CPDI has a triplet ground state,[40,41] nevertheless it reacts in an excited singlet state,[48] especially when it is generated photochemically, which also explains the stereoselectivity of its reactions involving addition to multiple bonds.[40,41,49]



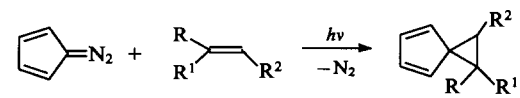
The availability of DACPD, which can be readily obtained[50] in 70%–80% yields from cyclopentadiene (CPD) and toluene-*p*-sulfonyl azide in the presence of diethylamine at 0 °C, as well as the simplicity of its carbene decomposition, promoted the synthesis of an appreciable proportion of the SHD derivatives known at the present time precisely by this method (Table 1).

Table 1. The yields of SHD derivatives **1** in the reactions of diazocyclopentadiene with olefins.

R	R^1	R^2	Yield of **1** (%)	Ref.
Me	Me	Me[a]	33	38, 51
Bu^t	H	H	46	38, 51
Bu	H	H	30	38, 51
Ph	H	H	18–20	45, 51
Me	H	Me	40	52, 53
Et	H	Et	50	52, 53
Me	H	Cl	[b]	54
4-$MeOC_6H_4$	H	H	17	45
4-MeC_6H_4	H	H	12	45
4-ClC_6H_4	H	H	12	45
3-BrC_6H_4	H	H	7	45
$MeSiCH_2$	H	H	[b]	46
$MeOCH_2$	H	H	[b]	46
$ClCH_2$	H	H	[b]	46
$NCCH_2$	H	H	[b]	46
Me	H	Pr^i	70	49
H	Me	Pr^i	70	49
$EtOCH_2$	H	H	35	55
Me	Me	H	15	56–59
$CH_2=CH$	H	H	59–68	60, 61
$CH_2=CH$	H	Me	[b]	61
H	$-(CH_2)_2-$		[b]	62
H	$-(CH_2)_4-$		23	38, 51
H	$-(CH=CH)_3-$		40–50	60, 63
H	$-(CH=CH)_2-$		25–35	60, 63
$CH_2=$	H		[b]	64

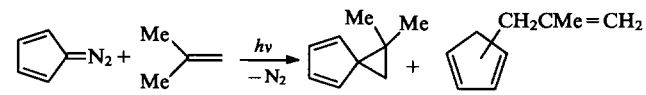
[a] In the reaction with tetramethylethylene, the yield of SHD is 35%.[38,51]
[b] The yield of SHD derivatives is not indicated.

The reaction is usually carried out in the presence of a (30–40)-fold molar excess of the initial unsaturated compound, its mixture with the DACPD being irradiated for several hours at 0–30 °C.



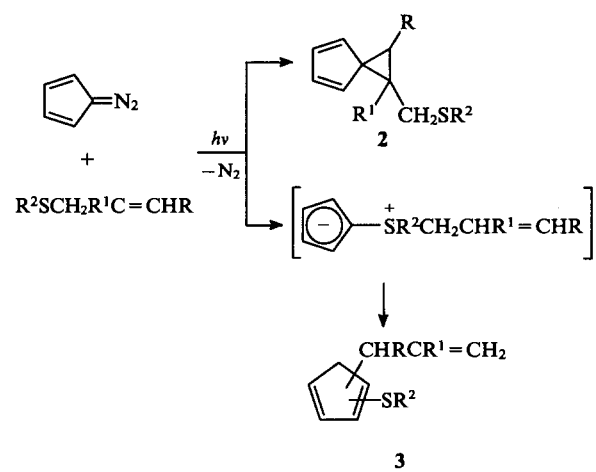
1

It is noteworthy that such reactions involve a side process in which the intermediate CPDI is inserted in different single bonds of the initial unsaturated acceptor.[55,59] For example, the insertion of CPDI in a C–H bond in the initial olefins leads to substituted cyclopentadienes.[59]



1 : 0.14–0.29

However, in the reaction of DACPD with allyl sulfides under similar conditions, the usual addition of CPDI to the double bonds is accompanied by the formation of unstable S ylides, which are subsequently converted into disubstituted cyclopentadienes (Table 2).[55]

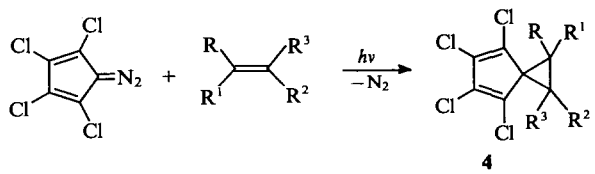


3

Table 2. The yields of SHD derivatives **2** and disubstituted cyclopentadienes **3** in the reaction of diazocyclopentadiene with allyl sulfides.

R	R^1	R^2	Yield (%)	
			2	**3**
H	H	Et	13	31
H	H	Bu^t	24	37
Me	H	Et	8	35
H	Me	Et	17	40
H	Me	Me	18	28

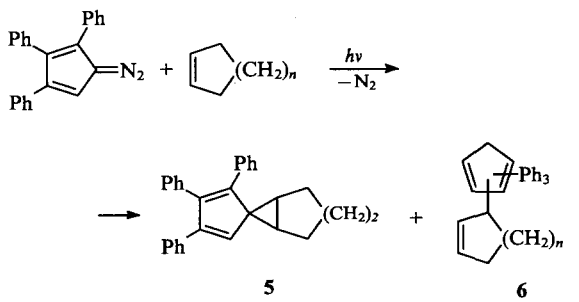
The reactions of substituted DACPD with unsaturated compounds, leading to SHD derivatives, have been studied only occasionally. Thus photolysis of tetrachlorodiazocyclopentadiene in the presence of a (30–40)-fold excess of the unsaturated compound afforded a series of 4,5,6,7-tetrachlorospiro[2.4]hepta-4,6-dienes (Table 3).[53,65,66]



4

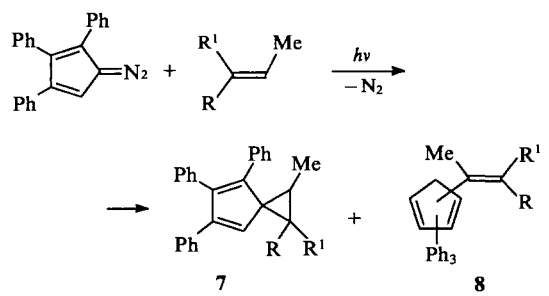
On the whole, the same behaviour has been observed for tetrachlorodiazocyclopentadiene as for the unsubstituted DACPD: first, the presence of electron-withdrawing groups (for example, COOMe) at the double bond of the unsaturated acceptor lowers significantly the yield of SHD derivatives and, second, the addition of the tetrachlorodiazocyclopentadiene takes place stereoselectively (Table 3).

The reactions of 2,3,4-triphenyldiazocyclopentadiene with cyclic and acyclic olefins,[42] leading to the formation, together with compounds of the SHD series, of the products of the insertion of the corresponding carbene into a C–H bond in the initial olefin, have also been described.



5 6

n	Yield of 5+6 (%)	5:6 ratio
1	71	1.85
2	73	1.70
3	63	1.15
4	62	1.22



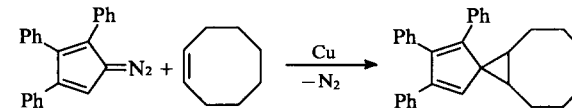
7 8

R	R^1	Yield of 7 + 8 (%)	7:8 ratio
Me	Me	49	4:1
H	Pr^i	85	19:1
Pr^i	H	58	2.8:1

Table 3. The yields of 4,5,6,7-tetrachlorospiro[2.4]hepta-4,6-dienes **4** in the reaction of tetrachlorodiazocyclopentadiene with olefins.

R	R^1	R^2	R^3	Yield of compound **4** (%) (*cis*/*trans* ratio)	Ref.
COOMe	H	COOMe	H	11	53, 65
COOMe	H	H	COOMe	8	53, 65
COOMe	H	H	H	42	65
H	—(CH$_2$)$_4$—		H	89	66
Bu	H	H	H	54	66
Me	Me	Me	H	87	66
Me	Me	Me	Me	80	66
Me	H	Me	H	63	66
Me	H	H	Pr	87 (77/23)	66
Me	H	H	Et	81 (78/22)	66
Me	H	H	Me	83.5 (79/21)	66

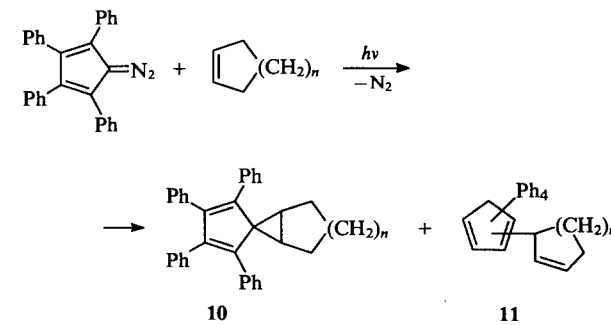
The catalytic decomposition of 2,3,4-triphenyldiazocyclopentadiene in the presence of cyclooctene also led to the formation of the corresponding substituted SHD **9**.[42]



9 (24%)

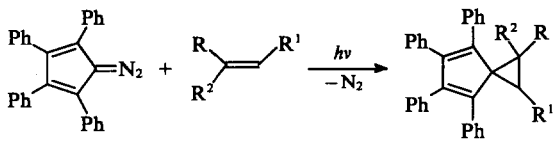
Although in the catalytic decomposition of triphenyldiazocyclopentadiene the yield of SHD derivatives is lower than on photolysis, nevertheless this example indicates the possibility of using the more convenient and simpler catalytic methods, in comparison with photolytic methods, for the generation of the corresponding carbenes from DACPD and its derivatives.

Tetraphenyldiazocyclopentadiene interacts with cyclic and acyclic olefins under the conditions of photolytic decomposition [(20–30)-fold excess of the initial unsaturated compound], which leads to the corresponding SHD derivatives **10** and **11**.[65, 67, 68]

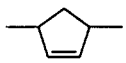


10 **11**

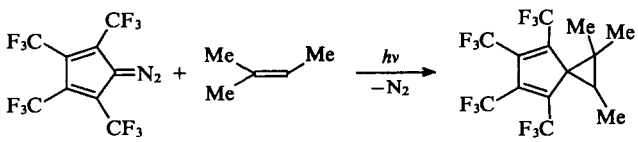
n	Yield of 10+11 (%)	10:11 ratio
1	47–55	9:1
2	60	2:1
3	74	1:1



12

R	R^1	R^2	Yield of 12 (%)	Ref.
Et	H	Me	48	67
Pr^i	Me	H	47–50	67
H	Pr^i	Me	60	67
Me	Me	Me	45–52	67
COOMe	H	H	–	65
COOMe	COOMe	H	–	65
		H	16	68

Finally there is an instance of the formation of the corresponding derivative **13** from tetrakis(trifluoromethyl)-diazocyclopentadiene under the conditions of photolytic decomposition.[69]

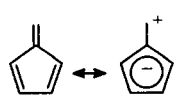


13

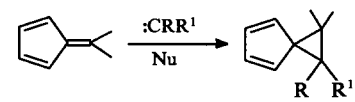
It follows from the data presented that the method of synthesis of compounds of the SHD series by the addition of cyclopentadienylidenes, generated photolytically from DACPD and its derivatives, to the double bonds of unsaturated compounds is fairly universal. At the same time, it suffers from a series of significant limitations. These are, in the first place, the low yields of the cycloaddition products and also the large number of side processes, in particular the insertion of the intermediate CPDI and its derivatives into the single bonds of the initial unsaturated compounds, especially when these contain heteroatoms (for example, sulfur and oxygen atoms). Furthermore, by virtue of the electrophilic nature of the cyclopentadienylidenes, electron-withdrawing functional groups in the initial unsaturated compounds lower significantly the rate of their addition to the double bonds, which increases the amount of side products, in particular the products of insertion in single bonds, and, since the majority of the known functional groups are electron accepting, the method may be relatively unsuitable for the synthesis of SHD with such functional-group substituents. Finally, the method is experimentally complex and has no preparative value because DACPD and its derivatives are extremely explosive, which necessitates the use of only small amounts of these substances (only 50–200 mg of DACPD are normally employed in the experiments). Nevertheless, the method is convenient for the synthesis of many complex SHD derivatives.

2. Cyclomethylenation of the exocyclic double bond in fulvenes

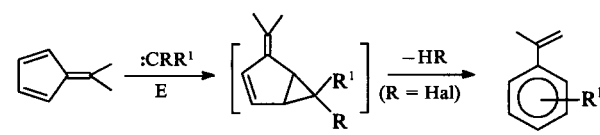
The high polarity of fulvene, which is responsible for the difference between the chemical properties of its double bonds, is generally known.[70–72]



The exocyclic double bond in fulvene is electrophilic, whereas the endocyclic double bond is nucleophilic. Therefore, as shown by Moss et al.,[73] electrophilic and nucleophilic carbenes react differently with fulvenes. Nucleophilic carbenes (Nu) add to the exocyclic double bond of the fulvene, affording SHD derivatives, but the range of such carbenes is extremely small, since it is restricted by the small number of electron-releasing substituents at the carbene centre (R = OAlk, OCOAlk).

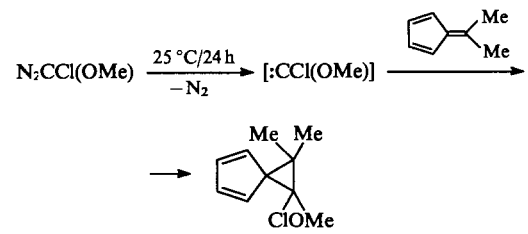


On the other hand, electrophilic carbenes, which constitute the vast majority of the known carbenes, add to the endocyclic nucleophilic double bonds, the product of such an addition usually being unstable and isomerising under the reaction conditions to aromatic derivatives.[73,74]

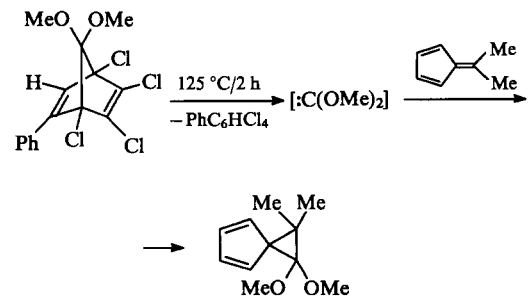


R, R^1 = Hal, COOMe, COMe, CN, etc.

Thus the addition of nucleophilic carbenes to the exocyclic double bond in fulvenes can be used to synthesise compounds of the SHD series containing electron-releasing groups in the cyclopropane ring. For example, nucleophilic carbenes such as chloromethoxycarbene and dimethoxycarbene, generated by the decomposition of chloromethoxyazirine and 1,2,3,4-tetrachloro-7,7-dimethoxy-5-phenylbicyclo[2.2.1]hepta-2,5-diene,[73] afford derivatives **14** and **15** respectively in their reaction with fulvene.

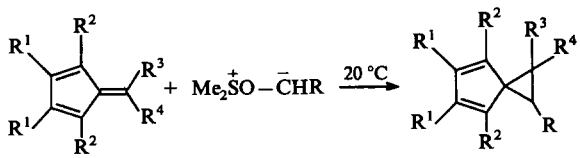


14 (35%)



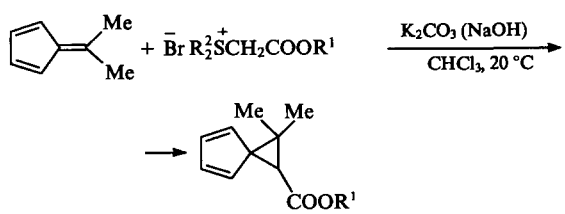
15 (8%)

Like nucleophilic carbenes, sulfur ylides, in which the reaction centre (the carbon atom linked to sulfur) has a negative charge, convert the exocyclic double bond in fulvenes into a cyclopropane group.[75,76] A series of derivatives **16** have been obtained in this way (Table 4).[77,78]



16

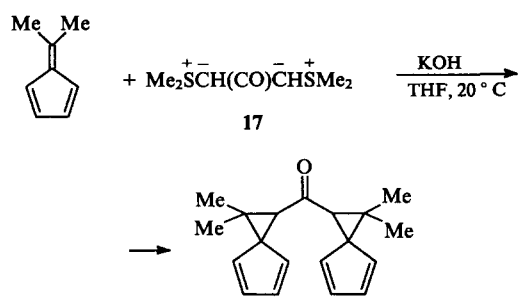
Special mention should be made of the use of the ylide method for the synthesis of a number of highly effective insecticides of the pyrethroid series (in 40%–80% yield); their toxicity to warm blooded animals is low.[1–8]



R^1 = CH_2—(OPh),[7] CH_2—(O)—CH_2Ph,[6]

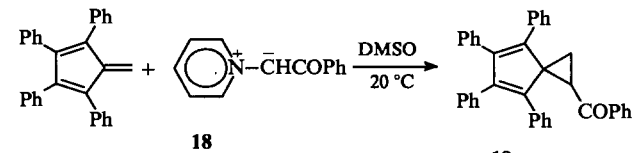
R^1 = —$CHRC_6H_4OPh$-*m*, where R = H, CN,[2–5]
R^2 = Me, R^2_2 = —$(CH_2)_4$—.[4]

The use of the diylide **17** in this reaction made it possible to obtain a compound with two SHD systems in 50% yield.[79]



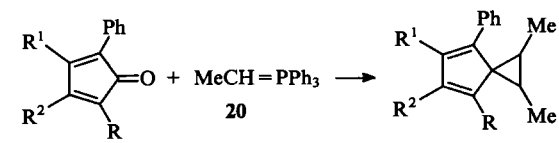
17

Nitrogen and phosphorus ylides (X^+-C^-, X = P, N) convert the exocyclic double bond of fulvenes into a cyclopropane group similarly to sulfur ylides. Thus the substituted SHD **19** has been obtained in 75% yield from the N ylide **18**.[77]

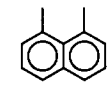


18 **19**

When the phosphorus ylide **20** was used, the corresponding substituted SHD **21** were obtained in 15%–30% yields from cyclopentadienones by the Wittig reaction with a subsequent secondary reaction involving the conversion of fulvenes into cyclopropane derivatives by reaction with the same phosphorane.[80]



20 **21a–c**

21a: R = R^1 = R^2 = Ph
21b: R = Ph, $R^1 + R^2$ = 
21c: R = Me, R^1 = R^2 = Ph

However, the attempt to synthesise SHD derivatives unsubstituted in the three-carbon ring from triphenylmethylenephosphorane was unsuccessful—the reaction stopped at the fulvene formation stage.[80]

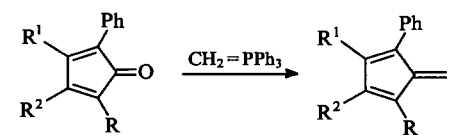
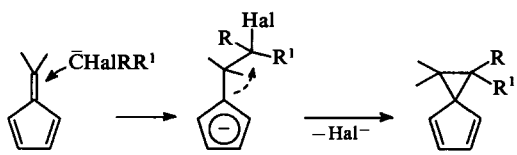


Table 4. The yields of SHD derivatives **16** in the reactions of fulvenes with sulfur ylides.

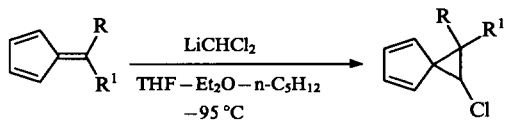
R^1	R^2	R^3	R^4	R	Solvent	Yield (%)
H	H	Me	Me	H	DMSO	80
H	H	H	4-$MeOC_6H_4$	H	DMSO	79
H	H	Me	4-$MeOC_6H_4$	H	DMSO	76
Ph	Ph	H	H	H	DMSO	70
4-MeC_6H_4	Ph	H	H	H	DMSO	64
4-$MeOC_6H_4$	Ph	H	H	H	DMSO	84
H	H	Me	Me	PhCO	$CHCl_3$	76
Ph	Ph	H	H	PhCO	$CHCl_3$	86
H	H	Me	Me	COOEt	THF	90
H	H	Et	Me	COOEt	THF	90
H	H	Me	*cyclo*-C_3H_5	COOEt	THF	60
H	H	Me	$(CH_2)_3OAc$	COOEt	THF	70
H	H	—$(CH_2)_4$—		COOEt	THF	40
H	H	H	α-C_4H_3O	COOEt	THF	35
H	H	Me	Ph	COOEt	THF	10
H	H	SMe	SMe	COOEt	THF	60
H	H	SEt	SEt	COOEt	THF	54
H	H	— $S(CH_2)_2S$ —		COOEt	THF	30
Cl	Cl	H	α-C_4H_3O	COOEt	THF	30
Cl	Cl	H	Ph	COOEt	THF	90

A series of reactions are known in which the carbanions generated with the aid of highly basic agents and containing a halogen atom at the carbanionic centre ($-CHalRR^1$) add to the electrophilic exocyclic bond of fulvenes, forming the anion **22**, the intramolecular cyclisation (S_N) of which leads to compounds of the SHD series.

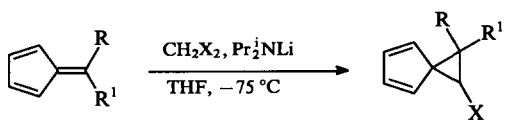


22

The interaction of fulvenes with equimolar amounts of an organolithium derivative $Li^+CHX_2^-$, generated in different ways, also leads to compounds of the SHD series.[54]

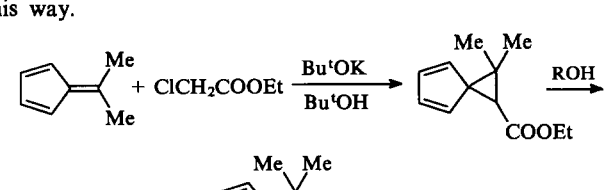


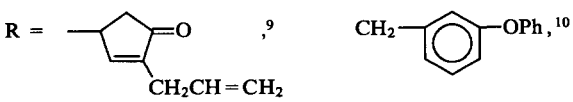
R	R^1	Yield (%)
H	H	56
Me	H	75
Ph	H	65
Pr^i	H	37
Bu^t	H	90
Me	Me	56
Ph	Ph	0



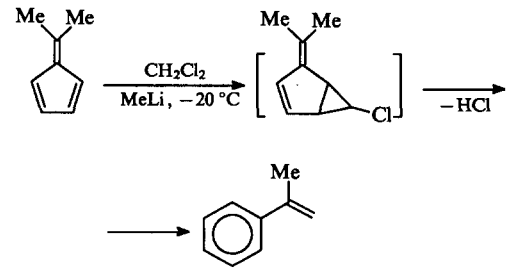
R	R^1	Yield (%)	
		X = Cl	X = Br
H	H	37	–
Me	H	63	72
Ph	H	63	–
Pr^i	H	33	30
Bu^t	H	90	72
Me	Me	80	92
Ph	Ph	0	0

The carbanion generated from ethyl chloroacetate reacts similarly with dimethylfulvene, affording the corresponding SHD in 13% yield.[9,10] A series of pyrethroids have been obtained in this way.

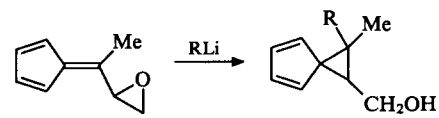


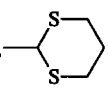


An alternative mechanism for the synthesis of compounds of the SHD series, involving the formation of monohalocarbenes or alkoxycarbonylcarbenes, is unlikely because in this case the nucleophilic endocyclic double bond of fulvene should be converted into a cyclopropane group by virtue of the electrophilic nature of these carbenes.[40,41,46] Thus it has been shown[54] that the monochlorocarbene, generated at −20 °C from CH_2Cl_2 by treatment with MeLi, does indeed add to the endocyclic double bond of fulvene, but the product of such addition is unstable and readily isomerises to methylstyrene under the reaction conditions.

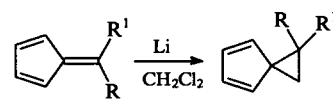


The rearrangements of the cyclopentadienyl anion, generated from alkyllithium and fulvene, constitute the basis of the synthesis of hydroxymethyl-substituted SHD (in 31%–55% yield).[81,82]



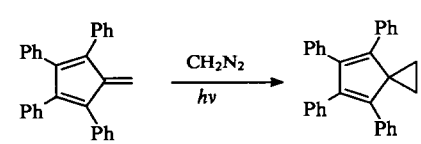
R = Me, Bu, CHMeEt, $CH=CH_2$, 

Finally, the anion of 6,6-diarylfulvenes enters into a nucleophilic substitution reaction with CH_2Cl_2, affording 1,1-diaryl-substituted SHD.[83]

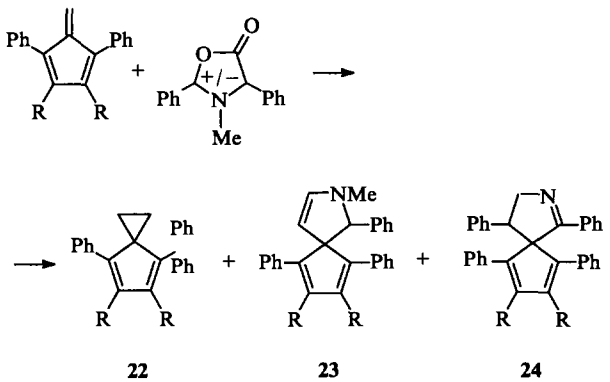


R = Ph, 4-$MeOC_6H_4$, 4-ClC_6H_4;
R^1 = Ph, 4-$MeOC_6H_4$, 4-ClC_6H_4, 2-C_5H_4N.

Among other reactions of fulvenes, mention should be made of the synthesis of the tetraphenyl derivative of SHD in a quantitative yield (99%) by the photolysis of the pyrazoline formed as a result of the 1,3-dipolar addition of a fourfold excess of diazomethane to tetraphenylfulvene.[77]



Finally, the synthesis of SHD derivatives (in 17%–27% yield) from fulvenes and 3-methyl-2,4-diphenyl-1,3-oxazolidinium-5-olate has been described.[84]



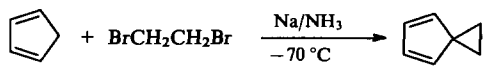
22 **23** **24**

R	Yield (%)		
	22	**23**	**24**
Ph	27	30	11
4-MeC_6H_4	24	22	19
4-$MeOC_6H_4$	17	30	17

Thus the methods of synthesis of compounds of the SHD series by the cyclomethylenation of the exocyclic double bonds in fulvenes, which have been examined above, have a number of characteristic features. In speaking of the carbene methods, one should emphasise that the formation of SHD derivatives is characteristic only of nucleophilic carbenes, which have an extremely limited range, while the methods of their generation are rather complex for wide-scale use in the synthesis of SHD derivatives. However, such methods do in fact make it possible to obtain most effectively derivatives of SHD with electron-releasing groups. Similar reactions are also characteristic of sulfur ylides, but the number of the latter is likewise small [75,76] and the syntheses of compounds of the SHD series from them involve multiple stages. In addition, it has to be mentioned that reactive ylides enter readily also into side reactions. For example, when the initial compounds or the products contain carbonyl groups, epoxidation side reactions take place to a significant extent. [75,76] Nevertheless, ylides have been used successfully in the synthesis of aryl- and carboxy-substituted SHD.

3. Cyclialkylation of cyclopentadiene by 1,2-dibromo derivatives and similar 1,2-difunctional compounds

As mentioned above, SHD was first obtained in 25% yield [37] by the cyclialkylation of cyclopentadiene (CPD) by 1,2-dibromoethane on treatment with sodium in liquid ammonia.



This method of synthesis of SHD still remains the most convenient preparative procedure, its improvement involving mainly the simplification of the method and an increase in the SHD yield (Table 5).

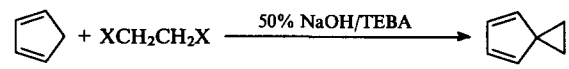
The appearance of a new method in organic synthesis—phase transfer catalysis (PTC) [100,101]—also made it possible to simplify significantly the cyclialkylation of cyclopentadiene, leading to the formation of SHD and its derivatives. [95–99,102,103] The advantages of the PTC method are not only its simplicity and the high yield of SHD but also the possibility of using ordinary NaOH instead of expensive bases and of carrying out the reaction in the absence of a solvent, which facilitates in its turn the isolation of SHD.

Under the conditions of phase-transfer catalysis, SHD can be obtained by the reaction of cyclopentadiene with 1,2-dichloroethane or ethylene glycol di(benzenesulfonate). [102–104]

Table 5. Conditions in the cyclialkylation of cyclopentadiene by 1,2-dibromoethane and the yield of SHD.

Base	*T*/°C	*t*/h	Yield of SHD (%)	Ref.
Na/NH_3	−70–35	3–5	18–75	37, 85–88
Na/THF	0	–	[c]	89
$NaNH_2/NH_3$	–	–	69	90
$NaNH_2$/THF	20	3	54	91, 92
$NaH/MeO(CH_2CH_2O)_2H$	–	–	78	93
NaH/diglyme	0	4	38	94
NaOH (50%), TEBA[a]	30–50	4	76–85	95–97
NaOH, PEG[b]	20	–	–	98
KOH (solid), TEBA	0–20	3	80	97
K_2CO_3/DMSO	20	8	70	99

[a] TEBA = triethylbenzylammonium chloride. [b] PEG = poly(ethylene glycol). [c] The yield of SHD is not indicated.

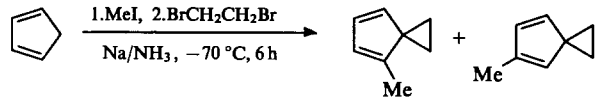


X = Cl, OSO_2Ph.

The reaction with dichloroethane can be carried out also on treatment with NaH as the base (THF, 20 °C, yield 83%). [105]

The use of the more readily available and cheaper 1,2-dichloroethane instead of 1,2-dibromoethane opens up new prospects for investigators. The possibility of using di(benzenesulfonate) in this reaction is of special interest in its turn, because di(benzenesulfonates) (together with ditosylates) are intermediates in the synthesis of the corresponding dihalo-derivatives.

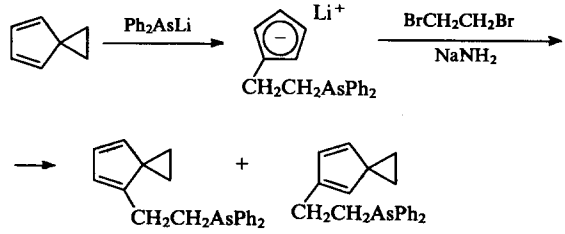
The use of substituted cyclopentadienes in the reaction with 1,2-dibromoethane makes it possible to obtain the corresponding SHD derivatives. Thus a mixture of 4- and 5-methyl-substituted SHD is formed in 30%–55% overall yield on successive alkylation of cyclopentadiene by methyl iodide and 1,2-dibromoethane. [87,106]



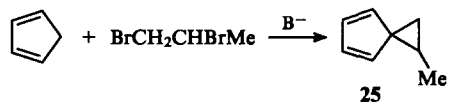
2.8 : 1

This evidently involves the initial formation of a mixture of isomeric methylcyclopentadienes in which the thermodynamically most stable 1- and 2-methyl derivatives predominate. [107] These are subsequently cyclialkylated by 1,2-dibromoethane.

Similar cyclialkylation by 1,2-dibromoethane of an arsenic derivative of cyclopentadiene has been described. [108] In this case, a mixture of the 4- and 5-substituted SHD is likewise formed.



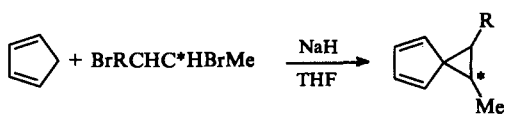
Apart from 1,2-dibromoethane, 1,2-dibromopropane, its closest homologue, is used in the cyclialkylation of cyclopentadiene.



25

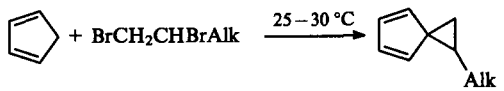
Base	Yield of **25** (%)	Ref.
Na/NH_3, −35 °C	54	57, 109
$NaNH_2/NH_3$	–	110
NaH/THF	–	111
NaOH (50%), TEBA	76–85	96, 97

The use of the optically active 1,2-dibromopropane in this reaction makes it possible to obtain the optically active 1-methyl-substituted SHD.[111]



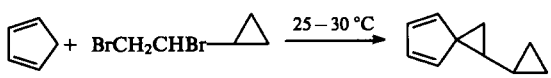
R = H, D.

Under the conditions of phase transfer catalysis, the cyclialkylation of cyclopentadiene by 1,2-dibromo-n-alkanes, in which one bromine atom is at a primary carbon atom and the other at a secondary carbon atom, proceeds just as smoothly as the reaction with 1,2-dibromoethane itself and leads to the corresponding 1-alkylspiro[2.4]hepta-4,6-dienes (in 65%–75% yield).[96, 97, 102, 103]

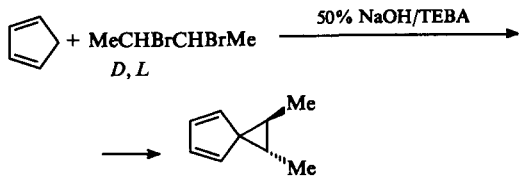


Alk = Me, Pr, Bu, Pe.

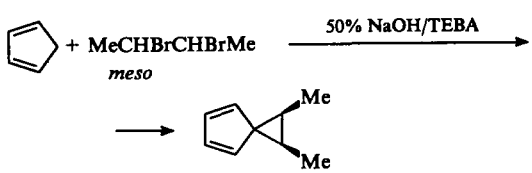
1-Cyclopropylspiro[2.4]hepta-4,6-diene has been obtained in 80% yield from 1,2-dibromo-1-cyclopropylethane under similar conditions.[96]



The possibility of using 1,2-dibromo-derivatives with the two bromine atoms at secondary carbon atoms in this reaction under PTC conditions has also been demonstrated. Thus the interaction of cyclopentadiene with *D,L*-2,3-dibromobutane readily affords *trans*-1,2-dimethylspiro-[2,4]hepta-4,6-diene in 70% yield.[96, 102, 103]

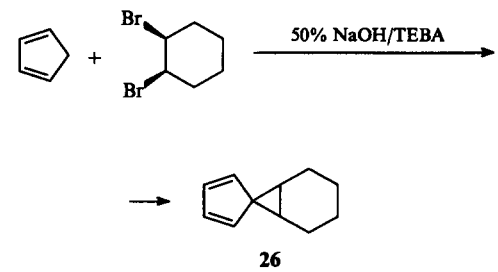


On the other hand, the reaction of cyclopentadiene with *meso*-2,3-dibromobutane leads to the corresponding *cis*-isomer in 60% yield.[96, 102, 103]



The formation of only one isomer of 1,2-dimethyl-SHD on reaction of cyclopentadiene with *meso*- or *D,L*-2,3-dibromobutane is evidence in support of the S_N2 mechanism of cyclialkylation of cyclopentadiene under PTC conditions and leads to the possibility of obtaining optically active derivatives of SHD in this way.[102, 103]

Under the same conditions, another dibromo-derivative — *cis*-1,2-dibromocyclohexane — reacts similarly with cyclopentadiene under the same conditions and leads to spiro(bicyclo-[4.1.0]heptane-7,5′-cyclopentadiene) **26**.[102, 103]

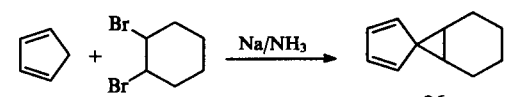


26

On the other hand, the reaction of cyclopentadiene with *trans*-1,2-dibromocyclohexane affords, instead of the corresponding SHD derivative, isomeric bromocyclohexylcyclopentadienes (the products of the monoalkylation of cyclopentadiene) as well as the products of the dehydrobromination of the latter and of the initial dibromocyclohexane.[97]

Thus the difference between the reactivities of *cis*- and *trans*-1,2-dibromocyclohexanes confirms the S_N2 mechanism of the cyclialkylation reaction.[102, 103]

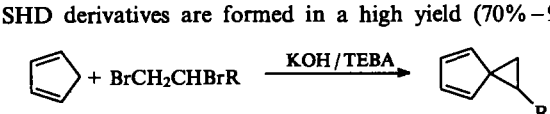
The cyclialkylation of cyclopentadiene by 1,2-dibromocyclohexane takes place also when the Na/NH_3 system is used as the base, which results in the formation of the corresponding tricyclic derivatives of SHD **26** in 10% yield.[86]



26

In contrast to primary and secondary dibromo- derivatives, dibromoalkanes containing at least one bromine atom at a tertiary carbon atom do not form SHD derivatives under the conditions of phase transfer catalysis because of the ease of their dehydrobromination.[96, 102, 103]

The cyclialkylation of cyclopentadiene under conditions of phase transfer catalysis by 1,2-dibromoethane with functional group substituents makes it possible to obtain various SHD derivatives.[102, 103, 112] The use of powdered KOH in CH_2Cl_2 in the presence of TEBA under these conditions fully rules out side reactions involving functional groups, for example hydrolysis. The yields of SHD derivatives depend significantly on the electronic properties of the functional group R in the initial 1,2-dibromoethane. Thus, when the group R linked directly to the reaction centre is an aryl substituent or possesses electron-withdrawing properties (COOMe, COMe, CN, Ph, 4-MeC_6H_4, 4-$MeOC_6H_4$, 4-BrC_6H_4, 4-$NO_2C_6H_4$, Cl), then the corresponding SHD derivatives are formed in a high yield (70%–95%).[112]

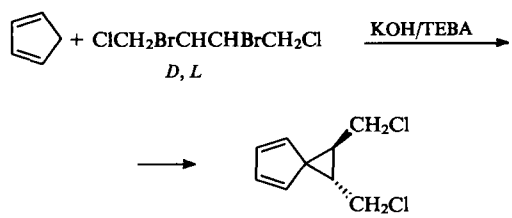


On the other hand, if the functional group in the initial 1,2-dibromoethane is markedly electron-releasing (R = OAc, OEt), then the yields of the SHD derivatives are significantly lower (25%–50%).[112]

However, if the functional group is separated from the reaction centre by a methylene unit, its electronic properties hardly affect the yields of the SHD derivatives, which in this case are 60%–80% for 1,2-dibromopropanes containing functional group substituents in the 3-position with both electron-withdrawing (R = CN, Cl) and electron-donating (R = OMe, OAc) properties.[112]

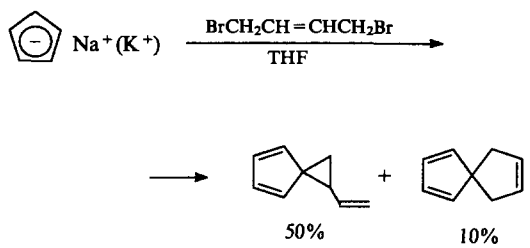


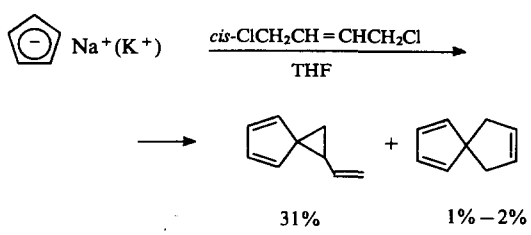
The possibility of synthesising SHD disubstituted in the 1,2-positions by functional groups has been demonstrated for the reaction of cyclopentadiene with *D,L*-2,3-di-bromo-1,4-dichlorobutane. The main product obtained in this case in 55% yield was *trans*-1,2-di(chloromethyl)spiro[2.4]hepta-4,6-diene.[112]

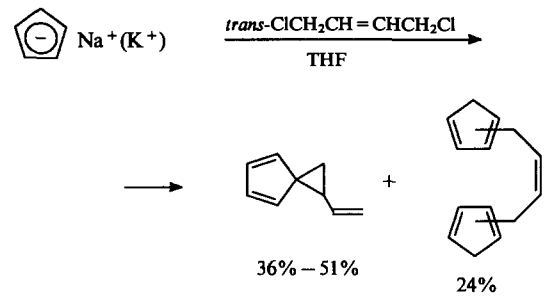


The exclusive formation of *trans*-1,2-bis(chloromethyl)-SHD is fully consistent with the S_N2 mechanism of cyclialkylation of cyclopentadiene under phase transfer catalysis conditions and at the same time indicates a higher reactivity of the bromo-derivatives compared with the chloro-derivatives, although bromine is attached to a secondary carbon atom whereas chlorine is attached to a primary carbon atom.[102,103,112]

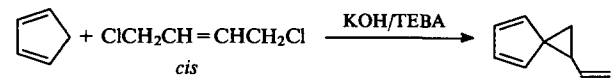
Among other alkylating agents used to obtain SHD derivatives by the cyclialkylation of cyclopentadiene, mention should be made of 1,4-dihalobut-2-enes and epichlorohydrin. Thus the interaction of cyclopentadiene with 1,4-dihalobut-2-enes is accompanied by the allyl rearrangement and leads mainly to 1-vinyl-substituted SHD.[60,113,114]



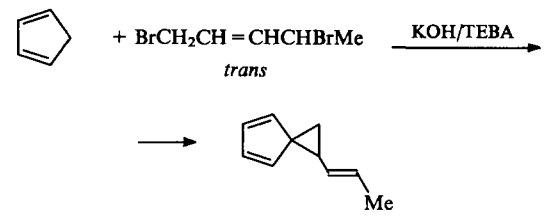




Under PTC conditions, the interaction of cyclopentadiene with *cis*-1,4-dichlorobut-2-ene on treatment with solid KOH in CH_2Cl_2 proceeds similarly, leading to 1-vinylspiro-[2.4]hepta-4,6-diene in 60% yield.[115]

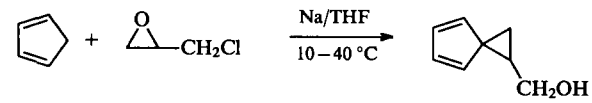


The cyclialkylation of cyclopentadiene by *trans*-1,4-dibromopent-2-ene also proceeds similarly, leading to the formation of propen-1-ylspiro[2.4]hepta-4,6-diene in 55% yield.[115]



The formation of vinyl-substituted SHD in these reactions indicates the possibility of using derivatives of 1,4-dihaloalk-2-enes for the synthesis of alken-1-ylspiro[2.4]hepta-4,6-dienes.[102,103]

Finally, the cyclialkylation of cyclopentadiene by epichlorohydrin leads to 1-hydroxymethylspiro[2.4]hepta-4,6-diene in 64%–77% yields.[116–118]

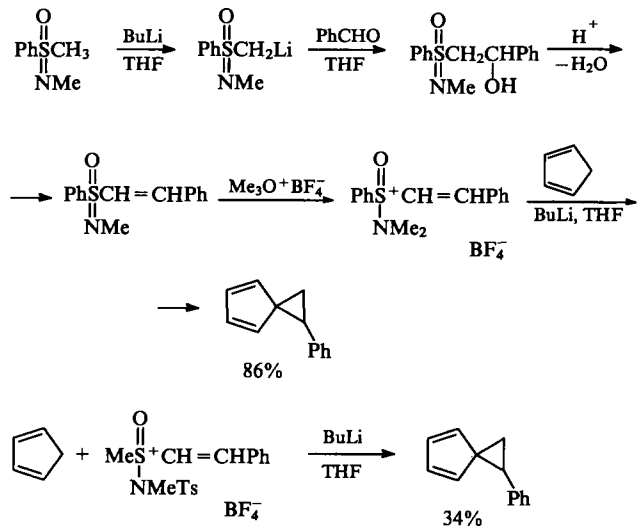


Thus the method involving the cyclialkylation of cyclopentadiene is universal and makes it possible to obtain easily and in high yield SHD derivatives with various functional groups, which renders these compounds readily available synthons for wide scale employment in specific organic synthesis. This method of preparation of SHD and its derivatives is the simplest and most effective compared with other procedures examined in previous sections of the review. The cyclialkylation of cyclopentadiene under the conditions of phase transfer catalysis with formation of compounds of the SHD series proceeds via an S_N2 mechanism,[102,103] which can be used in the synthesis of optically active SHD derivatives. The method is ineffective in the synthesis of SHD with electron-releasing substituents and of *gem*-disubstituted SHD.

4. Other methods of synthesis of spiro[2.4]hepta-4,6-dienes

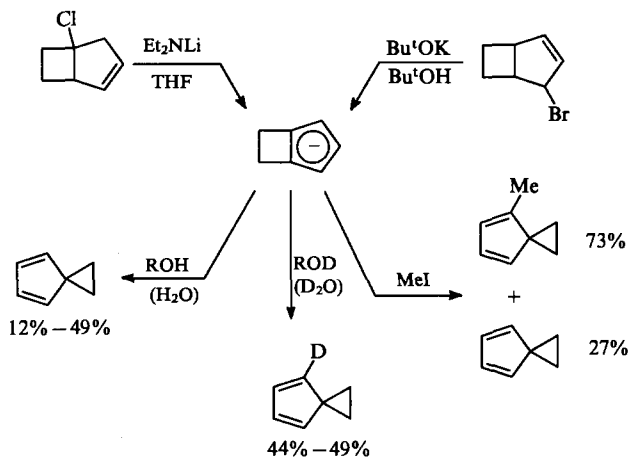
Certain further examples of the construction of the SHD system are considered below. They are frequently random in character and as a rule have no preparative value.

Thus the synthesis of the 1-phenyl derivative of SHD by the reaction of cyclopentadiene with derivatives of vinylsulfoxyimines on treatment with butyllithium has been described.[119]

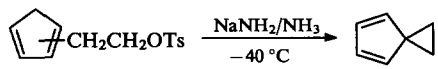


Apparently the mechanism of this reaction is similar to that of the addition of a nucleophile to a Michael acceptor,[119] the cyclopentadienyl anion, formed as an intermediate from cyclopentadiene on treatment with BuLi, acting as the nucleophile.

Several examples of the synthesis of SHD and its derivatives as a result of intramolecular reactions have been described. Thus halo-derivatives of bicyclo[3.2.0]hept-2-ene readily give up a hydrogen halide molecule on treatment with strong bases, affording the corresponding bicyclo[3.2.0]hepta-1,3-dienyl carbanion, which combines with a proton or a methyl group and rearranges to SHD and its derivatives.[120, 121]

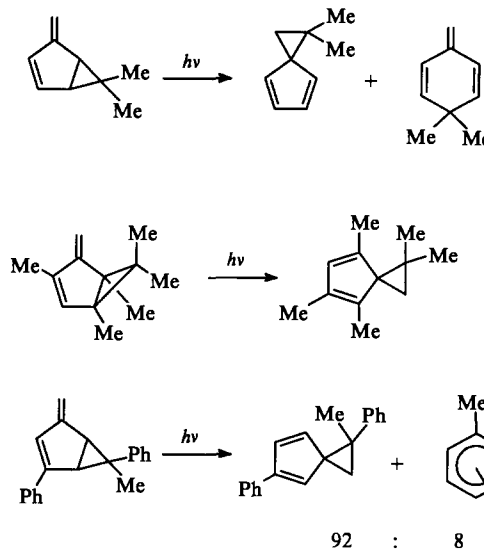


Furthermore, intramolecular alkylation of the β-tosylethyl derivative of cyclopentadiene also results in the formation of SHD.[122]

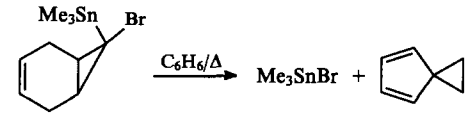


This reaction is very similar to those described in the previous Section.

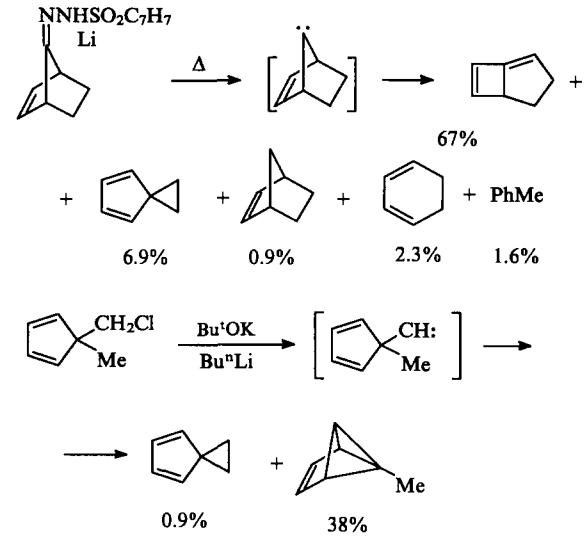
Examples also exist of the formation of compounds of the SHD series as a result of the photochemical isomerisation of derivatives of 4-methylenebicyclo[3.1.0]hex-2-ene.[56, 58, 123–126]



Spiro[2.4]hepta-2,6-diene has been synthesised in 76%–86% yield by the thermolysis (101–162 °C) of a derivative of norcarene[127] (degree of conversion 75%–85%). It has been suggested that the reaction proceeds via the intermediate formation of carbene.



Finally, the formation of SHD has been observed, although only as a side product, in the following carbene reactions.[128–131]



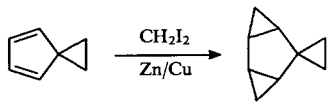
Whereas in the first case[128–131] the mechanism of the formation of SHD is not altogether clear, in the second reaction[131] SHD is apparently obtained as a result of the insertion of the intermediate carbene in a C–H bond of the methyl group.[128, 129, 131]

III. Chemical reactions of spiro[2.4]hepta-4,6-dienes

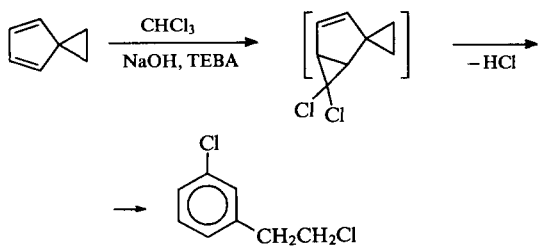
The [2 + 1]-, [2 + 2]-, [2 + 3]-, and [2 + 4]-cycloaddition reactions involving compounds of the SHD series as well as oxidation, reduction, and thermal isomerisation reactions will be considered in this Section. The review does not include the numerous thoroughly investigated complex formation[92, 132–151] (only

studies published during the last ten years are quoted), polymerisation,[14–24] and dehydrochlorination[152] reactions as well as the reactions of SHD and its derivatives with organolithium compounds of arsenic and other elements.[153]

In the [2 + 1]-cycloaddition reactions, i.e. in the reactions with carbenes, SHD yields the products of conversion into one or two cyclopropane groups. Thus the product resulting from the conversion of both double bonds of SHD into cyclopropane groups is formed from the latter in 50% yield under the conditions of the Simmons–Smith reaction.[154]

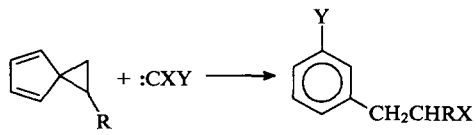


In the reaction of SHD with dichlorocarbene, generated under the conditions of phase transfer catalysis, the intermediate product of conversion of one of the double bonds of SHD into a dichlorocyclomethylene group is unstable, like the analogous monoadduct of dichlorocarbene and cyclopentadiene, and rearranges to the *meta*-derivative of benzene under the existing reaction conditions.[155,156]



50%

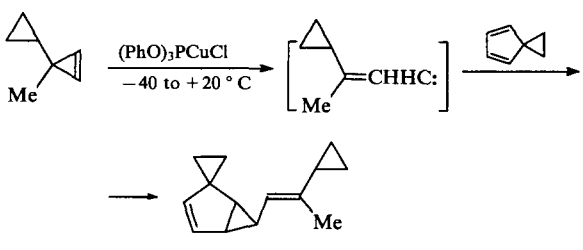
SHD and its substituted derivatives react similarly with other halocarbenes generated under of PTC conditions.[157,158]



X = Y = Cl, Br; X = Cl, Br, Y = F;
R = H, Ph, 3-ClC_6H_4, 4-ClC_6H_4, 4-MeC_6H_4.

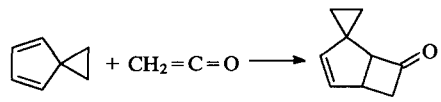
The exclusive formation of *meta*-substituted benzenes in these reactions is very important, since it opens up prospects for the creation of new convenient methods of synthesis of *meta*-substituted benzenes, which are of great practical value, from SHD derivatives (*meta*-substituted benzenes are usually obtained as a result of multistage synthesis). This demonstrates that compounds of the SHD series are likely to be useful as synthons in organic synthesis.

The reaction of SHD with vinylcarbene, generated from methylcyclopropylcyclopropene, leads to the formation of the stable product of the conversion of one of the double bonds of SHD into a cyclopropane group.[159]



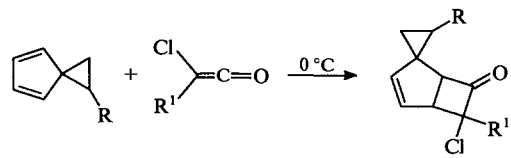
65%

The [2 + 2]-cycloaddition of SHD to ketene affords the corresponding cyclobutanone **27**, which may serve as a convenient intermediate for the synthesis of a series of analogues of natural icosanoids, for example thromboxane A_2 and prostaglandin D_2.[160]



27

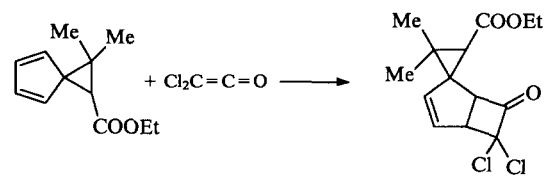
The reactions of SHD and 1-methyl-SHD with chloroketenes, obtained from dichloroacetic acid chloride on treatment with a (3–5)-fold excess of triethylamine, proceed similarly.[161–163]



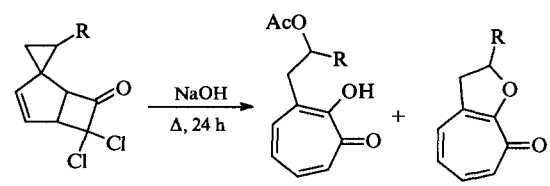
28

R	R^1	Yield of **28** (%)
H	Me	88
H	Pr^i	82
H	Ph	95
H	Cl	85
Me	Cl	92.5

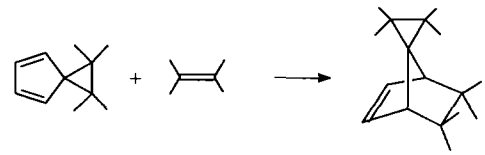
The addition of dichloroketene to trisubstituted SHD also proceeds in this way.[164]



The cyclobutanone derivatives obtained in the [2 + 2]-cycloaddition reaction isomerise with the opening of the four-membered carbon ring on treatment with alkali. The tropolones formed in 35%–40% yield are convenient intermediates for the synthesis of a series of important biologically active compounds and natural products.[162]



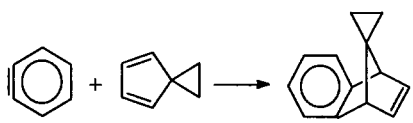
The majority of the reactions investigated, proceeding with participation of compounds of the SHD series, are [2 + 4]-cycloaddition reactions in which SHD and its derivatives usually react as the diene component, affording derivatives of spiro-(bicyclo[2.2.1]hept-2-ene-7,1′-cyclopropane).



The vast majority of reactions of this type have been achieved for SHD itself and its 1-hydroxymethyl derivative. Reactions involving 1-vinyl-substituted SHD and certain other SHD derivatives are also known. The available literature data concerning the involvement of SHD itself in the [2 + 4]-cycloaddition reaction, summarised in Table 6, indicate its high reactivity. This opens up extensive prospects for the employment of SHD in the synthesis of skeletal structures.

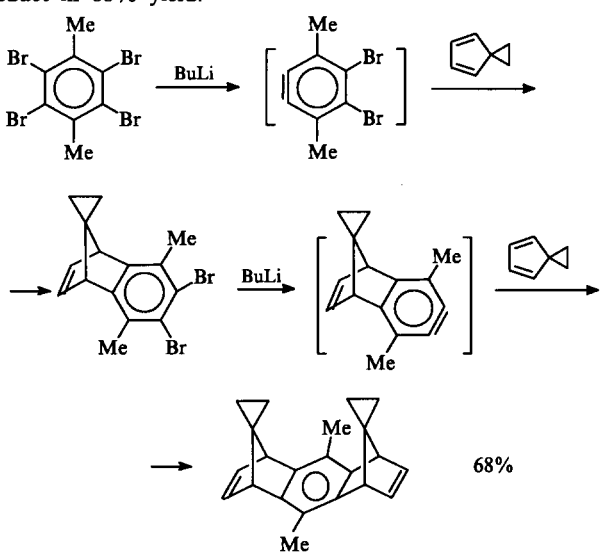
The Diels–Alder reaction involving SHD can proceed both via the usual thermal pathway and catalytically. For example, SHD and 1-methyl-SHD form exclusively cyclic *endo*-[2 + 4]-adducts (in 70%–75% yield) with 1,4-benzoquinone and 1,4-naphthoquinone under the conditions of micellar catalysis (an analogue of phase transfer catalysis) in an aqueous medium in the presence of cetyltrimethylammonium bromide as the micelle forming agent.[175–177] SHD may dimerise in the presence of Lewis acids[165] and on photoinduced electron transfer.[31,32]

SHD readily gives rise to cyclic [2 + 4]-adducts **28** on reaction with dehydrobenzene and its derivatives.[88,164,187]



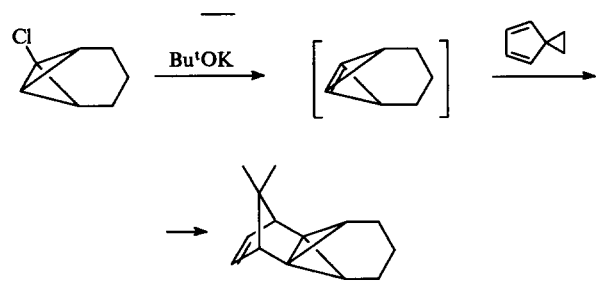
28 (50%–70%)

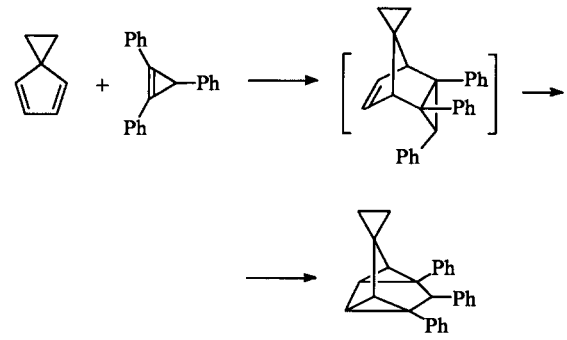
SHD reacts similarly with 1,2,4,5-tetrabromo-3,6-dimethylbenzene, affording the corresponding double cyclic [2 + 4]-adduct in 68% yield.[190]



The reactions of SHD with 1,2,4,5-tetrabromobenzene and 2,3,6,7-tetrabromonaphthalene proceed similarly, affording both mono- and di-adducts of dehydrobenzene derivatives.[191]

SHD is an effective 'trap' for highly reactive unstable unsaturated molecules, for example cyclopropenes. The intermediate unstable strained molecules, containing a double bond, readily afford in this case cyclic [2 + 4]-adducts with SHD. Similar products are also formed in the reactions with stable cyclopropenes. This is illustrated by the following examples.[192,193]

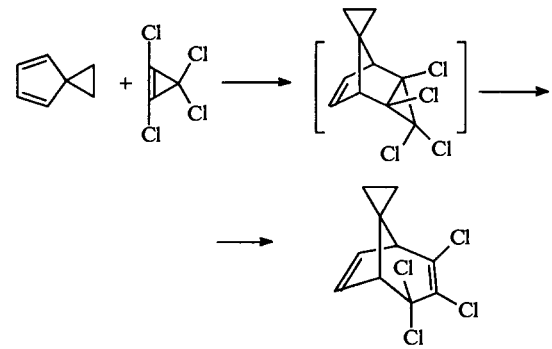




A series of highly strained polycyclic hydrocarbons have been obtained from SHD and its dimer (see, for example, Khusnutdinov et al.[165] and de Meijere et al.[194]).



In many cases, the primary adducts formed are labile and rearrange to thermodynamically stable products under the reaction conditions. Thus the product of reaction of SHD with tetra-chlorocyclopropene derives from the opening of the three-carbon ring of the intermediate chlorocyclopropane.[195]



Derivatives of SHD enter into the Diels–Alder reaction similarly to SHD itself (Table 7, see page 464)).

It is interesting to note that the adduct formed in the Diels–Alder reaction of tetracyanoethylene with dicyclopropyl-substituted SHD undergoes an unusual isomerisation under the conditions of its formation, in contrast to SHD itself and its other alkyl-substituted (methyl- and propyl-substituted) derivatives.[197,198]

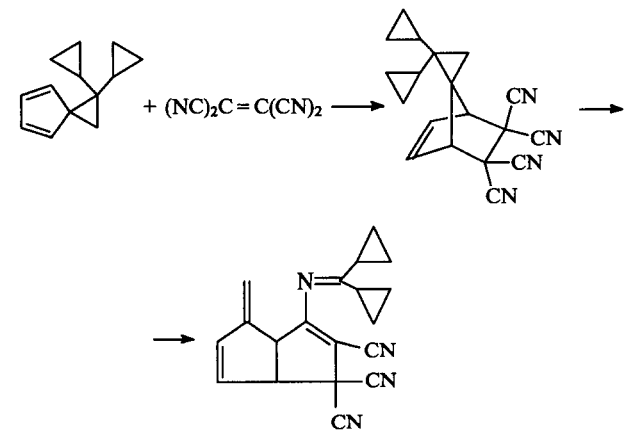


Table 6. The yields of the products of the [2 + 4]-cycloaddition reaction (the Diels–Alder reaction) of dienophiles with SHD.

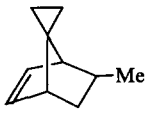
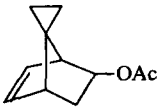
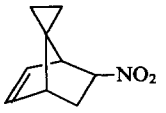
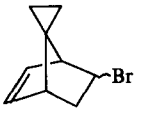
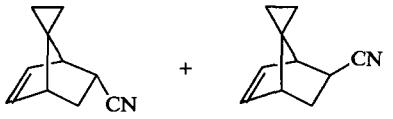
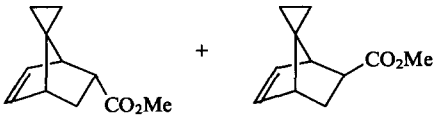
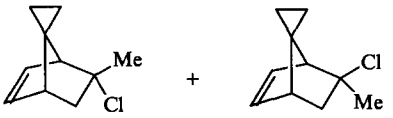
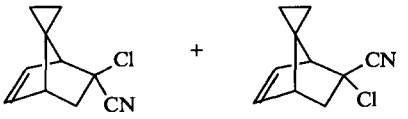
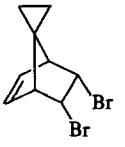
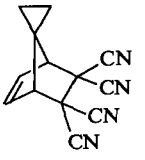
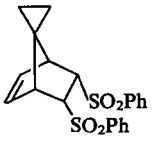
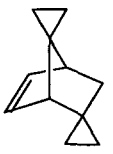
Dienophile	Final product	Yield (%)	Ref.
$CH_2=CHCH_3$		76	165
$CH_2=CHOAc$		60	87
$CH_2=CHNO_2$		89	166
$CH_2=CHBr$		62	167
$CH_2=CHCN$		71 (65:35)	168
$CH_2=CHCO_2Me$		77 (95.8:4.2)	168
$CH_2=CCIMe$		– (90:10)	168
$CH_2=CClCN$		– (94:6)	168
$BrCH=CHBr$		38	87, 105
$(CN)_2C=C(CN)_2$		90	130
$PhSO_2CH=CHSO_2Ph$		85	169
		29	170

Table 6 (continued).

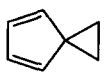
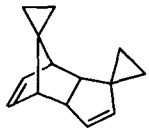
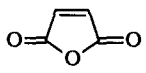
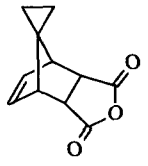
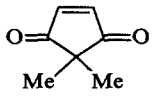
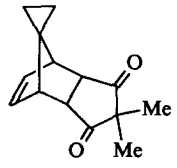
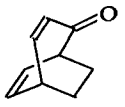
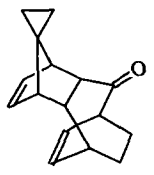
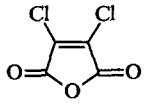
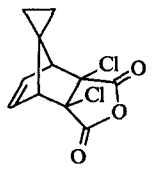
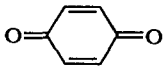
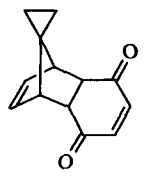
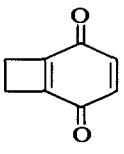
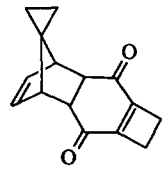
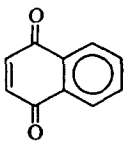
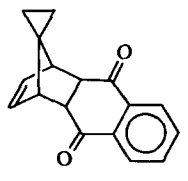
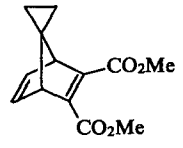
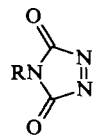
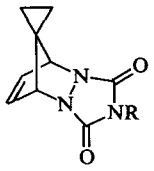
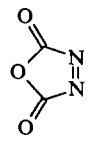
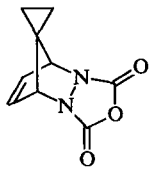
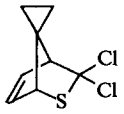
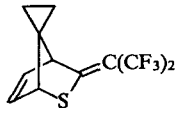
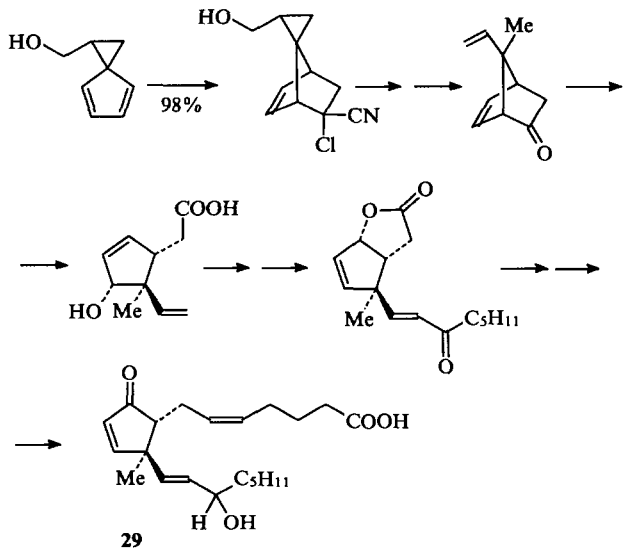
Dienophile	Final product	Yield[a] (%)	Ref.
		–	87, 165
		74–90	37, 87, 91
		73	171
		58	172
		–	109, 173, 174
		–	94, 175–177
		89	178
		100	179, 175–177
$MeO_2CC{\equiv}CCO_2Me$		64	180, 181
$PhCH_2N{=}CH_2$		62	182

Table 6 (continued).

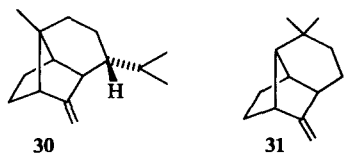
Dienophile	Final product	Yield[a] (%)	Ref.
		50–60	183, 184
		–	185
$S=CCl_2$		74	186
$S=C=C(CF_3)_2$		91	186

[a]A dash shows that the yield is not indicated; the *endo* : *exo* isomer ratio is indicated in brackets.

In speaking of useful practical properties of compounds of the SHD series, one should note that some of the Diels–Alder adducts of SHD possess physiological activity,[11,12] including insecticidal properties.[183] Interesting polymers have been obtained from the adducts of SHD with fluoroolefins.[16,17] The diene adducts of 1-hydroxymethyl-substituted SHD are of great interest as chemical intermediates. The simplest and most effective methods of synthesis of prostaglandins, for example prostaglandin A_2 (compound **29**) (overall yield 9%)[13] and their analogues,[199] as well as certain natural products such as cinularene **30**[118,200–202] and longifolene **31**,[118,202–204] have been proposed on the basis of the chemical reactions of such adducts.



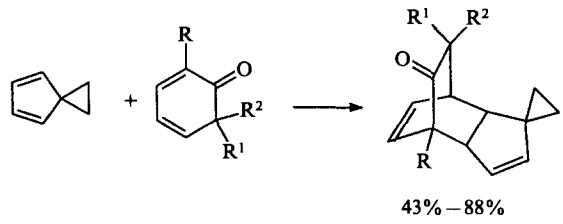
29



30 **31**

Such products are also convenient intermediates in the synthesis of norbornenes disubstituted by functional groups in the 7,7-positions.[205]

SHD and its derivatives can also enter into [2 + 4]-cycloaddition reactions as the dienophile, especially in reactions with highly reactive dienes such as 2,4-cyclohexadienones that are generated in situ.[206–210]

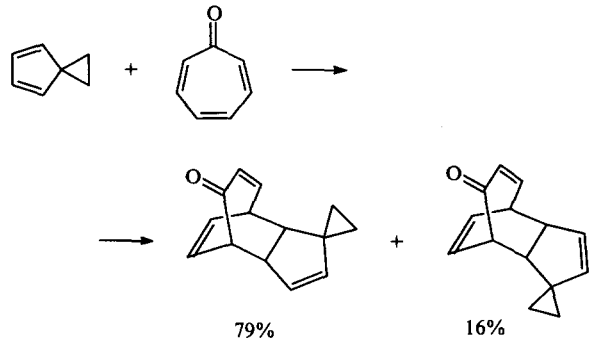


43%–88%

R = H, Me; R^1 = OH, OAc; R^2 = Me, CH_2Cl; $R^1+R^2 = CH_2O$.

The adducts of SHD with 6-hydroxymethylenecyclohexa-2,4-dienone are convenient intermediates in the stereoselective synthesis of natural polyquinane products[210] and compounds of the sesquiterpene series.[209]

SHD also reacts as the dienophile with tropone.[211]



79% 16%

Table 7. The yields of the products of the Diels–Alder reaction with substituted SHD.

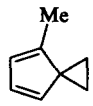
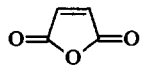
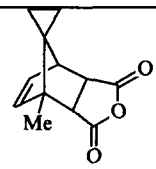
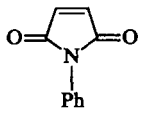
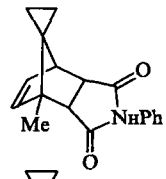
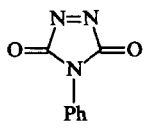
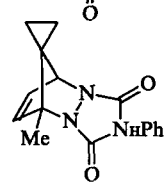
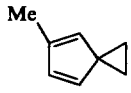
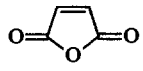
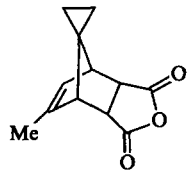
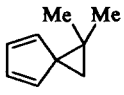
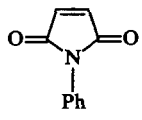
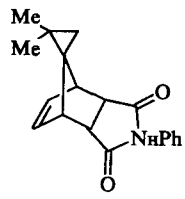
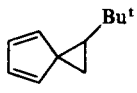
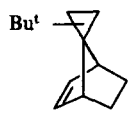
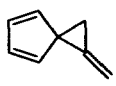
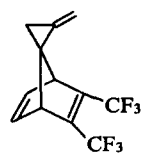
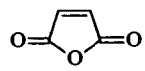
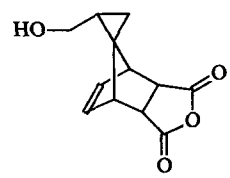
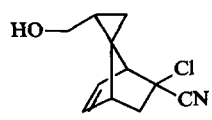
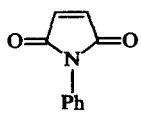
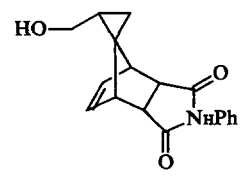
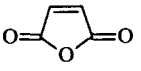
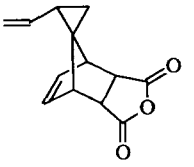
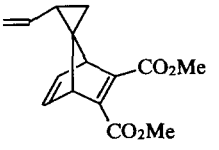
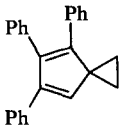
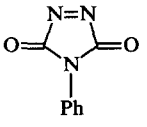
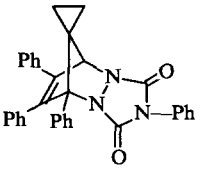
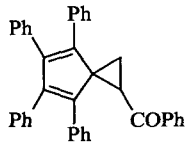
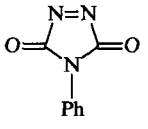
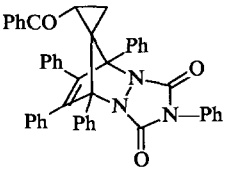
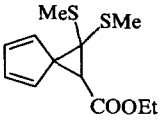
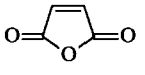
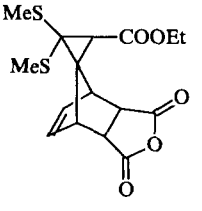
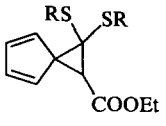
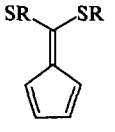
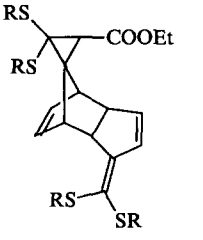
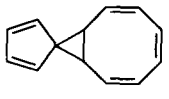
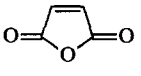
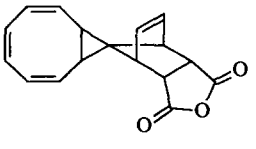
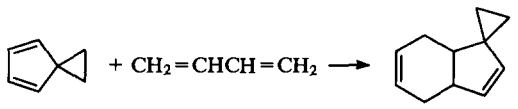
Diene	Dienophile	Product	Yield[a] (%)	Ref.
			80	106
			–	106
			50–60	121
			–	106
			–	124
	$CH_2=CH_2$		70	196
	$CF_3C\equiv CCF_3$		–	64
			–	22
	$CH_2=CClCN$		98	13
			–	116

Table 7 (continued).

Diene	Dienophile	Product	Yield[a] (%)	Ref.
			69	60
	$MeO_2CC{\equiv}CCO_2Me$		–	60
			94	77
			40–57	77
			94	78
			40	78
			76	60

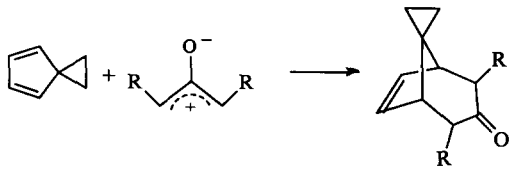
[a] A dash shows that the yield is not indicated.

SHD again assumes the role of the dienophile in a series of reactions with simple dienes. Thus its reaction with butadiene leads to the exclusive formation of spiro(bicyclo[4.3.0]nona-3,7-diene-9,1′-cyclopropane) (in 40% yield).[165]



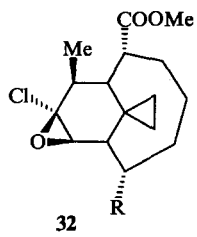
The reaction with cyclopentadiene proceeds similarly.[165]

The reactions involving the dipolar [3 + 4]-cycloaddition of propen-2-oxides, generated in situ, to SHD are also known; for example:[212–214]



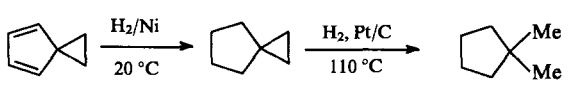
R = Cl, Me; R+R = CH_2CH_2.

The adducts obtained in this way are convenient intermediates in the synthesis of various natural products, for example taxane diterpenes **32**.[215]

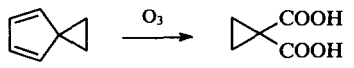


32

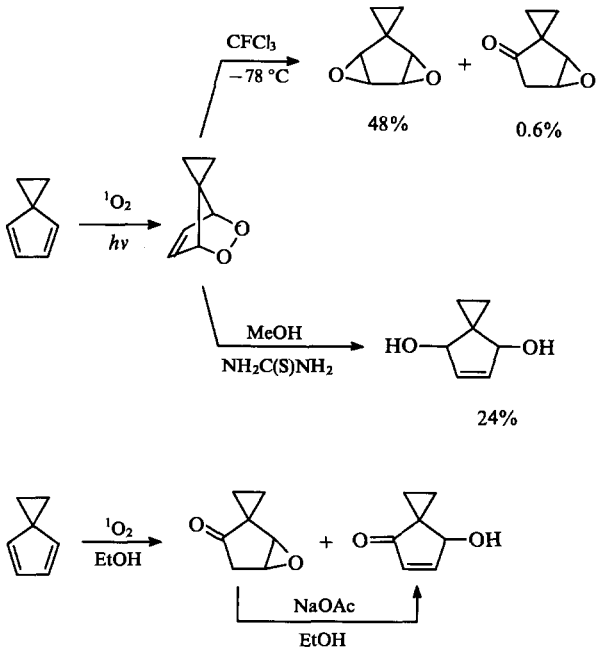
Among other reactions involving SHD, mention should be made of its catalytic hydrogenation, which, in the presence of Raney nickel at 20 °C, leads to the reaction of only the double bonds and yields the associated products, whereas at higher temperature the hydrogenolysis of the three-carbon ring also occurs.[86,216]



The ozonolysis of SHD involves both double bonds of the cyclopentadiene ring and leads to the formation of cyclopropane-1,1-dicarboxylic acid.[85]

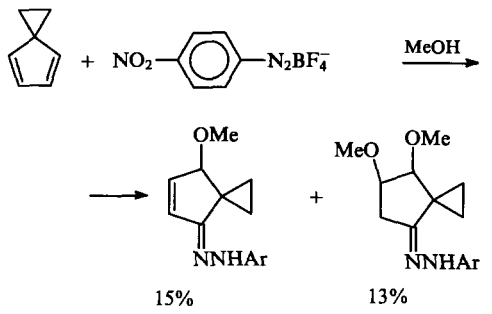


On the other hand, oxidation of SHD by singlet oxygen leads initially to the product of the 1,4-addition of oxygen to the diene system of SHD, which then undergoes further transformations under the reaction conditions.[217,218,219]

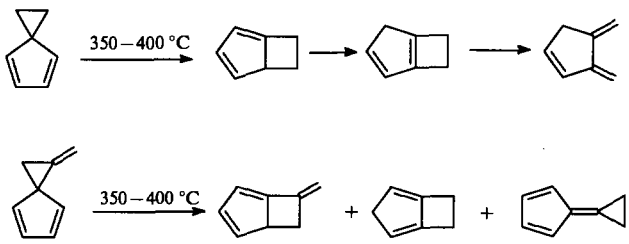


These reactions constitute the basis of the synthesis of natural pederol.[219]

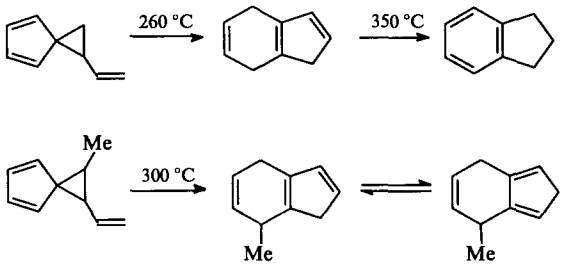
The reaction of SHD with 4-nitrobenzenediazonium fluoroborate in methanol likewise leads to 1,4-adducts.[220]



Finally, certain thermal reactions of compounds of the SHD series have been investigated. At 300–400 °C, SHD and its derivatives undergo irreversible isomerisation, similarly to 5,5-disubstituted cyclopentadienes, as a result of the 1,2-shift of the methylene unit of the three-carbon ring accompanied by 1,2-hydride transfer. Isomerisation leads to the thermodynamically more stable isomeric bicyclo[3.2.0]hepta-1,3-dienes, which may be subsequently trapped by reactive dienophiles in the Diels–Alder reaction.[64,151,220–225]



On the other hand, the thermal reactions of vinyl-substituted SHD are accompanied by the allyl rearrangement, which results in the formation of derivatives of bicyclo[4.3.0]nonatriene.[61]



These bicyclo[3.2.0]heptadienes formed in thermal reactions of SHD can participate subsequently in various [2 + 4]-cycloaddition reactions.[224,225]

The thermolysis of 1-substituted and 1,2-disubstituted SHD at temperatures above 200 °C can also entail their epimerisation.[111]

IV. Conclusion

As can be seen from the literature data examined in the present review, compounds of the SHD series constitute an extremely interesting class of chemical substances with considerable potential synthetic possibilities, both as such and as intermediates in the synthesis of physiologically active and other products of practical value. SHD derivatives have found applications in the synthesis of polyfunctional compounds[226,227] and skeletal structures. Furthermore, such compounds have been arousing an unflagging interest in connection with the problem of spiroconjugation[228–230] and complex formation.

The development of the chemistry of compounds of the SHD series depends to a large extent on the availability of effective methods for their synthesis. The methods of synthesis of SHD and its derivatives developed hitherto, principally the cyclialkylation of cyclopentadiene under the conditions of phase transfer catalysis, have made mono- and 1,2-disubstituted SHD derivatives readily available. It may be expected that further studies in this field will be directed to the development of new preparative methods of synthesis of such compounds by means of reactions involving the cyclomethylenation of the exocyclic double bond of fulvenes.

Finally, the above survey of literature data demonstrates that the chemical reactions of SHD and its derivatives have been studied mainly in relation to the most readily available compounds. Evidently the high availability of these interesting compounds will also stimulate a comprehensive study of their properties, including their chemical properties.

References

1. German P. 2 727 909; *Chem. Abstr.* **89** 6 015f (1978)
2. US P. 4 087 523; *Chem. Abstr.* **89** 108 818z (1978)
3. German P. 2 723 236; *Chem. Abstr.* **88** 89 403w (1978)
4. German P. 2 724 734; *Chem. Abstr.* **88** 74 129n (1978)
5. German P.2 713 651; *Chem. Abstr.* **88** 7 422m (1978)
6. Jpn. P. 76 148 024; *Chem. Abstr.* **86** 166 407p (1977)
7. US P. 3 966 959; *Chem. Abstr.* **85** 123 660c (1976)
8. US P. 3 962 458; *Chem. Abstr.* **85** 105 432a (1976)
9. US P. 4 045 469; *Chem. Abstr.* **88** 190 463r (1978)
10. US P. 3 823 177; *Chem. Abstr.* **81** 77 562q (1974)
11. Eur. P. 486 280; *Chem. Abstr.* **117** 111 477q (1992)
12. German P. 2 939 660; *Chem. Abstr.* **95** 114 914t (1981)
13. E J Corey, C S Shiner, R P Volante, C R Cyr *Tetrahedron Lett.* **16** 1161 (1975)
14. V K Singh, P T Deota, A V Bedekar *J. Chem. Soc., Perkin Trans. 1* 903 (1992)
15. T Kunitake, T Ochiai *Macromol. Synth.* **9** 61 (1985)
16. N Seehof, S Grutke, W Risse *Macromolecules* **26** 695 (1993)
17. N Seehof, C Mehler, S Breunig, W Risse *J. Mol. Catal.* **76** 53 (1992)
18. T Kunitake, T Ochiai, O Ohara *J. Polym. Sci., Polym. Chem. Ed.* **13** 2581 (1975)
19. H Sugimoto, M Takayanagi, T Kunitake *Polym. J.* **9** 95 (1977)
20. T Kunitake, K Takarabek *Asahi Garasu Kogyo Gijutsu Shoreikai Kenkyu Hokoku* **29** 289 (1976)
21. M Takayanagi, T Maijyama *Henkyu Hokoku-Asahi Garasu Kogyo Gijutsu Shoreikai* **37** 355 (1980); *Chem. Abstr.* **94** 175 756u (1981)
22. Jpn. P. 7 411 867; *Chem. Abstr.* **81** 49 338c (1974)
23. Jpn. P. 7 367 391; *Chem. Abstr.* **81** 26 439x (1974)
24. Jpn. P. 7 347 980; *Chem. Abstr.* **80** 4 073a (1974)
25. V K Mavroznev, I I Furlei, E A Burmistrov, F Z Galin, S N Lakeev, V K Ignatyuk, G A Tolstikov *Izv. Akad. Nauk SSSR, Ser. Khim.* 576 (1989)
26. I I Furlei, E A Burmistrov, F Z Galin, V N Iskandarova, V K Mavroznev, G A Tolstikov *Izv. Akad. Nauk SSSR, Ser. Khim.* 1783 (1986)
27. I I Furlei, A Sh Sultanov, R I Khusnutdinov, V A Dokichev, G A Tolstikov, U M Dzhemilev *Izv. Akad. Nauk SSSR, Ser. Khim.* 73 (1985)
28. R Benn, H Butenskhoen, R Mynott, W Wisniewski *Magn. Reson. Chem.* **25** 653 (1987)
29. A J Ragauskas, J B Stothers *Can. J. Chem.* **63** 2961 (1985)
30. J Salazar, M Marques, A Barriola *Acta Cient. Venez.* **38** 505 (1987)
31. H D Roth, M L M Schilling, C J Abelt *Tetrahedron* **42** 6157 (1986)
32. H D Roth, M L M Schilling, C J Abelt *J. Am. Chem. Soc.* **108** 6098 (1986)
33. S W Staley, J T Strnad *J. Phys. Chem.* **98** 116 (1994)
34. K K Irikuka, W A Goddard III, J L Beauchamp *J. Am. Chem. Soc.* **114** 48 (1992)
35. W R Roth, O Adamczak, R Breuckmann, H W Lennartz, R Boese *Chem. Ber.* **124** 2499 (1991)
36. E Gey, B Ondruschka, H Boegel *J. Prakt. Chem.* **332** 519 (1990)
37. R Ya Levina, N N Mezentsova, O V Lebedev *Zh. Obshch. Khim.* **25** 1097 (1955)
38. R A Moss *J. Chem. Soc., Chem. Commun.* 622 (1965)
39. M S Baird, I R Dunkin, N Hacker, M Poliakoff, J J Turner *J. Am. Chem. Soc.* **103** 5190 (1981)
40. O M Nefedov, A I Ioffe, L G Menchikov *Khimiya Karbenov* (Carbene Chemistry) (Moscow: Khimiya, 1990)
41. M Jones, R A Moss *Carbenes* Vol. 1 (New York: Wiley, 1973)
42. H Durr, L Schrader *Chem. Ber.* **102** 2026 (1969)
43. O M Nefedov, P S Zuev, A K Mal'tsev, Y V Tomilov *Tetrahedron Lett.* **30** 763 (1989)
44. A K Mal'tsev, P S Zuev, Yu V Tomilov, O M Nefedov *Izv. Akad. Nauk SSSR, Ser. Khim.* 2202 (1987)
45. H Durr, F Merndorff *Angew. Chem.* **86** 413 (1974)
46. T Migita, K Kurino, W Ando *J. Chem. Soc., Perkin Trans. 2* 1094 (1977)
47. R Gleiter, R Hoffmann *J. Am. Chem. Soc.* **90** 5457 (1968)
48. E Wasserman, L Barash, A M Trozzolo, R W Murrau, W Yager *J. Am. Chem. Soc.* **86** 2304 (1964)
49. R A Moss, J R Przybyla *J. Org. Chem.* **33** 3816 (1968)
50. T Weil, M Cais *J. Org. Chem.* **28** 2472 (1963)
51. R A Moss *J. Org. Chem.* **31** 3296 (1966)
52. P Bischof, R Gleiter *Chem. Ber.* **109** 1412 (1976)
53. H Durr, K-H Albert, M Kausch *Tetrahedron* **35** 1285 (1979)
54. A Amaro, K Grohmann *J. Am. Chem. Soc.* **97** 3830 (1975)
55. W Ando, Y Saiki, T Migita *Tetrahedron* **29** 3511 (1973)
56. H E Zimmerman, D F Juers, J M McCall, B Schroeder *J. Am. Chem. Soc.* **93** 3662 (1971)
57. S W Staley, J J Rocchio *J. Am. Chem. Soc.* **91** 1565 (1969)
58. H E Zimmerman, D F Juers, J M McCall, B Schroeder *J. Am. Chem. Soc.* **92** 3474 (1970)
59. R A Moss, C M Young *J. Am. Chem. Soc.* **105** 5859 (1983)
60. D Schonleber *Chem. Ber.* **102** 1789 (1969)
61. M Jones Jr, R N Hochman, J D Walton *Tetrahedron Lett.* **11** 2617 (1970)
62. L McElwee-White, D A Doudherty *J. Am. Chem. Soc.* **104** 4722 (1982)
63. D Schonleber *Angew. Chem.* **81** 83 (1969)

64. R D Miller, D Kaufmann, J J Mayerle *J. Am. Chem. Soc.* **99** 8511 (1977)
65. H Durr, B Ruge, T Ehrhardt *Liebigs Ann. Chem.* 214 (1973)
66. E T McBee, J A Bosoms, C J Morton *J. Org. Chem.* **31** 768 (1966)
67. H Durr, G Scheppers *Chem. Ber.* **100** 3236 (1967)
68. H Durr, G Scheppers, L Schrader *J. Chem. Soc., Chem. Commun.* 257 (1969)
69. E P Janulis Jr, A J Arduengo *J. Am. Chem. Soc.* **105** 3563 (1983)
70. J Thiec, J Wiemann *Bull. Soc. Chim. Fr.* 177 (1956)
71. N N Tyutyulkov, G D Neikov, I N K'nev *Izv. B'lg. Akad. Nauk Otd. Khim. Nauk* **10** 102 (1977)
72. S W Staley, M D Bjorke, J C Giordane, M R McMillan, J H Moore *J. Am. Chem. Soc.* **103** 7057 (1981)
73. R A Moss, C M Young, L A Perez, K Krogh-Jespersen *J. Am. Chem. Soc.* **103** 2413 (1981)
74. H Hart, R L Holloway, C Landry, T Tabate *Tetrahedron Lett.* **10** 4933 (1969)
75. B M Trost, L S Melvin Jr *Sulfur Ylides. Emerging Synthetic Intermediates* (New York: Academic Press, 1975)
76. A W Johnson *Ylid Chemistry* (New York: Academic Press, 1966) (Translated into Russian; Moscow: Mir, 1969)
77. W D Schroer, W Friedrichen *Liebigs Ann. Chem.* 1648 (1978)
78. G A Tolstikov, F Z Galin, V N Iskandarova, S N Lakeev, L V Spirikhin, L M Khalilov *Izv. Akad. Nauk SSSR, Ser. Khim.* 1373 (1990)
79. G A Tolstikov, F Z Galin, R K Sharipov *Izv. Akad. Nauk SSSR, Ser. Khim.* 1924 (1983)
80. W Ried, H Knorr, H Gurcan *Liebigs Ann. Chem.* 1415 (1976)
81. K Antczak, J F Kingston, A G Fallis *Tetrahedron Lett.* **25** 2077 (1984)
82. K Antczak, J F Kingston, A G Fallis *Can. J. Chem.* **62** 2451 (1984)
83. T Kawase, H Kurata, S Fujino, T Ekinaka, M Oda *Tetrahedron Lett.* **33** 7201 (1992)
84. T Debaerdemaeker, W-D Schroer, W Friedrichsen *Liebigs Ann. Chem.* 502 (1981)
85. B F Hallam, P L Pauson *J. Chem. Soc.* 646 (1958)
86. G Chiurdoglu, B Tursch *Bull. Soc. Chim. Belg.* **66** 600 (1957)
87. K Alder, H-J Ache, F H Flock *Chem. Ber.* **93** 1888 (1960)
88. J Ipaktschi *Chem. Ber.* **105** 1989 (1972)
89. E L Lentzner, W E Watts *Tetrahedron* **27** 4343 (1971)
90. V A Mironov, A P Ivanov, Ya M Kimel'fel'd *Izv. Akad. Nauk SSSR, Ser. Khim.* 2571 (1970)
91. C F Wilcox Jr, R R Craig *J. Am. Chem. Soc.* **83** 3866 (1961)
92. T Kauffmann, K Berghus, A Rensing *Chem. Ber.* **118** 3737 (1985)
93. S Takeshita, A Mori, S Hidaka *Yuki Gosei Kagaku Kyokai Shi* **32** 658 (1974); *Chem. Abstr.* **82** 31 001y (1975)
94. D Kosman, J M Stock *J. Org. Chem.* **40** 2255 (1975)
95. Pol. P. 55 571; *Ref. Zh. Khim.* 20 N 134P (1969)
96. A I D'yachenko, L G Menchikov, O M Nefedov *Izv. Akad. Nauk SSSR, Ser. Khim.* 1664 (1984)
97. L G Menchikov, Candidate Thesis in Chemical Sciences, Zelinskii Institute of Organic Chemistry, Academy of Sciences of the USSR, Moscow, 1984
98. G Rong, F Tao, L Xu *Gaodeng Xuexiao Huaxue Xuebao* **4** 576 (1983); *Chem. Abstr.* **100** 209196w (1984)
99. N S Zefirov, T S Kuznetsova, S I Kozhushkov, Z A Rashchupkina *Zh. Org. Khim.* **19** 541 (1983)
100. E V Dehmlow, S S Dehmlow *Phase Transfer Catalysis* (Berlin: Verlag Chemie, 1980)
101. W P Weber, G W Gokel *Phase-Transfer Catalysis in Organic Synthesis* (Berlin: Springer, 1977) (Translated into Russian; Moscow: Mir, 1980)
102. O M Nefedov, L G Menchikov, A I D'yachenko, S A Agre *Zh. Vses. Khim. O-va im. D.I.Mendeleeva* **31** 182 (1986)
103. L G Menchikov, O M Nefedov, in *Chemistry of Carbenes and Small-Size Cyclic Compounds* (Moscow: Mir, 1989) p. 225
104. A I D'yachenko, L G Menchikov, O M Nefedov *Izv. Akad. Nauk SSSR, Ser. Khim.* 1671 (1984)
105. R A Bartsch, J G Lee *J. Org. Chem.* **56** 2579 (1991)
106. S McLean, P Haynes *Tetrahedron* **21** 2333 (1965)
107. J M Jasinski, J K Frisoll, C B Moore *J. Phys. Chem.* **87** 2209 (1983)
108. K Berghus, A Hamsen, A Rensing, A Wolterman, T Kauffmann *Angew. Chem.* **93** 116 (1981)
109. S F Nelsen, E F Travecedo, E D Seppanen *J. Am. Chem. Soc.* **93** 2913 (1971)
110. F Meyer, P Haynes, S McLean, A G Harrison *Can. J. Chem.* **43** 211 (1965)
111. K E Gilbert, J E Baldwin *J. Am. Chem. Soc.* **98** 1593 (1976)
112. A I D'yachenko, L G Menchikov, O M Nefedov *Izv. Akad. Nauk SSSR, Ser. Khim.* 709 (1984)
113. M F Semmelhack, J S Foos, S Katz *J. Am. Chem. Soc.* **95** 7325 (1973)
114. T J Katz, N Acton, G Martin *J. Am. Chem. Soc.* **95** 2934 (1973)
115. L G Menchikov, A I D'yachenko, O M Nefedov *Izv. Akad. Nauk SSSR, Ser. Khim.* 949 (1984)
116. K Bangert, V Boekelheide *Tetrahedron Lett.* **4** 1119 (1963)
117. H Schaltegger *Helv. Chim. Acta* **45** 1368 (1962)
118. S K Attah-Poku, G Gallacher, A S Ng, L E B Taylor, S J Alward, A G Fallis *Tetrahedron Lett.* **24** 677 (1983)
119. C R Johnson, J P Lockard, E R Kennedy *J. Org. Chem.* **45** 264 (1980)
120. N K Hamer, M E Stubbs *Tetrahedron Lett.* **13** 3431 (1972)
121. M Oda, R Breslow *Tetrahedron Lett.* **14** 2537 (1973)
122. M Muhlstadt, R Schroder, G Zimmermann *Z. Chem.* **11** 67 (1971)
123. H E Zimmermann, T P Cutler *J. Org. Chem.* **43** 3283 (1978)
124. T Tabata, H Hart *Tetrahedron Lett.* **10** 4929 (1969)
125. H E Zimmermann, T P Cutler *J. Chem. Soc., Chem. Commun.* 232 (1978)
126. N K Hamer, M Stubbs *J. Chem. Soc., Chem. Commun.* 1013 (1970)
127. P M Warner, R D Herold *Tetrahedron Lett.* **25** 4897 (1984)
128. R A Moss, U-H Dolling, J R Whittle *Tetrahedron Lett.* **12** 931 (1971)
129. R A Moss, H Chi-Tang *Tetrahedron Lett.* **17** 3397 (1976)
130. S-I Murahashi, O Kumura, Y Maeda, A Sonoda, I Moritani *Bull. Soc. Chem. Jpn.* **47** 2420 (1974)
131. U Burger, G Gandillon, J Mareda *Helv. Chim. Acta* **64** 844 (1981)
132. R T Kettenbach, W Bonrath, H Butenschoen *Chem. Ber.* **126** 1657 (1993)
133. M D Butts, R G Bergman *Organometallics* **12** 4269 (1993)
134. H Lehmkuhl, J Naeser, G Mehler, T Keil, F Danowski, R Benn, R Mynott, G Schroth, B Gabor, C Krueger, P Betz *Chem. Ber.* **124** 441 (1991)
135. R T Kettenbach, H Butenschoen *New J. Chem.* **14** 599 (1990)
136. C G Kreiter, M Wenz, W Michels *Z. Naturforsch., B Chem. Sci.* **44** 1247 (1989)
137. A M Z Slawin, D J Williams, J Crosby, J A Ramsden, C White *J. Chem. Soc., Dalton Trans.* 2491 (1988)
138. M L H Green, L L Wong *J. Chem. Soc., Dalton Trans.* 411 (1987)
139. C G Kreiter, W Michels, M Wenz *Chem. Ber.* **119** 1994 (1986)
140. V C Gibson, C E Graimann, P M Hare, M L H Green, J A Bandy, P D Grebenik, K Prout *J. Chem. Soc., Dalton Trans.* 2025 (1985)
141. T Kauffmann, M Bisling *Chem. Ber.* **118** 4517 (1985)
142. T Kauffmann, K Berghus, J Ennen *Chem. Ber.* **118** 3724 (1985)
143. P Eilbracht, W Fassmann, W Diehl *Chem. Ber.* **118** 2314 (1985)
144. T Kauffmann, E Antfang, J Olbrich *Chem. Ber.* **118** 1022 (1985)
145. T Kauffmann, A Rensing *Chem. Ber.* **118** 380 (1985)
146. T Kauffmann, R Kriegesmann, A Rensing *Chem. Ber.* **118** 370 (1985)
147. T Kauffmann, J Ennen, K Berghus *Tetrahedron Lett.* **25** 1971 (1984)
148. T Kauffmann, E Antfang, J Olbrich *Tetrahedron Lett.* **25** 1963 (1984)
149. M L Green, L L Wong *J. Chem. Soc., Chem. Commun.* 1442 (1984)
150. M L H Green, in *Proceedings of the 4th Int. Conf. on Chem. Uses Molybdenum 1982* p. 74; *Chem. Abstr.* **100** 85 862p (1984)
151. K P Angermund, P Betz, H Butenschoen *Chem. Ber.* **126** 713 (1993)
152. A H Amaro, K Grohmann *J. Am. Chem. Soc.* **97** 5946 (1975)
153. T Kauffmann, J Ennen, H Lhotak, A Rensing, F Steinseifer, A Woltermann *Angew. Chem.* **92** 321 (1980)
154. A M Magerramov, Sh T Akhmedov, L A Dadasheva, N S Sadykhov, S G Bektashi *Nauchn. Tr. Azerb. Inst., Ser. Khim.* 35 (1979)
155. M Makosza, I Gajos *Rocz. Chem.* **48** 1883 (1974)
156. A P Molchanov, I S Vorob'eva, L V Koroleva, R R Kostikov *Zh. Org. Khim.* **26** 2523 (1990)
157. A P Molchanov, R R Kostikov *Zh. Org. Khim.* **28** 1197 (1992)

158. N V Volchkov, A V Zabolotskikh, M B Lipkind, O M Nefedov *Izv. Akad. Nauk SSSR, Ser. Khim.* 1935 (1989)
159. Yu V Tomilov, V G Bordakov, N M Tsvetkova, A Ya Shteinshneider, I E Dolgii, O M Nefedov *Izv. Akad. Nauk SSSR, Ser. Khim.* 336 (1983)
160. S W Jones, D Middlemiss, R F Newton, F Scheinmann, B J Wakefield *J. Chem. Res. (S)* 392 (1988)
161. P R Brook, J M Harrison *J. Chem. Soc., Perkin Trans. 1* 778 (1974)
162. J Tsunetsuqu, M Asai, S Hiruma, Y Kurata, A Mori, K Ono, H Uchiyama, M Sato, S Ebine *J. Chem. Soc., Perkin Trans. 1* 285 (1983)
163. A Hassner, R M Cory, N Sartoris *J. Am. Chem. Soc.* **98** 7698 (1976)
164. G A Tolstikov, L M Khalilov, N V Nazimova, O A Kolchin, E V Vasil'eva, R R Akhmetvaleev, F A Valeev, M S Miftakhov, A A Panasenko *Zh. Org. Khim.* **25** 2105 (1989)
165. R I Khusnutdinov, V A Dokichev, D K Galeev, N F Asylduzhina, S Z Sultanov, U M Dzhemilev *Izv. Akad. Nauk SSSR, Ser. Khim.* 2152 (1988)
166. D Ranganatan, C B Rao, S Ranganathan, A K Mehrotra, R Iyengar *J. Org. Chem.* **45** 1185 (1980)
167. P Yates, G F Hambly *Can. J. Chem.* **57** 1668 (1979)
168. B C C Cantello, J M Mellor, C F Webb *J. Chem. Soc., Perkin Trans. 2* 22 (1974)
169. I V Kazimirchik, K A Lukin, I L Taranyuk, G F Bebikh, N S Zefirov *Zh. Org. Khim.* **21** 313 (1985)
170. W Adam, M Doerr, K Hill, E M Peters, K Peters, H G von Schnering *J. Org. Chem.* **50** 587 (1985)
171. L A Paquette, K E Green, R Gleiter, W Schaefer, J C Gallucci *J. Am. Chem. Soc.* **106** 8232 (1984)
172. H Takeshita, T Hatsui, I Shimooda, H Memetsuka *Bull. Chem. Soc. Jpn.* **55** 2291 (1982)
173. R L Blankespoor, D Gollehon *J. Org. Chem.* **42** 63 (1977)
174. R L Blankespoor *J. Am. Chem. Soc.* **96** 6196 (1974)
175. V K Singh, B N S Raju, P T Deota *Synth. Commun.* **18** 567 (1988)
176. V K Singh, B N S Raju, P T Deota *Synth. Commun.* **17** 1103 (1987)
177. V K Singh, B N S Raju, P T Deota *Synth. Commun.* **16** 1731 (1986)
178. M Oda, Y Kanao *Chem. Lett.* 1547 (1981)
179. R G F Giles, I R Green *J. Chem. Soc., Perkin Trans. 1* 228 (1974)
180. H Prinzbach, W Eberbach, M Klaus, G von Veh *Chem. Ber.* **101** 4066 (1968)
181. C F Wilcox, R R Craig *J. Am. Chem. Soc.* **83** 4259 (1961)
182. S M Roberts, C Smith, R J Thomas *J. Chem. Soc., Perkin Trans. 1* 1493 (1990)
183. German P. 2 446 900; *Chem. Abstr.* **83** 58 835f (1975)
184. I Agmon, M Kaftory, S F Nelsen, S C Blackstock *J. Am. Chem. Soc.* **108** 4477 (1986)
185. R Jain, L McElwee-White, D A Dougherty *J. Am. Chem. Soc.* **110** 552 (1988)
186. M S Raasch *J. Org. Chem.* **40** 161 (1975)
187. R Criegee, B Bastani *Chem. Ber.* **103** 3942 (1970)
188. J Ipaktschi *Chem. Ber.* **103** 3944 (1970)
189. B M Trost *J. Org. Chem.* **34** 3644 (1969)
190. H Hart, C Lai, G Nwokogu, S Shamouilian, A Teuerstein, C Zlotogorski *J. Am. Chem. Soc.* **102** 6649 (1980)
191. H Hart, C Y Lai, G C Nwokogu, S Shamouilian *Tetrahedron* **43** 5203 (1987)
192. H-D Martin *Chem. Ber.* **107** 477 (1974)
193. U Szeimies-Seebach, A Schoffer, R Romer, G Szeimies *Chem. Ber.* **114** 1767 (1981)
194. A de Meijere, K Michelsen, R Gleiter, J Spanget-Larsen *Isr. J. Chem.* **29** 153 (1989)
195. A P Molchanov, R R Kostikov *Zh. Org. Khim.* **28** 278 (1992)
196. R A Moss, H Chi-Tang *Tetrahedron Lett.* **17** 1651 (1976)
197. S Nishida, N Asanuma, M Murakami, T Tsuji, T Imai *J. Org. Chem.* **57** 4658 (1992)
198. S Nishida, N Asanuma, T Tsuji, T Imai *Chem. Lett.* 495 (1991)
199. K Jarowicki, T Jaworski *Monatsh. Chem.* **115** 605 (1984)
200. K Antczak, J F Kingston, A G Fallis, A W Hanson *Can. J. Chem.* **65** 114 (1987)
201. K Antczak, J F Kingston, A G Fallis *Can. J. Chem.* **63** 993 (1985)
202. G Gallacher, A S Ng, S K Attah-Poku, K Antczak, S J Alward, J F Kingston, A G Fallis *Can. J. Chem.* **62** 1709 (1984)
203. Lei Bo, A G Fallis *J. Org. Chem.* **58** 2186 (1993)
204. Lei Bo, A G Fallis *J. Am. Chem. Soc.* **112** 4609 (1990)
205. A G Gonzalez, J Darias, F Diaz *Tetrahedron Lett.* **25** 2697 (1984)
206. V Singh, A V Bedekar *Synth. Commun.* **19** 107 (1989)
207. V Singh, B N S Raju, P T Deota *Indian J. Chem., Sect. B* **26** 301 (1987)
208. V K Singh, P T Deota, B N S Raju *Synth. Commun.* **17** 115 (1987)
209. V Singh, M Porinchu *J. Chem. Soc., Chem. Commun.* 134 (1993)
210. V Singh, B Thomas *J. Chem. Soc., Chem. Commun.* 1211 (1992)
211. H Tanida, T Yano, M Ueyama *Bull. Chem. Soc. Jpn.* **45** 946 (1972)
212. B Foehlisch, D Krimmer, E Gehrlach, D Kaeshammer *Chem. Ber.* **121** 1585 (1988)
213. B Foehlisch, R Joachimi *Chem. Ber.* **120** 1951 (1987)
214. B Foehlisch, E Gehrlach, B Geywitz *Chem. Ber.* **120** 1815 (1987)
215. J Oh, J R Choi, J K Cha *J. Org. Chem.* **57** 6664 (1992)
216. R Ya Levina, N N Mezentsova, E G Treshchova *Dokl. Akad. Nauk SSSR* **104** 549 (1955)
217. W Adam, I Erder *J. Org. Chem.* **43** 2737 (1978)
218. H Takeshita, H Kanamori, T Natsui *Tetrahedron Lett.* **14** 3130 (1973)
219. M C Pirrung, P M Kenney *J. Org. Chem.* **52** 2335 (1987)
220. R Huisgen, F Bronberger *Tetrahedron Lett.* **25** 61 (1984)
221. R A Clark, W J Hayles, D S Youngs *J. Am. Chem. Soc.* **97** 1966 (1975)
222. J M E Krekels, J W de Haan, H Kloosterziel *Tetrahedron Lett.* **11** 2751 (1970)
223. R D Miller, D Kaufmann *J. Chem. Soc., Chem. Commun.* 486 (1978)
224. Yu V Tomilov, A B Kostitsyn, E V Shulishov, O M Nefedov *Izv. Akad. Nauk SSSR, Ser. Khim.* 477 (1992)
225. Yu V Tomilov, A B Kostitsyn, E V Shulishov, O M Nefedov *Izv. Akad. Nauk, Ser. Khim.* 132 (1993)
226. L Bo, A G Fallis *Can. J. Chem.* **69** 1450 (1991)
227. L Bo, A G Fallis *Tetrahedron Lett.* **27** 5193 (1986)
228. H E Simmons, T Fukunaga *J. Am. Chem. Soc.* **89** 5208 (1967)
229. R Hoffmann, A Imamura, G D Zeiss *J. Am. Chem. Soc.* **89** 5215 (1967)
230. M J Goldstein, R Hoffmann *J. Am. Chem. Soc.* **93** 6193 (1971)

Russian Chemical Reviews **63** (6) 471 – 482 (1994)
©1994 Russian Academy of Sciences and Turpion Ltd

UDC 541.182.45 : 66.066.8

The mechanisms of antifoam action

P M Kruglyakov

Contents

I.	Introduction	471
II.	Methods for the investigation and estimation of the antifoam activities of substances	473
III.	The homogeneous (adsorption) mechanism of the antifoam action	473
IV.	The spreading of antifoams and the effectiveness of the antifoam action	475
V.	The antifoam effect of drops of organic liquids	476
VI.	The antifoam effect of solid hydrophobic particles	478
VII.	Concentration effects in antifoam processes	480

Abstract. The homogeneous and heterogeneous mechanisms of antifoam action are examined. The homogeneous mechanism involves the adsorption displacement of the molecules of the foam-forming agent from the surface layers of foam films with formation of mixed layers of the foam-forming agent and the antifoam; in this case, the foam films are in a nonequilibrium state. The heterogeneous mechanism of the destruction of the foam consists in the formation of unstable asymmetric aqueous films and the subsequent appearance, after their disruption, of 'bridges' consisting of drops or solid particles of the antifoam passing through the foam film. It is shown that the most important factors governing the instability of the asymmetric film are the low degree of adsorption of the foam-forming agent on the interface between the films and the drops of the antifoam and the solid particles, as well as the presence of rough regions on the solid particles. The antifoam action of solid particles or drops forming the 'bridges' is determined by the wetting angles. The foam film is ruptured when the establishment of an equilibrium three-phase foam film – antifoam – gas contact is impossible. In many systems, both mechanisms of the destruction of the foam operate simultaneously. The bibliography includes 66 references.

I. Introduction

Many industrial processes are accompanied by the formation of a foam, which creates serious difficulties in the technological process or spoils the product. The formation of a foam in the cellulose and paper industries, in the enzymic synthesis of antibiotics and other medicinal preparations, in the electroplating industry, in the dyeing of fabrics, in the preparation of food yeast, baker's yeast, and tomato juice, in blood transfusion, and in the pumping and treatment of bore hole, boiler, industrial, and domestic waste water is a list of only some examples of undesirable foam formation.[1,2]

In order to diminish foam formation, various measures are undertaken. Technological procedures (diminution of the entrainment of air, change in the composition of the solutions or their pH) are usually insufficient and it is necessary to resort to various physical (usually mechanical) and chemical methods to combat foam formation (antifoam action).

Mechanical antifoam equipment includes various rotating devices (stirrers, discs, blades, centrifuges, separators, etc.); in air, steam, or liquid streams, the foam is disrupted by the critical stresses and deformations in the film or as a consequence of the acceleration of the syneresis (drying) of the foam. A rational classification of these procedures for the destruction of the foam and the methods used in the design calculations for mechanical antifoam devices have been examined in detail by Vetoshkin.[3]

The physical procedures include the disruption of the foam by thermal action (heating, treatment with hot steam, freezing), by an electric current, by acoustic waves (mainly ultrasound), by vibration, by exposure to α-particles, by the creation of a high capillary pressure in the foam, etc.[1,2,4]

The most widely used procedure in the fight against foam involves the introduction into the foam-forming solution (or into the foam) of special substances — antifoams (chemical antifoam action). Fats, oils, waxes, aliphatic alcohols, acids, amines, ethers, organophosphorus compounds (in particular, tributyl phosphate), organosilicon compounds (silicone oils), nonionogenic surfactants with a low hydrophilic – lipophilic balance (HLB) [with a HLB number less than 6 (usually 1 – 3)], solid hydrophobic particles, as well as numerous types of waste containing the above and other components†.

'Filled' antifoams (hydrophobic particles, usually hydrophobic silica, dispersed in an oil), which can be emulsified in an aqueous medium, are regarded as some of the most promising.

Hitherto antifoams have been selected mainly empirically taking into account the purposes and nature of the industry. The mechanism of the action of antifoams, especially in the form of a separate phase (drops or hydrophobic particles), remains in many respects obscure.[2]

In terms of the principle governing their action, antifoams can be divided into two groups. The first includes substances that interact chemically with the foam-forming agent, which leads to the formation of insoluble or sparingly soluble compounds. Thus, when soluble aluminium or calcium salts are added to a foam or a foam-forming solution of the sodium or potassium salts of aliphatic acids or when cationic surfactants are added to a solution

† A detailed list of antifoams and their applications may be found in the relevant books.[1,5].

P M Kruglyakov Department of Chemistry, Penza State Architectural and Building Institute, ul. Titova 28, 440028 Penza, Russian Federation, Fax (7-841) 262 04 10

Received 4 April 1994
Uspekhi Khimii **63** (6) 493 – 505 (1994); translated by A K Grzybowski

of anionic surfactants, insoluble compounds are obtained, whereupon the foam is disrupted or ceases to form. The effectiveness of the antifoam is determined in this case by its ability to bind the foam-forming agent, converting it into a precipitate.

A procedure intensifying the disruption of an existing foam involves the supply of antifoams in the form of a foam.[2] For example, a foam produced from a solution of a cationic surfactant with added calcium and aluminium salts is supplied to a foam produced from a solution of anionic surfactants which it is proposed to destroy. The disadvantages of antifoams of this group are the large consumption of the substance and contamination of the working solution by the insoluble compounds formed. For this reason such antifoams are used very rarely.

The second, more common group of antifoams includes substances which do not interact chemically with the foam-forming agent. They disrupt the foam or prevent foam formation as a result of various physicochemical processes, so that they should probably not be referred to as chemical antifoams.

The mechanism of the action of the antifoams of the second group is more complex: it depends not only on the nature of the substance (composition, structure, etc.) and its concentration, but also on the state in which it exists in the foam-forming solution (in the form of molecules or ions or as a separate phase) and many other factors.

The mechanism of the antifoam action of dissolved antifoams will be referred to henceforth as homogeneous (or adsorption) and that of antifoams forming a separate phase will be called heterogeneous. The mechanism of the heterogeneous antifoam action operates in a pure form when liquid, nonpolar, and water-insoluble hydrocarbons or solid hydrophobic particles (Teflon, hydrophobic glass, or silica) are used. When diphilic sparingly soluble compounds are used, the foam may be destroyed as a result of the joint operation of the homogeneous and heterogeneous mechanisms of the antifoam action.

Antifoams in the form of a separate phase (such as drops of a pure substance, solutions in organic solvents, or emulsions) have long been used.[6] There exist various treatments of the mechanisms of the antifoam action including a homogeneous treatment involving the monolayer spreading of the antifoam on the surfaces of foam films and the adsorption displacement of the molecules of the foam-forming agent from their surfaces. The drops can then be regarded (like surfactant micelles) merely as an absorber (or 'reservoir') of the antifoam.

Various qualitative ideas concerning the operation of a special heterogeneous mechanism of antifoam action have been put forward in discussing the role of the spreading of drops in antifoam processes and in the prevention of the formation of optically black spots in microscopic foam films.[7,8]

An explanation of the heterogeneous mechanism of the antifoam action of drops, based on the conversion of stable foam films into unstable aqueous films on an antifoam support owing to the sharp decrease in the degree of adsorption of the foam-forming agent on one of the surfaces of the asymmetric film, was first put forward by Kruglyakov and coworkers.[9,10]

Another mechanism of the heterogeneous antifoam action has been proposed for hydrophobic solid particles.[11,12] Subsequently it was developed in detail in many other investigations.[13–16] This treatment came to be used also in relation to liquid drops.[13,15,16] Different mechanisms of antifoam action have not so far been compared.

The problem of the stability of foams (like that of other disperse systems) and of its regulation (increase in some systems and decrease in others) is crucial in colloid chemistry. Many aspects of this problem have not yet been elucidated.[2,17]

As a consequence of the excess surface energy, a foam is as a whole in a state of thermodynamic nonequilibrium. A consequence of this is spontaneous processes involving the segregation of the liquid from the foam (syneresis of the foam), diffusional transport of gas from small bubbles into larger ones, rupture of films with local coalescence, and the destruction of the foam as a whole, i.e. the separation of the disperse system into a liquid and a gas. However, individual constituents of the foam, in particular films and Plato–Gibbs channels, may be in equilibrium and may possess true stability (metastability).

Analysis of these processes and equilibrium states is outside the framework of this review (although it is important for the understanding of the mechanism of the action of antifoams). Individual questions concerning directly the influence of antifoams on the equilibrium in films or on the kinetics of the syneresis and disruption of the foam will be considered in the analysis of the mechanisms of the antifoam action.

The rate of syneresis of the foam as a function of time or simpler parameters, for example, the time required for the segregation of half of the initial volume of liquid, are used as characteristics of stability in relation to the segregation of the liquid.

The main parameter characterising the rate of internal disruption (aggregative instability) is the rate of decrease in the specific surface of the film and the parameter characterising the disruption of the foam as a whole is the rate of decrease in its volume or of the height of its column (provided that the cross-section of the column is identical along its height). The corresponding characteristics of the stability may be the reciprocals of the rates of the internal disruption and of the disruption of the foam as a whole. The simplest integral characteristic of the stability of a foam is the lifetime of the entire foam or of part of it.

The equilibrium in foam films and hence the prolonged existence of a foam are ensured, on the one hand, by the molecular, electrostatic, and short-range (adsorption or structural) components of the disjoining pressure (Π). On the other hand, various kinetic factors exert a significant influence on the rate of equilibration, the rate of the internal disruption of the foam (as a consequence of diffusion and coalescence), and on the response to the effect of various external perturbations (compressive and stretching deformations, changes in temperature, local changes in surfactant concentrations, etc.). These factors are determined by the stabilising effect of the surfact adsorption layers and by the volume properties of the solution[2]—the equilibrium and dynamic elasticity, the retardation of the rate of flow of the liquid along the films and the Plato–Gibbs channels with different mobilities of the adsorption layers, the volume and surface viscosities, and the electroosmotic pressure—as well as other properties combined in the concept of the structural-mechanical barrier.[18]

External physical influences (a change in temperature, an increase in capillary pressure, irradiation by a stream of α-particles, etc.) alter the rates of the above processes and lead to the breakdown of equilibria. The study of the mechanisms of certain influences helps to achieve a better understanding of the nature of the kinetic processes and equilibrium states and a specific regulation of the stability of the foam.

The method involving the creation of large pressure drops in the liquid phase of the foam and of the corresponding capillary (P_σ) and disjoining pressures in the foam films proved very effective in the study of various physicochemical processes and equilibria in a foam.[2,19,20] In this method, the foam is brought into contact with a porous hydrophilic partition under which a reduced pressure (relative to the atmospheric pressure), not exceeding the capillary pressure in the pores of the partition, is established. Only the liquid but not the gas flows out of the foam under these conditions. This form of external action is most 'natural' for a foam, since a reduced pressure in the Plato–Gibbs channels is an essential condition for the formation of any polyhedral foam. By regulating the pressure drop, it is possible to reduce the positive component of the disjoining pressure by $\Pi - P_\sigma$.

Comparison of the properties of microscopic foam films and the films in a real foam showed that the behaviour of the films in a foam and their response to external influences are more complex than in model films. This is associated both with the difference between the kinetics of various processes in the foam and with the

influence of the dimensions of the films, on the one hand, and with the existence of 'collective effects', arising as a result of the transmission of perturbations due to the rupture of individual films by neighbouring films and bubbles, on the other.[19,20] Various factors stabilising a real foam have been surveyed in a monograph.[2]

II. Methods for the investigation and estimation of the antifoam activities of substances

Various ways of using antifoams are known. They can be introduced beforehand into the working medium (foaming solution) in a pure form or as solutions and dispersions of solid particles in organic solvents (kerosene, turpentine, liquid paraffin) and also as emulsions of different composition in order to prevent the undesirable foam formation. Antifoams are sometimes introduced directly into the foam. The efficiency of antifoams is not the same under these conditions.[1,2]

In view of this, in estimating the antifoam activities of antifoams it is essential to distinguish their effectiveness in disrupting a foam which has already been formed (antifoam action proper) and in preventing foam formation in the foaming process. Substances which are effective in preventing foam formation usually effectively disrupt an existing foam at the same time. On the other hand, many antifoams which effectively disrupt a foam become relatively ineffective in preventing the formation of a foam when introduced into a solution. For example, when drops of butanol and silicone oil are added to a 0.024% solution of saponin, the foam is rapidly destroyed.[21,22] However, when the solution is subsequently shaken with butanol, abundant foam formation again takes place and the resulting foam is stable. On the other hand, the shaking of a solution containing a drop of the silicone antifoam does not induce foam formation.

Various methods are used to estimate the antifoam activities of substances. In the study of the mechanism of antifoam action and of the prevention of foam formation, a comprehensive qualitative assessment of the antifoam activity is very important. This is done in the first place by observing the behaviour of a model foam film (usually macroscopic) when a drop of the antifoam is deposited on it.[23,24] It can involve the observation of the characteristics of the behaviour of the foam or the foam film after the introduction of the antifoam (the nature and rate of attenuation, the lifetime, etc.) and of the behaviour of the antifoam (the form of spreading, fragmentation, the formation of 'bridges', etc.). The film is obtained by withdrawing frames of different size (for example 2 × 1.5 cm) or rings (6–10 mm in diameter). A drop of the test substance or a hydrophobic particle is deposited on the film or the latter is touched with a needle wetted with the antifoam. The film is also obtained from a solution containing the antifoam[13,14] and the nature and rate of its attenuation and disruption are observed.

Similar observations are also carried out when a drop of the antifoam is added directly to the foam investigated immediately after its formation or after a certain time (for example, after 2 or 20 min) or to a solution on the surface of which 'islands' of foam bubbles have been obtained.[7] This permits conclusions concerning the mechanisms of the antifoam action (homogeneous or heterogeneous), the rate of disruption of the foam, the role of the spreading of the antifoams, the influence of solvents on the antifoam activity, etc.

Yet another method for the investigation of the antifoam activity, useful in elucidating the mechanism of the antifoam action, involves the study of the suppression of the formation of optically black spots in microscopic foam films and the influence of the added antifoam.[8,9] This method is based on the fact that a sharp transition to films with a high stability with increase in the concentration of the antifoam is associated with the appearance of black spots in microscopic foam films.[2]

For the film to remain stable after the addition of the antifoams, i.e. in order to ensure the appearance of black spots, it is necessary to increase the concentration of the foam-forming agent. Conversely, with increase in the concentration of the foam-forming agent, the concentration of the antifoam necessary to suppress the formation of black spots must also be increased. Comparison of the ratio of the concentrations of the antifoam and of the agent producing black spots makes it possible to find a measure of the antifoam activity. Such a method for the estimation of the effectiveness of antifoams was first proposed by Ekserova and Buleva.[25]

A direct or indirect determination of the decrease in the stability (lifetime) of the foam or of the decrease in its volume under the influence of a definite dose of the antifoam are used to obtain quantitative characteristics of the antifoam activity. These are usually determined from the average lifetime of the foam or of the relative (compared with the foam without additives) lifetime of the foam in the presence of the antifoam.[1,2] The effectiveness of substances in preventing foam formation is frequently estimated from the decrease in the rate of foam formation for a constant supply of the gas, from the decrease in the height of a column of the foam compared with the height of the foam without the antifoam, etc.[1,2]

For industrial purposes, the antifoam activity (for example, the decrease in the volume of the foam) is referred to a unit volume or mass of the antifoam and sometimes the consumption of the antifoam is compared with the consumption of a standard substance.[1,2] The most complete estimate of the antifoam activity must take into account not only the effectiveness of the substance for different ways of its application but also the influence of the duration of its action (since the effectiveness usually diminishes greatly on contact with the solution) as well as the influence of the solvent and the form and concentration of the foam-forming agent.

III. The homogeneous (adsorption) mechanism of the antifoam action

Any decrease in the lifetime of a foam as the composition of the solution is altered may be regarded as the manifestation of antifoam activity and in this sense the process can be regarded as part of the problem of the stability of foams. However, antifoam action has come to be regarded as the rapid disruption of the foam by special additives and such a process and the mechanisms inducing it constitute a special theoretical and applied problem in colloid chemistry. It is at present difficult to predict theoretically the rate of disruption of a foam even in the simplest systems, for example, in foams for which the type of foam films and the internal structure and capillary (disjoining) pressure, determining the thickness of the films in the absence of an antifoam, are known. One of the main reasons why the mechanisms of the antifoam activity have not yet been fully elucidated is associated with this factor. Furthermore, antifoam activity is caused by many factors on which the effectiveness of antifoams also depends.

One of the possible mechanisms of the action of antifoams involves the adsorption displacement (complete or partial) of the molecules of the foam-forming agent from the interfaces of the foam films and the formation of mixed adsorption layers, which exhibit a poor stabilising activity.

The idea of the adsorption mechanism of the antifoam action was put forward in early studies by Quinke to account for the disruption of the foam on beer by ether vapour.[1] This idea is extremely widespread and is used to explain antifoam activity and de-emulsification,[1,4,26,27] although special studies designed to confirm and determine the details of the adsorption mechanism have been scarcely carried out.

As mentioned above, the disruption of a foam by antifoams introduced into the foam or the foam-forming solution as drops of the pure antifoam or its solutions in organic solvents immiscible with water or directly in the form of emulsions has been investigated in most of the studies. The spreading of the antifoam on the foam-forming solution (for a positive spreading coefficient

or a positive spreading pressure) does not permit an unambiguous conclusion concerning the mechanism of the antifoam action: it can be both homogeneous and heterogeneous.

The only reliable indication of a homogeneous mechanism of the antifoam action is provided by the results of a direct study of the decrease in the stability of foams in foam-forming systems containing an antifoam in an amount not exceeding its solubility (the true solubility or the colloidal solubility in the form of a solubilised system).

The disruption of foams by ethanol was already known to Plato. However, the antifoam activity of alcohol is low: the complete prevention of foam formation requires a concentration of about 25%. The properties of the solvent (mixture of water and alcohol) are markedly altered at such a high concentration.

The prevention of foam formation and the disruption of a foam obtained from a solution of sodium dodecyl sulfate (DDSNa) has been investigated under conditions where after the introduction of the antifoams (19 kinds in all) it was known exactly whether the system was homogeneous or heterogeneous.[28] When certain homogeneous systems (ethyl acetate, oleic acid) were used to prevent foam formation, virtually no decrease in the volume and stability of the foam was observed, but when the system became heterogeneous an appreciable suppression of foam formation was noted.

An almost complete prevention of foam formation in the homogeneous region is characteristic of other homogeneous systems (phenol, pentyl and butyl alcohols, butyric acid, ethyl ether, and triethyl phosphate)—when the antifoam was introduced, the height of the foam after 10 min did not exceed 0.4–0.5 cm, while the height of the foam in an aqueous DDSNa solution without additives was 10 cm. This confirms unambiguously the homogeneous mechanism of the antifoam action.

The antifoam activities of readily soluble antifoams—lower saturated alcohols—have been compared[29] over a wide range of concentrations, including the region of the transition from the homogeneous to the heterogeneous system. The effectiveness of the antifoams was estimated from their ability to prevent foam formation. The dependence of the decrease in the lifetime of the foam on the concentration of the antifoam is illustrated in Fig. 1 for certain foam-forming agents.

Comparison of the stabilities of foams in the homogeneous region showed that, in order to decrease the lifetime of the foam to the same value, for example to 20 min, the amount of butyl alcohol required is ~10–30 times greater than that of hexyl alcohol (depending on the nature and concentration of the foam-forming agent). This means that the antifoam activity of the lower homologous alcohols is approximately directly proportional to the surface activity of the alcohol. According to Traube's rule, the surface activity increases by a factor of 12 on passing from butyl to hexyl alcohol.[30] The most effective suppression of foam formation in the homogeneous region has been observed in a solution of saponin, which is probably associated with the fact that it has the lowest surface activity and with the poor stabilising activity of mixed adsorption layers. These results confirm, at least qualitatively, the fact that in the given homogeneous system the antifoam activity of the antifoam is determined by its adsorption capacity and that in a number of systems (DDSNa–isovaleric acid, OP-10‡–butyl alcohol) virtually complete suppression of foam formation is observed after the attainment of the concentration corresponding to the solubility limit (saturation). However, in other systems, for example DDSNa–hexyl alcohol and OP-10 (0.1%)–tributyl phosphate (TBP) and in all cases where higher homologues of alcohols are used,[29,31] an appreciable stability of the foam is retained (the lifetime is 10–25 min) up to the instant of saturation, but the subsequent increase in the concentration of the alcohols and transition to the heterogeneous region lead to the complete disruption of the foam and prevention of foam formation.

Convincing evidence for the inadequacy of the adsorption displacement of the foam-forming agent in antifoam action has also been obtained in studies of the suppression of the formation of black spots in microscopic foam films by the addition of aliphatic alcohols and acids.[8,9] It was shown experimentally[8,9] that this effect (i.e. the conversion of foam films into an unstable form) occurred in all the systems investigated only after the attainment of the limiting solubility of the antifoam in the solution of the foam-forming agent. These and the results mentioned previously[23,28] indicate the possible operation of two mechanisms of the antifoam action different from the adsorption-displacement mechanism and associated with the appearance of a new phase. In a number of systems (for example, in a mixture of saponin and soap), the antifoam action can be accounted for within the framework of the homogeneous mechanism but in a more complex specific form[32] with allowance for chemical interaction.[2]

In the homogeneous mechanism of the antifoam action, the effect of the antifoam reduces mainly to the alteration of the properties of the adsorption layers of the foam film, the rate of adsorption,[26,33] the elasticity, the surface viscosity,[26,34] and the positive component of the disjoining pressure. Antifoams sometimes influence indirectly the surface properties of foam films by altering the solubility of the foam-forming agent or its critical concentration for micelle formation (CCM). Thus it has been established[35,36] that the addition of 2-ethylhexanol, TBP, and tetradecanol increased the CCM of the foam-forming agent (sodium oleate, DDSNa, etc.) and hence reduced the surface activity.

Ross and Young[37] divided all antifoams into two groups: the first (for example, TBP) mainly accelerate the syneresis of foams by decreasing the surface viscosity and elasticity, while others (for example, isobutylcarbinol) increase the critical thickness of the films or more precisely convert the metastable foam films into unstable ones, which are ruptured at a certain critical thickness (in conformity with theory§; for further details, see Kruglyakov and Ekserova[2]).

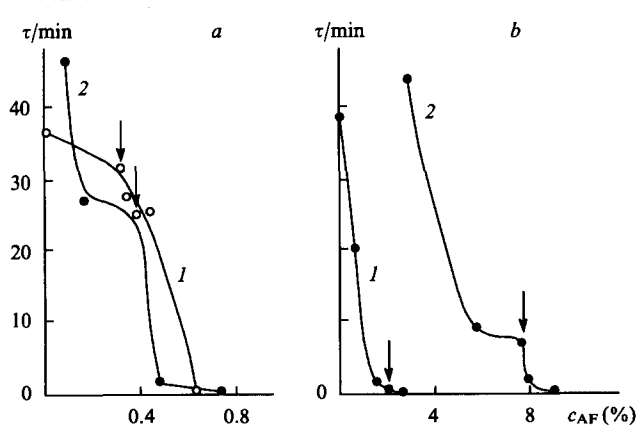


Figure 1. Dependence of the lifetime of the foam on the antifoam concentration. Antifoam: (*a*) 5 × 10^{-1} M DDSNa + 0.4 M NaCl + hexyl alcohol (curve *1*); 0.1% OP-10 + 0.1 M KCl + hexyl alcohol (curve *2*); (*b*) 5 × 10^{-5} M DDSNa + 0.4 M NaCl + isovaleric acid (curve *1*); 2.5 × 10^{-4} M DDSNa + 0.4 M NaCl + butyl alcohol (curve *2*). The limiting solubilities of the antifoams are indicated by arrows.

‡ Technical hydroxyethylated alkylphenol with ten hydroxyethyl groups.

§ See A Scheludko *Adv. Colloid. Interface Sci.* **1** 391 (1967); A Vrij *Discuss. Faraday Soc.* **42** 23 (1966).

IV. The spreading of antifoams and the effectiveness of the antifoam action

Antifoams frequently spread on the surface of the foam-forming solution (and foam films produced from this solution), destroying foam thereby, and for this reason many investigators explain the antifoam activity as being due to spreading.[2,21,25] Leviton and Leighton[38] were among the first investigators to relate the effectiveness of an antifoam to the spreading pressure. Ross and coworkers,[35,37,39] who investigated the influence of spreading on the antifoam action in greatest detail, concluded that there are several types of effects by the spreading substance on the stability of foam films.

The first type of effect involves the formation of a polymolecular spreading film. A condition for polymolecular spreading is a positive value of the initial spreading coefficient ($S_{B/A}$)¶:

$$S_{B/A} = \sigma_A - \sigma_{AB} - \sigma_B \ , \qquad (1)$$

where σ_A and σ_B are the surface tensions of the foam-forming solution A and of the antifoam B, while σ_{AB} is the interfacial tension between A and B.

Rapid spreading of an organic film on the surface of water is usually observed when this liquid has low surface and interfacial tensions. The coefficients $S_{B/A}$, calculated by Eqn (1) for several typical antifoams with a positive initial value of $S_{B/A}$ on the surface of foam-forming solutions, are listed in Table 1.

Table 1. Initial spreading coefficients.[7,31]

Antifoam	Surface tension of antifoam/mN m^{-1}	Foam-forming solution	
		I	II
Alcohols			
Butyl alcohol	24.6	3.0	4.7
Hexyl alcohol	25.3	1.1	1.7
Organosilicon compounds			
Polymethylsiloxane PMS-200	20.4	4.8	3.5
Polyhydrosiloxane liquid PGZh-891	20.2	6.3	6.9

Note. (I) σ_A = 28.5 mN m^{-1}; 1% solution of sulfonol (technical alkyl arenesulfonate) + 0.1% carboxymethylcellulose; (II) σ_A = 31.0 mN m^{-1}; 1% OP-10 solution.

Some time after the addition of the antifoam, the liquids are mutually saturated (at least in a thin layer) and the tensions σ_A and σ_{AB} vary up to the equilibrium values (σ'_A and σ'_{AB}), while the equilibrium spreading coefficient $S''_{B/A}$ becomes negative. Thus, for positive coefficient $S_{B/A}$, the liquid spreads in the form of a polymolecular film and soon after saturation the main bulk of the substance assumes the form of a lens, while the remainder exists in the form of a saturated monolayer.

The characteristic form of the lens is presented in Fig. 2. The shapes of such lenses and the equilibrium condition have been investigated in a number of studies (see, for example, Adamson[40]).

According to the Neuman equation, we have at equilibrium

$$\sigma'_A \cos\gamma = \sigma'_B \cos\beta + \sigma'_{AB} \cos\alpha \ . \qquad (2)$$

¶ A similar condition was used for a hypothetical film of condensed ether vapour in an early study by Quinke as a condition governing the displacement of the foam-forming agent by the antifoam.[4]

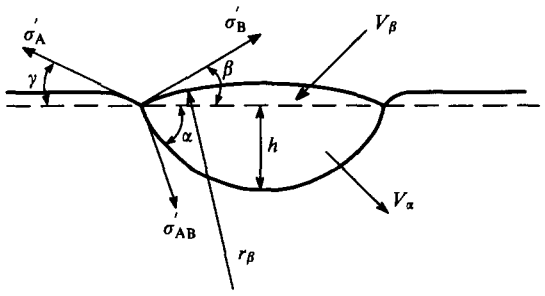


Figure 2. Profile of the organic liquid lens on water (for explanation, see text).

The angle γ is usually small and may be neglected in calculations of equilibria. The lens may be represented in the form of two spherical segments with volumes V_α and V_β. The volume of a segment is

$$V = \pi\left(r - \frac{h}{3}\right)h^2 \ , \qquad (3)$$

where h is the height of the segment and r the radius of curvature.

Furthermore, the radii of curvature of the upper (r_β) and lower (r_α) segments are related by the Laplace equation

$$r_\beta = r_\alpha \frac{\sigma'_B}{\sigma'_{AB}} \ . \qquad (4)$$

Table 2 presents the angles α and β for lenses floating on the surface of water.[41,42]

Table 2. The surface and interfacial tensions as well as the wetting angles for the lenses floating on the surface of water.

Substance	σ'_A/ mN m^{-1}	σ'_B/ mN m^{-1}	σ'_{AB}/ mN m^{-1}	α/ deg	β/ deg
Benzene	62.3	28.8	35	6	7.3
Chloroform	59.4	27.1	32.6	4.7	5.7
Heptyl alcohol	28.5	26.8	7.7	67	16
Octyl alcohol	28.8	26.2	8	70.5	16.7

Comparison of the data in Tables 1 and 2 shows that the tensions σ'_A and σ'_B in alcoholic systems are similar. Thus the angles α and β in typical antifoam systems (Table 1) are the same as for alcohols on the surface of water (Table 2). These angles may be used to predict the behaviour of the film (rupture or equilibrium) with a lens which covers the film.

The second type of effect is monomolecular spreading equivalent to the adsorption penetration by the molecules of the antifoam into the surface layer of the foam-forming agent. A necessary condition for monomolecular spreading is a positive surface pressure[40]

$$\pi^0_{BA} = \sigma_A - \sigma'_A = RT \int_{P(\Gamma=0)}^{P_0(\Gamma_\infty)} \Gamma \ln p \ , \qquad (5)$$

where Γ is the degree of adsorption of substance B, Γ_∞ the limiting degree of adsorption of substance B, and p the saturated vapour pressure of substance B for a negative initial spreading coefficient $S_{B/A} < 0$.

The surface pressure can also be determined from the difference between the initial ($S'_{B/A}$) and final (equilibrium $S''_{B/A}$) spreading coefficients:[40]

$$\pi^0_{B/A} = S'_{B/A} - S''_{B/A} \quad (6)$$

According to Ross's data, polymolecular spreading is most effective for the disruption of a foam, although Ross did not discover the mechanism of the action of such a film. Among the numerous systems investigated by Ross and coworkers,[21,37,39] Robinson and Woods,[43] and Pattle,[44] very many of those for which the conditions $S_{B/A} < 0$ and $\pi^0_{B/A} < 0$ hold proved to be effective antifoams (see, for example, Tables 3, 1, and 6 in the papers of Ross and Young,[37] Ross,[39] and Robinson and Woods[43] respectively). The effective disruption of a foam for $S_{B/A} < 0$ was also noted in later investigations.[7,13,45]

The possibility of the direct preparation of stable aqueous films on a support comprising certain antifoams[9] demonstrates that the condition for polymolecular spreading is not by itself either necessary or sufficient for the antifoam activity. Nevertheless, in a later study Ross[46] and a number of other investigators (see, for example, Pletnev[47] and Kozhanov et al.[48]) continued to assume that the antifoam activity in heterogeneous systems is a consequence of polymolecular spreading and suggested that the condition $S_{B/A} > 0$ be used as the principal criterion for the selection of effective antifoams. It is therefore useful to consider in greater detail the role of the spreading of antifoams in the prevention of the formation of foams and in the destruction of foams.

A study has been made[7] of the antifoam activity of aliphatic alcohols, acids, and polysiloxanes in two foam-forming systems with a high surfactant concentration (0.1% of OP-10 and 1% of sulfonol) with exact monitoring of the spreading. The antifoam activity was estimated both from the rate of disruption of the foam and from the ability to prevent its formation. The condition $S_{B/A} > 0$ served as the criterion of polymolecular spreading, while $\pi^0_{B/A} > 0$ combined with $S_{B/A} < 0$ served as the criterion of monomolecular spreading. In addition, the Wilhelmy balance was used to monitor the spreading directly.

An effective antifoam activity has been observed also for polymolecular (hexyl alcohol, PGZh-891) and monomolecular (heptyl and decyl alcohol in both systems, oenanthic and caprylic acids in solution in sulfonol) spreading and also in the absence of any spreading (caprylic and pelargonic acids). The nonpolar polysiloxane PMS-200 (without filler), having a high positive spreading coefficient, exhibits a very low antifoam activity.

In other experiments, the influence of antifoam drops on the disruption of foam 'islands' on the surface of the solution was observed.[7] It was established that only direct contact between the antifoam drops and the bubbles leads to the effective disruption of the foam. It was noted that polymolecular spreading of the polysiloxane PGZh-891 is completed by the fragmentation of its film into small droplets, which is an important factor, increasing the effectiveness of the antifoam.

It has also been shown that the antifoam activity of dispersions of solid stearic and palmitic acids[13] and of trialkylmelamine[49] is not due to spreading.

The results of a series of investigations[7,13,45,49] permit the conclusion that the effective action of antifoams in heterogeneous systems is not associated with any particular form of spreading and that an explanation of the partial association of positive values of $S_{B/A}$ and $\pi^0_{B/A}$ with effective antifoam activity can probably be found by comparing these conditions with the condition governing the instability of asymmetric aqueous films.

Yet another condition necessary for the manifestation of antifoam properties is believed to be a positive value of the so called disruption coefficient R,[26,43] for which the drops of the antifoam are believed[43] to penetrate the foam film between the bubbles. The positive disruption coefficient is given by[43]

$$R = \sigma_A - \sigma_B + \sigma_{AB} = -(\sigma_B - \sigma_A - \sigma_{AB}) > 0. \quad (7)$$

Evidently R is a negative coefficient for the spreading of the foam-forming solution on the antifoam, i.e. condition (7) is the condition for the nonwetting of B by a solution of A ($S_{A/B} < 0$). Condition (7), in the form of the negative spreading coefficient $S_{A/B}$, describes[50] yet another possible mechanism of the antifoam action, in which nonwetting is considered as a condition for the instability of the aqueous film.

However, it is known from the analysis of the stability of asymmetric films[51] that the fulfillment of the thermodynamic condition (7) is sufficient for the instability of an aqueous film on an antifoam support. It is then possible to obtain long-lived metastable aqueous films on an antifoam support stabilised by surfactant adsorption layers (similarly to stable foam films). The possibility of effective antifoam action should therefore be sought in the conditions for the instability of metastable films.

V. The antifoam effect of drops of organic liquids

Various organic liquids, sparingly soluble in water, appreciably diminish the stability of a foam on coming into contact with the latter.[28,45,48,50,52]

When a foam is formed in the presence of drops of an organic phase immiscible with the aqueous solution, there is a possibility of the formation of asymmetric aqueous films bounded by the gaseous medium on one side and by the antifoam phase on the other. Such aqueous films on an antifoam support can be obtained in the course of the attenuation of foam films if the solution of the foam-forming agent contains drops of an antifoam in the form of an emulsion (Fig. 3) and also when a solution of the antifoam is atomised in the form of an aerosol over the foam or when it spreads on the surface of the films and when the films containing drops of the antifoam are ruptured. The formation of an asymmetric film from a foam film containing drops of an organic liquid is promoted to a large extent by the absence of a charge on the drops, by a high concentration of the disperse phase, and by other conditions influencing heterocoagulation.

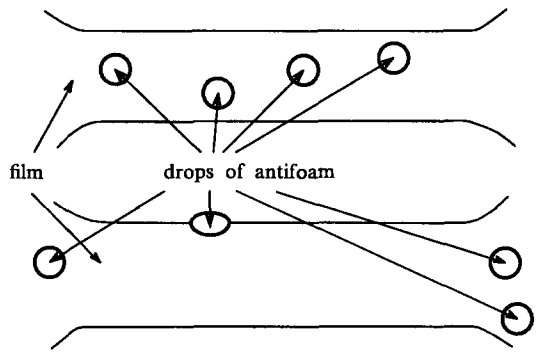


Figure 3. Schematic explanation of the formation of asymmetric films.

The asymmetric film (film on an antifoam support) can be part of the foam film or it can be fully bounded on one side by the organic phase, as in the polymolecular spreading of an antifoam on a film. If the asymmetric film formed is in a state of non-equilibrium for all thicknesses and is ruptured following the attainment of a critical thickness, its rupture leads to the disruption of the entire foam film of which it was a component. On the other hand, if the asymmetric film reaches equilibrium at a certain thickness (h), its influence on the stability of the foam film will depend on the height of the barrier on the disjoining pressure isotherm $\Pi(h)$. For the same height of the barrier, the lifetime of the foam film will evidently remain virtually unaltered. However, in the presence of antifoam drops the concentration of the foam-forming agent usually decreases in the aqueous phase as a consequence of its extraction by the drops of the organic liquid

and the additional adsorption on the drops. The adsorption of the surfactant on the water–antifoam interface is as a rule much smaller than on the water–gas interface, so that the energy repulsion barrier, generated by the interaction of the adsorption layers of the foam-forming agent on the water–antifoam and water–gas interfaces is significantly reduced compared with that in a two-sided film with adsorption layers on the water–air interface. Thus in this case too the antifoam exhibits a definite foam destroying capacity.

Analysis of the stability conditions shows that aqueous films on a support consisting of an organic phase are thermodynamically unstable.[4,51] Metastable asymmetric aqueous films can be obtained under certain conditions when the adsorption (Π_{ads}) or electrostatic (Π_{es}) components of the disjoining pressure, arising in the course of the attenuation of the film, exceed the molecular attraction Π_{vw} within a certain range of thicknesses:[51]

$$\Pi_{es}+\Pi_{ads} > \Pi_{vw}.$$

Model films of this type were first obtained from a solution of a nonionogenic surfactant—20-hydroxyethylated nonylphenol [NP-20, concentration $(1-5) \times 10^{-2}$%] with added magnesium sulfate on a cyclohexane support.[53] As in the case of foam and emulsion films, two types of equilibrium films were obtained in this case depending on the electrolyte concentration: the usual films and Newtonian black films.

In such films, the minimum surfactant concentration (c_{st}), necessary to obtain stable films (with a lifetime in excess of 10 min), depends greatly on the polarity of the organic phase (Table 3).

Table 3. Surfactant concentrations ensuring the formation of stable aqueous films on the surfaces of organic liquids.[9]

Organic phase	Surfactant concentration × 10^3 (%)	
	OP-10	Saponin
n-Decane	–	4
Benzene	3	3
Decyl alcohol	4	2
Heptyl alcohol	7	8
Butyl alcohol	Unstable films	

Note. The minimum surfactant concentrations for which thin (grey) films with a lifetime not less than 10 min were obtained.

In the case of a nonpolar organic phase, c_{st} does not differ greatly from the minimum concentration required to obtain a stable foam film, i.e. the concentration for the formation of black spots c_{bl} ($c_{bl} \approx c_{st}$). For example, $c_{bl} = 7 \times 10^{-4}$ % for a saponin solution and $c_{bl} = 1.2 \times 10^{-4}$ % for an OP-10 solution. This means that the effective disruption of the foam by nonpolar hydrocarbons due to the formation of unstable films is possible only at very low concentrations of the foam-forming agent (less than 0.003%–0.004% for saponin and OP-10). At higher concentrations of the foam-forming agent, the foam destroying capacity of the antifoam is determined by the slight decrease in the energy barrier and certain kinetic factors (for example, by additional adsorption).

The lifetime of a foam on an organic support diminishes greatly following the establishment of a reduced pressure in the Plato–Gibbs channels as a consequence of the decrease in the repulsion forces barrier by the amount $\Pi-\Delta P$ (where ΔP is the decrease in the pressure within the channels).[2,54] For alcohols, the difference between c_{bl} for foam films without and with added antifoam becomes significant and, on a support comprising lower alcohols, it is altogether impossible to obtain stable aqueous films as a consequence of the sharp decrease in the adsorption of the foam-forming agent on the water–antifoam interface (Table 3).

The simplest mechanism of the action of an antifoam (with barrier-free rupture whereupon the asymmetric film is in a state of nonequilibrium for all thicknesses) operates when highly polar organic liquids with a high affinity W_A for the aqueous medium are employed:

$$W_A = \sigma_A+\sigma_B-\sigma_{AB}.$$

In this case, the adsorption of the foam-forming agent at the water–antifoam interface is impossible (or its extent is very low) over the entire range of concentrations up to and including the CCM, because in such systems

$$\sigma^0_{AB} \approx \sigma_{AB} \approx 0, \quad (8)$$

where σ^0_{AB} is the interfacial tension on the antifoam–water interface and σ_{AB} is the interfacial tension on the interface with the aqueous solution of the foam-forming agent.

A low degree of adsorption of the foam-forming agent on the water–antifoam interface occurs in various foam-forming systems,[10] where lower alcohols (propyl and butyl) are used as antifoams at concentrations which exceed their solubility, and $\sigma^0_{AB} \sim 0$.

The same heterogeneous mechanism of the disruption of the foam with formation of unstable films on a support operates when the foam is introduced into highly polar liquids (partially or fully soluble in water): lower alcohols and acids, ketones, ethers, etc.[45] The rate-limiting stage in the disruption of the foam may be determined in this instance by various kinetic factors (the suction of the organic liquid into the foam, the rate of its dissolution in water, etc.), but the instability of the films is due to the sharp decrease or complete loss of the surface activity of the foam-forming agent on the water–antifoam interface.[45]

A heterogeneous mechanism of the antifoam action of drops has been described.[2,9,10,55] The second stage of the disruption of the foam film after the rupture of the asymmetric film and the appearance of a two-sided (symmetrical) antifoam lens within the foam film was not considered because the instability of such a system was regarded as evident.

Fig. 4 illustrates the possible behaviour of the antifoam lens after the rupture of the asymmetric film. It is seen that, when the lens shape is retained, the drop is continuously extended as a consequence of the inequality

$$\sigma'_B\cos\beta < \sigma'_A+\sigma'_{AB}\cos\alpha,$$

and is converted into a planar film of the substance. Without attaining mechanical equilibrium, the film of substance B and the foam film will be ruptured. On the other hand, if the drop rapidly assumes a shape close to spherical after the rupture of the asymmetric film, then, under the conditions of a temporary local mechanical drop–film equilibrium, the foam film forms a convex meniscus with an increased capillary pressure within it. The outflow of the liquid from the meniscus leads to a further rapid approach of the surfaces of the foam film and the drop until they touch and the foam film is then separated from the drop (slips off) and is destroyed. The instability of liquid drop 'bridges' within the foam film has also been indicated by Garrett.[12]

The disruption of a foam by diphilic antifoams as a consequence of the surface activity on the water–air interface takes place with the joint operation of two mechanisms–homogeneous (adsorption displacement) and heterogeneous. This is yet another of the causes of the greater effectiveness of diphilic antifoams compared with nonpolar liquids.

The contribution of the heterogeneous mechanism in the disruption of the foam in such systems can be isolated and estimated only in a quantitative study of the dependence of the foam destroying capacity of the antifoam on its concentration when passing from a homogeneous to a heterogeneous system.[29] The contribution of the heterogeneous mechanism usually increases at high surfactant concentrations, whereupon the homogeneous mechanism proves to be relatively ineffective.

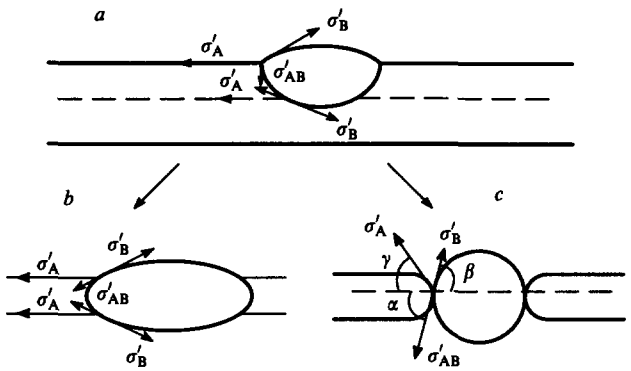


Figure 4. Schematic illustration of the behaviour of the antifoam lens on formation of a 'bridge' in the foam film: (*a*) initial stage after the rupture of the asymmetric film (the second side of the film is shown dashed); (*b*) extension of the lens with retention of the initial shape; (*c*) formation of a convex spherical meniscus near the antifoam drop.

A series of important features of foam formation and destruction in heterogeneous systems have been explained on the basis of the mechanism of the heterogeneous antifoam action:[2,55,56] the temperature dependence of the stability of foams produced from solutions of nonionogenic surfactants in the region of their turbidity temperature, the influence of solvents on the foam-destroying capacity of antifoams when they are used in the form of solutions, and, especially, the inversion of the antifoam activity in the series of aliphatic alcohols.[10]

VI. The antifoam effect of solid hydrophobic particles

Kurzendorfer[49] reported that, when particles of solid trialkylmelamine in suspension in alkyl benzenesulfonate fall on the surfaces of films, they cause their rapid rupture, which is not associated with the formation of mixed layers comprising trialkylmelamine and sulfonate molecules (with the adsorption displacement mechanism).

It has also been reported[57] that, when atomised silica particles which have been rendered hydrophobic enter a foam, they lead to the rapid disruption of the films in those bubbles which are in contact with the particles. Garrett later showed[11] that the chemically inert 5–40 μm particles of dispersed Teflon act as an effective antifoam on contact with a foam. He explained their antifoam properties by the appearance of hydrophobic 'bridges' made up of such particles and passing through the film and by their nonwettability. The formation of 'bridges' with subsequent rupture of the film near the hydrophobic particles (glass beads which have been rendered hydrophobic, lead sulfide, etc.) was demonstrated by Dippenaar[58] using a high speed filming technique.

The studies of the influence of hydrophobic particles on the stability of foams generated from aqueous surfactant solutions were later continued by other investigators.[12–16] The influence of the method used to form the foam and of the state of aggregation of the particles and of their shape on the effectiveness of the disruption of the foam was examined and the joint action of solid and liquid particles was investigated. In Garrett's experiments,[11] the foam was obtained from solutions of surfactants of different types (6-hydroxyethylated tetradecyl alcohol, tetradecyltrimethylammonium bromide, and DDSNa) by shaking in a 250 ml cylinder for 15 s. The three-phase contact wetting angles θ, measured on a plate wetted with water, were $\theta = 108° \pm 5°$ (incoming flow angle) and $\theta = 97° \pm 5°$ (outgoing flow angle). The volume of the foam in the presence of Teflon particles (40 mg per 50 ml of the solution) diminished by a factor of 2 and at low surfactant concentrations the foam was not obtained at all.

Garrett[11] deduced a thermodynamic justification of the critical value of the wetting angle at which the film ruptures spontaneously as a consequence of the formation of the hydrophobic particle 'bridge' between both surfaces of the foam film and the subsequent 'slipping off' (separation) of the menisci from the particles.

Garrett's analysis was based on the calculation of the change in the Helmholtz free energy when the particle passes from the incompletely or completely wetted state (immersion in the liquid) to a state where the foam film does not wet the elliptical particle at all, forming a point contact with the particle. An improved more realistic model of the rupture as a consequence of the nonwetting of the particle was developed by Frye and Berg.[14]

The mechanism of the rupture of the foam film by hydrophobic particles is explained by the scheme presented in Fig. 5. If the surfactant solution contains poorly wettable particles, then one (or several) may find itself on the surface (flotation by the surface), where it is rapidly oriented, occupying an equilibrium position. After the rupture of the asymmetric film under the particle, the latter moves, as shown by Dippenaar's direct measurements,[58] and occupies a symmetrical position relative to the film, so that the wetting angles on either side of the film are closer to the equilibrium values. the subsequent behaviour of the film around the particle depends on the equilibrium wetting angle. If $\theta < 90°$ (for a sphere), then the initially convex meniscus around the particle is converted, after the attainment of the equilibrium wetting angle, into a concave meniscus with a reduced pressure, which prevents further attenuation. If $\theta > 90°$, then after the formation of a 'bridge', a convex meniscus with an increased pressure $\Delta p = 2\sigma/R$, where R is the radius of curvature of the surface of the meniscus, appears. The increased pressure expels the liquid from the menisci and, since equilibrium is not attained under these conditions, the mutual approach of the surfaces around the particles continues until they come into full contact. This leads to the 'slipping off' (separation) of the meniscus, the 'liberation' of the particle, and the rupture of the film. This model has been used by Frye and Berg[14] to calculate the time required to disrupt such films. This time is made up of the attenuation time until the formation of a 'bridge' and the time required for the dewetting of the particle (direct rupture of the film). According to the authors,[14] the rupture time must be sufficiently short for the particle to behave as an effective antifoam. The attenuation time (τ) up to the formation of a 'bridge' was determined from the

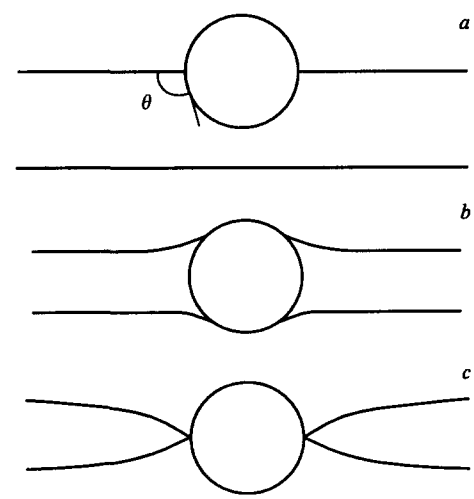


Figure 5. The influence of a solid hydrophobic spherical particle on the behaviour of the foam film: (*a*) equilibrium position on the surface; (*b*) local thickening of the film near the particle for $\theta < 90°$; (*c*) local attenuation of the film near the particle, inducing the rupture of the latter, for $\theta > 90°$.

Reynolds equation [2, 14] on the assumption that the surface of the film is fully retarded (immobile):

$$\tau = \frac{3\mu R}{2\Delta p h^2}, \quad (9)$$

where R is the radius of the circular film, μ the dynamic viscosity, Δp the capillary pressure, and h the thickness of the film at the instant of the appearance of the 'bridge'.

In the calculation of the rupture time (the time required for contact between the surfaces of the two menisci), it is assumed that the particle occupies a symmetrical position relative to the surfaces of the film. Fig. 6 illustrates the region of contact between the film and the particle and presents the designations of the quantities used to calculate the rupture time.

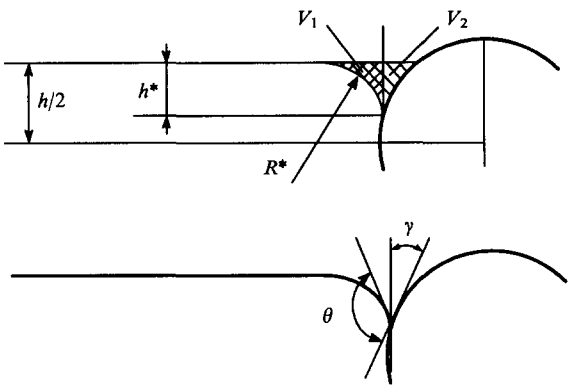


Figure 6. Schematic explanation of the significance of the parameters used to calculate the film rupture time.

In the initial state, the surface of the film is planar until there is contact with the solid particle; while at the instant of rupture, at which point the edges of the menisci come into contact, the thickness of the film becomes $h = 2h^*$. The rate of the mutual approach of the menisci depends on the volume rate of attenuation of the film and on the excess volume of the liquid ($V_1 + V_2$).

The calculation was based on Eqn (9) with substitution of the capillary pressure given by

$$\Delta p = \frac{\sigma}{R^*} = \frac{\sigma[1 - \sin(\theta + \gamma)]}{h^*}, \quad (10)$$

where γ is the angle between the vertical and the tangent at the point of contact between the surfaces of the solid and liquid phases. In this calculation, it is assumed that the excess liquid flows from the meniscus through the entire film, although Dippenaar's observations have shown [58] that the liquid flows only a short distance away from the particle at the instant of rupture. For particles with smooth surfaces without sharp angles (spheres, discs, ellipsoids, and rods oriented at right angles to the surface of the film), the calculation predicts the rupture of the film at $\theta > 90°$. A strong antifoam activity (a rupture time of the order of milliseconds) should be observed already for $\theta = 95° - 100°$.

Among particles of all shapes (to simplify the calculation, only figures of rotation are considered), conical particles alone are effective for $\theta < 90°$. The rupture time for conical particles depends both on the wetting angle θ and on the angle at the apex of the cone (β) and it is essential that $\beta < \theta$. The influence of the initial thickness of the film, the particle size, and other parameters on the film rupture time has also been considered. [14]

The results of the calculation agree well with experiment. The experiments involving the rupture of films obtained on a frame, by piercing the films with thin rods (d = 1 mm) of different materials, are especially instructive. In these experiments, only the shape, size, and orientation of the particles were known. The wetting angle could be measured accurately and it was an incoming flow angle. Furthermore, the problem of the probability of the penetration (entry) of particles onto the surface, which is not entirely evident in the disruption of a foam obtained from a suspension of particles, was in this instance solved unambiguously.

The results of such experiments are presented in Fig. 7. Despite some scatter in the range of angles 95° – 105°, it is readily seen, that for $\theta < 95°$, none of the films is ruptured and, for $\theta > 105°$, all the films are ruptured. Experiments with suspensions of solid particles (Teflon, glass beads which have been made hydrophobic, and ground glass) showed that in the case of 'smooth' particles, the antifoam activity begins to be manifested for $\theta = 35° - 45°$ and complete prevention of the formation of foam occurs for $\theta = 85°$. In the case of rough ground glass particles, effective antifoam action occurs already for 25° – 30° and, when $\theta = 50° - 55°$, a foam is not formed. The quantitative treatment of experiments with suspensions is more complex as a consequence of some uncertainty in the determination of the wetting angle during the rupture of films (owing to its uncertainty as the angle approaches the outflow value), the adsorption kinetics, and other factors.

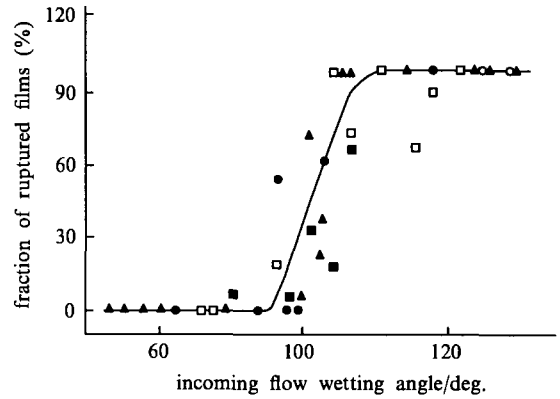


Figure 7. Dependence of the proportion of ruptured films on the incoming flow wetting angle. Antifoam: (*1*) hexadecyltrimethylammonium bromide; (*2*) sodium dodecylbenzenesulfonate; (*3*) Triton X-100. Open symbols — Teflon; filled symbols — glass which has been made hydrophobic.

The influence of the state of aggregation of the particles on the antifoam activity has been investigated by Aronson. [13] It was shown that, regardless of the type of solid particles (hydrocarbon or saturated aliphatic acids), the antifoam activity falls sharply with increase in temperature over a narrow range corresponding to the melting point.

Aronson believes that the most important cause of the large difference between the antifoam activities of liquids and solid particles is the influence of roughness on the stability of asymmetric films. Regardless of their shape, solid particles always have rough regions, which make it possible to overcome the energy barrier hindering the rupture of asymmetric films. However, the heights of the barriers are no less important for the wetting films on solid and liquid supports.

Various synergistic effects in the joint action of solid and liquid hydrophobic particles have been examined on the basis of the model of antifoam action described above. [15, 16] In particular, it has been shown [16] that an increase in the effectiveness of the antifoam action by solid particles in the presence of dodecane is associated with the decrease in the wetting angle θ required to disrupt the foam, while the decrease in the effectiveness of antifoams with increase in the concentration of the foam-forming agent is a consequence of the adsorption of the surfactant on the solid particles and the acquisition of hydrophilic properties by their surfaces.

Comparison of the two mechanisms of the antifoam action in heterogeneous systems permits the following conclusions. A necessary condition for the rupture of foam films in the model of drop antifoams is the instability of the film on the support as the drop approaches the interface. The cause of the instability may be a change in any of the components of the disjoining pressure. The simplest and clearest case of instability occurs when the energy barrier disappears due to the complete loss of surface activity at the water–polar antifoam (aliphatic alcohol or acid) interface.

The rupture stage after the formation of the drop 'bridge'-lens through the foam film is assumed to be evident in this case in view of the instability of the system produced for both lens-shaped and spherical initial drops (Fig. 4).

The second attenuation stage—extending from the formation of the hydrophobic 'bridge' up to equilibrium or rupture—is decisive for the mechanism of the antifoam action by solid particles. The first stage—the rupture of asymmetric films—is assumed to be evident at least for films on solid hydrophobic supports as a consequence of the influence of rough regions, although it has been shown experimentally [13] that, in the absence of such regions, films may be thermodynamically stable (metastable).

In the theory of the rupture of films by hydrophobic particles, the question of the influence of the particle size on the effectiveness of the antifoam action for $r < 1$ μm is not entirely clear. It follows from calculation [15] that the time required to attain rupture shortens with decrease in the particle size (from $r = 10^3$ to $r =$ 1 μm) as a consequence of the decrease in the volume of the meniscus and of the thickness of the film at the instant of formation of the 'bridges'. The experiments in which large particles ($r > 1$ μm) were separated by filtration demonstrated a sharp (almost complete) fall in the antifoam activity in systems without these particles. [13] Furthermore, when very small hydrophobic particles were used ($r = 20-1000$ nm), their pronounced stabilising action was observed and, according to data of Tang et al., [59] such particles behave to some extent like molecules, diminishing the surface tension.

VII. Concentration effects in antifoam processes

The effectiveness of antifoams in preventing foam formation diminishes sharply with increase in the concentration of foam-forming agents. However, as noted above, at high surfactant concentrations many substances effective in destroying foam lose this capacity fully or partially on entering the solution. These changes in antifoam activity, which are frequently extremely significant, may be a consequence of various physicochemical processes.

The mechanisms of antifoam action examined make it possible to explain, at least qualitatively, the various concentration effects in the prevention of foam formation and in the disruption of a foam by the addition of antifoams.

We shall consider certain characteristic instances of changes in antifoam activity following a change in the composition of the foam-forming agent and in the methods used to apply antifoams.

In the development of foam-forming compositions, used to extinguish fires arising on inflammation of liquids which are miscible with water, experiments are carried out on the disruption of the foam by these 'corrosive' liquids, the foam being supplied on to the surface of the liquid. The rate of such contact antifoam action is extremely high, but at the same time, when comparatively large amounts of these liquids (5%–10%) are added to aqueous solutions of surfactants, they cause a comparatively small decrease in the stability of the foam. A marked decrease in stability is observed only with increase in the concentration of the liquids to 20%–30%. The cause of the significant difference between the antifoam activities of these liquids in their contact interaction with the foam and when they are added to an aqueous solution in the given systems is evident: when a foam comes into contact with such liquids, unstable asymmetric films arise in the heterogeneous antifoam process [owing to the complete loss of surface activity by the foam-forming agent on the water–alcohol (ether, acetone) interface]. Furthermore, the surface is 'unstable' as a consequence of the complete miscibility of the phases in contact.

When such solvents are added to water, the stability of the foam does not change, owing to the low surface activity, until the foam-forming agents cease to be surface-active on the liquid–gas interface at very high concentrations owing to the marked change in the composition of the mixture (solvent). For this reason, the foam becomes completely unstable under these conditions.

Another example is the characteristic case involving the use of sparingly soluble diphilic additives (for example, aliphatic alcohols—pentyl, hexyl, heptyl, etc. [31]) as antifoams. With increase in the concentration of the foam-forming agent in systems [10, 31, 60] containing added antifoams in a molecular or drop form, the lifetime of the foam increases and the time required for the formation of its specified volume (Fig. 8), necessary to suppress the formation of black spots in foam films, achieving thereby the complete prevention of foam formation (Fig. 9), diminishes (or the amount of the antifoam increases). For low-molecular-mass diphilic antifoams (alcohols, acids, ethers, etc.), the loss of effectiveness is largely a consequence of the solubilisation of large volumes of the antifoam [31] which decreases the thermodynamic activity (for the dissolved component) and the number of drops, while for initial concentrations of the antifoam less than its colloidal solubility, it is a consequence of the change in the mechanism of the antifoam action (from the joint homogeneous and heterogeneous mechanism in the presence of drops to the homogeneous mechanism after dissolution).

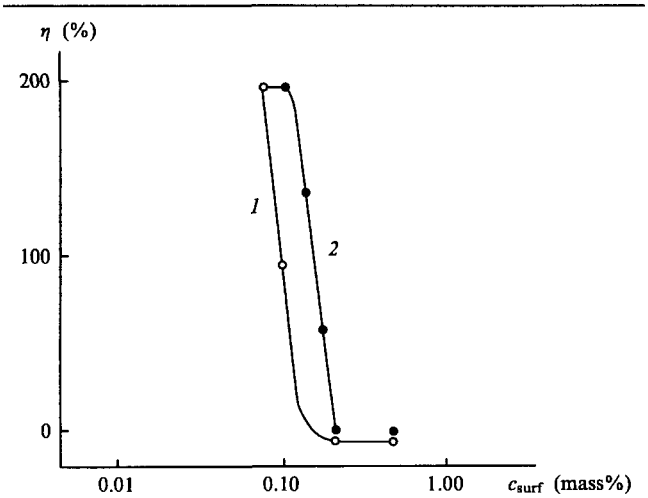


Figure 8. Dependence of the effectiveness of the antifoam action (η) on the concentration of the foam-forming agent (η is the ratio of the rate of foam formation without the antifoam to the rate in the presence of 0.016 vol.% of a 10% emulsion of polydimethylsiloxane as the antifoam): (*1*) 1% DDSNa solution; (*2*) 1% dodecylammonium chloride solution.

Another cause of the decrease in the antifoam activity may be an increase in the stability of the asymmetric films at high surfactant concentrations owing to the increase in the degree of adsorption on the interface between the solution of the foam-forming agent and the antifoam drops. [9, 10]

Yet another important cause of the loss of antifoam activity with increase in the concentration of ionogenic foam-forming agents, particularly when nonpolar (for example siloxane) antifoams are employed, is the appearance of a charge on the drops. Such a case has been studied in detail. [60]

The antifoam activity and the ζ-potential change markedly in the region of the 0.1% concentration of DDSNa, which corresponds approximately to the CCM (Fig. 10). Similar results have been obtained also for a solution of a cationic surfactant. The appearance of a charge stabilises the asymmetric film, the

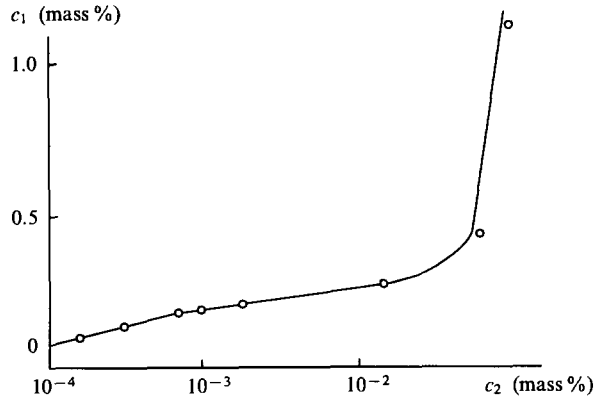


Figure 9. Dependence of the concentration of heptyl alcohol required to prevent foam formation (c_1) on the concentration of the OP-10 foam-forming agent (c_2).

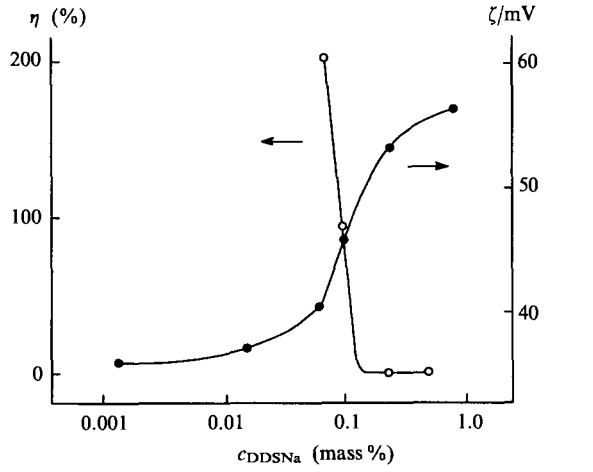


Figure 10. Dependence of the electrokinetic potential ζ and of the antifoam activity η on the DDSNa concentration (amount of added antifoam 0.016 vol.%).

drops cease to fall onto the surface, and the heterogeneous mechanism of the antifoam action becomes relatively ineffective.

The inversion of the antifoam activity in the series of aliphatic alcohols is associated with concentration effects. Systematic studies on higher aliphatic alcohols have shown that, at low concentrations of the foam-forming agents (OP-10, DDSNa, etc.), the effectiveness of the antifoam activity, estimated from the amount of alcohol required for the complete prevention of foam formation, increases along the homologous series with increase in the molecular mass of the alcohol (from butyl to undecyl).[9,10,55] With increase in the concentration of foam-forming agent, the maximum in the antifoam activity begins to shift towards lower homologues and finally, at the very highest concentrations, the lowest member of the series (butyl alcohol), which is fully insoluble in aqueous solution, becomes most effective.

The inversion of the antifoam activity of alcohols and the maximum in the antifoam activity corresponding to the middle homologues at 'medium' concentrations have been explained within the framework of the heterogeneous drop mechanism of the antifoam action.[10]

The effectiveness of the heterogeneous antifoam action is largely determined by two factors: the solubility of the antifoam (the lower the solubility, the sooner the heterogeneous mechanism is 'switched on') and the ability to prevent the adsorption of the foam-forming agent on the interface between the foam film and the antifoam and to destabilise thereby the asymmetric aqueous films.

The solubility of alcohols in the aqueous phase diminishes with increase in their molecular mass and the ability of the alcohols to prevent the adsorption of surfactants, which is determined by the interfacial tension on the interface between the aqueous solution of the foam-forming agent and the alcohol, decreases in the same direction.

At low concentrations of the foam-forming agent, when a minimal excess of any alcohol (relative to its solubility) is sufficient to destabilise foam films, the higher homologues are most effective. Conversely, at high concentrations of the foam-forming agent, the degree of its adsorption on the interface between the film and the alcohol drops is a maximum for the higher homologues, and it is sufficient to stabilise the asymmetric films, so that only films on supports comprising lower alcohols, for which the degree of adsorption of the surfactant is low, are unstable. This is precisely the reason why lower alcohols are the most effective. The inversion of the antifoam activity has been discussed in detail by the present author.[10,55]

In aqueous solutions with a high content of a solubilised organic phase, a marked influence of the amount of the oil on the solubility of foams is observed. By regulating the hydrophilic–lipophilic balance for the foam-forming agent by adding hydrophobic surfactants (for example, the esters of aliphatic acids and anhydrosorbitol, xylitol, and glycerol, aliphatic alcohols, acids, and amines) and also by varying the number of hydroxyethylene groups in the surfactant molecule and the electrolyte concentration, it is possible to obtain a water–oil–surfactant phase three-phase system in such solutions with high water and oil contents.[61,62] A significant increase in the stability of the foam with increase in the concentration of the oil is observed in systems of this kind already in the homogeneous micellar region. For example, the stability of the foam in a 15% solution of DDSNa with added butyl alcohol (up to 16%) decreased greatly on solubilisation of xylene: for a 20%–25% content of xylene, the foam became completely unstable.[63]

Similarly, in a foam formed from a solution of a mixture of technical alkylphenols (OP-10 and alfapol-4)[61] with an average number of hydroxyethyl groups $n = 7.8$ in the absence of an oil (kerosene), the lifetime of the foam exceeded two days, while for a kerosene content of ~20% (still in the homogeneous region) it was only 3 min. In another system,[61] water–kerosene–mixture of volgonate† and FM emulsifier‡ (concentration 30%), the lifetime of the foam fell from tens of hours when the volgonate : emulsifier concentration ratio was 4 : 1 and the kerosene content was 3.5% to 6 h for a concentration ratio of 2 : 3 and a kerosene content of 27%.

With increase in the concentration of pentyl alcohol in the system containing 1% of DDSNa, 1.75% of NaCl, and kerosene, the volume and stability of the foam fell sharply in the region of the hydrophilic–lipophilic balance close to the region corresponding to the appearance of the micellar phase of the surfactant, falling to zero on formation of this phase. The stability of the foam diminished similarly in a number of other systems on formation of the micellar phase.[62]

It is noteworthy that, also in the absence of oils, the stability of the foam is appreciably lower in this region of the hydrophilic–lipophilic balance compared with neighbouring regions. This means that not only the formation of the surfactant phase and the associated significant depletion of the aqueous solution in the surfactant, but also radical changes in the properties of the adsorption layers of the foam films are the causes of the instability of foams (and emulsions). As in many of the other cases considered above, in this instance the foam is disrupted via a mixed mechanism. The instability of asymmetric films is determined by the behaviour of the multilayer metastable foam films formed in these systems.

† Technical alkyl sulfate.
‡ Ester of oleic acid and triethanolamine.

The attenuation of the multilayer films does not take place continuously but with a discrete separation of the layers (stratification) with a thickness which is equal to (or is a multiple of) two surfactant bilayers containing a certain amount of a solubilised oil. [64] In conformity with this, the $\Pi(h)$ isotherm has an oscillating form. [65]

In nonaqueous nonpolar solutions, highly stable foams are usually obtained only in the presence of liquid crystals. [66] In such systems, water and certain other phases may be effective antifoams. The mechanism of the action of such antifoams is unknown.

References

1. V K Tikhomirov *Peny. Teoriya i Praktika Ikh Polucheniya i Razrusheniya* (Foams. Theory and Practice of Their Preparation and Destruction) (Moscow: Khimiya, 1983)
2. P M Kruglyakov, D R Ekserova *Pena i Pennye Plenki* (Foams and Foam Films) (Moscow: Khimiya, 1990)
3. A G Vetoshkin, Doctoral Thesis in Technical Sciences, Research Planning and Design Institute of Applied Biochemistry, Moscow, 1993
4. J J Bikerman *Foams* (New York: Springer, 1973)
5. I A Lichtman, T Gammon, in *Kirk-Othmer Encyclopedia of Science and Technology* Vol. 7 (Ed. M Grayson) (New York: Wiley-Interscience, 1980) p. 430
6. C H Fiske *J. Biol. Chem.* **35** 411 (1918)
7. P M Kruglyakov, T T Kotova *Dokl. Akad. Nauk SSSR* **188** 865 (1969)
8. P M Kruglyakov, T T Kotova *Izv. Sib. Otd. Akad. Nauk SSSR, Ser. Khim. Nauk* (1) 141 (1971)
9. P M Kruglyakov, T A Koretskaya *Izv. Sib. Otd. Akad. Nauk SSSR, Ser. Khim. Nauk* (2) 12 (1973)
10. P M Kruglyakov, T A Koretskaya *Kolloidn. Zh.* **36** 682 (1974)
11. P R Garrett *J. Colloid Interface Sci.* **69** 107 (1979)
12. P R Garrett *J. Colloid Interface Sci.* **76** 587 (1980)
13. M P Aronson *Langmuir* **2** 653 (1986)
14. G C Frye, J C Berg *J. Colloid Interface Sci.* **127** 222 (1989)
15. G C Frye, J C Berg *J. Colloid Interface Sci.* **130** 54 (1989)
16. R Aveyard, P Cooper, P D I Fletcher, C E Rutherford *Langmuir* **9** 604 (1993)
17. D A Fridrikhsberg *Kurs Kolloidnoi Khimii* (A Course of Colloid Chemistry) (Leningrad: Khimiya, 1984)
18. V N Izmailova, G P Yampol'skaya, in *Uspekhi Kolloidnoi Khimii i Fiziko-khimicheskoi Mekhaniki* (Advances in Colloid Chemistry and Physicochemical Mechanics) (Moscow: Nauka, 1992) p. 103
19. Khr Khristov, P M Kruglyakov, D Exerowa *Colloid Polym. Sci.* **257** 506 (1979)
20. Khr Khristov, D Exerowa, P M Kruglyakov *Colloid Polym. Sci.* **261** 265 (1983)
21. B T Sasaki, S Okasaki *Kolloid. Z.* **159** 11 (1958)
22. S Okasaki, B T Sasaki *Tenside* **3** 115 (1966)
23. S Ross, J W McBain *Ind. Eng. Chem.* **36** 570 (1944)
24. H Tsuge, J Ushida, S Hibino *J. Colloid Interface Sci.* **100** 175 (1984)
25. D Ekserova, M Buleva *Izv. Inst. Fiz. Khim. Bulg. Akad. Nauk* **4** 99 (1967)
26. D G Dervichian *Z. Elektrochem.* **59** 290 (1955)
27. L A Rauner, in *Encyclopedia of Polymer Science and Technology* Vol. 2 (Ed. H Mark) (New York: Interscience, 1965) p. 166
28. S Okasaki, K Hayashi, T Sasaki, in *Proceedings of the Fifth International Congress on Surface Active Substances, Barcelona, 1969* Vol. 3, p. 67
29. T A Koretskaya, P M Kruglyakov *Izv. Sib. Otd. Akad. Nauk SSSR, Ser. Khim. Nauk* (3) 129 (1976)
30. P M Kruglyakov *Kolloidn. Zh.* **38** 582 (1976)
31. P M Kruglyakov, P R Taube *Zh. Prikl. Khim.* **44** 129 (1971)
32. A M Shkodin, T P Tikhomirova *Kolloidn. Zh.* **13** 134 (1951)
33. S Ross, R V Haak *J. Phys. Chem.* **62** 1260 (1958)
34. S Ross, J N Butler *J. Phys. Chem.* **60** 1255 (1956)
35. S Ross, T H Bramfitt *J. Phys. Chem.* **61** 1261 (1957)
36. M J Schick, F M Fowkes *J. Phys. Chem.* **61** 1062 (1957)
37. S Ross, G J Young *Ind. Eng. Chem.* **43** 2520 (1951)
38. A Leviton, A Leighton *J. Dairy Sci.* **18** 105 (1935)
39. S Ross *J. Phys. Colloid Chem.* **54** 429 (1950)
40. A W Adamson *Physical Chemistry of Surfaces* (New York: Wiley, 1976) (Translated into Russian; Moscow: Mir, 1979)
41. N A Fuks *Zh. Fiz. Khim.* **2** 113 (1931)
42. J Donahue, F E Bartell *J. Phys. Chem.* **56** 480 (1952)
43. J V Robinson, W W Woods *J. Soc. Chem. Ind.* **67** 361 (1948)
44. R E Pattle *J. Soc. Chem. Ind.* **69** 363 (1950)
45. A F Sharovarnikov *Kolloidn. Zh.* **45** 616 (1983)
46. S Ross *Ind. Eng. Chem.* **61** 48 (1969)
47. M Yu Pletnev *Kolloidn. Zh.* **43** 826 (1981)
48. B P Kozhanov, M Yu Pletnev, I G Vlasenko *Kolloidn. Zh.* **45** 563 (1983)
49. C P Kurzendorfer, in *Trudy VII Mezhdunarodnogo Kongressa po PAV* T. 2 (Proceedings of the Seventh International Congress on Surface Active Substances, Vol. 2) (Moscow, 1976) p. 537
50. K Roberts, C Axberg, R Osterlund *J. Colloid Interface Sci.* **62** 264 (1977)
51. P M Kruglyakov *Izv. Sib. Otd. Akad. Nauk SSSR, Ser. Khim. Nauk* (1) 10 (1974)
52. B E Chistyakov, V N Chernin, I G Reznikov, A V Kulikova *Neftepererab. Neftekhim.* **10** 33 (1975)
53. P M Kruglyakov, Doctoral Thesis in Chemical Sciences, Inst. Inorg. Chem., Sib. Otd. Akad. Nauk SSSR, Novosibirsk, 1978
54. V N Chernin, Candidate Thesis in Chemical Sciences, Mosk. Gos. Univ., Moscow, 1981
55. P M Kruglyakov, in *Thin Liquid Films* (Ed. I B Ivanov) (New York: Marcel Dekker, 1990)
56. A F Koretskii, A V Smirnova, T A Koretskaya, P M Kruglyakov *Zh. Prikl. Khim.* **50** 84 (1977)
57. R D Kulkarni, E D Goddard, B Kanner *Ind. Eng. Chem., Fundam.* **16** 472 (1977)
58. A Dippenaar *Int. J. Miner. Process* **9** 1 (1982)
59. F Tang, Zn Xiao, J Tang, L Jiang *J. Colloid Interface Sci.* **131** 498 (1989)
60. R D Kulkarni, E D Goddard, B Kanner *J. Colloid Interface Sci.* **59** 468 (1977)
61. P M Kruglyakov, A G Baranova, N E Pul'ver, Kh I Khristov, T V Buzaeva, D R Ekserova *Kolloidn. Zh.*, **50** 275 (1988)
62. J Lachaise, T Breul, A Gracia, G Marion, A Monsalve, J L Salager *J. Dispersion Sci. Techn.* **11** (5) 443 (1990)
63. R Torres, M Podzimek, S Friberg *Colloid. Polym. Sci.* **258** 855 (1980)
64. Kh I Khristov, D R Ekserova, P M Kruglyakov, N G Fokina *Kolloidn. Zh.* **54** 173 (1992)
65. V Bergeron, C Y Radke *Langmuir* **8** 3020 (1992)
66. S J Ahmad, S Friberg *Acta Polytechn. Scand.* **102** 3 (1971)

Russian Chemical Reviews **63** (6) 483 – 489 (1994)
©1994 Russian Academy of Sciences and Turpion Ltd

UDC 541.128.3 : 542.941.8 : 541.412

Hydride forming metals and alloys as hydrogen acceptors in catalytic dehydrogenation

O V Chetina, V V Lunin

Contents

I. Introduction 483
II. Catalytic reactions using intermetallic hydrogen acceptors 484
III. Characteristic features of catalytic dehydrogenation coupled with hydride formation 485
IV. Conclusion 488

Abstract. The use of hydride forming metals and alloys as hydrogen acceptors in order to overcome the thermodynamic limitations in catalytic reactions involving the evolution of hydrogen is examined. The high effectiveness of intermetallic hydrogen acceptors in reactions involving the dehydrogenation of cycloalkanes, isobutane, and alcohols (C_1-C_3) and the aromatisation of alkanes (C_2-C_3) is noted. The bibliography includes 36 references.

I. Introduction

A unique feature of many transition metals and alloys based on them is the ability to absorb reversibly significant amounts of hydrogen at fairly high rates of absorption and desorption. This particular feature is in fact responsible for the wide scale application of metal hydrides in power and atomic engineering for the storage and purification of hydrogen.[1-3]

The incorporation of hydrogen in the metal or alloy lattice is preceded by dissociative chemisorption with formation of atomic hydrogen, while the evolution of hydrogen from the bulk of the hydride involves the recombination of atoms with subsequent desorption of H_2 molecules into the gas phase. The heterophase exchange of hydrogen between the hydride lattice and the hydrogen in the gas phase takes place continuously. The high activity of the surface centres as regards the dissociation of H_2 and the constant presence of activated hydrogen on the surfaces of hydrides makes it possible to employ compounds of this kind as highly effective hydrogenation catalysts in petrochemistry and petroleum processing.[4-6] The formation of hydrogenation products of hydrocarbons in the presence of hydrides of intermetallic compounds depleted in hydrogen was first observed more than 20 years ago by Lunin et al.[7]

In 1985, the absorption capacity of hydride forming metals and intermetallic compounds was used successfully to overcome thermodynamic limitations in catalytic dehydrogenation processes.[8,9] The reactions involving the dehydrogenation of alkanes, alkenes, and alcohols are known to be thermodynamically unfavourable at moderate temperatures. For example, the dehydrogenation of alkanes C_nH_{2n+2} to alkenes C_nH_{2n} at 298 K is accompanied by an increase in the standard Gibbs free energy.

$$C_nH_{2n+2} \longrightarrow C_nH_{2n} + H_2, \quad \Delta G^0 > 0 \qquad (1)$$

It was found that the introduction of a suitable metal or intermetallic compound (M) into the system displaces the equilibrium appreciably towards dehydrogenation, since the formation of the hydride (MH_2) entails the evolution of energy necessary to effect reaction (1).

$$M + H_2 \longrightarrow MH_2, \quad \Delta G^0 < 0 \qquad (2)$$

The absorption capacity of the initial alloy may be restored in the subsequent regeneration cycle. The combination of reactions (1) and (2) together with the regeneration of the initial alloy can be represented in the following form:

$$C_nH_{2n+2} + M \longrightarrow C_nH_{2n} + MH_2$$
$$\uparrow \qquad\qquad\qquad\qquad \downarrow$$
$$-H_2$$

Consequently the role of the hydride-forming alloy consists in binding the hydrogen evolved on dehydrogenation with the formation of a thermodynamically more favourable compound. This process is in many respects analogous to oxidative dehydrogenation:

$$C_nH_{2n+2} + O_2 \longrightarrow C_nH_{2n} + H_2O,$$

with the sole difference that in the former case a hydride is formed and may be regenerated to the initial alloy with evolution of hydrogen, while in the oxidative version water is formed as a side product.

The first studies using hydride forming metals and alloys as hydrogen acceptors were carried out in relation to the catalytic dehydrogenation of isobutane[8] and cyclohexane.[9] Subsequent investigations made it possible to discover a positive effect, which is attained when the hydrogenation of metals and intermetallic compounds is coupled with a whole series of thermodynamically restricted catalytic reactions proceeding with evolution of hydrogen. The principal results of such investigations are summarised in the present review and the characteristic features of the reactions in the presence of intermetallic hydrogen acceptors are considered.

O V Chetina Laboratory for the Study of the Mechanisms in Heterogeneous Catalysis by Spectroscopic Methods, Institute of Organic Chemistry, Russian Academy of Sciences, Leninskii prosp. 47, 117913 Moscow, Russian Federation. Fax (7-095) 135 53 28
V V Lunin Laboratory for Catalysis and Gas Electrochemistry, Faculty of Chemistry, Lomonosov Moscow University, Vorob'evy gory, 119899 Moscow, Russian Federation.
Fax (7-095) 939 00 67. Tel. (7-095) 938 35 20

Received 25 April 1994
Uspekhi Khimii **63** (6) 506 – 512 (1994); translated by A K Grzybowski

II. Catalytic reactions using intermetallic hydrogen acceptors

Tables 1 and 2 present the literature data on the application of hydride forming metals and alloys as hydrogen acceptors in catalytic reactions of various organic compounds. Intermetallic hydrogen acceptors have been tested mainly in the dehydrogenation reactions of alkanes and alcohols. Both oxide and zeolite systems with deposited metals and the activated surfaces of the intermetallic compounds themselves have been used as dehydrogenation catalysts. We shall examine in greater detail the reaction conditions and the principal results achieved.

1. Reactions of hydrocarbons

The first reaction in which a hydride forming metal (Ti) was used successfully to remove the hydrogen evolved was the dehydrogenation of isobutane to isobutene.[8] The reaction was carried out in a flow system on a platinum/alumina catalyst (5 mass% Pt) mixed mechanically with titanium powder at 641 K. The mass ratio of the catalyst and the acceptor was 1 : 1.5. As a result of the removal of 60 vol.% of the hydrogen formed, the ratio iso-C_4H_{10} : iso-C_4H_8 in the reaction product was 12.5 : 1, which corresponds to 7.4% conversion of isobutane into isobutene. Under these conditions but without the removal of hydrogen, the equilibrium ratio iso-C_4H_{10} : iso-C_4H_8, calculated from thermodynamic data is 19 : 1 and corresponds to 5.3% conversion. In a repeated dehydrogenation cycle after the regeneration of titanium, the conversion reached 10.4%. Thus, by carrying out the hydrogenation of the titanium powder jointly with the dehydrogenation of isobutane, it was possible to increase by a factor of 1.5 – 2 the yield of the alkene compared with the equilibrium value (without removing hydrogen).

The use under the same conditions of the intermetallic compound $Ti_{0.63}V_{0.27}Fe_{0.1}$, which functions simultaneously as a hydrogen acceptor and as a dehydrogenation catalyst, did not yield a positive result owing to the low catalytic activity of the intermetallic compound. The conversion to isobutane did not exceed 1% in this case although the hydrogen formed was fully absorbed by the acceptor.

The dehydrogenation of isobutane to isobutene has also been investigated in the presence of the ZrNi and ZrCo hydrogen acceptors on the Pt/Al_2O_3 and Pt/SiO_2 catalysts for a catalyst : acceptor mass ratio of 1 : 3.[10] The reaction was carried out at 300 and 350 °C. The calculated equilibrium yield of isobutene under these conditions, without the removal of hydrogen, was 1.5% and 4.2% respectively, while in the presence of the intermetallic compound ZrNi it reached 4.3% and 11.5%, i.e. exceeded the equilibrium yield by a factor of 2.5 – 3. The intermetallic compound ZrCo and the Pt/SiO_2 catalyst proved to be less effective in this reaction.

The highest yield of isobutene from isobutane, amounting to 45%, which exceeds by a factor of 2 the equilibrium yield under the same conditions without the removal of H_2, was achieved at 470 °C in the presence of the Cr_2O_3/ZrO_2 catalyst mixed with the intermetallic compounds Zr_2Fe.[10]

The effect of hydride-forming intermetallic compounds on the dehydrogenation of cycloalkanes to the corresponding aromatic hydrocarbons has been considered in a number of studies.[9,12–14] In the series of intermetallic compounds tested,[9,12] $CaNi_5$ proved to be the most effective hydrogen acceptor. In its presence, the yield of benzene from cyclohexane on the Pt/Al_2O_3 catalyst at 150 °C increased by a factor of 3.5 compared with the equilibrium yield (without the removal of hydrogen) and reached 32.2% (the equilibrium yield is 9.1%). The use of the intermetallic compound ZrNi as the hydrogen acceptor in a similar system made it possible to exceed by a factor of 5 the equilibrium yield of benzene from cyclohexane and of toluene from methylcyclohexane at 190 °C.[13,14] Under these conditions, 100% conversion of cycloalkanes into the corresponding aromatic products was observed (the equilibrium yield is about 20%).

The positive effect of the lanthanide intermetallic compounds Nd_2Co_7 and Sm_2Co_7, used simultaneously as catalysts and hydrogen acceptors, has been noted in the dehydrogenation of cyclohexene to benzene and of n-heptane to methylcyclohexane.[15] The latter reaction occurred at 398 K and only traces of the n-heptane cyclisation product were observed.

The intermetallic compound Zr_2Fe proved to be an effective hydrogen acceptor in the significantly more complex multistage aromatisation of C_2–C_3 hydrocarbons.[16–20] The reaction was studied in the temperature range 450 – 550 °C in the presence of catalysts based on the high-silica TsVM zeolite modified by zinc, gallium, or platinum cations. When the hydrogen evolved in the reaction was bound by the intermetallic acceptor, the yield of aromatic hydrocarbons from ethane was higher by a factor of 4 – 6 than in the absence of the intermetallic compound, and the selectivity of the aromatisation increased by a factor of 2 – 2.5 as a result of the suppression of the methane-forming side reaction.[16–18] In the aromatisation of propane in the presence of hydrogen acceptors, the yield of aromatic hydrocarbons increased by a factor of 2 – 5 and the sensitivity of the aromatisation increased by a factor of 1.5 – 3.5.[19,20]

An attempt was also made to influence the equilibrium in reactions involving the direct conversion of methane into C_2 hydrocarbons, which is thermodynamically least favourable but is of extremely great practical importance.[21] The reaction was carried out at 400 K with the use of Ti and TiFe as the hydrogen acceptor and deposited metallic catalysts containing Pt, Rh, or Ni. However, the only reaction product, for a very low conversion of methane (above 1%), was coke.

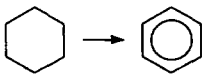
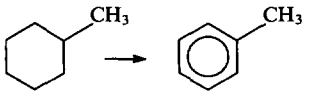
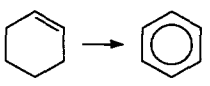
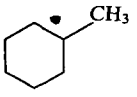
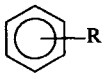
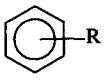
2. Reactions of alcohols

A large group of studies[15,22–27] has been devoted to the reactions of alcohols in the presence of intermetallic compounds of various compositions. In contrast to the reactions of hydrocarbons, hydride forming metals and alloys play the role of acceptors of the evolved hydrogen and of catalysts simultaneously in these processes. In certain cases, the surface of the alloys was modified by platinum, ruthenium, copper,[26] or rhodium[23] salts in order to increase the catalytic activity. The reactions were carried out in flow[24,25] and circulation systems[15,22,23,26] or in an auto-clave.[27] A direct quantitative estimate of the effect of hydride formation on the dehydrogenation of an alcohol is difficult and it can be inferred only indirectly from the decrease in the reaction temperature and the increase in the process selectivity.

In the presence of intermetallic compounds of different composition, methanol was dehydrogenated selectively under mild conditions (356 – 443 K) to CO and hydrogen, the latter forming part of the composition of the hydride.[15,22,23] The activity of the intermetallic compounds fell in the series $Zr_2Ni > M_2Co_7 > MFe_2$, where M is a lanthanide element. The authors explain this by the possible decrease in the catalytic activity of metals in the sequence Ni > Co > Fe. On the other hand, in terms of their absorption capacity the lanthanide intermetallic compounds were superior to Zr_2Ni: in their presence, complete removal of hydrogen from the reaction mixture was observed, whereas in the case where Zr_2Ni had been used, hydrogen was present in the gas phase from the very start and throughout the entire experiment. After the deposition of platinum or rhodium salts on the surfaces of the least active intermetallic compounds MFe_2, their properties were appreciably improved.[23] Thus the deposition of $RhCl_3$ on $DyFe_2$ increased the activity of the latter in the decomposition of methanol by a factor of 18.

Depending on the composition of the hydride-forming intermetallic compound used, the formation of various products was observed in the dehydrogenation of methanol at 523 K.[24,25] Thus the main product was formaldehyde in the presence of FeTi and $(Fe_{0.9}Mn_{0.1})Ti$. On nickel-containing alloys, methanol was con-verted into CO, while on Mg_2Cu methyl formate was also found among the reaction products in addition to CO.

Table 1. Reactions of hydrocarbons in the presence of intermetallic hydrogen acceptors.

Reaction	Intermetallic compound	Catalyst	Ref.
iso-C_4H_{10} ⟶ iso-C_4H_8	Ti	Pt/Al_2O_3	8
	$Ti_{0.63}V_{0.27}Fe_{0.1}$,	without catalyst	8
	$Ti_{0.63}V_{0.225}Fe_{0.1}Pt_{0.045}$		
	ZrNi, ZrCo	Pt/Al_2O_3	10
	Zr_2Fe	Cr_2O_3/ZrO_2	11
	FeTi, $(Fe_{0.9}Mn_{0.1})Ti$, $CaNi_5$, $LaNi_{4.7}Al_{0.3}$, Mg_2Ni, Mg_2Cu	Pt/Al_2O_3	9, 12
	ZrNi	Pt/Al_2O_3	13
	ZrNi, $ZrCr_2$, $ZrCr_2Ni_{0.1}$	Pt/Al_2O_3, Pt/SiO_2, Pd/Al_2O_3	14
	ZrNi	Pt/Al_2O_3	14
	Nd_2Co_7, Sm_2Co_7	without catalyst	15
n-C_7H_{16} ⟶ 	Nd_2Co_7, Sm_2Co_7	"	15
C_2H_6 ⟶ 	Zr_2Fe	Pt/HTsVM, Pt-Cr/HtsVM, Zn/HTsVM, Ga/HTsVM	16–18
C_3H_8 ⟶ 	Zr_2Fe	Zn/HTsVM, Ga/HTsVM, Pt/HTsVM	19, 20
CH_4 ⟶ C_2H_6	Ti, TiFe	Ni/Al_2O_3, Rh/SiO_2, Pt, Sn/Al_2O_3	21

The selective dehydrogenation of ethanol to acetaldehyde and hydride hydrogen occurred at 423 K [22] and 523 K [24] on all the intermetallic compounds tested by the authors with the exception of Mg_2Cu, in the presence of which a small amount of ethyl acetate was formed (the ethyl acetate : acetaldehyde ratio was 0.0047). The activities of the intermetallic catalysts in the reactions of ethanol and methanol depended to almost equal extents on the composition of the alloys, which indicates, according to the authors,[22,24] the similarity of the mechanisms of these reactions.

The dehydrogenation of isopropyl alcohol in the presence of the intermetallic compounds M_2Co_7 (where M = Pr, Nd, Sm) was quantitative and the selectivity in the formation of the corresponding hydride and acetone was close to 100% even at 317 K.[15,26] The rates of dehydrogenation of isopropyl alcohol on $Nd_2Co_7H_{0.1}$, $Nd_2Co_7H_{2.7}$, and $Nd_2Co_7H_{5.1}$ were respectively 1.1×10^{-3}, 6.0×10^{-4}, and 3.5×10^{-4} mmol min^{-1} per gram of the alloy. According to the authors,[15,26] this means that the formation of the hydride is the driving force of the dehydrogenation reaction. On the other hand, as in the case of methanol, modification of the surfaces of the alloys with platinum increases significantly their activity. For example, treatment of Pr_2Co_7 suspension with an aqueous solution of H_2PtCl_6 increased its activity in the dehydrogenation of isopropyl alcohol by a factor of 10.[26]

The effect of the hydride forming alloy $Mg_{2.4}Ni$ on the dehydrogenation of isopropyl alcohol in the presence of the Cu/CuO catalyst has been investigated[27] in a static system in an autoclave at 473 K and a pressure of 0.1–1.0 MPa. The absorption of hydrogen by the alloy altered appreciably the hydrogen balance in the system. However, as a consequence of the catalytic activity of the hydride in condensation reactions, the selectivity of the dehydrogenation reaction fell greatly.

Analysis shows that, in the vast majority of cases, the formation of the hydrides of transition metals and alloys under the conditions of catalytic dehydrogenation has a positive effect on the yields of the target products and on the selectivity of the dehydrogenation process.

III. Characteristic features of catalytic dehydrogenation coupled with hydride formation

Despite the wide variety of the initial organic reagents, the catalysts and the intermetallic compounds employed, and the experimental conditions, certain general features are characteristic of all the dehydrogenation reactions using intermetallic hydrogen acceptors.

1. Thermodynamics

It follows from Eqns (1) and (2) that the thermodynamic features of coupled dehydrogenation and hydride formation processes are equally important for the attainment of a positive effect.

For hydrogen to be absorbed, it is essential that its partial pressure in the gas phase should exceed the equilibrium dissociation pressure (p_{eq}) of the hydride. The pressure p_{eq} for a given metal or alloy is determined by the thermodynamics of the absorption–desorption equilibrium and tends to increase with increasing temperature.[28] The partial pressure of hydrogen in the reaction mixture is determined by the dehydrogenation equilibrium. When the temperature is reduced, thermodynamic

Table 2. Reactions of alcohols in the presence of intermetallic hydrogen acceptors.

Reaction	Intermetallic compound	Catalyst	Ref.
$CH_3OH \longrightarrow CO$	Nd_2Co_7, Sm_2Co_7	without catalyst	15
	$ErFe_2$, $DyFe_2$, Nd_2Co_7, Sm_2Co_7	"	22
	Zr_2Ni, Pr_2Co_7, Nd_2Co_7, Sm_2Co_7, $ErFe_2$, $DyFe_2$	$RhCl_3 \cdot 3H_2O$	23
	FeTi, $(Fe_{0.9}Mn_{0.1})Ti$	without catalyst	24, 25
$CH_3OH \longrightarrow HCHO$	$CaNi_5$, $LaNi_{4.7}Al_{0.3}$, Mg_2Ni	"	24, 25
$CH_3OH \longrightarrow HCOOCH_3$	Mg_2Cu	"	24, 25
$C_2H_5OH \longrightarrow CH_3COH$	$ErFe_2$, $DyFe_2$, Nd_2Co_7, Sm_2Co_7	"	22
	FeTi, $(Fe_{0.9}Mn_{0.1})Ti$, $CaNi_5$, $LaNi_{4.7}Al_{0.3}$, Mg_2Ni, Mg_2Cu	"	24
$CH_3CHCH_3 \longrightarrow$ (OH)	Nd_2Co_7, Sm_2Co_7	"	15
$\longrightarrow CH_3CCH_3$ (O)	$ErFe_2$, $DyFe_2$, Nd_2Co_7, Sm_2Co_7	"	22
	Pr_2Co_7, Nd_2Co_7, Sm_2Co_7	$RuCl_3$, $CuSO_4$, H_2PtCl_6	26
	$Mg_{2.4}Ni$	Cu/CuO	27

limitations to the dehydrogenation reactions arise (Fig. 1). In the dehydrogenation of alcohols, $\Delta G°$ shifts to the positive region at significantly lower temperatures than in the dehydrogenation of hydrocarbons, with the exception of the aromatisation of cycloalkanes (Table 3). Thus the equilibrium pressure p_{eq} and the temperature at which the free energies $\Delta G°$ for the dehydrogenation reactions shift to the positive region impose certain limitations on the choice of metals and intermetallic compounds as hydrogen acceptors. For example, the equilibrium dissociation pressure of the hydride of $Mg_{2.4}Ni$ [27] is such that this alloy can be used to remove the H_2 evolved in the dehydrogenation of ethanol or isopropyl alcohol but not propane or methanol.

The majority of binary and ternary metal hydrides have been synthesised and investigated in order to use them as hydrogen accumulators.[28] One of the main requirements which must be met by such systems is a low equilibrium dissociation pressure at room temperature. This restricts the search for intermetallic hydrogen acceptors suitable for the dehydrogenation of saturated hydrocarbons. Intermetallic compounds having the composition M(IV)$_2$M(VIII), the equilibrium dissociation pressures of the hydrides of which at 500 °C are much lower than 1 atm, appeared to be the most promising.

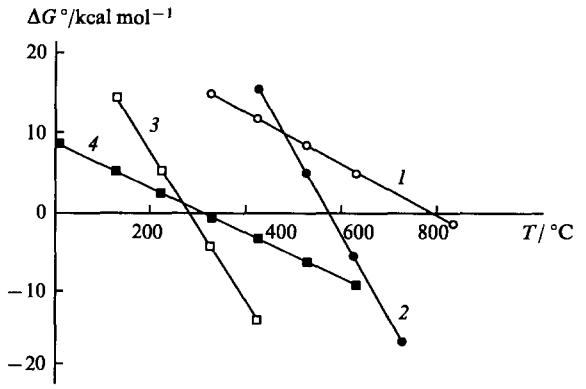


Figure 1. Temperature dependence of the change in the standard Gibbs free energy in the reactions involving the conversion of ethane into ethylene (line *1*), of ethane into benzene (line *2*), of cyclohexane into benzene (line *3*), and of ethanol into acetaldehyde (line *4*).

2. Absorption by metals and alloys of the hydrogen evolved in the dehydrogenation reaction

Evidently, for hydride formation to have a positive effect on the dehydrogenation reaction it is essential that the rate of absorption of hydrogen by the intermetallic acceptor should be equal to or greater than the rate of its formation as a result of the reaction. Indeed, in the dehydrogenation of isobutane,[10] cycloalkanes,[9,14] and alcohols[22] the rate of absorption of hydrogen by intermetallic compounds was one of the factors determining the effectiveness of their application.

The interaction of metals and alloys with hydrogen is a complex process including stages involving the dissociative adsorption of H_2, surface migration, transition from the adsorbed to the absorbed state, and finally bulk-phase diffusion.[28] Kinetic studies have shown that below 400 °C the rate of absorption is as a rule limited by the dissociation of H_2 molecules or the passage of H atoms through the surface oxide film,[30] which is formed when metals and intermetallic compounds come into contact with air under normal conditions.[31] This could have hindered the use of intermetallic hydrogen acceptors in low-temperature cycloalkane and alcohol dehydrogenation reactions. However, the presence on the surface of intermetallic compounds of Group VIII metals reduces appreciably the activation energy for the dissociative chemisorption of hydrogen, which facilitates absorption significantly even at room temperature.

The absorption of hydrogen may be promoted by sputtering isolated regions or monolayers of Ni, Pd, or Fe on to the surface of the intermetallic compound.[30,31] The introduction of Group VIII metals into intermetallic compounds at the stage where the metals are fused together does not always activate the absorption processes, since the surface oxide film is formed preferentially

Table 3. Thermodynamics of the dehydrogenation reactions of hydrocarbons and alcohols.

Reactant	Product	Temperature/ °C at which $\Delta G° = 0$ [a]
Ethane	ethylene	800
Ethane	benzene	580
Propane	propene	660
Butane	butene	540
Cyclohexane	benzene	260
Methanol	formaldehyde	430
Ethanol	acetaldehyde	330
Isopropyl alcohol	acetone	150

[a] Determined from thermodynamic data.[29]

from elements with a higher affinity for oxygen, so that the concentration of the Group VIII metal on the surface proves to be inadequate. In order to enrich the surface in the Group VIII metal, it is necessary to subject the intermetallic compound to a preliminary oxidation-reduction treatment under specific conditions[32] or to repeat the absorption-desorption cycles.[8,27]

One of the fairly important factors which determines the possibility of using particular intermetallic compounds as hydrogen acceptors is the retention of the ability to sorb H_2 under dehydrogenation conditions and after carrying out the desorption cycles. It was found that intermetallic hydrogen acceptors effectively retained their absorption properties under the conditions of catalytic reactions. In reactions involving hydrocarbons, this is probably associated with the catalytic inertness of the metals and alloys employed. In the reactions of alcohols, the dehydrogenation and H_2 absorption reactions take place at different active centres,[22,27] so that deactivation of the surface by the reaction products (observed in some cases) does not affect the absorption capacity of the acceptor.

As mentioned above, the repetition of the absorption-desorption cycles may increase the absorption capacity of the metals and alloys by activating their surfaces. For example, the acceptor properties of titanium are improved on repeating the isobutane dehydrogenation reaction after the desorption of hydrogen from the hydride.[8] On the other hand, the thermal desorption of hydrogen from the hydride of the intermetallic compound Zr_2Fe leads to an irreversible decrease in its absorption capacity as a consequence of the bulk-phase decomposition to $ZrFe_2$ and ZrH_2, which occurs at temperatures above 400 °C. However, the introduction of oxygen in the stage where the metals are fused together prevents the bulk phase decomposition of this intermetallic compound even at 850 °C.[33]

3. The activity of dehydrogenation catalysts and the change in the selectivity of catalytic processes

The yield of the products of dehydrogenation coupled with hydride formation is virtually unrestricted by the thermodynamic equilibrium and is therefore determined primarily by the rate of the reaction, i.e. by the activity of the hydrogenation catalyst. This was clearly demonstrated for the dehydrogenation of isobutane using Pt/Al_2O_3, $Ti_{0.63}V_{0.27}Fe_{0.1}$, or $Ti_{0.63}V_{0.225}Fe_{0.1}Pt_{0.045}$ as the catalyst.[8] In the aromatisation of cyclohexane,[14] the difference between the dehydrogenation activities of the Pt/Al_2O_3 and Pd/Al_2O_3 catalysts, which is not manifested in the absence of the hydrogen acceptor for thermodynamic reasons (the conversions of cyclohexane into benzene in the presence of these catalysts are respectively 19% and 21%), becomes very distinct if the product is removed by the intermetallic compound ZrNi (the conversions are 100% and 42% respectively). The yields of the dehydrogenation products of methanol[23] and isopropyl alcohol[26] increased by a large factor after deposition on the surfaces of intermetallic compounds of metals, such as platinum or rhodium, which are highly active in the dehydrogenation reactions.

The removal of hydrogen from the reaction mixture may exert a positive effect on reactions occurring with evolution of hydrogen, whereas reactions in which hydrogen is actually one of the reactants may be to a large extent suppressed in the presence of the intermetallic acceptor. The composition of the products of complex catalytic processes, in particular of the aromatisation of hydrocarbon gases, which includes several dehydrogenation stage as well as parallel hydrocracking, dealkylation, and hydrogen redistribution reactions, changes significantly in the presence of intermetallic compounds. For example, the selectivity of the aromatisation of ethane in the presence of pentasils modified by platinum increases by a factor of 2 in the presence of the intermetallic compound Zr_2Fe [18] as a result of the suppression of the methane formation side reaction and the displacement of the thermodynamic equilibrium in the rate-limiting stage involving the dehydrogenation of ethane to ethylene. The effect of the hydrogen acceptor on the secondary stage of the aromatisation reaction (the oligomerisation of ethylene) promotes the preferential formation of bicyclic aromatic products from ethane on Zn- and Ga-containing zeolites.[17]

The positive effect of the removal of hydrogen on the oligomerisation process was confirmed by the present authors in relation to the aromatisation of ethylene on the HTsVM zeolite (Table 4). In contrast to ethane, ethylene is readily activated on the acid centres of the H-form of pentasil, where rapid oligomerisation and aromatisation takes place. In the presence of Zr_2Fe, there is an appreciable increase in the yield of the aromatic products and of their content of bicyclic hydrocarbons for only a slight increase in the conversion of ethylene, but coke formation is not intensified. Evidently the removal of hydrogen has a positive effect on the stage involving the dehydrogenation of oligomers. On the other hand, the content of C_2-C_3 hydrocarbons in the gaseous reaction products diminishes. Consequently, as in the aromatisation of ethane, the removal of the hydrogen formed prevents the cracking of the intermediate and final reaction products. The slight increase in the yield of methane in the presence of the hydrogen acceptor is probably due to the demethylation of xylenes, the yield of which is reduced with a simultaneous increase in the yield of benzene.

Table 4. Aromatisation of ethylene on HTsVM (450 °C, 3600 h^{-1}) in the absence and presence of Zr_2Fe.

Parameter	Without acceptor	With acceptor
Conversion (mass%)	96.6	98.4
Yield of aromatic hydrocarbons (mass%)	38.2	44.9
Proportions of products (%):		
CH_4	1.4	3.7
C_2H_6	6.4	5.2
$C_3H_6+C_3H_8$	44.6	35.5
$C_4H_8+C_4H_{10}$	7.4	9.4
C_{5+}	0.6	0.6
Aromatic hydrocarbons	39.6	45.6
Proportions of aromatic hydrocarbons (%):		
Benzene	12.3	14.2
Toluene	39.5	40.1
Xylenes + ethylbenzene	43.7	37.6
C_{9+}	4.5	8.1
Content of coke on catalyst (mass%)	4.4	3.5
Content of hydrogen in the reaction stream (mol%)	11.8	0.2

Contrary to expectations, the removal of hydrogen by the hydrogen acceptors suppressed the dehydrogenation of ethane on oxide and on platinum-containing catalysts, both of which are inactive in the aromatisation reaction (Table 5), and at the same time no appreciable coke formation was observed.[18] This result shows that hydrogen plays a definite role in the dehydrogenation of ethane. One can postulate that it reduces to the acceleration of the desorption of the alkene from the surface of the catalyst. It has been shown[34] that the dehydrogenation of propane on gallium and zinc oxides is limited by the propene desorption stage, which is accelerated appreciably in the presence of the HZSM-5 zeolite as a result of the migration of $C_3H_7^+$ from gallium oxide to the acid centres of the zeolite, where a proton is fairly readily abstracted with the formation of propene. When H^+ is replaced by Na^+ in ZSM-5, the rate of dehydrogenation of propane diminishes by a factor of 100. It may be that this bifunctional mechanism operates in the dehydrogenation of ethane as well.

The change in the mode of reaction in the presence of hydrogen acceptors as a function of its mechanism and the catalyst composition has been observed in the aromatisation of

Table 5. The influence of the hydrogen acceptor Zr_2Fe on the dehydrogenation of ethane.

Catalyst	T/ °C	Reaction time/min	Yield of ethylene (mass %)	
			without acceptor	with acceptor
Ga_2O_3/SiO_2	550	6	5.1	5.7
	550	15	5.0	0.3
Cr_2O_3/ZrO_2	600	5	9.7	13.6
	600	22	9.8	1.9
Pt/SiO_2	550	7	7.9	1.2
	550	22	7.4	1.9
Pt/NaTsVM	550	5	7.2	1.0
	550	15	7.8	0.04

propane.[19,20] The authors suggest that, owing to the high activity of Ga/HTsVM in the dehydrogenation and oligomerisation processes, the displacement of the dehydrogenation equilibrium, occurring in the presence of the Zr_2Fe hydrogen acceptor, virtually precludes competition between the side reaction involving the hydrocracking of the intermediates and the aromatisation reaction, and the selectivity in the formation of aromatic hydrocarbons increases almost by a factor of 2. In the presence of the HTsVM and Pt/HTsVM catalysts, the removal of hydrogen from the reaction mixture activates the hydrogen redistribution processes, which increases the yield of aromatic products from propane but does not lower the amount of C_1-C_2 alkanes in the reaction products.

The dehydrogenation of methanol on intermetallic catalysts of different composition takes place with the formation of CO, formaldehyde, or methyl formate.[24,25]

Thus the activity and selectivity of the dehydrogenation catalyst as well as the process mechanism are of primary importance for the attainment of high yields of the target products when intermetallic hydrogen acceptors are used.

4. The spill-over of hydrogen

When the dehydrogenation and hydride formation reactions take place simultaneously, the catalytically active centres and hydrogen absorption centres are separated from one another by large distances. Presumably the hydrogen evolved migrates to the acceptor through the gas phase in the molecular state or it migrates on the surface in the atomic form. i.e. via spill-over.

The spill-over of hydrogen is more likely when the intermetallic compound functions simultaneously as a dehydrogenation catalyst and a hydrogen acceptor, since in this case the catalytic and absorption centres are close to one another and the transfer of hydrogen through the gas phase is energetically less favourable. The view exists[22,23,27] that the dehydrogenation of alcohols on hydride-forming intermetallic compounds is a pure example of the spill-over of hydrogen when the alcohol serves as the source of hydrogen atoms and the intermetallic compound is a solid acceptor. The activation of the surface of the intermetallic compound accelerates, according to the authors' view, not only dehydrogenation but also the spill-over of hydrogen to the absorption centres.

The ability to initiate the spill-over of hydrogen is characteristic of all hydride forming metals and alloys, because the H_2 absorption process involves the migration of the hydrogen dissociated on the surface into the bulk of the intermetallic phase. However, only some of them are active in dehydrogenation and this frequently requires a special treatment of the surface. Studies on the spill-over of hydrogen in various catalytic systems using different organic molecules as the hydrogen donors have shown that the ability of the catalysts to initiate this process depends on their activity in dehydrogenation.[35] In other words, the spill-over of hydrogen is closely related to dehydrogenation and apparently does really occur in the systems considered.

In the case where the intermetallic compound performs only the function of a hydrogen acceptor and the dehydrogenation reaction proceeds on an oxide, a deposited metal, or a zeolite catalyst, the involvement of spill-over in hydrogen transfer from the catalyst to the acceptor is less likely, but it cannot be ruled out on the basis of available data.

The appearance of molecular hydrogen in the reaction medium from the first minutes of the dehydrogenation of isobutane on Pt/Al_2O_3 in the presence of titanium presupposes, according to the authors,[8] that the transport of hydrogen takes place through the gas phase or in competition with the spill-over. The occurrence of the spill-over of hydrogen has been demonstrated indirectly in the dehydrogenation of cyclohexane in the presence of the intermetallic compound ZrNi and deposited platinum catalysts.[14] On Pt/Al_2O_3 and Pt/SiO_2 without a hydrogen acceptor, the yield of benzene was 19 mass% and 15 mass% respectively. After the removal of hydrogen, the maximum yield of benzene on the platinum/alumina catalyst reached 100%, while on Pt/SiO_2 it did not exceed 16 mass%, hydrogen being fully absent from the gas phase at the beginning of the experiment in the former case whilst in the latter it was present. This fact can be attributed to the different abilities of the Al_2O_3 and SiO_2 carriers to transfer the activated hydrogen along the surface.[36] Furthermore, for different proportions of Pt/Al_2O_3 and ZrNi in a mechanical mixture, the effectiveness of the hydrogen acceptor in the dehydrogenation of cyclohexane depends on the area of contact between the catalyst and the acceptor,[14] which can also be associated with the spill-over of hydrogen. Thus the maximum effect of hydride formation on the dehydrogenation reaction is probably attained when these processes are coupled, i.e. when the hydrogen acceptor reacts with the active hydrogen species formed as a result of dehydrogenation.

IV. Conclusion

The results examined in the present review reveal a new application of hydride-forming metals and intermetallic compounds as hydrogen acceptors for the displacement of the equilibrium in thermodynamically restricted catalytic reactions occurring with the evolution of H_2. The results indicate a high effectiveness of intermetallic hydrogen acceptors in the dehydrogenation reactions of cycloalkanes, isobutane, and C_1-C_3 alcohols and also in the aromatisation of C_2-C_3 hydrocarbon gases. This is manifested by the increase by a large factor in the yields of the target products, by the reduction of the reaction temperature by 100–150 °C, and by an increase in the selectivity of the processes.

In order to couple hydride formation with dehydrogenation, the hydrogen acceptor and the catalyst must satisfy certain requirements. It is essential that the metal or the intermetallic compound should be characterised by a low equilibrium dissociation pressure of the hydride at elevated temperatures, that the rate of absorption by the metal or the intermetallic compound should be high, and that it should retain its absorption capacity under dehydrogenation conditions and on repetition of the desorption cycles. The catalyst must have a high dehydrogenating activity and ability to initiate the spill-over of hydrogen. The process mechanism, which depends on the composition and properties of the catalyst, also affects the results of the dehydrogenation reaction occurring in the presence of an intermetallic hydrogen acceptor. All these factors create certain difficulties in the practical realisation of the processes and require additional search for new intermetallic compounds with the necessary properties and also the study of the reaction mechanisms under the conditions of hydrogen removal by the acceptor.

References

1. W M Mueller, J P Blackledge, G G Libowitz (Eds) *Metal Hydrides* (New York: Academic Press, 1969) (Translated into Russian; Moscow: Atomizdat, 1973)
2. H Wenzl *Int. Met. Rev.* **27** 140 (1982)
3. G D Sandrock, E L Huston *Chem. Tech.* **11** 754 (1981)
4. V V Lunin *Sci. USSR* 78 (1985)
5. W E Wallace *Chem. Tech.* **12** 752 (1982)
6. K Soga, H Imamura, S Ikeda *J. Phys. Chem.* **81** 1762 (1977)
7. V V Lunin, V I Deineka, A F Plate *Neftekhimiya* **16** 499 (1976)
8. A J Fanelli, A J Maeland, A M Rosan, R K Crissey *J. Chem. Soc., Chem. Commun.* 8 (1985)
9. H Imai, T Tagawa, M Kuraishi *Mater. Res. Bull.* **20** 511 (1985)
10. O V Chetina, V V Lunin, G V Isagulyants *Kinet. Katal.* **30** 1248 (1989)
11. O V Chetina, V V Lunin *Neftekhimiya* **30** 202 (1990)
12. H Imai, T Tagawa, M Kuraishi *Shokubai* **20** 511 (1985)
13. O V Chetina, V V Lunin, G V Isagulyants *Izv. Akad. Nauk SSSR, Ser. Khim.* 2405 (1988)
14. O V Chetina, V V Lunin, G V Isagulyants *Neftekhimiya* **27** 757 (1988)
15. H Imamura, K Uamada, K Nukui, S Tsuchiya *J. Chem. Soc., Chem. Commun.* 367 (1986)
16. O V Chetina, T V Vasina, V V Lunin, O V Bragin *Izv. Akad. Nauk SSSR, Ser. Khim.* 2871 (1990)
17. O V Chetina, V V Lunin, O V Bragin *Kinet. Katal.* **32** 1257 (1991)
18. O V Chetina, T V Vasina, V V Lunin, O V Bragin *Catal. Today* **13** 639 (1992)
19. O V Chetina, T V Vasina, V V Lunin *Catal. Lett.* **14** 101 (1992)
20. O V Chetina, T V Vasina, V V Lunin *Izv. Akad. Nauk, Ser. Khim.* 61 (1993)
21. A Andersen, J M Dahl, K J Jens, E Rytter, A Slagtern, A Slobakken *Catal. Today* **4** 389 (1989)
22. H Imamura, S Kasahara, T Takada, S Tsuchiya *J. Chem. Soc., Faraday Trans. 1* **84** 765 (1988)
23. H Imamura, T Takada, S Kasahara, S Tsuchiya *Appl. Catal.* **58** 165 (1990)
24. H Imai, T Tagawa, K Nakamura *Appl. Catal.* **62** 348 (1990)
25. H Imai, T Tagawa, K Nakamura *Rep. Res. Lab. Eng. Mater., Tokyo Inst. Technol.* **15** 61 (1990)
26. H Imamura, K Nukui, K Yamada, S Tsuchiya, T Sakai *J. Chem. Soc., Faraday Trans. 1* **83** 743 (1987)
27. W J T M Appelman, M Kuczynski, G F Versteeg *Appl. Catal., A* **81** 35 (1992)
28. K H J Buschow, P C P Bouten, A R Miedema *Rep. Prog. Phys.* **45** 937 (1982)
29. A A Vvedenskii *Termodinamicheskie Raschety Neftekhimicheskikh Protsessov* (Thermodynamic Calculations for Petrochemical Processes) (Leningrad: Gostoptekhizdat, 1960)
30. E Fromm, H Uchida *J. Less-Common Met.* **131** 1 (1987)
31. H Uchida, E Fromm *J. Less-Common Met.* **131** 125 (1987)
32. V V Lunin, O V Chetina *Zh. Fiz. Khim.* **64** 3019 (1990)
33. F Aubertin, U Gonser, S J Campbell *J. Phys., F* **14** 2213 (1984)
34. P Meriaudeau, C Naccache *J. Mol. Catal.* **59** L31 (1990)
35. P A Sermon, G C Bond *J. Chem. Soc., Faraday Trans. 1* **76** 889 (1980)
36. W C Conner, G M Pajonk, S J Teichner *Adv. Catal.* **34** 1 (1986)

Russian Chemical Reviews **63** (6) 491 – 505 (1994)
©1994 Russian Academy of Sciences and Turpion Ltd

UDC 541.15 + 541.117

Cryopolymerisation

I M Barkalov, D P Kiryukhin

Contents

I.	Introduction	491
II.	Crystals	492
III.	Glasses	497
IV.	Other metastable systems	500
V.	Autowaves	500
VI.	Oscillations in the rate of reaction	502

Abstract. The mechanism of cryochemical chain reactions is examined in relation to polymerisation. The study of such processes in crystals has led to the discovery of a low-temperature limit to the rates of chemical reactions. Polymerisation occurring under the conditions of a sharp change (by 5–6 orders of magnitude) in the molecular mobility of the medium in the region of the devitrification of the matrix has been investigated in vitreous systems. Unusual mechanoenergetic chains of chemical reactions have been observed in the study of systems immersed in liquid helium. The chemical reaction is initiated by a local brittle fracture and is propagated along the specimen in the form of an autowave. Auto-oscillations of the rate of cryopolymerisation have been observed under certain conditions. The bibliography includes 132 references.

I. Introduction

It is difficult to imagine an effective chemical reaction in a solid without a significant mass transfer of the reactants and products. At first sight it might turn out that chemical reactions in a solid occur in nature only on the geological time scale and even then not without the participation of liquid and gas phases, mechanical breakdown, and high pressures and temperatures.

Indeed, the classical picture of the elementary step in a chemical reaction is based on the following postulates: (1) an activation barrier must be overcome for the interaction reactions to be initiated; (2) reactants receive the energy required to overcome the activation barrier as a result of intermolecular interactions; (3) the time necessary for the reactions to accumulate this energy (the characteristic time of the elementary step) is determined by the temperature of the medium. It is easy to show that these postulates exclude the possibility of a chemical process in the vicinity of the absolute zero of temperature.

In the 1930s, communications were published in which the polymerisation of crystalline monomers was reported. It was found that crystalline trioxane polymerises in the presence of formaldehyde vapour with formation of polyoxymethylene fibres oriented along one of the crystallographic axes. The formation of rubber-like polymers of acetaldehyde was observed at the same time at the instant of its freezing (crystallisation) and fusion. The latter processes occur at low temperatures. Thus it was found that chain reactions can take place in a solid also at low temperatures.

Later investigators found new ways of initiating chemical reactions in the solid. One of them is based on the use of γ-radiation. Initiation of active centres, more or less uniform throughout the volume of the solid phase, takes place under these conditions and all the complications associated with the diffusion of the initiator molecules within the crystals are fully eliminated. However, the main advantage of radiation initiation is that its effectiveness is independent of temperature (in contrast to chemical initiation). The latter factor made it possible to proceed to the study of the polymerisation of solid monomers at low and ultralow temperatures.

All this led in the 1960s to a vigorous development of studies on solid-phase polymerisation. However, at the time most of the investigations were phenomenological in nature and theoretical generalisations and hypotheses were novel rather than experimentally well-founded.

It was found initially that the rigorous orientation of the monomer molecules in space, which is characteristic of crystals, may be reflected in the regularity of the macromolecules formed. Furthermore, hopes arose that the 'ordered military ranks' of the reactants in the crystal would promote the rapid occurrence of the process. In 1960, Semenov [1] proposed the energy chain mechanism for solid-phase polymerisation. The idea was that the energy evolved in each elementary chain propagation step is not scattered by being converted into heat, but, by virtue of the collective interaction of the monomeric 'precursors' in the crystal, ensures that the activation barrier is overcome in the next such step. One of the variants of the collective interaction may involve the movement of an exciton along the 'precursor'. In this case, the polymer chain may grow at the rate of propagation of the exciton. (The exciton chain model has been examined in detail by Adirovich [2].)

Here we shall not dwell on the analysis of the extensive factual data, with which the reader may become acquainted in the relevant communications, [1,3–8] and only the principal conclusions will be quoted. The formation of a polymer in a crystal of the initial monomer alters the average distances between the individual

I M Barkalov, D P Kiryukhin Laboratory of Cryochemistry and Radiation Chemistry, Institute of Chemical Physics in Chernogolovka, Russian Academy of Sciences, 142432 Chernogolovka, Moscow Region, Russian Federation. Fax (7-096) 515 35 88

Received 26 April 1994
Uspekhi Khimii **63** (6) 514 – 529 (1994); translated by A K Grzybowski

fragments, whereupon the spatial orientation of the monomer units may be changed. There is a wide variety of numerous systems in which these geometrical factors play a significant role. The transfer of classical ideas about the reaction mechanisms in the gas and liquid phases to solid-phase reactions proved fruitless; new ideas were needed.

In view of the extremely restricted translational displacements in a crystal, it is difficult to imagine the destruction of growing macroradicals as a result of recombination or disproportionation. In this case, the polymer chain gradually ceases to grow owing to progressive difficulties in the supply of the monomer to the growing active centre — a kinetic arrest of the process ('setting and revival' of the polymer chain) is observed.[9] This served as a basis for the development of the theory of 'polychronic kinetics'.[10]

The idea that chemical reactions are impossible near the absolute zero changed after *the low temperature limit to the rates of chemical reactions had been established* experimentally. This phenomenon was observed in the study of the mechanism of the polymerisation of solid formaldehyde in the temperature range 4–100 K.[11] The existence of the low-temperature limit to the rate was subsequently confirmed for a series of chain and nonchain chemical reactions.[12] Systems in which the chemical reaction takes place even at the temperature of liquid helium were found experimentally. Although the rate of such a reaction is low, it is nevertheless measureable and is independent of temperature.

Immediately after the discovery of the phenomenon of the low-temperature limit to the rate, it was suggested that its mechanism be interpreted within the framework of the concept of molecular tunnelling. This idea was subsequently developed taking into account the role of intermolecular vibrations.[12–15]

The present review describes only a small portion of the enormous amount of data concerning the mechanisms of solid-phase reactions.

II. Crystals

1. Formaldehyde

The possibility of the radiation polymerisation of solid formaldehyde at temperatures close to that of liquid nitrogen has been reported.[16–18] However, these studies were qualitative. Indeed, the yield of the polymer was determined only after the heating and fusion of the irradiated solid monomer (the rate of the process was determined by dividing the mass of the polymer isolated by the irradiation time of the system). This naturally did not allow the determination of the true rates of polymerisation at 77 K. Subsequently, it was found that, when the irradiated polycrystalline formaldehyde is heated, effective postpolymerisation takes place, masking completely the effect occurring directly during the radiolysis of the specimen at 77 K. Only the use of kinetic calorimetry made it possible to investigate these processes separately. The principal results of investigations of the solid-phase polymerisation of formaldehyde in the temperature range 5–150 K are presented below.[11,19–26]

The method for the purification and drying of gaseous formaldehyde, which has been thoroughly elaborated, made it possible to eliminate the problem of the reproducibility of kinetic measurements.[27] Calorimetric analysis showed that frozen formaldehyde forms a polycrystalline mass rapidly (~200 K min^{-1}) or slowly (~0.3 K min^{-1}) and undergoes no phase transitions of any kind in the temperature range 4.2–155 K. It melts at 155 K and its heat of fusion is $\Delta H = 1.80 \pm 0.05$ kcal mol^{-1}. The enthalpy of the polymerisation of solid formaldehyde was found to be 8.5 ± 1.0 kcal mol^{-1} and this value was used subsequently to calculate the rate of polymerisation.

The radiation polymerisation of formaldehyde proceeds extremely effectively, so that thermal explosion is observed when heat is removed inadequately.[16,17] For this reason, all the kinetic measurements were performed under conditions as close to isothermal conditions as possible, which was achieved by increasing the heat exchange area and by reducing the γ-radiation dose rate. After exposure to γ-radiation, the rate of heat evolution associated with polymerisation reaches a steady value during a period equal to the characteristic time of the calorimetric apparatus used in the experiments (Fig. 1).

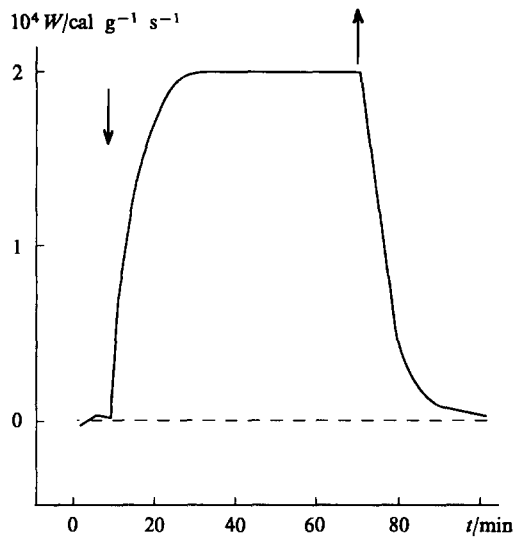


Figure 1. Variation of the rate of heat evolution in the polymerisation of formaldehyde in the field of γ-radiation. Temperature 100 K; dose rate 1.4×10^{-4} Gy s^{-1}. The arrows indicate the instants when γ-radiation was switched on and off. The dashed line represents the analogous experiment with polyformaldehyde.

However, the steady rate of polymerisation does not persist for a long time and an appreciable decrease in the rate is observed already for degrees of conversion of ~0.5%. The reason for the decrease can be only the kinetic arrest of the process when the access of the monomer to the growing polymer centre is hindered.

Experimental proof that the kinetic chain termination reaction is first order in the polymerisation process has been obtained. It is natural to attribute linear termination to the kinetic arrest of the growth of the polymer chain ('setting') and not to the destruction of active centres, because, when the temperature rises outside the radiation zone, effective postpolymerisation is observed, i.e. the chains which have set are 'revived'.

The radiation-chemical yield of the polymer is $G(-M) \geqslant 10^6$ molecules per 100 eV of the absorbed energy of the γ-radiation in the early stages of the process. One may assume that this is the highest recorded quantity for radiation polymerisation.

The temperature dependence of the steady rate in the range 80–150 K is described satisfactorily by the Arrhenius equation (the activation energy is 2.0 ± 0.6 kcal mol^{-1}). At temperatures above 140 K, the rate of polymerisation falls, apparently owing to the increase in the chain termination rate constant near the melting point of the monomer crystals. A negative activation energy for the polymerisation of formaldehyde ($E = -0.5$ kcal mol^{-1}) has been reported.[16,17] This value is clearly erroneous if only because the authors of the above communications observed the phenomenon of thermal explosion, which is impossible for a negative temperature dependence of the rate of polymerisation.

The following expression for the chain propagation rate constant has been obtained in the temperature range 8–140 K:

$$k_p \approx 0.03 \exp\left(-\frac{2000 \pm 100}{RT}\right).$$

On passing to the liquid phase, the steady rate of polymerisation of formaldehyde falls sharply (almost by a factor of 10). This is naturally associated with the significant increase in the rate of termination of polymer chains in the liquid phase compared with that in the crystal lattice.

The high radiation yield of the polymerisation of solid formaldehyde at the temperature of liquid nitrogen made it possible to proceed to the investigation of its polymerisation at still lower temperatures (5–80 K). The temperature dependence of the rate of polymerisation was studied. With decrease in temperature (below 80 K), the temperature dependence of the rate of polymerisation diminishes and then ceases altogether. A more marked deviation of the rate from the Arrhenius law is observed. However, even at 5 K polymerisation still occurs with a radiation yield $G(-M) \approx 1000$, which is characteristic of chain processes. Thus, the occurrence of a chain reaction at such low temperatures was observed for the first time by a direct method for the given process.

The characteristic chain propagation times in solid formaldehyde have also been measured in the temperature range 5–80 K. Two identical calorimetric experiments were performed: one with solid formaldehyde and another with polyoxymethylene. In the experiment with polyoxymethylene, the evolution of heat is associated solely with the heating of the system owing to the absorption of γ-radiation. Since γ-radiation is absorbed equally by the polymer and the monomer, in the experiments with the monomer the overall heat evolution due to the absorption of γ-radiation and the polymerisation reaction was detected.

Figure 2 presents the results of these measurements. The characteristic time of the process τ (the average kinetic chain propagation time) was determined by fitting the following relation to the rate of increase in the rate of polymerisation after exposure to initiating radiation:

$$W = W_{st}\left[1 - \exp\left(-\frac{t}{\tau}\right)\right].$$

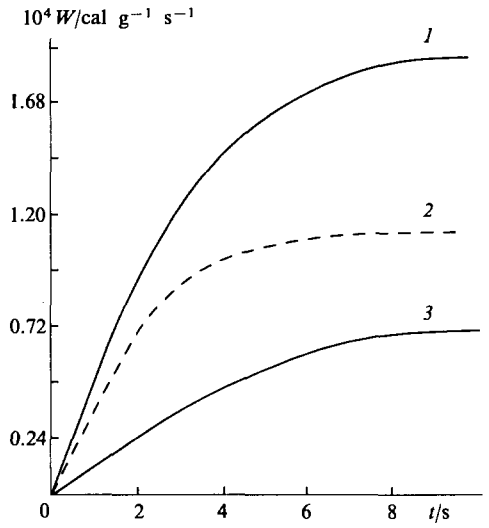


Figure 2. Time variation of the rate of heat evolution in the field of γ-radiation for formaldehyde (curve *1*) and polyformaldehyde (curve *2*) and variation of the rate of polymerisation of formaldehyde (curve *3*) (difference between the rates represented by curves *1* and *2*). Polymer sample 0.25 g; dose rate 0.45 Gy s^{-1}; temperature 5 K.

The intrinsic chain propagation characteristic time at temperatures below 10 K approached 10 s. The temperature dependence of the chain propagation time was obtained from the results of a series of similar experiments carried out at different temperatures. From the measured chain propagation characteristic times, one can proceed to the time required for the step involving an increment by one monomer unit:

$$\tau_o = \frac{\tau g}{G(-M)},$$

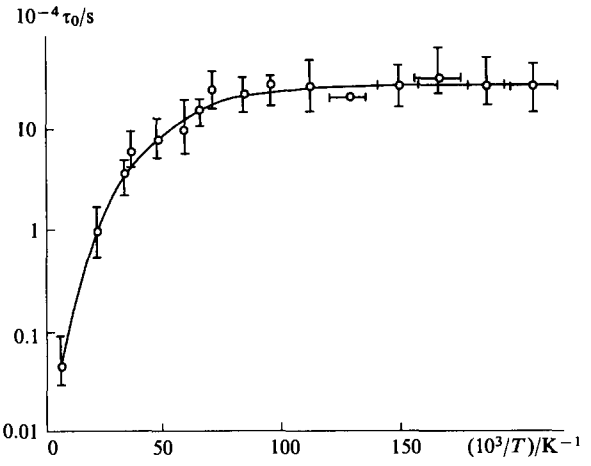


Figure 3. Temperature variation of the time required for the addition of one monomer unit in the polymerisation of formaldehyde.

where g is the radiation yield of the active centres initiating the polymerisation (usually $g \approx 1$). With decrease in temperature, a more marked deviation of the rate of polymerisation from the Arrhenius law is observed — the time required for the addition of one unit tends to the constant value $\tau_0 = 0.01$ s (Fig. 3), while extrapolation of the data for 80–140 K on the basis of the Arrhenius law would yield a value at 5 K, which would be much too high ($\tau_0 \approx 10^{100}$ years!).

A low-inertia calorimetric apparatus was used to investigate the possibility of polymerising formaldehyde at 5 K in the absence of radiation, but the reaction was carried out in this case under conditions where γ-radiation was switched off rapidly. After γ-radiation has been stopped, a decrease in the rate of polymerisation is observed with a characteristic time $\tau \approx 15$ s, which is significantly longer than the time corresponding to the inertia of the calorimeter (Fig. 4).

Thus it was shown clearly that the polymerisation chain continues to be propagated at helium temperatures also in the absence of a radiation field. Therefore the hypothesis that the

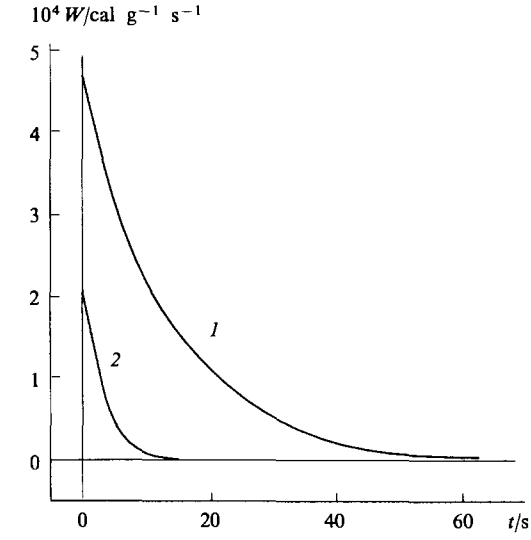


Figure 4. The postpolymerisation of formaldehyde after switching off γ-radiation: (*1*) monomer in the calorimetric cell; (*2*) analogous experiment with the polymer. Formaldehyde sample 0.25 g; temperature 5 K; dose rate 6 Gy s^{-1}.

radiant energy is used to activate each elementary addition step is incorrect. At the same time the hypotheses postulating that chain propagation takes place as a result of the transfer of short-lived excited states, that polymerisation takes place in tracks, etc. have to be abandoned. This significantly narrows the range of the possible hypotheses concerning the mechanism of the observed phenomenon.

The polyformaldehyde obtained by the radiation polymerisation of formaldehyde at 77 K has a supermolecular structure comprising monolithic crystalline domains.[28] The formation of this morphological type was not observed either on crystallisation of this polymer from solutions or melts or on crystallisation during synthesis.[29-31] Analysis of the IR spectra in the range 800–1300 cm^{-1}, where the vibration bands sensitive to changes in the angles of internal rotation of the CHO chain are located, demonstrated an unusual conformation of the chains in the polymer obtained by solid-phase polymerisation.

The known modifications of polyformaldehyde, named in accordance with the type of crystal lattice — hexagonal (I) and orthorhombic (II) — are characterised by a sequence of monomer units having the *gauche, gauche*-conformation with internal rotation angles of 77° (I) and 63° (II).[32] Such differences between the angles of internal rotation of the polymer chains do not lead to significant differences between the IR spectra. On the other hand, the spectrum of the polymer specimen obtained by solid-phase polymerisation contains bands additional to the absorption bands of the known modifications (I) and (II).[28] This finding shows that some of the monomer units of the polymer chains in the specimen are in a conformation different from the *gauche, gauche*-conformation. This can be only the uncoiled *trans*-conformation, since the coiled *cis*-conformation is prohibited by steric hindrance. One can therefore postulate that the chains in the new structural modification of the polymer are characterised by sequences of monomer units with the *gauche, trans*-conformation.

The new structural modification of the polymer, obtained by the solid-phase polymerisation of formaldehyde, proved to be metastable. Judging from the changes in the IR spectra, it passes to the known modification I on recrystallisation from melts and solutions and also under the influence of pressure. We may also note that a stable modification is formed in the radiation polymerisation of liquid formaldehyde.

The polymerisation of a monomer crystal entails a change in both the average distances between individual fragments (the intermolecular distances are replaced by chemical bond lengths) and in the spatial orientation of the monomer units. We may note two extreme cases: (1) the structure of the monomer crystal determines to a large extent the structure of the polymer (derivatives of conjugated diacetylenes, trioxane); (2) the polymer arises as an independent phase in the extended lattice defects, which leads to further fracture of the monomer crystal; the polymer phase is amorphous (acrylamide). There is a large number of intermediate cases between these extremes.

The polymerisation of crystalline acrylamide begins in the region of the extended defects and proceeds on the interface between the amorphous polymer and the crystalline monomer.[33] A decrease in the size of the crystals facilitates the polymerisation process. The average rates of polymerisation in fine defective acrylamide crystals are higher than in large perfect crystals.

An example of the first of the extreme cases listed above is the so called topochemical polymerisation.[34] A polymer phase, the crystallographic directions of the axes of which are determined by the directions of the axes of the initial crystal, is formed in such processes. The polymerisation in large crystals of monomers of this kind is faster than in small crystals, while the presence of noncrystallising additives reduces the rate of the process.

In this connection, it appeared important to elucidate the influence of the size of the formaldehyde crystals and of their defectiveness on the kinetics of the low-temperature radiation polymerisation. It was found[35] that the kinetics of the radiation polymerisation of formaldehyde depend significantly on their crystal size. The rate of polymerisation in small defective crystals is almost 20 times lower than in slowly grown large crystals. It is natural to assume that the decrease in the yield of the polymer on passing to highly defective formaldehyde crystals is associated with the decrease in the length of the kinetic chains in the polymerisation process, i.e. that the solid-phase polymerisation of formaldehyde takes place at a high rate only within large and perfect crystals.

Photoinitiation has also been used in the study of the low-temperature solid-phase polymerisation of formaldehyde. Thus the polymerisation of crystalline and amorphous formaldehyde at temperatures above 20 K on photoexcitation of added β-naphthol has been reported.[36,37] Such initiation entails the transfer of a proton from β-naphthol to formaldehyde with formation of a cation as the chain-transfer agent.

The low-temperature reactions of formaldehyde in amorphous formaldehyde–chlorine mixtures have been investigated.[38-40] Chlorine was photolysed by using an excimer laser (λ = 308 nm) or a mercury arc lamp (λ = 365 nm). The formation of oligomers with a chain length corresponding to 5–7 units was observed in the temperature range 10–77 K, whilst at temperatures $\geqslant$90 K the chain length increased by a factor of 2. The molecular mass of the polymer obtained in this way is much lower than that of the polymer formed in the crystal (chain length 10^3–10^6). This is caused by the molecular disorder in the amorphous state.

In order to account for the low-temperature limit to the rate of chain propagation, the concept of molecular tunnelling was introduced.[23,24] These investigations stimulated many studies on the theoretical development of ideas concerning the elementary chemical step in a solid†.

2. Acetaldehyde

Acetaldehyde is the closest homologue of formaldehyde. Rubber-like acetaldehyde polymers were first obtained by Travers[41] and Letort.[42] Pshezhetskii et al.[43] observed with the aid of thermographic and cine-film techniques the propagation of the polymerisation front in solid radiolysed acetaldehyde at relatively high temperatures (117–147 K) close to the melting point of the monomer (T_m = 150 K). Having made a series of assumptions and having restricted the treatment to one thermal conductivity equation, the authors[43] obtained an extremely short time for the addition of one monomer unit to the polymer chain (10^{-8} s). Such high rates stimulated further investigations of this system by the calorimetric method under slow temperature scanning conditions and directly in the field of γ-radiation under isothermal conditions.[44]

Even at the maximum rate of cooling of the liquid monomer to 77 K (~100 K min^{-1}), the latter does not form a vitreous state. As in formaldehyde, in polycrystalline acetaldehyde there are no phase transitions of any kind, the compound melting at 150 K (ΔH = 1.40 ± 0.07 kcal mol^{-1}).

Figure 5 presents the typical time dependence of the rate of polymerisation (rate of heat evolution) of solid acetaldehyde in the field of γ-radiation, indicating a distinct autoacceleration of the polymerisation process. Evidently, the autoacceleration is associated with the accumulation of active centres during the radiolysis of the solid monomer, i.e. with the increase in the rate of initiation. The expression for the time variation of the rate of the process is

$$W = -\frac{d[M]}{d[t]} = k_p g I t [M]_0 \exp(-0.5 k_p g I t^2),$$

where k_p is the polymer chain propagation rate constant, I the intensity of the radiation, and $[M]_0$ the initial monomer concentration. Two corollaries arise from this: (1) the experimental

† For further details, see the monograph of Gol'danskii et al.[12]

relation $W = f(t)$ (Fig. 5) should become linear in terms of the $\ln(W/t)$ against t coordinates; (2) the time required for the attainment of the maximum rate t_{max} is $k_p g I^{-0.5}$, which makes it possible to calculate k_p. This kinetic scheme does not take into account the possibility of the kinetic arrest of the growing chains, but it describes satisfactorily the relation obtained. Indeed, the function illustrated in Fig. 5 becomes satisfactorily linear in the appropriate coordinates.

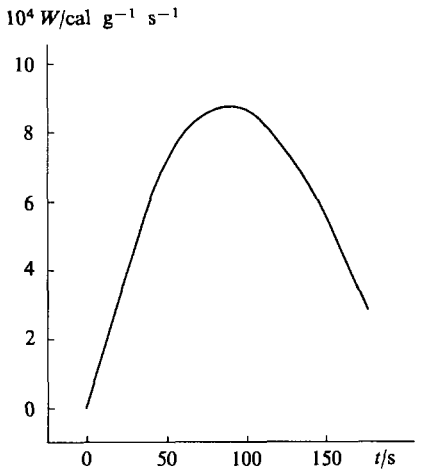


Figure 5. Time variation of the rate of heat evolution (polymerisation) in solid acetaldehyde in the field of γ-radiation. Dose rate 0.6 Gy s^{-1}; temperature 136 K.

A series of experiments, analogous to that described above, were then carried out at different temperatures, which made it possible to determine the chain propagation rate constant. The temperature variation of k_p in the range 130 – 144 K is described by an expression of the type

$$k_p = 5 \times 10^{-4} \exp\left(-\frac{11000}{RT}\right),$$

i.e. the average time required for the addition of the monomer unit in this temperature range is 0.1 – 0.001 s.

It is noteworthy that the activation energy (11 kcal mol^{-1}) is much higher for acetaldehyde than for formaldehyde (2 kcal mol^{-1}) in the same temperature range. However, we are apparently dealing here with an effective activation energy because its high values are compensated by the high values of the pre-exponential factor, which is characteristic of reactions occurring near the melting point.

Thus, in contrast to its nearest homologue, acetaldehyde hardly polymerises even at 77 K. An intense thermoactivated post-effect is characteristic of solid acetaldehyde, as for formaldehyde.

3. Glyoxal and tricarbon dioxide

We shall consider the polymerisation of crystalline glyoxal $(HCO)_2$.[45] In contrast to formaldehyde, the mechanism of the polymerisation of this monomer has been little investigated.[46] Calorimetric analysis showed that phase transitions of any kind do not occur in solid glyoxal in the temperature range 80 – 288 K. Glyoxal melts at 288 K and its heat of fusion is ΔH = 3.0 kcal mol^{-1}. The slightest traces of moisture lead to spontaneous polymerisation near the melting point of the monomer, which is clearly recorded on the calorimetric heating curve.

The rate of polymerisation of solid glyoxal in the field of γ-radiation slowly reaches a steady value and, with the initiating radiation switched off, it decreases with the characteristic time τ = 1300 s.

The heat of polymerisation of glyoxal is 5 ± 1 kcal mol^{-1}. This quantity is the mean of the heats of polymerisation of formaldehyde (8.5 kcal mol^{-1}) and acetaldehyde (2.5 kcal mol^{-1}). A series of measurements of the process dynamics at different temperatures made it possible, as in the case of other monomers, to determine the principal kinetic parameters. The chain propagation rate constant for the solid-phase polymerisation of glyoxal is different from that for formaldehyde.

$$k_p \approx 10^{-17} \exp\left(-\frac{4000}{RT}\right).$$

At 170 K, the rate of polymerisation of glyoxal becomes negligible. However, the postpolymerisation of this monomer can be observed even at temperatures slightly above 100 K. The supermolecular and molecular structures of the polymer formed depend significantly on the temperature at which glyoxal is polymerised. The particles of the polymer obtained at 100 – 170 K have a polygonal shape and exhibit double refraction, which indicates oriented growth of the polymer chains. The polymers obtained at higher temperatures (200 – 280 K) do not have this property. In both cases, the polymer is amorphous, because the formation of a three-dimensional network prevents crystallisation.

At low temperatures, predominantly one aldehyde group participates in the polymerisation of glyoxal. The IR spectrum contains an intense band due to the aldehyde group (1740 cm^{-1}). The spectrum of the polymer obtained at higher temperatures contains an absorption band due to hydroxy-groups in the range 3200 – 3400 cm^{-1}. Apparently, the polymerisation of the simplest dialdehyde proceeds via the mechanism of aldol condensation with formation of $-[CH(CHO)-CH(OH)]_n-$ chains. Since aldol condensation is characterised by a large volume of activation for chain propagation (compared with the formation of a polyacetal chain), this reaction becomes possible at high temperatures. Thus the closest analogues of the formaldehyde — glyoxal and acetaldehyde — polymerise in the crystalline state at comparatively high temperatures, the rate of their polymerisation decreases in conformity with the Arrhenius law, and a low-temperature plateau is not observed.

Continuing the search for monomers capable of chain polymerisation in the vicinity of the absolute zero of temperature, we considered a fairly exotic monomer — tricarbon dioxide O=C=C=C=O. The polymerisation of this monomer on thermal[47] and radiation[48] initiation as well as photoinitiation[49] has been reported in the literature. In all the studies, the investigators dealt with a complex set of reactions occurring in parallel, which hindered significantly the understanding of the polymerisation mechanism. When this reaction is carried out at low temperatures, the set of possible reaction pathways becomes significantly smaller. We shall consider the results of these investigations.[50,51]

The phase state of solid C_3O_2 has been subjected to calorimetric analysis. At 130 – 135 K a phase transition, apparently of the crystal – crystal type, takes place with ΔH = 1.4 ± 0.2 cal g^{-1}. Tricarbon dioxide melts at 160 K with the heat of fusion ΔH = 20.3 ± 1.7 cal g^{-1}. The enthalpy of polymerisation of C_3O_2 has been determined for the temperature range 160 – 310 K in a series of experiments; ΔH was 35 ± 5 kcal mol^{-1}.

The calorimetric experiments showed that the occurrence of the radiation polymerisation of C_3O_2 with measureable yields cannot be detected in the solid phase over the entire temperature range. This means that the radiation yield of the polymerisation reaction does not exceed $G(-M) \approx 100$ molecules per 100 eV of the absorbed energy.

The postpolymerisation of C_3O_2 specimens irradiated with different doses was investigated at 77 K. Evolution of heat due to the polymerisation of C_3O_2 begins to be observed on the calorimetric heating curve for the radiolysed specimen starting from the melting point of the monomer. In the temperature range 180 – 260 K, the polymerisation takes place at a low rate.

On further heating, the rate of polymerisation rises sharply, reaches a maximum, and then falls owing to the consumption of the monomer. The monomer specimen was heated in the experiments to 310 K, whereupon the overall yield of the polymer was 80% – 100%.[50]

The postpolymerisation was studied calorimetrically at a constant temperature of 297 ± 1 K (Fig. 6). It was found that the rate of the process initially increases with time, autoacceleration is observed, and then falls to zero owing to the exhaustion of the monomer. These experiments show that the active centres stored during the low-temperature radiolysis are retained in the postpolymerisation of not only solid but also liquid C_3O_2.

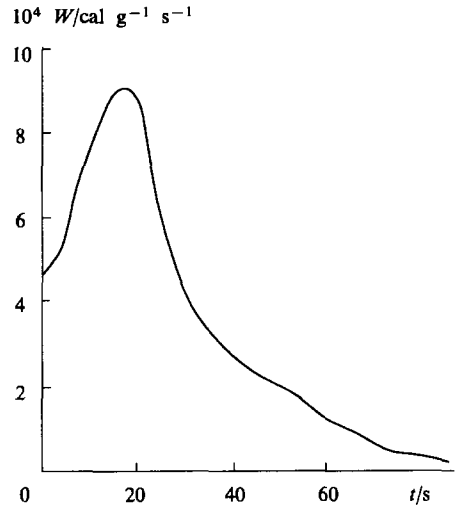


Figure 6. Time variation of the rate of heat evolution (postpolymerisation) in C_3O_2 at 297 K. Preliminary irradiation dose 10 kGy.

Unfortunately there are no experimental data of any kind concerning the nature of the active centres propagating the polymerisation. However, one can postulate that, as in the gas phase,[48] the polymerisation is propagated by ions. Apparently the long lifetime of the active centres, which are retained even in the liquid, is due to the following causes. The primary centres stabilised during the solid-phase radiolysis initiate the polymerisation of the monomer in its melting temperature range, forming oligomeric growing centres. The lifetime of such centres rises sharply owing to the appearance of steric hindrance, so that even in the liquid phase their concentration is sufficiently high to ensure effective polymerisation.

Another interesting feature of the postpolymerisation of C_3O_2 is the autoacceleration of the process at a constant temperature (Fig. 6). This phenomenon is unusual if only because the number of active centres generated during the preliminary irradiation can only decrease. The most probable cause of the autoacceleration is the increase in the rate of initiation apparently as a consequence of the branching of the chain reaction in the elementary monomer addition step. Without specifying in detail the branching mechanism, we may note that one may consider both material and energy branching. In one way or another, the question of the mechanism of the autoacceleration still remains open.

Thus the search for cryochemical chain polymerisation processes among the closest analogues of formaldehyde proved unsuccessful. The only example of a chain process occurring in the vicinity of the absolute zero of temperature and demonstrating the existence of a low-temperature limit to the rate still remains the polymerisation of formaldehyde. The next logical step was to switch the search to the chain reactions of compounds of other classes.

4. Hydrogen cyanide

It has been suggested that liquid hydrocyanic acid polymerises via an anionic mechanism under the influence of γ-radiation, affording a complex mixture of nitrogen compounds.[52] Furthermore, HCN is an extremely common molecular formation in the giant clouds of interstellar dust, in comets, and in other galactic structures. In general, the HCN molecule has come to be regarded as the basis of the prebiological chemical evolution, since its reactions constitute a direct pathway to the formation of purines, pyrimidines, and aminoacids.[53–57] It has been suggested[58] that the chain length of the cyanopolyene macromolecules arising on condensation of HCN be employed as an internal clock for the determination of the age of interstellar clouds. Other astrophysical aspects of the chemical reactions of hydrogen cyanide are developing vigorously.[59,60]

The chemical behaviour of this simple molecule under conditions approaching those in cosmic space (low temperatures and radiation) and its role in the 'cold' chemical evolution of the universe are of interest. The principal results of a series of experiments carried out on these lines recently are presented below.[61,62]

When hydrocyanic acid is cooled to 77 K, it passes to a crystalline state and, when it is heated, a phase transition of the crystal – crystal type (248 K) and fusion at 260 K (ΔH = 2.1 ± 0.1 kcal mol^{-1}) take place.

Calorimetric measurements directly in the field of γ-radiation at 77 K demonstrated the absence of appreciable heat evolution associated with a chain polymerisation reaction. When hydrocyanic acid radiolysed at 77 K is heated to room temperature, the formation of a polymer is observed. The heat change associated with the polymerisation of hydrocyanic acid is detected only in the fusion region. The yield of the polymer formed on heating to room temperature HCN specimens irradiated at 77 K increases with the preliminary irradiation dose and reaches 2.5% for a dose of 725 kGy. It is of interest that the radiation polymerisation of liquid HCN at 273 K proceeds significantly less effectively.

Prolonged maintenance of hydrocyanic acid in evacuated sealed tubes at room temperature does not lead to any changes in its colour or to the formation of polymeric products. But storage at room temperature of HCN specimens radiolysed at 77 K alters the colour (from pale-brown to almost black) and leads to the formation of polymeric products. The yield of polymer increases with increase in storage time, reaching 33.5% after 750 h.

Analysis of the IR absorption spectra of the freshly prepared polymer showed that, together with the absorption bands due to the stretching vibrations of the C≡N bond (2100–2200 cm^{-1}), which are also observed in the spectrum of monomeric HCN, absorption bands in the ranges 1600–1700 and 1200–1250 cm^{-1} appear in the spectrum. They are apparently due to the stretching vibrations of the C=N and C–N bonds respectively. When the system is maintained at room temperature, structure formation in the polymeric product together with an increase in its amount take place. A redistribution of the band intensities in the regions of 1250 and 2200 cm^{-1} is observed in the IR spectrum and the background in the range 1700–2200 cm^{-1} intensifies, but all the principal absorption bands are retained.

The polymer gives rise to a singlet EPR spectrum, characteristic of polyconjugated systems. The electrical conductivity of the polymer is typical for the majority of dielectric materials: $\sigma = 3 \times 10^6 \Omega^{-1}$ cm^{-1}. The appearance of colour in the polymeric product and its variation (up to black) during the radical reaction can be accounted for as a consequence of the formation of the –C=N–C=N– conjugation chain.

The appearance of the acicular crystals of the tetrameric hydrocyanic acid may be associated[63] with the formation of an intermediate biradical — aminocyanocarbene, the dimerisation of which actually leads to the appearance of the tetramer — 1,2-diaminomaleic acid dinitrile:

$$\begin{matrix} N{\equiv}C\text{-}C\text{-}NH_2 \\ \quad\quad\quad\

Indeed, photolysis of a vitreous solution of the lithium salt of the toluene-*p*-sulfonylhydrazone of 1-cyanoformamide in 2-methyltetrahydrofuran at 77 K led to the formation of a yellow product — aminocyanocarbene.[64] The biradical

$$H_2N-\overset{\delta+}{\ddot{C}}-C\equiv\overset{\delta-}{N},$$

exists in the singlet state.

The formation of appreciable amounts of the tetramer in our experiments on radiation polymerisation suggests the operation of the mechanism described above. Aminocyanocarbene apparently initiates further propagation of the hydrogen cyanide polymerisation chain, which leads to the formation of the polymeric product.

In the first place, it was necessary to discover when the tetramer crystals are formed: during the heating of the hydrocyanic acid radiolysed at 77 K, in the solid phase, or after its fusion. The radiolysed solid HCN specimen was therefore placed in vacuo and the unreacted monomer was sublimed at a temperature below the melting point (260 K). The residue obtained after such prolonged sublimation (2.5% of the initial mass) consisted of a mixture of the polymer and the crystalline tetramer. A noteworthy feature of fundamental importance is that these products were formed in the solid phase.

X-Ray diffraction analysis of the crystals selected from the residue obtained after the sublimation of the unreacted monomer described above showed that the crystals belonged to the monoclinic system.[65] The bond lengths and bond angles in the $(HCN)_4$ molecule have the standard values. The molecule is planar with localised triple $C\equiv N$ and double $C=C$ bonds and possesses an intrinsic plane of symmetry. Shortened intermolecular contacts or other specific interactions are absent from the crystal.

Thus it has been shown experimentally that crystals of 1,2-diaminomaleic acid dinitrile are formed together with a conjugated polymer of the type $-C=N-C=N-$ during the sublimation of the solid hydrocyanic acid matrix radiolysed at 77 K. These crystals are formed on recombination of biradicals of the aminocyanocarbene type, which are stabilised in the matrix during the low-temperature radiolysis. When the matrix sublimes in the vicinity of its melting point, these biradicals acquire molecular mobility and recombine.

In our experiments, 1,2-diaminomaleic acid dinitrile was formed with a radiation yield $G \approx 2$ molecules per gram per 100 eV of the absorbed energy. Such a yield is typical for the products of a primary radiation-induced reaction (for example, of the radicals). Consequently, 1,2-diaminomaleic acid dinitrile cannot be formed as a result of consecutive radiation-induced reactions. We suggest that dimers are formed in the solid HCN matrix via $C\equiv N\cdots H$ hydrogen bonds. The primary radiation excitation of these dimers actually leads to aminocyanocarbene. In one way or another, the formation of 1,2-diaminomaleic acid dinitrile under conditions approaching those in cosmic space appears to us to be extremely important because this compound may play a key role in prebiological organic synthesis, since the hydrolysis of 1,2-diaminomaleic acid dinitrile leads to the formation of an aminoacid.

From the standpoint of the problem of the cold chemical evolution of matter in cosmic space and the formation of complex polymeric macromolecules, the polymerisation of the closest analogue of HCN — cyanogen $(CN)_2$ — is of no less interest. It was found that the low-temperature radiation polymerisation of $(CN)_2$ proceeds less effectively than that of hydrogen cyanide. After $(CN)_2$ had been irradiated at 77 K with doses up to 10^3 kGy and was subsequently heated, the yield of the polymer was only 0.1%. However, polymerisation of this monomer in various solvents (alcohol, butyl chloride) leads to a severalfold increase in the yield. A significant increase in the yield of the polymer was also observed in the polymerisation of HCN in the presence of acetylene.

III. Glasses

Amorphous bodies are characterised by the presence of short-range order alone. Owing to the absence of long-range order, the macroscopic properties of amorphous bodies are independent of direction. However, on sufficiently rapid cooling, it is possible to obtain the state of a nonequilibrium supercooled liquid. Further cooling of the substance in this state below the glass point T_g leads to the formation of a nonequilibrium solid amorphous state frequently referred to as a glass. In reality, the transition from the supercooled liquid to the vitreous state usually occurs over a narrow temperature range. The glass point is not a thermodynamic characteristic of the substance and, depending on the conditions in the preparation of the specimen and the method of measurement employed, it can vary within a fairly wide range. In the vitreous state, the species comprising the substance are capable of only vibrational and small-scale rotational motions. The translational mobility, characteristic of the liquid state is almost completely lost in the vitreous state.

The fact that transitions from the supercooled liquid to the glass state and conversely (devitrification) are accompanied by a sharp alteration in properties is extremely important: the viscosity changes by 10–15 orders of magnitude, the modulus of elasticity changes by a factor of 10–1000, the coefficient of thermal expansion changes by a factor of 10–100, etc. The gigantic jump in viscosity over the narrow vitrification temperature range is naturally the most impressive. For the chemist, this means that the molecular mobility, which determines the dynamics of the chemical reaction, changes sharply in this region. The nature of the chemical process should change on passage through the glass softening region owing to the extremely sharp alteration of the mobilities of the reactants. The mobility of molecules changes very markedly following a very slight alteration in temperature (by only a few degrees).

Reactive radical and ionic species are formed on radiolysis of vitreous matrices, are stabilised in deeper or shallower traps, and can retain their reactivity for a very long time. The absence of molecular mobility in the glass prevents the mutual recombination of such stabilised radicals. When the matrix is heated and devitrified, the translational mobility increases sharply, which entails the recombination of the accumulated radicals.

Thus, following a sharp increase in translational mobility, which occurs over the narrow temperature range in the transition from the glass to the supercooled liquid, relatively small radicals undergo effective recombination. It is more accurate to say that those radicals recombine whose mobility is sufficient to ensure their encounter in a viscous supercooled liquid. In systems where radicals liberated on devitrification are capable of initiating a chain reaction, a chemical chain process does occur effectively, as will be shown below.

1. Radical polymerisation

Vinyl acetate can be obtained in both vitreous and crystalline states. The rate of polymerisation of vitreous vinyl acetate is an order of magnitude higher than that of the crystalline substance under identical conditions.[66] High rates of post-radiation polymerisation have been noted for a series of vitreous solutions of monomers in liquid paraffin and other glass-forming solvents.[67,68]

The use of the calorimetric method of measurement established that the polymerisation process in many radiolysed vitreous systems occurs when they are heated in the temperature range corresponding to the devitrification of the matrix.[69–71] We shall consider in greater detail the study of polymerisation in the acrylic acid–ethanol vitreous system.[72]

It has been established that, on cooling to 77 K, a 17% solution of acrylic acid in ethanol passes to the vitreous state. During the heating of the glass in the calorimeter, a transition of the system from the vitreous to the supercooled liquid state ($T_g \approx 103$ K) is observed. On further heating, the supercooled

liquid passes to the region of a thermodynamically stable liquid (without crystallisation and subsequent fusion). Direct calorimetric measurements in the field of γ-radiation showed that there is hardly any polymerisation in this system at $T \leqslant T_g$. Immediately after the devitrification step, intense heat evolution, associated with the polymerisation of acrylic acid, is observed on the calorimetric curve. The overall yield of the polymer then reaches 80%. EPR spectra recorded at 108 K indicate the conversion of the monomeric radicals and the radicals of the alcohol matrix, formed during radiolysis, into the radicals of the growing polymer chain.

The EPR spectra of these radicals and their conformational transformations have been analysed in detail.[73] Together with the initiation of the polymer chain, some of the monomeric radicals recombine and only half of them are converted into polymeric radicals. On further heating in the temperature range where acrylic acid polymerises vigorously, the concentration of the growing polymeric radicals remains unchanged. Later studies of the polymerisation dynamics in this system with the aid of Mössbauer spectroscopy confirmed the validity of the principal conclusions.[74]

It follows from the foregoing that the polymerisation process proceeds virtually without chain termination over a comparatively narrow temperature range in the region corresponding to the devitrification of the matrix. The radicals stabilised in the glass during radiolysis acquire translational mobility on passage through the devitrification region and begin to recombine. They also add simultaneously to the double bond of the monomer. *n*-Meric growing radicals, the mobility of which is so low in a viscous supercooled liquid that their encounters and recombination are hardly noticeable, are produced. Furthermore, the small monomer molecules are readily supplied to such *n*-meric growing centres and their termination-free propagation is observed. This unique situation has been widely used in various polymerisation processes.

The method involving polymerisation on devitrification of the matrix has been applied to the determination of the principal kinetic parameters (rate of chain propagation, activation energy) of the low-temperature polymerisation of tetrafluoroethylene.[75] Perfluoro-3-ethyl-2,4-dimethylpent-2-ene served as the vitrifying matrix. Solutions of tetrafluoroethylene in this solvent pass fully to the vitreous state on cooling. With increase in the tetrafluoroethylene concentration in the solution, the glass point shifts monotonically into the region of lower temperatures with a corresponding decrease in the temperature range of the polymerisation process.

It has been shown that chain termination occurs when the growing macroradical adds to the double bond of the solvent, whereupon a relatively inactive stable radical, incapable of further chain propagation, is produced.[76]

We may note that the method involving postpolymerisation on devitrification was subsequently used widely in the study of the kinetics and mechanisms of low-temperature polymerisation processes (see, for example, Barkalov[77] and Barkalov and Kiryukhin[78] and the literature quoted therein, as well as other communications by Barkalov and coworkers[79–81]). It would seem that the polymerisation process carried out on devitrification of the matrix should lead to the formation of polymers with an extremely high molecular mass. In reality this is not observed. Presumably even at such low temperatures chain transfer through the monomer or the solvent plays an appreciable role in limiting the length of the polymer chain owing to the long time of the mutual contact of the reactants. Here chain transfer is understood, for example, as the reaction involving the abstraction of hydrogen from the monomer or the solvent by the growing macroradical with formation of an inert macroradical and a radical which initiates the propagation of a new polymer chain.

Indeed, the results of a study of the polymerisation of acrylamide in a vitreous solution of acrylamide in glycerol have been published.[82] Kinetic chains with a length $\geqslant 10^7$ occur in this system. Effective polymerisation during heating takes place in the temperature range 220–260 K immediately after the softening of the glass. The initiation of polymerisation in this system requires an extremely low radiation dose—only 0.3 Gy. The number of growing polymeric radicals was measured by the EPR method and their radiation-chemical yield was calculated. It was found that a single chain initiation step leads to the reaction of more than ten million monomer molecules.

During polymerisation on devitrification of alcohol solutions, the reactivities of acrylic and methacrylic derivatives differ sharply.[83] Whereas the yield of the polymer reaches 80% in the polymerisation during the vitrification of alcohol solutions of acrylic acid, its amide, and its methyl ester, the yield of the polymer for methacrylic acid and its analogous derivatives does not exceed 3%–5% under identical conditions. Bearing in mind that the relative concentrations of the growing polymeric radicals proved to be similar for all the monomers investigated, one may conclude that the sharp difference between the rates of polymerisation of acrylic and methacrylic derivatives is not associated with the difference between the initiation efficiencies.

Figure 7 presents the temperature dependences of the relative concentrations of the radicals during the heating of radiolysed vitreous solutions. Evidently the concentration of the growing polymeric radicals for acrylic acid and its derivatives is constant within a certain temperature range. In this temperature range, acrylic acid undergoes effective polymerisation. In the case of methacrylic acid and its derivatives, a completely different picture is observed. The *n*-meric radicals initiated possess sufficient translational mobility, are not stabilised, and recombine rapidly.

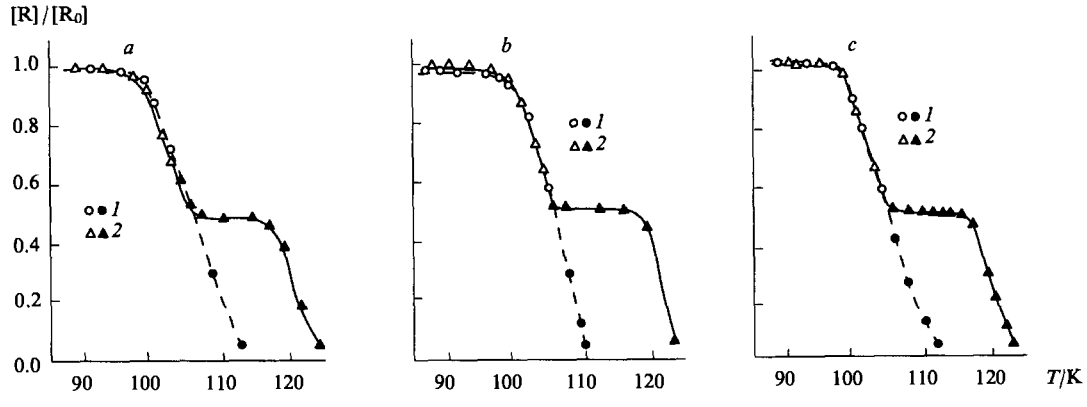


Figure 7. Variation of the relative concentration of radicals during the heating of radiolysed vitreous solutions: (*a*) methacrylic (*1*) and acrylic (*2*) acids; (*b*) methacrylamide (*1*) and acrylamide (*2*); (*c*) methyl methacrylate (*1*) and methyl acrylate (*2*). Filled symbols—growing *n*-meric radicals; initial radical concentration 1×10^{18} cm^{-3}.

In order to elucidate the causes of such a sharp difference between the rates of chain termination in the polymerisation reactions of acrylic and methacrylic acids, a study was made of the structure of the EPR spectra and the conformation of the growing terminal macroradicals was determined from the hyperfine splitting of the β-proton. The main factor responsible for the low translational mobility of macroradicals in a supercooled liquid is known to be their interaction with the alcohol molecules, which is indicated by the specific nonequilibrium conformation of the growing centre.[72,73] It was found that the presence of the CH_3 group near the reaction centre in the case of methacrylic acid prevents the interaction of the growing macroradical with the alcohol matrix, thereby preserving its mobility. This is apparently the main cause of the sharp difference between the rates of polymerisation of acrylic and methacrylic monomers on devitrification of their alcohol solution.

Thus, in contrast to the usual liquid-phase polymerisation, a sharp difference between the capacities of acrylic and methacrylic monomers for polymerisation is observed in polymerisation on devitrification, which is associated with the stronger interaction of the growing acrylic macroradicals with the medium. This difference between the reactivities of acrylic and methacrylic monomers is manifested only at fairly low temperatures.

2. Ionic polymerisation

The change in the physical properties of the matrix on passage through the devitrification region cannot fail to be reflected also in the dynamics of the propagation of the polymer chain via a cationic or anionic mechanism, since not only radicals but also trapped electrons and holes are stabilised during low-temperature radiolysis in glasses, i.e. the occurrence of the polymerisation process via an ionic mechanism is just as likely as its occurrence via a radical mechanism. The lifetime of the ions increases in the low-temperature region, while impurity water is segregated as its own crystalline phase and does not inhibit the polymerisation. Thus one may postulate that special methods for the drying of the monomer and the solvent are not needed under the conditions of postpolymerisation on devitrification of the matrix.

Cyclopentadiene was selected as the object for the study of low-temperature ionic polymerisation. The choice of cyclopentadiene was dictated by the fact that it had been earlier observed[84] that it undergoes cationic polymerisation on exposure to γ-radiation. Butyl chloride served as the vitrifying matrix in which the cationic centres arising on radiolysis are satisfactorily stabilised. On rapid cooling, solutions of cyclopentadiene in butyl chloride pass fully to the vitreous state. At 97 K, the glass is converted into a viscous supercooled liquid, which crystallises on heating and then melts at 140 K. Heating of a vitreous solution of cyclopentadiene in butyl chloride, γ-irradiated at 77 K, leads to the effective polymerisation of the monomer.[85,86] The heat evolution associated with the polymerisation of cyclopentadiene is observed over a narrow temperature range immediately after the transition of the system from the vitreous to the supercooled liquid state. On crystallisation and fusion of the system, polymerisation does not occur. The yield of the polymer increases with increasing preliminary irradiation dose and reaches a limiting value for extremely low doses (~30 kGy), which is characteristic of the accumulation of stabilised ionic centres in the course of the low-temperature radiolysis.

Epoxyethane is known to polymerise readily with the opening of the epoxide ring via a cationic or ionic mechanism in the presence of a large number of different catalysts. However, the epoxide ring proved to be extremely resistant to the action of high-energy radiation. The attempts to carry out the radiation polymerisation of epoxyethane in the solid and liquid phases were unsuccessful.[87] The effective polymerisation of epoxyethane with radiation initiation was achieved only by employing the post-polymerisation regime on devitrification of a butyl chloride matrix.[86,88] In contrast to the crystalline monomer, heating of vitreous solutions of epoxyethane in butyl chloride γ-irradiated at 77 K leads to effective polymerisation. The heat evolution associated with the postpolymerisation of epoxyethane is observed in the temperature range corresponding to the softening of the glass (~96 K).

The following evidence has been obtained for a cationic mechanism of the polymerisation of epoxyethane on devitrification of the matrix: (1) optical bleaching of the radiolysed specimens leads to a marked suppression of the postpolymerisation process; (2) the addition of small amounts of ethanol or pyridine (typical cationic inhibitors) fully inhibits the post-polymerisation; (3) the addition of hydroquinone (a typical inhibitor of radical polymerisation) to the initial solution does not affect the post-polymerisation reaction on devitrification.

Thus the use of the method of postpolymerisation on devitrification of the matrix makes it possible to achieve effective cationic polymerisation. A characteristic feature of this process is the lack of any special requirements as regards the drying of the monomer and the solvent.

3. Copolymerisation

On copolymerisation in the liquid and gas phases, the composition of the copolymer is determined by the reactivities of the comonomers (a homogeneous copolymer is obtained only in the initial stage of the polymerisation reaction). As the more reactive monomer is consumed, the resulting copolymer begins to be enriched, as a rule, in the less reactive monomer and the polymer chains acquire an inhomogeneous composition.

A characteristic feature of the supercooled liquid state obtained after the devitrification of the matrix is its comparatively high viscosity. In a highly viscous system of this kind, the duration of mutual contact between the reacting species is much longer than in the gas and liquid phases. It was therefore to be expected that the composition of the copolymer obtained under such conditions could be regulated by varying the composition of the initial mixture of monomers and that a homogeneous copolymer could be obtained for any degree of conversion.

Copolymerisation on devitrification in monomer–complex-forming agent systems has been investigated by Zubov and coworkers,[89–93] while similar copolymerisation in the absence of a complex-forming agent has been investigated by Bol'shakov et al.[94] It has been shown experimentally that copolymerisation in a supercooled viscous liquid makes it possible to obtain homogeneous copolymers and to regulate their composition.

It may be hoped that an increase in the time of contact between the reactants in the supercooled liquid will make it possible to involve compounds in copolymerisation which are not usually regarded as comonomers. In this connection, it is of interest to consider the copolymerisation of acetone with acrylic acid.[95] Heat evolution associated with copolymerisation was observed immediately after the transition of the system to a supercooled liquid state (110 K) on slow heating in a calorimeter of a vitreous solution of acrylic acid irradiated at 77 K.

In dilute acetone solutions of acrylic acid, the yield of the polymer isolated reached 250% relative to acrylic acid. Consequently the polymeric product contained two acetone molecules per acrylic acid molecule. Analysis of various mechanisms for the incorporation of acetone in the polymeric product showed that the copolymerisation of acrylic acid with the enolic form of acetone is most probable.

Thus the specific features of the supercooled liquid state, manifested by a significant increase in the contact time between the reactants, lead to a radical alteration of ideas concerning the reactivity of comonomers.

4. Graft polymerisation

Not only low-molecular-mass compounds but also polymers can be used as the vitrifying matrix. The use of the grafting method with devitrification of a polymer matrix proved effective for readily polymerising monomers such as tetrafluoroethylene.[96,97] The usual methods for the joint radiolysis of the monomer and

polymer in order to achieve graft polymerisation are difficult to use because the homopolymerisation of the monomer becomes the dominant process under these conditions.

IV. Other metastable systems

A large series of studies have been carried out also for other metastable solid systems. The low-temperature polymerisation of various monomers by condensing the monomer and the initiator onto a cooled surface (the molecular beam method) was achieved in 1959.[98-100] The initiators employed were metal couples (magnesium, potassium, sodium) and certain oxides and salts. In their presence, acrylamide, styrene, acrylonitrile, methyl methacrylate, and a series of other monomers polymerised at high rates. The low-temperature polymerisation occurred mainly in the vicinity of phase transitions, where the necessary mobility of the molecules was attained. The results of these studies have been surveyed in a review.[100]

Recently, the molecular beam method has been applied successfully in the low-temperature (77 K) polymerisation of frozen cocondensates initiated by a local mechanical action.[101-109] The polymerisation of cyclopentadiene and styrene in the presence of $TiCl_4$ has been investigated. The local mechanical action on the molecular mixtures of the monomer and the initiator involved impact by a steel needle with the aid of an electromagnetic gun. After the application of the mechanical impact, a rapid propagation of the polymerisation reaction through the specimen was observed at low temperatures. The dependence of the mechanical stresses in the low-temperature cocondensates of the monomer and the initiator on the conditions in the formation of the specimens and their role in the initiation of rapid polymerisation were demonstrated. These phenomena will be examined below in greater detail.

Photoinitiation has been used in a series of studies[105-109] of polymerisation and polycondensation at low temperatures. This procedure generally requires the application of photosensitisers; the systems obtained under these conditions are usually heterogeneous. It has been shown that in certain systems (with cinnamic acid derivatives and anthracene as sensitisers), the rate of addition at low temperatures ceases to depend on temperature and the polymerisation proceeds without activation as far as 4.2 K.

The photosensitised chain polymerisation reactions of acrylonitrile, formaldehyde, and xylene at low temperatures have been investigated. The sensitisers employed were *N,N'*-tetramethyl-*p*-phenylenediamine and β-naphthol and the specimens were prepared by the joint vacuum condensation of the monomer and the sensitiser onto an optical support. These reactions proceed as a result of the direct transformation of part of the radiant energy into the energy of the motion of the species along the reaction coordinate. Furthermore, it has been suggested that a proportion of the chemical energy is converted into mechanical stresses, which, for a certain structure of the solid system, induce the mutual approach of the reacting species and chain propagation at the very low temperatures employed.

Communications of this series report polymerisation at temperatures much lower than the glass point and the reactions are distinguished by a high yield of the polymer.

V. Autowaves

The mechanical energy of the elastic deformation of a solid at the instant of its disruption is concentrated in the region directly adjoining the newly formed surface. This energy transformation process is known to give rise to significant changes in the physicochemical properties of the substance on the freshly formed surface compared with the bulk-phase properties.[110]

Brittle breakdown is accompanied by phenomena such as the emission of electrons and ions, luminescence, the formation of radicals, and a sharp acceleration of transport processes on the cleavage surfaces. It appeared likely that the transition of the process from a homogeneous to a significantly heterogeneous regime via the brittle fracture of the specimen would include a nonequilibrium mechanism of energy transfer to the active centres previously stabilised in the solid matrix and would initiate the chemical reaction at low temperatures.

The ideas described above stimulated the study of the sensitivity of solid-phase processes to local perturbations which have been either introduced or have arisen spontaneously. These investigations led to the observation of highly intense autowave regimes in low-temperature solid-phase reactions. The principal conclusions have been surveyed in reviews.[111,112] The logic of the development of these studies will be traced below.

The objects of study were systems in which the spontaneous development of reaction chains is impossible in the solid state at radiolysis temperatures of 77 and 4.2 K, and the first task was to elucidate the activating role of the brittle fracture of the system. It was possible to show that the formation of the primary crack plays the role of an initiating device which switches on the positive feedback mechanism ensuring a self-supporting process regime. The following self-activation mechanism has been proposed. The chemical reaction arising on the cleavage planes and in the adjoining regions disturbs the monolithic nature of the sections of the solid matrix not involved in the reaction, thereby preparing the next layer for the reaction to take place. Such breakdown of monolithic structure can occur, for example, as a consequence of the appearance of temperature or density gradients during the reaction, which create stresses disrupting the specimen.

Autowave phenomena are known to be characteristic of systems described by nonlinear branched-chain models. Autowave reaction regimes should arise in sufficiently long specimens in response to a locally introduced perturbation. In the first experiments,[113] it was already possible to initiate the spontaneous propagation of the reaction wave throughout the specimen on formation of a local cleavage plane. The structure of the travelling front of the cryochemical reaction proved to be completely atypical for classical thermal self-propagation processes.

The qualitative picture of the propagation of the wave involved the concept of the movement in the solid specimen of a narrow zone highly truncated by an extensive network of freshly formed cracks. The chemical reaction arises in precisely this zone on the surface of the cracks (or close to it) and creates in its turn conditions for continuation of the breakdown in the adjoining layer of the solid matrix. Such layer-by-layer dispersion of the specimen is referred to as the travelling stress field. A stress of this kind may be caused, as already stated, either by the difference between the densities of the starting materials and the final products (isothermal mechanism) or by the appearance in the specimen of 'steep' temperature gradients as a result of the exothermicity of the reaction (nonisothermal mechanism). Naturally both factors can also operate simultaneously.

The studies carried out indicate the wide occurrence of autowave phenomena in cryochemical solid state reactions and the identity of their physical mechanism in a wide range of chemical systems. This gave grounds for the assumption that autowave reaction regimes can prove useful in the creation of new nontraditional chemical technologies. Indeed, the principal technological tasks (activation of the chemical system, supply of energy, and mixing of the reactants) are performed jointly by employing the energy of the autowave chemical proceses. The occurrence of very high rates of the chemical reaction in the autowave regime at low temperatures is also extremely attractive.

1. Acetaldehyde

The autowave polymerisation regime arises in polycrystalline acetaldehyde already at 4.2–77 K. Its principal characteristics have been investigated.[114] The polymerisation wave in the crystalline monomer was observed in massive (cylindrical) and thin-walled specimens immersed in both nitrogen and helium baths. The reaction wave was excited in response to the local brittle fracture of the frozen acetaldehyde.

Propagation of the polymerisation front in solid radiolysed acetaldehyde at relatively high temperatures (117 – 147 K), close to the melting point of the monomer (150 K), was observed with the aid of thermography and cine-filming.[43] This phenomenon was interpreted within the framework of the classical thermal combustion mechanism. The rate of propagation of the reaction front at these temperatures was 1 – 3 cm s^{-1} for preliminary irradiation doses of 5 – 100 kGy.

The development of ideas concerning autowave processes made it possible to analyse the characteristics of the polymerisation of acetaldehyde at a new qualitative level. Acetaldehyde is of special interest in connection with two factors. First, the autowave regime in the polymerisation of acetaldehyde is an example of the appearance of a cryochemical wave in a one-component system. Second, the heat of this reaction is almost an order of magnitude lower than for the systems investigated previously. This created preconditions for the development of ideas concerning the role of the isothermal and nonisothermal mechanisms and their inter-action in the autowave process.

When the autowave passed through the specimen in the helium bath, the maximum temperature in the front did not exceed 130 K, i.e. was significantly lower than the melting point of the monomer (Fig. 8). Thus here there are all the conditions for the analysis of the changes in the structure and phase state of the crystalline specimen induced by the passage of the mechanochemical cryo-wave through it. According to the ideas developed, the chemical reaction front represents a mechanical dispersion zone moving through the solid reactant. One may postulate that the passage of such a wave through the specimen results in its dispersion.

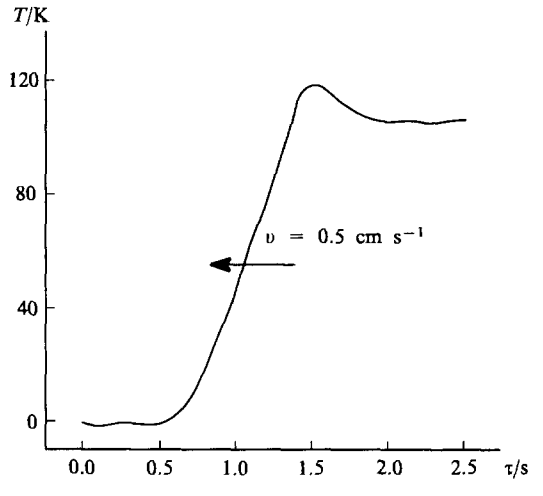


Figure 8. Time variation of the temperature profile of the acetaldehyde polymerisation travelling wave at 4.2 K. Preliminary γ-irradiation dose 700 kGy.

This hypothesis was tested by calorimetric analysis. To carry out such an analysis, the acetaldehyde specimen was transferred to a bath of liquid nitrogen after the passage of the auto-wave through it (in liquid helium) and was then cut up into several portions. Each of these was placed separately in a calorimeter at 77 K and the calorimetric heating curve was recorded. It was found that after the passage of the wave there was no crystalline phase in the specimen. Only a heat capacity jump, accompanying devitrification, was detected in the calorimetric experiments, and the signal corresponding to the heat of fusion was absent. When the process was carried out not in the autowave regime but in a regime involving the slow heating of the entire specimen in the calorimeter (without the brittle fracture initiating the autowave), the unreacted monomer retained its crystallinity. Thus the passage of the mechanochemical wave through the crystalline specimen does indeed lead to its conversion into an amorphous form.

The rate of propagation of the autowave depends on the preliminary γ-irradiation dose. As in the systems investigated previously,[111] there is a critical dose necessary for the attainment of the autowave regime. The magnitude of this dose increases with decrease in the thermostat temperature from 77 to 4.2 K. For specimens immersed in liquid nitrogen, the rate of propagation of the polymerisation wave increases linearly with the irradiation dose. It is logical to postulate that the increase in the rate of propagation of the wave with increasing irradiation dose is associated with the increased concentration of the active centres. However, the accumulation of paramagnetic centres (radical-ions and radicals) during the radiolysis of polycrystalline acetaldehyde at 77 K takes place linearly only in the region of small doses (only up to ~50 kGy) and then slows down. After the attainment of ~650 kGy, the stabilised active centres altogether cease to accumulate.

Even on rapid cooling, pure acetaldehyde cannot be converted into a vitreous state and its polymerisation in such a state has not therefore been investigated. A study has been made[115] of the polymerisation of a solid vitreous solution of acetaldehyde in butyl chloride. Local brittle fracture initiated the autowave polymerisation regime. The principal parameters of the autowave polymerisation process in the polycrystalline and vitreous matrices agreed only qualitatively. On the other hand, in quantitative terms, the critical dose of the preliminary γ-irradiation, above which it is possible to generate an autowave in glass, is 60 kGy, while in crystalline acetaldehyde it exceeds 300 kGy.

2. Cyclopentadiene

In the phenomenological description of the autowave processes considered above, the nature of the active centres arising on brittle fracture of the system were not specified in concrete terms. Since the majority of the cryochemical autowaves have been observed for typical radical chain reactions, it was of interest to establish the autowave regime for a typical ionic chain reaction.

Cyclopentadiene polymerises only via an ionic mechanism and this is why it was selected for the investigation of the characteristics of the autowave regimes in cryochemical reactions of this type.[116] It is noteworthy that the 'explosive' polymerisation reaction of cyclopentadiene was observed in films obtained by freezing them from molecular beams comprising the monomer and the catalyst ($TiCl_4$) and then pricking the film with a metallic needle at 77 K.[101]

On rapid cooling to 77 K, a solution of cyclopentadiene in butyl chloride passes to the vitreous state. On local brittle fracture of the radiolysed specimen immersed in liquid nitrogen, the polymerisation reaction, propagated through the specimen in the form of an autowave, begins. The velocity of the polymerisation wave and the form of its temperature profile depend significantly on the preliminary irradiation dose. The velocity of the wave increases with increasing dose, while the temperature profile of the wave becomes increasingly sharp.

The velocity of the polymerisation wave increases linearly with increasing preliminary irradiation dose up to 1200 kGy. This type of dependence of the velocity of the wave is evidently not associated with the dynamics of the accumulation of the cationic active centres, because such accumulation ceases for significantly lower doses.

The molecular mass and the yield of the polycyclopentadiene obtained in the autowave regime are higher than in thermo-activated postpolymerisation. The latter factor may prove useful in the development of technological regimes for the synthesis of polymers.

VI. Oscillations in the rate of reaction

Oscillations in the rate of reaction is an unusual phenomenon as regards the classical ideas concerning the nature of a chemical process. Many investigators are engaged nowadays in the study of its mechanism.[117-122]

The present authors encountered auto-oscillations in the rates of cryochemical reactions for the first time in a study of the solid-phase radiation-induced hydrobromination of ethylene.[123] The post-radiation process (for example, polymerisation), occurring under conditions where the temperature of the thermostat is scanned, is initiated by the active centres gradually liberated with increase in the temperature of the matrix. A definite number of active centres stabilised in the matrix are generated on γ-irradiation. The irradiation takes place at a fairly low temperature, the centres formed are stabilised in the matrix, and the reaction is not initiated. Only on raising the temperature of the medium are the active centres liberated and initiate the chemical reaction.

We shall consider the establishment of auto-oscillatory regimes in low-temperature radiation-induced thermokinetic chemical chain reactions.[123-128] For reactions occurring under isothermal conditions, the negative feedback necessary for the occurrence of oscillations in the reaction rate can be brought into operation only by chemical autocatalysis. For exothermic chain reactions, the heat evolved may play the role of the negative feedback under certain conditions. The evolution of heat can increase the temperature of the medium and hence the rate of the chemical reaction. Thus the evolution of heat can perform a function analogous to autocatalysis.

Cryochemical reactions are responsible for the appearance of thermokinetic oscillations: the defectiveness of solid matrices and their low heat capacities promote the appearance of non-uniformities in the temperature field. Thermokinetic models of the auto-oscillations in the rates of chemical reactions have been considered by Sal'nikov[129,130] and a detailed description of such reaction conditions may be found in monographs.[117,121,122] We shall consider certain examples of the auto-oscillatory regimes in cryochemical reactions in vitreous and crystalline matrices.

As an illustration, we may quote the results of a study of the polymerisation of crystalline heptyl acrylate. The process takes place during the heating of specimens γ-radiolysed at 77 K in both auto-oscillatory and the usual regimes. On rapid cooling of heptyl acrylate to 77 K, the monomer passes to the vitreous state. Heating of such specimens in a calorimeter makes it possible to observe the transition from the vitreous to the supercooled liquid (~138 K) state and then the crystallisation of the supercooled liquid in the temperature range 140–205 K and fusion of the monomer crystals at 205–210 K. If, however, the monomer is initially annealed at 205 K and then cooled to 77 K, then it passes fully to the crystalline state. The calorimetric heating curve for such specimens shows only the endothermic peak due to the fusion of the monomer at 208 K (Fig. 9). The postpolymerisation process was in fact investigated in precisely such specimens.

In order to accumulate the polymerisation active centres, the monomer was γ-irradiated at 77 K with a dose of 5–100 kGy. The calorimetric heating curves of the specimens subjected to preliminary irradiation are presented in Fig. 9 (curves *2–4*). The polymerisation reaction, recorded from the evolution of heat, begins at temperatures 15–20 K below the melting point of the monomer, where the molecules acquire translational mobility.

The rate of polymerisation exhibits a marked temperature dependence along the initial section and rapidly attains a maximum. After this, a sharp decrease and a further increase in the rate of the process are observed. Ultimately, several acceleration and retardation periods occur. The oscillations in the rate of reaction have a decaying amplitude. An increase in the preliminary irradiation dose shifts the onset of the process into the region of lower temperatures and increases the amplitude of the oscillations in the rate (cf. curves *2* and *3* in Fig. 9). When the preliminary

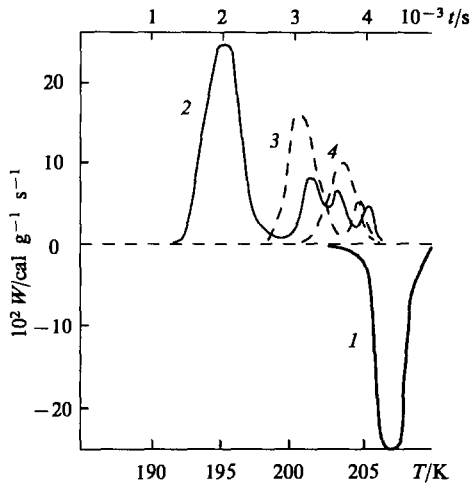


Figure 9. Calorimetric heating curve for nonirradiated heptyl acrylate (curve *1*) and variation of the rate of heat evolution on heating heptyl acrylate γ-irradiated at 77 K using different doses (kGy): (*2*) 100; (*3*) 17.5; (*4*) 5.

irradiation dose is sufficiently low, oscillations in the rate of post-polymerisation are no longer observed (curve *4*). The mathematical model of the postpolymerisation process proposed by Nefedov et al.[125] permits a qualitative explanation of the observed features of the polymerisation reaction of crystalline heptyl acrylate.

Oscillatory regimes in low-temperature radiation-initiated chain reactions have been observed also for polymerisation on devitrification of the matrix. As an example, we shall consider various regimes in the post-radiation polymerisation of acetaldehyde in a vitreous butyl chloride matrix.

On cooling to 77 K, a solution of acetaldehyde in butyl chloride passes fully to the vitreous state. When such a system is heated in a calorimeter in the temperature range 94–97 K, a transition from the vitreous to the supercooled liquid state is observed. This is followed by crystallisation (112–115 K) and then fusion (145 K). When the same system, subjected to preliminary γ-irradiation at 77 K, is heated, heat evolution due to the post-polymerisation of acetaldehyde is observed in the devitrification region. Various process regimes are possible depending on the conditions in the transfer of heat from the calorimetric cell.

Polymerisation can occur in the absence of appreciable superheating of the test substance in the cell relative to the calorimeter block (stationary conditions). For this regime to be achieved, it is necessary to establish a fairly rapid removal of heat from the cell. This can be done experimentally by altering a series of parameters. It is essential to decrease the rate of heating of the specimen, to improve the heat removal conditions by increasing the ratio of the surface of the specimen to its volume (by reducing the mass of the initial sample), and to reduce the preliminary irradiation dose, which leads to a diminution of the concentration of the active centres stabilised in the system, i.e. to a decrease in the rate of heat evolution due to the polymerisation reaction.

During the heating of the specimen in the absence of appreciable superheating of the latter in the cell, the rate of post-polymerisation of acetaldehyde increases with increasing temperature, reaches a maximum, and diminishes smoothly owing to the consumption of the monomer and the active centres for the reaction stored during the preliminary radiolysis (Fig. 10, curve *1*). The initial section of the calorimetric curve can be expressed satisfactorily in a linear form in terms of the Arrhenius variables under these conditions (the activation energy is 6 kcal mol^{-1}).

Another extreme case is the thermal explosion regime. It is observed when the conditions in the elimination of heat from the cell are impaired: an increase in the mass of the substance in the

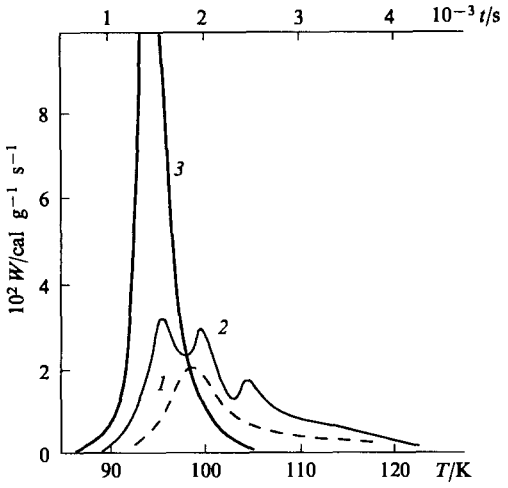


Figure 10. Variation of the rate of heat evolution in the devitrification region during the postpolymerisation of acetaldehyde (AA) in a butyl chloride (BC) matrix in different specimens: (*1*) 0.097 g of AA + 0.367 g of BC; (*2*) 0.138 g of AA + 0.549 g of BC; (*3*) 0.175 g of AA + 0.672 g of BC. Preliminary γ-irradiation dose at 77 K 120 kGy (curves *1* and *2*) and 300 kGy (curve *3*); *T*—temperature of the calorimeter block.

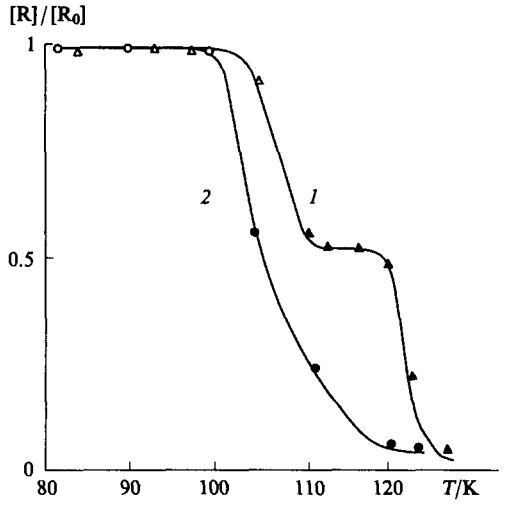


Figure 11. Variation of the relative concentration of radicals during the heating of 17% solutions of acrylic acid in ethanol irradiated at 77 K using doses of 20 kGy (curve *1*) and 50 kGy (curve *2*). Heating rate of the specimens 0.2 K min^{-1} (curve *1*) and 0.5 K min^{-1} (curve *2*). The filled symbols refer to the concentration of the growing polymer chain.

cell, in the rate of heating of the specimen, and in the preliminary irradiation dose (Fig. 10, curve *3*). Under the conditions of moderate heat removal, an oscillatory process regime has been recorded—several cycles involving an increase and a decrease in the rate of reaction were observed during the experiment (Fig. 10, curve *2*).

Thus, depending on the reaction conditions, different process regimes are realised: the stationary regime (in the absence of appreciable superheating of the test substance in the specimen), thermal explosion, and the oscillatory regime. Analysis of experimental data leads to the conclusion that the oscillations in rate in the acetaldehyde–butyl chloride system are associated with the thermokinetic mechanism described above. The following estimates of the limits of the existence of oscillatory regimes may be quoted: (1) $T_{th} < T_c < T_{th} + \Delta T$, where T_c is the temperature to which the reaction mixture has been superheated in the oscillatory regime in the cell relative to the thermostat temperature T_{th}, and ΔT represents the pre-explosion heating ($\Delta T = RT^2/E$); (2) $\tau > n\tau_{os}$, where τ is the average lifetime of the active centres ($\tau = 1/k$ in the case of unimolecular chain termination, $\tau = 1/k_t R_t$ in the case of bimolecular termination, k_t is the termination reaction rate constant, and R_t is the initial concentration of the polymerisation active centres), τ_{os} is the period of the oscillations, and n is the number of oscillation cycles. When the reaction takes place under stationary conditions (in the absence of appreciable superheating in the specimen), the growing macroradicals do not recombine in the temperature range 110–120 K; only the propagation of the polymer chain takes place (Fig. 11, curve *1*). When the quasi-isothermal regime is infringed and oscillations arise in the rate of postpolymerisation, the growing macroradicals are destroyed (Fig. 11, curve *2*). At high rates of heating of the system (~600 K min^{-1}), the growing polymer chains are not formed at all owing to the destruction of the active centres at an early stage in the process.

The different chemical reaction regimes are of interest in connection with the possibility of increasing the selectivity of complex processes and of expanding the technological procedures for controlling cryochemical synthesis. The thermal instability arising in the operation of chemical reactors is usually an undesirable phenomenon leading to a decrease in the quality of the production and possible breakdowns. The understanding of the process mechanism makes it possible to suppress the auto-oscillations and to maintain a stationary regime. However, oscillatory regimes may also prove convenient—they afford a significantly greater average yield of the product than stationary regimes. Such advantages are manifested particularly strikingly when the target product is an intermediate in a complex chemical chain reaction.[131]

As an example of the influence of various reaction regimes on the properties of the final product, we shall consider the low-temperature radiation polymerisation of 1,3-bis(dimethylamino)-isopropyl methacrylate.[132] Depending on the conditions in the removal of heat from the reaction volume, different polymerisation process regimes were realised on devitrification of the matrix: stationary, oscillatory, and thermal explosion.

In the case of the auto-oscillatory postpolymerisation regime, the mass-average molecular mass of the polymer diminishes from 2.8×10^6 to 1.4×10^6 with increase in the preliminary irradiation dose from 10 to 118 kGy. In the stationary regime, the molecular mass diminishes from 1.5×10^6 to 0.3×10^6. The high molecular mass of the polymer obtained in the oscillatory regime is evidently due to the fact that local superheating results in an increase in the mobility of the growing polymer chains, so that their bimolecular termination predominates.

Polymers with a different supermolecular structure, characterised by the presence of microheterogeneities, are obtained in the thermal explosion regime.[132] A more detailed analysis of the polymeric products obtained in this series of studies showed that the appearance of nonstationary conditions in the low-temperature polymerisation process (oscillatory regime and thermal explosion) leads to the broadening of the polymer molecular mass distribution in the direction of higher molecular masses.

References

1. N N Semenov *Khimiya i Tekhnologiya Polimerov* (7/8) 196 (1960)
2. E I Adirovich *Dokl. Akad. Nauk SSSR* **136** 117 (1961)
3. M Magat *Polymer* **3** 449 (1962)
4. A Chapiro *J. Polym. Sci., Part C, Polym. Symp.*, **4** 1551 (1964)
5. V A Kargin, V A Kabanov *Zh. Vses. Khim. O-va im. D.I. Mendeleeva* **9** 602 (1964)
6. V I Gol'danskii, N S Enikolopyan, in *Radiatsionnaya Khimiya Polimerov* (Radiation Chemistry of Polymers) (Moscow: Nauka, 1966) p. 7

7. A D Abkin, A P Sheinker, G N Gerasimov, in *Radiatsionnaya Khimiya Polimerov* (Radiation Chemistry of Polymers) (Moscow: Nauka, 1973) p. 7
8. V I Gol'danskii *Usp. Khim.* **44** 2121 (1975) [*Russ. Chem. Rev.* **44** 1019 (1975)]
9. A M Kaplan, D P Kiryukhin, I M Barkalov, V I Gol'danskii *Dokl. Akad. Nauk SSSR* **190** 1387 (1970)
10. A I Mikhailov, A I Bol'shakov, Ya S Lebedev, V I Gol'danskii *Fiz. Tverd. Tela* **14** 1172 (1972)
11. D P Kiryukhin, A M Kaplan, I M Barkalov, V I Gol'danskii *Vysokomol. Soedin., Ser. A* **14** 2115 (1972)
12. V I Gol'danskii, L I Trakhtenberg, V N Flerov *Tunnel'nye Yavleniya v Khimicheskoi Fizike* (Tunnel Phenomena in Chemical Physics) (Moscow: Nauka, 1986) p. 296
13. M Ya Ovchinnikova *Chem. Phys.* **36** 85 (1979)
14. V A Benderskii, V I Gol'danskii, A A Ovchinnikov *Chem. Phys. Lett.* **73** 492 (1980)
15. L I Trakhtenberg, V L Klochikhin, S Ya Pshezhetzky *Chem. Phys.* **59** 191 (1981); **69** 121 (1982)
16. C Chachaty, M Magat, L Ter-Minasian *J. Polym. Sci.* **48** 139 (1960)
17. C Chachaty, Theses, Paris, 1962
18. I M Barkalov, V I Gol'danskii, N S Enikolopian, S F Terekhova, G M Trofimova *J. Polym. Sci., Part C, Polym. Symp.*, **4** 909 (1963)
19. D P Kiryukhin, A M Kaplan, I M Barkalov, V I Gol'danskii *Vysokomol. Soedin., Ser. B* **12** 491 (1970)
20. D P Kiryukhin, A M Kaplan, I M Barkalov, V I Gol'danskii *Dokl. Akad. Nauk SSSR* **199** 857 (1971)
21. D P Kiryukhin, A M Kaplan, I M Barkalov, V I Gol'danskii *Dokl. Akad. Nauk SSSR* **206** 147 (1972)
22. D P Kiryukhin, A M Kaplan, I M Barkalov, V I Gol'danskii *Dokl. Akad. Nauk SSSR* **211** 632 (1973)
23. V I Gol'danskii, M D Frank-Kamenetskii, I M Barkalov *Dokl. Akad. Nauk SSSR* **211** 133 (1973)
24. V I Gol'danskii, M D Frank-Kamenetskii, I M Barkalov *Science* **182** 1344 (1973)
25. D P Kiryukhin, I M Barkalov, V I Gol'danskii *Vysokomol. Soedin., Ser. B* **16** 565 (1974)
26. V I Gol'danskii, D P Kiryukhin, I M Barkalov *Khim. Vys. Energ.* **8** 279 (1974)
27. N S Enikolopyan, S A Vol'fson *Khimiya i Tekhnologiya Formal'degida* (Chemistry and Technology of Formaldehyde) (Moscow: Khimiya, 1968)
28. V P Roshchupkin, T K Goncharov, D P Kiryukhin, I M Barkalov, V I Gol'danskii *Dokl. Akad. Nauk SSSR* **222** 396 (1975)
29. V P Roshchupkin, N S Andreeva, T K Goncharov *Vysokomol. Soedin., Ser. A* **14** 477 (1972)
30. V P Roshchupkin, Yu N Smirnov, T K Goncharov, V P Volkov, B A Rozenberg, N S Enikolopyan *Vysokomol. Soedin., Ser. A* **16** 1152 (1974)
31. L V Babare, T K Goncharov, A N Dremin, V P Roshchupkin *Vysokomol. Soedin., Ser. A* **16** 969 (1974)
32. V Zamboni, G Zerbi *J. Polym. Sci., Part C, Polym. Symp.* **7** 153 (1964)
33. G Adler, R Baysal *Mol. Cryst. Liq. Cryst.* **9** 361 (1969)
34. V E Shklover, N G Bokii, Yu T Struchkov *Usp. Khim.* **46** 1368 (1977) [*Russ. Chem. Rev.* **46** 706 (1977)]
35. D P Kiryukhin, I M Barkalov, V I Gol'danskii *Dokl. Akad. Nauk SSSR* **241** 134 (1978)
36. G N Gerasimov, A D Abkin *Khim. Fiz.* **3** 176 (1984)
37. S M Dolotov,O A Yuzhakova, G N Gerasimov, A D Abkin *Vysokomol. Soedin., Ser. B* **22** 575 (1980)
38. E S Mansueto, C Y Ju, C A Wight *J. Phys. Chem.* **93** 2143 (1989)
39. E S Mansueto, C A Wight *J. Am. Chem. Soc.* **111** 1900 (1989)
40. E Ya Misochko, V A Benderskii, V I Gol'danskii, V V Kononikhina *Dokl. Akad. Nauk SSSR* **316** 403 (1991)
41. M S Travers *Trans. Faraday Soc.* **32** 246 (1936)
42. M Letort *C. R. Acad. Sci.* **202** 767 (1936)
43. V S Pshezhetskii, V I Tupikov *Geterotsepnye Vysokomolekulyarnye Soedineniya* (Heterochain High-Molecular-Mass Compounds) (Moscow: Nauka, 1964) p. 220
44. D P Kiryukhin, I M Barkalov, V I Gol'danskii *Eur. Polym. J.* **10** 309 (1974)
45. D P Kiryukhin, I M Barkalov, V P Roshchupkin *Vysokomol. Soedin., Ser. B* **20** 550 (1978)
46. J Furukawa, T Saegusa *Polymerization of Aldehydes and Oxides* (Translated into Russian; Moscow: Mir, 1965)
47. R N Smith *Inorg. Chem.* **2** 829 (1963)
48. A R Blake, K E Hodgson *J. Chem. Soc., A* 533 (1966)
49. R N Smith, R A Smith, D A Young *Inorg. Chem.* **5** 145 (1966)
50. D P Kiryukhin, I M Barkalov, V I Gol'danskii *Vysokomol. Soedin., Ser. A* **18** 759 (1976)
51. I M Barkalov, I P Kim, A I Mikhailov, D P Kiryukhin *J. Polym. Sci., Polym. Chem. Ed.* **18** 1551 (1980)
52. D Hummel, O Janssen *Z. Chem.* **31** 111 (1962)
53. M Calvin *Chemical Evolution* (London: Oxford University Press, 1969)
54. R A Sanchez, J P Ferris, L E Orgel *Science* **154** 784 (1966)
55. J P Ferris, E H Edelson *J. Org. Chem.* **43** 3989 (1978)
56. J P Ferris, P C Joshi, E H Edelson, J G Lawless *J. Mol. Evol.* **11** 293 (1978)
57. J P Ferris, W J Hagan *Tetrahedron* **40** 1093 (1984)
58. S W Stahler *Astrophys. J.* **281** 209 (1984)
59. C Meisse, E T Arakawa, B N Khare, W R Thompson, C Sagan *Bull. Am. Astron. Soc.* **23** 1189 (1991)
60. C Sagan, C F Cyba *Bull. Am. Astron. Soc.* **23** 1211 (1991)
61. P S Mozhaev, D P Kiryukhin, G A Kichigina, I M Barkalov *Mendeleev Commun.* 17 (1994)
62. P S Mozhaev, G A Kichigina, D P Kiryukhin, I M Barkalov *Khim. Vys. Energ.* (1994) in the press
63. R M Kliss, C N Matthews *Proc. Natl. Acad. Sci. USA* **48** 1300 (1962)
64. R E Moser, J M Eritsch, T L Westman, R M Kliss, C N Matthews *J. Am. Chem. Soc.* **89** 5673 (1967)
65. P S Mozhaev, G A Kichigina, Z G Aliev, D P Kiryukhin, L O Atovmyan, I M Barkalov *Dokl. Akad. Nauk* (1994) in the press
66. I M Barkalov, V I Gol'danskii, N S Enikolopov, S F Terekhova, G M Trofimova *Dokl. Akad. Nauk SSSR* **147** 395 (1962)
67. A Chapiro *Chimia* **21** 454 (1967)
68. A Chapiro, A M Jendrychowska-Bonamour, L Perec *Adv. Chem. Series* **82** 513 (1968)
69. I G Gusakovsaya, V G Nikol'skii, V I Gol'danskii *Khim. Vys. Energ.* **4** 434 (1970)
70. I P Kim, A M Kaplan, I M Barkalov, V I Gol'danskii *Dokl. Akad. Nauk SSSR* **193** 855 (1970)
71. G S Georgiev, A M Kaplan, V P Zubov, V B Golubev, V I Gol'danskii, V A Kabanov, I M Barkalov *Vysokomol. Soedin., Ser. A* **14** 177 (1972)
72. A I Bol'shakov, A I Mikhailov, I M Barkalov, V I Gol'danskii *Dokl. Akad. Nauk SSSR* **205** 379 (1972)
73. A I Bol'shakov, A I Mikhailov, I M Barkalov *Teor. Eksp. Khim.* **9** 831 (1973)
74. R A Stukan, I L Arkhipov, V Ya Rochev, A I Bol'shakov, I M Barkalov *Vysokomol. Soedin., Ser. A* **28** 1446 (1986)
75. S R Allayarov, A I Bol'shakov, I M Barkalov *Vysokomol. Soedin., Ser. A* **29** 364 (1987)
76. V I Gol'danskii, I M Barkalov *Radiat. Phys. Chem.* **28** 189 (1986)
77. I M Barkalov *Usp. Khim.* **49** 362 (1980) [*Russ. Chem. Rev.* **49** 190 (1980)]
78. I M Barkalov, D P Kiryukhin *Int. Rev. Phys. Chem.* **11** 263 (1992)
79. I I Migunova, V S Ivanov, A I Bolshakov, I M Barkalov, in *Proceedings of the 5th Symposium on Radiation Chemistry, Budapest, 1982* p. 717
80. V M Munikhes, S I Kuzina, D P Kiryukhin, A I Mikhailov, I M Barkalov *Vysokomol. Soedin., Ser. A* **20** 810 (1978)
81. I V Vasil'eva, A I Bol'shakov, V K Smirnova, V S Ivanov, I M Barkalov *Vysokomol. Soedin., Ser. A* **26** 2186 (1984)
82. A I Bol'shakov, I M Barkalov, V I Gol'danskii *Dokl. Akad. Nauk SSSR* **255** 367 (1980)
83. A I Bol'shakov, A I Mikhailov, I M Barkalov *Vysokomol. Soedin., Ser. B* **19** 781 (1977)
84. M A Bonin, W R Busler, F Williams *J. Am. Chem. Soc.* **87** 199 (1965)
85. M R Muidinov, G A Kichigina, D P Kiryukhin, I M Barkalov *Vysokomol. Soedin., Ser. A* **25** 818 (1983)
86. I M Barkalov, D P Kirukhin, G A Kichigina *Eur. Polym. J.* **20** 1013 (1984)

87. A P Meleshevich *Usp. Khim.* **39** 444 (1970) [*Russ. Chem. Rev.* **39** 213 (1970)]
88. G A Kichigina, M R Muidinov, D P Kiryukhin, I M Barkalov *Khim. Vys. Energ.* **17** 249 (1983)
89. V P Zubov, V A Kabanov *Vysokomol. Soedin., Ser. A* **13** 1305 (1971)
90. G S Georgiev, N P Appolonova,V B Golubev, V P Zubov, V A Kabanov *Vysokomol. Soedin., Ser. A* **14** 643 (1972)
91. I L Stoyachenko, G S Georgiev, V B Golubev, V P Zubov, V A Kabanov *Vysokomol. Soedin., Ser. A* **15** 1899 (1973)
92. V B Golubev, V P Zubov, G S Georgiev, I L Stoyachenko, V A Kabanov *J. Polym. Sci., Polym. Chem. Ed.* **11** 2463 (1973)
93. I L Stoyachenko, E I Shklyarova, A M Kaplan, V B Golubev, V P Zubov, V A Kabanov *Vysokomol. Soedin., Ser. A* **18** 1420 (1976)
94. A I Bol'shakov, A I Mikhailov, I M Barkalov *Dokl. Akad. Nauk SSSR* **241** 1355 (1978)
95. A I Bol'shakov, A I Mikhailov, I M Barkalov, V I Gol'danskii *Dokl. Akad. Nauk SSSR* **222** 633 (1975)
96. T I Nevelskaja, I P Kim, I M Barkalov *J. Macromol. Sci., Chem.* **A11** 91 (1977)
97. M R Muidinov, D P Kiryukhin, M K Asamov, I M Barkalov *Vysokomol. Soedin., Ser. A* **20** 360 (1978)
98. V A Kargin, V A Kabanov, V P Zubov *Vysokomol. Soedin.* **1** 265 (1959)
99. V A Kargin, V A Kabanov, I M Papisov, V P Zubov *Dokl. Akad. Nauk SSSR* **134** 389 (1960)
100. V A Kargin, V A Kabanov *J. Polym. Sci.* **52** 71 (1961)
101. V A Kabanov, V G Sergeev, G M Lukovkin, V Yu Baranovskii *Dokl. Akad. Nauk SSSR* **266** 1410 (1982)
102. V G Sergeev, V Yu Baranovskii, G M Lukovkin, V A Kabanov *Vysokomol. Soedin., Ser. B* **24** 65 (1984)
103. G B Sergeev, V S Komarov *Vestn. Mosk. Univ., Ser. 2: Khim.* **29** 275 (1988)
104. V G Sergeev, V Yu Baranovskii, G M Lukovkin, V A Kabanov *Vysokomol. Soedin., Ser. A* **31** 502 (1989)
105. G N Gerasimov, A D Abkin *Khim. Fiz.* **3** 176 (1984)
106. G N Gerasimov, O B Mikova, A D Abkin *Vysokomol. Soedin., Ser. A* **27** 1280 (1985)
107. L N Aleksandrova, M I Gorilovskii, O B Mikova, G N Gerasimov, A D Abkin *Vysokomol. Soedin., Ser. A* **30** 982 (1988)
108. L N Aleksandrova, G N Gerasimov *Zh. Fiz. Khim.* **62** 2808 (1988)
109. L N Aleksandrova, K A Mailyan, A V Pebalk, G N Gerasimov, in *Tez. Dokl. 5 Vsesoyuz. Konf. po Khimii Nizkikh Temperatur* (Abstracts of Reports at the 5th All-Union Conference on Low Temperature Chemistry) (Moscow: Izd. Mosk. Gos. Univ., 1991) p. 35
110. N K Baramboim *Mekhanokhimiya Vysokomolekulyarnykh Soedinenii* (Mechanochemistry of High-Molecular Mass Compounds) (Moscow: Khimiya, 1978) p. 384
111. V V Barelko, I M Barkalov, V I Gol'danskii, D P Kiryukhin, A M Zanin *Adv. Chem. Phys.* **74** 339 (1988)
112. V V Barelko, I M Barkalov, V I Gol'danskii, A M Zanin, D P Kiryukhin *Usp. Khim.* **59** 353 (1990) [*Russ. Chem. Rev.* **59** 205 (1990)]
113. A M Zanin, D P Kiryukhin, I M Barkalov, V I Gol'danskii *Dokl. Akad. Nauk SSSR* **269** 1171 (1981)
114. G A Kichigina, A M Zanin, D P Kiryukhin, I M Barkalov, V I Gol'danskii *Khim. Fiz.* **7** 543 (1988)
115. G A Kichigina, A M Zanin, D P Kiryukhin, I M Barkalov *Vysokomol. Soedin., Ser. B* **30** 672 (1988)
116. G A Kichigina, D P Kiryukhin, A M Zanin, I M Barkalov *Vysokomol. Soedin., Ser. A* **32** 1094 (1990)
117. A M Zhabotinskii *Kontsentratsionnye Kolebaniya* (Concentration Oscillations) (Moscow: Nauka, 1974)
118. G Nicolis, I Prigogine *Self-Organization in Non-Equilibrium Systems* (New York: Wiley-Interscience, 1977) (Translated into Russian; Moscow: Mir, 1979)
119. D A Frank-Kamenetskii *Diffuziya i Teploperedacha v Khimicheskoi Kinetike* (Diffusion and Heat Transfer in Chemical Kinetics) (Moscow: Nauka, 1967)
120. H Haken *Synergetics* (Translated into Russian; Moscow: Mir, 1985)
121. R J Fiolg, M Burger (Eds) *Oscillation and Travelling Waves in Chemical Systems* (New York: Wiley, 1985) (Translated into Russian; Moscow: Mir, 1988)
122. B V Vol'ter, I E Sal'nikov *Ustoichivost' Rezhimov Raboty Khimicheskikh Reaktorov* (Stability of Operating Conditions in Chemical Reactors) (Moscow: Khimiya, 1981)
123. D P Kiryukhin, I M Barkalov *Khim. Vys. Energ.* **17** 301 (1983)
124. D P Kiryukhin, B A Nefedov, S I Khudyaev *Dokl. Akad. Nauk SSSR* **291** 1406 (1986)
125. B A Nefedov, D P Kiryukhin, A I Bol'shakov, S I Khudyaev *Khim. Fiz.* **6** 813 (1987)
126. D P Kiryukhin, G A Kichigina, I M Barkalov *Khim. Fiz.* **7** 864 (1988)
127. A I Bol'shakov, D P Kiryukhin, I M Barkalov *Vysokomol. Soedin., Ser. B* **31** 219 (1989)
128. D P Kiryukhin *Khimiya Nizkikh Temperatur i Kriokhimicheskaya Tekhnologiya* (Low Temperature Chemistry and Cryochemical Technology) (Moscow: Izd. Mosk. Gos. Univ., 1990) p. 27
129. I E Sal'nikov *Dokl. Akad. Nauk SSSR* **60** 405 (1948)
130. I E Sal'nikov *Zh. Fiz. Khim.* **23** 258 (1949)
131. I M Douglas, N Y Gaitonde *Ind. Eng. Chem., Fundam.* **6** 265 (1967)
132. S Yu Bondarenko, D P Kiryukhin, V N Ushakova, in *Vtoraya Konferentsiya po Teoreticheskoi i Prikladnoi Radiatsionnoi Khimii* (The Second Conference on Theoretical and Applied Radiation Chemistry) (Obninsk: NIITEKhim, 1990) p. 35

Russian Chemical Reviews **63** (6) 507 – 517 (1994)
©1994 Russian Academy of Sciences and Turpion Ltd

UDC 541.124

Characteristic features of the radical polymerisation of water-soluble monomers

V F Gromov, E V Bune, E N Teleshov

Contents

I. Introduction	507
II. Kinetics of the polymerisation of water-soluble monomers in various solvents	508
III. The role of solvation effects in the radical polymerisation of water-soluble monomers	511
IV. The influence of the solvent on the conformational characteristics of water-soluble polymers	513
V. Ideas concerning the mechanism of the influence of the solvent on the radical polymerisation of water-soluble monomers	514
VI. Conclusion	516

Abstract. The results of studies on the influence of the nature of the solvent on the kinetics of the radical polymerisation of water-soluble monomers are surveyed. It is noted that the rate of the process and the chain propagation rate constant in the polymerisation of monomers of this kind change sharply on passing from organic solvents to aqueous solutions. Comparative analysis of the kinetic data and the results of spectroscopic and viscometric studies made it possible to put forward a mechanism for the polymerisation of water-soluble monomers in various solvents. A distinctive feature of the polymerisation of water-soluble monomers is the hydrophobic interactions arising in aqueous solutions of the polymers and leading to a sharp difference between the kinetic parameters of the polymerisation of monomers of this class in water and organic solvents. The bibliography includes 76 references.

I. Introduction

The development of the classical theory of the radical polymerisation of vinyl monomers was completed towards the end of the 1950s. It was formulated in final form in the monographs of Bamford et al.[1] and Bagdasar'yan,[2] which appeared almost simultaneously. The theory is based mainly on the results of studies of the polymerisation of weakly polar hydrocarbon monomers (for example, styrene). The principal postulate of this theory is that the reactivity of the monomers and of the polymeric radicals formed from them, and hence the rate constant for the propagation of polymer chains (k_p), are determined solely by the chemical structure of the compounds and do not depend on the nature of the solvent in which the polymerisation takes place.

However, by the beginning of the 1960s studies had already been carried out in which it was established that the nature of the solvent affects not only the chain termination rate constant (k_t), as a consequence of a change in the viscosity of the reaction system, but also the propagation constant k_p in the polymerisation of monomers such as styrene, methyl methacrylate, and certain others.

Subsequently studies on the influence of the solvent and of various added compounds on the polymerisation of vinyl monomers were developed in a number of investigations (see, for example, Refs 3 – 15). They led to the establishment of new aspects of the field of radical polymerisation, in particular complex-radical polymerisation.[16] Studies on the influence of the nature of the solvent on the radical polymerisation of vinyl monomers published up to 1978 were examined in an earlier review.[17] The results of these investigations demonstrate that the influence of the solvent on the polymerisation of weakly polar monomers is associated with the formation of a donor – acceptor complex between the polymeric radicals and the solvent molecules, which alters the reactivity of the polymeric radicals. It is noteworthy, however, that the change in the overall rate of polymerisation and of the constant k_p for nonpolar monomers such as styrene is small (it does not usually exceed 30% – 50%). A more significant influence of the nature of the solvent is observed in the polymerisation of monomers containing functional groups capable of participating in a specific interaction with the solvent molecules. Such compounds include the esters of acrylic and methacrylic acids, vinyl acetate, and others. According to a series of data,[13–15] the overall rate of polymerisation of such monomers and the constant k_p may vary severalfold depending on the nature of the solvent.

The solvent exerts a much greater influence in the polymerisation of monomers containing atoms with a lone pair and functional groups capable of being involved in the formation of stronger complexes, in particular in the formation of hydrogen bonds. Such monomers include primarily water-soluble monomers incorporating amide, carboxy-, and carbonyl groups. In the polymerisation of these monomers, the replacement of the solvent may be accompanied by a change in the overall rate of polymerisation by a factor of several tens, an especially sharp change being observed on passing from an organic solvent to an aqueous solution.

The study of the influence of the nature of the solvent on the radical polymerisation of water-soluble monomers was initiated in the 1960s. Since then, numerous investigations of this problem have been published. The objects of study have been usually acrylamide, acrylic acid, *N*-vinylpyrrolidone, and the salts of the aminoesters of methacrylic and acrylic acids.

Apart from the elucidation of purely theoretical problems concerning the mechanism of the polymerisation of water-soluble

V F Gromov, E V Bune Radiation Polymerisation Laboratory,
E N Teleshov Department of Polymer Synthesis,
Karpov Physicochemical Institute, ul. Obukha 10, 103064 Moscow,
Russian Federation. Fax (7-095) 975 24 50

Received 25 March 1994
Uspekhi Khimii **63** (6) 530 – 541 (1994); translated by A K Grzybowski

monomers, the interest in this problem is also due to the fact that water-soluble anionic and cationic polymers, primarily acrylamide polymers and copolymers, have found extensive application in various branches of the economy as flocculants, for the purification of drinking and waste waters, in increasing the extraction of petroleum, in reducing the hydrodynamic resistance to friction, etc.

The fact that, for the monomers investigated above, the influence of the nature of the solvent not only on the overall rate of the process but also on the rate constants for the elementary polymer chain propagation and termination has been determined is especially important for the determination of the mechanism by which the nature of the solvent influences radical polymerisation. Studies on these lines, carried out up to 1980, were devoted mainly to the investigation of polymerisation in various individual solvents.[16–20] In the present review, we shall deal only briefly with the results of these studies, attention being concentrated on later studies, and an attempt will be made to formulate the principal characteristic features of the radical polymerisation of water-soluble monomers and the causes responsible for these features.

II. Kinetics of the polymerisation of water-soluble monomers in various solvents

According to the nature of the solvent, the overall rate of polymerisation of water-soluble monomers varies by 1.5–2 orders of magnitude. These effects were first observed and then studied in detail for acrylamide, acrylic acid, and their derivatives, as well as for the salts of the aminoesters of methacrylic and acrylic acids.[17,19]

In terms of the influence on the overall rate of polymerisation of acrylamide, the above solvents can be arranged in the sequence water > formamide > dimethylsulfoxide(DMSO) > tetrahydrofuran (THF). In the polymerisation of acrylamide in aqueous solution at 40 °C, the quantity $k_p/k_t^{1/2}$ is 12 times greater than in DMSO and 50 times greater than in THF. The decrease in the rate of polymerisation on passing from water to DMSO and THF is accompanied by a decrease in the molecular mass of the polymers.

A similar effect of the nature of the solvent has been established also in the polymerisation of methacrylamide.[17]

In order to elucidate the causes responsible for the observed kinetic effect, the absolute values of k_p and k_t were determined for the polymerisation of acrylamide under homogeneous conditions.[17] These data show that the change in the overall rate of polymerisation of acrylamide on passing from an aqueous solution to a solution in an organic solvent is caused mainly by the change in k_p. The chain termination constant changes in the same direction (albeit to a much lesser extent) and thus diminishes the influence of k_p on the overall rate.

An appreciable influence of the nature of the solvent on the overall rate of reaction and the constant k_p has also been established in the polymerisation of *N*-vinylpyrrolidinone. The solvents investigated can be arranged in the following sequence: tetrahydrofuran ≈ dichloroethane < methanol < *N*-vinylpyrrolidinone < water, the change from polymerisation in THF to polymerisation in an aqueous solution entailing a change in k_p by a factor of ~50.[21–23]

Qualitatively the same results have been obtained in the study of the homogeneous polymerisation of acrylic acid and its derivatives in various solvents (Table 1). In this case too, the polymerisation is fastest in aqueous solution, the overall rates as well as the constant k_p decreasing significantly on passing to polymerisation in formamide and DMSO. However, the data in Table 1 indicate a significant difference between the behaviour of the acids investigated in the polymerisation in different solvent. Whereas in the case of acrylic acid the sharp dependence of the overall rate of polymerisation and of the constant k_p on the nature of the solvent is observed, in the case of methacrylic and especially fluoroacrylic acid this dependence is much less pronounced. Nevertheless, in all the systems investigated the overall rate of polymerisation increases in the series of solvents DMSO < formamide < water. The increase in the rate of polymerisation in the above sequence is almost wholly determined, as in the case of acrylamide, by the increase in k_p, which is in its turn associated with the decrease in the activation energy for the chain propagation reaction.

According to the classical theory of radical polymerisation,[1,2] the rate of chain propagation is determined by the reactivity of the polymeric radical. Comparison of the data presented in Table 1 shows that the change in the nature of the solvent in the polymerisation of the acids investigated makes the reactive radical formed in the polymerisation of acrylic acid in water (the reactivity of this radical is characterised by the constant k_p) less reactive than the radicals derived from fluoroacrylic and methacrylic acids in DMSO. The different degrees of dissociation of these acids in water and DMSO as well as the ability of the acid polymeric radicals to participate in the formation of complexes with DMSO (which has basic properties) probably play a definite role in such alteration of the reactivity of polymeric radicals.

The homogeneous polymerisation of the aminoesters of acrylic or methacrylic acid and of their tertiary and quaternary salts is also much faster in water than in organic solvents (Table 2). As in the radical polymerisation of other water-soluble polymers, the increase in the overall rate of polymerisation in water is also caused by the increase in the chain propagation rate constant. Thus the constant k_p in the polymerisation of acetate salts of diethylaminoethyl methacrylate in water (72 000 litre mol^{-1} s^{-1}) is 240 times greater than k_p in the polymerisation of dioxane.[26] Furthermore, a very considerable change in k_t was established in this system on passing from an organic solvent to an aqueous solution: the constants k_t in water and dioxane are 65 × 10^7 and 0.1 × 10^7 litre mol^{-1} s^{-1} respectively.

There is no doubt that the polymerisation of ionogenic monomers such as acrylic and methacrylic acids and their salts or the salts of their aminoesters is influenced significantly by the degree of ionisation, which depends on the nature of the solvent.[18] Nevertheless, the principal features of the polymerisation of water-soluble ionogenic anionic and cationic monomers do not

Table 1. Polymerisation of acrylic (AA), methacrylic (MAA), and α-fluoroacrylic (FAA) acids in different solvents.[17]

Monomer	k_p (20 °C)/litre mol^{-1} s^{-1}	E_p/kcal mol^{-1}	$10^{-7} A_p$	$10^{-8} k_t$/litre mol^{-1} s^{-1}	E_t/kcal mol^{-1}	$10^{-8} A_t$
In water						
AA	27200	3.1	0.60	1.8	0	1.8
MAA	4100	4.3	0.67	0.12	1.0	0.16
FAA	2600	4.5	0.60	0.87	0.6	2.0
In formamide						
AA	4200	5.6	6.2	1.0	0	1.0
FAA	2200	4.9	0.75	0.74	0.4	1.5
In dimethyl sulfoxide						
AA	500	8.0	47	0.20	0	0.20

Table 2. The rates of polymerisation ($10^5 v_0$/mol litre^{-1} s^{-1}) of dialkylaminoethyl methacrylates and their salts in water and different organic solvents.[24–26]

Monomer	H_2O	DMSO	DMF	C_2H_5OH
DM	1.3	0.30	0.20	0.40
DE	1.5	0.25	0.20	0.30
DM.C_2H_5Br	7.0	2.7	–	2.0
DE.C_2H_5Br	9.6	6.2	–	3.6
DE.HBr	5.0	3.4	2.4	1.7
DE.CH_3I	4.0	–	1.1	–

Note. The following notation has been adopted: DM = dimethylaminoethyl methacrylate, DE = diethylaminoethyl methacrylate, and DMF = dimethylformamide. In all cases, the reaction was initiated by azobisisobutyronitrile at 60 °C; monomer concentration 0.25 M; initiator concentration 1 × 10^{-3} M.

differ from those of the radical polymerisation of nonionogenic water-soluble monomers of the type of acrylamide or *N*-vinylpyrrolidinone and are determined mainly by the same factors.

Analysis of the results obtained in the study of the polymerisation of water-soluble monomers in solvent mixtures of different composition is very important in elucidating the causes of the influence of the nature of the solvent on the polymerisation of such monomers. In our view, the study of the reaction in mixtures of water with organic solvents is especially important. Such investigations have been carried out in greatest detail for acrylamide.

The addition of even small amounts of an organic solvent in the homogeneous polymerisation of acrylamide in water–DMSO mixtures diminishes k_p significantly. A similar effect is exerted by the addition of dioxane or THF.[27,28] The addition of small amounts of benzene to a DMSO–H_2O mixture, which do not alter the homogeneity of the process, is also accompanied by a decrease in the overall rate of the process and in the constant k_p (Table 3).

Fig. 1 presents the dependence of the constants k_p and k_t and also of the relative viscosity of the reaction mixture on the water content in the solvent in the polymerisation of acrylamide in water–DMSO mixtures. Evidently there is no relation of any kind

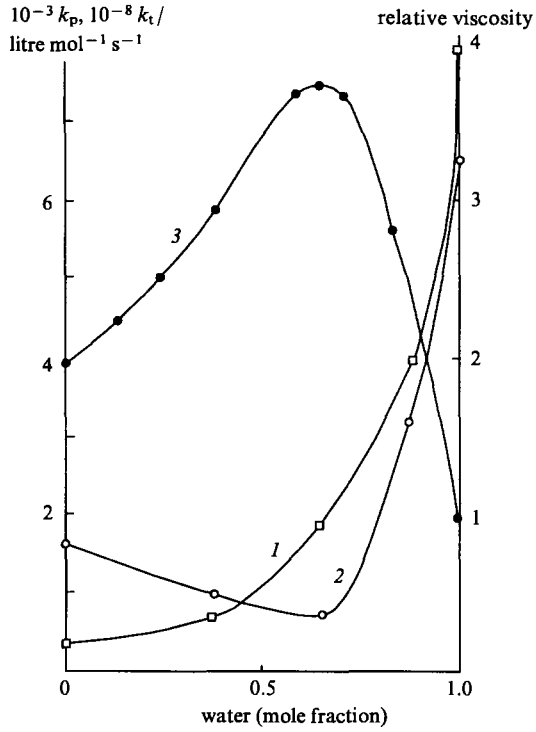


Figure 1. Dependence of k_p (curve *1*), k_t (curve *2*), and the viscosity of the initial reaction mixture (curve *3*) on the water content in the polymerisation of acrylamide in water–DMSO mixtures.[31] Monomer concentration 0.38 M.

between k_p and the viscosity of the reaction system: while k_p diminishes continuously on passing from water to DMSO, the viscosity of the reaction mixture passes through a maximum. The constant k_t also decreases with increase in the DMSO content in the solvent mixture, reaches a minimum for the water:DMSO = 65:35 molar ratio corresponding to the maximum viscosity of the reaction mixture, and then again increases somewhat. However, comparison of the data obtained in the polymerisation of acrylamide in individual and mixed solvents (Fig. 2) demonstrates the absence of a linear relation

Table 3. Polymerisation of acrylamide in different solvents.[27,28]

Solvent	$10^{-4} k_p$ (30 °C)/ litre mol^{-1} s^{-1}	E_p/ kcal mol^{-1}	$10^{-7} A_p$	$10^{-8} k_t$ (30 °C)/ litre mol^{-1} s^{-1}	E_t/ kcal mol^{-1}	$10^{-10} A_t$
Water (pH 7)	7.9	2.8	0.8	6.6	2.8	6.8
Formamide	1.2	5.0	4.4	2.3	0.8	0.072
Water–DMSO						
90:10	4.3	3.8	2.4	3.5	2.6	2.9
88:12	4.0	3.8	2.6	3.2	2.6	2.3
65:35	1.9	4.5	3.3	0.80	2.6	0.57
38:62	0.70	4.9	2.4	1.0	1.9	0.23
Water–DMSO–benzene						
64.4:34.7:0.9	1.4			0.70		
36.8:59.9:3.3	0.48			0.72		
DMSO	0.37	6.0	7.8	1.7	0	0.017
Water–dioxane						
95:5	5.7	3.5	1.9	4.5	2.6	3.4
90:10	3.3	4.2	3.4	2.3	2.5	1.5
Water–THF						
96:4	4.1	3.8	2.4	3.2	2.7	2.9
92:8	2.3	4.6	5.0	1.6	2.6	1.2
90:10	1.9	4.6	5.0	1.4	2.6	1.2

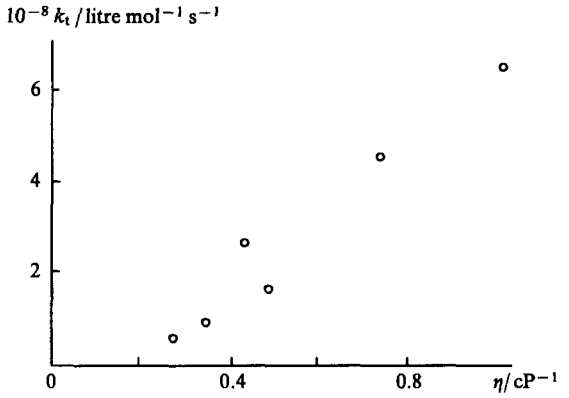


Figure 2. Dependence of k_t for the polymerisation of acrylamide in different solvents on the fluidity of the reaction mixture.[27]

between k_t and the fluidity of the initial polymerisation solution. Such a relation is characteristic of a diffusion-controlled chain termination reaction, for example, in the polymerisation of styrene and methyl methacrylate in various solvents.[1] The deviation from linearity shows that k_t for the polymerisation of acrylamide in the solvents investigated is not determined solely by diffusion. A similar relation has also been observed[29,30] in the polymerisation of vinyl benzoate and vinyl acetate in various solvents.

In the polymerisation of acrylamide in individual and mixed solvents, there is no definite relation between k_p and the relative permittivity of the solvent (ε). In particular, there is no linear correlation between the logarithm of k_p and the polarity parameter $(\varepsilon - 1)/(2\varepsilon + 1)$. This result shows that the solvent polarity is not in this case a factor which determines the reactivity of the reacting species.[31]

The addition of water to individual and mixed organic solvents (ethanol, ethanol–dioxane, DMSO) also increases significantly the overall rate of polymerisation of methacrylic acid and of the molecular masses of the polymers.[32] In this case too, the rate of reaction is almost independent of the relative permittivity of the reaction mixture and is determined by the amount of water present in it. The same pattern has been observed also in the polymerisation of diethylaminoethyl methacrylate and its salts. The addition of even 5 mol.% of water to methanol or dioxane is accompanied by an appreciable increase in the overall rate of polymerisation and also in the rate constant k_p both for the aminoester itself and for its acetate and chloride salts (Table 4).

Table 4. The influence of the nature of the solvent on the chain propagation and termination rate constants in the radical polymerisation of diethylaminoethyl methacrylate (DE) and its acetate (DE.HAc) and chloride (DE.HCl) salts.[26,33]

Monomer	Solvent	$10^{-3}k_p$/ litre mol^{-1} s^{-1}	$10^{-7}k_t$/ litre mol^{-1} s^{-1}
DE	dioxane	0.09	0.06
	dioxane–water	0.36	0.33
	methanol	0.70	1.3
DE.HAc	dioxane	0.30	0.10
	dioxane–water	1.8	1.2
	water	72	65
DE.HCl	methanol	3.3	0.90
	methanol–water	10.8	6.0

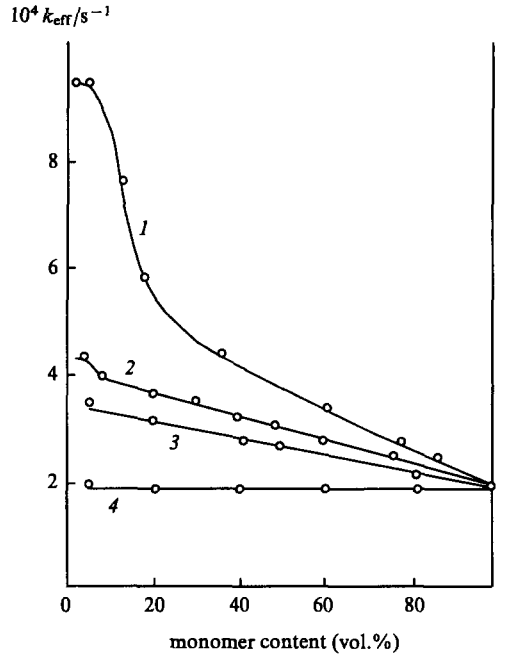


Figure 3. Dependence of k_{eff} on the *N*-vinylpyrrolidinone concentration in polymerisation in water (curve *1*), ethanol (curve *2*), 2-pyrrolidinone (curve *3*), and 2-methylpyrrolidinone (curve *4*) at 60 °C; concentration of azobisisobutyronitrile 1×10^{-3} M (data of Kirsh et al.[35]).

The influence of the composition of the reaction mixture on the effective overall rate of polymerisation constant $k_{eff} = V_o/[M]$, where V_o is the overall rate of polymerisation and [M] the monomer concentration, was established also in the polymerisation of *N*-vinylpyrrolidinone.[23,34,35] In the homogeneous polymerisation of this monomer in protic solvents such as water, ethanol, and 2-pyrrolidinone, the effective reaction rate constant decreases with decrease in the monomer concentration in solution. This effect is manifested to the greatest extent for aqueous solutions (Fig. 3). When the polymerisation is carried out in 2-methylpyrrolidinone, which is, as it were, a saturated analogue of the monomer, the constant k_{eff} remains unchanged over a wide range of monomer concentrations.

It is possible to distinguish three *N*-vinylpyrrolidinone concentration ranges depending on their influence on the rate of polymerisation in water: (1) the range from 100 to 30 vol.% of the monomer, where k_{eff} increases only slightly; (2) the range from 30 to 10 vol.% of *N*-vinylpyrrolidinone (in this range, a sharp rise in k_{eff} is observed with increase in the concentration of the monomer); (3) the range from 10 to 2 vol.% of the monomer, where the rate constant hardly changes.

Thus a sharp increase in k_{eff} in the polymerisation of *N*-vinylpyrrolidinone in aqueous solution is observed in the range of monomer mole fractions in the solution from 0.1 to 0.018, i.e. in the range where the number of water molecules per monomer molecule increases from 10 to ~60. For a higher water content in the reaction mixture, k_{eff} does not change. The ratio 60:1, established as a result of a kinetic study of the polymerisation, corresponds to the maximum number (55) of water molecules in the hydration shell of *N*-vinylpyrrolidinone in a dilute aqueous solution, i.e. to the maximum degree of solvation of the monomer by water molecules.[35] It is noteworthy that the maximum effective rate of polymerisation is observed in a medium with a minimal viscosity, which rules out the possible influence of the rate of the chain termination reaction on the overall rate of the process. The change in k_{eff} on passing from polymerisation in bulk to polymerisation in aqueous solution containing 10 vol. % of the monomer (~1 M) is wholly determined, as in the polymerisation of acrylamide, by the change in the constant k_p.

Thus k_p = 1200 litre mol^{-1} s^{-1} for the polymerisation of *N*-vinylpyrrolidinone in bulk,[22] while in the polymerisation in 10% aqueous solution $k_p = 2.2 \times 10^4$ litre mol^{-1} s^{-1}.[23]

The addition of small amounts of water to a solution of 1-vinyl-1,2,4-triazole in dimethylformamide or dimethylacetamide is accompanied by an appreciable increase in the molecular mass of the polymer obtained under the influence of radical initiators.[36]

Thus a distinctive feature of the polymerisation of water-soluble monomers is the marked dependence of the overall rate of polymerisation and also of the chain propagation rate constant and the molecular mass of the polymer on the nature of the solvent. The reaction proceeds at the highest rate and with formation of polymers having the maximum molecular mass in aqueous solution. The addition of even small amounts of an organic solvent to an aqueous solution of the monomer diminishes appreciably both the rate of polymerisation and the molecular mass of the polymers.

III. The role of solvation effects in the radical polymerisation of water-soluble monomers

The change in the kinetic parameters of the polymerisation of water-soluble monomers in various solvents may be influenced, as in the case of weakly polar monomers, by complex formation between the growing radicals and the solvent and also by the solvation of the monomers and radicals by the solvent. The role of the second factor is much more pronounced. This is associated with the fact that the water-soluble monomers, and especially amides and carboxylic acids, can exist in a self-associated form as a result of the formation of intermolecular hydrogen bonds even in dilute solutions,[37] the degree of association depending on the ability of the solvents to form hydrogen bonds. Cryoscopic studies have shown[27,28] that, at an acrylamide concentration of 1.0 M in water, acrylamide exists in the monomeric form, whereas in formamide and DMSO it is 15% or 30% dimerised respectively. The degree of dimerisation of acrylic acid in DMSO is ~10%, while fluoroacrylic acid exists exclusively in the monomeric form in both water and in solution in DMSO.[38] Different degrees of interaction with the solvent are also indicated by the heats of solution of acrylamide and acrylic acids in different solvents and by ^{1}H NMR spectroscopic data.[28] The difference between the degrees of self-association of the monomer molecules may be the cause of the observed difference between the activation energies for the chain propagation reaction and between the heats of polymerisation of water-soluble monomers.[38]

The formation of complexes between the polymeric radicals and solvent molecules can exert only an insignificant influence, as in the case of nonpolar vinyl monomers, on the kinetic parameters in the polymerisation of water-soluble monomers. Firstly, the energy of such interaction in not very great (thus it amounts to ~1 kcal mol^{-1} in the interaction of aromatic solvents with radicals). Secondly, the formation of a complex with an active centre is accompanied by the appearance of a compensation effect,[39] which should diminish the overall effect of the solvent on the overall rate of the process. Therefore, even when a complex is formed between the solvent and the unpaired electron of the radical via a hydrogen bond, the energy of which is higher than the energy of the donor–acceptor bond, the overall influence of the solvent should not be very great, particularly if one takes into account the fact that only a certain proportion of polymeric radicals are involved in the formation of the complex.

The solvation of the monomer by solvent molecules and especially the formation of hydrogen bonds between the monomer and the solvent can alter the electronic structure of the monomers and hence their reactivity. A distinctive feature of water-soluble monomers such as acrylamide, acrylic acids, and the salts of the aminoesters of methacrylic acid is conjugation between the C=C and C=O groups, which has been established experimentally for a series of water-soluble monomers by various spectroscopic methods.[26,40–43] Therefore the change in electron density at the carbon atom of the carbonyl group as a consequence of the formation of a hydrogen bond between the C=O group and the proton-donating solvents should naturally be accompanied by a change in electron density in the C=C double bond and hence by a change in the reactivity of the monomer.

According to IR spectroscopic data, the frequency $\nu_{C=O}$ in the spectra of the acetate salt of diethylaminoethyl methacrylate increases on passing from dioxane and acetonitrile to the dioxane–water mixed solvent and further to water, a linear relation being observed between the rates of polymerisation of this monomer and the frequency $\nu_{C=O}$ in the corresponding solvent.[26] A linear correlation between $k_p/k_t^{1/2}$ and $\nu_{C=O}$ for the monomer is observed in the polymerisation of certain other salts of the aminoesters of methacrylic acid, acrylamide, and *N*-vinylpyrrolidinone in various solvents.[26] The formation of a hydrogen bond between the monomer and the solvent diminishes the electron density on the protons and carbon nuclei of the CH_2 group of the monomer. This is indicated by the increase in the chemical shift of the proton and the carbon atom in the given group on passing from solutions of the monomers in an aprotic solvent (dioxane) to aqueous solutions. The decrease in electron density on the CH_2 group of the salt of the aminoester of methacrylic acid and hence the increase in the polarisation of the double bond of the monomer increases the rate of interaction between the monomer and the radical. As a consequence of the nucleophilic properties of alkyl radicals,[44] this leads to an increase in the rate of polymerisation on passing from a solution in dioxane to aqueous solutions, i.e. on formation of a hydrogen bond between the C=O group of the monomer and the solvent.

It is noteworthy that the formation of a hydrogen bond with the proton-donating solvent leads to some increase in the overall rate of polymerisation and in the constant k_p in the homogeneous polymerisation of a series of monomers which do not dissolve in water but contain the carbonyl group. Thus k_p for the polymerisation of methyl methacrylate in acetic acid is somewhat higher than in the polymerisation of the monomer in bulk.[45]

In the case of ionogenic monomers, a change in the nature of the solvent exerts a significant influence also on the degree of ionisation of the monomers and the polymeric radicals in the reaction system. The different degrees of ionisation as well as the presence of monomers in solution in the form of free ions or ion pairs lead in their turn to a change in the kinetic parameters of polymerisation of monomers such as methacrylic and acrylic acids or the salts of their aminoesters. The influence of ionisation on the polymerisation of ionogenic monomers has been examined in detail by Kabanov and Topchiev[18] and Bune et al.[19]

Valuable information for the determination of the mechanism of the polymerisation of water-soluble monomers in water–organic solvent mixtures of different composition has been obtained by comparing kinetic and spectroscopic data. A detailed study of the influence of the composition of the water–DMSO mixed solvent on the NMR spectra of acrylamide has been carried out[46] and it has been established that an increase in the concentration of water in the solvent mixture leads to an appreciable downfield displacement of the ^{13}C chemical shift of the C=O group of acrylamide ($\delta_{C=O}$). The comparatively slight alteration of the chemical shifts of the protons of the NH_2 group observed under these conditions shows that the strength of the intermolecular hydrogen bond between the NH_2 group of acrylamide and the solvent does not change very greatly on passing from DMSO to water and cannot be the cause of such a significant alteration of $\delta_{C=O}$. The change in $\delta_{C=O}$ is apparently caused mainly by the formation of a hydrogen bond between the carbonyl group of acrylamide and water molecules. An increase in the concentration of water in the acrylamide–DMSO system is not only accompanied by a change in $\delta_{C=O}$

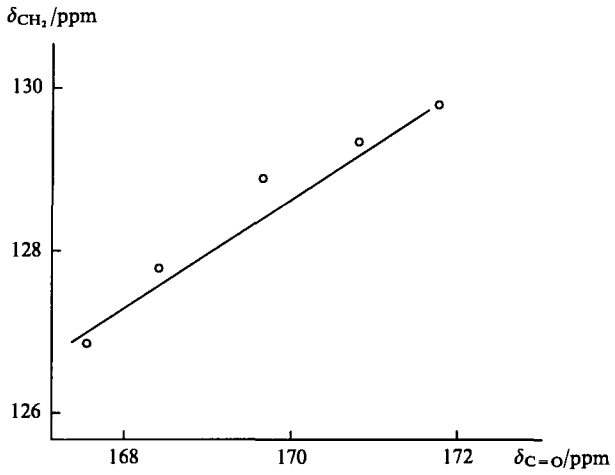


Figure 4. Relation between the ^{13}C chemical shifts of the CH_2 and C=O groups of acrylamide.[46] The measurements were performed in water–DMSO mixtures of different composition.

but also leads to an alteration of the chemical shifts of the hydrogen and carbon atoms involved in the double bond of acrylamide. There is a linear relation between the chemical shifts δ_{CH_2} and $\delta_{C=O}$ (Fig. 4), showing that the change in the electronic state of the C=O group as a consequence of the formation of a hydrogen bond between the groups and water alters the electronic state of the C=C group.

Indeed the formation of the C=O...H hydrogen bond between acrylamide and water is responsible for the enhancement of the electron-accepting properties of the amide group, the conjugation of which with the C=C double bond diminishes the electron density on the carbon atom of the CH_2 group. This conclusion follows from the correlation established[47–49] between the chemical shifts of the carbon atoms of the double bond and the elecron density in this bond. The change in the electron density in the C=C bond of the monomer should naturally alter its reactivity.

Assuming that both free acrylamide molecules and such molecules bound in a complex are present in the water–DMSO mixture and are characterised by different chain propagation rate constants, it was shown[46] that the effective chain propagation rate constant k_p^{eff} in the polymerisation of acrylamide in the water–DMSO mixture should vary linearly with $\delta_{C=O}$ or δ_{CH_2}. However, as can be seen from Fig. 5, this relation has a sharp break in the region of high concentrations of water in the mixed solvent. This type of curve indicates the existence of additional factors determining the reactivity of acrylamide in its polymerisation in the presence of water. The dependence of k_{eff} in the polymerisation of *N*-vinylpyrrolidinone in an aqueous solution on the ^{13}C chemical shift of the CH_2 group of this monomer is similar.

The relative contribution of the change in the electronic structure of the monomer as a consequence of its solvation by the solvent to the alteration of the reactivity of vinyl monomers and their radicals in radical polymerisation can be estimated approximately from the data of Sutyagin et al.[50] According to these data, a linear correlation is observed between the activation energy for chain propagation E_p in the polymerisation of vinyl monomers and the chemical shift of the β-carbon atom of the monomer in the ^{13}C NMR spectrum. The change in δ_{C_β} by ~25 ppm (transition from styrene to acrylonitrile) is accompanied by a change in E_p by 2.4 kcal mol^{-1} (Table 5). The maximum change in δ_{C_β} for acrylamide when the water content in the mixture with DMSO varies from 0% to 100% is 4.4 ppm.[46] Therefore, if account is taken only of the difference between the conditions in the solvation of acrylamide in water and DMSO, one may expect that E_p for the polymerisation of acrylamide in water should be lower by ~0.5 kcal mol^{-1} than in DMSO. On the other hand, the real difference between the values of E_p in these systems is more than 3 kcal mol^{-1}.[51] A similar situation is observed in the polymerisation of acrylic acid (the experimental change in E_p on passing from water to DMSO is ~5 kcal mol^{-1} [51]) and *N*-vinylpyrrolidinone in different solvents.[34,35]

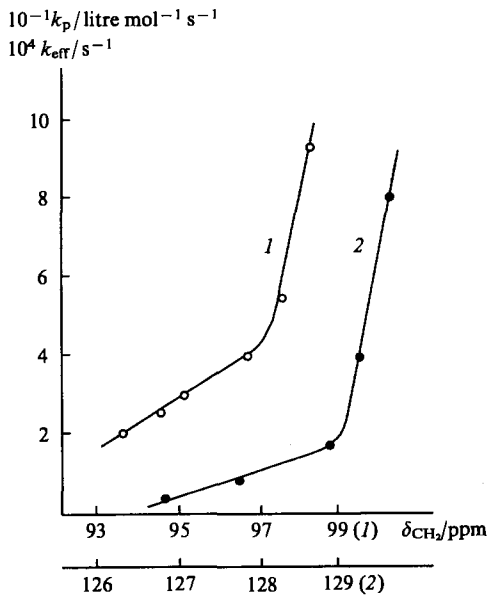


Figure 5. Dependence of k_p for the polymerisation of acrylamide (curve *1*) and k_{eff} for the polymerisation of *N*-vinylpyrrolidinone (curve *2*) on the ^{13}C chemical shift of the CH_2 group of the monomer.[55,56] Acrylamide was polymerised in water–DMSO mixtures of different composition; *N*-vinylpyrrolidinone was polymerised in aqueous solution at different monomer concentrations.

Table 5. Chemical shifts of the C_β atoms in the ^{13}C NMR spectra of vinyl monomers and certain parameters characterising their reactivity in radical polymerisation.[50]

Monomer	δ_{C_β}/ppm	Relative localisation energy of		E_p/kcal mol^{-1}
		monomer	radical	
Vinyl acetate	96.30	2.037	0.320	9.5
Vinylcarbazole	–	–	–	6.9
α-Methylstyrene	112.13	1.703	0.729	–
Styrene	113.20	1.704	0.720	6.3
Vinyl chloride	117.30	1.877	0.635	3.9
Methyl methacrylate	121.80	1.740	0.770	4.7
Ethylene	123.30	2.000	–	–
Methyl acrylate	132.30	1.704	0.645	4.1
Acrylonitrile	137.90	1.696	0.834	3.9

Thus the solvation of the monomer and the resulting change in its reactivity have a much greater influence on the overall rate of polymerisation and k_p than the formation of donor–acceptor complexes between the polymeric radical and the solvent. Nevertheless, this factor cannot fully explain the observed influence of the solvent on the radical polymerisation of water-soluble monomers.

IV. The influence of the solvent on the conformational characteristics of water-soluble polymers

The data presented above show that the hypotheses postulating different solvation conditions in water and organic solvents as well as the formation of complexes between polymeric radicals and the solvent cannot fully explain the results obtained in polymerisation in the presence of small amounts of added organic solvent. Indeed, it is difficult to postulate that such small amounts of the additive (up to 10 mol. %) can lower significantly the degree of dimerisation of acrylamide in solution. Nevertheless, as can be seen from Table 3, they appreciably diminish k_p. One can postulate that the change in the rate of chain propagation in such systems is partly caused by the change in the conformation of the polymer chains. This hypothesis is based on a comparison of the size of the polymer coil with the constant k_p for the polymerisation of acrylamide in various solvents.[52] It is seen from the data presented in Table 6 that the intrinsic viscosity of the same polymer and hence the size of the polymer coil in solution diminishes on passing from water to its mixtures with DMSO, dioxane, and THF containing 10 mol. % of the organic solvent.

Table 6. The influence of the solvent on the intrinsic viscosity of the polyacrylamide.[52]

Solvent in which polymerisation was carried out	Solvent in which the viscosity was measured	$[\eta]$/dl g^{-1}	
		25 °C	50 °C
Water	water	16.9	–
	water–DMSO (90 : 10)	10.0	–
	water–dioxane (90 : 10)	9.4	–
	water–THF (90 : 10)	9.2	–
Water–DMSO = 90 : 10	water	4.5	4.5
	water–DMSO (90 : 10)	3.4	3.6
	water–dioxane (90 : 10)	3.0	3.2
	water–THF (90 : 10)	2.9	3.5
Water–dioxane = 90 : 10	water	2.9	–
	water–DMSO (90 : 10)	2.2	–
	water–dioxane (90 : 10)	1.9	–
	water–THF (90 : 10)	1.8	–
Water–THF = 90 : 10	water	0.60	–
	water–DMSO (90 : 10)	0.46	–
	water–THF (90 : 10)	0.39	–
Water–DMSO = 65 : 35	water	2.5	–
	water–DMSO (65 : 35)	1.8	–
	water–DMSO (65 : 35) + + 0.25 M benzene	1.2	–
Water–DMSO = 38 : 62	water	1.6	–
	water–DMSO (38 : 62)	1.0	–
DMSO	water	0.88	–
	DMSO	0.65	–

It was found that the nature of the change in the size of the polymer coil as a function of the solvent is the same as for k_p (Fig. 6). An increase in temperature from 25 to 50 °C hardly affects the intrinsic viscosity of the polymer in aqueous solution (Table 6). On the other hand, in mixtures of water with organic solvents the viscosity $[\eta]$ increases somewhat as the temperature is raised. Consequently the size of the polymer coil formed in mixed solvents increases with increase in temperature relative to the size of the macromolecular coil formed on polymerisation in aqueous solution. Such a change in the morphology of the polymer coil as the temperature is altered may be one of the factors responsible for the marked temperature dependence of the overall rate of reaction and of the rate of chain propagation in mixtures of water with an organic solvent compared with the polymerisation of acrylamide in aqueous solution (Table 3).

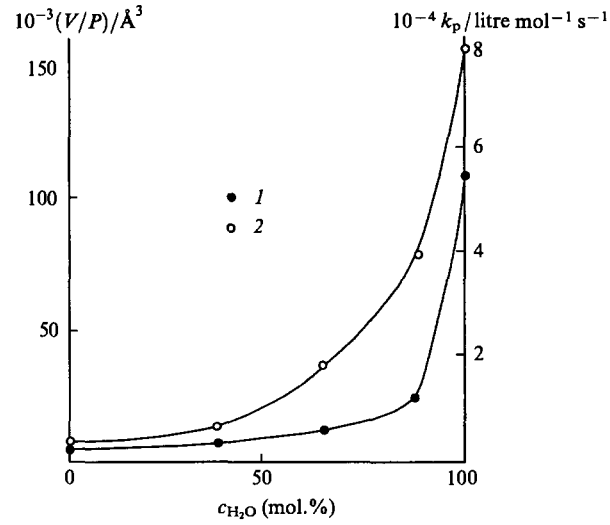


Figure 6. Dependence of the relative size of the polymer coil (curve *1*) and of the constant k_p (curve *2*) on the water content in the polymerisation of acrylamide in water–DMSO mixtures.[56] V = volume of polymer coil; P = degree of polymerisation.

An increase in the size of the polymer coil on passing from an organic solvent to water has also been observed for polymers of the tertiary salts of the aminoesters of methacrylic acid.[26,53] It is striking that in this case there is a sharp decrease in the size of the coil following the addition to water of even small amounts of an organic solvent. Thus the intrinsic viscosity of the solution of the acetate salt of poly(diethylaminoethyl methacrylate) (and hence also the volume of the polymer coil) diminishes from 1.3 in aqueous solution to 1.1 in the water–dioxane mixture containing 20 mol. % of dioxane and to 1.05 in dioxane.[33]

Calculations have shown that the density of the polyacrylamide coil synthesised in an organic solvent or in an aqueous organic medium exceeds by a factor of 30–40 the density of the polymer coil formed in aqueous solution.[27] A similar result has been obtained in a study[54] where it was shown that the addition of even small amounts of precipitants such as acetone or methanol to dilute aqueous solutions of high-molecular-mass polyacrylamide [$M_W = (2 - 3) \times 10^7$] diminishes the volume of the polymer coil by a factor greater than 100. The change in the density of the polyacrylamide coil on impairment of the quality of the solvent (the same picture has been observed also for other water-soluble polymers, in particular the polymers of the salts of dimethylaminoethyl methacrylate) indicates a possible conformational transition of the coil–globule type and may lead to the appearance of steric hindrance in the interaction between macroradicals and monomers.

The change in the conformation of polymer coils depends on the rigidity of the polymer chain. The introduction of a fluorine atom into the acrylic acid molecule increases the rigidity of polyfluoroacrylic acid compared with polyacrylic acid. Therefore the influence of the nature of the solvent on the conformational characteristics of the polymer and the kinetic parameters of the polymerisation of fluoroacrylic acid is much more pronounced than in the case of acrylic acid.

It is noteworthy that some influence by the conformational characteristics of the polymers on the constant k_p and k_t has been observed also in the polymerisation of butyl acrylate in different solvents.[14]

Thus the change in the overall rate of polymerisation of water-soluble monomers and of the rates of the elementary polymer chain propagation and termination reactions on passing from aqueous solutions to solutions in aqueous organic mixtures and organic solvents is caused both by a complex formation reaction of the solvent with the monomer molecules and growing

radicals as well as a number of physical factors, including the solvation of the monomeric and polymeric molecules, the change in the conformational characteristics of the macromolecules, etc. Ultimately all these factors lead to a change in the effective rates of chain propagation and termination.

V. Ideas concerning the mechanism of the influence of the solvent on the radical polymerisation of water-soluble monomers

Analysis of the kinetics of the polymerisation of acrylamide in water–DMSO mixtures, NMR spectroscopic data characterising the state of the monomer in these mixtures, as well as data on the conformational state of the polymer in solution permits a more accurate estimation of the role of various factors in the polymerisation of water-soluble monomers in different solvents.

It follows from the results in a number of investigations [27, 55, 56] that, on the one hand, a sharp increase in the overall rate of polymerisation of acrylamide, in the constant k_p, and in the volume of the polymer coil was observed after the addition of a large amount of water to DMSO (the water content in the solvent mixture was ~80–85 mol. %). On the other hand, the chemical shift δ_{CH_2} increased almost linearly with increase in the amount of water in the water–DMSO mixture up to 100%. In order to elucidate the causes of such discrepancy, the solvation of a number of water-soluble monomers and polymers in water, organic solvents, and water–organic solvent mixtures was investigated by NMR spectroscopy. [43, 56] It follows from the data presented in Tables 7 and 8 that the signals due to the carbon atoms of the C=O and CH_2 groups of the monomers are displaced downfield on passing from solutions in organic solvents to water–organic solvent mixtures and aqueous solutions, which is due to the formation of a hydrogen bond between the C=O group and water. Qualitatively the same picture has been observed also for $\delta_{C=O}$ for the polymers. However, whereas for acrylamide and *N*-vinylpyrrolidinone the change in $\delta_{C=O}$ is 4.4 and 5.0 ppm respectively on passing from a solution of the monomers in DMSO, which does not form a hydrogen bond with the carbonyl group, to an aqueous solution, for the polymers the replacement of DMSO by water is accompanied by a change in $\delta_{C=O}$ by only 2.3 and 3.6 ppm respectively. In the case of acrylic and polyacrylic acids, $\delta_{C=O}$ changes to almost the same extent on passing from DMSO to water (2.9 and 3.1 ppm respectively).

Analysis of the NMR spectroscopic data for a large number of low-molecular-mass compounds of the type RCOX (where X = OR', OH, NH_2) in solvents of different nature made it possible to establish [43, 57] that, regardless of the nature of the substituent R, the formation of a hydrogen bond between the carbonyl group and the solvent leads to a downfield displacement of the chemical shift $\delta_{C=O}$, which is rigorously defined for each type of compound. For different carboxylic acids, as well as their esters and amides, such displacements are 4.0, 4.0, and 5.0 ppm respectively. The results presented in Tables 7 and 8 show that the carbonyl groups of acrylamide, *N*-vinylpyrrolidinone, and dimethylaminoethyl methacrylate are almost fully linked by hydrogen bonds to water molecules, but in the case of the corresponding polymers only some of the carbonyl groups are involved in the formation of bonds of this kind.

A similar conclusion was reached for acrylic acid and its polymer. It is noteworthy that in this case analysis of the NMR spectroscopic data took into account the influence of the degree of ionisation of the ionogenic monomers and polymers on $\delta_{C=O}$. [43, 58] An estimate showed that, regardless of the nature of the polymer, ~70% of the carbonyl groups of the water-soluble polymers are involved in the formation of hydrogen bonds with water molecules in the aqueous solution. This difference between the numbers of carbonyl groups participating in the formation of hydrogen bonds with water molecules is due to the fact that the interactions of the monomer and polymer molecules with water are determined not only by the ability to form hydrogen bonds but also by the accessibility of the carbonyl groups for such interaction. Water-soluble monomers form a homogeneous solution in water, which is the reason for the ready accessibility of water for interaction with all the carbonyl groups of the monomer.

Another situation probably arises in the case of polymer solutions, where hydrophobic interactions begin to play a significant role. The unique properties of water-soluble polymers (in particular, polyacrylamide), which permit the use of these polymers as agents modifying the viscous and rheological properties of aqueous solutions, are apparently actually determined by the hydrophobic interactions, which lead to the formation of organised hydrophobic microdomains in the system. [59–63]

Table 7. The ^{13}C chemical shifts ($\delta_{C=O}$) of the monomers and polymers in different solvents and the increments in the influence of the hydrogen bond (Δ_{hb}). [43, 57]

Compound	Solvent	$\delta_{C=O}$	Δ_{hb}
MMA	dioxane	167.5	
	water	171.5	4.0
PMMA	dioxane	178.0	
DM	–	166.6	
	water	170.3	3.7
DE.HCl	acetone	167.0	
	water	169.1	2.1
AA	DMSO	168.3	
	water	171.2	2.9
PAA	DMSO	177.0	
	water	180.1	3.1
AM	DMSO	167.5	
	water	171.9	4.4
PAM	DMSO	178.3	
	water	180.6	2.3
VP	–	172.9	
	water	177.9	5.0
PVP	DMSO	175.2	
	water	178.8	

Note. The following notation has been adopted: MMA = methyl methacrylate; PMMA = poly(methyl methacrylate): PAA = polyacrylic acid; AM = acrylamide; PAM = polyacrylamide; VP = *N*-vinylpyrrolidinone; PVP = poly-*N*-vinylpyrrolidinone; $\Delta_{hb} = \delta_{H_2O} - \delta_{Solv.}$.

Table 8. The ^{31}C chemical shifts (ppm) of acrylamide, *N*-vinylpyrrolidinone, and their polymers in different solvents. [55]

Solvent	Monomer		Polymer	
	δ_{CH_2}	δ_{CH_2}	$\delta_{C=O}$	$\delta_{C=O}$
	Acrylamide			
DMSO : water				
100 : 0	126.8	133.2	167.5	178.3
62 : 38	127.7	132.5	168.4	178.6
35 : 65	128.9	131.9	169.7	179.4
12 : 88	129.3	131.3	170.9	180.2
0 : 100	129.7	130.4	171.9	180.6
Acetic acid	129.1	130.8	171.6	–
Dioxane	126.1	132.2	167.5	–
Methanol	127.2	131.7	170.2	–
	N-Vinylpyrrolidinone			
DMSO	93.4	130.5	172.9	175.2
Water	98.2	129.6	177.9	178.8
Dioxane	92.9	130.6	172.9	–
Chloroform	94.3	129.5	173.8	–
Methanol	95.5	129.9	175.5	–
VP	93.3	129.8	172.9	–

Water-soluble polymers containing a long main hydrocarbon chain and short hydrophilic side groups of the type of COX (where X = OH, NH_2, etc.) may be regarded to some extent as compounds exhibiting surface activity. In view of this, in aqueous solution they should tend to form microaggregates of the type of micelles containing the hydrophobic hydrocarbon chain of the polymer in their interior, while the hydrophilic groups are located on the outside as far as possible. The entry of water into the interior regions of these microaggregates is difficult because of their hydrophobic properties, so that only the carbonyl groups located in the aqueous phase participate in the formation of hydrogen bonds with water molecules. The appearance of aggregates of this kind in aqueous solutions has been established experimentally in the study of the fluorescence spectra of acrylamide polymers containing very small amounts of added (<0.5 mol. %) hydrophobically modified units, in particular acrylamide units with long alkyl substituents (C_8 and longer) or other hydrophobic substituents at the nitrogen atom of the amide group.[64-69]

The formation of micelle-like clusters has also been observed in aqueous solutions of hydrophobically modified poly(ethylene oxide).[70] The hydrophobic microaggregates are present in solution even at very low polymer concentrations. An attempt has been made[66] to determine experimentally the concentration of the polymers below which they do not aggregate but form monomolecular polymer solutions. Although the exact values of this 'critical concentration for aggregation' have not been determined for different hydrophobically modified acrylamide polymers, it has been established that hydrophobic microdomains exist in these systems at a very high dilution of the polymer solutions. Thus, in the case of the hydrophobically modified polyisopropylacrylamide, the presence of hydrophobic microdomains in aqueous solution has been observed at a polymer concentration of 10^{-3}%. The formation of interchain associated species of this kind depends on the extent to which the polymers are hydrophobic. Presumably in the case of unmodified water-soluble polymers the same situation occurs, while in aqueous solutions of these polymers different microaggregates of the type of micelles arise (albeit to a lesser extent). For example, the fact that only four polymer chains are sufficient for the formation of interchain associated species may serve as a basis for such a hypothesis.[71] Associated species of this kind can catalyse the reactions occurring within them and in particular the chain propagation reaction, i.e. a kind of micellar catalysis, capable of increasing the rates of various processes to a consider-able extent, may be observed.[72]

The associated species formed as a result of hydrophobic interactions solubilise the molecules of organic compounds, in particular those of the monomer, which may alter its local concentration in the vicinity of active centres — the growing polymeric radicals within the associated species. The preferential sorption of organic compounds by polymer chains is indicated by the results obtained in a study of the dissolution of polyisopropylacrylamide in water–methanol mixtures.[73] The favourable spatial disposition of the groups participating in the chain propagation reaction within their associated species evidently decreases the activation energy for this reaction in polymerisation in water. At the same time, association as a result of hydrophobic interactions should diminish the entropy of the system. Indeed the pre-exponential factor in the Arrhenius equation for the chain propagation reaction in the polymerisation of acrylamide and acrylic acid in aqueous solution is smaller than in other solvents investigated (Table 3).

The addition of even small amounts of an organic solvent to water should apparently lead to a decrease and then to a complete disappearance of the hydrophobic effect and hence to a decrease in the rate of chain propagation and in the overall rate of polymerisation. Precisely such a situation is observed in the polymerisation of acrylamide in mixtures of water with DMSO, dioxane, and THF, in the polymerisation of *N*-vinylpyrrolidinone in water at different monomer concentrations, and also in the polymerisation of salts of diethylaminothiomethacrylate [diethylaminoethyl methacrylate?] in mixtures of water with methanol or other organic solvents.

The ideas described above concerning the hydrophobic interaction in aqueous solutions of polymers combined with kinetic data, as well as the results of spectroscopic and viscometric studies, made it possible to put forward the following mechanism for the influence of the nature of the solvent on the radical polymerisation of water-soluble monomers.[52,56]

In the polymerisation of water-soluble monomers in various organic solvents and also in water–organic solvent mixtures containing up to ~70%–80% of water, the change in the overall rate of polymerisation and its k_p is caused mainly by the change in the reactivity of the monomer as a consequence of the alteration of the electron density in the C=C bond on formation of a hydrogen bond between the carbonyl group of the monomer and the solvent. This is confirmed by the linear dependence of the rate of polymerisation on δ_{CH_2} for many of the systems investigated.

The influence of the solvent on the kinetic parameters of the polymerisation of water-soluble monomers in such systems does not differ quantitatively from that in the polymerisation of acrylic acid esters, which, for example k_p, may vary by a factor of 3–4 depending on the nature of the solvent.[13-15,29,30] Approximately the same change in the rate of the process has been observed in the polymerisation of acrylamide in water–DMSO mixtures, where the water content increases to 60–70 mol. %[52,56] and also in the polymerisation of *N*-vinylpyrrolidinone, where the concentration of water in the reaction mixture does not exceed 70 mol. %.[34,35] A further increase in the amount of water in the reaction mixture leads, not withstanding the linear relation between the water content and δ_{CH_2}, to a sharp increase in the rate of polymerisation and in k_p, which is due to the hydrophobic interactions. The increase in the rate of copolymerisation of the hydrophobically modified salts of dimethylaminoethyl methacrylate with methyl methacrylate or styrene on passing from dimethylformamide to an aqueous solution has been explained[74] by the influence of the hydrophobic interaction in the aqueous systems.

Even at high water concentrations in the organic solvent–water mixture the organic solvent enters preferentially the microaggregates and the composition of the solvent within these microaggregates, i.e. in the vicinity of the active centres, remains almost constant. Therefore the solvation of the polymer, even at a relatively high concentration of water in the reaction mixture, and also the constant k_t (adjusted to the same viscosity of the reaction mixture) should remain unchanged. Indeed $\delta_{C=O}$ for polyacrylamide, characterising the formation of hydrogen bonds between the carbonyl group and water, as well as the constant k_t remain virtually unchanged when the water content in the mixture with DMSO is altered from 0 to 50 mol. % (Fig. 7). For a higher content of water in the mixture, the latter begins to penetrate into the polymer coil; the composition of the solvent in the coil, where the chain termination reaction takes place, begins to change, which is the reason for the experimentally observed change in the quantities $\delta_{C=O}$ and k_t.[55,56]

The characteristic features of the copolymerisation of water-soluble monomers which have been established comparatively recently are apparently also determined by the hydrophobic interactions in aqueous solutions of polymers. The study of the copolymerisation of acrylamide with water-soluble anionic and cationic monomers (ethylenesulfonic acid and the sulfate salts of dimethylaminoethyl methacrylate) in water established that the composition of the copolymers formed remains almost constant as the conversion increases up to a 70%–80% yield of the polymer.[75,76] Such behaviour can be explained by assuming that the compositions of the copolymerising monomer mixture within the active polymerisation zone (in the polymer coil) and outside it are different and that a constant ratio of the concentrations of the comonomers is maintained in the active zone.

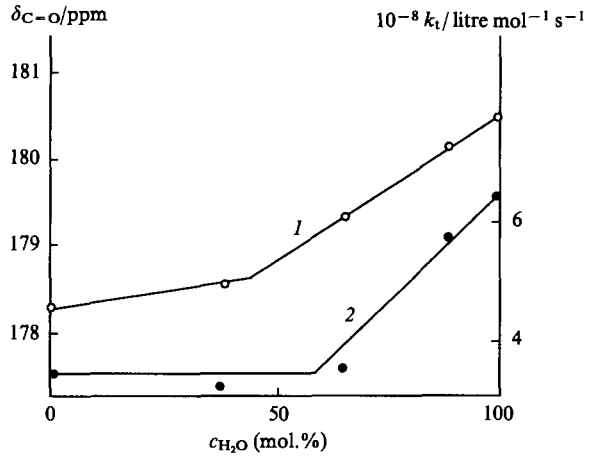


Figure 7. Dependence of the ^{13}C chemical shift of the C=O group of polyacrylamide (curve *1*) and of the constant k_t (curve *2*), adjusted to the same viscosity of the reaction system, on the water content in the polymerisation of acrylamide in a water–DMSO mixture.[55]

Such behaviour is probably a specific feature of the copolymerisation of water-soluble monomers in aqueous solutions and is associated with the formation of different interchain associated species resembling micelles, which solubilise preferentially the hydrophobic groups. A difference between the average composition of the initial monomer mixture and its composition in the active zone has been demonstrated in the emulsion copolymerisation of styrene and methyl methacrylate with long-chain alkyl salts of dimethylaminoethyl methacrylate,[74] which confirms the important role of the micellar structures in water in determining the distribution of the monomers in the reaction system.

Depending on the nature of the ionogenic comonomers, their copolymers with acrylamide are enriched either in the acrylamide units or in the units of the second comonomer. In the acrylamide–sulfate salt of dimethylaminoethyl methacrylate system, the copolymer is enriched in the cationic comonomer units, while in the copolymerisation of acrylamide with sodium ethylenesulfonate the enrichment of the copolymer in acrylamide units is observed. The rate of copolymerisation diminishes with increase in the content of the ionogenic comonomer in the initial monomer mixture regardless of the nature of the ionogenic monomer. This difference can be accounted for as follows. In the copolymerisation in an aqueous solution of monomers having different hydrophobic properties, a particular type of hydrophobic associated species is formed, depending on the composition of the copolymer, and determines the incorporation into the latter of definite amounts of the comonomers. Evidently the more hydrophobic (compared with acrylamide) cationic comonomer (the sulfate salt of dimethylaminoethyl methacrylate) enters the hydrophobic associated species more readily than acrylamide. Its local concentration in the vicinity of the active centre is therefore higher than in the initial monomer mixture. With increase in the amount of the polymer in solution, the role of the hydrophobic associated species should increase, which in fact probably leads to the observed constancy of the composition of the copolymer as the conversion is varied.

A somewhat different situation occurs in the acrylamide–sodium ethylenesulfonate system.[76] Since the hydrophilic properties of these comonomers are similar, one can postulate that, in contrast to the first system with a cationic comonomer, in this case the composition of the monomer mixture in the polymer coil differs little from the average composition of the mixture. Here one should bear in mind that sodium ethylenesulfonate was fully ionised under the copolymerisation conditions in the above study[76] and was present in the form of free ions solvated by water molecules. This factor probably hinders the incorporation of charged ethylenesulfonate anions in the hydrophobic associated species, so that the monomer mixture in these species is enriched in acrylamide compared with the average composition of the initial monomer mixture.

The independence of the composition of the copolymer of the conversion has also been established in the emulsion copolymerisation of the hydrophobically modified salt of an aminoester of methacrylic acid with styrene or methyl methacrylate. The idea that the compositions of the monomer mixture within and outside the active zone are different as a consequence of the sorption of the more hydrophobic comonomers by the polymer coil was also invoked to account for this finding.[74]

VI. Conclusion

The results presented above demonstrate convincingly that the nature of the solvent is an important factor determining the course of the radical polymerisation of water-soluble monomers. The influence of the solvent is significantly greater in the case of water-soluble monomers than in the case of the radical polymerisation of weakly polar monomers such as, for example, styrene. An especially large change in the overall rate of the reaction and in the constant k_p is observed on passing from polymerisation in organic solvents to polymerisation in an aqueous solution.

The influence of the nature of the solvent may be attributed to a number of causes, among which the following should be noted primariliy:

(1) The formation of donor–acceptor complexes between the polymeric radicals and the solvent molecules, which decreases the reactivity of the radicals.

(2) The solvation of the monomer molecules and the polymeric radicals or the specific interaction of these species with solvent molecules, in particular via the formation of hydrogen bonds, which alter the electron density in the C=C bond of the monomer or the unpaired electron density in the radical and hence alter the reactivity of the reacting species.

(3) The changes in the conformational characteristics of the polymer molecules in solvents possessing different solvent powers in relation to the polymer.

However, in our view, a distinctive feature of the polymerisation of water-soluble monomers is the hydrophobic interaction arising in aqueous solutions of the polymers. It leads to a sharp difference between the kinetic parameters of the polymerisation of monomers of this class in water and in solutions in organic solvents. The hydrophobic interaction is also responsible for the appreciable decrease in the rate of polymerisation and in the constant k_p following the addition of even small amounts of an organic solvent to water as a consequence of the preferential sorption of the organic solvent by the polymer coil.

Naturally, the formation of interchain associated species as a result of the hydrophobic interactions and hence their "catalytic" effect must depend on the hydrophobic properties of the monomers employed.

A fairly large number of studies devoted to the rheological properties of aqueous solutions of hydrophobically modified polymers have been published recently. However, there are virtually no data on the kinetics of the polymerisation of water-soluble monomers containing hydrophobic groups. At the same time, we believe that, in order to confirm the influence of the hydrophobic effect on the radical polymerisation of water-soluble monomers, it is necessary to expand the range of systems investigated, especially water-soluble monomers containing hydrophobic groups. The study of the polymerisation of monomers of this kind in water, organic solvents, and water–organic solvent mixtures of different composition will yield additional information about the role of hydrophobic interactions in radical polymerisation in aqueous solutions.

This review has been written with the financial support of the International Scientific Fund (Grant No. M8R000) and the Russian Fundamental Research Fund (Grant No. 93–03–1976).

References

1. C H Bamford, W J Barb, A D Jenkins, P F Onyon *The Kinetics of Vinyl Polymerization by Radical Mechanisms* (London: Butterworth, 1958) (Translated into Russian; Moscow: Inostr. Lit., 1961)
2. Kh S Bagdasar'yan *Teoriya Radikal'noi Polimerizatsii* (Theory of Radical Polymerisation) (Moscow: Nauka, 1966)
3. G Henrici-Olive, S Olive *Makromol. Chem.* **68** 219 (1963)
4. G Henrici-Olive, S Olive *Z. Phys. Chem.* **47** 286 (1965)
5. G Henrici-Olive, S Olive *Z. Phys. Chem.* **48** 35 (1966)
6. C H Bamford, S Brumby *Makromol. Chem.* **105** 122 (1967)
7. V A Kabanov *Usp. Khim.* **36** 217 (1967) [*Russ. Chem. Rev.* **36** 75 (1967)]
8. Yu L Spirin *Usp. Khim.* **38** 1201 (1969) [*Russ. Chem. Rev.* **38** 529 (1969)]
9. A N Pravednikov, S N Novikov *Vysokomol. Soedin., Ser. A* **13** 1404 (1971)
10. E White, M Zissel *J. Polym. Sci., Polym. Chem. Ed.* **1** 2181 (1963)
11. G M Burnett, G G Cameron, S N Joiner *J. Chem. Soc., Faraday Trans. 1* **69** 322 (1973)
12. J Barton, J Capek, V Juranicova, M Mlynarova *Makromol. Chem.* **181** 1289 (1980)
13. M Kamachi *Adv. Polym. Sci.* **38** 56 (1981)
14. M Kamachi *J. Polym. Sci., Polym. Chem. Ed.* **20** 1489 (1982)
15. E L Madruga, J S Roman *Makromol. Chem., Rapid Commun.* **7** 307 (1986)
16. V A Kabanov, V P Zubov, Yu D Semchikov *Kompleksnoradikal'naya Polimerizatsiya* (Complex Radical Polymerisation) (Moscow: Khimiya, 1987)
17. V F Gromov, P M Khomikovskii *Usp. Khim.* **48** 1943 (1979) [*Russ. Chem. Rev.* **48** 1040 (1979)]
18. V A Kabanov, D A Topchiev *Polimerizatsiya Ionizuyushchikhsya Monomerov* (Polymerisation of Ionisable Monomers) (Moscow: Nauka, 1975)
19. E V Bune, A P Sheinker, E N Teleshov *Vysokomol. Soedin., Ser. A* **31** 1347 (1989)
20. R A M Thomson, in *Chemistry and Technology of Water-Soluble Polymers* (Ed. C A Finch) (New York: Plenum, 1983) p. 31
21. Yu L Spirin, T S Yatsemirskaya *Vysokomol. Soedin., Ser. B* **11** 515 (1969)
22. V A Agasandyan, E A Trosman, Kh S Bagdasar'yan, A D Litmanovich, V Ya Shtern *Vysokomol. Soedin.* **8** 1580 (1966)
23. E V Shtamm, Yu I Skurlatov, T M Karaputadze, Yu E Kirsh, A P Purmal' *Vysokomol. Soedin., Ser. B* **22** 420 (1980)
24. A I Martynenko, Candidate Thesis in Chemical Sciences, Institute of Petrochemical Synthesis, Russian Academy of Sciences, Moscow, 1981
25. A I Martynenko, R Ruziev, A V Nechaeva, A T Dzhalilov, D A Topchiev, V A Kabanov *Uzb. Khim. Zh.* (2) 59 (1979)
26. E V Bune, A P Sheinker, A L Izyumnikov, E D Rogozhkina, A D Abkin *Vysokomol. Soedin., Ser. A* **25** 93 (1983)
27. V F Gromov, Doctoral Thesis in Chemical Sciences, Karpov Physico-chemical Institute, Moscow, 1989
28. V F Gromov, N I Galperina, T O Osmanov, P M Khomikovskii, A D Abkin *Eur. Polym. J.* **16** 529 (1980)
29. M Kamachi, J Satoh, S Nosakura *J. Polym. Sci., Polym. Chem. Ed.* **16** 1789 (1978)
30. M Kamachi, D J Liaw, S Nosakura *Polym. J.* **11** 921 (1979)
31. T O Osmanov, V F Gromov, P M Khomikovskii, A D Abkin *Vysokomol. Soedin., Ser. B* **20** 263 (1978)
32. F S De Schryer, G Smets, G J van Thielen *J. Polym. Sci., Polym. Chem. Ed.* **6** 547 (1968)
33. E V Bune, Candidate Thesis in Chemical Sciences, Karpov Physico-chemical Institute, Moscow, 1981
34. T M Karaputadze, V I Shumskii, Yu E Kirsh *Vysokomol. Soedin., Ser. A* **20** 1854 (1978)
35. Yu E Kirsh, A I Kokorin, T M Karaputadze, L A Kazarin *Vysokomol. Soedin., Ser. B* **23** 444 (1981)
36. L A Tatarova, T G Ermakova, Al Al Berlin, E F Razvodovskii, V A Lopyrev, N Ya Kedrina, N S Enikolopov *Vysokomol. Soedin., Ser. A* **24** 2205 (1982)
37. G C Pimentel, A McClellan *The Hydrogen Bond* (Ed. L Pauling) (Translated into Russian; Moscow: Mir, 1964)
38. N I Gal'perina, Candidate Thesis in Chemical Sciences, Karpov Physicochemical Institute, Moscow, 1976
39. A L Buchachenko, O P Sukhanova *Usp. Khim.* **36** 474 (1967) [*Russ. Chem. Rev.* **36** 192 (1967)]
40. I L Zhuravleva, E V Bune, Yu S Bogachev, N N Shapet'ko, A P Sheiker, A D Abkin *Vysokomol. Soedin., Ser. A* **27** 380 (1985)
41. E V Bune, I L Zhuravleva, A P Sheinker, Yu S Bogachev, E N Teleshov *Vysokomol. Soedin., Ser. A* **28** 1279 (1986)
42. I L Zhuravleva, E V Bune, Yu S Bogachev, A P Sheinker, E N Teleshov *Zh. Org. Khim.* **23** 2326 (1987)
43. Yu S Bogachev, I L Zhuravleva, V F Gromov, E V Bune, E N Teleshov *Zh. Fiz. Khim.* **64** 154 (1990)
44. V A Palm *Osnovy Kolichestvennoi Teorii Organicheskikh Reaktsii* (Fundamentals of a Quantitative Theory of Organic Reactions) (Translated into Russian; Leningrad: Khimiya, 1977)
45. A V Chernobai, A V Grinakovskaya *Izv. Vyssh. Uchebn. Zaved., Khim. Khim. Tekhnol.* **25** 1131 (1982)
46. I L Zhuravleva, E N Zav'yalova, Yu S Bogachev, V F Gromov *Vysokomol. Soedin., Ser. A* **28** 873 (1986)
47. G Miyajima, K Takahashi, K Nishimoto *Org. Magn. Reson.* **8** 413 (1974)
48. W Holzmuller *Plast. Kautsch.* **20** 121 (1973)
49. S Schlick, P A Narayana, L Kevan *J. Am. Chem. Soc.* **100** 3322 (1978)
50. V M Sutyagin, V P Lopatinskii, V D Filimonov *Vysokomol. Soedin., Ser. A* **24** 1968 (1982)
51. Yu D Semchikov, V F Gromov, E N Teleshov *Vysokomol. Soedin., Ser. A* **33** 1442 (1991)
52. T O Osmanov, V F Gromov, P M Khomikovskii, A D Abkin *Dokl. Akad. Nauk SSSR* **240** 910 (1978)
53. E V Bune, A P Sheinker, N V Kozlova, A D Abkin *Vysokomol. Soedin., Ser. A* **23** 1841 (1981)
54. S I Klenin, E N Bykova, I A Baranovskaya, V A Molotkov, V I Kurlyankina, in *Tezisy Dokladov 20 Nauchnoi Konferentsii po Khimii i Fizike Vysokomolekulyarnykh Soedinenii, Leningrad, 1983* (Abstracts of Reports at the 20th Scientific Conference on the Chemistry and Physics of High-Molecular-Mass Compounds, Leningrad, 1983) p. 5; *Ref. Zh. Khim.* 16 S 62 (1983)
55. V F Gromov, Yu S Bogachev, E V Bune, I L Zhuravleva, E N Teleshov *Dokl. Akad. Nauk SSSR* **309** 871 (1989)
56. V F Gromov, Yu S Bogachev, Ye V Bune, I L Zhuravleva, E N Teleshov *Eur. Polym. J.* **27** 505 (1991)
57. Yu S Bogachev, E V Bune, V F Gromov, I L Zhuravleva, E N Teleshov *Vysokomol. Soedin., Ser. A* **33** 1464 (1991)
58. Ye V Bune, A P Sheinker, Yu S Bogachev, I L Zhuravleva, E N Teleshov *Eur. Polym. J.* **27** 509 (1991)
59. M N Savitskaya, Yu D Kholodova *Poliakrilamid* (Polyacrylamide) (Kiev: Tekhnika, 1969)
60. F Franks, in *Chemistry and Technology of Water-Soluble Polymers* (Ed. C A Finch) (New York: Plenum, 1983) p. 157
61. D E Graham, in *Chemistry and Technology of Water-Soluble Polymers* (Ed. C A Finch) (New York: Plenum, 1983) p. 321
62. V F Gromov, E N Teleshov *Plast. Massy* (10) 9 (1984)
63. C L McCormick, R D Hester, S E Morgan, A M Safieddine *Macromolecules* **23** 2124 (1990)
64. C L McCormick, T Nonaka, C B Johnson *Polymer* **29** 731 (1988)
65. F M Winnik, A R Davidson, G R Hammer *Macromolecules* **25** 1876 (1992)
66. H Ringsdorf, J Simon, F M Winnik *Macromolecules* **25** 5353 (1992)
67. C L McCormick, C E Hoyle, M D Clark *Macromolecules* **24** 2397 (1991)
68. S A Ezzel, C L McCormick *Macromolecules* **25** 1881 (1992)
69. S A Ezzel, C E Hoyle, M D Clark, C L McCormick *Macromolecules* **25** 1887 (1992)
70. A Yekta, J Duhamel, P Brochard, H Adiwidjaja, M A Winnik *Macromolecules* **26** 1829 (1993)
71. C Maecheling-Strasser, J Francois, F Cloudet *Polymer* **33** 627 (1992)
72. I V Berezin, K Martinek, A K Yatsimirskii *Usp. Khim.* **42** 1729 (1973) [*Russ. Chem. Rev.* **42** 787 (1973)]
73. F M Winnik, M F Ottaviani, S H Bossmann, M Garcia-Garibay, N J Turro *Macromolecules* **25** 6007 (1992)
74. K Nagai, J Fujii, N Kuramoto *Polymer* **33** 3060 (1992)
75. V F Gromov, Yu S Bogachev, E V Bune, I L Zhuravleva, E N Teleshov *Polym. Sci.* **35** 3 (1993)
76. A I Baranova, V F Gromov, E V Bune, Yu S Bogachev, N V Kozlova, E N Teleshov *Polym. Sci.* **36** (1994) in the press

Russian Chemical Reviews **63** (6) 519 – 531 (1994)
©1994 Russian Academy of Sciences and Turpion Ltd

UDC 547.514.472.1 + 547.313

Marine prostanoids

M S Miftakhov, M E Adler, F A Akbutina, G A Tolstikov

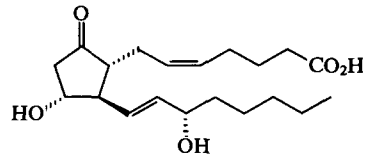
Contents

I. Introduction	519
II. Biosynthesis of marine prostanoids	521
III. Chemical syntheses of marine prostanoids	523
IV. Analogues of marine prostanoids	528
V. Biological properties of marine prostanoids	529

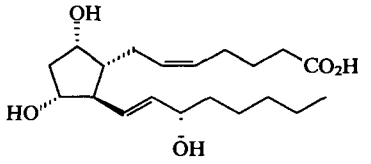
Abstract. The review describes the stages involving the isolation and the determination of the structures of marine prostanoids and their analogues, the problems of their biosynthesis, and their biological properties. The bibliography includes 76 references.

I. Introduction

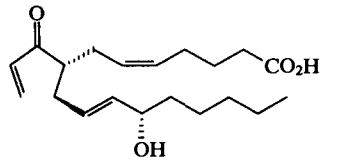
Prostaglandins (PG) were first discovered in the human seminal fluid by Kurzrok and Lieb[1] in 1930, but it was not until the beginning of the 1960s that Bergstrom and his coworkers[2–4] were able to isolate and identify a series of the main representatives of compounds of this class on the basis of the researches by Euler, who was Bergstrom's teacher. The structural formulae of the commonest series 2 prostaglandins are presented below.



PGE_2



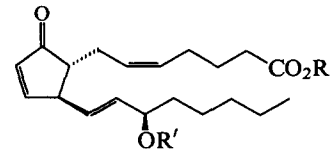
$PGF_{2\alpha}$



PGA_2

We may note that the content of total prostaglandins (more than ten prostaglandins of different types) in a rich source such as the plasma of human seminal fluid is only 300 μg ml^{-1}.[5] After the development of effective methods for the detection, isolation, and the determination of their structure, prostaglandins of different types and series as well as their derivatives were found at extremely low concentrations in virtually all mammalian organs and tissues and then in insects, plants, etc. (see the relevant reviews [6–10]).

Marine organisms, which are promising in this respect, did not prove an exception either. A major achievement of the period was the communication by Weinheimer and Sparings concerning the isolation of (15*R*)-PGA_2 (derivatives **1** and **2**) in 0.2% and 1.3% yields respectively from the coral *Plexaura homomalla*, which is common in the Caribbean Sea.[11] As can be seen from their structures, compounds **1** and **2** are the epimers of PGA_2 with respect to the allylic–alcoholic centre [C(15)] and they therefore lack the powerful hypotensive effects characteristic of PGA_2. Other workers[12] also isolated from corals of this species (15*R*)-PGE_2 and its ethyl ether in 0.1% – 0.2% yields. On the other hand, certain colonies of *Plexaura homomalla* contained only (15*S*)-prostaglandins identical to those isolated from mammals, while others contained approximately equal amounts of (15*R*)- and (15*S*)-PG.[13] Reasonable explanations of the lack of selectivity in the production of (15*R*)- and (15*S*)-PG by the coral were not proposed. Analysis of the lipids from both (15*R*)- and (15*S*)-prostaglandin-containing variants of *Plexaura homomalla* showed that 97% of the $C_{20:4}$ acid component comprises arachidonic acid. Therefore the formation of the (15*R*)-prostaglandins in some colonies of *Plexaura homomalla* and of (15*S*)-prostaglandins in other taxonomically identical colonies cannot be accounted for by the stereochemical differences between the initial $C_{20:4}$ acids.[14]



1, R = R′ = H
2, R = Me, R′ = Ac

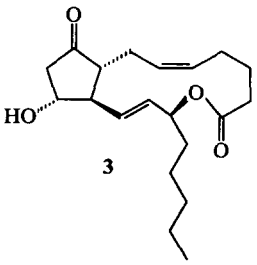
Schneider and coworkers[15,16] found 0.06% of PGE_2, traces of $PGF_{2\alpha}$, 13,14-dihydro-PGA_2, 5-*trans*-PGA_2, and other substances in Caribbean corals. Only insignificant amounts of (15*S*)-PG were discovered in specimens of *Plexaura homomalla* collected in the sea around Florida.[12] It was found that PGE_2 and $PGF_{2\alpha}$ are the most frequently encountered prostanoids in the marine organisms—coral, molluscs, seaweed, etc. Thus prostaglandin $F_{2\alpha}$, the 11-acetate of the methyl ester of $PGF_{2\alpha}$, and its 18-acetoxy-derivative were isolated from the soft

M S Miftakhov, M E Adler, F A Akbutina Laboratory for the Synthesis of Low-Molecular-Weight Bioregulators, Institute of Organic Chemistry
G A Tolstikov Institute of Organic Chemistry,
Ufa Scientific Centre, Russian Academy of Sciences, pr. Oktyabrya 71, 450054 Ufa, Russian Federation. Fax (7-347) 235 60 66

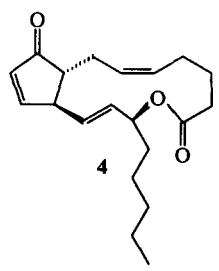
Received 31 May 1993
Uspekhi Khimii **63** (6) 543 – 556 (1994); translated by A K Grzybowski

coral *Lobophyton depressum*[17] and from the tissues of the molluscs *Tethys timbria* and *Aglisia californica*.[10] The content of PGE_2 in the Australian red seaweed *Gracularia lichenoides* is 0.05%–0.07% of the dry mass.[18] $PGF_{2\alpha}$ and 6-keto-$PGF_{1\alpha}$ were isolated together with PGE_2 from the aqueous extracts of the sea sponge *Teprios zeteki*.[19]

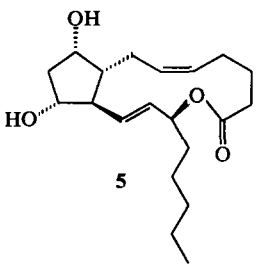
The 1,15-lactones of prostaglandins E_2, A_2, and $F_{2\alpha}$ (compounds **3**–**5**) and a series of their acyl derivatives, isolated from the tissues of the mollusc *Tethys timbria*, are of interest.[20] An unusual lactone **6**, related to prostanoids and called hybridalactone, was isolated from the red seaweed *Laurencia hybrida*. A mechanism of its biosynthesis from eicosapentaenoic acid has been postulated.[21] The structure of hybridalactone was confirmed by spectroscopic data and unambiguous synthesis.[22]



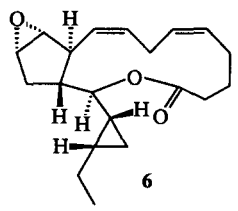
3



4



5

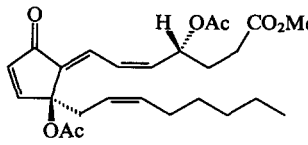


6

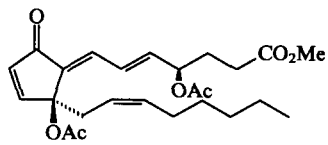
In order to identify the prostaglandins in the extracts from marine organisms, use was made of methods for their biological testing and their comparison with authentic specimens, immunochromatography and radioimmunology, thin-layer chromatography combined with biological testing for prostaglandin-like activity, etc.[10]

On the whole, it appears important that the above prostaglandins were detected and isolated in relatively large amounts from primitive nonmammalian sources (in contrast to mammals, in the tissues of which the content of prostaglandin does not exceed 1–2 ng g^{-1}, marine organisms are able to accumulate prostaglandins). The (15*R*)- and (15*S*)-PGA_2 substances produced by coral can be readily transformed chemically into prostaglandins of types E and F, which were used in its turn for the industrial manufacture of prostaglandins.[23] Several hypotheses concerning the biological functions of coral prostaglandins, including regulation of the ion and water transport in the coral as well as its protection against predators and parasites, have been put forward.

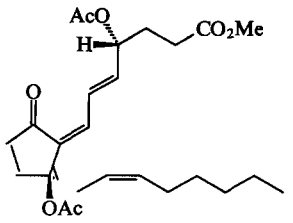
A group of Japanese scientists[24,25] published almost simultaneously in 1982 the results of studies devoted to the isolation from marine organisms and the determination of the structures of new prostanoids, which attracted attention because of their unusual structure and their antitumour activity. The prostanoids of this type detected in the corals of the Stolonifer *Clavularia virides* species were called clavulones by Yamada and coworkers.[24] Numerals ranging from I to IV were assigned, in order of decreasing polarity, to the related compounds **7**–**10** differing by the configuration of the double bonds at the C(5) and C(7) atoms. The names claviridenones D, C, B, and A, proposed for these structures by Kitagawa and coworkers[25] have not been widely used. Anticipating, we may note that clavulones and a series of similar structures — halovulones and punaglandins have been combined under the term marine prostanoids† in view of the unusual nature and uniqueness of their structures and this term also indicates the sources where they have been found and from which they have been isolated.



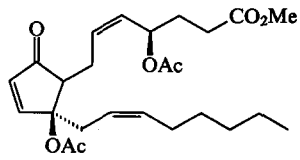
7, clavulone I



8, clavulone II



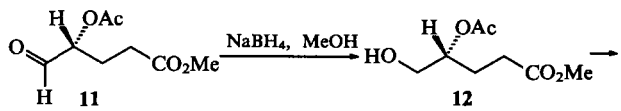
9, clavulone III



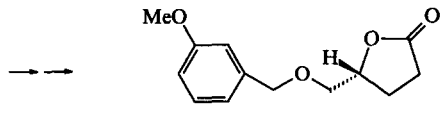
10, clavulone IV

The structure of the clavulones was established by thorough investigation of IR, UV, and ^1H and ^{13}C NMR spectroscopic data for these compounds, as well as of their chemical reactions. Additional evidence that compounds **7**–**10** are geometrical isomers was provided by the formation of the 1 : 6 : 12 : 2 mixture of all four compounds on UV irradiation of a benzene solution of any of these substances.[25] A similar result was achieved when one of the isomers was treated with a solution of oxalic acid in methanol (20 °C, 20 days).[26]

The absolute (*R*)-configuration of the C(4) chiral centre of clavulones was established by converting the aldehyde **11**, obtained by the ozonolytic cleavage of clavulone I, into the alcohol **12** and then into the lactone **13**, the enantiomer of which was obtained from the acetonide of D-glyceraldehyde.[26]



11 **12**

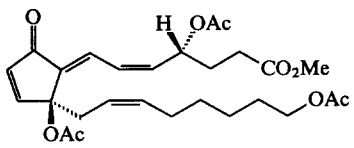


13

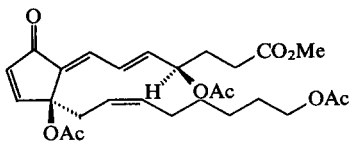
The study of ^1H NMR and circular dichroism spectra of the 9-(*p*-bromobenzoate) of clavulone I and its 12-deacetoxy-derivative established the (*S*)-configuration of the C(12) chiral centre.[26,27]

Subsequently three new C_{20}-acetoxyprostanoids **14**–**16** were isolated from the coral *Clavularia virides*.[28,29] Previously the C_{20}-hydroxyprostanoids were known as unstable prostaglandin metabolites detectable by gas–liquid chromatography or mass-spectrometrically. With the exception of the additional signal due to the CH_2OAc fragment, the spectroscopic characteristics of compounds **14**–**16** are identical with those of clavulones I–III, the absolute configuration of the chiral centres also remaining unchanged.

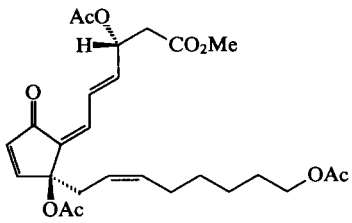
† As a consequence of a lack of appreciable structural differences from the classical prostaglandins isolated from mammals, it would be incorrect to combine the (15*R*)-PGA_2 and other prostaglandins (metabolites of C_{20} eicosapolyenoic acids) described previously with 'marine prostanoids' in terms of features defining this class. We shall therefore consider them only in terms of the historical aspect.



14

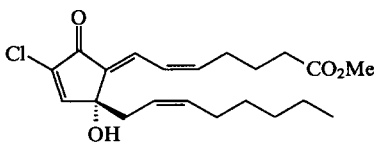


15

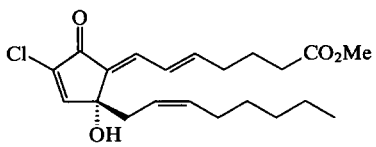


16

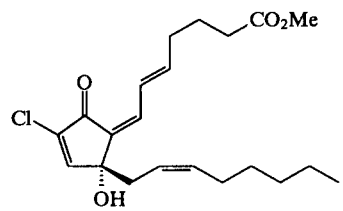
The next important stage of the studies on these lines was described in the communication published in 1985 concerning the isolation from *Clavularia virides* of 10-haloprostanoids exhibiting an anticancer activity—chlorovulones I–IV (compounds **17–20**).[30]



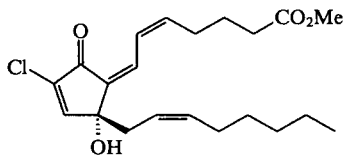
17, chlorovulone I



18, chlorovulone II



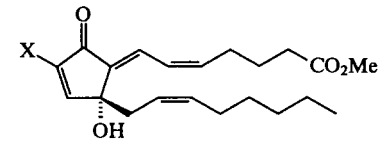
19, chlorovulone III



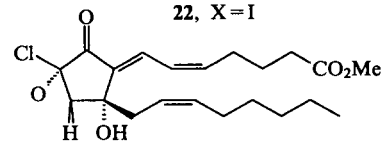
20, chlorovulone IV

The absolute configuration of the C(12) chiral centre in chlorovulones, determined from circular dichroism data of their derivatives and by comparing the spectroscopic characteristics as well as the specific angles of rotation of the natural chlorovulone II (compound **18**) and (−)-chlorovulone II obtained by enantioselective synthesis, was found to be the opposite of the configuration of the C(12) stereocentre of clavulones.[27]

In addition, prostanoids related to chlorovulones and containing Br and I atoms, which were called bromovulone I (compound **21**) and iodovulone I (compound **22**),[31,32] as well as the C(10,11)-epoxy-analogue **23**[33] were also identified among the series of compounds isolated from marine organisms. Like the parent chlorovulone I and clavulone I, they have the (5*Z*, 7*E*, 14*Z*)-configuration of the double bonds in the side chains.

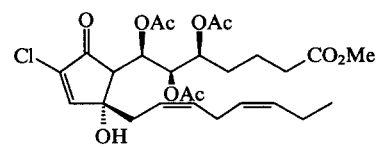


21, X = Br
22, X = I

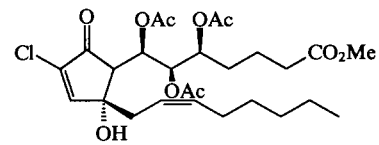


23

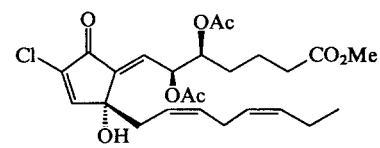
Representatives of halogenated eicosanoids with a more complex structure were isolated from the octocorals of the *Telesto riisei* species.[34,35] They have been called punaglandins I–IV (compounds **24–27**). The presence of vicinal acetate groups at the C(5) and C(6) atoms is characteristic of these compounds. The (*R*)-configuration of the C(12) chiral centre, refined by means of enantioselective synthesis, proved to be the opposite of that proposed initially and characteristic of clavulones.[35,36]



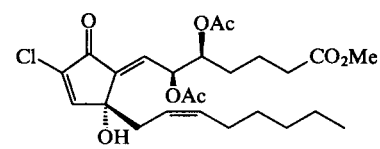
24, punaglandin I



25, punaglandin II



26, punaglandin III



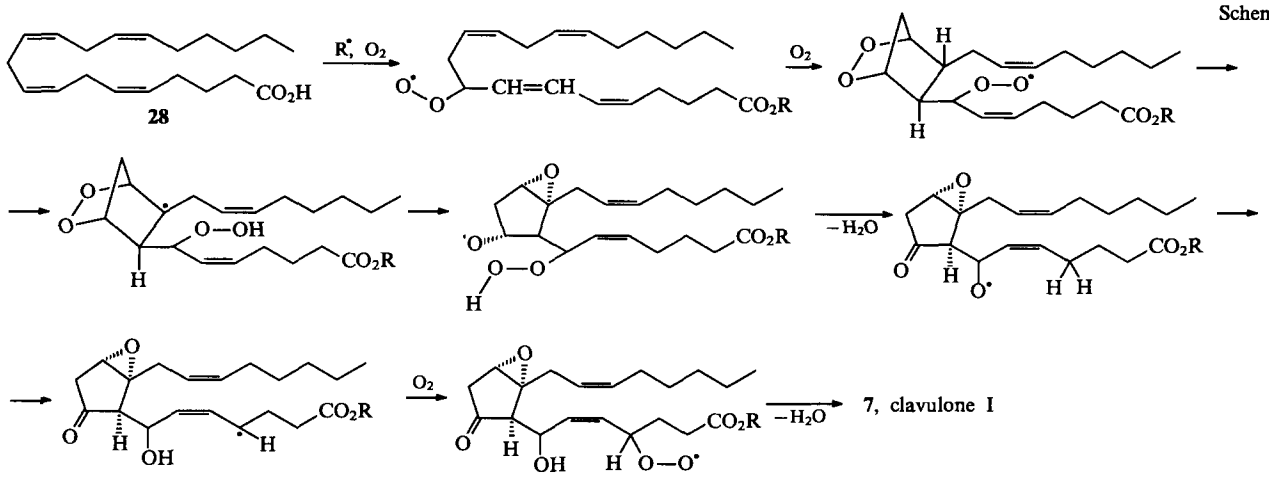
27, punaglandin IV

II. Biosynthesis of marine prostanoids

Arachidonic acid **28** is known to be synthesised by the 'endoperoxide pathway'. Initially Corey et al.[38] put forward the hypothesis that the biosynthesis of clavulones proceeds via a similar mechanism and that the key stage in this process is the ready transformation of the β-peroxyl radicals into cyclopentane epoxyketo-derivatives, which are formed as a result of the intramolecular attack by the radical on the nearest peroxide oxygen atom (Scheme 1, see over).

Somewhat later it was observed that, when arachidonic acid is treated with a homogenate of the coral of the *Clavularia virides* or *Pseudoplexaura porosa* species, the habitats of which are extremely remote from one another, a new eicosanoid **29**, called preclavulone A (PC-A), is formed.[35,39,40] Its structural similarity to 12-oxophytodienoic and *cis*-jasmonic acids suggested the similarity of the pathways leading to their biosynthesis, probably via a cationic mechanism through 8-hydroperoxyeicosatetraenoic acid [(8*R*)-HPETE] **30**, the allene oxide **31**, and the oxypentadienyl

Scheme 1

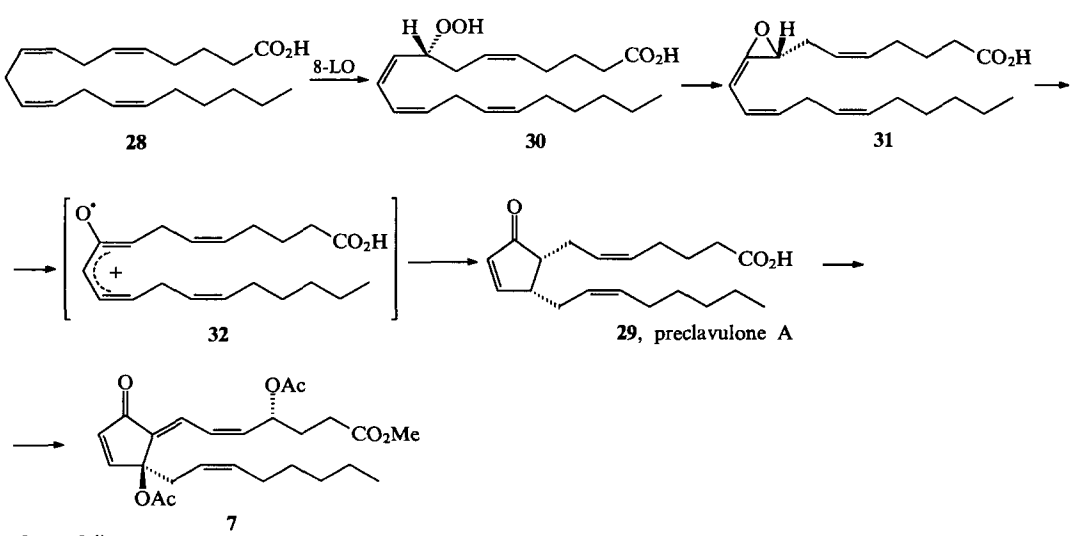


cation **32**.[40-42] Next, as a result of the successive enzymic hydroxylation of the C(4), C(7), and C(11) atoms, exhaustive acylation, and the elimination of the AcO group to the C(7) atom, preclavulone A is converted into clavulones (Scheme 2).

The formation of preclavulone A when the coral homogenate is kept in contact with tritium-labelled (8*R*)-HPETE confirms that the acid **30** is an intermediate in the biosynthesis of PC-A from arachidonic acid (radiochemical yield up to 13%).[42] The biosynthesis of PGA_2 in corals of the *Plexaura homomalla* species, which is known to be the richest source of prostaglandins (up to 2% of the dry residue), can take place via a similar chain of reactions (Scheme 3) from the acid **28** via the allene oxide **33**.[43] Thus, from the evolutionary point of view, the possibility of the biosynthesis of protanoids in mammals and marine organisms via different pathways is surprising.

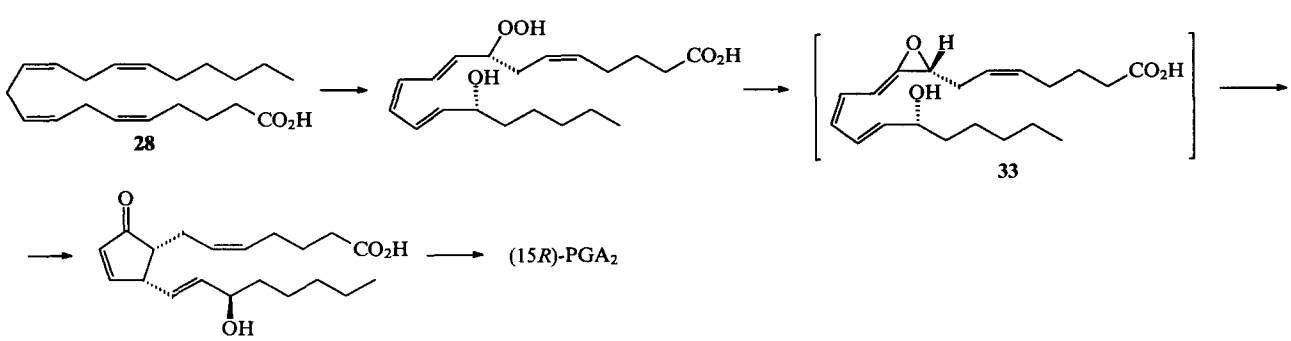
As already mentioned, the biomimetic synthesis of PC-A achieved by Corey[40] confirms the possibility, in principle, of the 'marine' pathway to the biosynthesis of prostanoids. The absolute configuration of the chiral centres of PC-A was established by the enantioselective synthesis of the methyl ester of (−)-preclavulone A.[44] The Cope rearrangement of the trimethylsilyl ether of the enone **34** undoubtedly constitutes a rational way of constructing the structures of the *cis*-joined tetrahydroindenes **35** and of achieving the synthesis of the key cyclopentanone derivative **36** with the required orientation and chemodifferentiation of the side substituents. The subsequent operations are standard and are well known from the chemistry of prostaglandins (Scheme 4).

Scheme 2

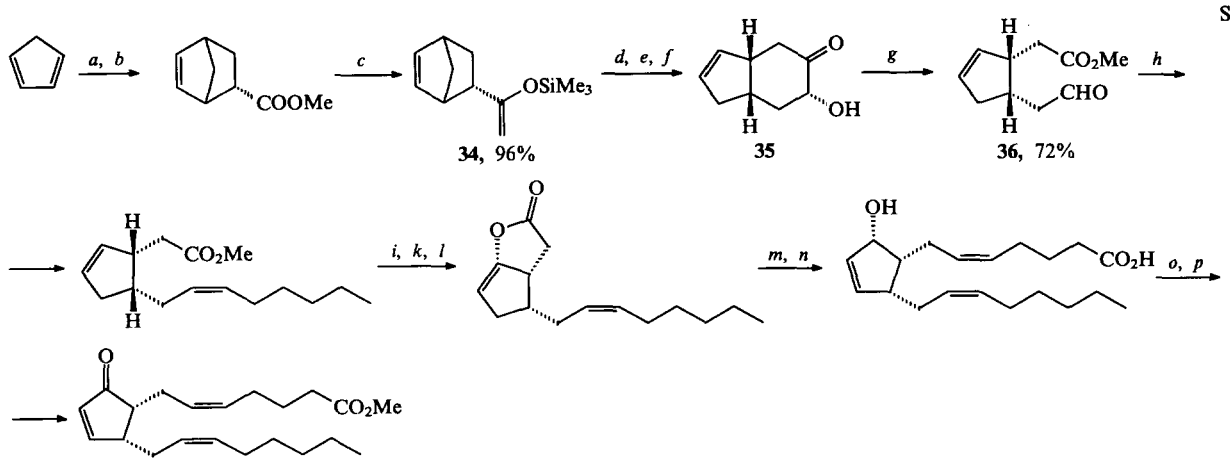


8-LO = 8-lipoxygenase.

Scheme 3



Scheme 4

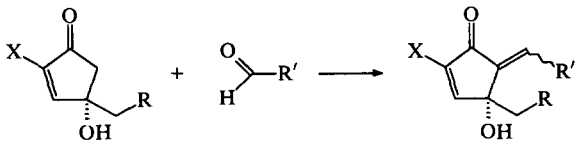


29a

(*a*) Acrylate of (*R*)-pentalactone, $TiCl_4$; (*b*) 3 equiv. of MeLi, from −25 to 0 °C, 1 h; (*c*) 2 equiv. of lithium diisopropylamide (LDA), 2.3 equiv. of Me_3SiCl, THF, −78 °C, 1.5 h; (*d*) 200 °C, toluene, 4 h; (*e*) 1.1 equiv. of *m*-$ClC_6H_4CO_3H$, 4 equiv. of $NaHCO_3$, CH_2Cl_2, −5 °C, 1 h; (*f*) 5 equiv. of 48% aqueous HF, 5 equiv. of NEt_3; (*g*) $Pb(OAc)_4$, MeOH, −5 °C, 1 h; (*h*) 1.6 equiv. of $Ph_3PC_6H_{13}Br$, 1.5 equiv. of sodio-derivatives of hexamethyldisilazane (HMDS-Na), THF, from −85 to 0 °C; (*i*) 1 M LiOH, H_2O–MeOH–THF (4 : 3 : 5), 23 °C, 24 h; (*k*) 3 equiv. of I_2, 5% aqueous $NaHCO_3$–THF, 0 °C, 2.5 h; (*l*) 2 equiv. of 1.5-diazabicyclo[5.4.0]undec-5-ene (DBU), dimethoxyethane (DME), refluxing for 12 h; (*m*) 2 equiv. of diisobutylaluminium hydride (DIBAH), CH_2Cl_2, −78 °C, 40 min; (*n*) $BrPPh_3(CH_2)_4CO_2H$, HMDS-Na, THF, 25 °C 2 h; (*o*) CH_2N_2, ether; (*p*) [O], CH_2Cl_2, 23 °C, 1 h.

III. Chemical syntheses of marine prostanoids

The stages involving the formation of the tertiary alcohol cyclopentane unit with a lower chain and the introduction of the polyoxygenated α-chain with an *exo*-methylene bond via the condensation of the enolate of the ketone **37** with the aldehyde **38** having the required structure are the most characteristic in the syntheses of marine prostanoids.



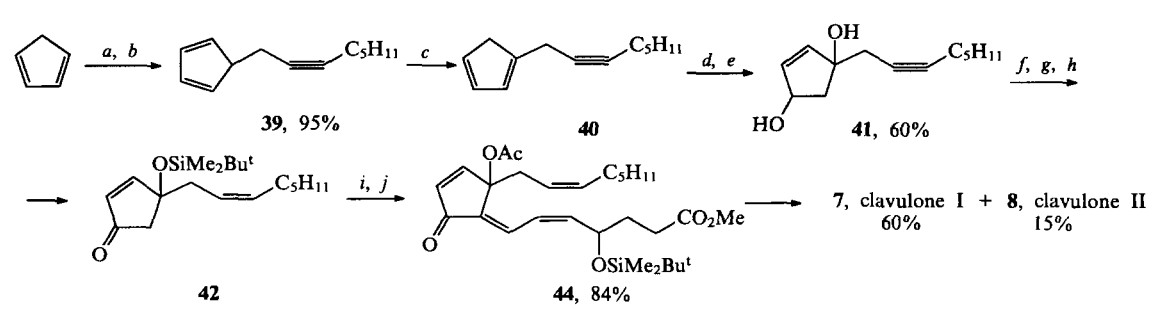
37, X = H, Cl **38**

Corey and coworkers[45] were the first to achieve the total synthesis of the racemic clavulone I. A synthetic scheme starting from cyclopentadiene is presented below.

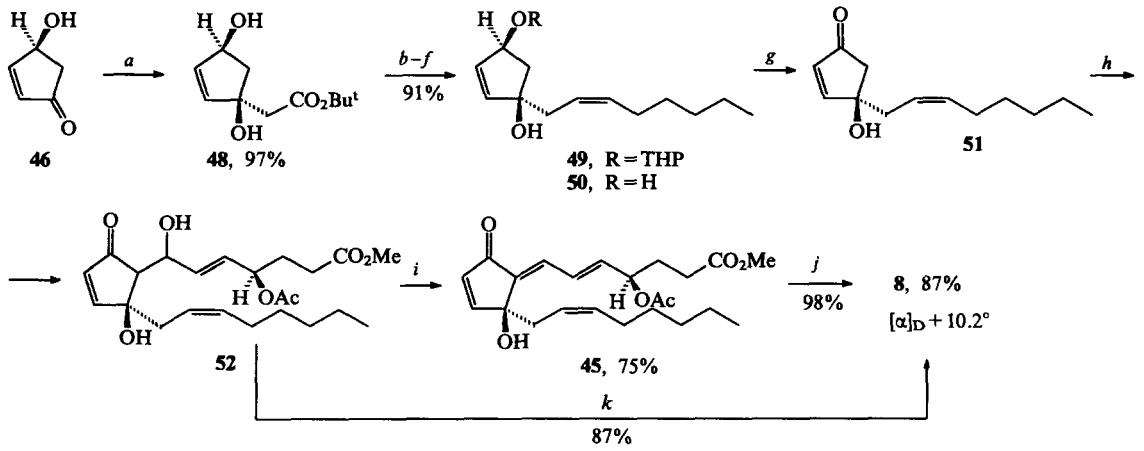
2-Alkylcyclopentadiene **40** was obtained by alkylating cyclopentadienyllithium with 1-iodooct-2-yne and subsequent 1,5-sigmatropic isomerisation of compound **39** under mild conditions. The key stage — photochemical oxidation of the diene **40** and the reduction of the intermediate endoperoxide by treatment with $NaBH_4$ — led to the diol **41**, which was converted by standard procedures into the synthon **42**. The second important stage — the condensation of the ketone enolate **42** with the aldehydoester **43** and the selective replacement of the Bu^tMe_2Si group protecting the tertiary hydroxyl by Ac — led to a mixture of the diastereoisomers **44** in proportions of 1 : 1, which was separated by column chromatography on SiO_2. The ^1H NMR spectrum confirmed the complete absence of the (7,8-*Z*) isomer. The less polar isomer was then smoothly transformed into a mixture of clavulones I and II, which were isolated by column chromatography on silica gel in 60% and 15% yields respectively and were identical as regards spectroscopic and chromatographic characteristics with the natural specimens.

The first enantioselective and stereoselective synthesis of clavulone II and of its 12-*O*-deacetyl derivative **45** has been described by Nagaoka et al.[46] The strategy of the synthesis is analogous to that presented above and consists in the successive introduction of the α-chain and of the chiral α,β-unsaturated aldehyde **47**, obtained from D-(+)-mannitol, into the structure of the optically active cyclopentenone **46** (Scheme 5).

The *cis*-diol **48** has been obtained with a high stereoselectivity by the interaction of (4*S*)-hydroxycyclopentenone **46** with the lithium enolate of *tert*-butyl acetate. The subsequent stages involving the blocking of the alcoholic groups, the conversion of the ester group into an aldehyde group, and the Wittig reaction, led to the alkene **49** in high yields. The oxidation of the diol **50** by Corey's reagent and condensation of the lithium enolate of the enone **51** with the aldehyde **47** afforded a diastereoisomeric



(*a*) BuLi, C_5H_{12}–THF; (*b*) 1.1 equiv. of $ICH_2C{\equiv}CC_5H_{11}$, from −78 to 30 °C, 3 h; (*c*) 23 °C, 4 h; (*d*) 0 °C, *hv*, MeOH, −40 °C, 2 h; (*e*) $NaBH_4$, MeOH; (*f*) pyridinium chlorochromate (PCC), CH_2Cl_2, 23 °C, 2 h; (*g*) H_2, $Pd/CaCO_3$, EtOAc–Py (9 : 1); (*h*) 2 equiv. of Bu^tMe_2SiCl, 3.5 equiv. of 2.6-lutidine, CH_2Cl_2, from 0 to 23 °C, 2.5 h; (*i*) LDA, THF, −78 °C, 5 min; (*j*) HOCCH=CHCH[OSi(Me$_2$)Bu^t]$CH_2CH_2CO_2Me$ **43**, from −78 to 10 °C, 6 h; (*k*) 5 equiv. of Bu_4^nNF, 20 equiv. of Ac_2O, 3 equiv. of 4-dimethylaminopyridine (4-DMAP), from 0 to 23 °C, 30 min; (*l*) column chromatography on SiO_2, Et_2O–C_6H_6 (6 : 4).



Scheme 5

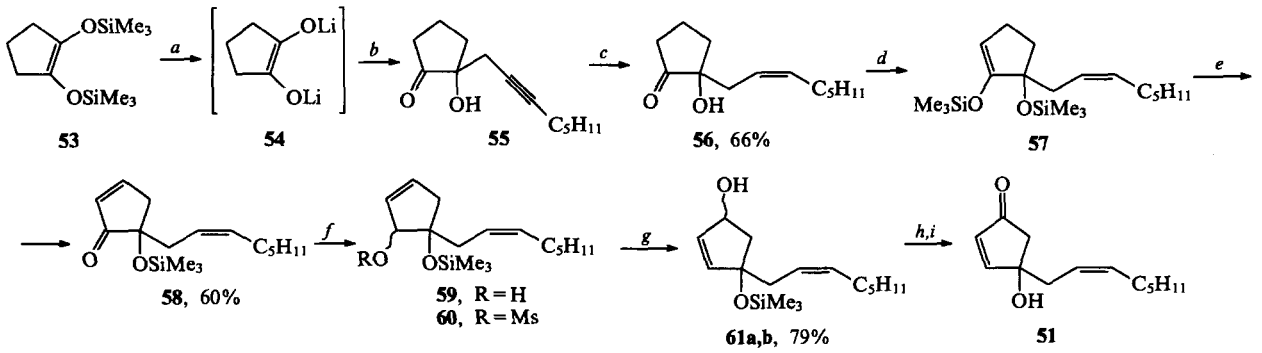
(*a*) $MeCO_2Bu^t$, LDA, THF, −78 °C; (*b*) dihydropyran (DHP), camphorsulfonic acid, Et_2O, 0 °C; (*c*) $LiAlH_4$, Et_2O, 20 °C; (*d*) DMSO–$(COCl)_2$, CH_2Cl_2, −78 °C, NEt_3; (*e*) $Ph_3PC_6H_{13}Br$, Bu^nLi, THF–HMPTA (hexamethylphosphoramide), −40 °C; (*f*) AcOH–H_2O (4 : 1); (*g*) PCC, molecular sieves (3 Å), CH_2Cl_2, 20 °C; (*h*) LDA, THF, −78 °C, HOCCH=CHCH(OAc)$CH_2CH_2CO_2Me$ **47**; (*i*) MsCl [Ms = methanesulfonyl (Translator)], NEt_3, CH_2Cl_2; (*j*) Ac_2O, Py, 30 °C; (*k*) Ac_2O, Py, 50 °C.

mixture of the alcohols **52**, the methanesulfonates of which are converted into 12-*O*-deacetylclavulone **45** on treatment with NEt_3. Standard acetylation of the latter afforded (+)-clavulone II, all the characteristics of which were identical with those of an authentic specimen of the natural product.

A fundamentally different pathway leading to the synthon **51** from the disilyl ether **53** has been proposed.[47] The key stage in this scheme—the interaction of the dilithium derivative of the 1,2-enediol **54** with 1-bromooct-2-yne, leading to a satisfactory yield of the hydroxyketone **55**, merits attention. Next, the ketoalcohol **56**, obtained by partial hydrogenation, is converted into the silyl ether of the enol **57**, which is oxidised by treatment with $Pd(OAc)_2$ in acetonitrile to the enone **58**. The boron hydride reduction of the latter, the methanesulfonation of the resulting allyl alcohol **59**, and subsequent hydrolysis of the methanesulfonate **60** afford a diastereoisomeric mixture of allyl alcohols **61a, b** in proportions of 1 : 1. The transformation of the enone **58** into an alcohol, formally regarded as 1,3-transfer of the oxygen-containing functional group, is possible as a consequence of the unidirectionality of the stages involving the hydrolysis and inversion of the sterically hindered allyl methanesulfonate **60**. The Collins oxidation of the alcohol **61** with subsequent hydrolysis of the protecting groups completes the synthesis of the enone **51**.

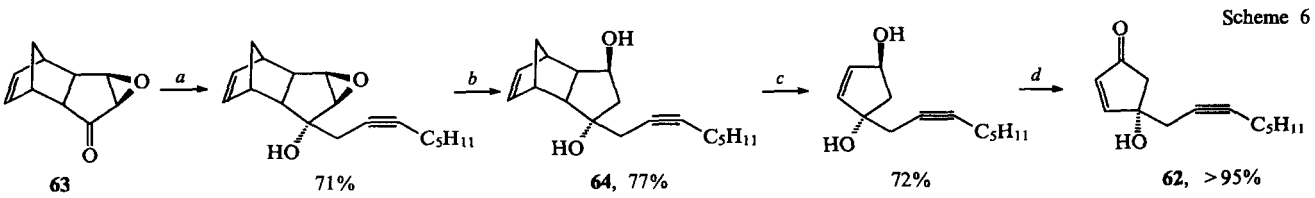
The acetylenic enone **62** described above, which is the equivalent of the synthon **51**, was obtained from the epoxyketone **63**, which is formed readily in its turn from *endo*-dicyclopentadiene.[48] The key stage in this scheme is the vacuum flash pyrolysis of the norbornene derivative **64** (Scheme 6).

The effective stereospecific synthesis of clavulones from Corey's lactone—a synthon popular in the synthesis of prostaglandins—is of special interest.[49] The polyfunctionalised cyclopentane synthon **65** is an extremely rational starting compound for the construction of the of clavulone structure. The main problem in work involving this compound is the stereoselective introduction of the C(12)-hydroxy-group. For this purpose, Corey's lactone was converted via the α,β-unsaturated lactone **66** into the allyl alcohol **67** and then into the epoxide **68**



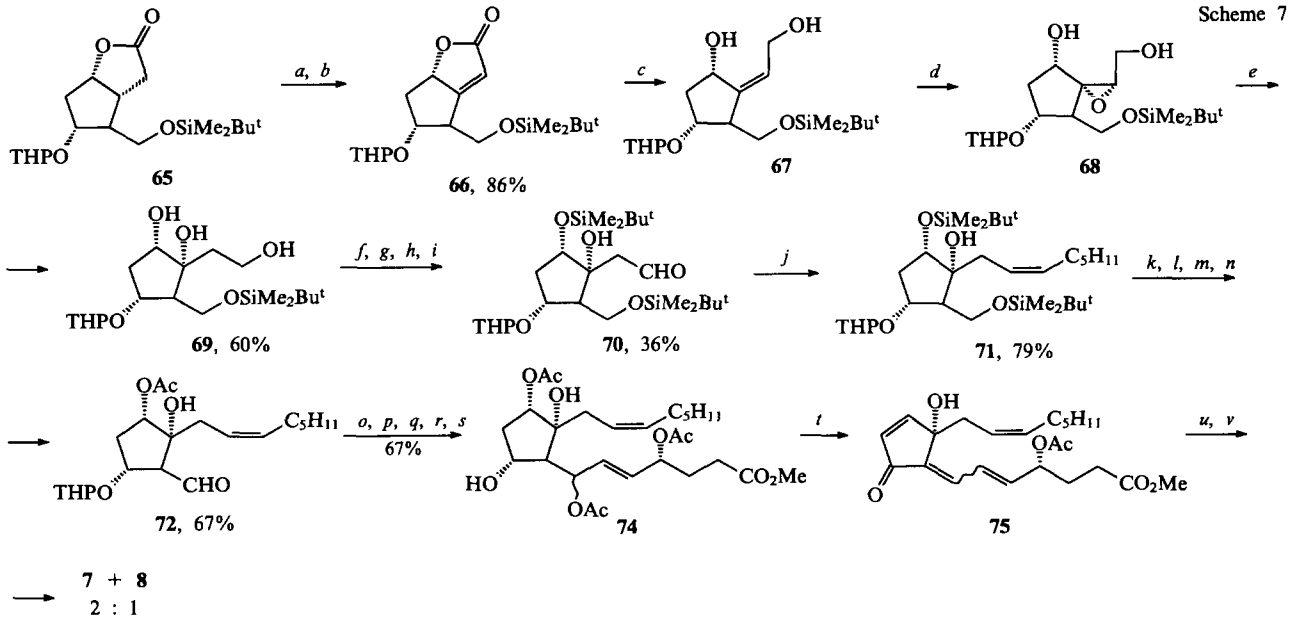
(*a*) MeLi, DME, Et_2O, −20 °C; (*b*) $BrCH_2C{\equiv}CC_5H_{11}$, HMPA, DME, −25 °C; (*c*) Lindlar H_2 catalyst, C_6H_{12}, 20 °C; (*d*) Me_3SiOTf [Tf = trifluoromethanesulfonate (Translator)], 2,6-Butidine, CH_2Cl_2, 25 °C; (*e*) $Pd(Ac)_2$, AcCN, 20 °C; (*f*) $NaBH_4$, $CeCl_3$, MeOH, 0 °C, Ms_2O, Py, 4-DMAP, CH_2Cl_2, 0 °C; (*g*) H_2O, Me_2CO, 25 °C; (*h*) $CrO_3.2Py$, CH_2Cl_2, 0 °C; (*i*) AcOH–H_2O–THF, 25 °C.

Scheme 6



(*a*) $BrZnCH_2C=C(CH_2)_4Me$, THF; (*b*) $LiAlH_4$, THF, 25 °C; (*c*) 550 °C, 0.05 Torr; (*d*) PCC, CH_2Cl_2, 25 °C.

Scheme 7

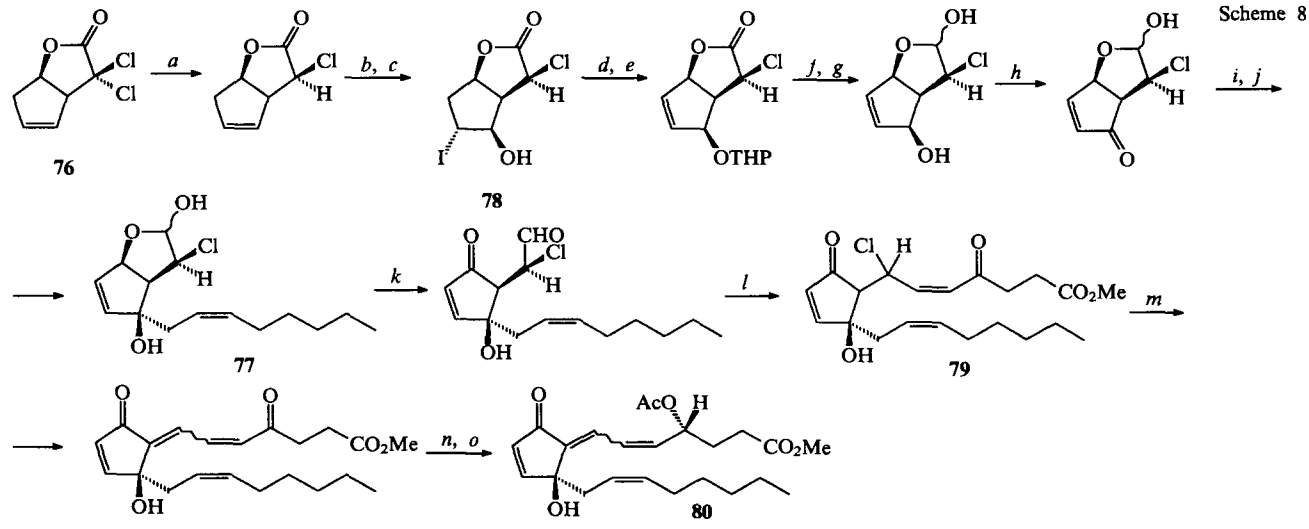


(*a*) LDA, PhSeCl, THF, −78 °C; (*b*) 10% aqueous H_2O_2, CH_2Cl_2, 1 h; (*c*) DIBAH, toluene, 0 °C, 30 min; (*d*) 2 equiv. of Bu^tOOH, $VO(acac)_2$; (*e*) 6 equiv of Red-Al, THF, 0 °C, 30 min; (*f*) PhCOCl, Py, CH_2Cl_2, −20 °C, 1 h; (*g*) Bu^tMe_2SiCl, Im (imidazole), DMF, 25 °C, 18 h; (*h*) K_2CO_3, MeOH, 40 °C, 1 h; (*i*) $CrO_3.2Py$, CH_2Cl_2, 0 °C, 15 min; (*j*) $PPh_3=CHC_5H_{11}$, THF− HMPTA (10 : 1), from −78 to 25 °C; (*k*) Bu_4NF, THF, 0 °C; (*l*) Ac_2O, Py, 25 °C; (*m*) Bu_4NF, THF, 0 °C; (*n*) $CrO_3.2Py$, CH_2Cl_2, 0 °C; (*o*) $LiCH=CHCH(OLi)(CH_2)_3OTHP$ **73** (THP = tetrahydropyran-2-yl), THF, −78 °C; (*p*) Ac_2O, Py, 25 °C, 18 h; (*q*) AcOH − H_2O (3 : 1), 80 °C, 8 min; (*r*) the Jones reagent, −20 °C, 30 min; (*s*) CH_2N_2, ether; (*t*) filtration through SiO_2; (*u*) Ac_2O, Py, 30 °C, 18 h; (*v*) high-pressure liquid chromatography.

(Scheme 7). On treatment with sodium bis(2-methoxyethoxy)-aluminium hydride (Red-Al), the epoxide afforded the tertiary alcohol **69** in 60% yield. The construction of the ω-chain from the triol **69** via the aldehyde **70** by the Wittig reaction does not present difficulties. Manipulation of the protecting groups in the resulting unit made it possible to arrive at compound **71**, the Collins oxidation of which led to the corresponding aldehyde **72**, which was then condensed with the dilithium intermediate **73**. By performing on the intermediate aldol the operations: acylation, hydrolysis of the protecting groups, the Jones oxidation, and methylation, the ketoester **74** was obtained. During the slow filtration of the latter through a layer of silica gel, the labile C(7)- and C(12)-acetoxy-groups were smoothly split off, which led to the thermodynamically favourable conjugated polyene structure **75** in the form of a mixture of isomers. Acylation of the tertiary alcoholic functional group at the C(12) atom in compound **75** gave rise to a mixture of clavulones I and II in proportions of 2 : 1, which were separated by high-pressure liquid chromatography (HPLC).

The initial compound in another effective scheme for the stereospecific synthesis of clavulones is the readily available *gem*-dichlorolactone **76**.[50,51] The key synthon **77** with a tertiary alcoholic group was obtained by a ten-stage sequence of reactions including the selective dechlorination of the lactone **76**, the preparation of the iodohydrin **78**, dehydroiodination with formation of a double bond, reduction to the lactol, the Jones oxidation, introduction of the ω-chain, and the selective hydrogenation of the triple bond (Scheme 8). In order to form the α-chain, the lactol **77** was converted into the corresponding aldehyde and was subjected

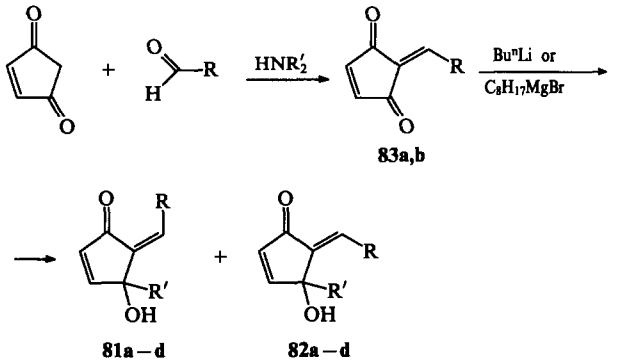
Scheme 8



(*a*) Zn, AcOH, 15–20 °C, 0.5 h; (*b*) 5% Na_2CO_3, 25 °C, 0.5 h; (*c*) 5 N AcOH, KI, 25 °C, 3 h; (*d*) DHP, *p*-TsOH, CH_2Cl_2, 1.5 h; (*e*) DBU, THF, 25 °C, 15 h; (*f*) diisobutylphosphorus hydride (DIBPH), toluene, −70 °C, 0.5 h; (*g*) $BF_3.Et_2O$, MeOH, 0.5 h; (*h*) Jones reagent, 25 °C, 0.5 h; (*i*) $Me(CH_2)_4C\equiv CCH_2Li$, THF–$Et_2O$, from −78 to 15 °C; (*j*) H_2, $Pd/BaSO_4$, 25 °C; (*k*) Jones reagent, 60 °C, 1 h; (*l*) $(MeO)_2POCH_2CO(CH_2)_2Me$, NaH, THF; (*m*) OH^-; (*n*) $Zn(BH_4)_2$; (*o*) Ac_2O.

to Wittig condensation with dimethyl 4-methoxycarbonyl-2-oxobutylphosphonate. In conclusion, the diketone **79** obtained was converted into a mixture of clavulones **80** by dehydrochlorination, selective reduction of the keto-group in the α-chain, and exhaustive acylation.

A convergent approach to the synthesis of clavulone-like compounds **81a–d** and **82a–d**, fundamentally different from those described above, has been proposed by Tolstikov et al.[52] The scheme is based on the initial construction of a new synthon — cyclopentene-1,3-dione **83a,b** with an exocyclic double bond in the side chain — and the subsequent introduction of the ω-chain with the simultaneous generation of a tertiary hydroxy-group via the condensation of the enone with the corresponding organometallic reagents.



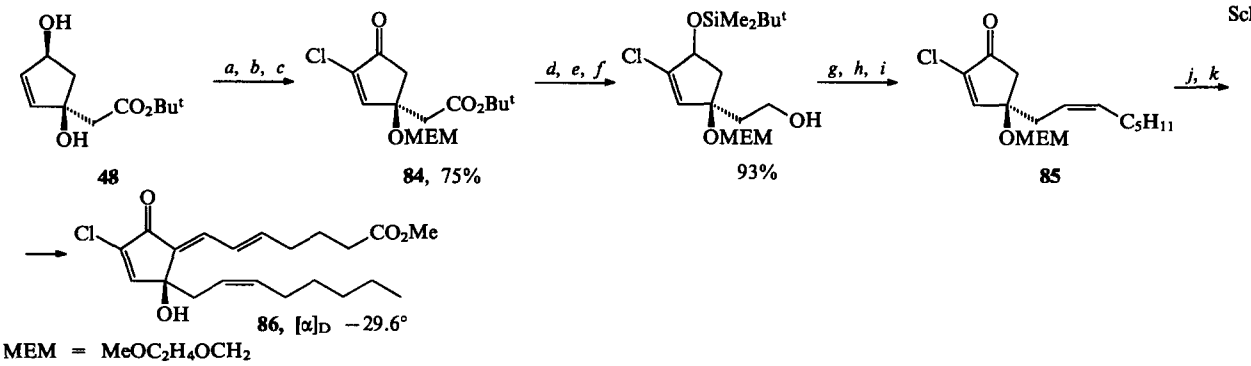
The enantioselective synthesis of (−)-chlorovulone II was undertaken by Yamada and coworkers[27] in order to establish the absolute configuration of the chiral centres in this natural product. The scheme for the synthesis reflects to an appreciable extent the strategy used by the same workers in the synthesis of clavulones.[46] The initial compound in this case is the optically active diol **48** obtained from (4*S*)-hydroxycyclopenten-2-one, which was converted in three stages into α-chlorocyclopentenone **84** and further into the key intermediate **85**. The subsequent transformation of this synthon led to (−)-chlorovulone II (compound **86**), identical in terms of all its spectroscopic characteristics, except for the sign of the angle of rotation, with a specimen of the natural product (Scheme 9).

Punaglandins II and IV have been obtained mainly in accordance with schemes similar to those described above for clavulones and chlorovulones.[27,46]

Thus, according to Nagaoka et al.,[35] the lithium enolate of the chiral cyclopentenone **87** is condensed with the chiral aldehyde **88**, synthesised from 2-deoxy-D-ribose via the acetonide **89** and the (*S*)-aldehyde **90**, which readily isomerises to compound **88** on treatment with catalytic amounts of K_2CO_3 in methanol (Scheme 10). The key condensation reaction and the subsequent standard transformations yielded a set of clavulones with different configurations of the chiral centres. The structures of punaglandins III and IV, which have the (5*S*, 6*S*, 12*R*)-configuration, were refined by comparing the spectroscopic (^{1}H NMR, IR, UV, and CD) as well as optical rotation data and the chromatographic characteristics of the synthetic and natural specimens.

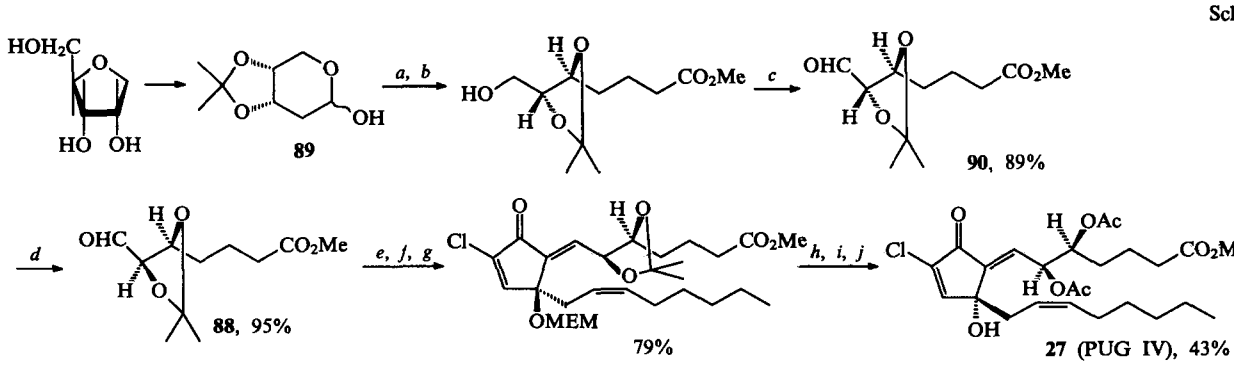
Another scheme for the preparation of punaglandins (IV) is based on the use of 1,2-bistrimethylsilylcyclopentene **53**, which was used earlier in the synthesis of clavulones.[53] The intermediate **91**, obtained by chlorinating the synthon **56**, was reduced after

Scheme 9



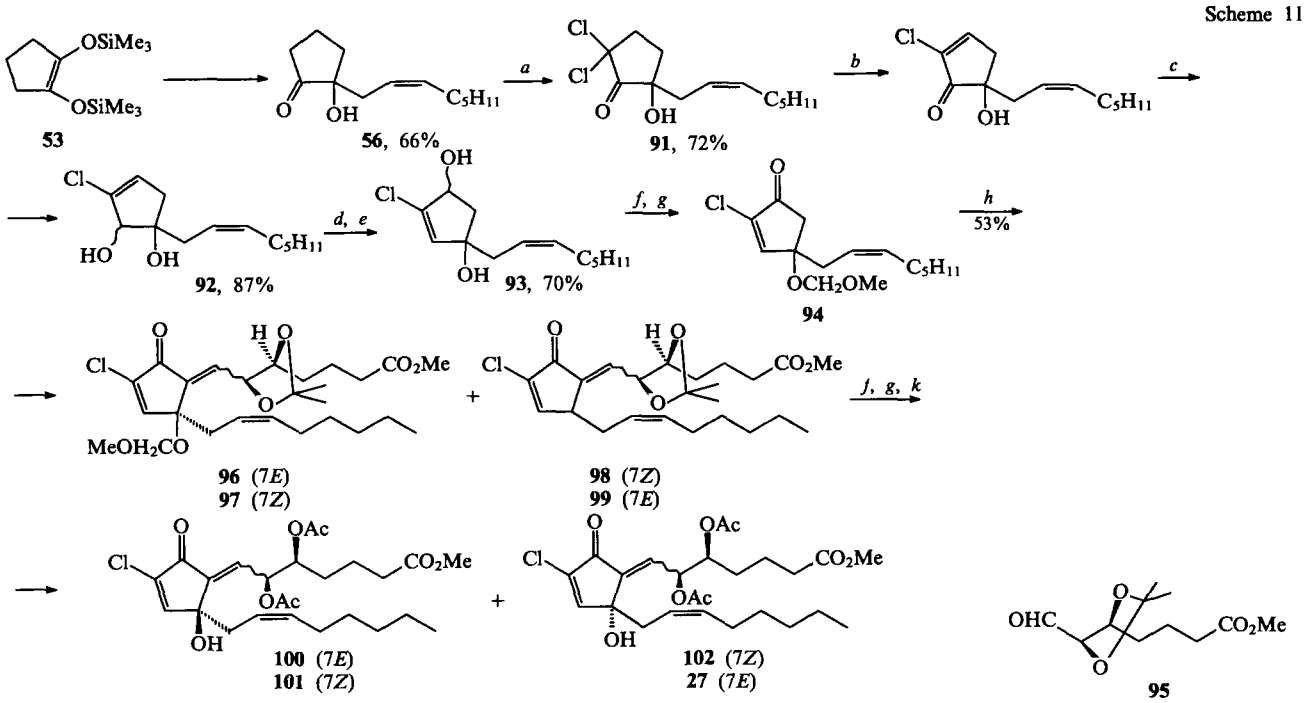
(*a*) Jones reagent, 0 °C; (*b*) $ClCH_2OMe$, Pr^i_2NEt, $(CH_2Cl)_2$, 60 °C; (*c*) Cl_2, Et_2O, 25 °C, NEt_3; (*d*) $NaBH_4$, $CeCl_3$, MeOH, 25 °C; (*e*) Bu^tMe_2SiCl, Im, DMF, 25 °C; (*f*) $LiAlH_4$, Et_2O, 0 °C; (*g*) $(COCl)_2$, DMSO; (*h*) $Ph_3P{=}CHC_5H_{11}$, THF–HMPTA, 42 °C; (*i*) H^+; (*j*) 1 equiv. of LDA, $OHC(CH{=}CH)_2CH_2CO_2Me$, THF; (*k*) conc. HCl–AcOH (1:50).

Scheme 10



(*a*) 1.1 equiv. of $Ph_3PCH{=}CHCH_2CO_2Me$, DME, refluxing, 6 h; (*b*) H_2, 10% Pd/C, EtOAc, 23 °C, 4 h; (*c*) 1.1 equiv. of $(COCl)_2$, 2 equiv. of DMSO, CH_2Cl_2, −78 °C, 10 min, NEt_3; (*d*) K_2CO_3–MeOH, 23 °C, (*e*) 1.2 equiv. of LDA, **87**, THF, −78 °C, 10 min; (*f*) Ac_2O, Py, 4-DMAP, 60 °C, 40 min; (*g*) SiO_2; (*h*) AcOH–H_2O (4:1), 60 °C, 1 h; (*i*) Ac_2O, Py, 70 °C, 40 min; (*j*) conc. HCl–AcOH (1:50), 40 °C, 15 min.

Scheme 11



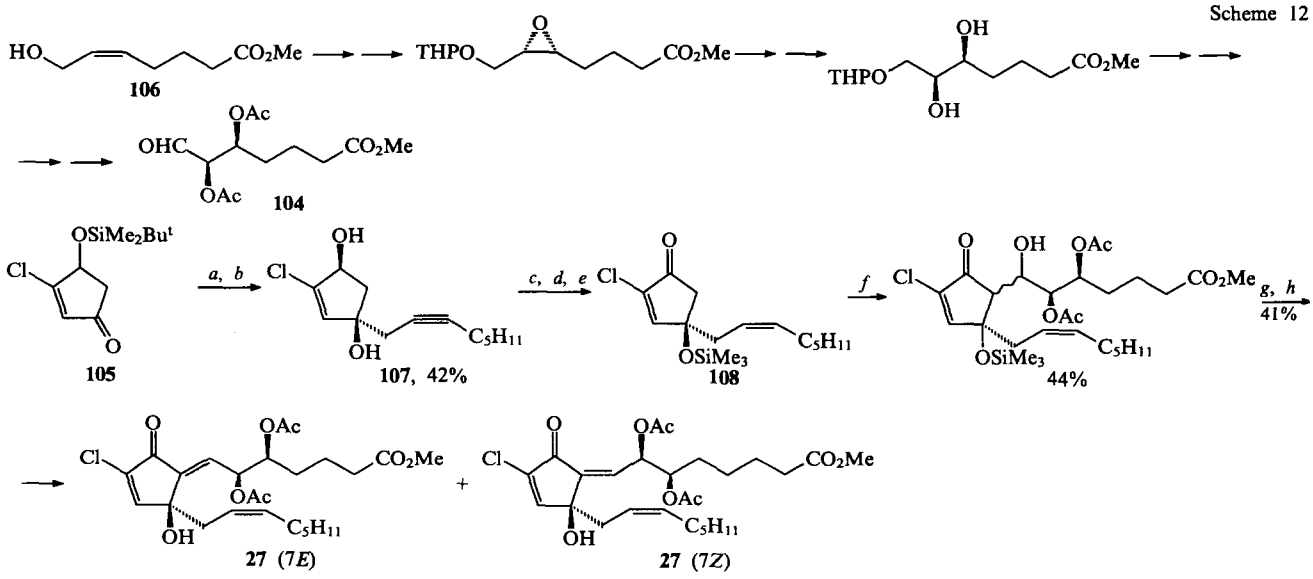
(*a*) *N*-chlorosuccinimide (NCS), NaOAc, dioxane, 25 °C; (*b*) LiCl, DMF, 120 °C; (*c*) $NaBH_4$, $CeCl_3$; (*d*) 1.3 equiv. of 4-DMAP, Py–CH_2Cl_2, 0 °C, 50 min; (*e*) 80% aqueous DMSO; (*f*) dipyridinium chromate (DPC), DMF; (*g*) $MeOCH_2Cl$, Pr^i_2NEt $(CH_2Cl)_2$, 60 °C; (*h*) LDA, **95**; (*i*) 80% aqueous AcOH, 100 °C.

dehydrochlorination to the diol **92**, which was converted into a secondary methanesulfonate and solvolysed in 80% aqueous DMSO (Scheme 11). The solvolysis of methanesulfonate proceeds with the allyl rearrangement and affords the alcohol **93** [a 1 : 1 mixture of the epimers at C(9)]. Oxidation of the crude mixture yielded a cyclopentanone derivative, which was converted into the corresponding methoxymethyl-blocked ketone **94**. The lithium enolate of the latter was treated with the aldehyde **95** and a mixture of the four diastereoisomers **96**–**99** obtained in equal amounts was separated by column chromatography. Their absolute configurations were determined by comparing the spectroscopic and optical rotation characteristics with those for authentic specimens. Selective hydrolysis of the isopropylidene protecting group in each of the products followed by acylation and acid hydrolysis afforded compounds **27** and **100**–**102** in 30%–40% yields, compound **27** being identical with the natural punaglandin IV.

A similar strategy (introduction of the ω-chain into the corresponding cyclopentenones, chlorination of the cyclopentane ring, and addition of a chiral aldehyde — the equivalent of the α-chain — by means of aldol condensation) has been used in the synthesis of 6-*epi*-14,15-dihydropunaglandin IV.[54]

Noyori's group[36] described a convergent synthesis of the natural (7*E*)- and (7*Z*)-punaglandins IV by means of the successive introduction of precursors of the ω-chain (compound **103**) and the α-chain (compound **104**) into (4*S*)-cyclopentenone **105**.

Scheme 12



(*a*) 1 equiv. of $H_2C{=}C{=}C(C_5H_{11})SnBu^n_3$ **103**, BuLi, THF, −78 °C; (*b*) Bu_4NF; (*c*) the Lindlar catalyst, MeOH; (*d*) Py.$2CrO_3$, DMF; (*e*) $MeSO_3SiMe_3$, Pr^i_2NH, CH_2Cl_2; (*f*) **104**, LDA, THF, −78 °C; (*g*) Ac_2O, 4-DMAP, CH_2Cl_2; (*h*) AcOH–THF–H_2O (6 : 3 : 1).

Tributylstannylallene **103** was obtained by the S_N2 reaction of 3-chloro-1-tributylstannylpropyne with tributylphosphine-pentylcopper at −78 °C in solution in THF. The chiral aldehydoester **104** was synthesised by the enantioselective Sharpless epoxidation of the unsaturated alcohol **106**. In the concluding stage of the synthesis, the crystalline diol **107** was obtained by condensing the stannyl derivative **103** with the enolate of the ketone **105**. The structure of the diol was confirmed by X-ray diffraction. The sequence of selective hydrogenation, oxidation and silylation reactions led to a satisfactory yield of the synthon **98**, in which the α-chain **104** was formed by standard methods (Scheme 12).

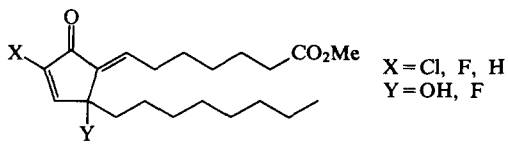
Overall, all the possible diastereoisomers with different configurations of the C(5), C(6), and C(12) chiral centres were obtained from the set of synthons **103**–**105** and their enantiomers. The involvement of the enantiomer **105** and compounds **103** and **104** in the above sequence of reactions led to a product all the characteristics of which (NMR, CD) agreed with those of the natural punaglandin IV having the (5*S*, 6*S*, 12*R*)-configuration. Thus the configuration of the C(12) chiral centre in punaglandins is identical with that in chlorovulones and is the opposite of the configuration of the C(12) centre in clavulones.

IV. Analogues of marine prostanoids

Immediately after the discovery of this class of prostanoids, studies were published on the synthesis and biological activity of their modified derivatives. Thus a group of Japanese investigators took out a series of patents[55–58] describing the isolation from *Clavularia virides* of clavulones and related compounds exhibiting anti-inflammatory and antitumour activities.

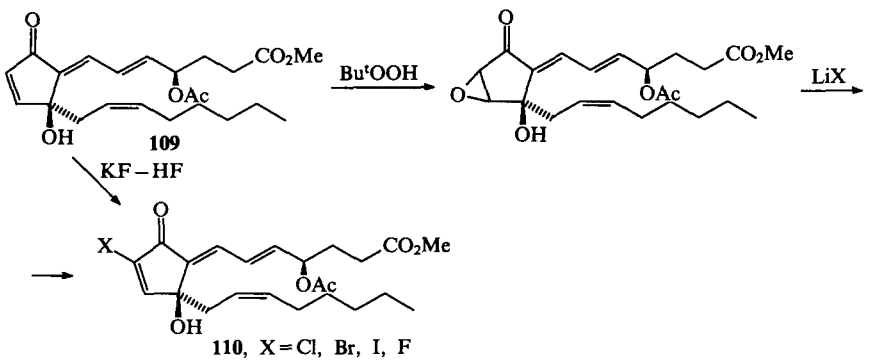
A patent[59] described the synthesis of analogues of clavulones by means of elimination reactions of sulfo-derivatives of 7-hydroxy-PGE_2. They exhibit anticancer and antiviral properties (IC_{50} = 0.4–1 μg ml^{-1}). The same workers[60] used the 7,8-dehydro-analogues of PGA to obtain the corresponding 1-chloro-derivatives, which can be regarded as modified clavulones. The compounds synthesised possessed antitumour, antibacterial and antiherpes activities.

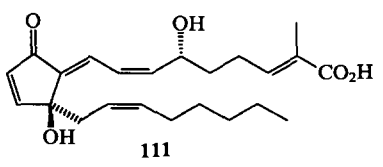
Derivatives of punaglandins have been patented[61] as effective anticancer and antiviral compounds. An attempt has been made[62] to modify the cyclopentane ring in prostaglandins by introducing powerful electronegative substituents—fluorine atoms—in the C(10) and C(12) positions. Unfortunately, comparative data on the biological activities of these compounds are not presented.

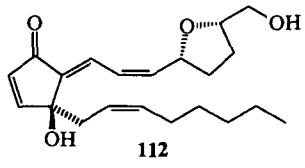


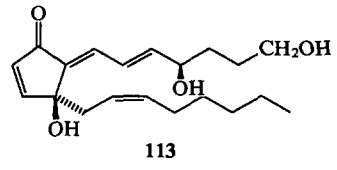
10-Haloclavulones **110** have been obtained from the cross-conjugated trienone **109**.[63]

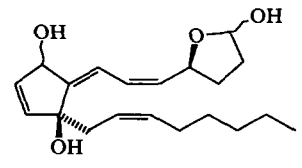
Modifications of the natural clavulones have been achieved.[64,65] Thus α-homologues of type **111**, γ-lactols **112**, the triols **113** and **114**, the lactone **115**, and derivatives **116** involving the modification of the carboxy-group have been synthesised from clavulone II.[64]

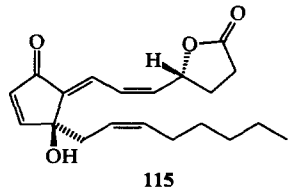


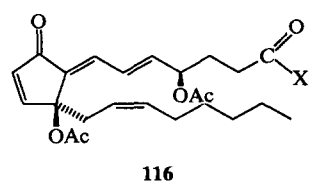






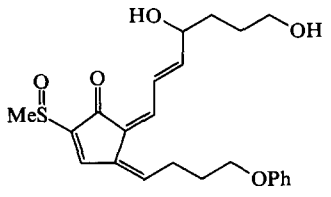




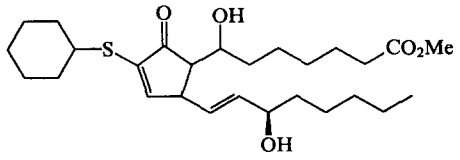


X = OH, OCH_2Ph, Bu^tO, Bu^iNH

Considerable attention has been devoted to the synthesis of the 10-thio-analogues of marine prostanoids.[66,67] In vitro experiments designed to test the activity against L-1210 cells demonstrated that the 10-methanesulfonyl derivative **117** had IC_{50} = 0.1 mg ml^{-1}, while compound **118** had IC_{50} = 0.02–2.30 mg ml^{-1}.



117



118

A series of other modifications have been achieved in order to investigate in detail the 'structure–activity' relation for this series of compounds.[68] This will be considered in detail in the next Section.

V. Biological properties of marine prostanoids

The antitumour activity of prostaglandins of types A and E was discovered as early as 1972. Subsequently, Suzuki et al.[62] found that the growth of cancer cells is also inhibited by PGD_2 and PGI_2 (9-deoxy-Δ^9-PGD_2), the activity of the latter exceeding by a factor of 3 that of PGA and PGE. Among the known prostaglandins, the most powerful antitumour agents are Δ^7-PGA_1 and Δ^{12}-PGI_2 and their derivatives. It was shown that the cyclopentane ring containing the α,β-unsaturated ketone fragment is responsible for this type of biological activity. Thus a promising field of study of prostaglandins concerns prostanoids with an alkylidenecyclopentane ring, which exhibit specific cytotoxic and antitumour activities. Clavulones (acetoxy-derivatives of Δ^7-PGA_2), discovered in 1982, and then the related punaglandins proved to be the most striking representatives of this class of prostaglandins. Tests on fertilised chicken eggs (30 μg ml^{-1}) showed that clavulones I–III possess anti-inflammatory properties.[69]

Clavulone I exhibited a distinctive antiproliferation activity in relation to HL-60 cells (ED_{50} = 0.4 μmol $litre^{-1}$), it is cytotoxic[70] at concentrations in excess of 1 μM, and it inhibits the synthesis of DNA.[71] Clavulone II manifested effective cytotoxic properties on L-1210 cells (IC_{50} = 0.6 μmol $litre^{-1}$)[71] and exhibited an antiviral activity in relation to the vesicular stomatitis virus in mice (IC_{50} = 1–1.5 μmol $litre^{-1}$).[72] Depending on the dose, punaglandins inhibit the growth of L-1210 cells in vitro (0.01–0.2 mg ml^{-1}), for which IC_{50} = 0.02 mg ml^{-1}; this is less than for vincristine and doxorubicin—the most powerful anticancer agents.[63,73,74] For clavulones, IC_{50} = 0.3 mg ml^{-1}, which is close to data for Δ^7-PGA_1.

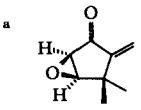
In vitro experiments showed[73] that, when mice infected with the L-1210 strain are administered punaglandins III and IV for five days using a dose of 5 mg per kilogram per day, their survival time increases by 50.5% and 78.9% respectively, while for clavulone II (10 mg per kilogram per day) the increase is by 50.8%; similar results are attained for Δ^7-PGA_1 using a dose of 20 mg per kilogram per day. Overall, the relative activities of the prostanoids in vitro and in vivo are correlated. It was also found that these compounds inhibit the synthesis of macromolecules containing leucine or thymidine: punaglandin IV causes 90% inhibition at a concentration of 5 mg ml^{-1} (L-1210), while clavulone II gives rise to a similar result at a concentration which is five times greater. It may be that these processes lead to the inhibition of the growth of tumours. The facts obtained also permit the hypothesis that one of the functions of eicosanoids in the vital activity of marine organisms may be the regulation of the growth of corals and other organisms growing in the immediate vicinity.

Yamada and coworkers[75,76] reported the results of biotests and elucidated certain features of the 'structure–activity' relation for a series of marine eicosanoids.

The decisive factor, necessary for the compounds to possess cytotoxic and antitumour (anti-HL-60 cells) activities, is the presence of an alkylidenecyclopentenone fragment in the structure. Comparison of the data in Table 1 for clavulone II and of its 10,11-dihydro-analogue shows that the presence of the C(10)–C(11) double bond is essential for the manifestation of cytotoxic activity. An exception to this rule is epoxyclavulone, which has no cross-conjugated cyclopentene system but which does exhibit a high activity. The epoxyketone fragment is probably a biological isostere of the enone system in this case (Table 1).

Table 1. The inhibiting effect of prostanoids of the clavulone type on the growth of HL-60 cells.[76]

Compound	X	R^1	R^2	IC_{50}/μmol $litre^{-1}$ (μg ml^{-1})	Cytotoxic effect/μmol $litre^{-1}$ (μg ml^{-1})
Clavulone II	H	MeCO	MeCO	0.40 (0.2)	>1.0 (0.5)
4-*O*-Deacetylclavulone II	H	MeCO	H	0.24 (0.1)	>1.2 (0.5)
12-*O*-Deacetylclavulone II[36]	H	H	MeCO	0.15 (0.06)	>0.5 (0.2)
4,12-*O*-Deacetylclavulone II	H	H	H	0.07 (0.025)	>0.3 (0.1)
10-Chloro-12-*O*-deacetylclavulone II	Cl	H	MeCO	0.03 (0.015)	>0.3 (0.15)
10,11-Epoxyclavulone II[a]	—	MeCO	MeCO	0.43 (0.2)	>1.08 (0.5)
10,11-Dihydroclavulone II[b]	—	MeCO	MeCO	2.23 (1.0)	>11.2 (5.0)
12-*O*-Methoxymethylclavulone II	H	$MeOCH_2$	MeCO	2.00 (0.90)	>4.5 (2.0)



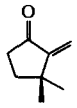
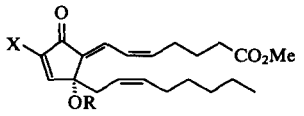
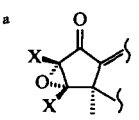


Table 2. The inhibiting effect of prostanoids of the chlorovulone type on the growth of HL-60 cells.



Compound	X	R	IC_{50}/ μmol litre^{-1} (μg ml^{-1})	Cytotoxic effect/ μmol litre^{-1} (μg ml^{-1})
Chlorovulone I	Cl	H	0.03 (0.01)	>0.3 (0.1)
Bromovulone I	Br	H	0.06 (0.025)	>0.9 (0.4)
Iodovulone I	I	H	0.06 (0.03)	>0.9 (0.4)
12-*O*-Acetyl-chlorovulone I	Cl	Bu^{t}O	0.19 (0.08)	>1.18 (0.5)
10,11-Epoxy-chlorovulone I[a]	Cl	H	0.10 (0.04)	>0.76 (0.3)

[a] 

The introduction of a halogen atom in the C(10) position increases the biological activity (Cl = F > Br = I > H) (Table 2).

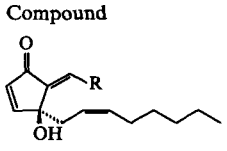
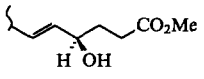
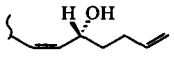
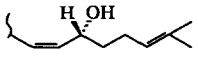
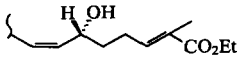
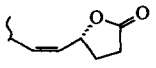
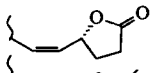
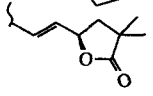
The introduction of a hydroxy-group at the C(12) atom increases the activity and the stereochemistry of the hydroxy-group does not exert an appreciable influence on the latter. The 12-hydroxy-group greatly increases the antiproliferation and cytotoxic activities. Thus the weak antiproliferation activity of PGA_2, Δ^7-PGA, PGI, and Δ^{12}-PGI has been explained precisely by the absence of the C(12)–OH group. When it is replaced by an acetyl group, the cytotoxic effect is diminished. Epoxidation decreases the activity compared with chlorovulone I, although it is nevertheless higher than that of clavulone II.

The introduction of groups blocking the β-oxidation of the α-chain does not induce an appreciable increase in activity. As shown in Table 3, the introduction of a cyclic γ-lactone or a hemiacetal group (d, e, f) does not have much influence on the β-oxidation process. On the basis of the data presented, one may note that the activity diminishes with increase in the length of the α-chain (chlorovulone I > a > b > c). The presence of eight carbon atoms is probably optimal, since the shortening of the chain also diminishes the activity.

The presence of the dienone fragment [C(5,6), C(7,8)] leads to an increase in activity.

Overall, the observed features of the 'structure–activity' relation in the series of marine prostanoids are undoubtedly important and necessary for studies directed specifically to the creation of a new class of anticancer medicinal preparations.

Table 3. The inhibiting effect of clavulones with a modified α-chain.

Compound 	R	IC_{50}/μmol litre^{-1} (μg ml^{-1})	Cytotoxic effect/μmol litre^{-1} (μg ml^{-1})
4,12-Deacetylclavulone II		0.07 (0.025)	>0.3 (0.1)
a		0.10 (0.033)	>0.6 (0.2)
b		0.11 (0.04)	>0.6 (0.2)
c		0.36 (0.15)	>1.2 (0.5)
d		0.09 (0.03)	>0.3 (0.1)
e		0.12 (0.04)	>0.6 (0.2)
f		0.11 (0.04)	>0.6 (0.2)

References

1. R Kurzrok, C C Lieb *Proc. Soc. Exp. Biol. Med.* **28** 268 (1930)
2. S Bergstrom, R Ruhage, B Samuelsson, J Sjovall *Acta Chem. Scand.* **16** 501 (1962)
3. S Bergstrom, B Samuelsson *J. Biol. Chem.* **237** PC 3005 (1962)
4. B Samuelsson *J. Biol. Chem.* **238** 3229 (1963)
5. M Humberg, B Samuelsson *J. Biol. Chem.* **241** 257 (1966)
6. E J Christ, D A van Dorp *Biochim. Biophys. Acta* **270** 537 (1972)
7. M P Murtaugh, D L Delinger *Insect. Biochem.* **12** 599 (1982)
8. T Nomura, H Ogata *Biochim. Biophys. Acta* **431** 127 (1976)
9. B W Nichols, R S Appleby *Phytochemistry* **8** 1907 (1969)
10. W H Gerwik *Chem. Rev.* **93** 1808 (1993)
11. A J Weinheimer, R L Sparrings *Tetrahedron Lett.* **10** 5185 (1969)
12. R J Light, B Samuelsson *Eur. J. Biochem.* **28** 232 (1972)
13. W P Schneider, R D Hamilton, L E Rhuland *J. Am. Chem. Soc.* **94** 2122 (1972)
14. R J Light *Biochim. Biophys. Acta* **296** 461 (1973)
15. W P Schneider, R D Hamilton, L E Rhuland *J. Am. Chem. Soc.* **94** 2122 (1972)
16. W P Schneider, R A Morge, B E Henson *J. Am. Chem. Soc.* **99** 6062 (1977)
17. S Carmely, V Kashman, V Loya, Y Benayahu *Tetrahedron Lett.* **21** 857 (1980)
18. R P Gregson, J F Marwood, R J Quinn *Tetrahedron Lett.* **20** 4505 (1979)
19. L Levine, T Kobayashi *Prostaglandins, Leukotriens Med.* **12** 357 (1983)
20. J Cimino, A Crispino, V Di Marzo, A Spinella, J Sodano *J. Org. Chem.* **56** 2907 (1991)
21. M D Higgs, L J Mulheirn *Tetrahedron* **37** 4259 (1981)
22. E J Corey, B De *J. Am. Chem. Soc.* **106** 2735 (1984)
23. W P Schneider, G L Bundy, F H Lincoln, E J Daniels, J E Pike *J. Am. Chem. Soc.* **99** 1222 (1977)
24. H Kikuchi, Y Tsukitani, K Iguchi, Y Yamada *Tetrahedron Lett.* **23** 5171 (1982)
25. M Kobayashi, T Yasuzawa, M Yoshihara, H Akutsu, Y Kyogoku, J Kitagawa *Tetrahedron Lett.* **23** 5331 (1982)
26. H Kikuchi, Y Tsukitani, K Iguchi, Y Yamada *Tetrahedron Lett.* **24** 1549 (1983)
27. H Nagaoka, K Iguchi, T Miyakoshi, N Yamada, Y Yamada *Tetrahedron Lett.* **27** 223 (1986)
28. K Iguchi, Y Yamada, H Kikuchi, Y Tsukitani *Tetrahedron Lett.* **24** 4433 (1983)
29. I Kitagawa, M Kobayashi, T Yasuzawa, B W Son, M Yoshihara, Y Kyogoku *Tetrahedron* **41** 995 (1985)
30. K Iguchi, S Kaneta, K Mori, Y Yamada, A Honda, Y Mori *Tetrahedron Lett.* **26** 5787 (1985)
31. K Iguchi, S Kaneta, K Mori, Y Yamada, A Honda, Y Mori *J. Chem. Soc., Chem. Commun.* 981 (1986)
32. D J Faulkner *Nat. Prod. Rep.* **4** 539 (1987)
33. K Iguchi, S Kaneta, K Mori, Y Yamada *Chem. Pharm. Bull.* **35** 4375 (1987)
34. B J Baker, R K Okuda, P T K Yu, P J Scheuer *J. Am. Chem. Soc.* **107** 2976 (1985)
35. H Nagaoka, H Miyaoka, T Miyakoshi, Y Yamada *J. Am. Chem. Soc.* **108** 5019 (1986)
36. M Suzuki, Y Morita, A Yanagisawa, R Noyori, B J Baker, P J Scheuer *J. Am. Chem. Soc.* **108** 5021 (1986)
37. S Bergstrom *Angew. Chem.* **95** 865 (1983)
38. E J Corey, G Schmidt, K Shimoji *Tetrahedron Lett.* **24** 3169 (1983)
39. E J Corey, P T Lansbury Jr, Y Yamada *Tetrahedron Lett.* **28** 4171 (1987)
40. E J Corey, K Ritter, M Yus, C Najera *Tetrahedron Lett.* **28** 3547 (1987)
41. E J Corey, S P T Matsuda *Tetrahedron Lett.* **28** 4247 (1987)
42. E J Corey, M d'Alarcao, S P T Matsuda, P T Lansbury Jr, *J. Am. Chem. Soc.* **109** 289 (1987)
43. W-C Song, A K Brash *Arch. Biochem. Biophys.* **290** 427 (1991)
44. E J Corey, Y B Xiang *Tetrahedron Lett.* **29** 995 (1988)
45. E J Corey, M M Mehrotra *J. Am. Chem. Soc.* **106** 3384 (1984)
46. H Nagaoka, T Miyakoshi, Y Yamada *Tetrahedron Lett.* **25** 3621 (1984)
47. M Shibasaki, Y Ogawa *Tetrahedron Lett.* **26** 3841 (1985)
48. A J H Klunder, B Zwanenburg, Z Y Liu *Tetrahedron Lett.* **32** 3131 (1991)
49. S Hashimoto, Y Arai, N Hamanaka *Tetrahedron Lett.* **26** 2679 (1985)
50. M Takemoto, A Koshida, K Miyazima, K Suzuki, K Achiwa *Chem. Pharm. Bull.* **39** 1106 (1991)
51. M Takemoto, K Miyazima, K Suzuki, K Achiwa, in *Abstracts of 16th International Symposium on the Chemistry of Natural Products, Japan, 1988* p. 422
52. G A Tolstikov, M S Miftakhov, N A Danilova, Ya L Vel'der, L V Spirikhin *Zh. Org. Khim.* **25** 438 (1989)
53. H Sasai, M Shibasaki *Tetrahedron Lett.* **28** 333 (1987)
54. H Nagaoka, T Miyakoshi, J Kasuga, Y Yamada *Tetrahedron Lett.* **26** 5053 (1985)
55. Eur. P.10 4631; *Chem. Abstr.* **101** 151 671z (1984)
56. US P. 4 560 703; *Ref. Zh. Khim.* 13 O 220 P (1987)
57. Jpn. P. 6 127 948; *Chem. Abstr.* **105** 133 641t (1986)
58. Jpn. P. 6 180 734; *Chem. Abstr.* **106** 49 657r (1987)
59. Jpn. P. 6 101 636; *Chem. Abstr.* **105** 60 465b (1986)
60. Eur. P. 131 441; *Chem. Abstr.* **103** 215 059g (1985)
61. Jpn. P. 6 259 258; *Chem Abstr.* **107** 39 505w (1987)
62. M Suzuki, M Mori, R Hirata Y Morita, R Noyori, in *Abstracts of 16th International Symposium on the Chemistry of Natural Products, Japan, 1988* p. 411
63. K Iguchi, S Kaneta, C Tsune, Y Yamada *Chem. Pharm. Bull.* **37** 1173 (1989)
64. K Iguchi, S Kaneta, H Nagaoka, Y Yamada *Chem. Pharm. Bull.* **38** 65 (1990)
65. Jpn. P. 02 270 836; *Chem. Abstr.* **114** 163 861t (1991)
66. Eur. P. 338 796; *Chem. Abstr.* **113** 114 932n (1990)
67. PCT P. 9 105 766; *Chem. Abstr.* **115** 255 889g (1991)
68. K Iguchi, S Kaneta, H Nagaoka, Y Yamada *Chem. Lett.* 157 (1989)
69. H Kikuchi, Y Tsukitani, K Iguchi, Y Yamada *Tetrahedron Lett.* **23** 5171 (1982)
70. A Honda, Y Yamamoto, Y Mori, Y Yamada, H Kikuchi *Biochem. Biophys. Res. Commun.* **130** 515 (1985)
71. M Fukushima, T Kato, Y Yamada, I Kitagawa, S Kurozumi, P Scheuer *Proc. Am. Assoc. Cancer Res.* **26** 980 (1985)
72. T Bader, Y Yamada, H Ankel *Antiviral Res.* **16** 341 (1991)
73. M Fukushima, T Kato, in *Advances in Prostaglandin, Thromboxane and Leukotriene Research* Vol. 15 (New York: Raven Press, 1985) p. 415
74. M Suzuki, Y Morita, A Yanagisawa, B J Baker, P J Scheuer, R Noyori *J. Org. Chem.* **53** 286 (1988)
75. A Honda, Y Mori, K Iguchi, Y Yamada *Mol. Pharm.* **32** 530 (1987)
76. A Honda, Y Mori, K Iguchi, Y Yamada *Prostaglandins* **36** 621 (1988)

Russian Chemical Reviews **63** (7) 533 – 549 (1994)
©1994 Russian Academy of Sciences and Turpion Ltd

UDC 548.736

The structures of new germanates, gallates, borates, and silicates with laser, piezoelectric, ferroelectric, and ion-conducting properties

E L Belokoneva

Contents

I.	Introduction	533
II.	Brief characteristics of the methods for the preparation and study of the new compounds	534
III.	The garnet structural type	534
IV.	The $A_3M_xT_{6-x}O_{14}$ structural type	535
V.	The melilite structural type	537
VI.	The $Pb_3GeAl_{10}O_{20}$ and $NdAlGe_2O_7$ structural types	538
VII.	The stillvellite – datolite structural type in the $LnBGeO_5$ series	539
VIII.	Lanthanide borates with the huntite structure and their polytypic derivatives	540
IX.	The $KTiOPO_4$ structural type	541
X.	The sphene (titanite) structural type	545
XI.	Germanate-zeolites and zeolite-like germanates	546

Abstract. The results of studies on the structures of more than 50 new crystals of germanates, gallates, borogermanates, borates, and silicates, possessing laser, piezoelectric, ferroelectric, and ion-conducting properties, are presented. The structure–property relations are considered. The bibliography includes 71 references.

I. Introduction

The needs of modern engineering for new materials, which are promising by virtue of their unusual physical properties, are increasing with each year. Inorganic single crystals occupy an important place among such materials. The interest in them has been aroused by the developing modern technologies. Thus the enormous possibilities arising in the application of the new optical properties of crystals have been demonstrated in a communication [1] reviewing the results of studies involving the search for new nonlinear optical materials of the $KTiOPO_4$ structural type. The large band widths available in the optical transmission of data make it possible to move and store specimens with an information density in excess of 10^8 bits cm^{-2}. The generation of the third harmonic can be used to improve significantly the density of optical discs. The fibre optics used in telecommunications permits a relatively free transmission of signals subject to a minimal noise due to the external electromagnetic field. This also means that the modulations of the light wave carriers are nontrivial and that chemists specialising in materials science should play an important role in the creation of an optical system (crystal) with a predetermined amplitude and response time.

In a study [2] of the relation between the structures of new crystalline phases and their ferroelectric properties, the structure–properties problem was designated as crucial in chemistry and structural crystallography. Ferroelectrics, i.e. crystals capable of spontaneous polarisation, are materials in which structure–property relations are clearly manifested and are being actively investigated. Such materials frequently also possess ionic conductivity.

Studies in recent years have shown that solid electrolytes or superionic crystals have a specific structure — they contain large channel-cavities in which cations migrate. This has led to the specific search for and synthesis of such compounds.

Compounds in which, for example, luminescent, piezoelectric, and nonlinear optical properties are combined with a high mechanical and thermochemical stability are especially valuable. This review is devoted to the consideration of the characteristics of the steric structures of such compounds which have been obtained and whose structures have been investigated during the last 10–15 years. For example, in the case of solid state lasers, the search for compounds has been governed by problems involving the adoption of new spectral ranges and expansion of the stimulated radiation frequency ranges. Problems associated with the improvement of the effectiveness of energy conversion and of thermal stability are of current interest for piezoelectric single crystals.

The problem of the preparation of large and perfect single crystals for their subsequent study (in particular of their optical properties) and use is extremely important in such investigations. For this purpose, it is essential to know the conditions for the crystallisation of the corresponding phases. The determination of the regions of stability of structural types make it possible to achieve optimum compositions for the manifestation of the given physical properties by means of isomorphous substitution of atoms at different sites.

In the present review, attention is concentrated on the question of the relation between the structural characteristics of the new phases and physical properties. Mainly studies by Russian investigators, who have contributed greatly to the preparation and study of the properties and structures of new laser, piezoelectric, ferroelectric, and ion-conducting crystals, will be considered.

The majority of the germanate, gallate, and borogermanate crystals were obtained by B V Mill' in the Faculty of Physics at Moscow State University, the germanate-zeolites were obtained by L N Dem'yanets at the Institute of Crystallography of the Russian Academy of Sciences, and lanthanide borates were

E L Belokoneva Department of Crystallography and Crystal Chemistry, Faculty of Geology, M V Lomonosov Moscow State University, Vorob'evy gory, 119899 Moscow, Russian Federation.
Fax (7-095) 939 01 26. Tel. (7-095) 939 38 75

Received 28 April 1994
Uspekhi Khimii **63** (7) 559 – 575 (1994); translated by A K Grzybowski

prepared by L I Leonyuk in the Faculty of Geology at Moscow State University. The optical, piezoelectric, and mechanical properties were measured by A A Kaminskii and coworkers at the Institute of Crystallography of the Russian Academy of Sciences, while the measurements concerned with second harmonic generation and measurements of the electrical and ion-conducting properties were performed by S Yu Stefanovich of the Physicochemical Institute.

II. Brief characteristics of the methods for the preparation and study of the new compounds

The majority of the compounds, the crystals of which will be considered below, belong to the class of germanates and the related gallates. Crystallisation has been investigated for the $A_2O(AO)-M_2O_3(MO_2)-GeO_2(Ga_2O_3, SiO_2)$ systems, where A are alkali, alkaline earth, or lanthanide elements, i.e. large cations, and M are predominantly trivalent cations (Ga, Al, In, Fe, Sb, Ta), smaller in size and with higher electronegativities. The crystals were obtained by solid-phase synthesis,[3] i.e. by sintering in air-pressed mixtures of the oxides at 1100–1500 °C for 3–5 h (the temperatures used in the preparation of the single-phase specimens will be given below on the basis of the literature quoted in describing the data). The single crystals of a number of congruently melting compounds were grown by Czochralski's method. The boules were 8–9 cm long and 3 cm thick. The germanate-zeolites were obtained by hydrothermal synthesis[4] in autoclaves from alkaline solutions in the $NaAlO_2-GeO_2-Na_2CO_3-NaOH-H_2O$ systems at 300–500 °C. The lanthanide borates were synthesised by the solution-melt method in the $Ln_2O_3-Al_2O_3-B_2O_3-K_2Mo_3O_{10}$ systems by spontaneous crystallisation on cooling from 1500 °C.[5]

Crystalline elements in the form of rods up to 70 mm long and up to 5 mm in diameter with plane-parallel (5") end-faces were prepared for the investigation of the optical properties from the boules obtained by Czochralski's method.[6] The crystals were pumped by the pulsed radiation from neodymium (LaF_3, $Y_3Al_5O_{12}-Nd^{3+}$) and praseodymium ($Y_3Al_5O_{12}-Pr^{3+}$) laser crystals and also using Xe lamps. The spectral-lasing characteristics of the stimulated radiation, the optical transmission, absorption, and Raman spectra and the optical activity were investigated for the specimen synthesised, and measurements were also made of their elastic, dielectric, and piezoelectric characteristics. The measurements concerned with second harmonic generation and the measurements of the electrical and ion-conducting properties were performed by means of a specially developed method (see, for example, Belokoneva and Timchenko[5]).

Full X-ray diffraction studies of the single crystals of the new compounds were carried out in order to investigate their crystal structures. A correct allowance for the absorption of X-rays is extremely important in the study of objects containing germanium, gallium, the lanthanides, barium, strontium, and other heavy elements. In most cases, the single crystal specimens were prepared in the form of spheres with radii determined by the linear absorption coefficient ($\mu r \leqslant 4$).

The compounds will be considered in accordance with their structural types, most of which are known. New, previously unknown structural types or their modifications were also obtained and investigated in the course of the structural studies.

III. The garnet structural type

Many compounds with valuable properties crystallise with a garnet-type structure, for example, the garnet-ferrites $M_3Fe_5O_{12}$ with lanthanide elements at the dodecahedral M sites[8] or the familiar $Y_3Al_5O_{12}:Nd^{3+}$ laser crystal.[9] Isomorphous substitutions in the crystals can lead to the formation of new promising compounds.

By analogy with the work of Gibbs and Novak[10] on silicate garnets, in which the crystal-chemical characteristics and the region of stability were characterised as a function of the size of the ion at the dodecahedral (*c*) and octahedral (*a*) structural sites, the corresponding germanate analogues were investigated.[11] The garnet-germanate crystals were grown by Czochralski's method. The X-ray diffraction characteristics of the representatives of this series investigated are presented in Table 1. In the diffraction experiments, only the reflections for which the contribution of the cations is small or zero were scanned, this yielded from 58 to 86 observed independent reflections. The positional and thermal parameters of the O atom were refined on their basis, after which the interatomic distances in the polyhedra of the cations, located at the specific 24*c*, 16*a*, and 24*d* sites in the cubic lattice (the dodecahedron, octahedron, and tetrahedron) and their distortions were calculated. The quantities obtained from the structural data made it possible to deduce the region of stability of the germanium garnets (Fig. 1), i.e. to determine the combinations of ions in conformity with their ionic radii at the 24*c* and 16*a* sites of the *Ia*3*d* group when the germanium atoms are located at the 24*d* sites. These characteristics were deduced on the basis of the existence of common edges in the garnet structure between the tetrahedron and the octahedron, on the one hand, and the dodecahedra on the other.

Table 1. X-Ray diffraction characteristics of the phases investigated with the structure of the garnet type (space group *Ia*3*d*).

Compound	*a*/Å	μr	N_{refl}	R_{hkl} (%)
$Mn_3Al_2Ge_3O_{12}$	11.891(3)	2.5	84	7.8
$Ca_3Al_2Ge_3O_{12}$	12.116(3)	1.3	86	5.2
$Ca_3Ga_2Ge_3O_{12}$	12.247(3)	2.5	79	5.7
$Ca_3Fe_2Ge_3O_{12}$	12.338(3)	1.0	72	5.2
$Cd_3Sc_2Ge_3O_{12}$	12.449(3)	2.7	73	6.1
$Ca_3Sc_2Ge_3O_{12}$	12.506(3)	2.0	73	3.9
$Ca_3In_2Ge_3O_{12}$	12.595(3)	1.7	76	6.7
$Ca_3Lu_2Ge_3O_{12}$	12.738(3)	2.1	58	9.5
$Sr_3Sc_2Ge_3O_{12}$	12.750(4)	4.0	31	11.8

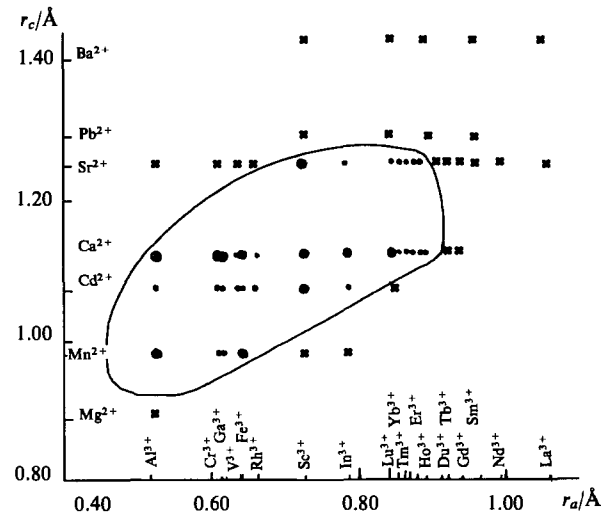


Figure 1. The region of stability of germanium garnets.

As regards practical applications (for the production of stimulated radiation), the $Ca_3Ga_2Ge_3O_{12}$ crystal activated by Nd^{3+} at concentrations from 0.05 to 16 at.% proved to be most promising. The position of the Nd^{3+}-activated ion was unambiguously determined as 24*c*, while that of the Cr^{3+} sensitiser ion was determined as 16*a*. The luminescence spectra of

this specimen have been analysed.[12] The question of the usefulness of polycationic garnets with heterovalent isomorphism for the formation of disordered Nd^{3+}-containing laser garnet crystals of the type $\{Ca_{1-x}Nd_x\}_3[Ga_2](Ge_{1-x}Ga_x)_3O_{12}$ was discussed in the same communication.

As a development of the possibilities of the heterovalent isomorphism discussed previously,[12] the cation-deficient garnet $Ca_{3.02}Nb_{1.67}Ga_{3.2}O_{12}$ (space group $Ia3d$, a = 12.507 Å) was synthesised and its structure was investigated.[13] The initial nonstoichiometry of the specimen compared with the standard $A_3B_2T_3O_{12}$ stoichiometry and also the unusually pronounced broadening of the lines in the luminescence spectra indicated a complex isomorphism and the presence of unoccupied cationic sites. Partial incorporation of Ca at the octahedral sites occupied predominantly by Nb and the excess Ga as well as the inclusion of a small proportion of Nb at Ga tetrahedral sites have been postulated. The ionic radii of the elements permit isomorphous mixing of this kind. In addition it was found that all the cationic sites in the structure are unoccupied. Successive refinement of various structural models of the crystal for different compositions (with specification of mixed atomic scattering curves) and populations of the atomic sites made it possible to obtain satisfactory thermal corrections for the atoms and the optimum divergence factor (R = 0.020) for the structural formula $\{\square_{0.05}.Ca_{2.95}\}[\square_{0.025}Ca_{0.07}Nb_{1.62}Ga_{0.275}](\square_{0.025}Nb_{0.05}Ga_{2.925})O_{12}$.

The existence of cationic vacancies was also established for V-garnets, but the Ca, Nb, Ga-garnet investigated by Kaminskii et al.[13] is the first disordered crystal with the garnet structure used to excite stimulated radiation. The statistical nature of the distribution of the heterovalent Ca^{2+}, Ga^{3+}, and Nb^{5+} ions among crystallographic sites, obtained as a result of X-ray diffraction study, was fully confirmed by the results of the study of the Raman spectra (Fig. 2), the luminescent properties, and the stimulated emission from this crystal containing Nd^{3+} ions. The high quality of experimental X-ray diffraction data and the reliability of the results for this crystal were confirmed by the investigation of the electron density distribution[14] and $\delta\rho$ maps, which proved to be comparable to those obtained for other garnets.

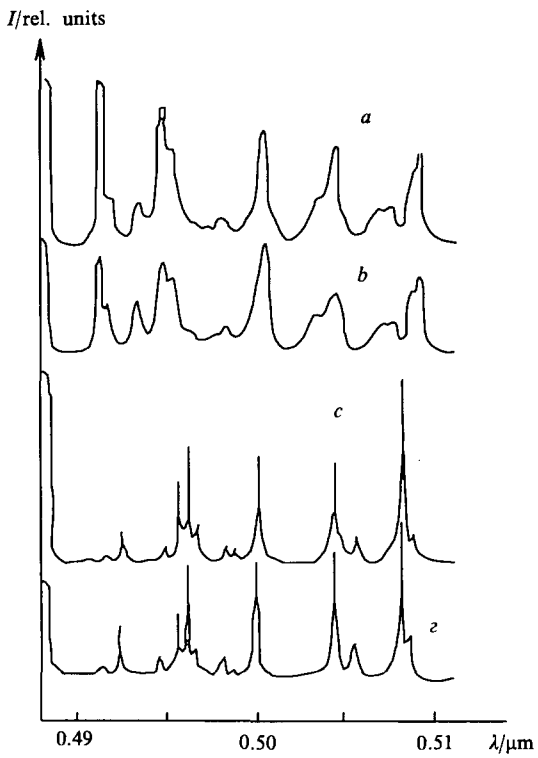


Figure 2. Raman spectra of the $Ca_{3.02}Nb_{1.67}Ga_{3.2}O_{12}$ garnets[13] with a disordered structure (a, b) and the $Ca_3Ga_2Ge_3O_{12}$ garnet with an ordered structure (c, d).

IV. The $A_3M_xT_{6-x}O_{14}$ structural type

In the study of the crystallisation of the $Ca_3Ga_2Ge_3O_{12}$ garnet, the compound $Ca_3Ga_2Ge_4O_{14}$ was obtained and subsequently became the parent compound of a series of compounds of a new structural type. The small amount of added oxides of certain tetravalent and pentavalent elements stabilises this new structural type for different compositions.[3] In the main, the compounds were obtained by solid-phase synthesis and those which melt congruently were synthesised by Czochralski's method. In all, more than 50 compounds were synthesised. The phase diagrams for the $CaO-Ga_2O_3-GeO_2$, $SrO-Ga_2O_3-GeO_2$, $Ln_2O_3-Ga_2O_3-SiO_2(GeO_2)$ (Ln = La, Nd), and $La_2O_3-Ga_2O_3-Nb_2O_5$ systems have been described.[15] The structures of seven compounds were investigated, the relevant data being presented in Table 2. In the acentric trigonal Fedorov group $P321$, which is characteristic of these phases, the cations are distributed among four regular point systems a, d, e, and f with different symmetries and with coordination to the oxygen atoms: a—octahedron with 32 symmetry; e—Thompson cube with 2 symmetry, and d and f—tetrahedra with 3 and 2 symmetry respectively (Table 2, Fig. 3). The true diffraction symmetry of $A_3M_xT_{6-x}O_{14}$ is trigonal ($P\bar{3}1m$), and the diffraction pseudosymmetry is hexagonal ($P6/mmm$). In the crystal structure, the Ge tetrahedra on the threefold and twofold axes form layers (Figs 3 and 4) perpendicular to the c axis. The Ge octahedra, strengthening the tetrahedra by forming a mixed framework, are distributed among them. The unshared ('hanging') apex of the d tetrahedron, viewed from above or downwards along the 3 axis (Fig. 3), makes it necessary to assign such a framework to the class of pseudoframeworks; the formula of the framework is $[M_1T_5O_{14}]$. The 'double-decker' structure of the framework is clearly seen in side projection (Fig. 4). The large A cations, the coordination polyhedra of which are the so called Thompson cubes in which the two square bases have been rotated relative to one another approximately by an angle of 45°, are located in the large cavities between the tetrahedral layers (Fig. 3). The most characteristic detail of the pseudoframework of the structural type considered is the group with 32 symmetry made up of the a octahedron and the three apices of the f tetrahedra linked to it.

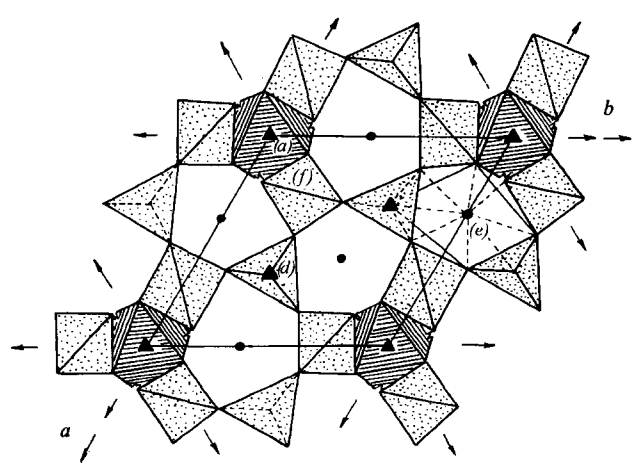


Figure 3. Projection of the crystal structure of the $A_3M_xT_{6-x}O_{14}$ type onto the ab plane. The regular systems of points for the positions of the cations and the symmetry elements are indicated.

Table 2. X-Ray diffraction characteristics of the phases investigated with structures of the $A_3M_xT_{6-x}O_{14}$ type.

Compound	a/Å	c/Å	Positions of cations[a]				μr	N_{refl}	R_{hkl} (%)
			e Thompson cube	a octahedron	d tetrahedron	f tetrahedron			
$Ca_3Ga_2Ge_4O_{14}$	8.076(3)	4.974(1)	Ca (2.549)	Ge (1.919)	Ge (1.752)	Ge+Ga=1:2 (1.826)	1.8	1516	6.3
$(Na_2Ca)Ge_6O_{14}$	8.183(3)	4.836(1)	Na+Ca=2:1 (2.579)	Ge (1.893)	Ge (1.747)	Ge (1.766)	2.2	1075	5.5
$Sr_3Ga_2Ge_4O_{14}$	8.270(3)	5.040(1)	Sr (2.654)	Ge+Ga=3:2 (1.924)	Ge (1.735)	Ge+Ga=7:8 (1.812)	3.7	1308	6.5
$Ba_3Fe_2Ge_4O_{14}$	8.541(5)	5.214(1)	Ba (2.783)	Fe (2.015)	Ge (1.763)	Fe+Ge=1:2 (1.812)	1.5	967	6.8
$La_3Ga_5SiO_{14}$	8.168(3)	5.095(1)	La (2.586)	Ga (1.997)	Ge+Si=1:1 (1.741)	Ga (1.861)	2.5	1979	4.5
$La_3Ga_5GeO_{14}$	8.204(4)	5.109(1)	La (2.592)	Ga (1.993)	Ga+Ge=1:1 (1.803)	Ga (1.852)	3.2	1693	4.0
$La_3Ga_{5.5}Nb_{0.5}O_{14}$	8.235(5)	5.129(2)	La (2.598)	Ga+Nb=1:1 (1.997)	Ga (1.829)	Ga (1.835)	2.4	1985	5.3

[a]The mean interatomic cation–oxygen distance (in Å) in the polyhedron is given in brackets.

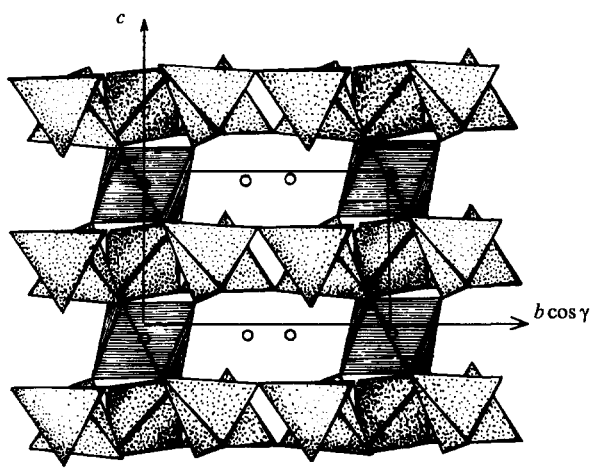


Figure 4. Projection of the crystal structure of the $A_3M_xT_{6-x}O_{14}$ type onto the *bc* plane.

Similar structural blocks are fundamental for mixed frameworks and pseudoframeworks of a large group of compounds with Ge atoms in octahedral and tetrahedral coordination such as $Li_2Ge_4O_9$, $LiNaGe_4O_9$, $Li_2Ge_7O_{16}$, $Li_4Ge_9O_{20}$, $Cd_2Ge_7O_{16}$, $BaGe_4O_9$, $K_2Ba(Ge_4O_9)_2$, and $Ba_3Ge_9O_{20}(OH)_2$.[16] The symmetry of the microblocks may be varied: 32, $\bar{3}m$, $3m$, $\bar{3}$, i.e. they may or may not have a centre of symmetry.

A similar structure, involving the existence of layered tetrahedral elements and different combinations of tetrahedra and octahedra, is characteristic of a large group of germanates, which nevertheless differ in the symmetry of their structures (the tetragonal Cd germanate, the trigonal Ca, Ga and K, Ge germanates, the orthorhombic $Li_2Ge_4O_9$ and $Li_2Ge_7O_{15}$, and the monoclinic $Li_4Ge_9O_{20}$) and in the topology of the tetrahedral layer. The axes perpendicular to the layered elements have the same dimensions in all the structures as that of the c = 4.7 Å axis of the structural type investigated or are a multiple of it (Fig. 5).

All these phases contain large interlayer cavities which can be filled by cations. Such cavities constitute convenient sites for activator ions. This can lead to the appearance of laser properties in the crystal. One can also postulate that phases such as $Cd_2Ge_7O_{16}$ (sp. gp $P\bar{4}b2$), $BaGe_4O_9$ (sp. gp $P31m$),

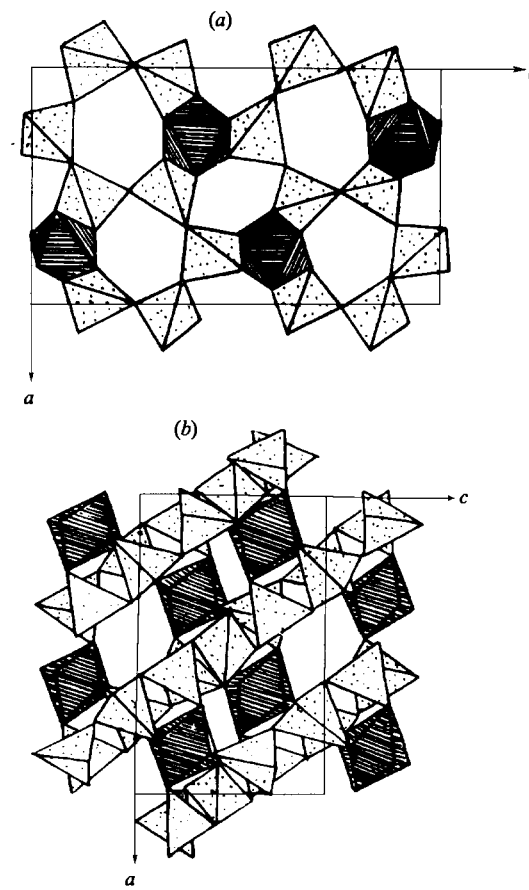


Figure 5. The crystal structures of $Li_2Ge_4O_9$ (*a*) and $Li_4Ge_9O_{20}$ (*b*). The anionic framework is illustrated.

and $Li_4Ge_9O_{20}$ (sp. gp $C2_1$) are promising as regards possible ferroelectric (for polar crystals) properties. Thus it has been established[17] that the compound $Li_2Ge_7O_{15}$ in this group undergoes a phase transition at 283.5 K ($Pbcn$—$Pbc2_1$) to a polar ferroelectric modification, which is accompanied by spontaneous polarisation along the c axis of the structure.

The synthesis and X-ray diffraction structural studies established that in crystals of the $A_3M_xT_{6-x}O_{14}$ structural type there is a possibility of extensive isovalent and heterovalent isomorphism which would enhance the laser and piezoelectric properties of those crystals which possess them.

The region corresponding to the stability of the compounds has been constructed in accordance with the crystal-chemical results in terms of the radii of ions with C.N. = 8 and the average radii of the ions of the framework as variables (Fig. 6).[16] Table 2 shows that isomorphic substitutions take place at all the cationic structural sites: (Na + Ca), Ca, Sr, Ba, and La for *e*; Ge, (Ge + Ga), Fe, and (Ga + Nb) for *a*; Ge, (Ga + Si), and Ga for *d*; Ge, (Ge + Ga), (Fe + Ge), and Ga for *f*. In the presence of isomorphism, the charge on the framework varies from −4 to −9: $[Ge_6O_{14}]^{4-}$, $[Ga_2Ge_4O_{14}]^{6-}$ and $[Fe_2Ge_4O_{14}]^{6-}$, $[Ga_5SiO_{14}]^{9-}$. One of the two independent tetrahedra, the *f* tetrahedron on the twofold axis, forming a microblock with the octahedron, is larger than the *d* tetrahedron on the threefold axis. In the *f* tetrahedron, the average interatomic distance varies from 1.766 Å (Ge) to 1.861 Å (Ga) with a possible inclusion at this site of up to 30% of the Fe atoms ($Ba_3Fe_2Ge_4O_{14}$). (In the structurally similar tetragonal gehlenites, which will be considered below, there is also a difference between the sizes of the two independent tetrahedra.) The tetrahedron on the threefold axis represents a cell for the smallest cations in the given structural type, in particular for Si^{4+} in $La_3Ga_5SiO_{14}$.

Octahedra with a mixed framework are also distinguished by 'flexibility' as regards size [the mean cation–oxygen distance varies from 1.893 Å (Ga) to 2.015 Å (Fe)] and, as already noted, can be occupied by germanium, gallium, niobium (to the extent of 50%), and iron cations. The fairly loose framework which is susceptible to isomorphism is readily distorted, and this may be the reason for the appearance of polarity in the structure and of the spontaneous polarisation vector P_s. The introduction of the Nd^{3+} activator ion at sites with lanthanide elements makes it possible to obtain satisfactory lasing characteristics.[18] The compound $La_3Ga_5SiO_{14}$ proved to have the best spectroscopic characteristics and piezoelectric properties among all those investigated.[3,15] $La_3Ga_5SiO_{14}$ single crytals are nowadays grown by a number of western and Russian firms. In accordance with the structural results, these crystals have been assigned to the class of materials with a disordered structure and a single activation quasi-centre. The fully substituted (La^{3+}–Nd^{3+}) compound $Nd_3Ga_5SiO_{14}$, i.e. a compound with a very high Nd^{3+} concentration, has been obtained from $La_3Ga_5SiO_{14}$.[6] Crystals of lanthanum gallate containing niobium (Table 2), which is incorporated in the *a* octahedron, are promising as regards the manifestation of nonlinear optical properties.

All the crystals of this group exhibit a piezoactivity higher by a factor of 3–8 than that of quartz.[15] The acoustic Q-factor of the crystals is also higher. Although the symmetry space groups of the new phases ($P321$) and quartz ($P3_121$) differ, they are both acentric and belong to the same 32 point group.

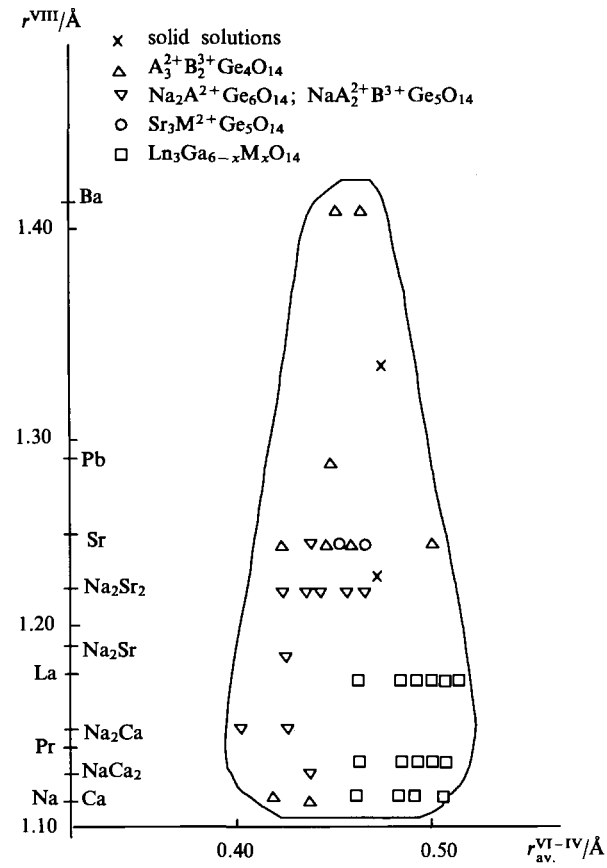


Figure 6. The region of stability of the compound $A_3M_xT_{6-x}O_{14}$.

The unique combination of physical properties (luminescent, laser, nonlinear optical, piezoelectric, and elastic) in this structural type of germanates makes it possible to regard them as multifunctional elements for technological purposes.

V. The melilite structural type

In the study of the $CaO–Ga_2O_3–GeO_2$ ternary system, crystals of the Ca, Ga, Ge-gehlenite $Ca_2Ga_2GeO_7$, belonging to the melilite structural type, were obtained. The interest in compounds with the melilite structure is due to the fact that stimulated emission from Ba,Zn and Ba,Mn germanates with the melilite structure and containing Nd^{3+} ions has been excited. A structural study of $Ca_2Ga_2GeO_7$ confirmed[19] that it belongs to the melilite structural type with the $P\bar{4}2_1m$ group. Apart from this compound, two further representatives of this structural type have been

Table 3. X-Ray diffraction characteristics of the phases investigated with structures of the gehlenite type.

Compound	*a*/Å	*c*/Å	Positions of cations[a]			μr	N_{refl}	R_{hkl} (%)
			e Thompson cube	*a* tetrahedron	*e* tetrahedron			
$Ca_2Ga_2GeO_7$	7.896(4)	5.207(2)	Ca (2.58)	Ga (1.85)	Ga + Ge = 1 : 1 (1.80)	0.9	392	5.5
$Ca_2Ga_2SiO_7$	7.793(3)	5.132(2)	Ca (2.580)	Ga (1.815)	Ga + Si = 1 : 1 (1.723)	0.8	722	4.2
$CaNdGa_3O_7$	7.903(3)	5.231(2)	Ca + Nd = 1 : 1 (2.591)	Ga (1.816)	Ga (1.824)	2.35	842	5.2

[a]The mean interatomic cation–oxygen distance in the polyhedron (in Å) is given in brackets.

synthesised and their structures have been investigated—$Ca_2Ga_2SiO_7$ and $CaNdGa_3O_7$ (Table 3)[20] (the low accuracy of the structural data obtained previously[21] for $Ca_2Ga_2SiO_7$ precluded a complete interpretation of the physical properties). The calcium or calcium + neodymium cations in the compounds synthesised are accommodated in Thompson cubes with the *m* symmetry. The larger *a* tetrahedra on the inversion axes, filled in the given structures with gallium atoms, are occupied by magnesium atoms in melilites and by iron atoms in åkermanites. The smallest *e* tetrahedra with *m* symmetry are occupied by Ga, Ga + Ge, and Ga + Si. The cationic polyhedra of gehlenites and $A_3M_xT_{6-x}O_{14}$ are identical (Tables 2 and 3). Despite the significant difference between symmetries (trigonal and tetragonal), the two structural types of Ca gallogermanates have features in common as regards coordination polyhedra, isomorphous relations (Tables 2 and 3), and the alternation along the *c* axes of layers of tetrahedra and A polyhedra in the large interlayer cavities.

The increased germanium content in the trigonal phase revealed, as mentioned previously by many investigators, its amphoteric nature, cationic character, and the manifestation of the octahedral as well as tetrahedral environments. The tetrahedral layers of both gallogermanates also have similar structures. The tetrahedral melilite layer can be described as made up of translationally identical bands extended along the *a*(*b*) axis (Fig. 7*a*). Five-membered tetrahedral rings can be distinguished in each band. The tetrahedral layer in the trigonal phase is made up of similar bands twisted in succession around the 2 axes (Fig. 7*b*). As a result of the presence of germanium atoms in the octahedra in this structure, the tetrahedral five-membered rings are ruptured and the band is converted into a chain. One of the melilite tetrahedra has rotated and occupies a position on the 2 axis (Fig. 7*b*). The relative dimensions of both *a*(*b*) axes and the *c* axis in both structures are in full agreement.

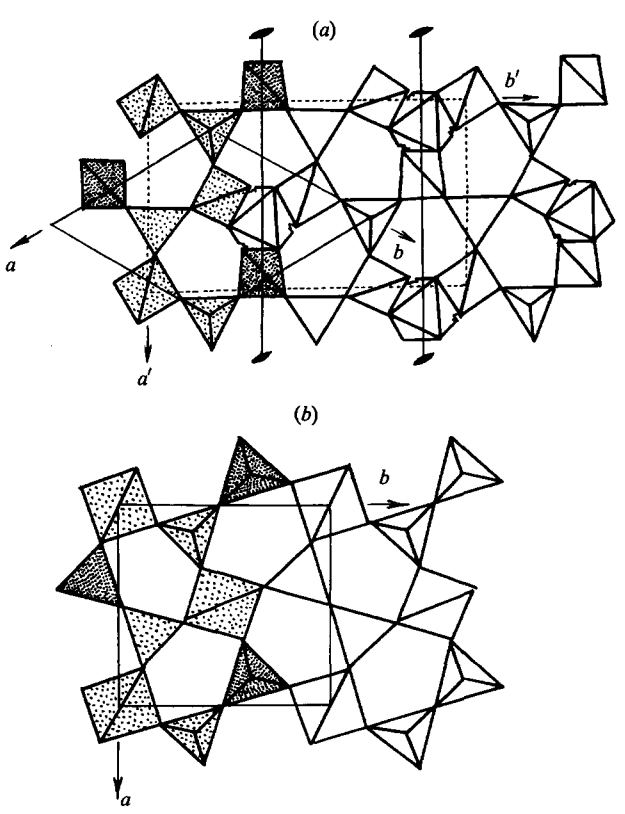


Figure 7. Comparison of the structures of $Ca_3Ga_2Ge_4O_{14}$ (*a*) and $Ca_2Ga_2GeO_7$ (*b*).

Thus the similar crystal structures involving the presence of layered elements and large cavities between them—the positions of the cations A and the impurity activator ions Nd^{3+}—made it possible to use the crystals of both structural types in lasers. Stimulated emission has been investigated.[20] According to X-ray diffraction data, crystalline $Ca_3Ga_2Ge_4O_{14}$ and $Ca_2Ga_2GeO_7$ are disordered compounds with a single activation quasi-centre.

VI. The $Pb_3GeAl_{10}O_{20}$ and $NdAlGe_2O_7$ structural types

The compound $LaSr_2Ga_{11}O_{20}$ crystallises in the $SrO-La_2O_3-Ga_2O_3$ system and its structure is similar to that of $Pb_3GeAl_{10}O_{20}$ (Table 4).[22] The results of an X-ray diffraction study showed that the Ga atoms, like the Ge and Al atoms in the structure of the prototype phase, form a mixed framework. It is made up of Ga octahedra joined into bands and Ga tetrahedra forming a highly puckered three-dimensional double-decker layer with large cavities (Fig. 8). In the tetrahedral layer, it is possible to distinguish vinogradovite bands linked in pairs by the mirror *m* planes (Fig. 8). In the cavities of the mixed framework, which has many features in common with the vinogradovite structure, there are two sites for the large La and Sr cations: sites *a* (2/*m* symmetry) at which Sr atoms are located and *i* sites (*m* symmetry) occupied isomorphously by the La and Sr atoms in proportions of 1 : 1. Calculation of the mean interatomic distances showed that a Sr–O distance of 2.691 Å is characteristic of the larger *a* cavity (distorted octahedron), whereas in the heptagon of the *i* site the mean (La, Sr)–O distance is 2.628 Å. It follows from X-ray diffraction data that the Nd^{3+} activator ion occupies the 4*i* site. The La–Sr disorder is manifested also in spectroscopic data.[22] Analysis of the parameters of the anisotropic thermal vibrations shows that the Sr atoms vibrate more freely in the *bc* plane in the intertetrahedral layer, whereas the Sr, La atoms vibrate in the direction of the *c* axis in the communicating open-network cavities (Fig. 8). The La,Sr gallate, which appears promising for use in lasers, has structural features in common with $A_3M_xT_{6-x}O_{14}$—a mixed framework made up of octahedra and tetrahedra with large cavities for identical large cations.

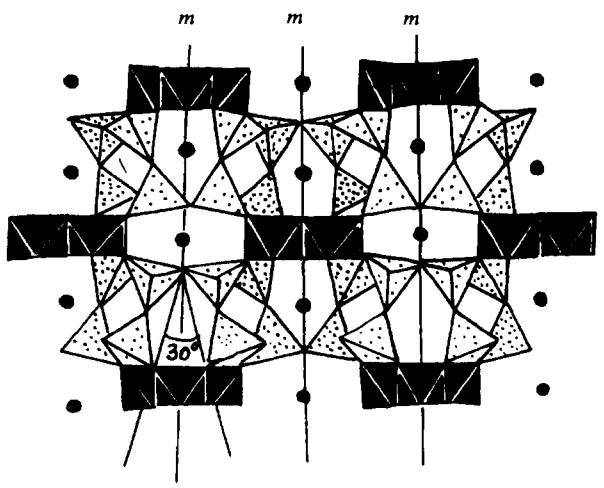


Figure 8. The crystal structure of La,Sr gallate.

Crystals of $LaGaGe_2O_7$ have been obtained in the study of the conditions for the crystallisation of $La_3Ga_5GeO_{14}$ in the $La_2O_3-Ga_2O_3-GeO_2$ system. X-Ray phase analysis[23] showed that they belong to the $NdAlGe_2O_7$ structural type. X-Ray structural study of the single crystals (Table 4) confirmed this similarity. Apart from the La gallogermanate, the Gd gallogermanate was obtained and its structure was investigated (Table 4). In the

Table 4. X-Ray diffraction characteristics of the phases investigated with structures of the $Pb_3GaAl_{10}O_{20}$ and $NdAlGe_2O_7$ types.

Compound	a/Å	b/Å	c/Å	β	Space group	μr	N_{refl}	R_{hkl} (%)
$LaSr_2Ga_{11}O_{20}$	14.576(5)	11.637(3)	5.070(1)	91.27	$I2/m$	2.4	2319	4.3
$LaGaGe_2O_7$	7.307(2)	6.635(1)	12.962(4)	117.41	$P2_1/c$	2.9	3419	7.3
$GdGaGe_2O_7$	7.160(3)	6.571(2)	12.763(4)	117.5	$P2_1/c$	2.0	3212	3.8

crystal structures of both phases, the Ge tetrahedra, combined into diortho-groups, and the Ga pentagons (distorted trigonal bipyramids) form a mixed framework as in the phases investigated previously. It is possible to distinguish in them six-sided window-rings made up of two Ga pyramids and two diortho-groups $[Ge_2O_7]$ as well as four-sided window-rings made up of two tetrahedra and two Ga pyramids (Fig. 9). The lanthanide cations (La, Gd), C.N. = 9, coordinated to O atoms are accommodated in the large cavities. The interatomic distances are La–O = 2.558 Å and Gd–O = 2.481 Å. When the crystals were activated by Nd^{3+} ions, occupying the sites for the lanthanide element, stimulated emission was obtained.[23,24]

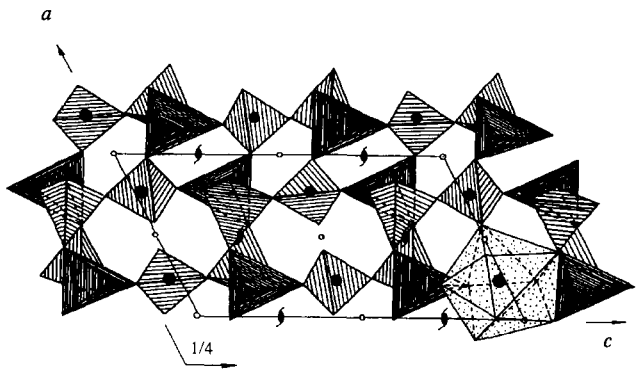


Figure 9. Projection of the crystal structure of $LaGaGe_2O_7$ onto the *ac* plane.

VII. The stillvellite–datolite structural type in the $LnBGeO_5$ series

In terms of their structures, the compounds $LnBGeO_5$ are divided into two groups: compounds with Ln = La–Pr (at low temperatures also with Nd and Eu), which crystallise with the structure of the type of the mineral stillvellite $CeBSiO_5$; the compounds with Ln = Nd–Er and Y (with Nd–Eu in the high-temperature form) have a monoclinic structure, which was assumed similar to that of stillvellite before a structural study had been carried out.

The crystal structures of $LaBGeO_5$ and $NdBGeO_5$ have been investigated.[25] The stillvellite structural type with the $P3_1$ polar space group has been confirmed for $LaBGeO_5$ (Table 5). In a study of the structure of stillvellite, it had been noted earlier[26] that it has a pseudosymmetry corresponding to the space group $P3_121$ but photographic experimental data and extremely limited diffractometer data cast doubts on the correctness of the choice of the space group $P3_1$ and precluded the determination of the deviations from the pseudosymmetry. The determination of the crystal structure of $LaBGeO_5$ made it possible to achieve this.

The positions of the heavy La and Ge atoms are very similar to the specific positions on the twofold axes in the space group $P3_121$,[24] in which the O(1, 2) and O(3, 4) atoms are linked in pairs by the twofold axes. The B and O(5) atoms are furthest away from the postulated specific positions on the twofold axes of the space group $P3_121$ and remain independent (Fig. 10). According to the literature,[27–29] the phase transition observed at T_c = 530 °C may correspond to the phase transition from the space group $P3_1$ to the space group $P3_121$ with loss of polarity by the crystals but with retention of acentricity. We may note that deviations from pseudosymmetry are significant for all the atoms in the $LaBGeO_5$ structure at room temperature and appreciably exceed the errors.[25]

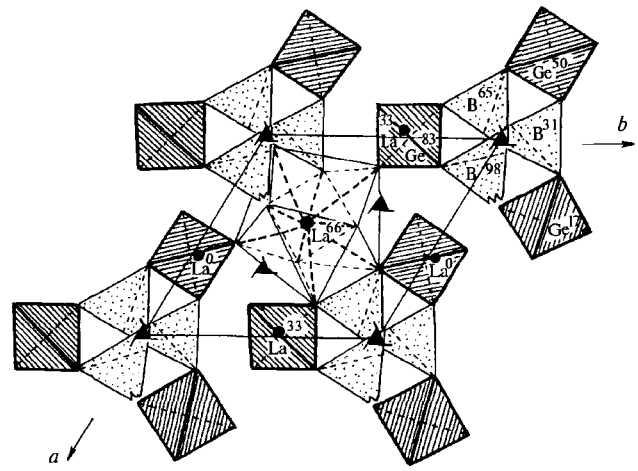


Figure 10. Projection of the crystal structure of $LaBGeO_5$-stillvellite onto the *ac* plane.

The $P3_1$–$P3_121$ phase transition belongs to the class of second-order phase transitions of the displacement type. The $LaBGeO_5$ structure can be described as made up of columns of La nonagons and Ge tetrahedra (Fig. 10) extended along the c axis. Chains made up of $[BO_4]$ tetrahedra, forming together with the Ge tetrahedra the $[BGeO_5]$ chain radical, are extended between the columns in the same direction along the c axis.[26] In an independent accurate study of the crystal structure of stillvellite,[30] difficulties were noted in refining the positional and thermal parameters of the O(5) atom and additional electron density peaks in the vicinity of this atom were observed. The authors[30]

Table 5. X-Ray diffraction characteristics of the $LaBGeO_5$ phases investigated with structures of the stillvellite and datolite types.

Compound	a/Å	b/Å	c/Å	β	Space group	μr	N_{refl}	R_{hkl} (%)
$LaBGeO_5$	7.020(5)	–	6.879(4)	–	$P3_1$	0.95	1407	2.9
$NdBGeO_5$	10.048(20)	7.610(10)	4.964(7)	92.0	$P2_1/a$	3.00	2367	3.0

concluded that the crystal investigated is twinned and is obtained as a result of rotation about an axis along the [110] direction. The polar individuals are linked in opposite directions along the c axis, their volumes amounting to 0.605 and 0.395 respectively.

Numerous studies of the physical properties of the $LaBGeO_5$ crystal, in particular the laser, nonlinear optical,[31] and ferroelectric[28,29] properties, have shown that this material possesses all three properties. For example, the intensity of the generation of the second harmonic in this crystal exceeds by a factor of 50 the intensity in $La_3Ga_{5.5}Nb_{0.5}O_{14}$ (see above). The possibility of obtaining large high-quality single crystals from the melt constitutes an advantage of $LaBGeO_5$ over, for example, other likely materials for the creation of effective lasers with self-multiplication of the lasing frequency, such as $LiNbO_3$ and $YAl_3(BO_3)_4$ with Nd^{3+}. Structural data make it possible to explain the occurrence of the spontaneous polarisation P_s in the given crystal and its ferroelectric properties.

The crystal structure of $NdBGeO_5$ differs from that of stillvellite[25] but is close to the structure of another natural borosilicate—datolite $CaBSiO_4(OH)$ and it involves the replacement in the latter of Ca by Nd, of Si by Ge, and of OH^- by O^{2-}. It can be described as a layered structure (Fig. 11) in which the large-cation layers alternate with tetrahedral layers along the c axis. Tetrahedral layers, the structure of which is similar to that of the datolite layers, are also present in melilite, the structural type of which was described above. A similarity between the melilite and $A_3M_xT_{6-x}O_{14}$ layers was noted at the same time (Fig. 7). The Nd and Ca coordination polyhedra are identical—they are all the same Thompson cubes. As regards the manifestation of physical properties, the presence of the centrosymmetrical space group for members of the lanthanide series ranging from Nd and beyond rules out the nonlinear optical and ferroelectric properties, but the possibility of the manifestation of laser properties is retained.

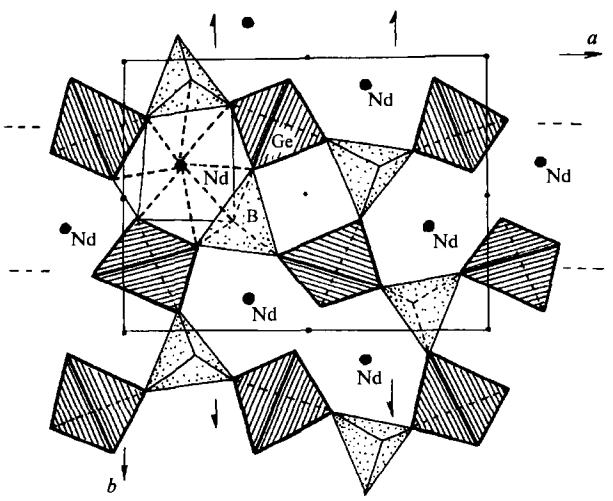


Figure 11. Projection of the crystal structure of $NdBGeO_5$-datolite onto the *ab* plane.

Two polymorphic modifications of $LnBGeO_5$—the chain (stillvellite) and layered (datolite) modifications—have significantly different structures. The polymorphism of $LaBGeO_5$ is associated with the variation of the sizes of the Ln^{3+} ions (the lanthanide contraction). The stillvellite structure is characteristic of compounds with large ions accommodated in coordination polyhedra (nonagons), whereas for members of the series with smaller ions, the stability of the stillvellite structure diminishes and in the datolite structure the coordination polyhedra are octagons—Thompson cubes. Both structures obtain for cations of average size ($Nd^{3+}-Eu^{3+}$).

The sharp difference between the structures of the two polymorphic modifications of $LnBGeO_5$ is manifested in absorption luminescence spectra.[25] In both structures, the Nd^{3+} ions form activator centres of the same type. On the other hand, the coordination numbers, coordination polyhedra, and the symmetries of sites differ markedly in the structures of these centres. In conformity with the structural results, the spectroscopic data show that both phases belong to the class of simple crystals with an ordered structure.

VIII. Lanthanide borates with the huntite structure and their polytypic derivatives

The compound $YAl_3(BO_3)_4:Nd^{3+}$ with the huntite $CaMg_3(BO_3)_4$ structure already attracted the attention of investigators a long time ago—since the beginning of the 1960s. The crystals of Y,Al-huntite possess a combination of laser and nonlinear optical properties.

Studies on the solution-melt crystallisation of the Y, Al borate made it possible to obtain crystals of this compound of satisfactory quality; structural studies have been carried out for the compounds $NdAl_3(BO_3)_4$[32] and $GdAl_3(BO_3)_4$,[33] directly for $YAl_3(BO_3)_4$,[34] and also for $NdGa_3(BO_3)_4$[35] and $(Nd,Bi)Fe_3(BO_3)_4$.[36] It was observed that, apart from the huntite modification,[34–36] further monoclinic high-temperature modifications[32,33] are characteristic of $LnAl_3(BO_3)_4$. They were investigated in relation to $NdAl_3(BO_3)_4$ and $GdAl_3(BO_3)_4$. The crystallisation regions of the high-temperature modifications of the neodymium and gadolinium borates differ appreciably. The high-temperature monoclinic modification of the Nd,Al borate is stable over a wide temperature range (from 870 to 1150 °C). The high-temperature monoclinic modification of Gd,Al borate was noted in the crystallisation of highly supersaturated solution-melts at a temperature above 1060 °C. It was shown[5] that the two monoclinic modifications of Nd,Al and Gd,Al borates are different polytypic modifications having the same parameters a and b but different parameters c, structures, and space groups (Table 6).

In the rhombohedral cell of huntite, it is possible to select the monoclinic C cell in accordance with familiar rules. One of the $a(b)$ axes of the trigonal cell then becomes the monoclinic axis, one of the R translations becomes a C translation, and the a and c axes with the corresponding angle β may be selected on the basis of the R lattice sites in the plane perpendicular to b. In both monoclinic borates, it is possible to select cells with the same monoclinic angle β in which the parameters c'_2 and c'_3 are greater by factors of 2 and 3 respectively than the parameters c'_1 of the huntite modification ($c'_1 = 5.9$ Å) considered in the monoclinic aspect.

Dornberger-Schiff[37] devised a theory of OD structures the symmetry relations of which have been applied widely and clearly for the description of the characteristics of polytypic structures with differentiation of one or more types of layers and consideration of different kinds of neighbours. Thus it is possible to differentiate layers of two types (L_{2n} and L_{2n+1}; Fig. 12) in the monoclinic cells of three modifications of lanthanide borates (huntite, Nd,Al and Gd,Al borates). The layers of the first type (L_{2n}) are made up of pairs of edge-linked Al octahedra combined by B triangles into a layer. The formula of the layer is $[Al_2B_2O_{10}]$ and its symmetry is higher than that of each structure and can be described in terms of the $C2/m$ symmetry group. Layers of the second type (L_{2n+1}) are made up of Ln trigonal prisms and Al octahedra linked via their apices into columns extended along the a axis; the columns are also bound by the B triangles. The formula of the layer is $[LnAlB_2O_{10}]$ and its symmetry is $C2$. When two layers are combined in the structure, sixteen oxygen atoms are shared and a compound with the formula $LnAl_3B_4O_{12}$ is obtained. The subsequent odd L_{2n+1} layers are obtained from the initial layer by multiplication involving symmetry operations on the even L_{2n} layers: by the twofold axes in the case of huntite, by the centres of symmetry $\bar{1}$ in the case of Nd,Al borate, and by the twofold axes and the centres of symmetry $\bar{1}$ simultaneously with the

Table 6. X-Ray diffraction characteristics of the $LnAl_3(BO_3)_4$ phases investigated.

Compound	a/Å	b/Å	c/Å	β	Space group	μr	N_{refl}	R_{hkl} (%)
$YAl_3(BO_3)_4$	9.295(3)	–	7.243(2)		$R32$	0.8	450	3.7
$NdGa_3(BO_3)_4$	9.500(1)	–	7.502(2)		$R32$	2.0	464	3.0
$(Nd_{0.5}Bi_{0.5})Fe_3(BO_3)_4$	9.587(3)	–	7.608(2)		$R32$	2.4	654	3.9
$NdAl_3(BO_3)_4$	7.262(3)	9.365(3)	11.138(7)	103.41	$C2/c$	1.4	3641	5.0
$GdAl_3(BO_3)_4$	7.262(3)	9.315(3)	16.184(4)	90.37	$C2$	1.5	5063	5.2

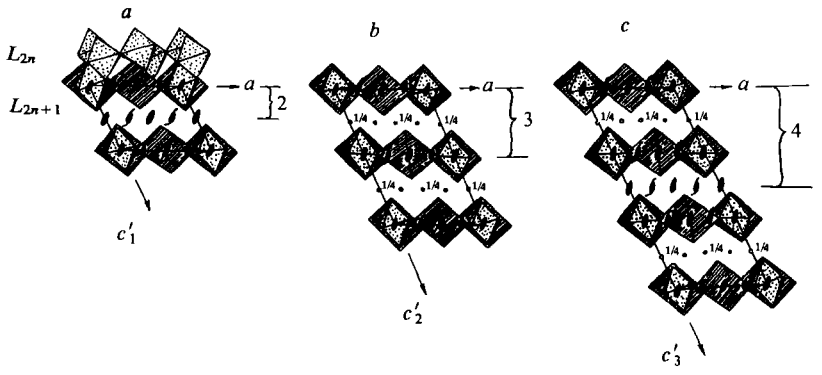


Figure 12. Polytypic diversity in the family of Ln,Al borates: (*a*) huntite (222...); (*b*) the Nd,Al modification ($\bar{1}\bar{1}\bar{1}$...); (*c*) the Gd,Al modification ($\bar{1}\bar{1}2\bar{1}\bar{1}2$...).

$\bar{1},\bar{1},2,\bar{1},\bar{1}$... alternation in the case of Gd,Al borate. Thus the odd layers in the structures with the C_2 symmetry are multiplied by the $C2$ and $C\bar{1}$, subgroups belonging to the $C2/m$ group of the even layer.

L_{2n}	L_{2n+1}
$[Al_2B_2O_{10}]$	$[LnAlB_2O_{10}]$
C 1 2/m (1)	C 1 2 (1)
[P 1 2 (1)]	[C 1 2/$\bar{1}$ (1)]

The result obtained expresses the operation of the familiar Dornberger-Schiff theorem, according to which the number of combinations of two layers Z is equal to the ratio of the multiplicity of the symmetry group of the initial layer N and the multiplicity F of the symmetry group of a pair of layers, i.e. $Z = N/F$. In the given case, $Z_{2(1)} = 4/2 = 2$. The sequence 222... corresponds to a structure with a period c in one pair of layers (Fig. 12, braces) — this is the huntite structure, which can be described in terms of the rhombohedral setting. The sequence $\bar{1}\bar{1}\bar{1}$... corresponds to a structure with a period c in two pairs of layers — this is the high-temperature $NdAl_3(BO_3)_4$ modification. The sequence $T\,\bar{1}\bar{1}2\bar{1}\bar{1}2$... corresponds to the third, $GdAl_3(BO_3)_4$ structure and has a period in three pairs of layers.

The different sequences of operations afford hypothetical structures with different periods and symmetries. The possible variants for 10-layer polytypes with a symbolic-literal description have been specified by Zvyagin and Belokoneva.[38]

The Laue diffraction patterns for Nd huntite, obtained (in contrast to the remaining lanthanide borates) by rapid quenching, showed, together with point reflections also distinct diffuse reflections. Out of the three equally legitimate a axes in the trigonal cell, one axis, which possesses a plane of symmetry according to the diffuse reflections, was selected. The $h0l$ and $h1l$ layer lines, corresponding to the monoclinic setting of the trigonal phase, were recorded along this axis. Distinct diffuse lines, along which the index l varies continuously, were observed on the Weissenberg diffraction pattern. Point reflections, corresponding to integral values of l for c in the huntite structure were distinguished against their background. This type of picture indicates the breakdown of a rigorous order in the alternation of layers and the existence of a disorder superimposed on the ordered structure.

It is seen from the foregoing that the decisive factors in the formation of borate polytypes and in the breakdowns of order in the latter are the crystallisation temperatures and the rate of cooling of the melt. The higher the crystallisation temperature, the more complex the polytypes. Polytypes even more complex than those established hitherto may be found among them. Strictly ordered polytypes are formed on slow cooling, while at a high cooling rate a nonordered structure also arises against the background of the simplest ordered structure (as in trigonal huntite)

The nature of the lanthanide element also plays a definite role in polytypicism. It has been noted[39] that the statistics of the morphotropic transitions in tetrahedral compounds (silicates, germanates, phosphates) with lanthanide elements makes it possible to differentiate a single common region around Nd (in the case of germanates this also applies to Gd). The $LnBGeO_5$ and $LnAl(BO_3)_4$ series provide a good illustration of the empirical rule noted above. The reason for it is the magnitudes of the ionic radii of the lanthanide elements.

The phase transitions between the polytypic modifications examined above, which occur at different temperatures and sometimes coexist (for example, in the case of Pr, Al borate[40]) are second-order phase transitions of the 'order–disorder' type and are accompanied by very slight changes in structure.

Structural studies made it possible to account for the absence of nonlinear optical properties in $NdAl_3(BO_3)_4$, unlike $YAl_3(BO_3)_4$, and also for the impairment of their laser properties†. The former is associated with the presence in the Nd,Al borate crystals of the monoclinic centrosymmetric space group $C2/c$, while the latter is associated with the polytypic nature of the phases, which entails a tendency towards disorder and inhomogeneity in the crystal, particularly with increase in the crystallisation temperature.

IX. The $KTiOPO_4$ structural type

Potassium titanyl phosphate $KTiOPO_4$ (PTP) is nowadays one of the most effective nonlinear optical crystals.[1] The germanate and silicate analogues of $KTiOPO_4$ having the general formula

† In all the crystals, the positions of the activator ions correspond to the positions of Ln or Y.

Table 7. X-Ray diffraction characteristics of the phases investigated with structures of the $KTiOPO_4$ type.

Compound	a/Å	b/Å	c/Å	Space group	μr	N_{refl}	R_{hkl} (%)
$KSbOGeO_4$	13.224(2)	6.597(1)	10.759(2)	$Pna2_1$	1.35	3044	2.6
$KTaOGeO_4$	13.386(3)	6.658(3)	10.997(2)	$Pna2_1$	3.10	2110	3.3
$RbNbOGeO_4$	13.382(3)	6.708(2)	10.746(2)	$Pna2_1$	1.70	1747	3.9
$NaSbOGeO_4$	13.008(5)	6.433(2)	10.736(3)	$Pna2_1$	0.73	2328	2.6
$TlSbOGeO_4$ at T/K							
293	13.369(2)	6.668(1)	10.758(1)	*Pnan*	3.9	764	3.7
280	13.331(2)	6.659(1)	10.740(3)	*Pnan*	3.9	1705	7.7
253	13.368(3)	6.669(2)	10.767(3)	$Pna2_1$	3.9	1331	4.5
123	13.358(2)	6.664(1)	10.762(1)	$Pna2_1$	3.9	1429	4.3
$AgSbOSiO_4$ at T/K							
293	12.832(9)	6.331(4)	10.727(6)	$Pna2_1$	0.66	1300	4.3
973 + slow cooling	12.786(6)	6.305(5)	10.717(7)	$Pna2_1$	0.72	1133	5.1
673 + quenching	12.781(4)	6.307(2)	10.754(3)	*Pnan*	0.55	1148	4.8

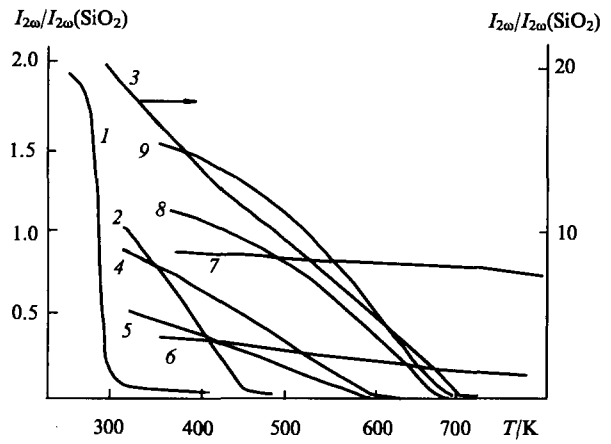


Figure 13. Temperature variation of the intensity of the second harmonic generation signal[7,44] for different powders: (*1*) $TlSbGeO_5$; (*2*) $RbSbGeO_5$; (*3*) $KTaGeO_5$; (*4*) $KSbGeO_5$; (*5*) $KSbSiO_5$; (*6*) $NaSbSiO_5$; (*7*) $NaSbGeO_5$; (*8*) $AgSbSiO_5$; (*9*) $AgSbGeO_5$.

$AMOXO_4$ (A = Na, K, Rb, Tl, Ag; M = Sb, Ta; X = Ge, Si) have been obtained recently and their structures have been investigated.[41,42] On the basis of results of measurements of the temperature dependence of the generation of the second harmonic of laser radiation[7] (Fig. 13), as well as dielectric and microcalorimetric studies,[43] the phase transitions were assigned to the class of second-order transitions. The possibility of a weak first-order transition has also been considered for $TlSbOGeO_4$ and $AgSbOSiO_4$.[44,45] The Curie points T_c, determined by various methods, agree satisfactorily and the entire group of compounds has as a whole significantly lower T_c than the phosphates and arsenates known up to that time.

The study of the phase transitions in new compounds of the $KTiOPO_4$ structural type makes it possible to discover the structural features responsible for the ferroelectric and nonlinear optical properties. According to the results of measurements of second harmonic generation (SHG), the crystal structures of K,Sb germanate, Rb,Sb germanate, K,Ta germanate, and also $NaSbOGeO_4$ obtained from $KSbOGeO_4$ by ion exchange in a $NaNO_3$ melt (the sold-phase synthesis affords a sphene structure) proved to be polar (Table 7) like that of $KTiOPO_4$.[41,45–47] According to the results of French investigators,[48,49] Na, Sb and K, Sb silicates are also polar at room temperature with the space group $Pna2_1$.

The study of the crystal structures of $KFeFPO_4$ and $KSnOPO_4$ showed that the mixed framework made up of Fe(Sn) octahedra and P tetrahedra possesses a pseudosymmetry corresponding to the space group *Pnan* (Fig. 14).[50,51] It follows from this that there is a possibility that a highly symmetrical prototype phase may exist. SHG measurements have shown[7] that Tl, Sb germanate should have the structure of the centrosymmetric modification at room temperature, since T_c = 272 K for this compound.

The structure of $TlSbOGeO_4$ at room temperature has been investigated by Belokoneva and Mill'[52] and then reinvestigated by Belokoneva et al.[53] Within the framework of the *Pnan* group, the position of the Tl atom was found to be split (the Tl – Tl′ distance is 0.6 Å for populations of 0.65 and 0.35 respectively). The splitting of the positions of the cations in the large cavities of the mixed framework made up of M octahedra and P tetrahedra was first established for $KFeFPO_4$ and $KTiOPO_4$, where additional split positions were noted for the K(1) and K(2) atoms but with significantly smaller populations: 0.1 (in the additional position) compared with 0.9 (in the main position).[50] Crystal-chemical analysis showed that the splitting originates from the main positions along the direction of two additional pseudosymmetrical positions (Fig. 14).[52]

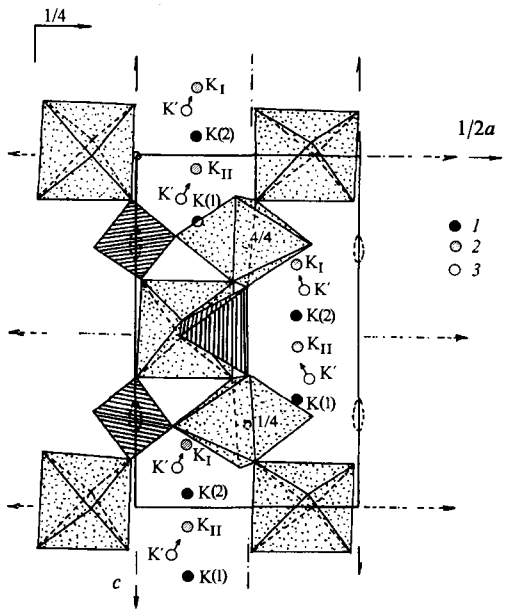


Figure 14. The pseudosymmetry of the framework in $KTiOPO_4$-like phases. The continuous lines represent the true symmetry elements of the space group $Pna2_1$, while the dashed lines represent the symmetry pseudoelements of the space group *Pnan*: (*1*) principal positions of K atoms; (*2*) additional positions; (*3*) unoccupied pseudosymmetrical positions.

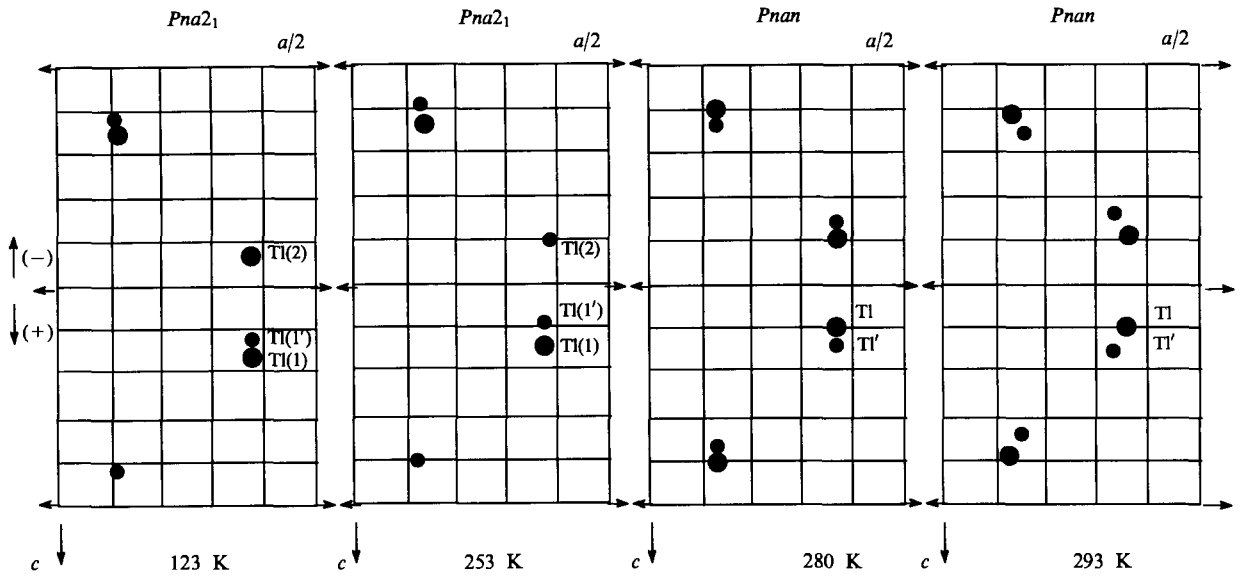


Figure 15. Disposition of Tl atoms at four temperatures in the $TlSbOGeO_4$ structure. The true axes in the space group *Pnan* and the twofold pseudoaxes in the space group $Pna2_1$ are shown at the 1/2 level on the *c* axis (at 123 and 253 K).

For the $TlSbOGeO_4$ crystal structure, the polar modification should exist also at a low temperature. It was expected that the Tl atoms would then be displaced from their positions in the structure to form an acentric modification. In order to determine the polar modification of the Tl, Sb germanate, low-temperature studies were carried out. At 123 K, the structure did indeed prove to be acentric[53] and the maximum displacement [to a greater extent for Tl(2) than for Tl(1)] was ~0.8 Å.

It was of interest to follow the dynamics of the phase transformation in the vicinity of the Curie point (272 K). For this purpose, a low-temperature X-ray diffraction experiment was carried out at 253 K. A study was also made of the structural state at 280 K, corresponding to an intermediate point between T_c and a second extremum at 286 K, observed in measurements of the relative permitivity and the electrical conductivity of $TlSbOGeO_4$ single crystals.[44] The results of the measurements and structural calculations at the above four temperatures are presented in Fig. 15 and Table 7.[53,54] The positions of the Tl atoms and the positions symmetrical to them in the two modifications are linked by either a true twofold axis or a twofold pseudoaxis. The distances from the ½ level along the *c* axis, (+) and (−), are given in Table 8. It is seen from the data in Table 8 that, compared with room temperature, the populations of the positions at 280 K remain unchanged, the atoms being slightly displaced towards the twofold axis. Overall, the structure determined from the system of sharp reflections (diffuse ring reflections with a texture similar to that of metals were also observed on the rocking X-ray diffraction pattern) retains the centrosymmetric space group and its principal characteristics. At 253 K, after passage through T_c = 272 K, the space group changes and becomes acentric, one of the Tl positions (−) is no longer split and the (+) and (−) distances are not strictly equal (Table 8), although they are in fact similar to one another [Tl(2) and Tl(1′)] and to the distances for the Tl and Tl′ positions at 280 K. The populations of the Tl−Tl′ positions (280 K) and Tl(1′)−Tl(1) positions (253 K) also change. With decrease in temperature, the polarity of the *c* axis increases owing to further displacement of the Tl atoms. The difference between the (+) and (−) distances increases and is now appreciably different from that in the initial (293 K) state (Table 8). As mentioned above, the overall shift is ~0.8 Å. The thermal corrections for the Tl and O atoms at 253 K indicate the instability of the structure near the phase transition.

One may conclude that the thallium atoms are most responsible for the paraelectric⇆ferroelectric phase transitions. The calculated displacements of the remaining atoms of the structure are an order or two orders of magnitude smaller.[54] The phase transitions are most probably mixed second-order phase transitions, being simultaneously of the displacement and order–disorder type, since not only are the thallium atoms displaced but there is a change in the splitting of the positions and their populations [Tl(1) ⇆ Tl(1′)]. The appearance of structural polarity along the *c* axis is directly responsible for the occurrence of the spontaneous polarisation P_s in the same direction, which has been attributed to the manifestation of ferroelectric and nonlinear optical properties. We may note that a high ionic conductivity is characteristic of $TlSbOGeO_4$.

Such treatment of the structural transformations is consistent with the approaches developed by Abrahams[2] in order to account for the structure–ferroelectric properties relation. The Abrahams–Kurtz–Jamieson (AKJ) criterion relates the square of the maximum displacement of the atom along the polar direction from the position with zero spontaneous polarisation to the

Table 8. The distances between the Tl atoms in $TlSbOGeO_4$ and the true twofold axis or twofold pseudoaxis.

Atom	Space group $Pna2_1$		Atom	Space group *Pnan*	
	123 K	253 K		280 K	293 K
			Tl′	−0.1441 (1.55)	−0.1502 (1.62)
Tl(2)	−0.0827 (0.89)	−0.0985 (1.06)	Tl	−0.0959 (1.03)	−0.1029 (1.11)
Tl(1′)	−0.1242 (1.34)	+0.0938 (1.01)	Tl	+0.0959 (1.03)	+0.1029 (1.11)
Tl(1)	+0.1562 (1.68)	+0.1464 (1.58)	Tl′	+0.1441 (1.55)	+0.1502 (1.62)

Note. Values expressed as fractions of the cell are quoted, the same values in Ångstroms being given in brackets.

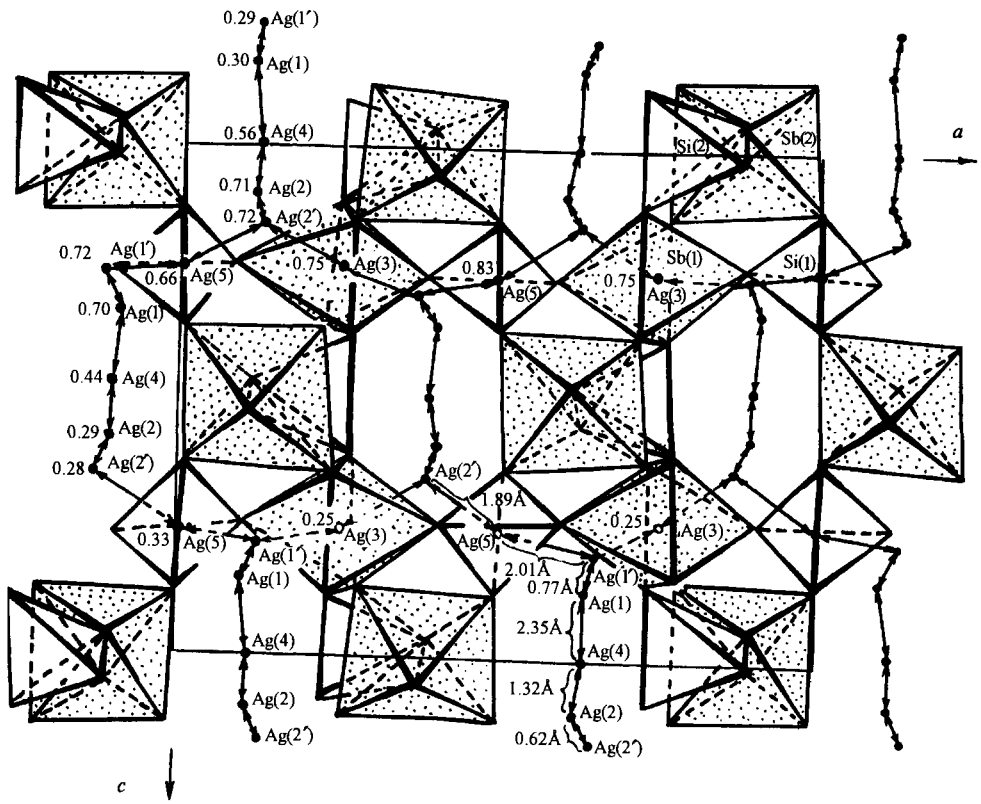


Figure 16. The cation migration pathways in $AgSbOSiO_4$ (projection onto the *ac* plane). The heights of the atoms and the distances between the positions in the independent increment are shown.

Curie point T_c.[2] According to this criterion, the group of germanates investigated, belonging to the $KTiOPO_4$ structural type and having in the polar state a higher pseudosymmetry than $KTiOPO_4$ and other phosphates and arsenates, should be distinguished by smaller atomic displacements in phase transitions and should have a correspondingly lower Curie point T_c, which has in fact been observed in measurements.

The higher pseudosymmetry and the very slight distortion of the octahedra in the germanates investigated (with which the non-linear optical properties are traditionally associated) compared with the Ti octahedra in $KTiOPO_4$ are responsible for the significantly lower intensity of the SHG signal in these compounds than in 'record holders' such as $KTiOPO_4$ and $KTiOAsO_4$.

The results of the study of the $AgSbOSiO_4$ structure (Table 7) constitutes an extremely remarkable example confirming that the cations in compounds of the given structural type are responsible for the course of the phase transitions and the ionic conductivity. Like $NaSbOGeO_4$ crystals, those of $AgSbOSiO_4$ have been obtained by ion exchange in a nitrate melt.[45] Despite the clear acentricity of the structure at room temperature, both positions, Ag(1) and Ag(2), are split, the components having similar populations, as in the case of $TlSbOGeO_4$, i.e. the Ag atoms occupy virtually all four possible positions[50,55] for cations in the cavities. The electron density difference maps unexpectedly show peaks at positions corresponding to cavities joining the large cavities within the skeleton, i.e. to passages between the tetrahedra and octahedra and also at the centres of the largest cavities between the four positions occupied by cations. This made it possible to discover the real ion-exchange channels. Previously their existence in structures of the $KTiOPO_4$ type was merely postulated in view of the manifestation of ion-exchange properties by the latter.[56]

Fig. 16 illustrates the ion-exchange channels in the $AgSbOSiO_4$ structure. The Ag(5) position, located in the widest passages between the tetrahedra, is populated to the greatest extent in the structure (population coefficient $f = 0.07$). Some of the silver atoms have 'settled' at the centres of the cavities at the Ag(4) position ($f = 0.04$). Traces of silver have been detected also at the Ag(3) position ($f = 0.01$) in the narrower passages between the more bulky octahedra (compared with tetrahedra). Accordingly, the populations of the three principal positions of the Ag atoms in the structure are found to be deficient.

The schematic representation of the potential relief profile in Fig. 17 for the principal conductivity channel along the *c* axis

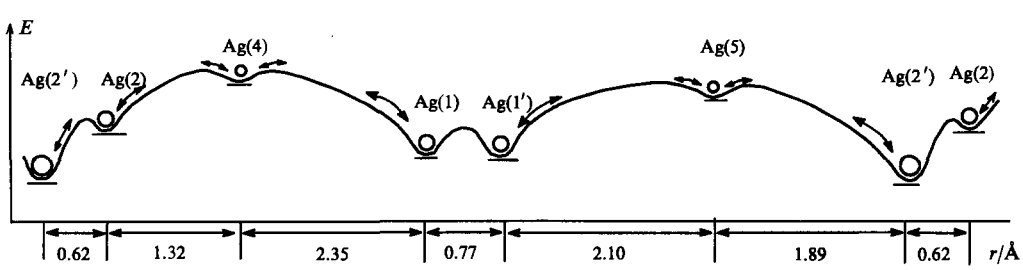


Figure 17. Schematic profile of the potential relief of the main ion-exchange channel in the $AgSbOSiO_4$ structure.

(a second possible path is along the *a* axis; there is no path along the *b* axis) illustrates the jumps of Ag atoms during ion migration. This state is unstable and one may expect that, for example on heat treatment of the crystals, the Ag(3, 4, 5) positions will be vacated.

Annealing of the specimens with subsequent quenching and slow cooling yielded interesting results. Slow cooling from 973 K leads to the same polar structure but with vacated Ag(3, 4, 5) positions and with some redistribution of the silver atoms relative to the initial ion exchange state at the main positions.

Fixation by quenching at 673 K afforded the high-temperature centrosymmetric modification. In contrast to the positions of the Tl atoms in $TlSbOGeO_4$, the positions of the Ag atoms in $AgSbOSiO_4$ (space group *Pnan*) are hardly split (f = 0.02) (Fig. 18). The population of the position corresponding to the tetrahedral passage diminished appreciably and the positions at the centre of the cavity and between the octahedra were vacated.

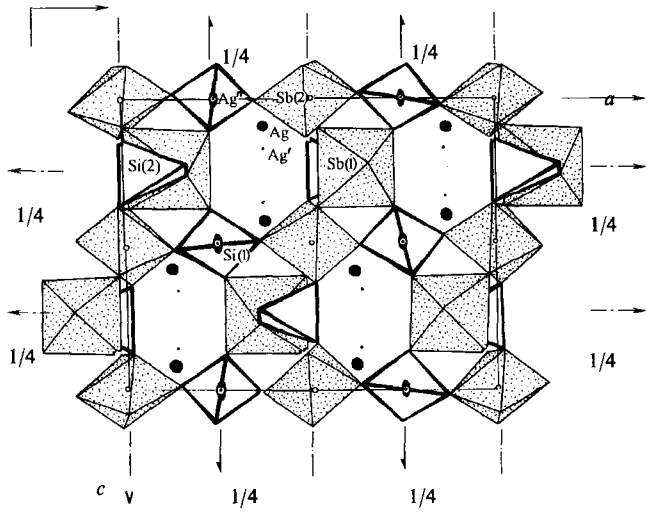


Figure 18. Projection of the centrosymmetric modification of $AgSbO.SiO_4$ onto the *ac* plane after annealing at 673 K and quenching. The positions of the Ag atoms and the symmetry elements of the space group *Pnan* are shown.

The course of the phase transformations in $AgSbOSiO_4$ is also reflected in Fig. 19, where the state at 293 K and that quenched at 673 K are the extreme possible states, while the state obtained on slow cooling from 973 K is intermediate. The Ag(2′)–Ag(2′)–Ag positions populated to the maximum extent are retained together with the Ag(1)–Ag(1)–Ag positions. The Ag(1) position (973 K) begins to split only on cooling, but does not return to the initial state Ag(1′) at 293 K. The pseudosymmetry of the crystal annealed at 973 K is much higher than the pseudosymmetry of the crystal cooled to 293 K. This is also seen from the comparison of the coordinates of the (+) and (−) positions of the Ag atoms, as for the Tl atoms in the case of $TlSbOGeO_4$.

This confirms the conclusion reached previously for the Tl compound that the disposition of the cations in the cavities of structures of the $KTiOPO_4$ type is the principal determinant of their symmetry and hence of their properties. X-Ray diffraction studies[55] made it possible for the first time to locate the pathways followed in the migration of the cations in structures of the $KTiOPO_4$ type and to explain the preferred conduction along the *c* axis, the weak conduction along the *a* axis, and its absence along the *b* axis.

A tetragonal pseudosymmetry is also characteristic of $KTiOPO_4$, which had been noted already by Tordjman et al.[57] The tetragonal modification has also been detected[58] for the compound $K(Mg_{1/3}Nb_{2/3})PO_5$. The results make it possible to conclude that the isomorphous substitutions play an important role in the manifestation of nonlinear optical properties, in particular that they are sharply impaired when Mg atoms are incorporated in the structure.

X. The sphene (titanite) structural type

As already mentioned above, the solid-phase synthesis of $NaSbOGeO_4$ leads to the sphene structure. This indicates a similarity of the regions corresponding to the existence of these two structural types. Among the four crystalline sphene structures (Table 9), only one has the $P2_1/c$ space group characteristic of the low-temperature modification. Note that $LiTaGeO_5$ has in addition a strongly pseudohexagonal symmetry[59] ($KTiOPO_4$-like phases have a pseudotetragonal symmetry). The formation of high-pressure modifications at

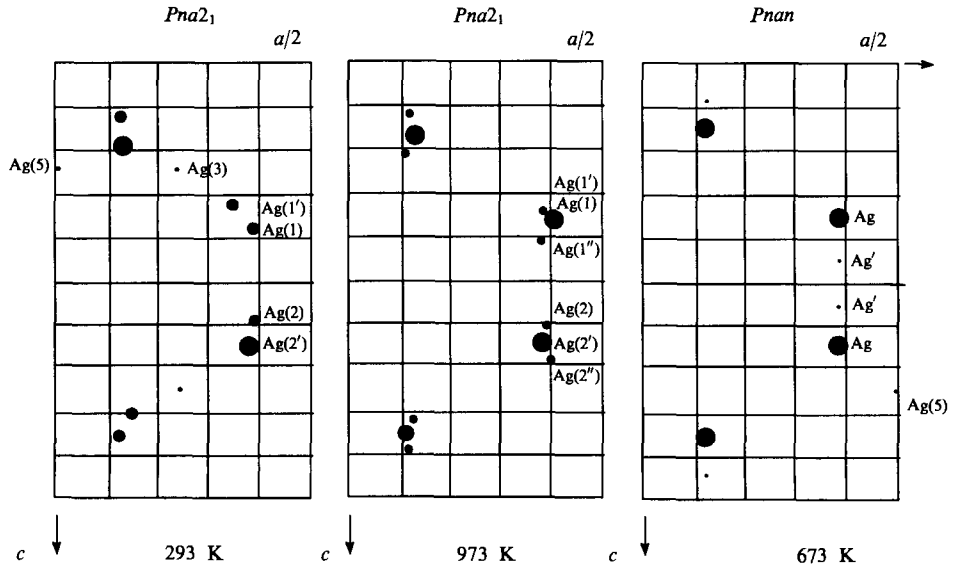


Figure 19. Disposition of the Ag atoms in the $AgSbOSiO_4$ structure at three temperatures.

Table 9. X-Ray diffraction characteristics of the phases investigated with structures of the sphene and sillimanite types.

Compound	a/Å	b/Å	c/Å	β	Space group	μr	N_{refl}	R_{hkl} (%)
$NaNbGeO_5$	6.798(4)	8.913(3)	7.523(2)	115.42	$P2_1/c$	0.7	2445	2.6
$NaTaGeO_5$	6.843(4)	8.916(4)	7.417(7)	114.77	$C2/c$	1.3	600	6.3
$LiTaGeO_5$	7.589(5)	8.130(4)	7.509(6)	119.55	$C2/c$	1.35	918	4.9
$NaSbGeO_5$	6.722(6)	8.892(7)	7.220(7)	114.76	$C2/c$	0.9	1517	3.3
$LiNbGeO_5$	7.738(1)	7.512(1)	6.706(6)	–	$Pnam$	1.1	1694	2.0

pressures significantly lower than for silicates is characteristic of germanates. The high-temperature modifications are formed with a $KTiOPO_4$ type of structure at much lower temperatures than, for example, those of phosphates. The sphene germanates also crystallise preferentially with the space group $C2/c$ (the high-temperature modification). The reason for this is the unusual crystal-chemical properties of the Ge atoms (large ionic radius, smaller electronegativity compared with Si), which are manifested, in particular, by the much greater ease of the formation of compounds with Ge atoms in the octahedra.

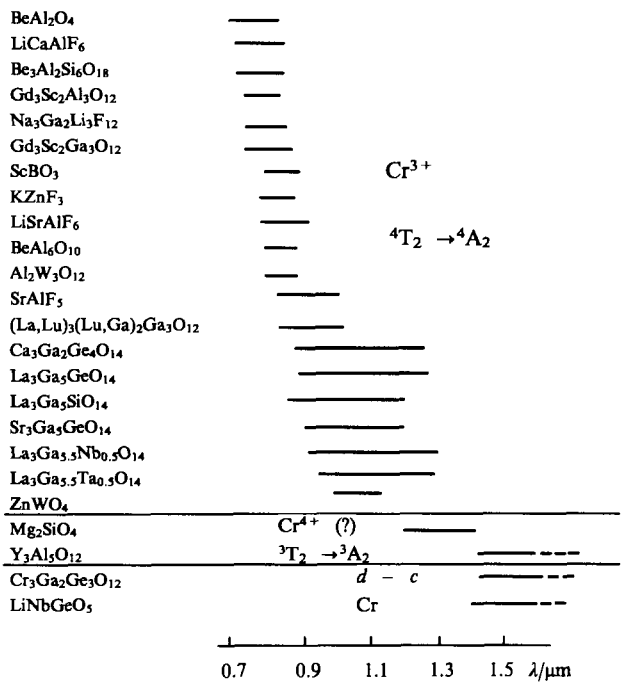


Figure 20. The spectral ranges corresponding to the retuning of the lasing wavelength for chromium-containing laser crystals.[61]

In the study of niobium-containing compounds, it was observed that the compound $LiNbGeO_5$ crystallises in the fairly unexpected sillimanite (Al_2SiO_5) type structure. The two structures are similar, when account is taken of the replacement of Li by Al, of Nb by Al, and of Ge by Si and of the change in the symmetry space group. Chains of Nb, Sb, and Ta octahedra, equivalent to the Ti octahedra in natural sphene, are differentiated in the $LiNbGeO_5$ structure, as in the sphene structure. According to the spectroscopic data of Dutch investigators[60] as well as our own data,[61] stimulated emission can be excited from $LiNbGeO_5$, especially in the presence of a Cr^{3+} admixture. Consequently, this crystal can be used in lasers. The spectroscopic characteristics of 24 chromium-containing compounds (Fig. 20) and of well known laser crystals (Y,Al and Gd, Sc garnets, fluorides, and oxides) and of the new phases examined in the present review have been compiled and compared.[61]

XI. Germanate-zeolites and zeolite-like germanates

In a study of compounds which are potential ferroelectric materials, Abrahams[2] considered also the crystal structure of natural cancrinite (space group $P6_3$). The germanium analogue of cancrinite was obtained by hydrothermal synthesis. Whilst retaining the size of the unit cell and the space group (Table 10), the synthetic Ge-cancrinite contains the octahedral $Ge(OH)_6^{2-}$ group instead of CO_3 (Fig. 21).[4] The positions occupied in the lattice by the Ge, Al, O(1, 2, 3, 4) as well as Na(1, 2) atoms are completely filled while the Ge^{VI} position is half-filled. The change in coordination from plane-trigonal for the C atom to octahedral for the Ge atom following the replacement of CO_3 by $Ge(OH)_6^{2-}$ induces a slight shift of the Ge atom from the position occupied by the C atom on the c axis. The positions of the water molecules in the structure have also been determined. It was found that the large cavity-channels along the c axis ensure the ion-exchange properties of the synthetic cancrinite. In natural cancrinite, these cavities are blocked by OH groups, while in the synthetic Ge-cancrinite the cavity is occupied by the $[Ge(OH)_6]^{2-}$ groups, which are, as it were, trapped by the structure—the $Ge(OH)_6$ octahedra had been observed earlier in the mineral stottite $Fe[Ge(OH)_6]$. Thus the synthetic germanium cancrinite possesses ion-exchange properties and is a potential ferroelectric material.

Table 10. X-Ray diffraction characteristics of the zeolite-germanates and zeolite-like germanates investigated.

Compound	a/Å	b/Å	c/Å	Space group	μr	N_{refl}	R_{hkl} (%)
Cancrinite	13.023(5)	–	5.204	$P6_3$	1.0	792	5.5
$Na_8Al_6Ge_6O_{24} \cdot Ge(OH)_6 \cdot 2H_2O$	–	–					
Sodalites							
$Na_8Al_6Ge_6O_{24}(OH)_2$	9.029(5)	–		$P\bar{4}3n$	1.0	455	4.8
$Na_8Al_6Ge_6O_{24} \cdot (Br_{1.5}OH_{0.5})$	9.089(1)	–		$P\bar{4}3n$	1.0	495	5.1
$K(H_3O)_3Ge_7O_{16}$	7.707(4)			$P\bar{4}3n$	0.6	220	6.8
$Rb_3Sb_3[Si_3O_9]O_6$	7.296(2)	10.295(2)	20.166(4)	$P\bar{2}_12_12_1$	1.3	2070	4.1
$Cs_4Sb_4[Ce_4O_{12}]O_8$	7.240(2)		20.022(5)	$P\bar{4}m2$	1.8	1328	7.6
$K_{3.8}Nb_5[Ge_3O_9]O_{11.4}$	7.064(2)	12.177(2)	22.113(5)	$Pbc2_1$	1.0	1637	7.9

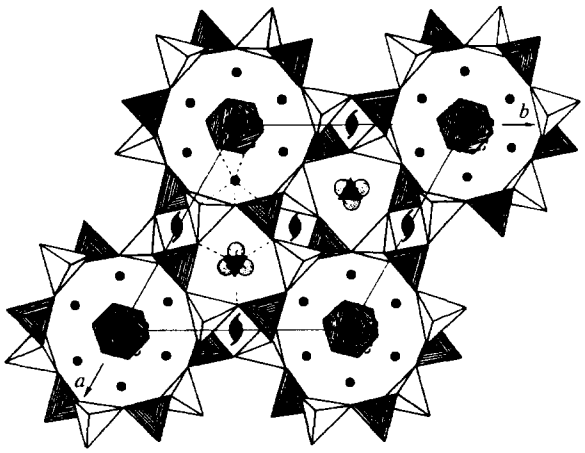


Figure 21. Projection of the structure of Ge-cancrinite onto the *ab* plane.

Sodalite also has germanium analogues (Table 10)[62,63] in which the positions of the Al, Na, and O (1, 2) atoms are retained while the Si atom is replaced by Ge. In the Ge-hydrosodalite, the OH groups of the natural mineral have been displaced from the 2*a*(000) positions of the Cl atoms to the 8*e*(*xxx*) positions and, for a statistical distribution, there is one OH group per cavity. The positions of the Br atoms are identical with those of the Cl atoms. Isomorphous substitutions in the anionic component makes it possible to improve the cathodochromic properties. Sodalites may prove promising for use where crystals with electrooptical and piezoelectric properties are required.[63]

Zeolites having the composition $M_3HGe_7O_{16} \cdot 4H_2O$ were described by Novotnyi[64] as early as 1958. It was noted that the combination of Ge octahedra and tetrahedra leaves room for large channels in the direction of coordinate axes, while the alkali metal cations are distributed statistically. This accounts for the zeolitic properties of these phases. The Ge-zeolite investigated (Table 10) contains the atoms of potassium as the metal, the deficiency of K atoms being compensated by the excess number of H atoms (or H_3O^+ groups).[65] The structural type of the Ge-zeolite belongs to the leucophosphite–pharmacosiderite group. Thus the crystal structure of $Cs_3Mo_4P_3O_{16}$ in this family[66] may be compared with the structure of $K_3Ge_7O_{16} \cdot 4H_2O$ (investigated by Sturua et al.[65]), where the positions of the Ge(2) atoms in the octahedron have been occupied by Mo atoms, while those of the Ge(1) atoms in the tetrahedron have been occupied by P atoms. The Cs atom is at the centre of the large channels. The diameters of the channels are ~5 Å in the $Cs_3Mo_4P_3O_{16}$ zeolite, exceed 6 Å in cancrinite, and are ~4 Å in sodalites.

We shall examine a further three structures of germanates and a silicate having the general formula $AMTO_5$ with the alkali metals A = K, Rb or Cs, M = Nb or Sb, and T = Ge or Si. Whilst differing in symmetry (Table 10), all three crystals have one feature in common, namely the large cavities in which the A atoms are accommodated. These cavities communicate with one another via channels which facilitate the ion-exchange in these compounds.

In the orthorhombic $RbNbSiO_5$[67] containing the chain radical $[Si_3O_9]_\infty$, the mixed framework $\{Nb_3[Si_3O_9]\}^{6-}$ was obtained by combining the three-dimensional bands of Nb octahedra with Si chains (Fig. 22). The crystal contains tubular cavities, where Rb atoms are accommodated.

In the tetragonal $CsSbGeO_5$,[63] the pattern of the cross-junction of the octahedra (Fig. 23) is close to that in $RbNbSiO_5$. The difference is that in $CsSbGeO_5$ one series of apex-linked octahedra, located below the main rod, has been omitted. Furthermore, the octahedra in this compound form a framework and no longer a band. In this framework, joined to the four-membered $[Ge_4O_9]$ rings, there are large communicating cavities in which Cs atoms are accommodated (Fig. 24), and it is possible to

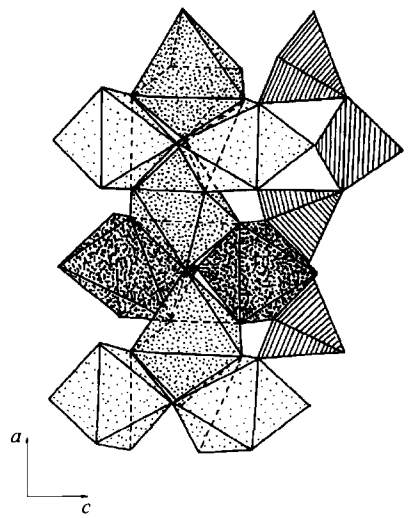


Figure 22. A band of Nb octahedra in the $RbNbSiO_5$ structure. The dot density reflects the height of the Nb octahedra along the *b* axis; the Si tetrahedra in the $[Si_3O_9]_\infty$ chain are shown shaded.

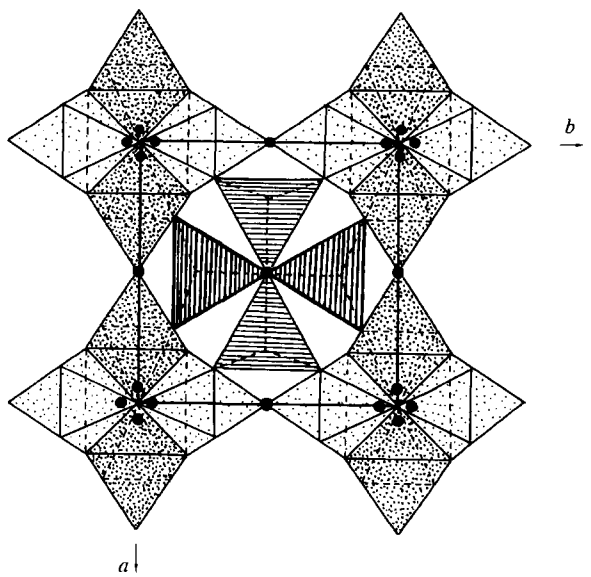


Figure 23. Projection of the $CsSbGeO_5$ structure onto the *ab* plane. The dot density reflects the height of the Sb octahedra along the *c* axis.

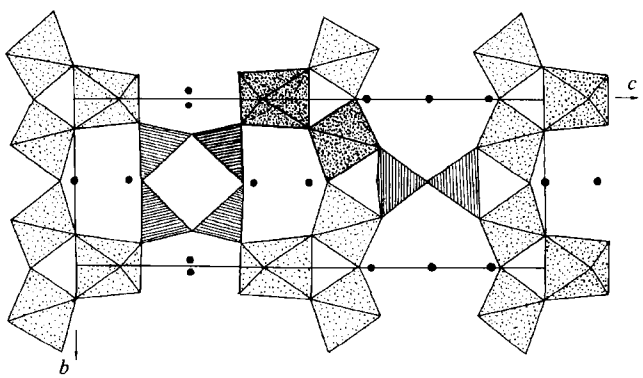


Figure 24. Projection of the $CsSbGeO_5$ structure onto the *bc* plane. The $KTiOPO_4$-like fragment is differentiated.

differentiate fragments close to the $KTiOPO_4$-like phases and sphenes. The crystal structure of $CsSbGeO_5$ was also solved in another study,[69] where the likely usefulness of this compound as an ion exchanger was likewise noted.

The crystal structure of the orthorhombic '$KNbGeO_5$'[70] with a slight deficiency of potassium and oxygen atoms (Table 10) proved to be derived from the structure of hexagonal $Cs_8Nb_{10}.Si_6O_{41}$.[71] In both structures, the tetrahedral radical is a three-membered $[T_3O_9]$ (T = Si, Ge) ring. In the structures, it is possible to differentiate the benitoite and pyrochlore fragments. The reason for the distortion of the '$KNbGeO_5$' structure and for the decrease in its symmetry from hexagonal to orthorhombic is the replacement of the Si atom by the large Ge atom in the tetrahedral position. To maintain the structure, the $[Ge_3O_9]$ ring in '$KNbGeO_5$' must be greatly distorted compared with $[Si_3O_9]$ in $Cs_8Nb_{10}Si_6O_{41}$ in order fit in the framework which has also been 'compressed' by replacement of Cs the by K. Like the two phases described above, K,Nb silicate should exhibit ion-exchange properties, i.e. it is possible to identify channels for the migration of cations along the *b* and *c* axes of the crystal.

* * *

More than 50 structures of germanates, gallates, borates, and silicates have been examined in the present review. The class of germanates (gallates), which predominates, provides analogues of the known structures of the silicate type such as garnet, melilite, sphene, cancrinite, and sodalite. Borogermanates are analogues of the borosilicates stillvellite and datolite. The tendency of germanium to be involved in octahedral coordination, particularly when it is present in excess in the initial systems, is responsible for the wide variety of germanates and their ability to form new structural types such as $A_3M_xT_{6-x}O_{14}$. An important factor is that the formation of high-temperature modifications at lower temperatures than, for example, in the case of phosphates, is typical for germanates. This makes it possible to investigate successfully the phase transitions in $KTiOPO_4$-like phases.

The study of the structures of the new phases is extremely important for the interpretation of their physical properties and for the understanding of their nature and hence in the search for phases having these properties and for the improvement of the already existing physical characteristics, for example by means of isomorphism.

The crystals of germanates, gallates, borates, and silicates investigated have a wide range of physical properties and can serve as multifunctional elements in engineering.

References

1. G D Stucky, M L F Phillips, T E Gier *Chem. Mater.* **1** 492 (1989)
2. S C Abrahams *Acta Crystallogr., Sect. B* **46** 311 (1990)
3. B V Mill', A V Butashin, G G Khodzhabagyan, E L Belokoneva, N V Belov *Dokl. Akad. Nauk SSSR* **264** 1385 (1982)
4. E L Belokoneva, T G Uvarova, L N Dem'yanets *Kristallografiya* **31** 874 (1986)
5. E L Belokoneva, T I Timchenko *Kristallografiya* **28** 1118 (1983)
6. A A Kaminskii, B V Mill', G G Khodzhbagyan, A F Konstantinova, A J Okorochkov, I M Silvestrova *Phys. Status Solidi A* **80** 387 (1983)
7. B V Mill', S Yu Stefanovich, A V Butashin *Kristallografiya* **36** 1481 (1991)
8. F Bertaut, F Forrat *C. R. Hebd. Seances Acad. Sci.* **243** 382 (1956)
9. J E Geusic, H M Marcos, L G Van Hitert *Appl. Phys. Lett.* **4** 182 (1964)
10. G A Novak, G V Gibbs *Am. Mineralogist* **56** 791 (1971)
11. B V Mill', E L Belokoneva, M A Simonov, N V Belov *Problemy Kristallologii* (Problems of Crystallology) (Moscow: Izd. Mosk. Gos. Univ., 1982) p. 161
12. A A Kaminskii, B V Mill', A V Butashin *Phys. Status Solidi A* **78** 723 (1983)
13. A A Kaminskii, E L Belokoneva, A V Butashin, K Kurbanov, A A Markosyan, B V Mill', O K Nikol'skaya, S E Sarkisov *Izv. Akad. Nauk SSSR, Neorg. Mater.* **22** 1061 (1986)
14. N N Lobanov, V G Tsirel'son, E L Belokoneva *Zh. Neorg. Khim.* **33** 3021 (1988)
15. In *Fizika i Spektroskopiya Kristallov* (The Physics and Spectroscopy of Crystals) (Moscow: Nauka, 1986) Ch. 9, p. 197
16. In *Kristallokhimicheskaya Sistematika Mineralov* (Systematic Crystal-chemical Classification of Minerals) (Moscow: Izd. Mosk. Gos. Univ., 1985) p. 140
17. S Haussuhl, F Wallrafen, K Recker, J Eckstain *Z. Kristallogr.* **153** 329 (1980)
18. A A Kaminskii, E L Belokoneva, B V Mill', Yu V Pisarevskii, S E Sarkisov, I M Silvestrova, A V Butashin, G G Khodzhabagyan *Phys. Status Solidi A* **86** 345 (1984)
19. E L Belokoneva, N V Belov *Dokl. Akad. Nauk SSSR* **260** 1363 (1981)
20. A A Kaminskii, E L Belokoneva, B V Mill', S E Sarkisov, K Kurbanov *Phys. Status Solidi A* **97** 279 (1986)
21. P Korzak, F Raaz *Österr. Akad. Wiss. Sitzungen Math. Naturwiss. Klasse* **13** 383 (1967)
22. A A Kaminskii, E L Belokoneva, S E Sarkisov, K Kurbanov, B V Mill' *Izv. Akad. Nauk SSSR, Neorg. Mater.* **22** 1869 (1986)
23. A A Kaminskii, E L Belokoneva, B V Mill', K Kurbanov, E S Dosmagambetov, S A Tamazyan, A V Butashin *Izv. Akad. Nauk SSSR, Neorg. Mater.* **22** 2013 (1986)
24. A A Kaminskii, B V Mill', A V Butashin, E L Belokoneva, K Kurbanov *Phys. Status Solidi A* **103** 575 (1987)
25. E L Belokoneva, B V Mill', A V Butashin, A A Kaminskii *Izv. Akad. Nauk SSSR, Neorg. Mater.* **27** 1700 (1991)
26. A A Voronkov, Yu A Pyatenko *Kristallografiya* **12** 258 (1967)
27. S Yu Stefanovich, B V Mill', A V Butashin *Kristallografiya* **37** 965 (1992)
28. Y Uesu, N Horiuchi, E Osakabe, S Omori, B A Strukov *J. Phys. Soc. Jpn.* **62** 2522 (1993)
29. A Onodera, B A Strukov, A A Belov, S A Taraskin *J. Phys. Soc. Jpn.* **62** 4311 (1993)
30. A Callegary, G Ginseppetti, F Mazzi, C Tadini *N. Jb. Mineral. Mh.* **2** 49 (1992)
31. A A Kaminskii, A V Butashin, A Masljanizin *Phys. Status Solidi A* **125** 671 (1991)
32. E L Belokoneva, M A Simonov, A V Pashkova, T I Timchenko, N V Belov *Dokl. Akad. Nauk SSSR* **255** 854 (1980)
33. E L Belokoneva, A V Pashkova, T I Timchenko, N V Belov *Dokl. Akad. Nauk SSSR* **261** 361 (1981)
34. E L Belokoneva, A V Azizov, N I Leonyuk, M A Simonov *Zh. Strukt. Khim.* **22** 196 (1981)
35. E L Belokoneva, L I Al'shinskaya, M A Simonov, N I Leonyuk, T I Timchenko, N V Belov *Zh. Strukt. Khim.* **19** 382 (1978)
36. E L Belokoneva, L I Al'shinskaya, N I Leonyuk, M A Simonov, N V Belov *Zh. Strukt. Khim.* **20** 542 (1979)
37. K Dornberger-Schiff *Grundzüge einer Theorie der OD-Strukturen aus Schichten* (Berlin: Deutsch. Akad. Wissensch., 1964)
38. B B Zvyagin, E L Belokoneva *Kristallografiya* **29** 291 (1989)
39. E A Pobedimskaya, D Yu Pushcharovskii, O G Karpov *Strukturnye Tipy Redkozemel'nykh Silikatov, Germanatov i Fosfatov* (Structural Types of Rare-earth Silicates, Germanites and Phosphates) (Moscow: Izd. Mosk. Gos. Univ., 1984)
40. E L Belokoneva, L I Leonyuk, A V Pashkova, T I Timchenko *Kristallografiya* **33** 1287 (1988)
41. E L Belokoneva, B V Mill', A V Butashin *Izv. Akad. Nauk SSSR, Neorg. Mater.* **27** 1708 (1991)
42. C Pagnoux, D Guyomard, A Verbaere, Y Piffard, M Tournoux *C. R. Acad. Sci., Ser. 2* **312** 611 (1991)
43. A Simon, J Ravez, J F Favard, A Verbaere, Y Piffard *C. R. Acad. Sci., Ser. 2* **317** 179 (1993)
44. S Yu Stefanovich, B V Mill', A V Butashin *Kristallografiya* **38** 121 (1993)
45. B V Mill', A V Butashin, S Yu Stefanovich *Zh. Neorg. Khim.* **38** 947 (1993)
46. J F Favard, A Verbaere, Y Piffard, M Tournoux *C. R. Acad. Sci., Ser. 2* **315** 305 (1992)
47. E L Belokoneva, B V Mill' *Zh. Neorg. Khim.* **37** 998 (1992)

48. M P Crosnier, D Guyomard, A Verbaere, Y Piffard *Eur. J. Solid State Inorg. Chem.* **27** 845 (1990)
49. C Pagnoux, J F Favard, A Verbaere, Y Piffard, M Tournoux *C. R. Acad. Sci., Ser. 2* **314** 151 (1992)
50. E L Belokoneva, O V Yakubovich, V G Tsirel'son, V S Urusov *Izv. Akad. Nauk SSSR, Neorg. Mater.* **26** 595 (1990)
51. P A Thomas, A M Glazer, B E Watts *Acta Crystallogr., Sect. B* **46** 333 (1990)
52. E L Belokoneva, B V Mill' *Zh. Neorg. Khim.* **37** 252 (1992)
53. E L Belokoneva, F M Dolgushin, M Yu Antipin, B V Mill', Yu T Struchkov *Zh. Neorg. Khim.* **38** 631 (1993)
54. E L Belokoneva, F M Dolgushin, M Yu Antipin, B V Mill', Yu T Struchkov *Zh. Neorg. Khim.* **39** 40 (1994)
55. E L Belokoneva, B V Mill' *Zh. Neorg. Khim.* **39** 355; 363 (1994)
56. S Furusava, H Hayasi, H Y Ishibashi, A Mijamoto, T Sasaki *J. Phys. Soc. Jpn.* **62** 181 (1993)
57. P A Tordjman, R Masse, J C Guital *Z. Kristallogr.* **139** 103 (1974)
58. E M McCarron III, J C Calabrese, T E Gier, L K Cheng, C M Foris, J D Bierlein *J. Solid State Chem.* **102** 354 (1993)
59. B V Mill', E L Belokoneva, A V Butashin *Kristallografiya* **35** 316 (1990)
60. G Blasse, G J Dirksen *J. Solid State Chem.* **65** 283 (1986)
61. A A Kaminskii, B V Mill', E L Belokoneva, A V Butashin *Izv. Akad. Nauk SSSR, Neorg. Mater.* **27** 1899 (1991)
62. E L Belokoneva, L N Dem'yanets, T G Uvarova, N V Belov *Kristallografiya* **27** 995 (1982)
63. E L Belokoneva, T G Uvarova, L N Dem'yanets *Kristallografiya* **30** 800 (1985)
64. Kh Novotnyi *Usp. Khim.* **27** 996 (1958)
65. G Sturua, E L Belokoneva, M A Simonov, N V Belov *Dokl. Akad. Nauk SSSR* **242** 1078 (1978)
66. R C Haushalter *J. Chem. Soc., Chem. Commun.* 1566 (1987)
67. E A Genkina, E L Belokoneva, B V Mill', A V Butashin, B A Maksimov *Kristallografiya* **37** 606 (1992)
68. E L Belokoneva, B V Mill', A V Butashin *Zh. Neorg. Khim.* **37** 2435 (1992)
69. C Pagnoux, A Verbaere, A Kanno, Y Piffard, M Tournoux *J. Solid State Chem.* **99** 173 (1992)
70. E L Belokoneva, A V Butashin, B V Mill' *Zh. Neorg. Khim.* **38** 1455 (1993)
71. M P Crosnier, C Pagnoux, D Guyomard *Eur. J. Solid State Inorg. Chem.* **28** 71 (1991)

Russian Chemical Reviews **63** (7) 551 – 557 (1994)
©1994 Russian Academy of Sciences and Turpion Ltd

UDC 541.128.13

The role of adsorbed hydrogen species in the dehydrogenation and hydrocracking of saturated hydrocarbons on supported metal catalysts

L V Babenkova, I N Naidina

Contents

I. Introduction 551
II. The mechanism of the activation of H – H, C – H, and C – C bonds in the molecules of hydrogen and hydrocarbons 551
III. The role of hydrogen in the reactions of hydrocarbons 552
IV. Relation between the adsorption characteristics of hydrogen, the state of the metals, and catalyst activity in the reactions of saturated hydrocarbons 553
V. Conclusion 556

Abstract. The role of certain hydrogen adsorption complexes in the dehydrogenation and hydrocracking of hydrocarbons on low-percentage one-component, (Pt, Pd/Al_2O_3) and bimetallic (Pd – Co, Pd – Ce, Pt – Co, $Pt-Sn/Al_2O_3$) catalysts is discussed. It is shown that the combination of metals in reduced forms and forms oxidised to different extents on the catalyst surfaces is responsible for their high capacity for the chemisorption of hydrogen, the wide range of its energetic inhomogeneity, and the high activity of the catalysts in the conversion of saturated hydrocarbons. Catalysts containing on the surface mainly sites for the type $H^{\delta-}$ chemisorption are the most active in the dehydrogenation of hydrocarbons, whereas specimens chemisorbing hydrogen mainly in the $H^{\delta+}$ form are the most active in the hydrocracking of hydrocarbons. It is concluded that the strongly bound atomic hydrogen $H^{\delta+}$ plays a dual role, since it not only participates directly in the dehydrogenation reaction but also promotes the reduction of the electron-deficient surface centres, which optimises the number of centres for the activation of C – H bonds. The bibliography includes 75 references.

I. Introduction

Hydrogen strongly affects the course of the processes involved in the heterogeneous catalytic conversion of saturated hydrocarbons. It alters the capacity of hydrocarbons for adsorption, participates in the hydrogenation of highly dehydrogenated molecules, enters into the composition of intermediate adsorption complexes, etc.[1-3]

In the present review, attention is concentrated on the role of hydrogen in the dehydrogenation and hydrocracking of hydrocarbons on supported metal catalysts. Mainly platinum catalysts, including those modified by doping with other elements, containing both zerovalent and oxidised metals are used as dehydrogenation catalysts.[1] The participation of adsorbed hydrogen in dehydrogenation and hydrocracking and also the nature of the adsorbed state, which is determined by the composition and structure of the active centres on the catalyst surface, have been scarcely investigated hitherto.

L V Babenkova, I N Naidina Petrochemistry Laboratory,
D V Sokol'skii Institute of Organic Catalysis and Electrochemistry,
National Academy of Sciences of the Kazakhstan Republic,
ul. K. Marksa 142, 480100 Alma-Ata, Kazakhastan.
Fax (7-327) 261 57 22

Received 5 April 1994
Uspekhi Khimii **63** (7) 577 – 584 (1994); translated by A K Grzybowski

II. The mechanism of the activation of H – H, C – H, and C – C bonds in molecules of hydrogen and hydrocarbons

The mechanism of the chemisorption of hydrogen on the surfaces of Group VIII metals has been discussed in detail in a number of communications, in particular in reviews.[4,5]

In considering the mechanism of the activation of hydrogen on metal oxides, one should bear in mind that experimental estimation of the sorption state of hydrogen is possible only in the case of metal oxides which are difficult to reduce — those of molybdenum, zirconium, strontium, barium, and cerium.

As a consequence of the highly ionic character of such metal oxides, the interaction of hydrogen with the latter leads to the polarisation of the hydrogen molecule:

$$\begin{matrix} H^{\delta-} & \cdots & H^{\delta+} \\ \vdots & & \vdots \\ H^{\delta+} & \cdots & H^{\delta-} \end{matrix}$$

This is followed by heterolysis.[6-11] The existence of the $M^{m+}-O^{n-}$ pairs on the surfaces of the oxides of the metals indicated above[12-18] with different coordinative unsaturation of the metal and oxygen (surface defects) is responsible for the presence of several types of pairs of active centres differing in the strength of bonding of the chemisorbed hydrogen.[7,18]

The chemisorption of hydrogen on readily reducible metal oxides (including Group VIII metal oxides) and its energy characteristics have been investigated mainly by theoretical methods.[7,12,19-22]

Quantum-chemical calculations for the chemisorption of a hydrogen molecule on the (001) face of NiO indicate that the binding of hydrogen to Ni^{2+} ions is very weak in a perfect lattice (E_b = 0.65 eV).[19,22] Only a positively charged molecular form of chemisorbed hydrogen arises on a positively charged iron ion in the hematite (Fe_2O_3) lattice.[20] The presence of defects — cationic or anionic vacancies — on the oxide surface leads to strong binding of hydrogen (E_b = 4.5 – 7.7 eV).[7,19,22]

Calculations for the chemisorption of a hydrogen molecule on an oxygen ion of the Fe_2O_3 cluster showed that the H–H bond energy diminishes greatly on interaction with an O^{n-} anion.[20] When the hydrogen molecule is oriented parallel to the metal–oxygen bond, the interaction is repulsive, i.e. there is no chemisorption of hydrogen on Fe_2O_3 via a heterolytic mechanism.

Analysis of the H–H and C–H bond activation processes on metallic surfaces and on transition metal complexes showed that these processes proceed via similar mechanisms.[6,18,23,24] The activation of hydrocarbon molecules, like that of hydrogen molecules, involves electron transfer from the bonding σ_g orbitals of the H–H and C–H bonds to the metal and the reverse electron transfer from the occupied orbitals of the metals to the antibonding unoccupied σ_u^* orbitals of the molecule of hydrogen or the saturated hydrocarbon.[23] The electron-donating or electron-accepting nature of the interaction of metals with hydrogen or hydrocarbons is determined by the oxidation states of the metals, i.e. by the position of the Fermi level of the metal relative to the highest occupied or lowest unoccupied level of the reactant molecule, which is in fact the reason for the preferential charge transfer either to the adsorbed molecule or to the transition metal.[23]

In the case of zerovalent metals, the high energies of the highest occupied molecular orbitals (HOMO) of their surface atoms give rise to interaction involving mainly electron transfer from the metal to the σ_u^* levels of the hydrogen or saturated hydrocarbon molecule. Quantum-chemical calculations of the heats of chemisorption of saturated hydrocarbons (CH_4, C_2H_6) on 3*d* transition metals showed[24] that the difference between the energies of the Fermi level of the metal and the σ_g levels of the hydrocarbon molecules are fairly large for the majority of these metals. It is therefore evident that the electron-accepting properties of saturated hydrocarbons will predominate in the interaction with metals.

In oxides and metal complexes (in contrast to heterogeneous metal catalysts), the metal ions exhibit a higher coordinative unsaturation and the energies of their frontier orbitals are higher.[23,24] Thus the typical Fermi energies, established from the electron work functions of the reduced transition metals, range from −4.5 to −5.5 eV, while the ionisation potentials of the atomic *d* orbitals in complexes range from −8 to −12 eV.[23] As a consequence of the lower HOMO energies of the metals in complexes or oxides compared with H–H and C–H bonds, electron transfer from the σ_g orbitals of the H–H and C–H orbitals to the metal predominates in the early stages.[25,26]

The dominant role of electron-donating properties of saturated hydrocarbons in their interaction with metals in a high oxidation state, for example, with organometallic clusters, has been demonstrated.[24] The author[24] calculated a critical point $\varepsilon_d \approx -9.1$ eV on the energy scale. He showed that, when the HOMO energy of the metal is greater than this quantity, then the molecule, for example of CH_4, is an electron acceptor, whilst if it is lower than the critical point the molecule is an electron donor. Since the HOMO energies of the majority of transition metals are above −9.1 eV, the methane molecule is an electron acceptor in relation to them.

The frontier orbital energies of the molecules of hydrogen and the hydrocarbons involved in the chemisorption on the surface metal atoms determine the difference between the activations of the H–H and C–H bonds: the CH_4 molecule is a better electron donor, since its HOMO lies 2 eV higher than in hydrogen. The electron-accepting properties of hydrogen and methane molecules are similar, since the energy of the bonding σ_g hydrogen orbital is −17.56 eV, while that of the antibonding σ_u^* orbital is +4.17 eV; the energies of the corresponding orbitals in CH_4 are −15.4 and +3.6 eV.[23]

The deposition of the metal on a carrier exerts a significant influence on the donor–acceptor character of the interaction of the metal with hydrogen and hydrocarbons. According to Beran et al.,[27] the C–H bond dissociation energy in the CH_4 molecule on supported nickel catalysts diminishes with increase in the electronegativity of the carrier. The transfer of electrons from the carrier to the metal is hindered by the higher electron density in the latter (for example 10^{23} cm^{-3} in platinum and 10^{20} cm^{-3} in titanium dioxide).[28] However, in the case of highly dispersed particles of the deposited metal, which are electron-deficient,[29–31] paraffinic hydrocarbons exhibit electron-donating properties, coordinating very strongly to these particles, reducing catalytic activity in their reactions.[29,31,32]

In the reactions of hydrocarbons on the surfaces of heterogeneous catalysts, the C–C bond is activated together with C–H, which leads to a nonselective course of the reaction in the dehydrogenation of hydrocarbons. The ratio of the dehydrogenation and hydrocracking products is determined by the ratio of the energies of the bonds formed (M^+–H, M^+–C) and dissociated (C–C, C–H).[33]

It has been shown in a study of the hydrogenolysis kinetics of C_2–C_5 alkanes on supported rhodium and nickel catalysts and also on the surface of single crystal iridium[34–36] that the activation of the C–C bond is a structure-sensitive reaction. According to Dorfman,[37] because of symmetry considerations the dissociation of the C–C bond takes place on pairs of coordinatively unsaturated atoms of *d* metals located at the apices, on the edges, and in high-index planes of small crystallites.

Systematic data on the ability of metals to break the C–C bond as a function of their position in the Periodic System are not to be found in the literature; only isolated results have been published. Thus it has been shown[38] that the C–C and C–H bond dissociation energies decrease in the sequence Pt > Ni > Fe/W. The strength of the bond between the metal and carbon increases on passing from Pt to Ir and Os; the frequency of the C–C bond increases in the same direction.[34] It has been established for fission exchange involving deuteriated methane that cobalt and iridium preferentially form multiple bonds to a carbon atom, whereas on platinum the formation of single M–H bonds is preferred.[39,40] The ability of cobalt and iridium to form multicentre bonds explains their high activity in the hydrogenolysis processes.

Certain ideas about the mechanism of the fission of C–C bonds have arisen in the study of the high-temperature activation of saturated hydrocarbons by metal complexes.[33] Several C–C bond activation pathways are possible on coordinatively unsaturated transition metal (metals in the zerovalent or a low oxidation state) complexes. For example, activation takes place on direct insertion of the metal in the C–C bond via the oxidative addition mechanism or in the initial oxidative addition of a C–H bond to the metal complex and the subsequent cleavage of the C–C bond in the σ-alkylmetal hydride complex.

Thus the activation of hydrogen and hydrocarbon molecules on the surfaces of supported catalysts proceeds either via oxidative addition (the formation of negatively charged complexes) or via a donor–acceptor mechanism with charge transfer from the molecule to the metal (the formation of positively charged complexes) predominating depending on the degree of reduction of the metals on the surface.

III. The role of hydrogen in the reactions of hydrocarbons

In the numerous studies of the reactions of saturated hydrocarbons in the presence of hydrogen (dehydrogenation, dehydrocyclisation, hydrogenolysis, hydrocracking, etc.) published hitherto, it has merely been shown that hydrogen, without being a stoichiometric reactant, has a positive effect at certain concentrations both on the rate and selectivity of the process. Thus it has been observed[2,41] that the addition of hydrogen to the reaction medium suppresses the dissociative chemisorption of hydrocarbons on the surfaces of metals, which prevents self-poisoning of the catalyst surfaces and the deposition of carbon on the latter. On the other hand, at relatively high concentrations of the gas phase,

hydrogen promotes both the hydrogenation of the alkenes formed and the cleavage of the C–M bond, reducing thereby the fraction of the surface involved in the reaction of the hydrocarbons and lowering the overall degree of conversion.[2,41,42] The forms of hydrogen firmly retained on the catalyst surface insulate the surface metal atoms from direct contact with the reactant molecules,[43] which can alter the mechanism of their interaction.

The change in the size of the working metal assemblies, induced by the change in the amount of carbonaceous deposits, has also been explained[44] by the involvement of hydrogen in the reactions of alkanes on the surfaces of platinum catalysts. In the presence of a deficiency of hydrogen, the catalyst surface is largely covered by hydrocarbons, retained mainly on the platinum centres. The H–Pt–C system formed under these conditions breaks up the large platinum assemblies and the centres active in the dissociation of the C–C bond are blocked. In the presence of an excess of hydrogen in the mixture, whereupon the surface coverage by the hydrocarbons is low (the H–Pt system), the main reaction path involves the fragmentation of the alkane molecules.[44,45]

It has been established[46] that the reaction of n-hexane on the surface of a platinum–tin catalyst freed from adsorbed hydrogen proceeds nonselectively with formation of light saturated hydrocarbons. If the catalyst surface has been covered with hydrogen, then the selectivity with respect to alkenes increases.

The role of the energy characteristics of hydrogen, which influence the rate and mode of the reactions of hydrocarbons, have been discussed in a number of publications. Thus Volter and coworkers[47,48] observed a satisfactory correlation between the activity of platinum and platinum–tin catalysts in the dehydrogenation of cyclohexane and their content of hydrogen retained on the surface in the temperature range 0–300 °C.

The hydrogen initially adsorbed on the platinum/alumina catalyst can participate directly in the reactions of cyclohexane, effecting the hydrogenation of its extensively dehydrogenated strongly bound molecules with formation of a high-temperature form of benzene.[49] The chemisorbed hydrogen does not participate directly in the formation of the low-temperature form of benzene, but in the absence of hydrogen from the catalyst surface this form of benzene is not formed and the thermoprogrammed desorption (TPD) spectrum shows only the peaks of the strongly bound form of benzene.[49]

The direct involvement of atomic forms of hydrogen in the dehydrogenation of cyclohexane adsorbed on the surfaces of palladium or nickel catalysts has been demonstrated.[50] As a result of the study of the dehydrogenation of cyclohexane on specimens with preadsorbed deuterium, a reaction mechanism was proposed in which the adsorbed hydrogen and the hydrogen in the chemisorbed cyclohexane molecule recombine with elimination of a hydrogen molecule. Analysis of the activation energy for the reaction involving the deposition of carbonaceous deposits led Masai et al.[50] to conclude that the forms of hydrogen which can increase the activity of catalysts in the dehydrogenation of cyclohexane are also responsible for the high degree of carbon deposition on the surface.

The C_5-dehydrocyclisation reaction proceeds via a similar mechanism, presupposing the recombination of a hydrogen atom belonging to a hydrocarbon transition complex with a hydrogen atom adsorbed on the surface.[2]

It has been suggested in a number of investigations[51–53] that the C–H bonds in the cyclohexane molecule are activated on the centres for the adsorption of weakly bound hydrogen because the dehydrogenation reaction on the Pt/Al_2O_3 and $Pt–Sn/Al_2O_3$ catalysts begins at temperatures at which the surface of the specimens is freed from hydrogen (T_{des} < 350 °C).

A correlation between the content in the catalyst of the hydrogen desorbed in the temperature range 320–480 °C and the catalyst activity has been observed in a study of the dehydrogenation of n-dodecane on platinum catalysts promoted with indium and gallium.[54] The observed relation can be explained by the fact that the centres for the activation of the dissociatively chemisorbed hydrogen serve simultaneously as the sites for the adsorption of intermediate products formed on dissociation of a C–H bond.

Comparison of the reactivity of hydrogen in the dehydrogenation of cyclohexane and its thermodesorption characteristics in low-percentage promoted Pt and Pd catalysts on Al_2O_3 showed[55,56] that the most active specimens chemisorb two energetically different atomic forms of hydrogen—with T_{des} = 160–480 °C and 480–900 °C respectively. The weakly active catalysts are characterised by the absence from the surface of the form of hydrogen with a lower bond energy.

Thus analysis of the available literature data shows that hydrogen is an obligatory participant in the catalytic reactions of saturated hydrocarbons. However, as a consequence of the nonuniformity of the energy characteristics of the hydrogen chemisorbed on the surfaces of catalysts, it is necessary to discover the role of each form of hydrogen in the catalytic reactions of unsaturated hydrocarbons.

The nature of the adsorption complexes of hydrogen, determined by the state of the active centres of the catalyst surface, can be discovered from the relation between the oxidation state of the metals in supported low-percentage catalysts and the adsorption characteristics of the hydrogen on their surfaces.

IV. Relation between the adsorption characteristics of hydrogen, the state of the metals, and catalyst activity in the reactions of saturated hydrocarbons

It is essential to note that towards the beginning of the 1980s there had been virtually no experimental studies on the chemisorption of hydrogen and its energy characteristics on Group VIII metal oxides. The reason for this was the relative ease of the reduction of the oxidised metals in hydrogen.

The metals can retain their oxidation state during the reduction process if the oxides are part of the composition of low-percentage supported catalysts [in the presence of a strong metal–carrier interaction (SMCI)]. The H–H bond is activated via the heterolytic mechanism for high oxidation states or via the donor–acceptor mechanism for low oxidation states of the metal in the oxide and for chemisorption on highly dispersed electron-deficient particles of the metal on a carrier.[23,33,37]

It has been shown[1,57–61] that metals deposited on a carrier at low concentrations (0.02–0.1 mass% Pd; 0.5–1.0 mass% Co; 0.05–0.1 mass% Pt; 2.1 mass% Ce), corresponding to the SMCI region, are mainly in the oxidised state (Pt^{2+}, Co^{2+}, Pd^{2+}, Ce^{4+}) and in the case of Pd/Al_2O_3 partially in the atomically disperse[58,60] state after high-temperature (400–500 °C) treatment in hydrogen. The highly dispersed particles of the deposited metals with an increased concentration of the active phase are also electron-deficient.[29–31,62,63] In the above catalyst, virtually all the atoms of the deposited metal are on the surface and are accessible for chemisorption. Thus, according to data obtained by the paramagnetic probe method (PPM), after the deposition of 0.02–0.1 mass% Pd, 0.6×10^{13} palladium atoms cover 2×10^{13} Al^{3+} centres,[57] whereupon a sharp decrease (up to 50%) in the number of coordinatively unsaturated Al^{3+} atoms on the surface is observed (Fig. 1*a*, curve *1*).

The degree of coverage of the active phase of the catalysts by hydrogen in the SMCI region, determined by the TPD method,[57,58] is negligible: the ratio H : M $\leqslant$ 0.01 (M = Co, Ce, Pt) with the exception of Pd/Al_2O_3, for which H : Pd is somewhat higher—H : Pd = 0.01–0.2 (Fig. 1*a*, curve *2*; Fig. 2*a*, curve *1*). This is evidently induced by the presence on the catalyst surface of palladium in the atomically dispersed electron-deficient state.[58]

In catalysts with an active phase concentration higher than in the SMCI region (Pd $\geqslant$ 0.01–0.3 mass%; Pt > 0.1 mass%; Co > 1.0 mass%; Ce $\geqslant$ 2.1 mass%), the deposited metal is adsorbed on the previously occupied parts of the surface, because the number of coordinatively unsaturated Al^{3+} centres does not

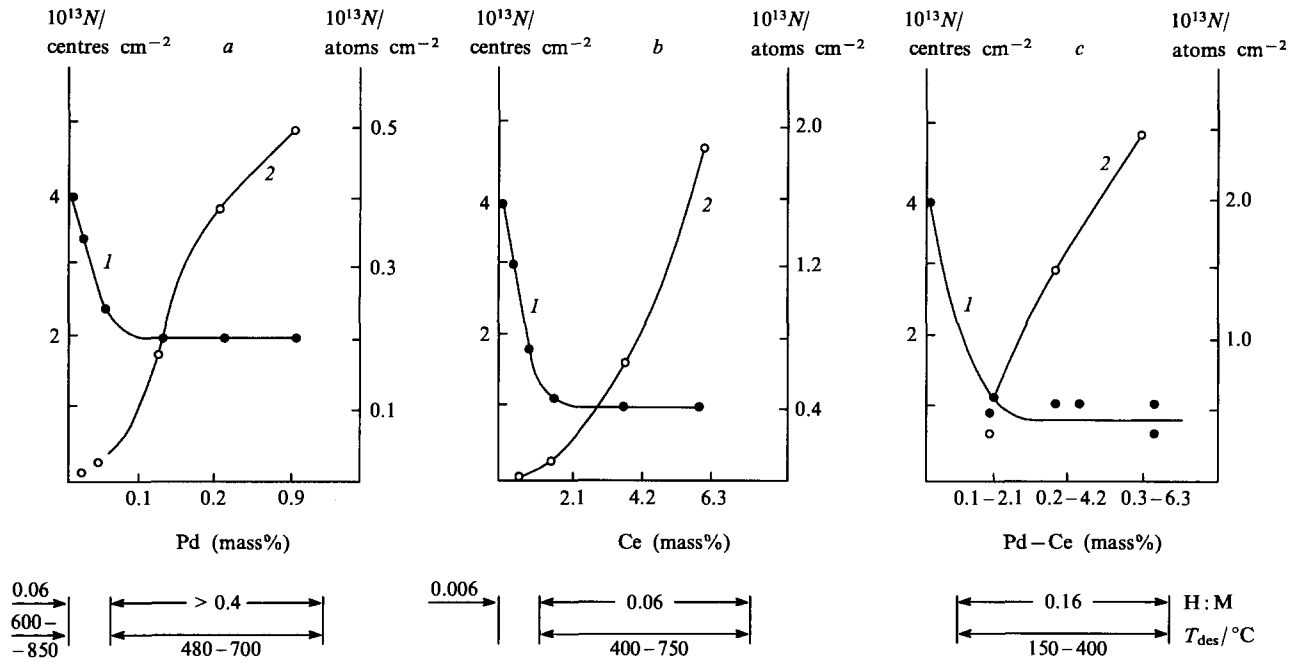


Figure 1. Effect of concentration of deposited Pd (*a*), Ce (*b*), and Pd–Ce (*c*) on the number of Al^{3+} acceptor centres on the Al_2O_3 surface (curves *1*) and on the overall content of the hydrogen adsorbed by the catalyst (curves *2*). The H : M ratios and the temperature ranges in which hydrogen is desorbed, corresponding to regions of strong and weak interaction of the metal with the carrier, are indicated on the scale parallel to the abscissa axis.

diminish with increase in the metal content, according to PPM data (Figs 1*a* and 1*b*, curves *1*).[57] After high-temperature reduction in hydrogen, metals in a more reduced form as well as highly dispersed metallic particles are detected in such specimens.[58,61,64–67] For example, it has been demonstrated by X-ray photoelectron spectroscopy (XPES) that in the 6% Co/Al_2O_3 and 0.35% Pt/Al_2O_3 catalysts 37% and 20% of the metal atoms relative to the overall content exist on the surface in the reduced form.[67,68] Catalysts of this type interact with H_2 and produce mainly strongly bound forms of the chemisorbed hydrogen ($T_{des} \geqslant 480-500$ °C; Fig. 2*a*, curves *2* and *3*), the ability of the specimens to chemisorb hydrogen increasing significantly with increase in the concentration of the deposited metal (from 0.1–0.3 mass% Pd, from 1.7–4.3 mass% Co, and $\geqslant$ 4.2 mass% Ce): the ratio H : M increases by a factor of 8–10 (Figs 1*a* and 1*b*, curves *2*; Fig. 2*a*, curves *1–4*; Fig. 3*a*, curves *1–3*) and hydrogen less strongly bound to the catalyst surface appears (Fig. 2*a*, curve *4*).[57–59]

For bimetallic catalysts, there is a mutual facilitation of the reduction of the metals.[56,58,64–72] Therefore in the platinum/alumina and palladium/alumina catalysts with the noble metal concentrations corresponding to the SMCI region ($\leqslant$ 0.1%) and promoted by the oxides of cobalt (1.0–1.7 mass%),[55,56] cerium (1.0–2.5 mass%; Fig. 1*c*, curve *1*),[56,57,59] and tin (2.0 mass%),[68] the degree of reduction of the metals is higher than in the corresponding monometallic catalyst. For example, the fraction of Pt^0 rises to 40% in $Pt-Sn/Al_2O_3$ compared with 20% in Pt/Al_2O_3. A characteristic feature is also an appreciable increase in the overall capacity for the chemisorption of hydrogen and the appearance of the form of hydrogen weakly bound to the surface (Fig. 1*c*, curve *2*; Fig. 2*a*, curve *5*; Fig. 4*a*, curves *2* and *3*).

Thus there is virtually no chemisorption of hydrogen on oxides of transition metals in a high oxidation state incorporated in the carrier matrix (in the SMCI region). Following the appearance in the specimens of weakly oxidised forms of the metal (highly dispersed electron-deficient metallic particles and the oxides of metals in a low oxidation state), the chemisorption of H_2 is observed with the formation of atomically adsorbed forms firmly bound to the surface (T_{des} > 480–500 °C). When the supported catalysts contain metallic bulk phases, the chemisorption of relatively weakly bound forms of hydrogen with $T_{des} \gtrsim 300$ °C is observed together with the chemisorption of the strongly bound forms.[56,58] This means that, as increasingly more reduced forms and bulk phases of the reduced metal appear in the catalysts, the energetic nonuniformity of the adsorbed hydrogen complexes increases as a result of the formation of the weakly bound $H^{\delta-}$ forms.

The absence of chemisorbed hydrogen from catalysts with the concentration of the active phase corresponding to the SMCI region, in which the oxidised forms of the metals are retained after the high-temperature treatment in hydrogen, may be a consequence of both thermodynamic difficulties induced by the greater difference between the energy levels of the oxidised metals and hydrogen and by the coordinative saturation of the metal oxides in the carrier matrix (Al_2O_3). The chemisorption of hydrogen on the more reduced metals can be regarded[23,33,37] as a result of the activation of hydrogen via the mechanism involving the donor–acceptor interaction with transfer of electron density in both directions $H \rightleftarrows M^{n+}$.

Analysis of the oxidation states of the metals and of the thermodesorption characteristics of the chemisorbed hydrogen permits a conclusion concerning the charge distribution in the adsorbed forms of hydrogen. Thus the chemisorption of hydrogen in the strongly bound atomic form (the $H^{\delta+}$ form with T_{des} > 480 °C), which occurs on electron-deficient metallic particles and on oxides of metals in a low oxidation state, may be associated with the activation of hydrogen via the donor–acceptor mechanism with the preferential transfer of electron density from the hydrogen molecule to the unoccupied *d* orbitals of the metal.[23,37] The presence of relatively weakly bound forms of hydrogen (the $H^{\delta-}$ form with $T_{des} \geqslant 300$ °C), which are characteristic of monometallic catalysts with a high metal concentration and of bimetallic systems containing bulk phases of the reduced metal, is due to the activation of hydrogen via a mechanism involving oxidative addition with electron transfer

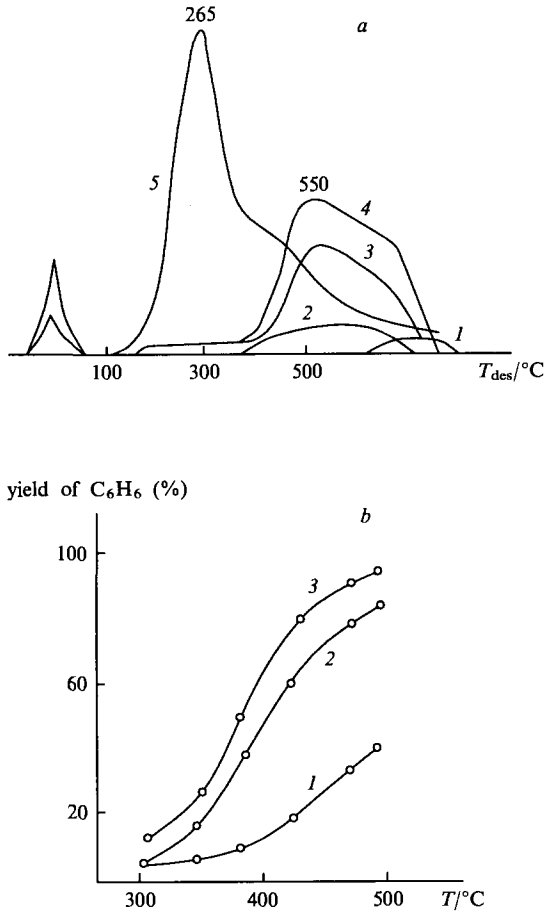


Figure 2. Spectra of the thermodesorption of hydrogen from catalysts on Al_2O_3 (*a*) and the activity of hydrogen in the dehydrogenation of cyclohexane when different catalysts are used (*b*). Metal concentration (mass%): (*a*) 0.04 Pd (curve *1*), 0.3 Pd (curve *2*), 4.2 Ce (curve *3*), 6.3 Ce (curve *4*), and Pd–Ce (curve *5*); (*b*) 0.05 Pd (curve *1*), Pd–Ce/Al_2O_3 (curve *2*); Ce content 1.0 mass% (curves *2*) and 2.5 mass% (curves *3*).

from the metal to the antibonding σ_u^* orbital of the hydrogen molecule.[23,27] The different degrees of dispersion of the reduced metallic particles create in their turn a set of energetically different desorption centres on the surface. Thus it has been shown [73] that, depending on their size, the monodisperse platinum particles on Al_2O_3 (23, 45, or 90 Å) chemisorb hydrogen with different bond energies (E_{des} = 204, 113.4, or 96.6 kJ mol^{-1}).

We shall consider the influence of the state of the metals and of the associated characteristics of the adsorption complexes of hydrogen on the activity of the catalyst in the hydrocracking and dehydrogenation reactions of hydrocarbons (cyclohexane [55,56] and n-propane [68]). In the cobalt/alumina catalyst with a low concentration of the deposited metal (1.7 mass%), containing cobalt mainly in the oxidised state (the SMCI region) and partly in the atomically disperse form, the amount of chemisorbed relatively strongly bound hydrogen in the $H^{\delta+}$ form is small. This catalyst exhibits a low activity in the hydrocracking of cyclohexane [~10% of C_1-C_5 hydrocarbons can be detected in the products (Fig. 3*b*, curve *1*)] and the parallel dehydrogenation reaction (~6% of benzene). The ratio of the yields of the hydrocracking and dehydrogenation products is 1.7. With increase in the cobalt content in the catalyst to 3.0 mass% – 4.3 mass% accompanied by a sharp increase, not proportional to the increase in the concentration of the deposited metal, in the amount of strongly bound hydrogen chemisorbed on weakly oxidised and finely dispersed particles of reduced cobalt, the hydrocracking of cyclohexane proceeds very readily (the yield of C_1-C_5 hydrocarbons is 95% – 99%; see Fig. 3*b*, curves *2* and *3*), while dehydrogenation is almost completely suppressed (the yield of benzene is 3.0% – 0.4%); the ratio of the yields of the hydrocracking and dehydrogenation products increases by a factor of 32 – 246 respectively.

The experimental data presented show that the hydrocracking reaction requires the presence of weakly oxidised forms of the metals on which hydrogen is chemisorbed with formation of strongly bound $H^{\delta+}$ complexes (E_{des} > 250 kJ mol^{-1}; Fig. 3*a* and 4*a*). With increase in E_{des} for the chemisorbed hydrogen, the ability of the catalyst to cleave the hydrocarbon molecule increases and the temperature corresponding to complete conversion diminishes (Fig. 3*b*, curves *2* and *3*; Fig. 4*c*).

While analysing the relation between the state of the chemisorbed hydrogen and the activity of the catalysts investigated, it is essential to note that at 500 °C, where saturated hydrocarbons such as cyclohexane and n-propane react, only hydrogen with T_{des} > 500 °C remains on the surface according to data obtained by the stepwise thermodesorption method (Figs 2*a*, 3*a*, and 4*a*). The $H^{\delta+}$ form of hydrogen cannot evidently be displaced from the catalyst surface during the reaction by the organic component of the reaction mixture (H_2 + saturated hydrocarbon) as a consequence of the lower reactivity of the C–C and C–H bonds compared with the H–H bond. [33] Retained on the surface in this form, hydrogen promotes an increase in the degree of reduction of the weakly oxidised highly dispersed metallic particles, i.e. it behaves as a modifying additive able to alter the electronic properties of the catalyst surface.

Consequently the catalysts containing on their surface an appreciable amount of strongly bound atomic hydrogen in the $H^{\delta+}$ form exhibit an increased activity in the hydrocracking of cyclohexane. This agrees well with the finding that the structure-sensitive C–C bond dissociation reaction takes place readily on pairs of coordinatively unsaturated metal atoms via the

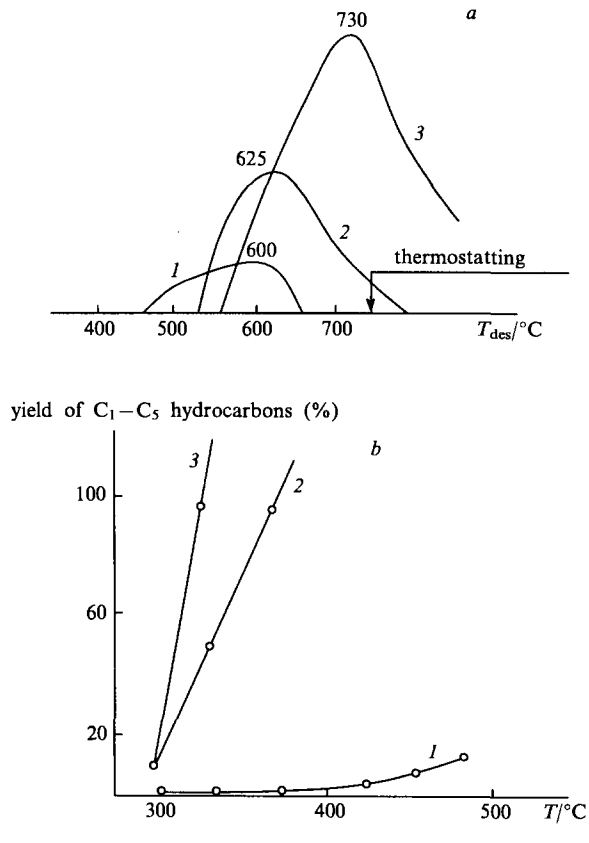


Figure 3. Hydrogen thermodesorption spectra (*a*) and the activity of the Co/Al_2O_3 catalysts in the hydrocracking of cyclohexane (*b*). Cobalt concentration (mass%): (*1*) 1.7; (*2*) 3.0; (*3*) 4.3.

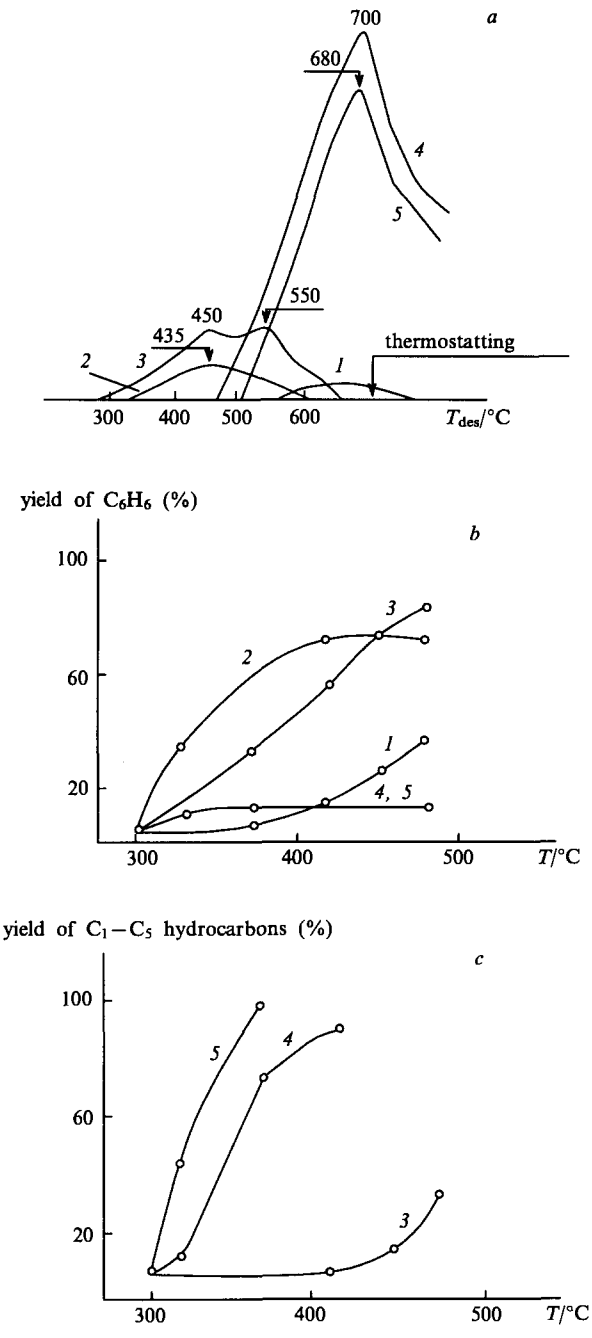


Figure 4. Hydrogen thermodesorption spectra (*a*) and activities in the dehydrogenation (*b*) and hydrocracking (*c*) of cyclohexane of the 0.1 mass% Pd/Al_2O_3 catalyst (curves *1*) and the $Pd-Co/Al_2O_3$ catalysts with various cobalt contents (mass%) [(*2*) 1.0; (*3*) 1.7; (*4*) 3.0; (*5*) 4.3].

oxidative addition mechanism with formation of negatively charged hydrocarbon fragments $(R_3C)^-$.[37] The hydrogen in the $H^{\delta+}$ form also promotes an increase in the degree of reduction of the coordinatively unsaturated electron-deficient metal atoms, accelerating thereby the dissociation of the C–C bonds in the hydrocarbon molecule. Furthermore, it evidently participates in the hydrogenation of the $(R_3C)^-$ fragments that are formed on cleavage of the C–C bonds. The possibility of the simultaneous activation of the H–H and C–C bonds on the same metal atom (centre) has been demonstrated.[37]

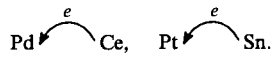
In the dehydrogenation reactions of cyclohexane and n-propane, the most active are bimetallic platinum/alumina and palladium/alumina catalysts containing low concentrations of the promoting agent [1.0–1.7 mass% Co (Fig. 4*b*, curves *2* and *3*), 1.0–2.5 mass% Ce (Fig. 2*b*, curve *3*), or 2.0 mass% Sn],[68] in which the degree of reduction of both the noble and nonnoble metals is higher. Their oxidised forms are less electron-deficient than in the corresponding monometallic specimens. These catalysts are characterised by the chemisorption of both the $H^{\delta+}$ form of the hydrogen and of the $H^{\delta-}$ form (Figs 2*a* and 4*a*).

In the dehydrogenation reaction, a significant fraction of the relatively weakly bound atomic hydrogen $H^{\delta-}$ in the modified catalysts is desorbed from the surface of the specimens, liberating the chemisorption centres on which the C–H bonds in the hydrocarbon molecules are activated. This stage is rate-limiting in the dehydrogenation reaction.[74, 75] The concentration of the centres for the activation of C–H bonds can be estimated quantitatively on the basis of the presence and content of the $H^{\delta-}$ form of hydrogen with E_{des} = 125–250 kJ mol^{-1}, which is chemisorbed on the most reduced surface centres of the catalyst, and the activity of the catalyst in the dehydrogenation of hydrocarbons can be inferred.

The hydrogen in the $H^{\delta+}$ form ($T_{des} > T$) chemisorbed on weakly oxidised and highly dispersed metallic particles is retained on the surface of the catalyst at the temperature of the dehydrogenation reaction. Evidently the hyrogen can participate directly in the catalytic dehydrogenation step, recombining with the atomic hydrogen $H^{\delta-}$ formed on dissociation of the C–H bonds as a result of their activation on the reduced surface centres via the oxidative addition mechanism.[37] Furthermore, the degree of reduction of the electron-deficient surface centres increases during the formation of the $H^{\delta+}$ form. Hence, the number of centres for the activation of the C–H bonds is increased.

V. Conclusion

The combination of reduced metals and metals oxidised to different extents in the bimetallic catalysts investigated, which chemisorb hydrogen via different mechanisms, ensures their high capacity for the chemisorption of hydrogen. The degree of reduction of the metals in bimetallic catalysts, which determines the strength of the bonding and the charge state of the different forms of chemisorbed hydrogen and hence the mode of the reactions of saturated hydrocarbons, depends on the chemical nature of the modifying additive (the electron work function, the oxidation-reduction potential, etc.) which weakens or intensifies the electron-donating properties of the noble metal, for example:



Catalysts containing on their surface centres for the chemisorption of complexes of the type $H^{\delta-}$ exhibit a fairly high activity in the dehydrogenation of hydrocarbons ($Pd-Ce/Al_2O_3$ with 2.5 mass% Ce). On catalysts containing centres for the chemisorption of both types, namely $H^{\delta+}$ and $H^{\delta-}$ ($Pd-Co$, $Pt-Sn/Al_2O_3$), alkanes react via two pathways: dehydrogenation and hydrocracking, whereas catalysts which chemisorb hydrogen only in the $H^{\delta+}$ form (Co/Al_2O_3) drive the process mainly along a single path — the hydrocracking of the molecule.

Chemisorbed hydrogen can be regarded not only as a participant in the dehydrogenation or hydrocracking reaction (hydrogenation of fragments of the hydrocarbon molecule in the hydrocracking process or recombination with the hydrogen atom formed on dissociation of a C–H bond) but also as a modifying agent, which gives rise to a definite degree of oxidation or reduction of the metals on the catalyst surface.

References

1. N R Bursian, S B Kogan *Usp. Khim.* **58** 451 (1989) [*Russ. Chem. Rev.* **58** 272 (1989)]
2. O V Bragin, A L Liberman *Prevrashcheniya Uglevodorodov na Metallsoderzhashchikh Katalizatorakh* (Conversions of Hydrocarbons on Metal-Containing Catalysts) (Moscow: Nauka, 1981)
3. T N Bondarenko, L M Kustov, A A Dergachev, A Yu Khodakov, V B Kazanskii, Kh M Minachev *Kinet. Katal.* **31** 912 (1990)
4. Z Knor *Catal. Sci. Technol.* **3** 231 (1983)
5. L V Babenkova, N M Popova, I N Blagoveshchenskaya *Usp. Khim.* **54** 177 (1985) [*Russ. Chem. Rev.* **54** 105 (1985)]
6. O V Krylov, V F Kiselev *Adsorbtsiya i Kataliz na Perekhodnykh Metallakh i Oksidakh* (Adsorption and Catalysis on Transition Metals and Oxides) (Moscow: Khimiya, 1981)
7. D A Dowden *Annu. Rep. Prog. Chem., Sect. C* **79** 99 (1982)
8. S Roy Morrison *The Chemical Physics of Surfaces* (New York: Plenum Press, 1977) (Translated into Russian; Moscow: Mir, 1980)
9. P C Richardson, D R Rossington *J. Catal.* **14** 157 (1969)
10. P P M M Wittgen, C Groeneveld, J H G J Janssens, M L J A Wetzels, G C A Schuit *J. Catal.* **59** 168 (1979)
11. W C Millman, M Crespin, A C Cirillo Jr, S Abdo, W Keit Hall *J. Catal.* **60** 404 (1979)
12. P Meriaudeau, M Primet *J. Mol. Catal.* **61** 227 (1990)
13. S Colluccia, F Boccuzzi, G Ghiotti, C Morterra *J. Chem. Soc., Faraday Trans. 1* **78** 2111 (1982)
14. T Ito, M Kuramoto, M Yoshioka, T Tokuda *J. Phys. Chem.* **87** 4411 (1983)
15. J Kondo, H Abe, Y Sokata, K Maruya *J. Chem. Soc., Faraday Trans. 1* **84** 511 (1988)
16. S Bernal, F J Botana, R Garcia *Catal. Today* **2** 73 (1983)
17. R J Levy, M Primet *Appl. Catal.* **70** 263 (1991)
18. D A Dowden, D Wells, in *Actes 2me Congres International de Catalyse, Paris, 1961* p. 1489
19. G T Surrat, A B Kunz *Phys. Rev. Lett.* **40** 347 (1978)
20. L I Rodriges, F Ruette, M Rosa-Brussin *J. Mol. Catal.* **62** 199 (1990)
21. Z Zsoldos, T Hoffer, L Guczi *J. Phys. Chem.* **95** 798 (1991)
22. G G Wepfer, G T Surrat, R S Weidman, A B Kunz *Phys. Rev. B* **21** 2596 (1980)
23. J Y Sailard, R Hoffman *J. Am. Chem. Soc.* **106** 2006 (1984)
24. R C Baetzold *J. Am. Chem. Soc.* **105** 4271 (1983)
25. E Shustorovich, R C Baetzold *Science* **227** 876 (1985)
26. Ying H Pan, D P Ridge *J. Phys. Chem.* **93** 3375 (1989)
27. S Beran, Z Slanina, N Neshev, E Proinov, in *Heterogeneous Catalysis, Proceedings of the 6th International Symposium, Part 1* (Sofia: Bulg. Acad. Sci., 1987) p. 330
28. J-M Hermann *J.Catal.* **118** 43 (1989)
29. H R Aduris, P Bodnariuk, B Coq, F Figueras *J.Catal.* **119** 97 (1989)
30. H R Aduriz, P Bodnariuk, M Dennehy, C E Gigola *Appl. Catal.* **58** 227 (1990)
31. G C Bond, R Yahua, B Coq *J. Chem. Soc., Faraday Trans.* **86** 2297 (1990)
32. S Hub, L Hilaire, R Touroude *Appl. Catal.* **36** 307 (1988)
33. I S Akhrem, M E Vol'pin *Usp. Khim.* **59** 1906 (1990) [*Russ. Chem. Rev.* **59** 1118 (1990)]
34. J H Sinfelt *J. Phys. Chem.* **90** 4711 (1986)
35. C Lee, L D Schmidt *J. Catal.* **101** 123 (1986)
36. I R Engstrom, D W Goodman, W H Weinberg *J. Am. Chem. Soc.* **110** 8305 (1988)
37. Ya A Dorfman *Katalizatory i Mekhanizmy Gidrirovaniya i Okisleniya* (Catalysts and Mechanisms of Hydrogenation and Oxidation) (Alma-Ata: Nauka, 1984)
38. E Shustorovich, A T Bell *Surf. Sci.* **205** 492 (1988)
39. M J Dess, V Ponec *J. Catal.* **119** 376 (1989)
40. E H Van Brockhoven, V Ponec *J. Mol. Catal.* **25** 109 (1984)
41. Z Paal *Mekhanizm Kataliza, Ch.2. Metody Isledovaniya Kataliticheskikh Reaktsii* (The Mechanism of Catalysis, Methods for the Investigation of Catalytic Reactions, Part 2) (Novosibirsk: Nauka, 1984)
42. O V Bragin, S A Krasavin *Usp. Khim.* **52** 1108 (1983) [*Russ. Chem. Rev.* **52** 625 (1983)]
43. G A Somorjai *Science* **227** 902 (1985)
44. A Sarcany, in *Heterogeneous Catalysis, Proceedings of the 6th International Symposium, Part 1* (Sofia: Bulg. Acad. Sci., 1987) p. 193
45. F Zaera, G A Somorjai *J. Catal.* **84** 375 (1983)
46. L Margitfalvi, P Seedlacsec, M Hegedms, E Talas, F Nagy, in *Proceedings of the IXth International Congress on Catalysis, Calgary, 1988* p. 1283
47. J Volter, H Lieske, G Lietz *React. Kinet. Catal. Lett.* **16** 87 (1981)
48. J Volter, G Lietz, M Uhlemann, M Herman *J. Catal.* **68** 42 (1981)
49. V V Rozanov, A V Sklyarov *Kinet. Katal* **24** 909 (1983)
50. M Masai, N Khondaku, T Ando, S Onaka, K Nakakhara *Sekubai* (Catalyst) **19** 56 (1977)
51. V K Duplyakin, in *Nanesennye Metallicheskie Katalizatory Prevrashcheniya Uglevodorodov. Materialy Vsesoyuznoi Konferentsii "Sibirskie Chteniya po Katalizu, Novosibirsk, 1987" T. 1* (Supported Metal Catalysts for the Conversion of Hydrocarbons, Proceedings of the All-Union Conference Novosibirsk, 1987 "Siberian Lectures on Catalysis" Vol. 1) p. 74
52. A S Belyi, V K Duplyakin, Yu V Fomichev *React. Kinet. Catal. Lett.* **7** 461 (1977)
53. Z Pall, H Zimmer, P Tetenyi *J. Mol. Catal.* **25** 99 (1984)
54. A V Zaitsev, A P Tyupaev, V Yu Borovkov, E A Timofeeva, G V Isagulyants, V B Kazanskii *Izv. Akad. Nauk SSSR, Ser. Khim.* 759 (1986)
55. L V Babenkova, I N Blagoveshchenskaya, N M Popova, N K Nadirov, L F Lykova, N I Kondratkova *Khim. Tekhnol. Topliv i Masel* **10** 20 (1985)
56. L V Babenkova, I N Naidina, in *Razvitie Rabot v Oblasti Kataliza v Kazakhstane* (Development of Research into Catalysis in Kazakhstan) (Alma-Ata: Nauka, 1990) p. 12
57. L V Babenkova, N M Popova, E V Lunina, O A Kryukova, A G Sarmurzina, K M Kurbanova *Zh. Fiz. Khim.* **61** 2984 (1987)
58. L V Babenkova, I N Blagoveshchenskaya, N V Vorob'ev, K M Kubanova *Kinet. Katal.* **28** 1132 (1987)
59. L V Babenkova, A G Sarmurzina, K M Kubanova, L M Kurashvili *Izv. Akad. Nauk Kaz. SSR, Ser. Khim.* (3) 53 (1986)
60. K Kh Razikov, V N Vorob'ev, E A Sapozhnikova, in *Trudy I Sovetsko-Indiiskogo Seminara po Katalizu, Novosibirsk, 1985* (Proceedings of the First Soviet – Indian Seminar on Catalysis, Novosibirsk, 1985) p. 74
61. L V Babenkova, I N Blagoveshchenskaya, N M Popova, L M Kurashvili *Zh. Fiz. Khim.* **58** 1378 (1984)
62. H Kobayashi, M Yamaguchi, T Ito *J. Phys. Chem.* **94** 7206 (1990)
63. A N Mansoeir, J W Gook, D E Sayers *J. Catal.* **89** 462 (1984)
64. A S Sass, V A Shvets, G A Savel'eva, V B Kazanskii *Kinet. Katal.* **26** 1149 (1985)
65. E M Moroz, W A Drozdov, V A Ushakov, A K Dzhunusov, P G Tsyrulnikov *React. Kinet. Catal. Lett.* **41** 104 (1990)
66. L S Kravchuk, N I Ivashchenko, S V Markevich, I P Stremok, T V Khorlashina, M V Zaretskii *Izv. Akad. Nauk BSSR, Ser. Khim. Nauk* (4) 72 (1978)
67. G V Antoshin, E S Shpiro, V N Belyatskii, O P Tkachenko, Kh M Minachev *Izv. Akad. Nauk SSSR, Ser. Khim.* 1913 (1983)
68. L V Babenkova, S Szabo, Yu G Kulievskaya, V G Shalyuhin *Acta Chim. Hung.-Models in Chemistry* **129** (6) 831 (1992)
69. N M Popova *Vliyanie Nositelya i Struktury Metallov na Adsorbtsiyu Gazov* (The Influence of the Carrier and the Metal Structure on the Adsorption of Gases) (Alma-Ata: Nauka, 1980)
70. E S Shpiro, O P Tkachenko, N V Belyatskii, V B Kazanskii, Kh M Minachev *Kinet. Katal.* **31** 950 (1990)
71. Z Zhang, W M Sachtler *J. Chem. Soc., Faraday Trans.* **86** 2313 (1990)
72. L V Babenkova, I N Naidina, N M Popova, N R Bursian, S B Kogan, N M Podkletnova *Zh. Prikl. Khim.* **63** 158 (1990)
73. L V Babenkova, N M Popova, D V Sokol'skii, Sh A Dushabaev *Dokl. Akad. Nauk SSSR* **273** 1152 (1983)
74. Lyu Kam Lok, N G Gaidai, S L Kiperman, S B Kogan *Kinet. Katal.* **32** 72 (1991)
75. V P Sitnik, N V Nekrasov, T V Vasina, V I Yakerson, O V Bragin *Izv. Akad. Nauk SSSR, Ser. Khim.* 727 (1990)

Russian Chemical Reviews **63** (7) 559 – 574 (1994) ©1994 Russian Academy of Sciences and Turpion Ltd

UDC 541.128

Intermediates and mechanisms of heterogeneous catalytic reactions. The simplest reactions of hydrocarbons, alcohols, and acids

O V Krylov, V A Matyshak

Contents

I.	Introduction	559
II.	Certain problems concerning the methods for the study of processes on the surfaces of solids	560
III.	Isomerisation of alkenes	563
IV.	Oligomerisation of alkenes and certain other reactions	565
V.	Metathesis of alkenes	567
VI.	Decomposition of alcohols	568
VII.	Decomposition of acids	570
VIII.	Conversion of methanol into hydrocarbons	571
IX.	Conclusion	572

Abstract. The structures of the intermediate surface compounds in heterogeneous-catalytic reactions of hydrocarbons, alcohols, and acids, established by spectroscopic (mainly IR spectroscopic) measurements, are examined. The evidence obtained concerning the role of particular structures in catalysis is differentiated: from spectroscopic data obtained before or after catalysis; from spectroscopic data obtained in situ but without kinetic measurements; from spectroscopic data obtained in situ by comparing the kinetics of the heterogeneous-catalytic reactions with the kinetics of the changes in the concentrations of the surface compounds. The mechanisms of heterogeneous catalytic reactions obtained on the basis of the available information about the surface complexes are presented. The bibliography includes 89 references.

I. Introduction

In order to understand the mechanism of heterogeneous catalysis, it is necessary to know the sequence of the elementary stages through which the catalytic reaction proceeds. For this purpose, information on the structures and reactivities of the intermediates is first needed.

In the general case, a large set of complexes may exist on the catalyst surface. For example, in the reaction $A \rightleftharpoons B$, occurring on a catalyst K in accordance with the mechanism

$$\begin{array}{l} \quad\quad\quad\

the catalytic reaction. Therefore they cannot be regarded as proven. Furthermore, the majority of investigators confined themselves merely to stating that a particular compound is formed (it was later referred to as the intermediate) under the catalytic conditions without studying the rate of its formation and consumption.

Nevertheless, it is precisely by measuring the rates of formation and consumption of the different compounds in the reaction medium and by comparing them with the rates of the catalytic reaction proper that one can demonstrate whether a particular compound, found under the catalytic conditions, is an intermediate. In heterogeneous catalysis most of the stages of the overall processes occur on the surface. The concentration of the reactive species on the surface, calculated per unit volume, is much lower than in homogeneous reactions. Therefore sensitive spectroscopic methods must be resorted to in order to detect the intermediates on the surface.

The high resolving power of spectroscopic methods as regards time is also very important. Under stationary conditions in catalytic reactions, direct comparison of the concentration of complexes of any kind with the rate of the overall reaction cannot provide a direct answer to the question whether such complexes are intermediate or 'dead-end'. This can be done by carrying out the reaction under non-stationary conditions using methods involving the pulsed introduction of the reactants, a sharp variation of the reactant concentrations (the 'response method'), a jump in temperature, irradiation, etc. The turnover number of a catalytic reaction (i.e. the number of reaction steps occurring on a single active catalyst centre per second) is known[2] to be as a rule $10^{-2}-10^{2}$ s^{-1}†. The characteristic times of a catalytic reaction are correspondingly in the range from 10^{-2} to 10^{2} s. Evidently the resolving power of the spectroscopic methods employed in situ as regards time must not be less than this. However, in the majority of cases spectroscopic measurements are performed with interruption of the catalytic reaction, the interruption time greatly exceeding the characteristic time of the catalytic reaction.

This review presents data (mainly from communications published after 1980) concerning the intermediates in catalysis obtained by spectroscopic methods, mainly by IR spectroscopy. UV spectroscopy, spectroscopy in the visible region, X-ray photoelectron spectroscopy, low-energy electron scattering spectroscopy, NMR, and EPR have been used in individual investigations. Unfortunately, in the vast majority of studies, the above criterion, based on the correspondence between the kinetic characteristics of the concentration variation of a possible intermediate and the kinetics of the catalytic reaction itself, was not considered. Therefore the conclusions reached in them concerning the structure of the intermediates and the sequence of their reactions must be regarded as tentative and not proven.

Apart from spectroscopic methods, other procedures also exist for the investigation of the catalytic reaction mechanism: temperature-programmed desorption (TPD) and temperature-programmed reaction (TPR), isotopic methods (exchange of isotopes under catalytic conditions, kinetic isotopic effect), kinetic transient response methods, the so called 'time analysis of the products' (TAP-reactor), and others. Without dwelling especially on the description of these methods and the results obtained with their assistance, we shall use these data as well in a number of cases.

The present review presents data concerning intermediates in the simplest heterogeneous-catalytic polymerisation and oligomerisation reactions, the metathesis of hydrocarbons, and the decomposition of alcohols and acids. The single starting material in these reactions is converted into one or several reaction products. More complex oxidation–reduction reactions will be considered in future reviews.

† These figures refer to reactions occurring under flow or static conditions at pressures not too remote from atmospheric. At ultralow and high pressures, smaller and larger turnover numbers are obtained respectively.

We shall not deal with the spectroscopic proof of the existence of a particular intermediate and so the numerical vibration frequencies will not therefore be quoted as a rule.

II. Certain problems concerning the methods for the study of processes on the surfaces of solids

IR spectroscopy in the frequency range 400–5000 cm^{-1} is usually employed to investigate the nature of the complexes arising on the surfaces of the catalysts. This is associated not only with the fact that molecular IR spectroscopy yields information directly concerning the structure of surface compounds but also with the fact that, in contrast to the majority of other physical methods, it permits a wide scale variation of the temperature and pressure in the spectrometer cell.

The amount of information derivable from IR spectroscopy may actually increase in the study of complexes on the surfaces of solids (compared with molecules in the gas phase). The point is that a fairly large number of vibrations are inactive in the IR spectrum and are manifested only in the Raman spectrum. When molecules interact with the surface, their symmetry is reduced, so that virtually all the vibrations become active in the IR spectrum. Adsorbed nitrogen, hydrogen, oxygen, etc. molecules may be successfully detected on the surfaces of solids by IR spectroscopy.

Transmission spectroscopy, reflectance spectroscopy, emission spectroscopy, and diffuse reflectance spectroscopy are used nowadays to a greater or lesser extent in the study of processes on the surface.

Massive metals are one of the commonest types of catalyst. The surface processes on such objects cannot be investigated by the traditional transmission spectroscopic methods. Emission spectroscopy is promising in this instance.

The measurement of the transmission spectra of surface compounds is frequently hindered by the intrinsic absorption of the catalyst. Difficulties of this kind can be overcome by applying the diffuse reflectance method in the IR region of the spectrum.We shall consider briefly the principal features of each of the methods listed above.

1. Infrared transmission spectroscopy

The principles of this method have been described in detail in numerous monographs (see, for example, Refs 3–5). Spectrophotometers record the transmittance T:

$$T = \frac{I}{I_0} = \exp(-kl), \tag{1}$$

where I and I_0 are the intensities of the transmitted and incident light, k is the linear absorption coefficient, and l the thickness of the absorbing layer. According to the Beer–Lambert–Bouguer law, the optical density is given by

$$D = \ln\frac{1}{T} = \ln\frac{I_0}{I} = \varepsilon c l, \tag{2}$$

where ε is the extinction coefficient and c the concentration of the absorbing layer. Eqn (2) constitutes the basis of quantitative analysis by means of spectroscopy.

The sensitivity of the method is determined both by the characteristics of the radiation detector and by the absorption coefficient of the medium. It is possible to estimate the number of absorbing molecules necessary to obtain sufficiently intense absorption bands on tranditional instruments. For example, a reliable determination requires $\sim 10^{17}$ CO molecules in the sample or 10^{12} molecules cm^{-2} for a specific surface of the specimen of 100 $m^2 g^{-1}$. Since other vibrations (C–H, C–C, etc.) are characterised by lower (by two–three orders of magnitude) absorption coefficients, the sensitivity with respect to them is significantly lower.

The appearance of the Fourier technique improved somewhat the situation in this field. Calculations have shown[5] that the use of

an interferometer instead of a dispersing element should result in an approximately 100-fold gain in sensitivity. In practice, however, the use of an interferometer with Fourier transformation yields a gain in sensitivity by a factor of only 10. The intrinsic noise of the detector precludes the attainment of the calculated gain in sensitivity.

A significant obstacle to the application of transmission spectroscopy under the conditions of a catalytic reaction is the intrinsic emission by the specimen. As a result of this, instead of the true absorption spectrum, one records a resultant spectrum due to the superposition of absorption and emission spectra. Emission can be excluded by modulating the emission in front of the specimen.

It is noteworthy that Fourier spectrometers permit measurements at high temperatures. Distortions of the spectra are possible only due to the fact that the emission by the heated specimen can alter the glow bar temperature. A very important advantage of Fourier spectroscopy is the possibility of working with low radiant energies. This means that the surface compounds can be investigated even on catalysts with a high intrinsic absorption.

Since spectroscopic measurements are performed under stationary and nonstationary conditions, the question arises of the characteristic times of the processes which can be investigated by this method. Processes with characteristic times $> 1\ s^{-1}$, which constitutes the upper limit to the range of characteristic times of catalytic reactions, are accessible to study by spectroscopic methods.

The same time constant applies also to Fourier spectroscopy (the time of a single scan is ~ 1 s). In studying specimens with a high intrinsic absorption, a large number of scans is necessary in order to obtain a high quality spectrum of the surface compounds (the signal to noise ratio increases in proportion to the square root of the number of scans). In this case, the time of the measurement of one spectrum may reach 1 h. Clearly, such systems can be investigated only under stationary conditions. A Fourier spectrometer capable of performing 25 scans per second has been described recently.[6] With the aid of such instruments, it is possible to investigate reactions with characteristic times significantly less than 1 s.

It is noteworthy that the application of transmission spectroscopy has made it possible hitherto to accumulate an enormous amount of information about the structures and properties of surface compounds. However, the question of their role in the catalytic reaction remains open.

2. Infrared diffuse reflectance spectroscopy

In experiments using infrared transmission spectroscopy, it is essential to employ sufficiently thin (from the standpoint of transmission) discs of the test substance. Very often success depends precisely on the possibility of preparing such a disc (the formation of discs is necessary to suppress scattering). Furthermore, in the spectral range above 2000 cm^{-1} the transmittance is fairly low owing to the fairly considerable intrinsic absorption by the catalyst. Finally, as a result of the large optical path length in the cell, the absorption bands of the molecules in the gas phase and on the surface compounds are superimposed.

Diffuse reflectance spectroscopy is free from the above disadvantages.[7,8] Its essential feature is that the detector detects the light scattered by a powdered specimen.

The Kubelka–Munk formula,[7] which relates the fraction of the light reflected by an infinitely thick medium to the absorption and scattering coefficients, is used for the quantitative description of diffuse reflectance spectra.

$$\frac{K}{S} = \frac{(1 - R_\infty)^2}{2R_\infty}, \tag{3}$$

where K is the absorption coefficient of the specimen, S its scattering coefficient, and R_∞ the fraction of the light reflected by the infinitely thick medium.

For the adsorption of molecules on an infinitely thick specimen, the Kubelka–Munk formula assumes the form

$$\frac{K + \varepsilon c}{S} = \frac{(1 - R)^2}{2R}, \tag{4}$$

where ε is the extinction coefficient of the adsorbed substance, c its concentration, and R the fraction of the light reflected by the infinitely thick specimen with the adsorbed layer. The quantities R and R_∞ are determined from the spectrum.

The line intensity is found from the formula

$$I = \frac{R_\infty - R}{R_\infty}. \tag{5}$$

After obtaining the difference between Eqns (4) and (3) and taking into account Eqn (5), we obtain the relation between the intensity of the band due to the adsorbed substance and its concentration (the Kubelka–Munk function):

$$F(R) = I\left(\frac{1}{R - R_\infty}\right) = \frac{2\varepsilon c}{S}. \tag{6}$$

The optical path length for the light in the material of the catalyst can be estimated from this formula.

It has been shown[8] that the optical path length is 2–3 mm when this method is used, which is much greater than in the transmission method. The greater path traversed by light in the specimen is apparently in fact one of the causes of the high sensitivity of diffuse reflectance spectroscopy. Theoretical estimates indicate that, when effectively scattering specimens are investigated, diffuse reflectance spectroscopy is more sensitive (by more than an order of magnitude) than the traditional transmission spectroscopy.

Under real conditions, the sensitivity relation is less favourable owing to the difference between the scattering capacities of the powders (scattering spectra) and the discs (transmission spectra). Furthermore, the attachments used to measure the diffuse reflectance spectra are nonideal and are incapable of collecting all the light scattered by the specimen. However, despite this, even when only a few per cent of the scattered light reaches the detector, in the analysis of effectively scattering substances ($R_\infty \sim 1$) diffuse reflectance spectroscopy has an advantage, as regards sensitivity, over transmission spectroscopy.

It follows from the Kubelka–Munk function (3) that quantitative measurements require the determination of the scattering coefficient. However, it has been shown[8] that in the case of low-intensity bands the concentration of the absorbing substance and the intensity of the corresponding band in the spectrum are linked by a relation analogous to the Beer–Lambert–Bouguer law:

$$-\varepsilon c l_{ef} = \ln\left(\frac{R}{R_\infty}\right), \tag{7}$$

where l_{ef} is the optical path length for the light in the specimen. Eqn (7) is valid when

$$\frac{R_\infty - R}{R_\infty} \ll \frac{2(1 - R_\infty)}{(R_\infty)^{1/2}}.$$

In the analysis of intense bands for the determination of concentration characteristics, it is essential to know the scattering coefficient. The procedures for the independent determination of S have been examined.[8]

The characteristic times of the processes which may be investigated with the aid of diffuse reflectance spectroscopy are the same as in measurements involving the use of transmission spectroscopy.

3. Emission spectroscopy

A large proportion of the early studies on energy emission processes were devoted to blackbody emission. The frequency distribution of the energy emitted on heating a blackbody depends on temperature but is independent of the material of the body itself, i.e. information about the substance cannot be obtained from the emission spectrum of a blackbody. However, real materials are not blackbodies. For example, the emission spectrum of a gas at a low pressure consists of a set of lines which carry information about the nature of the gas.

The expression for the distribution of the radiant energy on a non-blackbody can be obtained with the aid of the Kirchhoff–Planck laws. The emittance of a grey medium (ε_ν) at a temperature T and a frequency ν is defined as the ratio of the radiant intensities of the emission by the grey medium [$I(\nu, T)$] and blackbody [$I_B(\nu, T)$]:[9,10]

$$\varepsilon_\nu = \frac{I(\nu, T)}{I_B(\nu, T)}. \quad (8)$$

The Kirchhoff law establishes the fact that $\varepsilon_\nu = a_\nu$, where a_ν is the absorptance of the substance.

The simplest case is that of emission by a gas whose molecules are distributed uniformly in a certain volume. We shall calculate the emittance from a thin layer of molecules located at a distance d from the boundary of the emitting volume. If $I_0(\nu, T)$ is the emittance from this layer, then the emittance which has reached the boundary is $I(\nu, T) = I_0 \exp[-K(\nu, T)d]$, where $K(\nu, T)$ is the absorption coefficient of the medium. The fraction of the energy transmitted through the layer d is equal to the ratio I/I_0, so that $a = 1 - I/I_0$.

Using the Kirchhoff law and eliminating I_0, we obtain the expression

$$I(\nu, T, d) = I_B(\nu, T)\{1 - \exp[-K(\nu, T)d]\}, \quad (9)$$

which describes the emittance from a layer of gas parallel to the boundary and at a distance d from the latter. There is a possibility that I may depend on the pressure because the quantity $K(\nu, T)$ may change owing to an intermolecular interaction.

Calculation of the emittance from liquids or solids constitutes a more difficult task, because it is essential to take into account the reflection of the radiation emitted in the direction towards the boundary of the substance.

Catalytic systems partly transmit IR radiation. According to the theory of emission by semitransparent substances,[9,10] the sum of the emittance (ε_ν), reflectance (r), and transmittance (T) is approximately unity:

$$\varepsilon_\nu + r + T \approx 1. \quad (10)$$

Eqn (10), which can be derived thermodynamically, is at present the principal expression for quantitative measurements. Emission spectroscopy is much more rarely used than transmission and diffuse reflectance spectroscopy. The reason for this is the difficulty of measuring low-intensity emittances with the aid of dispersion spectrometers. The possibilities of emission spectroscopy have increased significantly only recently following the development of the Fourier technique.

If the reflectance of the specimen is low, then, according to Eqn (10), the following expression is sufficiently accurate:

$$\varepsilon_\nu(\nu) = 1 - T(\nu).$$

The absorptance of the specimen $a(\nu)$ is related to the concentration of the absorbing substance by the Beer–Lambert law:

$$a(\nu) = -\lg T(\nu) = Kcl. \quad (11)$$

In this case, the emittance from the specimen may be related to the concentration of the absorbing substance as follows:

$$c = \frac{\lg[1 - \varepsilon_\nu(\nu)]}{Kl}. \quad (12)$$

This relation holds satisfactorily for gases and semitransparent bodies.[10]

Analogous expressions exist for the calculation of emittance when the emitting substance is on the surface of a metal.[11] Certain characteristics of various IR spectroscopic methods are presented in Table 1. For a comparative assessment of the sensitivities of the dispersion and Fourier spectroscopic methods, we may recall that a reliable determination of CO requires the presence in the sample of 10^{17} and 10^{16} molecules of this substance respectively.

Table 1. Comparative characteristics of the IR methods for the study of catalytic processes.

Characteristics	Spectral range/cm^{-1}	Time resolution/s^{-1}	Equation for quantitative treatment
Transmittance	400–5000	> 1	$D = \varepsilon cl$
Diffuse reflectance	1800–5000	> 1	$F = \frac{2\varepsilon}{S}c$
Emittance	400–2500	> 1	$F = \frac{2\varepsilon}{S}c$ (for highly reflecting objects) $D = \varepsilon cl$ (for weakly reflecting objects)

4. Raman spectroscopy

The radiation scattered by the specimen is investigated in Raman spectroscopy. Suppose that the specimen is irradiated by light at a frequency ν_0. Then most of it undergoes Rayleigh scattering in which the frequency of the scattered light is also ν_0. However, the frequency of a small proportion of the scattered light changes and assumes a new value ν such that the quantity $h(\nu_0 - \nu)$ is exactly equal to the energy of the vibrational or rotational transition. The frequency shifts $\Delta\nu$ give rise to the vibrational–rotational spectra of the specimen. However, the selection rules in Raman spectroscopy differ from those in IR spectroscopy. The main requirement is that the polarisability of the molecule should change during the vibration. Vibrations active in the IR spectrum may be active or inactive in the Raman spectrum and conversely. IR and Raman spectra supplement each other, so that their joint employment makes it possible to obtain virtually complete information about the objects investigated.

The Raman spectra of many molecules adsorbed on oxide systems have now been described. The application of this method at elevated temperatures encounters a series of technical difficulties associated with the emission of light from the heated walls. This is apparently the reason why Raman spectroscopy has so far been used in catalysis to investigate the state of the catalyst itself but not of the adsorbed phase.[12] For example, the reduction of deposited molybdenum oxide catalysts has been investigated from the variation of the intensity of the Mo=O absorption band. Studies[13,14] in which it was claimed that adsorbed CH_3 and CH_2 groups are formed on oxide catalysts during high-temperature oxidative condensation of methane are an exception. This observation is apparently an artefact and is associated with the intense heating and decomposition of the organic molecules in the light beam.

An appreciable increase in the sensitivity of Raman spectroscopy has been achieved with the use of laser sources. Hence the name of the method—laser Raman spectroscopy. Its sensitivity reaches 10^{18} molecules in the specimen, which is as a rule much greater than the number of molecules in the monolayer. A further increase in sensitivity was achieved by the discovery of the SERS (surface-enhanced Raman spectroscopy) or GRS

(giant Raman spectroscopy) effect.[15] Following adsorption on Ag, Au, Cu, and certain other metals, the sensitivity (scattering cross-section) increases by a factor of 10^4-10^6.

5. X-Ray photoelectron spectroscopy, Auger spectroscopy, and electron energy loss spectroscopy

X-Ray photoelectron spectroscopy (XPES) and Auger spectroscopy make it possible, in principle, to investigate the composition of adsorbed compounds and, when the spectral resolution is satisfactory, their structures as well. Electron energy loss spectroscopy (EELS) yields information about the vibrational levels of the absorbed molecule, i.e. in principle the same information as IR spectroscopy. Its advantages are high sensitivity (0.01–0.1 of a monolayer even on smooth surfaces) and the possibility of using it in the low-frequency range of vibrations (10–800 cm^{-1}). At the same time, the EELS method is characterised by a much poorer resolution (at best 25 cm^{-1}, usually 50 cm^{-1}) than IR spectroscopy (1–2 cm^{-1}).

An evident disadvantage of all the varieties of electronic spectroscopy is the impossibility of using them at a high pressure, which usually occurs in catalytic processes. The maximum possible pressure is 10^{-3} Pa (10^{-5} torr). However, even at a pressure below 10^{-3} Pa, the mechanism of the catalytic reaction must be studied on surfaces cleaned in an ultrahigh vacuum. Here one has to bear in mind that the catalytic reaction under the usual conditions, i.e. at higher pressures, can proceed via a different mechanism. The problem of the pressure gap is widely discussed in the literature on catalysis. There are cases where the kinetic data obtained at a low pressure can be referred to high pressures, but the converse cases also occur.

6. Spectroscopy in the visible and ultraviolet regions

The spectroscopy in the visible and ultraviolet regions (UV-VIS) is distinguished by a fairly high sensitivity. In particular, the intensity of the absorption for allowed one-electron $d-d$ transitions is characterised by a molar absorption coefficient of the order of $\sim 10^4$. For this absorption coefficient, it is possible to detect $\sim 10^{16}$ molecules of the test substance in a 1 cm^3 sample. The absorption coefficient for $d-d$ transitions in complexes with a high symmetry is significantly lower and hence the sensitivity is appreciably worse.

The advantage of UV-VIS spectroscopy over IR spectroscopy is the simplicity of the design of the cell-reactors: there is no need to use 'windows' made from special materials and quartz cells can be employed. This method is widely used to determine the electronic state and the coordination of transition metal ions forming part of the composition of the catalysts. It is fairly rarely used to investigate the catalytic reaction intermediates and surface compounds. Organic compounds with C=C, C≡C, C=O, etc. multiple bonds, specially with conjugated bonds, and aromatic compounds are mainly investigated. The electronic transitions in compounds with C–C, C–H, and C–O single bonds occur in the far UV region and are therefore difficult to observe under the conditions of the catalytic reaction. The studies are usually carried out at room temperature, since technical difficulties, associated with light emission from the heated walls, arise at an elevated temperature.

7. Electron paramagnetic resonance

Electron paramagnetic resonance has by a high sensitivity; the presence in the specimen of 10^{11} spins is sufficient for the measurement.

The EPR method is used widely to investigate transition metal ions and other radical centres in catalysts. Its application to the investigation of adsorbed compounds in situ is limited, firstly, by the fact that the lifetime of the free radicals on the surface is as a rule short under catalytic conditions (high temperatures and pressures) and because of this the sensitivity of the method proves to be insufficient. Secondly, the EPR signal from the surface paramagnetic complexes is frequently broadened under catalytic conditions (up to complete disappearance) involving physical adsorption of O_2, H_2O, etc. molecules on the surface due to the dipole–dipole interaction.

The EPR method is frequently employed to observe the radical states of oxygen, NO, and certain other molecules on the surface. For this purpose, the cell-reactor is usually cooled rapidly to low temperatures. Accordingly the time required for the observation of the test molecules increases to ~10 s.

8. Nuclear magnetic resonance

The NMR method has been finding increasing application in catalysis during recent times.[16] The NMR method with a magic angle of rotation is used in the study of solids, especially catalysts.

When applied to catalysis in situ, the NMR method has been used successfully to investigate reactions such as catalytic polarisation under the conditions of an isolated static reactor. However, the technical difficulties associated with the necessity for the continuous introduction of the reactants into a rotating tube-reactor have so far precluded the wide scale employment of NMR.

* * *

Among all the spectroscopic methods listed above, IR spectroscopy has remained the most widely used procedure since it has been most thoroughly developed. Therefore it is in fact recommended that IR spectroscopy be used to determine the intermediates and to investigate the dynamics of catalytic reactions.[17]

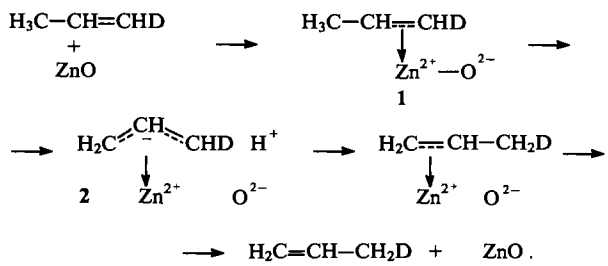
A large proportion of the studies published nowadays concern the measurement of the spectra of adsorbed molecules at room temperature (these investigations were initiated by Terenin and coworkers[18]) and the spectra of surface compounds after 'freezing' the reaction. Evidently, conclusions concerning the role of surface complexes in the reaction, based on such measurements, are to a large extent tentative. The application of IR spectroscopy in the study of the dynamics of heterogeneous catalysis was pioneered by Tamaru,[19,20] who drew attention to the need for the simultaneous measurement of the rate of the catalytic reaction and the rate of reaction of the surface compounds. Together with his coworkers, he investigated the intermediates formed during the decomposition of HCOOH on Al_2O_3, SiO_2, and ZnO and also during the oxidation of methanol on ZnO.

The extents to which the involvement of particular surface compounds as intermediates in catalysis has been demonstrated are differentiated in the present review. In most studies, the conclusion concerning the participation of surface compounds in catalysis is based on spectroscopic measurements before and after the reaction. The reliability of such conclusions will be designated by the letter L (lowest). Measurements of IR spectra in situ are resorted to much more rarely in order to establish the role of the surface compound in the reaction. The reliability of the conclusions reached on the basis of such measurements will be designated by the letter M (moderate). Publications in which the role of the surface complex in the reaction is estimated by comparing the rate of its reaction with the rate of formation of the reaction product are altogether rare. It is quite evident that agreement between these quantities serves as an adequate basis for the claim that the surface compound detected is an intermediate in the reaction. The reliability of such conclusions will be designated by the letter H (highest).

III. Isomerisation of alkenes

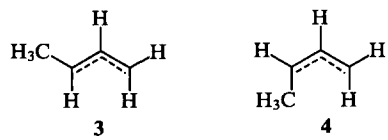
The simplest type of catalytic reaction is A → B, where A and B are substances of similar chemical nature. The isomerisation of alkenes belongs to reactions of this type.

The isomerisation of deuteriopropenes on zinc oxide results in the formation of an equilibrium mixture of $CH_2D-CH=CH_2$, $CH_3-CH=CHD$, and $CH_3-CD=CH_2$.[21] A band corresponding to the vibration of the OH group and five bands corresponding to the formation of the symmetrical π-allyl are observed in the IR spectrum. This indicates that the isomerisation proceeds via dissociative cleavage of a C–H bond. The intermediate (π-allyl) probably exists in the anionic form $C_3H_5^-$:



The first stage of the reaction is evidently the formation of the π-complex **1**. Bands corresponding to the formation of π-complexes following the adsorption of alkenes on a series of oxides have indeed been observed in the IR spectra.[22] In chemical terms, one can also imagine the formation of π-complexes of the alkene with the acid OH groups and the subsequent formation of the carbonium ion $C_3H_7^+$. However, the formation of such ions has not been detected in any of the investigations.

In the isomerisation of but-1-ene to but-2-ene on ZnO, bands corresponding to the π-complexes of but-1-ene and *cis*- and *trans*-butenes as well as π-allyl complexes were observed in the IR spectra.[23] Of the two possible methyl-π-allyls

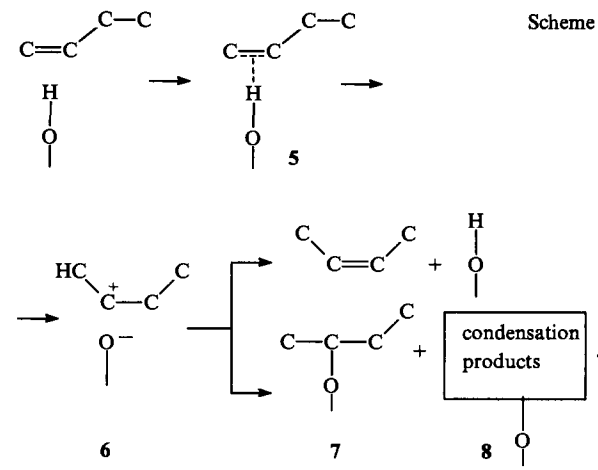


the allyl **3** may be a precursor of *trans*-butene, while the allyl **4** may be a precursor of *cis*-butene. However, only complex **4** was detected on the surface. The most intense absorption bands in the spectra of the π-complexes are those of the *cis*-butene π-complex, although a greater amount of *trans*-butene is formed in the equilibrium gas mixture. Consequently, the form **3** exists only as a short-lived precursor in the reaction **4** ⇌ **3** ⇄ *trans*-butene. Under catalytic conditions, the intensity of the signal due to π-C_4H_8-1 diminishes slowly, while that of the signals of π-*cis*- and π-*trans*-C_4H_7 increases slowly. At the same time, complex **4** is formed initially at a rate close to the overall rate of isomerisation, which then remains constant. Hence one may conclude that π-allyl is a true intermediate.

The formation of a π-complex with acid OH groups was observed in a study of the isomerisation of but-1-ene to *cis*-butene on HY zeolites and other acid silicates at 0–200 °C.[24] The attempts to detect the $C_4H_9^+$ carbonium ions failed in this case too, although a correlation was observed between the rate of reaction and the number of acid OH groups. It is suggested that the reaction proceeds in acordance with scheme 1. According to Paukshtis et al.,[24] the conversion of complex **5** into complex **6** is the rate-limiting stage. In a kinetic study, it was observed that the continuous increase in the intensity of the absorption bands of the saturated complexes **7** and **8** is accompanied by a decrease in the rate of isomerisation. Evidently complexes **7** and **8** are 'dead-end' compounds which deactivate the catalyst.

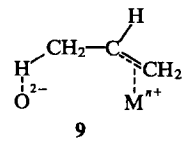
A band at 1510 cm^{-1}, characteristic of a C=C bond with an OH group, was observed in the IR spectra in the isomerisation of hex-1-ene to hex-2-ene and the subsequent *cis–trans* isomerisation on the HZSM-5 zeolite at 200 °C. At the same

Scheme 1



time, the spectrum of the OH groups changed also. On this basis, the authors[25] concluded that the reaction proceeds via the intermediate formation of a carbonium ion (a reaction of the **5** → **6** type)‡.

The formation of stable carbonium ions of the type $(CH_3)_2C^+CH_2CH_3$ has been postulated in the adsorption of isoalkenes on zeolites.[22] The possibility of the isomerisation of the double bonds via cyclic complexes of the type



9

in accordance with an associative, 'concerted' mechanism was considered in the same investigation.

Table 2 presents a compilation of data concerning the intermediates formed in the adsorption of alkenes on heterogeneous catalysts; the reliability of the evidence for the role of a particular complex in the isomerisation reaction, in conformity with the criteria described above, is indicated.

A dissociative isomerisation mechanism, involving the cleavage of a C–H bond with formation of π-allyl anions or carbonium ions, has been postulated in all the studies considered. We may note, however, that virtually no direct spectrokinetic confirmations of such a mechanism exist (apart from the detection of the π-allyl complex itself). The observed changes in the IR spectra of the adsorbed molecules are associated in most cases with dead-end compounds not involved in the main reaction.

The data presented in table 2 refer to the isomerisation of alkenes involving the double bond. As regards their skeletal isomerisation, there have been virtually no investigations in which intermediates were identified with the aid of IR spectroscopy. The mechanisms of the skeletal isomerisation quoted in individual communications (see, for example, Cuong Pham-Hun et al.[26]) are based on indirect data.

‡The migration of carbon along the chain of carbon atoms in octane at 20–70 °C on the HZSM-5 zeolite has been recently demonstrated by ^1H and ^{13}C NMR methods [A G Stepanov, M V Luzgin, V N Romannikov, K I Zamaraev *Catal. Lett.* **24** 271 (1994)]. The authors believe that this proves the formation of a carbenium ion. The direct spectroscopic detection of this ion is impossible because it is in equilibrium with an alkyl silyl ether.

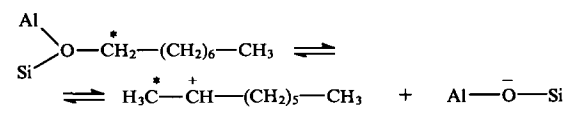
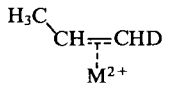
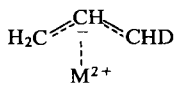
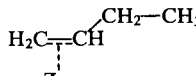
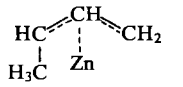
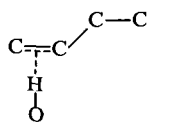
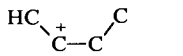
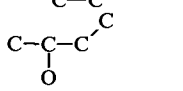
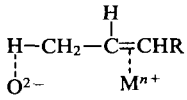
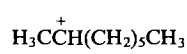


Table 2. Intermediates formed in the isomerisation of alkenes.

Reaction, catalyst	Intermediate complex	Reliability	Ref.
Isomerisation of deuteriopropenes on oxides		M	21, 22
		M	21, 22
Isomerisation of butenes on ZnO		H	23
		H	23
Isomerisation of butenes and higher alkenes on zeolites and other acid silicates		M	24, 25
		L	22, 25
		L	22, 25
		L	22
Isomerisation of oct-1-ene on HZSM-5 zeolite		M	

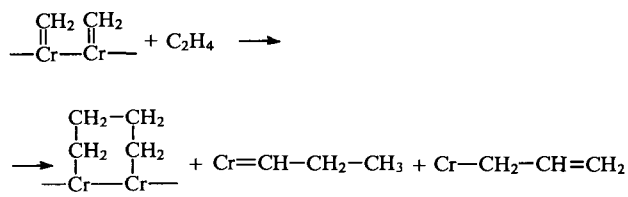
IV. Oligomerisation of alkenes and certain other reactions

1. Oligomerisation, alkylation, and aromatisation of alkenes

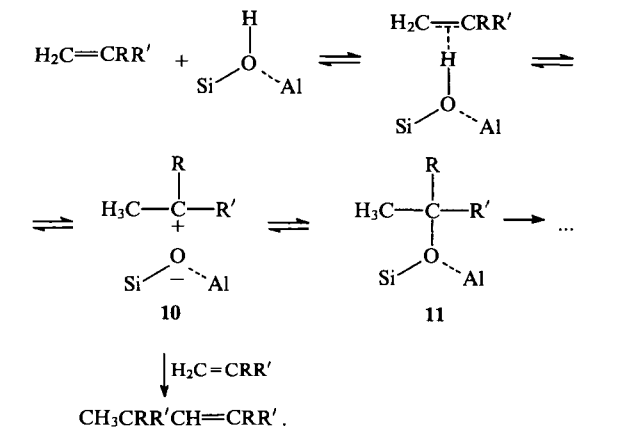
The oligomerisation of alkenes $n\mathrm{A} \rightarrow \mathrm{B}$ formally belongs to the class of reactions of a more complex type than isomerisation. However, the fact that the reaction product—an oligomer or a polymer—is not desorbed into the gas phase facilitates the spectrokinetic investigation and this renders the results more unambiguous. UV-VIS and NMR spectroscopy have been used together with IR spectroscopy to identify the intermediates.

Mainly the stable starting materials and oligomers as well as stable long-lived alkoxy-derivatives have been dectected in situ by IR [25,27–29] and NMR [30–32] spectroscopy in the oligomerisation of C_2H_4, C_3H_6, and C_4H_8 on zeolites at 0–200 °C.

The initial stage of the interaction—the formation of a π-complex with an OH group—was discovered in a study of the NMR spectra of isobutene on the HY and HZSM zeolites at a low temperature (−150 °C). [31] The oligomerisation of propene to 4-methylpentene and hex-1-ene on NiO/SiO_2 involves the formation of a π-complex between C_3H_6 and Ni^{2+}. [33] The nature of the IR spectra, obtained in situ in a study of the polymerisation of C_2H_4 on Cr/SiO_2, [27] indicates the existence of dissociative forms of ethylene adsorption. This provided grounds for the hypothesis that carbenes participate in the reaction, although these intermediates were not detected directly.

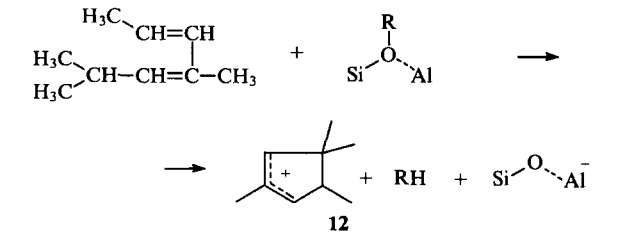


The π-complex of the alkene with an OH group can be converted into a carbonium ion. It can be formed as a transition state, but carbonium ions have not been detected in the study of the reactions of alkenes by IR and NMR spectroscopic methods even at low temperatures. [31–32] Apparently they are immediately converted into long-lived alkoxide groups $\equiv Si-OR$ on alumino-silicates. A study of the kinetics of the oligomerisation of C_2H_4 and C_3H_6 on the TsVK zeolite and silicalite [29] from the change in the IR band at 2935 cm^{-1} (due to CH_2 groups in the reaction products) showed that the rate of reaction initially diminishes and then increases. This is due to the fact that the CH_3O groups are relatively unreactive, although the $O(CH_2)CH_3$ groups are reactive in relation to the alkene. The band due to the CH_3O group (2977 cm^{-1}) gradually disappears from the spectrum. The initial stages of the oligomerisation reaction may be represented by the following scheme: [31–33]



This is followed by the formation of the alkoxide $\equiv Si-O-CH_2-CRR'-CH_2-CHRR'$ and a further increase in the chain length of the oligomer. The rate-limiting stage may be the conversion of the intermediate carbonium ion **10** into a dimer, after which both linear and branched polyalkenes are produced.

Stable cyclic carbonium ions **12**, formed via the scheme

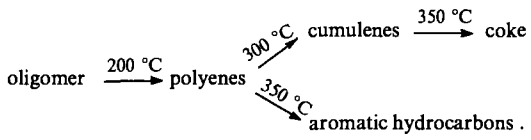


after the consumption of the entire monomer, have been detected in a study of the oligomerisation of C_3H_6 by the NMR method. [32] However, they are not intermediates in the oligomerisation reaction.

The oligomer chain is apparently terminated via β-limination. Peaks corresponding to the products of the interaction of the terminal $-CH=CH_2$ group of the growing oligomer with an OH group of the catalyst have been observed in the IR spectra obtained in the polymerisation of C_2H_4 on 0.5% Cr/SiO_2. [34]

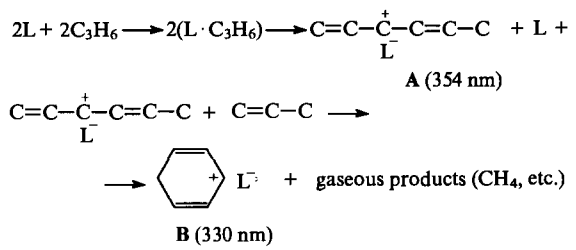
The subsequent stages of the reaction of oligomers at a higher temperature (260–400 °C) were investigated by UV-VIS spectroscopy. [29,35–37] Polyenyl and other condensed structures

were then detected. Starting from 250–300 °C, aromatisation takes place, while at a still higher temperature (350 °C) coke is formed. The overall scheme of the reactions of oligomers on zeolites assumes the following form:[29]



Polyenes are stabilised under catalytic conditions on the same OH groups as oligomers. It has been confirmed by the IR [28] and NMR [38] spectroscopic methods that coke and aromatic hydrocarbons are formed via independent pathways.

The formation of stable unsaturated cations has also been observed by UV-VIS spectroscopy. It has been shown [35] that C_3H_6 is aromatised on the Lewis acid centres of γ-Al_2O_3 at 180–300 °C via the mechanism



where L is a Lewis acid centre. The rate of formation of compound **B**, characterised by the 330 nm vibration frequency, is proportional to the concentration of compound **A** (354 nm vibration frequency) and the pressure of C_3H_6 in the gas phase. After the reaction has occurred, various condensed compounds are detected on the surface.[23,35,36]

It has also been shown by the EPR method that, when HM, HY, etc. zeolites with adsorbed alkenes are heated, free-radical products are formed. For example, C_3H_6 affords the radicals[39]

$$CH_2{=}\dot{C}H{=}CH_2 \text{ and } CH_2{=}\dot{C}H{=}CH{-}CH(CH_3)_2.$$

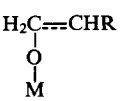
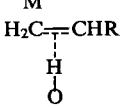
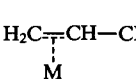
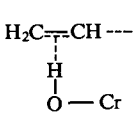
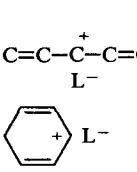
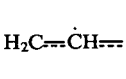
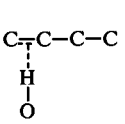
The EPR spectra were recorded after extensive cooling and not under catalytic conditions.

Alkylation on zeolites proceeds via a mechanism analogous to the oligomerisation mechanism. The π-complexes of C_4H_8 and alkoxide compounds were detected in situ in a study of the alkylation of isobutane by butenes on the HNaCaX zeolite by IR spectroscopy. According to the authors,[40] butane can also give rise to the intermediate carbonium ion $(CH_3)_3C^+$, which participates in hydride (H^-) transfer to $C_4H_9^+$ with formation of the alkoxy-group $(CH_3)_3C{-}O{-}$ or a C–C bond in oligomers via an associative mechanism. Isobutane is capable of being adsorbed mainly on the basic (nucleophilic) centres of the zeolite, whereas butenes are adsorbed on the acid centres.

We may note that the oligomerisation examined above probably proceeds via an associative mechanism (for example, by the reaction of the carbonium ion **10** with the alkoxide **11**). Its occurrence apparently requires two active centres: one with the alkoxide chain and the other with the carbonium ion. The lack of a direct relation between the concentration of the alkoxide structure and the rate of oligomerisation indicates the possible existence of equilibria of the type **10** $\rightleftharpoons$ **11**. The main bulk of the surface may serve as a reservoir supplying the reaction when its conditions are varied. It may be that cyclic carbonium ions **12** play the same role.

A compilation of data on the intermediate compounds formed in the oligomerisation of alkenes, aromatisation, and alkylation is presented in Table 3.

Table 3. Intermediates formed in the oligomerisation and certain other reactions of alkenes.

Reaction, catalyst	Intermediate complex	Reliability	Ref.
Oligomerisation of alkenes on zeolites		L	25, 27–33
		M	31
Oligomerisation of propene on NiO/SiO_2		L	33
Polymerisation of ethylene on Cr^{3+}/SiO_2		L	27, 33
Aromatisation of propene on Al_2O_3		H	35
Aromatisation of propene on zeolites		L	39
Alkylation of isobutane by butenes on zeolites		L	40

The polymerisation of alkenes, for example on Ziegler–Natta catalysts, apparently proceeds via a coordination mechanism. The alkene molecule forms a π-complex with the transition metal ion, which simultaneously retains the polymer chain. CH_2 groups, interacting with the catalyst to some extent, have been detected in a high concentration in an IR spectroscopic study of this process.

2. The cracking of hydrocarbons

The cracking of hydrocarbons can be regarded as a reaction which is to some extent the reverse of oligomerisation. It too proceeds on aluminosilicates. However, cracking occurs at much higher temperatures and therefore the intermediates may be different. A generally accepted view is that carbonium ions are formed as intermediate species. The application of spectroscopic methods in situ to investigate the cracking is difficult owing to the high process temperatures. The same intermediates as in oligomerisation have been detected by the NMR method among the cracking products of propene oligomers on HY at 220 °C.[38] Dissociative mechanisms are more probable at higher temperatures.

In the cracking of the methylcyclohexane and 3-methylpentane on H-mordenite above 100 °C, adsorbed free radicals were detected by the EPR method.[41] They are stable up to 100 °C, while at a higher temperature they are converted into the final products, possibly via the formation of intermediate carbonium ions. The EPR signal is not observed at room temperature. The authors suggest that a strong Lewis acid centre abstracts an electron from a tertiary C–H bond in the first stage of the reaction with formation of a radical-cation. The latter loses a H atom and gives rise to a free radical. This is followed by the two-stage elimination of the hydride ion.

The cracking on metals proceeds via a different mechanism. On decomposition of C_2H_6 on Pt/SiO_2, absorption due to ethylidyne structures $CH_3C{\equiv}Pt$ and possibly $PtCH_2-CH_2Pt$ were observed in the IR spectra. At 200–300 °C, these compounds decompose with formation of CH_4 and a carbon residue.[42]

V. Metathesis of alkenes

The metathesis of alkenes

$$2A \rightarrow B + C$$

is formally a reaction of a more complex type than those examined above. However, in reality its mechanism is simple, since all the reactants (A, B, and C) belong to the same class of alkenes (for example A may be propene, B ethylene, and C butene). Therefore the intermediates should also be of the same type. Intermediate carbene complexes have been detected in this reaction.

The present authors investigated the UV-VIS diffuse reflectance spectra of molybdenum, tungsten, and rhenium oxides deposited on Al_2O_3 and SiO_2.[43,44] The mechanisms of the metathesis of propene in the presence of such a catalyst are different at low (50–250 °C) and high (300 °C) temperatures judging from the content of the butene isomers. It was postulated that the metathesis can proceed via quasi-cyclobutane and carbene mechanisms at low and high temperatures respectively.

$$H_3C-CH=CH_2 + 2M \longrightarrow H_3C-CH{:}M + H_2C{:}M$$

$$H_2C{:}M + H_3C-CH=CH_2 \longrightarrow \underset{\text{13}}{H_3C-\underset{\displaystyle CH_2}{\overset{\displaystyle M}{\overset{\diagup\!\diagdown}{CH}}}-CH_2} \longrightarrow$$

$$\longrightarrow H_3C-\underset{\displaystyle CH_2}{\overset{\displaystyle \diagup\!\diagdown}{CH}}-CH_2 + CH_3CH=CHCH_3 + C_2H_5CH=CH_2$$

$$H_2C{:}M + H_3C-CH=CH_2 \longrightarrow H_3C-CH{:}M + C_2H_4$$

$$H_3C-CH{:}M \longrightarrow M + C_2H_4$$

M = metal

However, conclusions concerning the mechanism were reached on the basis of indirect data, namely by analysing changes in the coordination in the Mo, W, and Re complexes, which are reflected in the nature of the UV-VIS spectra.

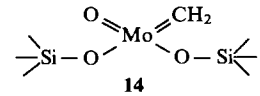
UV-VIS spectroscopy has been applied[45,46] directly under the conditions of the propene metathesis reaction. The rate of reaction was determined simultaneously with the measurement of the spectra. Comparison of these data made it possible to establish that the activation of the $Mo(CO)_6/\gamma\text{-}Al_2O_3$ catalyst is associated with the formation and rearrangement of subcarbonyl structures on the surface. The formation of the $Mo_2(CO)_6$ active centre may be represented schematically as follows:

$$Mo(CO)_6 \rightleftharpoons Mo(CO)_4 \underset{-CO}{\overset{L}{\rightleftharpoons}} Mo(CO)_3L \underset{-L}{\rightleftharpoons} Mo_2(CO)_6,$$

where L is the ligand (possibly a surface OH group).

The kinetic parameters of the formation of the active centre in the metathesis reaction have been established as a function of the state of the hydroxyl coating of the surface. The decrease in the activation energy for the formation of $Mo_2(CO)_6$ active centre is associated with the decrease in the energy expenditure on overcoming the hydroxy-group barrier when it arises. The nature of the temperature dependence of the activity of the catalyst is determined by the ratio of the rates of evolution of CO and of the rearrangement of the subcarbonyl surface structures.

The formation of the carbene complex



14

stable in vacuo up to 400–450 °C, has been observed by IR and UV-VIS spectroscopy in the adsorption of cyclopropane on MoO_3/SiO_2, in which Mo^{6+} had been reduced photochemically to Mo^{4+}.[47] Isotope exchange between complex **14** and C_2D_4 is observed at room temperature.

$$Mo{=}CH_2 + C_2D_4 \rightleftharpoons Mo{=}CD_2 + D_2C{=}CH_2.$$

At 0–350 °C, complex **14** interacts with alkenes via the mechanism

$$Mo{=}CH_2 + H_2C{=}CH-CH_3 \rightleftharpoons$$

$$\rightleftharpoons Mo{=}CH-CH_3 + C_2H_4\uparrow \rightleftharpoons \overset{H_2C}{\underset{Mo}{\overset{\|}{\underset{|}{}}}}CH_2.$$

There is also a possibility of the formation of the cyclobutane complex **15**, which has been confirmed by the appearance of new bands in the spectrum.

$$Mo{=}CH_2 + H_2C{=}CH-CH_3 \rightleftharpoons \underset{\text{15}}{\overset{CH_3}{Mo\diagup\!\diagdown}} \rightleftharpoons$$

$$\rightleftharpoons Mo{=}CH-CH_3 + C_2H_4$$

The same bands appear also in the interaction of cyclopropane with the Mo=O bond. The energy of the $Mo{=}CH_2$ bond in complex **14** is 435 kJ mol^{-1}.[48]

It is noteworthy that the catalyst in the study of Vikulov et al.[47] was subjected to photochemical reduction. However, in the usual thermal metathesis of alkenes there is also a possibility of the appearance of carbenes. In the metathesis of propene on Nb/SiO_2, the intermediate carbene complex $Nb{=}CH_2$ was formed.[49] Its structure was investigated by IR spectroscopic and EXAFS methods. It was found that the Nb–C distance in the complex is 0.195 nm, which corresponds to the length of the Nb=C double bond (whereas the length of the normal Nb–C bond is 0.210 nm). The IR bands correspond to vibrations of the CH_2 group.

Data concerning the intermediates formed in the metathesis of alkenes are compiled in Table 4.

The kinetics of the formation and decomposition of the carbene were not compared in the above studies[43,44,47–49] with the kinetics of the overall metathesis reaction.

Table 4. Intermediates formed in the metathesis of alkenes.

Reaction, catalyst	Intermediate complex	Reliability	Ref.
Metathesis of propene on MoO_x/SiO_2	$\equiv Mo{=}CH_2$	M	43,44, 47,48
	$\equiv Mo{=}CH-CH_3$	M	
	$\equiv Mo\diagup\!\diagdown CH_3$	L	48
Metathesis of propene on Nb_2O_5/SiO_2	$\equiv Nb{=}CH_2$	L	49

VI. Decomposition of alcohols

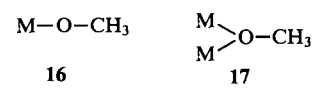
Alcohols decompose via two principal pathways: with dehydration and the formation of an alkene and water or with dehydrogenation and the formation of hydrogen and an aldehyde (or ketone). Both pathways involve reactions of the type

$$A \rightarrow B + C.$$

On dehydration of the first member of the series of aliphatic alcohols (methanol), formaldehyde CH_2O or dimethyl ether $(CH_3)_2O$ may be formed. The dehydration of methanol to CO and H_2 will not be considered here. The conversion of methanol into hydrocarbons will be examined below in Section VIII.

1. Dehydration of alcohols

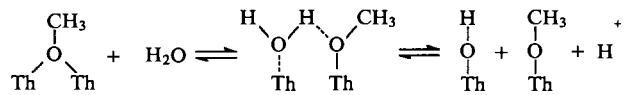
Surface methoxy-groups were detected in situ by IR spectroscopy in all the studies on the decomposition of methanol on oxides. They are present on α-Fe_2O_3,[50] CeO_2 and ThO_2,[51] Cr_2O_3,[52] ZnO,[53] and ThO_2.[54] Linear (compound **16**) and bridging (compound **17**) methoxy-groups were distinguished on CeO_2 and ThO_2.



16 **17**

The decomposition of complex **16** results in the reformation of methanol, while the decomposition of complex **17**, or more precisely the decomposition of two such complex species next to one another, affords the $CH_3OH + (CH_3)_2O + CO$ mixture.[52]

There is also a possibility of the interconversion of complexes **16** and **17**.[54]



17 **18** **16**

The interconversion of the methoxide complexes **16** and **17** proceeds in essence via the associative catalytic dehydration mechanism.

Methanol bound to the oxide by the CH_3OH ... OM hydrogen bond was also detected at a low temperature (150 °C). It may be a precursor of the methoxide.[50] Heating to high temperatures (> 200 °C) leads to the conversion of the alkoxides into formates and carbonates.[50,53]

Periodic modulation of the free stream of CH_3OH with a 1 s resolution made it possible[55] to distinguish two mechanisms of the dehydration of methanol on γ-Al_2O_3—the dissociative mechanism

$$CH_3OH_{ads} + CH_3O_{ads} \longrightarrow CH_3OCH_3(g) + OH_{ads}$$

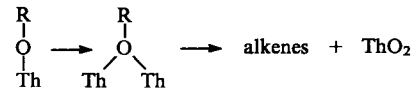
$$2\,OH_{ads} \longrightarrow H_2O(g) + O_{ads},$$

and the associative mechanism

$$CH_3OH_{ads} + O_{ads} \longrightarrow CH_3O_{ads} + OH_{ads} \longrightarrow$$

$$\longrightarrow CH_3OCH_3(g) + H_2 + H_2O.$$

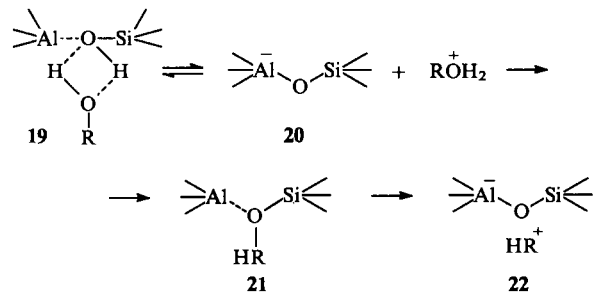
Alkoxy-groups are also formed in the dehydration of higher alcohols: isopropyl alcohol on ThO_2,[54] isobutyl alcohol on Al_2O_3,[56] and various alcohols on the HZSM-5 zeolites.[57] An attempt has been made[54] to correlate the kinetics of the dehydration of *tert*-butyl alcohol and isopropyl alcohol, based on the measurement of the rate of evolution of gaseous products, with the kinetics of the decomposition of linear and bridged alkoxides. The authors proposed the following scheme:



However, bearing in mind that the curves obtained[54] are insufficiently distinct, the reaction may also proceed via a bimolecular mechanism.

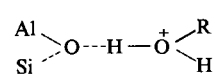
The change in the diffuse IR spectra in situ and the kinetics of dehydration of a series of alcohols (C_2H_5OH, iso-C_3H_7OH, *tert*-C_4H_9OH) on Al_2O_3 have been investigated by the response method at 140–280 °C.[56] The removal of alcohol from the gas phase at 260 °C leads immediately to the disappearance of the bands due to the hydrogen-bonded or coordinated alcohol; the bands of the alkoxide vanish somewhat more slowly, while those of the carboxylates remain unchanged. The dehydration rate constants, found from the analysis of the IR spectra and from the yield of the gaseous products, are the same. Hence the authors concluded[56] that the alkoxide is an intermediate.

In the adsorption of various alcohols, ranging from C_1 to C_4, on the HZSM-5 zeolite,[57,58] each alcohol molecule is adsorbed near an Al atom, which is indicated by the disappearance from the IR spectrum of the band due to the acid OH group. The results of exchange studies in isopropyl alcohol and *tert*-butyl alcohol, on the one hand, and D_2O, on the other, indicate that the alcohol molecules are dehydrated with formation of a carbonium ion before desorption. However, 1-butanol does not exchange with D_2O, which can be explained, according to the authors,[57] by a bimolecular mechanism in which two alcohol molecules are involved. A hydrogen bond is formed in the first stage of the interaction (complex **19**), after which the oxonium ion **20** and then the carbonium ion **22** appear.



19 **20** **21** **22**

The covalent structure **21** predominates in zeolites with nucleophilic centres, whilst the ionic structure **22** predominates in zeolites with more acid centres. The ionic structures **20** and **22** are not manifested in the IR spectra (at any rate it is difficult to distinguish them from the covalent structures), but the authors[57] assume that they may arise as a result of stabilisation due to interaction with the zeolite lattice, for example with formation of the bridged ions



as in homogeneous catalysis.[58] Such stabilisation helps to overcome the energy barrier in the endothermic stages of the reaction.

We may note that the formation of association complexes in the dehydration of isopropyl alcohol on Al_2O_3 was demonstrated previously by kinetic and calorimetric methods.[59] A four-stage scheme was proposed:

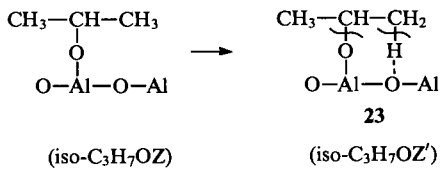
$$\text{iso-}C_3H_7OH + ZOH \rightleftharpoons [\text{iso-}C_3H_7OH \cdot ZOH],$$

$$[\text{iso-}C_3H_7OH \cdot ZOH] \rightleftharpoons \text{iso-}C_3H_7OZ + H_2O,$$

$$\text{iso-}C_3H_7OZ \xrightarrow{Z'} \text{iso-}C_3H_7OZ + Z,$$

$$\text{iso-}C_3H_7OZ' \longrightarrow C_3H_6 + Z'OH.$$

A complex of type **19** is formed in the first stage, whilst the third stage (possibly rate-limiting) represents surface diffusion of the isopropoxide groups to another active centre Z′ incorporating a surface oxygen atom.

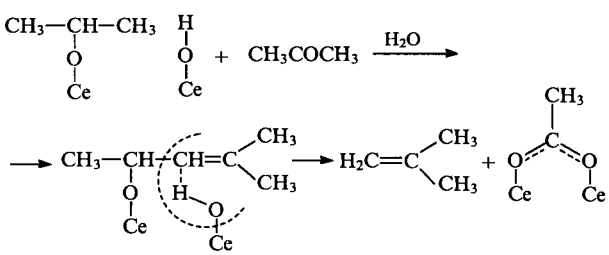


(iso-C_3H_7OZ) (iso-C_3H_7OZ')

The activation energy for this stage is 106 kJ mol^{-1}. The measured enthalpy of the first stage (26 kJ mol^{-1}) corresponds approximately to the energy of two hydrogen bonds in the type **19** complex or to a lifetime of the complex of $\sim 10^{-10}$ s.

Consequently the mechanisms proposed[57,60] agree with one another as regards the formation of hydrogen-bonded association complexes and alkoxy-groups, which do in fact largely cover the surface under stationary conditions. On the other hand, the formation of propene (the concluding stage of the reaction) proceeds, according to Aronson et al.,[57] with participation of a carbonium ion, while Sadovnikov and Gefter[60] believe that it proceeds with participation of basic centres. The question whether all the alkoxy-groups (Z centres) or only some of them (Z′ centres) participate in the formation of the final product while the remaining ones serve as a reservoir for the latter remains unresolved.

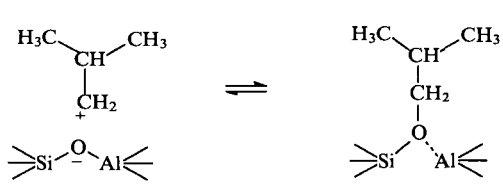
According to the view of Zaki and Sheppard,[61] based on the analysis of the IR spectra recorded after heating CeO_2 in isopropyl alcohol at 150–400 °C, the dehydration also proceeds via an associative mechanism. Apart from the direct dehydration, aldol condensation with the acetone formed on dehydrogenation of the alcohol takes place.



24

At a low temperature, close to room temperature, the aldol condensation proper, with formation of the unsaturated ketone $CH_3COCH=C(CH_3)_2$ from complex **24**, takes place. A similar process involving CH_3CHO on Na/SiO_2 has been investigated by Raman spectroscopy at room temperature.[61] Enolate complexes and complexes retained on the surface by two C–O–M bonds were detected. Physically adsorbed 2,4-dimethyl-1,3-dioxane was also found. On heating to 130 °C, it decomposes, affording crotonaldehyde $CH_3CH=CH-CHO$, acetaldehyde (or the adsorbed enolate $CH_3=CHOH$), and water.

The mechanism of the alcohol dehydration has also been investigated by the NMR method in situ.[63–69] The dehydration of *tert*-butyl alcohol and isobutyl alcohol at 100 °C, proceeds with formation of isobutene, water, and a C_8 oligomer according to the NMR data. The short-lived carbonium ion **25** may be an



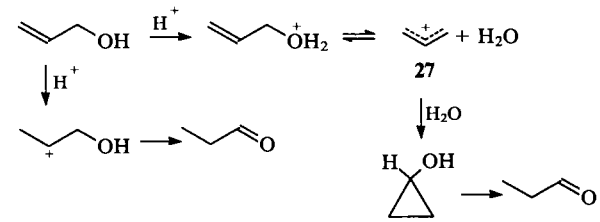
25 **26**

intermediate.[64,65] The alcohol molecule is localised at an intersection of the zeolite channels. Under these conditions, the alkoxide **26** (C_4H_9OSi) is an intermediate in the dehydration of isobutyl alcohol but not *tert*-butyl alcohol.§

The stable triphenylmethyl carbonium ion was detected in the dehydration of triphenylcarbinol on acid catalysts.[67]

The formation of the isobutyl carbonium ion, also in the dehydration of *tert*-butyl alcohol on HZSM-5, could not be detected by the NMR method,[62] although the same authors[57] had previously postulated the appearance of complex **22** in this process on the basis of IR spectroscopic data. Only type **21** alkoxide was detected. The same complex was found by these investigators also in the adsorption of methylpropane. The carbonium ion formed as a result of the adsorption of C_3H_8 on the zeolite[68] likewise belongs, according to Stepanov et al.,[64] to the class of ethers Si–O–R. The formation of a carbonium ion on the HY zeolite is more probable than on HZSM-5 owing to its higher relative permittivity and nucleophilicity.

NMR study of the dehydration of allyl alcohol on the HZSM-5 zeolite made it possible to detect the intermediate oxonium and carbonium compounds and to establish the sequence of the reactions.[69]



27

The interaction of the allyl cation **27** with allyl alcohol afforded diallyl ether $(CH_2=CH-CH_2)_2O$.

The formation of the isopropoxide was likewise observed in a study of the decomposition of isopropyl alcohol on metallic molybdenum by the EELS method.[70] C_3H_6, C_3H_8, H_2, and H_2O were also found among the reaction products.

A compilation of data concerning the intermediates formed in the dehydration of alcohols is given in Table 5.

Summarsing the data presented above on the dehydration of alcohols, we may note that the formation of linear and bridged alkoxides is acknowledged in all the investigations and in some of them also the formation of carbonium ions. Spectrokinetic measurements have scarcely been made with the exception of some not very clear-cut data.[54,56] However, on the basis of the combination of a large number of results, one may assume that the above complexes are very probably reaction intermediates.

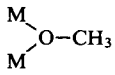
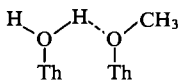
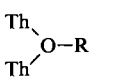
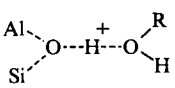
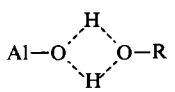
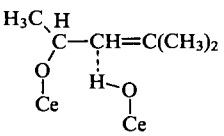
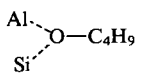
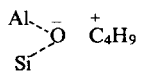
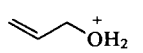
2. Dehydrogenation of alcohols

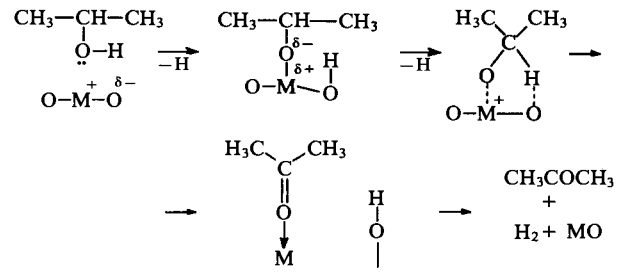
When alcohols are dehydrogenated on an oxide surface, bands corresponding to alkoxide structures are also observed in the IR spectra,[60,71] but the presence of a strong basic (nucleophilic) centre next to an acid centre is essential for the occurrence of this reaction pathway.

According to Efremov and Davydov,[71] the conversion of isopropyl alcohol occurs only in the absence of the weakly bound alcohol, blocking the neighbouring centres (possibly O^{2-}), i. e. the occurrence of the reaction via an associative mechanism is impossible in this case.

§It has been possible to demonstrate by the NMR method that the decomposition of isobutyl alcohol on the HZSM-5 zeolite involves the transfer of the $^{13}CH_2$ label from isobutyl alcohol to isobutyl silyl ether **26** and a further redistribution of ^{13}C among the C atoms in butane[J Kokes, A L Dent *Adv. Catal.* **22** 1 (1972)]. According to the authors, this demonstrates the occurrence of the transition **26** → **25** and the participation of the carbonium ion **25** in the dehydration of C_4H_9OH.

Table 5. Intermediates formed in the dehydration of alcohols.

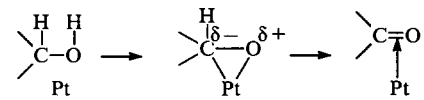
Reaction, catalyst	Intermediate complex	Reliability	Ref.
Dehydration of methanol on oxides	$M-O-CH_3$	M	50–55
		M	50–55
Dehydration of methanol on ThO_2		M	54
	$Th\cdots H-O-CH_3$	L	50
Dehydration of isopropyl and isobutyl alcohols on ThO_2	$Th-O-R$	H	54
		H	54
Dehydration of alcohols on Al_2O_3	$Al-O\cdots H-O-R$	H	56
	$Al-O-R$	H	56
Dehydration of C_1-C_4 alcohols on zeolites		L	57
Dehydration of isopropyl alcohol on Al_2O_3		M	59
Ditto on CeO_2		L	60
Dehydration of isobutyl alcohol on HZSM-5		L	64, 65
		L	64, 65
Dehydration of allyl alcohol on HZSM-5		L	69
		L	69
Dehydration of triphenyl-carbinol on acid catalysts	$(C_6H_5)_3C^+$	L	67



The IR bands at 2910 and 2960 cm^{-1}, observed when isopropyl alcohol was dehydrogenated on Fe_2O_3 at 150 °C,[72] were attributed to the enolate, which is evidently an intermediate between the alkoxide complex and the final product.

The formation of the $C_2H_5O^-$ and the $C_4H_8O^-$ alkoxides as well as acetates and carbonates, which are apparently side products, was noted in a ^{13}C NMR study of the decomposition of C_2H_5OH on MgO.[73]

On dehydrogenation of cyclohexanol to cyclohexanone on Pt/SiO_2, a shift of the C=O vibration bands was observed in the IR spectra and was attributed to the occurrence of the process

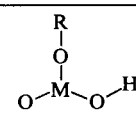
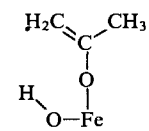
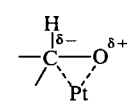


The broad bands at 1400 and 1610 cm^{-1} were assigned to the enol group.

Aldehydes and ketones may also be formed in the oxidation of alcohols with participation of the oxygen of the oxide lattice.

Data on the dehydrogenation of alcohols are compiled in Table 6.

Table 6. Intermediates formed in the dehydrogenation of alcohols.

Reaction, catalyst	Intermediate complex	Reliability	Refs
Dehydrogenation of alcohols on oxides		L	60, 71
Dehydrogenation of isopropyl alcohol on Fe_2O_3		L	72
Dehydrogenation of cyclohexanol on Pt/SiO_2		L	74

Thus the number of reliable data on intermediate compounds participating in the dehydrogenation of alcohols is much smaller than for their dehydration. The formation of enolates or enolate anions is more probable.

VII. Decomposition of acids

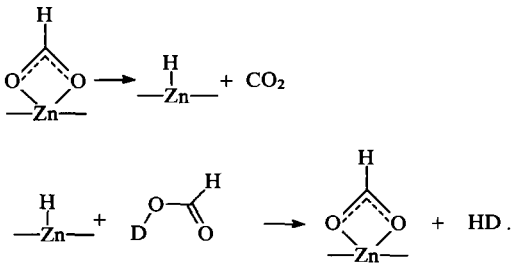
Like alcohols, formic acid may decompose via two pathways: dehydration and dehydrogenation. The principal substances formed on the catalyst surface are formates.[19, 20, 50, 75–77]

In the studies by Tamaru and coworkers already mentioned,[19, 20, 77] a catalyst disc was heated in the cell to the reaction temperature and then DCOOD was introduced until the attainment of a steady rate of decomposition. After this,

the DCOOD in the gas phase was rapidly replaced by HCOOH and the reaction was continued, observing simultaneously both the behaviour of the chemisorbed species and the rate of the overall reaction. The experiments on the dehydration of formic acid at 150–190 °C on Al_2O_3 showed that most of the adsorbed $DCOO^-$ ions vanish during the reaction, but the corresponding number of molecules appear in the gas phase as HCOOH, i.e. a rapid exchange takes place. A correlation was observed between the rate of dehydration of HCOOH and the number of proton centres on the surface. It was concluded that the $HCOO^-$ groups are not intermediate complexes and that the dehydration of formic acid proceeds when HCOOH molecules interact with the H^+ centres. The adsorption of molecular HCOOH on SiO_2 was observed, but formates were not detected under these conditions. According to the authors,[20] in this case too HCOOH molecules in the gas phase react with OH groups.

The dehydration of HCOOH on TiO_2 and zeolites has been investigated by ^{13}C NMR.[73] A monodentate formate, bound to an OH group, was detected on TiO_2, while on the zeolite a bidentate formate was found. The rate-limiting stage may be the removal of H_2O from the surface on condensation of the surface OH groups.

On the other hand, study of the dehydrogenation of HCOOH on ZnO at 145–220 °C confirmed the hypothesis that the reaction proceeds via intermediate formates.[19,20] When HCOOH was removed from the gas phase, evolution of H_2 ceased, but the rate of evolution of CO_2 did not change. On reintroduction of HCOOH into the gas phase, the rate of evolution of H_2 was restored. Almost the entire surface of ZnO was coated by the formate during the reaction. On the basis of these data, the following mechanism of the dehydrogenation of HCOOH on ZnO was proposed:



When HCOOH was dehydrogenated on α-Fe_2O_3, vibration bands of the bidentate formates, OH groups, and HCOOH molecules bound to the surface via the O–H and C=O groups were found in the IR spectra.[50] When the reaction was carried out in a closed vessel, a decrease in the intensity of the formate bands was observed.

The data on the decomposition of formic acid are compiled in Table 7.

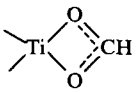
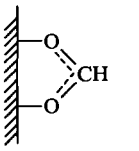
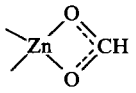
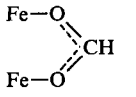
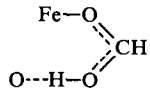
Thus the formates frequently detected under conditions for the decomposition of formic acid are most probably intermediates in the dehydrogenation of HCOOH, which proceeds via an associative mechanism. On dehydration of HCOOH, the protons are such intermediate forms.

VIII. Conversion of methanol into hydrocarbons

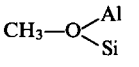
On zeolite catalysts, methanol is dehydrated to dimethyl ether, which is subsequently converted into hdyrocarbons. These reactions are referred to as the Mobil or the MTG (methanol to gasoline) process. The first stage, the formation of the ether $(CH_3)_2O$ on simple oxides, has already been considered in Section VI.

The mechanism of the conversion of methanol into hydrocarbons on the HZSM-5, HY, and SAPO-34 zeolites was investigated by the IR,[78,79] EPR,[80] and NMR[81–84] spectroscopic methods.

Table 7. Intermediates formed in the decomposition of HCOOH.

Reaction, catalyst	Intermediate complex	Reliability	Ref.
Dehydration on Al_2O_3	HCOOH	M	19, 20, 77
Dehydration on TiO_2		L	75
Dehydration on zeolites		L	75
Dehydrogenation on ZnO		M	19, 20
Dehydrogenation on Fe_2O_3		L	50
		L	50

When methanol interacted with the HZSM-5 zeolite in the absence of CH_3OH in the gas phase, the vibration bands due to different methoxy-groups were detected in the IR spectrum, viz.: the zeolite group CH_3O_{Zeol}, the oxygen atom of which is linked to the Al and Si atoms, i.e.



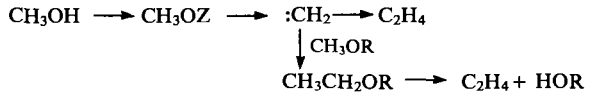
the CH_3O–Al and CH_3O–Si groups, and also weakly coordinated CH_3OH.[78] When CH_3O_{Zeol} is heated, methane and formaldehyde are formed. According to Novakova et al.,[78] this reaction proceeds via the mechanism

$$CH_3O_{Zeol} + (CH_3O-Al)^{n+} \longrightarrow CH_2O + CH_4 + Al^{(n+1)+} + O^-_{Zeol}$$

$$2\,CH_2O_{ads} + O^-_{Zeol} \longrightarrow CH_3OH + COO^-_{ads.\,Zeol}.$$

In the presence of methanol in the gas phase, C_2–C_5 hydrocarbons, mainly C_2H_4 and C_3H_6, were detected in the reaction products. Their formation was attributed to the associative interaction of CH_3OH with CH_3OZ, the details of which were not discussed.

The stage involving formation of the C–C bond is the most problematical. According to a hypothesis,[85] it is achieved via the intermediate formation of carbenes.

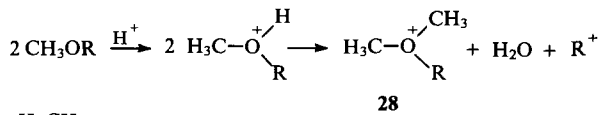


Under the conditions of the interaction of CH_3OH with C_3H_6 on the HTsVK and HY zeolites at 200–240 °C, absorption bands of various substances, attributed to oligomeric alkyl, allyl, and polyenyl cations, were observed in the IR and UV spectra.[79]

The study of the conversion of CH_3OH into hydrocarbons on zeolites by the ^{13}C and ^1H NMR methods in situ with rapid freezing of the reactor at the temperature of liquid nitrogen made it possible to follow the formation of the reaction products.[81–83]

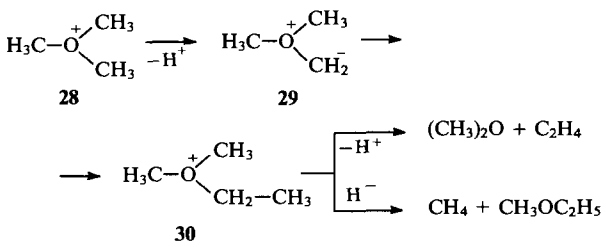
The compositions of the products in the gas phase and within the zeolite cavities were different. When HZSM-5 was used, mainly aromatic hydrocarbons were obtained. Mostly toluene, *m*- and *p*-xylenes, and 1,2,4-trimethylbenzene were found in the reaction products, while the adsorbed phase contained *o*-xylene and 1,2,4,5-tetramethylbenzene. Hence it follows that the molecules within the cavities are formed in equilibrium proportions and their emergence into the gas phase depends on the size of the windows in the zeolite.[82] On the SAPO-34 zeolite, which has even narrower channels, C_1-C_3 hydrocarbons emerge into the gas phase, while branched C_4-C_8 hydrocarbons remain in the intercrystalline space. In contrast to HZSM-5, aromatic products are not formed here.[81]

The hypothesis of the intermediate formation of oxonium ions in the synthesis of hydrocarbons from methanol was first put forward on the basis of isotopic and chemical data and not spectroscopic measurements.[86,87] According to Mole and Whiteside,[86] the oxonium ion **28** is formed in the interaction of methanol or dimethyl ether with the CH_3O^+RH surface group.



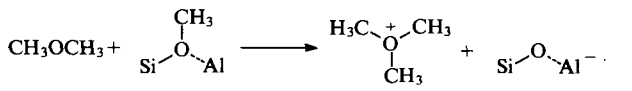
R = H, CH_3

This process was investigated using the WO_3/Al_2O_3 bifunctional catalyst with the aid of the ^{13}C carbon label. According to the authors' hypothesis,[87] in the presence of basic centres on the surface the trimethyloxonium ion **28** is converted into methylene-methyloxonium ylide **29** and the latter undergoes intramolecular methylation in the excess of dimethyl ether with formation of dimethylethyloxonium **30**.

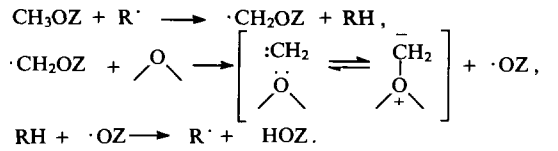


This results in the formation of a C–C bond.

The kinetics of the conversion of CH_3OH into hydrocarbons on zeolites at 250 °C were investigated by the NMR method in situ.[84] An induction period was observed initially, after which the rate of reaction attained a steady level. The authors suggest[84] that the induction period is associated with the formation from $(CH_3)_2O$ of trimethyloxonium ion, first discovered by Hunter and Hutchings.[88] However, when ether and CH_3OH were adsorbed jointly, the trimethyloxonium ions were not detected and their kinetic role is therefore not clear. Manson et al.[84] postulated that the trimethyloxonium ion **28** is formed as a result of the activated interaction of $(CH_3)_2O$ with an alkoxide group:



Another, radical mechanism of the formation of the C–C bond has been put forward.[89] Free radicals had been previously detected by the EPR method in the decomposition of $(CH_3)_2O$ on HZSM-5.[80] It had also been shown[89] that the addition of NO inhibits the synthesis of hydrocarbons via a free-radical mechanism. Paramagnetic centres had been found in heat-treated HZSM-5. The following reaction mechanism was proposed:



The radical R· can be an alkyl, alkoxyl, alkoxyalkyl, etc. The reactive carbene species participates in the formation of the C–C bond, possibly via an oxonium ion.

Consequently the formation of the alkoxides ROZ as intermediates in the synthesis of hydrocarbons from CH_3OH may be regarded as more or less demonstrated (degree of reliability M), while the formation of oxonium ions is rather tentative (degree of reliability L). Their real kinetic role has not been elucidated. An associative mechanism, i. e. the participation of two molecules or fragments in the rate-limiting stage, is most likely.

IX. Conclusion

The results of studies of the intermediates in the simplest heterogeneous catalytic reactions of hydrocarbons, alcohols, and acids, obtained by spectroscopic methods during the last 15 years, were described above. We may note that in the vast majority of the studies quoted the reliability is low. The level of sophistication of even recent studies does not exceed that in the fundamental studies by Tamaru,[19,20,76,77] in which a parallel relationship between the rate of a catalytic reaction and the changes in the IR spectra of the adsorbed species under the reaction conditions was first noted.

The most reliable evidence concerning the real role of an intermediate is provided by the agreement between the rate of reaction of the surface complex and the rate of formation of the product.

There have been very few studies in which this approach has been employed. This is associated with the considerable experimental difficulties, among which the following may be noted: (1) the need to construct reactor-cells for the simultaneous study of the spectroscopic and catalytic properties of the system; (2) the need to develop methods for the determination of absorption coefficients; (3) inadequate time resolution in both kinetic and spectroscopic measurements; (4) the presence on the surface of a large number of different surface compounds, some of which are intermediates, whilst others are dead-end complexes.

The majority of the possible intermediate complexes listed above are chemical compounds with a saturated valence; these are alkoxides, formates, acetates, etc. The π-alkene and π-allyl complexes detected in the reactions with participation of alkenes are also fairly stable.

Free radicals were detected by the EPR method only on zeolites at low temperatures, while carbonium ions, which should be more reactive than the saturated intermediates, were found by the NMR method. By resorting to shorter measurement times, at least millisecond times (the lower limit of the characteristic times of catalytic reactions), it is possible to detect short-lived (and hence more reactive) intermediates.

It is also noteworthy that the low reliability of results obtained in the study of the catalytic reactions of hydrocarbons is associated with low intensity (low extinction coefficients) of the C–H and C–C vibrations. The adsorbed substances can be detected in these reactions only when their concentration is fairly high. This explains the small number of data referring to very familiar catalytic reactions such as oligomerisation, isomerisation, and the metathesis of hydrocarbons.

References

1. J E Germain, in *Catalytic Conversion of Hydrocarbons* (London: Academic Press, 1969) (Translated into Russian; Moscow: Mir, 1972) p. 308
2. M Boudart *Usp. Khim.* **43** 317 (1974) [Translated into Russian from *AIChE J.* **18** 465 (1972)]
3. L H Little *Infrared Spectra of Adsorbed Species* (New York: Academic Press, 1966) (Translated into Russian; Moscow: Mir, 1969)
4. K Nakamoto *Infrared Spectra of Inorganic and Coordination Compounds* (New York: Wiley, 1965) (Translated into Russian; Moscow: Mir, 1966)
5. A Lee Smith, in *Applied Infrared Spectroscopy Fundamentals, Techniques, and Analytical Problem-Solving* (New York: Wiley-Interscience) (Translated into Russian; Moscow: Mir, 1982) p. 37
6. A Zecchina, G Spoto, S Bordiga, in *Europa Cat-1 (Abstracts of Reports)* (Montpellier, 1993) Vol. 1, p. 71
7. W W Wendlandt, H G Hecht *Reflectance Spectroscopy* (New York: Interscience, 1966)
8. V Yu Borovkov, Doctoral Thesis in Chemical Sciences, Institute of Organic Chemistry, Russian Academy of Sciences, Moscow, 1989
9. P R Griffiths *Chemical Infrared Fourier Transform Spectroscopy* (London: Wiley, 1975) p. 308
10. J B Bates, in *Fourier Transform Infrared Emission Spectroscopy* Vol. 1 (New York: Academic Press, 1978) p. 99
11. E Steger, D Rasmus *Appl. Spectrosc.* **28** 376 (1974)
12. R P Cooney, G Curthoys, Nguen The Tam *Adv. Catal.* **24** 293 (1975)
13. A V Bobrov, A A Kadushin, Ya M Kimel'fel'd, S E Plate *Kinet. Katal.* **29** 1006 (1988)
14. A A Kadushin, O V Krylov, S E Plate, Yu P Tulenin, V A Seleznev, A V Boborov, Ya M Kimelfeld, in *Proceedings of the International Congress "New Developments in Selective Oxidation"* (Amsterdam: Elsevier, 1989) p. 447
15. M Fleischman, P J Hendra, A J McQuillan *Chem. Phys. Lett.* **26** 163 (1974)
16. V M Mastikhin, O B Lapina, I L Mudrakovskii *Yadernyi Magnitnyi Rezonans v Geterogennom Katalize* (Nuclear Magnetic Resonance in Heterogeneous Catalysis) (Moscow: Nauka, 1992)
17. W H Delgass, G L Haller, R Kellerman, J H Lunsford *Spectroscopy in Heterogeneous Catalysis* (New York: Academic Press, 1979)
18. N G Yaroslavskii, A N Terenin *Dokl. Akad. Nauk SSSR* **66** 885 (1949)
19. K Tamaru *Adv. Catal.* **15** 65 (1964)
20. Yu Noto, K Fukuda, T Onishi, K Tamaru, in *Trudy IV Mezhdunarodnogo Kongressa po Katalizu, T. 1* (Proceedings of the IVth International Congress on Catalysis, Vol. 1) (Moscow: Nauka, 1970) p. 389
21. R J Kokes, A L Dent, C C Chang, L T Dixon *J. Am. Chem. Soc.* **94** 4429 (1972)
22. A A Davydov *IK-Spektroskopiya v Khimii Poverkhnosti Oksidov* (Infrared Spectroscopy in the Chemistry of Oxide Surfaces) (Novosibirsk: Nauka, 1984)
23. C C Chang, W C Conner, R J Kokes *J. Phys. Chem.* **77** 1957 (1973)
24. E A Paukshtis, A V Malysheva, N S Kotsarenko, L B Karakchiev *Kinet. Katal.* **21** 455 (1980)
25. A Bezoukhanova, H Lechert, G Tarabanska, A Meyer *React. Kinet. Catal. Lett.* **40** 209 (1989)
26. Cuong Pham-Hun, M J Ledoux, J Guille *J. Catal.* **143** 249 (1993)
27. P Zielinski, I G Dalla Lana *J. Catal.* **137** 368 (1992)
28. A K Ghosh, R A Kydd *J. Catal.* **100** 185 (1986)
29. A S Medin, V Yu Borovkov, V B Kazanskii, in *Trudy IV Vsesoyuznoi Konferentsii po Mekhanizmu Kataliticheskikh Reaktsii, T. 1* (Proceedings of the IVth All-Union Conference on the Mechanisms of Catalytic Reactions, Vol. 1) (Moscow: Nauka, 1986) p. 275
30. K P Datema, A R Nowale, J Van Branm, J Houekqeest, A F Wielers *Catal. Lett.* **11** 267 (1991)
31. N D Lazo, B R Richardson, P D Schettler, J L White, E J Munson, J F Haw *J. Phys. Chem.* **95** 9420 (1991)
32. J F Haw, B R Richardson, I S Oshiro, N D Lazo, J A Speed *J. Am. Chem. Soc.* **111** 2052 (1989)
33. D Deininger, G Wendt *React. Kinet. Catal. Lett.* **17** 277 (1981)
34. P Jozwink, I G Dalla Lana, W Przystajko, R Fredorow, in *Proceedings of the 9th International Congress on Catalysis* (Ottawa Chem. Inst. Canada, 1988) Vol. 3, p. 1340
35. R B Akhverdiev, A P Mamedov, F V Aliev, G N Asmolov, O V Krylov *Kinet. Katal.* **21** 999 (1980)
36. M Laniecki, H S Karge, in *Proceedings of the 6th International Symposium on Heterogeneous Catalysis* (Sofia: Bulg. Acad. Sci., 1987) Part 2, p. 129
37. I Kiriczi, S Kh Akopyan, A V Mikhailov, H Forster *React. Kinet. Catal. Lett.* **42** 145 (1990)
38. J L White, N D Lazo, B R Richardson, J F Haw *J. Catal.* **126** 260 (1990)
39. A V Kucherov, A A Slinkin *Kinet. Katal.* **24** 947, 955 (1983)
40. G M Tel'biz, V M Gun'ko, P N Galich, L M Roev, in *Trudy IV Vsesoyuznoi Konferentsii po Mekhanizmu Kataliticheskikh Reaktsii, T. 1* (Proceedings of the IVth All-Union Conference on the Mechanisms of Catalytic Reactions, Vol. 1) (Moscow: Nauka, 1986) p. 270
41. F R Chen, J J Fripiat *J. Phys. Chem.* **97** 5796 (1993)
42. C Della Cruz, N Sheppard *J. Catal.* **127** 445 (1991)
43. R K Aliev, I L Tsitovskaya, A A Kadushin, K N Spiridonov, O V Krylov *React. Kinet. Catal. Lett.* **8** 347 (1978)
44. A A Kadushin, R K Aliev, O V Krylov, A A Andreev, R M Edreva- Kardzhieva, D M Shopov *Kinet. Katal.* **23** 276 (1982)
45. A A Kadushin, V A Matyshak, N A Kutyreva, A V Sklyarov, A G Vlasenko *Kinet. Katal.* **23** 1167 (1982)
46. V A Matyshak, A A Kadushin, N A Kutyreva, R M Edreva-Kardzhieva *Kinet. Katal.* **24** 1255 (1983)
47. K A Vikulov, I V Elev, B N Shelimov, V B Kazansky *J. Mol. Catal.* **55** 126 (1989)
48. V B Kazansky, B N Shelimov, K A Vikulov, in *New Frontiers in Catalysis (Proceedings of the 10th International Congress on Catalysis, VA)* (Amsterdam: Elsevier, 1993) p. 515
49. K Asakura, M Nishimura, Y Iwasawa *J. Mol. Catal.* **55** 159 (1989)
50. G Busca, V Lorenzelli *J. Catal.* **66** 155 (1980)
51. J Lamotte, V Moravek, M Bensitel, J C Lavalley *React. Kinet. Catal. Lett.* **36** 113 (1988)
52. K Yamashita, S Naito, K Tamaru *J. Catal.* **94** 353 (1985)
53. D L Roberts, G L Griffin *J. Catal.* **95** 617 (1985)
54. V Moravek, J Lamotte, J C Lavalley, in *Proceedings of the 6th International Symposium on Heterogeneous Catalysis* (Sofia: Bulg. Acad. Sci., 1987) Part 2, p. 377
55. R S Schiffino, R P Merrill *J. Phys. Chem.* **97** 6425 (1993)
56. T Hattori, K Shirai, M Niwa, N Murakami *React. Kinet. Catal. Lett.* **15** 193 (1980)
57. M T Aronson, R J Gorte, W E Farneth *J. Catal.* **105** 455 (1987)
58. W R Moser, C C Chiang, R W Thompson *J. Catal.* **115** 532 (1989)
59. N B Librovich, V D Maiorov, V A Savel'ev *Dokl. Akad. Nauk SSSR* **225** 1388 (1975)
60. V V Sadovnikov, A M Gefter *Izv. Akad. Nauk SSSR, Ser. Khim.* 1220 (1976)
61. M I Zaki, N Sheppard *J. Catal.* **80** 114 (1983)
62. A W Klaassen, C G Hill *J. Catal.* **69** 299 (1981)
63. M T Aronson, R J Gorte, W E Farneth, D White *J. Am. Chem. Soc.* **111** 840 (1989)
64. A G Stepanov, V N Maryasov, V N Romannikov, K I Zamaraev, in *New Frontiers in Catalysis (Proceedings of the 10th International Congress on Catalysis, VA)* (Amsterdam: Elsevier, 1993) p. 621
65. A G Stepanov, K I Zamaraev *Catal. Lett.* **19** 153 (1993)
66. C Williams, M A Makarova, L V Malysheva, E A Paukshtis, E P Talsi *J. Catal.* **127** 377 (1991)
67. W K Hall, in *New Frontiers in Catalysis (Proceedings of the 10th International Congress on Catalysis, VA)* (Amsterdam: Elsevier, 1993) p. 631
68. M Zardkoohi, J F Haw, J H Lunsford *J. Am. Chem. Soc.* **109** 5287 (1987)
69. A I Biaglow, R J Gorte, D White *J. Chem. Soc., Chem. Commun.* 1164 (1993)
70. P Uvdal, B C Wiegand, J G Serafin, C M Friend *J. Chem. Phys.* **97** 8727 (1992)
71. A A Efremov, A A Davydov *React. Kinet. Catal. Lett.* **18** 363 (1981)
72. G Busca *React. Kinet. Catal. Lett.* **20** 373 (1982)
73. S H C Liang, I D Gay *J. Catal.* **101** 293 (1986)

74. T Szilagyi, A Sarcani, J Mink, P Tetenyi *J. Catal.* **66** 91 (1980)
75. T W Root, T M Duncan *J. Catal.* **101** 527 (1986)
76. K Tamaru, in *Plenary Lectures at the 7th International Congress on Catalysis, Tokyo, 1980* p. 41
77. B Y Soma, T Onishi, K Tamaru *Trans. Faraday Soc.* **65** 2215 (1969)
78. J Novakova, L Kubelkova, Z Dolejšek *J. Catal.* **108** 208 (1987)
79. A A Demidov, A A Davydov, L N Kurina, in *Trudy IV Vsesoyuznoi Konferentsii po Mekhanizmu Kataliticheskikh Reaktsii, T. I* (Proceedings of the IVth All-Union Conference on the Mechanisms of Catalytic Reactions, Vol. 1) (Moscow: Nauka, 1986) p. 295
80. J K A Clarke, R Darcy, B F Hegarty, E O'Donoghue, V Amir-Ebrahimi, J J Rooney *J. Chem. Soc., Chem. Commun.* 425 (1986)
81. M W Anderson, B Sulikowski, P J Barrie, J Klinowski *J. Phys. Chem.* **94** 2730 (1990)
82. M W Anderson, J Klinowski *Nature (London)* **339** 200 (1989)
83. J Klinowski *Chem. Rev.* **91** 1459 (1991)
84. E J Manson, A A Kheir, N D Lazo, J F Haw *J. Phys. Chem.* **96** 7640 (1992)
85. C D Chang, A J Silvestry *J. Catal.* **47** 249 (1977)
86. T Mole, J Whiteside *J. Catal.* **75** 284 (1982)
87. G A Olah, H Doggweiler, J D Felberg, S Frohlich, H J Grdina, R Karpeles, T Keumi, S Inaba, W M Ip, K Lammertsma, G Salem, D C Tabor *J. Am. Chem. Soc.* **106** 2143 (1984)
88. R Hunter, G J Hutchings *J. Chem. Soc., Chem. Commun.* 886 (1985)
89. C D Chang, S D Hellring, J A Pearson *J. Catal.* **115** 282 (1989)

Russian Chemical Reviews **63** (7) 575 – 609 (1994)
©1994 Russian Academy of Sciences and Turpion Ltd

UDC 547.953 + 547.91

Trivalent phosphorus acid amides as phosphorylating agents for alcohols and amines

E E Nifant'ev, M K Grachev

Contents

I. Introduction	575
II. Phosphorylation of alcohols and phenols	575
III. Phosphorylation of amines	596
IV. Conclusion	602

Abstract. The principal results of studies on trivalent phosphorus acid amides (TPAA) as phosphorylating agents for alcohols, phenols, and amines are summarised and discussed. Problems concerning the catalysis and mechanism of the phosphorylation of proton-donating nucleophiles by TPAA are considered and new possibilities for the development of investigations on these lines are analysed. The preparative advantages of TPAA and the specific prospects for their use in fine organic synthesis and macromolecular chemistry are demonstrated. The bibliography includes 560 references.

I. Introduction

Phosphorylation, i.e. the introduction of a phosphorus-containing functional group in place of hydrogen atoms into a molecule of an organic nucleophile, is one of the most important problems in organophosphorus chemistry. Pentavalent and trivalent phosphorus reagents have been used traditionally in laboratory research and in industry. More attention was devoted initially to pentavalent phosphorus compounds and then in the subsequent period to trivalent phosphorus compounds. There were important reasons for such switching of interest. It was established that the use of trivalent phosphorus compounds ensures the maximum rates of phosphorylation and makes it possible to avoid side processes such as dealkylation and elimination. The usefulness of trivalent phosphorus reagents is also due to the creation of a modern strategy for the synthesis of organophosphorus compounds. According to the latter, in the first stage of the synthetic scheme the trivalent phosphorus reagents interact with nucleophiles to form only the key substances for subsequent reactions. When necessary, in the second stage of the scheme the key substances may be oxidised, iminated, and alkylated and may combine with sulfur, selenium, chlorine, etc. All these features lead to the formation of a large set of target compounds, including those which are inaccessible within the framework of the classical preparative methods based on the use of pentavalent phosphorus reagents.

E E Nifant'ev, M K Grachev Department of Organic Chemistry, Faculty of Chemistry, V I Lenin Moscow State Pedagogic University, Nesvizhskii per. 3, 119021 Moscow, Russian Federation.
Fax (7-095) 248 01 62.
Tel. (7-095) 246 57 90 (E E Nifant'ev), 246 54 53 (M K Grachev)

Received 23 May 1994
Uspekhi Khimii **63** (7) 602 – 637 (1994); Translated by A K Grzybowski

Among the phosphorylating agents which have come to be used vigorously during the last 10 – 15 years, mention should first be made of trivalent phosphorus acid amides (TPAA). Their advantages are ready availability, high reactivity, and the mild conditions in their preparative application. It is very important that the phosphorylating activity of these reagents can be increased significantly by catalysts, for example amine hydrochlorides.

By virtue of these qualities, TPAA are widely used nowadays for the solution of many problems in fine organic synthesis, for example for the preparation of higher oligonucleotides and other phosphorus-containing natural products and their analogues. Furthermore, they are used to obtain valuable high-molecular-mass compounds.

The number of communications describing phosphorylations by phosphoramides runs into thousands. Nevertheless, many important theoretical questions associated with their reactivity have still not been solved, although fairly numerous hypotheses concerning this topic have been put forward in the literature. Thus the phosphorylation mechanism has been elucidated only in broad outline, the relation between the structure and reactivity of the reagents has not been elucidated, and the role of solvation has been poorly investigated. Thus a clear contradiction has arisen between the breadth and depth of the investigation of the problem. In our view, further progress in the study of the phosphorylation of proton-donating nucleophiles by TPAA could be assisted by the writing of an analytical survey of literature data with emphasis on the latest advances. Bearing this in mind, the present review was prepared. In order to differentiate clearly the most important aspects of the problem, we made a selection from the published data and, instead of including data on the phosphorylation of all the proton-donating nucleophiles investigated, only those on the most popular nucleophiles are dealt with: alcohols, phenols, and amines. In the study of precisely these compounds, quantitative measurements have been made of the rates of phosphorylation and reliable results have therefore been obtained concerning both the synthetic aspects of the reactions and their mechanisms.

II. Phosphorylation of alcohols and phenols

The reaction of TPAA with alcohols and phenols was discovered at the very end of the 1950s independently in three laboratories simultaneously.[1-3]

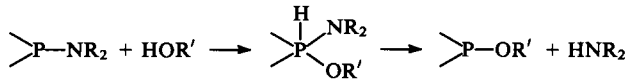
$$>P{-}NR_2 + HOR' \longrightarrow >P{-}OR' + HNR_2$$

This phosphorylation method has important synthetic advantages (see above), but much time was required for investigators to become 'used to it'. It appears that the new method being chemically unusual had an effect. Indeed, until its discovery it had no evident analogies: the amides of pentavalent phosphorus acids phosphorylate alcohols and phenols with a low effectiveness and only at a high temperature, while the amides of carboxylic acids (and even sulfenic acids[4]) altogether failed to interact with alcohols (on the other hand, the corresponding esters are smoothly converted into amides on treatment with ammonia and primary and secondary amines)†. The new method had not been resorted to for some time also because the synthetic problems in which its best aspect would be manifested had not been clearly formulated and included in the range of those dealt with by chemists concerned with organophosphorus chemistry. Nevertheless, this induction period was not wasted. During this period, studies were carried out which established the catalytic nature of the reaction and its principal features as well as the most promising ways of using it. Ultimately, the TPAA came to be firmly included among organophosphorus reagents and began to be used vigorously for the phosphorylation of labile natural products, in the creation of new types of polymers, and in the solution of other complex scientific problems. Bearing this in mind, the present section of the review has been subdivided into individual subsections devoted to the basic problems and questions in the phosphorylation of alcohols and phenols by TPAA and also in the modern synthetic use of this reaction.

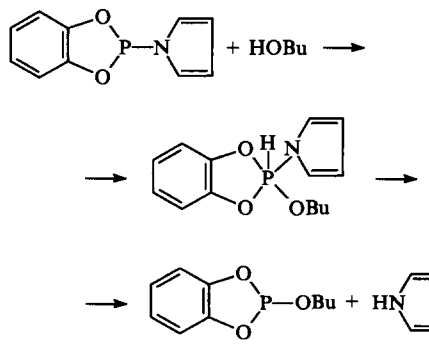
1. The mechanism of the phosphorylation reaction. Catalysis

a. History of the problem

In the first paper devoted to the alcoholysis and phenolysis of the simplest TPAA,[3] certain considerations concerning its mechanism were already put forward. Subsequently, this problem was dealt with by different investigators, but it was discussed only at a speculative level. A version of the mechanism of the 'addition–elimination' type was usually put forward in publications. Thus the intermediate formation of a hydrophosphorane, which decomposes with liberation of an amine, was postulated.[3]

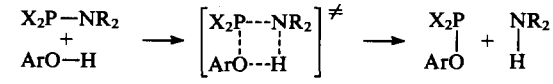


The principal features of this scheme were subsequently confirmed experimentally in a study with cyclic systems,[7–13] for example:[10]



A variant of this scheme is the hypothesis of the P-protonation of the phosphoramide by the alcohol with formation of a quasi-phosphonium adduct, which splits off the amine and is converted into an ester.[3,14–20] An alternative hypothesis is that the TPAA undergoes N-protonation.[3,17,19–23] None of these variants was confirmed experimentally.

At the same time, a view concerning the mechanism of the phenolysis of TPAA has been expressed in the literature according to which a four-centred transition state is formed.[24,25]



This hypothesis is supported by certain thermodynamic data (the activation energies and entropies). Unfortunately experimental errors were made in the relevant studies[25,26] which vitiated the conclusions reached.

When studies of the rates of phosphorylation were undertaken, it proved possible in a number of investigations to elucidate important problems concerning the chemistry of the reaction. Thus it was confirmed that the process is bimolecular for equimolecular proportions of the reactants[10,25,27–31] and that the medium[10,25,26,31] and temperature[32] influence the reaction. The interesting fact that the phosphorylation is inhibited following the accumulation in the medium of the amine produced in the course of the substitution reaction was established; apparently the inhibition is caused by the complex formation reaction between the amine and the alcohol, which reduces the rate of the main reaction.[10,29,31,33,34]

b. Catalysis of the phosphorylation by amine hydrohalides

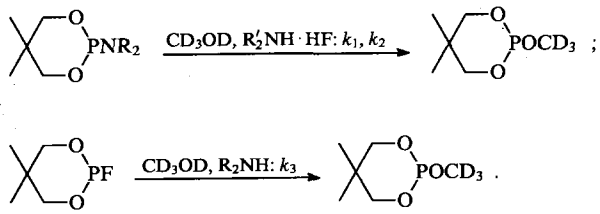
The study of the rate of alcoholysis of TPAA made it possible to determine the catalytic character of many reactions of this type. The catalytic effect was observed in 1965 on comparing the rates of phosphorylation of the simplest alcohols by phosphorus(III) acid amides freed from possible impurities and by phosphoramides which were obtained by the usual procedure and were contaminated by a certain amount of amine hydrochlorides (AHC).[35,36] The observed catalytic effect was subsequently confirmed in many laboratories,[10,18,22,25,28,37–41] the concentrations of the initial compounds and of the products of their reactions being usually determined by ^1H and ^{31}P NMR spectroscopy.[10,25,28,37–42]

The chemical aspect of the catalysis was the subject of prolonged discussion, the outcome of which has been described by Nifant'ev and Borisov.[43]

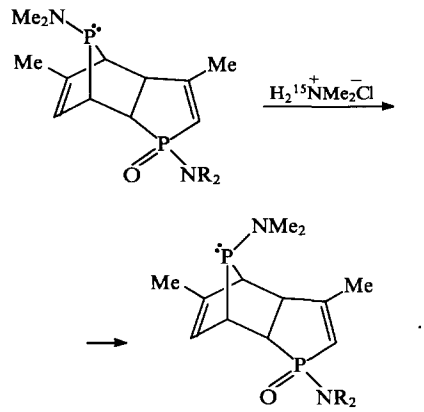
Two hypotheses were discussed. One of them was that acid substances protonate the phosphoramide at the phosphorus or nitrogen atom or at the phosphorus–nitrogen bond. As a result of such protonation, the phosphorus atom of the onium compound becomes more electrophilic and reacts with the alcohol more readily. According to the second hypothesis, the phosphoramide must be protonated at the nitrogen atom. The phosphorammonium cation produced is attacked by an anion (the chloride ion when AHC are used) and is converted into a mixed anhydride, which in fact constitutes the direct phosphorylating agent. The anhydride hypothesis was based on a known fact: on intense heating with diethylamine hydrochloride, phosphorous hexaethyltriamide affords the hydrochloride of *N,N,N',N'*-tetraethylphosphorodiamidite and diethylamine, which is distilled away from the reaction mixture. We may note that, after a lapse of time, the second hypothesis began to be considered by some investigators (see, for example, Refs 44–50) as fully wellfounded. At the same time, it became customary to resort to a speculative description of the mechanisms of the TPAA reaction instead of securing evidence for them. Nevertheless, the anhydride hypothesis was questioned[38,51–54] and was subsequently subjected to a specific criticism. Thus it has been demonstrated experimentally that the cleavage of the phosphoramide linkage in TPAA by amine hydrohalides is not a general phenomenon. For example, phosphorous hexaethyltriamide is cleaved much less effectively than the hexamethyltriamide, while higher amides do not interact

† The unusual character of alcoholysis by TPAA is due to the fact that this reaction had in fact been described twice[5,6] before its 'official discovery', but initially it had not been assessed as a novel and promising phosphorylation method.

preparatively with amine hydrohalides. On the other hand, the effectiveness of catalysis is high for all the amides indicated.[43] An even more interesting result was obtained on comparing the rates of deuteriomethanolysis of the imidazolide (k_1) and *N*-ethylanilide (k_2) of neopentylene phosphite in the presence of amine hydrofluorides and of deuteriomethanolysis of neopentylene phosphorofluoridite (k_3):

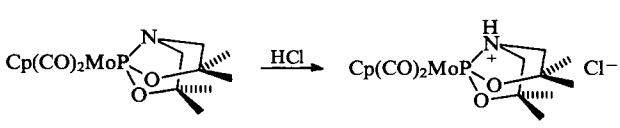


It was found that k_1 and $k_2 \gg k_3$.[55,56] It is significant that the catalytic activities of diethylamine hydrofluoride and other corresponding halides are comparable under standard conditions.[55,56] Such a situation would be impossible if the reaction pathway included a stage involving the formation and alcoholysis of phosphorohalidites. We shall complete the analysis of the hypothesis by quoting the data of Szewczyk and Quin,[57] who investigated the inversion at the phosphorus atom in the presence of dimethylamine hydrochloride enriched in the ^{15}N isotope:



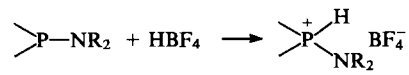
The authors observed the complete inversion of the phosphorus(III) acid amide centre only in the presence of a catalyst (15 h, 25 °C). It was established that the ^{15}N label does not appear in the phosphoramide. Thus the activation of the phosphoramide is associated with some kind of interaction of the substrate and the reagent which does not include an acid chloride formation stage. Otherwise, labelled dimethylamine would have appeared in the medium and its reaction with the acid chloride would have afforded phosphorous [^{15}N]dimethylamide.

The hypothesis of the protonation of TPAA to give onium compounds as a means of their activation for subsequent reaction with alcohols and other nucleophiles was revived at one time and was discussed in the literature. This possibility was specified in detail: the N-protonation pathway was initially considered to be the most probable.[22,23,44] Indeed, in a series of quantum-chemical studies on model >P–N< systems this pathway was specified as energetically preferable.[54,58,59] Nevertheless, convincing evidence for N-protonation in TPAA–AHC–alcohol systems was not obtained. At the same time, data secured in a successful experiment on the N-protonation of a metal complex derivative of one of the bicyclic TPAA were published:[60]

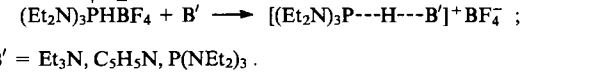


The lone pair of the phosphorus atom in the initial complex formed the phosphorus–molybdenum bond, which fact determines the course of the protonation.

Recently, many investigators indicated the probability of parallel P- and N-protonation[20,47–50] or selective P-protonation.[14,16,30] Evidence for this reaction pathway, obtained by IR[16,61–63] and NMR[20,64–67] spectroscopy, was quoted in the corresponding publications. A group of salts was recently synthesised by the reaction of TPAA with anhydrous fluoroboric acid.[68–72]



These salts are semicrystalline or crystalline. It was of interest that some of them are entirely stable on storage. The interaction of the salts with bases stronger than the initial phosphorus(III) acid amides leads to their deprotonation. By estimating the degree of the latter, it is possible to establish approximately the basicity of the TPAA.[71,72] The structures of certain initial phosphoramides and their quasi-phosphonium salts have been investigated by X-ray diffraction.[70–72] The structural parameters of these substances were determined. Among them, the anomalous shortening of the P–H bonds is striking. Conversely, it was established at the same time that the P–N bond in these salts is anomalously long. For example, its length in the fluoroborate of phosphinous di-*tert*-butylpyrrolide is 1.75 Å.[72] Additional studies demonstrated that treatment of solutions of the quasi-phosphonium salts with bases (B′), including TPAA, leads to the formation of dynamic complexes in which a proton migrates between two donor centres:[71,72]



Experiments were carried out on the alcoholysis of the salts and it was established[70–72] that they do not really react with alcohols‡.

Thus the hypothesis that the products of the protonation of TPAA are intermediates in the alcoholysis of phosphoramides is likewise not true. It was of interest to compare the tendencies of the products of the protonation and alkylation of TPAA to undergo alcoholysis, since these salt-like substances are isoelectronic. It was found that they all remain unchanged on treatment with alcohol§.[70,73]

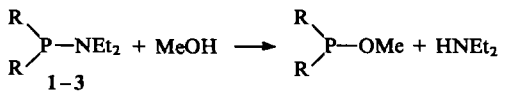
Further study of the alcoholysis of TPAA in the presence of AHC involved investigation of the rates of reaction in the presence of selected concentrations of various catalysts¶.

The quantitative characteristics of the effect of amine salts on the rate of alcoholysis of the amides **1–3** were established in preliminary experiments.[78]

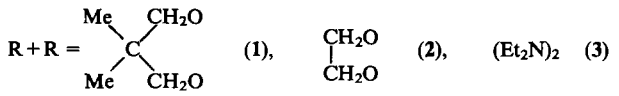
‡ Thus the P(III)–N bond length and the factors influencing it are not decisive criteria of the phosphorylating capacity, which has been occasionally implied.[24,48]

§ In this connection, we may note another important fact, namely that the phosphorammonium salts alkylated at the nitrogen atom undergo alcoholysis at the P–N bond.[74]

¶ For accurate kinetic studies of the acid-catalysed reactions of TPAA, the procedures for the removal of AHC impurities from TPAA already known[75,76] were supplemented by developing a purification procedure using phase transfer principles,[77] which made it possible to achieve a residual concentration of the chloride ions of 0.11×10^{-3} M. The residual content of chloride ions was monitored by potentiometric titration.[70,78] An attempt had been made previously[29] to monitor quantitatively the residual content of AHC and TPAA by a conductimetric method.



1–3



Thus the rate constants for the first stage of methanolysis were determined as a function of the content of the AHC in the ranges of concentrations corresponding to their amounts usually present in TPAA. The quantitative composition of the reaction mixture was determined by NMR spectroscopy — by integrating the ^{31}P signals. The pseudofirst-order rate constants (k_I^{ψ}) were determined from the decrease in the concentration of the initial amide by means of the linear plot of $-\ln([\gtrdot P-NEt_2]/[\gtrdot P-NEt_2]_0) = f(\tau)$, where $[\gtrdot P-NEt]_0$ is the initial concentration of the amide. The second-order rate constant was found from the values of k_I^{ψ} obtained by means of the equations $k_{II} = k_I^{\psi}/[MeOH]$.

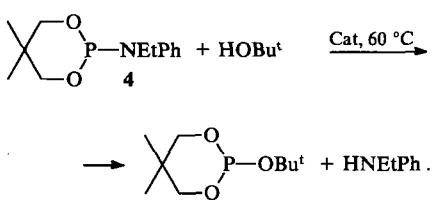
The results of the kinetic measurements can be represented by Eqns (1) and (2):[29]

$$-\frac{d\left[\gtrdot P-NEt_2\right]}{d\tau} = k_{II}\left[\gtrdot P-NEt_2\right][MeOH], \quad (1)$$

$$k_{II} = k_0 + k_c[Et_2\overset{+}{N}H_2], \quad (2)$$

where k_0 is the rate constant for the noncatalysed reaction, k_c a catalytic coefficient taking into account the activating effect of diethylamine hydrochloride, and $[Et_2\overset{+}{N}H_2]$ and [MeOH] are the concentrations of the salt and methanol, which remain constant during the reaction. The linearity of the dependence of k_{II} on the salt concentration demonstrated that the reaction is first order with respect to the catalyst. Thus the fundamental importance of the quantitative monitoring of the purity of the amides in the study of the alcoholysis of TPAA was established[70,78] and conditions were selected for the investigation of a crucial feature of the acid-catalysed reactions of TPAA — the nature of the interaction of AHC with TPAA.

For this purpose, a study was made of the influence of the nature of AHC on the catalytic activity in the alcoholysis of TPAA. The experiment was performed in the neopentylene *N*-ethylphosphoroanilidite – *tert*-butyl alcohol system.[70,79]



The catalysts employed were the hydrochlorides of diethylamine (**5**), dimethylamine (**6**), triethylamine (**7**), trimethylamine (**8**), benzyldiethylamine (**9**), benzylmethylamine (**10**), *N*,*N*-diethylaniline (**11**), and imidazole (**12**). The choice of the amide **4** and of the catalysts **5**–**12** was dictated by the fact that the basicity of the amines should be not less than that of the amine produced on alcoholysis, i.e. *N*-ethylaniline. Otherwise the catalyst would change during the reaction.

Graphical treatment of the data in accordance with equations (1) and (2) above showed that there is a linear relation between $\lg k_c$ and the acidity of the salts **5**–**12**. In the case of salts of secondary and tertiary amines, it is expressed by two independent straight lines (Fig. 1). The introduction of the statistical factor *S* (the number of protons bound to the nitrogen atom of the ammonium salt[80]) combines the two lines into one (Fig. 2).

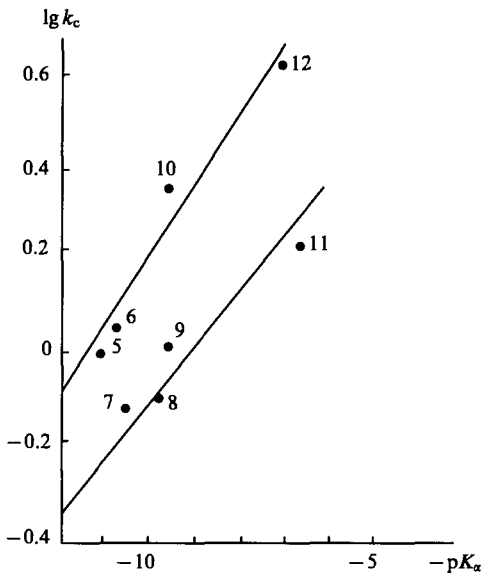


Figure 1. Dependence of $\lg k_c$ on the acidity of catalysts **5**–**12**.

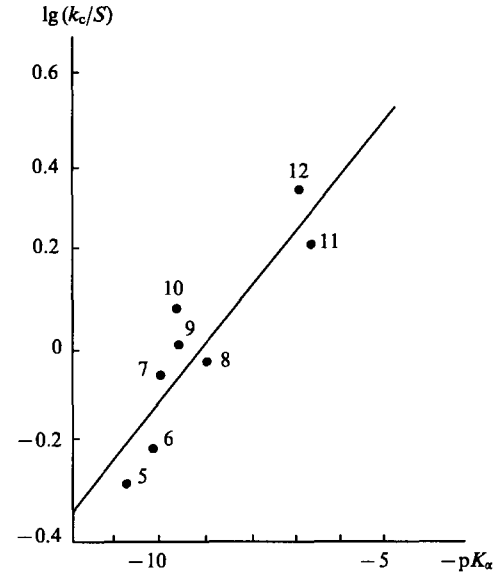
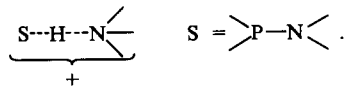


Figure 2. Dependence of $\lg(k_c/S)$ on the acidity of catalysts **5**–**12**.

The Brønsted equation (3) was used to analyse the results. For the process investigated, it was expressed in the following form:[81]

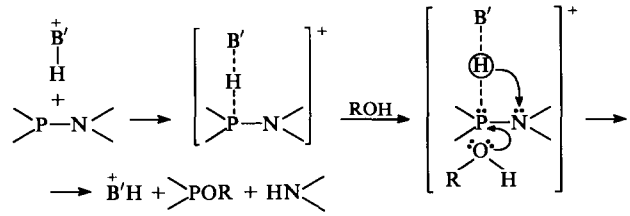
$$\lg\left(\frac{k_c}{S}\right) = \lg G_A - \alpha pK_a, \quad (3)$$

where G_A and α are constants characterising the reaction series. The slope α is a measure of the sensitivity of the reaction to the acid catalyst. It was found that $\alpha = 0.13$ ($r = 0.95$), which indicates *general acid catalysis* of the phosphorylation reaction. In this case, it is best to interpret α as an approximate measure of the change in the charge on the proton-donating or proton-accepting atom in the transition state.[82] Thus the catalytic process proceeds not via the protonation of the phosphoramide substrate (the formation of a phosphonium or phosphorammonium salt postulated previously) but via the formation of the catalytic hydrogen-bonded complex incorporating the substrate (S) and the catalyst as a whole:

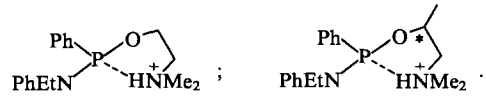


In contrast to the onium salts this complex is a proton-labile system, which apparently determines also its tendency to undergo alcoholysis.

Summarising the foregoing, one may conclude that the alcoholysis of TPAA in the presence of AHC includes stages involving the formation of the catalytic hydrogen-bonded complex. In the latter, the proton fulfills two functions: firstly, it activates the phosphorus atom in the electrophilic reaction, for example with an alcohol, and secondly, during the reaction the proton migrates from the phosphorus to the nitrogen atom, thereby assisting the dissociation of the P–N bond.[70–72]



An important stereochemical consequence follows from this: if a chiral catalyst is employed, then the catalytic hydrogen-bonded complex is also chiral. Therefore, when chiral catalysts are used, one may expect the manifestation of stereoselectivity in the phosphorylation reaction. Correspondingly, the interaction of the racemic 1,3-butylene *N*-ethylphosphoranilidite with 1,2;5,6-diisopropylidene-α-D-glucofuranose (in molar proportions of 2 : 1) was carried out in the presence of the racemic hydrochloride of α-phenylethylamine and its (+)- and (−)-enantiomers. It was shown by ^{31}P NMR that, when a racemic catalyst is used, approximately equal amounts of the two diastereoisomers are formed. When the hydrochloride of the laevorotatory amine is employed, 10% more of one of the diastereoisomers is obtained. The dextrorotatory hydrochloride ensures approximately the same preferential formation of the other diastereoisomer. Thus it has been shown[70,79] that the use of optically active catalysts can ensure stereoselectivity in the phosphorylation of TPAA. Subsequently this fact was used to attain a more effective 'contact' between the phosphoramide and the hydrochloride forming part of its composition (compound **13**), which ensured effective intramolecular catalysis resulting in a sharp increase in the rates of phosphorylation and in a significant stereoselectivity of the process following the inclusion of a chiral fragment in the composition of the 'catalytic' component of the phosphorus(III) acid amide **14**:[83]

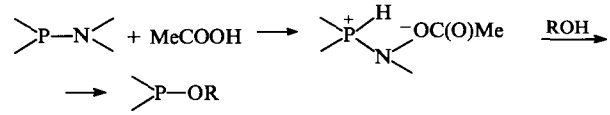


13 **14**

c. Phosphorylation in the presence of carboxylic acids and azoles

The discovery of the catalytic effect of AHC in the alcoholysis of TPAA led to the search for new ways of accelerating this type of phosphorylation. AHC and phenols are known to have comparable acid properties. Taking this into account, successful experiments were carried out on the phosphorylation of alcohols by TPAA in the presence of phenol.[84] The catalysis of the alcoholysis of TPAA by phenol was thus confirmed experimentally. Unfortunately this version of the catalysis is not promising in preparative terms, since the reaction resulted in the formation not only of the compounds sought but also of the corresponding phenyl esters.

The next stage in the development of the acid catalysis involved the study of the alcoholysis of TPAA in the presence of carboxylic acids, acceleration of phosphorylation by acetic acid being observed.[16,25,85] In a number of instances, the acceleration was very significant. Thus it has been shown[16] that phosphorous tripiperidide does not react with ethanol even on refluxing but, when acetic acid is added to the reaction mixture, phosphorylation occurs even at 20 °C. The formation of a quasi-phosphonium cation was initially postulated as the first stage.



Subsequent study of the catalytic effect of acetic acid showed that it not only accelerates but also alters the mode of certain reactions of phosphoramides. Thus the reaction of the amides with aliphatic mercaptans in the presence of acetic acid proceeds with dissociation of the P–N bond[85] and not via the addition of sulfur to the initial amides, noted in experiments without added catalyst.[86]

The mechanism of catalysis by carboxylic acids has been investigated only to a first approximation. It may be that the mechanism corresponding to the catalysis by AHC operates under certain conditions, but other variants are also possible. It has been shown[37] that the phenolysis of TPAA in the presence of carboxylic acids involves the formation of acyl phosphites, which were detected by ^{31}P NMR. Apparently the acyl phosphites phosphorylated phenol with formation of phenyl phosphites and carboxylic acids.[87,88] The latter again interact with TPAA, affording acyl phosphites, etc. At the present time, this mechanism is not well founded. We may draw attention to the fact that acyl phosphites can undergo not only phenolysis (alcoholysis) but also aminolysis with formation of carboxylic acid amides and hydrophosphoryl compounds.[87–93] Furthermore, it is essential to take into account also the neutralisation of the carboxylic acid by the secondary amines formed. Yet another important factor may be noted: there are data indicating the catalytic nature of the conversion of TPAA into acyl phosphites.[90,91,94] Hence, in the acyl phosphite variant, there may be two catalytic stages.

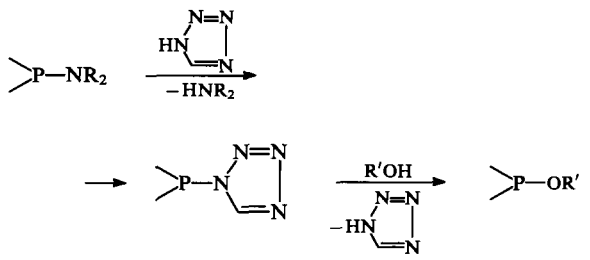
The alcoholysis of TPAA can also be catalysed by other acids, for example amidodithiocarbamic acids and also their ammonium salts.[95]

The search for new variants of the phosphorylation reaction led to the investigation of the activation of the alcoholysis with the aid of free azoles, which are weak N–H acids. These are usually 1*H*-tetrazole ($pK_a \approx 4.8$) (see, for example, Refs 96–99) and more rarely 1,2,4-triazole ($pK_a \approx 10$)[100,101] or azoles the acidity of which has been enhanced by the introduction of electronegative substituents into the azole ring (4,5-dichloroimidazole, 3-chloro-1,2,4-triazole,[100,102] 5-*p*-nitrophenyltetrazole, and certain others[103,104])†. The salts of azoles, mainly diisopropylammonium tetrazolide, are used for a similar purpose (see, for example, Refs 106–114). Very satisfactory results — complete phosphorylation in 2–3 min at 20 °C — have been achieved under the optimised conditions for the phosphorylation of complex systems. Because of this, the azolide variant has come to be especially widely used, including its employment in automatic synthesisers for the preparation of important oligonucleotides (see below).

The situation is less satisfactory as regards the understanding of the chemistry of the azolide variant of the phosphorylation reaction. It is significant that the amounts of azoles in relation to TPAA used in the experiments described were not catalytic but equimolar or even greater than equimolar. This makes it difficult to classify the reactions considered as catalytic. In view of the

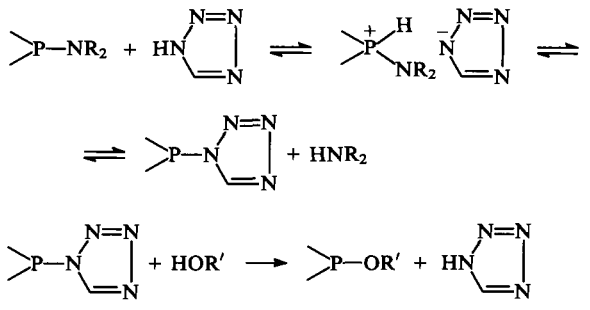
† The use of the last activator has been criticised.[105]

foregoing, we may note the observation in the ^{31}P NMR spectra of reaction mixtures containing an excess of tetrazole of a signal corresponding to the transamidation product—a phosphorus(III) tetrazolide, which is regarded as an intermediate.[115-117]



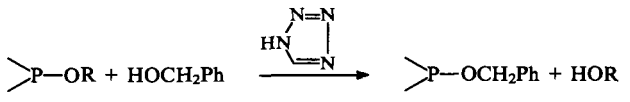
The possibility of the formation of phosphorus(III) tetrazolides has been the subject of certain special investigations, in which the role of the acidity of the activators was emphasised. According to the authors of these studies,[100,115,117,118] the activators are capable of protonating the initial TPAA. It is of interest that it has been possible to perform kinetic measurements in the TPAA—tetrazole system and to devise a scheme for the overall alcohol phosphorylation process (Scheme 1).[118]

Scheme 1



Unfortunately this scheme has not been analysed in depth. Two comments may be made on this question. The first is that the authors of the scheme do not prove but merely postulate the protonation of TPAA by tetrazole. The second is that the authors have not demonstrated that the phosphorus(III) tetrazolide is an 'on-going' and not a dead-end product in the system of stages involved in the phosphorylation of alcohols using the usual TPAA. The second comment is especially important in connection with the publication of data[119] on the transesterification of neutral phosphites in the presence of tetrazole (Scheme 2). There are also data concerning the activation of the transesterification of neutral phosphites by 1,2,4-triazole.[120]

Scheme 2



The reaction described is related to that discussed by ourselves because it too involves nucleophilic substitution at the trivalent phosphorus atom in the presence of tetrazole. However, it is difficult to postulate that the stage involving the conversion of the alkyl phosphite ester into the tetrazolide is obligatory, since in fact reactions of the opposite type are well known. Consequently, it is essential to analyse not only the tetrazolide but also other activation procedures. The authors of the present review believe that the most probable form of activation of the alcoholysis of an alkyl phosphite is the formation of a complex between this ester and tetrazole.

We shall return to the question of the phosphorylation of alcohols by TPAA in the presence of tetrazole. Taking into account the foregoing, we suggest that general acid catalysis may operate in this instance in the conversion of the dialkyl amides into the required esters or into tetrazolides. If, on the other hand, the tetrazolides prove to be intermediates in the synthesis of the esters, then they too probably require cooperation from tetrazole. The main factor in the catalysis in all these cases may be the formation and reaction of the corresponding tetrazole complexes. Unfortunately more far reaching kinetic studies with introduction of catalytic amounts of tetrazole into the reaction mixture have not yet been carried out. Nevertheless, a study has been published very recently on the application of triazole, indicating the existence of an acid catalytic stage in this process.[101]

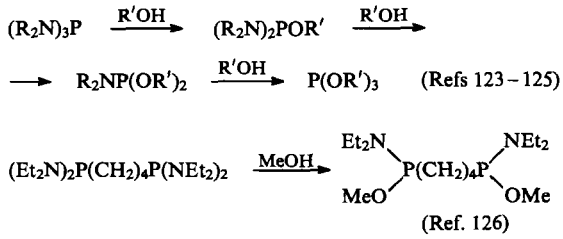
2. General characteristics of the phosphorylation of alcohols and phenols

The dependence of the phosphorylating capacity of TPAA on their structure and certain related problems will be considered in this subsection of the review. The second part of the subsection is devoted to the stereochemical features of the phosphorylation reaction.

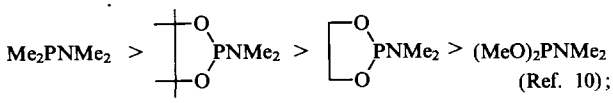
There have been few kinetic studies on the alcoholysis of TPAA and for this reason reliable correlations between the reactivity of phosphoramides and their structure have not so far been established. The situation is complicated also by the fact that in most of the published communications the problem of catalysis was overlooked and for this reason acid admixtures were not specially eliminated from the phosphoramides and a definite amount of a selected catalyst was not added to the substrate. Nevertheless, one can already speak of certain qualitative features, since the phosphoramides most often employed for phosphorylation have been usually obtained by a standard method in different laboratories and they were therefore contaminated by approximately equal amounts of identical activator impurities (these were most often AHC). The range of alcohols employed almost always comprised the most readily available standardised representatives.

Taking into account these comments, one may note that as a rule branched alcohols had a lesser tendency to undergo phosphorylation than linear alcohols, while secondary alcohols were inferior in this respect to the primary ones.[10,28,84] There exist data indicating a higher reactivity of phenols[10,24,25,28,84] and acid alcohols[84] in phosphorylation compared with the usual alcohols. However, it has been noted that the phosphorylation of phenols in bulk may be complicated by the formation of intermolecular hydrogen bonds, which, however, are ruptured on heating the phenol–TPAA system in aromatic solvents. The use of this procedure makes the phosphorylation of phenols more effective.[121] Intramolecular hydrogen bonds have a smaller inhibiting effect on phosphorylation; however, when these bonds are strengthened, as happens on passing from 8-hydroxyquinoline to 5,7-dibromo-8-hydroxyquinoline, the phosphorylation is impaired.[122]

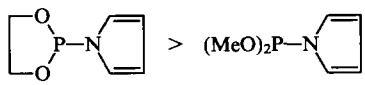
The influence of the TPAA structure on phosphorylation is expressed by more complex relations. It has been established that the amino-groups in phosphorous triamides can be substituted stepwise by alkoxy-groups.[123-126]



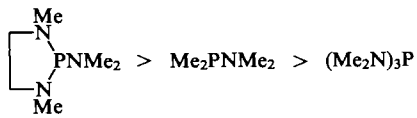
Consequently the full amides are more reactive than the amidoesters. Certain detailed features of the phosphorylation reactions have also been discovered, but these are based on a relatively narrow range of experimental data.[10,28] In terms of reactivity, amines can be arranged in the following sequence:

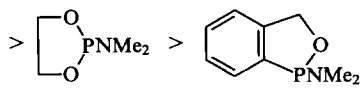


(Ref. 10);

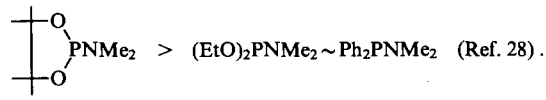


(Ref. 10);





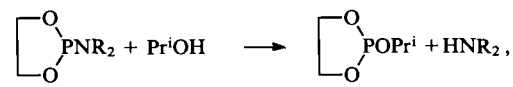
(Ref. 28);



(Ref. 28).

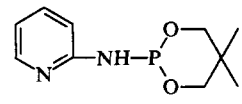
We may draw attention to the fact that the phosphorylating capacity of TPAA is in some way correlated with their basicity. One can apparently now state that the tendency of TPAA to form a complex with the acid catalyst plays a decisive role, i.e. that these substances are ready to form catalytic complexes.

The second aspect of the problem of the reactivity of TPAA, involving the elucidation of the role of substituents at the phosphorus atom, has been examined in greater detail. Thus it has been established for the reaction,

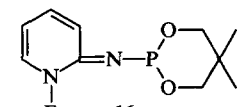


that the phosphorylating activity increases in the following sequence of substituents at the phosphorus atom:[28] $N(Pr^i)_2$ < NMe_2 < NMePh < NPh_2. The high phosphorylating activity of monophenyl- and diphenyl-amides, noted previously,[127] is striking. The phosphopyrrolides, which exhibit an increased resistance to alcoholysis, are an exception.[10,71,127,128] It has been shown[71] that this is associated with the passivity of the lone pair of pyrrole as regards the formation of a hydrogen bond and prototropism. We may note further that data have been published on the high phosphorylating capacity of the vinyl amides of trivalent phosphorus acids.[47] Summarising the foregoing, we may conclude that in phosphorylation there is an inverse relation between the tendency of the amino-group to leave the phosphorus atom and its basicity. It is of interest that, according to the data of Evdakov et al.,[25] the phenolysis of TPAA does not obey the rules presented above. Apparently such data should be subjected to additional analysis.

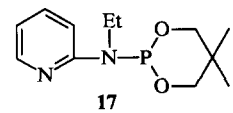
The observation of a high reactivity of anilides in alcoholysis led to the extension of the studies initiated to the field of related heterocyclic phosphoramides.[129,130] Thus phosphorylated 2-aminopyridine **15** and its two derivatives **16** and **17**, ethylated at different nitrogen atoms, have been subjected to methanolysis.[131,132]



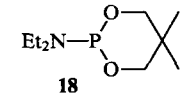
15



16



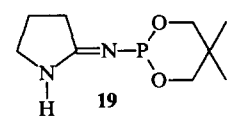
17



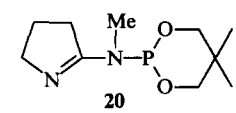
18

Study of the rates of methanolysis of these compounds made it possible to formulate several important conclusions. (1) The phosphoramides **15** and **17** are more reactive than neopentylene *N,N*-diethylphosphoramidite **18**. Thus the early observation that the reactivity of phosphoranilides is high has been reliably confirmed. (2) The phosphoramides **15** and **17** are more reactive than the phosphorimide **16**, so that the electronic structure in the P–N–C–N fragment is important for the alcoholysis of the P–N bond. (3) The phosphoramide **15**, the molecules of which contain secondary hydrogen atoms, is much more reactive than its *N*-ethyl derivatives **16** and **17**. Furthermore, compound **15** does not require a catalyst in alcoholysis, whilst compounds **16** and **17** do require it. This means that the reactions of compound **15** involve autocatalysis.[132]

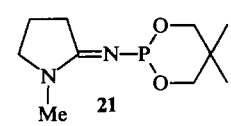
Thus it follows from the data presented that the tendency of TPAA to undergo alcoholysis can be effectively regulated by the structural features of these compounds. An even more interesting picture of this phenomenon has been observed in a study of the alcoholysis of phosphorylated 2-aminopyrrolines.[131,133,134] The rates of methanolysis of the three related derivatives **19**–**21** were compared in this instance and it was shown that compound **19** exhibits the greatest susceptibility to substitution.



19



20



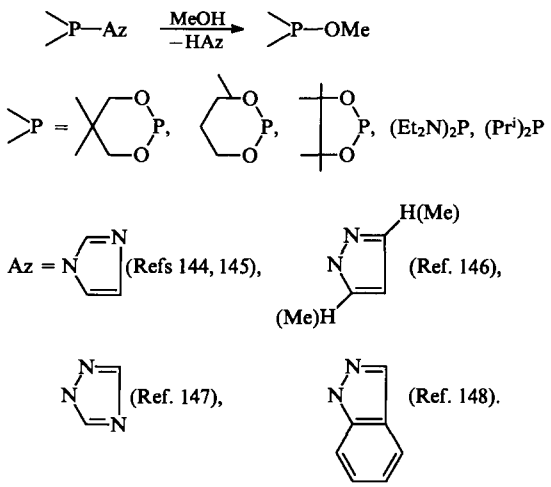
21

A distinctive feature of this compound is the presence of a mobile hydrogen atom. In this connection, we may note the greater reactivity of the pyrrolidine derivative **19** compared with that of the pyridine derivative **15**. This finding suggests an important role for prototropism in phosphorylation, which is more probable for the phosphopyrrolidine **19** than for the aromatic phosphopyridine **15**.

Comparison of compounds **20** and **21** revealed a relation which had already been discovered earlier for pyridines: the imine **21** is inferior in reactivity to the amide **20**. Nevertheless, comparison of the conditions in phosphorylation by these substances led to an unexpected observation — compound **21** does not require a catalyst in alcoholysis. Apparently, being one of the phosphorylated forms of an amidine, this compound exhibits a high reactivity and, together with an alcohol molecule, constitutes a catalytic complex for the phosphorylation reaction. Naturally, compound **19** is also a phosphorylated amidine but here the phosphorus atom is at the imine end of the amidine system, which lowers its basicity.

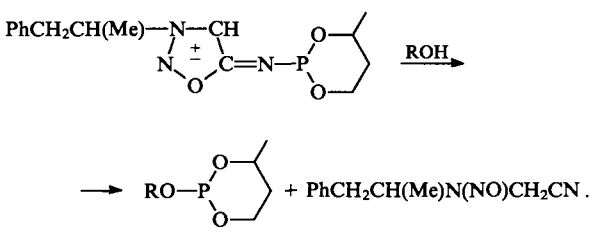
The interest in phosphorylated derivatives of heterocycles as phosphorylating agents for fine organic synthesis has become particularly marked nowadays in the study of phosphorazolides and related systems. Investigations on these lines began with the publication of the papers of Birkofer et al.[135] and Nifant'ev[136] and were vigorously continued in other studies[137–143] in which

phosphorimidazolides were identified as the most reactive preparations. The tendency has arisen recently to expand this research and to treat the results systematically. In this connection, we may note a series of communications on the synthesis of various phosphorazolides and their phosphorylating capacity.[144-148]



It has been established that the reactivity of phosphorus(III) acid azolides decreased significantly in this case in the series diester phosphorazolidites > phosphorous diamide azolides > phosphinazolidites and, depending on the nature of the azole, in the series imidazolide > pyrazolide > triazolide > benzimidazolide.[120] A very marked influence of the solvent polarity on the phosphorylating capacity of the phosphorus(III) acid azolides was unexpected. It decreased sharply on passing from acetonitrile to chloroform and even more so on passing to dioxane and benzene.[120] Azoles are known to exist in nonpolar solvents in the form of linear oligomers or cyclic trimers.[149,150] With increase in solvent polarity, these self-associated species can decompose and the catalytic function of azoles comes to the fore, which accelerates the alcoholysis.

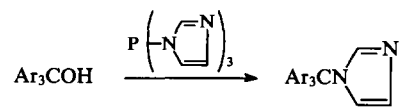
Continuing the consideration of the alcoholysis of heterocyclic phosphorus(III) acid amides and imides, we may point to the results of the phosphorylation of alcohols by phosphosydnone imine obtained in the following instance:[151,152]



This reaction has no special preparative advantages, but it is interesting because it is not accompanied by the accumulation of a nitrogenous base in the system, since the sydnone imine produced isomerises immediately to *N*-nitroso-1-phenylisopropylaminoacetonitrile. This product has optical properties differing strongly from those of phosphosydnone imine, so that it is easy to investigate the kinetics of its reactions by UV spectroscopy, including dilute solutions.

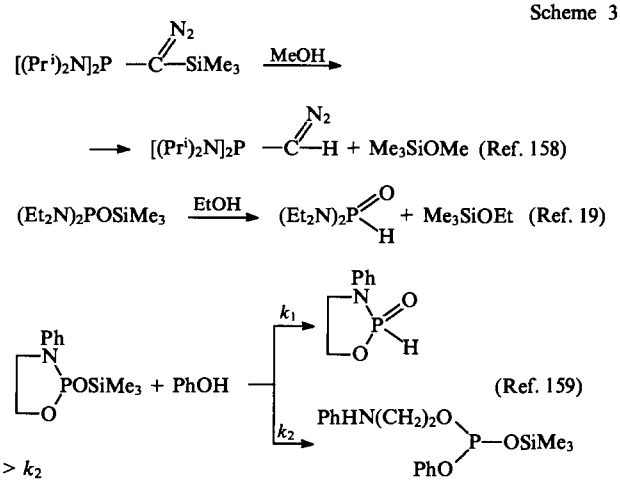
The first data have now been obtained also on the alcoholysis of the hydrazides,[153] hydroxyamides,[154] benzamidides,[155] and guanidides[156] of certian trivalent phosphorus acids. All these compounds exhibit an effective phosphorylating capacity, which intensifies with acid catalysts, but no characteristic features making them specially valuable have yet been noted.

The advantages of the phosphoramide phosphorylation method were indicated above: the mildness of the conditions and the absence of side reactions. This general rule has a few exceptions, which must be stated in the review. Thus it has been established that the phosphorylation of triarylcarbinols by phosphorous acid triimidazolide leads to triarylimidazolylmethanes and not to the expected product.[157]



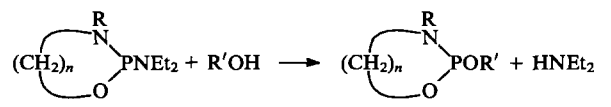
A deficiency of the phosphorus(III) acid amide method is also the unpredictability of the reactions of certain organoelement TPAA derivatives. Thus systems containing the C–Si[158] and O–Si[19,159] bonds can undergo cleavage at precisely these bonds on alcoholysis and phenolysis (Scheme 3)‡.

Scheme 3



We shall consider the influence of structural factors on the mode of alcoholysis and phenolysis of cyclic systems, the molecules of which contain both exophosphoramide and endophosphoramide bonds. There are literature data on the interaction of alcohols and phenols, in equimolar amounts relative to the substrate, with 2-dialkylamino-1,3,2-oxazaphospholane[162-165] and [the corresponding] phosphorinane.[166-170] These reactions lead mainly to the dissociation of the exocyclic bond (Scheme 4).

Scheme 4

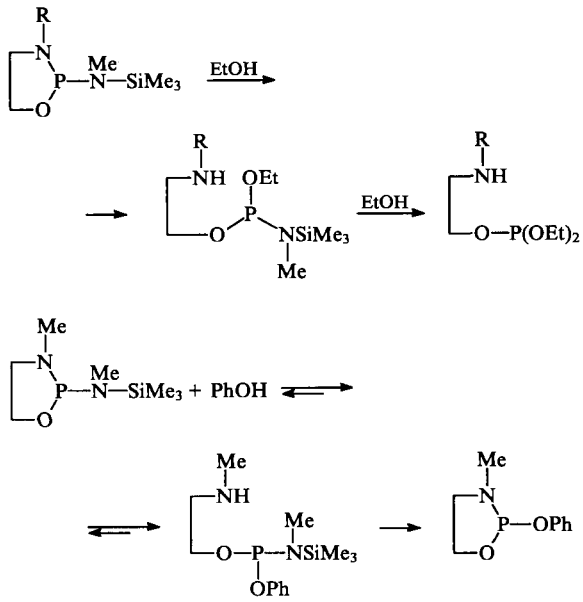


n = 2, 3; R,R′ = Alk, Ph

Oxazaphospholanes having a P–C exocyclic bond are much more reactive in the alcoholysis of the endocyclic P–N bond than the corresponding 2-alkoxy-derivatives, the introduction of an alkyl substituent in the 5-position in the oxazaphospholane ring resulting in a significant stability of the P–N bond.[171]

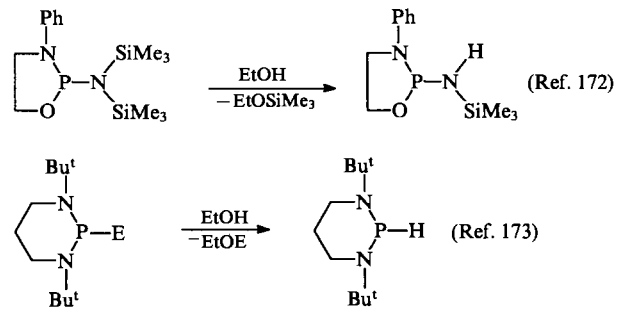
However, alcoholysis of oxazaphospholanes containing an exocyclic *N*-methyl-*N*-trimethylsilylamino-group begins with the rupture of the endocyclic P–N bond and only then of the exocyclic bond. In phenolysis, the ring is reformed in the second stage.[172]

‡ The acid catalyst (tetrazole) can, however, alter the mode of the reaction towards the dissociation of the P–N bond.[160,161]



When the molecules contain an exocyclic *N,N*-bistrimethylsilylamino-group[172] and trisubstituted P-silyl and P-germyl groups,[173] alcoholysis does not involve the cyclic skeleton of the molecules and begins with the dissociation of the N–Si and P–Si(Ge) exocyclic bonds (Scheme 5).

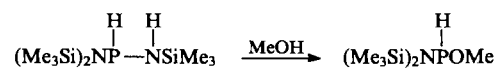
Scheme 5



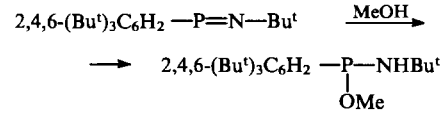
E = $SiEt_3$, $SiPh_3$, $GeEt_3$.

We may note the unusual nature of the alcoholysis of the P–N–Si acyclic systems. In the presence of two types of trimethylsilylamino-groups — secondary and tertiary — in the molecules of such TPAA, a secondary silylamino-group is the first to undergo alcoholysis (Scheme 6).

Scheme 6

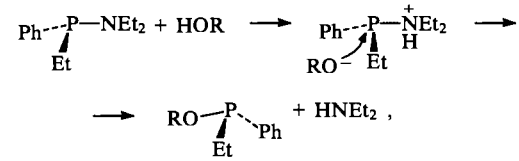


Finally, mention should be made of the possibility of the alcoholysis of the P=N π-bond in iminophosphine derivatives.[175,176]

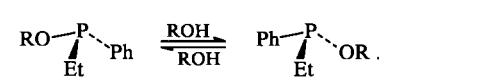


When an excess of the alcohol is used, there is a possibility of further alcoholysis, this time involving the P–N σ-bond.

The results of the study of the stereochemistry of substitution of the amino-group at the phosphorus(III) atom are difficult to interpret because it is essential to take into account the possibility of inversion at the phosphorus centre (especially at elevated phosphorylation temperatures) both in the initial TPAA and in the products of their reaction. Such inversion can occur readily under the influence of acid impurities[177,178] and other factors, for example owing to the presence of an excess of the alcohol (transesterification). Therefore the early studies, where the purity of the initial reactant was not rigorously monitored, must be treated with caution. This applies in the first place to the publications on the mechanisms of the reactions of optically active compounds, where the conclusions about their chemistry were reached solely on the basis of measurements of the angle of rotation of the reaction mixtures. As an example, we may point to a study[179] of the interaction of the optically active ethylphenylphosphinous diethylamide with methyl, ethyl, n-propyl, and isopropyl alcohols. A decrease in the angle of optical rotation was observed in these experiments. The above results were explained by two reactions. Firstly, by the substitution proper involving the inversion of the configuration at the phosphorus(III) atom:

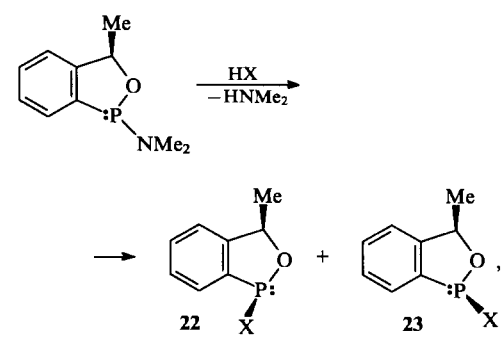


and secondly, by the racemisation effected by the excess alcohol:



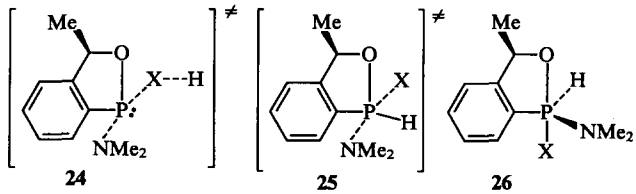
Under these conditions, retention of the configuration was observed in the reaction of *p*-cresol, which served as a basis for an explanation of the mechanism in terms of a four-membered transition state. In this connection, we emphasise that the authors[179] carried out the reaction with cresol for 1 h at 100 °C and were therefore unable to observe the primary inversion. Furthermore, the monitoring procedure they used enabled them to observe only the overall optical rotation of the mixture, while the influence of the initially inverted product might have been small owing to its insignificant amount.

More reliable results were obtained in the analysis of the stereochemical transformations of diastereoisomers by NMR spectroscopy. Thus, in the interaction of certain derivatives of phospholanes with phenol, Nielsen and Dahl[41,180] observed by ^1H NMR the initial inversion of the configuration of the phosphorus atom and the subsequent inversion in the reaction product. The latter led to the formation of a thermodynamically stable isomer (< 5 min). The data obtained in a study by ^1H and ^{31}P NMR of the nucleophilic substitution of a diastereoisomerically pure benzoxaphospholene, i.e.



where X = OMe, OBu^t, OPh, NMe_2, $N(CH_2)_5$, or NHPh, showed that the reaction with HX [X = OMe, OPh, $N(CH_2)_5$] at 25 °C in $CDCl_3$ proceeds with formation of two products, **22** and **23**, the product with the inverted configuration at the phosphorus atom being initially obtained preferentially. Subsequent reactions evidently lead to an equilibrium mixture of the diastereoisomers **22** and **23**. For X = OBu^t and NHPh, the rate of reaction is lower

than the rate of inversion and in this case an equilibrium mixture of compounds **22** and **23** was therefore immediately obtained. The authors believe that the $S_N2(P)$ type substitution mechanism at phosphorus(III) usually proposed (see, for example, Zavlin et al.[27]) is improbable because of the unfavourable diequatorial disposition of the phospholene ring in the transition states of two different types, **24** and **25**, and postulate the formation of a new type intermediate **26**.

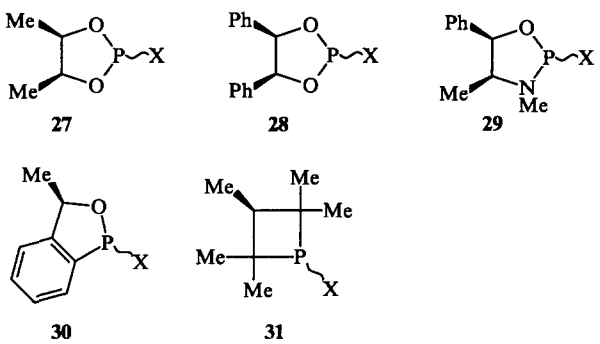


24 **25** **26**

Thus the stereochemical result of the reaction will depend on which pseudorotation (which is necessary to place the NMe_2 group in the axial position favourable for its elimination) in compound **26** has the lower energy barrier. In their analysis of possible pseudorotations, the authors conclude that the reaction proceeds with preferential inversion if the hydrogen is more apicophilic than NMe_2, which is known to be the case for phosphoranes of this kind.[181]

As a development of their research, Dahl and Nielsen investigated the stereochemistry of nucleophilic substitution in substrates **27–31** in their reactions with MeO^-, MeOH + NEt_3 (for compounds **27–31** with X = Cl), Et_2NH, PhOH, HCl, and MeOH (Scheme 7).[41]

Scheme 7

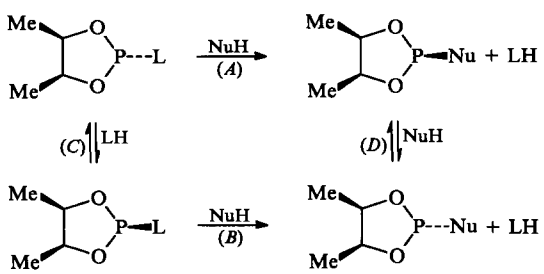


27 **28** **29**

30 **31**

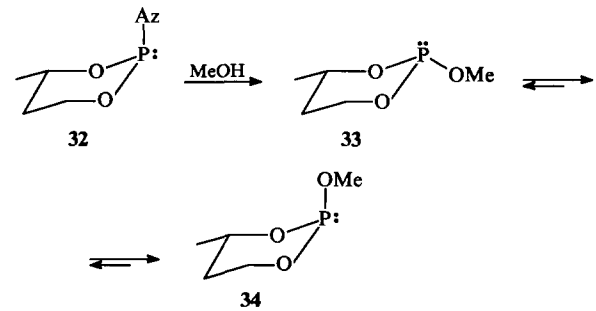
X = Cl (a), NMe_2 (b), NEt_2 (c), OMe (d), OPh (e),  .

The majority of the compounds investigated were configurationally stable (with the exception of the compounds with X = Cl) at 25 °C only in a pure form and their isomerisation was readily accelerated by nucleophilic and acidic impurities (atmospheric moisture, alcohol, amines, acids, etc.). The scheme below reflects the different possibilities in the isomerisation of compounds **27–31**.



According to the authors, pure inversion is possible only when the substitution reactions (*A* and *B*) are much faster than the isomerisation reactions (*C* and *D*) (see also Horner and Jordan[179]). It was concluded that nucleophilic substitution in TPAA proceeds in most cases with complete inversion. We may note that this conclusion is to some extent arbitrary. Indeed, many cyclic compounds of trivalent phosphorus containing amino-groups are usually configurationally unstable and therefore the reactions of these substances are not stereoselective.

More clear-cut results were obtained in a study of the stereodynamics of the methanolysis of cycloasymmetric trivalent phosphorus acid (TPA) azolides **32**, which have been shown[145–148] to exist in the *trans*-configuration with the azolide substituent in the axial position.



32 **33** **34**

It has been demonstrated by ^{31}P NMR spectroscopy that, in contrast to TPA dialkylamides, alcoholysis takes place rapidly even at 20 °C (inversion of configuration) and a labile ester (isomer **33**) is formed and is then slowly converted into a stable ester—isomer **34**.

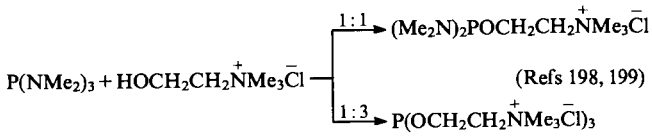
3. Trivalent phosphorus acid amides in fine organic synthesis

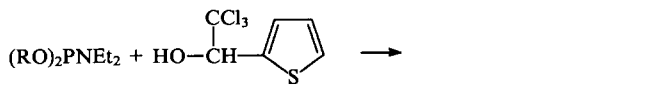
A considerable proportion of the publications on the chemistry of TPAA are devoted to problems of using these compounds in fine organic synthesis. This is due to their ready availability, high reactivity, convenience, and the mildness of the conditions under which they can be applied. The last fact permits specific phosphorylation of complex polyfunctional systems, avoiding at the same time isomerisations, dehydrations, and other unfavourable side reactions, which frequently occur in work involving phosphorochloridites and related reagents.

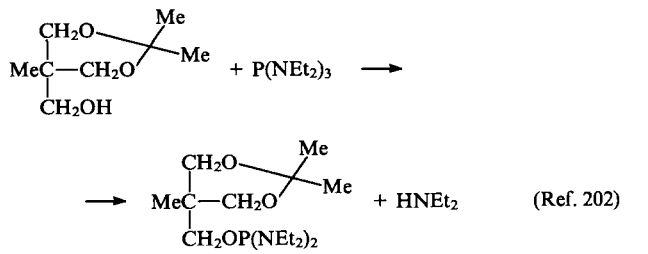
The principal synthetic results, arranged in terms of the types of hydroxy-compounds employed in phosphorylation will be examined below.

a. Phosphorylation of alkanols, phenols, and their functional derivatives

Phosphorylation of alkanols and phenols by TPAA is of a more general importance and is used to obtain the esters (amidoesters) of phosphorous, phosphonous, phosphinous, and hypophosphorous acids. This reaction was used initially to synthesise the simplest derivatives of compounds of the above classes and in this field has been recognised as not only convenient but also as preparatively useful[123–125] for purposes including the synthesis of sterically hindered phenol derivatives.[182,183] Subsequently the phosphoramide method came to be widely employed to obtain various functionalised systems, the molecules of which contain a trivalent phosphorus atom: phosphorylated aminoalcohols,[2,184–189] amidoalcohols,[190–197] cholines,[198,199] polyhalogenated alcohols,[200,201] partially acetalised triols,[167,168,183,184,202–211] etc. Certain examples are presented overleaf as an illustration.

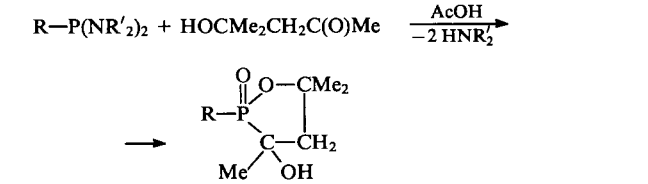




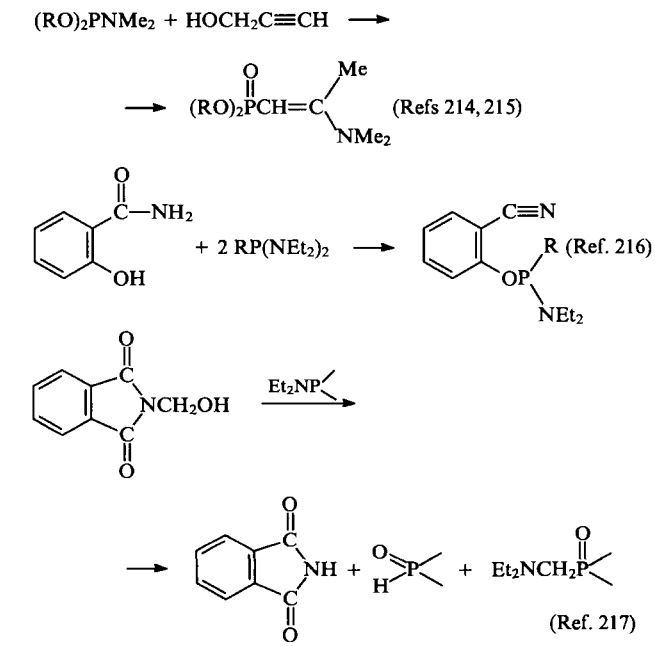


The phosphorylation of functionalised alcohols may be accompanied by additional reactions, which extend the possibilities of the classical synthesis and lead to simple procedures for the preparation of very interesting compounds (Scheme 8).[212,213-217]

Scheme 8

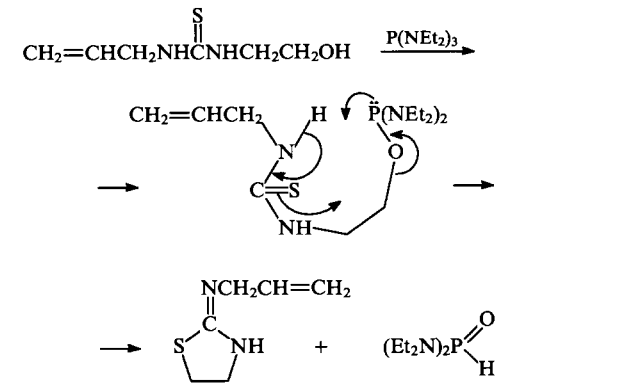


R = Alk_2N, AlkO, Alk; R' = Alk (Ref. 213).

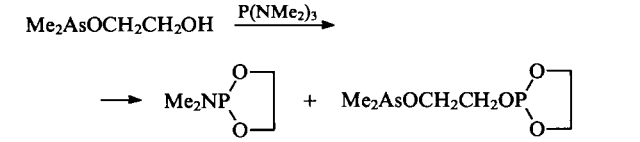


In a number of instances, phosphorylation leads to the creation of complex systems, which subsequently undergo the elimination of hydrophosphoryl compounds. In particular, it has been suggested that 2-allyliminothiazolidine be obtained in this way (Scheme 9).[218]

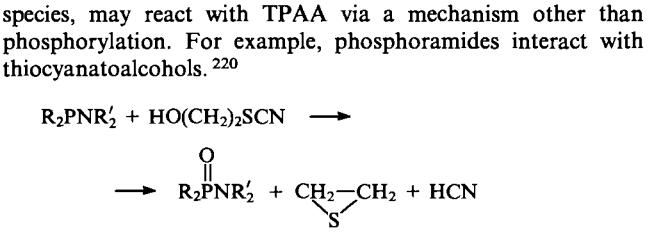
Scheme 9



The modes of the above reactions are treated quite clearly by the authors quoted. Nevertheless, some of the phenomena described in the literature have still not been adequately explained; these include, for example, the double phosphorylation of dimethylarsenylated ethylene glycol.[219]



Functionalised alcohols, capable of generating electrophilic species, may react with TPAA via a mechanism other than phosphorylation. For example, phosphoramides interact with thiocyanatoalcohols.[220]

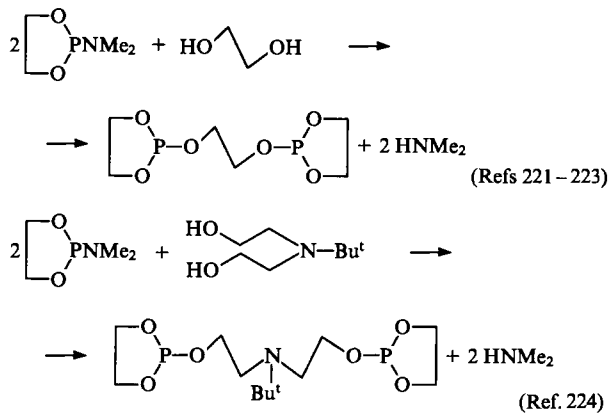


b. Phosphorylation of diols

Numerous publications have been devoted to the study of the reactions in the TPAA–diol system, which can be accounted for by the chemical diversity of the processes carried out and the importance of the products. The phosphorylation reaction is influenced by many factors: the nature of the reactants, their proportions, the reaction conditions, and also the characteristic features of the products. In many instances, this led to difficulties in the analysis of the results and then to erroneous conclusions. Subsequently these conclusions were revised.

It is possible to differentiate the following aspects of the phosphorylation of diols: (1) bisphosphorylation involving both hydroxy-groups of the diol and ending with the formation of a diphosphorous system; (2) monophosphorylation leading to phosphorylated hydroxy-compounds; (3) cyclophosphorylation and cyclooligophosphorylation. In addition, it is necessary to point out also the possibility of the combination of various aspects and also of polycondensations leading to polymeric esters. The last possibility will be examined separately.

The bisphosphorylation of glycols and dihydric phenols has been widely investigated. A series of studies devoted to the use of trivalent phosphorus acid monoamides in reactions with glycols in molar proportions of 1 : 2 have been published. They result in the formation of diesters, for example:[221-224]



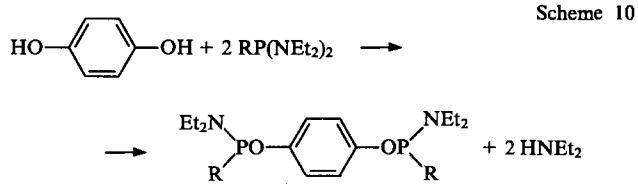
(Refs 221–223)

(Ref. 224)

We may note that the alternative method (the phosphorochloridite method) yields poor results owing to the interaction of the hydrogen chloride produced with the new reaction centre.

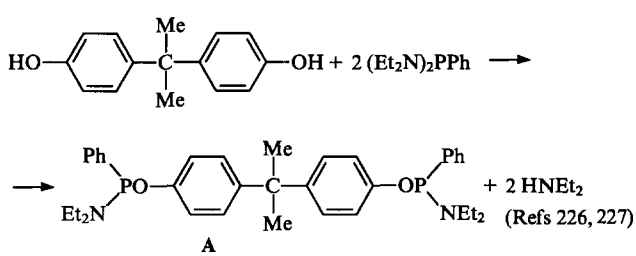
Many reactions with TPA diamides and triamides take place effectively (Scheme 10).[225–227]

Scheme 10



(Ref. 225)

R = NEt_2, OAlk

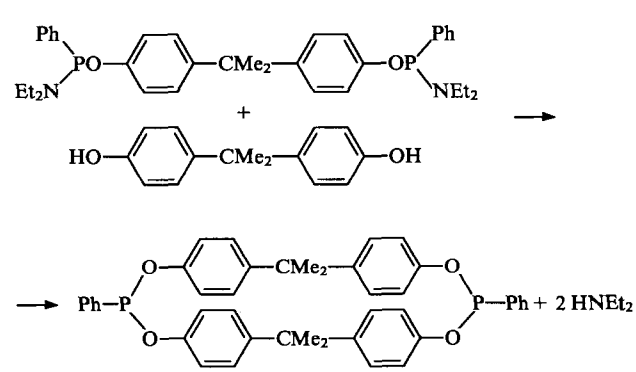


(Refs 226, 227)

A

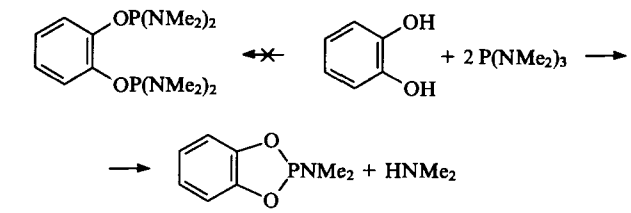
Compound A is interesting because, under the conditions discovered, it can react with an equimolar amount of 2,2-di-*p*-hydroxyphenylpropane (DIAN) and is converted into a phosphorus-containing cyclic system, which is the first representative of the new class of crown-ethers in the molecules of which arylene residues and trivalent phosphorus atoms alternate (Scheme 11).[226]

Scheme 11

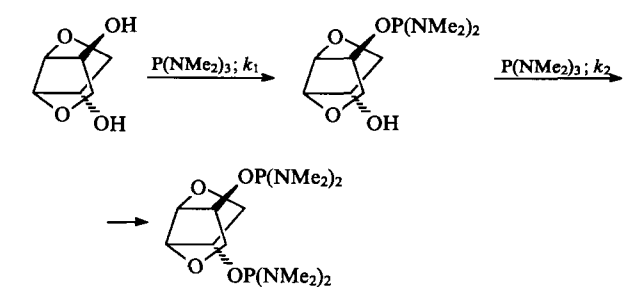


Cyclisation and not bicyclophosphorylation reactions are typical for experiments with diols in which the hydroxy-groups are close to one another in space. Half of the phosphoramide introduced into the reaction fails to react under these conditions. An example is provided by the phosphorylation of catechol and its derivatives by phosphorous acid hexaalkyltriamides (Scheme 12).[228–234]

Scheme 12



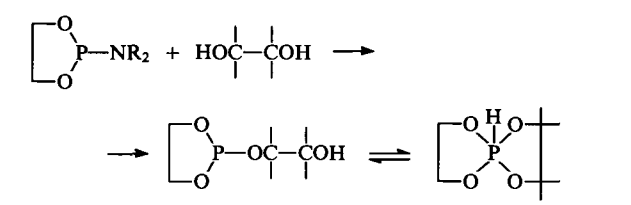
The interaction of phosphorous triamides with 1,4;3,6-dianhydromannitol merits special consideration. In this case, alcoholic hydroxyls in the initial compound are not quite so close in space as in catechol, so that phosphacyclisation is difficult.[235,236] On the other hand, the primary phosphorylation step leads to a novel situation: the free hydroxyl of the intermediate is apparently more reactive than the hydroxyl of the initial diol, the reactivity of which diminishes owing to the formation of intramolecular hydrogen bonds. The reactivity of the intermediate is manifested by the fact that in the interaction of even equimolar amounts of dianhydromannitol and phosphorous hexamethyltriamide results in the formation of mainly the bisphosphorylated product and residual unreacted dianhydromannitol remains.[237]



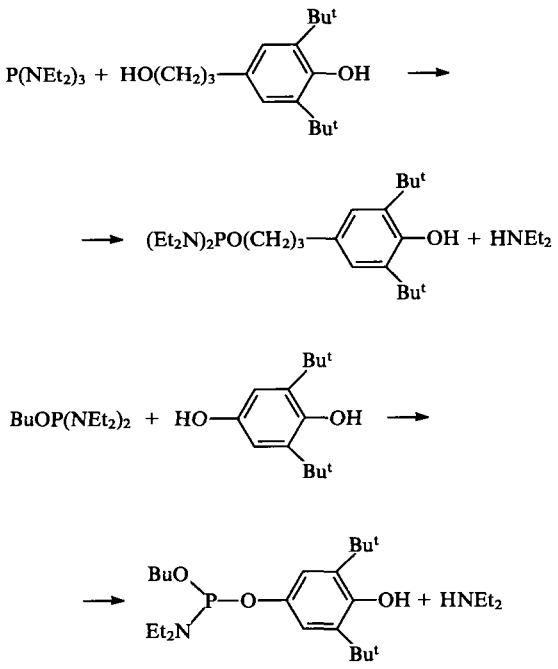
$k_2 \gg k_1$

Thus the geometrical characteristics of the initial diols may regulate significantly the nature of their phosphorylation.

The monophosphorylation of diols by an equimolecular amount of phosphorus(III) acid amides rarely affords satisfactory results. The group of reactions of cyclic TPAA with 1,2-diols has been investigated in greatest detail. The phosphoalcohols formed in this case as the primary product exhibited a tendency to undergo ring–chain tautomerism.



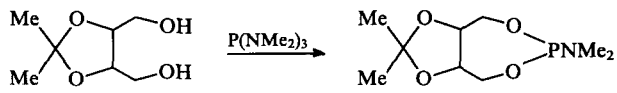
The position of the tautomeric equilibrium is determined by the structure of the compound, the solvent, and temperature. It is usually fully or largely displaced towards the formation of the form with pentacoordinate phosphorus—hydrospirophosphoranes. The history of this problem and the extent to which it has been investigated have been described in a series of reviews.[238–242] A different result was noted in the phosphorylation of diols the hydroxy-groups of which are of a different chemical nature: one of them is sterically exposed whilst the other is shielded. 4-(γ-Hydroxypropyl)-2,6-di-*tert*-butylphenol[243] and 2,6-di-*tert*-butylhydroquinone[210] may be included among these diols. In this case, phosphorous diamides and triamides interact regioselectively with an equimolecular amount of the diol.



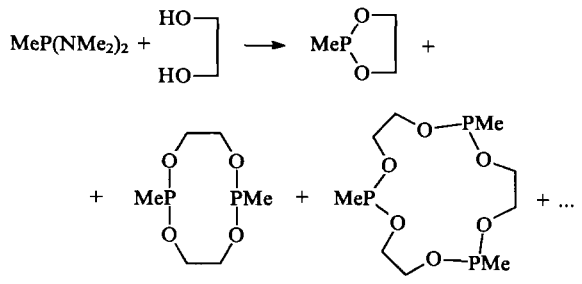
The phenyl phosphorodiamidites obtained are entirely stable. They can be distilled in a high vacuum and phosphorylate extraneous nucleophiles by virtue of their phosphoramide fragment.

The cyclophosphorylation and cyclooligophosphorylation of diols by TPAA has been comprehensively investigated. It has been shown that phosphorous diamides and tiramides effect the preparative phosphorous cyclisation of alkane-1,2 diols,[142,229,244-247] alkane-1,3-diols,[142,244,248,249] and alkane-1,4-diols[142,250-253] with formation of the corresponding 1,3,2-dioxaphosphacyclanes.

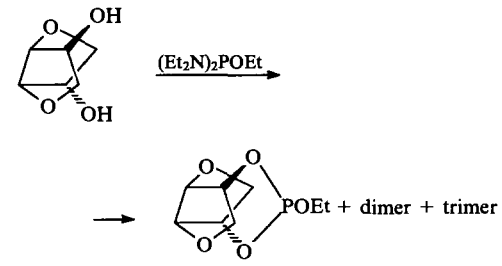
These phosphoramides cyclophosphorylate similarly also functional derivatives of diols,[254-257] for example, 2,3-isopropylidene-D-threitol.[257]



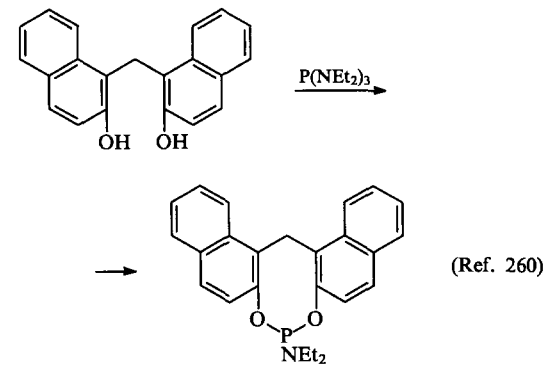
Many of the phosphacyclic compounds obtained in this way are used in the solution of stereochemical problems and in the synthesis of compounds of practical importance. It is very interesting that phosphorylation of alkane-1,2-diols and alkane-1,3-diols by phosphonous diamides leads to compositions comprising monocyclic and oligocyclic compounds which are in equilibrium, for example:[258]



It has recently been possible to extend the cyclophosphorylation reaction to 1,4;3,6-dianhydromannitol and to establish also the parallel formation of mono- and tri-cyclophosphorylated systems (this time phosphorous and not phosphonous).[236]

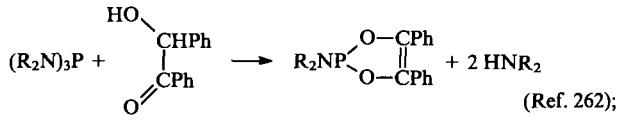


Normal cyclophosphorylation has been observed for catechols,[228-232] *o*-naphthalenediols,[259,260] and other dihydric phenols containing hydroxy-groups which are close in space.

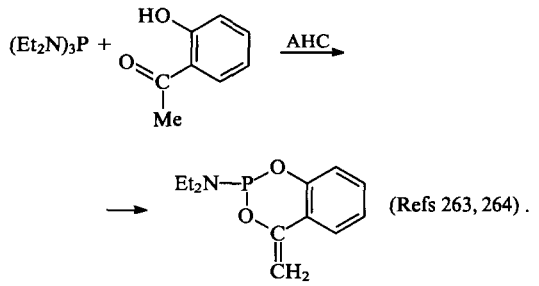


Aromatic heterocyclic *o*-diols—2,3-dihydroxypyridine[261] and 2,3-dihydroxyquinoxaline[259]—also form phosphacyclic compounds on reaction with TPAA. We may note, however, that the preparative conditions in these cyclisations are not identical. The latter diol is formed with considerable difficulty apparently owing to the great strength of its intermolecular hydrogen bonds.

The ready cyclophosphorylation of hydroxyketones, which readily react in their enolic forms when the hydroxy-groups are close together in space, also merits attention:[262]

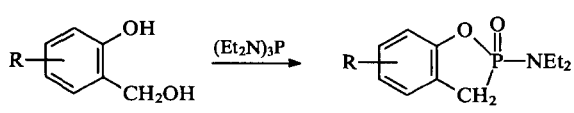


(Ref. 262);

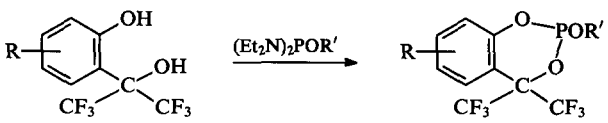


The last reaction is of interest because it leads to cyclisation only in the presence of amine hydrochlorides. Pure phosphoramides react with *o*-acetylphenol to form benzoxaphospholanes.[263,264]

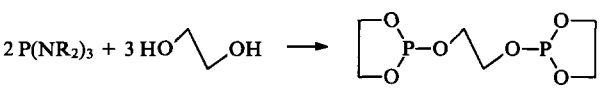
A number of investigators have attempted to cyclophosphorylate saligenin or related *o*-hydroxymethylphenols with formation of benzophosphorinanes. These attempts were unsuccessful: benzoxaphospholanes were obtained instead of the expected compound.[265]



It was postulated that the benzyl cations, formed readily after the primary phosphorylation, play a crucial role in such reactions. Taking this into account, bistrifluoromethyl derivatives of saligenins were used in the cyclophosphorylation reaction, which led to the successful synthesis of previously unknown benzodioxaphosphorinanes.[266]



In conclusion of the subject of the cyclophosphorylation of diols, we may point to interesting instances of the combination of reactions leading ultimately to the formation of cyclic diphosphites. An appropriate reactant ratio is needed for this purpose. Such combination is particularly successful with 1,2-diols, for example ethylene glycol.[221,222]

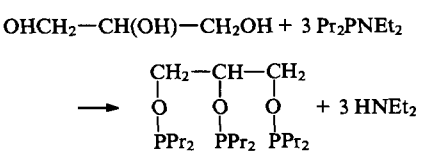


c. Phosphorylation of triols and higher oligools

TPAA were introduced into the range of popular phosphorylating agents during the period when the problem of the study of skeletal systems became of current interest in organic chemistry. It became necessary to develop specific procedures for the synthesis of phosphorus-containing skeletons. This was achieved in a series of leading scientific centres via the cyclophosphorylation of oligools by phosphorous and phosphonous amides. An extremely important feature is that, even in the first stages of the work involving the design and study of the properties of phospha-skeletal compounds, fundamentally important results were obtained, including the discovery of novel stereoelectronic interactions and other structural effects.

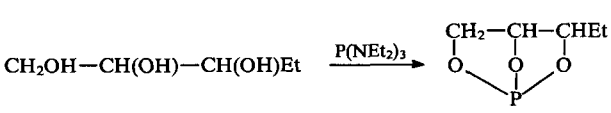
Studies on these lines are frequently experimentally complex and this is why there is still no well structured set of data. In view of this, we have arranged the published data in terms of a formal characteristic — the number of hydroxy-groups in the molecules of the phosphorylated oligools.

Phosphorylation of triols. The phosphorylation of glycerol with formation of open-chain triesters and phosphacyclic compounds has been described in the literature. Only one publication, reporting the interaction with dipropylphosphinous diethylamide, has been devoted to the triesters.[267]



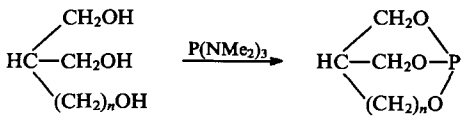
It was noted that the phosphoramide employed exhibits in this case a lower reactivity than in the phosphorylation of other alcohols.

It is noteworthy that glycerol is a poor coreactant in the bicyclophosphorylation reaction using trifunctional derivatives of phosphorous acids. The instability of the target product, having a strained central unit, adds to the difficulties in phosphorylation under these conditions.[268] On the other hand, terminally substituted glycerols, for example pentane-1,2,3-triol, are smoothly bicyclophosphorylated with formation of stable esters.[269]



It may be that in this case the molecules of bicyclophosphites interact stereoelectronically with participation of terminal substituents, which alters the parameters of the valence bonds and hence diminishes the angular strain. Furthermore, an effect of the Thorpe–Ingold type may exert some influence in this instance.

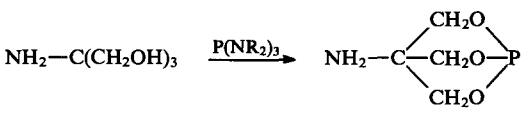
The related bicyclophosphites are obtained even more effectively on treating with phosphorous triamides linear triols having more widely separated hydroxyls: butane-1,2,4-triol,[270–273] pentane-1,2,5-triol,[274] and also related or branched systems — 1,1,1-tris(hydroxymethyl)methane[270] and 1,1,2-tris-(hydroxymethyl)ethane.[275]



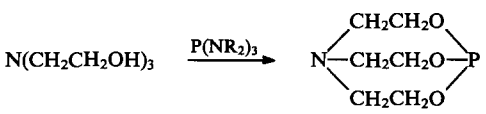
$n = 1, 2$

Stable skeletal bicyclophosphites, in the molecules of which 1,3,2-dioxaphospholane, 1,3,2-dioxaphosphorinane, and 1,3,2-dioxaphosphepane rings are condensed, are formed in all cases. Such skeletal systems have come to be widely used in fine organic synthesis and in coordination chemistry. They have attracted the attention also of physicochemical biologists[276] in connection with their ability to regulate membrane transport §.

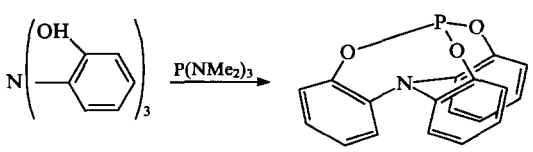
Phosphorous triamides can also interact with tris(hydroxymethyl)methylamine.[277]



A phosphorus-containing skeleton, the molecules of which contain two condensed six-membered rings and a free amino-group, is formed in this case. This aminoalkyl phosphite is a valuable ligand for the preparation of metal complex catalysts soluble in aqueous systems.[277] A formally, structurally similar, very labile system, which has been called phosphatrane, has been synthesised by the reaction of triethanolamine with phosphorous triamides.[278–282]



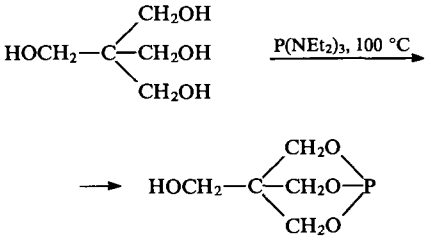
A skeletal amino-substituted phosphite, similar to that described above but containing *o*-phenylene groups and not ethylene groups as the main alkylene elements, has been synthesised by phosphorylating tris(*o*-hydroxyphenyl)amine with phosphorous hexamethyltriamide.[283]



This phosphite belongs to the class of rigid skeletal compounds of the 'cage' type. Its phosphorus and nitrogen atoms are not close to one another and do not therefore interact, as happens in phosphatrane. It is apparently of interest for the creation of supermolecular constructions.

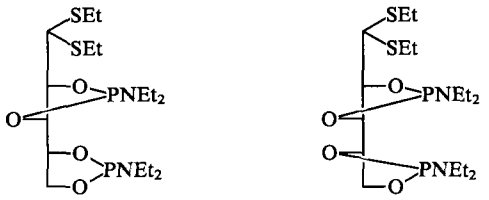
§ The synthesis of phosphaskeletal compounds is examined in greater detail in the section devoted to carbohydrate phosphites.

Phosphorylation of tetraols. All the publications dealing with 'tetraols' were concerned only with the problem of cyclophosphorylation. Pentaerythritol may be specified in the first place as a promising substrate for cyclophosphorylation. This symmetrical tetraol is readily available and various syntheses have been planned on its basis. Some of them have already been achieved. Thus it has been reported that, when pentaerythritol is heated with an equimolecular amount of phosphorous hexaethyltriamide, a symmetrical skeletal phosphite is formed—4-hydroxymethyl-2,6,7-trioxa-1-phosphabicyclo[2.2.2]octane.[270]

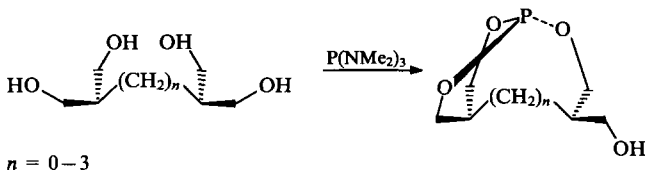


This compound is of great interest for subsequent reactions and also for use as a stabiliser of materials and as a ligand in the synthesis of metal complexes.

The 1,1-diethylthioacetals of aldopentoses—D-xylose and L-arabinose—are also bicyclophosphorylated with formation of compounds **35** and **36**.[284]

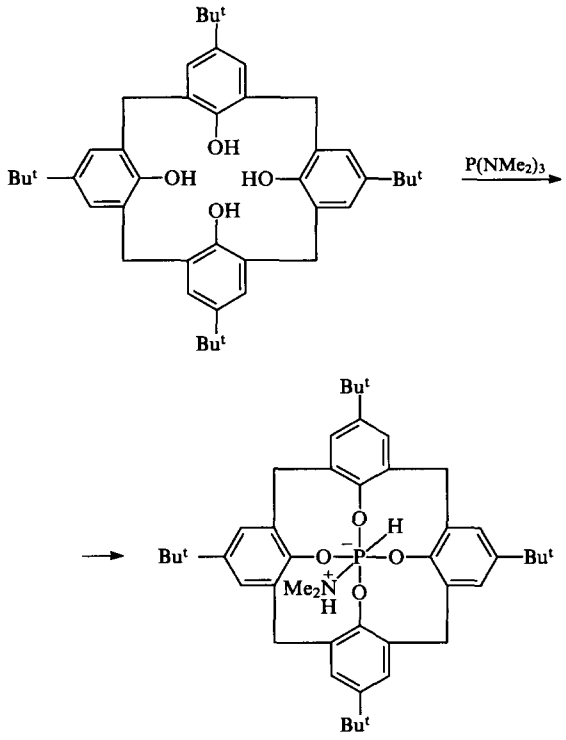


The group of α,α,ω,ω-tetrakis(hydroxymethyl)alkanes has been investigated in the reaction with an equimolecular amount of phosphorous hexamethyltriamide.[275]

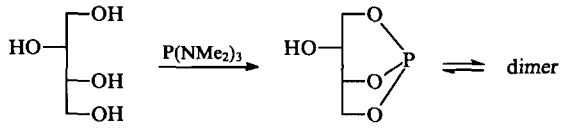


$n = 0-3$

The interaction of *p*-(*tert*-butyl)calix[4]arene with phosphorous hexamethyltriamide in equimolecular proportions is very interesting.[285] Triple phosphorylation of the calixarene occurs in this case and leads to the formation of a bicyclophosphite the phosphorus atom of which is very close to the phenolic hydroxyl which has not reacted. Owing to the spatial proximity of these groups, they readily react, which leads to the appearance of the phosphorane structure. The latter combines with a molecule of the dimethylamine produced. Naturally, the pathway described is only one of those possible in the reaction. A detailed study of this process can lead us to the discovery of new characteristics of the reactions of flattened skeletal phosphacyclic compounds.



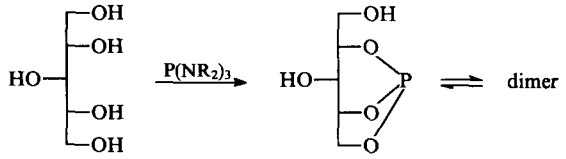
The phosphorylation of threitol, which is a conformationally labile tetraol, by TPAA is of a different kind. The interaction of equimolecular amounts of the reactants results in the initial formation of a mixture of products. Subsequently, it is converted into a 1,2,4-bicyclophosphite, which may dimerise reversibly.[286]



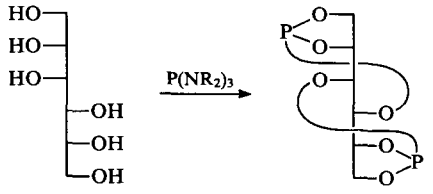
The entire information about these reactions has been obtained by ^{31}P NMR spectroscopy.[286]

Phosphorylation of higher polyols. The phosphorylation of higher polyols by TPAA leads to the formation of complex products[287-289] the structure of which has been reliably established only with the aid of NMR spectroscopy and X-ray diffraction.

Thus xylitol in contact with an equimolecular amount of phosphorous triamide behaves similarly to threitol.[286]



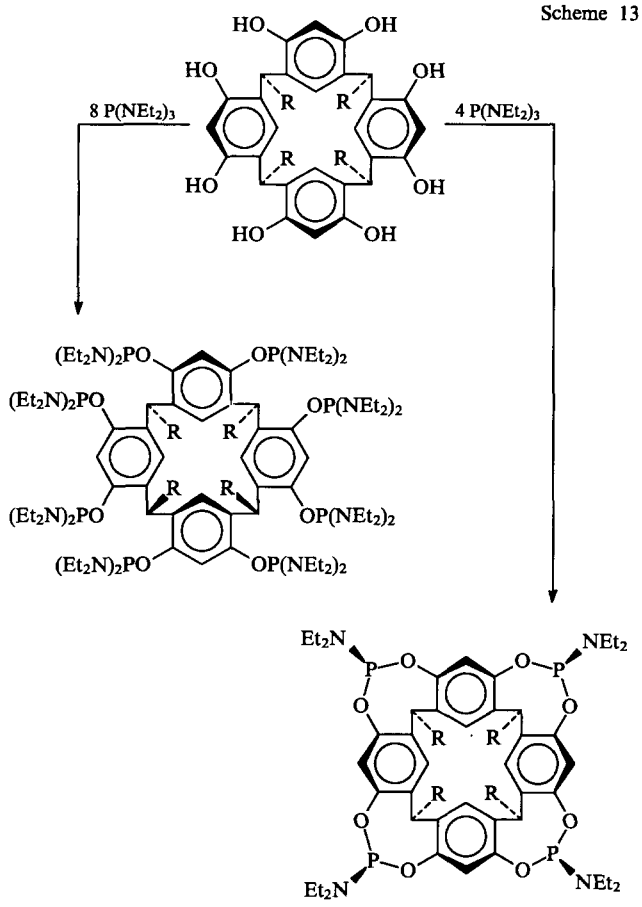
The reaction of mannitol with phosphorous triamide is more promising: in this case it was possible to obtain a bisbicyclophosphite—the product of the complete phosphorylation of the hexaol.[290]



We may note that a similar reaction with phosphorus trichloride affords much poorer results owing to the partial substitution of the hydroxyls by chlorine atoms. The structure and steric configuration of the compound obtained have been demonstrated by X-ray diffraction.[291]

Phosphorylation and cyclophosphorylation have been investigated also in the series of aromatic octaols in connection with the synthesis of ligands for the formation of supramolecular systems. Thus it has been shown[292,293] that octahydroxy[1$_4$]metacyclophane affords an octaamidophosphite on treatment with an eightfold molecular amount of phosphorous hexaethyltriamide, while treatment with a fourfold amount of this reagent gives rise to a tetracyclic derivative, which is the first reliably described representative of phosphorus-containing cavitands (Scheme 13).

Scheme 13



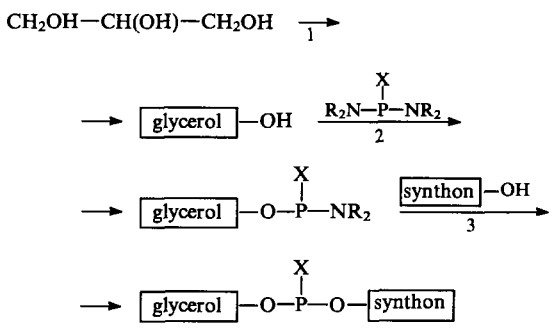
4. Trivalent phosphorus acid amides in the chemistry of natural products

The development of the methods of organophosphorus chemistry has in many respects determined the progress in physicochemical biology. Thus, by virtue of the active employment of trivalent phosphorus reagents, especially TPAA, fundamentally important results have been obtained during the last 10–15 years in the synthesis of oligonucleotides, phosphorylated sugars, phospholipids, and other phosphorus-containing natural products as well as their analogues as regards the phosphorus-containing functional groups. This has been reflected in the publication of a series of reviews in which problems of the employment of phosphoramides in the design of specific classes of natural products have been discussed.[294–304] The publication of these reviews helped us in writing the present review, because it obviated the need for a difficult task and for the exhaustive quotation of a large set of communications, which are of the same type from the standpoint of organophosphorus chemistry, and thus made it possible to draw the reader's attention to the principles of phosphoramide synthesis and the current trends in its employment.

a. The synthesis of phospholipids

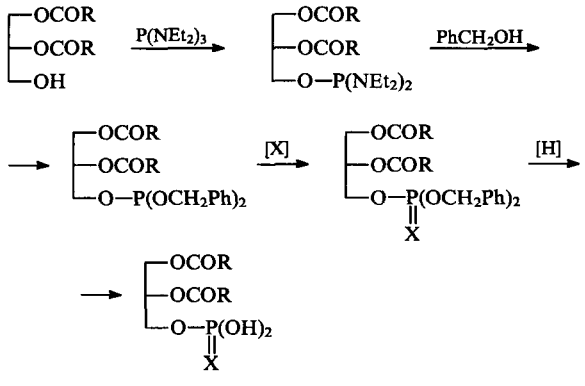
The commonest phospholipids in nature are glycerophosphates, especially phosphatidic acids and their various derivatives. These compounds perform exceptionally important biological functions and an enormous amount of attention has been devoted to their synthesis.[304–306]

We therefore begin the present section of the review with the consideration of the use of TPAA in the design of glycerophosphatides and their P-analogues. The strategy for these syntheses developed in recent years usually presupposes the carrying out of the following stages: (1) the synthesis of monohydroxy-derivatives of glycerol—either 1,2- or 1,3-acetals or 1,2- or 1,3-diacylates; (2) phosphorylation of glycerol derivatives via the alcoholysis of the phosphoramide linkage of a suitable TPAA; (3) oxidative and other necessary reactions leading to phosphatidic acids or other very simple phosphoglycerides, and construction of the complex phosphoglyceride by introducing into the glycerophosphite unit of an additional synthon as a result of the alcoholysis of the second phosphoramide linkage by a selected synthetic equivalent of this synthon.



This process is completed by oxidation reactions and the necessary reactions leading to the formation of the required complex glycerophospholipids.

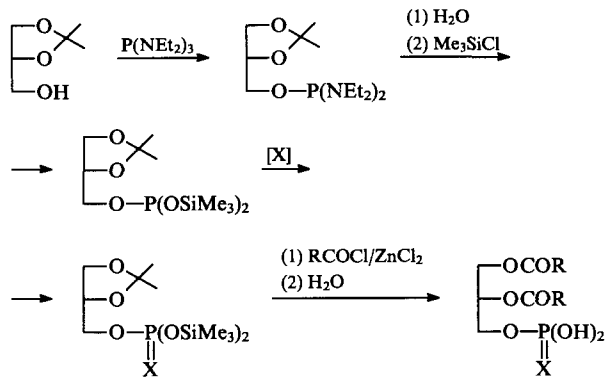
The general scheme presented above has now been embodied in numerous syntheses of various phospholipids and they have all been carried out on the basis of a narrow set of initial reagents and using convenient synthetic procedures.[304] We shall examine the syntheses of phosphatidic acids. These compounds can be obtained from 1,2- or 1,3-acylglycerols which are made to react with TPAA, this being followed by oxidation reactions and the removal of protecting groups, for example:[307,308]



X = O, S

The use of diacylglycerols in phosphorylation entails a risk, because the secondary amine produced can, generally speaking, add to the carbonyl group of acylates, which leads to their partial deacylation or isomerisation. Special studies were carried out which showed how it is possible to avoid these complications.[308,309] At the same time an analogous variant of the synthesis, based on the use of glycerol acetals instead of acylates, was proposed. Glycerol acetals are readily available compounds

which are convenient to handle. They are readily phosphorylated by TPAA without side reactions, after which they are converted by hydrolysis into diols. These are subsequently acylated. Unfortunately, this procedure is preparatively difficult and requires a scrupulous selection of conditions.[187] Therefore a much simpler and effective process has developed—direct acylation of acetals.[310-313] Subsequently the general scheme for the synthesis of phosphatidic acids was supplemented also by other improvements.[304]



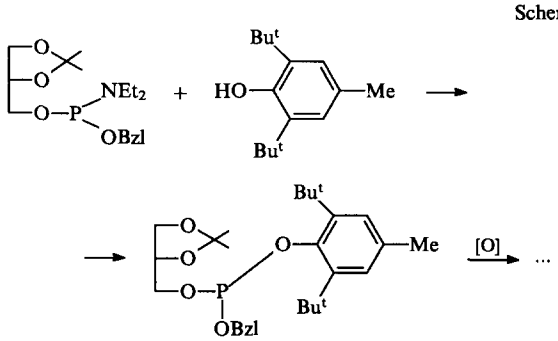
We emphasise that the proposed solution made not only phosphatidic acids but also their thio- and seleno-analogues really available. These analogues immediately began to be used successfully for the solution of important scientific problems, for example for the ^{31}P NMR study of phase transitions in lipid membranes.[314-315]

The use of the phosphoramidite synthesis is even more promising for the preparation of complex natural phosphatides and their analogues. For this purpose, glycerophosphoramidites are made to react[295,304] with aminoalcohols, glycerols, sugars, myoinositol, aminoacids, etc., which leads to the formation of the corresponding phosphatidic acid esters and amides¶. As an illustration, we present (above right) a scheme for the synthesis of 6'-(1,2-distearoylglycero-3-phospho)-D-galactose.[204,207]

Glycophospholipids containing D-glucose[185,207] and disaccharide (maltose)[316] residues were obtained in a similar way.

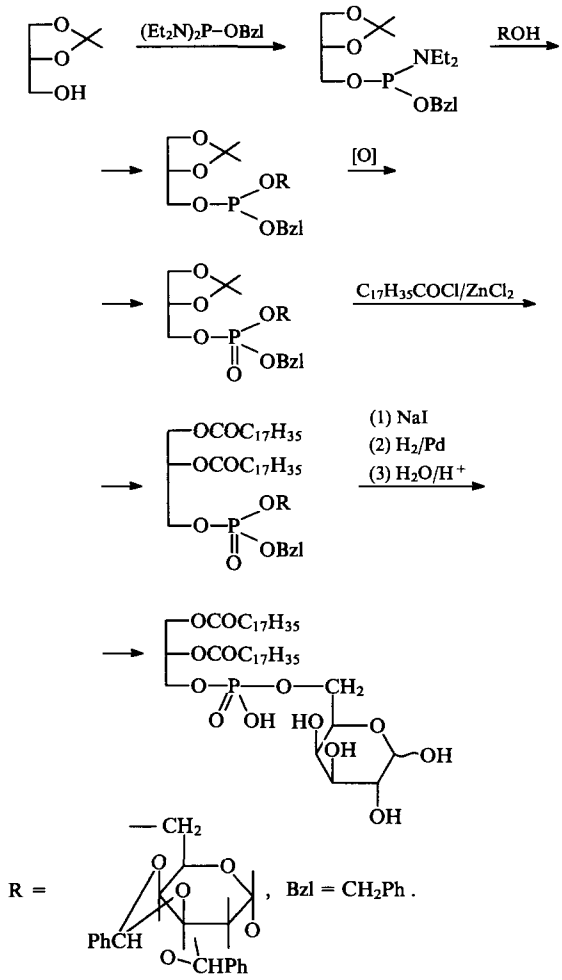
The method considered has been applied also to the synthesis of new constructions of fundamental importance, for example phosphatidyl derivatives of sterically hindered phenols (Scheme 14).[182,183] The preparations thus obtained are membranoaddressed bioantioxidants.

Scheme 14



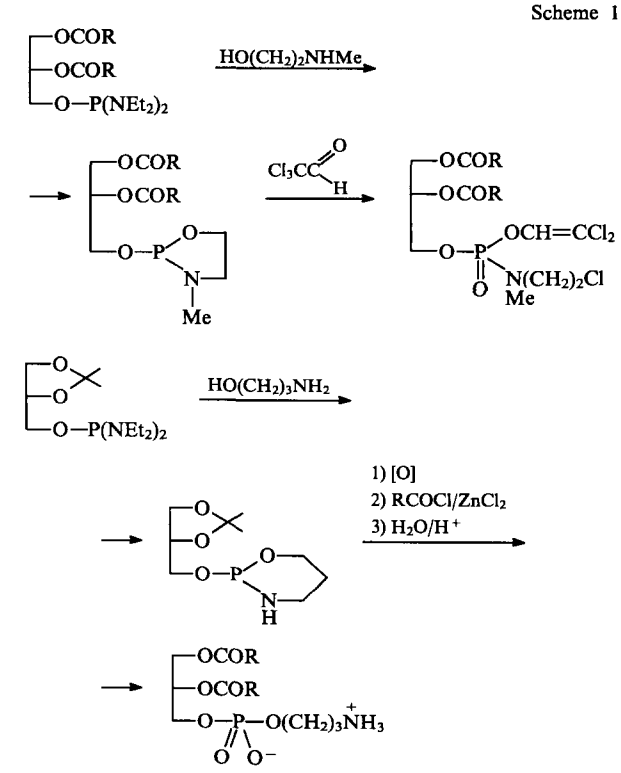
Reactions of glycerophosphorodiamidites with diols[188,206,317] and aminoalcohols[186,187] also merit attention. As in the phosphorylation of substituted glycerols by the amides of the

¶ In many cases an alternative approach may be useful. According to this procedure, the substituted glycerol incorporating sugar, aminoalcohol, etc. residues is phosphorylated by phosphoramidites.

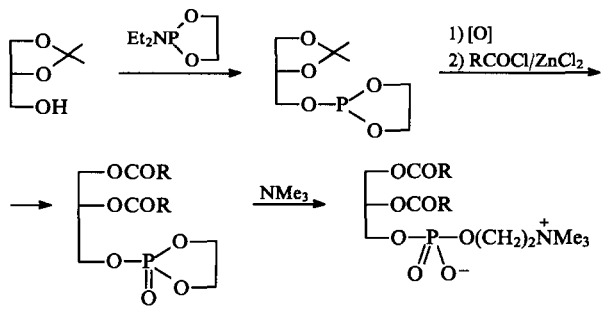


corresponding alkyl or alkylene phosphoramidites, various glycerophosphacyclanes are formed in such cases. There are good prospects for the use of phosphacyclanes for synthetic purposes (Scheme 15).

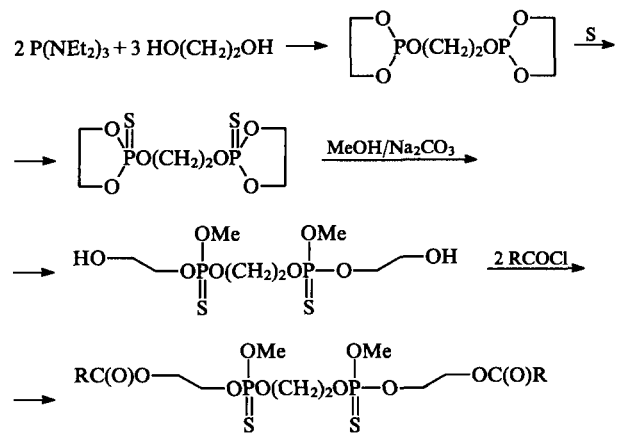
Scheme 15



During the study of such glycerophosphacyclic compounds, a promising reaction was discovered—alkylation of tertiary amines and other nucleophiles by alkylene cyclophosphites.[188, 206, 317–325] A simple method of synthesis of lecithins based on this reaction is presented below.

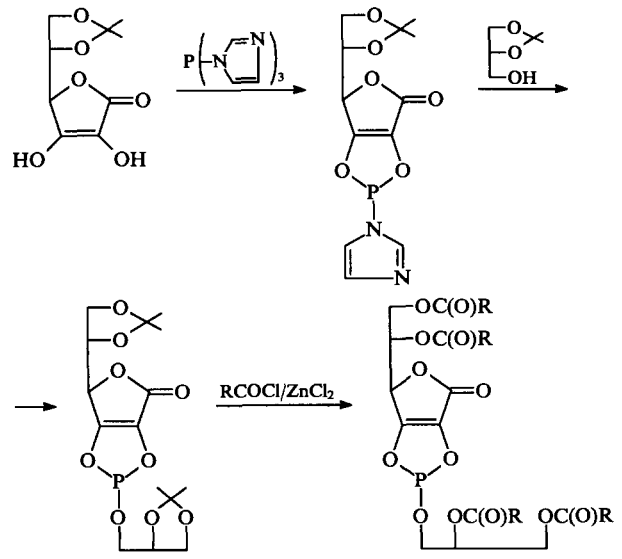


The successful development of glycerophosphoramidite syntheses stimulated research into the chemistry of diol phospholipids. A series of useful reactions leading both to the simplest diphosphites and to extremely complex substances which are difficult to obtain by other methods have been achieved.[326]



R = $C_{17}H_{35}$

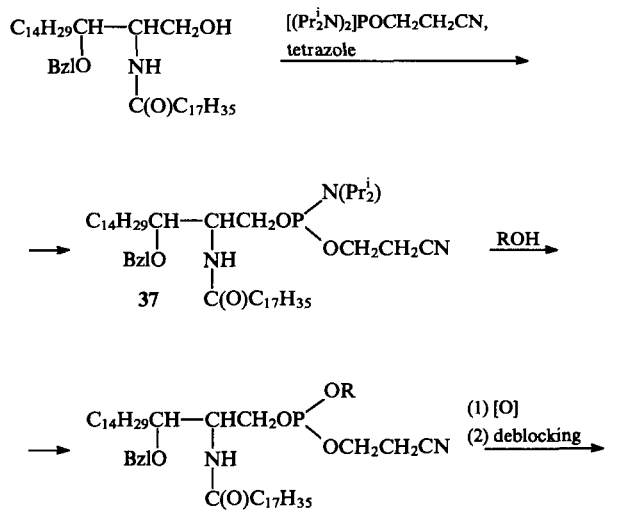
The synthesis of lipid systems from ascorbic acid is much more difficult.[327] For this purpose, 5,6-isopropylideneascorbic acid was cyclophosphorylated by phosphorazolidites, which act under mild conditions, to form an ascorbophospholene. The product was used subsequently as a phosphorylating agent in the reaction with 1,2-isopropylideneglycerol.



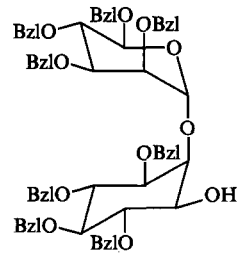
R = $C_{17}H_{35}$

Elegant studies have been carried out recently on the use of TPAA for the preparation of ceramidophosphoric systems. It was shown that the interaction of 3-benzoylceramide with β-cyanoethyl *N,N*-diisopropylphosphorodiamidite in the presence of tetrazole affords a phosphoramidite which can be converted by the methods mentioned above into extremely complex phosphate and phosphorothioate systems. As an illustration, we present the results of one of the latest studies[328] (Scheme 16).

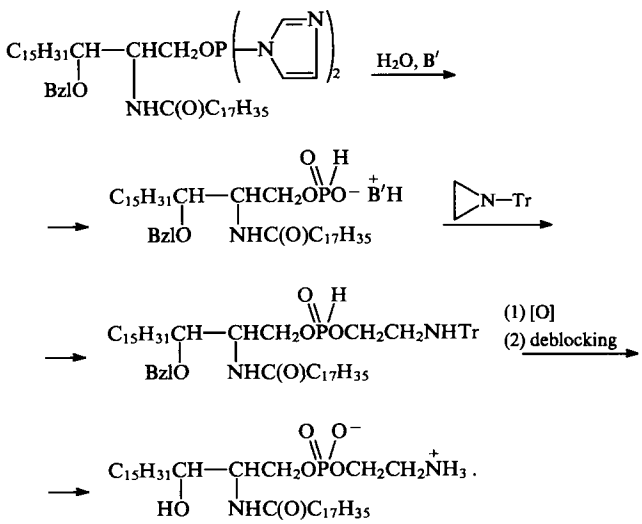
Scheme 16



ROH =



We may note that intermediate **37** and the corresponding phosphorodiamidite may be hydrolysed to form hydrophosphoryl compounds, which are phosphorous monoesters and diesters. These compounds are also promising for phospholipid syntheses: they have been introduced into a series of reactions, both those which have already proved useful in phospholipid practice[329, 330] and comparatively new ones, for example:[328]



Tr = CPh_3

b. Phosphorylation of nucleosides and the formation of an internucleotide linkage

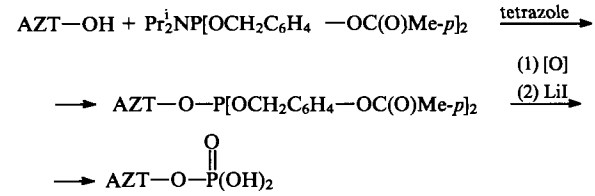
The methods of phosphate chemistry, intricately refined in many scientific centres, have been used for a long time for the phosphorylation of nucleosides, the formation of the internucleotide linkage, and the solution of other related problems. Nevertheless, owing to the low rates of phosphorylation, these methods do not meet the needs of modern research. Furthermore, the classical methods lead to poor results in the synthesis of thiophosphoryl and other nucleotide derivatives which are nonstandard in the phosphorus component. The employment of the highly reactive trivalent phosphorus derivatives and in the first place TPAA was seen as a method of overcoming the difficulties which have arisen.

The possibility, in principle, of resorting to amides of phosphorous, phosphonous, and phosphinous acids in order to phosphorylate nucleotides was demonstrated at the end of the 1960s and the beginning of the 1970s.[331,332] Unfortunately, time was needed to become accustomed to the new reagents and they have only now, i.e. much later, been introduced into laboratory practice. TPAA are nowadays widely employed in different chemical, molecular biological, and gene engineering aspects of nucleotide syntheses. It must be emphasised that TPAA are used not only for the synthesis of oligonucleotides but also of a wide variety of their P-analogues, which have extended the possibilities of research involving biopolymers.

The use of TPAA in the chemistry of nucleic acids has been described in a series of interesting monographs and reviews,[300-302,333] and in the present review we shall consider only the key aspects of the problem.

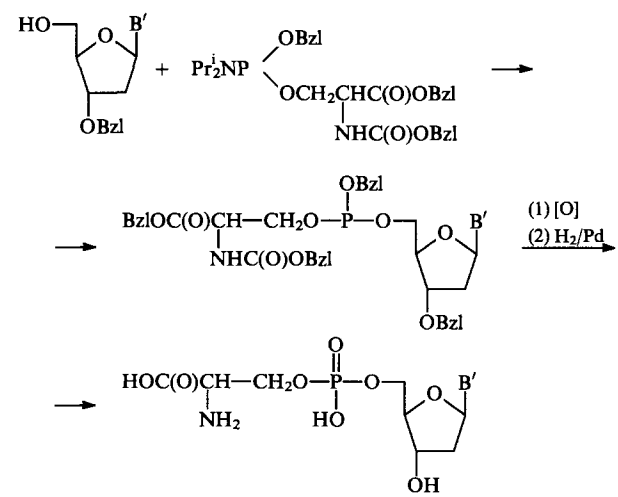
We may note that especially reactive phosphorazolides, such as the triazolides,[111,334-338] tetrazolides,[103,104,334,339-341] imidazolides†,[140-143,334,342] or the 'usual' TPAA, are frequently employed for the phosphorylation of deoxyribo- and ribo-nucleotides in the presence of acid activators — usually tetrazole,[300-302] diisopropylammonium tetrazolide,[106-114] 4,5-dichloroimidazole,[100,102] and certain others. In most studies, the phosphorylation is combined with oxidation reactions and manipulations involving protecting groups. As a rule, in contrast to the acid chloride method,[343] in the phosphoramide method the phosphorylation of nucleosides hardly involves their nitrogen-containing heterocycles. However, this version of the reaction is nevertheless possible in certain situations, which has been specially noted in the literature.[99,344]

We shall consider the most fruitful procedures for the phosphorylation of nucleosides using TPAA. In many instances, this reaction has served as the basis of the synthesis of nucleotides of especially great importance, for example the synthesis of phosphorylated azidothymidine (AZT):[345,346]

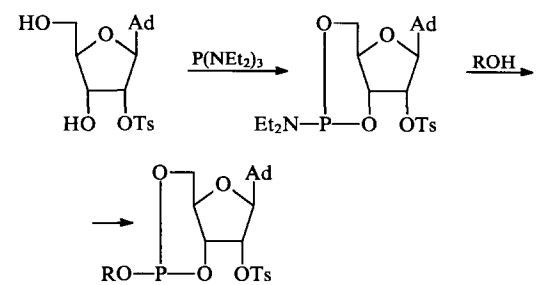


It has been suggested that nucleotide-sugars, including derivatives of sialic acids, which are of interest in the fight against AIDS, can be synthesised using TPAA.[347] In addition, it has been possible to synthesise compounds the molecules of which include the so called 'reporter' groups, for example aminoxyl radicals which assist in the performance of detailed structural studies on the functions of nucleotide compositions.[348,349]

Phosphorylation by TPAA which contain residues comprising aminoacids or other biomolecules have also attracted the attention of investigators. In this case, the synthesis leads to the formation of the link component of nucleoproteins or other complex systems. As an illustration we present the synthesis of the phosphoserine link.[350]



In view of the great importance of adenosine (thymidine) monocyclophosphates, studies have been made on the synthesis of their phosphite and phosphonite analogues.[332,351-357]

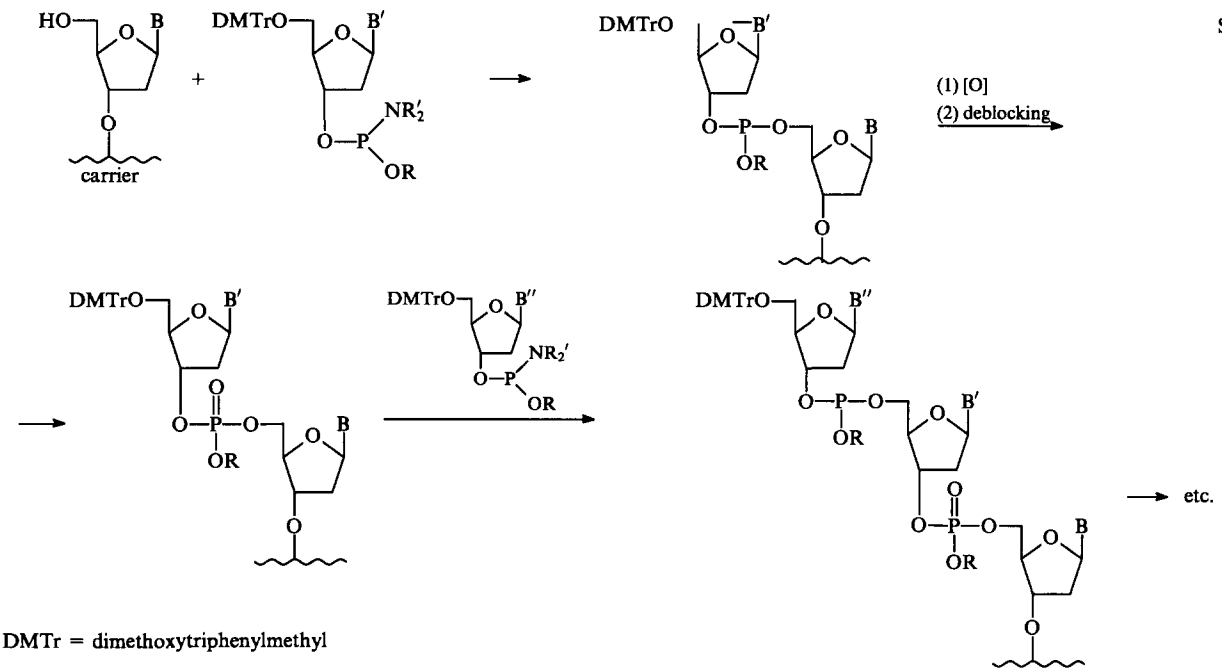


The compounds obtained were used in Arbuzov alkylation, oxidation, and other reactions.

Apparently most publications have been devoted to the use of phosphoramides to form the internucleotide linkage and especially for the synthesis of oligonucleotides by this procedure. The relatively easy and rapid methods for the synthesis of a wide variety of higher oligonucleotides have nowadays revolutionised a number of aspects of molecular biology and gene engineering.[300-302,333] The most widely used scheme for the synthesis of oligodeoxyribonucleotides is presented overleaf in a general form (Scheme 17).

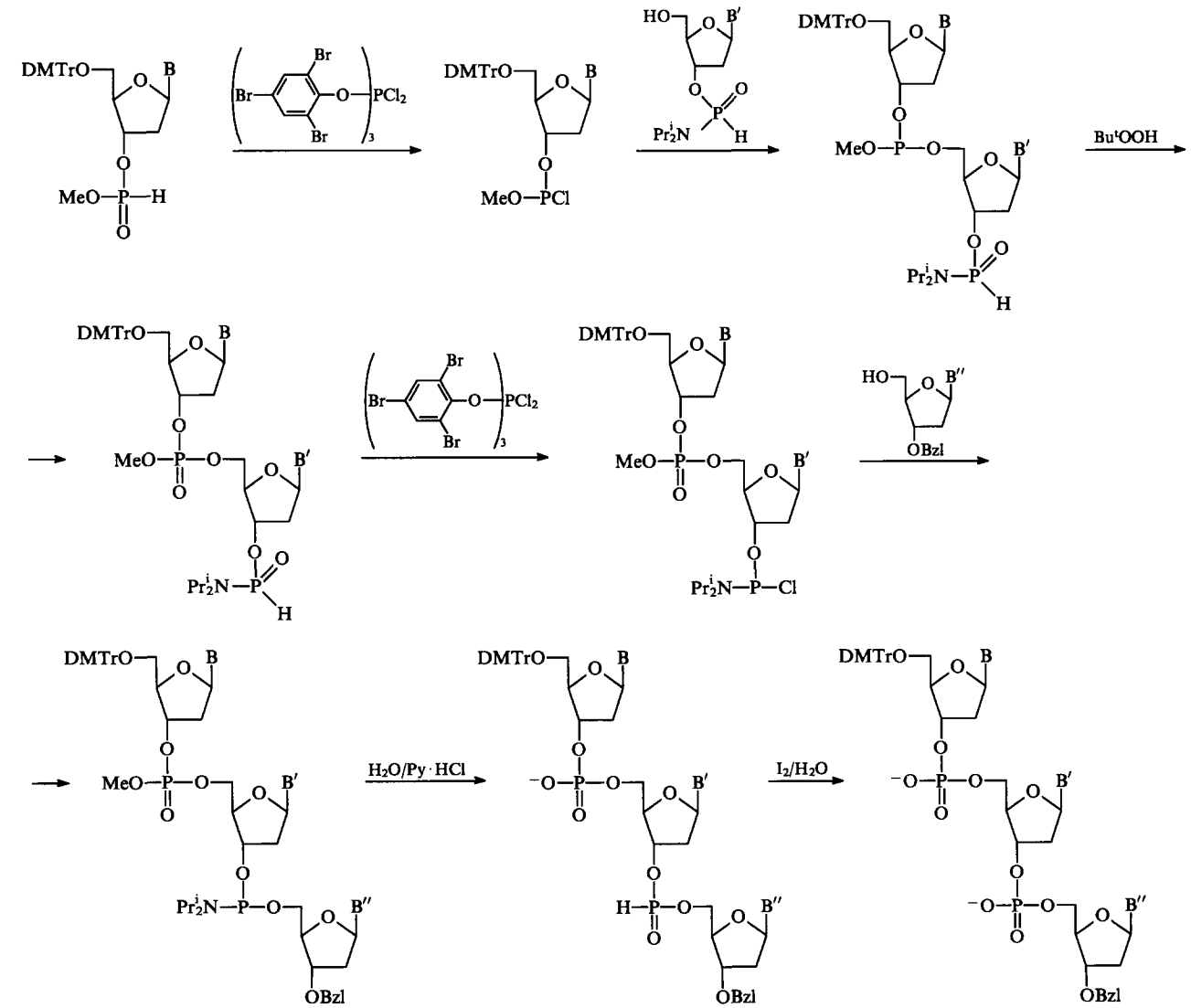
† The imidazolides are the most effective phosphorylating agents, but they are very sensitive to traces of moisture and are therefore unstable.

Scheme 17



DMTr = dimethoxytriphenylmethyl

Scheme 18



We may note that oligonucleotide condensations are most often carried out on solid carriers using automatic synthesisers which ensure a high process efficiency. It is sufficient to state that the typical phosphorylation step requires several minutes at 20 °C in these instruments. It is significant that nucleoside phosphoramidites, which are the principal reagents in the above condensations, have now become available as commercial preparations.[358, 359]

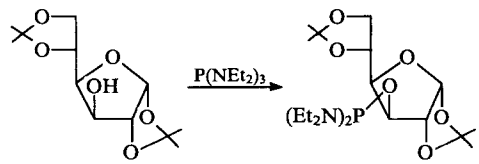
Oligoribonucleotides are also synthesised in accordance with a more complex programme.[104, 340, 359-361] It is very significant that, together with oligonucleotides, their phosphonate,[362-364] phosphoramidate,[106, 344, 365-367] phosphorothioate,[344, 365, 368-370] and phosphorodithioate[371-375] analogues can be obtained by the phosphoramidite method using the extensive procedures of the chemistry of trivalent phosphorus.

In molecular biology, the greatest interest attaches to solutions which make it possible to assemble from nucleoside phosphoramidites and diol oligomers [oligo(ethylene glycols) for example] complex constructions in which oligonucleotide and other chains are combined. A special review[302] published in 1993 was devoted to this current problem.

Finally, the phosphorylation of nucleosides by TPAA, supplemented by hydrolysis, sulfohydrolysis, or acidolysis, makes it possible to obtain primary[338, 376-383] and secondary[342, 367] nucleoside phosphites, phosphoramidites,[384] and phosphorothioites,[371] which are nowadays actively employed in a wide variety of hydrophosphoryl and thiophosphoryl syntheses. A new scheme for the synthesis of oligonucleotides with the aid of two different types of hydrophosphoryl compounds is presented (Scheme 18).[384]

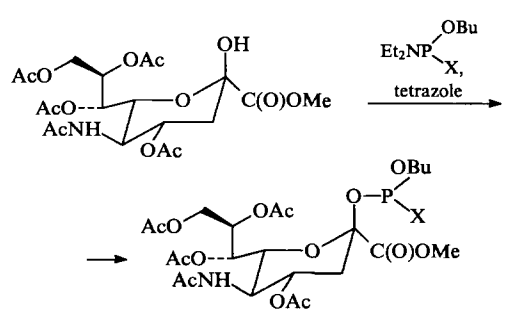
c. Phosphorylation of monosaccharides

Trivalent phosphorus acid esters and monosaccharides became the objects of independent systematic studies only after their synthesis began to be based on the phosphoramide method.[294, 298] TPAA of different nature readily phosphorylate monosaccharides the molecules of which contain a free alcoholic hydroxyl,[385, 390] for example, 1,2;5,6-diisopropylidene-D-glucofuranose.[386]



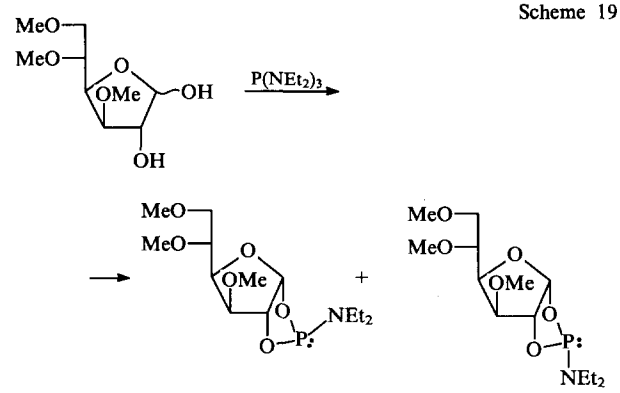
The products can be used subsequently as phosphorylating agents for various nucleophiles or can be introduced into a reaction with electrophiles (oxidants, alkyl halides, the simplest transition metal complexes, etc.).[185, 207, 391-393]

Monosaccharide derivatives are effectively phosphorylated also at the glycosidic hydroxyl,[394-396] whereupon the stereochemistry of the phosphorylated centre does not change during the reaction.[397] Such phosphorylation began to be extended to extremely complex systems in the most recent times. For example, β-sialyl phosphites and β-sialyl phosphoramidites have been obtained with the aid of TPAA.[347]

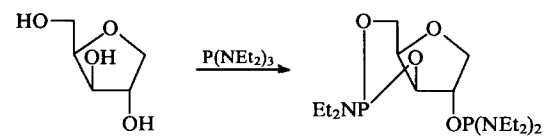


Treatment of monosaccharide derivatives containing two close hydroxyls can involve cyclophosphorylation. If one of the above hydroxyls is glycosidic, then stereochemical selection may take place (Scheme 19).[398]

Scheme 19

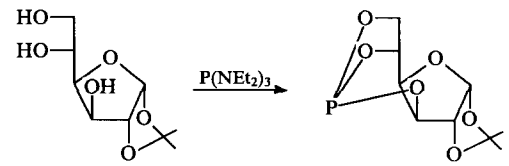


In this case, the selection concerns only the glycosidic and not the phosphoramide component of the system and therefore leads to the formation of two geometrical isomers the ratio of which may change on heating. The phosphorylation of triol systems takes place in different ways. Hydroxyls which are separated in space, as is the case in xylitan, are phosphorylated with formation of diphosphites.[392]

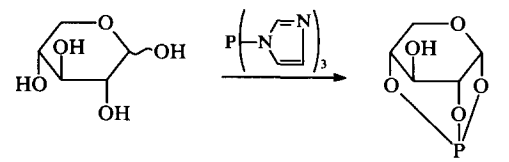


Such diphosphites began to be investigated as ligands for the preparation of chelate metal complex systems, which are likely to be used in enantioselective catalysis.[392, 393]

Monosaccharides—triols and tetraols with hydroxy-groups in close proximity—are phosphorylated particularly readily, being converted under these conditions into bicyclophosphites, for example:



(Ref. 399);



(Ref. 400).

As can be seen from the reaction presented, the latter case involves selective bicyclophosphorylation, the mode of which is determined by the steric characteristics of the sugar.

In the course of the development of the phosphoramide method for the bicyclophosphorylation of partly substituted and unsubstituted monosaccharides, a large group of skeletal systems was obtained. They proved to be interesting objects to study as regards stereochemistry, reactivity, and also practical use. The results of studies on the synthesis, steric organisation, and reactions of these new phosphaskeletal compounds have been recently summarised in a special review.[303]

d. Phosphorylation of other natural products

Aminoacids and peptides containing pentavalent phosphorus acid residues are widely investigated. Such studies involve the search for reactions based on new methods of organophosphorus chemistry.[401-403] The development of these investigations led to the study of the phosphorylation of carboxylic aminohydroxyacids by various TPAA, for example di(4-chlorobenzyl) *N,N*-diisopropylphosphoramidite[404] and benzyl bis(*N,N*-diisopropyl)phosphorodiamidite.[350,405] Subsequently the aminoacid phosphites obtained were introduced into oxidation reactions or were used as phosphorylating agents.

Steroid compounds have been relatively little studied in the phosphorylation reaction. It is noteworthy that studies were initiated recently on the phosphorylation of cholesterol and other steroids by various phosphorous amides.[95,406-409] Apparently there are good prospects for the synthesis from these derivatives of a wide variety of bioregulators, which can be addressed by means of the steroid component of the molecular system.

Simultaneously with steroids, α-tocopherol has been phosphorylated.[95,407,410,411] These studies are probably of interest for the development of research into bioantioxidants and other systems.

The specific phosphorylation of myoinositol[251-253,412-415] and its deoxy-derivatives[413,416] by phosphoramidite esters has clearly aroused interest recently. These studies were initiated mainly in connection with the development of effective methods of synthesis of complex phospholipids and the creation of cytostatic substances which are not targeted on DNA.[417]

TPAA have become the usual reagents for the phosphorylation of monosaccharides and other oligols in connection with the synthesis of the corresponding primary phosphites. The latter are successfully used nowadays in the synthesis of teichoic acids[418,419] and capsular polysaccharides.[420,421] Finally, TPAA have been used in the synthesis of a wide variety of biotin-containing phosphoramidites,[422-424] phosphoramidite derivatives of the alkaloid fagaronine,[425] and macrocyclic oligoester-oligodeoxynucleotide hybrid compounds in order to be able to 'recognise' DNA.[426] Unfortunately, the phosphorylation of alkaloids, a wide variety of plant phenols, terpenoids, and other polyfunctional natural products with the aid of TPAA has been scarcely investigated.

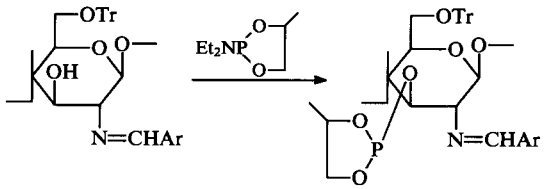
5. Trivalent phosphorus amides in the synthesis of phosphorus-containing polymers

TPAA have also begun to be used in macromolecular chemistry. The studies in this field can be divided into two aspects: (1) the introduction of phosphorus into hydroxylated polymers; (2) a polycondensation process with participation of diols and other oligools.

The first aspect has been investigated in greatest detail in relation to natural polymers. Thus it has been shown that anhydrous cellulose in a heterogeneous system is phosphorylated on heating to 80–120 °C by phosphorous hexaethyltriamide, various phosphoramidites, and also diethylphosphinous diethylamide.[427,428] In the reaction with the last reagent, it was possible to follow the degree of substitution and to achieve the degree of phosphorylation $\gamma = 180$. It is of interest that, in contrast to the initial cellulose, the phosphinite obtained is soluble in certain organic solvents.

The best phosphorylating agents proved to be the azolides of phosphorous and diphenylphosphinous acids, which modify cellulose at 20–50 °C with attainment of high degrees of phosphorylation.[429] The products obtained in the interaction with solutions of palladium chloride or bis(π-allylpalladium chloride) afford heterogeneous hydrogenation subcatalysts. Such systems exhibited a high catalytic activity in the hydrogenation of styrene under mild conditions.[429] A very important feature is that the above polymeric complexes are more effective than the complexes obtained using the chlorides of the corresponding trivalent phosphorus acids.[430]

The phosphorylation of chitosan derivatives soluble in organic solvents has been achieved very recently.[431]



The above communication is the first on the phosphorylation of chitosan in general. Among other natural hydroxylated polymers, only lignin was phosphorylated by TPAA.[432] The properties of the esters obtained have not been studied in detail.

There have been indications also of the phosphorylation by TPAA of synthetic hydroxylated oligomeric and high-molecular-mass resins[433-435] and poly(allyl alcohol).[436] The products synthesised have been investigated as regards the formation of polymeric pesticides and in other promising technical applications.[437]

The second aspect of the use of TPAA in macromolecular chemistry includes studies on the phosphorylation of glycols[244] and dihydric phenols[438] by equimolecular amounts of phosphonous diamides and alkyl phosphorodiamidites. Unfortunately, this outwardly simple instance of polycondensation is supplemented by the simultaneous formation of monophosphorus-containing rings[244] and the corresponding macrocyclic systems,[438] as a result of which the molecular masses of the products are low. Presumably the use of the latest generation phosphoramides, for example phosphorus(III) acid azolides, makes it possible to carry out the polycondensation effectively at low temperatures, avoiding thereby the conversion of linear systems into cyclic systems.

$$n\,R{-}P(NEt_2)_2 + n\,HOR'OH \longrightarrow$$

$$\longrightarrow -(-R'{-}O{-}\underset{\displaystyle R}{\overset{\displaystyle |}{P}}{-}O{-})_n + 2n\,HNEt_2$$

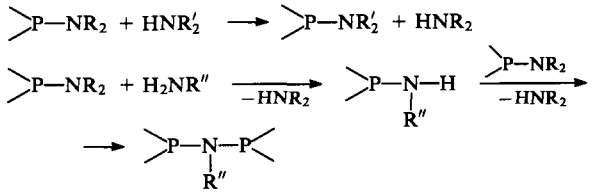
Hexitols[288] as well as methyl glucoside[439] have been used in polycondensations with TPAA. For selected reactant ratios, under the conditions discovered, oligomers and high-molecular-mass phosphorus-containing polymers were obtained in such cases. They are of practical interest, for example as additives to lubricants and as stabilisers.[440]

Overall, the field under consideration has not yet been adequately developed in view of the complications noted above and the fact that the attention of phosphorylation specialists has been to a large extent diverted to the striking problems posed by molecular biology and gene engineering. However, the logic of the development of the chemistry of trivalent phosphorus and macromolecular chemistry leads us to execute the tasks associated with the second stage in the development of the problem. This also arises from the needs of related sciences, especially coordination chemistry. Indeed, despite all the attention devoted to macromolecular ligands and complexes based on them, the very promising polyphosphite, phosphoramidite, and phosphonite ligands have been neglected nowadays. The optimum procedures for the synthesis of such ligands may be based primarily on the achievements in the chemistry of TPAA.

III. Phosphorylation of amines

The alcoholysis, phenolysis, and aminolysis of TPAA are in principle related reactions. Furthermore they are comparable as regards their effectiveness and experimental conditions. However, preliminary analysis of these reactions indicates also differences between them. Firstly, in contrast to the alcoholysis and phenolysis, the aminolysis can include not only single but also

double phosphorylation steps when secondary and primary amines are used as substrates‡. Secondly, the structures of the intermediates in the reactions enumerated differ significantly. In the alcoholysis and phenolysis, the leaving and entering groups are based on different atoms (nitrogen and oxygen), whilst in the case of aminolysis they are based on the same atoms. This situation hinders the elucidation of the pathway followed in the migration of the hydrogen forming part of the composition of the intermediate, this being particularly difficult when several hydrogen atoms, occupying different positions in space, are attached to the nitrogen atom.



These factors have apparently contributed to the delay in research into the transamination of TPAA behind the study of the corresponding reactions with alcohols and phenols. Nevertheless, the transamination methods already employed made it possible to solve a series of interesting and promising problems, especially in the chemistry of complex phosphacyclic compounds and nitrogen-containing natural products.

1. The history of the problem. Principal features of the reactions of trivalent phosphorus acid amides with amines

The first mentions of the possibility of the interaction of TPAA with amines leading to transamination date back to the end of the 1950s and the beginning of the 1960s.[135,441] Initial studies were on the simplest instances of transamination and were not associated with the solution of complex scientific problems. In the experiments, the low-boiling amine (usually diethylamine), which was one of the reaction products, was as a rule distilled away.[15,36,123,124,442–446] Approximately the same results were obtained in studies with the amides of phosphinous, phosphonous, and phosphorous acids.[447] The di- and tri-amides of these acids were used for complete and partial transamination. Mono- and polyfunctional amines of different chemical nature were selected as the substrates.

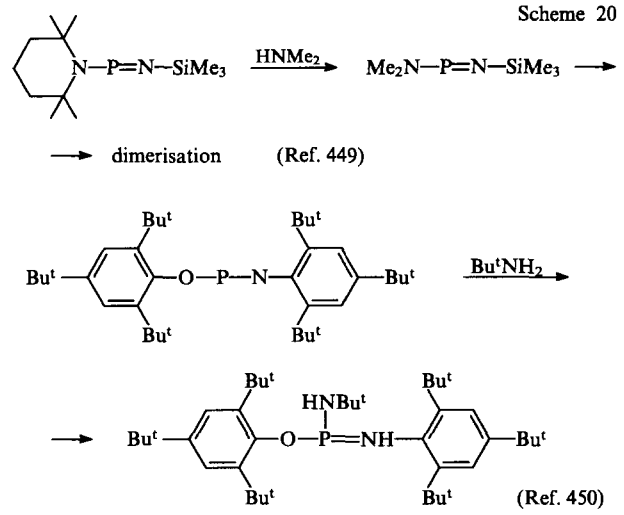
A high reactivity of the phosphoramide group was recorded in all the investigations. In this connection, we may note that even phosphorodifluoridous dimethylamide interacts with higher secondary amines via this group and not the phosphorofluoridite group.[448]



Studies on the interaction of primary and secondary amines with phosphenimidous compounds have been initiated recently. Various possibilities in the cleavage of the P–N σ- and π-bonds have been demonstrated in this connection: either substitution of a secondary amino-group[449] or the addition of an amine to the multiple bond (Scheme 20).[450] When an excess of the amine is used, more far reaching transamination processes can also occur.

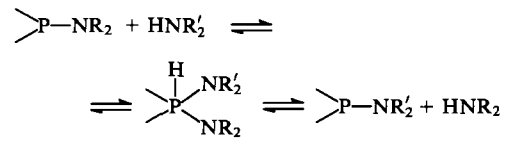
‡ Generally speaking, triple steps are also possible when ammonia is used as a substrate, but such reactions have so far been very little investigated.[441]

Scheme 20



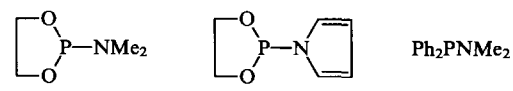
2. The chemistry of the transamination of trivalent phosphorus acid amides

On the basis of their own observations or merely on the grounds of general consideration, many investigators have expressed views concerning the dependence of the mechanism of the transamination of TPAA and of the rate of reaction on the structure of the reagent and the substrate. A mechanism involving addition of the phosphoramide to the amine with formation of a phosphorane and decomposition of the latter to the products detected has been proposed.[12,41,180,451,452]



Mechanisms involving a four-centre transition state[23,24] and direct nucleophilic substitution at phosphorus have also been discussed. The second variant is most common in the usual reactions. It has been related recently to the experimental observation of acid catalysis—the acceleration of the phosphorylation reaction by the addition of amine hydrochlorides[15,22,23,36,189] and acids.[38]

Convincing arguments in support of the nucleophilic substitution mechanism were first put forward in a study[33] in which the influence of the basicity of the entering and leaving amines on the rate of reaction was estimated. The authors investigated the interaction of ethylene *N,N*-dimethylphosphoramidite **38** with amines having different basicities and observed an increase in the rate of phosphorylation with increase in the basicity of the reacting amine. Thus, on passing from morpholine (pK_a = 8.70) to pyrrolidine (pK_a = 11.27), the rate increases, while in attempted reactions with *N*-methylaniline (pK_a = 4.85) and pyrrole (pK_a = −0.27), dimethylamine (pK_a = 10.77)§ is not displaced. Accordingly pyrrolidine displaces pyrrole more readily in experiments with ethylene phosphoropyrrolidite **39** than dimethylamine in experiments with the amide **38**.



38 **39** **40**

We may also point to the higher reactivity of the amide **38** than that of diphenylphosphinous dimethylamide **40**, which is consistent with the general principles of nucleophilic substitution at a trivalent phosphorus atom.[453] Unfortunately, the results of

§ The values of pK_a in water at 25 °C are quoted.

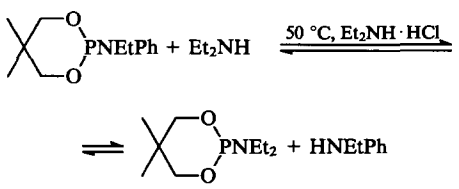
the transamination of the amide **38** were not obtained under equilibrium conditions, while those with the amide **39** were obtained under equilibrium conditions, so that strictly speaking their comparison is not valid. The difficulties in the interpretation of the results obtained with the pyrrolidite **39** have been noted also by other investigators.[31] We may note that the problem of the equilibrium nature of the transamination reaction has not been duly taken into account also in studies carried out in other laboratories (see, for example, Batyeva et al.[23]). Mosbo's study,[38] in which the transamination of the amino-derivatives of 1,3,2-dioxa- and 1,3,2-diaza-phosphorinanes was rigorously examined, is therefore especially important.



X = O, NMe; R = Et, $R_2 = (CH_2)_4$

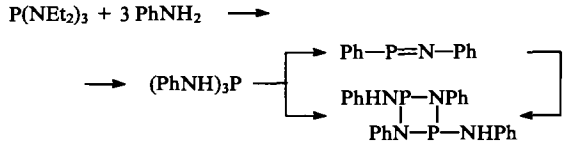
It was shown in this series of reactions that equilibrium can be attained when aminolysis is carried out in both forward and reverse directions. The conclusion that the high basicity of the amine substrate is important for the substitution reaction was confirmed. The results of this investigation do not confirm the necessity for the intermediate conversion of the initial amide into the corresponding acid chloride with subsequent phosphorylation by the chloride of the amine (substrate).[22,23,454]

The acid chloride concept has also been rejected in another study[189] where acid-catalysed aminolysis was investigated at the kinetic level.



The occurrence of catalysis was clearly demonstrated in this investigation and the dependence of the rate of reaction on the basicity of the amine was confirmed, but the influence of the solvent polarity on the rate of phosphorylation was not observed. In addition, the ability of the substrate, taken in excess, to inhibit the phosphorylation reaction was established. Thus, the study of the transamination of TPAA at the kinetic level established certain characteristics of this process, which distinguish it from the corresponding alcoholysis reactions.

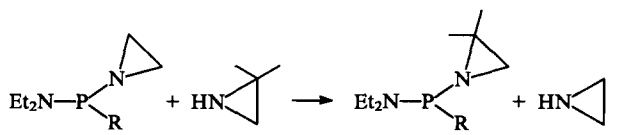
Comparison of the rates of phosphorylation and transamination of TPAA made it possible to make definite preparative recommendations. Thus it became clear that the best phosphorylating agents among the available phosphoramides are the anilides (*N*-alkylanilides).[127,189,209,447,455] We may note that the dialkylamides can react with aniline but only on heat treatment and with distillation of the dialkylamine evolved,[51,53] which shifts the equilibrium in the desired direction. The reaction considered is experimentally very complex and requires careful maintenance of constant phosphorylation conditions. Otherwise, elimination of self-phosphorylation reactions take place.[51,53,456-459]



The phosphorylation of dialkylamines by phosphorazolides merits attention.[145-148] The effectiveness of phosphorazolides increases in the sequence phosphinazolidite > phosphorodiamidous azolide > phosphorazolidite diester. The reverse reactions, i.e. the interaction of phosphorus acid dialkylamides with azoles, do not always take place. For example, they do not occur in the interaction of trivalent phosphorus acid diethylamides with imidazole.[145] The reason why this autocatalytic phosphorylation is impossible is the fact that the reaction involving the abstraction of a proton together with the imidazole residue by the intermediate is clearly preferred. We may note, however, that the problem of the chemical behaviour of phosphorus acid azolides, which are very unusual substances, has not yet been duly developed.

The rates of reactions of phosphorazolides under consideration depend definitely on the type of substituents at the phosphorus atom. Alkoxides ensure the maximum rates and alkyls the minimum rates,[145-148] which is also consistent with the concept of P-nucleophilic substitution. Nevertheless, a detailed description of the mechanism of the transamination of TPAA in the presence of acid catalysts is lacking in the literature. One may postulate that it is in principle analogous to the description of the alcoholysis of TPAA but differs by the migration of a proton between the linked nitrogen centres.

The problem of steric factors in the phosphorylation of TPAA has also been discussed in the literature, contradictory results being published. Thus the preferential phosphorylation of amines with less bulky substituents at the nitrogen atom has been reported.[38] On the other hand, the following reaction has been described:[445]

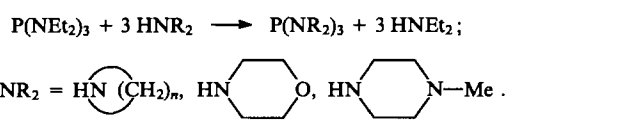


Thus our knowledge about the characteristic features of the transamination of TPAA requires further development.

3. The use of the transamination of trivalent phosphorus acid amides for the purposes of fine organic synthesis

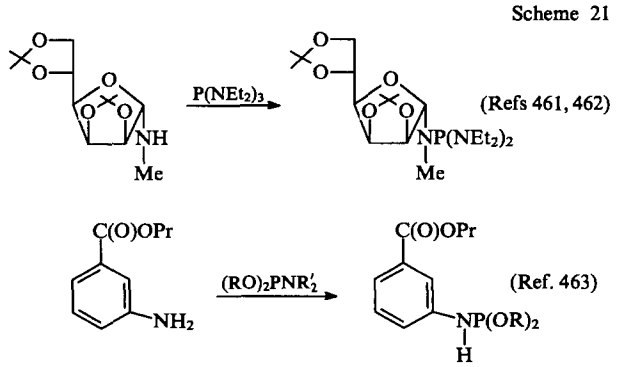
a. Phosphorylation of higher and functionalised primary and secondary amines

A useful preparative method of synthesis of higher and other complex phosphoramides is the aminolysis of the simplest representatives of substances of this class. Thus phosphorous hexamethyl(ethyl)triamides, which are readily available commercial products, perform the function of key substances in the synthesis of various more complex triamides, for example:[123,124,460]



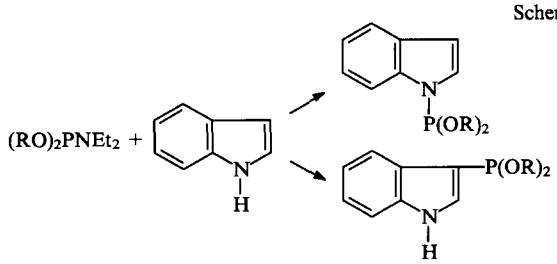
Complex asymmetric systems, including phosphorylated glucosylamines[461,462] and derivatives of *m*-aminobenzoic acid (Scheme 21),[463] can also be obtained in this way.

Scheme 21



Transamination may be supplemented by C-phosphorylation, as happened in experiments with indole (Scheme 22).[464] In the case of 3-mercaptoindole, phosphorylation can occur both at the nitrogen and at the sulfur depending on the conditions.[465]

Scheme 22



Higher primary α,ω-alkylenediamines are smoothly phosphorylated by *N,N*-dialkylphosphoramidites with formation of phosphorodiamidites which are difficult to obtain in other ways (Scheme 23).[447]

Scheme 23

$$2\,(RO)_2PNEt_2 + H_2N(CH_2)_6NH_2 \longrightarrow$$

$$\longrightarrow (RO)_2PNH(CH_2)_6NHP(OR)_2 + 2\,HNEt_2$$

For equimolecular reactants oligomeric or polymeric phosphoramidites may be formed.[442] This aspect has been investigated for cystamine.[444]

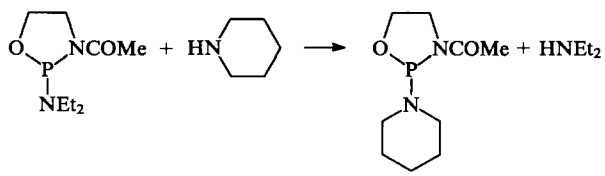
$$n\,RP(NEt_2)_2 + n\,H_2NCH_2CH_2SSCH_2CH_2NH_2 \longrightarrow$$

$$\longrightarrow \left[\begin{array}{c} \\ PHNCH_2CH_2SSCH_2CH_2NH \\ | \\ R \end{array}\right]_n$$

R = Alk, OAlk, Et_2N.

When phosphorous hexaethyltriamide is used, it is possible to obtain network and not linear polymers. All these compounds are of interest as long-acting radioprotectors [radiation protectives? Ed.].

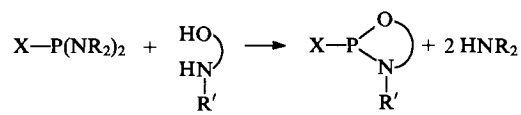
The result of transamination using phosphoramides with partially functionalised amino-groups, which are usually inert, is very interesting.[191]



There are data on the reactions of phosphoramides, the structures of which incorporate a polymeric amine having a N–P bond, with a nucleoside phosphite oligomer. It has been established that the oligonucleotide unit can be conveniently removed from the support in many instances by treatment with an excess of an amine, for example tetrazole.[466,467]

b. Phosphorylation of aminoalcohols and *o*-aminophenols

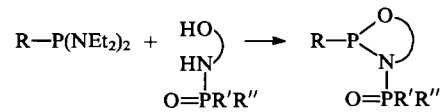
As mentioned above, the phosphorylation of tertiary aminoalcohols by treatment with TPAA leads to the formation of tertiary phosphoramidites and related compounds. The corresponding secondary aminoalcohols with functional groups in the 1,2- and 1,3-positions, including derivatives of 1,2-ethanolamine,[162,163,165,203,229,468–478] 1,3-propanolamine,[168,186,479–481] ephedrine,[473,482–486] prolinol,[484,487] etc. usually undergo phosphacyclisation on reacting with trivalent phosphorus acid diamides and triamides.



Aminomercaptans,[488] 1-alkylamino-1-deoxysugars,[489] and 3-imino-1-*N*-hydroxyethylpyrazoline[490] phosphacyclise in a similar manner.

Such reactions of aminoalcohols with TPAA are of extensive synthetic importance and are actively employed in the solution of many scientific and technical problems. We may point to the synthesis of phosphacyclic ligands for metal complex catalysis,[393,491,492] phospholipid systems (see the review by Nifant'ev and Predvoditelev[304]), and phosphacyclane derivatives of sugars.[303]

N-Phosphorylated aminoalcohols react similarly with TPAA.[194]

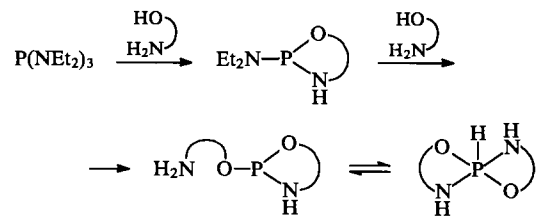


We may note that this scheme describes reactions for R = Alk or $NAlk_2$. When phosphorodiamidites are used, mono-*O*-phosphorylation turns out to be more probable.[194]

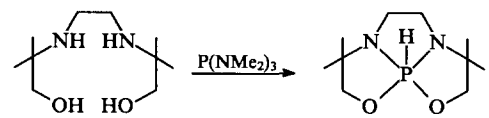
$$ROP(NEt_2)_2 + HO(CH_2)_3NHP(O)(OR')_2 \longrightarrow$$

$$\longrightarrow \begin{array}{c} NEt_2 \quad\quad O \\ | \quad\quad\quad \| \\ ROPO(CH_2)_3NHP(OR')_2 \end{array}$$

Many primary and certain secondary 1,2- and 1,3-aminoalcohols interact in a more complex manner with phosphorous triamides for a reactant molar ratio of 2 : 1; viz. 2-amino-1,3,2-oxazaphospholanes (phosphorinanes) are formed in the first stage of the synthesis and are then converted into phosphoramidites. The latter can be fully or partly converted into hydrospirophosphoranes (ring–chain tautomerism).[124,245,246,472,482,493–500]

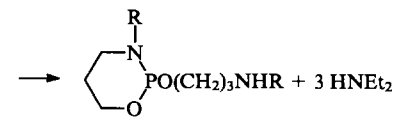


Similar, but this time tricyclic, hydrospirophosphoranes may be formed also in the phosphorylation of bisaminoethanols.[501]

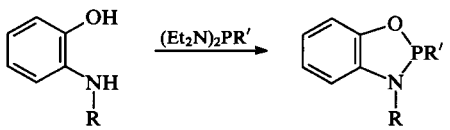


The ease of formation of the hydrospirophosphoranes is in many respects determined by the structure of the aminoalcohols. Vicinal, especially primary, aminoalcohols participate vigorously in this process. Secondary 1,3-aminoalcohols do not form spirosystems.[168]

$$P(NEt_2)_3 + 2\,HO(CH_2)_3NHR \longrightarrow$$

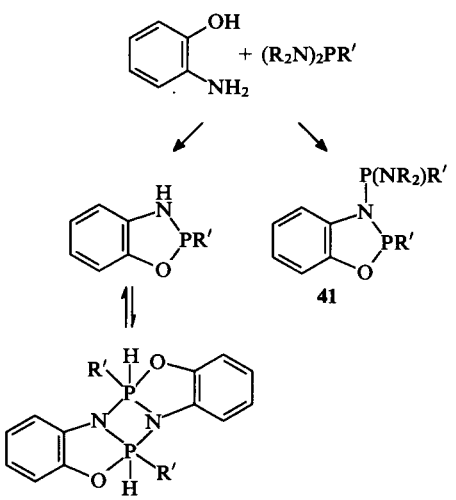


TPAA with two and three amino-groups effectively phosphorylate *o*-*N*-alkylaminophenols with formation of 4,5-benzo-1,3,2-oxazaphospholanes.[502,503]

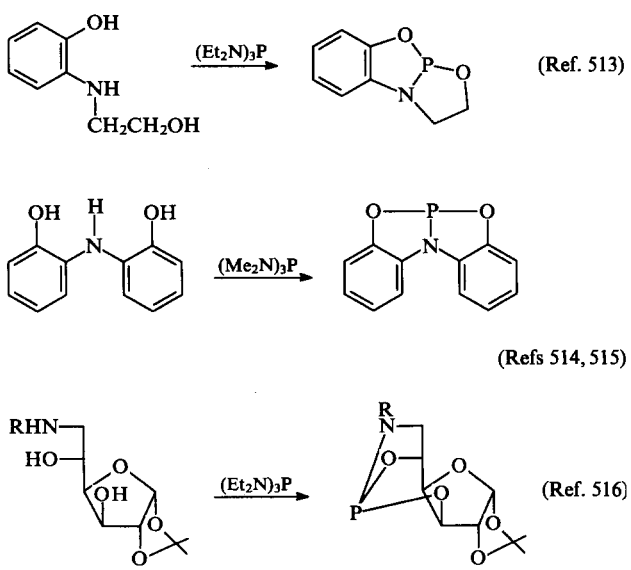


o-Aminothiophenols[229,504–507] and derivatives of *N*-acylaminophenols[508] are cyclophosphorylated in a similar manner.

Depending on the phosphorylation conditions and the reactant ratio, *o*-aminophenol itself can be either converted, in its reactions with trivalent phosphorous diamides, into a benzoxazaphospholane, which is capable of dimerising, or it affords a diphosphorus product.[509–512]



Aminophenols, namely *o*-(*N*-β-hydroxyethylamino)phenol[513] and di(*o*-hydroxyphenylene)amine[514,515] as well as 6-amino-6-deoxy-1,2-isopropylideneglucofuranose and 3-amino-3-deoxy-1,2-isopropylideneglucofuranose[516] are phosphorylated in an interesting manner. Rigid condensed systems are formed in such cases.



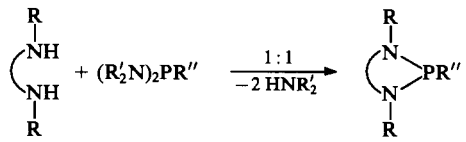
(Ref. 513)

(Refs 514, 515)

(Ref. 516)

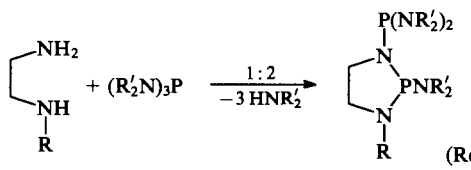
c. Phosphorylation of di, tri-, and tetra-amines

Alkylenediamines (1,2-alkylenediamine[517–519] and 1,3-alkylenediamine[520–522]), which include diprimary, primary-secondary, and disecondary representatives, are effectively phosphorylated by phosphorous and phosphonous diamides and triamides; in a few instances, the reaction has been achieved with 1,4-alkylenediamines.[523–527]

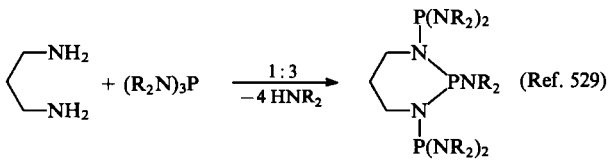


R = H, Alk.

When two or three molar amounts of the phosphoramide relative to the diamide are used, it is possible to obtain diphosphaheterocycles[518,519,528] and triphosphaheterocycles.[529]

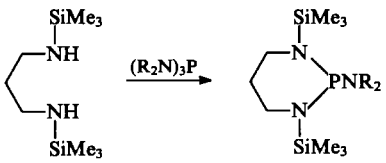


(Refs 518, 519, 528)

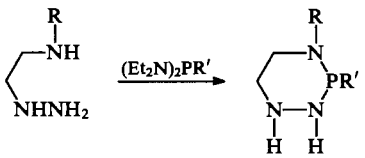


(Ref. 529)

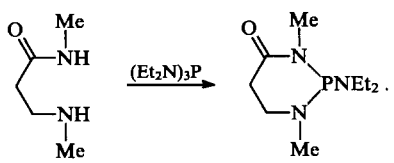
1,3-Disilylamines enter similarly into such reactions.[530]



It is interesting that β-aminoethylhydrazines can undergo the same phosphacyclisations, affording triazaphosphorinanes.[18]

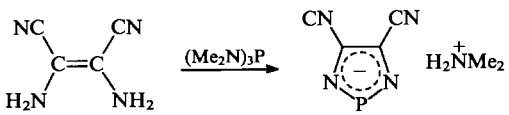


Certain aminoamides also enter into the phosphacyclisation reaction, for example:[531,532]

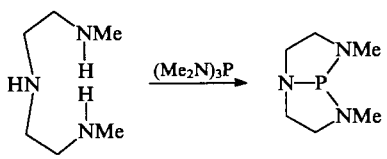


In the phosphacyclisation of diaminodicyanoethylene by phosphorous triamide, a stable anion may be formed—the isoelectronic 1,3,2-diazaphospholane (Scheme 24).[533]

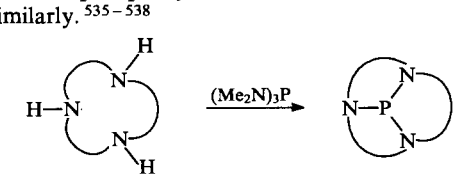
Scheme 24



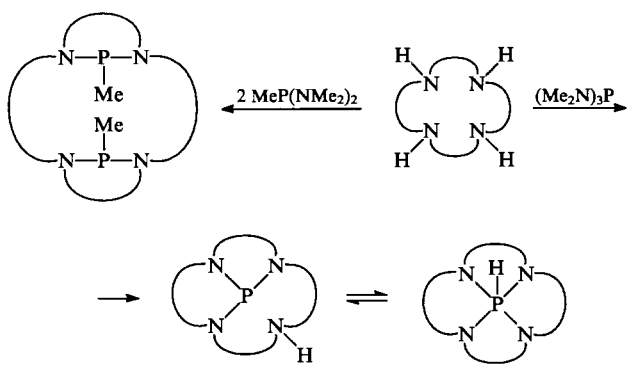
Mention must be made of the study of the phosphorylation of linear and alicyclic triamines and tetraamines, to which much attention has been devoted recently. It has been established that reaction of 2,5,8-triazanonane with an equimolar amount of phosphorous hexamethyltriamide affords a condensed bicyclic compound.[534]



The phosphorylation of trialkylenetriamines takes place similarly.[535-538]

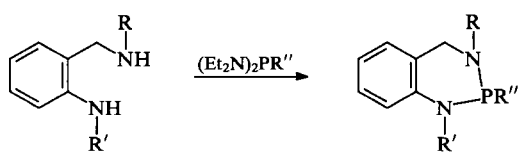


The phosphorylation of alkyenetetraamines has been studied even more extensively.[539-543]



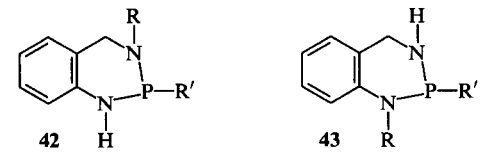
An interesting case of prototropism, leading to a symmetrical hydrospirophosphorane, has been observed in this series of studies. The position of the equilibrium described depends on the nature of the solvent and of the alkylene group linking the nitrogen atoms into a single system.

Aliphatic-aromatic diamines have been investigated even more vigorously in cyclophosphorylation by TPAA. Thus *N,N'*-dialkyl(aryl)-2-aminobenzylamines react with phosphorous diamides and triamides, forming readily and in high yields 1,3-disubstituted 4,5-benzo-1,3,2-diazaphosphorinanes.[544-547]



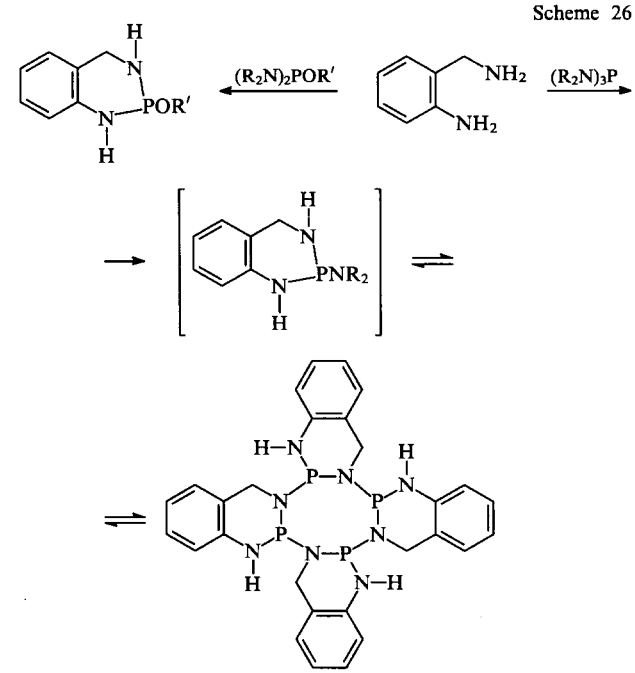
There are two types of 2-aminobenzylamines monosubstituted at the nitrogen atom. Each has been successfully phosphacyclised with formation of 4,5-benzo-1,3,2-diazaphosphorinanes of two classes—**42** and **43** (Scheme 25).[544-547]

Scheme 25



Unsubstituted 2-aminobenzylamine also reacts with TPAA. Phosphorodiamidite esters give rise in this case to 2-alkoxy-4,5-benzo-1,3,2-diazaphosphorinanes, while phosphorous triamides afford 2-dialkylamino-4,5-benzo-1,3,2-diazaphosphorinanes, which immediately undergo cyclotetracondensation (Scheme 26).[548]

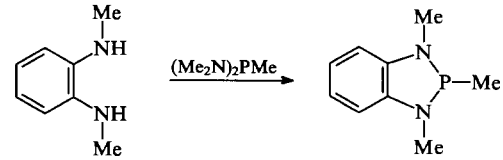
Scheme 26



The high efficiency (yield about 90%) and regiospecificity of the reaction [products containing only aminobenzyl nitrogen atoms in the tetraazaphosphacyanogen (tetraazatriphosphacyclooctane? Ed. of translation) ring] is striking. X-Ray diffraction data showed that a molecule of the product consists of a symmetrical crown in which the nitrogen atoms lie in a plane parallel to the plane of the phosphorus atoms. One can postulate that this and similar systems will be of considerable interest for the synthesis of new coordination systems.

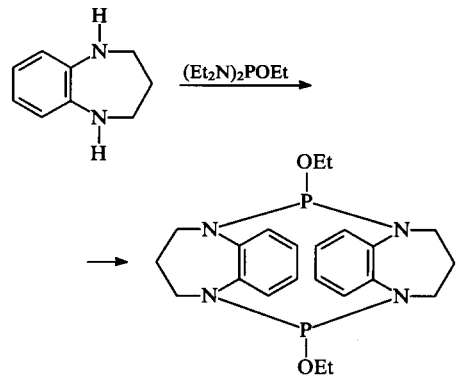
It is essential to note that as a rule all the phosphacyclisations examined above are more efficient than the corresponding reactions with phosphorous acid chlorides.

We shall now turn to the phosphorylation of aromatic diamines. Secondary *o*-diaminobenzenes interact readily with TPAA.[549]



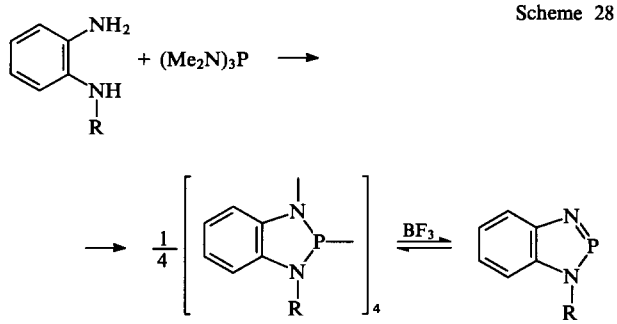
In the case of the cyclophosphorylation of *o*-phenylenediamine, in the molecules of which the nitrogen atoms are linked via a 1,3-propylene bridge, the process is more complex and leads to the formation of a diphosphorus system (Scheme 27).[550]

Scheme 27



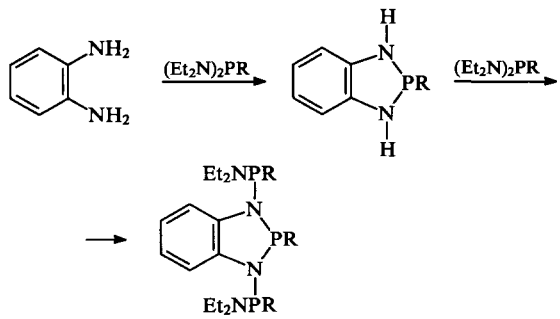
Primary-secondary diamines afford tetramers on reaction with phosphorous acid hexamethyltriamide (Scheme 28).[508,551-553]

Scheme 28

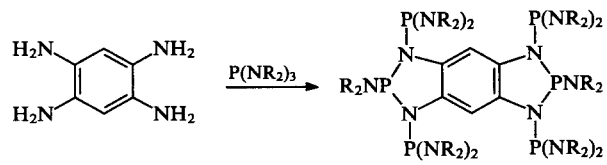


On heating with boron trifluoride, this tetramer decomposes. The monomer has been detected in solution by ^{31}P NMR spectroscopy.

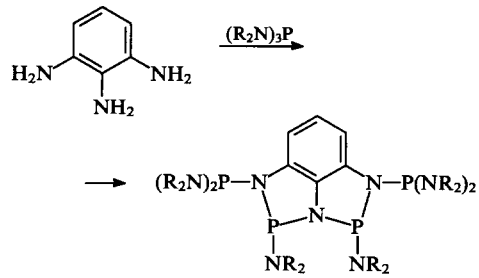
On phosphorylation with phosphorous diamides and triamides, unsubstituted *o*-phenylenediamine can give rise to the usual phosphacycles or the products of their additional phosphorylation at the nitrogen atom depending on the reaction conditions and the reactant ratio.[529,554-557]



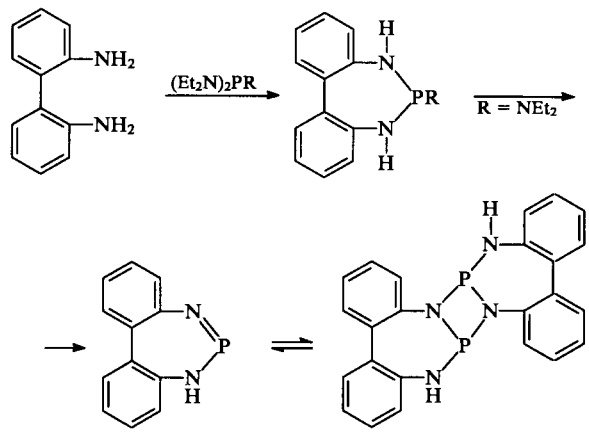
The second phosphorylation pathway has also been achieved in a study with 1,2,4,5-tetraminobenzene.[558]



We may also note that 1,2,3-triaminobenzene affords a phosphacyclic system of a different chemical nature in an analogous situation.[558,559]



The interaction of a more complex aromatic amine — *o,o'*-diaminobiphenyl — with phosphorous diamides and triamides affords 4,5,6,7-dibenzo-1,3,2-diazaphosphorinanes.[560]



R = OAlk, NEt_2

When R = NEt_2, the primary product can undergo the elimination of the amine with formation of a derivative of dicoordinate phosphorus, which apparently dimerises as a result of the regular 1,2;1,2-cycloaddition.[560]

IV. Conclusion

It is seen from the data presented that TPAA have found extensive application for the phosphorylation of alcohols, phenols, and amines of a wide variety of chemical types. Virtually all the types of these proton-donating nucleophiles have already served as substrates in the synthesis of derivatives of phosphorous, phosphonous, and phosphinous acids. The success of the syntheses is apparently due to the experimental formulation of the reactions and primarily the use of optimum catalysts (activators) and solvating agents.

The discovery of a high reactivity in TPAA brought modern organophosphorus chemistry closer to other chemical disciplines and eliminated the barriers which have traditionally arisen between them. The most important result of such a mutual approach has been a radical alteration in strategy for the synthesis of natural products, including the most complex of these, namely nucleic acids and phospholipids. Furthermore, there has been a change in the principles governing the design of phosphorus-containing skeletal compounds and other complex phosphorus heterocycles. There has been a revival also in other interdisciplinary fields.

Nevertheless, the considerable chemical potential of TPAA has not yet been fully realised. It is sufficient to state that studies on the application of these reagents in macromolecular chemistry, both for the modification of polyfunctional polymers and the polycondensation of oligools and amines, have been dealt with only in outline. Nevertheless we may state that certain fundamental problems, the solution of which will apparently lead to useful recommendations, have been found in this field.

It has now been established that, apart from the nucleophiles already named, TPAA can readily phosphorylate also other compounds — various derivatives of acids, mercaptans, phosphines, transition metal hydrides, etc. They give rise to interesting results in reactions of other types as well. All this makes TPAA valuable reagents for fine organic synthesis.

References

1. BRD P. 1 079 022; *Ref. Zh. Khim.* 18 L 94P (1961); BRD P. 1 098 940; *Ref. Zh. Khim.* 16 N 181P (1963)
2. M Furdik, J Mašek *Acta Fac. Rerum. Nat. Univ. Comen. Chim.* **6** 611 (1961)
3. K A Petrov, E E Nifant'ev, T N Lysenko, V P Evdakov *Zh. Obshch. Khim.* **31** 2377 (1961)
4. D A Armitage, M J Clark, A C Kinsey *J. Chem. Soc., Ser. C* 3867 (1971)
5. B A Arbuzov, N I Rizpolozhenskii, M A Zvereva *Izv. Akad. Nauk SSSR, Ser. Khim.* 1021 (1955)
6. S Goldschmidt, H Krauss *Liebigs Ann. Chem.* **595** 193 (1955)
7. R Burgada, D Berbard *C. R. Acad. Hebd. Seances Sci., Ser. C* **273** 164 (1971)
8. S A Terent'eva, M A Pudovik, A N Pudovik, Kh E Kharlampidi *Zh. Obshch. Khim.* **45** 2559 (1975)
9. S A Terent'eva, M A Pudovik, A N Pudovik *Izv. Akad. Nauk SSSR, Ser. Khim.* 1897 (1976)
10. R Burgada, L Lafaille, F Mathis *Bull. Soc. Chim. Fr.* 341 (1974); L.Lafaille, F Mathis, J Barrans *C. R. Hebd. Seances Acad. Sci., Ser. C* **285** 575 (1977)
11. M T Boisdon, C Malavaud, F Mathis, J Barrans *Tetrahedron Lett.* **18** 3501 (1977)
12. M A Pudovik, S A Terent'eva, A V Il'yasov, A N Chernov, A A Nafikova, A N Pudovik *Zh. Obshch. Khim.* **54** 2448 (1984)
13. M Haddad, Th N'Gando, M'Pondo, C Malavaud, L Lopez, J Barrans *Phosphorus Sulfur* **20** 333 (1984)
14. E E Nifant'ev, N L Ivanova *Vestn. Mosk. Univ., Ser. II: Khim.* 104 (1968)
15. E E Nifant'ev, A I Zavalishina, M R Ter-Ovanesyan *Zh. Obshch. Khim.* **39** 360 (1969)
16. E E Nifant'ev, N L Ivanova, I V Fursenko *Zh. Obshch. Khim.* **39** 854 (1969)
17. B E Ivanov, S V Samurina, S S Krokhina, L A Valitova, in *Khimiya i Primenenie Fosforoorganicheskikh Soedinenii (Tr. V Konf.)* [The Chemistry and Applications of Organophosphorus Compounds (Proceedings of the Fifth Conference)] (Moscow: Nauka, 1974) p. 119
18. G S Gol'din, S G Fedorov, G S Nikitina, N A Smirnova *Zh. Obshch. Khim.* **44** 2668 (1974)
19. E S Batyeva, V A Al'fonsov, A N Pudovik *Izv. Akad. Nauk SSSR, Ser. Khim.* 463 (1976)
20. A N Pudovik, E S Batyeva, E N Ofitserov *Dokl. Akad. Nauk SSSR* **232** 1092 (1977)
21. F Mathis, L Lafaille, R Burgada *Spectrochim. Acta, Part A* **30** 357 (1974)
22. E S Batyeva, E N Ofitserov, V A Al'fonsov, A N Pudovik *Dokl. Akad. Nauk SSSR* **224** 339 (1975)
23. E S Batyeva, V A Al'fonsov, G U Zamaletdinova, A N Pudovik *Zh. Obshch. Khim.* **46** 2204 (1976)
24. F Mathis *Phosphorus* **1** 109 (1976)
25. V P Evdakov, V P Beketov, B I Bryantsev *Zh. Obshch. Khim.* **47** 1726 (1977)
26. V P Evdakov, V P Beketov *Zh. Obshch. Khim.* **45** 1642 (1975)
27. P M Zavlin, A N D'yakonov, V M Al'bitskaya *Zh. Obshch. Khim.* **45** 2113 (1975); A N D'yakonov, P M Zavlin, V M Al'bitskaya *Zh. Obshch. Khim.* **47** 2178 (1977)
28. O Dahl *Phosphorus Sulfur* **18** 201 (1983)
29. E V Borisov, N L Ivanova, T B Aksenova, L K Vasyanina, M K Grachev, A R Bekker, E E Nifant'ev *Zh. Obshch. Khim.* **55** 2270 (1985)
30. O S Diallo, J-F Brazier, A Klaebe, R Wolf *Phosphorus Sulfur* **22** 93 (1985)
31. L Lafaille, F Mathis *C. R. Acad. Sci., Ser. 2* **300** 939 (1985)
32. E S Batyeva, V A Al'fonsov, V D Nesterenko, A N Pudovik *Zh. Obshch. Khim.* **47** 550 (1977)
33. L Lafaille, F Mathis, R Burgada *C. R. Hebd. Seances Acad. Sci., Ser. C* **270** 1138 (1970)
34. E V Borisov, N L Ivanova, E E Nifant'ev *Zh. Fiz. Khim.* **53** 2803 (1979)
35. E E Nifant'ev, N L Ivanova, N K Bliznyuk *Zh. Obshch. Khim.* **36** 765 (1966)
36. E E Nifant'ev, A I Gavrilova, N K Bliznyuk *Zh. Obshch. Khim.* **36** 363 (1966)
37. V P Evdakov, V P Beketov, V I Svergun *Zh. Obshch. Khim.* **43** 55 (1973)
38. J A Mosbo *Phosphorus Sulfur* **4** 273 (1978)
39. F S Mukhametov, E E Korshin, R R Shagidullin, N I Rizpolozhenskii *Zh. Obshch. Khim.* **53** 2703 (1983)
40. P S Thorstenson, H S Aaron *Phosphorus Sulfur* **22** 145 (1985)
41. J Nielsen, O Dahl *J. Chem. Soc., Perkin Trans. 2* 553 (1984)
42. E E Nifant'ev, N L Ivanova, A A Borisenko *Zh. Obshch. Khim.* **40** 1420 (1970)
43. E E Nifant'ev, E V Borisov *Zh. Obshch. Khim.* **55** 1660 (1985)
44. V N Eliseenkov, A N Pudovik, S G Fattakhov, N A Serkina *Zh. Obshch. Khim.* **40** 498 (1970)
45. N A Andreev, O N Grishina, V N Smirnov *Zh. Obshch. Khim.* **49** 332 (1979); N A Andreev, O N Grishina *Zh. Obshch. Khim.* **49** 718 (1979)
46. V N Eliseenkov, T N Shumilina *Zh. Obshch. Khim.* **52** 825 (1982)
47. A M Kibardin, P I Gryaznov, T Kh Gazizov, A N Pudovik *Izv. Akad. Nauk SSSR, Ser. Khim.* 1826 (1987)
48. T Kh Gazizov, L K Sal'keeva *Dokl. Akad. Nauk SSSR* **302** 1380 (1988)
49. T Kh Gazizov, L K Sal'keeva, E K Gafurov, A V Kazantsev *Zh. Obshch. Khim.* **58** 944 (1988)
50. E S Batyeva, V A Al'fonsov, A N Pudovik *Dokl. Akad. Nauk SSSR* **303** 632 (1988)
51. Yu G Trishin, V N Chistokletov *Zh. Obshch. Khim.* **52** 2476 (1982)
52. O Dahl, in *Conference de Chimie du Phosphor (Résumes Abstracts) Nice, France, 1982* N 67
53. Yu G Trishin, V N Chistokletov, A A Petrov *Zh. Obshch. Khim.* **53** 664 (1983)
54. A A Korkin, E N Tsvetkov *Zh. Obshch. Khim.* **57** 2155 (1987)
55. E E Nifant'ev, M K Grachev, A R Bekker *Dokl. Akad. Nauk SSSR* **291** 1383 (1986)
56. E E Nifantyev, M K Gratchev, E V Borisov, A R Bekker *Phosphorus Sulfur* **34** 105 (1987)
57. J Szewczyk, L D Quin *J. Org. Chem.* **52** 1190 (1987)
58. A A Korkin, A M Mebel', E N Tsvetkov *Zh. Obshch. Khim.* **58** 1015 (1988)
59. A A Korkin, E N Tsvetkov *Bull. Soc. Chim. Fr.* 335 (1988)
60. J Febvay, F Casabianca, J G Riess *J. Am. Chem. Soc.* **106** 7985 (1984)
61. L M Epshtein, Z S Novikova, L D Ashkinadze, V N Kostylev *Dokl. Akad. Nauk SSSR* **184** 1346 (1969)
62. L M Epshtein, A N Zhdanova, N S Dolgopyat, D A Bochvar, N P Gambaryan, L A Kazitsina *Izv. Akad. Nauk SSSR, Ser. Khim.* 2487 (1979)
63. V I Shibaev, A V Garabadzhiu, A N Lavrent'ev, E G Sochilin *Zh. Obshch. Khim.* **50** 309 (1980)
64. O Dahl *Tetrahedron Lett.* **23** 1493 (1982)
65. T A Van der Knaap, F Bickelhaupt *Phosphorus Sulfur* **21** 227 (1984)
66. A N Marchenko, G N Koidan, A M Pinchuk, A V Kirsanov *Zh. Obshch. Khim.* **54** 1774 (1984)
67. J Szewczyk, J Lloyd, L D Quin *Phosphorus Sulfur* **21** 155 (1984); E Niecke, D Gudat, E Symalla *Angew. Chem.* **98** 817 (1986)
68. S Yu Burmistrov, L K Vasyanina, M K Grachev, E E Nifant'ev *Zh. Obshch. Khim.* **59** 2639 (1989)
69. E E Nifantyev, M K Gratchev *Phosphorus Sulfur* **49/50** 203(1990)
70. E E Nifantyev, M K Gratchev, S Yu Burmistrov, L K Vasyanina, M Yu Antipin, Yu T Struchkov *Tetrahedron* **47** 9839 (1991)
71. E E Nifant'ev, M K Grachev, S Yu Burmistrov, A R Bekker, L K Vasyanina, M Yu Antipin, Yu T Struchkov *Zh. Obshch. Khim.* **62** 1461 (1992)
72. E E Nifantyev, M K Gratchev, S Yu Burmistrov, M Yu Antipin, Yu T Struchkov *Phosphorus Sulfur* **70** 159 (1992)
73. E E Nifant'ev, N L Ivanova *Zh. Obshch. Khim.* **40** 1992 (1970)

74. H Sliwa, J P Picavet *Tetrahedron Lett.* **18** 1583 (1977)
75. USSR P. 827 491; *Byull. Izobret.* **17** (1981)
76. USSR P. 1 235 869; *Byull. Izobret.* **21** (1986)
77. USSR P. 1 558 918; *Byull. Izobret.* **15** (1990)
78. E E Nifant'ev, M K Grachev, S Yu Burmistrov, L K Vasyanina *Zh. Obshch. Khim.* **58** 1011 (1988)
79. E E Nifant'ev, M K Grachev, S Yu Burmistrov, L K Vasyanina *Dokl. Akad. Nauk SSSR* **303** 115 (1988)
80. W P Jencks, in *Catalysis in Chemistry and Enzymology* (New York: McGraw-Hill, 1969) p. 173
81. W P Jencks, in *Catalysis in Chemistry and Enzymology* (New York: McGraw-Hill, 1969) p. 170
82. W P Jencks, in *Catalysis in Chemistry and Enzymology* (New York: McGraw-Hill, 1969) p. 241
83. E E Nifant'ev, M K Grachev, L K Vasyanina *Zh. Obshch. Khim.* **63** 575 (1993)
84. E E Nifant'ev, N L Ivanova *Zh. Obshch. Khim.* **41** 2192 (1971); L M Epshtein, Z S Novikova, L D Ashkinadze, L M Rubashova, L A Kazitsina *Izv. Akad. Nauk SSSR, Ser. Khim.* 963 (1971)
85. E E Nifant'ev, N L Ivanova, I P Gudkova, I V Shilov *Zh. Obshch. Khim.* **40** 1420 (1970)
86. K A Petrov, V P Evdakov, G I Abramtseva, A K Strautman *Zh. Obshch. Khim.* **32** 3070 (1962)
87. V P Evdakov, K A Bilevich, G P Sizova *Zh. Obshch. Khim.* **33** 3770 (1963)
88. K A Bilevich, V P Evdakov *Zh. Obshch. Khim.* **35** 365 (1965)
89. E E Nifant'ev, I V Fursenko *Zh. Obshch. Khim.* **37** 511 (1967)
90. E E Nifant'ev, I V Fursenko *Zh. Obshch. Khim.* **38** 1285 (1968)
91. E E Nifant'ev, I V Fursenko *Zh. Obshch. Khim.* **38** 1295 (1968)
92. I V Fursenko, G T Bakhvalov, E E Nifant'ev *Zh. Obshch. Khim.* **38** 1299 (1968)
93. E E Nifant'ev, D A Predvoditelev, M K Grachev *Zh. Obshch. Khim.* **44** 2779 (1974)
94. R Burgada *Bull. Soc. Chim. Fr.* 4161 (1972)
95. S D Stamatov, S A Ivanov *Phosphorus Sulfur* **37** 213 (1988)
96. S L Beaucage, M H Caruthers *Tetrahedron Lett.* **22** 1859 (1981)
97. L J McBride, M H Caruthers *Tetrahedron Lett.* **24** 245 (1983)
98. A D Barone, J Y Tang, M H Caruthers *Nucl. Acids Res.* **12** 4051 (1984)
99. R T Pon, M J Damha, K K Ogilvie *Tetrahedron Lett.* **26** 2525 (1985)
100. M F Moore, S L Beaucage *J. Org. Chem.* **50** 2019 (1985)
101. E E Nifant'ev, M K Grachev, S Yu Burmistrov, N M Rososhanskaya, L K Vasyanina *Dokl. Akad. Nauk* (1994) (in the press)
102. S L Beaucage *Tetrahedron Lett.* **25** 375 (1984)
103. B C Froehler, M D Matteucci *Tetrahedron Lett.* **24** 3171 (1983)
104. R T Pon *Tetrahedron Lett.* **28** 3643 (1987)
105. M Sekine, N Masuda, H Hata *Bull. Chem. Soc. Jpn.* **59** 7181 (1986)
106. Sh Hamamoto, H Takaku *Chem. Lett.* 1401 (1986)
107. T Tanaka, S Tamatsukuri, M Ikehara *Chem. Pharm. Bull. Jpn.* **34** 2044 (1986)
108. B S Sproat, B Beijer, P Rider, P Neuner *Nucl. Acids Res.* **15** 4837 (1987)
109. S M Gryaznov, V V Gorn, V F Zarytova, V P Kumarev, A S Levina, A S Polishchuk, V K Potapov, G A Potemkin, Yu G Sredin, Z A Shabarova *Izv. Sib. Otd. Akad. Nauk SSSR, Ser. Khim. Nauk* 119 (1987)
110. H Takaku, T Watanabe, S Hamamoto *Nucleosides, Nucleotides* **6** 293 (1987)
111. J C Schulhof, D Molko, R Teoule *Tetrahedron Lett.* **28** 51 (1987)
112. H Takaku, T Watanabe, S Hamamoto *Tetrahedron Lett.* **29** 81 (1988)
113. C J Malasco, Jr, J R Sufrin *J. Org. Chem.* **57** 6363 (1992)
114. C Sergheraet, C Pierlot, A Tartar, Y Henin, M Lamaitre *J. Med. Chem.* **36** 826 (1993)
115. S Berner, K Mühlegger, H Seliger *Nucleosides, Nucleotides* **7** 763 (1988)
116. S Berner, K Mühlegger, H Seliger *Nucl. Acids Res.* **17** 853 (1989)
117. J Helinski, W Dabkowski, J Michalski *Tetrahedron Lett.* **32** 4981 (1991)
118. B H Dahl, J Nielsen, O Dahl *Nucl. Acids Res.* **15** 1729 (1987)
119. Y Watanabe, S Machara, S Ozaki *J. Chem. Soc., Perkin Trans. 1* 1879 (1992)
120. M K Grachev, V Yu Mishina, L K Vasyanina, E E Nifant'ev *Zh. Obshch. Khim.* **63** 1526 (1993)
121. E E Hifant'ev, Yu I Blokhin, F S Galiaskarova *Zh. Obshch. Khim.* (1994) (in the press)
122. E E Nifant'ev, A P Tuseev, D I Val'dman, P A Morozov, A I Val'dman *Zh. Prikl. Khim.* **52** 1343 (1979)
123. K Smeyral, H Baltz, H Fischer *J. Pract. Chem.* **22** 186 (1963); L Maier *Helv. Chim. Acta* **47B** 2129 (1964); D Houalla, M Sanchez, R Wolf *Bull. Soc. Chim. Fr.* 2368 (1965)
124. R Burgada, M G Martin, G Mavel *Bull. Soc. Chim. Fr.* 2154 (1963); R Burgada, H Normant *C. R. Hebd. Seances Acad. Sci.* **257** 1943 (1963); R Burgada *Ann. Chim.* 15 (1966)
125. M Zentil, S Senges, J-P Faucher, M-C Labarre *Bull. Soc. Chim. Fr.* 376 (1971)
126. K Diemert, W Kuchen, J Ketter *Phosphorus Sulfur* **15** 155 (1983)
127. E E Nifant'ev, N L Ivanova, D A Predvoditelev *Dokl. Akad. Nauk SSSR* **228** 357 (1976)
128. S Fischer, J Hoyano, I Johnson, L K Peterson *Can. J. Chem.* **54** 2706 (1976)
129. M K Grachev, G I Kurochkina, S G Sakharov, A R Bekker, E E Nifant'ev *Zh. Obshch. Khim.* **61** 1701 (1991)
130. E E Nifantyev, V V Negrebetsky, M K Gratchev, G I Kurochkina, A R Bekker, L K Vasyanina, S G Sakharov *Phosphorus Sulfur* **66** 261 (1992)
131. M K Gratchev, E E Nifantyev, in *The XIIth International Conference on Phosphorus Chemistry (Abstracts of Posters) Toulouse, France 1992*, I-73
132. M K Grachev, G I Kurochkina, A R Bekker, L K Vasyanina, E E Nifant'ev *Zh. Obshch. Khim.* **63** 338 (1993)
133. E E Nifant'ev, M K Grachev, G I Kurochkina, L K Vasyanina *Zh. Obshch. Khim.* **63** 947 (1993)
134. M K Gratchev, G I Kurochkina, V V Negrebetsky, E E Nifantyev *Phosphorus Sulfur* (1994) (in the press)
135. L Birkofer, W Gilgenberg, A Ritter *Angew. Chem.* **73** 143 (1961)
136. E E Nifant'ev *Zh. Obshch. Khim.* **34** 3850 (1964)
137. T Shimidzu, K Yamana, A Murakami, K Nakamichi *Tetrahedron Lett.* **21** 2717 (1980)
138. T Shimidzu, K Yamana, K Nakamichi, A Murakami *J. Chem. Soc., Perkin Trans. 1* 2294 (1981)
139. D A Predvoditelev, M K Grachev, M B Smirnov, E E Nifant'ev *Zh. Obshch. Khim.* **18** 1326 (1982)
140. T Shimidzu, K Yamana, K Nakamichi, S Maikuma, M Kanda *Nucl. Acids Res., Symp. Ser.* **11** 89 (1982)
141. T Shimidzu, K Yamana *Polym. J. Jpn.* **15** 727 (1983)
142. T Shimidzu, K Yamana, N Kanda, S Kitagava *Bull. Chem. Soc. Jpn.* **56** 3483 (1983)
143. T Shimidzu, K Yamana, A Murakami, S Maikuma *Heterocycles* **21** 546 (1984)
144. E E Nifant'ev, M K Grachev, A R Bekker, L K Vasyanina, A M Koroteev *Zh. Obshch. Khim.* **58** 312 (1988)
145. M K Grachev, V Yu Iorish, A R Bekker, E E Nifant'ev *Zh. Obshch. Khim.* **60** 66 (1990)
146. V Yu Iorish, M K Grachev, A R Bekker, E E Nifant'ev *Zh. Obshch. Khim.* **61** 106 (1991)
147. M K Grachev, V Yu Iorish, A R Bekker, E E Nifant'ev *Zh. Obshch. Khim.* **62** 1032 (1992)
148. V Yu Iorish, M K Grachev, A R Bekker, E E Nifant'ev *Zh. Obshch. Khim.* **63** 783 (1993)
149. V N Babin, E B Zavelovich *Khim. Geterotsikl. Soedin.* 781 (1977)
150. S-M Wang, L-Y Lee, J-T Chen *Spectrochim. Acta* **35A** 765 (1979)
151. E V Borisov, A K Akhlebinin, A A Borisenko, E E Nifant'ev *Zh. Obshch. Khim.* **53** 1406 (1983)
152. E V Borisov, A K Akhlebinin, E E Nifant'ev *Zh. Obshch. Khim.* **54** 2345 (1984)
153. M K Grachev, A R Bekker, E E Nifant'ev *Zh. Obshch. Khim.* **61** 1572 (1991)
154. M K Grachev, E E Nifant'ev *Zh. Obshch. Khim.* **59** 1729 (1989)
155. E E Nifant'ev, V V Negrebetskii, M K Grachev *Zh. Obshch. Khim.* **61** 1581 (1991)
156. M K Grachev, G I Kurochkina, A R Bekker, L K Vasyanina, E E Nifant'ev *Zh. Obshch. Khim.* **63** 948 (1993)

157. Jpn. P. 80 53 274; *Chem. Abstr.* **94** 30 752e (1981); Jpn. P. 80 62 070; *Chem. Abstr.* **94** 4 010s (1981); Jpn. P. 81 73 073; *Chem. Abstr.* **95** 187 253m (1981); Jpn. P. 81 73 074; *Chem. Abstr.* **95** 203 952w (1981)
158. M Granier, A Baceiredo, Y Dartiguenave, M Dartiguenave, M-J Menu, G Bertrand *J. Am. Chem. Soc.* **112** 6277 (1990)
159. L K Kibardina, M A Pudovik, A N Pudovik *Izv. Akad. Nauk SSSR, Ser. Khim.* 1133 (1981)
160. W Dabkowski, J Michalski, W Oing *Angew. Chem.* **102** 565 (1990)
161. J Michalski, W Dabkowski, in *The XVth International Conference on Organometallic Chemistry (Programme, Abstracts and Participants) Warsaw, 1992* p. 26
162. T Mukaiyama, Y Kodaira *Bull. Chem. Soc. Jpn.* **39** 1297 (1966)
163. Y Kodaira, T Mukaiyama *J. Org. Chem.* **31** 2903 (1966)
164. A N Pudovik, M A Pudovik, O S Shulyndina, Kh Kh Nagaeva *Zh. Obshch. Khim.* **40** 1477 (1970)
165. D A Predvoditelev, G A Podzhunas, E E Nifant'ev *Zh. Obshch. Khim.* **41** 2195 (1971)
166. USSR P. 469 710; *Byull. Izobret.* **17** (1975)
167. USSR P. 502 900; *Byull. Izobret.* **6** (1976)
168. E E Nifant'ev, D A Predvoditelev, M K Grachev *Zh. Obshch. Khim.* **46** 477 (1976)
169. M K Grachev, D A Predvoditelev, E E Nifant'ev *Zh. Obshch. Khim.* **46** 1677 (1976)
170. E E Nifant'ev, A A Borisenko, S F Sorokina, M K Grachev, A I Zavalishina *Zh. Obshch. Khim.* **47** 2474 (1977)
171. M A Pudovik, L K Kibardina, A N Pudovik *Zh. Obshch. Khim.* **52** 781 (1982)
172. M A Pudovik, L K Kibardina, A N Pudovik *Zh. Obshch. Khim.* **52** 1481 (1982)
173. E E Nifantyev, N S Vyazankin, S F Sorokina, L A Vorobieva, O A Vyazankina, D A Bravo-Zhivotovsky, A R Bekker *J. Organomet. Chem.* **277** 211 (1984)
174. E Niecke, G Ringel *Angew. Chem.* **89** 501 (1977)
175. L N Markovskii, V D Romanenko, E O Klebanskii, M I Povolotskii *Zh. Obshch. Khim.* **56** 1721 (1986)
176. L N Markovskii, V D Romanenko, A D Drapailo, A V Ruban *Zh. Obshch. Khim.* **56** 2231 (1986)
177. C L Bodkin, P Simpson *J. Chem. Soc., B* 1136 (1971)
178. L L Chang, D B Denney *J. Org. Chem.* **42** 782 (1977)
179. L Horner, M Jordan *Phosphorus Sulfur* **8** 235 (1980)
180. O Dahl *Tetrahedron Lett.* **22** 3281 (1981)
181. B M Dahl, O Dahl, S Trippett *J.Chem. Soc., Perkin Trans. 1* 2239 (1981)
182. E E Nifant'ev, D A Predvoditelev, A P Tuseev, M K Grachev, M A Zolotov *Zh. Obshch. Khim.* **50** 1702 (1980)
183. E E Nifant'ev, D A Predvoditelev, M A Zolotov *Bioorg. Khim.* 7 1100 (1981)
184. D A Predvoditelev, T G Chukbar, E E Nifant'ev *Zh. Obshch. Khim.* **46** 291 (1976)
185. E E Nifant'ev, D A Predvoditelev, V A Shin *Zh. Obshch. Khim.* **46** 2369 (1976)
186. E E Nifant'ev, D A Predvoditelev, M K Grachev *Bioorg. Khim.* 3 68 (1977)
187. M K Grachev, V A Sukhanov, D A Predvoditelev, V I Shvets, E E Nifant'ev *Zh. Obshch. Khim.* **13** 1830 (1977)
188. D A Predvoditelev, E N Rasadkina, M K Grachev, E E Nifant'ev *Zh. Org. Khim.* **18** 1115 (1982)
189. E E Nifant'ev, M K Grachev, S Yu Burmistrov, L K Vasyanina *Zh. Obshch. Khim.* **62** 2439 (1992)
190. L I Mizrakh, L Yu Polonskaya *Zh. Obshch. Khim.* **45** 2343 (1975)
191. L I Mizrakh, L Yu Polonskaya, L N Kozlova, T A Babushkina, B I Bryantsev *Zh. Obshch. Khim.* **45** 1469 (1975)
192. L I Mizrakh, L Yu Polonskaya, T A Babushkina, B I Bryantsev *Zh. Obshch. Khim.* **45** 549 (1975)
193. D A Predvoditelev, V B Kvantrishvili, E E Nifant'ev *Zh. Obshch. Khim.* **11** 1190 (1975)
194. M A Pudovik, A N Pudovik *Zh. Obshch. Khim.* **46** 222 (1976)
195. D A Predvoditelev, V B Kvantrishvili, E E Nifant'ev *Zh. Org. Khim.* **12** 38 (1976)
196. D A Predvoditelev, V B Kvantrishvili, E E Nifant'ev *Zh. Org. Khim.* **13** 1392 (1977)
197. L I Mirzakh, L Yu Polonskaya, N O Ulanovskaya *Zh. Obshch. Khim.* **49** 2393 (1979)
198. USSR P. 486 022; *Byull. Izobret.* **5** (1976)
199. I P Andrianova, G V Gridasova, A S Lapin *Izv. Sib. Otd. Akad. Nauk SSSR, Ser. Khim. Nauk* (6) 77 (1975)
200. K V Nikonorov, E A Gurylev, F F Martsalova *Izv. Akad. Nauk SSSR, Ser. Khim.* 182 (1981)
201. I V Konovalova, E N Ofitserov, V F Mironov, A N Pudovik *Izv. Akad. Nauk SSSR, Ser. Khim.* 1432 (1983)
202. K A Petrov, E E Nifant'ev, L V Khorkhoyanu, I G Shcherba *Zh. Obshch. Khim.* **34** 70 (1964)
203. E E Nifant'ev, G A Podzhunas, D A Predvoditelev, Yu B Filippovich *Zh. Obshch. Khim.* **42** 1842 (1972)
204. E E Nifant'ev, D A Predvoditelev, V A Shin *Zh. Vses. Khim. O-va im. D. I. Mendeleeva* **23** 200 (1978)
205. V A Shin, D A Predvoditelev, E E Nifant'ev *Zh. Org. Khim.* **14** 948 (1978)
206. Kh Kh Alarkon, D A Predvoditelev, E E Nifant'ev *Bioorg. Khim.* **4** 1513 (1978)
207. E E Nifant'ev, D A Predvoditelev, M K Grachev, V A Shin *Bioorg. Khim.* **4** 1213 (1978)
208. L I Smirnova, M A Malenkovskaya, D A Predvoditelev, E E Nifant'ev *Zh. Org. Khim.* **16** 1170 (1980)
209. D A Predvoditelev, M K Grachev, E E Nifant'ev *Bioorg. Khim.* **7** 601 (1981)
210. E E Nifant'ev, D A Predvoditelev, M A Zolotov *Bioorg. Khim.* **8** 1263 (1982)
211. S D Stamatov, S Gronovitz *Lipids* **25** 149 (1990)
212. F S Mukhametov *Zh. Obshch. Khim.* **61** 10 (1991)
213. F S Mukhametov, R M Eliseenkova, N I Rizpolozhenskii *Izv. Akad. Nauk SSSR, Ser. Khim.* 915 (1980)
214. Ya S Arbisman, Yu A Kondrat'ev, S Z Ivin *Zh. Obshch. Khim.* **37** 509 (1967)
215. Yu A Kondrat'ev, O N Emel'yanova, K D Shvetsova-Shilovskaya, V V Negrebetskii, S F Dymova *Zh. Obshch. Khim.* **47** 2707 (1977)
216. A K Kuliev, V V Moskva, D A Akhmedzade *Zh. Obshch. Khim.* **57** 230 (1987)
217. B E Ivanov, S V Samurina, S S Krokhina, N P Anoshina *Izv. Akad. Nauk SSSR, Ser. Khim.* 2075 (1974)
218. L I Mizrakh, L Yu Polonskaya, A N Gvozdetskii, A M Vasil'ev, L B Karpunina *Zh. Obshch. Khim.* **58** 2246 (1988)
219. F Kober *Z. Chem.* **16** 406 (1976)
220. O N Nuretdinova, V G Novikova, F F Guseva *Izv. Akad. Nauk, Ser. Khim.* 2816 (1992)
221. R Burgada, D Houalla, R Wolf *C. R. Hebd. Seances Acad. Sci., Ser. C* **264** 356 (1967)
222. H Germa, M Willson, R Burgada *C. R. Hebd. Seances Acad. Sci., Ser. C* **270** 1474 (1970)
223. USSR P. 504 779; *Byull. Izobret.* **8** (1976)
224. F H Osman, W S El-Hamouly, M M Abdel-Gawad, M M Abbasi *Phosphorus Sulfur* **14** 1 (1982)
225. E E Nifant'ev, V I Kodolov, E P Nonishev *Zh. Obshch. Khim.* **41** 482 (1971)
226. E E Nifant'ev, Yu I Blokhin, M E Ergashev *Dokl. Akad. Nauk* **325** 731 (1992)
227. Yu I Blokhin, L K Vasyanina, M E Ergashev, E E Nifant'ev *Izv. Akad. Nauk, Ser. Khim.* 2777 (1992)
228. J F Brazier, R Wolf, R Burgada *Bull. Soc. Chim. Fr.* 2109 (1966)
229. M Sanchez, R Wolf, R Burgada, F Mathis *Bull. Soc. Chim. Fr.* 773 (1968)
230. L Beslier, M Sanches, D Houalla, R Wolf *Bull. Soc. Chim. Fr.* 2563 (1971)
231. M A Pudovik, S A Terent'eva, A N Pudovik *Zh. Obshch. Khim. (Sb. Khimiya Elementoorganicheskikh Soedinenii)* (Collection. The Chemistry of Organoelement Compounds) (1976) p. 129
232. M A Pudovik, S A Terent'eva, A N Pudovik *Dokl. Akad. Nauk SSSR* **228** 363 (1976)
233. E E Nifant'ev, T S Kukhareva, I A Soldatova, T G Chukbar *Zh. Obshch. Khim.* **56** 2487 (1986)
234. E E Nifant'ev, T S Kukhareva, I A Soldatova, I S Belostotskaya, V V Ershov, L K Vasyanina *Zh. Obshch. Khim.* **58** 2242 (1988)
235. O M Plotnikova, N S Magomedova, N G Ruchkina, A N Sobolev, V K Bel'skii, E E Nifant'ev *Metalloorg. Khim.* **5** 1288 (1992)

236. E E Nifant'ev, O M Plotnikova, N G Ruchkina, L K Vasyanina, A R Bekker *Zh. Obshch. Khim.* **62** 2456 (1992)
237. E E Nifant'ev, M K Grachev, K L Anfilov, L K Vasyanina *Zh. Obshch. Khim.* (1994) (in the press)
238. R Burgada, in *Khimiya i Primenenie Fosfororganicheskikh Soedinenii (Tr. V Konf.)* [The Chemistry and Applications of Organophosphorus Compounds (Proceedings of the Fifth Conference)] (Moscow: Nauka, 1974) p. 232
239. R Burgada *Phosphorus Sulfur* **2** 237 (1976)
240. A Klaebe, A Carrelhas, J-F Brazier, D Houalla, R Wolf *Phosphorus Sulfur* **3** 61 (1977)
241. M A Pudovik, V V Ovchinnikov, R A Cherkasov, A N Pudovik *Usp. Khim.* **52** 640 (1983) [*Russ. Chem. Rev.* **52** 350 (1983)]
242. N A Polezhaeva, R A Cherkasov *Usp. Khim.* **54** 1899 (1985) [*Russ. Chem. Rev.* **54** 1126 (1985)]
243. M A Zolotov, D A Predvoditelev, E E Nifant'ev *Zh. Obshch. Khim.* **50** 2380 (1980)
244. K A Petrov, E E Nifant'ev, R G Gol'tseva, L M Solntseva *Vysokomol. Soedin.* **5** 1691 (1963)
245. R Burgada *Ann. Chim.* **8** 347 (1963)
246. N P Grechkin, R R Shagiddulin, G S Gubanova *Izv. Akad. Nauk SSSR, Ser. Khim.* 1797 (1968)
247. Y Germa, M Sanchez, R Burgada, R Wolf *Bull. Soc. Chim. Fr.* 612 (1970)
248. E E Nifant'ev, A A Borisenko, I S Nasonovskii, E I Matrosov *Dokl. Akad. Nauk SSSR* **196** 121 (1971)
249. J A Mosbo, J G Verkade *J. Am. Chem. Soc.* **94** 8224 (1972)
250. B A Arbuzov, R A Kadyrov, V V Klochkov, R P Arshinova, A V Aganov *Izv. Akad. Nauk SSSR, Ser. Khim.* 588 (1982)
251. Y Watanabe, Y Komoda, K Elisuyu, S Ozaki *Tetrahedron Lett.* **31** 255 (1990)
252. Y Watanabe, T Shinohara, T Fujimoto, S Ozaki *Chem. Pharm. Bull. Jpn.* **38** 562 (1990)
253. S Ozaki, Y Kando, N Shiotai, Y Watanabe *J. Chem. Soc., Perkin Trans. 1* 729 (1992)
254. J P Dutasta, J B Robert *J. Am. Chem. Soc.* **100** 1925 (1978)
255. F N Osman, G M M Abdel, M M Abbasi *J. Chem. Soc., Perkin Trans. 1* 1189 (1984)
256. USSR P. 1 172 927; *Byull. Izobret.* **30** (1985)
257. E E Nifant'ev, D A Predvoditelev, M A Malenkovskaya, A R Bekker, S V Meshkov *Zh. Obshch. Khim.* **63** 2452 (1993)
258. J P Albrand, J P Dutasta, J B Robert *J. Am. Chem. Soc.* **96** 4584 (1974)
259. L M Voropai, N G Ruchkina, E E Milliaresi, E E Nifant'ev *Zh. Obshch. Khim.* **55** 65 (1985)
260. I A Litvinov, O N Kataeva, V A Naumov, R P Arshinova, B A Arbuzov *Izv. Akad. Nauk SSSR, Ser. Khim.* 1985 (1987)
261. A Munoz, M-T Boisdon, J-F Brazier, R Wolf *Bull. Soc. Chim. Fr.* 1424 (1971)
262. F S Mukhametov, V N Volkova, N I Rizpolozhenskii, M A Pudovik *Izv. Akad. Nauk SSSR, Ser. Khim.* 2841 (1976)
263. F S Mukhametov, E E Korshin *Zh. Obshch. Khim.* **55** 2013 (1985)
264. F S Mukhametov, E E Korshin, V M Nekhoroshkov, Yu Ya Efremov *Zh. Obshch. Khim.* **59** I309 (1989)
265. B E Ivanov, S V Samurina, N N Lebedeva, A B Ageeva, E I Gol'dfarb *Izv. Akad. Nauk SSSR, Ser. Khim.* 1825 (1973)
266. E E Nyfantyev, T S Kukhareva, V I Dyachenko, A O Kolomietz, N S Magomedova, V K Belskiy, L K Vasyanina *Phosphorus Sulfur* (1994) (in the press)
267. K A Petrov, E E Nifant'ev, L V Khorkhoyanu *Zh. Obshch. Khim.* **32** 3720 (1962)
268. S A Shaidullin V A Naumov, N A Makarova *Zh. Obshch. Khim.* **19** 942 (1978)
269. E E Nifant'ev, M P Koroteev *Zh. Obshch. Khim.* (1994) (in the press)
270. E E Nifant'ev, I M Petrova *Zh. Obshch. Khim.* **40** 2196 (1970)
271. R S Edmundson, E W Mitchell *J. Chem. Soc., C* 3179 (1971)
272. N K Kochetkov, E E Nifantyev, M P Koroteev, Z K Zhane, A A Borisenko *Carbohydr. Res.* **47** 221 (1976)
273. E E Nifant'ev, M P Koroteev, A M Koroteev, N S Magomedova *Zh. Obshch. Khim.* **61** 2505 (1991)
274. A M Koroteev, M P Koroteev, A R Bekker, M Yu Antipin, B K Sadybakasov, Yu T Struchkov, E E Nifant'ev *Zh. Obshch. Khim.* **63** 69 (1993)
275. R V Davis, D J Wintergrass, M N Janakiraman, E M Hyatt, R A Jacobson, L M Daniels, A Wroblewski, J Padmakumari, S K Das, J G Verkade *Inorg. Chem.* **30** 1330 (1991)
276. V P Zinchenko, M P Koroteev, E E Nifant'ev, N K Kochetkov *Dokl. Akad. Nauk SSSR* **297** 1482 (1987)
277. E E Nifant'ev, R K Magdeeva *Zh. Obshch. Khim.* (1994) (in the press)
278. J C Clardy, D S Milbrath, J P Springer, J G Verkade *J. Am. Chem. Soc.* **98** 623 (1976)
279. D S Milbrath, J G Verkade *J. Am. Chem. Soc.* **99** 6607 (1977)
280. L E Carpenter II, J G Verkade *J. Org. Chem.* **51** 4287 (1986)
281. C Lensink, S K Xi, L M Daniels, J G Verkade *J. Am. Chem. Soc.* **111** 3478 (1989)
282. M A H Laramay, J G Verkade *J. Am. Chem. Soc.* **112** 9421 (1990)
283. E Müller, H-B Bürgi *Helv. Chem. Acta* **70** 1063 (1987)
284. V N Nabiullin, E T Mukmenev, B A Arbuzov *Zh. Org. Khim.* **22** 2007 (1986)
285. D V Khasnis, M Lattman *J. Am. Chem. Soc.* **112** 9422 (1990)
286. A Munoz, L Lamande *Phosphorus Sulfur* **51/52** 380 (1990)
287. O V Voskresenskaya, N A Makarova, P A Kirpichnikov, E T Mukmenev *Izv. Akad. Nauk SSSR, Ser. Khim.* 1833 (1969)
288. T G Shestakova, E A Kirichenko, E E Nifant'ev *Zh. Prikl. Khim.* **44** 1620 (1971)
289. N A Makarova, E T Mukmenev, B A Arbuzov *Izv. Akad. Nauk SSSR, Ser. Khim.* 1167 (1979)
290. E E Nifant'ev, R K Magdeeva, D Da Koshta *Zh. Obshch. Khim.* (1994) (in the press)
291. I A Litvinov, V D Cherepinskii-Maslov, Yu T Struchkov, B A Arbuzov, L I Gurarii, A Kh Plyamovatyi, E T Mukmenev *Izv. Akad. Nauk SSSR, Ser. Khim.* 2068 (1983)
292. E E Nifant'ev, B I Maslennikova, L K Vasyanina, E V Panina *Zh. Obshch. Khim.* **64** 154 (1994)
293. E E Nifant'ev, B I Maslennikova, L K Vasyanina, A R Bekker, E V Panina *Zh. Obshch. Khim.* (1994) (in the press)
294. E E Nifant'ev, I P Gudkova *Usp. Khim.* **41** 1824 (1977) [*Russ. Chem. Rev.* **41** (1977)]
295. E E Nifant'ev, D A Predvoditelev *Bioorg. Khim.* **7** 1285 (1981)
296. S A Narang *Tetrahedron* **39** 3 (1983)
297. E E Nifantyev, M P Koroteev *Soviet Sci. Rev., Sect. B Chem.* 399 (1984)
298. E E Nifant'ev, in *Progress Khimii Uglevodov* (Progress in Carbohydrate Chemistry) (Moscow: Nauka, 1985) p. 174
299. A E Stepanov, Y I Shvetz *Chem. Phys. Lipids* **41** 1 (1986)
300. N N Karpyshev *Usp. Khim.* **57** 1546 (1988) [*Russ. Chem. Rev.* **57** 886 (1988)]
301. S L Beaucage, R P Iyer *Tetrahedron* **48** 2223 (1992)
302. S L Beaucage, R P Iyer *Tetrahedron* **49** 1925 (1993)
303. M P Koroteev, E E Nifant'ev *Zh. Obshch. Khim.* **63** 481 (1993)
304. E E Nifant'ev, D A Predvoditelev *Usp. Khim.* **63** 73 (1994) [*Russ. Chem. Rev.* **63** 71 (1994)]
305. R P Evstigneeva, E N Zvonkova, G A Serebrennikova, V I Shvets, in *Khimiya Lipidov* (The Chemistry of Lipids) (Moscow: Khimiya, 1983) p. 78
306. O V Bogomolov, A P Kaplun V I Shvets *Usp. Khim.* **57** 684 (1988) [*Russ. Chem. Rev.* **57** 382 (1988)]
307. L I Smirnova, M A Malenkovskaya, D A Predvoditelev, E E Nifant'ev *Zh. Org. Khim.* **16** 1170 (1980)
308. D A Predvoditelev, L I Smirnova, M B Smirnov, E E Nifant'ev *Dokl. Akad. Nauk SSSR* **256** 402 (1981)
309. D A Predvoditelev, M K Grachev, M B Smirnov, E E Nifant'ev *Zh. Org. Khim.* **18** 1326 (1982)
310. E E Nifant'ev, D A Predvoditelev, L I Smirnova, I V Fursenko *Bioorg. Khim.* **6** 1346 (1980)
311. D A Predvoditelev, I V Fursenko, E E Nifant'ev *Bioorg. Khim.* **7** 1426 (1981)
312. E E Nifantyev, D A Predvoditelev, I V Fursenko, L I Smirnova *Synthesis* 132 (1982)
313. D A Predvoditelev, L I Smirnova, E E Nifant'ev *Zh. Org. Khim.* **15** 2223 (1979)
314. V V Chupin, I A Vasilenko, D A Predvoditelev, G A Serebrennikova, R P Evstigneeva *Dokl. Akad. Nauk SSSR* **248** 235 (1979)
315. V V Chupin, I A Vasilenko, G A Serebrennikova, R P Evstigneeva *Bioorg. Khim.* 7 768 (1981)

316. D A Predvoditelev, M K Grachev, M B Smirnov, E E Nifant'ev *Bioorg. Khim.* **5** 1509 (1979)
317. E E Nifant'ev, D A Predvoditelev, Ch Ch Alarkon *Zh. Org. Khim.* **14** 63 (1978)
318. N H Phuong, N T Thuong *C. R. Hebd. Seances Acad. Sci., Ser. C* **283** 229 (1976)
319. V A Vaver, T A Simonova, G V Titeeva *Bioorg. Khim.* **6** 146 (1980)
320. D A Predvoditelev, Ch Ch Alarkon, E E Nifant'ev *Zh. Org. Khim.* **16** 1549 (1980)
321. K S Bruzik, S M Gupte, M-D Tsai *J. Am. Chem. Soc.* **104** 4682 (1982)
322. K S Bruzik, R-T Jiang, M-D Tsai *Biochemistry* 2478 (1983)
323. R Garrigues *Helv. Chim. Acta* **71** 274 (1988)
324. USSR P. 577 211; *Byull. Izobret.* **39** (1977)
325. USSR P. 586 643; *Byull. Izobret.* **38** (1978)
326. E N Rasadkina, D A Predvoditelev, E E Nifant'ev *Bioorg. Khim.* **18** 1559 (1992)
327. M A Malenkovskaya, D A Predvoditelev, E E Nifant'ev *Zh. Org. Khim.* **27** 1668 (1991)
328. A Yu Zamyatina, Candidate Thesis in Chemical Sciences, Lomonosov Moscow Institute of Fine Chemical Technology, Moscow, 1992
329. K S Bruzik *J. Chem. Soc., Chem. Commun.* 329 (1986)
330. K S Bruzik *J. Chem. Soc., Perkin Trans. 1* 423 (1988)
331. E E Nifant'ev, S M Markov, A P Tuseev *Zh. Obshch. Khim.* **34** 3126 (1964)
332. I P Andrianova, E E Nifant'ev *Zh. Obshch. Khim.* **45** 488 (1975)
333. S A Narang *Synthesis and Applications of DNA and RNA* (Orlando: Academic Press, 1987)
334. M D Matteucci, M H Caruthers *J. Am. Chem. Soc.* **103** 3185 (1981)
335. J L Fourrey, J Varenne *Tetrahedron Lett.* **24** 1963 (1983)
336. R G K Schneiderwind-Stlcklein, I Ugi *Z. Naturforsch.* **39B** 968 (1984)
337. J L Fourrey, J Varenne *Tetrahedron Lett.* **26** 2663 (1985)
338. T Tanaka, S Tamatsukuri, M Ikehara *Nucl. Acids Res.* **15** 7235 (1987)
339. T M Cao, S E Bingham, M T Sung *Tetrahedron Lett.* **24** 1019 (1983)
340. J Lekschas, J Kind, D Cech *Z. Chem.* **27** 338 (1987)
341. H Ozaki, K Yamana, T Shimidzu *Tetrahedron Lett.* **30** 5899 (1989)
342. T Wada, R Kato, T Hata *J. Org. Chem.* **56** 1243 (1991)
343. M J Damha, K K Ogilvie *J. Org. Chem.* **51** 3559 (1986)
344. J Nielsen, O Dahl, G Remaud, J Chattopadhyaya *Acta Chim. Scand., Ser B* **41** 633 (1987)
345. C Meier, T Huynh-Dinh *Bioorg. Med. Chem. Lett.* **1** 527 (1991)
346. W Thomson, D Nicholls, J S Al-Mushadani, W J Irwin, S Freeman, A Karpas *J. Pharm. Pharmacol.* **44** 1080 (1992)
347. K Ikeda, Y Nogoi, K Achiwa *Carbohydr. Res.* **224** 122 (1992)
348. C A A Claesen, C J M Daemen, G I Tesser *Recl. Trav. Chim. Pays-Bas* **104** 190 (1985)
349. C A A Claesen, C J M Daemen, G I Tesser *Recl. Trav. Chim. Pays-Bas* **106** 116 (1986)
350. C M Druf-Tromp, A W Lefel, G A Van der Marel, J H Van Boom *Synthesis* 1269 (1992)
351. G Baschang, V Kvita *Angew. Chem.* **85** 44 (1973)
352. USSR P. 483 397; *Byull. Izobret.* **10** (1976)
353. G S Bajwa, W G Bentrude *Tetrahedron Lett.* **19** 421 (1978)
354. G S Bajwa, W G Bentrude *Tetrahedron Lett.* **21** 4683 (1980)
355. A E Sopchik, W G Bentrude *Tetrahedron Lett.* **21** 4679 (1980)
356. K A Nelson, A E Sopchik, W G Bentrude *J. Am. Chem. Soc.* **105** 7752 (1983)
357. J-C Wu, C-G Wang, L-H Zhang *Huaxue Xuebao, Acta Chim. Sinica* **44** 635 (1986); *Ref. Zh. Khim.* 22 E 233 (1986)
358. Sh Iwai, T Sasaki, E Ohtsuka *Tetrahedron* **46** 6673 (1990)
359. E Rozners, R Renhofa, M Petrova *Nucleosides, Nucleotides* **11** 1579 (1992)
360. N Usman, R T Pon, K K Ogilvie *Tetrahedron Lett.* **26** 4567 (1985)
361. A G Ven'yaminova, Z A Kosolapova, A S Levina *Bioorg. Khim.* **13** 125 (1987)
362. A Jäger, J Engels *Tetrahedron Lett.* **25** 1437 (1984)
363. S Agrawal, J Goodchild *Tetrahedron Lett.* **28** 3539 (1987)
364. T Löschner, J W Engels *Nucleosides, Nucleotides* **7** 729 (1988)
365. T Tanaka, S Tamatsukuri, M Ikehara *Tetrahedron Lett.* **27** 199 (1986)
366. M Mag, J W Engels *Nucleosides, Nucleotides* **7** 725 (1988)
367. Y Kazushige, N Yoshitaka, O Atsushi, N Hidehiko, S Osamu, O Hiroaki, S Takeo *Tetrahedron* **45** 4135 (1989)
368. W Pfleiderer, M Schwarz, H Schirmeister *Chem. Scr.* **26** 147 (1986)
369. K A Gallo, K Shao, L R Phillips, J B Judith, M Koziolkiewicz, B Uznanski, W J Stec, G Zon *Nucl. Acids Res.* **14** 7405 (1986)
370. M W Schwarz, W Pfleiderer *Nucleosides, Nucleotides* **6** 537 (1987)
371. J Nielsen, W K-D Brill, M H Caruthers *Tetrahedron Lett.* **29** 2911 (1988)
372. W K-D Brill, J Nielsen, M H Caruthers *Tetrahedron Lett.* **29** 5517 (1988)
373. W K-D Brill, J-Y Tang, Y-X Ma, M H Caruthers *J. Am. Chem. Soc.* **111** 2321 (1989)
374. B H Dahl, K Bjergarde, V B Sommer, O Dahl *Acta Chem. Scand.* **43** 896 (1989)
375. K H Peterson, J Nielsen *Tetrahedron Lett.* **31** 911 (1990)
376. M J Nemer, K K Ogilvie *Tetrahedron Lett.* **21** 4153 (1980)
377. A Kume, M Fuji, M Sekine, T Hata *J. Org. Chem.* **49** 2139 (1984)
378. B C Froehler, M D Matteucci *Tetrahedron Lett.* **27** 469 (1986)
379. J E Marugg, A Burik, M Tromp, G A Van der Marel, J H Van Boom *Tetrahedron Lett.* **27** 2271 (1986)
380. B C Froehler, P G Ng, M D Matteucci *Nucl. Acids Res.* **14** 5399 (1986)
381. R I Garegg, T Regberg, J Stawinsky, K Stroemberg *Tetrahedron Lett.* **27** 4051 (1986)
382. R I Garegg, T Regberg, J Stawinsky, K Stroemberg *Chem. Scr.* **26** 59 (1986)
383. J E Marug, M Tromp, E Kuylyeheskiely, G A Van der Marel, J H Van Boom *Tetrahedron Lett.* **27** 2661 (1986)
384. T Wada, K Ishikawa, T Hata *Tetrahedron* **49** 2043 (1993)
385. K A Petrov, E E Nifant'ev, A A Shchegolev *Zh. Obshch. Khim.* **32** 1006 (1962)
386. E E Nifant'ev, A P Tuseev *Zh. Obshch. Khim. (Sb. Sintez Prirodnykh Soedinenii, Ikh Analogov i Fragmentov)* (Collection. The Synthesis of Natural Products, Their Analogues and Fragments) 34 (1965)
387. E E Nifant'ev, A P Tuseev, V V Tarasov *Zh. Obshch. Khim.* **36** 1124 (1966)
388. N K Kochetkov, E E Nifant'ev, I P Gudkova, N L Ivanova, N Ts Vlasov, V A Leskin *Zh. Obshch. Khim.* **42** 450 (1972)
389. E E Nifant'ev, D A Predvoditelev, M K Grachev, V A Shin *Dokl. Akad. Nauk SSSR* **235** 595 (1977)
390. D A Predvoditelev, M K Grachev, M V Galakhov, E E Nifant'ev *Zh. Obshch. Khim.* **49** 285 (1979)
391. N K Kochetkov, E E Nifant'ev, M P Koroteev *Dokl. Akad. Nauk SSSR* **194** 587 (1970)
392. E E Nifantyev, S A Rumyantseva, M P Koroteev, E M Abbasov, A T Teleshev, V A Pavlov, E I Klabunovsky *Phosphorus Sulfur* **12** 27 (1981)
393. E E Nifant'ev, A T Teleshev, Yu I Blokhin *Usp. Khim.* **56** 558 (1987) [*Russ. Chem. Rev.* **56** 326 (1987)]
394. E E Nifant'ev, I P Gudkova, I K Golovnikova *Vestn. Mosk. Univ., Ser. 2: Khim.* 129 (1966)
395. I P Gudkova, I K Golovnikova, E E Nifant'ev *Zh. Obshch. Khim.* **38** 1340 (1968)
396. Sh Hashimoto, Y Yahagiya, T Honda, Sh Ikegami *Chem. Lett.* 1511 (1992)
397. H Kondo, Y Ichikawa, Ch Wong *J. Am. Chem. Soc.* **114** 8748 (1992)
398. E E Nifant'ev, S A Rumyantseva, K L Sisneiros, M P Koroteev, N K Kochetkov *Zh. Obshch. Khim.* **53** 2619 (1983)
399. N K Kochetkov, E E Nifantyev, M P Koroteev, Z K Zhane, A A Borisenko *Carbohydr. Res.* **47** 221 (1976)
400. M P Koroteev, S B Makasheva, A R Bekker, E E Nifant'ev *Bioorg. Khim.* **19** 376 (1993)
401. H R Krichelderf, M Fehrle, J Kaschig *Angew. Chem.* **88** 337 (1976); H B A de Bont, J H Van Boom, R M J Liskamp *Recl. Trav. Chim. Pays-Bas* **109** 27 (1990)
402. Y-Ch Li, Y-F Zhao *Phosphorus Sulfur* **60** 233 (1991)
403. A B Uryupin, V Yu Komissarov, P V Petrovskii, Yu A Davidovich, T A Mastryukova, M I Kabachnik *Izv. Akad. Nauk, Ser. Khim.* 1694 (1992)

404. J W Perich, R B Johns *Synthesis* 701 (1989)
405. K Misiura, I Durrant, M Evans, M Gait *Nucleosides, Nucleotides* **10** 671 (1991)
406. E E Nifant'ev, S A Ivanov, S D Stamatov, M P Koroteev *Dokl. Akad. Nauk SSSR* **287** 356 (1986)
407. S D Stamatov, S A Ivanov *Phosphorus Sulfur* **40** 167 (1988)
408. S D Stamatov, S A Ivanov *Phosphorus Sulfur* **45** 73 (1989)
409. Bulgarian P. 42 582; *Ref. Zh. Khim.* 21 N 221 (1988)
410. S D Stamatov, V I Staneva, S A Ivanov *Chem. Phys. Lipids* **46** 199 (1988)
411. D Will, T Brown *Tetrahedron Lett.* **33** 2729 (1992)
412. K-L Yu, B Frazer-Reid, M Paul *Tetrahedron Lett.* **29** 979 (1988)
413. N J Noble, D Dubreuil, V L B Potter *Bioorg. Med. Chem. Lett.* **2** 471 (1992)
414. A Yu Zamyatina, A E Stepanov, A S Bushnev, E N Zvonkova, V I Shvets *Bioorg. Khim.* **19** 347 (1993)
415. C E Dreef, G W Mayr, J-P Jansze, H C P F Roelen, G A Van der Marel, J H Van Boom *Bioorg. Med. Chem. Lett.* **1** 239 (1991)
416. F Seela, K Kaiser *Nucleosides, Nucleotides* **6** 447 (1987)
417. A P Karikowski, W Tuckmantel, G Pawis *Angew. Chem.* **104** 1408 (1992)
418. P Westerduin, G H Veeneman, Y Pennings, G A Van der Marel, J H Van Boom *Tetrahedron Lett.* **28** 1557 (1987)
419. K Fukase, T Matsumoto, N Ifo, T Yoshimura, S Kotani, S Kusumoto *Bull. Chem. Soc. Jpn.* **65** 2643 (1992)
420. C J J Elie, H J Muntendam, H Elst, G A Van der Marel, P Hoogerhout, J H Van Boom *Recl. Trav. Chim. Pays-Bas* **108** 219 (1989)
421. L Chan, G Just *Tetrahedron* **46** 151 (1990)
422. A M Alves, D Holland, M D Edge *Tetrahedron Lett.* **30** 3089 (1989)
423. A J Cocurra *Tetrahedron Lett.* **30** 6287 (1989)
424. R T Pon *Tetrahedron Lett.* **32** 1715 (1991)
425. J-K Chen, D V Carlson, H L Weith, J A O'Brien *Tetrahedron Lett.* **33** 2275 (1992)
426. Rumney IV Squire, E T Kool *Angew. Chem.* **104** 1686 (1992)
427. K A Petrov, E E Nifant'ev, L V Khorkhoyanu, V F Voblikov *Vysokomol. Soedin.* **5** 348 (1963)
428. D A Predvoditelev, E E Nifant'ev, Z A Rogovin *Vysokomol. Soedin.* **8** 213 (1966)
429. V Yu Mishina, A T Teleshev, M K Grachev, E E Nifant'ev *Vysokomol. Soedin.* (1994) (in the press)
430. K Kaneda, H Yamamoto, T Imanaka, S Teranishi *J. Mol. Catal.* **29** 99 (1985)
431. E E Nifant'ev, A V Vasil'ev, M P Korotev, A I Gamzazade *Dokl. Akad. Nauk* (1994) (in the press)
432. USSR P. 181 108; *Byull. Izobret.* **9** (1966)
433. E E Nifant'ev, S G Fedorov *Vestn. Mosk. Univ.* 90 (1964)
434. E E Nifant'ev, S G Fedorov *Dokl. Akad. Nauk SSSR* **164** 1327 (1965)
435. S G Fedorov, E E Nifant'ev *Zh. Prikl. Khim.* **39** 1881 (1966)
436. L M Kolesova, E E Nifant'ev, V P Zubov *Vysokomol. Soedin., Ser. B* **14** 249 (1972)
437. E E Nifant'ev, S G Fedorov, A F Vasil'ev *Zh. Prikl. Khim.* **40** 1066 (1967)
438. E E Nifant'ev, Yu I Blokhin, M Ya Ergashev, I I Tverdokhlebova *Izv. Akad. Nauk SSSR, Ser. Khim.* 1198 (1991)
439. K A Petrov, E E Nifant'ev, T N Lysenko, A I Suzanskii *Vysokomol. Soedin.* **5** 712 (1963)
440. USSR P. 376 435; *Byull. Izobret.* **17** (1973)
441. A B Burg, P J Slota *J. Am. Chem. Soc.* **80** 1107 (1958)
442. K A Petrov, V A Parshina, G M Tsypina, M B Luzanova *Plast. Massy* 20 (1964)
443. E E Nifant'ev, S M Markov, A P Tuseev, A F Vasil'ev *Zh. Obshch. Khim. (Sb. Sintez Prirodnykh Soedinenii, Ikh Analogov i Fragmentov)* (Collection. The Synthesis of Natural Products, Their Analogues and Fragments) 42 (1965)
444. E E Nifant'ev, S M Mapkov, A P Tuseev *Vysokomol. Soedin.* **7** 1020 (1965)
445. I A Nuretdinov, N P Grechkin *Izv. Akad. Nauk SSSR, Ser. Khim.* 1363 (1968)
446. N P Grechkin, I A Nuretdinov, N A Buina *Izv. Akad. Nauk SSSR, Ser. Khim.* 1141 (1968)
447. K A Petrov, V P Evdakov, K A Bilevich, V I Chernykh *Zh. Obshch. Khim.* **32** 3065 (1962)
448. O Adler, F Kober *J. Fluor. Chem.* **5** 231 (1975)
449. V D Romanenko, A V Ruban, S V Iksanova, L N Markovskii *Zh. Obshch. Khim.* **54** 313 (1984)
450. V D Romanenko, A V Ruban, A B Drapailo, L N Markovskii *Zh. Obshch. Khim.* **57** 128 (1987)
451. D Houalla, F H Osman, M Sanchez, R Wolf *Tetrahedron Lett.* **18** 3041 (1977)
452. F Jeanncaux, J G Riess, J Wachter *Inorg. Chem.* **23** 3036 (1984)
453. R F Hudson, in *Structure and Mechanism in Organophosphorus Chemistry* (Translated into Russian; Moscow: Mir, 1967) p. 159
454. A N Pudovik, E S Batyeva, E N Ofitserov, V A Al'fonsov *Zh. Obshch. Khim.* **45** 2338 (1975)
455. V A Gilyarov, M I Kabachnik *Zh. Obshch. Khim.* **36** 282 (1966)
456. H-J Vetter, H Nöth *Chem. Ber.* **96** 1308 (1963); G Peiffer, A Guillemonat, J-C Traynard *C. R. Hebd. Seances Acad. Sci., Ser. C* **266** 400 (1968); E Fluck, P Wachther *Liebigs Ann. Chem.* 1125 (1979)
457. Yu G Trishin, V N Chistokletov, V V Kosovtsev, A A Petrov *Zh. Org. Khim.* **11** 1752 (1975); Yu G Trishin, V N Chistokletov, A A Petrov *Zh. Obshch. Khim.* **49** 48 (1979)
458. M M Yusupov, Sh Egamberdiev, N K Rozhkova, K L Seitanidi, M R Yagudaev *Uzb. Khim. Zh.* (6) 48 (1980)
459. A Tarassoli, M L Thompson, R C Haltiwanger, T G Hill, A D Norman *Inorg. Chem.* **27** 3382 (1988)
460. L A Hussain, A J Elias, M N Rao *Tetrahedron Lett.* **29** 5983 (1988)
461. E E Nifant'ev, S A Rumyantseva, M P Koroteev, K L Sisneiros, N K Kochetkov *Zh. Obshch. Khim.* **51** 2806 (1981)
462. E E Nifant'ev, S A Rumyantseva, M P Koroteev, K L Sisneiros, A S Shalimov, N K Kochetkov *Zh. Obshch. Khim.* **53** 221 (1983)
463. N P Grechkin, L K Nikanorova, L A Zhelonkina *Zh. Obshch. Khim.* **53** 1054 (1983)
464. A I Razumov, P A Gurevich, S A Muslimov, T V Komina, T V Zykova, R A Salakhutdinova *Zh. Obshch. Khim.* **50** 778 (1980)
465. P A Gurevich, A I Razumov, T V Komina, G Yu Klimentova, T V Zykova *Zh. Obshch. Khim.* **55** 1327 (1985)
466. H Seliger, K Gupta *Nucleosides, Nucleotides* **4** 169 (1985)
467. H Seliger, K Gupta *Angew. Chem.* **97** 711 (1985)
468. T Mukaiyama, Y Yokota *Bull. Chem. Soc. Jpn.* **38** 858 (1965)
469. O Mitsunobu, T Ohashi, M Kikuchi, T Mukaiyama *Bull. Chem. Soc. Jpn.* **40** 2964 (1967)
470. Jpn. P. 18 608; *Ref. Zh. Khim.* 19 H 255 (1968)
471. Jpn. P. 23 330; *Ref. Zh. Khim.* 15 H 249 (1969)
472. A N Pudovik, M A Pudovik, S A Terent'eva, V E Bel'skii *Zh. Obshch. Khim.* **41** 2407 (1971)
473. R Burgada, C Laurenço *C. R. Hebd. Seances Acad. Sci., Ser. C* **273** 1536 (1971)
474. D A Predvoditelev, G A Urvantseva, E E Nifant'ev *Zh. Obshch. Khim.* **43** 948 (1973)
475. L I Mizrakh, L Yu Polonskaya, B I Bryantsev, N V Stepanchikova *Zh. Obshch. Khim.* **46** 1490 (1976)
476. M A Pudovik, G Yu Gadzhiev, E Yu Dzhalilov, A N Pudovik *Izv. Akad. Nauk SSSR, Ser. Khim.* 2158 (1979)
477. M A Pudovik, S A Terent'eva, A N Pudovik *Zh. Obshch. Khim.* **51** 518 (1981)
478. M A Pudovik, G Yu Gadzhiev, E Yu Dzhalilov, M D Medvedev, A N Pudovik *Zh. Obshch. Khim.* **51** 514 (1981)
479. M A Pudovik, O S Shulyndina, L K Ivanova, S A Terent'eva, A N Pudovik *Zh. Obshch. Khim.* **44** 501 (1974)
480. USSR P. 469 710; *Byull. Izobret.* **17** (1975)
481. W G Bentrude, W N Setzer, A A Kergaye, V Ethridge, M R Saadein, A M Arif *Phosphorus Sulfur* **57** 37 (1991)
482. R Contreras, R Wolf, M Sanchez *Synth. Inorg. Metal-Org. Chem.* **3** 37 (1973)
483. M R Marre, J F Brazier, R Wolf, A Klaebe *Phosphorus Sulfur* **11** 87 (1981)
484. W J Richter *Chem. Ber.* **117** 2328 (1984)
485. S Juge, J P Genet *Tetrahedron Lett.* **30** 2783 (1989)
486. S Juge, M Stephan, J Laffitte, J P Genet *Tetrahedron Lett.* **31** 6357 (1990)

487. B Faure, A Archavlis, G Buono *J. Chem. Soc., Chem. Commun.* 805 (1989)
488. E E Nifant'ev, A P Tuseev, S M Markov, G F Didenko *Zh. Obshch. Khim.* **36** 319 (1966)
489. S A Rumyantseva, K L Sisneiros, M P Koroteev, E E Nifant'ev *Zh. Obshch. Khim.* **54** 204 (1984)
490. G Yu Gadzhiev, M P Koroteev, V A Budagov, S I Ibragimov *Zh. Obshch. Khim.* **56** 2648 (1986)
491. E E Nifant'ev , I D Rozhdestvenskaya *Koord. Khim.* **5** 1846 (1979)
492. V A Pavlov, E I Karpeiskaya, G V Chel'tsova, L N Kaigorodova, E I Klabunovskii, E N Rasadkina *Izv. Akad. Nauk SSSR, Ser. Khim.* 1087 (1980)
493. G Quesnel, A Thiot, H Coates, R Burgada *C. R. Hebd. Seances Acad. Sci.* **256** 717 (1963)
494. M Sanchez, J-F Brazier, D Houalla, R Wolf *Bull. Soc. Chim. Fr.* 3930 (1967)
495. A N Pudovik, M A Pudovik, S A Terent'eva *Zh. Obshch. Khim.* **41** 2177 (1971)
496. J Ferekh, A Munoz, J F Brazier, R Wolf *C. R. Hebd. Seances Acad. Sci., Ser. C* **272** 797 (1971)
497. C Laurenço, D Bernard, R Burgada *C. R. Hebd. Seances Acad. Sci., Ser. C* **275** 237 (1972)
498. D Bernard, R Burgada *C. R. Hebd. Seances Acad. Sci., Ser. C* **277** 433 (1973)
499. D Bernard, R Burgada *Phosphorus Sulfur* **3** 187 (1974)
500. R Burgada, C Laurenço *J. Organomet. Chem.* **66** 255 (1974)
501. Y Vannoozenberghe, G Buono *J. Am. Chem. Soc.* **112** 6142 (1990)
502. M P Koroteev, E E Nifant'ev *Zh. Obshch. Khim.* **41** 2364 (1971)
503. M A Pudovik, S A Terent'eva, A A Karelov, E I Gol'dfarb, A N Pudovik *Zh. Obshch. Khim.* **50** 740 (1980)
504. M A Pudovik, N P Morozova, A N Pudovik *Izv. Akad. Nauk SSSR, Ser. Khim.* 2837 (1976)
505. M A Pudovik, Yu B Mikhailov, A N Pudovik *Izv. Akad. Nauk SSSR, Ser. Khim.* 1108 (1981)
506. M A Pudovik, Yu B Mikhailov, T A Mironova, A N Pudovik *Izv. Akad. Nauk SSSR, Ser. Khim.* 1624 (1982)
507. P Jacob, W Richter, I Ugi *Liebigs Ann. Chem.* 519 (1991)
508. M A Pudovik, S A Terent'eva, M D Medvedeva, A N Pudovik *Zh. Obshch. Khim.* **43** 679 (1973); M A Pudovik, S A Terent'eva, I V Nebogatikova, A N Pudovik *Zh. Obshch. Khim.* **44** 1020 (1974); X-B Ma, J-L Zhang *Phosphorus Sulfur* **53** 227 (1990)
509. A N Pudovik, M A Pudovik, S A Terent'eva, E I Gol'dfarb *Zh. Obshch. Khim.* **42** 1901 (1972)
510. USSR P. 395 369; *Byull. Izobret.* **5** (1974)
511. S A Terent'eva, M A Pudovik, A N Pudovik *Izv. Akad. Nauk SSSR, Ser. Khim.* 1150 (1979)
512. M A Pudovik, S A Terent'eva, Yu Yu Samitov, A N Pudovik *Zh. Obshch. Khim.* **45** 266 (1975); M A Pudovik, Yu A Mikhailov, T A Malykh, V A Al'fonsov, G U Zamaletdinova, E S Batyeva, A N Pudovik *Zh. Obshch. Khim.* **50** 1677 (1980)
513. S A Terent'eva, M A Pudovik, A N Pudovik *Izv. Akad. Nauk SSSR, Ser. Khim.* 221 (1983)
514. D B Denney, D Z Denney, P J Hammond, C Huang, K-S Tseng *J. Am. Chem. Soc.* **102** 5073 (1980)
515. A Murillo, L Chiquete, P Joseph, R Contreras *Phosphorus Sulfur* **53** 87 (1990)
516. S A Rumyantseva, M P Koroteev, S A Lysenko, A S Shashkov, E E Nifant'ev *Zh. Obshch. Khim.* **52** 418 (1982)
517. R Burgada *Bull. Soc. Chim. Fr.* 136 (1971)
518. USSR P. 523 104; *Byull. Izobret.* **10** (1977)
519. M A Pudovik, N P Morozova, M D Medvedeva, A N Pudovik *Izv. Akad. Nauk SSSR, Ser. Khim.* 1637 (1978)
520. V V Kurochkin, A I Zavalishina, E I Orzhekovskaya, A R Bekker, E E Nifant'ev *Zh. Obshch. Khim.* **57** 311 (1987)
521. E E Nifant'ev, A I Zavalishina, E I Orzhekovskaya, L K Vasyanina *Zh. Obshch. Khim.* **59** 816 (1989)
522. E E Nifant'ev, A I Zavalishina, V G Baranov, E I Orzhekovskaya, L K Vasyanina, M Yu Antipin, B K Sadybakasov, Yu T Struchkov *Zh. Obshch. Khim.* **63** 1748 (1993)
523. E E Nifant'ev, A I Zavalishina, E I Smirnova, N V Kofanova *Zh. Obshch. Khim.* **54** 1207 (1984)
524. E E Nifant'ev, A I Zavalishina, E I Orzhekovskaya, A R Bekker *Zh. Obshch. Khim.* **59** 2497 (1989)
525. N N Nurkulov, A I Zavalishina, E I Orzhekovskaya, A R Bekker, E E Nifant'ev *Zh. Obshch. Khim.* **62** 1186 (1992)
526. E E Nifant'ev, A I Zavalishina, N N Nurkulov, E I Orzhekovskaya, A R Bekker *Zh. Obshch. Khim.* **63** 1726 (1993)
527. E E Nifant'ev, A I Zavalishina, N N Nurkulov, E I Orzhekovskaya, A R Bekker, N S Magomedova, V K Bel'skii *Zh. Obshch. Khim.* **63** 1739 (1993)
528. M A Pudovik, N P Morozova, M D Medvedeva, A N Pudovik *Izv. Akad. Nauk SSSR, Ser. Khim.* 1637 (1978)
529. V V Moskva, A K Kuliev, D A Akhmedzade, M A Pudovik, E B Sakhnovskaya *Zh. Obshch. Khim.* **55** 935 (1985)
530. V V Kurochkin, A I Zavalishina, E I Orzhekovskaya, A R Bekker, A G Agranovich, E E Nifant'ev *Zh. Obshch. Khim.* **57** 311 (1987)
531. E E Nifant'ev, A I Zavalishina, E I Smirnova, M M Blasova *Zh. Obshch. Khim.* **50** 459 (1980)
532. E E Nifantyev, A I Zavalishina, E I Smirnova *Phosphorus Sulfur* **10** 261 (1981)
533. A Schmidpeter, K Karaghiosoff *Z. Naturforsch. B* **36** 1273 (1981)
534. D B Denney, D Z Denney, D M Gavrilovic, P J Hammond, C Huang, K-S Tseng *J. Am. Chem. Soc.* **102** 7072 (1980)
535. B L Laube, R D Bertrand, G A Casedy, R D Compton, J G Verkade *Inorg. Chem.* **6** 173 (1967)
536. US P. 3 996 276; *Ref. Zh. Khim.* 17 N 214 (1977); US P. 4 038 312; *Ref. Zh. Khim.* 7 N 282 (1978)
537. T J Atkins *Tetrahedron Lett.* **19** 4331 (1978)
538. D W White, U A Karcher, R A Jacobson, J G Verkade *J. Am. Chem. Soc.* **101** 4921 (1979)
539. J E Richman, T J Atkins *Tetrahedron Lett.* **19** 4333 (1978)
540. T J Atkins, J E Richman *Tetrahedron Lett.* **19** 5149 (1978)
541. H Hope, M Viggiano, B Moezzi, P Power *Inorg. Chem.* **23** 2550 (1984)
542. J-M Dupart, A Grand, J G Riess *J. Am. Chem. Soc.* **108** 1167 (1986)
543. A Filali, J J Yaouanc, J Jean, H Handel *Angew. Chem.* **103** 563 (1991)
544. E E Nifant'ev, A I Zavalishina, V V Kurochkin, E I Smirnova, A A Borisenko *Zh. Obshch. Khim.* **59** 2031 (1985)
545. E E Nifant'ev, A I Zavalishina, S S Dorogotovtsev, E I Orzhekovskaya, A R Bekker, N N Nevskii *Dokl. Akad. Nauk SSSR* **312** 372 (1990)
546. E E Nifant'ev, A I Zavalishina, S S Dorogotovtsev, E I Orzhekovskaya, N N Nurkulov, A R Bekker, L K Vasyanina *Zh. Obshch. Khim.* **62** 1994 (1992)
547. E E Nifant'ev, A I Zavalishina, S S Dorogotovtsev, E I Orzhekovskaya, A R Bekker, N S Magometova, A N Sobolev, V K Bel'skii *Zh. Obshch. Khim.* **62** 289 (1992)
548. E E Nifant'ev, A I Zavalishina, S S Dorogotovtsev, E I Orzhekovskaya, S P Sirotinkin, N N Nevskii *Dokl. Akad. Nauk SSSR* **312** 377 (1990)
549. M Wieber, O Mulfinger, H Wunderlich *Z. Anorg. Allg. Chem.* **477** 108 (1981)
550. E E Nifant'ev, A I Zavalishina, E I Smirnova, V F Filimonov *Zh. Obshch. Khim.* **55** 2806 (1985)
551. C Malavaud, M T Boisdon, Y Charbannel, J Barrans *Tetrahedron Lett.* **20** 447 (1979)
552. C Malavaud, T N M'Pondo, L Lopez, J Barrans, J-P Legros *Can. J. Chem.* **62** 43 (1984)
553. E G Bent, R C Haltiwanger, A D Norman *Inorg. Chem.* **29** 4310 (1990)
554. M A Pudovik, T A Pestova, A N Pudovik *Zh. Obshch. Khim.* **46** 230 (1976)
555. M M Yusupov *Zh. Obshch. Khim.* **48** 1424 (1978)
556. J M Barendt, R C Haltiwanger, A D Norman *J. Am. Chem. Soc.* **108** 3127 (1986)
557. A D Norman, E Bent, R C Haltiwanger, T Prout *Phosphorus Sulfur* **41** 63 (1989)
558. J M Barendt, R C Haltiwanger, C A Squier, A D Norman *Inorg. Chem.* **30** 2342 (1991)
559. J M Barendt, R C Haltiwanger, A D Norman *Inorg. Chem.* **25** 4323 (1986)
560. E E Nifant'ev, A I Zavalishina, E I Orzhekovskaya, N N Nurkulov *Zh. Obshch. Khim.* (1994) (in the press)

Russian Chemical Reviews **63** (7) 611 – 622 (1994)
©1994 Russian Academy of Sciences and Turpion Ltd

UDC 57.11; 57.083.3

Immunochemical methods for the assay of herbicides of the 1,3,5-triazine group

S A Eremin, Zh V Samsonova, A M Egorov

Contents

I. Introduction	611
II. Principal components of the immunochemical assay methods	612
III. Solid-phase immunoenzyme assay using polyclonal antisera	614
IV. Solid-phase immunoenzyme assay using monoclonal antibodies	618
V. Quantitative determination of several herbicides in one sample	619
VI. Alternative immunoassay methods	620

Abstract. The review deals with studies published during the last 10 years on the development of immunochemical methods for the assay of herbicides of the 1,3,5-triazine group. Questions concerning the optimisation of methods for the immunoenzyme assay and their application in the determination of 1,3,5-triazines in various samples (water, soil, food products etc.) are discussed. The bibliography includes 75 references.

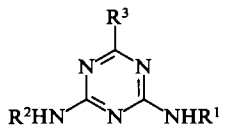
I. Introduction

The contamination of the environment as a result of man's economic activity has long become one of the contemporary global problems. An important aspect of this problem is the universal application of pesticides in agricultural practice. On the one hand, chemical protection of plants is the most radical method for combating pests, diseases, and weeds, but, on the other hand, nonrational application of pesticides can lead to their accumulation within objects in the environment and can induce the breakdown of relationships in ecosystems. For example, in the EEC member countries, norms has been established for the content of pesticides in drinking water: not more than 0.1 ng ml^{-1} for one pesticide and 0.5 ng ml^{-1} for all pesticides.[1] This is why it is important to have assay methods which permit a rapid and exact determination of residual amounts of pesticides in the soil, water, and food products. Ecological problems have in fact stimulated further development and improvement of the methods for the assay of physiologically active substances. The review deals with studies published during the last 10 years on immunochemical methods (ICM) for the assay of herbicides of the 1,3,5-triazine group within objects in the environment.

Herbicides of the 1,3,5-triazine group, used in agriculture to destroy weeds, comprise the largest group of herbicides in terms of the scale of their worldwide manufacture and consumption.[2]

S A Eremin, Zh V Samsonova, A M Egorov Department of Chemical Enzymology, Faculty of Chemistry, M V Lomonosov State University, Vorob'evy gory, 119899 Moscow, Russian Federation.
Fax (7-095) 939 27 42, Tel. (7-095) 937 34 07

Received 28 April 1994
Uspekhi Khimii **63** (7) 638 – 649 (1994); translated by A K Grzybowski



The main representatives of this group are presented in Table 1. Mainly simazine, atrazine, and prometryn are used in Russia.[3] The following limiting permissible concentrations (LPC) in water reservoirs for sanitary–domestic purposes have been adopted in our country: 0.5 mg $litre^{-1}$ for atrazine and 3.0 mg $litre^{-1}$ for prometryn; the presence of a residual amount of simazine is not allowed. Physicochemical assay methods (PCM), namely thin-layer chromatography (TLC), gas chromatography (GC) gas–liquid chromatography (GLC), and high performance liquid chromatography (HPLC), are employed traditionally for the assay of residual amounts of herbicides, including 1,3,5-triazines in air, water, soil, and food products.[4–7] These methods are irreplaceable in cases where it is necessary to identify rigorously the substance being sought, but they suffer from a number of significant disadvantages. These include their laborious nature, complex preparation of the specimen, long assay time, stringent requirements as regards the qualifications of the

Table 1. The structures of the herbicides of the 1,3,5-triazine group, their metabolites, and analogues.

Compound	R^1	R^2	R^3
Atrazine	Et	Pr^i	Cl
Simazine	Et	Et	Cl
Propazine	Pr^i	Pr^i	Cl
Terbutylazine	Et	Bu^t	Cl
Cyanazine	Et	$C(CN)Me_2$	Cl
Ametryn	Et	Pr^i	SMe
Prometryn	Pr^i	Pr^i	SMe
Terbutryn	Et	Bu^t	SMe
Aziprotryn	N_3	Bu^t	SMe
Atrazine mercaptourate	Et	Pr^i	$SCH_2CH(NHCOMe)COOH$
Hydroxyatrazine	Et	Pr^i	OH
Hydroxysimazine	Et	Et	OH
De-ethylatrazine	H	Pr^i	Cl
Deisopropylatrazine	Et	H	Cl

personnel, and the high cost of the equipment used. The technical equipment employed in physicochemical assay is being constantly improved, which increases its sensitivity and accuracy, but at the same time it also raises the cost of such equipment. It is therefore necessary to recognise that physicochemical assay methods are completely unsuitable for routine analyses and operational monitoring. The endeavour to create more effective methods for the analysis of air, soil, and food products for residual amounts of pesticides to reduce the cost of the determination has led to the development of immunochemical assay methods.

The possibility of employing immunochemical methods for the assay of pesticides in water, soil, and food products has been justified in detail in a number of reviews.[8-15] The advantages of immunochemical assay methods include specificity, sensitivity, accuracy, ease of application, high speed, the possibility of automation and use in routine analyses under field conditions, and easy preparation of the specimen (if it is required at all) which rules out the degradation of the test substance. Immunochemical methods are also characterised by a relatively low cost of the determination; for example, a single determination of the herbicide diflubenzuron by the immunoenzyme assay (IEA) method is 20 times cheaper than the determination by the HPLC method and 55 times cheaper than the determination by gas chromatography.[16] The disadvantages of the immunochemical assay methods include the following: the need for appropriate qualifications of the personnel and for the ability of antibodies to react with substances having related structures, which in many instances renders a rigorous qualitative determination of the test substance problematical. At the present time, immunochemical assay methods have been firmly introduced into analytical practice and are used in various branches of medicine, agriculture, and the microbiological and food industries and also for the monitoring of the environment.

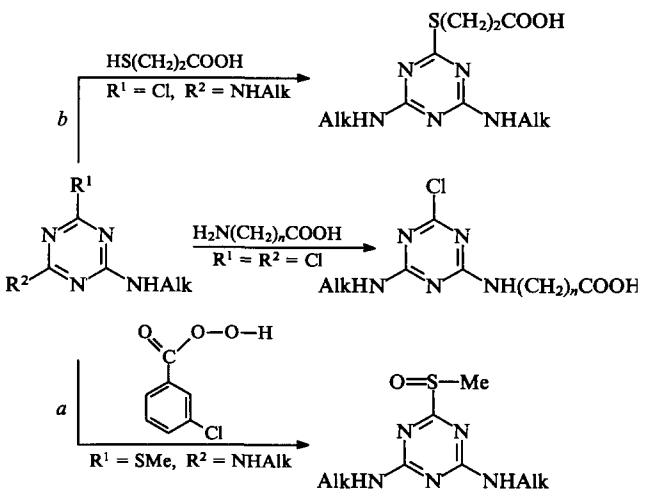
II. Principal components of the immunochemical assay methods

The immunochemical assay methods are based on the specific binding of a particular compound to the corresponding antibodies. The complex form is detected by introducing a label (enzyme, fluorescence) into one of the initial components of the reaction system. If one of the components of the system is bound chemically (covalently) or by sorption to a solid carrier in order to separate a specific complex from the components of the reaction mixture, then the methods are referred to as heterogeneous. Otherwise, if there is no need to separate the components of the immunochemical reaction, the methods are called homogeneous.

Numerous studies devoted to the development and different aspects of the optimisation of immunochemical methods for the assay of herbicides of the 1,3,5-triazine group in objects within the environment and in food products have been published in recent years. The vast majority of the investigations are devoted to methods for the solid-phase immunoenzyme assay—ELISA (enzyme-linked immunosorbent assay). In order to carry out such an assay, it is necessary to have specific antibodies, a conjugate of the substance to be determined with a protein or an enzyme, as well as a solid phase on which one of the components of the immunochemical complex is adsorbed.

The principal components in any immunochemical assay method are specific antibodies—polyclonal and monoclonal. Like all pesticides, 1,3,5-triazines are haptens, i.e. they are incapable of inducing the production of antibodies when introduced into the organism and therefore, in order to obtain antibodies, they are conjugated with proteins. In the 1,3,5-triazine molecule there are no suitable reaction groups for binding to a high-molecular-mass carrier (a protein or an enzyme), so that investigators have to resort to the modification of the herbicide. The questions concerning the selection of the correct structure of the hapten in the synthesis of the pesticide immunogens for the successful production of antibodies have been described in detail.[16] We shall consider the procedures for the modification of 1,3,5-triazines. A carboxy-group is usually introduced into the *N*-alkyl side chain or in the 2-position in the trazine ring (see the Scheme below).

Scheme



2,4-Dichloro-1,3,5-triazines are conjugated to unbranched aminoacids with a terminal amino-group (the 2,4-dichloro-derivatives can be used immediately for conjugation).[17-19] 2-Methylthio-1,3,5-triazines are modified by oxidising them to the sulfoxides by 3-chloroperbenzoic acid (pathway *a*),[18,20-22] while 2-chloro-1,3,5-triazines are conjugated with 3-thiopropionic acid (pathway *b*). The reasons for using the latter modification method are as follows: the sulfur atom is most suitable for the simulation of a chlorine atom as it contains, like chlorine, two lone pairs; the resonance interaction between the sulfur atom and the triazine ring is limited; the atomic radii of sulfur and chlorine are similar; proteins do not add to sulfur just as they do not add to oxygen or nitrogen: the nucleophilicity of the thiolate anion facilitates the substitution of chlorine; finally, all the reagents can be synthesised.[17]

Table 2 presents the structures of the modified 1,3,5-triazines which were used, after conjugation with proteins, to obtain polyclonal antisera and monoclonal antibodies. The table shows that the polyclonal antisera and the monoclonal antibodies exhibit an appreciable percentage of cross-reaction with structurally similar herbicides. Furthermore, one may note the following features: an appreciable percentage of cross-reaction with atrazine is observed for antisera against a simazine derivative (hapten **2**); the antibodies obtained against atrazine derivatives (hapten **3**) exhibit an appreciable percentage of cross-reaction with propazine. The antibodies obtained to the conjugates of 1,3,5-triazines with 3-thiopropionic acid (haptens **9** and **10**) recognise also 2-methylthio-derivatives of herbicides (for example, ametryn and prometryn). In certain cases, the specificity of the antibodies obtained was unexpected.[18,19] Both homologous and heterologous haptens may be used for the synthesis of conjugates with an enzyme and a protein and also in analysis. We recall that, if a single hapten is used to obtain the immunogen and the conjugate and the method used to achieve its addition to the high-molecular-mass carrier is the same, then such a system is referred to as homologous. If, however, the haptens are different in the two cases the system is heterologous. The structure of the hapten used for conjugation to high-molecular-mass carriers can then exert an appreciable influence on the sensitivity of the assay. As will be seen below, heterologous systems are more sensitive than homologous ones.[17,23-26]

The conjugation of the modified carboxylated 1,3,5-triazine with the amino-groups of a protein or an enzyme to form a peptide linkage is carried out by the traditional methods used in protein

Table 2. The structures of the modified 1,3,5-triazines, the methods for the conjugation of derivatives with a carboxy-group, and the characteristics of the specificity of the monoclonal antibodies and polyclonal antisera obtained.

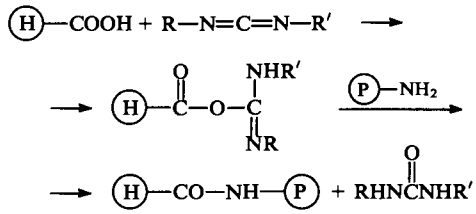
Compound	R^1	R^2	R^3	Method of conjugation with protein	Antibodies	Herbicide	Cross reaction (%)	Ref.
1	Pr^i	Cl	Cl	–	mAb	aziprotryn	100	18
						propazine	70	
					mAb	terbutylazine	100	19
						atrazine	7	
2	Et	$(CH_2)_nCOOH$ $n = 1-5$	Cl	AE	pAb	simazine	100	17, 23
						propazine	180	
						atrazine	250	
						hapten **2**	1830	
				CD (CMC)	mAb	atrazine	100	39
						propazine	136	
						cyanazine	28	
3	Pr^i	$(CH_2)_nCOOH$ $n = 1-5$	Cl	AE	pAb	atrazine	100	17, 23
						hapten **3**	700	
						propazine	260	
						simazine	12	
				AE	mAb	–	–	24
				MA	pAb	atrazine	100	28
						propazine	87	
						simazine	10	
				AE	pAb	atrazine	100	42
						propazine	90	
				CD (CMC, DCC)	pAb	atrazine	100	47
						propazine	195	
						simazine	20	
				CD (CMC)	pAb	atrazine	100	68
						propazine	116	
						prometryn	10	
				CD (CMC)	pAb	–	–	75
4	Et	$(CH_2)_2COOH$	OH	AE	pAb	hydroxysimazine	100	25
						hapten **3**	96	
						hydroxyatrazine	38	
5	Pr^i	$(CH_2)_5COOH$	OH	AE	mAb	hydroxyatrazine	100	42
						hydroxypropazine	100, 83[a]	
6	H	$(CH_2)_5COOH$	Cl	CD(CMC)	pAb	de-ethylatrazine	100	40
						deisopropylatrazine	100	
7	Pr^i	Et	SOMe	–	mAb	terbutryn	100	18
						terbutylazine	64	
				–	mAb	prometryn	100	18
						ametryn	25	
				–	pAb	atrazine	100	22
						ametryn	106	
						propazine	57	
8	Et	Bu^t	SOMe	–	pAb	terbutryn	100	21
						hydroxyterbutryn	78	
						terbutylazine	64	
9	Pr^i	Et	$S(CH_2)_2COOH$	AE	pAb	ametryn	100	17, 23
						hapten **9**	200, 670[a]	
				AE	mAb	–	–	24
				AE	pAb	–	–	72
10	Et	Et	$S(CH_2)_2COOH$	AE	pAb	simetryn	100	17, 23
						hapten **10**	1050, 157[a]	
11	Pr^i	$C(CN)Me_2$	$S(CH_2)_2COOH$	MA	pAb	cyanazine	100	29
						terbutylazine	3	
12	$(CH_2)_3COOH$	$C(CN)Me_2$	Cl	–	pAb	–	–	48, 49

Note. Notation adopted: pAb = polyclonal antisera, mAb = monoclonal antibodies, DCC = dicyclohexylcarbodiimide, CMC = 1-cyclohexyl-3-(2-*N'*-methylmorpholinoethyl)carbodiimide toluene-*p*-sulfonate, AE = activated esters method, CD = carbodiimide method, MA = mixed anhydride method.

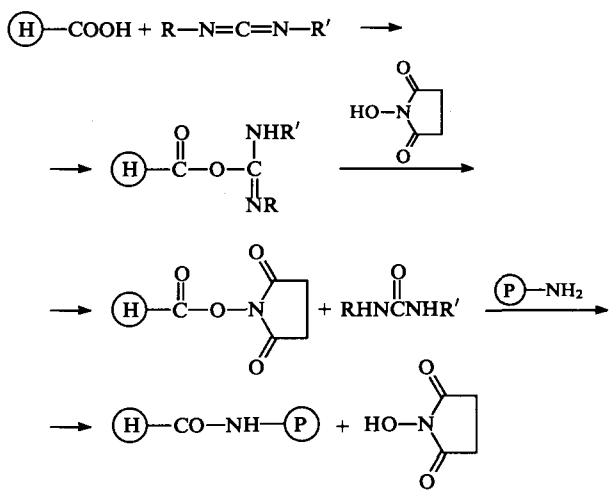
[a] The values for different antibodies or the values obtained by different methods for the determination of specificity are quoted.

chemistry. Among these we may specify the carbodiimide method, the activated esters method (the *N*-hydroxysuccinimide ester is used),[27] and the mixed anhydride method employing isobutyl chloroformate.[28,29]

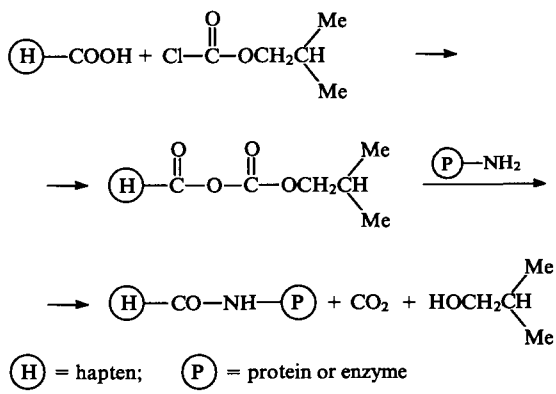
Carbodiimide method



Activated esters method



Mixed anhydride method



(H) = hapten; (P) = protein or enzyme

In most of the studies on the development of ELISA methods for 1,3,5-triazines, 96-well polystyrene trays are used. A number of investigators have also reported the employment of polystyrene test tubes,[30-37] spheres,[20-22] and magnetic particles.[29,38] The methods used to carry out the competitive enzyme-linked immunosorbent assay (formats) are also different (Fig. 1). Format I is usually employed for the screening of the antibodies obtained and is distinguished by a large number of stages. One of the modifications of format III involves preliminary adsorption of the antispecies antibodies or the protein A on the solid phase. It has been noted that an advantage of formats II and III over format I is a higher sensitivity and the fact that less time is required for the assay,[24-26,39] but they are more sensitive to the effect of the matrix and solvents.[24] The studies concerned with the comparative assessments of different forms of the ELISA method will be examined in greater detail below.

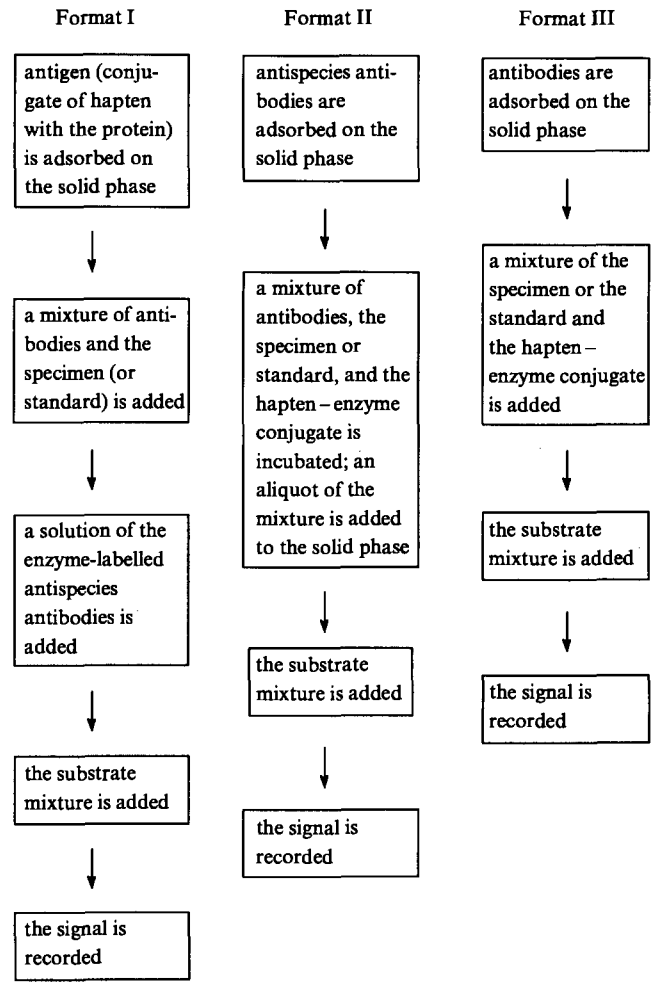


Figure 1. The ELISA formats used in the assay of haptens. After incubation, the unreacted components are washed off in each stage with a wash buffer containing clean Tween 20. Modification of format III: IIIa—antispecies antibodies are adsorbed on the solid phase in the first stage; IIIb—a protein A is adsorbed on the solid phase in the first stage.

A survey of published literature shows that 1,3,5-triazines are usually assayed by the ELISA method in water and soil although there have been reports also of other objects of study (Tables 3 and 4). Water is used for analysis without preliminary preparation, since its matrix does not as a rule affect the results of the assay. The data obtained by the ELISA and gas-chromatographic methods,[24,29,39-41] by the HPLC method,[26,30,36,37,42-44] and by gas chromatograph-linked mass spectrometry (GC/MS) [35] are satisfactorily correlated and the ELISA method does not afford any false negative results. A correlation of the results with HPLC data in the assay of liquid food products has been reported.[31] Herbicides from the soil, solid food products, and other objects are extracted with organic solvents or water. The results of such measurements are also satisfactorily correlated with physicochemical analytical data (Table 4).

III. Solid-phase immunoenzyme assay using polyclonal antisera

1. Determination of 1,3,5-triazines in objects within the environment

Among 1,3,5-triazines, most attention is devoted to atrazine, this being the most common herbicide of the given group used abroad, and its metabolites (Table 3). Assay methods developed on the basis of polyclonal antisera have been described in a series of publications.

Table 3. Characteristic of ELISA for 1,3,5-triazines.

Substance assayed	Detection limit/ng ml^{-1}	Samples	ELISA format[a]	Solid phase	Antibodies	Ref.
Atrazine	0.01	water	III	assay tray	pAb	20, 22
	0.1	"	III	spheres	pAb	20, 22
	0.05	water, soil	I, II, **IIIa**	assay tray	mAb	24
	0.5 – 10	water, soil	III	test tubes	pAb	30, 31
		food products			pAb	36, 37
	0.2 – 6.4	milk	III	"	pAb	32
	20 – 1000	soil	III	"	pAb	33, 34
	0.05	water		magnetic particles		38
	0.03	water, soil	II, III, **IIIa, IIIb**	assay tray	mAb	39
	0.05	" "	I	" "	mAb	42
	1 – 10	water, soil, algae	I	"	pAb	43
	1[b]	soil	III	" "	pAb	52
		water	**II**, IIIa	" "	mAb	55
	0.03 – 1	" "	IIIa	" "	mAb	58
	0.01 – 10	" "	I	" "	pAb	75
Deisopropylatrazine	0.01	" "	III	" "	pAb	40
De-ethylatrazine	0.01	" "	III	" "	pAb	40
	2[b]	soil	III	" "	pAb	52
Hydroxyatrazine	0.1	water, soil, manure, fungal micro-organisms	I, II, **IIIa**	" "	pAb	25
	0.1[c]	water, soil	I	" "	mAb	42
Hydroxysimazine	0.1[c]	water, soil, manure fungal micro-organisms	I, II, **IIIa**	" "	pAb	25
		soil	II, IIIa	" "	mAb	55
Atrazine mercaptourate	0.5	urine	IIIa	" "	mAb	57
Simazine		water, soil	I, II, **IIIa**	" "	mAb	24
		soil	**II**, IIIa	" "	mAb	55
Cyanazine	0.035	water	III	magnetic particles	pAb	29
	3.5	soil	III	" "	pAb	29
	0.5	water	I	assay tray	pAb	48, 49
	10	soil	I	" "	pAb	48, 49
Terbutryn	25 – 1500	water	III	" "	pAb	21
	0.1 – 600	" "	III	spheres	pAb	21
Atrazine, simazine, cyanazine	1[c]	" "	I, II, **IIIa**	assay tray	mAb	26

[a] The formats used for the assay are specified.
[b] The detection limit is expressed in μg kg^{-1}.
[c] The detection limit is expressed in μmol litre^{-1}.

The first studies on the ELISA of atrazine were published in 1985.[20,45] The radioimmunoassay method was used to characterise the antiserum described in a patent.[45] The conjugate of the hapten with the methyl ester of tyrosine, which was suitable for the introduction of the ^{125}I label, was synthesised by the mixed anhydride method; the atrazine detection limit was 1 ng in the sample. An ELISA with a lower atrazine detection limit of 0.1 ng ml^{-1} was developed later.[28] In assay by format I of ELISA use was made of secondary antibodies conjugated with biotin which interacted with the streptavidin – horseradish peroxidase conjugate in the following stage.

Polystyrene trays and spheres were used in the development of a homologous ELISA for atrazine.[20,22] Purification of the polyclonal antiserum by immunoaffinity chromatography made it possible to lower the detection limit by a factor of 100. It was noted that, when spheres are used as the solid phase, the assay is less sensitive (Table 3). The characteristic features of this procedure are the different ratio between the volume of the specimen and the area of the solid phase, a possible increase in sensitivity with increase in the volume of the specimen only within a limited range (a large volume of the specimen is then required for the assay), a long assay time (5 h), and difficulties in mechanisation and automation. The same procedure has been used in the development of a homologous ELISA for terbutryn.[21] The terbutryn detection limit was improved by a factor of 250 using polystyrene spheres as the solid phase.[46] A similar range of measurable concentrations was obtained using ^{14}C-labelled terbutryn in radioimmunoassay.[46]

Wittmann and Hock[47] used different carbodiimides to synthesise the immunogen: 1,3-dicyclohexylcarbodiimide (DCC), 1-ethyl-3-(3-dimethylaminopropyl)carbodiimide hydrochloride (EDC), and CMC as well as various hapten : protein and carbodiimide : hapten ratios. A number of the immunogens proved to be insoluble (especially when EDC was used). An immunogen having the hapten : protein = 4 : 1 composition was used for immunisation in the initial stage (hapten : protein = 200 : 1 and DCC : hapten = 1 : 2), but, since the titres of the antisera were low, an immunogen with the maximum number of attached molecules (hapten : protein = 35 : 1; reactant ratios — hapten : protein = 100 : 1, and DCC : hapten = 1 : 1) was employed for subsequent immunisation. Also synthesised were homologous conjugates with enzymes such as horseradish peroxidase (by the activated esters method) and alkaline phosphatase (using CMC). The hapten : enzyme and hapten : carbodiimide ratios were also varied in the synthesis. The conjugate with peroxidase exhibited a higher sensitivity of assay and was used for subsequent

Table 4. The extractants and the procedures used in the preparation of the specimen for the assay of 1,3,5-triazines by the ELISA method.

Specimen analysed	Extractant and procedure for preparation of specimen [a]	PCM for correlation	Ref.	Specimen analysed	Extractant and procedures for preparation of specimen [a]	PCM for correlation	Ref.
Soil	water, aqueous methanol, dilution with buffer	GC	23	soil	water, tenfold dilution	–	52
	ethyl acetate; acetonitrile : water (9 : 1), evaporation reconstitution with buffer	GLC	24		ethyl acetate, evaporation and dilution with buffer	CC [b]	55
	acetonitrile, evaporation to dryness, reconstitution with buffer	–	25		water : methanol (3 : 2), dilution with buffer	GC	56
	methanol : water (3 : 1), 50-fold dilution with buffer	–	29	manure	methanol : ethyl acetate (1 : 1), evaporation, reconstitution with buffer	–	25
	aceonitrile : water (9 : 1), evaporation to dryness, reconstitution with buffer	HPLC	30	fungal microorganisms	methanol : water (1 : 10)	–	25
	water; methanol; water : methanol (3 : 2); acetonitrile, dilution with buffer	GC	34	solid food products (maize, pineapple)	acetonitrile : water (9 : 1), evaporation to dryness, reconstitution with buffer	HPLC	31
	methanol : water (4 : 1), 40-fold dilution with buffer	GLC, HPLC	42	algae	organic solvents, dilution with buffer to 1%	HPLC	43
	water, electro-ultrafiltration	GC	43	urine	chloroform, evaporation to dryness, reconstitution with buffer	–	57
	methanol : water (4 : 1), 0.5 M ammonium acetate, acetonitrile : water (9 : 1), dilution of organic-extracts with buffer	–	51				

[a] The extractants used for the assay are specified.
[b] Probably column chromatography (Ed. of Translation).

optimisation. The method developed was applied to the analysis of water, soil, and algae.[43] In the last case, an ecosystem model with algae and organisms into which specific amounts of atrazine had been introduced was employed. The authors note that the method is fast and convenient, but appreciable cross-reactivity with propazine is one of its disadvantages. Three types of ELISA, based on various combinations of two antisera obtained against immunogens of different structure, and two enzyme conjugates, were subsequently assessed.[41] In the most sensitive assay, the cross-reactivity was 195% for propazine and 20% for simazine.

The use of magnetic particles as the solid phase in the development of ELISA for atrazine has been reported.[38] The degree of cross-reaction was 171% for ametryn, 132% for propazine, and 105% for prometryn. It was shown that the presence of various salts, metal ions, or a change in pH from 2 to 12 do not affect the results of the analysis of water specimens. The authors note the advantages of the assay developed: the assay time is 45 min and there are no problems with the coverage of the solid phase by antibodies (the antibodies are attached to magnetic particles via glutaraldehyde).

Investigators of the Shell Development Company obtained a highly specific antiserum to cyanazine which was used to develop the ELISA.[48,49] Cross-reaction was demonstrated only for cyanazine metabolites. The method was used to monitor water and soil and the analytical results were well correlated with gas-chromatographic data. The ELISA for cyanazine in water and soil on magnetic particles has been developed[29] by the method of Rubio et al.[38] A high specificity of the method for cyanazine and tolerance towards the matrix as well as sensitivity to changes in pH and different components of the medium (organic solvents, salts) were noted.

In Western countries, some firms already manufacture kits of immunochemical reagents for the assay of 1,3,5-triazines,[16] for example: Res-I-Mune™, Res-I-Quant™ ("Immunosystems"); Triazin-ELISA ('Riedel-de-Haen'); RaPID Assays® ('Ohmicron'); EnviroGard™, Triazine Test Kit ('Millipore'). Studies have been published where such kits have already been applied successfully. Bushway and coworkers developed an ELISA for atrazine in water,[30,36,37] soil,[30] liquid and solid food products,[31] and milk[32] using Res-I-Mune™, which incorporates polystyrene test tubes coated with polyclonal antibodies and all the necessary reagents. In one assay, it is possible to analyse eight specimens and the assay time is 15 min. The study of a large number of water, soil, food products, and milk specimens containing both natural and introduced herbicides demonstrated the high accuracy and satisfactory reproducibility of the results. In the analysis of food products, positive results were obtained for

two specimens. However, the HPLC method demonstrated the absence of herbicides from these samples. In the analysis of milk specimens, the authors noted that unduly low results are obtained for samples with a high fat content. They put forward a hypothesis according to which atrazine dissolves partly in the fat and becomes inaccessible to the antibodies. The authors divided milk into three groups in terms of its fat content: > 3.5%, 1.5%–3.5%, and < 0.5% and proposed that the milk specimens should be diluted to give a fat level of the order of 1%, although this lowers the detection limit. The cross-reactions of polyclonal antibodies have been investigated[32] and it has been observed that ametryn, propazine and simazine give rise to the highest percentage of cross reactions. In view of the simplicity and rapidity of the proposed method, the authors suggest that it be used also for assay under field conditions. It has shown that the assay is relatively insensitive to changes in pH, temperature, and the concentrations of calcium, sodium, and nitrate ions.[50]

An attempt to apply the Res-I-Mune™ kit to the assay of atrazine in the soil has been described.[33,34] It has been reported[33] that coextracted substances interfere with the determination. When extraction with water was used, atrazine was determined at concentrations of 0.5–5 ng ml^{-1}, while in the case where methanol was used as the solvent the concentration range was 5–20 ng ml^{-1}. Various solvents for extraction have been investigated (Table 4).[34] A water–methanol mixture and methanol were selected taking into account the ability of the solvents to extract the herbicide. However, the authors abandoned the use of methanol, since it affected the results of the assay at atrazine concentrations less than 50 ng ml^{-1}. The authors note that this assay is suitable for use in fields subjected to a known chemical treatment. The same kit has been used to analyse water specimens.[35]

A commercial kit for the immunoenzyme assay of atrazine on Res-I-Quant™ 96-well trays has been described.[51] The authors tested two different methods and three solvents (Table 4) in the extraction of atrazine from the soil. The presence of organic solvents begins to affect the results of the assay at concentrations greater than 3.5%. It was shown that the best solvent as regards the percentage detection of the herbicide is acetonitrile.

The metabolites of 1,3,5-triazines have not been neglected either. A study has been devoted to the development of a homologous ELISA for deisopropyl- and de-ethyl-atrazine.[40] The calibration curves for both compounds virtually coincided. The method using a conjugate of the hapten to horseradish peroxidase proved to be more sensitive than the one employing a conjugate with alkaline phosphatase. The method developed for the assay of atrazine[43] and of its principal metabolite (de-ethyl-atrazine)[40] has been used to study the degradation of atrazine in the soil in the course of a year.[52] It was suggested that a simplified scheme be used for the extraction of the herbicide with water, which makes it possible to achieve its extraction from the soil at the level of 1/3–2/3 of the extraction with methanol. The ELISA for de-ethylatrazine has been used successfully in the analysis of water specimens.[44]

The application of ELISA for the determination of hydroxysimazine and hydroxyatrazine in various media (water, soil, and manure) and for the investigation of the degradation of atrazine by micro-organisms resistant to UV light has been demonstrated.[25] For use in the assay, haptens **2** ($n = 2$), **4**, and **5**, were conjugated to bovine serum albumin (BSA) and alkaline phosphatase by the activated esters method. The attempt to develop homologous and heterologous (conjugate based on hapten **5**) systems for hydroxysimazine was unsuccessful for all formats of ELISA. An unexpectedly high sensitivity was achieved using the enzyme conjugate based on hapten **2** ($n = 2$). The study of the antisera obtained by means of this system showed that three of the antisera recognise effectively hydroxysimazine and one recognises hydroxyatrazine. By using different modifications of format III, it was established that the direct coating of the tray with antibodies reduces the sensitivity by a factor of 2–5. The antiserum responding to both metabolites was selected to develop assay methods. It was shown that different salts and metal ions over a wide range of concentrations, pH (5–9), and matrices do not affect the results in the analysis of water specimens. It was suggested that this method be used to investigate ecosystems as regards their tolerance and ability to degrade xenobiotics.

Interesting data on two interlaboratory tests have been published.[53] For the first test, ten water specimens of different composition were sent to thirteen laboratories. Each laboratory analysed the specimens by the ELISA method, and the results were confirmed by GC/MS data. It was reported that only some laboratories were able to determine the correct amount of atrazine and none of the laboratories were able to determine correctly the total amount of 1,3,5-triazines. For the second test, six water specimens of different composition were analysed in twelve laboratories with the aid of the three ELISA procedures which were most successful in the first test. These results were also compared with gas chromatographic and GC/MS data and showed that among the three ELISA methods, one determines atrazine specifically, while the others determine the total amount of 1,3,5-triazines in the sample. Some useful comments were made: (1) it is necessary to certify immunochemical laboratories (the personnel working in these laboratories must be highly qualified); (2) it is necessary to describe the assay procedure in detail; (3) the working concen-tration range must be close to the middle of the calibration curve; (4) at least 6 standard solutions must be employed to plot the calibration curve; (5) if the matrix is unknown [?known (Ed. of Translation)], the substances analysed should be introduced into it; (6) four replicate measurements must be made for each specimen in order to avoid erroneous results.

2. The influence of the structure of the immunoreagents and of the format of the analysis on the sensitivity of the determination

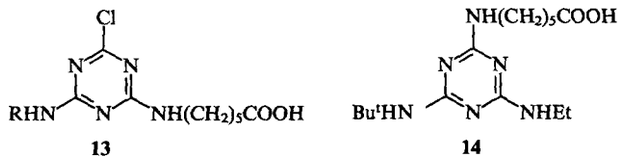
It is seen from the foregoing that homologous systems are used as a rule in the development of ELISA. Hammock's group carried out a fundamental study designed to develop and optimise the ELISA methods for herbicides of the 1,3,5-triazine class and to determine the influence of the structure of the immunoreagents on the parameters of the analysis.[17,23] Two types of atrazine and simazine derivatives were synthesised and characterised: (a) haptens **9** and **10**; (b) haptens **2** and **3** with different lengths of the spacer, ranging from $n = 1$ to $n = 5$. Conjugates of haptens **2**, **3**, **9**, and **10** as well as dichlorosimazine and dichloroatrazine with BSA, conalbumin (CONA) and tyroglobulin (TG) were synthesised. Since problems concerning the solubility of the conjugates with TG and CONA arose, those with BSA were used as antigens in the analysis.

During the screening of the antibodies, the authors[17,23] noted the following features: the maximum binding was observed for all the antibodies in homologous systems, the majority of the antibodies exhibiting appreciable binding to at least one heterologous antigen. When immunogens based on atrazine were used, the sera were obtained with higher titres than in the case when simazine derivatives were used. For the former, high titres were observed in many instances when a heterologous antigen was applied, while in the latter this happened in only one case. Next, the assay was optimised for antisera with the highest titre in relation to a large number of heterologous systems using atrazine and simazine as inhibitors. It was shown that homologous systems are least sensitive. In a study of the conjugation site, of the length of the 'foot' (the length of the alkyl chain), and of the changes in the *N*-alkyl groups, it was observed that the sensitivity depends to the greatest extent on the conjugation site, although this rule has not always been observed. For example, the highest sensitivity of the antisera obtained against the protein conjugate of hapten **5** was attained using a protein conjugate of hapten **1** (in which the 'foot' was altogether absent).

In the study of the specificity of the antisera obtained, it was noted that homologous haptens induce the greatest inhibition. The authors note that the antisera can be divided into two groups: antisera obtained against protein conjugates of haptens **9** and **10**, which recognise not only atrazine but also other 2-methylthio-1,3,5-triazines, and antisera obtained against protein conjugates of haptens **2** and **3**, which effectively recognise the 2-chloro-compounds and hardly react with the 2-methylthio-derivatives. The loss of an alkyl group on substitution of a chlorine atom (methylthio-group) by a hydroxy-group led to an appreciable decrease of recognition by all the antisera.

The influence of the matrix and solvents in the sample has been examined[17,23] in the assay of water and soil specimens. It was observed that the most sensitive systems proved least resistant to the influence of the matrix and solvents in the extract. The authors note that, in the development of any assay method, it is necessary to find a compromise solution: between the most sensitive assay and the greatest tolerance to the influence of the matrix. The authors also emphasise that, in the presence of a set of well characterised antibodies and antigens of different structure, it becomes possible to determine quantitatively structurally similar substances in specimens of complex composition.

An attempt has been made[54] to follow the influence of the structure of the enzyme conjugate on the sensitivity of the assay. Conjugates with horseradish peroxidase were synthesised by the activated esters method. The haptens employed were compounds **13** with various side groups (ethyl, isopropyl, cyclopropyl, *tert*-butyl, cyclopentyl) and 2-*tert*-butylamine-4-(1-carboxypent-5-yl)amino-6-ethylamino-1,3,5-triazine **14**.



R = Et, Pr^i,  , Bu^t,  .

A distinct dependence of the sensitivity of the assay on the structure of the conjugates could not be found. For the antibodies obtained against the protein conjugate of hapten **3**,[47] the sensitivity decreased in the sequence (the substituents R are indicated) isopropyl > ethyl > cyclopropyl > *tert*-butyl > cyclopentyl when conjugates based on compound **13** were used. The same antibodies were scarcely bound to the conjugates obtained from compound **14**. For the antibodies to the protein conjugate of hapten **7**,[22] the greatest sensitivity was achieved when the enzyme conjugate of the hapten with an isopropyl side group was employed, while for the remaining conjugates scarcely any binding was observed.

As can be seen from the foregoing, the use of polyclonal antisera makes it possible to attain low detection limits for 1,3,5-triazines in various objects. However, the fact that the number of antisera obtained is limited and their quality (affinity, specificity) depends on the animal immunised precludes their standardisation. The last disadvantage can be avoided by using monoclonal antibodies for the assay.

IV. Solid-phase immunoenzyme assay using monoclonal antibodies

Monoclonal antibodies have found extensive application in the assay of 1,3,5-triazines. One of their advantages is the possibility of their standardisation and production in a virtually unlimited amount. Monoclonal antibodies to atrazine and its metabolite hydroxyatrazine have been described.[42] In the homologous ELISA, format I was used and the mixture of antibodies and the specimen was subjected to preliminary incubation before adding them to the tray.

Karu et al.[24] summarised the results of studies in three laboratories on the development of ELISA methods for 1,3,5-triazines using monoclonal antibodies. Three formats were investigated—I, II, and IIIa. They all exhibited approximately the same sensitivity (conjugates with hapten **3** were used), but the application of the enzyme conjugate of hapten **2** ($n = 2$) in format IIIa increased the sensitivity of the assay by a factor of 5. The study of the specificity of the antibodies obtained showed that monoclonal antibodies bind preferentially to 1,3,5-triazines containing an isopropyl group in the 4- or 6-position and a methylthio-group in the 2-position; *N*-dealkyl and hydroxy-derivatives hardly react with the antibodies. It was shown that the results of the assay of 75 water specimens by gas chromatography for atrazine and of 48 soil specimens by gas–liquid chromatography for simazine were satisfactorily correlated with ELISA results. The method was used to determine atrazine and simazine in sewage.

A whole series of studies have been carried out in which the monoclonal antibodies proposed by Karu et al. were used.[24] Lucas et al.[55] compared the advantages of two ELISA methods for simazine and atrazine using monoclonal antibodies[24] and polyclonal antisera.[17] One of the polyclonal antisera and the monoclonal antibodies were employed against the protein conjugate of hapten **9**, while another polyclonal antiserum was used against the protein conjugate of hapten **3**. Two ELISA formats were investigated (II and IIIa) using the conjugate of hapten **3** ($n = 2$) with alkaline phosphatase for the monoclonal antibodies and the conjugate of hapten **3** ($n = 3$) for polyclonal antisera. Comparison of the antibodies showed that the polyclonal antisera were more specific to atrazine than to simazine, while the monoclonal antibodies recognised both herbicides to approximately the same extent. The monoclonal antibodies showed a greater sensitivity, a weaker background, a more intense colour of the product of the enzymic reaction, and a greater resistance to the influence of the solvent on the matrix compared with the polyclonal antisera. They were therefore selected for the assay.

In the study of different assay formats, it was observed that the use of format IIIa increases the sensitivity by a factor of 10. However, format II proved to be more resistant to the influence of the matrix and gave rise to a weaker background. For example, the presence of methanol, acetonitrile, acetone up to 10%, and tetrahydrofuran up to 2.5% did not affect the results of the assay. Format II was selected for the analysis of water and soil specimens. The assay developed subsequently[55] was used successfully in the study of the leaching of simazine.[56] Soil specimens were collected from different depths after irrigation, the highest concentration of the herbicide being observed in the upper layers of the soil (0.2 m). The application of this assay method in the study of the content of atrazine and its metabolites in urine has been reported;[57] gas chromatography, mass spectrometry, and HPLC have been used to supplement and confirm the ELISA data in qualitative and quantitative determinations of the atrazine metabolites. It was shown that the main atrazine metabolites in the urine of people working with herbicides is atrazine mercaptourate. This metabolite was found at concentrations ten times greater than atrazine or its *N*-dealkyl derivatives. Atrazine mercaptourate was isolated from urine by affinity extraction using polyclonal antisera.[17,25] After monitoring for ten days the level of atrazine mercaptourate in the urine of people working with atrazine and who have received different doses of the herbicide through the skin or via the respiratory pathways, it was suggested that ELISA be used to determine atrazine mercaptourate as a biomarker of the dose received.

The influence of the ELISA format and of the structure of the enzyme conjugate on the sensitivity of the method has been analysed in detail;[39] the optimum variant was used to analyse water and soil specimens. Enzyme conjugates with horseradish peroxidase and alkaline phosphatase were synthesised for haptens **2** and **3** ($n = 2, 5$) by the activated esters method. Four formats were investigated — II, III, IIIa, and IIIb. Different

antigen : enzyme ratios were used in the synthesis of the enzyme conjugates. It was found that the sensitivity of the assay depends little on the antigen : enzyme ratio, although an increase in the amount of the hapten entailed a proportional increase in the optical density of the product of the enzymic reaction. Comparison of the enzyme conjugates showed that the use of haptens with the longest 'foot' ($n = 5$) for conjugates with horseradish peroxidase increases the sensitivity by a factor of 3–5 compared with haptens having a short 'foot' ($n = 2$). For conjugates with alkaline phosphatase, the opposite picture was obtained. In general, the conjugates with alkaline phosphatase proved inferior to the conjugates with horseradish peroxidase, since they required a smaller dilution and a longer time for the development of the colour of the product of the enzyme reaction. Ultimately the enzyme conjugate of hapten **3** with horseradish peroxidase proved to be best. The authors[39] note that this feature, found for different enzymes, is somewhat surprising and attribute it to the different molecular masses of the enzymes and hence to different dispositions of the hapten on their surfaces and to possible steric hindrance.

Comparison of different formats of the assay showed that format II was least sensitive and economical as regards the consumption of the reagent. Formats III, IIIa, and IIIb had approximately equal sensitivities but a longer time was required for format III to develop the colour of the same intensity as for formats IIIa and IIIb. In addition, the greatest scatter of the results from tray to tray was observed for this format. As regards formats IIIa and IIIb, the former was selected for the assay as being more economical. The greatest percentages of cross-reaction were observed for atrazine (100%), propazine (147%), ametryn (70%), and simazine (32%).

The preparation of monoclonal antibodies and an extremely simple semiquantitative method for the assay of atrazine on strips have been reported.[58] The duration of the assay is 20 min. The strips are coated in succession by antispecies antibodies, monoclonal antibodies, and casein. For the assay, an aliquot of the specimen assayed and the enzyme conjugate are mixed and placed on the strips for 5 min. After washing, the colour is developed. This method makes it possible to determine visually the content of atrazine in water at a concentration in excess of 0.5 ng ml^{-1}. Monoclonal antibodies have also been used in the development of ELISA. The employment of conjugates of haptens **2** and **3** with horseradish peroxidase involved hardly any differences in their calibration curves and the conjugate of hapten **3** was used for the assay.

After the use of atrazine had been prohibited in Germany, it began to be replaced universally by terbutylazine. This is the reason why a series of studies on the development of ELISA for this herbicide have appeared recently. Giersch and Hock[18] described the synthesis of homologous conjugates of terbutylazine with alkaline phosphatase involving the use of format III. Somewhat unexpected results were obtained. For antibodies synthesised against the conjugate of hapten **7**, the greatest cross-reactivity was shown by terbutryn and prometryn (the detection limits were 0.1 and 0.3 ng ml^{-1} respectively), while the antibodies to the protein conjugate **1** (Table 2) recognised aziprotryn most effectively (detection limit 1 ng ml^{-1}). The monoclonal antibodies obtained[18] were used in numerous investigations. It has been suggested[59] that dextran be employed as the high-molecular-mass carrier. When protein conjugates and the conjugate with dextran were used in format I, it was shown that the sensitivity of the determination is approximately the same in both cases. The advantages of the conjugates with dextran were noted: resistance to denaturation and resistance to high temperatures, different pH values, and salts.

The influence of the incubation time of the enzyme conjugate on the sensitivity of ELISA has been investigated. Monoclonal antibodies,[18,42] polyclonal antisera,[22,47] and format III were used. In order to obtain antibodies to the protein conjugates of haptens **3**, a homologous enzyme conjugate was employed, whilst for the remaining antibodies use was made of the conjugate of compound **14**. Conjugates with horseradish peroxidase were obtained by the activated esters method. The incubation time of the conjugate was varied from 1 min to 40 h. For the polyclonal antibodies, the variation in the position of the central point on the calibration curve was appreciable (by five orders of magnitude). The authors explained this by the presence in the polyclonal antiserum of antibody fractions with different affinities. It was noted that such a large range of measurable concentrations permits the analysis of an undiluted specimen over a wide range of concentrations solely by varying the incubation time of the enzyme conjugate. For monoclonal antibodies, the variation was much less (by about one order of magnitude). A decrease in the incubation time led to a decrease in the optical densities of the product of the enzymic reaction. It was observed that a decrease in the assay time did not diminish the cross-reactivity. For the optimised assay of atrazine based on the polyclonal antiserum, the detection limit was 2 ng $litre^{-1}$ (incubation time 1 min), whereas for monoclonal antibodies the detection limit in the assay for terbutylazine was 30 ng $litre^{-1}$ (incubation time 7 min).

Monoclonal antibodies to the protein conjugate of hapten **1** have been obtained.[19] ELISA for terbutylazine was optimised using various formats (I, modification of I by labelling monoclonal antibodies with biotin and subsequent interaction with the streptavidin–horseradish peroxidase conjugate, IIIa). A protein conjugate of hapten **2** was used in the assay involving format I, whereas for format IIIa use was made of the enzyme conjugate of hapten **2** with an isopropyl side group. It was shown that the sensitivity increased in the following series of formats: I, modified I, IIIa.

Thus the employment of monoclonal antibodies in the assay of 1,3,5-triazines make it possible as a rule to obtain a higher sensitivity of the assay compared with polyclonal antibodies. However, it is not possible to improve radically the specificity of the assay, since monoclonal antibodies also exhibit an appreciable cross-reaction with related 1,3,5-triazines. This may be associated with only slight differences between the structures of the herbicides of the given group, which as a rule involve only the alkyl substituent in the side chain.

V. Quantitative determination of several herbicides in one sample

Owing to the appreciable cross-reaction with structurally similar 1,3,5-triazines when the sample contains several related herbicides, it is impossible to determine quantitatively just one of them. We shall consider below the results of two studies in which ways of solving this problem have been proposed.

The application of a set of characterised monoclonal antibodies for the quantitative determination of atrazine, simazine, and cyanazine in a single specimen in the analysis of waste and wash liquids has been described.[26] Five monoclonal antibodies,[24] three formats [I (with preincubation of a mixture of a solution of antibodies and the specimen or standard), II, and IIIa], and various (homologous and heterologous) structures of the ELISA antigens were investigated. From the five antibodies proposed initially, three with different cross-reactivities in relation to atrazine, simazine, and cyanazine were selected. The highest sensitivity was observed for the heterologous systems. In terms of sensitivity, format II was best, while the sensitivity for format IIIa was slightly lower but the assay time was then shorter by 2 h. Initially all the antibodies were analysed by means of format I using the protein conjugates of haptens **3** and **9** with BSA, by means of format II using the enzyme conjugate of haptens **2** ($n = 2$) and **3** ($n = 2$), and by means of format IIIa using the enzyme conjugate of hapten **2** ($n = 2$). Three ELISA methods (with different antibodies) in format IIIa were used to analyse water specimens employing a conjugate of hapten **2** ($n = 2$). An approach to a quantitative determination of several herbicides was based on the assumption that the observed response and the

response measured in the immunoassay (i.e. in ELISA) of the antibodies binding to the antigens present in the sample represents an 'overall response' to all the reacting antigens. The observed response is represented by the equation

$$\text{ELISA response} = A(X_A) + B(X_B) + C(X_C) + \ldots + Z(X_Z),$$

where the ELISA response is the amount of substance assayed determined on the basis of the calibration curve for the antigen selected as the standard, A, B, C, and Z are the concentrations of different antigens, and X_A, X_B, X_C, and X_Z are the reactivity coefficients for these antigens.

In this case, the ELISA response was expressed in micromoles of atrazine, the reactivity coefficient for which was adopted as unity. The reactivity coefficients for other herbicides were determined from the slope of the plot of the linear dependence of the ELISA response on the antigen (simazine or cyanazine) concentration. In the analysis of specimens containing three herbicides, equations were derived for each ELISA:

$$\text{ELISA response 1} = A(X_{A1}) + B(X_{B1}) + C(X_{C1}),$$

$$\text{ELISA response 2} = A(X_{A2}) + B(X_{B2}) + C(X_{C2}),$$

$$\text{ELISA response 3} = A(X_{A3}) + B(X_{B3}) + C(X_{C3}),$$

where A, B, and C are the unknown concentrations of atrazine, simazine, and cyanazine and X_{Ai}, X_{Bi}, and X_{Ci} are respectively the reactivity coefficients of atrazine, simazine, and cyanazine when different antibodies are used ($i = 1-3$).

The amount of each herbicide in the sample was determined by solving three equations with three unknowns. Analysis of water specimens showed that atrazine and the total amount of herbicides are determined with a satisfactory accuracy and reproducibility, whereas the determination of simazine and cyanazine is less accurate.

The application of two antibodies with different specificities for the detection of a known pesticide in the sample has been reported.[61] A polyclonal antiserum (the cross-reactivities with respect to atrazine and terbutylazine were 100% and 4% respectively)[47] and monoclonal antibodies (the cross-reactivities for terbutylazine and atrazine were 100% and 25% respectively)[18] were used in the analysis of water specimens. In the assay of atrazine, the cross-reactivity in relation to terbutylazine (4%) was used to calculate the concentration equivalent of terbutylazine. Similar calculations were performed in the assay of terbutylazine. Next, the ratio of the smaller and higher concentration equivalents was determined for each herbicide. If the ratio was in the range 0.4–1, it was concluded that the herbicide was present in the sample. A satisfactory correlation of the results with gas-chromatographic data was obtained. Thus it was shown that the type of herbicide employed can be determined rapidly in the sample by the ELISA method.

VI. Alternative immunoassay methods

Apart from the spectrophotometric detection of the enzymic reaction product usually employed, it is possible to detect its fluorescence or luminescence.

Two versions of the immunoassay of atrazine and simazine with enhanced luminescence have been described.[62,63] In the former case, the peroxidase-labelled hapten competed with the substance assayed for the binding centres of polyclonal antibodies adsorbed on test-tubes. The test-tubes were then washed and the amount of peroxidase remaining with the antibodies was determined using the isoluminol reagent. When assay trays were used, the range of measurable concentrations was 0.01–1 ng ml^{-1}. The concentrations of the reagents were increased compared with the usual method in order to shorten the incubation time and make the assay suitable for field conditions.

Ulrich and Niessner[64] used a fluorogenic substrate for alkaline phosphatase in the development of an immunoassay for terbutylazine with fluorescence detection of the label. For a homologous assay on monoclonal antibodies,[18] the required incubation time of the substrate mixture was 20 h. Later is was possible to shorten the incubation time to 20 min by synthesising the enzyme conjugate by means of a modified method.[65] Glyme was used as the solvent for the synthesis of the enzyme conjugate, while, instead of the traditional *N*-hydroxysuccinimide, di(*N*-succinimidyl) carbonate was employed.[66]

The study of Seare et al.[67] was devoted to the application of fluorescence immunoassay (FIA) in the quantitative determination of 1,3,5-triazines. For this purpose, the hapten was conjugated with fluorophors (dansyl chloride or fluorescein).

Recently increasing attention has been devoted to versions of the immunochemical assay methods where the procedure is simplified to the maximum extent and which are most suitable for routine analyses under field conditions. The development of a semiquantitative method for the determination of atrazine on strips was described above.[58]

It has been suggested that immunobiosensors be used to assay atrazine in drinking water.[68] The immunobiosensor consists of a piezo-crystal with a vibration frequency of 10 MHz, which is coated in succession with a protein A and polyclonal antibodies. When the immunobiosensor is bound to atrazine, the mass of the crystal and hence the frequency of its vibrations changes, the effect being proportional to the content of the pesticide in water. After the removal of the antigen from the surface, such an immunobiosensor can be used for 8–9 measurements. The linear range of the measurable concentrations is 0.03–100 μg ml^{-1}.

The first description of flow-injection immunoassay for pesticide determination in water was published in 1991.[69] A polyclonal antiserum to atrazine[47] was immobilised on immunoaffine membranes. The 'stop-go' method was used when the reagents were passed through the membrane and a fluorimeter was employed to detect the product of the peroxidase oxidation of hydroxyphenylpropionic acid. The linear range of the calibration curve was 0.02–0.3 ng ml^{-1}. The reproducibility of the results was poorer than in the corresponding immunoenzyme assay method. This might have been due to the nature of the flow–injection reaction, the nonequilibrium reaction conditions, and the immobilisation method used.

The optic fibre immunosensor has been employed to assay atrazine in water.[70] The hapten was immobilised on the surface of the optic fibre via glutaraldehyde. The immunosensor was placed in a cell containing a mixture of the specimen to be analysed and monoclonal fluorescein-labelled antibodies[18] and the fluorescence was measured. In a later study,[71] it was possible to reduce the detection limit by a factor of 100 (0.01 nM atrazine concentration) by selecting the hapten for immobilisation.

An immunochromatographic method for the assay of atrazine in which ABICAP (antibody immunocolumn for analytical processes, Abion, Germany) immunochromatographic columns with a microheterogeneous medium, containing antispecies antibodies, are used, has been developed.[72] In the assay, the reagents are passed in succession through the column in the course of 10 min; the lower limit in the detection of atrazine is 0.1 ng ml^{-1}. Various detection methods (spectrophotometric, fluorescence, and chemiluminescence) are considered in the above communication.

The present authors are conducting studies designed to develop a polarisation fluorescence immunoassay (PFIA) for herbicides of the 1,3,5-triazine group and to investigate the influence of the structure of the labelled hapten on the sensitivity of the assay. The method is homogeneous, simple, and rapid. It is based on the competition between the antigen to be determined and the antigen with a fluorescence label for the limited number of binding centres of the antibody and on the measurment of the degree of polarisation of the reaction mixture. A PFIA has been developed[73] for simazine on the basis of a polyclonal antiserum with a lower detection limit of 5 ng ml^{-1}. The influence of the structure of the labelled antigen on the sensitivity of the assay has been studied.[74] It was shown that the assay employing

heterologous labelled antigen with the shortest chemical bridge is the most sensitive. The PFIA method is less sensitive than the ELISA method, but it is simpler and rapid.

One may conclude that immunochemical methods for the assay of herbicides of the 1,3,5-triazine group are used successfully in the analysis of various specimens. The results obtained by immunochemical and physicochemical analytical methods are as a rule satisfactorily correlated. The simpler and fast immunochemical methods will apparently also soon find extensive application in our country.

References

1. *European Communities, Council Directive of 15th July 1980 Relating to the Quality of Water Intended for Human Consumption [80/778/EEC], Drinking Water Directive* N L 229
2. V A Kasparov, V K Promonenkov *Primenenie Pestitsidov za Rubezhom* (Application of Pesticide Abroad) (Moscow: Agropromizdat, 1990)
3. V A Zakharenko *Gerbitsidy* (Herbicides) (Moscow: Agropromizdat, 1990)
4. D Soniassy (Ed.) *Environmental Analysis. Instrumental Techniques* (Moscow: Mir, 1993)
5. M A Klisenko, A A Kalinina, K F Novikova (Comps) *Metody Opredeleniya Mikrokolichestv Pestitsidov v Produktakh Pitaniya, Kormakh i Vneshnei Srede: Spravochnik* (Methods for the Determination of Microamounts of Pesticides in Foodstuffs, Animal Feed, and the Environment: Handbook) (Moscow: Kolos, 1992)
6. A Di Corcia, M Marchetti *Anal. Chem.* **63** 580 (1991)
7. G Felding *Pestic. Sci.* **35** 39 (1992)
8. S G Zhemchuzhin, R P Gorobets *Agrokhimiya* (1) 149 (1990)
9. E A Korostyleva, O A Mel'nichenko, A A Tumanov *Zh. Anal. Khim.* **46** 2314 (1991)
10. B D Hammock, R O Mumma, in *Pesticide Analytical Methodology (ACS Symposium Series)* Vol. 136 (Eds J Harvey, G Zweig) (Washington DC: American Chemical Society, 1980) p. 321
11. R O Harrison, S J Gee, B D Hammock, in *Biotechnology in Crop Protection (ACS Symposium Series)* Vol. 379 (Eds P Hedin, J J Menn, R M Hollingworth) (Washington DC: American Chemical Society, 1988) p. 316
12. F Jung, S J Gee, R O Harrison, M H Goodrow, A E Karu, A L Braun, Q X Li, B D Hammock *Pestic. Sci.* **26** 303 (1989)
13. J Van Emon, J N Seiber, B D Hammock, in *Analytical Methods for Pesticides and Plant Growth Regulators: Advanced Analytical Techniques* Vol. XVII (Ed. J Sherma) (New York: Academic Press, 1989) p. 217.
14. W H Newsome *J. Assoc. Off. Anal. Chem.* **69** 919 (1986)
15. J P Sherry *Crit. Rev. Anal. Chem.* **23** 217 (1992)
16. R O Harrison, M H Goodrow, S J Gee, B D Hammock, in *Immunoassays for Trace Chemical Analysis: Monitoring Toxic Chemicals in Humans, Food and Environment (ACS Symposium Series)* Vol. 451 (Eds M Vanderlaan, L H Stanker, B E Watkins, D W Roberts) (Washington DC: American Chemical Society, 1991) p. 14.
17. M H Goodrow, R O Harrison, B D Hammock *J. Agric. Food Chem.* **38** 990 (1990)
18. T Giersch, B Hock *Food Agricul. Immunol.* **2** 85 (1990)
19. T Giersch, K Kramer, B Hock *Total Envir.* **132** 435 (1993)
20. S J Huber *Chemosphere* **14** 1795 (1985)
21. S J Huber, B A Hock *J. Plant Dis. Prot.* **92** 147 (1985)
22. S J Huber, B Hock, in *Methods of Enzymatic Analysis, Drugs and Pesticides* Vol. XII (Ed. H U Bergmeyer) (Weinheim: VCH, 1986) p. 438
23. R O Harrison, M H Goodrow, B D Hammock *J. Agric. Food Chem.* **39** 122 (1991)
24. A E Karu, R O Harrison, D J Schmidt, C E Clarkson, J Grassman, M H Goodrow, A Lucas, B D Hammock, J M Van Emon, R J White, in *Immunoassays for Trace Chemical Analysis: Monitoring Toxic Chemicals in Humans, Food and Environment (ACS Symposium Series)* Vol. 451 (Eds M Vanderlaan, L H Stanker, B E Watkins, D W Roberts) (Washington DC: American Chemical Society, 1991) p. 59
25. A D Lucas, H K M Bekheit, M H Goodrow, A D Jones, S Kullman, F Matsumura, J E Woodrow, J N Seiber, B D Hammock *J. Agric. Food Chem.* **41** 1523 (1993)
26. M T Muldoon, G F Fries, J O Nelson *J. Agric. Food Chem.* **41** 322 (1993)
27. P Tijssen *Laboratory Techniques in Biochemistry and Molecular Biology, Practice and Theory of Enzyme Immunoassay* Vol. 15 (Eds R H Burdon, P H Knippenberg) (Amsterdam: Elsevier, 1985)
28. B Dunbar, B Riggle, G Niswender *J. Agric. Food Chem.* **38** 433 (1990)
29. T S Lawruk, C E Lachman, S W Jourdan, J E Fleeker, D P Herzog, F M Rubio *J. Agric. Food Chem.* **41** 747 (1993)
30. R J Bushway, B Perkins, S A Savage, S J Lekousi, B S Ferguson *Bull. Environ. Contam. Toxicol.* **40** 647 (1988)
31. R J Bushway, B Perkins, S A Savage, S J Lekousi, B S Ferguson *Bull. Environ. Contam. Toxicol.* **42** 899 (1989)
32. R J Bushway, L B Perkins, H L Hurst, B S Ferguson *Food Chemistry* **43** 283 (1992)
33. K S Goh, J Hernandez, S J Powell, C D Greene *Bull. Environ. Contam. Toxicol.* **45** 208 (1990)
34. K S Goh, J Hernandez, S J Powell, C Garretson, J Troiano, M Ray, C D Greene *Bull. Environ. Contam. Toxicol.* **46** 30 (1991)
35. E M Thurman, M Meyer, M Pomes, C A Perry, A P Schwab *Anal. Chem.* **62** 2043 (1990)
36. R J Bushway, B Perkins, L Fukal, R O Harrison, B S Ferguson *Arch. Environ. Contam. Toxicol.* **21** 365 (1991)
37. R J Bushway, H L Hurst, B Perkins, L Tian, C G Cabanillas, B E S Young, B S Ferguson, H S Jennings *Bull. Environ. Contam. Toxicol.* **49** 1 (1992)
38. F M Rubio, J A Itak, A M Scutellaro, M Y Selisker, D P Herzog *Food Agric. Immunol.* **3** 113 (1991)
39. R J Schneider, B D Hammock *J. Agric. Food Chem.* **40** 525 (1992)
40. C Wittmann, B Hock *J. Agric. Food Chem.* **39** 1194 (1991)
41. S Wuest, U Doht, T Giersch, C Wittmann, B Hock *GIT Fachz. Lab.* **34** 99 (1990)
42. J-M Schlaeppi, W Fory, K Ramsteiner *J. Agric. Food Chem.* **37** 1532 (1989)
43. C Wittmann, B Hock *Food Agric. Immunol.* **2** 65 (1990)
44. C Wittmann, B Hock *J. Agric. Food Chem.* **41** 1795 (1993)
45. US P. 4 530 786; 1985
46. S J Huber, B Hock *GIT Fachz. Lab.* **10** 969 (1985)
47. C Wittmann, B Hock *Food Agric. Immunol.* **1** 211 (1989)
48. M J Wraith, D W Britton, in *Brighton Crop Protection Conference, 1988. Pests and Diseases (1)* (London: British Crop Protection Council) p. 131
49. K M Robotti, J K Sharp, P R Ehrmann, L J Brown, B W Hermann, in *Abstracts of Papers Presented at the 192nd ACS National Meeting* (Washington DC: American Chemical Society, 1986) AGRO 42
50. P A Schulze, P D Capel, "Utility and Limitations of Immunoassay Tests as a Field Screening Method for Triazine Herbicides". Paper presented at the U.S. Geological Survey's 2nd National Symposium on Water Quality, Orlando, FL, Nov. 12–17, 1989
51. G K Stearman, V D Adams *Bull. Environ. Contam. Toxicol.* **48** 144 (1992)
52. R J Schneider, L Weil, R Niessner *Intern. J. Environ. Anal. Chem.* **46** 129 (1992)
53. B Hock *Anal. Lett.* **24** 529 (1991)
54. P Ulrich, M Weller, L Weil, R Niessner *Vom Wasser* **76** 251 (1991)
55. A D Lucas, P Schneider, R O Harrison, J W Biggar, D E Rolston, J N Seiber, B D Hammock *Food Agric. Immunol.* **3** 155 (1991)
56. K S Goh, S J Richman, J Troiano, C L Garretson, J Hernandez, J Hsu, J White, T A Barry, M Ray, D Tran, N R Miller *Bull. Environ. Contam. Toxicol.* **48** 554 (1992)
57. A D Lucas, A D Jones, M H Goodrow, S G Saiz, C Blewett, J N Seiber, B D Hammock *Chem. Res. Toxicol.* **6** 107 (1993)
58. T Giersch *J. Agric. Food Chem.* **41** 1006 (1993)
59. M Bocher, T Giersch, R D Schmid *J. Immunol. Methods* **151** 1 (1992)
60. M G Weller, L Weil, R Niessner *Mikrochim. Acta* **108** 29 (1992)
61. R J Schneuder, L Weil, R Niessner *Fresenius Z. Anal. Chem.* **343** 145 (1992)
62. G W Aherne *Anal. Proc.* **27** 100 (1986)

63. A Hardcastle, G W Aherne, V Marks *J. Biolumin. Chemilumin.* **2** 209 (1988)
64. P Ulrich, R Niessner *Fresenius Envir. Bull.* **1** 22 (1992)
65. P Ulrich, L Weil, R Niessner *Fresenius Z. Anal. Chem.* **343** 50 (1992)
66. M G Weller, L Weil, R Niessner *Fresenius Z. Anal. Chem.* **343** 51 (1992)
67. N J Seare, J N Miller, E R Cole, A J Samuel, A P Woodbridge *Anal. Proc.* **23** 220 (1986)
68. G G Guilbault, B Hock, R Schmid *Biosens. Bioelectron.* 7 411 (1992)
69. P Kramer, R Schmid *Biosens. Bioelectron.* **6** 239 (1991)
70. F F Bier, W Stocklein, M Bocher, U Bilitewski, R D Schmid *Sens. Act.* **B7** 509 (1992)
71. R Jockers, F F Bier, R D Schmid *J. Immunol. Methods* **163** 161 (1993)
72. B B Kim, E V Vlasov, P Miethe, A M Egorov *Anal. Chim. Acta* **280** 191 (1993)
73. Zh V Samsonova, A M Egorov, S A Eremin *Agrokhimiya* (1) 95 (1994)
74. Zh V Samsonova, S A Eremin, A M Egorov, M Franek *Bioorg. Khim.* **10** (1994)
75. S Wust, B Hock *Anal. Lett.* **25** 1025 (1992)

Russian Chemical Reviews **63** (8) 623–639 (1994)
©1994 Russian Academy of Sciences and Turpion Ltd

UDC 536.212.2

The chemistry of the compound semiconductor–intrinsic insulator interface

N N Berchenko, Yu V Medvedev

Contents

I.	Introduction	623
II.	Thermodynamic analysis of the compound semiconductor–intrinsic insulator interface	624
III.	Experimental data on the oxidation of semiconducting compounds	628
IV.	Electrophysical properties and chemistry of the compound semiconductor–intrinsic oxide interface	632
V.	Current trends in the development of insulators for metal–insulator–semiconductor devices and protection of the surfaces of compound semiconductors	636

Abstract. Processes leading to the growth of intrinsic insulators (oxides, sulfides, and fluorides) on the surfaces of semiconductors of the III–V, II–VI, and IV–VI groups as well as their solid solutions are analysed with the aid of classical thermodynamics. Their phase compositions, found from the equilibrium phase diagram, are compared with the compositions found as a result of experimental studies of the semiconductor–insulator interface. It is shown that there is a relation between the characteristic features of the equilibrium phase diagram (in particular the segregation of a metal or nonmetal at the interface), the type of intrinsic lattice defects, and the electrophysical properties of the interface. The possible ways of creating an ideal compound semiconductor–insulator interface are considered. The bibliography includes 171 references.

I. Introduction

Oxidation is one of the first chemical reactions which humanity encountered at the dawn of history. With time, the number of known metals increased and the requirements which they had to meet became more stringent, but the problem remained in essence the same: how to protect finished articles from the destructive effect of the environment. Two main approaches were used. The first reduced to the search for a metal which would not be oxidised at all and it is not fortuitous that such metals have been called noble. The second involved the transformation of the enemy into a friend, i.e. the finding of an oxide which would serve as a protection. Aluminium oxide may serve as a successful example.

When it was proposed that the surface of silicon semiconductor devices be protected by silicon dioxide SiO_2, nothing new took place. However, when the first transistor based on a metal–oxide–semiconductor (MOS) system was created, the layer of oxide became an active component of the device itself and fundamentally new requirements, concerning primarily electrical parameters, were formulated for it. Almost all the electrical properties of the semiconductor–oxide interface are determined not by the bulk-phase characteristics of the oxides but by the extremely thin transition region, with a thickness of several nanometers, between the oxide and silicon, which contains a boundary phase with unusual composition and coordination of the silicon and oxygen atoms. Chemical engineering was therefore faced with the problem of regulating, with hitherto unheard of accuracy, the composition and structure of the interface formed on the surface of the conductor during oxidation.[1]

The problem of optimising the properties of the $Si–SiO_2$ interface was solved successfully and for the best MOS transistors the concentration of the electrically active defects on the interface does not nowadays exceed one defect per $10^4–10^6$ surface silicon atoms.† Nowadays the structure and properties of the $Si–SiO_2$ interface have been investigated in great detail, which is best indicated by the advances in silicon electronics. The relative simplicity of the technology, compactness, and the low power required by circuits based on MOS transistors made them irreplaceable in the manufacture of microprocessors and memory circuits, the wide scale employment of which determines in many respects the current progress in science and engineering.

The advance achieved in the development of silicon electronics permits one to hope that it will be repeated in the creation of devices based on binary semiconductors, particularly bearing in mind that the problems of regulating the bulk-phase properties have already been solved for most of them. This applies primarily to GaAs, in which the electron mobility is six times higher, its radiation stability is greater, and its working temperature range is wider (from −200 to 200 °C) compared with silicon. All this leads to most extensive prospects for the creation of ultrafast integrated circuits. The reason why these prospects have not been fully realised hitherto is mainly associated with the failure of the attempts, over a period of almost 30 years, to create a gallium arsenide–insulator interface the parameters of which would be close to those of the $Si–SiO_2$ interface.‡ In many respects this is

N N Berchenko Department of Semiconductor Electronics, 'Lvov Polytechnic' State University, ul. Mira 12, 290646 Lvov, Ukraine.
Fax (7-032) 274 43 00
Yu V Medvedev Institute of Applied Physics, I Franko Lvov State University, ul. Pushkina 49, 290044 Lvov, Ukraine.
Fax (7-032) 272 28 01. Tel. (7-032) 275 93 38

Received 6 June 1994
Uspekhi Khimii **63** (8) 655–672 (1994); translated by A K Grzybowski

† We may note that a method for the modulation of the electrical conductivity in the surface layer of the material, which constitutes the basis of the operation of MOS transistors, was patented as early as 1926, but, owing to the lack of ability to regulate the properties of the surface, it could not be applied in practice for a long time.

‡ At the Jubilee XXth Conference on the Physics and Chemistry of Interfaces in Semiconductors (USA, 1992), it was noted that the reason for the failures is the complexity of the chemistry of the GaAs surface.[2]

associated with the much more complex chemical composition of the boundary phases. Thus the chemistry of interfaces has become a crucial problem in the creation of microelectronic devices based on compound semiconductors.

Valuable results of this kind have been obtained for III–V semiconductors using the methods of classical thermodynamics. With the aid of these methods, it has been possible to predict at the microlevel the phase composition of the interfaces, which is, generally speaking, unexpected for a macroapproach of this kind. There has been recently a certain renaissance of thermodynamic methods. Nowadays, when it is possible to determine experimentally with the aid of electronic and ionic spectroscopy the composition and structure of interfaces at the atomic level, it has been found that thermodynamic calculations make it possible to analyse extremely effectively such complex systems. Thus thermodynamic calculations have in fact successfully predicted the sequence in the formation of phases on interaction in metal–silicon structures.[3] Thermodynamic analysis of the oxidation of the test material in order to determine the phase composition of the intrinsic oxide on the semiconductor–oxide interface is of interest for MOS structures. One of the simplest procedures used successfully in such analysis involves the calculation of phase equilibrium diagrams for the semiconductor–oxygen system. This approach was in fact first used to analyse the oxidation of the surfaces of semiconductors of the III–V group by Schwartz[4] and members of the Institute of Inorganic Chemistry of the Siberian Division of the USSR Academy of Sciences[5] at the beginning of the 1980s; later it was extended to other semiconducting compounds.

It must be emphasised that at the present time the range of insulators which are potentially suitable for the creation of devices based on metal–insulator–semiconductor (MIS) systems has greatly expanded. These are not only oxides but also other intrinsic insulators, i.e. compounds during the formation of which the semiconductor atoms are incorporated in the composition of the growing layer of the insulator.[6] The interface between the semiconductor and such compounds has also been analysed successfully with the aid of the phase equilibrium diagram.

This review is devoted primarily to the analysis of the application of phase equilibrium diagrams in the description of the interaction of oxygen with binary semiconductors and solid solutions based on them. Attention is concentrated on the establishment of a relation between the chemistry of the interface and its electrophysical parameters since only the understanding of this relation will make it possible to create promising devices based on compound semiconductors.

II. Thermodynamic analysis of the compound semiconductor – intrinsic insulator interface

There is a definite relation between the advances in the silicon MOS technology and the relative simplicity of the chemical processes occurring in the oxidation of silicon.[1,7–9] Indeed, in terms of their chemical composition and structure, the SiO_2 layers on silicon resemble vitreous silicon dioxide (fused quartz), are characterised by a high degree of chemical uniformity, and correspond to the stoichiometric formula SiO_2 almost throughout the thickness of the layer. Only at the interface between the Si and SiO_2 phases, which have different crystal structures and chemical compositions, the surface regions of both materials are reconstructed, some of the surface chemical bonds are rehybridised, and new chemical groups (characteristic of the interface alone), in which silicon has the Si^{3+}, Si^{2+}, and Si^{+} oxidation states, are formed. The thickness of the transitional region, having the composition SiO_x ($x < 2$), does not exceed several nanometers. Although the SiO_2 layer, having a thickness of 1.5–3.0 nm, adjoining this transitional region does have the stoichiometric composition, it is nevertheless mechanically strained owing to the nonidentity of the lattice constants of silicon and SiO_2. The structure of two monolayers of silicon atoms adjoining the interface is disturbed on the side of the silicon support. It is assumed that the defects in the transitional SiO_x region actually determine many of the electrical parameters of the interface.§ Bearing in mind the deficiency of oxygen in the transition layer, one can assume that such intrinsic defects may be oxygen vacancies and the ruptured bonds involving silicon atoms (the so called trivalent silicon).

Overall, the picture of the $Si–SiO_2$ interface proved to be fairly complex and it was necessary to develop unique experimental methods in order to be able to characterise it fully.

Proceeding to the consideration of the chemistry of interfaces involving compound semiconductors, it must be emphasised that the problem of the formation of the $Si–SiO_2$ interface actually reduces merely to the correspondence between the crystal lattices of two single-phase stoichiometric materials, the problem being facilitated by the fact that one of them possesses fairly flexible interatomic bonds, the angle between which can vary within wide limits.

In the case of a binary semiconductor, the problem is immeasurably more complex: two elements are now oxidised, each of which can have several oxides and some of the oxides can be variable-composition phases. Furthermore, if the oxide of one of the elements is highly basic whilst that of the other is highly acidic, a salt is formed and the number of complex oxide phases, for example phosphates, can also be large. All this leads to a multiphase structure of the oxide layer, which is usually accompanied also by a spatial nonuniformity. Furthermore, under certain conditions, chemical interaction of the oxide phases not only with one another but also with the semiconductor support becomes possible. As will be shown below, by employing phase equilibrium diagrams, it is possible to predict the composition of the oxide layer and, what is especially important, of the compound semiconductor–intrinsic insulator interfaces.

The method of phase equilibrium diagrams is based on the analysis of the possible interactions in the test materials–oxygen system. For a two-component compound AB, the interaction of the phases in the A–B–O ternary system, represented by the Gibbs triangle, is considered. The specific form of the phase equilibrium diagrams for the III–V, II–VI, and IV–VI compounds considered in this review is presented in Fig. 1.

All the oxide phases in the A–B–O system are assumed to be pure individual compounds and only condensed phases under standard conditions are considered. The miscibility of the phases is neglected. The chemical reactions occurring between pure phases are therefore studied, so that the phase equilibrium diagram for the A–B–O system contains only straight lines connecting the phases pairwise. These lines represent the thermodynamic equilibrium states between the phases. The stability of the lines is estimated from the Gibbs free energies of the chemical reactions (ΔG) recorded at the point of intersection of the lines, the line connecting the products of the reactions with $\Delta G < 0$ being regarded as stable. The calculation of ΔG requires a knowledge of the standard molar Gibbs free energies of formation ΔG° of all the phases belonging to the A–B–O system. Since the free energies ΔG° are by no means known for all substances, a series of methods have been developed for the estimation of these quantities (see, for example, Barin et al.[14]).

The phase equilibrium diagram can be used, firstly, for the estimation of the phase composition of the oxide film formed on the surface of the test compound during reversible oxidation in dry oxygen. The number of phases and their spatial distribution in the bulk of the oxide film can be found by analysing the line connecting oxygen and the test material and by analysing the question of which phase regions are intersected by this line.

§ The properties of the interface, like those of the insulator itself, can be regulated with the aid of impurity atoms. A review has been devoted to this problem.[10]

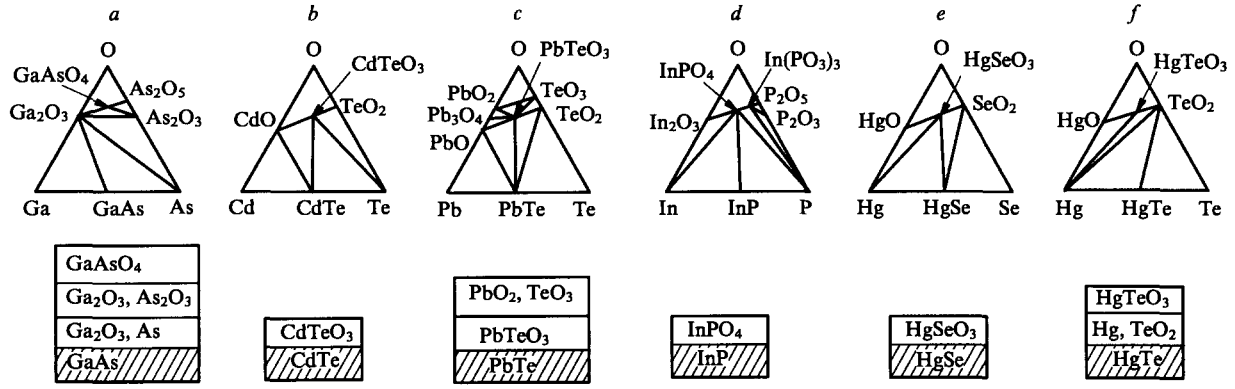


Figure 1. Phase equilibrium diagrams and phase composition profiles for the intrinsic oxides in various systems: (*a*) Ga–As–O;[4] (*b*) Cd–Te–O;[11] (*c*) Pb–Te–O;[12] (*d*) In–P–O;[4] (*e*) Hg–Se–O;[13] (*f*) Hg–Te–O.[11]

The chemical potential of oxygen is lowest at the semiconductor–oxide interface, increases monotonically along the thickness of the oxide film, and reaches a constant value in the gas phase. Consequently, movement along the line from the test compound, located at the base of the phase equilibrium triangle, to the apex of the diagram describes in succession the phase composition of the semiconductor–oxide interface and of the bulk-phase and surface components of the oxide film.

Another important practical application of phase equilibrium diagrams involves the possibility of predicting the chemical interaction of the oxide films formed with the support. It was noted above that the chemical potential of oxygen decreases monotonically from the oxide–gas phase interface to the support–oxide interface. The oxide film is formed until its thickness reaches a value for which the chemical potential of oxygen diminishes to a critical value which is insufficient for further growth of the oxide. If gaseous oxygen is removed (such a situation actually arises when the oxidised material is annealed *in vacuo* or under an inert gas atmosphere), then the oxide phases which are not linked by stable lines on the phase equilibrium diagram with the semiconductor may serve as the oxidant.

At the same time the method suffers from a fundamental limitation. The phase equilibrium diagram refers to a state of thermodynamic equilibrium and in no way describes the kinetics of the oxidation process. It provides a fundamental answer to the question of the possibility of the spontaneous occurrence of chemical reactions in the material–oxygen system investigated but does not indicate the time during which they take place. In practice, this means that the phase equilibrium diagram describes adequately the composition of the oxide film when the growth of the latter is sufficiently slow, so that its phase composition is determined by thermodynamic and not kinetic factors.

Additional complications in comparing data obtained by the method of phase equilibrium diagrams with experimental results may arise from the volatility of the oxide phases and their thermal decomposition or solubility, depending on the specific method used to oxidise the material.

A multiplicity of different versions of the structure of phase equilibrium diagrams is possible. For the binary semiconductors considered, six fundamentally different types of such diagrams are so far known. They are arranged in Fig. 1 in an order which reflects the transition from the preferential oxidation of the metal at the semiconductor–oxide interface in GaAs (Fig. 1*a*), through the synchronous oxidation of both components of the semiconductor with formation of a single complex oxide compound (Figs. 1*b*–1*e*), to the preferential oxidation of the nonmetal in HgTe (Fig. 1*f*).

We shall deal in greater detail with the diagram for GaAs bearing in mind that indium arsenide, indium and gallium antimonides,[4] as well as tin,[12] zinc,[13] and manganese[15] selenides and tellurides have qualitatively similar phase diagrams. When GaAs is oxidised, Ga_2O_3 and elemental arsenic are formed near the interface and the oxide consists of Ga_2O_3, As_2O_3, and $GaAsO_4$ (Fig. 1*a*). Thus, using the Ga–As–O phase equilibrium diagram it is possible to predict the formation of elemental arsenic at the GaAs–oxide interface as the phase corresponding to thermodynamic equilibrium. A similar conclusion concerning the preferential oxidation of the metal and the possible presence of the nonmetallic component in an elemental form at the semiconductor–oxide interface is also reached from the analysis of the analogous phase equilibrium diagrams for InAs, InSb, GaSb, SnTe, SnSe, ZnTe, ZnSe, MnTe, and MnSe. The phase equilibrium diagram for the Ga–As–O system also permits the technologically important conclusion that chemical reactions are possible between the semiconductor and the intrinsic oxide. Indeed, GaAs is linked on the phase equilibrium diagram by a stable line only with Ga_2O_3, i.e. the contacts between GaAs and arsenic oxides correspond to thermodynamic disequilibrium. If GaAs is linked by imaginary straight lines to As_2O_3, As_2O_5, or $GaAsO_4$, then the latter all intersect the stable Ga_2O_3–As line. This means that the oxidised arsenic is unstable in contact with GaAs and the chemical reactions occurring lead to the enrichment of the interface in elemental arsenic.

The phase equilibrium diagram for the Cd–Te–O system (Fig. 1*b*) has a fundamentally different structure. It contains the stable CdTe–$CdTeO_3$ line, which means that the oxidation of CdTe results in the formation of only one oxide compound — $CdTeO_3$. As for GaAs, the metal oxide is linked to the semiconductor by a stable line on the phase equilibrium diagram and the reaction between CdTe and TeO_2 can lead to the appearance of elemental tellurium in the region of the interface. Thus the CdTe–oxide interface is thermodynamically stable when the entire oxidised tellurium is in $CdTeO_3$.¶

PbTe undergoes yet another important change on the phase equilibrium diagram (Fig. 1*c*). Here the semiconductor is linked by stable lines to the first oxides of lead and tellurium and also to lead tellurite $PbTeO_3$. The PbTe–oxide interface is single-phase on either side and is thermodynamically stable relative to both PbO and TeO_2. Only when higher lead and tellurium oxides appear in the oxide film do reactions become possible in the semiconductor–oxide system, but in this case the components of the semiconductor should not be segregated at the interface in the elemental form.

The phase equilibrium diagram for the In–P–O system has a different structure (Fig. 1*d*). It contains the stable InP–$InPO_4$ line, but InP is not linked by stable lines with either phosphorus

¶ The possibility of formation of the compounds $CdTe_2O_5$ and $HgTe_2O_5$, the presence of which has been mentioned in a number of studies,[16–18] has not been taken into account in Fig. 1 for CdTe and HgTe.

oxides or with In_2O_3. The InP–interface formed under equilibrium conditions is also single-phase on either side. If the composition of the oxide layer differs from $InPO_4$, there is a possibility of the occurrence of chemical reactions between the support and the oxide layer, which probably results in the appearance of both indium and phosphorus in the elemental form in the region of the interface.

The phase equilibrium diagram for the Hg–Se–O system (Fig. 1*e*) is a mirror image of the analogous phase equilibrium diagram for Cd–Te–O. The HgSe–oxide interface is single-phase but is unstable relative to mercury oxide. Elemental mercury may appear at the HgSe–oxide interface as a result of chemical reactions between the support and HgO.

Similarly the phase equilibrium diagram for the Hg–Te–O system (Fig. 1*f*) is the mirror image of the corresponding diagram for the Ga–As–O system. In the region of the HgTe–oxide interface, the chalcogen is oxidised preferentially, while mercury remains in the elemental form. The HgTe–oxide interface is unstable, since the only stable line on the diagram is HgTe–TeO_2, linking HgTe to the oxide phases. It follows from the phase equilibrium diagrams that the reactions between the support and the oxide should lead to the enrichment of the HgTe–oxide interface in metallic mercury.

Thus, judging from the phase equilibrium diagrams for the III–V, II–VI, and IV–VI binary semiconductors, there is a possibility of different variants of the phase composition and thermodynamic stability on semiconductor–oxide interfaces.

No less interesting results have been obtained with the aid of phase equilibrium diagrams for semiconductor solid solutions. The first three-dimensional diagrams, consisting of tetrahedra, have been constructed for the $In_xGa_{1-x}As$ [19] and $Hg_{1-x}Cd_xTe$ [11,16] solid solutions. The methods used to construct such diagrams were supplemented by several important postulates compared with the methods used to construct the phase equilibrium diagrams for binary semiconductors.[11] Stable triangular planes in the three-dimensional diagram play the role of the stable lines in the two-dimensional diagram. Each apex of such a triangle must correspond to one of the phases of the test system, each side of the triangle represents a stable line of the phase equilibrium diagram, and at least one apex of the triangle is located on a face of the tetrahedron. All possible planes are considered and their stability is estimated from the calculated free energies ΔG.

As an example, Fig. 2 presents the phase equilibrium diagram for the Hg–Zn–Te–O system. We may note that, apart from the phase equilibrium diagrams for the Hg–Te–O and Zn–Te–O systems, the estimation of the form of the phase equilibrium diagrams for the Hg–Zn–O and Hg–Zn–Te systems was needed in order to construct the phase equilibrium diagram for the $Hg_{1-x}Zn_xTe$–O system. Such three-dimensional diagrams can be used to determine the phase composition of the solid solution–oxide interface. The phase composition profile is estimated from the points of intersection of the straight line connecting the solid solution to oxygen with the stable lines and planes of the phase equilibrium diagram. A definite compound corresponds to each such point. The phase composition profiles are presented for the diagrams considered. Such analysis can be carried out conveniently by considering the cross-section through the three-dimensional diagram along the plane connecting the binary compounds of the solid solution and oxygen.

The most interesting variants of such cross-sections are presented in Fig. 3. Analysis can be usefully begun with the thoroughly investigated Hg–Cd–Te–O system. In the oxidation of the $Hg_{1-x}Cd_xTe$ solid solutions, CdTe is initially oxidised (the $Hg_{1-x}Cd_xTe$–O straight line belongs to the stable HgTe–$CdTeO_3$–CdTe plane) (Fig. 3*a*). After the completion of the oxidation of CdTe (the $Hg_{1-x}Cd_xTe$–O straight line intersects the stable HgTe–$CdTeO_3$ line), the oxidation of HgTe begins with the preferential formation of the chalcogen in the initial stage, mercury being segregated in the elemental form at the interface.

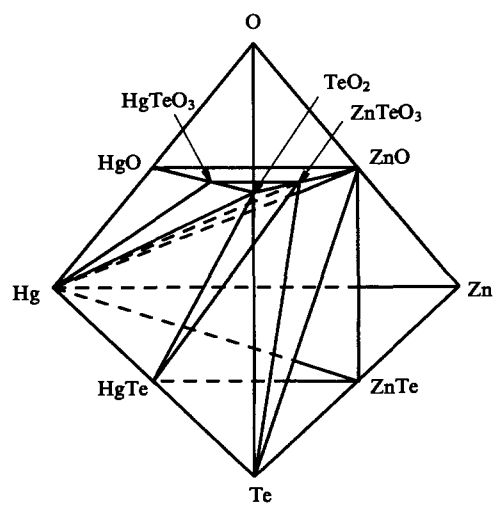


Figure 2. Phase equilibrium diagram for the Hg–Zn–Te–O system.[13]

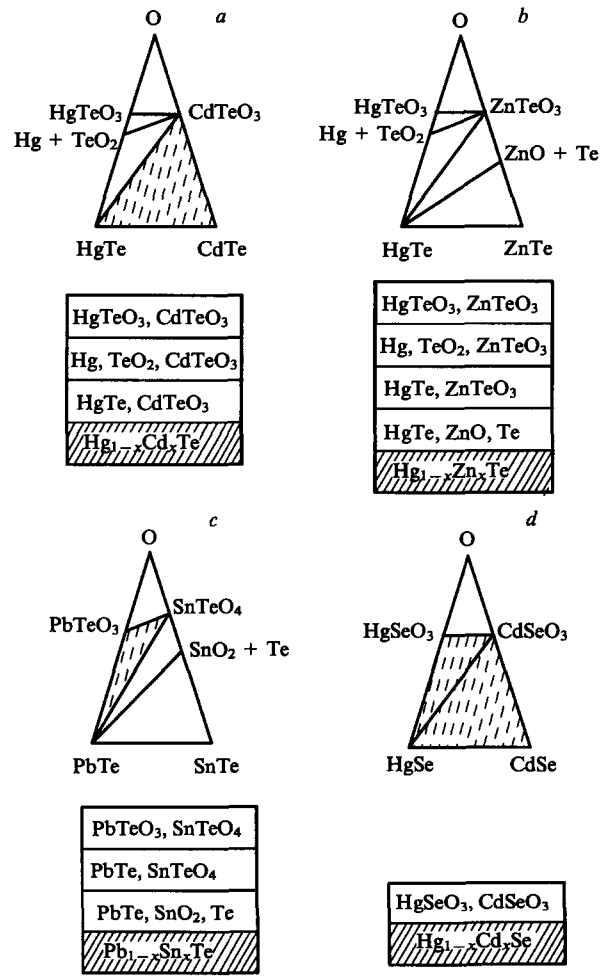


Figure 3. Sections through phase equilibrium diagrams for various systems:
(*a*) Hg–Cd–Te–O along the HgTe–O–CdTe plane;[11]
(*b*) Hg–Zn–Te–O along the HgTe–O–ZnTe plane;[13]
(*c*) Pb–Sn–Te–O along the PbTe–O–SnTe plane;.[12]
(*d*) Hg–Cd–Se–O along the HgSe–O–CdSe plane.[13]
The corresponding phase composition profiles for the intrinsic oxides are shown under the sections.

Thus the solid solution–oxide interface is multiphase and contains metallic mercury (Fig. 3*a*).

The opposite oxidation pattern is characteristic of the $Pb_{1-x}Sn_xTe$ solid solution (Fig. 3*c*). Here SnTe is oxidised first, giving rise to SnO_2 and elemental tellurium. Thus, in contrast to $Hg_{1-x}Cd_xTe$, the solid solution–oxide interface for $Pb_{1-x}Sn_xTe$ contains the elemental chalcogen.

An even more complex situation obtains for the $Hg_{1-x}Zn_xTe$ solid solution. Analysis of the HgTe–O–ZnTe section (Fig. 3*b*) shows that, in the oxidation of the $Hg_{1-x}Zn_xTe$ solid solution, ZnTe is the first to be oxidised with formation of ZnO and elemental tellurium [the $Hg_{1-x}Zn_xTe$–O line intersects the Hg–ZnO–Te plane (Fig. 2)]. Then tellurium is oxidised to zinc tellurite $ZnTeO_3$ (the $Hg_{1-x}Zn_xTe$–O line intersects the Hg–$ZnTeO_3$ line). Next, the oxidation of HgTe begins, tellurium being oxidised preferentially, and elemental mercury is evolved at the interface. Consequently the simultaneous presence of elemental tellurium and mercury in the region of the solid solution–oxide interface is characteristic of the $Hg_{1-x}Zn_xTe$ solid solution.

Analysis of the HgSe–O–CdSe section (Fig. 3*d*) shows that the $Hg_{1-x}Cd_xSe$ solid solution is unique. By virtue of the presence of the stable CdSe–$CdSeO_3$ and HgSe–$HgSeO_3$ lines on the phase equilibrium diagrams for the Cd–Se–O and Hg–Se–O systems, the corresponding HgSe–O–CdSe section represents a stable plane. The equilibrium oxidation of the $Hg_{1-x}Cd_xSe$ solid solution reduces to the oxidation of CdSe and HgSe to $CdSeO_3$ and $HgSeO_3$ respectively. Because of this, the solid solution–oxide interface should exhibit thermal stability. As regards other solid solutions considered above, the solid solution–oxide interface is multicomponent and thermodynamically unstable. In view of the absence of any stable planes in, for example, the HgTe–O–ZnTe section, the solid solution–oxide interface is multicomponent and potentially unstable. However, as will be shown below, this multicomponent property has a mutually compensating character (Hg^0 and Te^0) and paradoxically can actually improve the properties of the interface.

Similar phase equilibrium diagrams can also be constructed for even more complex systems. For example, the phase diagram for the $(PbSe)_{1-x}(SnTe)_x$ four-component solid solution has been published.[20] It was shown that in this system both chalcogens are present as a phase in thermodynamic equilibrium in the region of the solid solution–oxide interface.

The method of phase equilibrium diagrams can be employed also for the analysis of the processes occurring when a metal is deposited on the oxidised surface of a semiconductor.[21]

Fig. 4 presents as an example the phase equilibrium diagram for the Pb–Te–O–Al system. Analysis of sections through this diagram along the PbTe–O–Al plane makes it possible to estimate the phase composition of the PbTe–Al interface depending on the initial chemical state of the semiconductor surface. The composition of the PbTe surface is represented along the base of the PbTe–O–Al triangle by a point the movement of which, within the limits of the PbTe–$PbTeO_3$ segment, corresponds to the change in the state of the surface from that of a completely unoxidised semiconductor to a continuous oxide film. When aluminium is deposited on the unoxidised PbTe surface, chemical interaction takes place, which results in the formation of Al_2Te_3 and metallic lead (when the PbTe–Al straight line is drawn, it intersects the stable Al_2Te_3–Pb line). When aluminium is deposited on an oxidised PbTe surface, it initially interacts with the oxide, which results in the formation of Al_2O_3 and PbTe and then (depending on the thickness of the oxygen layer) it interacts with the semiconductor support or with the products of the first reaction. If the point on the PbTe–$PbTeO_3$ segment is connected with the apex of the PbTe–O–Al triangle, then the straight line is initially located in the PbTe–$PbTeO_3$–Al_2O_3 plane and then intersects the Pb–Al_2Te_3–Al_2O_3 plane. Thus, when aluminium is deposited on the oxidised PbTe surface, chemical interaction between the metal and the oxide is to be expected. This results in a decrease in the thickness of the oxide film and in the formation of

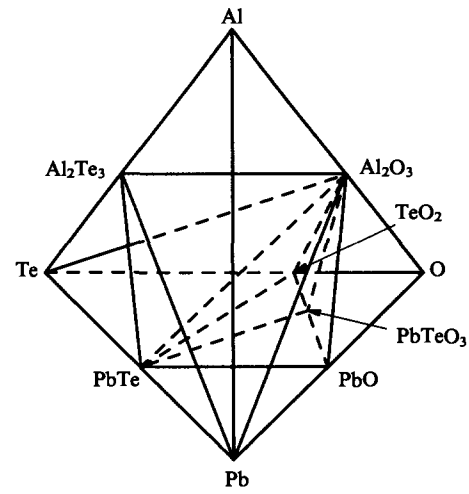


Figure 4. Phase equilibrium diagram for the Pb–Te–O–Al system.[21]

a boundary layer containing Al_2O_3, Al_2Te_3, and metallic lead and there is a possibility of the complete disappearance of the initial oxide.

It has been observed experimentally that different variants of the sulfidation † of the surfaces of semiconductors greatly improve their electrophysical properties. Phase equilibrium diagrams were constructed for certain semiconductor–sulfur systems (Fig. 5). None of them differ fundamentally from the phase equilibrium diagram for the Ga–As–O system, i.e. in this case the elemental nonmetal phase is formed at the semiconductor–sulfide interface. At the same time, the phase equilibrium diagram for the In–P–S system contains the stable InP–In_2S_3 line, while the phase equilibrium diagram for the Ga–As–S system contains the stable GaAs–GaS line, i.e. in each system there is a sulfide and the interface between the latter and the semiconductor is thermodynamically stable. An exchange reaction takes place in the Cd–Te–S and Hg–Te–S systems (Fig. 5*c*).

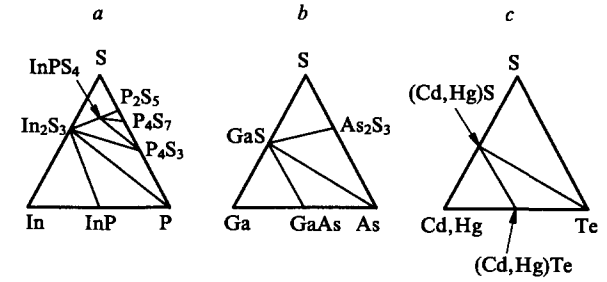


Figure 5. Phase equilibrium diagrams for different systems: (*a*) In–P–S;[22] (*b*) Ga–As–S;[23] (*c*) (Cd,Hg)–Te–S.[24]

Useful information about the composition and thermodynamic stability of the intrinsic insulator has been obtained with the aid of the phase equilibrium diagram for the $Hg_{1-x}Cd_xTe$–F system.[24] It was established that, as in the sulfidation of the III–V semiconductors, in the fluorination of CdTe at the CdTe–CdF_2 interface the elemental nonmetal is evolved and the CdTe–CdF_2 line is thermodynamically stable. On the other hand,

† The problem of the sulfidation of the surfaces of III–V semiconductors is one of the crucial problems in semiconductor materials science at the present time. We shall be concerned only with those aspects of the problem which are linked directly with the aim of this review.

on fluorination of HgTe the liberation of the components of the material in the elemental form should not be observed at all. Comparison of the sections through the Hg–Cd–Te–F diagram along the HgTe–F–CdTe plane, through the Hg–Cd–Te–S diagram along the HgTe–S–CdTe plane,[24] and through the Hg–Cd–Te–O diagram along the HgTe–O–CdTe plane (Fig. 3*a*) permits the conclusion that the principal feature of the $Hg_{1-x}Cd_xTe$–intrinsic insulator interface in the sulfidation and fluorination reactions is the absence of elemental mercury. On the other hand, the phase equilibrium diagram predicts the liberation of the elemental chalcogen in both cases. Its amount in the fluorination reaction should be significantly smaller, since the source of Te^0 is only CdTe, the content of which does not exceed 30% in the compositions of the $Hg_{1-x}Cd_xTe$ solid solution of the greatest practical importance.

It will be shown below whether the differences in the phase equilibrium diagrams presented above lead to different properties of the MIS materials based on these systems.

III. Experimental data on the oxidation of semiconducting compounds

Thin oxide films ($\leqslant 5$ μm) are used in semiconductor electronics, the thickness becoming continuously smaller with progress in the technology. For example, in modern MOS transistors the thickness of the oxide under the gate is ~25 nm. The composition of the semiconductor–oxide interface itself, whose thickness in most cases does not exceed several nanometers, is of greatest interest to investigators. This must be borne in mind in comparing the chemical compositions of the oxide films predicted by the phase equilibrium diagram and obtained experimentally.

Electronic and ionic spectroscopic methods, which make it possible to investigate the composition and structure of the surface and interfaces at the atomic level, are usually employed in the study of such oxide films.[25] In the first place these are methods, such as electronic Auger spectroscopy (EAS) combined with ionic etching, which make it possible to determine the distribution of the elements in the bulk of the structure. The particles of the specimen atomised by the primary ionic beam are analysed by secondary ion mass spectrometry (SIMS). The Rutherford back scattering (RBS) method has almost no disruptive effect, but is resolution as a function of depth is poorer.

Photoelectron spectroscopy (PES) affords the most valuable information about the chemical bonds linking the elements on the surface and the interface. Ultraviolet (UPES) and X-ray photoelectron spectroscopy (XPES) are distinguished by the energy range of the primary radiation beam.

Valuable information, particularly in the presence of Group V and VI nonmetals, has also been obtained with the aid of Raman spectroscopy and the voltammetric method.

For the purpose of analysis, it is convenient to divide the theoretical and experimental results into three groups depending on the oxidation conditions: 'natural' oxidation (at room temperature), thermal oxidation, and anodic electrochemical oxidation (photochemical oxidation and oxidation in an oxygen plasma are also usually included here). One should bear in mind that, for each of these oxidation procedures, there exist technological factors which lead to the deviation of the composition of the oxide films from the equilibrium composition — for example, thermal decomposition in thermal oxidation, different solubilities of the oxide phases in the electrolyte in anodic oxidation, etc. Only correct allowance for these factors makes it possible to achieve a correct comparison.

1. Gallium arsenide

The natural oxidation processes were initially investigated mainly on chemically etched surfaces, but the results obtained by different investigators proved to be extremely contradictory; this was associated primarily with the fact that etching can appreciably disturb the stoichiometry of the surface. In addition, oxidation is a component of the etching process which leads to the growth of insoluble oxide films of different composition depending on the composition of the etch. This has been demonstrated clearly for the InP surface.[26] According to data obtained by the XPES and RBS methods, the thickness of the grown oxide layer varied from 0.7 to 2.4 nm depending on the composition of the etch and the etching time, while the ratio of phosphorus and indium, normalised with respect to $InPO_4$, ranged from 0.2 to 1.5. Similar results have been obtained from GaAs[27] and $Hg_{1-x}Cd_xTe$.[18]

This is why the study of the oxidation of an atomically clean surface (ACS), usually obtained by cleaving the crystal in an ultrahigh vacuum or by ion bombardment, is of greatest interest. Electron spectroscopy makes it possible to observe the oxygen adsorption process at the monolayer level on such a surface. However, one should bear in mind that the thickness of the oxide, growing on the ACS of III–V and II–VI compounds, does not usually exceed 2–3 monolayers, i.e. it is too small to permit a description of these films by means of the thermodynamic parameters obtained for bulk phase specimens. Furthermore, the differences between the electronic and lattice subsystems of the atomic layers on the free surface and in the parallel layers in the bulk of the semiconductors are particularly strongly manifested precisely in the initial stages of the interaction of oxygen with the semiconductor.[28] These differences actually explain, for example, the finding that, when the ACS on silicon was oxidised for an oxide thickness of ~1 nm, unstable oxidation states of silicon were observed by the UPES method.[1]

Despite these limitations, it is possible to establish a definite relation between the phase equilibrium diagram and the oxidation of the ACS of semiconductors at room temperature. It has been established with the aid of electronic spectroscopy that the unexcited oxygen molecules interact with the surface of GaAs, InAs, and InP in three stages.[29–32] Adsorption takes place in the first stage but only on surface defects formed on cleavage or on cleaning the surface by ion bombardment. In the second stage, the oxygen molecule dissociates with formation of bridge bonds of the Ga–O–As type. The interaction accompanied by a chemical shift of the skeletal levels begins only in the third stage. For all three compounds, the atoms of both the metal and the nonmetal participate equally in the formation of bonds with oxygen, since the amplitude of the PE peaks due to oxidised indium (gallium) and arsenic (phosphorus) increases equally with increase in the surface coverage by oxygen in the range from 0.1 to 1.5 monolayers.[32,33] However, after brief annealing of InP in vacuo at 350 °C, the PE peaks for indium, phosphorus, and oxygen remain unchanged, whereas after annealing GaAs the peak for oxidised gallium increases and that for oxidised arsenic diminishes while the amplitude of the oxygen peak remains unchanged.

According to the phase equilibrium diagrams (Fig. 1), the oxide layer on InP consists of the compound $InPO_4$, which is stable on heating, while that on GaAs comprises a mixture of oxides,[34] the heating of which gives rise to the reaction

$$2GaAs + As_2O_3 = Ga_2O_3 + 4As. \quad (1)$$

On the other hand, on oxidation of the ACS on gallium arsenide by ionised oxygen, the chemical interaction is accelerated (peaks corresponding to Ga_2O_3 and As_2O_3 appear in the photoelectron spectrum) and a peak corresponding to elemental arsenic appears.[29] The appearance of elemental antimony has been observed in the oxidation of the ACS of gallium and indium antimonides.[35,36] The difference between even the initial stages of the oxidation of GaAs and InP is indicated by the analysis of the composition of thin ‡ layers obtained by the natural, chemical, and thermal oxidation of GaAs and InP specimens.[37,38] All the

‡ Thin layers are understood as layers whose thickness is comparable to the depth from which photoelectrons emerge (< 5 nm). Their composition, like that of the interface, can be analysed in depth without resorting to etching.

specimens were subjected to the same preliminary surface treatment and the composition was investigated by the XPES method with angular resolution, which makes it possible to vary the depth of the probed layer from 2 to 4 nm. Both elemental arsenic and gallium and arsenic suboxides were observed in all the oxide layers on GaAs under these conditions, whereas both elemental phosphorus and indium and phosphorus suboxides were absent from the oxidised InP surface and the entire oxidised phosphorus was present in the form of complex compounds.

Studies on the thermal oxidation of GaAs (see Wilmsen's review[39]) showed that elemental arsenic is present on the interface under different annealing conditions (dry and moist oxygen, O_2/As_2O_3 mixture) over a wide temperature range ($\leqslant 620$ °C). Only at higher temperatures does its concentration diminish and $GaAsO_4$ appears on the interface in addition to Ga_2O_3. The oxide layer at $T \leqslant 500$ °C consists largely of amorphous Ga_2O_3, which crystallises as β-Ga_2O_3 at higher temperatures; As_2O_3 is present in much smaller amounts. This is associated both with the consumption of As_2O_3 via reaction (1) and with its high volatility. The concentration of As_2O_3 in the bulk phase can be increased by growing the oxide in the vapour of As_2O_3 or the O_2/As_2O_3 mixture. The exact spatial disposition of arsenic remained unelucidated for a long time. It was assumed that it may accumulate in the form of a continuous film directly on the interface. However, the latest studies have shown that elemental arsenic is present throughout the bulk of the thermal oxide,[40] while analysis of the cross-sections through structures with the thermal oxide with the aid of transmission microscopy and microdiffraction confirmed that, for example after oxidation at 500 °C, the interface consists of an epitaxial layer of γ-Ga_2O_3 on GaAs, beween which are injected 5–10 nm precipitates of hexagonal arsenic with a density of $(2-5) \times 10^{11}$ cm^{-2}.[41] In addition, it was shown that arsenic may be formed not only in reaction (1) but also in the direct GaAs oxidation reaction

$$4GaAs + 3O_2 = 2Ga_2O_3 + 4As, \quad (2)$$

first put forward by Smirnova et al.[42]

One of the controversial questions is whether elemental arsenic is or is not formed at the interface in the low-temperature oxidation (electrochemical anodic, plasma, etc. oxidation). The majority of investigators believed that it appears at the interface only after the annealing of the grown oxides at $T > 250$ °C as a result of a secondary reaction. However, it was later shown[42] that As^0 could not be detected in the initial film as a consequence of the inadequate sensitivity of the Raman technique ($\sim 10^{15}$ atoms cm^{-2}). Thus, when solid-phase voltammetry having a sensitivity of $10^{11}-10^{12}$ atoms cm^{-2} was used, it was possible to detect elemental arsenic and antimony in the initial anodic oxide films (AOF) on GaAs, InAs, and InSb,[5,40,42] i.e. reaction (1) occurs also at room temperature under these conditions. Furthermore, it has been possible to carry out a layer-by-layer investigation using this method of not only the phase composition but also of the structure of the oxide layers and to establish its relation with the conditions governing the growth of the anodic oxide.[42]

Thus the anodic oxide film, approximately 100 nm thick, grown under galvanostatic conditions ($j \approx 5.0$ mA cm^{-2}) on the GaAs surface, has the following distribution of composition as a function of its thickness:[40]

Layer	Chemical composition
1	ε-Ga_2O_3, As_2O_3(cryst.), As_2O_3(amorph.), $GaAsO_4$(cryst.)
2	ε-Ga_2O_3, As_2O_3(amorph.), As_2O_3(cryst.), As_2O_5(cryst.), As_2O_4(cryst., traces)
3	α-Ga_2O_3, ε-Ga_2O_3, As_2O_3(amorph.), As_2O_5(cryst., traces)
4	α-Ga_2O_3, As_2O_3(amorph.), As_2O_5 (cryst., traces)
5	δ-Ga_2O_3, As_2O_3(cryst.), As(amorph.), As(cryst.)

Layer 5 adjoins the GaAs surface. Evidently, Ga_2O_3, As_2O_3, and As are formed at the interface, which agrees with the phase equilibrium diagram. On moving away from the interface, oxides appear in which arsenic has the highest oxidation state (As_2O_4, As_2O_5, $GaAsO_4$), and the nonequilibrium combinations of phases $As_2O_3 + As_2O_5$, and $Ga_2O_3 + As_2O_5$ are observed, which is most probably associated with kinetic factors. After a time or on heat treatment, this leads to the following solid-phase reactions:

$$As_2O_3 + As_2O_5 = 2As_2O_4, \quad (3)$$

$$Ga_2O_3 + As_2O_5 = 2GaAsO_4, \quad (4)$$

$$Ga_2O_3 + 2As_2O_4 = 2GaAsO_4 + As_2O_3. \quad (5)$$

Under these conditions, structural transformations also occur in the films—the amorphous forms of As and As_2O_3 crystallise and the less stable crystalline forms of Ga_2O_3 are converted into the more stable ones. The chemical state is in many respects determined by the conditions in the anodic oxidation.[40,43] Thus an increase in current density leads to additional oxidation of arsenic to the pentavalent state and to the appearance of As^0 at the interface in both amorphous and crystalline forms. Comparison of the spectra of the analytical signals due to the electrochemical transformations of the anodic oxide, the thermal oxide, and mixtures of reference compounds shows that none of these oxides are homogeneous, consisting of a mixture of phases of different structural modifications with a grain size greater than 5 nm.[40] This agrees well with the existing data showing that the oxides are initiated in isolated regions on exposure to an electron beam[44] and in the initial stages of the growth of the anodic oxide.[45]

The chemical composition of the oxide layer on GaAs, obtained by oxidation in an oxygen plasma,§ does not actually differ from the composition of the layer obtained on anodic oxidation and also represents a mixture of As_2O_3 and Ga_2O_3. Its composition is then influenced quantitatively by factors such as the rate of growth of the oxide, the degree of ionisation of the plasma, and the anodic current density. The concentration of arsenic in the plasma oxides is found to be higher than in the electrochemical oxides and can reach 4%–5% of the overall composition.[47] It is determined to a large extent by the dynamics of the growth of the oxide layer: the more intense the oxidation process, the smaller the amount of arsenic displaced to the interface. Its total amount at a high rate of growth (300 nm min^{-1}) is equivalent to a layer 4.2 nm thick, while at a low rate of oxidation it corresponds to 41 nm for an overall thickness of the layer of 160 nm.[48] One cannot rule out the possibility that the appearance of such a large amount of elemental arsenic is associated with the preferential oxidation of gallium as a consequence of the difference between the activation energies for the gallium and arsenic oxidation reactions in the plasma.[49]

2. Indium phosphide

XPES analysis of thin oxide films grown under an oxygen atmosphere at temperatures in the range 340–400 °C showed that they are a mixture of amorphous In_2O_3 and $InPO_4$ and that phosphorus is present as the phosphate and not P_2O_5 over the entire experimental temperature range (up to 650 °C), but, with increase in the oxidation time, i.e. for thicker films, elemental phosphorus appears at the interface.[39] With increase in the oxidation temperature from 350 to 550 °C, the amount of accumulated P^0 increases and then falls.[50] At ~ 650 °C, elemental phosphorus was not detected[39] and only $InPO_4$ was found at the interface, which is consistent with the phase equilibrium diagram. The appearance of P^0 is probably associated with the fact that at $T < 600$ °C the oxide grows as a result of the diffusion of indium and phosphorus to the oxide surface, the diffusion of phosphorus being appreciably slower than that of indium. The extent of the

§ The preparation of the oxides of compound semiconductors by plasma anodisation and their properties have been described in detail.[46]

diffusion of oxygen at these temperatures is low and the oxidation occurs on the surface, which in fact leads to the accumulation of unoxidised phosphorus at the interface. Furthermore, according to Mittova et al.,[51] unoxidised (or insufficiently oxidised) indium is formed in the bulk of the oxide during thermal oxidation at 575–675 °C. On the other hand, in general the excess indium present in the thermal oxide on InP, especially in the outer layer, is due to the evaporation of phosphorus from the surface.[52] Thus, in a certain temperature range, kinetic factors become dominant. Experiments on the oxidation of InP at oxygen pressures in the range from 1 to 500 atm confirmed that this is in fact so and that the appearance of P^0 is not associated with the reactions of types (1) and (2). At pressures of 150 atm and above, the interface consists of $InPO_4$, In_2O_3, and P_2O_5. Such a change in the composition of the interface can be explained by the increase in the rate of diffusion of oxygen, which in fact leads to the complete oxidation of the elements.[53] It is of interest to note that P^0 is not formed on oxidation of InP by oxygen in the presence of water vapour.[39]

A detailed comparison of the elemental compositions of the thermal, chemical, and anodic oxides of InP has been carried out with the aid of XPES using precision layer-by-layer chemical etching, which ruled out all the effects associated with the action of the ion beam.[50, 54–56] A sufficiently reliable identi-fication of different oxide phases was achieved by comparing the chemical shifts of the peaks for different levels of the skeleton, their intensities, and the spectra of the valence bands of the oxide films and reference compounds. If the thermal oxides represent a mixture of amorphous In_2O_3 and $InPO_4$ particles with the P^0 present at the interface, then they also include polyphosphates of the type $In(PO_3)_x$. The oxides grown in concentrated nitric acid under strong illumination are homogeneous throughout their thickness. Their average atomic composition corresponds to $In(PO_3)_{2.6}$ and is independent of the thickness of the oxide layer, time, and the temperature ($\leqslant 80$ °C) of the growth process. Anodic oxides have been grown in the familiar AGW electrolyte,[57] the pH of which was varied in the range from 2 to 12 by adding NH_4OH. They all consist of two layers, the outer layer being enriched in indium (P : In = 0.4) and representing apparently a hydrated mixture of $InPO_4$ and In_2O_3 or $In(OH)_3$. The inner layer, adjoining the interface, is enriched in phosphorus and has the average composition $In(PO_{3.2})_{3.9}$. This distribution remains unchanged for all anodic oxides with a thickness between 10 and 50 nm and is independent of both the pH of the electrolyte and the current density. The distributions of the elements in the anodic oxide and in the oxides grown in other electrolytes[58, 59] are quantitatively the same. This has been attributed to the growth mechanism specific for the anodic InP oxide, which cannot operate in, for example, GaAs, because the anodic oxide on GaAs is not a vitreous compound but a mixture of polycrystalline oxides.

Analysis of the photoelectron spectra of the valence band has shown that the inner part of the anodic oxide on the side of the interface consists of single-phase nonstoichiometric phosphate $In(PO_x)_y$ with x and y close to 3. Studies by the fast electron diffraction method showed that the oxides are amorphous. This agrees with the existence of vitreous $In(PO_3)_3$.[60] The study of the crystalline metaphosphate $In(PO_3)_3$ showed that the P–O–P bond angle in the PO_4 tetrahedron can vary within wide limits, like the O–Si–O angle in the SiO_2 structure, i.e. these structures are sufficiently flexible to ensure a good agreement between the phosphate and InP lattices, as happens in the Si–SiO_2 system. Annealing at temperatures up to 350 °C does not alter the chemical composition of the anodic oxide or of the interface with InP and, furthermore, according to data obtained by transmission electron microscopy, somewhat smoothes out the roughness of the interface at the atomic level. The change in the composition of the interface (the formation of a P^0 layer up to 0.5 nm thick) is observed only after annealing at 450 °C. The appearance of phosphorus can be explained, in conformity with the phase equilibrium diagram (Fig. 1*d*), by the fact that the InP–anodic oxide interface is nevertheless unstable and the reaction

$$4In(PO_3)_3 + 5InP = 8P + 9InPO_4, \quad (6)$$

takes place on it. One cannot rule out the possibility that, as a consequence of the presence of hydrates in the anodic oxide layer, additional reactions take place at high temperatures and result in the liberation of phosphorus.

An oxide consisting mainly of a polymeric polyphosphate phase has been obtained on indium phosphide by plasma oxidation.[61]

3. Semiconductor solid solutions

A few studies have shown that the oxidation reactions of solid solutions of III–V compounds can be regarded as a superposition of the oxidation reactions of the binary semiconductors. The appearance of a new As_zP_{1-z} phase in the oxidation of the $InAs_xP_{1-x}$ solid solution may be regarded as the most interesting result.[62]

It is noteworthy, in connection with the widescale use of $Hg_{1-x}Cd_xTe$ (x = 0.2, 0.3) and $Pb_{1-x}Sn_xTe$ (x = 0.2) in IR techniques, that mainly the solid solutions have been investigated, whereas the initial binary compounds HgTe and CdTe, as well as PbTe and SnTe, were considered only for a better understanding of the oxidation reactions of the solid solutions.

The study of the oxidation of the ACS of epitaxial $Pb_{1-x}Sn_xTe$ (x = 0, 0.2, and 1.0) showed that[63] SnTe is oxidised much more vigorously than PbTe. The rapid oxidation of tin is also characteristic of the solid solution and is accompanied by the enrichment of the surface in this element as a result of the sublimation of free tellurium. Vacuum annealing leads to the complete transition of tin to the oxidised state and hence to a decrease in the XPES peak associated with TeO_2. Bearing in mind the low temperature of the sublimation of elemental tellurium, the experimental data are seen to agree well with the phase equilibrium diagram (Fig. 3*c*).

The oxidation of the ACS of HgTe and $Hg_{0.7}Cd_{0.3}Te$ begins with the rupture of the Hg–Te bonds and the subsequent oxidation of tellurium but not mercury, the atoms of which leave the surface of this semiconductor, while both elements are oxidised in CdTe.[64] Comparison of the kinetics of the oxidation of all three materials showed that the solid solution is not oxidised as a simple mixture of two binary compounds. This can be explained by the fact that, on formation of the solid solution, a charge redistribution takes place between the mercury and cadmium ions and leads to the weakening of the Hg–Te bonds and to the strengthening of the Cd–Te bonds.[65]

Thermal oxidation has been investigated only for CdTe in view of the low thermal stability of mercury chalcogenides.[66] According to AES and XPES data, the thermal oxide, grown in both dry and moist oxygen at temperatures in the range 350–500 °C, consists of $CdTeO_3$ and no traces of enrichment of the interface in cadmium or tellurium were found. Furthermore, electron diffraction data show that epitaxial layers of cubic $CdTeO_3$ grow on CdTe at these temperatures. Complex cadmium and mercury oxide compounds are also present in the $Hg_{1-x}Cd_xTe$ oxides.[67]

Among all the variants of the oxidation reaction used to protect the $Hg_{1-x}Cd_xTe$ surface, anodic oxidation, carried out in 0.1 M KOH solution in 9 : 1 ethylene glycol–water mixture at a current density of 0.3 mA cm^{-2} under galvanostatic conditions, has unquestionably been most thoroughly investigated.[68] The composition and mechanisms of the growth of the anodic oxide have been studied by various methods. Fairly contradictory results have been obtained. At the present time, one can regard it as reliably established[69, 70] that the anodic oxide on $Hg_{1-x}Cd_xTe$ grows at the semiconductor–oxide interface as a result of the interaction of the atoms of the oxide with oxygen migrating to the interface via a vacancy mechanism. Oxygen vacancies migrate under the influence of the electric field in the direction towards the

outer boundary of the anodic oxide. At the oxide–electrolyte interface, the vacancies are filled with oxygen as a result of the electrochemical reaction. At this boundary, the oxide only dissolves in the electrolyte but does not grow.

Taking into account the available experimental data, the following model of the $Hg_{1-x}Cd_xTe$–anodic oxide interface has been proposed (Fig. 6*a*).[71,72] The $CdTeO_3$ layer is in direct contact with the semiconductor. The layer is formed because the binary components of the solid solution of CeTe and HgTe are oxidised separately — CdTe is oxidised preferentially, while HgTe remains partly unoxidised (private communication by Seelmann-Eggebert and H Richter — see Stahle et al.[73]). The anodic oxide grows into the semiconductor support, while the unoxidised HgTe remains in the layer adjoining the interface. The oxygen concentration is higher here, so that gradual further oxidation of HgTe takes place. In the bulk of the anodic oxide, all the components are fully oxidised and it is homogeneous as regards elemental composition. Comparison of the elemental composition determined experimentally by different methods with the composition calculated on the assumption that the entire oxidised semiconductor has been converted into a stoichiometric mixture of $HgTeO_3$ and $CdTeO_3$ has shown that more mercury than tellurium dissolves during the anodic oxidation. The anodic oxide has the following phase composition: 52% $HgTeO_3$, 30% TeO_2, and 18% $CdTeO_3$.[72] It is fully amorphous with the exception of the layer at the interface, where 2–5 nm crystalline particles are encountered. They have been identified as particles of unoxidised HgTe.

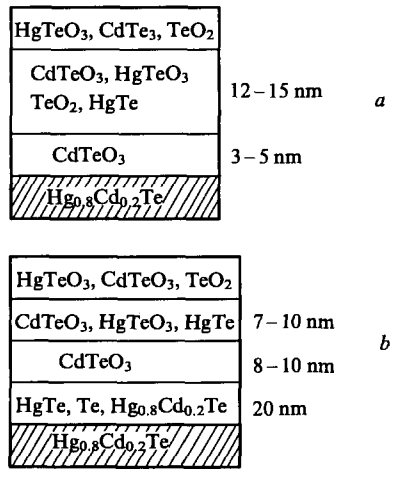


Figure 6. Phase composition profiles for the anodic oxide on $Hg_{0.8}Cd_{0.2}Te$: (*a*) after growth (before annealing; (*b*) after annealing at 220 °C.[72]

Annealing at relatively low temperatures (150 °C and above) leads to an appreciable redistribution of the elements at the interface, primarily to a decrease in the cadmium content in the semiconductor and an increase in its content of the oxide, the change in the composition involving HgTe being of the opposite kind.[71] This is unquestionably associated with the thermodynamic instability of the $Hg_{1-x}Cd_xTe$–oxide interface (Fig.3*a*). However, in the model illustrated in Fig. 6*a* the interface itself is thermodynamically stable, since $Hg_{1-x}Cd_xTe$ is in contact only with $CdTeO_3$, which is thermodynamically stable, and with HgTe and CdTe (continuous lines in Fig. 3a). It has therefore been suggested[72] that the $CdTeO_3$ layer in too porous and thin to prevent the interaction of TeO_2 with $Hg_{1-x}Cd_xTe$:

$$3TeO_2 + 10Hg_{0.8}Cd_{0.2}Te = 2CdTeO_3 + 8HgTe + 3Te. \quad (7)$$

This leads to some thickening of the $CdTeO_3$ layer and to the appearance of mercury telluride and tellurium in the semiconductor support (Fig. 6*b*). However, no account is taken of the possibility of the appearance of metallic mercury at the interface either directly during the period of oxidation or during subsequent heating as a consequence of a whole series of other thermodynamically feasible reactions, for example the interaction of $HgTeO_3$ with $Hg_{1-x}Cd_xTe$. However, in the presence of metallic mercury, it is impossible to account for the change in the electrical properties of the $Hg_{1-x}Cd_xTe$ surface layer (protected by the anodic oxide) during annealing.[71,74–76] According to RBS data, an appreciable increase in the mercury content after annealing at 200–250 °C is observed in the surface layer of the semiconductor approximately 20 nm thick.[76] The concentration of excess mercury under these conditions is up to 2×10^{21} cm^{-3}. Part of the mercury is actually segregated as HgTe, which alters the composition of the surface layer of the solid solution (according to optical absorption spectra, x diminishes to 0.125). The remainder accumulates in the form of mercury atoms in the interstices, which diffuse into the bulk of the semiconductor during annealing.

As in the case of GaAs and InP, the plasma oxide on $Hg_{1-x}Cd_xTe$ does not differ from the anodic oxide either as regards composition or the structure of the interface.[77] On the other hand, depending on the process conditions during photochemical oxidation, the compositions of both the oxide itself and of the interface, in particular their depletion or enrichment in mercury, can vary within wide limits. This is associated with the complexity of the oxide growth mechanisms.[78] Furthermore, it has been shown in relation to the photochemical oxide how greatly the composition of the interface for a compound semiconductor may depend on the preliminary treatment of the oxidised surface.[18]

An AES study of the anodic oxide on PbTe showed[79] that the distributions of the metal and the chalcogen in it agree fully with the distributions of cadmium and tellurium in the CdTe oxide.[67] This can be attributed to the fact that in both cases oxidation leads to the formation of the tellurite. RBS data indicate that the oxygen content in the bulk of the anodic oxide corresponds to lead in the Pb^{4+} oxidation state and not to Pb^{2+}, i.e. the appearance of the higher lead oxides — PbO_2 or $PbTeO_4$ — in the final stages of the oxidation reaction, predicted on the basis of the phase equilibrium diagram, has been confirmed experimentally for PbTe.

Comparison of the distributions of the elements at the oxide–semiconductor interface for the oxides on $Pb_{0.8}Sn_{0.2}Te$, obtained by the anodic,[80] plasma,[81] chemical,[82,83] and thermal[84] oxidation, yields interesting results. It shows that, although the compositions in the bulk of the oxides and especially in their outer layer differ appreciably, all the characteristics of the interface, which are already manifested on natural oxidation and, as stated above, are associated with the preferential oxidation of tin, are retained and actually intensify for all the oxidation methods. This concerns primarily the redistribution of tin and lead at the interface, which has been observed[85] in the oxidation of Pb–Sn alloys and which can be explained by topochemical substitution reactions typical for the initial stages of the oxidation of binary alloys of metals with different oxygen affinities.[86] However, also the appearance of elemental tellurium should be observed in the oxidation of tellurides (Fig. 3*c*).

Studies by Raman spectroscopy have made it possible to detect Te^0 on the naturally oxidised surface of only SnTe.[87] For $Pb_{0.8}Sn_{0.2}Te$, elemental tellurium can be detected only after thermal oxidation at $T \geqslant 250$ °C. For the anodic oxide on $Pb_{0.8}Sn_{0.2}Te$, elemental tellurium is also detected after annealing at this temperature. As in the case of As^0 in GaAs, its appearance here is associated primarily with the thermodynamically favourable secondary process

$$SnTe + TeO_2 = SnO_2 + 2Te. \quad (8)$$

At the same time, elemental tellurium could not be detected in the chemical oxide even on annealing. This is apparently associated with the characteristic features of the growth of the oxide film by this method.[83] The oxide always contains unoxidised PbTe, which

accumulates, in combination with SnO_2, at the interface, ensuring its thermodynamic stability.

Electrochemical anodisation has been used successfully to produce on the $Hg_{1-x}Cd_xTe$ surface other intrinsic insulators—sulfides[88] and fluorides.[89] The process is in both cases similar to anodic oxidation and is carried out respectively in Na_2S and KF + KOH solutions in ethylene glycol. During the growth of the anodic sulfide, HgS and TeS_2 are dissolved preferentially. The growing layer consists of 30% HgS and 70% CdS with some excess of tellurium in the form of hexagonal ~5 nm particles.[90] The $Hg_{1-x}Cd_xTe$–anodic sulfide interface is sharp and the change in composition is observed at appreciably higher annealing temperatures than for the anodic oxide (350 °C for annealing in air in the course of 15 days). The changes are mainly associated with the evaporation of mercury.[91]

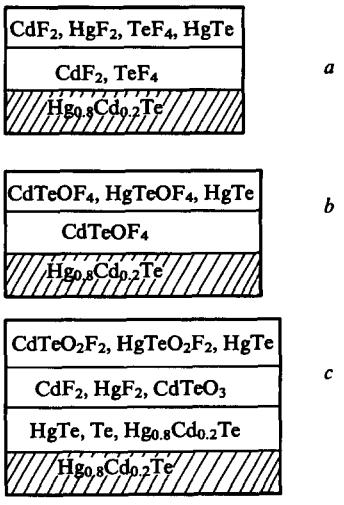


Figure 7. Phase composition profiles for the anodic fluoride on $Hg_{0.8}Cd_{0.2}Te$: (*a*) after growth; (*b*) after storage in air at room temperature; (*c*) after annealing at 220 °C.[92]

The study of the composition of the anodic fluoride on $Hg_{1-x}Cd_xTe$ showed,[92,93] that it consists mainly of 14% CdF_2, 21% HgF_2, 35% TeF_4, and 30% HgTe, i.e. the entire HgTe is not fluorinated. It is very significant that the interface is depleted in mercury fluoride and actually consists of only CdF_2 and TeF_4 (Fig. 7*a*). This should have promoted the thermal stability of the $Hg_{1-x}Cd_xTe$–anodic fluoride interface, but it has been found that the anodic fluoride is so sensitive to the presence of oxygen that oxide fluorides are formed even at room temperature (Fig. 7*b*). On heating, they react further with oxygen, which leads to the loss of fluorine:

$$2MTeOF_4 + O_2 = 2MTeO_2F_2 + 2F_2, \qquad (9)$$

where M = Hg or Cd. A reaction similar in many respects to that occurring in the annealing of the anodic oxide on $Hg_{1-x}Cd_xTe$ takes place at the interface, i.e.

$$3MTeO_2F_2 + 10Hg_{0.8}Cd_{0.2}Te = \\ = 3MF_2 + 2CdTeO_3 + 8HgTe + 3Te, \qquad (10)$$

which results in the formation of a multiphase interface similar to the $Hg_{1-x}Cd_xTe$–anodic oxide interface. It must be emphasised that the formation of metallic mercury is characteristic of only the $Hg_{1-x}Cd_xTe$–anodic oxide interface. As will be shown below, this is responsible for the fundamental differences between the electrophysical properties of these interfaces.

Owing to the instability of the anodic fluoride on $Hg_{1-x}Cd_xTe$ in the presence of not only oxygen but also water vapour, it is essential to provide additional protection to the anodic fluoride in practical applications, for example, by depositing ZnS.[94] Here it is necessary to take into account the possibility of chemical interaction between these compounds, leading to the appearance of ZnF_2, HgTe, and Te. When the anodic fluoride is sufficiently thick, its interaction does not affect the properties of the interface.

Similar chemical reactions, leading to partial reduction of the components of the anodic oxide on $Hg_{1-x}Cd_xTe$, occur also when ZnS[95] or metals (indium,[96] platinum, and gold[97]) are deposited on it. This must be taken into account in selecting the optimum thickness of the intrinsic insulator.

The knowledge of the possible chemical interactions in the semiconductor, the oxide, and the metal (Fig. 4) makes it possible to regulate specifically the properties of the metal–semiconductor interface with the aid of a thin intervening layer of oxide having a specified composition. Thus, by employing the chemical oxide, it has been possible to prevent the undesirable interaction of the metal with the semiconductor and to improve significantly the electrical and photoelectric properties of $M-Pb_{1-x}Sn_xTe$ (M = metal) barrier structures.[82]

IV. Electrophysical properties and chemistry of the compound semiconductor–intrinsic oxide interface

In the analysis of the requirements imposed on MOS (or MIS) structures by investigators developing electronic devices, the $Si-SiO_2$ system, which ideally satisfies all these requirements, may serve as a natural reference standard.[1]

The operation of MOS transistors is based on the possibility of inducing in the surface layer of the semiconductor an electric field which regulates the concentration of charge carriers up to the inversion of the type of conduction. The influence of the surface of the semiconductor is especially important in MOS transistors and other devices where the interface is an active region of the device (Schottky barriers, heterojunctions, superlattices). In practice, in order to optimise the parameters of any semiconductor device (dipolar transistor, photodiode, photoresistor), it is neces-sary to protect its surface by an insulator with fully defined characteristics.

Localised surface electronic states (SES),¶ the nature of which may be various, play the main role in all electronic phenomena on the surface and on the interface between the semiconductor and another material. In the first place, these are intrinsic SES arising due to the distortion of the periodic potential of the crystal lattice and the rupture of the chemical bonds involving surface atoms (the Tamm–Shockley levels). In addition, the appearance of SES may be caused by local surface imperfections of the type of structural defects, impurities, and their complexes.

The influence of the SES on the properties of the interface is determined by their charge state, disposition relative to the Fermi level (E_F) and distance from the interface.

A high SES concentration of the order of $10^{14}-10^{15}$ cm^{-2}, which is only a little less than the number of surface atoms, is observed on an atomically clean surface of silicon. The times of the electron exchange between the SES and the bulk phase are very short (less than 10^{-5} s) and such SES are called fast. Their high concentration leads to firm stabilisation of E_F (the so called 'pinning' of the Fermi level) on the surface near the centre of the forbidden gap E_g and it is almost impossible to regulate the properties of the surface with the aid of an external electric field.

During the thermal oxidation of the surface of silicon under optimum conditions, the SES concentration diminishes appreciably (to 10^9 cm^{-2}). This is probably associated with a certain degree of saturation of the ruptured bonds and a weakening of the

¶ The term 'surface electronic states' can be understood literally only for an atomically clean surface. For real interfaces, the SES are distributed in a finite three-dimensional layer.

Tamm factor in the perturbation of the periodic variation of the crystal lattice potential, which diminishes the degree of pinning of the Fermi level and makes it possible to modulate the bending of the bands at the $Si-SiO_2$ interface. However, the presence of structural defects in the oxide leads to the appearance of electron traps (the so called slow SES with a charge transfer time of $10^{-1}-10^{2}$ s).

A characteristic feature of the $Si-SiO_2$ interface is the presence of a built-in charge localised in a narrow (< 2 nm) region, the size and magnitude of which are most important characteristics. In fact it specifies the initial bending of the bands at the silicon surface and hence the conditions in the operation of the MOS transistor (depletion or enrichment). As regards the fast SES, their concentration should be minimal to ensure the maximum efficiency of the regulation of the surface conductivity. As already mentioned, for a high SES density (such as, for example, that at the ACS silicon), this effect is altogether absent. The SES charge transfer times, on which the frequency characteristics of the devices depend, are also important. The number of traps in the oxide should likewise be minimised, since their presence leads to instability of the parameters of the devices as a function of time.

In industrial manufacture, the decisive factor becomes not simply the development of processes ensuring the required parameters of the interface but also their technological suitability and, what is most important, their reproducibility. This requires a deeper understanding of the chemistry of the process in purely empirical developments. The initial advances in the creation of silicon MIS devices, which in the case of binary semiconductors proved useless, are associated with precisely such developments. This is confirmed by the fact that, as early as the 1970s, reports appeared concerning the development of MOS transistors based on GaAs and InP with parameters close to those of the silicon devices but in reality such devices had not been created at the time.

1. Gallium arsenide

Studies of the problem of the segregation of elemental arsenic at the GaAs–oxide interface must be regarded as fundamental. At the beginning of the 1980s, it began to be suspected that it is in fact the presence of As^0 at the interface that makes it unsuitable for the formation of GaAs-based MOS devices.[98] Analysis of the electrical parameters of the GaAs-based MIS structure showed that the concentration of surface electronic states and the position of E_F on the surface are independent of the method of preparation and even of the nature of the insulator (intrinsic oxides grown by means of the electrochemical, anodic, and plasma oxidation, SiO_2, Si_3N_4, $Si_xO_yN_z$, and Al_2O_3), although some dependence of the preliminary treatment of the GaAs surface was noted.[98,99] The density of the surface electronic states, fixing E_F in the vicinity of the middle of E_g, is so high that the bending of the semiconductor bands by the external electric field can be varied within limits insufficient for the attainment of the enrichment conditions or the inversion of surface conductivity.

Studies were carried out on the properties of the ACS of gallium arsenide and the changes in the latter when subjected to controlled influences. It has been established experimentally that there are no surface electronic states in the forbidden gaps of the absolutely clean GaAs and InP surfaces, so that, in contrast to silicon, there is no pinning of E_F on the surface in GaAs and its position is the same as in the bulk phase. However, when extraneous atoms are deposited onto the ACS in amounts appreciably less than a monolayer, the Fermi level in both *n*- and *p*-GaAs shifts approximately to the middle of E_g, where it is fixed and remains unchanged on further increase in the number of adsorbed atoms. Such behaviour of E_F is observed in the adsorption of both different metals and nonmetals, including oxygen.[100]

This made it possible to postulate that the pinning of E_F is caused by the surface electronic states associated with the intrinsic lattice defects and arising on adsorption of extraneous atoms. In the UDM (unified defect model),[101] it was initially assumed that such defects are gallium and arsenic vacancies. However, subsequently calculations and experiments on GaAs bulk phase specimens with different deviations from stoichiometry showed that antistructural defects of the type involving the transfer of arsenic to a Ga sublattice site (As_{Ga}) and conversely the transfer of gallium to an As sublattice site (Ga_{As}) are thermodynamically more favourable in GaAs. In particular, the EL2 trap, which determines many of the characteristic features of GaAs, represents either an isolated As_{Ga} defect or contains an interstitial arsenic atom on the {111} axis.[102] Whereas the appearance of an excess of As in the bulk phase of GaAs is related to the characteristics of its phase diagram,[103] in the oxidation reaction it is related to the GaAs–O structural diagram. Therefore in the approved version of the UDM model — the ADM (advanced defect model)[104] — the main cause of the pinning of E_F is believed to be the antistructural As_{Ga} defect which gives rise to two donor levels. The Fermi level is located between them and the position of E_F depends on the degree of compensation for As_{Ga} by the second defect Ga_{As}, which is an acceptor. An increase in the arsenic content on the surface shifts E_F to the conductivity band, whilst a decrease shifts it in the opposite direction.

One cannot claim that the ADM model fully explains the entire mechanism of the appearance of surface electronic states regulating the position of E_F on the interfaces with GaAs. It may be that effects associated with the presence of impurities, in the given instance adsorbed oxygen [the MIGS (metal induced gap states) model][105] and the disordering of the crystal lattice of the semiconductor in adsorption [the DIGS (defect induced gap states) model],[106] also make a definite contribution.

Convincing evidence that the pinning of E_F is in fact associated with the antistructural defects arising as a consequence of the liberation of arsenic on oxidation has been obtained in a study of thin (~5 nm) epitaxial GaAs layers.[107] The change in the position of E_F can be readily found from the change in the electrical conductivity of such layers on oxidation in air (after their removal from the growth chamber). It has been established that E_F for high-quality epitaxial *n*-GaAs layers, grown at 530 °C, varies nonmonotonically following an increase of exposure in air before becoming fixed. On the other hand, the position of the Fermi level for a similar layer grown at 300 °C does not change at all after exposure to air. Layers obtained at such a low temperature contain up to 5×10^{19} cm^{-3} As_{Ga} defects and their E_F is fixed from the beginning. High-temperature annealing of such layers is known to decrease the concentration of As_{Ga} by more than an order of magnitude. Indeed, the shift of E_F on oxidation for a similar specimen grown at a low temperature but then annealed at 530 °C occurred in the same way as for the usual specimens.

It has been established[108] that the position of E_F for layers grown at low temperatures with an excess of arsenic may be fixed not only by As_{Ga} point defects but also by As^0 precipitates segregated in the bulk of the material.† The position of E_F changes by more than 0.2 eV on passing from one pinning mechanism to another.

The changes in the electrophysical parameters of the GaAs-based MOS transistors may be caused not only by their thermodynamic instability, due to reaction (1), but also by the precipitation of As^0 on the interface described above.

The relation between the presence of As^0 and As_2O_3 on the GaAs surface and the fixation of the Fermi level has been confirmed by experiments involving the washing of the GaAs surface with water.[111] As_2O_3 is soluble in water, whereas As^0 dissolves in water only if the specimen has been illuminated with fairly intense light inducing photochemical reactions or if the water has been saturated with oxygen. In this case, As^0 is initially oxidised to As^{3+}, which then dissolves in water. Experiment shows that the intensity of the photoluminescence, which depends on the degree of fixation of E_F, increases appreciably only when

† The so called internal Schottky barrier model,[109] which permits a new approach to the problem of semi-insulating semiconductors.[110]

the GaAs specimens have been washed in a stream of water saturated with O_2 or under illumination. This leads to the washing away of both As_2O_3 and As^0. However, after storage for several minutes in air, especially at an elevated temperature, the photoluminescence intensity falls to the previous level, which is associated with the reoxidation of the GaAs surface. The new stage involving washing with water again increases the brightness of the luminescence and this cycle can be repeated several times.

Treatment of the GaAs surface with a $Na_2S.9H_2O$ solution also leads to an appreciable increase in the effectiveness of the photoluminescence.[112,113] A series of methods have been developed for the treatment of the GaAs surface with sulfides, which greatly diminishes the rate of surface recombination. After such treatment, the oxides are removed from the GaAs surface and an ideal crystal lattice is created on the latter, in the first layer of which the sulfur atoms substitute all the arsenic atoms and form thermodynamically stable bonds with gallium atoms (Fig. 8).

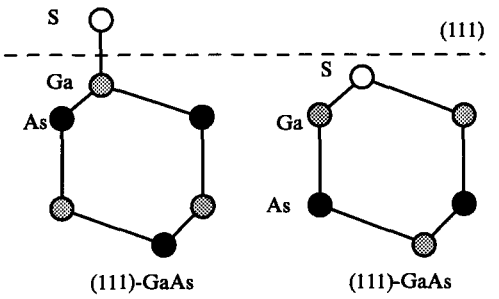


Figure 8. Distribution of sulfur atoms on the (111) surface of GaAs passivated with sulfur.[2,149]

The importance of the complete removal of arsenic is indicated by the comparison of the efficiencies of the treatment of the GaAs surface with Na_2S and $(NH_4)_2S$ solutions.[114] Experiments with a layer of arsenic especially sputtered on showed that, in contrast to Na_2S, the $(NH_4)_2S$ solution effectively dissolves arsenic. Sulfidation with this solution actually leads to a more than twofold decrease in the density of surface traps and hence to a decrease in the rate of surface recombination. However, since the heats of formation of sulfides are lower than those of the corresponding oxides, a GaAs surface treated with sulfide solutions is unstable on storage in air and in the course of several days the initial properties of the surface are restored.

All the experiments involving the study of the stability of the GaAs surface freed from As by different methods have shown that the reason for the subsequent appearance of arsenic is reoxidation. Therefore all the technological processes for the creation of an insulator–GaAs interface must be devised in such a way that the oxidation of the GaAs surface is ruled out.

In the plasmochemical etching methods, it is technologically easy to combine in a single cycle the cleaning of the GaAs surface and the deposition of insulators. An example is provided by the etching of the surface in a hydrogen HF plasma with subsequent deposition of Ga_2O_3,[115] which is thermodynamically stable in relation to GaAs. The protecting layer is generated by evaporating gallium in an oxygen plasma. In order to rule out the reoxidation of GaAs under these conditions, the GaAs specimens are additionally etched in a nitrogen plasma, which creates a thin layer of arsenic nitride saturating the free arsenic bonds. The interfaces thus obtained have a low density of surface electronic states and the E_F level is not fixed. Under these conditions, degradation of the parameters was not observed even after storage of the specimens for several months in air.

It has been established[116] that treatment of the GaAs surface in a CF_4 plasma before depositing Si_3N_4 leads to the effective removal of As^0 and As_2O_3 and also to the formation of a passivating layer made up of Ga_2O_3 and GaF_3. Such a passivating coating greatly improves the characteristics of high-power GaAs-based transistors and prolongs their working life. The stability of the interface can be achieved also by the direct deposition of GaF_3 if the GaAs surface has been subjected to a preliminary treatment in $(NH_4)_2S$ solution.[117]

Another method for producing an ideal interface involves not the removal of the oxides from the GaAs surface but their reduction. This can be carried out by depositing a thin layer of silicon on the GaAs surface. For a correctly selected thickness of the layer (~0.8 nm) and of the temperature of the subsequent annealing, it is possible to reduce the oxides on GaAs completely and a layer of SiO_2 with a specified thickness can be deposited on the structure thus obtained.[118]

It is noteworthy that the understanding of the chemistry of all processes leading to the oxidation of the GaAs surface has actually made it possible in recent years to take definite steps towards the creation of GaAs-based MIS devices.

2. Indium phosphide

It follows from the phase equilibrium diagram that the chemistry of the InP–intrinsic oxide interface is qualitatively different. It is of interest to elucidate how this is reflected in the electrophysical properties of MOS structures.

When oxygen is adsorbed, E_F on the InP surface is also fixed but not in the middle of E_g, as in GaAs, but closer to the bottom of the conductivity band (as a result of an intrinsic lattice defect different from that in GaAs).[101] In combination with the fact that the density of surface electronic states on the interface involving InP is an order of magnitude lower than in GaAs, this makes it possible to achieve different versions of InP-based MOS transistors.[99] Slow surface electronic states and traps, which lead to a prolonged drift of the characteristics, are always present on the interfaces obtained between InP and intrinsic oxides as well as other insulators.

The effects associated with the instability of the characteristics can be eliminated by employing thin (< 30 nm) oxide layers[119] consisting only of the phosphate $In(PO_3)_3$, in which the width of the forbidden gap is fairly considerable ($E_g \simeq 7$ eV). Under these conditions, the edge of the conduction band E_c in the oxide is higher by 2.3 eV than in InP, which ensures an adequate potential barrier preventing the injection of electrons from InP into the oxide.[56] In the case of thick oxide films, the outer layer of which consists partly of In_2O_3 having an appreciably lower E_g (~ 3.5 eV), the difference $E_c(In_2O_3) - E_c(InP)$ is apparently also small. This leads to the possibility of the tunnelling of electrons from InP through $In(PO_3)_3$ and into In_2O_3.[120] This factor is apparently the cause of the marked frequency dispersion and the hysteresis characteristics of the MOS capacitors prepared on the basis of thick oxides. Having etched away the outer layer of the anodic oxide leaving only the layer consisting of $In(PO_3)_3$, it is possible to eliminate the deficiencies noted above. Furthermore, this operation greatly diminishes the hygroscopicity of the specimens. Thus, whereas after the storage of unetched specimens for several hours in air an appreciable increase in the thickness of the initial anodic oxide (up to 40%) is observed, for the anodic oxide with an etched outer layer such a change is much slower (up to 30% in one month). Furthermore, annealing of an anodic oxide of this kind at 250 °C in nitrogen for 30 min stabilises its properties. Having sputtered a layer of Al_2O_3 onto it with a thickness of 100 nm, it was possible to obtain, on the basis of a semi-insulating InP substrate, a transistor with significantly more stable characteristics.[56]

Having selected the plasma oxidation conditions in such a way that the contents of In_2O_3 and P_2O_5 are reduced to a minimum, it is possible to obtain an interface with nearly theoretical electrical parameters.[61]

Under optimal conditions, the interface between InP and an intrinsic oxide is sufficiently ideal. During its formation, it is important to eliminate (bearing in mind the low thermal and

radiation stabilities of the InP surface) the possibility of both a general structural disordering[106, 121] and of the appearance of intrinsic lattice defects. For example, the phosphorus vacancies arising during the annealing of an absolutely clean (100) surface of InP in vacuo lead to an appreciable alteration of its properties and, in the view of a number of investigators, are responsible for the pinning of E_F.[122] One cannot also exclude the possibile formation on the InP surface of other types of intrinsic defects which may exist in the bulk of InP in the presence of an excess of one of the components.[123–125] This has been clearly demonstrated by Hu et al.,[127] who obtained the oxide by plasma oxidation under the conditions which excite electron cyclotron resonance. This process is closer to thermal than to anodic oxidation, although it does occur at room temperature. Indeed, after the formation in the plasma of an oxide film 9 nm thick, an appreciable amount of elemental phosphorus appears at the InP – intrinsic oxide interface according to XPES data. It was possible to eliminate this effect by placing a screen between the source of plasma and the InP surface, which greatly reduced the rate of growth of the oxide film (by a factor greater than 2) but eliminated the direct bombardment of the InP surface by high-energy ions. A layer of SiO_2 having a thickness of 70 nm was grown by the same method on the oxide 3 nm thick obtained in this way. The structures with the oxide grown in shielded plasma have a very low density of fast and slow surface electronic states.

3. Semiconductor solid solutions

Fairly satisfactory properties of the interface were obtained already in the first experiments on the formation of CdTe-based MOS structures. The phase equilibrium diagram for this compound also predicts equilibrium oxidation with formation of only one compound (Fig. 1*b*). Anodic,[128] thermal, chemical, and plasma[129] oxidation reactions were tested, but the best parameters of the interface and of the insulator itself were obtained for the thermal oxide. The properties of the MOS structures depend in many respects on the initial treatment of the semiconductor surface. It is not fortuitous that the best parameters were obtained after the preliminary annealing of CdTe under an atmosphere of hydrogen, which restores the stoichiometry of the CdTe surface disturbed by chemical polishing.

Despite the complexity of the chemical reactions occurring in the oxidation of $Hg_{1-x}Cd_xTe$, only $CdTeO_3$ is present at its interface with the anodic oxide (Fig. 6*a*). This is precisely why the interface before annealing has a very low density of the fast and slow surface electronic states, which is actually comparable to the density at the $Si-SiO_2$ interface.[24, 72] It has been shown[24] that the (100) surface of $Hg_{1-x}Cd_xTe$ can be brought into virtually ideal conformity with the (011) surface of $CdTeO_3$, which has the perovskite crystal lattice. This minimises the number of ruptured bonds at the interface. The interfaces between $Hg_{1-x}Cd_xTe$ and the anodic sulfide[88] and fluoride[89] also have a low density of the fast and slow surface electronic states. In the former case, this is associated with the fact that the interface actually represents a heterojunction formed by II–VI solid solutions, while the reason for the latter is that the cadmium oxide fluoride (Fig. 7*b*), the parameters of which are close to those of $CdTeO_3$, is always actually present at the $Hg_{1-x}Cd_xTe$–fluoride interface.

A high built-in charge, which always has a positive sign, is characteristic of the $Hg_{1-x}Cd_xTe$–anodic oxide interface. It has been suggested that the positive sign is due to positively charged oxygen vacancies.[72] This agrees well with the mechanism of ion transport during the growth of the anodic oxide and also with data for the cathodoluminescence of the anodic oxide on $Hg_{1-x}Cd_xTe$.[130] The latter data show that the radiative recombination centres are associated with the deficiency of oxygen in TeO_2 or in more complex compounds based on it. A significant disadvantage of the anodic oxide on $Hg_{1-x}Cd_xTe$ is its low thermal stability. Heating of *n*-type specimens at relatively low temperatures leads to an increase in the built-in charge, while heating of the *p*-type specimens results in the inversion of the type of conductivity, the thickness of the *n*-type layer produced reaching 40 μm depending on the temperature and duration of the annealing.[74–76] The mercury accumulated at the interface during anodic oxidation diffuses during annealing to the bulk of the crystal and is annihilated on recombining with mercury vacancies. This accounts for the inversion of the type of conductivity. The reactions occurring at the interface during annealing may serve as an additional source of mercury.

The $Hg_{1-x}Cd_xTe$ surface acquires *n*-type conductivity during natural, anodic, and plasma oxidations. On the other hand, the conductivity of the surfaces of PbSe, $Pb_{1-x}Sn_xSe$,[131] and $Pb_{1-x}Sn_xTe$ [132] is always of the *p*-type. Comparison of the phase equilibrium diagrams for $Hg_{1-x}Cd_xTe$ and lead and tin chalcogenides suggested[133] that the preferential oxidation of the chalcogen in the former case and of the metal in the latter is in fact responsible for the opposite type of surface conductivity in these materials. The presence of free chalcogen or metal atoms at the interface, appearing as a consequence of such oxidation, can exert a decisive influence on the entire assembly of defects in the oxide responsible for the built-in charge. This is indicated by data on the cathodoluminescence of the anodic oxides on $Hg_{1-x}Cd_xTe$ [130] and $Pb_{1-x}Sn_xTe$,[134] demonstrating the different nature of the radiative recombination centres. Furthermore, differences are manifested also in the mechanisms of mass transfer during the growth of anodic oxides on the surfaces of both materials.[69, 135] As a consequence of the excess of one of the components on the interface, as in the case of As in GaAs, the concentration of the intrinsic lattice defects increases. Different point defects, whose electrical behaviour and influence on the diffusion processes in the semiconductor have not yet been finally established, may occur in mercury and lead chalcogenides.[136–138] However, one may expect that their contributions to the properties of the interface will be different.

The same phenomena have been observed in the study of the $Hg_{1-x}Zn_xTe$–anodic oxide interface, where both the metal and the chalcogen are liberated according to the phase equilibrium diagram (Fig. 3*b*). The differences between the properties of the $Hg_{1-x}Zn_xTe$–anodic oxide and $Hg_{1-x}Cd_xTe$–anodic oxide interfaces can be accounted for by the competing influence of the elemental tellurium appearing in the region of the interface.[133] Firstly, the magnitude of the built-in charge in the $Hg_{1-x}Zn_xTe$-based MOS structures is smaller than in the analogous $Hg_{1-x}Cd_xTe$-based structures.[139–141] Secondly, the layer with *n*-type conductivity on $Hg_{1-x}Zn_xTe$ arises at higher annealing temperatures and its thickness is smaller by a factor of 2 than that of the anodic oxide on $Hg_{1-x}Cd_xTe$ obtained under similar conditions. This indicates a small amount of mercury liberated at the $Hg_{1-x}Zn_xTe$–anodic oxide interface. Similar changes are also observed during annealing for the $Hg_{1-x}Mn_xTe$–anodic oxide system.[75, 142] Since the zinc and manganese contents in the solid solutions investigated are low compared with the mercury contents, the liberation of tellurium is insignificant compared with mercury and there is a correspondingly small compensating effect.

The changes in the properties of the $Hg_{1-x}Cd_xTe$–anodic sulfide (or fluoride) interface are greater than the changes in the properties of the $Hg_{1-x}Cd_xTe$–anodic oxide interface. According to the phase equilibrium diagrams, mercury should not be liberated at all at the interface in such systems. Indeed, the sign of the built-in charge for the anodic sulfide is reversed,[88] while that for the fluoride, although remaining positive, is an order of magnitude smaller compared with the anodic oxide and its magnitude is to a large extent regulated by the conditions in the electrochemical process.[89] Finally, on heating both the sulfide and fluoride on $Hg_{1-x}Cd_xTe$, an *n*-type layer does not arise,[75, 142] which indicates the absence of the liberation of mercury at the $Hg_{1-x}Cd_xTe$–intrinsic insulator interface.

V. Current trends in the development of insulators for metal – insulator – semiconductor devices and protection of the surfaces of compound semiconductors

1. Gallium arsenide

In the development of a technology for the formation of GaAs-based insulators, it was necessary to exclude the possibility of the fortuitous oxidation of the semiconductor surface, for example on contact with the atmosphere between individual operations, and of a side oxidation reaction as a consequence of some kind of secondary process. New intrinsic defects of the As_{Ga} antistructural defect type must not arise under these conditions and structural disordering of the interface must not occur, i.e. it is essential to exclude all factors inducing the appearance of surface electronic states.

A theoretically ideal semiconductor–insulator interface can be obtained by growing epitaxial layers of a single crystal insulator on the semiconductor. Such insulators may be the alkaline earth metal fluorides CaF_2 and SrF_2. On evaporation in an ultrahigh vacuum, these materials sublime without dissociating, which makes it possible to obtain stoichiometric single crystal layers with the aid of molecular beam epitaxy. MIS structures based on the GaAs–SrF_2 and GaAs–CaF_2 systems have been investigated.[144,145] The differences between the types of chemical bonds as well as the lattice constants and thermal expansion coefficients of these fluorides and III–V semiconductors are responsible for the high density of surface electronic states at the interface, although it can in fact be diminished by rapid annealing. Best results have been obtained with the aid of the epitaxy of cubic gallium sulfide.[146,147] Bearing in mind that the discrepancy between the lattice constants of the two compounds is small and that the sulfur in gallium sulfide is satisfactorily compatible with the GaAs lattice (Fig. 8), it is possible to obtain an ideal interface with parameters indicating that there are good prospects for the practical employment of such structures.

An ideal interface can also be obtained by employing semiconductors of the same III–V group in which the width of the forbidden gap is large (quasi-insulators). The lattice constants of these semiconductors and GaAs should agree. A satisfactory interface with a low density of surface electronic states and a high stability has been obtained for the GaAs–$Al_xGa_{1-x}As$ structure,[148] but the gap between the bands of the insulator and the semiconductor is then too narrow (only 0.4 eV) to prevent the transfer of electrons from the semiconductor to the insulator. A larger gap between the bands exists in another couple, namely GaAs–ZnSe.[2]

Two-layer structures, in which the first layer, without adequate chemical stability primarily towards atmospheric oxygen, forms an interface with the required electrical parameters, while the second performs protecting functions, are promising.[2] According to the authors,[2] interfaces with GaAs having nearly ideal parameters are ensured by a monolayer of antimony, which gives rise to an ordered structure of the (110) surface of GaAs in which there are no ruptured bonds. The principal problem under these conditions is the creation of a second layer: it must be formed without disturbing the properties of the GaAs–Sb interface. This is achieved by sputtering on CaF_2. At any rate the GaAs surface passivated by sulfur remains stable after the deposition of CaF_2 even on annealing at temperatures up to 410 °C.[149]

Amorphous or crystalline germanium or silicon layers can also be employed as an intervening layer. The GaAs–Si–SiO_2, GaAs–Si–Si_3N_4, and GaAs–Si–AlN structures have been vigorously investigated recently.[150] The best results were obtained for GaAs–Si–Si_3N_4 when a layer of silicon was grown in the presence of atomic hydrogen. The parameters of such MIS structures approach those of the Si–SiO_2 system. This permits the hope that, by employing precisely this technology, it will be finally possible to create GaAs-based MIS devices.

2. Indium phosphide

The parameters of the InP–oxide interface are significantly higher than those of the GaAs–oxide interface. It is believed[150] that further improvement of the characteristics may be achieved only by employing a technology which excludes any kind of oxidation. Therefore many of the methods described above are used also for InP. These include epitaxy of the alkaline earth metal fluorides CaF_2[151] and $Ba_{1-x}Sr_xF_2$[152] and of the quasi-insulators $In_xAl_{1-x}As$.[144] Interesting results have been obtained for InP (as for GaAs) on deposition of an antimony monolayer.[122] However, it is still too early to speak of InP-based devices.

More promising results have been obtained on deposition of phosphorus[153] or boron[154] nitrides. However, it is then necessary to carry out the process under mild conditions which rule out a disturbance of the stoichiometry of the InP surface.

At the same time, the form of the phase equilibrium diagram for the InP–O system suggests that, in order to improve the parameters of InP-based MIS devices, there is no need at all to avoid oxidation but it is necessary to optimise the process in such a way that a thermodynamically stable phosphate phase is grown on the InP surface. This view is supported by the continuing development of different methods for the creation of oxide films — by anodic,[56] plasma,[61,155] photochemical,[156] and thermal[51] oxidation and by the thermal evaporation of P_2O_5.[157]

3. Semiconductor solid solutions

Intrinsic insulators are used quite widely for the passivation of the surfaces of devices based on $Hg_{1-x}Cd_xTe$ as a layer forming an interface with the semiconductor. The anodic oxide combined with thermally sputtered ZnS is used in photoresistors,[158,159] whilst the anodic sulfide in the same combination is employed in photodiodes.[6,160] Their main disadvantage is their low thermal stability. Some improvement is afforded by the replacement of the anodic oxide by the anodic fluoride.[6]

It is believed that a radical improvement of the properties of the $Hg_{1-x}Cd_xTe$–intrinsic insulator interface and of the thermal stability will be achieved by employing as the quasi-insulator wide-band semiconductors of the same group — CdTe and $Cd_{1-x}Zn_xTe$[159–162] and of $Cd_{1-x}Mn_xTe$ for $Hg_{1-x}Mn_xTe$.[163] These materials have a much higher E_g compared with the protected semiconductor, which makes the use of quasi-insulators in this case much more effective than for III–V semiconductors. The satisfactory correspondence of the crystal lattices makes it possible to obtain, using different epitaxial methods, an almost ideal interface between such semiconductors and $Hg_{1-x}Cd_xTe$.

The electrochemical methods for the generation of CdTe[164,165] on the $Hg_{1-x}Cd_xTe$ surface are also of interest. A single crystal interface cannot be obtained with their aid owing to the low process temperature, but it is possible to combine in one technological operation the precision chemical cleaning of the $Hg_{1-x}Cd_xTe$ surface and the deposition of CdTe. Interesting results have been obtained on electrochemical reconstruction of the $Hg_{1-x}Cd_xTe$ surface layer on ZnTe on which a layer of ZnS was subsequently deposited by means of gas-phase epitaxy.[166]

In conclusion one should note that the possibilities of generating on $Hg_{1-x}Cd_xTe$ a high-quality interface with the aid of classical insulators such as Al_2O_3,[167] SiO_2,[168] and their combinations[169] cannot be regarded as fully exhausted. Thus the best parameters of the interface for the $Hg_{1-x}Zn_xTe$ solid solution have in fact been obtained with the aid of SiO_2.[140] Incidentally, despite the disadvantages mentioned above, even oxidation has found an application in the creation of lasers based on $Al_xGa_{1-x}As$–GaAs quantum-well heterostructures[170,171] by virtue of the excellent optical characteristics of the oxides.

* * *

Comparison of the entire set of experimental data obtained in studies of compound semiconductor–intrinsic insulator interfaces with the corresponding phase equilibrium diagrams has shown that in many instances there is a direct relation between the characteristics of the phase diagrams such as segregation of the metal or the nonmetal and the intrinsic lattice defects arising under these conditions, on the one hand, and the electrophysical parameters of the interface, on the other.

All this demonstrates that the ideas underlying the models of intrinsic defects[101,104] for the III–V compounds are fully applicable also to the analysis of the interfaces involving the II–VI and IV–VI semiconductors.

References

1. V S Vavilov, V F Kiselev, B N Mukashev *Defekty v Kremnii i na Ego Poverkhnosti* (Defects in Silicon and on Its Surface) (Moscow: Nauka, 1990)
2. A M Green, W E Spicer *J. Vac. Sci. Technol. A* **11** 1061 (1993)
3. R Pretorius, T K Marais, C C Theron *Mater. Sci. Eng. Rep.* **10** 1 (1993)
4. G P Schwartz *Thin Solid Films* **103** 3 (1983)
5. T P Smirnova, A N Golubenko, N F Zakharchuk, V I Belyi, G A Kokovin, N A Valisheva *Thin Solid Films* **76** 11(1981)
6. Y Nemirovsky, G Bahir *J. Vac. Sci. Technol. A* 7 450 (1989)
7. C R Helms, in *Proceedings of the 4th International Symposium on Silicon Materials Science and Technology, Pennington 1981* p. 455
8. V G Litovchenko *Osnovy Fiziki Poluprovodnikovykh Sloistykh Sistem* (Fundamentals of the Physics of Layered Semiconductor Systems) (Kiev: Naukova Dumka, 1980)
9. A P Baraban, V V Bulavinov, S P Konorov *Elektronika Sloev SiO_2 na Kremnii* (The Electronics of SiO_2 Layers on Silicon) (Leningrad: Izd. Leningrad. Univ., 1988)
10. I Ya Mittova, V R Pshestanchik *Usp. Khim.* **60** 1898 (1991) [*Russ. Chem. Rev.* **60** 967 (1991)]
11. D R Rhiger, R E Kvaas *J. Vac. Sci. Technol. A* **1** 1712 (1983)
12. Yu V Medvedev, N N Berchenko, Yu P Kostikov, A V Matveenko, A O Olesk *Izv. Akad. Nauk SSSR, Neorg. Mater.* **23** 108 (1987)
13. Yu V Medvedev, N N Berchenko *Zh. Neorg. Khim.* **38** 1940 (1993)
14. I Barin, O Knacke, O Kubashewski *Thermochemical Properties of Inorganic Substances* (Berlin: Springer, 1977)
15. Yu V Medvedev, N N Berchenko *Zh. Neorg. Khim.* **39** 846 (1994)
16. A I Evstigneev, Yu P Kostikov, K R Kurbanov, M V Pashkovskii, B M Repchak *Elektron. Tekh. Mater.* (1/174) 78 (1983)
17. G Brandt, R Moritz *Mater. Res. Bull.* **20** 49 (1985)
18. M Seelmann-Eggebert, G Carey, V Krishnamurthy, C R Helms *J. Vac. Sci. Technol. B* **10** 1297 (1992)
19. G P Schwartz, J E Griffiths, G J Gualtieri *Thin Solid Films* **94** 213 (1982)
20. Yu V Medvedev *Poverkhnost'* (8) 151 (1987)
21. Yu V Medvedev, N N Berchenko *Izv. Akad. Nauk SSSR, Neorg. Mater.* **26** 2080 (1990)
22. M Gendry, J Durand, J M Villeneuve, L Cot *Thin Solid Films* **139** 53 (1986)
23. Yu V Medvedev *Appl. Phys. Lett.* **64** 1917 (1994)
24. C R Helms *J. Vac. Sci. Technol. A* **8** 1178 (1990)
25. N N Berchenko, N R Aigina *Metody Elektronnoi i Ionnoi Spektroskopii dlya Issledovaniya Poverkhnosti i Granits Razdela v Poluprovodnikovoi Elektronike. Zarubezhnaya Elektronnaya Tekhnika* (Methods of Electronic and Ionic Spectroscopy for the Investigation of Surfaces and Interfaces in Semiconductor Electronics. Electronic Engineering Abroad) No. 9, 10 (1986)
26. G Hollinger, E Bergignat, J Joseph, Y Robach *J. Vac. Sci. Technol. A* **3** 2082 (1985)
27. H J Yoon, M H Choi, J S Park *J. Electrochem. Soc.* **139** 3229 (1992)
28. B A Nesterenko, O V Snitko *Fizicheskie Svoistva Atomarnochistoi Poverkhnosti Poluprovodnikov* (Physical Properties of Atomically Clean Surfaces of Semiconductors) (Kiev: Naukova Dumka, 1983)
29. C Y Su, I Lindau, P R Skeath, P W Chye, W E Spicer *Phys. Rev. B* **25** 4045 (1982)
30. H U Baier, L Koenders, W Mönch *Surf. Sci.* **184** 345 (1987)
31. G Hollinger, G Hughes, F J Himpsel, J L Jordan, J F Morar, F Houzay *Surf. Sci.* **168** 617 (1986)
32. W Mönch *Surf. Sci.* **168** 577 (1986)
33. K A Bertness, J J Yeh, J J Friedman *Phys. Rev. B* **38** 5406 (1988)
34. G Hughes, R Ludeke *J. Vac. Sci. Technol. B* **4** 1109 (1986)
35. P W Chye, C Y Su, I Lindau, C M Garner, P Pianetta, W E Spicer *Surf. Sci.* **88** 439 (1979)
36. V M Bermudez, V H Ritz *Phys. Rev. B* **26** 3297 (1982)
37. T Ishikawa, H Ikoma *Jpn. J. Appl. Phys.* **31** 3981 (1992)
38. N Shibata, H Ikoma *Jpn. J. Appl. Phys.* **31** 3976 (1992)
39. C W Wilmsen *J. Vac. Sci. Technol.* **19** 279 (1981)
40. T P Smirnova, N F Zakharchuk, V I Belyi *Izv. Akad. Nauk SSSR, Neorg. Mater.* **26** 492 (1990)
41. T Sands, J Washburn, R Gronsky *Mater. Lett.* **3** 247 (1985)
42. T P Smirnova, V I Belyi, N F Zakharchuk *Poverkhnost'* (2) 94 (1984)
43. V G Aleshin, V V Nemoshkalenko, E M Semashko, A I Senkevich *Poverkhnost'* (2) 111 (1985)
44. A K Petford-Long, D J Smith *J. Electron. Microsc.* **35** 1355 (1986)
45. W H Makky, F Cabrera, K M Geib, C W Wilmsen *J. Vac. Sci. Technol.* **21** 417 (1982)
46. V P Parkhutik, V A Labunov *Plazmennoe Anodirovanie* (Plasma Anodizing) (Minsk: Navuka i Tekhnika, 1990)
47. Y Mizokawa, O Komoda, H Iwasaki, S Nakamura *Oyo Butsuri* **51** 831 (1982)
48. J B Theeten, R P Chang, D E Aspnes, T E Adams *J. Electrochem. Soc.* **125** 481 (1978)
49. R P Chang *Thin Solid Films* **56** 89 (1979)
50. E Bergignat, G Hollinger, J Robach *Surf. Sci.* **189/190** 353 (1987)
51. I Ya Mittova, G V Borzakova, V A Terekhov, O N Mittov, V R Pshestanchik, V M Kashkarov *Izv. Akad. Nauk SSSR, Neorg. Mater.* **27** 2047 (1991)
52. M Yamaguchi, K Ando *J. Appl. Phys.* **51** 5007 (1980)
53. C W Wilmsen, K M Geib, R Gann, J Costello, G Hryckowian, R J Zeto *J. Vac. Sci. Technol. B* **3** 1103 (1985)
54. G Hollinger, J Joseph, Y Robach, E Bergignat, B Commere, P Victorovich *J. Vac. Sci. Technol. A* **3** 2082 (1985)
55. G Hollinger, J Joseph, Y Robach, E Bergignat, B Commere *J. Vac. Sci. Technol. B* **5** 1108 (1987)
56. Y Robach, M P Besland, J Joseph, G Hollinger, P Victorovich, P Ferret, M Pitaval, A Falcon, G Post *J. Appl. Phys.* **71** 2981 (1992)
57. H Hasegawa, H L Hartnagel *J. Electrochem. Soc.* **123** 173 (1976)
58. M Salvi, P N Eavennec, H L Haridon, G P Pelous *Thin Solid Films* **87** 13 (1982)
59. M P Besland, Y Robach, J Joseph *J. Electrochem. Soc.* **140** 104 (1993)
60. S J Sferko, G Allan, J Lefebre, M Lannou, E Bergignat, G Hollinger *Phys. Rev. B* **42** 11232 (1990)
61. E D Belyakova, A D Gabaraeva, A T Gorelenok, R V Karzhavin, V M Mikushin, S E Sysoev, N M Shmidt *Poverkhnost'* (7) 88 (1992)
62. G P Schwartz, F A Thiel, G J Gualtieri *J. Vac. Sci. Technol. A* **2** 1252 (1984)
63. M Bettini, H J Richter *Surf. Sci.* **80** 334 (1979)
64. J A Silberman, D Laser, I Lindau, W E Spicer, J A Wilson *J. Vac. Sci. Technol. A* **3** 222 (1985)
65. A-B Chen, A Sher, W E Spicer *J. Vac. Sci. Technol. A* **1** 1674 (1983)
66. F Wang, A Schwartzman, A L Fahrenbruch, R Sincleir, R B Bube, C M Stahle *J. Appl. Phys.* **62** 1469 (1987)
67. U Solzbach, H J Richter *Surf. Sci.* **97** 191 (1980)
68. US P. 3 997 018 (1976)
69. G V Beketov, V F Bibik, E A Sal'kov, in *Poluprovodniki s Uzkoi Zapreshchennoi Zonoi i Polumetally. Materialy VII Vsesoyuznogo Simpoziuma, L'vov, 1986, T. 1* (Narrow-Gap Semiconductors and Semimetals. Proceedings of the VIIth All-Union Symposium, Lvov, 1986, Vol. 1) p. 12
70. R L Strong *J. Vac. Sci. Technol. A* **5** 2003 (1987)
71. C M Stahle, C R Helms, A Simmons *J. Vac. Sci. Technol. B* **5** 1092 (1987)
72. C M Stahle, C R Helms, H F Schaake, R L Strong, A Simmons, J B Pallix, C H Becker *J. Vac. Sci. Technol. A* 7 474 (1989)
73. C M Stahle, C R Helms, H F Schaake, R L Strong, A Simmons, J B Pallix, C H Becker *J. Vac. Sci. Technol. A* 7 477 (1989)
74. B P. 1 600 599 (1981)

75. P Brogowski, J Piotrowski *Semicond. Sci. Technol.* **5** 530 (1990)
76. N Kh Talipov, V P Popov, V G Remesnik, Z A Nal'kina *Fiz. Tekh. Poluprovodn.* **26** 310 (1992)
77. Y Nemirovsky, R Goshen, I Kidron *J. Appl. Phys.* **53** 4888 (1982)
78. G H Winton, K Prasad, L Faraone, M A C Hotchkiss *J. Electron. Mater.* **22** 365 (1993)
79. O F Afonin, N N Berchenko, A I Vinnikova, A V Matveenko, Yu V Medvedev, D A Sakseev *Pis'ma Zh. Tekhn. Fiz.* **18** (7) 45 (1992)
80. N N Berchenko, A I Vinnikova, A V Matveenko, Yu V Medvedev, D A Sakseev *Poverkhnost'* (10) 92 (1988)
81. V P Parkhutik, Yu E Makushok, S Yu Borisov, N N Berchenko, A I Vinnikova, A V Ermakov, D A Sakseev, in *Fizika i Khimiya Poverkhnosti i Granits Razdela Uzkoshchelevykh Poluprovodnikov. Tez. Dokl. Resp. Konf., L'vov, 1990* (Physics and Chemistry of the Surfaces and Interfaces of Narrow-Gap Semiconductors. Abstracts of Reports at the Republic Conference, Lvov, 1990) p. 72
82. T A Grishina, N N Berchenko, G D Goderdzishvili, I A Drabkin, A V Matveenko, T D Mkheidze, D A Sakseev, E A Tret'yakova *Zh. Tekhn. Fiz.* **57** 2355 (1987)
83. N N Berchenko, T A Grishina, I A Drabkin, Yu P Kostikov, A V Matveenko, D A Sakseev, E A Tret'yakova *Pis'ma Zh. Tekhn. Fiz.* **14** 1071 (1988)
84. Yu A Aleshchenko, N N Berchenko, A I Vinnikova, L K Vodop'yanov, Yu V Medvedev, D A Sakseev, S V Fadeev, in *Poluprovodniki s Uzkoi Zapreshchennoi Zonoi i Polumetally. Materialy VIII Vsesoyuznogo Simpoziuma, L'vov, 1991, T. 2* (Narrow Gap Semiconductors and Semimetals. Proceedings of the VIIIth All-Union Symposium, Lvov, 1991, Vol. 2) p. 200
85. E E DeKlutzenaar *J. Vac. Sci. Technol. A* **1** 480 (1983)
86. A G Akimov *Poverkhnost'* (10) 5 (1984)
87. Yu A Aleshchenko, N N Berchenko, A I Vinnikova, L K Vodop'yanov, A V Matveenko, Yu V Medvedev, E A Tret'yakova *Pis'ma Zh. Tekhn. Fiz.* **15** (3) 17 (1989)
88. Y Nemirovsky, L Burstein *Appl. Phys. Lett.* **44** 443 (1984)
89. E Weiss, N Mainzer *J. Vac. Sci. Technol. A* **6** 2765 (1988)
90. R L Strong, J D Luttmer, D D Little, T H Teherani, C R Helms *J. Vac. Sci. Technol. A* **5** 3207 (1987)
91. Z Ma, R Li *Appl. Phys. Lett.* **56** 2417 (1990)
92. E Weiss, C R Helms *J. Electrochem. Soc.* **138** 993 (1991)
93. I Esquivias, D Brink, M Dal Colle, J Baars, M Bruder *Mater. Sci. Eng. B* **9** 207 (1991)
94. E Weiss, C R Helms *J. Vac. Sci. Technol. A* **9** 2235 (1991)
95. S Jin, W M Lau *Appl. Phys. Lett.* **55** 209 (1989)
96. W M Lau *Appl. Phys. Lett.* **53** 2161 (1988)
97. W M Lau, J-W He, P R Norton *Appl. Phys. Lett.* **54** 772 (1989)
98. H C Gatos, J Lagowski, T E Kazior *Jpn. J. Appl. Phys. Suppl.* **22** 11 (1983)
99. H H Wieder, C M Wilmsen *Thin Solid Films* **56** 5 (1979)
100. W E Spicer, A M Green *J. Vac. Sci. Technol. B* **11** 1347 (1993)
101. W E Spicer, I Lindau, P R Skeath, C Y Su, P W Chye *Phys. Rev. Lett.* **44** 420 (1980)
102. G A Baraff *Acta Phys. Pol. A* **82** 664 (1992)
103. O Oda, H Yamamoto, M Seiwa, G Kano, T Inoue, M Mori, H Shimakura, M Oyake *Semicond. Sci. Technol.* **7** 2115 (1992)
104. W E Spicer, Z Liliental-Weber, E Weber, N Newman, T Kendelewicz, R Cao, C McCants, P Mahowski, K Miyano, I Lindau *J. Vac. Sci. Technol. B* **6** 1245 (1988)
105. J Tersoff *Phys. Rev. Lett.* **52** 465 (1984)
106. H Hasegawa, H Ohno *J. Vac. Sci. Technol. B* **4** 1130 (1986)
107. I Ohbu, M Takahama, H Mizuta *Appl. Phys. Lett.* **62** 3279 (1993)
108. A C Warren, J M Woodall, P D Kirchner, Y Yin, F Pollak, M R Melloch, N Otsuka, K Mahalingam *Phys. Rev. B* **46** 4617 (1992)
109. A C Warren, J M Woodall, J L Freeouf, D Grischkowski, D T McInturff, M R Melloch, N Otsuka *Appl. Phys. Lett.* **57** 1331 (1990)
110. R P Leon, E R Weber *Acta Phys. Pol. A* **82** 664 (1992)
111. N A Ives, G W Stupian, M S Leung *Appl. Phys. Lett.* **50** 256 (1987)
112. C J Sandroff, R N Nottenburg, J-C Bischoff, R Bhat *Appl. Phys. Lett.* **51** 33 (1987)
113. E Yablonovich, C J Sandroff, R Bhat, T Gmitter *Appl. Phys. Lett.* **51** 439 (1987)
114. E Yablonovich, B J Scromme, R Bhat, J P Harbison, T J Gmitter *Appl. Phys. Lett.* **54** 555 (1989)
115. A Callegari, P D Hoh, D A Buchanan, D Lacey *Appl. Phys. Lett.* **54** 332 (1989)
116. M Taniguchi, T Murakawa, Y Kajitani *Appl. Surf. Sci.* **56/58B** 827 (1992)
117. H Ricard, K Aizawa, H Ishiwara *Appl. Surf. Sci.* **56/58B** 888 (1992)
118. I Jimenez, F J Palomares, J Avila, M T Cuberes, F Soria, J L Sacedon, K Horn *J. Vac. Sci. Technol. A* **11** 1028 (1993)
119. K Yamasaki, T Sugano *J. Vac. Sci. Technol.* **17** 959 (1980)
120. J F Wager, K M Geib, C W Wilmsen, L L Kazmerski *J. Vac. Sci. Technol. B* **1** 278 (1983)
121. B I Bednyi, N V Baidus', I A Karpovich, M V Laganina, I I Tsyplenkov, R N Shchukin *Poverkhnost'* (12) 47 (1991)
122. M Yamada, A W Wahi, T Kendelewicz, W E Spicer *Phys. Rev. B* **45** 3600 (1992)
123. R E Allen, T J Humphreys, J D Dow, O F Sankey *J. Vac. Sci. Technol. B* **2** 449 (1984)
124. R W Jansen *Phys. Rev. B* **41** 7666 (1990)
125. G V Semenova, T P Sushkova, E G Goncharov, N A Khoroshilova *Zh. Neorg. Khim.* **38** 887 (1993)
126. V P Kamenushkin, V A Yur'ev *Fiz. Tekh. Poluprovodn.* **25** 798 (1991)
127. Y Z Hu, M Li, Y Wang, E A Irene, M Rowe, H C Casey *Appl. Phys. Lett.* **63** 1113 (1993)
128. R T Talasek, A J Syllaios *J. Electrochem. Soc.* **132** 887 (1985)
129. T L Chu, S S Chu, S T Ang *J. Appl. Phys.* **58** 3206 (1985)
130. N N Berchenko, A V Voitsekhovskii, N Yu Izhnina, I I Izhnin, O G Lanskaya, E P Lilenko, V P Savchin *Poverkhnost'* (5) 107 (1991)
131. J D Jensen, R B Schoolar *J. Vac. Sci. Technol.* **13** 920 (1976)
132. A Rogalski *Thin Solid Films* **74** 59 (1980)
133. N N Berchenko, Yu V Medvedev, D A Sakseev *Pis'ma Zh. Tekhn. Fiz.* **18** (20) 68 (1992)
134. N N Berchenko, M M Batenchuk, A I Vinnikova, I I Izhnin, V P Savchin *Zh. Tekhn. Fiz.* **63** 183 (1994)
135. N N Berchenko, A I Vinnikova, A P Kovarskii, A V Matveenko, Yu V Medvedev, N L Chernyus *Elektrokhimiya* **27** 1207 (1991)
136. D M Zayachuk, V A Shenderovskii *Ukr. Fiz. Zh.* **36** 1692 (1991)
137. M A Berding, M Van Schildegaarde, A Sher *J. Electron. Mater.* **22** 1005 (1993)
138. C L Littler, E Maldonado, X N Song, Z Yu, J L Elkind, D G Seiler, J R Lowney *J. Vac. Sci. Technol. B* **10** 1466 (1992)
139. I Esquivias, J Baars, D Brink, D Eger *Semicond. Sci. Technol.* **8** S71 (1993)
140. K H Khelladi, D Lemoine, S Rolland, R Granger, R Triboulet *Semicond. Sci. Technol.* **8** 56 (1993)
141. A Sher, A-B Chen, W E Spicer, C K Shin *J. Vac. Sci. Technol. A* **3** 105 (1985)
142. O G Lanskaya, V I Kalenik, E P Lilenko, O A Yakubtsov, I N Gorbatyuk, A V Voitsekhovskii *Poverkhnost'* (8) 101 (1991)
143. S E Schacham, E Finkman *J. Vac. Sci. Technol. A* **8** 1171 (1990)
144. H H Wieder *J. Vac. Sci. Technol. B* **11** 1331 (1993)
145. S Sinharoy, R A Hoffman, R F C Farrow, J D Warner, K Basin, in *Proceedings of the Symposium on Dielectric Films on Compound Semiconductors* Vol. 86-3 (Pennington: Electrochemical Society, 1985) p. 313
146. A N MacInnes, M B Power, A R Barron, P P Jenkins, A F Hepp *Appl. Phys. Lett.* **62** 711 (1993)
147. M Tabib-Azar, S Kang, A N MacInnes, M B Power, A R Barron, P P Jenkins, A F Hepp *Appl. Phys. Lett.* **63** 625 (1993)
148. P M Solomon, T W Hickmott, H Morkoç, R Fisher *Appl. Phys. Lett.* **42** 82 (1983)
149. M Sugiyama, S Maeyama, M Oshima, H Oigawa, Y Nannichi, H Hashizume *Appl. Phys. Lett.* **60** 3247 (1992)
150. D S L Mui, Z Wang, H Morkoç *Thin Solid Films* **231** 107 (1993)
151. W Weiss, R Hornstein, D Schmeisser, W Gopel *J. Vac. Sci. Technol. B* **8** 715 (1990)
152. T K Paul, D N Bose *J. Appl. Phys.* **67** 3744 (1990)
153. A Astino, A Foucaran, G Bastide, M Rouzeyre, J L Leclercq, J Durand *J. Appl. Phys.* **70** 2584 (1991)

154. A Bath, P J Van Der Put, J G M Becht, J Schoonman, B Lepley *J. Appl. Phys.* **70** 4366 (1991)
155. H Lim, J A Baglio, N DeCola, H L Park, J I Lee, K N Kang *J. Appl. Phys.* **69** 7918 (1991)
156. M P Besland, P Louis, Y Robach, J Joseph, G Hollinger, D Galled, P Victorovich *Appl. Surf. Sci.* **56/58B** 846 (1992)
157. K Hattori, Y Torii *J. Appl. Phys.* **69** 3130 (1991)
158. A V Voitsekhovskii, V N Davydov *Fotoelektricheskie MDP-Struktury iz Uzkozonnykh Poluprovodnikov* (Photoelectric MIS-Structures Comprising Narrow-Band Semiconductors) (Tomsk : Radio i Svyaz', 1990)
159. W E Tennant, C A Cockrum, J B Gilpin, M A Kinch, M B Reine, R P Ruth *J. Vac. Sci. Technol. B* **10** 1359 (1992)
160. Y Nemirovsky, A Unikovsky *J. Vac. Sci. Technol. B* **10** 1602 (1992)
161. G Sarusi, G Cinader, A Zemel, D Eger, Y Shapira *J. Appl. Phys.* **71** 5070 (1992)
162. P H Zimmermann, M B Reine, K Spignese, K Maschhoff, J Schirripa *J. Vac. Sci. Technol. A* **8** 1182 (1990)
163. P Becla, S Motakef, T Koehler *J. Vac. Sci. Technol. B* **10** 1599 (1992)
164. S Menezes, W L McLevige, E R Blazejewski, W E Tennant, J P Ziegler *J. Vac. Sci. Technol. B* **9** 1874 (1991)
165. J M Fisher, L E A Berlouis, B N Rospendowski, P J Hall, M G Astles *Semicond. Sci. Technol.* **8** 1459 (1993)
166. C Wei, K Rajeshwar, J D Luttmer *J. Electrochem. Soc.* **140** 829 (1993)
167. A Yu Nikiforov, E V Shimanskaya, M S Nikitin, A I Dirochka, in *Poluprovodniki s Uzkoi Zapreshchennoi Zonoi i Polumetally. Materialy VIII Vsesoyuznogo Simpoziuma, L'vov, 1991, T. 1* (Narrow-Gap Semiconductors and Semimetals. Proceedings of the VIIIth All-Union Symposium, Lvov, 1991, Vol. 1) p. 153
168. I V Klochko, E G Petrova, V P Ponomarenko, V I Stafeev, in *Poluprovodniki s Uzkoi Zapreshchennoi Zonoi i Polumetally. Materialy VIII Vsesoyuznogo Simpoziuma, L'vov, 1991, T. 2* (Narrow-Gap Semiconductors and Semimetals. Proceedings of the VIIIth All-Union Symposium, Lvov, 1991, Vol. 2) p. 39
169. I V Shimanskii, V P Ponomarenko, V I Stafeev, in *Poluprovodniki s Uzkoi Zapreshchennoi Zonoi i Polumetally. Materialy VIII Vsesoyuznogo Simpoziuma, L'vov, 1991, T. 2* (Narrow-Gap Semiconductors and Semimetals. Proceedings of the VIIIth All-Union Symposium, Lvov, 1991, Vol. 2) p. 44
170. F A Kish, S J Caracci, S A Maranowski, N Holonyak, Jr, S C Smith, R D Burnham *Appl. Phys. Lett.* **60** 1582 (1992)
171. R S Burton, T E Schlesinger, D J Holmgren, S C Smith, R D Burnham *Appl. Phys. Lett.* **60** 1776 (1992)

Russian Chemical Reviews **63** (8) 641 – 659 (1994)
©1994 Russian Academy of Sciences and Turpion Ltd

UDC 547.413

Trichloroethylene in organic synthesis

R V Kaberdin, V I Potkin

Contents

I.	Introduction	641
II.	Addition reactions	641
III.	Elimination reactions	649
IV.	Substitution reactions	649
V.	Oxidation reactions	654
VI.	Other reactions	655
VII.	The practical use of trichloroethylene and its derivatives	656

Abstract. The literature data on the chemistry of trichloroethylene are surveyed. Reactions involving the addition of inorganic and organic reagents to trichloroethylene are examined and cycloaddition reactions with participation of trichloroethylene are classified. A systematic account is given of the reactions of trichloroethylene with various nucleophiles occurring with the substitution of 1 – 3 chlorine atoms by nucleophilic residues. The elimination and oxidation reactions of trichloro-ethylene as well as aspects of the practical application of its derivatives are considered. The analysis demonstrates the extensive possibilities for the synthesis of polyfunctional organic compounds of various classes from trichloroethylene. The bibliography includes 310 references.

I. Introduction

Trichloroethylene (TCE) is nowadays one of the main products of organochlorine synthesis, the annual production of which is more than 1 million tonnes.[1] Its practical applications are exceptionally extensive and are being continually expanded. It is one of the most important technical solvents and is used in various branches of industry and for domestic purposes. It is employed as an inhalation agent for narcosis and anaesthesia in medicine. Industrial methods of synthesis from trichloroethylene of a number of important products, including chloroacetic acid, pentachloroethane, and dichloroacetyl chloride, have been developed.

The synthetic possibilities of TCE as a polyfunctional compound containing three chlorine atoms and a carbon – carbon double bond are very great. It enters into chemical reactions of various types (substitution, elimination, addition, oxidation, etc.), which makes it a valuable and in certain cases an irreplaceable intermediate in organic synthesis.

R V Kaberdin Laboratory of Organoelement Compounds, Institute of Physical Organic Chemistry, Academy of Sciences of Belarus, ul. Surganova 13, 220072 Minsk, Belarus. Fax (7-017) 239 46 79. Tel (7-017) 239 46 00.
V I Potkin Institute of Physical Organic Chemistry, Academy of Sciences of Belarus, ul. Surganova 13, 220072 Minsk, Belarus. Fax (7-017) 239 46 79. Tel (7-017) 239 59 72.

Received 10 May 1994
Uspekhi Khimii **63** (8) 673 – 692 (1994); translated by A K Grzybowski

The publication of a large number of studies on TCE chemistry, which have revealed various new aspects of its synthetic and practical use, required a systematic survey. The very first data on TCE chemistry were briefly described in two communications.[2,3] The state of research in TCE chemistry towards the beginning of the 1980s was given in greater detail in a monograph.[4] Extensive information about the reactions of TCE, published during the last 10 – 15 years, have still not been surveyed and analysed critically. Only reactions involving the addition to TCE of compounds containing N – Cl bonds and the thiylation of TCE have been considered in recently published reviews.[5-7]

Experimental data on the chemical reactions of TCE collected and dealt with systematically in the present review include communications and patent data up to 1993.

II. Addition reactions

Addition to TCE has been used to synthesise a wide variety of polyfunctional organochlorine compounds. This reaction of TCE is one to have been most thoroughly investigated.

1. Halogenation

Initial studies of the reaction of halogens (chlorine, bromine, and fluorine) with TCE showed that it leads mainly to the formation of the corresponding adducts — 1,2,2-trichloro-1,2-dihaloethanes.[2-4] Iodine does not react with TCE; positive results were not obtained even when the reaction was initiated by γ-radiation.[8]

Pentachloroethane **1** can be synthesised by the addition of chlorine to TCE in both gas and liquid phases.[9] The chlorination of TCE in the dark proceeds only slightly, but the rate of reaction increases sharply in the presence of ethylene.[10] When TCE is chlorinated with a solution of chlorine in carbon tetrachloride (under illumination from an incandescent filament lamp), pentachloroethane is formed in a quantitative yield.[11] The role of radical addition increases significantly in the presence of complex-forming solvents (benzene, carbon disulfide).

The interaction of TCE with chlorine in liquid hydrogen fluoride proceeds by an electrophilic mechanism via the formation of ion pairs and leads to compound **1** and the coupled chlorofluorination products — 1,1,2,2-tetrachloro-1-fluoroethane. The overall yield of pentachloroethane and tetachlorofluoroethane relative to the TCE which has reacted is 82% and their ratio is 85 : 15.[12]

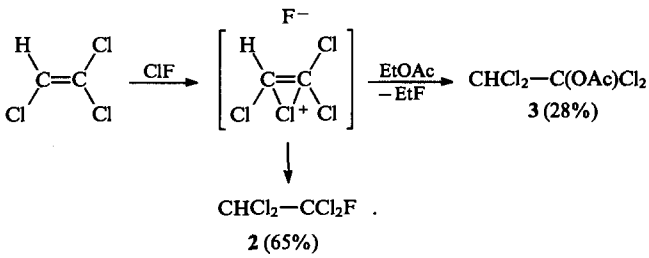
Under pressure and in the presence of free radical initiators, chlorination of TCE is more far reaching, leading ultimately to the formation of CCl_4 and C_2Cl_6.[13]

Other chlorinating agents have no advantages over chlorine. Thus the chlorination of TCE with a solution of trichloroamine in methylene chloride (molar ratio NCl_3 : TCE = 0.04 : 0.09) in the presence of small amounts of added benzoyl peroxide (BP) affords pentachloroethane in 41% yield.[14] In the interaction of perchloryl fluoride with TCE in the presence of aluminium halides, addition of two halogen atoms from the aluminium halide is observed. When $AlCl_3$ is used, pentachloroethane is produced.[15] The oxychlorination reaction of TCE in the presence of hydrogen chloride, oxygen, and the Deacon catalyst involves additive chlorination with formation of compound **1**, which is subsequently dehydrochlorinated to tetrachloroethylene.[16] When epoxyethane or epoxycyclohexane reacts with TCE and liquid chlorine, coupled chlorination of TCE accompanied by telomerisation is observed.[17]

Bromine adds readily to TCE both in the presence and absence of catalysts, affording a 1,2-adduct — 1,2-dibromo-1,1,2-trichloroethane.[2,18]

The interaction of TCE with fluorine proceeds less selectively than with chlorine and bromine, a mixture of chlorofluoroalkanes being formed; the main product is 1,1,2-trichloro-1,2-difluoroethane.[2] The formation of side products is appreciably reduced when the reaction is carried out at 70–85 °C.[19,20] Data on the gas-phase fluorination of TCE in the presence of chromium catalysts have been published.[21,22]

The reactions of TCE with mixed halogens have been investigated for the reaction with chlorine monofluoride, which added readily to TCE.[23] It is suggested that, owing to the appreciable polarity of the Cl–F bond and the high electrophilicity of the chlorine atom in the ClF molecule, the addition is electrophilic. In order to establish the mechanism of this reaction, the chlorofluorination was carried out in the presence of an external nucleophile (ethyl acetate).[24] The reaction gave a mixture of products **2** and **3**, the formation of which may be represented by the following scheme:



The results demonstrate that the mode of addition of both the internal (F^-) and the external (EtOAc) nucleophiles to TCE is virtually the same.

The reaction of TCE with the SbF_5–HF–Cl_2 system has been investigated[25] and it has been shown that this system is a source of stoichiometric equivalents of chlorine monofluoride. The reaction afforded the coupled halofluorination product $CHCl_2CCl_2F$ in a quantitative yield. When the SbF_5–HF–Br_2 system was used, the product was 2-bromo-1,1,2-trichloro-1-fluoroethane.

2. Hydrohalogenation

On reaction with excess gaseous dry hydrogen chloride in the presence of small amounts of $FeCl_3$ at room temperature, TCE gives 1,1,1,2-tetrachloroethane **4** in 49% yield. When $FeCl_3$ is replaced by $AlCl_3$ (5%–10%), the yield of the adduct **4** increases to 86%–88% (reaction temperature 30–40 °C). At a higher temperature (50 °C and above), the yield of compound **4** falls and the formation of 1,1,2,2-tetrachloroethane, 1,1,2,4,4- and 1,1,2,3,4-pentachlorobutadienes, and hexachlorobenzene is observed.[2] A method has been proposed recently for the synthesis of tetrachloroethane **4** by hydrochlorination of TCE in the presence of $FeCl_3$ or $AlBr_3$ at a pressure exceeding 500 kPa and at a temperature in the range 10–160 °C. Thus, when gaseous HCl was introduced into a mixture of 2 moles of TCE and 1% of $FeCl_3$ (relative to the weight of TCE) up to a pressure of 3.46 MPa and the mixture was heated for 3 h at 70–80 °C, the target product was obtained in 96.4% yield.[26]

Hydrogen bromide adds to TCE only in the presence of catalysts. Ionic addition (small amounts of added $FeCl_3$ and $AlCl_3$) follows the Markovnikov rule and leads to the formation of 1-bromo-1,1,2-trichloroethane (80%). In the presence of peroxides, anti-Markovnikov addition of hydrogen bromide to TCE occurs (the Kharasch 'peroxide effect') with the exclusive formation of 2-bromo-1,1,2-trichloroethane (yield 91%).[27]

The interaction of hydrogen fluoride with TCE under the influence of various catalysts has been described in the patent literature.[28–36] These reactions proceed in a complex manner and lead to a mixture of chlorofluoro-compounds, among which derivatives containing 3–4 fluorine atoms predominate. Thus, when a gaseous stream of TCE and HF (1 : 3.5) is passed over γ-Al_2O_3 on a metallic support at 230 °C, mainly 2-chloro-1,1,1-trifluoroethane **5** is formed (yield 91.5%).[28] Reaction of TCE with hydrogen fluoride proceeds similarly in the presence of chromium(III) halides on activated charcoal.[29] When HF is brought into contact with TCE over a chromium catalyst [1%–10% chromium(III) oxide] deposited on β- and/or α-AlF_3 and treated with 1,2-dichloro-1,1,2,2-tetrafluoroethane, 1,1,1-trifluoroethane is formed at 350 °C in 95% yield.[30] When the 6% CrO_3 + 3% $TiCl_3/Al_2O_3$ catalyst treated beforehand with hydrogen fluoride is used, the products of the reaction of TCE with HF at 500 °C are compound **5** (50%) and 1,1,1,2-tetrafluoroethane (20%).[31] According to other data,[32,33] the halides TaF_5, NbF_5, $MoCl_5$, and $TiCl_4$ are also catalysts of the reaction of HF with halogenated alkenes, including TCE.

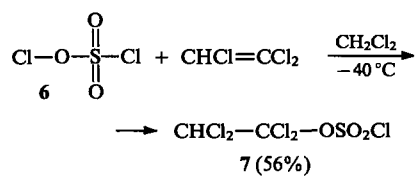
The reaction of TCE with anhydrous HF under pressure in an autoclave takes place at 115–130 °C. In the presence of fluorination catalysts (arsenic and antimony compounds to which transition metal derivatives have been added[34–36]), the yield of the main reaction product — 2-chloro-1,1,1-trifluoroethane **5** — reaches 87%–92%.

Methods for the synthesis of monofluoro- and difluoro-derivatives from TCE have been proposed in recently published patents.[37,38] It has been shown[37] that, in the presence of an aluminium oxide–magnesium oxide catalyst (Al_2O_3 : MgO = 3 : 1) subjected to a preliminary treatment with HF, the main products of the interaction of TCE with HF were 1,1,2-trichloro-1-fluoroethane (53%) and 1,2-dichloro-1,1-difluoroethane (41.5%). The formation of compound **5** was observed in this process, but its yield did not exceed 1.1%. 1,1,2-Trichloro-1-fluoroethane — the product of the Markovnikov addition of hydrogen fluoride to TCE — was obtained in 80% yield in the presence of WF_6 at 50–150 °C and at a pressure of 137 kPa.[38]

Hydrogen iodide does not add to TCE. After prolonged illumination of a mixture of TCE with hydrogen iodide, only partial reduction of TCE to 1,1,2-trichloroethane was observed.[2]

3. Addition of certain other reagents

Chlorine chlorosulfonate **6**, which has become available recently, readily undergoes Markovnikov addition to TCE to form 1,1,2,2-tetrachloroethyl chlorosulfonate **7**.[39,40]



Chlorine and fluorine fluorosulfonates react similarly with TCE, affording respectively 1,1,2,2-tetrachloroethyl fluorosulfonate (yield 80.7%) and 1,1,2-trichloro-2-fluoroethyl fluorosulfonate (yield 70%).[41,42] After brief heating of a mixture of TCE and sulfur dichloride (2:1) in the presence of Bu_3PO_4 at 110 °C, 1,1,2,2-tetrachloroethanesulfenyl chloride is formed.[43] Under radical conditions this reaction gives a similar product only after prolonged irradiation of the mixture, in the presence of small amounts of added phosphorus trichloride, by light from a mercury lamp.[44]

UV irradiation of equimolar amounts of thiocyanogen chloride and TCE in acetic acid gave two α-chloro-β-thiocyanato-derivatives with preferential formation of the anti-Markovnikov isomer: $CHCl_2C(SCN)Cl_2$ (yield 52%) and $CHCl(SCN)CCl_3$ (yield 6%).[45] It is noteworthy that TCE does not react with thiocyanogen chloride heterolytically.[46]

In the presence of SbF_3, the reaction of trifluoromethyl hypochlorite with TCE gives a high yield of 1,1,2,2-tetrachlorotrifluoromethoxyethane.[47]

4. Addition reactions leading to the formation of new C–C bonds

Reactions involving the condensation of various organic compounds with TCE have opened a pathway to the synthesis of compounds with dichloro- and trichloro-vinyl groups which are difficult to synthesise. Such reactions proceed both in the presence of radical initiators and under the influence of the Friedel–Crafts catalysts.

a. Radical condensation

The chlorovinylation of saturated hydrocarbons with the aid of TCE, which proceeds on treatment with organic peroxides, was first achieved by Schmerling[48] in 1949. He later investigated the condensation of TCE with alkenes,[49–51] alicyclic compounds,[52] and benzene derivatives.[53] The products of these reactions — compounds with β,β-dichlorovinyl groups — have found applications in the synthesis of alkenynes,[49] chlorinated alkenylbenzenes,[50] and cycloalkenes containing a triple bond in a side chain.[52]

A series of patents have been devoted to the development of methods of synthesis of the practically important 1,1-dichloro-4-methylpenta-1,3-diene, which is based on the condensation of TCE with isobutene (or a *tert*-butyl halide).[54–58]

This reaction can be achieved both in the liquid and gas phases (125–550 °C) in the presence of 0.05–5 mol% of radical initiators. However, it is noteworthy that a high yield of the target product is attained only when a twofold to threefold excess of TCE is employed. On the other hand, in the presence of an excess of isobutene, preferential formation of 2,5-dimethylhexa-1,5-diene is observed.

The photochemical addition of bromotrichloromethane to TCE leads to the formation of a complex mixture of products, among which the following have been found: $CHClBr-CBrCl_2$ (2%), $CCl_3-CHCl-CBrCl_2$ (< 1%), CCl_3-CCl_3 (30%), $CBrCl=CHCl$ + $CHBr=CCl_2$ (26.5%), $CCl_3-CCl=CHCl$ (0.9%), $CCl_3-CH=CCl_2$ (29.1%), and $CHCl_2-CBrCl_2$ (11.9%).[59] The kinetics and mechanism of this reaction have been investigated.[60]

The interaction of TCE with hexane in the presence of *tert*-butyl peroxide (TBP) has been studied in detail.[61] It has been established that the reactivities of the hydrogen atoms of the first, second and third carbon atoms in hexane are respectively 0.04, 1.68, and 1.0. The chlorovinylation of hexane occurred mainly in the 2-position and to a lesser extent in the 3-position. The formation of the main products of this reaction can be represented schematically as follows:

$$ROOR \longrightarrow 2\,RO^{\cdot}$$

$$RO^{\cdot} + C_6H_{14} \longrightarrow ROH + {}^{\cdot}C_6H_{13}$$

$${}^{\cdot}C_6H_{13} + CHCl{=}CCl_2 \longrightarrow C_6H_{13}{-}CHCl{-}{}^{\cdot}CCl_2$$

$$C_6H_{13}{-}CHCl{-}{}^{\cdot}CCl_2 + C_6H_{14} \longrightarrow$$

$$\longrightarrow C_6H_{13}{-}CH{=}CCl_2 + HCl + {}^{\cdot}C_6H_{13}$$

R = Bu^t; ${}^{\cdot}C_6H_{13}$ = $MeC^{\cdot}HBu^n$ or $EtC^{\cdot}HPr^n$.

When hexane is treated with a mixture of TCE and carbon tetrachloride, the main reaction product is 2-chlorohexane and dichlorovinyl derivatives are not then formed.

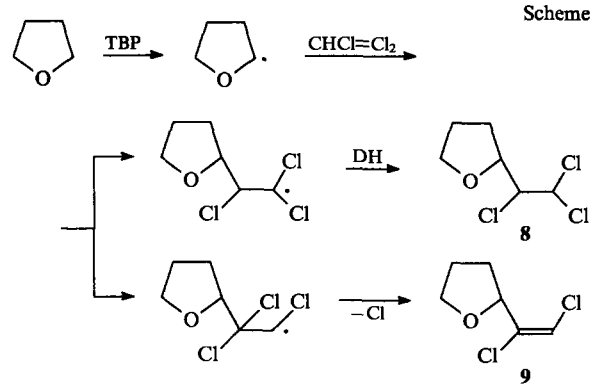
The high-temperature condensation of TCE with naphthalene at 535 °C leads to a complex mixture of isomeric products — *cis*-RCCl=CHCl, *trans*-RCCl=CHCl, $RCH=CCl_2$, *cis*-R'CCl=CHCl, *trans*-R'CCl=CHCl, and $R'CH=CCl_2$ (R = β-$C_{10}H_7$, R' = α-$C_{10}H_7$).[62] The isomer $RCH=CCl_2$ predominates, but it could only be isolated in 10.6% yield in a pure form, which undoubtedly lowers the preparative value of this reaction.

Reaction of TCE with 1- and 2-methylnaphthalenes proceeds via the side chain to form a mixture of the corresponding dichloropropenylnaphthalenes.[63] Under these conditions, the main products contained the α,α-dichloropropenyl fragment (yield ~90%), which makes this reaction preparatively promising.

The addition to TCE of *m*-carbaboran-9-yl radicals, formed on photolysis of bis(*m*-carbaboran-9-yl)mercury, has been achieved recently.[64] The radical-adduct obtained is stabilised by elimination of a chlorine atom, affording 9-(2,2-dichlorovinyl)-*m*-carbaborane in 50% yield; 9-chloro-*m*-carbaborane (8%) and *m*-carbaborane (10%) were also isolated.

In the presence of TBP, tetrahydrofuran reacts with TCE to form 1,2,2-trichloro-1-(tetrahydro-2-furyl)ethane **8** (main product), 1,2-dichloro-1-(tetrahydro-2-furyl)-ethylene **9**, and 1,2-dichlorohex-1-en-3-one.[65] The presence of 1,2-dichlorohex-1-en-3-one among the reaction products confirms that hydro-2-furyl radicals arising on treatment with the peroxide are consumed in both addition and isomerisation reactions. The formation of the first two products is presented in Scheme 1.

Scheme 1



DH = hydrogen donor.

It has been shown that the phenyl radicals obtained on decomposition of 2-phenylazopropan-2-ol add to the less-substituted carbon atom of TCE. The $PhCHCl-{}^{\cdot}CCl_2$ radicals are formed and stabilised in this case by hydrogen atom abstraction, and not by chlorine atom loss, affording trichlorophenylethane in 48% yield. The interaction of TCE with 1-cyclohexenyl radicals, formed on decomposition of 1-(1-azacyclohexenyl)cyclohexanol, gives a product with a similar group in the side chain — cyclo-$C_6H_9CHClCHCl_2$ (23%).[66]

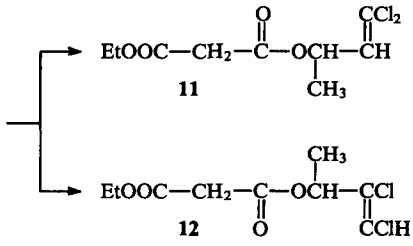
Syntheses based on the reaction of TCE with alcohols, acids, ethers, and amines have opened a pathway to the preparation of a whole series of polyfunctional compounds which were previously difficult to obtain. Thus the reaction of TCE with methanol (525–540 °C), initiated by CCl_4 and $CHCl_3$ in a quartz flow reactor, leads to $CCl_2=CHCH_2OH$ in 22% yield.[67] A method has been developed for the synthesis of chlorinated alcohols of the type $CHCl_2CCl_2CRR'OH$ and $CCl_2=CClCRR'OH$ on the basis of the reaction of alcohols RR'CHOH (where R and R' = Alk or H) with TCE in the presence of organic peroxides.[68,69]

2-Alkyl-3,4-4-trichlorobutyric acids have been synthesised in preparative yields from TCE and carboxylic acids, having an α-hydrogen atom, in the presence of peroxide initiators at 40–200 °C.[70]

Esters react with TCE under similar conditions, mainly the α-carbon atom of the alcohol component of the ester molecule participating under these conditions in the formation of a new carbon–carbon bond in the adducts.[71,72] The reaction of diethyl malonate **10** with TCE proceeds via two pathways with formation of compounds **11** and **12**.

$$CH_2(COOEt)_2 + CHCl=CCl_2 \longrightarrow$$

10



11 **12**

Dichlorovinyl-substituted amines $C_7H_{15}CH(CH=CCl_2)NH_2$ and *cyclo*-$C_6H_{10}(CH=CCl_2)NH_2$ have been obtained by the reaction of TCE with the corresponding amines in the presence of TBP.[73]

b. Heterolytic addition

The synthesis of the practically important nonachloro-pentene is based on the reaction of hexachloropropene with TCE on heating in the presence of catalysts [$AlCl_3$ and metallic aluminium in proportions of (2–6):1].[74]

Aromatic compounds interact with TCE to form condensation products. However, one should note that the reactions of benzene and ethylbenzene with TCE are accompanied by appreciable tar formation and are of no practical value.[75,76] Benzene derivatives **13**, containing between 2 and 4 substituents, react with TCE, affording substituted α,β-dichloro-styrenes **14** in preparative yields.[77]

$$R_nC_6H_{6-n} + CHCl=CCl_2 \xrightarrow{AlCl_3} R_nC_6H_{5-n}CCl=CHCl$$

13 **14**

R = Alk, Hal, Alk_{Hal}; n = 2–4.

Polychlorotoluenes **15** react with TCE to form the chlorinated propenylbenzenes **16** and **17**.[78,79]

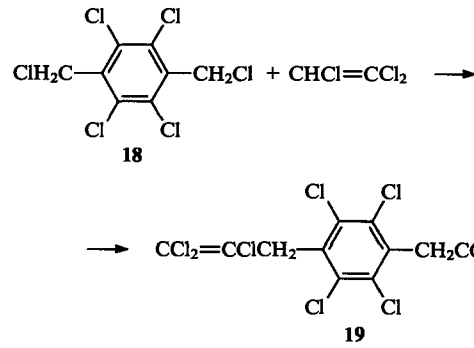
$$RCl + CHCl=CCl_2 \longrightarrow RCCl=CCl_2 + HCl$$

15 **16, 17**

R = $C_6Cl_5CH_2$ (**16**), $C_6Cl_5CCl_2$ (**17**).

It is noteworthy that, apart from compound **17**, *cis*- and *trans*-$C_6Cl_5-CCl=CCl-CCl_3$, $C_6Cl_5\overline{C=CCl(CCl_2)_2}CCl_2$ and *trans*-$C_6Cl_5-CCl=CClCCl_2CHClCCl_3$ are also formed in the reaction of TCE with perchlorotoluene.

2,3,5,6-Tetrachloro-1,4-bis(2,3,3-trichloroprop-2-enyl)-benzene **19** is a product of the interaction of 2,3,5,6-tetrachloro-1,4-bis(chloromethyl)benzene **18** with TCE. Its formation may be represented by the following scheme:[80]



18 **19**

Substituted chlorodiphenylethylenes (p-$ROC_6H_4)_2C=CHCl$ (R = H, Me) are obtained by the reaction of PhOR with TCE in the presence of trifluoromethanesulfonic acid.[81]

In the presence of sulfuric acid, trichloroethylene and formaldehyde condense, (the Prins reaction), with formation of α-chloro-β-hydroxypropionic acid **20**, which is dehydrated under the reaction conditions, giving α-chloroacrylic acid **21**. In the presence of alcohol, the reaction product is methyl α-chloro-acrylate **22**.[82]

$$CH_2O + CHCl=CCl_2 \xrightarrow{80\%\ H_2SO_4} HOCH_2-CHCl-COOH \longrightarrow$$

20

$$\xrightarrow{H^+,\ T} CH_2=CCl-COOH$$

21

$$\xrightarrow{H^+/EtOH} CH_2=CCl-COOEt$$

22

The condensation of TCE with bis(chloromethyl)ether in methylene chloride or carbon disulfide in the presence of aluminium chloride proceeds readily. The reaction product is bis-(2,3,3,3-tetrachloropropyl) ether **23** (yield 87.5%).[83,84] The ether **23** can be obtained using 1,3,5-trioxane instead of bis(chloromethyl) ether, which is a powerful lachrymator. When dry hydrogen chloride was passed through a mixture of TCE, 1,3,5-trioxane, and aluminium chloride, the yield of the ether **23** was 92%.



$$+ CHCl=CCl_2 \xrightarrow{HCl,\ AlCl_3} (CCl_3CHClCH_2)_2O$$

23

On treatment with zinc, perfluoroalkyl iodides and TCE condense with formation of β,β-dichlorovinylperfluoroalkanes $R_FCH=CCl_2$, which are the starting compounds in the synthesis of valuable perfluoroalkanoic acids.[85]

5. Addition reactions leading to the formation of a carbon–heteroatom bond

a. Radical thiylation

The reaction of aromatic thiols **24** with TCE in the presence of benzoyl peroxide (BP) leads to aryl β,β-dichlorovinyl sulfides **25**.[86–89]

$$XC_6H_4SH + CHCl=CCl_2 \xrightarrow[-HCl]{BP} XC_6H_4S-CH=CCl_2$$

24 **25**

X = 4-MeO, 4-Me, 3-Me, H, 4-Cl, 4-NO_2.

Diaryl disulfides are side products in this reaction, while in the interaction of TCE with *p*-nitrothiophenol oxidation products of β,β-dichlorovinyl *p*-nitrophenyl sulfide—the corresponding sulfone and sulfoxide—were detected.

Thiylation of TCE by aliphatic thiols, which leads also in this case to the formation of the corresponding β,β-dichlorovinyl sulfides, can be more conveniently carried out with irradiation by UV light and heating of the reaction mixture (the TCE : thiol ratio varies from 3 : 1 to 4 : 1).[88,89] The free-radical chlorovinylation of diaryl disulfides **26** by TCE leads to the formation of a complex mixture of products.[90,91]

$$ArSSAr + CHCl{=}CCl_2 \xrightarrow{h\nu} ArS{-}CH{=}CCl_2 + ArS{-}CCl{=}CHCl + ArS{-}CCl{=}CCl_2 + ArS{-}CHCl{-}CCl_3 + CCl_2{=}CH{-}CCl_2{-}CHCl_2$$

26 **25** **27** **28** **29** **30**

Ar = *p*-MeC_6H_4, Ph, *p*-ClC_6H_4.

Earlier studies on the free-radical thiylation of TCE and other polychloroalkenes and diaryl sulfides have been surveyed by Voronkov et al.[7]

b. Synthesis of compounds with C–N and C=N bonds

Voronkov and coworkers[92,93] investigated the addition of compounds containing a N–Hal bond to TCE and demonstrated its extensive synthetic possibilities. Thus, the reaction of *N,N*-dichloroarenesulfonamides **31** with TCE leads to pentachloroethane and (trichloroethylidene)arenesulfonamides **32**.[92,93]

$$RNCl_2 + CHCl{=}CCl_2 \longrightarrow RN{=}CHCCl_3 + CHCl_2{-}CCl_3$$

31a–c **32a–c** **1**

R = $PhSO_2$ (**a**), *p*-$MeC_6H_4SO_2$ (**b**), *p*-$ClC_6H_4SO_2$ (**c**).

The reactions of TCE with *N,N*-dibromobenzenesulfonamide,[94] *N,N*-dibromourethane,[95] and *N,N*-dichloroethylphosphoramide[96] proceed similarly. They afforded respectively *N*-(2-bromo-2,2-dichloroethylidene)benzenesulfonamide, *N*-(2-bromo-2,2-dichloroethyl)ethoxycarbonylimine, and 1,1,1-trichloro-2,2-bis(diethylphosphoramido)ethane. The interaction of *N,N*-dichlorourethane with TCE leads to chloral *N*-ethoxycarbonylimine.[97] When water is introduced into the reaction mixture, chloral reacts with it and the urethane formed as a side product, giving 2,2,2-trichloro-1,1-bis(*N*-ethoxycarbonylamino)ethane (50%) and 2,2,2-trichloro-1-(*N*-ethoxycarbonylamino)-1-hydroxyethane (20%).[98] The free-radical mechanism of the reactions involving the addition of *N,N*-dichlorobenzenesulfonamide and *N,N*-dichlorourethane to TCE was subsequently confirmed.[99]

It has been shown[100] that the reactions of *N,N*-dichloroacetamide **33a** and *N,N*-dichlorobenzamide **33b** with TCE under an inert atmosphere give reaction products of the corresponding chloral acylimines **34a** and **34b**—1,1-diacetamido-2,2,2-trichloroethane **35a**, 1,1-dibenz-amido-2,2,2-trichloroethane **35b**, *N*-(2,2,2-trichloro-1-hydroxy-ethyl)acetamide **36a**, *N*-(2,2,2-trichloro-1-hydroxyethyl)benzamide **36b**, and pentachloroethane:

$$RCONCl_2 + CHCl{=}CCl_2 \longrightarrow RCON{=}CHCCl_3 + CHCl_2{-}CCl_3$$

33a,b **34a,b** **1**

$RCONH_2$ | H_2O

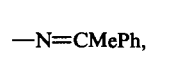
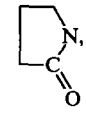
$(RCONH)_2CHCCl_3$ **35a,b** $RCONHCH(OH)CCl_3$ **36a,b**

R = Me (**a**), Ph (**b**).

The high electrophilicity of the acylimines obtained from trichloroethylidenearenesulfonamides and TCE made it possible to introduce them into reactions with nucleophiles, without preliminary isolation, and to develop ways of obtaining different polyfunctional compounds having the general formula

$CCl_3CHR'(NHSO_2R)$ (Refs 101–104)

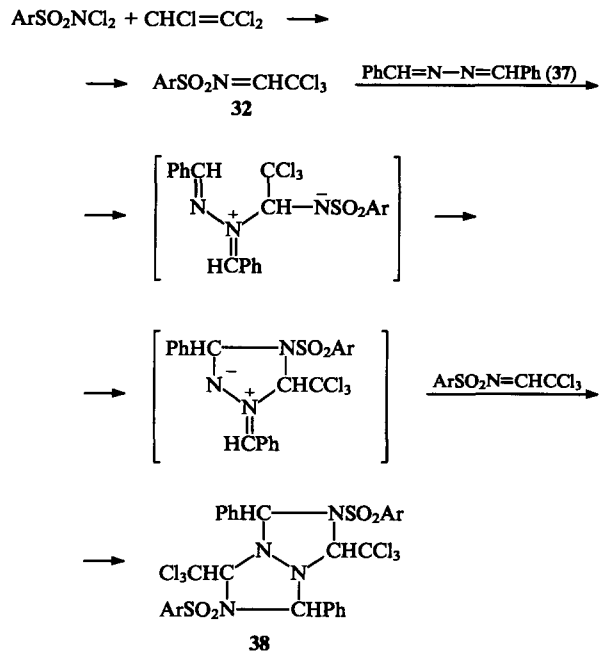
R = Ph, 4-MeC_6H_4;

R′ = OH, OMe, OEt, OPh, $PhSO_2NH$, 4-$MeC_6H_4SO_2NH$, PhC(O)NH, MeC(O)NH, OBu^n, OCH_2CH_2Cl, O—N=CMePh,  , O—N=CMeBu^t, MeCOO, SCH_2COOH,  , PhNH,  , PhNHNH, PhNHC(O)NH, MeNH, Bu^tNH.

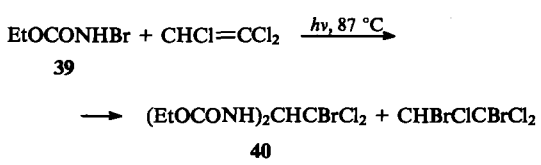
The reaction of *N*-(2,2,2-trichloroethylidene)arenesulfonamides, obtained from *N,N*-dichloroarenesulfonamides and TCE, with bifunctional nucleophiles such as mercaptoethanol and monoethanolamine proceeds via the mercapto- and hydroxy-groups respectively, giving the corresponding adducts—*N*-[2,2,2-trichloro-1-(2-hydroxyethylthio)ethyl]- and *N*-[1-(2-aminoethoxy)-2,2,2-trichloroethyl]-arenesulfonamides; in reactions with ethylene glycol, the products of both mono- and bis-*o*-amidoalkylation of the latter were obtained: *N*-[2,2,2-trichloro-1-(2-hydroxyethoxy)ethyl]arenesulfonamides and 1,2-(1-arenesulfonamido-2,2,2-trichloroethoxy)ethanes. The products of the reactions of *N*-(2,2,2-trichloroethylidene)arenesulfonamides with mercaptoethanol—*N*-[2,2,2-trichloro-1-(2-hydroxyethylthio)ethyl]arenesulfonamides—give rise to 3-arenesulfonyl-2-trichloromethyl-1,3-thiazolidines on successive treatment with thionyl chloride and then alkali.[105]

In the reactions of chloral arenesulfonylimines **32** with benzylideneazine **37**, the latter behaves as a 1,3-dipolar reagent, which combines with 2 moles of the imine to form 1,3,5,7-tetraazabicyclo[3.3.0]octanes **38**.[106]

It has been shown recently[107] that the product of the interaction of *N*-bromourethane **39** with TCE is 2-bromo-2,2-dichloro-1,1-di(ethoxycarbonylamino)ethane **40**. The reaction mechanism includes a series of processes—disproportionation of *N*-bromourethane to *N,N*-dibromourethane and urethane, the reaction of *N,N*-dibromourethane with TCE to form *N*-(2-boromo-2,2-dichloroethylidene)ethoxycarbonylamine, and the addition of urethane to the latter—which lead to the final product **40**.

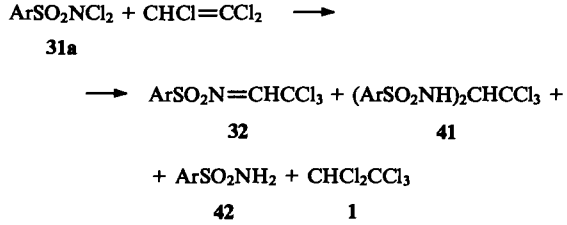


Ar = Ph, 4-MeC_6H_4, 4-ClC_6H_4.



The reactions of *N*-haloamides with TCE have been considered in greater detail in two reviews,[5,6] covering studies up to and including 1987.

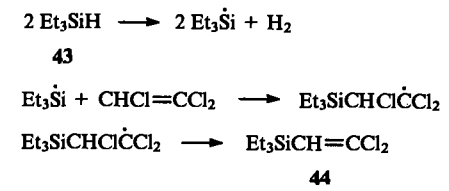
The ionic addition of *N*-haloamides to unsaturated compounds, including TCE, has been studied inadequately compared with the radical addition. It is known only that the interaction of *N*,*N*-dichloroarenesulfonamide **31a** with TCE in the presence of Lewis acids gives a complex mixture of compounds **1**, **32**, **41**, and **42**.[108,109]



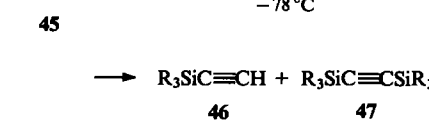
The reaction of TCE with the amide **31a** on heating and subsequent addition of acetamide to the reaction mixture leads to $PhSO_2NHCH(NHCOMe)CCl_3$. When acetoxime was used instead of acetamide, the product $PhSO_2NHCH.(ON=CMe_2)CCl_3$ was obtained.[108] It has been shown that *N*-(2,2,2-trichloro-ethylidene)arenesulfonamides can be used, without isolating them from the reaction mixture, as arenesulfonamidoalkylating agents. The *C*-alkylation of thiophene[110] and aromatic compounds[111] has been achieved with their aid.

c. Synthesis of compounds with a C–Si bond

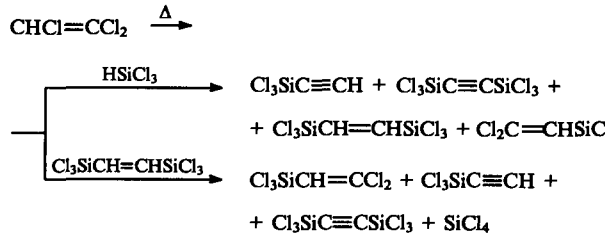
The dichlorovinylation of triethylsilane **43** has been carried out with the use of TCE (the reaction is initiated by γ-radiation). The formation of dichlorovinyltriethylsilane **44** can be represented as a free-radical addition–elimination mechanism.[112]



The interaction of trialkylchlorosilanes **45** with TCE in the presence of lithium gives the trialkylethynylsilanes **46** in 44%–54% yield. The side products of this reaction are bis(trialkylsilyl)alkynes **47**.[113]



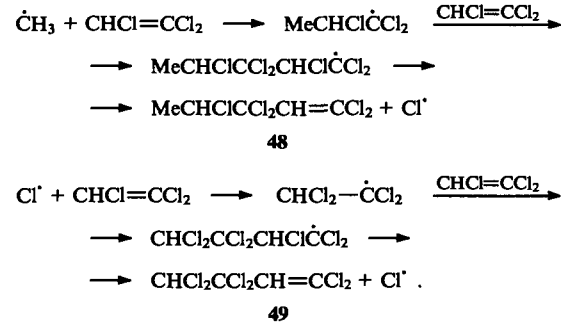
The gas-phase thermal reactions of TCE with trichlorosilane[114] and 1,2-bis(trichlorosilyl)ethylene[115] are more complicated.



Other organosilicon compounds with ethynyl groups—diorganoethynylchlorosilanes and diorganoethynylalkoxysilanes—have been obtained by the reaction of TCE with diorganodichlorosilanes and diorganoalkoxychlorosilanes respectively in $PO(NMe_2)_3$ in the presence of zinc dust.[116]

6. Dimerisation of trichloroethylene

On treatment with various initiators, TCE can dimerise to form $C_4H_2Cl_6$ or products of its dehydrochlorination having the composition C_4HCl_5.[117–121] Despite the fact that numerous studies were devoted to these processes, in particular the reactions occurring in the presence of free-radical initiators, the available information about the structure of the dimer formed remained contradictory for a long time.[117] It has been shown recently that the products of the reaction of acetyl peroxide with TCE are 1,1,3,3,4-pentachloropent-1-ene **48** and 1,1,3,3,4,4-hexachlorobut-1-ene **49** (in yields of 0.6 and 4.0 mole per mole of the peroxide respectively). The formation of these substances can be explained in terms of the following scheme:[122]



Hexachlorobutene **49** is a readily available and extremely valuable organic intermediate. The synthetic possibilities of compound **49** and of its derivatives have been reflected in a large series of studies by the authors of the present review.[123–133]

The dimerisation of TCE under the influence of fluorosulfonic acid proceeds differently: two hexachlorobutenes containing the CCl_3, $CHCl=CClCHClCCl_3$, and $CCl_3CH=CClCHCl_2$ groups are formed in an overall yield of 37%.[134] At high temperatures (460–530 °C) trichloroethylene dehydrodimerises, giving principally hexachlorobutadiene (30%) and hexachlorobenzene (24%).[135,136]

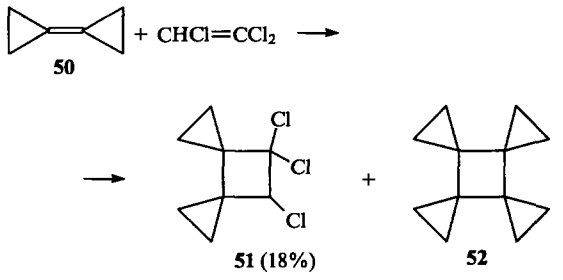
The results of early studies of the interaction of TCE with aluminium chloride are contradictory.[137–139] Detailed investigation of this reaction showed that 2*H*-pentachlorobuta-1,3-diene predominates among the three isomers of C_4HCl_5 formed.[140]

7. Cycloaddition reactions

Cycloaddition reactions with participation of TCE opened a synthetic pathway to chlorine-containing cyclic compounds which were previously difficult to obtain. Methods for cyclobutane ring construction have been most thoroughly developed in this series.

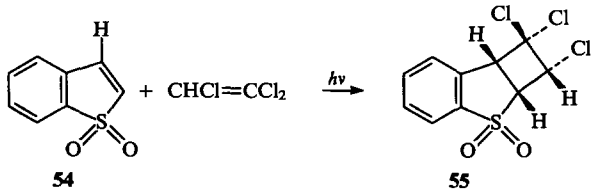
a. [2+2]-cycloaddition reactions

When a mixture of bicyclopropylidene **50** and TCE was heated (at 180 °C) for 96 h, 7,7,8-trichlorodispiro[2.0.2.2]octane **51** and the cyclopropylidene cyclic dimer **52** were obtained.[141,142]

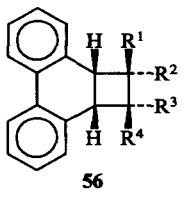


The cycloaddition reaction of dehydrobenzene, generated in situ from benzenediazonium-2-carboxylate, with TCE gives 1,1,2-trichlorobenzocyclobutene **53** in 18% yield. The use of dehydrobenzene, generated in 1,2-dichloroethane and containing a 15-fold excess of TCE, increased the yield of the target trichloro-derivative **53** to 42%, but it was contaminated by 2% of biphenyl.[143]

On irradiation of a mixture of benzo[*b*]thiophene 1,1-dioxide **54** and TCE with light at a wavelength of 300 nm and above, the adduct **55** was obtained in 52% yield.[144]

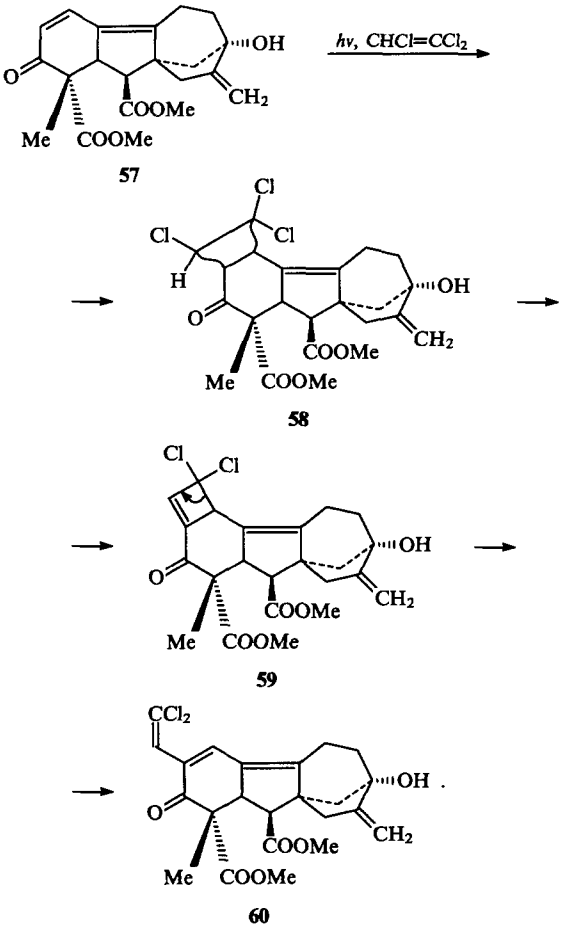


The photochemical reaction between phenanthrene and TCE leads to two cyclic adducts—the *anti*- and *syn*-isomers of 1,1,2-trichloro-1,2,2a,10b-tetrahydrocyclobuta[*e*]phenanthrene **56**—in an overall yield of 55%. Each adduct has *cis*-stereochemistry at the 2a- and 10b-positions and the *anti*-isomer ($R^1 = R^2 = R^4 = Cl$, $R^3 = H$) and the *syn*-isomer ($R^1 = R^2 = R^3 = Cl$, $R^4 = H$) were isolated in 48% and 7% yields respectively.[145]



1,4,5,8-Tetraazaphenanthrene also undergoes the cycloaddition reaction. When its mixture with TCE was irradiated with UV light, a cyclic adduct was obtained in 32% yield.[146]

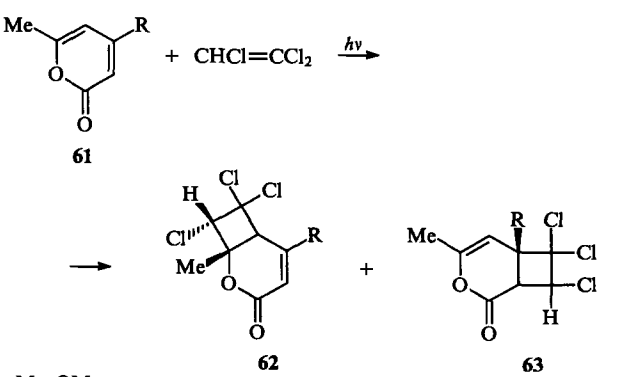
Photolysis of the dimethyl ester of 3-dehydrogibberellenic acid **57** in the presence of an excess of TCE in methylene chloride leads to two dimers (50%) and the photoadduct **58**.[147] Apparently owing to the presence of a chlorine atom in the β-position relative to the CO group, the latter is unstable and, after elimination of HCl and isomerisation of the highly strained cyclobutene derivative **59**, is converted into the stable final product **60** in 43% yield in accordance with the following scheme:



It is noteworthy that the photocycloaddition of the dienone **57** to TCE is distinguished by a high stereospecificity and leads to only one adduct.

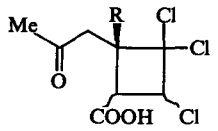
The photochemical syntheses of a series of new heterocyclic systems from 2-pyrones and 2-pyridones have been achieved. These reactions proceed in the presence of various sensitisers.

2-Pyrones **61** afford two types of cyclic adducts—**62** and **63**.[148]

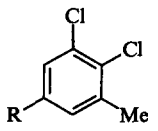


R = Me, OMe.

Hydrolysis of the cyclic adducts formed as a result of TCE addition to the C(3)=C(4) double bond of 2-pyrones yielded compounds **64** and **65**.



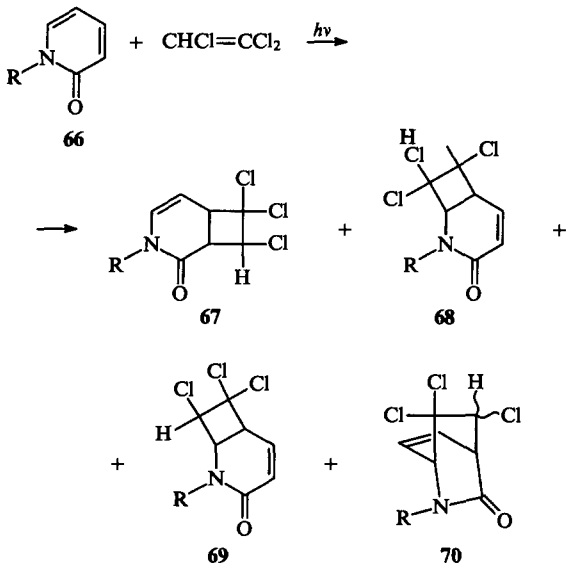
64



65

The reactions of 2-pyridones **66** with TCE gave a complex mixture of cyclic adducts **67**–**70**, among which the 5,6-adducts **68** and **69** predominate.[149]

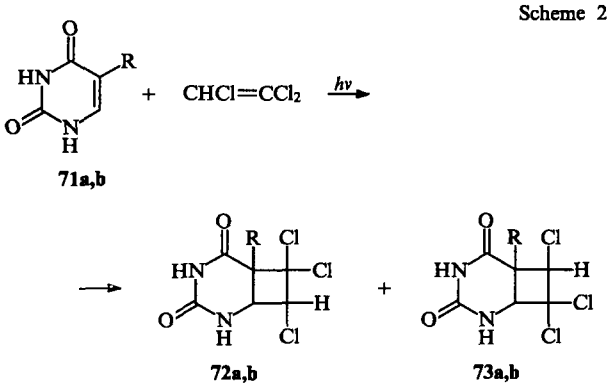
7,7,8-Trichloro-2-R-2-azabicyclo[2.2.2]oct-5-en-3-one **70**, formed as a result of the Diels–Alder reaction, is a [4+2]-adduct.



66 **67** **68** **69** **70**

The photochemical reactions of TCE with thymine **71a** and 5-fluorouracil **71b** opened a pathway to the synthesis of the corresponding cyclobutapyrimidinediones **72** and **73** (Scheme 2).[150]

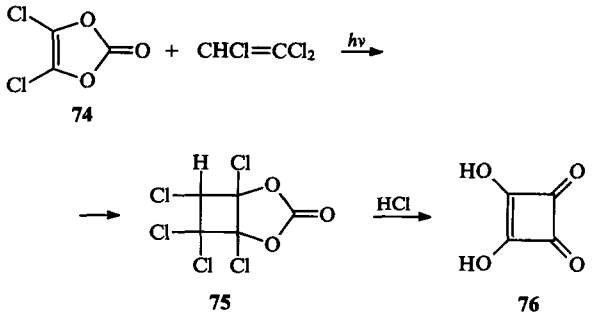
Scheme 2



71a,b **72a,b** **73a,b**

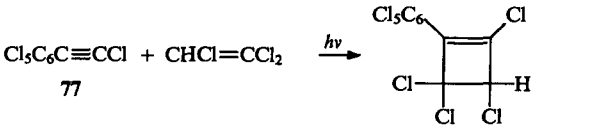
R = Me (a); R = F (b).

Quadratic acid **76**, which is of practical value, has been synthesised by the reaction of TCE with dichlorovinyl carbonate **74** and subsequent hydrolysis of the cyclic adduct — 1,2-carbonyldioxy-1,2,3,3,4-pentachlorocyclobutane **75**.[151]



74 **75** **76**

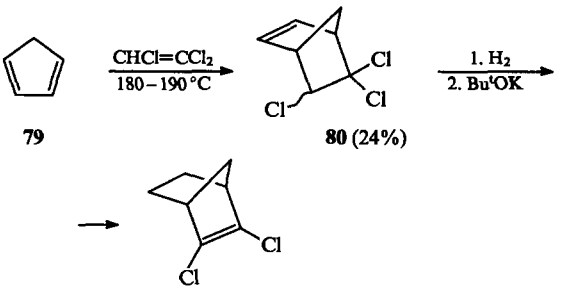
TCE has been used to achieve the direct synthesis of cyclobutene derivatives in the reaction of perchlorophenylacetylene **77** with TCE. When a mixture of the alkyne **77** with TCE, present in large excess in a sealed Pyrex tube, was irradiated with UV light, 3*H*-nonachloro-1-phenylcyclobutene **78** was obtained.[152]



77 **78** (58%)

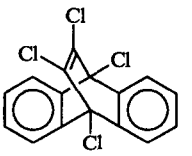
b. The Diels–Alder reaction

The [4+2]-cycloaddition reaction of TCE has been investigated only for certain cyclic dienes. Thus cyclopenta-1,3-diene **79** reacts with TCE to form 5,5,6-trichloronorbornene **80**.[153] Successive hydrogenation of the adduct **80** and dehydrochlorination of the saturated compound obtained yielded 2,3-dichloro-2-norbornene **81**.[154,155]



79 **80** (24%) **81** (17%)

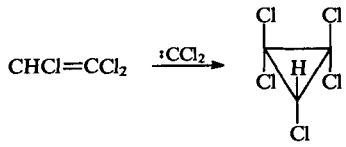
When 9,10-dichloroanthracene is treated with TCE (autoclave, 230 °C, 48 h), a mixture of Diels–Alder adducts is formed, the main one being 1,4,7,8-tetrachlorodibenzobicyclo[2.2.2]octatriene **82**.[156]



82 (10%)

c. Cyclopropane formation reactions

The formation of cyclopropane rings by reaction with dihalocarbenes is known to be one of the best methods for this purpose. Since both TCE and dihalocarbenes have pronounced electrophilic properties, it might have been expected that reaction between them would proceed with difficulty. Indeed pentachlorocyclopropane **83** has been obtained only after prolonged refluxing (~$2^1/_2$–5 days) of a mixture of TCE and sodium trichloroacetate in 1,2-dimethoxyethane.[157]



83 (22.4%)

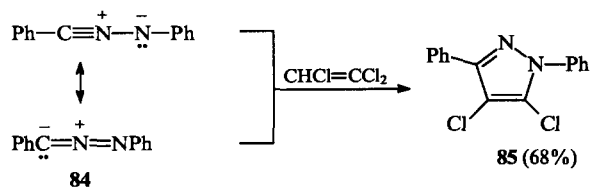
By varying the conditions in the cyclopropane formation reaction, it was later possible to raise the yield of the adduct **83** to 45%.[158,159] By generating dichlorocarbene from organomercury compounds, it is possible to carry out the cyclopropane formation reaction at room temperature. Thus, cyclopropane **83** has been obtained in 22% yield by the reaction of bromodichloromethyl-(cyclohexyl)mercury with TCE.[160]

The simpler method for the generation of $:CCl_2$ from sodium trichloroacetate in the presence of phase transfer catalysts makes it possible to carry out the cyclopropane formation reaction in an aqueous medium, but the adduct **83** is formed in a low yield (~9%).[161]

Methods for the synthesis of halocyclopropenes and halocyclopropanes,[158,162] which were previously scarce, and a convenient method for the synthesis of 7,7-difluorocyclopropabenzene[163] and other compounds have been developed which involve the use of pentachlorocyclopropane **83**.

e. Other cycloaddition reactions

It has been found[164] that, on interaction with TCE, diphenylnitrile imine **84** behaves as a 1,3-dipolar reagent. This reaction is completed by the formation of 4,5-dichloro-1,3-diphenylpyrazole **85** and is an example of the [3+2]-cycloaddition reaction.



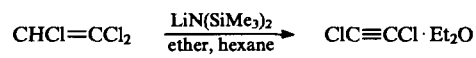
84

85 (68%)

III. Elimination reactions

Among elimination reactions, the dehydrochlorination of TCE and to a lesser extent its dechlorination have been investigated in the greatest detail. The elimination of a hydrogen chloride molecule from TCE proceeds on treatment with alkalies and leads to the formation of dichloroethyne **86**, which is an extremely explosive product.[165] When the dehydrochlorination of TCE is carried out in diethyl ether, dichloroethyne is isolated in the form of the stable complex $ClC{\equiv}CCl \cdot Et_2O$ **87**. Various modifications of this method have been described.[166-169]

Under laboratory conditions, small amounts of compound **86** can be obtained by treating a TCE–ether mixture with lithium hexamethyldisilazide in hexane, but this procedure requires the use of an expensive base and careful drying of the reactants.[170]



87

Two improved methods for the synthesis of dichloroethyne have been proposed recently. One of them is based on the phase transfer catalytic method. Makosza and coworkers[171] showed earlier that, in the presence of ammonium catalysts, TCE gives rise to the trichlorovinyl anion, which decomposes above 40 °C to form dichloroethyne.[172] Treatment of a mixture of TCE and ether with a 50% aqueous solution of NaOH in the presence of triethylbenzylammonium chloride (TEBA) at 70 °C led to the formation of complex **87** in a high yield.

Another rapid method for the synthesis of pure dichloroethyne, also in a high yield, is based on the reaction of TCE with potassium hydride in tetrahydrofuran (THF) in the presence of catalytic amounts of methanol.[173] When TCE is exposed to laser radiation, the dehydrochlorination reaction predominates and dechlorination is a side process.[174-179] When low pressures are employed, the yield of dichloroethyne **86** diminishes, whereas that of chloroethyne **88** increases. On exposure to an electric discharge at a reduced pressure, TCE gives rise to chloroethyne **88**.[180-182]

The reaction of TCE with naphthalenesodium in pentane or THF leads to the complete dechlorination of TCE with formation of ethyne and ethene (overall yield 97%).[183]

IV. Substitution reactions

1. Interaction of trichloroethylene with nucleophiles

Nucleophilic substitution at a vinyl carbon atom is known to be difficult. In some studies, one can encounter the claim even nowadays that TCE does not enter into nucleophilic substitution reactions. Indeed, under the usual conditions, TCE is not hydrolysed by aqueous solutions of alkalies, which makes it possible to employ them for the purification of TCE. However, under certain conditions TCE does react with nucleophiles of different nature, which can be accounted for by the presence in its molecule of the C=C electrophilic bond. The synthesis of a wide variety of products has been achieved by using nucleophilic substitution reactions of TCE.

The reactions of nucleophiles with chloroethenes can proceed via at least two pathways: (1) via the addition–elimination mechanism;[184] (2) via the elimination–addition mechanism.[185] TCE apparently reacts with nucleophiles via the second mechanism. Dichloroethyne is formed initially and the nucleophile then adds to it. The nucleophilic addition stage proceeds stereoselectively and constitutes an anti-process, which leads in most cases to final products with the (*E*)-configuration.

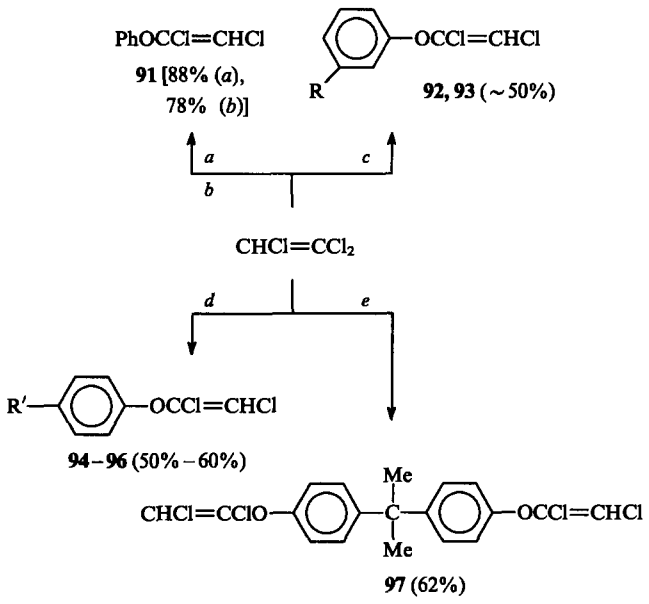
a. Interaction with O-nucleophiles

The reaction of O-nucleophiles with TCE was first investigated in its reaction with sodium ethoxide: the product was 1,2-dichlorovinyl ethyl ether **89**.[2]

The interaction of sodium alkoxides with TCE has been studied recently in very great detail in connection with the use of alkyl dichlorovinyl ethers **90** for the synthesis of various derivatives of alkoxyalkynes.[186] It was found that alkoxides of primary and secondary alcohols react with TCE on refluxing to form the ethers **90** in moderate yields (34%–54%).

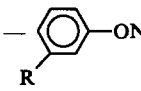
According to a patent,[187] ether **89** is obtained by treating TCE with an alcoholic solution of alkali and is used subsequently in the synthesis of 2-bromo-2-chloro-1,1,1-trifluoroethane. The reactions of sodium phenoxide and its derivatives with TCE proceed readily in aprotic solvents.[188-190] It has been shown recently that TCE interacts with various phenols also under phase-transfer catalytic conditions in the presence of Makosza's catalysts.[191] The products of these reactions are the 1,2-dichlorovinyl ethers **91–97** having the (*E*)-configuration. The simplest and most convenient method for the synthesis of the ethers is under the conditions of phase-transfer catalysis.

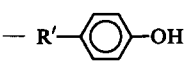
When two chlorine atoms in the TCE molecule are replaced by nucleophilic residues, chloroketene acetals are formed. It was found that potassium *tert*-butoxide interacts extremely vigorously with TCE, affording the acetal **98**,[186] whereas the acetal **99**—the product of the reaction of sodium β-methoxyethoxide and TCE—takes place under fairly severe conditions.[192]

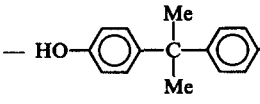


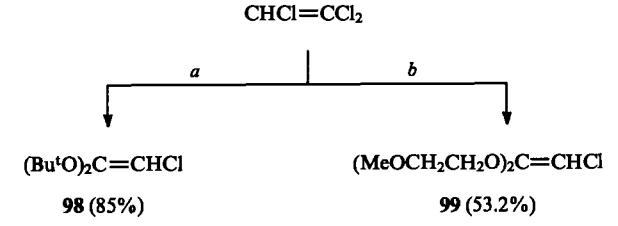
a — PhOH; Na + MeOH, DMFA;[188]

b — PhONa; DMSO;[189]

c —  (R = NO_2, Me); DMFA;[190]

d —  (R' = Me, Et, NO_2); H_2O, NaOH, $C_6H_5CH_2\overset{+}{N}(Pr^n)_3Cl^-$;[191]

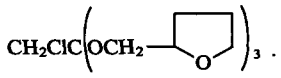
e —  ; H_2O, NaOH.[191]



a — Bu^tOK, THF, −60 °C;[186]

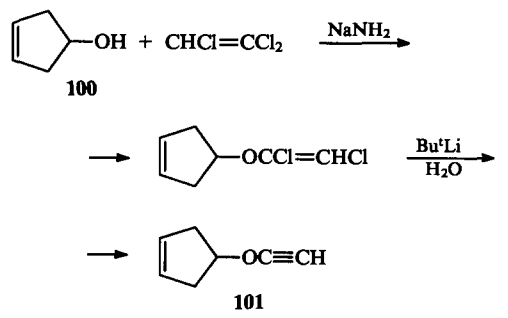
b — $MeOCH_2CH_2ONa$, xylene, 100–130 °C.[192]

The product of the interaction of TCE with tetrahydrofurfuryl alcohol and sodium under a nitrogen atmosphere is the orthoester

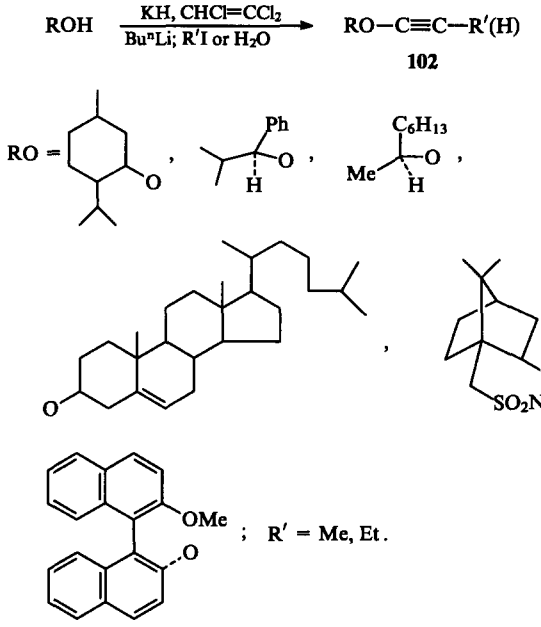


which indicates the possibility of the addition of a molecule of the nucleophile to the intermediate chloroketene.[193]

Convenient methods for the synthesis of acetylenic esters from TCE have been proposed recently.[194,195] The possibility of the synthesis of the alkyne **101** has been demonstrated in the reaction of cyclopentenol **100** with TCE.[194]



A simple and general method of synthesis of acetylenic ethers **102** has been developed on the basis of secondary alcohols and TCE.[195]

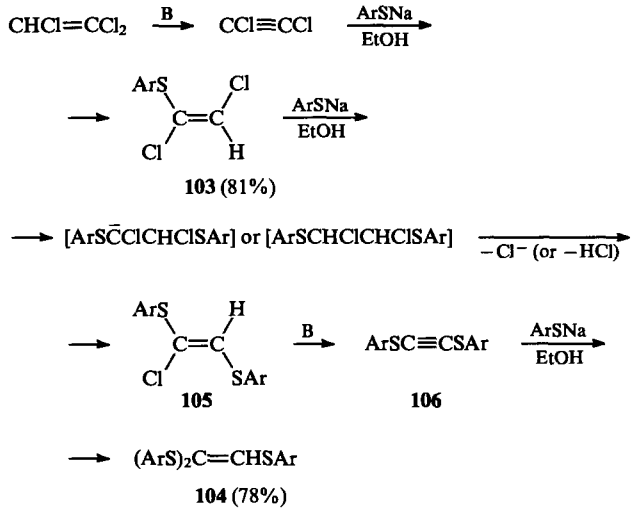


; R' = Me, Et.

A new and effective two-stage synthesis of propargyl ethers $ROCH_2C{\equiv}CH$ [R = cyclohexyl, (−)-menthyl, (−)-bornyl, or 1-adamantyl] has been achieved by isomerising 1-propynyl ethers $ROC{\equiv}CMe$, obtained from the corresponding secondary alcohols and TCE, on treatment with potassium 3-aminopropylamide.[196] According to a patent,[197] TCE and other alkenyl polyhalides are used in the esterification of resin acids and their derivatives.

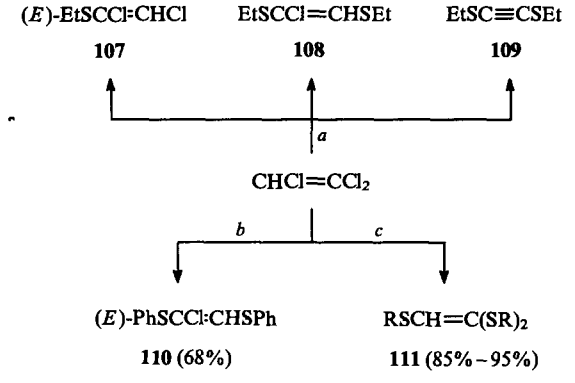
b. Interaction with S-nucleophiles

When TCE interacts with S-nucleophiles, products containing one or several thiolate residues are formed depending on the reaction conditions. A detailed study has been made of the reaction of sodium *p*-methylthiophenoxide with TCE, which proceeds only in the presence of sodium ethoxide.[198] For a 1 : 1 reactant ratio and after brief heating of the mixture, the main reaction product is 1,2-dichloro-1-(*p*-tolylthio)ethylene **103**. In the presence of a four-fold excess of the thiolate and after prolonged heating of the reactant mixture, 1,1,2-tris(*p*-tolylthio)ethylene **104** was obtained. By varying the reaction conditions, it was also possible to isolate the intermediates in this reaction: 1-chloro-1,2-di(*p*-tolylthio)-ethylene **105** and di(*p*-tolylthio)ethylene **106**. The results show that the reaction of TCE with sodium toluene *p*-thiolate proceeds via elimination–addition and addition–elimination mechanisms:



B = base, Ar = *p*-MeC_6H_4.

The reaction of other thiolates with TCE in aprotic solvents also leads to the initial formation of (*E*)-1,2-dichlorovinylation products, for example compound **107**, which can be involved in further reactions, giving compounds with two and three thiolate groups, for example, compounds **108–111**.

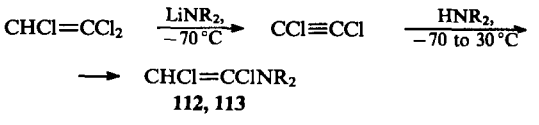


a — EtSNa, DMF;[188]
b — PhSNa, PhSNa : TCE = 3 : 1, DMF;[199]
c — Pr^{i}SNa or MeSNa, DMF.[199]

c. Interaction with N-nucleophiles

TCE reacts with amines only in the presence of strong bases, which shows that the reaction proceeds via the elimination–addition mechanism. The 1,2-dichlorovinylation of certain amines has been achieved with TCE, and convenient methods have also been developed for the formation of chloroketene aminals, diaminoalkynes, and glycine and its derivatives.

The dichlorovinylation of aliphatic amines has been investigated in relation to dimethyl- and diethyl-amines. 1,2-Dichloro-1-(*N*,*N*-dialkylamino)ethylenes **112** and **113** have been obtained by treating TCE initially with lithium dialkylamide in ether and then with the amine.[200]

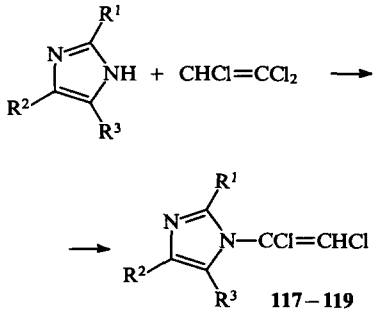


R = Me (**112**, yield 75%); R = Et (**113**, yield 85%).

On heating (60–70 °C) with an excess of dimethyl- and diethyl-amine, the enamines **112** and **113** are converted into the corresponding chloroketene aminals $CHCl=C(NR_2)_2$ [R = Me (compound **114**), R = Et (compound **115**)].[200] The mono- and di-substituted products **112–115** have found applications in the synthesis of diaminoalkynes of the type $R_2N-C\equiv C-NR_2$,[200,201] which are important synthons.[202]

The direct synthesis of these compounds has been developed only for bis(dimethylamino)ethyne **116**, which is obtained via the reaction[203]

The interaction of TCE with heterocyclic amines has been more widely investigated. Thus treatment of TCE with a mixture of potassium hydride and imidazole in THF in the presence of catalytic amounts of methanol leads to the formation of *N*-(1,2-dichlorovinyl)imidazole in 80% yield.[173] Another method has been proposed[204] for the alkenylation of imidazole and its derivatives, which involves treatment of the reaction mixture with an aqueous solution of NaOH in the presence of dimethyl sulfoxide (DMSO). The reaction proceeds stereoselectively with formation of the corresponding (*E*)-derivatives of imidazole **117–119** in 60%–62% yield.

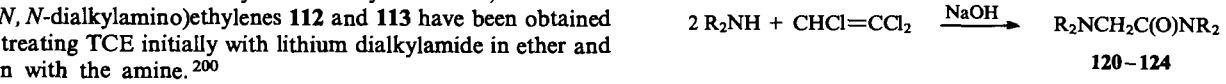


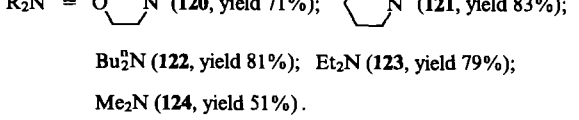
$R^1 = R^2 = R^3 = H$ (**117**); R^1 = Ph, $R^2 = R^3 = H$ (**118**);
$R^1 = H$, $R^2 = R^3$ = Ph (**119**).

N-[(*E*)-1,2-dichlorovinyl]benzimidazole is formed in 60% yield from benzimidazole and TCE under similar conditions.

The interaction of carbazole and its derivatives with TCE under phase-transfer catalytic conditions has been investigated recently.[205] On treatment with aqueous NaOH and catalytic amounts of triethylbenzylammonium chloride, this reaction proceeds stereoselectively via the intermediate formation of dichloroacetylene **86**, affording high yields (~80%) of 9-[(*E*)-1,2-dichlorovinyl]carbazole derivatives.

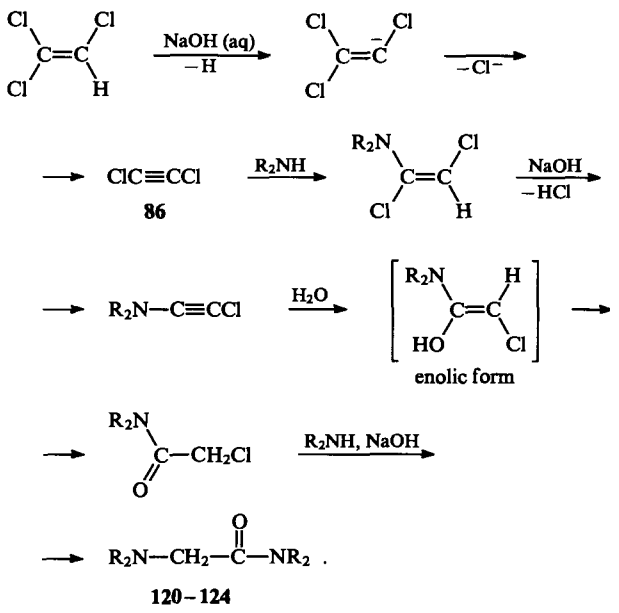
A new general method of synthesis of symmetrically substituted, *N*,*N*,*N*′,*N*′-tetraalkylglycine amides **120–124** has been developed based on the reaction of TCE with more nucleophilic secondary amines under phase-transfer catalytic conditions.[172,206]





The less nucleophilic aromatic amines do not react with TCE under these conditions.

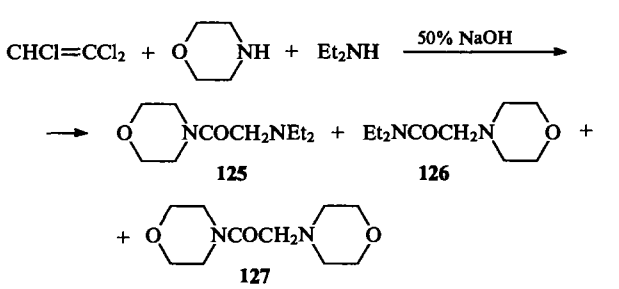
It has been suggested that the reaction takes place via the intermediate trichlorovinyl anion,[171] which is converted into the alkyne **86** and the latter reacts with the amine in accordance with the mechanism



120–124

In order to confirm the postulated mechanism, an attempt was made to isolate the intermediates, but R_2NCOCH_2Cl was isolated only in the reaction of TCE with morpholine.

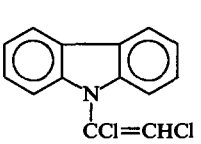
The reactions of TCE with a mixture of two unequally nucleophilic amines in the presence of phase-transfer catalysts is of definite synthetic interest. Thus, when a mixture of morpholine and diethylamine was used, the glycine amide derivatives **125–127** were obtained, the main product being compound **125**.[207]



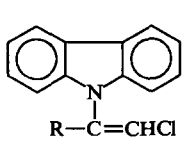
125 **126**

127

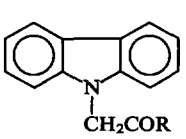
Treatment of TCE with carbazole and a secondary aliphatic amine leads to the formation of the products **128–130**, the yields of which depend on the nature of the aliphatic amine and the ratios of all the reactants.[208]



128



129



130

R = Et_2N, Pr_2N, , .

The synthesis of glycine, **131**, based on the reaction of TCE with an aqueous ammonia solution is important.[209,210] The reaction takes place in an autoclave on treatment with various alkaline catalysts, among which the most effective is $NaHCO_3$. Under optimum conditions (14% aqueous ammonia, pressure 294 kPa, temperature 180 °C, 4 h), the yield of glycine is 71.6%.

It has been suggested that the reaction proceeds via the initial formation of aminoacetonitrile **132** in accordance with the mechanism

$$2NH_3 + CHCl{=}CCl_2 \longrightarrow \underset{\mathbf{132}}{NH_2CH_2CN} \xrightarrow{H_2O} NH_2CH_2COOH\,.$$

131

Indeed, when anhydrous ammonia and lower temperatures (70–80 °C) are used, the main reaction product is the nitrile **132** (yield 70%).[211]

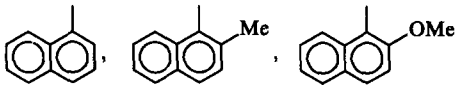
d. Reactions with C-nucleophiles

Study of the reactions of TCE with C-nucleophiles is of undoubted interest because the problem of new C–C bond formation is extremely pressing.

The reaction of TCE with organomagnesium compounds leads to the formation of a complex mixture of substances.[189] Grignard reagents are known to be fairly strong bases and moderate nucleophiles, so that the occurrence of competing elimination and substitution reactions is possible. In the presence of catalysts, TCE reacts with Grignard reagents more selectively and the nature of the catalyst influences the mode of the reaction more significantly. Thus aromatic Grignard reagents and TCE afford diarylalkynes **133** and biaryls **134** (by reduction of the Grignard reagent) on treatment with cobalt(II) or nickel(II) salts.[212]

$$ArMgBr + CHCl{=}CCl_2 \xrightarrow{CoCl_2\ (or\ NiCl_2)} \underset{\mathbf{133}}{Ar{-}C{\equiv}C{-}Ar} + \underset{\mathbf{134}}{Ar{-}Ar} + ArH$$

Ar = Ph, *p*-MeC_6H_4, 1,3,5-$Me_3C_6H_2$,



The yields of the alkynes **133** depend on the structure of the reagent employed. For example, in the reaction of TCE with 1,3,5-$Me_3C_6H_2MgBr$ the yield of the corresponding alkyne is 48%, whereas when phenylmagnesium bromide was used the target product was obtained in a yield of only 5%.

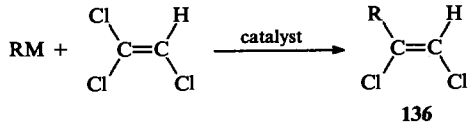
The interaction of TCE with organomagnesium compounds proceeds differently in the presence of phosphinepalladium-(nickel) catalysts. A simple method of synthesis of substituted 1,1-dichloroalkenes **135** has been developed which employs the reaction of a Grignard reagent with TCE catalysed by tetrakis-(triphenylphosphine)palladium (or nickel).[213] It has been suggested that the reaction proceeds via the initial formation of intermediates involving the oxidative addition of the catalyst in a monosubstituted position in TCE. The intermediate then reacts with the Grignard reagent and is converted into the corresponding alkene after reductive elimination.

$$RMgCl + CHCl{=}CCl_2 \xrightarrow[or\ Ni(PPh_3)_4]{Pd(PPh_3)_4} \underset{\mathbf{135}}{RCH{=}CCl_2}$$

R = n-C_8H_{17} (65%–75%), n-C_6H_{13} (60%–72%), Bu^i (55%), Pr^i (52%), cyclo-C_6H_{11} (81%).

The reaction proceeds under mild conditions (room temperature, solvent—mixture of ether with benzene), but we may note that phenylmagnesium bromide gives a mixture of three products in 40% yield under these conditions.

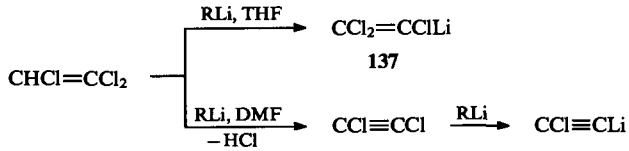
The regio- and stereo-selective monoalkylation and monoarylation of TCE by Grignard reagents or organozinc reagents was achieved for the first time in the presence of the phosphinepalladium catalyst $\{PdCl_2[Ph_2P(CH_2)_4PPh_2]\}$.[214] In this case, the reaction involves the CCl_2 group of TCE and is completed by the formation of monosubstituted (*Z*)-1,2-dichloroethylenes **136** in good or high yields.



136

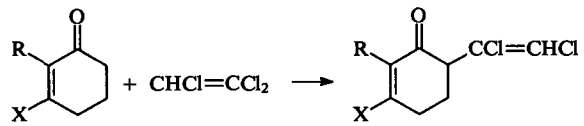
R = Ph, 4-ClC_6H_4,  M = MgBr or ZnCl.

When TCE was treated with organolithium compounds, metallation products of both TCE (trichlorovinyllithium **137**)[215] and dichloroethyne (chloroethynyllithium **138**) were obtained.[189]



The carboxylation of vinyllithium **137** leads to the formation of trichloroacrylic acid in 81% yield.[179]

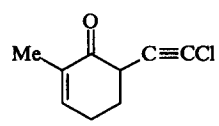
It has been shown in a number of studies[216–218] that TCE is an effective agent for the alkenylation of tertiary conjugated enolates. Although the latter are in fact ambident nucleophiles, only their tertiary carbon atoms are subjected to electrophilic attack. Thus lithium enolates, obtained from the substituted cyclohexenones **139** and **140** (lithium dialkylamide, THF, −78 °C), react with TCE under mild conditions, giving the 1,2-dichlorovinylation products—the dichlorovinyl ketones **141** and **142**.[216]



139, 140 **141, 142**

X = OEt, R = H (**139, 141**); X = H, R = Me (**140, 142**).

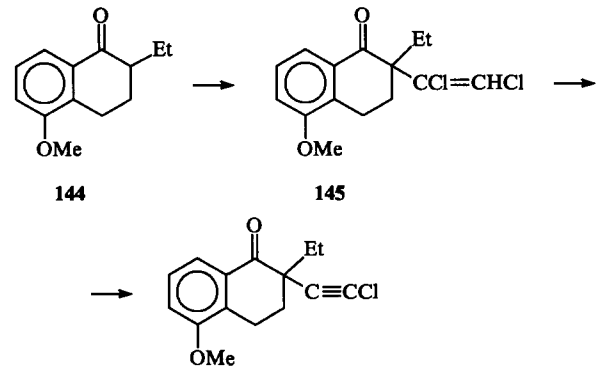
When the enolate **140** is used, the chloroalkyne **143** is formed as well.



143

It has been shown with the aid of X-ray diffraction that the ketone **142** has the (*E*)-configuration.

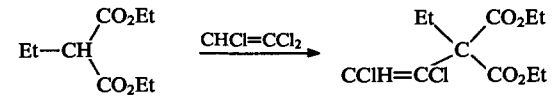
Two products are formed in the reaction of the lithium enolate of the substituted tetralinone **144** with TCE: the dichloroalkyne **145** and the chloroalkyne **146**. The complete conversion of compound **144** into the chloroalkyne derivative **146** (yield 44%) is achieved by repeated treatment of the mixture of products with lithium dialkylamide (THF, −78 to 20 °C).



144 **145**

146

Diethyl ethylmalonate **147** condenses with TCE under more severe conditions (NaH, THF, HMPA, refluxing), forming compound **148**.

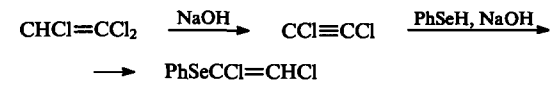


147 **148**

The dichlorovinylation of ethyl 2-acetylpropionate proceeds similarly. The reactions with participation of deuteriated TCE have shown that the dichlorovinylation of the tertiary enolates investigated takes place by the elimination–addition mechanism via dichloroethyne as an intermediate.[217] The condensation of enolates with TCE can be formally regarded as a reaction involving substitution of a chlorine atom in the dichloromethylene group of TCE. The attempt to extend this reaction to other types of enolates was unsuccessful.[218]

e. Reactions with other nucleophiles

It has been shown[219,220] that selenophenol reacts with TCE in concentrated NaOH solution to form 1,2-dichlorovinyl phenyl selenide **149** in a high yield. The reaction is catalysed by ammonium salts and leads to the (*Z*)-isomer for an equimolar ratio of the catalyst and the selenol. In the presence of a tenfold excess of the selenol, a mixture of the (*Z*)- and (*E*)-isomers is formed. It has been suggested that the interaction of the selenol with TCE takes place by the elimination–addition mechanism and subsequent isomerisation of the (*Z*)-selenide, formed initially, to the thermodynamically more stable (*E*)-isomer.



(*Z*, *E*)-**149**

Diethyl ether is used to bind the dichloroethyne formed *in situ*. The nucleophilic substitution of chlorine in TCE by the PhSe-ion in ethanol and DMF also leads to a mixture of the (*Z*)- and (*E*)-selenides, but the product yields are appreciably lower than in a two-phase system.

The interaction of TCE with diphenyl and dimethyl diselenides **150** in the presence of tributylbenzylammonium chloride as the phase-transfer catalyst proceeds, on the whole, similarly to the reaction with the selenol. However, under these conditions, an appreciable amount of trichlorovinyl selenides **151** and 1,2-dichloro-1,2-bis(organoseleno)ethylenes **152** is formed together with the expected (*Z*)-1,2-dichlorovinyl selenides and the products of their isomerisation [the (*E*)-isomers].[221]

$$CHCl{=}CCl_2 + RSeSeR \xrightarrow{(10\%-15\%)\ NaOH\ -\ Et_2O}$$

150

$$\longrightarrow RSeCCl{=}CClSeR + RSeCCl{=}CCl_2 + Z(E)\text{-}RSeCCl{=}CHCl$$

152 **151**

R = Ph, Me.

The data obtained can be accounted for by the formation, in the course of the reaction, of selenolate ions RSe^- by heterolytic cleavage of the selenides in an alkaline medium, the ions adding to the $CCl{\equiv}CCl$ generated in situ from TCE.

TCE is phosphonylated by the sodium salts of dialkyl phosphites. Depending on the structure of the phosphites employed and the reaction conditions, the esters of tri- and/or tetra-phosphonic acids are produced.[222]

f. Hydrolysis

When TCE vapour is passed through concentrated sulfuric acid heated to 180 °C, a technically valuable product is formed — monochloroacetic acid **153**.[1] In order to increase the yield of the acid **153** and to reduce the process temperature, it is recommended that the hydrolysis be carried out at a reduced temperature.[1,223]

A method has been proposed for the synthesis of monochloroacetyl chloride through hydrolysis of TCE in the liquid phase in the presence of partly suspended iron(II) chloride with continuous passage of hydrogen chloride under pressure. The acid **153** is in this case a side product of the reaction.[224,225] Alkaline hydrolysis of TCE (steel reactor, sodium methoxide, 60–65 °C) leads to the formation of methyl monochloroacetate.[226]

2. Interaction with electrophiles

The reactions examined above confirm that TCE has pronounced electrophilic properties. One can therefore postulate that its interaction with electrophiles is difficult and is possible only with electrophiles stronger than TCE itself.

According to patent data,[227,228] TCE reacts with nitric acid. Thus, when TCE is refluxed with 30%–80% aqueous HNO_3 and also on slow addition of 90%–100% HNO_3 to TCE at 65–75 °C, trichloronitroethylene is formed in a preparative yield. However, together with the nitration of TCE, the molecules of the latter are degraded, which results in the formation of dichlorodinitromethane.

Trichloroethylenesulfonyl chloride has been obtained in high yield by the reaction of TCE with chlorosulfonic acid.[229] The reaction is carried out at the boiling point of TCE (87 °C), the hydrogen chloride formed being removed by passing dry nitrogen through the reaction mixture.

V. Oxidation reactions

1. The effect of oxygen

The oxidation of TCE by oxygen, the study of which was begun as early as 1911,[220] is nowadays being investigated in fair detail commercially. Its main products are dichloroacetyl chloride **154** and trichloroepoxyethane **155**, the yields of which depend to a considerable extent on the oxidation reaction conditions.

The studies on the oxidation of TCE published up to 1970 have been examined in a monograph.[4] The oxidation of TCE under the influence of ionising radiation has been described in a recent monograph.[231]

The patents, published during the last 10–15 years and devoted to this problem, are concerned primarily with improvement of the synthesis of compound **154**.[232–241] It has been shown[233] that the photochemical oxidation of TCE at 70–80 °C in the presence of catalytic amounts of a chloride in DMF makes it possible to obtain compound **154** in 90% yield with ~90% conversion of TCE. Compound **154** has been obtained in a high yield also by oxidising TCE in the presence of azobisisobutyronitrile (AIBN) or benzoyl peroxide and trialkylamines,[234] pyridines,[235,236] quinoline, and isoquinoline.[237] The rate of oxidation increases appreciably when TCE containing small amounts of added compound **154** is irradiated by short-wavelength light.[238] The target product **154** was obtained with 99.47% purity and 99.9% conversion by varying the power of the UV irradiation.[239]

There are data showing that haloalkenes are oxidised on heating under pressure without a catalyst.[240] In industry, dichloroacetal chloride is obtained by the continuous oxidation of TCE with air or an oxygen–air mixture at 170 °C under a pressure of 491 kPa in the presence of benzoyl peroxide and amide catalysts.[241]

Trichloroepoxyethane **155** — the second main product formed on oxidation of TCE — is extremely reactive and is used in the synthesis of a wide variety of substances. It is obtained by McKinney's method[242] involving the autoxidation of TCE in methanol in the presence of RCOOOH under irradiation with light from an Hg lamp[243] or as a result of radiation-chemical oxidation.[244]

Study of the low-temperature photoinitiated oxidation of TCE showed that selectivity in epoxide formation increases after the addition of aromatic ketones and on irradiation with light at $\lambda = 300$ nm for low (15%–20%) conversions of TCE. An increase in the yield of the epoxide is also promoted by carrying out the process at low temperatures.[245] The radiation-chemical method of synthesis of the epoxide **155** is promising because in this case the oxidation reaction proceeds at low temperatures.[246]

The characteristic features of the oxidation of haloalkenes, including TCE, have been examined in communications[247–250] and monographs.[231,251–253]

Results of kinetic studies on the oxidation of TCE in both liquid and gas phases indicate a radical-chain oxidation mechanism. However, the mechanism of the oxidation of TCE has not hitherto been fully elucidated.

Certain quantitative characteristics of the liquid-phase AIBN-initiated oxidation of TCE have been established recently.[254,255] It has been shown that, in the presence of the above initiator, TCE is oxidised via a radical-chain mechanism, compounds with long chains ($n \gg 10$) without degenerate branching being obtained. The epoxide **155** and dichloroacetyl chloride **154** are formed simultaneously, their ratio remaining constant at ~3, i.e. the selectivity with respect to the epoxide is ~75%–80%.

Taking into account the literature data on the oxidation kinetics of alkenes[252,253] and haloalkenes,[250,251] Kucher et al.[255] proposed on the basis of the results obtained a mechanism for TCE oxidation in which, together with the radical pathway, a molecular pathway leading to the formation of the epoxide **155** is described. In the gas-phase oxidation of TCE, the main reaction product is also dichloroacetyl chloride.[256] Various modifications of the gas-phase oxidation reactions of TCE have been examined.[257]

Interesting data have been obtained for the joint oxidation of certain organic compounds with TCE. It was concluded[258] that the co-oxidation of cyclohexane with TCE, which gives rise to very reactive peroxyl radicals, can serve as an effective method for the regulation of both the rate and selectivity of the oxidation of cyclohexane to alcohol, a ketone, and adipic acid. The co-oxidation of cyclohexane with TCE at 75 °C has been investigated[259] and it has been shown that cyclohexanol and cyclohexanone are formed simultaneously in the chain termination reaction. It was established that, when the TCE concentration is varied from zero to 50 vol.% in a mixture with cyclohexane, the cyclohexanol : cyclohexanone ratio can be varied in the range from 1.75 to 3.3.

It has been established[260] that the presence of two chlorine atoms in the terminal $-CCl_2OO^{\cdot}$ fragment of the peroxyl radicals

leads to an appreciable increase in their electrophilicity and reactivity in the dehydrogenation of organic compounds. It has been shown that the reactivity of secondary C–H bonds in n-alkanes is independent of the length of the carbon skeleton of the molecule.

The co-oxidation of TCE with aromatic alkyl compounds [261] and oxygen-containing aliphatic compounds [262] has been recently investigated and it has also been shown that the reactions involved in hydrocarbon processing, which proceed via a radical mechanism, can be facilitated by their co-oxidation with TCE, which generates highly reactive peroxyl radicals.

The main product of the reaction of TCE with PCl_3 in the presence of oxygen is acetyl chloride **154** (yield 45%), while the phosphorus-containing compounds **156** and **157**, formed as a result of the rupture of the C = C bond of TCE, were found among the side products. [263]

$$CHCl{=}CCl_2 \xrightarrow{PCl_3 + O_2} CHCl_2COCl\ (\mathbf{154}) + Cl_2P(O)CHCl_2\ (\mathbf{156}) + Cl_2P(O)OCHCl_2\ (\mathbf{157})$$

2. The effect of ozone

On treatment with ozone, TCE undergoes oxidative cleavage. The main products of this reaction are phosgene, hydrogen chloride, and carbon oxides. [247,264,265] The kinetics of the ozonisation reaction in various media have been investigated. [266,267] Peroxyformic acid has been detected among the products of the gas-phase reaction of ozone with TCE. [268]

3. The effect of peroxide reagents

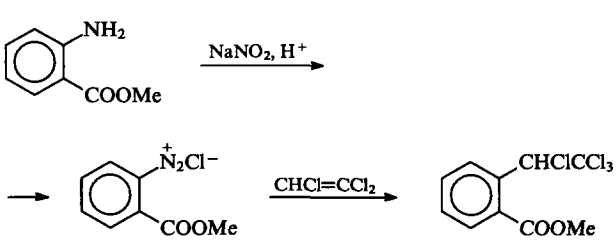
The main products of the reaction of TCE with peracetic acid are dichloroacetic acid and pentachloroethane. The optimum conditions for this reaction have been investigated and possible pathways leading to the formation of the main and side products have been proposed. [269]

The interaction of TCE with benzoyl peroxide leads to the formation of trichloroepoxyethane **155**, which readily isomerises to $CHCl_2COCl$ in the presence of catalysts (for example, Et_4NBr). [270]

VI. Other reactions

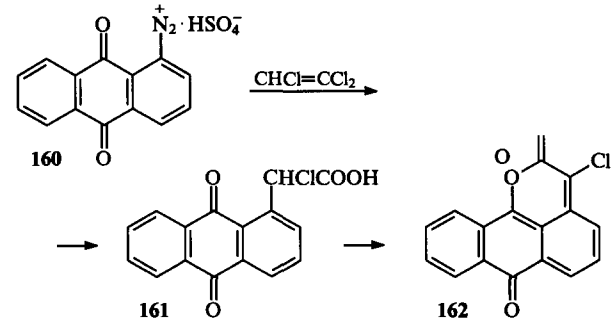
1. Reaction with diazonium compounds

The diazonium derivative of methyl anthranilate **158** reacts with TCE to form methyl *o*-(α,β,β,β-tetrachloroethyl)benzoate **159**. [271]



158 **159**

The reaction of anthraquinonediazonium sulfate **160** with TCE in acetic acid leads to the highly reactive 3-chloro-2*H*,7*H*-dibenzo[*de*,*h*]chromene-2,7-dione **162**, possibly as a result of cyclisation and dehydration of the anthraquinone-1-chloroacetic acid **161** formed initially. [272]



160 **161** **162**

2. The Bott reaction

Bott [273–275] showed that compounds of the adamantane and norbornane series, which form stable carbonium ions in sulfuric acid, react with TCE, affording substituted chloroacetic acids **163**.

$$R^+ + CHCl{=}CCl_2 \xrightarrow{H_2SO_4} RCHCl{-}\overset{+}{C}(Cl)Cl \xrightarrow{\text{solvolysis}} RCHClCOOH\ (\mathbf{163})$$

The syntheses of numerous adamantylchloroacetic acids in preparative yields have been achieved in this way. When the acids formed contain a hydrogen atom at the bridgehead carbon atom of the bridged system, new carbonium ions arise, which results in the appearance of dibasic adamantane-1,3-bis(chloroacetic) acids among the reaction products.

The reaction of norbornene with TCE leads to 2-*exo*-norbornylchloroacetic acid in 66% yield. [273] Numerous substituted benzyl alcohols and their ethers **164**, which give rise to stable benzyl cations in sulfuric acid at temperatures above 80 °C, react with TCE, affording derivatives of α-chlorohydrocinnamic acids **165** in 30%–85% yield. [274,275]

$$RC_6H_4CH_2OR'\ (\mathbf{164}) + CHCl{=}CCl_2 \xrightarrow{H_2SO_4,\ 85-95\ ^\circ C} RC_6H_4CH_2CHClCOOH\ (\mathbf{165})$$

R = *p*-O_2N, *m*-O_2N, *p*-HOOC, *m*-HOOC, *p*-$MeSO_2$, *p*-$PhSO_2$, *p*-Bz; R′ = H or Ac.

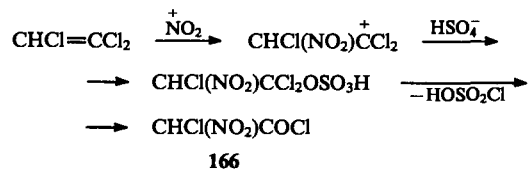
The substituted 1,1,2-trichloroalkenes $RC_6H_4CH_2CCl{=}CCl_2$ are side products in this reaction.

The Bott reaction has undergone further development recently. Thus the interaction of hydroxyadamantanes with TCE in concentrated H_2SO_4 leads to a mixture of the corresponding diadamantylchloroacetic and diadamantanebis(chloroacetic) acids. [276] A method has been proposed for the synthesis of various derivatives of diamantane-4,9-bis(chloroacetic) acid. [277]

We may note, however, that, in the interaction of diamantane-3-spiro-3′-diazirine with TCE under the conditions of the Bott reaction, the corresponding acids are formed in only trace amounts, while the principal products are diamantane, diamantanone, 3-chlorodiamantane, and 1-chlorodiamantane. [278]

3. Reaction with nitric acid and its oxides

The interaction of nitric acid and its oxides with TCE proceeds in a complex manner. The main product of the reaction of TCE with the $HNO_3 + H_2SO_4$ nitrating mixture is the chloride of chloronitroacetic acid **166**, obtained in 80%–85% yield. [279] The acid chloride **166** is apparently formed as a result of the initial addition of the nitronium cation to the double bond of TCE and the subsequent reactions of the carbonium ion. [280]



166

Dichloroacetyl chloride, pentachloroethane, and nitryl chloride were found among the side products of this reaction. The influence of the composition and amount of the nitrating mixture on the nitration process has been investigated.[281]

The interaction of TCE with nitrogen monoxide involves nitration, nitrosation, oxidative degradation, and chlorination reactions, which lead to the formation of 1,1,1,2-tetrachloro-2-nitroethane **167**, dichloroacetic acid **168**, pentachloroethane **1**, 1,1,3,3,4-pentachloro-4-nitrobut-1-ene, and also carbon dioxide and monoxide. The same set of products has been obtained also in the reaction of N_2O_3 with TCE.

In the dark and at a temperature above 100 °C, nitrosyl chloride behaves only as a chlorinating agent. In the reaction of TCE with nitrosyl chloride in sunlight at room temperature, pentachloroethane **1**, 1,1,1,2-tetrachloro-2-nitrosoethane, the nitroalkane **167**, the acid **168**, and a pentachloronitrobutene, whose structure has not been established, were obtained. Consequently, under conditions promoting the formation of free radicals, nitrosyl chloride exhibits nitrosating, nitrating, and oxidising activities.[283]

VII. The practical use of trichloroethylene and its derivatives

By virtue of its high reactivity, incombustibility, and inappreciable toxicity, TCE is an excellent solvent and is used widely in the national economy.[1] In addition, it is used in medicine as a powerful narcotic.[284,285] According to patent data,[286,287] the addition of TCE improves the properties of insecticidal preparations. One of the ways of eliminating hexachloroethane from hexachlorobutadiene is based on the fractional distillation of the mixture in the presence of TCE.[288] The use of this compound as a solvent in the pentafluorobenzylation of organic acids appreciably increases the yield of benzyl esters.[289] In the synthesis of *m*-chloroperbenzoic acid, TCE has also been recognised as the best inert solvent.[290] A new reaction involving the thermal heterocyclisation of arylchlorosilanes in the gas phase, which proceeds in the presence of TCE (and certain other halo-derivatives), has been discovered.[291] Thus the pyrolysis of dichlorodiphenylsilane in a mixture with TCE (1 : 1 ratio) leads to 9,9-dichloro-9-silafluorene (yield 35%).[292,293]

The chemical properties and in particular the poly-functionality of TCE have led to extensive possibilities for its employment in organic synthesis (see the present review) and in chemical engineering[294] as a most valuable intermediate. Industrial methods of synthesis of monochloroacetic acid, which is an intermediate in the synthesis of dyes and pesticidal and medicinal preparations, have been developed on the basis of TCE.[295] The chloride of dichloroacetic acid, formed in the oxidation of TCE, is the main intermediate in the synthesis of the antibiotic levomycetin.[295]

Further examples of the practical use of other TCE derivatives have now been discovered. Thus it has been suggested that 1,2-dibromo-1,1,2-trichloroethane be used as an anaesthetic.[18] The product of the interaction of TCE with HF—1,1,1,2-tetra-fluoroethane—is a potential blood substitute.[31] According to patent data,[296,297] the steroids synthesised with participation of TCE, containing the chloroethynyl group in the C(17) position, possess a broad spectrum of physiological activity. Other TCE derivatives are physiologically active as well, such as—chlorine-containing amines,[73] 2-bromo-2-chloro-1,1,1-trifluoro-ethane,[298] and substituted vinylthioacetamidooxacephalo-sporins.[299]

Many of the compounds obtained with participation of TCE have been proposed as pesticides. Derivatives of urea[190,300,301] and chlorine-containing aromatic compounds[77] exhibit a herbicidal activity. 4-(Diphenylacryloyl)morpholines are used as fungicides[302] and 4-chlorobenzyl 2,2-dichlorovinyl sulfide is a nematocide.[303] Insecticidal activity has been discovered in chloronorbornenes. Trichloronitroethylene,[228] bis(dichlorovinyl) sulfide,[304,305] bis(dichlorovinyl) disulfide,[306] and 1,1-dichloro-4-methylpenta-1,3-diene, which is a product of the condensation of TCE with isobutene (it is used in the synthesis of pyrethroids[56–58]), have a broad spectrum of activity.

Fireproofing agents[307] and flame extinguishers[308] as well as regulators of molecular mass in the manufacture of silicone rubbers and oils[116] have been found among TCE derivatives. The polylactones obtained from TCE and paraformaldehyde are used in the manufacture of insulating materials and detergents.[309]

* * *

The claim that TCE is a relatively unreactive compound can still be encountered in the literature. For example, in a recently published monograph[310] it is noted that TCE does not enter into nucleophilic substitution reactions. However, our analysis demonstrated the extensive synthetic possibilities of TCE, including their use in processes involving the formal nucleophilic substitution of chlorine atoms. Convenient methods of synthesis of polyfunctional compounds of different classes have been developed on the basis of TCE, substances with useful properties, which were previously difficult to obtain, have been synthesised, and new nontrivial features of certain chemical processes have been discovered.

References

1. *Promyshlennye Khlororganicheskie Produkty (Spravochnik)* [(Industrial Chlororganic Products) (Handbook)] (Ed. L A Oshin) (Moscow: Khimiya, 1978)
2. E H Huntress *The Preparation, Properties, Chemical Behavior, and Identification of Organic Chlorine Compounds* (New York: Wiley; London: Chapman and Hall, 1948)
3. *Methoden der Organischen Chemie (Houben–Weyl)* Vol. V/3 (Stuttgart: Georg Thieme, 1962)
4. *Metody Elementoorganicheskoi Khimii. Khlor. Alifaticheskie Soedineniya* (Methods of Organoelement Chemistry. Chlorine. Aliphatic Compounds) (Eds A N Nesmeyanov, K A Kocheshkov) (Moscow: Nauka, 1973)
5. A N Mirskova, G N Drozdova, G G Levkovskaya, M G Voronkov *Usp. Khim.* **58** 417 (1989) [*Russ. Chem. Rev.* **58** 250 (1989)]
6. N N Labeish, A A Petrov *Usp. Khim.* **58** 1844 (1989) [*Russ. Chem. Rev.* **58** 1048 (1989)]
7. M G Voronkov, A V Martynov, A N Mirskova *Sulfur Rep.* **6** 77 (1986)
8. T Manek, H K Wankhade, D V Parvate, A N Garg *Radiochem. Radioanal. Lett.* **58** 373 (1983)
9. R Atkinson, S M Aschmann *Int. J. Chem. Kinet.* **19** 1097 (1987)
10. French P. 2 057 604; *Chem. Abstr.* **76** 58 943 (1972)
11. M L Poutsma, R L Hinman *J. Am. Chem. Soc.* **86** 3807 (1964)
12. N B Mel'nikova, E N Krom, V R Kartashov, L A Ternovskii *Izv. Vyssh. Uchebn. Zaved., Khim. Khim. Tekhnol.* **24** 810 (1981)
13. Jpn. Appl. 79-122 206; *Chem. Abstr.* **92** 93 880 (1980)
14. K W Field, P Kovacic *J. Org. Chem.* **36** 3566 (1971)
15. I V Vigalok, A V Ostrovskaya *Zh. Obshch. Khim.* **41** 1410 (1971)
16. V N Paraskevov, I V Pimenov, Yu G Treger, G S Dasaeva *Kinet. Katal.* **24** 1007 (1983)
17. G A Sidakova, A S Kyazimov *Sopryazhennoe Galogenirovanie Olefinov i Ikh Proizvodnykh s Kislorodsoderzhashchimi Soedineniyami* (Coupled Halogenation of Olefins and Their Derivatives with Oxygen-Containing Compounds) (Baku: AzINNEFTEKhIM, 1973)
18. US P. 3 637 874; *Chem. Abstr.* **76** 85 375 (1972)
19. Eur. Appl. 219 823; *Chem. Abstr.* **107** 58 492 (1987)
20. L Conte, G P Gambaretto, M Napoli, C Gervasutti *J. Fluorine Chem.* **38** 319 (1988)

21. L Marangoni, G Rasia, C Gervasutti, L Colombo *Chim. Ind.* **64** 135 (1982)
22. Jpn. Appl. 60-12910; *Chem. Abstr.* **104** 5 561 (1986)
23. G P Gambaretto, M Napoli *J. Fluorine Chem.* 7 569 (1976)
24. L S Boguslavskaya, N N Chuvatkin, I Yu Panteleeva *Zh. Org. Khim.* **18** 2082 (1982)
25. B V Kunshenko, Nagib Mukhtar Mokhamed, V O Omarov, N N Muratov, L M Yagupol'skii *Zh. Org. Khim.* **28** 672 (1992)
26. Fr. Appl. 2 647 439; *Ref. Zh. Khim.* 18 N 17P (1991)
27. M S Kharasch, J A Norton, F R J Mayo *J. Org. Chem.* **3** 48 (1938)
28. BRD Appl. 2 108 951; *Chem. Abstr.* **77** 139 405 (1972)
29. Jpn. Appl. 73-72105; *Chem. Abstr.* **80** 59 424 (1974)
30. Jpn. Appl. 81-33039; *Chem. Abstr.* **95** 97 010 (1981)
31. Eur. Appl. 295 885; *Chem. Abstr.* **110** 195 124 (1989)
32. A E Feiring *J. Fluorine Chem.* **14** 7 (1979)
33. US P. 4 258 225; *Chem. Abstr.* **95** 6 482 (1981)
34. BRD Appl. 2 719 021; *Chem. Abstr.* **90** 54 453 (1979)
35. BRD Appl. 2 739 621; *Chem. Abstr.* **90** 203 466 (1979)
36. BRD Appl. 2 737 950; *Chem. Abstr.* **90** 168 040 (1979)
37. US P. 4 374 289; *Chem. Abstr.* **98** 197 593 (1983)
38. US P. 4 766 259; *Chem. Abstr.* **110** 97 549 (1989)
39. N S Zefirov, A S Koz'min, V D Sorokin *J. Org. Chem.* **49** 4086 (1984)
40. N S Zefirov, A S Koz'min, V D Sorokin, V V Zhdankin *Zh. Org. Khim.* **22** 898 (1986)
41. A V Fokin, Yu N Studnev, A I Rapkin, I N Krotovich *Izv. Akad. Nauk SSSR, Ser. Khim.* 2374 (1981)
42. L F R Cafferata, J E Sicre *Inorg. Chem.* **13** 242 (1974)
43. Dutch Appl. 76-00091; *Chem. Abstr.* **86** 16 278 (1977)
44. Hungarian Appl. 3 282; *Chem. Abstr.* **76** 112 689 (1972)
45. R G Guy, I Pearson *Bull. Chem. Soc. Jpn.* **50** 541 (1977)
46. R G Guy, I Pearson *Bull. Chem. Soc. Jpn.* **49** 2310 (1976)
47. W A Kamil, F Haspel-Hentrich, J M Shreeve *Inorg. Chem.* **25** 376 (1986)
48. L Schmerling, J P West *J. Am. Chem. Soc.* **71** 2015 (1949)
49. US P. 3 799 997; *Chem. Abstr.* **80** 132 771 (1974)
50. US P. 3 810 947; *Chem. Abstr.* **81** 25 323 (1974)
51. L Schmerling *J. Org. Chem.* **40** 2430 (1975)
52. US P. 4 005 152; *Chem. Abstr.* **87** 39 007 (1977)
53. US P. 3 998 895; *Chem. Abstr.* **86** 106 155 (1977)
54. BRD Appl. 2 629 868; *Chem. Abstr.* **86** 155 188 (1977)
55. Br. P. 1 532 676; *Chem. Abstr.* **90** 186 329 (1979)
56. Br. P. 1 546 804; *Ref. Zh. Khim.* 23 O 433 (1979)
57. Hung. P. 182 860; *Ref. Zh. Khim.* 4 N 9 (1987)
58. W Hewertson, D Holland, D L Milner *J. Chem. Soc., Perkin Trans. 2* 1062 (1978)
59. D P Johari, H W Sidebottom, J M Tedder, J C Walton *J. Chem. Soc., B* 95 (1971)
60. A Horowitz, G Baruch *Int. J. Chem. Kinet.* **12** 883 (1980)
61. F F Rust, Ch S Bell *J. Am. Chem. Soc.* **92** 5530 (1970)
62. R V Kereselidze, V G Tsitsishvili, E D Lubuzh, D B Razmadze *Izv. Akad. Nauk Gruz. SSR, Ser. Khim.* **16** 152 (1990)
63. G I Nikishin, R V Kereselidze, D B Razmadze, E D Lubuzh, A A Dzamukashvili *Soobshch. Akad. Nauk Gruz. SSR* **134** 325 (1989)
64. F K Velichko, V Ts Kampel', V I Dostovalova, V L Antonovich, V I Bregadze *Metalloorg. Khim.* **4** 39 (1991)
65. S V Komarova, D E Kruglov, E V Pastushenko, in *V Vsesoyuz. Nauch. Konf. "Sovremennoe Sostoyanie i Perspektivy Razvitiya Teoreticheskikh Osnov Proizvodstva Khlororganicheskikh Produktov", Baku, 1991 (Tez. Dokl.)* [The Vth All-Union Scientific Conference "The Current State and Prospects for the Development of the Theoretical Principles of the Production of Organochlorine Derivatives, Baku, 1991 (Abstracts of Reports)] p. 122
66. J-M Chang, R Profetto, J Warkentin *J. Am. Chem. Soc.* **103** 7189 (1981)
67. M I Dyusenov, G I Nikishin, B T Dzhetpisov, in *3 Respublikanskaya Nauch.-Tekhn. Konf. po Neftekhimii Akad. Nauk Kaz. SSR, Gur'ev, 1974 (Tez. Dokl.) T. 1* [The Third All Republic Scientific and Technical Conference on Petrochemistry of the Acad. Sci. Kaz. SSR, Gur'ev, 1974 (Abstracts of Reports) Vol. 1] p. 308
68. Jpn. Appl. 53-21111; *Ref. Zh. Khim.* 4 N 28P (1979)
69. USSR P. 694 486; *Byull. Izobret.* **40** 86 (1979)
70. USSR P. 636 222; *Byull. Izobret.* **45** 79 (1978)
71. Jpn. Appl. 58-140 042; *Ref. Zh. Khim.* 4 N 12P (1985)
72. G I Nikishin, Yu N Ogibin, V N Lebedev *Izv. Akad. Nauk SSSR, Ser. Khim.* 1066 (1971)
73. USSR P. 810 670; *Ref. Zh. Khim.* 4 O 336P (1982)
74. USSR P. 515 732; *Ref. Zh. Khim.* 7 O 339P (1977)
75. M M Guseinov, T A Kambarova, Z K Mekhtieva, Z G Yartseva *Dokl. Akad. Nauk Az. SSR* **22**(8) 38 (1966)
76. M M Guseinov, T A Kambarova, Z K Mekhtieva, M T Dzhafarova *Dokl. Akad. Nauk Az. SSR* **25**(8) 37 (1969)
77. US P. 3 957 891; *Chem. Abstr.* **85** 77 845 (1977)
78. BRD Appl. 2 425 991; *Chem. Abstr.* **84** 121 402 (1976)
79. M Ballester, J Castaner *An. R. Soc. Esp. Fis. Quim.* **66** 487 (1970); *Ref. Zh. Khim.* 23 Zh 70 (1972)
80. BRD Appl. 2 333 650; *Chem. Abstr.* **83** 43 004 (1975)
81. US P. 4 139 721; *Chem. Abstr.* **90** 168 275 (1979)
82. D R Adams, S P Bhatnagar *Synthesis* 661 (1977)
83. BRD Appl. 2 057 057; *Chem. Abstr.* **77** 87 853 (1972)
84. Pol. P. 131 012; *Chem. Abstr.* **110** 192 251 (1989)
85. Fr. P. 2 559 479; *Chem. Abstr.* **104** 206 723 (1986)
86. S J Cristol, B B Jarvis *J. Am. Chem. Soc.* **88** 3095 (1966)
87. DDR P. 93 552; *Ref. Zh. Khim.* 13 O 34P (1975)
88. A N Mirskova, A V Martynov, M G Voronkov *Zh. Org. Khim.* **16** 2076 (1980)
89. USSR P. 690 013; *Byull. Izobret.* **37** 89 (1979)
90. A N Mirskova, A V Martynov, M G Voronkov *Zh. Org. Khim.* **18** 1555 (1982)
91. A V Martynov, A N Mirskova, M G Voronkov *Zh. Org. Khim.* **20** 23 (1984)
92. USSR P. 899 543; *Byull. Izobret.* **3** 98 (1989)
93. A N Mirskova, G G Levkovskaya, T I Drozdova, I D Kalikhman, M G Voronkov *Zh. Org. Khim.* **18** 452 (1982)
94. T I Drozdova, A N Mirskova, G G Levkovskaya, I D Kalikhman, M G Voronkov *Zh. Org. Khim.* **24** 1240 (1988)
95. A N Mirskova, I T Gogoberidze, G G Levkovskaya, M G Voronkov *Zh. Org. Khim.* **20** 2235 (1984)
96. A N Mirskova, G G Levkovskaya, M G Voronkov *Zh. Org. Khim.* **23** 1119 (1987)
97. Ya T Bal'on, V E Paranyuk *Zh. Org. Khim.* **19** 1346 (1983)
98. A N Mirskova, G G Levkovskaya, I T Gogoberidze, T I Drozdova, I D Kalikhman, M G Voronkov *Zh. Org. Khim.* **19** 1110 (1983)
99. M B Taraban, V I Mar'yasova, T V Leshina, A N Mirskova, G G Levkovskaya, T I Drozdova, I T Gogoberidze, M G Voronkov *Zh. Org. Khim.* **22** 925 (1986)
100. A N Mirskova, G G Levkovskaya, I T Gogoberidze, I D Kalikhman, M G Voronkov *Zh. Org. Khim.* **21** 269 (1985)
101. USSR P. 803 361; *Byull. Izobret.* **36** 259 (1987)
102. A N Mirskova, T I Drozdova, G G Levkovskaya, S A Guseva, I D Kalikhman, M G Voronkov *Zh. Org. Khim.* **23** 2184 (1987)
103. A N Mirskova, T I Drozdova, G G Levkovskaya, O B Bannikova, I D Kalikhman, M G Voronkov *Zh. Org. Khim.* **18** 1407 (1982)
104. A N Mirskova, G G Levkovskaya, A A Bryuzgin, T I Drozdova, I D Kalikhman, M G Voronkov *Zh. Org. Khim.* **26** 140 (1990)
105. A A Bryuzgin, G G Levkovskaya, A N Mirskova, I D Kalikhman *Zh. Org. Khim.* **26** 1296 (1990)
106. A N Mirskova, G G Levkovskaya, A A Bryuzgin, I D Kalikhman, M G Voronkov *Zh. Org. Khim.* **22** 2173 (1986)
107. T I Drozdova, A N Mirskova, G G Levkovskaya *Zh. Org. Khim.* **26** 1002 (1990)
108. A N Mirskova, T I Drozdova, G G Levkovskaya, E E Kuznetsova, G S Vavil'chenkova, T A Pushechkina, T I Malkova, S K Suslova, M G Voronkov *Khim.-Farm. Zh.* **16** 1479 (1982)
109. A N Mirskova, T I Drozdova, G G Levkovskaya, I D Kalikhman, M G Voronkov *Zh. Org. Khim.* **22** 763 (1986)
110. I T Gogoberidze, G G Levkovskaya, A N Mirskova, M G Voronkov *Zh. Org. Khim.* **20** 1100 (1984)
111. I T Gogoberidze, G G Levkovskaya, A N Mirskova, I D Kalikhman, O B Bannikov, M G Voronkov *Zh. Org. Khim.* **21** 633 (1985)
112. R Aloni, L A Raibenbach, A Horowitz *J. Organomet. Chem.* **171** 155 (1979)
113. R West, L C Quass *J. Organomet. Chem.* **18** 55 (1969)

114. V D Sheludyakov, V I Zhun', V G Lakhtin, V V Shcherbinin, E A Chernyshev *Zh. Obshch. Khim.* **53** 1192 (1983)
115. V D Sheludyakov, V G Lakhtin, V I Zhun', V V Shcherbinin, E E Chernyshev *Zh. Obshch. Khim.* **51** 1829 (1981)
116. Jpn. Appl. 76-19729; *Chem. Abstr.* **85** 108 761 (1976)
117. C Walling *Free Radicals in Solution* (Translated into Russian; Moscow: Izd. Inostr. Lit., 1960)
118. A Roedig, R Kloss *Chem. Ber.* **90** 2902 (1957)
119. W Miller, W H Stafford, W H Taylor, D Laever, A H McQuillan *J. Chem. Soc.* **4485** (1961)
120. E I Babkina *Zh. Obshch. Khim.* **44** 953 (1974)
121. W J Howard, R E Gilbert *J. Org. Chem.* **27** 2685 (1962)
122. Yu A Ol'dekop, R V Kaberdin, E E Buslovskaya *Zh. Org. Khim.* **17** 272 (1981)
123. R V Kaberdin, V I Potkin *Polikhlor-1,3-butadieny* (Polychlorobuta-1,3-dienes) (Minsk: Nauka i Tekhnika, 1991)
124. R V Kaberdin, V I Potkin, Yu A Ol'dekop *Izv. Akad. Nauk B. SSR, Ser. Khim. Nauk* 105 (1985)
125. V I Potkin, R V Kaberdin, E Yu Dubova, Yu A Ol'dekop *Zh. Org. Khim.* **26** 256 (1990)
126. Yu A Ol'dekop, R V Kaberdin *Zh. Org. Khim.* **12** 2039 (1976)
127. Yu A Ol'dekop, R V Kaberdin, E E Buslovskaya, I A Shingel' *Zh. Org. Khim.* **15** 691 (1979)
128. R V Kaberdin, V I Potkin, Yu A Ol'dekop *Zh. Org. Khim.* **26** 1560 (1990)
129. V I Potkin, R V Kaberdin, Yu A Ol'dekop *Zh. Org. Khim.* **27** 56 (1991)
130. R V Kaberdin, V I Potkin, E Yu Dubova, Yu A Ol'dekop *Zh. Org. Khim.* **24** 1618 (1988)
131. V I Potkin, R V Kaberdin, Yu A Ol'dekop *Zh. Org. Khim.* **22** 1389 (1986)
132. V I Potkin, R V Kaberdin *Zh. Org. Khim.* **29** 56 (1993)
133. V I Potkin, R V Kaberdin, Yu A Ol'dekop *Izv. Akad. Nauk B. SSR, Ser. Khim. Nauk* 57 (1992)
134. French Appl. 2 092 817; *Chem. Abstr.*, **77** 113 785 (1972)
135. USSR P. 626 090; *Byull. Izobret.* **36** 101 (1978)
136. V I Perevalova, E N Deryagina, M G Voronkov *Zh. Org. Khim.* **14** 1557 (1978)
137. F Kaufler *Annalen* **433** 48 (1923)
138. A E Kulikova, N M Pinchuk, E N Zil'berman *Zh. Org. Khim.* **3** 1388 (1967)
139. A E Kulikova, N M Pinchuk, A Ya Lazaris *Zh. Org. Khim.* **9** 861 (1973)
140. M Carrega *Bull. Soc. Chim. Fr.* 4163 (1968)
141. W Weber, I Erden, A De Meijere *Angew. Chem.* **92** 387 (1980)
142. A De Meijere, I Erden, W Weber, D Kaufman *J. Org. Chem.* **53** 152 (1988)
143. O Abou-Teim, M C Goodland, J F W McOmie *J. Chem. Soc., Perkin Trans. 1* 2659 (1983)
144. D N Harp, C Heitner *J. Org. Chem.* **38** 4184 (1973)
145. N P Hacker, J F W McOmie *Tetrahedron* **40** 5249 (1984)
146. Park Seung Ki, Shim Sang Chul *Bull. Korean Chem. Soc.* **8** 27 (1987)
147. H K Al-Ekabi, G A W Derwisch, G Adam, K Schreiber *Tetrahedron* **37** 1741 (1981)
148. T Shimo, K Somekawa, Y Wakikawa, H Uemura, O Tsuge, K Imada, K Natabe *Bull. Chem. Soc. Jpn.* **60** 621 (1987)
149. K Somekawa, R Imai, R Furukido, S Kumamoto *Bull. Chem. Soc. Jpn.* **54** 1112 (1981)
150. S Kumamoto, K Somekawa, H Uemura, T Shimo *Kenkyu Hokoku-Asahi Garasa Kogyo Gijutsu Shoreikai* **41** 185 (1982); *Chem. Abstr.* **99** 139 892 (1983)
151. D Bellus, H Fischer, H Greuter, P Martin *Helv. Chim. Acta* **61** 1784 (1978)
152. M Ballester, J Castaner, J Riera, I Tabernoro *J. Org. Chem.* **51** 1413 (1986)
153. G Nagendrappa *Org. Synth.* **53** 173 (1973)
154. Europ. Appl. 283 719; *Chem. Abstr.* **110** 115 542 (1989)
155. E Lewars, S Siddiqi *J. Org. Chem.* **50** 135 (1985)
156. T Miettinen *Acta Chem. Scand., Ser. B* **32** 359 (1978)
157. S W Tobey, R West *J. Am. Chem. Soc.* **88** 2478 (1966)
158. J Sepiol, R L Soulen *J. Org. Chem.* **40** 3791 (1975)
159. W Weber, A Meijere *Chem. Ber.* **118** 2450 (1985)
160. D Seyferth, C K Haas, D Dagani *J. Organomet. Chem.* **104** 9 (1976)
161. E V Dehmlow *Tetrahedron Lett.* **17** 91 (1976)
162. S K Choi, W K Suk *Bull. Korean Chem. Soc.* **2** 83 (1981)
163. C Glueck, V Poignee, H Schwager *Synthesis* 260 (1987)
164. J S Cloves, W Fliege, R Huisgen *Chem. Ber.* **116** 3062 (1983)
165. E Ott *Berichte* **75** 1517 (1942)
166. J H Wotiz, F Huba, R Vendley *J. Org. Chem.* **26** 1626 (1961)
167. R Reimschneider, K Brendel *Liebigs Ann. Chem.* **640** 1 (1961)
168. J Siegel, R A Jones, L Kurlansik *J. Org. Chem.* **35** 3199 (1970)
169. E Kloster-Jensen *Tetrahedron* **27** 33 (1971)
170. A S Kende, P Fludzinski *Synthesis* 455 (1982)
171. A Jonczyk, A Kwast, M Makosza *J. Org. Chem.* **44** 1192 (1979)
172. J Pielichowski, R Popielarz *Synthesis* 433 (1984)
173. J N Denis, A Moyano, A E Greene *J. Org. Chem.* **52** 3461 (1987)
174. A Sudbo, P A Schulz, E R Grant, Y R Shen, Y T Lee *J. Chem. Phys.* **68** 1306 (1978)
175. C Reiser, E M Lussier, C C Jensen, J I Steinfeld *J. Am. Chem. Soc.* **101** 350 (1979)
176. K Walzer, M Tacke *J. Chem. Phys.* **73** 3045 (1980)
177. US P. 4 165 269; *Chem. Abstr.* **91** 147 811 (1979)
178. K Y Choo, T J Kang, Q Won Choi *Chem. Phys. Lett.* **102** 321 (1983)
179. P Kubat, J Pola *Z. Phys. Chem.* **268** 849 (1987)
180. A E Laird, J K Tyler *J. Chem. Soc., Chem. Commun.* 335 (1978)
181. J S Uppal, R H Staley *J. Am. Chem. Soc.* **102** 4144 (1980)
182. J F Caballero, C Wittig *J. Chem. Phys.* **78** 7169 (1983)
183. A Oku, K Kimura *Chem. Express* **5** 181 (1990)
184. W E Truce, M M Boudakian *J. Am. Chem. Soc.* **78** 2748 (1956)
185. W E Truce, M M Boudakian, R F Heine, R J McManimie *J. Am. Chem. Soc.* **78** 2743 (1956)
186. A Loffler, G Himbert *Synthesis* 495 (1992)
187. Polish P. 96 979; *Chem. Abstr.* **90** 86 709 (1979)
188. J Normant *Bull. Soc. Chim. Fr.* 1876 (1963)
189. S Tanimoto, R Taniyasu, T Takahashi, T Miyake, M Okano *Bull. Chem. Soc. Jpn.* **49** 1931 (1976)
190. US P. 3 937 726; *Chem. Abstr.* **85** 192 415 (1976)
191. J Pielichowski, D Bogdal *Pol. J. Chem.* **62** 483 (1988)
192. W C Kurula *J. Org. Chem.* **30** 3926 (1965)
193. W C Kurula, D G Leis *J. Org. Chem.* **29** 2773 (1964)
194. M A Kesselmayer, P S Sheridan *J. Am. Chem. Soc.* **109** 5029 (1987)
195. A Moyano, F Charbonnier, A Greene *J. Org. Chem.* **52** 2919 (1987)
196. C Almansa, A Moyano, M A Pericas, F Serratosa *Synthesis* 707 (1988)
197. US P. 4 405 514; *Chem. Abstr.* **99** 196 905 (1983)
198. W E Truce, R Kassinger *J. Am. Chem. Soc.* **80** 1916 (1958)
199. M Tiecco, L Testaferri, M Tingoli, D Chianelli, M Montanucci *J. Org. Chem.* **48** 4795 (1983)
200. R Van der Heiden, L Brandsma *Synthesis* 76 (1987)
201. S Y Delavarenne, H G Viehe *Chem. Ber.* **103** 1209 (1970)
202. J Ficini *Tetrahedron* **32** 1 (1976)
203. L Rene, Z Janousek, H G Viehe *Synthesis* 645 (1983)
204. J Pielichowski, D Bogdal *Bull. Pol. Acad. Sci., Chem.* **37** 123 (1989)
205. J Pielichowski, D Bogdal *Liebigs Ann. Chem.* 595 (1988)
206. J Pielichowski, R Popielarz *Tetrahedron* **40** 2671 (1984)
207. J Pielichowski, R Popielarz *Stud. Org. Chem. (Amsterdam)* **18** 225 (1984)
208. J Pielichowski, D Bogdal *Bull. Soc. Chim. Belg.* **100** 561 (1991)
209. M Inoue, S Enomoto *Chem. Lett.* 1231 (1978)
210. M Inoue, S Enomoto *Bull. Chem. Soc. Jpn.* **55** 33 (1982)
211. Jpn. Appl. 82-95952; *Chem. Abstr.* **97** 162 405 (1982)
212. A Collet, J Jacques *Synthesis* 38 (1972)
213. V Ratovelomanana, G Linstrumelle, J F Normant *Tetrahedron Lett.* **26** 2575 (1985)
214. A Minato, K Suzuki, K Tamao *J. Am. Chem. Soc.* **109** 1257 (1987)
215. G Kobrich, K Flory *Chem. Ber.* **99** 1773 (1966)
216. A S Kende, M Benechie, D P Curran, P Fludzinski, W Swenson, J Clardy *Tetrahedron Lett.* **20** 4513 (1979)
217. A S Kende, P Fludzinski *Tetrahedron Lett.* **23** 2369 (1982)
218. A S Kende, P Fludzinski, J H Hill, W Swenson, J Clardy *J. Am. Chem. Soc.* **106** 3551 (1984)
219. A V Martynov, N A Mirskova, M G Voronkov *Zh. Org. Khim.* **21** 2467 (1985)
220. A V Martynov, A N Mirskova, I D Kalikhman, M D Voronkov *Zh. Org. Khim.* **24** 509 (1988)
221. A V Martynov, A N Mirskova, M G Voronkov *Zh. Org. Khim.* **25** 1773 (1989)
222. BRD Appl. 3 111 152; *Chem. Abstr.* **98** 126 378 (1983)

223. Rom. P. 58 033; *Chem. Abstr.* **85** 123 353 (1976)
224. Eur. Appl. 4 496; *Chem. Abstr.* **92** 58 239 (1980)
225. Fr. Appl. 2 420 521 (1980); *Izobret. za Rubezhom* **7** 48 (1980)
226. V Sarca, A Magyari, A Buzasiu, V Szebeni, M Paska *Rev. Chim.* **36** 862 (1985)
227. US P. 3 054 828; *Chem. Abstr.* **58** 3 315 (1963)
228. Jpn. P. 14 002; *Ref. Zh. Khim.* 4 N 599P (1967)
229. French P. 2 094 444; *Ref. Zh. Khim.* 8 N 504P (1973)
230. E Erdman *J. Prakt. Chem.* **85** 78 (1911)
231. V V Saraeva *Okislenie Organicheskikh Soedinenii pod Deistviem Ioniziruyushchikh Izluchenii* (Oxidation of Organic Compounds by the Action of Ionising Radiation) (Moscow: Izd. Mosk. Univ., 1991)
232. Pol. P. 106 693; *Chem. Abstr.* **95** 6 527 (1981)
233. BRD Appl. 2 533 181; *Chem. Abstr.* **84** 164 189 (1976)
234. Rom. P. 78 153; *Chem. Abstr.* **99** 121 837 (1983)
235. Rom. P. 75 601; *Chem. Abstr.* **99** 121 832 (1983)
236. Rom. P. 78 095; *Chem. Abstr.* **99** 121 836 (1983)
237. Rom. P. 77 963; *Chem. Abstr.* **99** 121 834 (1983)
238. Jpn. Appl. 59-48435; *Chem. Abstr.* **101** 9 093 (1984)
239. Jpn. Appl. 63-51352; *Chem. Abstr.* **109** 169 876 (1988)
240. US P. 3 959 367; *Chem. Abstr.* **85** 108 280 (1976)
241. Hung. Appl. 31 631; *Chem. Abstr.* **101** 229 996 (1984)
242. L L McKinney, E H Uhing, J L White *Agric. Food Chem.* **3** 413 (1955)
243. S A Kline, B L van Duuren *J. Heterocycl. Chem.* **14** 455 (1977)
244. V A Poluektov, I V Dobrov, A V Chertorizhskii, Yu Ya Mekhryushev *Khim. Promst. (Moscow)* 197 (1976)
245. I P Shevchuk, O I Makogon, T M Tomashevskii, in *6 Vsesoyuzn. Nauch. Konf. po Okisleniyu Organicheskikh Soedinenii v Zhidkoi Faze, L'vov, 1986 (Tez. Dokl.)* [The Sixth All-Union Scientific Conference on the Liquid-Phase Oxidation of Organic Compounds, Lvov, 1986 (Abstracts of Reports)] p. 27
246. V A Poluektov, Yu Ya Mekhryushev *Zh. Fiz. Khim.* **45** 2338 (1971)
247. E Sanhueza, I C Hisatsune, J Heicklen *Chem. Rev.* **76** 801 (1976)
248. A C Razus, A M Glatz, Zs Arvay, F Iordache, F Baded *Rev. Roum. Chim.* **25** 547 (1980)
249. A L Shevchenko, A Yu Ivanov, G M Ostrovskii, V S Levshanov, I V Dobrov *Zh. Prikl. Khim.* **53** 382 (1980)
250. V A Poluektov, A I Chernyavskii *Neftekhimiya* **18** 558 (1978)
251. V A Poluektov, I V Dobrov, Yu Ya Mekhryushev *Teoriya i Praktika Zhidkofaznogo Okisleniya* (Theory and Practice of Liquid-Phase Oxidation) (Moscow: Nauka, 1974)
252. R V Kucher, V I Timokhin, I P Shevchuk, Ya M Vasyutin *Zhidkofaznoe Okislenie Nepredel'nykh Soedinenii v Okisi Olefinov* (Liquid-Phase Oxidation of Unsaturated Compounds to Olefin Oxides) (Kiev: Naukova Dumka, 1986)
253. E A Blyumberg, T V Filippova, V G Dryuk *Kinetika i Kataliz T. 18 (Ser. Itogi Nauki i Tekhniki)* [Kinetics and Catalysis, Vol. 18 (Ser. Advances in Science and Engineering)] (Moscow: Izd. VINITI, 1988)
254. R V Kucher, R I Flyunt, V I Timokhin *Kinet. Katal.* **28** 979 (1987)
255. R V Kucher, R I Flyunt, Yu A Pazderskii, V I Timokhin, I P Shevchuk, O I Makogon, Ar A Berlin *Dokl. Akad. Nauk SSSR* **309** 875 (1989)
256. G Hyubrechts, L Meyers *Trans. Faraday Soc.* **62** 2191 (1966)
257. E Sanhueza, I C Hisatsune, J Heicklen *Adv. Environ. Sci. Technol.* **8** 155 (1977)
258. R V Kucher, V I Timokhin, N A Kravchuk, A P Pokutsa, R I Flyunt, D S Lutsyk *Neftekhimiya* **27** 661 (1987)
259. R V Kucher, V I Timokhin, A P Pokutsa, R I Flyunt *Neftekhimiya* **28** 701 (1988)
260. R V Kucher, V I Timokhin, R I Flyunt *Dokl. Akad. Nauk SSSR* **305** 134 (1989)
261. R I Flyunt, O I Makogon, in *2 Konf. Molodykh Uchenykh-Khimikov, In-t Fiz.-Org. Khimii i Uglekhimii AN USSR, Donetsk, 1990 (Tez. Dokl.)* [The Second Conference of Young Research Chemists, Inst. Phys.-Org. Chem. and Coal-Chem., Acad. Sci. Ukr. SSR, Donetsk, 1990 (Abstracts of Reports)] p. 196
262. O I Makogon, A P Pokutsa, in *Materialy Nauch. Konf. Molodykh Uchenykh Khim. Fakul'teta Uzhgorodskogo Universiteta, Uzhgorod, 1990* (Proceedings of the Scientific Conference of Young Scientists in the Faculty of Chemistry of Uzhgorod University, Uzhgorod, 1990), p. 18
263. C B C Boyce, S B Webb, L Phillips *J. Chem. Soc., Perkin Trans. 1* 1650 (1974)
264. E Mathias, E Sanhueza, I C Hisatsune, J Heicklen *Can. J. Chem.* **52** 3852 (1974)
265. L A Hull, I C Hisatsune, J Heicklen *Can. J. Chem.* **51** 1504 (1973)
266. B I Tarunin, Yu A Aleksandrov, V N Perepletchikova, N V Baklanov *Kinet. Katal.* **18** 1329 (1977)
267. W A Pryor, D Giamalva, D F Church *J. Am. Chem. Soc.* **105** 6858 (1983)
268. H Niki, P D Maker, C M Savage, L P Breitenbach, R I Martinez, J T Herron *J. Phys. Chem.* **86** 1858 (1982)
269. G M Shakhnazaryan *Arm. Khim. Zh.* **27** 111 (1974)
270. Polish P. 122 341; *Chem. Abstr.* **102** 184 732 (1985)
271. L M Yagupol'skii, V B Milevskaya, G I Matyushecheva *Zh. Org. Khim.* **11** 2580 (1975)
272. M V Gorelik, M V Kazankov, M I Bernadskii *Zh. Org. Khim.* **12** 2041 (1976)
273. K Bott *Angew. Chem.* **79** 943 (1967)
274. K Bott *Tetrahedron Lett.* **9** 4979 (1968)
275. K Bott *Chem. Ber.* **103** 3850 (1970)
276. L Vodička, J Burkhard, J Janku *Collect. Czech. Chem. Commun.* **51** 1086 (1986)
277. Czech. P. 240 246; *Chem. Abstr.* **109** 169 923 (1988)
278. L Vodichka, I Burkkhard, P Zakharzh, S D Isaev, S I Saichenko, A G Yurchenko, I Yanku *Zh. Org. Khim.* **21** 2569 (1985)
279. I V Martynov, Yu L Kruglyak, S P Makarov *Zh. Obshch. Khim.* **33** 3382 (1963)
280. Z G Ovsyannikova, M K Baranaev, V K Kurochkin, T A Vasilevskaya, I V Martynov, Yu L Kruglyak *Zh. Org. Khim.* **4** 1209 (1968)
281. V I Anufriev, I V Martynov *Zh. Prikl. Khim.* **63** 1889 (1990)
282. J Tuaillon, R Perrot *Helv. Chim. Acta* **59** 171 (1976)
283. Y Calvez, J Tuaillon, R Perrot *Helv. Chim. Acta* **57** 1433 (1974)
284. M D Mashkovskii *Lekarstvennye Sredstva. T. 1* (Medicines, Vol. 1) (Minsk, Belarus', 1987)
285. D L Hewer *Cah. Anesthesiol* **24** 163 (1976); *Chem. Abstr.* **85** 13 548 (1976)
286. Jpn. Appl. 76-48436; *Chem. Abstr.* **85** 88 539 (1976)
287. Jpn. Appl. 76-48439; *Chem. Abstr.* **85** 138 606 (1976)
288. Jpn. P. 48-42615; *Ref. Zh. Khim.* 16 N 50P (1974)
289. J M Rosenfeld, S Veroushalmi, E Y Osei-Twum *Anal. Chem.* **58** 3044 (1986)
290. Jpn. Appl. 211 565; *Ref. Zh. Khim.* 6 N 92P (1991)
291. E A Chernyshev, N G Komalenkova, L N Shamshin, I A Shashkov *Zh. Org. Khim.* **55** 2317 (1985)
292. USSR P. 571 486; *Byull. Izobret.* **33** 68 (1979)
293. USSR P. 649 720; *Byull. Izobret.* **8** 87 (1979)
294. W C McNeill, in *Kirk–Othmer Encyclopedia of Chemical Technology* Vol. 5 (Eds M Grayson, D Eckroth) (New York: Wiley, 1979) p. 745
295. *Kratkaya Khimicheskaya Entsiklopediya, T. 5* (A Short Chemical Encyclopedia, Vol. 5) (Ed. I L Knunyants) (Moscow: Sov. Entsiklopediya, 1967)
296. US P. 4 447 424; *Chem. Abstr.* **101** 130 975 (1984)
297. Can. P. 1 199 907; *Chem. Abstr.* **105** 79 225 (1986)
298. M-H Yang, H-E Wang, T-Y Ou, H-Ch Wu *K'o Hsuch Fa Chan Yueh K'an* **9** 251 (1981); *Chem. Abstr.* **95** 61 359 (1981)
299. Br. Appl. 2 121 825; *Chem. Abstr.* **101** 151 677 (1984)
300. G Hoerlein, H Schoenowsky, A Studeneer, P Langelueddeke *Z. Naturforsch., C* **28** 653 (1973)
301. US P. 4 013 452; *Chem. Abstr.* **87** 5 675 (1977)
302. Eur. P. 21 975; *Chem. Abstr.* **107** 134 314 (1987)
303. Jpn. P. 73-03368; *Chem. Abstr.* **80** 824 (1974)
304. Belg. P. 627 096; *Chem. Abstr.* **60** 11 899 (1964)
305. US P. 3 790 683; *Chem. Abstr.* **81** 46 373 (1974)
306. US P. 3 109 032; *Chem. Abstr.* **60** 2 769 (1964)
307. BRD Appl. 2 354 001; *Chem. Abstr.* **83** 98 494 (1975)
308. Jpn. P. 74-02108; *Chem. Abstr.* **81** 151 781 (1974)
309. Jpn. Appl. 62-72707; *Chem. Abstr.* **107** 237 573 (1987)
310. N Freemantle *Chemistry in Action, Part 2* (Translated into Russian; Moscow: Mir, 1991)

Russian Chemical Reviews **63** (8) 661 – 666 (1994)
©1994 Russian Academy of Sciences and Turpion Ltd

UDC 547.812.5

Organoelement derivatives of 2-pyrone and their applications in organic synthesis

V N Kalinin, O S Shilova

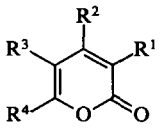
Contents

I. Introduction
II. The synthesis and properties of organoelement σ-derivatives of 2-pyrone
III. η^4-Iron tricarbonyl complexes of 2-pyrones

Abstract. The methods of synthesis and properties of organometallic (Li, Cu) and organoelement (Si, N, S) σ-derivatives and η^4-iron tricarbonyl complexes of 2-pyrone are considered. The Diels-Alder reactions of the organoelement derivatives of 2-pyrone with dienophiles take place stereoselectively and under mild conditions, which opens new pathways to the specific synthesis of polyfunctional cyclohexenes and cyclohexadienes. The bibliography includes 40 references.

I. Introduction

2-Pyrone systems **1** [1] form part of the composition of steroid,[2-4] nor- and dinor-diterpenoid[5-9] and many monocyclic[10] natural products with a broad spectrum of physiological activity.



1

Thus steroid bufadienolides exhibit cardiotonic and antineoblastic[3] properties while certain nor- and dinor-diterpenoid of 2-pyrones are insecticides[9] and cytotoxic agents.[5-7]

The use of 2-pyrones as dienes in Diels-Alder reactions with acetylenic[11,12] or olefinic dienophiles[13] gives rise to extensive possibilities for the stereoselective synthesis of cyclohexene and cyclohexadiene derivatives. Derivatives of 2-pyrone and the methods of their synthesis are therefore of great interest for organic chemists engaged in synthesis.

The chemistry of 2-pyrones has been reviewed,[1,14] but organoelement derivatives of 2-pyrones have been little studied. Two types of organoelement derivatives of 2-pyrones are known: Li, Cu, Si, N, S compounds with a σ-bond between the element and the carbon atom of the pyrone ring and η^4-iron tricarbonyl complexes of 2-pyrones.

The present review is an attempt at a systematic treatment of the available literature data on organoelement compounds of 2-pyrones, the methods of their synthesis, their reactivities, and the prospects for their use in organic synthesis.

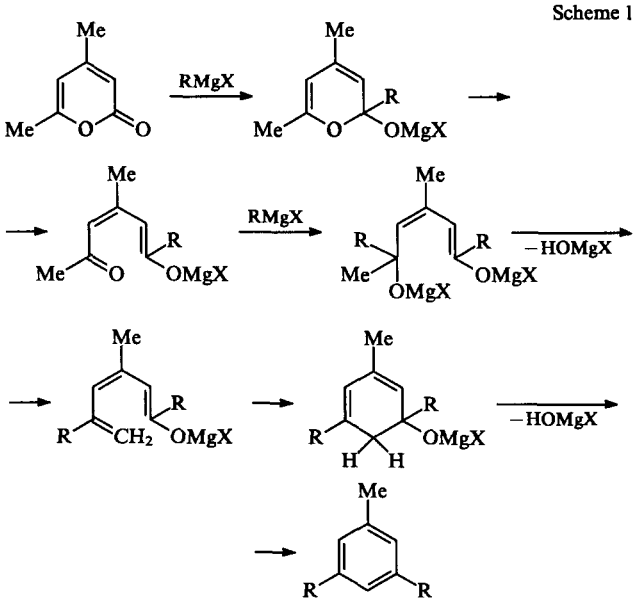
V N Kalinin, O S Shilova Laboratory of Fine Organic Synthesis, Nesmeyanov Institute of Organoelement Compounds, Russian Academy of Sciences, ul. Vavilova 28, 117813 Moscow, Russian Federation. Fax (7-095) 135 50 85, Tel. (7-095) 135 92 51

Received 22 February 1994
Uspekhi Khimii **63** (8) 693 – 699 (1994); translated by A K Grzybowski

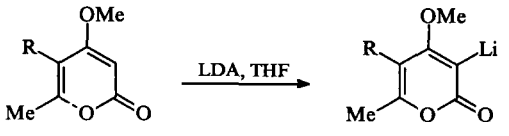
II. The synthesis and properties of organoelement σ-derivatives of 2-pyrone

The synthesis of organolithium derivatives of 2-pyrone is associated with certain difficulties since the pyrone ring is extremely sensitive to nucleophiles. The nucleophile attacks the carbonyl carbon atom of 2-pyrone,[15-19] which leads to the opening of the pyrone ring and its recyclisation to a ring of a nonpyrone type, for example a benzene ring (Scheme 1).[16]

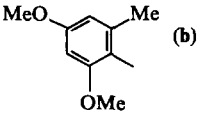
Scheme 1



However, it has been found that lithium can be substituted in the 3-position of 4-methoxy-2-pyrones **2** under mild conditions on treatment with lithium diisopropylamide (LDA) with formation of organolithium derivatives **3**.[17]



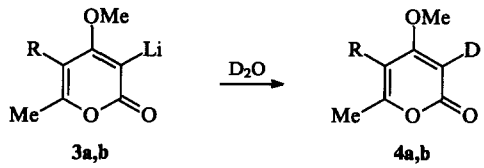
2a,b **3a,b**

R = H (**a**),  (**b**)

The authors suggest that the simultaneous presence of 4-methoxy- and 2-oxo-groups in compounds **2** can influence both the mode of the lithium substitution reaction and the stability of the carbanion formed.

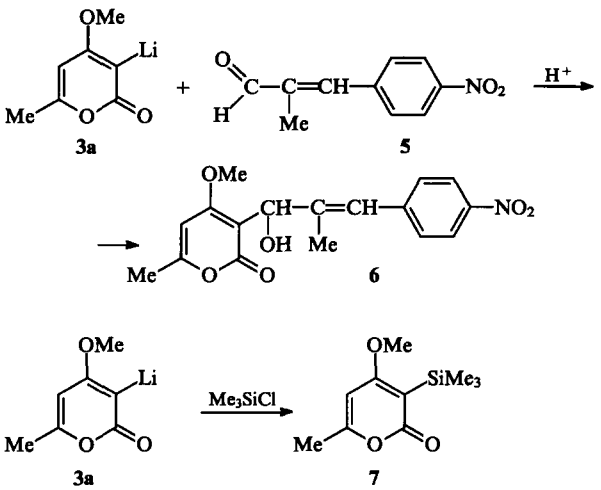
The lithio-derivative **3a** has also been obtained in 70% yield from compound **2a** by treatment with n-butyllithium.[18]

Lithium-substituted pyrones **3a, b** interact with heavy water to form the 3-deuterio-derivatives **4a, b**.[17]



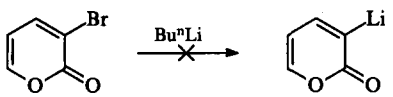
3a,b **4a,b**

The lithio-derivative **3a** interacts with 2-methyl-3-(4-nitrophenyl)-prop-2-enal **5**, affording the secondary alcohol **6**,[18] and also with chlorotrimethylsilane to form 4-methoxy-6-methyl-3-trimethylsilylpyrone **7**.[17] 4-Methoxy-6-phenyl-2-pyrone can also be lithium-substituted in the 3-position but the yield of products obtained from it has not been stated.[17]

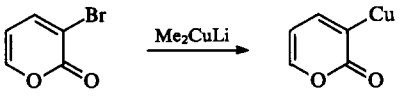


3a **5** **6** **3a** **7**

The attempt to obtain 3-lithio-2-pyrone without other substituents in the pyrone ring, by treating 3-bromo-2-pyrone with n-butyllithium, was unsuccessful.[19]

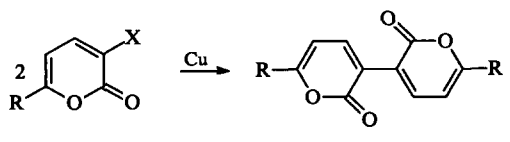


In 1985 Posner et al.[19] obtained for the first time 3-cuprio-pyrone **8** by the reaction of 3-bromopyrone with lithium dimethylcuprate.



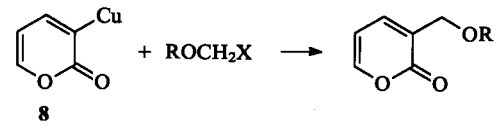
8

Previously Sokolovskaya and Moldovanova[20] synthesised a series of bispyrones by the Ullmann reaction, which proceeds via the intermediate formation of organocopper compounds.[21]



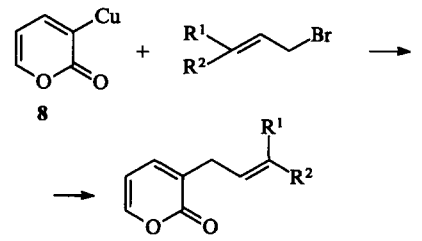
R = Ph, 4-MeC_6H_4, 4-$MeOC_6H_4$, 2-$C_{10}H_7$; X = Br, I.

3-Cuprio-2-pyrone **8** reacts under mild conditions with chlorobenzyl and bromomethyl ethers[19] and with allyl bromides.[19,22]

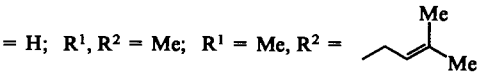


8

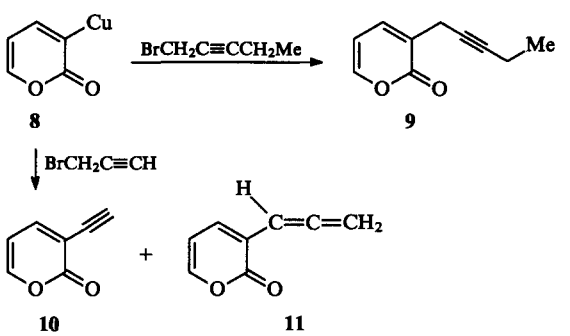
R = Me, X = Br; R = $PhCH_2$, X = Cl.



8

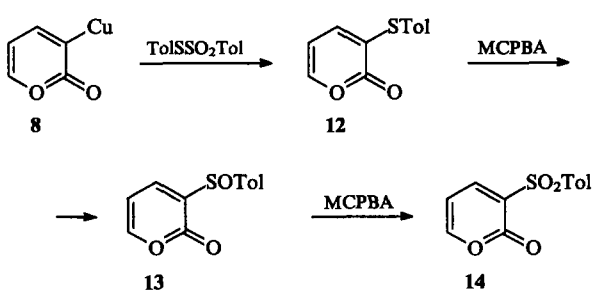


3-Cuprio-2-pyrone reacts with 1-bromopent-2-yne to form 3-(pent-2-yn-1-yl)pyrone **9** while its reaction with propargyl bromide affords a mixture of 3-propargylpyrone **10** and 3-allenylpyrone **11** in proportions of 3:1, but it does not react with alkyl, benzyl, and benzoyl halides and is thus an appreciably less nucleophilic agent than the majority of the organocopper compounds described previously.[19]



8 **9** **10** **11**

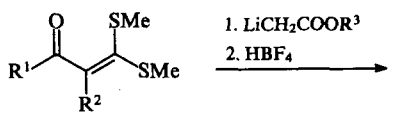
3-Cuprio-2-pyrone **8** reacts with $TolSSO_2Tol$ (Tol = 4-MeC_6H_4) to form 3-tolylthiopyrone **12**, which can be oxidised with *m*-chloroperbenzoic acid (MCPBA) to 3-tolylsulfinylpyrone **13** and 3-tolylsulfonylpyrone **14** respectively.[19]



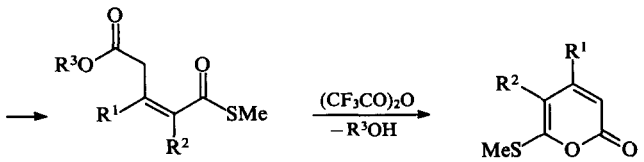
8 **12** **13** **14**

Another method of synthesis of organosulfur derivatives of pyrone involves the cyclisation of the thioesters of unsaturated dicarboxylic acids.[23-25]

Dieter and Fishpaugh[24] observed that α-oxoketene dimethyl thioacetals **15** react with *tert*-butyl or isopropyl lithioacetates to form the monothioesters of pent-2-ene-1,5-dioic acids **16**, which cyclise to substituted 6-methylthiopyrones **17** on treatment with trifluoroacetic anhydride.



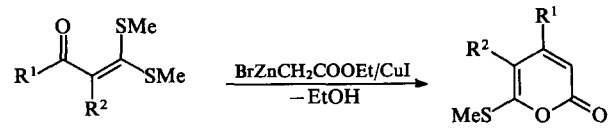
15

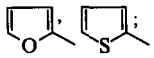


16 17

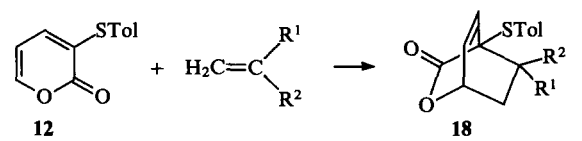
R^1, R^2 = $-(CH_2)_3-$, $-(CH_2)_4-$; R^1 = Et, R^2 = Me;
R^3 = Bu^t, Pr^i.

Bromozinc acetates in the presence of univalent copper may be used instead of lithioacetates.[23]



R^1 = Me, Ph, Tol, α-$C_{10}H_7$,  ;
R^2 = H, Me

A review by Posner is devoted to the reactivity of organosulfur derivatives of 2-pyrones.[26] The introduction of the electron-donating 4-tolylthio- and electron-accepting toluene-4-sulfinyl and toluene-4-sulfonyl substituents alters sharply the reactivity of 2-pyrones towards dienes. Thus, whereas 2-pyrones without organosulfur groups react with dienes at 100–200 °C, 3-(4-tolylthio)-2-pyrone **12** interacts with electron-deficient dienes (for example, with nitroethylene and acrolein) even at 85–90 °C. Mild reaction conditions make it possible to isolate the intermediate bicyclic lactones **18**, which lose CO_2 at high temperature.[27] The reactions of tolylthiopyrone **12** with nitroethylene, acrolein, 2-methylpropenal, and but-3-en-2-one take place stereoselectively (the ratio of *endo*- and *exo*-isomers is 98:2).[27]



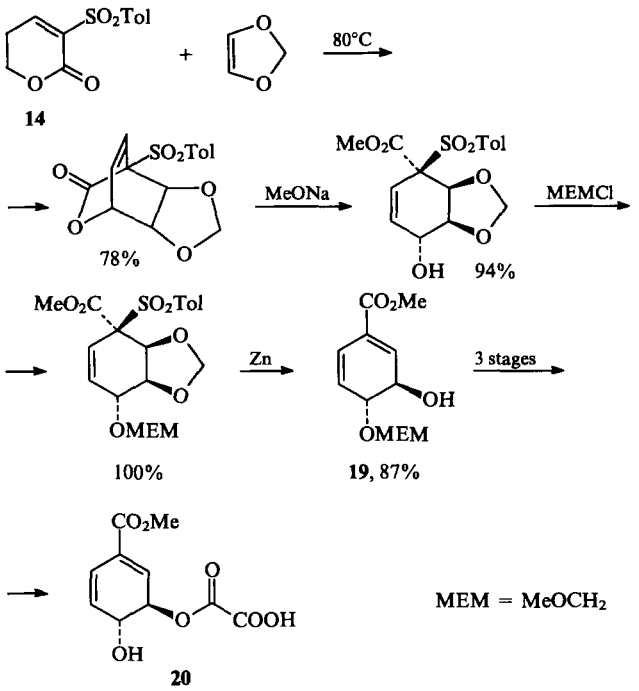
12 18

R^1 = H, Me; R^2 = NO_2, CHO, COMe

Stereoselectivity is much lower in the reactions of compound **12** with acrylonitrile, methylacrylate, methylmethacrylate, and benzyl acrylate, but the *endo*-isomer is still the main product of the reaction.[27]

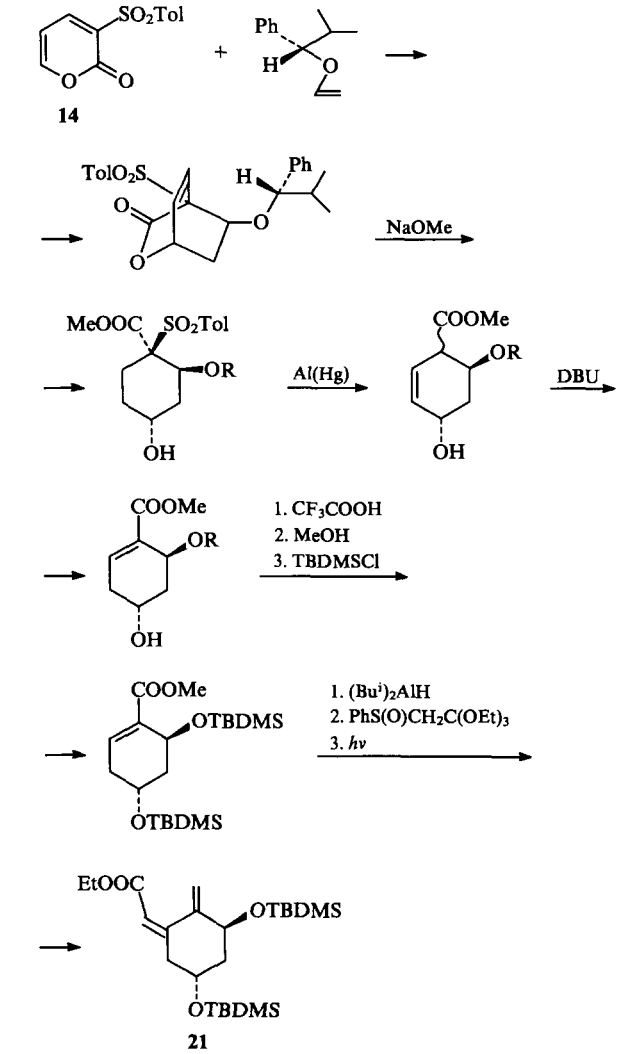
The introduction of electron-accepting sulfinyl and especially sulfonyl substituents into the pyrone ring greatly facilitates the reaction of the pyrone with electron-donating alkenes such as vinyl ethers and dioxoles.[28] As in the case of 3-(4-tolylthio)-2-pyrone **12**, in the reactions of 3-(toluene-4-sulfonyl)-2-pyrone **14** with dienes it is possible to isolate bicyclic intermediates. These reactions also proceed stereoselectively, which fact has been used successfully in the synthesis of the cyclic compounds **19**. The scheme constitutes a convenient method of synthesis of the cyclic compound **19**, which is a precursor of chorismic acid **20**.[26] Chorismic acid is in its turn a key intermediate in the shikimate biosynthetic pathway which bacteria and lower plants use to convert carbohydrates into aromatic compounds.[29,30]

The toluenesulfonylpyrone **14** has also been used in the synthesis of the A ring of hydroxyvitamin D_3 **21**.[26]



20

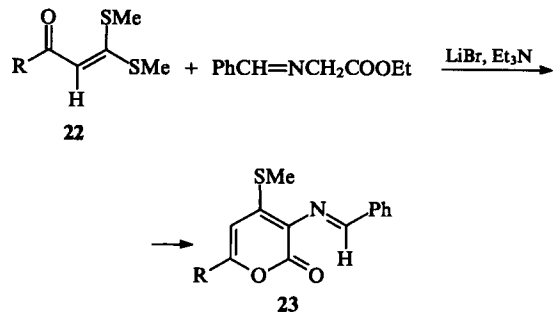
MEM = $MeOCH_2$



21

TBDMS = Bu^tSoMe_2;
DBU = 1,5-diazabicyclo[5.4.0]undec-5-ene.

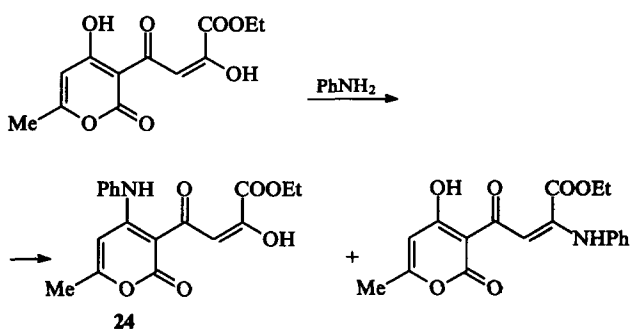
The reaction of the bis(methyl thioacetal) **22** with benzylideneaminoacetate leading to pyrones containing thio- and imino-substituents (compound **23**) is interesting.[31]



22 **23**

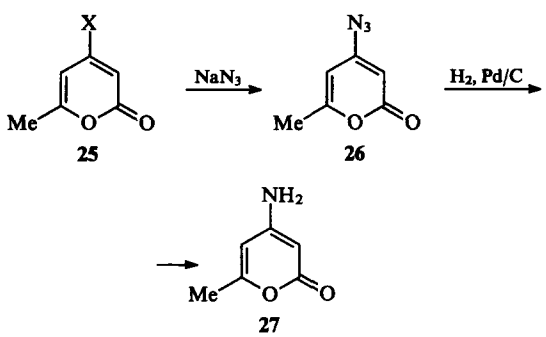
R = Alk, Ar

Ammonia and amines are known to open the pyrone ring with formation of acyclic products, which then recyclise to benzene derivatives or pyridones.[32,33] However, phenylaminopyrone **24** was obtained in the reaction of substituted 4-hydroxypyrone with aniline.[34]



24

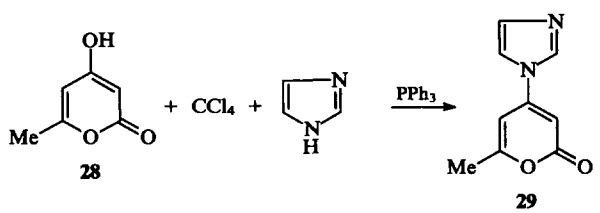
The pyrone **27**, containing a primary amino-group, was synthesised by the exchange of the halogen in 4-halo-6-methylpyrones **25** for the azido-group and the subsequent reduction of the 4-azidopyrone **26** with hydrogen over a palladium catalyst.[35]



25 **26** **27**

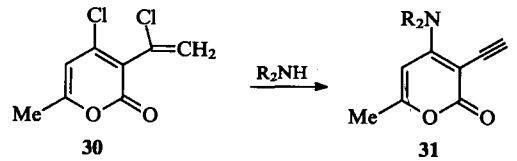
X = Cl, Br

When an attempt was made to obtain 4-chloro-6-methylpyrone by substituting the OH group in the pyrone **28** for chlorine on refluxing with CCl_4, imidazole, and triphenylphosphine, only 4-(1-imidazolyl)-6-methylpyrone **29** was isolated.[35]



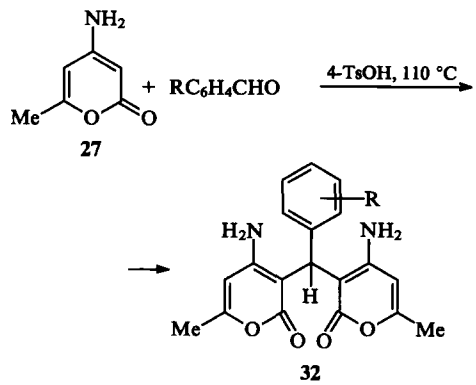
28 **29**

There are literature data showing that the reaction of 4-chloro-3-(1-chlorovinyl)-6-methylpyrone **30** with secondary alkylamines leads to 4-dialkylamino-3-ethynyl-6-methylpyrones **31**.[36]



30 **31**

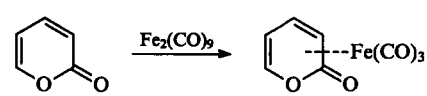
In the presence of toluene-4-sulfonic acid, 4-amino-6-methyl-2-pyrone **27** reacts with aldehydes at the 3-position in the pyrone ring to form bis(4-aminopyron-3-yl)methanes **32**.[34]



27 **32**

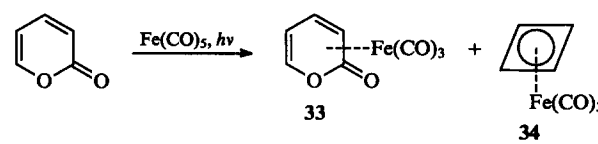
III. η^4-Iron tricarbonyl complexes of 2-pyrones

The diene system of the pyrone ring can form complexes with transition metal atoms. Thus the first organometallic derivative of 2-pyrone—the η^4-diene complex **33**—was obtained in 1967 by heating 2-pyrone and diiron nonacarbonyl in heptane.[37]



33

Irradiation of the pyrone and iron pentacarbonyl with UV light leads to the formation of a mixture of complex **33** and cyclobutadieneiron tricarbonyl **34**. (The overall yield of the products **33** and **34** is 10%–15%.)

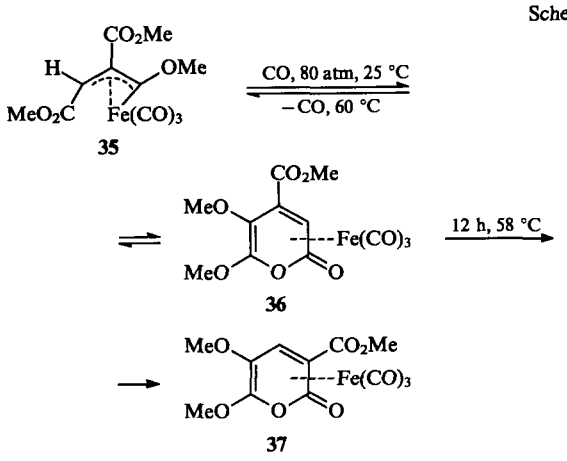


33 **34**

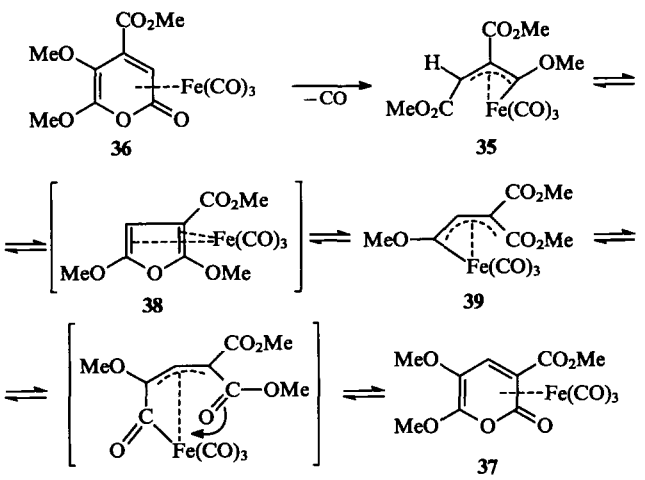
The authors confirmed the structure of the pyroneiron tricarbonyl complex by IR and ^1H NMR spectroscopic data. The product **33** is the only η^4-diene complex of pyrone obtained by the interaction of the latter with a metal carbonyl. In the remaining cases, the η^4-pyrone ligands were formed as a result of the cocyclisation of ligands having a simpler structure in the coordination sphere of the transition metal.

Mitsudo et al.[38] described the synthesis of the η^4-pyrone ligand by carbonylating the σ,π-allyliron tricarbonyl derivative **35** under pressure (Scheme 2). On heating in dichloroethene, the η^4-pyrone complex **36** is converted into the isomeric product **37** in 21% yield. The structures of compounds **36** and **37** were established by X-ray diffraction. On heating to 60 °C, complex **36** is decarbonylated and reconverted into the initial σ,π-allyl derivative **35**.

Scheme 2

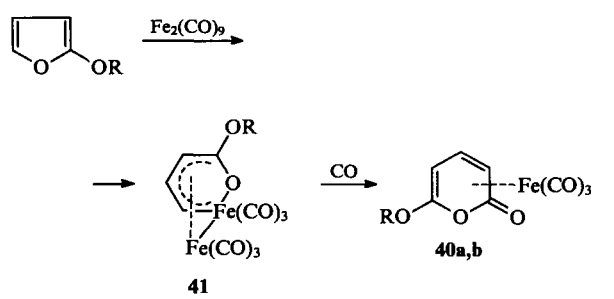


Scheme 3



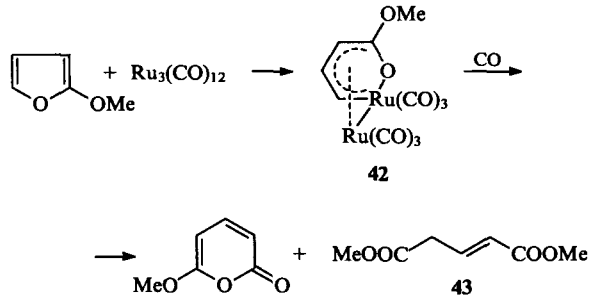
Bearing in mind that on heating under CO pressure complex **36** does not isomerise to complex **37** Mitsudo et al.[38] proposed the mechanism of the rearrangement presented in Scheme 3. In the initial stage, the η^4-pyrone complex **36** is decarbonylated to the σ,π-allyl derivative **35**, which rearranges to the σ,π-allyl derivative **39** via the intermediate formation of the fairly unstable 2,5-dimethoxyfuran complex **38**. The derivative **39** is probably carbonylated and is then converted into complex **37**. If account is taken of the fact that complex **37** is formed on carbonylation of compound **35** under pressure, then the authors' hypothesis that compound **39** is carbonylated in solution in the absence of pressure appears doubtful, but is nevertheless probable since the rearrangement product **37** is obtained in a low yield.

Mitsudo et al.[38] mention the formation of the 6-methoxypyroneiron tricarbonyl complex in the reaction of 2-methoxyfuran and diiron nonacarbonyl, which evidently proceeds via the insertion of CO in the furan ring.

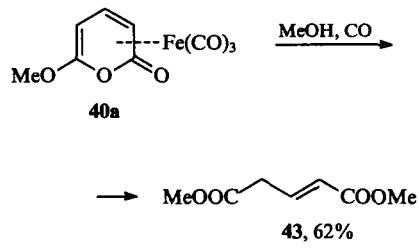


R = Me (**a**), Bu^t (**b**).

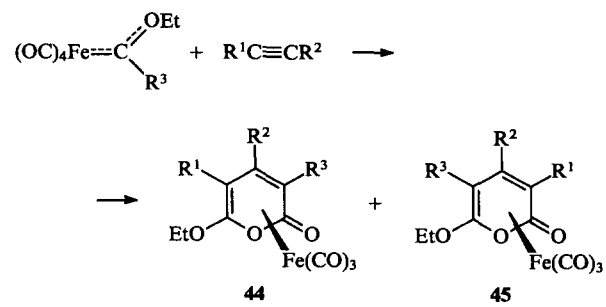
In a later study, Mitsudo et al.[39] showed that 2-alkoxyfurans interact with diiron nonacarbonyl to form η^4-(6-alkoxypyrone)iron tricarbonyl complexes **40**. It is postulated that complexes **41**, containing a metallacycle and an iron-iron bond, are formed initially. Their carbonylation leads to compounds **40**. In contrast to diiron nonacarbonyl, triruthenium dodecacarbonyl reacts with 2-methoxyfuran at 120 °C, affording only the ruthenacyclic compound **42**. Under more severe conditions (150 °C) and under CO pressure, appreciable amounts of 6-methoxypyrone and dimethyl glutaconate **43** were obtained together with compound **42**.[39]



The mechanism of the formation of compound **43** is not entirely clear, but the authors[39] suggest that it is obtained by the reaction of 6-methoxypyrone with the methanol formed as a result of the decomposition of 2-methoxyfuran. In order to confirm their hypothesis, the authors carried out the reaction of the pyroneiron tricarbonyl derivative **40a** with methanol under CO pressure and obtained dimethyl glutaconate **43**.[39]

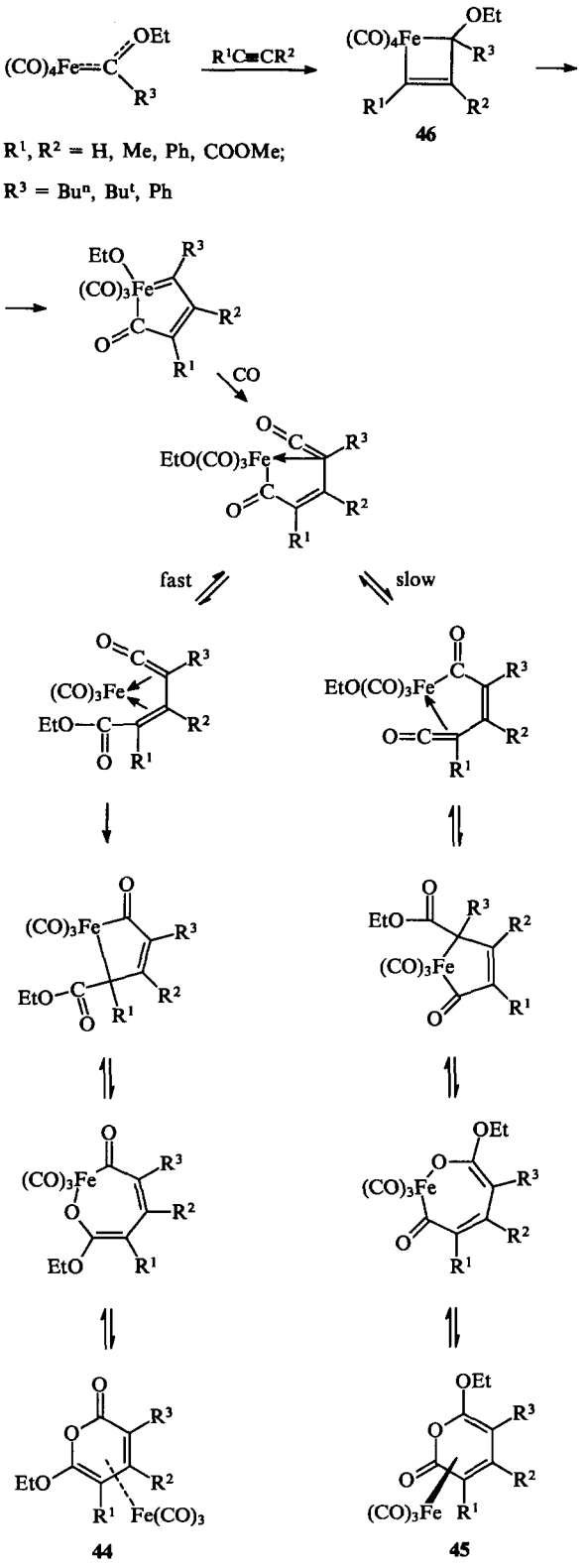


The η^4-pyroneiron tricarbonyl complexes **44** and **45** were obtained by the reaction of the carbene complexes of iron with acetylenes under CO pressure.[40] The pyrone ligand is formed in this case from the carbene ligand, two CO molecules, and an acetylene molecule. η^4-Pyrone complexes were isolated in high yields, the isomer **44** predominating. The authors proposed the following scheme for the formation of the pyrone complexes (Scheme 4), although they believe that the reaction mechanism has not been established exactly. However, rapid chromatography of the reaction mixture on silica gel led to the isolation of the product **46**, to which a metallacyclobutene structure may be assigned on the basis of ^{13}C NMR spectroscopic data. The product **46** is unstable and decomposes readily with formation of the pyroneiron tricarbonyl complex **44** and other compounds.[40]



R^1, R^2 = H, Me, Ph, COOMe; R^3 = Bu^n, Bu^t, Ph

Scheme 4



The reactions involving the formation of the η^4-pyrone ligand from the allyl fragment and a CO molecule[38] and also from an acetylene molecule and the carbene and carbonyl ligands in the coordination sphere of the iron atom[40] have no analogies in the organic chemistry of 2-pyrones. Presumably the use of transition metals will significantly expand the scope of the synthesis of 2-pyrones and their derivatives.

The review has been prepared with the support of a European grant INTAS-93-1588 ISF MA8000 and a grant from the Russian Fundamental Research Fund No.93-03-4403.

References

1. J Staunton, in *Comprehensive Organic Chemistry* Vol. 4 (Ed. P G Sammes) (Oxford: Pergamon Press), 1979, p. 624
2. M A Goetz, J Meimerald, T Eisner *Experientia* **37** 679 (1981)
3. S M Kupchan, J L Moniot, C W Sigel, P J Hemingway *J. Org. Chem.* **36** 2611 (1971)
4. K K Chem, A Kovarikova *J. Pharm. Sci.* **56** 1535 (1967)
5. Y Hayashi, T Matsumoto, T Sakau *Heterocycles* **10** 123 (1978)
6. Y Hayashi, Y Yuki, T Matsumoto, T Sakau *Tetrahedron Lett.* **18** 3637 (1977)
7. Y Hayashi, Y Yuki, T Matsumoto, T Sakau *Tetrahedron Lett.* **18** 2953 (1977)
8. J W Loder, R H Nearn *Tetrahedron Lett.* **16** 2497 (1975)
9. G B Russell, P G Fenemore, P Singh *J. Chem. Soc., Chem. Commun.* 166 (1973)
10. N Adityachaudhury, A K Das *J. Sci. Ind. Res.* **38** 265 (1979)
11. T A Bryston, D M Donelson *J. Org. Chem.* **42** 2930 (1977)
12. J A Reed, C L Schilling, R F Tarvin, T A Retting, J K Stille *J. Org. Chem.* **34** 2188 (1969)
13. A P Kozikovski, E J Corey *Tetrahedron Lett.* **16** 2389 (1975)
14. A R Katritzky, in *Comprehensive Heterocyclic Chemistry* Vol. 3 (Eds A J Boulton, A McKillop) (Oxford: Pergamon Press), 1984, pp 675, 789
15. R Gompper, O Christmann *Chem. Ber.* **94** 1784 (1961)
16. R Gompper, O Christmann *Chem. Ber.* **94** 1795 (1961)
17. T A Carpenter, P J Jenner, F J Leeper, J Staunton *J. Chem. Soc., Chem. Commun.* 1227 (1980)
18. M Moreno-Mañas, R Pleixats *J. Heterocycl. Chem.* **28** 2041 (1991)
19. G H Posner, W Harrison, D G Wettlaufer *J. Org. Chem.* **50** 5041 (1985)
20. S V Sokolovskaya, L K Moldovanova *Khim. Geterotsikl. Soedin.* 173 (1979)
21. T Cohen, T Poeth *J. Am. Chem. Soc.* **94** 4363 (1972)
22. G H Posner, W Harrison *J. Organomet. Chem.* **285** C27 (1985)
23. A Datta, H Ila, H Junjappa *J. Org. Chem.* **55** 5589 (1990)
24. R K Dieter, J R Fishpaugh *Tetrahedron Lett.* **27** 3823 (1986)
25. X Huang, G Wu *Youju Huaxue* **9** 460 (1989); *Chem. Abstr.* **113** 6090c (1990)
26. G H Posner *Pure Appl. Chem.* **62** 1949 (1990)
27. G H Posner, T D Nelson, C M Kinter, N Johnson *J. Org. Chem.* **57** 4083 (1992)
28. G H Posner, T D Nelson *Tetrahedron* **46** 4573 (1990)
29. U Weiss, J M Edwards *The Biosynthesis of Aromatic Compounds* (New York: Wiley), 1974
30. E Haslam *The Shikimate Pathway* (New York: Wiley), 1974
31. M P Balu, H Ila, H Junjappa *Tetrahedron* **46** 6771 (1990)
32. N P Shusherina, V L Lapteva *Zh. Org. Khim.* **10** 849 (1974)
33. N P Shusherina, N D Dmitrieva, E A Luk'yanets, R Ya Levina *Usp. Khim.* **36** 437 (1967) [*Russ. Chem. Rev.* **36** 175 (1967)]
34. A Brbot-Saranovic, B Katusin-Razem *Heterocycles* **29** 1559 (1989)
35. M Cervera, M Moreno-Mañas, R Pleixats *Tetrahedron* **46** 7885 (1990)
36. Y Azuma, A Sato, K Tanno, M Madarame, S Hisamichi *Annu. Rep. Tohoku Coll. Pharm.* **36** 219 (1989); *Chem. Abstr.* **114** 143052b (1991)
37. M Rosenblum, C Gatsonis *J. Am. Chem. Soc.* **89** 5074 (1967)
38. T Mitsudo, H Watanabe, T Sasaki, Y Watanabe, V Takegami *J. Chem. Soc.* 22 (1981)
39. T Mitsudo, Y Ogino, Y Komiya, H Watanabe, Y Watanabe *Organometallics* **2** 1202 (1983)
40. M F Semmelhack, R Tamura, W Schnatter, J Springer *J. Am. Chem. Soc.* **106** 5363 (1984)

Russian Chemical Reviews **63** (8) 667 – 684 (1994)
©1994 Russian Academy of Sciences and Turpion Ltd

UDC 542.952.6 : 541.127

Kinetic nonuniformity in radical polymerisation processes

S S Ivanchev, V N Pavlyuchenko

Contents

I. Introduction	667
II. Polymerisation in homogeneous systems	667
III. Kinetic nonuniformity in emulsion polymerisation processes	670
IV. Kinetic nonuniformity in polymerisation processes in the presence of a dispersed solid phase	678
V. Conclusion	681

Abstract. The characteristic features of radical polymerisation in homogeneous and heterogeneous systems are considered from the standpoint of the kinetic nonuniformity of the elementary reactions. The kinetic nonuniformity is due to the variation of the properties of the reaction system during the process and to the appearance of kinetically nonequivalent zones for certain critical conversions. The kinetic nonuniformity in heterogeneous systems is examined in relation to emulsion polymerisation and polymerisation in the presence of a solid dispersed phase. It is shown that the specific formation in the reaction systems of kinetically nonuniform zones makes it possible to control effectively the polymerisation process and the properties of the polymers formed. The bibliography includes 143 references.

I. Introduction

The theory of radical polymerisation was created over several decades and was largely formulated in its classical version towards the end of the 1950s. Its principal postulates have been reflected in a series of monographs (see, for example, Refs 1 – 4). Many kinetic features predicted by the theory have been confirmed experimentally. However, at the same time results have accumulated which do not fit fully within the framework of the classical theory. The theory was supplemented by the concept of the gel effect and by studies of the influence of the cage effect and of diffusional control on the characteristic features of polymerisation at high conversions of the monomer into polymer.[3,4]

Analysis of the kinetics of radical polymerisation was based on the idea that the polymerisation system is homogeneous and on the use of approaches and concepts typical for liquid-phase reactions. Even in studies carried out during recent years,[5–7] the kinetics have been analysed without taking into account the possible kinetic nonequivalence of individual zones in the polymerisation system, although the concept of macromolecular effects in polymerisation had in fact been introduced.

S S Ivanchev, V N Pavlyuchenko 'Plastopolimer' Joint Stock Company, Polyustrovskii pr. 32, 195108 St Petersburg, Russian Federation.
Fax (7-812) 540 30 01

Received 24 May 1994
Uspekhi Khimii **63** (8) 700 – 718 (1994); translated by A K Grzybowski

During the last decade significant changes have taken place in our ideas about chemical processes in polymer systems. The essential features of these changes have been described in the monograph by Emanuel' and Buchachenko[8] and somewhat later in that of Denisov.[9] It has been shown that a chemical reaction in a solid polymer phase differs appreciably from that in the liquid phase. There is a possibility that the relative rates of various competing reactions and the criteria governing the diffusion and kinetic regimes may differ significantly and the rate-limiting stages and the physical significance of the kinetic constants may change. Together with changes in the energy state of the molecules and the kinetic nonequivalence (nonuniformity) arising on this basis, other causes of nonequivalence appear in such systems — the differences in the conformational state of the species, in the structure of their environment, in their disposition in space, and in the mobility of molecules or their fragments. Such kinetically nonequivalent states lead to an arbitrary distribution of species among assemblies differing in kinetic parameters. As a result, the reaction system may be characterised by a certain set of rate constants, activation energies, and pre-exponential factors in the Arrhenius equation. The kinetics of the reactions in such a system are polychromatic and sensitive to the structural-physical properties of the polymer.

The question arises of the stage in which the above features of chemical reactions in polymer systems should be used in the analysis of the kinetics of radical polymerisation. Can one assume the kinetic nonuniformity of the system and to what extent can it affect the molecular characteristics, structure, and hence the properties of the polymer formed? The answers to these questions are not unambiguous if one takes into account the presence in the polymerisation system, together with the polymer formed, of one or several monomers, which can eliminate or weaken the effect of the kinetic nonuniformity, and the permanent dynamic behaviour of the system as a consequence of the chemical conversion of the monomer into the polymer.

In the present review, an attempt is made to consider the possibilities of the appearance and manifestation of the kinetic nonequivalence of individual zones in homogeneous (in the initial system) and heterogeneous radical polymerisation.

II. Polymerisation in homogeneous systems

The view that the theory of radical polymerisation is complete, expressed in the 1960s, proved to be unjustified. This has been demonstrated by numerous publications which appeared in 1970 – 1980 and which were devoted to the analysis and improvement of the theory of radical polymerisation. Nevertheless, despite

the significant progress in the development of ideas concerning the kinetics and mechanism of radical polymerisation, it has still not been possible to create a quantitative theory which could describe the diverse polymerisation systems for different conversions of the monomers from a single standpoint. The main reason for this is apparently the difficulty of taking into account and describing the changes in the physical properties of the reaction system during polymerisation.

We shall analyse briefly the most interesting, from our standpoint, studies concerning the characteristic features of the kinetics of polymerisation in homogeneous systems which have appeared during the last two decades.

In 1982, Soh and Sundberg[10] introduced the concept of four stages of radical polymerisation in homogeneous systems. The first, ideal polymerisation stage fully obeys the classical equations of radical polymerisation. The second stage is characterised by autoacceleration due to the change in the rate constants for elementary reactions, primarily the chain termination reaction. In the third stage, autoacceleration ceases whilst a high overall rate of polymerisation is maintained and the molecular mass of the polymer formed is reduced. In the last (fourth) stage, the rate of polymerisation diminishes (or the polymerisation comes to a stop). It has been found that, as the polymer is formed in the reaction mixture, the kinetic parameters of virtually all the processes (initiation and chain termination, propagation, and transfer reactions) change.

For a long time, the efforts of many investigators were directed to the search for equations describing the kinetic changes in advanced stages of polymerisation and the models explaining these changes. It is possible to distinguish two types of approach to the explanation of the characteristic features of polymerisation for high conversions of the monomer into the polymer: (a) kinetic; (b) structural (the free volume concept).

The kinetic approaches or models reduced to the establishment of the dependences of the rate constants for elementary reactions on the viscosity of the polymerisation system.[3,4,6,9,11-13] In the structural models, an attempt was made to take into account the changes in the physical properties of the reaction medium on attainment of the critical concentrations and dimensions of the macromolecules. Under these conditions, there is mutual interpenetration and overlap of the macromolecular coils with formation of a stable network of entanglements.[10,14-17]

For polymerisation systems characterised by the segregation of a polymer phase during the reaction, the explanation of the kinetic deviations was associated both with the possibility of occlusion of the growing radicals of the polymers and with the appearance of a two-phase model of the propagation of polymerisation.[3]

The kinetic constants for radical polymerisation obtained by various experimental methods have been analysed.[18,19] It has been proposed that one should distinguish not four stages, as in the study of Soh and Sandberg,[10] but three stages of polymerisation depending on the degree of conversion and the type of reaction systems. The first stage represents the low conversion regime (the dilute solution regime), in which nonoverlapping macromolecular coils are formed (entanglements do not arise in this system). The low conversion regime continues until the onset of an increase in the rate. The high conversion regime begins from the instant when the chain propagation becomes diffusion-controlled and the effectiveness of initiation falls sharply. There is a transitional regime between the above two regimes, during which the reaction mechanism changes. Buback et al.[19] emphasised that it is fairly difficult to establish the boundaries of the above regimes. They depend on the type of polymerisation system, the nature of the monomer, and the rate of initiation and these are difficult to determine by measuring some characteristic of the system. In the same study, attention was drawn to the significant discrepancies between the experimental data obtained in the determination of the kinetic parameters and the rate constants for the elementary reactions in radical polymerisation.

The existence of a transitional regime and the associated change in the radical polymerisation mechanism are usually explained by a transition from the chemical control of the polymerisation kinetics to physical control. Chemical control should be understood as the activation barrier to the reaction and physical control as the predominance of diffusional limitations over activation limitations.[8,19] Analysis of the simple equation

$$\frac{1}{k} = \frac{1}{k_{\text{chem}}} + \frac{1}{k_{\text{diff}}}$$

shows that the rate of reaction is controlled by one mechanism, since we have either $k_{\text{chem}} \gg k_{\text{diff}}$, or $k_{\text{diff}} \gg k_{\text{chem}}$, where k_{chem} and k_{diff} are respectively the activation and diffusional components of the reaction rate constants k. On passing from one regime to another, the rate-determining stage changes for at least one of such elementary reactions. One may assume[19] that $k_{\text{t chem}} \gg k_{\text{t diff}}$ for all the regimes, $k_{\text{p}} \approx k_{\text{p chem}}$ for the low conversions regime and the intermediate regime, and $k_{\text{p}} \approx k_{\text{p diff}}$ for the high conversions regime, where k_{t} is the chain termination rate constant and k_{p} the chain propagation rate constant.

The kinetics of radical polymerisation and the changes in the constants for the elementary reactions have been analysed in numerous investigations[6,7,11,13] from the standpoint of the influence of diffusional limitations. At the same time, with increased conversion a change has been observed in the distribution of the concentrations of the system components in the polymerisation of methyl methacrylate[20,21] and in the polymerisation and copolymerisation of divinyl derivatives.[22]

This finding already indicates directly the nonuniformity of the distribution of the components in the system and hence the appearance of kinetically nonuniform zones. The appearance and growth of the nonuniformity of the distribution of the concentrations of the components (the monomer and initiator) with increase in conversion has also been mentioned.[23,24]

Deviations from the principal rules in radical polymerisation have been noted. Thus two groups of investigators observed independently a change in the composition of the copolymers formed in radical copolymerisation as a function of the change in the rate of initiation of the polymerisation.[25-29] The authors attribute this effect to the influence of the copolymer formed and also to the change in the relative concentrations of the comonomers in the chain propagation reaction zone as a consequence of the selective sorption of the comonomers by the macromolecular coils formed. This is one of the manifestations of the macromolecular effects in radical polymerisation noted by Semchikov et al.[5]

We believe that the above features of the kinetics and mechanism of radical polymerisation and copolymerisation should be considered from a single standpoint, i.e. should be related to the characteristics of the macromolecules formed during the reaction, the nonuniformity of the reaction medium produced, and the dynamics of its variation with conversion and hence with the kinetic nonequivalence of the zones.

The theory of radical polymerisation was formulated before the appearance of ideas concerning the characteristic features of the reactions in polymers and polychromatic reaction kinetics.[8,9] According to these ideas, any polymer system is a 'motley mosaic' of regions with different packing densities of the macromolecules, sometimes differing in the alternation of the amorphous and crystalline sections, molecular mobility, and average size and mobility of the holes through which molecules or species diffuse during chemical reactions. The cause of polychromatic kinetics or kinetic nonuniformity is the 'rigid cage' of the polymer, which is responsible for the hindrance to the diffusion of species and which leads to the levelling of the reactivities of the reactants. The 'cage effect' has been related mainly to unimolecular radical formation reactions. However, it has been shown recently[30] that it influences also slow bimolecular reactions. It is important to note that the principal postulate of the theory of radical polymerisation, which

is that the reactivity of the monomers and radicals is determined by their structure and is independent of their molecular mass, does not hold for reactions in polymer systems.

The results of studies of the influence of solvents on the rate of polymerisation of water-soluble monomers and on the rate constants for the elementary chain propagation and termination reactions merit special attention in this sense.[31-34] It has been shown that the change in the density of the polymer coil and the conformational transitions of the coil–globule type can lead to the appearance of steric hindrance to the interaction of the macroradicals and the monomer. The possibility of such transitions naturally depends on the rigidity of the macrochain.

Thus one should bear in mind the possibility, for certain critical conversions in the formation of the polymer phase during polymerisation, of both the appearance of concentration nonuniformities (the nonuniformity of the distribution of the components in the system) and of a change in the conformational state of the macromolecules and hence in the reactivity of the growing chains. These two factors may lead to the kinetic nonequivalence (nonuniformity) of the zones in the system.

The possibility of the appearance of kinetic nonuniformity has been confirmed in Khokhlov's study,[35] in which the fluctuations in local density in the macromolecular system have been attributed to specific entropy effects arising on formation of the macromolecular system. The local concentration gradients of the units lead to entropy losses, which can affect the free energy of the chain propagation reaction.

The above analysis suggests a new approach to the characteristics of radical polymerisation, taking into account the possibility of the appearance during the monomer–polymer transformation of kinetically nonequivalent (nonuniform) zones associated with the nonuniformity of the system as regards both concentration and composition. This approach presupposes initially homogeneous uniform kinetics in the polymerisation system up to a critical conversion. Such critical conversion should depend on the nature of the polymer, the rigidity of the polymer formed, the polymerisation temperature, and the compatibility in the monomer–polymer system. At this instant, the polymerisation system can be represented as an assembly of kinetically nonequivalent dynamically varying zones where the polymerisation process is propagated.

We shall understand kinetic nonuniformity (KN) as the manifestation of the variability of the kinetic constants and parameters of the polymerisation process in time and space (in the microzones of the reaction system). Under these conditions, KN may not be observed experimentally owing to the difficulty of finding the zones and determining their kinetic parameters, but it must influence the structure and molecular characteristics of the polymer formed. As a consequence of the dynamic nature of the system, the experimental kinetic parameters are average quantities characterising the kinetic behaviour in different microregions.

The proposed concept is supported by experimental data on the nonuniform distribution of the components in the polymerisation process.[23,24] The specification of three regimes in the polymerisation process proposed by Buback et al.[19] can also be accounted for from the standpoint of KN.

In the low conversion regime, the polymerisation system is virtually homogeneous. The formation of the polymer phase and the appearance of concentration nonuniformities, initially as a result of the fluctuations in density and in the concentrations of the reactants and subsequently owing to the change in the polymerisation conditions and the type of system, begin in this regime. The process involving the appearance of concentration nonuniformities gradually reaches a critical stage and the system passes to the intermediate regime. The change in the characteristics of the kinetically nonuniform zones continues and the number of denser zones, formed by the polymer molecules, increases. In the high conversion regimes, a polymerisation system nonuniform in space is fully formed.

The change in the mechanism of chain termination from bimolecular to linear can be fully accounted for within the framework of the KN concept.[12,23,24]

On the basis of the foregoing, it is possible to formulate the principal factors responsible for the appearance of KN in radical polymerisation processes.

1. The formation and accumulation of the polymer and the appearance of fluctuations in the density of macromolecules in the reaction system.

2. The change in the distribution of the concentrations of the components of the polymerisation system (monomer, initiator, regulator, etc.) under the influence of the macromolecular nonuniformities which have arisen.

3. The possible phase separation during polymerisation.

4. The change in the thermodynamic conditions and rate constants for the elementary reactions of the polymerisation process.

It is possible to put forward the following classification of polymerisation systems in terms of the type of the kinetic and structural nonuniformities arising in them.

1. Polymerisation systems in which the polymer formed is compatible with its monomer. For these systems, the appearance of KN is latent in character and depends on the properties of the monomer–polymer system (for example, on the glass point) and the reaction conditions (temperature, rate of initiation, etc.). Such systems are formed in the polymerisation of styrene and methacrylic and acrylic monomers.

2. Polymerisation systems in which the polymer formed is insoluble or its solubility in its own monomer is limited (or in the reaction medium when solvents or precipitants are used). Starting from a certain degree of conversion of the monomer, microheterogeneities begin to be produed in such systems. The polymer or macromolecular aggregates segregated to form a zone comprising grains of the polymer phase in which the rate constants for the elementary reactions and the concentrations of the reactants can differ from their values in another zone. The quantitative ratio of these zones varies with the degree of conversion of the monomer in favour of the polymer zone, which is reflected in the dynamics of the heterogeneity and the kinetics and mechanism of the reaction. The systems used in the polymerisation of vinyl chloride and fluorinated monomers and many copolymer systems may serve as examples. The characteristic features of the polymerisation in such systems have been described.[36,37]

3. Systems in which monomers with several polymerisable groups are polymerised. With increase in the degree of conversion of the monomer in such systems, the structure formation process in the reaction medium intensifies, which leads to the appearance of microheterogeneity and KN. The characteristic features of the polymerisation of such systems have been noted by Berlin and Korolev.[38,39]

4. Emulsion polymerisation systems in which the heterogeneity and hence the possibility of the appearance of KN are specified by the polymerisation conditions. The characteristic features of the polymerisation in such systems have been described in a series of monographs and reviews[4,40-42]. For such systems, it is of interest to analyse the role of KN in the establishment of the properties of the polymerisation products formed.

5. Heterogeneous systems in which polymerisation proceeds in the presence of the surface of a solid phase. Such systems have been vigorously investigated.[4,43,44] They are of interest as model systems for the investigation of polymerisation in adsorption layers of the monomer and also in the formation of filled polymers (polymerisation filling). Systems of this kind are of interest from the standpoint of the specific generation of KN in order to create complex preplanned heterogeneous structures of different kinds.

In proposing the above classification of polymerisation systems, we take into account the fact that KN is a consequence of the concentration or phase nonuniformity. However, the change

in the mechanisms of elementary reactions is not always manifested in the study of the polymerisation macrokinetics as a consequence of the possible compensation effects.

For the first two groups of polymerisation systems, the characteristics of the accumulation of the kinetic and spatial nonuniformities were examined above. We may note that hitherto no attempts have been made to apply the phenomenological models of polychromatic kinetics to homogeneous polymerisation processes, although they might yield interesting results.

For the third group of systems, interesting generalisations concerning the characteristic features of the kinetics of the polymerisation process are available in the literature.[38,39]

A multiphase structure and the presence of an interface already in the initial state are combined in systems of the fourth and fifth groups. On the one hand, this complicates the study of such systems and, on the other hand, there is a possibility that microheterogeneities may arise in these systems, with parameters which can be predicted beforehand. Taking this factor into account and also the fact that there has been no systematic analysis of such systems from the standpoint of KN, in the subsequent sections we shall concentrate on the consideration of precisely such systems and we shall attempt to establish the specific factors characteristic of these systems alone and also to determine the possibility of using them to regulate the kinetics of the processes and the properties of the products.

III. Kinetic nonuniformity in emulsion polymerisation processes

The factors responsible for KN which were examined above are manifested with certain characteristic features in emulsion polymerisation (EP). The very nature of the emulsion creates preconditions for the appearance of additional factors in KN. The first precondition is due to the distribution of the reactants between two phases: the continuous phase (usually water) and the discrete phase, while the second precondition is due to the physical and chemical natures of the phases.

Attention should be drawn to the ambiguity of the very concept of 'discrete phase' in the study of the characteristics of emulsion polymerisation. According to the familiar ideas of Harkins,[45] Yurzhenko and Kolechkova,[46] and Smith and Twart,[47] in the initial stages the reaction system consists of several types of particles: drops of the monomer, micelles of the emulsifier containing the solubilised monomer, and polymer-monomer particles (PMP) formed as a result of the entrainment of free radicals by the micelles and the polymerisation of the solubilised monomer. The nucleation centres are emulsifier micelles into which the monomer diffuses from the drops.

There are also other ideas[48,49] concerning the nucleation of particles according to which PMP are formed via a homogeneous mechanism, namely as a result of the polymerisation of the part of the monomer which is dissolved in water, the precipitation of the oligomeric radicals from the aqueous phase after they have attained a certain size, and agglomeration to primary particles which undergo further limited coagulation. The particles arising in this way are stabilised by the emulsifier molecules and sorb the monomer from the drops, after which they are converted into the PMP.

There is a possibility also of a third variant of the nucleation — the creation with the aid of special emulsifying systems or with the aid of special procedures of microemulsions the particles of which are the nucleation centres.[50-52]

Evidently the conditions for the occurrence of the elementary reactions may differ significantly in the PMP formed via different mechanisms. The situation is complicated because certain elementary steps in the course of the entire polymerisation process can develop not only in the PMP or in the aqueous phase but also at the interface. The above reaction zones are kinetically nonequivalent.

Thus additional factors in the KN in emulsion polymerisation processes are the nucleation of the PMP and the characteristic features of the elementary steps occurring in particles of different type and in other reaction zones. We shall analyse the causes of the appearance of KN from the standpoint of the above factors concentrating attention particularly on the KN arising in the PMP already formed, since precisely this form of KN determines to a large extent the molecular characteristics of the polymer, the dispersity of the latex formed, and the morphology of the latex particles.

1. Nucleation of the particles

The latexes formed as a result of emulsion polymerisation are as a rule polydisperse systems. The diameter of the PMP and the nature of their size distribution usually change during the process. It is known from the theory of emulsion polymerisation that the kinetics of polymerisation in a separate particle are influenced to a large extent by the particle size, which is associated with the dependence of the monomer concentration in the PMP on its radius.[53]

Another group of factors is associated with the differences between the kinetic parameters of polymerisation in particles of different size. In particular, the rate of capture of the free radicals generated in the aqueous phase when water-soluble initiators are used depends on the radius or surface area of the PMP. It has been shown[54] that, in the seeded emulsion polymerisation of styrene, initiated by potassium persulfate, the rate constant for the incorporation of the free radicals in the PMP at similar initiator concentrations increases by a factor greater than 10 with increase in the radius of the seeding particles from 40 to 100 nm. A consequence of this is the nonidentity of the chain termination conditions in PMP differing in size. Furthermore, the different volumes of the particles presuppose different contents of the radicals in the PMP,[55] which is also reflected in the characteristics of the chain termination. A fundamental feature is that, in the presence of a single free radical in the PMP, the incorporation of the next radical induces chain termination. If the particle attains a size sufficiently large to accommodate two radicals, the possibility of a bimolecular termination of the macroradicals with all its consequences (dependence of k_t on the microviscosity in the PMP and the appearance of the gel effect) arises.

One should also note that the total number of the PMP, i.e. the number of reaction sites and hence the concentration of the free radicals, varies as a function of the mechanism and kinetics of the nucleation in the polymerisation system.

In discussing the mechanisms of the nucleation of the PMP, we may note that one common feature is characteristic of each of them — the particles are not formed instantaneously but during a definite time interval. This can be explained by the fact that the rate of generation of free radicals is as a rule insufficiently high to convert simultaneously all the potential nucleation centres into the PMP. Indeed, in emulsion systems the rates of initiation do not usually exceed $10^{-9}-10^{-7}$ mol litre^{-1} s^{-1} or $10^{14}-10^{16}$ free radicals formed in 1 s in 1 litre of the reaction volume, whereas the total number of reaction sites (micelles or microemulsion particles) reaches $10^{20}-10^{21}$ litre^{-1}. In homogeneous nucleation, the particles are formed over a definite period and their nucleation ceases only after the disappearance of the free emulsifier.

The presence on the kinetic curves for the accumulation of the polymer in emulsion systems of a section involving an acceleration of the process (usually up to a 5%–10% conversion) before the curve attains the stationary stage has in fact been explained by the nucleation of particles over a period of time.[4] In certain systems, the stationary section on the curve is altogether absent, which has been accounted for by the continuous nucleation of the particles throughout the process. An example of such a process is provided by the emulsion polymerisation of styrene in a microemulsion generated with the aid of the sodium dodecyl sulfate–1-pentanol emulsifying system.[50]

The long duration of the nucleation process leads to different growth times of various particles. This results in the polydispersity of the latex formed and the KN of the emulsion polymerisation as a consequence of the differences between the rates of polymerisation of particles of different size.

There are also other causes responsible for the polydispersity of the latex formed. Such phenomena are as a rule associated with the use of surfactants which are relatively readily soluble not only in water but also in the monomer phase. For example, in the potassium persulfate-initiated emulsion polymerisation of styrene in the presence of hydroxyethylated tridecyl alcohol,[56] in the first stage the PMP are initiated in the micelles of the emulsifier dissolved in water. After this, polymerisation takes place in the presence of a constant number of particles at a constant rate of up to 30%–40% conversion. As the monomer is consumed, the emulsifier dissolved in the monomer phase is liberated and a secondary nucleation of the particles, leading to a bimodal size distribution of the latter, takes place. Similar results have been obtained when the emulsion polymerisation of styrene was carried out using a block copolymer [poly(ethylene oxide)–poly(propylene oxide)] as the emulsifier.[57]

Periodic nucleation of the particles is characteristic of continuous and semicontinuous emulsion polymerisation processes. The latter version presupposes a continuous supply of the components, for example of the monomer, and periodic removal of the reaction product. Cyclic oscillations in the number of particles in the continuous processes have been explained by the periodic variation of the concentration of the free emulsifier in the reactor,[42] which has been confirmed experimentally by measuring the surface tension of the latex formed in the polymerisation of styrene in the presence of sodium alkanesulfonate and potassium persulfate.[58] For an average residence time in the reactor of 40 min, the surface tension varied in the range 30–50 mJ m^{-2}, which corresponded to a transition from the complete adsorption saturation of the PMP to unsaturation. Such effects are associated with the fact that the rate of formation of the interface in the continuous emulsion polymerisation of nonpolar monomers is usually higher that the rate of supply of the emulsifier to the reactor. As a result, at certain stages of the polymerisation the formation of PMP ceases and the process proceeds in particles already formed, whereupon the rate of increase in the overall surface area of the particles diminishes. Fresh portions of the emulsifier supplied after saturation of the surfaces of the growing particles induce a new nucleation of the PMP and a decrease in the degree of adsorption saturation of the interface, the cycle being repeated.

Oscillations in the surface tension of latexes and in the number of particles formed occur also in the semicontinuous emulsion polymerisation of acrylic esters (ethyl and butyl acrylates) in the presence of the ammonium persulfate–sodium metabisulfite initiating system.[59] However, the explanation of the appearance of oscillations is different and the authors[59] attribute them to characteristic features of the emulsion polymerisation of polar monomers partially soluble in water. The oscillations in the surface tension indicate a periodic variation of the system between two states. The first state is characterised by the presence in the reaction system of an excess of the free emulsifier. In the second state, the emulsifier is almost fully adsorbed on the surface of the particles and its content in the aqueous phase is below the critical concentration for micelle formation (CCM). These oscillations are associated with the variation of the overall surface area of the particles. At a certain stage of the process, the surface of the particles adsorbs the entire micellar emulsifier. The further increase in the surface area as a result of the growth of the particles and the formation of new PMP via a homogeneous mechanism render the surface adsorption unsaturated, which lowers the stability of the system towards aggregation and leads to the flocculation of the particles. As a result of this process, the overall surface area of the particles diminishes, the emulsifier is liberated, and conditions suitable for nucleation of new particles arise, which leads to the repetition of the cycle. Thus both the number and size of the particles vary periodically during the process.

There is yet another cause responsible for the expansion of the size distribution of the particles and in certain cases for the appearance of a polymodal distribution. It is associated with the possibility of the nucleation of the PMP via several simultaneous mechanisms.

Evidently the micellar nucleation mechanism can operate only in the presence of emulsifier micelles in the aqueous phase. The nature of the initiator employed is less significant than the concentration of the emulsifier. However, one should note that the use of oil-insoluble initiators increases the probability of polymerisation in monomer drops. The formation of the polymer in two different reaction zones leads to a bimodal molecular mass distribution (MMD) of the polymer formed,[60,61] which is a consequence of the KN in such systems.

Homogeneous nucleation is more probable for the emulsion polymerisation of monomers which are relatively readily soluble in water, such as vinyl acetate or lower acrylic acid esters. In carrying it out, use of water-soluble initiators of the type of persulfates is preferable, although in the presence of enough emulsifier the homogeneous nucleation of PMP is possible also when compounds of the type of azobisisobutyronitrile (AIBN), which are only partly soluble in water, are used.[62,63] The PMP are formed exclusively via a homogeneous mechanism in the polymerisation of nonpolar monomers sparingly soluble in water (for example, styrene) in systems without an emulsifier or in the presence of a surfactant at concentrations below the CCM. In other cases, it is fairly difficult to distinguish the homogeneous mechanism from the micellar one.[64–66]

Certain ideas concerning the mechanism of nucleation or the contributions of the micellar and homogeneous mechanisms to the formation of PMP can be derived from the kinetic dependence of the rate of emulsion polymerisation on the emulsifier concentration. Presumably the absence of such a dependence, which is characteristic of the polymerisation of monomers comparatively readily soluble in water,[67] can be explained by the homogeneous nucleation of the particles. One may assume that, when the reaction order with respect to the emulsifier is close to 0.6 (the value corresponding to the Smith–Ewart theory[47]), the PMP are formed via the micellar mechanism. Intermediate reaction orders between 0 and 0.6 suggest the occurrence of nucleation via two mechanisms simultaneously.[67] However, the conclusions concerning the nature of the nucleation based on kinetic data require additional confirmation, since it has been shown[64,65] that this kind of reaction order can be explained also by homogeneous nucleation.

There are data concerning the emulsion copolymerisation of monomers differing greatly in their solubility in water,[68] which may be treated from the standpoint of the micellar or homogeneous nucleation of particles or of the variation of the relative contributions of these mechanisms depending on the reaction conditions. It has been shown[68] that the effective constants for the copolymerisation of vinyl acetate (VA) and n-butyl acrylate (BA) depend on the method of preparation of the reaction system. When the system is carefully freed of dissolved atmospheric oxygen, the copolymerisation constants have values characteristic of the copolymerisation of these monomers under homogeneous conditions ($r_{VA} = 0.074$ and $r_{BA} = 4.89$).[69] The copolymerisation takes place either in microdrops or in micelles containing the solubilised monomers. If the copolymerisation is carried out in a system containing oxygen solubilised by the emulsifier micelles, then the copolymerisation constants assume different values ($r_{VA} = 0.67$ and $r_{BA} = 0.91$). The values obtained can hardly be explained by a change in the reactivities of the monomers. It is most likely that vinyl acetate and n-butyl acrylate copolymerise in conformity with their true relative reactivities and the observed anomalies are due to a change in the relative concentrations of the monomers in the reaction zone. On this assumption the ratio VA : BA = 7.60, derived from the composition of the copolymer

at low conversions, is approximately consistent with the ratio of the solubilities of the monomers in water. The latter results suggest that the copolymer is formed as a result of the copolymerisation of the monomer dissolved in water, i.e. the nucleation proceeds via the homogeneous mechanism. The example presented demonstrates that, even in the emulsion polymerisation of the same monomers, the nucleation mechanism may vary as a function of specific conditions.

Other combinations of nucleation mechanisms are also possible. For example, when the polymerisation is carried out in microemulsions, it is by no means always possible to achieve the process exclusively in microdrops and the PMP may be partly formed via other mechanisms (micellar or homogeneous). In discussing the microemulsion mechanism of the nucleation of PMP, it has become usual nowadays to distinguish two types of microemulsions: miniemulsions (particle diameter greater than 50 nm) and microemulsions proper (particle diameter 10–50 nm). In contrast to the first type, emulsions of the second type constitute a thermodynamically stable system, which is usually formed when high concentrations of special emulsifying systems based on ionogenic surfactants and higher aliphatic alcohols or hydrocarbons are used.[50] Miniemulsions are formed in the presence of traditional surfactants under the conditions of intense hydrodynamic forces[42] or when the emulsifying systems mentioned above are used but at relatively low concentrations.[70] Miniemulsions can also be produced in systems where the emulsifier is first dissolved in the monomer phase[71] or is obtained in situ at the interface.[72,73]

As a consequence of the low rate of formation of the PMP, KN arises for any of these variants of the preparation of microemulsions or miniemulsions. The low rate of nucleation when the process is initiated by water-soluble initiators is due to the low rate of transfer of radicals from the aqueous phase as a consequence of the appearance at the interface of ionogenic surfactant–aliphatic long-chain alcohol complexes in the form of liquid-crystal formations.[50,70]

For the reasons stated, nucleation during emulsion polymerisation continues in some cases throughout the polymerisation process.[50] For this reason, not all the particles of the microemulsion are converted into the PMP. An appreciable fraction of the particles serve merely as a source of the monomer, which is transported into the reactive PMP (containing the free radical). This results in a wide size distribution of the particles despite the narrow distribution in the initial microemulsion. Similar effects arise also in miniemulsion polymerisation.[74]

There are data indicating the possibility of the simultaneous nucleation of PMP in miniemulsions or microemulsions via two mechanisms. For example, such effects have been observed in the emulsion polymerisation of methyl methacrylate (MMA) in miniemulsions obtained using the stabilised sodium lauryl sulfate–hexadecane system.[75] The simultaneous formation of particles in microdrops and via the micellar mechanism leads to the formation of latexes with a wide size distribution of the particles. When the miniemulsions are produced in the presence of ionogenic surfactants, it is also impossible to avoid fully the micellar nucleation as a consequence of the vigorous hydrodynamic action, which is indicated by the formation of latexes with a bimodal size distribution of the particles.[76,77]

The particles formed via different mechanisms are kinetically nonuniform not merely because of the differences between their sizes. Firstly, the monomer concentrations in such particles are different. For example, the monomer : polymer ratio in the PMP formed via the homogeneous mechanism is lower than in the particles obtained from micelles.[78] Secondly, the rate of incorporation of the radicals in the PMP and hence also many other kinetic parameters also depend on the method of nucleation. If under the conditions of the microemulsion nucleation mechanism a proportion of the particles are formed homogeneously, there is no doubt that the PMP obtained from the microemulsion are characterised by a significantly lower rate of capture of the radicals.

Thus nucleation is a powerful factor influencing the emulsion polymerisation kinetics. By regulating the rate and mechanism of the nucleation process, it is possible to carry out the polymerisation under kinetically uniform or extremely nonuniform conditions and to regulate thereby the characteristics of the products formed. Evidently, the occurrence of emulsion polymerisation under uniform conditions requires the maximum reduction of the nucleation period and the process must be carried out via a single mechanism. There are a number of ways of regulating these parameters.

It has been shown[79] that, by altering the emulsifier and initiator concentrations or the rate or initiation, it is possible to influence effectively the polydispersity of the latex formed, i.e. the particle nucleation time can be changed. The decrease in the emulsifier concentration and the increase in the rate of initiation as a result of the increase in the initiator content in the reaction system or in temperature ensure the formation of latexes with particles which are most uniform as regards size (Figs 1, 2).

An effective procedure for accelerating the PMP nucleation involves the use of active chain-transfer agents.[80] The low-molecular-mass radical formed when the chain is transferred to

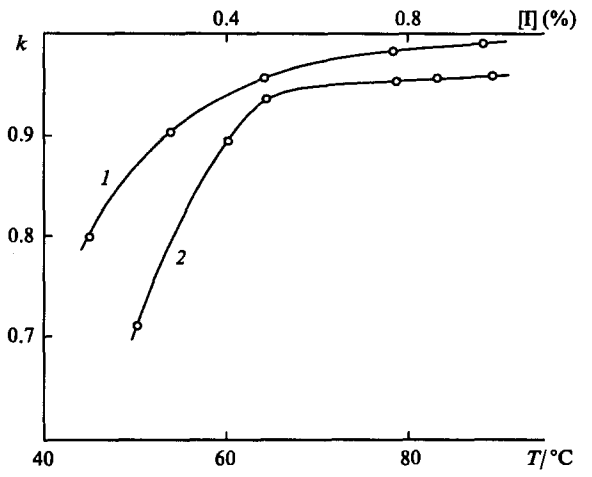


Figure 1. Dependence of the coefficient of the monodispersity of PMMA latex particles on the initiator (ammonium persulfate) concentration (curve *1*) and on temperature (curve *2*); emulsifier concentration — 0.1% relative to the mass of the monomer; T = 80 °C (curve *1*).

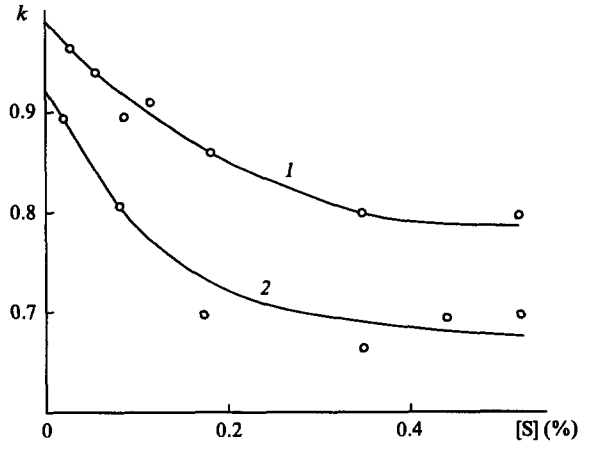


Figure 2. Dependence of the coefficient of the monodispersity of PMMA (curve *1*) and PMA (curve *2*) latex particles on the emulsifier (sodium dodecyl sulfate) concentration; T = 80 °C; initiator concentration — 0.5% of the mass of the monomer.

the molecular mass regulator can leave the PMP. As a result of such processes, each primary radical initiates a large number of PMP, which significantly shortens the nucleation stage.

Morrison et al.[65] established that the rate of nucleation varies in the emulsion polymerisation of styrene in the presence of indifferent electrolytes (NaCl) or inert solvents (ethylbenzene). In the former case, the nucleation period is shortened and in the latter lengthened, which is reflected in the polydispersity of the latex formed.

The possibility of regulating the process by inhibiting (with oxygen) the nucleation of the PMP in the micellar phase was examined above in the discussion of the copolymerisation of vinyl acetate and n-butyl acrylate. It was shown that the transition from the micellar to the homogeneous mechanism of the formation of particles makes it possible, in principle, to vary the effective copolymerisation constants and to obtain copolymers with a more homogeneous composition.[68]

The approach based on the use of inhibitors capable of excluding selectively a particular nucleation mechanism has been developed recently in the studies by Barton and coworkers.[62,63,81] By carrying out the emulsion polymerisation of styrene or methyl methacrylate in the presence of a water-soluble inhibitor (potassium nitrososulfonate) and an oil-soluble initiator (benzoyl peroxide), Barton and Juranicova[81] succeeded in fully excluding the possibility of homogeneous nucleation. On the other hand, in the emulsion polymerisation of the same monomers in the presence of an oil-soluble inhibitor (4-stearoyloxy-2,2,6,6-tetramethylpiperidine 1-oxide) and a water-soluble initiator or an initiator partially soluble in water (AIBN)[62,63] nucleation proceeded only via the homogeneous mechanism. It is of interest to note that in both cases the polymerisation occurred without an induction period.

Oganesyan et al.[82] proposed a simpler method for the regulation of the nucleation of particles. It consists in altering the water/monomer phase ratio (φ) and the particle radius (r). The rate of adsorption (z) of the radical growing in water is described by the equation[82]

$$z = 4\pi\bar{r}DN,$$

where $\bar{r}$ is the reduced radius of the monomer drops and of the growing radical ($\bar{r} = r$), D is the sum of their diffusion coefficients, and N is the number of particles defined by the formula

$$N = \frac{3}{4\pi r^3(1+\varphi)}.$$

The rate of growth of a single radical in water (w_p) is

$$w_p = k_p[M]_w,$$

where k_p is the chain propagation rate constant and $[M]_w$ the monomer concentration in water. The ratio of the rate of adsorption of the radical to the rate of its growth, i.e.

$$\theta = \frac{z}{w_p} = \frac{3D}{k_p[M]_w r^2(1+\varphi)},$$

determines the probability of the formation of particles in the aqueous phase or of the capture of radicals by the monomer drops.

Evidently, when $\theta \gg 1$, the growing radicals pass from the aqueous phase to the monomer drops already in the early stages and for $\theta \ll 1$ polymerisation develops in the aqueous phase. Calculation shows that chain propagation in the aqueous phase is possible for the emulsion polymerisation of styrene when $r \gg 10^{-4}$ cm. In the remaining cases, the growing radicals are adsorbed by the surfaces of the monomer drops having failed to recombine rapidly enough in the aqueous phase regardless of the value of φ. For vinyl acetate, the probability of the growth of the radical in water increases greatly for $r > 10^{-5}$ cm. For $r < 10^{-5}$ cm, the polymerisation of both styrene and vinyl acetate occurs in the monomer drops whatever the phase ratio.

2. Kinetic nonuniformity and elementary reactions in emulsion polymerisation

a. Initiation

The problem of the initiation of emulsion polymerisation has a direct bearing on the mechanism of the nucleation of PMP because the type of initiator determines to a large extent the region of the emulsion system where the particles are formed. Until recently, the accepted procedure was to distinguish two types of initiating systems: water-soluble and oil-soluble. However, it is now possible to differentiate also a third type — initiators with distinct surface-active properties.[67,83–85] Such initiators are located in the region of the interface.

The above classification is in a certain sense arbitrary, since many initiators are able to dissolve in both phases, and organic hydroperoxides, which possess some surface activity, can also be concentrated in the region of the emulsifier adsorption layers. The distribution of the initiator between different zones of the reaction system leads to the appearance of several types of nucleation centres, which renders the process kinetically nonuniform.

When the emulsion polymerisation of styrene in the presence of AIBN is considered as an example, it is possible to note three possible radical-formation zones: monomer drops, emulsifier micelles, and the aqueous phase (bearing in mind some solubility of AIBN in water).[86] The presence of several nucleation zones leads to the appearance of a polymer nonuniform with respect to molecular characteristics (bimodal molecular mass distribution). However, the nonuniformity diminishes during the polymerisation process, since following the appearance of a large number of PMP the contribution of the processes occurring in the monomer drops becomes insignificant.[86]

Another type of KN may be due to the difference between the kinetic parameters of the radical formation reaction in different reaction zones. Such effects are most marked when hydroperoxides are used as initiators of emulsion polymerisation.[87,88] Table 1 shows that the kinetics of the decomposition of isopropylphenyl hydroperoxide vary appreciably as a function of the reaction conditions. The most significant changes then occur when an interface appears in the system (in the isopropylbenzene–water emulsion). Even more marked differences between the kinetic parameters of the decomposition of the initiators as a function of the zones in which they are located in the latex system are observed for peroxides which are copolymers of vinyl monomers with the methacrylic acid ester of α-hydroxyethyl-*tert*-butyl peroxide.[83] The decomposition constants for the peroxy-groups located in the surface zone of the particles are 2–3 orders of magnitude higher than those for the same functional groups located in the bulk of the latex particles.

When water-soluble initiators such as potassium or ammonium persulfate are employed, it is usual to assume that at temperatures in the range 50–70 °C they generate free radicals at an almost constant rate, because only a small proportion of the initiator decomposes during polymerisation at moderate temperatures and its concentration changes little from its initial value. The persulfates are almost insoluble in organic media, so that free radicals are generated only in the aqueous phase. The second step in the initiation reaction — the interaction of the primary radical

Table 1. Kinetic parameters of the thermal decomposition of isopropylphenyl hydroperoxide at 95 °C.

Decomposition medium	k_d^a/min^{-1}	E_a/kcal mol^{-1}	Refs
Isopropylbenzene	5.0×10^{-4}	23.6	87
Water	3.3×10^{-4}	–	88
Isopropylbenzene–water emulsion (2:3) stabilised by potassium palmitate	1.1×10^{-3}	18.0	88

[a] k_d = thermal decomposition rate constant.

with a monomer molecule—also occurs in the aqueous phase according to the existing ideas for the commonest systems in which anionic surfactants are used as emulsifiers.[89] The above considerations should seemingly indicate the kinetic uniformity of the process involving initiation by persulfates. However, the results of studies by Okubo and Mori[90] and Georgescu et al.[91] suggest that the conditions governing the decomposition of the initiator into free radicals may vary during polymerisation. These hypotheses are based on the mechanism, discovered by the authors, by which the rate of decomposition of the persulfate is influenced by the emulsifier in the free state, in the micellar state, and in the state where it is adsorbed on the surface of the particles.

According to Okubo's data,[90] the mechanism of the decomposition of persulfates in the presence of an emulsifier, for example sodium dodecyl sulfate (SDS), can be represented as follows:

$$S_2O_8^{2-} \longrightarrow 2\,SO_4^{\cdot-},$$

$$SO_4^{\cdot-} + CH_3CH_2(CH_2)_{10}OSO_3^- \longrightarrow HSO_4^- + CH_3\dot{C}H(CH_2)_{10}OSO_3^-,$$

$$CH_3\dot{C}H(CH_2)_{10}OSO_3^- + S_2O_8^{2-} \longrightarrow SO_4^{\cdot-} + SO_4^{2-} + [X].$$

The activating effect of the emulsifier consists in inducing the decomposition of persulfates by the surfactant radicals. If the emulsifier is present in the form of micelles or in the adsorbed state on the surface of the PMP, then the interaction of the radical-anions with the hydrocarbon fragments of the surfactant is inhibited by electrostatic and steric hindrance. Furthermore, exchange reactions of the type

$$^{\cdot}SDS_{free} + SDS_{mic} \rightleftharpoons {}^{\cdot}SDS_{mic} + SDS_{free},$$

$$^{\cdot}SDS_{free} + SDS_{adsorb} \rightleftharpoons {}^{\cdot}SDS_{adsorb} + SDS_{free},$$

lower the concentration of the $^{\cdot}SDS$ radicals in a free state.

Thus, with increase in the surface area of the particles during polymerisation, the free emulsifier and its radicals are removed from the aqueous phase, which diminishes the rate of decomposition. Indeed the increase in the surface tension of the latex during emulsion polymerisation described above indicates the disappearance of the free emulsifier, while the presence of latex particles, for example those of poly(vinyl chloride),[91] diminishes the rate of decomposition of the persulfate approximately by a factor of 4 compared with the rate of decomposition at a surfactant concentration in the aqueous phase close to the CCM.

The effects examined should alter appreciably the rate of initiation of the emulsion polymerisation especially in those stages where the formation of the PMP has been completed (the micellar emulsifier has been exhausted). If the process proceeds in the presence of a constant number of PMP, then the rate of emulsion polymerisation also changes little because the stationary concentration of free radicals in the system is constant (the second case of the Smith–Ewart theory, $n = 0.5$).[47] However, as a consequence of the change in the overall surface area of the particles and in the rate of initiation, a varying frequency of the entry of free radicals into the particles alters the molecular characteristics of the polymer formed.

The increase in microviscosity in the PMP with increase in conversion after the disappearance of monomer drops should also change the initiation conditions. It is known from the theory of radical polymerisation[3] that, at advanced conversions of the monomer, the initiator decomposition rate constant and the initiation efficiency diminish. Clearly this phenomenon can occur only for compounds which are almost insoluble in water. For water-soluble initiators, the above effect is of no importance, since free radicals are generated outside the PMP.

Thus the KN in the emulsion polymerisation initiation reaction is determined primarily by colloidal-chemical causes: the presence of an interface, the change in the overall area of the interface and its adsorption saturation, and the existence of the emulsifier in several states (free, micellar, and adsorbed).

b. Chain propagation and termination reactions

When the KN in the chain propagation and termination reactions is considered, three aspects must be discussed:

1. the nonuniformities arising in connection with the possible occurrence of these reactions in the PMP produced and in the aqueous phase.

2. The nonuniform distribution of the concentrations of the monomer and of the growing radicals in the bulk of the PMP.

3. The variation during polymerisation of the chain propagation and termination rate constants.

In discussing the homogeneous PMP nucleation processes, we drew attention to the fact that the chain propagation reaction develops partially in the aqueous phase up to the instant of the capture of an oligomeric radical by the particle. The nature of this reaction depends on the nature of the monomer employed. Depending on the solubility of the monomer in water, from several to several tens of monomer units can add to the primary free radical before the oligomeric radical enters the PMP and its growth continues under other conditions. This means that the chain propagation reaction in emulsion polymerisation is kinetically extremely nonuniform. It occurs initially at very low monomer concentrations (10^{-3}–10^{-1} M) in the aqueous phase and then continues at a concentration of 5–7 M in the PMP. Despite this two-stage mechanism of the chain propagation (in water and in the PMP), the molecular characteristics of the polymer formed are largely determined by the processes in the PMP, because, for 10^3–10^4 additions of the monomer to the free radical in the particle, there are not more than several tens of chain propagation steps in water.

The latter claim is valid only provided that the growing radicals have insufficient time to undergo bimolecular termination in the aqueous phase before being trapped by the PMP. It has been shown[92,93] that the probability of chain termination exists and is most marked in the emulsion polymerisation of monomers sparingly soluble in water, characterised by low chain propagation rate constants (such as styrene), and also at high initiator concentrations, i.e. under the conditions of a low rate of chain propagation and a high rate of generation of free radicals in the aqueous phase. The bimolecular chain termination in water leads to an appreciable nonuniformity of the polymer with respect to molecular mass. This is indicated by experimental data which confirm the presence in the polymer of a low-molecular-mass fraction ($M_n = 10^3$) together with the high-molecular-mass fraction ($M_n = 10^5$–10^6).[94–96] The formation of two polymer fractions can be explained not only by the different monomer concentrations in water and in the PMP but also by different chain termination rate constants (k_t) in different media. Whereas in the PMP, where the polymer concentration is usually 40% to 50%, termination takes place in a highly viscous medium with $k_t = 10^3$–10^5 litre mol^{-1} s^{-1},[89] in the aqueous phase this reaction has been shown recently to be characterised by the constant $k_t = 10^9$ litre mol^{-1} s^{-1}.[64]

The rate constants for the elementary reactions change appreciably in the third stage of emulsion polymerisation, where the process proceeds with formation of PMP in the absence of monomer drops. Under these conditions, the microviscosity in the PMP rises rapidly, as a result of which the chain propagation reaction becomes diffusion-controlled at a certain degree of conversion. As regards chain termination, this reaction is the same as in the stationary stage of emulsion polymerisation, where the polymer content in the PMP reaches high values. The increase in conversion in the third stage leads to a further lowering of k_t, which induces the gel effect. It is noteworthy that the gel effect manifested in emulsion systems is fairly unusual. It is known that in emulsion polymerisation the gel effect usually arises for conversions in excess of 40%–50%, whereas in homogeneous systems this phenomenon occurs for lower conversions of the monomer. Furthermore, the explicit appearance of the gel effect (increase in the rate of polymerisation) is not always observed in emulsion polymerisation, because the increase in the average

number of radicals in the PMP, responsible for the increase in the rate of polymerisation, can occur only when the particle reaches a certain size (usually more than 100 nm). If the latter condition is not fulfilled, then the gel effect is absent even in the polymerisation of methyl methacrylate.[67]

The chain propagation reactions in emulsion systems differ significantly from those in homogeneous systems. If methyl methacrylate is polymerised in an oil at 50–60 °C, then the reaction ceases for a conversion of 84%–85%, because the reaction system approaches the vitreous state,[97] whereupon the chain propagation rate constant tends to zero, as shown by Marten and Hamielec.[98] In the emulsion polymerisation of methyl methacrylate at similar temperatures, it is possible to attain a conversion of 97% and above[97] and the constant k_p remains fairly high (of the order of 10^1 litre mol^{-1} s^{-1}) even for such conversions of the monomer.

The differences between the homogeneous and emulsion systems can be explained by two causes.

Firstly, the data presented by Marten and Hamielec[98] were obtained without taking into account the appreciable change in initiation efficiency at high conversions. It has been shown[99] that for azo-compounds the initiation efficiency decreases from 10^{-4} at 80% conversion to 10^{-6} at 82%–83% conversion. The latter factor shows that the data of Marten and Hamielec[98] are incorrect. The constants k_p listed in Table 2 are more reliable, because they were calculated from direct measurements of the concentration of active centres by EPR. The decrease in initiation efficiency can then be disregarded, since free radicals are generated in the aqueous phase, the viscosity of which remains virtually constant during polymerisation.

Secondly, the rate constants for the diffusion-controlled chain propagation reaction under homogeneous conditions and in emulsion polymerisation may indeed differ owing to the different conditions governing the transport of the monomer molecules to the active centres. During polymerisation in an oil, the average distance between the free radicals is ~100 nm. In an emulsion system for a PMP diameter of ~50 nm, the pathway which the monomer molecule must traverse before encountering a free radical is approximately four times shorter,[97] which suggests a higher value of k_p for the same diffusion coefficient.

The characteristic features of the chain propagation reaction at high monomer conversions examined above make it possible to formulate the principal conditions governing the formation of latexes with a minimal content of the residual monomer.

1. The use of water-soluble initiators. This rules out a decrease in the initiator decomposition rate constant and in initiation efficiency with increase in the microviscosity in the PMP.

2. The increase in the reaction temperature above the glass point of the polymer formed.

3. The introduction of solvents which reduce the glass point of the reaction system.

4. The increase in the monomer concentration in the PMP. This is needed particularly for monomers which are readily soluble in water (methyl acrylate, vinyl acetate, acrylonitrile). A change in the distribution of the monomer between the aqueous phase and the particles can be achieved by reducing the surface tension at the PMP–water interface and by selecting conditions ensuring the formation of a latex with particles having a minimal size. The last recommendation follows Morton's equation,[53] which relates the equilibrium monomer concentration in the PMP to a series of physicochemical parameters of the system.

In considering the polymerisation process developing in the PMP, one should note that the particles formed, like the reaction system as a whole, are nonuniform. In the discussion of the initiation reactions, it was shown that the surface of the particle and its bulk phase are kinetically nonequivalent. For the chain propagation and termination steps, these factors are less important. The polymerisation of monomers with surface-active properties is an exception. Their location in the adsorption layer influences significantly the kinetic parameters.[100] In other cases, it is possible to restrict the treatment to the consideration of the inhomogeneities associated with the nonuniform distribution of the reactants in the bulk of the PMP.

According to the ideas of Williams and coworkers[101,102] concerning the monomer concentration gradient in PMP, the polymerisation process develops mainly in the shell of the particles as a consequence of the higher monomer concentration in the surface layers. For the majority of simple systems, the concept of a thermodynamically improbable monomer concentration gradient has not received reliable experimental confirmation, although in certain cases an equilibrium monomer concentration may in fact not be established throughout the bulk of the PMP by virtue of kinetic causes (for example, the rate of diffusion of the monomer into the reaction zone may be lower than the rate of its polymerisation). Such a situation arises in the polymerisation of polar monomers characterised by high constants k_p[67] or when the monomer is supplied to the reactor at a rate lower than the rate at which it reacts.[78] Under these conditions, the monomer, having insufficient time to penetrate into the core of the particle, polymerises in its shell. For example, Kao et al.[103] showed that, in seeded emulsion polymerisation of styrene with a low rate of supply of the monomer, the thickness of the shell does not exceed 16% of the particle radius.

Another cause which explains the formation of particles of the core–shell type in the PMP during emulsion polymerisation without resorting to the concept of the monomer concentration gradient is associated with the nature of the initiator generated in the decomposition of the radical-anions, for example $SO_4^{\cdot-}$ formed on decomposition of persulfates. The electrical charge arising at one end of the growing macromolecule maintains it in the surface zone of the PMP, which restricts or altogether prevents the translational mobility of the macromolecule. Similar effects occur when surface-active initiators are used. Simple calculation shows that the statistical average size of the polymer coil with a degree of polymerisation of 10^4 should not exceed 10^2 Å even in a dilute solution. It has been shown[95] that, in the emulsifier-free, seeded potassium persulfate-initiated emulsion polymerisation of styrene, the polymerisation reaction proceeds in a shell ~100 Å thick on seed particles 2000 Å and more in diameter.

It is noteworthy that, in order to account for the possibility of the formation of PMP of the core–shell type, the concept of the fixation of one end of the growing macroradical is not always adequate. It is well known,[104,105] that by no means all

Table 2. Kinetic parameters of the emulsion polymerisation of methyl methacrylate initiated by $K_2S_2O_8$ at 50 °C.[97]

Time/min	$[M]_p$/mol litre^{-1}	Fraction of polymer in PMP	Rate of polymerisation/mol litre^{-1} s^{-1}	$10^7[\dot{R}]$/mol litre^{-1}	$10^{-16}N$/litre^{-1}	$\bar{n}$	k_p/ litre mol^{-1} s^{-1}
14	6.6	0.38	2.71	0.27	7.8	0.21	1500
29	5.1	0.51	7.10	0.44	7.9	0.72	1490
37	1.8	0.84	17.4	11.8	8.6	8.9	800
46	0.54	0.86	1.48	111	8.0	84	24.8
53	0.30	0.97	0.68	166	8.0	125	13.6

Key. $[\dot{R}]$ = concentration of free radicals; $[M]_p$ = concentration of the monomer in the particle; $\bar{n}$ = number of radicals in the particle.

macromolecules have terminal SO_4^- groups formed as a consequence of the reaction

$$SO_4^- + HOH \longrightarrow HSO_4^- + HO^\cdot ,$$

and the subsequent initiation of the polymerisation by hydroxyl radicals. One cannot rule out the hydrolysis of the SO_4^- end groups, which also leads to the appearance of electrically neutral terminal fragments. The SO_4^- groups may be partly 'buried' in the bulk of the PMP.

Chern and coworkers[106] proposed the concept of a nonuniform distribution of free radicals in the bulk of PMP regardless of the type of end groups. The authors calculated the radical distribution function along the particle radius assuming that the movement of the radical is random and is caused by the chain propagation, i.e. polymerisation. The movement of the growing radical stops as a result of chain termination or after the radical is completely surrounded by segments of the inactive polymer. Modelling of such movement by the Monte Carlo method showed that the distribution function is exponential and that it assumes the highest values for the surface layers of PMP, tending to zero for regions close to the centre of the particle.

The nonuniformities arising in the formation of PMP can be used in the formation of polymer dispersions with particles having a complex morphology and in securing specified properties of the polymeric product. A typical case is that of the synthesis of ABS copolymers by the seeded copolymerisation of styrene and acrylonitrile on polybutadiene particles. This type of technology, ensuring the formation of particles of the core–shell type, is widely used for the synthesis of different polymeric materials.[67, 107, 108] It actually makes it possible to obtain materials with opposite properties from the same monomeric raw material: plates with rubber inclusions which are distinguished by a high impact strength; elastomers reinforced by particles of rigid-chain polymers; latexes with a low minimum film-formation temperature due to the formation of a soft shell on hard particles. Studies have been carried out recently on the synthesis of latexes with particles containing inclusions of mineral pigments or fillers[109, 110] and dispersions of particles with microcavities.[111, 112]

The required properties of latexes or of the polymeric materials based on them are attained when particles with a specified morphology are obtained. The creation of the required core–spherical shell structure involves serious difficulties in many cases. The first problem — the carrying out of the process on seed particles — is solved relatively easily. It is sufficient to create conditions which exclude the formation of new particles. This is attained by carrying out the seeded emulsion polymerisation in the absence of the free emulsifier, the presence in the system of seed particles reducing sharply the probability of forming new PMP via the homogeneous mechanism.[113]

It is more difficult to guarantee the formation of a polymer solely on the surface of the seed particles. Under the conditions of equilibrium swelling of the particles in the monomer, polymerisation can occur also in the bulk of the PMP with formation of a new polymer in the form of inclusions in the seed particles. Such a process can be fully excluded, provided that the monomer and the polymer formed are thermodynamically incompatible with the polymer of the seed. In this case, seeded emulsion polymerisation on mineral microparticles is ideal. However, even when the conditions listed above are fulfilled, the correct core–shell structure is not always attained. Sometimes the polymer is formed on the seed particles in the form of excrescences[114] or has the raspberry fruit shape.[115]

The causes responsible for a particular morphology can be elucidated on the basis of thermodynamic and kinetic analysis of the processes occurring in the formation of heterogeneous particles. A complete analysis of the thermodynamics of the formation of particles with a complex structure has been carried out by Sundberg and coworkers[116, 117] in terms of the free surface energy (G) of the three-phase system (polymer 1, polymer 2, and water):

$$G = \sum \gamma_{ij} A_{ij} ,$$

where γ_{ij} is the interfacial tension between phases i and j and A_{ij} is the area of the interface between phases i and j. In such analysis, each morphology of the particle should be associated with its own free energy. For example, the free energies for particles with two extreme structures of the core–shell type can be represented by the following equations:

$$G = \gamma_{12} 4\pi r_1^2 + \gamma_{2w} 4\pi r_2^2 , \quad (1)$$

polymer 2 is polymerised in the form of a shell with a radius r_2 on seed particles of polymer 1 with a radius r_1);

$$G = \gamma_{12} 4\pi r_2^2 + \gamma_{1w} 4\pi r_1^2 , \quad (2)$$

(polymer 2 is polymerised in the bulk of the seed particles and forms a core with a radius r_2 surrounded by a shell of polymer 1 with a radius r_1).

In the above equations, γ_{12} is the interfacial tension between polymers 1 and 2 and γ_{1w} and γ_{2w} are the interfacial tensions at the polymer 1–water and polymer 2–water boundaries respectively.

Using similar equations, Sundberg and coworkers[116, 117] demonstrated the possibility of predicting the morphology of the particles. Naturally, the most probable morphology is that which has the minimum free energy. Indeed it has been demonstrated in practice[107, 108] that, when polymer 2 is more polar and hydrophilic than polymer 1, then it forms a shell on cores comprising the seed particles. If polymer 2 is hydrophobic while polymer 1 has hydrophilic properties, then the formation of the opposite morphology is more probable.

The interfacial tension may be influenced with the aid of surfactants. The usual low-molecular-mass surfactants are known to diminish effectively the polymer–water interfacial tension. Therefore the use of surfactants, especially for the preparation of particles with a hydrophobic shell, is an essential procedure. It has been shown[118] that the use of more effective surfactants in the formation of particles in which the core consists of poly(methyl methacrylate) while the shell consists of polystyrene promotes the attainment of the required morphology. The interfacial tension at the polymer 1–polymer 2 interface can be regulated by forming during the synthesis graft copolymers on the interface, which play the role of surfactants capable of stabilising emulsions of the oil in oil type. As an example, one may quote yet again the synthesis of the ABS copolymers during which a certain amount of a graft copolymer is produced as a result of the grafting of styrene and acrylonitrile to polybutadiene macromolecules.

Yet another thermodynamic factor is the compatibility of the polymers. It would seem that the ideal case is that of complete incompatibility of the seed polymer and the polymer formed in the second stage. However, it is then difficult to count on the formation of a continuous shell. The heterogeneous particles formed can have a mushroom or raspberry shape. A limited compatibility of the polymers is therefore desirable. It is achieved, for example, by the partial grafting of the shell polymer to the core polymer already mentioned. The problem of the incompatibility of the polymer arises only at a certain stage of the process after a certain degree of conversion of the monomer, because in the initial state the PMP is as a rule homogeneous (the monomer is a solvent for the seed polymer).

In order to predict the morphology of the particles, it is necessary to take into account kinetic as well as thermodynamic factors. We shall consider certain kinetic factors which determine the possibility of achieving the polymerisation process in the shell of the particle. These factors are associated either with the localisation of the active centres in the surface zone of the PMP or

with the creation of conditions preventing the penetration of the monomer and of the polymer formed in the second stage into the bulk of the seed particle and promoting the appearance of new interfaces: polymer 1–polymer 2 and polymer 2–water. As an example, we shall consider the most complex thermodynamically unfavourable case — the creation of a hydrophobic shell on hydrophilic seed particles.

As shown above, the localisation of the active centres in the PMP shell is promoted by the use of initiators generating radical-ions on thermal decomposition, which fix one end of the growing macroradical in the surface zone of the particle. In the polymerisation of styrene on poly(methyl methacrylate) (PMMA) seed particles in the presence of potassium persulfate, it is not possible to obtain a continuous polystyrene (PS) shell, but an appreciable proportion of the polystyrene domains are on the surface of the PMMA particles.[118] A similar picture is observed in the polymerisation of styrene on poly(vinyl acetate) particles, but, in contrast to the first case, only under the conditions of a slow supply of the monomer to the reaction system.[113] If AIBN is used to initiate the seeded emulsion polymerisation of styrene in the presence of PMMA particles, then a completely inverted structure arises (the polystyrene is present in the form of a core within the bulk of the PMMA seed particle).[118]

The use of initiators linked by covalent bonds to the surface of the seed particles is an effective method for the preparation of core–shell particles. Such a possibility has been demonstrated[67] in the polymerisation of n-butyl acrylate on seed particles comprising the styrene–methacrylic acid ester of α-hydroxyethyl-*tert*-butyl peroxide (MEP) copolymer. The formation of a continuous poly(butyl acrylate) shell is indicated by the low minimum latex film formation temperature (the film was obtained even at 0 °C). It is noteworthy that in this case the MEP units ensure not only the initiation of the process but also the grafting of n-butyl acrylate, which assists in the formation of a regular structure.

Particles with a regular core–shell morphology are formed when purely kinetic approaches are used. These are based on introducing the monomer into the seed latex at a rate equal to or lower than the rate of its polymerisation. The polymerisation of styrene on seed particles comprising hydrophilic polymers [poly-acrylates, poly(vinyl acetate)] under the conditions of a reduced rate of supply of the monomer to the reactor ('monomer starvation') ensures the formation of surface polystyrene domains and in certain cases of a continuous shell.[113, 118, 119]

Another procedure, which also hinders the diffusion of the monomer into the bulk of the seed particles, involves the use of cross-linked polymers as the seed.[118] If the cross-linking agents are also used in the seeded emulsion polymerisation stage, then a continuous shell of the hydrophobic polystyrene on the particles of the cross-linked poly(butyl acrylate) is formed even when an oil-soluble initiator is employed.[119] When seeded emulsion polymerisation is carried out at a reduced temperature, the rate of diffusion of the monomer is also lowered, which makes it possible to obtain sometimes a regular core–shell morphology without resorting to the 'monomer starvation' procedures.[120]

The procedures described above for the regulation of the morphology of heterogeneous particles are listed in Table 3. Analysis of the data presented makes it possible to differentiate the following factors governing the structure of the particles formed: the degree of compatibility of the polymers in the core and in the shell; the existence of a chemical bond between the polymers (grafting) or the formation of interpenetrating networks (the use of cross-linked agents); the relation between the hydrophilic and

Table 3. The influence of the conditions in seeded emulsion polymerisation on the morphology of the heterogeneous particles.

Seed	Monomer	Initiator	Surfactant	Method for emulsion polymerisation	Morphology of particles	Ref.
PMMA	Styrene	$K_2S_2O_8$	P-8	Single introduction of all components	Incomplete inversion. PS domains within and on the surface of particles	118
PMMA	Styrene	AIBN	P-8	Ditto	Complete inversion	118
PMMA	Styrene	AIBN	P-40	"	Incomplete inversion. PS domains within and on the surface	118
Styrene–MEP copolymer	n-Butyl acrylate	MEP units	E-30	"	Core — copolymer, shell — poly(butyl acrylate)	67
PMMA cross-inked by AM	Styrene	AIBN	P-80	Semicontinuous emulsion polymerisation ('monomer starvation')	PS domains on the surface of PMMA	118
Poly(vinyl acetate)	Styrene (monomer : seed = 0.3–0.35)	$K_2S_2O_8$	–	Ditto	PS domains on the surface of poly-(vinyl acetate)	113
Poly(butyl acrylate) cross-linked by AM (1%)	Styrene + divinyl-benzene (0.5%)	AIBN	–	"	Core–shell (PS shell)	119
Poly(vinyl acetate)	Styrene (monomer : seed = 0.7	$K_2S_2O_8$	–	"	Core–shell (PS shell)	113
Polystyrene	Methyl methacrylate	–	–	Once only introduction of components	Core–shell (PMMA shell)	120
Polystyrene	Methyl methacrylate	–	–	Ditto	Core–shell (PS domains in the core)	120

Note. The following notation has been adopted: AM = allyl methacrylate; P-8 = hydroxyethylated nonylphenol (8 hydroxyethylene units); P-40 = hydroxyethylated nonylphenol (40 hydroxyethylated units); E-30 = sodium alkanesulfonate (alkane = $C_{15}H_{31}$).

hydrophobic properties of the polymers of the core and the shell; the nature of the surfactant; the type of initiator; the method used in carrying out the seeded emulsion polymerisation (by introducing the monomer into the seed latex in one go or by carrying out the process under the conditions of 'monomer starvation'); the process temperature; the seed polymer : monomer ratio.

Thus emulsion polymerisation is kinetically an extremely nonuniform process. It is characterised by the same elements of KN which obtain in radical polymerisation under homogeneous conditions, namely the change in the elementary reaction rate constants at high conversions. However, this type of KN in emulsion polymerisation is manifested in a fairly unusual manner (the gel effect arises at higher conversions and under certain conditions is absent even in the polymerisation of methyl methacrylate). When the emulsion polymerisation is initiated by water-soluble compounds, viscous effects do not influence the initiation reaction.

The fundamental difference between emulsion polymerisation and other radical systems, even heterogeneous ones, is associated with the characteristics of the nucleation of the PMP. The polydispersity of the particles, the different mechanisms of their nucleation, and the possibility of the nucleation of the particles via several mechanisms simultaneously lead to a new type of KN which is not characteristic of other types of radical polymerisation. The KN of this type introduces additional elements which are responsible for the nonuniformity of the molecular characteristics of the polymers formed. On the one hand, the KN in emulsion systems induces appreciable nonuniformities in the properties of the polymerisation product (polydispersity of the latex, a broad molecular mass distribution, nonuniformity of the composition of the copolymers) and, on the other, can be used to establish and regulate the properties of new polymeric materials. The most interesting approaches, which can be employed in emulsion systems, involve the formation of particles of the core–shell type having a heterogeneous structure.

In conclusion of this section of the review, we may note that analysis of the causes responsible for the KN in emulsion polymerisation permits a specific selection of the process conditions ensuring the minimum (or maximum) manifestation of KN or its complete elimination. Emulsion polymerisation on radicals, separated in space on individual PMP, may serve as an example. The polymers formed under these conditions are almost monodisperse.[121]

IV. Kinetic nonuniformity in polymerisation processes in the presence of a dispersed solid phase

Systems with a dispersed solid phase have been introduced into research practice comparatively recently. The results have been surveyed in a number of reviews.[43,44,122,123] As in emulsion polymerisation, the heterogeneity of the system is specified by the initial polymerisation conditions (degree of dispersion of the solid phase and its permeability to the monomer, the nature of the monomer and other system components, etc.).

One of the principal problems is that of the state of the monomer and initiator molecules and of the growing radicals in different zones of the polymerisation system and of their role in the polymerisation kinetics in the creation of the structure of the macromolecules formed.

If dispersed inorganic materials incompatible with and impermeable to the monomer, initiator, etc. are used as the initial solid phase, we can differentiate three zones in which the elementary polymerisation reactions take place (Fig. 3): I—zone located in the immediate vicinity of the surface of the solid phase where the monomer (or the initiator) can be bound chemically or physically to the solid surface; II—transitional zone; III—the bulk phase (of the monomer or its solution) zone.

Near the surface zone, the components of the polymerisation system (the monomer, the initiator, etc.) can have reactivities

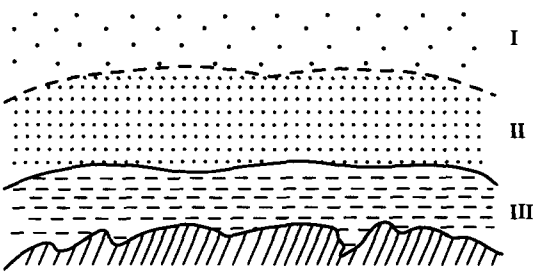


Figure 3. Schematic illustration of the establishment of the concentration nonuniformity in heterogeneous polymerisation in the presence of a dispersed solid phase: (I) bulk phase (monomer vapour or solution); (II) transitional layer; (III) layer of monomer physically adsorbed or chemisorbed on the surface or in the immediate vicinity of the surface of the dispersed phase.

different from those of the same components in the bulk of the liquid phase, which is the cause of the KN.

If the solid phase (for example, the polymer phase dispersed in the polymerisation system) is permeable to the polymerising monomer, then the reaction zone may arise there during polymerisation and may spread directly in the polymer phase.[124–128]

It has been shown[122,123] how significant is the adsorption and molecular transport of the monomers (or other components) on the surface in determining the characteristics of heterogeneous polymerisation. In the model proposed for the reaction zone, the monomers are divided into systems with strong and weak bonding depending on the adsorption mechanism and the adsorption bonding forces. Examples of such systems are presented in Table 4.

A mobile nonlocalised adsorption, which is reversible close to room temperature, is characteristic of systems weakly bound to the surface. The surface diffusion coefficients in these systems are fairly high (10^{-4}–10^{-5} cm^2 s^{-1}). For systems with strong bonding, the distribution of the monomer on the surface is of a localised type and the adsorption is irreversible and activated.

In systems with strong bonding to the surface, the surface of the dispersed solid phase is modified by the chemical interaction and is fully covered by a molecular monomer (or initiator) layer. Thus dispersed inorganic fillers with surface (anchoring) monomer groups or initiating peroxy-groups of the type of macromonomers or macroinitiators can be obtained by the interaction of the hydroxy-groups of aerosil with alkoxy- or halo-groups of organosilicon compounds containing polymerisable (vinyl) bonds or initiating groups.[43,44,130–132]

In polymerisation systems with such components, we encounter an artificial nonuniform distribution of the concentrations of the initiator or the comonomer established beforehand in the polymerisation system (Fig. 4). Naturally, in such systems the KN underlies the very structure of the distribution of the initial components of the recipe and makes it possible to some extent to predict beforehand or to establish the microheterogeneity of the polymer systems or compositions formed and to obtain polymer-inorganic compositions or block copolymers with a satisfactory enforced compatibility of the solid phase with the polymer phase produced during polymerisation. Such compatibility is achieved by the chemical grafting of the polymer to the solid phase.[44,133–135]

The study of the kinetics of polymerisation in the heterogeneous systems considered is far from complete and there is virtually no theory of heterogeneous radical polymerisation. The characteristics of the elementary reactions constitute a key to the understanding of the experimentally observed kinetic features. Therefore, in analysing the KN of such systems, we shall concentrate on the characteristics of their occurrence in some of the most thoroughly investigated systems.

Table 4. The mechanisms of the adsorption of vinyl monomers in certain systems.[129]

Monomer	Adsorbent	Characteristics of sorption mechanism	Characteristics of adsorption bonding force
Alkenes and dienes	SiO_2	Formation of weak π-complexes between C=C bonds (or a system of C=C bonds) and surface OH groups	$\Delta\nu(OH) \approx 100-120$ cm^{-1}
Carbonyl-containing compounds (VA, MMA, MA, OMA)	SiO_2	Formation of hydrogen bonds between carbonyl and silanol groups. At low coverages, the oxygen of the methoxy-group may participate in the adsorption interaction	$\Delta\nu(OH) \approx 300$ cm^{-1} $\Delta H_\alpha \approx 49-53$ kJ mol^{-1}
Carbonyl-containing compounds (VA, MMA, MA, OMA)	MgO Al_2O_3	Chemisorption as a result of strong coordination of C=O group to the surface	$\Delta\nu(C=O) = 170$ cm^{-1}
Unsaturated carboxylic acids	SiO_2	Possibility of the interaction of the carboxy-group with two OH surface groups	$\Delta\nu(OH) = 350$ cm^{-1}
Unsaturated carboxylic acids	Aminated aerosil	Ionisation of acids in the presence of adsorbed water	
Nitrogen-containing vinyl monomers (4-VP, 2-VP, *N*-VPD, etc.)	SiO_2	Acid–base interaction with surface OH groups	$\Delta\nu(OH) \approx 700-950$ cm^{-1} $\Delta H_\alpha = 140$ kJ mol^{-1}
4-VP	Carboxylated aerosil	Formation of ionic bonds in the presence of adsorbed water	
Styrene	SiO_2	Formation of weak π-complexes with surface OH groups. Resolution of the rotational structure in IR spectra	$\Delta\nu(OH) = 120$ cm^{-1}

Note. The following notation has been adopted: OMA = octyl methacrylate, VP = vinylpyridine, *N*-VPD = *N*-vinylpyrolidinone.

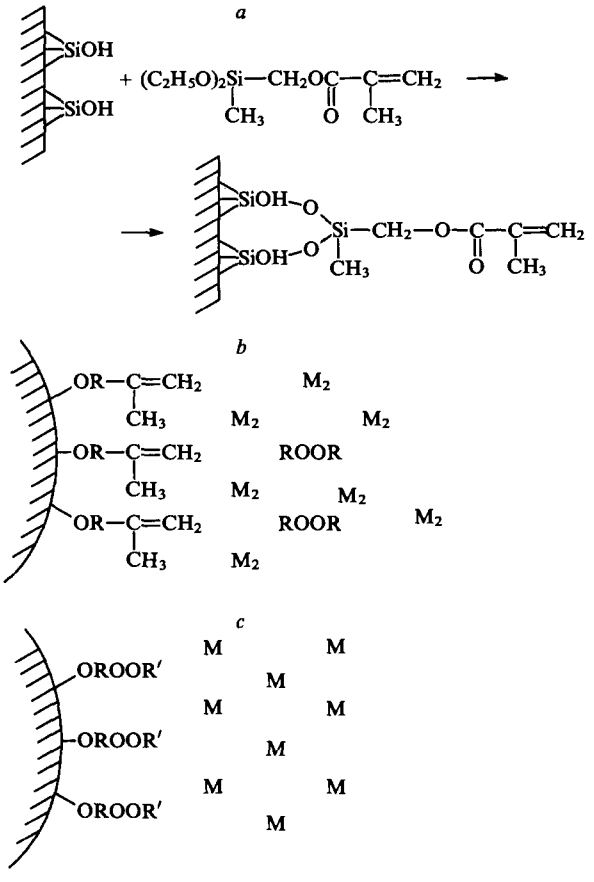


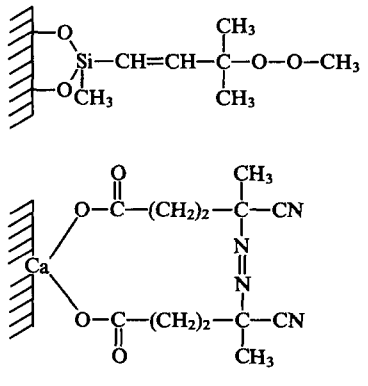
Figure 4. Schematic illustration of the formation of anchoring compounds on the aerosil surface (*a*) and illustration of the concentration nonuniformity in the distribution of the comonomer (*b*) and the initiator (*c*) in a heterogeneous polymerisation system.

1. Initiation of heterogeneous radical polymerisation in the presence of a dispersed solid phase

Such a reaction can be achieved in several ways.

1. By means of the functional group of the initiator fixed on the solid surface (as a result of a chemical reaction with the surface groups of the solid phase).[130–132, 136, 137]

Such initiating systems may be assigned to the class of macroinitiators.



2. By means of initiators deposited on the solid surface as a result of preliminary physical adsorption from solution.

3. By means of an initiator introduced into the monomer phase.

4. By means of radiation initiation or photoinitiation.

The choice of the type of initiation of heterogeneous polymerisation is frequently determined by the endeavour to obtain the maximum amount of the polymer grafted to the solid surface.

For the first two versions, we may note the nonuniformity of the distribution of the initiator and hence the localisation of the initiation reaction in the zone adjoining directly the surface, which by itself leads to KN. It has been shown in a number of studies[23, 131, 136–138] that, together with this feature, the localisation of the initiator in the surface zone can alter significantly the

Table 5. The constants k_p and k_t for the polymerisation reactions of vinyl acetate and methyl methacrylate on the surface (monolayer coverage) and in the liquid phase (in bulk) at 50 °C.

Parameter	Vinyl acetate			Methyl methacrylate		
	on the surface		in the liquid phase	on the surface		in the liquid phase
	AS/400	MAS		AS/400	AS/200	
k_p/litre mol^{-1} s^{-1}	34	160	1500–2600	22	15.4	350–410
$10^{19} k_p$/cm^3 molecule^{-1} s^{-1}	1.4	2.7	25–43	0.39	0.26	5.8–6.8
k_t/litre mol^{-1} s^{-1}	–	5.4×10^3	2.5×10^7	–	–	2×10^7
$10^{19} k_t$/cm^3 molecule^{-1} s^{-1}	–	0.9	4.2×10^3	–	–	3.3×10^3

Note. The following notation has been adopted: AS/400, AS/200 = aerosil; MAS = methylated aerosil.

kinetics of radical formation. We noted the acceleration of the decomposition of hydroperoxides in heterogeneous systems (Table 1) in the analysis of the characteristic features of emulsion polymerisation. Similar data have been obtained[138] for the decomposition of cumenyl hydroperoxide on the surfaces of particles of titanium compounds.

The kinetics of the decomposition of initiators (derivatives of azonitriles and peroxides) fixed by covalent bonds on the surface of copper or aerosil have been studied in greatest detail.[131,136,137,139] The initiators fixed on the surface decompose much faster (with the exception of 4-azobis-4-cyanopentanoic acid[129,136]) and the activation energy for the decomposition reaction is lower than for the decomposition in the liquid phase under similar conditions. However, as for emulsion systems,[83] a decrease in the effectiveness of initiation is observed. Such a decrease depends on the way in which the initiator is fixed on the solid surface (via one or both ends of the initiator) and can differ by an order of magnitude.

A mechanism which explains these results has been proposed. Its essential feature reduces to the orientation effect on the surface as a function of the method of fixation of the initiator and to the increase in the role of the cage effect in connection with the hindrance to the separation of the radical pair by diffusion and hence a greater probability of a radical acceptor mechanism of the liberation of the initiating radicals.

When an initiator introduced into the monomer phase of the system is used, the initiation reaction differs little from that in homogeneous systems if a distribution of the initiator concentration does not occur under the influence of the solid surface.

The radiation initiation and photoinitiation in heterogeneous systems have been analysed in detail.[122,123,129] One may note the coupled influence of the nature of the dispersed solid phase and of the polymerising monomer on the initiation reactions and on the appearance of nonuniform zones in the system and hence on the KN.

2. Chain propagation reactions

The elementary chain propagation and chain termination reactions in radical polymerisation in the presence of dispersed solids have been surveyed by Bruk and Pavlov,[122,123] and also by Krul'.[124] The experimental polymerisation rate constants in a number of heterogeneous systems have shown that the reactivity of the monomers in the region of the surface of the solid is significantly lower (by 1–2 orders of magnitude) than in the liquid phase.[123,129] We obtained similar data for monomers grafted to the aerosil surface.[140] The possible energetic nonuniformity of the surface relative to the adsorbed or bound monomer and the lateral interactions in the absorption layer must be regarded as the main causes of this behaviour.

The elucidation of the role of diffusional inhibition is important for the determination of the causes of the decrease in the reactivity of the monomers in the region of the surface. The possibility of diffusional inhibition is indicated by the dependence of k_p on the degree of surface coverage by the monomer. However, it has been shown[141] that an appreciable influence of diffusional retardation on k_p in polymerisation on the surface can be assumed only for systems characterised, together with a low surface mobility of the monomers, by a low equilibrium monomer vapour pressure. This is possible only for certain systems with strong bonding of the monomer to the surface and provided that the polymerisation is carried out from the gas phase at low monomer partial pressures. Certain kinetic parameters of the polymerisation of vinyl acetate and methyl methacrylate adsorbed on a surface and in the liquid phase, taken from a monograph,[123] are presented in Table 5.

Evidently, the chain propagation rate constants expressed in comparable units are at least an order of magnitude lower on the surface than in polymerisation in the liquid phase. This difference is greater in systems with strong bonding of the monomer to the surface. One may assume that an increase in the volume of the monomer molecules (an increase in the length of the substituent) can lower k_p and enhance the stereocontrol on the surface in the chain propagation steps.

In the adsorption layer, the monomer copolymerisation constants may change significantly.[123] These changes are most marked for monomers differing in the strength of their adsorption to the surface. Table 6 presents the copolymerisation constants for certain monomers taken from the monograph of Bruk and Pavlov.[123]

Table 6. Copolymerisation constants in the liquid phase and on the surface of aerosil.[123]

VA/4-VP	MMA/4-VP	VA/VPD
Liquid phase		
0/30	0.57/0.79	0.20/3.3
AS surface, 70 °C		
0.14/0.11	0.50/0.50	0.27/3.0
AS surface, 20 °C		
0.25/3.5	0.45/0.15	0.65/1.3

3. Kinetic chain termination processes

One of the principal features of the polymerisation in heterogeneous systems in the presence of dispersed solids is the inhibition of the quadratic chain termination processes in the interaction of the growing radicals. This can be caused by the decreased capacity for diffusion and by the possibility of the insulation of the growing radicals in space. The quantitative data presented in Table 5 and obtained in the determination of the quadratic termination constants for the growing radicals in the region of the surface in the polymerisation of vinyl acetate are 3–4 orders of magnitude lower than in the liquid phase. The low values of k_t give rise to long average lifetimes of the kinetic chains. The low translational mobility and the long average lifetimes of the kinetic chains enhance the role of alternative chain termination mechanisms, for example the linear mechanism.

The mechanism of the linear termination is usually related [123] to the immobilisation of the growing macroradical at a certain propagation stage without the chemical destruction of the growing radical. The loss of the reactivity of the radicals in the propagation reaction is observed when they attain certain chain lengths or as a result of a conformational transition with localisation of the active centre within the globule or as a result of the immobilisation or enclosure in a structural trap — a micropore. This is promoted by an increase in the rate of termination with increase in the content of micropores in the solid phase.

The immobilisation effect is manifested to a lesser extent for macroradicals characterised by a high reactivity (for example, in the case of vinyl acetate). The probability of chain transfer to the monomer as a variant of the linear termination mechanism may increase for such systems.

In any polymerisation system, there is a possibility of the simultaneous retention of conditions for the quadratic and linear termination of the growing chains. Mixed termination, expressed by an initiation reaction order between 0.5 and 1.0, frequently obtains in practice.

It is of interest to note the results obtained in the study of the dependence of the fraction of the immobilised radical α on the average distance between the initial active centres r and on the nature of the polymerising monomer.[129] For high values of r, the fraction α is close to 1 (Table 7). With decrease in r, the fraction α diminishes monotonically as a consequence of the interaction of the growing macroradicals. Quadratic termination begins to compete with the linear termination at a radical concentration of $(1.5-2) \times 10^{14}$ m^{-2}, which can be adopted as the onset of the effective overlap of the coils on the surface.

Table 7. The influence of the nature of the monomer, the average distance between the growing chains r, and the polymerisation temperature on the capacity of the growing macroradicals for immobilisation on the surface of aerosil modified by methacrylic acid (monomer temperature in the feeding device 0 °C).

Monomer	Fraction of immobilised chains		
	r = 30 nm, T = −78 °C	r = 114 nm, T = 25 °C	r = 7 nm, T = 25 °C
Methyl methacrylate	1	0.98 [a]	0.40
Methacrylic acid	1	0.44	0.41
α-Methylstyrene	0.5 [b]	0.60	0.22
Acrylonitrile	0.27	0.36	0.20
Methyl acrylate	0.22	0.39	0.14
Vinyl acetate	0.30	0.23	–
Styrene	0.18	0.33	0.16

[a] Temperature of liquid monomer in the feeding device: 25 °C.
[b] Temperature of liquid monomer in the feeding device: −23 °C.

4. Characteristic features of the chain propagation and termination in the polymerisation of monomers sorbed in polymer matrices

The polymerisation of monomers sorbed in polymer matrices is one of the variants of heterogeneous polymerisation in which the reaction zone [apart from the monomer (liquid) phase] can spread through the polymer phase. It has now been established [128, 129] that the characteristic dimensions of the microheterogeneity arising in the polymer matrix are comparable with the dimensions of the individual macromolecules formed. This justifies the consideration of the polymerisation processes in polymer matrices as typically heterogeneous reactions with segregation of a polymer microphase.

The study of the polymerisation of methyl methacrylate sorbed in polypropylene and PTFE matrices [129] led to the conclusion that the initial radicals are converted quantitatively into the PMMA chain propagation radicals and that the reaction ceases at a constant concentration of the growing radicals and of the sorbed monomer. With increase in the monomer vapour pressure in the gas phase, polymerisation is renewed at the previous rate. It has been found by a special method and with the aid of deuteriated methyl methacrylate that the equilibrium in the chain propagation reaction is established after the attainment of a definite length of the macroradical. Detailed analysis of the experimental data permitted the conclusion that the 'self-entombment' or immobilisation of the growing radicals is associated not with the diffusional hindrance of the monomer transport and the decrease in the mobility of the macroradical but with the decrease in the true reactivity of the growing macroradicals after they attain a certain chain length.[129] The restriction of the reactivity of the macroradical concerns only the chain propagation reaction and does not extend to the chain transfer reaction. These kinetic effects are a consequence of the thermodynamic conditions and are characteristic of both polymer matrices and of disperse inorganic systems.

V. Conclusion

The theoretical ideas and experimental data examined permit the claim that, in the determination of kinetic parameters, especially at advanced stages of the polymerisation reaction, it is essential to take into account the KN and the factors which determine it. In many cases the KN may be regarded as an effective instrument for controlling the polymerisation process and the characteristics and operating properties of the polymer formed. The latter may be confidently considered to apply to emulsion polymerisation and polymerisation in the presence of a dispersed solid phase. This is associated with the fact that the elements of the KN in heterogeneous polymerisation systems can be generated comparatively readily even before the onset of polymerisation (a specified distribution of the components in different kinetically nonequivalent reaction zones and their predicted reactivity in these zones).

In homogeneous systems, the KN is not always manifested explicitly, which hinders the use of the structural-kinetic approach in calculations for specific technological polymerisation processes. Nevertheless, in terms of the structural-kinetic aspect, the problems considered lead to definite prospects for the development of approaches which will make it possible to describe from a single standpoint the set of complex phenomena accompanying the polymerisation process. The creation of such an approach is complicated by the fact that the radical polymerisation process is characterised by a large set of interdependent parameters, the variation of which it is at present fairly difficult to predict.

One may assume that the most fruitful route to the solution of the problem involves a further development of ideas about the reactivity of molecules. Speaking of the latter, we draw attention yet again to the complexity of this concept for polymer systems and to the need to take into account not only the purely chemical factors (the electronic state of the molecules and radicals and the steric factors due to the presence of various substituents in the molecules) but also physical (diffusion) factors.

In conclusion we may note a further two considerations.

Firstly, in the development of kinetic mechanisms for radical polymerisation, it is necessary to take into account the possibility of a change as a function of conversion in not only the initiation, propagation, and termination reaction rate constants but also in the rate constants for other possible elementary reactions, for example the chain transfer rate constants. A simple approach has been proposed [142] to the calculation of the constants for chain transfer to the monomer as a function of the degree of conversion of the monomer into the polymer and it has been shown that, for example in the polymerisation of methyl methacrylate, a change in conversion from 80% to 90% lowers the rate constants for chain transfer to the monomer by a factor of approximately 3.

Secondly, in estimating the decrease in k_t with conversion only the change in the translational and segmental mobility of the macroradicals has been taken into account hitherto. Nevertheless,

there exists yet another form of motion of the macroradical—due to the polymerisation chain propagation. Buback et al.[143] noted a significant contribution of the latter type of motion to the overall decrease in k_t with conversion, having demonstrated the actual dependence of k_t on k_p at advanced stages of the polymerisation process.

We hope that the proposed approach to the generalisation of the ideas about the KN in radical polymerisation processes and about the polymerisation mechanism at different conversions will stimulate further studies in this field.

References

1. C H Bamford, W G Barb, A D Jenkins, P F Onyon *The Kinetics of Vinyl Polymerisation by Radical Mechanisms* (Translated into Russian; Moscow: Izd. Inostr. Lit., 1961)
2. Kh S Bagdasar'yan *Teoriya Radikal'noi Polimerizatsii* (Theory of Radical Polymerisation) (Moscow: Nauka, 1966)
3. G P Gladyshev, V A Popov *Radikal'naya Polimerizatsiya pri Glubokikh Stepenyakh Prevrashcheniya* (Radical Polymerisation at High Degrees of Conversion) (Moscow: Nauka, 1974)
4. S S Ivanchev *Radikal'naya Polimerizatsiya* (Radical Polymerisation) (Leningrad: Khimiya, 1985)
5. Yu D Semchikov, V U Gromov, E N Teleshov *Vysokomol. Soedin., Ser. A* **33** 1428 (1991)
6. V I Ivanov, V A Kaminskii, E B Brun, B A Korolev, M B Lachinov *Vysokomol. Soedin., Ser. A* **33** 1442 (1991)
7. J A Maxwell, G T Russel *Macromol. Chem., Theory Simul.* **2** 95 (1993)
8. N M Emanuel', A L Buchachenko *Khimicheskaya Fizika Stareniya i Stabilizatsii Polimerov* (Chemical Physics of the Ageing and Stabilisation of Polymers) (Moscow: Nauka, 1982)
9. E T Denisov *Okislenie i Destruktsiya Karbotsepnykh Polimerov* (Oxidation and Destruction of Carbon-Chain Polymers) (Leningrad: Khimiya, 1990)
10. S K Soh, D C Sundberg *J. Polym. Sci., Polym. Chem. Ed.* **20** 1299 (1982)
11. A Nort, in *Reactivity, Mechanisms of Reactions and Structure in Polymer Chemistry* (Eds A Jenkins, A Redvis) (Translated into Russian; Moscow: Mir, 1977) p.162
12. M B Lachinov, B A Korolev, B E Dreval', E I Cherep, V P Zubov, G V Vinogradov, V A Kabanov *Vysokomol. Soedin., Ser. A* **24** 2220 (1982)
13. M B Lachinov, R A Simonian, T G Georgieva, V P Zubov, V A Kabanov *J. Polym. Sci., Polym. Chem. Ed.* **17** 613 (1979)
14. A B Lee, D T Turner *Macromolecules* **10** 226 (1977)
15. S A Arzhakov, N F Bakeev, V A Kabanov *Vysokomol. Soedin., Ser. A* **15** 1154 (1973)
16. V P Zubov, L I Efimov, V A Arulin, V A Kabanov *Vysokomol. Soedin., Ser. B* **15** 588 (1973)
17. T J Tulig, M Tirrel *Macromolecules* **15** 459 (1982)
18. M Buback, L H Garcia-Rubio, R G Gilbert, D H Napper, J Gullot, A E Hamilec, P Hill, K F O'Driscoll, O F Olaj, J Shen, D Solomon, G Moad, M Stickler, M Tirrell, A Winnik *J. Polym. Sci., Part C, Polym. Lett.* **26** 293 (1988)
19. M Buback, R G Gilbert, G T Russel, D Y T Hill, G Moad, K F O'Driscoll, J Shen, M A Winnik *J. Polym. Sci., Part A, Polym. Chem.* **30** 851 (1992)
20. I M Bel'govskii, G N Kornienko, N S Enikolopyan *Vysokomol. Soedin., Ser. B* **13** 564 (1971)
21. L Matisova-Richla, J Richly, M Lazar *Makromol. Chem.* 176 2701 (1975)
22. V M Lagunov, I V Golikov, G V Korolev *Vysokomol. Soedin., Ser. A* **24** 131 (1982)
23. G A Bugrova, A I D'yachkov, A L Efimov, L N Efimov, V I Zubov *Vysokomol. Soedin., Ser. B* **26** 646 (1984)
24. A L Efimov, T A Bugrova, A I D'yachkov *Vysokomol. Soedin., Ser. A* **32** 2296 (1990)
25. L A Smirnova, Yu D Semchikov, N A Kopylova, V V Izvolinskii, M V Grebneva *Dokl. Akad. Nauk SSSR* **317** 410 (1991)
26. Yu D Semchikov, L A Smirnova, T E Knyazeva, S A Bulgakova, T A Voskoboinik, V I Sherstyanykh *Vysokomol. Soedin., Ser. A* **25** 704 (1984)
27. Yu D Semchikov, L A Smirnova, S A Bulgakova, T E Knyazeva, V I Sherstyanykh, N N Slavnitskaya *Dokl. Akad. Nauk SSSR* **298** 411 (1988)
28. H J Harwood *Makromol. Chem. Macromol. Symp.* **10/11** 331 (1987)
29. K Plochocka, H Horwood *J. Am. Chem. Soc., Div. Polym. Chem., Polym. Prepr.* **19** 240 (1978)
30. R R Rakhimov, A I Prokof'ev, Ya S Lebedev *Usp. Khim.* **62** 547 (1993) [*Russ. Chem. Rev.* **62** 509 (1993)]
31. T O Osmanov, V F Gromov, P M Khomikovskii, A D Abkin *Dokl. Akad. Nauk SSSR* **240** 910 (1978)
32. E V Bune, A P Sheinker, N V Kozlova, A D Abkin *Vysokomol. Soedin., Ser. A* **23** 1941 (1981)
33. E V Bune, A P Sheinker, A L Izyumnikova, E D Rogozhkina, A D Abkin *Vysokomol. Soedin., Ser. A* **25** 93 (1983)
34. M Kamochi *Makromol. Chem., Rapid Commun.* **7** 307 (1986)
35. A R Khokhlov *Statisticheskaya Fizika Makromolekul* (Statistical Physics of Macromolecules) (Moscow: Izd. Mosk. Gos. Univ., 1985)
36. D N Bort, S I Kuchanov, V I Zegel'man *Vysokomol. Soedin., Ser. A* **17** 2742 (1975); D N Bort, S A Arzhanov *Vestn. Akad. Nauk SSSR* (11) 79 (1979)
37. Yu A Panshin, S G Malkevich, Ts S Dunaevskaya *Ftoroplasty* (Fluoroplastics) (Leningrad: Khimiya, 1978)
38. A A Berlin, G V Korolev, T Ya Kefeli, Yu Ya Sivergin *Akrilovye Oligomery i Materialy na Ikh Osnove* (Acrylic Oligomers and Materials Based on Them) (Moscow: Khimiya, 1983)
39. M P Berezin, G V Korolev *Vysokomol. Soedin., Ser. A* **22** 1872 (1980)
40. V I Eliseva, S S Ivanchev, S I Kuchanov, A V Lebedev *Emul'sionnaya Polimerizatsiya i Ee Primenenie v Promyshlennosti* (Emulsion Polymerisation and Its Application in Industry) (Moscow: Khimiya, 1976)
41. D C Blackley *Emulsion Polymerisation. Theory and Practice* (London: Applied Science Publisher, 1975)
42. V I Eliseeva *Polimernye Dispersii* (Polymeric Dispersions) (Moscow: Khimiya, 1980)
43. S S Ivanchev, A V Dmitrienko *Usp. Khim.* **51** 1178 (1982) [*Russ. Chem. Rev.* **51** 670 (1982)]
44. V A Dmitrienko, S S Ivanchev, in *Reaktsii v Polimernykh Sistemakh* (Reactions in Polymeric Systems) (Ed. S S Ivanchev) (Leningrad: Khimiya, 1987) p. 201
45. W D Harkins *J. Am. Chem. Soc.* **69** 1428 (1947)
46. A I Yurzhenko, M Kolechkova *Dokl. Akad. Nauk SSSR* **47** 354 (1945)
47. W V Smith, R H Ewart *J. Am. Chem. Soc.* **16** 592 (1948)
48. C P Roe *Ind. Eng. Chem.* **60** 20 (1968)
49. R M Fitch, C-H Tsai, in *Polymer Colloids* (Ed. R M Fitch) (New York, London: Plenum, 1971) p. 73
50. J S Guo, E D Sudol, J W Vanderhoff, M S El-Aasser, in *Polymer Latexes* (Eds E S Daniels, E D Sudol, M S El-Aasser) (Washington DC: American Chemical Society, 1992) p. 99
51. J Ugelstad, F K Hansen *Rubber Chem. Technol.* **49** 536 (1976)
52. G A Simakova, V A Kaminskii, I A Gritskova, A N Pravednikov *Dokl. Akad. Nauk SSSR* **276** 151 (1984)
53. M Morton, S Kaizerman, M V Altier *J. Colloid. Sci.* **3** 300 (1954)
54. S Fu, Y Qian, F Rai, T Yu *Makromol. Chem. Macromol. Symp.* **63** 117 (1992)
55. W H Stockmeyer *J. Polym. Sci.* **24** 314 (1957)
56. I Piirma, M Chang *J. Polym. Sci., Polym. Chem. Ed.* **20** 489 (1982)
57. W D Hergeth, P Bolss, F Biedenweg, P Abandroth, K Schmutzer, S Warrewig *Makromol. Chem.* **191** 2949 (1990)
58. G Ley, H Gerrens *Makromol. Chem.* **175** 563 (1974)
59. J Snuparek, J Skoupil, S Podzimek, A Kastaned *Makromol. Chem. Macromol. Symp.* **31** 81 (1990)
60. I A Gritskova, L I Sedakova, D S Muradyan, B M Sinekaev, A V Pavlov, A N Pravednikov *Dokl. Akad. Nauk SSSR* **243** 403 (1978)
61. P E Il'menev, G I Litvinenko, V A Kaminskii, I A Gritskova *Vysokomol. Soedin., Ser. A* **30** 814 (1988)
62. J Barton, V Juranikova, Z Hlouskova *Makromol. Chem.* **189** 501 (1988)
63. J Barton *Makromol. Chem. Macromol. Symp.* **31** 11 (1990)
64. B S Casey, I A Maxwell, B Morrison, R G Gilbert *Makromol. Chem. Macromol. Symp.* **31** 1 (1990)

65. B R Morrison, I A Maxwell, R G Gilbert, D H Napper, in *Polymer Latexes* (Eds E S Daniels, E D Sudol, M S El-Aasser) (Washington DC: American Chemical Society, 1992) p. 28
66. F K Hansen, in *Polymer Latexes* (Eds E S Daniels, E D Sudol, M S El-Aasser) (Washington DC: American Chemical Society, 1992) p. 12
67. V N Pavlyuchenko, S S Ivanchev *Acta Polym.* **9** 521 (1983)
68. S S Ivanchev, P G Bagdasaryan, V N Pavlyuchenko *Dokl. Akad. Nauk SSSR* **275** 653 (1984)
69. I S Avetisyan, K A Pospelova, K E Onikul, P I Zubov *Lakokras. Mater. Ikh Primen.* (2) 13 (1964)
70. P L Tang, E D Sudol, M E Adams, C A Silebi, M S El-Aasser, in *Polymer Latexes* (Eds E S Daniels, E D Sudol, M S El-Aasser) (Washington DC: American Chemical Society, 1992) p. 72
71. S A Nikitina, V A Spiridonova, O S Mochalova, in *Uspekhi Kolloidnoi Khimii* (Advances in Colloid Chemistry) (Eds P A Rebinder, G I Fuks) (Moscow: Nauka, 1973) p. 268
72. A N Pravednikov, G A Simakova, I A Gritskova, N I Prokopov *Kolloidn. Zh.* **47** 189 (1985)
73. A N Pravednikov, G A Simakova, I A Gritskova, N I Prokopov *Kolloidn. Zh.* **47** 192 (1985)
74. J Delgado, M S El-Aasser *Makromol. Chem. Macromol. Symp.* **31** 63 (1990)
75. K J Fentenot, J Reiners, F I Schork *DECHEMA Monogr.* **127** 429 (1992)
76. V I Eliseeva, N N Zhukov *Vysokomol. Soedin., Ser. A* **23** 1540 (1981)
77. D F Durbin, M S El-Aasser, G W Poechlein, J W Vanderhoff *J. Appl. Polym. Sci.* **24** 703 (1971)
78. J W Vanderhoff, J M Park, M S El-Aasser, in *Polymer Latexes* (Eds E S Daniels, E D Sudol, M S El-Aasser) (Washington DC: American Chemical Society, 1992) p. 272
79. A V Zuikov, Yu V Solov'ev *Kolloidn. Zh.* **42** 549 (1980)
80. V I Lukhovitskii, V V Polikarpov *Tekhnologiya Radiatsionnoi Emul'sionnoi Polimerizatsii* (Technology of Radiation Emulsion Polymerisation) (Moscow: Atomizdat, 1980)
81. J Barton, V Juranicova *Makromol. Chem., Rapid Commun.* **12** 669 (1991)
82. A A Oganesyan, A V Gukasyan, G A Manukyan *Arm. Khim. Zh.* **43** 598 (1990)
83. S S Ivanchev, V N Pavljuchenko, N A Byrdina *J. Polym. Sci., Part A, Polym. Chem.* **25** 47 (1987)
84. K Tauer, K-H Boebel, S Kosnella, K Staehler, J Neelsen *Makromol. Chem. Macromol. Symp.* **31** 107 (1990)
85. J M H Kuster, D H Napper, R G Gilbert *Macromolecules* **25** 7043 (1992)
86. M Nomura, J Ikoma, K Fujita, in *Polymer Latexes* (Eds E S Daniels, E D Sudol, M S El-Aasser) (Washington DC: American Chemical Society, 1992) p. 55
87. N I Solomko, V F Tsepalov, A I Yurzhenko *Kinet. Katal.* **10** 527 (1969)
88. N I Solomko, V F Tsepalov, A I Yurzhenko, A D Shaposhnikova *Kinet. Katal.* **10** 735 (1969)
89. V N Pavlyuchenko, S S Ivanchev, in *Reaktsii v Polimernykh Sistemakh* (Reactions in Polymer Systems) (Ed. S S Ivanchev) (Leningrad: Khimiya, 1987) p. 78
90. M Okubo, T Mori *Makromol. Chem. Macromol. Symp.* **31** 148 (1990)
91. C-S Georgescu, A Stabu, M Tanaka, V Butucea *Makromol. Chem. Macromol. Symp.* **47** 337 (1991)
92. M J Ballard, D H Napper, R G Gilbert *J. Polym. Sci., Polym. Chem. Ed.* **22** 3225 (1984)
93. B C Hawkett, D H Napper, R C Gilbert *J. Polym. Sci., Polym. Chem. Ed.* **19** 3173 (1981)
94. J Hearn, H C Wilkinson, A R Goodall, H Ghainey *J. Polym. Sci., Polym. Chem. Ed.* **23** 1869 (1985)
95. S-A Chen, H-S Chang *J. Polym. Sci., Part A, Polym. Chem.* **30** 2077 (1992)
96. B R Morrison, J A Maxwell, D H Napper, R G Gilbert, J L Ammerdorffer, A L German *J. Polym. Sci., Part A, Polym. Chem.* **31** 467 (1993)
97. M J Ballard, R G Gilbert, D H Napper, P J Pomery, P W O'Sullivan, J H O'Donnel *Macromolecules* **19** 1303 (1986)
98. F L Marten, A E Hamielec *Am. Chem. Soc., Ser. Symp.* **104** 43 (1979)
99. M E Adams, B S Casey, M F Mills, G T Russel, D H Napper, R G Gilbert *Makromol. Chem. Macromol. Symp.* **35/36** 1 (1990)
100. Yu N Egorov, V P Zubov *Usp. Khim.* **56** 2076 (1987) [*Russ. Chem. Rev.* **56** 1153 (1987)]
101. M R Grancio, D J Williams *J. Polym. Sci., A-1* **8** 2617 (1970)
102. D J Williams *J. Polym. Sci., Polym. Chem. Ed.* **11** 103 (1973)
103. C-I Kao, D I Lee, E F Stevens *J. Dispersion Sci. Technol.* **5** 283 (1984)
104. H J Hul, J W Vanderhoff *J. Electroanal. Chem.* **37** 161 (1972)
105. B M Jayasuria, M S El-Aasser, J W Vanderhoff *J. Polym. Sci., Polym. Chem. Ed.* **23** 2819 (1985)
106. C-S Chern, G W Poehlein *J. Polym. Sci., Part A, Polym. Chem.* **25** 617 (1987)
107. V I Eliseeva *Usp. Khim.* **57** 307 (1988) [*Russ. Chem. Rev.* **57** 174 (1988)]
108. S Lee, A Rudin, in *Polymer Latexes* (Eds E S Daniels, E D Sudol, M S El-Aasser) (Washington DC: American Chemical Society, 1992) p. 234
109. P Espiard, A Revillon, A Guyot, J E Mark, in *Polymer Latexes* (Eds E S Daniels, E D Sudol, M S El-Aasser) (Washington DC: American Chemical Society, 1992) p. 387
110. C H M Caris, R P M Kuijpers, A M van Reck, A L German *Makromol. Chem. Macromol. Symp.* **35/36** 535 (1990)
111. J W Vanderhoff, J M Park, M S El-Aasser, in *Polymer Latexes* (Eds E S Daniels, E D Sudol, M S El-Aasser) (Washington DC: American Chemical Society, 1992) p. 272
112. M Okubo, K Ichikawa, M Fujimura, in *Polymer Latexes* (Eds E S Daniels, E D Sudol, M S El-Aasser) (Washington DC: American Chemical Society, 1992) p. 282
113. C Schorlemmer *Makromol. Chem. Macromol. Symp.* **31** 123 (1990)
114. M Okibo, Y Katsuta, T Matsumoto *J. Polym. Sci., Polym. Lett. Ed.* **20** 45 (1982)
115. M Okibo, Y Katsuta, T Matsumoto *J. Polym. Sci., Polym. Lett. Ed.* **18** 481 (1980)
116. D Sundberg, A P Casassa, J Pantazopoulos, M R Muscato, B Krenberg, B Berg *J. Appl. Polym. Sci.* **41** 1425 (1990)
117. E J Sundberg, D C Sundberg *J. Appl. Polym. Sci.* **47** 1277 (1992)
118. S Lee, A Rudin *Makromol. Chem., Rapid Commun.* **10** 655 (1989)
119. D G Cook, A Rudin, A Plumtree *J. Appl. Polym. Sci.* **46** 1387 (1992)
120. S Lee, A Rudin *J. Polym. Sci., Part A, Polym. Chem. Ed.* **30** 2211 (1992)
121. D Mikulasova, V Chrastova, P Citovicky, K Horie *Makromol. Chem.* **178** 429 (1977)
122. M A Bruk *Usp. Khim.* **56** 148 (1987) [*Russ. Chem. Rev.* **56** 81 (1987)]
123. M A Bruk, S A Pavlov *Polimerizatsiya na Poverkhnosti Tverdykh Tel* (Polymerisation on the Surfaces of Solids) (Moscow: Khimiya, 1990)
124. L P Krul' *Geterogennaya Struktura i Svoistva Privitykh Polimernykh Materialov* (Heterogeneous Structure and Properties of Graft Polymer Materials) (Minsk: Izd. Minsk. Univ., 1986)
125. I Yu Babkin, Yu M Gordeev *Khim. Vys. Energ.* **21** 418 (1987)
126. A V Dmitrienko, M I Serushkin, A M Mesh, T G Agnivtseva, S S Ivanchev *Vysokomol. Soedin., Ser. A* **34** 60 (1992)
127. A V Dmitrienko, A M Mesh, M I Serushkin, T G Agnivtseva, A G Korchagin, S S Ivanchev *Vysokomol. Soedin.* **35** 646 (1993)
128. E A Rogol'skaya, S G Prutchenko, S G Pavlov, E N Teleshov *Vysokomol. Soedin., Ser. A* **32** 495 (1990)
129. S A Pavlov, Doctoral Thesis in Chemical Sciences, L Ya Karpov Physicochemical Institute, Moscow, 1992
130. USSR P. 787 411; *Byull. Izobret.* **46** 97 (1980); USSR P. 765 271; *Byull. Izobret.* **35** 144 (1980)
131. Yu A Zvereva, V A Popov, V V Guzeev, E P Shvarev, S S Ivanchev, G P Gladyshev *Dokl. Akad. Nauk SSSR* **252** 1174 (1980)
132. S S Ivanchev, B O Polozov, A V Dmitrienko, V A Demidova, A M Krupnik, A K Litkovets *Vysokomol. Soedin., Ser. A* **23** 2064 (1981)
133. A V Dmitrienko, S S Ivanchev, A M Volkov, N E Shadrina, L P Kastorskii *Vysokomol. Soedin., Ser. A* **30** 2255 (1988)
134. A V Dmitrienko, N N Ulinskaya, A M Volkov, S S Ivanchev *Vysokomol. Soedin., Ser. A* **31** 1591 (1989)

135. A V Dmitrenko, N E Shadrina, S S Ivanchev, N N Ulinskaya, A M Volkiv *J. Chromatogr.* **520** 21 (1990)
136. V A Popov, Yu A Zvereva, E S Klimov, T V Palaeva, A A Grishin *Vysokomol. Soedin., Ser. A* **24** 729 (1982)
137. V A Popov, A N Grishin, Yu A Zvereva, T V Palaeva, V A Fomin, S S Ivanchev *Vysokomol. Soedin., Ser. A* **24** 760 (1983)
138. A V Sukin, M A Bulatov, V I Kononenko, B V Mitrofanov, G P Shveikin *Vysokomol. Soedin., Ser. B* **22** 552 (1980)
139. S S Ivanchev, A V Dmitrienko, A M Krupnik *Vysokomol. Soedin., Ser. A* **30** 1951 (1988)
140. A V Dmitrienko, V A Demidova, V P Sass, S S Ivanchev *Vysokomol. Soedin., Ser. B* **30** 172 (1988)
141. S A Pavlov, M A Bruk *Dokl. Akad. Nauk SSSR* **236** 1148 (1983)
142. B S Casey, M F Mills, D F Sungster, R G Gilbert, D H Napper *Macromolecules* **25** 7063 (1992)
143. M Buback, B Huckestein, G T Russel *Macromol. Chem. Phys.* **195** 539 (1994)

Russian Chemical Reviews **63** (8) 685–694 (1994)
©1994 Russian Academy of Sciences and Turpion Ltd

UDC 678 : 043.044.048 : 002.237

Modification of chemical additives to elastomeric compositions

A A Mukhutdinov, B S Grishin

Contents

I. Introduction 685
II. Physical modification of chemical additives 686
III. Physicochemical modification of chemical additives 689
IV. Conclusion 693

Abstract. The physicochemical principles of the modification of crystalline chemical additives to elastomeric compositions are examined. A classification of various types of modifications based on scientific principles is given. The modifications are subdivided into physical and physicochemical depending on the configuration of the molecules in the crystals, the defectiveness and dispersity of the crystalline particles, the melting points of the crystals, and the presence of nucleophilic and electrophilic centres in the molecules of the components of binary and complex eutectic mixtures. The effectiveness of the modification of the chemical additives is determined by the manifestation in binary systems of these components in elastomeric compositions of physical and chemical synergism due to the occurrence of the relevant processes in such systems. A relation has been discovered between the physical and chemical phenomena accompanying the modification of the chemical additives in binary and complex eutectic mixtures, their influence on the properties of the elastomeric composition is examined, the ecological problems associated with the processing of such materials are discussed, and the relation between the structure and properties of the molecules of the additives is analysed using quantum-chemical calculations. The bibliography includes 92 references.

I. Introduction

Chemical additives to elastomeric compositions, i. e. the components of sulfur-based vulcanising systems and antiageing agents, constitute molecular crystals (zinc oxide and liquid accelerators are an exception) whose structures are formed via intermolecular forces in accordance with the close packing principle.[1] In the processing of elastomeric compositions, it is essential that the crystalline chemical additives should be well dispersed and dissolved in the elastomer and that they should manifest at a certain instant a high chemical reactivity as moderators of prevulcanisation and as accelerators of the vulcanisation of elastomeric compositions and as antiageing and antifatigue agents in rubbers.

A A Mukhutdinov Department of Engineering Geology, Kazan State Technological University, ul. K. Marksa 68, 420015 Kazan, Russian Federation.
B S Grishin Institute of the Tyre Industry, ul. Burakova 27, 105118 Moscow, Russian Federation.

Received 4 April 1994
Uspekhi Khimii **63** (8) 719–729 (1994); translated by A K Grzybowski

In the existing methods for the preparation of elastomeric compositions, the main criterion of the uniform distribution of crystalline chemical additives in the elastomer is their solubility. According to Gardiner[2] and Ikeda et al.,[3] the limiting solubilities of crystalline accelerators and sulfur in elastomers depend greatly on temperature. However, not the limiting but current solubilities of the components in the elastomers are more important. It has been established[4] that the times required for the dissolution of sulfur, di(2-benzothiazolyl) disulfide (DBTD), and *N*,*N*′-diphenylguanidine (DPG) with a 0.2 mm particle size in butadiene rubber at 130 °C are respectively 2.8, 11.4, and 4.6 min. Similar times are characteristic also of other chemical additives.

Crystalline accelerators and sulfur are introduced into elastomeric compositions at a temperature below 112 °C and the mixing time is 2.5 min. Under such conditions, a proportion of the additives introduced into the elastomer remains in the form of small crystalline particles, which behave as centres for the formation of defects in rubbers.[5]

Another important index of the effectiveness of chemical additives in elastomeric compositions is the extent to which they manifest their functional properties. In order to attain the maximum effectiveness of the chemical additives, compounds of different classes have been synthesised.[6] It was found that the effective manifestation of the properties of chemical additives cannot be achieved by using traditional methods for their introduction into elastomeric compositions. The use of chemical additives in the form of dustlike powders and readily fragmented grains leads to the impairment of the environment in the processing of elastomeric compositions[7–13] and polymers.

Various methods for the modification of chemical additives are used to improve their effectiveness. Some of them are listed below.

1. The preparation of dispersions of powdered components in mineral oils in the form of pastes of different consistencies.[14,15] The use of such pastes facilitates the dispersion of the components in elastomeric compositions as a result of their preliminary wetting by the oil and prevents the formation of a dust during mixing.[16] However, the preparation and application of viscous pastes is associated with technological difficulties.

2. The mixing of the powdered components with polymeric binders, including encapsulation in microcapsules made from high-molecular-mass amino-compounds,[17–19] which melt during the vulcanisation of the elastomeric compositions, and also in capsules made from a polymer based on cellulose acetate.[20] However, the preparation of such microcapsules is difficult.

3. The use of binary and complex synergistic chemical additive systems (for example accelerators of the sulfur-based vulcanisation of elastomers[21] and antioxidants[22]). The synergistic effect, manifested by such systems in elastomeric compositions and rubber, has a both physical and chemical nature.[23] The chemical interaction of the components of synergistic systems takes place in the highly viscous elastomer under diffusional conditions, which lowers the probability of encounters of the molecules and prevents the complete manifestation of the synergistic effect.

4. The preparation on the basis of binary and complex chemical additive systems of simple eutectic mixtures, substitutional solid solutions, molecular complexes, and new chemical compounds,[21,24-26] which can form strong and readily diffusable granules at the temperature corresponding to eutectic fusion. The molecules retain their individuality in the eutectic mixtures and substitutional solid solutions, whilst in the molecular complexes there is a redistribution of electron density.[27]

In contrast to synergistic systems of chemical additives, introduced into the polymer compositions in the form of individual powders, in the eutectic mixtures and molecular complexes the components interact in the kinetic region in both the crystalline and fused states, which promotes the most complete manifestation of the synergistic effect.

Depending on the extent of the processes in the binary and complex chemical additive systems promoting an increase in their effectiveness in elastomeric compositions, physical and physicochemical modification procedures are distinguished.[28]

II. Physical modification of chemical additives

The physical modification of chemical additives is based on the increase in the defectiveness and dispersity of the crystals and the increase in the melting points of the components in the binary and complex eutectic systems and substitutional solid solutions.[28] All these factors tend to increase their effectiveness in elastomeric compositions.

The aim of the physical modification of chemical additives is the most complete manifestation of the synergism of their functional properties, which promotes a more complete and rapid (compared with the use of individual solvents) vulcanisation reaction of elastomeric compositions, an increase in the duration of the induction period for the process, and a decrease of reversion in the vulcanisation process. This ensures the formation of rubbers with effective physicomechanical parameters.

Physical synergism is manifested when the accelerators in the binary systems form only simple eutectic mixtures or substitutional solid solutions. These binary systems include CBS (*N*-cyclohexylbenzothiazole-2-sulfenamide)–OBS (morpholinobenzothiazole-2-sulfenamide), TMTD (tetramethylthiuram disulfide)–TMTM (tetramethylthiuram monosulfide), CBS–DBTD, TMTD–TETD (tetraethylthiuram disulfide), TMTD–DPG, TBTD–MBT (2-mercaptobenzothiazole), etc. The synergism of the properties of these systems of accelerators in elastomeric composition is due to the following causes.

The increase in the defectiveness and dispersity of the crystalline particles in the eutectic mixtures, which leads to an increase in the surface free energy and hence in the chemical reactivity of the accelerator, and the latter increases the rate of vulcanisation of elastomeric compositions.

The increase in the solubility of one accelerator in the elastomeric composition in the presence of another accelerator.

The sharp decrease in the melting points of the accelerators in the eutectic mixtures, which promotes their dispersion and improves their distribution in the elastomeric compositions and hence ensures a more complete vulcanisation with formation of a uniformly distributed and less defective three-dimensional network in rubbers.

The possibility and the effectiveness of the physical modification of chemical additives is determined primarily by the following characteristics of the components of binary and complex mixtures: the structure of the molecules in the crystals, the defectiveness of the crystals in eutectic mixtures, the dispersity of the crystalline particles, and the melting points of the components.

1. The conformation of the molecules in crystals of chemical additives

Analysis of the results of X-ray diffraction studies on the components of sulfur-based vulcanising systems[21] indicates different configurations of their molecules (with the exception of MBT and DBTD).

Even activated molecules are known[29] to react with one another only when they are oriented relative to one another in a specific manner. The configuration of the molecules in organic crystals is determined in its turn by the spatial disposition of the bonded atoms making up the molecule.[30] Thus the thiocarbamic acid residue in dithiocarbamate and thiuram accelerators has a planar structure.[31-33] The same configuration is characteristic also of stearic acid[34] and the benzothiazolyl group in MBT and DBTD.[35] On the other hand, the benzothiazolyl group in CBS–OBS has the chair configuration.[36,37]

Simple eutectic mixtures in binary systems of accelerators are formed when the molecules have significantly different configurations and are characterised by approximately the same nucleophilicity or electrophilicity (for example, the TMTD–TETD and CBS–DBTD systems). If the molecules of the components have similar configurations, as in the DBTD–MBT system, a substitutional solid solution is formed. When the energy of the interaction of unlike molecules is appreciable, i. e. when they contain nucleophilic and electrophilic centres and have a favourable orientation, molecular complexes (π- and *n*-complexes) may be formed in the eutectic mixtures. Then the composition of one of the phases will correspond fairly closely to an integral molar ratio of the components within certain temperature limits.[38]

The addition of zinc oxide to binary mixtures of accelerators may promote a change in the conformation of the molecules as a result of their adsorption.[39,40] This alters the ratio of the components in the eutectic mixtures or the substitutional solid solution and hence increases or lowers the eutectic melting point (T_{eu}) and the enthalpy of fusion (ΔH_m), which has been confirmed by studies on binary and ternary mixtures of the components of sulfur-based vulcanising systems by differential scanning calorimetry (Table 1).[28]

Table 1. Variation of the properties of the eutectic mixtures as a function of composition.

Binary or ternary mixture	Mass ratio of components	T_{eu}/ °C	ΔH_m/kJ mol^{-1}
MBT–TMTD	0.5:0.5	103	18.40
MBT–ZnO–TMTD	0.5:2.0:0.5	102	24.07
DBTD–TMTB	0.5:0.5	106	29.47
DBTD–ZnO–TMTD	0.5:2.0:0.5	112	27.08
CBS–TMTD	0.7:0.3	76	24.47
CBS–ZnO–TMTD	0.7:2.0:0.3	84	26.75

2. Defectiveness of crystals of chemical additives in eutectic mixtures

Crystal defects include dislocations and point, volume, and surface defects.[41] In organic crystals, dislocations are crystal lattice defects which disturb the regular disposition of molecular planes. Point defects comprise vacancies and interstitial impurity molecules introduced by substitution and volume effects comprise pores, cracks, and inclusions of other phases. Surface defects are defects in the packing of the crystals and in their surface relief.

The state corresponding to an ideally regular crystal is the most stable.[42] Such a crystal has the minimum entropy and free energy. Structural defects diminish the stability of the crystal because they lead to an increase in entropy and free energy.

Substances with more defective crystals exhibit a higher chemical reactivity. A mixture of defective crystals is characterised by a higher reactivity than a mixture of crystals with an ideal structure.

Surface, volume, and point defects, the number of which may be increased by the physical modification of the components leading to the formation of simple eutectic mixtures and substitutional solid solutions, promote an increase in the effectiveness of crystalline chemical additives in elastomeric compositions.

Table 2 presents the principal characteristics of binary mixtures of crystalline components of sulfur-based vulcanising systems obtained by the method of thermal analysis.[25,28] Evidently the formation of equilibrium eutectic systems is accompanied by a significant decrease in the enthalpy of fusion and an increase in the activity coefficients of the components, which is due to the increase in the defectiveness and dispersity of the crystals.

The increase in the defectiveness of the crystals (up to 42%) during the formation of simple eutectic systems, substitutional solid solutions, and molecular complexes (Table 3) has been confirmed quantitatively by the results of investigations by NMR (analysis of broad lines) and differential scanning calorimetric methods.[25]

According to Zalkin,[43,44] the increase in the defectiveness of the crystals in eutectic mixtures of the components of sulfur-based vulcanising systems is caused by the following factors. In the solid eutectic mixtures, the surfaces of two crystals 'trap one another' via intermolecular forces, which leads to the elastic deformation of the crystal lattices in the boundary regions. The surface of the crystal with a higher melting point is then the 'active substrate' and tends to distort the surface of the low-melting crystals in conformity with its surface relief. As a result, the excess free energy is concentrated in the contact zone together with the increased number of surface and volume defects, such free energy being the cause of the increased chemical reactivity of the components of the eutectic mixture.

In the solid solutions, the substitution of one molecule in the crystal lattice of the first component by a larger molecule of the second component leads to loosening of the packing and to the appearance of strains and distortions in neighbouring molecules, the number of which may reach 400 and more.[1] When a larger molecule is substituted by a smaller one, contraction takes place, whereupon the number of molecules subjected to strain and distortions does not exceed 350. Accordingly, the increase in the activity coefficient of DBTD in the DBTD–MBT substitutional solid solution (Table 3) is due to the fact that, when one DBTD molecule in the DBTD unit cell is substituted by two MBT molecules (the volume of two MBT molecules is greater than the volume of the DBTD molecule by the volume of two hydrogen atoms), the structure is loosened, which is accompanied by an increase in the free energy of DBTD and hence also in its activity coefficient. On the other hand, the replacement of two MBT molecules by one smaller DBTD molecule leads to contraction of the unit cell of MBT and to some decrease in the free energy and in the activity coefficient of MBT.[28] The introduction of such eutectic mixtures and substitutional solid solutions into elastomeric compositions makes it possible to increase the rate of vulcanisation whilst retaining the duration of the prevulcanisation period at the level of control specimens. The rubbers thus obtained have a higher tensile strength, a greater wear resistance on repeated deformations, and a greater resistance to thermal ageing.

Table 3. Defectiveness of the crystals of binary mixtures of accelerators.

Binary mixture	Degree of defectiveness of crystals			Increase in degree of defectiveness of crystals in eutectic mixture compared with additive value (%)
	A	M	E	
MBT–TMTD	0.365	0.44	0.51	39.72
DBTD–TMTD	0.305	0.36	0.42	37.70
CBS–TMTD	0.370	0.42	0.46	24.32
OBS–TMTD	0.360	0.38	0.38	5.55
MBT–DBTD	0.365	0.48	0.52	42.46
DBTD–ZDMDTC	–	0.46	0.48	–

Remarks. The following notation has been adopted: A—additive mixture, M—mechanical mixture, E—eutectic mixture..

3. The dispersity of crystalline particles of chemical additives

An increase in the dispersity of a crystal is known to diminish its stability owing to the increase in the surface free energy. As a result of this, more highly dispersed crystals exhibit a higher chemical reactivity. For this reason, the properties of elastomeric compositions depend to a large extent on the dispersity of the particles of the powdered chemical additives; the smaller the particle size the more effectively are they dispersed in the elastomeric compositions and the greater their functional effectiveness.[16,45,46]

The distribution of the powdered accelerators, sulfur, and antiageing agents in elastomeric compositions occurs most effectively at the level of crystalline particles, which cannot ensure

Table 2. Certain thermodynamic characteristics of the components of the binary systems for the sulfur-based vulcanisation of elastomers.

Binary mixture	Molar ratio of components	T_{eu}/ °C	T_{per}/ °C	Enthalpy of fusion/kJ mol^{-1}			Activity coefficients of components[a]		Type of mixture formed
				ΔH_{ad}	ΔH_{mix}	ΔH_{eq}	1	2	
Sulfur–MBT	0.49:0.51	104	–	18.70	17.00	15.20	1.816	1.686	Simple eutectic
Sulfur–OBS	0.30:0.70	77	–	20.00	18.00	12.60	2.070	1.750	" "
Sulfur–CBS	0.50:0.50	80	–	22.47	18.35	15.05	1.250	1.180	" "
DBTD–MBT	0.33:0.67	137[b]	–	26.63	13.10	8.36	1.296	0.891	Solid solution
OBS–TMTD	0.80:0.20	76	90	23.34	17.20	16.69	1.320	2.200	Molecular complex
DBTD–TMTD	0.42:0.58	106	111	35.65	29.47	18.33	1.522	2.100	" "
CBS–DTDM	0.57:0.43	79	83	25.50	18.00	11.80	1.220	2.150	" "
DBTD–ZDMDTC	0.56:0.42	144	151	–	22.60	4.50	1.360	1.950	" "
TMTD–ZDMDTC	0.84:0.16	136	142	–	30.00	16.72	1.266	1.900	" "

Remarks. ΔH_{ad} is the additive enthalpy of fusion; ΔH_{mix} and ΔH_{eq} are the enthalpies of fusion of mechanical and equilibrium eutectic mixtures; T_{eu} and T_{per} are the eutectic and peritectic melting points. [a] The activity coefficients of the components were calculated from Wilson's equation for the known eutectic conditions.[49] [b] The lowest temperature of a liquidus with a minimum is quoted.

Table 4. The structure of the particles of certain crystalline powdered components of sulfur-based vulcanising systems.

Component	Average particle size $10^2 d$/mm	Volume of spherical particle $10^8 V$/mm^3	Volume of unit cell $10^{18} V$/mm^3	Number of unit cells in particle $10^{-12} n$	Number of molecules	
					in unit cell	in spherical particle $10^{-11} N$
TMTD	2.33	662	1.138	5.81	4	232
MBT	2.27	612	0.768	7.97	4	318
DTDM	2.40	723	1.171	6.178	4	247
Orthorhombic sulfur	2.07	464	3.296	1.40	16	225
Monoclinic sulfur	2.07	464	1.298	3.57	6	214
Stearic acid	–	–	2.349	–	–	–
Zinc oxide	1.89	353	–	–	–	–

the same concentration gradients of these components throughout the bulk of the elastomer because in the vicinity of the particles themselves an increase in the concentration of dissolved molecules is maintained.[4,28] This is indicated also by the structure of the particles of certain powdered components established on the basis of crystal-chemical data (Table 4).

If it is assumed that the particles of crystalline components are approximately spherical,[47] it is possible to calculate the number of unit cells in them and, knowing the number of molecules in each cell,[21] it is possible to determine the total number of molecules in each spherical particle. It is seen from the data presented in Table 4 that the particles of the powdered components contain an enormous number of molecules and their uniform distribution in the particles solely as a result of dissolution is hardly possible despite the fairly high solubility of sulfur and of the accelerators in elastomers at the mixing temperatures.[3,4] Under these conditions, a uniform distribution of the chemical additives in the bulk of the elastomeric composition can be attained by increasing their dispersibility in the fused state.

By analogy with the diffusion of gases in liquids,[48] the following equation is used for the mathematical description of the distribution and diffusion of chemical additives in an elastomer:[28]

$$\frac{dc}{dt} = D\frac{d^2c}{dx^2},$$

where dc/dt is the rate of accumulation of the molecules of the component in a unit elementary volume, D the diffusion coefficient of the molecules of the component in the elastomer, and d^2c/dx^2 the derivative of the concentration gradient characterising the distribution of the component in the elastomer.

Evidently the rate of increase in the concentration of the component is dissolved in the elastomer depends on the rate of distribution of its molecules, and the more effectively the component is dispersed in the bulk of the elastomer in the form of small fused particles, the faster the equalisation of the concentration gradient of its molecules throughout the bulk of the elastomer.

The dispersion of powdered and fused components during the mixing of chemical additives and the diffusion of the dissolved molecules of the component accompanied by the equalisation of the concentration throughout the entire bulk of the substance are illustrated schematically in Fig. 1.

It follows from the foregoing that, in order to improve the distribution of chemical additives in elastomeric compositions, it is necessary to fuse them at the very beginning of the mixing process. The fusion of the particles after their dispersion in the crystalline state does not promote an improvement in the dissolution of the components because, in conformity with thermodynamic ideas, under identical conditions a solid and its melt dissolve in the same way.[49] On the other hand, the component fused initially is dispersed in the elastomeric composition much more effectively than the same component in the powdered state and it executes its functional task more effectively, for example as an accelerator,[50] a vulcanising agent, an antiageing agent, etc. Nevertheless, the melting points of the majority of the widely used chemical additives, except for CBS, OBS, and stearic acid (StA), are higher than the temperatures corresponding to their introduction into elastomeric compositions. The dispersion of such chemical additives in elastomeric compositions is improved in the presence of zinc stearate, which is capable of forming reversed micelles in the nonpolar elastomer; these solubilise the accelerators and sulfur in the polar core.[51] The low critical concentration for micelle formation (2×10^{-3} M) confirms the possibility of accumulating sufficient zinc stearate for the formation of micelles in elastomeric compositions as a result of the reaction of stearic acid with ZnO at the very beginning of the mixing process.[53]

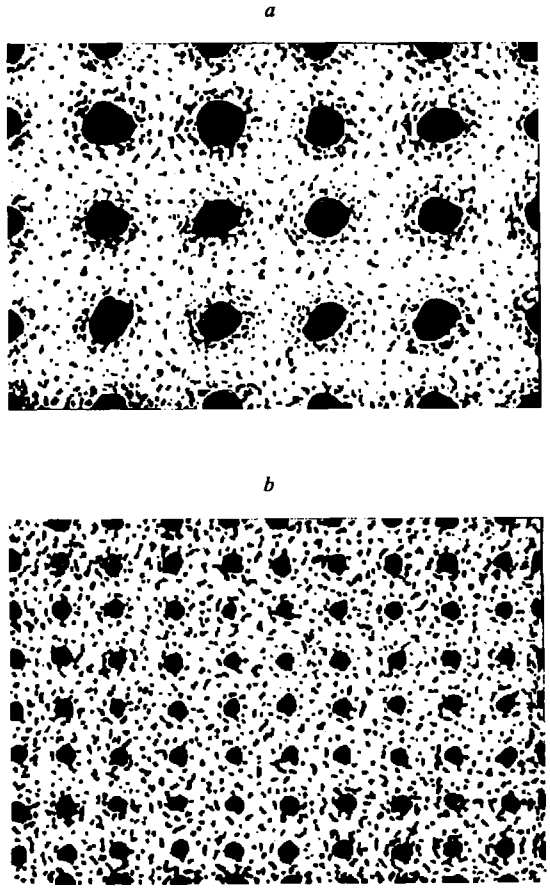


Figure 1. Schematic illustration of the dispersion and dissolution of powdered (*a*) and fused (*b*) components in the elastomer during the mixing process.

When the components of sulfur-based vulcanising systems are used in the form of readily fusible eutectic mixtures, the dispersity of the particles can influence the properties of the elastomeric compositions and rubbers if the mixing temperature is lower than the temperature of eutectic fusion or the equilibrium temperature on the liquidus of the phase diagram, determined by the ratio of the concentrations of the initial accelerators in the binary eutectic system. If the temperature of the preparation of the elastomeric composition is above the liquidus line, the eutectic mixture is dispersed in the elastomeric composition in the fused state and the dispersity of the particles of the components constituting the eutectic mixtures does not affect the properties of the elastomeric compositions and rubbers.

The formation of eutectic mixtures is known[49] to be accompanied by an increase in the dispersity of the crystalline particles of the constituent components, which increases their chemical reactivity as a consequence of the increase in the surface free energy. Hence it follows that, when the eutectic mixtures are introduced into elastomeric compositions at temperatures below the temperature of eutectic diffusion, the accelerators are more highly dispersed and are more chemically reactive than in the initial state. This applies also to the case where the temperature of the preparation of the elastomeric composition is below the liquidus line of one of the components. The crystalline particles of the accelerator in equilibrium with the melt are more highly dispersed than the particles of the initial accelerator.

In those cases where the accelerators and sulfur are adsorbed in the form of eutectic mixtures on zinc oxide, the dispersity of the particles of these components undergoes an additional increase as a consequence of the retardation of the crystallisation of the adsorbed components and the formation of a large number of nuclei.[54]

4. The melting points of crystals of chemical additives

In simple eutectic systems, the eutectic temperature (T_{eu}) is lower and closer to the centre of the phase diagram the smaller the difference between the melting points (T_m) of the components. The greater the difference between the melting points T_m of the components of eutectic mixtures the greater the displacement of T_{eu} towards the low-melting component. This type of variation of T_{eu} as a function of the T_m of the constituent components makes it possible to attain the maximum synergistic effect by varying the proportions of the accelerators with different T_m within wide limits (by virtue of the better dispersion and distribution of the accelerators in the elastomeric compositions in the fused form and the increase in the defectiveness and dispersity of the crsytalline particles). This promotes an increase in the free surface energy and hence in the chemical reactivity of the components.

Furthermore, the properties of the binary eutectics are influenced by the polymorphic transformations of the crystals of the chemical additives[34,56,57] occurring following an increase in temperature and promoting a change in the miscibility of the components in the solid state.

* * *

Thus the effectiveness of the physical modification of chemical additives in binary and complex eutectic mixtures and substitutional solid solutions is determined by the differences between the configurations of the molecules and the melting points of the components as a result of the increase in the defectiveness and dispersity of the crystalline particles. The physical modification not only improves the distribution of the components in elastomeric compositions and increases their chemical reactivity but also facilitates the formation of strong (0.35–0.4 MPa) and readily fusible granules of the eutectic melts of the chemical additives without the introduction of binders.[28] This is one promising way of solving the environmental problems in the processing of elastomeric compositions and polymers.

III. Physicochemical modification of chemical additives

An increase in the chemical reactivity of the components of binary eutectic mixtures, exhibiting nucleophilic and electrophilic properties relative to one another, leads to the formation of molecular π- and n-complexes or new more active accelerators exhibiting a high thiophilicity in relation to free sulfur and hence increasing the rate of vulcanisation of the elastomeric compositions and reducing the activation energy for the process. The physical and chemical transformations occurring under these conditions can be regarded as the physicochemical modification of the chemical additives.[28]

The synergistic effect in the binary systems on formation of molecular complexes and new accelerators may intensify also as a result of the retardation of the migration of the molecules of the complexes to the surfaces of the elastomeric compositions as a consequence of the increase in molar volume and the more complete functional utilisation of the system of accelerators.

The combination of physical and chemical synergism is characteristic of binary systems such as OBS–TMTD, DBTD–TMTD, CBS–TMTD, OBS–DTDM (*N,N'*-dithiodimorpholine), CBS–ZDMDTC (zinc dimethyldithiocarbamate), CBS–MBT, etc., whose components form molecular complexes and new compounds—more active accelerators of the sulfur-based vulcanisation of the elastomers than the initial compounds.[28,58,59]

Thus the presence in the crystals of the components of active centres capable of interacting with one another is very important in the physicochemical modification of chemical additives.

1. The active centres in the molecules of chemical additives

The molecular diagrams of components of sulfur-based vulcanising systems have been obtained[60–63] by quantum-chemical methods. Analysis of the results of the quantum-chemical calculations and of the molecular diagrams presented in a number of studies[59–62,64–66] makes it possible to arrange the components of the sulfur-based vulcanising systems in the following series in terms of the increase in their nucleophilicity:

$$ZnO < ZnX_2 < S_8 < DTDM < OBS < CBS \leqslant DBTD \leqslant MBT < DPG < TMTD.$$

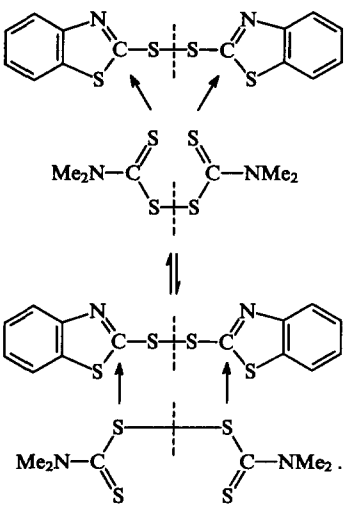
Zinc oxide, zinc mercaptide, zinc dialkyldithiocarbamates, sulfur, and DTDM exhibit electrophilic properties in relation to CBS, DBTD, MBT, DPG, and TMTD. In binary systems containing the zinc salts of mercaptobenzothiazole or dialkyldithiocarbamic acid, on the one hand, and thiazole, sulfenamide, or thiuram accelerators, on the other, the latter behave as ligands coordinated to the zinc atom and bound to it both as a result of the partial shift of the n electrons of the nitrogen or sulfur atoms to the unoccupied p orbitals of the zinc atom[67] and also as a result of the formation of a π-bond when the occupied d orbitals of zinc overlap with the antibonding π^* orbital of the ligand.[68] The involvement of the zinc atom in the formation of a π-bond has been confirmed by the fact that the transfer of one of its d electrons to a higher energy level requires an energy of only 15.5×10^{-19} J cm^{-1}.[69]

2. The formation of molecular complexes

Together with the eutectic point, a peritectic point appears on the phase diagrams of binary systems of accelerators exhibiting donor–acceptor properties relative to one another, which confirms the formation of a molecular complex in the mixture.[55] This shows that the charge transfer from the donor to the acceptor molecule in a mixture of crystalline substances is facilitated on eutectic fusion. Consequently the formation of π- and n-complexes is preceded by an increase in the chemical reactivity of the components in the eutectic mixtures. The light hypsochromic shift characteristic of the UV spectra of dilute solutions of such binary systems indicates the preferential formation of n-complexes in the latter.[63]

The nature of the molecular complexes formed and the factors promoting the mutual activation of their components can be discovered by comparing the crystal-chemical properties of the initial components and the binary systems.

In the TMTD–DBTD binary system, the nucleophilic centres are the sulfur atoms of TMTD, while the electrophilic centres are the carbon atoms of the benzothiazolyl fragments of DBTD.[62] The TMTD molecule can be represented by several structures,[70] which form the following *n*-complexes:



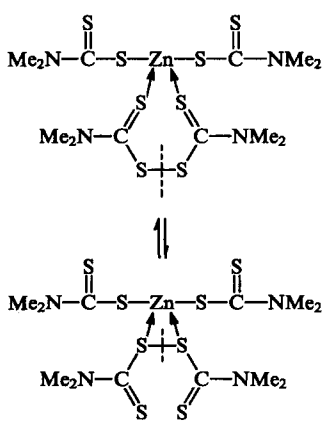
The enhancement of the accelerating function of such complexes can be explained by the weakening of the disulfide linkage in the latter and by the more ready addition of free sulfur to the complex.

The interaction of the accelerators in the TMTD–CBS and TMTD–OBS binary systems is accompanied by the formation of similar complexes with the sole difference that the electrophilic centres in the CBS and OBS molecules are the carbon atoms involved in the double bond of the benzothiazolyl fragment, the carbon atoms in the cyclohexyl group,[65] and the nitrogen atom in the morpholine fragment.[71]

The synergistic effect of the accelerators in the *n*-complexes is caused by, firstly, their more effective functional employment as a consequence of the better dispersion of the eutectic mixture in the fused form and, secondly, by the facilitation of the interaction of the complexes with S_8. Such interaction leads to the formation of tetramethylthiuram polysulfide, polythiobissulfenamide, and dibenzothiazolyl polysulfide,[72] as well as the hydroammonium polysulfides $[H_3NR]^+S_x^-$ and $[H_2NR']^+S_x^-$ (R = cyclohexyl, R′ = morpholinyl), which ensure a high rate of vulcanisation of elastomeric compositions.[71]

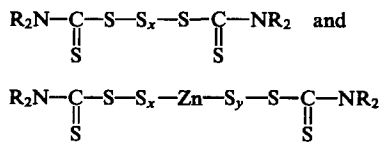
In binary systems where one of the accelerators is zinc dialkyldithiocarbamate or zinc mercaptide, the electrophilic zinc atom plays a significant role in the formation of molecular complexes.

Scheme 1

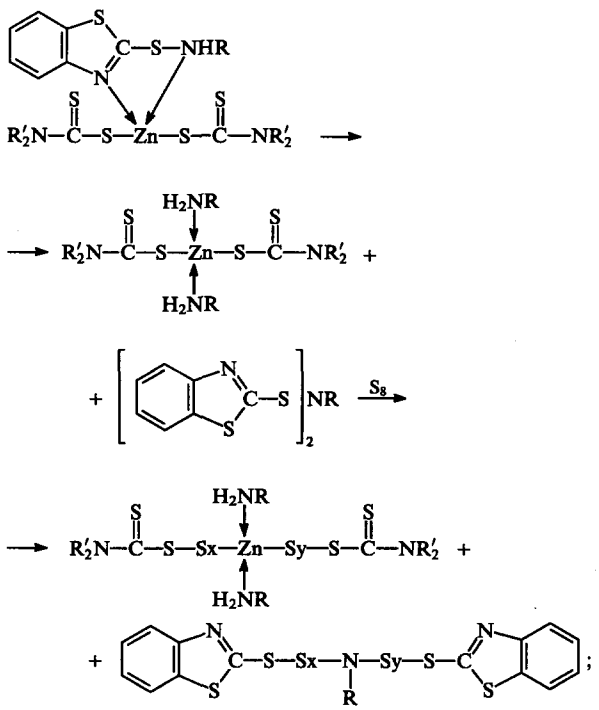


The structure of the ZDMDTC–TMTD complex is presented in Scheme 1.[73]

Complexes of this type prevent premature vulcanisation[70] and also ensure a higher rate of vulcanisation compared with the accelerators taken separately, owing to the weakening in the latter of the Zn–S and S–S bonds and facilitation of the interaction with S_8 leading to the formation of polysulfide compounds.[74]



The formation of a *n*-complex, an amine complex, and a number of other compounds in the ZDMDTC–CBS system can be represented as follows:[73]



R = cyclo-C_6H_{11}; R′ = Me.

The properties of the molecular complexes described above are determined by the nature of the orbitals provided by the components of the complexes for the formation of intermolecular bonds.[75] The nucleophilic centres are the sulfur atoms in the TMTD molecules, the nitrogen atoms in the MBT and DBTD molecules, the nitrogen atoms in the benzothiazolyl and exocyclic HN groups in CBS, and the nitrogen atoms of the secondary amino- and imino-groups in DPG. As regards the excess negative charge, the accelerators containing the benzothiazolyl group hardly differ from one another.[62] On the other hand, the carbon atoms involved in the double bond of the benzothiazolyl fragment of BD and BTD, the carbon atoms of the cyclohexyl group in CBS, and the nitrogen atom in the morpholine fragment of OBS relative to TMTD and DPG, as well as the zinc atoms in ZDMDTC and zinc mercaptide relative to CBS, DBTD, MBT, DPG, and TMTD differ significantly in their electrophilicity.[62,67,71] Therefore the greatest overlap of the molecular orbitals of the donor and the acceptor and hence the formation of the most stable π- and *n*-complexes is to be expected in the ZDMDTC–X and ZnS–X binary systems, where X = TMTD, DPG, CBS, DBTD, or MBT. This is confirmed by the presence of an appreciable convexity in the phase diagrams for these systems between the peritectic and

eutectic points,[28] which indicates the formation of stable complexes[55] and also that some of them exist in an individual state.[76] The absence of a convexity between the peritectic and eutectic melting points on the phase diagrams for the OBS–TMTD, DBTD–TMTD, CBS–TMTD, etc. binary systems[28] is evidence for the low stability of such complexes and for the possibility of their existence only in the presence of the initial components.[55]

The comparative stability of the molecular complexes formed in the physicochemical modification of binary systems of accelerators promotes synergism in their action in elastomeric compositions because, according to the theory of molecular complexes, the more intense the interaction of the molecules of the complexes the more marked their activation on dissociation.[77]

When complex mixtures of the components of sulfur-based vulcanising systems are used, it is essential to take into account the presence in them of zinc oxide, which adsorbs the molecules of the accelerators, sulfur, and aliphatic acids.[53,78] Zinc oxide is not a molecular crystal and cannot therefore form simple eutectic mixtures or substitutional solid solutions with accelerators and sulfur. On the other hand, the electrophilicity of the zinc atoms ensures the physical and chemical adsorption of the accelerators, stearic acid, and sulfur on zinc oxide as a result of the formation of the corresponding zinc salts of the accelerators and of zinc stearate and through them of dialkyldithiocarbamate, amine, and carboxylate complexes.[78–81]

The adsorption of the accelerators and stearic acid on zinc oxide can be selective and dissociative. In those cases where the components exhibit approximately the same nucleophilic or electrophilic properties, the selective adsorption depends on the configuration of the molecules, which determines the accessibility of the active centres of the interaction with the surface of zinc oxide.

Dissociative adsorption on zinc oxide is characteristic of TMTD, DBTD, and DTDM, which contain disulfide bonds.[53] It is known[75] that aliphatic disulfides react with acceptors (metal oxides) to form 1:1 complexes, which increases the length of the disulfide bond and weakens it. The interaction of aromatic disulfides, having relatively weak S–S bonds, with strong acceptors leads to the homolytic dissociation of these bonds. One can therefore postulate that zinc mercaptide is formed initially in the DBTD–TMTD–ZnO mixture and then the dimethyldithiocarbamate complex is produced. This was subsequently confirmed by other data.[28,79]

The conventional heats of adsorption of chemical additives on zinc oxide, presented in Table 5 and obtained by differential scanning calorimetry,[28] indicate the dependence of the selectivity of the adsorption on the nucleophilicity and configuration of the molecules and also on their ability to be dissociatively adsorbed with formation of the corresponding zinc salts.

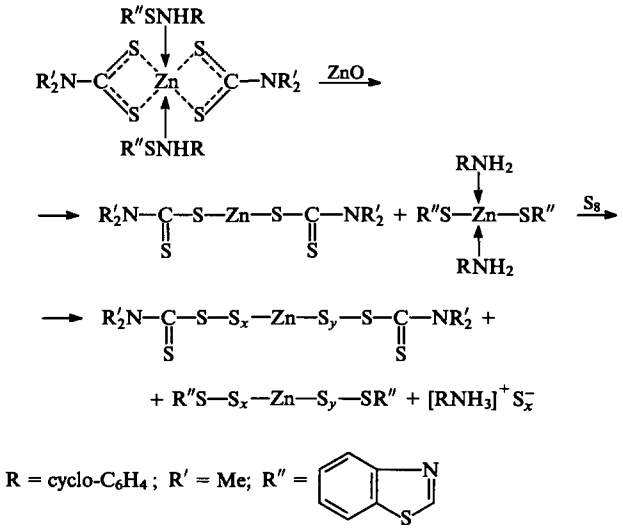
The foregoing suggests the following consecutive mechanism of the physicochemical modification of chemical additives in binary and complex eutectic systems.

In the first stage, the crystalline components interact, which is accompanied by an increase in the free energy of the system in the region of contact between the surfaces of unlike crystals. This results in the eutectic fusion of the mixture.

In the second stage, the components pass to the activated state on eutectic fusion, which results in the formation of π- and *n*-complexes between the nucleophilic and electrophilic molecules. This leads to an increase of their reactivity relative to free sulfur.[75]

In the third stage, the molecules to the π- and *n*-complexes interact chemically on raising the temperature with formation of amine, dialkyldithiocarbamate, and carboxylate complexes, whereas in the presence of free sulfur polysulfide compounds with hydroammonium polysulfides are produced.

The interaction of the components of sulfur-based vulcanising systems in complex mixtures can be described schematically in relation to the CBS–ZDMDTC–ZnO–S_x system.



The hydrogen adsorbed in the atomic or ionic form on zinc oxide may participate in the formation of amine ligands and hydroammonium polysulfides.[39]

$$H_2 \longrightarrow 2H \longrightarrow 2H^+ + 2e^-$$

The above mechanism of the physicochemical modification of chemical additives may be applied also to the highly effective synergistic systems of antioxidants obtained in the form of granules from eutectic melts of binary and complex mixtures of components and used in the synthesis of polymers.

Scheme 2

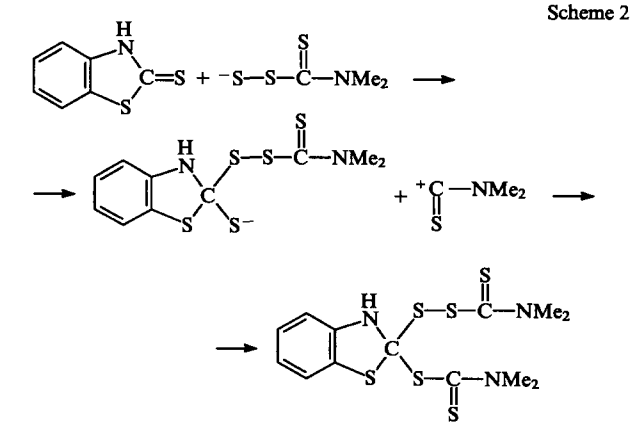


Table 5. Conventional heats of adsorption of the crystalline components of elastomeric compositions on zinc oxide.

Component	Heat of fusion/kJ mol^{-1}		Conventional heat of adsorption[a]/kJ mol^{-1}
	of individual component	in mixture with zinc oxide	
TMTD	33.2	4.8	28.4
MBT	20.4	4.3	16.1
Stearic acid	43.4	29.9	14.5
Phthalic anhydride	19.7	14.0	5.7
Diafen FP	27.9	23.7	4.8
CBS	27.4	23.8	3.6
DBTD	35.3	32.6	2.7
Sulfur	16.2	15.2	1.0
Santogard PVI	21.4	20.6	0.8
OBS	21.2	21.2	0.0

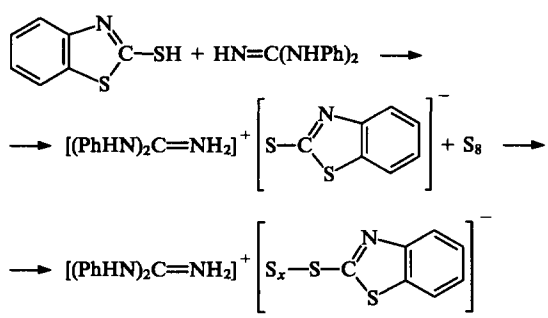
[a] The measurements were performed at the melting points of the adsorbed components.

3. The formation of new accelerators

On chemical interaction of the accelerators and binary eutectic systems, two eutectic melting points and a singular point, corresponding to the melting point of the new compound formed, appear on the phase diagram.

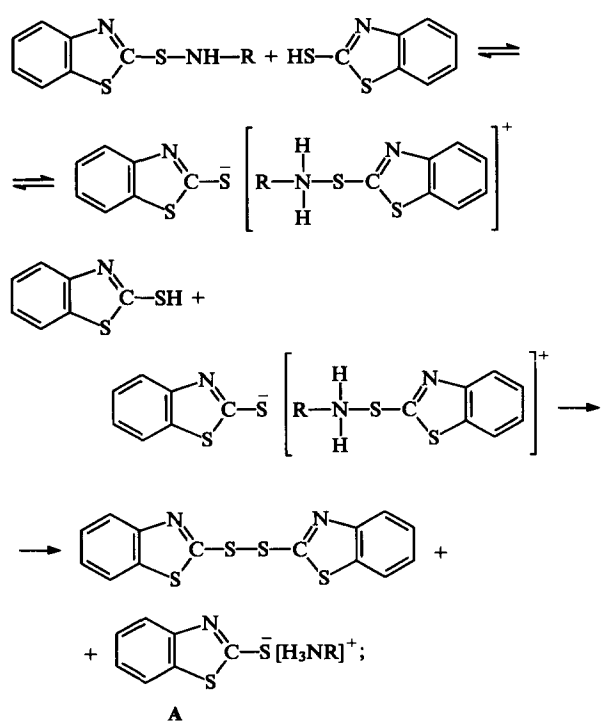
In the TMTD–MBT eutectic mixture, the products of the heterolytic decomposition of TMTD which occurs at 100–110 °C interact with the thiono-form of MBT (Scheme 2).[58] This increases the duration of the induction period for the vulcanisation of elastomeric compositions. The higher rate of vulcanisation can be explained by the decomposition of the compound obtained on raising the temperature into the highly reactive benzothiazolyl and dimethyldithiocarbamate fragments. Quantum-chemical cal-culations of the electronic characteristics of the accelerators[62] confirm the possibility of the nucleophilic addition reaction between the products of the heterolytic decomposition of TMTD and MBT.

The reaction between the accelerators in the MBT–DPG binary eutectic mixture leads to the formation of the diphenylguanidinium salt of mercaptobenzothiazole (DSMB), which, as a consequence of the increased nucleophilicity of the benzothiazolyl ion, is more thiophilic relative to free sulfur and is capable of forming an ionic polysulfide compound.[26]



Like hydroammonium polysulfides,[71] this compound exhibits a high vulcanising activity.

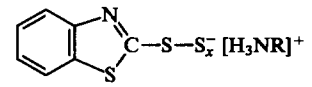
According to Ignatov's data,[59] the accelerators CBS and MBT in the CBS–MBT binary eutectic mixture interact in accordance with the following schemes:



A

R = cyclo-C_6H_{11}.

The chemical synergism manifested by this system in elastomeric compositions is due to the formation of more active accelerators than the initial MBT and CBS. Like DSBM, the ionic complex A can interact readily with S_8 to form hydro-ammonium polysulfides



which ensure a high rate of vulcanisation of elastomeric compositions.

The mutual activation of chemical additives, caused by the formation of eutectic mixtures, molecular complexes, and new chemical compounds, also occurs when they are introduced separately into elastomeric compositions. The eutectic mixtures are then obtained only as a result of the collision of the crystalline particles of the components on shear deformations arising during the preparation of the elastomeric compositions, while the main bulk of the components interact with one another in the diffusion regime, i. e. after the dissolution of the accelerators and sulfur and by diffusion of their molecules to the surface of zinc oxide with formation of molecular complexes and polysulfide compounds. Part of the sulfur and of the accelerators fail to interact with one another under these conditions and migrate to the surface on cooling of the elastomeric compositions.

Thus the physical and physicochemical modifications of the crystalline components of sulfur-based vulcanising systems in binary and complex mixtures do not alter the principal characteristics of the sulfur-based vulcanisation of unsaturated elastomers. They merely induce a decrease in the activation energy and a change in the kinetics of the process because its rate-limiting stage—the chemical activation of sulfur by molecular, amine, dialkyldithiocarbamate, and carboxylate complexes—takes place in the kinetic region under favourable conditions and is more effective than in the separate introduction of the chemical additives into the elastomeric compositions.

Furthermore, the modification of chemical additives ensures the most complete fulfillment by the latter of their functions, which makes it possible to diminish the concentrations of the components in the elastomeric compositions (the concentration of zinc oxide in the modified sulfur-based vulcanising systems can be decreased by a factor of 2–2.5 and that of the accelerators by a factor of 1.1–1.3).[28]

4. The influence of the crystal-chemical characteristics of chemical additives on the structure–property relation in the specific formation of their molecules

The attempts to employ quantum-chemical calculations to achieve the deliberate formation of the molecular structure of the chemical additives, starting with the specified properties of polymer compositions, which have been undertaken in recent years,[62,82–85] have not led to the desired results because in these calculations no account was taken of the change in the physical and chemical properties of the components as a result of their interaction with one another in the crystalline state.

Therefore, in the quantum-chemical calculations it is essential to take into account the presence of other crystalline components and the possibility of their interaction with the initial compounds to form eutectic compositions and molecular complexes.

Theoretical studies of the mechanism of the antioxidant activity of sterically hindered phenols in polyalkenes established[83] that their antioxidant activity is determined by the donor–acceptor properties of the *para*- and *ortho*-substituents. It is known[86–87] that the effectivenss of the accelerator increases with increase in its nucleophilicity. On the other hand, studies on the inhibiting effect of aromatic amines for different types of ageing of rubbers have shown[85] that the experimental molecular reactivity indices, characterising the ability of amines to enter into heterolytic and homolytic reactions, differ from the calculated values.

This is due to the physicochemical interaction of aromatic amines in elastomeric compositions with the components of sulfur-based vulcanising systems. Such interaction results in the formation of eutectic mixtures and molecular complexes in which the configuration and orbital state of the molecules[75] and hence the π-electron density and the free valence index have been altered relative to those in the initial components. This hypothesis has been confirmed by the satisfactory correlation between the calculated and experimental data obtained in the study of the influence of sterically hindered phenols in polyalkenes (in the absence of other crystalline components) and in elastomeric compositions—thiophthalimide derivatives—on the vulcanisation processes.[88] They exhibit a low reactivity relative to the nucleophilic and electrophilic components of the vulcanising systems as a consequence of their tendency to enter into homolytic reactions.[89]

The effectiveness of antioxidants and antiozonants in polymer ageing processes is determined by the formation of hydrogen bonds in these systems. It has been established[90] that the presence of hydrogen bonds in crystalline antioxidants and antiozonants is one of the causes of their relatively low solubility in elastomers. An increase in the polarity of the elastomer increases the solubility of the antiageing agent by intensifying the intermolecular interaction up to the formation of hydrogen bonds between the elastomer macromolecules and the molecules of the antioxidants and antiozonants. On the other hand, the formation of hydrogen bonds in the polymer–antioxidant system reduces the effectiveness of the antioxidant.[91]

The functional effectiveness of chemical additives diminishes on formation of hydrogen bonds between the molecules of different components. Thus hydrogen bonds decrease the activity of the amine accelerator in the sulfur-based vulcanisation and the inhibiting activity of resorcinol in the oxidation of rubber.[92]

The molecules of chemical additives incapable of forming hydrogen bonds but exhibiting nucleophilic and electrophilic properties relative to one another can form π- and *n*-complexes, which induces an increase in the effectiveness of the components. The increase in the reactivity of molecules in such complexes compared with their ground state[63] occurs as a result of the interaction of the π^* antibonding orbitals of one component with the nonbonding orbitals of the nitrogen, sulfur, or oxygen atoms of the other component or with the occupied 3*d* orbitals of the zinc atom.[68]

Thus, in order to increase the functional effectiveness of chemical additives to elastomeric compositions, it is useful to achieve a decrease in the probability of the formation of hydrogen bonds between the components and an increase in the probability of the formation of molecular complexes. This can be done by selecting chemical additives on the basis of a comparison of their molecular structures and crystal-chemical characteristics and the phase diagrams for binary systems of the components.[28]

IV. Conclusion

The above analysis shows that comparison of the melting points of the chemical additives, the configurations of their molecules, and the π-electron densities and free valence indices of the atoms in the molecules makes it possible to regulate the formation in the binary and complex mixtures of these components of simple eutectic systems, substitutional solid solutions, molecular complexes, and polysulfide compounds and also to determine the optimum conditions for the formation of systems with prespecified properties. Such systems and compounds are more effective than the initial components, since they ensure a greater defectiveness and dispersity of the crystalline particles and this increases the chemical reactivity of the components. The formation of molecular complexes and new compounds in the eutectic mixtures increases still further the effectivenss of the crystalline accelerators in vulcanisation processes, because this leads to their thiophilicity and facilitates their interaction with sulfur molecules in the formation of polysulfide compounds and hydroammonium polysulfides, which exhibit a high vulcanising activity.

The formation of polysulfide compounds in such mixtures makes it possible to reduce the concentrations of the accelerators and of zinc oxide in sulfur-based vulcanising systems without a decrease or even with an increase in their effectivenss compared with control vulcanising systems.[28] Furthermore, the sharp fall in the melting points of the chemical additives in eutectic mixtures makes it possible to granulate the melts without introducing binders, obtaining thereby strong, friable, and readily fusible granules. The use of such granules eliminates the formation of dust from the powdered components and improves the environmental situation in the processing of elastomeric compositions and polymers.

An important advantage of the physical and physicochemical modification of chemical additives is the possibility of predicting on the basis of the crystal-chemical characteristics and molecular structures of the components the formation in binary and complex systems of simple eutectic mixtures, substitutional solid solutions, and molecular complexes and of estimating their influence on the properties of the elastomeric compositions and rubbers. This advantage may be used for the development of a fundamentally new scientifically based approach to the creation of recipes for elastomeric compositions.

References

1. A I Kitaigorodskii *Molekulyarnye Kristally* (Molecular Crystals) (Moscow: Nauka, 1971)
2. I B Gardiner *Rubber Chem. Technol.* **41** 13129 (1968)
3. M Ikeda, T Yamamoto, Y Shinozaki, N Wada, Y Kaneko *Radioisotopes* **22** 556 (1973)
4. B S Grishin, I A Tutorskii, E E Potapov *Vysokomol. Soedin., Ser. A* **16** 130 (1974)
5. I A Landa, A S Kuz'minskii, S A Reitlinger, N G Kolyadina *Kauch. Rezina* (9) 12 (1973)
6. *Khimicheskie Dobavki k Polimeram. Spravochnik* (Chemical Additions to Polymers. Handbook) (Moscow: Khimiya, 1973)
7. B Spiegelhalder, R Preussman *Carcinogenesis* **4** 1147 (1983)
8. J M Fajen, G A Carson, D P Rounbehler, T Y Fan, R Vita, V E Goff, G S Edwards, D H Fine, V Reinhold, K Biemann *Science* **205** 1262 (1979)
9. W Hoffman *GAK: Gummi, Fasern, Kunstst.* **43** 562 (1990)
10. D W Chasar, P D Matheny *Kautsch. Gummi Kunstst.* **44** 435 (1991)
11. I Zieltow *Kunststoffberater* **81** 427 (1991)
12. G Catania *Umwelt* **20** 631 (1990)
13. A V Acaraglu *Proc. Eng. News* **15** 52 (1987)
14. Yu N Neienkirkhen, A A Dontsov, B S Grishin, G V Insarova *Kauch. Rezina* (2) 35 (1983)
15. BRD P. 1 570 125; *Ref. Zh. Khim.* 5 T 570P (1978)
16. D L Fedyukin, T I Vinogradova, L A Danchenko, N V Ermilova *Kauch. Rezina* (1) 11 (1973)
17. A A Dontsov, B S Grishin *Kauch. Rezina* (2) 40 (1984)
18. Jpn. Appl. 59-80438; *Ref. Zh. Khim.* 8 U 27P (1985)
19. Jpn. Appl. 62-537; *Ref. Zh. Khim.* 24 U 52P (1987)
20. US P. 4 895 884; *Ref. Zh. Khim.* 6 U 30P (1991)
21. A A Mukhutdinov *Modifikatsiya Sernykh Vulkaniziruyushchikh Sistem i Ikh Komponentov* (Modification of Sulfur Vulcanising Systems and Their Components) (Moscow: TsNIITEII, 1989)
22. N M Emanuel' *Usp. Khim.* **50** 1721 (1981) [*Russ. Chem. Rev.* **50** (901) (1981)]
23. G V Karpukhina, N M Emanuel' *Dokl. Akad. Nauk SSSR* **276** 1163 (1984)
24. A A Mukhutdinov, V N Zelenova *Kauch. Rezina* (7) 28 (1988)
25. A A Mukhutdinov, S L Smol'yaninov, V S Minkin, I G Shaikhiev *Kauch. Rezina* (4) 22 (1989)
26. A A Mukhutdinov, I G Shaikhiev, R Z Musin *Khimiya i Tekhnologiya Elementoorganicheskikh Soedinenii i Polimerov* (Chemistry and Technology of Organoelement Compounds and Polymers) (Kazan: KKhTI, 1991)

27. V M Bilobrov *Vodorodnaya Svyaz'. Vnutrimolekulyarnye Vzaimodeistviya* (Hydrogen Bond. Intramolecular Interactions) (Kiev: Nauk Dumka, 1991)
28. A A Mukhutdinov, Doctoral Thesis in Chemical Sciences, KGTU, Kazan, 1993
29. P Saike *Mekhanizm Reaktsii v Organicheskoi Khimii* (The Mechanisms of Reactions in Organic Chemistry) (Moscow: Khimiya, 1971)
30. J Mathieu, R Panico *Mécanismes Réactionnels en Chimie Organique* (Translated into Russian; Moscow: Mir, 1975)
31. A Walberg *Acta Crystallogr.* **34** 392 (1978)
32. T Adzami, X Sudzuka, F Ono *J. Soc. Rubber Ind. Jpn.* **39** 62 (1966)
33. K Marry *Acta Chem. Scand.* **19** 1509 (1965)
34. V Malta, R Celotti, R Zannetti, A F Martelli *J. Chem. Soc., B* **3** 548 (1971)
35. J P Chesik, J Donohue *Acta Crystallogr., Sect. B* **27** 1441 (1971)
36. T Adzami, I Imazu *J. Soc. Rubber Ind. Jpn.* **37** 413 (1964)
37. A Radha *Z. Kristallogr.* **171** 225 (1985)
38. S P Popkov *Fiziko-Khimicheskie Osnovy Pererabotki Rastvorov Polimerov* (Physicochemical Principles of the Processing of Polymer Solutions) (Moscow: Khimiya, 1976)
39. L H Little *Infrared Spectra of Adsorbed Species* (Translated into Russian; Moscow: Mir, 1969)
40. A F Wells *Structural Inorganic Chemistry* (Translated into Russian; Moscow: Mir, 1987)
41. *Fizicheskaya Entsiklopediya* (Physical Encyclopedia) (Moscow: Sov. Entsiklopediya, 1990)
42. A I Kitaigorodskii *Smeshannye Kristally* (Mixed Crystals) (Moscow: Nauka, 1983)
43. V M Zalkin *Zh. Fiz. Khim.* **43** 299 (1969)
44. V M Zalkin *Zh. Fiz. Khim.* **57** 499 (1983)
45. A Ya Erchenkova, M Z Rakhman, M A Shtern, L N Gogina *Kauch. Rezina* (11) 12 (1973)
46. T Yanon, M Macno, S Maeda *J. Soc. Rubber Ind. Jpn.* **64** 605 (1991)
47. P A Kouzov, A D Mal'gin, G M Skryabin *Ochistka ot Pyli, Gazov i Vozdukha v Khimicheskoi Promyshlennosti* (Purification from Dust, Gases and Air in Chemical Industry) (Moscow: Khimiya, 1982)
48. P V Danckwerts *Gas–Liquid Reactions* (Translated into Russian; Moscow: Khimiya, 1973)
49. S M Walas *Phase Equilibriums in Chemical Technology* (Translated into Russian; Moscow: Mir, 1989)
50. E V Zimin, A B Kusov *Kauch. Rezina* (6) 23 (1968)
51. I D Khodzhaeva, V V Markov, G V Insarova, L D Filippovich, Z N Tarasova, G M Plavnik *Kolloidn. Zh.* **41** 315 (1979)
52. B S Grishin, V I Borisov, I D Khodzhaeva, V A Shershnev, Z N Tarasova *Kolloidn. Zh.* **40** 972 (1978)
53. A A Dontsov, V A Shershnev *Zh. Vses. Khim. O-va im. D I Mendeleeva* **31** 88 (1986)
54. P A Rebinder *Poverkhnostnye Yavleniya v Dispersnykh Sistemakh* (Surface Phenomena in Dispersed Systems) (Moscow: Nauka, 1978)
55. I Hauben-Weyl *Methoden der Organischen Chemie* (Translated into Russian; Moscow: Khimiya, 1967)
56. L P Bondar', V A Borokhovskii, G I Brolinskii *Fiziko-Khimicheskie Svoistva Sery* (Physicochemical Properties of Sulfur) (Moscow: TsNIITEII, 1985)
57. M A Menkovskii, V T Yavorskii *Tekhnologiya Sery* (Technology of Sulfur) (Moscow: Khimiya, 1985)
58. L B Simanenkova, K V Markushevskaya, M N Voloktrub, G V Tarkhov *Kauch. Rezina* (7) 18 (1982)
59. V A Ignatov *Zh. Obshch. Khim.* **49** 1122 (1979)
60. A I Zubenko, A G Pilipenko, L I Savranskii *Koord. Khim.* **10** 1219 (1984)
61. N V Mel'nikova, A I Zubenko, A G Pilipenko *Ukr. Khim. Zh. (Russ. Ed.)* **53** 472 (1987)
62. A A Shurkus, P P Pipiraite, A B Bolotin, L B Simanenkova *Teor. Eksp. Khim.* **20** 627 (1984)
63. K Higasi, H Baba, A Rembaum *Quantum Organic Chemistry* (Translated into Russian; Moscow: Mir, 1967)
64. V A Ignatov, L S Degtyarev, L F Protopopova, M S Fel'dshtein *Kauch. Rezina* (9) 18 (1975)
65. S I Satava *J. Soc. Rubber Ind. Jpn.* **44** 356 (1971)
66. A B Bolotin, P P Pipiraite, A Yu Ruzhene, B N Gorbunov, G V Tarkhov, L B Simanenkova *Zh. Strukt. Khim.* **29** 19 (1988)
67. A S Kuz'minskii, S M Kavun, V P Kirpichev *Fiziko-Khimicheskie Osnovy Polucheniya, Pererabotki i Primeneniya Elastomerov* (Physicochemical Principles of the Preparation, Processing, and Application of Elastomers) (Moscow: Khimiya, 1976)
68. L J Andrews, R M Keefer *Molecular Complexes in Organic Chemistry* (Translated into Russian; Moscow: Mir, 1967)
69. G Zundel *Hydration and Intermolecular Interaction* (Translated into Russian; Moscow: Mir, 1972)
70. V I Ovcharov, B L Pikalov, M V Bykov *Kauch. Rezina* (5) 20 (1985)
71. T V Shestakova, A M Evdokimov, E V Korotyshev, V O Reikhsfel'd, A B Kusov *Zh. Org. Khim.* **6** 1929 (1970)
72. T V Tarasov, I I Vishnyakov, B S Grishin *Kauch. Rezina* (5) 39 (1991)
73. A A Mukhutdinov *Kauch. Rezina* (6) 38 (1993)
74. A A Dontsov *Protsessy Strukturirovaniya Elastomerov* (Structure Formation Processes in Elastomers) (Moscow: Khimiya, 1978)
75. E N Gur'yanova, I P Romm *Zh. Fiz. Khim.* **62** 2687 (1988)
76. T D Skinner, A A Watson *Rubber Age* **99** 76 (1967)
77. A V Mashkina *Geterogennyi Kataliz v Khimii Organicheskikh Soedinenii Sery* (Heterogeneous Catalysis in the Chemistry of Organic Compounds of Sulfur) (Novosibirsk: Nauka, 1977)
78. V A Shershnev *Rubber Chem. Technol.* **55** 537 (1982)
79. V Dukhachek, R Sh Frenkel' *Tr. Mezhdunar. Konf. po Kauchuku i Rezine* (Proceedings of International Conference on Raw and Cured Rubber) (Kiev, 1978)
80. B Milligan *Rubber Chem. Technol.* **39** 1115 (1966)
81. R N Campbell, R M Wise *Rubber Chem. Technol.* **37** 650 (1964)
82. A B Bolotin, B N Gorbunov, A A Efimov, P P Pipiraite, A Yu Ruzhene *Teor. Eksp. Khim.* **25** 594 (1989)
83. A B Bolotin, P P Pipiraite, A Yu Ruzhene, L B Simanenkova *Teor. Eksp. Khim.* **26** 73 (1990)
84. A B Bolotin, P P Pipiraite, B N Gorbunov *Teor. Eksp. Khim.* **27** 165 (1991)
85. P K Liplyanin, in *Tez. Dokl. Pervoi Rossiiskoi Nauch.-Prakt. Konf. Rezinshchikov "Syr'e i Materialy dlya Rezinovoi Promyshlennosti: Nastoyashchee i Budushchee"* (Abstracts of Reports of the First Russian Scientific Practical Conference of Rubber Specialists "Resources and Materials for the Rubber Industry: The Present and The Future") (Moscow, 1993) p. 68
86. L B Simanenkova, K V Makushevskaya, G V Tarkhov, A A Shurkus *Kauch. Rezina* (5) 23 (1983)
87. G Mathew, B Kuriakose, A C Kuriakose *Kautsch. Gummi Kunstst.* **45** 490 (1992)
88. S M Kavun, V A Palyulin, M M Donskaya, Yu M Genkina, in *Tez. Dokl. Pervoi Rossiiskoi Nauch.-Prakt. Konf. Rezinshchikov "Syr'e i Materialy dlya Rezinovoi Promyshlennosti: Nastoyashchee i Budushchee"* (Abstracts of Reports of the First Russian Scientific Practical Conference of Rubber Specialists "Resources and Materials for the Rubber Industry: The Present and The Future" (Moscow, 1993) p. 65
89. G A Blokh *Organicheskie Uskoriteli Vulkanizatsii i Vulkanizuyushchie Sistemy dlya Elastomerov* (Organic Vulcanisation Accelerators and Vulcanising Systems for Elastomers) (Leningrad: Khimiya, 1978)
90. L S Fel'dshtein, A S Kuz'minskii *Kauch. Rezina* (10) 16 (1970)
91. M L Andropov, G E Zaikov, Z K Maizus, N M Emanuel' *Zh. Fiz. Khim.* **41** 2002 (1967)
92. E E Potapov, I A Tutorskii, L E Chernukha, E T Golovin, B A Dogadkin *Kauch. Rezina* (11) 18 (1970)

Russian Chemical Reviews **63** (8) 695 – 710 (1994)
©1994 Russian Academy of Sciences and Turpion Ltd

UDC 547.963.3

The synthesis and transformations of uronic acid nucleosides

V A Timoshchuk

Contents

I. Introduction	695
II. Catalytic oxidation of nucleosides to uronic acid nucleosides	695
III. Oxidation of nucleosides by nonspecific oxidants	696
IV. Glycosylation of purine and pyrimidine heterocycles by uronic acids	698
V. Synthesis of uronic acid nucleosides by modifying the sugar and heterocyclic base residues	704
VI. Transformations of uronic acid nucleosides	706

Abstract. The results of studies on the synthesis and transformations of uronic acid nucleosides are surveyed. Various pathways leading to the synthesis of uronic acid nucleosides are examined, including methods involving specific and nonspecific oxidation of nucleosides, and the glycosylation and modification of the sugar residue or the heterocyclic base. The bibliography includes 97 references.

I. Introduction

Uronic acid nucleosides occupy a special place among the numerous modified nucleosides. Replacement of the primary hydroxy-group in nucleosides by a carboxy-group induces appreciable changes in the reactivities of other functional groups due both to the redistribution of electron density in the molecule and to conformational factors. Furthermore, the presence of a carboxy-group extends the possibilities of the syntheses based on nucleosides.

The interest in uronic acid nucleosides is caused primarily by the fact that they are a component of many antibiotics exhibiting a broad spectrum of biological activity.[1] There is much promise for derivatives of adenosine-5′-carboxylic acid, which are agonists of adenosine receptors and in the future may find extensive application in medical practice as hypotensive, cardiotonic, and thrombolytic agents.[2]

Progress in the synthesis of natural antibiotics, in devising new antibiotics, and also in the study of the biological action of uronic acid nucleosides with a wide variety of structures is in many respects determined by current advances in the development of methods for their preparation. The aim of the present review is to examine and treat systematically the existing methods of synthesis of uronic acid nucleosides and their transformations.

V A Timoshchuk Radiation Chemistry Laboratory,
Faculty of Chemistry, Belarus State University, prosp. F Skoriny 4,
220050 Minsk, Belarus
Fax (7-017) 220 82 72. Tel (7-017) 220 67 56

Received 10 May 1994
Uspekhi Khimii **63** (8) 730 – 746; translated by A K Grzybowski

II. Catalytic oxidation of nucleosides to uronic acid nucleosides

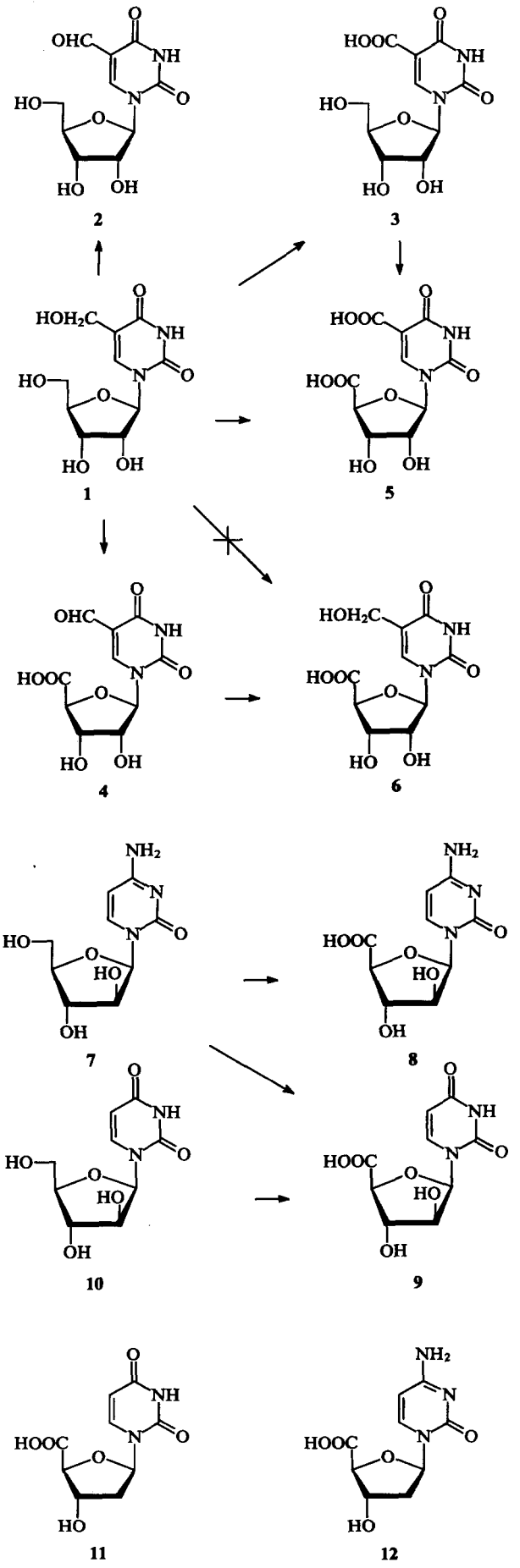
A general method of synthesis of uronic acid nucleosides, involving the selective oxidation of the primary hydroxy-group of the nucleoside to a carboxy-group by oxygen over a platinum catalyst, has been proposed by Todd and coworkers[3] in connection with the solution of the problem of the stepwise degradation of polynucleotides. The catalytic oxidation of uridine, thymidine, adenosine, guanosine, 3′-bromo-3′-deoxy-3-methylthymidine, 3-methylthymidine, thymidine 3′-phosphate and thymidylyl-(3′→5′)-thymidine was investigated. The corresponding nucleoside-5′-carboxylic acids were obtained and characterised. The oxidation of nucleosides to acids is usually carried out in a weakly alkaline medium at 50 – 60 °C by bubbling with finely dispersed oxygen in the presence of platinum on charcoal. The maintenance of a specified solution pH (~7.5) and a high rate of stirring are extremely important factors in the process.

It has been shown[4] that, when the reaction is carried out at room temperature in 50% acetic acid, three oxidation products are formed from 5-hydroxymethyluridine **1**: uridine-5-carboxaldehyde **2**, uridine-5-carboxylic acid **3**, and the aldehydoacid **4**. The oxidation of nucleosides **1** and **3** in the presence of sodium bicarbonate leads to the acid **5**. The reduction of compound **4** with sodium tetrahydroborate affords the nucleoside **6**, which cannot be obtained by direct oxidation of compound **1**.

Together with the acid **8**, its uracil analogue **9** was isolated from the reaction mixture in the oxidation of the arabino-nucleoside **7**. Compound **9** can also be obtained by oxidising the uracil nucleoside **10**.

In the oxidation of 5-halo-derivatives of 2′-deoxyuridine and 2′-deoxycytidine, it was noted that the rate of reaction increases in the sequence H < Br < I.

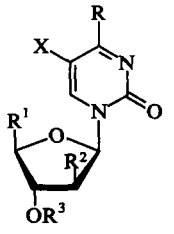
2′-Deoxyuridine-5′-carboxylic acid **11** and 2′-deoxycytidine-5′-carboxylic acid **12** were obtained by catalytic oxidation.



5-Fluoro-2′-deoxyuridine (FUDR) is known to exhibit an antitumour activity. However, the toxic 5-fluorouracil, formed as a result of its hydrolysis by phosphorylase, impairs the therapeutic properties of this preparation. Various attempts have been made to modify FUDR in such a way that it is stable toward phosphorylase and at the same time its ability to penetrate cell membranes is retained. It was found that these requirements are satisfied by 5-fluoro-2′-deoxyuridine-5′-carboxylic acid and its esters. These compounds are more resistant to hydrolysis, their toxicity is relatively low, and they exhibit a higher antitumour activity than FUDR.[5] When FUDR was oxidised in a weakly alkaline medium, the reaction products could not be isolated. Positive results were obtained on oxidation in a weakly acid medium (pH 6.81 ± 0.2).

Thymidine-5′-carboxylic acid has been obtained by the catalytic oxidation of nucleosides. Its nitriles, amides, and esters are inhibitors of thymidylate kinase of Walker 256 carcinoma.[6,7]

Catalytic oxidation of uracil and cytosine nucleosides afforded uronic acids and their derivatives having the general formula **13**.[8]



13

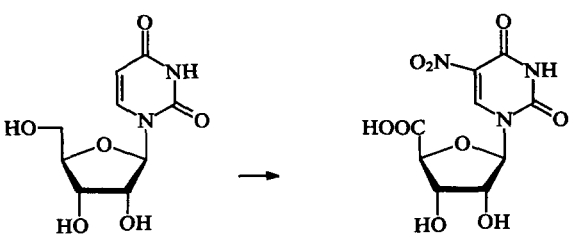
R = OH, NH_2;
R^1 = COOH, COOMe, CN;
R^2 = H, OH;
R^3 = H, COMe;
X = H, F, Br, I, Me.

It was observed that uracil nucleosides are oxidised at a higher rate than cytosine nucleosides. The ease of oxidation depends on the nature of the substituent in the 5-position in the pyrimidine ring and decreases in the sequence H > Me > F > Br > I. Thirty five compounds were obtained; the 5-bromo- and 5-iodouracil nucleosides of 2′-deoxyriburonamides possess an antiviral activity.

It is noteworthy that the method involving the catalytic oxidation of nucleosides suffers from disadvantages as well as having evident advantages. Thus the yields of the acids obtained by this method are as a rule fairly moderate (20%–50%), although they sometimes reach 70%–80%. Appreciable deviations from the activities of catalysts obtained by the same procedure, which results in a poor reproducibility of the results, have been noted. Compounds containing sulfur and amino-groups deactivate platinum catalysts. This method is relatively unsuitable for the preparative synthesis of amounts of nucleosides. A significant disadvantage is also the high cost of the catalyst. Methods for the synthesis of uronic acid nucleosides in which oxidants with a nonselective activity are used therefore merit attention.

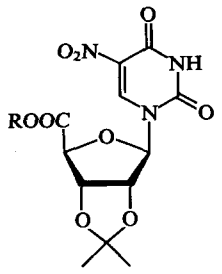
III. Oxidation of nucleosides by nonspecific oxidants

One of the first examples of uronic acid nucleoside synthesis was the oxidation of uridine **14** by nitric acid to 5-nitrouridine-5′-carboxylic acid **15**.[9]

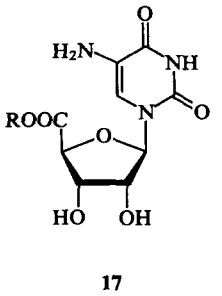


14 15

Later Fox and coworkers, [10] who repeated the synthesis of the acid **15**, confirmed its structure and obtained a series of its derivatives, including the acetonides of the esters **16** and the amine **17**.



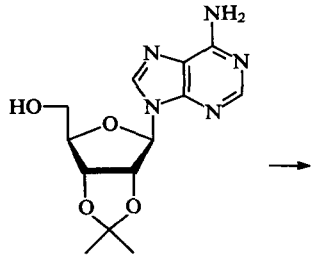
16



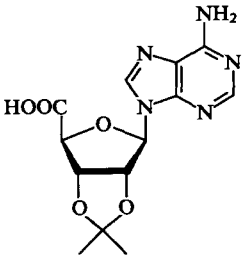
17

Oxidation of thymidine and 2′-deoxyadenosine by chromium trioxide afforded a low yield (~14%) of the corresponding acids. [11] Owing to the low selectivity of the oxidant, the secondary hydroxy-group is oxidised as well as the primary hydroxy-group. The ketoacids synthesised under these conditions are extremely unstable and decompose with formation of thymine and adenine. 2′-Deoxyadenosine-5′-carboxylic acid has been obtained in higher yield (28%) by oxidising 2′-deoxyadenosine with potassium permanganate in an alkaline medium. [12]

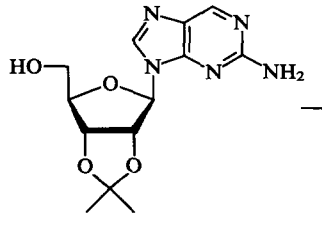
After an unsuccessful attempt at the catalytic oxidation of the adenosine acetonide **18** (the yield of the acids was 2%–5%), Harper and Hampton [13] oxidised it with chromium trioxide in various solvents. In all cases, the reaction mixtures contained several oxidation products. The acids **19** and **21** were obtained in satisfactory yields by oxidising the nucleosides **18** and **20** with potassium permanganate. [14, 15]



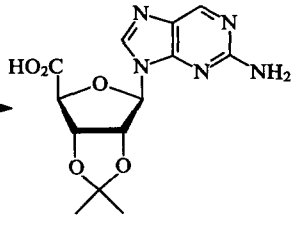
18



19



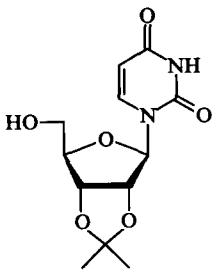
20



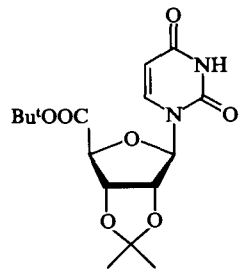
21

In the oxidation of isopropylidene derivatives of guanosine, inosine, and uridine by potassium permanganate, the only reaction product isolated has been oxalic acid. 2′,3′-*O*-Isopropylideneinosine-5′-carboxylic acid has been obtained in high yield using chromium peroxide in glacial acetic acid as the oxidant. [16]

A method of synthesis of guanosine-5′-carboxylic acid has not been described hitherto. In order to obtain derivatives of uridine-5′-carboxylic acid, Corey and Samuelsson [17] developed an unusual variant of the oxidation of 2′,3′-*O*-isopropylidene-uridine **22** coupled with esterification. Treatment of compound **22** with four equivalents of pyridinium dichromate in methylene chloride and dimethylformamide in the presence of acetic anhydride and *tert*-butyl alcohol leads to the formation of the *tert*-butyl ester of the acid **23**.

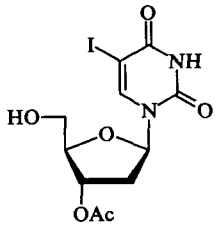


22

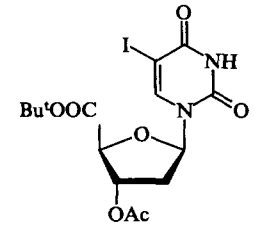


23

The ester **25** was obtained by this method from the deoxynucleoside **24**. [18]

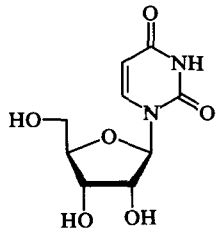


24

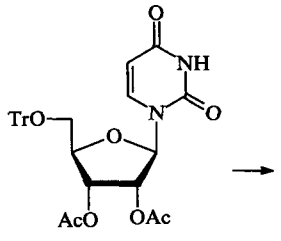


25

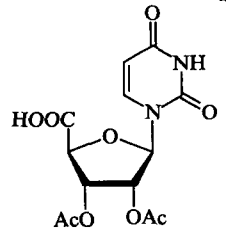
A scheme has been developed for the synthesis of pyrimidine nucleosides of uronic acids involving the treatment of uridine **14** in pyridine initially with chlorotriphenylmethane and then with acetic anhydride, this being followed by the oxidation of the resulting fully substituted nucleoside **26** with chromium peroxide [chromium trioxide? (Ed.)] in acetone in the presence of 50% sulfuric acid (the Jones reagent). The diacetate **27** was obtained by this procedure in 50% yield. [19]



14



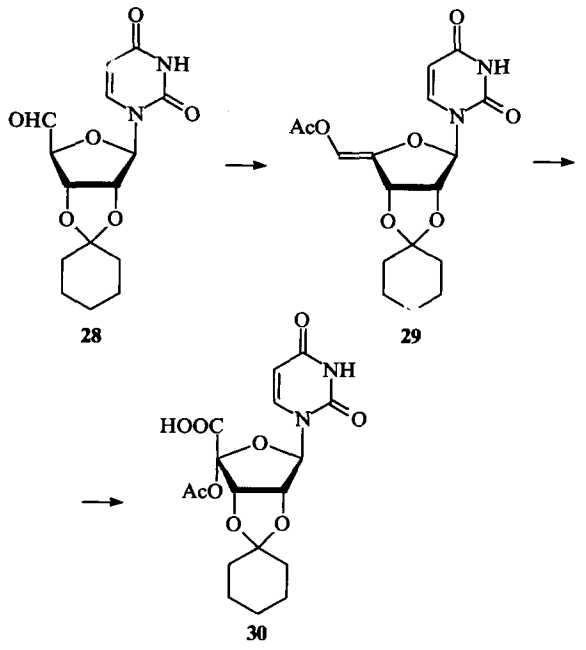
26



27

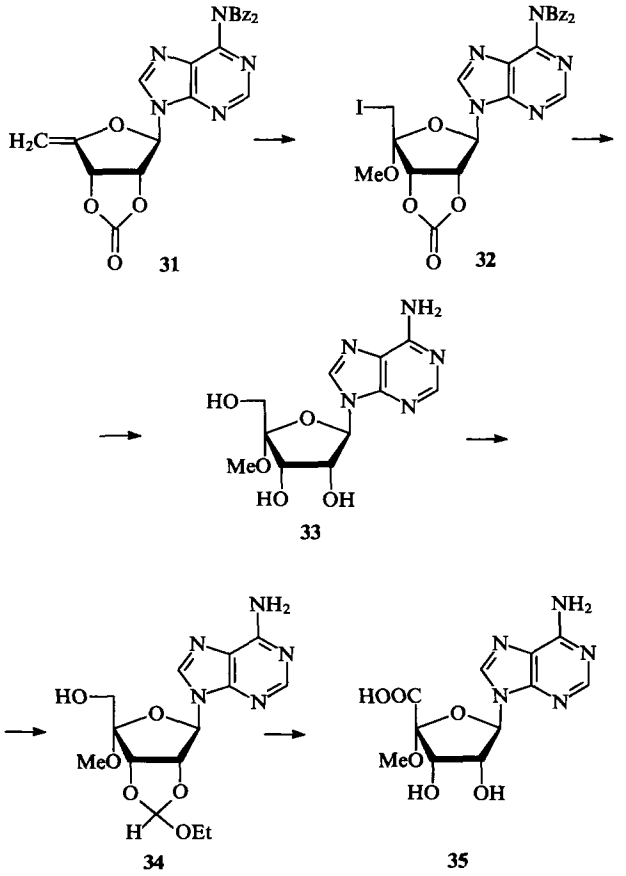
Tr = $C(Ph)_3$.

Nucleosides with an exocyclic double bond are convenient precursors in the synthesis of 4′-acetoxy- and 4′-methoxy-derivatives of nucleoside-5′-carboxylic acids. When the aldehyde **28** is heated with potassium carbonate in acetic anhydride, the enol acetate **29** is formed readily and its oxidation with *m*-chloroperbenzoic acid in methylene chloride gives the 4′-acetoxy-acid **30**. [20]



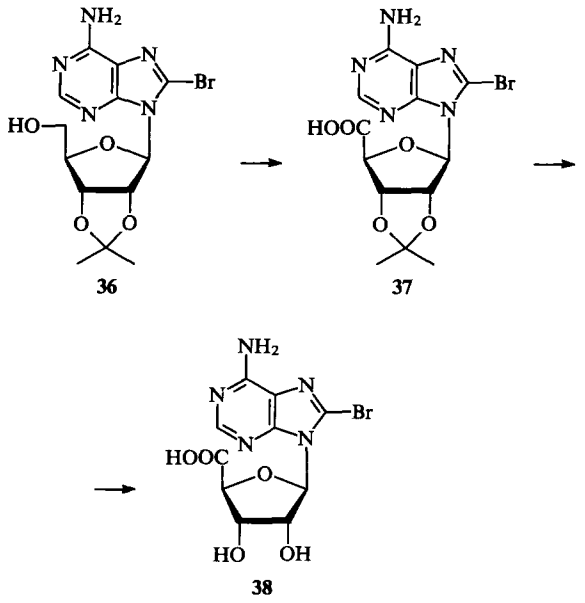
28 29 30

Treatment of the unsaturated nucleoside **31** with iodine leads to the selective formation of the iododeoxynucleoside **32**, which is converted into 4′-methoxyadenosine **33** as a result of hydrolysis, benzoylation, substitution of iodine by the benzyloxy-group, and ammonolysis. The oxidation by potassium permanganate of the ethoxymethylidene derivative **34** obtained from compound **33**, esterification, and the removal of the protecting group lead to the 4′-methoxy-acid **35**.[21]



31 32 33 34 35

Derivatives of adenosine-5′-carboxylic acid with various substituents in the 8-position in the adenine residue are of interest as potential agonists of adenosine receptors.[22] The acid **37** was obtained by oxidising the bromo-derivative **36** with potassium permanganate in an alkaline medium. Its controlled hydrolysis made it possible to remove the isopropylidene protecting group without appreciable cleavage of the *N*-glycosidic linkage, which in the presence of a bulky substituent in the 8-position is very sensitive to the action of acids. The esters obtained from the acids **37** and **38** were found to be able to form only primary amides on treatment with a mixture of primary and secondary amines. The secondary amines substitute the bromine atoms with a high degree of selectivity under these conditions, giving tertiary amines.[23]



36 37 38

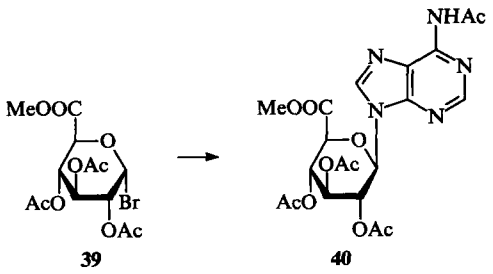
Oxidation of the acetonides of 8-aminoadenosine derivatives with potassium permanganate led to the complete decomposition of the purine residue.[22]

As can be seen from these examples, the oxidation of nucleosides by nonspecific oxidants encounters difficulties due to both the necessity for the preliminary protection of the secondary hydroxy-groups and the sensitivity of the heterocycles to oxidation, which appreciably limits the scope of this method.

The method involving the glycosylation of a wide variety of purine and pyrimidine heterocycles by uronic acid derivatives, for the preparation of which the range of oxidants employed in organic chemistry is in principle suitable, gives rise to extensive prospects for the synthesis of uronic acid nucleosides. The glycosylation of heterocycles by uronic acid derivatives has its specific features associated with the presence of a carboxy-group, which induces an appreciable redistribution of electron density in the molecule.

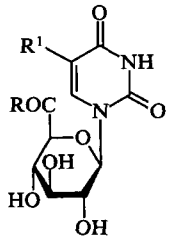
IV. Glycosylation of purine and pyrimidine heterocycles by uronic acids

There are numerous examples in the literature of the synthesis of nucleosides via the glycosylation of a wide variety of nitrogen-containing heterocycles by carbohydrate derivatives. At the same time, the use of uronic acid derivatives as glycosylating agents has only recently been systematically studied. Early attempts to synthesise uronic acid nucleosides include the condensation of the bromo-derivative **39** with 6-acetamido-9-chloromercuriopurine in the presence of cadmium carbonate and celite, which gave nucleoside **40** in 57% yield.[24]



39 40

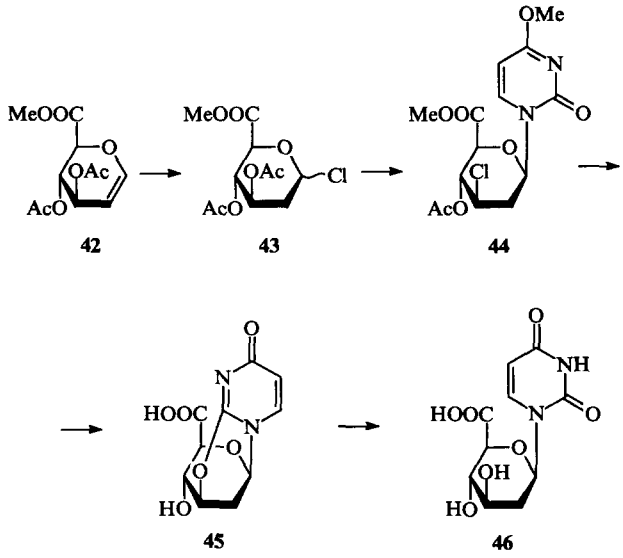
Hilbert and Johnson's method has been used to synthesise the pyrimidine nucleosides of D-glucopyranouronic acid: the glycosylation of 2,4-dialkoxypyrimidines by the bromo-derivative **39** gave the corresponding *N*-glycosides in 40%–60% yield, their methanolysis, ammonolysis, and alkaline hydrolysis giving rise to the uracil and thymine nucleosides of D-glucuronic acid and its methyl ester and amide having the general formula **41**.[25]



41

R = OH, OMe, NH_2;
R^1 = H, Me, Br, I.

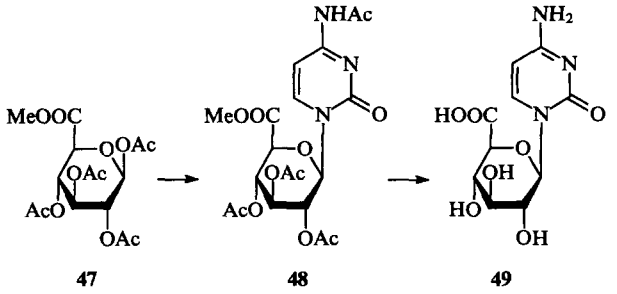
An interesting scheme for the synthesis of the nucleosides of 2-deoxypyranouronic acid has been described.[26] The chloro-derivative **43**, obtained by adding hydrogen chloride to the glycal **42**, was condensed with 2,4-dimethoxyuracil at 90–95 °C. Subsequent treatment of 3'-chloro-2',3'-dideoxy-β-nucleoside **44** with hydrogen chloride in methanol and with alkali afforded the cyclic nucleoside **45**. The opening of the anhydride ring by treatment with alkali led to the formation of the 2'-deoxynucleoside **46**.



42 43 44

45 46

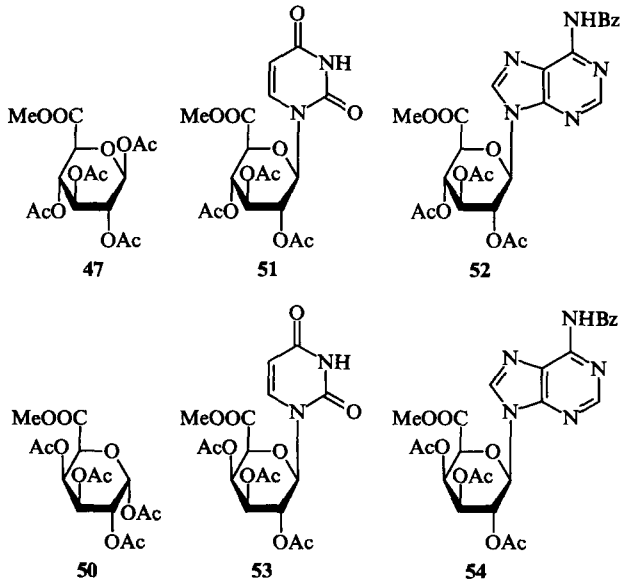
Fox and coworkers[27] synthesised the acid **49**, which is the cytosine nucleoside of D-glucuronic acid detected among the products of the biosynthesis of the antibiotic blasticidin S. Glycosylation of the silyl derivative of *N*(4)-acetylcytosine by the acetate **47** in the presence of $SnCl_4$ gave the nucleoside **48** in a low yield (20%). The required acid **49** was obtained by the alkaline hydrolysis of the latter.



47 48 49

The glycosylation of the silyl derivative of *N*-benzoylcytosine by the acetate **47** in the presence of three equivalents of $SnCl_4$ led to the benzoyl analogue of compound **48** in 70% yield.[28]

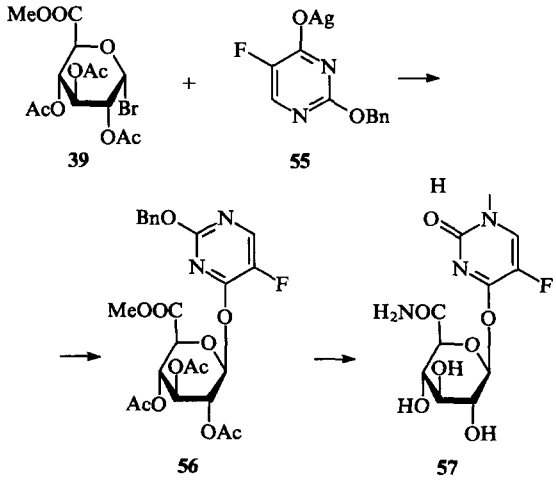
Lichtenthaler and coworkers[29,30] investigated the condensation of silyl derivatives of nitrogen-containing heterocycles with peracylated uronic acid esters in the presence of Lewis acids. It was found that, in the glycosylation of uracil and *N*(6)-benzoyladenine by the acetates **47** and **50**, the corresponding nucleosides **51**–**54** are formed in satisfactory yields only in the presence of 2.6 equivalents of $SnCl_4$.



47 51 52

50 53 54

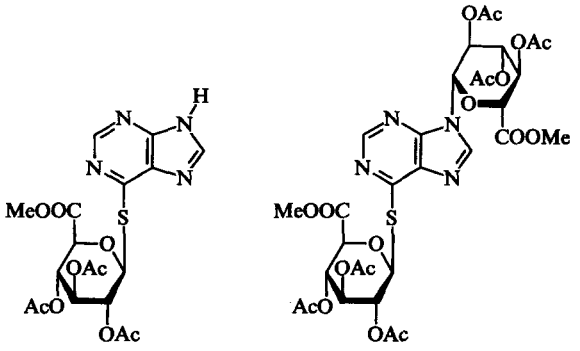
The *O*-glucuronide of 5-fluorouracil **57** has been obtained by condensing the silver salt of 5-fluorouracil **55** with the bromo-derivative **39** and by the subsequent removal of the protecting groups of the nucleoside **56**.[31]



39 55

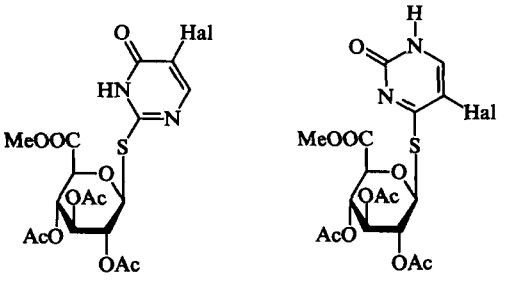
56 57

The reaction of bromo-derivative **39** with 6-mercaptopurine in DMF containing potassium carbonate afforded the *S*-glucuronide **58**. The reaction of **39** with the silver salt of 6-mercaptopurine and also the transglycosylation of the *S*-glucuronide **58** in the presence of $HgBr_2$ led to the formation of *N*(9),*S*-bisglucuronide **59**.[32,33]

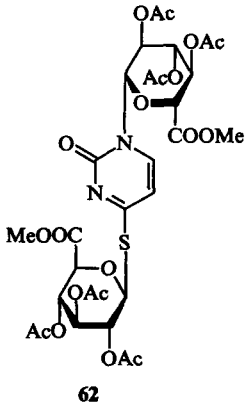


58 **59**

Methods for the synthesis of the *S*-glucuronides of 2- and 4-thiouracils, containing halogen atoms in the 5-position of the pyrimidine group, have been developed.[34] The best synthetic procedure was found to be the glycosylation of thiouracils by the acetate **47** in acetonitrile in the presence of 3.3 equivalents of $SnCl_4$. Together with the *S*-monoglucuronides **60** and **61**, a small amount of the *N*(1),*S*-bisglucuronide **62** was found, the latter being formed probably as a result of transglycosylation of the *S*-glucuronides.



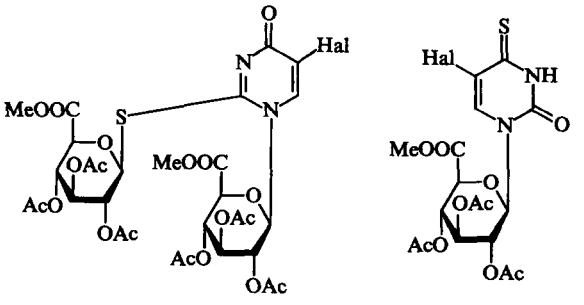
60 **61**



62

The corresponding 5-halo-derivatives have been obtained by halogenating the *S*-glucuronides and it was shown that 4-thiouracil glucuronides are halogenated less effectively than 2-thiouracil glucuronides. The fluorination of 4-thiouracil glucuronides led to cleavage of the *S*-glycosidic linkage.

The reactions of the *S*-glucuronides of 2, and 4-thiouracils and of their 5-halo-derivatives on treatment with Lewis acids have been investigated.[35] Refluxing of the *S*-glucuronides of 2-thiouracil and of its 5-halo-derivatives **60** in benzene in the presence of $HgBr_2$ led to the *N*(1),*S*-bisglucuronide **63** as a result of the transglycosylation reaction, whereas the *S*-glucuronides of the 5-halo-derivatives of 4-thiouracil gave predominantly the *N*(1),*S*-bisglucuronides **62** and insignificant amounts of the *N*(1)-glucuronides **64** as a result of the S → N transglycosylation of the nucleoside **61**.



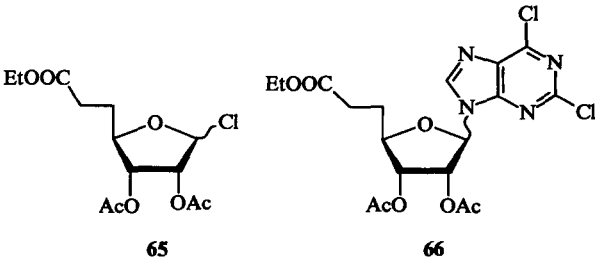
63 **64**

Mahrwald and Wagner[36] examined synthetic approaches to glucuronides of 2-hydroxy and 4-hydroxy- as well as 2-mercapto- and 4-mercaptopyrimidines.

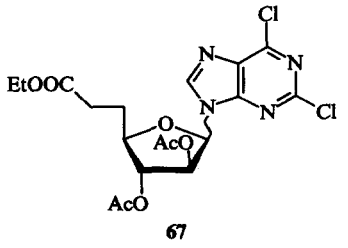
Glycosylation of 5-halouracils (Hal = F, Cl, Br, I) by the bromo-derivative **39** and the acetate **47** has been investigated.[37] The interaction of the bromo-derivative with silyl derivatives of 5-halouracils in benzene in the presence of $HgBr_2$ and $Hg(CN)_2$ led to the corresponding *N*(1)-nucleosides; the formation of small amounts of *N*(1), *N*(3)-bisglucuronides was observed. An increase in the yield of the *N*(1)-nucleosides on passing from uracil to 5-iodouracil was noted. The authors attributed this finding to the decreasing electronegativity of the halogens and the increasing basicity of the *N*(1) atom of the heterocycle.

The condensation of the silyl derivatives of 5-halouracils with the sugars **39** and **47** in acetonitrile and dichlorobutane in the presence of $SnCl_4$ afforded predominantly the *N*(1)-nucleosides, the *N*(3)-nucleosides being found in only two cases.

When the chlorosugar **65**, synthesised in six stages from allofuranose, was fused together with 2,6-dichloropurine in the presence of catalytic amounts of toluene-*p*-sulfonic acid with a yield of 47%, the formation of the α- and β-anomeric nucleosides of the D-ribose (compound **66**) and D-arabinose (compound **67**) series was observed.[38]

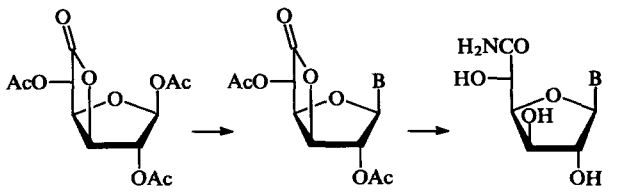


65 **66**



67

The condensation of silyl derivatives of uracil (U), *N*(4)-benzoylcytosine [*N*(4)-BzC], and also *N*(6)-benzoyladenine [*N*(6)-BzA] with the completely acetatoxylated glucurone **68** in the presence of three equivalents of $SnCl_4$ gave the nucleosides **69**–**71**, the ammonolysis of which led to the amides **72**–**74**.[39–41]



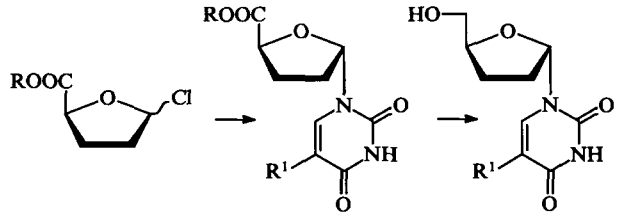
68

69: B = U; **72**: B = U;
70: B = *N*(4)-BzC; **73**: B = *N*(4)-BzC;
71: B = *N*(6)-BzA; **74**: B = *N*(6)-BzA.

The high stereospecificity of the condensation, leading to the formation of nucleosides only in the β-anomeric configuration, was demonstrated.

The nucleosides of glucurone and their derivatives have been synthesised by condensing the lactone **68** with the silyl derivatives of 5-fluoro-, 5-bromo-, and 5-iodo-uracil.[42] The condensation of the lactone with silylated uric acid, xanthine, and *N*(2)-acetylguanine has been investigated in dichlorobutane in the presence of trimethylsilyltrifluorosulfonic acid.[43] The formation of a mixture of the *N*(3)-, *N*(7)-, and *N*(9)-nucleosides was observed under these conditions.

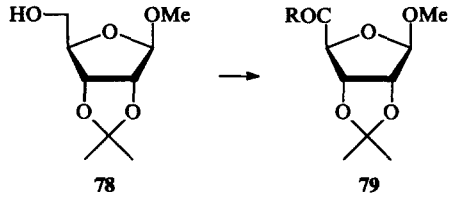
The nucleosides **76** have been synthesised by alkylating silylated pyrimidines by the chloro-derivatives of tetrahydrofurancarboxylic acid **75**. The reaction takes place at 20–30 °C with formation of racemic nucleosides having the *trans*-configuration. Reduction of the esters gave the dideoxynucleosides **77**. A small amount of the *cis*-isomer together with the *trans*-isomer was isolated following the alkylation of 5-fluoro-uracil by the chloro-derivative **75** at 100 °C with distillation of the chlorotrimethylsilane formed during the reaction.[44]



75 76 77

R^1 = Me, H, F.

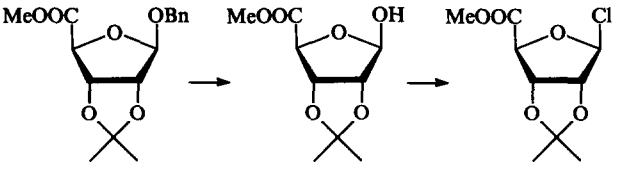
Schmidt and coworkers[45–47] have studied the glycosylation of pyrimidine and purine heterocycles by uronic acid derivatives. They developed methods for the preparation of derivatives of riburonic acid by oxidising the methyl riboside **78** with potassium permanganate. Because of their low reactivity in glycosylation reactions, the esters and amides **79** were found unlikely to be useful in the synthesis of nucleosides.[45]



78 79

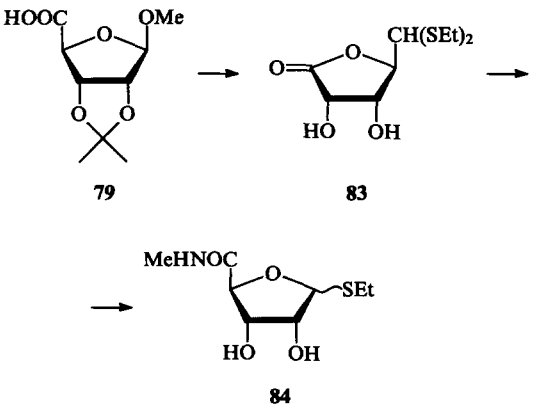
R = OH, OR^1, NR_2^2.

Chlorosugars are more active glycosylating agents. The sugar **81** with a free hemiacetal hydroxy-group was obtained by the hydrogenolysis of the riburonide **80**. Its treatment with thionyl chloride led to the β-anomer of the glycosyl chloride **82**.[46]



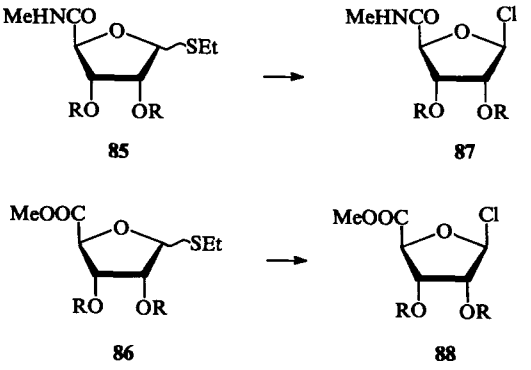
80 81 82

The use of the chloro-derivative **82** in order to obtain nucleosides proved to be of limited applicability for the following reason. In contrast to the isopropylidene derivatives of nucleosides, where the protecting group can be removed under the conditions of mild acid hydrolysis, the hydrolytic removal of the isopropylidene protecting group from uronic acid nucleosides requires severe conditions, which leads to appreciable cleavage of the glycosidic linkage. Methods have been described[47] for the synthesis of halo-derivatives of riburonic acid with benzylidene, benzyl, and benzoyl protecting groups. Treatment of the acid **79** with ethanethiol led to the synthesis of the diethylmercaptoacetal of the lactone **83**, which was transformed in two stages into the amide **84**.



79 83 84

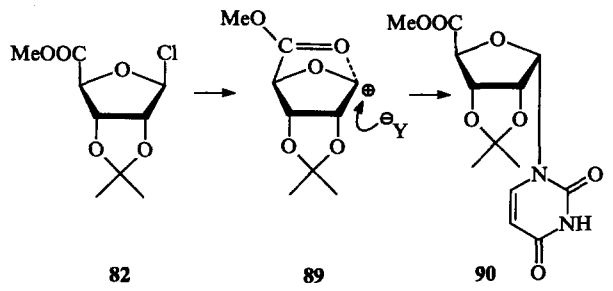
On treatment with chlorine, the benzylidene, benzyl, benzoyl, and acetyl derivatives of the amide **85** and the ester **86** were converted smoothly into the chloro-derivatives **87** and **88**.



85 87

86 88

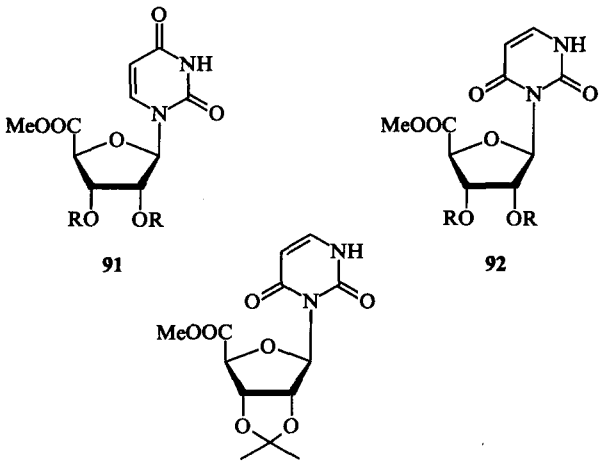
The stereochemical features of the glycosylation of pyrimidine heterocycles by the halo-derivatives of riburonic acid esters and amides with different protecting groups have been investigated. The method involving fusion of the chloro-derivative **82** with silylated uracil in the absence of a catalyst gave only the α-anomeric nucleoside **90**. The stereochemical result of this reaction is probably determined by the steric influence of the methoxycarbonyl group, which prevents the attack on the carbonium ion **89** by the nucleophile from the β-region.[48]



82 89 90

On fusion with uracil, the acetyl and benzoyl derivatives of the chloro-derivative **88** afforded a mixture of anomeric nucleosides, in which the β-anomer predominated. In this case, the stereochemical result was determined by neighbouring group participation, i.e. by the directing effect of the 2-*O*-acyl group.

When the condensation was carried out in benzene in the presence of silver perchlorate, the same behaviour was observed, but an increase in the fraction of the β-anomer was also noted in all cases. When $SnCl_4$ was used as the catalyst, the condensation led only to β-nucleosides, but appreciable amounts of the *N*(3)-nucleosides **92** were found in the reaction mixture under these conditions together with the *N*(1)-nucleosides **91**. Condensation of chloride **82** with uranyl gave only *N*(3) nucleoside **93**. Substitution of chlorine by the acetyl group produced the same result.

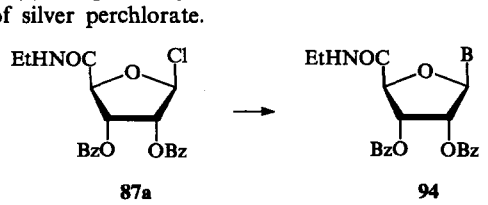


91 92

R = Ac, Bz. 93

The *N*(1)-α-, *N*(1)-β-, and *N*(3)-β-nucleosides have been obtained in proportions of 2 : 15 : 3 respectively by glycosylation of the silylated *N*(4)-acetylcytosine by the chloro-derivative **82** in the presence of $SnCl_4$. The condensation of the benzoate **88** led to the α- and β-anomers in proportions of 1 : 3 and the *N*(3)-nucleoside was not formed. Fusion with silver perchlorate did not alter significantly the stereochemical result of the reaction.

The ethylamides **94** were obtained in satisfactory yields by glycosylating silylated derivatives of uracil, *N*(4)-acetylcytosine [*N*(4)-AcC], and thymine (T) by the diethylamide **87a** in presence of silver perchlorate.



87a 94

B = U, *N*(4)-AcC, T.

The condensation of activated derivatives of D-riburonic and D-lyxuronic acids with various purines was investigated by Schmidt et al.[49] in order to estimate the effectiveness of the glycosylation of purines as a general method of synthesis of uronic acid nucleosides. The anomeric and regioisomeric [*N*(7),*N*(9)] nucleosides were separated by high performance column chromatography and structural assignments were reliably made on the basis of ^1H and ^{13}C NMR data.

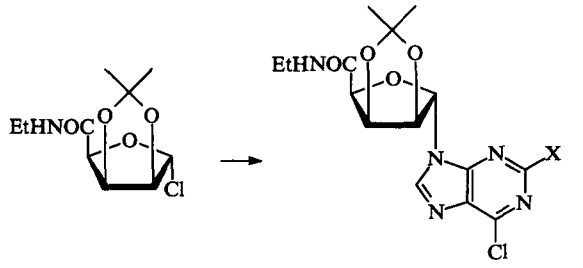
It was established that catalysis by mercury salts and also by $SnCl_4$ and $AgClO_4$ gave nucleosides in acceptable yield only in rare cases. Satisfactory results were obtained by fusing silylated purines with the methyl esters of chloro-derivatives of riburonic and lyxuronic acids with an isopropylidene protecting group. Together with the α- and β-anomers of the *N*(9)-nucleosides, the anomers of *N*(7)-nucleosides were isolated. The ratio of the anomers of the nucleo-sides obtained was shown to be independent of the anomeric configuration of the sugar. Condensation of the riburonic acid derivative with 6-chloropurine led to only one isomer—the α-*N*(7)-nucleoside.

In contrast to the esters, the amides of riburonic acid form exclusively the *N*(9)-nucleosides with approximately equal proportions of the anomers as a result of fusion with purines.

The use of acyl derivatives of riburonamides for condensation with halo-derivatives led to the preferential formation of the β-*N*(9)-nucleosides, as was in fact to be expected in view of the involvement of the 2-*O*-acyl groups.

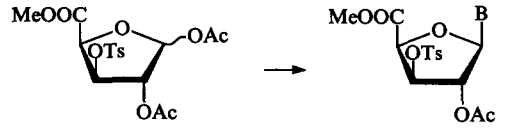
The condensation of purines with the methyl ester of the chloro-derivative of lyxuronic acid carrying an isopropylidene protecting group obeys in the main the same rules, but the formation of a considerable proportion of the β-nucleoside is somewhat unexpected, since all the substituents are then located on one side of the furanose ring.

Purine nucleosides of the ethylamide of lyxuronic acid **96** have also been obtained by fusing the chloro-derivative **95** with 6-chloro- and 2,6-dichloropurines. In contrast to the esters of lyxuronic acid, the condensation of the amide led to the formation of *N*(9)-nucleosides (with a 2 : 1 ratio of the α- and β-anomers) and only trace amounts of the *N*(7)-isomers.[50]



95 96, X = H, Cl.

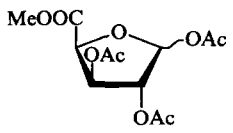
The reaction of alkoxyuronides with silylated nitrogen-containing heterocycles affords nucleosides in lower yields.[51] The 1-*O*-acetyl derivatives of sugars are less active glycosylating agents than alkyl glycosides and are more stable than halo-derivatives of sugars.[52] The condensation of acetate **97** with silylated uracil in the presence of an equimolar amount of $SnCl_4$ leads to the formation of the nucleoside **98** in 32% yield. When the amount of $SnCl_4$ was increased to three equivalents, the yield rose to 85%. The interaction of the acetate **97** with silylated derivatives of 5-fluorouracil, *N*(4)-benzoylcytosine, and *N*(6)-benzoyladenine afforded the corresponding nucleosides **99**–**101**. The formation of only the β-anomeric nucleosides was observed in all cases.[51,53]



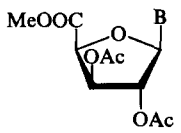
97, Ts = $MeC_6H_4SO_2$.

98: B = U;
99: B = 5-F-U;
100: B = *N*(4)-BzC;
101: B = *N*(6)-BzA.

On glycosylation with the xyluronic acid ester **102** in acetonitrile in the presence of three equivalents of $SnCl_4$, the silyl derivatives of uracil, 5-fluorouracil, and *N*(6)-benzoyladenine give the corresponding nucleosides **103**–**105** in moderate yields.[54]

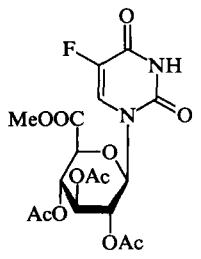


102

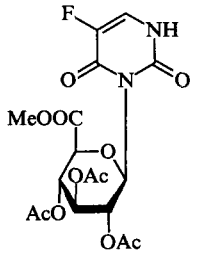


103: B = U;
104: B = 5-F-U;
105: B = *N*(6)-BzA.

The donor–acceptor complexes formed between the silylated pyrimidines and the Lewis acids, the so called *N*(1)-σ-complexes, are capable of reacting slowly with the sugar cation to form *N*(3)-nucleosides.[55]



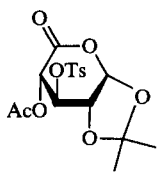
106



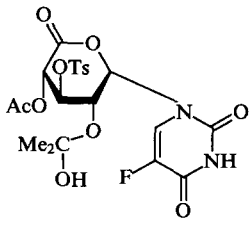
107

The glycosylation of 5-fluorouracil by the acetate **47** using three equivalents of $SnCl_4$ affords the *N*(1)-nucleoside **106** and the *N*(3)-nucleoside **107** in 36% and 6% yields respectively. The replacement of $SnCl_4$ by boron trifluoride etherate gave rise to approximately equal amounts (30.5% and 30%) of the isomeric nucleosides **106** and **107**.[56,57]

The formation of the α-anomeric nucleoside **109** was observed as a result of the glycosylation of 5-fluorouracil by the products of the acetolysis of the lactone **108**.[58,59]

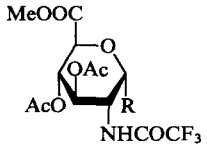


108

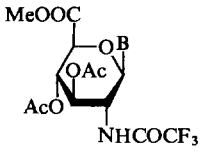


109

The first example of the synthesis of the nucleosides of 2-amino-2-deoxyuronic acids has been described by the present author and Kulinkovich.[60] The glycosylation of uracil by the acetate **110** in the presence of $SnCl_4$ proved to be unsuccessful. The condensation of the bromo-derivative **111** was also relatively ineffective. The nucleosides **112**–**114** were obtained in 26%, 36%, and 25% yields respectively by fusing the bromo-derivative **111** with the silylated heterocycles at 130 °C at a reduced pressure (40 Torr).

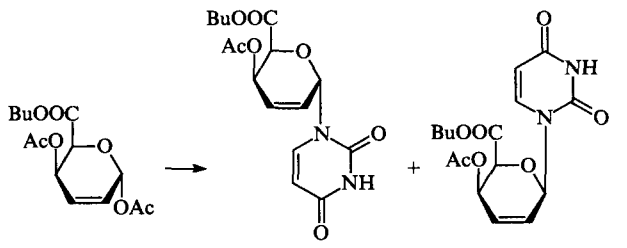


110: R = Ac;
111: R = Br;

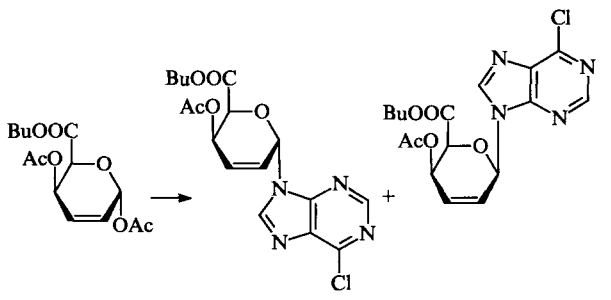


112: B = U;
113: B = 5-Br-U;
114: B = *N*(6)-BzA.

The ready availability of esters of the acid **115**, which are obtained in a single stage from diacetoxybuta-1,3-diene and alkyl glyoxylate, makes them convenient precursors in the synthesis of unsaturated uronic acid nucleosides.[61] The antimony pentachloride-catalysed reaction of the acetate **115** with silylated uracil afforded a mixture of the α-nucleoside **116** and the β-nucleoside **117** (overall yield 80%) with a 3:2 anomer ratio. In the case of thymine, the anomer ratio was 2. The α-nucleoside **118** and the β-nucleoside **119** were obtained in an overall yield of 75% and with the anomer ratio α:β = 2:1 by refluxing the acetate **115** in nitromethane with 6-chloropurine in the absence of a catalyst.

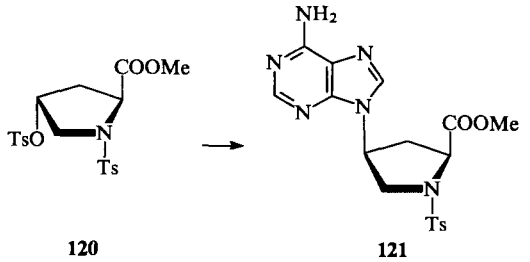


115 **116** **117**



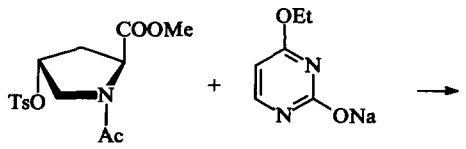
115 **118** **119**

Noncarbohydrate analogues of nucleosides are of undoubted interest as potential biologically active compounds. Certain derivatives of L-hydroxyproline have been used to synthesise them. Thus nucleophilic substitution of the *O*-tosyl group in compound **120** by the sodium salt of adenine led to the nucleoside analogue **121**.[62]

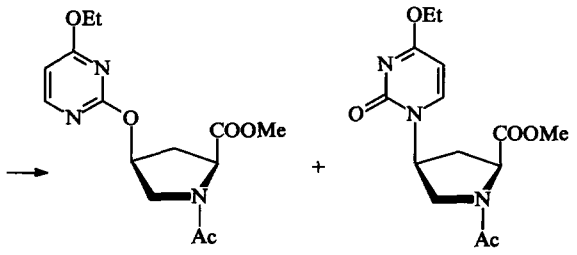


120 **121**

The similar substitution by the sodium salt of 4-*O*-ethyluracil in the pyrrolidine **122** afforded a low yield of the *O*-pseudoglycoside **123** and the *N*-pseudoglycoside **124**.[63]

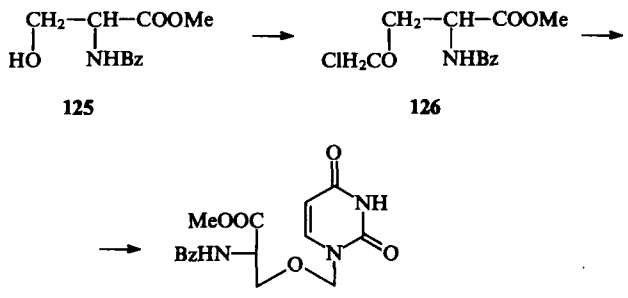


122



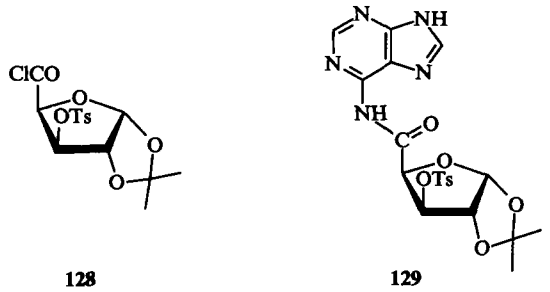
123 124

The possibility of using suitably substituted serine in the synthesis of acyclic analogues of polyoxine antibiotics has been demonstrated.[64] The unstable chloromethyl ether **126** has been obtained by chloromethylating the *N*-benzoyl-DL-serine ester **125**. The condensation of the ether with silylated uracil in acetonitrile led to the acyclic analogue **127** of polyoxine C.



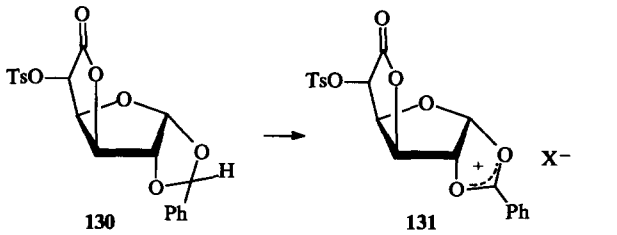
125 126 127

The uronic acid chloride **128** readily reacts with silylated *N*(6)-benzoyladenine to form the xyluronoyl derivative **129**.[65]

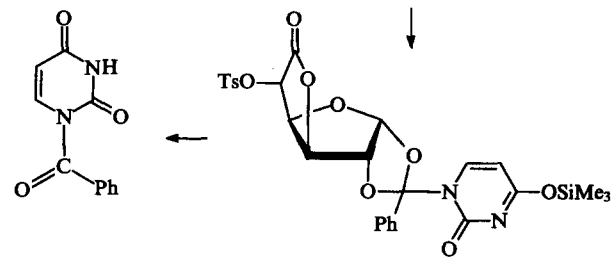


128 129

The intermediate formation of an acyloxonium salt has been postulated as the key stage in the mechanism of the synthesis of nucleosides via glycosylation. The generation of such a salt from the benzylidene derivative of the glucuronolactone **130** has been described.[66] The lactone was treated in acetonitrile with an equivalent amount of Ph_3CBF_4 or $Ph_3CCl/SnCl_4$ and the resulting salt **131** was condensed with silylated uracil. This led to the isolation of *N*(1)-benzoyluracil **132**, the yield of which varied from 30% to 50% in different experiments. Contrary to expectation, nucleoside products were not detected in the reaction mixture. The formation of the intermediate **133**, the hydrolysis of which leads to compound **132**, from the benzoxonium salt **131** appears most probable in this reaction.



130 131



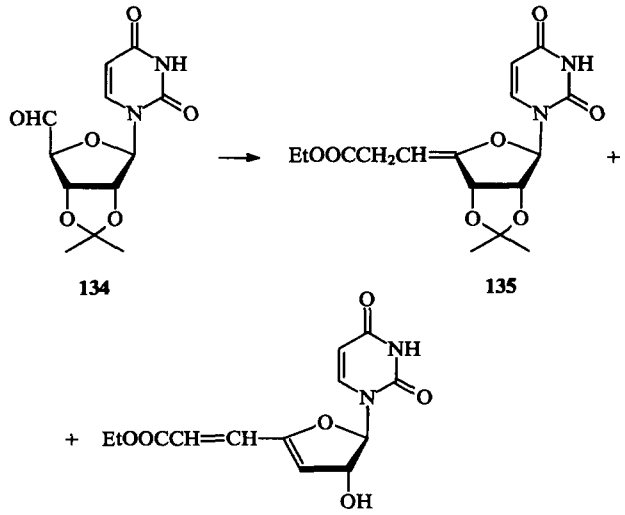
132 133

The structures of the intermediates in the glycosylation reaction differ from the canonical carbonium ion and the acyloxonium ion, although both structures can be formed sometimes, depending on the reaction conditions, which is indicated by the formation of α-anomeric nucleosides and acylated heterocycles.

As can be seen from these data, the glycosylation of heterocycles by uronic acids has characteristic features due to the electron-accepting properties of the alkoxycarbonyl group, which is capable of forming stable complexes with Lewis acids. As a result, an excess of the condensing agent is required to obtain acceptable yields of the nucleosides. The presence of the alkoxycarbonyl group in the sugar molecule can appreciably influence the stereochemical result of the glycosylation reaction.

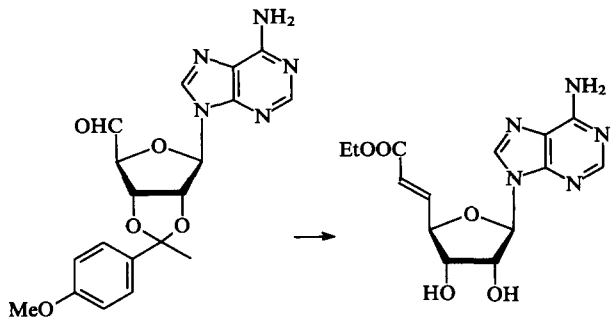
V. Synthesis of uronic acid nucleosides by modifying the sugar and heterocyclic base residues

One of the procedures in the synthesis of uronic acid nucleosides is the condensation of phosphoranes with nucleoside-5'-carboxaldehydes. The reaction of the aldehyde **134** with ethoxycarbonylmethylenetriphenylphosphorane afforded the two unsaturated nucleosides **135** and **136**.[67]



134 135 136

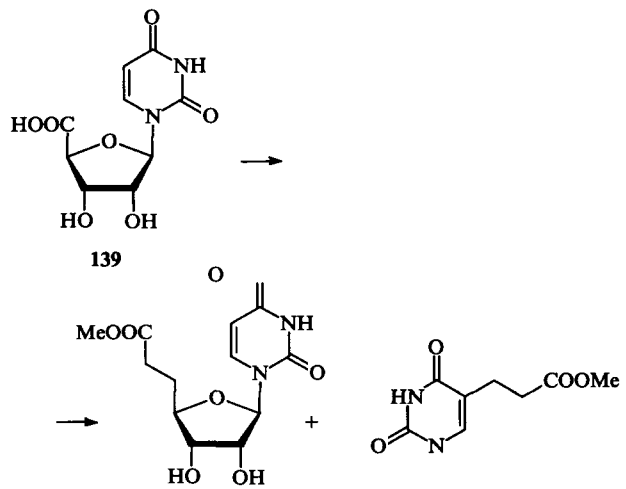
In contrast to the example quoted above, interaction of the aldehyde **137** and the phosphorane under similar conditions gave the nucleoside **138** in a low yield.[68]



137 138

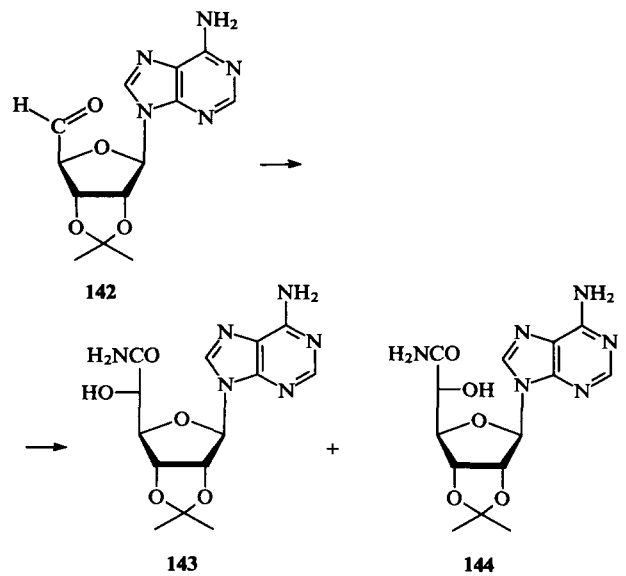
The synthesis of purine and pyrimidine nucleosides having a similar structure has been described.[69-72]

Nucleosides of this type can be obtained by the Kolbe anodic condensation of the acid **139** and the monomethyl ester of succinic acid.[67] The nucleoside **140** and the uracil derivative **141** were obtained by this reaction.



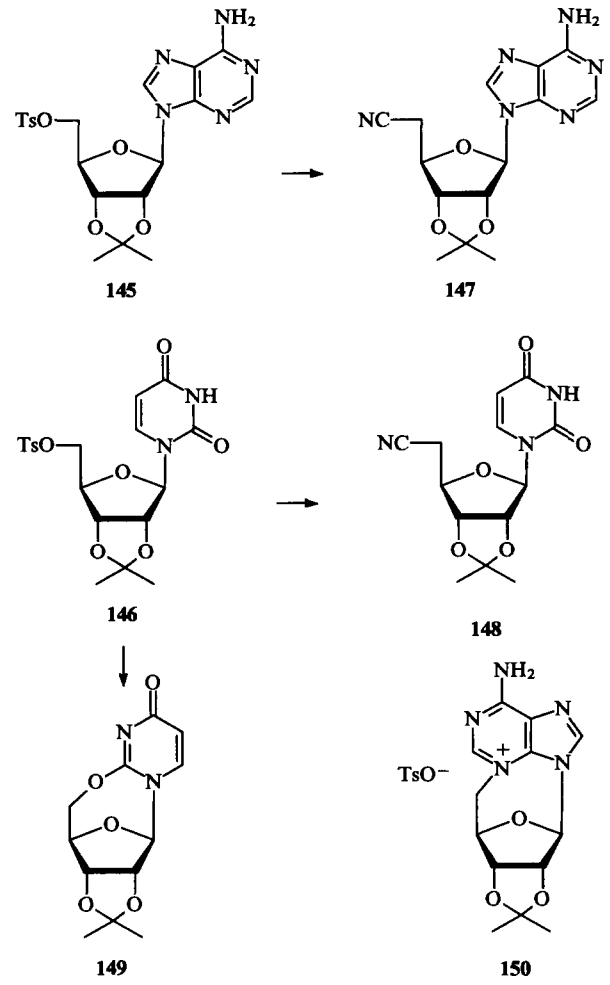
139 140 141

The exocyclic carbon chain of the nucleoside can be developed with simultaneous introduction of a carboxy-group by adding nucleophiles to the carbonyl group of nucleoside-5'-carboxaldehydes. The reaction between the aldehyde **142** and acetone cyanohydrin followed by treatment with hydrogen peroxide at pH 10 of the unstable α-hydroxynitriles formed led irreversibly to the two epimeric amides **143** and **144**.[73]



142 143 144

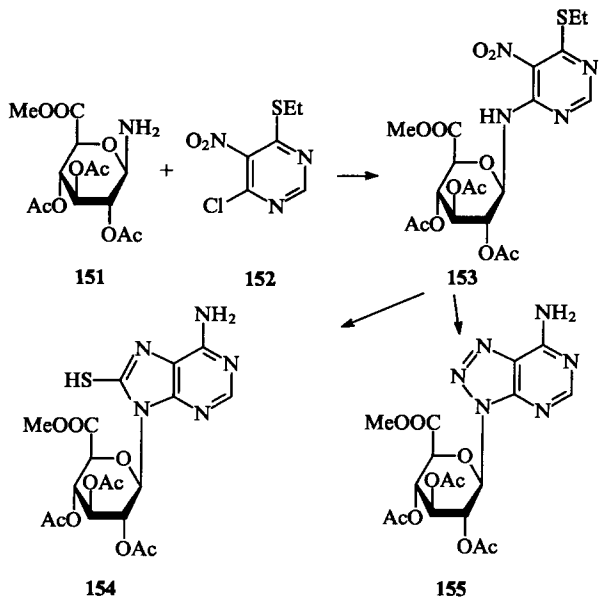
A method has been developed for the synthesis of nucleosides with a lengthened carbon chain from readily available 5'-*O*-tosyl derivatives of nucleosides.[74] The nitriles **147** and **148**, which were previously difficult to obtain, have been synthesised by treating tosylates of adenosine (compound **145**) and uridine (compound **146**) with potassium cyanide in the presence of a crown-ether. In the case of nucleoside **146**, the crown-ether-activated cyanide acts as a base and deprotonates the *N*(3) atom of the pyrimidine; intramolecular nucleophilic substitution results in the formation of a small amount of the cyclic nucleoside **149**. The purine cyclic nucleoside **150** has also been detected.



145 147 146 148 149 150

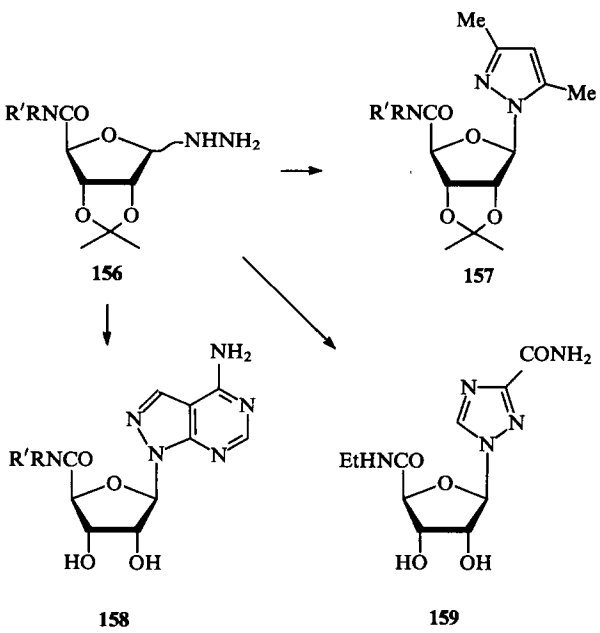
Another route to uronic acid nucleosides, involving modification of the sugar and heterocyclic base residues (the building-on method), is also possible. This variant was applied for the first time in the interaction of the amine **151** with the pyrimidine **152** in the presence of triethylamine.[75] The hydrogenolysis of the *N*-glycoside **153** and refluxing of the resulting amine in a carbon disulfide–pyridine mixture afforded the nucleoside **154**. The reduction of compound **153** with sodium nitrate in aqueous acetic acid led to the 8-azanucleoside **155** (see over).

The building-on method has been used successfully by Schmidt and coworkers[76] to synthesise a wide variety of heterocyclic derivatives of riburonic acid amides. The hydrazinoriburonamides **156** have been used as key compounds for their synthesis. Their condensation with acetylacetone, ethoxymethylenemalononitrile, and oxalic ester thioamide led to the formation of the pyrazole nucleoside **157**, the pyrazolopyrimidine nucleoside **158**, and the virazole analogue **159**.



151 152 153

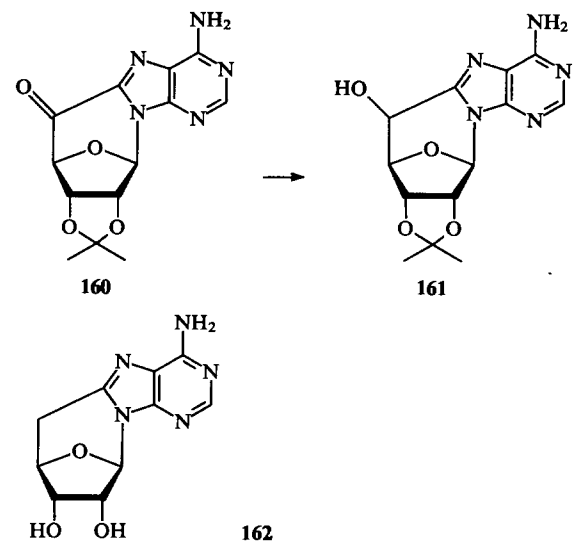
154 155



156 157 158 159

VI. Transformations of uronic acid nucleosides

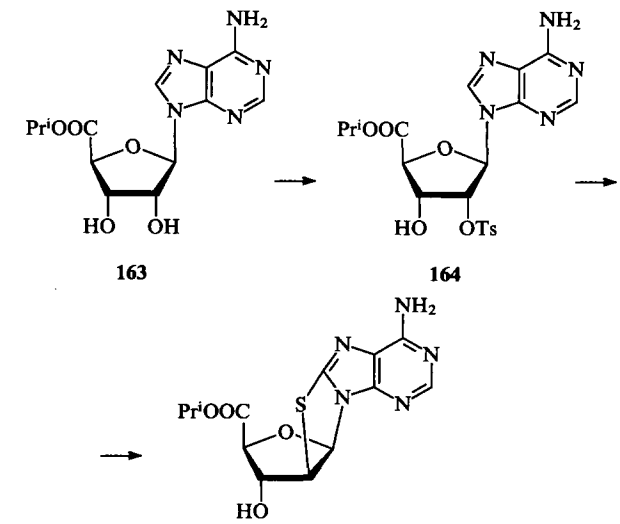
The presence of the carboxy-group in nucleosides is significantly reflected in their chemical and conformational properties, which has led to new possibilities for the synthesis of diverse nucleosides, the preparation of which by traditional methods involves considerable experimental difficulties. The use of reactions characteristic of the carboxy-group makes it possible to synthesise a whole series of nucleosides with unusual structures. The synthesis of cyclic purine nucleosides may serve as confirmation of the foregoing. Treatment of the acid **19** with methyllithium afforded the ketone **160**, the reduction of which with sodium tetrahydroborate led to the cyclic nucleoside **161**, which is an analogue of deoxycycloadenosine **162**—the product of the photolysis of coenzyme B_{12}.[77] Adenosine-5'-carboxylic acid has been obtained by the photolytic oxidation of the nucleoside **162**.[78]



160 161

162

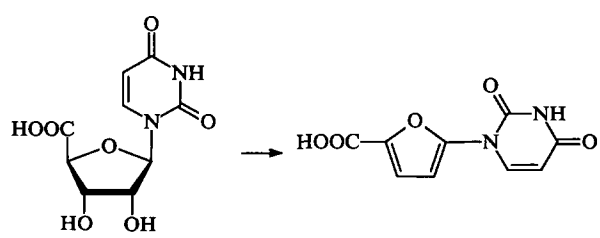
The use of the alkoxycarbonyl group of compound **163** as a kind of protecting group has made it possible to develop an alternative method of synthesis of 2'-deoxyadenosine.[79] Successive bromination and tosylation of the ester **163** afforded the nucleoside **164**, the treatment of which with thiourea gave rise to the *S*-anhydronucleoside **165**. Its reduction over Raney nickel gave 2'-deoxyadenosine in an overall yield of 10%.



163 164 165

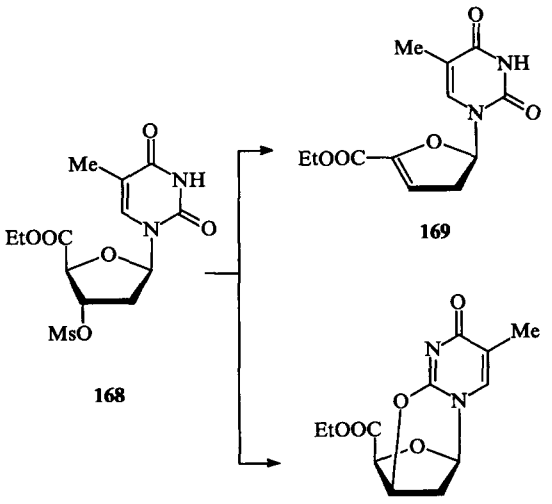
Uronic acids and their nucleosides are known[80] to be capable of giving, by β-elimination, unsaturated compounds, which are of undoubted interest for use in a wide variety of chemical reactions and also for the study of their unusual spectroscopic characteristics.

The β-elimination reaction is observed after brief heating of the acid **166** in acetic anhydride, whereupon the furan derivative **167** is formed.[3]



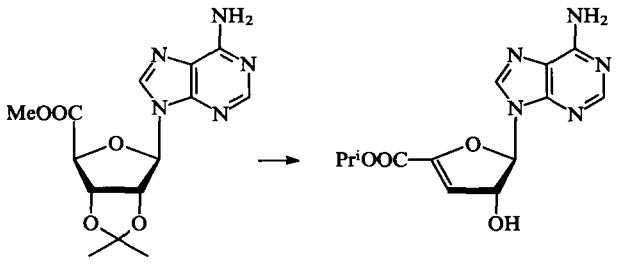
166 167

Uronic acid nucleosides are convenient precursors of 3',4'-unsaturated-nucleosides. Heating of the methanesulfonate **168** with triethylamine or sodium benzoate in DMF leads to the unsaturated nucleoside **169**, while heating with barium carbonate gives the cyclic nucleoside **170**.[81-83]



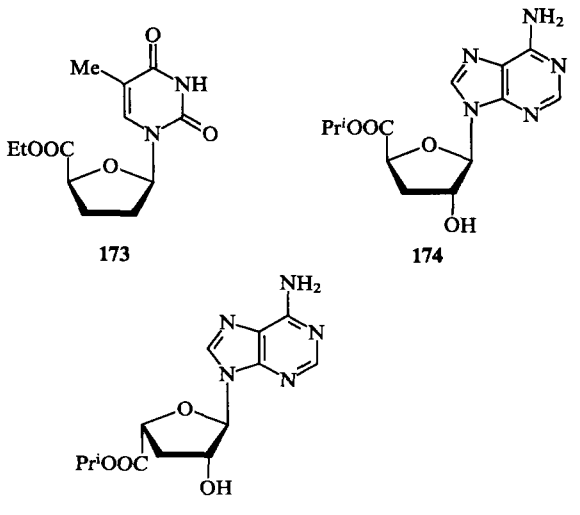
168 **169** **170**

The elimination reaction of acetonide **171** with formation of the unsaturated nucleoside **172** occurred only when sodium isopropoxide was used as the base.[84]



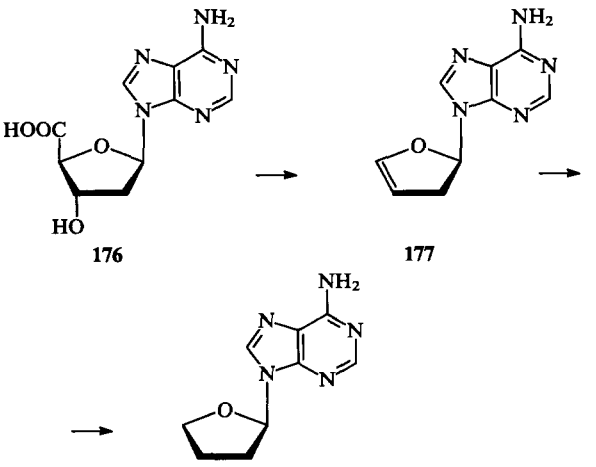
171 **172**

The nucleosides thus obtained were used in the synthesis of the D- and L-series of deoxynucleosides. The catalytic reduction of nucleoside **169** led stereoselectively to the D-isomer **173**, while reduction of nucleoside **172** gave the D- and L-isomers **174** and **175**. Deoxythymidine and deoxyadenosine have been obtained by reducing the esters **174** and **175**.[81,84]



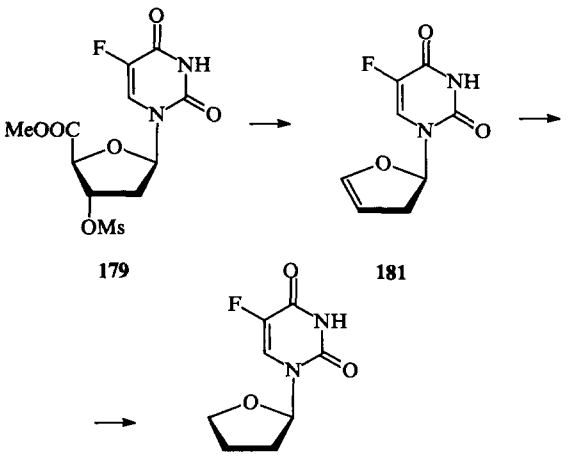
173 **174** **175**

An elimination reaction coupled with decarboxylation has been observed in a series of uronic acid nucleosides.[12] The interaction of nucleoside **176** with the dineopentyl acetal of dimethylformamide in DMF at 80-90 °C leads to a satisfactory yield of the unsaturated nucleoside **177**, the reduction of which makes it possible to obtain the optically active tetrahydrofuran nucleoside **178**.



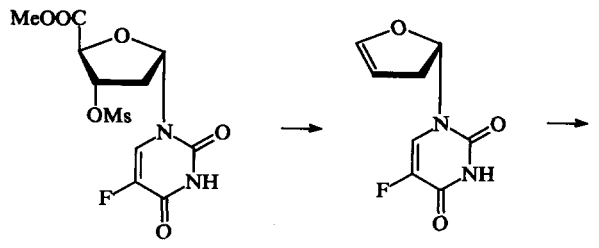
176 **177** **178**

An elimination reaction coupled with dealkoxycarbonylation has been described.[85] Heating of the α- and β-nucleosides **179** and **180** in aqueous pyridine with sodium bicarbonate gave the unsaturated nucleosides **181** and **182**, hydrogenolysis of which led to the optically active nucleosides **183** and **184** (ftorafur).

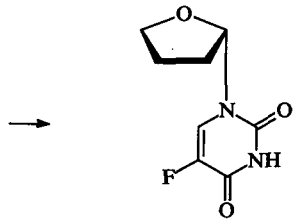


179 **181** **183**

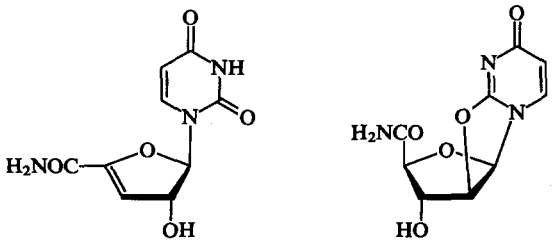
Nucleosides containing derivatives of 3-TsO-D-xyluronic acid as the carbohydrate fragment are readily converted into 3',4'-unsaturated and cyclic nucleosides on treatment with bases.[51,53] The nucleosides **185** and **186** were synthesised by treating the nucleoside **98** with a solution of ammonia in methanol. The nucleoside **185** was also obtained by treating compound **98** with sodium bicarbonate in boiling benzene with subsequent ammonolysis of the unsaturated nucleoside produced. The unsaturated purine nucleoside **187** was synthesised similarly from the tosylate **101**.



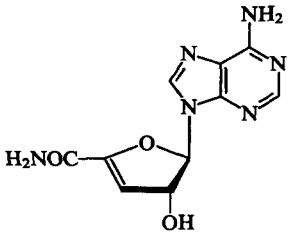
180 182



184

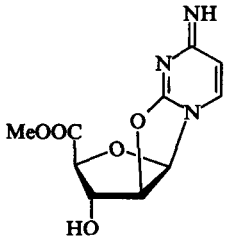


185 186



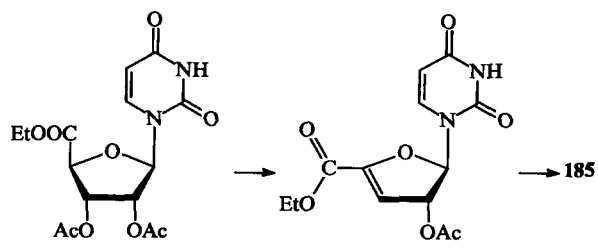
187

For the specific synthesis of the cyclic nucleoside **188**, the nucleoside **100** was initially deacetylated with hydrogen chloride in methanol and then treated with sodium bicarbonate. Under the selected conditions, the dominant process is the intermediate formation of the 2',3'-*O*-anhydronucleoside, which is subsequently converted into the *O*(2),2'-anhydronucleoside **188**.[86]



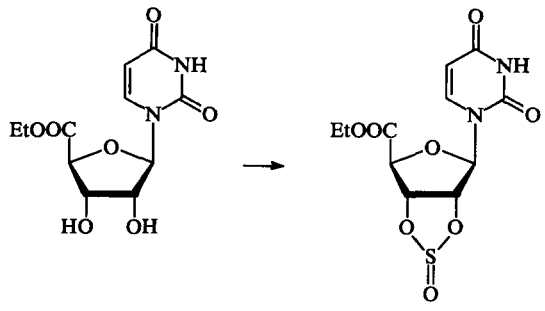
188

The amide **185** has been synthesised by a shorter route from the ester **189**, which was converted into the unsaturated nucleoside **190** on treatment with 1,5-diazabicyclo[5.4.0]undec-5-ene (DBU). Ammonolysis gave the amide **185** in a satisfactory yield.[87]

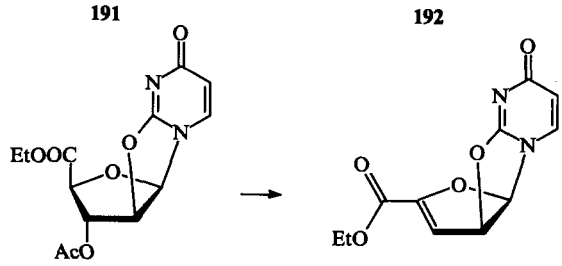


189 190

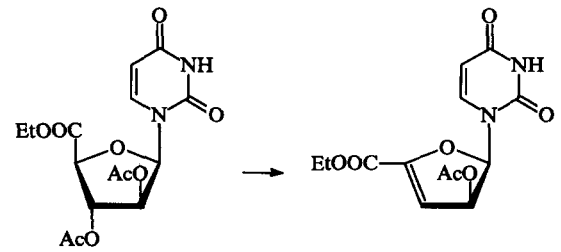
The synthesis of a nucleoside containing an anhydro-ring and a double bond together has been described.[87] Treatment of the ester **191** with thionyl chloride in acetonitrile led to the formation of the sulfite **192**, the heating of which with phthalimide in DMF led to cyclic and arabinosyl nucleosides. The acetates **193** and **194**, obtained from them, gave on treatment with DBU the unsaturated cyclic nucleoside **195** and the nucleoside **196**, which is isomeric in relation to compound **190**.



191 192

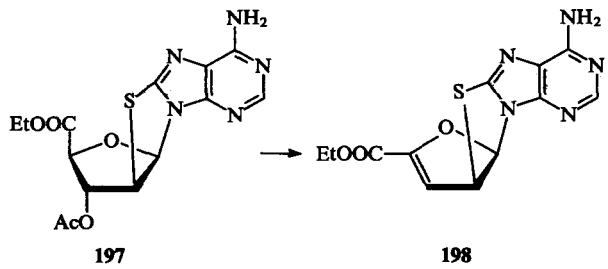


193 195



194 196

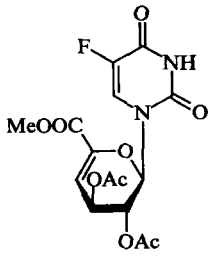
The unsaturated cyclic purine nucleoside **198** was obtained from the *S*-anhydronucleoside **197** on treatment with DBU.[88]



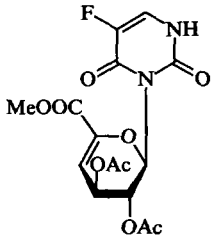
197 198

The Cotton effects observed in the circular dichroism (CD) spectra of the unsaturated nucleosides **195** and **198** are characterised by extremely high molar ellipticities, typical of systems with an internally dissymmetric chromophore.[87,88]

The 4',5'-unsaturated nucleosides **199** and **200** have been obtained by treating the *N*(1)- and *N*(3)-isomeric nucleosides **106** and **107** with DBU.[89,90]



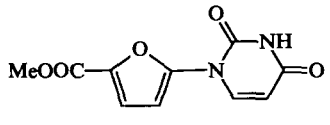
199



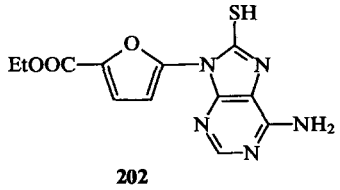
200

There exists in the literature a single point of view on the cause of the anomalies in the CD spectra of unsaturated nucleosides. It has been shown[87] that the sign and amplitude of the Cotton effect in the CD spectra of purine and pyrimidine nucleosides with a double bond in the carbohydrate fragment of the molecule depend on the position of the double bond, the asymmetry of the glycosidic carbon atom, and the sign of the pitch of the weakly or strongly bound internally disymmetric chromophore.

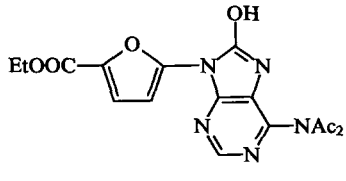
In the presence of an excess of DBU, unsaturated cyclic nucleosides are readily converted into the furancarboxylic acid derivatives **201**–**203**.[87,88,91]



201



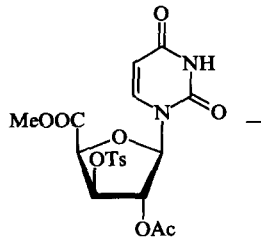
202



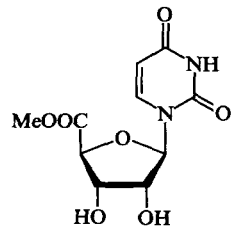
203

Compounds **201**–**203**, which have no asymmetric carbon atom, were found to be optically active.[92] The antiperiplanar conformation of the lone pair of the nitrogen atom (the sp^3-orbital) and of the σ(CO) orbital and their conjugation on passing from anhydronucleosides to furans stabilised the structure with a mutually perpendicular arrangement of the planes of the furan ring and of the nitrogenous base. The stabilisation of such structures as a result of the hindered rotation of the C–N bond leads to the appearance of stereoisomerism, which may be classified as related to the isomerism of allenes and biphenyls but is caused by the stereoelectronic anomeric effect.

Nucleophilic substitution of the halogens and of the methanesulfonyl and tosyl groups, which proceeds with inversion of the configuration, is one of the most widely used methods for specific transformations in the chemistry of carbohydrates and nucleosides. This method is unsuitable in the series of uronic acids when the group to be substituted is in the β-position relative to the alkoxycarbonyl group. The competing β-elimination reaction then takes place. It has been observed[93] that the nucleosides of 3-TsO-D-xyluronic acid can be converted smoothly into nucleosides with the D-ribo-configuration on treatment with phthalimide. Treatment of the nucleoside **98** with phthalimide in DMF at 130 °C gives rise to a mixture of positional acetate isomers, the deacetylation of which leads to the ribonucleoside **204**.

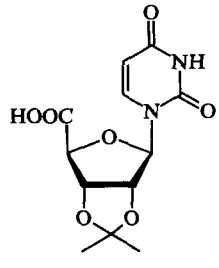


98

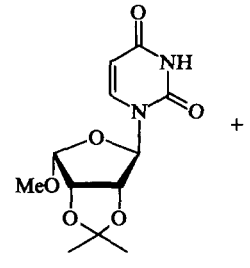


204

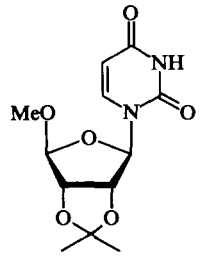
The results of the anodic oxidation of the acid **205** are interesting.[94] A mixture of the methoxynucleosides **206** and **207** has been obtained in a 35% overall yield by the electrolysis of the acid in methanol. The cyclic nucleoside **208** with an unusual structure was isolated from the reaction mixture together with the above compounds. Electrolysis of the nucleoside **205** in acetic acid afforded the acetates **209** and **210**.



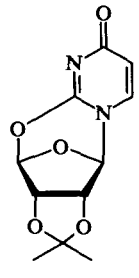
205



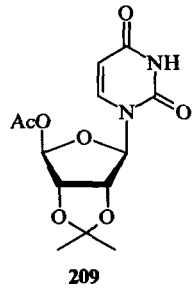
206



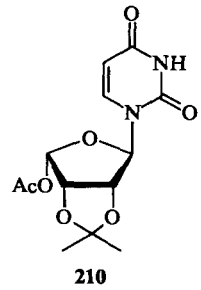
207



208



209



210

It is essential to note one other feature of uronic acid nucleoside. Anisochronicity of the diastereotopic protons in the ^{1}H NMR spectra of the ethyl and isopropyl esters has been observed only in nucleosides with an anhydro-ring or an isopropylidene protecting group. It has been shown that the observed anisochronicity, caused by the presence of anisotropic heterocycles in the chiral molecule, depends on the distance between the alkoxycarbonyl group and the anisotropic group and on their orientation relative to one another in space.[95–97]

References

1. K Isono *J. Antibiot.* **41** 1711 (1987)
2. J W Daly *J. Med. Chem.* **25** 197 (1982)
3. G P Moss, C B Reese, K Schofield, R Shapiro, L Todd *J. Chem. Soc.* 1149 (1963)
4. K Imai, M Honjo *Chem. Pharm. Bull.* **13** 7 (1965)
5. K C Tsou, N J Santora, E E Miller *J. Med. Chem.* **12** 173 (1969)
6. J P Neenan, W Rohde *J. Med. Chem.* **16** 580 (1973)
7. J J Baker, P Mellish, C Riddle, A R Somerville, J R Tittensor *J. Med. Chem.* **17** 764 (1974)
8. R F Schinazi, M S Chen, W H Prusoff *J. Med. Chem.* **21** 1141 (1978)
9. P A Levene, F B La Forge *Berichte* **45** 608 (1912)
10. J Wempen, J L Doerr, L Kaplan, J J Fox *J. Am. Chem. Soc.* **82** 1624 (1960)
11. A S Jones, A R Williamson, M Winkley *Carbohydr. Res.* **1** 187 (1965)
12. J Žemlička, R Gasser, J V Freisler, J P Horwitz *J. Am. Chem. Soc.* **94** 3213 (1972)
13. P J Harper, A Hampton *J. Org. Chem.* **35** 1688 (1970)
14. R E Harmon, C V Zenarosa, S K Gupta *Chem. Ind.* 1141 (1969)
15. R R Schmidt, U Schloz, D Schwille *Chem. Ber.* **101** 590 (1968)
16. R R Schmidt, H-J Fritz *Chem. Ber.* **103** 1867 (1970)
17. E J Corey, B Samuelsson *J. Org. Chem.* **49** 4735 (1984)
18. B Classon, B Samuelsson *Acta Chem. Scand., Ser. B* **39** 501 (1985)
19. V A Timoshchuk *Zh. Org. Khim.* **28** 1512 (1992).
20. S L Cook, J A Secrist *Carbohydr. Res.* **52** C3 (1976)
21. C M Richards, J P H Verheyden, J G Moffatt *Carbohydr. Res.* **100** 315 (1982)
22. A A Akhrem, T M Ermolenko, V A Timoshchuk *Zh. Org. Khim.* **21** 1795 (1985)
23. A A Akhrem, T M Ermolenko, V A Timoshchuk *Zh. Org. Khim.* **21** 1800 (1985)
24. M L Wolfrom, P McWain *J. Org. Chem.* **30** 1099 (1965)
25. T Kishikawa, T Yamazaki, H Yuki *Chem. Pharm. Bull.* **14** 1354 (1966)
26. T Kishikawa, K Furuta, S Takitani *Tetrahedron Lett.* **10** 1961 (1969)
27. K A Watanabe, D H Hollenberg, J J Fox *J. Antibiot.* **29** 597 (1976)
28. L N Kulinkovich, V A Timoshchuk *Khim. Prir. Soedin.* 617 (1983)
29. F W Lichtenthaler, A Heerd, K Strobel *Chem. Lett.* 449 (1974)
30. F W Lichtenthaler, P Voss, A Heerd *Tetrahedron Lett.* **15** 2141 (1974)
31. M Kaneko, H Tanaka, M Kimura, B Schimizu *Chem. Pharm. Bull.* **25** 2458 (1977)
32. A Parker, L Fedor *J. Med. Chem.* **25** 1505 (1982)
33. C K Zercher, L R Fedor *Carbohydr. Res.* **165** 299 (1987)
34. G Wagner, R Mahrwald *Pharmazie* **35** 663 (1980)
35. G Wagner, R Mahrwald *Pharmazie* **36** 12 (1981)
36. R Mahrwald, G Wagner *Pharmazie* **37** 257 (1982)
37. R Mahrwald, G Wagner *Pharmazie* **35** 587 (1980)
38. J A Montgomery, K Hewson, A G Laseter, M C Thorpe *J. Am. Chem. Soc.* **94** 7176 (1972)
39. A A Akhrem, V A Timoshchuk, I F Mikhailopulo *Zh. Obshch. Khim.* **45** 956 (1975)
40. A A Akhrem, E K Adarich, L N Kulinkovich, I A Mikhailopulo, E B Posshchast'eva, V A Timoshchuk *Dokl. Akad. Nauk SSSR* **219** 99 (1974)
41. A A Akhrem, V A Timoshchuk, L N Kulinkovich, I A Mikhailopulo *Bioorg. Khim.* **2** 513 (1976)
42. M K Kilevitsa, Yu A Maurin'sh, R A Paegle, E E Liepin'sh, A A Zidermane, M Yu Lidak *Khim. Geterotsikl. Soedin.* 1532 (1981)
43. Yu A Maurin'sh, R A Paegle, M Yu Lidak, E I Kvasyuk, I A Mikhailopulo *Bioorg. Khim.* **12** 1514 (1986)
44. R A Zhuk, A E Berzinya, V N Silinya, E E Liepin'sh, S A Giller *Khim. Geterotsikl. Soedin.* 1128 (1979)
45. R R Schmidt, D Heermann, K-H Jung *Liebigs Ann. Chem.* 1856 (1974)
46. R R Schmidt, K-H Jung, P Hermentin *Chem. Ber.* **111** 3311 (1978)
47. K-H Jung, R R Schmidt *Liebigs Ann. Chem.* 1426 (1979)
48. K-H Jung, R R Schmidt *Chem. Ber.* **113** 1775 (1980)
49. R R Schmidt, G R Losch, P Fischer *Chem. Ber.* **113** 2891 (1980)
50. P Fischer, G R Losch, R R Schmidt *Chem. Ber.* **114** 2947 (1981)
51. A A Akhrem, V A Timoshchuk, I A Mikhailopulo *Carbohydr. Res.* **43** 195 (1975)
52. U Niedballa, H Vorbrüggen *Angew. Chem.* **82** 449 (1979)
53. A A Akhrem, L N Kulinkovich, A G Lapko, I A Mikhailopulo, V A Timoshchuk *Bioorg. Khim.* **2** 621 (1976)
54. V A Timoshchuk, L N Kulinkovich, T I Olimpieva, E I Boreko, G V Vladyko *Khim. Farm. Zh.* 49 (1988)
55. H Vorbrügen, U Niedballa, K Krolikiewicz, B Bennua, G Höfle *Chemistry and Biology of Nucleosides and Nucleotides* (New York: Academic Press, 1978)
56. L N Kulinkovich, V A Timoshchuk *Zh. Obshch. Khim.* **53** 1649 (1983)
57. L N Kulinkovich, V A Timoshchuk *Zh. Obshch. Khim.* **53** 1652 (1983)
58. V A Timoshchuk *Carbohydr. Res.* **145** 131 (1985)
59. V A Timoshchuk *Zh. Obshch. Khim.* **57** 2375 (1987)
60. V A Timoshchuk, L N Kulinkovich *Zh. Obshch. Khim.* **58** 1144 (1988)
61. R R Schmidt, R Angerbauer *Carbohydr. Res.* **72** 272 (1979)
62. F M Kaspersen, U K Pandit *J. Chem. Soc., Perkin Trans. 1* 1617 (1975)
63. F M Kaspersen, U K Pandit *J. Chem. Soc., Perkin Trans. 1* 1798 (1975)
64. V A Timoshchuk, T I Olimpieva *Zh. Obshch. Khim.* **58** 2404 (1988)
65. L N Kulinkovich, V A Timoshchuk *Zh. Obshch. Khim.* **53** 1645 (1983)
66. L N Kulinkovich, V A Timoshchuk *Zh. Obshch. Khim.* **53** 1439 (1983)
67. P Howgate, A S Jones, J R Tittensor *Carbohydr. Res.* **12** 403 (1970)
68. T E Walker, H Follmann, H P C Hogenkamp *Carbohydr. Res.* **27** 225 (1973)
69. T Ishida, T Miyazaki, M Inoue, A Ota, T Kurichara, M Sugiura *J. Chem. Soc., Perkin Trans. 1* 1325 (1983)
70. J A Montgomery, A G Laseter, K Hewson *J. Heterocycl. Chem.* **11** 211 (1974)
71. J A Montgomery, H J Thomas *J. Org. Chem.* **46** 594 (1981)
72. D C Baker, R P Grews, T H Haskell, S R Putt, G Arnett, W M Shannon, C M Reinke, H B Katlama, J C Drach *J. Med. Chem.* **26** 1530 (1983)
73. A Hampton, P Howgate, P J Harper, F Perini, F Kappler, R K Preston *Biochemistry* **12** 3328 (1973)
74. W Meyer, H Follmann *Chem. Ber.* **113** 2530 (1980)
75. T Kishikawa, H Yuki *Chem. Pharm. Bull.* **14** 1360 (1966)
76. K-H Jung, R R Schmidt, D Heermann *Chem. Ber.* **114** 2834 (1981)
77. P J Harper, A H Hampton *J. Org. Chem.* **37** 795 (1972)
78. A W Johnson, N Shaw *J. Chem. Soc.* 4608 (1962)
79. R R Schmidt, R Machat, U Schloz *Chem. Ber.* **106** 1256 (1973)
80. J Kiss *Adv. Carbohydr. Chem. Biochem.* **29** 229 (1974)
81. J Žemlička, J V Freisler, R Gasser, J P Horwitz *J. Org. Chem.* **38** 990 (1973)
82. J Žemlička, R Gasser, J P Horwitz *J. Am. Chem. Soc.* **92** 4744 (1970)
83. J Zemlicka, J P Horwitz *J. Am. Chem. Soc.* **97** 4089 (1975)
84. K L Nagpal, J P Horwitz *J. Org. Chem.* **36** 3743 (1971)
85. J Kiss, P Taschner *J. Carbohydr. Nucl. Nucl.* **1** 279 (1974)
86. L N Kulinkovich, V A Timoshchuk *Zh. Obshch. Khim.* **53** 1901 (1983)
87. V A Timoshchuk *Zh. Org. Khim.* **26** 559 (1990)
88. A A Akhrem, T M Ermolenko, V A Timoshchuk *Zh. Org. Khim.* **21** 2185 (1985)
89. V A Timoshchuk, L N Kulinkovich *Carbohydr. Res.* **145** 123 (1985)
90. V A Timoshchuk, L N Kulinkovich *Zh. Obshch. Khim.* **58** 1651 (1988)
91. A A Akhrem, T M Ermolenko, V A Timoshchuk *Zh. Org. Khim.* **21** 2190 (1985)
92. V A Timoshchuk, A A Akhrem *Dokl. Akad. Nauk SSSR* **302** 105 (1988)
93. A A Akhrem, A G Lapko, I A Mikhailopulo, V A Timoshchuk *Carbohydr. Res.* **54** C1 (1977)
94. K Kondo, I Inoue *J. Org. Chem.* **44** 4713 (1979)
95. V A Timoshchuk, T M Ermolenko, A A Akhrem *Zh. Org. Khim.* **24** 1214 (1988)
96. V A Timoshchuk, T M Ermolenko, A A Akhrem *Zh. Org. Khim.* **24** 1703 (1988)
97. V A Timoshchuk *Zh. Org. Khim.* **26** 498 (1990)

Russian Chemical Reviews **63** (9) 711 – 734 (1994)
©1994 Russian Academy of Sciences and Turpion Ltd

UDC 541.16

The chemical bonding and electronic properties of metal borides

G P Shveikin, A L Ivanovskii

Contents

I. Introduction	711
II. Group I and II metal and aluminium borides	712
III. Transition *d* metal borides	716
IV. Metal–nonmetal–boron ternary systems	724
V. Metal–metal–boron ternary systems	727
VI. Amorphous metal borides	728

Abstract. The results of theoretical and experimental studies on the electronic structure, and nature of interatomic interactions, and the properties of binary metal borides, ternary boron-containing compounds and alloys, and also amorphous binary and multicomponent borides are examined. The prospects for employing the methods of solid-state quantum-chemistry in the description of the fundamental electronic properties of metal borides are discussed. The bibliography includes 255 references.

I. Introduction

Metal borides belong to one of the most interesting classes of solid compounds and possess a set of important physicochemical properties (thermomechanical, magnetic, electrophysical, and others), which permits their wide scale employment as components of refractory alloys, in the development of special purpose ceramics and metalloceramics, as protective coatings for high-temperature alloys, as a base for composite materials, as solid solders, and as corrosion-resistant and abrasive materials.[1–14]

In terms of their thermal properties, strength, plastic properties, and electrical and thermal insulating characteristics, borides compete with other classes of high-temperature compounds—carbides and nitrides.[15,16] The borides possess a series of specific properties determined, in particular, by the nature of the chemical bonding and the electronic structure.

Boron is known to form predominantly covalent compounds with metals, an important role being assumed in this process not only by M–B and M–M bonds (M = metal) but also by direct B–B interactions. The latter are evidently responsible for the great diversity of the structural types of borides,[5,7,9,11,12] in which boron atoms can be both surrounded by metallic centres and can form linear, planar, or three-dimensional structures (Fig. 1).

The ability of many metals to form, in their interaction with boron, a large set of phases with a considerable variation of the M/B ratio—ranging from hemiborides (M_2B) to dodecaborides (MB_{12})—as well as amorphous alloys, is well known.[1–14]

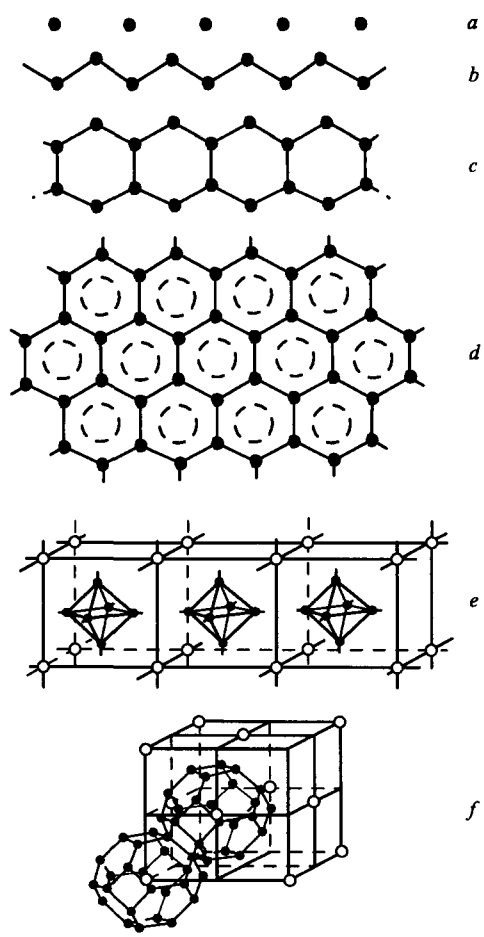


Figure 1. The possible configurations of boron atoms in the structures of the metal borides M_2B (*a*), MB (*b*), M_3B_4 (*c*), MB_2 (*d*), MB_4–MB_6 (*e*), and MB_{12} (*f*).

Relations of the composition–property type are therefore of extreme interest for metal–boron systems.

In the early stages of the relevant investigations, several alternative phenomenological models were proposed for the description of the nature of the interatomic bonds and charge states in borides. Thus the formation of borides containing planar

G P Shveikin, A L Ivanovskii Institute of Solid State Chemistry, The Urals Division of the Russian Academy of Sciences, Pervomaiskaya 91, 620219 Ekaterinburg, Russian Federation, Fax (7-343) 244 44 95

Received 27 June 1994
Uspekhi Khimii **63** (9) 751 – 775 (1994); translated by A K Grzybowski

networks made up of boron atoms has been attributed[17,18] to the formation of sp^2 configurations of the boron atoms, while the appearance in the higher borides of three-dimensional groups of boron atoms (octahedra, cubooctahedra, etc.) has been attributed to the formation of the electronic sp^3 configuration. The existence of graphite-like motifs of boron atoms in a type AlB_2 lattice has been explained[19] by the presence of metal atoms as electron donor and of boron atoms as electron acceptors. Conversely, in the 'interstitial alloy' model,[20] the transfer of additional electron density to metal atoms is postulated.

The correlation of the properties with the specific features of the chemical bonding in borides has been interpreted from the standpoint of the dominant character of the B–B bonds in the overall system of interactions in the crystals,[19,21] whereas in other studies[22,23] preference has been given to covalent metal–boron bonds. Dempsey[20] believed that M–M bonds play a decisive role in bonding (especially for the lower borides). It is noteworthy that, although each of the models examined has had some success in the treatment of the characteristic features of the variation of a specific set of properties of individual groups of borides, they are nevertheless far from being universal.

The aim of the present review is to attempt a consideration of the current state of the theory of the electronic structure, the chemical bonding, and the most important physicochemical properties of the main groups of *s*, *p*, and *d* metal borides on the basis of the study of their fundamental electronic properties within the framework of computational solid state quantum-chemical methods and the most correct experimental methods for the investigation of the electronic structure of crystals—X-ray emission, electronic, and optical spectroscopy and a series of other methods.

The borides have been segregated into individual groups in conformity with the classification adopted and are considered in the following sections:[14,24,25] Group I and II binary metal borides in Section II, *d* metal borides in Section III, ternary metal–nonmetal boron systems in Section IV, metal–metal–boron systems in Section V, and amorphous metal borides (metallic glasses) in Section VI.

II. Group I and II metal and aluminium borides

1. Sodium and potassium borides

The study of the phase diagrams for the alkali metal–boron systems indicates[1–11] the greatest probability of the formation and stability of the borides MB_6. The band structure of the hypothetical sodium hexaboride (CsCl type lattice with interatomic distances corresponding to those found for CaB_6)[7] has been calculated[26] by the tight binding method. The valence band contains 10 partly occupied subbands, the dispersion of which is significantly smaller than in the isostructural calcium hexaboride (see below), the highest occupied states including also the 2*s* states of boron. The 3*s* states of sodium are located predominantly in the conduction band.

There is no forbidden gap in NaB_6. The concentration of valence electrons per unit cell is 19 e, so that some of the highest bonding bands (forming a planar section in the vicinity of the Fermi level) remain unoccupied, which may be the reason for the instability of the phase. The lowest virtual NaB_6 bands are separated from the system of valence states, which makes it likely that the type of conductivity of NaB_6 is intermediate between that of semicon-ductor systems based on Group II metals and that of the quasi-metallic lanthanum hexaborides.

The electronic spectrum of KB_6 has been calculated[26] by the tight binding method. A considerable similarity between the topologies of the NaB_6 and KB_6 bands has been noted. The introduction of the *d* states of potassium into the basis set in the calculation diminishes the width of the forbidden gap at the point *X*. The Fermi level (−8.1 eV) is located near the lower edge of the forbidden gap in the region of a high concentration of electronic states. It is postulated that the stability of the KB_6 lattice is caused primarily by the transfer of some of the 'metallic' electrons (the effective charges on the component atoms are +0.74 e for K and −0.74 e for B) to the bonding states between the boron atoms in the B_6 octahedra and the bonds between the given groups, which are manifested by two intense maxima in the distribution of the density of 2*p* states of boron (Fig. 2). We may note that this treatment conflicts with the Longuet-Higgins and Roberts model,[27] which postulates the existence of the doubly charged anions B^{2-} in the structure of stable hexaborides. The insignificant concentration of holes in the valence band may indicate that the boride is a semiconductor.

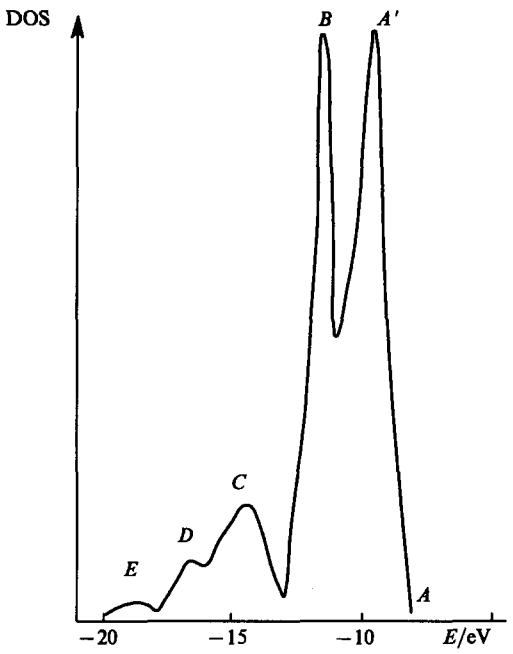


Figure 2. Distribution of the density of B 2*p* states for KB_6.[26]

2. Beryllium borides

According to the literature,[2,7,10] there are at least six individual compounds in the Be–B system (ranging from Be_5B to BeB_9), which differ sharply in their crystal structures and physicochemical properties. However, the increase with increasing boron content of the melting point and of the enthalpy of atomisation of the phase, as well as the change in the type of conductivity (from metallic to semiconducting), etc. still cannot be explained from the standpoint of electronic properties.

The treatment of the electronic processes accompanying the diffusion of boron and beryllium was initially based on the ideas of the configuration theory,[1,17] in which the primary single-electron transition $s \rightarrow p$ with formation of the Be $2s^12p^1$ configuration and subsequent 'trapping' of the boron electrons with the formation of stable sp^2 or sp^3 configurations is postulated.

In the single calculation[28] known to us, the cubic Be_2B phase (structure of the *anti*-CaF_2 type) was considered. Calculations were performed by the self-consistent method of the linearised muffin-tin orbitals (LMTO) and the chemical bonding was analysed within the framework of the self-consistent field X_α-discrete variation (SCF X_α-DV) method.

The calculated data[28] show that the valence band of the boride contains two segregated subbands separated by a minimum in the density of states (DOS) and comprising mainly the *s* and *p* states of the components. The Fermi level is located in the region of the (B, Be) 2*p*-like band. Both the *s* and *p* states of the component atoms overlap significantly, which indicates the formation of covalent bonds of the mixed *s*–*s*, *s*–*p*, and *p*–*p* types.

Comparative analysis of the involvement of individual atomic orbitals in such covalent mixing permits the calculation of the Mulliken bond populations.[28] It follows from these that the greatest contribution to the B–B and Be–Be bonding in Be_2B comes from the overlap of the $2p$ functions; the overlap populations of the s–s orbitals are also of comparable magnitude. The involve-ment of all (s, p) valence states is observed in the Be–B interaction, the outer $2p$ orbitals overlapping to the greatest extent under these conditions.

It is seen from the calculations of the electronic configurations and the effective atomic charges of the [BBe_4B_6] cluster that the unoccupied (in the atomic states) $2p$ orbitals of beryllium are appreciably populated (~1 e) with formation of configurations close to Be $2s^12p^1$. Estimation of the effective atomic charges indicates the partial transfer of charge density to the boron atoms, which indicates the presence of an ionic bond component.

Thus the calculations[28] make it possible to claim that a covalent-ionic type of chemical bonding is characteristic of Be_2B. The covalent component arises due to the overlap of the outer $2s$ and $2p$ functions of the component atoms involved in the Be–Be, Be–B, and B–B interactions. The contribution of the ionic component is due to the polarisation of electron density in the crystals with partial charge transfer in the direction Be → B.

The ideas about the principal effects of orbital hybridisation yield contour maps of the wave functions of the cluster [BBe_4B_6] for which the calculation has been made (Fig. 3). Evidently the lowest valence molecular orbitals $7a_1$ and $3b_2$ are non-bonding and are largely made up of the B $2s$ states with addition of Be $2s$ orbitals. The contours of the molecular orbitals with $9a_1$ symmetry embrace Be–Be pairs of atoms, illustrating the formation of directed covalent σ^{Be-Be}-bonds, in which the $2s$ and $2p$ states of beryllium participate, while the boron states hardly contribute to this molecular orbital. The wave functions of the $2a_1$ molecular orbital (consisting to the extent of 85% of Be s states) have a typical nonbonding character: the contours of the atomic orbitals of the individual centres are separated by lines with a zero value of the wave function. The Be $2s$, Be $2p$, and B $2p$ atomic orbitals contribute to the $11a_1$ molecular orbital, the configuration of the wave function contours indicating the occurrence in the given energy range of combined (Be–B, B–B) interactions. Finally the wave function contours of the highest occupied $12a_1$ molecular orbital (of the B $2p$ type) are distorted in the direction of the 'outer' (in the cluster) boron atoms, which can be treated as indicating the presence of B–B bonds.

Summarising the foregoing, one may claim that 'covalent interactions occur in Be_2B both between the individual components (Be–Be, B–B) and in the Be–B bond.

There is no doubt that further systematic studies are essential in order to gain a complete idea about the electronic properties of beryllium borides.

3. Calcium, strontium, and barium borides

Calcium, strontium, and barium borides have the composition MB_6 (cubic lattice of the NaCl type). It was in fact because of the simplicity of their crystal structure that calcium hexaboride became one of the first boron-containing compounds the energy structure of which was considered within the framework of theoretical approaches.[27,29–31]

The calculation for CaB_6 was performed by the linear combination of atomic orbitals (LCAO) method with a basis set incorporating the $2s$ and $2p$ orbitals of boron without taking into account the Ca–B interactions.[27] Thus in essence only the structure of the bands formed by the states of the boron sublattice was examined,[27] while the presence of the metal was taken into account in the filling of the energy levels in terms of the rigid band approximation.

Solutions of the secular equation for the crystal made it possible to devise a qualitative scheme for the structure of the energy bands of CaB_6,[27] which showed that a forbidden gap (~4.4 eV) appears between the bonding and antibonding orbitals. Since CaB_6 is a conducting substance,[1–4] the authors[27] explained these contradictions both by the possibility of the population of the lowest unoccupied states by the metal electrons and by the probable transfer of valence electrons to the conduction band on irradiation of the crystal.

In describing the energy bands of CaB_6, Yamazaki[29] took into account the Ca $4s$ states in addition to the B s and B p states. It was shown that the bonding bands of the hexaboride are fully occupied while the antibonding ones are unoccupied. This explains the stability of this structural type of borides (in conformity with phenomenological ideas,[32] the hexaborides can be regarded as the complexes $M^{2+}B_6^{2-}$ containing doubly charged metal cations). According to Yamazaki,[29] the width of the forbidden gap is ~1.5 eV.

In Flodmark's calculations,[30,31] the CaB_6 band structure was considered as a function of the choice of the exponent $z/3$ for the d orbitals (z = 1–5). It was noted that the inclusion of the M shells in the basis set has a very appreciable effect on the energies of the valence bands, leading, in particular, to a further decrease in the width of the forbidden gap.

The conclusions reached[27,29] about the structure of the CaB_6 valence band are consistent with the results of the calculation performed by the LCAO method taking into account only the boron functions[33] and also by the semiempirical

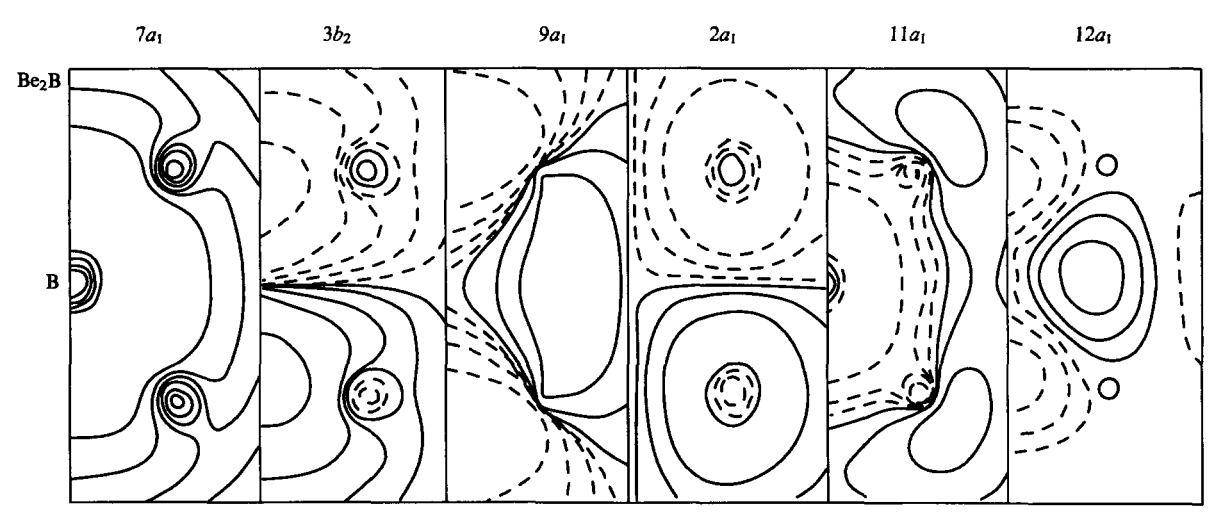


Figure 3. Contour maps for the wave functions of the valence orbitals of the BBe_4B_6 cluster according to the X_α-DV calculation.[28]

LCAO method in terms of the Gaussian orbitals basis set (GO-LCAO),[34] using a basis set comprising the *sp* functions of boron and calcium.

The LCAO method in terms of the tight binding approximation has been used[35] in calculations for CaB_6, where account was taken of the B 2*s*, B 2*p*, and Ca 3*s* states. At the same time, in order to discover the role of calcium in the organisation of the electronic centre of the hexaboride, a band calculation was performed[35] for a hypothetical 'boride' with the parameters of the CaB_6 lattice in which the metal sublattice sites remained unoccupied.

As the energy bands of this 'boride' are filled on the hypothesis that the number of valence electrons of the system (per formula unit) corresponds to that for MB_6 (20 e), it is found that the lowest ten bands are fully occupied. In this case, the minimum 'straight' forbidden gap corresponds to the splitting of the states at the point *X* and its width is 2.11 eV, which exceeds somewhat the values obtained by Johnson and Daane.[36] This discrepancy may be eliminated by including the highest states of the metal (*p* and *d*) in the basis set.[35]

Comparison of the 'B_6' and CaB_6 bands indicates an appreciable role of the metallic states in bonding, which is manifested by an increase in dispersion for a series of bands (along the Λ, Σ, and Δ directions) and also by the initiation of the appearance of new levels in the conduction band.

Calculations have shown[35] that the Ca → B_6 charge transfer does not exceed 0.9–1.0 e, although according to Longuet-Higgins and Roberts[27] the transfer of two electrons is required to stabilise the CaB_6 structure—for the complete filling of the bonding states band. This electron deficiency leads mainly to a weakening of the $p_\sigma p_\sigma$ and $p_\pi p_\pi$ bonds between the B_6 groups without having a significant influence on the 'intracluster' interaction, i.e. without leading to a critical destabilisation of the structure as a whole. This situation is analogous to that for alkali metal hexaborides, where the M → B_6 charge transfer does not exceed 1 e.[35]

The CaB_6 band structure, calculated by the augmented plane wave (APW) method with a Slater exchange-correlation contribution (α = 2/3),[37] differs significantly from that presented in other communications.[27,29–31,35] The absence of a forbidden gap between the valence and conduction bands and also the appreciable concentration of pre-Fermi states (at the point Γ), which conflicts with X-ray electron spectroscopic data, are noteworthy. These discrepancies have been explained[37] by the absence of self-consistency in the calculation for the boride.

A self-consistent study of the influence of metallic *d* states on the electron spectrum of CaB_6 has been carried out by Hasegawa and Yanase,[38] who carried out the calculation by the self-consistent symmetrised APW method. The relativistic effects were described in terms of the scheme presented by Koelling and Harman.[39] The calculations were performed in terms of both the standard muffin tin (MT) approximation and with a correction for the nonsphericity of the potential.

Both calculations yield fairly similar structures of the CaB_6 valence band (Fig. 4), containing a low-energy (lower by ~1.05 Ryd than E_F; Ryd = Rydberg number) B 2*s* band and a system of occupied bands (which are filled by 18 electrons per unit cell) in the range E_F–0.70 Ryd. The lowest virtual band is characterised by an appreciable dispersion due to the effect of the *p*–*d* hybridisation typical for the hexaborides with a very significant contribution by the Ca 3*d* function at the point *X*. The resolution of the states in the MT spheres into individual components also indicates the involvement of the Ca 3*d* orbitals in the pre-Fermi level X_3.

The most remarkable difference in the results of the calculation taking into account the nonsphericity of the potential is the increase in the energy of the X_3 state with appearance of a forbidden gap [$\Delta E(X_3 - X_{3'}) \approx 0.02$ Ryd (Fig. 4)]. The observed changes in the fine structure of the density of states are caused, in particular, by the increase in the amplitude of the Ca *d* states with decrease in the potential, whereupon the given functions assume the form of plane waves.

According to the MT calculation,[38] the surface of the CaB_6 Fermi level consists of electron and hole layers (Fig. 5). The number of carriers is ~2×10^3 electrons and the same number of holes are present in the unit cell. The role of the spin–orbital interactions in the establishment of the pre-Fermi bands has been analysed.[38] It was noted that, when the spin–orbital interactions are taken into account for a slight (~0.01 Ryd) overlap of the valence and conduction bands (according to

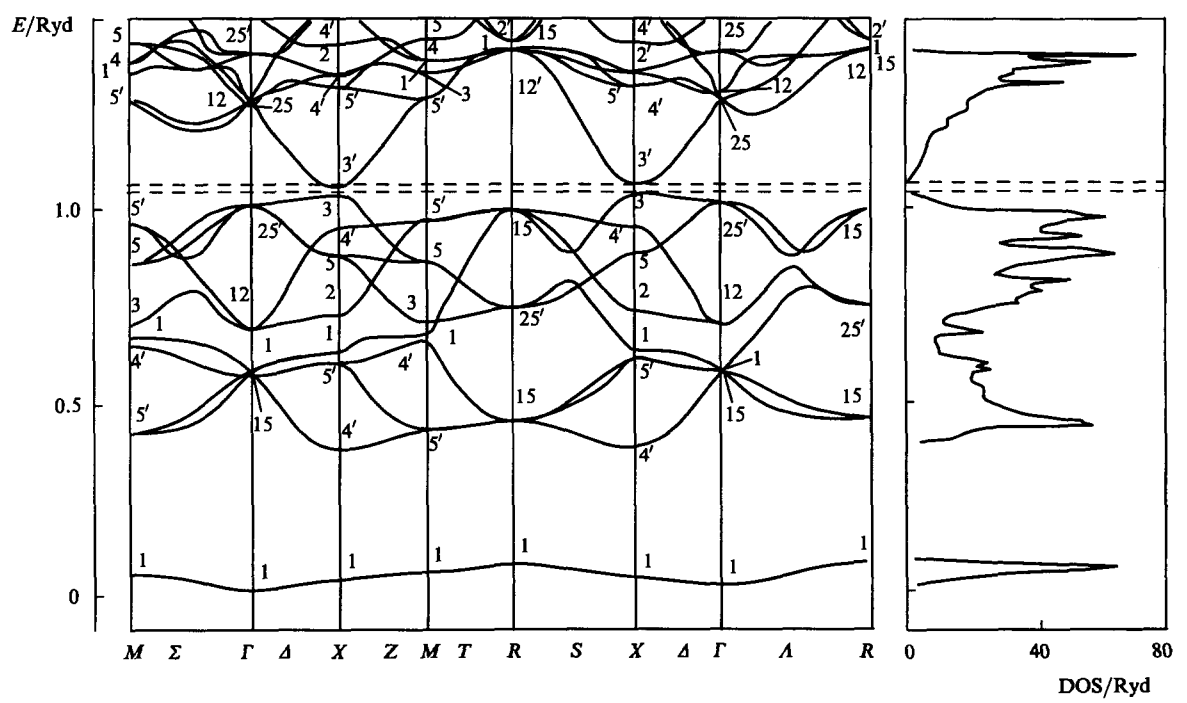


Figure 4. The band structure and the total density of states in CaB_6. SCF-APW calculation with a correction for the nonsphericity of the potential.

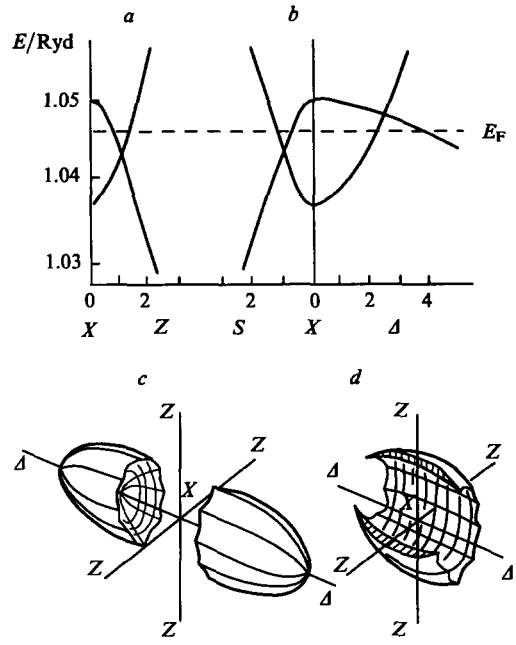


Figure 5. Energy bands near the bottom of the conduction band (*a*) and the upper edge of the valence band (*b*) and schematic representation of the hole (*c*) and electrons (*d*) layers on the Fermi surface in the vicinity of the symmetry point *X* for CaB_2.[38]

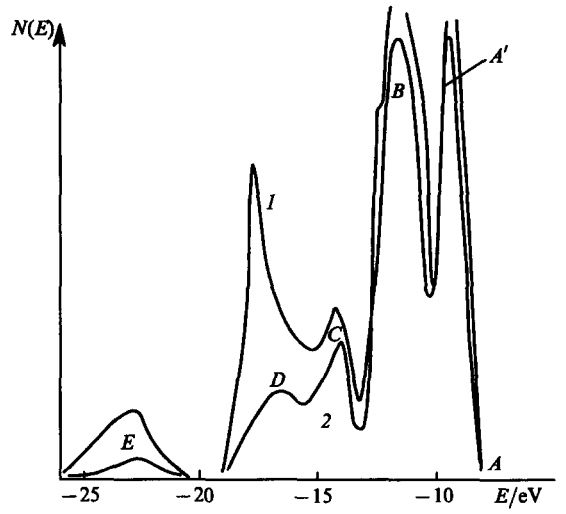


Figure 6. The total (curve *1*) and local (curve *2*) densities of B 2*p* states in BaB_6.[35]

calculations with the MT approximation), a forbidden gap should appear with an indirect transition energy of $\sim 0.001\ R_\infty$, which makes it possible to assign CaB_6 to the class of semiconductors.

The following borides have been investigated by X-ray emission, absorption, and electron spectroscopy: CaB_6,[37,40] BaB_6,[41] ScB_2,[44,46,78] TiB_2,[42–46] VB_2,[46–53] Cr_2B, CrB, CrB_2,[44–46,49,51,54,56,79] Mn_4B, Mn_2B, MnB, Mn_3B_4, MnB_2, MnB_4,[46,54,57,58] Fe_2B, FeB,[43–45,55,58–68] Co_3B, Co_2B, CoB,[44,54,60,65,67,69,70] Ni_3B, Ni_2B, Ni_4B_3, NiB,[44,45,54,58,59,67,71,78,80–82] YB_6,[40] ZrB_2,[37,51,74–76] Nb_2B, Nb_3B_2, Nb_3B_4, NbB, NbB_2,[51,72,73] MoB,[77] HfB_2,[51] and TaB_2.[51,74]

The conducting properties of calcium hexaboride have been treated[1–14] as being either of the semimetallic or semiconducting type. The dependence of the forbidden gap on the method of synthesis of the specimens[83] and on the presence of a wide variety of impurity centres or crystal defects,[83] in particular vacancies in the metal sublattice, is evident. The possibility of the formation of the latter for CaB_6 has been noted, for example, in the study of the fusion of CaB_6, whereupon dissociation takes place with the preferential evaporation of calcium.[84,85] This finding can be readily accounted for by the specific features of the energy structure of CaB_6, because the bonds between the atoms of the nonmetal sublattice of the boride play a dominant role in the organisation of the inter-species interaction.

Calculations for strontium and barium hexaborides within the framework of the LCAO formal treatment[35] indicate that the structures of their electronic spectra are similar to that for CaB_6 (Fig. 4). Therefore, without going into their details, we shall only note that the form of the valence DOS is determined primarily by the type of the distribution of states in the B_6 groups (Fig. 6) and is characterised by five principal maxima *A*–*E*. Comparison with the data obtained by X-ray emission BK_α spectra of BaB_6 shows (when account is taken of the simplifications used in the calculation)[41] a fairly reasonable agreement between the energies of the principal B 2*p* maxima with the exception of the intense peak *A* manifested on the spectral line in the form of a weak high-energy bulge.

4. Aluminium borides

The phase diagrams for the Al–B system indicate[86–95] the existence of at least two stable binary phases—aluminium diboride AlB_2 and aluminium dodecaboride AlB_{12}. Two possible modifications have been identified for the latter compound—monoclinic and tetragonal.[10] The existence of the AlB_{10} phase,[90–92,95] found by Kuz'ma,[11] was not unambiguously confirmed.

In terms of the aspect under discussion, the most interesting compound is the diboride AlB_2—a phase the structural type of which (or one related to it) is characteristic of a large number of binary and more complex *d* metal borides (see below). Aluminium diboride has one of the simplest structures and contains two alternating networks of atoms—the metal and boron (Fig. 1).

General ideas about the nature of the metal–metal bond in the diborides AlB_2 have been discussed within the framework of the Hückel model.[96,121] It is claimed that the system of chemical bonds in such crystals is based on the M–B and B–B interactions, whereas the M–M interactions (in the direction perpendicular to the network of B atoms) are antibonding.

The band structure of AlB_2 (calculation by the LCAO method)[97] is determined by the presence of filled boron bands (the structure of which is found to be similar to that for graphite) split into states with σ are π symmetries. Part of the charge density is transferred to the latter from the metal atom, whereupon the metal atoms acquire the effective charges +1.884 e (Al) and −0.942 e (B). The B–B bonds have a stabilised π component; the $Alp_{x,y}$ functions are mixed with the band comprising these states, giving rise to the B–Al bond. We may note, however, that in the calculations[97] the basis set did not include the Al 3*d* states, allowance for which (see above) may significantly amend the fine structure of the band in the energy spectrum of the crystals.

Overall, the calculations[97] are in satisfactory agreement with X-ray emission spectroscopic data[98] and have been used to interpret the anisotropy of the electrical properties of AlB_2 (on the basis of the analysis of the topology of the Fermi surface and estimates of the differences between the effective masses of the carriers for different directions in *k* space).

The molecular orbital scheme for the fragment modelling AlB_{12}, for which semiconducting properties have been predicted, has been calculated[99] by the LCAO method in terms of the Gaussian orbital basis set (GO LCAO).

III. Transition *d* metal borides

Transition *d* metal borides constitute one of the most numerous and thoroughly investigated groups of binary boride phases, and numerous monographs and reviews have been devoted to their crystal chemistry and physicochemical properties.[1-14]

The analysis of the possible approaches to the description of the electronic structure and properties of compounds of this type will be begun with the Ti–B system.

1. Titanium borides

Numerous studies have been devoted to phase formation in the Ti–B system.[1-3,5,7,9,11-14] It is suggested that not less than five individual phases exist in the Ti–B system.

Most of the investigations of the electronic properties of the boride phases of titanium refer to titanium mono- and di-borides. However, before turning to the consideration of the results, we shall mention the calculations of the perturbations in the electronic states of titanium when boron atoms are introduced into its interstices (the corresponding region in the binary system with a low content of the nonmetal is designated as the α-phase on the phase diagrams).[100]

The LMTO Green function method (LMTO-GF) has been used[100] in the calculation for the Ti–B system, in which the nonmetal atom was placed at the centre of an octahedral interstice of the face-centred cubic structure of titanium. It follows from the analysis of the distribution of the local density of states (LDOS) of boron that the quasi-core B 2*s* functions form a discrete impurity peak near the lower edge of the valence band of the matrix, while the B 2*p* function overlaps the lower part of the valence band of titanium, promoting the formation of Ti–B bonds.

The perturbing effect of the impurity on the electronic states of the matrix (ΔN) has also been considered. It was established that in the region of energies corresponding to the localisation of the impurity states, two positive $\Delta N(E)$ peaks are observed. The first and second peaks correspond respectively to the states of titanium mixing with the 2*s* and 2*p* orbitals of the interstitial atom respectively.[100] In the pre-Fermi region, a characteristic oscillating $\Delta N(E)$ structure is observed, reflecting the redistribution of the high-energy states of the metal atoms in the vicinity of the interstitial element. Negative values of $\Delta N(E)$ correspond to spectral ranges with a lower electron density $N(E)$ than for pure titanium and conversely. We then have $\Delta N(E_F) > 0$, i.e. the doping of titanium with small amounts of added boron leads to some increase in $N(E_F)$ for the alloy primarily owing to the disturbance of the bond system in the ideal crystal. Nonequivalent Ti–B and Ti–Ti bonds are formed in this case in the vicinity of the impurity *p* centre. Concentration of electron density in the region of energies of the B 2*s* and B 2*p* functions corresponds to bonds of the first type, whilst positive pre-Fermi $\Delta N(E)$ maxima correspond to bonds of the second type.

The next step was to investigate the effect of the interstitial elements on the electronic states of titanium atoms in the face-centred cubic structure constituting the first and second coordination spheres of the impurity atoms.[100] The γ-Fe_4N structure was used as a model.

The total and local DOS of the hypothetical Ti_4B are presented in Fig. 7. In contrast to the isolated impurity, the B 2*s* and B 2*p* states now form bands of finite width. It is especially interesting to emphasise that the LDOS for titanium atoms at nonequivalent (relative to the centre of insertion) sites are markedly different. Thus, whereas the titanium atoms in the closest sphere make appreciable contributions to the subbands of the nonmetallic 2*p* states, the extent of such mixing is smaller for the Ti atoms in the next sphere, which indicates the local character of the Ti–B bond. This is also reflected in the charge and energy states of the crystallographically nonequivalent metal atoms.

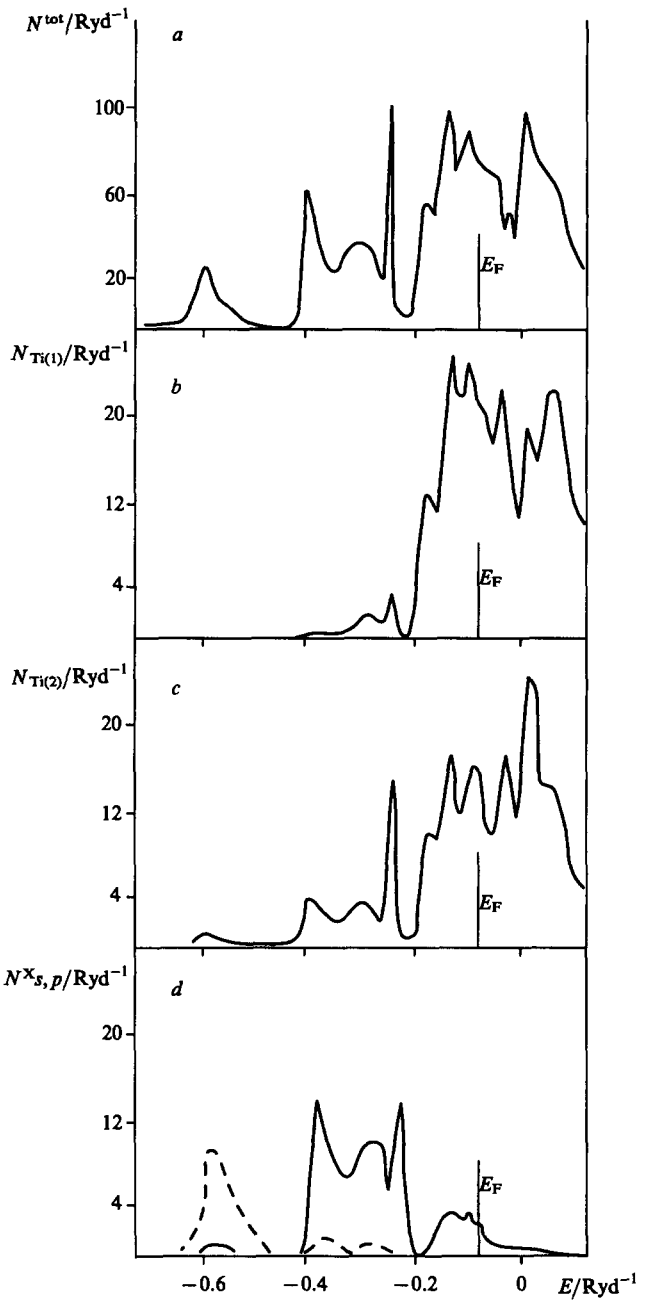


Figure 7. The band structure of Ti_4B (γ-Fe_4N structural type) according to LMTO calculations:[100] (*a*) total density of states; (*b*) and (*c*) LDOS for titanium atoms in the second and first (relative to the nonmetal) spheres; (*d*) densities of B 2*s* (dashed curve) and B 2*p* (continuous curve) states.

Analysis of the valence subbands showed that the maximum contribution to the hybrid Ti_4B band comes from the *d* states of the nearest atoms, i.e. the Ti–B bonds are organised in conformity with the *p*–*d* hybridisation mechanism typical for refractory phases.[101-104] One cannot also neglect the involvement of the *s* and *p* functions of titanium in these interactions. Thus it is mainly the Ti 4*s* functions of the titanium atoms constituting the second metal sphere which enter into the interaction with the nonmetals. In other words, both the energies and the nature of the bonds between the interstitial elements and the titanium atoms in the first and second spheres are different.

These differences in the nature of the Ti–B bonds are reflected in the distribution of the states of the metal band, i.e. lead to the anisotropy of the Ti–Ti bonds.

We may note that the calculated data[100] have been used for a qualitative treatment (in relation to the Ti–B and Ni–B systems) of the phase relations observed on the phase diagrams for metal–boron systems. For this purpose, use was made of the changes in the total energy (ΔE) of the face-centred cubic titanium matrix when a nonmetal atom is introduced into an interstice. These changes were obtained by solving the single-impurity problem by the method proposed by Anisimov et al.[105] It was found that $\Delta E < 0$ for the systems considered, i.e. the introduction of nickel and boron atoms, involved in covalent interactions with the matrix, into the interstices of the face-centred cubic titanium and nickel structures is energetically favourable. However,

$$|\Delta E^{Ti-B}(-0.767\ \text{Ryd})| > |\Delta E^{Ni-B}(-0.673\ \text{Ryd})|\ .$$

In other words, the boron in the octahedral positions in titanium is more strongly bound than in the nickel matrix. This agrees with the known fact that compounds up to the diborides are formed in the Ti–B system, whereas the maximum content of boron in the nickel compound does not exceed Ni/B $\approx$ 1. Naturally, in analysing the results[100] one cannot fail to take into account the direct B–B interactions arising in the boride phases, which should introduce significant corrections to the overall energy relations of the systems under discussion. However, the above data[100] make it possible to gain a general idea about the role of the metal–nonmetal interactions in the boride phases considered.

With increase in boron content, the compound Ti_2B (orthorhombic structure of the Al_2Cu type) was detected on the Ti–B phase diagram. In its structure, all the boron atoms are surrounded by metal atoms.[5,11] The increase in the B/M ratio is accompanied by a further transformation of the electron energy spectra (EES) of the matrix [calculation by the method of augmented spherical waves (ASW)].[106] The B 2*p* states are then mixed in throughout the width of the occupied part of the valence band, which is predominantly of the Ti 3*d*, *s* type. In addition, the valence band contains near its lower edge two subbands of the B 2*s* type separated by a narrow energy gap. The bonds are formed as a result of two types of interactions: Ti–Ti and Ti–B; direct B–B bonds were not detected. The Fermi level is located on the high-energy slope of the intense Ti *d* type DOS peak.

The further genesis of the band structure of titanium boride as the boron content increases will be considered by comparing the EES of the higher borides—TiB and TiB_2.

Titanium monoboride crystallises with a structure of the FeB type.[11] There are also data concerning monoborides crystallising with structures of the NaCl and ZnS types.[7–10] It has likewise been suggested[11] that the cubic monoboride (NaCl structural type) can be obtained either in the form of a high-temperature phase or in the form of a phase stabilised by added carbon.

Calculations for the orthorhombic TiB have been carried out.[107–109] The dispersion of the bands and the total density of states (TDOS) in TiB have been investigated[107] by the nonself-consistent LCAO method in the tight binding approximation.[35,110] A broadening of the dispersion in the k_z direction ($\Gamma-Z$, $T-Y$, $R-S$, $U-X$) compared with k_x and k_y was noted. This should indicate the predominance of the bonding effects along the *c* axis of the crystal, along which the chains of boron atoms are oriented, i.e. a pronounced cohesion anisotropy. The TDOS in TiB comprises (in order of decreasing binding energy) the B 2*s*, B 2*p*, and Ti *d*, *s* states (Fig. 8). The Fermi level is located at the DOS minimum in the vicinity of the intense virtual *d* type resonance. Calculations of the populations of the atomic orbitals made it possible to estimate the charge states of titanium (−1.31 e) and boron (+1.31 e).

The bond indices of various atoms, forming layers in the TiB crystals, have been calculated[107] in the cluster approximation by the method proposed by Bell and Perkins.[111] The calculation was carried out taking into account all the interacting neighbours in accordance with the Born–Carman principle.

The results show that the B–B covalent bonds are most highly populated.[107] In the calculations of the bond indices in other similar

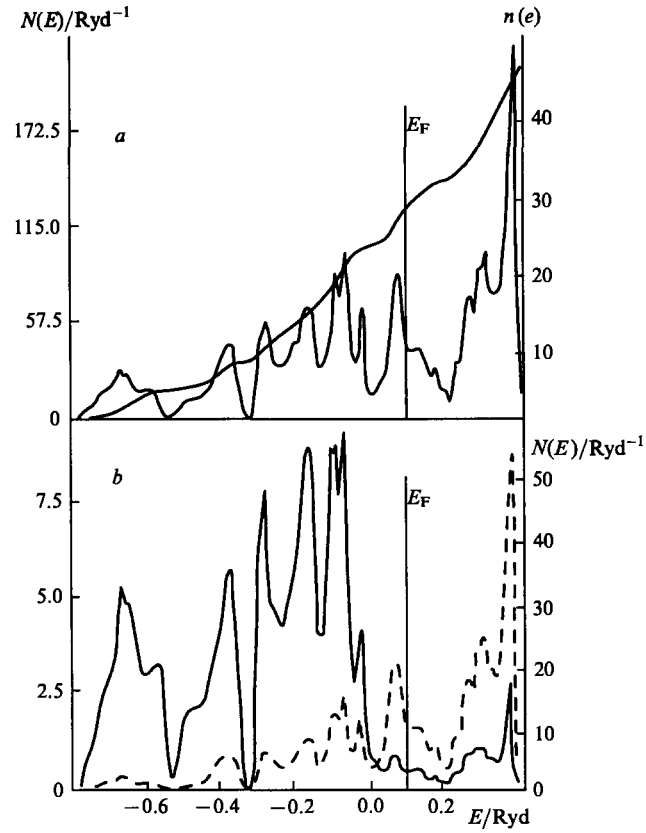


Figure 8. The total (*a*) and local (*b*) densities of states in TiB (FeB structural type). Calculation by the LMTO method.[109]

TiB clusters, where the lowest unoccupied levels lying 0.01 and 0.1 eV above E_F (this simulated the thermal excitation of the boride) were filled, the bond indices of the B–B and Ti–B types remained virtually unchanged, but the index of the Ti–Ti type diminished significantly. Consequently, heating of the specimens affects primarily the bond system in the metal sublattice of the boride.

Calculations for TiB using the more accurate self-consistent augmented spherical waves method[112,113] have been performed.[108] Here a study was made of the structural stability of 3*d* metal monoborides for five possible crystallographic modifications (structures of the FeB, CrB, NaCl, CsCl, and CuAu types). For this purpose, the total crystal lattice energies were calculated for the six cell volumes differing by ±15% from the equilibrium value in the case of all the structures listed above (Fig. 9). Evidently, in conformity with experiment, the orthorhombic modification is energetically most favourable for the boride under discussion, while the CsCl and CuAu structural types are least likely; an intermediate value was obtained for the NaCl type. The equilibrium volume of the TiB unit cell was reasonably well produced and the volume modulus of elasticity was calculated (Table 1).

Table 1. Theoretical (I)[108] and experimental (II)[114–116] unit cell volumes *v*, atomic magnetic moments μ, and volume moduli *b* of titanium monoboride.

Compound	v/Å^3		μ/μ_B		*b*/kbar
	I	II	I	II	
ScB	25.6	—	0	—	3100
TiB	22.6	21.3	0	0	2400
VB	19.5	18.8	0	0	2800
CrB	18.0	17.1	0	0	3400
MnB	17.3	17.2	2.00	1.83	2600
FeB	16.8	16.4	1.25	1.12	2500

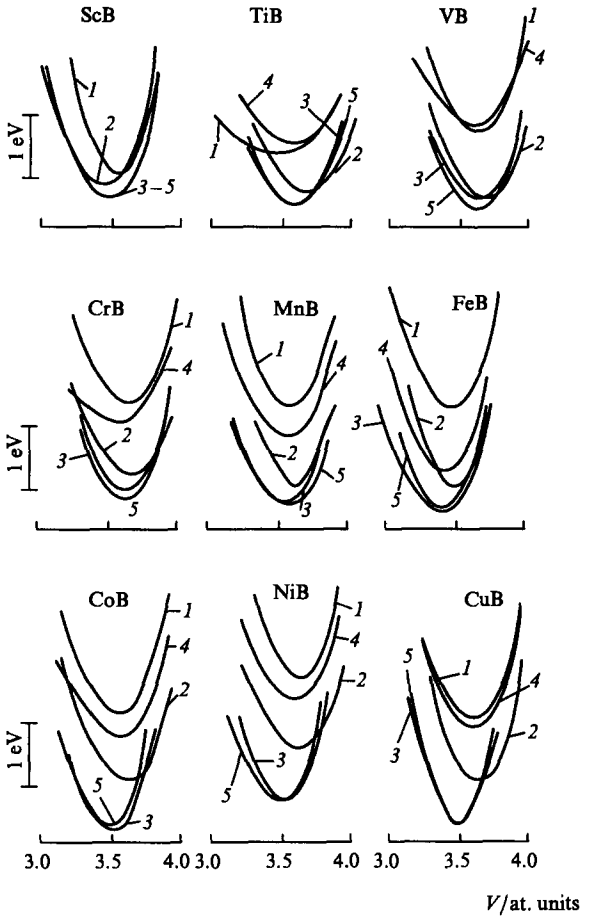


Figure 9. Variation of the total one-electron energy of 3*d* metal borides as a function of the crystal structure of the phase and the volume of the unit cell (calculation by the ASW method).[108] Type of structure: (*1*) CuAu; (*2*) NaCl; (*3*) FeB; (*4*) CsCl; (*5*) CrB.

A somewhat different approach to the discussion of the relative stabilities of the structural modifications of TiB, based on the calculations of the band spectrum of the crystals, has been used in a study[109] where the calculation for TiB with structures of the NaCl and FeB types was carried out by the LMTO method in the atomic spheres approximation in terms of the formal treatment of Sabiryanov et al.[117]

A multipeak TDOS structure was obtained for the orthorhombic monoboride TiB (FeB structural type) (Fig. 8). Taking into account the decomposition of the TDOS into atomic components, one can segregate arbitrarily two low-energy bands, predominantly of the B *s* and B *p* types, separated by a narrow forbidden gap from the band with an energy lower by approximately −3.14 to −0.1 Ryd than E_F and having a mixed $p-d$ character. The intense resonance of the Ti *d* and Ti *s* states in the vicinity of the Fermi level is also noteworthy. A significant difference between the results of the calculation by the self-consistent LMTO method[109] and the data of Armstrong and Perkins[107] concerns the position of the lowest unoccupied *d* band, which is separated from E_F by a deep DOS minimum according to Sabiryanov and Ivanovskii[109] (Fig. 8).

The DOS of the cubic monoboride (NaCl structural type)[117-119] differs significantly from that examined above for the orthorhombic TiB (FeB type). It has a two-band form[101-104] characteristic of NaCl-like phases (carbides, nitrides, etc.) with a distinct separation of the bands of the B 2*s* and B 2*p* states. Adjustment for self-consistency[119] then leads to the appearance of a forbidden gap between the bands, whereas in the absence of such adjustment their overlap is observed.[118]

We shall now analyse the energy relations of the paired bonds (E_b) in TiB (with structures of the FeB and NaCl type) using the method described by Sabiryanov et al.[117] The energies E_b for the orthorhombic borides are listed in Table 2. Evidently the interactions between boron atoms located in the closest layers of the crystal make the greatest contribution to the energy of the covalent bonds. This result differs fundamentally from the conclusions reached by Armstrong and Perkins,[107] who postulate that the interaction between boron atoms located in one layer predominates. Evidently, the analysis of the cohesive properties of crystals, based solely on the calculations of the parameters of the overlap of wave functions,[107] may not be always correct.

Table 2. Pair energies of the covalent bond in titanium borides.[102]

Pair	Energy of covalent bond/mRyd	Pair	Energy of covalent bond/mRyd
TiB (NaCl)		**TiB (FeB)**	
Ti(1)–Ti(1)[a]	−56.16	Ti(3)–Ti(2)	−33.18
Ti(1)–B(2)	−674.04	Ti(3)–Ti(3)[a]	−15.06
B(2)–B(2)[a]	8.12	Ti(3)–Ti(3)[b]	−98.92
		Ti(3)–Ti(1)	−210.14
TiB_2		B(7)–Ti(1)	−341.74
Ti(1)–B(2)	−350.40	B(7)–Ti(2)	−246.22
Ti(1)–Ti(1)[a]	−21.14	B(7)–Ti(4)[a]	−48.70
Ti(1)–Ti(1)[b]	−95.02	B(7)–Ti(3)	−212.00
B(2)–B(3)	−975.42	B(7)–B(8)	−705.40

[a] Atom from the cell displaced by unit translation vector along the *a* axis.
[b] Atom from the cell displaced by unit translation vector along the *c* axis.

In conclusion, we may note that the total covalent interaction energy is 1887.9 mRyd for the cubic boride and 1907.1 mRyd for the orthorhombic boride,[109] which indicates unambiguously the greater stability of the orthorhombic phase and is fully consistent with the conclusions reached by Mohn and Pettifor.[108]

Proceeding now to the consideration of the energy spectra of the higher titanium boride TiB_2 (AlB_2 structural type), we may note the calculation for the diboride[120] carried out by the LCAO cluster method in the tight binding approximation[18] as one of the first approximate calculations. The calculations were performed for a lattice fragment (with D_{3h} symmetry) taking into account the fourth- and fifth-order neighbours in terms of a basis set comprising the B *s*, *p* and Ti *s*, *p*, *d* orbitals. The resolution of the resulting molecular orbitals into atomic contributions makes it possible to estimate the width of the TiB_2 valence band (~13.56 eV), the lower edge of which is made up mainly of the *s* and *p* states of boron with progressively increasing contributions by the Ti *s* orbital as the energy of the molecular level decreases. Analysis of the parameters of the electronic structure of TiB_2, calculated by Samsonov et al.,[120] indicates the Ti → B charge transfer as additional p_x states of boron are filled. The latter form B–B bonds both within planes (π-bonds) and between layers (σ-bonds), the maximum filling of the p_x states (in the TiB_2–VB_2–CrB_2 series) being responsible, according to Samsonov et al.,[120] for the extrema in the melting point, the coefficient of thermal expansion, the microhardness, and the phonon component of the thermal conductivity.

Band calculations for TiB_2 have been carried out by the LCAO method[26] in terms of Hückel's formal scheme,[121] the augmented spherical wave method,[37] and the LMTO method.[109,122] The electron energy spectrum of the diborides has been investigated by spectroscopic methods.[42-46] The $E(\vec{k})$ dispersion relations for TiB_2 have a number of characteristic features compared with the monoborides (Fig. 10). There is no forbidden gap between B 2*s* and the hybrid B 2*s*, B 2*p*, and Ti *d*, *s* bands and there are random degeneracy points in the vicinity of E_F in the $\Gamma-K$, $K-M$, and

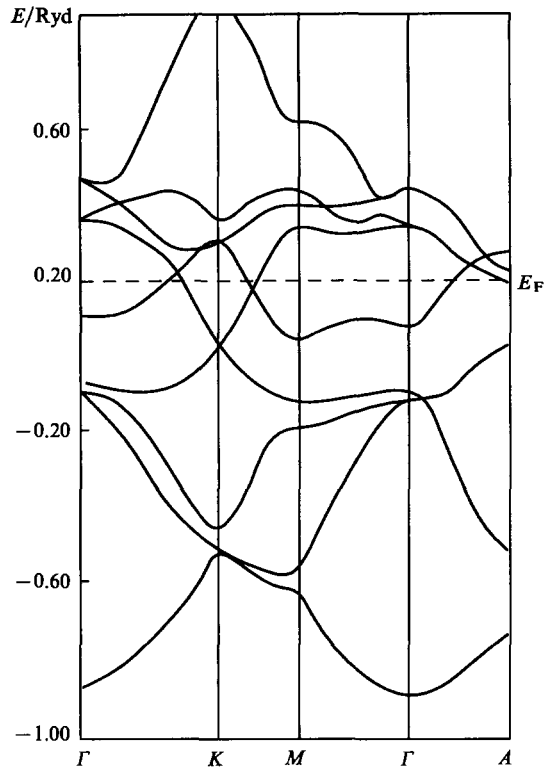


Figure 10. The band structure of TiB_2.[109]

$\Gamma-A$ directions. Three principal subbands, made up of the B 2*s* state, the B 2*s*, 2*p* and Ti *d*, *s* states, and the Ti *d*, *s* states respectively, can be differentiated in the TiB_2 valence band. The Fermi level is located in a deep DOS minimum separating the valence and conduction bands, which agrees well with the results of X-ray emission analysis.[41]

Analysis of the energy relations of the paired bonds (Table 2) shows that the interaction between the boron atoms located in one plane (network) is most significant whereas bonds between networks were not detected. The next in magnitude is a type Ti–B interaction, the Ti–Ti bond energy being an order of magnitude smaller. The results of calculations of the partial energies of the pair interactions proved somewhat unexpected.[109] According to these calculations, the Ti 4*p*–B 2*p* (72 mRyd) and Ti 4*p*–B 3*s* (66 mRyd) bond energies are comparable to the Ti 3*d*–B 2*p* (92 mRyd) bond energy.

Estimates of the charge polarisation,[120,122] indicating a displacement of the electron density to the nonmetal atoms, are consistent with experimental X-ray diffraction data.[123]

The possibility of the appearance of high-temperature superconductivity in layered titanium borides has been examined[124] on the basis of the generalised Hubbard–Emery model[125,126] (taking into account the integrals of the jumps between nearest neighbours). The presence in such borides of separated $d_{xz,yz}$ states, tunnelling through boron ions in the degenerate $p_{x,y}$ states, has been postulated. Calculations of the amplitude of the kinematic interaction (by Dyson's method) taking into account the possible filling of the bands for the hexagonal TiB_x phases showed that superconductivity can occur in the composition range $TiB_{26/17}$–TiB_2 (Fig. 11). The conclusions reached by Zaitsev[124] agree qualitatively with the results of other studies,[127,128] in which the possibility of superconductivity in the $TiB_{1.5-1.6}$ phases and its absence in the TiB_2 and Ti_3B_4 phases was indicated.

The quantitative microscopic description of the parameters of the superconducting state of the borides undoubtedly requires special consideration.

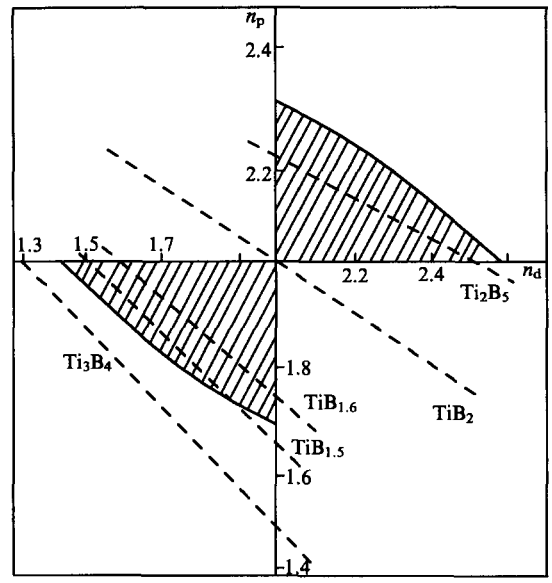


Figure 11. Phase diagram for the compound TiB_x. The regions of possible superconductivity are shown cross-hatched.

2. 3*d* Metal borides

Proceeding now to the discussion of the electronic properties of the borides of other 3*d* metals, we may note that the boride phases formed by specific 3*d* metals have been investigated to significantly different extents. Systematic calculations have been performed only for the hemiborides[106] and monoborides.[108] It follows from them that the dispersion relations and the energy distributions for these phases are similar to those for Ti_2B and TiB (see above), provided that account has been taken of the increase in the filling of the *d* bands as a function of the concentration of the valence electrons (CVE) and of the consistent low-energy shift of the metallic subbands with increase in the atomic number of the transition metal along the Period.

Most studies carried out hitherto have been devoted to the description of the characteristic features of the electronic structures of iron and nickel borides. We shall consider in greater detail their principal results.

The hemiboride Fe_2B and the monoboride FeB have been differentiated in the Fe–B system as equilibrium phases.[1,2,9,11]

The hemiboride has a body-centred tetragonal structure of the Al_2Cu type ($a = b = 4.249$ Å, $c = 5.110$ Å, space group *I4/mcm*), where the boron atoms are located between layers of iron atoms.[11] Iron monoboride crystallises with formation of an orthorhombic structure in which there are four molecules in the unit cell.[1]

The spectroscopic properties of iron borides have been investigated.[43–45,54] The results of numerical quantum-chemical calculations for Fe_2B and FeB have been published.[106,108,129–131]

One of the most complete calculations of the electron energy spectra of Fe_2B has been carried out[131] by the linearised APW-(LAPW) method, in which the energies of the core electrons were calculated in accordance with the full relativistic Dirac–Slater scheme. A semirelativistic approach, taking into account the contributions to the Dirac equation of the Darvin and mass–velocity terms, was used to calculate the energy of the valence electrons. In the solution, account was taken of plane waves (~270) with energies of up to 6.15 Ryd and angular momenta $l \leqslant 8$. Adjustment for self-consistency (with respect to energies) was carried out until the attainment of the condition $\Delta E \leqslant 4$ mRyd.

Analysis of the dispersion curves and of the total and partial densities of states in Fe_2B shows that the bands due to the B 2*s* and B 2*p* states lie below the partially filled Fe 2*s* states. Two lowest bands are made up of 2*s* states of two boron atoms in a unit cell.

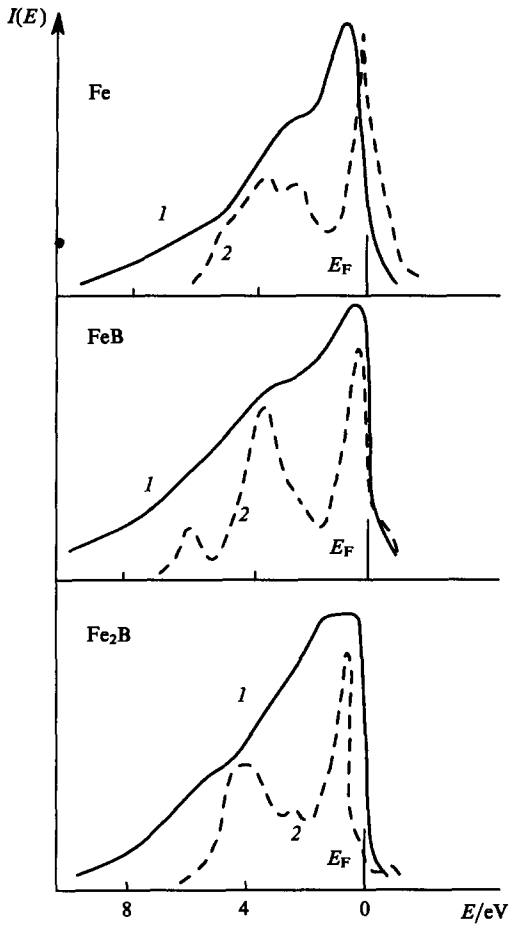


Figure 12. Fe 3*d* electron spectra (curves *1*) and densities of Fe 3*d* states (curves *2*) in Fe, Fe_2B, and FeB.

The degenerate B *p* states are located in the range −0.6 to 0.2 Ryd. An appreciable superposition of the iron and boron states occurs higher along the energy scale. Finally, the highest energy peak reflects the concentration of the bonding Fe 3*d* orbitals, while a further two resonances, corresponding to the nonbonding Fe 3*d* states, are observed in the immediate vicinity of E_F.

Comparison of the DOS and the photoelectron spectra of Fe_2B (Fig. 12) shows that they are acceptably consistent with one another.[131] Evidently the Fermi level coincides with the local Fe 3*d* resonance band, where the DOS (calculated per iron atom) reaches ~1 Ryd^{-1}. If account is taken of the fact that the Stoner parameter *I* (for pure iron) is ~0.92, it becomes evident[131] that, since $IN(E_F) \gg 1$, the manifestation of ferromagnetic properties is to be expected for Fe_2B. Unfortunately the calculations[131] were performed solely in the spin-limited variant, which made it impossible for the authors to estimate the atomic magnetic moments.

Table 3. Distribution of valence electrons among the MT spheres of Fe_2B and FeB (calculated by the LAPW method).[131]

Compound	Type of sphere	Number of electrons		
		s	*p*	*d*
Fe_2B	Fe	0.3205	0.3907	6.0726
	B	0.3654	0.6329	0.0161
FeB	Fe	0.2973	0.4027	6.1631
	B	0.3667	0.6785	0.0171

Analysis of the interatomic bonds in Fe_2B, based on the calculation of the distribution of states in the MT spheres (Table 3) and charge density maps [in the (120) plane] for the boride leads to the conclusion that there is significant B 2*p*–Fe 3*d* hybridisation between the boron atoms and the eight nearest iron atoms. Thus the charge density contours indicate the concentration of charge density along the B–Fe line and also between the nonmetallic centres, which is evidence for the existence of direct B–B bonds.

We may also note that charge transfer between the iron atoms in the hemiboride was not observed.[131] The formation of direct covalent Fe–B and B–B bonds enhances the cohesive properties of Fe_2B compared with Fe.[131]

Direct calculations of the Fe_2B core orbital energies (Table 4) and of electron densities on the iron nuclei, which have been used to calculate the isomeric shifts (measured by Mössbauer spectroscopy), are of interest.

The spin-labelled LAPW calculation for FeB has been performed by the method described above. The boron 2*s* states are concentrated in the vicinity of the bottom of the valence band. The higher-energy *A* and *B* maxima correspond to the hybridised Fe 3*d*–B 2*s* states, whereas in the vicinity of the Fermi level predominantly the Fe 3*d* functions make the main contribution to the DOS (Fig. 13). Comparison of the results of the calculation with emission spectroscopic data[61–63] shows that they are in agreement.

The formation of covalent bonds (as a result of *sp*–*sp* hybridisation) between boron atoms constituting the linear chains is characteristic of iron monoboride as well as Fe_2B. Charge transfer between the iron and boron atoms in FeB has not been observed (Table 3). It is seen from the data presented in Table 4 that the calculation in the study of Joyner et al.[131] correctly reproduced the sequence of the energies of the core levels of FeB, which are somewhat displaced in the direction towards E_F relative to the experimental results.[62,63] We may note that, following the transition $Fe_2B \rightarrow FeB$, the energy relations for these levels remains virtually unchanged (within the limits of ±0.1 eV), which is also consistent with experiment. The Fe_2B and FeB valence band schemes are presented in Fig. 14.

Table 4. The energies (Ryd) of the core levels of Fe_2B and FeB.

Compound	Fe 2*s*[a]	Fe $2p_{1/2}$	Fe $2p_{3/2}$	Fe 3*s*	Fe $3p_{1/2}$	Fe $3p_{1/2}$	B 1*s*
Calculated data[131]							
Fe_2B	−59.588	−51.385	−50.471	−6.348	−3.951	−3.837	−12.432
FeB	−59.584	−51.384	−50.469	−6.338	−3.960	−3.846	−12.352
Experimental data[61,63,66]							
Fe	−62.14	−52.94	−51.98	−6.71	−3.90	—	−13.83
Fe_2B	−62.11	−52.96	−51.99	−6.74	−3.90	—	−13.82
FeB	−62.14	−52.96	−52.00	−6.74	−3.92	—	−13.82
B	—	—	—	—	—	—	—

[a] The energies are quoted relative to the Fermi level.

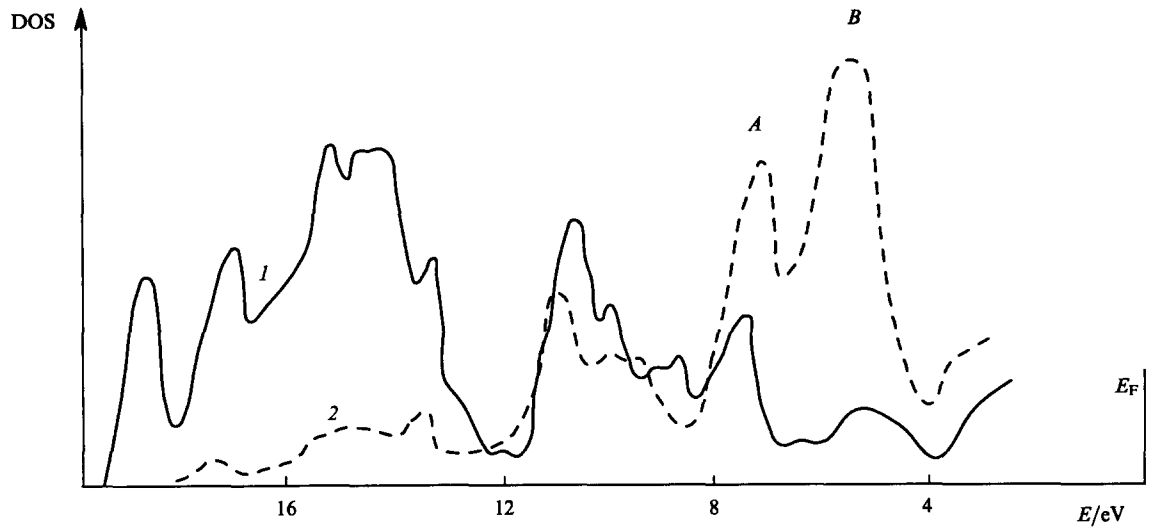


Figure 13. The local densities of B 2*s* (curve *1*) and B 2*p* (curve *2*) states in FeB.[131]

The energy structure of nickel monoboride (type CrB structure)[11] has been calculated[106] by the ASW method (Fig. 15). The relative positions of the total and local DOS make it possible to differentiate the sections of the electronic state spectrum corresponding to the *p*–*p* bonds in the chains of metalloid atoms (peak *A*), to the Ni–B interactions (peaks *B* and *B'*), and to nonbonding *d*–*d* states (peak *C*). The calculated value of the volume modulus [of elasticity] and of the unit cell volume are presented in Table 2.

The value of $N(E_F)$ for crystalline NiB is not quoted in Mohn's study,[106] although it is seen from Fig. 15 that it is insignificant and is much smaller than for manganese and iron monoborides. Measurements of magnetic susceptibility made it possible to assign NiB to the class of weak paramagnetic materials and to estimate $N(E_F) \approx 0.18$ state eV^{-1} $atom^{-1}$,[132,133] in which the contributions of the *s* and *p* states predominate.

The parametrised LCAO method with the Slater–Coster (SC) tight binding approximation has been used[134] in calculations for the lowest nickel boride Ni_3B (Fe_3C structural type).

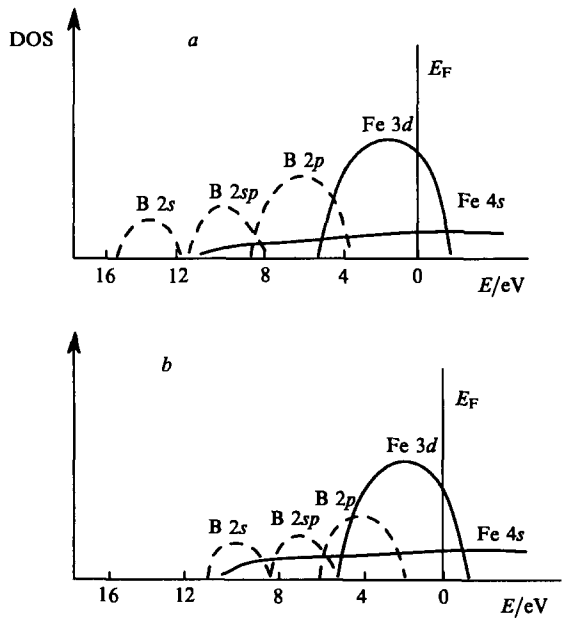


Figure 14. Schematic illustrations of the structures of the valence bands of FeB (*a*) and Fe_2B (*b*).

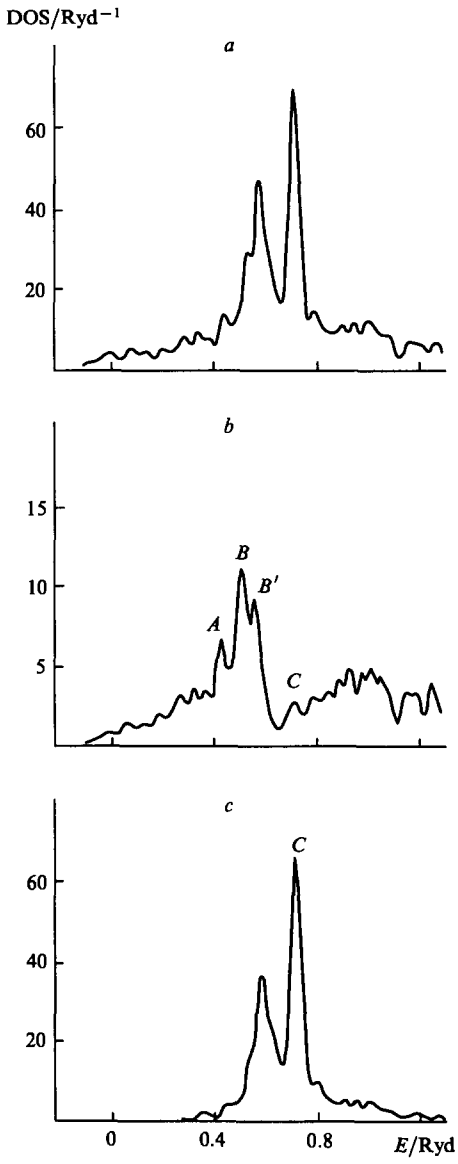


Figure 15. The total (*a*) and partial densities of B 2*p* (*b*) and Ni 3*d* (*c*) states in NiB.

The *B* 2*s*, B 2*p*, and Ni 3*d* functions were included in the basis set and account was taken of the interaction of only the nearest neighbours. The SC parameters for the Ni–Ni bond were taken from calculations performed for metallic nickel,[135,136] while the parameters of the B–B bond were obtained by extrapolating the SC parameters for carbon.[134]

The energy spectrum of the valence electrons of Ni_3B is typical of binary borides and contains two lowest bands (E = 0.0315 and 0.0607 Ryd) made up of B 2*s* states. The following twelve bands (0.433–0.569 Ryd) reflect the hybrid Ni 3*d*–B 2*p* states, the upper band having predominantly the *d* character. The higher energy free bands ($E \geqslant 1.135$ Ryd) also have a mixed B 2*p*–Ni *d*, *s* character.

The band structure in the vicinity of E_F makes it possible to assign Ni_3B to the class of paramagnetic materials, which is consistent with the available experimental data.[138,139]

3. 4*d* Metal borides

Proceeding now to the discussion of 4*d* metal borides, we may note that the energy structure of these compounds has been investigated in much less detail than that of the 3*d* analogues. Zirconium diboride, which has a series of valuable physicochemical properties, namely a high melting point, high electrical and thermal conductivities, and a high hardness, has attracted most attention hitherto.[1–4,8–11] This makes it possible to employ it as a cathodic material, as an abrasive, and as a component of heat-resistant alloys, composite materials, etc.

Nonself-consistent calculation for ZrB_2 by the APW method using the exchange potentials specified by Slater and Kohn-Shem[140] showed that the density of states in ZrB_2 is defined by three characteristic maxima. The first is linked genetically to the bands of the B 2*s* states, while the next two correspond to the 2*p* states of the nonmetal.

The ZrB_2 band structure has been investigated[141] by the self-consistent Korringa–Kohn–Rostoker (KKR) method in terms of the MT spheres approximation. The initial potential was determined by the Mattheiss method[142] with the initial atomic configurations Zr $4d^{2.5}5s^{1.5}$ and B $2s^22p^1$. The exchange-correlation parameters α were taken from Schwarz,[143] whilst the remaining parameters were taken from Ham and Segal[144] and Segal.[145] Adjustment for self-consistency proved most critical in relation to the energies of a series of virtual DOS peaks and the distribution of the Zr *d* electrons. Their number in the MT sphere of the metal (compared with the nonself-consistent calculation) increased by ~0.667 e.

The dispersion $E(k)$ proved extremely complex, which hindered a clear interpretation of the nature of the interatomic bonding. In describing the structure of the energy bands, Johnson et al.[141] confine themselves to only several preliminary remarks. In particular, it is noted that the lowest bands (T_1, T_4, Z_1, Z_4) resemble the sp^2 σ-bonding states in graphite[146] and can be made up of the bonding states of boron (s, p_x, p_y). Nevertheless, one cannot fail to take into account the admixture of metal functions in this region.

By analogy with 'two-dimensional' graphite, it is suggested that the band intersecting the Fermi level (T_1) is associated with the π band of boron, while the lowest unoccupied Σ_3 and all the s_4 bands are made up of the antibonding B π states significantly hybridised with the Zr *d* orbitals. A detailed analysis of the remaining states has been carried out by Johnson et al.,[141] who examined also the principal differences between the energy structure of ZrB_2 and the intercalated layered phases of the KC_8 and LiC_8 types.[147,148] They also analysed the composition of the orbitals forming the pre-Fermi region — the predominance of the Zr *d* states was noted.

The results of the calculation[141] were also used for the theoretical interpretation of the optical properties of zirconium diboride. Fig. 16 presents the imaginary part of the relative permittivity of the ZrB_2 film[149] and the calculated curve (calculated on the hypothesis of constant matrix elements).

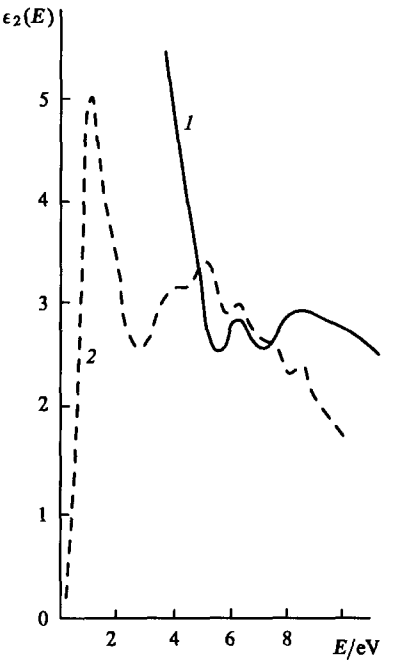


Figure 16. The energy dependence of the dielectric function for ZrB_2:[141] (*1*) experiment; (*2*) calculation.

Evidently, within the framework of the approximations adopted, the most reasonable description of the relative permittivity is attained in the range 6–7 eV. Its variation in the given energy range may be correlated with the transitions between sets of one-electron band states located directly above and below the Fermi level.

The melting point of ZrB_2 has been estimated[141] (from the Lindemann equation).[150] It was noted that the high melting point $T_m \approx 3000$ °C is due primarily to the significant covalent Zr–B interactions.

A fairly good agreement has also been observed between the quantity $N(E_F) = 0.20$, calculated using the low-temperature heat capacity γ data, and the values obtained in calculations:[141] 0.31 eV (nonself-consistent calculation) and 0.26 eV (self-consistent calculation) per unit cell. In conclusion, we may note that the results of the above study[141] have also been used for the qualitative interpretation of the X-ray electron spectra, the Hall effect, the conductivity, and the ^{11}B NMR spectra of the diboride. As regards the problem of charge transfer in ZrB_2, the data obtained permit the claim that there is partial charge polarisation in the crystal in the B → Zr direction.

The remaining 4*d* metal borides have been investigated to a much lesser extent or not at all. Among the available results, we may note the LMTO calculations for the hypo-thetical cubic ZrB,[118,119] in relation to which the problem of the effect of point defects — zirconium and boron vacan-cies — on the spectrum of the monoboride (calculations by the LMTO-GF method) was considered. The marked *s*-type resonance in the region of the minimum in the DOS for the matrix between the *p*, *d* and *d*-like bands of two additional low-energy peaks (in the region of the *s* and *p*–*d* bands of the boride) was established on the LDOS distribution curve of the B defect.[151] Their appearance may be accounted for (by analogy with the similar effects in non-stoichiometric carbides and nitrides)[103] by the increase in the energy of a series of Zr 4*d* states (on dissociation of some of the Zr–B bonds) with appearance of 'lateral' Zr–Zr interactions, which is manifested in the ZrB_x spectrum by the 'vacancy' resonances already mentioned.

The behaviour of $\Delta N(E)$ (the change in the electronic states of the matrix under the influence of vacancies) (Fig. 17) reflects the electronic processes accompanying the removal of a boron atom:

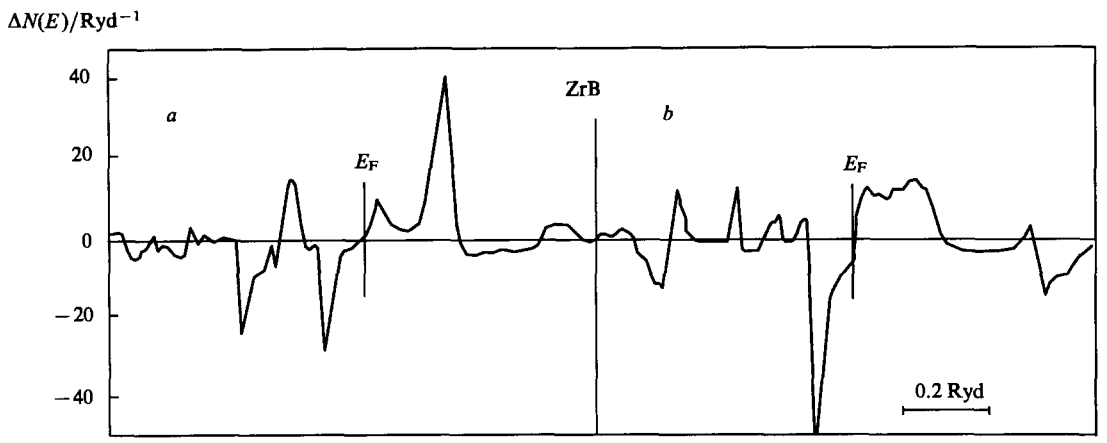


Figure 17. Variation of the density of states in ZrB following the introduction of B (*a*) and Zr (*b*) vacancies.[151]

negative values of $\Delta N(E)$ predominate in the region of the $p-d$ band of the valence band. In other words, the overall DOS of the nonmetallic band of the nonmetal-deficient phase decreases both as a result of the subtraction of the p states of the boron atoms removed and as a result of the transition of some of the d states of the metal to a higher-energy state. This is indicated by the positive $\Delta N(E)$ resonances in the pre-Fermi region (the region of the Zr–Zr bonds).

The nature of the states of the vacancies in the metal sublattice proved to be generally similar.[151] The 'vacancy peaks' are in this case caused by the subtraction of some of the B s,p states ('ruptured B–Zr bonds'), by the increase in their energy, and by a transition to a nonbonding state. The concentration of additional electron density is observed in this range (near E_F).

Estimates of the change in the one-electron energy of the system ΔE in the presence of boron of zirconium vacancies (by the method developed in the study of Ivanovskii et al.[103]) showed that $\Delta E(\text{Zr}) = 0.459$ Ryd and $\Delta E(\text{B}) = 0.508$ Ryd,[131] i.e. $\Delta E(\text{Zr}) < \Delta E(\text{B})$, which reflects the specific features of the bonding in borides. Indeed, the formation of Zr vacancies requires the rupture of only six nearest Zr–B bonds, whereas the formation of boron vacancies presupposes the dissociation of a further twelve B–B bonds. This is the reason why the formation of metallic defects is relatively favoured on energy grounds and in the general case ensures the possibility of the existence in the system of boron-rich phases (up to dodecaborides).[11]

With increase in the atomic number of the 4*d* metal, the ratio $x = \text{B/M}$ diminishes sharply and does not exceed $x = 1/3$ in the case of palladium for example. This fact can be qualitatively attributed to the destabilisation of the structures of the higher borides of the metals at the end of the 4*d* series, while the increase in the CVE leads to a progressive filling of the band of the antibonding s and d functions of the metal. This can be clearly traced by comparing the ZrB_2 (see above) and TcB_2 band structures.[152]

The energy structure of the hexagonal TcB_2 (space group $P4/mnc$, $a = 2.892$ Å and $c = 7.453$ Å)[153,154] has been calculated[152] in terms of the approximate Hoffmann scheme[155] and a basis set comprising Bloch functions including the B 2*s*, 2*p* and Tc 4*d*, 5*s*, 5*p* orbitals. The number of unit cells for which account was taken of the interaction with the 'central' cell was 2024.

In the analysis of this dispersion of the TcB_2 bands along certain symmetrical directions of the Brillouin band, the compact group of bands, made up of Tc 4*d* states, in the range −5 to 10 eV is striking. According to Armstrong,[152] this determines the conducting properties of the phase. At the same time the $k_{x,y}$ components of the wave vectors form fairly broad (in terms of energy) $\Gamma-M$, $\Gamma-K$, $A-H$, and $A-L$ bands.

The Fermi level has an energy of about −7.5 eV and is located in the region of *d* resonance. The most distinct pre-Fermi valence band maxima with energies of −8.0, −8.6, and −10.3 eV are also generated by the *d* functions of the metal. Charge transfer takes place in the Tc → B direction and reaches 0.87 e per boron atom, the electronic configuration of boron assuming the form $s^{1.30}p_\sigma^{1.61}p_\pi^{0.96}$.

The nature of the Tc–B bonds may be inferred from the composition of the occupied levels, the decomposition of which into orbital contributions has been examined for the point k with the coordinates 1/3, 3/9, and 1/4 (Table 5). Thus, whereas the four lowest levels mainly include the boron functions and

Table 5. The Mulliken populations (in %) of the occupied TcB levels.[152]

Level	E/eV	B s	B p_σ	B p_π	Tc s	Tc p	Tc d_σ	Tc d_π
1	−18.68	54	39	3	1	0	1	2
2	−18.58	57	34	0	4	0	2	2
3	−14.20	26	62	0	2	0	8	2
4	−13.84	21	62	2	1	0	2	12
5	−12.16	18	7	40	8	0	23	4
6	−11.70	5	60	3	0	0	14	19
7	−11.50	2	65	10	3	0	17	14
8	−10.65	0	15	40	1	0	43	2
9	−10.32	1	10	35	2	0	8	44
10	−9.85	0	8	26	0	0	10	56
11	−8.63	0	5	4	0	1	38	51
12	−8.30	1	3	6	2	5	80	2
13	−7.61	0	14	2	2	1	49	32

the three highest the technetium functions, the middle (5–10) are of a mixed type and indicate the hybridisation of the corresponding states.

Finally a qualitative conclusion about the energy of the Tc–B bonds can be reached by comparing the total energies of the boride and of the initial components.[152] Judging from the data presented, the stabilising role in the formation of technetium diborides can be attributed precisely to the bonds noted above.

4. 5*d* Metal borides

The available information about the electronic structure of binary 5*d* metal borides is extremely limited. A LMTO calculation for the hypothetical cubic HfB (NaCl structural type) has been carried out;[119] the charges on the MT spheres were analysed for a qualitative description of the nature of the interatomic bonds.

The bands of the hexagonal ReB_2 (a = 2.900 Å, c = 7.478 Å) have been calculated[152] by Hoffman's method.[155] The $E(k)$ relation is on the whole a repetition of that for the isostructural and isoelectronic TcB_2. Fundamental differences are not observed also for the TDOS. One may note only a closer disposition in terms of energy of the principal Re 5*d*-like maxima (−9.0, −9.8, and −10.3 eV), a smaller charge transfer from Re to B (0.44 e), and some differences between the atomic configurations of boron (B $s^{1.26}p_\sigma^{1.38}p_\pi^{0.79}$).

For the analysis of the role of individual components (B and Re) in the formation of the overall band structure, calculations were performed for the hypothetical 'Re' and 'B_2' crystals with the ReB_2 structure.[152] A system of bands, concentrated in a narrow energy range, was obtained for 'Re'. On the other hand, the dispersion of the bands of 'Re' and 'B_2' with the energy structure of the real boride indicates a greater dispersion of the states of the latter, which is associated with the 'inclusion' of the direct Re–B interaction.

The analysis of the composition of the occupied Re_2B levels, carried out[152] by analogy with that described previously, and calculation of the total energy of the boride make it possible to postulate that the Re–B interactions are important in the stabilisation of the ReB_2 lattice.

The data on the electronic structure of osmium and iridium borides are limited at the present time to those of the study of Novikov et al.,[156] in which the Os_3B_{14} fragment was used within the framework of the nonself-consistent X_α-DV method in the calculation for the $OsB_{1.2}$ phase (hexagonal system, WC structural type). A calculation was performed for a cluster of a similar composition in the case of the hypothetical hexagonal iridium boride. It was established that, in contrast to the isostructural molybdenum and tungsten borides in which the M–C bond predominates, the (Os, Ir)–B interaction is antibonding and the interatomic interactions are based on the B–B bonds, the populations of which are smaller for 'IrB' (~9.04) than for 'OsB' (~11.63). The stability of the structures of the borides has been attributed[156] to this fact: in contrast to osmium boride, iridium boride with the WC structure has been obtained only in the form of the high-temperature modification.[9]

IV. Metal–nonmetal–boron ternary systems

Together with binary systems, ternary and more complex compounds and solid solutions constitute an extensive group of boron-containing phases. The crystallographic and certain physicochemical properties of these systems have been investigated in fair detail.[1,2,5–11] However, the general microscopic models of the conditions governing their formation, stability, the nature of chemical bonding, and properties, based on the results of quantum-chemical calculations, are lacking at the present time. The principal results of the studies of the electronic properties of ternary borides will be examined below within the framework of theoretical and experimental approaches.

1. The M–B–C systems

Studies on the interactions of metal borides with carbon demonstrated that continuous solid solutions (SS) are as a rule not formed in the M–B–C systems (where M is a metal).[157–166] The reasons for this are the significant differences between the atomic radii of boron and carbon and also between their energy characteristics.[157,158] Thus the products of the reactions of Group IV and V metals with boron and carbon are as a rule mixtures of boride, carbide, and borocarbide phases. Their structures, compositions, and proportions are determined by many factors (the annealing temperature, the duration of annealing, the pressing conditions, etc.).[162–166]

In the search for materials to be used in the manufacture of instruments and in construction, a study has been made of the Ti–C–B system.[157–166] An appreciable solubility of the diboride in TiC, an increased microhardness of the TiC_x-based phase, and some increase in the lattice parameter of the carbide have been noted for the TiB_2–TiC_x section.[157,158]

The conclusion reached initially[158] that the TiB and TiC_x components are infinitely miscible was not confirmed subsequently in the study of the section of the Ti–C–B phase diagram bounded by the TiB and TiC_x straight lines (x = 0.48–1.00). Three phases were identified in the specimens obtained: TiB_2, TiC_xB_4, and TiB (FeB structural type).

The phase formation process in the TiB–$TiC_{0.93}$ pseudobinary systems in the temperature range 1670–2070 K can be divided into two components according to X-ray diffractometric and scanning electron microscope data. Such subdivision is due to the different nature of the TiC_x interactions with the cubic and orthorhombic modifications of the monoboride.[165,166] The dominant involvement of the orthorhombic TiB in reactions leading to the formation of the higher borides Ti_3B_4 and TiB_2 has been postulated.

The quantum-chemical description of the heterophase systems is an extremely complex problem, which has not so far been solved. Only a few attempts[167–169] at calculations of the energy states of one of the components of the given polycrystalline materials—a borocarbide phase (a solid solution of the MC_xB_{1-x} type)—are known to have been made.

The local perturbation of the electron density of the hypothetical TiB following the introduction of a single carbon atom into the boron sublattice has been examined.[167] This simulated the initial stage in the formation of the $TiB_{1-x}C_x$ solid solution. The calculations were performed by the LMTO–GF method. The results indicate that the valence *s* and *p* functions of the carbon admixture are located in the region of the B 2*s* and Ti *d*,*s*–B 2*p* bands of the boride and the occurrence of the hybrid C–Ti–B interaction in the alloy cannot therefore be ruled out. Estimation of the perturbation of the LDOS of the titanium atoms (by the method described by Anisimov et al.[105]) shows, however, that the most marked effect, occurring when a boron atom is replaced by carbon, is the appearance of localised σ(Ti–C) bonds in the CTi_6 octahedron, as happens in refractory monocarbides.[103]

The converse problem, involving a single boron impurity atom at a C site of $TiC_{1.0}$, has been solved.[168] It is noted that the impurity states form two subbands. The lower subband has a markedly pseudoatomic form and corresponds to the localisation of the B 2*s* functions in the energy range between the C 2*s* and C 2*p*–Ti 3*d* bands. On the other hand, the B 2*p* states form a broad subband which overlaps almost fully the *p*–*d* hybrid band to TiC, indicating the formation of bonds of the Ti–B type in the TiC–B system.

A similar problem for the VC–B system has been solved by the LMTO-GF method.[169] Taking into account the uncertainty in the data concerning the processes involving the formation of the intergrain boundaries in the V–C–B system, the calculation was made for the case where boron substitutes both carbon and metal centres in $VC_{1.0}$. Whereas for the first type of substitution the LDOS of the impurity is similar to that for TiC–B, in the replacement of V by B (the formation of type

BC_6 'microclusters') the valence states of boron shift significantly into the region of lower bond energies, being partly superimposed on the C 2*s* states. Estimates of the change in the overall single-electron energy of the system show that ΔE in the latter is positive (~0.09 Ryd). This can be evidently attributed to the incomplete energy compensation for the 'rupture' of the strong V–C bonds due to the formation of new, weaker B–C bonds. Consequently, according to Sabiryanov,[169] in the solid-phase interaction of VC_x and boron (borides) the formation of borocarbides is less likely than that of vanadium borides.

A cluster analysis of the nature of the bonding in the Ti–C–B system has been carried out,[168] adopting titanium monocarbide as a basis. Its carbon sublattice was doped with boron atoms (the TiC_6Ti_{12}, TiC_5BTi_{12}, $TiC_4B_2Ti_{12}$, and $TiC_3B_3Ti_{12}$ fragments). The calculations were peformed in terms of the extended Hückel method (EHM). It was established that, when a carbon atom is replaced by a boron atom, the system of Ti–X (X = C, B) paired bonds is significantly transformed. Thus, if it is assumed that σ_{2p}(Ti–C) and π_{2p}(Ti–C) participate in the Ti–C interaction, then the Ti–B interaction includes the σ_{2s}(Ti–B), σ_{2p}(Ti–B), and π_{2p}(Ti–B) bonds, the populations of which (estimated in accordance with Mulliken's scheme) are comparable. In addition, the occurrence of a significant B–B interaction was established.

Hence, when account is taken of the known criteria of the formation of homogeneous solid solutions,[169–179] one may conclude that the absence of a continuous series of borocarbide solid solutions is associated with the specific features of the chemical bonds formed in the M–B–C systems apart from the dimensional factors.

Together with the variable-composition M–C–B solid solutions, fairly numerous crystalline *p* and *d* metal borocarbides have now been synthesised and their structures and some of their properties have been determined.[9,11] However, there have been no systematic studies of their microscopic properties and the available literature data refer solely to individual representatives of these compounds.

Table 6. The electron populations of bonds (e) in yttrium borocarbides.

Bond	YC_2	YBC	YB_2C_2	YB_2C	YB_4
Y–Y	0.351	0.165	0.235	0.302	0.121
Y–C	0.254	0.582	0.011	0.053	—
Y–B	—	0.196	0.372	0.400	0.827
C–C	1.785	0.012	1.236	0.012	—
C–B	—	1.339	0.976	1.321	—
B–B	—	1.457	1.245	2.132	2.736

A series of yttrium borocarbide phases, formed in the Y–B–C system and including the compounds YBC, YB_2C_2, and YB_2C, have been investigated[169] within the framework of the extended Hückel method. It was noted that there is a significant superposition of the (B, C) *s,p* and Y *s,p,d* states, the form of the LDOS of the individual centres depending critically on the type of their coordination in the crystal. This situation leads to the appearance of a complex system of interatomic bonds differing greatly in their nature and populations. The results presented in Table 6 show that, whereas the C–C interactions between pairs of nearest carbon atoms predominate in YC_2, in YBC there is competition between the B–B and C–B bonds, the role of the B–B bonds increasing with increase in the B/C ratio, which results in the formation of ordered structural motifs made up of the given atoms. It has been noted[169] that the B–B and B–C bonds arise as a consequence of the hybridisation of the B 2*s*,2*p*–C 2*p* orbitals, while the involvement of the metal atoms is secondary.

The Sc_2BC_2 alloy is yet another representative of borocarbides the electronic structure of which has been calculated within the framework of the extended Hückel and tight binding methods.[170] This phase (space group *I4/mmm*, lattice parameters $a = 3.300$ Å and $c = 10.691$ Å)[171] differs from most of the known lanthanide borocarbides, which have a layered structure,[172] by the fact that it contains in the bulk phase BC_2 groups similar to those present in the boron carbide $B_{13}C_2$.[173]

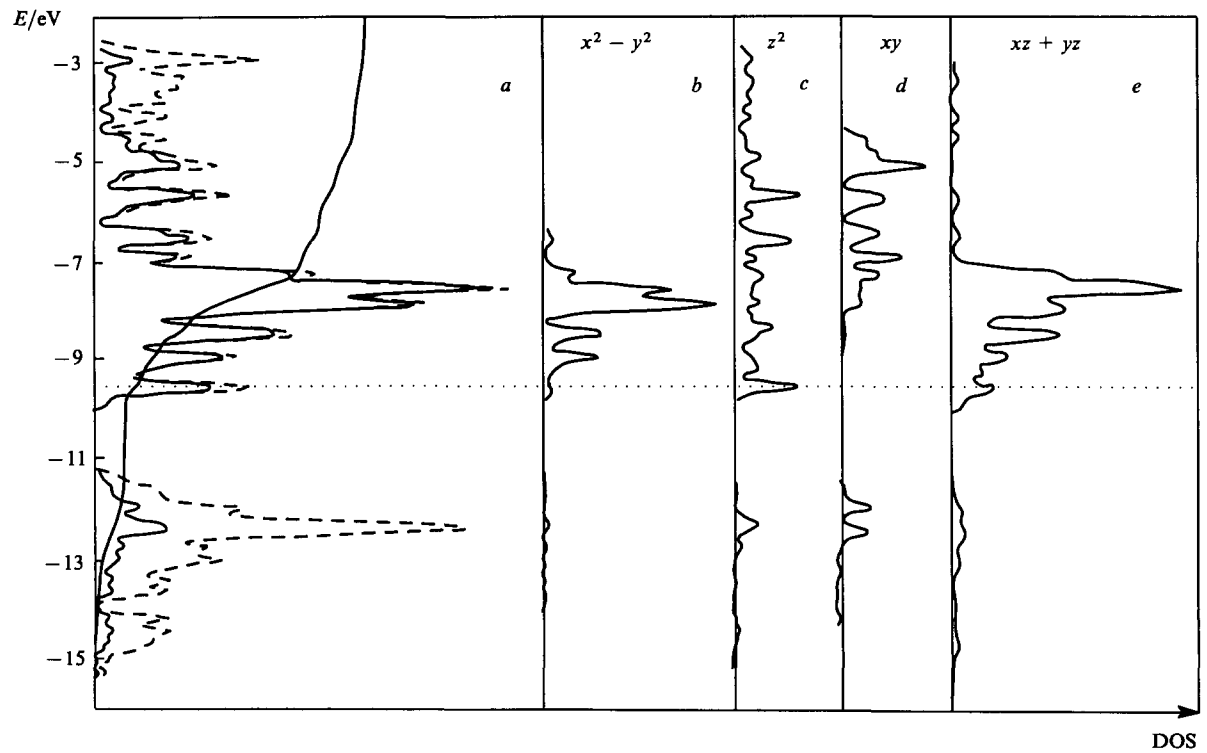


Figure 18. Densities of states in Sc_2BC_2:[170] (*a*) the total density of states of scandium (dashed curve) and the density of Sc 3*d* states (continuous curve); (*b*)–(*e*) partial contributions of the scandium *d* states.

EHM calculations for the BC_2 'molecule' indicate an appreciable separation of the nonbonding π_u- and antibonding π_u^* levels. The molecular charge has been estimated as approximately -5 e, i.e. this borocarbide can be regarded as a crystal containing the BC_2^{5-} anions. Allowance for the contribution by the atomic orbitals of the metal leads to a somewhat smaller overall charge (-2.48 e). The splitting of the electronic levels of the metal atom in the ligand field has been considered in relation to calculations for the $[ScB_5C_{10}]^{22-}$, $[Sc_2B_6C_{12}]^{25-}$, and $[Sc_2B_8C_{16}]^{35-}$ fragments with different configurations of the BC_2 groups.

The energy spectrum of Sc_2BC_2, obtained with the aid of the tight binding method, is presented in Fig. 18 (see previous page). Evidently, the low-energy bands are made up largely of the (B, C) 2*p* functions with an admixture of the Sc 3*d* orbitals and are separated from the nonbonding partly occupied bands by an energy gap. The Fermi level ($E_F \approx -9.5$ eV) is located in the region of the peak corresponding to the Sc 3*d* states, which is the reason for the metallic type of conductivity of the borocarbide.[171]

The energy dispersion of the bands in the pre-Fermi region suggests the anisotropy of the conductivity of Sc_2BC_2 when the Fermi level is intersected by the bands along the $\Sigma(M \rightarrow \Gamma)$ and $\Delta(\Gamma \rightarrow X)$ lines, which corresponds to the [010], [100], and [110] directions in the crystal. These bands are made up to the extent of 80%–100% of the Sc $d_{xz,yz,zz}$ states. Thus conduction is predominantly effected by Sc atoms separated by 3.144 Å distances in the (110) plane.

2. The M–B–N systems

As for the borocarbides, the available information about the phase relations in the M–B–N systems has remained extremely scattered and refers mainly to systems with participation of Group IVA and VA 3*d* and 4*d* metals. The efforts of investigators have been concentrated mainly on two aspects: on the creation of boronitride compositions of the TiB_2–TiN, ZrB_2–ZrN, and similar types[180–182] in order to improve the parameters of the initial phases and on the study of the formation of the boundary of the region of homogeneity in variable-composition boronitride phases.[183–187]

From the standpoint of the electronic theory, the description of the boronitride systems repeats that of borocarbide phases examined above and the difficulties arising are caused by the lack of correct methods permitting theoretical calculations for heterophase systems. The calculations of the energy states in the M–N–B systems carried out hitherto either involve the consideration of the problem of the single boron impurity in the nitride[167,168] or they resort to fragmentary approaches for the description of the transformation of the electronic states at the grain boundaries in composite boronitrides.[187,188]

In the first group of calculations, performed by LMTO-GF method for the TiN : B, ZrN : B, VN : B, and NbN : B impurity (as regards boron) systems, the form of the LDOS in boron was considered as a function of the EES of the matrix.[167,168] As in the case of the boron impurity in the carbides, the LDOS in the boron impurity in the nitrides has a two-peak structure comprising the B 2*s* and B 2*p* states, the degree of localisation of which (taking into account their position relative to the TiC and TiN valence bands) is found to be significantly more marked.

The rearrangement of the charge states and the system of orbital functions arising when a boron atom is incorporated in the cubic titanium nitride have been considered within the framework of the Mulliken–Wolfsberg–Helmholtz (MWH)[186,187] and X_α-DV[168] methods.

We may note that, according to the data of Zainulin et al.[185] the region of the existence of the homogeneous boronitride TiN_zB_y is extremely narrow: $z+y = 0.62-0.94$, $y \leqslant 0.03$. It follows from other data[186,187] that the electron energy spectrum of TiN_zB_y is markedly different from that of TiN. The lower group of orbitals, corresponding to the band of the quasi-core N 2*s* states, becomes narrower. The form of the rearrangement of the principal valence-bonding band is especially interesting. Whereas in TiN this band is made up predominantly of the N 2*p* states, which are significantly hybridised with metallic e_g-like orbitals, in TiN_zB_y an appreciable admixture of the B 2*s* states and a small admixture of B 2*p* states appears in TiN_zB_y in the region of the same energies. In the region of energies close to the edge of the filled part of the spectrum, there is an appreciable admixture of the 2*p* states of boron together with the Ti 3*d* type-t_{2g} atomic orbital.

Consequently, together with the Ti *d*–N 2*p* interaction, the Ti *d*–B 2*s* and Ti *d*–B 2*p* interactions play a significant role in TiN_zB_y. This becomes evident from an analysis of the bond populations and electronic configurations of the fragments for which calculations have been made.[186,187] The charge on the metal atom diminishes when boron atoms are introduced into its closest sphere. This finding is correlated with the results of a study[188] where the chemical shifts of the internal levels of the component atoms of a series of homogeneous TiN_xB_{1-x} solid solutions were investigated by electron microscopy.

Calculations have been made for simple octahedral clusters[186] in the Ti–N–B system for an increasing B/N ratio (the TiN_4B_2–TiN_2B_4 fragments). These groups can arise at the intergrain boundaries in polycrystalline boronitrides. It has been noted[186] that a steady increase in the number of states of the B *s,p* type entails a sharp alteration in the mechanism of interatomic bonding where Ti–B bonds of π_{2p} and σ_{2s} types predominate. Conversely, the Ti–N paired bonds are negligibly weak, which may affect the mutual diffusional mobility of the nitrogen and boron atoms and thus determine the processes involving the mutual dissolution of the boride and nitride phases.

3. The M–B–O system

A series of studies[167–169,187] have been devoted to the possibility of the partial substitution of oxygen atoms by boron atoms (in the TiO, VO, and ZrO structures) and to the formation of ternary solid solutions of the type MB_xO_{1-x}. Calculations for the VO : B system by the LCAO method have indicated, in particular, the appearance of a sharp anisotropy of the V–O and V–B bonds and also of significant B–B interactions, which may lead to the 'clustering' of the boron impurities in the bulk of the oxide.

Calculations by the LMTO method have been used[189] to predict the compositions of the possible stable cubic phases in the Ti–O–B system. The estimated energy of the substitution of B atoms by O atoms as well as the dependence of the total pressure and of the bonding and antibonding pressures on the number of valence electrons (in the range 6.5–9 e) indicate the probable existence of the stable phase $TiB_{0.75}O_{0.25}$.

A series of phases of the M–B–O systems with individual structural types have been examined.[190,191] The electronic spectrum of $Li_2B_4O_7$—a promising material for acousto-electronics—has been calculated.[190] Taking into account the characteristic features of the crystal structure of $Li_2B_4O_7$[192] and on the basis of phonon spectra,[193] a series of structural fragments (BO_3, BO_4, LiO_4, LiO_6) were identified in the crystal and for each of them a secular equation was set up. The effect of environment was taken into account within the framework of the perturbation theory. The interband intervals were corrected on the basis of the maxima in the imaginary component of the relative permittivity.

The band structure of $Li_2B_4O_7$ thus obtained represents in essence a superposition of the electronic states of the structure-forming elements of the phase, included in the consideration and arranged in an energy sequence.[190] It was noted that the covalent bonds in the boron–oxygen groups are the most significant (degree of covalence ~ 0.94, Harrison's data[194]), but the maximum mount of ionic character (~ 0.17) was found in the LiO_{4-6} fragment.

Problems concerning the chemical bonding in $LiBO_2$, which is formed in the Li–B–O system, have been examined[191] with the aid of the X-ray diffraction method and dynamic deformation electron density (DED) maps.[195–197] The crystal structure of

$LiBO_2$ can be represented as an assembly of BO_3 'triangles' making up the chain and oriented in the $(\bar{1}05)$ plane, the lithium atoms being located in their vicinity.[198] There are different B–O distances in the BO_3 groups, varying in the range from 1.324 to 1.409 Å. The differences in the distance from the lithium atom to the oxygen atoms constituting its closest sphere (1.955–2.473 Å) are extremely significant.

The published[191] DED maps indicate the formation of B–O covalent bonds in the BO_3 groups. The estimated amount of ionic character of the bonding indicates the B → O charge transfer. The charges are (assuming +1 for Li) 2.6+ for B, 1.8– for O^1, and 1.9– for O^2. The DED maps for planes incorporating lithium demonstrate only a slight overlap of the cationic and oxygen states. The interaction of lithium with its environment in the metaboride is therefore largely electrostatic.

4. The M–B–P systems

The preparation of the crystalline borophosphide $Fe_3(P_xB_{1-x})$ has been reported.[199] The initial interpretation of its properties was based on a simplified model postulating charge transfer from nonmetal atoms to the iron atom.[200,201]

The ternary $Fe_3B_{0.9}P_{0.1}$ alloy (Fe_3B structural type) has been investigated[202] by photoelectron X-ray spectroscopy (AlK_α radiation, ~0.2 eV resolution) with the aid of the method described by Wertheim and coworkers.[203,204] The binding energies for the Fe 3*s*,3*p*, P 2*p*, and B 1*s* core levels were determined and were found to be similar to those for the pure elements (within the limits of experimental error), which precludes the hypothesis of an ionic model for the given alloy. The X-ray photoelectron spectra of Fe, Fe_3P, and $Fe_3B_{0.9}P_{0.1}$ demonstrate a fairly complex profile of the spectral lines.[202] Taking into account the degrees of photoionisation of states of different symmetry, one may claim that the most intense pre-Fermi maxima correspond to emission from the band of *d* states. The lower energy maxima correspond to states similar to B *s*,*p*. The widths of the valence bands, which are ~17 eV for Fe_3P and ~14 eV for $Fe_3B_{0.9}P_{0.1}$, differ appreciably.

On the basis of calculations,[201] the high-energy maxima were assigned to the *s* states of iron and nonmetals, while the lower-energy peaks reflect the splitting of the *d* functions of the iron atoms in structurally nonequivalent positions and their mixing with the *p*-type subbands of phosphorus and boron. Finally, the greater width of the spectrum at the half maximum level in the case of $Fe_3B_{0.9}P_{0.1}$ (5.1 eV) compared with Fe_3P (4.5 eV) is treated as a consequence of the shorter Fe–B distances and greater hybridisation of their valence orbitals. Hence it follows that the observed change in the magnetic moments and parameters of the hyperfine fields on formation of the ternary iron alloys is associated with the reordering of the orbitals of the iron atoms as a result of interactions with the atoms in the immediate environment and not with electron transfer effects.[198]

V. Metal–metal–boron ternary systems

All the ternary compounds formed in metal–metal–boron systems can be arbitrarily divided into two groups.[11] The first comprises ternary boride phases having individual crystal structures, while the second consists of solid solutions with limited or infinite miscibility on formation of which the substitution of part of the metal atoms of the binary phase by metal atoms of a different kind takes place statistically.

Most of the studies on the electron energy spectra of ternary ordered phases by quantum-chemical methods have been devoted to compounds containing *f* elements. Their consideration is outside the scope of the present review. We shall only mention studies[205–207] in which band calculations were performed for the borides $Y_2Fe_{14}B$ and $Y_2Co_{14}B$. By virtue of their magnetic characteristics, the latter have attracted attention as promising materials for the construction of permanent magnets.[208,209]

Calculations by the LCAO method[205] and in terms of the tight binding model,[206,207] carried out for the above borides, lead to similar electron energy spectra of these compounds: the valence band is made up predominantly of a complex superposition of Fe(Co) states which are significantly different for structurally

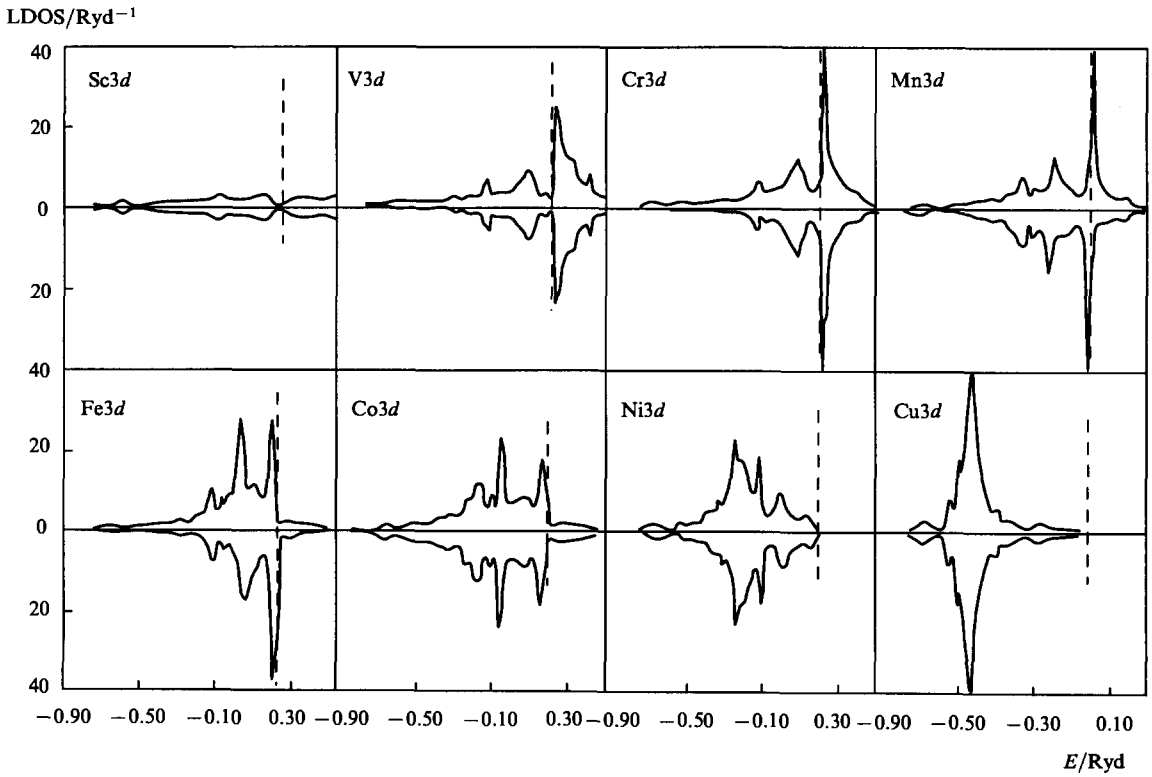


Figure 19. The local densities of states of 3*d* impurities in TiB_2. Spin-polarised calculation by the LMTO-GF method.

nonequivalent centres (six positions) with an admixture of yttrium and boron states. Most attention has been devoted in the above investigations[205-207] to calculations of the magnetic parameters of the phases. It was established that, depending on the type of the immediate environment, the local magnetic moments (LMM) on the iron atoms in $Y_2Fe_{14}B$ can vary appreciably (from 2.11 to 2.74 μ_B); the local magnetism for $Y_2Co_{14}B$ is appreciably weaker — the LMM on the cobalt atoms vary in the range 1.28 to 1.48 μ_B.

The energy states of the 3*d* metal impurities in TiB_2 (these systems can be treated as the starting materials in the formation of $M_xTi_yB_2$ solid solutions) have been investigated[210] by the LMTO-GF method. The local densities of states of the impurity elements make it possible to trace the rules governing their formation throughout the series of 3*d* metals (Fig. 19).

Evidently, the similarity of the orbital energies of the dopand metal atoms at the beginning of the *d* series (Sc, V) to the energies of the states of the titanium atom promotes the establishment of a LDOS similar to that for titanium. The LDOS for the *d* metals at the end of the series assume a significantly different form. With increase in the valence of the impurity (on passing from Cr to Cu), there is a progressive low-energy shift of the occupied states of the dopand atoms with generation of additional (nonbonding) DOS lines in the region of a local minimum in the spectrum of the matrix (between the *s*- and *p*-like bands) and also in the vicinity of the lower edge of the valence band of the diboride. This effect can be traced most distinctly for the LDOS in copper.

The increase in the concentration of the impurity states in the region of the principal bonding bands of TiB_2 indicates an increase in the covalent component of the bonding in the ternary systems. The estimated changes in the total one-electron energy of the matrix following the introduction of the dopands (ΔE) are presented in Fig. 20. Although in terms of the single-site approximation these quantities can reflect only the qualitative behaviour in the series of such systems, we may note that the substitution of Ti atoms by Sc and V atoms leads (as for the *d* metals at the end of the series) to the destabilisation of the system of interatomic bonds in the crystal. Conversely, it follows from the data obtained that doping of the diborides with admixtures of Cr, Mn, Fe, and Co tends to decrease the one-electron energy. This can indicate stronger binding of the additives in the bulk of TiB_2 compared with the centre being substituted.

The transformation of the high-energy *d* band of the impurity (which is unoccupied for Sc and V) is of interest. With increase in the atomic number of the impurity element, the energy of the *d* band falls sharply and, for example, in the case of chromium, is located in the immediate vicinity of E_F, being subsequently partly (Mn, Fe) or completely (Co, Cu) filled. Such behaviour of the LDOS leads to the appearance of spin polarisation with splitting of the bands corresponding to the opposite spin orientation and hence the formation of appreciable LMM on centres comprising *d* metals in the middle of the series (Fig. 20). This finding can be accounted for on the basis of Stoner's criteria, according to which one of the conditions for the formation of the LMM in the crystal is a high DOS in the vicinity of E_F, which is in fact observed for chromium, manganese, and iron. For cobalt, nickel, and copper, these states are fully occupied and there are therefore no magnetic moments on the given atoms.

In conclusion, we may note that the results agree with those obtained for the series of 3*d* and 4*d* metal carbides and nitrides. This suggests that the characteristics of the band structure of the matrix, in the first place the presence of a deep DOS minimum in the vicinity of the Fermi level, are decisive in the generation of local magnetic moments on *d* impurities in binary phases. One may expect that a similar situation occurs also in the ZrB_2: M and HfB_2: M systems (M = 3*d* metal), while the 4*d* impurities in diborides are nonmagnetic in the vast majority of cases.

VI. Amorphous metal borides

We shall consider yet another class of boron-containing systems — amorphous metal borides [metallic glasses (MG)], which exhibit interesting mechanical properties, a high corrosion resistance, and a series of unusual magnetic characteristics.[210,211]

There are several phenomenological theories which explain the stability of the amorphous state of the glasses near the composition $M_{80}X_{20}$. In the model proposed by Nagel and Tauc,[212] the metallic glasses are described as systems with almost free electrons. Their stability is explained by the position of the Fermi level in a deep DOS minimum, which is attained by introducing nonmetal atoms into the alloy. The role of such atoms reduces to the regulation of the electron concentration in the system. In the statistical theory taking into account the degree of packing of 'hard spheres' (metal atoms), the involvement of *p* elements is accounted for by the need to fill the cavities in the polyhedra of the 'matrix'. This is manifested most effectively for the ratio $M/X \approx 4$.[213] The possible role of chemical metal–nonmetal bonding in the transition of the system to the amorphous state has been pointed out by Shen and Park.[214]

The role of chemical bonding has been analysed within the framework of fragment models.[215,216] A calculation has been carried out[215] for the $[Ni_2Fe_2B]$ group in the $Ni_{40}Fe_{40}B_{20}$ structure by the spin-polarised multiple scattering method (Fig. 21). The structure is represented with the aid of Bernal polyhedra, the

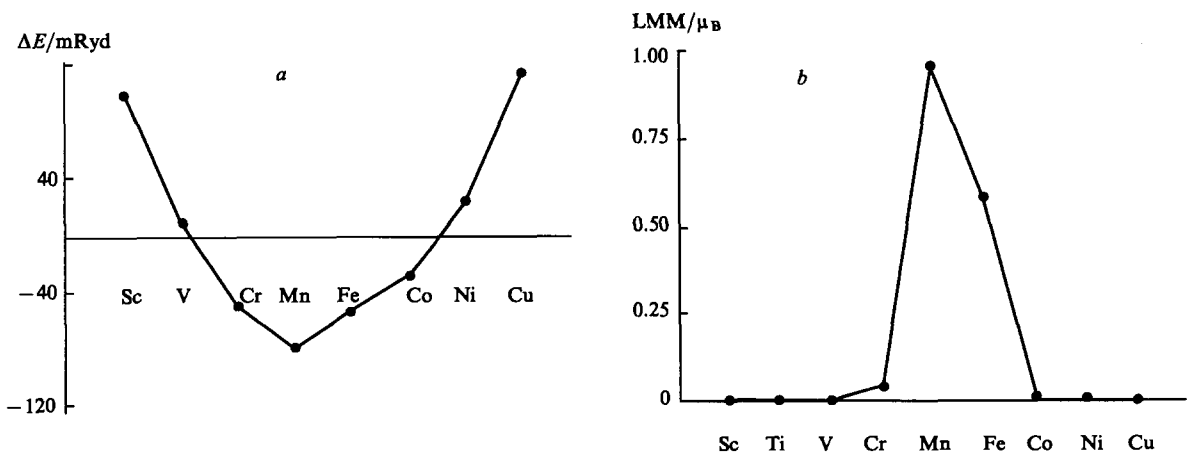


Figure 20. The changes in the total one-electron energy of TiB_2 on introduction of *d* metal impurities (*a*) and in the local magnetic moment on the 3*d* centres in TiB_2 (*b*).

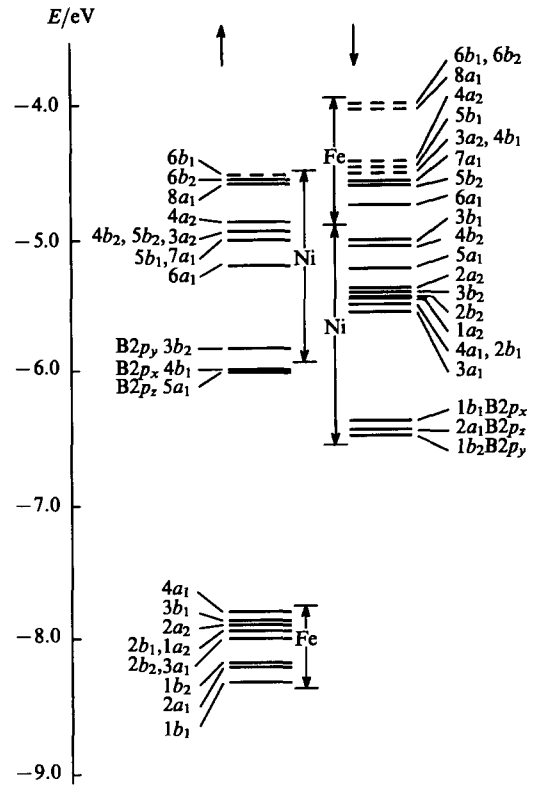


Figure 21. Molecular orbital diagram for the Ni_2Fe_2B cluster. Spin-polarised calculation by the scattered wave method.

smallest cluster (a tetrahedron) simulating the alloy being employed. A significant hybridisation of the boron *p* states with a series of low-energy molecular orbitals containing an appreciable contribution due to Ni *d* orbitals has been established. The boron–iron states exhibit a much smaller overlap. The local nature of these bonds and their anisotropy have been emphasised.[215] In this case, the charge density is concentrated mainly in the BNi_2 plane, which indicates the preferential bonding of boron to one of the metals, namely nickel. This results in the formation of microclusters of the type BNi_x in the metallic glass region.[217]

A similar approach has been used in calculations for the $[Co_8B_2]$, $[Co_4Fe_4B_4]$, $[Co_8B_4]$, and $[Fe_8B_4]$ clusters taking into account the possible formation of direct B–B bonds.[216] The greater stability of the $[Co_8B_2]$ system, compared with $[Co_8]$, has been interpreted[217] as a consequence of the decrease in the energy of a series of molecular orbitals (by ~1 eV) genetically related to the Co 3*d* states. This is due to their mixing with the B 2*p* functions accompanied by a weakening of the Co–Co bonds. The introduction of the iron impurity into the alloy hardly affects the energy states of cobalt, i.e. the decisive role of the Co–B bonds is retained, which leads to the appearance of local Co_nB ordering in the bulk of the metallic glass. It has been concluded[217] that cluster type boride metallic glasses (Co_3B, Fe_3B) are more stable than the corresponding crystal structures.

An attempt has been made to apply to the description of the amorphous $Fe_{80}B_{20}$ alloy the spin polarised LMTO method developed for calculations relating to invariant crystals.[218] A structure of the Fe_4N type, in which the coordination numbers of the Fe and N atoms are closest to those in the amorphous alloy, was selected as a model.[219–221] It was established that the conductivity band of the 'Fe_4B' metallic glass is determined by the states of the iron atom while the Fe 3*d*–B 2*p* hybridised states are concentrated near the bottom of the conductivity band (Fig. 22).

A fairly extensive series of studies have been carried out in recent years on the modification of the band approaches to calculations on amorphous systems.[222–231] Thus the problem of the relation between atomic structure and electron distributions in the $Fe_{100-x}B_x$ amorphous alloys has been considered.[222] The structure of the metallic glass was described in terms of an assembly of particles (several hundreds) interacting in accordance with the Morse function. The densities of states were calculated by the recursion method for a tight binding Hamiltonian with Harrison's parametrisation. A satisfactory agreement was obtained between the calculated data and experimental atomic radial distribution functions. The agreement between theoretical electronic and photoemission data is satisfactory.

The magnetic properties of $Fe_{100-x}B_x$ valence bonds amorphous alloys have been calculated.[230] Using the spin-polarised LMTO tight binding method and the recursion technique, the hyperfine fields on the iron nuclei as well as the isomeric shifts were calculated. The results agree quite well with Mössbauer spectroscopic data. A correlation was established between the directions of the shifts and the local environment of the ^{57}Fe nuclei (the number of boron atoms in the first coordination sphere of iron).

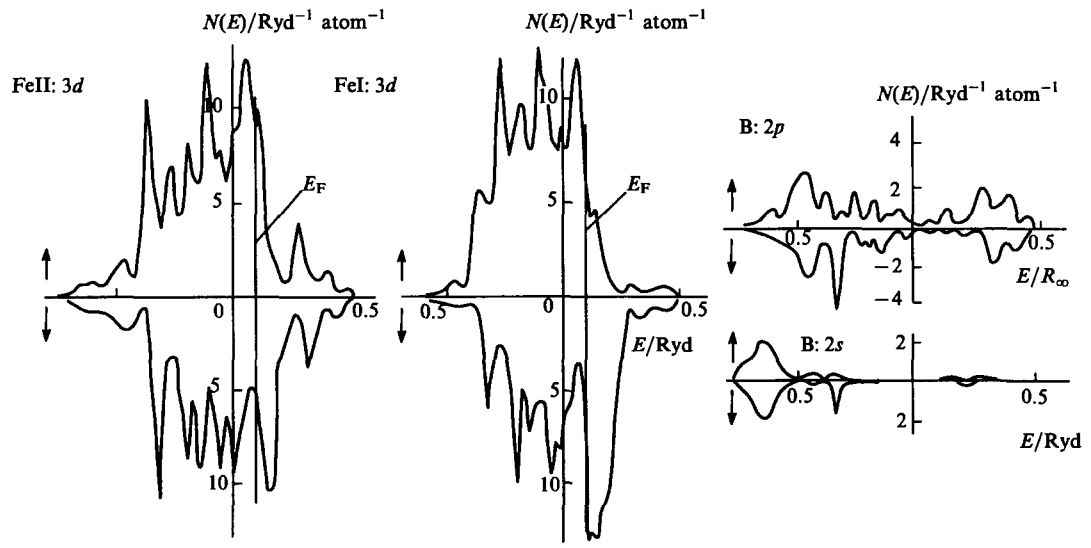


Figure 22. Partial densities of states in Fe_4B. The designations FeII and FeI correspond to iron atoms in the first and second coordination spheres of boron.

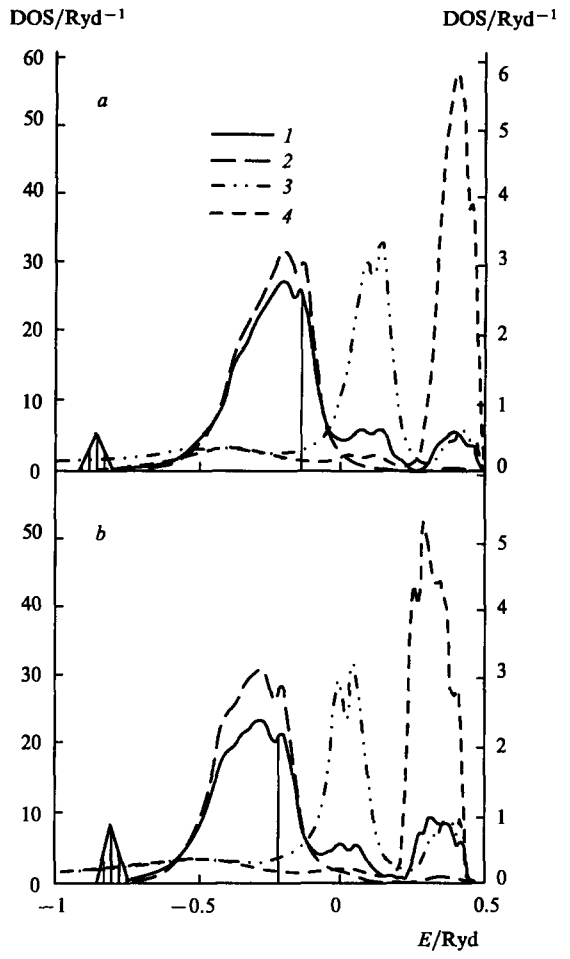


Figure 23. The total density of states (curve *1*) and the partial densities of Fe 3*d* (curve *2*), Fe 4s (curve *3*), and B 2*p* (curve *4*) states in the $Fe_{85}B_{15}$ (*a*) and $Fe_{75}B_{25}$ (*b*) amorphous alloys. The cross-hatched triangles indicate the position and 'centre of gravity' of the B 2*s* bands.

The structures of the $Fe_{85}B_{15}$ and $Fe_{75}B_{25}$ valence bands (Fig. 23) have been calculated by the LMTO method in terms of the atomic spheres approximation (LMTO ASA) and the recur-sion method.[228] The valence band of the alloy is made up of hybridised Fe 3*d*–B 2*p* states, the contributions of which to the occupied part of the spectrum vary in accordance with the composition of the boride. With increase in the boron content, the local magnetic moment diminishes from 1.795 μ_B for $Fe_{85}B_{15}$ to 1.705 μ_B for $Fe_{75}B_{25}$. The relation between the electronic parameters and the atomic configurations of the metallic glass has also been discussed in other investigations.[224–226]

The LMTO ASA method combined with the recursion technique has been used in calculations for a metallic glass of the $Co_{100-x}B_x$ (x = 17, 23, and 32) type.[231] As in the case of $Fe_{100-x}B_x$, the valence band of cobalt boride is of the Co 3*d*–B 2*p* hybrid type and the bonds between unlike atoms are determined by the Co–B covalent interactions. The charge transfer from Co to B is insignificant (~0.68 e) and is stable for the concentrations considered. The local magnetic moment diminishes sharply as the alloy becomes enriched in boron (for example, from 1.32 μ_B for $Co_{83}B_{17}$ to 0.94 μ_B for $Co_{68}B_{32}$).

Whereas the range of metallic glasses for which theoretical calculations have been made is fairly limited, the class of such glasses whose electronic structure has been investigated experimentally is much more extensive:

Alloy	Ref.
$Fe_{80}B_{20}$	234, 243, 247
Fe_xB_{100-x} (x = 88, 87, 86, 80, 75)	239, 255
$Fe_{1-x}B_x$ ($x \leqslant 0.2$)	246
Fe_xB_{100-x} (x = 86, 82, 28, 24, 20)	248
$Co_{80}B_{20}$	232
$Fe_{82}B_{18}$; $Ni_{81.5}B_{18.5}$	253
$Co_{81.5}B_{18.5}$	248
$Co_{76}Fe_4B_{20}$; $Co_{70}Fe_{10}B_{20}$	233
$Co_{80-x}Fe_xB_{20}$ (x = 6, 10, 20)	232
$Co_{85-x}Fe_xB_{15}$ (x = 65, 73)	235
$Fe_{80}M_3B_{17}$ (M = Fe, Co, W, Pt)	235
$Fe_{40}Ni_{40}B_{20}$	234, 243
$Fe_{75}Si_{10}B_{15}$; $Ni_{75}Si_{10}B_{15}$	253
$Fe_{76}Si_{12}B_{12}$; $Fe_{76}Si_{18}B_{12}$	248
$FeSi_{10}B_{12}$; $Fe_{45}Ni_{45}P_{8.5}B_{1.5}$	244
$Fe_{40}Ni_{40}P_{14}B_6$; $Fe_{32}Ni_{36}Cr_{14}P_{12}B_6$	252
$Fe_{82}B_{18-x}Be_x$	254
$Ni_{40}Fe_{40}P_{14}B_6$	251
$Fe_{70}Ni_8Si_{10}B_{12}$	250
$Co_{78}P_{14}B_8$	249
$Fe_{40}Ni_{40}P_{16}B_6$	234, 242, 245
$Fe_{67}Co_{18}B_{14}Si_{12}$	236
$Fe_{40}Ni_{38}Mo_4B_{18}$; $Ni_{76}Si_{12}B_{12}$	237
$Fe_{32}Ni_{32}Cr_{14}P_{12}B_6$	238
$Ni_{36}Fe_{32}Cr_{14}P_{12}B_6$	240, 241

The main problem discussed in the above investigations involves the consideration of the energy structure of the amorphous alloys, the establishment of the differences between the electron energy spectra of the amorphous and crystalline states, and also the determination of relations of the composition–property type for a fairly representative set of systems.

The BK_α-XES presented as an example in Fig. 24 for a series of metallic classes and crystalline phases based on iron and nickel and their joint representation in terms of a single energy scale with K_β and L_α lines[253] illustrate the main results obtained within the framework of the approaches mentioned above. Thus the following points have been noted:[253] (1) the valence band of the metallic

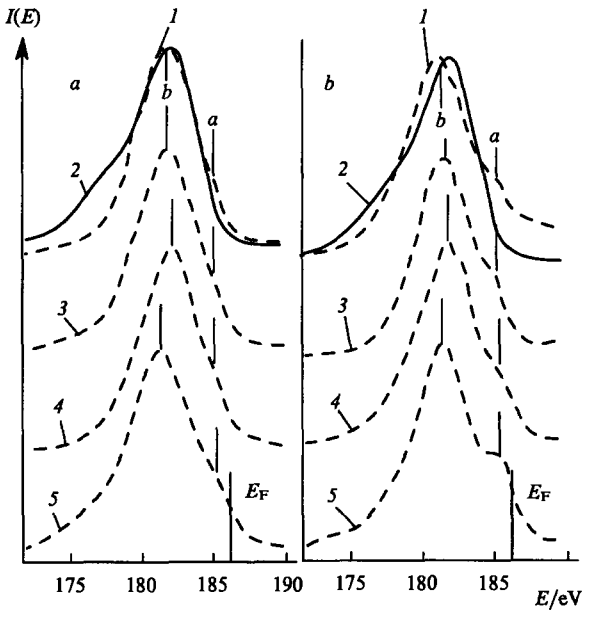


Figure 24. The BK_α X-ray emission spectra of amorphous iron and nickel borides and the spectrum of crystalline boron. (*a*): (*1*) α-$Fe_{82}B_{18}$; (*2*) B (crystalline); (*3*) α-$Fe_{75}Si_{10}B_{15}$; (*4*) Fe_2B; (*5*)FeB; (*b*): (*1*) α-$Ni_{81.5}B_{18.5}$; (*2*) B (crystalline); (*3*) α-$Ni_{75}Si_{10}B_{15}$; (*4*) Ni_2B; (*5*) NiB.

glass is made up of overlapping subbands of the B $2p$–(Fe, Ni) $3d$ states; (2) the maximum in the BK_α spectrum (peak *b*) is located near the bottom of the valence band and the substructure *a* [the intensity of which diminishes with increase in the (Fe, Ni)/B ratio], can be clearly traced on the short-wavelength slope of the line; (3) apart from the main maximum (located in the pre-Fermi region, which indicates the predominance of states with $3d$ symmetry near E_F), bulges, which have the same energies as the *a* and *b* maxima of the BK_α line, can be clearly seen in the L_α spectra, indicating an appreciable hybridisation of the B $2p$–(Fe, Ni) $3d$ states; (4) the peaks in the BK_α spectra of nickel-based metallic glasses, corresponding to the bonding states of NiB, are the most intense and are displaced into the long-wavelength part of the spectrum relative to the Fe-containing metallic glasses (this is probably the reason why Ni–B interactions are preferred in more complex systems containing simultaneously the Fe and Ni components); (5) comparison of the characteristics of the XES of the metallic glasses [similar to those noted in (4)] with those of binary crystals may indicate the probable cause of the transition to the amorphous state and its stability.

The XES, ES, and ESCA methods have also been used to investigate the chemical shifts of the inner levels (charge states) in metallic glasses,[233,235,238,239,252] for the description of the effects of the doping of the metallic and nonmetallic 'sublattices' of the glasses,[232,235,238,240–242,244,245,250,255] and for the oxidation of surfaces of amorphous materials.[238,250] The optical properties of boride metallic glasses have been considered, for example, by Lustig et al.[246]

In conclusion, we may note a series of studies[234,236,241] in which transitions from the crystalline to the amorphous state in a series of binary iron, cobalt, and nickel alloys and the compositions of the surfaces of the latter were investigated by Auger electron spectroscopy. In particular, the concentration profiles constructed for the distribution of the elements in the 'bulk' of $Fe_{80}B_{20}$ and $Fe_{40}Ni_{40}P_{16}B_4$ specimens[234] indicate the enrichment of their surface layers in the nonmetals during crystallisation.

This review has been written with the financial support of the Russian Fundamental Research Fund (Project No. 94-03-09524).

References

1. G V Samsonov, L Ya Markovskii, A F Zhigach, M G Valyashko *Bor, Ego Soedineniya i Splavy* (Boron, Its Compounds and Alloys) (Kiev: Izd. Akad. Nauk Ukr. SSR, 1960)
2. G V Samsonov, Yu B Paderno *Boridy Redkozemel'nykh Metallov* (Borides of Rare-earth Metals) (Kiev: Nauk. Dumka, 1961)
3. B Post, F W Glaser *Refractory Binary Borides* (New York: Interscience, 1963)
4. T Lundstorm, S Rundqvist *Borides, Silicides and Phosphides* (London: Methuen, 1965)
5. W G Wyckoff *Crystal Structures* Vol. 1 (New York: Wiley, 1963)
6. B Post *Refractory Binary Borides, Metallo-Boron Compounds and Boranes* (New York: Wiley, 1964)
7. E L Muetterties *The Chemistry of Boron and Its Compounds* (New York: Wiley, 1967)
8. R Thompson *Prog. Boron Chem.* **2** 173 (1970)
9. J Goldschmidt *Interstitial Phases* (Translated into Russian; Moscow: Mir, 1971)
10. G V Samsonov, T I Serebryakova, V A Neronov *Boridy* (Borides) (Moscow: Atomizdat, 1975)
11. Yu B Kuz'ma *Kristallokhimiya Boridov* (Crystal Chemistry of Borides) (Lvov: Vishcha Shkola, 1983)
12. T Ya Kosolapova (Ed.) *Svoistva, Poluchenie i Primenenie Tugoplavkikh Soedinenii: Spravochnik* (Properties, Preparation and Applications of Refractory Compounds: Handbook) (Moscow: Metallurgiya, 1986)
13. T Lindstrom *Pure Appl. Chem.* **57** 1383 (1985)
14. *Boridy i Materialy na Ikh Osnove. Sbornik Trudov* (Borides and Materials Based upon Them. Collected Works) (Kiev: Nauk. Dumka, 1986)
15. G V Samsonov, G Sh Upadkhaya, V S Neshpor *Fizicheskoe Materialovedenie Karbidov* (Physical Materials Technology of Carbides) (Kiev: Nauk. Dumka, 1974)
16. G V Samsonov, I M Vinitskii *Tugoplavkie Soedineniya* (Refractory Compounds) (Moscow: Metallurgiya, 1976)
17. G V Samsonov, I F Pryadko, L F Pryadko *Elektronnaya Lokalizatsiya v Tverdom Tele* (Localisation of Electrons in Solids) (Moscow: Nauka, 1976)
18. Yu M Goryachev, B A Kovenskaya, G V Samsonov *Izv. Vyssh. Uchebn. Zaved. Fiz.* **8** 86 (1974)
19. W N Lipscomb, D Britton *J. Chem. Phys.* **33** 275 (1960)
20. E Dempsey *Philos. Mag.* **8** 285 (1983)
21. G V Samsonov, Y M Goryachev, B A Kovenskaya *J. Less-Common Met.* **47** 147 (1976)
22. K E Spear *J. Less-Common Met.* **47** 123 (1976)
23. J Piper *J. Phys. Chem. Solids* **27** 1907 (1966)
24. R Kiessling *Fortschr. Chem. Forsch.* **3** 41 (1954)
25. S T Serebryakova *J. Less-Common Met.* **67** 499 (1979)
26. P G Perkins, A V J Sweeney *J. Less-Common Met.* **47** 165 (1976)
27. H S Lonquet-Higgins, M V Roberts *Proc. R. Soc. London, Ser. A* **224** 336 (1954)
28. A L Ivanovskii, I V Shein *Izv. Akad. Nauk SSSR, Neorg. Mater.* **27** 2103 (1991)
29. M Yamazaki *J. Phys. Soc. Jpn.* **12** 1 (1957)
30. S Flodmark *Ark. Fys.* **18** 49 (1960)
31. S Flodmark *Ark. Fys.* **14** 513 (1959)
32. S Flodmark *Ark. Fys.* **9** 1357 (1955)
33. W N Lipscomb, D Britton *J. Chem. Phys.* **33** 275 (1960)
34. Yu B Paderno, Yu M Goryachev, E S Graf, in *Redkozemel'nye Metally i Ikh Soedineniya* (Rare-earth Metals and Their Compounds) (Kiev: Nauk Dumka, 1970) p. 101
35. P G Perkins, D R Armstrong, A Breeze *J. Phys. C, Solid State Phys.* **8** 3558 (1975)
36. R W Johnson, A H Daane *J. Phys. Chem.* **65** 909 (1961)
37. H Ichara *Res. Electrotech. Lab.* **125** 775 (1977)
38. A Hasegawa, A Yanase *J. Phys. C, Solid State* **12** 5431 (1979)
39. D D Koelling, B N Harman *J. Phys. C, Solid State Phys.* **10** 3107 (1977)
40. M Aono, S Kawai, S Kono *J. Phys. Chem. Solids* **37** 215 (1976)
41. I I Lyakhovskaya, T M Zimkina, V A Fomichev *Fiz. Tverd. Tela* **12** 174 (1970)
42. L Ramqvist, B Ekstig, E Kallne, E Noreland, R Manne *J. Phys. Chem. Solids* **30** 1849 (1969)
43. D W Fisher, W L Baum *J. Appl. Phys.* **39** 4757 (1968)
44. V G Aleshin, T Ya Kosolapova, V V Nemoshkalenko, T I Serebryakova, N G Chudinov *J. Less-Common Met.* **67** 173 (1979)
45. V G Alyoshin, T I Serebryakova, A I Kharlamov *Phys. Status Solidi B* **83** 537 (1977)
46. I I Lyakhovskaya, T M Zimkina, V A Fomichev *Izv. Akad. Nauk SSSR, Ser. Fiz.* **36** 393 (1972)
47. E Z Kurmaev, S A Nemnonov, V P Belash, Yu V Efimov *Fiz. Met. Metalloved.* **33** 578 (1972)
48. J Wong, F W Lytle, R P Messmer, D H Maylotte *Phys. Rev. B, Condens. Matter* **30** 5596 (1984)
49. E A Zhurakovskii, V P Dzeganovskii, T N Bondarenko *Metallofizika* **7** 37 (1971)
50. E A Zhurakovskii, V P Dzeganovskii, T N Bondarenko *Ukr. Fiz. Zh. (Russ. Ed.)* **15** 1477 (1970)
51. I N Frantsevich, E A Zhurakovskii, N N Vasilenko *Ukr. Fiz. Zh. (Russ. Ed.)* **14** 1065 (1970)
52. S I Salem, C N Chang, T J Nash *Phys. Rev. B, Solid State* **18** 5168 (1978)
53. C Senenaud, C Hagne *J. Phys. (Paris)* **4** 193 (1971)
54. T B Shashkina, B I Kotlyar, E A Zhurakovskii *Teor. Eksp. Khim.* **7** 686 (1971)
55. E A Zhurakovskii *Dokl. Akad. Nauk Ukr. SSR, Ser. B* **3** 240 (1967)
56. R B Singh, S K Händel, B Stenerhag *Z. Phys.* **249** 241 (1972)
57. T B Shashkina, B I Kotlyar, E A Zhurakovskii *Izv. Vyssh. Uchebn. Zaved. Fiz.* **6** 16 (1970)
58. V V Nemoshkalenko, A I Kharlamov, T I Serebryakova, V G Aleshin *Kinet. Katal.* **19** 1567 (1978)
59. A V Koval', S M Karal'nik *Izv. Vyssh. Uchebn. Zaved. Fiz.* **8** 17 (1978)

60. S Falch, G Rainer-Harbach, F Schmuckle, S Steeb *Z. Naturforsch. A* **36** 937 (1981)
61. D J Joyner, O Johnson, D M Hercules *J. Am. Chem. Soc.* **102** 1910 (1980)
62. O Johnson, D J Joyner, D M Hercules *J. Phys. Chem.* **84** 542 (1980)
63. D J Joyner, O Johnson, D M Hercules *J. Phys. F, Met. Phys.* **10** 169 (1980)
64. V G Alyoshin, A I Kharlamov, V M Prokopenko *J. Solid State Chem.* **38** 105 (1981)
65. G Mavel, J Escard, P Costa, J Castaing *Surf. Sci.* **35** 109 (1973)
66. D J Joyner, R F Willis *Philos. Mag.* **43A** 815 (1981)
67. M P Arbuzov, B I Kotlyar, T B Shashkina, et al. *Izv. Vyssh. Uchebn. Zaved. Fiz.* **6** 52 (1972)
68. D J Joyner, O Johnson, D M Hercules, D W Bullett, J H Weaver *Phys. Rev. B, Condens. Matter* **24** 3122 (1981)
69. A Amamon, G Krill *Solid State Commun.* **31** 971 (1979)
70. E A Zhurakovskii, T B Shashkina, B I Kotlyar *Izv. Vyssh. Uchebn. Zaved., Fiz.* **1** 24 (1970)
71. K Tanaka, T Saito, K Suzuki, R Hasegawa *Phys. Rev. B, Solid State* **32** 6853 (1985)
72. M I Korsunskii, Ya E Genkin *Izv. Akad. Nauk Kaz. SSR, Ser. Fiz.-Mat.* **2** 77 (1967)
73. M I Korsunskii, Ya E Genkin, V G Lifshits *Izv. Akad. Nauk Kaz. SSR, Ser. Fiz.-Mat.* **4** 62 (1975)
74. E V Petrov, V V Tsvetkov *Metallofizika* **40** 98 (1972)
75. P H Middleton, A J Paul, P M A Sherwood *J. Chem. Soc., Faraday Trans. 1* **80** 2549 (1984)
76. E V Petrov *Metallofizika* **44** 83 (1973)
77. Yu M Shul'ga, S Yu Zasedatelev, Yu G Borodko, E A Blyumberg *Metallofizika* **44** 787 (1973)
78. E A Zhurakovskii, A A Vladimirova, V P Dzeganovskii *Dokl. Akad. Nauk SSSR* **170** 548 (1966)
79. D R Wheeler, W A Brainard *J. Vac. Sci. Technol.* **15** 24 (1978)
80. E A Zhurakovskii, V V Gorskii *Dokl. Akad. Nauk Ukr. SSR* **11** 1428 (1966)
81. E A Zhurakovskii, V I Kotlyar, T B Shashkina *Dokl. Akad. Nauk Ukr. SSR* **7** 654 (1969)
82. T B Shashkina *Phys. Status Solidi B* **44** 571 (1971)
83. E S Konovalova, Yu V Paderno, in *Vanadaty i Boridy RZM. Sintez i Svoistva* (Vanadates and Borides of Rare-earth Metals. Synthesis and Properties) (Sverdlovsk: Ural'sk. Nauch. Tsentr Akad. Nauk USSR, 1982) p. 28
84. K Spear *Refract. Mater.* **6** 91 (1976)
85. S Gajima, K Niihara, in *Abstracts of Reports at the IXth RE Research Conference, Blackburg, Virginia, 1971* p. 23
86. W Hoffmann, W Janiche *Z. Metallkd.* **28B** 1 (1936)
87. V A Neronov *Zh. Neorg. Khim.* **14** 1704 (1969)
88. V T Serebryanskii, V A Epel'baum, G S Zhdanov *Zh. Neorg. Khim.* **12** 2486 (1967)
89. V T Serebryanskii, V A Epel'baum, G S Zhdanov *Dokl. Akad. Nauk SSSR* **141** 885 (1967)
90. G Will *Nature (London)* **212** 175 (1966)
91. G Will *J. Am. Chem. Soc.* **85** 2335 (1963)
92. G Will *Acta Crystallogr.* **23** 1071 (1967)
93. V N Gurin, M M Korsukova, in *Boron and Refractory Borides* (Berlin: Springer, 1977) p. 293
94. R Greatrex *Annu. Rep. Prog. Chem., Sect. A* **81** 29 (1984)
95. J A Kohn, A A Giardini *Z. Kristallogr.* **111** 53 (1958)
96. J K Burdett, E Canadell, G J Miller *J. Am. Chem. Soc.* **108** 6561 (1986)
97. D R Armstrong, A Breeze, P G Perkins *J. Chem. Soc., Faraday Trans. 2* **7** 952 (1977)
98. I I Lyakhovskaya, T M Zimkina, V A Fomichev *Fiz. Tverd. Tela* **12** 138 (1970)
99. V V Odintsov, Yu B Paderno, Yu M Goryachev *Zh. Strukt. Khim.* **2** 344 (1971)
100. A L Ivanovskii, D L Novikov, V I Anisimov *Zh. Strukt. Khim.* **30** 32 (1989)
101. A Neckel *Int. J. Quantum Chem.* **23** 1317 (1983)
102. V P Zhukov, N I Medvedeva, V A Gubanov *Phys. Status Solidi B* **151** 407 (1989)
103. A L Ivanovskii, V P Zhukov, V A Gubanov *Elektronnoe Stroenie Tugoplavkikh Karbidov i Nitridov Perekhodnykh Metallov* (Electronic Structures of Refractory Carbides and Nitrides of Transition Metals) (Moscow: Nauka, 1990)
104. A L Ivanovsky, G P Shveikin *Phys. Status Solidi B* **181** 251 (1994)
105. V I Anisimov, V P Antropov, V A Gubanov, A L Ivanovskii, A I Likhttenshtein, E Z Kurmaev *Elektronnaya Struktura Defektov i Primesei v Metallakh, Splavakh i Soedineniyakh* (The Electronic Structure of Defects and Admixtures in Metals, Alloys and Compounds) (Moscow: Nauka, 1989)
106. P Mohn *J. Phys. C, Solid State* **21** 2841 (1988)
107. D R Armstrong, P G Perkins *Theor. Chim. Acta* **64** 41 (1983)
108. P Mohn, D G Pettifor *J. Phys. C, Solid State Phys.* **21** 2829 (1988)
109. R F Sabiryanov, V L Ivanovskii *Metallofizika* **14** 7 (1992)
110. D R Armstrong, P G Perkins *J. Chem. Soc., Faraday Trans. 2* 12 (1979)
111. T N Bell, P G Perkins *J. Phys. Chem.* **81** 2102 (1977)
112. A R Williams, J Kubler, C D Gelatt *Phys. Rev. B, Solid State* **19** 6094 (1979)
113. M C Cadeville, A J P Meyer *C. R. Acad. Sci.* **255** 3391 (1962)
114. N S Miryasov, A P Parsanov *Izv. Akad. Nauk SSSR, Ser. Fiz.* **23** 285 (1959)
115. N Lundquist, H P Myers *Ark. Fys.* **20** 30 (1961)
116. R Hocart, M Fallot *C. R. Hebd. Seances Acad. Sci.* **203** 1062 (1936)
117. R F Sabiryanov, O N Mryasov, A L Ivanovskii, G P Shveikin *Metallofizika* **13** 71 (1991)
118. A L Ivanovskii, V I Anisimov, V A Gubanov, E Z Kurmaev *Zh. Strukt. Khim.* **27** 3 (1986)
119. A L Ivanovsky *Phys. Status Solidi B* **157** 129 (1990)
120. G V Samsonov, Yu M Goryachev, B A Kovenskaya, E Ya Tel'nik *Izv. Vyssh. Uchebn. Zaved. Fiz.* **6** 37 (1972)
121. J K Burdett, E Canadell, G J Miller *J. Am. Chem. Soc.* **108** 6561 (1986)
122. V M Anishchik, N N Dorozhkin *Phys. Status Solidi B* **160** 173 (1990)
123. G Will, A Kirfel, in *Proceedings of the International Conference on Boron-rich Solids, Albuquerque, New York, 1986* p. 88
124. R O Zaitsev *Sverkhprov. Fiz. Khim. Tekh.* **2** 36 (1989)
125. J Hubbard *Proc. R. Soc. London, Ser. A* **281** 401 (1964)
126. V Emery *Phys. Rev. Lett.* **58** 2797 (1987)
127. F Vahldiek *New Technol. Week* **9** 6 (1989)
128. B Ahern *Supercond. Week* **23** 9 (1989)
129. P J Brown, J L Cox *Philos. Mag.* **23** 705 (1971)
130. R S Perkins, P J Brown *J. Phys. F, Met. Phys.* **4** 906 (1974)
131. D J Joyner, O Johnson, D M Hercules, D W Bullett, J H Weaver *Phys. Rev. B, Solid State* **24** 3122 (1981)
132. R H Multu, A Aidimuraz *J. Magn. Magn. Matter* **68** 328 (1987)
133. I Bakonyi *J. Magn. Magn. Matter* **73** 171 (1988)
134. E J O Garba, R L Jacobs *J. Phys. Chem. Solids* **50** 101 (1989)
135. N E Solov'ev, V S Makarov, Ya A Ugai, in *Boridy i Materialy na Ikh Osnove* (Borides and Materials Based upon Them) (Kiev: Inst. Poroshk. Metallurg. Akad. Nauk Ukr. SSR, 1986) p. 36
136. E I Zornberg *Phys. Rev. B, Solid State* **2** 224 (1970)
137. D G Dempsey, W R Grise, L Kleinman *Phys. Rev. B, Solid State* **17** 1209 (1978)
138. I I Kostetskii, S N L'vov *Fiz. Met. Metalloved.* **34** 475 (1972)
139. I I Kostetskii, S N L'vov *Fiz. Met. Metalloved.* **33** 773 (1972)
140. H Ichara, M Nirabayashi, H Nakagava *Phys. Rev. B, Solid State* **16** 726 (1977)
141. D L Johnson, B N Harman, S H Liu *J. Chem. Phys.* **73** 1989 (1980)
142. L F Mattheiss *Phys. Rev.* **33** 1399 (1964)
143. K Schwarz *Phys. Rev.* **8** 2466 (1957)
144. F S Ham, B Segal *Phys. Rev.* **124** 1786 (1961)
145. B Segal *Phys. Rev.* **105** 108 (1957)
146. G S Painter, D E Ellis *Phys. Rev. B, Solid State* **1** 4747 (1970)
147. T Inoshita, K Nakoo, H Kamimura *J. Phys. Soc. Jpn.* **43** 1237 (1977)
148. N A Holzwarth, S Rabii, L A Girifalco *Phys. Rev. B, Solid State* **18** 5190 (1978)
149. R C Linton *Thin Solid Films* **20** 17 (1974)
150. J M Ziman *Principles of the Theory of Solids* (New York: Cambridge University Press, 1972)
151. A L Ivanovskii, Thesis in Chemical Sciences, Institute of Chemistry, Urals Div. Acad. Sci. USSR, Sverdlovsk, 1988

152. D R Armstrong *J. Less-Common Met.* **67** 191 (1979)
153. S La Placa, B Post *Acta Crystallogr.* **15** 97 (1962)
154. W Trzebiatowski, J Rudzinski *J. Less-Common Met.* **6** 244 (1964)
155. R Hoffmann *J. Chem. Phys.* **39** 1397 (1963)
156. D L Novikov, A L Ivanovskii, V A Gubanov *Zh. Neorg. Khim.* **33** 2673 (1988)
157. A N Pilyankevitsh, V K Rasovenov, G L Zhounkovsky, in *VI Int. Pulvermetal. Tagung B. 2, Dresden, 1977* p. 441
158. S S Ordan'yan, V I Unrod, A K Avgustinnik *Poroshk. Metall.* **9** 40 (1975)
159. J D Venables *Philos. Mag.* **16** 873 (1967)
160. G L Zhunkovskii, T M Evtushok, S A Shvab, in *Boridy i Materialy na Ikh Osnove* (Borides and Materials Based upon Them) (Kiev: Inst. Poroshk. Metallurg. Akad. Nauk Ukr. SSR, 1986) p. 91
161. O F Chernysheva, V S Sinel'nikov, T Ya Kosolapova *Izv. Akad. Nauk SSSR, Neorg. Mater.* **15** 614 (1979)
162. G V Samsonov, in *Voprosy Poroshkovoi Metallurgii i Prochnosti Materialov* (Problems in Powder Metallurgy and the Strength of Materials) No VII (Kiev: Izd. Akad. Nauk Ukr. SSR, 1959) p. 72
163. G G Smirnov, Author's Abstract of Candidate Thesis in Technical Sciences, Leningrad Technol. Inst., Leningrad, 1971
164. A L Borisova *Sovmestimost' Tugoplavkikh Soedinenii s Metallami i Grafitom* (Compatibility of Refractory Compounds with Metals and Graphite) (Kiev: Nauk. Dumka, 1985)
165. R Kiffer, F Benzenovskii *Tverdye Materialy* (Solid Materials) (Moscow: Metallurgiya, 1968)
166. V V Pakholkov, I V Brettser-Portnov, I G Grigorov, Yu G Zainulin *Izv. Akad. Nauk SSSR, Neorg. Mater.* **16** 873 (1993)
167. V I Anisimov, A L Ivanovskii, V A Gubanov, E Z Kurmaev *Zh. Strukt. Khim.* **27** 3 (1986)
168. A L Ivanovsky, V I Anisimov, A I Lichtenstein, V A Gubanov *J. Phys. Chem. Solids* **49** 479 (1988)
169. R F Sabiryanov, Author's Abstract of Candidate Thesis in Physicomathematical Sciences, Inst. Chem. Solids, Urals Div. Russ. Acad. Sci., Ekaterinburg, 1993
170. J F Halet, J Y Saillard, J Bauer *J. Less-Common Met.* **158** 239 (1990)
171. J Bauer, M Potel, J Geogeon, in *Proceedings of the IXth International Conference on Solid Compounds of Transition Elements, Dalton Division, Oxford, 1988* p. 112
172. J Bauer, O Bars *Acta Crystallogr., Sect. B* **36** 1540 (1980)
173. W N Lipscomb *J. Less-Common Met.* **82** 1 (1981)
174. W Hume-Rothery, G V Raynor *The Structure of Metals and Alloys* (Translated into Russian; Moscow: Metallurgiya, 1959)
175. I I Kornilov *Izv. Akad. Nauk SSSR, Metall. Gorn. Delo* **6** 19 (1964)
176. I I Kornilov *Metally i Vzaimodeistviya mezhdu Nimi* (Metals and Interactions between Them) (Moscow: Nauka, 1964)
177. E S Makarov *Dokl. Akad. Nauk SSSR* **186** 313 (1969)
178. I I Kornilov *Dokl. Akad. Nauk SSSR* **81** 597 (1951)
179. I I Kornilov, N M Matveeva, L I Pryakhina, R S Polyakova *Metallokhimicheskie Svoistva Elementov Periodicheskoi Sistemy* (Metallochemical Properties of the Elements) (Moscow: Nauka, 1966)
180. V N Troitskii, B N Grebtsov, M I Aivazov *Poroshk. Metall.* **3** 6 (1973)
181. Ya A Krestin'sh, U A Tsielen, V Ya Bondars, in *Dispersionnye Kristallicheskie Poroshki v Materialovedenii* (Dispersed Crystalline Powders in Materials Technology) (Kiev: Inst. Poroshk. Metallurg. Akad. Nauk Ukr. SSR, 1980) p. 16
182. T Ya Kosolapova, E M Dudnik, O P Kulik, in *Boridy i Materialy na Ikh Osnove* (Borides and Materials Based upon Them) (Kiev: Inst. Poroshk. Metallurg. Akad. Nauk Ukr. SSR, 1986) p. 13
183. J Y Cautarel, H Pastor, R Meyer, in *Plansee Seminar, Reutte Austria, 1974* p. 12
184. H Nowotny, F Benesovsky, C Brukl, O Schob *Monatsh. Chem.* **92** 403 (1961)
185. Yu G Zainulin, S I Alyamovskii, G P Shveikin *Izv. Akad. Nauk SSSR, Neorg. Mater.* **12** 1581 (1976)
186. A L Ivanovskii, Yu G Zainulin, V A Gubanov *Zh. Neorg. Khim.* **30** 579 (1985)
187. A L Ivanovsky, V A Gubanov, G P Shveikin, V I Anisimov *J. Phys. Chem. Solids* **47** 275 (1986)
188. A Lebugle, R Nyholm, N Martensson *J. Less-Common Met.* **82** 265 (1981)
189. V P Zhukov, N I Medvedeva, G P Shveikin *Izv. Akad. Nauk SSSR, Neorg. Mater.* **28** 1402 (1992)
190. Ya V Buran, Ya O Dovgii, I V Kityk *Fiz. Tverd. Tela* **31** 275 (1989)
191. G Will, A Kirfel, B Josten *J. Less-Common Met.* **82** 255 (1981)
192. M Krogh *Acta Crystallogr., Sect. B* **24** 179 (1968)
193. Ya V Burak, Ya O Dovgii, I V Kityk *Zh. Prikl. Spektrosk.* **51** 745 (1989)
194. W Harrison *Electronic Structure and the Properties of Solids* Vol. 2 (Translated into Russian; Moscow: Mir, 1983)
195. A Kirfel, A Gupta, G Will *Acta Crystallogr., Sect. B* **38** 1311 (1980)
196. A Kirfel, A Gupta, G Will *Acta Crystallogr., Sect. B* **35** 1052 (1979)
197. A Kirfel, A Gupta, G Will *Acta Crystallogr., Sect. B* **35** 2291 (1979)
198. W H Zacharasen *Acta Crystallogr., Sect. B* **17** 749 (1964)
199. A Amamon *Phys. Status Solidi A* **54** 565 (1979)
200. L Tokacs *Solid State Commun.* **21** 611 (1977)
201. A C Switendick *Solid State Commun.* **19** 511 (1976)
202. A Amamon, G Krill *Solid State Commun.* **33** 1087 (1980)
203. P H Citrin, G K Wertheim, Y Boer *Phys. Rev. Lett.* **41** 1425 (1978)
204. G K Wertheim, G Crecelius *Phys. Rev. Lett.* **40** 813 (1978)
205. Zong-Quan Gu, W Y Ching *J. Magn. Magn. Mater.* **54/57** 525 (1986)
206. J Inoue, M Shimizu *J. Phys. F, Met. Phys.* **16** 1051 (1986)
207. J Inoue, M Shimizu *J. Phys. F, Met. Phys.* **16** 1157 (1986)
208. M Sagawa, S Fujiwara, N Tagawa, H Yamamoto, Y Matsuura *J. Appl. Phys.* **55** 2083 (1984)
209. H Yamaguchi, M Yamada, Y Yamaguchi, H Yamamoto, S Hirosawa, M Sagawa *J. Magn. Magn. Mater.* **54/57** 413 (1986)
210. K Handrik, S Kobe *Amorphous Ferro- and Ferrimagnetic Substances* (Translated into Russian; Moscow: Mir, 1982)
211. D S Boudreaux *Phys. Rev. B, Solid State* **18** 4039 (1978)
212. C R Nagel, J Tauc *Phys. Rev. Lett.* **35** 380 (1975)
213. D E Polk *Acta Metall.* **20** 485 (1972)
214. H S Shen, B P Park *Acta Metall.* **21** 395 (1973)
215. R P Messmer *Phys. Rev. B, Solid State* **23** 1616 (1981)
216. V V Nemoshkalenko, A P Shpak, I P Nagibin, A N Yares'ko V L Karbovskii *Metallofizika* **4** 82 (1990)
217. J Wong, F W Lytle, R B Greegor, in *Rapidly Quenched Metals III* Vol. 2 (Ed. B Cantor) (London: Metal Society, 1978) p. 345
218. A V Postnikov, Candidate Thesis in Physicomathematical Sciences, Inst. Phys. Math. Urals Div. Acad. Sci. USSR, Sverdlovsk, 1985
219. P Lamparter, E Nodl, G Rainer *Hartbach. Ztschr. Naturforsch.* **A36** 165 (1981)
220. N Cowlan, G E Carr *J. Phys. F, Met. Phys.* **15** 1117 (1985)
221. D S Boudereaux, H J Frost *Phys. Rev. B, Solid State* **23** 1506 (1981)
222. M Krajci, P Mrafko *J. Phys. F, Met. Phys.* **18** 2137 (1988)
223. I Turek, J Yafner, Ch Hausleitner *J. Magn. Magn. Mater.* **109** L145 (1992)
224. Y Kakehashi *Phys. Rev. B, Solid State* **43** 10 820 (1991)
225. D N Manh, G D Hoai, A Pasturel, C Colinet *Physica B* **173** 293 (1991)
226. H J Nowak, O K Andersen, T Fujiwara, O Jepsen *Phys. Rev. B, Solid State* **44** 3577 (1991)
227. I Turek *J. Phys., Condens. Matter* **2** 10 559 (1990)
228. T Fujiwara *J. Phys. F, Met. Phys.* **12** 661 (1982)
229. T Fujiwara, H S Chen, Y Wasada *J. Phys. F, Met. Phys.* **11** 1327 (1981)
230. I Turek *J. Magn. Magn. Mater.* **98** 119 (1991)
231. H Tanaka, S Takayama, M Hasegawa *Phys. Rev. B, Solid State* **47** 2671 (1993)
232. V V Nemoshkalenko, A P Shpak, V L Karbovskii *Metallofizika* **12** 24; 129 (1990)
233. E Majkova, P Duhaj *Phys. Status Solidi B* **146** K17 (1988)
234. T I Bratus', M A Vasil'ev, V T Cherepin *Metallofizika* **5** 71 (1983); **6** 77 (1984)
235. P Marko, O Dusha, L Pototski *Poverkhn. Fiz. Khim. Mekhan.* **3** 68 (1984)
236. P P Karve, S K Kulkarnai, A S Nigavekar *Solid State Commun.* **49** 719 (1984)
237. P Sen, A Srinivasan, M S Hedge, C N O Rao *J. Mater. Sci.* **18** 173 (1983)
238. D R Baer, M T Thomas *J. Vac. Sci. Technol.* **18** 722 (1981)
239. M Matsuura, T Namoto, F Itoh, K Suzuki *Solid State Commun.* **33** 895 (1980)

240. D R Baer, D A Petersen, L R Pederson, M T Thomas *J. Vac. Sci. Technol.* **20** 957 (1982)
241. P P Karve, M G Thube, S K Kulkarnai, A S Nigavekar *Solid State Commun.* **50** 1027 (1984)
242. V V Nemoshkalenko, D E Ovsienko, D Yu Paderno, in *"Issledovanie Struktury Amorfnykh Metallicheskikh Splavov". Tezisy Dokladov Vsesoyuznoi Konferentsii, Moskva, 1990* (Abstracts of Reports at the All-Union Conference "Investigation of the Structures of Amorphous Metal Alloys", Moscow, 1990) p. 119
243. S Kapusta, K E Heusler *Z. Metallkd.* **72** 785 (1981)
244. B V Molotilov, A I Zakharov, A G Narmonev, in *"Rentgenovskie i Rentgenoelektronnye Spektry i Elektronnaya Struktura Splavov i Soedinenii". Tezisy Dokladov Vsesoyuznoi Konferentsii, Izhevsk, 1979* (Abstracts of Reports at the All-Union Conference "X-Ray and X-Ray Electron Spectra and the Electronic Structures of Alloys and Compounds", Izhevsk, 1979) p. 105
245. B V Molotilov, A I Zakharov, A G Narmonev *Fiz. Met. Metalloved.* **51** 1106 (1981)
246. N Lustig, L J Pilione, K C Woo, J S Lannin *J. Non-Cryst. Solids* **61/62** 1295 (1984)
247. S Ray, J Tauc *Solid State Commun.* **34** 769 (1980)
248. S Falch, G Rainer-Harbach, F Schmueckle, S Steeb *Z. Naturforsch. A, Phys. Sci.* **36** 937 (1981)
249. A Amamon, G Krill *Solid State Commun.* **31** 971 (1979); **33** 1087 (1980)
250. V V Nemoshkalenko, A I Senkevich, S I Latynov, A G Dmitriev *Metallofizika* **7** 18 (1985)
251. J L Walter, F Bacon, F E Liborsky *Mater. Sci. Eng.* **24** 239 (1976)
252. E Cartier, Y Baer, M Liard, H-J Guentherodt *J. Phys. F, Met. Phys.* **10** L21 (1980)
253. K Tanaka, M Yoshino, K Suzuki *J. Phys. Soc. Jpn.* **51** 3882 (1982)
254. A J Bevolo, C S Severin, C W Chen *J. Vac. Sci. Technol.* **20** 852 (1982)
255. K Hricovind, J Krempasky *J. Phys. F, Met. Phys.* **15** 1321 (1985)

Russian Chemical Reviews **63** (9) 735–750 (1994)
©1994 Russian Academy of Sciences and Turpion Ltd

UDC 547.541.521.07

The chemistry of disulfides

I V Koval'

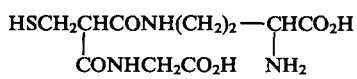
Contents

I. Introduction	735
II. The structure and physicochemical properties of disulfides	736
III. Methods of synthesis of disulfides	736
IV. Reactions with participation of disulfides	739

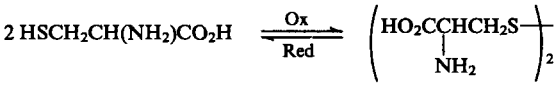
Abstract. The results of studies in the chemistry of disulfides during recent years are surveyed and treated systematically. The structures, methods of synthesis, and the physicochemical and chemical properties of disulfides are examined. The bibliography includes 151 references.

I. Introduction

Disulfides play an important role in living organisms. In the formation of the tertiary structure of proteins, covalent disulfide bonds are known [1] to ensure the formation of cross-links, which are much stronger than hydrophobic interactions and hydrogen bonds. The disulfide cross-link renders relatively permanent the disposition of the peptide chains established initially as a result of weaker bonding forces. The biochemical importance of the disulfide bond is also determined by the uniqueness of the nature of the thiol–disulfide system, in which the S–S bond can be formed under conditions appropriate for biological processes — via disulfide exchange with participation of glutathione. [2]

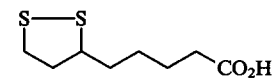


Cystine, which contains a disulfide bond, is a component of aerobic systems. [1] It is formed as a result of the ready oxidation of cysteine.



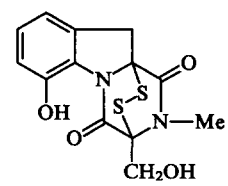
In the hormone insulin, the disulfide bonds of cystine join two different peptide chains, one of which contains 21 and the other 30 aminoacid residues. [1] The composition and form of the protein of hair are to a large extent determined by the cystine S–S bonds and the chemical permanent wave in hair is based on this fact. [1] Hair is initially treated with a reductant in order to cleave the S–S bonds and convert them into sulfhydryl groups. Hair, the proteins of which no longer have cross-links, readily assumes the required form by virtue of the regeneration of the protein S–S cross-links as a result of oxidation by air or a chemical oxidant, and retains it for a long time.

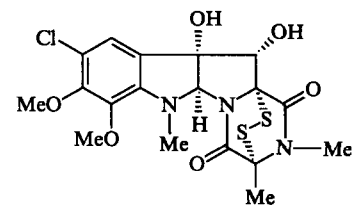
Lipoic acid



participates in the oxidative decarboxylation of α-oxoacids and is a common unit in two fundamental biochemical processes in which the thiol–disulfide system participates: electron transfer and generation of thioester linkages. [2,3]

Disulfides such as glyotoxin and sporidesmin





are the main representatives of the group of metabolites of fungi. [1] Many disulfides enter into the composition of various natural products. For example, (−)-bis(3-acetoxyundec-5-enyl) disulfide has been isolated from Hawaiian seaweed of the genus *Dictyopteris*. [4] Di-n-propyl disulfide is a component of the mixture of substances responsible for the specific smell of the onion. [2]

Certain disulfides can be used as accelerators of the vulcanisation of rubber, [5] as chain transfer agents in radical polymerisation processes, [6] as biologically active substances, [7] and as complex-forming agents. [8] A very important application of disulfides is in fine organic synthesis. The lability of the S–S bond in disulfides and its ability to be cleaved by both nucleophiles and electrophiles as well as the active reaction centre with a variable valence (sulfur) impart to disulfides the properties of extremely valuable synthons, which are widely used in multistage organic syntheses and in particular for the introduction of the sulfide functional group.

The interest shown by many investigators gave rise at one point to the appearance of a series of reviews [2,3,9–15] reflecting to some extent the state of the chemistry of disulfides during that period. Unfortunately, the reactions occurring with an increase in the valence of sulfur and in particular the oxidative imination reactions and the formation of sulfonium complexes were hardly considered in these communications. On the other hand, since the publication of these reviews many new experimental data on

I V Koval' Department of the Chemical Technology of High-Molecular-Mass Compounds, Ukrainian Chemical-Technological University, prosp. Gagarina 8, 320005 Dnepropetrovsk, Ukraine.
Fax (7-056) 247 33 16. Tel. (7-056) 247 24 91

Received 11 January 1994
Uspekhi Khimii **63** (9) 776–792 (1994); translated by A K Grzybowski

the chemistry of disulfides have accumulated and these are surveyed in the present review. The literature is covered up to 1992 inclusive.

II. The structure and physicochemical properties of disulfides

Virtually all the possible physicochemical research methods have been used in the study of the structure of disulfides and also of the main characteristics of the S–S bond in disulfides.[2,3,15–17] In particular, it has been established[2,15,16] that the molecules of disulfides have a zig-zag shape with a X–S–S–X dihedral angle of ~90°.

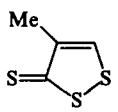
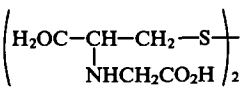
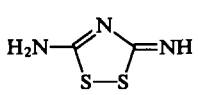
The strongest bonds between two identical atoms are formed by Group V–VII elements of the Third Period, which has been explained[17] by the contribution of the $p-\pi$ and $d-\pi$ interactions. By virtue of these interactions, the S–S bond in disulfides is much stronger than the O–O, Se–Se, and Te–Te bonds in the isostructural peroxides, diselenides, and ditellurides. The S–S bond dissociation energies for certain disulfides are listed in Table 1.

Table 1. The S–S bond dissociation energies.[3,17]

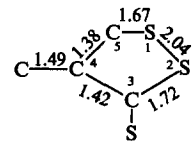
Disulfide	E_{dis}/kcal mol^{-1}
PhS–SPh	55.0 ± 1.5
FS–SF	60.0 ± 4.0
PhS–SMe	65.0 ± 1.5
HS–SH	66.0 ± 2.0
EtS–SEt	70.0 ± 2.0
EtS–SMe	72.0 ± 2.0
MeS–SMe	74.0 ± 2.0

As can be seen from the data in Table 1, the structures of the alkyl groups linked directly to sulfur in disulfides have little influence on the strength of the S–S bond. Aryl groups exert a greater influence on the strength of the bond, which has been explained by the involvement of the sulfur p electrons in conjugation with the π electrons of the benzene ring (p,π conjugation). The enthalpy of the S–S bond is 63 kcal mol^{-1}. The S–S bond lengths in certain disulfides are listed in Table 2.

Table 2. The S–S bond lengths.[3]

Compound	S–S bond length/Å
	2.03
MeS–SMe	2.04
	2.04
HS–SH	2.04
ClS–SCl	2.05
CF_3S-SCF_3	2.05
	2.09

By comparing the S–S bond lengths in Table 2 with the values calculated by Pauling's equation,[3] it is possible to estimate the amount of double-bond character in the S–S bond. In 4-methyl-1,2-dithiacyclopent-4-ene-3-thione, it amounts to 20%, which indicates the aromatic nature of such trithione compounds and hence their high stability, which is also indicated by the results of the structural analysis of 1,2-dithiolane-3-thione.



The C(5)–S(1) bond (1.67 Å) in 4-methyl-1,2-dithiacyclopent-4-ene-3-thione is much shorter than the usual C–S bond (1.83 Å), while the C(4)–C(5) bond (1.38 Å) has virtually the same length as the C–C bond in aromatic hydrocarbons.

The structure of the terminal alkyl groups in disulfides hardly affects their dipole moments, which is apparently associated with the retention of the configuration of the C–S–S–C group.[3] The experimental molecular refractions of certain disulfides are numerically greater than the values calculated from atomic refractions.[3]

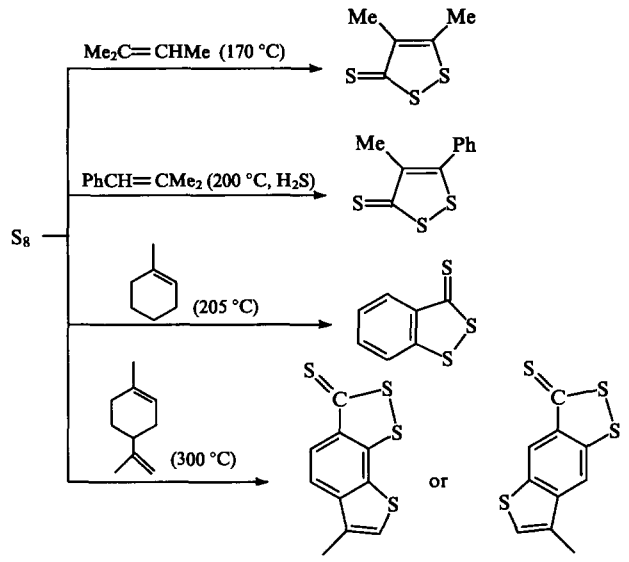
The absorption maximum in the UV spectra of dialkyl disulfides is in the range 240–280 nm. It undergoes a hypsochromic shift on passing from Me to Et, to Pr^i, and then to Bu^t, which is believed[3] to be associated with hyperconjugation. The absorption maximum in the UV spectra of *para*-substituted diphenyl disulfides *p*-$XC_6H_4SSC_6H_4Y$-*p* (X = H, Cl, NO_2, MeO; Y = NO_2, MeO) is in the range 240–324 nm (ε = 4.07–4.34). As the electron-accepting properties of the substituents in the benzene ring become more pronounced, a bathochromic shift of the absorption maximum is observed. The S–S bond stretching vibrations in disulfides are manifested in the range 470–503 cm^{-1}.[3] The chemical shift δ of the protons in the H_3C-S group is in the region of 2 ppm and that of the protons in the >CH–S group is in the region of 3.2 ppm.[18] UV irradiation of diphenyl disulfide at −200 °C leads to the formation of a radical product, the EPR spectrum of which is characterised by an axially anisotropic g-factor. This is apparently due to the localisation of the unpaired electron on the sulfur atom in the PhS$^\cdot$ radical. The absorption spectrum of this radical contains bands at 355 and 380 nm and its luminescence spectrum has bands at 374 and 240 nm.[17]

When diaryl disulfides react with strong electron acceptors (aluminium and gallium halides), the S–S bonds undergo homolytic cleavage with formation of the stable radical-complexes $ArS^\cdot \cdot MCl_3$ (Ar = Ph, *p*-MeC_6H_4, *o*-$NO_2C_6H_4$, α-$C_{10}H_7$; M = Al, Ga), which are solid deeply coloured substances capable of being stored under a nitrogen atmosphere for a long time.[19] It has been suggested that the donor–acceptor bond in the radical-complex is formed with participation of the lone pair of the sulfur atoms. In contrast to diaryl disulfides, dialkyl disulfides form under similar conditions 1:1 complexes with the above electron acceptors without the homolytic cleavage of the S–S bond. When the radical-complexes react with stronger electron donors, for example with pyridine, the thiyl radical is displaced and forms a disulfide as a result of recombination.

III. Methods of synthesis of disulfides

1. Syntheses based on sulfur and its inorganic derivatives

The use of sulfur in the synthesis of disulfides has been known for a relatively long time.[3] For example, a preparative method of synthesis of bis(*p*-aminophenyl) disulfide involves the heating of sulfur with aniline. A series of cyclic disulfides have been obtained by heating sulfur with unsaturated hydrocarbons.[3]



One of the preparative methods of synthesis of dialkyl disulfides involves the interaction of sulfur with alkyl iodides and sodium in liquid ammonia.[2]

$$RI + S_8 + 2\,Na \xrightarrow[NaI]{NH_3} RSSR$$

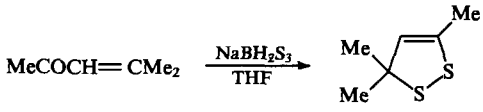
The interaction of elemental sulfur with trialkylboranes and subsequent alkaline hydrolysis of the products also lead to the formation of dialkyl disulfides.[2]

$$R_3B \xrightarrow{S_8\,(\Delta)} RSBR_2 \xrightarrow{OH^-} RSSR$$

On treatment with sulfur-containing sodium tetrahydroborate, aldehydes and ketones are converted into disulfides, while 1,2-epoxides and α,β-unsaturated ketones are converted into bis(1,2-hydroxyethyl) disulfides and cyclic disulfides respectively.[2,20]

$$PhCHO \xrightarrow{NaBH_2S_3} PhCH_2S-SCH_2Ph$$





The interaction of alkyl halides with sulfur in the presence of alkoxides leads to the formation of the corresponding dialkyl disulfides and dialkyl trisulfides.[21]

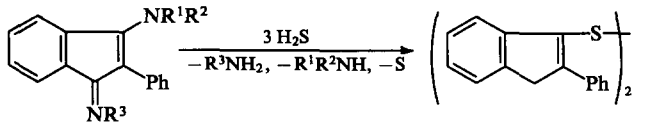
$$RCH_2Hal + S_8 + RO^- \longrightarrow (RCH_2)_2S_n$$

$n = 2, 3.$

The synthesis of alkynyl disulfides based on the reaction of elemental sulfur with lithium acetylides and subsequent sulfenylation of lithium thiolates by sulfenyl chlorides has been described.[22]

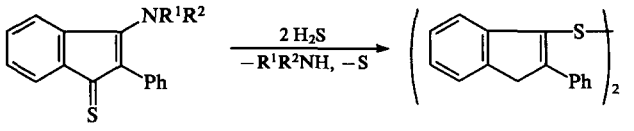
$$RC{\equiv}CLi + S_8 \longrightarrow RC{\equiv}CSLi \xrightarrow[-LiCl]{R^1SCl} RC{\equiv}CSSR^1$$

Among the inorganic derivatives of sulfur, sodium disulfide has found the most extensive application in the synthesis of disulfides. A whole series of preparatively very easy methods of synthesis of dialkyl and diallyl disulfides, described in handbooks and in the scientific literature, have been developed on the basis of the reactions involving the alkylation and arylation of sodium disulfide by alkyl halides and activated aryl halides as well as arenediazonium salts. Dialkenyl disulfides are obtained similarly from sodium disulfide.[23] Among other inorganic derivatives of sulfur, hydrogen sulfide and sulfur monochloride are also used in the synthesis of disulfides. For example, it has been noted[24,25] that bis(indenyl) disulfide is formed in the reaction of hydrogen sulfide with 3-amino-1-imino-2-phenylindenes in an alcoholic medium in the presence of piperidine.

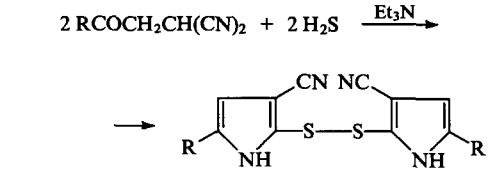


$R^1 = R^2 = H$; R^3 = Alk.

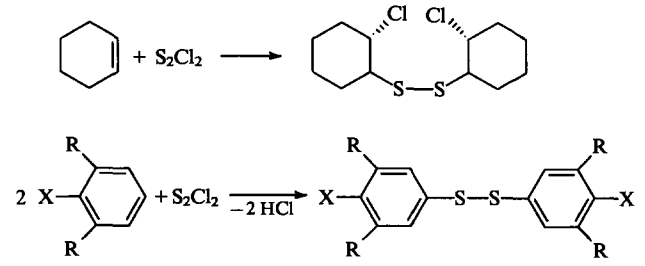
The same disulfide is obtained in the reaction of hydrogen sulfide with 3-amino-2-phenylindene-1-thiones.[25]



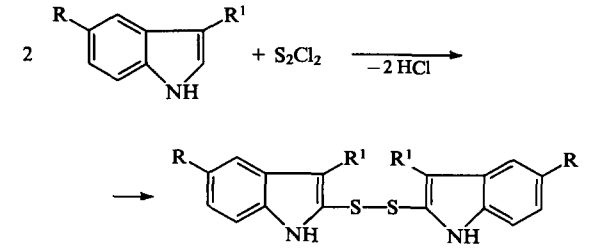
The reaction of hydrogen sulfide with alkyl(aryl) β,β-dicyanoethyl ketones in an organic solvent in the presence of triethylamine affords bis(5-R-3-cyanopyrrol-2-yl) disulfides.[26]



The use of sulfur monochloride in the synthesis of disulfides is based on the reactions involving its addition to unsaturated bonds[27] and also on substitution reactions involving aromatic and heterocyclic compounds.[2,3]



R = H, Bu^t; X = OH, NMe_2.



R, R^1 = Alk.

It has been noted[28] that the interaction of malonic ester with the $SF_4-HF-S_2Cl_2$ system leads to the formation of bis-[di(ethoxycarbonyl)fluoromethyl] disulfide.

2. Synthesis of disulfides from thiols

a. Oxidation of thiols

Thiols are relatively readily oxidised by various oxidants to disulfides. A whole series of preparatively extremely convenient methods of synthesis of disulfides have been developed on the basis of this reaction. The oxidation of thiols by oxygen catalysed by metal ions (Fe^{3+}, Cu^{2+}), UV irradiation, and other initiators of radical processes, is used very often in the synthesis of disulfides. Despite the great importance of this reaction in biological processes and its importance for the removal of sulfur from petroleum products, its mechanism has not been ultimately elucidated.[2] The stoichiometric equation of this reaction in a basic medium is as follows:

$$4RSH + O_2 = 2RSSR + 2H_2O.$$

Flavins oxidise anaerobically the excess thiol to the disulfide in a high yield and are simultaneously reduced to dihydroflavins.[2]

Hydrogen peroxide,[3] iron trichloride,[3] potassium hexacyanoferrate(III),[29] hypohalites,[29] cobalt-disulfophthalocyanine,[29] manganese tris(acetylacetonate),[29] iodine,[30] carbon tetrachloride,[31] *N*-chloro-compounds,[32–34] yeast,[35] and other compounds are also used as oxidants.

b. Photolysis of thiols

In the synthesis of asymmetric disulfides, both individual thiols and their mixtures with disulfides are photolysed. For example, the photolysis of a mixture of ethanethiol and dimethyl disulfide leads to the formation of ethyl methyl disulfide.[36]

$$EtSH \xrightarrow{h\nu} EtS^{\cdot} + H^{\cdot},$$

$$EtS^{\cdot} + Me_2S_2 \xrightarrow{h\nu} EtSSMe + MeS^{\cdot},$$

$$EtS^{\cdot} + MeS^{\cdot} \longrightarrow EtSSMe.$$

c. Sulfenylation of thiols

The sulfenylation of thiols by sulfenyl halides is a preparative method of synthesis of asymmetric disulfides.[29,37–39]

Alkali metal[29] and silver[40] thiolates as well as alkyl(aryl)-thiotrimethylsilanes[41] are sometimes used instead of thiols.

$$RSSiMe_3 + R^1SCl \xrightarrow[-Me_3SiCl]{} RSSR^1$$

R = Ph, $PhCH_2$; R^1 = Et, Ph, 4-MeC_6H_4.

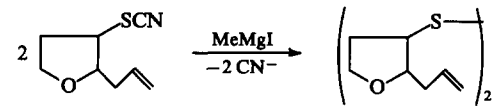
Thiols may be sulfenylated also by sulfenamides,[42–44] carboxylic acid thioloesters,[2] phosphonyl dithioformates,[45] phosphine sulfides,[46] alkyl(aryl)dithiopyridine *N*-oxides,[47] and other divalent sulfur compounds.[48,49] However, these methods have not found extensive application owing to the formation of side products which hinder the isolation of the disulfides.

3. Synthesis of disulfides from thiocyanates

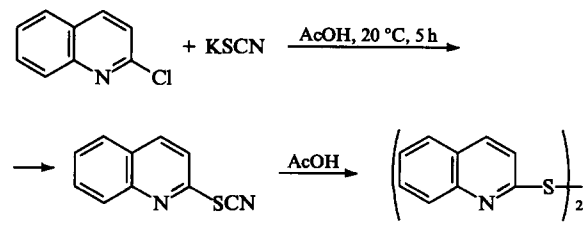
Symmetrical disulfides can be obtained relatively easily by cleaving thiocyanates with alkali.[3]

$$RSCN \xrightarrow{OH^-} RSSR + NH_3 + CO$$

The similar cleavage of 2-allyl-3-tetrahydrofuryl thiocyanate in the presence of methylmagnesium iodide affords bis(2-allyl-3-tetrahydrofuryl) disulfide.[50]



The synthesis of bis(quinolin-2-yl) disulfide by the reaction of 2-chloroquinoline with potassium thiocyanate in acetic acid has been described.[51]



The reaction of thiols with dithiocyanogen affords sulfenyl thiocyanates, the interaction of which with thiols leads to disulfides. This sequence of reactions has been used in the synthesis of cystine derivatives.[29]

$$RSH \xrightarrow[-HSCN]{(SCN)_2} RSSCN \xrightarrow[-HSCN]{R^1SH} RSSR^1$$

$R = HO_2CCHCH_2$ (NH_2); $R^1 = HO_2CCHCH_2$ ($NH_2 \cdot HCl$).

4. Syntheses of disulfides based on tetravalent and hexavalent sulfur compounds

The reduction of sulfinic acids by hydrogen bromide or of their chlorides by a mixture of trichlorosilane and tripropylamine is sometimes used to obtain symmetrical disulfides.[2] The chlorides of aromatic sulfonic acids are reduced comparatively readily to disulfides by hydrogen iodide in acetic acid. The preparation of asymmetric disulfides by the reaction of thioloesters of sulfinic acids with alkylthiotrimethylsilanes has been described.[52]

$$RS(O)SR + R^1SSiMe_3 \xrightarrow[-RSOSiMe_3]{} RSSR^1$$

5. Other methods of synthesis of disulfides

Asymmetric disulfides are frequently obtained by the thiol–disulfide exchange reaction.[2] For example, treatment of thiols with an excess of dimethyl disulfide in the presence of triethylamine leads to the formation of the corresponding alkyl methyl disulfides.

$$RSH + MeSSMe \xrightarrow{Et_3N} MeSSR + MeSH$$

The reaction of silyl sulfides with disulfides involves the exchange of the RS groups and the formation of asymmetric disulfides.[52]

$$RSSiMe_3 + R^1SSR^1 \rightleftharpoons R^1SSiMe_3 + R^1SSR$$

Asymmetric disulfides have also been obtained by treating alkyl disulfide anions, generated electrochemically from thiolate ions, with haloalkanes.[54]

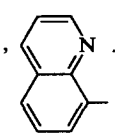
$$ArSS^- + RX \longrightarrow ArSSR$$

Ar = Ph, 2-$NO_2C_6H_4$, 4-$NO_2C_6H_4$; R = Alk.

It has been noted[54] that alkoxy- and acetoxy-disulfides are formed as a result of the ring opening and dimerisation of thiiranes in alcohols and acetic acid in the presence of germanium salts.

The monodesulfurisation of trisulfides by treatment with phosphines is sometimes used in the synthesis of symmetrical disulfides.[2] Depending on the nature of the phosphine, this entails either the removal of the terminal or the central sulfur atom. Thus, when tris(dimethylamino)phosphine is used, the terminal sulfur atom is mainly removed, whereas triphenylphosphine displaces the central sulfur atom. In order to retain the configuration in the conversion of sporidesmin trisulfide into the corresponding disulfide, triphenylphosphine is therefore employed. Disulfides are also formed in the interaction of sodium thiolates with chlorodiphenylmethane in an alcoholic medium.[55]

$$RSNa + Ph_2CHCl \xrightarrow[-NaCl]{O_2} RSSR + Ph_2C{=}O$$

R = 2,4-$(NO_2)_2C_6H_3$,  .

IV. Reactions with participation of disulfides

All the reactions with participation of disulfides can be divided into three large groups: (1) reactions occurring with cleavage of the S–S bond; (2) reactions occurring with cleavage of a C–S bond; (3) reactions leading to an increase in the valence of sulfur.

1. Reactions occurring with cleavage of the S–S bond

a. Cleavage by nucleophiles

The cleavage of the S–S bond in disulfides by nucleophiles proceeds via a S_N2 mechanism.[2]

$$RSSR + Nu^- \longrightarrow \left[RS{-}\underset{\displaystyle Nu}{\overset{\displaystyle -}{S}}R\right] \longrightarrow NuSR + RS^-$$

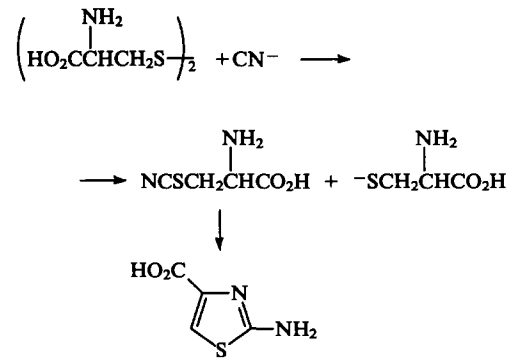
In the absence of steric influences, the sequence based on the relative S-nucleophilicities (thiophilicities) for reactions with aryl disulfides is as follows: $P(EtO)_3 > R^-$, HS^-, $EtS^- > PhS^- > PPh_3$, $CN^- > SO_3^{2-} > OH^- > 2,4\text{-}(NO_2)_2C_6H_3S^- > N_3^- > SCN^-$, I^-, $PhNH_2$. This sequence is not identical with that based on the relative C-nucleophilicities and depends to a much greater extent on the polarisability of the nucleophile.[2]

Cleavage by C-nucleophiles. The cleavage of disulfides by C-nucleophiles has been thoroughly investigated for reactions with the cyanide anion and carbanions generated by various methods.

The rate of cleavage of disulfides by the cyanide anion as well as the composition and structure of the reaction products are determined primarily by the nature of the initial disulfide. For example, simple dialkyl disulfides do not react with the cyanide anion, while diphenyl disulfide does react with it and forms an equilibrium mixture of products.

$$PhSSPh + CN^- \rightleftharpoons PhSCN + PhS^-$$

The interaction of the cyanide anion with cystine results in the formation of 2-aminothiazoline-4-carboxylic acid.[2]



On treatment with the cyanide anion, tetramethylthiuram disulfide undergoes monodesulfurisation,[3] which proceeds via a S–S bond cleavage stage.

$$Me_2NC(=S)SC(=S)NMe_2 + CN^- \longrightarrow Me_2NCS^- + Me_2NC(=S)SCN \longrightarrow$$

$$\longrightarrow Me_2NC(=S)SC(=S)NMe_2 + SCN^-$$

The cleavage of asymmetric disulfides by the cyanide anion proceeds relatively smoothly.[3]

$$ArSSR + CN^- \longrightarrow RSCN + ArS^-$$

Ar = 2-$NO_2C_6H_4$, 4-$NO_2C_6H_4$, 2,4-$(NO_2)_2C_6H_3$; R = Alk.

The rate of cleavage then depends directly on ΔpK_a—the difference between the pK_a for the thiols the residues of which form part of the disulfide molecule. The cleavage of disulfides with ΔpK_a = 1.8 proceeds in one direction. Disulfides with ΔpK_a = 1.65 to 1.05 can be attacked by the cyanide ion at both sulfur atoms. Disulfides with ΔpK_a = 0, i.e. symmetrical disulfides, do not react with the cyanide anion.[56]

The composition and nature of the products of the cleavage of asymmetric disulfides by the cyanide ion are also determined by thermodynamic factors, i.e. the cleavage takes place with formation of the thermodynamically more stable thiolate anion. The electronic factor (the cyanide anion attacks the sulfur atom with a lower electron density) and steric factors can also play a significant role.

In the presence of strong bases (KOH, Bu^tOK), dialkyl disulfides react with acetylene and its homologues to form mono- and di-(alkylthio)ethenes.[57,58]

$$RSSR + R^1C{\equiv}CH \xrightarrow[H_2O\ (or\ DMSO)]{ROH\ (or\ Bu^tOK)}$$

$$\longrightarrow RSC(R^1){=}CHSR + RSCH{=}CHR^1$$

R = Et, Pr^n, Bu^n; R^1 = H, Pr^n, Bu^n, Bu^t, Ph.

The mechanism of this reaction includes a stage in which the S–S bond is cleaved by the acetylide anion.

$$R^1C{\equiv}CH + OH^- \longrightarrow R^1C{\equiv}C^- + H_2O,$$

$$R^1C{\equiv}C^- + RSSR \longrightarrow [R^1C{\equiv}CSR] + RS^-,$$

$$RS^- + R^1C{\equiv}CH \longrightarrow R^1\bar{C}{=}CHSR \xrightarrow{R^1C{\equiv}CH} \longrightarrow R^1CH{=}CHSR,$$

$$[R^1C{\equiv}CSR] + RS^- \longrightarrow \underset{\displaystyle SR}{R^1C{=}\bar{C}SR} \xrightarrow{R^1C{\equiv}CH} \longrightarrow \underset{RS}{\overset{R^1}{}}\!\!>C{=}C<\!\!\overset{H}{}_{SR}.$$

The cleavage of the S–S bond in disulfides by organolithium compounds[27] leads to thiolates and sulfides as in the case of organomagnesium compounds.[29]

$$PhLi + PhSSPh \longrightarrow PhSLi + PhSPh$$

The carbanions generated by treatment with Pr^i_2NLi also cleave the S–S bond in disulfides. This is one of the procedures most widely used in fine organic synthesis for the introduction of the sulfide functional group. It is used, for example, in the syntheses of α,β-unsaturated carbonyl compounds and α-oxoesters.[59,60]

$$R_2CHCHCO_2R \xrightarrow[2.\ PhSSPh]{1.\ LiN(Pr^i_2)} R_2CHCCO_2R \xrightarrow[MeOH]{NaIO_4} \longrightarrow R_2CHCCO_2R \xrightarrow{\Delta} R_2C{=}CCO_2R$$

$$RCH_2CO_2R \xrightarrow[2.\ PhSSPh]{1.\ LiN(Pr^i_2),\ THF\ (-78\ ^\circ C)} R{-}C(SPh)_2{-}CO_2R \xrightarrow[2.\ CF_3CO_2H]{1.\ I_2,\ MeOH} \longrightarrow RC(=O){-}C(=O)R$$

The nucleophilic substitution of the tributylstannate group by the thiolate anion obtained from disulfides by treatment with butyllithium has been described.[61]

$$Bu_3SnCH{=}CHSnBu_3 \xrightarrow[-Bu_3SnLi]{RSSR\ (BuLi,\ -78\ ^\circ C)} Bu_3SnCH{=}CHSR$$

The addition of disulfides to the double bonds of cyclopentadiene in the presence of sodium hydride[62] also evidently proceeds via a stage involving the cleavage of the S–S bond by the carbanion.

Cleavage by O-nucleophiles. The reaction of disulfides with OH^- ions can proceed via one of three mechanisms depending on the structure of the initial disulfide.[2] In the absence of active α- or β-hydrogen atoms in the disulfide molecule, nucleophilic substitution takes place at a sulfur atom with formation of a thiolate anion and a sulfenic acid,[63] which disproportionates to the sulfinic acid.

$$2ArSSAr + 4OH^- = 3ArS^- + ArSO_2^- + 2H_2O$$

In the case of asymmetric disulfides, the hydroxide ion attacks the sulfur atom furthest from the electron-accepting group and the cleavage proceeds more readily the more stable the anion split off.

In the presence of an acid α-hydrogen atom, there is a possibility of a 1,2-elimination reaction with the initial formation of a thione, which hydrolyses to a ketone or isomerises to an enethiol.[2]

$$RS{-}S{-}\underset{Me}{\overset{H{\leftarrow}OH^-}{C}}CO_2^- \longrightarrow RS^- + S{=}\underset{Me}{C}{-}CO_2^- \xrightarrow{H_2O} \longrightarrow \underset{Me}{O{=}C}{-}CO_2^-$$

R = $CHMeCO_2^-$.

The cleavage of aryl diphenylmethyl disulfides on treatment with an alkoxide anion proceeds similarly.[2]

$$RO^- + Ph_2CHSSAr \longrightarrow \left[RO^{\delta-}\cdots H^{\delta+}\cdots \underset{Ph}{\overset{Ph}{C}}\cdots S^{\delta+}\cdots SAr^{\delta-}\right] \longrightarrow Ph_2C{=}S + ROH + ArS^-$$

In the presence of an acid β-hydrogen atom, 1,2-elimination results in the formation of an alkene and a hydrodisulfide anion, which is converted into a thiolate anion and further into a sulfide.[2]

$$^-OOC{-}\underset{H_2N}{\overset{H{\leftarrow}OH^-}{C}}{-}CH_2{-}SSR \longrightarrow {}^-OOC{-}\underset{H_2N}{C}{=}CH_2 + RSS^-$$

$$RSS^- \longrightarrow RS^- + S$$

$$^-OOC{-}\underset{H_2N}{C}{=}CH_2 + RS^- + H_2O \longrightarrow {}^-OOC{-}\underset{H_2N}{CH}{-}CH_2SR$$

R = $CH_2CH(NH_2)COO^-$.

Cleavage by P-nucleophiles. The composition and structure of the products of the cleavage of disulfides by phosphorus compounds are determined by the nature of the organophosphorus compounds. Thus the cleavage of disulfides in the presence of dialkylaminophosphines proceeds with formation of sulfides and *N,N*-dialkylphosphoramidothioates.[27] The reaction takes place stereospecifically with inversion at one of the α-carbon atoms.

$$(R_2N)_3P + \cdots\!\!>\!\!C{-}S{-}SR^1 \longrightarrow \cdots\!\!>\!\!C{-}S{-}\overset{+}{P}(NR_2)_3 + R^1S^-$$

$$R^1S^- + \cdots\!\!>\!\!C{-}\overset{+}{S}{-}P(NR_2)_3 \longrightarrow R^1S{-}C\!<\!\cdots + (R_2N)_3P{=}S$$

Symmetrical diallyl disulfides are more reactive than dialkyl disulfides, while asymmetric disulfides react even at room temperature.

Primary and secondary phosphines convert disulfides into thiols.[3]

$$RPH_2 + 2\,R^1SSR^1 \longrightarrow RP(SR^1)_2 + 2\,R^1SH$$

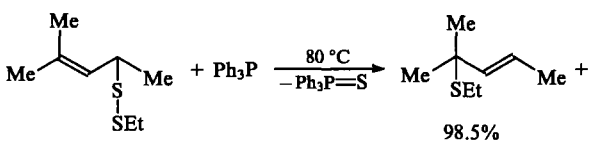
$$R_2PH + R^1SSR^1 \longrightarrow R_2PSR^1 + R^1SH$$

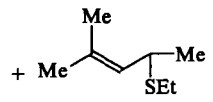
Triphenylphosphine in aqueous dioxane reduces disulfides to thiols;[64] triphenylphosphine oxide is formed simultaneously owing to the hydrolysis of the cation formed in the first stage of the reaction. In the absence of a solvent, a monosulfide and triphenylphosphine sulfide are formed.[3]

$$RSSR + Ph_3P \longrightarrow RSR + Ph_3P{=}S$$

R = $CH_2{=}CHCH_2$, $MeCH{=}CHCH_2$, $Me_2C{=}CHCH_2$ etc.

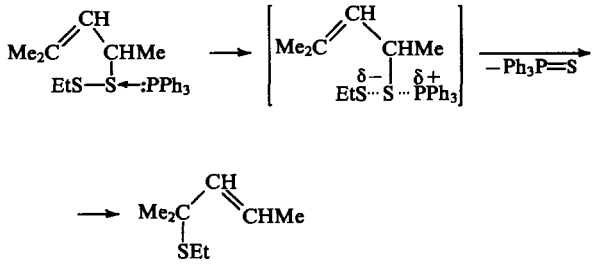
When dialkenyl and alkenyl alkyl sulfides are heated with triphenylphosphine, a mixture of two sulfides and triphenylphosphine sulfide is formed.[65]



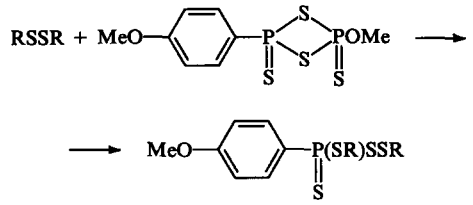


1.5%

The authors[65] believe that the reaction proceeds via an intermediate polarised complex formed as a result of the nucleophilic attack by triphenylphosphine at one of the sulfur atoms, further cleavage occurring via a S_Ni mechanism with migration of the double bond.



It has been noted[66] that the interaction of disulfides with dithiadiphosphetanes in anhydrous toluene at 120–130 °C proceeds with formation of phosphonotrithioates.



Cleavage by S-nucleophiles. The cleavage of disulfides by the thiolate anion — the thiol–disulfide exchange reaction — plays a very important role in biological processes. For example, it has been suggested[3] that the permeation of a bacteriophage through the wall of the rectum in animal organisms occurs as a result of the cleavage of the S–S bond by the thiolate anion. Asymmetric disulfides are cleaved more readily by the thiolate anion than symmetrical ones. In this case, the thermodynamic factor, i.e. the thermodynamic stability of the newly formed thiolate anion, plays an important role. The steric factor is likewise important. For example, the cleavage of di(*tert*-butyl) disulfide is approximately 10^6 times slower than that of di(n-butyl) disulfide, which is evidence in support of a S_N2 mechanism of this reaction. 1,2-Dithiolanes exhibit an anomalously high reactivity in their reaction with the thiolate anion, which has been explained[3] by the removal of the torsional strain as a result of ring opening.



The behaviour of lipoic acid in biological systems has also been explained by a similar anomalous reactivity.

Cleavage by N-nucleophiles. The cleavage of the S–S bond in bis(dialkoxyphosphonyl) and bis(dialkoxythiophosphonyl) disulfides in the presence of amines leads to sulfenamides.[67]

$$RSSR + 2\,R^1R^2NH \longrightarrow RSNR^1R^2 + RS^- + R^1R^2\overset{+}{N}H_2$$

R = CN, $(AlkO)_2P(S)$, $(AlkO)_2P(O)$.

$R^1 = R^2 = Me, H$.

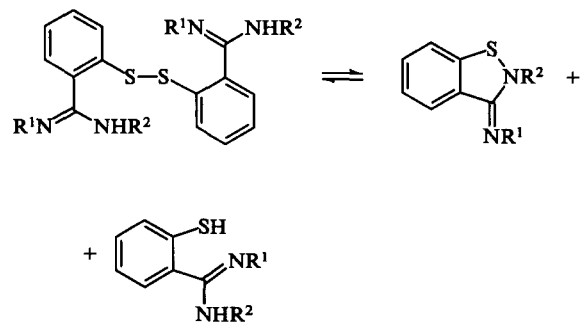
The reactivity of amines in this reaction diminishes in accordance with their basicity in the following sequence: $Me_2NH > MeNH_2 > NMe_3 > NH_3$.

The cleavage of diaryl disulfides by *N*-arenesulfonylsulfilimines in chlorobenzene leads to the formation of *N,N*-bis(arylthio)arenesulfonamides.[68]

$$ArSSAr + Ph_2S{=}NR \xrightarrow[PhCl]{\Delta} (ArS)_2NR + Ph_2S$$

Ar = 4-MeC_6H_4, Ph; R = Ts, $PhSO_2$.

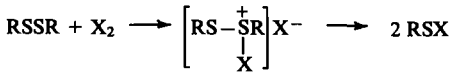
Diaryl disulfides containing amidine groups in the *ortho*-position are cleaved at the S–S bond on heating, with participation of the more nucleophilic nitrogen atom of the amidine group.[69]



$R^1 = R^2 = H$, Alk, Ar.

b. Cleavage of the S–S bond by electrophiles

The cleavage of the S–S bond in disulfides by the halogens and halogenating agents has long been known and has been thoroughly investigated. A series of preparative methods of synthesis of sulfenyl halides have been developed on the basis of this reaction.[70–72] The reaction proceeds with formation of chlorosulfonium intermediates, the cleavage of which leads to two



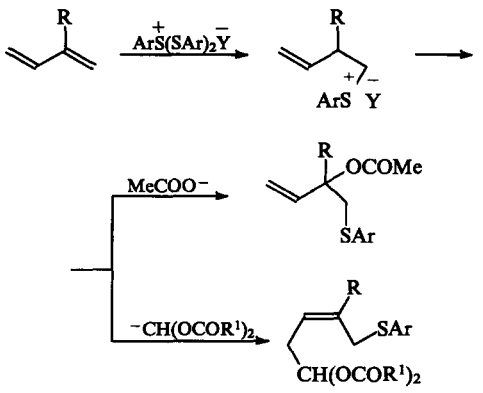
molecules of a sulfenyl halide.[70]

The interaction of disulfides with sulfenyl halides can proceed in different ways depending on the conditions. In the absence of catalysts, the reaction between diaryl disulfides and arenesulfenyl chlorides takes place with cleavage of the S–S bond and the exchange of arenesulfenyl groups.[2]

$$ArSSAr^1 + ArSX \longrightarrow \left[ArS-\overset{+}{\underset{Ar}{S}}-SAr^1\right]X^- \longrightarrow$$

$$\longrightarrow ArSSAr + Ar^1SX$$

In the presence of Lewis acids, diaryl disulfides and arenesulfenyl halides form the complexes $ArS^+(SAr)_2Y^-$ ($Y = SbCl_6$, $SbCl_4$, SbF_6, BF_4), which are effective agents for the transfer of the arylthio-cation in reactions with alkenes.[73-75]

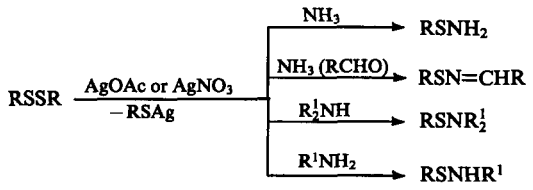


R = H, Me; R^1 = Me, Et;

Ar = Ph, 4-ClC_6H_4, 4-MeC_6H_4, C_6F_5;

Y = BF_4, SbF_6, $SbCl_6$.

In the syntheses of various sulfenamides from disulfides, the joint action of electrophiles and nucleophiles (for example Ag^+ ions and amines) is used to cleave the S–S bond.[2,76,77]



R = 4-MeC_6H_4, 3-$NO_2C_6H_4$, 4-$NO_2C_6H_4$ etc.;

R^1 = Me, Et, Pr^i, Bu, etc.

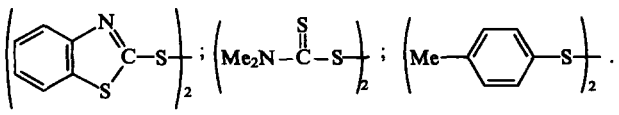
It has been noted[78] that, on heating in acetic anhydride, diphenyl disulfide is cleaved, affording the following products: PhSH, PhSAc, and $(PhS)_3CMe$.

c. Homolytic cleavage of the S–S bond

Many disulfides exhibit thermochromism (they are reversibly coloured on heating). In order to account for this phenomenon, the erroneous hypothesis has been put forward that the thermochromism is due to the reversible dissociation of disulfides into thiyl radicals, which are present at an appreciable concentration.

$$RSSR \rightleftarrows 2RS^{\bullet}$$

When disulfides are heated, the homolysis of the S–S bond does indeed take place but with very low rate constants (k), which have the following values at 100 °C:[2]



$k = 8.3 \times 10^{-5}\ s^{-1}$ $k = 5.5 \times 10^{-6}\ s^{-1}$ $k \leqslant 2 \times 10^{-8}\ s^{-1}$

The pyrolysis of dialkyl disulfides in the gas phase begins at 200 °C. The thermal decomposition temperature is then reduced with increase in the length of the alkyl groups and the degree of their branching.[79] The pyrolysis of dimethyl disulfide in the gas phase at 316–317 °C under reduced pressure (3.2 to 3.0 kPa) takes place with formation of hydrogen sulfide, ethylene, sulfur, and other products. It has been suggested[27] that the pyrolysis begins with the homolytic cleavage of the S–S and C–S bonds; the radicals MeS$^{\bullet}$ and atomic sulfur, formed under these conditions, react subsequently with the initial disulfide. (In a high vacuum, dimethyl disulfide dissociates into thioformaldehyde and methanethiol.)

$$MeSSMe \longrightarrow CH_2{=}S + MeSH$$

Judging from the nature of the final products, the pulsed vacuum pyrolysis of diisopropyl disulfide at 500 °C begins with the homolytic rupture of a C–S bond accompanied by the formation of isopropyldisulfane as an intermediate, which subsequently decomposes into propene, hydrogen sulfide, and sulfur.[80]

$$Me_2CHSSCHMe_2 \longrightarrow [Me_2CHSSH] \longrightarrow$$

$$\longrightarrow MeCH{=}CH_2 + HSSH$$

$$HSSH \longrightarrow H_2S + S$$

The pyrolysis of di(*tert*-butyl) disulfide also begins with the homolysis of a C–S bond and is completed by the formation of H_2S, CS_2, CH_4, and $CH{\equiv}CH$.[27,79] Hence, on passing from dimethyl disulfide to diisopropyl and di(*tert*-butyl) disulfides, the probability of the cleavage of a C–S bond increases owing to the decrease in the dissociation energy of this bond in the above series.

The vacuum pyrolysis of diphenyl and di(naphth-2-yl) disulfides at 400–700 °C takes place with formation of thiyl radicals owing to the homolytic cleavage of the S–S bond.[27]

The thiyl radicals obtained by the pyrolysis of disulfides are used in organic synthesis as highly reactive intermediates. For example, the thiyl radicals generated from the diphenyl disulfide in the liquid phase at 125–230 °C react with bromoarenes in hydrogen sulfide to form the corresponding asymmetric sulfides.[81]

$$2\,ArBr + Ph_2S_2 \xrightarrow{H_2S} 2\,ArSPh + 2\,HBr$$

$$PhSSPh \xrightarrow{\Delta} 2\,PhS^{\bullet}$$

$$ArBr \longrightarrow Ar^{\bullet} + Br^{\bullet}$$

$$PhS^{\bullet} + H_2S \longrightarrow PhSH + HS^{\bullet}$$

$$Br^{\bullet} + H_2S \longrightarrow HBr + HS^{\bullet}$$

$$Ar^{\bullet} + H_2S \longrightarrow ArH + HS^{\bullet}$$

$$PhSH + Br^{\bullet} \longrightarrow PhS^{\bullet} + HBr$$

$$PhSH + Ar^{\bullet} \longrightarrow PhS^{\bullet} + ArH$$

$$ArBr + PhS^{\bullet} \longrightarrow \left[R\text{–}\langle\rangle\text{(SPh, Br)}\right] \xrightarrow[-HBr]{PhSH}$$

$$\longrightarrow ArSPh + PhS^{\bullet}$$

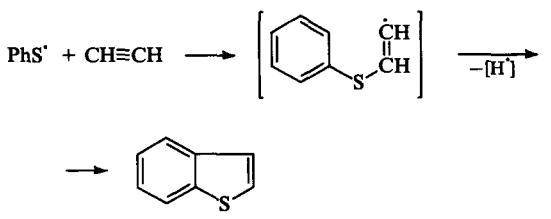
The radicals PhS$^{\bullet}$ play also the role of agents transferring hydrogen atoms from H_2S to the Br$^{\bullet}$ and Ar$^{\bullet}$ radicals in this reaction. The temperature of the thiylation of bromoarenes in

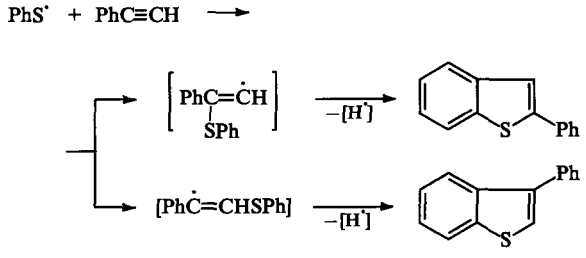
accordance with this scheme decreases after the introduction of a π-dative substituent into the benzene ring. Chloro-derivatives of benzene, thiophene, and naphthalene react with disulfides at higher temperatures than the bromo-derivatives owing to the greater resistance of the C–Cl bond to thermal homolysis.[82–84]

$$RSSR + R^1Cl \xrightarrow{600-630\ ^\circ C} RSR^1 + RSCl$$

R = Alk; R^1 = Ph, 4-MeC_6H_4, $C_{10}H_7$, C_4H_3S, 2-ClC_6H_4, 4-$CF_3C_6H_4$, 3,4-$Cl_2C_6H_3$.

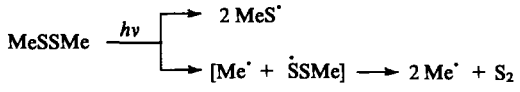
The thiyl radicals generated by the thermolysis of diphenyl disulfide at 550 °C react with acetylene and phenylethyne to form benzo[*b*]thiophene and 2- and 3-phenylbenzo[*b*]thiophenes respectively.[85]





At higher temperatures, the addition of the phenylthiyl radical to phenylethyne and other acetylene homologues leads to phenyl vinyl sulfides.[86,87]

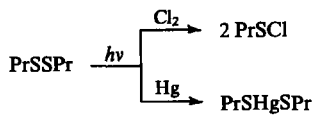
Depending on the wavelength of the radiation, the gas-phase photolysis of disulfides can proceed with homolytic cleavage of both the S–S and C–S bonds.[27] Thus, on irradiation of dimethyl disulfide with UV light at a wavelength < 195 nm, the ratio of the products formed as a result of the homolysis of the C–S and S–S bonds is 1.35 : 1.



When sources of radiation with a wavelength of 254 nm are used, the photolysis of the C–S bond becomes insignificant provided that the alkyl radical is not stabilised by the corresponding functional groups. The main process in this case becomes the homolysis of the S–S bond with formation of thiyl radicals. In the case of primary and secondary dialkyl disulfides, these radicals readily recombine in solution; this is used in the synthesis of asymmetric dialkyl disulfides.

$$RSSR + R^1SSR^1 \overset{h\nu}{\rightleftharpoons} 2\,RSSR^1$$

The equilibrium position is determined by the nature of the alkyl group. In the case of alkyl groups having the normal structure, the ratios RSSR : $RSSR^1$: R^1SSR^1 are 1 : 2 : 1.[27] The photochemical homolysis of the S–S bond in disulfides in the presence of chlorine or elemental mercury leads respectively to sulfenyl chlorides and mercury thiolates.[27]



The thiyl radicals generated in the photolysis of diaryl disulfides enter into the homolytic chlorine substitution reaction in trichloro- and tetrachloroethenes, affording $ArSCH=CCl_2$, $ArSCCl=CHCl$, and $ArSCCl=CCl_2$.[88] In liquid ammonia, on UV irradiation in a quartz bulb for 12 h diaryl disulfides react with trifluoromethyl iodide, forming the corresponding aryl trifluoromethyl sulfides.[89]

$$XC_6H_4S-SC_6H_4X \xrightarrow{2\,CF_3I\ (h\nu)} 2\,XC_6H_4SCF_3$$

X = H, 4-Cl, 2-NO_2, 4-NO_2.

After prolonged irradiation of diphenyl disulfide and its *para*-chloro-derivative, a series of side products are formed, so that the yields of the corresponding sulfides are 12% and 36% respectively. The presence of the nitro-group hinders the radical side processes and the yields of *p*- and *o*-nitrophenyl trifluoromethyl sulfides reach 58% and 72%.

The homolytic cleavage of the S–S bond in disulfides also takes place in the presence of free radicals and compounds which are sources of free radicals (peroxides, diazo-compounds, azo-compounds, etc.). The homolytic cleavage of the S–S bond in disulfides by free radicals constitutes the basis of the polymer chain transfer process in radical polymerisation.[6]

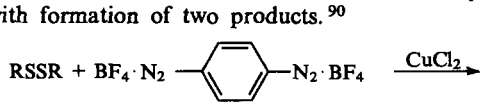
The aryl radicals formed as a result of the cleavage of diazonium salts afford sulfides on reaction with symmetrical disulfides.[90]

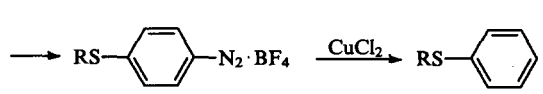
$$4\text{-}ClC_6H_4N_2X \xrightarrow[-N_2,\ -X^-]{CuCl_2} 4\text{-}ClC_6H_4^{\bullet}$$

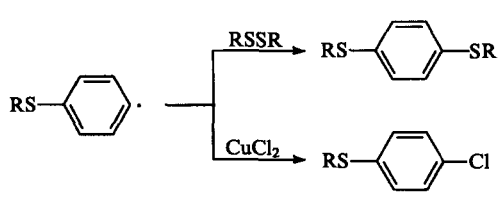
$$4\text{-}ClC_6H_4^{\bullet} + RSSR \longrightarrow 4\text{-}ClC_6H_4SR + RS^{\bullet}$$

R = Bu, $PhCH_2$, Ph; X = Cl, BF_4.

Benzenebisdiazonium tetrafluoroborates arylate disulfides with formation of two products.[90]







R = Bu, Ph, $PhCH_2$.

d. Reduction of disulfides

The reduction of disulfides takes place with cleavage of the S–S bond and the formation of thiols.

$$RSSR \xrightarrow{Red} 2\,RSH$$

A series of preparative methods of synthesis of thiols, described in the scientific literature and in handbooks, have been developed on the basis of this reaction. Zinc in acetic, hydrochloric, and sulfuric acids,[70] metallic sodium in xylene,[70] sodium hydrogen sulfide in alcohol,[29] lithium tetrahydroaluminate in ether or tetrahydrofuran,[91] and the $BF_3 \cdot H_2O - Et_3SiH$ system[92] are used as the reductants. Bis(trifluoromethyl) disulfide is relatively easily reduced in the presence of powdered activated copper in dimethylformamide[89] or acetonitrile.[93]

$$CF_3SSCF_3 \xrightarrow{2\,Cu\ (DMF\ or\ MeCN)} 2\,CF_3SCu \cdot DMF(MeCN)$$

In dimethylformamide, the reaction is exothermic and is completed after 1 h, whereas in acetonitrile the reduction takes place over a period of 14–16 h. The ease of the cleavage of the S–S bond in bis(trifluoromethyl) disulfide in the presence of copper has been explained[93] by the high oxidising capacity of this compound.

The traditional method for the reduction of disulfide bonds in proteins involves the treatment of the protein with a large excess of a thiol. The thiol–disulfide exchange reaction then takes place.[2]

$$RSSR + 2\,R^1SH \rightleftharpoons 2\,RSH + R^1SSR^1$$

Dithiothreitol $HSCH_2CH(OH)CH(OH)CH_2SH$ is used nowadays for such purposes. The reduction of cystine to cysteine in living organisms takes place mainly as a result of the action of the enzyme glutathionecystine-oxidoreductase.[2]

e. Insertion of sulfur and other reagents in the S–S bond

Certain cyclic sulfides and disulfides are converted into trisulfides on interaction with a dihydrodisulfide. It has been suggested[2] that the reaction proceeds via the insertion of sulfur in the S–S bond and not via nucleophilic substitution at a carbon atom.

$$RSSR \xrightarrow{HSSH} \left[RS-\overset{S}{\overset{\|}{S}}R\right] \longrightarrow RSSSR$$

This hypothesis has been confirmed to some extent by the fact that the conversion of sporidesmin (S_2 bridge) into sporidesmin E (S_3 bridge) in the presence of dihydrodisulfide takes place with retention of configuration.

The insertion of carbenes in the S–S bond of disulfides leads to the formation of thioacetals.[94]

$$RSSR + :CH_2 \longrightarrow RSCH_2SR$$

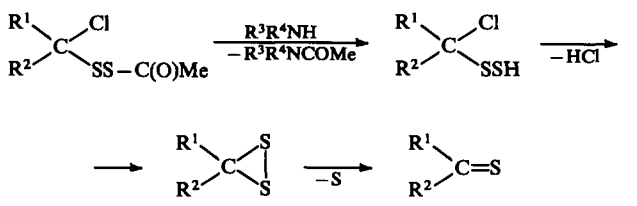
2. Reactions involving the cleavage of a C–S bond

The cleavage of a C–S bond is less characteristic of disulfides than the cleavage of the S–S bond. The cleavage of the S–S bond is sometimes accompanied by the cleavage of a C–S bond, which has already been noted in the case of the photolysis or the thermolysis of disulfides.

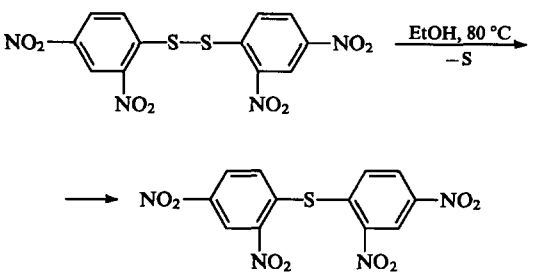
Disulfides containing readily removable groups at the sulfur atom, such as RCO, $PhCH_2$, $HOOCCH_2$, $2,4\text{-}(NO_2)_2C_6H_3$, etc. show the greatest tendency towards the cleavage of a C–S bond. For example, when a diacyl disulfide is acted upon by chlorine, the S–S bond and not a C–S bond is cleaved with formation of acyldisulfenyl chlorides.[72]

$$RC(O)SSC(O)R \xrightarrow{Cl_2} RC(O)SSCl + RC(O)Cl$$

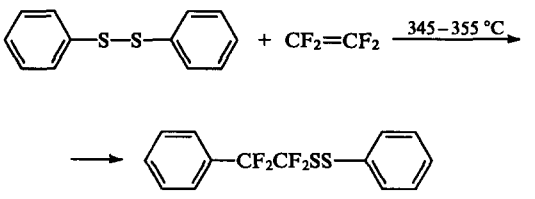
A C–S bond in acetyl α-chloroalkyl disulfides is cleaved by secondary amines with formation of α-chloroalkyl disulfones, which are converted into unstable cyclic disulfides as a result of the elimination of hydrogen chloride.[95]



On heating in alcohol, bis(2,4-dinitrophenyl) disulfide is readily converted into the corresponding sulfide, as a result of the cleavage of the C–S and S–S bonds.[96]

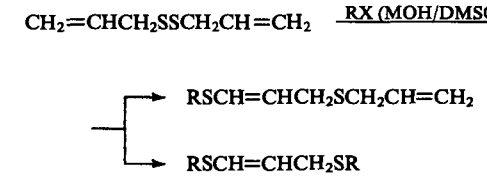


The thermal insertion of tetrafluoroethene in a C–S bond of diphenyl disulfide with formation of phenyl β-phenyltetrafluoroethyl disulfide has been described.[97]



40%

The cleavage of a C–S bond also occurs in various rearrangements of disulfides. Thus diallyl disulfide and its substituted derivatives rearrange to the thioanion $CH_2{=}CHCH_2.SCH_2CH{=}CHS^-$ on treatment with the dimethyl sulfoxide (DMSO)–MOH (M = K, Na) superbasic system.[98] Under the same conditions, the disulfides $RSSCHCH{=}CH_2$ (R = Et, Pr) rearrange to the corresponding thioanions, the subsequent alkylation of which by alkyl iodides leads to the bissulfides $RSCH_2CH{=}CHSR^1$ (R^1 = Pr, Pr^i). The alkylation of diallyl disulfides by alkyl halides in the DMSO–NaOH(KOH) superbasic system leads to 1-alkylthio-3-allylthio-1-propenes and 1,3-di(alkylthio)-1-propenes.[99]



Under similar conditions, 1-alkylthiobuta-2,3-dienes rearrange to 2-alkylthio- and 1-alkylthio-buta-1,3-dienes.[99]

3. Reactions involving an increase in the valence of sulfur

a. The formation of sulfonium complexes

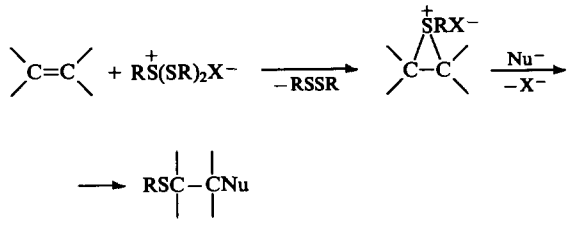
As already mentioned, the interaction of disulfides with sulfenyl halides in the presence of Lewis acids leads to the formation of sulfonium complexes in which the sulfonium cation is stabilised by the anionoid fragment of the Lewis acid.[27,73–75]

$$RSSR + RSCl + SbCl_5 \longrightarrow R\overset{+}{S}(SR)_2SbCl_6^-$$

Complexes of a similar structure are also formed in the interaction of disulfides with the alkyl esters of trifluoromethanesulfonic acid.[100]

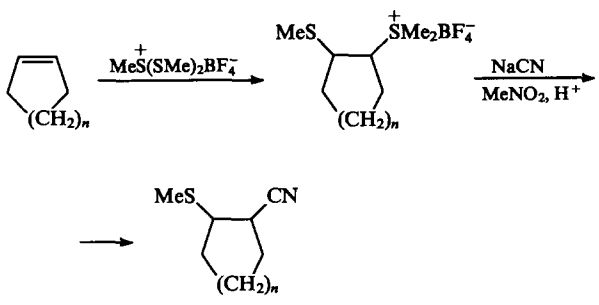
$$(MeS)_2 + CF_3SO_3Me \xrightarrow{CH_2Cl_2,\ 0\,^\circ C,\ N_2} Me\overset{+}{S}(SMe)_2CF_3SO_3^- \quad 84\%$$

Such complexes have found applications in organic synthesis as RS^+ group transfer agents. The interaction of sulfonium complexes with alkenes can proceed differently. In some cases, the reaction involves the formation of episulfonium ions, which undergo ring opening on treatment with nucleophiles, giving rise to sulfides.[100-102]



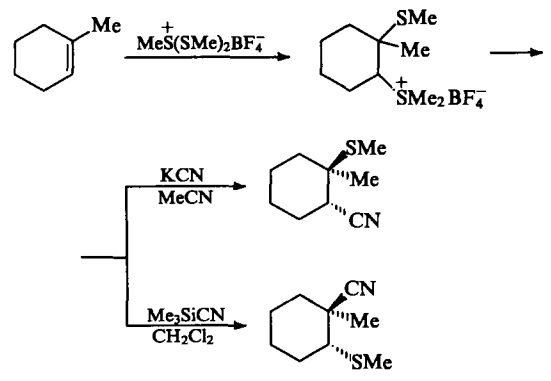
R = Alk, Ar; X = CF_3SO_2, $SbCl_6$, BF_4, etc.

In other cases, for example in the addition of sulfonium complexes to cycloalkenes, adducts are formed, their behaviour in reactions with nucleophiles being similar to that of episulfonium salts. A general mild cyanosulfenylation method has been developed on the basis of this reaction.[27]

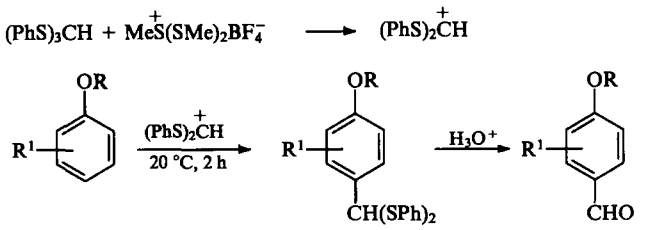


n = 1, 2.

Depending on the conditions in the reaction with nucleophiles, both regioisomers may be obtained.[27]



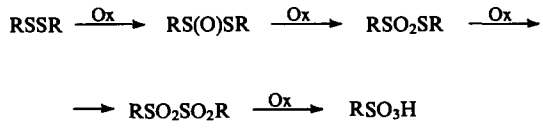
A method for the regioselective formylation of phenols and naphthols has been developed using sulfonium complexes and thioacetals.[103]



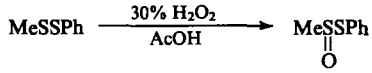
35%-87%

b. Oxidation of disulfides

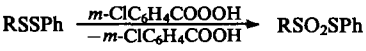
Depending on the nature of the oxidant and the reaction conditions, the oxidation of disulfides can lead to the formation of thiolosulfinates, thiolosulfonates, disulfones, and sulfonic acids.



Symmetrical thiolosulfinates are formed as a result of the oxidation of symmetrical disulfides by peroxyacids, sodium metaperiodate, and ammonium persulfate or by photosensitised oxidation in the presence of Methylene Blue.[70] Asymmetric thiolosulfinates are formed in the oxidation of asymmetric disulfides by 30% hydrogen peroxide in acetic acid.[104] The oxidation then proceeds regioselectively at the more nucleophilic sulfur atom.



The use of an excess of hydrogen peroxide leads to thiolosulfonates, which are also formed in the oxidation of disulfides by cold nitric acid and vanadium pentoxide[70] or by chlorine in acetic acid with subsequent hydrolysis.[105] The oxidation of asymmetric disulfides by *m*-chloroperbenzoic acid also takes place regioselectively at the more nucleophilic sulfur atom.[106]



The oxidation of disulfides RSSR (R = Me, Bu, Ph, $PhCH_2$) by the $H_2O_2-Na_2WO_4$ system in the presence of acetyltrimethylammonium chloride leads to the formation of the disulfones RSO_2SO_2R in 46%-81% yield.[107]

Disulfides are oxidised by hot nitric, chromic, and performic acids or potassium permanganate to sulfonic acids.[2] The reaction of disulfides with the radical-anion $^-O-O^-$, generated from KO_2 and anhydrous 18-crown 6-ether in dry pyridine at 25 °C, leads to the formation of a mixture of RSO_2^- and RSO_3^-.[108]

The standard method for the cleavage of disulfide bonds in proteins involves treatment of the latter with performic acid. The cysteine and cystine residues are then converted after hydrolysis[2] into cysteic acid $HO_2CCH(NH_2)CH_2SO_3H$. Chlorination of disulfides by chlorine in acetic acid leads to the formation of the chlorides of sulfinic[109] or sulfonic[2] acids.

c. Oxidative imination of disulfides

The reactions accompanied by the oxidation of an element and the formation of the imino-group have come to be called oxidative imination.[110] The oxidative imination of disulfides by *N*-chloro- and *N,N*-dichloro-compounds can lead to the formation of the chlorides, amides, and esters of iminosulfinic acids.

The formation of the chlorides of iminosulfinic acids. The interaction of disulfides with *N,N*-dichloroamides or

N,N-dichloroamines in anhydrous aprotic organic solvents for a 1 : 1 reactant ratio leads to the formation of the chlorides of *N*-substituted iminosulfinic acids and sulfenyl chlorides.[112–115]

$$RSSR + R^1NCl_2 \longrightarrow RS(=NR^1)Cl + RSCl$$

R = Ph, $PhCH_2$, 4-ClC_6H_4, 4-$NO_2C_6H_4$, 2-$NO_2C_6H_4$;
R^1 = $ArSO_2$, ArCO, Bu^t, $Me_2C(CN)$, CF_3SO_2.

In the case of asymmetric disulfides, the sulfenyl chlorides formed contain more highly electron-accepting groups, since the sulfur atom with a high electron density undergoes oxidative imination. The sulfenyl chlorides formed can react further under more severe conditions with *N,N*-dichloro-compounds to form *N*-substituted chlorides of iminosulfinic acids, so that for preparative purposes the reaction is carried out in a single stage without isolating the sulfenyl chlorides. The chlorides of *N*-(benzenesulfonyl)areneiminosulfonic acids are formed in the reaction of diaryl disulfides with chlorine in acetic acid and subsequent treatment of the reaction mixture with the *N,N*-dichloroamide of benzenesulfonic acid.[116]

$$ArSSAr \xrightarrow[AcOH]{Cl_2} 2\,ArS(O)Cl \xrightarrow[-Cl_2]{2\,PhSO_2NCl_2} 2\,ArS(Cl)(O)=NSO_2Ph$$

In the reaction of disulfides with the *N*-chloroamides of carboxylic acids, the chlorides of *N*-acyliminosulfinic acids are obtained.[117]

$$ArSSAr + 3\,RCONHCl \longrightarrow 2\,ArS(=NCOR)Cl + RCONH_2 + HCl$$

The reaction takes place in stages. For a 1 : 1 reactant ratio, *N*-acylsulfenamides and sulfenyl chlorides are formed initially and then react further with the *N*-monochloroamide.

$$ArSSAr + RCONHCl \longrightarrow ArSNHCOR + ArSCl$$

$$ArSNHCOR + RCONHCl \longrightarrow ArS(=NCOR)Cl + RCONH_2$$

$$ArSCl + RCONHCl \longrightarrow ArS(=NCOR)Cl + HCl$$

The interaction of diaryl disulfides with the alkyl esters of *N*-chlorobenzenecarboxyimidic acid for a 1 : 1 reactant ratio leads similarly to the formation of the corresponding alkyl esters of *N*-(arylthio)benzenecarboxyimidic acid and arenesulfenyl chlorides. The latter react further with the *N*-chloroimino-ester, affording the chlorides of *N*-benzoylareneiminosulfinic acids.[118]

$$ArSSAr + ClN{=}C(OAlk)Ph \longrightarrow ArSN{=}C(OAlk)Ph + ArSCl$$

$$ArSCl + ClN{=}C(OAlk)Ph \longrightarrow ArS(=NCOPh)Cl + AlkCl$$

The oxidative imination of disulfides by sodiochloroamides of sulfonic acids in aqueous media leads to the amides of aminosulfinic acids.[119–121] As in the oxidation of thiols to disulfides,[122] the reactivity of the disulfides with respect to the sodiochloroamides of sulfonic acids is then directly related to the pK_a of the corresponding thiols the residues of which form the disulfides. Consequently the acid properties of thiols can be used as a quantitative criterion for the estimation of the reactivities of disulfides with respect to the sodiochloroamides of sulfonic acids. Indeed, it has been shown[121] that the disulfides for which the pK_a for the corresponding thiols are in the range 7–11 are relatively easily iminated by the sodiochloroamides of sulfonic acids. A decrease in the pK_a for the thiols to 5–6 leads to a decrease in the rate of the imination reaction and in the yield of the amides of iminosulfinic acids. The disulfides where the pK_a for the corresponding thiols are less than 5 are not iminated by the sodiochloroamides of sulfonic acids. Such disulfides contain as a rule highly electron-accepting groups at the sulfur atoms which reduce the nucleophilicity of the latter. The imination of asymmetric disulfides by the sodiochloroamides of sulfonic acids takes place regioselectively at the more nucleophilic sulfur atom.[123] From the standpoint of the acid properties of the corresponding thiols, this means that the pK_a for the thiol the residue of which is iminated is higher than that for the thiol the residue of which is eliminated. This residue gives rise to symmetrical disulfides.

$$RSSR^1 + 2\,PhSO_2NNaCl\cdot xH_2O \xrightarrow[-0.5\,R^1SSR^1,\ -2\,NaCl]{} RS(=NSO_2Ph)NHSO_2Ph$$

R = Bu; R^1 = 4-$NO_2C_6H_4$, 2,4-$(NO_2)_2C_6H_3$;
R = Ph; R^1 = 4-$NO_2C_6H_4$, 2,4-$(NO_2)_2C_6H_3$;
R = 4-MeC_6H_4; R^1 = 2,4-$(NO_2)_2C_6H_3$;
R = $PhCH_2$; R^1 = 2,4-$(NO_2)_2C_6H_3$.

The interaction of *N,N*-dichloro-compounds with sodium thiolates, which results in the formation of the sodium salts of the amides of iminosulfinic acids,[125–133] proceeds via a disulfide formation stage.

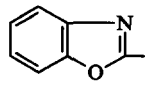
$$5\,RSNa + 2\,R^1NCl_2 \xrightarrow[-2\,RSSR,\ -2\,NaCl]{} RS(=NR^1)N(Na)R^1$$

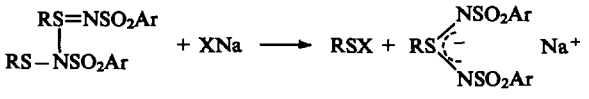
R = Alk, Ar, Het, $AlkOCOCH_2$, $ArNHCOCH_2$;
R^1 = $ArSO_2$, ArCO, $(PhO)_2P(O)$, $(NCCH_2CH_2)_2NC(O)$.

In inert solvents and in the absence of moisture, diaryl disulfides react with the sodiochloroamides of sulfonic acids, forming *N*-arylthio-*N,N'*-bis(arenesulfonyl)arenesulfinamidines,[134–136] which are also obtained on interaction of sodium thiolates with the dichloroamides of sulfonic acids for a 2 : 1 reactant ratio.[137–140] These compounds have found applications in organic synthesis as ArS^+ transfer agents in reactions with nucleophiles[138] and unsaturated compounds.[135]

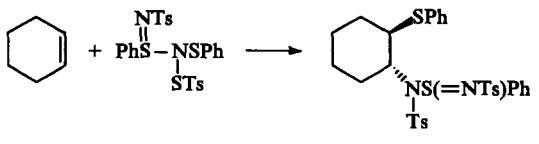
$$RSSR + 2\,ArSO_2NNaCl \xrightarrow[-NaCl]{} RS(=NSO_2Ar)N(SR)SO_2Ar$$

$$4\,RSNa + 2\,ArSO_2NCl_2 \xrightarrow[-RSSR,\ -4\,NaCl]{} RS(=NSO_2Ar)N(SR)SO_2Ar$$

R = Ph, 4-MeC_6H_4, 



X = OH, RS, RO, $ArSO_2NH$.



It is believed[124,133,138] that *N*-arylthio-*N,N'*-bis(arenesulfonyl)arenesulfinamidines are intermediates in the reactions of disulfides with the sodiochloroamides of sulfonic acids in aqueous media and also of sodium thiolates with the dichloroamides of sulfonic acids for a 5 : 2 reactant ratio. The sequence of the reactions in the imination of thiols by the sodiochloroamides of sulfonic acids is therefore as follows:

$$2\,RSH + ArSO_2NNaCl\cdot xH_2O \longrightarrow RSSR + ArSO_2NH_2 + NaCl$$

$$RSSR + 2\,ArSO_2NNaCl \longrightarrow$$

$$\longrightarrow RS(=NSO_2Ar)N(SR)SO_2Ar + 2\,NaCl$$

$$RS(=NSO_2Ar)N(SR)SO_2Ar + H_2O \longrightarrow$$

$$\longrightarrow RS(=NSO_2Ar)NHSO_2Ar + RSOH$$

$$RSOH \longrightarrow 0.2\,RSO_3H + 0.4\,RSSR + 0.4\,H_2O.$$

The introduction into the reaction of yet another mole of the sodiochloroamide of the sulfonic acid can lead to the formation of an additional amount of the iminosulfinamide, but the disulfide does not fully disappear from the reaction mixture, since it is reformed as a result of the disproportionation of the sulfenic acid. The formation of an appreciable amount of side products naturally reduces the yield of the amides of iminosulfinic acids, which does not as a rule exceed 60% in this case.

The interaction of disulfides with the *N*-chloroamides of carboxylic[117,141,142] and phosphonic acids[143] in anhydrous organic solvents (CH_2Cl_2, CCl_4) in the presence of pyridine leads to the formation of *N,N'*-disubstituted amides of iminosulfinic acids.

$$RSSR + 4\,AcNHCl + 3\,C_5H_5N \xrightarrow[-2\,C_5H_5N\cdot HCl \\ -\,C_5H_5N\cdot Cl_2]{} 2\,RS(NAc)-NHAc$$

R = Me, Bu, C_5H_{11}, C_7H_{15}, Ph, 4-MeC_6H_4, 4-$NO_2C_6H_4$;

Ac = PhCO, $(PhO)_2PO$.

In the absence of bases and for a 1 : 2 reactant ratio, diazasulfonium salts are formed. They decompose on heating with formation of *N,N'*-diacylsulfinamidines.[117]

$$ArSSAr + 2\,RCONHCl \longrightarrow Ar\overset{+}{S}(NHCOR)_2Cl^- \xrightarrow[-\,HCl]{\Delta}$$

$$\longrightarrow ArS(=NCOR)NHCOR$$

The formation of iminosulfinic acid esters. The interaction of disulfides with the sodiochloroamides of sulfonic acid in alcoholic media leads to the formation of a mixture of amides and alkyl esters of iminosulfinic acids.[144] The formation of iminosulfinic acid esters is due to the interaction, according to the authors,[144] of the intermediate chlorides of the iminosulfinic acids with alcohols.

$$RSSR + TsNNaCl \longrightarrow \left[RS(Cl)=NTs\right] \longrightarrow$$

$$\xrightarrow[-Cl^-]{TsNH^-} RS(=NTs)NHTs$$

$$\xrightarrow[-HCl]{R^1OH} RS(=NTs)OR^1$$

On the other hand, according to Levchenko,[124] the formation of iminosulfinic acid esters is caused in this case by the imination of the sulfenic acid esters formed as a result of the cleavage of *N,N'*-bis(arenesulfonyl)-*N*-(R-sulfenyl)sulfinamidines in the presence of alcohols.

$$RSSR + 2\,TsNNaCl \xrightarrow[-2NaCl]{} RS(=NTs)N(SR)Ts$$

$$RS(=NTs)N(SR)Ts + R^1OH \longrightarrow$$

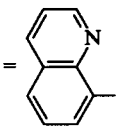
$$\longrightarrow RS(=NTs)NHTs + RSOR^1$$

$$RSOR^1 + TsNNaCl \xrightarrow[-NaCl]{} RS(=NTs)OR^1$$

The formation of the alkyl esters of iminosulfinic acids has been noted[145,146] in the reaction of disulfides with the *N,N'*-dichloroamides of sulfonic acids in the presence of alkalis in alcoholic media.

$$RSSR + 2\,PhSO_2NCl_2 + 2\,R^1OH + Na_2CO_3 \xrightarrow[-2NaCl,\,-2CO_2,\\ -Cl_2,\,-H_2O]{}$$

$$\longrightarrow 2\,RS(=NSO_2Ph)OR^1$$

R =  ; R^1 = Me, Et.

4. The applications of disulfides

a. Biological activity

Disulfides occur to a much lesser extent in many biologically active preparations than other compounds of divalent sulfur. They are used much more often as initial compounds or intermediates in the manufacture of biologically active substances.[7] However, individual representatives of disulfides exhibiting a relatively high biological activity are also encountered. For example, it has been noted[2,3] that 1-methylthiopropyl propenyl and *sec*-butyl 3-methylthioallyl disulfides, isolated from the resin of *Asa foetida*, exhibit a relatively high insecticidal activity. Glyotoxin and sporidesmin possess antifungal, antibacterial, and antiviral activities.[147]

b. The use of disulfides in polymer chemistry

Certain disulfides, in particular bis(2-benzothiazolyl) disulfides have found extensive applications as accelerators of the vulcanisation of rubbers.[5] Bis(*o*-benzamidophenyl) disulfide is used as the accelerator of the plasticisation of cured rubbers and bis(2,4-dimethylphenyl) disulfide is employed as an accelerator of the regeneration of cured rubbers.[148]

Disulfides are effective polymer chain transfer agents in radical polymerisation reactions,[6] since the thiyl radical formed as a result of chain transfer is relatively reactive and participates in the initiation of a new chain.

$$\sim CH_2\dot{C}H(R) + RSSR \longrightarrow \sim CH_2CH(R)SR + RS^{\cdot}$$

$$RS^{\cdot} + CH_2{=}CHR \longrightarrow RSCH_2\dot{C}H(R)$$

The ability of disulfides to transfer a polymer chain is characterised by the transfer constant *C*, which is equal to the ratio of the transfer rate constant K_f to the chain propagation constant K_p:

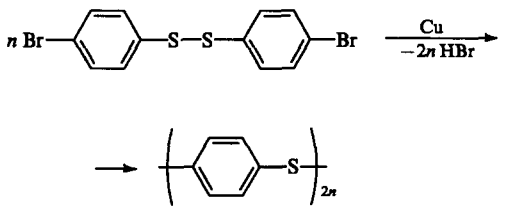
$$C = K_f / K_p$$

The higher the transfer constant, the more readily are disulfides subjected to attack by a free radical.

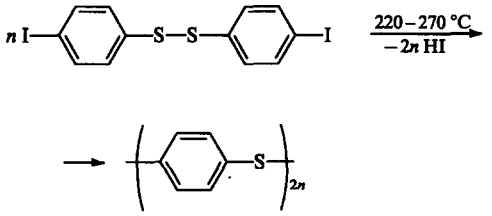
The chain transfer constants for disulfides are lower than for the corresponding peroxide compounds. For example, the chain transfer constant for dibenzoyl disulfide is five times lower than for benzoyl peroxide, which can be explained, on the one hand, by the smaller strength of the O–O bond in peroxides compared with that of the S–S bond in disulfides and, on the other, by a different chain transfer mechanism in the case of peroxide compounds. The main reaction for disulfides is the cleavage of the S–S bond by the macroradical, while for peroxide compounds it is the abstraction of a hydrogen atom.

It has been noted [149] that bis(glycylaminophenyl) disulfides are iniferters, which make it possible to obtain hydrophobic [poly(methylmethacrylate), polystyrene] and hydrophilic (poly-*N*-methylmethacrylamide) macroinitiators with a wide set of molecular masses, which can be used for the synthesis of block-copolymers of the A–B–A type.

The synthesis of poly(1,4-phenylene sulfide) in which bis-(4-bromophenyl) disulfide is used as a monomer has been described. [150]



The synthesis is carried out in a boiling mixture of quinoline and pyridine in the presence of equimolecular amounts of copper powder. The reaction takes place over a period of 8 h with formation of poly(phenylene sulfide) with a molecular mass $\leqslant 4000$ and in 76% yield. The synthesis of poly(1,4-phenylene sulfide) by the thermolysis of bis(4-iodophenylene) disulfide has been described. [151]



The thermolysis is carried out at 220–270 °C in diphenyl ether. The polymer formed has a molecular mass of 20 000 and a high mechanical strength and thermal stability.

* * *

Thus the studies in the chemistry of disulfides during the last 10–15 years have been largely directed to further development of the methods of synthesis of disulfides already known and to the search for new ones (syntheses based on alkylthiotrimethylsilanes, thiocyanates, sulfenyl thiocyanates, etc.). Much attention has been devoted to the study of the reactivity of disulfides and in particular of reactions occurring with formation of sulfonium complexes and imino-compounds of tetravalent sulfur. The previous studies on the use of disulfides in polymer chemistry underwent further development in recent years.

References

1. D Epplequist, C H DePuy, K Rinehart *Introduction to Organic Chemistry* (third edition) (New York: Wiley, 1982) (Translated into Russian; Moscow: Mir, 1985)
2. D R Hogg, in *Comprehensive Organic Chemistry* Vol. 5 (Eds D Barton, W D Ollis)(Translated into Russian; Moscow: Khimiya, 1983) p. 445
3. S Oae, in *Organic Chemistry of Sulfur* (New York: Plenum) (Translated into Russian; Moscow: Khimiya, 1975) p. 155
4. Y Kishi, S Nahatsuka, T Fukuyama, M Havel *J. Am. Chem. Soc.* **95** 6493 (1973)
5. G A Blokh, in *Organicheskie Uskoriteli Vulkanizatsii i Vulkaniziruyushchie Sistemy dlya Elastomerov* (Organic Accelerants of Vulcanisation and Vulcanising Systems of Elastomers) (Leningrad: Khimiya, 1973) p. 25
6. V R Gawariker, N V Visvanathan, J Shridhar *Polymers* (Translated into Russian; Moscow: Nauka, 1990)
7. N N Mel'nikov, K V Novozhilova, T N Pylova *Khimicheskie Sredstva Zashchity Rastenii* (Chemical Agents for the Protection of Plants) (Moscow: Khimiya, 1980)
8. Yu A Bankovskii *Khimiya Vnutrikompleksnykh Soedinenii Merkaptokhinolina i ego Proizvodnykh* (Chemistry of Chelate Compounds of Mercaptoquinoline and Its Derivatives) (Riga: Zinatne, 1978)
9. A J Parker, N Kharasch *Chem. Rev.* **59** 583 (1959)
10. O Foss, in *Organic Sulfur Compounds* Vol. 1 (Ed. N Kharasch) (Oxford: Pergamon Press, 1961) Chs 8, 9
11. M Schmidt, in *Polysulfides* (Translated into Russian; Moscow: Mir, 1965) p. 25
12. J L Kice, in *Sulfur in Organic and Inorganic Chemistry* Vol. 1 (Ed. A Senning) (New York: Dekker, 1971) Ch. 6
13. A L Fluharty, in *The Chemistry of the Thiol Group* Part 2 (Ed. S Patai) (London: Interscience, 1974) Ch. 13
14. G Capozzi, G Modena, in *The Chemistry of the Thiol Group* Part 2 (Ed. S Patai) (London: Interscience, 1974) Ch. 17
15. L A Sorokina, Author's Abstract of Candidate Thesis in Chemical Sciences, Kazan State Univ., Kazan, 1975
16. L A Sorokina, S G Vul'fson, L M Kataeva, A N Vereshchagin, E G Kataev, R I Vinokurova *Izv. Akad. Nauk SSSR, Ser. Khim.* 2371 (1977)
17. M G Voronkov, E N Deryagina *Usp. Khim.* **59** 1338 (1990) [*Russ. Chem. Rev.* **59** 778 (1990)]
18. K Reid *Course of Physical Organic Chemistry* (Translated into Russian; Moscow: Mir, 1972)
19. E N Gur'yanova, I P Romm, L A Ganyushin, A A Vyazgina, in *IX Mezhdunarodnyi Simpozium po Khimii Organicheskikh Soedinenii Sery, Riga, 1980 (Tezisy Dokladov)* (Abstracts of Reports at the IXth International Symposium on the Chemistry of Organic Sulfur Compounds, Riga, 1980) p. 188
20. H Viola *Z. Chem.* **27** 15 (1987)
21. M G Voronkov, A N Mirskova *Zh. Vses. Khim. O-va im. D I Mendeleeva* **30** 294 (1985)
22. K Norkjarr, A Senning, in *Abstracts of Reports at the XVth International Symposium on the Organic Chemistry of Sulfur, Caen, 1992* p. 28
23. S V Amosova, V V Nasyreva, M V Sigalov *Zh. Org. Khim.* **28** 927 (1992)
24. V A Usov *Izv. Akad. Nauk Latv. SSR, Ser. Khim.* **1** 94 (1986)
25. V A Usov, L V Timokhina, M G Voronkov *Usp. Khim.* **55** 1761 (1986) [*Russ. Chem. Rev.* **55** 1003 (1986)]
26. I V Moiseeva, P M Lukin, O E Nasakin, V N Romanov, V A Tafeenko, A Kh Bulat, P A Sharbatyan *Khim. Geterotsikl. Soedin.* 277 (1992)
27. L I Belen'kii (Ed.) *Khimiya Organicheskikh Soedinenii Sery* (Chemistry of Organic Compounds of Sulfur) (Moscow: Khimiya, 1989)
28. L A Alekseeva, A I Burmakov, D V Ivanov, B V Kunshenko, N N Muratov, V O Omarov, in *XVI Ukrainskaya Konferentsiya po Organicheskoi Khimii, Ternopol', 1992 (Tezisy Dokladov)* (Abstracts of Reports at the XVIth Ukrainian Conference on Organic Chemistry, Ternopol', 1992) p. 185
29. I V Koval' *Usp. Khim.* **62** 813 (1993) [*Russ. Chem. Rev.* **62** 769 (1993)]

30. H Bock, P Pittmeyer *Phosphorus Sulfur Silicon Relat. Elem.* **68** 261 (1992)
31. M Heydenreich, I Kmhn, R Runge, E Wenschuh *Sulfur Lett.* **2** 65 (1989)
32. I V Koval', T G Oleinik, M M Kremlev *Vopr. Khim. Khim. Tekhnol.* **54** 24 (1979)
33. I V Koval', A I Tarasenko, T G Oleinik, M M Kremlev *Zh. Org. Khim.* **15** 1004 (1979)
34. I V Koval', A V Kharchenko, M M Kremlev *Vopr. Khim. Khim. Tekhnol.* **54** 29 (1979)
35. K Rao Rama, S H M Sampath *Bioorg. Med. Chem. Lett.* 1 507 (1991)
36. Yu A Razskazovsky, M Ya Melnikov *Radiochem. Radioanal. Lett.* **46** 129 (1981)
37. N B Islam, H Kwart, S Khan *J. Chem. Eng. Data* **30** 509 (1985)
38. R M De Marinis, W M Bryan *J. Org. Chem.* **42** 2024 (1977)
39. I V Koval' *Usp. Khim.* **60** 1645 (1991) [*Russ. Chem. Rev.* **60** 830 (1991)]
40. T Endo, H Tasai, T Ishigami *Chem. Lett.* 813 (1975)
41. D N Harpp, B T Friedlander, C Larsen, K Steliou, A Stockton *J. Org. Chem.* **43** 3481 (1978)
42. B Vielsen, B Jensen, A K Jensen, A Senning *Sulfur Lett.* **10** 165 (1989)
43. L Craine, M Raban *Chem. Rev.* **4** 689 (1989)
44. I V Koval' *Usp. Khim.* **59** 681 (1990) [*Russ. Chem. Rev.* **59** 396 (1990)]
45. A Bulpin, S Masson *J. Org. Chem.* **57** 4507 (1992)
46. M Wada, M Kanzaki, M Fujiwara, K Kajihara, T Erabi *Repts Asahi Glass Found.* **57** 31 (1990); *Ref. Zh. Khim.* 4 Zh 388 (1992)
47. D H R Barton, Chen Chen, G M Wall *Tetrahedron* **47** 6127 (1991)
48. D H R Barton, R H Hesse, A C O'Sullivan, M M Pechet *J. Org. Chem.* **56** 6697 (1991)
49. M Ohtani, M Narisada *J. Org. Chem.* **56** 5475 (1991)
50. Yu N Polivin, R A Karakhanov, T S Sheveleva, V I Kelarev, A A Bratkov *Metalloorg. Khim.* **5** 1364 (1992)
51. C Iijima, E Hiyoshi, A Miyashita *Chem. Pharm. Bull.* **40** 1090 (1992)
52. G Capozzi, S Menichetti, A Rosi, in *Abstracts of Reports at the XVth International Symposium on the Organic Chemistry of Sulfur, Caen, 1992* p. 33
53. M Benaichoucke, G Bosser, J Paris, in *Abstracts of Reports at the XVth International Symposium on the Organic Chemistry of Sulfur, Caen, 1992* p. 92
54. N Iranpoor, J Owji *Tetrahedron* **47** 149 (1991)
55. I V Koval', A I Tarasenko, I S Panchenko *Vopr. Khim. Khim. Tekhnol.* **84** 54 (1987)
56. R G Hiskey, F I Carroll *J. Am. Chem. Soc.* **83** 4644 (1961)
57. S V Amosova, N K Gusarova, B A Trofimov, in *XII Nauchnaya Sessiya po Khimii i Tekhnologii Organicheskikh Soedinenii Sery i Sernistykh Neftei, Riga, 1971 (Tezisy Dokladov)* (Abstracts of Reports at the XIIth Scientific Session on the Chemistry and Technology of Organic Sulfur Compounds and Sulfurous Petroleum, Riga, 1971) p. 322
58. B A Trofimov, N K Gusarova, A S Atavin, S V Amosova, A V Gusarov, N I Kazantseva, G A Kalabin *Zh. Org. Khim.* **9** 8 (1973)
59. B M Trost, in *Organic Sulfur Chemistry: Structure, Mechanisms and Synthesis* (Ed. C J M Stirling) (London: Butterworths, 1975) p. 252
60. E Vedejs, D A Engler *Tetrahedron Lett.* **17** 3487 (1976)
61. V Farina, S I Hauck *J. Org. Chem.* **56** 4317 (1991)
62. K Hartke, K-H Lee, W Massa, B Schwarz *Liebigs Ann. Chem.* 243 (1991)
63. D R Hogg, A Robertson *J. Chem. Soc., Perkin Trans. 1* 1125 (1979)
64. L E Overman, E M O Connor *J. Am. Chem. Soc.* **98** 771 (1976)
65. A V Anisimov, E A Viktorova, T A Danilova *Molekulyarnye Peregruppirovki Seroorganicheskikh Soedinenii; Organicheskie Sul'fidy* (Molecular Rearrangements of Organic Compounds of Sulfur: Organic Sulfides) (Moscow: Izd. Mosk. Univ., 1989)
66. I S Nizanov, L A Al'metkina, E S Batyeva, V A Al'fonsov, A N Pudovik *Izv. Akad. Nauk Ser. Khim.* 1932 (1992)
67. N N Mel'nikov, B A Khaskin, N A Torgasheva *Zh. Obshch. Khim.* **45** 2856 (1972)
68. S Oae, Y Tsuchida, K Tsujihara, N Furukawa *Bull. Chem. Soc. Jpn.* **45** 2856 (1972)
69. H Boeshagen, W Gaiger, in *IX Mezhdunarodnyi Simpozium po Khimii Organicheskikh Soedinenii Sery, Riga, 1980 (Tezisy Dokladov)* (Abstracts of Reports at the IXth International Symposium on the Chemistry of Organic Sulfur Compounds, Riga, 1980) p. 124
70. C Weygand, G Hilgetag, *Organisch-chemische Experimentierkunst* (Translated into Russian; Moscow: Khimiya, 1968)
71. T Nagase, K Akama, S Ozaki *Chem. Lett.* **8** 1385 (1988)
72. Yu G Gololobov, N I Gusar' *Sul'fenilkhloridy* (Sulfenyl Chlorides) (Moscow: Nauka, 1989)
73. A S Gybin, V A Smit, V S Bogdanov, M Z Krimer, Yu B Kal'yan, in *IX Mezhdunarodnyi Simpozium po Khimii Organicheskikh Soedinenii Sery, Riga, 1980 (Tezisy Dokladov)* (Abstracts of Reports at the IXth International Symposium on the Chemistry of Organic Sulfur Compounds, Riga, 1980) p. 47
74. M Z Krimer, Yu B Kal'yan, V A Smit, in *IX Mezhdunarodnyi Simpozium po Khimii Organicheskikh Soedinenii Sery, Riga, 1980 (Tezisy Dokladov)* (Abstracts of Reports at the IXth International Symposium on the Chemistry of Organic Sulfur Compounds, Riga, 1980) p. 48
75. M C Caserio, J K Kim *J. Am. Chem. Soc.* **104** 3231 (1982)
76. F A Davis, J A Friedman, E W Kluger, T B Skibo, E R Fretz, A P Milicia, W C Le Masters, M D Bentley, J A Lacadie, I B Douglass *J. Org. Chem.* **42** 967 (1977)
77. F A Davis, A J Friedman, U K Nadir *J. Am. Chem. Soc.* **100** 2844 (1978)
78. M Aslam, K G Davenport, W F Stansbury *J. Org. Chem.* **56** 5955 (1991)
79. H Bock, S Mohmand *Angew. Chem.* **89** 105 (1977)
80. G Martin, N Barroeta *J. Chem. Soc., Perkin Trans. 2* 1421 (1976)
81. L K Papernaya, E N Deryagina, M G Voronkov *Zh. Org. Khim.* **26** 147 (1990)
82. M G Voronkov, E N Deryagina, E N Sukhomazova *Zh. Org. Khim.* **18** 1736 (1982)
83. M G Voronkov, E N Deryagina, E N Sukhomazova *Zh. Org. Khim.* **22** 846 (1986)
84. M G Voronkov, E N Deryagina *Usp. Khim.* **59** 1338 (1990) [*Russ. Chem. Rev.* **59** 778 (1990)]
85. E N Sukhomazova, E N Russavskaya, N V Korchevin, E N Deryagina, M G Voronkov *Zh. Org. Khim.* **25** 1506 (1989)
86. L Benati, P C Montevecchi, P Spagnolo *J. Chem. Soc., Perkin Trans. 1* 2103 (1991)
87. L Benati, C P Montevecchi, P Spagnolo *J. Chem. Soc., Perkin Trans 1* 1659 (1992)
88. A V Martynov, A N Mirskova, M G Voronkov *Zh. Org. Khim.* **20** 23 (1984)
89. L M Yagupol'skii *Aromaticheskie i Geterotsiklicheskie Soedineniya s Ftorsoderzhashchimi Zamestitelyami* (Aromatic and Heterocyclic Compounds with Fluorine-containing Substituents) (Kiev: Naukova Dumka, 1988)
90. B V Kopylova, L V Yashkina, R Kh Freidlina, in *IX Mezhdunarodnyi Simpozium po Khimii Organicheskikh Soedinenii Sery, Riga, 1980 (Tezisy Dokladov)* (Abstracts of Reports at the IXth International Symposium on the Chemistry of Organic Sulfur Compounds, Riga, 1980) p. 68
91. E Bald, in *IX Mezhdunarodnyi Simpozium po Khimii Organicheskikh Soedinenii Sery, Riga, 1980 (Tezisy Dokladov)* (Abstracts of Reports at the IXth International Symposium on the Chemistry of Organic Sulfur Compounds, Riga, 1980) p. 267
92. M Eckert-Maksic, D Margetic *Energy Fuels* **5** 327 (1991)
93. S Munavalli, I D Bossman, K Rohzbaugh, P C Ferguson, Fu-Lian Hsu *Heteroatom Chem.* **3** 189 (1992)
94. L Field, C H Banks *J. Org. Chem.* **40** 2774 (1975)
95. A Senning, in *IX Mezhdunarodnyi Simpozium po Khimii Organicheskikh Soedinenii Sery, Riga, 1980 (Tezisy Dokladov)* (Abstracts of Reports at the IXth International Symposium on the Chemistry of Organic Sulfur Compounds, Riga, 1980) p. 9
96. B I Stepanov, V Ya Rodionov, T A Chibisova, in *XIII Nauchnaya Sessiya po Khimii i Tekhnologii Organicheskikh Soedinenii Sery i Sernistykh Neftei, Riga, 1974 (Tezisy Dokladov)* (Abstracts of Reports at the XIIIth Scientific Session on the Chemistry and Technology of Organic Sulfur Compounds and Sulfurous Petroleum, Riga, 1974) p. 272

97. K V Dvornikova, A M Maksimov, V E Platonov, G G Yakobson, in *IX Mezhdunarodnyi Simpozium po Khimii Organicheskikh Soedinenii Sery, Riga, 1980 (Tezisy Dokladov)* (Abstracts of Reports at the IXth International Symposium on the Chemistry of Organic Sulfur Compounds, Riga, 1980) p. 170
98. S V Amosova, V V Nasyreva, in *XVIII Konferentsiya po Khimii i Tekhnologii Organicheskikh Soedinenii Sery, Kazan', 1992 (Tezisy Dokladov)* (Abstracts of Reports at the XVIIIth Conference on the Chemistry and Technology of Organic Sulfur Compounds, Kazan, 1992) p. 14
99. S V Amosova, G K Musorin, V V Nasyreva, V V Keiko, in *VI Mezhdunarodnaya Konferentsiya po Organicheskomu Sintezu, Moskva, 1986 (Tezisy Dokladov)* (Abstracts of Reports at the VIth International Conference on Organic Synthesis, Moscow, 1986) p. 72
100. K Okuma, T Koike, I S Yamamoto, H Takeuchi, Y Kazuki, O Masaaki, H Ohta *Bull. Chem. Soc. Jpn.* **65** 2375 (1992)
101. G Capozzi, O De Lucchi, V Lucchini, G Modena *Tetrahedron Lett.* **16** 2603 (1975)
102. G Capozzi, O De Lucchi, V Lucchini, G Modena *Synthesis* **10** 677 (1976)
103. I Degani, R Fochi *J. Chem. Soc., Perkin Trans. 1* 1133 (1978)
104. S Oae, T Takata, H Y Kim *Bull. Chem. Soc. Jpn.* **55** 2484 (1982)
105. G J Kasperek, J G Kasperek *J. Org. Chem.* **43** 3393 (1978)
106. A Bhattacharva, A G Hortmann *J. Org. Chem.* **43** 2728 (1978)
107. A V Anisimov, R M Ahmad, A V Tarakanova, in *Abstracts of Reports at the XVth International Symposium on the Organic Chemistry of Sulfur, Caen, 1992* p. 142
108. T Tahata, Y H Kim, S Oae *Tetrahedron Lett.* **20** 821 (1979)
109. J T Maricich, L V Hoffman *J. Am. Chem. Soc.* **96** 7770 (1974)
110. I V Koval' *Usp. Khim.* **59** 1409 (1990) [*Russ. Chem. Rev.* **59** 819 (1990)]
111. E S Levchenko, L V Budnik *Zh. Org. Khim.* **9** 212 (1973)
112. T N Dubininina, L N Markovskii, E S Levchenko *Zh. Org. Khim.* **13** 1621 (1977)
113. E S Levchenko, L V Budnik, T N Dubinina *Zh. Org. Khim.* **14** 1846 (1978)
114. E S Levchenko, L V Budnik, T N Dubinina *Zh. Org. Khim.* **13** 212 (1977)
115. L M Yagupolski, R Yu Garlyauskajte, N V Kondratenko *Synthesis* **8** 749 (1992)
116. V N Khabashesku, N S Zefirov *Phosphorus Sulfur* **1** 87 (1976)
117. E S Levchenko, T N Dubinina, L V Budnik *Zh. Org. Khim.* **19** 2158 (1983)
118. E S Levchenko, T N Dubinina, S V Sereda, M Yu Antipin, Yu T Struchkov, I E Boldeskul *Zh. Org. Khim.* **23** 86 (1987)
119. M M Campbell, G Johnson *Chem. Rev.* **78** 65 (1978)
120. I V Koval', A I Tarasenko, M M Kremlev *Zh. Org. Khim.* **14** 111 (1978)
121. I V Koval', M M Kremlev, V A Aleksenko *Vopr. Khim. Khim. Tekhnol.* **75** 111 (1984)
122. M S Kharasch, W Nudenberg, G J Mantell *J. Org. Chem.* 524 (1951)
123. I V Koval', T G Oleinik, M M Kremlev *Vopr. Khim. Khim. Tekhnol.* **64** 17 (1980)
124. E S Levchenko *Ukr. Khim. Zh. (Russ. Ed.)* **55** 929 (1989)
125. M M Kremlev, I V Koval' *Zh. Org. Khim.* **5** 2014 (1969)
126. M M Kremlev, I V Koval', A V Kharchenko *Vopr. Khim. Khim. Tekhnol.* **30** 36 (1972)
127. A V Kharchenko, M M Kremlev, I V Koval' *Vopr. Khim. Khim. Tekhnol.* **48** 6 (1977)
128. A V Kharchenko, M M Kremlev, I V Koval' *Vopr. Khim. Khim. Tekhnol.* **45** 24 (1976)
129. A V Kharchenko, M M Kremlev, I V Koval' *Zh. Org. Khim.* **13** 459 (1977)
130. A V Kharchenko, I V Koval', M M Kremlev *Zh. Org. Khim.* **15** 443 (1979)
131. I V Koval', N D Borodavko *Zh. Org. Khim.* **17** 2022 (1981)
132. R P Naumenko, I V Koval', M M Kremlev, L I Bondar', S I Guseinov *Vopr. Khim. Khim. Tekhnol.* **82** 12 (1986)
133. I V Koval', A I Tarasenko, M M Kremlev *Zh. Org. Khim.* **2** 410 (1986)
134. E S Levchenko, B V Budnik *Zh. Org. Khim.* **11** 2293 (1975)
135. D H R Barton, M R Britten-Kelly, D Ferreira *J. Chem. Soc., Perkin Trans. 1* 1090 (1978)
136. E S Levchenko, N P Pel'kis *Zh. Obshch. Khim.* **57** 2744 (1986)
137. USSR P. 245 771; *Byull. Izobret.* **20** (1969)
138. M M Kremlev, I V Koval' *Zh. Org. Khim.* **6** 1457 (1970)
139. USSR P. 384 827; *Byull. Izobret.* **25** (1974)
140. I V Koval' *Vopr. Khim. Khim. Tekhnol.* **59** 58 (1980)
141. A V Kharchenko, I V Koval', M M Kremlev *Zh. Org. Khim.* **13** 2385 (1977)
142. I V Koval', A V Kharchenko, M M Kremlev *Vopr. Khim. Khim. Tekhnol.* **57** 83 (1979)
143. A V Kharchenko, I V Koval', M M Kremlev *Zh. Org. Khim.* **16** 754 (1980)
144. E Fischer *Sulfur Lett.* **6** 191 (1987)
145. I V Koval', R P Naumenko, M M Kremlev, A Yu Romanenko *Zh. Org. Khim.* **22** 457 (1986)
146. I V Koval', A I Tarasenko, T G Panasenko, A Yu Romanenko, R M Naumenko, I S Panchenko, in *XV Ukrainskaya Respublikanskaya Konferentsiya po Organicheskoi Khimii, Uzhgorod, 1986 (Tezisy Dokladov)* (Abstracts of Reports at the XVth Republic Conference on Organic Chemistry, Uzhgorod, 1986) p. 320
147. Y Kishi, S Nakatsuga, T Fukuyama, M Havel *J. Am. Chem. Soc.* **95** 6493 (1973)
148. G N Shalygina, G F Shalygin, Z N Nudel'man, in *Spravochnik Rezinshchika* (Rubber Specialist's Handbook) (Moscow: Khimiya, 1971) p. 279
149. B M Shabsel's, G D Rudkovskaya, G P Vlasova *Vysokomol. Soedin., Ser. B* **30** 278 (1988)
150. P A Lovell, R H Still *Br. Polym. J.* **22** 2737 (1990)
151. S H Allan, Y Z Wang *Macromolecules* **24** 333 (1991)

Russian Chemical Reviews **63** (9) 751 – 766 (1994)
©1994 Russian Academy of Sciences and Turpion Ltd

UDC 541.422:542.943:678.019.3

Degradation of the carbon chain in the liquid-phase oxidation of saturated compounds

A L Perkel', S G Voronina, B G Freidin (deceased)

Contents

I.	Introduction	751
II.	Dissociation of C – C bonds in the stages involving the formation and decomposition of hydrocarbon hydroperoxides	751
III.	Degradation of the carbon chain in the oxidation of secondary alcohols and in the interaction of ketones with peroxide compounds	752
IV.	Reactions of α-ketohydroperoxides in the radical-chain oxidation of ketones	753
V.	Oxidative degradation of α-ketoalcohols	756
VI.	Oxidation of α-diketones by peroxide compounds	758
VII.	The formation of esters in autoxidation processes	760
VIII.	Certain aspects of the decarbonylation and decarboxylation reactions in the oxidation reactions of hydrocarbons and their oxygen-containing derivatives	762
IX.	Conclusion	764

Abstract. The reaction pathways leading to the degradation of the carbon chain in the liquid-phase oxidation reactions of saturated hydrocarbons and their oxygen-containing derivatives are examined. The relative importance of the pathways and their dependence on the structure of the substrate and of the oxidation conditions are discussed. The bibliography includes 151 references.

I. Introduction

Reactions involving the extensive oxidation of saturated hydrocarbons by molecular oxygen in the liquid phase lead to a wide variety of oxygen-containing compounds. The formation under these conditions of compounds with a lower molecular mass than that of the initial hydrocarbon is associated with the degradation of the carbon chain, which occurs to some extent in virtually all the stages of these complex radical-chain processes.

In conformity with the ideas which arose in the 1950s – 1960s and which have been quite fully surveyed in monographs [1,2] and reviews, [3,4] it was assumed that the carbon chain is ruptured mainly in the stages following the formation of ketones, for example in the stage involving the decomposition of α-ketohydroperoxides. However, later experimental data were obtained indicating that, in the oxidation of alicyclic, [5] aliphatic, [6] and to a lesser extent aromatic [7–9] ketones, the decomposition of α-hydroperoxyketones leads preferentially to α-ketoalcohols and α-diketones and that the reactions of these substances actually provide the main routes to the degradation of the carbon chain, including those associated with the formation of carboxylic acid anhydrides. [10–20]

A L Perkel', S G Voronina, B G Freidin
Department of the Technology of Fundamental Organic Synthesis, Kuzbass State Technical University, Vesennyaya 28, 650026 Kemerovo, Ukraine. Fax (7-384) 223 08 08

Received 5 April 1993
Uspekhi Khimii **63** (9) 793 – 809 (1994); translated by A K Grzybowski

The possibilities for the occurrence of reactions leading to the dissociation of the C – C bond in liquid-phase oxidation processes are discussed in the present review. An attempt is made to trace the influence of the structure of the substrate, temperature, and the medium on the probability of the occurrence of such reactions. The principal pathways leading to the formation of esters in autoxidation reactions are examined.

II. Dissociation of C – C bonds in the stages involving the formation and decomposition of hydrocarbon hydroperoxides

The oxidation reactions of hydrocarbons and their oxygen-containing derivatives in the absence of initiating additives are known to include [1,2,21,22] the chain initiation (1), propagation (2, 3), and termination (4) stages:

$$RH + O_2 \longrightarrow R^{\cdot} + HO_2^{\cdot}, \quad (1)$$

$$R^{\cdot} + O_2 \longrightarrow RO_2^{\cdot}, \quad (2)$$

$$RO_2^{\cdot} + RH \longrightarrow ROOH + R^{\cdot}, \quad (3)$$

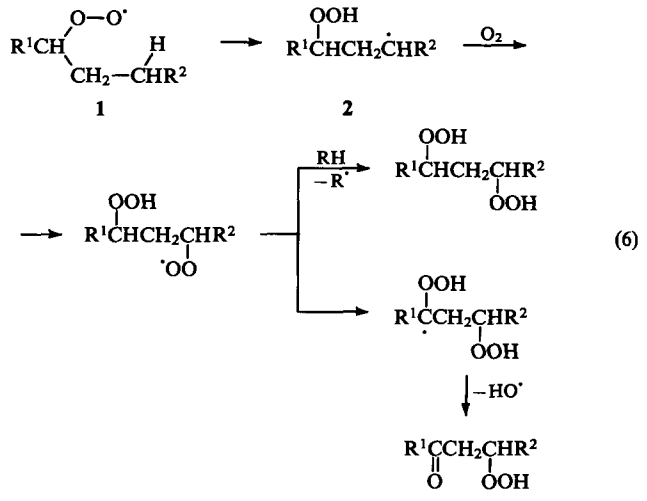
$$2\,RO_2^{\cdot} \longrightarrow \text{molecular products}. \quad (4)$$

They also involve the degenerate branching stage — unimolecular decomposition of hydroperoxides, i.e.

$$ROOH \longrightarrow RO^{\cdot} + HO^{\cdot}, \quad (5)$$

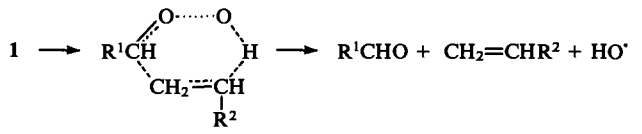
or decomposition with participation of the substrate and the oxidation products, which leads, incidentally, also to the radicals $RO^{\cdot}$. [21,22]

The peroxyl radicals $RO_2^{\cdot}$, formed by reaction (2), are capable of abstracting hydrogen from the substrate molecules [1,2,21–25] [reaction (3)] and of isomerising to type **2** radicals, which are subsequently converted into β- or γ-dihydroperoxides or hydroperoxyketones. [25]



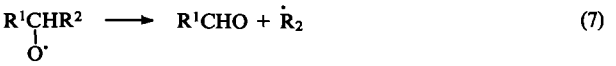
(6)

There are data indicating that the secondary peroxyl radicals can decompose with degradation of the carbon chain.[26]



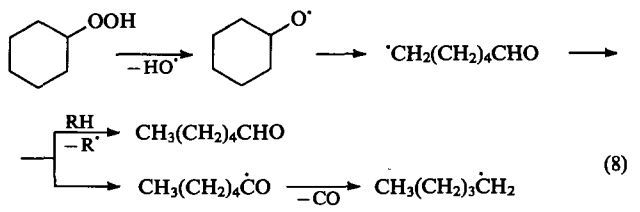
Incidentally, the probability of the degradation via this route is apparently low; it has been shown[26] that, in the sensitised oxidation of pentadecane at 130 °C, the rate of accumulation of unsaturated compounds is only 0.04% of the rate of the radical-chain oxidation.

Secondary monohydroperoxides decompose predominantly without the cleavage of the carbon skeleton, affording approximately equal amounts of alcohols and ketones. The reaction products were then found to include also those whose origin can be explained by the degradative decomposition of oxyl radicals.[27,28]



(7)

Thus the cyclohexyl hydroperoxide decomposition pathway leads to caproic aldehyde[27-29] and carbon monoxide.[29]



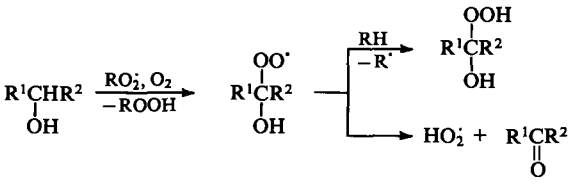
(8)

It has been shown[29] that 56% of the cyclohexyloxyl radicals generated from *tert*-butyl cyclohexyl peroxide (TBCHP) in cyclohexane are converted into cyclohexanol and only 8% decompose with decarbonylation. This factor as well as data[21] indicating a low contribution of the homolytic pathway to the overall decomposition of hydroperoxides indicate a low contribution of type (7) reactions to the formation of the hydrocarbon chain degradation products in the extensive oxidation process. Incidentally, their role may increase when the radical decomposition of hydroperoxides is stimulated, for example in the presence of cobalt salts,[21] and also with increase in temperature and in an inert solvent.[29]

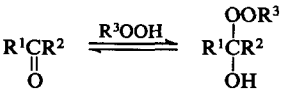
Reliable data concerning the mechanism of the reaction of the dihydroperoxides formed via reactions (6) have apparently not been obtained hitherto. It is postulated that they are less stable than the secondary monohydroperoxides.[30]

III. Degradation of the carbon chain in the oxidation of secondary alcohols and in the interaction of ketones with peroxide compounds

The secondary alcohols formed on decomposition of monohydroperoxides readily undergo the radical-chain oxidation at the α-C–H bonds, the reactivity of which is significantly higher than in hydrocarbons.[1,2,29] The reaction proceeds via the intermediate formation of the α-hydroxyperoxyl radical, which either abstracts hydrogen from a substrate molecule and is converted into a α-hydroxyhydroperoxide or decomposes into a ketone and a hydroperoxyl radical.[2,31]



Secondary α-hydroxyhydroperoxides can also be formed as a result of the acid-catalysed reversible nucleophilic addition of H_2O_2 to ketones; in the analogous addition of hydroperoxides or peracids, α-hydroxyperoxides or α-hydroxyperesters are formed respectively.[2]

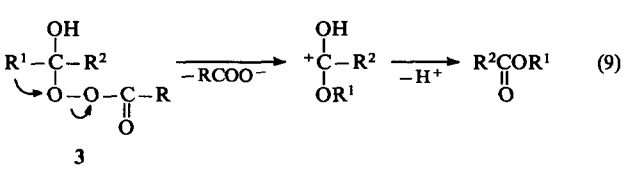


R^3 = H, Alk, Ac.

The mechanism of the subsequent reactions of the α-hydroxyperesters differs significantly from the mechanisms of the decomposition of α-hydroxyhydroperoxides and α-hydroxyperoxides.

The principal aspects of the oxidation of ketones by peracids (the Baeyer–Villiger reaction), leading to the rupture of the carbon chain, have been considered in reviews.[32-34] The reaction takes place under the conditions of general acid catalysis.[35-37] The peroxide 3 (the Criegee intermediate) formed in the first stage [reaction (9)] undergoes a rapid 1,2-rearrangement. In hydrocarbon solvents, the first stage of the process is rate-limiting.[35] In the oxidation of cyclic ketones by perbenzoic acid, the rate of reaction decreases in the sequence cyclohexanone > cyclopentanone > cycloheptanone, which is consistent with the decrease in the reactivity of the carbonyl groups of the above ketones in the same sequence.[36]

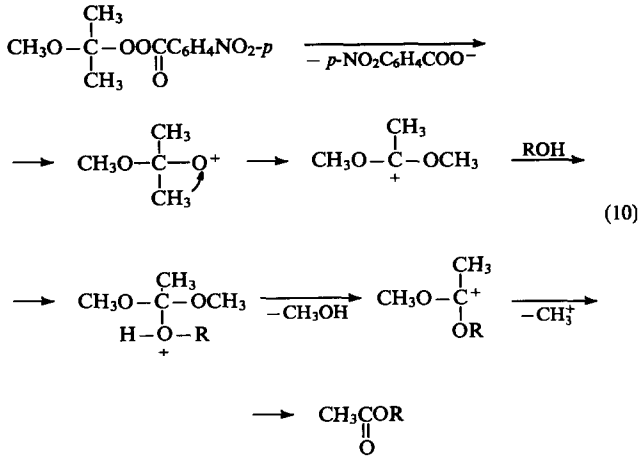
The rearrangement of the Criegee intermediate proceeds via an ionic mechanism[32,37,38] [reaction (9)], which is consistent with data indicating the transfer of the carbonyl oxygen of the ketone to the carbonyl group of the ester.[37]



(9)

3

The ionic nature of reaction (9) has been quite convincingly demonstrated by studying the decomposition of 2-methoxy- and 2-ethoxy-2-propyl *p*-nitroperbenzoates in methanol or ethanol.[38] Methyl acetate is formed in a ~100% yield in the decomposition of 2-methoxy-2-propyl *p*-nitroperbenzoate in methanol, whereas in the case where the reaction is carried out in ethanol up to 93% of ethyl acetate is obtained. Similarly, methyl acetate is formed preferentially from 2-ethoxy-2-propyl *p*-nitroperbenzoate in methanol. It has been suggested[38] that the carbonium ion formed in the stage involving the rearrangement of 2-alkoxy-2-propyl *p*-nitroperbenzoates interacts with the solvent and is converted into an orthoester and then into an ester.



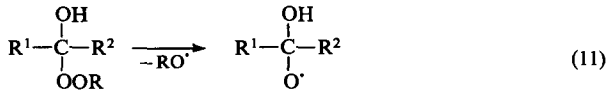
(10)

Robertson and Swelin [39] concluded that the homolytic decomposition of the Criegee intermediate can take place in parallel with the ionic decomposition, but this hypothesis apparently requires an additional experimental test.

The ability of the radicals to migrate in the Baeyer–Villiger reaction depends on their structure [40–43] and decreases in the sequence *tert*-butyl > cyclohexyl > isopropyl > benzyl > cyclopentyl > neopentyl > ethyl > methyl. [40]

In contrast to α-hydroxyperesters, α-hydroxyperoxides are in all probability incapable of undergoing heterolytic decomposition under the conditions of liquid-phase oxidation in nonpolar media because its products should be, as in reaction (9), esters or lactones which are not formed in appreciable amounts in this instance. [44,45] This factor is evidently associated with the fact that the HO and RO groups are poorer leaving groups compared with RCOO. [46] The heterolysis of the O–O bond in the α-hydroxyhydroperoxide or α-hydroxyperoxide is therefore possible only after the modification of the leaving groups, for example by protonation. Aliphatic carboxylic acids are probably incapable of participating in such a modification. However, it is known that esters or lactones are formed in the oxidation of ketones by hydrogen peroxide in the presence of inorganic acids [32] and also in the oxidation by a hydroperoxide + Lewis acid mixture. [47]

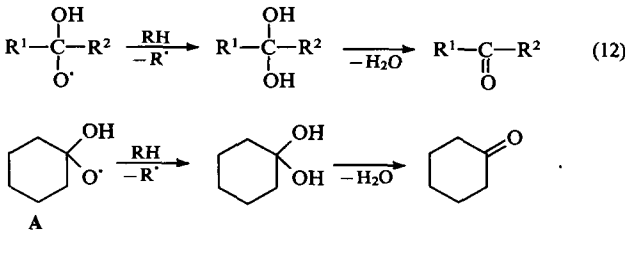
The principal pathway to the formation of products of the degradation of α-hydroxyhydroperoxides and α-hydroxyperoxides involves homolytic decomposition and leads initially to α-hydroxyoxyl radicals.



(11)

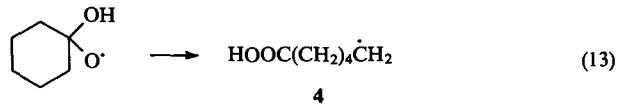
The rate constant for reaction (11) is known to be approximately an order of magnitude greater than the rate constant for the homolytic decomposition of hydrogen peroxide or hydroperoxides. [2,48–52]

The subsequent reactions of the α-hydroxyoxyl radicals depend on the reaction conditions. [29,53] It has been shown for the 1-hydroxycyclohexyloxyl radical **A** [29] that, in a reactive solvent at a temperature below 80 °C, it is converted preferentially into a ketone via the reaction



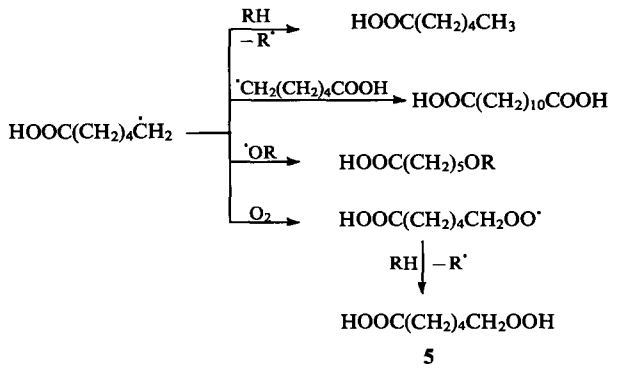
(12)

With increase in temperature [29] and in an inert solvent (for example, in benzene), [53] the isomerisation of the radical **A** to the ω-carboxyalkyl radical **4**, occurring with dissociation of the C–C bond, is more probable.



(13)

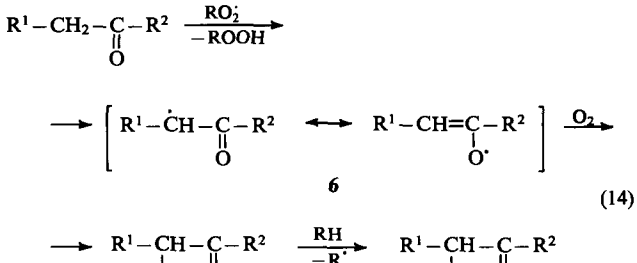
The radical **4** can combine with oxygen, being converted subsequently into the ω-carboxyhydroperoxide **5**, can dehydrogenate the substrate with formation of caproic acid, [54,55] can dimerise to decanedicarboxylic acid [54–56] (which, incidentally, is unlikely under oxidation conditions), and can recombine in a solvent cage with the oxyl radical [52,57] formed simultaneously with the radical **4** via a type (11) reaction.



The role of type (11) reactions should increase on stimulation of the radical decomposition of α-hydroxyperoxides, for example in the presence of variable-valence metal salts. It is significant that this route to oxidative degradation can lead to carboxylic acids, bypassing the ketone formation stage. [53]

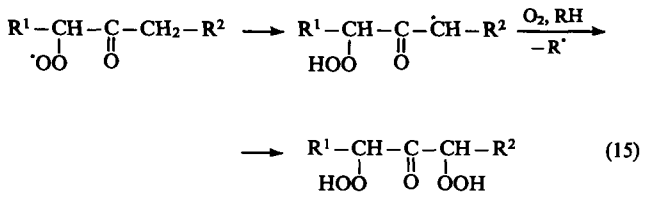
IV. Reactions of α-ketohydroperoxides in the radical-chain oxidation of ketones

Apart from the nonchain interactions with peroxide compounds, ketones are capable of undergoing oxidation via a free-radical mechanism preferentially at the α-C–H bonds. [1,2] The reactivity of the α-C–H bonds of ketones is 12–16 times higher than in hydrocarbons, [1,29,58–60] which is due to the resonance stabilisation of the intermediate radical **6** (stabilisation energy ~17 kJ mol^{-1}) [61]



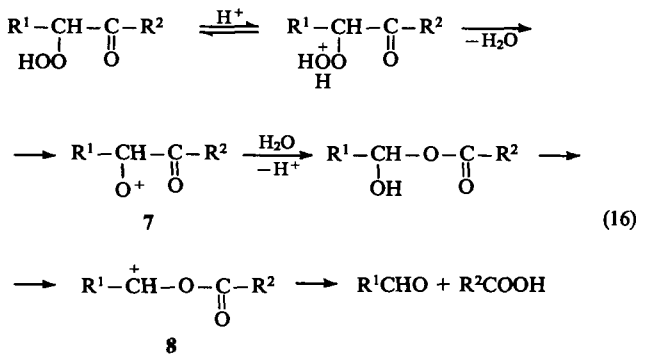
(14)

In the oxidation of long-chain aliphatic ketones, [62–65] significant deviations of the composition of the products from that postulated on the basis of the α-mechanism are observed, which is a consequence of the involvement in the oxidation process of C–H bonds remote from the carbon atom of the carbonyl group, and of the isomerisation of α-ketoperoxyl radicals [a type (6) reaction], [1,24] which can also proceed via the intermediate formation of a six-membered reaction ring incorporating the carbonyl group. [24,66–67]



(15)

It was assumed that the α-ketohydroxyperoxides formed via reaction (14) decompose preferentially with degradation of the carbon chain, which leads, in conformity with the familiar acid-catalytic Langenbeck–Pritzkov mechanism, to compounds with functional carbonyl and carboxy-groups.[2,68–76]



(16)

Results casting doubt on the universality of the Langenbeck–Pritzkov mechanism as the principal route to the degradation of the carbon chain in liquid-phase oxidation processes have been obtained comparatively recently. Pritzkov's data[69,70] indicating the preferential formation of 6-oxo-1-hexanoic acid in the decomposition of 2-hydroperoxycyclohexanone were not confirmed in the studies of Perkel' and Freidin[5] and Korsak et al.;[77] the yield of the acid in this reaction did not exceed 15%. The yield of 6-oxo-1-hexanoic acid did not increase also when the reaction was carried out in the presence of cobalt salts[5,77] and acetic acid.[77] These factors are associated with the fact that 2-hydroperoxycyclohexanone is largely converted into 2-hydroxycyclohexanone.[5]

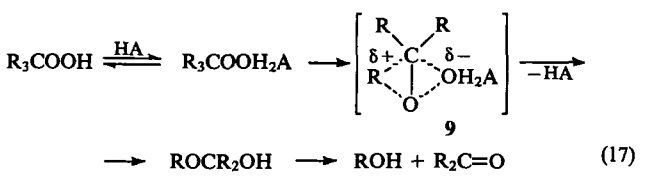
The yield of the ketoalcohol in the thermal decomposition (at 120 °C) of hydroperoxycyclohexanone, obtained by the oxidation of cyclohexanone, depends on the conversion of the ketone and averages 60%.[5] Together with 2-hydroxycyclohexanone (74%), another compound, also formed from the hydroperoxide without the degradation of the carbon chain, namely cyclohexane-1,2-dione (12%), was found among the products of the cobalt naphthenate-catalysed decomposition of 2-hydroperoxycyclohexanone at 80 °C.[5] The conversion of 2-hydroperoxycyclohexanone into 2-hydroxycyclohexanone not only on decomposition of the hydroperoxide under an inert atmosphere but also under oxidation conditions is indicated by the formation, in the initial stages of the noncatalysed and chromium and cobalt salt-catalysed oxidation of cyclohexanone, of a ketoalcohol as the main product.[11,78]

Decomposition without the destruction of C–C bonds is not characteristic solely of 2-hydroperoxycyclohexanone.[6–9] Thus the main products of the thermal reaction of 3-hydroperoxybutanone in oxidised butanone were found to be diacetyl and acetoin.[6] Although the yield of the products (benzoin and benzil) formed without the rupture of the carbon chain in the thermal decomposition of 2-hydroperoxy-1,2-diphenylethanone in oxidised 1,2-diphenylethanone was in fact lower than in the decomposition of 2-hydroperoxycyclohexanone or 3-hydroperoxybutanone, nevertheless it reached 38%–40% in this case also relative to the hydroperoxide which has reacted.[7–9]

It follows from the data presented above that the yield of the products associated with the dissociation of C–C bonds is significantly lower in the decomposition of aliphatic and alicyclic α-ketohydroperoxides than had been supposed earlier. On the other hand, in the decomposition of the hydroperoxides of aromatic ketones the degradation of the carbon chain may predominate.[45,67,79–82]

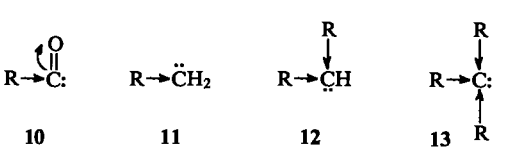
The mechanism of the degradation of the hydrocarbon chain in the decomposition of α-ketohydroperoxides is apparently obscure. Apart from the acid-catalytic mechanism mentioned above [Eqn (16)] postulated by Langenbeck and Pritzkov, homolytic[3,29,67,79–82] and dioxetane[83–85] mechanisms have been described.

The main evidence in support of the acid-catalytic mechanism is the similarity of the yields of compounds with carbonyl and carboxy-groups observed in the oxidation of a series of ketones and the acceleration of the decomposition of α-ketohydroperoxides in the presence of acids. However, the formation of the oxonium cation **7** has not yet been confirmed experimentally. Yablokov[86,87] demonstrated quite convincingly in relation to cumenyl hydroperoxide that hydrocarbon peroxides do not decompose via the acid-catalytic mechanism [Eqn (16)], since even in a strongly acid medium (HA) the rearrangement of cumenyl hydroperoxide proceeds most probably via the cyclic activated state **9** and not via the type **7** oxonium cation.[86,87]

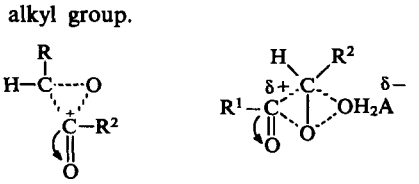


(17)

The mechanism (16) presupposes the preferential migration of the acyl carbanion. This hypothesis is controversial for the following reasons. In the mechanisms (16) and (17), the most nucleophilic group, which stabilises most effectively the transition state and the carbonium ion **8** formed after the migration, should migrate to the electron-deficient oxygen atom.[89] However, the acyl carbanion **10** is a weaker nucleophile than the primary, secondary, and especially tertiary hydrocarbon carbanions **11**–**13** respectively, and the probability of its migration should therefore be minimal from the standpoint of nucleophilicity.



The second cause is that the transition states formed on migration of the acyl group are less stable than those formed on migration of the hydrocarbon carbanion, because the sp^2-hybridised carbon atom of the acyl group, the valence bonds of which are disposed at an angle of 120°, produces a greater strain in the reaction ring than the sp^3-hybridised carbon atom in the alkyl group.



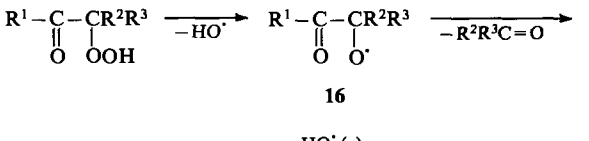
Furthermore, the transition state in the rearrangement of α-ketohydroperoxides is less stable than that obtained in the reaction of alkyl hydroperoxides because the oxygen atom increases the partial positive charge on the acyl carbon atom.

There are three possible types of the 1,2-rearrangement of the oxyl cation **7** which lead to the carbonium ions **8**, **14**, and **15** (Scheme 1).

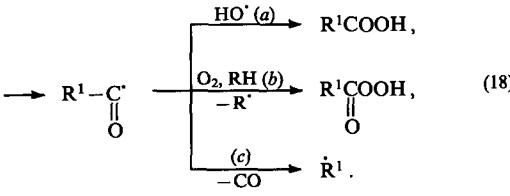
Examination of the resonant structures **8a, b, 14a–c**, and **15a–c** shows that they can be arranged in the following sequences in order of decreasing stability: **8a** > **14a** ~ **15a**, **14b** ~ **15b** > **8b**, and **14c** > **15c**. At first sight, it appears that the structure **8a** should be more stable than the structures **14a** and **15a**, but the cation **8** is apparently less stable than the cations **14** and **15** because it can have only two limiting structures and there is no structure which would make it possible to stabilise it in the way typical of the allyl carbonium ion, as happens in the cations **14** and **15**.

Thus the existing theoretical ideas [the mechanisms (16) and (17)] concerning the mode of the oxidative degradation reaction of hydrocarbons are in poor agreement with the preferred conversion of the α-ketohydroperoxide into a carboxylic acid and a carbonyl compound. Consequently they are inconsistent with the Langenbeck–Pritzkov mechanism.

The homolytic mechanism of the degradative reaction of α-ketohydroperoxides has been justified in a number of studies.[29,45,67,79–82] Thus the composition of the products of the oxidation of isopropyl methyl ketone indicates, according to Itoh et al.,[82] the decomposition of the primary reaction product (3-hydroperoxy-3-methylbutan-2-one) via the mechanism



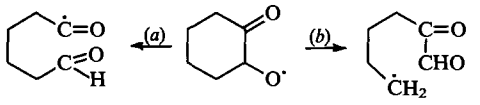
16



(18)

The reactions of tertiary α-ketohydroperoxides, studied by Ogata and Savaki,[79–81] proceed via a similar mechanism. α-Diketones are then formed in a small amount, probably via the elimination of hydrocarbon groups from the radical **16**. It has been shown that the photolysis of α-ketohydroperoxides in the presence of oxygen leads to a peracid (pathway *b*).[81] The rate of decomposition of α-acyloxyl radicals with destruction of a C–C bond is approximately two orders of magnitude higher than the rate of abstraction of a hydrogen atom from the solvent by this radical with formation of a α-ketoalcohol. This factor is apparently associated with the increased stability of the benzoyl radicals obtained on fragmentation. They are stabilised by the $+E$ effect of the aromatic ring.

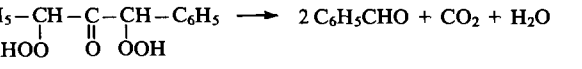
The study of the composition of the products of the oxidation of cyclohexanone led Pritzkov and Hahn[29] to the conclusion that two pathways are possible in the reaction of the 2-oxocyclohexyloxyl radical with degradation of the carbon chain.



(19)

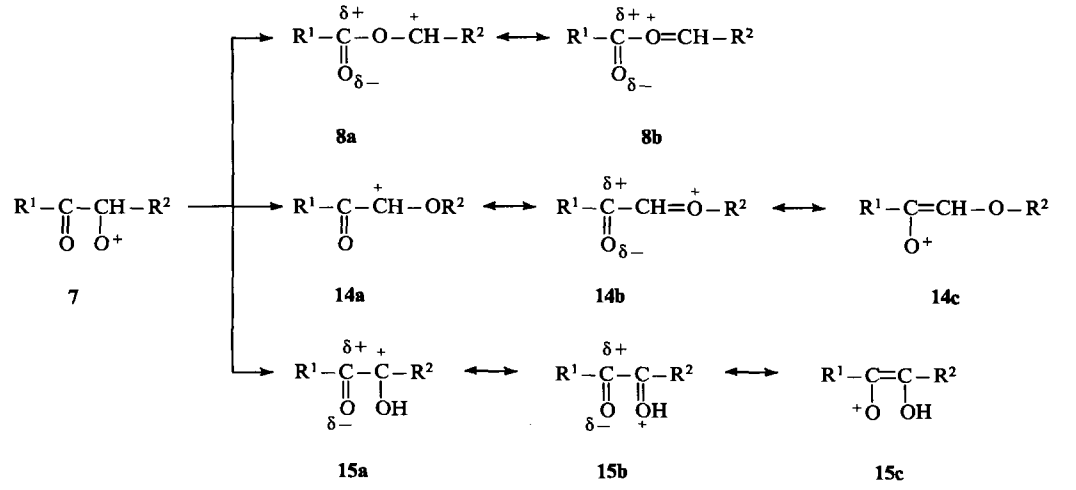
Pathway *a* explains the formation in the oxidation reaction of 6-oxo-1-hexanoic, monoperadipic, and adipic acids,[29] whilst pathway *b* accounts for the formation of glutaric acid, δ-valerolactone, and valeric acid.[29,90]

The homolytic decomposition of the secondary α-ketohydroperoxide (the β′-mechanism) has been observed in the oxidation of dibenzyl ketone.[45,67,91] This is indicated by the deviation of the composition of the product from that expected on the basis of the Langenbeck–Pritzkov mechanism (the α-mechanism). The phenylacetyl radical formed via reaction (18) is almost completely decarbonylated to the benzyl radical (pathway *c*); pathways *a* and *b* do not occur. Therefore, on the basis of the ratio of the initial rates of accumulation of phenylacetic acid and of benzyl hydroperoxide together with benzyl alcohol (the benzyl radical reaction products), it is possible to estimate the contribution of the homolytic mechanism to the overall decomposition of the α-ketohydroperoxide. In the noncatalysed oxidation of dibenzyl ketone at 100 °C, the contribution of the homolytic decomposition is not less than 50% according to Perkel' et al.[45] The composition of the products of the decomposition of dibenzyl ketone α-dihydroperoxide, formed in the oxidation of dibenzyl ketone [a type (15) reaction, β″-mechanism],[20,67] also deviates from that expected on the basis of the α-mechanism.

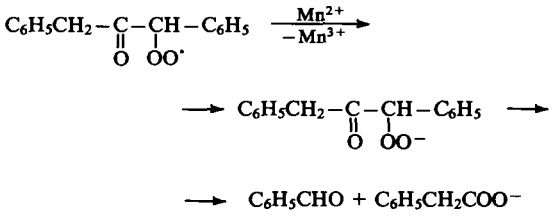


The relative contributions of the different routes to the oxidative degradation of ketones can be altered by introducing catalytic amounts of variable-valence metals.[20,67] According to the data of Perkel' and co-workers,[20,67] the relative contributions of the α-, β′-, and β″-mechanisms (expressed as percentages) in the oxidative degradation of dibenzyl ketone at 100 °C in chlorobenzene are 9 : 49 : 42 in the presence of cobalt(II) naphthenate as the catalyst, 26 : 27 : 47 in the presence of chromium(III) naphthenate, and 40 : 50 : 10 in the presence of manganese(II) naphthenate. Since the contribution of the α-mechanism in the noncatalysed oxidation

Scheme I



under the same conditions is only 18%, the above data demonstrate that chromium and manganese naphthenates increase the selectivity of the dibenzyl ketone oxidation reaction as regards the formation of phenylacetic acid compared with the noncatalysed process.[20,67] In the case of chromium naphthenate, the increase in the contribution of the α-mechanism to the overall process is associated with the decrease in the proportion of the homolytic decomposition of the α-ketohydroperoxide, whilst in the case of manganese naphthenate it is associated with the suppression of reaction (15).[20,67]

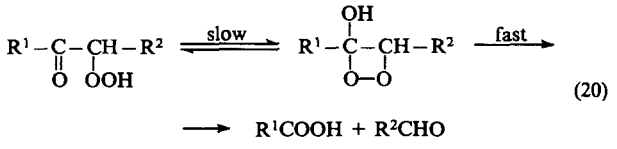


The yield of the products of the degradation of α-ketohydroperoxides in conformity with the Langenbeck–Pritzkov mechanism can also be explained satisfactorily by resorting to the dioxetane mechanism. The formation of 1-hydroxy-1,2-dioxetanes (Kohler peroxides[48]) was already postulated in early investigations of the oxidation of the enolic forms of ketones. However, after evidence had been obtained in support of the existence of ketone α-hydroperoxides predominantly in the acyclic keto-form, these ideas were abandoned for a long time.

The interest in the dioxetane mechanism was manifested anew in the 1970s–1980s when chemiluminescence characteristic of 1,2-dioxetanes (this class of organic compounds had been well investigated by that time) was observed[83–85] in the base-catalysed oxidation of ketones and in the decomposition of α-ketohydroperoxides in an alkaline medium.[92] These ideas have not gained wide currency as the explanation of the oxidation reaction in a neutral medium.

The dioxetane mechanism of the reaction of α-ketohydroperoxides does not conflict with the available experimental data on the decomposition of these hydroperoxides and it accounts for some of them more satisfactorily than the acid-catalytic and homolytic mechanisms.

The formation of 1-hydroxy-1,2-dioxetanes from α-ketohydroperoxides is energetically unfavourable owing to the ring strain arising under these conditions.[92] The equilibrium in the reversible first stage of the reaction should therefore be displaced towards the keto-form, which is additionally stabilised by an intramolecular hydrogen bond.[93] The sequence of the slow reversible and rapid irreversible reactions should be manifested kinetically as an irreversible first-order reaction,[94] which is in fact usually observed in the decomposition of α-ketohydroperoxides of different structure.[1,2]



(20)

Although the base catalysis in reactions involving nucleophilic addition to the carbonyl group is usually preferred,[46,89] the interaction of carbonyl compounds with hydroperoxides takes place readily also without a catalyst[95] and under the conditions of general acid catalysis by weak acids such as carboxylic acids.[20] Furthermore, the carbonyl group of α-ketohydroperoxides should be significantly activated by the $-I$ effect of the hydroperoxide group and by the intramolecular bond, as happens in the case of α-ketoalcohols.[13]

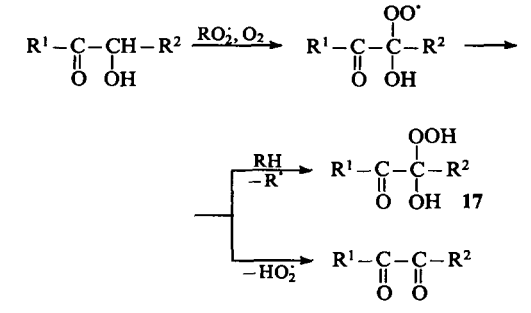
Evidently, when the dioxetane mechanism operates, a correlation should be observed between the reactivity of the carbonyl groups of the α-ketohydroperoxides and the stability of the latter. Indeed, tertiary α-ketohydroperoxides the carbonyl group of which is linked to an aromatic ring are the most stable (and therefore have been most thoroughly investigated).[3] Aromatic groups are known to reduce the reactivity of the carbonyl group in nucleophilic addition reactions because, when the ketone is converted into the adduct, the stabilisation via delocalisation is disturbed.[46] The presence of substituents at the α-carbon atom also lowers significantly the reactivity of the carbonyl groups owing to steric effects.[46] Evidently this is the reason why 2-hydroperoxy-2,4-dimethylpentanone is much more stable than the α-ketohydroperoxides of normal aliphatic ketones.[2]

In the decomposition of tertiary aromatic α-ketohydroperoxides in the presence of alkoxide ions[96] taken in large amounts, or in the presence of trifluoroacetic acid,[97] 1,2-dioxetanes are not formed. This finding may be associated with the low reactivity of such hydroperoxides in intramolecular nucleophilic addition reactions accompanied by the competing reaction of the carbonyl group with a stronger nucleophile—the alkoxide ion, and also with the suppression of reaction (20) as a consequence of the associative interactions of trifluoroacetic acid with the hydroperoxy- and carbonyl groups of the hydroperoxide. The possibilities of the dioxetane mechanism for the explanation of the characteristic features of the decomposition of α-ketohydroperoxides in autoxidation reactions are apparently still not exhausted.

V. Oxidative degradation of α-ketoalcohols

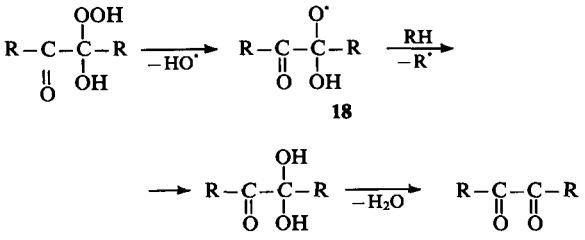
It was noted above that α-ketoalcohols are the principal products of the decomposition of α-ketohydroperoxides not involving the degradation of the carbon chain. The reactions of α-ketoalcohols in hydrocarbons undergoing oxidation involve both a radical-chain process[10,11,13–17,20,98–101] and their interactions with peroxide compounds.[13,17,20]

The mechanism of the radical-chain oxidation of α-ketoalcohols has been investigated in relation to 2-hydroxycyclohexanone,[10,11,13–17,20,98] 11-hydroxy-10-eicosanone,[20] and benzoin.[99–101] As secondary alcohols, α-ketoalcohols are oxidised via the reactive α-C–H bond, which is additionally activated by the carbonyl group. The intermediate α-hydroxy-α-oxoperoxyl radicals in the oxidation of ketoalcohols either abstract hydrogen from the substrate with formation of α-hydroperoxy-α-hydroxyketones **17** or decompose to the radical $HO_2^{\cdot}$ and a diketone.[13,16,20,99–101]



α-Hydroperoxy-α-hydroxyketones dissociate reversibly in their turn into hydrogen peroxide and an α-diketone[15,20,98–101] or undergo degradation via homolytic and nonhomolytic mechanisms[14,17,20,99] with formation of α-diketones, carboxylic acid anhydrides, or free carboxylic acids.

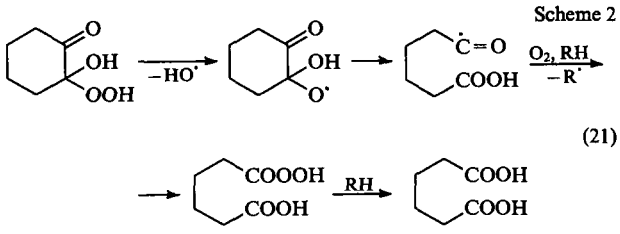
The homolytic decomposition of α-hydroperoxy-α-hydroxyketones proceeds via 1-hydroxy-2-oxoalkoxyl radicals **18**,[14,17,19] the principal pathway in the reaction of which does not involve the formation of a new carbonyl group, as in the case of α-hydroxyalkoxyl radicals (see Section III), but takes place with dissociation of the carbon chain.[14,17,20,99]



18

It has been shown in relation to 2-hydroperoxy-2-hydroxycyclohexanone that such degradation in the presence of oxygen leads to adipic acid via a monoperacid (Scheme 2).[14,17,20]

Scheme 2

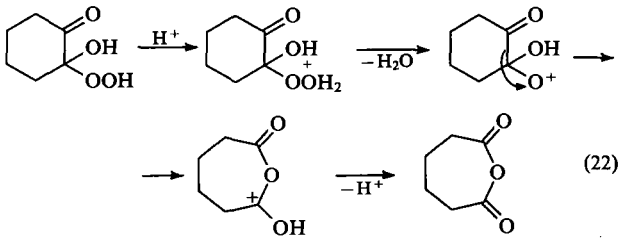


(21)

By comparing the potential yield of the peracid with the yield of adipic acid formed in the oxidation of 2-hydroxycyclohexanone at 50 °C, it was found that about 50% of the adipic acid is obtained via reaction (21).[17,20]

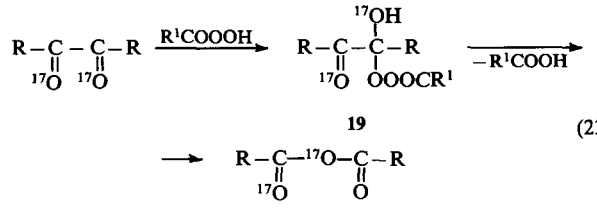
Mechanisms involving both the heterolytic[14,16] and pericyclic[17,20] rearrangements have been put forward to account for the formation of adipic anhydride from 2-hydroperoxy-2-hydroxycyclohexanone.

A heterolytic rearrangement of the Baeyer–Villiger type,



(22)

which presupposes the migration of the acyl carbon atom, is unlikely for the same reason as in the acid-catalytic decomposition of α-ketohydroperoxides (see Section IV). Furthermore, there are data[102] showing that, in the oxidation of ^{17}O- or ^{18}O-labelled benzil by *m*-chloroperbenzoic acid, which proceeds via the α-acylperoxy-α-hydroxyketone **19**, one of the carbonyl atoms of the α-diketone becomes the bridging atom of the anhydride, i.e.



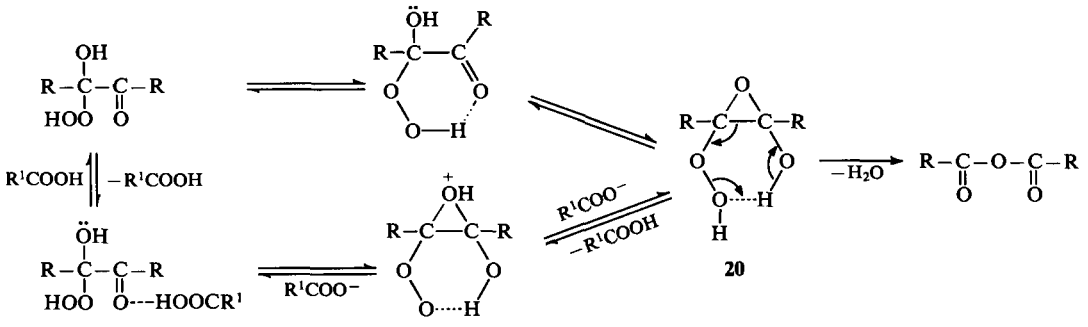
19 (23)

which cannot be explained by a Baeyer–Villiger rearrangement [reactions (10) and (22)].

The data on the distribution of the labelled oxygen agree well with the hypothesis that the peroxides **17** and **19** are converted into the anhydride via the slow reversible intramolecular nucleophilic addition of the hydroxy-group to the carbonyl group with subsequent rapid pericyclic rearrangement of the oxirane intermediate **20** (Scheme 3).[17,20]

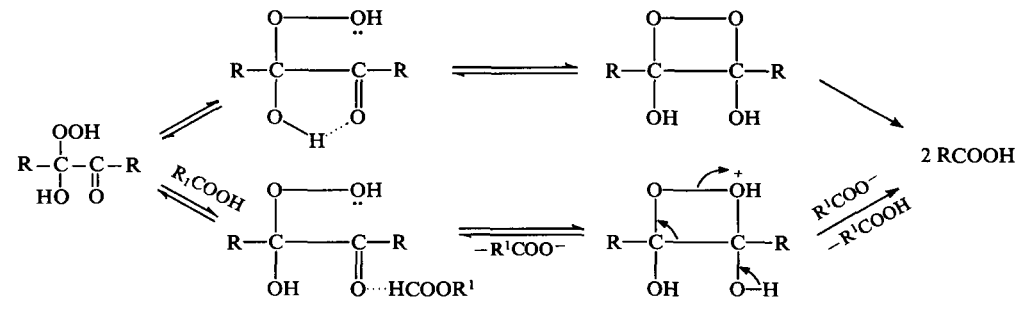
Reaction (24) takes place under the conditions of general acid catalysis; the effective rate constant for the first-order reaction involving the decomposition of 2-hydroperoxy-2-hydroxycyclohexanone to adipic anhydride in 2-hydroxycyclohexanone undergoing oxidation varies linearly with the concentration of carboxy-groups.[17,20] The mechanism (24) explains fairly satisfactorily the influence of the solvent and of the structure of the α-hydroperoxy-α-hydroxyketone on the yield of anhydrides. It has been established that adipic anhydride is hardly formed in the oxidation of 2-hydroxycyclohexanone in a solvent such as dimethylformamide,[17,20] which suppresses the nucleophilic addition of the hydroxy- and hydroperoxy-groups[17] to the carbonyl group, preventing thereby the formation of the intermediate **20**. One of the causes of the low yield of benzoic anhydride in the oxidation of benzoin may be the reduced reactivity of the carbonyl group of the α-hydroperoxy-α-hydroxyketone linked to the aromatic ring.[46]

Scheme 3



(24)

Scheme 4



(25)

It has been concluded [17,20] that the adipic acid formed in the oxidation of 2-hydroxycyclohexanone is produced mainly not via reaction (21) but as a result of the rearrangement of 2-hydroperoxy-2-hydroxycyclohexanone [reaction (25)] similar to that examined above the α-hydroperoxides [reaction (20)], i.e. the dioxetane mechanism operates (Scheme 4).

The carbonyl group of α-hydroperoxy-α-hydroxyketones is additionally activated (compared with α-ketohydroperoxides) by the $-I$ effect of the hydroxy-group. [17,20] As in reaction (24), carboxylic acids accelerate the conversion of the peroxide. [17,20]

Thus the possibility of the selective preparation of anhydrides from α-hydroperoxy-α-hydroxyketones is determined by the contribution of reactions (24) and (25) to the overall oxidation process. On the grounds that these reactions have stages with similar mechanisms and virtually identical activation energies, [16,17,20] it was concluded that the process selectivity is low. Data on the oxidation of 2-hydroxy-cyclohexanone in chlorobenzene at 95 °C [16] showed that the ratio of the yields of adipic anhydride and adipic acid reaches 2.2 under these condtions, i.e. reaction (24) predominates. An increase in the selectivity of the conversion of α-hydroperoxy-α-hydroxyketones into carboxylic acids can be achieved by stimulating their homolytic decomposition and(or) by suppressing reaction (24). Thus, in the oxidation of 2-hydroxycyclohexanone the significance of reaction (21) increases with increase in the initial concentration of the ketoalcohol, when the reaction is carried out in a reactive solvent, and when variable-valence metal salts are used as catalytic additives. [14-17,20]

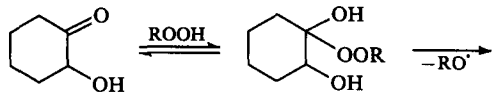
When the concentration of 2-hydroxycyclohexanone is varied in the range from 0.24 to 1.47 M (95 °C, chlorobenzene), the ratio of the initial rates of accumulation of adipic acid and its anhydride increases from 0.5 to 1.05. [16,20] In the oxidation of 2-hydroxycyclohexanone in ethylbenzene (95 °C, 1.2 M), this ratio reaches 1.8. [16] The increase in the yield of adipic acid in the cases indicated above is associated with the increase in the contribution of the homolytic decomposition of the α-hydroperoxy-α-hydroxyketone, with participation of compounds R^1H containing reactive C–H bonds, as a result of the occurrence of reaction (26). [16,20,56]

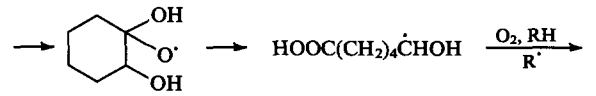
$$ROOH + R^1H \longrightarrow RO^{\cdot} + H_2O + \dot{R}^1 \qquad (26)$$

In the study of the influence of cobalt(II), nickel(II), chromium(III), and iron(III) naphthenates on the oxidation of 2-hydroxycyclohexanone, it was established that the yield of adipic acid in the presence of all the catalysts is higher than in the noncatalysed reaction, while the yield of adipic anhydride is correspondingly lower, especially in the presence of the cobalt salt. [11,20] The results of the decomposition of the peroxide compounds formed in the oxidation of 2-hydroxycyclohexanone under a nitrogen atmosphere showed that the mode of the decomposition and oxidation reactions is as a rule the same. [20] The decrease in the yield of the anhydride with simultaneous formation of the acid in the presence of variable-valence metals has been explained by the increasing role of a type (21) reaction. [20]

An increase in the relative yield of adipic acid has been observed also in the oxidation of 2-hydroxycyclohexanone in dimethylformamide, although the rate of its formation was lower than in the oxidation in chlorobenzene. [17,20] It has been suggested [17,20] that this phenomenon is associated with the suppression of reactions (24) and (25) in dimethylformamide as a consequence of the suppression of the intramolecular nucleophilic addition to the carbonyl group in this solvent. [17,20]

α-Ketoalcohols can not only participate in the radical-chain oxidation but can also interact with peroxide compounds. (The rate of decomposition of peroxide compounds in the presence of ketoalcohols is much higher than in the presence of monofunctional alcohols and ketones. [13,20]) Apart from reactions (26), such interaction can include the addition of the peroxide compounds to the carbonyl group of the α-ketoalcohol, [13,20] which has been observed, for example, in the cooxidation of 2-hydroxycyclohexanone together with ethyl methyl ketone [13] and cyclohexanol [17] and also in the oxidation of benzoin. [99] Thus, when 2-hydroxycyclohexanone is introduced into ethyl methyl ketone undergoing oxidation, ε-caprolactone, ε-hydroxycaproic acid, and 6-oxo-1-hexanoic acid are formed in a yield of about 40% relative to the ketoalcohol which has reacted. The reaction probably proceeds via the following mechanism: [13]

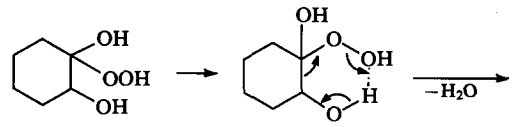




(27)

$$\longrightarrow HOOC(CH_2)_4CH(OH)OOH \xrightarrow{-H_2O_2} HOOC(CH_2)_4CHO.$$

It has been suggested [17] that, in the cooxidation of 2-hydroxycyclohexanone together with cyclohexanol, 6-oxo-1-hexanoic acid is obtained both as a result of reaction (27) and as a result of the pericyclic rearrangement of 1-hydroperoxy-1,2-dihydroxycyclohexane **21**.



21

$$\longrightarrow HOOC(CH_2)_4CHO$$

The formation of benzaldehyde in the liquid-phase oxidation of benzoin is associated with the reaction of the latter with peroxide compounds. [99] This possibility is supported also by data for the oxidation of benzoin by *m*-chloroperbenzoic acid. [103]

VI. Oxidation of α-diketones by peroxide compounds

α-Diketones, which together with α-ketoalcohols are the main products of the reaction of α-ketohydroperoxides without the degradation of the carbon chain (see Section IV), are also capable of interacting with peroxide compounds in hydrocarbons undergoing oxidation.

There are few data on the radical-chain oxidation of α-diketones. The oxidation of diacetyl by oxygen at 80 °C has been investigated. [104] It is suggested that the reaction proceeds via the intermediate formation of acetic anhydride, which, however, was not identified. [104] The main product of the reaction is acetic acid.

In the oxidation of cyclohexane-1,2-dione by oxygen in solution in chlorobenzene, only tarry products were detected. [105] This finding is probably associated with the fact that cyclohexane-1,2-dione exists predominantly as the monoenol (2-hydroxycyclohex-2-en-1-one), [12] which can be readily oxidised at the carbon atom in the α-position relative to the double bond and evidently polymerises under the influence of free radicals. Since there are no data on the enolic form of cyclohexane-1,2-dione in the cyclohexane oxidation reaction, the selection of the latter as a model reaction appears controversial. There is no doubt that

problems concerning the radical-chain oxidation of α-diketones still await solution.

Problems associated with the reactions of α-diketones with peroxide compounds (H_2O_2, hydroperoxides, peracids), used for preparative purposes, have been investigated to a greater extent. A study has been made of the influence of equimolar amounts of added oxygen-containing compounds of different classes on the rate of the thermal decomposition of *tert*-butyl hydroperoxide (TBHP) in benzene at 160 °C under a N_2 atmosphere. The effective rate constants for the decomposition of THBP in the presence of various additives have the following values:[13,20]

Additive	$10^4 k_{eff}/s^{-1}$
Eicosane-10,11-dione	25.0
Cycloheptane-1,2-dione	11.0
2-Hydroxycyclohexanone	10.0
11-Hydroxyeicosan-10-one	5.0
2-Hydroxycyclohex-2-en-1-one	1.27
Cyclohexanone	0.20
Cyclohexanol	0.17
Nonan-5-ol	0.14
Nonadecan-10-one	0.13
Without additive	0.025

It is seen from the data presented that, in terms of their capacity to decompose hydroperoxides, α-diketones are more effective than not only monofunctional alcohols and ketones but also α-keto-alcohols.

The interaction of α-diketones with peroxide compounds in autoxidation reactions is not only an important route to the conversion of the latter but also serves as a pathway to the formation of degradation products, in particular carboxylic acid anhydrides. It was found that these reactions proceed at fairly high rates even in nonpolar solvents close to room temperature. The first stage of the interaction of hydroperoxides and peracids with α-diketones involves their reversible nucleophilic addition to one of the carbonyl groups of the α-diketone with formation of α-hydroperoxy-α-hydroxy-, α-alkylperoxy-α-hydroxy-, and α-acylperoxy-α-hydroxy-ketones.[12,18,19,32,102,106–110] The rate-limiting stage is the subsequent degradative composition of α-hydroperoxy-α-hydroxy- and α-alkylperoxy-α-hydroxy-ketones.[20,111]

The main products of the oxidation of hexadecane-8,9-dione by hydrogen peroxide are caprylic anhydride and caprylic acid.[18,20] Caprylic anhydride is formed via reaction (24), whilst the acid is formed via reactions (21) and (25).[20] In the interaction of hexadecane-8,9-dione with TBHP, *tert*-butyl caprylate was obtained in addition to caprylic anhydride and caprylic acid.[18,20] The yield of caprylic anhydride is in this case significantly higher than in the reaction with hydrogen peroxide, whilst caprylic acid is formed either in the homolytic decomposition of the peroxide [reaction (21)] or from caprylic anhydride simultaneously with *tert*-butyl percaprylate, and not via reaction (25).[18,20] The effective decomposition rate constants increase linearly under these conditions as the degradation products accumulate,[18] which is apparently associated with the catalytic effect of caprylic acid.

The high equilibrium constants in the interaction of hexadecane-8,9-dione with hydrogen peroxide and TBHP at 23 °C (41.5 and 49.0 litre mol^{-1}) are due to the stabilisation of the adducts by the formation of an intramolecular hydrogen bond.[20,112]

Di-*tert*-butyl peradipate was detected together with mono-*tert*-butyl peradipate among the products of the oxidation of cyclohexane-1,2-dione by TBHP.[12] The formation of the former has been explained by the interaction of the hydroperoxide with a polymeric form of adipic anhydride.[12]

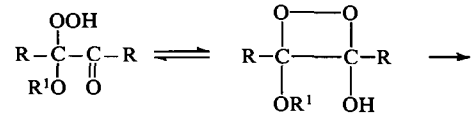
Acetic anhydride is formed selectively in the oxidation of diacetyl by TBHP in solution in acetic acid, while in the case where the reaction is carried out in *tert*-butyl alcohol the acid is formed predominantly.[112] Evidently acetic acid accelerates the conversion of the corresponding α-alkylperoxy-α-hydroxyketone via reaction (24), while *tert*-butyl alcohol has the opposite effect, suppressing this degradation pathway (as a result of the competing interactions of the OH group of the alcohol with the carbonyl group of the α-alkylperoxy-α-hydroxyketone); acetic acid is then formed homolytically via reaction (21).

In the interaction of diacetyl with 2-hydroperoxy-2-methyltetrahydrofuran or 2-hydroperoxytetrahydropyran in chlorobenzene, the homolytic decomposition of α-alkylperoxy-α-hydroxyketones predominates.[106] The reaction products are formed as a result of the recombination of the acyl radical of the α-diketone and oxyl or carbon-centred radicals of the hydroperoxide within a cage.[106] Thus the relative contributions of the different routes to the degradation of α-alkylperoxy-α-hydroxyketones are affected not only by the medium but also by the structure of the α-diketones and hydroperoxides.

In the oxidation of α-diketones by peracids, the rate-limiting stage is the acid-catalysed nucleophilic addition of the peracid to the carbonyl group of the α-diketone. The effective rate constants for the second-order reaction (given in brackets in litre $mol^{-1} s^{-1}$) involving the oxidation of α-diketones by perlauric acid at 23 °C diminish on passing from hexadecane-8,9-dione (0.37) to 1-phenylpropane-1,2-dione (0.036) and then to benzil (0.0071) as a consequence of the decrease in the reactivity of the carbonyl groups of the α-diketones under the influence of aromatic substituents.[20,111] Lauric acid increases the effective rate constant for the reaction of hexadecane-8,9-dione with perlauric acid almost by a factor of 100.[19,20,111] Consequently the importance of such reactions increases at advanced stages in the autoxidation reactions of hydrocarbons.

It was first established in Karrer's studies[32,113–117] that the main products of the oxidation of α-diketones by peracids are carboxylic acid anhydrides. It was postulated that such reactions proceed via a heterolytic rearrangement of α-acylperoxy-α-hydroxyketones [reaction (22)][32] or via oxirane intermediates.[20,102,111]

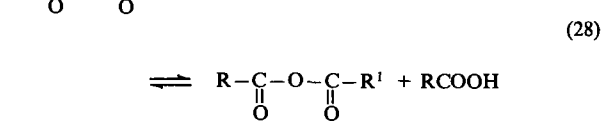
The data[102] indicating the preferential conversion of the α-acylperoxy-α-hydroxyketones into an anhydride [see reaction (23)] cannot be accounted for by resorting to heterolytic rearrangement, but the formation of the anhydride is described satisfactorily by Eqn (24), which involves the oxirane intermediates **20**. The important role of the OH group in the formation of the anhydride is indicated also by the fact that esters and not anhydrides are formed in the decomposition of α-alkoxy-α-hydroperoxyketones **22**.[118] The mechanism (24) does not operate in this case and the ester is formed via a reaction analogous to reaction (25).



22

$$\longrightarrow RCOOR^1 + RCOOH$$

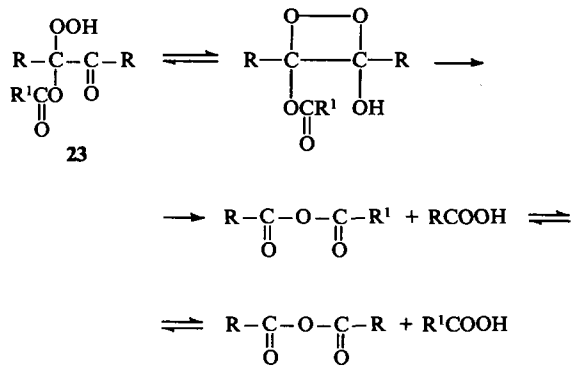
Together with the expected symmetric anhydride [reaction (24)], mixed anhydrides, including acylperacids, were also found in the reactions of hexadecane-8,9-dione and benzil with perlauric acid.[19,20,111] Their formation is associated with the transacylation of the symmetrical anhydride by reaction with lauric acid obtained by the reduction of the peracid.[19]



(28)

The occurrence of reaction (28) leads to a decrease in the selectivity of the overall reaction with respect to the target anhydride. This is probably why the yield of the expected anhydrides did not as a rule exceed 50% in the early studies.[32,113-117]

The formation of symmetrical anhydrides in the decomposition of α-acyloxy-α-hydroperoxyketones **23** is probably associated with transacylation.[119]



23

Thus not only the composition of the products of the reactions of α-hydroperoxy-α-hydroxy-,α-alkylperoxy-α-hydroxy-, and α-acylperoxy-α-hydroxy-ketones, formed in the radical-chain oxidation of α-ketoalcohols and in the oxidation of α-diketones by peroxide compounds, but also the composition of the related peroxides **22** and **23** can be explained on the basis of the mechanisms (21), (24), and (25).

The importance of different mechanisms of the oxidative degradation of the hydrocarbon chain, examined in Sections V and VI, for the hydrocarbon oxidation reactions is still to be assessed. However, there is no doubt that the reactions leading to carboxylic acid anhydrides occupy a special place among them. The formation of the anhydrides was detected not only in the oxidation of the α-ketoalcohols and α-diketones but also in the oxidation reactions of cyclohexane,[10] cyclohexanone,[11,78] ethyl methyl ketone,[120,121] dibenzyl ketone,[45,91] and benzyl phenyl ketone.[7-9,45] Being highly reactive in nucleophilic addition reactions, carboxylic acid anhydrides interact during the autoxidation processes with the water produced in the reaction, alcohols, hydroperoxides, and carboxylic acids[20] and this is why it is usually difficult to establish the amount in which they are actually formed in the reaction. According to the data of Bogomol'nyi and Freidin,[121] not less than 20% of acetic acid is obtained during the oxidation of ethyl methyl ketone as a result of the hydrolysis of acetic anhydride. The problems associated with the participation of the anhydrides in the formation of esters and other oxidation products will be examined in Sections VII and VIII.

VII. The formation of esters in autoxidation processes

Esters are side products of the reactions involving the autoxidation of hydrocarbons and their oxygen-containing derivatives to carboxylic acids.[1,2] To facilitate the consideration of the mechanisms of the formation of esters, the latter will be divided into three groups.

The first group includes the esters of primary (more rarely secondary) alcohols containing the same total number of carbon atoms as the compound oxidised (for example, ethyl acetate and ε-caprolactone obtained in the oxidation of butane and cyclohexane respectively, or isopropyl acetate, which is a side product in the oxidation of isopropyl methyl ketone,[82] etc.).

The esters of secondary alcohols (with the same number of carbon atoms as in the initial compound) and acids containing as a rule fewer carbon atoms than the alcohols (for example, *sec*-butyl acetate—the product of the oxidation of butane or *sec*-butyl alcohol,[1] the cyclohexyl esters of mono- and di-carboxylic acids—the products of the oxidation of cyclohexane, cyclohexanol,[19] etc.) should be included in the second group.

Finally, the third group incorporates γ- and δ-lactones containing the same or a smaller number of carbon atoms than the initial compound (for example, γ-methyl- and γ-ethyl-butyrolactones obtained by the oxidation of undecan-6-one[24,62] and γ-octyl-butyrolactone and δ-heptylvalerolactone formed in the oxidation of lauric acid[2]).

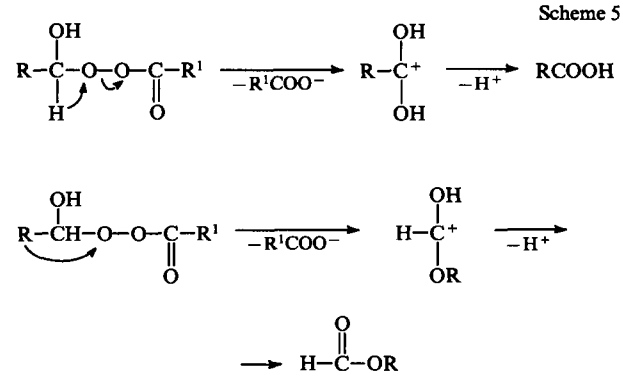
Since the esters of the first group can be formally obtained by inserting an oxygen atom into the C–C bond closest to the carbonyl group, it was postulated that they are formed in the oxidation of the corresponding ketones by peracids,[44,45,68,82,122] The peroxyl radical,[2] and hydroperoxides[123] and also as a result of the homolytic rearrangement of α-ketohydroperoxides.[1]

The fairly high rate of oxidation of ketones by peracids in nonpolar solvents and at moderate temperatures (see Section III) as well as the existence of theoretical preconditions for the formation of peracids in liquid-phase oxidation processes makes it possible to give preference to the Baeyer–Villiger reaction. An experimental test of the importance of this reaction was achieved comparatively recently for the oxidation reactions of cyclohexanone[44] and aromatic ketones.[45]

In a study of the influence of added diphenyl sulfide and diphenyl sulfone (reagents which reduce peracids) on the composition of the cyclohexanone oxidation products, it was established that the main side product of this reaction—ε-caprolactone—is formed predominantly by the interaction of the ketone with the peracid.[44] It was shown that the alternative mechanisms of the formation of ε-caprolactone, presupposing the oxidation of the ketone by peroxyl radicals or hydroperoxides, as well as the reactions of α-ketohydroperoxides unrelated to the appearance of peracids do not occur on an appreciable scale under the conditions of the process.[20,44] It was found that benzyl benzoate and benzyl phenylacetate are also formed as a result of the oxidation of benzyl phenyl ketone and dibenzyl ketone respectively by the peracid.[20,45]

The formation of formic acid esters in the oxidation of aldehydes is apparently also associated with the Baeyer–Villiger reaction. In this case, the 1,2-rearrangement of the α-hydroxyperester may entail the migration of both a hydride ion and of a hydrocarbon group, which lead respectively to an acid and an ester (Scheme 5).[2]

Scheme 5



The mechanism of the formation of the esters of secondary alcohols, which we assigned to the second group, remained obscure for a long time. The esterification of alcohols by carboxylic acids, postulated in a number of studies (see, for example, Emanuel' et al.[1]) as the main reaction, makes only a 10%–25% contribution to the observed rate of accumulation of esters even according to the most optimistic estimates.[126-129] This is evidence in support of the existence of a nonacid (unrelated to carboxylic acids) route to the formation of esters.

Such a route is apparently provided by the esterification of alcohols by anhydrides. This hypothesis has been tested[10] in relation to the oxidation of cyclohexane. A satisfactory agreement

was found between the rate of accumulation of monocyclohexyl adipate observed in the oxidation of cyclohexane at 150 °C, and the rate of formation of this ester calculated from kinetic data for the reaction of adipic anhydride with cyclohexanol.

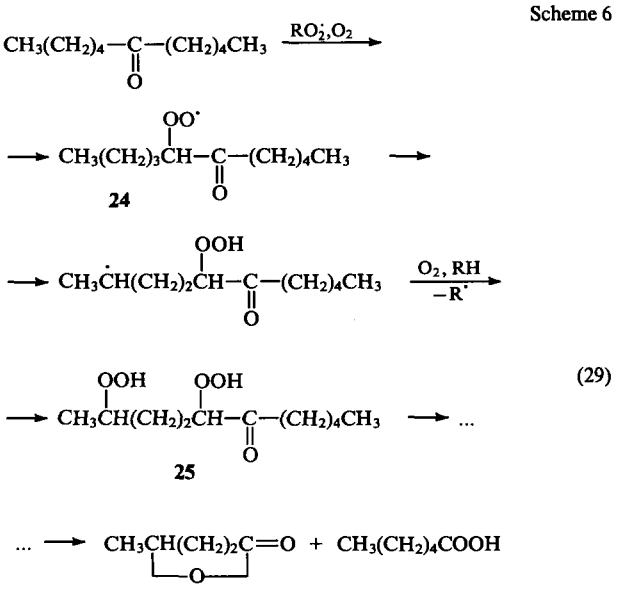
The transacylation of the anhydrides with the free acids results in the formation of mixed anhydrides [reaction (28)]. Their interaction with alcohols leads to esters incorporating the acyl residues from the carboxylic acid participating in the transacylation. It has been demonstrated for the oxidation reactions of cyclohexane, cyclohexanol, and cyclohexanone that cyclohexyl or 2-oxocyclohexyl esters of mono- and di-carboxylic acids are formed with participation of adipic anhydride.[19,20]

The pathways leading to the formation of γ- and δ-lactones in the oxidation of long-chain hydrocarbons are still insufficiently clear and are apparently associated with the multistage nature of such reactions and with the difficulty of identifying and determining the intermediates. According to the most widely held view, the lactones are formed from the corresponding hydroxyacids.[1,2]

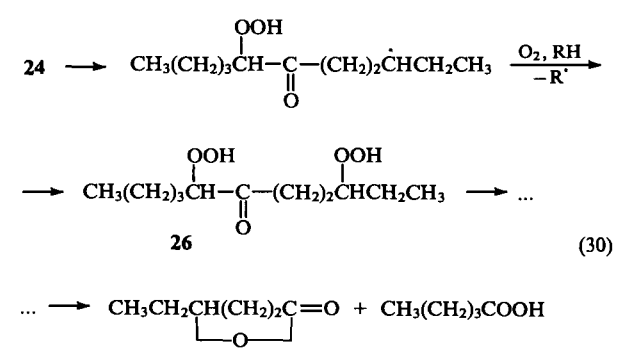
It has been suggested[24,62] that the γ-lactones arise in the stages which follow the formation of the ketones. The products of the oxidation of undecan-6-one were found to contain γ-methyl- and γ-ethyl-butyrolactones, the origin of which has been attributed[24,62] to the intramolecular isomerisation of the ketoperoxyl radical **24** and the subsequent reaction of the dihydroperoxides **25** and **26** (Scheme 6).

The intramolecular isomerisation of the radical **24** in conformity with reaction (29) is entirely realistic, while the isomerisation of this radical via reaction (30) is improbable.[1] If it is supposed that such isomerisation is possible, then it should lead to δ-lactones in the oxidation of long-chain ketones, for example tridecan-7-one (Scheme 7). However, only γ-lactones were found among the tridecan-7-one oxidation products.[24]

Scheme 6

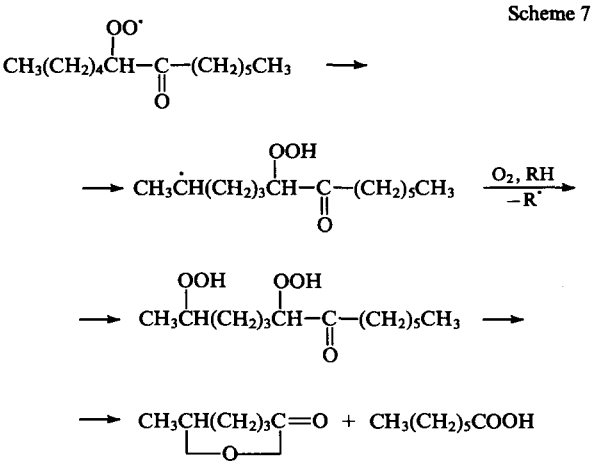


(29)



(30)

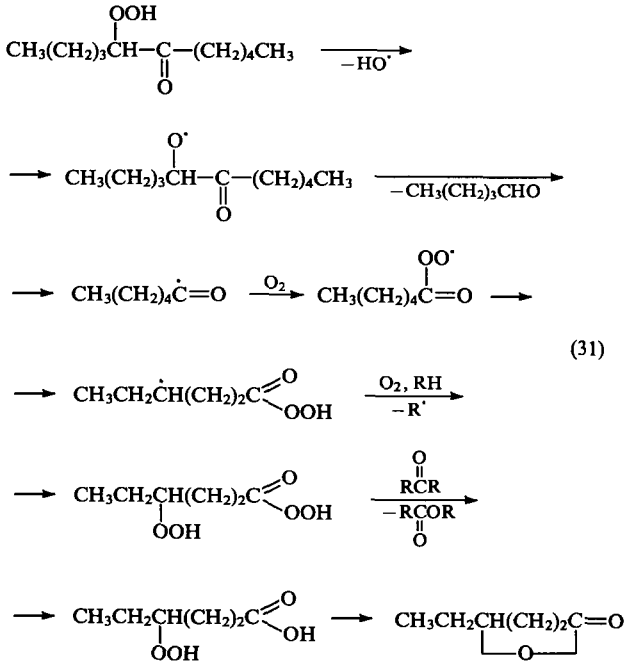
Scheme 7



The hypothesis has been put forward that the formation of γ-lactones is associated not only with the intramolecular isomerisation of the α-ketoperoxyl radical[24] but also with the oxidation of ketones at the γ- and δ-C–H bonds.[1,2] The possibility of these reaction pathways is not open to doubt, but, in order to achieve the formation of γ- and δ-lactones, it is essentially to subject γ- and δ-ketohydroperoxides to a secondary oxidation at the α- C–H bonds, which is unlikely to occur in the initial stage of the process. Incidentally, the intramolecular isomerisation of the δ-ketoperoxyl radical can also lead to a hydroperoxide of type **25**. The probability of the latter reaction should be fairly high in view of the enhanced reactivity of the α-C–H bonds of ketones.

The oxidation of carboxylic acids at the γ- and δ-C–H bonds can also lead to the formation of γ- and δ-lactones. The reactivities of these bonds are approximately the same[130] and hardly differ from the reactivities of the methylene C–H bonds of hydrocarbons. Indeed, the products of the oxidation of lauric acid were found to contain γ-octylbutyrolactone and δ-heptylvalerolactone.[2] However, the parallel formation of acids and γ-lactones in the oxidation of undecan-6-one and tridecan-7- one[24] as well as the absence of δ-lactones among the tridecan-7-one oxidation products mentioned above cannot be explained by the occurrence of this reaction.

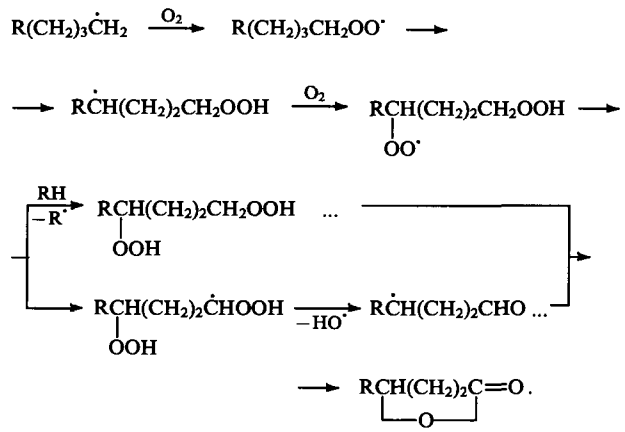
It appears that the formation of γ-ethylbutyrolactone in the oxidation of undecan-6-one can be associated with the



(31)

homolytic decomposition of α-ketohydroperoxide in the presence of oxygen and with subsequent intramolecular isomerisation of the hexanoylperoxyl radical. The fact that the possibility of the occurrence of such a reaction in the oxidation of aldehydes is usually disregarded[1,2] is apparently associated with its suppression in the presence of readily oxidisable substances such as aldehydes. Since acyl radicals may be formed in the oxidation of aldehydes, α-ketoalcohols, and α-diketones (see Sections V and VI), it follows that reaction (31) is an important source of the accumulation of γ-lactones in autoxidation processes.

One cannot rule out the possibility that γ-lactones may be obtained also from primary alkyl radicals via the mechanism



The homolytic decomposition of secondary hydroperoxides and α-hydroxyhydroperoxides [reactions (7) and (13)] as well as decarbonylation and decarboxylation reactions, which will be examined below, lead to primary alkyl radicals.

The experimental data presented show that the structure of the esters formed in the oxidation reactions depends on the method of their synthesis. The esters of primary alcohols (as well as lactones) with the same number of carbon atoms as in the initial hydrocarbon are obtained mainly in the oxidation of ketones by peracids, whereas the esters of secondary alcohols are produced as a result of the esterification of the alcohols by carboxylic acid anhydrides. The formation of γ-lactones is apparently associated with intramolecular isomerisation reactions of the peroxyl radicals.

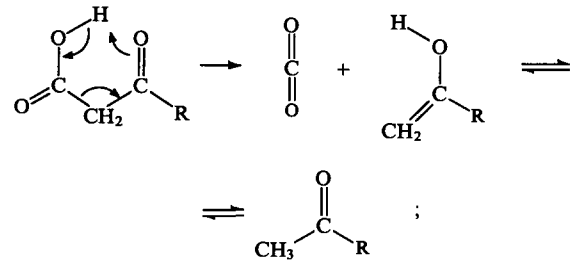
VIII. Certain aspects of the decarbonylation and decarboxylation reactions in the oxidation reactions of hydrocarbons and their oxygen-containing derivatives

The decarbonylation and decarboxylation reactions occur in virtually all the stages of the oxidative degradation of the carbon chain[1,2] and lower the selectivity of the autoxidation processes.

The available literature data permit the conclusion that the decarbonylation process is associated predominantly with the homolytic reactions of the oxidation products.

Under the autoxidation conditions, the acyl radicals formed in reactions (8) (18), and (21) either combine with oxygen [reaction (18, b)] or are decarbonylated [reaction (18, c)] when aldehydes are treated with peroxyl radicals. The relative contributions of these pathways depend both on temperature and on the structure of the hydrocarbon radical.[131,132] Since the activation energy for reaction (2) is close to zero[1] and that for reaction (18, c) involving aliphatic acyl radicals with a normal structure is of the order of 40–91 kJ mol^{-1},[131] one may conclude that the relative importance of the decarbonylation reactions should increase with increasing temperature. The rate constant for reaction (18, c) depends significantly on the stability of the hydrocarbon radicals formed on decarbonylation and increases in the sequence $C_6H_5^{\cdot} \ll CH_3^{\cdot} < CH_3CH_2CH_2^{\cdot} \ll C_6H_5CH_2^{\cdot}$ at 25 °C.[131] The decarbonylation reaction is favoured by the branching of the chain at the α-carbon atom.[132]

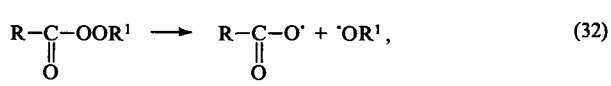
With the exception of the cleavage of β-oxoacids and β-dicarboxylic acids, which proceeds readily via a cyclic transition state,[46,89] i.e.



R = Alk, OH;

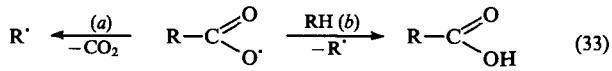
the decarboxylation reactions in autoxidation processes are mainly associated with the homolytic reactions of the oxidation products.[1,2] Certain features of the decarboxylation resulting from the reactions of peracids, peresters, and carboxylic acids are examined below.

The homolytic decomposition of peracids and peresters leads to acyloxyl radicals,[54] i.e.



(32)

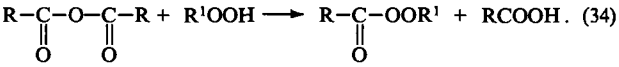
the subsequent reactions of which proceed via two competing pathways—decarboxylation (pathway *a*) and abstraction of hydrogen atoms from the substrate (pathway *b*).[2]



(33)

The relative contributions of these pathways depend on the structure of the radical R$^{\cdot}$, temperature, concentration and the reactivity of the C–H bond of the substrate. Reaction (33, a) is promoted by the stability of the hydrocarbon radical formed on decarboxylation,[21] by unreactive or weakly reactive solvents, and also by a high temperature.[133] Reactive substrates, for example, aldehydes, suppress the decarboxylation reaction.[133]

Since peracids are able to oxidise readily carbonyl compounds, being themselves converted into the acids, the role of reactions (32) and (33, a) in decarboxylation processes is probably small. The influence of the perester formation and decomposition reactions on the autoxidation processes is still being elucidated at the present time. Thus the presence in the reaction medium of carboxylic acid anhydrides makes the following reaction probable:



(34)

The study of the kinetics of the accumulation of products in the cyclohexane oxidation reactions and in the interaction of adipic anhydride with cyclohexanol and *tert*-butyl hydroperoxide led to the conclusion that the reaction with the hydroperoxide is an important route to the consumption of the anhydride in the oxidation of cyclohexane. The decomposition of the peresters formed in this process should lead to products with less than 6 carbon atoms.[20] On the hypothesis that peresters are formed in the autoxidation processes, it is possible to account also for the characteristic features of the decarboxylation reactions of carboxylic acids.

Numerous studies, examined in detail in a monograph,[2] have been devoted to the problem of the decarboxylation of carboxylic acids coupled with the oxidation reaction. It was postulated that, in the case of mono- and di-carboxylic acids with a normal structure, the acyloxyl radical, formed on treatment with peroxyl radicals, is decarboxylated.[2]

$$RCOOH + R^1OO^{\cdot} \xrightarrow[-R^1OOH]{} RCOO^{\cdot} \longrightarrow R^{\cdot} + CO_2 \qquad (35)$$

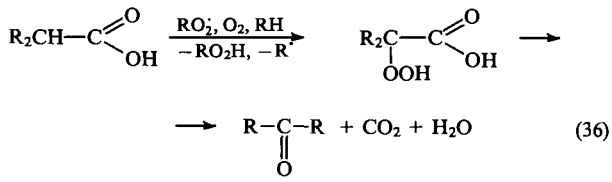
On the basis of the comparatively low values of the kinetic isotope effect (KIE) in the replacement of the carboxyl hydrogen by deuterium and the acceleration observed on the kinetic curves for the evolution of CO_2 in the cooxidation of carboxylic acids together with cumene or other reactive substrates, it was later concluded that the decarboxylation proceeds not only via reaction (35) but also via the intermediate formation of molecular products of the type of hydroperoxyacids and α- or β-oxoacids.[2]

Such a molecular product may be evidently also a perester. The perester can be obtained via reactions (28) and (34). The anhydrides required for these reactions are apparently formed as a result of the oxidative degradation of both the hydrocarbon group of the acid and of the substances employed as the cooxidants.

The hypothesis of the involvement of peresters in the decarboxylation of acids explains satisfactorily a series of experimentally observed facts. The low relative yields of $^{14}CO_2$ in the decarboxylation of acids labelled in the carboxy-group[1,2] may be associated with the possibility of attack by the hydroperoxide on both the initially formed anhydride and on the anhydride incorporating the acyl group of the labelled acid; in the latter case, a perester not containing ^{14}C may also be formed. As nonradioactive acids accumulate in the reaction medium, the probability of the formation of labelled peresters and hence of $^{14}CO_2$ should diminish, as in fact has been observed.[1,2] As was to be expected, the rate of formation of the nonradioactive CO_2 increased under these conditions.[2] The carbon-centred radical obtained by reaction (35) should be readily converted into a carboxylic acid under the oxidation conditions. The similarity of the rates of formation of valeric acid and CO_2 in the oxidation of caproic acid therefore becomes understandable.[2]

In the transacylation of anhydrides by carboxylic acids, the stage involving the attack on the carbon atom of the anhydride group by the oxygen atom of the acid hydroxyl should be rate-limiting.[44,89] The O–H bond is then ruptured in a nonrate-limiting stage and the replacement of the carboxyl hydrogen by deuterium should not therefore lead to an appreciable kinetic isotope effect, which in fact has been established in the case of acids with a normal structure.[2]

In order to explain the characteristic features of the decarboxylation of acids containing a tertiary hydrogen atom in the α-position, a mechanism involving the oxidation of the acids at the α-C–H bonds and unimolecular decomposition of α-hydroperoxyacids was proposed.[2]

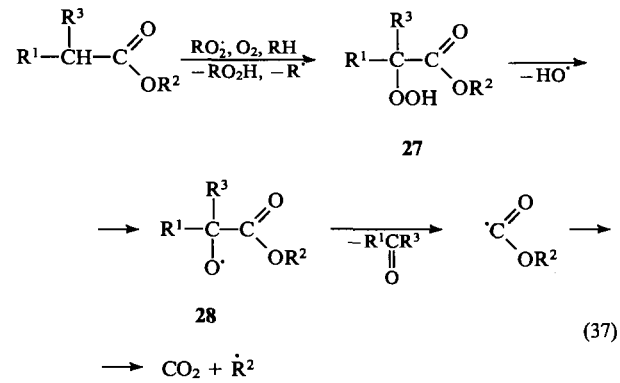


(36)

The proposed mechanism agrees well with the decrease in the rate of decarboxylation of isobutyric acid on replacement of a tertiary hydrogen atom by deuterium (KIE = 6.6).[2] Data indicating a low kinetic isotope effect (1.1) in the replacement of the carboxyl hydrogen by deuterium indicate in their turn an insignificant contribution of the mechanism (35) to the decarboxylation of this acid.[2]

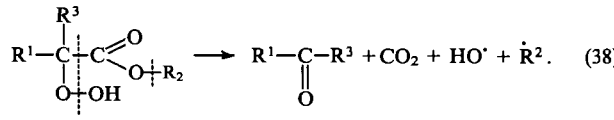
The decarboxylation of isobutyric and trimethylacetic acids apparently proceeds without the participation of peresters, since there are certain difficulties in the formation of anhydrides on oxidation of branched short-chain acids and in addition the probability of the attack on the acyl residues of such acids in the molecules of mixed anhydrides by hydroperoxides diminishes as a consequence of the steric factors mentioned above. The preferential formation of one of the two possible esters in the alcoholysis of mixed anhydrides has been noted.[45,134]

The formation of CO_2 is observed in the oxidative degradation of the ester group.[2,135–139] Carbon dioxide is obtained as a result of the homolytic decomposition of the primary molecular product of the oxidation of the ester at the acyl α-C–H bonds — the α-alkoxycarbonylhydroperoxide **27** [Eqn (37)].



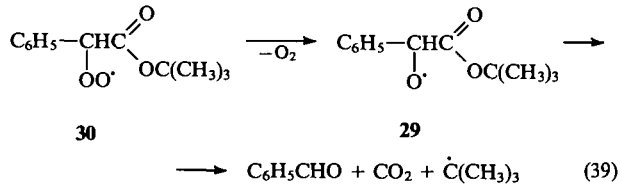
(37)

According to Denisov,[21] such a reaction may occur as a result of the concerted dissociation of several bonds in the hydroperoxide molecule [Eqn (38)]



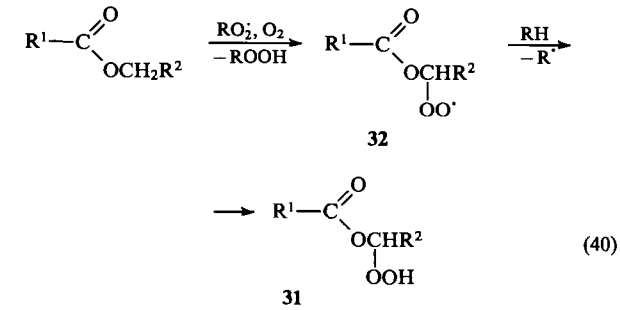
(38)

The high relative yield of benzaldehyde in the autoxidation of *tert*-butyl phenylacetate at 140 °C indicates the importance of the homolytic route to the decomposition of the intermediate *tert*-butyl α-hydroperoxyphenylacetate with the degradation of the carbon chain via reactions (37) and (38).[140] The formation of α-*tert*-butoxycarbonylbenzyloxyl radicals **29** and their degradation, leading to benzaldehyde, take place on recombination of the α-*tert*-butoxycarbonylbenzylperoxyl radicals **30** without chain termination.[140]



(39)

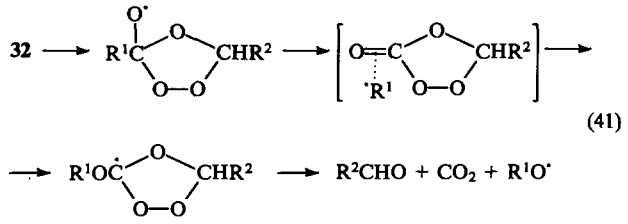
The α-acyloxyhydroperoxides **31**, obtained on oxidation of esters,[2,138,141–145] decompose preferentially via a nonhomolytic pathway.



(40)

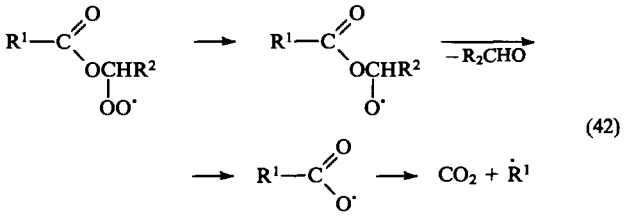
This was demonstrated in relation to the oxidation of the esters of polyhydric alcohols by Martem'yanov[138,142-145] and was later confirmed in the oxidation of benzyl benzoate[146] and benzyl phenylacetate.[147] The formation of CO_2 from compound **31** in these cases is unlikely.

It has been suggested[138] on the basis of kinetic data and the detection among the ester oxidation products of alcohols of the type R^1OH that CO_2 may be formed in these reactions as a result of the transformations of the α-acyloxyperoxyl radicals **32** [Eqn (41)].



(41)

The formation of CO_2 from compound **31** is also possible as a result of the recombination of the latter without chain termination[146] and the decomposition of the oxyl radicals **33** obtained under these conditions.



(42)

The importance of reactions (37)-(42) for hydrocarbon oxidation processes is still insufficiently clear. There is no doubt that it cannot be considerable because the data on the reactivity of the α-C-H bonds of aromatic esters in relation to the *tert*-butylperoxyl radical[148,149] and of pentaerythritol esters in the reaction with cumenylperoxyl radicals[138,150] indicate the deactivation of the C-H bonds in both α-positions of the ester molecule compared with the hydrocarbon molecule. The oxidation of esters at the C-H bonds remote from the functional group is therefore more probable.[151] In such cases, the degradation of the carbon chain evidently occurs in conformity with the rules examined above for hydrocarbons.

IX. Conclusion

The experimental data obtained during the last 15-20 years permit a fresh look at the importance of the known reaction pathways leading to the rupture of the carbon chain and make it possible to justify new routes to oxidative degradation in autoxidation processes.

When the homolytic decomposition of hydroperoxides is stimulated, for example on catalysis, the degradation of the carbon chain to an appreciable extent can apparently occur already in the stages involving the reaction of the α-hydroxyhydroperoxides formed on oxidation of alcoholic functional groups.

On the other hand, the principal pathways in the oxidative degradation reaction include a stage in which ketones react. The ketones are oxidised by peroxide compounds and are involved in the radical-chain process. The oxidation of ketones by hydroperoxides proceeds via a stage involving the formation of α-hydroxyperoxides, which decompose like α-hydroxy- α-hydroperoxides. When ketones are acted upon by peracids, the carbon chain is degraded with formation of esters. In the radical-chain oxidation of ketones at the most reactive α-C-H bonds, the products are α-ketohydroperoxides, which decompose both with and without the degradation of the carbon chain. The available data show that aliphatic and alicyclic α-ketohydroperoxides react preferentially without the rupture of the carbon chain, affording α-ketoalcohols and α-diketones. The fraction of α-ketohydroperoxides decomposing with destruction of the C-C bonds depends on the reaction conditions and the structure of the α-ketohydroperoxides.

α-Ketohydroperoxides decompose via homolytic and nonhomolytic mechanisms with formation of compounds having functional carbonyl and carboxy-groups. It is not clear what is the principal route to the nonhomolytic degradation of α-ketohydroperoxides. Some preference is given to the dioxetane mechanism, which explains more effectively than the familiar acid-catalytic Langenbeck-Pritzkov mechanism the available experimental data on the characteristic features of the reactions of α-ketohydroperoxides. In the oxidation of ketones at other C-H bonds and also in the intramolecular chain transfer and in the decarbonylation of acyl radicals during the homolytic reactions of α-ketohydroperoxides, the latter do not decompose via the α-mechanism.

In their turn, α-ketoalcohols and α-diketones interact with peroxide compounds in hydrocarbons undergoing oxidation and are themselves subjected to radical-chain oxidation. The influence of these bifunctional compounds on the rate of decomposition of hydroperoxides is much greater than that of monohydric alcohols and monoketones.

The radical-chain oxidation of α-ketoalcohols leads to α-hydroperoxy-α-hydroxyketones, which are also formed on reversible nucleophilic addition of hydrogen peroxide to α-diketones. The interaction of the latter with hydroperoxides and peracids affords α-alkylperoxy-α-hydroxy- and α-acylperoxy-α-hydroxy-ketones, which, like α-hydroperoxy-α-hydroxy-ketones, also decompose with degradation of the carbon chain even at room temperature. The principal products of the degradation of these compounds are carboxylic acid anhydrides and the free acids. The anhydrides are evidently formed as a result of the pericyclic rearrangement of the oxirane intermediate, while the acids are formed via the dioxetane mechanism or on homolytic decomposition of the above peroxides. The relative importance of each of these three main mechanisms for the reactions of α-hydroperoxy-α-hydroxyketones is determined by the relative yields of the corresponding anhydrides and acids and depends on the structure of the peroxide, the medium, and the additives stimulating the homolytic decomposition of the peroxide.

Being extremely reactive, carboxylic acid anhydrides interact during the autoxidation processes with the water produced by the reaction, alcohols, acids, hydroperoxides, and other nucleophiles, participating thereby in the formation of numerous degradation products. In particular, not less than 20% of acetic acid is obtained in the oxidation of ethyl methyl ketone via acetic anhydride, while the cyclohexyl esters of mono- and di-carboxylic acids are formed in the oxidation of cyclohexane predominantly with participation of adipic anhydride. The influence of the homolytic decomposition reactions of the peresters, formed on esterification of hydroperoxides by acid anhydrides, on the rate of initiation and decarboxylation in the autoxidation processes is still to be estimated. However, it is believed that it may be extremely significant.

References

1. N M Emanuel', E T Denisov, Z K Maizus *Tsepnye Reaktsii Okisleniya Uglevodorodov v Zhidkoi Faze* (Chain Oxidation Reactions of Hydrocarbon in the Liquid Phase) (Moscow: Nauka, 1965)
2. E T Denisov, N I Mitskevich, V E Agabekov *Mekhanizm Zhidkofaznogo Okisleniya Kislorodsoderzhashchikh Soedinenii* (The Mechanism of the Liquid-phase Oxidation of Oxygen-containing Compounds) (Minsk: Nauka i Tekhnika, 1975)
3. V Ya Karnozhitskii *Usp. Khim.* **50** 1693 (1981) [*Russ. Chem. Rev.* **50** 888 (1981)]
4. W Pritzkov *Wiss. Z. Tech. Hochsch. Chem.* **27** 702 (1985)
5. A L Perkel', B G Freidin *Zh. Prikl. Khim.* **54** 1376 (1981)

6. G M Bogomol'nyi, B G Freidin *Zh. Prikl. Khim.* **57** 1164 (1984)
7. A A Fokin, B G Freidin *Zh. Prikl. Khim.* **58** 346 (1985)
8. A A Fokin, B G Freidin, N I Volosatova, I V Bundina *Zh. Prikl. Khim.* **61** 341 (1988)
9. A A Fokin, B G Freidin *Zh. Org. Khim.* **25** 1501 (1989)
10. B G Freidin, A L Perkel' *Zh. Prikl. Khim.* **53** 861 (1980)
11. B G Freidin, A L Perkel', O V Borodina *Zh. Prikl. Khim.* **58** 2689 (1985)
12. A L Perkel', B G Freidin *Zh. Prikl. Khim.* **52** 1829 (1979)
13. A L Perkel', G M Bogomol'nyi, R V Neginskaya, B G Freidin *Zh. Prikl. Khim.* **60** 1590 (1987)
14. B G Freidin, A L Perkel' *Zh. Prikl. Khim.* **54** 2733 (1981)
15. A L Perkel', B G Freidin *Zh. Prikl. Khim.* **55** 395 (1982)
16. A L Perkel', B G Freidin, L F Novokreshchenova *Zh. Prikl. Khim.* **55** 402 (1982)
17. A L Perkel' *Zh. Prikl. Khim.* **64** 1533 (1991)
18. O V Gol'dman, A L Perkel', T Ya Smirnova, B G Freidin *Zh. Prikl. Khim.* **57** 1830 (1984)
19. A L Perkel', B G Freidin, R V Neginskaya, S P Stolyankova, L E Ivanova *Zh. Prikl. Khim.* **58** 1572 (1985)
20. A L Perkel', Author's Abstract of Doctoral Thesis in Chemical Sciences, St Petersburg Technological Institute, St Petersburg, 1992
21. E T Denisov *Kinetika i Kataliz T. 9 (Itogi Nauki i Tekhniki)* [Kinetics and Catalysis, Vol. 9 (Advances in Science and Engineering)] (Moscow: Izd. VINITI, 1981)
22. E T Denisov, G I Kovalev *Okislenie i Stabilizatsiya Reaktivnykh Topliv* (Oxidation and Stabilisation of Reactive Fuels) (Moscow: Khimiya, 1983)
23. N K Voskresenskaya, B G Freidin *Zh. Prikl. Khim.* **50** 1315 (1977)
24. V M Potekhin, Author's Abstract of Doctoral Thesis in Chemical Sciences, Leningrad Technological Institute, Leningrad, 1972
25. R K Jensen, S Korcsek, L R Mahoney, M Zinbo *J. Am. Chem. Soc.* **101** 7574 (1979)
26. N F Trofimova, V V Kharitonov, E T Denisov *Dokl. Akad. Nauk SSSR* **241** 416 (1978)
27. W Pritzkov, K A Muller *Chem. Ber.* **89** 2321 (1956)
28. D G Hendry, C M Gould, D Schuetzle, M G Syz, F R Mayo *J. Org. Chem.* **41** 1 (1976)
29. W Pritzkov, I Hahn *J. Prakt. Chem.* **16** 287 (1962)
30. A S Lyavinets, K A Chervinskii, V I Belenkov *Zh. Prikl. Khim.* **61** 588 (1988)
31. J Andre, J Lemaire *Bull. Soc. Chim. Fr.* 4231 (1969)
32. V N Belov, L A Kheifits, S I Virezub, in *Reaktsii i Metody Issledovaniya Organicheskikh Soedinenii, T. 10* (Reactions and Methods for Investigation of Organic Compounds, Vol. 10) (Ed. B A Kazanskii) (Moscow: Goskhimizdat, 1961) p. 7
33. C H Hassall, in *Organic Reactions* Vol. 9 (Translated into Russian; Moscow: Izd. Inostr. Lit., 1959) p. 82
34. J B Lee, B C Uff *Q. Rev.* **21** 429 (1967)
35. Y Ogata, Y Sawaki *J. Org. Chem.* **37** 2953 (1972)
36. S L Friess *J. Am. Chem. Soc.* **71** 2571 (1949)
37. J March *Advanced Organic Chemistry* Vol. 4 (Translated into Russian; Moscow: Mir, 1988)
38. E Hedaya, S Winstein *Tetrahedron Lett.* **3** 563 (1962)
39. J C Robertson, A Swelin *Tetrahedron Lett.* **8** 2871 (1967)
40. M F Hawthorne, W D Emmons, K S McCallum *J. Am. Chem. Soc.* **80** 6393 (1958)
41. R V White, W D Emmons *Tetrahedron Lett.* **3** 2953 (1962)
42. M A Winnik, V Stoute *Can. J. Chem.* **51** 2788 (1973)
43. B W Palmer, A Fry *J. Am. Chem. Soc.* **92** 2580 (1979)
44. A L Perkel' *Zh. Prikl. Khim.* **62** 1111 (1989)
45. A L Perkel', B G Freidin, S G Voronina, S V Ginter, A A Fokin *Zh. Prikl. Khim.* **62** 2560 (1989)
46. P Saiks *Mekhanizmy Reaktsii v Organicheskoi Khimii* (Mechanisms of Reactions in Organic Chemistry) (Moscow: Khimiya, 1991)
47. US P. 3 660 433; *Ref. Zh. Khim.* 2 N 70P (1973)
48. E T Denisov, V V Kharitonov, E N Raspopova *Kinet. Katal.* **5** 981 (1964)
49. E T Denisov *Zh. Fiz. Khim.* **37** 1896 (1963)
50. E T Denisov *Dokl. Akad. Nauk SSSR* **146** 394 (1962)
51. L K Kazantseva, V V Lipes, V I Morozova, M S Furman *Kinet. Katal.* **13** 216 (1972)
52. V V Lipes, Author's Abstract of Doctoral Thesis in Chemical Sciences, Division of Institute of Chemical Physics, Academy of Sciences, Chernogolovka, 1987
53. R V Neginskaya, Author's Abstract of Candidate Thesis in Chemical Sciences, Kemerovo State University, Kemerovo, 1986
54. V L Antonovskii *Organicheskie Perekisnye Initsiatory* (Organic Peroxide Initiators) (Moscow: Khimiya, 1972)
55. E G E Hawkins *Organic Peroxides. Their Formation and Reactions* (Translated into Russian; Moscow, Leningrad: Khimiya, 1964)
56. E K Starostin, A V Aleksandrov, G I Nikishin *Izv. Akad. Nauk SSSR, Ser. Khim.* 85 (1986)
57. S Chubashi, H Matsui, K Yamamoto, S Ishimoto *Bull. Chem. Soc. Jpn.* **42** 789 (1969)
58. V K Tsyskovskii, B G Freidin, Yu L Moskovich *Zh. Prikl. Khim.* **39** 870 (1961)
59. I V Berezin, V L Ivanov, L F Kazanskaya, N N Ugarova *Zh. Fiz. Khim.* **39** 3011 (1965)
60. N L Budeiko, V E Agabekov, N I Mitskevich *Vestsi Akad. Navuk BSSR, Ser. Khim. Navuk* (6) 21 (1983)
61. S W Benson *Thermochemical Kinetics* (Translated into Russian; Moscow: Mir, 1971)
62. Yu N Martynov, N A Gudova, I I Rif, V M Potekhin *Zh. Prikl. Khim.* **45** 1837 (1972)
63. A M Syroezhko, V M Potekhin, V A Proskuryakov *Zh. Prikl. Khim.* **43** 2295 (1970)
64. I I Rif, V M Potekhin, V A Proskuryakov *Zh. Prikl. Khim.* **45** 2043 (1972)
65. A M Syroezhko, V M Potekhin, V A Proskuryakov, V V Serov *Zh. Prikl. Khim.* **44** 597 (1971)
66. I A Opeida, V I Timokhin, V F Galat *Teor. Eksp. Khim.* **14** 554 (1978)
67. A L Perkel', S G Voronina, E I Shimko, B G Freidin *Zh. Prikl. Khim.* **64** 592 (1991)
68. W Langenbeck, W Pritzkov *Chem. Technol.* **4** 391 (1952)
69. W Pritzkov *Chem. Ber.* **87** 1668 (1954)
70. W Pritzkov *Chem. Ber.* **88** 572 (1955)
71. A Rieche *Angew. Chem.* **50** 520 (1937)
72. A Rieche *Angew. Chem.* **70** 251 (1958)
73. A Robertson, W A Waters *J. Chem. Soc.* **10** 1574 (1948)
74. R C Fuson, H L Jackson *J. Am. Chem. Soc.* **72** 1637 (1950)
75. A G Pinkus, W C Servoss, K K Lum *J. Org. Chem.* **32** 2649 (1967)
76. A G Pinkus, M Z Hag, J G Lindberg *J. Org. Chem.* **35** 2555 (1970)
77. I I Korsak, V E Agabekov, N I Mitskevich *Neftekhimiya* **15** 130 (1975)
78. B G Freidin, A L Perkel' *Zh. Prikl. Khim.* **53** 1611 (1980)
79. Y Ogata, Y Savaki *J. Org. Chem.* **41** 373 (1976)
80. Y Savaki, Y Ogata *J. Org. Chem.* **41** 2340 (1976)
81. Y Savaki, Y Ogata *J. Am. Chem. Soc.* **98** 7324 (1976)
82. K Itoh, S Sakai, Y Ishii *J. Chem. Soc. Jpn., Ind. Chem. Soc.* **68** 2404 (1965)
83. W H Richardson, G Ranney, F C Montgomery *J. Am. Chem. Soc.* **96** 4688 (1974)
84. W H Richardson, V F Hodge, D L Stiggall, M B Yelvington, F C Montgomery *J. Am. Chem. Soc.* **96** 6652 (1974)
85. I Kamiya, T Sugimoto *Bull. Chem. Soc. Jpn.* **50** 2442 (1977)
86. V A Yablokov *Usp. Khim.* **49** 1711 (1980) [*Russ. Chem. Rev.* **49** 833 (1980)]
87. V Ya Yablokov, in *Khimiya Organicheskikh Peroksidov* (Chemistry of Organic Peroxides) (Ed. N M Emanuel') (Volgograd: Izd. Volgograd. Politekh. Inst., 1982) p. 103
88. M S Kharasch, A Fono, W J Nudenberg *J. Org. Chem.* **15** 748 (1950)
89. H Becker *Einführung in die Elektronentheorie Organisch-Chemischer Reaktionen* (Translated into Russian; Moscow: Mir, 1977)
90. J D Druliner *J. Org. Chem.* **43** 2069 (1978)
91. V A Voroshilov, N M Voroshilova, A L Perkel', B G Freidin, T I Orlova *Zh. Prikl. Khim.* **57** 1568 (1984)
92. G L Sharipov, V P Kazakov, G A Tolstikov *Khimiya i Khemilyuminestsentsiya 1,2-Dioksetanov* (The Chemistry and Chemiluminescence of 1,2-Dioxetanes (Moscow: Nauka, 1990)
93. O P Yablonskii, V L Belyaev, A N Vinogradov *Usp. Khim.* **41** 1260 (1972) [*Russ. Chem. Rev.* **41** 565 (1972)]
94. R Schmid, V N Sapunov *Non-formal Kinetics* (Translated into Russian; Moscow: Mir, 1985)

95. V L Antonovskii, V A Terent'ev, in *Uspekhi Khimii Organicheskikh Perekisnykh Soedinenii i Autookisleniya* (Advances in the Chemistry of Organic Peroxide Compounds and Autooxidation) (Ed. N M Emanuel') (Moscow: Khimiya, 1969) p. 442
96. Y Sawaki, Y Ogata *J. Am. Chem. Soc.* **99** 5412 (1977)
97. Y Sawaki, Y Ogata *J. Am. Chem. Soc.* **100** 856 (1978)
98. I I Korsak, V E Agabekov, N I Mitskevich *Vestsi Akad. Navuk BSSR, Ser. Khim. Navuk* (6) 28 (1974)
99. I A Belkov, B G Freidin *Zh. Prikl. Khim.* **62** 1596 (1989)
100. I A Belkov, B G Freidin *Kinet. Katal.* **32** 23 (1990)
101. I A Belkov, B G Freidin *Kinet. Katal.* **30** 1224 (1989)
102. P M Cullis, J R P Arnold, M Clarke, R Howell, M De Mira, M Naylor, D Nicholls *J. Chem. Soc., Chem. Commun.* 1088 (1987)
103. T Greibrokk *Acta. Chem. Scand.* **27** 3365 (1973)
104. G E Zaikov, Z K Maizus *Zh. Fiz. Khim.* **40** 211 (1966)
105. I I Korsak, V A Agabekov, N I Mitskevich *Vestsi Akad. Navuk BSSR, Ser. Khim. Navuk* (4) 18 (1974)
106. V G Glukhovtsev, Yu V Il'in, A V Ignatenko, N V Slavinskii, G I Nikishin *Izv. Akad. Nauk SSSR, Ser. Khim.* 2156 (1980)
107. L P Stepovik, V A Dodonov, G N Smyslova *Zh. Obshch. Khim.* **62** 123 (1992)
108. W Frankvoort *Thermochim. Acta* **25** 35 (1978)
109. C Bunton *Peroxide Reaction Mechanisms* (Ed. L Edwards) (New York, London: Int. Publ., 1962)
110. H Kwart, N J Wegemer *J. Am. Chem. Soc.* **83** 2746 (1961)
111. A L Perkel', in *Khimiya Dikarbonil'nykh Soedinenii(Tezisy Dokladov VII Vsesoyuznoi Konferentsii Posvyashchennoi 100-letiyu so Dnya Rozhdeniya Prof. G.Vanaga, Riga, 1991)* [The Chemistry of Dicarbonyl Compounds (Abstracts of Reports at the VIIth All-Union Conference on the Occasion of the Centenary of Prof. G. Vanag's Birth, Riga, 1991)] p. 151
112. B G Freidin, G M Bogomol'nyi, in *IX Vsesoyuznaya Konferentsiya po Khimii Organicheskikh i Elementoorganicheskikh Peroksidov, Tezisy Dokladov, Gor'kii, 1990* (Abstracts of Reports at the IXth All-Union Conference on Chemistry of Organic and Organoelement Peroxides, Gorky, 1990) p. 160
113. P Karrer, C Cochand, N Neuss *Helv. Chim. Acta* **29** 1836 (1946)
114. P Karrer, L Schneider *Helv. Chim. Acta* **30** 859 (1947)
115. P Karrer, R Schwyzer, A Neuwirth *Helv. Chim. Acta* **31** 1210 (1948)
116. P Karrer, T Hohl *Helv. Chim Acta* **32** 1932 (1949)
117. P Karrer, F Haab *Helv. Chim. Acta* **32** 950 (1949)
118. P S Bailey, Y-G Chang *J. Org. Chem.* **27** 1192 (1962)
119. R Criegee, M V Lederer *Liebigs Ann. Chem.* **583** 29 (1953)
120. G M Bogomol'nyi, B G Freidin *Zh. Prikl. Khim.* **54** 1261 (1981)
121. G M Bogomol'nyi, B G Freidin *Zh. Prikl. Khim.* **61** 2597 (1988)
122. R V Kucher, I A Opeida, L G Nechitailo, M A Simonov *Kinet. Katal.* **22** 332 (1981)
123. O A Borislavskii, V V Reutskii, E N Mokryi, T I Drozdova, L V Petrov, V M Solyanikov *Neftekhimiya* **28** 90 (1988)
124. I V Berezin, A N Ragimova *Zh. Fiz. Khim.* **35** 842 (1961)
125. I V Berezin, L S Vardanyan, B G Dzantiev, N F Kazanskaya, N M Emanuel' *Zh. Fiz. Khim.* **31** 340 (1957)
126. B G Freidin *Zh. Prikl. Khim.* **36** 1101 (1963)
127. Kh F Fakhrf, M P Manakov *Izv. Vyssh. Uchebn. Zaved., Khim. Khim. Tekhnol.* **13** 705 (1970)
128. B G Freidin, Author's Abstract of Doctoral Thesis in Chemical Sciences, Institute of Chemical Physics, Academy of Sciences, Moscow, 1972
129. D Yu Brodskii, L A Dement'eva, A V Iogansen, G A Kurkchi, N I Fainovich, M S Furman, A I Khomunaya, in *Khimiya i Tekhnologiya Produktov Organicheskogo Sinteza. Proizvodstvo Kaprolaktama, Vyp. 38* (Chemistry and Technology of Organic Synthesis Products. Production of Caprolactam, No. 38) (Moscow: Izd. Gos. Inst. Azot. Promst., 1976) p. 86
130. W Pritzkow, V Voerckel *Oxid. Commun.* **4** 223 (1983)
131. J K Vollenweider, H Paul *Int. J. Chem. Kinet.* **18** 791 (1986)
132. V Haisman, P Stampachova, Y Vselak, V Chvanovsky *Oxid. Commun.* **4** 229 (1983)
133. S A Maslov, E A Blyumberg *Usp. Khim.* **45** 303 (1976) [*Russ. Chem. Rev.* **45** 155 (1976)]
134. A L Perkel', B G Freidin *Zh. Anal. Khim.* **48** 353 (1993)
135. K Itoh, S Sakai, Y Ishii *J. Chem. Soc. Jpn., Ind. Chem. Soc.* **68** 2401 (1965)
136. E Rafii, L Lena, J Metzger *Bull. Soc. Chim. Belg.* **84** 21 (1975)
137. E Rafii, L Lena, J Metzger *Bull. Soc. Chim. Belg.* **84** 35 (1975)
138. V S Martem'anov, Author's Abstract of Doctoral Thesis in Chemical Sciences, Institute of Petrochemical Synthesis, Academy of Sciences, Moscow, 1987
139. B I Chernyak, G I Donets *Zh. Org. Khim.* **17** 2294 (1981)
140. S G Voronina, A L Perkel', B G Freidin *Zh. Prikl. Khim.* **65** 2079 (1992)
141. G M Bogomol'nyi, N A Mirantsova, N N Pintegova, B G Freidin *Zh. Prikl. Khim.* **56** 627 (1983)
142. V S Martem'anov *Neftekhimiya* **26** 753 (1986)
143. V S Martemyanov, V N Khlebnikov, J A Chushkina *React. Kinet. Catal. Lett.* **25** 357 (1984)
144. V S Martem'anov, V N Khlebnikov, L M Lapkin, Z F Sharafutdinov, L N Gaisina *Kinet. Katal.* **25** 781 (1984)
145. V S Martem'anov, V N Khlebnikov, Z F Sharafutdinova *Dokl. Akad. Nauk SSSR* **276** 1416 (1984)
146. S G Voronina, A L Perkel', B G Freidin *Kinet. Katal.* **33** 266 (1992)
147. S G Voronina, A L Perkel', B G Freidin *Zh. Prikl. Khim.* **65** 2084 (1992)
148. J A Howard, S Korcsek *Can. J. Chem.* **48** (1970)
149. E I Buneeva, S G Voronina, A L Perkel', B G Freidin *Kinet. Katal.* **31** 1330 (1990)
150. N N Pozdeeva, E T Denisov, V S Martem'anov *Kinet. Katal.* **22** 912 (1981)
151. P J Sniegoski *ASLE Trans.* **20** 282 (1977)

Russian Chemical Reviews 63 (9) 767 – 780 (1994)
©1994 Russian Academy of Sciences and Turpion Ltd

UDC 541.64; 536.7;542.952

The reactions of polycarboxylic acid *o*-dinitriles with aromatic diamines

S A Siling, S V Vinogradova

Contents

I.	Introduction	767
II.	Interaction of phthalodinitrile with aromatic diamines	768
III.	Macroheterocycles with a system of five- or six-membered heterocycles condensed with the isoindole ring	772
IV.	Polycondensation of tetracarboxylic acid tetranitriles and unsubstituted diamines in phenol	775
V.	The properties of solutions of polyhexazocyclanes	777
VI.	Polycondensation of tetracarboxylic acid tetranitriles and diamines in phenols with electron-accepting substituents	777
VII.	Polycondensation of tetracarboxylic acid tetranitriles and weakly basic diamines	778
VIII.	Polycondensation of tetracarboxylic acid tetranitriles and bisanthranilic acids in polyphosphoric acid	778

Abstract. Experimental data on the interaction of phthalodinitriles and bis(phthalodinitriles) with aromatic diamines are surveyed. The dependence of the mechanism of the reaction of phthalodinitriles with diamines on the structure of the diamine and the phthalodinitrile as well as the nature of the reaction medium is examined and general ideas concerning the mechanism of this reaction are formulated. The principal features of the polycondensation of bis(phthalodinitriles) with diamines are specified and the possibility of using this reaction to obtain a series of new classes of heterocyclic polymers with benzopyrrole fragments in the chain is demonstrated. The bibliography includes 70 references.

I. Introduction

A leading aspect of polymer chemistry is the synthesis and study of polyheteroarylenes with a cyclochain structure,[1-7] which have a series of valuable thermal, physicochemical and electrical properties. This review is devoted to a nontraditional approach to the synthesis of heterocyclic polymers, namely the polycondensation of tetracarboxylic acid *o*-dinitriles and aromatic diamines.

Studies on the chemistry of the interaction of *o*-dinitriles of aromatic di- and poly-carboxylic acids with diamines were initiated by the researches of Elvidge and coworkers[8,9] into the condensation of phthalodinitrile with aniline and diamines. Unfortunately, these very interesting reactions did not initially attract the attention of other investigators. It was not until 1967 that Packham and coworkers[10-13] turned their attention to these reactions and attempted to investigate them in greater detail in relation to the interaction of phthalodinitrile with 2,6-diaminopyridine and to use it for the synthesis of polymers with macroheterocycles in the chain. Siegel[14] and Balahura and Purcell[15] studied the mechanism of the condensation of phthalodinitrile with diamines in the presence of metal salts. The condensation of phthalodinitrile with diamines has been used as a preparative method of synthesis of macroheterocyclic compounds.[16,17]

These isolated communications in essence exhaust the studies of the interaction of *o*-dinitriles with the amino-group carried out hitherto.

Studies by Gaumans et al.[18] and Packham and Rackley[19] were devoted to the polycondensation of tetracarboxylic acid tetranitriles and diamines, which results in polymer formation with benzopyrrole fragments in the chain. Fusion of tetracarboxylic acid tetradinitriles with diamines at 300 °C leads to black insoluble and infusible polymers to which a macrocyclic structure has been assigned solely on the basis of IR spectroscopic data.[20] For a long time, there had been no systematic studies whatsoever of the effect of the structure of the starting materials, nature of the reaction medium, and the reaction conditions on the structure and properties of the compounds formed. Clearly, investigation of these problems is essential for the determination of the synthetic possibilities of the reaction, the elucidation of the reaction mechanisms occurring in the interaction of phthalodinitriles and tetracarboxylic acid tetranitriles with diamines, and the determination of the general characteristics of the process.

The few literature data on the model reaction of phthalodinitrile with aromatic diamines,[11,14,15] show that polycondensation of aromatic tetracarboxylic acid tetranitriles with aromatic diamines is an extremely complex process, which may lead to the formation of macrocyclic polymers, polymers without macrocycles, as well as polymers with a mixed structure. Therefore, in order to be able to specify the reaction, it was first essential to investigate in detail the main features of the condensation of phthalodinitriles with aromatic diamines. The macroheterocyclic compounds formed under these conditions in a number of instances were called hexazocyclanes, and polymers containing macroheterocycles with the corresponding structure in the chain were called polyhexazocyclanes.[7,21]

S A Siling, S V Vinogradova Heterochain Polymer Laboratory, Nesmeyanov Institute of Organoelement Compounds, Russian Academy of Sciences, ul. Vavilova 28, 117813 Moscow, Russian Federation. Fax (7-095) 135 50 85. Tel (7-095) 135 93 61 (S A Siling) and (7-095) 135 61 78 (S V Vinogradova)

Received 21 June 1994
Uspekhi Khimii 63 (9) 810 – 824 (1994); translated by A K Grzybowski

II. Interaction of phthalodinitrile with aromatic diamines

From literature data,[22,23] one may postulate that, when the condensation is carried out in an alcoholic medium, diamines react not with phthalodinitrile but with the product of its interaction with alcohol — 1-alkoxy-3-iminoisoindole. We studied the role of the hydroxylated solvent, and hence also the structure of the 1-alkoxy-3-iminoisoindole on the composition of the products of the condensation reaction between phthalodinitrile and *p*-phenylenediamine.[7,21,24-26] Butyl alcohol, cyclohexanol, phenol, and its derivatives with electron-donating substituents (cresols, dimethylphenol) and electron-accepting substituents (chloro-, bromo-, nitro-, and methoxy-phenols) were used as the reaction medium. The reaction products were investigated by the mass spectrometry and thin-layer chromatography (TLC) with the use of reference substances synthesised by specially developed methods. The results made it possible to put forward mechanisms of the condensation of phthalodinitrile with *p*-phenylenediamine in solvents of different nature.

Thus it was found that chloro- and nitrophenols function not only as the reaction medium but also as one of the reactants and enter into the composition of the reaction products (Scheme 1).

The condensation products of phthalodinitrile with *p*-phenylenediamine in aliphatic and alicyclic alcohols contain a wide range of compounds in which the content of the macroheterocycles **1** is only 50% (Scheme 2).

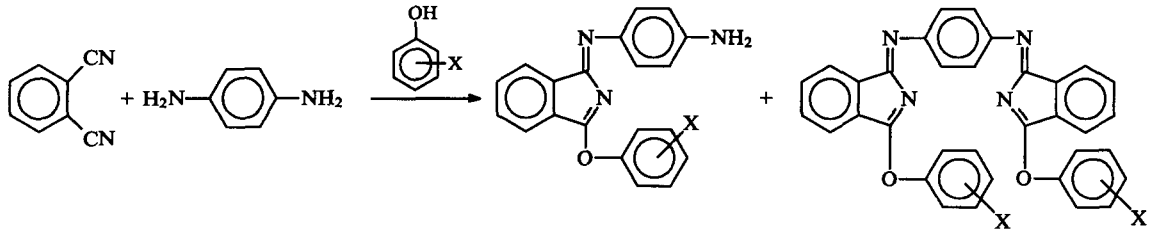
In the reaction of phthalodinitrile with *p*-phenylenediamine in phenol and its derivatives with electron-donating substituents, the yield of the macroheterocycle increases to 85%. The process is extremely selective and, apart from the macroheterocycle **1**, only compound **2** was found among the reaction products. In the reaction of phthalodinitrile with *p*-phenylenediamine, it was established at various stages of the latter that, when the reaction is carried out in solvents other than phenols with electron-accepting substituents, the intermediates contain compounds with m/z = 236, 327, and 455.

The following expanded mechanism of the reaction of phthalodinitrile with *p*-phenylenediamine in phenol, where the macroheterocycle was obtained in maximum yield, was proposed on the basis of these data (Scheme 3).

The results presented permit the fundamentally important conclusion that one of the decisive factors determining the composition of the products of the condensation of phthalodinitrile with aromatic diamines in hydroxylated solvents is the nature of the reaction medium. Since the condensation of phthalodinitrile with diamines in phenol is the most selective process in the formation of hexazocyclanes, the kinetics and mechanism of this reaction were investigated in detail.

The thermodynamics of the process were investigated for the condensation of phthalodinitrile with *m*-phenylenediamine.[27] Table 1 presents the enthalpies, entropies, and Gibbs free energies as well as equilibrium constants for this reaction at different temperatures. The negative Gibbs free energies indicate that the synthesis of the hexazocyclane is thermodynamically

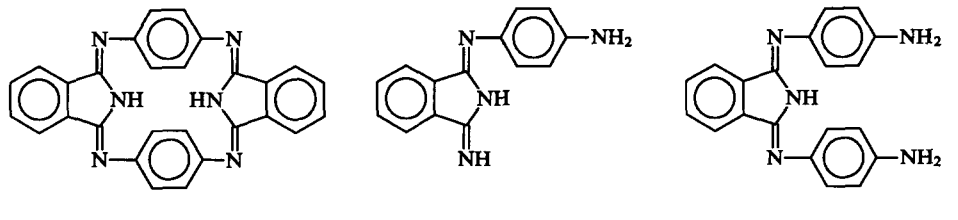
Scheme 1

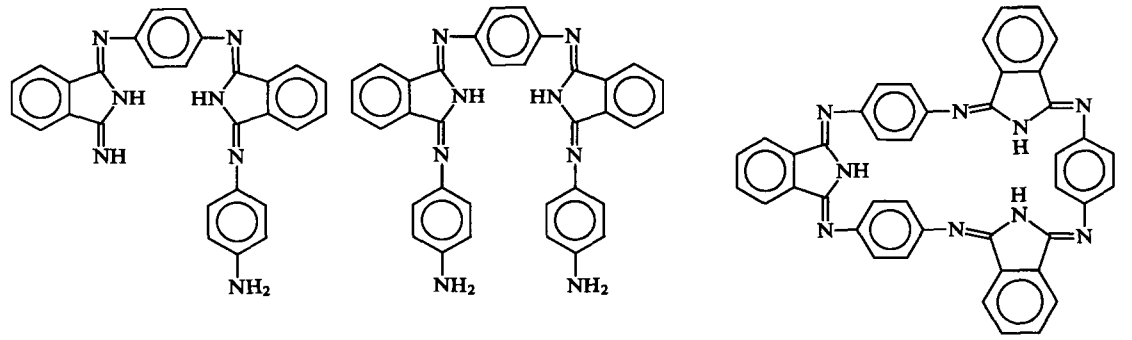


X = Cl, m/z = 347; X = NO_2, m/z = 358;

X = Cl, m/z = 586; X = NO_2, m/z = 597.

Scheme 2





Scheme 3

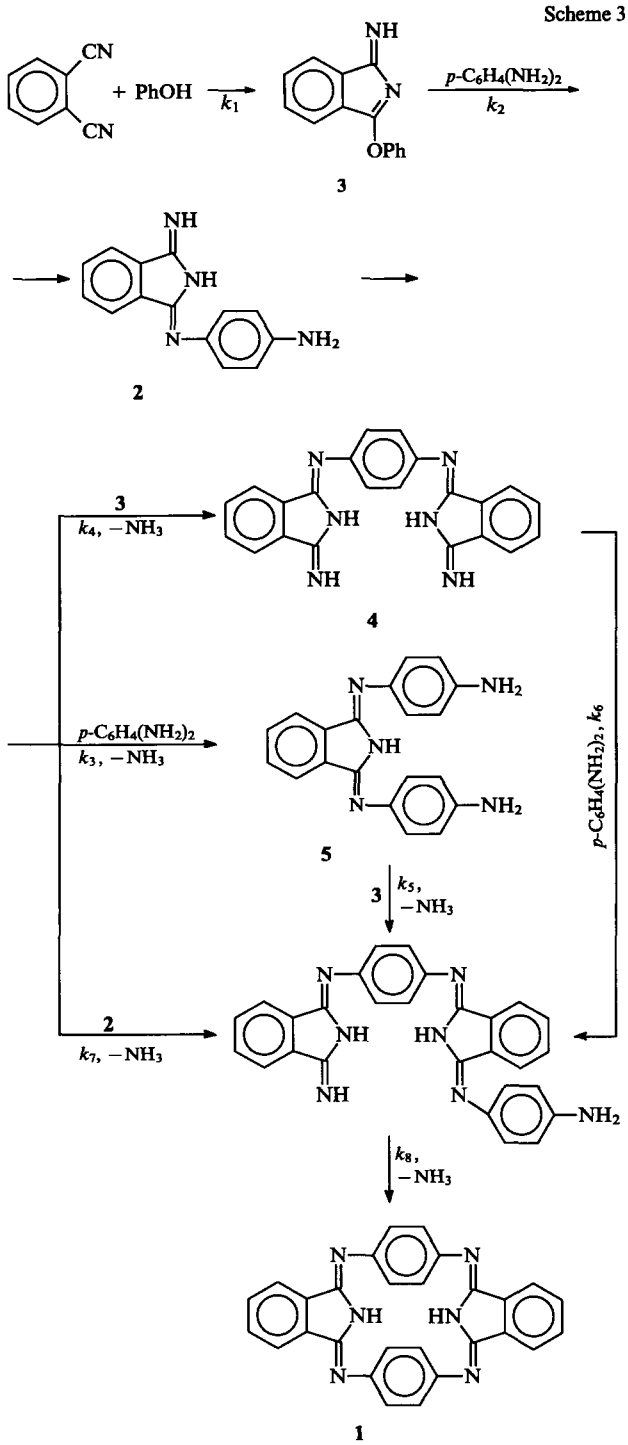


Table 1. The enthalpies, entropies, Gibbs free energies, and equilibrium constants for the condensation of the dinitrile of *o*-phthalic acid (DN) with *m*-phenylenediamine (*m*-PDA) (p = 101.325 kPa).

T/K	$-\Delta H_r^\circ(T)$/ kJ mol^{-1}	$-\Delta S_r^\circ(T)$/ J mol^{-1} K^{-1}	$-\Delta G_r^\circ(T)$/ kJ mol^{-1}	lgK_e
2DN(c) + 2*m*-PDA(c) → HC(c) + 2NH$_3$(g)				
250	5.88	−134.6	39.53	8.258
298.15	11.38	−115.8	45.83	8.027
2DN(c) + 2*m*-PDA(l) → HC(c) + 2NH$_3$(g)				
350	50.74	1.92	50.07	7.472
400	62.40	32.35	49.46	6.456
2DN(l) + 2*m*-PDA(l) → HC(c) + 2NH$_3$(g)				
420	106.4	139.2	48.00	5.969
440	110.4	148.4	45.06	5.349
460	114.1	156.7	42.01	4.770
480	117.7	164.1	38.87	4.229
500	121.1	170.9	35.66	3.725

Note. The following notation has been adopted: c = crystal, l = liquid, g = gas, HC = hexazocyclane.

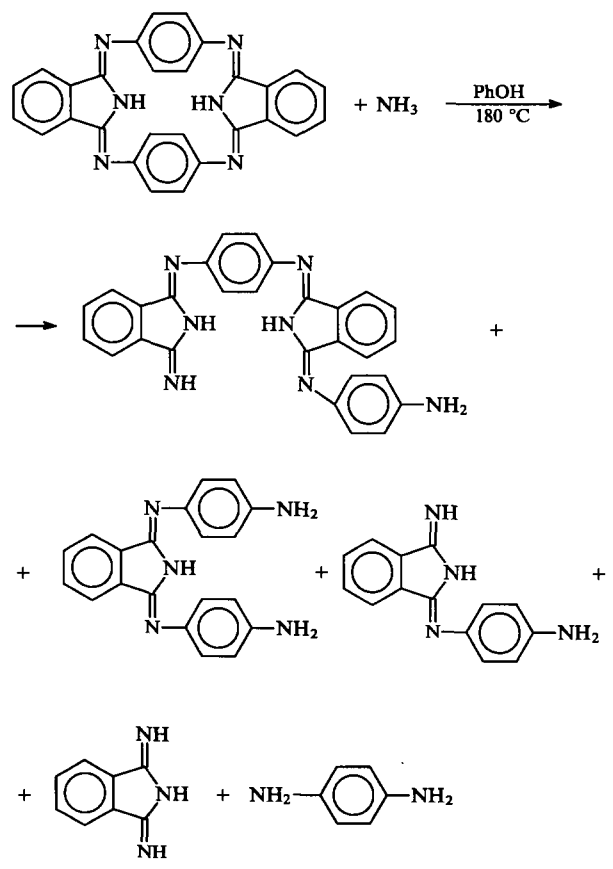
allowed throughout the temperature range investigated. The equilibrium constant of the reaction is $9.3 \times 10^5 - 5.3 \times 10^3$, so that the condensations of phthalodinitrile with diamines are irreversible. In the temperature range 420–500 K, the entropy of reaction is negative. The high negative enthalpy of the process is responsible for its being thermodynamically allowed and for its irreversibilty.

Since the formation of the hexazocyclane is a multistage process, its overall irreversibility does not rule out the reversibility of individual stages. The study of the composition of the products of the reaction of the hexazocyclane with ammonia—a low-molecular-mass product of this reaction—under the conditions of the synthesis[28] made it possible to put forward Scheme 4 for the ammonolysis of the hexazocyclane.

Comparison of the reactions involving the synthesis and ammonolysis of the hexazocyclane provided grounds for the hypothesis that the stages in its formation which take place with evolution of ammonia are reversible, i.e. that the process irreversibility should be attributed to its initial stages.

The kinetics and mechanism of the formation of the hexazocyclane were investigated for the reaction of phthalodinitrile with *p*-phenylenediamine. The process was followed from the decrease in intensity of the C≡N absorption band of phthalodinitrile in the IR spectrum of the reaction solution and

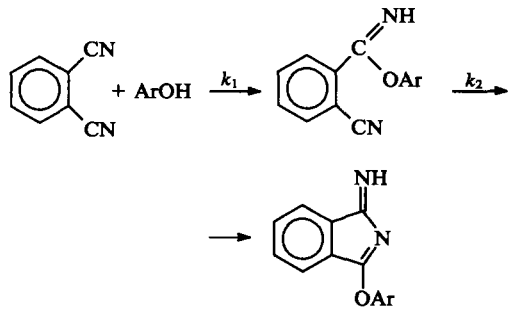
Scheme 4



from the evolution of ammonia. In order to determine the contribution of the individual stages to the formation of the macroheterocycle and to establish the most probable mechanism, mathematical modelling was used with preliminary estimation of the rate constants for those stages where it was possible.

In terms of Scheme 3, the first stage of the reaction is the interaction between phthalodinitrile and phenol. According to literature data,[29,30] there is an excess electron density in the phthalodinitrile molecule on one of the nitrogen atoms and a deficiency on the carbon atoms of the nitrile groups, the positive charge on the carbon atom on one of the nitrile groups being much higher than that on the carbon atom of the other group. This justifies the hypothesis that the reaction begins with nucleophilic attack by the phenol on the carbon atom with the greater positive charge.

The next stage is apparently nucleophilic attack by the nitrogen of the imino-group on the carbon atom of the second nitrile group with subsequent isomerisation and cyclisation.

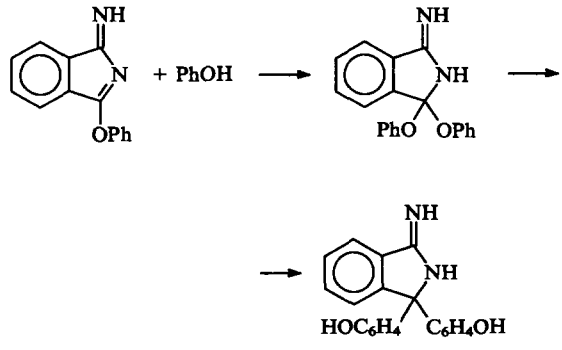


6

However, it was found that the reaction product is 1-(4-hydroxyphenyl)-1-(2-hydroxyphenyl)-3-iminoisoindoline **7** and not 1-aryloxy-3-iminoisoindole **6**.[31] This gives grounds for the assumption that the 3-imino-1-phenoxyisoindole formed is an unstable compound, which, having combined with a phenol molecule, undergoes a rearrangement, which is consistent with the hypothesis put forward by Bartlett.[32]

Judging from the fact that there is no compound **7** among the products of the reaction of phthalodinitrile with diamines in phenol, the rate of reaction of the aryloxy-group with the amino-group is higher than the rate of its reaction with phenol.

Taking into account the proposed mechanism for the additional polarisation of the nitrile groups, it was decided to employ LiCl as the catalyst (the polarising effect of the Li^+ ion amounts to 1.7).[33]



7

Studies of the kinetics of the interaction of phthalodinitrile with phenol have shown[34] that there is an induction period in the reaction, which becomes shorter after the introduction of LiCl. The fact that the rate of reaction increases as a function of time is extremely important. This justifies the hypothesis that the process is autocatalytic.

Indeed, it was found that, when 1-(4-hydroxyphenyl)-1-(2-hydroxyphenyl)-3-iminoisoindoline is introduced into the reaction mixture, the induction period is markedly shortened. This is apparently associated with the presence in compound **7** of a secondary cyclic amino-group, the interaction of which with the phenolic hydroxyl increases the electron density on the oxygen atom, thereby increasing the rate of the reaction of phenol with the electrophilic carbon atom.

Other cyclic amines exhibit in this reaction a catalytic activity,[34] which increases with increase in the basicity of the amine. When a tertiary amine and LiCl are introduced simultaneously into the reaction, both reagents are activated and the induction period virtually vanishes.

The following reaction rate constants have been obtained from kinetic data with the aid of the mathematical model:

$$k_1/h^{-1} = 0.004 + 1.6\,c_{LiCl} + 7\,c_7,$$

$$k_2/h^{-1} = 5.$$

The results show that both LiCl and compound **7** are catalysts of the first stage of the reaction, the catalytic activity of the latter being higher. The cyclisation stage is noncatalytic. The proposed mechanism of the reaction of phthalodinitrile with phenol is confirmed indirectly by the shortening of the induction period with increase in the nucleophilicity of phenols caused by the introduction of electron-donating substituents into the benzene ring.

The product of the reaction of a substituted phthalodinitrile containing an electron-accepting substituent with phenol is 3-imino-1-phenoxyisoindole. The latter compound does not combine with a second phenol molecule and does not rearrange. Kinetic studies have shown[34] that the rate of reaction of phenol with substituted phthalodinitriles depends on the nature of the substituent in the phthalodinitrile and increases as its electron-accepting properties become more pronounced. The equations for the rate constants for the reaction of 4-nitrophthalodinitrile with phenol have the following form:

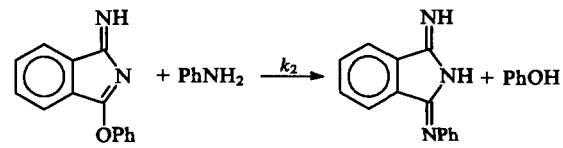
$$k_1/h^{-1} = 0.075 + 25\,c_{LiCl} + 11\,c_7,$$

$$k_2/h^{-1} = 9.$$

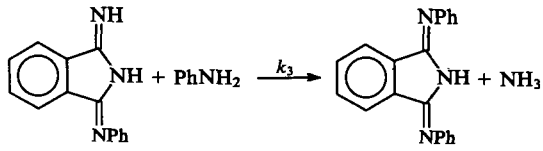
From the above equation for k_1, when the nitro-group is introduced into the phthalodinitrile ring, the contribution of the catalytic reaction increases appreciably (compared with the unsubstituted phthalodinitrile). This is accompanied by a sharp increase also in the catalytic activity of LiCl. Evidently, the increase in the positive charge on the carbon atoms of the nitrile groups facilitates their nucleophilic attack by phenol in the first stage of the reaction by the nitrogen of the free C≡N group in the second stage.

When the electron-donating OH group is introduced into the ring of phthalodinitrile, a sharp decrease in the reaction rate is observed, which is fully consistent with the proposed mechanism.

The next stage of macroheterocycle formation, the interaction of 3-imino-1-phenoxyisoindole with the diamine, was investigated for the reaction of phthalodinitrile with aniline at 20–180 °C in view of the complexity of the process.[35] It was found that, at temperatures below 70 °C, 3-imino-1-phenoxyisoindole interacts with aniline via the phenoxy-group.

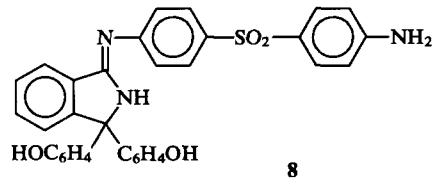


At a temperature above 70 °C, aniline behaves as a nucleophilic relative to the carbon atom of the C≡N group. The reaction of aniline with 1,3-diiminoisoindole results in the evolution of ammonia, which is apparently formed by the addition of the aniline protons to the exocyclic NH group.[36]

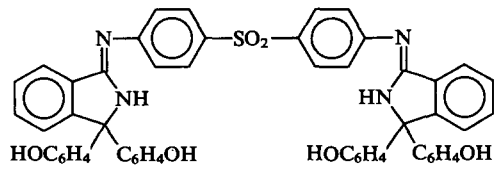


Calculation of the reaction rates by means of the mathematical model for the process showed[37] that the rate of reaction of phthalodinitrile with phenol diminishes sharply in the presence of aniline. Comparison of the equations for the rate constants showed that aniline appreciably lowers the catalytic activity of LiCl, apparently due to the formation of the complex $LiCl-PhNH_2$. The rate-limiting stage of the process is the formation of this complex.

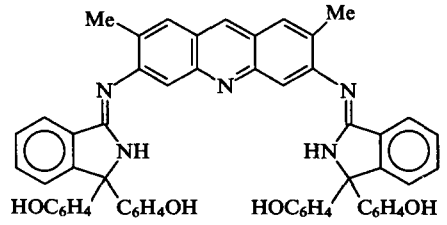
Since the condensation of the amino-group with the phenoxy- and imino-groups takes place via a nucleophilic substitution mechanism, the basicity of the amine should influence significantly the rate and mode of the reactions. The study of the composition of the products of the reaction of phthalodinitrile with 3,6-diamino-2,7-dimethylacridine ($pK_a = 1.5$), di(4,4-aminophenyl) sulfone ($pK_a = 2.7$), 9,9-bis(4-aminophenyl)-fluorene ($pK_a = 3.3$), and *p*-phenylenediamine ($pK_a = 6.2$) in phenol showed that, instead of the macroheterocycles, the corresponding compounds **8–11** are formed in the first two cases.



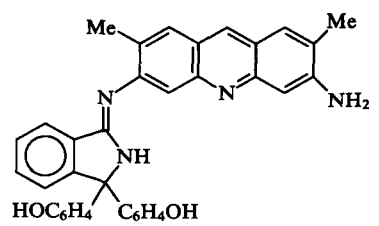
8



9

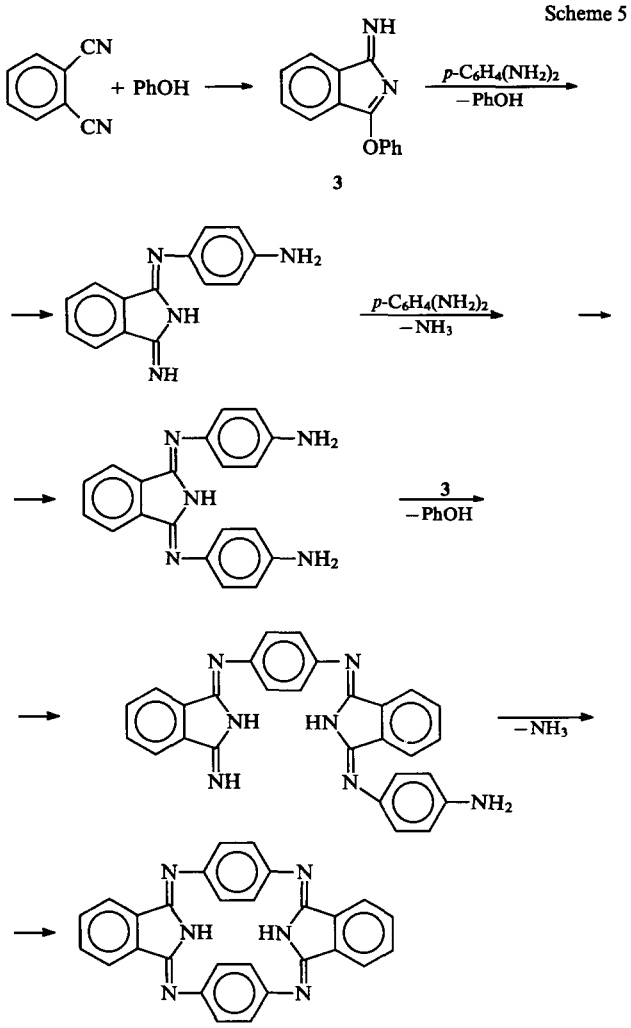


10, $m/z = 835$

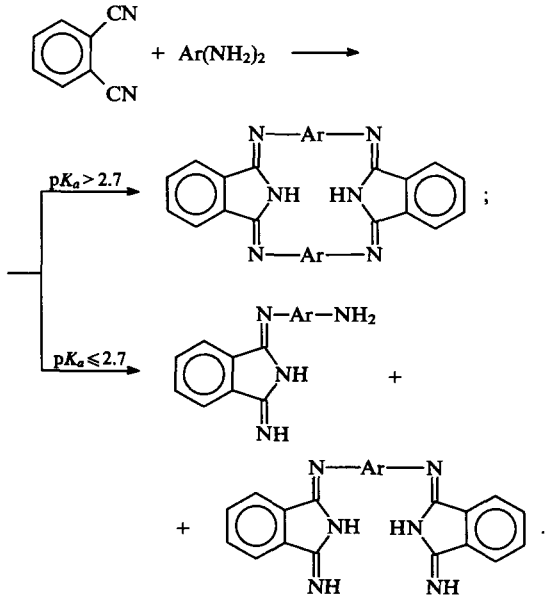


11, $m/z = 537$

Scheme 5



Apparently, owing to the low basicity of these diamines, the rate of reaction of the amino-groups with the phenoxy-group in compound **3** (see Scheme 3) is lower than the rate of formation of compound **2**, which actually reacts with the diamine. In all the remaining cases, macroheterocycles are formed. From these data, the interaction of phthalodinitrile with diamines can be represented by the following general scheme as a function of the basicity of the diamines:



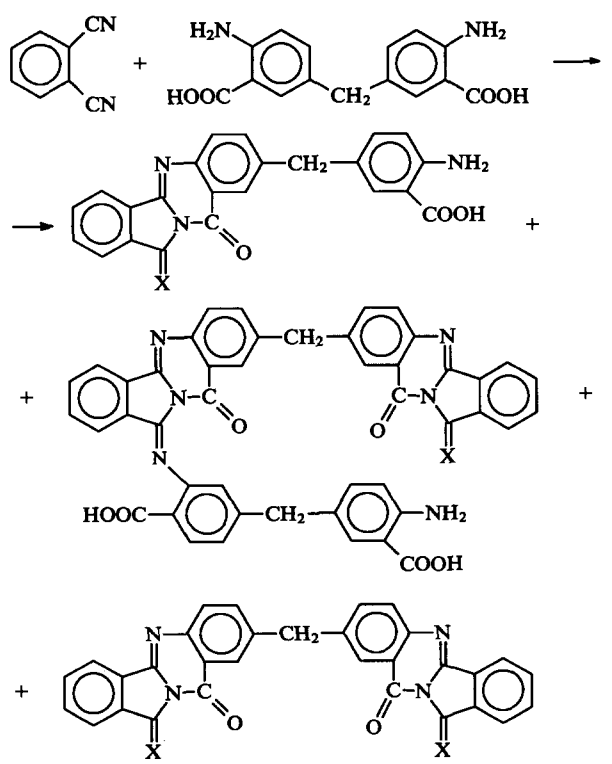
The kinetics of the formation of the macroheterocycle have been investigated for the condensation of phthalodinitrile with *p*-phenylenediamine.[40] The mathematical description of the process made it possible to calculate the rates of all the reactions constituting the formation reaction of the hexazocyclane and to determine its principal aspects (Scheme 5, see previous page).

Direct experimental confirmation of the macrocyclic structure of the hexazocyclane was obtained by X-ray diffraction study of the hexazocyclane based on phthalodinitrile and di(4,4-aminophenyl) ether.[31] The geometry of the principal groups of atoms is close to the usual geometry, i.e. the formation of the macroheterocycle hardly requires the distortion of the bond angles and bond lengths. The conformation of the five-membered nitrogen-containing heterocycles is nearly planar (the endocyclic torsional angles do not exceed 4.4°). However, in combination with some twisting about the endocyclic C–N bonds, this proves sufficient for a significant deviation of the conformation of the macrocycle itself from planarity.

Hexazocyclanes contain water in the endocyclic space, i.e. they are clathrate compounds. In contrast to the majority of known clathrate compounds, for hexazocyclanes the guest molecule inclusion cage consists of a single molecule; hexazocyclanes based on mononuclear diamines contain one water molecule in the endocyclic space, whilst the remaining hexazocyclanes contain two such molecules regardless of the size of the macroheterocycle.[41]

III. Macroheterocycles with a system of five- or six-membered heterocycles condensed with the isoindole ring

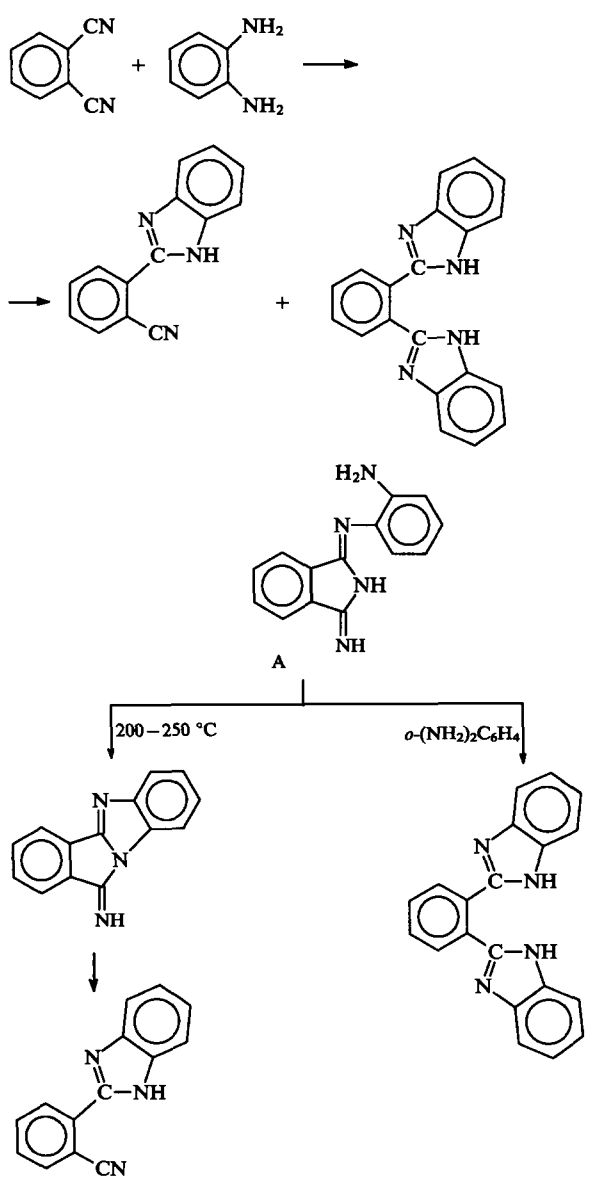
Macroheterocycles with a system of condensed heterocycles can be formed if a diamine, containing *ortho*-substituents capable of interacting with the secondary amino-groups of the isoindole ring, is used as one of the initial reactants. Such reactions proceed both with the evolution of volatile products and via isomerisation cyclisation. This requires a high reactivity of the *ortho*-substituents. For example, they may contain a labile hydrogen atom, the interaction of which with the NH group of the isoindole ring is accompanied by water or ammonia evolution.



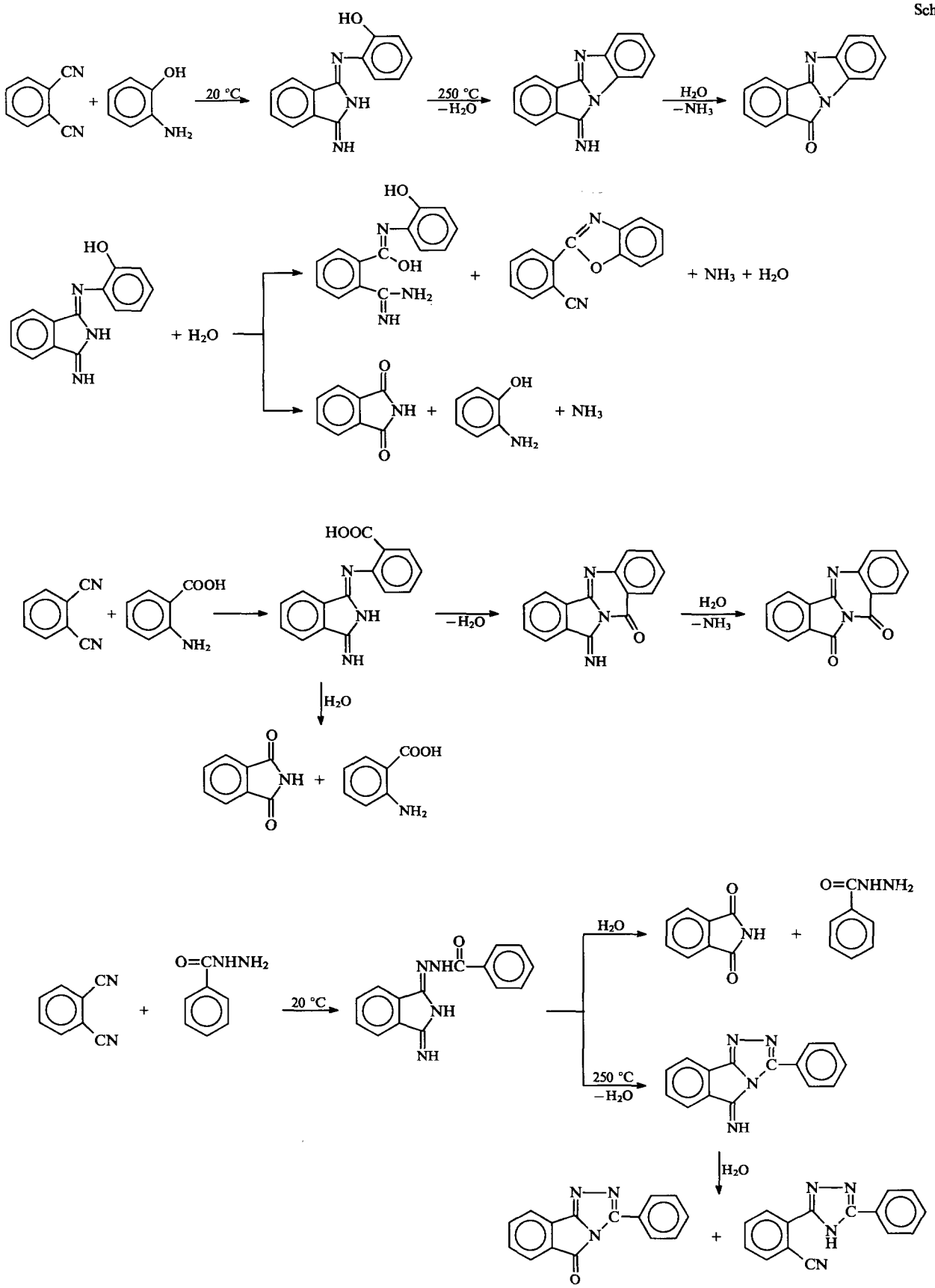
X = O, NH

The mechanism of this process has been studied for the condensation of phthalodinitrile with *ortho*-substituted monoamines—*o*-aminophenol, anthranilic acid, and benzohydrazide.[42] When these diamines interact with the imino-group of the isoindole ring, water is liberated. The thermal cyclisation process was investigated using compounds obtained by condensing phthalodinitrile with a monoamine at room temperature. At 200–250 °C both the formation of compounds with condensed heterocycles and the hydrolysis of the final and intermediate products take place (Scheme 6). Therefore, the possibility of using polyphosphoric acid (PPA) as the reaction medium, which binds the water evolved on cyclisation, was investigated in the condensation of phthalodinitrile with anthranilic acid. The composition and structure of the products of this reaction were found to be determined by the temperature and the order in which the reactants are added. The selectivity of the reaction of phthalodinitrile with anthranilic acid is ensured by introducing the acid at $T > 180$ °C into a solution of phthalodinitrile.

However, the reaction of phthalodinitrile with methylenedianthranilic acid proceeds under these conditions without the formation of a macroheterocycle.[43] (See bottom left.)



Scheme 6

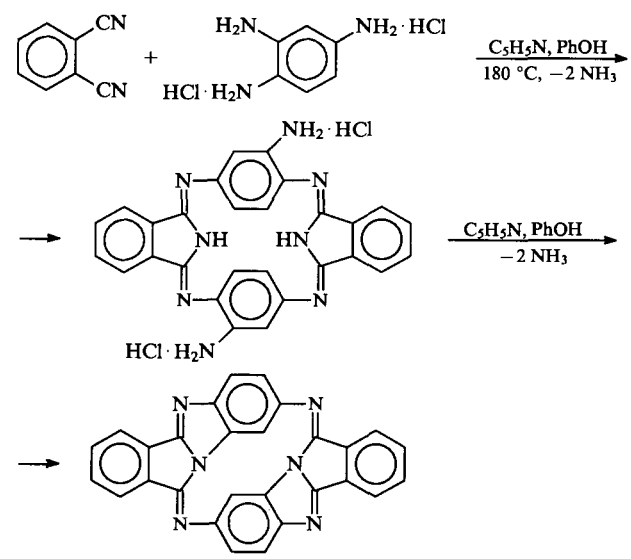


The fact that, instead of the macroheterocycle, only the intermediates in its synthesis are formed in the condensation of phthalodinitrile and *p*-phenylenediamine in PPA is extremely important. The same products, isolated from PPA and then placed in phenol, interact with the latter, affording a hexazocyclane. In the condensation of phthalodinitrile with 1,2,4-triaminobenzene, the formation of a system of condensed isoindole and benzimidazole rings should be accompanied by ammonia evolution. To find out whether such a reaction occurred, a comparison was made of the product composition of the condensation of *o*-phenylenediamine with phthalodinitrile in phenol at 180 °C [44] and of the cyclisation products of 1-*N*-(2-aminophenyl)-3-iminoisoindoline at 200–250 °C in the presence and absence of *o*-phenylenediamine (see page 772, bottom right).

It follows from a comparison of the results that the factors preventing the formation of compounds with a system of condensed isoindole and benzimidazole rings are the isomerisation of compound A with participation of the exocyclic NH group during the cyclisation process as well as the interaction of the intermediate — 1-*N*-(2-aminophenyl)-3-iminoisoindoline — with *o*-phenylenediamine. This required as the initial reactant not *o*-phenylenediamine itself but a derivative with a substituted amino-group. Furthermore, it is necessary that substitution of the exocyclic NH groups should precede formation of the benzimidazole ring.

Therefore, 1,2,4-triaminobenzene in the form of the 1,4-dihydrochloride was used as the amine component for the synthesis of a hexazocyclane with condensed benzimidazole and isoindole rings. During the synthesis, the hydrochloride groups were neutralised in two stages. Judging from literature data,[44] the 4-amino-group is the first to be neutralised, which is the reason for the possibility of macroheterocycle formation. After the neutralisation of the second amino-group, the latter reacts quantitatively with the NH group of the isoindole ring to form condensed heterocycles.[45] (See above right.)

In order to obtain compounds with a system of condensed heterocycles without the isolation of volatile products, the dinitrile of methylenedianthranilic acid was used as the amine component in the reaction with phthalodinitrile in phenol, because in this case the quinazoline ring is formed via isomerisation cyclisation.[46] A quantitative estimate by IR showed that the hexazocyclane

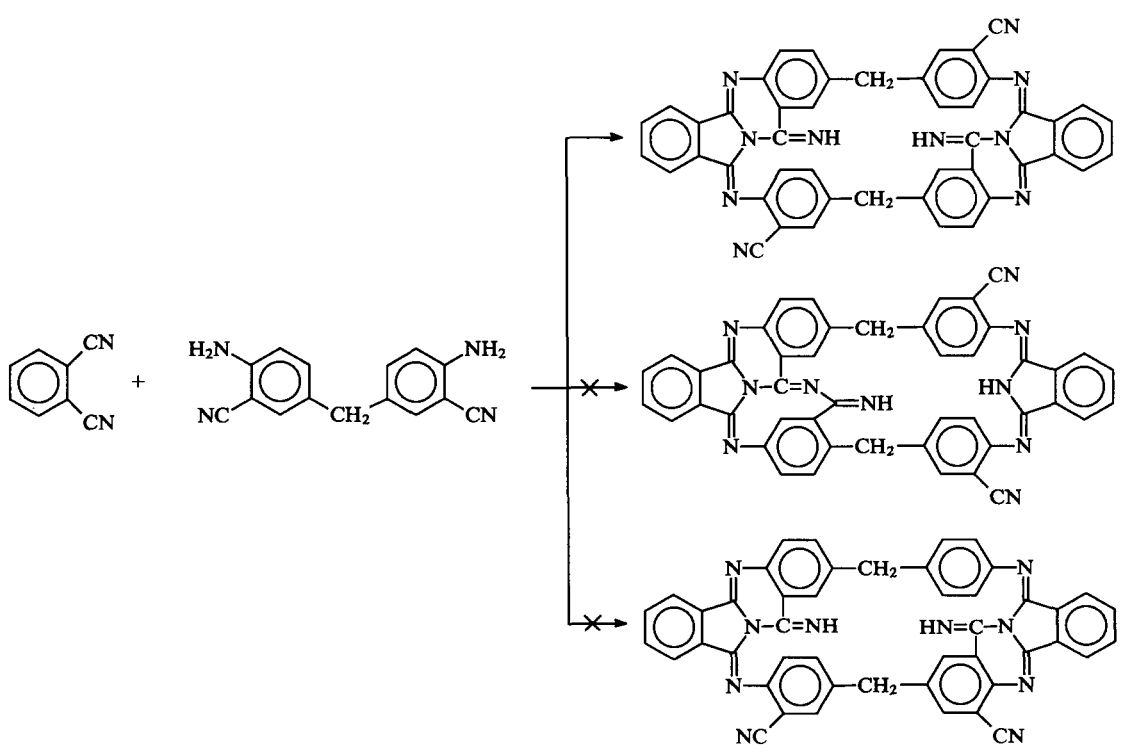


contained two free C≡N groups, which justifies the hypothesis that three isomers of the macroheterocycle differing in the position of the C≡N groups are formed. Studies showed that the reaction proceeds strictly selectively only via a single pathway with formation of a macroheterocycle having the structure presented in Scheme 7.

The selectivity of the reaction is evident because, as a result of the interaction of one of the nitrile groups with the imino-group of the isoindoline ring, the benzene ring incorporating this nitrile group rotates until it coincides with the average plane of the macroheterocycle. The plane of the second benzene ring should then be inclined relative to the average plane of the macroheterocycle. The distance between the nitrile group of this ring and the imino-group of the isoindole ring increases, which rules out the possibility of intramolecular cyclisation.

The data obtained in the study of model reactions of phthalodinitriles with diamines served as a basis for the development of specific methods of synthesis, from tetracarboxylic acid tetranitriles and diamines, of polymers both having a macrocyclic structure and without macroheterocycles.

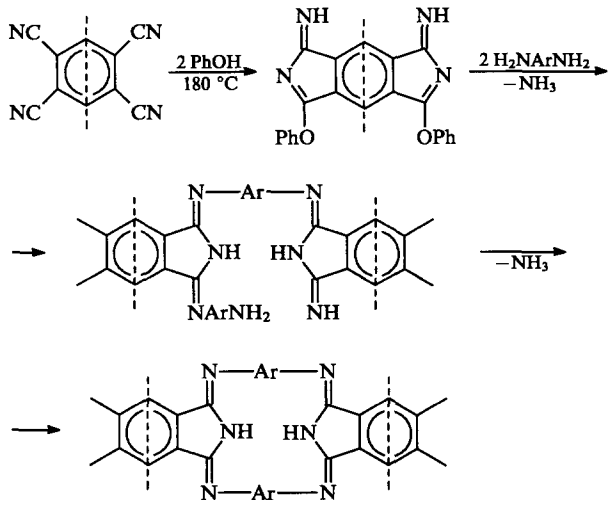
Scheme 7



IV. Polycondensation of tetracarboxylic acid tetranitriles and unsubstituted diamines in phenol

The data obtained in the study of model reactions of phthalodinitriles with diamines give grounds for the assumption that polymers with the maximum content of macroheterocycles in the chain can be obtained by the polycondensation of tetracarboxylic acid tetranitriles and highly basic ($pK_a > 3.3$) aromatic diamines in phenols ($pK_a > 9.8$). The polycondensation process can be represented by the multistage Scheme 8.

Scheme 8



The polymer chain grows by accumulation in the latter of macroheterocycles, the formation of which is accompanied by ammonia evolution. Hence, the amount of ammonia evolved is used as a measure of the degree of reaction and of the propagation of the polymer chain. The structure of the polymers has been confirmed by ^1H NMR spectroscopic data[26] obtained in the study of a polyhexazocyclane (PHC) based on pyromellitic acid tetranitrile and *p*-phenylenediamine.

Kinetic studies of the reaction of tetracarboxylic acid tetranitriles and diamines show that the polycondensation process is autocatalytic. By analogy with the model reaction, one can postulate that the autocatalysts of the polycondensation process are intermediates containing a cyclic imino-group. The use as the catalyst of a tertiary cyclic amine with LiCl leads to the disappearance of the induction period and to an increase in reaction rate.

The set of monomers which has been used to synthesise PHC made it possible to trace in succession the influence of their structure on the properties of the polymers.

It follows from Table 2 that a high degree of reaction and a high yield are characteristic of all the PHC. The solubility of the polymers is determined by their structure. The introduction into the monomer of a cardo-group and of an oxygen bridge between the benzene rings increases the range of solvents in which the PHC dissolve.[21]

All the PHC possess a high thermal stability and heat resistance. According to dynamic thermogravimetric analyses (TGA), the temperature of the onset of their vigorous decomposition in air exceeds 400 °C. A more complete idea about the thermal transformations of PHC has been obtained in the study of the composition of the products of the thermal and thermohydrolytic degradation of the macrocycle based on phthalodinitrile and *p*-phenylenediamine as well as a series of PHC at 350–600 °C.[47]

The presence in the thermal degradation products of the macrocycle of carbon oxides, ammonia, phthalimide, and *p*-phenylenediamine suggested that carbon oxides [carbon dioxide only? (Ed. of Translation)] are formed as a result of the hydrolytic cleavage of the hexazocyclane (Scheme 9).

The main hydrolysing agent is apparently the water enclosed in the macroheterocycle. This hypothesis is supported by the finding that the products of degradation (at 400–450 °C) of a hexazocyclane, the endocyclic space within which was occupied by other groups[41] or of a hexazocyclane from which the occluded water had been removed by sublimation, contained only traces of CO_2.

The overall data obtained in the study of the degradation products justified the hypothesis that hydrolytic decomposition processes dominate in the thermal degradation of hexazocyclanes and polymers up to 450 °C, while above 450 °C homolytic decomposition processes assume this role, as indicated by the appearance of hydrogen, methane, and carbon monoxide in the decomposition products.

One of the real routes to increasing the thermal stability of the PHC involves the synthesis of polymers the endocyclic part of the space within which is occupied by groups of some kind, which rules out the presence of occluded water. The preparation of polymers containing five- or six-membered heterocycles condensed with the isoindole ring is most promising in this respect.

Scheme 9

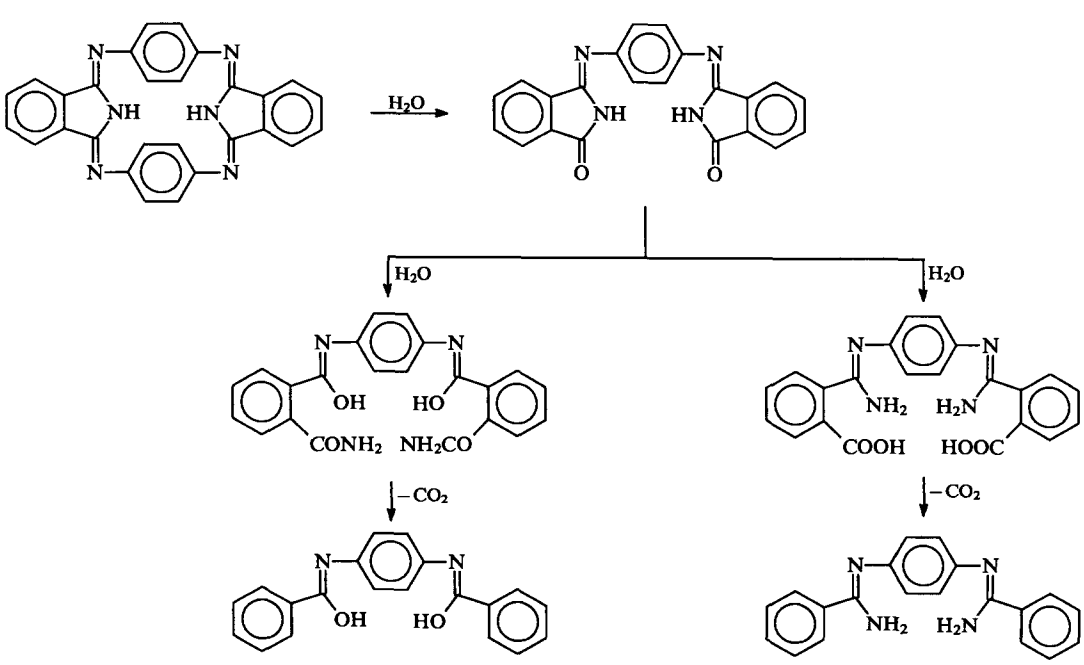
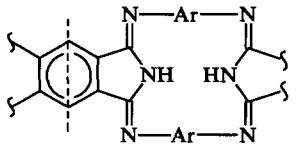
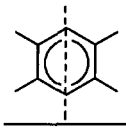
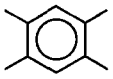
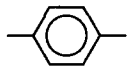
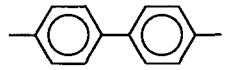
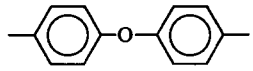
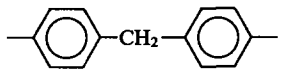
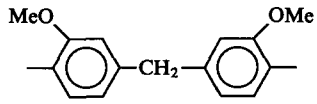
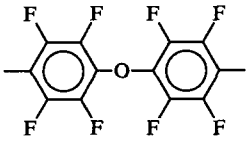
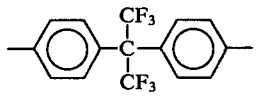
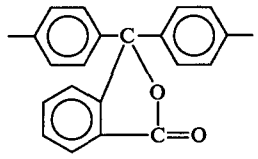
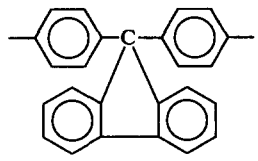
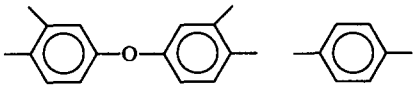


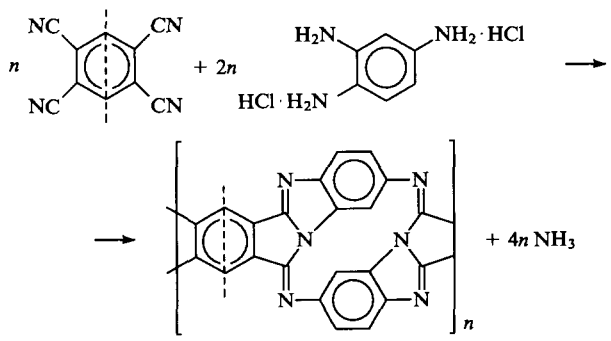
Table 2. The properties of polyhexazocyclanes having the general formula



	—Ar—	Degree of reaction (%)	Yield of polymer (%)	Solvents [a] in which polymers dissolve	Temperature of onset of softening [b]/°C	Temperature of onset of decrease in mass [c] in air/°C
		98	99	H_2SO_4	Does not soften	400
		98	99	H_2SO_4	"	420
		95	95	DMF, HMPA, DMSO, *N*-MP	225	400
		98	99	H_2SO_4	370	410
		97	98	DMF, HMPA, DMSO, *N*-MP	180	350
		91	95	DMF, DMA, *N*-MP, DMSO, acetone, dioxane	210	410
		95	95	"	180	380
		98	97	DMF, HMPA, DMSO, *N*-MP	380	410
		99	98	DMF, DMSO, *N*-MP, dioxane	220 (p = 19.6 MPa)	430
		97	92	DMF, DMSO, *N*-MP, HMPA	180	410

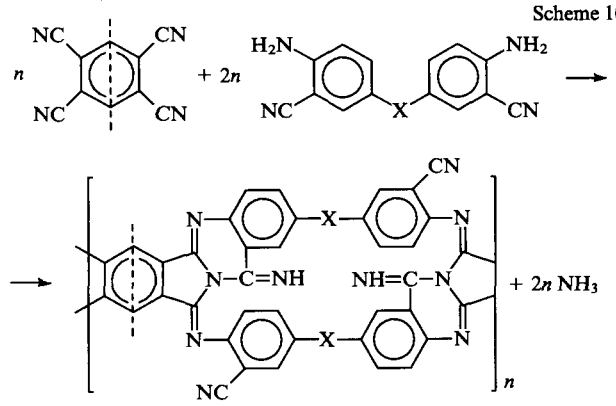
[a] DMF = dimethylformamide, HMPA = hexamethylphosphoramide, DMSO = dimethyl sulfoxide, *N*-MP = *N*-methylpyrrolidinone [DMA = dimethylacetamide (Ed. of Translation)].
[b] Rate of temperature rise 10 °C min^{-1}, p = 9.8 MPa.
[c] Rate of temperature rise 4.5 °C min^{-1}.

Polyhexazocyclanes with condensed isoindole and benzimidazole rings have been obtained by polycondensation of tetracarboxylic acid tetranitriles and diamine dihydrochlorides,[48] the latter being neutralised during the synthetic process.



Polyhexazocyclanes with condensed isoindole and quinazoline rings have been synthesised using bis(*o*-cyanoarylamines) (Scheme 10).[48]

Scheme 10



The thermal stability of such polymers is much higher than that of the usual polyhexazocyclanes.[49] Hydrolytic processes in polymers with condensed heterocycles are extremely slight. The amount of CO_2 evolved during their thermal degradation is smaller by a factor of 4–6 at 450 °C and by a factor of 2–4 at 500–550 °C than in the degradation of the PHC based on *p*-phenylenediamine. In this case, the hydrolysing agent is apparently adsorbed water, the content of which in the polymers, determined by the Fischer method, does not exceed 1%.

V. The properties of solutions of polyhexazocyclanes

The presence of macroheterocycles in the PHC chain determines the specific properties of dilute and concentrated solutions of these polymers.[50] Thus when the degree of reaction is quantitative, the intrinsic viscosity of 0.3%–1.0% solutions of the polymers in *N*-methylpyrrolidinone (*N*-MP) and dimethylformamide (DMF) is low and independent of concentration. Centrifugation results in the complete precipitation of the polymers from the solutions. This provides grounds for the hypothesis that solutions of PHC in aprotic solvents are not true solutions but approach colloidal or are colloidal solutions. This hypothesis has been confirmed by studies of solutions of PHC in *N*-MP by electron microscopy,[51] according to which the polymers in solution exist in the form of aggregates up to 1.5 μm in size, which is evidently associated with a weak polymer–solvent interaction.

In view of the presence in the macroheterocycle of the tertiary amino-group and on the basis of the available data on the solubility of rigid-chain nitrogen-containing polymers,[52,53] it was postulated that the interaction of the polymers with formic acid, which exhibits protogenic properties, is more intense than the interaction with *N*-MP. Indeed, it was found that the absolute intrinsic viscosities of solutions of the polymers in HCOOH are appreciably higher than those of the solutions in *N*-MP. According to electron microscope data, the polymers exist in formic acid in the form of individual 10–20 nm globular particles.

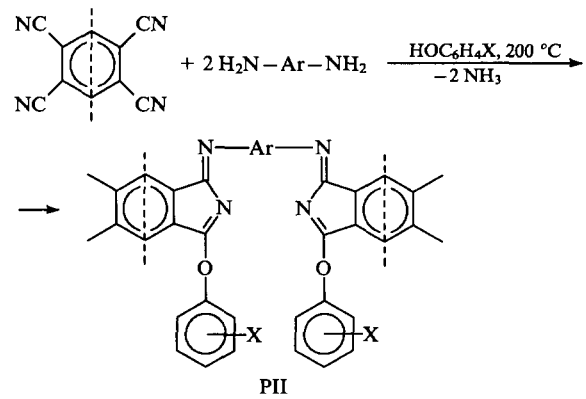
Polymers with charged nitrogen atoms have also been obtained by quaternising them with alkyl halides.[50] The dependence of the viscosity of solutions of such polymers in *N*-MP on the concentration is characteristic of molecularly disperse solutions, while the size of the polymer particles in solution does not exceed 20 nm.

The viscous characteristics of concentrated solutions of PHC are determined by their structure and by the nature of the solvent. Thus, up to a 25%–30% concentration of the PHC in *N*-MP, there is no interaction between the aggregates and the viscosity of the solutions is low and almost independent of concentration. Newtonian flow is characteristic of solutions of PHC in this concentration range. At concentrations above 30% the viscosity rises sharply, evidently at a consequence of the mutual interaction of the aggregates, which leads to a non-Newtonian type of flow.

Starting with a 10% concentration of a solution in formic acid of a rigid-chain polymer, the preparation of which is illustrated in Scheme 10, gel formation takes place which is apparently associated with the mutual arrangement of the extended macromolecules. The modulus of elasticity of a 10% solution of the gel is 6.2×10^{-4} Pa. The high elasticity of the gel is due to the presence in the polymer of nitrile side groups, which are additionally polarised as a result of complex formation with the carboxy-group, intensifying the intermolecular interaction. The modulus of elasticity remains constant up to 70 °C, which distinguishes this gel from the usual heat-treated gels produced as a result of the formation of physical bonds.

VI. Polycondensation of tetracarboxylic acid tetranitriles and diamines in phenols with electron-accepting substituents

Polymers with side aryloxy-groups in the chain, called polyisoindoxazenes (PII) are formed in the polycondensation of tetracarboxylic acid tetranitriles and diamines in phenols with electron-accepting substituents.[54]



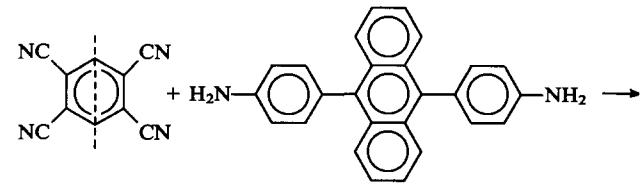
PII

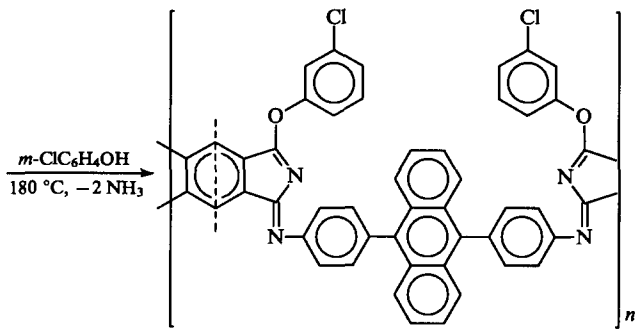
X = Cl, Br, NO_2.

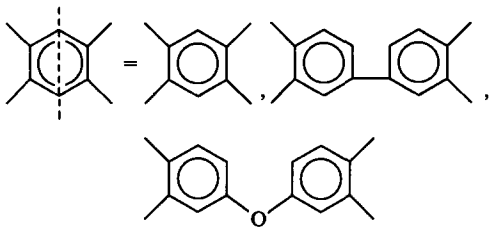
Kinetic studies show that the reaction has an induction period. With increase in the pK_a for a phenol, the duration of the induction period diminishes and the rate of polycondensation rises. From data obtained on model reactions, it is suggested that the process under consideration is autocatalytic, the product of the interaction of the tetranitrile with the phenol playing the role of the autocatalyst. The reaction of the phenol with the *o*-dinitrile is a nucleophilic process, so that the acidity of the phenol determines the rate of formation of the autocatalyst, which is simultaneously a reaction intermediate, and hence the rate of the reaction as a whole.

Polyisoindoxazenes have fairly high thermal stabilities and heat resistances, their thermal stabilities being somewhat inferior to those of the PHC. The temperature corresponding to a 5%

decrease in the mass of these polymers in air does not exceed 400 °C according to dynamic TGA data. As a rule, these polymers are readily soluble in organic solvents. The polymer based on pyromellitonitrile and bis(4,4'-aminophenol)anthracene, which precipitates during synthesis and does not dissolve even in sulfuric acid, is an exception.





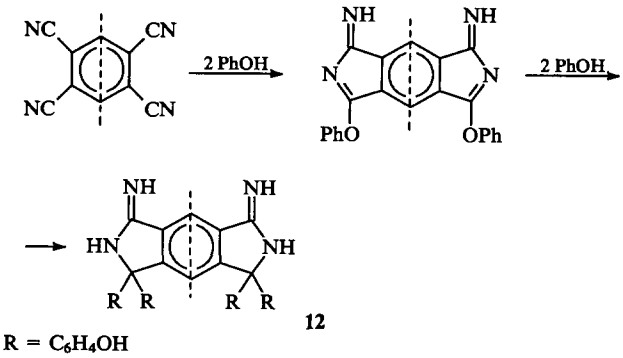


Calculations of the conformational parameters of this PII showed[55] that the rigidity of its macromolecule is such that it cannot form a coil and retains the shape of a straight rigid rod whatever the number of units, which is due to the presence of only a single virtual bond around which rotation is possible. The polymer having this structure has the most rigid chain among all those known at the present time and the concept of the Kuhn segment is not applicable to it. The replacement of pyromellitonitrile by the tetranitrile of oxybis(benzenedicarboxylic) acid results in the appearance in the polymer of additional virtual bonds around which rotation is possible. Under these conditions, the size of the Kuhn segment diminishes to 40 Å and the polymer becomes soluble in organic solvents.

VII. Polycondensation of tetracarboxylic acid tetranitriles and weakly basic diamines

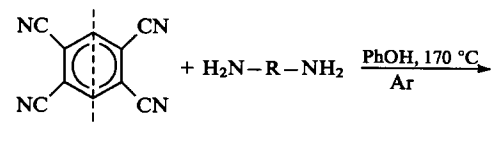
Judging from model reaction studies, in the polycondensation of the tetranitriles and weakly basic ($pK_a < 2.7$) diamines in phenol[56] the first stage in polymer formation is the interaction of the tetranitrile with four phenol molecules and subsequent rearrangement of the phenoxide groups. Compound **12**, formed at this stage, reacts with the diamine.

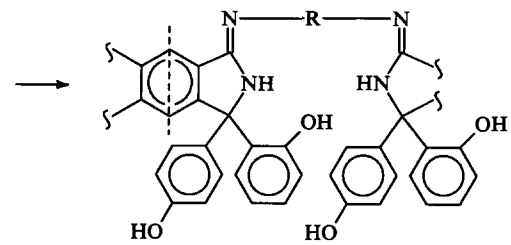
The polymers obtained in this way have been called polyoxyphenylisoindazenes. Their solubilities are higher than those of PHC and PII, whilst their thermal stabilities are comparable with those of the latter compounds. The presence in the polymers of free hydroxy-groups leads to the possibility of extensive modification of their properties by means of further polymer-analogue reactions.

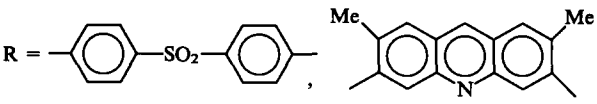


12

R = C_6H_4OH







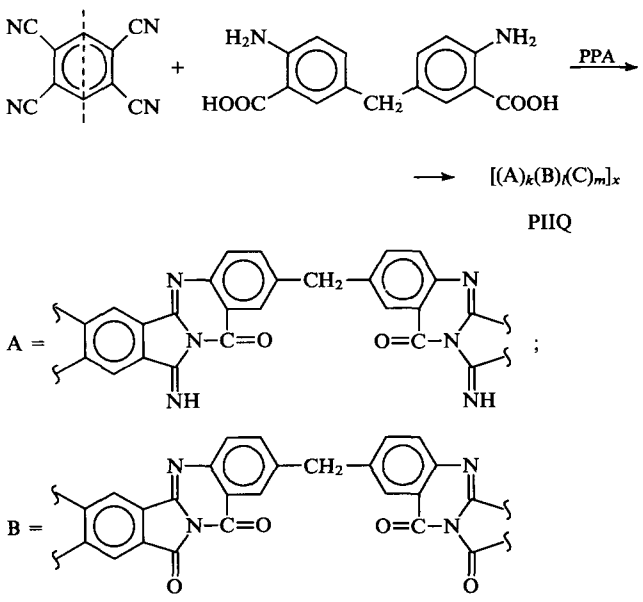
VIII. Polycondensation of tetracarboxylic acid tetranitriles and bisanthranilic acids in polyphosphoric acid

Polymers with a nonmacrocyclic structure, containing condensed isoindole and quinazolinone rings in the chain, have been obtained by the polycondensation of tetracarboxylic acid tetranitriles and bisanthranilic acids in polyphosphoric acid.[42] Such polymers have been called polyisoindolequinazolinones (PIIQ).

Polyisoindolequinazolinonediones, the structure of which is similar to that of the PIIQ, have been obtained by the polycondensation of bis(*o*-aminoamides) [?bis(*o*-aminobenzenecarboxamides) (Ed. of Translation)] with tetracarboxylic acid dianhydrides and also by the interaction of diaminodicarboxylic acids with the dianhydrides and chlorides of tetracarboxylic acid half-esters.[57-61] The possibility of the synthesis of such polymers by polycondensation of derivatives of tetracarboxylic acids with diaminodicarboxylic acids has also been demonstrated.[62,63]

This aspect developed appreciably after the polycondensation of 2,5-dicyanoterephthaloyl chloride with dicarboxy- and bis(methoxycarbonyl)-amines as well as bis(*o*-aminonitriles) had been achieved.[64,65] The use of these compounds made it possible to obtain polyiminoquinazolinepyrrolones via an isomerisation mechanism without the isolation of volatile products.[66]

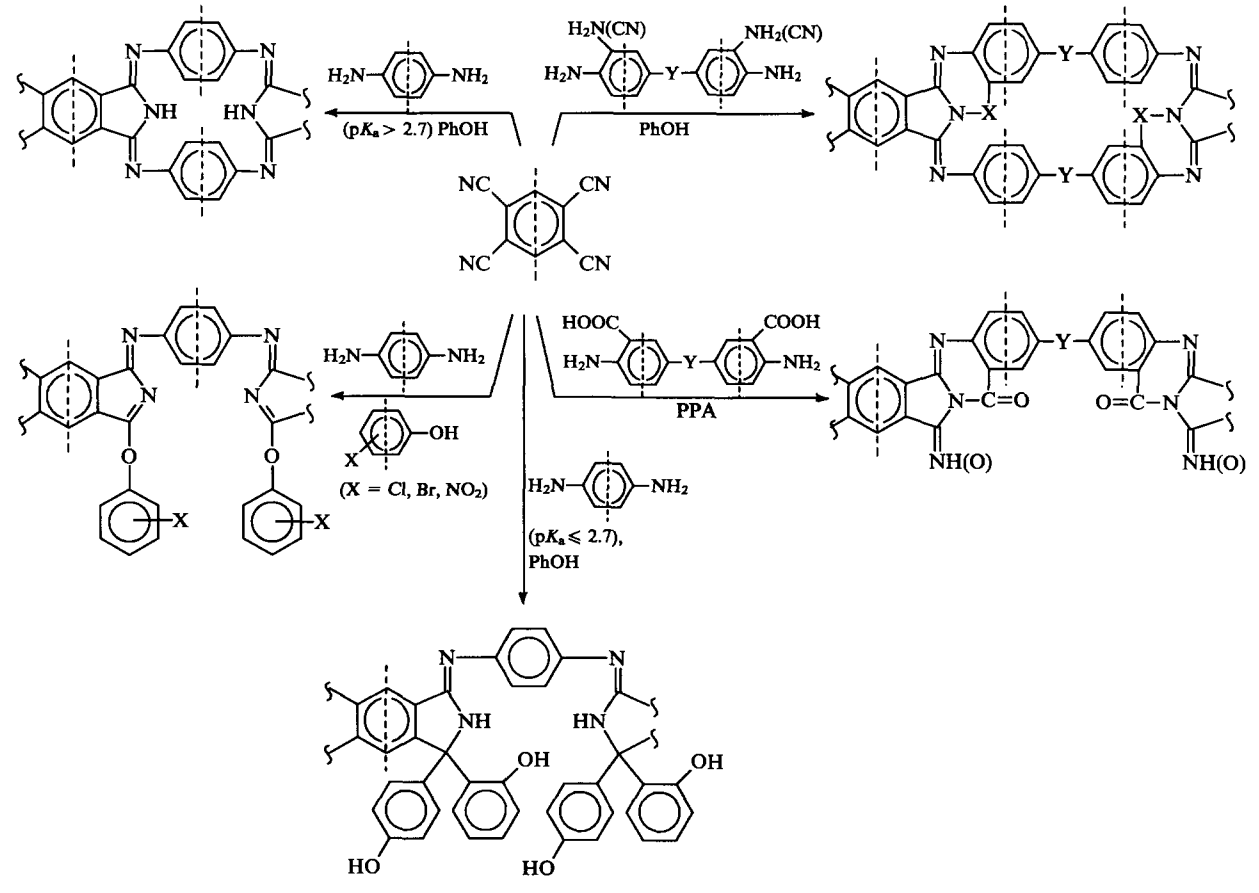
Polyisoindolequinazolinones are readily soluble in organic solvents and in inorganic acids. Their thermal stability is high: according to dynamic TGA data, the temperature of a 5% decrease in their mass in air is 420–440 °C. Carbon monoxide is completely absent from the products of the degradation of the polymers in vacuo at 400 °C, while at 450 °C its amount is insignificant, which indicates the virtually complete cyclisation of the polymer under the conditions of the synthesis.



At 500 °C, gas evolution is greater by a factor of 4–5 for polyisoindolequinazolinones than for PHC, indicating an appreciable contribution of the macrocyclic structure to the thermal stability of the polymers (Scheme 11).

Thus the study of the condensation and polycondensation of phthalodinitriles and bis(phthalodinitriles) with diamines demonstrated the extensive synthetic possibilities of these reactions. The determination of the physicochemical characteristics of the processes made it possible to formulate general ideas concerning the mechanisms of these reactions, which provided a basis for the synthesis of a series of new classes of polymers.[6,7,21,42,43,48,67–70]

Scheme 11



References

1. A L Rusanov, in *Advances in Polymer Chemistry* (Moscow: Mir, 1986) p. 159
2. A L Rusanov, D S Tugushi, V V Korshak *Uspekhi Khimii Poligeteroarilenov* (Advances in Chemistry of Polyheteroarylenes) (Tbilisi: Izd. Tbil.Univ., 1988)
3. J P Critcheley, C J Knight, W W Wright *Heat Resistant Polymers* (London: Plenum, 1983)
4. A L Rusanov, G S Matvelashvili, G V Kazakova *Plast. Massy* (11) 3 (1992)
5. B Sillon, in *Comprehensive Polymer Science* Vol. 5 (Oxford, New York: Pergamon Press, 1989) p. 499
6. S V Vinogradova, V A Vasnev *Chem. Rev.* (1994) (in the press)
7. S A Siling, S V Vinogradova *Sov. Sci. Rev. B, Chem.* **16** 1 (1992)
8. P F Clark, J A Elvidge, P P Linsted *J. Chem. Soc.* 3593 (1953)
9. US P. 2 765 380; *Chem. Abstr.* **51** 8143g (1957)
10. D L Packham, J C Haydon *Polymer* **11** 385 (1970)
11. D L Packham, J D Davis, F A Rackley *Polymer* **11** 533 (1970)
12. Br. P. 1 174 352; *Chem. Abstr.* **71** 92298v (1970)
13. D L Packham, F A Rackley *Chem. Ind.* 1254 (1967)
14. W O Siegl *J. Org. Chem.* **42** 1872 (1977)
15. R I Balahura, W L Purcell *J. Inorg. Chem.* **18** 937 (1979)
16. V E Maizlish, M K Islyaikin, V S Borodkin *Izv. Vyssh. Uchebn. Zaved., Khim. Khim. Tekhnol.* **22** 1441 (1979)
17. M K Islyaikin, V E Maizlish, V S Borodkin *Izv. Vyssh. Uchebn. Zaved., Khim. Khim. Tekhnol.* **22** 151 (1979)
18. R L Gaumans, K A Hold, W A Holmes-Walker *Polymer* **12** 400 (1971)
19. D L Packham, F A Rackley *Chem. Ind.* 1566 (1967)
20. Z K Timokhina, R P Smirnov *Tr. Ivanov. Khim.-Tekhnol. Inst.* (20) 57 (1976)
21. S V Vinogradova, S A Siling, W N Solowjov *Makromol. Chem.* **177** 1905 (1976)
22. J A Elvidge, R P Linsted *J.Chem. Soc.* 5000 (1952)
23. F Baumann, B Bienert, A Rosch, H Vollman, W Wolf *Angew. Chem.* **68** 133 (1956)
24. S V Vinogradova, V V Korshak, B V Rozynov, S A Siling *Zh. Org. Khim.* **8** 1305 (1972)
25. V V Korshak, S V Vinogradova, S A Siling, V N Solov'ev *Dokl. Akad. Nauk SSSR* **221** 114 (1975)
26. V V Korshak, S V Vinogradova, S A Siling, L A Fedorov *Dokl. Akad. Nauk SSSR* **195** 1113 (1970)
27. N B Rabinovich, N V Karyakin, E S Dzharimova, S A Siling, I I Ponomarev, S V Vinogradova *Izv. Akad. Nauk SSSR, Ser. Khim.* 779 (1984)
28. S V Vinogradova, S A Siling, V N Solov'ev *Zh. Org. Khim.* **10** 2437 (1974)
29. O E Polancky, M A Grassbirger *Monatsh. Chem.* **94** 677 (1963)
30. H E Popkie, J B Moffat *Can. J. Chem.* **43** 624 (1965)
31. S V Lindeman, V E Shklover, Yu T Struchkov, I I Ponomarev, S A Siling, S V Vinogradova, V V Korshak *Izv. Akad. Nauk SSSR, Ser. Khim.* 2015 (1984)
32. L Bartlett, V Renny, K Chan *J. Chem. Soc.* 129 (1969)
33. A A Grinberg *Vvedenie v Khimiyu Kompleksnykh Soedinenii* (Introduction to the Chemistry of Complex Compounds) (Leningrad: Khimiya, 1971)
34. S A Siling, I I Ponomarev, V V Kuznetsov, B V Lokshin, S V Vinogradova, V V Korshak *Vzaimodeistvie Ftalodinitrilov s Aromaticheskimi Aminami v Fenolakh. Kinetika i Mekhanizm Reaktsii o-Ftalonitrilov s Fenolami* (Interaction of Phthalodinitriles with Aromatic Amines in Phenols. Kinetics and Mechanism of the Reaction of *o*-Phthalonitriles with Phenols (Moscow, 1983); Article deposited at the All-Union Institute of Scientific and Technical Information (VINITI), No. 2858 (1983)
35. S A Siling, I I Ponomarev, V V Kuznetsov, B V Lokshin, V V Korshak, S V Vinogradova *Izv. Akad. Nauk SSSR, Ser. Khim.* 1762 (1984)
36. B A Geller *Usp. Khim.* **47** 537 (1978) [*Russ. Chem. Rev.* **47** 297 (1978)]
37. S A Siling, I I Ponomarev, V V Kuznetsov, B V Lokshin, S V Vinogradova *IX Mezhdunarodnyi Simpozium po Polikondensatsii. Tezisy Dokladov, Budapesht, 1983* (Abstracts of Reports at the IXth International Symposium on Polycondensation, Budapest, 1983)
38. S A Siling, S V Vinogradova *Kondensatsiya Ftalodinitrila s Diaminami v Fenolakh* (Condensation of Phthalodinitrile with Diamines in Phenols) (Moscow 1987); Article deposited at the All-Union Institute of Scientific and Technical Information (VINITI), No. 7478 (1987)
39. S A Siling, S V Vinogradova, N A Klyuev *Izv. Akad. Nauk SSSR, Ser. Khim.* 2145 (1983)
40. S A Siling, I I Ponomarev, V V Kuznetsov, S V Vinogradova, V V Korshak *Izv. Akad. Nauk SSSR, Ser. Khim.* 771 (1984)
41. S A Siling, N N Godovikov, I I Ponomarev, V V Korshak, S V Vinogradova *Izv. Akad. Nauk SSSR, Ser. Khim.* 1371 (1985)
42. S A Siling, I I Ponomarev *Izv. Akad. Nauk SSSR, Ser. Khim.* 1871 (1978)
43. S V Vinogradova, S A Siling, I I Ponomarev, V V Korshak *Vysokomol. Soedin., Ser. A* **21** 138 (1979)
44. V V Korshak, A L Rusanov *Izv. Akad. Nauk SSSR, Ser. Khim.* 289 (1970)
45. S A Siling, I I Ponomarev, N Ya Vasyukova, V V Korshak, S V Vinogradova *Izv. Akad. Nauk SSSR, Ser. Khim.* 2335 (1980)
46. I I Ponomarev, N Ya Vasyukova, S A Siling, B V Lokshin, S V Vinogradova, V V Korshak *Izv. Akad. Nauk SSSR, Ser. Khim.* 1866 (1980)
47. R N Gribkova, T N Balykova, S A Siling, V N Solov'ev, S A Pavlova, S V Vinogradova, V V Korshak *Vysokomol. Soedin., Ser. A* **21** 1294 (1979)
48. V V Korshak, S V Vinogradova, S A Siling, I I Ponomarev *Vysokomol. Soedin., Ser. A* **23** 1120 (1981)
49. S A Siling, P N Gribkova, I I Ponomarev, T N Balykova, I V Vlasova, S A Pavlova, S V Vinogradova *J. Polym. Sci.* **21** 2675 (1983)
50. S A Siling, I I Ponomarev, V G Vasil'ev, L Z Rogovina, G L Slonimskii, S V Vinogradova, V V Korshak *Vysokomol. Soedin., Ser. A* **29** 162 (1987)
51. S A Siling, E F Titova, S V Vinogradova *Vysokomol. Soedin., Ser. B* **30** 357 (1988)
52. C P Wong, G C Berry *Am. Chem. Soc., Polym. Prepr.* **17** 413 (1976)
53. D Y Chen, G M Vekatesh, D J Burchel *J. Polym. Sci., Polym. Phys. Ed.* **20** 509 (1982)
54. V V Korshak, S V Vinogradova, S A Siling, V N Solov'ev *Dokl. Akad. Nauk SSSR* **222** 114 (1975)
55. S A Siling, I A Ronova, G M Tseitlin, S V Vinogradova, S A Pavlova, V V Korshak *Vysokomol. Soedin., Ser. A* **29** 1539 (1987)
56. S A Siling, S V Vinogradova, B N Feofanova, V V Korshak, G M Tseitlin *Dokl. Akad. Nauk SSSR* **299** 633 (1988)
57. French P. 1 504 425; *Chem. Abstr.* **70** 496 (1969)
58. G Rabilloud, B Sillion, G De Gaudemaries *Makromol. Chem.* **108** 18 (1967)
59. M Kurihara *J. Org. Chem.* **34** 2123 (1963)
60. M Kurihara, N Yoda *J. Polym. Sci., Part B, Polym. Lett.* **6** 875 (1968)
61. M Kurihara *Makromolecules* **3** 722 (1970)
62. V V Korshak, Yu E Doroshenko, N K Kharitonova *Dokl. Akad. Nauk SSSR* **200** 114 (1971)
63. V V Korshak, Yu E Doroshenko, N K Kharitonova, N M Chelyzova, V N Muzykantov *Vysokomol. Soedin., Ser. A* **17** 2205 (1975)
64. V N Yarosh, N N Voznesenskaya, E N Teleshov, A N Pravednikov *Vysokomol. Soedin., Ser. A* **18** 1360 (1976)
65. V N Yarosh, N N Voznesenskaya, E N Teleshov, A N Pravednikov *Vysokomol. Soedin., Ser. B* **17** 471 (1975)
66. I V Vasil'eva, E N Teleshov, V N Yarosh, V I Berendyaev, N N Voznesenskaya, B V Kotov, A N Pravednikov *Vysokomol. Soedin., Ser. B* **16** 779 (1974)
67. S V Vinogradova *Vysokomol. Soedin., Ser. A* **27** 2243 (1985)
68. S A Siling *Rev. Roum. Chim.* **34** 585 (1989)
69. S V Vinogradova, in *Advances in Polymer Chemistry* (Moscow: Mir, 1986) p. 75
70. S V Vinogradova, V V Korshak, S A Siling, V N Solov'ev *J. Polym. Sci.* **22** 1043 (1984)

Russian Chemical Reviews **63** (9) 781–796 (1994)
©1994 Russian Academy of Sciences and Turpion Ltd

UDC 577.15.035

Tritium planigraphy of biological systems

A V Shishkov, L A Baratova

Contents

I.	Introduction	781
II.	Fundamentals of the method	782
III.	Study of the accessible surface of proteins. Limits of application of the method	785
IV.	Conformational transitions in proteins	788
V.	Accessible surface and intramolecular dynamics of proteins	789
VI.	Modelling the three-dimensional structure of proteins	790
VII.	Three-dimensional organisation of supermolecular systems	791

Abstract. The transfer of the ideas and methods of nuclear physics and nuclear chemistry to the study of structural biology has led to the creation of a new method of studying the accessible surface and the three-dimensional structure of biological materials. We shall review the papers which have formed a basis for the tritium planigraphy method and the main directions in which the method has developed in its applications to molecular biology problems. The bibliography includes 129 references.

I. Introduction

Recent advances in the study of many biological phenomena at the molecular level have stimulated the search for and development of new approaches to the study of the structure of supermolecular systems, to the determination of the size and composition of the surface of the interacting components in the system, and to the study of the mechanism of specific protein–protein and protein–nucleic acid interactions.

High-resolution (1–2 Å) X-ray structural analysis is the only experimental method capable of giving wide-ranging data on the three-dimensional structure, and therefore also on the surface area of the object. However, its range of applications is limited to a relatively narrow choice of materials, available as highly ordered crystals. In addition to the purely technical problems associated with the growth of these crystals (especially in the case of large and labile complexes) there are difficulties in the interpretation of their complex diffraction patterns. Furthermore, demonstrating the identity in structure of a given compound in a crystalline sample and in solution (the natural working medium of biological systems) remains an unsolved problem.

Because of these difficulties methods such as NMR are still used in studies of relatively low-molecular peptides and proteins.[1]

A V Shishkov N N Semenov Institute of Chemical Physics, Russian Academy of Sciences, 4 Ul. Kosygina, 117334 Moscow, Russian Federation, Fax (7-095) 938 21 56
L A Baratova A N Belozersky Institute of Physicochemical Biology, M V Lomonosov Moscow State University, Vorob'evy Gory, 117400 Moscow, Russian Federation, Fax (7-095) 939 31 81

Received 8 June 1994
Uspekhi Khimii **63** (9) 825–841 (1994); translated by J I Carasso

In the case of large-scale objects (100 nm or more) structural information can be obtained by electron microscopy methods, which (in conjunction with the most recent data processing techniques) offer a resolution of the order of 20 Å, increasing to 5 Å in cryoelectron crystallographic studies.[2,3] This method allows the molecular architecture of complexes to be studied, together with the distribution of the component masses in the complex, the relative localisation of the molecules, and the quaternary structure of the protein (see, for example, Holzenburg et al.[4]).

The new scanning electron microscopy method, which offers the highest reported resolution (~1 Å), must also be mentioned among the methods of studying the surface, but it has not yet achieved the status of a generally usable method. So far its application to biological materials is mainly in general illustration of areas of interest, but we may well find that with some further development the method will provide information at the level of localisation of individual atoms.[5]

Traditional approaches, based on the introduction of various types of probe and of modifier, are widely used in studies of the surface topography and the structure of biological systems. The recently produced low-frequency ESR spectrometers have allowed whole cells and even fragments of tissue to be studied *in vivo*.[6] However, the structural information obtained in this way applies exclusively to local fragments of the object, or (in the most favourable case) to the nearest surroundings of the tracer species, and is totally unrelated to the structure of the sample as a whole. Perturbations which can seriously alter the native structure of the object can be induced by the introduction of probes of various kinds, and should not be ignored when this information is interpreted.

In all the studies listed above the use of modifying agents labelled with radioactive isotopes increases the sensitivity of the detection by a large factor. Successful studies of the selective iodination of surface proteins in cell membranes[7] and of intact hepatitis A virus particles[8] are good examples of this effect.

However, there is also another group of methods based on the use of radioactive indicators. In these methods structural data are obtained directly from the method used to introduce the label, which establishes the accessibility of the various groups in the three-dimensional structure to the particular test label.

A good example of this approach is the study of the surface of specific protein-transfer RNA complexes, in which the label was introduced into the H-8 position of the purine bases of RNA by exchange with HTO water.[9] Of course, there are many cases in

which both groups of methods can be applied: in these, the steric accessibility of the reactive group is established (from the yield of the labelled product) together with its structural surroundings (for example, from the spectral characteristics).

The tritium planigraphy method belongs essentially to the second group. It is characterised by lack of selectivity of the labelling. As will be shown below, it can be used to determine the steric accessibility of the hydrocarbon groups ($-CH$, $-CH_2$, $-CH_3$) to attack by a hot tritium atom under free flight conditions. The result of this attack is the replacement of ^1H hydrogen by its radioactive isotope tritium, which takes place in all the sterically accessible fragments of the object with approximately equal probability and does not affect their properties: the labelled product and the unlabelled initial molecule are chemically identical. The range of application of this method is quite wide, since practically all the biological molecules are derivatives of hydrocarbons. It should be pointed out that the small size of the tritium atom results in a higher level of structural discrimination than can be achieved by using larger probes or labels.

In this review we shall not discuss the various methods of introducing the tritium label: interested readers are referred to the monograph by Neiman et al.[10] We shall instead confine the discussion to the tritium planigraphy method, in which the hot tritium atoms are generated by thermal dissociation of molecular tritium.

II. Fundamentals of the method

The tritium planigraphy method is based on chemical reactions involving fast particles (the so-called hot-atom chemistry), which began to be studied in the 1950s and 1960s. The most important result of these studies was the concept of the excitation function of a chemical reaction, i.e. the dependence of the probability (or cross-section) of the reaction on the energy of the particles. It was shown that in many cases this function has a limiting character, and the cross-section of the reaction increases from zero over a relatively narrow range of energies. Obviously, if several reactions (with different thresholds) can occur together in a given system the process can be shifted in the required direction by varying the energy. Thus, if the particles X and Y can interact by three channels having activation energies E_1, E_2, and E_3, where $E_1 < E_2 < E_3$, all three products can be formed in the system when $E > E_3$. However, if $E_2 < E < E_3$ only two channels are available to the reaction, and lastly for $E_1 < E < E_2$ only one reaction is possible (Fig. 1).

The most important chemical process taking place during the interaction of hot hydrogen atoms with saturated hydrocarbons is the substitution reaction, which (according to the energy of the atoms) can proceed by the direct substitution mechanism (activation energy 1.5 eV)[11,12]

$$RH + \overset{*}{H} \longrightarrow R\dot{H} + H, \quad (1)$$

or through a free radical formation stage

$$RH + \overset{*}{H} \longrightarrow \dot{R} + H_2, \quad (2)$$

$$\dot{R} + \dot{H} \longrightarrow RH, \quad (3)$$

where the asterisk denotes a hot atom and the dot denotes a free radical. The limiting step is the removal of the hydrogen atom, whose activation energy lies between 0.3 and 0.4 eV (depending on the bond type).[13] The recombination reaction (3) has a zero activation energy, and takes place with the participation of hot hydrogen atoms. The nonreactive collision is accompanied by loss of energy (thermalisation) of the hot atom:

$$RH + \overset{*}{H} \longrightarrow (RH)' + H, \quad (4)$$

where $(RH)'$ is an excited molecule. The probability of the collision and the amount of energy transferred in a single collision depend on the velocity of the incident particle, and also on the structural and energy characteristics of the partner molecule. When ordinary hydrogen is replaced by its isotope (tritium) the product of the substitution reaction is labelled. As a method of studying the accessible surface and the three-dimensional structure of the object tritium planigraphy is applicable only under conditions in which the chemical substitution reaction leading to the incorporation of the label occurs at the first collision between the hot atom and the hydrocarbon molecule. Obviously, this requires a source of atoms having energies which satisfy the condition $0.3 < E < 1.5$ eV and $E - \Delta E < 0.3$ eV, where ΔE is the loss of energy accompanying a nonreactive collision. In this case one nonreactive collision makes the subsequent reaction impossible, and only reaction (2) (hydrogen removal) is observed in the system.

The ideal variant would seem to be the presence of a source of monoenergetic particles having energies in the required range, but this is extremely difficult to realise in practice. The tritium planigraphy method relies on the atomisation of diatomic gases on heated metal filaments, first studied by Langmuir.[14] On the surface of an incandescent filament the gas molecules dissociate into atoms, which are emitted from the surface with an energy corresponding to the temperature of the filament. This method was used in studies[15,16] of the reactions between oxygen and hydrogen atoms.

At a filament temperature of 2000 K the average energy of the emitted atoms is 0.17 eV, and in the Maxwell spectrum of the atomic beam ~25% of the atoms have an energy sufficient to displace hydrogen ($E \geqslant 0.3$ eV).[17] The proportion of the particles having energies of 1.5 eV, and therefore able to replace hydrogen by the direct substitution mechanism [reaction (1)], is small (<3%), and therefore reaction (1) can be ignored.

Attempts to use the thermal activation method to prepare labelled compounds began in the middle 1960s. Moser et al.[18] bombarded films of sugars with tritium atoms, and obtained labelled products, but the high yield of decomposition products even then raised serious doubts as to the practical value of the method. For the same reason other similar studies (for example, early attempts to label whole granules of starch)[19] have not been developed further. It was found that the main decomposition mechanism was the use of excessively thick targets, which suppressed the removal of heat from the reaction zone. The surface of the target became heated by absorbing the luminous radiation of the filament, by heat transfer through the molecular gas, and also by the heat evolved by the reaction of the tritium atoms with the substance. It was subsequently shown that by using effective heat removal procedures almost 100% of the substance

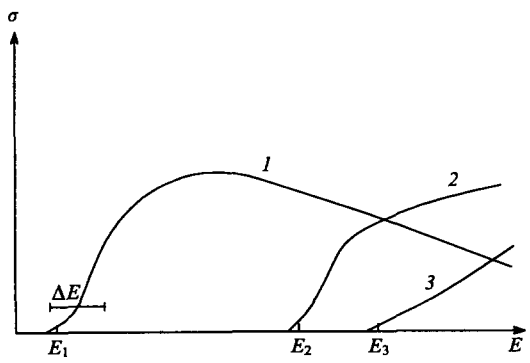


Figure 1. Dependence of the probability of a chemical reaction (σ) on the energy of the interacting particles (E) for three possible channels with thresholds E_1, E_2, and E_3: ΔE is the loss of energy for a single nonreactive collision.

could be preserved.[20] This required working with thin layers of organic materials and cooling the target with liquid nitrogen. Even after a long exposure the temperature of the target was not more than 10–15 K higher than the liquid nitrogen temperature.[21] A low target temperature (77 K) suppresses the mobility of the free radicals formed by hydrogen removal, and therefore the main path for their disappearance is the recombination with thermalised tritium atoms with formation of the labelled initial molecule [reaction (3)].

The possibility of studying the accessible surface and the three-dimensional structure of the macromolecules is due to the small penetration depth of the tritium atoms which are able to react with the target atoms. The direct measurement of the depth of penetration of the reactive tritium atoms is experimentally difficult. However, this quantity can be calculated by making certain assumptions, and it can also be obtained from some indirect results. The calculations show that for tritium hot-atom initial energies close to the threshold energy of the removal reaction even a single nonreactive collision is sufficient to transfer the particle to a region in which hydrogen removal becomes impossible. Fig. 2 shows the dependence of the fractional number of tritium atoms with an energy $E \geqslant 0.3$ eV upon the depth of penetration into a layer of organic compound. It can be seen that whereas at X = 0 (i.e. at the surface of the object or at the first collision of the tritium atom with the molecule) the fractional number of reactive atoms is 26% this value decreases to 0.4% when the atoms have penetrated within the layer to a depth of only 6 Å. In practice the free path of the reactive atoms (the thickness of the reaction layer) is even smaller, since their number in the beam passing through the target is lowered also by a chemical reaction whose cross-section is comparable to the collision cross-section in the case of atoms with an energy higher than the threshold value.[10] This means that if a macromolecule is used as the target the distribution of the label over its fragments becomes a measure of its steric accessibility for a collision with the primary bombarding particle, i.e. it characterises the surface area of the macromolecule accessible to the tritium atoms. The thickness of the reaction layer can also be estimated from the results of experiments on the introduction of a tritium label into adsorption layers of surface-active substances with hydrocarbon chains of different lengths

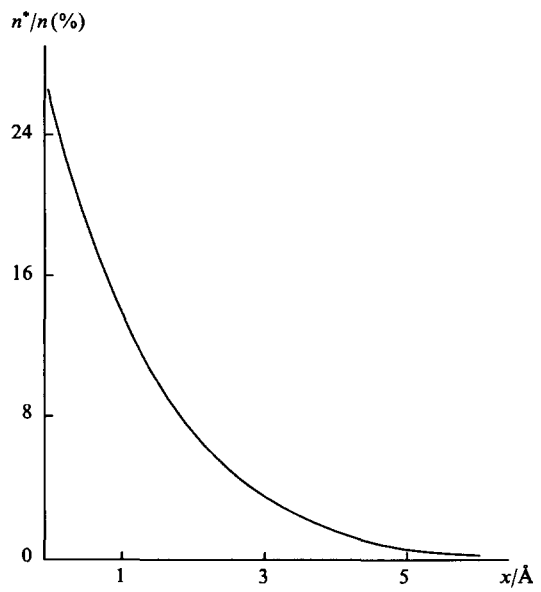


Figure 2. Decrease in the relative number of reactive particles during the passage through a layer of thickness x in a condensed organic substance (calculated for atoms with a temperature of 2000 K under conditions of elastic retardation, $E_{act} = 0.3$ eV).

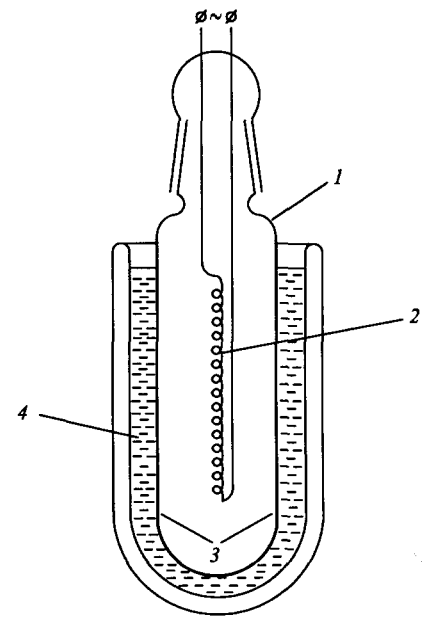


Figure 3. Glass reactor for tritium bombardment.

(from C_1 to C_{16}).[22] From the dependence of the yield of labelled product (incorporation of the label) on the length of the molecule and on its orientation at the interface it was concluded that a change in layer thickness by one methylene group, i.e. by ~3 Å, has a marked effect on the yield of labelled product. This length can be used as a quantitative characteristic of the thickness of the reaction layer. A similar value is suggested by experiments on the incorporation of tritium into myoglobin, which will be discussed below.

The apparatus used in all the experiments on tritium labelling is shown in Fig. 3. The central part of the apparatus (the reactor) is a cylindrical glass vessel (*1*) fitted with an axial tungsten wire (*2*) heated by an electric current. The target material (*3*) is deposited as a thin film on the side wall of the vessel, which is cooled in liquid nitrogen (*4*). The reactor is evacuated to a residual pressure of 10^{-5} Torr, and gaseous tritium is then admitted into the system. In the reaction vessels used in the majority of experiments (60 mm in diameter) the pressure of molecular tritium was 5×10^{-3} Torr. When the filament was heated to 2000 K the tritium was atomised on its surface, and the resulting atoms (formed under conditions of free flight to the target) were allowed to bombard the walls of the reactor. Experimental details and the sequence of operations have already been discussed in some depth,[10] and in this review we shall confine ourselves to examining the methods of preparation of the target and the general methodology adopted for analysing the distribution of the label.

The simplest method is the lyophilisation of a solution of the substance. However, if this method is chosen it is essential to ensure that the resulting film is firmly attached to the reactor walls over the whole of its internal surface. Furthermore it should not be forgotten that the lyophilic drying process may itself influence the structure of the substance under study.

In order to study the structure of the macromolecule in solution a target can be prepared by 'smearing' the experimental solution as a thin film by rapidly rotating the reactor immersed in liquid nitrogen. In many cases this method gives good results, but there are at least two aspects which limit its application. The first is the crystallisation of the water induced by the relatively low rate of cooling. When the vessel is immersed in liquid nitrogen the latter boils, forming a layer of gas bubbles close to the wall which slows down the cooling. This effect can be avoided by choosing other cooling agents (for example, liquid ethane), but working with this

gas has some undesirable features. The formation of a crystalline phase of ice must be avoided in work with materials containing 'internal' water, such as macromolecules and their complexes (including clusters) including more than 10 water molecules, liposomes, and whole cells.

The second limitation is due to the specific features of the method. Since the incorporation of the label is confined to a zone accessible to the first collision of the tritium atom incident from the gas phase, i.e. to the surface of the target, and in practical experiments the specific radioactivity is measured, it is essential to know, or at least to be able to control, the concentrations of the solute at the surface and in the bulk of the sample. In the method of target preparation described above a liquid solution exists for a certain time, giving a water–air interface. Therefore the bombardment by atomic tritium is experienced by an adsorption layer of molecules, whose parameters are determined by the adsorption process. The concentration of solute molecules in this layer is described by the adsorption isotherm. It is most convenient to work under conditions of complete saturation of the surface layer: these offer adequately reproducible results even when the surface concentration of the substance is not known. Calculations show that for solutions of macromolecules the time of formation of the saturated layer is a few minutes ($\sim 2-5$ min), which is of the same order as the time of preparation of the sample. The formation of a saturated layer is confirmed by the observed dependence of the time on the concentration of the solution.[22] In the case of amphiphilic substances the use of this method of target preparation can lead to the orientation of the molecules with respect to the phase separation boundary, and in this case the distribution of the label will represent the character of the orientation rather than the structural features of the object. In substances of low-molecular mass the orientation effects are especially clearly displayed. The orientation of macromolecules requires long times, and their amphiphilicity is weaker.

Both these difficulties (crystallisation of the water and the contribution from adsorption processes) can be avoided by rapidly freezing the solution using a 'spraying' technique. The solution is sprayed as very small droplets onto the inner surface of the reactor previously cooled in liquid nitrogen by using a specially designed nebuliser. The lifetime of each drop, and therefore also of the water–air interface, is small (equal to the time of flight from the nozzle of the nebuliser to the wall), and adsorption cannot take place. However, the rate of cooling of the drop incident on the reactor surface at 77 K is so high that the solution solidifies as a glass. Under these conditions we find a state of affairs similar to that which exists on a freshly cleaved solid surface. The concentration of molecules on the cleaved surface can be related to that in the bulk by the simple expression $C_s = C_v^{2/3}$. The dependence of the activity taken up by the sample on the concentration ($I = C_v^{0.67}$) is found to be consistent with the above relationship in experiments with both substances of low-molecular mass and solutions of proteins.[10,22,23].

Yusupov and Spirin[24] proposed an original method of target preparation which avoided the artefacts associated with the crystallisation of water and with the adsorption of the solute on the phase separation surface. A solution or suspension of the sample was introduced dropwise into liquid nitrogen. The very small particles of ice formed in this way were crushed directly in the liquid nitrogen, and this 'slurry' was deposited on the reactor walls. The liquid nitrogen quickly boiled off, and the ice particles were left firmly adhering to the reactor wall. The results obtained confirm the effectiveness of the proposed method, but its practical application requires special skills.

When considering the technique of the method we must particularly note the special factors which determine the reproducibility of the results obtained. Among customary factors, such as the precision of radioactivity measurement and of the determination of temperature of the wire, of the pressure of molecular tritium, of the exposure time, and also of the errors introduced by the chosen method of analysis, we should include the reproducibility of the total surface area of the target bombarded by the tritium atoms. When the techniques of solution spraying or evaporation from a suspension are used it is difficult to achieve good reproducibility of the total target area. To ensure a correct comparison of the results of independent experiments we must normalise the reported values with respect to the total flux of tritium atoms reacting with the target surface. Obviously, the latter quantity corresponds to the total radioactivity of the sample, including the activity of the sample itself and that of the solvent. If all the other standardisation conditions are observed (for example, the mass of the label attached to the C–H bond) the assignment of the radioactivity of the substance under study to the flux of tritium atoms should be constant for a given substance. An additional method (in some cases, the only possible method) of standardising the experiment is to use a different kind of monitor: organic substances placed at a fixed distance from the filament. Monitors of this type include various polymer films, cellulose or paper filters, etc.

In studies of proteins the transition from the amount of label included to the determination of the steric accessibility (or, in other words, of the accessible surface area) requires an allowance for the probability of the incorporation of tritium into aminoacid residues of different types under identical exposure conditions. These calibrating coefficients are needed also in all other cases of experimental samples consisting of components of different chemical nature. Several attempts have been made to determine the relative reactivities of aminoacid residues by comparing free aminoacids[25] and short peptides,[23] and determining the inclusion of the label in the aminoacid residues and in proteins with known three-dimensional structures in which the accessibility (exposure response) of the residues could be calculated from X-ray structural analysis results. Though the results of different workers, obtained for different systems, show some discrepancies they can be summarised as follows:

(1) in proteins we find a linear relationship between the amount of label incorporated and the accessible surface area calculated for the hydrocarbon fragments of the aminoacid residue;

(2) the nature of the neighbouring residue on the polypeptide chain does not affect the amount of label which is taken up (if normalised for unit area of accessible surface); this amount is also independent of the site on which the residue is located (the N or the C end of the peptide);

(3) the inclusion of the label in the residues of different aminoacids has almost equal probabilities when calculated for a single C–H bond or for unit area of accessible surface.

The results obtained by Gedrovich and Badun[23] deserve a special mention: these workers found that in the composition of di- and tripeptides the relative reactivities of three aminoacids (valine, leucine, and isoleucine) are several times higher than those of other aminoacids. This effect was ascribed to the presence (in the side group) of tertiary carbon atoms, from which the removal of hydrogen is substantially easier than in other configurations.[26] Table 1 shows the probabilities of including the label into the residues of aminoacids, established experimentally for the model protein lysozyme. We consider these results to be among the most reliable.

In conclusion we should dwell briefly on the general methodology used in the analysis of the distribution of the label in the experimental object. It varies according to the particular problem being studied, and it is determined by the required level of 'resolution'. Even the first stage [the determination of the overall amount of label remaining in the sample after removal of the labelled solvent, i.e. the sum of the labile (exchangeable) and of the stable labels (held in the C–H bond), and also the labelled water strongly bound to the surface of the macromolecule] allows us to determine the total area of accessible surface of the sample. Since the overall amount of label is usually 2–3 orders of magnitude

Table 1. Probability of including the label (K) in the aminoacid residues of lysozyme, normalised for unit area of accessible surface of the hydrocarbon fragment ($C_\alpha - H$, side groups).[45]

Aminoacid residue	K[a]	Aminoacid residue	K[a]
Lys	0.12	Pro	0.11
His	0.16	Ala	0.12
Arg	0.10	Val	0.11
Asx	0.10	Ile	0.10
Glx	0.20	Leu	0.08
Thr	0.10	Tyr	0.07
Ser	0.10	Phe	0.09
Gly	0.09		

[a] Standard deviation 20%.

greater than the amount of stable label in the C–H bonds the differences between the probabilities of interaction of tritium with aminoacids of different types are quite unimportant.

Preliminary estimates can be made, and a fairly wide range of problems whose solution requires a knowledge of the total aminoacid content of the solvent can be examined, by determining the label incorporated in aminoacids of different types. To this end the protein freed from the labile label (by dialysis, chromatography, electrophoresis, etc.) is hydrolysed, and the inclusion of the label in individual aminoacids is determined by analysing the hydrolysates and at the same time measuring their radioactivity.

Often we need to know the distribution of the label along the polypeptide chain of a protein. In this case the protein is fragmented into peptides, the mixture of peptides is separated, the peptides are identified and hydrolysed, and lastly the inclusion of label in each aminoacid is determined. Obviously, in an ideal situation, peptides in which each aminoacid occurs only once are produced by the fragmentation of the protein. In practice this state of affairs is very seldom met, but every effort is made to minimise the number of repeat occurrences. Lastly, a sequence of peptides with an analysis of the activity in each of the aminoacids removed is also possible.

Thus, by correctly preparing the target, labelling the sample, and choosing an appropriate strategy for analysis of the distribution of the label, the latter parameter can be used to construct a model of the three-dimensional structure. This possibility was first demonstrated in a study of labelled myoglobin.[27] According to the X-ray structural analysis results the N end of the protein fractions is an α-helix A, including the residues 3–18 (Fig. 4) and oriented so that part of its surface is directed outwards, and part is in the 'shadow' produced at its contact with the G and H helices where A connects them with a chain fragment.[28] The distribution of the label in the N end of the protein (aminoacid residues 1–20) shows that the label is incorporated only in the aminoacid residues pointing outwards, and not in those localised in the region of contact and therefore not accessible to the tritium. A reasonably good correlation was obtained in comparisons of the incorporation of the label with the area of the accessible surface in the same residues, calculated by the method of Lee and Richards[29] from X-ray structural analysis data. This experiment confirmed earlier reports of the dependence of the take-up of the label on the three-dimensional structure in peptides, and predicted the possibility of developing a new experimental method of studying the structure and the topography of the accessible surface of macromolecules and of supermolecular systems: the tritium planigraphy method.

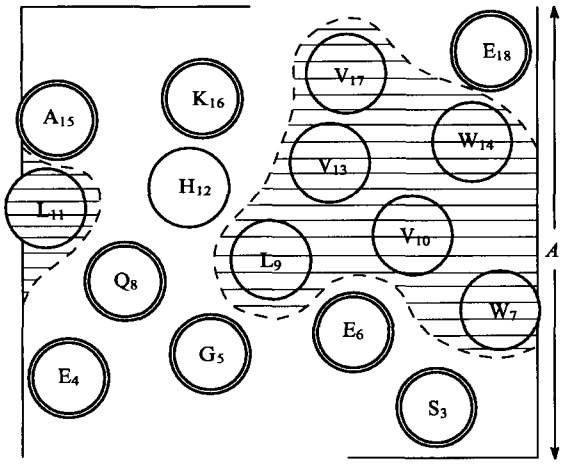


Figure 4. Schematic of the 'unfolding' of the surface of the α-helix region A of the whale myoglobin protein (residues 4–18). The one-letter code is used for the aminoacids. The cross-hatched regions are aminoacid residues sterically inaccessible to the tritium atoms (regions of 'shadow').

III. Study of the accessible surface of proteins. Limits of application of the method

The interaction of polymeric molecules takes place through groups of atoms localised on their surface. Methods proposed to describe the surface (Fig. 5) include determining the area of the macromolecule surface accessible to water molecules: this was found to be a very important concept, because this surface plays a fundamental role in the formation, stabilisation, and operation of the native structure of biopolymers. A new term was created by Lee and Richards[29] to describe it: the 'accessible surface'. It denotes the surface which can accommodate the centres of spherical test species (probes) with a radius of 1.4 Å (approximately equal to the radius of water molecules) in contact with the van der Waals surface of the macromolecule. The macromolecule itself is treated as an assembly of atoms approximating van der Waals spheres, and the coordinates of their centres are determined by high-resolution (1–2 Å) X-ray structural analysis. Lee and Richards obtained a quantitative description of the accessible surface by applying a specially developed computational algorithm, which they used to calculate the accessible surface area of three globular proteins: lysozyme, ribonuclease A, and myoglobin.[29] These calculations were subsequently applied to a series of other globular proteins, whose three-dimensional structure was thus determined with an acceptably high resolution.

The great functional importance of the surface of macromolecules, and its relationship with the characteristics of their three-dimensional structure, stimulated a large number of studies (mainly theoretical) of various aspects of the correlation of the area, composition, and topography of the surface with the globule

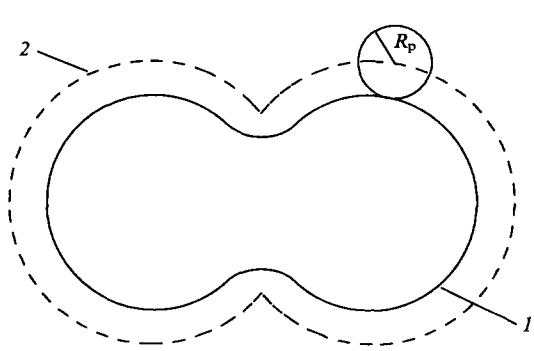


Figure 5. Description of the 'surface' by testing with a spherical probe of radius R_p in a two-centre system.[30] (*1*) contact surface; (*2*) accessible surface.

volume, the molecular mass of the protein, its packing density, and other parameters of the three-dimensional structure (see, for example, Refs 31–36).

In recent years the surface of macromolecules has been analysed increasingly by the molecular cartography method, which allows almost the whole of the protein surface to be 'viewed' simultaneously.[37] By using these charts Barlow and Thornton[38] studied the distribution of charged groups, and Fanning et al.[39] and Novotny et al.[40] studied the topography of the protein surface with the aim of localising the antigenic centres. An analysis of the surface features can be carried out by super-imposing three different charts.[41] This analysis of the nature of the accessible surface provided an unambiguous interpretation of the hydrophobic properties of proteins, calculated exclusively from their aminoacid composition. The concept of an accessible surface has proved very fruitful in the construction of models of the self-organisation of the polypeptide chain.[42–44]

Without belittling the value of the computational methods of determining the accessible surface we note that all the calculations are based on high-resolution X-ray structural analysis results. There is no doubt that the tritium planigraphy method now offers the fullest possible information on the accessible surface of the object. As stated above, this method relies on establishing the steric accessibility of the hydrocarbon groups (CH, CH_2, and CH_3) of all the component units (in the case of proteins, the aminoacid residues) in the substance under study, and provides information on its surface. As could have been expected, a simple relationship has been observed between the specific radioactivity (A) and accessible surface area calculated by the Lee and Richards algorithm (S): $A = kS$, where k is the probability of finding the label in the aminoacid residue of a given type, normalised for the accessible surface area. By using model proteins with known three-dimensional structures it was shown that this relationship applies for the majority of protein residues.[27,45] In most cases the results corresponded to those given by calculations of the accessible surface by the Lee and Richards algorithm.[29] However, some discrepancies were noted: these were associated with special features of the mechanism chosen to introduce the label and with the difference in size between the tritium atom and the water molecule. A new model, proposed to eliminate these contradictions, describes the accessibility to tritium atoms of fragments of the sample on the assumption that any scattering event must result in loss of reactivity.[46] A calculation by this model for the 20 N end residues of myoglobin gave a better agreement with previously reported[27] experimental data. The effective radius of the tritium atom (1.1 Å) was found, as expected, to be smaller than the radius assumed for a water molecule.

It should not be forgotten that the surface defined by the tritium planigraphy method differs in principle from the accessible surface in its generally accepted sense. In the surface accessible to the incorporation of the label there are no atoms not directly linked to hydrogen atoms (in the proteins these are the oxygen atoms of the carbonyl groups, =C=O, in disulfide bonds and in methionine they are the sulfur atoms). There are also no groups from which the label is readily removed by exchange with water (the −OH, −SH, $-NH_2$, =NH, and −COOH groups). The fragments which are sterically inaccessible to reactions with tritium atoms incident on the surface with a rectilinear trajectory are also not included. As a result, the surface determined by tritium planigraphy includes breaks associated with the regions containing the atoms and groups of atoms listed above, whereas the surface calculated by the Lee and Richards algorithm is free from discontinuities.

It is legitimate to ask to what extent and between what limits the tritium planigraphy data can be correlated with calculations of the accessible surface by the 'sliding' probe method. To answer this question the radius of the probe approximating the tritium atom, for which the calculation by the algorithm which assumes 'lining' of the van der Waals surface agrees most accurately with experiments on the incorporation of the label, had to be determined. It was also necessary to determine the limits between which these data can be extrapolated to test probes having other radii. These studies were carried out with the model protein lysozyme, for which high-resolution X-ray structural analysis data are available, and the accessibility profile of the aminoacids towards the introduction of the tritium label was established.[47]

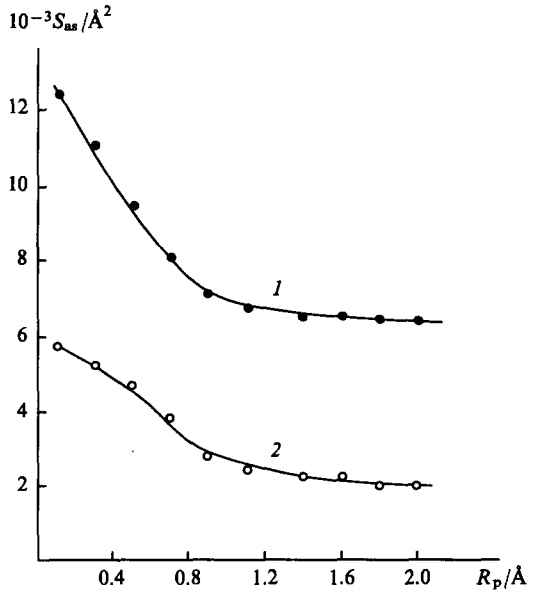


Figure 6. Dependence of area of accessible surface in a lysozyme globule upon the radius of the test probe (R_p). (*1*) Accessible surface of the globule (S^{Σ}_{as}), (*2*) accessible surface of the hydrocarbon fragments (S^{CH}_{as}).

By using a slightly modified algorithm (as compared with that proposed by Lee and Richards) the surface area of the protein accessible to probes with radii between 0.1 and 2.0 Å (and even 10.0 Å) was calculated for each aminoacid residue and for the protein globule as a whole. The calculation was carried out separately for each residue, including the 'labile' hydrogen-containing groups (S^{Σ}_{as}), and only for the hydrocarbon fragment (S^{CH}_{as}) of the aminoacid. Fig. 6 shows the dependence of the accessible surface area of the protein globule upon the radius of the test probe. It can be seen that for low radii (from 0.1 to 1.0 Å) the accessible surface decreases sharply (by ~40%) as the radius is increased, an effect ascribed to the smoothing of the surface topography. For probe radii greater than 1.0 Å the S^{Σ}_{as} value stays almost constant until it begins to increase again for the largest probes (10 Å) as a result of the increased radius of the 'sliding' trajectory. For a probe with a radius of 1.4 Å (the water molecule) the calculated value of S^{Σ}_{as} stays practically constant at the level of 6510 Å^2, which is close to the value of 6710 Å^2 obtained by Lee and Richards.[29] The best agreement between experiment and calculation is obtained by assuming a sphere with a radius of 0.9 Å as an approximation to the tritium atom (Fig. 7).

Fig. 8 shows experimental and calculated accessibility profiles for the peptide chain of the protein. Data on the inclusion of the label are presented as the ratio A/K, which is equivalent to the accessible surface area (in Å^2). It can be seen that on the whole the correlation between the two distributions is acceptably good. Accessibility calculations for probes having different radii showed that the results obtained for a tritium atom assumed to have a radius of 0.9 Å can be extrapolated with reasonable assurance to probes having radii of up to 2 Å for aminoacid residues with a high (> 50%) or a moderately high (20% – 50%) average level of accessibility if the ratio of the residue areas (in the composition of the protein molecule) to the area of a hypothetical fully unfolded

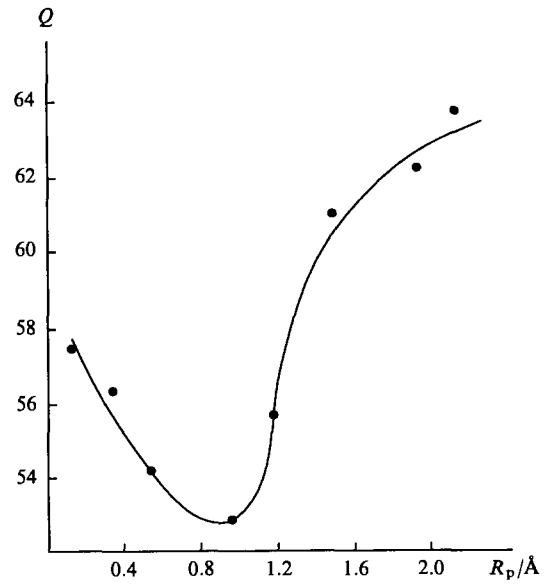


Figure 7. Deviation function Q, describing the discrepancy between calculated and experimental data for test probes having different radii. The minimum of the function corresponds to an effective radius of the tritium atom of R = 0.9 Å.

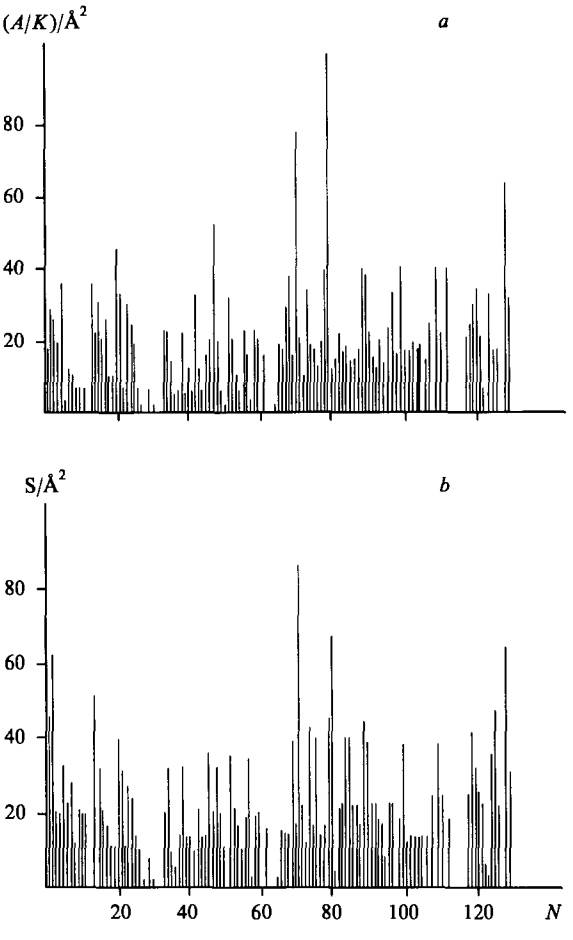


Figure 8. Accessibility profile of the polypeptide chain in lysozyme, obtained experimentally by introducing the label (*a*) and calculated for a test probe of radius 0.9 Å (*b*). A/K is the specific activity of the aminoacid residues, normalised for the probability of incorporating the label, S is the accessible surface area in Å², N is the number of the aminoacid residue in the protein sequence.

polypeptide chain for a probe with a radius of 1.4 Å is taken as a measure of the accessibility (the *trans*-peptide Ala–X–Ala is a suitable model compound). In the case of poorly accessible residues (< 20%) the data on the incorporation of the label should be interpreted with some caution. However, the proportion of these residues on the surface of the macromolecule is not large, and it cannot introduce a significant error into the final result. In the determination of the total area of the protein their contribution balances out.

In the same investigation the coefficients needed to convert the accessible surface area of the hydrogen fragment into the total area of the residue ($S_a^{CH} = \gamma S_{as}^{\Sigma}$) were determined. It was found that the parameter γ depends not only on the nature of the residue (which is not surprising) but also on its level of accessibility in the tertiary structure. However, at the level of the entire globule this quantity remains constant over a wide range of probe radii (0.4 ± 0.06). We note that according to Chothia[81] the fractional amount of accessible surface formed by nonpolar atoms (mainly, the hydrocarbon fragments) depends on the molecular mass of the protein: it decreases as the latter increases. In the work of Lee and Richards[29] this fraction was 0.392 for lysozyme, which corresponded to the value obtained by Bogacheva et al.[47]

Gedrovich et al.[55] suggested an approach which allows quantitative estimates of the total accessible surface area of the protein from the amount of label included in the aminoacid residue groups which are free to exchange and in the water molecules firmly bound to the surface (hydration shell). They examined a group of proteins having known three-dimensional structures (lysozyme, ribonuclease S, myoglobin, papain, subtilisin, and α-chymotrypsin), and obtained a linear dependence in $\lg I - \lg S$ coordinates. The straight line thus obtained can be treated as a calibrating plot, and used to determine the accessible surface area of globular proteins of unknown structure (Fig. 9). Calculations of this type carried out for the globular protein parvalbumin III found in the pike gave an accessible surface area of 5700 ± 900 Å². Using the empirical dependence of the accessible surface area on the molecular mass of the protein gave[34] an area of 5800 Å².

The results of experiments with proteins whose three-dimensional structure had been determined by high-resolution X-ray structural analysis allowed the method to be extended to objects on which structural information was inadequate or totally absent.

Thus an analysis of the specific labelling of aminoacids in the overall hydrolysate of the protein led to reasonable conclusions on various parameters of the periphery of human serum albumin,[45,49] for which available X-ray structural analysis data had a resolution of 6 Å which was insufficient for the calculation.[48] It was found that (as compared with that of lysozyme) the accessible surface of the albumin was enriched in hydrophobic aminoacid residues, which accounted for 63% of the total aminoacid content

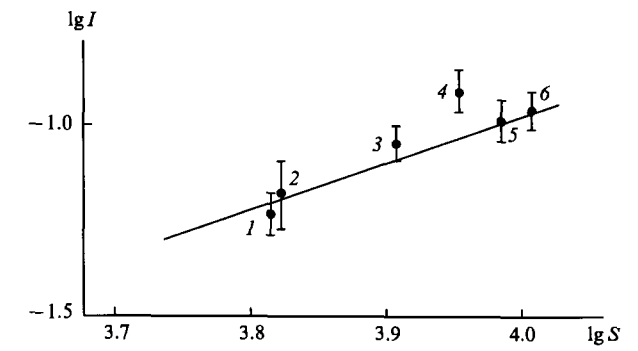


Figure 9. Dependence of the reduced radioactivity on the accessible surface area of proteins. (*1*) Lysozyme, (*2*) ribonuclease S, (*3*) myoglobin, (*4*) papain, (*5*) subtilisin, (*6*) α-chymotrypsin. The I value includes the label in the C–H bonds, in the labile groups, and in the strongly held water, normalised for the flow of tritium atoms.

of the surface (whereas in lysozyme the amount was 18%). Summing the accessible surface areas in the aminoacids and allowing for the number of residues of each type gives[45] a total area $S_{as}^{CH} = 19\,900$ Å^2. Using the ratio $S_{as}^{CH}/S_{as}^{\Sigma}$, whose value is 0.4 for lysozyme, gave a total area of 49 000 Å^2 for the protein. Using the empirical dependence of the accessible surface area of a fully unfolded polypeptide chain on the molecular mass gave a coefficient of 0.48 for the degree of unfolding of the polypeptide chain. By treating the albumin globule as an ellipsoid of revolution with axes of 140:40:40 Å important structural parameters of the surface were determined:[50] for example, the 'roughness coefficient' of the native protein was found to be 2.7. For the lysozyme molecule the corresponding unfolding and roughness coefficients were 0.68 and 1.7. From these results we may conclude that the packing is less compact (and the surface topography is more broken) in the polypeptide chain of human serum albumen than in lysozyme, in good agreement with the known physicochemical properties of this protein and above all with its strong hydrophobicity.[51] The openwork appearance of its three-dimensional structure is confirmed by many data on the capacity of albumin to bind low-molecular hydrophobic substances (for example, fatty acids), and is consistent with reports of the presence of several hydrophobic cavities in the molecule of this protein.[52] The rough packing of the albumin globule is also consistent with views on the flexibility of this molecule and on its tendency to undergo volume fluctuations.

Bobkova et al.[53,54] reported a comparative study of the surfaces accessible to label introduction in two important enzymes of protein biosynthesis (aminoacyl-tRNA-synthetase). The two enzymes (phenylalanine-tRNA-synthetases from *E. coli* and *Thermus thermophilus*) have complex quaternary structures. The similarity in structure (at least, in the region of the active centres of these enzymes) suggests that the thermophilic enzyme catalyses the aminoacylation reaction of tRNA from *E. coli*, whereas the enzyme from *E. coli* can catalyse the aminoacylation of the thermophilic tRNA. The enzyme from *Thermus thermophilus* was obtained in the form of crystals suitable for use in X-ray structural analysis, but attempts to prepare crystalline phenylalanine-tRNA-synthetase from *E. coli* were unsuccessful. In these circumstances the tritium planigraphy method is one of the few methods available for studying the surface structure of the enzyme from *E. coli* and for comparing it with that of its thermophilic analogue. Fig. 10 shows the diagrams defining the surface areas of the aminoacid residues for the two proteins, obtained from data on the specific activity of the aminoacids and of the total hydrolysates of the proteins. We note a fairly high level of hydrophobicity in the surface of the proteins (60% for the enzyme from *E. coli* and 67% for the thermophilic protein). Comparing the data for the degree of hydrophobicity and for the overall sum of hydrophobic residues in the two proteins shows that this distribution is approximately the same for the mesophilic and the thermophilic synthetase being studied. The proportionate increase in hydrophobicity on the surface and in the inner parts of the protein globule on passing from the mesophilic to the thermophilic enzyme is a very interesting effect. However, the possibility of identifying the difference in the aminoacid residues localised on the surface of the protein is even more important. The increased accessibility of the arginine residues in the identifiable composition of the aminoacyl-tRNA-synthetase led to an explanation[53,54] of the increased sensitivity to exposure of the charged residues on the globule surface in terms of the tendency of the thermophilic tRNA-synthetase to compensate the destabilising action of the high temperature by using additional electrostatic interactions with the substrate.

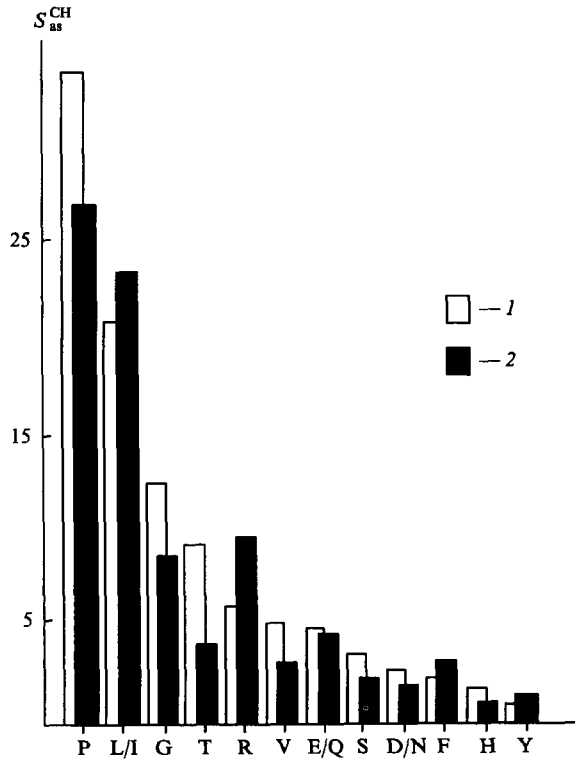


Figure 10. Aminoacid composition of the accessible surface phenylalanine–tRNA–synthetase from *E. coli* (*1*) and from *Thermus thermophilus* (*2*) expressed as a percentage of the total area of the globule.

Similar studies had been previously carried out with the Fe- and MoFe-proteins of the azotobacter nitrogenase.[10] Without discussing these results in detail we shall only point out that they yet again confirm the possibility of obtaining valuable structural information from a relatively simple experiment.

IV. Conformational transitions in proteins

Obviously, any changes in the three-dimensional structure of a macromolecule must affect the topography of its accessible surface. This suggests very promising applications of the tritium planigraphy method in studies of conformational transitions. Volynskaya et al.[56,57] demonstrated this prospect in a study of the denaturation of lysozyme by 8 M urea with reduction of the disulfide bonds. Distribution of the label on the aminoacid residues in the denatured form differs markedly from the native distribution and approaches random distribution. The latter was calculated by using the tripeptide Ala–X–Ala as a model,[29] allowing for the probability of incorporating the label. Of course, this model can only be accepted as a crude approximation. In the analysis of the real structure of the denatured state we must allow for the mutual screening of the residues by their nearest neighbours, and also for the possible orientation of the polypeptide chain on the surface of the target. Nevertheless the calculated and the experimental distribution of the label in the fully denatured form are reasonably close.

We note that, under the influence of 8 M urea only, a state having a well-defined structure is formed without breaking the S–S bonds. It is characterised by an accessibility of the hydrophobic aminoacid residues greater than in the native material, coupled with a small change in the accessibility of the hydrophilic groups. This is interpreted[56,57] as a breakdown of the hydrophobic contacts although the globular structure as a whole is retained. The interpretation is consistent with independent data on the viscosity of the protein solutions in the presence of 8 M urea, on the circular dichroism (CD) spectra, and on optical rotary dispersion.[58,59]

The high sensitivity of tritium planigraphy led to the detection of intermediate states of the protein, formed as a result of weak denaturing interactions and not revealed by traditional

methods.[56] One of these states can be induced by adding 1 M lithium chloride and is characterised by an accessibility of the polar aminoacid residues substantially lower than in the native conformation, while the accessibility of the hydrophobic residues is almost unchanged. This transition can be treated as a 'compression' of the globule. Conversely, another state is characterised by an increased accessibility of all the types of aminoacid residue, and is induced by the addition of 1 M urea and guanidine·HCl. This transition is similar to an unfolding of the globule while retaining all the other structural characteristics (viscosity, CD spectra, etc.). Obviously, in this case we are dealing with a slight 'loosening' of the packing of the elements in the secondary structure without dissociation and without changes in the overall architecture of the globule. A similar type of intermediate state was detected also in ribonuclease.[60]

The conformational transitions observed in lysozyme have been compared with the changes in enzyme activity. By using the rate of lysis of *Micrococcus lysodecticus* as a test it was shown that the 'compression' and the 'loosening' of the lysozyme globule result in a decreased enzyme activity, the 'compression' effect being the stronger. Similar changes were observed in ribonuclease A.[60] Low salt concentrations (0.1–0.2 M) produced compression of the protein globule, accompanied by a rapid decrease in the enzyme activity. Under these conditions the intramolecular mobility of the protein, monitored as its mean-square deviation $\langle X^2 \rangle$ from Rayleigh scattering data for the Mössbauer radiation, is also substantially lowered. Unlike the addition of salts, low concentrations of urea produce a loosening of the protein globule also accompanied by a decrease in the enzyme activity. In this case complete loss of enzyme activity was observed only in the presence of 8 M urea.

The results of studies by tritium planigraphy of pH-dependent conformational transitions in proteins call for a detailed discussion. These changes often play a key role in the functioning of macromolecules, and in this case changes in the pH of the medium are one of the factors which control their biological activity.

Human serum albumin is one of the most important proteins in blood plasma, whose function is mainly to control the transport of various kinds of biologically active substances. It is known to undergo various pH-dependent conformational changes, of which the most striking are the N–F and the N–B transitions, taking place in acid (pH 3.5–4.5) and in alkaline media (pH 7.0–9.0) respectively.[61,62] In spite of extensive studies the nature of these structural transitions is not well understood.

A comparative study by tritium planigraphy of the accessible surface of a protein in the N, F, and B form produced some valuable structural information.[63,64] It was found that in the N–F transition the total accessible surface is increased 2-fold, in good agreement with the change in size of the molecule, determined by low-angle scattering and by viscosity measurements.[65,66] Broadening of the globule in the F form is indicated by an increase in the ratio of the molecular axes[67] from 3.3 to 5.8, and also by a 50% increase in the hydration of the molecules.[68] In the F form of the protein the hydrophobic residues are more accessible to labelling than in the N form. This effect is well correlated with the greater hydrophobicity of the protein in the F form as compared with the native form. An analysis of the distribution of the label in the B form of the protein indicates a greater accessibility of the aminoacid residues in this form than in the native state, but the scale of this increase and the number of residues undergoing a change in accessibility are much smaller than in the N–F transition.

Unfortunately in all the above studies the label incorporated in the sum of the aminoacids of various types was determined, and no attempt was made to analyse the distribution of tritium over the chain of the protein. This allowed the occurrence of a conformational transition to be established, and the most general characteristics of the states thus produced to be identified, but none of the information was helpful in identifying the detailed structure.

Interesting results were obtained in studies of pH-dependent conformational transitions in hemagglutinin, a functionally important protein of the virus membrane group. It is now firmly established that the fusion of the viral and of the endosomal membrane induced by pH changes (the most important contribution to the infection of the cell) takes place with the participation of this protein.[69] However, in spite of wide-ranging studies by biochemical, biophysical, genetic, and immunologic methods,[70] the molecular mechanisms and the intermediate states of the fusion of the membranes are still a problem to be solved. Glushakova et al.[71] proposed a sensitive experimental model for studying pH-dependent conformational changes in proteins leading to their interaction with the membrane.[71]

The model system consisted of liposomes with the ionophore nigericine attached to the lipid membrane and containing hemagglutinin in their bulk. Lowering the pH of the surrounding medium produced a corresponding change in the pH within the liposome and induced a transition of the protein to a conformation able to interact with the liposomal membrane. Tritium labelling was used to visualise the outer surface of the liposomes. By comparing the specific labelling of the protein and the distribution of radioactivity in the aminoacids in control samples (at a neutral pH) and in the experimental samples (at the fusion pH) of the liposomes the authors were able to explain the nature of the protein–membrane interaction. It was found that in an acid medium the specific activity of the protein is increased (the activities of the hydrophobic aminoacids Ile, Phe, and Tyr increased 2–3-fold). This indicates the introduction of a protein molecule (or a part of it) into the membrane, and possibly also that part of the molecule is exposed on the outer surface, and it confirms the widely held opinion that the hydrophobic N-end peptide in a small subunit of the protein (the so-called fusion peptide) is responsible for the interaction of the membranes. An analysis of the intramolecular distribution of the label along the protein chain from control and from experimental liposomes should unambiguously establish the detailed pattern of the lipid–protein interaction. The model can be treated as universal for studies of lipid–protein interactions of any type, since any protein (and even an entire virus) can be incorporated within the liposome.

The tritium planigraphy method has been used to study the pH-dependent conformational change of hemagglutinin in the composition of the whole virus, leading to its inactivation. So far attempts have been made to calculate the change in the conformation of the hemagglutinin after acid preincubation of the virus from the change in the antigenic properties of the protein, in its sensitivity to proteinases, and above all from changes in the exposure of its 'fusing peptide'. An attempt to study this phenomenon by tritium planigraphy was reported by Ksenofontov et al.,[72] who showed that on the one hand the small subunit of hemagglutinin in the virus inactivated in an acid medium is readily accessible, as shown by the approximate doubling of its specific labelling as compared with the active virus; on the other hand inactivation in an acid medium of the target without membrane does not produce a strong exposure of the 'fusion peptide'. These results led the authors to propose a new model of the conformation of hemagglutinin in the composition of the inactive virus.

V. Accessible surface and intramolecular dynamics of proteins

Several published papers suggest a relationship between the intramolecular dynamics of biopolymers and their functional properties.[73] Clearly, the intramolecular mobility (at least the large-scale segmental mobility) should be reflected by the structure of the accessible surface. However, only a few calculations aiming to demonstrate this relationship have been published so far. In particular, Levit[74,75] showed by a computer modelling experiment that in dynamic calculations the accessible surface of several aminoacid residues may differ from the static value by

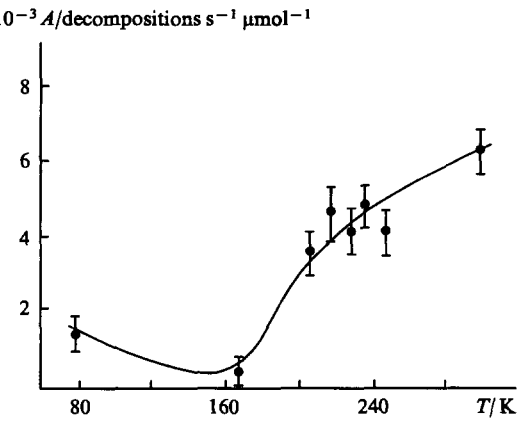


Figure 11. Temperature dependence of the inclusion of the label in lysozyme. *A* is the radioactivity of the protein normalised for the activity of the monitor.

50%–60%. No direct experimental data on the relationship between the accessible surface and the dynamic parameters have been published so far.

We know that the intramolecular mobility of biopolymers is substantially dependent on two parameters: the water content of the sample and its temperature.[76,77] This suggests the possibility of studying the relationship between the accessible surface and the molecular dynamics by the tritium planigraphy method by analysing the distribution of the label for different target temperatures and a constant humidity, or vice-versa.

A similar attempt was reported by Bogacheva et al.,[78] who chose the protein lysozyme as the model substance and determined the temperature dependence of the incorporation of the label in both the protein as a whole and the aminoacid residues of each type. The target temperature was varied between 77 K and room temperature.[79] In Fig. 11 we show the temperature dependence of the specific radioactivity of the protein, normalised for the flux of tritium atoms (*A*) in the temperature range 77–293 K. Two regions can be distinguished in the curve: a decreasing incorporation of the label at 77–163 K followed by an increase at 163–293 K. The increased level of labelling above 163 K cannot be explained in terms of the temperature dependence of the rate constant of the reaction leading to an increased incorporation of the label, since the temperature of the hot tritium atoms incident on the target surface (2000 K) is much higher than the temperature of the sample. An increase in temperature from 77 to 293 K can increase the incorporation of the label by not more than a factor of 1.2, but the observed increase in activity is 3-fold. According to data on the Rayleigh scattering of the Mössbauer radiation, and by using paramagnetic probes, it was shown[76,80] that an 'unfreezing' of the intramolecular mobility takes place at 170 to 190 K. This observation is well correlated with the observed[78] increase in the accessibility. The greater incorporation of the label (corresponding to an increased accessible surface area) upon lowering the temperature from 163 to 77 K is inexplicable in terms of dynamic effects. It may be due to a change in the three-dimensional structure of the protein as a result of the freezing of the internal water, firmly bound to the protein, which destroys the balance of forces stabilising the three-dimensional structure and leads to its breakdown.

The temperature dependence of the probability of incorporating the label was studied also at the level of the individual aminoacid residues. According to the features of this dependence all the residues can conveniently be divided into three groups. Most of the residues of the first group, whose accessibility increases in the range of 170–293 K, lie outside the region of enhanced mobility of the polypeptide chain. They are usually located on the N and C ends of the structured regions, near the sites of rotation of the polypeptide chain. The residues of the second type have a lower accessibility, independent of the temperature in this region. As a rule they are found in the middle of α-helix regions, in the immediate vicinity of the residues forming the inner region of the protein globule. Lastly 70% of the residues, which form the regions of enhanced mobility, are residues of the third type. Their accessibility changes only slightly in the range 160–270 K, but increases steeply at 293 K.

Unfortunately these results, like the results of the studies of conformational transitions discussed above, are averaged over the types of aminoacid and do not allow a detailed picture to be established. We are only at the first stage in the attempt to show that the accessible surface is a function of the molecular dynamics and that this relationship can be studied by applying the present method.

VI. Modelling the three-dimensional structure of proteins

As was stated above, X-ray structural analysis and the NMR method are laborious and have a number of fundamental limitations which seriously hinder the study of the three-dimensional structure of macromolecules. These shortcomings stimulated numerous attempts to develop theoretical predictions of the tertiary structure of proteins on the basis of data on the primary structure, of a statistical and evolutionary analysis of objects having a known structure, etc.[82–85] Unfortunately we must conclude that (in contrast to the methods of predicting the secondary structure) the theoretical modelling of the three-dimensional structure is still an unresolved problem, even at the level of predicting the general outline of the polypeptide chain.

Clearly, the most promising approaches are those which use, in addition to the theoretical predictions, parameters obtained directly from experiments (for example, data on the topography of the accessible surface). In fact, since an unambiguous linkage exists between the three-dimensional structure and the accessible surface, and since this linkage can be calculated from the coordinates of atoms, it is legitimate to formulate the inverse problem, namely to construct a model of the three-dimensional structure of the protein molecule from the accessibility of the constituent aminoacid residues. The algorithm for the solution of this problem can be defined in the following general form:

(1) determine the accessibility profile of the aminoacid residues of the protein molecule labelled with tritium;

(2) predict the elements of the secondary structure of the protein by using existing theoretical approaches;

(3) find a method of packing together the elements of the secondary structure while ensuring their surface localisation on the model of the chain fragments accessible to the tritium atoms, and (conversely) identify the inaccessible regions within the model of the globule.

Modelling greatly facilitates the acquisition of additional information: for example, data on the number and localisation of disulfide bonds, on the binding sites of ligands, substrates, and metals, on the localisation of individual functional groups, and antigenic mapping data. Taken as a whole this information may be sufficient for the choice of the optimum method of packing the elements of the secondary structure at all stages in the assembly of the model.

The first attempt to construct a model of the three-dimensional packing of a polypeptide chain was undertaken for the protein in the shell of the tobacco mosaic virus.[86] The simplicity of the object, containing only four α-helix portions, made it easy to construct a three-dimensional model satisfactorily consistent with the X-ray diffraction analysis data.[87]

More recently the scope of this approach was tested on the globular protein, pike parvalbumin, belonging to the family of Ca^{2+} binding proteins[88] (a relatively small protein containing 108 aminoacids). Two widely used methods were used to calculate the elements of the secondary structure: those of Chow and Fasman[89]

and Lim.[90] The five-predicted α-helices included 69 aminoacids, corresponding to 64% of the whole number of aminoacids. This feature greatly facilitated the modelling. Models of the three-dimensional structure of the protein were constructed by the method of Ptitsyn and Rashin,[91] which includes as an essential step a search for the contacts between neighbouring α-helices (using rigid cylinders as an approximation to the α-helices in this case). The stacking of the polypeptide chain was carried out by first searching for the contacts between the inner C and D helices (classified as inner from the standpoint of their accessibility to tritium labelling), and then successively adding to the resulting complex the helices E, F, B, and A. The choice of the relative orientation of the helices was helped by a knowledge of the calcium binding regions, which imposes strict limitations on the mutual disposition of the residues which coordinate the calcium ions.[92] The model of the three-dimensional structure of pike parvalbumin (Fig. 12) was found to be very similar to that of the homologous protein carp parvalbumin.[93]

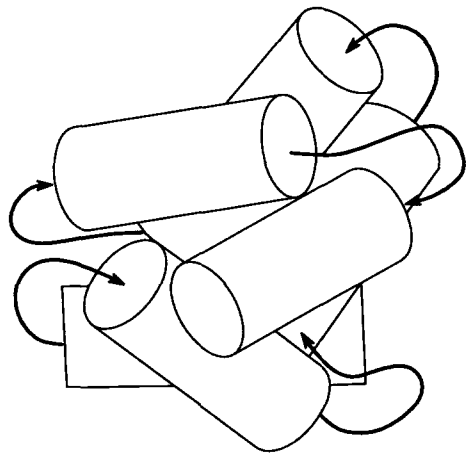


Figure 12. Model of the three-dimensional structure of the protein, pike parvalbumin III.

The similarity in structure of these two proteins is seen also in the similar topographies of their accessible surfaces, observed by comparing calculated data for carp parvalbumin with experimental data for pike parvalbumin.[87]

The results examined in this section cannot be treated as a complete concept, allowing three-dimensional models of proteins to be constructed from a combination of experimental data on the topography of the accessible surface and of theoretical predictions of the elements of the secondary structure. However, there are good reasons to hope that the further development of this approach and the application to it of the appropriate elements of computer modelling will provide researchers with a new and fruitful method of obtaining information on the three-dimensional structure of macromolecules.

VII. Three-dimensional organisation of supermolecular systems

The relationship between label distribution and structure of the accessible surface demonstrated above for proteins is seen even more clearly in studies of supermolecular systems, in which the mutual screening effects of the components play a substantial role. Depending on the experimental plan, information was obtained on the most general characteristics of the structure (general architecture of the complex, relative distribution of the components of the system in three dimensions, localisation of the contact surfaces, etc.) as well as on structural details such as determining the accessibility of the individual monomer units of the protein in the composition of the complex system.

As far as can be established the first attempt to use the tritium planigraphy method to study the three-dimensional structure of a complex supermolecular object was the tritiation of the ribosome from *E. coli*. As we know, a ribosome is a nucleoprotein complex which contains two molecules of highly polymeric RNA: 16S-RNA in the smaller moiety and 23S-RNA in the larger. The composition of the large 50S-subparticle also includes the low-molecular 5S-RNA. In the small 30S-subparticle, 21 proteins are associated with the 16S-RNA, and the large subparticle contains 32 different proteins.

By comparing the amounts of label incorporation in the proteins of the isolated subparticles of the 30S and 50S ribosomes and in the whole 70S ribosome, the proteins exposed on the surface could be identified and the absence of proteins on the contacting surface of the subparticles was demonstrated.[24,94-96] As was shown in separate experiments, under these conditions the RNA molecules retain their integrity and their ability to undergo specific interactions with proteins.[97] However, when considering the absence of proteins from the contacting surface of ribosomal subparticles, we should not forget that in practice the contact of two ribosomal subparticles is not very tight and cannot prevent the incorporation of tritium in the protein in the region between the subunits.

An interesting attempt to determine the accessibility of a polypeptide chain synthesised on the ribosome has been reported.[98,99] It has been suggested that the first units of the growing peptide are accommodated in a channel whose geometry allows the polypeptide chain to unfold into a helix. However, experimental approaches aimed at demonstrating the existence of the channel mostly relied on large macromolecules (protease and its antibody) as test reagents applied to the proteins synthesised by the ribosome. It was found that the small size of the tritium atom offers information with the required detail. The data on the inclusion of the label showed that a polypeptide chain already three or more residues long is exposed on the ribosome surface. Unfortunately these workers used a synthetic poly-(Y)-dependent cell-free translation system, i.e. they did not allow for the initiation of the translation in the form found in the translation of natural mRNAs. This may account for the discrepancy between the results and current views on the presence of a channel.

Another example of a nucleoprotein complex which has been studied by tritium planigraphy are the chromosomes from mouse fibroblast.[100] It was found that in the metaphase chromosomes both the chromosome proteins and the RNA are accessible to tritium. An analysis of the take-up of label by the protein showed that the 'scaffold' proteins are the most exposed, which suggests that they are located on the outer surface of the metaphase chromosomes.

A substantial volume of work has been devoted to applying the tritium planigraphy method to studies of the three-dimensional architecture of protein complexes having many subunits. Thus, Mironov and coworkers[101,102] tried to determine the relative accessibility of the protein subunits in the composition of cytochrome oxidase and in its complex with cytochrome C. Cytochrome oxidase is the terminal enzyme of the respiratory chain of living cells. It is a transmembrane protein, consisting (in the higher mammals) of 12 different subunits. Tritiation of the free enzyme and of the enzyme incorporated in the complex was carried out in order to establish, confirm, and add some detail to the existing model of the structural organisation of the subunits in cytochrome oxidase, and also to identify the regions of interaction of the enzyme with cytochrome C. Comparing the specific labelling values of the subunits showed that in the formation of the complex the cytochrome molecule is partially screened by the subunits I, II, VIc, and VIIa–VIIc of the protein, which agrees with previous reports.[103]

Applications of tritium planigraphy to the study of membrane structures (in particular to the study of the topography of transmembrane proteins) are of special interest because the presence of a lipid bilayer should lead to marked differences in

the accessibility to tritium between the exposed and the intramembrane parts of the polypeptide chain. In fact, as was shown in the experiments with liposome loaded with hemagglutinin discussed above, the bilayer lipid membrane weakens the flow of tritium atoms by a factor of 10.[72] The cell membrane almost completely screens the contents of the cell from the incident tritium atoms. Thus, in the case of erythrocytes it was observed that the level of incorporation of the label into the hemoglobin within the cell is more than two orders of magnitude lower than the same level in the free protein.[104]

The first example of the study of membrane structures by tritium planigraphy was applied to bacteriorhodopsin.[104-106] This is one of the best characterised membrane proteins, for which the type of three-dimensional organisation has been established in general traits and various exposed residues have been identified (see, for example, Ovchinnikov et al.[107]). This work allowed the prospects of the method to be assessed, and (in the case of favourable results) it also allowed additional experimental data, needed for checking and more detailed characterisation of existing models of the protein location in the membrane, to be obtained. A packing scheme (Fig. 13) was proposed by analysing the incorporation of label in the aminoacid residues of the protein in the membrane composition, and shown to agree satisfactorily with the model constructed from theoretical predictions.[108] As a result of this work the positions of the tryptophan residues were accurately established (positions 10 and 12), and shown to lie near the surface rather than within the membrane, as had been suggested earlier.[109,110] The new model allows for the partial screening of the fragments not included in the composition of the intramembrane α-helix segments.[111]

The fact that residues within the membrane, at least 5 Å distant from the surface (i.e. at a distance greater than the mean free path of the tritium atoms), nevertheless include some tritium can be attributed to the number of lipids in the purpuric membrane (10 molecules per molecule of protein[112]) being insufficient to make the inner part of the polypeptide chain wholly inaccessible to tritium.

Ostrovskii et al.[113] tritiated the intact cells and the protoplasts of *Micrococcus luteus* bacteria with the aim of localising the components of the membrane (potential antigens) exposed on the cell envelope. It was shown that over 90% of the non-exchanged tritium is included in cytoplasmatic membranes, and that 98% of this amount is associated with lipids, suggesting good prospects for studying the asymmetric distribution of lipids in the cell membrane. It was also found that in the case of protoplasts the tritium is incorporated preferentially in three membrane proteins, but in the case of cells in a single protein.

In most of the work discussed above the information on the structure of the supermolecular object was limited to the determination of the accessibility of whole molecular complexes (with the exception of bacteriorhodopsin). A more detailed study was carried out with the tobacco mosaic virus (TMV). Data for the virus from an X-ray diffraction analysis[114,115] with a resolution of 3.6 Å, and a detailed antigenic characterisation of the virus capsid,[116] show that this object can be used as the ideal model system.

Whole virus particles were exposed to tritium bombardment.[117-119] In Fig. 14 we show the distribution of the label over the aminoacid residues of the polypeptide chain of the protein.

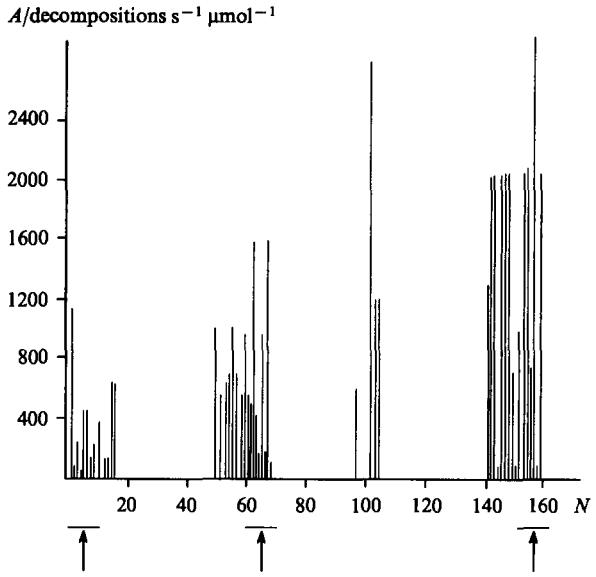


Figure 14. Experimental accessibility profile of the polypeptide chain in the protein of the tobacco mosaic virus shell in the virion composition. *N* is the number of the aminoacid residue in the polypeptide chain.

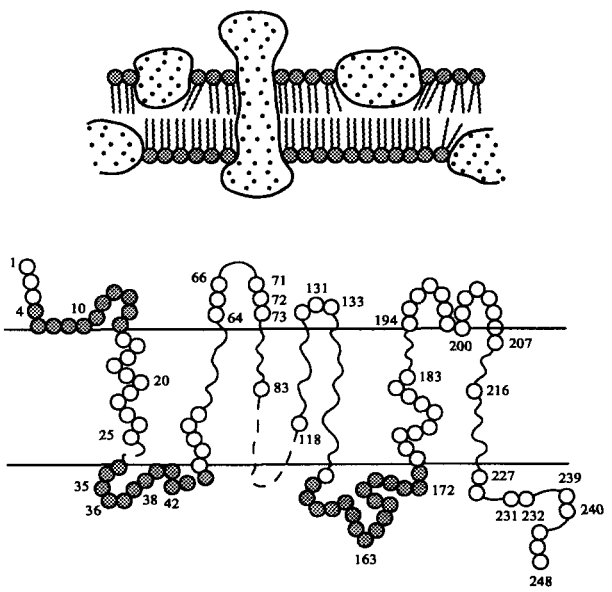


Figure 13. Schematic diagram of the 'placement' of the polypeptide chain of bacteriorhodopsin in the membrane. Filled circles denote aminoacid residues in which incorporation of the label has been observed. The sections 25-33, 66-71, 83-118, 207-231, 232-239, and 240-246 have not been analysed.

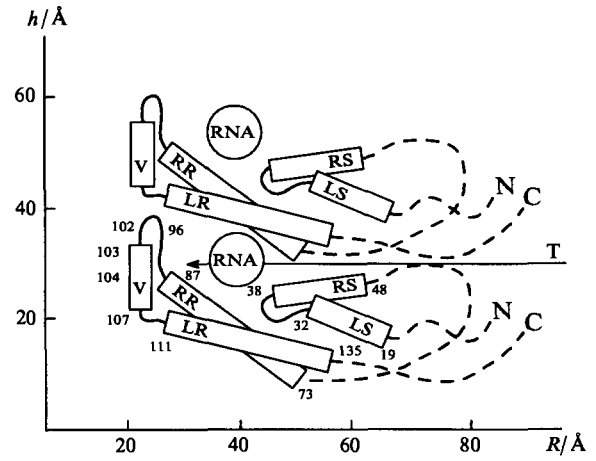


Figure 15. Schematic diagram of the placement of protein subunits in the TMV virion, demonstrating the possibility of penetration by the tritium atoms into the inner region of the virion.[115]

Relatively extensive regions can be observed, in which the amino-acid residues are not accessible to the tritium atoms. Fig. 15 shows a schematic view of the packing of the polypeptide chain for the protein coat of the virus. Comparing the experimental results on the distribution of the label in the protein with those given by this scheme shows that the N and C end fragments of the protein, located on the outer side of the virus particle, are the most accessible; the part of the protein not accessible to the labelling is found in the contact region between subunits. Surprisingly, at first sight the label was found to be included in residues 93–112 of the polypeptide chain, which (according to the X-ray structural analysis data) is remote from the surface of the virus and in contact with the RNA molecule. The authors suggested that channels are present at the 'joint' between three shell protein subunits, and that the tritium atoms can penetrate into the bulk of the virion and interact with the 93–112 residues and the virus RNA located on its 'bottom'. On the X-ray diffraction pattern these regions, 3–5 Å in diameter, appear as regions of low electron density.[114–116] It appears that channels of this type have been observed by Neiman et al.[120] in a study of the structure of the MS2-phage. According to their results 25% of the label is combined with RNA within the bacteriophage, which also suggests the presence of a relatively large number of 'pores' in the capsid of the phage between the protein molecules, through which the tritium atoms can interact with the internal regions of the phage.

It is of interest to compare the information on the surface of the virion obtained in this way with data on the localisation of the antigenic determinants. In Fig. 14 we have marked the regions 1–10, 62–68, and 153–158, which are the antigenic determinants of the protein in the composition of the virus.[116] It can be seen that they all fall among the fragments accessible to labelling by tritium. There can be no doubt that the tritium atoms are not the best indicator of the location of antigenic determinants. The small size (~1 Å) of the tritium atoms allows them to 'see' too much. However, a knowledge of the surface regions undoubtedly helps this work by narrowing the circle of possibilities.

The results obtained for the model object stimulated studies of a virus on whose structure (mainly the conformation of the subunits of the shell protein and their packing in the virion) very little was known. This was the X potato virus (XPV), one of the most widespread members of the potato virus group. Its flexible rod-like virion contains single-chain RNA, and the capsid of the virion is composed of identical protein subunits containing 236 aminoacid residues. When this work was begun data on the surface of the virion were scarce, and to some extent contradictory. Immunological studies indicated the localisation of the N-end region of the protein on the virion surface.[121] By predicting the elements of the secondary structure of the protein in the shell of XPV, using the three-dimensional structure of TMV as a first approximation, Sawyer et al.[122] were able to postulate a certain generality in the formation of the architecture of virions, namely the surface localisation of the N and C end regions in all the rod-like vegetable viruses. Subsequently Schukla et al.[123] suggested that the deflection of the polypeptide chains in proteins was a general phenomenon, leading to surface localisation of their N and C end regions in all the rod-like vegetable viruses.

In a comparative study by tritium planigraphy of intact XPV particles and of XPV degraded in situ (lacking the first 19 aminoacids through the action of the protease in the cell sap[126]) it was shown that the distribution of the label (Fig. 16*a*) differs

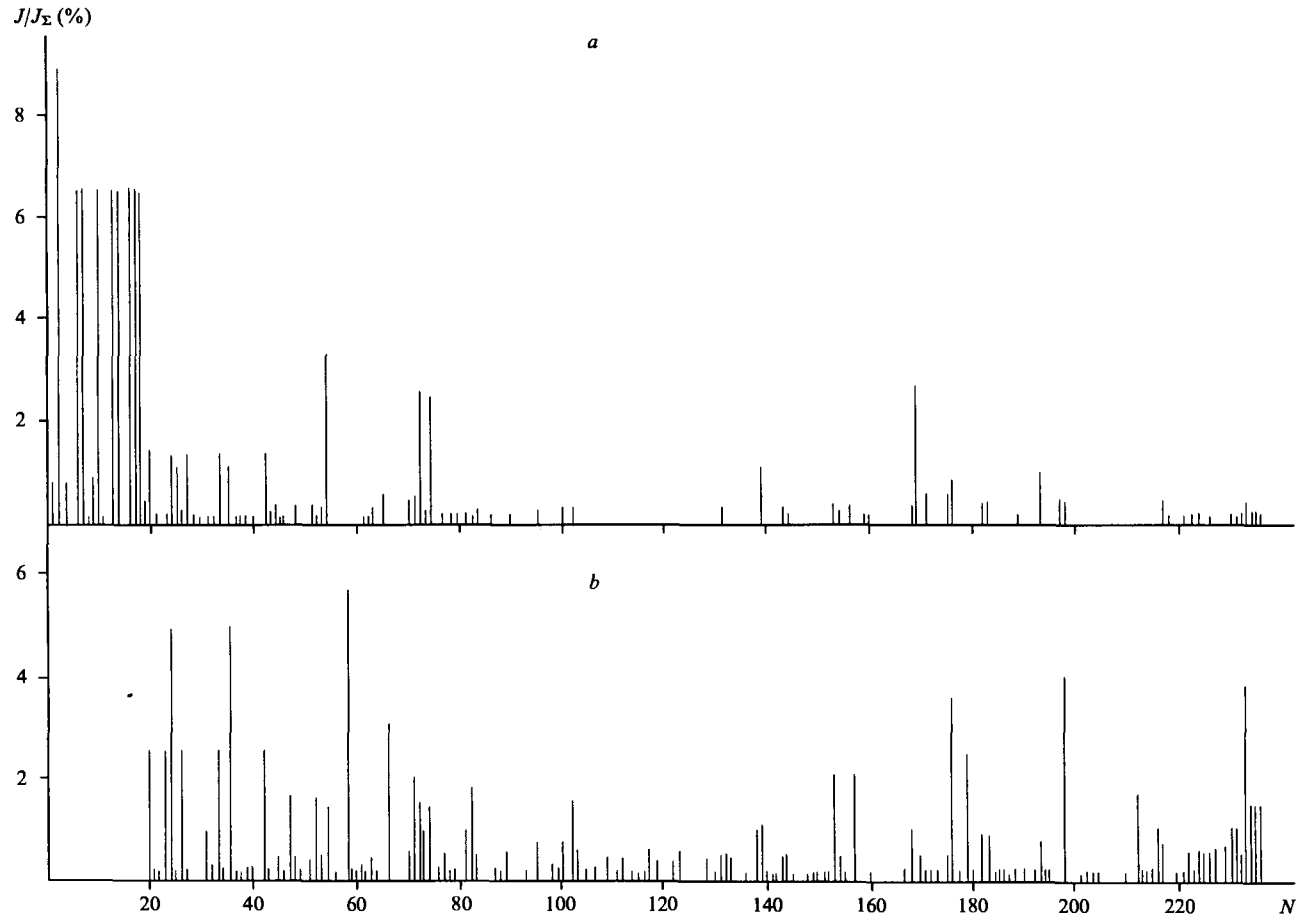


Figure 16. Experimental accessibility profile of the polypeptide chain in the X potato virus (XPV) in the native form (*a*) and partially degraded by proteases of the cell sap (*b*). J/J_Σ is the portion of the activity attributable to the respective aminoacid residue; N is the number of the aminoacid residue in the polypeptide chain.

from the distribution observed for TMV (see Fig. 14): the sharp boundaries between accessible and inaccessible regions have disappeared. This suggests that XPV has a much 'rougher' surface than TMV.[124,125] We note that 85% of the total amount of label incorporated by the preparation is located in the first 19 amino-acids in the intact virus: this shows that the entire N-end region of the protein is exposed on the virus surface. The absence of the first 19 end aminoacids (Fig. 16*b*) in the coat protein of the virus preparation degraded in situ produces a qualitative change in the labelling process. Evidently, the C-end region of the protein, which apparently had been previously 'covered' by the N-end part of the protein in the coat, has become accessible to the tritium atoms.

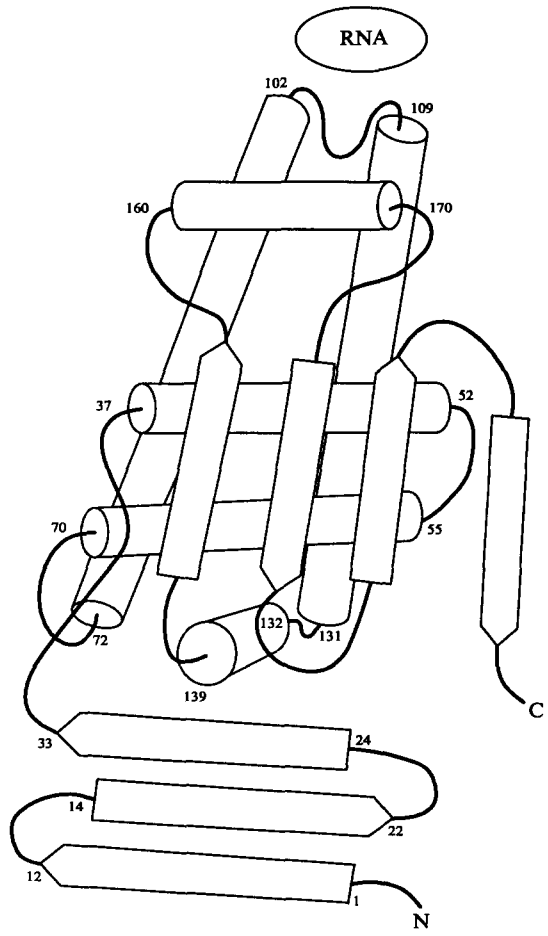


Figure 17. Model of the three-dimensional packing of the polypeptide chain in the protein of the XPV shell. The α-helices are shown as cylinders; the β structural regions are indicated by arrows. The numbers denote the boundaries of the structured regions.

On the basis of the result obtained by tritium planigraphy, of existing biochemical and immunological data, and also of the basic principles governing the packing of the predicted elements of the secondary structure in globular proteins Baratova et al.[125] proposed a model of the tertiary structure of the protein in the coat of XPV (Fig. 17). In this model one β group, containing the β structural regions 1–12, 14–22, and 24–33, lies alongside the molecule and forms the outer surface of the virus particles.

To conclude this review we shall briefly mention another group of problems which could be solved effectively by the application of tritium planigraphy. The concept of linear or conformational antigenic determinant proteins is widely adopted in modern immunology and immunochemistry. It is assumed that linear determinants are composed of several aminoacid residues, amounting to a substantial proportion of the residues in the protein sequence, whereas the conformational determinants contain aminoacid residues from different parts of the sequence, lying close together in the native structure of the protein globule.

However, recent work suggests that all the antigenic determinants are conformational.[127,128] Thus, the surface of the protein obtained from X-ray structural analysis data is always complex and has a very broken outline. Even a visual analysis of any structure shows that most of the residues on the protein surface have neighbours which are quite removed in the primary structure of the protein. Furthermore the most 'unbroken' parts are mostly loops and/or projecting regions. This explains why surface properties such as hydrophilicity, accessibility, and mobility can be used to predict possible antigenic determinants. This concept is well illustrated by the correlation between the accessibility to tritium atoms and the antigenic properties of these parts of the structure, observed in the TMV and XPV viruses and (earlier) in globular proteins. By describing the structure of the object in terms of data on its surface (provided by an analysis of the tritium labelling), and also by a comparative analysis of the surfaces of the free protein and of the protein complexes with a monoclonal antibody, it should be possible, we believe, to identify the conformational determinants. So far this possibility has been realised only at the level of the X-ray structural analysis of structures such as complexes with site-directed mutagenesis.[129]

References

1. G M Clore, M A Robien, A M Gronenborn *J. Mol. Biol.* **231** 82 (1993)
2. R Henderson, J M Baldwin, T M Ceska, F Zemlin, E Beckmann, K H Downing *J. Mol. Biol.* **213** 899 (1990)
3. D N Wang, W J Kuhlbrandt *J. Mol. Biol.* **217** 691 (1991)
4. A Holzenburg, F H Wilson, M E Finlow, R C Ford *Biochem. Soc. Trans.* **20** 591 (1992)
5. H Arakawa, K Umemura, A Ikai *Nature (London)* **358** 171 (1992)
6. S Colacicchi, M Ferrari, A Sotgin *Int. J. Biochem.* **24** 205 (1992)
7. J A Thompson, A L Lau, D D Cunningham *Biochemistry* **26** 743 (1987)
8. B H Robertson, V K Brown, B P Holloway, B Khanna, E Chan *Arch. Virol.* **104** 117 (1989)
9. P R Schimmel, H J P Schoemaker *Methods Enzymol.* **59** 332 (1979)
10. L A Neiman, V S Smolyakov, A V Shishkov *Obshchie Problemy Fiziko-khimicheskoi Biologii, T. 2 (Itogi Nauki i Tekhniki)* [Common Problems of Physicochemical Biology, Vol. 2 (Advances in Science and Engineering)] (Moscow: Izd. VINITI, 1985)
11. M Menzinger, R Wolfgang *J. Chem. Phys.* **50** 2991 (1969)
12. M Menzinger, R Wolfgang *J. Am. Chem. Soc.* **89** 5992 (1967)
13. V N Kondrat'ev *Konstanty Skorosti Gazofaznykh Reaktsii. Spravochnik* (Rate Constants of Gas-phase Reactions. Handbook) (Moscow: Nauka, 1970)
14. I Langmuir *J. Am. Chem. Soc.* **34** 1310 (1912)
15. R Klein, M D Sheer *J. Phys. Chem.* **62** 1011 (1958)
16. A N Ponomarev, V L Tal'roze *Dokl. Akad. Nauk SSSR* **130** 120 (1960)
17. L A Neiman, V S Smolyakov, L P Antropova, I A Gedrovich, I A Kashirin, A V Shishkov, in *I Vsesoyuznyi Biofizicheskii S'ezd, Moskva, 1982 (Tezisy Dokladov, Stendovye Soobshcheniya 1690-2318)* [The First All-Union Biophysical Congress, Moscow, 1982 (Abstracts of Reports, Posters 1690-2318)] p. 214
18. H C Moser, P Nordin, J K Senne *Int. J. Appl. Radiat. Isot.* **15** 557 (1964)
19. P Nordin, H C Moser, J K Senne *Biochem. J.* **96** 336 (1965)
20. A V Shishkov, E S Filatov, E F Simonov, M S Unukovich, V I Gol'danskii, A N Nesmeyanov *Dokl. Akad. Nauk SSSR* **228** 1237 (1976)
21. A K E Hagopian, R H A Johnsen *J. Chem. Soc., Chem. Commun.* 837 (1974)
22. A V Volynskaya, A Yu Skripkin, A V Shishkov, V I Gol'danskii *Dokl. Akad. Nauk SSSR* **266** 871 (1982)
23. A V Gedrovich, G A Badun *Mol. Biol. (Moscow)* **26** 558 (1992)
24. M M Yusupov, A S Spirin *Methods Enzymol.* **164** 426 (1988)

25. L A Baratova, V I Gol'danskii, Yu M Rumyantsev, M S Unukovich, A V Shishkov *Mol. Biol. (Moscow)* **16** 117 (1982)
26. A F Trotman-Dickenson, G S Milne *Natl. Stand. Res.-Natl. Bur. Stand.* **9** 41 (1967)
27. V I Gol'danskii, Yu M Rumyantsev, A V Shishkov, L A Baratova, L P Belyanova *Mol. Biol. (Moscow)* **16** 528 (1982)
28. S E V Philips *Nature (London)* **273** 247 (1978)
29. B K Lee, F M Richards *J. Mol. Biol.* **55** 379 (1971)
30. S A Islam, D L Weaver *Proteins: Structure, Function and Genetics* **10** 300 (1991)
31. E Stellwagen, M Wilgus *Nature (London)* **275** 342 (1978)
32. S H Bryant, S A Islam, D L Weaver *Proteins: Structure, Function and Genetics* **6** 418 (1989)
33. R E Gates *J. Mol. Biol.* **127** 345 (1979)
34. S Miller, J Janin, A M Lesk, C Chothia *J. Mol. Biol.* **196** 641 (1987)
35. J Janin, S Miller, C Chothia *J. Mol. Biol.* **204** 155 (1988)
36. C Chothia *Nature (London)* **254** 304 (1975)
37. D J Barlow, J M Thornton *Mol. Graphics* **4** 97 (1986)
38. D J Barlow, J M Thornton *Biopolymers* **25** 1717 (1986)
39. D W Fanning, J A Smith, G D Rose *Biopolymers* **25** 863 (1986)
40. D M Novotny, M Handschumacher, E Haber, R E Brucoletti, W B Carlson, D W Fanning, J A Smith, G D Rose *Proc. Natl. Acad. Sci. USA* **83** 226 (1986)
41. Yu Chirgadze, N Kurochkina, S Nikonov *Protein Eng.* **3** 105 (1989)
42. G Neweths, H A Scheraga *Q. Rev. Biophys.* **10** 239 (1977)
43. M Levit, C Chothia *Nature (London)* **261** 552 (1976)
44. C Chothia *Ann. Rev. Biochem.* **53** 537 (1984)
45. A V Volynskaya, A Yu Skripkin, A V Shishkov, E S Dzhafarov, Yu M Rumyantsev, V I Gol'danskii *Mol. Biol. (Moscow)* **19** 1294 (1985)
46. A B Ivlev, A V Gedrovich, A V Shishkov *Mol. Biol. (Moscow)* **26** 1047 (1992)
47. E N Bogacheva, A A Shishkov, A V Shishkov, L A Baratova *Mol. Biol.* (Moscow) (1994) (in the press)
48. D C Carter, He Hiao-min, S H Munson, F D Twigg, K M Gernett, M B Broom, T Y Miller *Science* **244** 1195 (1989)
49. A V Volynskaya, E A Kasumov, E N Bogacheva, A V Shishkov, V I Goldanskii *Eur. J. Biophys.* 1994 (in the press)
50. T Peters *Adv. Clin. Chem.* **13** 37 (1970)
51. E Keshavarz, S Nakai *Biochim. Biophys. Acta* **576** 269 (1979)
52. A V Volynskaya, V N Izmailova, V A Pchelin *Biofizika* **18** 210 (1973)
53. K E Bobkova, A V Gedrovich, V N Ankilova, O I Lavrik, L A Baratova, A V Shishkov *Biokhimiya* **55** 1570 (1990)
54. E V Bobkova, A V Gedrovich, V N Ankilova, O I Lavrik, L F Baratova, A V Shishkov *Biochem. Int.* **20** 1001 (1990)
55. A V Gedrovich, L A Baratova, E N Bogacheva, V N Medvedkin, A V Shishkov *Mol. Biol. (Moscow)* **27** 309 (1993)
56. A V Volynskaya, S A Murashova, A Yu Skripkin, A V Shishkov, V I Gol'danskii *Mol. Biol. (Moscow)* **23** 356 (1989)
57. A Yu Skripkin, A V Volynskaya, A V Shishkov, V I Gol'danskii *Mol. Biol. (Moscow)* **23** 365 (1989)
58. K Hamaguchi, K Rokkaku *J. Biochem.* **48** 358 (1960)
59. H Edelhoch, R F Steiner *Biochim. Biophys. Acta* **60** 359 (1962)
60. E A Kasumov, A V Volynskaya, A V Shishkov, V I Goldanskii *Stud. Biophys.* **136** 167 (1990)
61. Ch N Cornell, L J Kaplan *Biochemistry* **17** 1750; 1755 (1978)
62. J Welting, M M Weideman, A C-J Roomer, J H Perrin *Biochim. Biophys. Acta* **579** 469 (1979)
63. E S Dzhafarov *Mol. Biol. (Moscow)* **25** 1412 (1991)
64. E S Dzhafarov, L A Aliev, A Yu Skripkin, A V Volynskaya, A V Shishkov, L A Baratova, V I Gol'danskii *Izv. Akad. Nauk Azerb. SSR* (3) 102 (1985)
65. S F Sun *Arch. Biochem. Biophys.* **129** 411 (1969)
66. V Luzzati, J Witz, A Nicholaieff *J. Mol. Biol.* **3** 379 (1961)
67. M Ioly, in *A Physico-chemical Approach to the Denaturation of Proteins* (Translated into Russian; Moscow: Mir, 1968) p. 38
68. V A Kashpur, V Ya Maleev, T Yu Shchegoleva *Mol. Biol. (Moscow)* **10** 568 (1976)
69. J White, M Kielian, A Helenius *Q. Rev. Biophys.* **16** 151 (1983)
70. D Hoekstra, J W Kok *Biosci. Rep.* **9** 273 (1989)
71. S E Glushakova, A L Ksenofontov, N V Fedorova, L A Mazhul, O N Ageeva, L B Margolis, L A Baratova, A V Shishkov *Biosci. Rep.* **11** 131 (1991)
72. A L Ksenofontov, A L Danilov, S E Glushakova, L B Margolis, L A Baratova, A V Shishkov *Biochem. Int.* (1994) (in the press)
73. M Karplus, J A McCammon *CRC Crit. Rev. Biochem.* **9** 293 (1981)
74. M Levit *J. Mol. Biol.* **168** 595 (1983)
75. M Levit *J. Mol. Biol.* **168** 621 (1983)
76. E N Frolov, O V Belonogova, G I Likhteinshtein, in *Ravnovesnaya Dinamika Nativnoi Struktury Belka* (Equilibrium Dynamics of Native Protein Structure) (Pushchino: Sci. Centre Biol. Inv., 1977) p. 99
77. V I Goldanskii, Yu F Krupyanskii *Hyperfine Interact.* **39** 341 (1988)
78. E N Bogacheva, N D Zhukov, A V Shishkov *Mol. Biol. (Moscow)* **27** 1044 (1993)
79. A V Shishkov, L A Neiman, V S Smolyakov *Usp. Khim.* **53** 1125 (1984) [*Russ. Chem. Rev.* **53** 656 (1984)]
80. I V Kurinov, Yu F Krupyanskii, I P Suzdalev, V I Goldanskii *Hyperfine Interact.* **33** 223 (1987)
81. C Chothia *J. Mol. Biol.* **105** 1 (1976)
82. M E Snow *Proteins; Structure, Function and Genetics* **15** 183 (1993)
83. F E Cohen, S R Presnell, L M Gregoret, I D Kuntz, in *Protein Folding: Deciphering the Second Half of the Genetic Code* (Eds L Gierasch, J King) (Washington, DC/AAAS, 1990) p. 251
84. R Unger, J Moult *J. Mol. Biol.* **231** 75 (1993)
85. S Saitoh, T Nakai, K Nishikawa *Proteins: Structure, Function and Genetics* **15** 191 (1993)
86. A V Shishkov, Yu M Rumyantsev, M S Unukovich, V I Gol'danskii, E F Simonov, E S Filatov, L A Baratova, L P Belyanova, R K Ledneva, in *IV Vsesoyuznyi Simpozium po Khimii Belkov i Peptidov, Minsk, 1977 (Tezisy Dokladov)* (Abstracts of Reports at the IVth All-Union Symposium on the Chemistry of Proteins and Peptides, Minsk, 1977) p. 23
87. G J Stubbs, S G Warren, K S Holmes *Nature (London)* **267** 216 (1976)
88. A V Gedrovich, A V Shishkov, V I Goldanskii, L A Baratova, N I Grebenshchikov, A V Efimov *Eur. Biophys.* **19** 283 (1991)
89. P V Chow, G D Fasman *Annu. Rev. Biochem.* **47** 251 (1978)
90. V I Lim *J. Mol. Biol.* **88** 872 (1974)
91. O B Ptitsyn, A A Rashin *Biophys. Chem.* **3** 1 (1975)
92. R H Tufty, R H Kretsinger *Science* **187** 167 (1975)
93. P C Moews, R H Kretsinger *J. Mol. Biol.* **91** 210 (1975)
94. A V Gedrovich, M M Yusupov, A V Shishkov, V I Gol'danskii, A S Spirin *Dokl. Akad. Nauk SSSR* **267** 1255 (1982)
95. M M Yusupov, A S Spirin *Biokhimiya* **51** 1858 (1986)
96. M M Yusupov, A S Spirin *FEBS Lett.* **197** 229 (1986)
97. I A Kashirin, A V Gedrovich, A V Shishkov, V K Kagramanova, L A Baratova *Bioorg. Khim.* **9** 1531 (1983)
98. V A Kolb, A A Kommer, A S Spirin *Dokl. Akad. Nauk SSSR* **296** 1497 (1987)
99. V A Kolb, A A Kommer, A S Spirin *Mechanism and Control of Translation* (Netherlands: Noordwijkerhout, 1990)
100. N D Belyaev, V G Budker, V A Dubrovskaya, A A Kim, E V Kiseleva, V N Sidorov *FEBS Lett.* **297** 43 (1992)
101. I A Filatov, M A Kulish, A F Mironov, E V Nozhevnikova, L A Neiman *Bioorg. Khim.* **13** 623 (1987)
102. N G Kotlova, M A Kulish, A F Mironov *Bioorg. Khim.* **14** 1695 (1988)
103. B Kadenbach, A Stroh *FEBS Lett.* **173** 374 (1984)
104. L V Gordeeva, L A Baratova, L B Margolis, A V Shishkov *Biofizika* **34** 971 (1989)
105. A B Kuryatov, V V Shemyakin, L P Antropova, in *XVI Konferentsiya FEBS, Moskva, 1984 (Tezisy Dokladov)* (Abstracts of Reports at the XVIth FEBS Conference, Moscow, 1984) p. 335
106. A B Kuryatov, A S Arsen'ev, T N Alenycheva, L A Neiman, V I Tsetlin, in *Mezhdunarodnyi Simposium "Retinal'soderzhashchie Belki", Moskva, 1986 (Tezisy Dokladov)* (Abstracts of Reports at the International Symposium "Retinene-containing Proteins", Moscow, 1986) p. 76
107. Yu A Ovchinnikov, N G Abdulaev, R G Vasilov, I Yu Vturina, A B Kuryatov, A V Kiselev *FEBS Lett.* **179** 343 (1985)
108. J K Mohana Rao, P Argos *Biochim. Biophys. Acta.* **869** 197 (1986)
109. Yu A Ovchinnikov, N G Abdulaev, M Yu Feigina, A V Kiselev, N A Lobanov *FEBS Lett.* **100** 219 (1979)
110. D M Engelman, R Henderson, A D Mclachlan, B A Wallace *Proc. Natl. Acad. Sci. USA* **77** 2023 (1980)

111. T N Alenycheva, A B Kuryatov, L P Antropova, V V Shemyakin, L A Neiman, V I Tsetlin, V T Ivanov *Bioorg. Khim.* **13** 898 (1987)
112. R Henderson *J. Mol. Biol.* **93** 123 (1975)
113. D N Ostrovskii, V A Eremin, I G Zhukova, A A Masyagin, A V Shishkov *Mikrobiologiya* **57** 875 (1988)
114. K Namba, G Stubbs *Science* **231** 1401 (1986)
115. G Stubbs, S Warren, K Holmes *Nature (London)* **267** 216 (1977)
116. D Altschuh, D Hartman, J Reinbolt, M H V Van Regenmortel *Mol. Immunol.* **20** 271 (1983)
117. I A Kashirin, N I Grebenshchikov, L A Baratova, A V Shishkov, V I Gol'danskii *Mol. Biol. (Moscow)* **20** 1264 (1986)
118. I V Kashirin, N I Grebenshchikov, L A Baratova, A V Shishkov, V I Gol'danskii *Mol. Biol. (Moscow)* **21** 456 (1986)
119. V I Goldanskii, I A Kashirin, A V Shishkov, L A Baratova, N I Grebenshchikov *J. Mol. Biol.* **201** 567 (1988)
120. L A Neiman, L P Antropova, M A Zalesskaya, E I Budovskii *Bioorg. Khim.* **12** 1070 (1986)
121. J Sober, L V Jarvekulg, I E Toots, Yu L Radavsky, R Villems, M Saarma *J. Gen. Virol.* **69** 1799 (1988)
122. L Sawyer, P Tollin, H R Wilson *J. Gen. Virol.* **68** 1229 (1987)
123. D D Shukla, P M Strike, S L Tracy, K H Gough, C M Ward *J. Gen. Virol.* **69** 1497 (1988)
124. L A Baratova, N I Grebenshchikov, A V Shishkov, I A Kashirin, Yu L Radavsky, L Jarvekulg, M Saarma *J. Gen. Virol.* **73** 229 (1992)
125. L A Baratova, N I Grebenshchikov, E N Dobrov, A V Gedrovich, I A Kashirin, A V Shishkov, A V Efimov, L Jarvekulg, Yu L Radavsky, M Saarma *Virology* **188** 175 (1992)
126. M I Gol'shtein, N I Grebenshchikov, S V Kust, A S Kaftanova, E N Dobrov, I G Atabekov *Mol. Gen., Mikrobiol. Virusol.* (2) 9 (1990)
127. M H V Regenmortel *Hybridonia Technology in Agriculture Veterinary Research* (Eds N J Stern, H R Gramble) (New Jersey: Rowman and Allanheld, 1984) Ch. 3
128. D J Barlow, M S Edwards, J M Thornton *Nature (London)* **322** 747 (1986)
129. J M Nuss, P B Whitaker, G M Air *Proteins: Structure, Function and Genetics* **15** 121 (1993)

Russian Chemical Reviews **63** (10) 797–814 (1994)
©1994 Russian Academy of Sciences and Turpion Ltd

UDC 547.796.1

Tetrazoles

G I Koldobskii, V A Ostrovskii

Contents

I. Introduction	797
II. Methods of synthesis of tetrazoles	797
III. Physicochemical properties	801
IV. Reactions of tetrazoles	803
V. Applications of tetrazoles	809
VI. Conclusion	809

Abstract. A systematic account is given of the latest data on the methods of synthesis, physicochemical properties, and practical applications of tetrazoles. New results obtained in the study of the electronic structures, acid–base properties, tautomerism, reactivities, and thermal stabilities of tetrazoles are discussed. The bibliography includes 369 references.

I. Introduction

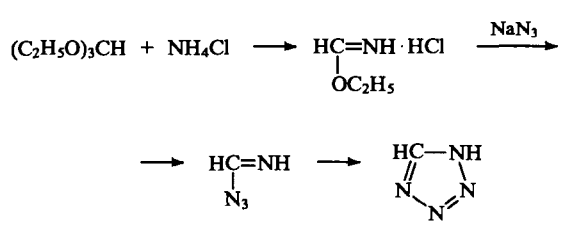
The development of the chemistry of tetrazoles during the last decade has been largely associated with the wide-scale employment of these compounds in medicine,[1–12] biochemistry,[13–17] agriculture,[18–20] and photography,[21,22] and also as components of systems for the recording of information.[23–25] Novel[26–29] methods of synthesis of substituted tetrazoles have been developed during these years and existing methods have been significantly improved.[30–35] As a result of this, tetrazoles, which had been difficult to obtain and were rather exotic, became the subject of detailed investigation and in many instances their practical applications were recommended. New results obtained in the study of the electronic structures,[36–40] acid–base properties,[41–43] tautomerism,[44] reactivities,[45–47] and thermal stabilities[48–50] of tetrazoles are of great interest. Original studies published up to 1981 have been described schematically in other reviews.[46,51] The latest data on methods of synthesis, physicochemical properties, and practical applications of tetrazoles are discussed below.

II. Methods of synthesis of tetrazoles

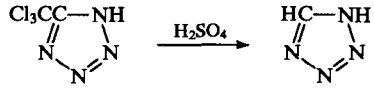
1. Tetrazole

Several methods of synthesis of tetrazole are known: the interaction of hydrocyanic acid with hydrazoic acid, the interaction of ethyl formate with sodium azide and ammonium chloride in acetic acid, the diazotisation of 5-aminotetrazole in the presence of reductants, the oxidative degradation of mono- and di-substituted tetrazoles, and certain others.[51]

Among these methods, the commonest involve the diazotisation of 5-aminotetrazole and the interaction of ethyl orthoformate with sodium azide. In the latter case, the reaction evidently proceeds via the formation of the iminoester hydrochloride and its subsequent conversion into tetrazole on treatment with sodium azide.[52]



The electrochemical reduction of 5-trichloromethyltetrazole is known to afford a low yield of tetrazole (~16%).[53] On the other hand, according to our data, tetrazole is formed in 75% yield on heating 5-trichloromethyltetrazole in 85% sulfuric acid.



The synthesis of a tetrazole containing a ^{13}C carbon isotope atom in the ring has been described recently.[54]

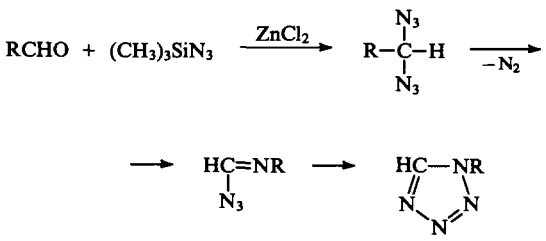
2. 1-Substituted tetrazoles

The choice of synthetic methods for 1-substituted tetrazoles is limited. The main procedure again involves addition of hydrazoic acid to isonitriles. Together with this procedure, use is also made of coupling reactions between diazonium salts and diformylhydrazine or the interaction of imidoyl chlorides, obtained from monosubstituted formamides, with hydrazoic acid.[51] Among the new methods of synthesis of 1-substituted tetrazole, mention should be made of the reaction of aldehydes with trimethylsilyl azide (TMSA)[55] and of amines with ethyl orthoformate and sodium azide.[56–59] In the former case,[55] the interaction of an aldehyde with TMSA leads to the initial formation of a diazide which is then converted into an imidoyl azide by scission of a nitrogen molecule and a rearrangement.

G I Koldobskii Department of the Chemical Technology of Organic Dyes and Phototropic Compounds,
V A Ostrovskii Department of the Chemistry and Technology of Organic Compounds of Nitrogen,
St Petersburg State Technological Institute, Moskovskii prosp. 26, 198013 St Petersburg, Russian Federation.
Fax (7-812) 110 62 85. Tel. (7-812) 316 53 49 (G I Koldobskii)

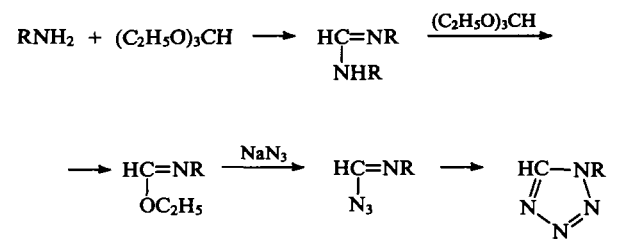
Received 27 May 1993
Uspekhi Khimii **63** (10) 847–865 (1994); translated by A K Grzybowski

The imidoyl azide cyclises to the 1-substituted tetrazole.



The mode of reaction depends on the aldehyde : TMSA ratio. In the presence of a threefold excess of TMSA, 1-substituted tetrazoles are formed, while for a reactant ratio ranging from 1 : 1 to 1 : 1.5 the products are disubstituted tetrazoles.

One of the most promising methods of synthesis of 1-substituted tetrazoles involves the reaction of amines with ethyl orthoformate and sodium azide. This method may be regarded as universal, since aliphatic and aromatic amines having different structures can be used for the preparation of tetrazoles. It is believed[58] that 1-substituted tetrazoles are formed in accordance with the following scheme:



1-Substituted tetrazoles can also be obtained by alkylating tetrazole. This reaction will be examined in detail in the discussion of the chemical properties of tetrazoles.

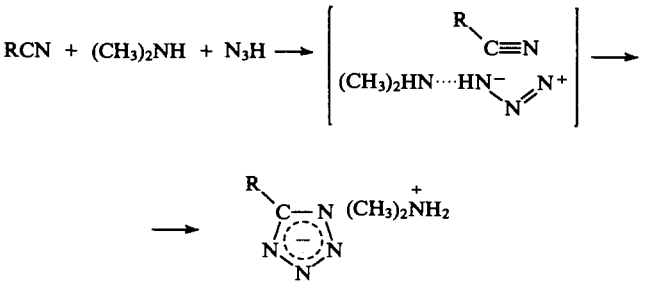
3. 2-Substituted tetrazoles

The development of simple and effective methods of synthesis of 2-substituted tetrazoles is one of the problems in the chemistry of tetrazoles of greatest current interest. As before, the only method of synthesis of 2-substituted tetrazoles involves the alkylation of tetrazole.[47,51] On the other hand, we should bear in mind that, although a wide variety of 2-substituted tetrazoles may be obtained in the alkylation of tetrazole, the application of this method usually entails difficulties in the separation of the isomeric 1- and 2-substituted tetrazoles formed as a result of the reaction.

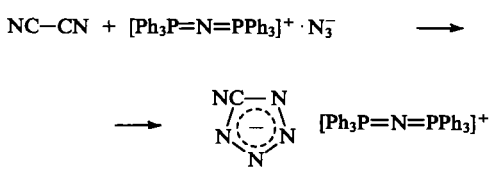
4. 5-Substituted tetrazoles

The commonest method of synthesis of 5-substituted tetrazoles involves the reaction of nitriles with salts of hydrazoic acid.[51] Both the simplest aliphatic and aromatic nitriles and nitriles with a complex structure, including those containing N-, O-, and S-heterocyclic substituents, may be used for such purposes.[60-68] The most suitable solvents for such reactions are dimethyl formamide[51] and butanol.[69]

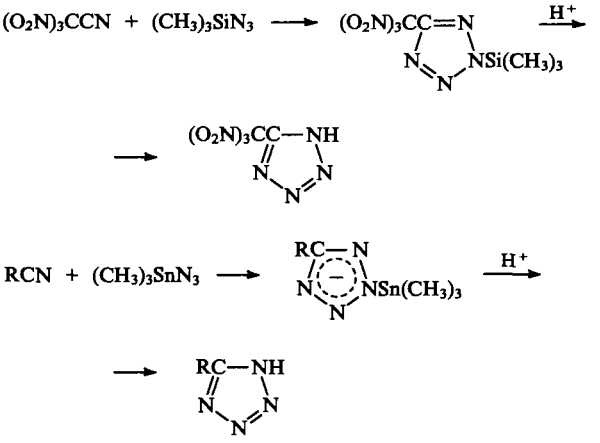
It was postulated previously that the interaction of nitriles with ammonium azides is accompanied by the formation of an imidoyl azide as a result of nucleophilic attack of the azide ion on the carbon atom of the nitrile group; the imidoyl azide cyclises to the tetrazole.[70] However, subsequently it was established in the study of the kinetics of this reaction that 5-substituted tetrazoles are formed via a 1,3-dipolar cycloaddition mechanism. In this process, the dipolarophile is the nitrile, while the hydrogen-bonded complex of the amine with hydrazoic acid serves as the 1,3-dipole.[71,72]



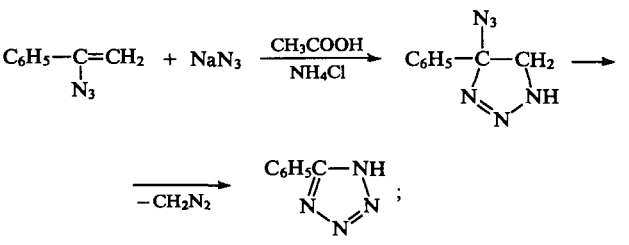
On the other hand, the possibility of the formation of 5-substituted tetrazoles via a two-stage mechanism is not ruled out. This mechanism apparently operates for substrates in which the nitrile group is linked to a powerful electron-accepting substituent, for example for trifluoro- and fluorodinitroacetonitriles[73-75] and also for oxalodinitrile.[76] It is therefore appropriate to note that oxalodinitrile reacts at a high rate with $[Ph_3P=N=PPh_3]^+N_3^-$ affording 5-cyanotetrazole in 96% yield.[76]



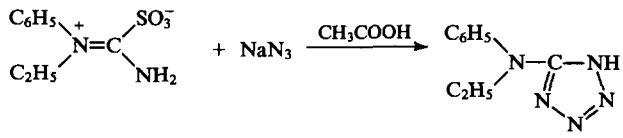
Instead of the salts and complexes of hydrazoic acid, trimethylsilyl azide[29,74] as well as trimethyl- and tributyl-stannyl azides[77,78] may be employed in the reaction with nitriles. In such cases, 1-trimethylsilyl- and 1-trimethyl(butyl)stannyl-5-R-tetrazoles are formed in the first stage, being converted into 5-R-tetrazoles on acid hydrolysis.



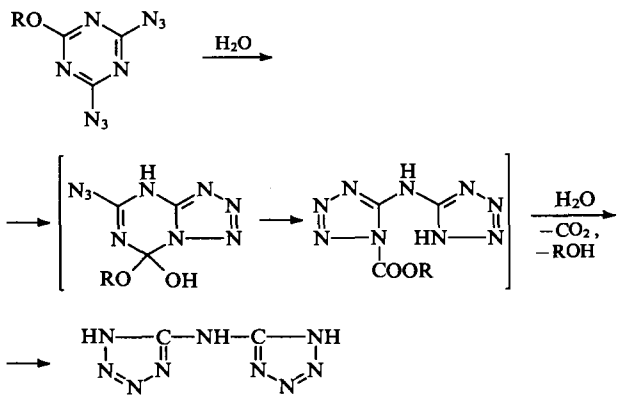
One should include among the novel methods of synthesis of 5-substituted tetrazoles the reaction of 1-azido-1-phenylethene with sodium azide in acetic acid or in dimethylformamide (DMF),[27] i.e.



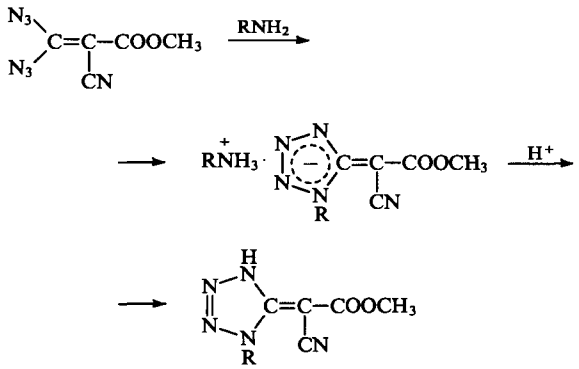
as well as the interaction of aminoiminomethanesulfonic acids with sodium azide in acetic acid.[28]



An interesting method of synthesis of di(tetrazol-5-yl)amine has been proposed.[79] When 6-alkoxy-2,4-diazido-1,3,5-triazines are heated in water, a ring carbon atom and the alkoxy-group linked to it are eliminated, which leads to di(tetrazol-5-yl)amine.



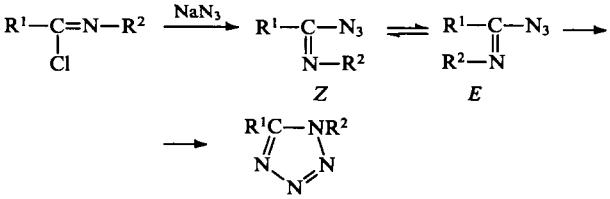
The synthesis of 5-substituted 4,5-dihydrotetrazoles from methyl 3,3-diazido-2-cyanoacrylate and ammonia or amines in a satisfactory yield has been reported recently.[80,81]



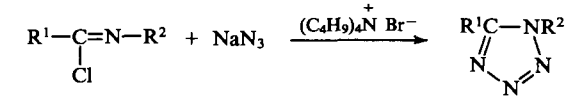
R = H, Alk

5. 1,5-Disubstituted tetrazoles

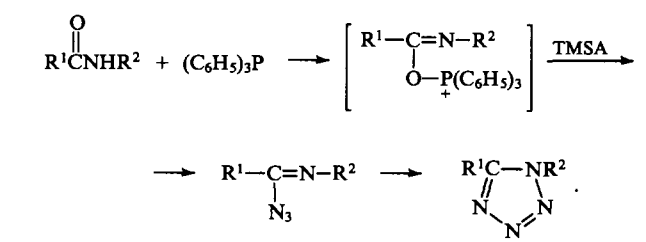
The reactions of imidoyl chlorides with hydroazoic acid or inorganic azides is again one of the most commonest methods of synthesis at 1,5-disubstituted tetrazoles. This method is universal and can be used to synthesise 1,5-disubstituted tetrazoles containing a wide variety of functional groups.[82-91] The kinetics and mechanism of this reaction have been investigated.[92,93] It has been shown that the interaction of an imidoyl chloride with sodium azide involves the formation in the first stage of a mixture of the (*Z*)- and (*E*)-conformers of the imidoyl azide in which only the (*E*)-conformer is converted into the tetrazole.



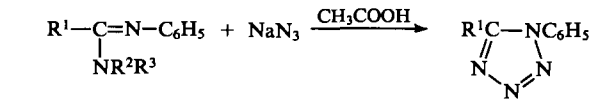
In the synthesis of 1,5-disubstituted tetrazoles from imidoyl chlorides and hydrazoic acid, one should bear in mind that certain precautions must be taken in working with hydrazoic acid, which is highly toxic and explosive. The use of inorganic azides instead of hydrazoic acid enables these difficulties to be avoided to a large extent, but, owing to the limited solubility of these reagents, the reaction must be carried out in DMF.[94,95] Other solvents—dry dioxane, ethanol, or acetone—are less effective.[96-99] The addition of water to the reaction mixture makes it possible to increase somewhat the solubility of alkali metal azides, but, owing to the hydrolysis of the imidoyl chloride, the yield of 1,5-disub-stituted tetrazoles diminishes.[100] This conflict was resolved with the aid of phase transfer catalysis. It was shown that imidoyl chlorides react at a high rate with sodium azide in the methylene chloride (chloroform)–water two-phase system in the presence of phase transfer catalysts (tetrabutylammonium bromide, 5-butyl-2,3-diphenyltetrazolium bromide, or hexa-decyltributylphosphonium bromide). Under these conditions, tetrazoles are formed in 87%–92% yields.[33-35]



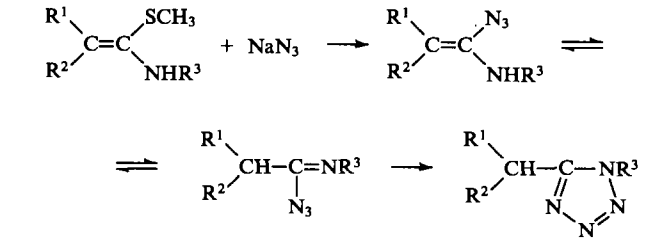
It has recently been reported that trimethylsilyl azide may be used in the reaction with imidoyl chloride instead of hydrazoic acid or inorganic azides.[101] It has been stated[78] that trimethylsilyl azide has been used successfully in the synthesis of 1,5-disub-stituted tetrazoles from amides and triphenylphosphine. The reaction evidently proceeds in accordance with the following mechanism:



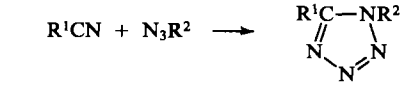
A convenient method of synthesis of 1,5-disubstituted tetrazoles has been proposed by Gaponik et al.,[102] who found that the reaction of amidines with sodium azide in acetic acid results in the formation of the corresponding tetrazoles in a high yield.



Finally, 1,5-disubstituted tetrazoles may be obtained from *S,N*-acetals of ketene on heating the latter with sodium azide in dimethyl sulfoxide.[26]



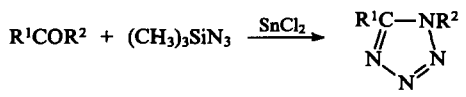
One of the fairly thoroughly investigated methods of synthesis of 1,5-disubstituted tetrazoles involves the reaction of nitriles with aliphatic and aromatic azides.



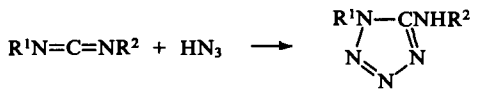
Nitriles having different structures have been used to obtain 1,5-disubstituted tetrazoles.[103-105] The process is significantly accelerated when the reaction is carried out at an increased pressure (10 kbar).[30,31,106,107]

The transition state in the reaction of nitriles with organic azides is formed by the interaction of the HOMO of the azide and the LUMO of the nitrile.[108] This conclusion agrees with experimental data and also accounts for the influence of steric factors on the reactivity of nitriles and organic azides.

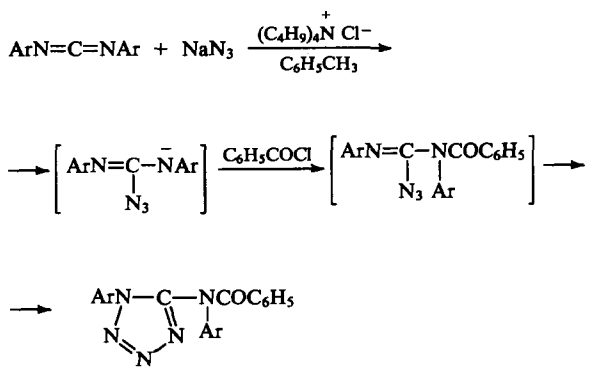
The reaction of ketones with hydrazoic acid is very important for the synthesis of 1,5-disubstituted tetrazoles.[51] The mechanism and synthetic possibilities of this reaction have been investigated in very great detail. It has been shown that ketones of various structures, including steroid ketones, may be used in the synthesis of 1,5-disubstituted tetrazoles. The reaction is carried out in the presence of catalysts such as sulfuric or trichloroacetic acids,[109,110] boron trifluoride etherate,[111,112] and titanium tetrachloride.[113] For a long time, the principal limitation of the method was the need to use hydrazoic acid. These difficulties were overcome by using trimethylsilyl azide with tin chloride[114] or trifluoroacetic acid[115] instead of hydrazoic acid.



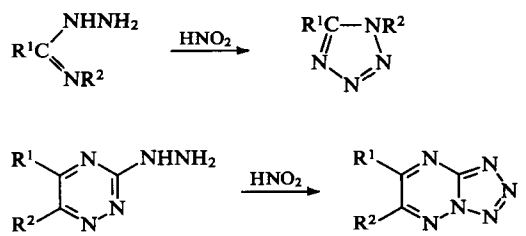
Yet another common method of synthesis of 1,5-disubstituted tetrazoles involves the reaction of carbodiimides with hydrazoic acid.[116-118]



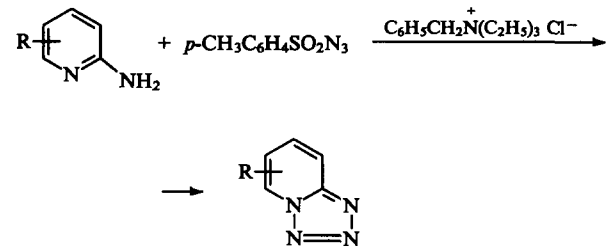
If the reaction is carried out under the phase transfer catalysis conditions in the presence of benzoic acid chlorides, then sodium azide may be used instead of hydrazoic acid.[32]



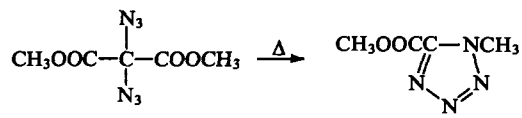
1,5-Disubstituted tetrazoles may be obtained by treating hydrazides,[119] 4-hydrazino-1,2,3-triazines,[120] or 3-hydrazino-1,2,4-triazines[121] with hydrazoic acid.



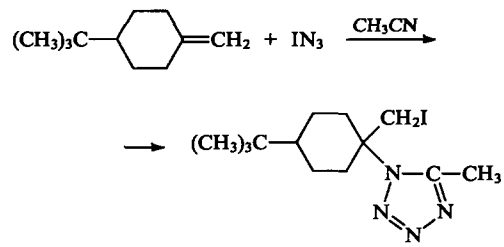
An interesting method of synthesis of annelated tetrazoles by the interaction of 2-aminopyridine or 2-aminoquinoline with toluene-*p*-sulfonyl azide under phase transfer catalysis conditions has been proposed.[122]



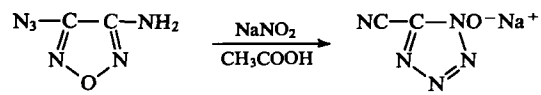
Finally, mention should also be made of a series of methods of synthesis which have so far been used to a limited extent. In the first place, this includes the reaction of isocyanates with sodium azide[123] or trimethylsilyl azide[124] and the thermal rearrangement of 5-azido-1,2,3-triazoles[125,126] and the diesters of 3,3-diazidomalonic acid.[127]



This group of syntheses also includes the addition of iodine azide to norbornene[128] and 4-(*tert*-butyl)-1-methylenecyclohexane[129] acetonitrile.

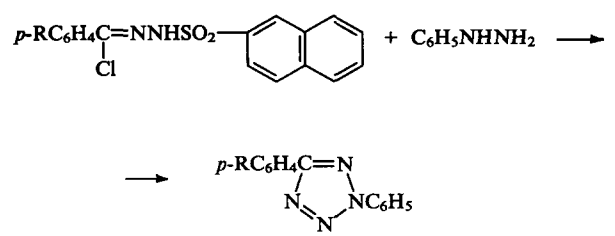


Several further methods of synthesis of 1,5-disubstituted tetrazoles have been proposed recently: the reaction of 1,3-oxazinium salts with sodium azide,[130] the reaction of benzotriazole with glyoxal and sodium azide,[131] and the diazotisation of 3-amino-4-azido-1,2,5-oxadiazole.[132]



6. 2,5-Disubstituted tetrazoles

The methods of synthesis of 2,5-disubstituted tetrazoles have been developed inadequately. Not even one fundamentally new method of synthesis of these compounds of a general character has been proposed during the last decade. Nevertheless, the reaction of imidoyl chlorides with phenylhydrazine is noteworthy.[133]

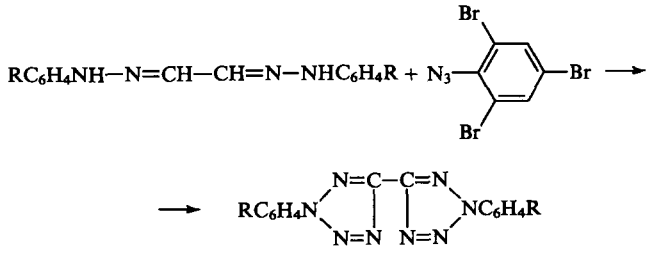


R = H, CH_3, OCH_3, NO_2

N-(Naphthalenesulfonyl)benzohydrazides were used to synthesise the imidoyl chlorides.

A novel method of synthesis of 2-aryl-5-(2-aryltetrazol-5-yl)tetrazoles, based on the reaction of glyoxal bisarylhydrazones with 2,4,6-tribromoazidobenzene, has been proposed (Scheme 1).[134]

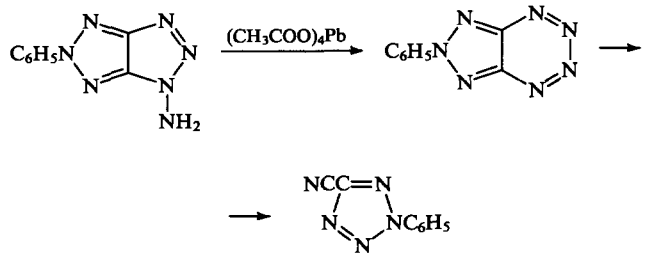
Scheme 1



R = H, OCH_3, Br, Cl

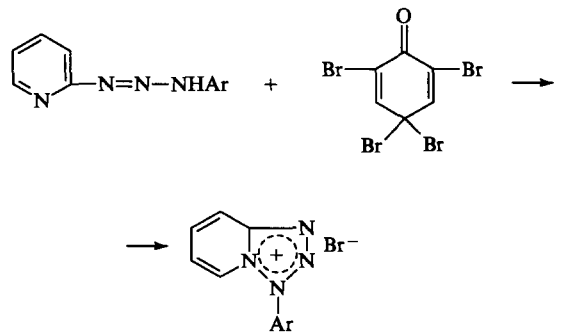
Finally, mention should be made of an interesting example of the conversion of condensed 4-amino-2-phenyl-1,2,3-triazolo-[4,5-*d*]-1,2,3-triazole into 5-cyano-2-phenyltetrazole on treatment with lead tetraacetate (Scheme 2).[135]

Scheme 2

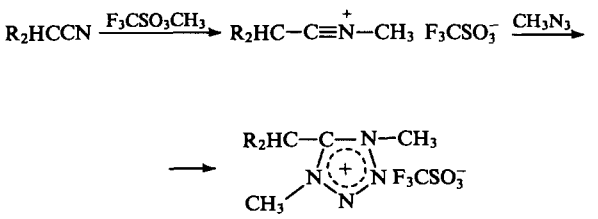


7. Tetrazolium salts

Isomeric 1,2,5-, 1,3,5-, 1,4,5-, and 2,3,5-trisubstituted tetrazolium salts are known. The synthesis of these compounds has been reviewed.[136] Studies published after 1986 are considered below. The syntheses of a series of 1,2,5-trisubstituted tetrazolium salts by oxidising 3-aryl-1-(2-pyridyl)triazenes with 2,4,4,6-tetrabromocyclohexa-2,5-dien-1-one have been described.[137,138]



The alkylation of 1,5- and 2,5-disubstituted tetrazoles is a convenient method of synthesis of tetrazolium salts.[136] It has been shown recently[139] that 1,4,5-trisubstituted tetrazolium salts are formed in a satisfactory yield in the alkylation of 1,5-disubstituted tetrazoles by dialkyl sulfates or alkyl iodides. The above tetrazolium salts have also been obtained by the successive treatment of nitriles with methyl trifluoromethanesulfonate and methyl azide.[140]



The oxidation of formazans having different structures with potassium permanganate in an organic solvent–water two-phase system leads to the corresponding tetrazolium salts in a high yield. A significant feature of this reaction is the fact that the role of the phase transfer catalyst is assumed by the tetrazolium hydroxide formed in the first stage of the reaction—in the oxidation of the formazan at the interface.[34,141,142]

The synthesis of mesoionic tetrazoles has been described.[143–145]

III. Physicochemical properties

1. Electronic structure

Nonempirical quantum-chemical methods have been used successfully during the last decade to study the electronic structure of tetrazoles. Attention has been concentrated on the problem of prototropic tautomerism in the solution of which an ab initio method was employed. The total energies of 1*H*- and 2*H*-tautomers of tetrazoles have been calculated in terms of the 6-31G** and 6.311+G(2*d*, 2*p*) basis sets. It follows from these data that the 2*H*-tautomer is more stable in the gas phase.[146,147] The vertical ionisation potential of the 2*H*-tautomer of tetrazole, calculated by quantum-chemical methods, agrees with the experimental value obtained by photoelectron spectroscopy.[148] It is noteworthy that the higher stability of the 2*H*-tautomer in the gas phase is indicated by the results of quantum-chemical calculations for the radical-cations of the two prototropic tautomers, carried out by the semiempirical CNDO/2 method, and also by mass-spectrometric data.[149,150] On the other hand, calculations by the modern semiempirical MNDO method indicate a greater stability of the 1*H*-tautomers of tetrazole and 5-fluorotetrazole in the gas phase.[36,37]

Objectively, the choice of the basis set does not play a fundamental role in the analysis of the prototropic tautomerism of tetrazole by a nonempirical method. However, the situation changes on passing to the protonated tetrazole (the tetrazolium cation). Here one should bear in mind that, in the calculation of the energy of the protonation of tetrazole in terms of a minimal basis set, unduly high values are obtained. It follows from the calculation that the tetrazolium cation containing protons in the 1- and 4-positions in the heterocycle is the most stable and that the relative stability of this tautomer diminishes by 29.3 kJ mol^{-1} on passing from the STO-3G basis set to the 6-31G**/6-31G basis set.[38,151] A similar analysis has been carried out for the protonation of 1-methyl- and 2-methyl-tetrazoles, in which the basicity centre is also the N(4) atom of the heterocycle according to the ab initio (6-31G) calculation.[152]

The extensive application of quantum-chemical methods made it possible to obtain valuable information not only about the prototropic tautomerism of tetrazoles but also about many other interesting questions. Thus a topological analysis of the structures of complexes of tetrazole with Li^+, Na^+, K^+, and Al^{3+} has been carried out by an ab initio method. The possibility of different relative dispositions of the heterocyclic ligand and the metal ion in space has been demonstrated.[40]

Modern semiempirical methods have also been used successfully in the analysis of the electronic structures of tetrazole and its derivatives. It has been shown that the MNDO method describes adequately the electronic structures of tetrazoles and that the application of this method is sometimes preferable to the use of the ab initio method in terms of a minimal basis set.[153]

At the same time, it has been noted that the method yields enthalpies of formation which are too low by 83.8 kJ mol^{-1}: 230.5 and 248.0 kJ mol^{-1} for 1*H*- and 2*H*-tetrazoles respectively.[36]

We may list a further several studies in which the electronic structures of tetrazoles have been investigated. Thus a study has been made[154,155] of the electronic structures of various alkyl- and alkenyl-tetrazoles (MNDO). The proton affinities of tetrazole and substituted tetrazoles have been calculated.[156] The azidoazomethine–tetrazole equilibrium has been analysed[36] and the structure of a dipolar diazonium tetrazolate has been considered in another study.[157] One should include here also the recently published results of an ab initio calculation of the potential energy profile for the Dimroth rearrangement of 1-substituted 5-aminotetrazoles[158] and the stability of the relatively unstable electronic states of tetrazole[159] as well as the results of semiempirical calculations of the electronic parameters of the reactants and products in the alkylation reactions of salts of 5-substituted tetrazoles (CNDO, CNDO/2),[160,161] the exhaustive alkylation of isomeric *N*-alkyltetrazoles,[162] and the aminomethylation of *N*-alkyl-5-aminotetrazoles (CNDO/2).[163]

Quantum-chemical calculations have been used effectively for the interpretation of the UV spectra of 1,4-dihydro-5*H*-tetrazoles (CNDO/S-CI),[164] the ^{15}N NMR spectra of tetrazole (MNDO), *N*-alkyltetrazoles (INDO/S-SOS),[165,166] *N*-aminotetrazoles (INDO),[167,168] and tetrazolopyridines (INDO/S-SOS),[169] and also of the mass spectra of the isomeric methyltetrazoles (CNDO, CNDO/2).[150,170]

The joint analysis of experimental data and results obtained by quantum-chemical methods will probably persist.

2. Electronic, photoelectron, and vibrational spectra

Communications concerning the application of UV spectroscopy as an analytical method in the study of protolytic equilibria, reactivities, and compositions of multicomponent mixtures of tetrazoles have occupied a leading position among publications of recent years. Thus UV spectroscopy has been used successfully to determine the acidity and basicity constants of 5-(*o*-, *m*-, and *p*-carboxyphenyl)tetrazoles in aqueous solutions of different acidity,[171] in the study of the rates and regioselectivities of the reactions of tetrazolate anions with dimethyl sulfate,[172,173] ethyl bromoacetate,[174] and methyl vinyl ketone,[175,176] and also in the study of equilibria involving ion pairs of the salts of 5-aryltetrazoles in acetonitrile.[174] Finally, bearing in mind the sensitivity of the UV spectra of the tetrazolate anions to the addition of small amounts of water, one may investigate quantitatively the specific solvation of tetrazolate ions in binary systems and also estimate the reactivities of specifically solvated tetrazole substrates.[173]

The luminescence spectra of 5-aryltetrazoles have been discussed.[177]

The photoelectron spectra (PES) of tetrazoles have their specific features and differ from those of other azoles, which is associated with the high ionisation potentials of tetrazoles by virtue of the enhanced stabilisation of the π levels.[178] According to photoelectron spectroscopic data, tetrazole exists in the gas phase almost exclusively as the 2*H*-tautomer.[148,179] A satisfactory agreement between spectroscopic data and the results of non-empirical calculations has been noted.[148,179] A publication[180] on the photoelectron spectra of certain condensed tetrazoles should be added to the studies quoted above.

Finally, we shall consider investigations of the vibrational spectra of tetrazoles. Thus the frequencies and the normal modes of vibration of 1-methyl- and 2-methyl-tetrazoles, 1-vinyl- and 5-vinyltetrazoles, 2-methyl-5-vinyltetrazole, and 5-phenyltetrazole have been analysed.[181,182] Detailed studies have been made of the vibrational spectra of the hydrazides of tetrazolylacetic acids[182] and tetrazole-containing polymers[183] and also of the IR and Raman spectra of 5-aminotetrazole.[184,185] Levchik et al.[185] interpreted the bands due to the stretching-deformation vibrations of 5-aminotetrazole (1000–1100 cm^{-1}) in terms of Fermi resonance. These data permit a reliable interpretation of the experimental spectra of tetrazoles, which extends the possibilities of vibrational spectroscopy as a method for the identification of compounds containing the tetrazole ring. Vibrational spectroscopy and ^{1}H and ^{13}C NMR spectroscopy can be used jointly in the analysis of tetrazoles having a complex structure. This approach has been demonstrated successfully in the analysis of polyvinyltetrazoles.[186]

3. NMR spectra

NMR spectroscopy has been used widely for the identification, structural study, and the prediction of the properties of tetrazoles. In a number of recent investigations the exceptional possibilities of ^{15}N NMR spectroscopy as a promising method for the investigation of polynitrogen heterocycles, and in particular tetrazoles, have been clearly demonstrated. This method proved extremely effective in the study of the prototropic tautomerism of tetrazole, since the chemical shifts of the ^{15}N nuclei of the pyrrole [N(1)] and pyridine [N(2)] atoms differ significantly.[187] According to Woffold et al.[187] and Bojarska-Olejnik et al.,[188] tetrazole in solution in DMSO-d_6 and $CDCl_3$ exists predominantly as the 1*H*-tautomer. The study of the ^{15}N NMR spectra of tetrazole and isomeric *N*-alkyltetrazoles led to the same conclusion.[189] It was shown that, for solutions of tetrazoles in DMSO or dioxane at concentrations not exceeding 0.5 M, it is possible to identify reliably the 1*H*- and 2*H*-tautomers and the isomeric *N*-alkyltetrazoles[166,189] and to demonstrate convincingly that 5-mercapto- and 5-hydroxy-tetrazoles exist mainly as the thiono- and oxo-derivatives respectively.[189] The structures of mono- and di-alkyl(alkenyl)tetrazoles,[190,191] complex condensed systems incorporating the tetrazole ring,[169] and also tetrazolium salts[191,192] have been established with the aid of ^{15}N NMR spectroscopy. The results of these investigations agree well with X-ray diffraction and gas electron diffraction data.[193] Interesting results have been obtained in a study[194] of tetrazoles by ^{15}N NMR spectroscopy. ^{15}N chemical shifts for a series of mono- and bicyclic tetrazoles and also for the salts and complexes of 5-substituted tetrazoles were determined. Together with the solution of the traditional problem — the determination of the individuality of the N(1)- and N(2)-isomers — ^{15}N chemical shifts were obtained for the tetrazolate anions taking into account data on the NH acidity of 5-substituted tetrazoles. A later study[190] dealt with the influence of the protonation of the tetrazole ring at the N(4) atoms on the ^{15}N chemical shift.

^{13}C NMR spectroscopy has also been used widely for the solution of structural problems in the chemistry of tetrazoles. The available information about the ^{13}C NMR spectra of isomeric *N*-substituted tetrazoles and other azoles has been surveyed and the data have been compared.[195] The torsional angles between the phenyl and azolyl fragments in *N*-aryltetrazoles have been estimated from ^{13}C NMR spectroscopic data,[196,197] and the electronic constants of the *N*(1)-tetrazolyl group have also been found.[196,198] ^{13}C NMR spectroscopy has been used in the study of 5-aryltetrazoles,[199] derivatives of 5-furyltetrazole,[200] and isomeric vinyltetrazoles[154,201,202] and also in the analysis of complex amino-imino equilibria involving 5-alkylamino-1-phenyltetrazoles.[203]

The most complete information about the structure of tetrazoles can be obtained by the joint application of ^{1}H, ^{15}N, and ^{13}C NMR spectroscopy. The tendency to carry out such studies is clearly manifested in recent publications.[154,168,169,191] It is noteworthy that the spin–spin coupling constants $J(^1H, ^1H)$,[204] $J(^{15}N, ^1H)$,[205] and $J(^{13}C, ^{13}C)$[206] as well as the nuclear Overhauser effect[207] are used together with the ^{1}H, ^{15}N, and ^{13}C NMR chemical shifts for the solution of structural problems, including the problem of the prototropic tautomerism and the identification of the isomeric *N*-alkyl(aryl)tetrazoles.

4. Thermolysis, combustion, and detonation

Tetrazoles possess extreme thermochemical characteristics among the azoles. The enthalpies of formation of tetrazole in the crystalline and gaseous states are ΔH_f(cr) = 236.1 kJ mol^{-1} and ΔH_f(g) = 327.2 kJ mol^{-1} respectively,[208,209] while the enthalpy of formation of crystalline 5-(tetrazol-5-yl)tetrazole is ΔH_f(cr) = 532.1 kJ mol^{-1}.[210] The standard enthalpies of combustion ΔH_c of tetrazole and 5-(tetrazol-5-yl)tetrazole are −916.1 and −1605.6 kJ mol^{-1} respectively.[208,210] The thermal decomposition of tetrazoles takes place in the temperature range 150–250 °C with dissociation of the N–N bonds.[211] According to the results of thermogravimetric analysis, the intense decomposition of tetrazoles is accompanied by an exothermic effect and a marked decrease in mass.[185] The thermal stability of tetrazoles is determined by the nature and location of the substituents in the heterocycle.[212–214] Thus an increase in the number of nitro-groups in nitroaryltetrazoles lowers their thermal stability.[214] The decomposition of the tetrazole ring is usually accompanied by the evolution of molecular nitrogen. However, the routes to the fragmentation of isomeric tetrazoles differ significantly. The thermolysis of 1,5-disubstituted tetrazoles leads to intermediate nitrenes,[215] while nitrile imines are formed from 2,5-disubstituted tetrazoles.[216,217] In all cases, the elimination of nitrogen proceeds via a highly polar transition state.[218] The rate-limiting stage of the thermal decomposition of 1,5- and 2,5-disubstituted tetrazoles is the homolytic dissociation of the N(1)–N(2) and N(2)–N(3) bonds respectively. The activation energies for these processes are in the range E_a = 162–200 kJ mol^{-1}. There is a linear relation between the logarithms of the rate constants for the thermal decomposition of tetrazoles and the Coulombic component of the perturbation energy (E_N). This makes it possible to predict the rate constants for the homolytic thermal decomposition of tetrazoles of different structure.[219] The characteristic features of the thermal decomposition of amino- and nitroamino-tetrazoles have been considered.[220,221]

It has been established that the rate-limiting stage in the thermolysis of poly-1-vinyltetrazole is the opening of the tetrazole ring. The activation energy for this process is 140–148 kJ mol^{-1}.[222] The thermal decomposition of the salts of 5-alkyl-2,3-diaryl- and 2,3,5-triaryl-tetrazolium salts has been discussed.[34,141]

In conclusion, it is essential to note that the fragmentation reactions of the tetrazole ring under the influence of a thermal pulse and electron impact have common features.[51] Joint examination of the thermal decomposition and mass spectra of tetrazoles yields valuable information about the nature of the reacting and intermediate species and about their reactivities.[223–227]

The characteristic features of the structure of the high-energy tetrazole ring predetermine the specific features of the combustion processes involving tetrazole and tetrazole-containing substances. These processes sometimes take place with unusual external effects, as happens in the combustion of mixtures of tetrazole and sodium tetrazolate.[50,228–230] A detailed study of the combustion of tetrazole has been carried out[231] and it has been shown that the process proceeds mainly in the condensed phase.

The characteristics of the transition of the combustion of the tetrazoles to detonation have been investigated in relation to the isomeric 1-methyl- and 2-methyl-5-nitrotetrazoles. Moulded 2-methyl-5-nitrotetrazole has much more effective detonation characteristics. The average time required for the transition from combustion to detonation is longer for 2-methyl-5-nitrotetrazole than for lead azide but shorter than for lead styphnate.[232] The capacity for detonation of complexes of 5-cyano-, 5-nitro-, and 5-nitroamino-tetrazoles as initiating explosives has been investigated experimentally.[233–235] Theoretical predictions of the detonation properties of tetrazoles have been made[236] and the methods for the analysis of the explosive properties of tetrazole derivatives have been discussed in a monograph.[237]

5. Acid–base properties

Tetrazole and 5-substituted tetrazoles are NH acids and weak organic bases, the acidity and basicity constants of which vary within wide limits depending on the nature of the substituent. Thus, on passing from 5-methyl to 5-nitro-tetrazole, the acidity constant increases while the basicity constant decreases approximately by seven orders of magnitude. The results of an experimental study of the acid-base properties of tetrazoles published up to 1990 have been surveyed in reviews[41,42] and in a monograph.[43] The same publications present tabulated acidity and basicity constants for a large number of tetrazoles. Among the studies in recent years, mention must be made of those in which the acidity and basicity have been investigated by various quantum-chemical methods and the proton affinities PA and PA^- of tetrazole and monosubstituted tetrazoles have been calculated.[160,168,238] The values of PA^- for the tetrazolate anion, calculated by the MNDO, AM1, and PM3 methods, are respectively 1567.5, 1351.3, and 1325.7 kJ mol^{-1}.[238]

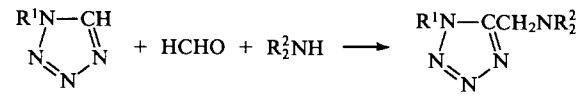
The calculations by Ostrovskii et al.[160] and Claramunt et al.[168] agree with the earlier experimental data for the basicity of tetrazoles. The protonation of tetrazoles of different structure at the nitrogen atom in the 4-position has been explained by the greater stability of the corresponding tetrazolium cation. It has also been shown[160] that there is a linear correlation between the calculated (MNDO) affinities PA and the experimental pK_{BH^+} for 5-substituted tetrazoles: pK_{BH^+} = 0.323PA − 49.01.

Unfortunately there have been as yet no experimental studies of the acidity and basicity of tetrazoles in the gas phase.

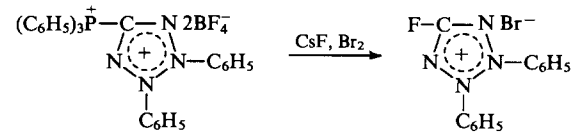
IV. Reactions of tetrazoles

1. Electrophilic substitution at a ring carbon atom

The reactions involving electrophilic substitution at a ring carbon atom in tetrazoles have been inadequately investigated. It has been shown recently that 1-alkyltetrazoles are smoothly iodinated by iodine in solution in sulfuric acid in the presence of potassium permanganate.[239] The corresponding 1-alkyl-5-iodotetrazoles are formed in 55%–75% yield. It has also been established that, when 1-methyltetrazole is treated with *tert*-butyllithium in tetrahydrofuran (THF), the hydrogen atom at a ring carbon atom in substituted by lithium.[240] The hydrogen at a ring carbon atom in 2,3-diaryltetrazolium salts is also substituted on treatment with *tert*-butyllithium in hexane.[241,242] 1-Substituted tetrazoles react with formaldehyde and amines under mild conditions, affording aminomethylation products.[59,243]

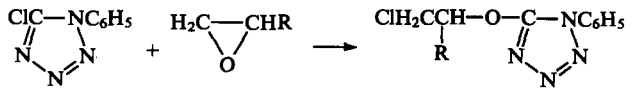


Finally, it is noteworthy that the triphenylphosphonium group in 2,3-diaryl-5-triphenylphosphoniotetrazolium is substituted by fluorine on treatment with caesium fluoride in the presence of bromine.[241]



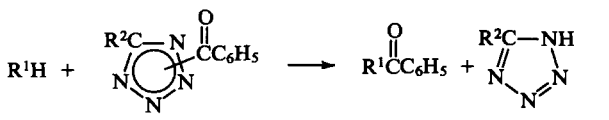
2. Nucleophilic substitution

The chlorine atom in 5-chloro-1-phenyltetrazole is readily substituted by treatment with alkali metal phenoxides in acetonitrile.[244] Similarly the chlorine atom in 5-chloro-1-phenyltetrazole is substituted by the SeH group on interaction of the tetrazole with sodium selenide in DMF at 100 °C.[245] Under phase transfer catalysis conditions, the corresponding ethers are formed in a satisfactory yield from 5-chloro-1-phenyltetrazole and various epoxy-compounds.[246]

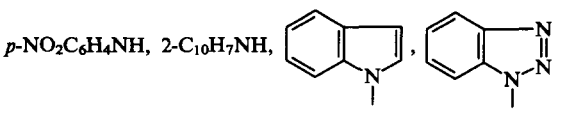


The bond between the sulfur and carbon atoms in 1-aryl-5-mercaptotetrazoles is cleaved on alkaline hydrolysis, which leads to the formation of 1-aryl-5-tetrazolols.[245]

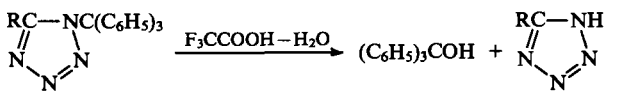
The tetrazole ring in 5-aryl-1-benzoyl- and 5-aryl-2-benzoyltetrazoles is readily substituted by various nucleophiles.[247] *N*-Benzoyltetrazoles are mild acylating agents, which are effective in reactions with primary and secondary aliphatic and aromatic amines as well as alcohols, benzimidazoles, and benzotriazole.



R^1 = C_2H_5O, C_6H_5O, *p*-$NO_2C_6H_4O$, 2-$C_{10}H_7O$, C_6H_5NH,



Compared with the widely used acylating agents *N*-benzoylimidazole and *N*-acylimidazoles,[248] 5-aryl-*N*-benzoyltetrazoles have significant advantages. The reactivity of *N*-benzoyltetrazoles is superior to that of *N*-acylimidazoles and these compounds also have a higher selectivity towards primary and secondary hydroxy- and amino-groups.[249] The use of *N*-benzoyl-tetrazoles is especially effective when the reactants and products are sensitive to acids and alkalis and are also thermally relatively unstable. The tetrazole ring in 1-triphenylmethyl-5-R-tetrazoles is readily substituted on treatment with trifluoroacetic acid in aqueous tetrahydrofuran.[78]

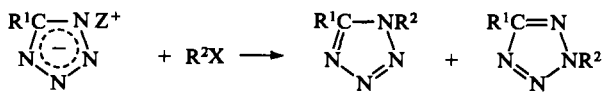


3. Alkylation

Alkylation belongs to the group of reactions of tetrazoles which have been investigated in greatest detail. It constitutes a simple method of synthesis of mono- and di-substituted tetrazoles of different structure, the preparation of which by other procedures is frequently impossible. Theoretically this reaction is of great interest, since it can serve as a convenient model for the study of heterocyclic substrates with dual reactivity.

Depending on the properties of the reaction medium, tetrazole, 5-substituted tetrazoles, as well as their salts enter into the alkylation reaction. Alkyl halides,[250-255] esters of sulfuric and aromatic sulfonic acids,[254] the acetates of nitroaminoalcohols,[256] and compounds containing activated double bonds [175,176,257,258] are used as the alkylating agents. Data on the application of alcohols, [259-262] unsaturated compounds (propene and isobutene),[263] certain nitrylium ions,[264] and vinyl ethers [265] for such purposes have been published recently. Separate mention should be made of the reactions of 5-substituted tetrazoles with aldehydes (formaldehyde) and amines, which result in the formation of *N*-aminomethyl(*N*-hydroxymethyl) derivatives of tetrazoles.[266-269]

It was postulated previously that, regardless of the nature of the alkylating agent and the properties of the reaction medium, the alkylation of tetrazole and 5-substituted tetrazoles always results in the formation of the corresponding 1- and 2-substituted tetrazoles.



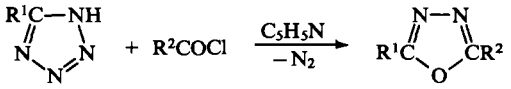
Z^+ = cation.

It was noted that the electronic nature of the substituents in the 5-position in the tetrazole ring exerts the main influence on the selectivity of this reaction—electron-donating and electron-accepting substituents promote respectively an increase and a decrease in the fraction of the *N*(1)-isomer in the alkylation products.[51] However, according to the latest data, exclusively 2-substituted tetrazoles are formed in the alkylation of tetrazole and 5-substituted tetrazoles by *tert*-butyl, isopropyl, or cyclohexyl alcohols in 96% sulfuric acid regardless of the nature of the substituent in the 5-position in the tetrazole ring.[262] Consequently, the selectivity of the alkylation of the tetrazoles depends also on the form (neutral or ionised) in which the substrate reacts with the alkylating agent. The high selectivity of the alkylation of the triethylammonium salts of 5-aryltetrazoles by methyl vinyl ketone in aprotic dipolar solvents [only the corresponding 4-(5-aryltetrazol-2-yl)butan-1-ones are formed] can be explained by the steric blocking of the N(1) atom of the tetrazole ring.[175,176]

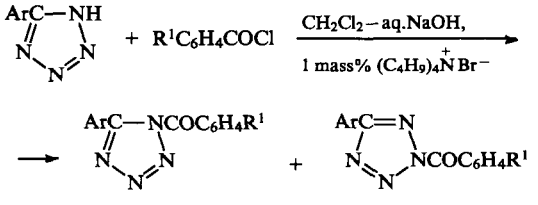
In the alkylation of tetrazoles under conditions of phase transfer catalysis and in homogeneous media, appreciable differences between the reaction selectivities were not discovered.[162] On the other hand, alkylation employing phase transfer catalysis is preparatively an extremely promising method, which makes it possible to obtain a wide variety of *N*-mono- and *N*,*N*′-disubstituted tetrazoles under mild conditions and in high yields using simple and readily available reagents and solvents.[270]

4. Acylation and imidoylation

Reactions of tetrazoles with acylating agents and imidoyl chlorides have recently acquired special importance, mainly because 2,5-disubstituted 1,3,4-oxadiazoles of different structure [142,247,270-273] as well as the previously unavailable 3*H*-1,3,4-benzotriazepines [274-277] can be obtained with their aid. Thus tetrazole and 5-substituted tetrazoles are converted into the corresponding 1,3,4-oxadiazoles in high yields on acylation by the chlorides of organic acids in the presence of organic bases at 100–120 °C.



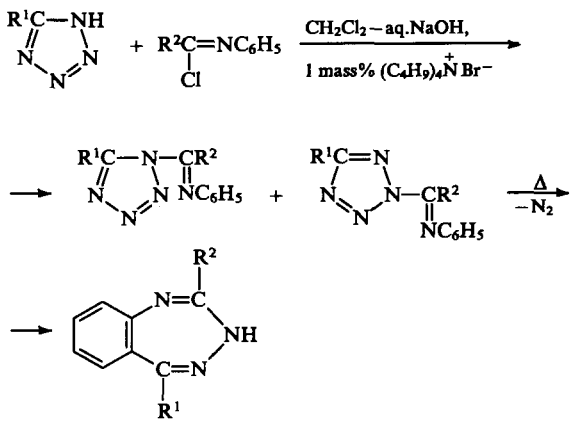
Previously it had been assumed that the first stage of this reaction involves the formation of an unstable 2-acyltetrazole, the cleavage of which with evolution of a nitrogen molecule leads to 1,3,4-oxadiazole.[278] However, subsequently it was demonstrated as a result of the application of phase transfer catalysis that the acylation of 5-aryltetrazoles by substituted benzoic acid chlorides affords not only 2-benzoyltetrazoles but also the isomeric 1-benzoyltetrazoles.[247,271]



The formation of oxadiazoles from 1-benzoyltetrazoles is preceded by isomerisation of the latter to 2-benzoyltetrazoles. It is suggested that, as a result of thermal cleavage and the elimination of a nitrogen molecule, 2-benzoyltetrazole is converted into an acylnitrile imine, the cyclisation of which leads to the oxadiazole.

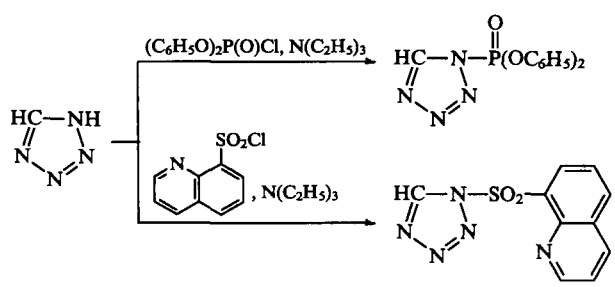
The results obtained in the study of the acylation of 5-substituted tetrazoles by carboxylic acid anhydrides are of greatest practical interest.[273] This reaction can be regarded as one of the most effective and simple methods of synthesis of 2(5)-mono- and 2,5-disubstituted 1,3,5-oxadiazoles.

During the last 30 years, it has come to be assumed that the reaction of 5-substituted tetrazoles with imidoyl chlorides, leading to 3,4,5-trisubstituted 1,2,4-triazoles, proceeds via a mechanism similar to that of the acylation reaction.[279] It was postulated that, on heating 5-substituted tetrazoles with imidoyl chlorides in pyridine, an unstable 2-imidoyl tetrazole is formed initially and is then converted into an imidoylnitrile imine as a result of thermal cleavage and elimination of a nitrogen molecule. The subsequent cyclisation of the imidoylnitrile imine leads to the 1,2,4-tetrazole. The study of this reaction under phase transfer catalysis conditions established that not only 2-imidoyltetrazole but also the isomeric 1-imidoyltetrazole is formed in the first stage. It is of fundamental importance that heating of the isomeric imidoyltetrazoles thus obtained in solutions in toluene, *m*-xylene, or dioxane and also in the absence of solvents results in the formation of the previously unknown 3*H*-1,3,4-benzotriazepines instead of the expected 3,4,5-trisubstituted 1,2,4-triazoles.[276,277]



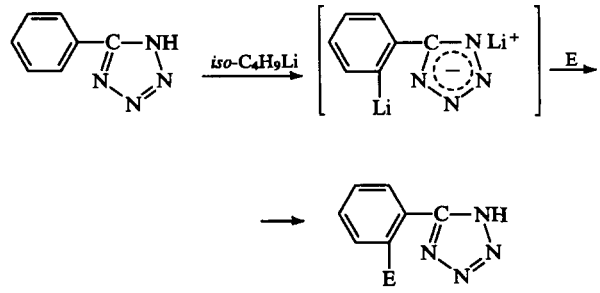
5. Silylation, phosphorylation, and sulfonylation

The interaction of the sodium salts of tetrazole with chlorotrimethylsilane results in the formation of trimethylsilyltetrazole in 85% yield.[47] The best solvent for this reaction is methylene chloride, while acetonitrile and DMF are virtually unsuitable. Begtrup and Larsen[47] do not discuss the problem of the selectivity of the silylation reaction, but one cannot rule out the possibility of the formation of two isomers — 1- and 2-trimethylsilyltetrazoles. It is surprising that the problem of regioselectivity has also not been discussed in the study of the phosphorylation[279] and sulfonation[280] of tetrazole. It is assumed that these reactions result in the formation of only 1-substituted tetrazoles.



6. Reactions of electrophiles with substituted tetrazoles

The reactions of 5-aryltetrazoles as well as 1-alkyl- and 2-alkyl-5-phenyltetrazoles with electrophiles of different nature have been investigated.[240,281–284] For example, it has been shown that, when 5-phenyltetrazole is treated with isobutyllithium in THF at −35 to −30 °C in the presence of tetramethylethylenediamine, the corresponding ionic intermediate is formed and reacts in situ with methyl iodide, acetaldehyde, or acrolein.[284]



It is striking that electrophilic substitution takes place only in the benzene ring and does not involve the tetrazole ring.

It is interesting that, when 5-alkyl-*N*-methyltetrazoles react under similar conditions, electrophilic substitution takes place in both *N*-methyl and *C*-alkyl groups.[285]

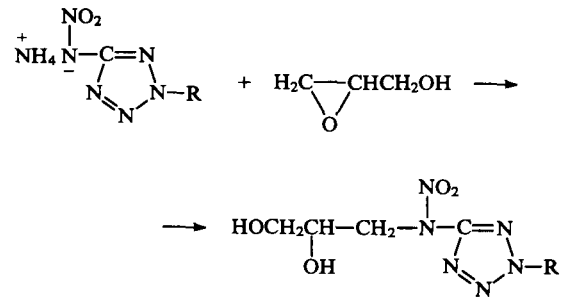
The nitration of 5-aminotetrazole and also of 1-alkyl- and 2-alkyl-5-aminotetrazoles by tetranitromethane in an alkaline medium leads to the corresponding 5-nitroaminotetrazoles.[286,287] Data exist on the nitration of condensed systems—5,6-dihydro-7*H*-imidazolo[1,2-*d*]tetrazole, 7,8-dihydrotetrazolo-[1,5-*b*]1,2,4-triazine, and 5,6,7,8-tetrahydrotetrazolo-[1,5-*b*]-1,2,4-triazine[288]—as well as certain tetrazolium salts.[289]

Treatment of 5-aminotetrazoles with orthoesters results in the formation of the corresponding iminoesters,[290] whilst heating with nitriles in the presence of organoboranes affords amidines.[291] On treatment with thionyl chloride, 1-alkyl-5-aminotetrazoles are unexpectedly converted into 1,2,4-thiadiazoles.[292]

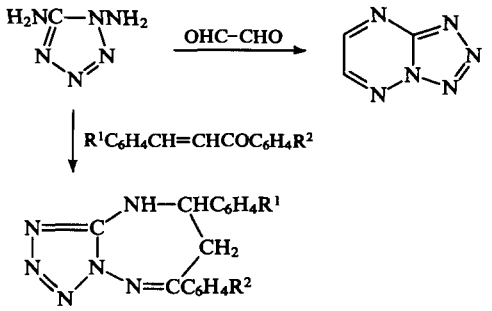


The acylation of 5-aminotetrazole at the amino-group by the chlorides of aromatic carboxylic acids[293,294] as well as the interaction of 5-aminotetrazole with *p*-cyanophenylcarbonylimidoyl chloride[295] have been described. In the latter case, the reaction also involves the exocyclic amino-group.

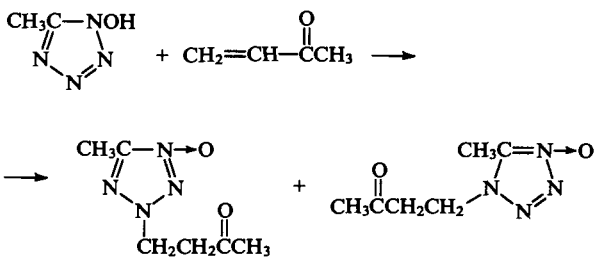
The salts of 2-alkyl-5-nitroaminotetrazole are alkylated by glycidol under mild conditions.[296] The tetrazole ring is not involved in this case.



1,5-Diaminotetrazole is an interesting reagent in the synthesis of heterocycles of various structures. Thus the interaction of 1,5-diaminotetrazole with glyoxal or unsaturated ketones leads to the formation of tetrazolo[1,5-*b*]-1,2,4-triazines and 5,7-disubstituted 5,6-dihydro-4*H*-tetrazolo[1,5-*b*]-1,2,4-triazepines respectively.[288,296]



When 1-hydroxy-5-phenyltetrazole is treated with epoxyalkanes, the reaction involves both the hydroxy-group and the tetrazole ring.[297] On the other hand, the reaction of 1-hydroxy-5-methyltetrazole with methyl vinyl ketone affords the corresponding isomeric *N*-oxides.[298]

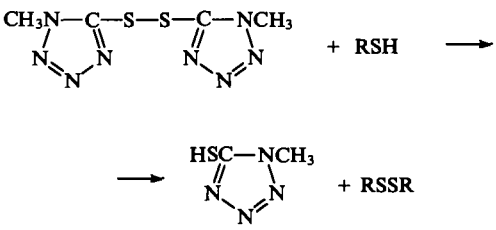


The tetrazole ring is not involved in the alkylation of bis(1-aryltetrazol-5-yl)methanes by methyl iodide,[299] in the arylation and alkylation of 1-phenyltetrazole-5-thiol by 1-chloro-2,4-dinitrobenzene[300] and *tert*-butyl isonitrile[301] respectively, and in the interaction of tetrazole-containing glyoximes with bromocyanogen.[302]

7. Reactions of nucleophiles with substituted tetrazoles

The interaction of tetrazole-5-diazonium chloride with substituted anilines affords a high yield of 3-aryl-1-(tetrazol-5-yl)triazepines.[302] Treatment of 1-alkyl- and 2-alkyl-5-chloroethyltetrazoles with an alcoholic solution of sodium hydroxide led to the formation of the corresponding 5-vinyltetrazoles.[303]

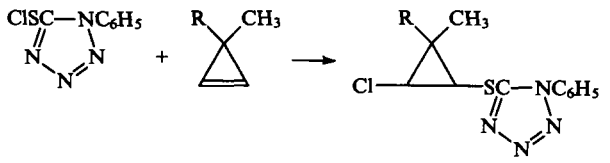
The reactions of 1-alkyl(aryl)tetrazole-5-thiols with nucleophiles (thiols, alcohols) have attracted continuous attention. This is because they can be used to synthesise substances with biological activity.[304] Thus it has been observed that bis(1-methyltetrazol-5-yl) disulfide exhibits an exceptionally high reactivity in relation to thiols.[305-307]



This reaction[306] is a convenient method of synthesis of both symmetrical and asymmetric disulfides.

S-Heteroaryl derivatives of 1-phenyltetrazole-5-thiols are also readily cleaved by potassium hydroxide in the water–acetonitrile system.[245]

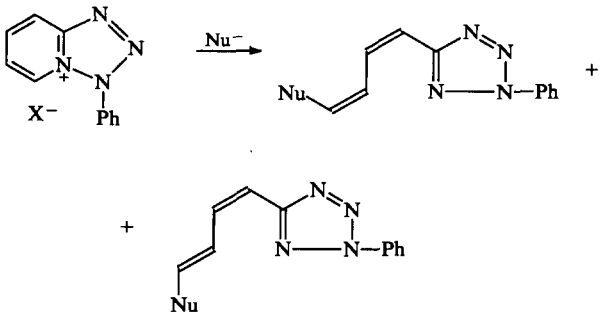
3,3-Disubstituted cyclopropenes interact with 1-phenyltetrazole-5-sulfenyl chloride in solution in methylene chloride at −20 °C.[308]



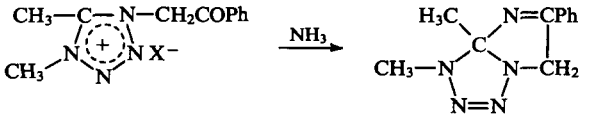
On treatment with unsaturated alcohols in the presence of tertiary amines, *S*,*S*′-bis(1-phenyltetrazol-5-yl) dithiocarbonate is hydrolysed under mild conditions.[309,310]

Grignard reagents may be used to obtain a series of tetrazole derivatives with functional group substituents.[311-313]

Finally, it is noteworthy that treatment of tetrazolylpyridinium salts with nucleophiles entails the dissociation of the N–C bond in the six-membered heterocycle.[314]

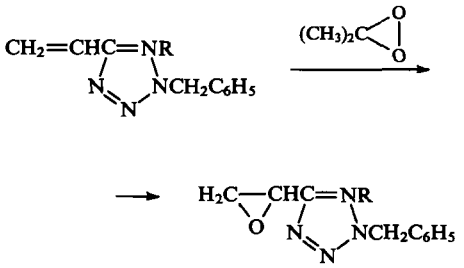


On the other hand, 2,3-dimethyl-4-benzoylmethyltetrazolium salts are converted into dihydro-3*H*-imidazo[1,2-*d*]-tetrazoles on treatment with ammonia.[315]

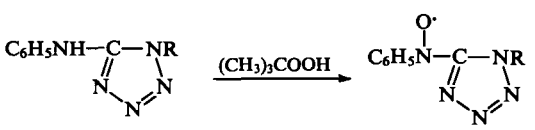


8. The effect of oxidants and reductants

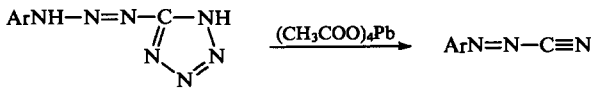
The tetrazole ring is resistant to the action of oxidants. The nature of the reactions between tetrazoles and oxidants depends on the nature and position of the substituent in the heterocycle. Thus interaction of 2-benzyl-5-vinyltetrazole with dimethyldioxirane results in the formation of the corresponding epoxide.[316]



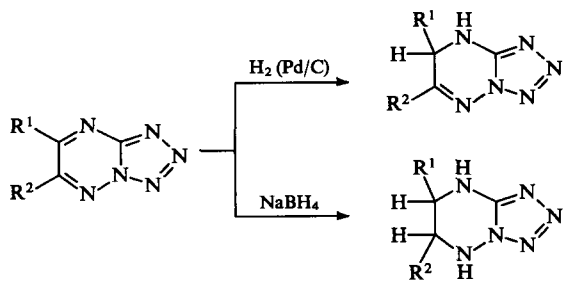
while the oxidation of 5-arylaminotetrazoles by *tert*-butyl peroxide afforded stable nitroxyl radicals.[317]



On the other hand, treatment of 1-aryl-3-(tetrazol-5-yl)triazenes with lead tetraacetate results in the degradation of the heterocycle.[318]



The ring is usually not involved in the reactions with reductants. It has been shown[288] that the reduction of tetrazolo-[1,5-*b*]-1,2,4-triazines by hydrogen (Pd/C) entails only partial hydrogenation of the six-membered ring, whereas in the reduction by sodium tetrahydroborate in methanol the corresponding 5,6,7,8-tetrahydrotetrazolo[1,5-*b*]-1,2,4-triazines are formed in a high yield.

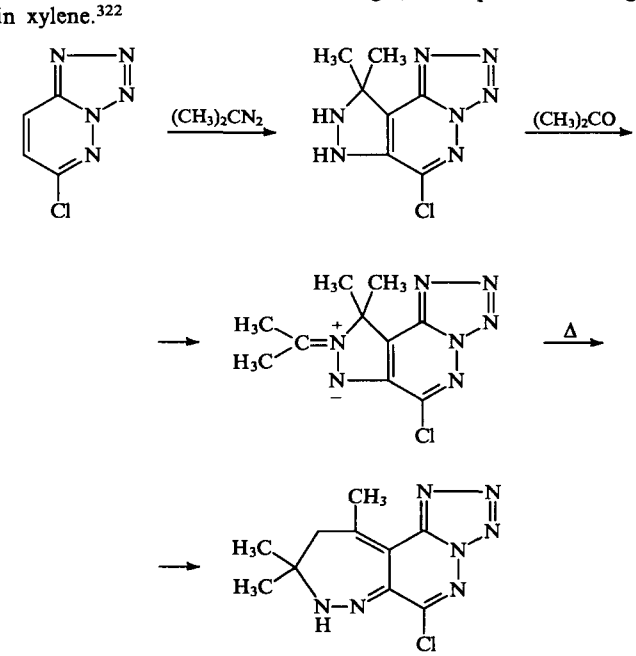


Satisfactory results have been obtained in the catalytic (Pd) reduction of 5-(2-naphthoxy)-1-phenyltetrazole by tetrabutylammonium hypophosphite in the benzene–water two-phase system.[319]

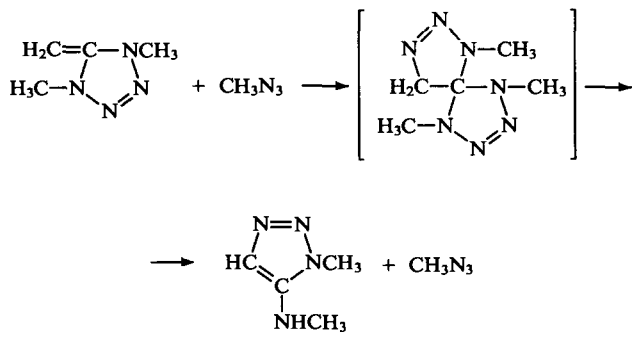
A small number of studies on the electrochemical reduction of tetrazoles have been published in recent years. It has been found that the electrochemical reduction of 1-vinyl- and 5-vinyltetrazoles in acetonitrile proceeds with the transfer of one electron.[320] The electrochemical reduction of 5-trichloromethyltetrazole leads to the formation of tetrazole and 5-chloromethyl- and 5-dichloromethyl-tetrazoles in 16%, 5%, and 28% yields respectively.[53]

9. Cycloaddition reaction

In connection with the active search for methods of synthesis of new heterocyclic systems, there has been an appreciable growth of interest in cycloaddition reactions with participation of tetrazoles as dipolarophiles.[321] It has been shown that the interaction of 6-chlorotetrazolo[1,5-*b*]pyridazine with diazoalkanes results in the formation of the corresponding cyclic adducts. The interaction of the latter with acetone leads to stable azomethine imines, which are converted into tetrazole-containing 1,2-diazepines on heating in xylene.[322]



On treatment with methyl azide, 4,5-dihydro-1,4-dimethyl-5-methylenetetrazole isomerises to 1-methyl-5-methylamino-1,2,3-triazole.[140] It is believed[140] that an unstable cyclic adduct is formed in the first stage of this reaction and then decomposes to the corresponding triazole and methyl azide.



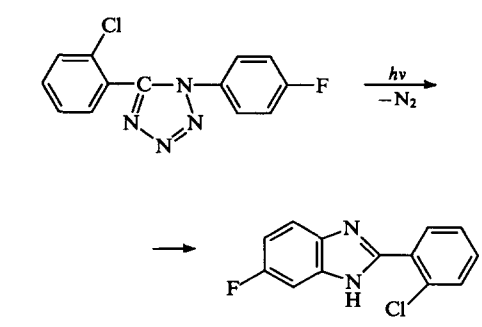
The formation of a stable cyclic adduct can be detected in the reaction of phenyl azide with 4,5-dihydro-1-methyl-5-(1-methylethylidene)-4-phenyltetrazole in cyclohexane.

10. Polymerisation of vinyltetrazoles

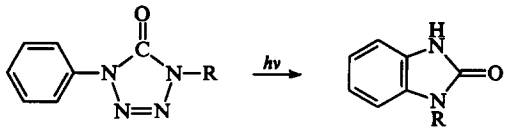
Vinyltetrazoles polymerise fairly readily in solution or in bulk in the presence of radical catalysts, for example azobisisobutyronitrile. Important data for the understanding of the mechanism of the polymerisation of vinyltetrazoles and for the prediction of the polymers formed have been obtained in a study of the polymerisation of 1-vinyl-, 5-methyl-1-vinyl-, and 2-methyl-5-vinyltetrazoles in aqueous solutions of sodium thiocyanate.[323] It was shown that the polymerisation of these compounds is in many respects similar to the polymerisation of acrylonitrile under similar conditions and is apparently of a complex-radical type. The use of sodium thiocyanate solutions as the reaction medium makes it possible to obtain tetrazole-containing polymers with a high molecular mass and the polymerisation process is much faster than in organic solvents. Together with the homopolymerisation, a study was made of the copolymerisation of 1-vinyl- and 2-methyl-5-vinyltetrazoles with acrylic and methacrylic acids, their derivatives, and styrene.[324–326] It was established that very long blocks of homopolymer units may be formed in the copolymer macrochain in the copolymerisation of 2-methyl-5-vinyltetrazole with acrylonitrile, which indicates a tendency by vinyltetrazole to undergo homopolymerisation. On the other hand, the probability of the formation of copolymer blocks is higher in the copolymerisation of 2-methyl-5-methylenetetrazole with methacrylic acid and its esters.

11. Photochemical reactions

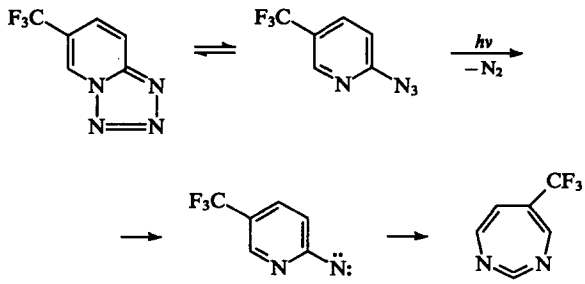
The photolysis of tetrazoles entails their fragmentation with liberation of a nitrogen molecule and the formation of a new heterocyclic system. Thus satisfactory yields of the corresponding benzimidazoles can be obtained from 1,5-diaryltetrazoles.[327]



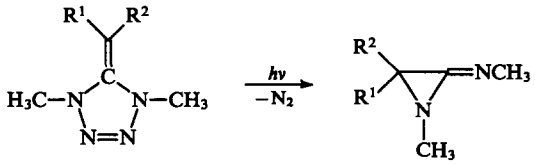
1,4-Disubstituted 4,5-dihydrotetrazol-5-ones undergo similar reactions.[328-330]



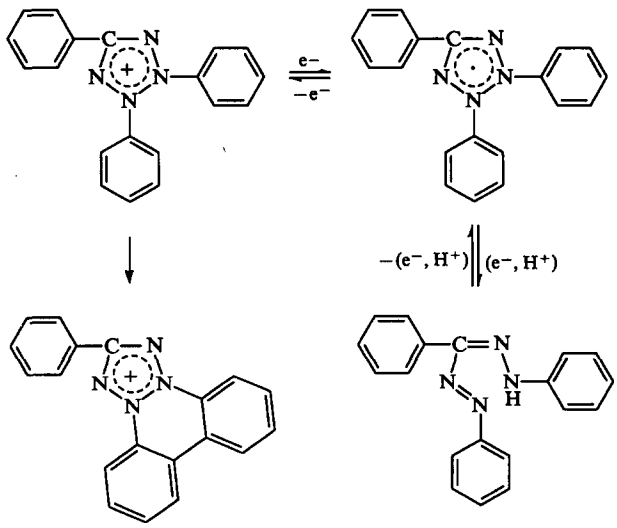
Interesting results have been obtained in a study of the photolysis of tetrazolopyridines containing the trifluoromethyl group in the six-membered ring.[331] This reaction can be regarded as a method of synthesis of 1,2-didehydro-1,3-diazepines, which are difficult to obtain.



The mechanism of the photolysis of 2,5-disubstituted tetrazoles has been investigated.[332] It has been shown that the corresponding nitrile imines are intermediates in these reactions. The formation of iminoaziridines has been detected in the photolysis of 5-alkylidene-4,5-dihydrotetrazoles.[333]



The mechanism of the photochemical reduction of 2,3,5-triphenyltetrazolium chloride has been investigated in aqueous solutions at pH 9–11.5 by the method of flash photolysis. A mechanism involving the formation of an intermediate tetrazolium radical has been proposed for this reaction.[334]



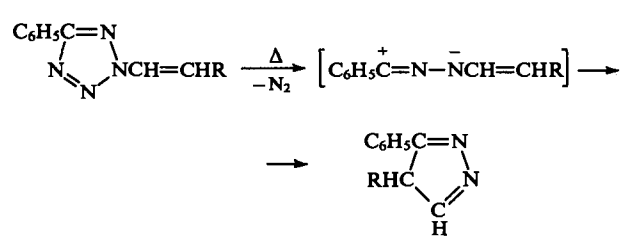
12. Metal complexes of tetrazoles

Systematic studies on the structures and properties of metal complexes of tetrazoles and also the capacity for complex formation of the corresponding heterocyclic ligands were not initiated until the beginning of the 1980s.[335-338] The unsubstituted tetrazole readily forms complexes with cobalt(II), nickel(II), copper(II), and cadmium(II) chlorides.[335] It has also been shown that 1- and 2-monoalkyltetrazoles interact with copper(II) chloride and thiocyanate, affording crystalline complexes. Regardless of the reactant ratio and the nature of the tetrazole ligand (T), complexes having the general formula CuT_2X_2 are formed.[339,340] Tetrazoles substituted in the 1- and 2-positions are monodentate ligands which are coordinated to the central copper atom via one of the nitrogen atoms. It is significant that 1-alkyltetrazoles show a greater tendency to form complexes than the 2-isomers.[336] The cobalt(II) and cobalt(III) complexes of 5-substituted tetrazoles have been investigated in detail.[341-343] It has been shown that the interaction of 5-aminotetrazole with pentamminecobalt nitrate results in the formation of the complex $[Co(NH_3)_5T](NO_3)_3$.[343] The indium(III) and iron(III) complexes PMT, where P is the octaethylporphyrin dianion and M the corresponding metal ion, have been obtained by the reaction of azidoporphyrins with nitriles.[344,345] Numerous complexes of 1,5-disubstituted tetrazoles with cobalt(II), nickel(II), copper(II), and iron(III) chlorides have been obtained. It has been shown that the crystalline complexes $CuTCl_2$ are formed in a high yield in the interaction of 1,5-disubstituted tetrazoles with $CuCl_2$ in organic solvents at 25–30 °C.[340] The molecules of the 1,5-disubstituted tetrazoles apparently serve as bridging ligands in such complexes. Each molecule of the tetrazole ligand is bound simultaneously to two neighbouring Cu^{2+} ions linked to one another by Cl^- bridging ions. Barium complexes of 1,5-disubstituted tetrazoles have been described.[346] 1,5-Disubstituted 4,5-dihydrotetrazoles proved to be effective siderophores.[347,348] When the methyl esters of 2-(1-R-4,5-dihydrotetrazol-5-yl-alphaidene)cyanoacetic esters are treated with iron(III) chloride ether, blue cryptocrystalline complexes FeT_3 are formed. Each of the three molecules of the tetrazole ligand in such complexes is coordinated to the central Fe^{3+} ion via a nitrogen atom of the heterocycle and the carbonyl oxygen atom. When iron(III) chloride is replaced by $FeSO_4$, the polymeric complex $(FeT_2)_n$ is produced.

The complexes of 2,5-disubstituted tetrazoles have been investigated to a much lesser extent. The complexes of 2-methyl-5-vinyltetrazoles with chromium(III), nickel(II), cobalt(II), and palladium(II) chlorides have been recently described. It has been shown that the metal ion in such complexes is coordinated to the N(4) atom of the tetrazole ligand.[349,350] The mercury(II) and palladium(II) complexes of tetrazolium salts have been described.[351,352]

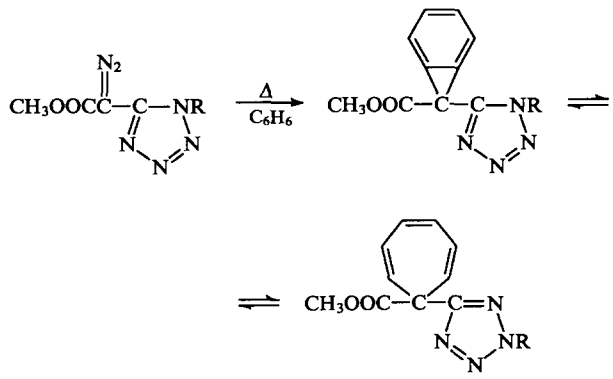
13. Other reactions

In this section, it is necessary to mention primarily the conversion of 2-alkenyl-5-phenyltetrazoles into the corresponding 4-alkenyl-3-phenylpyrazoles.[282] The alkenyltetrazoles are fragmented on heating in 1,2-dichlorobenzene, the yield of pyrazoles being 79%–98%.

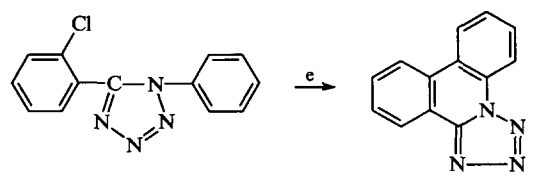


This reaction can be regarded as a method of synthesis for 3,4-disubstituted pyrazoles which are difficult to obtain.

The isomeric *N*-substituted 5-(methoxycarbonyldiazomethyl)tetrazoles undergo interesting reactions on heating.[353] The different influences of the isomeric tetrazolyl substituents on the functional groups in the side chain can be clearly traced in this example.



The electrochemical cyclisation of 5-(*o*-chlorophenyl)-1-phenyltetrazole to tetrazolo[1,5-*a*]phenanthridine has been investigated.[354]



Finally, it has been shown recently that trichloroacetonitrile adds smoothly to 1-methyl- and 2-methyl-5-vinyltetrazoles,[355,356] that 4,6-dinitrotetrazolo[1,5-*a*]pyridine forms stable adducts with alkoxide anions,[357] and that the acid hydrolysis of 5-diazomethylazotetrazole results in the formation of 5-hydrazinotetrazole.[358]

V. Applications of tetrazoles

There has been a steady growth of publications devoted to the applications of tetrazoles during the last decade. A systematic analysis of this problem, involving the examination of 700 patents published in 20 countries, has been carried out.[359] It follows from this analysis that the main applications of tetrazoles are in medicine, biochemistry, agriculture, analytical chemistry, information recording systems, and energy consuming processes as corrosion inhibitors and energy consuming materials. The most significant results have been obtained in the synthesis of tetrazole-containing β-lactam antibiotics of the cephalosporin series.[1,3,360,361] Such antibiotics exhibit a high antimicrobial activity, a prolonged action, and a low toxicity. Highly effective antiviral preparations have been found among tetrazoles.[362] 3-Tetrazole analogues of azidothymidine (AZT) have been obtained recently. It has been predicted that they should be active against the AIDS virus.[118] *C*-Glycosyltetrazoles—potential inhibitors of *E. coli* dehydrokinase-synthetase—have been described.[68] Preparations possessing antitubercular activity have been widely investigated.[4,6,8] Studies devoted to the creation of tetrazole-containing antihypertensive (losartan) and antiangina preparations, which belong to the new generation of regulators of cardiovascular activity, merit special attention.[7,11] Certain tetrazolium salts exhibit a high radioprotecting activity. The use of these compounds ensures the survival of up to 60% of animals irradiated with a lethal dose.[363]

Tetrazole is a condensing agent in the synthesis of oligonucleotides and also in systems for the automated synthesis of polynucleotides. In a number of instances, it is superior to other nitrogen-containing heterocycles used for these purposes.[16,17,364,365] Date have been published recently concerning the preparation of new generation herbicides on the basis of tetrazole-containing compounds.[20] Tetrazolium salts are widely used in analytical chemistry as extractants for the lanthanide metals[366] and in information recording systems, including their use as components of low-silver photographic materials.[21,25] 5-Mercapto-1-phenyltetrazole is a DIR component in modern photoprogramming systems and is one of the best antifogging agents.[22] Finally, highly effective corrosion inhibitors,[367] components of pyrotechnic and gas-generating compositions, and explosives[368,369] have been found among tetrazoles.

VI. Conclusion

Little more than a hundred years have elapsed since the discovery of tetrazoles. Interest in these compounds was aroused at the beginning of the 1950s when the principal methods of synthesis of tetrazoles were developed and studies on their physicochemical properties were initiated. Some diminution of interest in tetrazoles towards the end of the 1960s was rapidly replaced by its rearousal, and active studies on the chemistry of these compounds have been continued to the present.

Tetrazoles are exceptionally important in synthetic chemistry. They are used in the syntheses of many nitrogen-containing heterocycles—pyrazoles, imidazoles, 1,2,4-triazoles, 1,3,4-oxadiazoles, and what is especially important, the previously unavailable 3*H*-1,3,4-benzotriazepines.

Unfortunately no new advances have been made recently in the development of new general methods of synthesis of tetrazoles. This problem still awaits solution.

There have been considerable achievements in the practical application of tetrazoles, especially in medicine and biochemistry. An increase in the production of tetrazoles in industrially developed countries has been noted.

References

1. G Lancini, F Parenti *Antibiotics* (Translated into Russian; Moscow: Mir, 1985)
2. D H Klaubert, J Sellstedt, C J Guinosso, S C Bell, R P Capetola *J. Med. Chem.* **24** 748 (1981)
3. W Durckheimer, J Blumbach, R Lattrel, K H Scheunemann *Angew. Chem.* **97** 183 (1985)
4. J Vanzura, A Hrabalek, Z Odlerova, K Waisser, M Celadnik *Cesk. Farm.* **34** 271 (1985)
5. M V Aleksanyan, M S Kramer, S G Akopyan, R V Agababyan, Yu Z Ter-Zakharyan, L G Akopyan, G M Paronikyan, Sh L Mndzhoyan *Khim.-Farm. Zh.* **24** (10) 56 (1990)
6. J Nevidkova, P Stolba, V Strabak, J Vanzura, A Hrabalek, J Vinsova *Cesk. Farm.* **40** 75 (1991)
7. J V Duncia, D J Carini, A T Chiu, A L Johnson, W A Price, P C Wong, R R Wexler, P Timmermans *Med. Res. Rev.* **12** 149 (1992)
8. K Waisser, J Vanzura, A Hrabalek, J Vinsova, S Gresak, J Hruska, Z Odlerova *Collect. Czech. Chem. Commun.* **56** 2389 (1991)
9. M D Milecan, R J Sorenson, D T Konnor, D O Thueson, J A Kennedy, M C Konroy *J. Med. Chem.* **34** 2186 (1991)
10. S R Watson *Synth. Commun.* **22** 2971 (1992)
11. M E Pierce, D J Carini, G F Huhn, G J Wells, J F Arnett *J. Org. Chem.* **58** 4642 (1993)
12. P L Ornstein, D D Schoepp, M B Arnild, N D Jones, J B Decter, D Lodge, J D Leander *J. Med. Chem.* **35** 3111 (1992)
13. A N Sinyakov, A V Lebedev *Bioorg. Khim.* **12** 1129 (1986)
14. A N Markaryan, Ya V Voznyi, B B Dzantiev, A M Egorov *Bioorg. Khim.* **13** 236 (1987)
15. P J Garegg, J Stawinski, R Stromberg *J. Org. Chem.* **52** 284 (1987)
16. N N Karpyshev *Usp. Khim.* **57** 1546 (1988) [*Russ. Chem. Rev.* **57** 886 (1988)]
17. S L Beaucage, R P Iyer *Tetrahedron* **48** 2223 (1992)

18. V M Ostrovskaya, I A D'yakonova, T D Nikolaeva *Zh. Vses. Khim. O-va im. D I Mendeleeva* **30** 585 (1985)
19. B A Khaskin *Zh. Vses. Khim. O-va im. D I Mendeleeva* **33** 698 (1988)
20. G Theodoridis, F M Hotzman, L W Scherer, B A Smith, T M Tymonko, M J Wyle, in *Synthesis and Chemistry of Agrochemicals, III* (Eds D R Baker, J G Fenyes, J J Steffens) (Washington, DC: American Chemical Society, 1992) p. 122
21. L V Krasnyi-Admoni *Maloserebryanye Fotograficheskie Materialy i Protsessy Ikh Obrabotki* (Low-Silver Photographic Materials and the Processes in Their Treatment) (Leningrad: Khimiya, 1986)
22. K V Chibisov *Fotograficheskoe Proyavlenie* (Photographic Development) (Moscow: Nauka, 1989)
23. Jpn. P. 90 287 346; *Chem. Abstr.* **115** 18 522z (1991)
24. Jpn. P. 90 280 140; *Chem. Abstr.* **115** 18 528f (1991)
25. T Habu, N Mil, K Kuge, H Manto, Y Takamuki *J. Imaging Sci.* **35** 202 (1991)
26. R T Chakrasali, H Ila, H Junjappa *Synthesis* 453 (1988)
27. P K Kadaba *Synlett.* **6** 349 (1990)
28. A E Miller, D J Feenly, Y Ma, L Zarcone, M A Aziz, E Magnuson *Synth. Commun.* **20** 217 (1990)
29. S J Wittenberger, B G Donner *J. Org. Chem.* **58** 4139 (1993)
30. M M Krayushkin, A M Beskopyl'nyi, S G Zlotin, V V Son, N I Vainberg, O A Luk'yanov, V M Zhulin *Izv. Akad. Nauk SSSR, Ser. Khim.* 640 (1982)
31. M M Krayushkin, A M Beskopyl'nyi, E B Zhuravleva, V M Zhulin *Izv. Akad. Nauk SSSR, Ser. Khim.* 461 (1985)
32. Yi-Xiang Ding, W P Weber *Synthesis* 823 (1987)
33. I V Nikonova, G I Koldobskii, A B Zhivich, V A Ostrovskii *Zh. Obshch. Khim.* **61** 1483 (1991)
34. I V Nikonova, G I Koldobskii, A B Zhivich, V A Ostrovskii *Zh. Obshch. Khim.* **61** 2104 (1991)
35. L Bruche, L Garanti, G Zecchi *Synth. Commun.* **22** 309 (1992)
36. E Fos, J Vilarrasa, J Fernandez *J. Org. Chem.* **50** 4894 (1985)
37. J Garcia, J Vilarrasa *Heterocycles* **27** 1803 (1988)
38. M Alcami, O Mo, M Yanez *J. Phys. Chem.* **93** 3929 (1989)
39. I Jano *J. Phys. Chem.* **95** 7694 (1991)
40. M Alcami, O Mo, M Yanez *J. Phys. Chem.* **96** 3022 (1992)
41. J Catalan, J L M Abboud, J Elguero, in *Advances in Heterocyclic Chemistry* Vol. 41 (New York: Academic Press, 1987) p. 187
42. G I Koldobskii, V A Ostrovskii *Khim. Geterotsikl. Soedin.* 579 (1988)
43. V A Ostrovskii, G I Koldobskii *Slabye Organicheskie Osnovaniya* (Weak Organic Bases) (Leningrad: Izd. Leningr. Gos. Univ., 1990)
44. G I Koldobskii, V A Ostrovskii, B V Gidaspov *Khim. Geterotsikl. Soedin.* 867 (1980)
45. F R Benson *The High Nitrogen Compounds* (New York: Wiley, 1984) p. 263
46. R N Butler, in *Comprehensive Heterocyclic Chemistry* Vol. 5 (Eds A R Katritzky, C W Rees) (Oxford: Pergamon Press, 1984) p. 791
47. M Begtrup, P Larsen *Acta Chem. Scand., Ser. B* **44** 1050 (1990)
48. A I Lesnikovich, O A Ivashkevich, V A Lyutsko, G V Printsev, K K Kovalenko, P N Gaponik, S V Levchik *Termochim. Acta* **145** 195 (1989)
49. A I Lesnikovich, O A Ivashkevich, P N Gaponik, V A Shandakov *Termochim. Acta* **171** 207 (1990)
50. A I Lesnikovich, G A Printsev, O A Ivashkevich, P N Gaponik, V A Shandakov *Termochim. Acta* **184** 221 (1991)
51. G I Koldobskii, V A Ostrovskii, V S Poplavskii *Khim. Geterotsikl. Soedin.* 1299 (1981)
52. P N Gaponik, V P Karavai *Vestn. Beloruss. Gos. Univ. Ser. 2* 51 (1980)
53. M E Niyazymbetov, V A Petrosyan, V V Kozlov, M S Pevzner *J. Electroanal. Chem.* **338** 239 (1992)
54. R S Roweltt, T Klysa, W Shiraki *J. Labelled Compd. Radiopharm.* **28** 1437 (1990)
55. K Nishiyama, M Oba, A Watanabe *Tetrahedron* **43** 693 (1986)
56. P N Gaponik, V P Karavai *Khim. Geterotsikl. Soedin.* 841 (1983)
57. P N Gaponik, V P Karavai *Khim. Geterotsikl. Soedin.* 1521 (1985)
58. P N Gaponik, V P Karavai, Yu V Grigor'ev *Khim. Geterotsikl. Soedin.* 1521 (1985)
59. P N Gaponik, V P Karavai, N E Davshko, M M Degtyarik, A N Bogatikov *Khim. Geterotsikl. Soedin.* 1528 (1990)
60. D S Lingenfelter, R C Helgeson, D J Gram *J. Org. Chem.* **46** 393 (1981)
61. P S Bevan, G P Ellis, H K Wilson *J. Chem. Soc., Perkin Trans. 1* 2552 (1981)
62. J M Adam, T Winkler *Helv. Chim. Acta* **66** 411 (1983)
63. L I Vereshchagin, T M Filipova, R L Bol'shedvorskaya, L D Gavrilov, G A Pavlova *Zh. Org. Khim.* **20** 142 (1984)
64. J R Maxwell, D A Wasdahl, A C Wolfson, V I Stenberg *J. Med. Chem.* **27** 1565 (1984)
65. R G Dubenko, I M Bazavova, E F Gorbenko *Zh. Org. Khim.* **20** 577 (1984)
66. P R Bernstein, E P Vacek *Synthesis* 1133 (1987)
67. C G Zlotin, A I Podgurskii, N V Airapetova, O A Luk'yanov *Izv. Akad. Nauk SSSR, Ser. Khim.* 1647 (1991)
68. J G Buchanan, A P W Clelland, T Johnson, R A C Rennie, R H Wightman *J. Chem. Soc., Perkin Trans. 1* 2593 (1992)
69. R K Russel, W V Murray *J. Org. Chem.* **58** 5023 (1993)
70. W G Finnegan, R A Henry, R Lofquist *J. Am. Chem. Soc.* **80** 3908 (1958)
71. I E Titova, V S Poplavskii, G I Koldobskii, V A Ostrovskii, V D Nikolaev, G B Erusalimskii *Khim. Geterotsikl. Soedin.* 1086 (1986)
72. V A Ostrovskii, V S Poplavskii, G I Koldobskii, G B Erusalimskii *Khim. Geterotsikl. Soedin.* 1214 (1992)
73. W P Norris *J. Org. Chem.* **27** 3248 (1962)
74. V Grakauskas, A Albert *J. Heterocycl. Chem.* **18** 1477 (1981)
75. A V Fokin, Yu N Studnev, A I Rapkin, V A Komarov, O V Varenikin, T M Potarina *Izv. Akad. Nauk SSSR, Ser. Khim.* 1592 (1981)
76. J Sundermeyer, H W Roesky, M Noltemeyer *Z. Naturforsch., B* **45** 77 (1990)
77. D M Gapinski, C R Roman, L E Rinkema, J H Fleisch *J. Med. Chem.* **31** 172 (1988)
78. J V Duncia, M E Pierce, J B Santella *J. Org. Chem.* **56** 2395 (1991)
79. Yu A Azev, I P Loginova, B V Golomolzin, I I Mudretsova, V L Rusinov *Khim. Geterotsikl. Soedin.* 135 (1990)
80. R W Saalfrank, C-J Lurz, U Wirth, H G Schnering, K Peters *J. Heterocycl. Chem.* **28** 1863 (1991)
81. R W Saalfrank, C-J Lurz, J Hassa, D Danion, L Toupet *Chem. Ber.* **124** 595 (1991)
82. S Rault, M Sevricourt, M Robba *J. Heterocycl. Chem.* **18** 739 (1981)
83. D Meth-Cohn, B Narine, B Tarnowski, R Hayes, A Keyzod, S Rhouti, A Robinson *J. Chem. Soc., Perkin Trans. 1* 2509 (1981)
84. V N Bodnar, M O Lozinskii, P S Pel'kis *Ukr. Khim. Zh. (Russ. Ed.)* **48** 1308 (1982)
85. K Makina, G Sakata, K Morimoto, Y Ochiai *Heterocycles* **23** 2025 (1985)
86. A F Shivanyuk, E V Dashkovskaya, M O Lozinskii *Zh. Org. Khim.* **22** 200 (1986)
87. O B Smolii, V S Bovarets, B S Drach *Zh. Obshch. Khim.* **56** 2802 (1986)
88. Yu Kuo-Lang, R L Johnson *J. Org. Chem.* **52** 2051 (1987)
89. J Zabroski, D Smith, J B Dunbar, J H Iijima, G Marshall *J. Am. Chem. Soc.* **110** 5875 (1988)
90. C K Lowe-Ma, R A Nissan, W S Wilson *J. Org. Chem.* **55** 3755 (1990)
91. J Zabroski *Wiad. Chem.* **44** 831 (1990)
92. A F Hegarty, E P Ahern *J. Org. Chem.* **46** 1342 (1981)
93. A F Hegarty, M Mullane *J. Chem. Soc., Chem. Commun.* 913 (1984)
94. E V Dashkovskaya, A F Shivanyuk, M O Lozinskii, Yu A Sokolova, O A D'yachenko, L O Atovmyan *Izv. Akad. Nauk SSSR, Ser. Khim.* 2427 (1988)
95. A F Shivanyuk, E V Dashkovskaya, A B Rozhenko, M O Lozinskii, N P Onishchuk, O A Bukreev, O A D'yachenko, L O Atovmyan *Zh. Org. Khim.* **26** 1629 (1990)
96. S Ito, Y Tanaka, A Kakehi *Bull. Chem. Soc. Jpn.* **57** 539 (1984)
97. R Galli, O Palla, F Gozzo *J. Chem. Soc., Perkin Trans. 1* 2813 (1982)
98. G A Bhat, L B Townsend *J. Chem. Soc., Perkin Trans. 1* 2378 (1981)
99. G Weber, J Hartung, L Beyer *Z. Chem.* **26** 70 (1986)
100. O B Smolii, V S Bravarets, V V Pirozhenko, B S Drach *Zh. Obshch. Khim.* **58** 2465 (1988)
101. Yu I Matveev, V I Gorbatenko, L I Samarai, S V Sereda, Yu T Struchkov *Zh. Org. Khim.* **24** 2216 (1988)

102. P N Gaponik, Yu V Grigor'ev, V P Karavai *Khim. Geterotsikl. Soedin.* 566 (1985)
103. P H Benders, D N Reinhoudt, D M W van den Ham *Recl. Trav. Chim. Pays-Bas* **100** 330 (1981)
104. D H Klaubert, J Sellstedt, C J Guinosso, S C Bell, R J Capetola *J. Med. Chem.* **24** 748 (1981)
105. D H Klaubert, S C Bell, T W Pattison *J. Heterocycl. Chem.* **22** 333 (1985)
106. M M Krayushkin, A M Beskopyl'nyi, S G Zlotin, G A Stashina, V M Zhulin *Dokl. Akad. Nauk SSSR* **259** 370 (1981)
107. M M Krayushkin, V N Yarovenko, O A Luk'yanov, V M Zhulin *Izv. Akad. Nauk SSSR, Ser. Khim.* 2764 (1981)
108. N N Vainberg, M M Krayushkin, V M Zhulin *Izv. Akad. Nauk SSSR, Ser. Khim.* 2014 (1984)
109. M W Majchrzak, A Kotelko, R Guryn, J V Lambert, S M Wharry *Tetrahedron* **37** 1075 (1981)
110. J A Valderrama, H Pessoa-Mahana, R Tapia *Synth. Commun.* **22** 629 (1992)
111. C W Bird, Y P S Chauhan, D R Turton *Tetrahedron* **37** 1277 (1981)
112. G I Georg, X Guan *Tetrahedron Lett.* **33** 17 (1992)
113. A Hassner, R Fibiger, A S Amarasekara *J. Org. Chem.* **53** 22 (1988)
114. K Nishiyama, A Watanabe *Chem. Lett.* 455 (1984)
115. G Litkei, T Patonay *Acta Chim. Acad. Sci. Hung.* **114** 47 (1983)
116. E Zbiral, W Schorkhuber *Liebigs Ann. Chem.* 1870 (1982)
117. H Knotz, E Zbiral *Monatsh. Chem.* **117** 1437 (1986)
118. D Habich *Synthesis* 358 (1992)
119. S N Dehuri, P C Pradhan, A Nayak *J. Indian Chem. Soc.* **60** 475 (1983)
120. J Clark, G Varvounis, M Bakavoli *J. Chem. Soc., Perkin Trans. 1* 711 (1986)
121. M M Goodman, J L Atwood, I G Carlin, W Hunter, W W Paudler *J. Org. Chem.* **41** 2860 (1976)
122. B Stanovnik, M Tisler, D Gabrijelcic, M Kunaver, J Zmitek *J. Heterocycl. Chem.* **16** 1567 (1979)
123. F Janssen, J Torremans, P A J Janssen *J. Med. Chem.* **29** 2290 (1986)
124. M Tosseli, P Zanirarto *J. Chem. Soc., Perkin Trans 1* 1101 (1992)
125. G L L'abbe, P V Stappen *Bull. Soc. Chim. Belg.* **92** 912 (1983)
126. G L L'abbe, P V Stappen, S Toppet *Tetrahedron* **41** 4621 (1985)
127. P M Moriarty, B R Bailey, I Prahash, R S Miller *J. Org. Chem.* **50** 3710 (1985)
128. R C Cambie, G Dixon, P S Rutledge, P D Woodgate *J. Chem. Soc., Perkin Trans. 1* 961 (1982)
129. R C Cambie, J L Jurlina, P S Rutledge, P D Woodgate *J. Chem. Soc., Perkin Trans. 1* 315 (1982)
130. J Cherton, P Desbene, M Bazinet, M Lanson, O Convert, J Basselier *Can. J. Chem.* **63** 86 (1985)
131. A R Katritzky, W Q Fan, V Greenhill *J. Org. Chem.* **56** 1299 (1991)
132. A M Churakov, S L Ioffe, V S Kuz'min, Yu A Strelenko, Yu T Struchkov, V A Tartakovskii *Khim. Geterotsikl. Soedin.* 1666 (1988)
133. H M Hassaneen, A A Fahmi, H Abdelhamid, A A Yassin, A S Shawali *J. Heterocycl. Chem.* **21** 797 (1984)
134. P Weinberg, C Csongar, G Tomaschewski *Z. Chem.* **27** 407 (1987)
135. T Kaihoh, T Itoh, K Yamaguchi, A Ohsawa *J. Chem. Soc., Chem. Commun.* 1608 (1988)
136. A B Zhivich, G I Koldobskii, V A Ostrovskii *Khim. Geterotsikl. Soedin.* 1587 (1990)
137. A Messmer, A Gelleri, G Hajos *Tetrahedron Lett.* **42** 4827 (1986)
138. A Messmer, A Gelleri, G Hajos *Tetrahedron Lett.* **42** 5415 (1986)
139. G W Fischer *J. Prakt. Chem.* **331** 885 (1989)
140. H Quast, T Hergenrother *Liebigs Ann. Chem.* 581 (1992)
141. A B Zhivich, Yu E Myznikov, G I Koldobskii, V A Ostrovskii *Zh. Obshch. Khim.* **58** 1906 (1988)
142. G I Koldobskii, A B Zhivich, V A Ostrovskii *Zh. Obshch. Khim.* **62** 3 (1992)
143. C G Newton, C A Ramsden *Tetrahedron* **38** 2965 (1982)
144. D Moderhack, A Lembcke *J. Chem. Soc., Perkin Trans. 1* 1157 (1986)
145. R W Saalfrank, U Wirth *Chem. Ber.* **122** 969 (1989)
146. A P Mazurek, R Osman *J. Phys. Chem.* **89** 460 (1985)
147. M Wah Wong, R Leung-Toung, C Wentrup *J. Am. Chem. Soc.* **115** 2465 (1993)
148. M N Palmer, I Simpson, J R Wheller *Z. Naturforsch. A* **36** 1246 (1981)
149. A Razynska, A Tempczyk, E Malinski, J Szafranek, Z Grzonka, P Herman *J. Chem. Soc. Perkin Trans. 2* 379 (1983)
150. A Razynska, A Tempczyk, Z Grzonka *J. Chem. Soc., Faraday Trans. 1* **81** 1555 (1985)
151. O Mo, J L G de Paz *J. Phys. Chem.* **90** 5597 (1986)
152. R M Claramunt, D Sanz, G Boyer, J Catalan, J L G de Paz, J Elguero *Magn. Reson. Chem.* **31** 791 (1993)
153. B Ya Simkin, M N Glukhovtsev *Khim. Geterotsikl. Soedin.* 1587 (1989)
154. P N Gaponik, O A Ivashkevich, O N Bubel', M M Degtyarik, V N Naumenko *Teor. Eksp. Khim.* 33 (1989)
155. V G Kharatyan, V B Gavalyan, N Sh Mailyan, G V Asratyan, O N Bubel', E M Rakhman'ko, E G Darbinyan, S G Matsoyan *Arm. Khim. Zh.* **38** 751 (1985)
156. O A Ivashkevich, P N Gaponik, A O Koren, O N Bubel, E V Fronchek *Int. J. Quantum Chem.* **43** 813 (1992)
157. M Cabre, J Farras, J F Sanz, J Vilarrasa *J. Chem. Soc., Perkin Trans. 2* 1943 (1990)
158. M Nguen, G Leroy, M Sana, J Elguero *J. Heterocycl. Chem.* **19** 943 (1982)
159. J Farras, S Olivella, A Sole, J Vilarrasa *J. Phys. Chem.* **95** 10623 (1991)
160. V A Ostrovskii, N S Panina, G I Koldobskii, B V Gidaspov, I Yu Shirobokov *Zh. Org. Khim.* **15** 844 (1979)
161. T F Osipova, V A Ostrovskii, G I Koldobskii, G B Erusalimskii *Zh. Org. Khim.* **20** 398 (1984)
162. I Yu Shirobokov, M V Chekushina, V A Ostrovskii, G I Koldobskii, G B Erusalimskii *Khim. Geterotsikl. Soedin.* 502 (1988)
163. A L Kovalenko, V A Ostrovskii, I V Tselinskii *Zh. Org. Khim.* **28** 573 (1992)
164. R Gleiter, T Veszpremi, H Quast *Chem. Ber.* **122** 985 (1989)
165. V N Naumenko, A D Koren, P N Gaponik *Magn. Reson. Chem.* **30** 558 (1992)
166. L Stefaniak, J D Roberts, M Witanowski, G A Webb *Org. Magn. Reson.* **22** 215 (1984)
167. M Foces-Foces, F H Cano, R M Claramunt, D Sauz, J Catalan, F Fabero, A Fruchier, J Elguero *J. Chem. Soc., Perkin Trans. 2* 237 (1990)
168. R M Claramunt, D Sauz, J Catalan, F Fabero, N A Garcia, M Foces-Foces, A L Liamus-Saiz, J Elguero *J. Chem. Soc., Perkin Trans. 2* 1687 (1993)
169. L Stefaniak, J D Roberts, M Witanowski, B T Hamdi, G A Webb *Org. Magn. Reson.* **22** 209 (1984)
170. Yu V Shurukhin, N A Klyuev, V A Ostrovskii, G I Koldobskii, G B Erusalimskii *Zh. Org. Khim.* **20** 2458 (1984)
171. I Janic, M Kakas *J. Mol. Struct.* **142** 189 (1986)
172. V A Ostrovskii, I Yu Shirobokov, G I Koldobskii *Zh. Org. Khim.* **17** 146 (1981)
173. L N Agarkova, V A Ostrovskii, G I Koldobskii, G B Erusalimskii *Zh. Org. Khim.* **18** 1043 (1982)
174. V S Poplavskii, I E Titova, V A Ostrovskii, G I Koldobskii *Zh. Org. Khim.* **18** 1981 (1982)
175. I E Titova, V S Poplavskii, V A Ostrovskii, G B Erusalimskii, G F Tereshchenko, G I Koldobskii *Zh. Org. Khim.* **23** 1082 (1987)
176. V S Poplavskii, I E Titova, V A Ostrovskii, G I Koldobskii *Zh. Org. Khim.* **25** 2182 (1989)
177. I Cryczynski, A Kawski, A Razynska, Z Grzonka *Z. Naturforsch. A* **32** 1259 (1982)
178. V I Vovna, in *Elektronnaya Struktura Organicheskikh Soedinenii po Dannym Fotoelektronnoi Spektroskopii* (The Electronic Structure of Organic Compounds According to Photoelectron Spectroscopic Data) (Moscow: Nauka, 1991) p. 244
179. M N Palmer, A J Beveridje *Chem. Phys.* **111** 243 (1987)
180. B Kovac, L Klasinc, B Stanovnik, M Tisler *J. Heterocycl. Chem.* **17** 689 (1980)
181. N I Sushko, N I Makarevich, N A Matveeva, O A Ivashkevich, P N Gaponik *Zh. Prikl. Spektrosk.* **54** 923 (1991)
182. N A Matveeva, N I Sushko, N I Makarevich, P N Gaponik, O A Ivashkevich, A O Koren' *Zh. Prikl. Spektrosk.* **57** 442 (1992)
183. V P Sinditskii, M D Dutov, A E Fogel'zong *Khim. Geterotsikl. Soedin.* 72 (1991)

184. O A Ivashkevich, P N Gaponik, T B Kovalyova *Makromol. Chem.* **193** 1369 (1992)
185. S V Levchik, O A Ivashkevich, A I Balabanovich, A I Lesnikovich, P N Gaponik, L Costa *Termochim. Acta* **207** 115 (1992)
186. A Bigotto, G Castellani *J. Raman Spectrosc.* **15** 232 (1984)
187. D S Woffold, J D Forkey, J G Russel *J. Org. Chem.* **47** 5132 (1982)
188. E Bojarska-Olejnik, L Stefaniak, M Witanowski, B T Hamdi, G A Webb *Magn. Reson. Chem.* **23** 166 (1985)
189. E Bojarska-Olejnik, L Stefaniak, M Witanowski, G A Webb *Bull. Chem. Soc. Jpn.* **59** 3263 (1986)
190. V N Naumenko, A O Koren, P N Gaponik *Magn. Reson. Chem.* **30** 558 (1992)
191. P N Gaponik, O A Ivashkevich, V N Naumenko, T V Kovalyova, T N Andreeva, A O Koren *Spectrochim. Acta, Part A* **49** 135 (1993)
192. W Kozminski, J Jazwinski, L Stefaniak, G A Webb *Magn. Reson. Chem.* **28** 1927 (1990)
193. N I Sadova, A A Ivanov, I F Popik, I F Shishkov, L V Vilkov, Yu F Pankrushev *Zh. Strukt. Khim.* **30** 56 (1989)
194. J H Nelson, N E Takach, R A Henry, D W Moore, W M Tolles, G A Gray *Magn. Reson. Chem.* **24** 984 (1986)
195. M Begtrup, J Elguero, R Foure, P Camps, C Estopa, D Ilavsky, A Fruchier, C Marzin, J de Mendoza *Magn. Reson. Chem.* **26** 134 (1988)
196. C W Fong *Aust. J. Chem.* **33** 1763 (1980)
197. V M Bzhezovskii, E V Dashkovskaya, A B Rozhenko, S V Iksanova, A F Shivanyuk, M O Lozinskii *Zh. Org. Khim.* **25** 1852 (1989)
198. V P Karavai, P N Gaponik, O A Ivashkevich *Magn. Reson. Chem.* **27** 611 (1989)
199. P J Kathari, V I Sternberg, S P Singh, S S Parmar, R W Zoelener *J. Heterocycl. Chem.* **17** 637 (1980)
200. J Svetlik, I Goljer, L Landa *Collect. Czech. Chem. Commun.* **49** 1895 (1984)
201. M V Signalov, G A Kalabin, A G Proidakov, E S Domnina, G G Skvortsova *Izv. Akad. Nauk SSSR, Ser. Khim.* 2676 (1981)
202. L B Krivdin, A G Proidakov, V V Shcherbakov, G A Kalabin *Zh. Org. Khim.* **21** 1138 (1985)
203. I Goljer, J Svetlik, I Hrusovsky *Monatsh. Chem.* **114** 65 (1983)
204. J Elguero, A Fruchier, A Konnecke *Monatsh. Chem.* **11** 775 (1980)
205. B Wrackmeyer, E Kupce, A Schmidpeter *Magn. Reson. Chem.* **29** 1045 (1991)
206. L B Krivdin, V V Shcherbakov, G A Kalabin *Zh. Org. Khim.* **23** 2070 (1987)
207. W Holzer, C Jager *Monatsh. Chem.* **123** 1027 (1992)
208. A A Balepin, V P Lebedev, E A Miroshnichenko, G I Koldobskii, V A Ostrovskii, B P Larionov, B V Gidaspov, Yu A Lebedev, in *Svoistva Veshchestv i Stroenie Molekul* (The Properties of Substances and Molecular Structure) (Kalinin: Izd. Kalinin. Gos. Univ., 1977) p. 93
209. A A Kozyro, V V Simirskii, A P Krasulin, V M Sevruk, G Ya Kabo, M L Frenkel', P N Gaponik, Yu V Grigor'ev *Zh. Fiz. Khim.* **64** 656 (1990)
210. E E Barboody, J A Carpenter *J. Chem. Eng. Data* **24** 3 (1979)
211. M F Marshalkin, L N Yakhontov *Usp. Khim.* **55** 1785 (1986) [*Russ. Chem. Rev.* **55** 1016 (1986)]
212. R J Spear, M Maksacheff *Termochim. Acta* **105** 287 (1986)
213. R J Spear, P P Elischer *Aust. J. Chem.* **135** 1 (1982)
214. G OmReddy, V K Nochan, B K Mohan Muraly, A K Chatterejee *Thermochim. Acta* **43** 61 (1981)
215. R A Evans, C Wentrup *J. Chem. Soc., Chem. Commun.* 1062 (1992)
216. P D Croce, C La Rote, G Zecchi *J. Chem. Soc., Perkin Trans. 1* 2621 (1985)
217. L M Gelmi, D Pocar, R Riva *Heterocycles* **34** 315 (1992)
218. A I Lesnikovich, S V Levchik, A I Balabanovich, O A Ivashkevich, P N Gaponik *Termochim. Acta* **200** 427 (1992)
219. Yu Yu Nikishev, I Sh Saifullin, O R Klyuchnikov *Kinet. Katal.* **34** 969 (1993)
220. A Gao, A L Rheingold, T B Brill *Prop. Expl. Pyrotech.* **16** 97 (1991)
221. A Gao, Y Oyumi, T B Brill *Combust. Flame* 345 (1991)
222. A I Lesnikovich, S V Levchik, O A Ivashkevich, E E Bolvanovich, P N Gaponik, B L Korsunskii, S V Kurmaz, T S Larikova, V V Nedelko, V P Roshchupkin *Termochim. Acta* **215** 303 (1993)
223. E Constantin, A Schnell, in *Mass-Spectrometry. Ellis Horwood Series in Analytical Chemistry* (Chichester: Ellis Horwood, 1990) p. 184
224. Yu V Shurukhin, N A Klyuev, V A Ostrovskii, G I Koldobskii, G B Erusalimskii *Zh. Org. Khim.* **20** 2458 (1984)
225. Yu V Shurukhin, N A Klyuev, I I Grandberg *Khim. Geterotsikl. Soedin.* 723 (1985)
226. C Csongar, P Weinberg, G Slezak, G Tomaschewski *J. Prakt. Chem.* **330** 629 (1988)
227. Yu V Shurukhin, A V Dovgilevich, I I Grandberg, B P Baskunov *Khim. Geterotsikl. Soedin.* 925 (1988)
228. A I Lesnikovich, G V Printsev *Khim. Fiz.* **9** 1648 (1990)
229. A I Lesnikovich, V V Sviridov, G V Printsev, O A Ivashkevich, P N Gaponik *Nature (London)* **323** 706 (1986)
230. V V Sviridov, G V Printsev, O A Ivashkevich, P N Gaponik *Dokl. Akad. Nauk BSSR* **30** 1002 (1986)
231. A I Lesnikovich, G V Printsev, O A Ivashkevich, V A Lyutsko, K K Kovalenko *Fiz. Goreniya Vzryva* 48 (1988)
232. K Tarver, T Gudeil, R Shou, M Kupperveit, in *Proceedings of the Sixth International Symposium on Detonation, Coronado, CA* (Translated into Russian; Moscow: Mir, 1981) p. 76
233. A S Tompa *Termochim. Acta* **80** 367 (1984)
234. T M Massis, P K Morenus, D H Huskesson, R M Merill *J. Hazard. Mater.* **5** 309 (1982)
235. S F Palopoli, S I Geig, A L Pheingold, T B Brill *Inorg. Chem.* **27** 2963 (1988)
236. M A Schroeder, R A Henry *Gov. Rep. Announce. Index (U.S.)* **82** 1250 (1982); *Chem. Abstr.* **97** 22 882u (1982)
237. J Yinon, S Zitrin *The Analysis of Explosives* (Oxford: Pergamon Press, 1981)
238. V A Ostrovskii, G B Erusalimskii, M B Shcherbinin *Zh. Org. Khim.* **29** 1297 (1993)
239. P N Gaponik, Yu V Grigor'ev, A O Koren' *Khim. Geterotsikl. Soedin.* 1699 (1988)
240. C J Moody, C W Rees, R G Young *J. Chem. Soc., Perkin Trans. 1* 323 (1991)
241. R H Lowack, R Weiss *J. Am. Chem. Soc.* **112** 333 (1990)
242. R Weiss, R H Lowack *Angew. Chem., Int. Ed. Engl.* **30** 1162 (1991)
243. V P Karavai, P N Gaponik *Khim. Geterotsikl. Soedin.* 66 (1991)
244. E R Civitello, H Rapaport *J. Org. Chem.* **57** 834 (1992)
245. J R Bartels-Keith, J B Mahoney, A J Puttick *J. Org. Chem.* **50** 980 (1985)
246. Ren-Hua Jin, T Nishikubo *Synthesis* 28 (1993)
247. Yu E Myznikov, G I Koldobskii, I N Vasil'eva, V A Ostrovskii *Zh. Org. Khim.* **24** 1550 (1988)
248. L Fieser, M Fieser, in *Reagents for Organic Synthesis* Vol. 2 (Translated into Russian; Moscow: Mir, 1970) p. 29
249. J Stawinski, T Hozumi, S A Narang *J. Chem. Soc., Chem. Commun.* 243 (1976)
250. S Shimizu, M Ogata *J. Org. Chem.* **51** 3897 (1986)
251. S R Buzilova, Yu V Brekhov, A V Afonin, G F Gareev, L I Vereshchagin *Zh. Org. Khim.* **25** 1524 (1989)
252. J Torres, J L Lavandera, P Cabildo, R M Claramunt, J Elguero *J. Heterocycl. Chem.* **25** 771 (1988)
253. V V Semenov, B I Ugrak, S A Shevelev, M I Kanishchev, A T Baryshnikov, A A Fainzil'berg *Izv. Akad. Nauk SSSR, Ser. Khim.* 1827 (1990)
254. M Begtrup, P Larsen *Acta Chem. Scand.* **44** 1050 (1990)
255. R N Butler, K F Quinn, B Welke *J. Chem. Soc., Chem. Commun.* 1481 (1992)
256. G A Gareev, L P Kirillova, V M Shul'gina, S R Buzilova, L P Vologdina, L I Vereshchagin *Zh. Org. Khim.* **24** 2221 (1988)
257. L I Vereshchagin, S R Buzilova, T K Mityukova, L G Proidakov, V N Kizhnyaev, V V Il'ina, G T Sukhanov, G A Gareev, A K Bognes *Zh. Org. Khim.* **22** 1979 (1986)
258. A de la Cruz, J Elguero, P Goya, A U Martinez *J. Heterocycl. Chem.* **25** 225 (1988)
259. A V Sachivko, V P Tverdokhlebov, I V Tselinskii *Zh. Org. Khim.* **22** 1112 (1986)
260. I Yu Shirobokov, A V Sachivko, V P Tverdokhlebov, V A Ostrovskii, I V Tselinskii, G I Koldobskii *Zh. Org. Khim.* **22** 1763 (1986)
261. A O Koren', P N Gaponik *Khim. Geterotsikl. Soedin.* 1643 (1990)
262. A O Koren', P N Gaponik *Khim. Geterotsikl. Soedin.* 1280 (1991)

263. A O Koren', P N Gaponik *Khim. Geterotsikl. Soedin.* 1280 (1991)
264. R N Butler, K J Fitzgerald *J. Chem. Soc., Perkin Trans 1* 1587 (1988)
265. G A Gareev, V M Nikitin, M A Shafeev, L P Kirillova, L I Vereshchagin *Zh. Org. Khim.* **27** 2261 (1991)
266. I V Tselinskii, A A Mel'nikov, L G Varyagina, I G Zhigadlova *Khim. Geterotsikl. Soedin.* 415 (1983)
267. W Ried, S Aboul-Fetouh *Chem.-Ztg.* **112** 135 (1988)
268. A R Katritzky, A Jozwiak, P Lue, K Yannakopoulou, G J Polenik, Ze-Ying Zhang *Tetrahedron* **46** 633 (1990)
269. M Binda, A Dziklinska, A F Hachiam, J Plenkiewicz *Pol. J. Chem.* **66** 1257 (1992)
270. G I Koldobskii, Yu E Myznikov, A B Zhivich, V A Ostrovskii, V S Poplavskii *Khim. Geterotsikl. Soedin.* 754 (1992)
271. T F Osipova, G I Koldobskii, V A Ostrovskii *Zh. Org. Khim.* **20** 2468 (1984)
272. E O John, R L Kirchmeier, J M Shreeve *J. Fluorine Chem.* **47** 333 (1990)
273. Yu E Myznikov, G I Koldobskii, V A Ostrovskii, V S Poplavskii *Zh. Obshch. Khim.* **62** 1367 (1992)
274. G V Boyd, J Cobb, P F Lindley, J C Mitchell, G A Nicolaou *J. Chem. Soc., Chem. Commun.* 99 (1987)
275. P F Lindley, G V Boyd, G A Nicolaou *Acta Crystallogr., Sect. C* **46** 1693 (1990)
276. G I Koldobskii, I V Nikonova, A B Zhivich, V A Ostrovskii, V S Poplavskii *Zh. Obshch. Khim.* **62** 194 (1992)
277. S E Ivanova, G I Koldobskii, V A Ostrovskii *Khim. Geterotsikl. Soedin.* 907 (1993)
278. R Huisgen, H J Sturm, J H Markgraf *Chem. Ber.* **93** 2106 (1960)
279. T V Mal'tseva, E M Ivanova, I K Korobeinicheva *Izv. Sib. Otd. Akad. Nauk SSSR, Ser. Khim. Nauk* (1) 112 (1985)
280. H Takaku, M Yoshida *J. Org. Chem.* **46** 589 (1981)
281. C J Moody, C W Rees, R G Young *Synlett.* 413 (1990)
282. C J Moody, C W Rees, R G Young *J. Chem. Soc., Perkin Trans. 1* 329 (1991)
283. C J Moody, C W Rees, R G Young *J. Chem. Soc., Perkin Trans. 1* 335 (1991)
284. L A Flippin, *Tetrahedron Lett.* **32** 6857 (1991)
285. E W Thomas, M M Cudahy *J. Org. Chem.* **58** 1623 (1993)
286. A G Mayants, K G Pyreseva, S S Gordeichuk *Zh. Org. Khim.* **24** 884 (1988)
287. A G Mayants, V S Klimenko, V V Erina, K G Pyreseva, S S Gordeichuk, V N Leibzon, V S Kuz'min, Yu N Burtsev *Khim. Geterotsikl. Soedin.* 1067 (1991)
288. R L Willer, R A Henry *J. Org. Chem.* **53** 5371 (1988)
289. V V Semenov, S A Shevelev, L G Mel'nikova *Mendeleev Commun.* 58 (1993)
290. A P Winogradoff, N P Peet *J. Heterocycl. Chem.* **26** 97 (1989)
291. V A Dorokhov, A R Amamchan, V S Bogdanov, T A Shchegoleva *Izv. Akad. Nauk SSSR, Ser. Khim.* 2622 (1987)
292. R N Butler, D A O'Donoghue, G A O'Halloran *J. Chem. Soc., Chem. Commun.* 800 (1986)
293. N P Peet, L E Baugh, S Sunder, J E Lewis, E H Matthews, E L Olberding, D N Shah *J. Med. Chem.* **29** 2403 (1986)
294. N P Peet *J. Heterocycl. Chem.* **24** 223 (1987)
295. S Nagarajan, Tse-Lok Ho, G E Du Bois *Synth. Commun.* **22** 1191 (1992)
296. S M Desnenko, P N Orlov, P N Gaponik, V P Karavai *Khim. Geterotsikl. Soedin.* 1533 (1990)
297. O A Luk'yanov, N I Shlykova, Yu A Strelenko *Izv. Akad. Nauk SSSR, Ser. Khim.* 2376 (1987)
298. O A Luk'yanov, N I Shlykova, Yu A Strelenko *Izv. Akad. Nauk SSSR, Ser. Khim.* 1619 (1989)
299. E V Dashkovskaya, N V Ignat'ev, A F Shivanyuk, M O Lozinskii *Zh. Org. Khim.* **26** 205 (1990)
300. S K Sagnal, A Kumar *Chem. Acta Turc.* **17** 263 (1989)
301. U Schmidt, M Dietsche *Angew. Chem.* **93** 786 (1981)
302. R N Butler, D P Shelly, V C Garvin *J. Chem. Soc., Perkin Trans. 1* 1589 (1984)
303. O R Buzilova, V M Shul'gina, G A Gareev, L I Vereshchagin *Khim. Geterotsikl. Soedin.* 842 (1980)
304. N Chino, K Y Kumagaye, Y Noda, T X Watanabe, T Kimura, S Sanakibara *Biochem. Biophys. Res. Commun.* **141** 665 (1986)
305. M Narisada, Y Terui, M Yamakawa, F Watanabe, M Ohtani, H Miyazaki *J. Org. Chem.* **50** 2794 (1985)
306. M Ohtani, M Narisada *J. Org. Chem.* **56** 5475 (1991)
307. T L Gilchrist, J E Wood *J. Chem. Soc., Chem. Commun.* 1460 (1992)
308. R R Khaliullin, V V Plemenkov *Zh. Obshch. Khim.* **63** 874 (1993)
309. K Takeda, K Tsuboyama, K Torii, M Muzata, H Ogura *Tetrahedron Lett.* **29** 4105 (1988)
310. K Tsuboyama, K Takeda, K Torii, H Ogura *Chem. Pharm. Bull.* **38** 2357 (1990)
311. R A W Johnstone, W N McLean *Tetrahedron Lett.* **29** 5553 (1988)
312. D Moderhack, A Beissner *Z. Naturforsch., B* **47** 1803 (1992)
313. R K Russel, W V Murray *J. Org. Chem.* **58** 5023 (1993)
314. A Messmer, G Hajos, G Timari *Tetrahedron* **48** 8451 (1992)
315. D Moderhack, D-O Bode, D Schomburg *Chem. Ber.* **126** 129 (1993)
316. E S Yoo, R H Kim, N Jeong *Korean J. Med. Chem.* **1** 65 (1991)
317. L Omelka, M Meske, V Cholvad, J Svetlik, M Schulz *Collect. Czech. Chem. Commun.* **57** 1065 (1992)
318. R N Butler, D P Shelly *Tetrahedron Lett.* **26** 3401 (1985)
319. A F Brigas, R A W Johnstone *J. Chem. Soc., Chem. Commun.* 1041 (1991)
320. V A Lopyrev, T G Ermakova, T N Kashik, L E Protasova, T I Vakul'skaya *Khim. Geterotsikl. Soedin.* 315 (1986)
321. B Stanovnik *Tetrahedron* **47** 2925 (1991)
322. M Zlicar, B Huc, B Stanovnik, M Tisler *Synlett.* 707 (1990)
323. P N Gaponik, O A Ivashkevich, T N Andreeva, T B Kovaleva *Vestn. Beloruss. Gos. Univ. Ser. 2* 24 (1990)
324. P N Gaponik, O A Ivashkevich, T V Kovalyova, T N Andreeva *J. Appl. Polym. Sci.* **33** 769 (1987)
325. P N Gaponik, O A Ivashkevich, T B Kovaleva, V A Morozov, A G Kriger, E V Fronchek, V L Tsailingol'd, V V Grachev *Vysokomol. Soedin., Ser. B* **7** 39 (1988)
326. O A Ivashkevich, P N Gaponik, O N Bubel, T B Kovalyova *Makromol. Chem.* **189** 1363 (1988)
327. S Donnelly, J Grimshaw, J Trocha-Grimshaw *J. Chem. Soc., Perkin Trans. 1* 1557 (1993)
328. H Quast, U Nahr *Chem. Ber.* **117** 2761 (1984)
329. H Quast, U Nahr *Chem. Ber.* **118** 526 (1985)
330. H Quast, A Fuss, U Nahr *Chem. Ber.* **118** 2164 (1985)
331. R A Evans, C Wentrup *J. Chem. Soc., Chem. Commun.* 1062 (1992)
332. P Leichkauf, V Lohse, C Csongar, M Siegmund, G Tomaschewski *Z. Chem.* **27** 371 (1987)
333. H Quast, T Hergenrother *Chem. Ber.* **125** 2095 (1992)
334. M C Gonzales, E San Roman *J. Phys. Chem.* **93** 3536 (1989)
335. L G Lavrenova, S V Larionov, V N Ikorskii, Z A Grankina *Zh. Neorg. Khim.* **30** 964 (1985)
336. L G Lavrenova, A N Bogatikov, L A Sheludyanova, V N Ikorskii, S V Larionov, P N Gaponik *Zh. Neorg. Khim.* **36** 1220 (1991)
337. N I Vorob'eva, N S Frumina, S N Eremenko *Zavod. Lab.* **50** 13 (1984)
338. A I Vrublevskii, P N Gaponik, M M Degtyarik, A I Lesnikovich, R S Luk'yanova *Koord. Khim.* **7** 213 (1981)
339. M M Degtyarik, P N Gaponik, A I Lesnikovich, A I Vrublevskii *Zh. Obshch. Khim.* **55** 516 (1985)
340. A O Koren', V A Ostrovskii, P N Gaponik, I E Titova, V S Poplavskii, G B Avetikyan, G I Koldobskii *Zh. Obshch. Khim.* **58** 825 (1988)
341. L G Lavrenova, A R Amamchan, S V Larionov, V A Dorokhov *Izv. Akad. Nauk, Ser. Khim.* 2311 (1992)
342. W R Ellis, W L Purcell *Inorg. Chem.* **21** 834 (1982)
343. T G Leonova, S V Larionov, N I Bratchenko, A A Sheludyakova *Zh. Obshch. Khim.* **59** 1660 (1989)
344. R Guilard, N Jagerovic, A Tabard, P Richard, L Courthaudon, A Louati, C Lecomte, K M Kadish *Inorg. Chem.* **30** 16 (1991)
345. R Guilard, N Jagerovic, A Tabard, P Richard, C Lecomte, Y H Liu, K M Kadish *Inorg. Chem.* **30** 27 (1991)
346. F A Banbury, M G Davidson, A Martin, P R Raithby, R Snaith, K L Verhorevoort, D S Wright *J. Chem. Soc., Chem. Commun.* 1152 (1992)
347. R W Saalfrank, C-J Lurz, K Schobert, O Struck, E Bill, A X Trautwein *Angew. Chem.* **103** 1449 (1991)
348. R W Saalfrank, O Struck, K Nunn, C-J Lurz, R Harbig, K Peters, H G Schnering, E Bill, A X Trautwein *Chem. Ber.* **125** 2331 (1992)
349. Z G Aliev, T K Goncharov, V P Grachev, S V Kurmaz, V P Roshchupkin *Koord. Khim.* **17** 1101 (1991)

350. A G Starikov, G I Dzhardimalieva, I E Uflyand, T K Goncharov, A D Pomogailo *Izv. Akad. Nauk, Ser. Khim.* 76 (1993)
351. S Araki, Y Wanibe, F Uno, A Morikawa, K Yamamoto, K Chiba, Y Butsugan *Chem. Ber.* **126** 1149 (1993)
352. S Araki, Y Butsugan *Chem. Ber.* **126** 1157 (1993)
353. G L'abbe, M Gelinne, Z Toppet *J. Heterocycl. Chem.* **25** 1741 (1988)
354. J Grimshaw, S A Hewitt *J. Chem. Soc., Perkin Trans. 1* 2995 (1990)
355. G A Shveikhgeimer, K I Kobrakov, O G Mityagina, V A Korolev, V K Promonenkov *Khim. Geterotsikl. Soedin.* 711 (1986)
356. G A Shveikhgeimer *Khim. Geterotsikl. Soedin.* 1443 (1993)
357. I E Filatov, G L Rusinov, O N Chupakhin *Khim. Geterotsikl. Soedin.* 1145 (1992)
358. A G Mayants, L M Tishchenko, V N Vladimirov, V A Shlyapochnikov *Khim. Geterotsikl. Soedin.* 1351 (1992)
359. V A Ostrovskii, V S Poplavskii, G I Koldobskii, in *Perspektivnye Napravleniya Khimii i Khimicheskoi Tekhnologii* (Future Trends in Chemistry and Chemical Technology) (Eds A S Dudyrev, V V Bogdanov) (Leningrad: Khimiya, 1991) p. 103
360. J A Weber, W J Wheller, in *Chemistry and Biology of 3-Lactam Antibiotics* Vol. 1 (New York: Academic Press, 1982) p. 371
361. V Nagata, in *Current Trends in Organic Synthesis* (Ed. H Nozaki) (Translated into Russian; Moscow: Mir, 1986) p. 117
362. G D Diana, D Cutcliffe, D L Volkots, J P Mallamo, T R Railey, N Vescio, R C Oglesby, T J Nitz, J Wetzel, V Giranda, D C Pevear, F J Dutko *J. Med. Chem.* **36** 3240 (1993)
363. V G Yashunskii, V Yu Kovtun *Usp. Khim.* **54** 126 (1985) [*Russ. Chem. Rev.* **54** 76 (1985)]
364. S L Beaucage, R P Iyer *Tetrahedron* **49** 6123 (1993)
365. S L Beaucage, R P Iyer *Tetrahedron* **49** 10441 (1993)
366. Z K Karlova, E A Lavrinovich, B F Myasoedov *Radiokhimiya* **33** 70 (1991)
367. L Horner, E Pliefke *Werkst. Korros.* **36** 545 (1985)
368. J H Boyer, in *Organic Nitro Chemistry* Vol. 1 (Ed. H Feuer) (Deerfield Beach, FL.: VCH, 1986) p. 268
369. R J Spear, P P Elischer *Aust. J. Chem.* **35** 1 (1982)

Russian Chemical Reviews **63** (10) 815–832 (1994)
©1994 Russian Academy of Sciences and Turpion Ltd

UDC 547.759.3.5

The chemistry of pyrroloindoles

Sh A Samsoniya, N L Targamadze, N N Suvorov

Contents

I.	Introduction	815
II.	Methods of synthesis of pyrroloindoles	815
III.	Electrophilic substitution reactions of pyrroloindoles	824
IV.	Side chain reactions of derivatives of 1*H*, 6*H*-pyrrolo[2,3-*e*]indole	828

Abstract. The methods of synthesis of isomeric pyrroloindoles are surveyed. The characteristic features of electrophilic substitution reaction of the pyrroloindole ring and certain side chain reactions are discussed. The bibliography includes 60 references.

I. Introduction

Pyrroloindoles are striking representatives of indole-containing condensed systems. Chemically they are the closest analogues of indole. A wide variety of bifunctional analogues of biologically active indole derivatives have been obtained from pyrroloindoles.

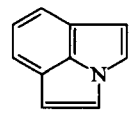
Substances with bactericidal, antimicrobial, and antitumour activities as well as other properties of value for medicine and the national economy have been found among pyrroloindole derivatives.[1–3] The highly active antitumour antibiotic CC-1065, the principal structural fragment of which is the pyrroloindole system, was isolated in 1987 from *Streptomyces zebensis*. Its antitumour activity in vitro is many times greater than that of other known preparations.[4] This stimulated further development of synthetic methods for the preparation of pyrroloindoles. Research on these lines is being continued.

Pyrroloindole is a typical representative of heteroaromatic systems. Its molecule consists of three conjugated rings with 14π electrons which satisfy the aromaticity rule ($4n + 2$) in Dewar's treatment. Like indole itself, the pyrroloindoles **1–4** belong to systems with an excess of π electrons, since the total number of π electrons of the aromatic system exceeds the number of atoms in the ring.[35] In contrast to indole, there are two nitrogen atoms in the molecules of the pyrroloindoles **1–4** which contribute four π electrons to the aromatic system. Simple calculations have shown that the number of π electrons corresponding to each ring atom is 1.17 in the pyrroloindoles **1–4** and 1.11 in indole. Thus the excess of π electrons in pyrroloindoles is greater than in indole. Approximately the same relation between their reactivities with respect to weak electrophiles may be expected.

Sh A Samsoniya, N L Targamadze Department of Organic Chemistry and the Chemistry of Natural Products, Organic Synthesis Laboratory, Dzhavakhishvili Tbilisi State University, prosp. I Chavchavadze 3, 380028 Tbilisi, The Georgian Republic. Fax (7-883) 222 11 03
N N Suvorov Department of Organic Chemistry, Mendeleev Russian Chemical-Technological University, Miusskaya pl. 9, 125820 Moscow, Russian Federation. Fax (7-095) 200 42 04

Received 1 July 1994
Uspekhi Khimii **63** (10) 866–884 (1994); translated by A K Grzybowski

The pyrroloindoles described in the literature can be divided into three groups. Those in the molecules of which pyrrole is condensed with indole via the benzene ring (type I) or the carbon atoms in the pyrrole ring (type II) and also pyrroloindoles in the molecules of which there is one common nitrogen atom and all three rings are linked directly to one another (type III), for example as in the following formula:

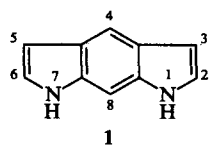


The properties of type I pyrroloindoles differ from those of type II and III compounds, which will not be considered in the present review.

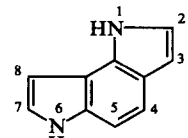
Type I pyrroloindoles are particularly interesting because they contain two reactive centres in the β-positions in the pyrrole rings. This makes it possible to obtain bifunctional analogues of the known physiologically active indole compounds.

II. Methods of synthesis of pyrroloindoles

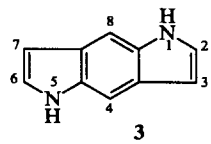
The following pyrroloindole systems are known at present:



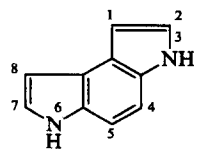
1



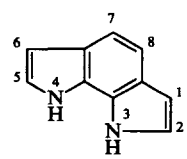
2



3



4

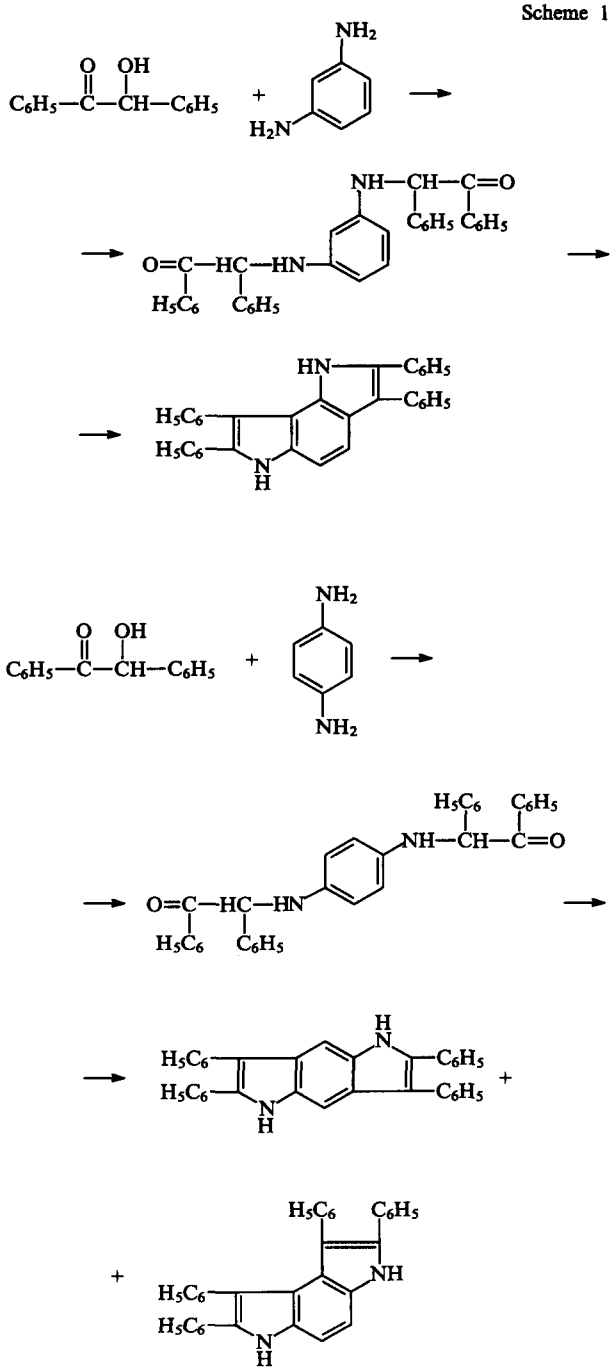


5

Pyrroloindoles may be synthesised in two ways: the first procedure involves simultaneous closure of both pyrrole rings, the second involves the attachment of a pyrrole ring to the benzene ring of indoline or indole.

The first pyrroloindoles were obtained as early as the past century. Thus Japp and Meldrum[5] synthesised tetraphenylpyrroloindoles from *m*- and *p*-phenylenediamines and benzoin by the Bischler reaction (the yields are not indicated) (Scheme 1).

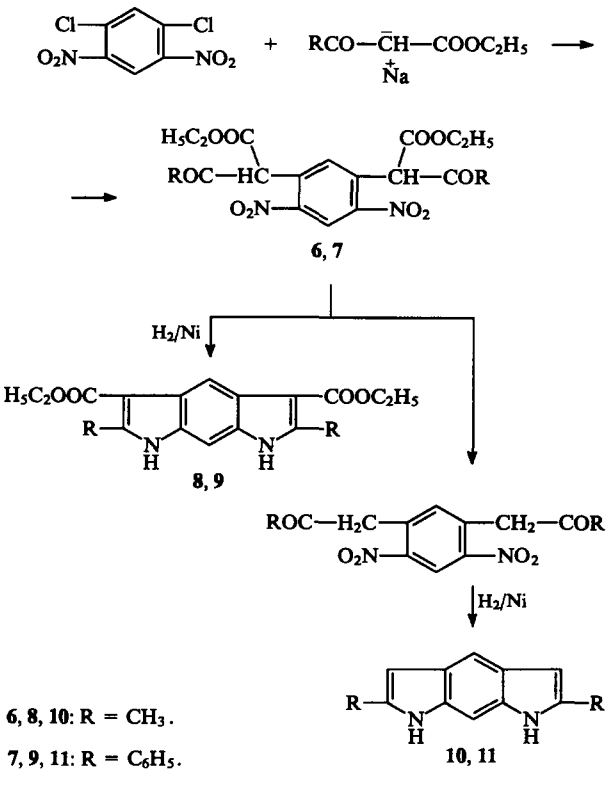
Scheme 1



Another scheme for the synthesis of pyrroloindoles using the Bischler method involves the condensation of 4-, 5-, 6-, and 7-aminoindoles with benzoin and subsequent cyclisation. Various isomeric pyrroloindoles obtained in accordance with this scheme are listed in Table 1.

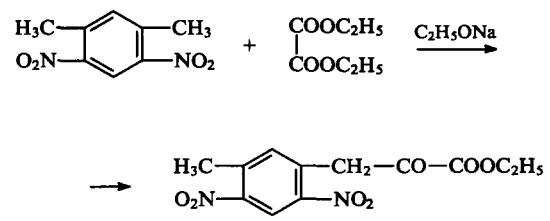
However, these reactions are only of historical significance: they are restricted because only aryl- or arylalkyl-substituted derivatives can be obtained and the yields of the cyclisation products are low.

The German investigator Ruggli and his students[7,8] used a different method for the synthesis of pyrroloindoles, which is based on a modified Reissert reaction.



The condensation of 2,4-dichloro-1,5-dinitrobenzene with the enolates of certain ketoacid esters takes place stepwise; the substitution of the second chlorine atom is difficult. The reductive cyclisation of the diketones **6** and **7** in the presence of 'Ni Rupe' (a mixture of the crude catalyst with clay powder) under a hydrogen atmosphere leads to the pyrroloindoles **8** and **9**. Ketonic cleavage of compounds **6** and **7** and subsequent reduction afford the pyrroloindoles **10** and **11**. It is noteworthy that the target products were obtained in low yields owing to the considerable losses of these compounds during isolation and purification.

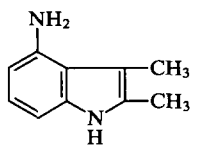
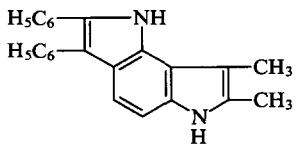
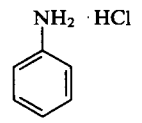
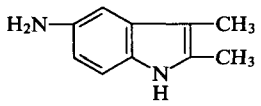
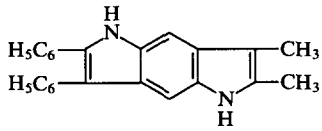
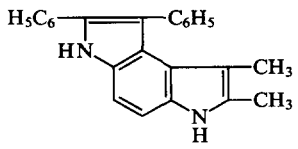
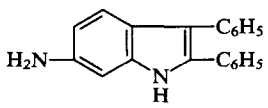
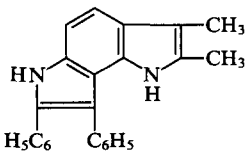
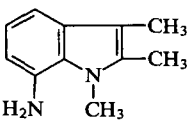
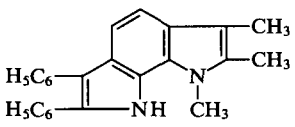
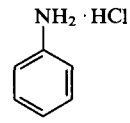
A disadvantage of the synthesis of pyrroloindoles by the Reissert reaction is also the fact that it cannot be used to obtain the unsubstituted pyrroloindole with a linear structure, since it has been established that in the condensation of diethyl oxalate with 4,6-dinitro-*m*-xylene only one methyl group reacts.

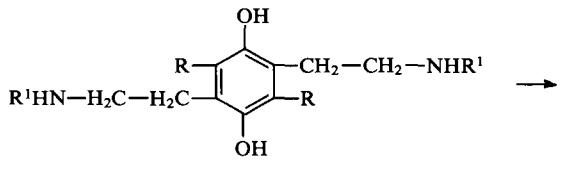


In 1973, Baird, Baxter, and coworkers[9] discovered a new method of synthesis of pyrroloindoles. It was found that the dihydrobromide of 2,5-bis(β-aminoethyl)hydroquinone **12a** is converted spontaneously into the dihydropyrroloindole **13a** in aqueous solution in air. The synthesis of compound **13a** was not the authors' aim, but they nevertheless investigated this process and put forward an hypothesis concerning the reaction mechanism. They also dehydrogenate compound **13a** to give the fully aromatised pyrroloindole **3**.

It was established subsequently[9] that the hydroquinones **12b** and **12c** undergo bicyclisation under similar conditions, forming respectively the dihydropyrroloindoles **13b** and **13c**. Compound **13c** was dehydrogenated to compound **14c**.

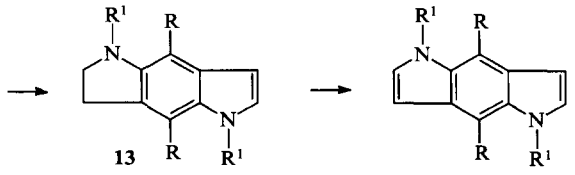
Table 1. Pyrroloindoles obtained from the products of the condensation of aminoindoles with benzoin.[6]

Initial aminoindole	Pyrroloindole	Cyclising agent	Yield (%)
			4
		HCl, H_2SO_4	6
		HCl, H_2SO_4	3
		HCl	7
			8



12a–c

R = R^1 = H (**a**);
R = Br, R^1 = H (**b**);
R = H, R^1 = CH_3 (**c**).

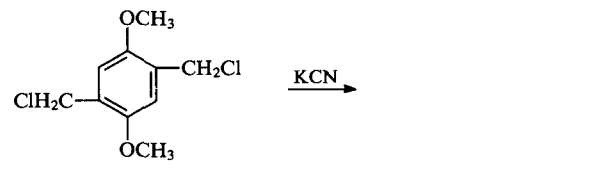


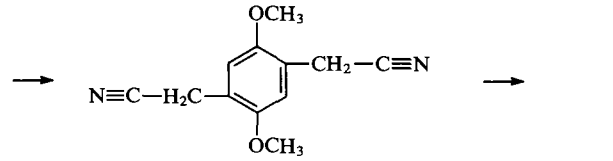
13

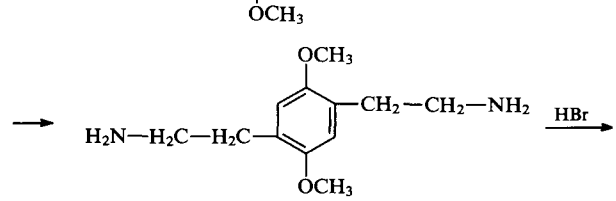
R = R^1 = H (**a**);
R = Br, R^1 = H (**b**);
R = H; R^1 = CH_3 (**c**).

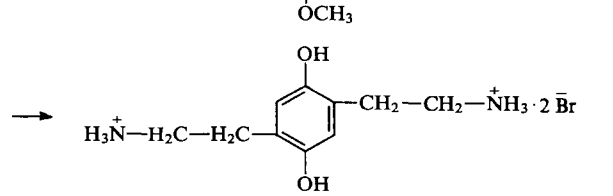
3: R = R^1 = H;

14c: R = H, R^1 = CH_3.



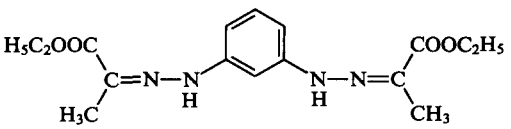
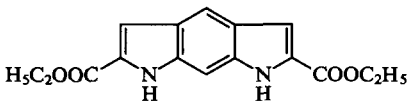
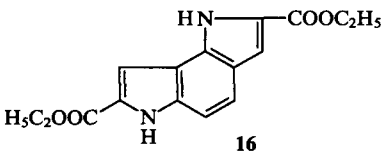
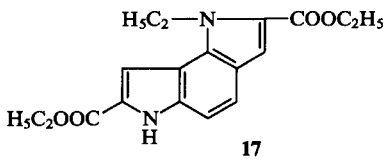
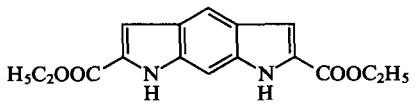
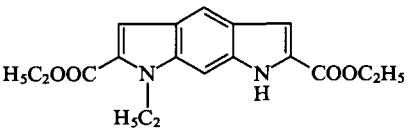
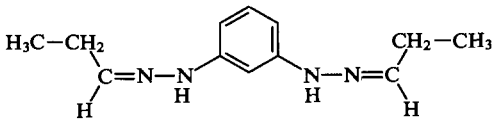
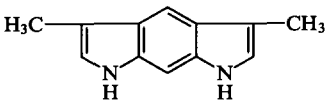
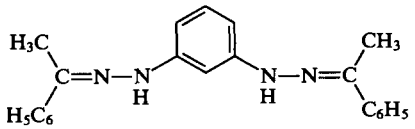
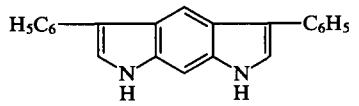
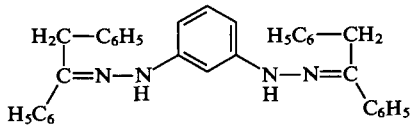
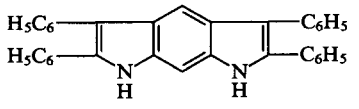
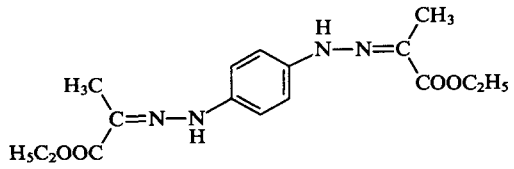
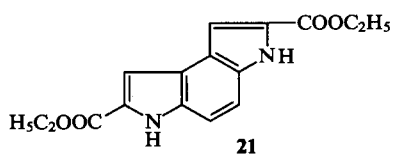






The initial hydroquinone **12a** was synthesised from 1,4-di(chloromethyl)-2,5-dimethoxybenzene.

Table 2. Pyrroloindoles obtained by cyclising certain *m*- and *p*-phenylhydrazones.

Hydrazone	Pyrroloindole	Cyclising agent	Yield (%)	Ref.
 **15**		12% H_2SO_4/C_2H_5OH	—	10
	 **16**	—	65	11–13
	 **17**	—	1	11–13
	 **18**	—	8	11–13
	 **19**	—	1	11–13
		5% H_2SO_4/C_2H_5OH	—	10
		12% H_2SO_4/C_2H_5OH	3	14
		H_2SO_4/ C_2H_5OH	50	14
 **20**	 **21**	EEPPA	6–9	15

Compound **12b** was obtained by brominating the hydroquinone **12a** and compound **12c** was synthesised by methylating it.[9]

However, in view of the low availability and instability of the initial compound and the large number of stages, this method cannot be regarded as preparative for the synthesis and further study of unsubstituted pyrroloindoles.[3]

The Fischer reaction has also been used in the synthesis of pyrroloindoles. The pyrroloindoles obtained by the cyclisation of certain *m*- and *p*-phenylenedihydrazones by the Fischer reaction are presented in Table 2.

It was found subsequently[11] that the first syntheses[10,14] suffered from significant disadvantages: the optimum reaction conditions were not selected (certain dihydrazones did not react even on prolonged refluxing, which indicated the low effectiveness of the catalyst employed); the cyclisation process was accompanied by appreciable charring and the reaction products were difficult to purify; the yield of the reaction products was very low. Furthermore, the cyclisation products were not characterised either by further reactions or by spectroscopic methods and a linear structure was attributed to them without proof. For example, when the cyclisation reaction of the dihydrazone **15** was reproduced under the conditions described by Giuliano and Leonardi[10] and the reaction product was investigated spectroscopically, it was found that it had an angular structure.[11]

For these reasons, there was a need for a detailed investigation of the Fischer reaction of phenylenedihydrazones, since this reaction was and remains the most convenient method of synthesis of indole and its analogues.

Studies were carried out on the cyclisation of ethyl pyruvates and *p*-phenylenedihydrazones and the optimum reaction conditions were selected.[11-13,15]

In the bicyclisation of *m*-phenylenedihydrazones, the formation of pyrroloindoles of two types, differing in the condensation of the rings, is theoretically possible. The cyclisation described above gives a mixture of the pyrroloindoles **16** and **18** having angular and linear structures, the angular isomer **16** predominating (yield 65%).[12,13] This can be explained by the fact that the angular structure is energetically more favourable than the linear structure in the formation of polynuclear condensed aromatic systems.[16] The *N*-ethyl derivatives **17** and **19** were also isolated from the cyclisation products in yields less than 1%.[13]

The conversion of various stereoisomers of the *m*-phenylenedihydrazone of ethyl pyruvate into indole derivatives takes place in virtually identical yields.

It is noteworthy that the development of convenient methods of synthesis of 2,7-diethoxycarbonyl-1*H*,6*H*-pyrrolo[2,3-*e*]indole **16** in high yields is a very important task, since this compound opens the way to the subsequent synthesis of the unsubstituted heterocycle.

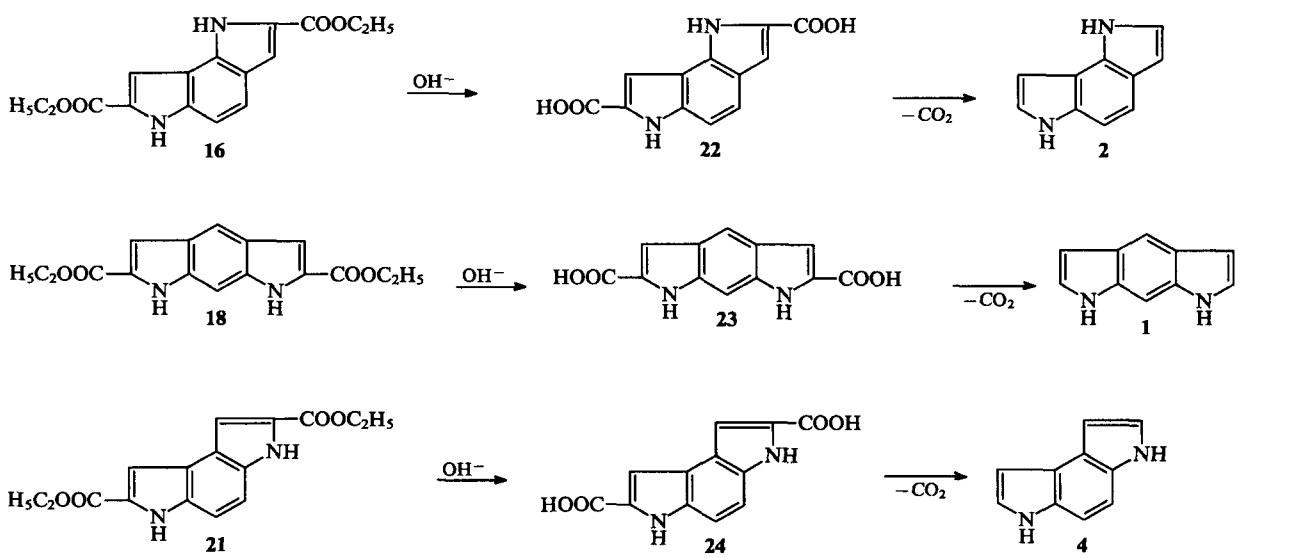
The ethyl ester of polyphosphoric acid (EEPPA) proved to be the most effective cyclising agent for the conversion of the *p*-phenylenehydrazone of ethyl pyruvate **20** into an indole derivative. However, in this case the yield of 2,7-diethoxycarbonyl-3*H*,6*H*-pyrrolo[3,2-*e*]indole **21** was only 6%–9%. In the remaining cases, charring of the reaction mass was observed.[15] The low yield of products in the cyclisation reaction can probably be explained by the fact that a crude dihydrazone **20** was employed, its purification involving considerable difficulties.[15]

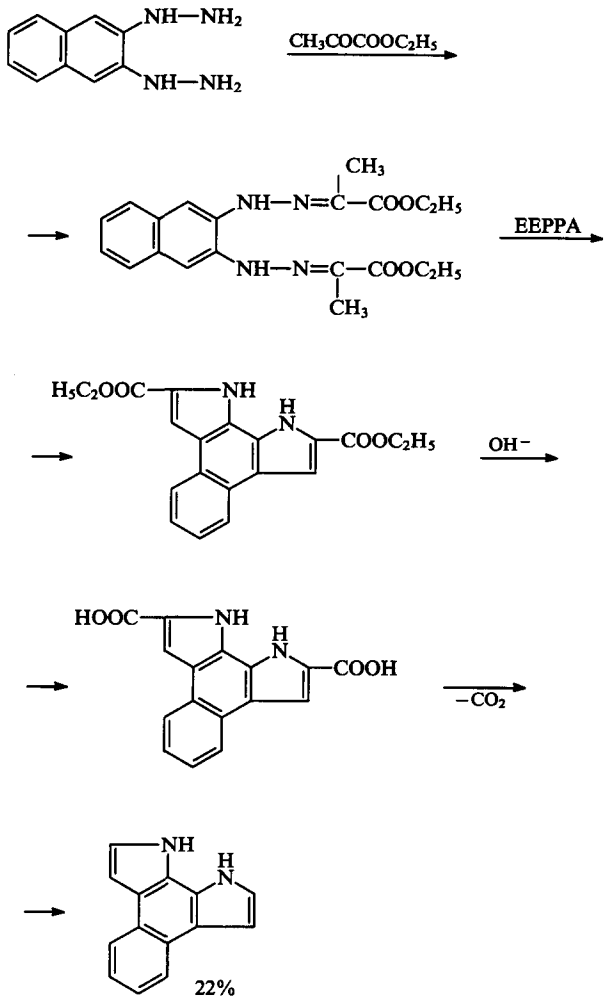
The hydrolysis of the diesters **16**, **18**, and **21** afforded high yields of the corresponding dicarboxylic acids **22**–**24** (Scheme 2).[11,12,15]

However, the methods for the bisdecarboxylation of dicarboxylic acids described in the literature (heating in quinoline or in dimethylacetamide in the presence of powdered copper[17] or copper salts[18]) proved unsuitable. The desired results were achieved only on thermal decarboxylation of the dicarboxylic acids **22**–**24** in a stream of an inert gas. The unsubstituted pyrroloindoles **1**, **2**, and **4** corresponding to compounds **22**–**24** were then obtained in 20%, 30%, and 25% yields respectively.[11,12,15]

The cyclisation of 2,3-naphthylenedihydrazone to 2,9-diethoxycarbonyl-1*H*,10*H*-benzo[*e*]pyrrolo[3,2-*g*]indole was achieved in 1984. Hydrolysis and subsequent decarboxylation of the dicarboxylic acid afforded the unsubstituted 1*H*,10*H*-benzo[*e*]-pyrrolo[3,2-*g*]indole.[19] The yields of the products were high in all the stages of the synthesis except the last.

Scheme 2



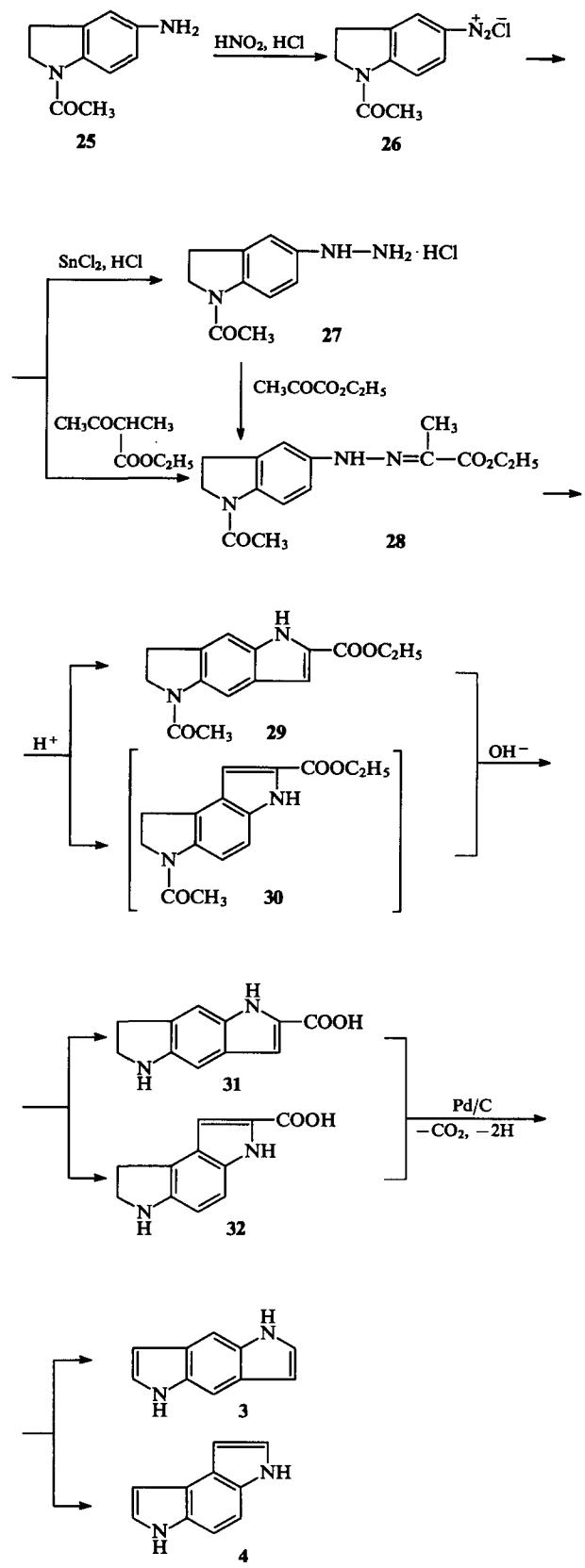


Thus it is seen that the unsubstituted pyrroloindoles **1**–**4** may be obtained with the aid of the Fischer reaction and the reaction of Baird and Baxter. However, these methods enable only 1*H*,6*H*-pyrrolo-[2,3-*e*]indole **2** to be synthesised in an amount sufficient for further study. The remaining three heterocycles **1**, **3**, and **4** are obtained in very low overall yields. Furthermore, the synthesis of the pyrroloindole **3** is complicated by the low availability and instability of the initial compound.

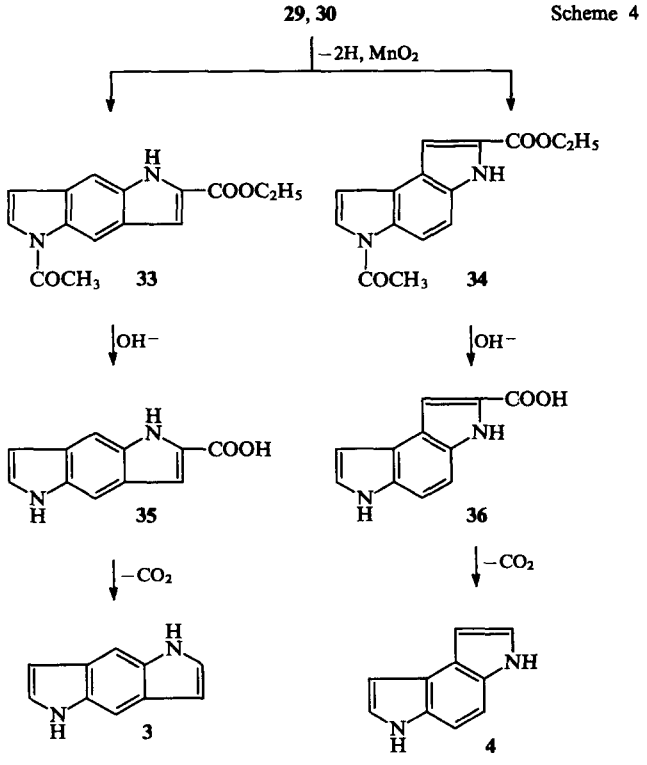
Continuing the search for convenient methods of synthesis of pyrroloindoles, Samsoniya, Suvorov, Kadzhrishvili, and coworkers[20] used a new procedure for the construction of the pyrroloindole system — the addition of the pyrrole ring to the benzene ring of the indoline system. The initial compounds chosen were 5- and 6-aminoindolines. The first of these was synthesised from indoline by the method of Terent'ev and Preobrazhenskaya[21] in acetic anhydride using nitric acid as the nitrating agent (yield 70%), while the second was obtained by nitration with a mixture of nitric and sulfuric acids (quantitative yield). The nitroindolines were acetylated with acetic anhydride and were reduced with hydrazine hydrate in the presence of Raney nickel (yield 95%) by the general method recommended for aromatic nitro-compounds.

The syntheses of 1*H*,5*H*-pyrrolo[2,3-*e*]indole **3**, 3*H*,6*H*-pyrrolo[2,3-*e*]indole **4**, and 1*H*,6*H*-pyrrolo[2,3-*e*]indole **2** are presented in Schemes 3–5.[20]

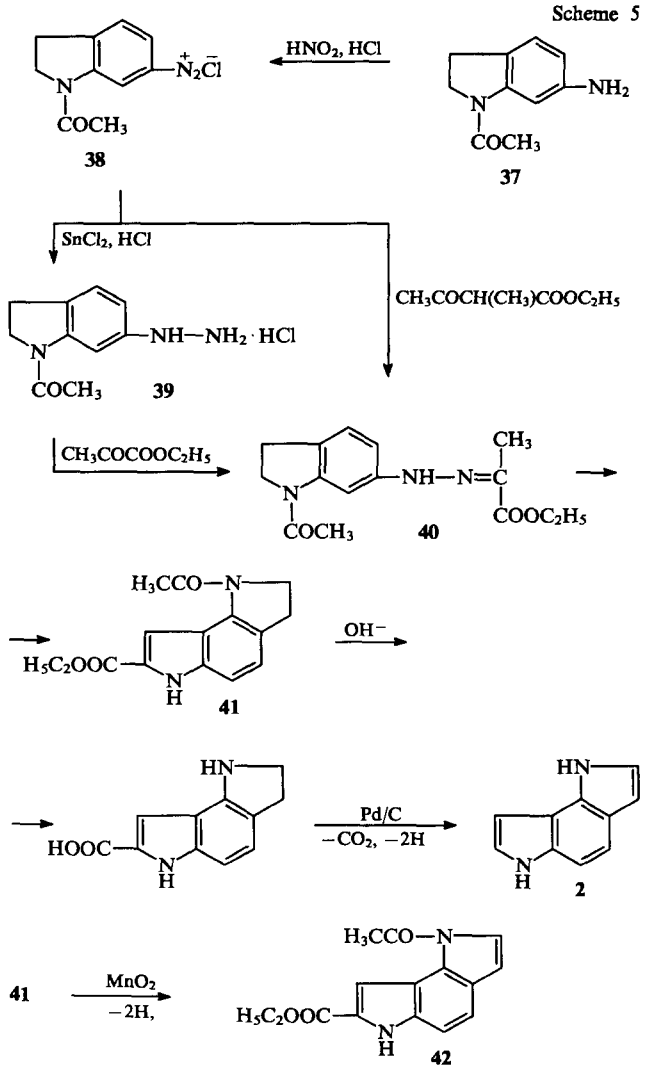
Scheme 3



Scheme 4



Scheme 5



Different compounds were tried as cyclising agents in the conversion of the hydrazones **28** (Scheme 3) and **40** (Scheme 5) into indole derivatives. The best results were obtained when EEPPA was used.

The cyclisation of the hydrazone **28** results in the formation of a mixture of pyrroloindolines having linear (compound **29**) and angular (compound **30**) structures (yield 74%). The main reaction product is the linear isomer. The attempts to separate the mixture of the isomers **29** and **30** were unsuccessful, but compound **29** can be isolated and characterised by means of column chromatography.

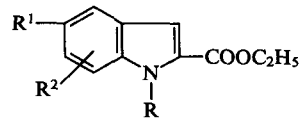
Hydrolysis of the mixture of esters **29** and **30** with aqueous alkali is very rapid and leads to a mixture of the acids **31** and **32** in 93% yield. The decarboxylation and simultaneous dehydrogenation of the acids in the presence of 10% Pd/C afforded a mixture of the isomeric pyrroloindoles **3** and **4** (yield 20%). The latter were separated by column chromatography.

The dehydrogenation of a mixture of the isomeric esters **29** and **30** by manganese dioxide in boiling xylene was also achieved (Scheme 4); compounds **33** and **34** were obtained in 75% yield. Separation of this mixture by column chromatography affords the angular ester **34** and the linear ester **33** in proportions of 1 : 6.

Hydrolysis of the esters **33** and **34** with aqueous alkali leads to high yields of the corresponding acids **35** and **36**, the thermal decarboxylation of which afforded the unsubstituted pyrroloindoles **3** and **4** in 20% and 26% yields respectively.[20]

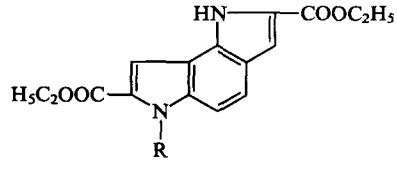
The unsubstituted pyrroloindole **2** was obtained similarly from the hydrazone **40** (Scheme 5) after the corresponding transformations. The dehydrogenation of the ester **41** gives the pyrroloindole **42**. The yields of the products of these reactions are approximately the same as in the previous syntheses.

Later (in 1983) Katti and Siddappa[22] achieved the synthesis of various pyrroloindole systems from *o*-, *m*-, and *p*-nitroanilines by the stepwise closure of one and then the other pyrrole rings using the familiar Fischer scheme. The 4-, 5-, 6-, and 7-nitroindoles obtained in this way are reduced with Raney nickel, diazotised under mild conditions, and coupled with methylacetoacetic ester. The diesters of the isomeric pyrroloindoles are obtained by cyclising the corresponding hydrazones. The overall yields of the pyrroloindoles are low. The subsequent reactions of the heterocycles were not described by the authors.



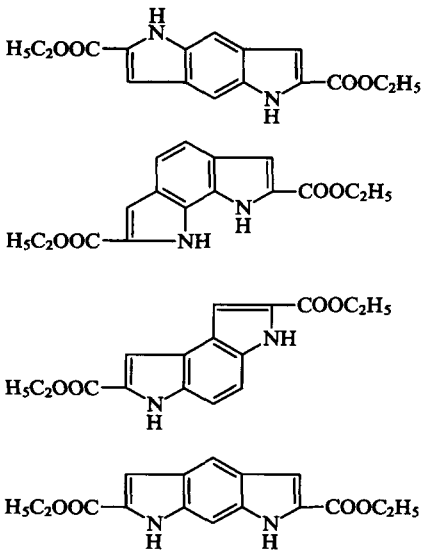
R = H, CH_3; R^1 = H, CH_3;

R^2 = NO_2, NH_2, —NH—N=C(CH3)COOC2H5.

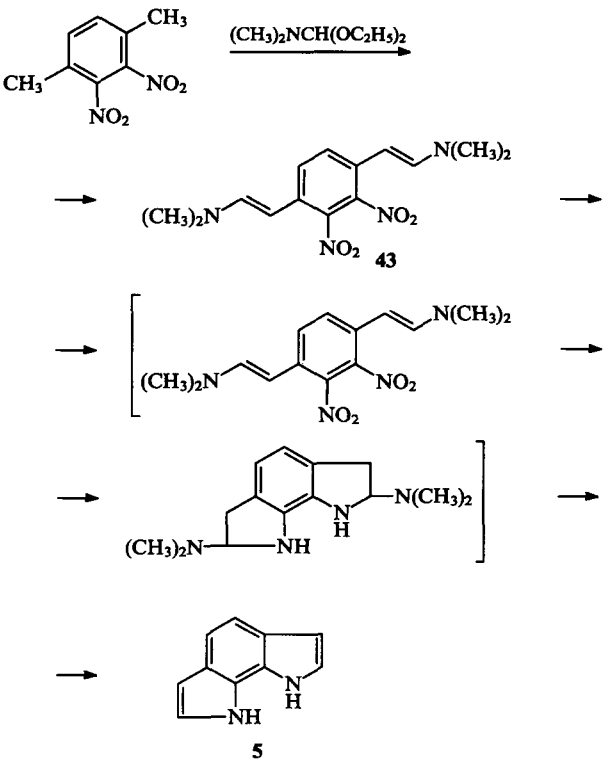


R = H, CH_3.

(continued over)



A convenient method of synthesis of certain pyrroloindoles has been proposed by Berlin et al.[23]



The synthesis was carried out by the Leimgruber – Batcho reaction and involved the following processes: the condensation of dinitro-*p*-xylene with the diethyl acetal of dimethylformamide and subsequent reductive cyclisation of the dinitroenamine **43**, obtained in the condensation reaction (yield 75%), to the unsubstituted pyrroloindole **5** (yield 70%).

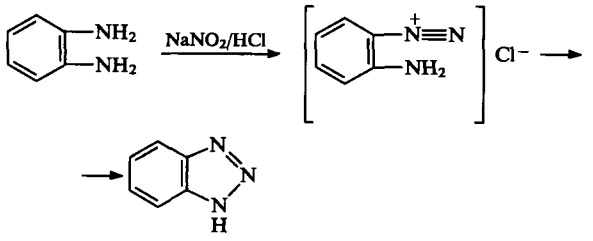
The linear pyrroloindole **1** was obtained similarly from 4,6-dinitro-*m*-xylene (yield 55%), while the isomer **3** was synthesised from 2,5-dinitro-*p*-xylene (yield 39%).

Only pyrroloindoles unsubstituted in the pyrrole rings can be obtained by this method, which limits its applications.

1. Synthesis of the initial hydrazones

The initial compounds for the Fischer reaction (arylhydrazones) are obtained by condensing arylhydrazines with the corresponding carbonyl compounds; the Japp – Klingemann reaction is sometimes used for this purpose. In both cases, it is necessary to have sufficiently pure aryldiazo-compounds.

The synthesis of benzene-1,2-bisdiazonium salts by the usual diazotisation of phenylenediamines is known to involve appreciable complications. Thus the diazotisation of *o*-phenylenediamine results in the initial formation of the *o*-aminobenzenediazonium salt, which is converted into a cyclic azimine (benzotriazole).



The diazotisation of *p*-phenylenediamine is accompanied by appreciable oxidation to quinone or quinone imine, while *m*-phenylenediamine readily couples during the diazotisation process with the mono- and bis-diazonium ions formed, affording the corresponding azo-dyes.[24-26]

Special diazotisation methods are used in the synthesis of the benzene-1,2-diazonium salt. Thus comparatively pure benzene-1,2-diazonium and benzene-1,4-diazonium chlorides are synthesised by diazotising the corresponding diamines with nitrosylsulfuric acid in the presence of concentrated phosphoric acid.[26,27] Since the synthesis of pure benzene-1,4-diazonium involves considerable difficulties, a two-stage process is employed as a rule in the synthesis of dyes — diazotisation and coupling of the amino-groups of *p*-phenylenediamine.[24]

In the diazotisation of *m*-phenylenediamine, the excess HCl and the brief contact between the reactants suppress the coupling reaction indicated above. The yield of benzene-1,3-diazonium chloride then increases.[24,28] The same result was achieved by introducing polyhydric alcohols or carbohydrates into the reaction.[29]

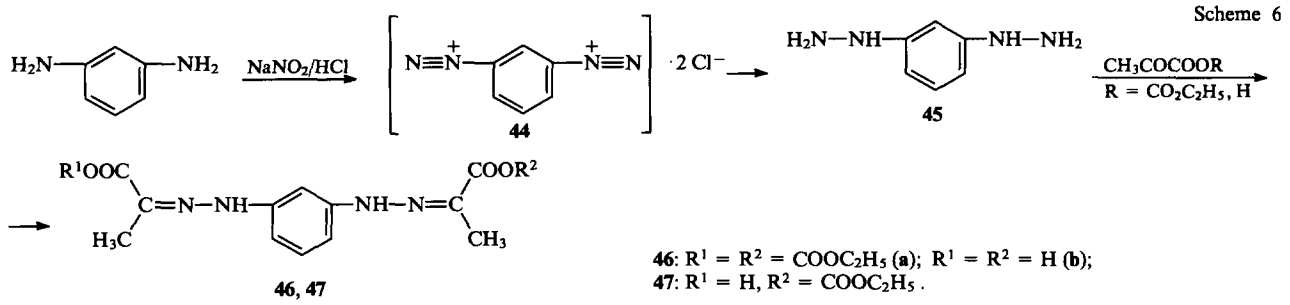
Thus only the *meta*-isomer is obtained in a high yield from all the isomeric benzenebisdiazonium chlorides, which makes it convenient to use it in the synthesis of phenylenedihydrazones.

The reduction of benzene-1,3-bisdiazonium **44** with tin dichloride in an excess of HCl leads to the corresponding dihydrazine **45**. However, the product is highly contaminated by tin salts, which creates difficulties for subsequent reactions. The purification of dihydrazine **45** is also difficult. It is carried out by passing gaseous H_2S through an aqueous solution of the compound.[10] However, the present authors were able to solve this problem by simple recrystallisation of compound **45** from water.[11] The *m*-phenylenedihydrazine purified in this way is entirely suitable for further reactions (Scheme 6).

The condensation of *m*-phenylenedihydrazine **45** with ethyl pyruvate in a weakly acid medium leads to a high yield of the *m*-phenylenedihydrazone of ethyl pyruvate **46a**. The mixed hydrazone **47**, containing both ester and acid groups, is formed as a side product of this reaction. It is apparently obtained as a result of the hydrolysis of the ethoxycarbonyl group of the initial ethyl pyruvate or of the dihydrazone **46b** formed.

p-Phenylenedihydrazine, which is suitable for the synthesis of *p*-phenylenedihydrazone, cannot be obtained in a pure form. It contains an appreciable amount of *p*-phenylenediamine.[15] Owing to the difficulty of separating this mixture and also the instability of *p*-phenylenedihydrazine, the latter could not be identified either in the form of a base or in the form of the dihydrochloride.

Scheme 6



46, 47

46: $R^1 = R^2 = COOC_2H_5$ (a); $R^1 = R^2 = H$ (b);
47: $R^1 = H$, $R^2 = COOC_2H_5$.

The m-phenylenedihydrazone of ethyl pyruvate is formed as a mixture of geometrical isomers having the *syn,syn-*, *syn,anti-*, and *anti,anti*-configurations. These isomers were separated by column chromatography and their structures were established from spectroscopic data. [11]

The usual diazotisation of 1-acetyl-5-aminoindoline **25** and 1-acetyl-6-aminoindoline **37** and the subsequent reduction of the diazonium salts **26** and **38** by tin(II) chloride lead to the hydrochlorides of 1-acetyl-5-hydrazinoindoline **27** and 1-acetyl-6-hydrazinoindoline **39**. The hydrazones **28** and **40** have been obtained in high yields by condensing the hydrazines **27** and **39** with ethyl pyruvate. [20]

The coupling of the diazonium salts **26** and **38** with methylacetoacetic ester via the Japp–Klingemann reaction also affords the hydrazones **28** and **40**.

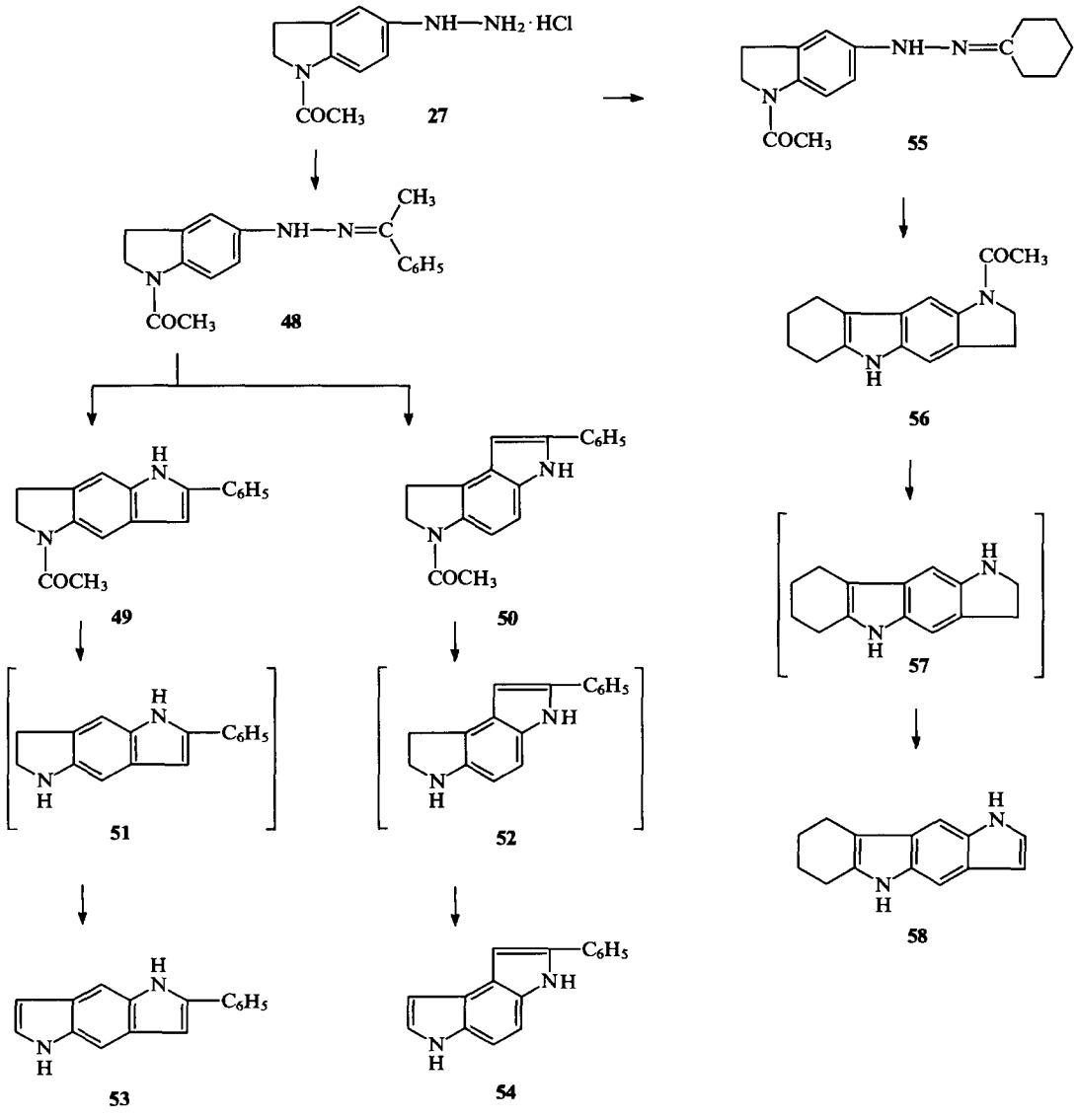
2. Synthesis of substituted pyrroloindoles from acetophenone and cyclohexanone

Apart from the cyclisation of the hydrazones of ethyl pyruvate, the conversion of the hydrazones of acetophenone and cyclohexanone into indole derivatives (Schemes 7 and 8) has been used to obtain pyrroloindole structures. [30]

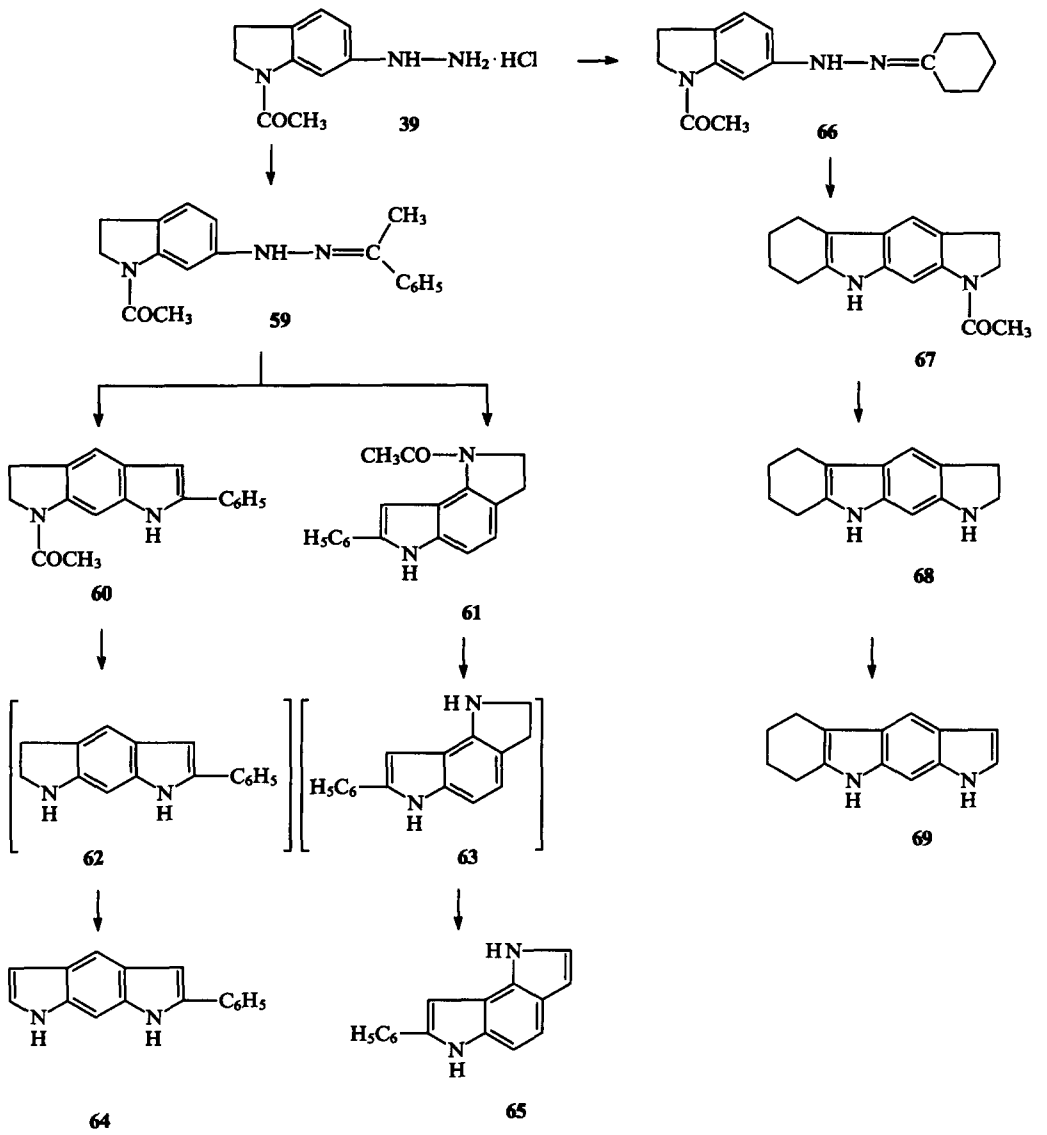
Condensation of compounds **27** and **39** with acetophenone and cyclohexanone yielded the corresponding hydrazones **48**, **55**, **59**, and **66**.

When the hydrazones were converted into indole derivatives, the best results were achieved using EEPPA as the cyclising agent.

Scheme 7



Scheme 8



It was established from spectroscopic data on the cyclisation products that conversion of the acetophenone hydrazones **48** and **59** into indole derivatives gives a mixture of the linear pyrroloindolines **49** and **50** and the angular pyrroloindolines **60** and **61**, while the conversion of the cyclohexanone hydrazones **55** and **66** into indole derivatives afforded only the linear isomers (compounds **56** and **67**). This has been explained by steric factors.[30] Hydrolysis of the pyrroloindolines **49**, **50**, **55**, **60**, **61**, and **66** leads to compounds **51**, **52**, **57**, **62**, **63**, and **68** and their subsequent dehydrogenation gives rise to the pyrroloindoles **53**, **54**, **58**, **64**, **65**, and **69** respectively.

III. Electrophilic substitution reactions of pyrroloindoles

The preparative methods described above have enabled the pyrroloindoles **1**–**4** to be obtained in amounts sufficient for various electrophilic substitution reactions to be studied in this series of compounds. The classical electrophilic substitution reactions characteristic of indoles were investigated: the Mannich, Vilsmeier, azo-coupling, and acetylation reactions.[13,31–34]

The effect of different types of condensation of the pyrrole and indole rings on the specific features of electrophilic substitution was of definite interest. Furthermore, the study of the above reactions was also of practical importance, since some of the pyrroloindole derivatives themselves possess physiological activity or can be used in the syntheses of other physiologically active substances.

The distribution of electron densities in the substrate is known to determine the mode of attack by electrophiles in electrophilic substitution reactions, although the site of preferential substitution depends greatly also on other factors promoting the stabilisation of the corresponding transition state.

In order to predict the most preferable directions of electrophilic attack in pyrroloindole molecules, quantum-chemical calculations were performed for compounds **1**–**4** in accordance with Maslov's program[36] on a BESM-6 computer by the SCF-MO method in the CNDO/2 approximation (Fig. 1).[37]

It is seen from the molecular diagrams that the highest overall ($\sigma + \pi$)- and π-electron densities are observed for atoms in the β-positions in the pyrrole rings. It was postulated that initial attack by electrophiles should take place at these sites. In the molecules of the pyrroloindoles **1**–**4**, there are also other reaction centres having fairly high electron densities. Nor can one rule out also the influence of other factors, especially steric factors, on the site of the initial electrophilic attack in these electrophilic molecules.

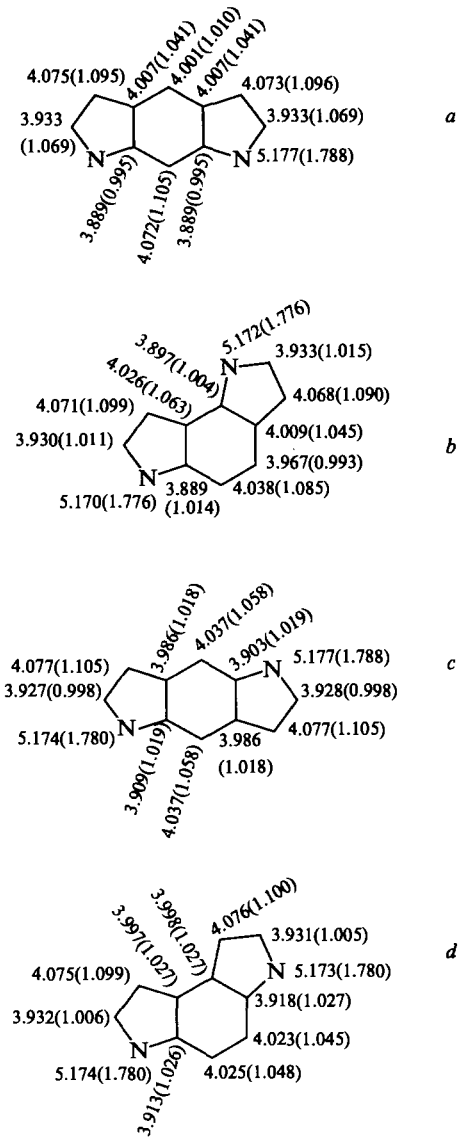


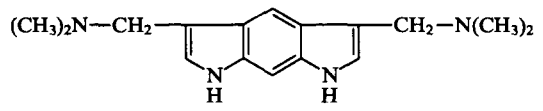
Figure 1. Molecular diagrams for the pyrroloindoles **1**–**4** (*a*–*d*); the overall ($\sigma + \pi$) charges are presented; the (σ^{**}-π)-electron densities are indicated in brackets.

1. The Mannich reaction

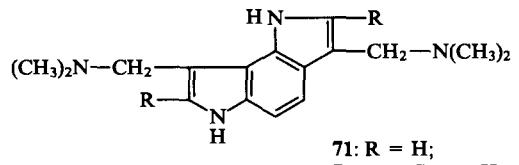
The great importance of the Mannich reaction for compounds of the indole series arises from the possibility of using the products of this reaction in the synthesis of a wide variety of biologically important compounds (tryptophan, heteroauxin, the series of tryptamines, etc.).

Among the indole Mannich bases, the alkaloid gramine (3-dimethylaminomethylindole) and its substituted derivatives have found the most extensive applications. The study of the Mannich reaction for the pyrroloindoles **1**–**4** is therefore of interest both from the standpoint of the possibility of obtaining bifunctional gramine analogues and for the investigation of their biological activity.

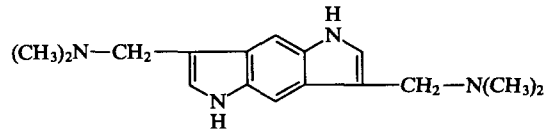
The aminomethylation of the unsubstituted pyrroloindoles **1**–**4** by freshly prepared Mannich bases (dimethylamine, formaldehyde, acetic acid) affords, apart from the bisgramine analogues **70**, **71**, **73**, and **74**, also compounds which are insoluble in the majority of organic solvents, which greatly reduces the yield of the target product.[31–33]



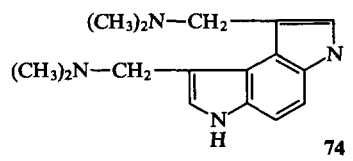
70



71: R = H;
72: R = $COOC_2H_5$.



73



74

The formation of side products can probably be accounted for by the interaction of the heterocycles with formaldehyde, similarly to the situation which obtains in the condensation of indole and its derivatives with formaldehyde in an acid medium with formation of bis(3-indolyl)methanes.[38,39]

This undesirable process is hindered in the case of 2,7-di-(ethoxycarbonyl)-1*H*,6*H*-pyrrolo[2,3-*e*]indole, apparently owing to the presence of the electron-accepting α-ethoxycarbonyl groups and their steric influence. The bisgramine **72** is formed in a high yield.

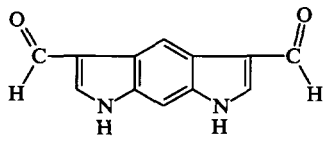
In the syntheses of the unsubstituted bisgramines **70**, **71**, **73**, and **74**, the desired result was achieved using as the electrophile *N*,*N*-dimethylmethyleneammonium chloride [$CH_2=N^+(CH_3)_2 . Cl^-$], synthesised from $[(CH_3)_2N]_2CH_2$ and CH_3COCl.[40] Best results were obtained when acetonitrile was used as the solvent. In this case, side products are not formed and the bisgramines **70**, **71**, **73**, and **74** were isolated in high yields.[31–33]

In order to investigate their physiological activity, the bifunctional gramine analogues synthesised were converted into the corresponding dihydrochlorides.[1]

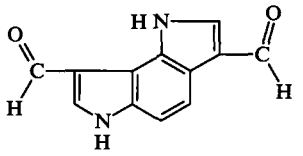
The blocking effect of the bisgramines on neuromuscular transmission was investigated by quaternising the tertiary nitrogen atoms in their molecules, which was achieved by converting them into the corresponding dimethosulfates.[1,2] The synthesis of the dimethosulfates is accompanied by formation of polyadducts as a result of interaction of the quaternary salts with the gramines. In order to suppress side reactions, the process is carried out in an acid medium. In the synthesis of the dimetho-sulfates of the diaminomethyl derivatives of the pyrroloindoles containing ethoxycarbonyl groups in the α-positions in the pyrrole rings, the formation of side products was not observed even in the absence of acetic acid, owing to the presence of electron-accepting groups.

2. The Vilsmeier reaction

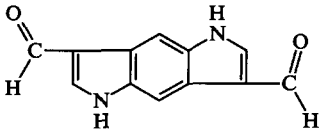
The formylation of the pyrroloindoles **1**–**4** by the dimethylformamide–$POCl_3$ complex proceeds readily at room temperature. When the reaction is carried out in the presence of a threefold excess of the Vilsmeier reagent, the hydrogen atoms in the β-positions in the pyrrole rings are substituted, as expected, and the dialdehydes **75**–**78** are formed in high yields.[31–33,41]



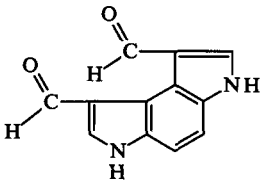
75



76

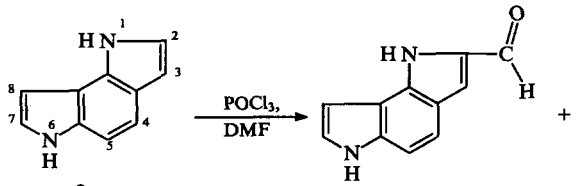


77



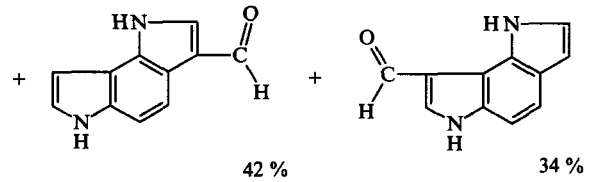
78

In the pyrroloindole **2**, the reactivities of the β-positions in the two different pyrrole rings are not the same. It follows from the model of the molecule of this compound that substitution in the 8-position is difficult owing to shielding by the neighbouring pyrrole ring. It was interesting to elucidate how these factors influence the electrophilic substitution reaction for an equimolar reactant ratio. It was established that three monosubstituted products are formed: 2-, 3-, and 8-formylpyrroloindoles.[42]



2

5 %



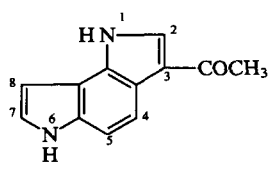
42 % 34 %

The ethoxycarbonyl groups in the α-positions in the pyrrole rings of the pyrroloindole **2** lower its reactivity, as expected. In this case, only the 3-substituted product is formed (yield 41%) and even then a fivefold excess of the Vilsmeier complex is required.[42]

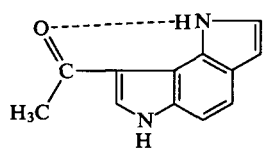
The formylation of 2,6-diethoxycarbonyl-1*H*,7*H*-pyrrolo-[3,2-*f*]indole under these conditions proceeds anomalously. Mainly the hydrogen atoms of the benzene ring are substituted (Scheme 9).[43]

In order to compare the reactivities of the β-positions of 1*H*,6*H*-pyrrolo[2,3-*e*]indole in the Vilsmeier reaction, a more selective electrophile was employed—a complex based on dimethylacetamide and $POCl_3$. This complex is known to react only with highly nucleophilic substrates. Certain indole-containing polynuclear heterocycles altogether fail to react with it,[44] while indole itself does react, affording 3-acetylindole in only 22% yield.[45]

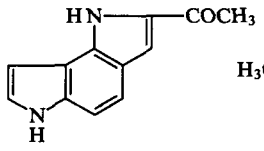
The pyrroloindole **2** has been acylated under the same conditions as those employed in the acetylation of indole. Four reaction products were isolated.[34] The main one is 3-acetyl-pyrroloindole **79**, which is formed at room temperature immediately after mixing the initial compounds. On heating the reaction mixture, the 8- and 2-acetyl-substituted derivatives **80** and **81** were also obtained and after some time 3,8-diacetyl-pyrroloindole **82** was produced. The overall yield of products is ~40%.



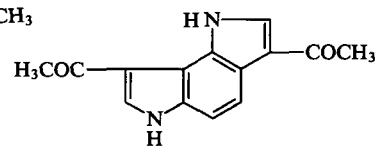
79



80

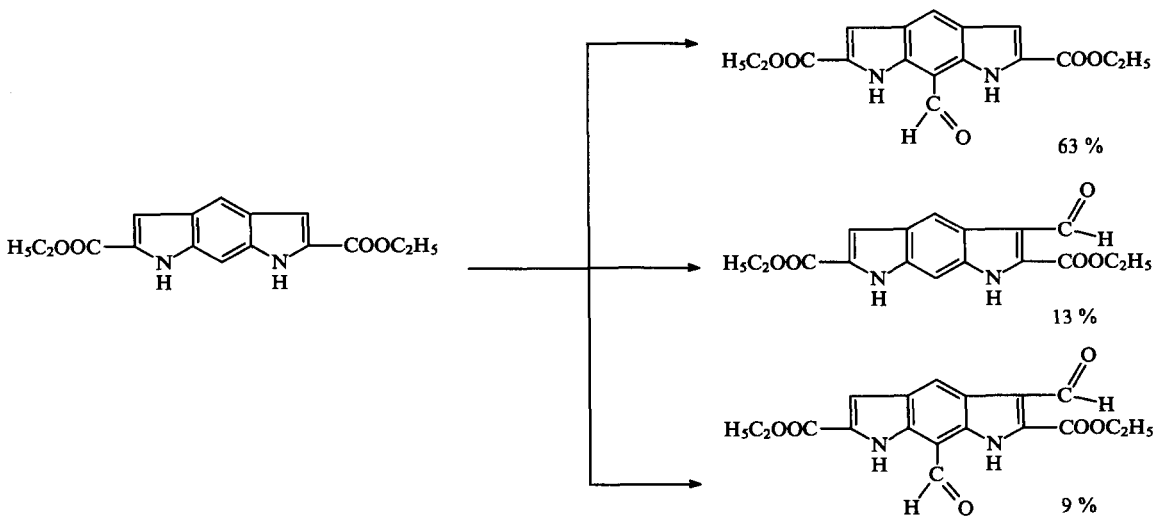


81

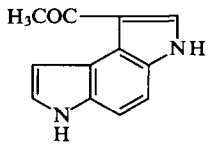


82

Scheme 9



As regards the remaining isomeric pyrroloindoles (compounds **1**, **3**, and **4**), the Vilsmeier reaction could be carried out only for compound **4**. 1-Acetyl-3*H*,6*H*-pyrrolo-[2,3-*e*]indole **83** is formed in 60% yield. In the remaining cases (compounds **1** and **3**), the reaction takes place with charring.[41]



83

Thus the acetylation of pyrroloindoles by the Vilsmeier complex showed that the angular structures are more stable than the linear isomers.

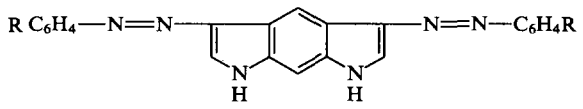
The reduced electrophilicity of the complex based on *N*,*N*-dimethylacetamide and $POCl_3$ compared with the dimethylformamide–$POCl_3$ complex makes it necessary to carry out the reaction at elevated temperatures, which leads to charring of the products of the reaction of linear pyrroloindoles.

3. The azo-coupling reaction

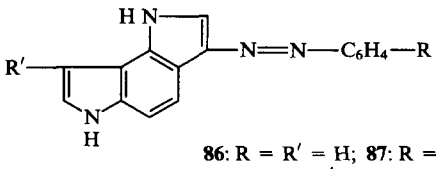
Arenediazonium salts are typical weak electrophiles. They are sensitive to small differences in the reactivities of substrates.

Benzenediazonium and *p*-chloro- and *p*-nitro-benzenediazonium chlorides have been used as the diazo-components in the azo-coupling of pyrroloindoles. Complex mixtures are formed in all cases, from which it has been possible to isolate by preparative column chromatography one product (probably the main one) in each case.

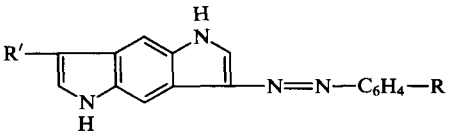
The azopyrroloindoles **83**–**93** are relatively unstable compounds which readily decompose during purification on a chromatographic column and on recrystallisation, which greatly hinders their isolation.



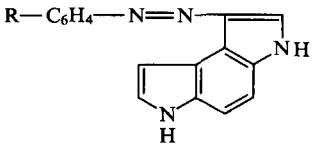
83: R = H; **84**: R = Cl; **85**: R = NO_2.



86: R = R′ = H; **87**: R = Cl, R′ = H;
88: R = Cl, R′ = N=N–C_6H_4–Cl.



89: R = NO_2, R′ = H;
90: R = H, R′ = N=N–C_6H_5;
91: R = Cl, R′ = N=N–C_6H_4–Cl.



92: R = Cl;
93: R = NO_2.

In the azo-coupling of the linear compounds **1**–**3**, mainly the formation of disubstituted products is observed.[32,33]

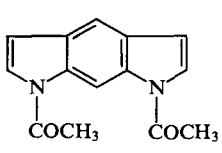
After the azo-coupling of the angular pyrroloindoles **2** and **4**, mainly monosubstituted products were isolated. In this case, the neighbouring pyrrole ring probably exerts a steric influence.[31,32]

4. The acetylation reaction

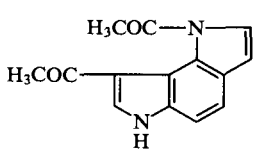
The acetylation of the pyrroloindoles **1**–**4** has been carried out without using the typical Friedel–Crafts catalysts: because these heterocycles are acidophobic, the use of strong catalysts induces the charring of the reaction mixture and lowers the yield of products.

The acetylation of the pyrroloindoles **1**–**4** under the conditions proposed for indole itself[46] leads to the formation of a mixture of the *N*- and *C*,*N*-acetylated derivatives **94**–**102**. The low yield of the reaction products (not more than 40%) can be explained by the partial charring of the reaction mixture.[31–33]

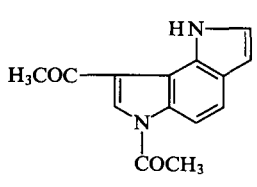
Thus electrophilic substitution reactions in the pyrroloindoles **1**–**4** take place mainly in the β-positions in the pyrrole rings, which agrees with the results of quantum-chemical calculations. In the Vilsmeier acetylation of the pyrroloindole **2**, the formation of 2-substituted products, for which there is no analogous reaction involving indole, is due to the increased excess of π electrons and hence the increased reactivity of the pyrroloindole compared with indole.



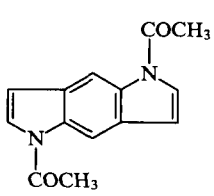
94



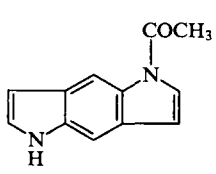
95



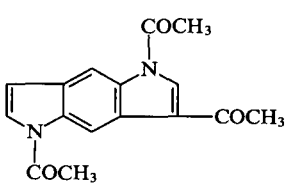
96



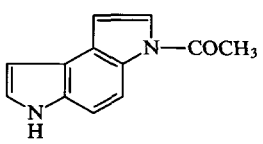
97



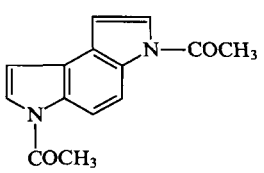
98



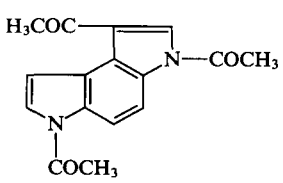
99



100



101



102

It has been established that the β-positions of both pyrrole rings in linear pyrroloindoles are equally reactive, which cannot be said of the angular isomers. In the interaction of the latter with weaker electrophiles (the azo-coupling reaction and the Vilsmeier acetylation), mainly monosubstituted products are formed, probably as a consequence of steric factors and of the reduced reactivity of the system due to the introduction of an electron-accepting substituent.

IV. Side chain reactions of derivatives of 1*H*,6*H*-pyrrolo[2,3-*e*]indole

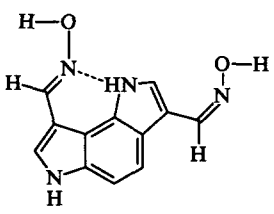
1. The condensation reactions of 3,8-diformyl- and 3-formyl-1*H*,6*H*-pyrrolo[2,3-*e*]indole

Among nucleophilic addition–elimination reactions, the condensation reactions with nitromethane, nitroethane, acetone, malonic and barbituric acids, aniline, and thiosemicarbazide have been investigated (for 3,8-diformyl-1*H*,6*H*-pyrroloindole) (Scheme 10).[47–49]

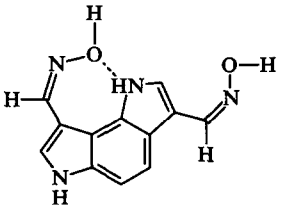
Under the conditions described,[47,48] the dialdehyde **76** reacts with CH acids mainly via one formyl group. The monocondensation products **103, 105**, and **107–110** are formed in high yields. The reduced reactivity of the formyl group in the 8-position can apparently be accounted for by the presence of an intramolecular hydrogen bond and also by steric factors.

In order to develop a convenient method of synthesis of the dinitrovinylpyrroloindoles **104** and **106**, various catalysts were employed (ammonium acetate, liquid ammonia, 50% NaOH solution, pyridine, $KHSO_4$). The desired result was achieved only when dimethylformamide was used as the solvent, in which the dialdehyde **76** is readily soluble.

The disubstituted products **111** and **112** are obtained when the dialdehyde **76** is condensed with hydroxylamine and thiosemicarbazide in a weakly acid medium. The dioxime **111** was formed as a mixture of geometrical isomers which were separated by column chromatography. It has been established by ^1H NMR spectroscopy that these isomers have the *anti,syn*-configuration (compound **111a**) and the *syn,syn*-configuration (compound **111b**) and the cisoid-transoid conformation of the side chains.[49]

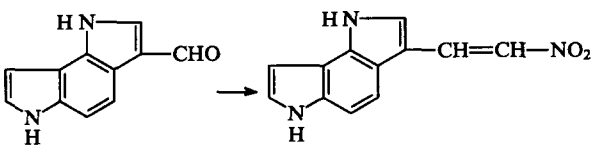


111a

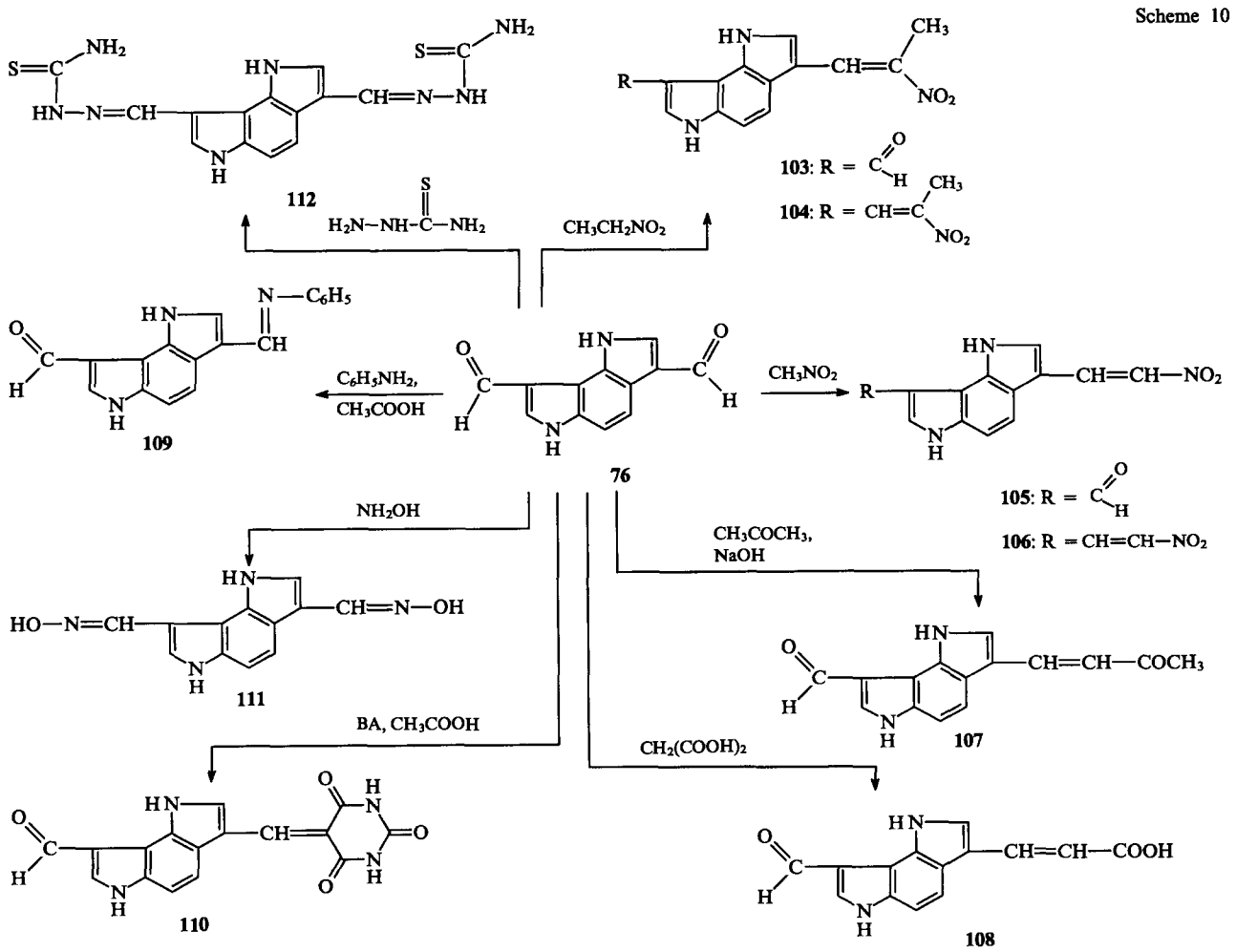


111b

In the reaction of the monosubstituted 3-formyl-1*H*,6*H*-pyrrolo[2,3-*e*]indole with nitromethane in the presence of ammonium acetate, 3-nitrovinyl-1*H*,6*H*-pyrrolo[2,3-*e*]indole is formed in a high yield.



Scheme 10



BA = barbituric acid.

2. Certain syntheses based on 3,8-bis(dimethylaminomethyl)-1*H*,6*H*-pyrrolo[2,3-*e*]indole and its diethoxycarbonyl derivative

3-Indolylacetonitrile (a natural product), is an effective stimulator of plant growth.[50] It has been used successfully in the syntheses of certain physiologically active indole derivatives.

3-Indolylacetonitrile can be conveniently obtained from quaternary salts of gramine and alkali metal cyanides. The use of a quaternised amino-group instead of a free amino-group facilitates the reaction and increases the yield of the target product.[51]

The bisgramines **71** and **72** were converted into the corresponding quaternary salts **113** and **114**. The subsequent reaction of these salts with KCN at 40 °C leads to the corresponding dinitriles **115** and **116**.[52] In the case of the salt **114**, the monosubstituted product **117** is also formed in a low yield. Its yield increases appreciably at high temperatures, accounted for, probably, by the increase in the rate of hydrolysis of KCN.[52]

Further studies showed that the dinitrile **116** can be more conveniently synthesised without the preliminary isolation of the quaternary salt, by adding solutions of KCN and CH_3I to the reaction mixture containing the Mannich base **72**. The application of this method in the synthesis of the dinitrile **115** did not yield positive results.[52]

The tetracarboxylic acid **118** is formed readily in the alkaline hydrolysis of the dinitrile **116**. Its structure was established by spectroscopic methods and by specific synthesis from the corresponding tetraester **119**.

The skatole analogue **120** has been synthesised by decarboxylating the acid **118**; acid alcoholysis of the dinitrile **116** in 33% alcoholic HCl afforded the tetraester **119** (Scheme 11).[52]

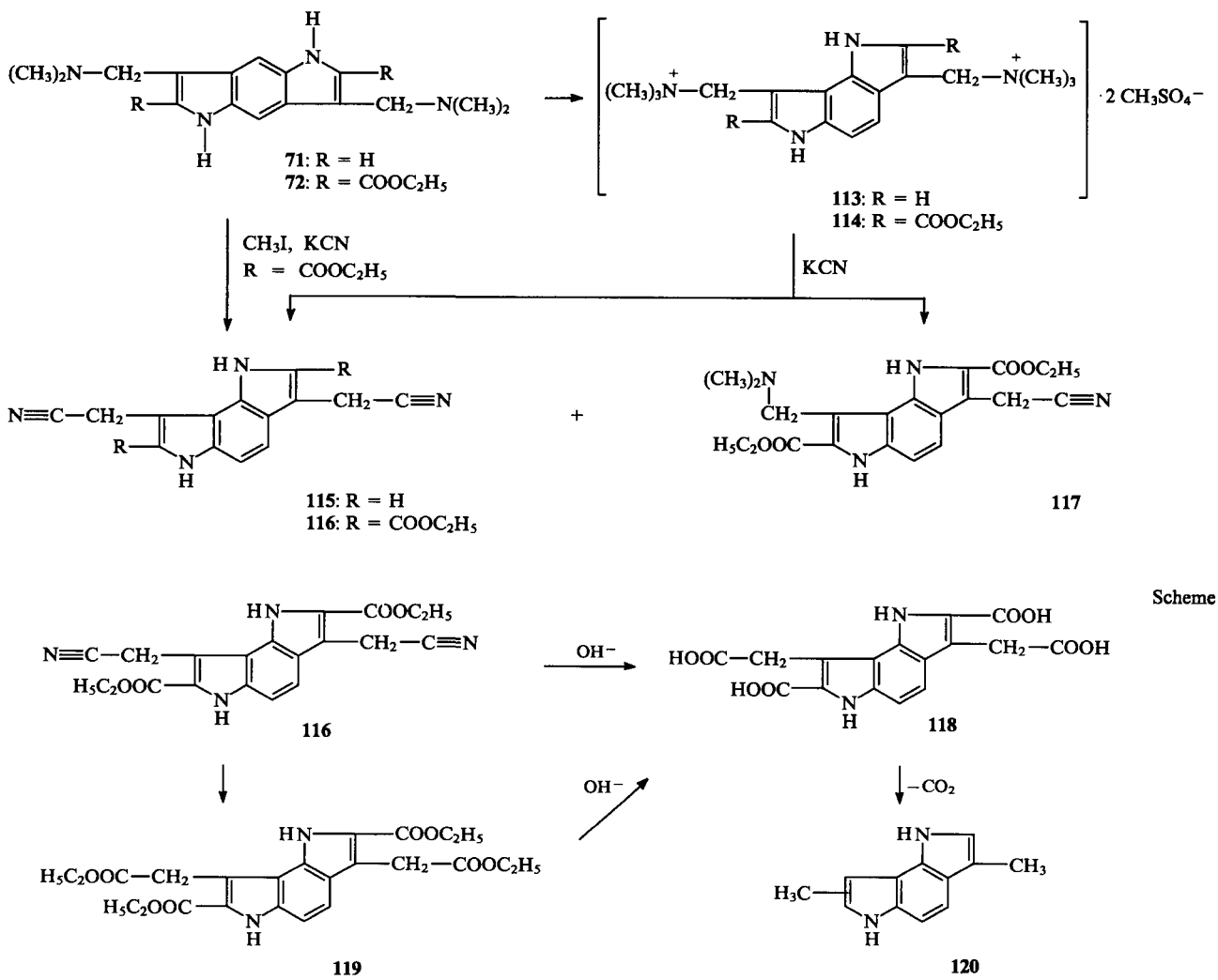
3. Synthesis of a tryptamine analogue from 1*H*,6*H*-pyrrolo[2,3-*e*]indole

It has been shown[48] that the bistryptamine **121** cannot be obtained by the direct reaction of the corresponding Grignard reagent, 1*H*,6*H*-pyrrolo[2,3-*e*]indolebismagnesium halide, and ethyleneimine.[48]

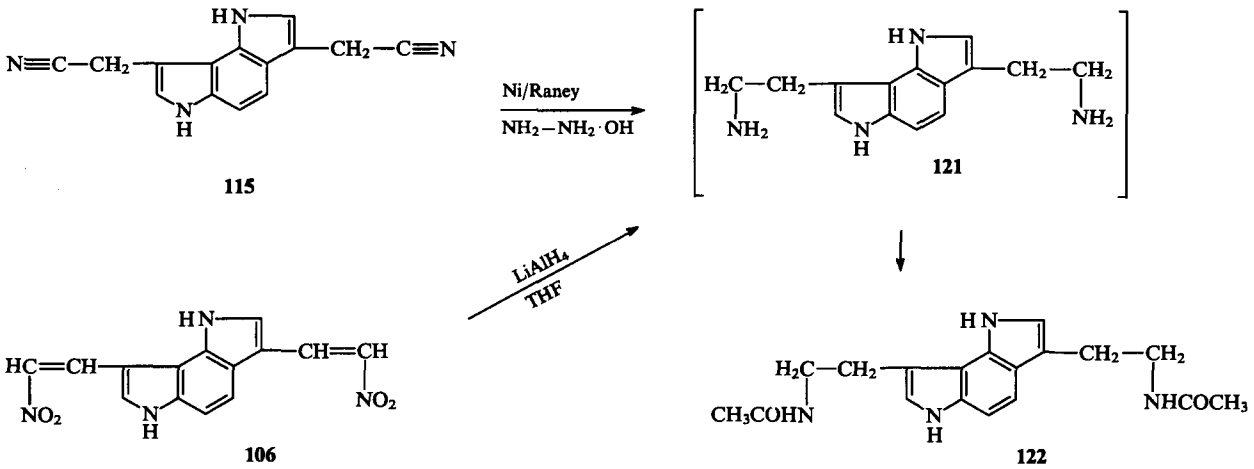
The bistryptamine **121** has been obtained in a high yield by reducing 3,8-di(cyanomethyl)-1*H*,6*H*-pyrrolo[2,3-*e*]indole **115** and 3,8-di(nitrovinyl)-1*H*,6*H*-pyrrolo[2,3-*e*]indole **106**. The product was purified by conversion into the diacetyl derivative **122** and was characterised in this form.[48]

In order to obtain the *N*-unsubstituted tryptamine in a pure form, 8-formyl-3-nitrovinyl-1*H*,6*H*-pyrrolo[2,3-*e*]indole **105** was used as the starting compound. However, the reaction took a completely different route. It was found that the reduction of compound **105** with diimide (hydrazine hydrate and Raney nickel) and subsequent acetylation of the product afford only the 3-*N*-acetylhydrazone of 3,8-diformyl-1*H*,6*H*-pyrrolo[2,3-*e*]indole **123**[48] (see over).

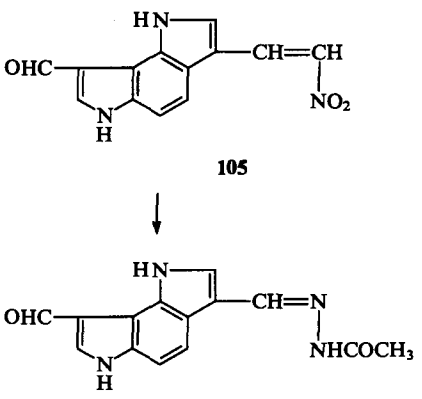
The reduction of the pyrroloindole **105** with lithium tetrahydroaluminate and subsequent acetylation lead to the formation of a gel-like mass, the components of which are difficult to isolate and identify. This is apparently associated with the formation, after the reduction of the aldehyde group, of an analogue of the unstable 3-indolylmethanol,[53] which is capable of both dimerising and of conversion into an oligomer in an acid medium or on standing.[48]



Scheme 11



115 121 106 122



105 123

4. Some syntheses based on 1*H*,10*H*-benzo[*e*]pyrrolo-[3,2-*g*]indole

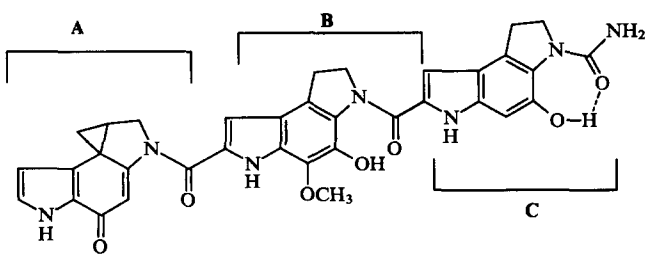
As expected, 1*H*,10*H*-benzo[*e*]pyrrolo[3,2-*g*]indole forms products disubstituted in the β-positions of the pyrrole rings in the Vilsmeier and Mannich reactions. In reactions with weaker electrophiles (azo-coupling reactions), only monosubstituted products are formed.[54]

Certain reactions of 2,9-di(carbohydrazido)-1*H*,10*H*-benzo-[*e*]pyrrolo[3,2-*g*]indole **124** have been described (Scheme 12).[55]

The reactions of the acid dichloride of 2,9-dicarboxy-1*H*,10*H*-benzo[*e*]pyrrolo[3,2-*g*]indole **125** merit attention. It has been obtained in a quantitative yield by refluxing the corresponding dicarboxylic acid with thionyl chloride. The condensation of the acid dichloride **125** with amines and phenols leads to various diamides and diesters.[56] In addition, high-molecular-mass compounds containing benzopyrroloindole fragments have been obtained from the pyrroloindole **125**.[57]

5. The antibiotic CC-1065 and its analogues

In the Introduction, we noted that the molecule of the powerful antitumour antibiotic CC-1065 contains the pyrrolo-indoline fragments **B** and **C**.[4]



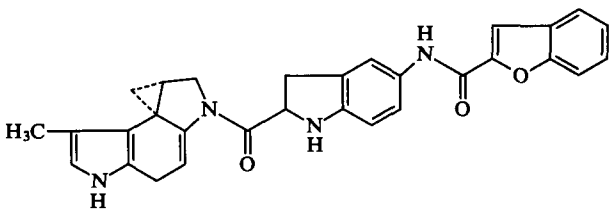
It was shown that this compound is bound covalently via the cyclopropane ring to the *N*(3)-position of adenine in a specific nucleotide sequence and is located within the limits of the small groove of DNA, suppressing selectively its synthesis. On the other hand, the antibiotic is not an intercalator; the cytotoxicity of the compound CC-1065 is approximately 400 times higher than that of adriamycin, which has been used successfully in the treatment of oncological diseases.[4] Unfortunately the antibiotic CC-1065 is also highly toxic, which precludes its clinical application.[58]

The data of Rawal et al.[4] initiated studies, directed towards the synthesis of the individual components (**A**, **B**, and **C**) of compound CC-1065. These investigations have been described in detail in the above review by the American investigators Rawal et al.[4]

A classical strategy was used in the synthesis of the pyrroloindole fragments **B** and **C** of the compound CC-1065. Indoline was obtained from substituted benzene and then the corresponding pyrroloindoline was obtained by the Fischer method or the pyrrole rings were attached stepwise to the benzene ring and the resulting pyrroloindole was hydrogenated to the corresponding pyrroloindoline.

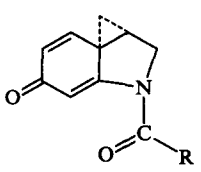
These skillfully performed complex syntheses include 14 stages each and the yields of the target products are < 7%.

An enormous amount of work was carried out on the synthesis of analogues of the antibiotic CC-1065. The benzofuran analogue I-73975 is promising.

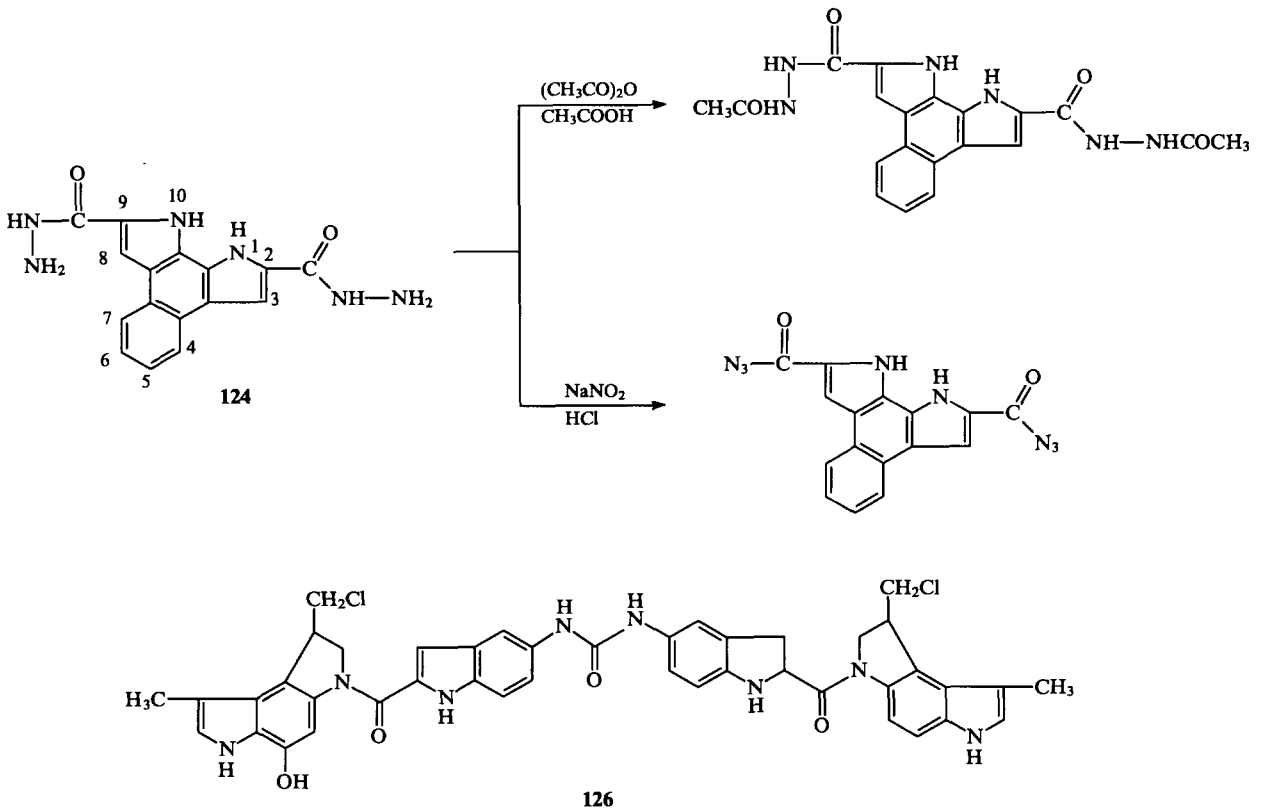


This compound is also a monoalkylating agent containing a cyclopropane ring in its structure. A highly active dialkylating agent, having the structure **126**, has also been synthesised.[59] However, it is not altogether clear whether the mechanism of its action is identical with that of the natural antibiotic.[59]

It was later observed,[60] that a whole class of antibiotics exist—duocarmycins—which are structurally and chemotherapeutically similar to CC-1065. They are all characterised by a common pharmacophore.[60]



Scheme 12



It is evident from the data presented that pyrroloindoles are extremely promising as regards the search for new antitumour preparations and merit further study.

References

1. Sh A Samsoniya, M V Trapaidze, N L Targamadze, I Sh Chikvaidze, R R Suvorov, N N Ershova, V A Chernov *Soobshch. Akad. Nauk Gruz. SSR* **100** 337 (1980)
2. Sh A Samsoniya, B A Medvedev, D O Kadzhrishvili, D M Tabidze M D Mashkovskii, N N Suvorov *Khim.-Farm. Zh.* 1335 (1982)
3. Sh A Samsoniya, Z Sh Lomtatidze, S V Dolidze, N N Suvorov *Khim.-Farm. Zh.* 1452 (1984)
4. V H Rawal, R J Jones, M P Gava *Heterocycles* **25** 701 (1987)
5. F R Japp, A N Meldrum *J. Chem. Soc.* **75** 1043 (1899)
6. D A Kinsley, S G P Plant *J. Chem. Soc.* 1 (1958)
7. P Ruggli, O Straub *Helv. Chim. Acta* **19** 326 (1936)
8. P Ruggli, O Straub *Helv. Chim. Acta* **21** 1084 (1938)
9. D B Baird, V Baxter, D W Cameron, W R Phillips *J. Chem. Soc., Perkin Trans. 1* 832 (1973)
10. R Giuliano, G Leonardi *Ric. Sci.* **27** 1843 (1957)
11. Sh A Samsoniya, N L Targamadze, L G Tret'yakova, T K Efimova, K F Turchin, I M Gverdtsiteli, N N Suvorov *Khim. Geterotsikl. Soedin.* 938 (1977)
12. Sh A Samsoniya, N L Targamadze, N N Suvorov *Khim. Geterotsikl. Soedin.* 849 (1980)
13. Sh A Samsoniya, Doctoral Thesis in Chemical Sciences, Mendeleev Moscow Chemical Technological Institute, 1984
14. P Ruggli, C Petitjean *Helv. Chim. Acta* **19** 928 (1936)
15. Sh A Samsoniya, D O Kadzhrishvili, N N Suvorov *Khim. Geterotsikl. Soedin.* 268 (1981)
16. N N Suvorov, T K Sergeeva, A N Gryaznov, V P Shabunova, L G Tret'yakova, T A Efimova, I A Morozova, R I Akhvediani, A M Vasil'ev, T K Trubitsina *Tr. Mosk. Khim. Tekhnol. Inst. im. D I Mendeleeva* **94** 23 (1977)
17. In *Organic Syntheses* Vol. 2 (Translated into Russian; Moscow: Mir, 1961) p. 76
18. L Fieser, M Fieser *Reagents for Organic Synthesis* Vol. 2 (Translated into Russian; Moscow: Mir, 1970) p. 305
19. Sh A Samsoniya, M V Trapaidze, N A Kuprashvili, A M Kolesnikova, N N Suvorov *Khim. Geterotsikl. Soedin.* 1222 (1984)
20. Sh A Samsoniya, D O Kadzhrishvili, E N Gordeev, V E Zhigachev, L N Kurkovskaya, N N Suvorov *Khim. Geterotsikl. Soedin.* 504 (1982)
21. A P Terent'ev, M N Preobrazhenskaya, A S Bobkov, G M Sorokina *Zh. Obshch. Khim.* **29** 2541 (1959)
22. H A Katti, S Siddappa *Ind. J. Chem.* **228** 1205 (1983)
23. A Berlin, S Bradamante, R Ferraccioli, G A Pagani, F Sannicolo *J. Chem. Soc., Chem. Commun.* 1176 (1987)
24. I M Kogan, in *Khimiya Krasitelei* (Chemistry of Dyes) (Moscow: Goskhimizdat, 1956) p. 696
25. H Zollinger, in *Khimiya Azokrasitelei* (Chemistry of Azo Dyes) (Leningrad: Goskhimizdat, 1960) p. 332
26. N N Vorozhtsov, in *Osnovy Sinteza Promezhutochnykh Produktov i Krasitelei* (Fundamentals of the Synthesis of Intermediate Products and Dyes) (Moscow: Goskhimizdat, 1955) p. 839
27. H A Schoutissen *J. Rec. Trav. Chim.* **57** 710 (1938)
28. H A Schoutissen *J. Rec. Trav. Chim.* **54** 253 (1935)
29. V V Kozlov, B I Stepanov *Zh. Obshch. Khim.* **10** 1510 (1940)
30. Sh A Samsoniya, D O Kadzhrishvili, E N Gordeev, N N Suvorov *Khim. Geterotsikl. Soedin.* 470 (1984)
31. Sh A Samsoniya, N L Targamadze, L N Kurkovskaya, Dzh A Kereselidze, N N Suvorov *Khim. Geterotsikl. Soedin.* 639 (1980)
32. D O Kadzhrishvili, Sh A Samsoniya, E N Gordeev, L N Kurkovskaya, V E Zhigachev, N N Suvorov *Khim. Geterotsikl. Soedin.* 1086 (1983)
33. Sh A Samsoniya, D O Kadzhrishvili, E V Gordeev, N N Suvorov *Khim. Geterotsikl. Soedin.* 1219 (1984)
34. Sh A Samsoniya, N L Targamadze, T A Kozik, N N Suvorov *Khim. Geterotsikl. Soedin.* 206 (1982)
35. A F Pozharskii *Khim. Geterotsikl. Soedin.* 723 (1977)
36. V G Maslov *Zh. Strukt. Khim.* **18** 414 (1977)
37. J A Pople, D L Reveridge, in *Advanced Chemistry* (New York: McGraw-Hill, 1970) p. 214
38. V Volter, J Clemen *J. Prakt. Chem.* **61** 249 (1900)
39. J Thesing *Chem. Ber.* **87** 692 (1954)
40. G Kinast, L-F Tietze *Angew. Chem.* **88** 261 (1976)

41. D O Kadzhrishvili, Candidate's Thesis in Chemical Sciences, Dzhavakhishvili Tbil. Gos. Univ., Tbilisi, 1983
42. S V Dolidze, Sh A Samsoniya, in *Tez. Dokl. V Vsesoyuznogo Kollokviuma "Khimiya, Biokhimiya i Farmakologiya Proizvodnykh Indola"* (Abstracts of Reports at the Fifth All-Union Colloquium "Chemistry, Biochemistry and Pharmacology of Indole Derivatives" (Tbilisi: Dzhavakhishvili Tbil. Gos. Univ., 1981) p. 54
43. S V Dolidze, Candidate's Thesis in Chemical Sciences, Dzhavakhishvili Tbil. Gos. Univ., Tbilisi, 1985, p. 64
44. L B Shagalov, T A Tkachenko, V N Eraskina, N N Suvorov *Tr. Mosk. Khim. Tekhnol. Inst. im. D I Mendeleeva* **80** (1974)
45. W C Anthony *J. Org. Chem.* **25** 2049 (1960)
46. J E Saxton *J. Chem. Soc.* 3592 (1952)
47. S V Dolidze, Sh A Samsoniya, N N Suvorov *Khim. Geterotsikl. Soedin.* 608 (1983)
48. S V Dolidze, N L Targamadze, Sh A Samsoniya, N N Suvorov *Zh. Org. Khim.* 326 (1983)
49. L N Kurkovskaya, N L Targamadze, Sh A Samsoniya, N N Suvorov *Khim. Geterotsikl. Soedin.* 646 (1981)
50. H B Henbest, E R H Jones, G F Smith *J. Chem. Soc.* 3796 (1953)
51. D K Brewster, E A Eliel, in *Organic Reactions* Vol. 7 (Translated into Russian; Moscow: Mir, 1956) p. 146
52. N L Targamadze, Sh A Samsoniya, N N Suvorov *Soobshch. Akad. Nauk Gruz. SSR* **96** 89 (1979)
53. E Leete, L Marion *Can. J. Chem.* **31** 775 (1953)
54. M V Trapaidze, Sh A Samsoniya, N A Kuprashvili, L M Mamaladze, N N Suvorov *Khim. Geterotsikl. Soedin.* 603 (1988)
55. Sh A Samsoniya, M N Basiladze, Dzh Zerkhugkh, in *Tez. Dokl. IV Vsesoyuznoi Nauchnoi Konferentsii po Khimii Azotsoderzhashchikh Geterotsiklicheskikh Soedinenii* (Abstracts of Reports at the Fourth All-Union Conference on the Chemistry of Nitrogen-Containing Heterocyclic Compounds) (Novosibirsk: Inst. Org. Khim., 1987) p. 100
56. N A Kuprashvili, M V Trapaidze, Sh A Samsoniya, in *Tez. Dokl. II Vsesoyuznoi Nauchnoi Konferentsii "Khimiya, Biokhimiya i Farmakologiya Proizvodnykh Indola"* (Abstracts of Reports at the Second All-Union Conference "Chemistry, Biochemistry and Pharmacology of Indole Derivatives") (Tbilisi: Dzhavakhishvili Tbil. Gos. Univ., 1991) p. 142
57. N A Kuprashvili, Author's Abstract of Candidate's Thesis in Chemical Sciences, Dzhavakhishvili Tbil. Gos. Univ., Tbilisi, 1991
58. G F Gauze, Yu V Dudnik, in *Protivoopukholevye Antibiotiki* (Antitumour Antibiotics) (Moscow: Meditsina, 1987) p. 92
59. W Wierenga *Drugs Future* **16** 745 (1991)
60. D Boger, T Ishizaki, H Zarrinmayeh, S A Munk, P A Kitos, O Suntornwat *J. Am. Chem. Soc.* **112** 8961 (1990)

Russian Chemical Reviews **63** (10) 833–851 (1994)
©1994 Russian Academy of Sciences and Turpion Ltd

UDC 541.64; 536,7; 542,952

Polyarylates. Synthesis and properties

S V Vinogradova, V A Vasnev, P M Valetskii

Contents

I. Introduction 833
II. Synthesis of polyarylates and their properties 833
III. Applications of polyarylates 846

Abstract. Data on the synthesis and properties of various types of polyarylates, including cardo-, self-coloured, self-protecting, carbaborane-containing, stereoregular, and block-polyarylates, etc., are examined and surveyed. It is shown that polyarylates represent a promising class of polymers with a valuable set of properties, which can be altered specifically by an appropriate design of the polymer chain. Certain aspects of the practical use of polyarylates are considered. The bibliography includes 320 references.

I. Introduction

In terms of their theoretical and practical importance, heterochain polyesters occupy an important place among synthetic high-molecular-mass compounds. The first representatives of these polymers had already been obtained in the last century.[1–4] Since then, there has been a continuous development of this field in polymer chemistry.

The study of the interrelation between the structure and properties of heterochain polyesters has led to the idea that the most interesting properties, and especially enhanced thermal characteristics, may be expected from polymers based on aromatic components. Thus the syntheses of a series of polyesters of aromatic dicarboxylic acids and aliphatic glycols have been achieved. Among these compounds, poly(ethylene terephthalates) and poly(butylene terephthalates) are of undoubted practical interest. The aromatic ring can be introduced into the polyester chain also via the diol component.

Polyarylates are heterochain polyesters of dihydric phenols. The first representatives of polyesters of this type were polycarbonates, i.e. polyarylates of dihydric phenols and carbonic acid, which were synthesised in 1898 by Einhorn[5] by the interaction of phosgene with resorcinol and hydroquinone. The study of polycarbonates developed during the 1960s because polymers of practical value were discovered among them, in particular the polycarbonate of 2,2-bis(4-hydroxyphenyl)propane.[6,7]

In 1957–1958 publications on the polyarylates of aromatic dicarboxylic acids, with a series of valuable properties, began to appear almost simultaneously in Belgium, the USSR, and the USA.[8–10] The studies on these polymers have continued to this day.

S V Vinogradova (Heterochain Polymers Laboratory),
V A Vasnev (Heterochain Polymers Laboratory),
P M Valetskii (Polymer Synthesis Laboratory),
Nesmeyanov Institute of Organoelement Compounds,
Russian Academy of Sciences, ul. Vavilova 28, 117813 Moscow,
Russian Federation. Fax (7-095) 135 50 85. Tel (7-095) 135 61 78

Received 23 June 1994
Uspekhi Khimii **63** (10) 885–904 (1994); translated by A K Grzybowski.

II. Synthesis of polyarylates and their properties

Polyarylates can be obtained by the interaction of dicarboxylic acids with dihydric phenols (method I), of the diacetates of dihydric phenols with dicarboxylic acids (method II), and of dihydric phenols with dicarboxylic acid esters (method III), but the synthesis of polyarylates using the chlorides of dicarboxylic acids as the acid reagents (method IV) has assumed the greatest importance.

In the synthesis of polyarylates by the first three methods,[4,10–31] the polycondensation is usually carried out in the melt in an inert gas stream; in the final stage, the reaction mixture is heated in vacuo. A disadvantage of these methods is their unsuitability for the synthesis of polyarylates with high softening temperatures. Furthermore, the polyarylates obtained by polycondensation in the melt frequently acquire a colour during the reaction.[32]

The last method is best for the synthesis of high-melting polyarylates as well as polyarylates containing reactive groups in their chains. The employment of highly reactive dicarboxylic acid chlorides makes it possible to carry out successfully the polycondensation in solution. This method is of great importance in the synthesis of high-melting polyarylates, since it is then possible to achieve successful polycondensation up to a high degree of reaction without the decomposition of the polymer formed.

The polycondensation of dicarboxylic acid chlorides with dihydric phenols can be achieved in several versions: (1) at an elevated temperature in a high-boiling solvent; (2) as interfacial polycondensation; (3) as acceptor-catalytic polyesterification.

The characteristics of the polycondensation of dicarboxylic acid chlorides with dihydric phenols in a high-boiling solvent have been investigated in a number of studies.[4,11,14,33–40] It was established that the reactivity of the starting materials is greatly influenced by their structure.[33,37–45]

For example, when the condensation is carried out in dinyl (azeotropic mixture of diphenyl ether with biphenyl) in the temperature range 150–210 °C, it was found that isophthalic acid chloride reacts with 2,2-bis(4-hydroxyphenyl)propane at a higher rate than terephthalic acid chloride (at 170 °C, the rate constants are 10.7×10^{-5} and 6.6×10^{-5} litre mol^{-1} s^{-1} respectively). At 170 °C, dihydric phenols can be arranged in the following sequence in terms of the rate of their reaction with terephthalic acid chloride: hydroquinone > resorcinol > 2,2′-dihydroxybiphenyl > 2,2-bis(4-hydroxyphenyl)propane.[41]

The study of the kinetics of the polycondensation of terephthalic acid chloride with bis(4-hydroxyphenyl)methane, 2,2-bis(4-hydroxyphenyl)propane, 2,2-bis(4-hydroxyphenyl)-hexafluoropropane, bis(4-hydroxyphenyl)phenylmethane, 2,2-bis(4-hydroxyphenyl)-2-phenylethane, bis(4-hydroxyphenyl)-trifluoromethylphenylmethane, and bis(4-hydroxyphenyl)-diphenylmethane in ditolylmethane in the temperature range 160–200 °C showed that the nature of the substituents at the central carbon atom of the bisphenol sometimes exerts a significant influence on the rate of polycondensation.[39] Thus the replacement of the electron-donating methyl groups in 2,2-bis-(4-hydroxyphenyl)propane by the strongly electron-accepting trifluoromethyl groups makes the rate of polycondensation of 2,2-bis(4-hydroxyphenyl)hexafluoropropane with terephthalic acid chloride higher by a factor of 2–2.5 than the rate of polycondensation of 2,2-bis(4-hydroxyphenyl)propane.

The introduction of side groups by substitution into the aromatic rings of the dihydric phenol in the *ortho*-position relative to the hydroxy-group diminishes the rate of reaction with aromatic dicarboxylic acid chlorides.[40,43] For example, when the extents of reaction of aromatic dicarboxylic acid chlorides with 2,2-bis(4-hydroxyphenyl)propane and 2,2-bis(3-allyl-4-hydroxyphenyl)propane are compared, it is found that the process is slower in the case of the diallyl-substituted bisphenol. Thus, whereas the degree of reaction of isophthalic acid chloride with 2,2-bis(4-hydroxyphenyl)propane at 220 °C (in dinyl) is 0.89 after only 1 h, in the case of the diallyl-substituted bisphenol the extent of reaction over the same period is only 0.34 and reaches 0.83 only after 9 h. Hence it follows that it is desirable to carry out the polycondensation of the diallyl-substituted bisphenol with terephthalic and isophthalic acid chlorides at an elevated temperature of the order of 220 °C over a long period.[43]

The rate of polycondensation of dicarboxylic acid chlorides with dihydric phenols containing substituents in the *ortho*-position relative to the hydroxy-group is influenced not only by the size but also by the chemical nature of the substituent. Thus the rate constants of the polycondensation of terephthalic acid chloride with 2,2-bis[3-methyl(propyl, chloro)-4-hydroxyphenyl] propanes are lower at the corresponding temperatures than the rate constants for the unsubstituted dihydric phenol in the same reactions.[40]

We shall also consider the synthesis of mixed block-polyarylates by high-temperature polycondensation in solutions of dicarboxylic acid chlorides, bis-phenols, and various low-molecular-mass polymers with terminal hydroxy-groups.[33,46–51] The block components employed were poly(ethylene oxide) $HO(CH_2CH_2O)_nH$, poly(propylene oxide) $HO[CH(CH_3).CH_2O]_nH$, poly[3,3-bis(chloromethyl)trimethylene oxide] $HO.[CH_2C(CH_2Cl)_2CH_2O]_nH$, and a silicon-containing oligomer having the structure $\{HOC_6H_4C(CH_3)_2C_6H_4[OSi(CH_3).(C_6H_5)]\}_2O$, i.e. polymers without reactive bonds in their chains with the exception of reactive terminal functional groups. Since the ether group is inert with respect to exchange reactions, such block components, used as one of the initial diols for the synthesis of the polyester, were introduced without change into the polymer chain of the final product, modifying it significantly. The properties of such mixed block-polyarylates are determined both by the composition and structure of the initial components and by the process conditions because the reactivities of the block component and of the dihydric phenol differ from one another. Comparative study of the kinetics of the polycondensation of terephthalic acid chloride with 2,2-bis(4-hydroxyphenyl)propane and the bifunctional block components listed above in ditolylmethane at 220 °C showed that these diols can be arranged in the following sequence in terms of their reactivity towards the acid chloride: poly(ethylene oxide) > poly(propylene oxide) > 2,2-bis(4-hydroxyphenyl)propane > poly[3,3-bis(chloromethyl)-trimethylene oxide] > silicon-containing oligomer.[47]

Apart from the synthesis of linear thermoplastic polyarylates, thermoreactive polymers can also be obtained by polycondensation in a high-boiling solvent. These include, for example, polyarylates containing free hydroxy-groups in the chain, obtained by the polycondensation of aromatic dicarboxylic acid chlorides with dihydric phenols and polyhydric aliphatic alcohols [glycerol, tris(hydroxymethyl)propane, pentaerythritol, tris(hydroxymethyl)ethane, etc.].[37,52–54]

Comparative study of the kinetics of the polycondensation of terephthalic and isophthalic acid chlorides with 2,2-bis(4-hydroxyphenyl)propane and tris(hydroxymethyl)ethane in dinyl showed that aromatic dicarboxylic acid chlorides react with polyhydric aliphatic alcohols much more vigorously than with dihydric phenols.[37] The extent of reaction is greatly influenced by the chemical nature of the diol component. Thus the extent of reaction of isophthalic acid chloride with tris(hydroxymethyl)-propane at 150 °C is 0.74 after 9 h, whereas in the case where 2,2-bis-(4-hydroxyphenyl)propane is used as the diol component it is only 0.21. In the latter case, the extent of reaction can be raised to 0.74 after 8 h only by carrying the polycondensation at 210 °C, i.e. at a higher temperature. In the polycondensation of isophthalic acid chloride with 2,2-bis(4-hydroxyphenyl)propane at 220 °C, the extent of reaction is 0.89 after only 1 h.

The above data show that it is desirable to synthesise mixed polyarylates containing free hydroxy-groups in the chain in two stages. The first stage — the polycondensation of the dihydric phenol with a dicarboxylic acid chloride — should be carried out at an elevated temperature (up to 220 °C). The second stage (after the entire dihydric phenol has reacted) — the polycondensation of the polyarylate formed with an aliphatic polyhydric alcohol — must be performed at lower temperatures (110–150 °C), which makes it possible to attain a fairly high degree of reaction without premature hardening of the product.[37,55]

Much attention has also been devoted to the study of processes occurring in the synthesis of polyarylates with the aid of interfacial and acceptor-catalytic polyesterification.[4,11,13,15,56–70]

Using all three variants, polymers with high molecular masses [for example up to 150 000 for the polyarylates obtained from 2,2-bis(4-hydroxyphenyl)propane and the chlorides of terephthalic and isophthalic acids by interfacial polycondensation, 60 000–100 000 for the polyarylates obtained by the high-temperature polycondensation in solution of phenolphthalein and aromatic dicarboxylic acid chlorides] can be obtained in nearly quantitative yields from dicarboxylic acid chlorides and dihydric phenols.[33,56]

The polycondensation of dicarboxylic acid chlorides with dihydric phenols has been used successfully for the synthesis of polyarylates having a wide variety of chemical structures.

As early as the 1930s, mention was made of the use of phenolphthalein for the synthesis of polyesters in a list of initial compounds published in an American patent.[71] Data on the synthesis of alkyd polymers using fluorescein and phenolphthalein were published in 1946.[72] However, a characteristic feature of these studies is that phenolphthalein was used simply as one of the representatives of the enormous number of diols without taking into account its specific contribution to the properties of the polymers.

Polyarylates derived from phenolphthalein and aromatic dicarboxylic acids were first obtained in 1961 and attention was turned to the specific contribution of the phthalide side group to a valuable set of properties of these polymers: the combination in the latter of an increased thermal stability with an effective solubility in organic solvents.[73,74] It was subsequently suggested that polymers of this type, i.e. those containing in the repeat unit at least one element entering into the composition of the cyclic side group, be called cardo-polymers,[75] from the Latin word 'cardo', which means loop, because such groups can be regarded as loops in relation to the main chain of the macromolecule. In subsequent years, the studies in the field of cardo-polyarylates developed extensively.[11,12,33,56,57,73–113]

In the synthesis of cardo-polyarylates, various dihydric phenols containing closed cyclic groups at the central carbon atom were used as the starting materials: phenolphthalein, phenolfluorene, phenolanthrone, phenolacenaphthylene, phenolphthalein imide, its *N*-β-hydroxyethyl and allyl derivatives, etc. The acid chlorides of aromatic dicarboxylic acids of the cardo-type, for example diphenylnaphthalide-4,4′-dicarboxylic acid, have also been used in a number of cases. For example, phenolphthalein polyarylates with a high molecular mass (up to ~100 000) have been obtained successfully by acceptor-catalytic polyesterification in an organic solvent at moderate temperatures (up to ~50 °C) in the presence of a tertiary amine or by polycondensation in an inert medium at an elevated temperature (100–200 °C) in a high-boiling solvent. Since the process takes place in the absence of a catalyst in the latter case, its completion requires approximately 10 h.

An interesting feature was discovered in the study of the formation reactions of phenolphthalein polyarylates in a high-boiling solvent. It was established that the properties of the polyarylate obtained from isophthalic acid and phenolphthalein varied appreciably depending on the nature of the solvent in which the process was carried out.[114]

The chemical structure of the polyarylates obtained from phenolphthalein and aromatic dicarboxylic acids ensures a high rigidity of their macromolecules. For this reason, in the synthesis of such polyarylates in ditolylmethane, which is not a solvent for the polymer obtained, the free energy of formation of the coiled macromolecules should be smaller than the free energy of formation of the uncoiled macromolecules. This results in the selection, during the synthesis, of globular forms of the macromolecules and ensures the globular type of supermolecular structure of the phenolphthalein polyarylates synthesised in ditolylmethane. On the other hand, in the synthesis of the phenolphthalein polyarylate in α-chloronaphthalene or nitrobenzene, which are solvents also for the polymer formed, uncoiled (extended) macromolecules are formed preferentially. Fibrillar supermolecular structures arise as a result of this. The polymers with such supermolecular structure have a better set of physicochemical properties. This follows from Table 1, which presents the characteristics of the isophthalic–phenolphthalein polyarylates synthesised in various media.

Table 1. The properties of phenolphthalein–isophthalic acid polyarylate.

Properties of polyarylate	Medium in which the polyarylate has been synthesised			
	ditolyl-methane	α-chloro-naphthalene		nitro-benzene
Molecular mass	28 000	28 000	48 000	26 000
Softening temperature/°C	270	290	300	275
Tensile strength/ kgf cm^{-2}	640	740	780	650
Elongation at rupture (%)	10–20	80	100	40–70
Specific impact strength/ (kgf cm) cm^{-2}	2–3	10	20	14

The synthesis of polyarylates based on 2-(β-hydroxyethyl)-3,3′-bis(4-hydroxyphenyl)phthalimidine or phenolphthalein imide at elevated temperatures is nonspecific, since infusible and insoluble polymers with a three-dimensional structure are then formed owing to the trifunctional nature of the initial bisphenols. At the same time, the interfacial polycondensation of these bisphenols with dicarboxylic acid chlorides, carried out under mild conditions, leads to linear high-molecular-mass polyarylates containing free hydroxy- or NH groups in the chain,[81,82,115] which do not interact with the acid chloride groups under the conditions of the given reaction.

The use of such bisphenols in the synthesis of polyarylates in a mixture with the usual bisphenols leads, for example, to the possibility of a clear-cut regulation of the content of the reactive group along the polymer chain. Such polymers have advantages over the widely known alkyd polymers because of their linear structure, high softening temperature, high molecular mass, and a uniform distribution of the free functional groups NCH_2CH_2OH or NH along the chain.

The development of the theory of nonequilibrium (irreversible) polycondensation and the advances in the field of its preparative methods of synthesis have created broad preconditions for the synthesis of block-copolymers of the polycondensation type. This applies in the first place to acceptor-catalytic polycondensation,[33,68,116,117] the mild conditions of which make it possible to synthesise block-copolymers with virtually complete suppression of exchange reactions. When the process characteristics are known adequately, this makes it possible to produce block-copolymers directly from the monomers.[68] Even greater prospects for controlling the microstructure of the polymer chain in block-copolymers and hence their properties arise when oligomers and polymers with terminal functional groups are used as the starting materials for their synthesis.[116–148]

At least three methods of synthesis of polycondensation block-copolymers are realistic, for example the synthesis of polyarylate-arylene sulfone oxide block-copolymers.

(1) The synthesis in two reaction volumes of oligomers, having different chemical structures, with a specified molecular mass and heterofunctional groups followed by their copolycondensation (Scheme 1).

Scheme 1

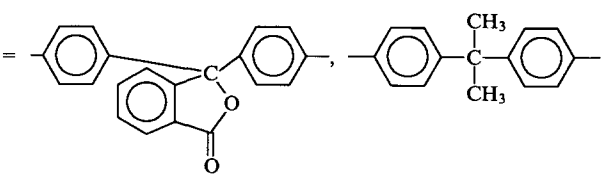
$$10n\,HOROH + 11n\,ClOCR'COCl \longrightarrow$$

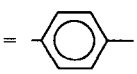
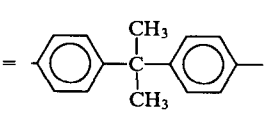
$$\longrightarrow n\,Cl(OCR'COORO)_{10}OCR'COCl$$

A

$$A + HOR''(OC_6H_4SO_2C_6H_4OR'')_{10}OH \xrightarrow{-2n\,HCl}$$

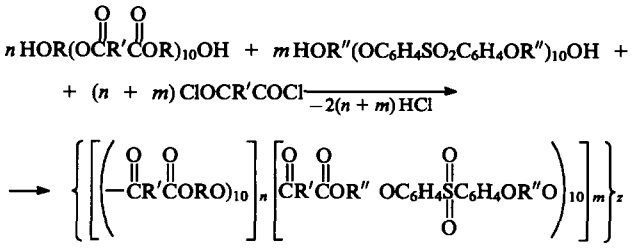
$$\longrightarrow \left\{\left[\left(-CR'CORO)_{10}\right]_n\left[CR'COR''\,OC_6H_4SC_6H_4OR''O\right)_{10}\right]_n\right\}_z$$

R = 

R′ =  ; R″ = 

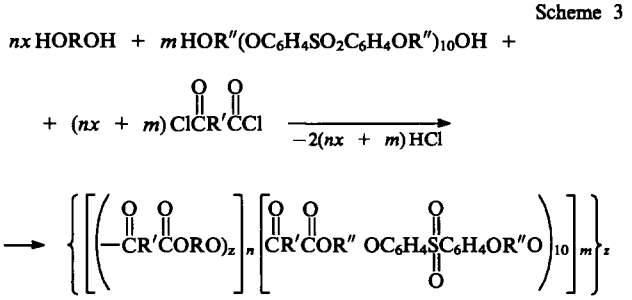
(2) The synthesis in two reaction volumes of oligomers, having different chemical structures, with a specified molecular mass and homofunctional end groups and their copolycondensation with the aid of an intermonomer (a chain lengthening agent) (Scheme 2).

Scheme 2



(3) The synthesis of an oligomer having a specified molecular mass and its copolycondensation with a low-molecular-mass monomer and an intermonomer, the interaction of which gives rise to polymer blocks having a different chemical structure (Scheme 3).

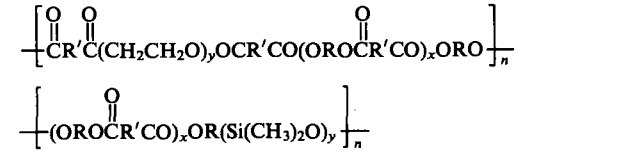
Scheme 3



Naturally, depending on the method of synthesis of the block-copolymers, the chemical structure of the monomers and the block components, their molecular mass, the length of blocks having different chemical structures and their distribution along the macrochain all vary, i.e. the nonuniformity of the composition of the block-copolymer and hence its properties vary. It follows from the three schemes presented above that the block-copolymers having the most regular structure are obtained as a result of acceptor-catalytic polyesterification in accordance with Scheme 1.

The polycondensation method makes it possible to vary widely the position of the block-copolymers. Thus various block-copolymers containing both polymer blocks having similar chemical structures (for example, polyarylate-arylene sulfone oxides [119-123, 136, 137]) and polymer blocks differing appreciably in their structure and properties from polyarylates [for example, polyarylate-ethylene oxides [120, 131, 137, 140, 141] or polyarylate-organosiloxanes [125-129, 137-139] (Scheme 4)] have been obtained (and investigated) on the basis of cardo-polyarylates incorporating terephthalic and isophthalic acids (polyarylate F-1 in the case of isophthalic acid) and the polyarylate obtained from 2,2-bis-(4-hydroxyphenyl)propane and terephthalic and isophthalic acids (polyarylate D).

Scheme 4



Deeper study of nonequilibrium condensation processes, especially acceptor-catalytic polyesterification, created theoretical preconditions for the synthesis of stereoregular polyarylates the molecules of which contain regular sequences of stable rotational isomers. [68, 145, 149-160]

The fundamental novelty of the synthesis of conformationally regular polyarylates consists in the fact that their regular steric microstructure is formed directly during the growth of the macromolecule when monomers which are neither conformational nor configurational isomers but their molecules contain fragments with hindered internal rotation are used in the reaction. An example of polyarylates of this kind is provided by the stereoregular polyterephthalates based on disubstituted 2,2-bis-(4-hydroxyphenyl)propanes, for example 2,2-bis(3-chloro-4-hydroxyphenyl)propane.

Comparison of the stereotacticities of the polymers obtained with the conditions of their synthesis made it possible to formulate a series of rules governing the formation of such macromolecules. Thus in the presence of weakly basic heterocyclic tertiary amines (nucleophilic catalysis), mainly polyarylates with the *cis*-disposition of the substituents in the bisphenol fragment are formed, whereas in the presence of highly basic trialkylamines (general base catalysis) polyarylates with the *trans*-isomers are produced, which is associated with the different geometries of the transition complexes. The presence of regular sequences of isomeric forms in the macromolecules of polyarylates influences significantly their properties. In particular, an increase in the stereotacticity of the polymers increases the degree of their crystallinity and their softening temperatures and diminishes their solubility. The synthesis of stereoregular polyarylates is illustrated schematically (Scheme 5).

A special series of studies have been carried out on the so called 'self-coloured' polyarylates. [161-166] Aromatic polyesters are known to be extremely difficult to dye. [161, 166] It has been found that in the case of polyarylates this problem can be solved by synthesising polymers the macromolecules of which contain chemically bound dye molecules.

The construction of such a polymer chain is achieved by employing chromophore-containing dihydric phenols and dicarboxylic acid chlorides together with the usual phenols and acids for the synthesis of polyarylates. Thus homogeneous and mixed polyarylates, containing anthraquinone residues or azo-groups in the chain, have been synthesised, and their properties investigated, from compounds such as the chlorides of azobenzene-3,3'- and azobenzene-4,4'-dicarboxylic acids, 2,2' and 4,4'-dihydroxy-, 4,4'-dihydroxy(ethoxy), and 4,4'-dihydroxy-(propoxy)-azobenzenes, quinizarin, alizarin, and Alizarin Blue. The use of fumaric acid chloride as the acid reagent in the synthesis of such polyarylates made it possible to obtain coloured polyarylates capable of copolymerising with various monomers. Table 2 (page 838) presents examples of the polymers obtained.

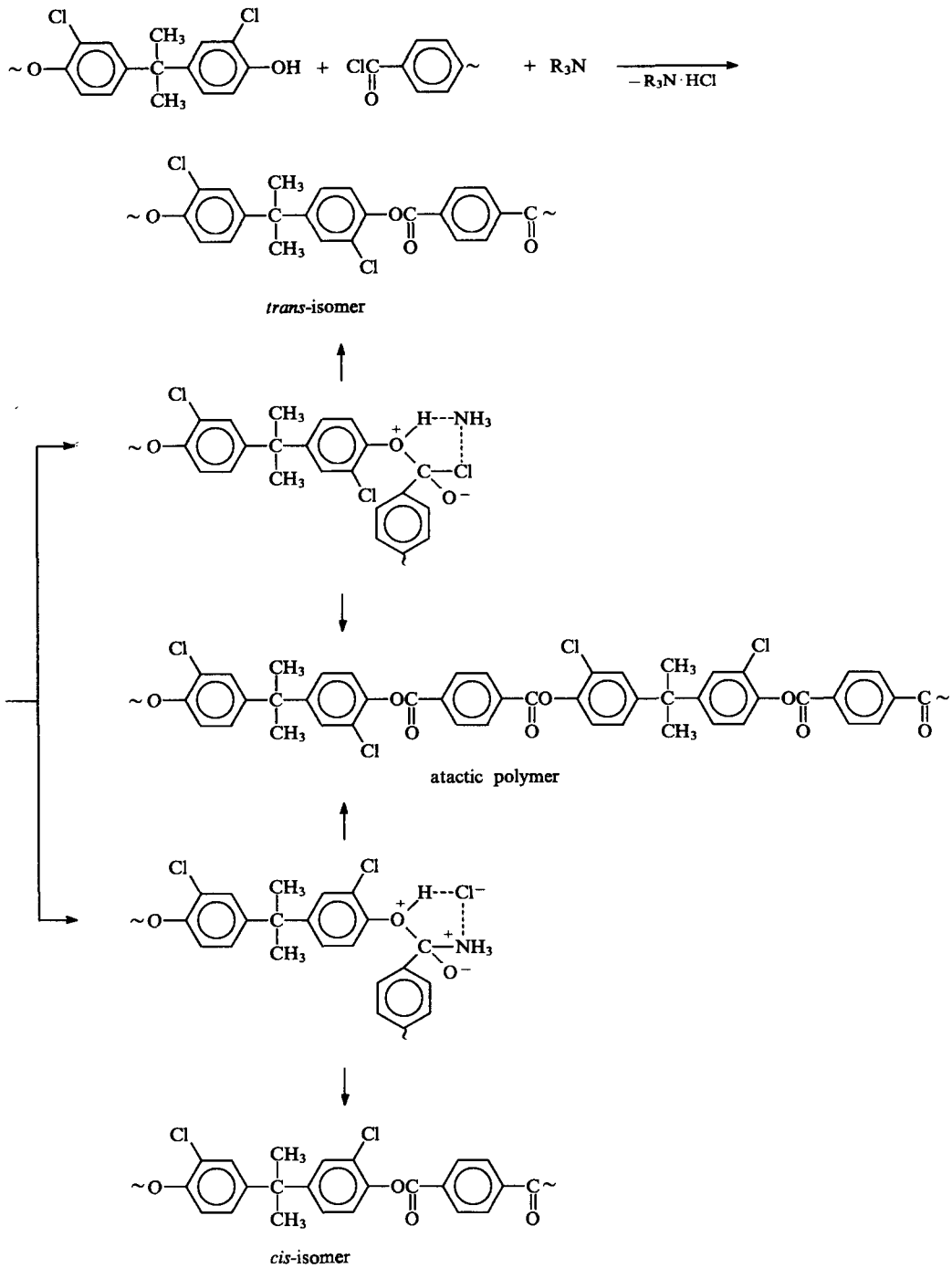
All these polyarylates are substances having colours corresponding to that of the starting material. It is noteworthy that, as part of the coloured component in the homopolyarylate is replaced by a colourless monomer, the colour of the polyarylate is usually retained and the intensity of the absorption in the visible region varies in proportion to the concentration of the coloured component in the polymer. The relatively high intensity of the absorption in the visible spectra of self-coloured polyarylates with even small amounts (for example 0.1-0.05 mole) of coloured chromophore-containing monomers in the mixture of the initial components suggests a technologically extremely simple solution of the problem of dyeing the known polyarylates. [163, 166]

The fact that molecules of the coloured substance in the self-coloured polyarylates are covalently linked to other components renders their colour stable towards various influences, including the action of light, which is one of the most important characteristics of the colour. For example, in the case of self-coloured homopolyarylates and copolyarylates containing only 0.05 mol.% (2-3 mass%) of a chromophore-containing substance, the photostability proved to be satisfactory.

It has been observed that the introduction of even small amounts of a chromophore-containing monomer into the polyarylate chain appreciably increases the resistance of solutions and films of these polymers to the action of UV radiation. [161]

Transparent coloured films, the tensile strength of which in the nonoriented state at room temperature varies in the range from 800 to 1300 kgf cm^{-2}, have been obtained from a series of coloured polyarylates containing different amounts of a chromophore-containing substance. Tests on these films at

Scheme 5



elevated temperatures showed that at 250 °C they retain up to 40% of the initial strength. The coloured polyarylates can be worked to produce cast and moulded articles. The specific impact strength of moulded specimens of the 4,4′-dihydroxyazobenzene polyarylate is 25 (kgf cm) cm^{-2}.[166]

A series of coloured polyarylates containing fumaric acid fragments in their macromolecules are satisfactorily compatible with various monomers (styrene, methyl methacrylate, diallyl isophthalate), forming with the latter under appropriate conditions coloured copolymers in the form of transparent coloured monolithic substances. Compositions comprising self-coloured unsaturated polyesters with unsaturated monomers have been used successfully in the preparation of yellow and red vitreous plastics possessing a high photostability and an effective chemical stability in addition to good mechanical parameters.[161,166]

Thus chromophore-containing bisphenols and dicarboxylic acids are of interest not only from the standpoint of the synthesis of new heat-resistant coloured polyesters but also from the standpoint of imparting a predetermined colour with a specified intensity to colourless polyarylates most interesting from the practical point of view and of an appreciable improvement of the photochemical stability of these polymers.[161]

In order to find polyarylate structures with an increased photostability, a study has been made of the effect of ultraviolet radiation on specifically synthesised homogeneous and mixed polyarylates based on phenolphthalein, phenolsulfophthalein, bis(4-hydroxyphenyl) sulfone, phenolphthalein anilide, phenolphthalein imide, phloroglucinol, and the chlorides of terephthalic, isophthalic, and methylphosphinic acids, bis(4-carboxyphenyl)-methyl ether, and a number of others.[167-174]

It has been found that the partial or complete replacement of the lactone ring by a lactam ring in phenolphthalein polyarylates as well as the presence of a cyclic substituent with a conjugated bond system (for example, the fluorenyl substituent) at the central

Table 2. Certain properties of coloured polyarylates.

Starting material		Temperature/°C		Colour of powdered polymer
acid chloride	dihydric phenol	softening	onset of decomposition[a]	
Azobenzene-3,3'-dicarboxylic acid	phenol-phthalein	250	310	yellow
Azobenzene-4,4'-dicarboxylic acid	"	295	360	red
Azobenzene-3,3'-dicarboxylic acid	2,2'-dihydroxy-azobenzene	230	350	bright yellow
Azobenzene-4,4'-dicarboxylic acid	"	235	380	orange
Azobenzene-3,3'-dicarboxylic acid	4,4'-dihydroxy-azobenzene	350	385 (380)	"
Azobenzene-4,4'-dicarboxylic acid	"	400[b]	410 (410)	yellow
Terephthalic acid	"	400[b]	415 (415)	yellow
	1,4-dihydroxy-anthraquinone	400[b]	420 (390)	green-yellow
	1,2-dihydroxy-anthraquinone	150	360 (360)	green
	7,8-dihydroxy-5,6-phthalyl-quinoline	190	300	blue-violet

[a] Obtained from the results of thermogravimetric analysis at a heating rate of 17 °C per minute; the values in brackets were obtained at a heating rate of 3 °C per minute.
[b] Softening takes place with decomposition.

carbon atom in the bisphenol residues appreciably increase the resistance of the polymer to the action of light. The inclusion of small amounts (~1%) of sulfur, phosphorus, and free phenolic groups in the polyarylate chain afforded polyarylates with increased resistance to light-induced ageing.

As shown above, the photostability of polyarylates can be increased also by introducing into their polymer chain the residues of bifunctional chromophore-containing substances (for example, 1,3-dihydroxyanthraquinone). It is also noteworthy that the high photostability of polyarylates, exhibited when their solutions are irradiated, may be due to the occurrence under these conditions of the Fries rearrangement, which leads to the appearance in the polymer chain of hydroxyketone groups stabilising the polymer.

The introduction of sulfur and phosphorus into the structure of phenolphthalein polyarylates increases not only the photostability of the polymers but also their thermal stability and in the case of phosphorus their fire resistance.

Thus polymers with 'self-protecting' properties as regards the action of light and heat can be obtained with the aid of specific design of the polyarylate chain.[174]

Polyarylates containing reactive groups in their chain, for example hydroxy-groups, and double bonds possess thermoreactive properties. They are capable of long-range chemical reactions and of undergoing a transition to an infusible three-dimensional state as a result of both heat treatment and various chemical reactions.

Thus polyarylates based on polyhydric alcohols containing free hydroxy-groups in their chain are capable of undergoing a transition to a three-dimensional state on additional heat treatment and as a result of their interaction with pyromellitic, maleic, and phthalic anhydrides, diisocyanates, metal derivatives, and other reagents,[52-54,175,176] whereupon the properties of the polymers are modified significantly, for example their thermal characteristics are improved.

The double bond-containing polyarylates based on 2,2-bis(3-allyl-4-hydroxyphenyl)propane (with added 2-allylphenol) and fumaric acid may be hardened on heating or as a result of copolymerisation with other unsaturated compounds.[177-186] This made it possible to modify within wide limits the properties of the polymers, in particular to improve their thermal characteristics. For example, high elastic deformation over a wide temperature range is characteristic of the hardened polyarylate obtained from isophthalic acid and 2,2-bis(3-allyl-4-hydroxyphenyl)propane; the decomposition of this polymer is observed at temperatures exceeding 500 °C.[11]

Polyarylates derived from aromatic dicarboxylic acids possess a valuable set of properties: high heat resistance and thermal stability, effective insulating properties over a wide temperature range, and resistance to the action of many chemical reagents, UV light, and ionising radiation.

The physicochemical properties of these polymers are closely related to their structure and depend on the disposition of the functional groups in the initial components and also on the presence and nature of substituents. The highest melting points are observed for polyarylates whose monomers contain functional groups in the *para*-positions and have no aliphatic units. Thus poly(hydroquinone terephthalate) and *o*-hydroxybenzoic acid polyarylate (econol) do not melt up to 500 °C, and the softening temperatures of phenolphthalein–terephthalic acid and phenolphthalein–isophthalic acid polyarylates are 340 and 275 °C respectively.

The high heat resistance of cardo-polyarylates[11,12,56,76-79,82,92,99,102] greatly exceeds that of polyarylates with similar chemical structures but not containing cardo-groups. For example, the softening temperatures of polyarylates of terephthalic acid combined with phenolphthalein, phenolfluorene, and phenolanthrone are 340, 350, and 360 °C respectively, whereas that of poly[bis(4-hydroxyphenyl)diphenyl methane terephthalate] is 280 °C. The heat resistance of polyarylates increases significantly with increase in the number of aromatic rings in the initial components.

The presence of alkyl substituents in the *ortho*-positions relative to the hydroxy-group of the bisphenol as it were promotes the 'internal' plasticisation of the polyarylates based on them.[187-191] Polyarylates obtained from terephthalic acid and such bisphenols have lower softening temperatures [for example, the softening temperature of the 2,2-bis(4-hydroxy-3-methylphenyl)propane polyarylate is 180 °C] and a greater impact resistance and they can be more readily worked to form monolithic articles than the polyarylates derived from the corresponding ring-unsubstituted bisphenols.

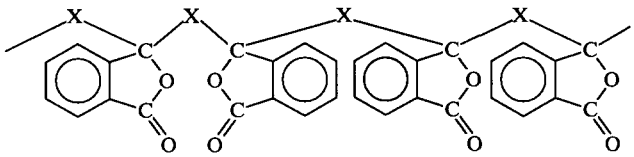
The properties of polyarylates are also closely related to the nature of the side substituents at the central carbon atom of the dihydric phenol.[192-199]

The decrease in the packing density of the polymer chains as a consequence of the presence of functional groups in the initial components in the *meta*- or *ortho*-positions rather than *para*-positions and the presence of side substituents in dihydric phenols promote the formation of amorphous polyarylates. The tendency of polyarylates to crystallise also diminishes with the appearance of an asymmetric substituent at the central carbon atom of the bisphenol.[4,11]

Since polyarylates based on phenolphthalein and an acid such as terephthalic it had always been obtained in the amorphous form, the impression was created initially that this is a specific feature of the cardo-polymers due to the large bulk of their cyclic substituents. However, deeper study of polyarylates with different cardo-groups made it necessary to revise this idea. It was found that, despite the large bulk of the cardo-group, these polymers are capable of crystallising. The conditions facilitating their crystallisation are the symmetry of the shape of the cardo-group (fluorene and anthrone groups) and the presence in the polymers of polar components (the anthrone group).

This made it necessary to look again at the lack of capacity for crystallisation in cardo-polyarylates containing cardo-groups with an asymmetric shape (phthalide and acenaphthene groups) and to attempt an explanation of this feature in terms of the atactic nature of the polyarylates obtained. As a consequence of the asymmetry of their shape and the statistical nature of the polycondensation reaction, the cardo-groups in such polymers are arranged in different nonordered ways relative to the main axis of the macromolecule (Scheme 6).

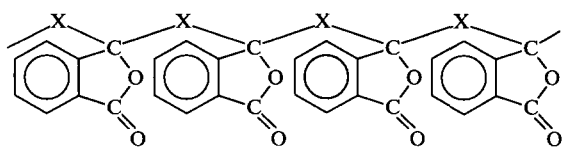
Scheme 6



Subsequently it was demonstrated for polyarylates with phthalimidine groups that polyarylates with asymmetric cardo-groups can also crystallise. This is apparently achieved by virtue of the presence of hydrogen bonds promoting a definite disposition and orientation of the macromolecules. A greater crystallinity can be achieved when the orientational mobility of the hydrogen is facilitated to the maximum extent (the H atom at the nitrogen atom is replaced by the CH_2CH_2OH group).[82]

The crystallisation of polyarylates with phthalimidine groups gives rise to the hope that, by an appropriate selection of the conditions in the synthesis or by subsequent treatment of the finished polymer, it may be possible to achieve the crystallisation also of polyarylates containing asymmetric cardo-groups such as the phthalide group. It is quite logical to suppose that this would be promoted by a regular disposition of the groups along the polymer chain (Scheme 7).

Scheme 7



The possibility of a deliberate change in structure is undoubtedly an important factor which will make it possible to achieve the desired modification of the properties of the polymers. For example, the heat resistance of the polyarylate obtained from phenolanthrone and terephthalic acid may be varied by altering the conditions in the synthesis and in the subsequent treatment of the polymer.[84,85,99] It increases significantly on passing from an amorphous polymer to one with an ordered structure: the amorphous polyarylate softens at ~340–360 °C, whilst the crystalline one does not soften before decomposition.[86]

Polyarylates with a definite structure also exhibit liquid crystal properties.[200–211]

The solubility of polyarylates is likewise associated with their chemical structure. Polyarylates derived from aromatic dicarboxylic acids such as terephthalic and isophthalic acids and biphenyl-4,4'-dicarboxylic acid and bisphenols such as hydroquinone and resorcinol are almost insoluble in organic solvents. The presence of side substituents in the bisphenol increases the solubility of the polyarylates. The polyarylates obtained from isophthalic acid, on the one hand, and 2,2-bis(4-hydroxyphenol)-propane, 2,2-bis(4-hydroxyphenyl)butane, and bis(4-hydroxy-phenyl)diphenylmethane, on the other, are soluble in cresol and chlorinated hydrocarbons. Compared with noncardo-polymers, cardo-polymers are much more readily soluble in organic solvents.[11,102] For example, the polyarylates obtained from phenolphthalein and aromatic dicarboxylic acids dissolve readily in methylene chloride, chloroform, dichloroethane, *sym*–tetra-chloroethane, tetrahydrofuran, cyclohexanone, etc., forming highly concentrated (> 25%) solutions.

The presence of mobile hydrogen atoms in the cardo-groups (for example, in the polyarylates of phenolphthalein imide), which are capable of involvement in the formation of hydrogen bonds, narrows the range of solvents. Such polyarylates no longer dissolve in chlorinated solvents but are readily soluble in solvents capable of forming hydrogen bonds with the mobile hydrogen atoms in the polyarylates (in dimethylformamide, tricresol, etc.).[81,82] Mixed polyarylates are more soluble than the homopolymers.[11]

Polyarylates possess film- and fibre-forming properties. In order to exhibit film-forming properties, the polymers must have an intrinsic viscosity (η_{int}) (in dichloroethane or tetrachloro-ethane) of the order of 0.4–0.5 dl g^{-1}, while the value required for fibre formation is approximately 1.0 dl g^{-1}. The breaking stress on extension of nonoriented polyarylate films is 600–1000 kgf cm^{-2}. The orientation of films in both directions can increase this value to 1500–2000 kgf cm^{-2}.

A valuable property of polyarylate films is their ability to retain effective mechanical parameters after prolonged heating at elevated temperatures. The breaking stresses on extension of nonoriented films of the cardo-polyarylates obtained by the reaction of diphenylphthalide-4,4'-dicarboxylic acid with phenol-phthalein and phenolphthalein anilide at 300 °C are 330 and 250 kgf cm^{-2} respectively. Films of mixed polyarylates obtained from 2,2-bis(4-hydroxyphenyl)propane and terephthalic and isophthalic acids withstand prolonged heating (for 1000 h) at 150–200 °C, retaining satisfactory mechanical parameters.

Polyarylates have effective dielectric parameters which do not change over a wide temperature range.[4,11,212,213] The relative permittivity of films of 2,2-bis(4-hydroxyphenyl)propane–phenolphthalein polyarylates is close to that of poly(ethylene terephthalate). The advantage of polyarylates over poly(ethylene terephthalate) and poly[2,2-bis(4-hydroxyphenyl)propane carbonate] consists in a smaller change in the dielectric loss angle and in the specific resistance of the bulk-phase material in the temperature range from −60 to 200 °C and above. The dielectric loss angle does not exceed $(4-5) \times 10^{-3}$ for 2,2-bis(4-hydroxy-phenyl)propane polyarylates and $(5-8) \times 10^{-3}$ for phenol-phthalein polyarylate in the same temperature range. Whereas the maximum in the dielectric loss angle is observed at 140 °C for poly(ethylene terephthalate) and at 200 °C for poly[2,2-bis-(4-hydroxyphenyl)propane carbonate], in the case of phenol-phthalein polyarylates it has not been observed even at 300 °C. The bulk-phase value of the resistivity of 2,2-bis(4-hydroxy-phenyl)propane and phenolphthalein polyarylate films is about $(1-3) \times 10^{13}$ Ω cm at 200 °C, which is 1.5–2 orders of magnitude higher than for poly(ethylene terephthalate) and the polycarbonate.

Polyarylates are resistant to the prolonged action of inorganic and organic acids (with the exception of sulfuric acid), oxidants, and dilute alkalis, but are inadequately resistant to the action of concentrated solutions of alkali and ammonia.[214]

The polyarylates of aromatic dicarboxylic acids are char-acterised by high thermal stability.[43,215] The polyterephthal-ates of 2,2-bis(4-hydroxyphenyl)propane, phenolphthalein,

phenolanthrone, and phenolfluorene under an inert atmosphere begins to lose mass at 350–360 °C for a heating rate of 5 °C per minute. The decrease in the mass of the phenolphthalein–biphenyl-4,4'-dicarboxylic acid polyarylate during isothermal heating in air at 400 °C for 1 h is about 7%.

Polyarylates burn but do not support combustion. The polymers containing chlorine (up to 13%) and phosphorus in the macromolecule exhibit an enhanced fire resistance and also a high resistance to the action of ionising radiation. The radiation yield of the gaseous products of the radiolysis of these polymers, obtained by the polycondensation of isophthalic acid chloride with 2,2-bis(4-hydroxyphenyl)propane and hydroquinone, is of the order of 0.02 of a molecule per 100 eV, which is appreciably less than the yield of gases on irradiation of poly(ethylene terephthalate) and the polycarbonate. The molecular structure of polyarylates does not change significantly for doses of the order of 10^{23} eV cm^{-3}.[216]

Table 3 presents certain properties of the phenolfluorene–terephthalic acid polyarylate. Evidently high heat resistance, thermal stability, and dielectric parameters are characteristic of this polymer over a wide temperature range.[108,109] Films of this polymer retain an appreciable strength even at 350 °C.

Table 3. The properties of the 9,9-bis(4-hydroxyphenyl)fluorene–terephthalic acid polyarylate.

Property	Value
Molecular mass	50000
Softening temperature/°C	~360
Glass point/°C	~290
Temperature of onset of decomposition (from thermogram)/°C	465
Tensile strength (of film), σ/kgf cm^{-2}, at	
20 °C	840
300 °C	440
350 °C	250
Elongation at rupture, ε (%), at	
20 °C	15
300 °C	32
Modulus of elasticity, E/kgf cm^{-2}, at	
20 °C	26000
300 °C	5400
Specific impact strength/(kgf cm) cm^{-2}	15–20
Tangent of dielectric loss angle at	
25 °C	0.0037
220 °C	0.0025
Relative permittivity at	
25 °C	3.3
200 °C	3.0
Bulk-phase specific resistance/Ω cm, at	
25 °C	10^{17}
200 °C	5×10^{13}

The cardo-polyarylates based on polycyclic bisphenols containing norbornane groups at the central carbon atom also possess a high heat resistance, effective physicomechanical and dielectric parameters, and a high solubility.[78,87,88]

The synthesis of mixed polymers based on several dicarboxylic acid chlorides or bisphenols as well as the synthesis of block-copolymers with polyarylate fragments in the chain have given rise to extensive possibilities for specific regulation of the properties of polyarylates. One of the methods for synthesis of the block-copolymers with polyarylate fragments involves, as mentioned above, their preparation from oligomers, previously synthesised, with a specific molecular mass and functional groups of different nature. By varying the molecular mass of the initial block components and their chemical nature, it is possible to regulate within wide limits the properties of such block-copolymers. We shall consider certain examples.

It is of interest that, despite the polyblock nature of their construction, polyarylate–siloxane block-copolymers possess a distinct microheterogeneous structure ensuring the retention of the high-temperature properties of the rigid block and the low-temperature properties of the flexible block. All the polyarylate–dimethylsiloxane copolymers have two glass points corresponding to the polydimethylsiloxane (−120 °C) and the polyarylate (for example, 320 °C in the case of the phenolphthalein–terephthalic acid polyarylate) and combine the properties of both homopolymers (strength, elasticity, gas-separating properties, etc.). Nonvulcanised films of such block-copolymers retain high ultimate strengths and relative elongations over a wide temperature range, which is related to the glass point of the rigid block and the phase incompatibility of the two blocks in the polyblock system. Table 4 shows that, after exposure to air at 250 °C for 10 h, the films of the block-copolymers remain elastic.[124]

Table 4. Mechanical properties of the polyarylate-siloxane block-copolymers $-[OROC(O)R'CO]_{10}ORO[Si(CH_3)_2O]_y-$.

y	σ/kgf cm^{-2}, at		ε (%), at	
	20 °C	200 °C	20 °C	200 °C
20–40	400–300	200–150	30–80	80–100
80–100	250–150	120–100	120–220	150–250
180–200	80–120	200–300	200–250	2–3
180–200[a]	40	–	120–150	–

[a] After ageing for 10 days at 250 °C.

In the case of polyarylate–arylene sulfone oxides,[119–123,136,137] microphase separation is difficult and a monotonic variation of the properties takes place over a wide range of compositions, as happens in the case of statistical copolymers. However, it has been found that, when the polyarylate–arylene sulfone oxide contains 10–15 mass% of arylene sulfone oxide blocks, a seemingly abrupt change in properties takes place, being manifested, in particular, by a sharp increase in the viscosity of their concentrated solutions and melts. This decrease reaches several orders of magnitude, the viscosity approaching the value for the poly(arylene sulfone oxide) melt. Thus, whereas the viscosities are $10^{4.0}$ P for the poly(arylene sulfone oxide) melt, $10^{7.0}$ P for the polyarylate F-1, and $10^{6.0}$ P for the polyarylate D, the viscosity of the block-copolymer based on the polyarylate F-1 and poly(arylene sulfone oxide) [obtained from 2,2-bis-(4-hydroxyphenyl)propane and bis(4-chlorophenyl) sulfone], in which the content of the latter is 10 mass%, amounts to $10^{4.5}$ P and that of the block–copolymer based on the polyarylate D and the same polysulfone for a content of the latter of 12 mass% is 10^4 P. This leads to the possibility of successful working of such block-copolymers by casting under pressure (which constitutes their advantage over homopolyarylates) whilst retaining a higher heat resistance than that of the initial polysulfone.

Table 5. Properties of polyarylate-arylene sulfone oxide block-copolymers.

Parameter	Brand of block-copolymer	
	FS-10	DS-12
Breaking stress/kgf cm^{-2}		
on extension	600–700	700–800
on compression	700–800	800–900
on static bending	800–900	900–1000
Relative elongation at rupture (%)	80	130
Modulus of elasticity in extension/kgf cm^{-2}	17000	14000
Specific impact strength/(kgf cm)cm^{-2}	30–40	70–90
Microhardness/kgf mm^{-2}	21–23	14–16
Absorption of water in 24 h (%)	0.20	0.18
Bulk phase resistivity/Ω cm	1×10^{15}	2×10^{16}
Tangent of dielectric loss angle at		
60 Hz	0.015	0.015
10^6 Hz	0.020	0.018
Insulating strength/kV mm^{-1}	25–30	25–30
Relative permittivity	4.2	4.0

Table 5 shows that polyarylate-arylene sulfone oxides have effective mechanical and electrophysical properties.[136] The properties of these block-copolymers can be altered specifically by varying the microstructure of the polymer chain and its chemical structure and composition.

A complex transformation of the phase composition from single-phase to three-phase takes place in polyblock polyarylate-ethylene oxide block-copolymers containing relatively short individual blocks with a definite compatibility.[140] In contrast to the block-copolymers with full phase separation, such as polyarylate-dimethylsiloxanes,[126,128] the phase separation in polyarylate-ethylene oxide block-copolymers depends on the mass ratios of the individual blocks and also on their molecular masses.[140]

Table 6 presents certain mechanical properties of polyarylate-ethylene oxide block-copolymers.[141] They show that, by varying the ratio of block sizes, it is possible to vary the properties of the block-copolymers within wide limits. Thus the strength of the films varies from 90 to 1000 kgf cm^{-2}, the deformation at rupture varies from 30% to 700%, and the modulus of elasticity varies from 400 to 17 000 kgf cm^{-2}. It is also noteworthy that the ratio of the reversible and irreversible deformations of the films likewise varies significantly under these conditions. For example, the high elastic deformation reaches 50% in the block-copolymer having the composition $x:y = 5:91$ (the molecular mass ratio is 2500:4000) and in terms of all their properties the block-copolymers having this composition approach an elastomer.[141]

Together with the synthesis of polycondensation block-copolymers containing block sequences of various heterochain polymers, block-copolymers based on block components comprising carbochain polymers have been synthesised. In particular, polyarylate-butadiene and polyarylate–arylene sulfone oxide–butadiene block-copolymers have been obtained and investigated using oligobutadiene and its derivatives as one of the block components.[142–144,147,148] Such construction of the polymer chain leads to new possibilities for the modification of polyarylate polymers. Thus it is known[12] that the deformation of

Table 6. Properties of the polyarylate-ethylene oxide block-copolymers $-OCR'CO(CH_2CH_2O)_yOCR'CO[OROC(O)R'CO]_xORO-$.

Composition of block-copolymers			η_{int}/dl g^{-1} (in $CHCl_3$)	σ/kgf cm^{-2}	ε (%)	E/kgf cm^{-2}
x	y	content of oligo-(ethylene oxide) (mass%)				
5	9	12.7	0.82	840	90	14000
5	14	17.9	0.98	800	110	9500
5	91	59.2	1.14	220	700	400
5	340	84.5	1.34[a]	90	5	3500
10	9	7.3	0.91	860	75	15000
10	14	10.6	0.96	880	94	13500
10	91	44.2	1.22	530	370	2000
10	340	74.8	1.45	200	15	4000
20	9	4.0	0.84	1000	110	17000
20	91	29.5	1.02	530	120	–
20	340	61.1	1.26	290	30	2800

[a] Molecular mass 70 000.

polyarylates takes place without the formation of a 'neck'. The appearance of a 'neck' has been observed in the deformation of polyarylate-butadiene block-copolymers containing up to 30% of polybutadiene blocks, which is associated with the increased mobility of the polyarylate phase owing to a kind of plasticisation of the latter by the polybutadiene blocks.[142]

We shall consider yet another type of polymer—carbaborane-containing polyarylates. The most interesting carbaborane-containing polyarylates have been synthesised from 1,2- and 1,7-bis(4-carboxyphenyl)carbaboranes combined with various bisphenols[216-229] or from 1,2-bis(4-hydroxyphenyl)-carbaborane (phenolcarbaborane) combined with the chlorides of various aromatic dicarboxylic acids.[230-233] These polyarylates have been synthesised by acceptor-catalytic and high-temperature polyesterification in solution.

Table 7 presents as an example data on the polyarylates derived from 1,2- and 1,7-bis(4-carboxyphenyl)carbaboranes. Polyarylates with diphenylcarbaborane fragments in the chain dissolve in a wide range of organic solvents. It must be emphasised that, in contrast to the usual cardo-polyarylates which are also readily soluble, many carbaborane-containing polyarylates exhibit a high solubility in solvents such as aromatic hydrocarbons (benzene, toluene, xylene), polyarylates derived from the less symmetrical and more polar isomer of bis(4-carboxyphenyl)-*o*-carbaborane being somewhat more soluble.[219] Like the usual polyarylates, strong colourless films can be obtained from the carbaborane-containing polyarylates by casting from solutions.

The softening temperatures of the polyarylates obtained from the *ortho*- and *meta*-isomers of bis(4-carboxyphenyl)carbaborane and dihydric phenols having the same composition are virtually identical under the conditions of a comparable phase state. The polyarylates derived from dihydric phenols of the cardo-type have the highest softening temperatures (340–360 °C).

In the case of a mononuclear dihydric phenol of the type of hydroquinone or a dinuclear one of the type of bis(hydroxyphenyl)propane the structure of the polyarylates derived from the more symmetrical *meta*-isomer of bis(4-carboxyphenyl)carbaborane is more ordered than that of the polyarylates of the *ortho*-isomer. Thus, whereas the polyarylate obtained from 1,2-bis-(4-carboxyphenyl)carbaborane and 2,2-bis(4-hydroxyphenyl)propane by acceptor-catalytic polycondensation is amorphous, the corresponding polymer based on the *meta*-isomer has a crystalline structure with a high degree of order. The polyarylates synthesised from 1,7-bis(4-carboxyphenyl)carbaborane and dihydric phenols of the cardo-type differ little from the analogous polymers based on the *ortho*-isomer as regards the degree of order. According to X-ray diffraction data, these polyarylates have a crystalline structure with an average degree of order.

The thermal properties of the polyarylates with the diphenylcarbaborane fragments in the chain described above have been considered in a number of studies.[217-219,221-225] According to the results of thermogravimetric analysis, in air the mass of the carbaborane-containing polyarylates begins to change at a temperature higher by 20–60 °C than for the usual polyarylates. Slower degradation processes are characteristic of the carbaborane-containing polyarylates and in a number of cases sections corresponding to the retardation or cessation of the degradation in the temperature range between 600 and 650 °C are observed on the thermogravimetric curve. The high 'coke' residue (from 50%

Table 7. The properties of polyarylates obtained by the acceptor-catalytic (A) and high-temperature (B) polycondensation of 1,2-bis-(4-carboxyphenyl)carbaborane (*ortho*) and 1,7-bis(4-carboxyphenyl)carbaborane (*meta*) with various dihydric phenols.

Dihydric phenol	Acid chloride	η_{int}/dl g^{-1} (in tetrachloroethane, 25 °C)		Softening temperature/°C[a]	σ/kgf cm^{-2}	ε (%)	Temperature of onset of decrease in mass/°C[b]	'Coke' residue on heating	
		A	B					to 900 °C[b]	to 400 °C[c]
Hydroquinone	*ortho*	0.6	–	320	brittle film		380	88	94
	meta	0.6	0.9	320	brittle film		380	85	91
Bis(4-hydroxy-phenyl) ether	*ortho*	0.6[d]	0.9	290	500	23	390	85	90
	meta	2.0	1.9	280	990	10	390	81	85
2,2-Bis(4-hydroxy-phenyl)-propane	*ortho*	0.9	–	290	570	4	400	62	96
	meta	0.6	2.3	320	650	2	420	50	86
9,9-Bis(4-hydroxy-phenyl)-fluorene	*ortho*	0.9	2.3	350	680	4	420	60	95
	meta	1.3	1.2	360	1050	5	400	58	90
9,9-Bis(4-hydroxy-phenyl)-10-anthrone	*ortho*	0.9	–	350	470	–	410	70	96
	meta	1.1	0.7	340	920	4	400	–	98
Phenolphthalein	*ortho*	1.2	–	350	570	2	400	78	98
	meta	2.0	2.4	340	1100	7	400	80	98

Remarks. All the polymers A were obtained in the presence of triethylamine in acetone over a period of 1 h at 45–50 °C. The polymers B were obtained in α-chloronaphthalene over a period of 10–16 h at 220 °C. The yields of the polymers were nearly quantitative. All the properties other than η_{int} are quoted for polymers obtained by method A.

[a] The temperature corresponding to the point of intersection of the tangents to the thermomechanical curve in the region of the onset of flow for a load of 0.8 kgf cm^{-2} was adopted as the softening temperature.

[b] The temperature was determined from the thermogravimetric curve at a heating rate of 4.5 °C per minute in air.

[c] Isothermal conditions in air over a period of 3 h.

[d] The molecular mass, determined by the light scattering method, was 116000.

to ~90% relative to the initial mass of the polymer), characteristic of the bis(4-carboxyphenyl)carbaborane polyarylates when the latter are heated in air to 900 °C should also be mentioned, as the usual polyarylate burns completely at 650–700 °C.

This difference is manifested even more clearly when carbaborane-containing polyarylates and the polyterephthalate of phenolfluorene are heated under isothermal conditions in air. Thus, after being heated at 400 °C for 3 h, the mass of the carbaborane-containing polyarylates (Table 7) diminishes by 2%–15%, whereas the polyterephthalate of phenolfluorene begins to decompose even before 400 °C is attained and the degree of decomposition increases monotonically, reaching 35% of the initial mass after 3 h.

Under an inert atmosphere, the mass of all the bis(4-carboxyphenyl)carbaborane polyarylates begins to change at the same temperature as in air, while the 'coke' residue amounts to ~80%–90% after thermal degradation, in many instances actually at higher temperatures than on heating in air.[219]

An appreciably lower content of carbon oxides and a high content of hydrogen in the gaseous products together with a lower degree of decomposition are characteristic of the thermal degradation processes involving polyarylates with diphenylcarbaborane fragments (compared with the usual polyarylates).[217,223,224] This difference is more striking for polyarylates with *o*-carbaborane groups in the chain. The evolution of hydrogen at comparatively low temperatures and with a low activation energy (~20 kcal mol^{-1}) and the results of the analysis of the thermal behaviour of compounds modelling fragments of the molecules of carbaborane-containing polyarylates and the products of the possible reactions led to the assumption that this phenomenon is due to heterolytic and not homolytic processes. The carbaborane ring exerts a stabilising influence on the thermal stability of the ester linkage. It has been noted that the thermal decomposition of the polyarylate obtained from bis-(4-carboxyphenyl)-*o*-carbaborane and phenolfluorene proceeds via two mechanisms: heterolytic reactions predominate up to 450 °C, whilst radical processes predominate at higher temperatures.[223]

Derivatives of dicarbaundecaborate have been detected in the products of the thermal degradation of carbaborane-containing polyarylates and the corresponding model systems in the presence of nucleophiles, including water.[221,223] This suggests that water, a certain amount of which is always present in polymers, behaves as a nucleophile disrupting the carbaborane ring to form the dicarbaundecaborate anion in the first stage of the degradation of the carbaborane-containing polyarylate. The consumption of water in this reaction with the carbaborane ring rules out the hydrolysis of the ester linkage, which plays the main role in the initial stage of the degradation of the usual polyarylates. This promotes in the case of the carbaborane-containing polyarylates the retention of the weak polyarylate link (the ester group) at higher temperatures.

Comparative study of the thermal and thermooxidative degradation of the 1,2-bis(4-carboxyphenyl)carbaborane–phenolfluorene polyarylate and the polyterephthalate of phenolfluorene revealed yet another characteristic feature of the behaviour of these polymers.[222] In vacuo, the onset of gel formation occurs sooner in the case of the *o*-carbaborane-containing polymer and a 100% degree of reaction is attained already at 350 °C, whereas the gel content in the case of the terephthalic acid polyarylate is only 2.7%. Under oxidation conditions, the *o*-carbaborane-containing polyarylate begins to lose its solubility much sooner and is fully cross-linked already at 275 °C, whereas the terephthalic acid polyarylate contains only 30% of the gel even at 350 °C.

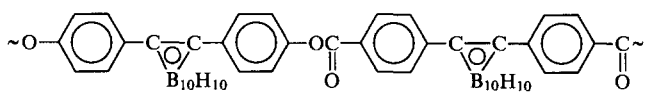
In the synthesis of polyarylates based on phenolcarbaborane and the chlorides of terephthalic, isophthalic, biphenyl-4,4′-carboxylic oxybis(benzene-4-carboxylic), and diphenylphthalide-4,4′-dicarboxylic acids, polyarylates with relatively high intrinsic viscosities were obtained only in the last two cases (0.92 and 0.62 dl g^{-1} respectively in tetrachloroethane).[230] Regardless of the conditions in the synthesis, the polyarylates derived from these dicarboxylic acids have an amorphous structure, whereas the terephthalic and biphenyl-4,4′-dicarboxylic acid polyarylates, obtained by high-temperature polycondensation, have a crystalline structure with a high degree of order according to X-ray diffraction data and are insoluble. The polymer obtained from isophthalic acid, which is less ordered and more soluble, occupies an intermediate position, but it too was obtained with low intrinsic viscosities of the solutions (0.20–0.31 dl g^{-1} in tetrachloroethane). In all cases, these polymers precipitated during polycondensation even for low degrees of conversion and subsequent polycondensation could take place only under heterogeneous conditions. The limited solubility, caused by the crystallisation of the polymers during their formation, is apparently the reason for their low molecular mass.

In comparing the properties of polyarylates derived from phenolcarbaborane polyarylates based on its carboxyl analogue — 1,2-bis(4-carboxyphenyl)carbaborane — one should note that the latter are readily soluble and are amorphous or are comparatively little ordered when dihydric phenols such as hydroquinone, 2,2-bis(4-hydroxyphenyl)propane, and bis(4-hydroxyphenyl) ether are used. Conversely, they are more ordered when dihydric cardo-phenols are employed: phenolphthalein, phenolfluorene, and phenolanthrone.[231] The softening temperatures of the amorphous polyarylates obtained by the polycondensation of phenolcarbaborane with oxybis(benzene-4-carboxylic) and diphenylphthalide-4,4′-dicarboxylic acids are 275 and 330 °C. The isomeric amorphous polyarylate obtained from 1,2-bis(4-carboxyphenyl)carbaborane and bis(4-hydroxyphenyl) ether softens at 290 °C, i.e. whether the *o*-carbaborane group is linked to the hydroxyphenyl or carboxyphenyl residues is immaterial as regards the softening temperatures of the amorphous polyarylates with an isomeric structure.

Under the conditions of dynamic thermogravimetric analysis, the mass of phenolcarbaborane polyarylates begins to change at 350–400 °C in air and at 360–410 °C in an inert medium. All these polymers contain a large 'coke' residue on heating to 900 °C both in air (70%–85%) and in an inert medium (85%–90%).

A polyarylate the polymer chain of which was made up only of alternating ester and 1,2-diphenylcarbaborane fragments has been synthesised by the polycondensation of 1,2-bis(4-hydroxyphenyl)-carbaborane with the acid chloride of 1,2-bis(4-carboxyphenyl)-carbaborane (Scheme 8).[232]

Scheme 8



It was found that, regardless of whether the polymer was synthesised by acceptor-catalytic polycondensation in acetone in the presence of triethylamine or by high-temperature polycondensation in chlorinated biphenyl or α-chloronaphthalene, the polymer formed had a crystalline structure (degree of crystallinity is 35%–55%) and was insoluble in any of the solvents known for polyarylates with the exception of tetrahydrofuran. The polymers obtained by high-temperature polycondensation in α-chloronaphthalene at 220 °C over a period of 15–18 h have the highest crystallinity. As already mentioned, by varying the polycondensation condition and also the subsequent treatment of the polymer, it is possible to alter its physical structure. Thus it has been observed that, after reprecipitation from solution in tetrahydrofuran in cold water or methanol, the polymer becomes amorphous and soluble in solvents such as chloroform, tetrachloroethane, cyclohexanone, and benzene. Depending on the degree of conversion into the amorphous form, the polymers soften at 260–290 °C, whereas the crystalline specimens do not melt up to 400 °C. Above this temperature, their thermal degradation begins.

Interesting results have been obtained in the study of the thermal stability of the polyarylate obtained from phenolcarbaborane and 1,2-bis(4-carboxyphenyl)carbaborane with different degrees of crystallinity [232,233] under the conditions of dynamic thermogravimetric analysis in air, under an inert atmosphere, and also under isothermal conditions at 400 °C for 3 h.

The highest-melting specimen usually has the highest thermal stability among polymers of the same or similar chemical structure which pass to the highly elastic or fused state at different temperatures. This can be accounted for by the diffusional inhibition of the degradative processes in the solid phase of the polymer. The opposite behaviour has been observed for the carbaborane-containing polyarylate considered: under the conditions of both dynamic (in the temperature range 400–500 °C) and isothermal (400 °C, 3h) thermogravimetric analysis, the specimen converted into the amorphous form exhibits the smallest weight loss.

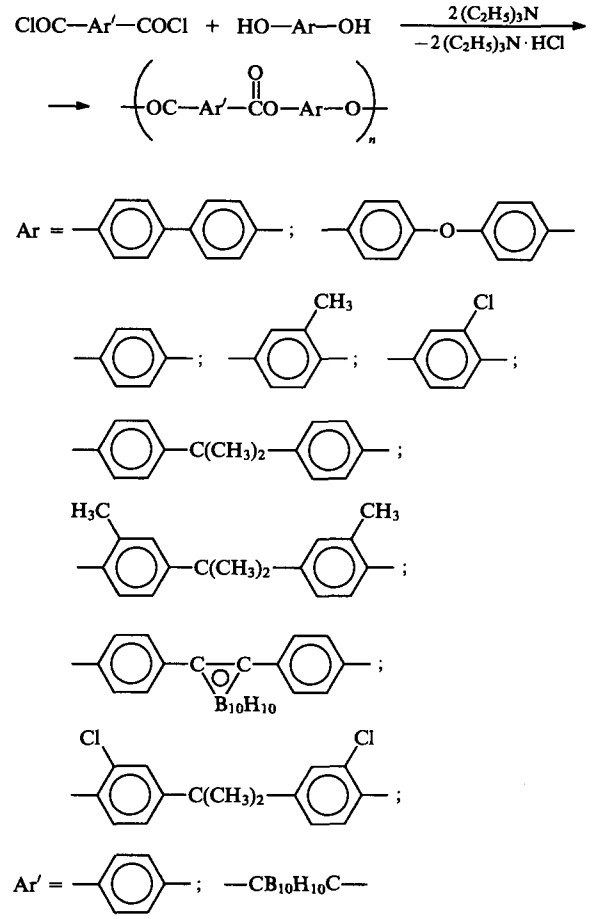
With increase in the degree of crystallinity of the polymer, the weight loss increases in all cases. Thus the mass of the specimen converted into the amorphous form does not change up to 650 °C, while the mass of the crystalline polymers diminishes already at 400 °C. It has been suggested that the different types of behaviour on heating of the crystalline carbaborane-containing polyarylate specimen and the specimen converted into the amorphous form may be caused by the difference between their molecular mobilities in the range 280–380 °C. [233] The increased thermal stability of the amorphous polymer with a relatively low softening temperature is caused either by the enhanced stabilising influence of the carbaborane groups in the polymer melt or by the formation of thermally more stable secondary structures as a result of the interaction of the carbaborane groups, the occurrence of which in the melt or in the highly elastic state is facilitated. In highly crystalline polymers with a high melting point, the manifestation of these effects is evidently hindered. [232]

The possibility of obtaining organoelement liquid crystal polymers from carbaborane-containing polyarylates has recently attracted the attention of investigators. [146,210,211,234]

Thus the polyarylates whose structures are presented in Schemes 9 and 10 have been obtained [146,234,235] by acceptor-catalytic polycondensation from bis(4-hydroxyphenyl)-*o*-carbaborane, the chloride of carbaborane-*m*-dicarboxylic acid (as the carbaborane-containing components), terephthalic acid chlorides, and various bisphenols.

The properties of carbaborane-containing polymers such as retarded thermal and thermo-oxidative degradation, effective mechanical properties, and high yields of the 'coke' residues in the products on heating, due to the involvement of the carbaborane fragments in the formation of three-dimensional structures, constitute a positive factor in the creation of thermostable and heat resistant materials. [229] Therefore one of the approaches to the preparation of new copolyarylate liquid crystal carbaborane-containing structures with an improved thermal stability involves the introduction of carbaborane-*m*-dicarboxylic acid and phenylcarbaborane fragments into the structures of various homo- and copolyarylates.

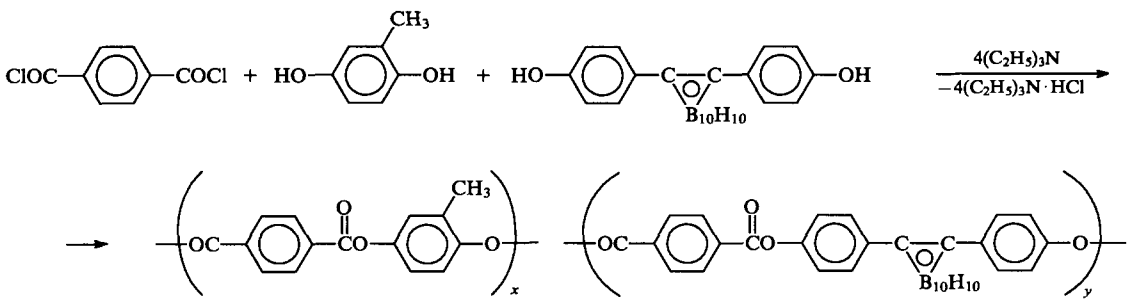
Scheme 9



The study of the properties of the polymers and copolymers obtained showed that, on passing from the high-melting polyterephthalate of 4,4′-dihydroxybiphenyl (does not melt up to 500 °C) to the carbaborane-*m*-dicarboxylic acid copolyarylates (i.e. on replacing some of the terephthalic acid units by the carbaborane-*m*-dicarboxylic acid units in the polyarylate structure), the softening temperature of the polymer falls appreciably (to 140 °C). A solid–liquid crystal transition (the temperature range of the mesophase is 260–350 °C) then appears in the copolymer with a molar content of the carbaborane-*m*-dicarboxylic acid (relative to the sum of the dicarboxylic acids) of 90 mol.% at 260 °C. On the other hand, the complete replacement of terephthalic acid residues by carbaborane-*m*-dicarboxylic acid residues in the polyester structure leads to the formation of poly(4,4′-dihydroxybiphenyl carbaborane-*m*-dicarboxylate) with a softening temperature of 240 °C and lacking liquid crystal properties.

The introduction of carbaborane-*m*-dicarboxylic acid fragments into the structure of the polyterephthalates of 2,2-bis-(4-hydroxyphenyl)propane, hydroquinone, or their chloro- or

Scheme 10



methyl-substituted derivatives leads to an appreciable decrease in the softening temperatures of the polymers. The presence or absence of the mesophase in the three-component copolyarylate structures depends on their quantitative content of carbaborane-*m*-dicarboxylic acid fragments. For example, the copolyarylate based on chlorohydroquinone and the chlorides of terephthalic and carbaborane-*m*-dicarbocyclic acids, introduced into the reaction in molar proportions of 1:0.8:0.2, has a softening temperature of 220 °C and the temperature range of the mesophase is 250–350 °C. In the case of four-component copolyarylates containing hydroquinone, 2,2-bis(4-hydroxyphenyl)-propane, and their chloro- or methyl-substituted derivatives, the introduction of small amounts of carbaborane-*m*-dicarboxylic acid (for example, 20 mol.%) leads to the loss of liquid crystal properties by the copolyarylates.

Table 8 presents as an example data on the homo- and co-polytetraphthalates of chlorohydroquinone and bis(4-hydroxyphenyl)-*o*-carbaborane.

It is noteworthy that the copolyterephthalates based on chlorohydroquinone and hydroxyphenylcarbaborane have lower softening temperatures than the copolyterephthalate of hydroquinone and hydroxyphenylcarbaborane owing to the introduction into the polymer structure of asymmetrically constructed fragments in the form of chlorohydroquinone residues. The transition to the mesophase occurs at a higher temperature the smaller the amount of hydroquinone introduced into the copolymer structure.

The temperature corresponding to the formation of the mesophase in carbaborane-containing copolyarylates based on hydroxyphenylcarbaborane shifts towards higher values (by 70–80 °C) compared with the copolyarylates containing carbaborane-*m*-dicarboxylic acid fragments.

The liquid crystal properties of carbaborane-containing copolyarylates based on asymmetric monomers having, as it were, a 'head' and a 'tail', in particular chlorohydroquinone and methylhydroquinone, are influenced not only by the ratio of the initial components in the copolymer structure but also by the microstructure of the copolymer: the sequence in which the comonomers alternate in the polymer chain and the direction in which the 'heads' and 'tails' of the asymmetric monomer are arranged. Thus, among the copolymers obtained from methylhydroquinone and the chlorides of terephthalic and carbaborane-*m*-dicarboxylic acids in molar proportions of 1.0:0.4:0.6[146] only those with a block structure are capable of undergoing a transition to a liquid crystal melt.

In order to investigate the effect of thermal influences on the structure and properties of copolymers containing carbaborane-*m*-dicarboxylic acid units, the copolyterephthalate of chlorohydroquinone carbaborane-*m*-dicarboxylate, containing 20 mol.% of carbaborane-*m*-dicarboxylic acid, was heated in air at 200 °C for 6 h. It was then found that the specimen retained its original composition, structure, and properties after the heat treatment.[146]

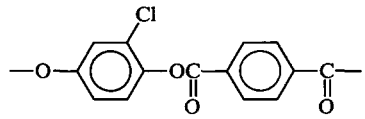
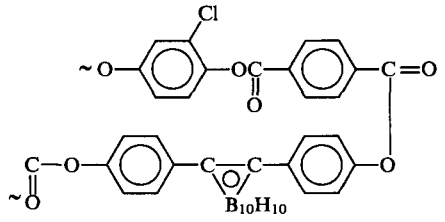
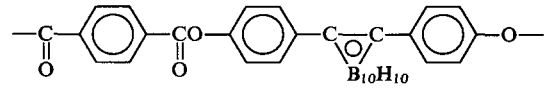
According to the results of a thermogravimetric study, chlorohydroquinone polyterephthalate decomposes totally in air at 600 °C (heating rate 5 °C min^{-1}), while the copolyarylate containing 20 mol.% of carbaborane-*m*-dicarboxylic acid affords a 65% yield of the 'coke' residue at the same temperature; the 'coke' residue of the copolyarylate containing 60 mol.% of carbaborane-*m*-dicarboxylic acid is 80%. Thus the presence of the carbaborane nucleus has a positive effect on the thermal properties of the liquid crystal copolyarylates obtained.

Together with their influence on the thermal characteristics, the carbaborane fragments in the macromolecules also alter the solubilities of the polymers. Thus the presence of 20 and 50 mol.% of carbaborane-*m*-dicarboxylic acid fragments (relative to the total acids) in the structure of the insoluble methylhydroquinone polyterephthalate led to the formation of soluble copolyarylates. Similarly, the introduction of bis(4-hydroxyphenyl)-*o*-carbaborane fragments into the structure of insoluble polyterephthalates of hydroquinone and its chloro- and methyl-substituted derivatives promotes an improvement in solubility and all the copolyarylates indicated are soluble in organic solvents.[146,234]

Thus the presence of carbaborane-containing fragments in the polymer structures lowers the softening temperatures of the copolyarylates and the temperatures corresponding to the transition to the liquid crystal state, improves their thermal properties, and helps to make them soluble.

It is useful to carry out further studies on carbaborane-containing liquid crystal polyarylates in order to establish the possibility of detecting the mesophase in the polymer on heating to 250 °C and above as a result of the thermal transformations of the *o*- and *m*-carbaborane nuclei which lead to the formation of a three-dimensional cross-linked structure.[229]

Table 8. The results of the synthesis and of the study of the properties of homo- and co-polyterephthalates of chlorohydroquinone and bis(4-hydroxyphenyl)-*o*-carbaborane.

Structure of homo- and co-polyarylates	Molar monomer ratio	η_{int}/dl g^{-1}	X-Ray diffraction data	T_{decomp}/ °C	Temperature range of mesophase/ °C
	1.0:1.0	insoluble	crystalline	160	none
	0.6:1.0:0.4	0.34	weakly-crystalline	195	230–400
	0.5:1.0:0.5	0.37	"	200	235–400
	0.4:1.0:0.6	0.40	"	210	245–400
	1.0:1.0	0.15	amorphous	215	none

The syntheses and properties of polyarylates of different structure were examined above and it was shown that the most promising method for their synthesis is the polycondensation of dicarboxylic acid chlorides with bisphenols carried out in different versions. However, attempts have been made to obtain polyarylates also in other ways.[146]

The new methods for synthesis of polyarylates include their preparation by the method of 'carbonylation' polycondensation resulting from the use of carbon monoxide and aromatic dihalocompounds combined with bisphenols in the presence of palladium catalysts, in place of the traditional dicarboxylic acids or their derivatives, as the acid component in the polycondensation process. Thus polyarylates with average intrinsic viscosities have been obtained by the reaction of 2,2-bis-(4-hydroxyphenyl)propane (or other bisphenols), bis(4-bromophenyl) ether, and carbon monoxide in the presence of palladium catalysts at 115 °C in chlorobenzene.[236-241]

The synthesis of polyarylates was also tried by comparatively new polycondensation methods such as 'direct',[69,146,242-258] 'activated',[69,146,259,260] and 'silylated'[146,261-271] polycondensation.

The 'direct' polycondensation leads to the possibility of carrying out the polycondensation process directly between the dicarboxylic acid (and not its derivatives) and the bisphenol in solution at a moderate temperature by employing special condensing agents (for example, triphenylphosphine dichloride, arenesulfonyl chloride, or hexachlorocyclotriphosphazene frequently in combination with other compounds).

The 'activated' polycondensation is based on the activation of the process by employing in the latter monomers having the appropriate structure [for example bis(2,5-dinitrophenyl) isophthalate or adipate, bis(pentachlorophenyl) isophthalate, etc.], containing groups which activate the terminal functional groups of the monomer in the part of the molecule which enters into the composition of the low-molecular-mass product during polycondensation and does not participate in the construction of the chain. This method makes it possible to carry out the process under comparatively mild conditions and is characterised by little tendency towards side reactions.

The 'silylated' polycondensation is based on the use of silylated nucleophilic monomers, in particular bisphenols and carboxylic hydroxyacids, as the starting materials in the polycondensation process. The silylation of the monomers leads to the possibility of altering their reactivity, frequently increasing it appreciably. The employment of silylated monomers instead of 'free' monomers makes it possible in a number of instances to carry out the polycondensation process under milder conditions, avoiding undesirable side reactions. However, in many cases the new methods do not lead to the desired results. There is no doubt that they still require further development and improvement.

III. Applications of polyarylates

Polyarylates are worked to produce articles by cast moulding, moulding under pressure, extrusion, vortical sputtering and, in the case of soluble polyarylates, also by employing their solutions.[11,56,214,272-278]

It was found that an infusible and insoluble polyarylate such as econol, can be used successfully to produce monolithic articles by sintering at 425–450 °C under a pressure of 350–1400 kgf cm^{-2} and also by high-speed forging. Econol coatings can be obtained by a plasma method (in a helium atmosphere).

The high heat resistance of polyarylates combined with their effective strength parameters have led to extensive possibilities for the use of these polymers as constructional articles (components for automation and other mechanisms); by virtue of their effective insulating properties, they are used successfully in radio engineering and electrical engineering (shells for coils, plugs, disconnecting devices, etc.) and in the electronic industry.[11,56,273,277,279,280]

Heat-resistant polyarylate films are obtained by extrusion or casting from solution and are used as electrically insulating materials. Polyarylates are also employed for the preparation of varnishes. By virtue of their high solubility and compatibility with various polymers, cardo- and other polyarylates are used successfully for the preparation of valuable composite materials.

For example, oligoepoxide-polyarylate compositions are used as casting compounds, sealing coatings, binders for reinforced plastics, etc. They exhibit enhanced heat resistance (~250 °C); the ultimate compressive strength of such systems reaches 800 kgf cm^{-2} and the ultimate bending strength is up to 1700–2000 kgf cm^{-2}, which is almost twice as high as the analogous parameters of systems hardened without using polyarylates.[309] In terms of their properties, such compositions are not inferior to materials containing mineral fillers and, in terms of a series of parameters, they are superior to them. Thus they are distinguished by a significantly higher specific gravity (by ~40%) and a high capacity to resist repeated thermal shocks following changes in temperature from −60 to 250 °C.

The introduction of a polymer such as the terephthalic acid–phenolphthalein polyarylate into an epoxide composition leads to the formation of not only strong and lighter materials but also of materials capable of being employed over a wide range of temperatures and loads.[310,311] The study of the properties of oligoepoxide-polyarylate compositions has demonstrated the extensive possibilities for the regulation of the mechanical properties of these network systems, including those associated with vibroabsorption.[310,312,313] Materials based on oligoepoxide polyarylate compositions exhibit a low creep when subjected to high loads.[313]

Filled materials such as antifriction products, which have a low coefficient of friction and can be employed for a long time without a lubricant at high temperatures (250 °C), *in vacuo*, and for high velocity gradients between friction surfaces (sliding and roller bearings) are also obtained from polyarylates. It has been suggested that highly heat-resistant antifriction self-lubricating coking plastics, ensuring the operation of dry friction units at temperatures in the range 350–500 °C, be prepared by employing in such plastics carbaborane-containing polymers including carbaborane-containing polyarylates which can be converted during preparation into a high-strength coke, constituting a sterically structured polymeric system, without altering the initial mass and shape of the article.[229,314-316]

For example, heat-treated materials comprising carbaborane-containing polyarylates [obtained from the acid chloride of 1,2-bis(4-carboxyphenyl)carbaborane and phenolfluorene or 1,2-bis(4-hydroxyphenyl)carbaborane] and graphite have the following physicomechanical parameters: coefficient of friction 0.05–0.09, intensity of linear wear $(2.5-5) \times 10^{-9}$, and limiting working temperature 500 °C.

It has been noted that compositions containing polyarylate, polyester imide, and a filler are technologically suitable for moulding and the preparation of impact-resistant articles.[281] The glass-reinforced polyarylates based on 2,2-bis(4-hydroxyphenyl)-propane and mixtures of terephthalic and isophthalic acid chlorides containing also a mineral filler possess a valuable set of properties.[290] Impact-resistant compositions with improved low-temperature properties (worked on a casting machine), which are used to manufacture motorcar components, are obtained from mixtures of polyarylates with poly(alkylene terephthalates) and other polymers.[292] Electrically conducting transparent polymer compositions have been developed. They were obtained by the crystallisation in situ of tetraselenatetracene chloride in a polyarylate matrix.[299]

It is noteworthy that filled polyarylate materials can be obtained not only by processing finished polyarylates with a filler but also directly during the synthesis of the polymer by polycondensation in the presence of fillers, which may play the role of a homogeneous or heterogeneous matrix.[270,317-320] For example,

mixtures of polyterephthalates of 2,2-bis(3-chloro-4-hydroxyphenyl)propane with graphite, obtained by polycondensation, are superior to blends obtained by the mechanical mixing of a finished polyarylate with a filler in terms of many properties (thermal characteristics, specific impact stength, specific electrical resistance, and a lower coefficient of friction).

The solubility of cardo-polyarylates leads to the possibility of their successful conversion from a solution into films and fibrous materials, which are used for the purification of gases and liquids and for the trapping of aerosols. Depending on the operating conditions, such filter materials can be employed at temperatures up to 300 °C.[11,56]

Polycondensation block-copolymers with a polyarylate base also possess useful properties.[56,145,146] Thus films of polyarylate-siloxane block-copolymers of the Silar type have a valuable set of physicomechanical and gas-separating properties. Their tensile strength reaches 500 kgf cm^{-2} in many cases. They possess a high elasticity and permeability to gases, the latter approaching that of polydimethylsiloxane, but their mechanical strength is higher than that of the latter material. This leads to the successful employment of such polymers in engineering and medicine (for example, as membrane gas oxygenators).

Polyarylate-arylene sulfone oxides with a small content of arylene sulfone oxide (~15%) exhibit a high heat resistance, which is close to that of polyarylates, but the viscosity of their melts is appreciably lower than that for the latter compounds, which significantly facilitates the working of such block-copolymers. Heat-resistant (prolonged heat resistance at 200–230 °C) polyarylate-arylene sulfone oxide cast thermoplastics, designed for constructional and electrical insulating purposes, can be used for the manufacture of articles for electronic engineering electrically insulating materials, and components subjected to appreciable loads at elevated temperatures.[136]

* * *

The foregoing review shows that polyarylates constitute an extremely promising class of polymers, which can be used successfully in many branches of engineering where a high heat resistance, photostability, and effective electrical insulating, mechanical, etc. parameters are needed.

The knowledge of the characteristic features of the formation of polyarylates and of the relation between their structure and properties leads to extensive prospects for the specific design of the polyarylate chain and hence for imparting a set of desired properties to such polymers.

This review has been written with the financial support of the Russian Fundamental Research Fund (grant 94-03-4288).

References

1. J G Lussak, J Pelouze *Annalen* **7** 40 (1833)
2. W Heintz *Jahresber.* 144 (1861)
3. V V Korshak, S V Vinogradova *Geterotsepnye Poliefiry* (Heterochain Polyesters (Moscow: Izd. Akad. Nauk SSSR, 1958)
4. V V Korshak, S V Vinogradova *Polyesters* (Oxford: Pergamon Press, 1965)
5. A Einhorn *Annalen* **300** 135 (1898)
6. H Schnell *Angew. Chem.* **68** 633 (1956)
7. H Schnell *Chemistry and Physics of Polycarbonates* (New York: Interscience, 1964)
8. A Conix *Belg. Chem. Ind.* **22** 1457 (1957)
9. V V Korshak, S V Vinogradova *Izv. Akad. Nauk SSSR, Ser. Khim.* 637 (1958)
10. M Levine, S C Temin *J. Polym. Sci.* **28** 179 (1958)
11. V V Korshak, S V Vinogradova *Poliarilaty* (Polyarylates) (Moscow: Nauka, 1964)
12. A A Askadskii *Fiziko-Khimiya Poliarilatov* (Physical Chemistry of Polyarylates) (Moscow: Khimiya, 1968)
13. V V Korshak, S V Vinogradova *Usp. Khim.* **30** 421 (1961) [*Russ. Chem. Rev.* **30** 171 (1961)]
14. V V Korshak, S V Vinogradova *Uspekhi Khimii Polimerov* (Advances in Polymer Chemistry) (Moscow: Khimiya, 1966)
15. B D Dean, M Matzer, J M Tibbitt, in *Comprehensive Polymer Science. The Synthesis, Characterization, Reactions and Application of Polymers* Vol. 5 (New York: Pergamon Press, 1989) p. 317
16. US P. 3 160 602; *Chem. Abstr.* **62** 5 415E (1965)
17. US P. 4 093 595; *Ref. Zh. Khim.* 6 S 359 (1979)
18. US P. 4 318 841; *Ref. Zh. Khim.* 3 T 679 (1983)
19. Jpn. Appl. 1-156 321; *Ref. Zh. Khim.* 17 S 630P (1990)
20. Jpn. Appl. 1-149 826; *Ref. Zh. Khim.* 23 S 594P (1990)
21. H R Kricheldorf, J Erxleben *Polymer* **31** 944 (1990)
22. Jpn. Appl. 1-294 731; *Ref. Zh. Khim.* 1 S 490P (1991)
23. H-B Tsai, C Lee, N-S Chang, S-J Chang, N-S Chen *Makromol. Chem.* **191** 1301 (1990)
24. US P. 4 895 928; *Ref. Zh. Khim.* 5 T 65P (1991)
25. Jpn. Appl. 2-60 920; *Ref. Zh. Khim.* 16 S 520P (1991)
26. US P. 4 958 000; *Ref. Zh. Khim.* 16 S 517P (1991)
27. US P. 4 959 449; *Ref. Zh. Khim.* 18 S 498P (1991)
28. Jpn. Appl. 2-208 319; *Ref. Zh. Khim.* 22 S 501P (1991)
29. Jpn. Appl. 2-138 334; *Ref. Zh. Khim.* 20 S 607P (1991)
30. US P. 4 957 996 SShA; *Ref. Zh. Khim.* 20 S 606P (1991)
31. BRD Appl. 3 918 690; *Ref. Zh. Khim.* 1 S 434P (1991)
32. W M Eareckson *J. Polym. Sci.* **40** 399 (1959)
33. V V Korshak, S V Vinogradova *Neravnovesnaya Polikondsensatsiya* (Nonequilibrium Polycondensation) (Moscow: Nauka, 1972)
34. S V Vinogradova, in *Progress Polimernoi Khimii* (Progress in Polymer Chemistry) (Moscow: Nauka, 1969) p. 113
35. V V Korshak, S V Vinogradova *Vestn. Akad. Nauk SSSR* (6) 72 (1965)
36. V V Korshak, S V Vinogradova, P M Valetskii, Yu V Mironov *Vysokomol. Soedin.* **3** 66 (1961)
37. S V Vinogradova, V V Korshak, P M Valetskii, Yu V Mironov *Izv. Akad. Nauk SSSR, Ser. Khim.* 70 (1966)
38. R S Velichkova, V V Korshak, S V Vinogradova, V I Ivanov, A P Ponomarenko, N S Enikolopov *Izv. Akad. Nauk SSSR, Ser. Khim.* 858 (1969)
39. S V Vinogradova, V V Korshak, V A Pankratov, D R Tur *Dokl. Akad. Nauk SSSR* **164** 563 (1965)
40. V V Korshak, S V Vinogradova, P M Valetskii, A N Baskakov *Dokl. Akad. Nauk SSSR* **174** 849 (1967)
41. S V Vinogradova, V V Korshak *Dokl. Akad. Nauk SSSR* **123** 848 (1958)
42. S V Vinogradova, V V Korshak, G Sh Papava, N A Maisuradze, R S Velichkova *Izv. Akad. Nauk SSSR, Ser. Khim.* 820 (1970)
43. S V Vinogradova, V V Korshak, Yu V Mironov, P M Valetskii *Izv. Akad. Nauk SSSR, Ser. Khim.* 245 (1966)
44. V V Korshak, I A Gribova, M A Andreeva *Vysokomol. Soedin.* **2** 427 (1960)
45. D Israilov, L A Rodivilova, M S Akutin *Plast. Massy* (9) 13 (1966)
46. V V Korshak, S V Vinogradova, G Sh Papava *Izv. Akad. Nauk SSSR, Ser. Khim.* 132; 149; 1296 (1964)
47. V V Korshak, S V Vinogradova, G Sh Papava, P D Tsiskarishvili *Dokl. Akad. Nauk SSSR* **156** 368 (1964)
48. S V Vinogradova, V V Korshak, G Sh Papava, P D Tsiskarishvili *Vysokomol. Soedin.* **8** 131 (1966)
49. S V Vinogradova, V V Korshak, G Sh Papava, P D Tsiskarishvili *Izv. Akad. Nauk SSSR, Ser. Khim.* 895 (1967)
50. G Sh Papava, B D Ageladze, P D Tsiskarishvili, V V Korshak, S V Vinogradova *Soobshch. Akad. Nauk GSSR* **18** 593 (1966)
51. G Sh Papava, N A Maisuradze, P D Tsiskarishvili, V V Korshak, S V Vinogradova *Soobshch. Akad. Nauk Gruz. SSR* **18** 349 (1966)
52. V V Korshak, S V Vinogradova, P M Valetskii *Vysokomol. Soedin.* **4** 987 (1962)
53. V V Korshak, S V Vinogradova, P M Valetskii, V A Ershova, V A Pankratov *Chem. Prum.* **13**(38) 265 (1963)
54. V V Korshak, S V Vinogradova, P M Valetskii, Ju V Mironov *Chem. Prum.* **13**(38) 489 (1963)
55. USSR P. 184 447; *Byull. Izobret.* **15** 89 (1966)
56. S V Vinogradova, in *Tekhnologiya Plasticheskikh Mass* (Technology of Plastics) (Moscow: Khimiya, 1985) p. 344
57. P W Morgan *Condensation Polymers by Interfacial and Solution Methods* (New York: Interscience, 1965)

58. V V Korshak, S V Vinogradova, A S Lebedeva *Vysokomol. Soedin.* **2** 61; 977; 1162 (1960); **3** 1117 (1961); **4** 968 (1962); **5** 674 (1963)
59. USSR P. 134 857; *Byull. Izobret.* **1** 43 (1961)
60. USSR P. 138 381; *Byull. Izobret.* **10** 45 (1961)
61. USSR P. 183 386; *Byull. Izobret.* **13** 77 (1966)
62. V V Korshak, S V Vinogradova, M A Iskenderov *Vysokomol. Soedin.* **4** 345; 637 (1962)
63. H-B Tsai, J T Jeng, R-S Tsai *J. Appl. Polym. Sci.* **39** 471 (1990)
64. US P. 4 910 285; *Ref. Zh. Khim.* 4 S 563 (1991)
65. C-H Yang, Y Oishi, M-A Kakimoto, Y Imai *J. Polym. Sci.* **28** 1353 (1990)
66. US P. 4 927 904; *Ref. Zh. Khim.* 7 S 560P (1991)
67. H-B Tsai, Y-D Lee *J. Polym. Sci., Polym. Chem. Ed.* **25** 1505 (1987)
68. V A Vasnev, S V Vinogradova *Usp. Khim.* **48** 30 (1979) [*Russ. Chem. Rev.* **48** 16 (1979)]
69. V V Korshak, V A Vasnev, in *Comprehensive Polymer Science. The Synthesis, Characterization, Reaction and Applications of Polymers* Vol. 5 (Oxford: Pergamon Press, 1989) p. 143
70. V V Korshak, V A Vasnev, in *Comprehensive Polymer Science. The Synthesis, Characterization, Reactions and Applications of Polymers* Vol. 5 (Oxford: Pergamon Press, 1989) p. 167
71. US P. 2 035 578; *Chem. Abstr.* **30** 3542 (1936)
72. I F Morozov *Khim. Promst. (Moscow)* **11** 22 (1946)
73. USSR P. 140 990; *Byull. Izobret.* **17** 51 (1961)
74. V V Korshak, S V Vinogradova, S N Salazkin *Vysokomol. Soedin.* **4** 339 (1962)
75. S V Vinogradova, S N Salazkin, G Sh Chelidze, G L Slonimskii, A A Askadskii, K A Bychko, L I Komarova, I V Zhuravleva, V V Korshak *Plast. Massy* (8) 10 (1971)
76. S V Vinogradova, Ya S Vygodskii *Usp. Khim.* **42** 1225 (1973) [*Russ. Chem. Rev.* **42** 55 (1973)]
77. V V Korshak, S V Vinogradova, Ya S Vygodskii *J. Macromol. Sci., Rev. Macromol. Chem.* **11C** 45 (1974)
78. Ya S Vygodskii, S V Vinogradova, in *Khimiya i Tekhnologiya Vysokomolekulyarnykh Soedinenii (Itogi Nauki i Tekhniki)* (Chemistry and Technology of High-Molecular-Mass Compounds. Advances in Science and Engineering) (Moscow: Izd. VINITI, 1975) Vol. 17, p. 14
79. S V Vinogradova, in *Polymer Science Contemporary Themes* Vol. 2 (New Delhi: Tata McGraw-Hill, 1991) p. 658
80. V V Korshak, S V Vinogradova *Usp. Khim.* **37** 2024 (1968) [*Russ. Chem. Rev.* **37** 885 (1968)]
81. S V Vinogradova, S N Salazkin, V V Korshak, S V Bereza, B V Lokshin, L I Komarova *Vysokomol. Soedin., Ser. A* **9** 1792 (1967)
82. V V Korshak, S V Vinogradova, S N Salazkin, L I Komarova *Eur. Polym. J.* **10** 967 (1974)
83. V V Korshak *Termostoikie Polimery* (Heat-Resistant Polymers) (Moscow: Nauka, 1969)
84. USSR P. 203 891; *Byull. Izobret.* **21** 81 (1966)
85. S V Vinogradova, S N Salazkin, L A Beridze, A I Mzhel'skii, G L Slonimskii, A A Askadskii, V V Korshak *Izv. Akad. Nauk SSSR, Ser. Khim.* 931 (1969)
86. V V Korshak, S N Salazkin, L A Beridze, S V Vinogradova *Vysokomol. Soedin., Ser. A* **15** 841 (1973)
87. S V Vinogradova, V V Korshak, G Sh Papava, N A Maisuradze, P D Tsiskarishvili *Izv. Akad. Nauk SSSR, Ser. Khim.* 433 (1969)
88. V V Korshak, S V Vinogradova, G Sh Papava, N A Maisuradze, P D Tsiskarishvili *Soobshch. Akad. Nauk Gruz. SSR* **51** 301 (1968)
89. USSR P. 507 595; *Byull. Izobret.* **11** 77 (1976)
90. USSR P. 241 013; *Byull. Izobret.* **13** 91 (1969); US P. 3 480 597; BRD P. 1 620 929; Jpn. P. 620 275; Br. P. 1 196 128
91. USSR P. 172 492; *Byull. Izobret.* **13** 70 (1965)
92. V V Korshak, S V Vinogradova, G L Slonimskii, Ya S Vygodskii, S N Salazkin, A A Askadskii, A I Mzhel'skii *Vysokomol. Soedin., Ser. A* **10** 2058 (1968)
93. S V Vinogradova, S N Salazkin, L A Beridze, A I Mzhel'skii, A A Askadskii, G L Slonimskii, V V Korshak *Vysokomol. Soedin., Ser. A* **11** 27 (1969)
94. S V Vinogradova V V Korshak, S N Salazkin, L A Beridze, G L Slonimskii, A A Askadskii *Izv. Akad. Nauk SSSR, Ser. Khim.* 2554 (1969)
95. S V Vinogradova, S N Salazkin, L A Beridze, A I Mzhel'skii, A A Askadskii, G L Slonimskii, V V Korshak *Izv. Akad. Nauk SSSR, Ser. Khim.* 931 (1969)
96. G L Slonimskii, A A Askadskii, A I Mzhel'skii, V V Korshak, S V Vinogradova, S N Salazkin, L A Beridze *Vysokomol. Soedin., Ser. A* **11** 2265 (1969)
97. V V Korshak, S V Vinogradova, V G Danilov, L A Beridze, S N Salazkin *Vysokomol. Soedin., Ser. B* **12** 129 (1970)
98. S V Vinogradova, L A Beridze, T M Pavlova, S N Salazkin, V V Korshak *Vysokomol. Soedin., Ser. B* **13** 681 (1971)
99. V V Korshak, S N Salazkin, L A Beridze, S V Vinogradova *Vysokomol. Soedin., Ser. A* **15** 841 (1973)
100. V V Korshak, S V Vinogradova, V G Danilov, S N Salazkin *Dokl. Akad. Nauk SSSR* **202** 1076 (1972)
101. S A Pavlova, L V Dubrovina, N B Klimanova, S N Salazkin *Vysokomol. Soedin., Ser. B* **19** 175 (1977)
102. A A Askadskii *Struktura i Svoistva Teplostoikikh Polimerov* (The Structure and Properties of Heat-Resistant Polymers) (Moscow: Khimiya, 1981)
103. USSR P. 159 030; *Byull. Izobret.* **23** 54 (1963)
104. USSR P. 176 401; *Byull. Izobret.* **22** 58 (1965)
105. S V Vinogradova, V V Korshak, S N Salazkin, S B Bereza *Vysokomol. Soedin.* **6** 1403 (1964)
106. P W Morgan *J. Polym. Sci., Part A* **2** 437 (1964)
107. USSR P. 231 120; *Byull. Izobret.* **35** 86 (1968)
108. V V Korshak, S V Vinogradova, V A Pankratov *Dokl. Akad. Nauk SSSR* **181** 1393 (1968)
109. V V Korshak, S V Vinogradova, V A Pankratov *Plast. Massy* (5) 21 (1967)
110. V V Rode, I V Zhuravleva, S R Rafikov, V V Korshak, S V Vinogradova, V A Pankratov *Vysokomol. Soedin.* **7** 1614 (1965)
111. *Advances in the Chemistry of Thermally Stable Polymers* (Ed. Z Jedlinski) (Warsaw: Pol. Sci. Publ., 1977)
112. Z Jedlinski *Thermal Stability of Polymers Containing Naphthalene Units in the Chain* (Warsaw: Pol. Sci. Publ., 1977)
113. V V Korshak, S V Vinogradova *Usp. Khim.* **39** 679 (1970) [*Russ. Chem. Rev.* **39** 308 (1970)]
114. G L Slonimskii, V V Korshak, S V Vinogradova, A I Kitaigorodskii, A A Askadskii, S N Salazkin, E M Belavtseva *Dokl. Akad. Nauk SSSR* **156** 924 (1964); *Vysokomol. Soedin., Ser. A* **9** 402 (1967)
115. S V Vinogradova *Vysokomol. Soedin., Ser. A* **19** 667 (1977)
116. S V Vinogradova, in *Polikondensatsionnye Protsessy i Polimery* (Polycondensation Processes and Polymers) (Nal'chik, 1979) p. 95
117. S V Vinogradova, in *Advances in Polymer Chemistry* (Moscow: Mir, 1986) p. 75
118. P M Valetskii, I P Storozhuk *Usp. Khim.* **48** 75 (1979) [*Russ. Chem. Rev.* **48** 42(1979)]
119. V V Korshak, P M Valetskii, I P Storozhuk *Makromol. Chem. Suppl.* **6** 55 (1984)
120. I P Storozhuk, P M Valetskii, E I Levin, L B Shirokova, S V Vinogradova, in *Abstracts of Reports at the International Symposium on Macromolecular Chemistry* (Tashkent: Nauka, 1978) Vol. 3, p. 140
121. I P Storozhuk, L B Shirokova, P M Valetskii, L Z Rogovina, S V Vinogradova, V V Korshak, G L Slonimskii *Vysokomol. Soedin., Ser. A* **21** 152 (1979)
122. L B Shirokova, I P Storozhuk, V S Voishchev, V A Beloglazov, V S Eremin, P M Valetskii, L Z Rogovina, G L Slonimskii, S V Vinogradova, V V Korshak *Vysokomol. Soedin., Ser. A* **24** 1974 (1982)
123. V S Voishchev, V A Beloglazov, I P Storozhuk, V V Mordvinov, P M Valetskii, S V Vinogradova, V V Korshak *Vysokomol. Soedin., Ser. A* **21** 2197 (1979)
124. S B Dolgoplosk, V P Mileshkevich, P M Valetskii, V V Korshak, S V Vinogradova *Vysokomol. Soedin., Ser. B* **19** 748 (1977)
125. V P Sidorov, Z V Gerashchenko, V F Blinov, I I Raigorodskii, V A Savin, P M Valetskii, S B Dolgoplosk, E I Levin, S V Vinogradova, V V Korshak *Plast. Massy* (12) 40 (1975)
126. P I Ivanov, E I Levin, S B Dolgoplosk, P M Valetskii, S V Vinogradova, V V Korshak, Yu V Zelenev *Dokl. Akad. Nauk SSSR* **221** 872 (1975)

127. A S Ramsh, A E Sidorovich, V V Korshak, S B Dolgoplosk, P M Valetskii, S V Vinogradova, A I Marei *Dokl. Akad. Nauk SSSR* **221** 361 (1975)
128. Yu K Godovskii, I I Dubovik, V S Papkov, P M Valetskii, S B Dolgoplosk, G L Slonimskii, S V Vinogradova, V V Korshak *Dokl. Akad. Nauk SSSR* **232** 105 (1977)
129. E A Nekhaenko, L Z Rogovina, Ya V Genin, G L Slonimskii, P M Valetskii, S B Dolgoplosk, L B Shirokova *Vysokomol. Soedin., Ser. A* **20** 1736 (1978)
130. G V Gryaznova, S B Dolgoplosk, V P Mileshkevich, L B Shirokova, A S Ramsh, I A Metkin, P M Valetskii *Vysokomol. Soedin., Ser. B* **21** 751 (1979)
131. Yu K Godovskii, L I Braude, Yu D Shibaev, E I Levin, P M Valetskii, S V Vinogradova, V V Korshak *Vysokomol. Soedin., Ser. A* **21** 127 (1979)
132. G Sh Papava, I S Khitarishvili, P D Tsiskarishvili, K A Andrianov, V V Korshak, S V Vinogradova *Soobshch. Akad. Nauk Gruz. SSR* **58** 341 (1970)
133. G Sh Papava, I S Khitarishvili, S V Vinogradova, V V Korshak *Soobshch. Akad. Nauk Gruz. SSR* **65** 345; 597; **66** 345 597; **68** 593 (1972)
134. S V Vinogradova, V V Korshak, K A Andrianov, G Sh Papava, I S Khitarishvili *Vysokomol. Soedin., Ser. A* **15** 1215 (1973)
135. M Kajiyama, M Kakimoto, Y Imai *Macromolecules* **22** 4143 (1989)
136. *Poliarilatarilensul'fonoksidy — Novye Lit'evye Termoplasty* (Polyarylate – arylene sulfone oxides — New Cast Thermoplastics) (Moscow: Nauka, 1977)
137. L Z Rogovina, P M Valetskii, G L Slonimskii *Plast. Massy* (5) 29 (1981)
138. L Z Rogovina, A E Chalykh, L V Adamova, A D Aliev, E A Nekhaenko, P M Valetskii, G L Slonimskii, A A Tager *Vysokomol. Soedin., Ser. A* **22** 428 (1980)
139. L Z Rogovina, A E Chalykh, P M Valetskii, E A Nekhaenko, Ya V Genin, N I Zakharov, E I Levin, S B Dolgoplosk, S V Vinogradova, G L Slonimskii, V V Korshak *Vysokomol. Soedin., Ser. A* **21** 393 (1979)
140. Yu K Godovskii, P M Valetskii, L M Braude, E I Levin, Yu D Shibaev, S V Vinogradova, V V Korshak *Dokl. Akad. Nauk SSSR* **244** 1149 (1979)
141. L Z Rogovina, N I Krotov, E A Nekhaenko, P M Valetskii, E I Levin, Ya V Genin, S V Vinogradova, G L Slonimskii, V V Korshak *Vysokomol. Soedin., Ser. A* **22** 526 (1980)
142. G G Nikiforova, I I Fatoev, V A Kim, E I Levin, L Z Rogovina, I P Storozhuk, P M Valetskii *Vysokomol. Soedin., Ser. A* **25** 2203 (1983)
143. G G Nikiforova, A E Chalykh, V V Matveev, I P Storozhuk, L Z Rogovina, G L Slonimskii *Vysokomol. Soedin., Ser. A* **25** 2210 (1983)
144. L Z Rogovina, G G Nikiforova, Ya V Genin, G L Slonimskii *Vysokomol. Soedin., Ser. A* **30** 509 (1988)
145. S V Vinogradova, V A Vasnev *Chem. Rev.* (1994) (in the press)
146. S V Vinogradova, V A Vasnev *Chem. Rev.* (1995) (in the press)
147. E N Zadorina, K S Isaev, G K Isaev, A K Mikitaev, Yu V Zelenev, A B Bashkirov *Kompozits. Polim. Mater.* **47** 5 (1990)
148. E M Pestryaev, I P Storozhuk, M V Filipenkova, L I Aksenov, L Z Rogovina, A I Maklakov *Vysokomol. Soedin., Ser. A* **23** 2276 (1981)
149. R C Shulz *J. Prakt. Chem.* **313** 447 (1971)
150. V V Korshak, T A Babushkina, V A Vasnev, S V Vinogradova, A V Vasil'ev, G K Semin *Izv. Akad. Nauk SSSR, Ser. Khim.* 1921 (1970)
151. V V Korshak, G L Slonimskii, S V Vinogradova, A A Askadskii, A V Vasil'ev, V A Vasnev, K A Bychko *Dokl. Akad. Nauk SSSR* **199** 607 (1971)
152. V V Korshak, S V Vinogradova, V A Vasnev, A V Vasil'ev *J. Polym. Sci., Polym. Lett.* **10** 429 (1972)
153. V V Korshak, S A Pavlova, L V Dubrovina, V A Vasnev, S V Vinogradova, A V Vasil'ev *Izv. Akad. Nauk SSSR, Ser. Khim.* 1409 (1972)
154. V V Korshak, S V Vinogradova, V A Vasnev, A V Vasil'ev, A A Askadskii, T A Babushkina, G K Semin, Yu K Godovskii, E S Obolonkova *Vysokomol. Soedin., Ser. A* **16** 291 (1974)
155. V V Korshak, S V Vinogradova, V A Vasnev, A P Gorshkov, G K Semin, E S Musaeva, L I Gvozdeva *Dokl. Akad. Nauk SSSR* **226** 350 (1976)
156. V V Korshak, S V Vinogradova, V A Vasnev, M G Keshelava, M M Dzhanashvili, L N Gvozdeva *Vysokomol. Soedin., Ser. A* **19** 2625 (1977)
157. V V Korshak, S V Vinogradova, V A Vasnev *Faserforsch. Textiltech.* **28** 491 (1977)
158. V V Korshak, S V Vinogradova, V A Vasnev, E B Musaeva, L N Gvozdeva, M M Dzhanashvili *Vysokomol. Soedin., Ser. A* **20** 888 (1978)
159. V V Korshak, S V Vinogradova, V A Vasnev *Izv. Akad. Nauk SSSR, Ser. Khim.* 2656 (1978)
160. V E Shklover, Yu T Stryuchkov, M M Dzhanashvili, V A Vasnev *Zh. Obshch. Khim.* **50** 2563 (1980)
161. S V Vinogradova, I P Antonova-Antipova, in *Progress Polimernoi Khimii* (Progress in Polymer Chemistry) (Moscow: Nauka, 1969) p. 375
162. V V Korshak, S V Vinogradova, I P Antonova-Antipova *Vysokomol. Soedin.* **6** 2174 (1964); **7** 322; 1543 (1965)
163. S V Vinogradova, V V Korshak, I P Antonova-Antipova *Vysokomol. Soedin.* **7** 2052 (1965)
164. V V Korshak, S V Vinogradova, I P Antonova-Antipova *Dokl. Akad. Nauk SSSR* **117** 120 (1967)
165. V V Korshak, S V Vinogradova, I P Antonova-Antipova *Izv. Akad. Nauk SSSR, Ser. Khim.* 1078 (1969)
166. USSR P. 184 445; *Byull. Izobret.* **15** 45 (1966)
167. V V Korshak, S R Rafikov, S V Vinogradova, Z Ya Fomina *Vysokomol. Soedin.* **7** 1908 (1965)
168. S R Rafikov, S V Vinogradova, V V Korshak, Z Ya Fomina, B V Lokshin, V V Rode *Vysokomol. Soedin.* **8** 2189 (1966)
169. S R Rafikov, S V Vinogradova, V V Korshak, Z Ya Fomina *Vysokomol. Soedin., Ser. A* **9** 98 (1967)
170. S R Rafikov, V V Korshak, S V Vinogradova, Z Ya Fomina, V A Pankratov *Vysokomol. Soedin., Ser. A* **9** 1903 (1967)
171. S V Vinogradova, S R Rafikov, V V Korshak, Z Ya Fomina *Vysokomol. Soedin., Ser. A* **9** 1797 (1967)
172. USSR P. 170 667; *Byull. Izobret.* **9** 68 (1965)
173. USSR P. 172 038; 175 656; *Byull. Izobret.* **12** 75 (1965); **20** 66 (1965)
174. V V Korshak, S V Vinogradova, S A Siling, S R Rafikov, Z Ya Fomina, V V Rode *J. Polym. Sci., Part A-1* **7** 157 (1969)
175. V V Korshak, S V Vinogradova, S A Siling *Vysokomol. Soedin.* **7** 701 (1965)
176. S V Vinogradova, S A Siling, V V Korshak, S A Pavlova *Vysokomol. Soedin., Ser. B* **9** 382 (1967)
177. USSR P. 156 680; 159 982; *Byull. Izobret.* **16** 52 (1963); **2** 54 (1964)
178. V V Korshak, S V Vinogradova, P M Valetskii, M G Deborin *Lakokras. Mater. Ikh Primen.* **1** 3 (1963)
179. USSR P. 197 164; *Byull. Izobret.* **12** 106 (1967)
180. V V Korshak, S V Vinogradova, M G Korchevei *Vysokomol. Soedin.* **7** 457 (1965)
181. S V Vinogradova, V V Korshak, M G Korchevei *Vysokomol. Soedin.* **7** 1884; 1889 (1965)
182. V V Korshak, S V Vinogradova, M G Korchevei, V I Kul'chitskii *Vysokomol. Soedin.* **8** 109 (1966)
183. V V Korshak, S V Vinogradova, V I Kul'chitskii *Vysokomol. Soedin.* **8** 1080 (1966)
184. S V Vinogradova, V V Korshak, V I Kul'chitskii, P N Gribkova, V G Danilov *Vysokomol. Soedin.* **10A** 1518 (1968)
185. S V Vinogradova, V V Korshak, V I Kul'chitskii, B V Lokshin, G Z Mirkin *Vysokomol. Soedin., Ser. A* **10** 1108 (1968)
186. V V Korshak, S V Vinogradova, S A Siling *Khim. Volokna* **3** 16 (1965)
187. V V Korshak, S V Vinogradova, A N Baskakov, P M Valetskii *Vysokomol. Soedin.* **7** 1633 (1965)
188. S V Vinogradova, V V Korshak, P M Valetskii, A N Baskakov, L M Gil'man *Vysokomol. Soedin., Ser. A* **9** 1298 (1967)
189. A A Askadskii, V V Korshak, S V Vinogradova, P M Valetskii, A N Baskakov *Vysokomol. Soedin., Ser. B* **9** 281 (1967)
190. V V Korshak, G L Berestneva, S V Vinogradova, A N Baskakov, P M Valetskii *Vysokomol. Soedin., Ser. A* **10** 1984 (1968)
191. K A Gol'dgammer, G G Pimenov, A I Maklakov, V V Korshak, S V Vinogradova, P M Valetskii, A N Baskakov *Vysokomol. Soedin., Ser. A* **10** 821 (1968)

192. V V Korshak, S V Vinogradova, V A Pankratov *Dokl. Akad. Nauk SSSR* **156** 880 (1964)
193. V V Korshak, S V Vinogradova, V A Pankratov, A N Baskakov *Izv. Akad. Nauk SSSR, Ser. Khim.* 141 (1964)
194. V A Pankratov, S V Vinogradova, R D Fedorova *Izv. Akad. Nauk SSSR, Ser. Khim.* 342 (1965)
195. V V Korshak, S V Vinogradova, V A Pankratov *Izv. Akad. Nauk SSSR, Ser. Khim.* 1649 (1965)
196. V V Korshak, I F Manucharova, S V Vinogradova, V A Pankratov *Vysokomol. Soedin.* **7** 1813 (1965)
197. V V Korshak, S V Vinogradova, V A Pankratov *Vysokomol. Soedin.* **7** 1689 (1965)
198. V V Korshak, S A Pavlova, G I Timofeeva, S V Vinogradova, V A Pankratov *Vysokomol. Soedin.* **7** 1679 (1965); *Dokl. Akad. Nauk SSSR* **160** 119 (1965)
199. V V Korshak, S V Vinogradova, V A Pankratov, S A Pavlova, G I Timofeeva *Izv. Akad. Nauk SSSR, Ser. Khim.* 747 (1967)
200. V Yu Voitekunas, G D Markova, V A Vasnev, S V Vinogradova *Sintez Termotropnykh Zhidkokristallicheskikh Poliefirov* (Synthesis of Thermotropic Mesomorphic Polyesters) (Moscow, 1991) Article deposited at the All-Union Institute of Scientific and Technical information (VINITI) No. 1783
201. G Schwarz, H R Kricheldorf *Macromolecules* **23** 1568 (1990)
202. Jpn. Appl. 170 529; *Ref. Zh. Khim.* 5 S 600P (1990)
203. Jpn. Appl. 1 229 033; *Ref. Zh. Khim.* 21 S 702P (1990)
204. D J Johnson, I Karacan, J G Tomka *Polymer* **31** 8 (1990)
205. S S Skorochodov, A Yu Bilibin *Makromol. Chem. Makromol. Symp.* **26** 9 (1989)
206. M C Gupta, A K Sharma *J. Sci. Ind. Res.* **49** 134 (1990)
207. T Schleeh, G Kossmehl, G Hinrichsen *Makromol. Chem.* **191** 1075 (1990)
208. H-B Tsai, C Lee, N-S Chang, M-S Chem, S-J Chang *J. Appl. Polym. Sci.* **40** 1499 (1990)
209. E Chiellini, R W Lent, in *Comprehensive Polymer Science. The Synthesis, Characterization, Reactions, and Applications of Polymers* Vol. 5 (Oxford: Pergamon Press, 1989) p. 701
210. V A Vasnev, V Yu Voitekunas, G D Markova, S V Vinogradova *Vysokomol. Soedin.* **37** (1995) (in the press)
211. V A Vasnev, V Yu Voitekunas, G D Markova, S V Vinogradova *Vysokomol. Soedin.* **37** (1995) (in the press)
212. T S Knyazeva, V V Korshak, M S Akutin, M M Kuleva, S V Vinogradova, L A Rodivilova, T P Nedopekina, P M Valetskii, S A Morozova, S N Salazkin *Plast. Massy* (12) 37 (1962)
213. USSR P. 132 399; *Byull. Izobret.* **19** 53 (1960)
214. M S Akutin, V V Korshak, L A Rodivilova, S V Vinogradova, Yu M Budnitskii, P M Valetskii, A S Lebedeva *Plast. Massy* (11) 20 (1962)
215. V V Korshak, S V Vinogradova, V G Danilov, L A Beridze, S N Salazkin *Vysokomol. Soedin., Ser. B* **12** 129 (1970)
216. S Ts Chzhao, P M Valetskii, S V Vinogradova, P Ya Glazunov, V V Korshak, S R Rafikov, B L Tsetlin *Vysokomolekulyarnye Soedineniya; Khimicheskie Svoistva i Modifikatsiya Polimerov* (High-Molecular-Mass Compounds; Chemical Properties and Modification of Polymers) (Moscow: Izd. Akad. Nauk SSSR, 1964) p. 126
217. P M Valetskii *Karbotsepnye i Geterotsepnye Polimery s Karboranovymi Gruppami v Tsepi* (Carbon-Chain and Heterochain Polymers with Carbaborane Groups in the Chain) (Gomel', 1972)
218. V V Korshak, S V Vinogradova, A I Kalachev, P M Valetskii, V I Stanko *Vysokomol. Soedin., Ser. A* **13** 848 (1971)
219. V V Korshak, S V Vinogradova, A I Kalachev, P M Valetskii, N S Titova, V I Stanko *Vysokomol. Soedin., Ser. A* **14** 1306 (1972)
220. L V Dubrovina, M M Ivanova, A I Kalachev, P M Valetskii, S V Vinogradova *Vysokomol. Soedin., Ser. B* **15** 834 (1973)
221. S R Rafikov, S A Pavlova, I V Zhuravleva, R S Ayupova, P M Valetskii, A I Kalachev, S V Vinogradova, V I Stanko, V V Korshak *Dokl. Akad. Nauk SSSR* **207** 1133 (1972)
222. S R Rafikov, S A Pavlova, I V Zhuravleva, R S Ayupova, P M Valetskii, A I Kalachev, S V Vinogradova, V V Korshak *Dokl. Akad. Nauk SSSR* **213** 603 (1973)
223. S R Rafikov, I V Zhuravleva, R S Ayupova, A I Kalachev, P M Valetskii, S V Vinogradova, V V Korshak *Vysokomol. Soedin., Ser. A* **15** 1706 (1973)
224. S R Rafikov, I V Zhuravleva, R S Ayupova, A I Kalachev, P M Valetskii, V I Stanko, S V Vinogradova, V V Korshak *Dokl. Akad. Nauk SSSR* **195** 1351 (1970)
225. V G Danilov, A I Kalachev, S V Vinogradova, P M Valetskii, V I Stanko, V V Korshak *Vysokomol. Soedin., Ser. A* **13** 2360 (1971)
226. V S Matochkin, A I Kalachev, Yu V Zelenev, P M Valetskii, S V Vinogradova, V V Korshak *Dokl. Akad. Nauk SSSR* **204** 1359 (1972)
227. I I Ivanov, V S Matochkin, A I Kalachev, Yu V Zelenev, P M Valetskii, S V Vinogradova, V V Korshak *Dokl. Akad. Nauk SSSR* **213** 338 (1973)
228. I I Ivanov, A I Kalachev, P M Valetskii, S V Vinogradova, V V Korshak, Yu V Zelenev *Vysokomol. Soedin., Ser. A* **21** 1264 (1979)
229. S V Vinogradova, P M Valetskii, N I Bekasova *Chem. Rev.* **18** 1 (1993)
230. P M Valetskii, E K Lyamenkova, S V Vinogradova *Vysokomol. Soedin., Ser. A* **16** 305 (1974)
231. USSR P. 316 708; *Byull. Izobret.* **12** 83 (1971)
232. P M Valetskii, E K Lyamenkova, T M Babchinitser, A I Kalachev, V P Lebedev, S V Vinogradova, V I Stanko, V V Korshak *Vysokomol. Soedin., Ser. A* **15** 2200 (1973)
233. E K Lyamenkova, R S Ayupova, I V Zhuravleva, V S Papkov, P M Valetskii, S V Vinogradova, S A Pavlova, V V Korshak *Vysokomol. Soedin., Ser. A* **17** 698 (1975)
234. V Yu Voitekunas, Candidate's Thesis in Chemical Sciences, Nesmeyanov Institute of Organoelement Compounds, Moscow, 1993
235. G D Markova, K R Papava, V Yu Voitekunas, V A Vasnev, S V Vinogradova *Vysokomol. Soedin., Ser. B* **34** 54 (1992)
236. M Yoneyama, M Kakimoto, Y Imai *Makromol. Chem.* **22** 2593 (1989)
237. Y Imai, in *Polymer Science Contemporary Themes* Vol. 1 (New Delhi: Tata McGraw-Hill Publ., 1991) p. 3
238. A L Rusanov, I A Khotina *Vysokomol. Soedin., Ser. A* **36** 1994 (in the press)
239. Y Imai *ACS Polym. Prepr.* **32**(1) 331 (1991)
240. Y Imai *Chem. Tech.* 560 (1991)
241. Y Imai *Makromol. Chem. Macromol. Symp.* **54/55** 151 (1992)
242. V A Vasnev, A L Rusanov, M L Keshtov, M K Ovechkin, in *Khimiya i Tekhnologiya Vysokomolekulyarnykh Soedinenii (Itogi Nauki i Tekhniki)* (Chemistry and Technology of High-Molecular-Mass Compounds. Advances in Science and Engineering) (Moscow: Izd. VINITI, 1987) Vol. 23, p. 3
243. Sh Kitayama, K Sanui, N Ogata *J. Polym. Sci., Polym. Chem. Ed.* **22** 2705 (1984)
244. F Higashi, K Kubota, M Sekizuka *Makromol. Chem., Rapid Commun.* 1 457 (1980)
245. F Higashi, K Kubota, M Sekizuka, M Higashi *J. Polym. Sci., Polym. Chem. Ed.* **19** 2681 (1981)
246. F Higashi, Y Ito, K Kubota *Makromol. Chem., Rapid Commun.* **2** 29 (1981)
247. F Higashi, K Kubota, M Sekizuka, M Goto *J. Polym. Sci., Polym. Lett. Ed.* **18** 385 (1980)
248. Sh Kitayama, K Sanui, N Ogata *J. Polym. Sci., Polym. Chem. Ed.* **22** 2705 (1984)
249. F Higashi, A Hoshio, J Kiyoshige *J. Polym. Sci., Polym. Chem. Ed.* **21** 3241 (1983)
250. H Tanaka, Y Iwanaga, G-C Wu, K Sanui, N Ogata *Polym. J.* **14** 643 (1982)
251. F Higashi, N Akiyama, T Koyama *J. Polym. Sci., Polym. Chem. Ed.* **21** 3233 (1983)
252. R D Katsarava *Usp. Khim.* **58** 1549 (1989) [*Russ. Chem. Rev.* **58** 891 (1989)]
253. S Yasuda, G-C Wu, H Tanaka *J. Polym. Sci., Polym. Chem. Ed.* **21** 2609 (1983)
254. Jpn. Appl. 1-167 329; *Ref. Zh. Khim.* 23 S 588 (1990)
255. F Pilati, in *Comprehensive Polymer Science. The Synthesis, Characterization, Reactions, and Applications of Polymers* Vol. 5 (Oxford: Pergamon Press 1989) p. 275
256. F Higashi, Y Yamada, A Hoshio *J. Polym. Sci., Polym. Chem. Ed.* **22** 2181 (1984)

257. F Higashi, Y Yamada *J. Polym. Sci., Polym. Chem. Ed.* **23** 2709 (1985)
258. F Higashi, A Hoshio, Y Yamada, M Ozawa *J. Polym. Sci., Polym. Chem. Ed.* **23** 69 (1985)
259. R D Katsarava *Vysokomol. Soedin., Ser. A* **31** 1555 (1989)
260. R D Katsarava, D P Kharadze, L M Avalishvili, M M Zaalishvili *Vysokomol. Soedin., Ser. B* **24** 198 (1982)
261. A L Rusanov *Usp. Khim.* **59** 1492 (1990) [*Russ. Chem. Rev.* **59** 868 (1990)]
262. H R Kricheldorf, G Schwarz *Polym. Bull.* **1** 383 (1979)
263. H R Kricheldorf, G Z Zang, G Schwarz *Polymer* **23** 1821 (1982)
264. H R Kricheldorf, G Schwarz *Makromol. Chem. Part B.* **184** 475 (1983)
265. R D Katsarava, Ya S Vygodskii *Usp. Khim.* **61** 1492 (1992) [*Russ. Chem. Rev.* **61** 629 (1992)]
266. H R Kricheldorf, G Schwarz, F Ruhser *J. Polym. Sci., Polym. Chem. Ed.* **26** 1621 (1988)
267. H R Kricheldorf, J Engelhardt *J. Polym. Sci., Part A, Polym. Chem.* **23** 2335 (1990)
268. H R Kricheldorf, in *Polymer Science Contemporary Themes* Vol. 1 (New Delhi: Tata McGraw-Hill Publ., 1991) p. 49
269. K Miyazawa, T Munetoh, T Matsumoto *Polym. Prepr. Jpn.* **36** 324 (1987)
270. V V Korshak, V A Vasnev, in *Comprehensive Polymer Science. The Synthesis, Characterization, Reactions and Applications of Polymers* Vol. 5 (Oxford: Pergamon Press, 1989) p. 131
271. H R Kricheldorf, G Schwarz *Polym. Bull.* **1** 383 (1979)
272. Jpn. Appl. 1-287 135; *Ref. Zh. Khim.* 1 S 519 (1990)
273. *Eng. Mater.* **36** 104 (1988); *Ref. Zh. Khim.* IC519 (1990)
274. B Miller *Plast. World* **48** 49 (1990)
275. J Zimmerman *J. Appl. Polym. Sci.* **39** 2067 (1991)
276. US P. 4 910 083; *Ref. Zh. Khim.* 9 T 197 (1991)
277. US P. 4 977 235; *Ref. Zh. Khim.* 23 S 532P (1991)
278. S P Suchilina, V N Sokolenko, in *Vsesoyuznoe Soveshchanie po Polimernym Opticheskim Materialam (Tez. Dokl.) Leningrad, 1991* [All-Union Conference on Polymeric Optical Materials (Abstracts of Reports)] (Leningrad, 1991) p. 111
279. Jpn. Appl. 1-287 134; *Ref. Zh. Khim.* 23 S 602P (1990)
280. Jpn. Appl. 1-263 113; *Ref. Zh. Khim.* 23S 600P (1990)
281. Jpn. Appl. 2-110 156; *Ref. Zh. Khim.* 6T 18P (1991)
282. US Appl. 4 908 419; *Ref. Zh. Khim.* 7 T 143P (1991)
283. Jpn. Appl. 2-16 152; *Ref. Zh. Khim.* 9 S 609P (1991)
284. US P. 4 908 418; *Ref. Zh. Khim.* 11 T 57P (1991)
285. US P. 4 879 534; *Ref. Zh. Khim.* 11 T 58P (1991)
286. Jpn. Appl. 1-261 454; *Ref. Zh. Khim.* 13 T 155P (1991)
287. G P Safonov, I Ya Kaplunov *4 Vsesoyuznaya Konferentsiya po Khimii i Fiziko-khimii Oligomerov (Tez. Dokl.) Chernogolovka, 1990* [The Forth All-Union Conference on the Chemistry and Physical Chemistry of Oligomers (Abstracts of Reports) (Chernogolovka, 1990)] p. 130
288. US P. 4 851 498; *Ref. Zh. Khim.* 2 T 85P (1991)
289. O I Sidorov, A F Matnik, M A Yusufov, in *Mezhdunarodnaya Konferentsiya po Kompozitam (Tez. Dokl.) Moscow, 1990* [International Conference on Composites (Abstracts of Reports) (Moscow, 1990)] Part 1, p. 73
290. D Osamu *Funct. Mater.* **10** 27 (1990); *Ref. Zh. Khim.* 4 T 61 (1991)
291. N Ogata, K Sanui, H Itaya *Polym. J.* **22** 85 (1990)
292. Jpn. Appl. 1 261 455; *Ref. Zh. Khim.* 13 T 156P (1991)
293. Jpn. Appl. 1 271 446; *Ref. Zh. Khim.* 16 T 133 (1991)
294. Jpn. Appl. 1 268 751; *Ref. Zh. Khim.* 17 T 114P (1991)
295. Jpn. Appl. 2-92 954; *Ref. Zh. Khim.* 18 T 88P (1991)
296. US P. 4 902 747; *Ref. Zh. Khim.* 9 T 55P (1991)
297. Jpn. Appl. 2-173 063; *Ref. Zh. Khim.* 21 P 86P (1991)
298. J P Runt, C A Barron, X-F Zhang, S K Kumar *Macromolecules* **24** 3466 (1991)
299. J Finter, C W Mayer, P Ansermet, H Bleier, B Hilti, E Minder, D Neuschifer *Int. Conf. Sci. and Technol. Synth. Metals* ICSM 90 Part 2; *Synth. Met.* **41** 951 (1991); *Ref. Zh. Khim.* 23 S 270 (1991)
300. US P. 4 942 200; *Ref. Zh. Khim.* 20 T 126P (1991)
301. Jpn. Appl. 2-169 664; *Ref. Zh. Khim.* 4 S 416P (1992)
302. M Kimura, R S Porter, G Salee *J. Polym. Sci., Polym. Phys. Ed.* **21** 367 (1983)
303. M Kumura, G Salee, R S Porter *J. Appl. Polym. Sci.* **29** 1629 (1984)
304. L M Robenson *J. Appl. Polym. Sci.* **30** 4081 (1985)
305. J I Eguiazabal, G Ucar, M Cortazar, J J Irvin *Polymer* **27** 2013 (1986)
306. I Mondragon, M Cortazar, G M Guzman *Makromol. Chem.* **184** 1741 (1983)
307. J Devaux, P Devaux, P Godard *Makromol. Chem.* **186** 1227 (1985)
308. I Mondragon, J Nozabal *J. Appl. Polym. Sci.* **32** 6191 (1986)
309. V V Korshak, S V Vinogradova, L I Komarova, Ya S Vygodskii, I A Bulgakova, M A Yusufov, E E Zaborovskaya, T I Kuznetsova, S N Salazkin *Plast. Massy* (6) 47 (1986)
310. L I Komarova, S N Salazkin, Ya S Vygodskii, S V Vinogradova *Vysokomol. Soedin., Ser. A* **32** 1571 (1990)
311. A A Askadskii, L N Belkina, K A Bychko, S N Salazkin, S V Vinogradova, I A Bulgakova, L I Komarova, G L Slonimskii, V V Korshak *Vysokomol. Soedin., Ser. A* **22** 1338 (1980)
312. A A Askadskii, Yu S Kochergin, L I Komarova, S N Salazkin, I A Bulgakova, G L Slonimskii, S V Vinogradova, V V Korshak, in *Struktura i Svoistva Polimernykh Materialov* (The Structure and Properties of Polymeric Materials) (Riga, 1979) p. 20
313. Yu S Kochergin, A A Askadskii, S N Salazkin, I A Bulgakova, V F Alekseev, S V Vinogradova, G L Slonimskii, V V Korshak *Vysokomol. Soedin., Ser. A* **20** 880 (1978)
314. W W Korshak, I A Gribova, A N Tschumaewskaja, S V Vinogradova, N I Bekasova, P M Valetskii *Plaste Kautsh.* **22** 324 (1975)
315. USSR P. 378 094; *Byull. Izobret.* **37** 232 (1973)
316. V V Korshak, I A Gribova, A N Chumaevskaya, B M Mgeladze *J. Appl. Polym. Sci.* **23** 1915 (1979)
317. V V Korshak, V A Vasnev, I A Gribova, A I Kuznetsov, S V Vinogradova, V N Ignatov, G I Gureeva, B D Lavrukhin, O A Lependina *Vysokomol. Soedin., Ser. A* **31** 86 (1989)
318. V A Vasnev, V N Ignatov, A I Kuznetsov, I A Gribova, S V Vinogradova, G I Gureeva *Dokl. Akad. Nauk SSSR* **310** 1379 (1990)
319. A I Kuznetsov, V N Ignatov, V A Vasnev, I A Gribova, S V Vinogradova, G I Gureeva, B D Lavrukhin *Acta Polymerica* **42** 76 (1991)
320. V N Ignatov, A I Kuznetsov, V A Vasnev, I A Gribova, S V Vinogradova, G I Gureeva, B D Lavrukhin, A I Krasnov *Macromolecules* **25** 1652 (1992)

Russian Chemical Reviews **63** (10) 853–867 (1994)
©1994 Russian Academy of Sciences and Turpion Ltd

UDC 615.462.011

Macrokinetic aspects of the biocompatibility and biodegradation of polymers

K Z Gumargalieva, G E Zaikov, Yu V Moiseev

Contents

I.	Introduction	853
II.	Reaction of the organism on the polymer	853
III.	Biocompatibility of polymers	854
IV.	Catalytic activity of biological media	855
V.	Products of the degradation in the organism	858
VI.	Biocompatibility and biodegradation of polymers of different classes	859
VII.	Conclusion	865

Abstract. We review the quantitative relationships between the degradation kinetics of the main classes of polymers (polyolefins, polyesters, polyamides, elastomers) used as implants. Their biocompatibility criteria and the reactions of the organism on the implants are considered, and the catalytic activity of biological media (water, salts, enzymes) are discussed together with problems in the metabolism and conjugation of the degradation products. The bibliography includes 127 references.

I. Introduction

The problem of producing special synthetic polymers to be used in contact with biological media first arose in the 1950s. It was created by the need by biology and medicine for synthetic polymeric materials to be used in the manufacture of various endoprostheses. This led to the development of a completely new area in technology: the production of polymers for medical applications.[1–3]

Both in the case of testing existing polymers for medical applications and when modified materials are used, the minimisation of the undesirable interactions between the material and the tissue of the living organism in implants of short or long duration as a function of the properties of the material is the most urgent problem.

Bioengineers who produce articles from these materials and doctors who use them in practice are interested in the biocompatibility of the polymers and in the retention time of desirable properties (mechanical, diffusional, optical, etc.).

When in contact with biologically active media (tissues) most polymers undergo two mutually related processes: degradation under the influence of the biologically active substances and interaction of the degradation products with the biological media responsible for the degradation (i.e. an influence of the metabolic and of the conjugation products on the life processes of the organism).

K Z Gumargalieva, G E Zaikov, Yu V Moiseev N N Semenov Institute of Chemical Physics, Russian Academy of Sciences, 4 ul. Kosygina, 117334 Moscow, Russian Federation. Fax (7-095) 938 21 56

Received 28 April 1994
Uspekhi Khimii **63** (10) 905–920 (1994); translated by J I Carasso

The study of the macrokinetic aspects of these processes ultimately allows the prediction of the lifetime of the polymer under stated operating conditions.

II. Reaction of the organism on the polymer

1. Initial reaction of the organism

A polymer in contact with the tissues of a living organism not only undergoes changes in its physical and chemical properties but also stimulates (as a foreign body) a corresponding reaction from the organism.

As a result of the damage produced in the tissues, the implantation of polymers into a living organism is accompanied by an inflammatory process.[4] This reaction consists, in the first stage of damage to the tissues, in a decrease in pO_2 and in pH, a decrease in the concentration of potassium, sodium, calcium, and magnesium ions, an accumulation of physiologically active substances resulting from the breakdown of the cell membranes and the evolution of circulating lymphocytes, and an increased accessibility of the microvessels.

In the second stage of the inflammatory process different forms of cell (neutrophils, monocytes, basophils, macrophages, etc.) are accumulated as a result of the directed motion of cells towards the inflammation region stimulated by the chemical irritants (chemotaxis). Chemical irritants include the physiologically active substances released by damaged cells and tissues (Table 1, see over), and also substances released by the polymeric materials (degradation products, residues of catalysts, stabilisers, fillers, etc.).[5]

Thus in this stage polymers can actively influence the progress of the inflammatory process.

If the process is not complicated by the onset of infections this stage of the inflammatory process is completed (on average) in three days, and the neutrophils (which were the predominant species initially) are replaced by monotcytes, plasma cells, lymphocytes, and macrophages.[6]

2. Formation of capsules round the polymer

After 4 to 5 days of contact the macrophages begin to predominate round the polymer, but lymphocytes, plasma cells, and fibroblasts are also present.[7]

If the polymer is biocompatible the number of macrophages decreases steeply after 1 or 2 weeks, and the fibroblasts form a collagen-like capsule on the surface of the polymer (Fig. 1). If the polymer is only partially biocompatible the microphages can

Table 1. Physiologically active substances contributing to inflammation reactions.

Substance	Chemical nature	Origin	Special features of the action
Histamine	β-Imidazolylethylamine	Fat cells, basophils, thrombocytes	Increased penetrability of the microvessels
Serotonin	5-Oxytryptamine	"	"
Catecholamines	Noradrenaline	"	"
Kinins	Polypeptides (metabolic products)	Plasma	Increased penetrability of the microvessels, pathogenic reactions
Hageman factor	Protease, globulin	"	"
Plasmin	Protease	"	"
Complement	Plasma proteins and metabolic products	Endothelium cells	Chemotaxis
Leucokinins	Polypeptides	Leucocytes	Increased penetrability of the microvessels
Lysosomal enzymes	Within-cell proteins	Neutrophils, macrophages, fat cells	Chemotaxis, phagocytosis
Lymphokinins	"	Lymphocytes	Immune reactions in the organism
Low-molecular regulators	Prostaglandins	Precursors present in all cells except erythrocytes	Increased penetrability of the microvessels, modulation of the inflammation, chemotaxis

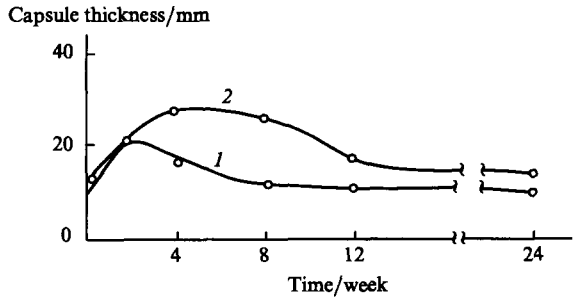


Figure 1. Plots of the thickness of the capsule against implantation time.[14] (*1*) Polydimethylsiloxane; (*2*) polystyrene coated with polydimethylsiloxane.

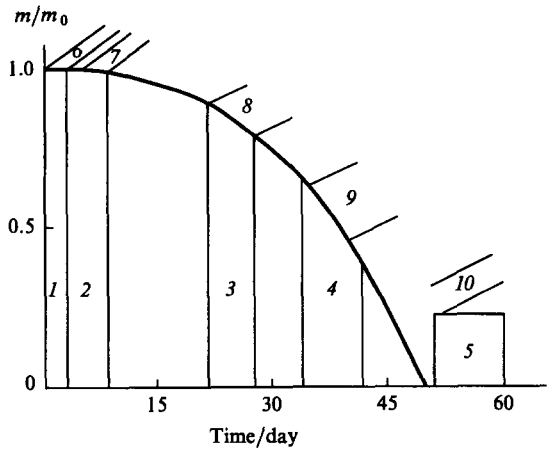


Figure 2. Dependence of the mass of the implant on time, and on its histoformological surroundings during the degradation of a polymer with satisfactory compatibility (polyglactin). (*1*) Macrophages round the implant: (*2*) macrophages containing phagocytes, fibroblasts; (*3*) giant cells and active macrophages; (*4*) macrophages and giant cells surrounding the polymer filaments with mitochondrial regions; (*5*) macrophages and giant cells surrounding the residues of the polymer fragments; (*6*) reaction on the polymer structure; (*7*) reaction to an operational trauma and healing, synthesis of collagen; (*8*) participation in the hydrolysis of the implant through the enzyme system; (*9*) participation of the cells in the metabolic process (increase in the respiratory functions); (*10*) complete resorption.

survive for longer times round the implanted polymer, and under these conditions giant cells can be formed.[8]

The thickness of the capsule depends on the biocompatibility of the polymer.[9] If the species responsible for the inflammation (for example, the degradation products) are produced at steady state we observe a chronic inflammation leading, after a long period, to the complete degradation of the polymer.

Being the main phagocyte cells of the organism the macrophages actively contribute to the degradation of most polymers. The macrophages contain lysosomes, which act as the 'alimentary canal' of the cell.[10] The lysosomal enzymes, mainly hydrolases, can destroy the polymer (phagocytosis) by two mechanisms. The first is exocytosis, in which liposomal enzymes are produced by the macrophage and the degradation takes place on the polymer surface. The second is endocytosis, in which the degradation process within the cell is preceded by the absorption of polymer particles by the macrophages. For example, Winter[11] detected metal particles within the macrophages by spectroscopic methods.

The dynamics of the morphological changes taking place on the surface of the polymer after implantation are illustrated in Fig. 2.

III. Biocompatibility of polymers

1. General definitions

We shall examine in general terms the response of the organism to a polymer after implantation, with special emphasis on the problems of biocompatibility.

When implanted into the organism polymers used in medical applications can fulfil special prosthetic or other functions (diagnostic, surgical or therapeutic) without undesirable interactions with the surrounding tissues or with the organism as a whole. At present we have no clear definition of biocompatibility, since there are no material parameters or biological tests which could be used as a quantitative measure of this property of polymers.[12]

Biocompatibility means that the polymer can exist in contact with blood and enzymes without undergoing degradation or causing thrombosis, breakdown of the tissues, or harmful immunological, toxicological, or allergenic effects.

Pure polymers with a high molecular mass usually have a low toxicity.[13] The degradation of the macromolecules produces fragments of lower molecular mass, down to the final degradation products (which could be the pure monomers). We know that the toxicity of the polymers of a given homologous series is inversely proportional to their molecular mass.[13]

Depending on the rate of degradation of the polymeric implant in the biological medium, its biocompatibility is found to change. In general the biocompatibility of the polymeric material is defined not only by the initial interactions but also by its chemical stability towards the surrounding biological medium.

2. Methods of determining the biocompatibility

A group of papers describing quantitative tests of the biocompatibility in various series of polymers has been published in the last few years.[14-18]

The in vitro experiments were mostly done by the 'tissue culture' method, which consists in growing cells on the surface of the experimental material. Two forms of the method are known: (1) depositing a layer of agar on the polymer, and observing the multiplication of the cells in the medium;[18-21] (2) depositing cells (usually fibroblasts) on the polymer and immersing the polymer inoculated with cells in the feed medium.[22,23]

The effect of the polymer on three functions of the cells is usually studied: their adhesion, survival, and multiplication.

Eleven phenomena were observed in a microscopic study.[15] Table 2 lists the polymers, the phenomena which were observed, and the doubling parameter (P_D) of the resulting fibroblast cells:

$$P_D = \frac{\lg(N/N_0)}{0.69}, \quad (1)$$

where N is the number of cells after 48 h incubation and N_0 is the initial number of cells deposited on the polymer.

From the results obtained in vitro all the polymers were divided into three arbitrary toxicity classes.

The in vivo measurements included 6 tests of the biocompatibility: (1) the extent of damage to the cells; (2) the thickness of the capsule; (3) the total number of cells; (4) the number of multinuclear leucocytes and erythrocytes; (5) the number of eosinophils, lymphocytes, and giant cells; (6) the number of fibrocytes from mononuclear phagocytes.

The number of cells is usually determined microscopically by defining a standard area.

An eight-point scale was adopted for each test.[16] The average index for each test (M) was found by adding the data obtained after two implantation cycles:

$$M_{STS} = (STS_{7\,\text{days}} + STS_{28\,\text{days}}) \times 10^{-1}, \quad (2)$$

where STS is the average sum of the marks on the scale for the tests.

The M_{STS} values for various polymers determined after implantation in the subcutaneous cellular tissues of the rat and their arbitrary assignment to the toxicity classes are shown in Table 3.

Table 2. Cytotoxicity of polymers in vitro.

Polymer	Phenomenon[a]	P_D	Toxicity class
Polypropiolactone	1	2.7	I
Polyhexamethylenediamine	1	1.9	I
Teflon	1	2.1	I
Polylactide	1	1.6	I
Poly(ethylene oxide)	1	2.1	I
Polyacrylamide	1	2.0	I
Polycaprolactone	1	2.1	I
Polyacrylonitrile	1	2.1	I
Polyglycollide	1	2.0	I
Poly(methyl methacrylate)	1, 11	–	II
Polymethyllactyl-2-cyano-acrylate	7, 8, 10	–	II
Polyisobutyl-2-cyanoacrylate	1	2.0	II
Poly(1,2-isopropylidene)-glycerolcyanoacrylate			
high-molecular	4	0.4	II
low-molecular	2, 5, 6, 7	–	III
Poly(acrylic acid)	5, 8, 9	–	III
Polydimethyl-2-cyanoacrylate	5, 7, 8	–	III

[a] The numbers refer to the following phenomena: 1, normal adhesion and multiplication of cells; 2, adhesion of a small number of cells; 3, normal growth of a small number of adhering cells; 4, the number of cells adhering after 48 h is negligible; 5, all cells in the medium have died; 6, all cells adhered to the growing surface have died after 48 h; 7, cells form a clump; 8, cells are not attracted to the surface; 9, sudden change in pH to 5.2; 10, there are some changes in the cells in the medium after 48 h; 11, the polymer adheres to the cells.

Table 3. Toxicity of polymers.

Polymer	M_{STS}	Toxicity class
Gelatin	2.1	I
Polyacrylamide	10.3	I
Polyglycollide	19.6	I
Polyacrylonitrile	52.0	I
Poly-α-lactide	34.7	I
Poly-β-propyllactone	69.1	I
Polycaprolactone	37.3	I
Poly(ethylene oxide)	21.8	I
Polymethyl-α-lactylcyanoacrylate	56.7	II
Poly(methyl methacrylate)	49.2	III
Polydimethyl-2-cyanoacrylate	59.1	III
Polyisobutyl-2-cyanoacrylate	49.7	III

IV. Catalytic activity of biological media

At the contact between polymers and biological media the latter usually show a catalytic activity towards the chemically unstable bonds in the polymers. Biological media contain a large number of low-molecular and high-molecular mass substances of different chemical nature, which interact with different polymers to different extents.

An analysis of published papers showed that the following substances should be considered from the standpoint of catalytic activity: water, salts, and enzymes. The choice of these substances was made partly because they are the most widespread and partly because their catalytic activity is now generally accepted.

1. Water

The water content of biological media is high. For example, the human organism contains approximately 75% of water, mainly in the intracellular fluid of the tissues and in the plasma. Thus polymers implanted into any part of the organism must be in contact with water.

Abundant information on the sorption and diffusion of water in various polymers is available. In Table 4 we show accepted data for the polymers used in medicine. As can be seen, water readily diffuses in all the polymers, but the amount of sorbed water varies widely as between the polymers. Three characteristic features can be noted.

In amorphous-crystalline polymers the sorbed water is located mainly in the amorphous regions. A dual sorption takes place in hydrophobic polymers at temperatures below the glass transition: volume filling of the micropores and dissolution in the polymer matrix.[28,29] Heterochain polymers and some carbon-chain polymers with heteroatoms in the side radicals are unstable towards water. Carbon-chain polymers without heteroatoms in the side chains are stable towards water.

Table 4. Values of the sorption ($c^0_{H_2O}$) and of the diffusion coefficient (D) of water in various polymers used in medicine.

Polymer	T/°C	$c^0_{H_2O}$/ g (100 g)$^{-1}$	$10^9 D$/ cm^2 s^{-1}
Segmented polyurethanes			
Avcotan-51	37	1.2	400
Biomer	37	1.0	700
Polyacrylonitrile [a]	25	7.5	
Poly(vinyl alcohol) [a]	25	4.0	0.051
Poly(vinyl chloride) [a]	30	0.5	23
Polydimethylsiloxane [a]	35	0.07	70000
Polydodecaneamide [b]	30	2.0	3.9
Poly(2-hydroxyethyl methacrylate), hydrone	37	40	100
Polyglycollide	37	8	5.0
Polycaproamide [b]	35	8	1.2
Polycarbonate	37	0.3	66
Polyglactin (copolymer of lactic and glycollic acids)	37	8.0	7.0
Poly(methyl methacrylate) [a]	50	1.2	130
Polypropylene [a]	25	0.007	240
Polytetrafluoroethylene [a]	20	0.01	–
Polyethylene (ρ = 0.923) [a]	25	0.006	230
Poly(ethylene terephthalate)	25	0.3	3.9

[a] Data from Ref. 26.
[b] Data from Ref. 27.

In the majority of polymers water diffuses relatively fast, and is sorbed in quite large quantities. Thus, in filaments and thin plates we can expect the degradation processes to take place in the inner kinetic region.

Table 5 shows the $k_{eff} c^0_{H_2O}$ values at 37 °C (where k_{eff} is the effective rate constant of the polymer degradation), and also the activation energy of the degradation for different heterochain polymers.

Partially cross-linked polydimethylsiloxane sorbs very small amounts of water, and its degradation takes place mainly in the outer diffusion-controlled kinetic region. The k_{eff} value at 37 °C and the activation energy are 2×10^{-5} g cm^{-2} day^{-1} and 14 kcal mol^{-1} respectively for this material.[35]

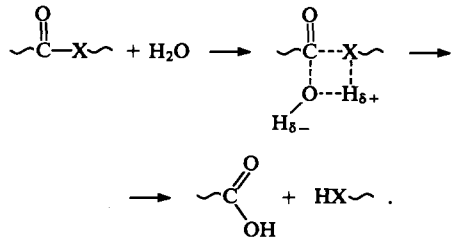
Thus in many polymers [for example polyglycollide, polygalactin, and poly(dimethylsiloxane)] degradation in water is relatively fast, and this must be allowed for when considering the overall kinetics of the resorption of these polymers in biological media, and also when choosing a sterilisation procedure (these polymers cannot be sterilised in steam).

Table 5. Values of $k_{eff} c^0_{H_2O}$ at 37 °C and activation energies for the degradation of various heterochain polymers.

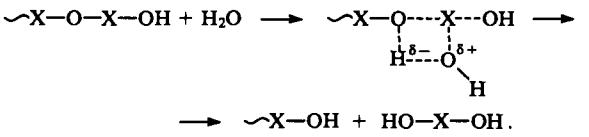
Polymer	$k_{eff} c^0_{H_2O}$/ min^{-1}	E_{H_2O}/ kcal mol^{-1}	Ref.
Polydodecaneamide	4.0×10^{-11}	–	see [a]
Polyglycollide	9.0×10^{-4}	–	
Polycaproamide	1×10^{-10}	–	32, 33
Polycarbonate	3.3×10^{-6} (at 70 °C)	23 ± 1	34
Polyglactin	1.5×10^{-3}	–	see [a]
Poly(ethylene terephthalate)	1×10^{-10}	25 ± 2	

[a] Reviewers' experimental results.

The hydrolytic degradation of carbonyl-containing polymers (polyamides, polyesters, polycarbonates) takes place by the bifunctional catalytic mechanism



The hydrolytic degradation of polymers containing oxygen (for example, polydimethylsiloxane) takes place only at the end of the chain (depolymerisation), and apparently by the following mechanism:[36]



2. Salts

Salts are found in large quantities in biological media. In Table 6 we show the ionic composition of liquids in the human organism.[37] The plasma and the intracellular liquid contain proteins present in the anionic form, because they include carboxylate groups. Detailed studies of the diffusion and sorption of salts in various polymers have been carried out in our laboratory.[24, 38] We shall mention only some of the most characteristic results.

In the diffusion of electrolytes in hydrogels [poly(2-hydroxyethyl dimethacrylate), poly(vinyl alcohol), etc.] the kinetic parameters (for example, the diffusion coefficient D) are close to the corresponding values for solutions. In hydrophilic polymers with only a moderate solubility for water the sorbed water does not form a continuous aqueous medium in the polymer matrix, and the ions diffuse by activated jumps between polar groups. This leads to a large decrease in the c^0 and D coefficients of the electrolyte as compared with the same parameters for the solution.

Electrolytes diffuse in hydrophobic polymers by a mechanism analogous to the transport of gases and vapours. Therefore in the case of electrolytes with a high vapour pressure (for example, hydrochloric acid) the c^0 and D values are close to the corresponding values for water in these polymers. For electrolytes with a low vapour pressure (for example, chlorides and phosphates) we find very low values of c^0 and D, i.e. these electrolytes are not sorbed on hydrophobic polymers to a significant extent.

Table 6. Ionic composition of the liquids in the human organism, mequiv l^{-1}.

Ion	Plasma	Liquid in tissues	Intracellular liquid
Na^+	138	141	10
K^+	4	4.1	150
Ca^{2+}	4	4.1	40
M^{2+}	3	3	40
Cl^-	102	115	15
HCO_3^-	26	29	10
PO_4^{3-}	2	2	100
SO_4^{2-}	1	1.1	20
Organic acids	3	3.4	–

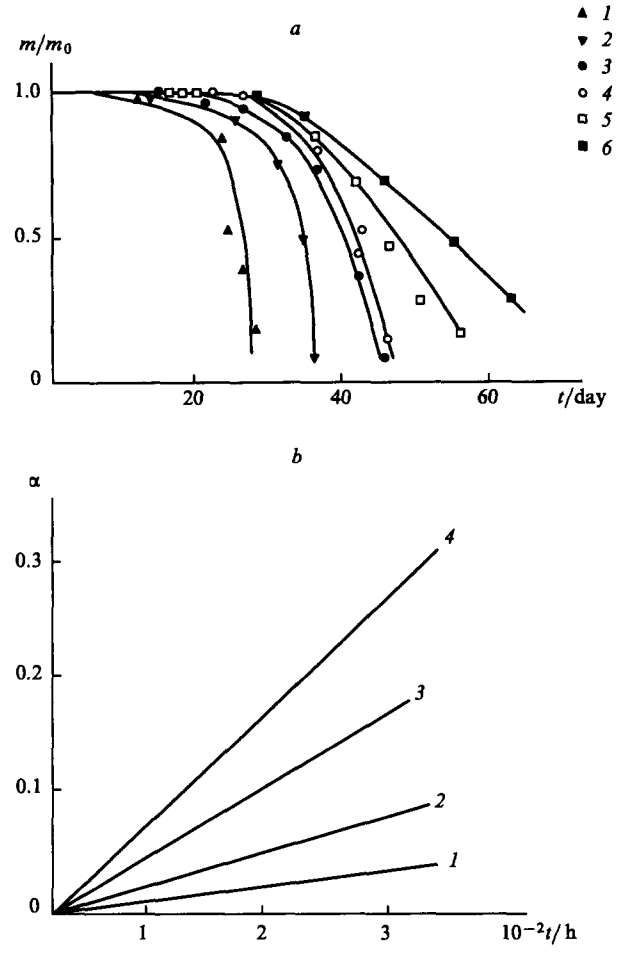


Figure 3. Plots of the relative mass of polyglycollide filaments against time since implantation and of exposure to model media (*a*) and change in the degree of conversion of the molecular mass of polycaproamide filaments incubated in a phosphate buffer solution (*b*). (*a*) pH 7.4, $T = 37$ °C; (*1*) 1 M phosphate buffer; (*2*) organism (subcutaneous tissue of rabbit): (*3*) 0.5 M phosphate buffer; (*4*) 0.1 M phosphate buffer; (*5*) 1 M salt solution; (*6*) water; (*b*) $M_{PCA} = 15000$, pH 7.4, $T = 37$ °C; concentration of phosphate buffer, M, (*1*) 0.1; (*2*) 0.3; (*3*) 0.6; (*4*) 0.1.

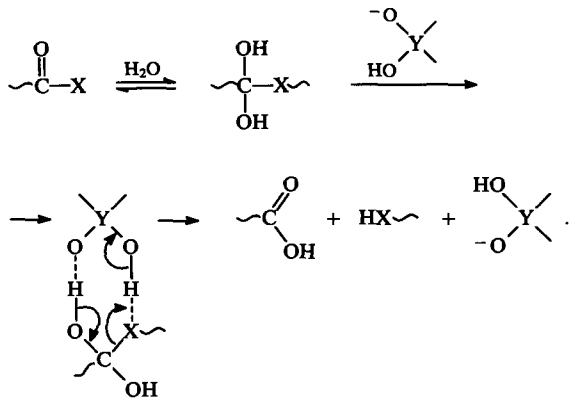
Thus all polymers can be nominally classified into two groups: those that dissolve water and those that do not. Polymers with $c^0_{H_2O} > 1\%$ are assigned to the first group; those with $c^0_{H_2O} < 1\%$ are assigned to the second.

Studies of the catalytic action of salts towards polymers are only just beginning. The effect of the salts listed in Table 6 on some polymers has been examined in our laboratory.

The degradation of moderately hydrophilic polymers (polyglycollide and polycaprolactam is markedly accelerated by an increase in the concentration of acid phosphates, bicarbonates, and bisulfates in buffer solutions of constant pH (Fig. 3). On these same polymers the salts of monobasic acids have a much smaller catalytic effect.[39]

Thus the ions so far examined can be arranged in the following sequence: the anions of polybasic acids are potentially catalytically active, the anions of monobasic acids and the cations listed in Table 6 are catalytically inactive.

The following overall scheme can be suggested for the catalysis by salts of the processes leading to the degradation of polymers containing carbonyl groups:[24]



Clearly, this bifunctional catalysis is impossible in polymers not containing carbonyl groups: for example polydimethylsiloxane.[35]

Thus salts (especially phosphates) have a strong catalytic influence on the degradation process in polymers containing carbonyl groups.

3. Enzymes

Enzymes play an active role in the degradation of polymers implanted in the organism. However, until very recently there was no clear experimental evidence of the reality of these effects. Typical results reported for medical polymers are shown in Table 7. Similar results have been obtained for some other polymers.[42]

Table 7. Rate of change of the relative intensity of the IR absorption bands ($10^2 W/\text{day}^{-1}$) of the polyurethane adhesive KL-3 in model media and in the subcutaneous tissue of rats.[40]

Medium	1110 cm^{-1}	1230 cm^{-1}	1730 cm^{-1}
Physiological solution	0.13	0.05	0.04
Ringer–Lock solution	0.13	0.04	0.03
Rabbit liver extract	0.10	0.04	0.02
Rabit muscle extract	0.10	0.02	0.03
Rabbit kidney extract	0.12	0.02	0.02
Trypsin solution (0.01%)	0.11	0.01	0.02
Chymotrypsin solution (0.01%)	0.12	0.01	0.02
Living organisms	0.59	0.39	0.34

We may conclude from these figures that the chosen media do not adequately model the high rate of degradation of polymers in the living organism. This can be explained by noting that the enzymes which catalyse the degradation are dissolved in a capsule and are essentially lysosomal enzymes produced by macrophages and other cells.

Salthouse[6] determined by quantitative histoenzymology the activity of various enzymes in a capsule on the surface of materials after implantation for different times into rats (Table 8, see over). An increase in the enzyme activity takes place in all the materials after 14 days, associated with an increased phagocytosis in the implantation region. After the healing of the surgical incision and the formation of a capsule from the connective tissue a stationary concentration of enzyme is apparently reached on the polymer surface.

Enzymes diffuse easily in the capsule, and are adsorbed on the surface of polymers in different concentrations. The surface concentration of catalytically active enzymes is determined not only by the number of enzyme species in the bulk of the capsule but also by the competitive adsorption of other proteins (catalytically inactive plasma proteins), lipids, etc. The mechanism of the action of enzymes on polymers is

Table 8. Activity of enzymes in the capsule on the surface of various materials.

Group of materials	Time after implantation	Activity		
		acid phosphatase	aminopeptidase	oxyreductase[a]
Polypropylene,	7	+	±	+
polyethylene,	14	+ +	+	+
polyurethane, poly-	28	±	±	±
tetrafluoroethylene	42	–	–	±
Silicone resin,	7	+ +	+	+
poly(vinyl chloride),	14	+ + +	+ +	+
polyethylene	28	+ +	+	+
(technical)	42	±	–	±
Poly(vinyl chloride),	7	+ +	+	+
plasticised with	14	+ + +	+	+
di-n-propyl and	28	+ +	±	±
decyl phthalates	42	±	–	±
Poly(vinyl chloride)	7	+ + +	+ +	+
plasticised with	14	+ + + +	+ +	+ +
di-n-amyl phthalate	28	+ + +	+ +	+
	42	+	+	+
Poly(ethylene	7	+	±	+
terephthalate)	14	+ +	±	+
	28	±	–	±
	42	–	–	–
Silk	7	+ +	+	+
	14	+ +	+ +	+ +
	28	+	+	+
	42	+	+	+
Polycaproamide	7	+	±	+
	14	+	+	+
	28	±	±	±
	42	±	±	±
Catgut	7	+ +	+	+
	14	+ + +	+ +	+
	28	+ +	+ + +	+
	42	+	+	+
	63	+	+	±
Polyglactin 910	7	+	+	+
	14	+	+	+ +
	28	+ +	+	+ +
	42	+	+	+
	63	–	–	–

Notes. The following symbols are used: – no activity; ± very low activity; + moderately high activity; + + substantial activity; + + + high activity; + + + + abnormally high activity.

[a] Combined activities of succino- and lactodehydrogenase and of cytochromeoxidase.

extremely complex because the majority of polymers are not specific substrates for the enzymes.

We have the results of experiments in vitro which confirm the action of enzymes on polyglycollide. Fig. 4 shows the kinetic curves for the evolution of glycollic acid during the degradation of polyglycollide fibres in solutions with different activities of β-glucouronidase.[43] The initial rate of degradation increases in proportion to the activity of the enzyme; if an inhibitor (iodoacetamide) is added to these solutions the catalytic effect of the β-glucouronidase is almost totally suppressed. Williams[44–46] studied the stability of polyglycollide filaments in solutions of various enzymes, and showed that carboxypeptidase A, physin, and leucineaminopeptidase can strongly accelerate the degradation of this polymer. In the case of other polymers catalytically active enzymes have not been identified beyond doubt, though they are often suggested as a possibility in published papers.

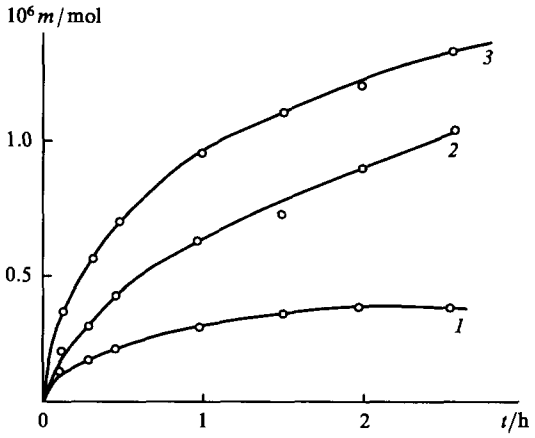


Figure 4. Kinetics of the production of glycollic acid during the incubation of polyglycollide filaments in a solution of the enzyme β-glucouronidase at a concentration of 1 mg ml^{-1} without inhibitor (*1*) and in the presence of the inhibitor iodoacetamide at concentrations 0.5 (*2*) and 1.8 mg ml^{-1} (*3*).

Thus enzymes, like water and the phosphates, are important catalytic agents in the degradation of polymers in biological media.

V. Products of the degradation in the organism

The degradation products are removed from the organism by a two-phase process: metabolic transformation and conjugation. This produces metabolites and conjugates, which are excreted with the urine and the bile or breathed out into the air.[47]

Metabolic transformations are reactions as a result of which the degradation products undergo one or more conversions (oxidative, hydrolytic, etc.) leading to the formation of functional groups which increase the polarity of the molecules.

Conjugation is a reaction which allows the degradation products or their metabolites to combine with biologically active substances in the organism, making the molecules more polar and less fat-soluble and therefore easily eliminated.

Table 9 shows the main heterochain medical polymers, the degradation products identified in model media, and their characteristic properties.

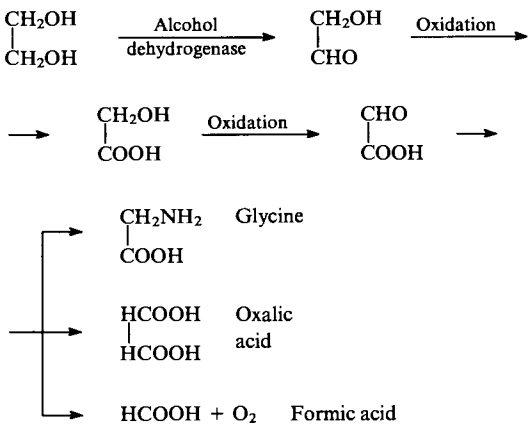
All the degradation products can be divided into three groups.

(1) Degradation products which contribute directly to the metabolic processes (cycles) of the organism: for example, lactic acid in the Corey cycle. These degradation products are almost nontoxic.

Table 9. Heterochain polymers used in medicine, their degradation products, and their characteristics.

Polymer	Degradation products	$10^5 k_{dis}$	Solubility in water
Polyglycollide	Glycollic acid	15	Good
Polyglactin	Glycollic and lactic acid	14	"
Polydodecaneamide	Aminoundecanoic acid	14	Poor
Polycaproamide	α-Aminocapronic acid	14	Good
Polydimethylsiloxane	Mixture of silols and their cyclisation products	–	–
Poly(ethylene terephthalate)	Terephthalic acid, ethylene glycol	29 35	Poor Good

(2) Degradation products able to undergo metabolic or conjugative transformations. For example, ethylene glycol is transformed in the organism by the scheme[47]



The toxic effect of the ethylene glycol is seen first of all in the kidneys, where oxalates are deposited in the channels.

(3) Degradation products eliminated from the organism in an unchanged form. For example, terephthalic acid ($k_{diss} \approx 3 \times 10^{-4}$) has a fairly high polarity and cannot easily penetrate into the tissues, and is therefore rapidly eliminated through the kidneys. It should not be forgotten that terephthalic acid can form a complex with albumin through the amino group of aspartic acid, and in this form it can be carried by the blood circulation system of the organism. Metabolically inert and nonpolar compounds such as vinyl chloride are eliminated with difficulty and tend to accumulate in the fatty tissues.

VI. Biocompatibility and biodegradation of polymers of different classes

Work on the biocompatibility and biodegradation of the main classes of polymers of medical importance is being currently reported. Various approaches to the study of these processes and the most important results obtained by various workers will be discussed below.

1. Polyamides

a. Polycaproamide

Polycaproamide (PCA) is one of the polymers first used for medical purposes. Its structure is similar to that of a polypeptide chain. At present this polymer has only limited applications, mainly as suture filaments (produced by the Ethicon Company, USA: a similar filament is produced in Russia as A122). Polycaproamide can be considered to be biocompatible as a polymer: histological data suggest a very slight inflammation round the implant.[48,49]

PCA has a moderately high resolution time in the organism. From this standpoint it can be used as a model for in vitro studies. For this reason detailed data are now available on the microkinetics of the decomposition of PCA not only in the organism but also in model media.[39,40,42] It follows from those data that the degradation of PCA takes place by a mixed mechanism: both on the surface and in the bulk of the polymer. The catalytic action of water and salts (phosphates, carbonates) on the degradation process should be examined first. In the organism the degradation of PCA takes place with a change in weight and in the molecular mass, due to the dissociation of the accessible amide bonds in the amorphous regions of the polymer (Fig. 5).

A remarkable feature of the degradation of PCA is the fact that the total surface of the polymer remains practically constant during the degradation as a result of the compensation of the normal decrease in diameter of the filaments by the increase in surface area produced by roughness and cracks on the surface.

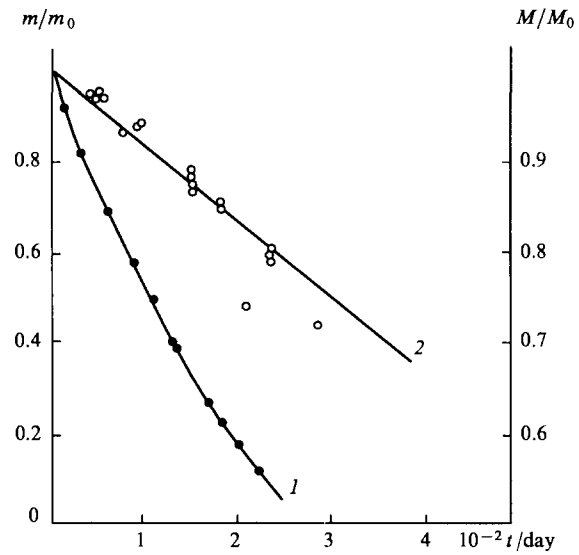


Figure 5. Change in the mass (*1*) and in the molecular mass (*2*) of PCA A122 (diameter = 24±2 μm, M = 15 000) after implantation for various times in the subcutaneous tissues of rabbits.

The change in mass of the polymer is described by the equation

$$m = m_0 - k_{eff}^S t .$$

Here m_0 and m are the initial and final mass respectively, and k_{eff}^S is the rate constant for the degradation of the polymer on the surface,

$$k_{eff}^S = kc_{cat} S ,$$

where c_{cat} is the concentration of catalyst and S is the area of the polymer surface.

The constant k_{eff}^S was determined by experiments on rabbit, and found to be $(1.6 \pm 0.2) \times 10^{-3}$ g day^{-1}. The rate constant of the decomposition of the amide linkages in the polymer matrix, determined by the law of chance [$k_{eff(l.ch.)}$] from data on the titration of the terminal amido groups in the implanted samples, was $(5.4 \pm 0.5) \times 10^{-5}$ day^{-1}.

An analysis of the action of catalytic agents showed that the bulk degradation of PCA takes place under the influence of water, whose solubility in PCA is 5.5% ± 0.5%. The large water content of the polymer allows the penetration of salts into the PCA with a diffusion coefficient[51] of 10^{-9} cm^2 s^{-1}. The rate constant of the decomposition of the amide bonds in the amorphous region in the presence of water at 37 °C is 1×10^{-7} day^{-1}; with this value of the rate constant only 0.5×10^{-4} of the amide bonds are dissociated in a year, which is much less than the rate constant for the decomposition in the organism.[32] This shows the important contribution made by salts to the degradation of polymers in the bulk. Model experiments in 0.1 M NaH_2PO_4 (the concentration of the liquid within the cells) at 37 °C gave

$$k_{eff(l.ch.)} = (0.5 \pm 0.1) \times 10^{-5} \text{ day}^{-1} .$$

Special experiments have shown that enzymes cannot penetrate effectively into films of PCA of thickness equal to the diameter of the filaments even over a period of 100 days. It is assumed that enzymes can contribute to the degradation process only from the surface. Thus the decomposition in the bulk of the polymer (V-type) takes place under the influence of water and salts, whereas the decomposition on the surface (S-type) takes place under the influence of enzymes in the organism.

These quantitative results allow us to predict the stability of PCA in the organism. In spite of the satisfactory compatibility with the tissues of the organism the use of PCA in suture threads is not very widespread; the prospects of using this material as rapidly resorbed threads have suffered from the more recent development of materials such as Dexon and polyglactin.

b. Polydodecaneamide

Polydodecaneamide (polyamide 12) is used as an endoprosthesis. This polymer is fairly stable in terms of its rate of resorption in the tissues of the organism, and therefore it is of interest as the foundation of various structural modifications aimed at preparing new materials for endoprosthetic purposes.[52-55]

The mechanism of the degradation of polyamide 12 was shown to be similar to the mechanism found in polycaproamide: implantation results in a decrease in molecular mass, in mass of the sample, and in the stability and diameter of the elementary filament, accompanied by the appearance of cracks on the polymer surface. As could have been expected the degradation mechanism is identical to that of the decomposition of PCA in the organism, i.e. the degradation takes place in the amorphous regions of the polydodecaneamide (according to IR spectroscopy and to X-ray structural analysis data[54]) under the influence of the same catalytic agents as in the case of PCA: salts and enzymes.

2. Polyesters

a. Polyglycollide

Polyglycollide (PGL), the polycondensation product of glycollic acid, was the first polymer specially synthesised for medical applications (in the late 1960s) by the American Cyanamid Company (USA). The principles of the synthesis and the structural features of PGL have been widely studied.[56-60] Polyglycollide is used in various fields of medicine: in orthopaedics and traumatology (pins, plates, pegs, needles, bone replacements), and in opthalmology as threads, fibre materials, sponges, and powders for wounds and burns. The principal advantage of PGL is its suitability for use in two-component systems as the resorbed member of the prosthesis.

The widespread use of PGL is explained by the good compatibility of the polymer at the initial implantation irrespective of its form (blocks, powders, filaments), and also by the fact that the only decomposition product, glycollic acid, contributes actively to the metabolism in the organism, breaking down[6] to H_2O and CO_2. Histological studies of this material (see Tables 2 and 3) in the initial, intermediate, and final stages of the implantation failed to detect any trend towards an increase in the size of the cells, characteristic of specific inflammation reactions. A well-formed capsule of connective tissue is found round the implant.[61-63]

Since the synthesis of PGL many studies of its degradation have been reported. The most detailed studies were made of suture threads of PGL commercially available under the name of Dexon produced by the firm Chek and Devis Cyanamid (USA).[8,46,64-66]

Some recent papers[43,46,67-71] discuss the kinetics of the decomposition of PGL in the organism and in model media. They include studies of the macrokinetics of the decomposition in the organism and in vitro and determinations of the main catalytic components of the medium in the living organism, and also of the relative contribution of each component to the degradation process.

Studies of the macrokinetic features of the degradation of the material in the living organism and in the separate components of the biological medium, coupled with quantitative studies of the contribution of each component of the medium allowing for the structural properties of the PGL filaments (established by electron microscopy and by X-ray diffraction analyses), led these workers[68,70] to propose a mechanism for the decomposition of PGL in the organism. The most significant results of this work are the following.

The filaments decompose by an unusual mechanism in the organism. After 15-18 days implantation the micrographs show a transverse distribution of the filaments on regions ~1 mm wide, without any change in the diameter of the elementary threads. However, a loss in mechanical strength of the PGL is observed.

The curves describing the loss in mass (Fig. 6) have a complex form: a slight change in the initial stages of the implantation followed by a rapidly increasing loss of mass after 20 days.

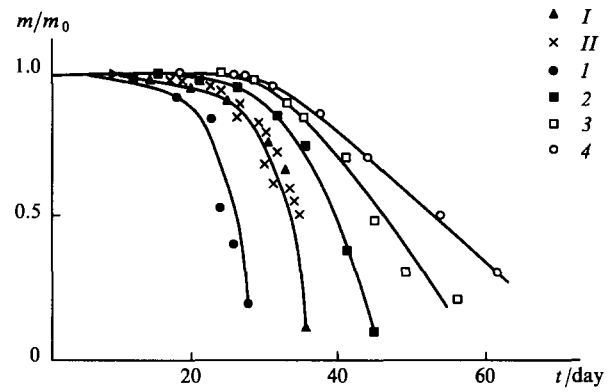


Figure 6. Changes in the relative mass of PGL filaments against time of implantation in the subcutaneous tissues of rabbits and time of treatment in a phosphate buffer of pH 7.4 at 37 °C. (*I*) In the organism, (*II*) theoretical curve for the organism as a medium; concentration of phosphate buffer, M: (*1*) 1; (*2*) 0.3; (*3*) 0.1; (*4*) water.

The kinetic weight loss curves in water, in phosphate buffer, and in carbonate buffer at pH 7.4 and 37 °C are similar to those observed in the organism, the salts of strong monobasic acids having practically no effect on the kinetic parameters whereas in the presence of phosphates we find a marked increase in the rate of degradation (curve *1* of Fig. 6).

In buffer solutions of pH 4.05 and 2.01 the PGL filaments are degraded at a rate close to that observed in water, i.e. in this range of pH the acid medium does not markedly affect the hydrolysis of the ester bonds.

In vitro experiments on the incubation of PGL in proteolytic enzyme solutions showed that the enzyme β-glucouronidase is active towards this reaction. The following values of the effective decomposition rate constant for the dissociation of esters bonds in PGL under the influence of the main components of the medium in the organism at 37 °C were reported.

Constant	$k \times 10^2$
$k^V_{H_2O}$	5.0
$k^{S-V}_{H_2O}$	4.2
$k^V_{H_2PO_4}$	5.0
$k^{S-V}_{H_2PO_4}$	4.2
k^{S-V}_{enz}	1.0

Here k^V is the effective rate constant for the decomposition of the ester bonds in PGL in the amorphous regions of the polymer under the influence of water and salts; k^{S-V} is the effective constant for rate of dissociation of ester bonds on the surface of the crystallites, depending on the type of decomposition of the fragments of the PGL macromolecule on the crystallite surface and on the adhesion and solubility in the surrounding medium of the decomposition products.

An analysis of these results suggests a two-stage mechanism for the degradation of PGL (a highly crystalline polyester, with an amorphous fraction of ~0.2 and a crystalline fraction of 0.8). In the initial period of the implantation water is sorbed in the amorphous regions, and the polymer degrades slowly, mainly under the influence of water. Then, after a conversion of the polymer of 0.2, the rate of degradation in the organism increases rapidly. This can be attributed to the breakdown of the crystallites on the surface under the influence of the sorbed water, salts, and enzymes. From in vitro experiments we can obtain the effective rate constants for the dissociation of the ester bonds under the influence of water, salts, and enzymes.

The general equation for the change in mass, obtained from the above results, is

$$\frac{m}{m_0} = 0.2 - v_i[1 - \exp(-k^V_{H_2O}\, c^V_{H_2O}\, t)]^2 + (1 - v_i)\left(1 - \frac{k^{S-V}_{H_2O}\, c^{S-V}_{H_2O}\, t}{Nb_0\rho}\right)^2 - v_i[1 - \exp(-k^V_{H_2PO_4^-}\, c^V_{H_2PO_4^-}\, t)]^2 + (1 - v_i)\left(1 - \frac{k^{S-V}_{H_2PO_4^-}\, c^{S-V}_{H_2PO_4^-}\, t}{Nb_0\rho}\right)^2 + (1 - v_i)\left(1 - \frac{k^{S-V}_{enz}\, c^{S-V}_{enz}\, t}{Nb_0\rho}\right)^2,$$

where m_0 and m are the initial and the time-dependent mass of the polymer, N is the number of crystallites in the transverse section, ρ is the density of the polymer, b_0 is the transverse dimension of the crystallites, $c^V_{H_2O,\,H_2PO_4^-}$ is the average concentration of water and of phosphate ions in the amorphous part of the polymer, 0.2 is the volume fraction of amorphous regions in the PGL, $c^{S-V}_{H_2O,\,H_2PO_4^-}$ is the average concentration of water and of phosphate ions on the side surface of the crystallite.

A computer solution of the inverse problem which used the above rate constants and a range of enzyme concentrations in the subcutaneous tissue of rabbits, undertaken because of the lack of accurate published data, gave a satisfactory agreement with the experimental curve for the weight loss in the organism.

The above quantitative analysis allows the kinetic curves for the decomposition and lifetime of PGL filaments of various diameters to be predicted for different parts of the organism (containing different enzymes and salts). The prospects for the application of this polymeric material in medicine are exceptionally good because of its good mechanical properties and biocompatibility and of its controllable resorption times.

b. Polyglactin

Polyglactin (PGLA) is a copolymer of glycollic and lactic acid produced by the Ethicon Company (USA). The decomposition products of this polymer in the organism are glycollic and lactic acid, which take part in the metabolic processes. Histomorphological tests on PGLA items in the form of suture threads or tablets show a good compatibility with the tissues of the organism.[6, 72–76]

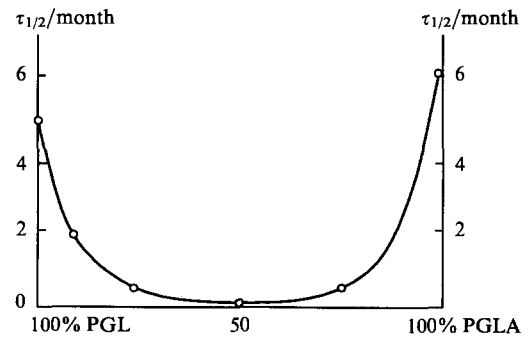


Figure 7. Plot of the time of half-decomposition of tablets of the copolymers PGL and PGLA implanted in rats.

The decomposition mechanisms and the rates of degradation of PGLA and its copolymers are identical. The homopolymer of lactic acid decomposes more slowly than PGL in the subcutaneous tissue of rats, evidently because of the lower solubility of water in the polylactide.[77] Tablets of the copolymer with different concentration ratios of glycollic and lactic acid have different half lives (measured from the concentration of ^{14}C in the organs of the rats), ranging from several months for the homopolymers to one week for the polymer with a concentration ratio of 50 : 50 (Fig. 7).

Salthouse and Matlaga[78] published a detailed study of the degradation of PGLA 910 in the subcutaneous tissues of rats, aimed at clarifying the role of cell enzymes in the resorption of the polymer. They concluded that in the initial stages the enzymes do not contribute to the degradation. A slight increase in the dehydrogenase and cytochrome oxidase activity after 40 days is explained by the participation of these enzymes in the breaking down of the dissociation products to metabolites by the scheme

PGLA 910 + water ⟶

⟶ Lactic and glycollic acids $\xrightarrow{\text{Oxyreductase}}$

⟶ $CO_2 + H_2O$.

We should stress that PGLA is the only polymer for which the decomposition kinetics and the metabolism of the degradation products have been investigated.

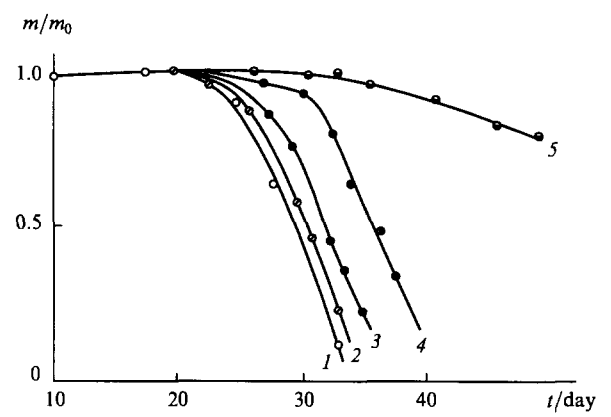


Figure 8. Changes in the relative mass of PGLA filaments with time of implantation in the subcutaneous tissues of rabbits and with the time of treatment in buffer systems of pH 7.4 at 37 °C. (*1*) 1 M carbonate buffer; (*2*) organism; (*3*) 1 M phosphate buffer; (*4*) 0.5 M phosphate buffer; (*5*) water.

The weight loss curves in the organism, in water, and in various buffer solutions are similar to the kinetic curves for PGL (Fig. 8).[68] We note a slight acceleration of the decomposition of PGLA as compared with the PGL filaments.[77] This can be explained by a slight disordering of the crystalline regions of the polymer due to the difference in the parameters of the unit cell of the copolymer.

Copolymers of this type have good prospects of applications in medicine because suture materials made from them offer a wider spectrum of resorption times than the materials made from PGL.

c. Poly(ethylene terephthalate)

Items made of poly(ethylene terephthalate) (PETP) as gauzes, suture threads, and vessel prostheses have a well established place in surgical practice because of their ability to retain their functional prosthetic properties over long implantation times as well as because of their good biocompatibility.[79–82]

Abundant information is available on its histological compatibility: it is well established that PETP implants always produce the smallest reaction from the tissues, consisting of a thin capsule and a normal connective tissue round the prosthesis for extended time periods (up to 5 years).[83-85] However, macrophages have been detected after long implantation times, apparently due to the influence of terephthalic acid on the surrounding tissues.[86]

There are reports of macroscopic observations of differences in the properties of vessel prostheses in the human organism implanted for different times, and it has been shown that periods in the organism of up to 5 years make effectively no difference to these properties.[81] After 8 and 11.5 years of residence in the organism cracks appears on the surface of the polymeric prosthesis, and the filaments becomes thinner.

Systematic studies of the degradation processes in PETP gauzes produced in Russia and implanted in the muscle tissues of rabbits, dogs, and humans have been aimed at establishing the lifetimes of the prostheses.[87-89]

As was pointed out above, at 37 °C PETP is stable towards hydrolysis in water, but it undergoes *S*-type decomposition in basic media (when the reaction rate is much greater than the rate of diffusion of the aggressive medium) and *V*-type decomposition in acid media (when the reaction rate is much smaller than the rate of diffusion of the aggressive medium). An analysis of data on the degradation of prostheses made from PETP used in soft tissues showed that both types of degradation can take place, depending on the conditions existing in the organism.

When the pH of the surrounding medium is between 7.0 and 7.4 the breaking load can be determined by the formula

$$P = P_0\left(1 - k_{\text{eff}}^{S}\,\frac{t}{r_0\rho}\right)^2,$$

where P_0 and P are the initial and the final breaking loads and r_0 is the radius of the elementary filaments. The linear dependence of $P^{1/2}$ on the time t allows the time for a 50% loss of strength under these conditions to be predicted (Fig. 9*a*).

The *V*-type decomposition of PETP was first detected in an analysis of the properties of prostheses implanted in the organism under conditions of strong inflammation. The medium had a pH of 4.8–6.8, and it appeared that these values were controlled by the action of bacteria observed on the prostheses and near them.[80] Under these conditions the samples completely lost their strength after 2 or 3 months in the organism, and their molecular mass fell steeply as a result of the dissociation of the ester bonds in the amorphous regions (Fig. 9*b*). The change in the molecular mass is described by the equation[90]

$$\frac{1}{M} - \frac{1}{M_0} = k_{\text{eff}}^{V}\,t,$$

where M_0 and M are the initial and the time-dependent number-average molecular masses, and k_{eff} is the effective rate constant of the dissociation of the bonds in the amorphous regions of the polymer.

As regards the participation of the catalysts present in the organism water does not appear to have any catalytic effect in the case of PETP: k_{eff} for water in PETP at 37 °C is 10^{-9}–10^{-10} min^{-1}, and after 10 years 0.1% of the ester bonds are decomposed.[24] Phosphate ions penetrate into the polymer matrix to a negligible extent, and therefore the degradation induced by these species is confined to the surface. The enzymes found in the organism should contribute (as in the case of PGL and PCA) to the degradation starting from the surface. Therefore under the conditions normally experienced by the prosthesis (pH 7.0–7.4) the degradation of the PETP will take place from the surface under the influence of salts and enzymes.

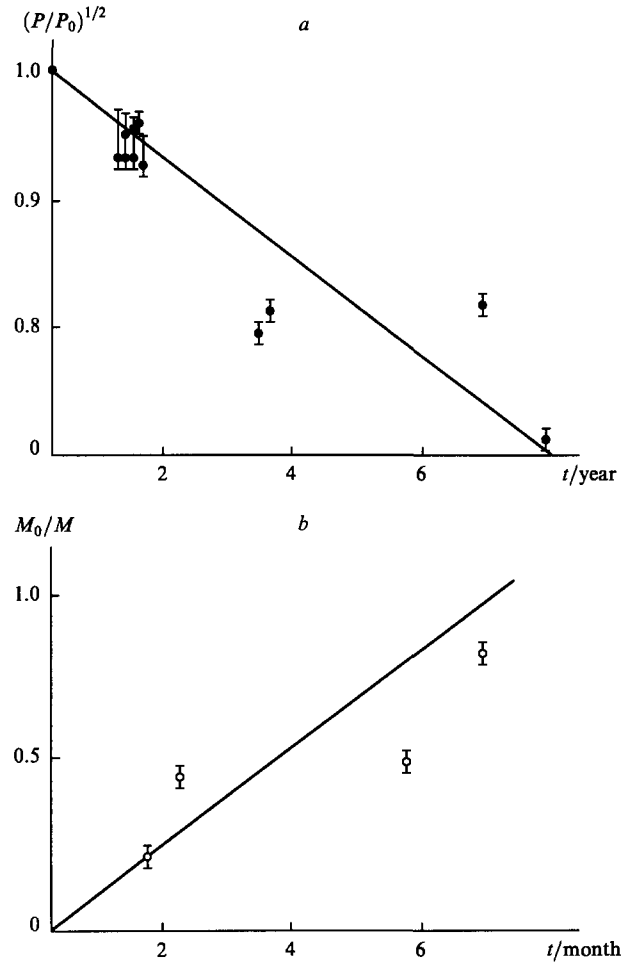


Figure 9. Changes in the breaking strength of elementary filaments of PETP recovered from the human organism for different times of residence of the prosthesis in the organism at pH 7.0–7.4 (*a*) and dependence of the relative molecular mass for samples of prostheses of PETP recovered from the human organism under infectious conditions, pH 4.8–6.8 (*b*).

In the case of a prosthesis in pathological surroundings (acidic medium) enzymes and acids can become catalytically active. Acids are the only really active substances able to induce degradation in the volume of the PETP because of the ability of volatile acids to diffuse in the polymer matrix. In this case the effective rate constant for the degradation of PETP in the organism[91] is 1.1 ± 0.5 year^{-1}.

These observations can explain the report[46] that PGL is degraded in the presence of bacteria. In fact, PGL (unlike PETP) dissociates in an acid medium at a rate close to its rate of decomposition in water (see Fig. 6). As reported,[89,92] the active degradation agents in a bacterial medium are mainly the enzymes produced by the bacteria, and various low-molecular products (mainly acids) which lower the pH of the medium. In the light of the main parameters of this material (biocompatibility and biodegradation) we may suggest that PETP will achieve a wide exploitation in medical practice for the fabrication of prostheses and other articles and materials.

3. Polyolefins

a. Polypropylene

Polypropylene (PP) was first used in medical practice because of its high chemical stability and favourable mechanical properties. In the early 1970s it was used for lining the valves of artificial hearts, and for ball joint prostheses. It is now commercially available as suture threads from the Ethicon Company (USA).

Histological results show that PP of 'medically pure' grade stimulates only a moderate reaction from the tissues of the living organism [6, 8, 93] as compared with PP containing traces of catalysts and stabilisers.[94]

Polypropylene can undergo only oxidative degradation. Therefore in the tissues of the living organism PP should be stable, and decompose slowly only under the influence of oxidative enzymes and oxygen dissolved in the living medium.

The overall picture of the degradation of PP filaments and films in the organism is characterised by the following phenomena: a worsening of the mechanical properties (a decrease in the breaking load and in the relative elongation);[84] crack formation in the initial stages of the implantation and fragmentation of the polymeric implant at longer times (the fragmentation being observed sooner in PP samples without an antioxidant);[84] constant molecular mass at all times during the implantation; appearance in the IR spectra of the PP samples after implantation of an absorption band corresponding to the C=O group;[95] an increased activity of oxyreductase and cytochrome oxidase in the capsule surrounding the implant.[6]

It follows from the above experimental observations on the degradation of PP in the organism that this polymer undergoes the *S*-type of degradation under the influence of oxidising enzymes, which cannot penetrate into the polymer matrix. As is well known, oxidative degradation is accompanied by the breaking of the main chain of the polymer and should lead to a decrease in the molecular mass, but since the catalytic agents are unable to penetrate into the bulk of the polymer the surface bond breaking produces a negligibly small decrease in the molecular mass of the whole article. The accumulation of carbonyl compounds as a result of oxidation also takes place on the surface of cracks rather than over the whole volume of the sample.

Special experiments with PP incubated in a solution of cytochrome oxidase did not produce the expected result because of the rapid inactivation of this enzyme in experiments in vitro. Therefore experiments with bacteria which produce oxidative enzymes able to open the C – C bond are needed to account for the role of these enzymes in the oxidation of this polymer.

b. Polyethylene

Articles made of polyethylene (PE) have been used in surgery for the past 30 years: for example, high-pressure polyethylene (HPPE) is used for fabricating pelvic joint prostheses. As a stable, undecomposed polymer this material has been used in emergency medical technology as packing and as circulatory vessels.

Histomorphological studies of PE have attracted extensive interest. It has been reported that the overall reaction of the organism to this polymer is favourable.[98–100]

The biodegradation of PE was established by solving the inverse problem with the aim of exploiting the polymeric by-products with the aid of microorganisms and bacteria. It was found that commercial polyethylenes (especially HPPE) undergo practically no biodegradation by the radical mechanism.[101, 102]

The following features of the biodegradation of PE have been established.

(1) The main condition for the biodissociation is an increase in the specific surface of the polymer (for example by using powders).[103]

(2) The dissociation process takes place with a decrease in mass, accelerating during the initial stages of incubation and then slowing down.

(3) Samples of low-pressure polyethylene (LPPE) incubated with microorganisms are found to include carbonyl groups, especially in the presence of fillers, which are sensitive to oxidases and esterases.[104, 105]

PE specially labelled with ^{14}C was used in studies of the rate of biodegradation of slowly decomposed PE.[105] Samples incubated with microorganisms for different times (up to 3 years) were irradiated with UV light in order to accelerate the degradation, and the weight loss caused by the action of the bacteria and microorganisms was determined. Extrapolation to zero time of irradiation gave the weight loss due to the biodegradation. The loss of mass of the powders determined by this method was 0.5% in 3 years.

It follows from these data that PE (like PP) is degraded by the *S*-type of mechanism, and that the decomposing species can be oxidative enzymes generated by bacteria and microorganisms, for which the PE acts as a carbon feed medium.

By combining the data for the degradation of PP and PE we may conclude that although these polymers decompose slowly the rearrangement of their structure during the oxidation process can lead to undesirable consequences for the organism.

4. Elastomers

a. Polydimethylsiloxane

Articles made from polydimethylsiloxane (PDMS) are used successfully in medicine. Its inertness, its favourable mechanical properties, and the ability to produce articles of almost any shape for introduction into the organism opened a wide range of applications for polyorganosiloxanes in various fields of medicine (in surgery as prostheses for various bone structures and for soft tissues, and as auxiliary items such as tubes, catheters, bypasses, medicine carriers). In the 1960s this polymer was industrially adopted for the production of various articles, now available under the trade name Silastic, by the Dow Corning Corporation (USA).

The good biocompatibility of PDMS is confirmed by the results of many quantitative studies. Histological and histochemical data obtained for silicone polymers are often used as tests for the biocompatibility in the evaluation of new polymers.[106–110]

In spite of the extensive studies and experimentation aimed at the practical application of siloxane polymers very few quantitative data on their degradation in the organism have been published. Systematic studies of the degradation of

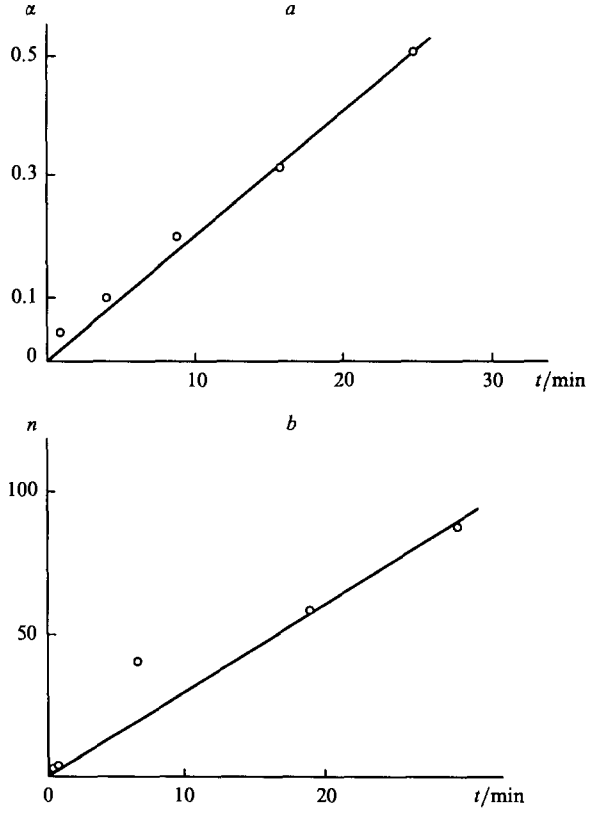


Figure 10. Plots of the extent of mass conversion of PDMS (*a*) and of the number of broken silanol bonds (*b*) against time during hydrolysis at 300 °C.

vulcanisates from dimethylsiloxane rubber of low molecular mass (SKTN) in living tissues have been carried out during the last 20 years at the Vishnevskii Surgery Institute.[109,111,112]

Fragments containing Si–O bonds can decompose in water.[113,114] Reported data[115] on the decomposition of SKTN at high temperatures in water vapour (Fig. 10) can be analysed quantitatively by postulating two simultaneous processes:
(1) decomposition by the laws of chance (with a rate constant $k_{l.ch.}$) with formation of silanol end groups

$$\frac{dn}{dt} = k_{l.ch.}(n_0 - n),$$

where n_0 is the initial concentration of silanol bonds, and n is the concentration of broken bonds at time t;
(2) depolymerisation at the silanol bonds (with a rate contant k_{dep}), resulting in loss of mass of the polymer

$$\frac{dm}{dt} = k_{dep} n .$$

On the assumptions that these two processes take place with comparable rates, that the decomposition by the laws of chance proceeds only to a small extent, and that the reaction itself is under activation control, the overall change in mass can be described by the equation

$$\Delta m = k_{dep} k_{l.ch.} t^2 .$$

Data on the degradation of PDMS are shown in Fig. 11.

The degradation of PDMS at temperatures below 100 °C has been discussed.[35] At these temperatures we can expect, in addition to the decomposition in the inner activation-controlled region, an active contribution from decomposition at the surface, since the concentration of water in the bulk of the polymer is extremely small. These types of degradation can be identified as follows. If a change in strength is observed the process is taking place mainly in the bulk, and conversely if the strength remains unchanged the surface decomposition is predominant. It was found that at high temperatures, when the water is in the vapour phase, the reaction is of the *V*-type, whereas at lower temperatures it is of the *S*-type.

Experiments on the degradation of PDMS in a phosphate buffer failed to detect a catalytic influence from the phosphate ions, thus excluding the possibility of a bifunctional catalysis reaction under the influence of the ions present in the organism.

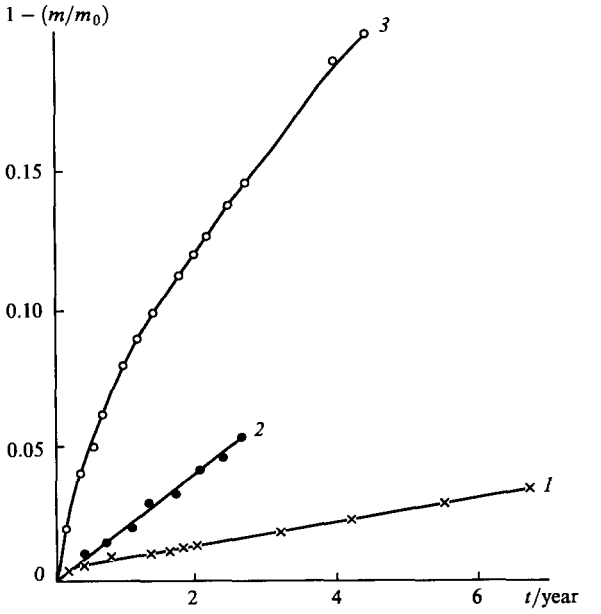


Figure 11. Plots of the extent of mass conversion of PDMS at 37 °C against time. (*1*) air; (*2*) water; (*3*) organism (subcutaneous rabbit tissue).

Therefore the contribution of water to the degradation of PDMS in the organism should manifest itself in the activation of the reaction leading to the depolymerisation of the end groups on the surface of the PDMS. However, the rates of degradation in the organism and in water are very different (see Fig. 11). This difference can be ascribed to the contribution from the enzyme component to the surface depolymerisation reaction. Unfortunately enzymes capable of breaking siloxane bonds have not so far been identified, and it is difficult to attempt a quantitative analysis of the contribution from enzymes.

The thinning of a PDMS plate owing to loss of mass (for example, during degradation in the organism) amounts to ~ 40 μm year^{-1}. Therefore the fabrication from PDMS of articles having a strictly prescribed form for long-term implantation is not recommended.

The prospects of articles based on polyorganosiloxane polymers in medicine are assured, especially in the solution of medical technology applications. Polydimethylsiloxane is also often used as an essential component for the modification of other polymers.

b. Polyurethanes

Polyurethane materials have found applications in medical practice because of their physicochemical properties, which can be varied over wide limits.

The polymer chain of polyurethanes (PU) contains the urethane group, whose structure is close to that of the peptide group in proteins: this may account for the successful application of this class of synthetic materials as biological plastics. Articles based on segmented PU with ether bonds are used as clot-resistant materials, catheters, intra-aortal bulbs, and components of artificial hearts.

Widely used items made from PU foam with ester bonds include adhesives and various alloplasts. Extensive studies have been devoted in our country as well as abroad to problems of biocompatibility and biodegradation in articles made from PU, especially adhesive compositions.[41,116–118] This work led to the conclusion that the main reaction is the hydrolysis of esters bonds, which results in the degradation of adhesives and other PU items in the tissues of the living organism.[119] These workers deny the involvement of enzymes in the degradation process on the basis of model experiments in solutions of trypsin, chitotrypsin, and elastase. Their results showed that in every case there was no difference between the rates of decomposition of PU in these media and in a physiological solution (the rates being determined from the change in molecular mass and from the strength of the IR absorption bands).

Enzymes which are found in a capsule of the given polymer must be used for experiments in vitro. In particular, aminopeptidase and acid phosphatase were found in the PU capsule.[6] This explains the negative effect reported[119] when using proteolytic enzymes, which often have an inhibiting action.

An analysis of kinetic data for PU with ester bonds showed that the degradation is caused by the hydrolytic dissociation of these bonds in water over the whole volume, as shown by the change in molecular mass of the polymer. The difference in the rates of decomposition can be explained by the participation of enzymes in the degradation from the surface of the polymeric material theough the breaking of the urethane bonds under the laws of chance, as was shown in the case of PGL.[68]

A systematic study of the degradation of low-molecular polyurethanes labelled with ^{14}C under the influence of a range of enzymes (from esterase to oxidative enzymes) also indicated a nonspecific degradation, mainly dependent on the molecular mass of the polymer. This work was done at a qualitative level.[120]

The role of the cell components in the degradation of PU foams from the surface (the so-called 'cell participation') has also been reported.[121,122] The cell involvement in the degradation of polymers is specially striking in polymers with a developed surface, such as PU, but nevertheless the active groups are the ultimate degradation agents.

Table 10. Main parameters of biocompatibility and biodegradation of polymers.

Polymer	Toxicity class of polymer	Toxicity of decomposition products	Type of decomposition and main catalyst	Notes
Polycaproamide	–	Moderately high	*S*, enzymes *V*, salts	$m/g = m_0/g - 1.6 \times 10^{-3} t/day$; a filament 24 ± 4 μm in diameter decomposes in 500 ± 50 days in the subcutaneous tissues of rabbits
Polydodecaneamide	–	Moderately high	*S*, enzymes *V*, salts	$m/g = m_0/g - 1 \times 10^{-3} t/day$
Polyglycollide	I	Very low	*S*, enzymes *V*, salts, water	$m/m_0 = 0.2 - 0.2[1 - \exp(-k_{H_2O}t) - \exp(-k_{salt}t)] + 0.8[(1 - k_{H_2O}t/A)^2 + (1 - k_{salt}t/A)^2] + (1 - k_{enz}t/A)^2$, where $A = Nb_0$. For a filament with a diameter of 18 ± 1 μm $P = 0$ after 20–25 days (subcutaneous rabbit tissues)
Polyglactin	I	Very low	*S*, enzymes *V*, water, salts	Similar equations apply to PGL
Poly(ethylene terephthalate)	–	Moderately high	*S*, enzymes, salts	$m/g = m_0/g - 4.0 \times 10 (t/day)(S/cm^2)$ $P = P_0[1 - 4.0 \times 10 (t/day)(S/cm^2)]^2$ After 30 ± 7 years a filament with a diameter of 19 ± 2 μm is completely decomposed and $P \approx 0$ (clinical data)
Polypropylene	–	Not determined	*S*, enzymes	–
Polyethylene	–	"	*S*, enzymes	$m/g = m_0/g - 2 \times 10^{-6} t/day$
Polydimethylsiloxane	I	"	*S*, water, enzymes	$m/g' = m_0/g - 1.5 \times 10^{-5} (t/day)(S/cm^2)$

5. Cyanoacrylate adhesives

Synthetic adhesive compositions based on cyanoacrylates have found wide applications in surgery for the sutureless connection of tissues. Cyanoacrylates, including the well known ethyl ester of α-cyanoacrylic acid, were first used in medical technology, but they were then modified for applications in medicine. At present adhesives based on alkyl(aryl)-α-cyanoacrylates are generally used in experimental and clinical surgery. A recent review [120] listed the main conclusions on the properties of cyanoacrylate adhesives. In general, according to a large group of results, cyanoacrylate adhesives are degraded rapidly (~60%–80% by weight in the first few months).[120] It is pointed out that the degradation products do not cause toxic of allergenic reactions in the organism,[120] and that the adhesives based on n-alkyl-α-cyanoacrylates are nontoxic, nonimmunogenic, biodegradable polymers.[121, 122] According to other workers (for example, Lipatova and Pkhakadze[123]) the degradation products of cyanoacrylate adhesives can induce local toxic reactions.

Unfortunately many studies of the biodegradation of cyanoacrylate adhesives do not include a quantitative analysis. Some interesting results were obtained [124] for the heterogeneous in vitro degradation of poly(n-alkyl-α-cyanoacrylates) of different molecular masses at 37 °C and different pH values (6–8). Under these conditions the degradation proceeds from the surface, and the experiments were made with films of sample having identical surface areas. The main product of the degradation is formaldehyde, and the dependence of the mass dissociation constant on the pH, molecular mass, and nature of the radicals (ethyl, butyl, hexyl) is linear.

Salts present in the organism catalyse the degradation, and therefore we expect the degradation of cyanoacrylate adhesives in the tissues of the living organism to proceed mainly from the surface.

Other polymers, such as polytetrafluoroethylene, poly(vinyl chloride), polycarbonate, poly(methyl methacrylate), cyanoacrylates, poly(vinyl alcohol), and poly(ethylene oxide) are used in medicine in addition to those mentioned above. The possibility of medical applications has been examined for polymers such as polydodecaneamide, polyglycollide, polyglactin, hydrogels, and segmented polyurethanes.

VII. Conclusion

At present polymers used in medicine cannot (unfortunately) be fully characterised in terms of their biocompatibility and biodegradation parameters (see Table 10). For PGL, PETP, and PDMS the lifetime and the mass durability in the organism can be determined with adequate precision. For PP and PE accurate data are not available at present, and must be obtained in the current research. Biocompatibility problems are the less well understood. With the exception of polymers specially synthesised for medical purposes, for which we may confidently expect that the degradation products cannot cause any complications in the organism, unambiguous and well founded conclusions on the biocompatibility of other polymers should become possible in the near future from a generalisation of the results of implantations and of experiments now in progress in many medico-biological research centres.

References

1. *Polymeric Biomaterials* (Eds S E Piskin, A S Hoffman) (Dordrecht: Martinus Nijhoff, 1986)
2. N A Plate, L I Valuev *Zh. Vses. Khim. O-va im. D I Mendeleeva* **30** 402 (1985)
3. *Fundamental Aspects of Biocompatibility* (Ed. D F Williams) (Boca Raton, FL: CRS Press, 1981)
4. A M Chernykh *Vospalenie* (Inflammation) (Moscow: Meditsina, 1979)
5. B Monis, T Weinberg, G J Spector *Br. J. Exp. Pathol.* **49** 302 (1968)
6. T N Salthouse *J. Biomed. Mater. Res.* **10** 197 (1976)
7. P A Ward, in *Principles of Pathobiology* (Eds M F Lavis, R D Hill) (New York: Oxford University Press, 1971) p. 115
8. T N Salthouse, B F Matlaga *J. Surg. Res.* **19** 127 (1975)
9. R E Wilsnack, D V M Bernadyn, B S Huntington *Biomater. Med. Devices Artif. Organs* **7** 527 (1979)
10. G M Frank (Ed.), in *Structure and Functions of the Cell* (Translated into Russian; Moscow: Mir, 1964) p. 90
11. G D Winter *J. Biomed. Mater. Res.* **5** 11 (1974)
12. D Bruck *J. Biomed. Mater. Res.* **11** 1 (1977)
13. R Lefaux, in *Chimie et Toxicologie des Matières Plastiques* (Ed. Y Champetier) (Paris: Compagnie Fran d'Éditions, 1964) p. 57

14. W L Guess, J Autian *Am. J. Hosp. Pharm.* **21** 261 (1964)
15. R M Rice, A F Hegyeli, C W R Wade, J G Dillon, H Jaffe, R K Kulkarni *J. Biomed. Mater. Res.* **12** 43 (1978)
16. S J Courlay, R M Rice, A F Hegyeli, C W R Wade, J G Dillon, H Jaffe, R K Kulkarni *J. Biomed. Mater. Res.* **12** 219 (1978)
17. M F Nichols *J. Biomed. Mater. Res.* **13** 299 (1979)
18. Y S Yeh, Y Iriyma, Y Matsuzawa *J. Biomed. Mater. Res.* **22** 795 (1988)
19. R F Wilsnack, D V M Bernadyn, B S Huntingdon *Biomater. Med. Devices Artif. Organs* **4** 235 (1976)
20. S A Rosenblath, G R Weddington, W L Guess, J Autian *J. Pharm. Sci.* **54** 156 (1965)
21. W L Guess, S A Rosenblath, J Autian *J. Pharm. Sci.* **54** 1545 (1965)
22. R I Johnsson, A F Hegyeli *Ann. N. Y. Acad. Sci.* **146** 66 (1968)
23. A Weninberg, G Haselgren, L Tronstad *J. Biomed. Mater. Res.* **13** 109 (1979)
24. Yu V Moiseev, G E Zaikov *Khimicheskaya Stoikost' Polimerov v Agressivnykh Sredakh* (Chemical Stability of Polymers in Aggressive Media) (Moscow: Khimiya, 1979)
25. M Shen, M B Bever *J. Mater. Sci.* **7** 741 (1972)
26. J A Barrie, in *Diffusion in Polymers* (Eds J Crank, G S Park) (London: Academic Press, 1968) p. 259
27. V I Lebedev, G P Andrianova, A E Chalykh, in *Difuzionnye Yavleniya v Polimerakh, Riga 1977 (Tez. Dokl.)* [Diffusion Phenomena in Polymers, Riga 1977 (Abstracts of Reports)] (Riga, 1977) Part 2, p. 323
28. W R Vieth, K J Sladek *J. Colloid Sci.* **20** 1014 (1965)
29. W R Vieth, K J Frangoulis, J A Rionda *J. Colloid Sci.* **22** 454 (1966)
30. G E Zaikov *J. Macromol. Sci. Chem. Phys.* **25C** 551 (1985)
31. A L Iordanski, G E Zaikov, in *Diffusion of Electrolytes in Polymers* (Utrecht: VSP, 1988) p. 385
32. Z Rogovin, E Khait, I Knunyants, Yu Rymashevskaya *Zh. Obshch. Khim.* **17** 1316 (1974)
33. V A Burshtein, L M Egorova, V V Solov'eva *Mekh. Polim.* (5) 854 (1977)
34. A A Khokhlov, Candidate's Thesis in Chemical Sciences, Mendeleev Chem. Technol. Inst., Moscow, 1980
35. N V Trostenyuk, B A Zhubanov, A A Adamyan, O S Voronkova *Vestn. Akad. Nauk Kaz. SSR* (1) 27 (1989)
36. L V Ivanova, Yu V Moiseev, G E Zaikov *Vysokomol. Soedin., Ser. A* **14** 1057 (1972)
37. E Laifut *Transfer Phenomena in the Living System* (Translated into Russian; Moscow: Mir, 1977)
38. A L Iordanskii, A D Shterenzon, Yu V Moiseev, G E Zaikov *Usp. Khim.* **48** 1460 (1979) [*Russ. Chem. Rev.* **48** 781 (1979)]
39. Yu V Moiseev, T T Daurova, O S Voronkova, K Z Gumargalieva, L G Privalova, in *17th Microsymposium on Medical Polymers, Prague, 1977* p. 113
40. K Z Gumargalieva, Yu V Moiseev, T T Daurova, O S Voronkova, I B Rozanova *Biomaterials* **1** 214 (1980)
41. E Lipatova, G A Pkhakadze, in *Primenenie Polimerov v Khirurgii* (Application of Polymers in Surgery) (Kiev: Naukova Dumka, 1977) p. 7
42. O S Voronkova, Candidate's Thesis in Chemical Sciences, Mendeleev Chem. Technol. Inst., Moscow, 1971
43. S Ya Karpukhina, E Z Gumargalieva, T T Daurova, V A Mironova *Vysokomol. Soedin., Ser. B* **25** 209 (1983)
44. D F Williams, in *Proceedings of the ASTM Conference, Kansas City, 1978;* ASTM Special Publ., 1979 (Eds B Syrett, A Acharya) p. 215
45. D F Williams *J. Biomed. Mater. Res.* **14** 329 (1980)
46. D F Williams, in *III International Conference on 'Plastics in Medicine and Surgery'* Netherlands, 1979
47. D V Park *Biokhimiya Chuzherodnykh Soedinenii* (Biochemistry of Alien Compounds) (Moscow: Meditsina, 1978)
48. D F Williams, R Roaf *Implants in Surgery* (Translated into Russian; Moscow: Meditsina, 1978)
49. K Schwertassek *Faserforsch. Textiltech.* **11** 125 (1960)
50. O V Voronkova, T T Daurova, M V Shablygin, L P Mil'kova, N M Mikhailov *Vysokomol. Soedin., Ser. A* **13** 677 (1971)
51. Yu V Moiseev, V S Markin, G E Zaikov *Usp. Khim.* **45** 510 (1976) [*Russ. Chem. Rev.* **45** 246 (1976)]
52. G E Titova, in *Fiziologicheski Aktivnye Sinteticheskie i Drugie Polimery Meditsinskogo Naznacheniya (Tez. Dokl. Simp.)* [Physiologically Active Synthetic and Other Medical Polymers (Abstracts of Reports)] (Leningrad: Nauka, 1975) p. 15
53. G E Titova, M S Akutin *Plast. Massy* **1** 73 (1976)
54. G E Titova, Candidate's Thesis in Chemical Sciences, Mendeleev Chem. Technol. Inst., Moscow, 1976
55. D J Heikens *J. Polym. Sci.* **35** 277 (1959)
56. V A Savin, O G Fortunatov *Promyshlennost' Meditsinskogo Stekla,* N 2 (Medical Glass Industry, N 2) (Moscow: TsBNTImedprom, 1976)
57. M N Noryan *Br. Med. J.* **1** 308 (1969)
58. T P Nuquid *Philipp. J. Surg.* **21** 215 (1969)
59. Y Chuja, K Suchiro, Y Okita, H Todokoto, K Chuio *Makromol. Chem.* **103** 215 (1968)
60. K Chuio, H Kobayaski, J Suzuki, S Tokuhara *Makromol. Chem.* **100** 267 (1967)
61. H Zilch, W Kleengel *Schwester* **10** 34 (1971)
62. R K Kulkarni, K C Pani, C Neuman, F Leonard *Arch. Surg.* **93** 839 (1966)
63. J M Brady, D E Cutright, R A Miller, G C Battistone, E E Hunsuck *J. Biomed. Mater. Res.* **7** 155 (1973)
64. D E Cutright, E E Hunsuck *J. Oral Surg.* **31** 134 (1971)
65. D E Cutright, E E Hunsuck, J D Brady *J. Oral Surg.* **29** 39 (1971)
66. D E Cutright, B Peres, J Beasley, W J Larson, W R Rasey *Oral Med., Oral Pathol.* **37** 142 (1974)
67. N S Snegireva, K Z Gumargalieva, L G Privalova, in *Starenie i Stabilizatsiya Polimerov, Tashkent 1976 (Tez. Dokl. IV Konf.)* [Ageing and Stabilisation of Polymers, Tashkent, 1976 (Abstracts of Reports at the Fourth Conference)] p. 64
68. Yu V Moiseev, T T Daurova, O S Voronkova, K Z Gumargalieva, L G Privalova *J. Polym. Sci., Polym. Symp.* **66** 269 (1979)
69. L L Razumova, T T Daurova, A A Veretennikova, L G Privalova, K Z Gumargalieva, O S Voronkova *Polim. Med.* **9** 119 (1979)
70. L G Privalova, K Z Gumargalieva, O S Voronkova, Yu V Moiseev, T T Daurova, L L Razumova, G E Zaikov *Vysokomol. Soedin., Ser. A* **22** 1891 (1980)
71. J Hermann, R I Kelly, G A Higgins *Arch. Surg.* **100** 486 (1970)
72. J D Bankroft *An Introduction to Histochemical Technique* (New York: Appleton Crofts, 1967)
73. R K Kulkarni, E G Moore, A F Hegueli, F Leonard *J. Biomed. Mater. Res.* **5** 169 (1971)
74. P H Craig, J A Williams, K W Davis, A D Magoun, A S Levy *Surg. Gynecol. Obstet.* **141** 1 (1975)
75. T N Salthouse, G K Kaminska, M L Murphy *Investig. Ophthalm.* **9** 844 (1970)
76. J Philippa, J Hocking *J. Macromol. Sci., Chem. Phys.* **32C** (1) 35 (1992)
77. R M Robert, J M Brady, D E Cutright *J. Biomed. Mater. Res.* **11** 711 (1977)
78. T N Salthouse, B F Matlaga *Surg. Gynecol. Obstet.* **142** 544 (1976)
79. K Schwertassek, J Dvorak *Faserforsch. Textiltech.* **24** 2 (1970)
80. K Schwertassek, J Dvorak *Textil. Praha* **26** 196 (1971)
81. K Schwertassek, J Dvorak *Faserforsch. Textiltech.* **25** 2 (1972)
82. H H Harrison *Am. J. Surg.* **95** 3 (1968)
83. R W Postlethwait *Ann. Surg.* **171** 892 (1970)
84. R W Postlethwait *Ann. Surg.* **190** 10 (1979)
85. Y Noishica *J. Biomed. Mater. Res.* **10** 759 (1976)
86. T T Daurova, S M Degtyareva *Byull. Eksp. Biol. Med.* **64** 366 (1977)
87. T T Daurova, O S Voronkova, S D Andreev, T E Rudakova, Yu V Moiseev, L L Razumova, G E Zaikov *Dokl. Akad. Nauk SSSR* **231** 919 (1976)
88. T E Rudakova, G E Zaikov, O S Voronkova, T T Daurova, S M Degtyareva *J. Polym. Sci., Polym. Symp.* **66** 277 (1979)
89. O S Voronkova, T T Daurova, Yu V Moiseev, K Z Gumargalieva *Vysokomol. Soedin., Ser. A* **24** 1412 (1982)
90. Z A Rogovin, in *Osnovy Khimii i Tekhnologii Khimicheskikh Volokon* (Fundamentals of the Chemistry and Technology of Chemical Fibres) (Moscow: Khimiya, 1964) p. 140
91. D A Ravens *Polymer* **1** 375 (1960)
92. J V Maxham, W J Maier *Biotechnol. Bioeng.* **20** 865 (1978)
93. N C Liebert, R P Cherthoff, S L Cosgrofe, R McCuskey *J. Biomed. Mater. Res.* **10** 939 (1976)

94. T I Vinokurova, I B Rozanova, S M Degtyareva, in *Sinteticheskie Polimernye Materialy Meditsinskogo Naznacheniya, Belgorod-Dnestrovskii 1977 (Tez. Dokl. III Simp.)* [Synthetic Polymer Medical Materials, Belgorod-Dnestrovskii, 1977 (Abstracts of Reports at the Third Symposium)] p. 32
95. J Dolezel *Plasty Kaut.* **13** 257 (1976)
96. N Grassie, in *Chemistry of High Polymer Degradation Processes* (Translated into Russian; Moscow: Izd. Inostr. Lit., 1959) p. 96
97. S N Levine *Ann. N. Y. Acad. Sci.* **146** 3 (1968)
98. Z Neuman *Br. J. Plast. Surg.* **9** 195 (1957)
99. N E Stinson *Br. J. Exp. Pathol.* **46** 135 (1965)
100. J Charniey, A Kamangar, M D Longfield *Med. Biol. Eng.* **7** 31 (1969)
101. A C Albertson, O A Svek, K Sigbritt *Polym. Degrad. Stability* **18** 73 (1987)
102. N B Nykvist *Plast. Polym.* **42** 195 (1974)
103. I P Fisher, in *First Biomaterials Congress* (Vienna: Hüthig, 1980) p. 20
104. M Mlinac, I Munjko, in *Second International Symposium on Degradation and Stabilization of Polymers, Dubrovnik, 1978* p. 8
105. A C Albertson, B Ranby, in *Proceedings of the 3rd International Symposium on Biodegradation, Kingston, RI, 1975* p. 743
106. R W Marck, Ch R H Wildevuur *J. Biomed. Mater. Res., Symp.* **1** 43 (1973)
107. J Autian *Ann. N. Y. Acad. Sci.* **146** 251 (1968)
108. E J Frazz, E E Schmidt *J. Biomed. Mater. Res., Symp.* **1** 43 (1973)
109. N I Ostretsova, Candidate's Thesis in Chemical Sciences, Mendeleev Chem. Technol. Inst., Moscow, 1980
110. W F Agnew, E M Todd, H Richmond, W S Chronister *J. Surg. Res.* **2** 357 (1962)
111. N I Ostretsova, A N Neverov *Vysokomol. Soedin., Ser. B* **16** 55 (1974)
112. N I Ostretsova, T T Daurova, A N Neverov *Polim. Med.* **6** 122 (1976)
113. M G Voronkov *Geterotsiklicheskie Reaktsii Rasshchepleniya Siloksanovykh Svyazei* (Heterocyclic Reactions in the Splitting of Siloxane Bonds) (Moscow: Khimiya, 1961)
114. D K Thomas, B B Moor *Polymer* **13** 109 (1972)
115. I A Metkin, K K Piotrovskii, Yu A Yuzhelevskii *Zh. Prikl. Khim.* **48** 1108 (1975)
116. J W Boretas, W S Pierse, R E Baier, A F Leroy, H I Donachy *J. Biomed. Mater. Res.* **9** 327 (1975)
117. D A Ulsen, H D Kletschka, E H Rafferty *Polym. Eng. Sci.* **13** 241 (1973)
118. H Hernauer *Plasty Kaut.* **10** 413 (1963)
119. T E Lipatova, T T Alekseev, L A Bakalo, T L Tereshchenko *Polim. Med.* **10** 19 (1980)
120. R Smith, D F Williams, C Oliver *J. Biomed. Mater. Res.* **21** 1149 (1987)
121. G A Pkhakadze, E L Tereshchenko, N A Galatenko, A K Kolomiitsev *Biosovmestimost'* **1** 33 (1994)
122. T E Lipatova, G A Pkhakadze *Primenenie Poliuretanov v Endoprotezirovanii* (Application of Polyurethanes in Endoprosthesis) (Kiev: Naukova Dumka, 1983)
123. T E Lipatova, G A Pkhakadze *Meditsinskie Klei* (Medical Glues) (Kiev: Naukova Dumka, 1979)
124. H Stricher *Arch. Pharm.* **300** 289 (1967)
125. V C Smith *J. Biomed. Mater. Res., Symp.* **1** 189 (1979)
126. R Lehman, G S Hays, F Leonard *Arch. Surg.* **93** 441 (1964)
127. W R Werin, A T Florence *J. Biomed. Mater. Res.* **14** 93 (1980)

Russian Chemical Reviews **63** (10) 869–882 (1994)
©1994 Russian Academy of Sciences and Turpion Ltd

UDC 547.915+547.996

Levoglucosenone: the properties, reactions, and use in fine organic synthesis

M S Miftakhov, F A Valeev, I N Gaisina

Contents

I. Introduction	869
II. The synthesis, structure, and mechanism of the formation of levoglucosenone	869
III. Chemical syntheses of levoglucosenone	871
IV. Reactions of levoglucosenone and its derivatives	871
V. The use of levoglucosenone in the synthesis of natural products	877

Abstract. The review deals with the synthesis, structure, chemical properties, and use of 1,6-anhydro-3,4-dideoxy-β-D-pyranosen-2-one (levoglucosenone) in the synthesis of natural products. The bibliography includes 67 referencces.

I. Introduction

Levoglucosenone (1,6-anhydro-3,4-dideoxy-β-D-pyranosen-2-one) is a sugar enone obtained in the acid-catalysed pyrolysis of cellulose and related materials which has attracted the attention of investigators by the unique nature of its structure and as a means for the introduction of chiral centres in the stereospecific synthesis of natural products. The 6,8-dioxabicyclo[3.2.1]octane skeleton, an enone system, and a highly activated keto-group and an acetal centre are combined in the structure of levoglucosenone. The effective facial differentiation of the attack by the reactants, induced by the 1,6-anhydro-bridge, as well as the coordinating and 'cooperative' effects of the 'chelate' acetal oxygen atoms ensure ease of occurrence and the high regio- and stereo-selectivity of the majority of the reactions involving levoglucosenone. Levoglucosenone is 'self-protected' in the form of an internal acetal, is thermally stable, and distils without appreciable decomposition. It forms readily dimeric and oligomeric condensation products and under certain conditions can generate highly reactive oxidopyrylium ylides. Levoglucosenone has proved useful as an effective Michael acceptor and as a powerful dienophile in Diels–Alder reactions, in dipolar cycloaddition, etc.

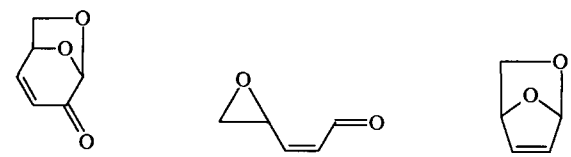
Although levoglucosenone has been known for more than 20 years,[1] it has still found only limited applications in organic synthesis. This is apparently associated with certain difficulties in the synthesis, purification, and handling of this compound and also with the lack of reviews on this topic. We hope that the data presented in this review will stimulate research by Russian chemists in this field.

M S Miftakhov, F A Valeev, I N Gaisina Laboratory for the Synthesis of Low-Molecular-Mass Bioregulators, Institute of Organic Chemistry, Ufa Scientific Centre, Russian Academy of Sciences, prosp. Oktyabrya 71, 450054 Ufa, Russian Federation.
Fax (7-347) 235 60 66. Tel (7-347) 235 52 88 (M S Miftakhov)

Received 10 May 1994
Uspekhi Khimii **63** (10) 921–935 (1994); translated by A K Grzybowski

II. The synthesis, structure, and mechanism of the formation of levoglucosenone

Since the 1970s, the attention of investigators has been directed to the study of the structure, mechanism of the formation, and the properties of levoglucosenone **1**, which is one of the principal volatile products of the acid-catalysed thermolysis of cellulose and related carbohydrates.[1] Other empirical and structural formulae were initially attributed erroneously to this compound; 4,5-epoxy-2(*Z*)-pentenal ($C_5H_6O_2$) **2**,[2] 1,5-anhydro-2,3-deoxy-β-D-pent-2-enofuranose ($C_5H_6O_2$) **3**,[3] etc. The principal difficulties in the determination of the structure **1** were associated with the incorrect interpretation of mass-spectrometric data; the *m/z* 98 peak, corresponding to the formula $C_5H_6O_2$, was assumed to be due to a molecular ion.



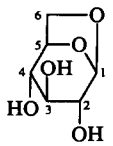
1 **2** **3**

Having investigated by NMR, UV, and IR spectroscopy as well as mass spectrometry and osmometry the products of the thermolysis of cellulose obtained under analogous conditions, Halpern et al.[4] concluded that it has the molecular formula $C_6H_6O_3$ and is 1,6-anhydro-3,4-dideoxy-β-D-pyranosen-2-one **1**, which was given the trivial name levoglucosenone.

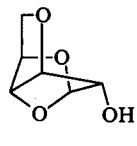
The structure of levoglucosenone was subsequently confirmed and adopted also by other investigators.[5–10] In particular, the exact mass of the molecular ion was determined[11] in 1985 as 126.0327, which corresponds to the empirical formula $C_6H_6O_3$, with the aid of chromatograph-linked mass spectrometry using both electron impact and chemical ionisation. The ion with *m/z* 98.0381 proved to be secondary and was produced as a result of fragmentation of levoglucosenone with ejection of CO. On the basis of ^1H and ^{13}C NMR spectroscopic data, it was also established that the six-membered ring of levoglucosenone has the envelope conformation.[12]

The pyrolysis of cellulose is a complex process, which leads to various products depending on the conditions.[13–18] Thus pyrolysis in vacuo (300–500 °C) affords a high yield of levoglucosan — 1.6-anhydro-β-D-glucopyranone **4**; at atmospheric pressure, levoglucosenone **1** and 1.4:3,6-dianhydro-β-D-glucopyranose **5** are formed as a result of the combination of

the reactions involving transglycosylation and dehydration of the D-glucose residues of cellulose.[17] The rapid removal of levoglucosan and other anhydrosugars prevents their further transformations into oligosaccharides, their decomposition into other volatile components, and salt formation. The presence of an acid catalyst promotes dehydration and charring accompanied by the formation of levoglucosenone, other unsaturated compounds, and carbon.[18]



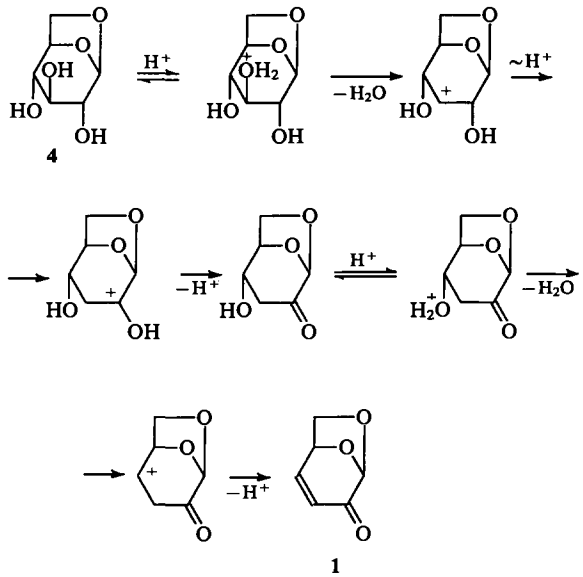
4



5

Studies of the influence of reaction conditions on the yield of levoglucosenone[17-21] led to the discovery of the optimum process parameters: 300 °C, atmospheric pressure, and 1% phosphoric acid concentration.

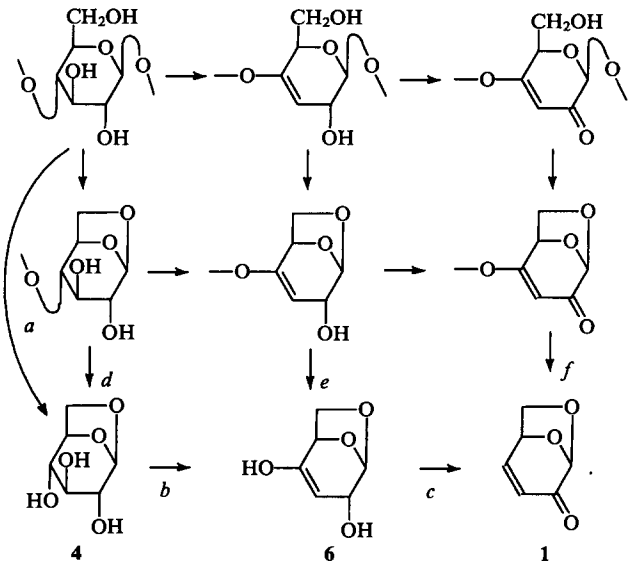
A mechanism has been proposed for acid-catalysed isotypical thermal decomposition reactions of cellulose, D-glucose, and levoglucosenone.[22] The C(1) and C(5) chiral centres of levoglucosan **5** are not involved in the transformations but the levoglucosenone obtained from the optically active levoglucosan {$[\alpha]_D^{25} = -55°$, $c = 0.5$, H_2O} is chiral {$[\alpha]_D^{25} = -52.7°$, $c = 1.0$, $CHCl_3$}.



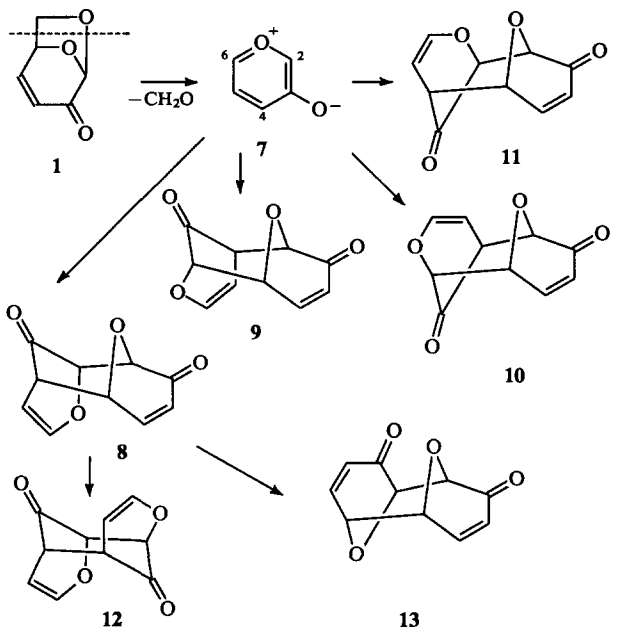
The third stage of the proposed mechanism, involving a 1,2-hydride shift from the C(2) atom to the carbenium centre C(3) and the formation of a more stable hydroxycarbenium ion, is the most important. The alternative 1,2-hydride shift leading to a hydroxycarbenium ion at C(4) apparently does not occur, since the corresponding levoglucosenone isomer was not found in the pyrolysate.[23]

The method involving pyrolysis at the Curie point was used subsequently to identify the primary products of the decomposition of cellulose and related compounds.[7] In this procedure, the specimen was heated briefly to a fixed temperature under an inert carrier gas atmosphere. As a result of the relatively low temperature, the reactions of the primary products were ruled out. The pyrolysis mechanism (top right) was proposed.[7]

Compounds **1**, **4**, and **6** can be formed not only via routes *a*, *b*, or *c* but also via polymeric anhydro- and deoxy-sugar units (stages *d*–*f*). However, direct evidence for this has not yet been obtained.

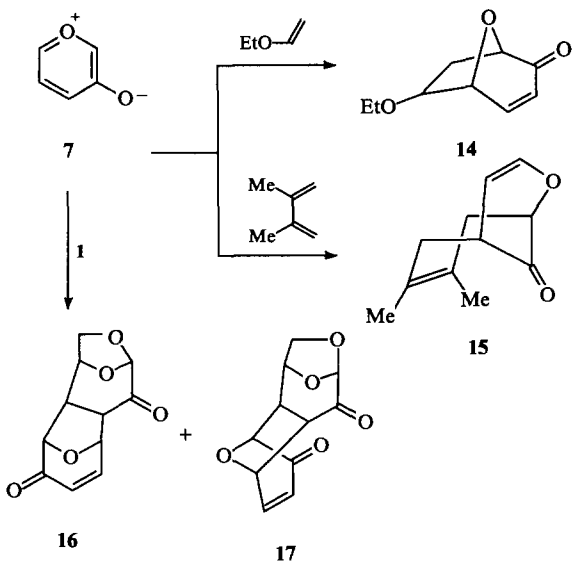


Levoglucosenone can undergo pyrolytic deformylation, affording the 3-oxidopyrylium intermediate **7**.[25] The highly reactive ylide **7** readily dimerises via a [6π + 4π] mechanism to form four regioisomeric adducts — the *endo*-compounds **8** and **9** and the *exo*-compounds **10** and **11** respectively. The situation is complicated by the fact that each of these adducts undergoes allyl rearrangements in its turn, affording two new dimers in each case. Thus the dimers for the primary adduct **8** are the bisvinyl ether **12** and the bisenone **13**.



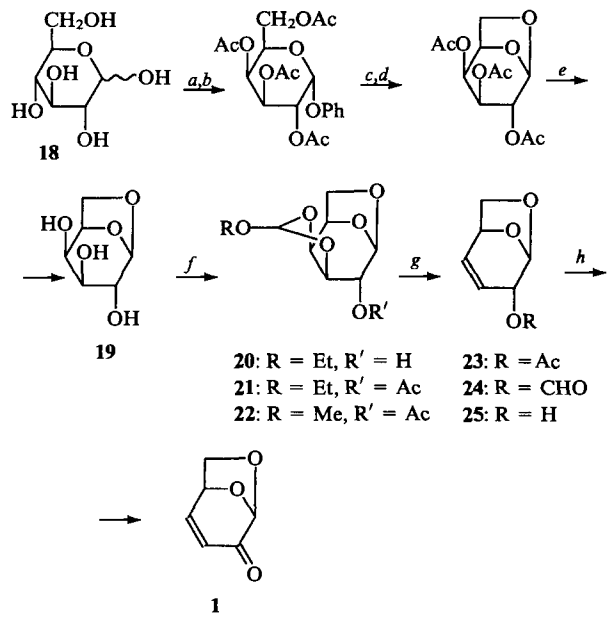
In thermal cycloaddition reactions, the 3-oxidopyrylium derivative **7** behaves both as a 4π-electron system (addition of ethyl vinyl ether and the formation of the bicyclic enone **14**) and as a 6π-electron component (addition in the 2- and 4-positions in the reaction with 2,3-dimethylbutadiene and the formation of the bicyclic vinyl ether **15**). In addition, the ylide **7** enters into a [4π + 2π]-cycloaddition reaction with levoglucosenone, affording the adducts **16** and **17**.

Thus the 3-oxidopyrylium intermediate **7** can condense with itself, with alkenes, and with dienes in electrocyclic reactions permitted by thermal conditions. All these factors are responsible for the diversity of the pyrolysis products.



III. Chemical syntheses of levoglucosenone

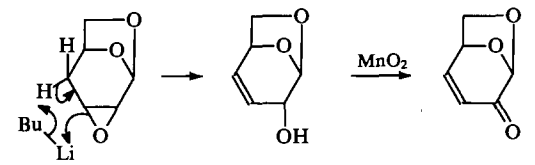
The synthesis of levoglucosenone from D-galactose **18** has been described.[26]



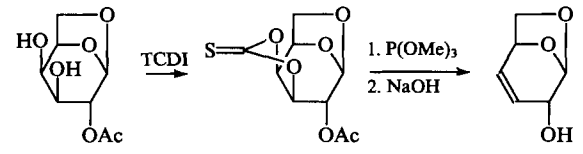
(*a*) AcONa–Ac_2O; (*b*) H^+, PhOH; (*c*) NaOH–H_2O; (*d*) Ac_2O, Py; (*e*) NaOMe; (*f*) $(RO)_3CH$, H^+, DMF; (*g*) Ac_2O, Cat; (*h*) MnO_2.

1,6-Anhydro-β-D-galactopyranose **19**, obtained from D-galactose, was mixed with 4 equivalents of triethyl orthoformate in solution in *N*,*N*-dimethylformamide in the presence of catalytic amounts of H_2SO_4 and was allowed to stand for 12 h. After appropriate treatment of the reaction mixture, the 3,4-ethoxyacetal of 1,6-anhydro-β-D-galactopyranose **20** was isolated in 95% yield. In the key reductive decarboxylation stage, the ethoxyacetal **20** or its acetyl derivatives **21** and **22** were refluxed in solution in acetic anhydride containing the catalyst. The highest yield of 2-acetyl-1,6-anhydro-3,4-dideoxy-β-D-*erythro*-hex-3-enopyranose **23** (in the absence of Ac_2O, the corresponding 2-formyl derivative **24** may be formed) was achieved when an aqueous solution of zirconium oxide was used (the yield of the alkene **23** was 88%). In the concluding stage, levoglucosenone was obtained as a result of the allylic oxidation of compound **25** by MnO_2.

Köll et al.[27] developed a scheme for the synthesis of levoglucosenone the key stage of which is the rearrangement of the epoxide **26**[28] to the allyl alcohol **25**.



The same workers proposed a more practical route to the enone **1** starting with the groundnut galactomannan. Pyrolysis of this polysaccharide followed by acetonation affords a monoisopropylidene derivative of 1,6-anhydro-β-D-galactopyranose. Its acetylation and treatment with aqueous acid lead to compound **27**. The crystalline thionocarbonate **28** was obtained from the latter by reaction with *N*,*N*′-thiocarbonyldiimidazole (TCDI) in boiling 2-butanone. On heating compound **28** with trimethyl phosphite for many hours and on treatment with alkali, the allyl alcohol **25** is produced.



A method for the synthesis of levoglucosenone from glucose has been described.[29] The reaction is carried out in dimethylformamide at 70–120 °C in the presence of concentrated H_2SO_4.

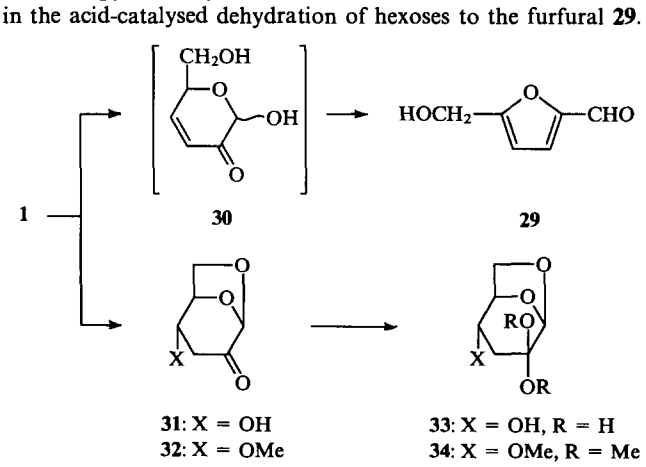
We may note that none of the methods of synthesis of levoglucosenone listed above can compete with the pyrolysis of cellulose, which remains the most economical and effective method for its preparation despite disadvantages such as the low yield of the product and the need to work with relatively large volumes of solid cellulose materials.

IV. Reactions of levoglucosenone and its derivatives

1. Acid- and base-catalysed reactions of levoglucosenone

Levoglucosenone has three reaction centres: the carbon–carbon double bond, the keto-group, and the glycosidic anhydro-linkage. Depending on the process conditions, each of these groups can react selectively.

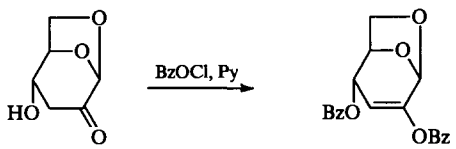
When levoglucosenone is heated with aqueous solutions of inorganic acids, 5-hydroxymethylfurfural **29** is formed.[17] This entails the initial rupture of the 1,6-anhydro-linkage of levoglucosenone and the formation of 3,4-dideoxy-D-*glycero*-hex-3-enopyranos-2-ylose **30**, which is in fact an intermediate in the acid-catalysed dehydration of hexoses to the furfural **29**.



Heating of levoglucosenone in aqueous acetic acid affords an intermediate resulting from the addition of water of the double bond — 1,6-anhydro-3-deoxy-D-*erythro*-hexopyranos-2-ylose **31**. Compound **31** can be readily separated from levoglucosenone **1** by extracting the latter with chloroform. The high solubility of compound **31** in water is due to the hydration of the keto-group and the formation of the *gem*-diol **33**, which has been confirmed by ^{1}H NMR spectroscopy.

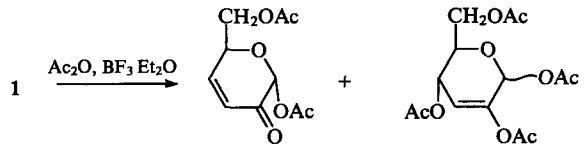
The acid-catalysed addition of methanol to the double bond of levoglucosenone using the MeOH – HCl system initially affords 4-*O*-methyl-2-ylose **32**, which is then rapidly converted into the dimethyl acetal **34** in an almost quantitative yield. Hydrolysis of compound **34** again leads to 4-*O*-methyl-2-ylose **32**.

The attempts to benzoylate the 4-hydroxy-group in compound **31** by benzoyl chloride in pyridine led to 1,6-anhydro-2,4-di-*O*-benzoyl-3-deoxy-β-D-*erythro*-hex-2-enopyranose **35** (via stages involving the successive enolisation and benzoylation of the keto-group).



31 **35**

The 1,6-anhydride ring of levoglucosenone is readily opened under acetolysis conditions in the presence of $BF_3.Et_2O$ as catalyst, which leads to the diacetate **36**. The anomeric tetraacetates **37** and **38** are formed in smaller amounts as a result of the exhaustive acetylation of the enone.



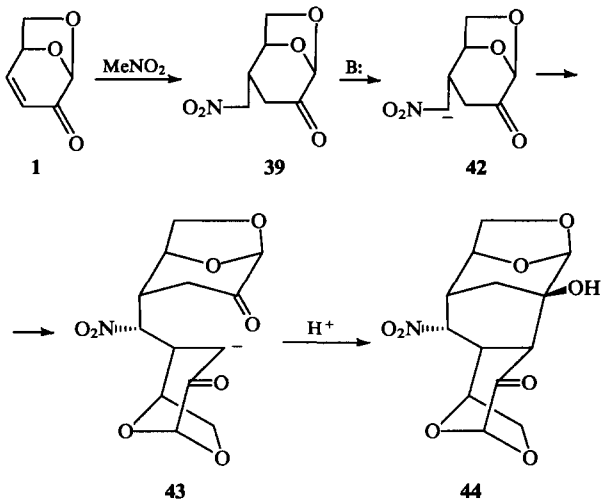
36 **37(α), 38(β)**

Reactions involving addition to the 3,4-double bond of levoglucosenone are also catalysed by bases. In the presence of small amounts of triethylamine, levoglucosenone affords satisfactory yields of the adducts **31** and **32** in water and anhydrous methanol respectively.

2. Michael addition

The reactions in which levoglucosenone serves as a Michael acceptor merit special attention.[30–33] Treatment of levoglucosenone with an excess of nitromethane in the presence of catalytic amounts of tetramethylguanidine gave rise to a mixture of two isomeric 2 : 1 adducts in an overall yield of 98%.[30] The reaction involves the initial 1,4-addition to the enone [the nitronate anion $^-CH_2NO_2$ adds to the C(4) atom of levoglucosenone from the side opposite to that of the 1,6-anhydro-bridge]; the subsequent base (B)-catalysed addition of a second nitromethane molecule to the carbonyl group of compound **39** leads to the formation of the diadducts **40** and **41** in proportions of 10 : 1.

When the reaction is carried out with an excess of levoglucosenone, 1 : 2 adducts are formed. The proposed mechanism of the formation of compound **44** represents the Michael addition of the nitromethyl anion **42** to levoglucosenone accompanied by the intramolecular aldol condensation of the intermediate diketone **43**. The high yield of the product **44** (95%) shows that each of the reaction stages is highly selective and that in each case the attack on the nucleophilic centre is directed exclusively to the *exo*-position.

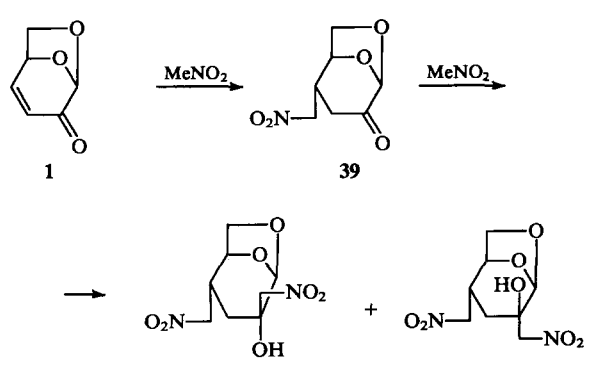


1 **39** **42**

43 **44**

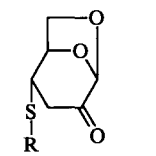
1,6-Anhydro-4-butylthio-3-deoxy-β-D-hexopyranos-2-ylose **45** has been obtained in a quantitative yield by the addition of butane-1-thiol to levoglucosenone.[31] Steric hindrance generated by the 1,6-anhydro-bridge interferes so much with equatorial attack on the thiol that the axial sulfide is formed exclusively. Other thiols behave similarly, affording the adducts **46**–**51**.

The same workers investigated the possibility of cross-coupling two levoglucosenone molecules via dithiols. Ethane-1,2-dithiol was chosen as the binding component, its reaction with levoglucosenone affording two products. The structure of one of them (compound **52**), obtained in 47% yield, was established by spectroscopic methods. The other reaction product could not be identified because of its instability (the compound decomposed rapidly at room temperature and it was shown by thin-layer chromatography that it afforded highly polar secondary products). Its ^{1}H and ^{13}C NMR spectra indicated the presence of three levoglucosenone molecules in its structure. The monoadduct was not detected.



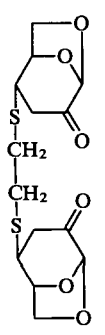
1 **39**

40 **41**



45: R = $(CH_2)_3CH_3$
46: R = $(CH_2)_5CH_3$
47: R = $(CH_2)_9CH_3$
48: R = $(CH_2)_{11}CH_3$
49: R = $CH_2CH(CH_3)_2$
50: R = $C(CH_3)_3$

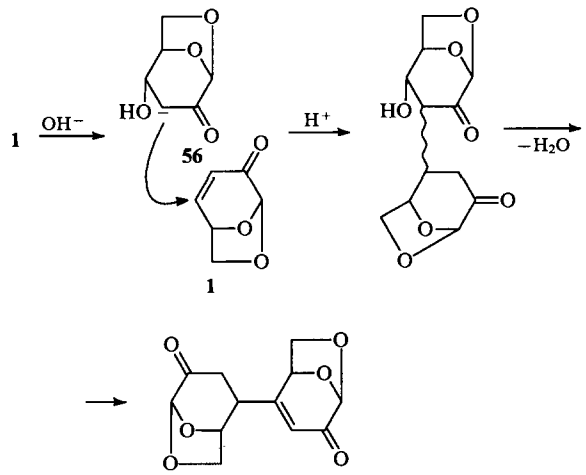
51: R = 



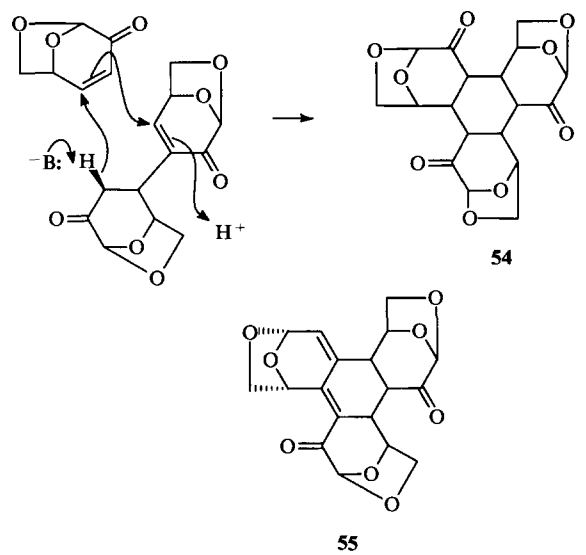
52

Heating levoglucosenone in aqueous triethylamine gives three principal oligomers: the dimer **53**, the saturated trimer **54**, and the unsaturated trimer **55**.[32]

The mechanism of the dimerisation of levoglucosenone is presented below. The base-catalysed hydration of compound **1** leads to the α-keto-stabilised carbanion **56**, which attacks a second levoglucosenone molecule in the *exo*-position. Subsequent dehydration affords the dimer **53**.

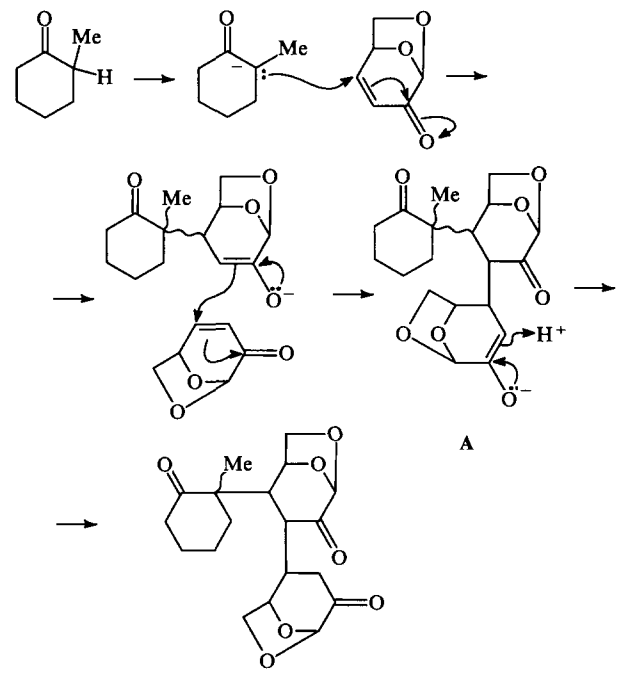


The mechanism of formation of the trimer **54** involves the condensation of three levoglucosenone molecules. The intramolecular condensation of the α-keto-stabilised carbanion **56** with a molecule of compound **1** is then accompanied by intramolecular cyclisation.

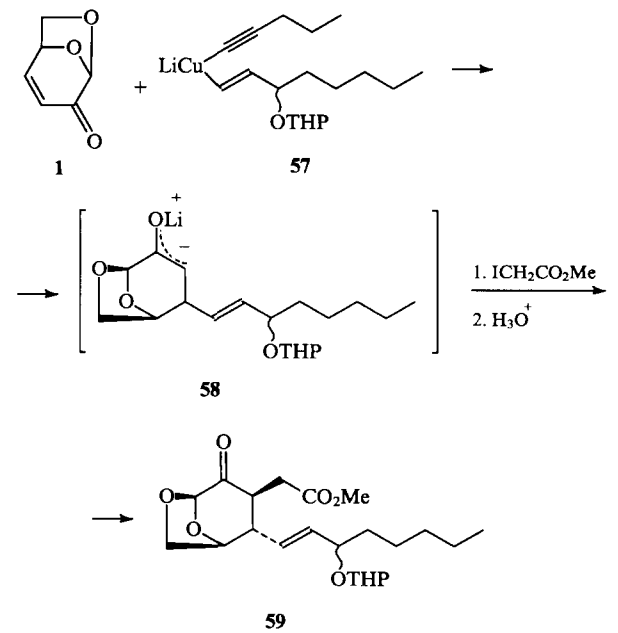


The formation of the alkene trimer **55** from compound **1** in aqueous triethylamine proceeds mainly via a similar mechanism. The crystal structures of the cyclic levoglucosenone trimers have been confirmed by X-ray diffraction.[33]

The Michael additions of diethyl malonate, ethyl cyanoacetate, 2-nitropropane, and 2-methylcyclohexanone to levoglucosenone using various catalysts have also been investigated.[34] The reaction of levoglucosenone with 2-methylcyclohexanone was carried out in *tert*-butyl alcohol in the presence of equimolar amounts of potassium *tert*-butoxide. The structure **A** was attributed to the product on the basis of spectroscopic data.

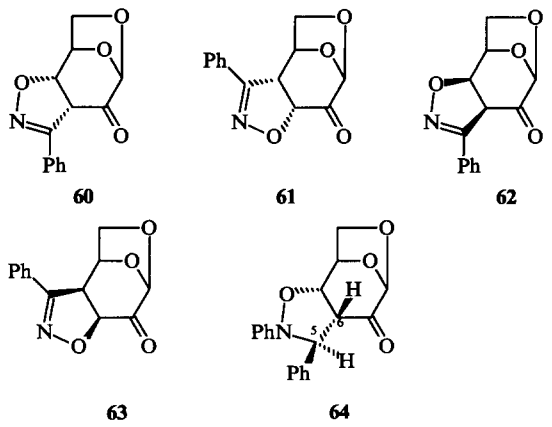


In order to obtain thromboxane-like structures, a study was made[35] of the coupled 1,4-addition of the racemic cuprate reagent **57** to levoglucosenone with subsequent alkylation of the intermediate enolate **58** by ethyl iodoacetate. The 'triple convergent coupling' sequence achieved ultimately led to compound **59** in 35% yield.



3. 1,3-Dipolar cycloaddition reactions

Levoglucosenone readily enters into cycloaddition reactions with benzonitrile oxide ($PhC{\equiv}N^{+}-O^{-}$) and with *C*,*N*-diphenylnitrone [$PhCH=N^{+}(Ph)-O^{-}$].[36] It was shown that, of the four possible adducts of levoglucosenone with benzonitrile oxide (the two *endo*-isomers **60** and **61** obtained when 1,3-dipolarophile is attacked from the side opposite to that of the 1,6-anhydro-bridge and the two alternative *exo*-isomers **62** and **63**), the *endo*-adduct **60** (yield 71%) and trace amounts (0.6%) of the *exo*-isomer **62** are formed.



60 61 62

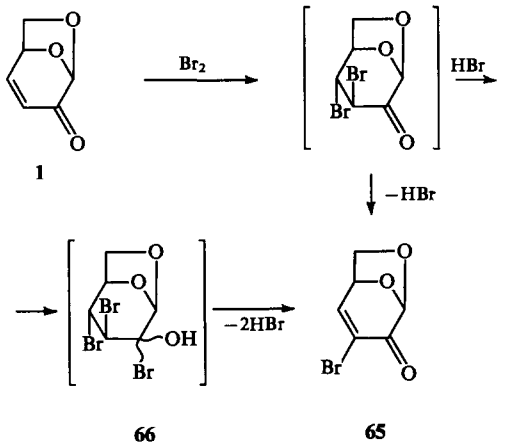
63 64

In the case of the *C,N*-diphenylnitrone, there is a possibility of the formation of eight adducts: the *exo*- and *endo*-isomers for each pair of regioisomers. However, refluxing of levoglucosenone with *C,N*-diphenylnitrone in toluene afforded only one 1 : 1 adduct in 68% yield. The absence of an appreciable Overhauser effect (< 2%) between the H(5) and H(6) protons is evidence in support of the *endo*-structure **64**, which was subsequently confirmed by X-ray diffraction. Thus the reaction also proved to be regio- and stereo-specific.

4. Bromination of levoglucosenone

The crystalline monobromo-derivative **65**, characterised by spectroscopic methods, has been obtained by brominating levoglucosenone with two equivalents of Br_2 in $CHCl_3$ and the subsequent removal of excess bromine by washing the organic phase with sodium hydroxide.[37]

The change in the type of treatment, i.e. the removal of the excess bromine by evacuation at 20 °C, led to the unstable crystalline tribromo-derivative **66**. In all probability, this anomalous course of the reaction is caused either by the presence in the reaction mass of HBr, formed owing to the presence of moisture in bromine, or by the radical reaction between bromine and chloroform. On heating in the solution, compound **66** splits off two HBr molecules, affording 3-bromolevoglucosenone **65**.

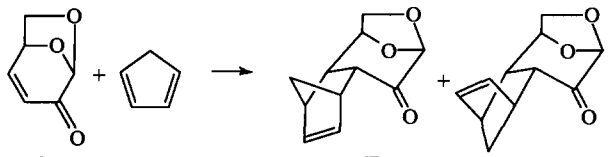


1 66 65

5. Levoglucosenone in the Diels–Alder reaction

The Diels–Alder reaction of levoglucosenone with cyclopentadiene, carried out in an excess of boiling dicyclopentadiene, affords a 47.8% yield of the crystalline adduct **67** and insignificant amounts of an unidentified carbohydrate.[38] Other investigators[39,40] carried out the reaction in boiling chlorobenzene and isolated the syrupy isomer **68** (in 16.5% yield) in addition to the crystalline compound **67** (in 65% yield).

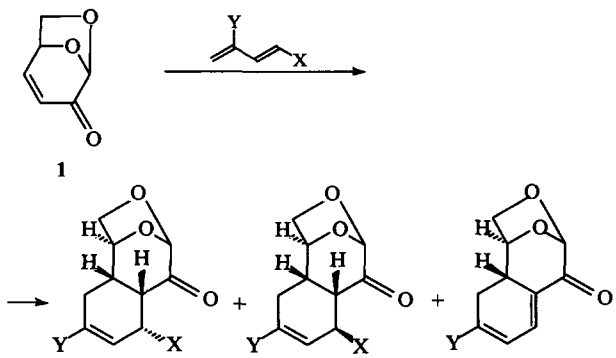
The structure of the adducts follows from spectroscopic data. Thus the absence of an appreciable interaction between H(4) and H(5) indicated by the ^1H NMR spectra of compounds **67** and **68** is evidence that these protons are diequatorial (the β-D-*ribo*-configuration) and that both adducts are formed when the diene is attacked 'from below'. The main adduct **67** is an *endo*-alkene (established with the aid of X-ray diffraction of the transformed product), while the minor adduct **68** is an *exo*-alkene (the configuration relative to the norbornene fragment is indicated).



1 67 68

The $ZnCl_2$-catalysed low-temperature Diels–Alder reaction of the above components, which makes it possible to obtain compound **67** in 75% yield without an admixture of the second isomer, is preparatively preferable.[41]

Subsequently various derivatives of cyclopentadiene, buta-1,3-diene, hexa-1,3-diene, and furan were tried as the diene component in the [4 + 2]-cycloaddition reactions of levoglucosenone.[38–40,42] In particular, in connection with the development of approaches to the synthesis of the indole alkaloid reserpine,[42] a study was made of the reaction of levoglucosenone with substituted buta-1,3-dienes. Unsubstituted buta-1,3-diene afforded a 98% yield of the adduct **69a**. In the case of 1-acetoxybuta-1,3-diene, the product of the elimination reaction **71** was formed together with the main product **69b** (in proportions of 3 : 1), whilst prolonged heating led to compound **71** as the only product formed in a quantitative yield. The reaction of levoglucosenone with 1-trimethylsiloxybuta-1,3-diene led to the formation of a mixture of the *endo*- and *exo*-adducts **69** and **70** in proportions of 2 : 1 in a 91% overall yield. the introduction of 5-benzyloxy-2-methoxypenta-1,3-diene, necessary for the formation of the basic reserpine synthons, into the reaction led to a stereoisomeric mixture of products in an overall yield of 38%.



1 69a–d 70a,b 71

Y = H: X = H (**a**), OAc (**b**), $OSiMe_3$ (**c**); Y = OMe, X = CH_2OCH_2Ph (**d**).

Y = H, X = $OSiMe_3$ (**a**); Y = OMe, X = CH_2OCH_2Ph (**b**)

Y = H, X = OAc (**a**); Y = OMe, X = CH_2OCH_2Ph (**b**).

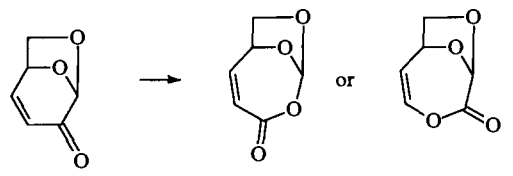
X	Y	Product ratios			Yield (%)
		69	**70**	**71**	
H	H	1	0	0	98
OAc	H	3	0	1	83
OAc	H	0	0	1	100
$OSiMe_3$	H	2	1	0	91
CH_2OCH_2Ph	OMe	1	1	1	38

6. The oxidation reactions of levoglucosenone and some of its derivatives

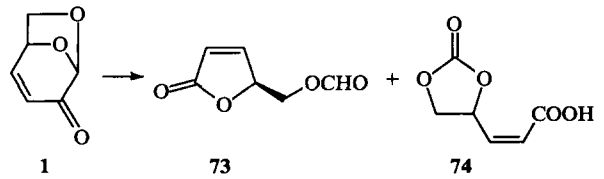
The unsaturated γ-lactone (*S*)-5-hydroxypent-2-en-4-olide **72**, containing one chiral centre, has found extensive applications in the manufacture of various medicinal drugs (burseran and isostegan), the antibiotic lasalocid A,[43] pheromones, aromatisers for whisky and cognac,[44] and also preparations suppressing the growth of the AIDS virus.[45]

In contrast to the approaches to the synthesis of the lactones **72** proposed previously and based on expensive and multistage syntheses using D-ribose and L-glutamic acid as the starting materials, the method developed by Koshi et al.[46] is extremely convenient and simple. The lactone **72** is obtained in one stage by oxidising levoglucosenone with *m*-chloroperbenzoic acid (MCPBA) by the Baeyer–Villiger method.

Shafizadeh and Furneaux,[17] who investigated the oxidation of levoglucosenone by *m*-chloroperbenzoic acid, demonstrated on the basis of spectroscopic data that the product of this reaction is either compound **A** or compound **B**, the formation of the enol-lactone **B** being most probable.



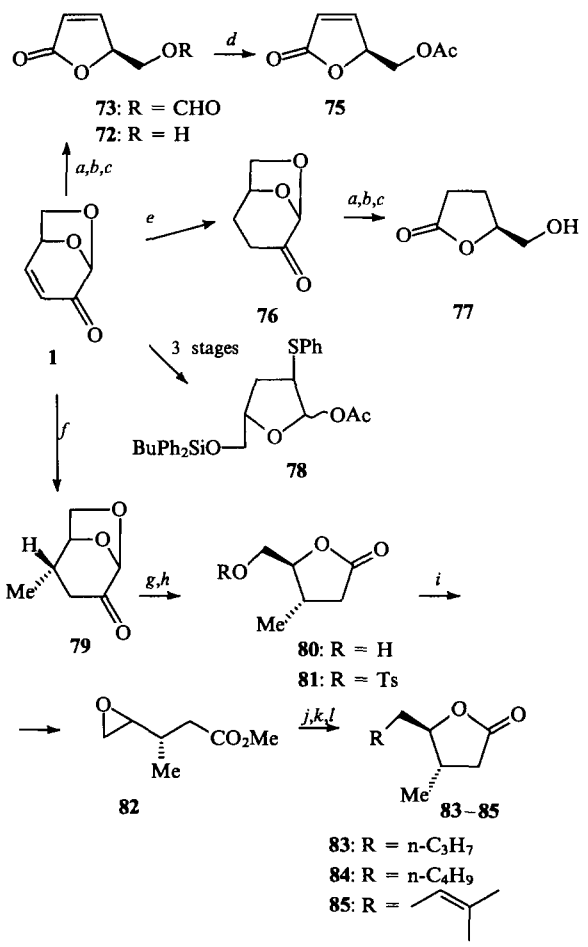
However, a more correct study of the oxidation reaction carried out by Koshi et al.,[46] established that the main reaction product is the formate **73** (yield 59%), while the cyclic carbonate **74** is a side product (yield 16%).



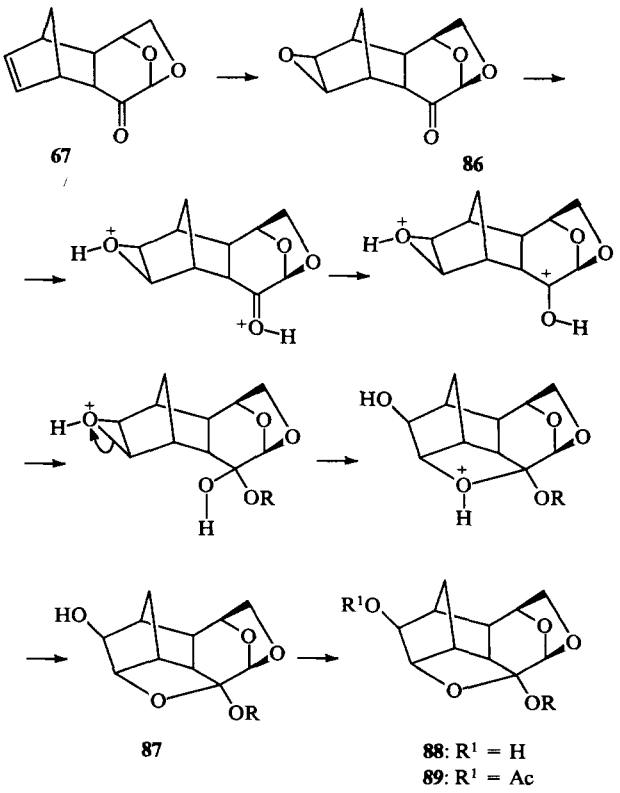
Subsequently peracetic acid was used to avoid oxidative rearrangements as side processes. After methanolysis and acetylation, the acetate **75** was synthesised as a result in 65% yield relative to levoglucosenone. (*S*)-5-Hydroxypentan-4-olide **77**[46,47] as well as 2-α-phenylthio-2,3-dideoxyribose **78** were obtained similarly from dihydrolevoglucosenone **76**.[48]

3,4-Dibsubstituted γ-lactones have been synthesised by the same procedure.[44] The methyl ketone **79** was oxidised to the lactone **80** and tosylated, the key epoxide **82** being obtained after the treatment of the tosylate **81** with alkali. The regioselective opening of the epoxide ring in compound **82** by means of appropriate cuprate reagents led to the 4-substituted γ-lactones **83**–**85**.

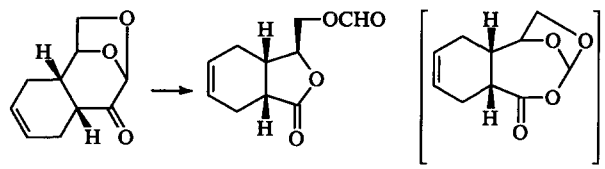
The oxidation of the principal cyclic [4 + 2]-adduct of levoglucosenone and cyclopentadiene **67** by *m*-chloroperbenzoic acid has been investigated.[43] The reaction afforded the *exo*-epoxide **86** in 86% yield. Its stereochemistry was elucidated by means of chemical reactions. Thus the hydrolysis of compound **86** does not entail the formation of a nonclassical ion characteristic of the norbornyl epoxide. Instead intramolecular cyclisation takes place and leads to the pentacyclic product **87**. Chemical proof of the involvement of the carbonyl group at the C(2) atom in the acid-catalysed solvolysis of compound **86** has been obtained by changing the solvent (water replaced by methanol). In order to determine the position of the hydroxy-group, compound **88** was acetylated. The spectra of the resulting acetate **89** indicated unambiguously that the hydroxy-group is at the C(9) atom while the methoxy-group is at the C(2) atom in compound **88**.



(*a*) AcOOH, AcOH; (*b*) Me_2S; (*c*) MeOH–HCl, 45 °C; (*d*) AcCl, Py, CH_2Cl_2; (*e*) H_2, Pd/C; (*f*) Me_2CuLi; (*g*) AcOOH, AcOH; (*h*) *p*-TsCl, Py; (*i*) K_2CO_3, MeOH; (*j*) Pr^n_2CuLi; (*k*) Bu^n_2CuLi; (*l*) $Me_2C{=}CHMgBr{-}CuBr$.



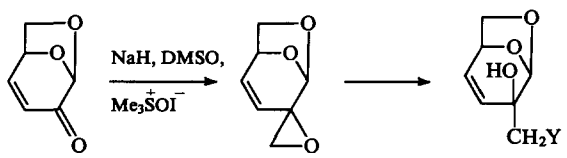
The Baeyer–Villiger oxidation of the tricyclic ketone **69a** afforded a high yield of the formyloxy-γ-lactone **90** with a *cis*-junction.[50] It was postulated that the formation of the formate is associated with the acid-catalysed rearrangement of the intermediate mixed inner orthoester **91**.



69a **90** **91**

7. Reactions involving the keto-group of levoglucosenone

In the course of the nucleophilic attack on the carbonyl group, the 1,6-anhydro-bridge of levoglucosenone exercises steric control, directing the approach of the reagent 'from below' the plane of the pyranose ring. Thus the interaction of the levoglucosenone with Cory's reagent, obtained by the reaction of NaH with $Me_3S^+OI^-$ in dimethyl sulfoxide, afforded a 50% yield of the epoxide **92**, which is obtained exclusively as a result of the *endo*-attack on the bulky reactant from the side of the levoglucosenone less shielded by the 1,6-anhydro-bridge.[51,52]



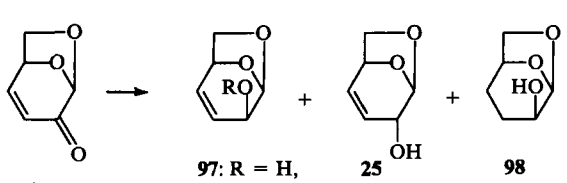
1 **92** **93–96**

Y = OH (**93**), H (**94**), N_3 (**95**), NH_2 (**96**).

Alkaline hydrolysis of the epoxide **92** by aqueous NaOH leads to the crystalline diol **93** in 71% yield. X-Ray diffraction of the specimen confirmed the structure **93** and hence also the structure of the epoxide **92**. Next the derivative **94** was obtained from the epoxide **92** by reduction with $LiAlH_4$, while azidolysis gave rise to the azide **95**, the reduction of which with $LiAlH_4$ led to the crystalline aminoalcohol **96**.

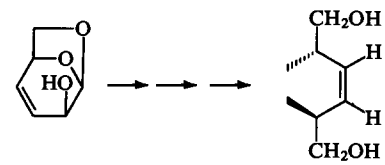
Thus the opening of the ring in the spiroepoxide **92** takes place entirely regiospecifically via an S_N2 mechanism.

It has been shown[13,27,53] that the double bond of levoglucosenone can be selectively hydrogenated. On the other hand, the reduction of the keto-group by $NaBH_4$ affords the allyl alcohols **97** and **25** as the main products, although the formation of minor unsaturated alcohols of type **98** is also possible depending on the reaction conditions.



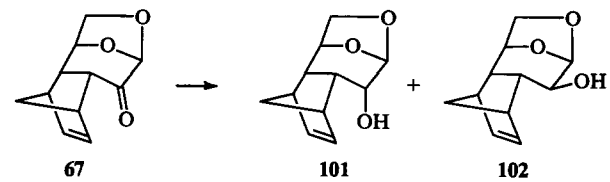
1 **97**: R = H, **99**: R = Ts. **25** **98**

On the basis of preliminary data obtained in Shafizadeh's laboratory,[13] the D-*erythro*-configuration (compound **25**) was attributed incorrectly to the product of the reduction of levoglucosenone by $LiAlH_4$. Subsequently the product was characterised as the D-*threo*-isomer **97** by comparing the alcohol obtained and its tosylate with authentic specimens[53,54] and also by the stereospecific conversion into (*Z*)-3,4-dideoxy-D-*threo*-hex-3-enitol **100**[17] with a known absolute configuration.

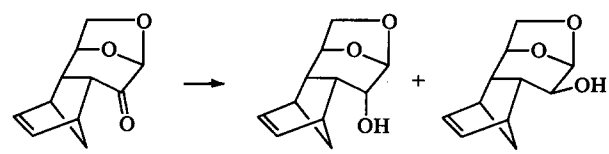


97 **100**

The reduction of the adduct **67** by sodium tetrahydroborate in 95% ethanol at 25 °C led to a mixture of the *endo*-alcohol **101** and the *exo*-alcohol **102** in 53% and 39% yields respectively.



67 **101** **102**



68 **103** **104**

Similarly the reduction of the minor adduct **68** with $NaBH_4$ afforded a mixture of the *exo*-alcohol **103** (yield 74%) and the less polar *endo*-alcohol **104** (yield 22%), the structures of which were established by spectroscopic methods. Axial attack on the *endo*-alkene **67** by the BH_4^- anion is more difficult, since in this case the carbonyl group occupies the *syn*-position relative to the bicyclo[2.2.1]hept-2-ene system.

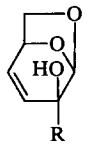
It had been reported earlier[13] that 1,2-adducts were obtained by the reaction of levoglucosenone with methylmagnesium iodide: 1,6-anhydro-3,4-dideoxy-2-*C*-methyl-β-D-*erythro*-hex-3-enopyranose **105** in 56% yield, its C(2)-epimer (1,6-anhydro-3,4-dideoxy-2-*C*-methyl-β-D-*threo*-hex-3-enopyranose **106**) in 6% yield, and the 1,4-adduct (1,6-anhydro-3,4-dideoxy-4-*C*-methyl-β-D-*erythro*-hexopyranos-2-ylose **79**) in 6% yield. When the reaction was carried out in the presence of Bu_3PCuI at −78 °C, the 1,4-adduct **79** was formed exclusively. The small spin–spin coupling constant between the H(4) and H(5) atoms obtained from the ^1H NMR spectrum of the adduct **79** indicated the *erythro*-configuration of the chiral centres. However, subsequently this claim was recognised as erroneous and, by analogy with the hydride reduction reaction, the D-*threo*-configuration was assigned to the main product of the Grignard reaction of levoglucosenone with methylmagnesium iodide.[17]



105: R^1 = Me, R^2 = OH. **106**: R^1 = OH, R^2 = Me. **79**

In order to attach long hydrocarbon chains, the reactions of levoglucosenone with tetradecyl- and octadecyl-magnesium bromides were carried out. Despite the fact that the target products **107** and **108** were obtained in 20% and 11% yields, the main products proved to be higher hydrocarbons formed via the

Wurtz reaction; the replacement of the Grignard reagent by alkyllithium reagents in order to suppress side reactions did not lead to the desired results.



107: R = $(CH_2)_{13}CH_3$;
108: R = $(CH_2)_{17}CH_3$.

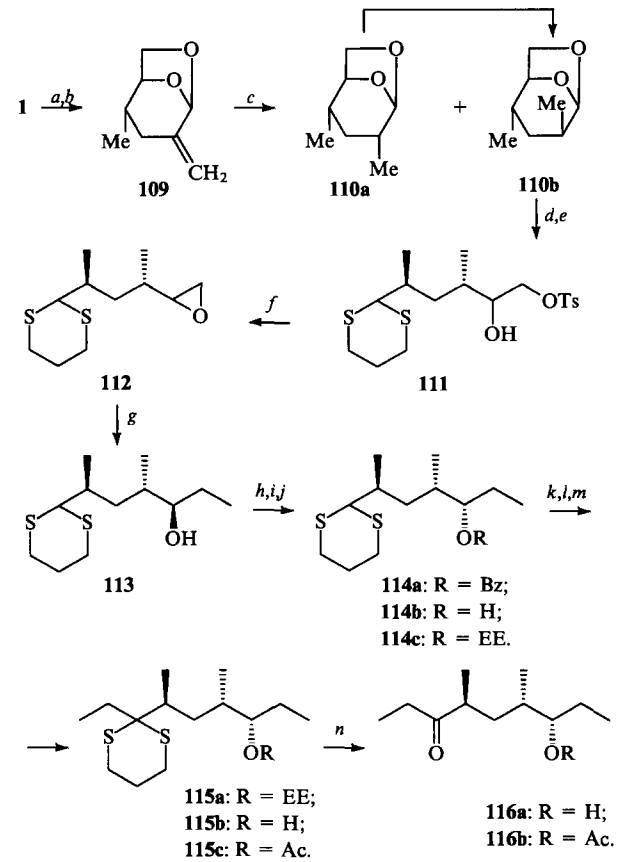
V. The use of levoglucosenone in the synthesis of natural products

The employment of sugars in the total syntheses of natural products has attracted the attention of investigators by the ready availability of the starting material with chiral centres and the universality of the approach, which are ensured by the diversity of the monomeric carbohydrates with a known configuration of the chiral centres. In contrast to other monosaccharides, levoglucosenone, which is a 1,6-anhydro-sugar, has a greater synthetic potential in view of its unusual structure and the conformational rigidity of the molecule. The characteristic features and advantages of levoglucosenone, noted in the Introduction and in the previous sections, were subsequently demonstrated on specific examples.

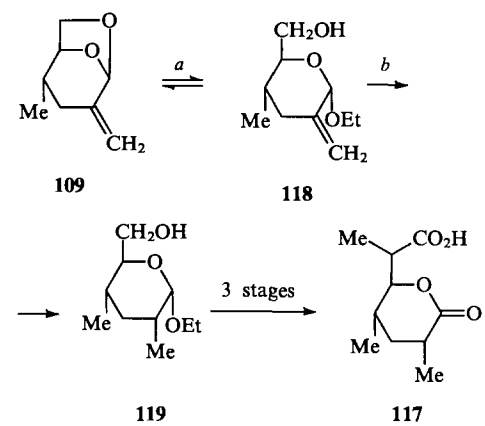
The stereoselective synthesis of serricornine, which is a sex pheromone of the tobacco beetle (*Lasioderma serricorne*—a pest on tobacco leaves), has been described.[55] Levoglucosenone was used as the starting material, its 1,6-anhydro bridge controlling unambiguously the stereoselective introduction of the methyl group at the C(4) atom. After the methylenation of the keto-group and hydrogenation of compound **109** in the presence of Pd/C, the 2,4-dimethyl derivatives **110a** and **110b** were obtained in proportions of 4:1. Compound **110b** (95% diastereoisomeric purity) was converted into the dithiane **111** and was then tosylated and the epoxide **112** was obtained after treatment with alkali. The epoxide reacted smoothly with 5 equiv. of Me_2CuLi in diethyl ether, affording the alcohol **113**. In order to obtain the alcohol having the desired configuration, Mitsunoba's method was used, the benzoate **114a** being hydrolysed to the alcohol **114b**. Compound **114b** was converted into acetylserricornine **116b** by a standard procedure: via stages involving the alkylation of dithiane, the replacement of the protecting group, and the hydrolysis of the dithiane **115c** with the aid of the $HgCl_2$–$CaCO_3$–aqueous MeCN system. The deacylated product **116a** exhibited the expected biological activity.

The *exo*-methylene derivative **109** proved to be a convenient starting material in the synthesis of the chiral synthon for the Prelog–Djerassi lactonoacid **117**.[56] Heating of the allyl glycoside **109** with trifluoroacetic acid in ethanol afforded an equilibrium mixture of compound **109** and the transglycosylation product **118**, isolated chromatographically. The stereoselective hydrogenation of the α-anomer **118** on a platinum catalyst led to ethyl 2,3,4-trideoxy-2,4-dimethyl-α-*ribo*-hexopyranoside **119** and its C(2) epimer in proportions of 6:1. Spectroscopic data confirmed the identity of compound **119** and of the key intermediate used in the synthesis of the Prelog–Djerassi lactonoacid. The method proposed makes it possible to reduce significantly the number of stages in the synthesis of the target lactone.

Pyranonaphthoquinones are compounds containing the naphtho[2,3-*c*]pyran ring system, which exhibit fungicidal, antibacterial, and anticancer activities. The fungal metabolite nanomycin A, altersolanol A, and the anthracycline antibiotic β-rhodomycinone are the best known representatives of these compounds.

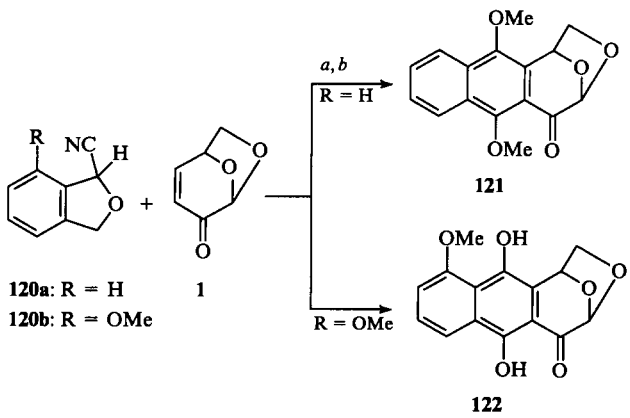


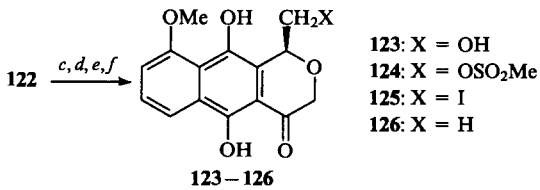
(*a*) Me_2CuLi, Et_2O; (*b*) Ph_3PCH_2, Et_2O; (*c*) H_2, Pd/C; (*d*) $HS(CH_2)_3SH$, $BF_3.Et_2O$, CH_2Cl_2; (*e*) *p*-TsCl, Py; (*f*) KOH, MeOH; (*g*) Me_2CuLi, Et_2O; (*h*) Ph_3P, BzOH, Et_2O; (*i*) KOH, MeOH; (*j*) EVE (EtOCH=CH_2), *p*-TsOH, CH_2Cl_2; (*k*) BuLi, TMEDA ($Me_2NCH_2CH_2NMe_2$), THF–EtI; (*l*) *p*-TsOH, EtOH; (*m*) Ac_2O, Py; (*n*) $HgCl_2$, $CaCO_3$, MeCN.



(*a*) 0.5% CF_3COOH–EtOH, 50 °C; (*b*) H_2, PtO_2, Et_2O.

The development of a new method for the construction of the rings of the naphthopyran ring system, which constitutes the central component of the above antibiotics, has been reported.[57] Levoglucosenone, which has the same stereochemistry as the dihydropyran fragments of the above antibiotics, was condensed with cyanotetrahydroisobenzofuran **120a**, affording an unstable naphthohydroquinone derivative, which was converted by methylation into compound **121** in 40% yield.





(*a*) $MeSCH_2Li$; (*b*) $Me_2SO_4.OH^-$; (*c*) Zn–Cu; (*d*) $MeSO_2Cl$; (*e*) NaI; (*f*) Zn–Cu.

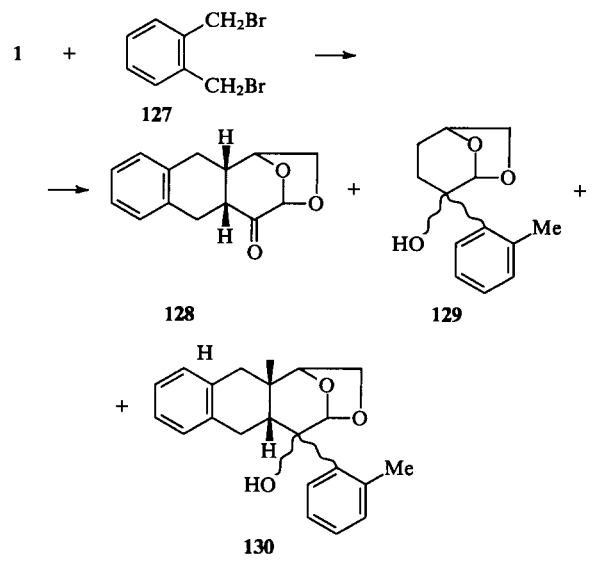
On the other hand, the reaction of compound **120b** with levoglucosenone gave rise to the stable crystalline naphthohydroquinone **122** in 65% yield. Its ring was subjected to reductive opening by the Zn–Cu couple in tetrahydrofuran. Having synthesised the chiral unit **123**, it was possible to construct in two stages the ring system of naphtho[2,3-*c*]pyran-5,10-quinones.

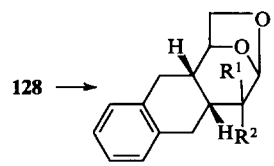
After several unsuccessful attempts to remove the primary hydroxy-group from compound **123**, the latter was converted via the methanesulfonate **124** into the iodide **125** and the required compound **126** was obtained by treatment with the Zn–Cu couple in moist THF. It is also noteworthy that the attachment of the lactone ring opened an easy route to calafungin, while the synthesis of the enantiomers **123–126** provided a short pathway to intermediates for the synthesis of nanomycin and its analogues. Overall, the sequence of reactions described above constitutes a promising method of synthesis of a series of substituted derivatives **123–126**, the hydroxyphthalides required for the synthesis of compound **120** being readily available.

It has been observed [57,58] that the interaction of levoglucosenone with the dibromo-derivative **127** in 1,4-dioxane in the presence of zinc powder in an ultrasonic bath affords compounds **128–130** in 53%, 3%, and 14% yields respectively.

The ^1H and ^{13}C NMR spectra of the main product **128** agree with the structure ascribed to it. The reduction of the ketone **128** with sodium tetrahydroborate leads to the epimeric alcohols **131** and **132**, which were isolated in 35% and 50% yields respectively. They were characterised as the acetates **133** and **134**; the H(4) and H(4a) atoms in compounds **131** and **133** are axial (according to ^1H NMR data), so that the compounds have the D-*altro*-configuration established by the *exo*-addition of the reagent to the double bond.

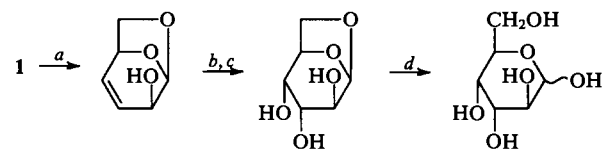
Compound **128** — a potential synthetic precursor of a series of representatives of pyranonaphthoquinone antibiotics — has been obtained by the Barton deoxygenation via the alcohols **131** and **132** and their thionocarbonates **135** and **136**. The side products **129** and **130** are believed tentatively to be formed from compound **127** via the Reformatskii reaction with participation of an organozinc intermediate, which attacks the carbonyl groups of the main product and levoglucosenone.





D-Altrose **139** is a rare sugar, for the preparation of which there is no readily available natural raw material. All the known syntheses of this compound consist of many stages. The method of synthesis of D-altrose via D-altrosan — 1,6-anhydro-β-D-altropyranose **138** — proposed by Chew and Ferrier [59] includes three stages and the overall yield is 29.1%.

1,6-Anhydro-3,4-dideoxy-β-D-*threo*-hex-3-enopyranose **97** has been synthesised from levoglucosenone by reduction using a standard method. [60] The *cis*-dihydroxylation of the double bond of the pyranose **97** by the OsO_4–*N*-methyl-morpholine *N*-oxide system proceeds stereoselectively, affording D-altrosan **138** in 86% yield; when stoichiometric amounts of $KMnO_4$ were used for the oxidation, the yield of the triol **138** was only 32.7%. Acid hydrolysis of compound **138** leads to D-altrose **139**.



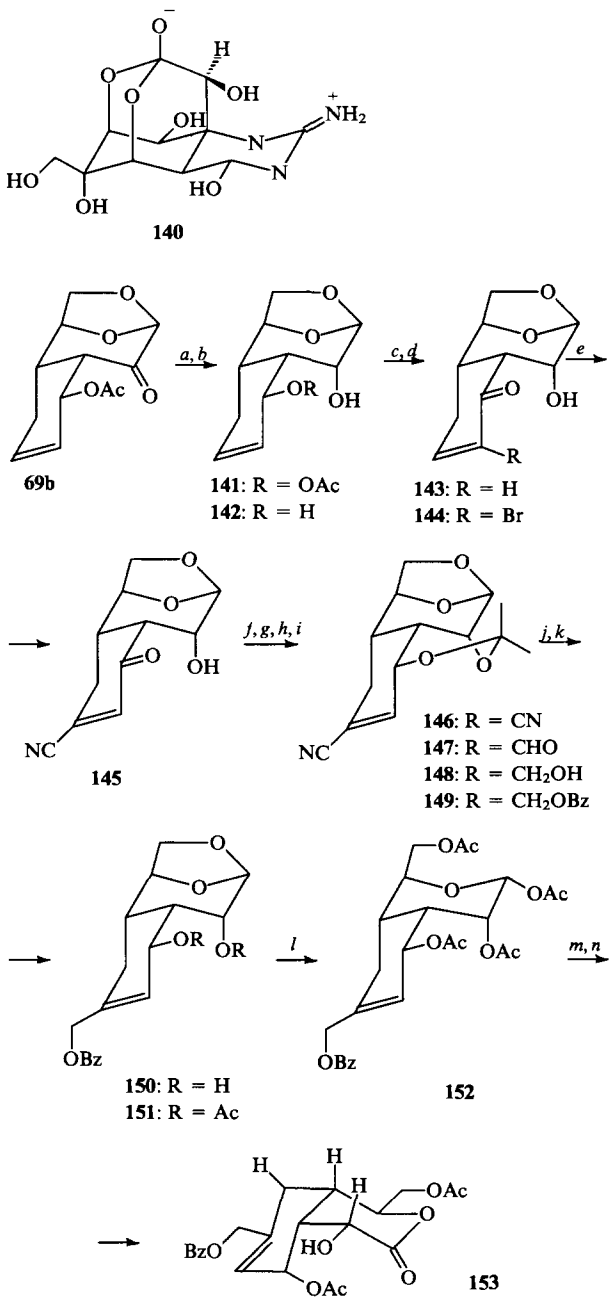
(*a*) $LiAlH_4$; (*b*) OsO_4–*N*-methylmorpholine *N*-oxide, Me_2CO, H_2O; (*c*) Na_2SO_3; (*d*) HCl–1,4-dioxane.

The same investigators obtained D-allosan and D-allose in six stages from levoglucosenone in 45% and 30% yields respectively. [61,62]

The key aspect of the approach to the synthesis of tetrodotoxin **140**, one of the best known of the food toxins, is the stage involving formation of the structure of the chiral cyclohexane via cycloaddition of acetoxybutadiene to the chiral dienophile — levoglucosenone. [63]

For this purpose, adduct **69b** was transformed into enone **143** via compounds **141** and **142**. The bromo-derivative **144** was obtained from the enone **143** by reaction with 1 equiv. of bromine in dichloromethane and subsequent treatment with triethylamine.

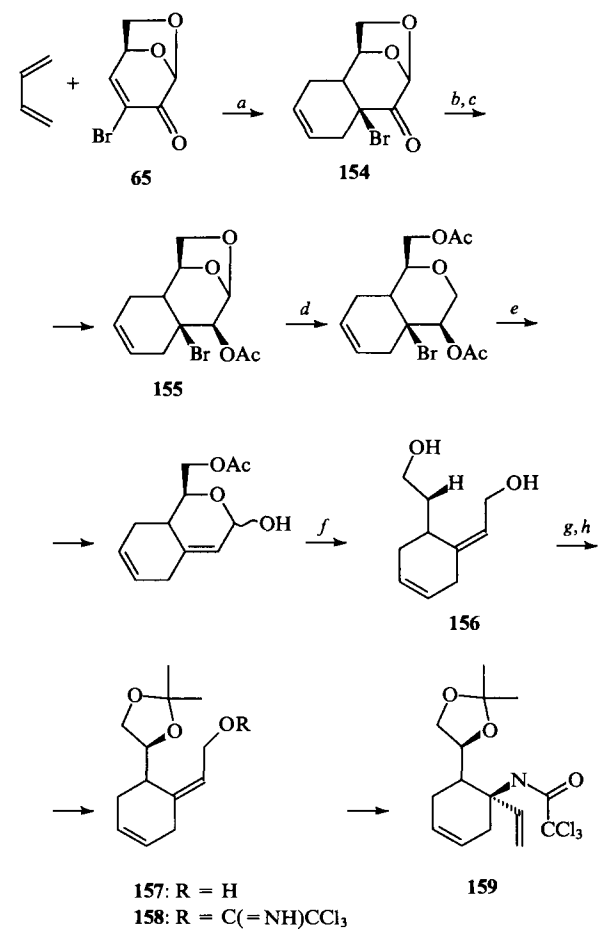
The addition of 2 equiv. of KCN at room temperature in the presence of ammonium chloride to the bromo-derivative **144** afforded the crystalline compound **145**. The reduction of the keto-group in compound **145** with sodium tetrahydroborate and protection of the diol group by 2,2-dimethoxypropane in camphorsulfonic acid (CSA) led to the acetonide **146**. Next followed the two-stage reduction of the nitrile group to the hydroxymethyl group via the aldehyde **147**. The alcohol **148** obtained was converted into the benzoate **149** and after acid hydrolysis the diacetate **151** was obtained from the diol **150**. The tricyclic compound **151** was solvolysed in the trifluoroacetic acid–acetic anhydride system. The yield of compound **152** was 96%.



(*a*) $NaBH_4$; (*b*) NaOMe; (*c*) MnO_2; (*d*) Br_2, CH_2Cl_2, Et_3N; (*e*) KCN–NH_4Cl; (*f*) $NaBH_4$, $Me_2C(OMe)_2$, CSA; (*g*) Bu^i_2AlH (DIBAL-H); (*h*) $LiAlH_4$; (*i*) BzCl–Py; (*j*) AcOH–THF–H_2O; (*k*) Ac_2O–Py; (*l*) Ac_2O–CF_3COOH; (*m*) $NH_2NH_2 \cdot H_2O$–DMF; (*n*) Jones reagent.

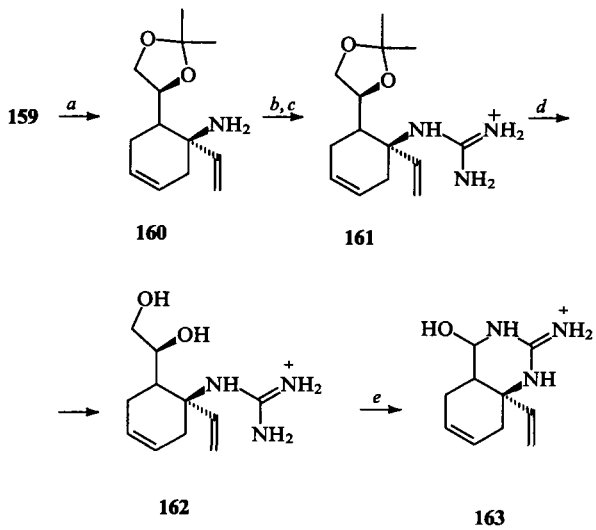
Acid hydrolysis of the anomeric acetate gave rise to the corresponding hemiacetal in a maximum yield of 70%, but this was accompanied by the formation of a side product. The hydrolytic stage was optimised by employing hydrazine (1.2 equiv. of $NH_2NH_2.H_2O$ in DMF at 60 °C). Oxidation of the hemiacetal by the Jones reagent completes the stage involving the formation of the cyclohexane unit **153**, into which suitable functional groups have been introduced.

The guanidine-containing part of tetrodotoxin was synthesised from the bromoketone **154**.[64] By opening the 1,6-anhydro-bridge and subsequent treatment with $NaBH_4$, the bromohydrin acetate **155** was transformed into the triol **156** and further into the *exo*-allyl alcohol **157**. The latter was treated with trichloroacetonitrile and NaH, the imide **158** formed was heated for 12 h in xylene, and the trichloroamidate **159** was obtained as a result of the successful Overman rearrangement.



(*a*) 110 °C, 12 h; (*b*) $NaBH_4$–MeOH; (*c*) Ac_2O, Py; (*d*) CF_3COOH, AcOH; (*e*) Zn–Cu; (*f*) $LiAlH_4$–THF; (*g*) $Me_2C(OMe)_2$, CSA; (*h*) Cl_3CCN, NaH, Et_2O; (*i*) 110 °C, 12 h.

The subsequent stages involved the hydrolysis of the trichloroacetamide group of compound **159** and the successive treatment of the amine **160** with bromocyanogen and ammonia, which led to the formation of the guanidine **161**. Next the acetonide protecting group was hydrolysed with trifluoroacetic acid, the glycol **162** was cleaved with periodic acid, and the guanidine derivative **163** was obtained in a satisfactory yield. Thus the optically active model tetrodoxin units **153** and **163** were synthesised from levoglucosenone.

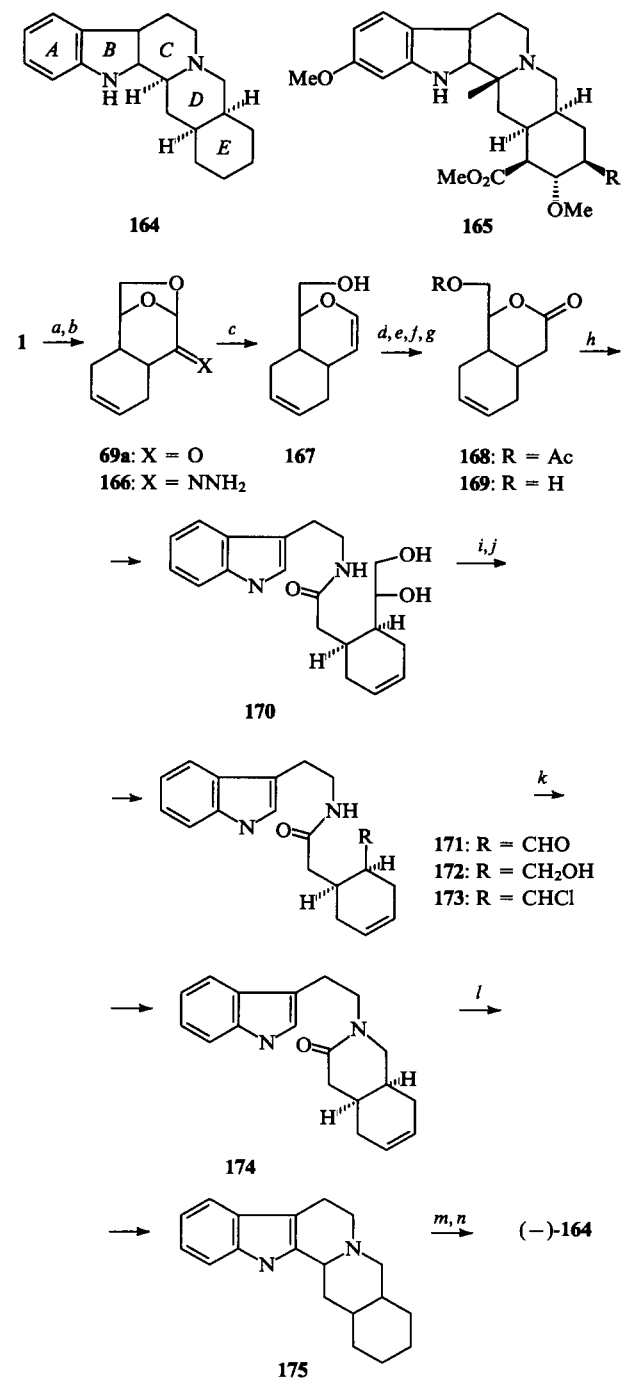


(*a*) KOH, EtOH, 50 °C; (*b*) BrCN–$NaHCO_3$; (*c*) NH_3, 100 °C; (*d*) CF_3COOH; (*e*) HIO_4.

The syntheses of the related optically active alkaloids alloyohimbane **164** and reserpine **165** from levoglucosenone have been described.[65] The crystalline Diels–Alder adduct of levoglucosenone with buta-1,3-diene **69a** was converted into the hydrazone **166**, the treatment of which with NaH in dimethyl sulfoxide (DMSO) afforded the vinyl ether **167**. Next followed stages involving acetylation, hydrolysis, and oxidation with the Jones reagent. The lactone **168** obtained was treated with MeONa in MeOH and compound **169** was heated with three equivalents of tryptamine in a 6:11 tetrahydrofuran–ethyldiisopropyl amine mixture. The glycol **170** produced was cleaved with HIO_4 to the aldehyde **171**. The reduction of the latter with $NaBH_4$ in methanol afforded the amidoalcohol **172**. The alcohol **172** was then converted by standard methods into the chloro-derivative **173**. Since compound **173** proved to be unstable, it was rapidly introduced into the reaction with lithium bis(trimethylsilyl)amide and the lactone **174** was obtained. In the concluding stage, cyclisation was achieved by heating compound **174** with $POCl_3$ and reduction of compound **175** with tetrahydroborate led to the target compound **164**.

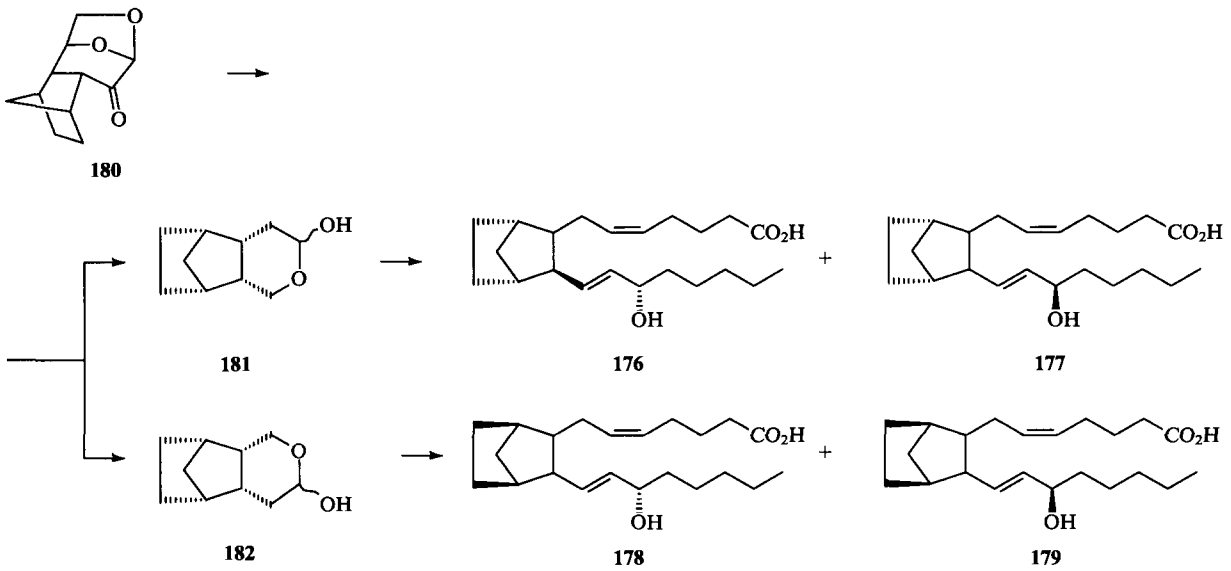
The enantiodivergent approach to the synthesis of the 9,11-ethano-analogues of the prostaglandin *endo*-peroxides (PGH_2) **176–179**, developed on the basis of the single chiral unit **180**, ensures a rational synthesis of the structures of both key enantiomeric precursors of the target compounds — the lactols **181** and **182** (see Scheme 1).[66,67]

The synthesis of nat-9,11-ethano-PGH_2 **176** and of its (15*R*)-diastereoisomer **177** is presented in Scheme 2. As can be seen from the latter, the transition **180** → **181** requires deoxygenation at the C(1) atom and the cleavage of the C(8)–C(9) bond in compound **180**. For this purpose, the ketone **180** was introduced into the Baeyer–Villiger reaction and the intermediate formate **183** was obtained in a high yield. It was hydrolysed to the alcohol **184**. The subsequent methanesulfonation, bromination (giving rise to compounds **185** and **186**), and then dehydrobromination with zinc



(*a*) $CH_2=CH-CH=CH_2$, 140 °C; (*b*) $NH_2NH_2 \cdot H_2O$, Et_3N; (*c*) NaH, DMSO; (*d*) Ac_2O–Py; (*e*) HCl–THF; (*f*) Jones reagent, 0 °C; (*g*) NaOMe–MeOH; (*h*) tryptamine, Pr^i_2EtN, THF; (*i*) HIO_4; (*j*) $NaBH_4$; (*k*) Ph_3P, CCl_4–LiN(SMe_3); (*l*) $POCl_3$, 100 °C; (*m*) $NaBH_4$; (*n*) H_2, Pd/C.

Scheme 1

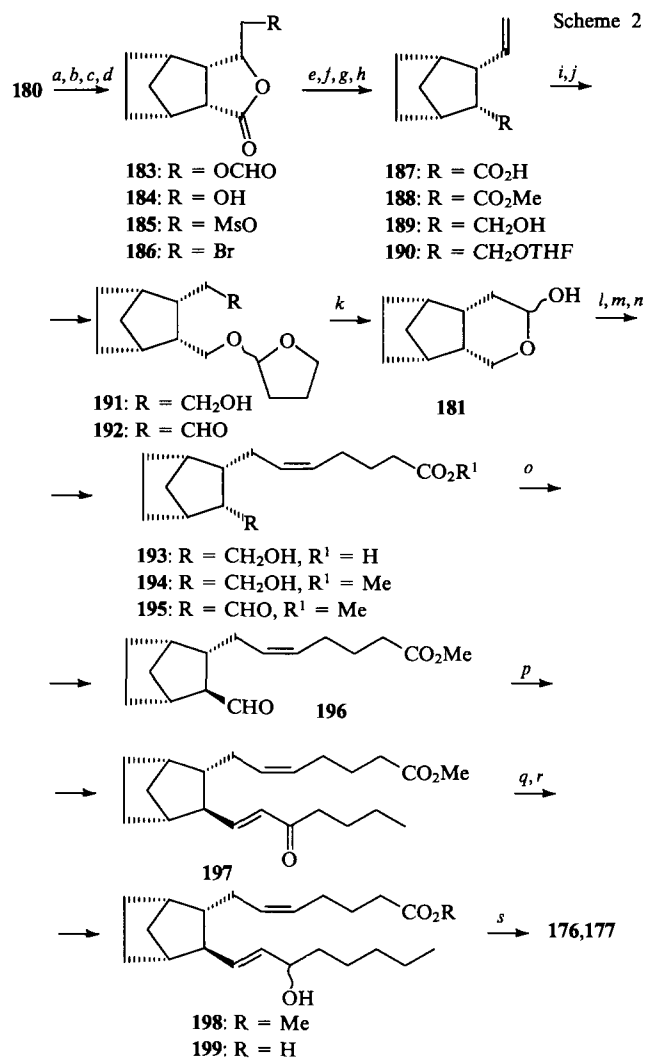


in Pr^iOH-H_2O led to the acid **187**. The latter was converted into the methyl ester **188** and treated with $LiAlH_4$ to form the alcohol **189**. After blocking the hydroxy-group in compound **189** by formation of the tetrahydrofuryl ether, the terminal double bond in compound **190** was functionalised with the aid of 9-bora-bicyclo[3.3.1]nonane (9-BBN) and the resulting diastereoisomeric mixture of alcohols **191** was oxidised with the Collins reagent and the acetal **192** was deblocked to form the lactol **181**. In view of its lability, the lactol **181** was converted, without purification, into an alkene by treatment with a phosphorane reagent and the alkene **193** was converted into the stable hydroxyacid **194** [the content of the 2'-(*Z*)-isomer was ~95%]. After methylation and oxidation by the P_2O_5-DMSO system, the hydroxyacid **194** afforded the *cis*-aldehyde **195**, which isomerises smoothly to the *exo*-aldehyde **196** on refluxing in toluene containing 1,5-diazabicyclo-[5.4.0]-undec-5-ene (DBU). Next the enone **197** was synthesised by the reaction of the aldehyde **196** with dimethyl 2-oxoheptyl-phosphonate under the conditions of the Wittig–Horner reaction. In the concluding stages, tetrahydroborate reduction of the enone **197** and hydrolysis of the ester **198** afforded a mixture of the 15α,β-epimeric alcohols **199** in proportions of ~1 : 1, which were separated by high performance liquid chromatography (HPLC).

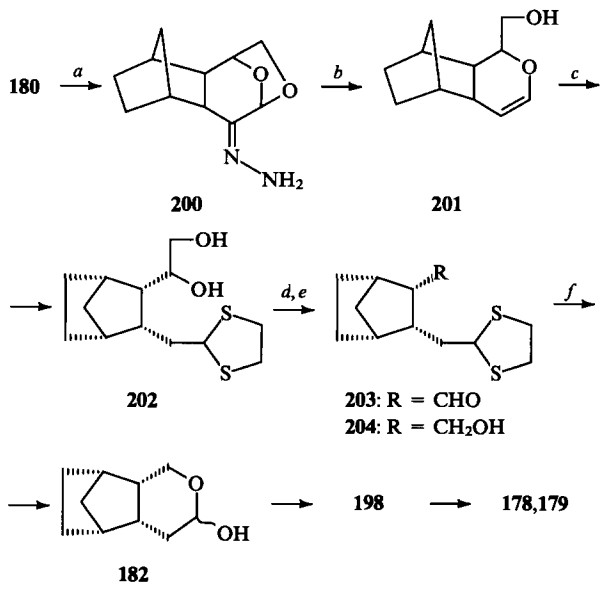
The synthesis of ent-9,11-ethano-PGH_2 **178** and of its (15*S*)-diastereoisomer **179** requires the C(8)-deoxygenation of the ketone **180**, which was achieved by the Huang–Minlon method. The conversion of the ketone **180** into the hydrazone **200** and then into the unsaturated ether **201** was achieved with an overall yield of 50% (see over). The following stages involved the conversion of compound **201** into the dithioacetal **202**, the cleavage of its diol group by $Pb(OAc)_4$, the reduction of the resulting *cis*-aldehyde **204** with sodium tetrahydroborate, and the Hg^{2+}-induced hydrolysis of the mercaptal **204** to the lactol **182**, which was transformed into the enone ent-**198** and further into substances of the ent-series **178** and **179**, as had been done in the case of compound **181**.

Thus the data presented demonstrate the extensive possibilities for the employment of levoglucosenone as a chiral precursor in the complex stereospecific synthesis of natural products and their analogues.

Scheme 2



(*a*) AcO_2H, $AcOH-H_2O$; (*b*) MeOH–MeONa; (*c*) MsCl–NEt_3, CH_2Cl_2; (*d*) LiBr–Me_2CO; (*e*) Zn, Pr^iOH-H_2O, ultrasound; (*f*) CH_2N_2; (*g*) $LiAlH_4$; (*h*) THF, H^+; (*i*) 1.1 equiv. of 9-BBN, H_2O_2–NaOH; (*j*) $CrO_3 \cdot 2Py$; (*k*) 10% HCl–dioxane; (*l*) $Ph_3P=CH(CH_2)_3CO_2Na$; (*m*) CH_2N_2; (*n*) P_2O_5– DMSO, CH_2Cl_2; (*o*) PhMe, 10% DBU, Δ; (*p*) $(MeO)_2POCH_2COC_5H_{11}$, 50% NaOH–CH_2Cl_2, $BnNEt_3Cl$–Cat; (*q*) $NaBH_4$, MeOH; (*r*) NaOH, $MeOH-H_2O$; (*s*) HPLC.



(*a*) NH_2NH_2. H_2O, 95 % Et_3N; (*b*) KOH–HOCH=CHOH; (*c*) $HSCH_2$. $.CH_2SH$, $BF_3.Et_2O$; (*d*) $Pb(OAc)_4$, CH_2Cl_2, −40 °C; (*e*) $NaBH_4$, MeOH; (*f*) $HgO-BF_3.Et_2O$, THF.

References

1. Y Tsuchiya, K Sumi *J. Appl. Polym. Sci.* **14** 2003 (1970)
2. L K M Lam, D P C Fung, I Tsuchiya, K Sumi *J. Appl. Polym. Sci.* **17** 391 (1973)
3. A E Lipsca, G E McCasland *J. Appl. Polym. Sci.* **150** 419 (1976)
4. Y Halpern, R Riffer, A Broido *J. Org. Chem.* **38** 204 (1973)
5. F Shafizadeh, P P S Chin *Carbohydr. Res.* **46** 149 (1976)
6. A Broido, M Evett, C C Hodges *Carbohydr. Res.* **44** 267 (1975)
7. A Ohnishi, K Kato, E Takagi *Polym. J.* 7 431 (1975)
8. US P. 480 107; *Ref. Zh. Khim.* 20 P 14 (1976)
9. F Wodly *J. Appl. Polym. Sci.* **15** 835 (1971)
10. G E Domburg, I Yu Berzinya, I Z Kirshbaum, M P Gavars *Khim. Drev.* **6** 105 (1978)
11. Y Halpern, J P Hoppech *J. Org. Chem.* **50** 1556 (1985)
12. G E Domburg, I Yu Berzinya, Z L Kupche *Khim. Drev.* 3 99 (1980)
13. F Shafizadeh, P P S Chin *Carbohydr. Res.* **58** 79 (1977)
14. F Shafizadeh, P P S Chin *Carbohydr. Res.* **46** 149 (1976)
15. A G Bradbury, F Shafizadeh, R H Furneaux, T G Cochran *J. Appl. Polym. Sci.* **23** 3271 (1979)
16. F Shafizadeh, A G Bradbury *J. Appl. Polym. Sci.* **23** 1431 (1979)
17. F Shafizadeh, R H Furneaux *Carbohydr. Res.* **71** 169 (1979)
18. F Shafizadeh, Y Z Lai, C R McIntyre *J. Appl. Polym. Sci.* **22** 1183 (1978)
19. F Shafizadeh, P P S Chin *Synth. Methods Carbohydr.* **39** 179 (1976)
20. P Köll, J Metzger *Angew. Chem.* **90** 802 (1978)
21. J J Miller, R Saunders *Fuel* **66** 123 (1987)
22. Y Halpern, R Riffer, A Broido *J. Org. Chem.* **38** 204 (1973)
23. R H Furneaux, G J Gainsford *Carbohydr. Res.* **146** 113 (1986)
24. K Kato, H Komorita *Agric. Biol. Chem.* **32** 21 (1968)
25. R H Furneaux, J M Mason, I J Miller *J. Chem. Soc., Perkin Trans. 1* 1923 (1984)
26. M Shibagaki, K Takahashi, H Kuno, I Honda, H Matsushita *Chem. Lett.* 307 (1990)
27. P Köll, T Shultek, R-W Rennecke *Chem. Ber.* **109** 337 (1976)
28. M Cerny, V Gut, J Pacak *Collect. Czech. Chem. Commun.* **26** 2542 (1961)
29. Russian P.1 710 563; *Ref. Zh. Khim.*19 O 115 (1992)
30. A C Forsyth *Tetrahedron Lett.* **30** 993 (1989)
31. M G Essig *Carbohydr. Res.* **156** 225 (1986)
32. F Shafizadeh, R H Furneaux *Carbohydr. Res.* **100** 303 (1982)
33. T T Stevenson, R E Stenkamp, L H Jensen, F Shafizadeh, R H Furneaux *Carbohydr. Res.* **104** 11 (1982)
34. F Shafizadeh, D D Ward, D Pang *Carbohydr. Res.* **102** 217 (1982)
35. G A Tolstikov, F A Valeev, A A Gareev, L M Khalilov, M S Miftakhov *Zh. Org. Khim.* **27** 565 (1991)
36. A J Blake, A C Forsyth, R M Paton *J. Chem. Soc., Chem. Commun.* 440 (1988)
37. D D Ward, F Shafizadeh *Carbohydr. Res.* **93** 284 (1981)
38. D D Ward, F Shafizadeh *Carbohydr. Res.* **95** 155 (1981)
39. P Bhat, D Horton *Carbohydr. Res.* **122** 189 (1983)
40. F Shafizadeh, M G Essig *Carbohydr. Res.* **114** 71 (1983)
41. G A Tolstikov, F A Valeev, I N Gaisina, L V Spirikhin, M S Miftakhov *Zh. Org. Khim.* **28** 2072 (1992)
42. M Isobe, N Fukami, T Nishikava *Heterocycles* **25** 521 (1987)
43. Jpn. P 411 403; *Chem. Abstr.* **114** 185 135m (1989)
44. E Takashi, M Katsuya, Y Hajime, K Koseki, H Kawakami, H Matsushita *Heterocycles* **31** 1585 (1990)
45. H Kawakami, T Ebata, K Koseki, K Statsumoto, H Matsushita, Y Naoi, K Itoh *Heterocycles* **31** 2041 (1990)
46. K Koshi, E Takashi, H Kawakami, H Matsushita, Y Naoi, K Itoh *Heterocycles* **31** 423 (1990)
47. Jpn. P. 418 925; *Chem. Abstr.* **115** 8 564a (1991)
48. H Kawakami, T Ebata, K Koseki, H Matsushita, Y Naoi, K Itoh *Chem. Lett.* 1459 (1990)
49. M G Essig, F Shafizadeh *Carbohydr. Res.* **127** 235 (1984)
50. F A Valeev, I N Gaisina, M S Miftakhov, G A Tolstikov *Zh. Org. Khim* **29** 105 (1993)
51. Y Gelas-Mialhe *Carbohydr. Res.* **199** 243 (1990)
52. Y Gelas-Mialhe, J Gelas, D Avenel, R Brahmi *Heterocycles* **24** 931 (1986)
53. J S Brimacombe, F Hunedy, L C N Tucker *Carbohydr. Res.* **60** C11 (1978)
54. J Pecka, M Cerny *Collect. Czech. Chem. Commun.* **43** 1720 (1978)
55. M Mori, T Chuman, K Kato *Tetrahedron Lett.* **23** 4593 (1982)
56. M Mori, T Chuman, K Kato *Carbohydr. Res.* **129** 73 (1984)
57. J N Freskos, J S Swenton *J. Chem. Soc., Chem. Commun.* 658 (1985)
58. S Chew, R J Ferrier *J. Chem. Soc. Chem. Commun.* 911 (1984)
59. S Chew, R J Ferrier *Carbohydr. Res.* **174** 161 (1988)
60. K Matsumoto, T Ebata, K Koseki, H Kawakami, H Matsushita *Bull. Chem. Soc. Jpn.* **64** 2309 (1991)
61. K Matsumoto, K Ebata, K Koseki *Heterocycles* **32** 2225 (1991)
62. K Matsumoto, K Ebata, K Koseki *Chem. Eng. News* **69** 36 (1991)
63. M Isobe, T Nishikawa, S Pikul, T Goto *Tetrahedron Lett.* **28** 6485 (1987)
64. M Isobe, Y Fukuda, T Nishikawa, Ph Chabert, T Kawai, T Goto *Tetrahedron Lett.* **31** 3327 (1990)
65. M Isobe, N Fukami, T Goto *Chem. Lett.* 71 (1985)
66. G A Tolstikov, F A Valeev, I N Gaisina, L V Spirikhin, M S Miftakhov *Zh. Org. Khim.* **28** 2072 (1992)
67. M S Miftakhov, F A Valeev, I N Gaisina, O V Shitikova, V R Sultanmuratova, G A Tolstikov *Zh. Org. Khim.* **29** 1122 (1993)

Russian Chemical Reviews **63** (11) 883–903 (1994)
©1994 Russian Academy of Sciences and Turpion Ltd

UDC 541.57; 541.124

Gradient lines on multidimensional potential energy surfaces and chemical reaction mechanisms

R M Minyaev

Contents

I.	Introduction	883
II.	Path of a chemical reaction on the potential energy surface	884
III.	Symmetry of the reaction path	888
IV.	Reaction paths consisting of several equivalent gradient lines	891
V.	Unimolecular reaction mechanisms	896
VI.	Collective processes	897
VII.	Biological systems	900
VIII.	Conclusion	901

Abstract. We show that the path of a chemical reaction on the potential energy surface of a chemical system can only be a gradient line between two critical points. Existing rules of symmetry conservation along the reaction path are analysed to establish their consistence with published experimental data and with ab initio calculations. In some systems the possible existence of reaction paths consisting of several gradient lines (both equivalent and nonequivalent) has been demonstrated. The relationship between the reaction mechanisms and the corresponding paths on the potential energy surface is discussed. The bibliography includes 238 references.

I. Introduction

The dynamics of chemical reactions on the appropriate potential energy surfaces (PES) are currently being studied in depth.[1–4] However, many problems relating to the structure of the PES and to the paths of chemical reactions on this surface are still controversial,[4–7] and in many cases have not yet been clearly and precisely formulated. Thus, studies of the dynamics of the thermo- and phototransformation of molecules (both in a gas and in a condensed medium) require a correct definition of the topology of the PES for both the ground and the excited state, as well as of their relative disposition over a reasonably wide range of changes in the intrinsic coordinates. Currently used one-dimensional models of various photoprocesses are far from offering a solution of these problems. A good example is provided by a study[8] of the dynamics of the photochromic behaviour of the indoline spiropyran **1** (1′,3′,3′-trimethyl-6-hydroxyspiro[2*H*-1-benzopyran]2,2′-indoline) in solution by nano- and femtosecond spectroscopy methods (Fig. 1). When the compound **1** is irradiated ($\lambda \approx 300$ nm) the C–O bond breaks in less than 100 fs with formation of the metastable compound **2**, which then isomerises to the merocyanine form **3**. The whole process is represented schematically by a one-dimensional energy diagram. This model cannot account for the many motions of a chemical system as complex as molecule **1** on the multidimensional surface of the ground and the excited state.

The dynamic behaviour of chemical systems in the classical or the quantum approximation is now being studied mainly in the one-channel approximation, although many examples of reactions taking place along several equivalent paths are

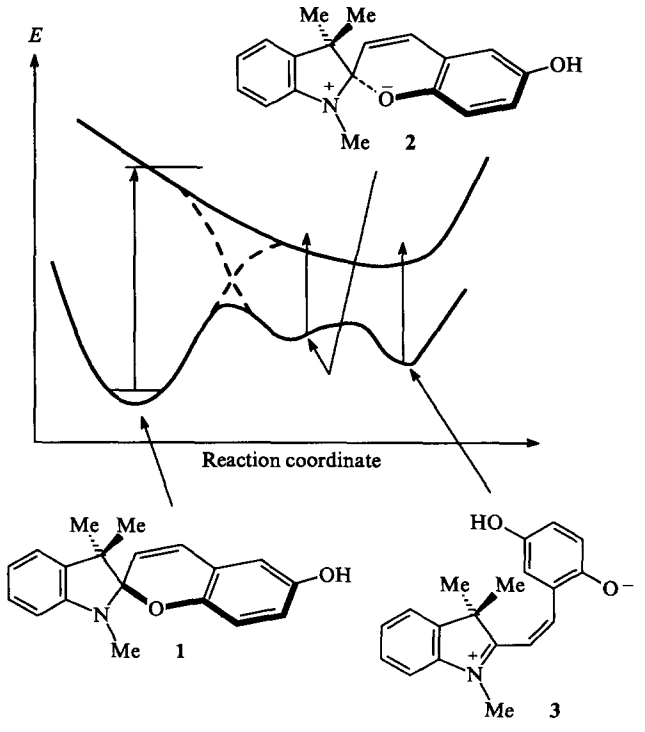


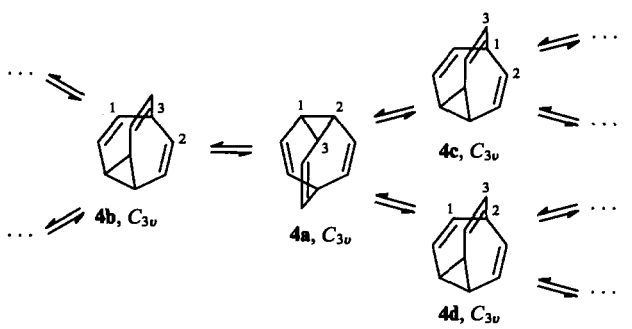
Figure 1. Scheme of the photochemical opening of 1′,3′,3′-trimethyl-6-hydroxyspiro[2*H*-1-benzopyran]-2,2′-indoline (**1**) (see Ref. 8). (**2**) initial metastable product, corresponding to the structure with a broken C–O bond but retaining the configuration of the fragments lying in perpendicular planes; (**3**) merocyanine form, which follows the reac-tion path along the diabatic surfaces (broken lines). Only one of the vari-ous possible merocyanine isomers (**3**) is shown in the figure as a product.

R M Minyaev Institute of Physical and Organic Chemistry, Rostov State University, 194/3 Prosp. Stachki, 344104 Rostov-on-Don, Russian Federation, Fax (7-863) 228 56 67

Received 20 September 1994
Uspekhi Khimii **63** (11) 939–961 (1994); Translated by J I Carasso

known,[9-22] for example the isomerisation of bulvalene **4** (Scheme 1),[9-12] the internal rotation of two or several groups in various systems,[13-19] the opening of cyclopropane[20,21] and ozone rings,[22] and other systems.[23-25] Clearly, changing to a multichannel representation of the reaction dynamics requires the development of new approaches to the description and the treatment of the PES, and also to the study of the system dynamics on such a surface.

Scheme 1



As shown by recent work,[26-37] the effect of a solvent on the mechanism and rate of the reaction is not so much a static effect as the effect of the direct participation of one or several solvent molecules in the reaction as discrete species. This undoubtedly requires the inclusion of the solvent molecules into the PES being considered for the chemical systems.

Studies of the structure of a solid surface,[38] of its interaction with adsorbed molecules, and of the chemical reactions taking place on the surface are impossible without a detailed knowledge of the structure of the PES for a combined system consisting of the adsorbed molecule and a model of the solid surface.[38-45] Configurational transitions of the solid from one symmetry group to another can be treated as transitions from one minimum to another in the appropriate PES.

The development of molecular devices for use in molecular electronics is greatly dependent on studies of the complex motion of the chemical system along the appropriate PES.[46,47] The problem of the transformation of one form of energy into another is far from solved,[48,49] and therefore studies of the direct molecular conversions of solar energy are important.[49-52] The search for molecular systems capable of storing solar energy, concentrating it, and converting it into forms convenient for practical applications relies on the study of the structure of the adiabatic PES of the appropriate chemical systems.[49]

A deeper understanding of the nature of biological systems and of their operating principles obviously requires a detailed study of the PES of model chemical systems simulating the totality of active centres and their collective properties.[53-56]

It follows from the above considerations that the study of the global PES is only beginning. The solution of many key theoretical and experimental problems is associated most closely with the study of the structure of the appropriate PES.

With the exception of the report by Bazilevskii and Ryaboi[4] there have so far been no reviews of the problems associated with the global structure of the PES in the Russian literature. Therefore the main aim of the present paper will be to fill this gap by stressing the many examples of inadequate studies of the PES, and thus to promote a wider understanding of the reaction path.

II. Path of a chemical reaction on the potential energy surface

The path of a chemical reaction on the PES,[57-59] which determines its mechanism, is one of the most important concepts in chemistry. This concept, first introduced[57] in the late 1930s immediately following the establishment of the concept of an adiabatic PES for the molecule,[60] is still controversial.[4-7,61-77] There are several different definitions of the reaction path, of which the most important are the minimum energy reaction path,[57-59,71-73] the path of steepest descent,[67-69,72,76] and the intrinsic reaction coordinate.[61,63,68]

The minimum energy path (MEP) is a line following the bottom of the reaction valley and connecting the energy minima of the reactants and products through the appropriate saddle point (transition state[78,79]) on the PES. The path of steepest descent is a gradient line originating at the saddle point and pointing towards the energy minima of the reactants or of the products. When mass-weighted coordinates are used the path of steepest descent becomes the intrinsic reaction coordinate (IRC).[61,63,68] In the construction of a topological PES structure, when the reaction valley connects the energy minima of reactants and products through a high saddle, all the above definitions of the reaction path are described by the same line on the PES (Fig. 2). In more complex topological structures of the PES the minimum energy path, the gradient line, and the IRC can be different, and therefore the mechanisms predicted for a given reaction may also differ. Of course, it becomes essential to choose the definition of the reaction path on the PES which is most appropriate to the physics and chemistry of the process being studied. Without denying the possible validity of the MEP or of the IRC this review will be concerned mainly with the gradient reaction path.[7,80] The choice of this definition of the path is most convenient in the case of a PES having a complex topological structure. We shall discuss only the PES of the electronic ground state, although the methodology developed in this review is equally applicable to the PES of any electronic state.

The potential energy surface $E(X)$ and its first and second derivatives are assumed to be finite and continuous functions at any point X (X_1, X_2, ..., X_{3N}) of the configurational space R^{3N} except at the poles (the points where the coordinates of two or more atoms in the molecule coincide). The chemically most important regions of the PES are the so-called nondegenerate critical (stationary or extremal) points, i.e. the points X_{cr} on the PES where the following relationships are satisfied simultaneously;

$$\nabla E(X_{cr}) = \operatorname{grad} E(X_{cr}) = 0\,, \tag{1}$$

$$\operatorname{rank}(H_{ij})_{X_{cr}} = \operatorname{rank}\left\|\frac{\partial^2 E}{\partial X_i \partial X_j}\right\|_{X_{cr}} = 3N-6\,, \tag{2}$$

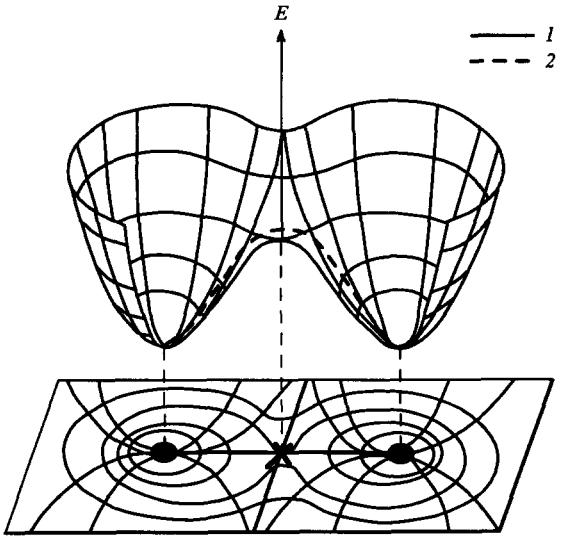


Figure 2. Potential energy surface of the molecule and its two-dimensional projection on the configurational space. (*1*) Path of the reaction on the PES, (*2*) projection of the reaction path on the configurational space. The curves emerging from the minima are gradient lines, the closed curves are equipotential lines.

where X and N are (respectively) the Cartesian coordinates of the nuclei and the number of atoms in the molecule.[64,65,78,79] Eqn (2) states that the Hessian (H_{ij}) has only six zero eigenvalues corresponding to the motion of the molecular system as a whole (three translations with respect to the three axes and three rotations round these same axes).

The point $X \in R^{3N}$, where the relationship (1) is not obeyed [$\nabla E(X) \neq 0$], is called a regular[81,82] (noncritical or normal[61,65]) point. All the critical points are characterised by the index λ (the number of negative eigenvalues of the Hessian). Thus, for a minimum $\lambda = 0$, for a saddle point $\lambda = 1$, for a critical point $\lambda = 2$, etc.[65]

The reaction path of the chemical system[57-59,61,83] is defined by a line on the PES which originates from the energy minimum for the reactant, passes through the saddle point corresponding to the transition state, and terminates at the energy minimum for the product (see line *1* of Fig. 2). The reaction path is defined in $(3N+1)$-dimensional R^{3N+1} space (the direct sum of the configurational space and of the energy coordinate $R^{3N+1} = R^{3N} \oplus E$),[81] which we shall call the entire space. A mutually single-valued correspondence exists between the points (and therefore also the curves) on the PES and in the configurational space. Thus the line in the configurational space directly defines the line on the PES, and vice versa. The orthogonal projection of the reaction path on the configurational space gives a curve in the R^{3N} space which is also called the reaction path (see line *2* in Fig. 2). We shall in most cases refer to the reaction path in the entire space.

In the adiabatic approximation[60] the PES is independent of the nuclear masses, and therefore any lines lying on the PES and its projection on the R^{3N} space are also independent of the nuclear masses. An infinitesimally small displacement along the PES from any point X_0 (produced by motion at an infinitesimally small speed) can only follow the direction of the gradient vector.[61,67,69] The result is that under conditions of infinitesimally small displacement the molecular system can slide on the PES only along the gradient lines between any two critical points.[61,63,68,69] Therefore of all the lines on the PES only the gradient line can act as the reaction path. In this case in order to identify the line on the PES corresponding to the path of the chemical reaction we must solve a system of ordinary differential equations defining the gradient lines on the PES, which can be written in Cartesian coordinates not weighed for mass in the well-known form,[61,63,68,81,82]

$$\frac{dX_1}{\partial E/\partial X_1} = \frac{dX_2}{\partial E/\partial X_2} = \cdots = \frac{dX_{3N}}{\partial E/\partial X_{3N}} = \text{const}, \qquad (3)$$

with the initial conditions $X_0 = (X_1, X_2, ..., X_{3N})_0$, and from the family of solutions of this system we must choose those which connect the appropriate critical points. Eqn (3) in mass-weighted coordinates was first used by Fukui[61] (in 1970) as a means of finding the reaction path. However, we should note that in studies of the dynamics of chemical systems it is convenient to work with mass-weighted coordinates,[61] though we shall not consider these in the present review, leaving interested readers to consult the original publications.[1-4,61,63,68]

For our purpose Eqn (3) is conveniently written as a system of $3N$ ordinary differential equations[4,61,67-69,80]

$$\frac{dX_i}{dt} = -\frac{\partial E[X_1(t), ... X_{3N}(t)]}{\partial X_i}, \quad i = 1, 2, ..., 3N, \qquad (4)$$

with the initial conditions $X(t_0) = (X_1, X_2, ..., X_{3N})_0$. The quantity t is a parameter for the length of the curve. The minus sign on the right-hand side of Eqn (4) means that the potential decreases as t increases. The integral curves of Eqn (4) are called the gradient lines $X = X(t)$ of the adiabatic potential.[68,69]

Thus under conditions of infinitesimally small displacement the molecular system can move on the PES only along gradient lines connecting any two critical points.[61,63,68] Only a gradient line can act as the reaction path among the lines belonging to the PES.

According to Ostgood's theorem[85,86] the system (4) with a right-hand side satisfying the Lipshits condition

$$\left| \frac{\partial E(X')}{\partial X_i} - \frac{\partial E(X'')}{\partial X_i} \right| \leqslant K \sum_i^{3N} |X_i' - X_i''|,$$

where X', $X'' \in R^{3N}$ and K is a positive constant, has a unique solution which passes through the given initial point X_0. Obviously the condition imposed on the PES ensure that the Lipshits conditions are obeyed by the right-hand side of (4), and therefore that for these condition the Ostgood theorem applies. Thus there is only one solution of the system (4), $X = X(t)$, which passes through the given regular point.[69,70,80,85,86] This means that the gradient line can neither disappear at nor emerge from a regular point, i.e. that gradient lines can have no bifurcations on the slopes of the PES.

The vector-gradient field ∇E behaves like an ordinary electrostatic field, whose integral lines of force do not intersect[84] (see also the quantum topology theory[87]).

In curvilinear coordinates $Q(X) \in R^{3N-6}$ (where R^{3N-6} is the configurational space of the intrinsic coordinates) the Eqns (4) can be written in the tensor form[4,6,68,74,88]

$$\frac{dQ^k}{dt} = -\sum_{l=1}^{3N-6} g^{kl} \frac{\partial E[Q^1(t), ..., Q^{3N-6}(t)]}{dQ^l}, \qquad (5)$$

$$k = 1, 2, ..., 3N-6,$$

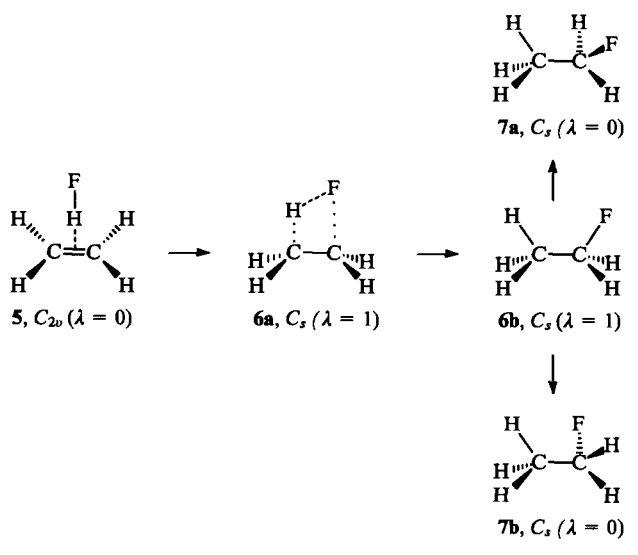
where the metric tensor g^{kl} (see Refs 81 and 88) is defined by the equation[4,74]

$$g^{kl} = \sum_{i=1}^{3N} \left[\frac{\partial Q^k}{\partial X_i}\right] \left[\frac{\partial Q^l}{\partial X_i}\right], \quad k = l = 1, 2, ..., 3N-6.$$

It is important to note that the functions $E(X)$ and $E(Q)$ define the same adiabatic PES, and the equations (4) and (5) give the same system of gradient lines.[4,6,67,74] The tensor form (5) ensures the invariance of the gradient lines for any transformation of the coordinates with a nonzero Jacobian. Thus the gradient lines, like the PES, are defined only by the given molecular system and are independent of the choice of coordinates.

A system of gradient lines connecting the energy minima of reactants and products and passing through one or several saddle points is called a gradient reaction path.[7,80] Thus in order to obtain the gradient reaction path we must have the solutions of Eqns (4) and (5), but this cannot be done in an explicit form since the functions $E(X)$ and $E(Q)$ are not known in an analytic form even

Scheme 2



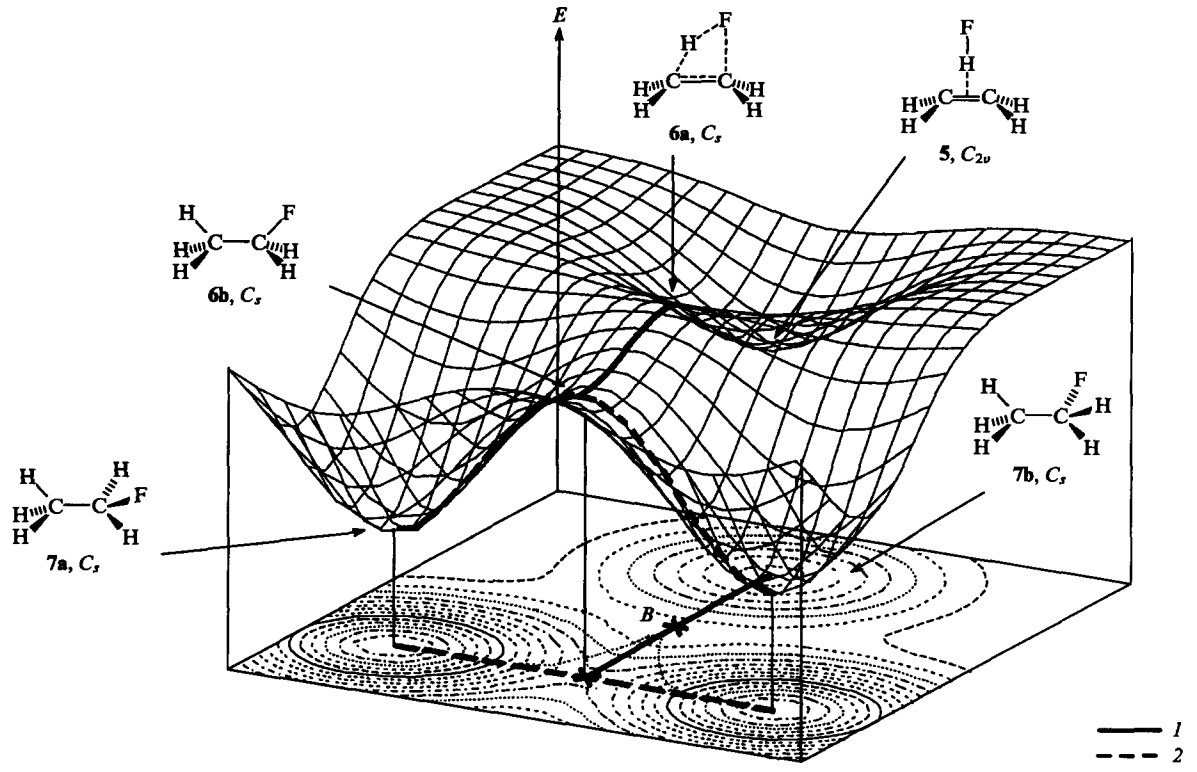


Figure 3. Potential energy surface for the electrophilic addition of HF to the C=C double bond of ethylene.[7] The line *1* corresponds to the initial part of the reaction **5** → **6a** → **6b**. The line *2* corresponds to the reaction **7a** ⇄ **6b** ⇄ **7b** for the internal rotation in the substituted ethane; the lines emerging from the bifurcation point *B* define the minimum energy path; the transition states are shown by crosses.

for the simplest triatomic systems.[71] However, numerical approximations to the gradient lines can now be obtained without great difficulty. We shall consider, as an example, the gradient path of the electrophilic addition of HF to a molecule of ethylene.[7] Nonempirical calculations (MP2/DZP) have predicted[7] that this reaction can be represented by the Scheme 2.

The structure of the PES for this reaction is shown in Fig. 3. The reaction, which begins with the formation of the metastable π-complex **5**, is described by the gradient line *1* in the region **5** → **6a** → **6b**. This line passes through the saddle point corresponding to the transition state **6a** and reaches the neighbouring saddle point corresponding to the other transition state **6b** for the internal rotation round the C–C bond.

At the point on the PES corresponding to the state **6b** the gradient path of the reaction changes direction in the configurational (entire) space and passes from the first gradient line to the second (line *2* of Fig. 3), reaching the minima of the states **7a** and **7b** along the two branches of the second line.

If the gradient line connects two critical points all the eigenvectors of the Hessian $\vec{q}_i$ of one critical point should smoothly change at the point of descent along the gradient line into the accompanying Frenet polyhedron,[81,82] which should itself be transformed into the appropriate eigenvectors of the Hessian for the other critical point.

In this case it is sufficient to consider the evolution of the two eigenvectors of the Hessian $\vec{q}_1$ and $\vec{q}_2$ along the first gradient line from the state **6a** to the state **6b** (see Fig. 4). The transition vector $\vec{q}_1$ of the state **6a** at the point of descent is converted into the tangential vector $\nabla E/|\nabla E|$ ($\vec{q}_1$ at the point *B*), which is further converted (for the state **6b**) into the eigenvector of the Hessian corresponding to the first positive eigenvalue ($\vec{q}_1$ at the point **6b**). At the same time the perpendicular vector $\vec{q}_2$, corresponding to the eigenvector of the Hessian for the first positive eigenvalue at the point **6a**, is continuously transformed along the gradient line, becoming the transition vector $\vec{q}_2$ for the structure **6b**.

Thus the gradient path of the addition of HF to ethylene consists of two nonequivalent gradient lines of which the first connects the points **5** → **6a** → **6b**, and the second the points **7a** → **6b** → **7b**. A characteristic feature of the PES is shown in Fig. 3: the first gradient line emerging from **6a** does not reach either of the minima at **7a** or **7b**. Along this gradient line and beyond the point *B* a shift in a perpendicular direction lowers the energy, i.e. a reaction valley develops beyond the bifurcation point *B* and therefore the MEP splits into two (broken lines in Fig. 3). The minimum-energy path begins at the point **6a** and leads to the minimum **7a** (or **7b**), missing the point **6b**. Thus the bifurcation point *B* exists only for the MEP, but not for the gradient line (∇E does not vanish at the point *B*, and therefore only one gradient line can pass through this point).

Gradient lines can be generated or disappear only at critical points,[85,86] and therefore the behaviour of the gradient lines in the infinitesimally small surroundings of the critical point denotes a relationship between the symmetry properties of the system on the reaction path and the symmetry properties of the system at a critical point (in particular, at the minimum points and at the saddle point).[80]

In the immediate surroundings of any critical point Q_{cr} the potential energy surface $E(Q)$ can be approximately represented by the quadratic term alone of a Taylor series[82]

$$E(Q) = \frac{1}{2}\sum_{l=1}^{3N-6}\left[\frac{\partial^2 E}{(\partial Q^l)^2}\right]_{Q_{cr}} \qquad (Q^l)^2 = \frac{1}{2}\sum_{l=1}^{3N-6}\alpha_l (Q^l)^2 . \qquad (6)$$

For this type of potential the equations (5) are easily integrated, giving solutions of two types:[67,69,74,80]

trivial

$$Q^k = 0, \quad k = 1, 2, ..., 3N-6 , \qquad (7)$$

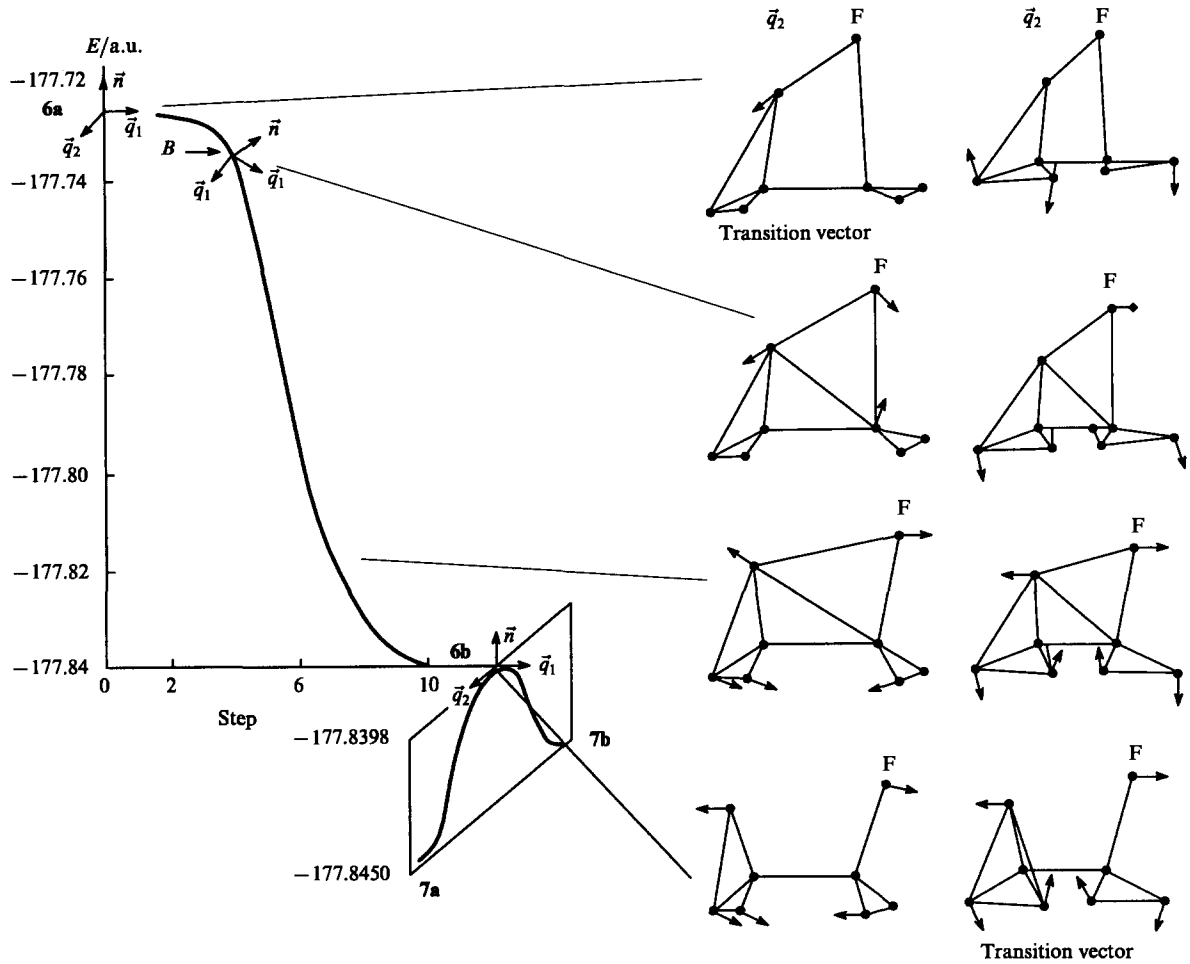


Figure 4. Evolution of the eigenvectors $\vec{q}_1$ and $\vec{q}_2$ of the Hessian along the gradient lines from the point **6a** (see Fig. 3) to the point **6b**. The vector $\vec{q}_1$ is the transition vector at the point **6a**, and the vector of the first positive eigenvalue of the Hessian at the point **6b**. The vector $\vec{q}_2$ is the vector of the first positive value of the Hessian at the point **6a** and the transition vector at the point **6b**. The forms of these vectors are shown on the right, $\vec{n}$ is the vector of the normal to the gradient line, and coincides with the direction of the E axis at the critical points.

and nontrivial

$$Q^k = (Q^k)_0 \exp(-\alpha_k t), \quad k = 1, 2, ..., 3N-6, \qquad (8)$$

where $(Q)_0$ is the initial point, corresponding to $t = 0$.

These curves are shown in Fig. 5 for the infinitesimally small surroundings of a minimum ($\lambda = 0$) and of a saddle point ($\lambda = 1$). They are asymptotic gradient lines for the total potential $E = E(Q)$ in an infinitesimally small region surrounding the nondegenerate critical points. Thus the gradient lines of any potential $E = E(Q)$ are described by the solution (7) or (8) as they approach the critical point.

For the quadratic potential (6), as for the total potential $E = E(Q)$, only one gradient line can exist in the infinitesimally small surroundings of the critical point. It passes through the given regular point Q_0 (the point X_0 in Fig. 5), and this line [a curve described by Eqn (7) or (8)] enters (or issues from) the critical point tangentially to one of the eigenvectors of the Hessian $\vec{q}_i$ ($i = 1, 2, ..., 3N-6$). In the special case of a saddle point we always find only one gradient line issuing from this point and tangential to the transitional eigenvector[79] corresponding to a negative eigenvalue of the Hessian.[67]

The eigenvectors of the Hessian $\vec{q}_i$ ($i = 1, 2, ..., 3N-6$) at the critical point are classified by irreducible representations of the symmetry point group of the molecular configuration corresponding to this critical point. It is important to note that whether or not the symmetry point group of this molecular configuration contains multidimensional representations the

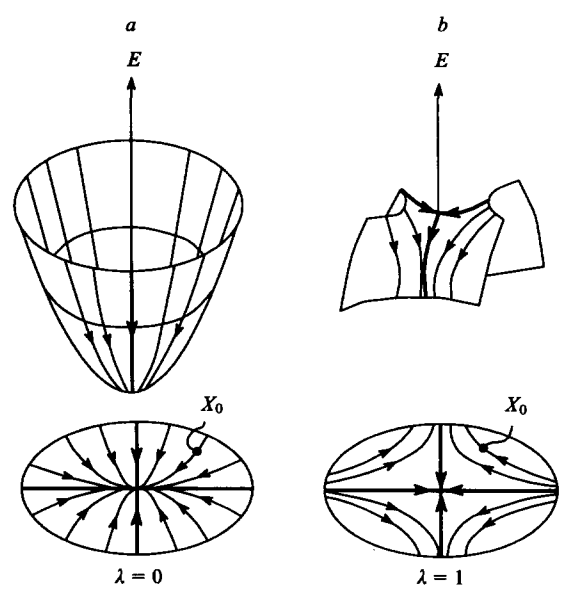


Figure 5. Principal (thick) and secondary gradient lines (thin) in the immediate vicinity of the minimum ($\lambda = 0$) and of the saddle point ($\lambda = 1$) in the entire space (*a*) and in the configurational space (*b*). X_0 are the initial points of the secondary gradient lines; the arrows on the gradient lines show the directions of decreasing potential.

gradient lines defined by the solution (8) can be tangential only to a vector belonging to a one-dimensional (nondegenerate) irreducible representation.[80]

The situations discussed above correspond to nondegenerate critical points, and in particular to minimum points and saddle points. However, there may be cases (said[4, 65] to be fairly rare) of degenerate critical points appearing on the PES, i.e. points where the condition (2) is not satisfied and one or several zero eigenvalues are found in the Hessian in addition to the six listed above. The study of the behaviour of the gradient lines in the immediate vicinity of degenerate points is one of the most important problems in the topological structure of the PES.[69, 70]

III. Symmetry of the reaction path

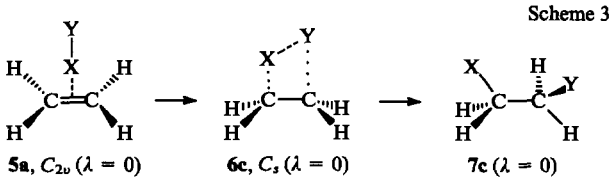
The conditions for symmetry conservation of the system along the reaction path are controlled by a theorem established by Pearson[89] in 1970, which states that the reaction path between two critical points (which are not included in the discussion) is strictly totally symmetric, i.e. that the symmetry point group of the molecular configuration is conserved over the whole length of the reaction path. It was later shown by Pechukas[67] that in practice the symmetry is conserved along the line of steepest descent (the gradient line) and that under these conditions the symmetry point group of the molecular structure of the transition state is conserved, i.e. the saddle point (upper critical point) is included in the discussion. However, Pechukas could not explain why in degenerate reactions (i.e. in reactions in which the reactant and the product are equivalent) this symmetry point group can vary at the critical points, and he was forced to treat these reactions as exceptions. Subsequently Rodger and Schipper[90, 92] also studied the conservation of symmetry along the reaction path by using the expression

$$G_q = G_R \cap G_T = G_P \cap G_T \subseteq G_R \cap G_P , \qquad (9)$$

where G_q, G_R, G_T, and G_P are respectively the symmetry point groups for the reaction, the reagent, the transition structure, and the product. Eqn (9) shows that the symmetry elements conserved along the reaction path should be symmetry elements of the reagent, of the product, and of the structure of the transition state. The expression was used[90] to formulate a hypothesis called the principle of maximum symmetry: all the symmetry relationships between reactants and products are conserved along the whole of the allowed reaction path, i.e. all the symmetry elements included in the symmetry groups of both the reactants and the products are conserved. However, examples have been reported of both degenerate and nondegenerate reactions on whose path the symmetry of the molecular configuration of the transition state can be perturbed and which do not satisfy the Pearson–Pechukas[67, 89] and the Rodger–Schipper[90] symmetry rules.

For example, as indicated by many quantum-chemical calculations in various approximations,[64, 93–102] the electrophilic addition of the XY molecule to the C=C double bond takes place according to the Scheme 3:

Scheme 3



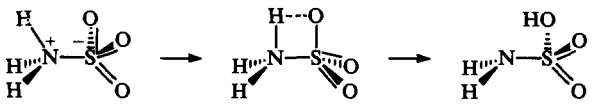
5a, C_{2v} ($\lambda = 0$) **6c**, C_s ($\lambda = 0$) **7c** ($\lambda = 0$)

where XY = HF (Refs 93–96, 98, 99), HCl (Refs 95, 96), F_2 (Ref. 97), Cl_2 (Ref. 97), HCN (Ref. 100), H_2O (Ref. 101), and MeLi, MeCu (Ref. 102).

This reaction begins with the formation of the metastable pre-reaction π-complex **5a**, followed by the transition structure **6c** with a C_s symmetry, and it ends at the minimum of the product **7c**.

It can be seen from Scheme 3 that the mirror plane of symmetry, which passes through the atoms X and Y and through the C=C bond and is retained in the initial part of the reaction (**5a** → **6c**), disappears in the final part **6c** → **7c**. But since no intermediate minima are found in the whole of the path (**5a** → **6c** → **7c**) this behaviour is inconsistent with both the Pearson[89] and Pechukas[76] theorems and the Rodger–Schipper relation.[90] A similar state of affairs has been observed[103] in the intramolecular proton transfer reaction of sulfamic acid from the zwitterion form **8** to the neutral form **10**, passing through the transition state **9** (Scheme 4):

Scheme 4



8, C_{3v} ($\lambda = 0$) **9**, C_s ($\lambda = 1$) **10**, C_1 ($\lambda = 0$)

Other examples of reactions on whose path the initial symmetry is altered through an intermediate state have been reported.[66, 104–112]

It has been shown[80] that the symmetry of a chemical system is preserved only during motions along gradient lines, and that this symmetry is determined by the symmetry of the eigenvectors of the Hessian $\vec{q}_i$ ($i = 1, 2, ..., 3N-6$) at the minimum and at the saddle point of the PES. Let us examine this problem in some detail.

The gradient lines entering an energy minimum[80] can be classified into two types: principal and secondary (see Fig. 5). The principal gradient lines define the main directions of the curvature[81, 82] at the minimum of the PES. By definition they are characterised exclusively by the eigenvectors of the Hessian $\vec{q}_i$ ($i = 1, 2, ..., 3N-6$) at the minimum, i.e. by the curvature properties of the PES in the infinitesimally small surroundings of the minimum, and they are independent of the initial conditions [the points $X_0(Q_0)$]. Evidently there are only $2(3N-6)$ principal gradient lines if allowance is made for the positive and the negative directions of each of the $\vec{q}_i$ vectors. The secondary gradient lines enter the minimum tangentially to $\vec{q}_i$ (corresponding to the lowest eigenvalue of the Hessian), and form an infinite series of gradient lines defined by the initial points $X_0(Q_0)$.

The symmetry point group of the molecular configuration at some point X on the gradient line defines the symmetry point group of the tangential vector $\nabla E(X)/|\nabla E|$, and this symmetry group (according to Pearson's theorem) is conserved over the entire length of the gradient line. Thus the symmetry of the gradient line, defined as the symmetry group of the vector $\nabla E/|\nabla E|$, is uniquely determined by this vector.

The direction of the principal gradient line in the configurational space coincides with that of one of the vectors $\vec{q}_i$ ($i = 1, 2, ..., 3N-6$) in the infinitesimally small surroundings of the minimum point. This means that the tangential vector $\nabla E(X)/|\nabla E|$ at the point X ($X \neq X_{min}$), which belongs to immediate surroundings of the minimum, has the symmetry of the corresponding vector $\vec{q}_i$. The symmetry point subgroup of the vector $\vec{q}_i$ is defined as the plurality of symmetry elements of this vector.

Thus the symmetry of the principal gradient line is given by the symmetry group of the Hessian vector $\vec{q}_i$, to which it is tangential at the minimum point. A similar analysis of the symmetry of a gradient line emerging from the saddle point tangentially to a transition vector shows that its symmetry group is determined by that of the transition vector. If the gradient line emerging from the saddle point enters the minimum along a principal direction the symmetry group of the transition vector coincides with that of the corresponding vector $\vec{q}_i$.

The direction of the secondary gradient lines in the configurational space does not coincide with the direction of the vector $\vec{q}_1$ in the infinitesimally small surroundings of the minimum

point. Therefore arguments similar to those used above for the principal gradient lines are not applicable to secondary lines. For the secondary gradient lines we may only conclude that the symmetry group cannot be higher than the symmetry group of the vector $\vec{q}_1$ to which they are tangential.

The rules for the conservation of symmetry along the reaction path can be formulated as follows.

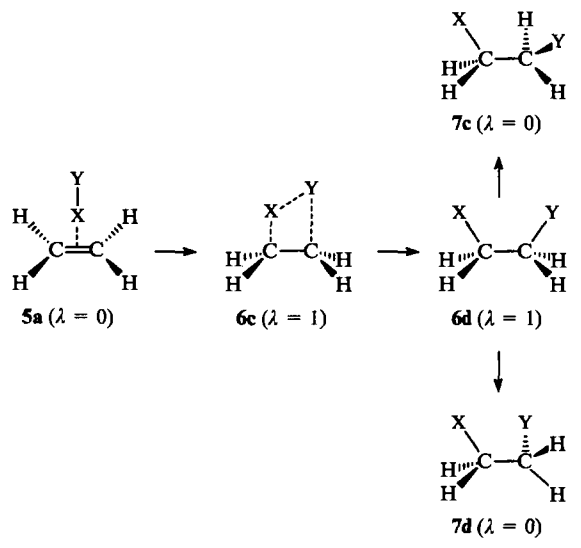
(1) The symmetry point group of the structure vector of the transition state is conserved along a gradient line. This symmetry group can either coincide with the symmetry group of the corresponding eigenvector of the Hessian for the minimum (if the gradient line enters the minimum along a principal direction) or it can have a lower value (if the gradient line enters the minimum along a secondary direction).[80]

(2) A change in the symmetry point group of the molecular configuration of the system is possible only at the critical points.[67, 113, 114]

(3) The symmetry point group of the transition vector, which is conserved along the gradient line, should also be a subgroup of the symmetry point groups of the reactant, of the transition state structure and that of the product, or of all three critical points connected by the given gradient line.[113]

The first rule states that the symmetry is conserved along the gradient line, and not along the MEP, and therefore we must first of all identify all the gradient lines which contribute to the reaction path of the given reaction by analysing the conservation of symmetry along each gradient line.

Scheme 5



Thus, if the reaction path consists of two gradient lines[7] (see Scheme 5, and also Scheme 3 and Fig. 3), the appropriate symmetry is retained along each of these lines. In the initial stage **5a** → **6c** → **6d** the reaction path is defined by the gradient line along which the mirror plane of symmetry passing through the atoms X and Y and through the two carbon atoms is conserved (C_s symmetry). In the final stage **7c** → **6d** → **7d** the reaction path is defined by the other gradient line (corresponding to internal rotation round the C–C bond, along which the symmetry conservation conditions are different from those which apply to the first gradient line.

The PES of sulfur tetrafluoride SF_4 has a more complex structure (Fig. 6). For this system the path of the enantiomerisation reaction consists of three nonequivalent gradient lines. The gradient line passing through the saddle point (corresponding to the planar transition structure with D_{4h} symmetry) connects three neighbouring saddle points (transition structures corresponding to two pyramidal structures with C_{4v} symmetry and one planar structure with D_{4h} symmetry).

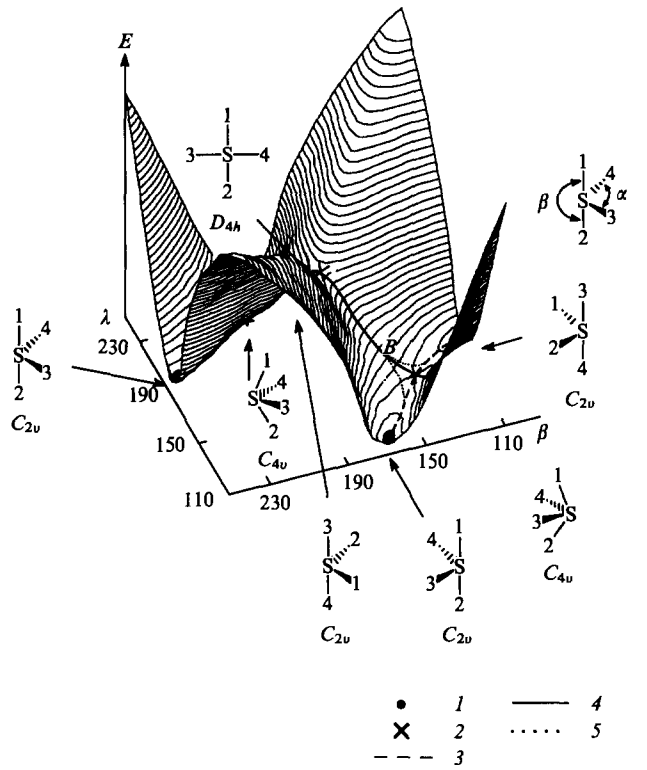
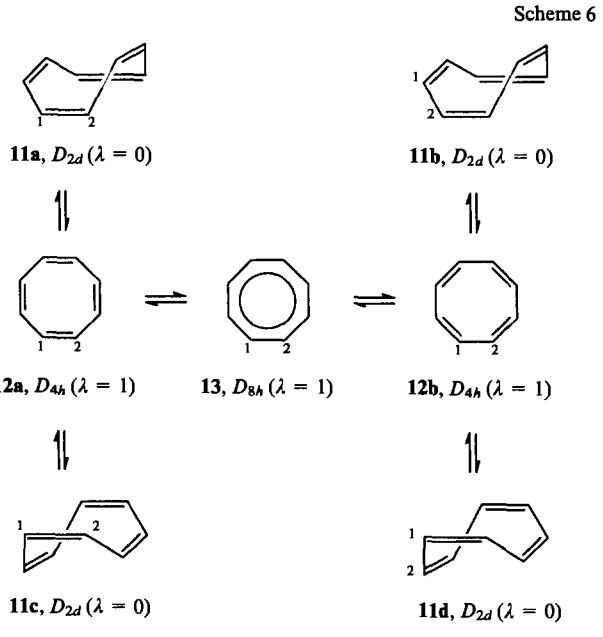


Figure 6. Potential energy surface of the enantiomerisation reaction of the sulfur tetrafluoride molecule in α, β coordinates according to ab initio calculations (STO 6-31G*).[108] The angles α and β are defined on the right of the figure.[108] (*1*) Minima; (*2*) saddle points (transition states); (*3*) Berry pseudorotation; (*4*) inversion of the C_{4v} structure of SF_4; *B* is the bifurcation point where the minimum energy path (*5*) breaks into two and diverges from the gradient line.

We should note that at the point *B* the minimum energy path is split into two and diverges from the gradient line. The other two gradient lines correspond to Berry's pseudorotation reaction[115] in sulfur tetrafluoride. A similar structure is observed in the PES for the 1,3 proton shift reaction in the zwitterion **8** (see Ref. 103) and in other reactions.[104, 105]

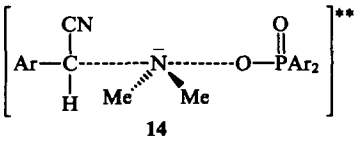
Scheme 6



The isomerisation of the cyclooctatetraene (COT) molecule,[116-121] first synthesised[118] by Willstätter in 1913, is a remarkable example of a reaction whose path consists of several nonequivalent gradient lines (Scheme 6). An unusual stereochemical lability (the fast valence isomerisation **11a** ⇄ **11b**, taking place through the planar structure **13** with an activation barrier of 14 kcal mol^{-1}) was detected by NMR more than 30 years ago.[112] Later studies[123,124] by dynamic NMR detected a lower-energy conformational transition in this system: the ring inversion **11a** ⇄ **11c**, with a barrier of ~10 kcal mol^{-1}. The transition structures in this process could be either the planar structure **12** (D_{4h}) or various nonplanar structures. The planar configuration **13** (D_{8h}) is a classical example of an antiaromatic system.[64,119] If the structure **12** corresponds to the transition state the difference in energy between the structures **12** and **13** will be the energy of the antiaromatic destabilisation (delocalisation) in the molecule. Therefore establishing the nature of the stationary points on the PES of cyclooctatetraene corresponding to the structures **12** (D_{4h}) and **13** (D_{8h}) has stimulated the interest of theoretical chemists for many years.[106,125-127] It was established relatively recently[106] by accurate ab initio calculations (CAS SCF/3-21G* and 6-31G* + ΔZPE) with full allowance for the force constants that these two planar structures are transition states ($\lambda = 1$) for the ring inversion and the valence isomerisation reaction respectively. In this case the structure of the PES is similar to that shown in Fig. 6. Surprisingly, however, though the vector of the transition state **13** shows unambiguously that the reaction path (gradient line) issuing from the PES point corresponding to **13** (D_{8h}) should arrive at the point **12** (D_{4h}), the authors[106] assume that the reaction path of the valence isomerisation misses this structure by branching on the slope of the PES.

The nucleophilic substitution (S_N2) at the nitrogen atom[128-133] is an interesting example of a reaction with a complex path. By using two isotopic labels it was shown experimentally[133] that the nucleophilic substitution reaction on the nitrogen atom of *N*, *N*-dimethyl-*O*-(diarylphosphinyl) derivatives passes through the structure of a transition state of the type **14**, which is similar to the transition structure of the S_N2 reaction at a carbon atom. This confirms the generality of the Walden inversion in tetrahedral or pseudotetrahedral configurations (in which the unshared pair of the central atom plays the role of a phantom ligand) in nucleophilic substitution reactions (Scheme 7).

Scheme 7



14

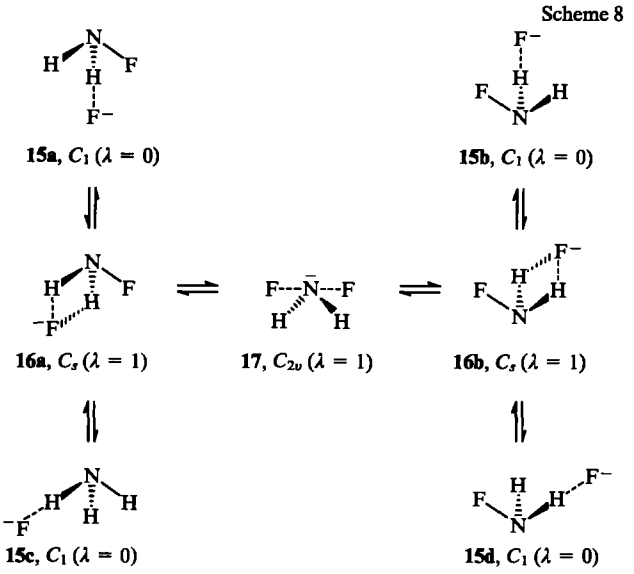
Ab initio calculations[107] (SCF TZP+/CISD) carried out with adequate precision within a year of the previous work[133] on the model reaction (Scheme 7)

$$F^- + H_2NF \rightleftarrows FNH_2 + F^-,$$

confirmed the original conclusions[133] and showed that the reaction begins with the formation of the nondipolar complex **15** having a linear F$^-\cdots$H–N bond and passes through the transition state **17** with a C_{2v} symmetry and an activation barrier of 24 kcal mol^{-1} (Scheme 8). This barrier is higher than the corresponding activation barrier for the S_N2 reaction on the carbon atom, calculated (by SCF DZDP/CISD methods) to be 17.1 kcal mol^{-1} (see Ref. 134). According to the proposed mechanism the fluoride ion can be transcoordinated between two NH bonds through the transition state **16** (C_s) by surmounting an activation barrier of 4.6 kcal mol^{-1}.

Thus, according to published calculations,[107,135] the general reaction path outlined in Scheme 6 is very similar to that of the sulfur tetrafluoride enantiomerisation and the cyclooctatetraene valence isomerisation reactions, and can be represented by the

Scheme 8



PES shown in Fig. 7. The gradient line issuing from the saddle point **17** transition state with C_{2v} symmetry) enters the neighbouring saddle point **16a** (or **16b**, transition state with C_s symmetry) corresponding to the peak of the activation barrier for the transcoordination of the fluoride ion from one NH bond to the next. At the point on the PES corresponding to the state **16a** the system passes from one gradient line to the next, and reaches the minima **15a** and **15c** (or **15b** and **15d**) along both branches of the line.

The conclusion that two (or more) saddle points cannot exist on the same gradient line follows from the Fernandez–Sinanoglu theorem.[136] It also follows that the reaction path must split into two before the second saddle point (the second transition state). The proof of the Fernandez–Sinanoglu theorem is based on the hypothesis that the reaction path always consists of a single gradient line connecting the saddle point with a minimum. However, there are no logical or physical reasons for this condition to be satisfied in general. As can be seen from the examples discussed above, the reaction path may consist of several gradient lines which the system follows sequentially. This means that the Fernandez–Sinanoglu theorem does not apply in general, and that there are no limitations (other than the Morse expressions,[137] which establish strict relationships between the numbers of nondegenerate critical points of different order in a defined region of the PES) on the character of the critical points lying on one gradient line (see also Refs 25 and 66).

According to the first rule of symmetry conservation along the reaction path (see above), the symmetry point group conserved along a gradient line is not that of the molecular configuration of the transition structure as had been suggested,[64,67,75,90-92,113,114] but that of the transition vector. This important difference from previously formulated rules[67,90] removes existing discrepancies in our understanding of the conservation of symmetry along the reaction path, including the exceptions from the Pechukas rules.[67] We shall illustrate this conclusion with two examples: the inversion in the ammonia molecule and the internal rotation in ethane. As can be seen from Fig. 8, the symmetry point groups of the vector of the rotational mode at the minimum and of the transitional vector at the saddle point coincide in the ethane molecule, and are equal to D_3. Similarly, in the ammonia molecule the symmetry point group C_{3v} is conserved. These symmetry groups do not change during the transition from the minimum of the reactants through the transition state to the minimum of the products. However, the corresponding point groups of the molecular configurations change from D_{3d} to D_{3h} and back to D_{3d} for ethane, and for ammonia they change in the sequence C_{3v}–D_{3h}–C_{3v}.

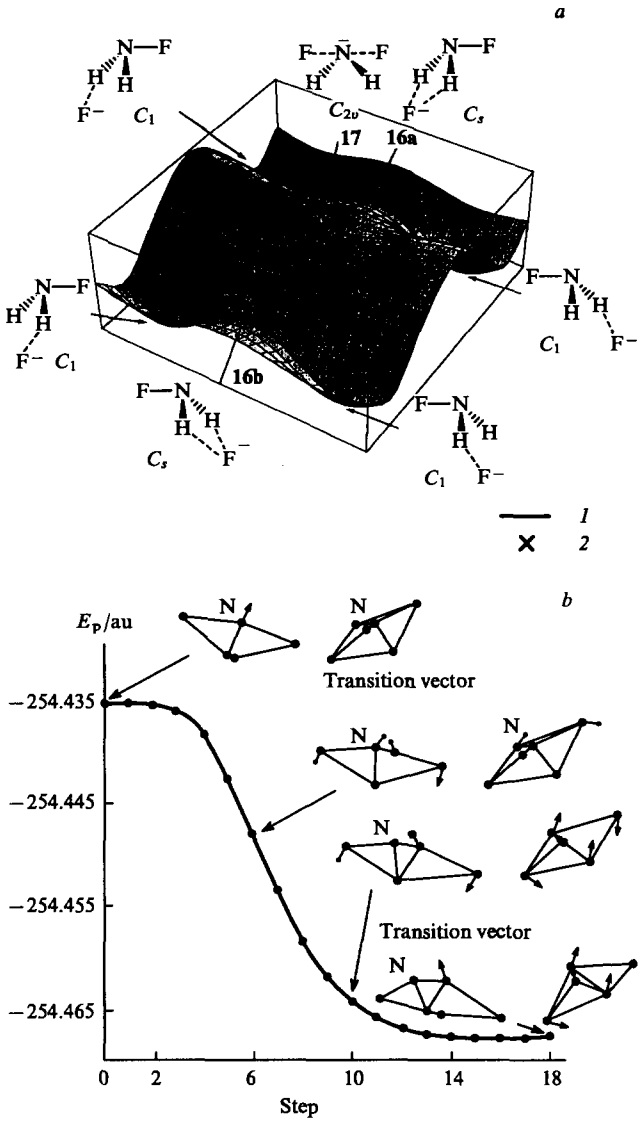


Figure 7. Potential energy surface (*a*) of the nucleophilic substitution reaction $F^- + H_2NF \rightleftarrows FNH_2 + F^-$ and evolution (*b*) of two eigenvectors of the Hessian along the gradient line (*1*) from the saddle point **17** to the neighbouring saddle point **16a** according to SCF/DZP ab initio calculations;[135] (*2*) are the saddle points.

Rule (2) [like rule (3)] is a corollary of rule (1). Unless used in conjunction with rule (1) it confuses our understanding of the principle of symmetry conservation along the reaction path.

We shall interpret the symmetry of a point on the PES (including a critical point) as the symmetry point group of the corresponding molecular configuration. The symmetry subgroup of each vector $\vec{q}_i$ is unambiguously determined by the symmetry point group of the molecular configuration at the critical point. Obviously, the inverse statement is equally valid: the symmetry subgroups of all the $\vec{q}_i$ vectors uniquely define the total symmetry group of the molecular configuration. In this case we may conclude that the symmetry of any critical point is determined by the symmetry of all the gradient lines entering or emerging from that point.[80] In other words each gradient line contributes to the given critical point its own symmetry subgroup, and the symmetry point group of the molecular configuration in the same critical point is determined by the combined symmetries of all three gradient lines. Therefore when the molecular system has reached a critical point (including a minimum) the order of its symmetry group can only rise.[114]

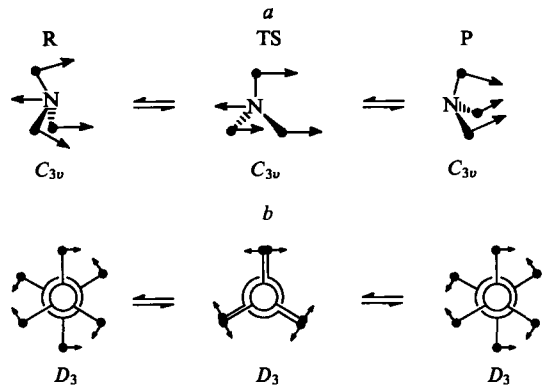


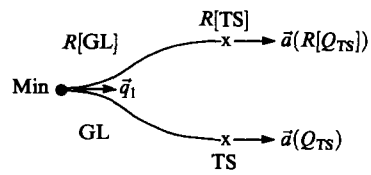
Figure 8. Reactions producing inversion of the pyramidal configuration of bonds in the ammonia molecule (*a*) and internal rotation around the C–C bond in ethane (*b*). The arrows show the components of the normal and of the transition vectors at the minima. R are the reactants, P are the products, TS is the saddle point.

IV. Reaction paths consisting of several equivalent gradient lines

1. Reaction paths consisting of two equivalent secondary gradient lines

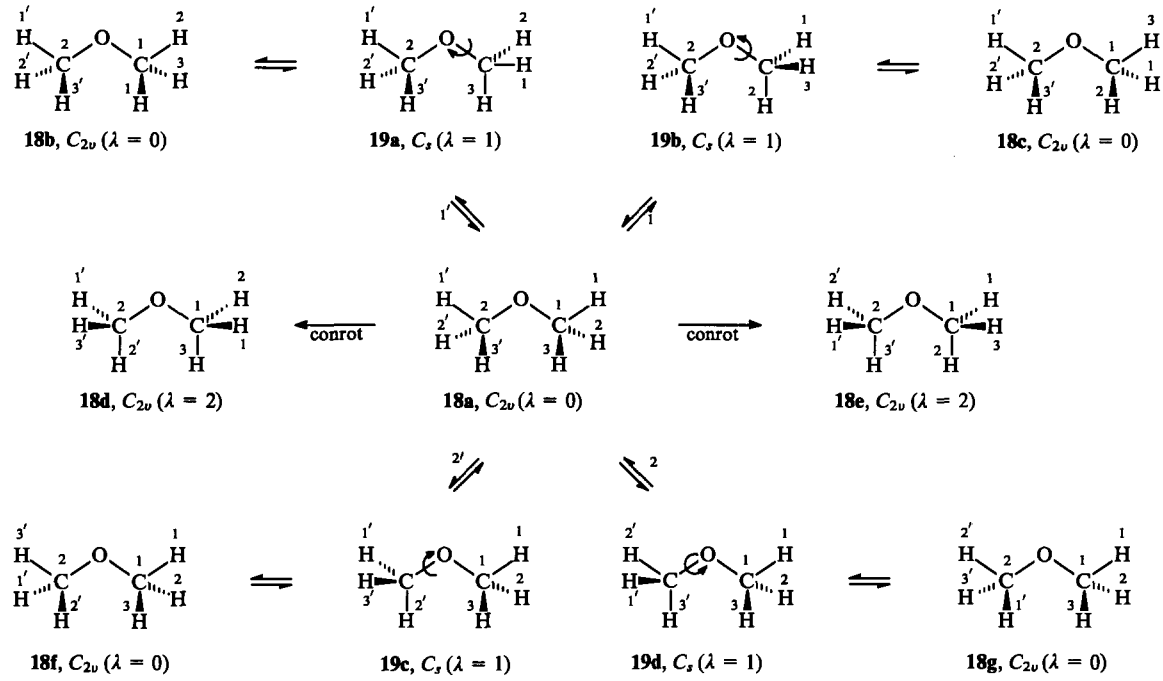
Unlike the symmetry group of principal gradient lines (see above) the symmetry group of a secondary gradient line entering a minimum can either coincide with the symmetry group of the Hessian vector $\vec{q}_1$ (corresponding to the lowest eigenvalue) or be its subgroup.[80] Therefore, if a secondary gradient line connects the minimum with any transition state the symmetry group of the transition state [according to the rule (1), see above] can either coincide with the symmetry group of the vector $\vec{q}_1$ at the minimum point or be its subgroup. We shall assume that $\vec{q}_1$ has at least one nontrivial symmetry element R, and that the transition state TS with the transition vector $\vec{a}(Q_{TS})$ is found on one of its secondary gradient lines. In this case the symmetry conditions require that in addition to the transition state TS an equivalent state R[TS] with a transition vector $\vec{a}(R[Q_{TS}])$ must exist. Then the minimum point is coupled with the two equivalent transition states TS and R[TS] by the two symmetry-equivalent secondary gradient lines GL and R[GL], as illustrated in Scheme 9.

Scheme 9



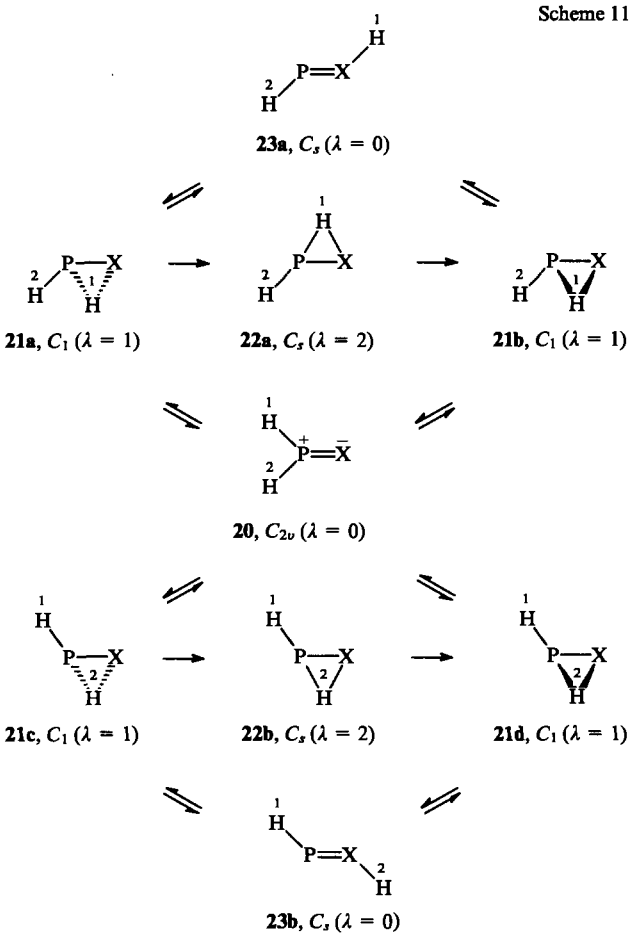
In this case the gradient path of the chemical reaction consists of two equivalent (physically indistinguishable) gradient lines. Various combinations are possible: each of the equivalent gradient lines leads to a different minimum (Figs 9*a* and 9*b*, see over), the lines lead in pairs to the same minimum (Figs 9*c* and 9*d*), etc. Examples of reactions whose equivalent paths lead to the same minimum[14,23,130,139] or to different minima[14–21,139–141] have been reported. If the molecule contains two stereochemically equivalent nonrigid groups which can independently undergo a conformational rearrangement (for example, rotation around single bonds, Scheme 9) we may observe a gradient reaction path consisting of two equivalent gradient lines. For example, in propane,[15] dimethyl ether,[16,17] and other molecules[18,19,138–141] two methyl groups can rotate independently of each other. Under these conditions each line in the gradient reaction path leads to a different minimum (see Fig. 9*b*). In particular, for the dimethyl ether molecule[16] this type of gradient reaction path can be illustrated by Scheme 10 (see over).

Scheme 10



Each of the methyl groups in this molecule can rotate independently. Four equivalent gradient lines, each passing through its own transition structure **19a–19d** and leading to a separate minimum **19b–19g**, emerge from the minimum **18a**. The routes 1 and 2 form one gradient reaction path, the routes 1′ and 2′ form another.

Scheme 11



An example of a reaction corresponding to the case shown in Fig. 8*c* is the 1–2 shift of the hydrogen atom in the $H_2P{=}N$ and $H_2P{=}P$ molecules (Scheme 11). Ab initio calculations[23] allowing for the correlation energy of the electrons in the $H_2P{=}N$ and $H_2P{=}P$ molecules show that in the migration process **20** ⇄ **23** the hydrogen atom moves out of the (initially) planar molecule. The out-of-plane (inversion) mode of the normal vibration of the structure **20** corresponds to the lowest frequency. In these reactions the transition states are the states **21a–21d**. The states **22a** and **22b** corresponds to a critical point with $\lambda = 2$ (see Refs 23 and 142). The potential energy surface of the system is shown in Fig. 10. The two secondary gradient lines emerging from the minimum **20** tangentially to the vectors $+\vec{q}_1$ and $-\vec{q}_1$ (out-of-plane inversion mode), which pass through the two saddle points **21a** and **21b** and terminate in the same neighbouring minimum **23a**, form two equivalent gradient reaction paths.

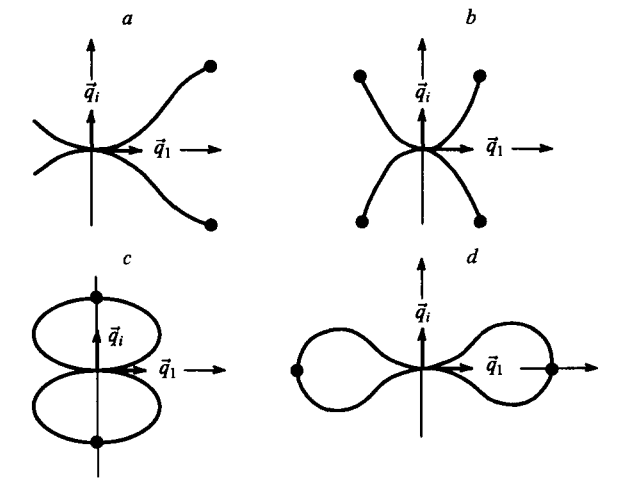


Figure 9. Variants of the two-line reaction paths. (*a*) Two branches of two equivalent secondary gradient lines enter two minima; (*b*) each of the branches of two gradient lines enters its own minimum; (*c*) two branches of one gradient line enter the same neighbouring minimum; (*d*) the branches of two different gradient lines enter the same neighbouring minimum.

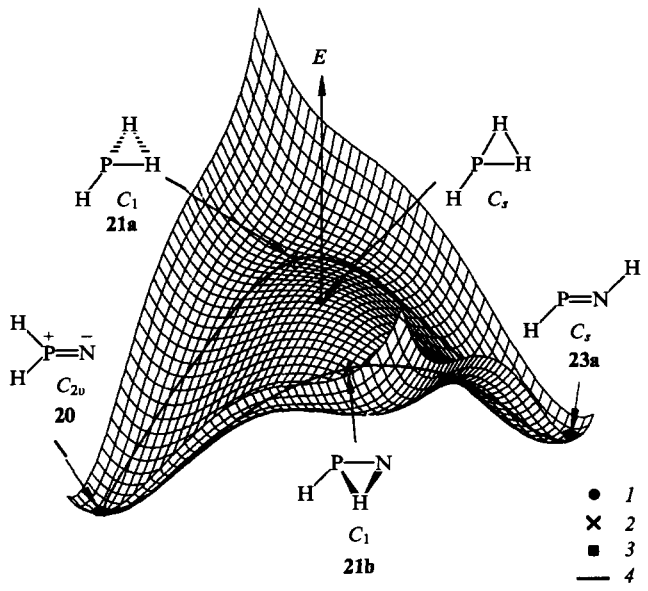
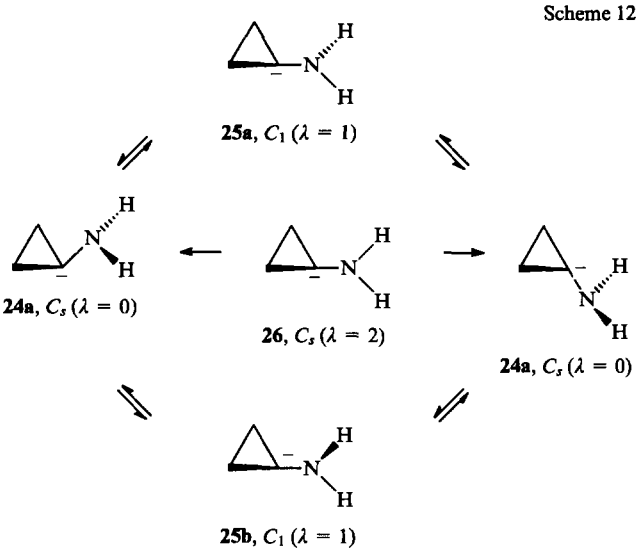


Figure 10. Potential energy surface of the 1,2 hydrogen atom shift in the H_2PN molecule (**20**) according to ab initio calculations.[23] (*1*) minima; (*2*) saddle points (transition states); (*3*) critical points with $\lambda = 2$; (*4*) gradient reaction path consisting of the two gradient lines **20** ⇄ **21a** ⇄ **23a** and **20** ⇄ **21b** ⇄ **23a**.

The principal gradient line issuing tangentially to $\vec{q}_2$ (the mode corresponding to the 1,2-H shift) passes through the critical point with $\lambda = 2$ (structure **22a**) and enters the minimum **23a**. This topology of the PES is consistent with the correlation of the atomic shift vectors along the whole length of the gradient line between two minima.[142]

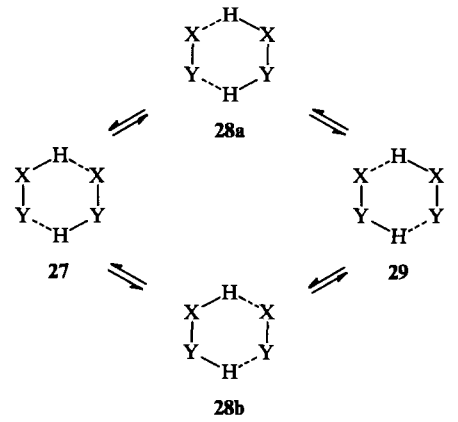
Scheme 12



The inversion reaction at the carbanion centre of the aminocyclopropyl anion **24** (Scheme 12) is an interesting example. Ab initio calculations [MP2/6-31 + G(d)//6-31 + G(d)][138] predict that the inversion reaction passes through two enantiomeric asymmetric (C_1) transition states **25a** and **25b** with an activation barrier of 30.1 kcal mol^{-1}. This means that the gradient path of the reaction is described by two equivalent gradient lines. The state **26** (C_s or C_{2v}), which unfortunately was not studied by Chou et al.,[138] should correspond to a critical point with $\lambda = 2$ on the PES of the carbanion.

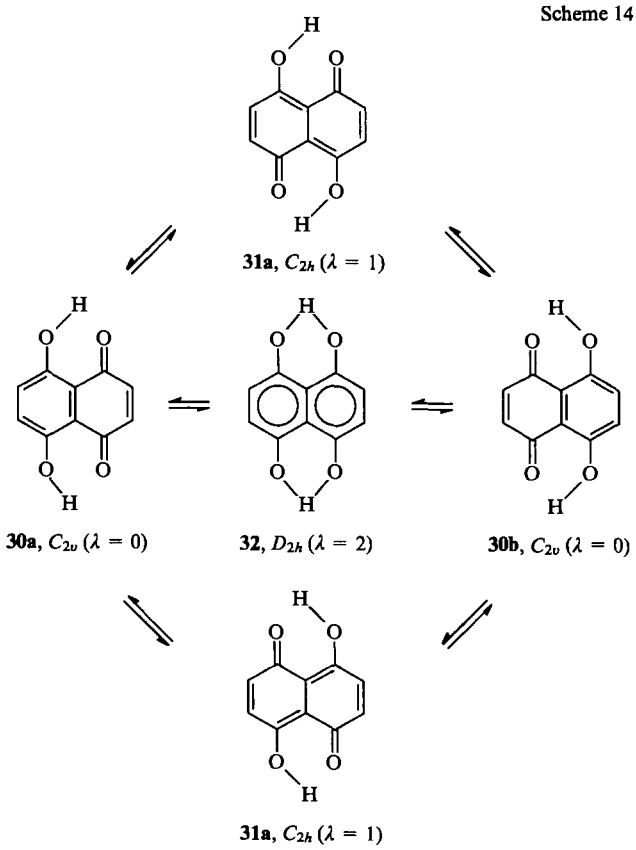
An important class of reactions described by two equivalent lines includes the double proton transfer reactions in various organic compounds,[143–167] such as porphyrin,[143–147] tetraphenylchlorin,[149] oxalamidine,[150,151] azophenone,[150–155] naphthazarin,[156–161] and the dimer of formamidine.[162–164] In all these systems the transfer of two protons occurs[149] by the general Scheme 13.

Scheme 13



The states **28a** and **28b** on the PES can be transition states (concerted process) or they can correspond to intermediate minima (multistage process). Nevertheless in both cases the chemical reaction **27** ⇄ **29** is described by two equivalent routes, **27** ⇄ **28a** ⇄ **29** and **27** ⇄ **28b** ⇄ **29**, along which the chemical system can decompose with equal probabilities. Thus, the double proton transfer in the naphthazarin molecule **30a** ⇄ **30b** (Scheme 14) passes through the transition state **31** with an activation barrier of 25 kcal mol^{-1}, calculated by an ab initio method in an STO-3G basis.[156] As was shown by the calculation[156] the symmetrical structure **32** (D_{2h}) corresponds

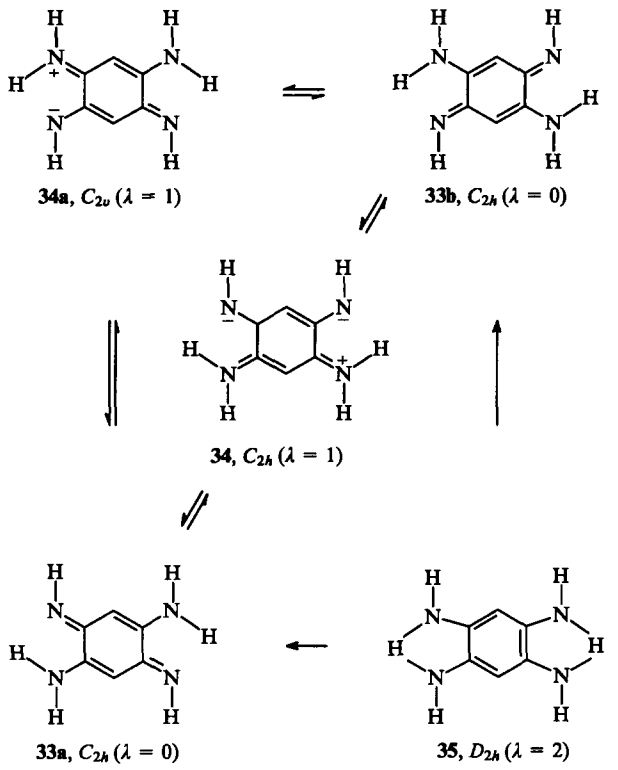
Scheme 14



to a critical point with $\lambda = 2$. These results agree with NMR data[158,159] and with IR spectroscopy results.[161] However, the small energy difference (3 kcal mol^{-1}) observed[156] between the structures **32** and **31**, which may be strongly affected by allowing for the correlation energy,[14] calls for a more careful examination of these results.

The next example of a reaction which has been studied in reasonable depth is the double proton transfer in the azophenine molecule **33** (Scheme 15).[150–155] The automerisation of this molecule was explained (from measurements[150] of the kinetic and isotopic effects in derivatives of azophenine) by the simultaneous synchronous (concerted) transfer of two protons through the transition state **35** with an activation barrier of 10 kcal mol^{-1}.

Scheme 15



However, later calculations by AMI[153] and by ab initio methods[155] (MP2/3-21G//3-21G) showed that the reaction **33a** ⇄ **33b** takes place in stages through the zwitterion intermediate structure **34** ($\lambda = 0$) with an activation barrier of 17.3 kcal mol^{-1}, which exceeds the experimental value by 7.3 kcal mol^{-1}. Under these conditions the structure **35** (D_{2h}), as in the case of naphthazarin, corresponds according to the calculations[153,155] to a critical point with $\lambda = 2$. The observed discrepancy between experimental and theoretical data stimulated a careful re-examination of the experimental measurements.[152] New experiments[152] carried out immediately after the theoretical calculations[155] confirmed the conclusion[153,155] that the reaction **33a** ⇄ **33b** takes place in stages through the zwitterion intermediate structure **34**. However, the difference between the theoretical height[155] of the activation barrier (17.3 kcal mol^{-1}) and the experimental value[150] (~10 kcal mol^{-1}) is attributed to the choice of an insufficiently broad basis[155] and to the failure to allow for the effect of substituents on the barrier height.

Thus the path of the reactions discussed above (Schemes 9–15) and of some other reactions consists essentially of two equivalent gradient lines along which the chemical system can move with equal probabilities.

The existence of these reaction paths was first predicted by Salem,[168] who used the term narcissistic to describe them.

2. Reaction paths consisting of three or more equivalent gradient lines

A chemical reaction gradient path consisting of three or more equivalent gradient lines can be realised for chemical systems having a point group symmetry containing a triad (or higher) symmetry axis.[80] In this case the gradient lines approach the minimum in a radial direction in the space generated by the $\vec{q}_k$ vectors from a multidimensional representation. Two situations may be realised in this way: in the first each equivalent gradient line leads to its own minimum, and in the second all the equivalent gradient lines enter the same neighbouring minimum. Good examples of the first case are the isomerisation (topomerisation) of bulvalene,[9] mentioned in the Introduction, and the opening of the three-membered ring of the ozone molecule.[22]

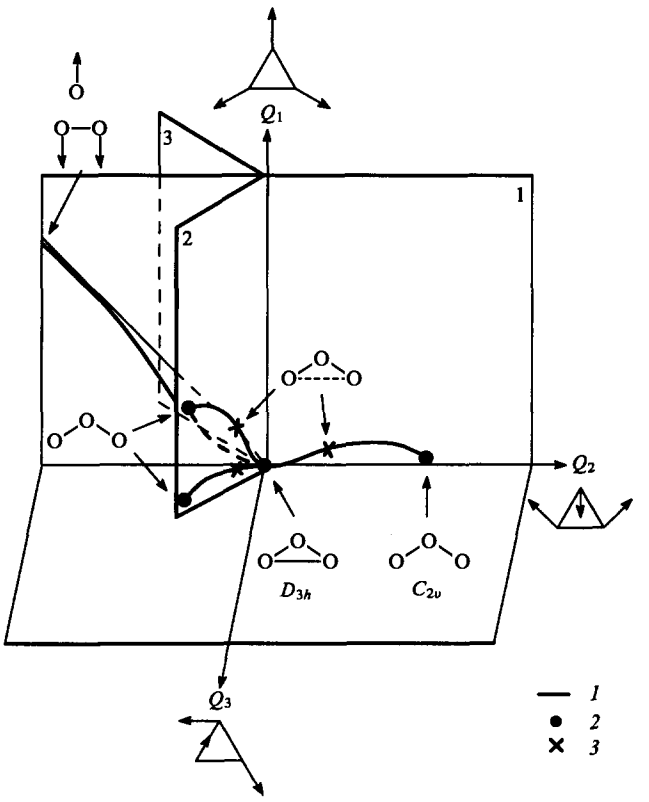
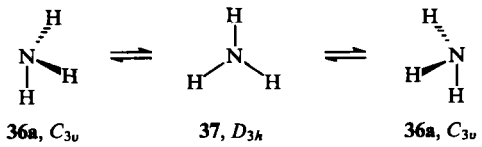


Figure 11. Equivalent gradient lines (*1*) leading to three equivalent transition states in the ring opening reaction of the D_{3h} form of the ozone molecule. The normal Q_i coordinates (i = 1, 2, 3) of the cyclic D_{3h} form are used as coordinates.[22] (*2*) Is a minimum; (*3*) is the transition state. The components of the normal $\vec{q}_i$ vectors (i = 1, 2, 3) are shown on the side of the coordinate axes.

Let us consider in more detail the opening of the three-membered ring (D_{3h}) of the ozone molecule. The gradient path of this reaction consists of three equivalent gradient lines connecting the central minimum (D_{3h}) with three equivalent minima (C_{2v}) corresponding to the open form of ozone (Fig. 11). In this case the global coordinates were taken to be the normal coordinates of the D_{3h} form. Unlike the local coordinates, which give an adequate description of the system only in a small region of the configurational space, the global coordinates fully describe the configurational space of the molecular system over the whole range of internal coordinates. The figure also shows how the gradient line corresponding to a motion opposite to that of the ring-opening reaction leads to the removal of an oxygen atom from the ozone molecule. Along this line the normal mode is converted into the local mode.[169,170] The theory of local modes was developed to explain the breaking of individual chemical bonds, for which the theory of normal modes could not account.

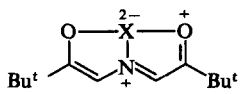
An example of a reaction in which all three gradient lines connect two neighbouring minima is provided by the inversion of the pyramidal bond configuration in the trifluorophosphine molecule.[24,25] The history of the discovery of this uncommon reaction path is instructive and we shall briefly dwell on it. We know[14,171-175] that the inversion of the ammonia molecule **33a** ⇄ **33b** takes place through a planar (D_{3h}) transition state **37** (Scheme 16).

Scheme 16



36a, C_{3v} **37**, D_{3h} **36a**, C_{3v}

It has long been assumed that a planar (D_{3h}) structure of the type **37** is the only possible transition state for the inversion of various three-coordinated pyramidal (C_{3v}) structure. This hypothesis is confirmed by the many published studies of inversion processes in different systems, and no exceptions to it have so far been reported.[13,14,171-175] However, the synthesis[176-178] of the compound **38**, containing a planar T-shaped bond configuration on the pnictogen atoms (P, As, Sb, and Bi) suggested that the T configuration may act as the transition state in the inversion of the XF_3 molecule (where X = P, As, Sb, Bi):



38

X = P, As, Sb.

In this way it was shown by ab initio calculations[179,180] that in the pyramidal molecules[179] PF_3 and SbF_3^+, and AsF_3 and SbF_3 (see Ref. 100) having a C_{3v} symmetry, the inversion takes place through the T-shaped C_{2v} form rather than through the planar (D_{3v}) form. This difference in the structure of the transition state between PF_3 and the ammonia molecule is unexpected. It can be attributed to the fact that the electrostatic repulsion between the unshared pair and the ligands is much smaller in the T-shaped form of the PF_3 molecule than in the D_{3h} form, whereas in the ammonia molecule (and in the other systems which invert through a planar D_{3h} state) the opposite is true.[179]

The appearance of a T-form as the transition state on the inversion path of the XF_3 molecule (X = P, S^+, As, Sb) requires the inversion mechanism to be reconciled with the microscopic reversibility principle,[181] according to which the path of the inversion reaction should contain three equivalent (topomeric) T-shaped transition structures[24] through which pass three equivalent gradient lines which form the gradient path of the reaction.

In the region between the two stable pyramidal C_{3v} forms the potential energy surface of PF_3 has a D_{3h} symmetry. The potential energy surface can be represented as a diagram of the gradient lines which connect the critical points (Fig. 12).[24]

The two axial corners of this bipyramid correspond to the two stable pyramidal structures **39a** and **39b** (C_{3v}), the three equatorial corners to the three T-shaped transition states **40a** – **40c** (C_{2v}). The centre of the bipyramid corresponds to the planar structure **41** (D_{3h}). All the lines in this figure are gradient lines issuing from a critical point with $\lambda \geq 1$ (structures **40**–**42**) in the direction of one of the imaginary frequency vectors. The gradient lines emerging from the transition structures **39a**–**39c** form (as a combined path) the gradient paths of the inversion reaction. In Fig. 12 they are shown as the edges of the pyramid. The axial line passing through the two axial corners and the centre of the bipyramid corresponds to the usual inversion (as in the ammonia molecule).

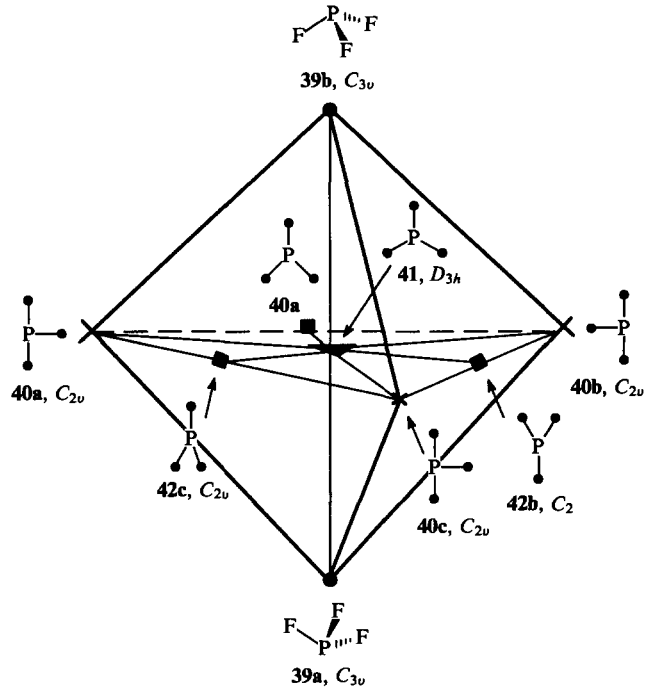
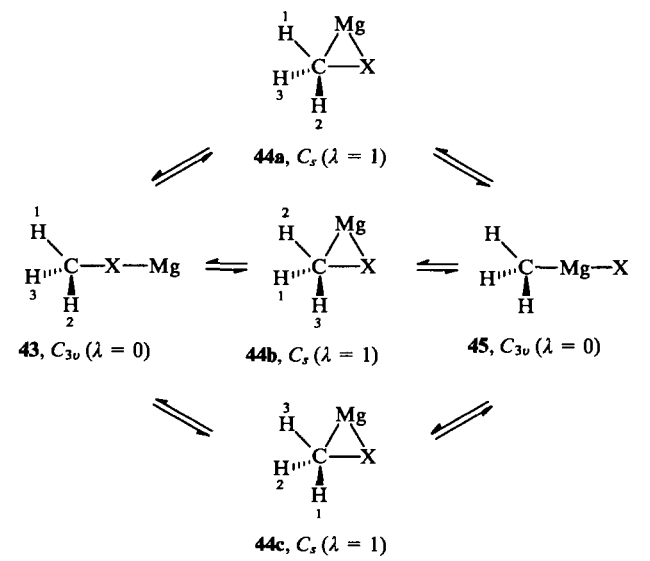


Figure 12. Diagram of the inversion reaction in the PF_3 molecule.[24] The thick lines denote three equivalent gradient lines passing through three equivalent transition states **40a**–**40c** (shown by crosses). The rectangles and the triangle show respectively the critical points of the second ($\lambda = 2$) and of the third order ($\lambda = 3$).

The lines joining the centre of the bipyramid with its equatorial corners correspond to three gradient lines on which the structure **41** (D_{3h}) becomes distorted into **40** (C_{2v}). All the transition structures are connected by a gradient line corresponding to the 'internal pseudorotation' of the T-shaped structure, simulating the true pseudorotation in ClF_3 (see Ref. 182) and other AX_3 systems (see Ref. 183).

Another interesting example of a reaction whose path consists of three equivalent gradient lines connecting two neighbouring minima is provided by the insertion of a magnesium atom into the C–X bond (X = F, Cl) of the halogenomethanes H_3C-X with formation of a Grignard reagent (Scheme 17). This reaction begins[184] with the formation of the complex **43**, after which

Scheme 17



44a, C_s ($\lambda = 1$)

43, C_{3v} ($\lambda = 0$) **44b**, C_s ($\lambda = 1$) **45**, C_{3v} ($\lambda = 0$)

44c, C_s ($\lambda = 1$)

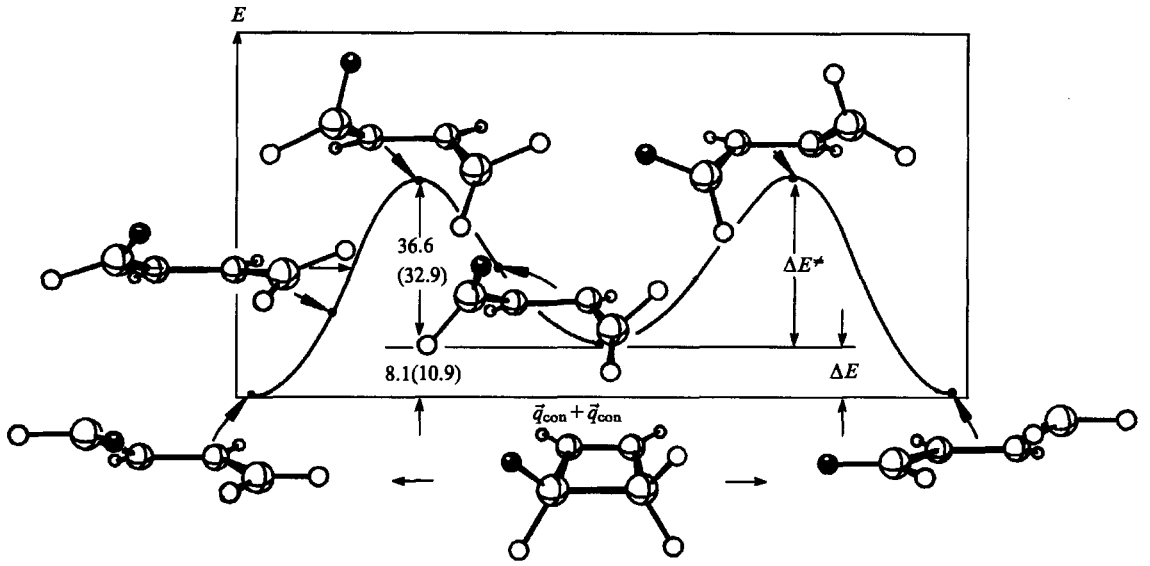


Figure 13. Mechanism of the pericyclic transformation reaction of the cyclobutene molecule into the gauche structure of 1,3-butadiene along the allowed conrotational path. The Figure shows the geometrical transformation of the water molecule along both directions of motion $+\vec{q}_{con}$ and $-\vec{q}_{con}$. Experimental [199-201] and calculated [188,193] values of the activation barrier and of the heat of reaction are given (numbers in parentheses and without parentheses respectively, kcal mol^{-1}).

[according to MP4 SDTQ/6-311G(dp) ab initio calculations [184]] the gradient path of the reaction passes simultaneously in three directions through the three equivalent transition states **44a–44c** and terminates at the minimum **45**. The activation barriers calculated for the reaction of (25) with X = F and Cl are 31.2 and 39.4 kcal mol^{-1} respectively.

V. Unimolecular reaction mechanisms

The term mechanism of a chemical reaction is usually applied to the totality of the elementary steps which contribute to the conversion of the reactants into the products.[185,186] For the purpose of this discussion it is more convenient to use the concept of the mechanism of an elementary reaction step,[187] which denotes the totality of the electronic–nuclear transformations of the molecular system on the reaction path from the given minimum to the neighbouring minimum. In Fig. 13 we show the mechanism of the pericyclic ring opening reaction of the cyclobutene molecule, including the geometric transformation of the system along the reaction path, established by various methods.[188-202] During the reaction the system moves along two equivalent gradient lines, which emerge from the minimum tangentially to the vectors $+\vec{q}_{con}$ and $-\vec{q}_{con}$ corresponding to the allowed[185] conrotation of the methylene end groups. These lines terminate in two different (enantiomeric) minima. If a substituent is introduced into the third position of cyclobutene these two paths become nonequivalent and we observe the so-called rotational stereoselectivity.[193,196]

If the elementary step of the reaction corresponds to two (or several) equivalent gradient lines connecting two minima the mechanism of the elementary step includes the transformations which the molecular system undergoes along all these equivalent gradient lines (see, for example, Fig. 12).

The mechanism of the elementary step is more complex in the case of the valence isomerisation reaction of the cyclooctatetraene molecule. As can be seen from Scheme 6 there is only one transition state **13** between the four equivalent minima **11a–11d**. The reaction in the chemical system takes place only when the latter is thermally excited to an energy corresponding to the transition state (ignoring the possibility of tunnelling), i.e. it is transferred from the zero vibrational level to an excited energy level located above the transition state (Fig. 14). If there are two equivalent transition states the reaction can take place through either. Therefore in order to induce the isomerisation of the cyclooctatetraene molecule from one of the minima (**11a**) into another (for example, **11b**) the system must be promoted to a vibrational energy level lying above the transition state **13**. However, in this case the system will rapidly become delocalised on this hypersurface with equal probabilities for the four minima **11a–11d**, and it can then relax to the zero vibrational level in each minimum. Therefore in this case the elementary step is described by three gradient lines: **11a** ⇄ **12a** ⇄ **11c**, **11b** ⇄ **12b** ⇄ **11d**, and **12a** ⇄ **13** ⇄ **12b** (see Scheme 6), and hence the mechanism of the elementary step is the totality of the transformations of the system along the three gradient lines. However, if we are concerned only with the inversion of the ring, the mechanism of the elementary step now becomes the totality of the transformations along only one of the lines, **11a** ⇄ **12a** ⇄ **11c** or **11b** ⇄ **12b** ⇄ **11d** (Scheme 18).

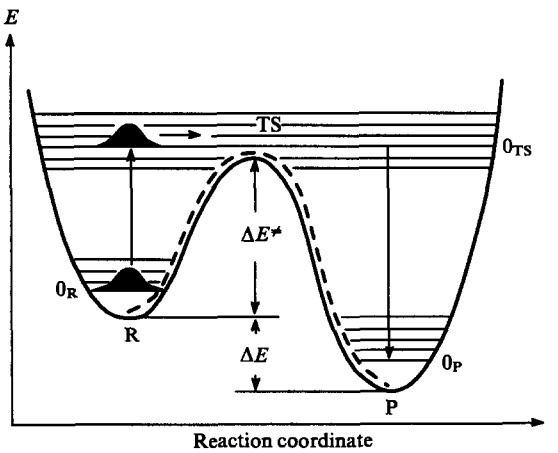
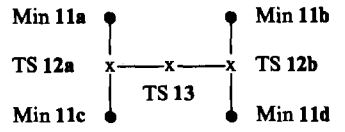


Figure 14. Classical reaction path (broken line joining the minima of the reactant R and of the product P through the saddle point of the transition state TS) and quantum transition (vertical arrows) from the vibrational ground state of the reactant (0_R) to the vibrational state (0_{TS}) lying above the energy of the transition state, and beyond to the vibrational ground state of the product (0_P).



Scheme 18

It is often assumed[61,75,203] that any unimolecular reaction begins along the 'softest mode', i.e. along the vector $\vec{q}_1$ corresponding to the minimum frequency. It is evident from the above discussion that this assertion is not entirely accurate, since in addition to the very large number of secondary gradient lines tangential to the vector $\vec{q}_1$ we have $2(3N-7)$ principal gradient lines tangential to the vectors $\pm\vec{q}_i$ ($i = 2, 3, ..., 3N-6$), which may also contain transition states. Of course, the chemical system can take part in all the reactions corresponding to these transition states, but the number of transition states which may be found on the secondary gradient lines entering a given minimum is still an unsolved problem. Therefore the problem of listing all the reaction mechanism available to a molecular configuration corresponding to a given minimum is also still unsolved. Obviously, the number of such mechanisms must be finite.

As was pointed out above, the chemical system can move away from a minimum only along the appropriate gradient line. This means that it can begin to move from the minimum only along one of the $\vec{q}_i$ vectors ($i = 1, 2, ..., 3N-6$), i.e. the chemical reaction can start only along a normal (collective) mode.[80] The idea of using a normal mode to describe a motion with a large amplitude was stimulated by the discovery by Pitzer and Kemp[204] (in 1937) of the restricted internal rotation in ethane. The idea was later developed and used to explain the mechanism of the internal pseudorotation in cyclopentane[205-209] and other molecules.[13,14,115] The same idea was recently extended to pericyclic reactions in the outstanding studies of Woodward and Hoffmann.[185] The case of unimolecular reactions of an arbitrary type has been discussed by the writer.[80]

The motion of the system from a minimum along a gradient line tangential to one of the $\vec{q}_i$ vectors ($i = 1, 2, ..., 3N-6$) helps us to understand the nature of the departure of the gradient path from the shortest path (in which the reaction follows the shortest path of each atom in the molecular system from the reactants to the products), proposed by Rice and Teller[210] in 1938 (see also Ref. 62). If the direction of the $\vec{q}_i$ vector coincides with that of the shortest distance path the reaction follows this path. However, the gradient path of the reaction may not coincide with the shortest distance path. For example, the transformation of the cyclobutene molecule into the gauche form of 1,3-butadiene (see Fig. 13) follows a path close to the shortest distance path, as can easily be seen by superimposing the structures along the reaction path. In this case the motion of each atom from its initial position (cyclobutene) to the final position (butadiene) is almost a straight line. In contrast to this reaction the elimination of a hydrogen molecule from 1,4-cyclohexadiene (according to MCSCF ab initio calculations in 6-31G and 6-31G** bases)[211] follows a path markedly different from the shortest distance path. As can be seen from Fig. 15, during the reaction the atoms follow fairly complex trajectories strongly different from straight lines. The normal vibration vector, shown by arrows in Fig. 15 and tangential to the reaction path, corresponds to the distortion of the planar structure into a bathtub conformation and does not agree (in this case) with the direction of shortest travel. An interesting characteristic of this process is the observation (in experimental studies of the distribution of vibrational and rotational energy in the products of the elimination reaction)[212] that a hydrogen molecule being removed from the benzene begins to rotate in a plane parallel to the benzene ring, which cannot be explained by the calculated[221] characteristics of the PES. In order to reconcile the experimental[212] and the theoretical data[211] we must postulate a second transition state on the reaction path (the point A in Fig. 15) with a structure of C_{2v} symmetry, corresponding to the rotation of the hydrogen molecule in a plane parallel to that of the benzene ring.

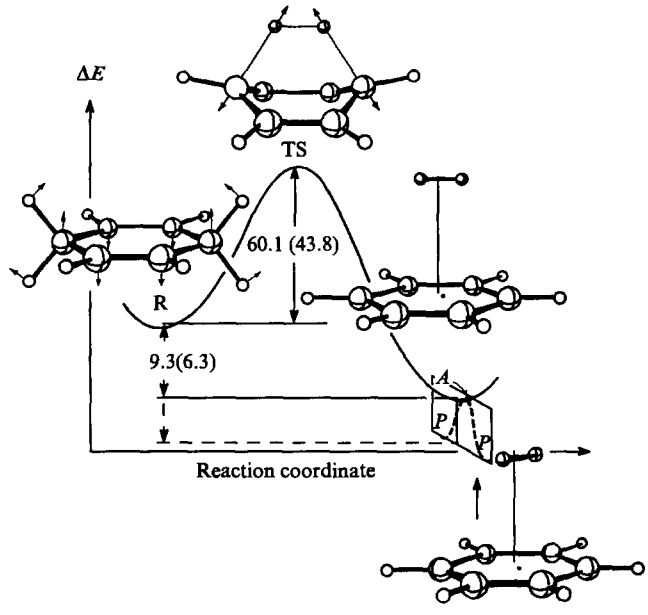


Figure 15. Transformation of the 1,4-cyclohexadiene molecule along the reaction path of the reaction for the removal of a hydrogen molecule according to ab initio calculations[211] (numbers without parentheses, kcal mol^{-1}). Experimental data for the activation barrier[213] and for the heat of the reaction[214] are given (numbers in parentheses). In order to reconcile the calculated PES [211] with the experimental data[212] we must assume that the point A corresponds to the second transition state on the path of the elimination reaction and that this structure is the transition state for the internal rotation of the hydrogen molecule in a plane parallel to the benzene molecule (broken line). The arrows show the components of the normal vibration vector at the minimum and of the transition vector at the saddle point.

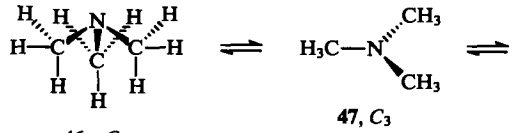
At the second transition state the translational motion of the hydrogen molecule with respect to the benzene becomes a rotational motion. In this case the gradient reaction path becomes analogous to the reaction path proposed in Scheme 2.

This approach also makes clear the nature of the strictly correlated conrotational or disrotational motion of the methylene end groups in the pericyclic ring opening reactions of polyenes,[185] and answers a number of other questions. For example, how does one methylene group at the beginning of the reaction 'sense' that another methylene group has started to move, and how does it establish the direction of this motion so as to align itself correctly with it? Why is the character of this correlated motion often different in similar systems? Answers to these questions can be given relatively simply by using existing data.[80] At a minimum point the molecular system initially has a limited choice of vibrational modes, corresponding only to the conrotational and the disrotational modes of the methylene group (see, for example, the calculations[215] of the rotational spectra of the *cis*- and *gauche*-conformers of 1,3-butadiene). Therefore in this system the gradient path of the reaction begins at a minimum tangentially to the vectors of these modes.

VI. Collective processes

Any single-stage process can be treated as a collective process. The most important collective processes are those consisting in the correlated (coordinated) motion of two or several groups (especially between not covalently bound fragments) with relatively minor changes in the other geometric parameters of the system. Equally important are the conditions under which the independent motion of these groups (multistage reaction) becomes single-stage. Let us make these statements clearer by considering some examples.

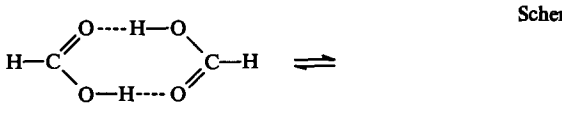
Scheme 19



46a, C_{3v} **47**, C_3 **46b**, C_{3v}

We shall discuss as a first example the inversion reaction of the trimethylamine molecule $(CH_3)_3N$ (Scheme 19). In the ground state this molecule has a C_{3v} symmetry.[216] In the transition structure during the inversion through a planar configuration of N–C bonds surrounding the nitrogen atom the molecule acquires the C_3 configuration. This means that all three methyl groups rotate simultaneously and synchronously during the reaction, so that a collective process of simultaneous and strictly correlated motion of all the stereochemically labile groups can take place in this reaction, i.e. the inversion of the bonds on the nitrogen atom induces a synchronous internal rotation of the methyl groups. A similar inversion process occurs in the $(CH_3)_3O^+$ (see Ref. 217) and the $(CH_3)_3S^+$ cations (see Ref. 216).

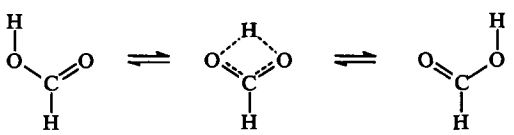
Scheme 20



48a **49** **48b**

We shall discuss as a second example the intermolecular double proton exchange in the dimers of formic acid[163,218,219] and pyrazole,[220–222] and the triple (in the trimer) and the four-fold proton transfer (in the tetramer) of pyrazole[220–222] (Scheme 20). As shown by theoretical and by experimental studies of the formic acid dimer[163,218,219] a double proton transfer takes place simultaneously in this system through the symmetrical transition structure **49** with an activation barrier of ~8 kcal mol^{-1} (see Ref. 163). At the same time the intramolecular transfer of a proton between oxygen atoms (Scheme 21) in the monomer **50** takes place, according to ab initio calculations,[223] with a much higher activation barrier: about 40 kcal mol^{-1}.

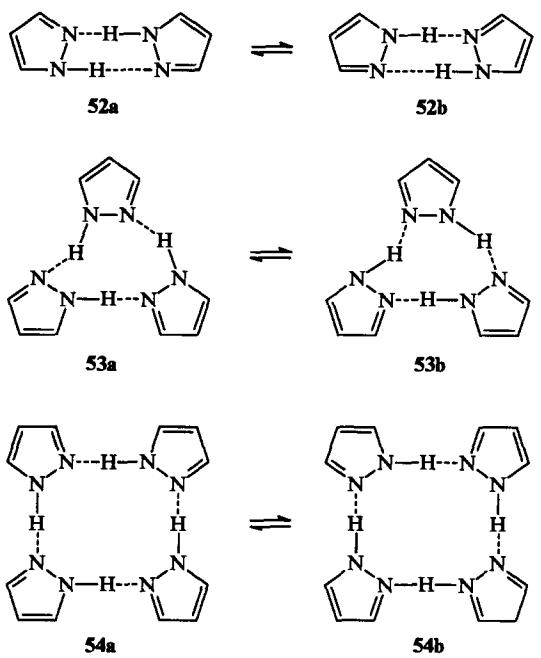
Scheme 21



50a **51** **50b**

Similar studies of the pyrazole dimers,[220,222] trimers,[220] and tetramers[222] showed that fast, reversible low-barrier proton transfer processes are possible in these systems. On the other hand the intramolecular proton transfer in pyrazole, as in formic acid, involves overcoming a substantially higher activation barrier (Scheme 22).

Scheme 22

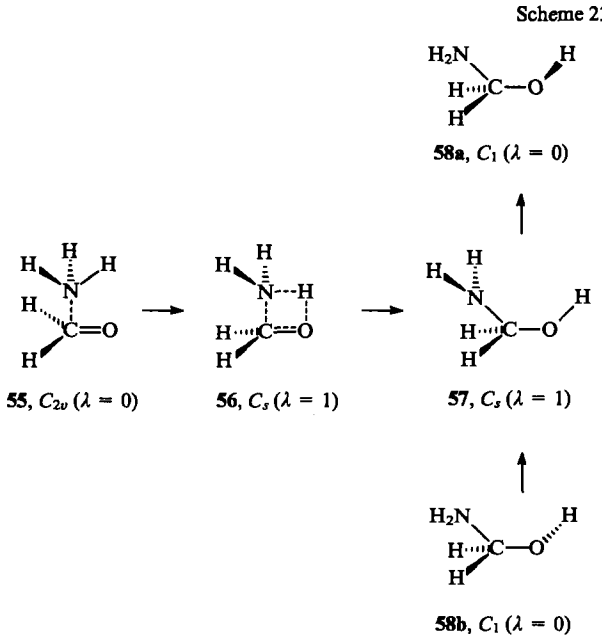


52a **52b** **53a** **53b** **54a** **54b**

According to experimental data[220–222] the rate of the proton transfer reaction in the series of compounds **52**–**54** decreases at first (on going from the dimer **52** to the trimer **53**), and then increases again in the tetramer **54**. This can be ascribed to the replacement of the concerted proton transfer in **52** by a multistage process in **54**.

The low activation barriers to the intermolecular double and triple proton transfer processes in these systems are due to two factors: the almost ideal stereochemical conditions found by the proton transfer[224–226] and the catalytic (acid–base) action of the second hydrogen bond, which greatly assists the reaction.[64]

Scheme 23



58a, C_1 ($\lambda = 0$) **55**, C_{2v} ($\lambda = 0$) **56**, C_s ($\lambda = 1$) **57**, C_s ($\lambda = 1$) **58b**, C_1 ($\lambda = 0$)

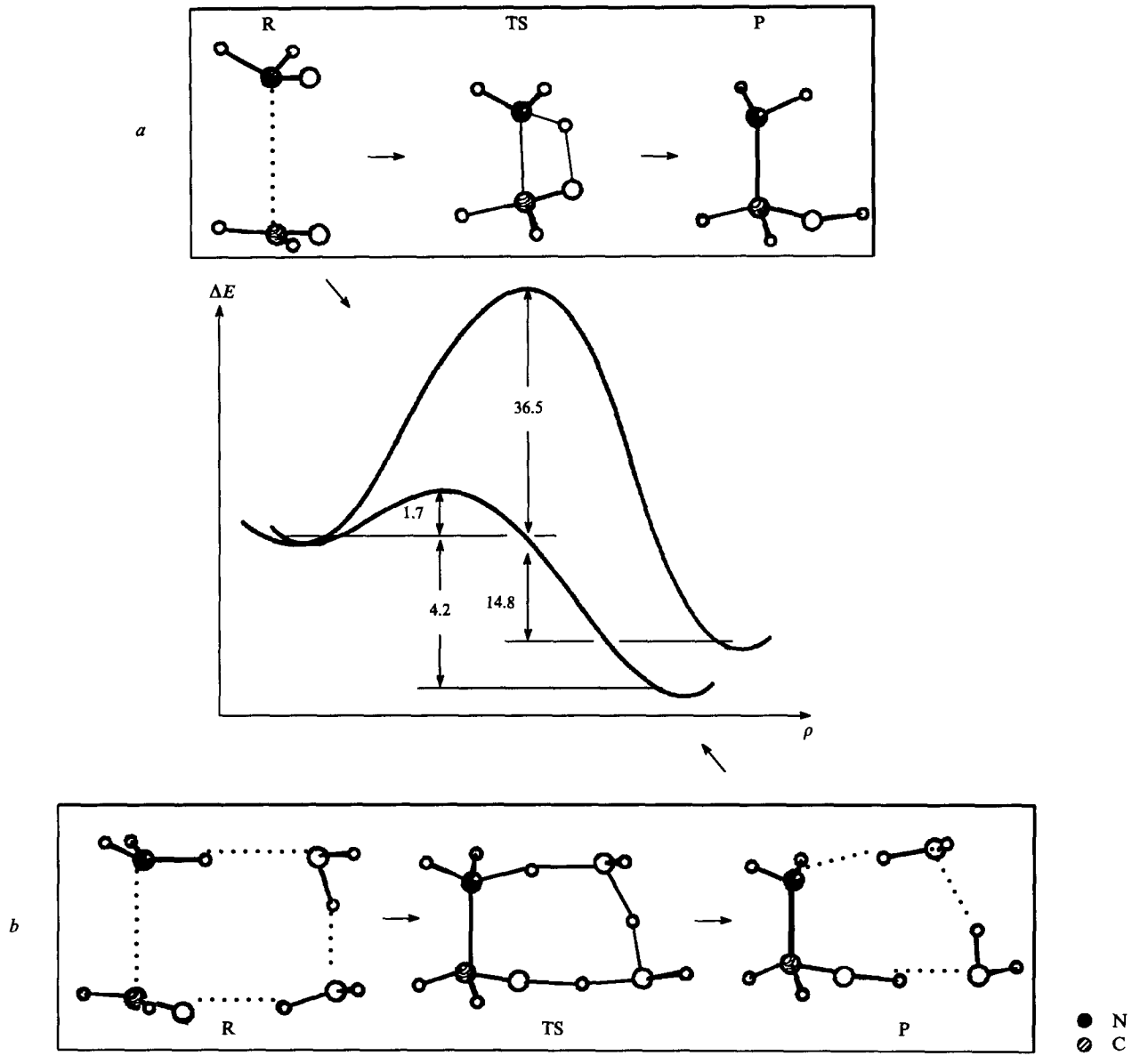


Figure 16. Mechanism of the addition of an ammonia molecule to formaldehyde according to ab initio calculations.[26] (*a*) Not allowing for solvation; (*b*) allowing for solvation by two water molecules. The relative energies are given in kcal mol^{-1}; ρ is the reaction coordinate.

Small differences in the distance between the hydrogen-bonded monomers lead to marked changes in the mechanism of the transfer process. Thus, the transition from the dimer of formic acid [163] to the dimers of formamide and of formamidine converts the proton transfer mechanism from single-stage (synchronous) to multistage (non-synchronous) as a result of the increased length of the H bond.

Our third example is the nucleophilic addition reaction of an ammonia molecule to formaldehyde with formation of aminomethanol and solvation by two water molecules (Scheme 23),[26,227] which is a model of the formation of peptide bonds in proteins.[228] The reaction begins with the formation of the complex **55**, in which the nitrogen atom of the ammonia molecule is oriented towards the carbonyl group. The reaction proceeds by the synchronous motion of all the atoms in the system through the multicentre transition state **56**. The energy profile of the reaction and its geometric evolution are shown in Fig. 16, together with data for the system which allow for the solvation by two water molecules. A comparison of the solvated and the nonsolvated system leads to the following conclusions.

First, in the nonsolvated system the reaction takes place along two gradient lines. Initially, from the pre-reaction complex **55** through the transition state **56** to the following transition state **57**, the system slides along a single gradient line. At the point corresponding to the structure **57** the system passes from the first line to the second, corresponding to the internal rotation of the O–H bond round the C–O single bond. In this way the two enantiomeric forms **58a** and **58b** appear as products in the nonsolvated system. Solvation with two water molecules lowers the initial symmetry C_s of the system to C_1, and the second (enantiomeric) reaction channel disappears.

Second, as the nitrogen atom approaches the carbon atom of the carbonyl group three protons are collectively transferred over the three hydrogen bridges in the system.

Third, in the pre-reaction solvated complex all the constituent single molecules are oriented in such a way that the stereochemical conditions most favourable to four simultaneous reactions [224–226,229–232] are satisfied: the nucleophilic addition to the carbonyl group [229–232] and three proton transfers over the hydrogen bridges.[224–226]

VII. Biological systems

The examples of various chemical reactions examined above have revealed some extremely branched (multichannel) mechanisms. Conversely, chemical reactions in living organisms follow strictly single paths.[228,233-236] This is because all living organisms (including the living cell) are essentially molecular machines,[233,235,236] and (accordingly) they function as machines, in a strictly determined rather than a random way. In this case the 'global' thermodynamics of biochemical processes (in particular the path of the reaction and its energy profile along this path) should be 'machine like'.[235,236]

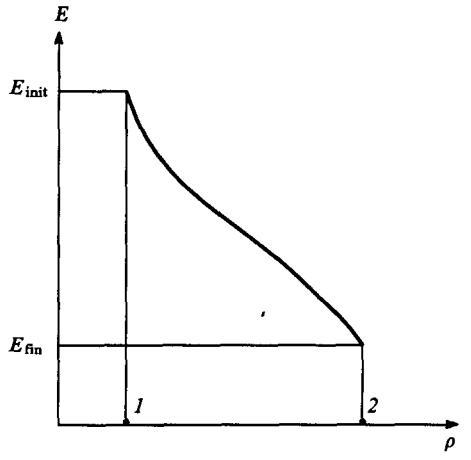


Figure 17. Energy profile of a living organism as a macroscopic body as a function of the internal reaction coordinate ρ. (*1*) and (*2*) are the initial and the final point of the motion along the reaction coordinate respectively. The reaction coordinate ρ is the length along the reaction path constructed in the coordinate system of the centre of mass.

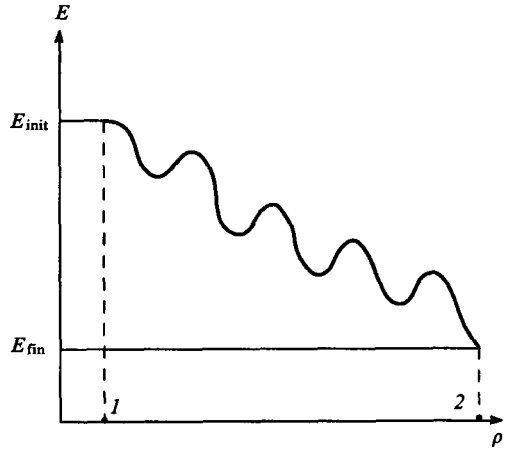


Figure 18. Energy profile of the system of a living organism as the combination of all the biochemical reactions along the reaction coordinate ρ. The points *1* and *2* correspond to those defined in Fig. 17.

The global energy profile of a living system is determined by examining its motion over a small enough time interval, during which the system can be treated as closed.[237] The motion of a system such as a macroscopic body as a whole is determined by the law of energy conservation (the first law of thermodynamics) irrespectively of the internal structure or of the nature of the internal interactions taking place in it.[237] The motion of the body over a small time interval satisfies the inequality

$$E_{init} > E_{fin},$$

where E_{init} and E_{fin} are the total energies of the system at the initial and the final moments. Therefore the dependence of the total internal energy of the system on the internal reaction coordinate (corresponding to a small time interval) is shown as a falling curve (Fig. 17). At the same time, any biological system is a plurality of chemical reactions strictly correlated in time and space. We know that the energy profile of the elementary step of any chemical reaction is defined by the Arrhenius curve.[59,83,238] A very large number of these elementary steps can occur in living cells. If they are mutually indepen-dent[228,238] the overall profile of the biological system consists of the independent profiles of the separate elementary chemical reactions, and it can be represented by the curve shown in Fig. 18. In this respect the profile of biological systems (interpreted as the combined profiles of many chemical reactions) does not coincide with the energy profile of Fig. 17. Thus we meet a difference in principle between the very complex energy profile of processes in biological systems and the energy profile of the macroscopic body (including biological bodies). In order to reconcile the profiles of biosystems (as macroscopic objects and as biochemical systems consisting of chemical reactions following microscopically separate paths) we must assume that the profile shown in Fig. 17 consists of a large number of separate parts corresponding to separate chemical reactions in the biosystem. This is possible if the final point of the previous reaction occurs after the activated barrier of the subsequent reaction, i.e. if the energy profile can be represented by the curve shown in Fig. 19. Only this reconciliation of the profiles of the elementary chemical reactions in the biological system can allow the development of functional systems such as molecular machines. Of course, this description is strictly schematic and oversimplified, and it cannot be offered as the final picture, but the arguments used above make clear the essential difference between chemical reactions and their biochemical analogues in the living organism. This difference suggests one possible direction for further studies of collective reactions.

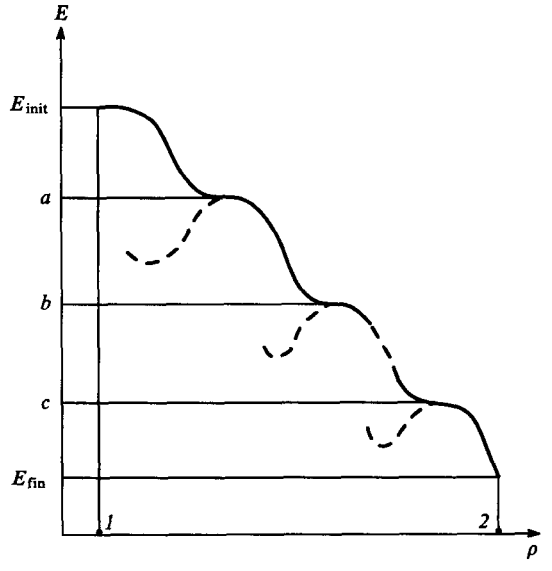


Figure 19. Full energy profile (thick line) of the system of a living organism as the combination of separate biochemical reactions (broken line) strictly correlated in space and time. Each reaction terminates at a point lying beyond the transition state of the 'next' reaction. E_{init} denotes the 'first' reaction (corresponding to the point *1* on the reaction coordinate ρ), which terminates at the point *a*. The second reaction begins at this point, and terminates at the point *b*. The point *c* denotes the initial point of the 'next' reaction, which terminates at the point *2*.

VIII. Conclusion

The stereochemical paths (mechanisms) of the elementary steps of the main types of chemical reaction, of which relatively few have so far been identified,[64, 185, 186, 232] have been studied in depth both experimentally and theoretically. Many workers[4, 13, 14, 22, 64, 185, 196, 202, 230] have successfully determined the stereochemical trajectories of their reaction paths, and the electronic nature of the driving force is now understood for most reactions. However, in practice chemical reactions are usually collective processes in a multicomponent system with a simultaneous or strictly correlated (relay mechanism) sequence of motions over the whole system. Biological reactions involving enzymes are a special case of these reactions. Therefore, in order to understand the nature of enzyme reactions we must progress from the study of the PES of simple systems to the study of the PES of chemical systems which model the course of several reactions at the same time. This calls, in turn, for the development of new methods of analysis of the topological structure of multidimensional PES, for the further development of nonempirical and semiempirical quantum-chemical methods of calculation, and lastly for an increase in the power and speed of response of the computers used in these studies.

The writer is grateful to the Russian Fund for Fundamental Studies for financial support (grant 93-03-4972).

References

1. D G Truhlar, M S Gordon *Science* **249** 491 (1990)
2. J T Hynes, in *Theory of Chemical Reaction Dynamics* (Ed. M Baer) (Boca Raton, FL: CRC Press, 1985) p. 171
3. T H Dunning Jr, L B Harding, E Kraka, in *Supercomputing Algorithms for Reactivity, Dynamics and Kinetics of Small Molecules* (Ed. A Lagana) (Dordrecht: Kluwer, 1989) p. 57
4. M V Bazilevskii, V M Ryaboi, in *Sovremennye Problemy Kvantovoi Khimii. Metody Kvantovoi Khimii v Teorii Mezhmolekulyarnykh Vzaimodeistvii i Tverdykh Tel* (Advanced Problems of Quantum Chemistry. Methods of Quantum Chemistry in the Theory of Intramolecular Interactions and Solids) (Ed. M G Veselov) (Leningrad: Nauka, 1987) p. 3
5. M V Basilevsky, A G Shamov *Chem. Phys.* **60** 371 (1968)
6. D Heidrich, W Kleiesch, W Quapp *Properties of Chemically Interesting Potential Energy Surfaces* (Berlin: Springer-Verlag, 1991)
7. R M Minyaev, D J Wales *Chem. Phys. Lett.* **218** 413 (1994)
8. J Z Zhang, B J Schwartz, J C King, C B Harris *J. Am. Chem. Soc.* **114** 1091 (1992)
9. W v E Doering, W R Roth *Tetrahedron* **19** 715 (1963)
10. J F M Oth, K Mallen, J-M Gilles, G Schröder *Helv. Chim. Acta* **57** 1415 (1974)
11. J J Titman, Z Luz, H M Spiess *J. Am. Chem. Soc.* **114** 3765 (1992)
12. S Schlik, Z Luz, R Poupko, H Zimmermann *J. Am. Chem. Soc.* **114** 4315 (1992)
13. W J Orville-Thomas (Ed.) *Internal Rotation in Molecules* (Translated into Russian; Moscow: Mir, 1977)
14. W J Hehre, L Radom, P v R Schleyer, J A Pople *Ab Initio Molecular Orbital Theory* (New York: Wiley, 1986)
15. A G Ozkabak, L Goodman *Chem. Phys. Lett.* **176** 19 (1991)
16. P Gomez, M Fernandez, L Sese, V Botella *J. Mol. Struct.* **142** 315 (1986)
17. H Guo, M Karplus *J. Chem. Phys.* **91** 1719 (1989)
18. J E Boggs, M Altman, F R Cordell, Y Dai *J. Mol. Struct.* **94** 373 (1983)
19. J R v Wazer, V Kello, B A Hess Jr, C S Ewig *J. Phys. Chem.* **94** 5694 (1990)
20. Y Yamaguchi, H F Schaefer III *Chem. Phys. Lett.* **185** 143 (1991)
21. S J Getty, E R Davidson, V T Borden *J. Am. Chem. Soc.* **114** 2085 (1992)
22. R M Minyaev *Zh. Strukt. Khim.* **32** 15 (1991)
23. M T Nguyen, T K Ha *Chem. Phys. Lett.* **158** 135 (1989)
24. R M Minyaev *J. Mol. Struct.* **262** 79 (1992)
25. R M Minyaev *Zh. Fiz. Khim.* **67** 1 (1993)
26. I H Williams *J. Am. Chem. Soc.* **109** 6299 (1987)
27. S C Tucker, D G Truhlar *J. Am. Chem. Soc.* **112** 3347 (1990)
28. E Clementi *J. Phys. Chem.* **89** 4426 (1985)
29. M Okumura, L I Yeh, J D Myers, Y T Lee *J. Phys. Chem.* **94** 3416 (1990)
30. S Schroder, N Buckley, N J Oppenheimer, P A Kollman *J. Am. Chem. Soc.* **114** 8232 (1992)
31. H S Rzepa, M Y Yi *J. Chem. Soc., Perkin Trans. 2* 531 (1991)
32. B J Gerner, R M Whitnell, K R Wilson *J. Am. Chem. Soc.* **113** 74 (1991)
33. M R Nimlos, D F Kelley, E R Bernstein *J. Phys. Chem.* **93** 643 (1989)
34. J R Alvarez-Idaboy, L A Montero *J. Mol. Struct.* **253** 243 (1992)
35. E M Duffy, D L Severance, W L Jorgensen *J. Am. Chem. Soc.* **114** 7535 (1992)
36. K M Merz Jr *J. Am. Chem. Soc.* **112** 7973 (1990)
37. M W Wong, K B Wiberg, W J Frish *J. Am. Chem. Soc.* **114** 1645 (1992)
38. R Hoffmann *Solids and Surfaces: a Chemist's View of Bonding in Extended Structures* (Translated into Russian; Moscow: Mir, 1990)
39. G A Somorjai *J. Phys. Chem.* **94** 1013 (1990)
40. J Rouxel *Acc. Chem. Res.* **25** 328 (1992)
41. J Sauer *Chem. Rev.* **89** 199 (1989)
42. W Weltner Jr, R J van Zee *Chem. Rev.* **89** 1713 (1989)
43. M-H Whangbo, C C Torardi *Acc. Chem. Res.* **24** 127 (1991)
44. S Lee *Acc. Chem. Res.* **24** 249 (1991)
45. A A Levin *Vvedenie v Kvantovuyu Khimiyu Tverdogo Tela* (Introduction to the Quantum Chemistry of Solids) (Moscow: Khimiya, 1974)
46. M Mehring, in *Electronic Properties of Conjugated Polymers III* (Eds H Kusmany, M Mehring, S Roth) (Heidelberg: Springer, 1989) p. 242
47. F L Carter, R E Siatkowdki, in *Molecular Electronic Devices* (New York: Marcel Dekker, 1989) p. 307
48. P L Kapitsa *Usp. Fiz. Nauk* **118** 307 (1976)
49. J Pimentel, J Coonrod *Opportunities of Chemistry Today and Tomorrow* (Translated into Russian; Moscow: Mir, 1992)
50. C D Mickey *J. Chem. Educ.* **58** 418 (1981)
51. V A Bren', A D Dubonosov, V I Minkin, V A Chernoivanov *Usp. Khim.* **60** 913 (1991) [*Russ. Chem. Rev.* **60** 451 (1991)]
52. M D Archer, J R Bolton *J. Phys. Chem.* **94** 8028 (1990)
53. V T D'Sonza, M L Bender *Acc. Chem. Res.* **20** 146 (1987)
54. J A Gerlt *Chem. Rev.* **87** 1079 (1987)
55. D Arad, R Langridge, P A Kollman *J. Am. Chem. Soc.* **112** 491 (1990)
56. F M Menger, M J Sherrod *J. Am. Chem. Soc.* **112** 8071 (1990)
57. H Eyring, M Polanyi *Z. Phys. Chem., Abt. B* **12** 279 (1931)
58. S Glasstone, K Laider, H Eyring *The Theory of Rate Processes* (Translated into Russian; Moscow: Inostr. Lit., 1948)
59. H Eyring, S H Lin, S M Lin *Basic Chemical Kinetics* (Translated into Russian; Moscow: Mir, 1983)
60. M Born, J R Oppenheimer *Ann. Phys. (Leipzig)* **84** 457 (1927)
61. R Fukui *J. Phys. Chem.* **74** 4161 (1970); *Acc. Chem. Res.* **14** 363 (1981)
62. M V Basilevsky *Chem. Phys.* **24** 81 (1977)
63. K Fukui, in *Applied Quantum Chemistry* (Eds V H Smith Jr, H R Schaefer, III, K Morokuma) (Dordrecht: Reidel, 1986) p. 1
64. V I Minkin, B Ya Simkin, R M Minyaev *Kvantovaya Khimiya Organicheskikh Soedinenii. Mekhanizmy Reaktsii* (Quantum Chemistry of Organic Compounds. Mechanisms of Reactions) (Moscow: Khimiya, 1986)
65. P G Mezey *Potential Energy Hypersurface. Studies in Physical and Theoretical Chemistry* Vol. 53 (Amsterdam: Elsevier, 1987)
66. R M Minyaev *Zh. Strukt. Khim.* **32** 127 (1991)
67. P Pechukas *J. Chem. Phys.* **64** 1516 (1976)
68. A Tachibana, K Fukui *Theor. Chim. Acta* **49** 321 (1978)
69. K G Collard, G G Hall *Int. J. Quantum Chem.* **12** 623 (1977)
70. P Valtazanos, K Ruedenberg *Theor. Chim. Acta* **69** 281 (1986)
71. K Müller *Angew. Chem., Int. Ed. Engl.* **19** 1 (1980)
72. E A McCullough Jr, D M Silver *J. Chem. Phys.* **62** 4050 (1975)
73. D M Silver *J. Chem. Phys.* **57** 586 (1966)
74. M V Basilevsky *Chem. Phys.* **67** 337 (1982)
75. R G Pearson *Symmetry Rules for Chemical Reactions* (Translated into Russian; Moscow: Mir, 1979)

76. A Banerjee, N P Adams *Int. J. Quantum Chem.* **43** 855 (1992)
77. R M Minyaev, D J Wales *J. Chem. Soc., Faraday Trans.* **90** 1839 (1994)
78. J N Murrel, K J Laidler *Trans. Faraday Soc.* **63** 371 (1968)
79. J W McIver Jr, R E Stanton *J. Am. Chem. Soc.* **94** 8618 (1972); R E Stanton J W McIver Jr *J. Am. Chem. Soc.* **97** 3632 (1975)
80. R M Minyaev *Int. J. Quantum Chem.* **49** 105 (1994); *Zh. Strukt. Khim.* **34** 3 (1993)
81. B A Dubrovin, S P Novikov, A T Fomenko *Sovremennaya Geometriya. Metody i Prilozheniya* (Advanced Geometry. Methods and Applications) (Moscow: Nauka, 1986)
82. A V Pogorelov *Geometriya* (Geometry) (Moscow: Nauka, 1984)
83. V N Kondrat'ev, E E Nikitin *Kinetika i Mekhanizmy Gazofaznykh Reaktsii* (Kinetic and Mechanisms of Gas-Phase Reactions) (Moscow: Nauka, 1974)
84. M E Tamm *Osnovy Teorii Elektrichestva* (Bases of the Theory of Electricity) (Moscow: Nauka, 1989)
85. I G Petrovskii *Lektsii po Teorii Obyknovennykh Differentsial'nykh Uravnenii* (Lectures on the Theory of Ordinary Differential Equations) (Moscow: Izd. Mosk. Gos. Univ., 1984)
86. L S Pontryagin *Obyknovennye Differentsial'nye Uravneniya* (Ordinary Differential Equations) (Moscow: Nauka, 1982)
87. R F W Bader *Acc. Chem. Res.* **18** 9 (1985)
88. L P Eizenkhart *Rimanova Geometriya* (Riemann Geometry) (Moscow: Izd. Inostr. Lit., 1948)
89. R G Pearson *Theor. Chim. Acta* **16** 107 (1970)
90. A Rodger, P E Schipper *Chem. Phys.* **107** 329 (1986)
91. A Rodger, P E Schipper *J. Phys. Chem.* **91** 189 (1987)
92. A Rodger, P E Schipper *Inorg. Chem.* **27** 458 (1988)
93. S Kato, R Morokuma *J. Chem. Phys.* **73** 3900 (1980)
94. D Volkmann, B Zurawski, D Heidrich *Int. J. Quantum Chem.* **22** 631 (1982)
95. A Hinchliffe *Chem. Phys. Lett.* **85** 531 (1982)
96. S Nagase, T Kudo *J. Chem. Soc., Chem. Commun.* 363 (1983)
97. S Yamabe, T Minato, S Inagaki *J. Chem. Soc., Chem. Commun.* 532 (1988)
98. C Clavero, M Duran, A Lledos, O N Ventura, J Bertran *J. Am. Chem. Soc.* **108** 923 (1986)
99. T-H Tang, W-J Hu, D-Y Yan, Y-P Cui *J. Mol. Struct.* **207** 319 (1990)
100. G Bouchoux, M T Ngueyn, P Longevialle *J. Am. Chem. Soc.* **114** 1000 (1992)
101. C Sosa, H B Schlegel *J. Am. Chem. Soc.* **109** 4193 (1987)
102. E Nakamura, M Nakamura, Y Miyachi, N Koga, K Morokuma *J. Am. Chem. Soc.* **115** 99 (1993)
103. M W Wong, K B Wiberg, M J Frisch *J. Am. Chem. Soc.* **114** 523 (1992)
104. D F Feller, M W Schmidt, K Ruedenberg *J. Am. Chem. Soc.* **104** 960 (1982)
105. M L McKee, P B Shevlin, H S Rzepa *J. Am. Chem. Soc.* **108** 5743 (1986)
106. D A Hrovat, W T Borden *J. Am. Chem. Soc.* **114** 5879 (1992)
107. B Bühl, H F Schaefer III *J. Am. Chem. Soc.* **115** 364 (1992)
108. R M Minyaev, I A Yudilevich *J. Mol. Struct.* **262** 73 (1992)
109. R G A Bone, T W Rowlands, N C Handy, A J Stone *Mol. Phys.* **72** 33 (1991)
110. S Koseki, M S Gordon *J. Phys. Chem.* **93** 118 (1989)
111. T L Windus, M S Gordon, L W Burggraf, L P Davis *J. Am. Chem. Soc.* **113** 4356 (1991)
112. A Tachibana, H Fueno, T Yamabe *J. Am. Chem. Soc.* **108** 4346 (1986)
113. D Liotard, in *Symmetries and Properties of Non-Rigid Molecules: A Comprehensive Survey. Studies in Physical and Theoretical Chemistry* Vol. 23 (Amsterdam: Elsevier, 1983) p. 323
114. P G Mezey *J. Am. Chem. Soc.* **112** 3791 (1990)
115. R S Berry *J. Chem. Phys.* **32** 932 (1960)
116. G Shröder, J F M Oth, R Mereni *Angew. Chem.* **77** 774 (1965) [Translated into Russian; *Usp. Khim.* **36** 993 (1967)]
117. L A Paquette *Tetrahedron* **31** 2855 (1975)
118. G I Fray, R G Saxton *The Chemistry of Cyclooctatetraene and Its Derivatives* (New York: Cambridge University Press, 1978)
119. P J Garratt *Aromaticity* (New York: Wiley, 1986)
120. P J Garratt, in *Comprehensive Organic Chemistry* Vol. 1 (Translated into Russian; Moscow: Khimiya, 1981)
121. D Lloyd *The Chemistry of Conjugated Cyclic Compounds* (New York: Wiley, 1989)
122. F A L Anet *J. Am. Chem. Soc.* **84** 671 (1962)
123. J F M Oth *Pure Appl. Chem.* **25** 573 (1971)
124. F A L Anet, A J Bourn, Y S Lin *J. Am. Chem. Soc.* **86** 3576 (1964)
125. M J S Dewar, K M Merz *J. Phys. Chem.* **89** 4739 (1985)
126. C Trindle, T Wolfskill *J. Org. Chem.* **56** 5426 (1991)
127. O Ermer, F-G Klarner, M Wette *J. Am. Chem. Soc.* **108** 4908 (1986)
128. E Erdik, M Ay *Chem. Rev.* **89** 1947 (1989)
129. M Famulok, G Boche *Angew. Chem., Int. Ed. Engl.* **28** 468 (1989)
130. B Singer, J T Kusmierek *Annu. Rev. Biochem.* **51** 655 (1982)
131. R Ulbrich, M Famulok, F Bosold, G Boche *Tetrahedron Lett.* **31** 1689 (1990)
132. M Novak, K A Martin, J L Heinrich *J. Org. Chem.* **54** 5430 (1989); J S Helmiek, K A Martin, J L Heinrich, M Novak. *J. Am. Chem. Soc.* **113** 3459 (1991)
133. P Beak, J Li *J. Am. Chem. Soc.* **113** 2796 (1991)
134. G E Scuseria, C C Janssen, H F Schaefer III *J. Chem. Phys.* **89** 7382 (1988)
135. R M Minyaev, D J Wales *J. Phys. Chem.* (1994) in the press
136. A Fernandez, O Sinanoglu *Theor. Chim. Acta.* **65** 179 (1984)
137. J Milnor *The Morse Theory* (Translated into Russian; Moscow: Mir, 1975)
138. P K Chou, G D Dahlke, S R Kass *J. Am. Chem. Soc.* **115** 315 (1993)
139. S Wolfe, H B Schlegel, I G Csizmadia, F Bernardi *J. Am. Chem. Soc.* **97** 2020 (1975)
140. J H Hammons, M B Coolidge, W T Borden *J. Phys. Chem.* **94** 5468 (1990)
141. A Nicalaides, W T Borden *J. Am. Chem. Soc.* **114** 8682 (1992)
142. R M Minyaev, D J Wales *J. Chem. Soc., Faraday Trans.* **90** 1831 (1994)
143. A Sarai *J. Chem. Phys.* **76** 554 (1982); **80** 5341 (1984)
144. Z Smedarchina, W Siebrand, T A Wildman *Chem. Phys. Lett.* **143** 395 (1988)
145. R J Abraham, G E Hawkes, K M Smith *Tetrahedron Lett.* **15** 1483 (1974)
146. H-H Limbach, J Hennig, R Kendrich, C S Yunnoni *J. Am. Chem. Soc.* **106** 4059 (1984)
147. M Schlabach, H-H Limbach, E Bunnenberg, A Y L Shu, B-K Tolf, C Djerassi *J. Am. Chem. Soc.* **115** 4554 (1993)
148. V M Mamaev, Doctoral Thesis in Chemical Sciences, Rostov Univ., Rostov-on-Don, 1988
149. M Sclabach, G Scherer, H-H Limbach *J. Am. Chem. Soc.* **113** 3550 (1991)
150. H-H Limbach, J Hennig, D Gerritzen, H Rumpel *Faraday Discuss., R. Soc. Chem.* **74** 229 (1982)
151. G Scherer, H-H Limbach *J. Am. Chem. Soc.* **111** 5946 (1989)
152. H Rumpel, H-H Limbach *J. Am. Chem. Soc.* **111** 5429 (1989)
153. M J S Dewar, K M Merz Jr *J. Mol. Struct.* **124** 183 (1985)
154. K M Merz Jr, C H Reynolds *J. Chem. Soc., Chem. Commun.* 90 (1988)
155. M K Holloway, C H Reynolds, K M Merz Jr *J. Am. Chem. Soc.* **111** 3466 (1989)
156. J R de la Vega, J H Busch, J H Schaable, K L Kunze, B E Haggert *J. Am. Chem. Soc.* **104** 3295 (1982)
157. S Bratan, F Strohbush *J. Mol. Struct.* **61** 409 (1980)
158. W-I Shiau, E N Duesler, I C Paul, D Y Curtin, W G Blann, C A Fyfe *J. Am. Chem. Soc.* **102** 4546 (1980)
159. C A Fyfe, L Bemi, R Childs, H C Clark, D Y Curtin, J Davies, D Drekler, R L Dudley, G C Gobbi, J S Hartman, P Hayes, J Klimowski, R E Lenkinski, G J Lock, I C Paul, A Rudin, W Tchir, J M Thomas, R E Wasylishen *Philos. Trans. R. Soc. London, A* **305** 591 (1982)
160. J R Lyerla, C S Yannoni, C A Fyfe *Acc. Chem. Res.* **15** 208 (1982)
161. C J H Schutte, S O Paul, D Röhm *J. Mol. Struct.* **232** 179 (1991)
162. K A Nguyen, M S Gordon, D G Truhlar *J. Am. Chem. Soc.* **113** 1596 (1991)
163. S Svensson, N-A Bergman, P Ahlberg *J. Chem. Soc., Chem. Commun.* 82 (1990)
164. K Fuke, K Kaya *J. Phys. Chem.* **93** 614 (1989)
165. B Wehrle, H Zimmermann, H-H Limbach *J. Am. Chem. Soc.* **110** 7014 (1988)
166. T J Zielinski, R A Poirier *J. Comput. Chem.* **5** 466 (1984)

167. M J Wojcik, A Y Hirakawa, M Tsuboi, S Kato, K Morokuma *Chem. Phys. Lett.* **100** 523 (1983)
168. L Salem *Acc. Chem. Res.* **4** 322 (1971)
169. B R Henry *Acc. Chem. Res.* **10** 207 (1977)
170. C Jaffe, P Brumer *J. Chem. Phys.* **73** 5646 (1980)
171. A I Boldyrev, O P Charkin *Zh. Strukt. Khim.* **26** 158 (1985)
172. M T Weiss, M W Ptranberg *Phys. Rev.* **83** 567 (1951)
173. J D Swalen, J A Ibers *J. Chem. Phys.* **36** 1914 (1962)
174. K Kuchitsu, J P Guillory, L S Bartell *J. Chem. Phys.* **49** 2488 (1968)
175. G Herzberg *Molecular Spectra and Molecular Structure* Vol. 2 (New York: Van Nostrand, 1945)
176. S A Culley, A J Arduengo III *J. Am. Chem. Soc.* **106** 1164 (1984)
177. S A Culley, A J Arduengo III *J. Am. Chem. Soc.* **107** 1089 (1985)
178. C A Stewart, R L Harlow, A J Arduengo III *J. Am. Chem. Soc.* **107** 5543 (1985)
179. D A Dixon, A J Arduengo III, T Fukunaga *J. Am. Chem. Soc.* **108** 2461 (1986)
180. D A Dixon, A J Arduengo III *J. Chem. Soc., Chem. Commun.* 498 (1987); *J. Am. Chem. Soc.* **109** 338 (1987)
181. R C Tolmen *Phys. Rev.* **23** 699 (1924)
182. R M Minyaev *Chem. Phys. Lett.* **196** 203 (1992)
183. R Hoffmann, in *IUPAC Frontier of Chemistry* (Ed. K J Laidler) (Oxford: Pergamon Press, 1982) p. 247
184. S R Davis *J. Am. Chem. Soc.* **113** 4145 (1991)
185. R Woodward, R Hoffmann *The Conservation of Orbital Symmetry* (Translated into Russian; Moscow: Mir, 1971)
186. N M Emanuel', D G Knorre *Kurs Khimicheskoi Kinetiki* (Course of Chemical Kinetics) (Moscow: Vysshaya Shkola, 1974)
187. C H Langford, B Gray *Ligand Substitution Processes* (Translated into Russian; Moscow: Mir, 1969)
188. J Breulet, H F Schaefer III *J. Am. Chem. Soc.* **106** 1221 (1984)
189. W J Leigh *Chem. Rev.* **93** 487 (1993); *Can. J. Chem.* **71** 147 (1993)
190. M Olivicci, I N Ragazos, F Bernardi, M A Robb *J. Am. Chem. Soc.* **115** 3710 (1993)
191. K B Wiberg, R E Rosenberg *J. Am. Chem. Soc.* **112** 1509 (1990)
192. K B Wiberg, R E Rosenberg, P A Rabin *J. Am. Chem. Soc.* **113** 2890 (1991)
193. D C Spellmeyer, K N Houk *J. Am. Chem. Soc.* **110** 3412 (1988)
194. C W Jefford, G Bernardinelli, Y Wang, D C Spellmeyer, A Buda, K N Houk *J. Am. Chem. Soc.* **114** 1157 (1992)
195. V A Pichko, B Ya Simkin, V I Minkin *J. Mol. Struct.* **235** 107 (1991)
196. K N Houk, Y Li, J D Evansek *Angew. Chem., Int. Ed. Engl.* **31** 682 (1992)
197. P W Mui, E Grunwald *J. Am. Chem. Soc.* **104** 6562 (1982)
198. M J S Dewar, C Jie *Acc. Chem. Res.* **25** 537 (1992)
199. W Cooper, W D Walters *J. Am. Chem. Soc.* **80** 4220 (1958)
200. R W Carr Jr, W D Walters *J. Phys. Chem.* **69** 1073 (1965)
201. K B Wiberg, R A Fenoglio *J. Am. Chem. Soc.* **90** 3395 (1968)
202. M Duran, J Bertran *Rep. Mol. Theory* **1** 57 (1990)
203. I B Bersuker *The Jahn-Teller Effect and Vibronic Interactions in Modern Chemistry* (Translated into Russian; Moscow: Nauka, 1987)
204. K S Pitzer, J D Kemp *J. Am. Chem. Soc.* **59** 276 (1937)
205. K S Pitzer, R Spitzer *J. Am. Chem. Soc.* **68** 2537 (1946)
206. J E Kilpatrick, K S Pitzer, R Spitzer *J. Am. Chem. Soc.* **69** 2483 (1947)
207. L E Bauman, J Laane *J. Phys. Chem.* **92** 1040 (1988)
208. J E Varigar, R A MacPhail *J. Phys. Chem.* **96** 576 (1992)
209. W Cui, F Li, N L Allinger *J. Am. Chem. Soc.* **115** 2943 (1993)
210. F O Rice, E Teller *J. Chem. Phys.* **6** 489 (1938)
211. R J Rico, M Page, C Doubleday Jr *J. Am. Chem. Soc.* **114** 1131 (1992)
212. E F Cromwell, D Liu, M J J Vrakking, F H Kung, Y T Lee *J. Chem. Phys.* **92** 3230 (1990)
213. S W Benson, R Shaw *Trans. Faraday Soc.* **63** 985 (1966)
214. J D Cox, G Pilcher *Thermochemistry of Organic and Organometallic Compounds* (London: Academic Press, 1970)
215. H Guo, M Karplus *J. Chem. Phys.* **94** 3679 (1991)
216. D A Armstrong, A Rauk, D Yu *J. Am. Chem. Soc.* **115** 666 (1993)
217. N Hartz, G Rasul, G A Olah *J. Am. Chem. Soc.* **115** 1277 (1993)
218. F Graf, R Meyer, T-K Ha, R R Ernst *J. Chem. Phys.* **75** 2914 (1981)
219. S Hayashi, J Umemura, S Kato, K Morokuma *J. Phys. Chem.* **88** 1330 (1984)
220. A Baldy, J Elguero, R Faure, M Pierrot, E J Vincent *J. Am. Chem. Soc.* **107** 5290 (1988)
221. J A S Smith, B Wehrle, F Aguilar-Parrilla, H-H Limbach, M de la C Foces-Foces, F H Cano, J Elguero, A Baldy, M Pierrot *J. Am. Chem. Soc.* **111** 7304 (1989)
222. F Aguilar-Parrilla, G Scherer, H-H Limbach, M de la C Foces-Foces, F H Cano, J A S Smith, C Toiron, J Elguero *J. Am. Chem. Soc.* **114** 9657 (1992)
223. W J Bouma, M A Vincent, L Radom *Int. J. Quantum Chem.* **14** 767 (1978)
224. S Scheiner *Acc. Chem. Res.* **18** 174 (1985)
225. R Taylor, O Kennard *Acc. Chem. Res.* **17** 320 (1984)
226. A C Legon, D J Millen *Acc. Chem. Res.* **20** 39 (1987)
227. C Kozmutza, E M Evleth, E Kapuy *J. Mol. Struct.* **233** 139 (1991)
228. A L Lehninger *Biochemistry* (Translated into Russian; Moscow: Mir, 1976)
229. H B Bürgi, J O Dunitz, J M Lehn, G Wipff *Tetrahedron* **30** 1563 (1974)
230. H B Bürgi, J O Dunitz *Acc. Chem. Res.* **16** 153 (1983)
231. E L Muetterties *Tetrahedron* **30** 1595 (1974)
232. V I Minkin, L P Olekhnovich, Yu A Zhdanov *Molekulyarnyi Dizain Tautomernykh Sistem* (Molecular Design of Tautomeric Structure) (Rostov-on-Don: Izd. Rostov Univ., 1977)
233. L A Blyumenfel'd *Problemy Biologicheskoi Fiziki* (Problems of Biological Physics) (Moscow: Nauka, 1974)
234. J Watson *Molecular Biology of the Gene* (Translated into Russian; Moscow: Mir, 1978)
235. L Peusner *Concepts in Bioenergetics* (Translated into Russian; Moscow: Mir, 1977)
236. M Eigen, P Schuster *The Hypercycle. A Principle of Natural Self-Organisation* (Translated into Russian; Moscow: Mir, 1982)
237. L D Landau, E M Lifshits *Statisticheskaya Fizika* (Statistical Physics) (Moscow: Nauka, 1976)
238. W P Jencks *Catalysis in Chemistry and Enzymology* (Translated into Russian; Moscow: Mir, 1972)

Russian Chemical Reviews **63** (11) 905–922 (1994)
©1994 Russian Academy of Sciences and Turpion Ltd

UDC 535.37; 546.63

The application of luminescence-kinetic methods in the study of the formation of lanthanide ion complexes in solution

V L Ermolaev, E B Sveshnikova

Contents

I. Introduction 905
II. The rate constants for nonradiative transitions in lanthanide ions as an indicator of the structure of their environment 905
III. The application of nonradiative energy transfer between lanthanide ions in the study of complex formation 913
IV. A luminescence-spectroscopic method for the determination of the rates of rapid ligand exchange in lanthanide ion complexes in liquid solutions 917

Abstract. The mechanisms of the nonradiative transitions in lanthanide ions in solutions are discussed. The results of the use of this phenomenon in the study of the structures and stability constants of complexes of lanthanide ions in solutions are described. The possible uses of the nonradiative energy transfer between lanthanide ions in the determination of the stability constants of their complexes and for the detection of unstable dinuclear bridged complexes are considered. The luminescence-spectroscopic methods for the determination of the rates of rapid ligand exchange in lanthanide complexes in solutions are discussed. The bibliography includes 62 references.

I. Introduction

The luminescence-kinetic methods for the study of lanthanide complexes in solution have been increasingly widely used by investigators in recent years. This is due both to the ready accessibility of luminescence-kinetic apparatus to investigators (pulse type fluorimeters, pulse type tunable laser sources) and to the employment of Ln^{3+} as luminescence labels in biology and medicine.[1] The progress in the understanding of the mechanism of the quenching of the luminescence of Ln^{3+} ions has also played an important role.

This review deals with the following questions: the methods for the determination of the composition of the environment of the luminescent Ln^{3+} ion based on the measurement of its luminescence decay time; a version of the method involving the use of the phenomenon of the nonradiative energy transfer between ions; the study by the same method of unstable dinuclear bridged complexes; the luminescence-spectroscopic kinetic methods for the determination of the rates of rapid ligand exchange in lanthanide complexes.

The chemical properties of Ln^{3+} ions are known to be similar although not identical. On the other hand, their luminescence-spectroscopic properties differ greatly. This enables experimenters to select experimentally suitable ions and to carry out investigations involving them in a manner depending on the problem formulated. The greatest number of luminescence studies have been performed on Tb^{3+} and Eu^{3+} ions.[1,2] On the one hand, these ions have an appreciable luminescence quantum yield in most of the solvents used. On the other hand, the long-wavelength bands in the absorption spectra of these ions are located in the region where effective tunable dye-based lasers emit radiation, which is convenient for the experimenter. Yet another positive feature of the employment of these ions is the marked influence of the deuteriation of the surrounding molecules on the quantum yields and decay times of their luminescence, which makes it possible in many instances to obtain important information about the structure of the environment of the Ln^{3+} ion.

V L Ermolaev, E B Sveshnikova Laboratory of Luminescence and Photochemistry, Institute of Optical Instrument Making at the All-Russian Scientific Centre "Vavilov State Optical Institute", Birzhevaya liniya 12, 199034, St Petersburg, Russian Federation. Fax (7-812) 218 21 33

Received 11 July 1994
Uspekhi Khimii **63** (11) 962–980 (1994); translated by A K Grzybowski

II. The rate constants for nonradiative transitions in lanthanide ions as an indicator of the structure of their environment

1. Modern ideas about the mechanism of nonradiative transitions in lanthanide ions in solutions

Ln^{3+} ions luminesce not only in crystals and glasses but also in aqueous solutions.[3] However, only Gd^{3+}, Tb^{3+}, and Eu^{3+} luminesce with an appreciable yield in water. The luminescence yields of the remaining lanthanide ions in water are low. The luminescence yields of Ln^{3+} ions in various media obey the general rule governing nonradiative transitions. The probability of the latter is lower the greater the electronic energy of the quantum converted into the energy of the vibrational or translational motion and the lower the maximum energy of the vibrational quanta in the molecular groups surrounding the ion.[4]

The most important step towards the understanding of the mechanism of the nonradiative transitions in Ln^{3+} ions was taken by Krop and Windsor.[5] They observed an appreciable increase (by a factor of several tens) in the decay time (τ) in the quantum yield (q) of the luminescence of Eu^{3+} ions from the $^5D_0$ level and of the Tb^{3+} ions from the $^5D_4$ level on passing from an aqueous to a deuteriated solution. This effect was explained by the smaller number of high-frequency quanta of the stretching vibrations of the H_2O molecules ($\nu_3^H \approx 3400$ cm^{-1}) compared with D_2O ($\nu_3^D \approx 2250$ cm^{-1}) required for the law of conservation of energy to hold in the nonradiative transitions. It was also established that the rate constant for the nonradiative transition (k_{nr}) in the Eu^{3+} and Tb^{3+} ions varies linearly with the mole fraction of H_2O in the H_2O-D_2O mixture as the solvent. The linear dependence of k_{nr} for the ions on the fraction of OH groups in the mixture was confirmed by Gallagher[6] and Heller[7] and by the latter also for Dy^{3+} and Sm^{3+}. These facts indicate that the

Table 1. The luminescence decay times for lanthanide ions in ordinary and deuteriated water and in hydrated crystals.

Ion (emitting level)	Base	T/K	τ/μs	Ref.
Tb^{3+}	H_2O	293	475	11
($^5D_4$)	D_2O	293	4000	11
	$TbCl_3 \cdot 6H_2O$	298	485	8
	$TbCl_3 \cdot 6D_2O$	298	2390	8
	$Y(C_2H_5SO_4)_3 \cdot 9H_2O$ (10% Tb^{3+})	300	429	9
	$YCl_3 \cdot 6H_2O$ (10% Tb^{3+})	300	482	9
Eu^{3+}	H_2O	293	125	11
($^5D_0$)	D_2O	293	4000	11
	$EuCl_3 \cdot 6H_2O$	298	130	8
	$EuCl_3 \cdot 6D_2O$	298	1650	8
	$Eu(C_2H_5SO_4) \cdot 9H_2O$	300	116	9
	$Eu(C_2H_5SO_4) \cdot 9D_2O$	300	750	9
Dy^{3+}	H_2O	293	3	10
($^4F_{9/2}$)	D_2O	293	60	10
	$GdCl_3 \cdot 6H_2O$ (1% Dy^{3+})	293	4	10
	$GdCl_3 \cdot 6D_2O$	293	67	10

quenching effects of each O–H oscillator around the Ln^{3+} ion are independent of one another. These results permit a choice to be made betwen two models of the exchange of the electronic excitation energy quantum; exchange with excitation of an individual high vibrational state of the molecular group surrounding the lanthanide ion; exchange for a set of vibrations of several molecular groups.

A similar effect of deuteriation in hydrated crystals of lanthanide ion salts has been observed by other workers.[8–10] Their data are presented in Table 1, which shows that τ for the Ln^{3+} ions in the hydrated crystals is close to τ for aqueous solutions and that the change in τ on passing from protonated to deuteriated crystals is similar to its change on deuteriation of aqueous solutions. These findings agree well with the fact that the inner (first) sphere surrounding the Ln^{3+} ion consists of water molecules both in water and in crystals.

2. The inductive-resonance theory of nonradiative transitions in lanthanide ions

Ideas concerning the nonradiative transitions in lanthanide ions have been developed[11] on the basis of inductive resonance energy transfer from the excited Ln^{3+} ion to the surrounding molecular groups, with their excitation to higher vibrational states. Questions concerning the energy transfer from the Ln^{3+} ion to water molecules have been discussed in the studies mentioned above,[5,9] but the mechanism of the interaction, initiating the energy transfer step and permitting semiempirical calculations of the constant k_{nr}, was not specified in them. In other investigations,[11–13] it was postulated that the nonradiative transitions are caused by electromagnetic interactions between the oscillator corresponding to the radiative downward electronic or vibronic transition from the deactivating level and the oscillator of the vibrational transition in the groups surrounding the ion and involved in energy resonance with the electronic (vibronic) oscillator.[11–13] The energy level scheme explaining this model is presented in Fig. 1.

Thus the model mentioned above is close to the energy transfer model in Förster's theory[14] with the difference that the energy acceptor is a purely vibrational oscillator. As in Förster's model, it is postulated that the energy transfer step is followed by the rapid (compared with the rate of transfer) deactivation of the vibrational oscillator excited in the transfer process. This hypothesis has been

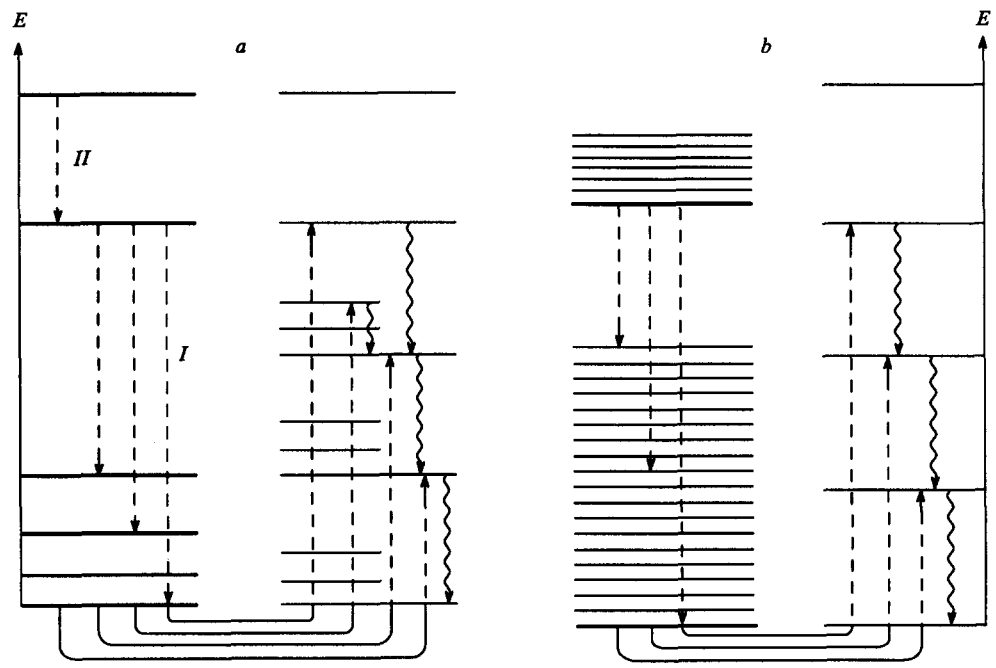


Figure 1. The energy level scheme explaining the inductive-resonance theory of nonradiative transitions: (*a*) weak vibronic linkage (Ln^{3+} ions) [(*I*) multiphonon nonradiative transition; (*II*) single-phonon nonradiative transition]; (*b*) strong (moderately strong) vibronic linkage (transition metal ions). The electronic (bold lines) and vibronic (thin lines) levels of the ions are shown on the left-hand sides of Figs *a* and *b*; the promoting-accepting vibrational levels of the molecules surrounding the ions are shown on the right; the vertical dashed lines designate the energy transfer inducing the nonradiative transition between the electronic levels of the ions and the excitation of the vibrational levels of the surrounding molecules.

confirmed experimentally in studies undertaken to estimate the rates of vibrational relaxation in solutions.[15] A further approximation, permitting specific calculations of the rate constants for nonradiative transitions, involves the selection of a multipolar interaction. In most cases, the treatment may be restricted to the approximation involving the interaction of electrical dipoles, as has been done in the derivation of Förster's familiar formula for the nonradiative electronic energy transfer between organic molecules.[14] Experimental confirmation of the possibility of using this approximation will be given below.

In the dipole–dipole approximation, the rate constant for the nonradiative transitions in the Ln^{3+} ions from the given excited level may be calculated provided the following features are known: the true luminescence spectrum (purely electronic or vibronic) associated with the transition from the given level to all the lower electronic levels of the given ion and the overall rate constant for emission from this level; the quantitative vibrational absorption spectra of the molecular groups, ligands, and solvent molecules surrounding the ion in the region of overlap with the luminescence spectrum of the ion; the distances from the ion to each molecular group responsible for the given vibrational absorption.

The expression for k_{nr} assumes the following form in this case:

$$k_{nr} = \sum \frac{8.8 \times 10^{-25} k_e \varkappa^2}{n^4 R_i^6} \int_0^\infty I^n(\nu)\, \varepsilon_i^{vibr}(\nu)\, \nu^{-4}\, d\nu , \qquad (1)$$

where k_e is the rate constant for the electrical dipole radiative transition from the given level to all the lower levels (s^{-1}), $\varkappa^2$ a coefficient which depends on the mutual orientation of the interacting dipoles (the average quantity $\overline{\varkappa^2} = 2/3$ is normally employed), n the refractive index of the medium, R_i the distance from the Ln^{3+} ion to the corresponding molecular groups (cm), $I^n(\nu)$ the luminescence spectrum, normalised for a unit area, emitted from the same level and expressed in terms of quantum intensities on the wave number ν scale (cm^{-1}), and $\varepsilon_i^{vibr}(\nu)$ the molar decadic vibrational absorption coefficient in the main and overtone regions for the molecular groups responsible for the absorption bands overlapping with the luminescence spectrum.

Naturally it is almost impossible to take into account all the molecular groups surrounding the Ln^{3+} ion in solution and even their position relative to the ion is usually not known exactly. However, one should bear in mind that the strongest interactions inducing the nonradiative transition involve groups adjoining directly the Ln^{3+} ions, i.e. located in the inner coordination sphere. Such molecular groups usually make the greatest contribution to k_{nr}. Only in the absence from the inner coordination layer of vibrating molecular groups capable of initiating the nonradiative transition, for example owing to the smallness of the vibrational quantum, is it necessary to take into account the influence of the second and more remote layers of molecular groups surrounding the ion as the main contribution to k_{nr}.

In many cases, it is useful to take into account only the first (inner) ordered sphere comprising molecules surrounding the ion [Eqn (1)], while the more remote molecules can be regarded as a continuous medium. The influence of remote molecules is taken into account by using the formula derived by Galanin and Frank[16] for the decay of a dipole in the absorping medium

$$k'_{nr} = \frac{k_e}{16\pi^4 n^4 a^3} \int_0^\infty I^n(\nu)\, \alpha(\nu)\, \nu^{-4}\, d\nu , \qquad (2)$$

where a is the radius of the sphere around the ion in which there are no oscillators absorbing the emission from the Ln^{3+} ion and $\alpha(\nu)$ is the linear absorption coefficient of the solvent (cm^{-1}). When account is taken of the effect of the molecules (groups) in the inner sphere of the ion in accordance with Eqn (1), a is the size of the inner sphere and the contribution of the remaining molecules outside the inner sphere is calculated by Eqn (2) in terms of the continuous medium approximation.

Calculations by Eqns (1) and (2) make it possible to take into account the influence on the nonradiative transitions by a factor such as the vibronic interaction in terms of the vibronic component of the luminescence spectrum. The vibronic spectra of Ln^{3+} ions usually have a low intensity and in most cases hardly affect k_{nr}. They can improve the resonance conditions if the narrow absorption bands of C–H group type do not overlap with the narrow band due to the electronic transition in the Ln^{3+} ion. However, in the calculation of k_{nr} for transition metal ions, characterised by extensive vibronic spectra, the overlap of the vibrational absorption spectra with the latter is in most cases decisive. As shown in a theoretical study,[17] it is then important to divide the vibrations into two types: vibrations contributing to the vibronic luminescence spectrum (accepting vibrations) and vibrations the absorption spectrum of which in the region of the main frequencies or overtones overlaps with the luminescence spectrum (promoting-accepting vibrations), since they initiate the nonradiative transition and accept part of the energy. Another component of the exchanging electronic energy quantum is accepted by the vibrations active in the vibronic spectrum. The vibronic levels illustrating this approach are presented schematically in Fig. 1.

Within the framework of this approach, the anharmonicity of the vibrations is taken into account: automatically, since for a multiphoton nonradiative transition the luminescence spectrum $I^n(\nu)$, included in Eqns (1) and (2), largely overlaps with the vibrational spectrum in the region of the overtones and compound frequencies, the latter spectrum being determined by the anharmonicity of the promoting-accepting vibrations of the molecular groups surrounding the ion.

We shall now consider how the inductive-resonance theory of nonradiative transitions agrees with the experimental decay times and luminescence quantum yields for Ln^{3+} ions in solutions and other media obtained by the present authors and available in the literature. The decay time of the luminescence of Ln^{3+} ions with an energy gap $20\,000 \geqslant \Delta E \geqslant 4000-5000$ cm^{-1} depends greatly on the replacement of protium atoms by deuterium atoms in the molecular groups located in the vicinity of the ion. The effect of deuteriation is undoubtedly associated with the change in the rate of the nonradiative transitions because the luminescence yield varies in parallel with τ and there are no physical grounds for such a sharp increase in the emission rate constant on deuteriation. From the standpoint of the inductive-resonance theory of nonradiative transitions, the influence of deuteriation is determined by the sharp change in the vibrational absorption owing to the decrease in the stretching vibration frequencies when H is replaced by D. Fig. 2 (see next page) presents the luminescence spectrum of Dy^{3+} in D_2O and the vibrational absorption spectra of H_2O and D_2O and of H_2O in a $GdCl_3.6H_2O$ crystal. Comparison of the luminescence (Fig. 2a) and absorption (Figs 2*b* and 2*c*) spectra of H_2O and D_2O shows that in the case of D_2O the overlap integral in Eqns (1) and (2) is many times smaller than in the case of H_2O.

Comparison of the overlap integrals of the spectra in Eqns (1) and (2) for the usual and deuteriated compounds makes it possible to calculate, provided that the luminescence and vibrational absorption spectra are known, the influence of deuteriation on the nonradiative transition rate constant for the given ion and its environment. Table 2 shows that, for the majority of Ln^{3+} ions, the effect of the deuteriation of the molecules surrounding the ion can be calculated by Eqns (1) and (2) with satisfactory accuracy. Table 2 also presents the experimental luminescence decay times

$$\tau = (k_e + k_{nr})^{-1} ,$$

where k_e is the rate constant for the emission from the given level of the ion and k_{nr} is the rate constant for the nonradiative transition from the same level. Since k_e does not change on deuteriation of the molecules surrounding the ion and only k_{nr} is altered, the dependence of τ on deuteriation for different energy gaps is as follows: for large gaps, $\Delta E \approx 30\,000$ cm^{-1} (for example, for

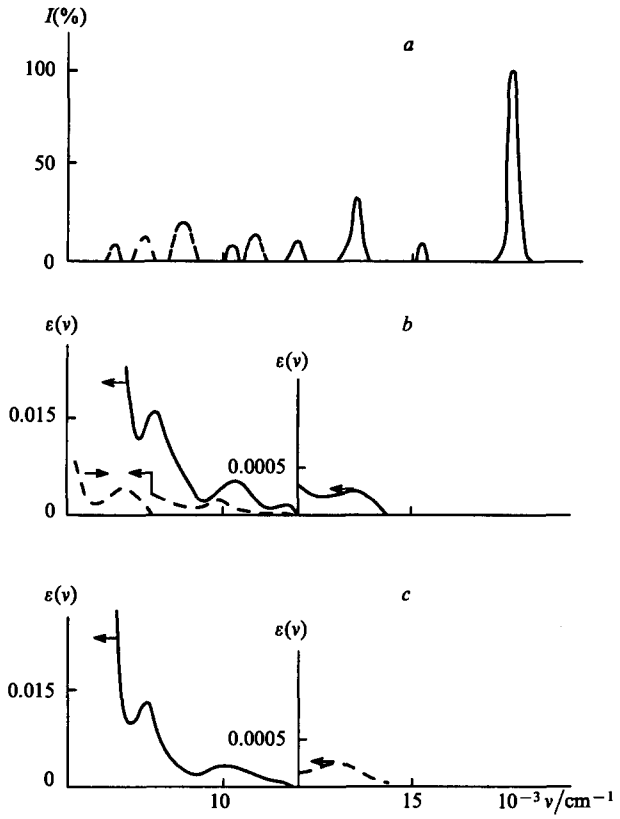


Figure 2. Luminescence spectra of the Dy^{3+} ion in D_2O (*a*) (the luminescence bands, the scale of which has been increased by a factor of 10, are shown by a dashed line), the absorption spectra of H_2O (continuous line) and D_2O (dashed line) in solution (*b*), and the spectra of H_2O in the $GdCl_3.6H_2O$ crystal (*c*) at 293 K.

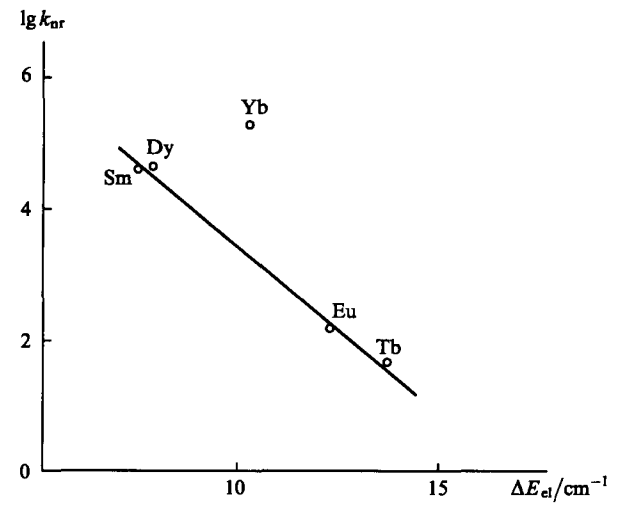


Figure 3. Dependence of the rate constant for the nonradiative transitions from the resonance levels of the Ln^{3+} ions in methanol-d_1 (293 K) on the difference between the energies of the emitting level and the lower level closest to it.

Gd^{3+}), the constant k_{nr} varies by many orders of magnitude, but τ is almost independent of deuteriation because in this region $k_e \geqslant k_{nr}$, so that $\tau \approx k_e^{-1}$. For gaps of medium size, $\Delta E = 20\,000-4000$ cm^{-1}, the constant k_{nr} depends less on deuteriation, but in this region $k_{nr} \geqslant k_e$ and τ increases markedly on deuteriation of the molecules surrounding the ion [$Eu^{3+}(^5D_0)$, $Yb^{3+}(^2F_{5/2})$, $Dy^{3+}(^4F_{9/2})$, $Nd^{3+}(^4F_{3/2})$]. In the region $\Delta E \leqslant 4000$ cm^{-1}, where $k_{nr} \gg k_e$ (for surrounding groups with H and D atoms), the dependence of k_{nr} and τ on such groups is determined by the overlap of the structural luminescence spectrum of the Ln^{3+} ion with the vibrational absorption spectrum, and may vary from a very large value for Er^{3+} ($^4I_{11/2}$) in water to low values for $Er^{3+}(^4I_{11/2})$ and $Pr^{3+}(^3P_0)$ in dimethyl sulfoxide, and even to an absence of the influence of deuteriation in $Eu^{3+}(^5D_1)$.

In this region, there is also the possibility of the opposite effect of deuteriation — a decrease in τ in deuterium-containing molecules.

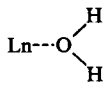
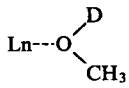
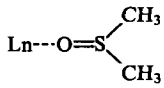
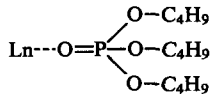
For Ln^{3+} ions surrounded by particular groups in the case where the nonradiative transition is of the multiphonon type, i.e. $\Delta E_{el} \geqslant 2h\nu_{vibr}^{max}$, a nearly inverse exponential dependence of k_{nr} on the energy gap ΔE_{el} between the emitting level and the nearest lower level is observed. Such an exponential dependence of k_{nr} on ΔE_{el} can be explained by the fact that the intensity of the overtones of the vibrational transitions diminishes approximately in a geometrical progression with increase in the number of the overtone.[18]

From the standpoint of the inductive-resonance theory of nonradiative transitions, the inverse exponential dependence of k_{nr} on ΔE for multiphonon transitions is a special case of a more general relation — the proportionality of k_{nr} to the overlap integral between the luminescence spectrum of Ln^{3+} ions and the vibrational absorption spectrum of the molecules surrounding the ion for an approximately constant k_e and a constant distribution of the quantum intensity in the luminescence spectrum. Fig. 3 illustrates such a relation. The appreciable deviation of the k_{nr} for ytterbium is due to the fact that an intense luminescence is observed for this ion in the region of the long wavelength band, whereas for the remaining ions (Sm^{3+}, Dy^{3+}, Eu^{3+}, and Tb^{3+}) the long wavelength bands constitute a small proportion of the overall luminescence intensity (see, for example, Fig. 2).

Table 2. The experimental constants k_{nr} (I) and their values calculated by Eqns (1) and (2) (II) for lanthanide ions in ordinary and deuteriated solvents.

Ln^{3+}	Transition	ΔE^{min}/cm^{-1}	Solvent	k_{nr}^H/k_{nr}^D		τ^D/τ^H	
				I	II	I	II
Eu^{3+}	$^5D_0-{}^7F_i$	12150	H_2O; D_2O	48	38	33	–
Yb^{3+}	$^2F_{5/2}-{}^2F_{7/2}$	10300	H_2O; D_2O	25	55	25	55
Dy^{3+}	$^4F_{9/2}-{}^6F_i$, ^6H_j	7000	H_2O; D_2O	20	18	20	18
Nd^{3+}	$^4F_{3/2}-{}^4I_i$	5000	H_2O; D_2O	5.0	9.0	5.0	9.0
Er^{3+}	$^4I_{11/2}-{}^4I_{13/2}$	3600	H_2O; D_2O	100	80	100	80
	$^4I_{11/2}-{}^4I_{13/2}$	3600	$(CH_3)_2SO$; $(CD_3)_2SO$	4.5	3.0	3.0	4.5
Pr^{3+}	$^3P_0-{}^1D_2$	3500	$(CH_3)_2SO$; $(CD_3)_2SO$	3.0	5.0	3.0	5.0
Eu^{3+}	$^5D_1-{}^5D_0$	1750	$(CH_3)_2SO$; $(CD_3)_2SO$	1.0	–	1.0	–

Table 3. Dependence of k_{nr} on the distance from the Ln^{3+} ion to the promoting-accepting vibrational oscillators.

Structural fragment of complex (Ln–O distance/Å)	$Dy^{3+}(^4F_{9/2})$			$Yb^{3+}(^2F_{5/2})$		
	$10^4 k_{nr}/s^{-1}$	$k_{nr}a^3$	$k_{nr}a^5$	$10^4 k_{nr}/s^{-1}$	$k_{nr}a^3$	$k_{nr}a^5$
 (2.2; 2.5)[a]	33	[b]	[b]	590	[b]	[b]
 (3.6; 3.9)[a]	5.0	3.0[c]	4.5[c]	22	10.0[c]	1.3[c]
 (5.0; 5.3)[a]	2.5	3.7	10.5	5.5	6.9	1.7
 (6.0; 6.3)[a]	1.5	3.8	15	4.5	9.7	3.5

[a] Here and henceforth the larger distance refers to Dy^{3+} and the smaller distance to Yb^{3+}.
[b] Aqueous solutions have not been included in the comparison column because the vibration frequency of the OH group differs appreciably from that of the CH group.
[c] Relative units.

According to the inductive-resonance theory of nonradiative transitions, for the interaction of the electrical dipoles in the Ln^{3+} ion and the ligands surrounding it [electrical dipoles comprising the Ln^{3+} ion and the ligand surrounding it?], the contribution to k_{nr} is inversely proportional to the sixth power of the distance between them. The electromagnetic interactions inducing the nonradiative transitions are universal and should be independent of the presence or absence of chemical bonds between them and the molecular group involved in the exchange.

Having postulated the occurrence of the dipole–dipole interaction, we compared the experimental and theoretical dependences of k_{nr} on the distances between the Ln^{3+} ion and the OH and CH groups most active in the exchange process. Eqn (2) was used for this purpose; the absorbing medium was assumed to be continuous and the dependence on the distance was expressed in terms of a sphere with a radius a. It was assumed that in the sphere there are no molecular groups with high frequency vibrations inducing the exchange of the electronic energy of the ion. Table 3 presents the values of k_{nr} for Dy^{3+} and Yb^{3+} in various solvents for increasing distances between the CH groups and the ion and the products $k_{nr}a^3$, which should remain constant if the electrical dipoles interact and hence Eqn (2) is valid. The products $k_{nr}a^5$, which would have remained constant if the interaction responsible for the nonradiative transition had been determined by the interaction between an electrical quadrupole and a dipole, i.e. if the formula for k_{nr} assumed the form

$$k_{nr}^q = \frac{9k_e}{32\pi^6 n^6 a^5} \int I^n(\nu)\,\alpha(\nu)\,\nu^{-6}\,d\nu,$$

are also presented.

The long-range and nonchemical nature of the interactions responsible for the nonradiative transitions in Ln^{3+} ions is confirmed by the influence on $\tau(k_{nr})$ by the solvent ion in the outer sphere of a bulky complex such as $Ln(NO_3)_3(TBP\text{-}d_{27})_3$ (here TBP-d_{27} is fully deuteriated tri-n-butyl phosphate).

Table 4 presents the values of τ and k_{nr} for lanthanide ion complexes with nitrate anions and the usual and fully deuteriated tri-n-butyl phosphate dissolved in CCl_4 and toluene-h_8. Toluene-h_8 is at a distance greater than 6 Å from the Nd^{3+} and Sm^{3+} ions and is not linked to them by any chemical bonds. However, it does affect appreciably τ and hence k_{nr} for the given ions.

The results of the study of the luminescence of the Dy^{3+} ion in the usual and fully deuteriated acetonitrile may be regarded as yet another confirmation of the inductive-resonance theory of nonradiative transitions. The point is that the frequency of the stretching vibration of the C≡N, group adjoining directly the Dy^{3+} ion (2254 cm^{-1}) is close to the stretching vibration frequency of the C–D bond (2257 cm^{-1}). It may be expected that τ for the Dy^{3+} ion in fully deuteriated acetonitrile is appreciably smaller than in the fully deuteriated dimethyl sulfoxide and acetone because the stretching vibration frequencies of the S=O and C=O groups are appreciably lower. However, measurements have shown that τ = 320 μs for Dy^{3+} in CD_3CN.[20] The value τ = 13.3 μs for Dy^{3+} in CD_3CN quoted by Haas et al.[19] is undoubtedly erroneous owing to the presence of the water impurity in this solution, the amount of which was not

Table 4. The influence of the outer-sphere solvent on τ and k_{nr} for the complexes $Ln(NO_3)_3(TBP)_3$ at 293 K.

Complex	τ/μs		k_{nr}/s^{-1}	
	toluene-h_8	CCl_4	toluene-h_8	CCl_4
$Nd(NO_3)_3(TBP\text{-}h_{27})_3$	2.1	3.0	4.8×10^5	3.3×10^5
$Sm(NO_3)_3(TBP\text{-}d_{27})_3$	350	1100	2.5×10^3	6×10^2
$Sm(NO_3)_3(TBP\text{-}h_{27})_3$	–	130	–	7.7×10^3
$Eu(NO_3)_3(TBP\text{-}d_{27})_3$	–	1600	–	0
$Eu(NO_3)_3(TBP\text{-}h_{27})_3$	1600	1600	0	0

Table 5. The energy and kinetic parameters and the decay times of the luminescence of lanthanide ions (μs) in solutions of the nitrate salts of the ions at 293 K.[1,10–13,20]

Parameter, solvent	Tb^{3+}	Eu^{3+}	Dy^{3+}	Sm^{3+}	Yb^{3+}	Eu^{3+}
	$^5D_4-\sum_i^6 {}^7F_i$	$^5D_0-\sum_i^6 {}^7F_i$	$^4F_{9/2}-\sum_{i,j} {}^6F_i, H_j$	$^4G_{5/2}-\sum_{i,j} {}^6F_i, H_j$	$^5F_{5/2}-{}^2F_{7/2}$	$^4I_{11/2}-{}^4I_{13/2}$
Parameters						
$\Delta E_{el}^{min}/cm^{-1}$	14800	12150	7850	7400	10300	3650
k_e/s^{-1}	100–550	70–600	750–2500	710–2000	2500	–
Decay times in						
H_2O	475	125	3	3	0.17	0.00012
D_2O	4000	4000	60	75	4.25	0.012
CH_3OH	1240	390	9	10.5	0.9	–
CD_3OH	1330	415	12	16	–	0.00077
CH_3OD	2600	2200	20	22	4.5	–
CD_3OD	3000	3300	150	175	12.5	0.033
$(CH_3)_2SO$	2600	1400	40	18	18	0.04
$(CD_3)_2SO$	–	–	235	255	149	0.18
$(CH_3)_2CO$	1200	1350	74	–	–	–
$(CD_3)_2CO$	–	–	235	–	–	–
CH_3CN	1900	1350	80	–	–	–
CD_3CN	–	–	320	–	–	–
$(C_3H_7O)_3PO$	1800	1600[a]	100[a]	130[a]	22	–
$(C_3D_7O)_3PO$	1800	1600[a]	500[a]	1100[a]	–	–
$POCl_3+SnCl_4$	–	3900	1300	2700	–	–

[a] Solution of the $Ln(NO_3)_3(TBP)_3$ complexes in CCl_4.

determined. The value of τ which we measured is greater by a factor of ~ 1.5 than τ for the Dy^{3+} ion in dimethyl sulfoxide-d_6 (235 μs) and acetone-d_6 (235 μs) and is twice as great as τ in fully deuteriated methanol (150 μs). This finding has been explained in a study[20] where it was shown, by comparing the IR spectra of the usual and deuteriated acetonitrile, that the anharmonicity of the vibrations and the intensity of its overtones are small for the C≡N bond, which has an intense absorption band at 2254 cm^{-1}. On the other hand, the C–D vibrations, for which the intensity in the region of the main frequency is smaller compared with the C≡N vibration, become the principal vibrations, determining the absorption spectrum, in the region of overtones owing to the greater anharmonicity. Consequently, they make the greatest contribution to the overlap integral with the Dy^{3+} luminescence spectrum and hence they make the main contribution to k_{nr} for the Dy^{3+} ion despite the greater distance from the latter. This is fully consistent with experimental data.

In conclusion, it is essential to discuss the errors in the calculations of k_{nr} in accordance with the inductive-resonance theory. Firstly, owing to the rapid liquid exchange with the surrounding groups, an average pattern is observed in the liquid solutions and $\bar{\tau}$ may be made up of the times τ for the rapidly varying different conformations of the environment of the ion. So long as the exchange time is shorter than τ, the decay is exponential. If the ligand exchange time becomes greater than or equal to τ, the decay of the luminescence is nonexponential because each form of the complex decays with its own τ. The ligand exchange time for Ln^{3+} ions in water is of the order of 10^{-7} s.[21] Thus, if different complexes coexist in solution, a nonexponential decay of the luminescence will be observed for times shorter than 100 ns.

The next source of error in the calculations of k_{nr} is the inaccurate knowledge of the mutual disposition of the ligands and the ion, especially in liquid solutions. Yet another source of error consists in the fact that in most cases the spectrum of the pure solvent and not of the molecules directly coordinated to the Ln^{3+} ion is adopted as the vibrational absorption spectrum. The spectra of the directly coordinated molecules, especially of the OH groups of water or alcohols where the oxygen atom is linked directly to the Ln^{3+} ion, differ in the frequencies and anharmonicity of the vibrations, which undoubtedly introduces a definite error into the calculation of k_{nr}. In a number of instances no account is taken of the mutual orientation of the dipole moment of the electronic transition of the ion and of the vibrational absorption in the surrounding groups because the average value $\varkappa^2 = 2/3$ is used in Eqn (1). The quantity k_e in Eqns (1) and (2) introduces an appreciable error into the calculations of k_{nr} especially when its experimental determination is difficult and it is necessary to employ the value calculated by the Judd–Offelt method. Nevertheless, comparison of the experimental and theoretical values of k_{nr} in water and hydrated crystals shows that, even for water, the variations in frequencies and anharmonicity do not play a decisive role in the calculations of k_{nr}.

Yet another doubt is associated with the size of the interacting dipoles and with the possibility of using an expansion in powers of the distance between the ion and the promoting-accepting groups. However, one should note that the size of the emitting dipole is less than 0.6 Å, i.e. is smaller than the size of the 4*f* shell of the Ln^{3+} ions; the size of the dynamic oscillator in the high frequency vibration is close to the amplitude of the displacement of a light atom, i.e. $b = (2\hbar/m\omega)^{1/2} \approx 0.1$ Å, while the distance between the interacting centres is greater than 2.4 Å.[22] Thus the conditions used in the derivation of Eqn (1) are satisfied.

Table 5 presents the luminescence decay times for the most frequently used Ln^{3+} ions in various solvents. The results of the interpretation of these data are presented in Table 6. They represent estimates of the contributions to k_{nr} by various molecular groups at different distances from the Ln^{3+} ion for six such ions. The estimates are naturally fairly approximate because in most cases we are dealing with the overall influence on k_{nr} of the inner and more remote spheres surrounding the ion. By replacing the molecules in the inner sphere, we as a rule alter simultaneously the absorption by the entire remaining mass of the solution and hence its contribution to k_{nr}. Furthermore, in order to estimate the contribution of an individual molecular group, it is necessary to know as exactly as possible the number of molecular groups in the inner coordination sphere of the ion, which is not always available.

Table 6. Approximate estimates of the contributions of the molecular groups located at different distances from the Ln^{3+} ions to k_{nr}/s^{-1} according to different data.[1,2,11-13,21-29]

Ln^{3+}	Level	O–H 2.2–2.5 Å	N–H 2.2–2.5 Å	CH_3 3.6–3.9 Å	CH_3 5.0–5.3 Å	C_3H_7 6.0–6.3 Å	C–D 2.2–2.5 Å
Tb^{3+}	$^5D_4$	100–200	70	12	–	–	–
Eu^{3+}	$^5D_0$	400–500	800–1000	40	–	–	10
Dy^{3+}	$^4F_{9/2}$	20000	–	9000	1700	900	1000
Sm^{3+}	$^4G_{5/2}$	18000	–	9000	4300	750	700
Yb^{3+}	$^4F_{5/2}$	3.5×10^5	–	36000	6000	5000	1.3×10^4
Er^{3+}	$^4I_{11/2}$	$(3-5) \times 10^8$	–	–	3.3×10^6	–	5×10^6

This quantity is influenced also by the change in the emission rate constant when the groups surrounding the Ln^{3+} ions are altered. The estimates of the contributions to k_{nr} by the first and all the remaining spheres based on Eqn (2) in terms of the dipole–dipole approximation for water molecules yield ~7:1 if the distances to the first and second coordination spheres are assumed to be 2.36 and 4.50 Å respectively (according to X-ray diffraction data[22]).

3. Determination of the stability constants of lanthanide ion complexes in liquid solutions by the method of nonradiative transitions

In one of the first studies devoted to the influence of the deuteriation of the solvent on the intensity (I) and decay time of the luminescence of Ln^{3+} ions, Kropp and Windsor[5] turned their attention to the dependence of τ and I on the presence of the anions of various acids in water and on the pH of the medium. In another study,[27] they were the first to suggest that the number of molecular OH groups attached directly to the Ln^{3+} ions and exhibiting high frequency vibrations be estimated from the changes in τ and I on complex formation. Here use was made of the property involving the independent effect of each oscillator on the deactivation of the ion (linear dependence of k_{nr} on the concentration of OH groups in the solution).

Kropp and Windsor[27] measured the dependence of the decay times of the luminescence of the Eu^{3+} and Tb^{3+} ions dissolved in ordinary and deuteriated water on the $KOOCCH_3$ and $KOOCCD_3$ concentrations (0–5 M). For the same concentrations of acetate and lanthanide ions, it is possible to formulate the following expression for the difference between the reciprocals of the luminescence decay times in ordinary and deuteriated water:

$$(\tau^H)^{-1} - (\tau^D)^{-1} = m(k_{nr}^{H_2O} - k_{nr}^{D_2O}) + \{k_e^H([Ac^-]) - k_e^D([Ac^-])\},$$

where m is the number of water molecules in the inner sphere of the ion at the given acetate concentration and $k_{nr}^{H_2O}$ and $k_{nr}^{D_2O}$ are the rate constants for the nonradiative transitions in the Ln^{3+} ions induced by H_2O and D_2O molecules respectively. The second expression in brackets on the right-hand side of the equation is zero because the constants k_e for the Ln^{3+} ion are the same in H_2O and D_2O in the presence of identical acetate concentrations. The estimation of the contribution by one water molecule to the quenching constant yielded the following results (k_{nr}/s^{-1}):

$$k_{nr}^{H_2O} = 9400/m_s; \quad k_{nr}^{D_2O} = 370/m_s;$$

for Eu^{3+} and

$$k_{nr}^{H_2O} = 2200/m_s; \quad k_{nr}^{D_2O} = 275/m_s,$$

for Tb^{3+}, where m_s is the number of water molecules in the inner hydration shell of the ion when no other ligands are present in it. Kropp and Windsor suggested that $k_{nr}^{H_2O}$ and $k_{nr}^{D_2O}$ are independent of the acetate concentration. From our point of view, this is incorrect, since according to Eqn (1) $k_{nr}^{H_2O}$ and $k_{nr}^{D_2O}$ are proportional to k_e and the latter constants for Eu^{3+} and Tb^{3+} have been shown by Kropp and Windsor themselves to depend on the concentration of acetate ions.

Later Horrocks and coworkers[2,28,29] used this method to determine the number of water molecules involved in complexes of Ln^{3+} ions, in particular in complexes of interest to biologists. The number of coordinated water molecules was determined from the formula

$$m = \frac{(\tau^H)^{-1} - (\tau^D)^{-1}}{k_{nr}^{H_2O}(Ln)},$$

where $k_{nr}(Eu) = 952\ s^{-1}$ and $k_{nr}(Tb) = 238\ s^{-1}$. A linear dependence of $(\tau^H)^{-1} - (\tau^D)^{-1}$ on the number of water molecules in the first coordination spheres of various complexes, determined from X-ray diffraction data, was observed. However, in our view, in this case too it is necessary to introduce a correction for the change in k_e and for the intensity distribution in the Ln^{3+} luminescence spectra, especially for the longest-wavelength bands.

In view of the foregoing, we believe it is more correct to use the luminescence decay time as an indicator in the method of corresponding solutions (as has been done by Gruzdev and Ermolaev[30]) rather than employing it directly to estimate the number of water molecules or other ligands in the first coordination sphere (as suggested by Kropp and Windsor and also by Horrocks). It is known[21] that ligand exchange in solution is fairly rapid for the majority of Ln^{3+} ion complexes compared with the decay times of the luminescence of ions exhibiting appreciable yields. In this case, the decay of the luminescence is exponential and the rate constant for the decay of the excited state of the Ln^{3+} ion is defined by the following expression:

$$\bar{k} = \bar{\tau}^{-1} = \frac{\sum_{n=0}^{N} \tau_n^{-1} \beta_n^* [L]^n}{\sum_{n=0}^{N} \beta_n^* [L]^n}, \quad (3)$$

where τ_n is the decay time of the luminescence of the corresponding complex, β_n^* the overall stability constant of the complex with n ligands and with the ion in the excited state, and [L] the equilibrium concentration of the free ligand. The rate constant for the decay of the excited state of the ion is the sum of two components: the emission rate constant and the rate constant for the nonradiative transitions. Both constants depend on the composition of the complex, but in the majority of cases the change in k_{nrn} when the structure of the complex is altered is appreciably greater than the change in k_{en}. Taking into account the data in Tables 5 and 6 and knowing the structure of the substituting and substituted ligands, it is possible to estimate the change in k_{nrn} following substitution for different Ln^{3+} ions. If k_{nr} changes little after substitution of, for example, an acetone molecule by a dimethyl sulfoxide molecule at Ln^{3+}, the sensitivity of the method can be increased sharply by employing as one of the ligands the fully deuteriated molecule,

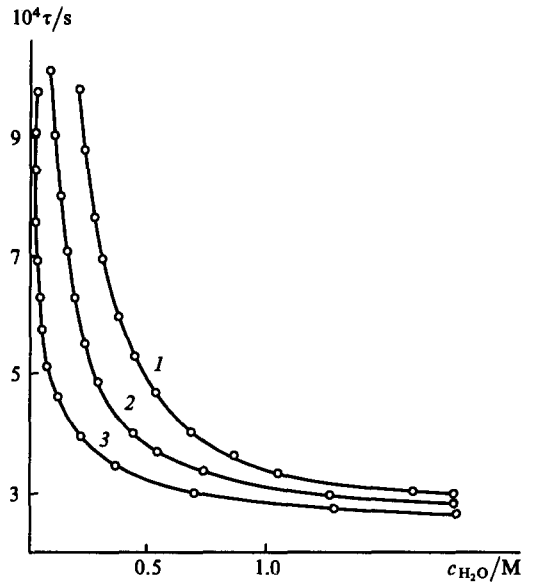


Figure 4. Dependence of the decay time of the luminescence of a europium nitrate solution in acetone on the overall concentration of water at 293 K; c_{Eu}/M: (*1*) 0.18; (*2*) 0.09; (*3*) 0.01.

i.e. $(CD_3)_2CO$ and $(CD_3)_2SO$ or conversely. One should then take into account the isotope exchange rate of hydrogen or deuterium.

As can be seen from Eqn. (3), the quantity $\bar{k}$ ($= \tau^{-1}$) is a function of the equilibrium free ligand concentration [L] only. Experiment showed that this function is unambiguous. In this case, it is possible to use the method of corresponding solutions for the determination of the stability constants.[31] The method has been used[30] to determine the stability constants of the Eu^{3+} complexes of water in acetone. Fig. 4 presents a series of curves reflecting the dependence of τ on the water concentration in dry acetone. Taking into account the material balance equation

$$c_L = \bar{n}c_{Eu} + \bar{n}^* c^*_{Eu^*} + [L], \qquad (4)$$

where c_L and [L] are the overall and equilibrium ligand concentrations respectively and $\bar{n}$ and $\bar{n}^*$ are the average numbers of ligands attached to the unexcited and excited ions, as well as the fact that in luminescence measurements the concentration of unexcited ions is always several orders of magnitude higher than that of excited ions, i.e. $c_{Eu} \gg c^*_{Eu^*}$, the second term on the right hand side of Eqn (4) may be neglected. The formation constant for the $Eu-H_2O$ system in acetone was determined with the aid of the curves presented in Fig. 4 and of Eqn (4). It is illustrated in Fig. 5. We emphasise that this expresses $\bar{n}$ as a function of [L] for unexcited Eu^{3+} ions, so that it may be compared with the results of traditional chemical methods.

Having a set of values $\bar{n}$ and [L], it is possible to calculate the stability constants of the complexes from the expression

$$\bar{n} = \frac{\sum n\beta_n[L]^n}{\sum \beta_n[L]^n}.$$

The calculation has been carried out by the least squares method (LSM) for three-ligand and four-ligand types of complexes. More accurate values were obtained for four-ligand types (i) of complexes.[30]

i	$\beta_i \times 10^{-(n+2)}/(\text{mol dm}^{-3})^i$	$K_i/(\text{mol dm}^{-3})^i$
1	1.27 ± 0.2	1.27 ± 0.2
2	5.6 ± 0.6	44.1 ± 8.6
3	4.4 ± 0.8	7.9 ± 1.6
4	5.9 ± 0.9	1.34 ± 0.4

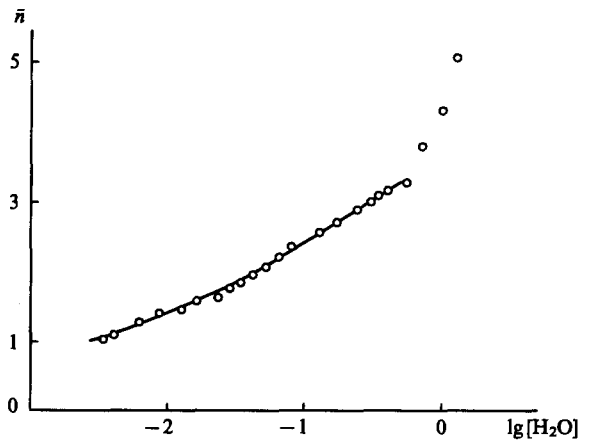


Figure 5. Dependence of the average number of water molecules in the first coordination sphere of the Eu^{3+} ion (europium nitrate solution in acetone) on the free ligand concentration [H_2O] at 293 K.

In the range $\bar{n} \geqslant 3$, the function $\bar{n} - \lg[H_2O]$ exhibits a sharp break (Fig. 5). It has been suggested that the displacement of the anion NO_3^- by water begins following an increase in the concentration of water in acetone and after the incorporation into the first coordination sphere of Eu^{3+} of more than three water molecules. The appearance in solution of free NO_3^- anions (a complex forming agent of the second type), which compete with Eu^{3+} for water molecules, is not taken into account in the method of corresponding solutions, so that the method yields unduly high values of $\bar{n}$ in this region.

This hypothesis that water displaces the NO_3^- anion for $\bar{n} \geqslant 2.5-3.0$ has been tested[30] by the energy transfer luminescence method. The dependence of the average rate of energy transfer from Eu^{3+} to Nd^{3+} in acetone on the average number of water molecules around Eu^{3+} is illustrated in Fig. 6. The concentration of Eu^{3+} (0.19 M) was 19 times greater than that of Nd^{3+} (0.01 M), which made it possible to use the values of $\bar{n}$ obtained above. For $\bar{n} = 2.5-3.0$, a sharp decrease in k'_t begins owing to the appearance of Coulombic repulsion between the complexes of the donor Eu^{3+} and the acceptor Nd^{3+} when their NO_3^- anions are substituted by water molecules. Therefore, only the values of $\bar{n} \leqslant 2.9$ were used in the calculation of the stability constants.

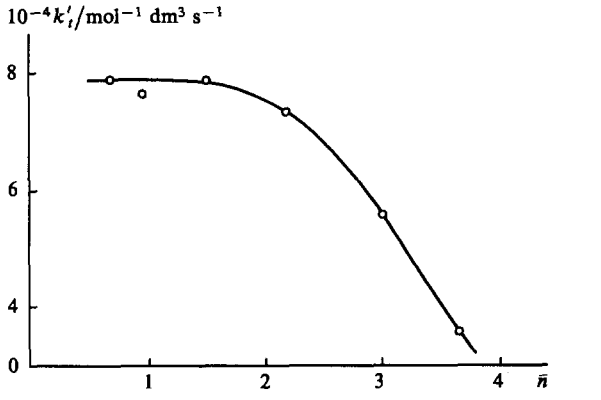


Figure 6. Dependence of the average rate constant for the energy transfer from europium to neodymium in acetone on the average number of water molecules in the first coordination sphere of Eu^{3+}. $c_{Eu} = 0.19$ M; $c_{Nd} = 0.01$ M.

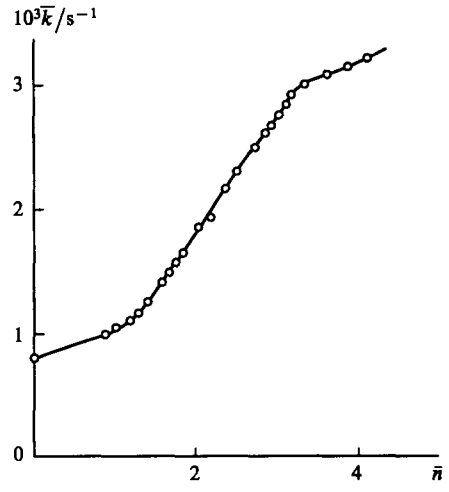


Figure 7. Dependence of the average rate constant for the deactivation of excited Eu^{3+} ions in acetone on the average number of water molecules in the first coordination sphere of the Eu^{3+} ion.

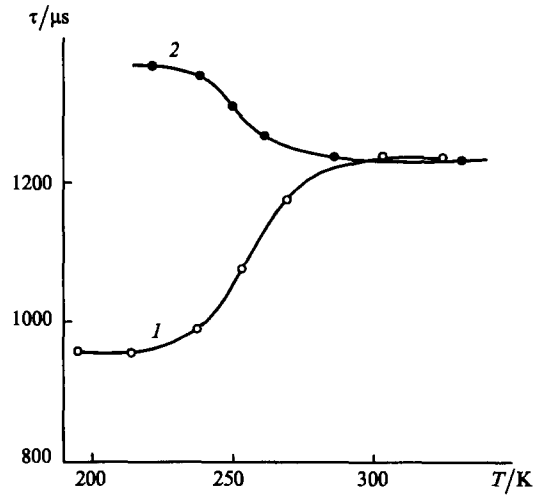


Figure 8. Temperature dependence of the decay time of the $Eu(NO_3)_3$ luminescence (c_{Eu} = 0.01 M) in partly dried acetone: (*1*) with added H_2O ($c_{H_2O} < c_{Eu}$); (*2*) with added D_2O ($c_{D_2O} < c_{Eu}$).

Fig. 7 presents the dependence of the average rate constant $\bar{k} = \bar{\tau}^{-1}$ for the deactivation of Eu^{3+} ions in acetone on the average number of water molecules $\bar{n}$ in the first coordination sphere of the ion. In the range of values of $\bar{n}$ from 1 to 3, the dependence of $\bar{k}$ on $\bar{n}$ is nearly linear. This shows that the emission constant k for complexes containing between one and three water molecules is invariant.

The luminescence-kinetic method also makes it possible to investigate the influence of the change in temperature on the structure of the environment of lanthanide ions in liquid solutions. It has been observed[32,33] that the decay times of the luminescence of Eu^{3+} and Tb^{3+} in weakly donating (according to Gutmann) solvents (acetonitrile, acetone, and ethyl acetate) increase with increase in temperature, in contrast to the usually observed temperature-induced quenching of the luminescence. On the other hand, in highly donating solvents (dimethyl sulfoxide, dimethylformamide, water), τ for the Eu^{3+} and Tb^{3+} ions is independent of temperature over a wide range of the latter.

It has been shown[32,33] that the increase in τ with temperature in weakly donating solvents is due to the removal of residual water molecules from the inner spheres of the ions and their replacement by solvent molecules which have lower deactivating capacities. Fig. 8 presents the curves describing the variation of τ for Eu^{3+} in partly dried acetone as a function of temperature. The activation energy for the splitting off of the last water molecule from the Eu^{3+} ion in acetone has been determined with the aid of these curves (36×10^3 J mol^{-1}).

Mention should be made of the method, proposed by Bünzli and Vuckovic, for the investigation of the inner coordination sphere of the Tb^{3+} ion in weakly donating solvents (acetonitrile) on the basis of the break in the Stern–Volmer linear plot for the quenching (or excitation) of the luminescence of the ion following the introduction of highly donating water molecules (quenching) or dimethyl sulfoxide molecules (excitation) into the solution.[34] The method is most effective when there is a large difference between the complex-forming capacities of the solvent and the added 'quenching agent' in relation to the Ln^{3+} ion. The complex nature of the quenching of the $Tb(NO_3)_3$ solution in acetonitrile by water[1,34] may be due to the fact that, after the displacement of three acetonitrile molecules from the outer sphere by water, the subsequent addition of water leads to the removal of NO_3^- anions.[30]

The possibility of using the inductive-resonance theory of nonradiative transitions for the study of complex formation involving the outer coordination sphere of lanthanide ions has been demonstrated.[35] Neutral neodymium complexes with three NO_3^- anions and three tributyl phosphate molecules were investigated. The quenching of the luminescence of the neodymium complex by water can be explained satisfactorily solely on the hypothesis that the water molecules hydrogen-bonded to a free tributyl phosphate molecule (asymmetric associated species) exert a quenching effect. On the other hand, the water molecules bound to two tributyl phosphate molecules (symmetrical associated species) have virtually no quenching effect on the luminescence of the neodymium complex. There are no free water molecules under these conditions. The high quenching constant can be explained by the protracted encounter between the neodymium complex and the asymmetric water associated species resulting from the formation of a hydrogen bond between the free hydroxy-group of water and a NO_3^- anion in the neodymium complex. The concentration of the asymmetric water associated species in solution was determined from the IR spectra.

III. The application of nonradiative energy transfer between lanthanide ions in the study of complex formation

The problem of the use of the phenomenon of nonradiative energy transfer between organic molecules and lanthanide ions for the investigation of the complex formation reaction between them in solutions has been examined in detail in a review.[36] Since the 17 years which have elapsed since then have not introduced appreciable corrections to the physical and chemical treatment of these phenomena, we shall not return to this problem and will concentrate attention on the application of the phenomenon of the nonradiative energy transfer between different lanthanide ions in liquid solutions to the study of complex formation.

In the first investigations of nonradiative energy transfer between different lanthanide ions in liquid solutions,[37–42] it was already noted that the bimolecular rate constants for the energy transfer (k_t'/dm^3 mol^{-1} s^{-1}) between Tb^{3+} and Eu^{3+} ions (energy donors), on the one hand, and Nd^{3+}, Ho^{3+}, Er^{3+}, etc. ions (energy acceptors), on the other, are five orders of magnitude lower than the rate constant for the process determined by diffusion in highly donating solvents, including water.[40,41] This is due to the low absorption coefficients of the energy acceptors and hence the low overlap integral (which enters into Förster's formula for the energy transfer rate constant) between the normalised luminescence spectra of the donors and the absorption spectra of the acceptors, the low emission rate constants for the energy donors, and the hindrance to the mutual approach of the energy donors and

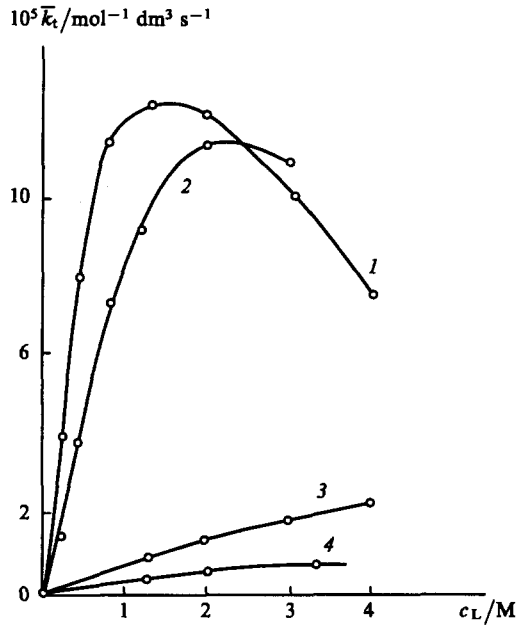


Figure 9. Dependence of the average rate constant for the nonradiative energy transfer from Tb^{3+} (0.03 M) to Nd^{3+} (0.015 M) in water at 293 K on the added carboxylic acid salts:[49] (*1*) CH_3COONa; (*2*) $CH_2ClCOOK$; (*3*) $CHCl_2COOK$; (*4*) CCl_3COOK.

acceptors owing to the Coulombic repulsion forces between the charged Ln^{3+} ion complexes surrounded by neutral solvent molecules.

It has been noted[41,42] that k'_t increases sharply after the addition to the aqueous solution of various alkali metal salts or acids whose anions form complexes with the lanthanide ions. Fig. 9 presents the dependence of the rate constant for energy transfer from Tb^{3+} ($^5D_4$) to Nd^{3+} in water on the concentration of various sodium and potassium salts and derivatives of acetic and other acids. The increase in the rate of transfer on formation of complexes between the lanthanides and the anions is caused both by the decrease in the Coulombic repulsion between the donor and acceptor owing to the neutralisation of the ionic charge on formation of complexes with the anions and by the formation of unstable bridged dinuclear donor Ln^{3+}–anion–acceptor Ln^{3+} complexes, which increase the duration of the encounter between the excited donor and acceptor.

The question of the influence of electrostatic repulsion and attraction of the charged donor and acceptor on the rate of energy transfer in solutions was first examined by Bodunov.[43,44] It was shown that this effect cannot explain quantitatively the experimental data.

The greatest increase in k'_t occurs in the inner-sphere complex formation reactions with anions which can give rise to bridged complexes. The outer-sphere complex formation also influences appreciably the energy transfer in certain cases.

The high sensitivity of k'_t to the inner-sphere complex formation made it possible to develop, using the phenomenon of energy transfer, a procedure for the determination of the stability constants of lanthanide ion complexes.[45] The method is a variant of Bjerrum's method of corresponding solutions,[31] extended to the case of the simultaneous presence in solution of two different central groups, and makes it possible to determine simultaneously the stability constants of complexes of two lanthanide ions—the energy donor and acceptor, where the indicator which depends unambiguously on the free ligand is k'_t. Using the experimental fact that the decay of the donor luminescence is exponential in the presence of the acceptor, it is possible to formulate the following expression for the rate of deactivation of the excited states of the donor in the presence of the acceptor:

$$-\frac{dc_{D^*}}{dt} = k_0^D c_{D^*} + k'_t c_{D^*} c_A ,$$

$$\bar{k}'_t = (k^D - k_0^D)c_A^{-1}; \quad k_0^D = \tau_{D0}^{-1}; \quad k^D = \tau_D^{-1} ,$$

$$\bar{k}'_t = \frac{\sum_{n=0}^{N}\sum_{m=0}^{M} k_t^{nm}\,\beta_n^{D^*}\,\beta_m^{A}\,[L]^{n+m}}{\left(\sum_{n=0}^{N}\beta_n^{D^*}\,[L]^n\right)\left(\sum_{m=0}^{M}\beta_m^{A}\,[L]^m\right)}, \qquad (5)$$

where c_{D^*} is the concentration of the excited energy donor (D^*), c_A the overall concentration of the unexcited energy acceptor (A), [L] the equilibrium concentration of the free ligand, and $\beta_n^{D^*}$ and β_m^A are respectively the overall stability constants of the complexes of the excited donor ions and unexcited acceptor ions

$$\beta_n^{D^*} = \frac{[D^*L_n]}{[D^*][L]^n}; \quad \beta_m^A = \frac{[AL_m]}{[A][L]^m}.$$

It follows from Eqn (5) that $\bar{k}'_t$ is an unambiguous function of the free ligand concentration [L] and can therefore be used as an indicator in the method of corresponding solutions. The quantity

$$\bar{\tau} = (\bar{k}_e^D + \bar{k}_{nr}^D)^{-1},$$

also depends on the free ligand concentration [L] and may be used to determine the stability constants. However, at the concentrations [L] employed it is small for aqueous solution (τ_0^D changes by not more than 2–3 units), while $\bar{k}'_t$ increases by 1–2 orders of magnitude following the addition of the ligand. Therefore $\bar{k}'_t$ was chosen as the parameter and the small changes in $\bar{\tau}_0^D$ were taken into account. For each acceptor concentration, $\bar{\tau}_0^D$ was measured at the donor concentration equal to the sum of the concentrations of the donor and acceptor at the point where the quenching was measured. This is legitimate bearing in mind the small variation of the stability constants in the series of lanthanides. When the donor gives rise to concentration-induced quenching, in the measurement of $\bar{\tau}_0^D$ it is necessary to add to the solution neutral [sic! (Ed. of Translation)] ions (La^{3+}, Gd^{3+}) at the concentration equal to that of the acceptor.

In order to determine the average numbers of ligands around the energy donor ($\bar{n}_D$) and acceptor ($\bar{m}_A$) and the equilibrium ligand concentration, two series of measurements are performed. In the first series, the dependence of $\bar{k}'_t$ on the energy donor concentrations c_D with c_A = const. is determined and plotted for several ligand concentrations c_L (Fig. 10*a*), while in the second series the dependences of $\bar{k}'_t$ on the acceptor concentration c_A with c_D = const. are plotted for the same ligand concentrations (Fig. 10*b*). The series of corresponding solutions for which $\bar{n}_D$, $\bar{m}_A$, and [L] are the same are found from the points of intersection of the experimental curves with the k'_t = const. straight lines. Under the conditions of the luminescence measurements, the concentrations of the excited donor and acceptor ions may be neglected compared with those of the unexcited ions, so that the material balance equation is written in the following form:

$$c_L = \bar{n}_D c_D + \bar{m}_A c_A + [L] .$$

The method described has been used[45] to investigate the formation of complexes between Tb^{3+} (energy donor) and Nd^{3+} (energy acceptor) ions and acetate ions CH_3COO^- in water at the ionic strength of the solution I = 2.0 and at a temperature of 293 K. A constant ionic strength was maintained by adding $NaClO_4$, so that the overall concentration of CH_3COONa and $NaClO_4$ was 2.0 M. The straight lines drawn through points corresponding to constant $\bar{k}'_t$ are presented in Fig. 11. The quantities $\bar{n}_D$ and $\bar{m}_A$ are determined from the slopes of the straight lines and [L] is determined from their intercepts on the ordinate axis, (c_L is the overall concentration of the ligand

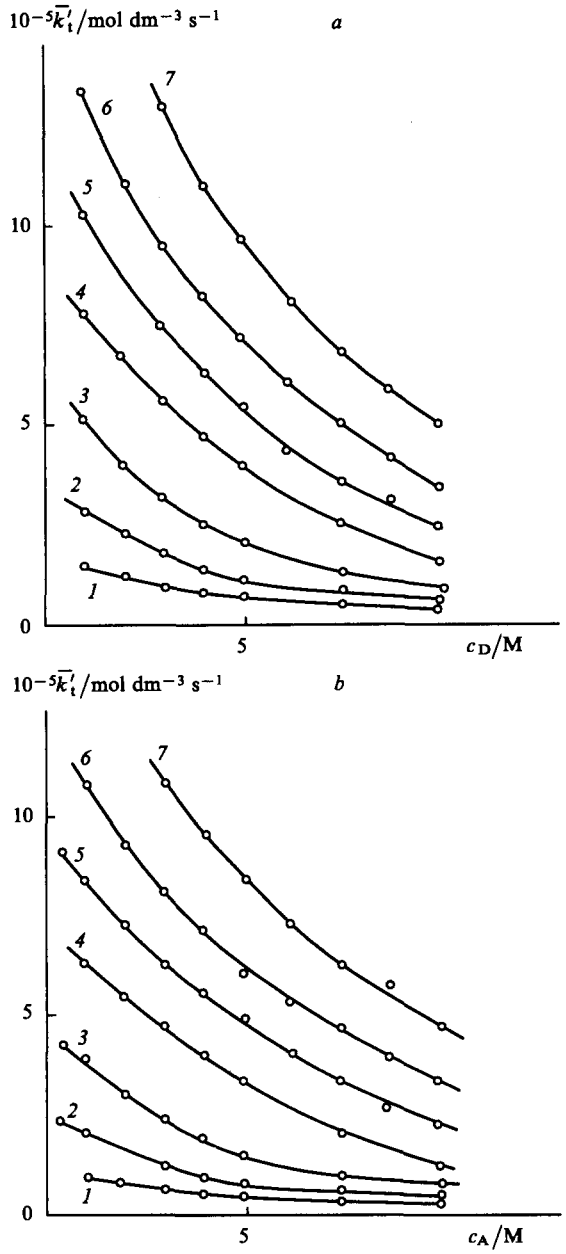


Figure 10. Dependence of the average rate constant for the energy transfer from $Tb^{3+}(^5D_4)$ to Nd^{3+} ions in water at 293 K and $I = 2.0$ on the concentration of the energy donor ions (*a*) at a constant concentration of the energy acceptor ions and on the concentration of the energy acceptor ions (*b*) at a constant concentration of the energy donor ions for different concentrations of sodium acetate (c_L/M): (*1*) 0.05; (*2*) 0.07; (*3*) 0.1; (*4*) 0.14; (*5*) 0.17; (*6*) 0.2; (*7*) 0.24.

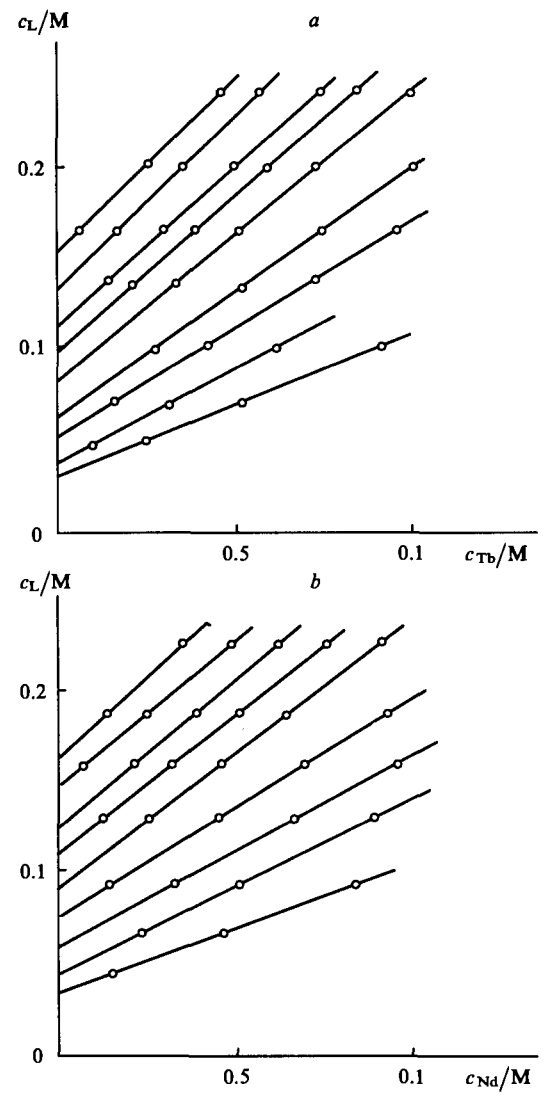


Figure 11. Dependence of the sodium acetate concentration on the concentrations of Tb^{3+} (*a*) and Nb^{3+} (*b*) for solutions with identical values of $\bar{k}'_t$ (corresponding solutions). The average numbers of the energy donors ($\bar{n}_{Tb}$) and the energy acceptors ($\bar{n}_{Nd}$) are determined from the slopes of the straight lines in Figs *a* and *b* respectively; the intercepts made by the straight lines on the ordinate axis yield the equilibrium ligand (acetate) concentrations.

CH_3COONa and c_D and c_A are respectively the overall concentrations of the Tb^{3+} donor and the Nd^{3+} acceptor). Fig. 12 presents the dependence of the average number of ligands around the donors (curve *1*) and acceptors (curve *2*) on the free ligand concentration [L]. The stability constants of the Tb^{3+} and Nd^{3+} complexes of CH_3COO^-, calculated from these data by the least squares method on the assumption that the first three complexes are formed, are presented in Table 7 (see following page). The stability constants obtained by the Fronaeus graphical method[31] were adopted as the zeroth approximation. For comparison, Table 7 presents the stability constants of neodymium acetate complexes obtained under similar conditions by the potentiometric method.[46] The stability constants of the neodymium complexes obtained by the luminescence energy transfer and potentiometric methods agree satisfactorily.

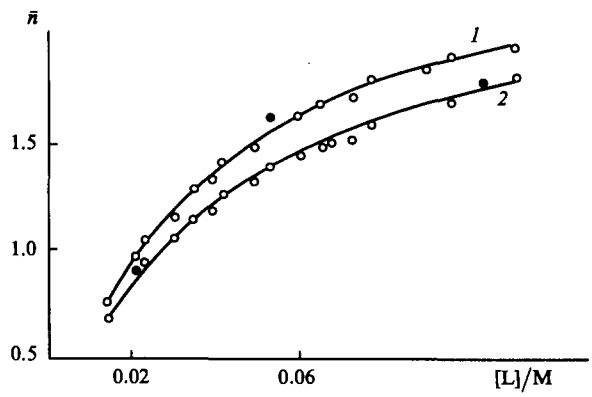


Figure 12. Dependence of the average number of acetate ions bound in the complexes with Tb^{3+} (curve *1*) and Nd^{3+} (curve *2*) on the equilibrium concentration of acetate ions [L]. The curves have been calculated from the stability constants obtained by the least squares method: (*1*) $\bar{n}_D = \bar{n}_{Tb}$; (*2*) $\bar{n}_A = \bar{n}_{Nd}$.

Table 7. The overall stability constants β_n, expressed in (M^{-n}), of the terbium and neodymium complexes of acetate ions in water at 293 K and $I = 2.0$.

Ln^{3+}	β_1	β_2	β_3	Treatment of data
Energy transfer method [45]				
Tb^{3+}	63 ± 6	1740 ± 60	5700 ± 630	LSM
Nd^{3+}	73 ± 8	1180 ± 60	3300 ± 550	"
Potentiometric method [46]				
Nd^{3+}	80 ± 3	1020 ± 100	2900 ± 500	Fronaeus graphical method

We shall not dwell on the application of the nonradiative energy transfer between lanthanide ions in the study of the structures of biological objects because this problem is dealt with elsewhere.[1,2]

1. Detection of unstable bridged lanthanide ion complexes by the nonradiative energy transfer method

The marked increase in k_t' [for energy transfer] between lanthanide ions in solutions in the presence of a series of acid anions cannot be explained solely by the decrease in the electrostatic repulsion. It has been suggested[47,48] that unstable bridged dinuclear lanthanide complexes exist in which the anion (for example, CH_3COO^-) is linked via one atom (in the case of acetate, it is an oxygen atom) to the energy donor ion (for example, to Tb^{3+}), whilst via another atom it is linked to the energy acceptor ion (for example, Nd^{3+}). The formation of this type of bridged complex leads to the arrest of the encounter between the excited ion and the energy acceptor and hence increases their residence time in close proximity, which in fact leads to a significant increase in k_t'.

Table 8 presents the measured average rate constants for energy transfer from terbium and europium ions to neodymium ions in water and alcohol in the presence of acetate anions at the concentration for which k_t' is a maximum.

The decay of the luminescence of the energy donor is exponential in all cases, which indicates a rapid ligand exchange. It is seen from the data in Table 8 that the maximum values of k_t' in the presence of CH_3COO^- anions increase in the sequence water < methanol < ethanol < n-propanol, k_t increasing by a factor of 20 on passing from water to n-propanol. This difference cannot be accounted for by electrostatic repulsion because the complexes are uncharged under these conditions. The formation of unstable bridged dinuclear complexes may be regarded as the only explanation.

Since the quenching of the luminescence of the donor by the acceptor in the presence of acetate is dynamic in all cases, i.e. $q_0/q = \tau_0/\tau$, two variants may be considered.

1. The rate of energy transfer in the bridged complex is high and exceeds the rate of its dissociation, but the equilibrium concentration of the complex is low because of the low value of its stability constant and we therefore do not see any difference between τ_0/τ and q_0/q.

2. The rate of dissociation in the bridged complex exceeds the rate of energy transfer in the latter and the acceleration of the bimolecular energy transfer reaction is associated with the prolongation of the encounter, i.e. with the increase in the average residence time of the acceptor in the vicinity of the excited donor. The quenching (transfer) step does not accompany each step involving the formation of the excited donor–ligand–unexcited acceptor complex.

The appreciable increase [by a factor of ~ 200 (Table 8)] in the average rate constant for energy transfer between lanthanide ions in the presence of acetate ions suggests that energy transfer in the bridged complexes makes the main contribution to the quenching and the reaction can be formulated thus:

$$[D^*L_j] + [AL_i] \underset{k_{diss}^{ji}}{\overset{k_{ass}'^{(ji)}}{\rightleftharpoons}} [D^*L_jAL_i] \xrightarrow{k_t^{ji}} [DL_jA^*L_i] \xrightarrow{k_{diss}^{ji}} [DL_j] + [A^*L_i],$$

$$k_t'^{(ji)} = \frac{k_{ass}'^{(ji)} k_t^{(ji)}}{k_{diss}^{ji} + k_t^{ji}},$$

where D and A are the energy donor and acceptor ions respectively, the asterisk designates the excited states, k_t^{ji} is the first-order intracomplex energy transfer rate constant, and $k_t'^{(ji)}$ is the second-order rate constant for energy transfer between donor complexes with j ligands and acceptor complexes with i ligands. The average energy transfer rate constant is then given by

$$\bar{k}_t' = \sum_j \sum_i k_t'^{(ji)} \alpha_j^{D^*} \alpha_i^A,$$

where $\alpha_j^{D^*}$ and α_i^A are respectively the relative concentrations of the complexes of the excited donor and the unexcited acceptor of each type.

For $k_t^{(ji)} \gg k_{diss}^{(ji)}$, the average energy transfer rate constant corresponds to the average rate constant for the formation of the bridged complexes and is almost independent of the acceptor ion. For $k_{diss}^{ji} \gg k_t^{ji}$, the average rate of transfer should depend greatly on the properties of the acceptor, namely on the overlap integral between the luminescence spectrum of the energy donor and the absorption spectrum of the energy acceptor.

Table 8. Rate constants for the nonradiative energy transfer from terbium and europium ions to neodymium ions at 293 K (according to Gruzdev's data[49]).

Solvent	c/M				$\bar{k}_t'$/mol^{-1} dm^3 s^{-1}	
	CH_3COONa	Tb^{3+}	Eu^{3+}	Nd^{3+}	Tb^{3+} ($^5D_4$)	Eu^{3+} ($^5D_0$)
H_2O	0.0	0.03	0.03	0.1	7.5×10^3	3×10^3
	1.4	0.03	0.03	0.02	1.3×10^6	1.2×10^6
CH_3OH	0.0	0.02	0.02	0.03	2.4×10^4	1.0×10^4
	0.3	0.02	0.02	0.005	4.4×10^6	2.3×10^6
C_2H_5OH	0.0	0.02	0.02	0.03	3.8×10^4	2.2×10^4
	0.04	0.005	–	0.001	1.3×10^7	–
n-C_3H_7OH	0.0	0.02	0.02	0.03	5.5×10^4	4.0×10^4
	0.02	0.001	0.001	0.0001	2.8×10^7	1.8×10^7

Note. All the ions were introduced into the solution in the form of the nitrates; the CH_3COONa concentrations at which the maximum value of $\bar{k}_t'$ is attained were employed.

Measurements have been made[49] of the maximum values of k_t' in the presence of CH_3COO^- ions at 293 K for three pairs of ions–energy donors and acceptors: $Dy^{3+}(^4F_{9/2})-Nd^{3+}$, $Tb^{3+}(^5D_4)-Nd^{3+}$, and $Tb^{3+}(^5D_4)-Eu^{3+}$. The following values have been obtained for these pairs (mol^{-1} dm^3 s^{-1}): 5×10^6; 1.3×10^6, and 9×10^4 respectively. They are correlated with the overlap integrals of the spectra for the above pairs, the ratios of which are $10:1.2:(\leqslant 0.1)$. This is unambiguous evidence in support of the second mechanism of the energy transfer in bridged complexes of the given type.

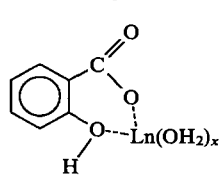
The important role of the bridged complexes in energy transfer between lanthanide ions has been confirmed.[49] A study was made of the energy transfer from salicylic (Sal^-), sulfosalicylic ($SSal^{2-}$), and anthranilic (Ant^-) acid complexes of samarium, terbium, and disprosium to the neodymium ion as the energy acceptor. At pH 5.9, the lifetimes of the Ln^{3+} complexes of Sal^- and $SSal^{2-}$ in water are more than 80 μs, which exceeds appreciably the lifetimes of the excited states of Dy^{3+} at the $^4F_{9/2}$ level and Sm^{3+} at the $^4G_{5/2}$ level [~3 μs (Table 5)]. The lifetime of the complex $[LnAnt]^{2+}$ in water exceeds 500 μs and is longer than the lifetime of Tb^{3+} at the $^5D_4$ level (475 μs). By creating in the solution a large excess of the Ln^{3+} ions (0.1 M) relative to the ligand concentration (10^{-4} M) and by exciting selectively only the Ln^{3+} ions bound in complexes via rapid ($\geqslant 10^8$ s^{-1}) intracomplex energy transfer from the ligands, this makes it possible to measure the rate constant for the reaction

$$[D^*L] + A \xrightarrow{k_t'} [DL] + A^*,$$

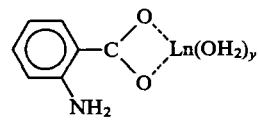
where $[D^*L]$ is the excited donor Ln^{3+} ion combined with the ligand and A the unexcited solvated energy acceptor Ln^{3+} ion. The following energy transfer reactions were investigated:

Reaction	$10^{-5}k_t'$/ mol^{-1} dm^3 s^{-1}
$(Dy^{3+})^* + Nd^{3+} \longrightarrow Dy^{3+} + (Nd^{3+})^*$	0.93
$[Dy^*Sal]^{2+} + Nd^{3+} \longrightarrow [DySal]^{2+} + (Nd^{3+})^*$	60
$[Dy^*SSal]^* + Nd^{3+} \longrightarrow [DySSal]^+ + (Nd^{3+})^*$	100
$[Dy^*Ant]^{2+} + Nd^{3+} \longrightarrow [DyAnt]^{2+} + (Nd^{3+})^*$	2.1
$(Tb^{3+})^* + Nd^{3+} \longrightarrow Tb^{3+} + (Nd^{3+})^*$	0.07
$[Tb^*Ant]^{2+} + Nd^{3+} \longrightarrow [TbAnt]^{2+} + (Nd^{3+})^*$	0.15
$(Sm^{3+})^* + Nd^{3+} \longrightarrow Sm^{3+} + (Nd^{3+})^*$	0.1
$[Sm^*Sal]^{2+} + Nd^{3+} \longrightarrow [SmSal]^{2+} + (Nd^{3+})^*$	3.4
$[Sm^*SSal]^+ + Nd^{3+} \longrightarrow [SmSSal]^+ + (Nd^{3+})^*$	4.6

Here the symbol for the lanthanide ion without brackets denotes a hydrate; the concentration of the Ln^{3+} ions was 0.1 M and that of the ligand 10^{-4} M. The rate constants for the nonradiative energy transfer between the lanthanide ion complexes in water at the ionic strength of the solution $I = 0.6$, 295 K, and pH 5.9 have been calculated[49] for the reactions listed above. The error in the determination of k_t' does not exceed 10%. The very marked acceleration of the energy transfer reaction for the complexes of lanthanide ions with salicylate and sulfosalicylate anions (by a factor of 35–100) and the very slight increase (by a factor of 2) in k_t' for the complex with the anthranilate anion are striking. The structure of the complex $[LnSal]^{2+}$ is



This complex is capable of giving rise to dinuclear bridged complexes via the free oxygen atom of the carboxy-group. On the other hand, the structure of the lanthanide complex with the anthranilate anion shows that it does not tend to form a dinuclear complex.



The slight increase in k_t' is in this case associated with the decrease in the electrostatic repulsion between the donor and the acceptor.

If it were possible to demonstrate unambiguously that the energy transfer in bridged complexes takes place via Förster's mechanism and to calculate the distance between the Ln^{3+} ions in the dinuclear complexes, one could estimate the rate constants for the intracomplex energy transfer in the bridged complex (k_t/s^{-1}). Then, having measured the rate constant for the energy transfer in solution k_t' (mol^{-1} dm^3 s^{-1}), it would be possible to calculate the equilibrium constant $K = k_t'/k_t$ for the bridged complex under the given conditions.

However, such calculations, which require reliable evidence for Förster's mechanism of energy transfer between lanthanide ions in solutions, the calculation of the overlap integral between the luminescence spectra of the energy donors and the absorption spectra of the acceptors, and a reasonable estimate of the relative disposition of the Ln^{3+} ions in the dinuclear bridged complex, have not so far been carried out.

IV. A luminescence-spectroscopic method for the determination of the rates of rapid ligand exchange in lanthanide ion complexes in liquid solutions

A new luminescence-spectroscopic method has been proposed[50] for the investigation of rapid ligand exchange reactions in lanthanide ion complexes. The main idea of the method is that one creates with the aid of a short light pulse a nonequilibrium distribution in the assembly of excited lanthanide ion complexes in solution. By following the kinetics of the variation of the luminescence spectra after the cessation of the exciting light pulse, it is possible to obtain information about the rate and, by altering the experimental conditions, also about the nature and mechanism of the relaxation processes. Such processes are the ligand exchange reactions (in particular, the dissociation and association reactions), electrophilic substitution reactions, conformational changes in the excited complexes, and the excitation energy migration process. Since the equilibrium constants for the excited and nonexcited lanthanide complexes differ only slightly, selective excitation of individual centres is essential in order to create a nonequilibrium distribution in the excited state.

The following conditions must be met for the successful application of the proposed method: 1. The rate of the transition of the complex from one form to another must exceed appreciably the rate of deactivation of the excited Ln^{3+} ions under the experimental conditions. 2. The two types of complexes, the kinetics of the transition reaction of which we have investigated, must have different spectral densities of the emission rate constant at the frequencies (wavelengths) at which the luminescence is recorded. 3. The duration of the selectively exciting light pulse must be appreciably shorter than the duration of the reaction investigated.

The simplest case of the coexistence in solution of only two types of complexes, $MLSolv_1$ and $MSolv_2$, has been examined.[50] Henceforth, for simplicity we shall omit the designations of the solvation shells of the complexes and the complexes will be designated by ML and M. The first type of complex (ML) can be converted into the second type (M) as a result of the ligand dissociation reaction and the second can be converted into the first as a result of the addition of the ligand during the lifetime of the

excited ions $\tau_1 = k_1^{-1}$ and $\tau_2 = k_1^{-1}$. It is then possible to formulate the following reaction scheme for the excited ions:

$$\begin{array}{ccc} M^*L & \underset{k_{as}[L]}{\overset{k_{diss}}{\rightleftharpoons}} & M^* + L \\ k_1 \downarrow & & \downarrow k_2 \\ ML & & M \end{array}$$

The system of differential equations describing the time variation of the concentrations of the excited complexes (c_1^*) and the solvates (c_2^*), taking into account the ligand exchange reactions, assumes the following form:

$$\frac{dc_1^*}{dt} = -(k_1 + k_{diss})\, c_1^* + k_{as}[L]\, c_2^*,$$

$$\frac{dc_2^*}{dt} = k_{diss}\, c_1^* - (k_2 + k_{as}[L])\, c_2^*, \qquad (6)$$

where [L] is the equilibrium ligand concentration. Eqns (6) are solved subject to the condition that k_{diss}, $k_{as}[L] \gg k_1$, k_2. The experimental luminescence intensity at a frequency ν is

$$I(t, \nu) = k_{e1}(\nu)\, c_1^* + k_{e2}(\nu)\, c_2^*,$$

where $k_{e1}(\nu)$ and $k_{e2}(\nu)$ are the spectral emission densities for the complex and the solvate at the frequency ν. After introducing the symbols N_1 and N_2 for the initial concentrations of the complex and the solvate at time $t = 0$, for which one can arbitrarily adopt the instant when the short exciting light pulse terminates, we obtain a solution in the following form:

$$I(t, \nu) \qquad (7)$$
$$= (N_1\alpha_2 - N_2\alpha_1)\{k_{e1}(\nu) - k_{e2}(\nu)\}\exp\{-(k_{diss}+k_{as}[L])t\}$$
$$+(N_1 + N_2)\{k_{e1}(\nu)\alpha_1 + k_{e2}(\nu)\alpha_2\}\exp\{-(k_1\alpha_1+k_2\alpha_2)t\},$$

where α_1 and α_2 are the fractions of the excited complex and solvate at equilibrium ($\alpha_1+\alpha_2 = 1$).

The first term in Eqn (7) describes the relaxation of the system to equilibrium via excited states and the second describes the kinetics of the decay of the luminescence of the system in the state of equilibrium. In order to be able to determine the sum of the rates of the forward and reverse complex formation reactions $\{k_{diss} + k_{as}[L]\}$ from the luminescence decay curve, the first term in Eqn (7) must be nonzero. An essential condition for this is that the excitation of one of the forms should be selective ($N_1\alpha_1^{-1} \neq N_2\alpha_2^{-1}$), and also that the spectral densities of the emission rate constant for the complex and solvate at the frequency corresponding to the observation of the luminescence should differ [$k_{e1}(\nu) \neq k_{e2}(\nu)$]. When the total luminescence light is recorded, Eqn (7) includes the integral of the product of the distribution of the spectral emission density for each complex and of the spectral sensitivity of the photoreceiver as well as the spectral transmission coefficient for the light filter employed. In order to be able to observe the effect, the above quantities must be nonzero.

The kinetics of the decay of the luminescence of labile complexes in solutions have been investigated.[51] Account was taken of the stepwise nature of the complex formation reaction and it was assumed that the rate of ligand exchange is appreciably higher than the rate of deactivation of the excited ions. When account is taken of these postulates, the solution of the equations for the luminescence intensity after pulse excitation consists of two parts, similar to the solution of the equations for two complexes. One part represents the sum of $n - 1$ 'fast' exponential functions corresponding to the establishment of equilibrium between different types of excited complexes and the second represents a significantly 'slower' exponential relation corresponding to the decay of the luminescence from the equilibrium state of the system of excited complexes. As in the simplest case, the observation of luminescence requires a nonequilibrium excitation of the system and a difference between the spectral densities of the emission rate constants for the test complexes at the observation frequency. It has also been concluded that, when three or more types of complexes with comparable rates of interconversion are present in solution, it is difficult to obtain quantitative data for the rates of ligand exchange. However, if the first stage of the complex formation is appreciably slower than the other stages, the measurement of the rate constants becomes possible.

The possibilities of the method proposed have been demonstrated.[50, 52, 53] In order to achieve the selectivity of the optical excitation, two procedures were used. In the first, the aromatic ligand in lanthanide ion complexes with such ligands (1,10-phenanthroline, 2,2′-bipyridyl, and naphthoic, salicylic, and sulfosalicylic acids) was excited by a nitrogen laser (λ_{exc} = 337 nm, $\Delta t \approx 20$ ns). This was followed by rapid ($t \leqslant 10^{-9}$ s) nonradiative energy transfer from the triplet state of the ligand to the lanthanide ion.[12, 36] In the second procedure, the excitation was achieved with the aid of a tunable laser based on the dye rhodamine 6G in the region of the $^5D_0 \leftarrow {}^7F_0$ transition of the europium ion. The selectivity was ensured by excitation in the spectral absorption band of the Eu^{3+} ion corresponding to the complex which it was necessary to excite.

Fig. 13 presents Eu^{3+} luminescence decay curves at the $^5D_0$ level (in D_2O at 295 K after pulse excitation by a nitrogen laser). Heavy water was used as the solvent because the lifetime of the excited state of the europium ion in it is many times greater than in H_2O (Table 5), so that the necessary condition is fulfilled — the rate of deactivation of the excited ion is many times lower than the rate of the ligand exchange.

The overall luminescence decay curve consists of two exponential components: the 'fast' component corresponding to the relaxation of the solution to the equilibrium state and the 'slower' exponential section corresponding to the decay of the equilibrium luminescence (Fig. 13). Since the concentration of 1,10-phenanthroline was 10^{-3} M and that of Eu^{3+} was 10^{-2} M and the absorption coefficient (λ = 334 nm) is 10^4 times greater

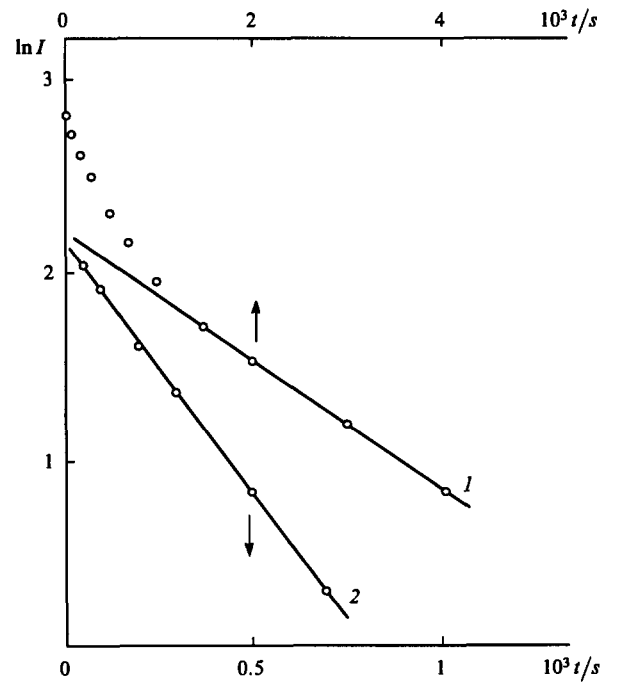


Figure 13. Time variation of the Eu^{3+} luminescence intensity corresponding to the λ = 613 nm emission band and sensitised by the intracomplex energy transfer from 1,10-phenanthroline (Phen). Solvent — D_2O, 295 K $c_{Eu(NO_3)_3 \cdot 6D_2O}$ = 0.01 M, c_{Phen} = 0.001 M, pulse excitation by a nitrogen laser (Δt = 20 ns, λ_{exc} = 337 nm); (*1*) equilibrium luminescence; (*2*) relaxation process.

Table 9. Rate constants for the dissociation of excited lanthanide ion complexes in solutions at 295 K.[49-53]

Ligand	Ion (level)	Solvent	k_{diss}/s^{-1} [a]	Reaction mechanism
Selective excitation by nonradiative energy transfer from the ligand to the lanthanide ion				
1,10-Phenanthroline	Eu^{3+} ($^5D_0$)	D_2O	2700 (44.4) [b]	dissociative opening of the chelate ring
2,2′-Bipyridyl	Eu^{3+} ($^5D_0$)	D_2O	22 000 (36) [b]	"
1-Naphthoate anion	Eu^{3+} ($^5D_0$)	CD_3OD	2.5×10^3	"
	Eu^{3+} ($^5D_0$)	$CD_3OD + D_2O$, 3:1	5.5×10^5	"
	Eu^{3+} ($^5D_0$)	$CH_3OH + H_2O$, 3:1	8.3×10^5	"
	Sm^{3+} ($^4G_{5/2}$)	$CD_3OD + D_2O$, 3:1	6.3×10^5	"
	Sm^{3+} ($^4G_{5/2}$)	$CD_3OD + D_2O$, 1:1	2.0×10^6	"
	Sm^{3+} ($^4G_{5/2}$)	D_2O	4.4×10^6	associative activation
	Sm^{3+} ($^4G_{5/2}$)	H_2O	5.5×10^6	associative activation
Salicylate anion	Tb^{3+} ($^5D_4$)	CH_3OH	4.0×10^3 [a]	"
	Tb^{3+} ($^5D_4$)	D_2O	7.6×10^9 [a]	acid catalysis
	Tb^{3+} ($^5D_4$)	H_2O	1.0×10^{10} [a]	acid catalysis addition of H^+
5-Sulfosalicylate dianion	Tb^{3+} ($^5D_4$)	CH_3OH	4.0×10^3	"
	Tb^{3+} ($^5D_4$)	D_2O	7.9×10^9 [a]	"
	Tb^{3+} ($^5D_4$)	H_2O	1.05×10^{10} [a]	"
Selective laser excitation at the wavelength corresponding to the $^5D_0 \leftarrow {}^7F_0$ transition of the Eu^{3+} ion				
1,10-Phenanthroline	Eu^{3+} ($^5D_0$)	D_2O	2.7×10^3	dissociative opening of the chelate ring
Acetate anion	Eu^{3+} ($^5D_0$)	H_2O	7.0×10^6 [d]	associative activation
	Gd^{3+} ($^8S_{7/2}$)	H_2O	7.0×10^6 [d]	associative activation
	Sm^{3+} ($^6H_{5/2}$)	H_2O	3.7×10^7 [e]	"
Iminodiacetate	[EuDCTA]$^-$ ($^5D_0$) [f]	H_2O	2.6×10^3	"

[a] The errors in k_{diss} do not exceed 20% – 30%.
[b] The numbers in brackets represent the activation energies for the reactions in kJ mol^{-1}.
[c] Second-order rate constant k' in mol^{-1} dm^3 s^{-1}.
[d] Value for the unexcited ion based on the data of Silber et al.[54] obtained by the temperature jump method.
[e] Value for the unexcited ion based on the data of Garza and Purdie[55] obtained by the acoustic absorption method.
[f] DCTA = 1,2-diaminocyclohexanetetraacetate.

for phenanthroline than for Eu^{3+}, there was a high excitation selectivity and the observed fast exponential function may be set equal to the dissociation rate constant (k_{diss}) for the complex. The value of this constant and also the value of the rate constant for the dissociation of the europium complex of 2,2′-bipyridyl in D_2O at 295 K are presented in Table 9.

The study of the dependence of k_{diss} for the above complexes on the temperature and the pH of the solution suggested a dissociative mechanism of the reaction in which the rate-limiting stage is the transfer of one of the donor nitrogen atoms to the second sphere of the Ln^{3+} ion (opening of the chelate ring), which is followed by rapid dissociation of the complex.

The study of the kinetics of the dissociation of europium and samarium complexes of the 1-naphthoate ion demonstrated that the rate of dissociation of the complex is greatly influenced by the solvent. On passing from pure methanol to a mixture of methanol and water and then to pure water, the rate of dissociation increases by three orders of magnitude (Table 9). One should bear in mind that, on excitation as a result of nonradiative energy transfer from the aromatic ligands, the $^5D_0$ level of the Eu^{3+} ion is populated via the $^5D_1$ level of europium. On the other hand, the rate of the nonradiative transition from the $^5D_1$ level to the $^5D_0$ level of europium is 10^6 s^{-1},[56] which limits the possibilities for the study of rapid dissociation reactions. Therefore the data for Sm^{3+}, where the rate of relaxation to the emitting $^4G_{5/2}$ level is appreciably higher, is quoted in Table 9 as the rate of dissociation of naphthoic acid [the naphthoic acid complex?] in water.

The dissociation reactions of the salicylic and sulfosalicylic acid complexes of the Tb^{3+} ion (the $^5D_4$ level) in methanol and water have been investigated. It has been shown that the rate of dissociation in water depends greatly on the pH of the solution, k_{diss} being directly proportional to the concentration of H^+ (H_3O^+) ions in water. Bimolecular constants, close in magnitude to the diffusion rate constant in water, are therefore quoted in Table 9 for these complexes. It is most likely that the first stage of the dissociation of these complexes involves the addition of a proton to the free oxygen of the COO^- group with subsequent departure of the ligand from the lanthanide ion. The constants k_{diss} have been measured by a similar method[57] for Tb^{3+} with the same ligands in water at $I = 0.06$ and pH 7.0. The constants k_{diss} exceeded by an order of magnitude those quoted by Gruzdev and Ermolaev[52,53] (Table 9). It may be that this is associated with the unduly high ligand concentration, comparable to the concentration of the Ln^{3+} ion. Complexes of lanthanide ions with different numbers of ligands coexist under these conditions and it is difficult to determine the values of k_{diss}. Furthermore, the authors[57] postulate that the rate of equilibration with respect to the excited ions is equal to the difference between the rates of dissociation and association, whereas it is in fact equal to their sum [see Eqn (7)]. These discrepancies are not discussed in the study quoted above.[57]

However, the selective excitation of the complexes via the excitation of the ligand and the nonradiative energy transfer to the Ln^{3+} ion is limited by the employment of mainly aromatic ligands. Therefore, in order to study the nonaromatic ligand exchange reactions, the second method for the creation of a high nonequilibrium distribution of the excited ion complexes — the method involving the selective excitation of specific complexes by illuminating the solution with the monochromatic light of a pulse-type tunable laser — was employed. The Eu^{3+} ion and its absorption band, corresponding to the $^5D_0 \leftarrow {}^7F_0$ transition, the position and strength of the oscillator of which are extremely sensitive to changes in the structure of the inner coordination sphere of the ion, are most suitable for these purposes.[1] The widely used rhodamine 6G-based tunable laser is also very suitable.

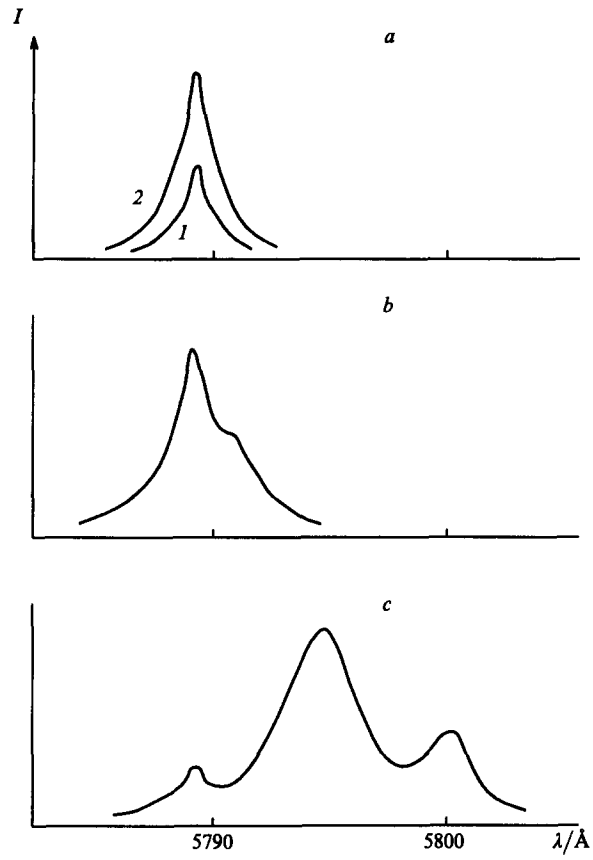


Figure 14. Luminescence excitation spectra in the $^5D_0 \leftarrow {}^7F_0$ transition in aqueous solutions containing Eu^{3+} ions (at the wavelength corresponding to the $^5D_0 \leftarrow {}^7F_0$ band) measured with the aid of a rhodamine 6G-based tunable laser: (*a*) $Eu(NO_3)_3$ (0.05 M) in H_2O (curve *1*) and $Eu(NO_3)_3$ (0.05 M)+NaAc (0.01 M) in H_2O (curve *2*); (*b*) $Eu(NO_3)_3$ (0.05 M)+Phen (0.01 M) in D_2O; (*c*) $Eu(NO_3)_3$ (0.05 M)+Na_2H_2EDTA (0.01 M) in D_2O, pD = 5.5; T = 295 K.

Fig. 14 presents the luminescence excitation spectra in the $^5D_0 \rightarrow {}^7F_1$ transition for various europium complexes in water by light corresponding to the $^5D_0 \leftarrow {}^7F_0$ band, measured with the aid of a rhodamine 6G-based tunable laser.[58] Such spectra correspond to the absorption spectra, the direct measurement of which is difficult owing to the extremely low oscillator strength of the transition. The rates of ligand exchange in the europium complexes of the acetate anion have been investigated by this method.[53,58] The selectivity of the excitation of the tunable laser was achieved because the molar absorption coefficient of the complex $(EuCH_3COO)^{2+}$ is approximately five times greater than that for the hydrate, although the positions of the $^5D_0 \leftarrow {}^7F_0$ absorption bands are identical. The luminescence decay curve for an aqueous solution of $Eu(NO_3)_3$ (5×10^{-2} M) + $NaCH_3COO$ (10^{-2} M) at 293 K, measured using the light corresponding to the hypersensitive $^5D_0 \rightarrow {}^7F_2$ band, is presented in Fig. 15. The relaxation time corresponding to the initial nonexponential section of the decay curve in Fig. 15 is 120 ns. Since the equilibrium is greatly displaced towards the solvates, the dissociation of the complex $(EuCH_3COO)^{2+}$ makes the main contribution to this quantity [see Eqn (7)]. Assuming that the stability constant of the complex (87 mol^{-1} dm^3) does not change appreciably on excitation, we obtain a dissociation rate constant of $(7 \pm 2) \times 10^6$ s^{-1}, which is close to the dissociation rate constant of the europium complex of the naphthoate anion and to the value found for the gadolinium acetate complex by the temperature jump method, but differs greatly from data obtained for samarium by the acoustic absorption method (Table 9).

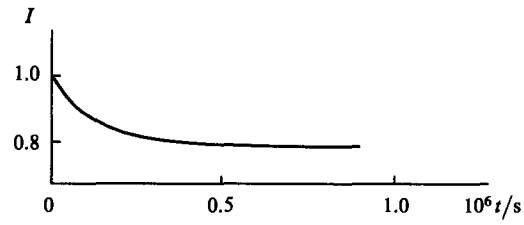


Figure 15. The luminescence decay curve for a solution of the europium complex of the acetate anion $(EuCH_3COO)^{2+}$ in water at the wavelength corresponding to the $^5D_0 \rightarrow {}^7F_2$ band (613 nm) on pulse excitation ($\Delta t \cong 20$ ns) by a rhodamine 6G-based tunable laser. The single-ligand complex $(EuCH_3COO)^{2+}$ is excited preferentially; $c_{Eu(NO_3)_3 \cdot 6H_2O}$ = 0.05 M; c_{CH_3COONa} = 0.01 M, T = 295 K.

Other processes may also lead to a nonexponential type of decay of the luminescence. Firstly, we have the reaction involving the substitution of the central atom in the excited state:
The contribution of this reaction may be determined from the

$$M^*L + M \longrightarrow M^* + ML\,.$$

dependence of the rate constant for the transition process on the concentration of the solvated ion.

Secondly, we have nonradiative electronic excitation energy transfer from the selectively excited complex to the unexcited solvate. As in the previous case, in order to distinguish the energy transfer from the dissociation of the complex, it is sufficient to investigate the dependence of the process on the concentration of solvated ions. It is more difficult to distinguish the energy transfer (migration) from the reaction involving the substitution of the central atom, since the rates of these processes increase with increasing concentration of the solvate. However, the energy transfer from the excited Ln^{3+} ions should not depend on the concentration of the lanthanum or lutetium added to the solution because the energy transfer to the latter is impossible for energetic reasons, whereas the central atom substitution reaction should accelerate in their presence.

It must be emphasised that the study of the transition process in connection with the kinetics of the decay of the luminescence after selective excitation makes it possible to obtain unique data concerning the migration (transfer) of energy between identical lanthanide ions in solutions. For example, the rate of migration of energy from the $^5D_0$ level of the Eu^{3+} ion in its complex with EDTA to the solvated Eu^{3+} ion in D_2O has been measured by this method.[59]

Thirdly, the nonexponential decay may be due to the presence of several types of complexes with different decay times which are not interconverted during the lifetime of the excited state of the ion. This process should be reflected in all the emission bands, whereas the dissociation reaction should be reflected only in the emission bands where the emission rate constant changes appreciably as a result of the dissociation. For example, under nonexponential conditions induced by several types of complexes, such conditions should be observed satisfactorily for europium on the basis of both the $^5D_0 \rightarrow {}^7F_1$ band and the $^5D_0 \rightarrow {}^7F_2$ band, whereas the dissociation of the complex can be observed only from the $^5D_0 \rightarrow {}^7F_2$ band.

The possibility of obtaining data on the kinetic parameters of the ligand exchange at excited lanthanide ions in solutions has also been considered.[1,2,60] Three variants were examined depending on the ratios of the rates of deactivation of the excited ions (complexes) and the rate of ligand exchange.

1. Slow exchange. The selective excitation of each complex in solution leads to luminescence involving exponential decay with τ characteristic of the given selectively excited complex, naturally provided that there is no energy transfer between the ions (complexes). In the case of incomplete (or in the total absence) of

selectivity of the excitation and also in the presence of energy transfer, a nonexponential decay of the luminescence is observed. Incidentally, this case can also be used to measure the rate of the slow ligand exchange, provided that the reaction leads to an appreciable shortening of τ. This method has been used[61] to investigate the rate constant for the incorporation of water in the inner sphere of chromium(III) hexathiocyanate. Later the same workers[62] used this method to determine the rates of the slow isotope exchange of hydrogen for deuterium in the complexes $Cr(en)_3^{3+}$ (where en = ethylenediamine) and $Cr(NH_3)_2(NCS)_4^-$ and their dependence on the pH(pD) of the solution.

2. Fast exchange. Having stated correctly that ligand exchange which is fast compared with the luminescence decay time leads to the exponential decay of the emission in later stages after the attainment of equilibrium with respect to the excited complexes. Horrocks and coworkers[2,60] for some reason neglected the transition process, which was later examined by Gruzdev and Ermolaev in 1977,[50] and did not point out the possibility of using it to measure the rates of rapid reactions.

3. The intermediate rate of exchange—corresponding to the case where the luminescence decay and exchange times are similar. In this case, differential equations have been formulated[60] for the concentrations of two types of complexes undergoing interconversion and deactivated at their own rates, similar to the equations quoted by Gruzdev and Ermolaev[50] [see Eqn (5)]. However, since the condition $\tau_1^{-1}, \tau_2^{-2} \ll k_{dis}, k_{as}[L]$ does not hold in this instance, a more complex solution is obtained than the solution based on the approximate formulae quoted by Gruzdev and Ermolaev[50] [Eqn (7)]. The intermediate case has been studied experimentally[60] in relation to the equilibrium between the europium complexes of 1,2-diaminocyclohexanetetraacetate ($DCTA^{4-}$) and iminodiacetate ($IMDA^{2-}$).

$$Eu(DCTA)^- + IMDA^{2-} \underset{k_{diss}}{\overset{k_{as}[IMDA^{2-}]}{\rightleftharpoons}} Eu(DCTA)(IMDA)^{3-}. \quad (8)$$

The experiment was performed at 293.5 K in aqueous solution at $EuCl_3$, H_4DCTA, and H_2IMDA concentrations of 0.4, 0.04, and 0.12 M respectively at pH 6–9 (NaOH) and $I = 1.0$ (KCl). Each complex was excited selectively by a dye-based laser at the wavelength corresponding to the $^5D_0 \leftarrow {}^7F_0$ band and each complex was detected selectively at the wavelengths of the $^5D_0 \rightarrow {}^7F_0$ bands of the Eu^{3+} ion. The decay of the luminescence was measured at three pH values for each pair of the combinations of the excitation wavelength (exciting mainly one of the complexes) and the observation wavelength characteristic of each complex—altogether four combinations. Using the solutions of the differential equations obtained and the expressions for the overall emission from the two complexes and including the fraction of the emission by each complex as a parameter, Horrocks et al.[60] found the constants k_{dis} and k'_{as}. The following values were obtained at pH 6.99:

$k_{diss}\{Eu(DCTA)(IMDA)^{3-}\} = 2.56 \times 10^3\ s^{-1}$;

$k_{as} = k'_{as}[IMDA^{2-}] = 13.4 \times 10^3\ s^{-1}$;

$\tau\{Eu(DCTA)^-\} = 0.32$ ms;

$\tau\{Eu(DCTA)(IMDA)^{3-}\} = 0.805$ ms.

It has been suggested that, instead of Eu^{3+}, the Sm^{3+} and Dy^{3+} ions be used in the study of faster ligand exchange reactions, as their luminescence in hydrogen-containing solvents decays faster by two orders of magnitude than that of Eu^{3+}.[2,60] However, in this case it is simpler and more accurate to employ Eu^{3+} complexes by carrying out measurements for the transition process on the basis of the decay of the Eu^{3+} luminescence using the method proposed by Gruzdev and Ermolaev.[50]

* * *

Luminescence research methods have been used recently in a wide variety of fields of science and engineering. This applies particularly to chemistry, photochemistry, and biology. Kinetic luminescence methods, in particular those involving laser excitation, have become more accessible to investigators. In the present review, we have attempted to draw the attention of chemists, with interests in the field of the chemistry of solutions of the lanthanide elements, to the possibilities of the study of these systems provided by the luminescence-kinetic methods.

In conclusion we thank the Russian Fundamental Research Fund for financial support (Project No. 94-02-06192).

References

1. *Lanthanide Probes in Life, Chemical and Earth Sciences. Theory and Practice* (Eds J-C G Bünzli, G R Choppin) (Amsterdam: Elsevier, 1989)
2. W DeW Horrocks Jr, M Albin, in *Progress in Inorganic Chemistry* Vol. 31 (Ed. S J Lippard) (New York: Wiley 1984) p. 1
3. P Pringsheim *Fluorescence and Phosphorescence* (New York, London, 1949)
4. R Englman *Non-radiative Decay of Ions and Molecules in Solids* (Amsterdam: North-Holland, 1979)
5. J L Kropp, M W Windsor *J. Chem. Phys.* **39** 2769 (1963); **42** 1599 (1965)
6. P K Gallagher *J. Chem. Phys.* **43** 1742 (1965)
7. A Heller *J. Am. Chem. Soc.* **88** 2058 (1966)
8. J J Freeman, G A Crosby, K E Lawson *J. Mol. Spectrosc.* **13** 399 (1964)
9. J Heber *Phys. Kondens. Mater.* **6** 381 (1967)
10. E B Sveshnikova, I B Neporent *Izv. Akad. Nauk SSSR, Ser. Fiz.* **37** 378 (1973)
11. E B Sveshnikova, V L Ermolaev *Opt. Spektrosk.* **30** 379 (1971); *Izv. Akad. Nauk SSSR, Ser. Fiz.* **35** 1481 (1971)
12. V L Ermolaev, E N Bodunov, E B Sveshnikova, T A Shakhverdov *Bezizluchatel'nyi Perenos Energii Elektronnogo Vozbuzhdeniya* (Nonradiative Transfer of Electronic Excitation Energy) (Leningrad: Nauka, 1977)
13. V L Ermolaev, E B Sveshnikova, in *Fizika i Spektroskopiya Lazernykh Kristallov* (Physics and Spectroscopy of Laser Crystals) (Ed. A A Kaminskii) (Moscow: Nauka, 1986) p. 30
14. Th Förster *Ann. Phys. (Leipzig)* **2** 55 (1948)
15. W Kaiser, A Laubereau *Pure Appl. Chem.* **50** 1231 (1978)
16. M D Galanin, I M Frank *Zh. Eksp. Teor. Fiz.* **21** 114 (1951)
17. E N Bodunov, E B Sveshnikova *Opt. Spektrosk.* **36** 340 (1974)
18. G Herzberg, in *Molecular Spectra and Molecular Structure. II Infrared and Raman Spectra of Polyatomic Molecules* (New York: Van Nostrand, 1966) pp 261, 281
19. Y Haas, G Stein, E Würzberg *J. Chem. Phys.* **60** 258 (1974)
20. V L Ermolaev, E B Sveshnikova, V S Tachin *Opt. Spektrosk.* **41** 343 (1976)
21. C Cossy, A E Merbach *Pure Appl. Chem.* **60** 1785 (1988)
22. G Johansson *Pure Appl. Chem.* **60** 1773 (1988)
23. Z Wang, G R Choppin, P DiBernardo, P-L Zanonato, R Portanova, M Tolazzi *J. Chem. Soc., Dalton Trans.* 2791 (1993)
24. P L Anelli, V Balzani, L Prodi, F Uggeri *Gazz. Chim. Ital.* **121** 359 (1991)
25. S Salama, F S Richardson *J. Phys. Chem.* **84** 512 (1980)
26. N A Kazanskaya, E B Sveshnikova *Opt. Spektrosk.* **28** 699 (1970)
27. J L Kropp, M W Windsor *J. Phys. Chem.* **71** 477 (1967)
28. W DeW Horrocks Jr, G F Schmidt, D R Sudnick, C Kittrell, R A Bernheim *J. Am. Chem. Soc.* **99** 2378 (1977)
29. W DeW Horrocks Jr, D R Sudnick *J. Am. Chem. Soc.* **101** 334 (1979)
30. V P Gruzdev, V L Ermolaev *Zh. Neorg. Khim.* **20** 2650 (1975)
31. F J C Rossotti, H Rossotti *The Determination of Stability Constants and Other Equilibrium Constants in Solution* (New York: McGraw-Hill 1961)
32. V L Ermolaev, V S Tachin *Opt. Spektrosk.* **35** 977 (1972)
33. V S Tachin, V L Ermolaev, E N Bodunov *Zh. Neorg. Khim.* **20** 341 (1975)
34. J-C G Bünzli, M M Vuckovic *Inorg. Chim. Acta* **73** 53 (1983)
35. E M Zimina, A V Shablya *Opt. Spektrosk.* **39** 686 (1975)

36. V L Ermolaev, E B Sveshnikova, T A Shakhverdov *Usp. Khim.* **45** 1753 (1976) [*Russ. Chem. Rev.* **45** 896 (1976)]
37. W W Holloway, M Kestigian *J. Chem. Phys.* **47** 1826 (1967)
38. G Alberti, M A Massucci *Gazz. Chim. Ital.* **95** 997 (1965)
39. J L Kropp *J. Chem. Phys.* **46** 843 (1967)
40. B M Antipenko, V L Ermolaev *Opt. Spektrosk.* **26** 758 (1969)
41. B M Antipenko, V L Ermolaev *Opt. Spektrosk.* **28** 931 (1970)
42. B M Antipenko, V L Ermolaev *Opt. Spektrosk.* **29** 90 (1970)
43. E N Bodunov *Izv. Akad. Nauk SSSR, Ser. Fiz.* **36** 996 (1972)
44. E N Bodunov *Spectrosc. Lett.* **11** 435 (1978)
45. V P Gruzdev, V L Ermolaev *Zh. Neorg. Khim.* **19** 2648 (1974)
46. A Sonesson *Acta Chem. Scand.* **12** 165 (1958)
47. V L Ermolaev, V P Gruzdev, V S Tachin *Izv. Akad. Nauk SSSR, Ser. Fiz.* **36** 984 (1972)
48. V L Ermolaev, V P Gruzdev *Spectrosc. Lett.* **11** 537 (1978)
49. V P Gruzdev, Candidate Thesis in Physicomathematical Sciences, S I Vavilov State Opt. Inst., Leningrad, 1978
50. V P Gruzdev, V L Ermolaev *Opt. Spektrosk.* **42** 586 (1977)
51. V P Gruzdev *Zh. Neorg. Khim.* **22** 3208 (1977)
52. V P Gruzdev, V L Ermolaev *Zh. Neorg. Khim.* **22** 3022 (1977); **23** 1221 1509 (1978)
53. V L Ermolaev, V P Gruzdev *Inorg. Chim. Acta* **95** 179 (1984)
54. H B Silber, R D Farina, J H Swinehart *Inorg. Chem.* **8** 819 (1969)
55. V L Garza, N Purdie *J. Phys. Chem.* **74** 275 (1970)
56. E B Sveshnikova, S P Naumov *Opt. Spektrosk.* **44** 127 (1978)
57. O Yu Pozharskaya, T A Privalova *Koord. Khim.* **17** 1146 (1991)
58. V P Gruzdev *Zh. Neorg. Khim.* **28** 3020 (1983)
59. V P Gruzdev *Opt. Spektrosk.* **56** 267 (1984)
60. W DeW Horrocks Jr, V K Arkle, F J Liotta, D R Sudnick *J. Am. Chem. Soc.* **105** 3455 (1983)
61. I B Neporent, E B Sveshnikova *Zh. Neorg. Khim.* **20** 673 (1975)
62. I B Neporent, E B Sveshnikova *Zh. Neorg. Khim.* **24** 700 (1979)

Russian Chemical Reviews **63** (11) 923–936 (1994)
© 1994 Russian Academy of Sciences and Turpion Ltd

UDC 66.097.3

Selective hydrogenation of unsaturated ketones and acetylene alcohols

E M Sul'man

Contents

I. Introduction 923
II. Selective hydrogenation of unsaturated ketones 923
III. Selective hydrogenation of acetylene alcohols 929

Abstract. The data on selective hydrogenation of unsaturated ketones and acetylene alcohols are analysed. The requirements for choosing selective catalytic systems are surveyed. The routes for the reduction of oxygen-containing compounds and factors affecting them are considered. The bibliography includes 177 references.

I. Introduction

In recent years the problem of selectivity became one of the primary problems of catalysis. High selectivity is an essential characteristic of a catalyst, in addition to its activity and stability.[1,2] Selectivity is characterised by the ratio between the rate of accumulation of the target product and the overall rate of conversion of one of the starting compounds, by different routes, at a given temperature and a given composition of the reaction mixture.[3] A decrease in the selectivity of a catalyst results in the formation of side products that contaminate the target product. This leads to heavy expenses for its purification, to excessive consumption of raw materials and energy, and to deterioration of the environment owing to increase in the amounts of harmful aqueous and gaseous waste products.[4] The most significant and interesting in the theoretical and practical respects among the catalytic processes is catalytic hydrogenation, which is widely used for production of monomers, intermediate products, medical preparations, etc.

This review is devoted to the reduction of unsaturated ketones and acetylene alcohols of various structures and to choosing and developing selective catalytic systems.

II. Selective hydrogenation of unsaturated ketones

1. Hydrogenation of α, β-unsaturated ketones

The catalysts used for the reduction of double bonds in unsaturated ketones may be divided into two groups: the catalysts incorporating platinum metals as the main component or a modifier, and those containing Ni, Co, or Cu.

Hydrogenation of methyl vinyl ketone (MVK), benzylidenelacetone (BA), and benzylidenelacetophenone (BAP) selectively occurs in the presence of Rh/Al_2O_3, Pt and Pd oxides, colloidal Pt, Pd/C, Ru/C, Raney Ni, or Raney-type Co.[5–10] The ethylene bond, keto-group, and benzene ring are consecutively saturated in this process. It has been noted[7,11] that the order of the reaction of hydrogenation of C=C bonds in α, β-unsaturated ketones is close to zero. Enones having two or more substituents at the carbon atoms of the C=C bond have been shown to be reduced with low yields.[12]

As the temperature is increased, hydrogenation of BA slows down,[11] owing to pronounced adsorption of the substrate on the catalyst and displacement of hydrogen from the catalyst surface by benzylideneacetone. Introduction of halogen-containing additives to Ni-based catalysts also decelerates hydrogenation of BA, especially of its C=O group.

In order to ascertain the relationship between the reactivity of a series of unsaturated ketones (MVK, BA, and BAP taken as model compounds) and their chemical structure, the changes in thermodynamic functions: Gibbs free energy (ΔG°_{298}), enthalpy (ΔH°_{298}), and bond order ($p_{C=C}$) during hydrogenation have been calculated (without regard to effects of the solvent and the catalyst under standard conditions), and the results have been then compared with the rates of hydrogenation of these ketones on Raney nickel.[13,14]

The specific rates (W_{sp}) of hydrogenation of MVK, BA, and BAP in the presence of Raney nickel in ethanol and dioxane correlate with the values of ΔG°_{298} and $p_{C=C}$. This led the authors[13–15] to simple correlation equations:

$$W_{sp} = W_0' \exp(-K' \Delta G^\circ_{298}), \quad (1)$$
$$W_{sp} = W_0'' \exp(-K'' p_{C=C}).$$

Experimental data on hydrogenation of C=C bonds in unsaturated ketones are formally adequately described by the following equation:

$$W_i = \frac{k_i x_i}{1 + Q_i x_i}, \quad (2)$$

where W_i is the reaction rate when the initial concentrations of a substrate and a catalyst are equal to unity; k_i and Q_i are kinetic and adsorption parameters, $x_i = c_i/c_0$, where c_i is the concentration of the i-th component and c_0 is the initial concentration of the substrate. The need to take into account adsorption of MVK, BA, and BAP has been shown in specially carried out runs on hydrogenation of a mixture of ketones.[15]

The empirical equation (1) made it possible to predict the initial rates of the reduction of C_{13} and C_{18} ketones under standard conditions. Later, the results were confirmed experimentally. The deviation of the calculated values from the experimental results amounted to 15%.[16]

E M Sul'man Tver' Polytechnic Institute, nab. A Nikitina, 22, 170026 Tver', Russian Federation.
Fax (7-082) 221 62 92. Tel (7-082) 224 93 17

Received 12 May 1994
Uspekhi Khimii **63** (11) 981–994 (1994); translated by Z P Bobkova

Hydrogenation of mesityl oxide on Pt-based catalysts involves the reduction of either the C=C bond (40 °C) or both this bond and the keto-group depending on the conditions under which the process is conducted. Under mild conditions (atmospheric pressure of H_2, 25 °C) on Pd/C, only the C=C bond is hydrogenated.[17,18] In the presence of platinum boride, hydrogenation of mesityl oxide is less selective.[19]

Palladium-based catalysts (Pd/SiO_2, Pd/C, Pd black) also ensure selective formation of methyl isobutyl ketone in the gaseous or liquid phase (methanol, ethanol).[20-23] Highly selective reduction of C=C bonds in α,β-unsaturated ketones has been observed on Pd/C at moderate temperatures and hydrogen pressures (75 °C, 0.5 MPa).[24] Hydrogenation of mesityl oxide on Pd/Al_2O_3 occurs selectively at 40 °C (the yield of the hydrogenation product is 99 %).[23] Increasing the temperature to 210 °C results in the formation of methylisobutylcarbinol, i.e. the C=O group is reduced, as well as the double bonds. In addition, the product of dehydration of methylisobutylcarbinol, viz. 2-methylpentane, has also been detected. Dzhaparidze et al.[25] have studied the kinetics and mechanism of selective hydrogenation of mesityl oxide yielding methyl isobutyl ketone in the presence of the industrial Pd catalyst in the vapour phase in a flow-circulation system. They showed that all the experimental data are adequately described by the following equation

$$W = \frac{k_1 P_1 P_{H_2}^{1/2}}{P_{H_2}^{1/2} + k_2 P_1 + k_3 P_2^2}, \quad (3)$$

where P_1 and P_2 are partial pressures of mesityl oxide and methyl isobutyl ketone, k_1, k_2, and k_3 are constants. Based on the analysis of the data on the H/D-isotope exchange in mesityl oxide and methyl isobutyl ketone, a multistage mechanism involving the formation of a semihydrogenated form has been proposed for this process.[25]

For selective reduction of mesityl oxide, as for the hydrogenation of methyl vinyl ketone, Rh-based catalysts are used.[8,9,26] To increase the rate of the reaction, Rh, Pt, and Pd are modified with rare earth metals (Y, Er, Yb).[27,28] Nitrogen-containing Rh complexes[29] and Ru, Rh, and Pd complexes with phosphines[30] are active and selective in the hydrogenation of mesityl oxide and methyl vinyl ketone. Borunova et al.[29] compared the catalytic activities of Rh/C and of Rh complexes with *N*-phenylanthranilic acid and tyrosine in the hydrogenation of α,β-unsaturated ketones and found that the activity of homogeneous catalysts is considerably higher than that of the heterogeneous Rh/C catalysts.

Reduction of α,β-unsaturated ketones in the presence of Rh, Ru, Pd, or Pt deposited on carbon has been shown to involve both direct hydrogenation of the C=C bond and 1,4-addition of hydrogen to the enone system.[10,31]

A large number of publications[32-37] are devoted to hydrogenation of mesityl oxide catalysed by Ni. In the presence of Raney nickel in various solvents, both the C=C bond and the carbonyl group are hydrogenated,[38,39] i.e. the reduction occurs nonselectively. It was assumed that the reaction, which occurs on the catalyst surface, between chemisorbed atomic hydrogen and adsorbed or nonadsorbed substrate is the rate-determining step of the process.[38] When supported Ni catalysts (30% Ni/Al_2O_3, 160–196 °C, without a solvent) are used, a yield of methyl isobutyl ketone of more than 96% can be achieved.[37]

Modification of Ni catalysts with halides of Group I, II, and III metals results in the increased selectivity of the process with respect to the saturation of C=C bonds.[35,36,40] According to the results obtained by Zhabrova,[41] modification is considered as a general phenomenon, which involves both promoting and poisoning of a catalyst. The use of NiI_2, ZnI_2, CdI_2, $FeBr_2$, $CdBr_2$, and $CoCl_2$ as modifying additives for Raney nickel has been patented.[33] The yield of methyl isobutyl ketone reached 94%. The authors of a paper,[40] who have compared the results of hydrogenation of mesityl oxide in the presence of unpoisoned Raney Ni and of Raney Ni poisoned with KI, concluded that adsorption of mesityl oxide on the catalyst is weaker than that of H_2.

Experiments have shown that the shielded double bond in mesityl oxide is hydrogenated at the same rate as the terminal C=C bond in methyl vinyl ketone.[42] Absorption of 1 mole of H_2 at 42 °C and an atmospheric pressure of hydrogen affords the saturated ketone with high selectivity. When the pressure is increased to 6 MPa, the C=O group is also reduced, but the second mole of H_2 is absorbed very slowly. It has been shown that the isolated double bond in 2-methylpent-1-en-4-one is hydrogenated four times more slowly than the C=C bond in mesityl oxide.

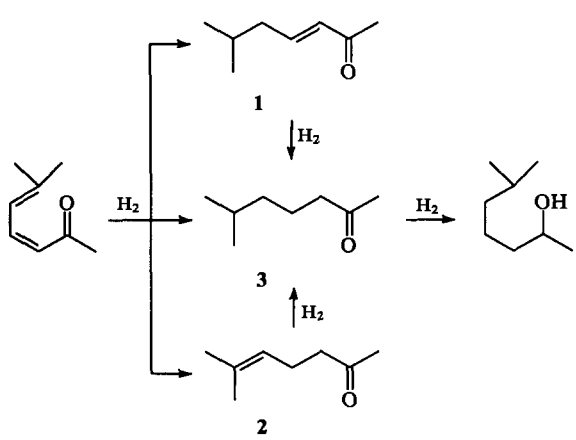
Hydrogenation of mesityl oxide in the presence of copper-based catalysts is not sufficiently selective.[43,44] The highest yield of methyl isobutyl ketone (86.5%) has been obtained at 180–220 °C, at a hydrogen : substrate molar ratio of approximately 1.2, in the presence of Cu_x-Cr_x-Mn oxides deposited directly on a carrier treated with a solution of H_2CrO_4. The process occurs more selectively in the presence of homogeneous catalysts: Cu compounds with additions of $LiAlH_4$.[45]

2. Hydrogenation of polyenones

When the conjugated system of unsaturated ketones is extended by one more double bond, hydrogenation products become more diverse. For example, reduction of 6-methylhepta-3,5-dien-2-one in hexane in the presence of $Pd/CaCO_3$ at atmospheric pressure of hydrogen and ambient temperature affords 67.6% of 6-methylhept-3-en-2-one and 30.2% of 6-methylheptan-2-one,[46] i.e. hydrogen adds initially at the C(5)=C(6) bond and then at the C(3)=C(4) bond. Hydrogenation of the diene alcohol on the same catalyst results in the initial saturation of the C(3)=C(4) bond. Apparently functional groups affect orientation of dienone molecules on the catalyst surface.

When dienones are hydrogenated in the presence of modified catalysts, hydrogen adds initially to the C(3)=C(4) bond and then to the C(5)=C(6) bond. A study[47] has been devoted to changes in the selectivity of the Pd-based catalyst occurring under the action of various modifying additives. Hydrogenation of 6-methylhepta-3,5-dien-2-one yields enones **1** and **2** and 6-methylheptan-2-one (**3**) (Scheme 1). To elucidate the route to the saturated ketone, hydrogenation was carried out in the presence of 5% $Pd/CaCO_3$, 1% Pd/Al_2O_3, or 1% Pd/TiO_2 at 1–5 MPa. In the case of unmodified Pd catalysts, the formation of ketone **3** is preceded by intermediate **1**. Modification of the catalysts with Cd promotes the preferential addition of H_2 to the C(3)=C(4) bond. Hydrogenation of 6-methylhepta-3,5-dien-2-one in the presence of Rh catalysts (Rh/Al_2O_3) with addition of 0.01%–1% Pb in methanol (70 °C, P_{H_2} = 5 MPa) or in the presence of Rh–Ru catalysts (2%–5% of the metal) deposited on carriers (Al, Ti, Zn, Zr, and Si oxides and aluminosilicate modified with 0.01%–1%

Scheme 1



Pb, Sn, Cd, or Bi[48]) affords enone **2** as the main product. In other words, as in the case of modified Pd catalysts, the C(3)=C(4) bond is the first to be saturated.

The route to the reduction of double bonds in a dienone system is determined not only by the nature of the catalyst and modifying agent and the number of these bonds, but also by the character of substituents in the dienone moiety. For example, in the case of cinnamylacetone in which the diene group is linked to an aryl group, the C(3)=C(4) bond is saturated first in the presence of Pd black, and then the saturation of the C(5)=C(6) bond takes place.[49]

Pseudoionone — 6,10-dimethylundeca-3,5,9-trien-2-one (A_1, a C_{13} unsaturated ketone), contains an isolated double bond in the 9,10 position, in addition to the dienone moiety. Several patents contain information on synthesis of hexahydropseudoionone — 6,10-dimethylundecan-2-one (A_4, a C_{13} saturated ketone) in the presence of 5% Pd/C, 5% $Pd/CaCO_3$, Pd/gauze, and Rh/gauze (50–70 °C, $P_{H_2} \leqslant 7$ MPa, yield 92.5%–96%).[50–53]

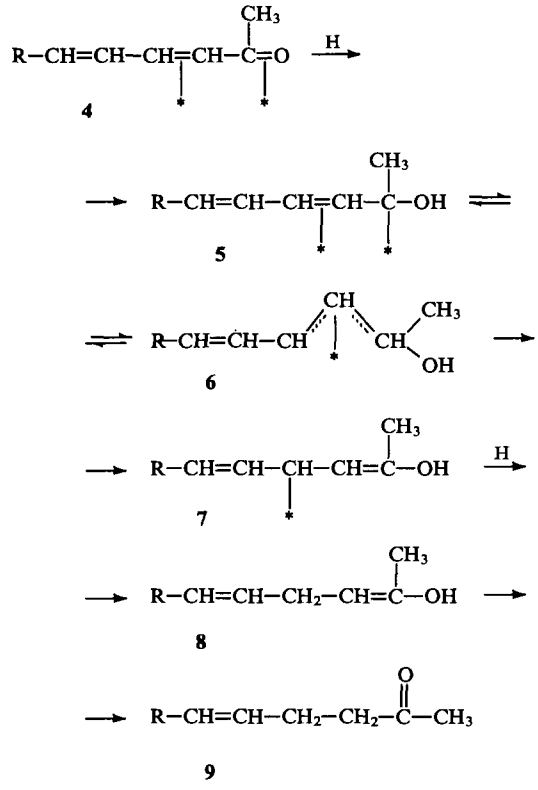
The liquid-phase hydrogenation of A_1 on 5% Pd/C has been found to yield products with various degrees of saturation: 3,4-dihydropseudoionone (*cis*- and *trans*-geranylacetone), 5,6-dihydropseudoionone (A_2), 3,4,5,6-tetrahydropseudoionone (A_3, citronellylacetone), and *cis*- and *trans*-isomers of 3,4,9,10-tetrahydropseudoionone.[54] Chromatographic analysis by the authors not only allowed them to detect these products in the reaction mixture but also confirmed that hydrogenation of ketone A_1 predominantly occurs via a multi-stage mechanism. Absorption of one mole of H_2 results in the formation of 70% of ketone A_2, and after absorption of two moles of H_2, 93% of ketone A_3 is produced.

In the hydrogenation of polyunsaturated and diene ketones in the presence of Ni[55] and Co catalysts,[56] as in the case of Pd catalysts,[46] H_2 adds mostly at the C(5)=C(6) double bond, and to a lesser degree it adds at the C(3)=C(4) bond. Modification of the Ni and Co catalysts with Pb, Cd, and Zn metals[48,49,55–59] or cations[60–62] changes the course of hydrogenation of this dienone: H_2 adds at the C(3)=C(4) bond conjugated with the keto-group. The catalysts used are Raney-type catalysts or blacks deposited on carriers (TiO_2, $Ca_3(PO_4)_2$, V_2O_5, ZnO, Al_2O_3, and MoO_3). Carriers affect the activity of catalysts without changing the reaction pathway.[57] Hydrogenation is carried out at temperatures of 20 to 125 °C and hydrogen pressures varying from atmospheric to 10.1 MPa; the amount of modifying additive is varied from 0.01% to 60% with respect to the weight of the catalyst. Modifiers not only affect the reaction pathway, but also lower activity of the catalyst and substantially decelerate hydrogenation of the carbonyl group.[49,59,62] The action of these additives cannot be reduced solely to poisoning the catalyst, they also promote it. Under severe conditions[59] the carbonyl group is reduced also on modified catalysts. Dienones (hepta-3,5-dien-2-one, 6-methylhepta-3,5-dien-2-one) and ketone A_1, the molecules of which contain diene groups, in the presence of both modified and unmodified catalysts behave in a similar way. This implies that the observed regularity is general: hydrogenation on catalysts modified with inorganic compounds begins with addition of hydrogen at the 3,4 positions. Introduction of pyridine leads to analogous results.[57]

It has been found that the structure of dienone influences the mode of addition of H_2.[59] For example, hydrogenation of hepta-3,5-dien-2-one and 6-methylhepta-3,5-dien-2-one in the presence of Ni catalyst modified with lead affords hept-3-en-2-one, hept-5-en-2-one, and 6-methylhept-5-en-2-one, respectively. Thus, in the latter case, hydrogen adds only at the C(3)=C(4) bond. This is probably due to the presence of a substituent at the C(6) atom and to a different orientation of the dienone molecule with respect to the surface of the catalyst.

Double bonds of a dienone are saturated either independently of each other or by 1,4-addition of hydrogen to the enone group. In fact, addition of hydrogen at the C(3)=C(4) bond, conjugated with the carbonyl group, may occur as the addition to the 1,4 positions of the enone system via intermediate formation of enol[60] (Scheme 2). In accordance with this Scheme, the final product, a ketone with a C(5)=C(6), is preceded by enol **8**, which is formed from the doubly-adsorbed substrate **4** via successive formation on the catalyst surface of semihydrogenated complex **5**, π-allylic complex **6**, σ-derivative **7**, and enol **8**. This Scheme has been confirmed by deuterium exchange. In the presence of the unmodified catalyst, enol is not produced.

Scheme 2



* is an active centre of the surface.

The results of these studies show that the change in the composition of the active catalyst surface caused by modification results in a change of its orienting properties and of the mechanism of the hydrogen addition to dienone.

A number of papers[16,63,64] present data on hydrogenation of pseudoionone under conditions excluding diffusion retardation. To increase selectivity of Ni catalysts the authors[63,64] used various modifying additives: K_2SO_4, KCl, KBr, and KI. It was found[63] that KI possesses the highest selectivity in the hydrogenation of the pseudoionone C=C bonds and all these modifiers, in terms of their selectivity, can be arranged in the sequence $K_2SO_4 < KCl < KBr \ll KI$.

When Zn and Cd halides were used, products of H_2 addition at the C(3)=C(4) bond of pseudoionone were detected in the catalysate. In the Fe^{2+}–Co^{2+}–Ni^{2+} series, the element with the greatest atomic number exhibits the highest catalytic activity.

The IR spectra of pseudoionone recorded after addition of $CoCl_2$ or $NiCl_2$ indicate that the additive interacts with the dienone system of the ketone: redistribution of the intensities of the absorption bands associated with the C=O group and the C=C–C=C bonds was observed.[16] Transition metal ions are likely to protect the ketone group against its reduction to an alcohol group.

To determine the optimum conditions for hydrogenation of the unsaturated ketone A_1 in the presence of the Ni–Co catalytic

system in isopropanol and to elucidate the reaction mechanism in detail, Sul'man[65,66] et al. investigated the kinetics of hydrogenation in a static system, varying the conditions of the process.

It was found that the reaction proceeds according to a parallel-sequential scheme [reactions (*1*)–(*4*), Scheme 3]. In addition to these reactions, transformation of the saturated ketone A_4 to the saturated alcohol A_5 ($A_4 \rightarrow A_5$) also occurs. The selectivity of hydrogenation of the C=C bonds in ketone A_1 diminished with increase in the temperature and hydrogen pressure. The highest selectivity with respect to ketone A_4 amounted to 95%–96%.

Hydrogenation of C_{13} and C_{18} polyene ketones in a dynamic regime in the presence of the Ni–Co catalytic system results in the accumulation of substantial amounts of saturated alcohols in the catalysate,[67] probably owing to retardation of internal diffusion.[68]

Hydrogenation of dienones is carried out not only on heterogeneous catalysts, but also in the presence of homogeneous catalysts, for example, Co complexes,[69,70] that are more selective in the formation of saturated ketones.

The saturation of polyenones in the presence of various catalysts may depend essentially on the initial concentration of the substrate and the nature of solvent. When the ketone concentration in the solution is increased from 10% to 50%, the reaction rate diminishes.[57] This can be attributed to adsorption of dienone from the catalyst surface with the displacement of hydrogen and to the complication of the process due to diffusion of hydrogen.

Experimental data on the kinetics of the hydrogenation of the ketone A_1 in Pr^iOH in the presence of 2% Pd/C are described by the linear relation[16,71–74]

$$\tau_{0.5} \sim q^n \quad (n = 1), \tag{4}$$

where $\tau_{0.5}$ is the time of half-conversion of ketone A_1 and $q = c_0/c_c$ (c_0 is the initial concentration of the substrate, c_c is the amount of the catalyst).

This relationship makes it possible to introduce the reduced time $\theta = t(c_c/c_0)$. Thus, the data obtained for different c_c values can be combined (Fig. 1).

To explain the experimental data, various kinetic models have been used.[75] Application of the equation

$$W_i = k_i x_i \tag{5}$$

for describing the kinetics of the consecutive conversion of ketone A_1 to the saturated ketone A_4 led to systematic deviations of the calculated results from the experimental data. This fact, together with the possibility of direct addition of two or three moles of H_2 to ketone A_1, required consideration of a parallel-sequential Scheme 3. It has been noted that in the consecutive conversion of ketone A_1 to A_4, the first mole of H_2 (according to chromatographic analysis) adds predominantly at the C(5)=C(6) bond of A_1 and to a slight extent at the C(3)=C(4) and C(9)=C(10) bonds. In addition, it has been shown in special experiments that the kinetic model should be constructed with due regard for adsorption of ketone A_3. Statistical analysis showed that the best results have been obtained by using Eqn (2) and parallel-sequential Scheme 3 [(reactions (*1*)–(*3*)] with due regard for the adsorption of ketone A_3. The curves calculated from Eqn (2) are in good agreement with experimental curves (see Fig. 1).

Hydrogenation of ketone A_1 in the presence of 5% Pd/C under dynamic conditions proceeded nonselectively with formation of the saturated alcohol. This is accounted for by the influence of the internal-diffusion retardation on the reduction of this ketone on Pd/C and by lyophilisation of the system when charcoal is used as the carrier.[76]

For hydrogenation of pseudoionone, ethanol[54,76] and methanol[53,57,59] have been used as solvents. In a study[16,64] of hydrogenation of ketone A_1 in the presence of the Ni–Co catalytic system, it was found that the selectivity of the process is

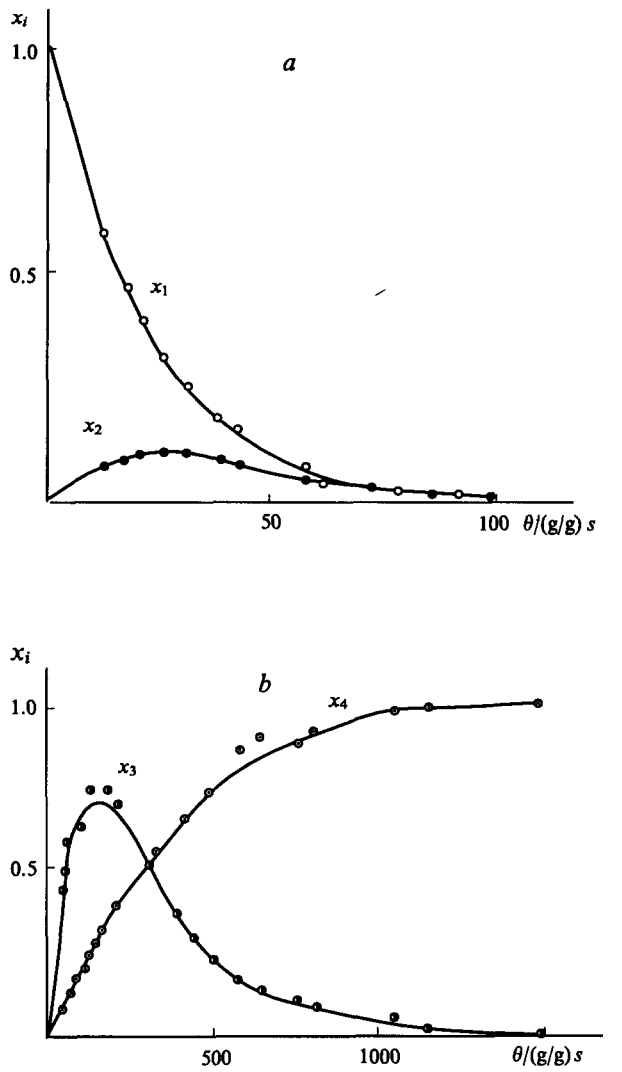
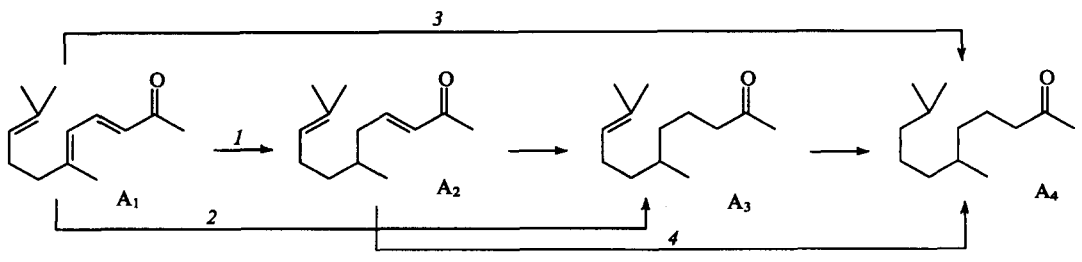


Figure 1. Composition of the catalysate in the hydrogenation of ketone A_1 in the presence of Pd/C ($T = 50\,^\circ C$, the hydrogen partial pressure is 2 MPa). Continuous lines show the results of the calculations; points correspond to experimental results.

Scheme 3



significantly affected by the nature of solvent (C_1-C_4 alcohols of normal and iso structures with addition of water were studied). In terms of the rate of the accumulation of ketone A_4, all these solvents can be arranged in the sequence: MeOH > EtOH > Pr^nOH + 15% H_2O > Pr^iOH + 5% H_2O > Pr^iOH > Pr^nOH > Bu^iOH > Bu^nOH. The optimum activity and selectivity (94%) of the Ni–Co catalytic system with respect to C=C bonds of pseudoionone were achieved in isopropanol. This is explained by the fact that isopropanol shows the least tendency to be adsorbed on Group VIII metals and, therefore, it weakens the interaction between the ketone and $CoCl_2$ in the solution bulk to a lesser degree.

The kinetics of hydrogenation of β-ionone in the presence of Pd and Ni catalysts have been studied both in open and in closed systems with varying conditions of the reaction and the nature of solvent.[77-80]

Of interest are papers dealing with hydrogenation of polyunsaturated ketones having more complex structures.[81-87] A method for preparing higher saturated ketones in the presence of the Pd/Al_2O_3 catalyst with a palladium content of 0.05 to 5 mass.% is described in a patent.[82] The yield of 6,10,14-trimethylpentadecan-2-one (A_8, a C_{18} saturated ketone) reached 95%. For selective reduction of unsaturated ketones to saturated ketones, an effective industrial Pd-based catalyst (ShPAK-0.5, 0.5% Pd/Al_2O_3) has been chosen.[16,84-87] The components used for its preparation, Pd/Al_2O_3 and Al_2O_3, were studied by various physicochemical methods [IR spectroscopy, X-ray photoelectron spectroscopy (XPS), extended X-ray absorption fine structure spectra (EXAFS), electron microscopy, and adsorption, analytical, and X-ray methods]. In conformity with EXAFS data,[88] it has been noted that the Pd–Pd distance increases upon deposition of palladium by 0.007 nm, which is due to the need for palladium to fit into the structure of the carrier. The free energy of the deposited palladium [$E_{fr}(Pd_{3d_{5/2}}) = 335.6$ eV] is close to that of massive palladium. The layers situated near the surface of palladium reduced in isopropanol contain carbon (Pd/C ~ 73). During thermal desorption (TDS), peaks due to hydrogen with T_{max} = 331 and 448 °C were detected, associated with destruction of hydrocarbons on the catalyst surface. Statistical analysis of the results of an electron-microscopic study of the catalyst active layer has shown that surface particles measure 2–5 nm; capillary impregnation of a sample with isopropanol made it possible to determine the average diameter of pores (9.5 nm) and porosity (0.57).[16]

In the presence of the ShPAK-0.5 catalyst, the kinetics of hydrogenation of pseudoionone have been studied, P_{H_2}, T_c, c_0, and c_c being varied over wide limits.[16,84] When the Pd/Al_2O_3 catalyst is used for the reduction of pseudoionone, the n value in Eqn (4) is 1, as in the case of Pd/C. The experimental results on the hydrogenation of pseudoionone under various reaction conditions are adequately described by Eqn (2), which suggests that hydrogenation of pseudoionone on Pd/Al_2O_3 and Pd/C proceeds via a common mechanism.

Hydrogenation of 6,10,14-trimethylpentadeca-3,5-dien-2-one (A_6, a C_{18} unsaturated ketone) in the presence of Pd/Al_2O_3 also occurs according to a parallel-sequential scheme (Scheme 4).

In this case, the n value in Eqn (4) is 1 or 2.[16,86] Experimental data were fitted using Eqn (4), and the optimum model for the process of hydrogenation of ketone A_6, which takes into account adsorption of the components of the reaction system, has been suggested.

$$W_1 = \frac{a_1 x_1}{(x_1 + Q_2 x_2 + Q_3 x_3)^n} \frac{P_{H_2}}{1 + b_1 P_{H_2}}, \quad (6)$$

$$W_2 = \frac{a_2 x_1}{(x_1 + Q_2 x_2 + Q_3 x_3)^n} \frac{P_{H_2}}{1 + b_2 P_{H_2}}, \quad (7)$$

$$W_3 = \frac{a_3 x_2}{(x_1 + Q_2 x_2 + Q_3 x_3)^n} \frac{P_{H_2}}{1 + b_3 P_{H_2}}, \quad (8)$$

where $n = 1, 2$ and x_1, x_2, and x_3 are reduced concentrations of the unsaturated ketone A_6, 6,10,14-trimethylpentadeca-3-en-2-one (A_7), and the saturated ketone A_8, respectively. Parameters of Eqns (6)–(8) are listed in Table 1.

Table 1. The results of solving the inverse problem in terms of equations (6)–(8) for hydrogenation of ketone A_6 (50 °C).

$10^3 \times a_i$/mol² g⁻² s⁻¹ MPa⁻¹			b_i/MPa⁻¹			Q_2	Q_3
a_1	a_2	a_3	b_1	b_2	b_3		
3.51	1.43	0.77	0.93	1.00	1.35	2.11	0.62

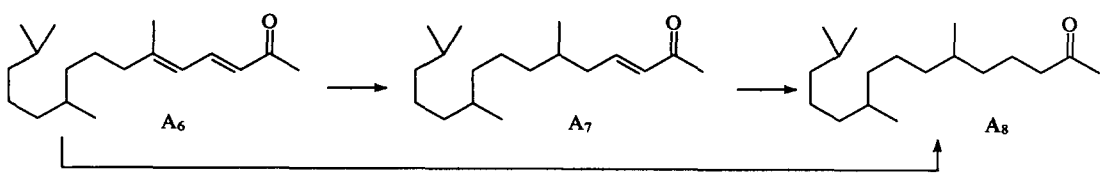
Comparison of the experimental and calculated curves (Fig. 2) showed that this model is in satisfactory agreement with the experimental observations: the error of the estimation of all the parameters of Eqns (6)–(8) lies within 10%. These equations attest to a complex mechanism of the hydrogenation reaction of ketone A_6.

In the physical justification of Eqns (6)–(8), we supposed[16] that the substrate is adsorbed on organometallic centres of the catalyst (Z')[89] that are formed as surface compounds, A_iZ' and $A_iZ'_2$, through the action of the substrate, solvent, and modifying additive. Hydrogen is activated on the metal atoms and diffuses to adsorbed substrate molecules.[90] Study of the influence of a competing inhibitor (pyridine) on the rate of hydrogenation of ketones A_1 and A_6, resorting to the XPS and TDS data, made it possible to conclude that the catalyst active centres have a complex structure; the IR spectra imply that the adsorption of ketones on the catalyst must be taken into account. The k_i, b_i, Q_i, and a_i parameters in Eqns (2) and (6)–(8) turned out to be complex combinations of constants.

It should be noted that in the presence of Pd/Al_2O_3, which is a selective catalyst of hydrogenation of polyunsaturated ketones, the saturated alcohol was formed neither under dynamic, nor under static conditions (the selectivity with respect to saturated ketones was 99.5%–99.7%).[91]

Metal-containing polymeric catalysts, for example those incorporating Rh, possess a number of advantages over traditional heterogeneous catalysts.[92,93] During the synthesis of a metallopolymer, formation of organometallic centres necessary for activation of the substrate is possible. To prepare rhodium-containing polymeric systems, the complex-formation reactions between rhodium chloride and rhodium carbonyl chloride and active olefin groups in a polymeric matrix have been

Scheme 4



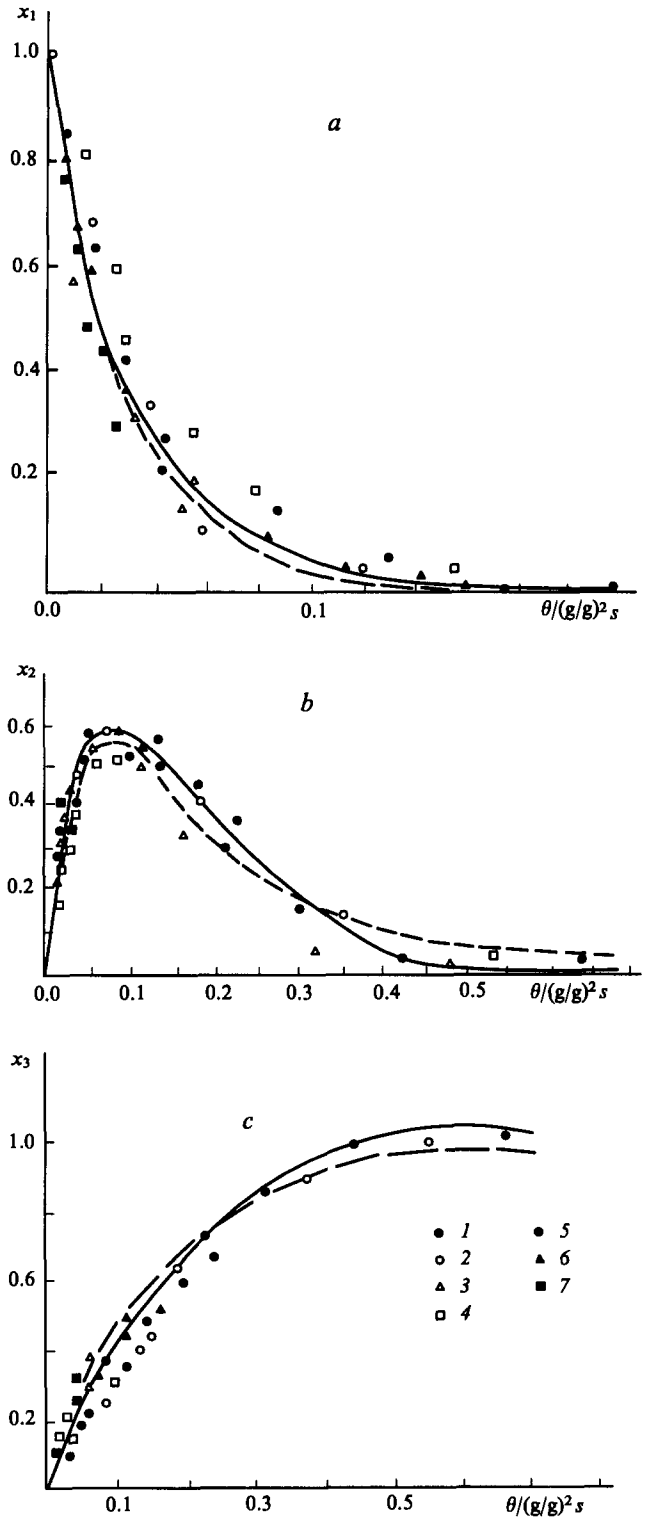


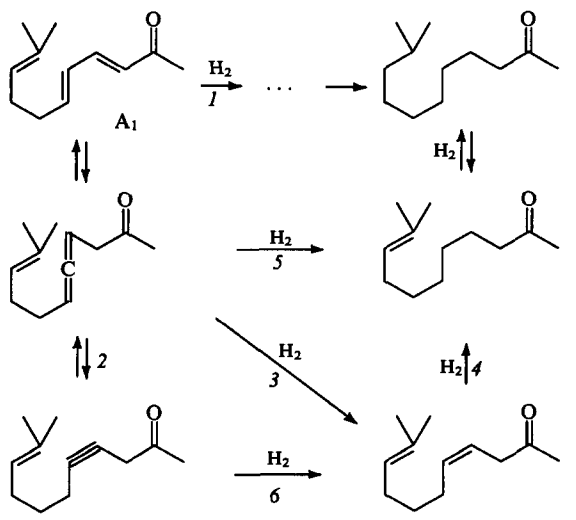
Figure 2. Generalised plots of the time variation of the composition of the reaction mixture during hydrogenation of ketones A_6 (*a*), A_7 (*b*), and A_8 (*c*) (Pd/Al_2O_3, $T = 25$ °C, $P_{H_2} = 2.5$ MPa). The continuous lines illustrate the results calculated according to model (6)–(8), the dashed lines correspond to the calculations according to the linear model, and the points are experimental results. q (g/g): (*1*) 37.5, (*2*) 71.4, (*3*) 75.0, (*4*) 107, (*5*) 143, (*6*) 250, (*7*) 750.

selected.[94] It was shown that the use of nonpolar solvents (benzene, toluene, hexane) results in deceleration of the hydrogenation. To the greatest degree this relates to hexane, possibly due to swelling of the polymeric catalysts in aromatic solvents, which results in increase in the number of available active centres. At the same time, polar aromatic compounds as well as THF, DMSO, and DMF are likely to be coordinated by the reactive centres of the catalyst, which leads to decrease in their activity. Good results were obtained when the hydrogenation of pseudoionone was carried out in alcohols. Isopropanol turned out to be the best, among the series of alcohols, as in the case of hydrogenation on the traditional heterogeneous catalyst, ShPAK-0.5 (Pd/Al_2O_3). Based on the study of the kinetics of hydrogenation of pseudoionone on a Rh-containing polymeric catalyst deposited on Al_2O_3 (Rh is twice deposited: on the polymer and on Al_2O_3), a kinetic model and a mechanism were proposed for the reaction. High stability of the Al_2O_3-deposited Rh-polymeric catalyst was noted.[95–97]

On an industrial scale, ketones A_1 and A_6 are produced by isomerisation of the corresponding allene ketones in ethanolic alkali. Hydrogenation of allene ketones in the presence of Ni and Pd catalysts was studied under static and dynamic conditions, the parameters of the process and the nature of solvent being varied over wide limits.[16] It was found that reduction of ketone A_1 occurs with a lower initial rate but much more selectively than that of ketone A_6. The selectivity of the hydrogenation of A_1 with respect to ketone A_4 in the presence of Raney Ni can be as high as 97.8%; that for the hydrogenation of A_6 with respect to A_8 is 53%.

The results of kinetic and spectroscopic studies suggest that in the presence of Pd/Al_2O_3 or the Ni–Co catalytic system, the reaction proceeds according to route (*1*) (Scheme 5) in all the solvents studied (C_1–C_4 alcohols of normal and iso structures, with or without addition of H_2O). In isopropanol in the presence of the Ni–Co catalytic system, route (*5*) is the predominant reaction path, and in the case of non-modified Raney Ni, routes (*2*) and (*6*) prevail.

Scheme 5



Analysis of the literature data on the selective hydrogenation of α, β-unsaturated and polyunsaturated ketones makes it possible to draw the following conclusions:

In the presence of platinum group catalysts, under mild conditions, the C = C bond in α, β-unsaturated ketones is reduced preferentially.

Pd- and Rh-containing polymeric and modified Ni catalysts (to a lesser degree) are the most selective catalysts of the hydrogenation of dienones and polyenones.

Highly selective addition of H_2 at the 1,2, 1,4, or 3,4 positions of the enone or dienone systems is possible, and C_{13} and C_{18} saturated ketones can be obtained from the corresponding allene ketones.

General features of the hydrogenation of unsaturated ketones have been identified:

Components of the reaction system affect significantly the selectivity and the activity of the catalyst with respect to double bonds of the ketone.

Interaction between the participants of the reaction, not only at the interface but also in the bulk of the solution, must be taken into account.

Heterogeneous catalysts can be modified not only by specially introduced additives but also by the solvent or substrate (this accounts for the observed nonlinear relations between kinetic parameters and the amount of catalyst).

Similar regularities are characteristic of the hydrogenation of acetylene alcohols.

III. Selective hydrogenation of acetylene alcohols

1. Catalysts for selective hydrogenation of C≡C bonds

A number of catalytic systems for selective hydrogenation of alkynes to alkenes have been described in the literature. Among these are homogeneous catalysts containing complexes of Group VIII metals (mostly Pd, Rh, Ni) with sulfur- and phosphorus-containing[98,99] ligands or nitrogen-containing organic chelating ligands (EDTA, ethylenamines, aminoacids, phenanthroline, morpholine, pyridine and its homologues, tertiary amines, etc).[100,101] Octylamine-based catalysts are most active in the hydrogenation of diphenylacetylene. Their selectivity with respect to the olefin amounts to 98%–100%. At the beginning of the reaction an induction period occurs, which disappears in the case where the complexes are first treated with hydrogen.[102]

However, homogeneous catalysts of the selective hydrogenation of acetylene compounds are not very effective from the technological standpoint. Therefore, in recent years studies on making them heterogeneous are being carried out.[103,104] In these studies, a modifying effect of oxygen and a substantial influence of a reduced hydrogen pressure ($\leqslant 0.01$ MPa) on the selective reduction of a C≡C bond to a C=C bond was found.[104] The selectivity with respect to olefin reaches 98%–99%. Unfortunately the above-mentioned papers contain no data on stability of the catalysts proposed.

Membrane catalysts based on Pd and its alloys have been considered as promising from the technological standpoint.[105–107] The high selectivity of conversion of acetylene alcohols in the presence of these catalysts is due to the fact that the concentration of hydrogen adsorbed on the catalyst surface and dissolved in its bulk can be controlled by varying the composition of the alloy and the hydrogen pressure at the operating side of the membrane. It was shown that these catalysts possess on average a 100-fold higher productivity per unit surface area than conventional catalysts,[108] the selectivity being 95%–99%.

However, supported catalysts are still the most technologically effective. One of the main lines of the search for selective catalysts of hydrogenation of acetylene compounds to ethylene compounds is modification of deposited Pd catalysts, which are most selective in the hydrogenation of a C≡C bond to a C=C bond. Heterogeneous catalytic systems for partial hydrogenation of a triple bond are listed in Table 2. Some authors (for example, Cerveny et al.[119]) attribute the enhanced activity and low selectivity of Pd/C with respect to formation of alkenes to the high degree of dispersion of the active metal on the carrier, however, they do not take into account the intensity of the interaction between the disperse phase and dispersion medium. On the contrary, Karturan et al.[128] have noted that Pd/SiO_2 possesses the maximum selectivity in the case where Pd is highly dispersed. Analysis of the data presented in Table 2 shows that the low-percentage Pd/Al_2O_3 catalyst modified with organic or inorganic substances is most widely used for the selective hydrogenation of C≡C bonds to C=C bonds.

Hydrogenation of dimethylethynylcarbinol. In a number of studies,[129–136] Pd catalysts modified with organic or inorganic additives were used for the selective hydrogenation of dimethylethynylcarbinol (DMEC, A_9, a C_5 acetylene alcohol) to the corresponding vinylic alcohol. For example, in a study of the reduction of carbinol A_9 yielding dimethylvinylcarbinol (DMVC, A_{10}, a C_5 ethylene alcohol) in the presence of 5%–20% $Pd/CaCO_3$ with addition of Zn, Cd, or Pb salts, it has been shown that the catalyst containing 20% Pd is the most selective. The dependence of the optimum modifier : catalyst ratio on the nature of the salt was noted; for Zn compounds this ratio is an order of magnitude higher, which is attributed to the lower adsorption ability of the Zn cation, as compared with Pb or Cd.[130]

It was found in a study of the hydrogenation of DMEC in the presence of 0.5% Pd/Al_2O_3 modified with the optimum amount of the specifically adsorbed Zn and Cd cations under static or dynamic conditions that the continuous process occurs with low selectivity, which, was suggested to be associated with transport phenomena.[129]

The selectivity of the reduction of DMEC to DMVC in the presence of the $Pd/CaCO_3$–$Zn(CH_3COO)_2$ catalytic system at a Zn : Pd atomic ratio of 0.75–5.87 was 92%–96% when 1 mole of H_2 had been absorbed; at this point the catalysate already contained 3.5%–5% of the saturated alcohol.[131] Introduction of nitrogen compounds (triethanolamine, triethylamine, NH_3) into this catalytic system suppresses hydrogenation of the C=C bond of the alcohol.

A catalyst for hydrogenation of DMEC to DMVC containing Pd and additives has been developed.[132] The laboratory and pilot

Table 2. Catalysts for the selective hydrogenation of C≡C bonds.

No. II/II	Catalyst, carrier, modifier, solvent, hydrogenation conditions	Ref.
1	Pd catalyst treated with alkali, 0–100 °C; 0.5–3.0 MPa	109
2	Pd/carrier (Al_2O_3, C, $CaCO_3$, $BaSO_4$, sepiolite), modified with heavy metal cations or organic amines	110, 111
3	the Lindlar catalyst, pyridine, in hexane	112
4	0.05% Pd/Al_2O_3	113, 114
5	0.05–5% Pd/Al_2O_3, $Pb(CH_3COO)_2$ or $Sn(CH_3COO)_2$ (modifier : catalyst = 2 : 5)	115
6	Pd/Al_2O_3 – Zn and/or, Cd, Bi and/or Tl	116
7	Pd/Al_2O_3 – Group VIB metals	117
8	Pd/Al_2O_3,$Pd/CaCO_3$, Pd/C	118
9	Pd/C, Pd/SiO_2 – Pb, Tl	119
10	0.1–60% of the hydrogenating Group VIII metal deposited on a carrier with 0.001%–10% of (Cd, Cu) oxides and 0.5–2% of K_2O added (relative to the overall weight of the catalyst)	120
11	Pd/carrier, Group IV elements (Sn or Pb)	121–123
12	Pd–Ag (Pd : Ag = 10 : 1)	124
13	Pd, modified with Ge, Sn, Pb or Sb	125
14	Pd/Al_2O_3 (0.3% Pd) with a Pd particle size of 8 nm	126
15	Zn – Cu, modified with alkali metals	127

tests on the hydrogenation of DMEC to DMVC showed that the Pd–Zn catalytic system is more active and selective than Pd–Pb.[133] The activity in the reduction of DMEC of low-percentage SiO_2-deposited Pd catalyst modified with chlorine-containing complexes of Ru(IV), Ir(IV), Rh(III) has also been studied.[134] In view of the fact that there is no additivity in the effect of the components of a catalyst on its activity and selectivity, it was suggested that heteronuclear metal complexes formed on the surface of the carrier are responsible for a definite reaction pathway. As has already been noted, the selectivity of the hydrogenation of DMEC to DMVC can be increased by using mixed catalysts. For this purpose, Pd–Cu/TiO_2 catalysts with various proportions of the active phase have been suggested.[135] The apparent activation energy for the hydrogenation of DMEC[136,137] varies from 16 to 50 kJ mol^{-1} and is determined by the nature of the components of catalytic system.

Hydrogenation of 3,7-dimethyloct-6-en-1-yn-3-ol. There are considerably fewer papers dealing with hydrogenation of 3,7-dimethyloct-6-en-1-yn-3-ol (DOL, A_{11}, a C_{10} acetylene alcohol). Interesting results have been obtained with Pd-based catalysts, which possess the highest selectivity.[138] When C_2–C_4 alcohols with the normal or branched structure are used as solvents, the proportion of linalool (LH, A_{12}, a C_{10} ethylene alcohol) in the catalysate is lower in the latter case. The selectivity of hydrogenation of DMEC to DMVC is higher than that of DOL to LH in all the alcohols. The apparent activation energy for the hydrogenation of DOL in the presence of Pd black amounts to 8.4–12.6 kJ mol^{-1}, i.e. it is lower than that for DMEC. At the same time, it has been shown[139] that lengthening of the hydrocarbon skeleton of acetylene alcohols from 5 to 8 atoms should be favourable for increase in the yield of the corresponding ethylene derivative in the hydrogenation process. Problems of selectivity of the catalytic hydrogenation of DOL have been considered in the literature.[118,140] Pd/$CaCO_3$ modified with Pb was used as the catalyst. However, the highest selectivity with respect to the conversion of DOL into LH is exhibited by γ-Al_2O_3-deposited Pd catalysts with a Pd content of 0.5%.[138] When the content of the active component is increased to 2%, the selectivity diminishes slightly, and when it is increased to 5%, the selectivity decreases substantially. Analysis of the degree of dispersion of Pd particles and their size distribution in the catalysts with different contents of the active component has shown that increase in the content of the active component results in increase in the proportion of particles of size 3.5–5 nm. The content of the dissolved hydrogen, promoting the saturation of a double bond,[128] in metal particles of diameter 5 nm corresponds to the ratio H : Pd = 1.[141,142] This is apparently the reason for the higher selectivity of 0.5% Pd/γ-Al_2O_3.

The influence of the hydrogen pressure in the range 1.01 to 5.05 MPa on the hydrogenation of DOL in the presence of Pd/Al_2O_3 has been studied.[138,143] A decrease in the selectivity at pressures above 3.03 MPa was observed. In the cases where the Pd/Al_2O_3 and Pd/$BaSO_4$ catalysts were used, the apparent activation energies were found to be approximately equal, while the reaction order with respect to the substrate is close to zero (in all the solvents) in the former case and is equal to unity (in EtOH) in the latter case. In addition, slight adsorption of the reaction products was observed.

The selectivity of hydrogenation of DOL, like that of DMEC, increases, when modifying additives are introduced into the reaction mixture.[144–146] A kinetic model for this reaction has been proposed.[147,148] Pd/C proved to be the least selective of the catalysts studied.[140,146]

Of interest are data on the hydrogenation of C≡C bonds of acetylene alcohols to C=C bonds in the presence of Pd immobilised in a polymeric matrix.[149]

This catalyst deposited on Al_2O_3[150] was used for preparing linalool. This system, like Rh-polymer/Al_2O_3 used for hydrogenation of unsaturated ketones,[95] possesses a series of advantages over the traditional heterogeneous catalysts, namely, high stability and mechanical strength, and requires no modifying additives (chemical poisons).

Hydrogenation of 3,7,11-trimethyldodec-1-yn-3-ol and 3,7,11,15-tetramethylhexadec-1-yn-3-ol. For hydrogenation of 3,7,11,15-tetramethylhexadec-1-yn-3-ol (dehydroisophytol, DHIP A_{13}, a C_{20} acetylene alcohol), the Lindlar catalyst prepared from commercial $Pb(CH_3COO)_2$ has been shown[151] to be more selective than this catalyst prepared from a preliminarily purified specimen. This fact led Rajaram and coworkers to the conclusion that microimpurities present in the commercial $Pb(CH_3COO)_2$ facilitate the selectivity of the process. In the list of these microimpurities they included Cu^{2+}, Cd^{2+}, Mn^{2+}, Fe^{3+}, and Co^{2+} ions and studied their effect on the selectivity of the Lindlar catalyst in the hydrogenation. The best results were obtained in the presence of $MnCl_2$, where the selectivity amounted to 97.2%.

A method has been patented for the selective reduction of acetylene alcohols in the presence of a Pd–M/carrier system (M is Zn, Bi, Cu, etc., the carrier is $CaCO_3$, $BaSO_4$, etc.) and a sulfur-containing or amino compound that are simply mixed with the Pd catalyst. The yield of isophytol was 98.3% and that of linalool was 98.6%.[152] Some authors recommend organophosphorus compounds as modifying additives for Pd catalysts of the hydrogenation of C_{20} acetylene alcohols and 3,7,11-trimethyldodec-1-yn-3-ol (dehydronerolidol, DHNL, A_{14}, a C_{15} acetylene alcohol).[153]

The hydrogenation reactions of C_5, C_{15}, and C_{20} acetylene alcohols to the corresponding ethylene analogues on Pd catalysts deposited on carriers of acidic or alkaline nature in the presence of iodides have been studied[154] under static and dynamic conditions in various solvents, varying the temperature, the hydrogen partial pressure, and the initial concentration of acetylene alcohol. An increase in the temperature and pressure was found to diminish the selectivity of the process. In the static system, the highest selectivity with respect to vinylcarbinol was achieved with Pd/$CaCO_3$ and Pd/ZnO–KI homogeneous-heterogeneous systems in MeOH. The author believe that the high selectivity observed with these carriers is due to their basic properties. They suggest that the reaction has the zeroth order with respect to substrate, though the relationships presented indicate that the reaction rate diminishes with decrease in the concentration of the substrate in the solution. The Pd/ZnO–KI system in EtOH was recommended for the reaction carried out under continuous conditions. However, the high starting selectivity of this catalyst (97.5%) quickly drops, due to gradual washing out of KI, which is readily soluble in EtOH.

A method of preparing ethylene alcohols from acetylene alcohols in the presence of the ShPAK-0.5 (0.5% Pd/Al_2O_3) catalyst modified with $Zn(CH_3COO)_2$, pyridine, and alkali has been developed.[16] The highest selectivity with respect to C_5, C_{10}, C_{15}, and C_{20} (99.2%–99.8%) ethylene alcohols in MeOH is achieved at a reduced hydrogen pressure. When catalysts with a controlled distribution of the active component[155] over a carrier grain have been used, high selectivity with respect to isophytol (98%) was achieved in the dynamic regime.[16] This is probably due to the absence of the internal-diffusion retardation.

Despite the fact that the use of modified Pd/Al_2O_3 for selective hydrogenation of the C_{15} and C_{20} acetylene alcohols is promising, studies aimed at the development of cheaper, more stable, more active, and no less selective catalysts are being carried out.[16] The research has several aims. The first of them is the development of novel Pd catalysts on polymeric carriers, the second is elaboration of methods for selective hydrogenation of acetylene alcohols in the presence of palladium-free catalysts, such as metal phthalocyanines (PcM) on oxides. PcM were chosen as the active component of the catalyst, in order to simulate the 'organometallic' active centre.

The selective hydrogenation of the A_{13} alcohol in the presence of Pd-containing polymeric catalysts with reaction parameters varying over wide ranges revealed the optimum substrate : catalyst

ratio, in terms of selectivity and duration of the reaction. This ratio confirmed that the formation of reactive complexes responsible for the reduction of the triple bond of the alcohol to the double bond is affected by the medium. Introduction of pyridine into the reaction system increases the selectivity of the conversion of the acetylene alcohol to the ethylene alcohol to 98%–99.3%.[149]

The selective hydrogenation of acetylene alcohols in the presence of PcM (M = Pd, Ni, Cu, Co) deposited on oxides (Al_2O_3, SiO_2) has been studied. The conditions in which the reaction was carried out, the nature of solvent, the method of the PcM deposition, and the content of the active component on the carrier have been varied. The experiments were carried out in the static and dynamic regimes.[16,156]

It was found[16] that transition from a polymolecular layer of PcM on the oxide carrier to a monomolecular layer results in an increase in the effectiveness of the catalytic action of immobilised PcM. The method of the PcM deposition on the oxide (from concentrated H_2SO_4 or from benzene) determines not only the activity of the catalyst but also the mechanism of its action. To elucidate the mechanism of the hydrogenation catalysis by PcM, kinetics of the hydrogenation of A_9 and A_{14} alcohols in the presence of $PcCo/SiO_2$ (0.2% Co, PcCo was deposited on the oxide from a solution in H_2SO_4) and $PcNi/Al_2O_3$ (0.2% Ni, PcNi was deposited on the oxide from a benzene solution) were studied. Under optimum conditions, the yield of the target product amounted to 99.2%–99.8%.

Analysis of the published papers allows the following conclusions to be drawn:

the most selective heterogeneous catalysts for hydrogenation of a triple bond to a double bond are Pd catalysts deposited on nonporous carriers ($BaSO_4$, $CaCO_3$) or on porous carriers (Al_2O_3, SiO_2) with small particles of the disperse phase (the latter has been satisfactorily confirmed by studies, which showed the dependence of the selectivity on the depth of the carrier porosity[128]);

modification of heterogeneous catalysts by inorganic additives of basic character, phosphorus- and sulfur-containing compounds, or salts of various metals favours an increase in the selectivity; the Pd–Zn system exhibits a fairly high activity with no loss in the selectivity;

catalytic systems based on PcM and Pd-containing polymers (on inorganic carriers) used for partial hydrogenation of C_5, C_{10}, C_{15}, and C_{20} acetylene alcohols possess high selectivities;

Pd/C has a low selectivity, which is attributed to the high degree of dispersion of this catalyst. The strength of the interaction between the disperse phase and the dispersion medium and thus the selectivity of the process can be controlled by varying the nature of the solvent and the concentration of the substrate.

2. The mechanism of the modification of catalysts for the selective hydrogenation of C≡C bonds

In a study of the selective hydrogenation of unsaturated ketones, interaction of the introduced additives with the solvent and the substrate within the bulk of the solution and an influence of the modifier on the heterogeneous catalyst have been observed.[16] The role of the modifier of catalysts of partial hydrogenation of C≡C bonds is that they poison the active centres at which further hydrogenation of the ethylene bond or hydrogenolysis of the substrate would have occurred[151,157,158] and promote the centres responsible for the saturation of the triple bond.[138] For example, it has been shown for Pd-containing catalytic systems that Pb, which blocks a part of the Pd surface, decreases the total adsorption of the hydrocarbon.[157] The centres with high bond energies are blocked first and, therefore, a sort of levelling of the substrate–metal bond energies occurs. The action of the modifying additives is explained as follows: the energies of metal–hydrogen and metal–substrate bonds and also the amount of hydrogen adsorbed change; the rate of release of the dissolved hydrogen decreases, since as a result of modification the activation energy of hydrogen desorption increases from 84 to 146.7 kJ mol^{-1}.[138,159] Thus, the addition of a modifying metal (for example, Pb or Zn) to the major component of the catalyst (for example, Pd) may change the electronic properties of the latter (the ligand effect) or the geometry of its surface.[160] The latter phenomenon is caused by a cluster effect or an ensemble effect.[161]

The cluster and ligand effects in bimetallic catalysts have been considered in detail in a review.[161] Clear-cut is the effect of modifying additives on the size of clusters of the active metal, which, in turn, determines the adsorption ability, activity, and selectivity of a catalytic system. The ligand effect, which is manifested as an electronic interaction between the modifier and the major component of the catalyst, causes the formation of strong bonds in the reactive complex. Charge transfer from the metal to the modifier or conversely is determined by the difference between the electronegativities of the components. In addition, the second component prevents carbonisation, poisoning, and agglomeration of a multicomponent catalyst. It also acts as a diluent of the surface, so that, of all the thermodynamically possible routes to the substrate transformation, only that reaction selectively occurs which requires a small ensemble. A definite concentration of the specifically adsorbed ions results, so that the dissolved hydrogen becomes the main hydrogenating agent.[159] However, this is inconsistent with the inferences of some researchers, who showed experimentally that the dissolved hydrogen exerts a negative effect on the selectivity of hydrogenation of acetylene compounds.[128]

Study of the thermal desorption of hydrogen and carbon monoxide from $Pd–Pb/Al_2O_3$ catalysts led Karski and Paryjczak[162] to the conclusion that the introduction of Pb into Pd/Al_2O_3 results only in a decrease in the amount of the gases sorbed, but causes no noticeable change in the activation energy of desorption.[162] In other words, these authors observed only the manifestation of the cluster effect.

Investigation of the mechanism of the action of poisons that enter in the composition of the Lindlar and Rosenmund catalysts is of some interest.[163] Analysis of the extensive literature data on the Lindlar catalyst and various methods for its modification, allowed the authors to conclude that the poisons are not involved in the catalytic process and do not occupy the active centres; they only change the structure of the catalyst surface. An electron-microscopic study showed that under the action of amines, species with low surface areas are formed.

Regarding the action of the Lindlar catalyst and the Lindlar catalyst–$MnCl_2$ catalytic system, two suggestions have been made:[151] 1) active ensembles for hydrogenation of a triple bond to a double bond and for hydrogenation of a double bond to a single bond are dissimilar; 2) there occurs a 'mobile' distribution of the cations of the modifying metal over the Pd surface. These suggestions have been confirmed by experimental results.

Effects of various substances, either present in the reaction mixture or added to it, on the selectivity of the catalytic hydrogenation of unsaturated compounds have been considered. It was noted that the mechanism of the action of additives is usually complex, nevertheless, in a number of cases it can be explained in terms of the ligand effect.[164] Introduction of electron-donor compounds, for example, piperidine, in a catalytic system results in an increase in its activity and selectivity with respect to the conversion of acetylenes to olefins.[165]

Comparing electronegativities,[166] electronic work functions, the first and second ionisation potentials, and standard electrode potentials[167] relative to Pd of the modifiers recommended in the literature, one may infer that the magnitudes of these parameters characterise to a certain extent the interaction between Pd and a modifier provided that there is information on the modification mechanism. For example, reasoning from electonegativities and assuming, as was done by Lindlar,[144] that a Pd–modifier catalytic system incorporates the modifier in the form of metal, one may conclude that modifiers act with respect to Pd as donor ligands.

A number of researchers, who have studied the action of a solution of $ZnCl_2$ (or $CdCl_2$) in a hydrogen atmosphere on the

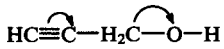
reduced 1% Pd/Al_2O_3 catalyst, inferred that complex surface clusters, $Pd-Zn/Al_2O_3$ and $Pd-Cd/Al_2O_3$, are formed.[168]

Of the possible modifiers for 0.5% Pd/Al_2O_3, $Zn(CH_3COO)_2$ was chosen.[16,169-171] The modified catalyst proved to be more selective in the hydrogenation of the A_{14} carbinol to isophytol (IP, A_{15}, a C_{20} ethylene alcohol) (93.2%) than the nonmodified catalyst (76%). Zn probably acts as a donor of electrons with respect to Pd and, therefore, it increases the possibility of the charge transfer to the acetylene alcohol. In addition, the metal–modifier bifunctional active centre levels the negative effect of the dissolved hydrogen. Finally, Zn prevents coke formation. All these effects ensure the higher selectivity of the modified catalyst. Modified Pd/Al_2O_3 was studied by various physicochemical methods. It was found that due to the modification of the catalyst, its porosity decreases from 0.57 to 0.04 and the effective pore radius decreases from 9.5 to 0.7 nm; this diminishes the influence of the internal diffusion in the hydrogenation of A_{14} in the kinetic regime. The increase in the degree of dispersion of surface Pd particles (2–3 nm) lowers the amount of the dissolved hydrogen and results in a higher selectivity of the conversion of the A_{14} alcohol to A_{15}. The decrease in $E_b(Pd_{3d_{5/2}})$ by 0.6 eV is attributed to the electron-donor properties of Zn. Based on the EXAFS spectra, the Pd–Zn distance was determined, and it was concluded that the interaction between Pd and Zn occurs via a ligand. Further modification of the catalyst with organic (pyridine) or inorganic (KOH) bases (base : catalyst = 1 : 10) made it possible to achieve the highest selectivity of the hydrogenation of the A_{14} acetylene alcohol to the A_{15} ethylene alcohol in the presence of this catalyst (99.2%).

3. Mechanism of the adsorption and catalysis of acetylene compounds

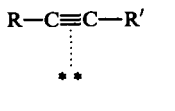
Acetylenic compounds, like ethylene compounds, can be adsorbed by both associative and dissociative mechanisms.[31,172] In the presence of hydrogen, acetylenes are adsorbed on the catalyst surface mostly by an associative mechanism.[173]

Considering adsorption of acetylene alcohols with various carbon chain lengths, one should take into account both inductive and mesomeric effects,[174] the latter withdrawing electron density from the triple bond to the oxygen atom.

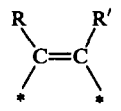


With increase in the carbon chain length, the inductive effect grows, which acts in the opposite direction, i.e. tends to increase the electron density at the C≡C bond. These effects, together with steric factors, govern the adsorption and catalysis in the case of acetylene alcohols.

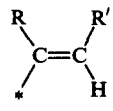
It has been suggested that selective catalytic hydrogenation of acetylene alcohols involves formation of the following surface structures:[151]



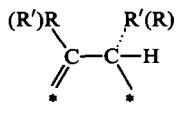
10



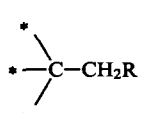
11



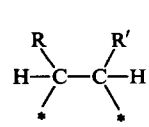
12



13



14



15

* is an active centre of the surface;

** is a diatomic active centre of the surface.

Intermediate compounds **10–12** may arise upon the reduction of an acetylene to an olefin, while structures **13–15** are intermediates on the way to the fully reduced products.

According to quantum-chemical calculations, the most probable mechanism of the hydrogenation of DMEC to DMVC involves formation of negatively charged forms of DMEC on the metal surface, though this does not rule out the possibility that the reaction occurs via an electronically excited form of DMEC, i.e. the participants of the catalytic system (modifiers, solvent) should be chosen in such a way as to provide the predominant electron transfer from the metal to the substrate.[175] Karavanov et al.[176] believe that the rate-determining factor in the hydrogenation of linalool is addition of the first mole of hydrogen.

All the foregoing attests to complexity of mechanisms of the catalysis and adsorption of acetylene compounds. This is probably due to the fact that active centres with different coordination numbers exist on the catalyst surfaces. The active centres with high coordination numbers, where a competing mechanism of adsorption is possible, are likely to prevail at faces of crystals. On the contrary, active centres with low coordination numbers, that favour formation of an involved multi-ligand complex on chemisorption, predominate at corners, edges, and defects. It should be noted that those alkynes[151] are involved in the complex formation, which change the surface structure of the catalyst in the course of the adsorption and catalysis.

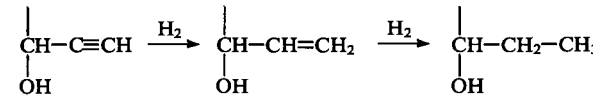
In order to identify details of the mechanism of the selective hydrogenation of acetylene alcohols, kinetics of hydrogenation of C_5, C_{15}, and C_{20} alcohols under static conditions have been studied, such parameters as T_c, P_{H_2}, c_O, c_C, and the nature of solvent being varied.[16]

Using Eqn (4) and taking into account the formal expression

$$W_1' = \frac{a_i x_i}{xX_1 + Qx_2} \frac{P_{H_2}}{1 + b_1 P_{H_2}}, \qquad (9)$$

where x_i are the reduced concentrations of acetylene ($i = 1$), ethylene ($i = 2$), and saturated alcohols ($i = 3$), for the reaction sequence depicted in Scheme 6, we managed to fit the experimental data on the hydrogenation of acetylene alcohols in methanol (Fig. 3).

Scheme 6



Based IR spectroscopic data, acetylene and ethylene alcohols were arranged, in terms of their adsorption ability, in the sequence $C_{20} > C_{15} > C_5$; the selectivity of their hydrogenation changes in the reverse order.

It should be noted that the generalised curves (Fig. 3) have an induction period at $0 \leqslant \theta \leqslant \theta_i$, the duration of which depends on the nature of alcohol. The above-given equation (9) does not hold in this region. The experimental data in this region are adequately described by the following relation:

$$\frac{dx_1}{d\theta} = -\frac{B}{x_1^n}, \qquad (11)$$

where B is a parameter.

The results of the interpretation of the experimental data on C_5, C_{15}, and C_{20} alcohols are presented in Table 3. The induction period has been attributed to the formation of a hetero-ligand reactive complex, which is responsible for the selectivity of the process, on the catalyst surface. The higher the molecular mass (M) of the alcohol, the stronger is its coordination with the catalyst, the lower is θ_i and the selectivity of the process.

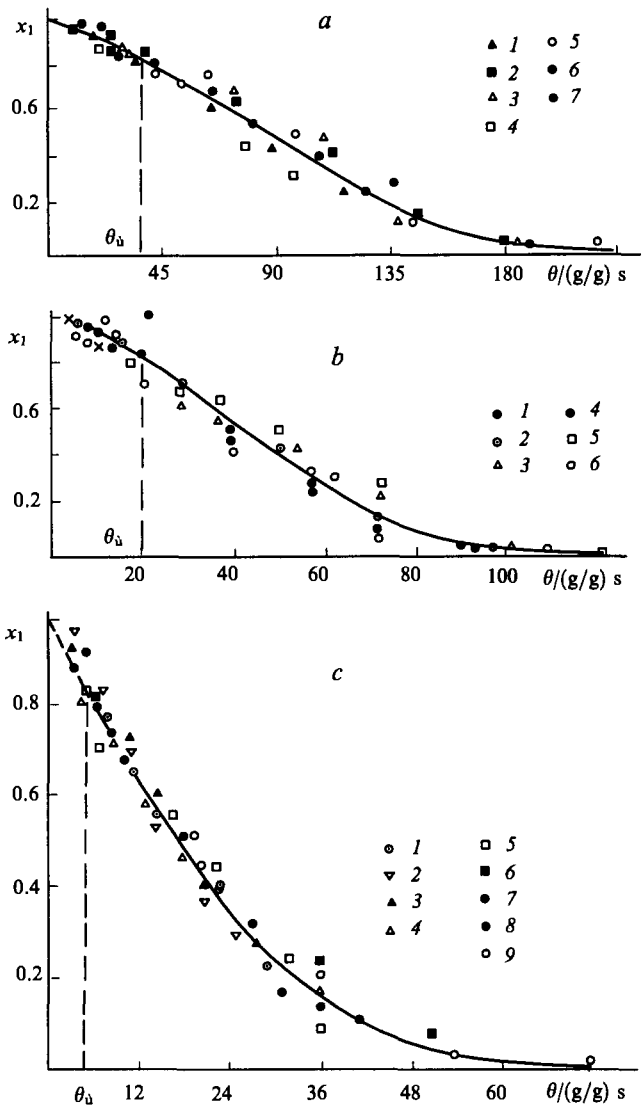


Figure 3. The dependence of x_1 on θ during hydrogenation of acetylenic alcohols A_9 (*a*), A_{13} (*b*), and A_{14} (*c*).
(*a*) T = 60 °C, P_{H_2} = 0.04 MPa, q(g/g): (*1*) 33, (*2*) 50, (*3*) 25, (*4*) 25, (*5*) 14, (*6*) 13, (*7*) 63;
(*b*) T = 40 °C, P_{H_2} = 0.07 MPa, q(g/g): (*1*) 55, (*2*) 50, (*3*) 30, (*4*) 15, (*5*) 15, (*6*) 100;
(*c*) T = 40 °C, P_{H_2} = 0.07 MPa, q(g/g): (*1*) 250, (*2*) 250, (*3*) 250, (*4*) 200, (*5*) 175, (*6*) 125, (*7*) 100, (*8*) 88.5, (*9*) 50.0

Table 3. The effect of the nature of alcohol on the characteristics of the induction period and the selectivity (S) of the process (T = 40 °C, P_{H_2} = 0.07 MPa).

Acetylenic alcohol	$n+1$	θ_i	S(%)
C_5	1.50	82.8	98.6
C_{15}	1.22	20.0	97.6
C_{20}	1.16	5.0	85.3

Analysis of the induction periods for acetylene alcohols affords the following relationship:

$$\theta_i = \frac{126\,764}{M^{1.65}} \quad (M^{n+1} = \text{const}). \tag{12}$$

On the basis of this equation, the θ_i and n values for dehydrolinalool were calculated: θ_i = 28 (g/g) s and $(n+1)$ = 1.32, which agrees with experimental results.[16]

Owing to the competing character of adsorption from solutions, the adsorption of substrates may be considerably affected by the ability of the solvent to solvate reactants and to be coordinated by the catalyst. When considering multi-component multiphase systems, one should take into account the strength of the interaction between the disperse phase and the dispersion medium and the phenomenon of drainage[177] of the dispersion medium from the gap (pore) formed by the lyophilic disperse phase. This accounts for the fact that the hydrogenation of A_{13} in isopropanol involves higher energetic barriers (45 kJ mol^{-1}) than that in methanol (25 kJ mol^{-1}) and that of all the solvents studied, methanol provides the optimum selectivity with respect to ethylene alcohols.

As a result of studies on adsorption and using IR spectroscopic data, we revised[16] the sites of the coordination of H_2 and acetylene alcohol to a PcM molecule. It turned out that the alcohol is coordinated by the nitrogen atoms of the azo bridges. At low P_{H_2} values, hydrogen is predominantly coordinated to the central metal atom, while at elevated P_{H_2} [10.1 MPa] it is coordinated to both the metal atom and the organic ligand.

Analysis of the literature data on the selective hydrogenation of acetylene alcohols in the presence of PcM attached to inorganic carriers, Pd-containing polymeric catalysts, and modified Pd catalysts made it possible to identify some general regularities: the reaction proceeds via a hetero-ligand reactive complex (solvent, substrate, hydrogen, catalyst, modifier, and carrier), which has a multilayer structure; all the participants of the complex (their nature and amount) exert a mutual influence on the catalytic activity and selectivity of the process; the reactants are activated on different active sites ('metallic' or 'organometallic'). The same regularities were found for the hydrogenation of unsaturated ketones. The catalytic system should be regarded as a homogeneous-heterogeneous system. The validity of this description is confirmed by the observed non-linear dependences of the reaction rates on the ratio between the concentrations of the participants of the reaction.

References

1. O V Krylov *Kinet. Katal.* **34** 250 (1993)
2. S L Kiperman, *Osnovy Khimicheskoi Kinetiki v Geterogennom Katalize* (Fundamentals of Chemical Kinetics in Heterogeneous Catalysis) (Moscow: Khimiya, 1979) p. 349
3. S L Kiperman *Kinet. Katal.* **22** 30 (1981)
4. K I Zamaraev *Usp. Khim.* **62** 1051 (1993) Original version in English in *Chemistry for the 21st Century Monographs. Perspectives in Catalysis* Eds J M Thomas, K I Zamaraev (Oxford: Blackwell Scientific) pp 35–65
5. J W Kern, R L Shrinen, S K Adams *J. Am. Chem. Soc.* **47** 1147 (1925)
6. R Cornubert, H G Eggert *Bull. Soc. Chim. Fr.* **21** 522 (1954)
7. A M Sokol'skaya, L Ya Iriskina *Uch. Zap. Kaz. Goz. Univ., Ser. Khim.* **22** 66 (1956)
8. French P. 2 247 445; *Chem. Abstr.* **83** 198 573k (1975)
9. E Ucciani, L Tanguy *C. R.Hebd. Seances Acad. Sci.* **284** 577 (1977); *Ref. Zh. Khim.* 18 Zh 125 (1977)
10. L Kh Freidlin, L I Gvinter, V A Zamureenko, L N Suvorova *Izv. Akad. Nauk SSSR, Ser. Khim.* 817 (1976)
11. D V Sokol'skii, A I Erzhanov *Dokl. Akad. Nauk SSSR* **93** 503 (1953)
12. P Four, F Guibe *Tetrahedron Lett.* **23** 1825 (1982)
13. M E Veselova, E M Sul'man, in *Raschetnye Metody v Fizicheskoi Khimii: Mezhvuzovskii Tematicheskii Sb. Nauch. Tr.* (Computational Methods in Physical Chemistry: Intercollegiate Topical Collection of Scientific Reports) (Kalinin: Kalinin Gos. Univ., 1988) p. 106
14. E M Sulman, M E Veselova *React. Kinet. Catal. Lett.* **37** 211 (1988)

15. M E Veselova, Candidate Thesis in Chemical Sciences, Institute of Organic Chemistry and Electrochemistry, Academy of Sciences of the Kaz. SSR, Alma-Ata, 1983
16. E M Sul'man, Doctoral Thesis in Chemical Sciences, Institute of Organic Chemistry, Academy of Sciences of the USSR, Moscow, 1989
17. G D Zakumbaeva, D V Sokol'skii *Izv. Akad. Nauk Kaz. SSR, Ser. Khim.* (1) 75 (1962)
18. C A Brown, H C Brown *J. Org. Chem.* **31** 3989 (1966)
19. Y Nitta, T Imanaka, S Teranisi *J. Chem. Soc. Jpn.* **72** 2363 (1969)
20. J Endrysova, M Kraus *Collect. Czech. Chem. Commun.* **35** 62 (1970)
21. I Jardine, F J McQuillin *J. Chem. Soc., C* 458 (1966)
22. K Brietner, E Roginsky, P N Eylander *J. Org. Chem.* **24** 1855 (1959)
23. V Macho *Chem. Prum.* **21** 9 (1971)
24. G Minmin, Z Shengyong, W Lifen *Org. Chem. (China)* (6) 454 (1984); *Ref. Zh. Khim.* 11 B 4 367 (1985)
25. G L Dzhaparidze, E Sh Kenchadze, T P Gegenava, N V Nekrasov, M M Kostyukovskii, S L Kiperman *Kinet. Katal.* **26** 673 (1985)
26. J A Cabello, J M Campelo, A Garcia, D Luna, J M Marianas *React. Kinet. Catal. Lett.* **26** 447 (1984)
27. A G Sarmurzina, D V Sokol'skii, in *Prikladnaya i Teoreticheskaya Khimiya* (Applied and Theoretical Chemistry) (Alma-Ata: Nauka, 1975) No. 6, p. 246
28. A G Sarmurzina, A F Razumkov, D V Sokol'skii, in *Prikladnaya i Teoreticheskaya Khimiya* (Applied and Theoretical Chemistry) (Alma-Ata: Nauka, 1975) No. 6, p. 241
29. N V Borunova, L Kh Freidlin, M L Khidekel', S S Danielova, V A Avilov, P S Chekryi *Izv. Akad. Nauk SSSR, Ser. Khim.* 434 (1968)
30. J Bo, Z Huanpei, J Zilin *Fenzi Chuihua* 7 (1) 73 (1993)
31. L Kh Freidlin, L I Gvinter, V A Zamureenko *Zh. Org. Khim.* **9** 3 (1973)
32. G D Zakumbaeva *Vzaimodeistvie Organicheskikh Soedinenii s Poverkhnost'yu Metallov VIII Gruppy* (Interaction of Organic Compounds with the Surface of Group VIII Metals) (Alma-Ata: Nauka, 1978)
33. Jpn. P. 5 226; *Ref. Zh. Khim.* 18 N 48 (1964)
34. J Hines, H F O'Driscol, G L Rempel *J. Catal.* **38** 435 (1975)
35. H Fukawa, V Izumi, S Kanatsu, S Akabori *Bull. Chem. Soc. Jpn.* **35** 1703 (1962)
36. V Izumi, S Akabori, H Fukawa, S Tatumi, M Imaida, T Fukuda, S Komatu, in *The Third International Congress on Catalysis, Amsterdam, 1965* Vol. 2, p. 1364
37. BRD P. 1 196 632; *Ref. Zh. Khim.* 9 H 47 (1967)
38. J Wisniak, M Herskowitz, D Roffe, S Smilovitz *Ind. Eng. Chem., Prod .Res. Dev.* **15** 163 (1976)
39. Bourdiol, Calcagni, Ducasse *Bull. Soc. Chim. Fr.* **8** 375 (1941)
40. S Kishida, S Teranishi *Bull. Chem. Soc. Jpn.* **41** 2528 (1968)
41. G M Zhabrova *Usp. Khim.* **20** 456 (1951)
42. L Kh Freidlin, N V Borunova, A S Nekrasov, S S Danielova, L G Emel'yanov, N A Nevolina *Izv. Akad. Nauk SSSR, Ser. Khim.* 135 (1968)
43. Jpn. P. 22 058; *Ref. Zh. Khim.* 16 N 47 (1967)
44. US P. 2 825 743; *Chem. Abstr.* **52** 11 895d (1958)
45. T Tsuda, T Fujii, K Kawasaki, T Saegusa *J. Chem. Soc., Chem. Commun.* **21** 1013 (1980)
46. M A Miropol'skaya, N I Fedotova, A Ya Veinberg *Zh. Obshch. Khim.* **32** 2214 (1962)
47. L Kh Freidlin, N V Borunova, L I Gvinter, S S Danielova *Zh. Fiz. Khim.* **42** 98 (1968)
48. USSR P. 163 172; *Byull. Izobret.* **12** 21 (1964)
49. L Kh Freidlin, L I Gvinter, N V Borunova, in *Kataliticheskie Reaktsii v Zhidkoi Faze: Mater. II Vsesoyuz. Konf. po Kataliticheskim Reaktsiyam v Zhidkoi Faze* (Catalytic Reactions in the Liquid Phase: Proceedings of the Second All-Union Conference on Catalytic Reactions in the Liquid Phase) (Alma-Ata: Nauka, 1967) p. 245
50. US P. 2 272 122; *Chem. Abstr.* **36** 3 514b (1942)
51. US P. 2 783 257; *Chem. Abstr.* **51** 14 787f (1957)
52. Br. P. 788 301; *Chem. Abstr.* **52** 12 914h (1958)
53. Jpn. P. 12 914; *Ref. Zh. Khim.* 4 R 447P (1967)
54. P Teisseire, B Corbier *Recherches* **12** 74 (1962)
55. L Kh Freidlin, N V Borunova, L I Gvinter *Dokl. Akad. Nauk SSSR* **163** 1173 (1965)
56. N V Borunova, L Kh Freidlin, L I Gvinter *Izv. Akad. Nauk SSSR, Ser. Khim.* 1568 (1966)
57. L Kh Freidlin, N V Borunova, G I Samokhvalov, M A Miropol'skaya, M Ts Yantonovskii, L I Gvinter, N I Fedotova *Izv. Akad. Nauk SSSR, Ser. Khim.* 996 (1964)
58. L Kh Freidlin, L I Gvinter, N V Borunova, S F Dymova, I N Kustanovich *Izv. Akad. Nauk SSSR, Ser. Khim.* 1052 (1972)
59. N V Borunova, L Kh Freidlin, L I Gvinter, T A Atabekov, V A Zamureenko, I N Kustanovich *Izv. Akad. Nauk SSSR, Ser. Khim.* 1299 (1972)
60. L Kh Freidlin, N V Borunova, L I Gvinter *Dokl. Akad. Nauk SSSR* **207** 1141 (1972)
61. N V Borunova, A A Slinkin, L Kh Freidlin, T A Atabekov *Izv. Akad. Nauk SSSR, Ser. Khim.* 1056 (1972)
62. N V Borunova, T Ya Rybinskaya, T A Atabekov, L Kh Freidlin, V A Zamureenko *Izv. Akad. Nauk SSSR, Ser. Khim.* 516 (1973)
63. O B Sannikov, E M Sul'man, O S Popov, T V Ankudinova, G I Samokhvalov, M K Shakhova, in *Voprosy Kinetiki i Kataliza* (Problems of Kinetics and Catalysis) (Ivanovo: Izd. Khim.-Technol. Inst., 1979) p. 53
64. E M Sul'man, O B Sannikov, O S Popov, T V Ankudinova, M K Shakhova, in *Voprosy Kinetiki i Kataliza* (Problems of Kinetics and Catalysis) (Ivanovo: Izd. Khim.-Technol. Inst., 1980) p. 108
65. E M Sul'man, O S Popov *Khim.-Farm. Zh.* **21** 1362 (1987)
66. E M Sul'man, O S Popov, G I Samokhvalov *Khim.-Farm. Zh.* **22** (1) 70 (1988)
67. A I Gontar', O S Popov, E M Sul'man, T V Ankudinova, O B Sannikov, M K Shakhova, G I Samokhvalov *Khim.-Farm. Zh.* **17** (2) 69 (1983)
68. K Frerich *Chem.Tech.* **45** (2) 67 (1993)
69. L I Gvinter, L Kh Freidlin, N V Borunova, G Ya Starodubskaya *Izv. Akad. Nauk SSSR, Ser. Khim.* 2318 (1972)
70. L I Gvinter, L Kh Freidlin, L N Suvorova *Izv. Akad. Nauk SSSR, Ser. Khim.* 2808 (1977)
71. E M Sul'man, O B Sannikov, T V Ankudinova, M K Shakhova, G I Samokhvalov, in *Voprosy Kinetiki i Kataliza* (Problems of Kinetics and Catalysis) (Ivanovo: Izd. Khim.-Technol. Inst., 1978) p. 44
72. E M Sul'man, O S Popov,O B Sannikov, T V Ankudinova, M K Shakhova, G I Samokhvalov, in *Kataliticheskie Reaktsii v Zhidkoi Faze: Tez. Dokl. V Vsesoyuz. Konf.* (Catalytic Reactions in the Liquid Phase. Abstracts of Reports at the Fifth All-Union Conference on Catalytic Reactions in the Liquid Phase) (Alma-Ata: Nauka, 1978) p. 124
73. O B Sannikov, E M Sul'man, G I Samokhvalov, T V Ankudinova, M K Shakhova, in *Voprosy Kinetiki i Kataliza* (Problems of Kinetics and Catalysis) (Ivanovo: Izd. Khim.-Technol. Inst., 1978) p. 51
74. A Ermakova, O B Sannikov, E M Sul'man *Kinet. Katal.* **23** 178 (1982)
75. O N Temkin, L G Bruk, A V Zeigarnik *Kinet. Katal.* **34** 445 (1993)
76. L I Gvinter, A V Ablov, L Kh Freidlin, L N Suvorova, V M Ignatov *Izv. Akad. Nauk SSSR, Ser. Khim.* 191 (1980)
77. USSR P. 701 990; *Byull. Izobret.* **45** 100 (1979)
78. Jpn. Appl. 58-19 656; *Izobret. Stran Mira* **3** 492 (1983)
79. T O Omarkulov, U S Suyunbaev, S V Goncharova, D V Sokol'skii *Zh. Fiz. Khim.* **59** 215 (1985)
80. D V Sokol'skii, T O Omarkulov, S V Goncharova, U S Suyunbaev *Dokl. Akad. Nauk SSSR* **289** 913 (1986)
81. BRD P. 2 640 026; *Chem. Abstr.* **87** 38 884a (1977)
82. BRD Appl. 3 006 867; *Chem. Abstr.* **5** 168 554u (1981)
83. Eur. Appl. 0 034 804; *Izobret. Stran Mira* 35 (1981)
84. A Yermakova, E M Sulman, O S Popov, O B Sannikov, A I Gontar, L B Dolzhenco *React. Kinet. Catal. Lett.* **29** 409 (1985)
85. E M Sul'man, in *Voprosy Kinetiki i Kataliza* (Problems of Kinetics and Catalysis) (Ivanovo: Izd. Khim.-Technol. Inst., 1985) p. 12
86. E M Sulman, A Yermakova, O S Popov *React. Kinet. Catal. Lett.* **33** 339 (1987)
87. E M Sul'man, O S Popov, A Ermakova *Kinet. Katal.* **29** 509 (1988)
88. D I Kochubei, T G Starostina, P G Tsyrul'nikov, K I Zamaraev *Kinet. Katal.* **34** 716 (1993)

89. A M Efstathiou, T Chafik, D Bianchi, C O Benneti, in *New Frontier Catalysis: Proceedings of the 10th International Congress on Catalysis, Budapest, 1993*, p. 1563
90. V V Rozanov, Tsao Yamin, O V Krylov *Kinet. Katal.* **34** 131 (1993)
91. E M Sul'man, O S Popov, O B Sannikov, G I Samokhvalov, T V Ankudinova, M K Shakhova, A I Gontar' *Khim.-Farm. Zh.* **20** (6) 727 (1986)
92. F R Hartley *A New Generation of Catalysts* (Translated into Russian; Moscow: Mir, 1989)
93. E Sh Mirzoeva, Candidate Thesis in Chemical Sciences, Institute of Organoelement Compounds, Academy of Sciences of the USSR, Moscow, 1988
94. E M Sul'man, L M Bronshtein, T V Ankudinova, E Sh Mirzoeva, A I Sidorov, P M Valetskii, S V Vinogradova, Yu E Avtushenko *Khim.-Farm. Zh.* **23** (12) 59 (1990)
95. A I Sidorov, E M Sulman, L M Bronshtein, T V Ankudinova, Yu E Avtushenko, E Sh Mirsoeva, E Yu Baukova, P M Valetsky *React. Kinet. Catal. Lett.* **44** 57 (1991)
96. A I Sidorov, E M Sul'man, L M Bronshtein, T V Ankudinova, Yu E Avtushenko *Kinet. Katal.* **34** 87 (1993)
97. A I Sidorov, Candidate Thesis in Chemical Sciences, Institute of Organic Chemistry, Russian Academy of Sciences, Moscow, 1992
98. L Kh Freidlin, Yu A Kopyttsev, N M Nazarova *Zh. Org. Khim.* **12** 934 (1976)
99. M A Esteruelas, A M Lopez, L A Oro, A Perez, M Schulz, H Werner *Organometallics* **12** 1823 (1993)
100. L P Shuikina, A I El'natanova, L S Kovaleva, O P Parenago, V M Frolov *Kinet. Katal.* **22** 177 (1981)
101. V M Frolov, O P Parenago, G N Bondarenko, L S Kovaleva, A I El'natanova, L P Shuikina, G M Cherkashin, E Ya Mirskaya *Kinet. Katal.* **22** 1356 (1981)
102. G M Cherkashin, L P Shuikina, O P Parenago, V M Frolov *Kinet. Katal.* **27** 1509 (1986)
103. A D Pomogailo *Kataliz Immobilizovannymi Kompleksami* (Catalysis by Immobilized Complexes) (Moscow: Nauka, 1991)
104. E Ya Mirskaya, A I El'natanova, L S Kovaleva, O P Parenago, V M Frolov *Selektivnoe Gidrirovanie Atsetilenovykh Soedinenii v Olefiny v Prisutstvii Nanesennykh Palladiikompleksnykh Katalizatorov s Azotsoderzhashchimi Ligandami* (Selective Hydrogenation of Acetylene Compounds to Olefins in the Presence of Deposited Palladium-Complex Catalysts with Nitrogen-Containing Ligands) (Moscow, 1983) . Article deposited at the All-Union Institute of Scientific and Technical Information (VINITI), No 5349 (in Russian)
105. A N Karavanov, I G Batirev *Mendeleev Commun.* 62 (1993)
106. A N Karavanov, V M Gryaznov *Kinet. Katal.* **25** 74 (1984)
107. V M Gryaznov *Kinet. Katal.* **23** 1358 (1982)
108. V M Gryaznov *Khim.-Farm. Zh.* **13** (7) 74 (1979)
109. Jpn. Appl. 56-150 022; *Ref. Zh. Khim.* 6 N 9P (1983)
110. M A Aramendia, V Borau, C Jimenez, J M Marinas, M E Sempere, F J Urbano, L Villar, in *New Frontier Catalysis: Proceedings of the 10th International Congress on Catalysis, Budapest, 1993*, p. 2435
111. Fr. Appl. 2 311 767; *Ref. Zh. Khim.* 3 N 275P (1978)
112. Jpn. Appl. 53-133 503; *Ref. Zh. Khim.* 17 N 4P (1981)
113. Jpn. Appl. 53-160 773; *Ref. Zh. Khim.* 20 N 9P (1981)
114. Jpn. Appl. 55-47 015; *Ref. Zh. Khim.* 24 N 13P (1981)
115. Jpn. Appl. 57-185 229; *Ref. Zh. Khim.* 23 N 11P (1983)
116. BRD P. 2 431 929; *Ref. Zh. Khim.* 8 L 249P (1982)
117. Jpn. Appl. 60-04 139; *Chem. Abstr.* **102** 148 862c (1985)
118. L Cerveny, B Vostry, V Ruzicka *Collect. Czech. Chem. Commun.* **46** 2676 (1981)
119. L Cerveny, N Thi Thang, V Ruzicka *Chem. Prum.* **33** 192 (1983)
120. BRD Appl. 3 312 252; *Ref. Zh. Khim.* 18 L 160P (1985)
121. Jpn. Appl. 59-196 828; *Ref.Zh. Khim.* 18 N 16P (1985)
122. Jpn. Appl. 59-196 829; *Ref. Zh. Khim.* 18 N 17P (1985)
123. Jpn. Appl. 59-227 829; *Ref. Zh. Khim.* 24 N 7P (1985)
124. US P. 4 484 015; *Ref. Zh. Khim.* 17 N 15P (1985)
125. H R Aduriz, B Coq, F Figueras *J. Catal.* **129** 47 (1991)
126. Fr. Appl. 2 458 524; *Ref. Zh. Khim.* 8 P 247 (1982)
127. U Myaeorg, Kh Timoteus *Izv. Akad. Nauk Est. SSR, Khim. Geol.* 180 (1985)
128. J Karturan, R Kampostrini, in *Kataliz Klasterami i Dispersnymi Metallami: Mezhdunar. Simp. po Svyazi mezhdu Gomogennym i Geterogennym Katalizom* (Catalysis by Clusters and Dispersed Metals: International Symposium on the Relation between Homogeneous and Heterogeneous Catalysis) (Novosibirsk: Nauka, 1986) Vol. 3, p. 146
129. V A Naidin, Candidate Thesis in Chemical Sciences, Institute of Chemical Sciences, Alma-Ata, 1972
130. Neth. P. 6 405 225; *Chem. Abstr.* **62** 9 005h (1965)
131. L N Ivanova, V F Kucherov *Dokl. Akad. Nauk SSSR* **178** 852 (1968)
132. USSR P. 417 151; *Ref. Zh. Khim.* 7 N 197P (1975)
133. G D Zakumbaeva, N A Zakarina, N F Toktabaeva, A V Ermolaev, A N Abramov *Zh. Prikl. Khim.* **54** 1192 (1981)
134. E A Kaznyshkin, I V Budnii, E P Stepanov, N I Borodina *Osn. Org. Sin. Neftekhim.* **20** 24 (1984)
135. T M Dukhovnaya, K K Dzhardamalieva, D T Nigmetova, D V Sokol'skii *Zh. Fiz. Khim.* **57** 617 (1983)
136. P B Wells *Platinum Met. Rev.* **7** 18 (1963)
137. S P Mel'nikov, A N Vorob'ev, A A Petrov *Zh. Org. Khim.* **9** 1586 (1973)
138. A M Pak, D V Sokol'skii *Selektivnoe Gidrirovanie Nepredel'nykh Oksosoedinenii* (Selective Hydrogenation of Unsaturated Oxo-Compounds) (Alma-Ata: Nauka, 1983)
139. US P. 2 516 826; *Chem. Abstr.* **45** 5 711h (1951)
140. L Cerveny *Chem. Eng. Commun.* **83** 31 (1989)
141. W Palczewska *Adv. Catal.* **24** 245 (1975)
142. A Janko, W Palczewska, I Samerska *J. Catal.* **61** 264 (1980)
143. A M Pak, O I Kartonozhkina, A Sh Kuanyshev, in *Kataliz i Kataliticheskie Protsessy Khim.-Farmatsevt. Proizvodstva: Tez. Dokl. II Vsesoyuz. Konf.* (Catalysis and Catalytic Processes in the Chemical and Pharmaceutical Industries: Abstracts of Reports at the Second All-Union Conference) (Moscow: All-Union Research Chem.-Technol. Inst. of Medical and Microbiological Industries, 1989) p. 126
144. H Lindlar *Helv. Chim. Acta* **35** 446 (1952)
145. USSR P. 730 674; *Byull. Izobret.* **16** 82 (1980)
146. L Cerveny, M Kuncova, V Ruzicka *Collect. Czech. Chem. Commun.* **46** 1258 (1981)
147. E M Sul'man, V G Matveeva, T V Ankudinova *Kinet. Katal.* **35** 385 (1994)
148. V G Matveeva, E M Sul'man, T V Ankudinova *Khim.-Farm. Zh.* **28** (1) 46 (1994)
149. E M Sul'man, L M Bronshtein, T V Ankudinova *Kinet. Katal.* **34** 61 (1993)
150. V G Matveeva, E M Sul'man, L M Bronshtein, T V Ankudinova *Khim.-Farm. Zh.* (1995) in the press
151. J Rajaram, A P S Narula, H P S Chawla, Sukh Dev *Tetrahedron* **39** 2315 (1983)
152. Appl. Jpn. 56-120 626; *Chem. Abstr.* **96** 8 580s (1982)
153. Appl. Jpn. 57-189 578 ; *Ref. Zh. Khim.* 13 P 11P (1985)
154. Zh Mukataev, Candidate Thesis in Chemical Sciences, Institute of Organic Chemistry and Electrochemistry, Academy of Sciences of the Kaz. SSR, Alma-Ata, 1987
155. I M Zhvanetskii, F D Klebanova, E A Katsman, A S Berenblyum *Kinet. Katal.* **31** 888 (1990)
156. E M Sul'man, B V Romanovskii, T V Ankudinova, I Yu Tyamina, S P Dorozhko, O S Popov, in *V Vsesoyuz. Konf. po Koordinatsionnoi i Fizicheskoi Khimii Porfirinov: Tez. Dokl.* (Abstracts of Reports at the Fifth All-Union Conference on the Coordination and Physical Chemistry of Porphyrins) (Ivanovo: Izd. Khim.-Technol. Inst., 1988) p. 207
157. M S Kharson, E M Davidov, S L Kiperman *React. Kinet. Catal. Lett.* **5** 125 (1976)
158. M S Kharson, S L Kiperman *React. Kinet. Catal. Lett.* **8** 383 (1978)
159. D V Sokol'skii, G D Zakumbaeva *Adsorbtsiya i Kataliz na Metallakh VIII Gruppy v Rastvorakh* (Adsorption and Catalysis on Group VIII Metals in Solutions) (Alma-Ata: Nauka, 1973)
160. W Sachtler *Chem. Tech.* **13** 434 (1983)
161. A A Slinkin *Kinetika i Kataliz (Itogi Nauki i Tekhniki)* [Kinetics and Catalysis (Advances in Science and Engineering)] (Moscow: Izd. VINITI, 1982) Vol. 10, p. 5
162. St Karski, Y Paryjczak *React. Kinet. Catal. Lett.* **18** 405 (1981)

163. A B McEwen, M J Guttieri, W F Maier, R M Laine, Y Shvo *J. Org. Chem.* **48** 4436 (1983)
164. J P Boitiaux, J Cosyns, G Martino, in *Metal-Support and Metal-Additive Effective Catalytic: Proc. Int. Symp., Amsterdam, 1982* p. 335
165. J P Boitiaux, J Cosyns, S Vasudevan *Appl. Catal.* **15** 317 (1985)
166. S S Batsanov *Elektrootritsatel'nost' Elementov i Khimicheskaya Svyaz'* (Electronegativity of the Elements and the Chemical Bond) (Novosibirsk: Izd. Sib. Otd. Akad. Nauk SSSR, 1962)
167. *Spravochnik Khimika* (The Chemist's Handbook) (Moscow; Leningrad: Izd. Khim. Lit., 1965) Vol. 4, p. 1919
168. G D Zakumbaeva, V A Naidin, T S Dagirov, in *Nauchnye Osnovy Prigotovleniya Katalizatorov: Tez. Dokl. Vsesoyuz. Soveshch.* (Scientific Principles of the Preparation of Catalysts: Abstracts of Reports at the All-Union Conference) (Novosibirsk: Nauka, 1983) p. 110
169. E M Sul'man, O S Popov, A Yermakova, A A Belyaev *React. Kinet. Catal. Lett.* **36** 59 (1988)
170. E M Sulman, A Ermakova, O S Popov *Khim.-Farm. Zh.* **21** 1124 (1987)
171. E M Sul'man, A I Sidorov, T V Ankudinova, B N Blinov, in *The 11th International Congress "SHISA '93", Prague, 1993* p. 42
172. S D Jackson, N J Casey *React. Kinet. Catal. Lett.* **49** 231 (1993)
173. D V Sokol'skii, L V Korolev, A U Alikhanova, in *Mekhanizm Kataliticheskikh Reaktsii: Mater. III Vsesoyuz. Konf.* (Mechanisms of Catalytic Reactions: Proceedings of the Third All-Union Conference) (Novosibirsk: Nauka, 1982) Part 1, p. 191
174. C K Ingold *Structure and Mechanism in Organic Chemistry* (London: Cornell University Press, 1969) (Translated into Russian; Moscow: Mir, 1973)
175. A D Chuvylkin, A M Pak, V B Kazanskii *Kinet. Katal.* **25** 1315 (1984)
176. A N Karavanov, V N Gryaznov, N R Roman, M G Botyrev *Kinet. Katal.* **32** 1162 (1991)
177. V V Yaminskii, V S Yushchenko, E A Amelina, E D Shchukin *Kolloidn. Zh.* **44** 956 (1982)

Russian Chemical Reviews 63 (11) 937–944 (1994)
©1994 Russian Academy of Sciences and Turpion Ltd

UDC 541.128.49.35

Metal-complex catalysts in the hydrogenation of unsaturated glycerides of natural oils

S R Savel'ev, N F Noskova

Contents

I. Introduction 937
II. Carbonyl, chelate, and other complexes of the Group VIII transition metals 937
III. Ziegler–Natta catalysts 938

Abstract. Information on the use of organometallic catalysts for the hydrogenation of natural oils published since 1979 is reviewed. Organometallic systems of the Ziegler–Natta type are shown to be the most promising. The nature of the catalytic activity of complex organometallic hydrogenation systems is discussed. The bibliography includes 84 references.

I. Introduction

Catalytic hydrogenation is the method mainly used in the treatment of natural oils and fats, and is widely used, for example, in the production of detergents and greases, in the oiling of leathers, and in the preparation of esters, especially in the food products industry.

The industrial production of hydrogenated fats for foodstuffs and for technical applications is carried out in the presence of heterogeneous, suspended catalysts, mainly based on nickel or on nickel–copper (with or without carriers), and also on stationary catalysts.[1] However, heterogeneous catalysts for the hydrogenation of fats have some serious shortcomings: their activity and selectivity are relatively low, and high temperatures and pressures are needed to obtain adequate performance.

In recent years studies of the hydrogenation of fats in the presence of metal-complex catalyts have attracted wide interest. Homogeneous organometallic catalysts offer a high selectivity in the hydrogenation of fats. The most promising metal-complex catalysts were found to be those of the Ziegler–Natta type, with an activity not only much greater than the activity of heterogeneaeous catalysts but also adequate for low-temperature operation. This feature not only safeguards the biological properties of the fats but also offers substantial savings in energy.

In the last 10–15 years there has been a marked jump in our understanding of the nature of the catalytic activity of organometallic catalytic complexes. The combined use of Mössbauer, EPR, and IR spectroscopy, of magnetic susceptibility methods, etc. have made it clear that associated polynuclear complexes are responsible for the catalytic effects.

The aim in this review is to assess the state and the prospects of this new field of study: the development and application of metal-complex catalysts for the hydrogenation of the unsaturated glycerides of oils and fats. Much of the work on the Ziegler–Natta catalysts discussed in the review was carried out at the laboratory for organometallic catalysts of the Institute for Organic Catalysis and Electrochemistry of the National Academy of Sciences of the Republic of Kazakhstan.

S R Savel'ev, N F Noskova Laboratory of organometallic catalysts of the Institute of Organic Catalysis and Electrochemistry, National Academy of Sciences of the Republic of Kazakhstan, 142 ul. K Marxa, 480100 Alma-Ata. Tel. (7-3272) 61-9874

Received 4 July 1994
Uspekhi Khimii 63 (11) 995–1003 (1994); translated by J I Carasso

II. Carbonyl, chelate, and other complexes of the Group VIII transition metals

The main constituents of fats and oils are the triglycerides, containing radicals of saturated (palmitic, stearic, etc.) and of unsaturated fatty acids (oleic, linoleic, linolenic, etc.).

The first review of studies of homogeneous hydrogenation was published by James.[2] It dealt mainly with the work of Shashimoto, Frankel, and Cecchi.

James pointed out that a stage of positional isomerisation of the non-conjugated substrate (triene, diene) into the conjugated analogue precedes the hydrogenation of linolenate and of linoleate in the presence of metal carbonyls and of the phosphine complexes of Pt, Pd, and Ni. The substrate can be activated either directly or after the formation of the mono- or dihydride of the transition metal. Active catalytic systems can be formed after the dissociation of the ligand (as in the case of metal carbonyls), or alternatively they can be formed after solvation (acetylacetonates) or as a result of ligand substitution (platinum tin chloride systems).

Later studies were devoted to the kinetic properties, to establishing the nature of the catalytically active complexes, and to formulating practically convenient catalytic systems.

Ucciani et al.[3] showed that $HCo(CO)_3$ is the active component of catalytic sytems based on $Co_2(CO)_8$. He proposed a catalytic hydrogenation cycle in which the first activation stage includes the conjugation of the unsaturated compound. The description of a cobalt catalyst protected by an envelope of fully hydrogenated palm oil[4] is also of interest.

Of the known metal carbonyls the most promising catalysts for the hydrogenation of fats and oils are the arenechromium complexes, characterised by a high selectivity and a strong suppression of the *cis–trans* isomerisation processes.[5] Hydrogenation takes place slowly [approximately 0.1–0.6 mol H_2 (g-at Cr)$^{-1}$ min^{-1}] at temperatures above 423 K and hydrogen pressures of 2–10 MPa, and the composition of the liquid hydrogenated product is close to the fatty acid composition of oleic acid.

During hydrogenation in the presence of benzoato and polystyrene metal complexes[6] the conjugated esters of soya bean oil showed an enhanced selectivity towards the formation of dienes from trienes in comparison with the hydrogenation of nonconjugated esters, the content of *trans* isomers being only 1%–3%.

The activity of chromium carbonyls is increased by the action of ultraviolet radiation on the catalyst,[7] and also by supporting the catalyst on the surface of poly(phenylsilicon).[8] In the latter case the selectivity of the hydrogenation is also enhanced.

High selectivity is also found in other chromium carbonyl catalysts based on $Cr(CO)_3PPh_3$, which were studied[9] in connection with the hydrogenation of canola oil at 473 K and 1.7 MPa.

Among the chelates the acetylacetonates and bissalicylaldiminates are most often used for the hydrogenation of fatty acids and their methyl esters. The main advantage of these systems is the almost complete absence of conjugated dienes and *trans* isomers among the products (<0.1%). In the presence of palladium acetylacetonates hydrogenation is carried out at 323–353 K and 0.5–5.0 MPa (see Refs 10 and 11). Chelates of Pd(II), Pd(0), Ni(0), and Rh(I) were studied in the hydrogenation of the methyl esters of the acids in soya bean oil.[12] The reaction with $NaBH_4$ was used to activate the complexes. With high metal contents in the substrate (1–2 mass%) the hydrogenation proceeds at 323–373 K and 0.5–1.0 MPa with a selectivity close to that of heterogeneous catalysts.

By supporting the palladium complexes on phosphinated polystyrene[13] the reaction could be carried out under mild conditions (213–353 K and 0.1 MPa) with a low Pd content in the substrate (40 mg Pd per 1 kg of ester).

Workers at the Petrochemicals Synthesis Institute of the Russian Academy of Sciences have recently synthesised new highly active catalysts, based on complexes of palladium with ligands containing nitrogen and supported on Al_2O_3, for the hydrogenation of the triacetylglycerides of fats.[14–16] The catalysts performed successfully in tests on a large laboratory pilot plant model of an industrial hydrogenation reactor. IR spectroscopy results led to the conclusion[14–16] that in this case the catalytic activity is due to the hydride forms of palladium produced during the reaction.

The properties of cationic rhodium catalysts have been studied in depth during the hydrogenation of methyl linoleate and its isomers under mild conditions, using $[Rh(NBO)L_2]^+PF_6^-$ (L = $P(i\text{-}C_4H_9)_3$, $P(C_2H_5)_2(C_6H_5)$, and $P(CH_3)_3$; NBO is norbornadiene).[17] The course of the reaction depends on the nature of the ligand (catalyst). Thus, whereas in the presence of a catalyst with L = $P(C_2H_5)_2(C_6H_5)$ the hydrogenation of methyl linoleate proceeds through a conjugated intermediate state, when a catalyst with L = $P(CH_3)_3$ is used one of the C=C bonds is directly hydrogenated.

Systems of the type of $RhBr[P(C_6H_5)_3]_3$ and $[Rh(NBO)diphos]^+$ [where diphos is $(C_6H_5)_2P-CH_2-CH_2-P(C_6H_5)_2$] are active catalysts for the hydrogenation of fats, and they give products containing only low amounts of the *trans* isomers.[18–20]

The use of ruthenium complexes has been discussed,[21–26] and their high selectivity towards the formation of monoenes has been stressed. By depositing the complex $RuCl_3[As(C_6H_5)_3]_2.CH_3OH$ on montmorillonite and then reducing it to $RuCl_2(H_2)[As(C_6H_5)_3]_2$ (see Ref. 23) those workers were able to hydrogenate jujube oil, which contains the esters of the C_{40-44} acids and C_{20-22} alcohols, and also unsaturated acids in dioxan at atmospheric pressure and 293–318 K. When supported on clay the catalyst is stable and can undergo many cycles without significant changes in structure or in activity.

It has been concluded[26] that the active ruthenium catalyst prepared by dissolving $RuCl_3$ in ROH (R = $i\text{-}C_3H_7$, $n\text{-}C_4H_9$, $n\text{-}C_6H_{13}$, $n\text{-}C_8H_{17}$) is a hydride complex of ruthenium formed by the dissociation of the alkoxide of ruthenium in a hydrogen atmosphere.

III. Ziegler–Natta catalysts

1. Use of the catalysts in the hydrogenation of fats

Systematic studies of the hydrogenation of fats with catalysts of the Ziegler type have recently been reported from laboratories in Czechoslovakia,[27–34] France,[35–39] the USA,[40–42] and Kazakhstan.[43–58]

The first of these groups of workers used the pentadionates,[31] carboxylates,[32] acetylacetonates,[27,28] and n-butyl-salicylaldiminates[29] of nickel and other metals as catalysts, and triethylaluminium and sodium bis-(2-metoxyethoxy)dihydroaluminate, $NaAlH_2(OCH_2CH_2OCH_3)_2$ as the alkylating component. The hydrogenation takes place both with and without a solvent. As reported,[28] the methyl esters of soya bean oil were hydrogenated under mild conditions for a catalyst concentration of 0.05% Ni in the substrate and an Al:Ni component ratio in the catalyst varying from 0.2 to 3.0. The need to use a molar excess of the organoaluminium component has been explained[28] by postulating the hydrogenation mechanism proposed by Sloane:[59]

$$AlR_3 + NiX_2 \longrightarrow R_2AlX + RNiX,$$

$$RNiX + H_2 \longrightarrow RH + HNiX,$$

$$\backslash C{=}C / + HNiX \longrightarrow HC(\backslash)-C(/)-NiX,$$

$$HC(\backslash)-C(/)-NiX + H_2 \longrightarrow HC(\backslash)-CH(/) + HNiX.$$

It is suggested that under the chosen conditions the alkylation of NiX_2 is acceptably fast only at high enough concentrations of triethylaluminium in the reaction mixture. The authors[28] do not limit the role of the aluminium alkyl to the initial activation of the system: they assume the possibility of alkylation of the dimeric nickel compound $(NiX)_2$ formed by the reaction

$$HC(\backslash)-C(/)-NiX + HNiX \longrightarrow HC(\backslash)-CH(/) + (NiX)_2.$$

Systems based on $NaAlH_2(OCH_2CH_2OCH_3)_2$, unlike those based on triethylaluminium, are effective in the hydrogenation of fats even with no solvent (353–423 K, 0.1–2.0 MPa).[27,28]

Since one of the main obstacles to the practical use of Ziegler catalysts in the hydrogenation of fats is the difficulty of separating them from the final product and of using them repeatedly there has been great interest in a method of hydrogenating the esters of unsaturated fatty acids using nickel bis-(n-butylsalicylaldiminate supported on oxide carriers (aluminosilicate or aluminium oxide), or activated $Al(C_2H_5)_3$ or $AlCl(C_2H_5)_2$ (see Ref. 29). At 293–298 K and hydrogen pressures of 0.1–0.15 MPa rapeseed oil was satisfactorily hydrogenated re-using the catalyst three times without any loss of activity [the specific rate of the hydrogenation was W_{sp} = 1.2–20.5 mol H_2 (g-at Ni)$^{-1}$ min^{-1}]. The catalyst was separated from the product by simple filtration.

In the case of an unsaturated catalyst the separation required special procedures such as treating the solution with concentrated phosphoric acid or an aqueous solution of the same acid,[34] and saponification with an aqueous solution of metal hydroxide or carbonate at 313–353 K (see Ref. 33).

French workers have made valuable contributions to studies of the hydrogenation of fats by assigning the Ziegler catalysts to the 'superactive' class.[35] By hydrogenating five tonnes of castor oil in an industrial plant at a relatively low temperature (433 K) and hydrogen pressure (1.5 MPa) they established that the activity of the Ziegler nickel catalysts is 22 times greater than the activity of heterogeneous industrial nickel.[35] They suggested[35] that the low concentration of the nickel (between 10 and 200 ppm) and its high activity should more than outweigh the cost of the Ziegler catalyst.

The hydrogenation of castor oil on these catalysts is selective, and the unwanted 12-ketostearic acid is formed in negligibly small amounts, which is an additional advantage of these systems over the heterogeneous nickel catalysts. Futhermore an original and economical way of separating the catalyst from the product was found. Vigorous stirring of the hydrogenation product with 10% of water at 373 K produces a precipitate from which a final product containing only 0.0001% of Ni can be separated by filtration with 0.2% of coactivator.

The work of the French scientists stimulated world-wide interest, and was patented in 10 countries. These disclosures [36,37] described the hydrogenation of solvent-free soya bean oil with a catalyst prepared from a transition metal salt and a hot concentrated solution of aluminium alkyl, which is undoubtedly the main drawback of this method. A wide range of transition metals was specified as hydrogenation catalysts (Ni, Cr, Ag, Cu, Ni–Ag, Ni–Mn, Ni–Fe, Ni–Cu) in the form of palmitates, stearates, oleates, octoates, etc. Metal complexes supported on oxide carriers (Al_2O_3, SiO_2, Cr_2O_3) were used in some experiments. It was shown that the most active of these catalysts is nickel stearate ($NiSt_2$) [W_{sp} = 16.3 mol H_2 (g-at Ni)$^{-1}$min^{-1}], and that with this catalyst the selectivity of the conversion of dienes into monoenes can reach 76%. Highly selective catalysts based on $NiSt_2$–$CuSt_2$ and on $Ni(acac)_2Py_2$ have a low activity [W_{sp} = 0.63 and 0.9 mol H_2 (g-at Ni)$^{-1}$ min^{-1} respectively].

A modelling method based on the chemical introduction of labels into linolenic, linoleic, and oleic acid chains has been used to explain the mechanism of the selective hydrogenation of fats. [38] It was shown that linolenic acid hydrogenated on a nickel catalyst to the complete conversion of the triene contains not only 3.5%–5.0% of the diene but also 3%–4% of the monoene (the initial concentration of linolenic acid was 7%–10%). Therefore the saturation of the triene is accompanied by saturation of the resulting diene.

Simultaneous saturation of the diene and the monoene takes place during the hydrogenation of the methyl esters of soya bean oil. [39] A catalytic cycle including a complex of Ni(0) with a coordinated diene and monoene has been proposed [39] on the basis of the observation that the oxidative addition of hydrogen takes place after the coordination of the substrate (with the metal) to the so-called 'exposed nickel' by the scheme

$$Ni(OOCR)_2 + Al(C_2H_5)_3 \longrightarrow \longrightarrow Ni(C_2H_5)_2 + Al(C_2H_5)(OOCR)_2,$$

$$Ni(C_2H_5)_2 \longrightarrow Ni^0 + 2(C_2H_5)^{\cdot},$$

$$2(C_2H_5)^{\cdot} \longrightarrow C_2H_4 + C_2H_6.$$

The main conclusion reached [39] in respect of the selectivity of these systems is that the final product contains an enhanced amount of stearate: this is thought to be an unavoidable disadvantage of the nickel Ziegler catalysts.

However, as will be shown below, by using some strictly defined catalyst preparation conditions and an Al-organic component (of the alumoxane type) we can obtain nickel systems in which the hydrogenation of a diene to a monoene takes place with a selectivity of 93%–100%.

A selective catalyst for the hydrogenation of the linolenate to the linoleate in soya bean oil, based on copper stearate with triethylaluminium and diethylmagnesium, has been described. [40] At 443 K, with a hydrogen pressure up to 1.5 MPa and a copper concentration in the oil of 0.1%–0.025%, the concentration of linolenate in the product could be lowered to 0.75% while the concentration of stearate increased from 3.9% to 5.2%. An increase in the activity of these systems was achieved by using trialkylsilicon as the alkylating component, but in this case the selectivity was slightly suppressed. [41]

A detailed description of the properties of copper catalysts and of the methods of increasing their activity has been published. [40] The activity of the copper catalysts is strongly influenced by the nature of the alkylating component, whose favourable effect increases in the sequence

$$Al(C_2H_5)_3 < Al(C_2H_5)_2(OC_2H_5) < < Mg(C_2H_5)_2 < AlH(i\text{-}C_4H_9)_2 < Al(n\text{-}C_4H_9)_3.$$

The addition of aluminium oxide to the $CuSt_2$–$Al(C_2H_5)_3$ catalyst increased its activity five-fold. [42] This activating action of the Al_2O_3 was explained by the adsorption on the carrier of harmful impurities (phosphatides, free fatty acids, etc.) which poisoned the catalyst. An experiment on the hydrogenation of soya bean oil with the addition of various amounts of ethanol has been described. [42] The addition of 0.5% of ethanol lowers the iodine number by 20 units (i.e. it activates the catalyst) as compared with the catalyst without the addition. Additions of 1%–2% of ethanol have the opposite effect, and in the presence of 5% of ethanol the hydrogenation of the oil is almost totally suppressed. According to Koritala [42] this is because of the interaction between ethanol and $Al(C_2H_5)_3$. A concentration of ethanol of 0.5% is sufficient to replace one ethyl group in the $Al(C_2H_5)_3$ by an ethoxy group; the resulting $Al(OC_2H_5)(C_2H_5)_2$ produces a better catalyst with the copper stearate than $Al(C_2H_5)_3$. At higher ethanol concentrations the triethylaluminium begins to decompose.

A programme of studies [43–53] of the hydrogenation of sunflower oil in a solvent (heptane) at 293–353 K involved a wide range of catalysts based on nickel, cobalt, chromium, copper, and iron stearates, and their mixtures with an alkylating agent (triethylaluminium). The following sequence of activities was noted: $NiSt_2 > CoSt_2 \gg FeSt_3 > CrSt_3 > CuSt_2$. The Al:M ratio needed to prepare the catalysts with the greatest hydrogenation activity was strongly temperature-dependent. The kinetic order was zero with respect to the substrate and close to unity with respect to the catalyst and the hydrogen. In every case the selectivity of the hydrogenation of linoleate to oleate increased with temperature and with the concentration of the substrate.

Supporting the stearates of Ni, Co, and Fe on Al_2O_3 increased the activity of the organometallic catalysts in solution, but lowered their selectivity. [45–48] The $NiSt_2/Al_2O_3$–$Al(C_2H_5)_3$ catalyst was proposed for the preparation of tristearin under mild conditions. [49]

The greatest increase in the activity of the catalyst by depositing it on a carrier (almost 60-fold as compared with the unsupported catalyst) was achieved in the $FeSt_3/Ni(OH)_2$–$Al(C_2H_5)_3$ system (see Ref. 50). The maximum rate [225.1 mol H_2 (g-at Fe)$^{-1}$ min^{-1}] was observed for a 50% content of the iron stearate on $Ni(OH)_2$.

With the aim of intensifying the hydrogenation of vegetable oils in solvents, Marusich and Noskova [51] examined the use of donor additives to the $NiSt_2$–$Al(C_2H_5)_3$ catalyst (water, glycerol, the tributyl ester of phosphoric acid, and ethanol). The additives increased the rate of the reaction by a factor of 1.2–1.8. The highest rates were observed for the following ratios between the additive and the nickel: 5:1 (water and ethanol), 1:1 (tributyl phosphate), and 5:1 (glycerol). Unlike Koritala, [42] who attributed the activating effect of ethanol to the formation of ethoxy groups, Marusich and Noskova [51] postulated the formation (in the case of water and ethanol) of alkylalumoxanes, i.e. of compounds containing an Al–O–Al group [$R_2Al(OAlR)_nOAlR_2$]. In fact, special experiments with different alkylalumoxanes [54–81] produced very active, selective, and thermally stable catalysts for the hydrogenation of fats.

Table 1. Effect of the nature of the Al-organic component of an organonickel catalyst on the activity, selectivity, and thermodynamic characteristics of the hydrogenation of the glycerides of sunflower seed oil (for the optimum Al : Ni ratios).

Al-organic catalyst	T/ K	Solvent	W_{sp}/ mol H_2 (g-at Ni)$^{-1}$ min^{-1}	S(%)	$10^2 k$/ min^{-1}	ΔE^*/[a] kJ mol^{-1}	ΔS^*/[b] e. u.
$Al(C_2H_5)_3$	313	Heptane	78.0	87.5	1.8	17.4	−0.24
	423	none	14.8	94.6	–	30.7	−0.20
$Al(i\text{-}C_4H_9)_3$	313	Heptane	76.0	89.0	1.2	24.6	−0.20
	423	none	21.8	93.0	–	26.1	−0.21
$Al(C_9H_{19})_3$	313	Heptane	48.0	90.5	0.29	30.1	−0.19
	423	none	9.0	94.6	–	28.3	−0.19
$Al_{21}O_{19}(C_2H_5)_{23}$	313	Heptane	24.5	91.0	0.9	24.0	−0.16
	353	none	5.9	99.8	–	33.1	−0.22
$Al_2O(i\text{-}C_4H_9)_4$	313	Heptane	72.0	84.5	1.2	19.6	−0.20
	423	none	49.8	99.8	–	22.5	−0.21
$Al_8O_7(i\text{-}C_4H_9)_{10}$	313	Heptane	42.0	85.0	0.5	27.1	−0.18
	423	none	27.7	98.3	–	–	–

[a] ΔE^* is the apparent activation energy. [b] ΔS^* is the entropy of activation.

Noskova and co-workers [69, 70] used a wide range of aluminium trialkyls (R = C_2H_5, i-C_4H_9, C_9H_{19}) and alumoxanes (R = C_2H_5 and i-C_4H_9 and n = 0, 2, 4, 8, 18, and 21) as alkylating components, and found that in the absence of a solvent the selectivity of the hydrogenation is almost unaffected by the nature of the alkyl radical (Table 1). Therefore the ratios of the stability constants of the complexes with linoleate and with oleate and those of the rate of transformation of linoleate and oleate are not very different for complexes with different R. On the other hand the suppression of the rate of hydrogenation at 313 K by increasing the molecular mass of the organoaluminium compound is explained by the decrease in reducing power in the series C_2H_5, i-C_4H_9, C_9H_{19} and by the increased steric hindrance to the activation of the substrate.

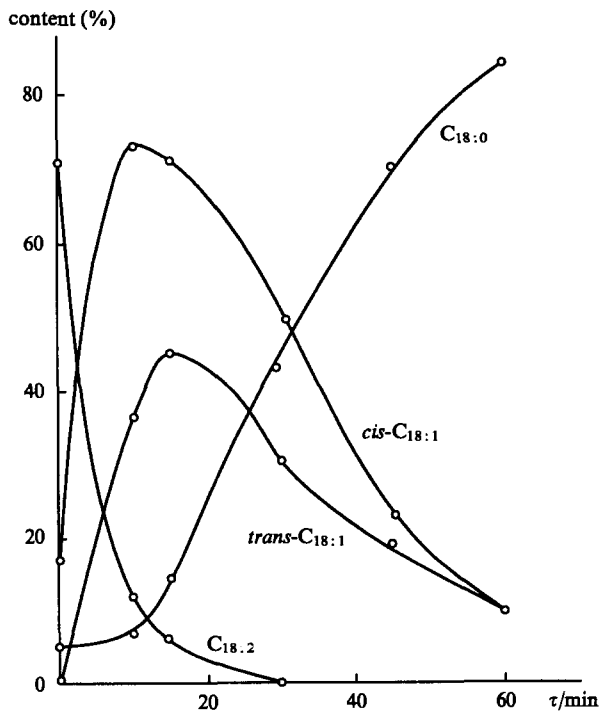


Figure 1. Kinetics of the hydrogenation of sunflower oil: changes in the fatty acid composition of the catalysate obtained on $NiSt_2-Al_2O(C_2H_5)_4$ (Al : Ni = 11, 423 K, 0.05% Ni in oil).

An oil without solvent is hydrogenated more slowly than in heptane (see Table 1). In the absence of a solvent the reaction takes place on all the catalysts with a selectivity of 92% – 100% towards the conversion of linoleate into oleate.

The kinetics of the hydrogenation of sunflower seed oil (1 kg) and the change in the fatty acid composition at 423 K and atmospheric pressure are shown in Fig. 1. The hydrogenation of the linoleate in the presence of 0.047% of Ni in the oil goes practically to completion in the first 15 minutes, during which the concentration of stearate increases from 4.5% to 16%. The rate of hydrogenation of the *trans* unsaturated isomers is lower than the rate of hydrogenation of the linoleate and of the *cis* isomers of oleic acid. After 60 min 11% of the *trans* isomer of oleic acid is the only unsaturated acid remaining in the oil.

Comparing the activities of the organometallic catalyst $NiSt_2-(i\text{-}C_4H_9)_2Al_2OAl(i\text{-}C_4H_9)_2$ with that of the industrial heterogeneous catalyst DM-3 (USA) showed that in the presence of the former a 60% – 63% conversion of the ester is achieved in 10 – 15 min of hydrogenation at 423 K, whereas in the presence of DM-3 the same extent of conversion requires 60 min at 473 K.

Using Ziegler catalysts based on $NiSt_2-Al(C_2H_5)_3$ at 423 K under a pressure of 1.0 – 9.0 MPa the hydrogenation of the ethyl esters of fatty acids can be controlled towards the formation of saturated fatty acids. [71]

A catalyst similar to the Ziegler systems was obtained [72] by activating $Ti(C_5H_5)Cl_2$ with magnesium. The authors stressed [72] that this catalyst is effective in the hydrogenation of methyl linoleate at room temperature, but only in the presence of triphenylphosphine.

2. Nature of the catalytically active complexes

A detailed study [69] of the catalysts based on $FeSt_3-Al(C_2H_5)_3$ by Mössbauer, IR and EPR spectroscopy, magnetic susceptibility, and other methods allowed their structure to be established. High-spin Fe(III) and Fe(II) complexes were detected, and also polynuclear (at the transition metal) associated formations containing bound iron ions. All the complexes are mutually in a dynamic equilibrium depending on the genesis of the catalyst (relative concentrations of aluminium and iron, temperature of the process, carrier, nature and concentration of the solvent and of the gases, atmosphere, time of formation of the complex, presence and nature of a substrate). Polynuclear associations are formed as a result of the interaction of complexes of different valencies between the transition metal and the trialkylaluminium. Calculations of the number of transition metal ions in the association showed that for an Al/Fe ratio of 7 – 9 up to several tens of iron ions may be present.

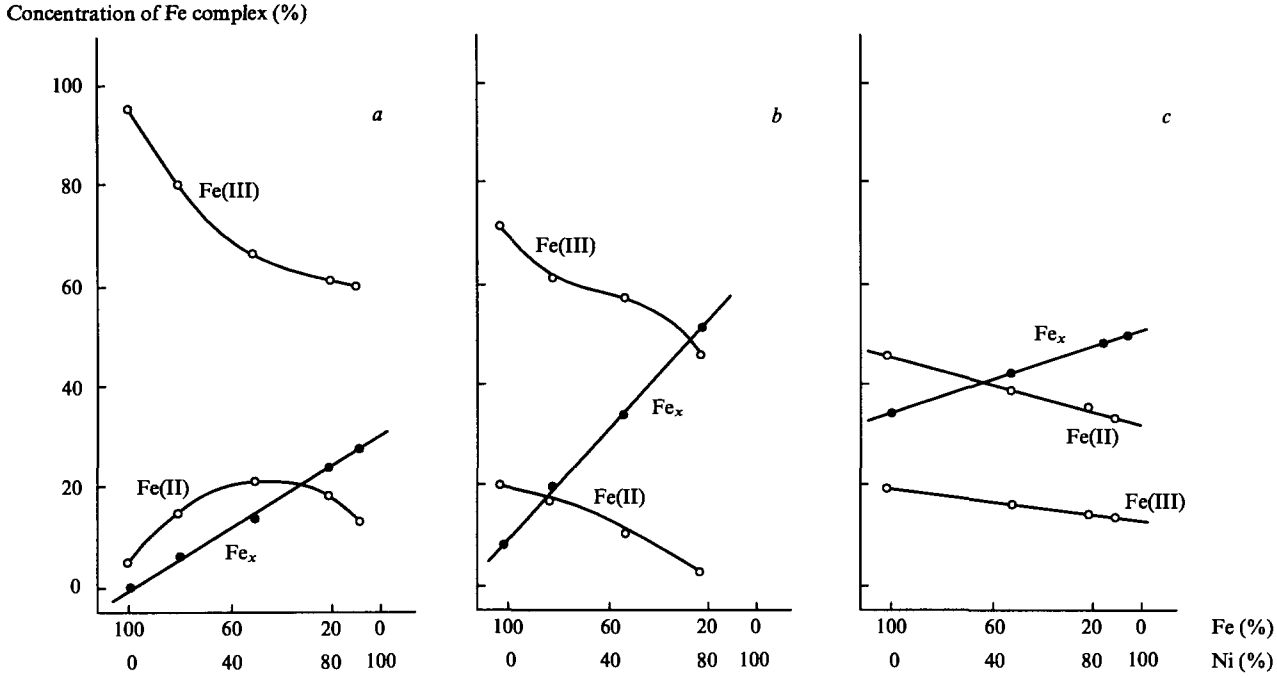


Figure 2. Changes in the concentration of the iron complexes as a function of the composition of the mixed $NiSt_2-FeSt_3-Al(C_2H_5)_3$ (293 K, $[\Sigma M] = 0.28 \times 10^{-3}$ mol); Al : ΣM: (*a*) 2; (*b*) 4; (*c*) 7.

An analysis of the dependence of the rates of hydrogenation of various unsaturated compounds on the concentration of the complex in the system showed unambiguously that the activity of organometallic catalysts is due to the presence of polynuclear complexes in the system.[60,61]

The polynuclear nature of the active complex was confirmed by a reverse synthesis which gave effective catalytic systems from undoubtedly polynuclear complexes of iron and of iron with chromium.[62-64] Active complexes of organometallic catalysts having a cluster nature have also been suggested.[65,66]

Ideas on the polynuclear nature of the active complexes of hydrogenation catalysts of the Ziegler–Natta type led to the belief that synergic systems could be obtained by mixing (in the synthesis) the salts of different transition metals or by supporting the salt of one transition metal on the hydroxide of another.[50,53,73] It was shown that mixed catalysts are not a simple mixture of the complexes of individual transition metals. The conclusion was that an ion of the second transition metal enters into the composition of the combined polynuclear complex, and forms a single system with the ion of the typical metal. As a result of partial reduction and electron transfer processes the transition metals in the conjugated system of the complex have a mixed valency, which enhances the reactivity of the complex.

The $^{57}FeSt_3-NiSt_2-Al(C_2H_5)_3$ catalysts have been studied by Mössbauer spectroscopy. Parallel tests of their catalytic activity towards the hydrogenation of sunflower oil were also carried out. By processing the spectra it was shown[67] that the system contains a set of iron complexes similar to that found in the system based on $^{57}FeSt_3-Al(C_2H_5)_3$ (see Ref. 60).

The Mössbauer parameters of the corresponding complexes in the two systems have similar values. The Fe : Ni ratio has little effect on the Mössbauer spectra of the complexes, but the relative concentration of the complexes is strongly dependent on this ratio. Fig. 2 shows the relative concentration of the various iron complexes [the high-spin Fe(III) and Fe(II), and the associated polynuclear Fe_x] in the $^{57}FeSt_3-NiSt_2-Al(C_2H_5)_3$ system with 10, 20, 50, and 80 mol% of Ni and a ratio of Al : ΣM = 2, 4, and 7. For each value of Al : ΣM the relative concentration of Fe(III) complexes decreases as the concentration of nickel stearate is increased, i.e. reduction processes are assisted by additions of $NiSt_2$. At the same time the relative concentration of associated polynuclear complexes increases almost linearly with the concentration of added stearate. The composition of the system is most strongly influenced by an increase in the content of $NiSt_2$ for a ratio of Al : ΣM < 4; for Al : ΣM = 7 these changes are much less marked, and for Al : ΣM > 7 they effectively vanish.

The increase in the content of polynuclear formations can be associated both with the fact that reduction processes are facilitated (as indicated by the most probable mechanism for the formation of polynuclear associations[60,61,68]) and with formation of stable polynuclear complexes when nickel is included in their composition. In the latter case the dynamic equilibrium between the associations and the other transition metal complexes is displaced towards the associations. This seems all the more likely in view of the tendency for mixed (heteroatomic) cluster complexes to be more stable than their analogues with atoms of one transition metal.[66]

The dependence of the composition of the $^{57}FeSt_3-NiSt_2-Al(C_2H_5)_3$ system and of its catalytic activity in the hydrogenation processes of fats on the amount of nickel stearate can be used to identify the complexes leading to hydrogenation. Property–composition correlation dependences show that [as in the systems[61] based on $^{57}FeSt_3-Al(C_2H_5)_3$] polar associated formations are responsible for the activity of the mixed systems, since a straight-line dependence is observed only between their concentration and the rate of hydrogenation (Fig. 3).

As can be seen from Table 1 the entropy of activation calculated for the formation of the intermediate active complex is negative for all the compositions of the catalyst and all the conditions of the process. Negative entropies are usually observed for the interaction of initial reactants including a bimolecular rate-limiting step, whose transition state is reached by the approach of the reactants (for example, the coordination of the substrate molecules with the metal ions),[74] i.e. for reactions passing through an associative transition state, probably by a concerted

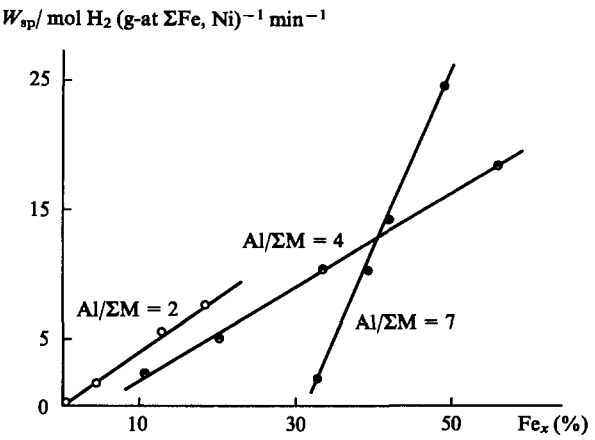


Figure 3. Dependence of the specific rate of hydrogenation of the linoleate from sunflower oil on the concentration of polynuclear Fe complexes in a mixed Ni–Fe catalyst.

(synchronous) mechanism. The latter is usually characterised by a zero or negative entropy of activation, and by a relatively low activation barrier, smaller than the dissociation energies of the weakest chemical bonds assumed in the adjusted process.[66] It can be seen from Table 1 that the apparent activation energy for the process is relatively low (17–34 kJ mol^{-1}). It seems probable that the coordination of hydrogen and of an unsaturated compound on a polynuclear complex involves their strict mutual orientation, with a decrease in the entropy of the active complex, and that a more or less synchronous exchange interaction of the coordinated substrate and hydrogen takes place during the rate-limiting step of the hydrogenation process.

Systematic studies of organometallic catalysts for the hydrogenation of fats, and the resulting evidence for the presence of catalytically active polynuclear and polyvalent complexes and of a dynamic equilibrium between the poly- and the mononuclear transition metal complexes, led to the suggestion[56,69,70,73] that

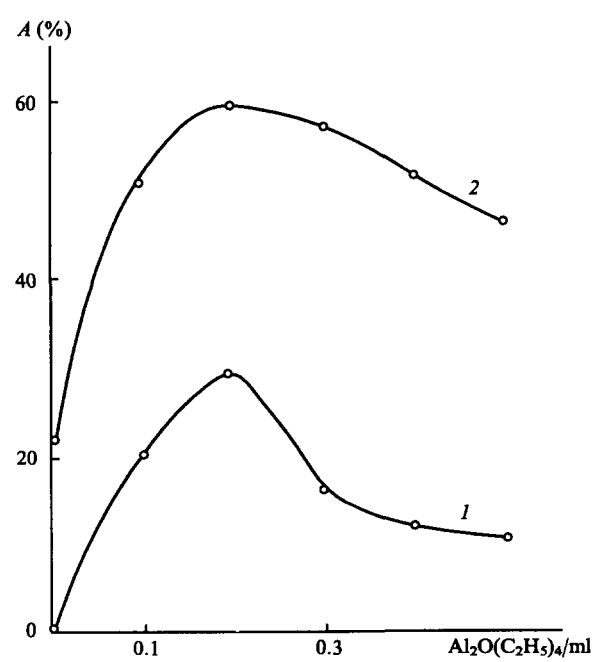


Figure 4. Effect of tetraethylalumoxane additions on the activity (*A*) of a Ni–Cu catalyst in the hydrogenation of sunflower oil at 473 K. Mass of Ni–Cu catalyst: (*1*) 0.03, (*2*) 0.1 g.

these catalysts (like organoaluminium compounds[56]) should be used as additives to heterogeneous catalysts in order to obtain heteropolynuclear and heterovalent complexes (clusters) on the surface of the latter. The following concepts were formulated: (1) the surface of heterogeneous metallic catalysts contains polynuclear (cluster) complexes; (2) there is a similarity between the coordinating powers of the metal atoms on the surface and in the metal complexes;[76–78] (3) like the compounds of the transition metals in solution the surface clusters can interact with Al-organic compounds and form active organometallic catalysts on the surface.

Thus, as shown in Fig. 4, the addition of tetraethylalumoxane to a low-activity nickel–copper heterogeneous catalyst of the VNIIZh-2 type (Ni:Cu = 1:2) increased its activity from 3%–20% to 30%–60%. The experimentally observed dependence of the activity of the catalyst on the amount of added alkyl-alumoxane can be explained by the similarly extremal relationships found in Ziegler catalysts.

Initially, at low concentrations of the Al-organic compound, the activity of the heterogeneous catalyst increased, both as a result of the faster reduction of the metals on the surface (according to ESCA data) and as a result of the formation of coordinated systems with the Al-organic compound on the surface. A further increase in the amount of Al-organic compound led to complex formation and blocking of the transition metal atoms on the surface by aluminium, which lowered the activity of the catalyst. This effect can be clearly seen at low concentrations of the heterogeneous catalyst (0.02%), when the Ni–Cu catalyst is almost completely inactive under the chosen conditions but the addition of tetraethylalumoxane can 'revive' it.

We shall complete our review of this series of papers[43–58,63,64,69,70,73] by summarising their most significant results.

The problem of synthesising a new generation of catalysts for the transformation of fats called for the development of concepts on the nature of the catalytically active complexes, for a detailed study of the changes in activity produced by changes in the genesis conditions (relative amount of the catalyst components, temperature, hydrogen pressure, concentration of catalyst, nature of the organic radical in the organoaluminium component of the catalyst, etc.), and for the determination of the kinetic and thermodynamic characteristics of the hydrogenation process and also of the selectivity and stability of the catalytic systems and of the composition of the final product.

Starting from a qualitative examination of the structure of the active polynuclear complex, and from Mössbauer spectroscopy data on the effect of the nature of the added compound on the irreversible or reversible (depending on the nature of the substrate) decomposition of this complex,[60] it was suggested that a substantial destabilisation of the polynuclear complex during the coordination of compounds such as fats in a solvent is caused by the localisation of charge on one bond of the resulting π complex induced by the strong π-acceptor properties of the substrate. In order to prevent the decomposition of the complex and to create an excess electron density on the conjugation chain in the polynuclear system it was suggested that donor additives should be used and that the nature of the aluminium component should be changed [replacing the traditional $Al(C_2H_5)_3$ by alkylalumoxanes]. These new concepts led to the development of a qualitatively new approach to the synthesis and production technology or organometallic Ziegler catalysts which overcame the serious shortcomings of AlR_3 catalysts (fire and explosion hazards) responsible for limitations and complications in the use of organometallic catalysts.

In the construction of catalytic systems it was possible to increase substantially the stability of the catalyst by creating conditions which suppressed the association of the polynuclear complexes (preparation of the catalyst in a vegetable oil, supporting the catalyst on a carrier). These changes allowed the catalysts to retain their initial activity for long periods.

Table 2. Hydrogenation of vegetable oils in n-heptane in the presence of metal-complex catalysts.

Catalytic system	Reaction conditions		% M in oil	Oil	W_{sp}/mol H_2, (g-at M)$^{-1}$ min^{-1}	S(%)	Ref.
	T/ K	p_{H_2}/ MPa					
$Co_2(CO)_8$	473	3.0[a]	0.09	Soya	1.0	83	3
$Pd(acac)_2$	333	1.5[a]	0.006	"	9.0	89	11
$H_2PtCl_2-SnCl_2$	313	0.1[a]	0.004	"	0.1	97	83
$Ni(acac)_2-Al(C_2H_5)_3$	293	0.12	0.05	MESO[b]	20.2	90	27
$Ni(acac)_2-NaAlH_2R_2$	293	0.12	0.05	"	17.2	91	27
$NiSt_2-Al(C_2H_5)_3$	373	1.0[c]	0.025	Soya	16.3	73	27
$NiSt_2-CuSt_2-Al(C_2H_5)_3$	393	2.0[c]	0.05	"	0.62	91	31
$Ni(acac)_2Py_2-Al(C_2H_5)_3$	333	3.0[c]	0.1	"	0.9	95	36
$CuSt_2-Al(C_2H_5)_3$	473	1.5[c]	0.05	"	2.0	95	42
$NiSt_2-Al(C_2H_5)_3$	293	0.1	0.1	Sunflower	21.0	84	84
	313	0.1	0.1	"	33.0	86	84
	333	0.1	0.1	"	79.0	92	84
$FeSt_3-Al(C_2H_5)_3$	293	0.1	0.4	"	1.2	82	47
	313	0.1	0.4	"	2.0	86	47
	333	0.1	0.4	"	2.8	90	47
$CoSt_2-Al(C_2H_5)_3$	293	0.1	0.1	"	20.0	81	45
	313	0.1	0.1	"	33.0	95	45
$CuSt_2-Al(C_2H_5)_3$	333	0.1	0.4	"	0.08	84	84
50%-$FeSt_3/Ni(OH)_2$ — $-Al(C_2H_5)_3$	313	0.1	0.1	"	59.0	83	50
	333	0.1	0.1	"	149.0	93	50
$NiSt_2-Al_2O(C_2H_5)_4$	333	0.1	0.05	"	200.0	93	55, 70
$NiSt_2-Al_2O(C_2H_5)_4$	353	0.1	0.05	"	4.8	99	55, 70
	473	0.1[c]	0.05	"	64.0	100	55, 70

[a] Solvent: acetic acid. [b] MESO are the methyl esters of soya bean oil. [c] The reaction was carried out without a solvent.

Thus, Ni-organic catalysts with alumoxanes in oil showed no loss of activity after three years' storage in closed vessels.

The new ideas on the polynuclear character of the catalytically active complex led to the synthesis of mixed Ni–M catalysts (M = Fe, Co, Cr, Cu). Using the $NiSt_2-FeSt_3-Al(C_2H_5)_3$ system an increase in the number of heteropolynuclear complexes was achieved, and a straight-line dependence of the activity of the complexes on the concentration of $NiSt_2$ was established. The position of the maximum on the rate–composition curve for mixed catalysts under different conditions is determined by the Ni : M ratio (M is the transition metals), i. e. we have a cluster effect.

Allowance for the polynuclear and polyvalent nature of the active complexes in catalysts of the Ziegler–Natta type, and also in the surface layers of heterogeneous catalysts, led to a method of activation of industrial heterogeneous catalysts by small additions of an organometallic catalyst or of an organic aluminium compound.

The 'construction' of organometallic systems by varying the composition of the cocatalyst, by supporting the active complex on a carrier, or by synthesising it on the surface of a low-activity heterogeneous catalyst allowed organometallic catalysts to be used in some processes of practical importance, such as the selective hydrogenation of fats and the transesterification of glycerides (aimed at accelerating the production and improving the quality of a group of food products manufactured by the 'margarine industry')[79] or the positional isomerisation of non-conjugated linoleate (aimed at accelerating the production of drying oils and of conjugated dienes for organic synthesis).[80–83]

Table 2 summarises the information from various sources on the use of metal-complex catalysts in the hydrogenation of the unsaturated glycerides of natural oils. By outlining the main results obtained since 1979 the Table allows us to compare the effectiveness of metal-complex catalysts of various types.

References

1. A G Sergeev (Ed.) *Gidrogenizatsiya i Pereeterifikatsiya Zhirov i Masel* (Hydrogenation and Ester Interchange of Fats and Oils) Vol. 3 (I) (Leningrad: Maslozhirprom, 1985)
2. B James *Homogeneous Hydrogenation* (Translated into Russian; Moscow: Mir, 1976)
3. E Ucciani, G Cecchi, G Mallet *Rev. fr. Corps Gras.* **24** 225 (1979)
4. E Ucciani, G Cecchi, A Bonfand *Rev. fr. Corps Gras.* **29** 219 (1982)
5. L L Diosady, W F Graidon, S S Koseoglu *Can. Inst. Food Sci. Technol.* **17** 218 (1984)
6. S Koritala, E N Frankel *J. Am. Oil Chem. Soc.* **58** 553 (1981)
7. I A Heldal, E N Frankel *J. Am. Oil Chem. Soc.* **62** 1044 (1985)
8. R A Awl, E N Frankel *J. Am. Oil Chem. Soc.* **58** 557 (1981)
9. P A Berstein, W F Graydon, L L Diosady *J. Am. Oil Chem. Soc.* **66** 680 (1989)
10. I A Heldal, E N Frankel *J. Am. Oil Chem. Soc.* **61** 756 (1984)
11. S Koritala *J. Am. Oil Chem. Soc.* **62** 517 (1985)
12. E N Frankel, J P Friedrich, T R Bessler *J. Am. Oil Chem. Soc.* **57** 349 (1980)
13. C Andersson, R Larsson *J. Am. Oil Chem. Soc.* **58** 675 (1981)
14. N G Bazhirova, A V Novikova, N V Komarov *Kinetika Gidrirovaniya Triatsilglitseridov v Prisutstvii Pd-soderzhashchikh Katalizatorov* (Moscow, 1989) (Kinetics of Hydrogenation of Triacetins in the Presence of Pd-containing Catalysts) Article deposited at the All-Union Institute of Scientific and Technical Information (VINITI), No 3042-I (in Russian)
15. N V Komarov, A N Arutyunyan, V Kh Paronyan *Tsis-transizomerizatsiya v Protsesse Gidrirovaniya Rastitel'nogo Masla na Pd-katalizatore* (*Cis-Trans*-isomerisation in the Hydrogenation of Vegetable Oil on a Pd catalyst) (Moscow, 1990) Article deposited at the All-Union Institute of Scientific and Technical Information (VINITI), No 2295-V (in Russian)
16. N V Komarov, L P Abramova, V Kh Paronyan *Issledovanie i Modelirovanie Protsessa Gidrirovaniya Podsolnechnogo Masla na Pd-katalizatore* (Investigation and Modelling of the Hydrogenation of Sunflower Oil on a Pd catalyst) (Moscow, 1990) Article deposited at the All-Union Institute of Scientific and Technical Information (VINITI), No 2296-V (in Russian)

17. P van der Plank, A van der Ent *J. Am. Oil Chem. Soc.* **57** 343 (1980)
18. W I Bland, T C Dine, R Iobanputra *J. Am. Oil Chem. Soc.* **62** 924 (1985)
19. M Berglund, C Andersson *J. Am. Oil Chem. Soc.* **61** 1351 (1984)
20. I A Heldal, E N Frankel *J. Am. Oil Chem. Soc.* **62** 1117 (1985)
21. T Nishiguchi, K Fukuzumi, F Kimura *Gukaguku* **32** 726 (1983)
22. C Bello, L Diosaky, W Graydon *J. Am. Oil Chem. Soc.* **62** 1587 (1985)
23. M Taqui Khan, M Siddiqui, in *V Mezhdunar. Simp. po Svyazi mezhdu Gomogennym i Geterogennym Katalizom (Tez. Dokl.)* (Abstracts of Reports at the Fifth International Symposium on the Bond between Homogeneous and Heterogeneous Catalysis) (Novosibirsk: Institute of Catalysis, Siberian Division of the Academy of Sciences, USSR, 1986) p. 226
24. M Taqui Khan, S Samad, M Siddiqui *J. Mol. Catal.* **50** 97 (1989)
25. US P. 4 963 295; *Ref. Zh. Khim.* 17 R 1 355P (1991)
26. D Mudesh, C S Narasimhan, K Ramnarayan *Ind. Eng. Chem. Res.* **28** 1261 (1989)
27. P Svoboda, J Hetfleijs, J Soucek *Chem. Prum.* **30** 89 (1980)
28. Z Vankova, P Svoboda, J Hetfleijs *Chem. Prum.* **31** 132 (1981)
29. Czech. P. 209 695; *Chem. Abstr.* **98** 34 276h (1983)
30. Czech. P. 197 143; *Chem. Abstr.* **97** 55 589g (1982)
31. Czech. P. 197 144; *Chem. Abstr.* **97** 109 783w (1982)
32. Czech. P. 209 573; *Chem. Abstr.* **98** 18 465p (1983)
33. Czech. P. 216 087; *Chem. Abstr.* **101** 24 073h (1984)
34. Czech. P. 214 531; *Chem. Abstr.* **101** 191 167w (1984)
35. G Cecchi, E Ucciani *Riv. Ital. Sostanze Grasse* **56** 235 (1979)
36. French P. 2 259 896; *Chem. Abstr.* **95** 63 729w (1980)
37. US P. 4 038 295; *Chem. Abstr.* **94** 9 712h (1980)
38. G Mallet, E Ucciani *Rev. fr. Corps Gras.* **27** 71 (1980)
39. G Cecchi, G Mallet, E Ucciani *Riv. Ital. Sostanze Grasse* **58** 228 (1981)
40. US P. 4 273 722; *Chem. Abstr.* **97** 13 826p (1982)
41. S Koritala *J. Am. Oil Chem. Soc.* **58** 701 (1981)
42. S Koritala *J. Am. Oil Chem. Soc.* **59** 309 (1982)
43. N F Noskova, D V Sokol'skii *Kinet. Katal.* **23** 1382 (1982)
44. N F Noskova, N I Marusich, G N Sharifkanova, in *V Vsesoyuz. Konf. po Kataliticheskim Reaktsiyam v Zhidkoi Faze (Tez. Dokl.)* (Abstracts of Reports at the Fifth All-Union Conference on Catalytic Reactions in the Liquid Phase) (Alma-Ata: Nauka, 1978) p. 144
45. G N Sharifkanova, N F Noskova, D V Sokol'skii *Zh. Prikl. Khim.* **52** 2422 (1979)
46. N I Marusich, N F Noskova, D V Sokol'skii *Zh. Prikl. Khim.* **52** 2558 (1979)
47. N F Noskova, A Zh Kazimova, D V Sokol'skii *Zh. Prikl. Khim.* **54** 653 (1981)
48. T A Petrova, N F Noskova *Izv. Akad. Nauk Kaz. SSR, Ser. Khim.* (5) 27 (1980)
49. USSR P. 1 062 251; *Byull. Izobret.* **47** (1983)
50. A Zh Kazimova, A R Brodskii *Zhidkofaznaya Ochistka Gaza Okisleniem i Vosstanovleniem Primesei* (Liquid-Phase Scrubbing of Gas by Oxidation and Reduction of Admixtures) (Alma-Ata: Nauka, 1985)
51. N I Marusich, N F Noskova *Izv. Akad. Nauk Kaz. SSR, Ser. Khim.* (5) 31 (1980)
52. N F Noskova, N I Marusich, A Zh Kazimova, in *XIV Chuguevskoe Vsesoyuz. Soveshchanie po Khimii Kompleksnykh Soedinenii (Tez. Dokl.)* (Abstracts of Reports at the XIVth Chuguev All-Union Conference on the Chemistry of Complex Compounds) (Ivanovo: Ivan. Chem. Technol. Inst., 1981) p. 396
53. N F Noskova, S R Savel'ev, T A Petrova *Izv. Akad. Nauk Kaz. SSR., Ser. Khim.* **6** 42 (1983)
54. S R Savel'ev, N F Noskova, N N Korneev, I M Khrapova, in *V Mezhdunar. Simp. po Svyazi mezhdu Gomogennym i Geterogennym Katalizom (Tez. Dokl.)* (Abstracts of Reports at the Fifth International Symposium on the Bond between Homogeneous and Heterogeneous Catalysis) (Novosibirsk: Institute of Catalysis, Siberian Division of the Academy of Sciences, USSR, 1986) p. 213
55. R S Savel'ev, R L Perkel', N F Noskova, in *VII Vsesoyuz. Konf. po Kataliticheskim Reaktsiyam v Zhidkoi Faze (Tez. Dokl.)* (Abstracts of Reports at the VIIth All-Union Conference on Catalytic Reactions in the Liquid Phase) (Alma-Ata: Nauka, 1988) Part 3, p. 144
56. S R Savel'ev, N F Noskova, N L Melamud, in *The VIIth International Symposium on Heterogeneous Catalysis, Part 2 (Abstracts of Reports), Bourgas, 1991* p. 793
57. S R Savel'ev, N F Noskova, N N Korneev, I M Khrapova *Zh. Prikl. Khim.* **64** 2190 (1991)
58. N F Noskova, A Zh Kazimova, S R Savel'ev *Zh. Prikl. Khim.* **28** 1352 (1992)
59. M F Sloan, A S Matlack, D S Breslow *J. Am. Chem. Soc.* **85** 4014 (1963)
60. A R Brodskii, Candidate Thesis in Chemical Sciences, Institute of Organic Catalysis and Electrochemistry, Academy of Sciences Kaz. SSR, Alma-Ata, 1987
61. A R Brodskii, N F Noskova, D V Sokol'skii, in *VI Evropeiskaya Konf. po Metalloorganicheskoi Khimii (Tez. Dokl.)* (Abstracts of Reports at the Sixth European Conference on Organometallic Chemistry (Riga: Institute of Organic Synthesis, Academy of Sciences Latv. SSR, 1985) p. 75
62. N F Noskova, A Zh Kazimova, N P Ovchinnikova, in *The XXVth Int. Conf. on Coordination Chemistry (Abstracts of Reports), Nanching, China, 1987* p. 734
63. N F Noskova, A Zh Kazimova, N P Ovchinnikova *Kinet. Katal.* **31** 213 (1990)
64. M M Mansurov, G L Semenova, N F Noskova *Zh. Prikl. Khim.* **63** 2003 (1990)
65. F K Shmidt *Kataliz Kompleksami Metallov Pervogo Perekhodnogo Ryada Reaktsii Gidrirovaniya i Dimerizatsii* (Catalysis of Hydrogenation and Dimerisation Reactions by Complexes of the Metals of the First Transition Row) (Irkutsk: Izd. Irk. Russ. Gos. Univ., 1986)
66. A Rufinska, R Giezynski *Wiadomosci Chem.* **34** 291 (1980)
67. A R Brodskii, S R Savel'ev, N F Noskova *Zh. Fiz. Khim.* **63** 1931 (1989)
68. A R Brodskii, V F Vozdvizhenskii, N F Noskova, N I Marusich, D V Sokol'skii *J. Organomet. Chem.* **178** 325 (1979); **179** 139 (1980)
69. S R Savel'ev, N F Noskova *Kinet. Katal.* **34** 1 (1994)
70. S R Savel'ev, N F Noskova, I M Khrapova, N N Korneev, in *IV Mezhdunar. Simp. po Gomogennomu Katalizu (Tez. Dokl.)* (Abstracts of Reports at the Fourth International Symposium on Homogeneous Catalysis) (Leningrad: Inst. Org. Chem. Phys. Acad. Sci. USSR, 1984) Vol. 4, p. 120
71. B Fell, A Kotoko *Fette Wiss. Technol.* **92** 338 (1990)
72. F Scott *J. Organomet. Chem.* **384** 17 (1990)
73. N F Noskova, A R Brodskii, S R Savel'ev *J. Mol. Catal.* **55** 94 (1989)
74. A Nakamura, M Tsutsui *Principles and Applications of Homogeneous Catalysis* (Translated into Russian; Moscow: Mir, 1983)
75. G Henrice-Olive, S Olive *Top. Curr. Chem.* **67** 107 (1976)
76. R Augustine, J Van Pappen *Ann. N. Y. Acad. Sci.* **172** 244 (1970)
77. R Ugo *The Vth International Congress of Catalysis (Abstracts of Reports), Palm-Beach, USA, 1972*
78. D V Sokol'skii, Ya A Dorfman *Koordinatsiya i Gidrirovanie na Metallakh* (Coordination and Hydrogenation on Metals) (Alma-Ata: Nauka, 1975)
79. S R Savel'ev, I M Khrapova, N F Noskova, N N Korneev *Zh. Org. Khim.* **25** 283 (1989)
80. S R Savel'ev, N F Noskova, in *Vsesoyuz. Konf. po Primeneniyu Metallokompleksnogo Kataliza v Organicheskom Sinteze (Tez. Dokl.)* (Abstracts of Reports at the All-Union Conference on the Application of Metallocomplex Catalysis in Organic Synthesis) (Ufa: Bashkir Scientific Centre, Ural Division of the Academy of Sciences of the USSR,1989) p. 54
81. S R Savel'ev, N F Noskova, in *III Vsesoyuzn. Konf. po Metalloorganicheskoi Khimii (Tez. Dokl.)* (Abstracts of Reports at the Third All-Union Conference on Organometallic Chemistry) (Ufa: Bashkir Scientific Centre, Ural Division of the Academy of Sciences of the USSR,1985) Part 2, p. 214
82. N F Noskova, D V Sokol'skii, N L Melamud *Zh. Prikl. Khim.* **53** 1830 (1980)
83. L P van't Hof, B G Linsen *J. Catal.* **7** 295 (1967)
84. N F Noskova, Doctoral Thesis in Chemical Sciences, Institute of Organic Catalysis and Electrochemistry, Academy of Sciences Kaz. SSR, Alma-Ata, 1985

Russian Chemical Reviews **63** (11) 945–964 (1994)
©1994 Russian Academy of Sciences and Turpion Ltd

UDC 547.963:541.6

The structural-functional organisation of natural peptides

E M Popov

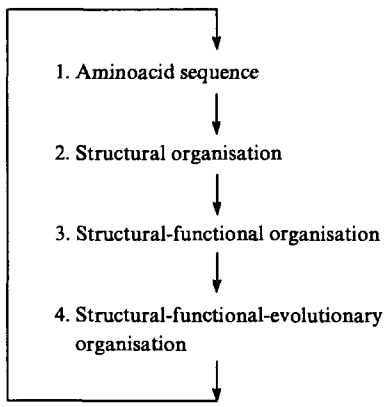
Contents

I.	Introduction	945
II.	Structural organisation of peptides	946
III.	Structural-functional organisation of peptides	949
IV.	The structure and functions of angiotensin II	952
V.	Synthetic analogues of angiotensin	956
VI.	Polyfunctionality of the hormone and heterogeneity of the receptors	958
VII.	Conclusion	963

Abstract. The principles of the structural and structural-functional organisation of the molecules of natural oligopeptides are discussed. The approach to the investigation of the biological activity of peptide hormones directed from structure to function is discussed in general terms and in relation to angiotensin II. It is shown that the polyfunctionality of peptides arises from their ability to exist in a series of conformational states under physiological conditions. A separate function of the peptide is achieved by means of a conformation characteristic of only this function among the conformations most preferred for the free molecule. The method of specific construction of artificial analogues, the steric structure of which corresponds to the set of low-energy physiologically active conformational states of the natural hormone, is examined. The bibliography includes 104 references.

I. Introduction

In the study of natural oligopeptides and proteins, investigators are faced with the need to solve four fundamental problems represented in the following scheme with an indication of the hierarchical relations between them:



E M Popov Department of Organic and Physical Chemistry, Moscow State Correspondence Institute of the Food Industry, Zemlyanoi val 73, 109803 Moscow, Russian Federation. Fax (7-095) 292 65 11. Tel. (7-095) 434 32 41

Received 25 August 1994
Uspekhi Khimii **63** (11) 1004–1025 (1994); translated by A K Grzybowski

The first task involves the establishment of the chemical structure of the compound, namely the determination of the order in which the standard aminoacids are arranged in the peptide chain. The second task involves the identification of the steric form and conformational dynamics of the molecule on the basis of the known aminoacid sequence. The third task involves the study of the dependence of the biological and physiological properties of peptides and proteins on their molecular-structural organisation. Finally, the last task is associated with the consideration of these compounds from the evolutionary standpoint as historical objects. The entire preceding information is now being integrated and the concept of the triunity of the structure, function, and evolution of natural peptides and proteins is being established.

The scheme presented embraces all aspects of the studies on peptides and proteins and classifies them in terms of groups forming a closed cycle in a system of four general coordinates (substance, three-dimensional form, function, and time). The arrows indicate subordinate relations and hence establish a logically justified order in which the fundamental tasks should be considered in the direction from simple to complex or in the given instance from structure to function. This communication describes the fundamentals of this approach and discusses its possibilities in the study of the properties of natural oligopeptides both in general terms and as regards the specific example of angiotensin II.

The theme of the structural and structural-functional organisation of natural oligopeptides has attracted attention for two reasons. Firstly, these compounds are intrinsically extremely interesting in both cognitive and applied respects. They possess unique properties and participate actively in many vital processes. Secondly, the enhanced interest in natural oligopeptides is also due to their genetic relations with proteins. They are close to the latter as regards their evolutionary origin and because they are compounds of the same chemical type. Furthermore, valence and nonvalence interactions between peptides and proteins frequently occur in biological processes, so that the knowledge of the properties of low-molecular-mass peptides is of primary importance in the study of high-molecular-mass compounds of the same nature.

In comparing the properties of natural peptides and proteins, one must bear in mind some uncertainty in their subdivision. The aminoacid sequences encountered in nature form a virtually continuous series of compounds with a gradually increasing number of residues in the chain ranging from several units to many hundreds. It is natural to expect that, on passing from

low-molecular-mass peptides to high-molecular-mass proteins, the conformational properties of the molecules change monotonically and not abruptly. For example, it is evident that the nonvalence interactions between the residues, localised on comparatively small sections of the aminoacid sequence, play the same role in the formation of oligopeptides and polypeptides. The understanding of the steric structure and mechanism of the spontaneous, rapid, and error-free assembly of a protein sequence into the native conformation is therefore impossible without the establishment of the principles of the structural organisation of the low-molecular-mass peptides selected by evolution. Since there are no clearly defined boundaries between natural oligopeptides and polypeptides, the conformational theory of simpler molecules becomes a natural component of the conformational theory of the more complex molecules of the same nature. A definite continuity apparently exists also with respect to the structural-functional organisation of natural oligopeptides and proteins.

II. Structural organisation of peptides

The steric structures of many tens of natural oligopeptides and their synthetic analogues, containing from 5 to more than 30 aminoacid residues, were previously investigated with the aid of the semiempirical method of conformational analysis.[1-3] This resulted in the formulation of the following principles governing the structural organisation of the molecules of these compounds:[2]

1. Under physiological conditions, the steric structure of a natural oligopeptide is determined by a limited set of low-energy compact structures, the stability of which depends on all the nonvalence interactions between the atoms within and between the residues being concerted.

2. The preferred structures of the oligopeptide may differ in the shapes of the peptide skeleton, in the forms of the main chain within the limits of one shape (one structural type), and in the orientations of the side chains, within the limits of one form.

3. The displacement of the equilibrium position between a few conformations of the oligopeptides takes place in accordance with a fully defined low-energy mechanism involving a series of consecutive conformational transitions.

4. The high sensitivity (ready adaptability) of the position of the conformational equilibrium in a natural oligopeptide to the environment (solvent, receptor, enzyme) is due to the rigorous selectivity of the low-energy conformational states as regards specific changes in external conditions.

The question arises what are the common features and what are the differences between the structural organisations of the molecules of natural oligopeptides and proteins. One difference between them is evident—the steric construction of the low-molecular-mass peptides is characterised by a set of structures, i.e. by the position of the conformational equilibrium, while that of the proteins is characterised by a single three-dimensional structure under native conditions. More detailed information about the structural organisation of protein molecules is required for further discussion of this question. We shall use for this purpose the bifurcation thermodynamic model of the spontaneous coiling of the polypeptide chain developed by the author and the physical conformational theory of proteins which makes it possible to predict on the basis of the known aminoacid sequence the geometry of the three-dimensional structure and to estimate quantitatively the capacity of the latter for conformational rearrangements. These data were presented in detail with proof in a monograph.[2] Here we shall deal only briefly with the requirements for the establishment of a genetic relation between the structural organisations of natural oligopeptides and proteins.

The most important feature of the protein chain is the specific conformational nonuniformity of the natural aminoacid sequence, which is responsible for the occurrence of irreversible fluctuations and the appearance of bifurcations (irreversible deviations[4,5]) and hence for the very possibility of the spontaneous formation of a highly organised structure from chaos. One may claim that the essential feature of this phenomenon consists in the existence of a clear-cut interdependence of chemical structure, conformational properties, and irreversible fluctuations. The heterogeneity of the aminoacid sequence is responsible for the difference between the conformational possibilities in its individual sections, which engenders in its turn the thermodynamic nonuniformity of the fluctuations and their differentiation into equilibrium (reversible) and nonequilibrium (irreversible) fluctuation. The combination of the fluctuations and the order in which they follow one another determine the nature and direction of the mechanism of the rapid and error-free self-assembly of the protein chain. This relation is characteristic only of aminoacid sequences selected by evolution.[6] On the other hand, in the case of regular homogeneous or even heterogeneous synthetic polypeptides with a random aminoacid sequence, this random process cannot develop and does not lead to the evolution of the chain from the state of a statistical coil.

In order that the random search mechanism should really lead to the coiling of the chain, the selection of the bifurcation fluctuations need not represent the sorting of all the possible combinations of all the random changes in the entire polypeptide chain, the number of which and the time required for their occurrence being improbably large. Coiling will occur only when structure formation in the protein globule is initiated and developed for a definite time independently in different sections of the sequence. This will occur when fragments differing significantly in their conformational properties alternate in the protein chain. They can be divided approximately into two groups. The first group includes the conformationally rigid fragments the steric structure of which is fully determined by the interactions of their constituent aminoacid residues. The second group includes conformationally labile sections of the chain. They acquire their final steric form after the occurrence of not only short-range but also long-range interactions between the residues. Calculations for a large number of complex natural oligopeptides (25–35 residues in the chain) and for two low-molecular-mass proteins (neurotoxin II and trypsin inhibitor) revealed the following characteristic features in the organisation of their steric structures, which are evidently common to protein aminoacid sequences:

1. The possible conformations of all the fragments of the protein chain are determined to a large extent by the nature and sequence of their constituent aminoacid residues.

2. The conformationally rigid and labile fragments alternate along the polypeptide chain of the protein and in the initial stage of the coiling process are almost independent of one another.

3. The rigid and labile fragments are comparatively small and include not more than 12 residues (the longer rigid fragments have several formation centres).

Subject to the maintenance of the above conditions, the assembly of the proteins begins simultaneously and almost independently on conformationally rigid fragments separated by labile sections of the sequence, i.e. takes place in essence as the assembly of several oligopeptide molecules linked by fairly flexible chains. Random and nonordered selection of all possible fluctuations of virtually autonomous rigid fragments leads sooner or later but inevitably to the appearance in each of them of a bifurcational combination of irreversible conformational changes corresponding to a unique combination of fluctuations of the residues in the fragment. The time necessary for the structural self-organisation of the peptide section from n residues via a random search mechanism is 10^{n-14} s according to Wetlaufer.[7] Consequently, the duration of the assembly of the conformationally rigid fragment with $n < 12$ does not exceed 10^{-2} s, i.e. is entirely realistic.

In proteins, the conformationally labile sections alternating along a chain of approximately the same length also undergo significant changes during this period. The occurrence of internal interresidue interactions in these sections leads to the limitation of conformational freedom. Only a limited set of relatively stable

and, in the absence of long-range interactions, isoenergetic states arises from the enormous set of random states by the same random selection of reversible and irreversible fluctuations during the period $t = 10^{-2}$ s.

It follows from the picture of the coiling of the polypeptide chain described that natural oligopeptide molecules have a structural organisation similar to that of the conformationally rigid fragments of the protein chain. The native conformation of the protein can be represented as an association of oligopeptide molecules in conformations corresponding to their low-energy states and ensuring most effectively the close packing of the protein globule, i.e. forming the maximum number of stabilising contacts between one another and with the sequences connecting them. The isolated conformationally rigid protein fragments, lacking an additional external stabilisation, have a structural organisation which fully corresponds to that of the natural oligopeptide molecules.

The steric structure of the natural polypeptides considered as well as the structure of synthetic oligo- and polyaminoacids depends on the position of the conformational equilibrium rather than being unambiguously determined. A very significant difference consists in the fact that in natural oligopeptides the conformational equilibrium involves a small number of low-energy bifurcational states, which are readily interconverted, and not an enormous number of reversibly fluctuating forms of the statistical coil, as in the artificial peptides.

The knowledge of the principles of the molecular-structural organisation and the ability to predict quantitatively the possible conformations in natural oligopeptides on the basis of the aminoacid sequence constitute the first necessary step towards the understanding of the structural-functional organisation of protein molecules. However, before taking the next step in this direction, it is necessary to consider at least briefly two further questions. The first concerns the reliability of the results of the theoretical conformational analysis and hence of the reliability of the generalisations based on them, while the second concerns the possibilities inherent in the existing experimental methods for the investigation of conformations and the likely success of the empirical approach employed which involves the transition 'from function to structure'.

One's attitude to theoretical calculated data naturally depends on one's certainty that they reflect correctly at least in qualitative terms, if not always strictly quantitatively, the characteristic features of the experimental facts, phenomena, and relations which they describe. An objective idea about the accuracy of the geometrical parameters of the molecules calculated a priori has a special significance in our discussion because the theoretical approach should in fact become the basis for a rigorous solution of the problem of the structural-functional organisation of natural oligopeptides.

The reliability of the calculation of the steric structure of the peptides can be rarely tested by direct comparison of theoretical results with experimental data. Low-molecular-mass peptides exhibit an enhanced, conformational lability, compared with proteins, and their preparation in a crystalline form is therefore a complex and usually an insoluble problem. Consequently the applicability of X-ray diffraction to the study of the steric structures of oligopeptides is extremely limited. Even if it is possible to grow crystals suitable for this purpose and to obtain a diffraction pattern, serious difficulties arise in its interpretation. The method of isomorphous substitution cannot be used in this case to decode the X-ray diffraction pattern, since the incorporation of heavy atoms in the oligomeric molecules constituting the crystal lattice can greatly distort their conformational state; in contrast to proteins, in the study of oligopeptides this method is not really the method of isomorphous substitution. On the other hand, oligopeptides are too complex for their structure to solve with the aid of the direct X-ray diffraction method usually employed in the study of simple organic molecules. Even if it is possible to overcome all the difficulties noted above, nevertheless the problem will still remain unsolved. At best, out of the entire set of low-energy potentially physiologically active conformations of the peptides, only one will become known, namely that tending to form a crystal lattice. There is a possibility that it may have no bearing on the functioning of the compound.

There are at present virtually no crystallographic data on the steric structures of linear low-molecular-mass peptides (with the exception of synthetic dipeptides and tripeptides). X-Ray diffraction analysis has been performed only for relatively rigid macrocyclic natural and artificial oligopeptides and oligodepsipeptides such as gramicidin S, antamanide, enniatin B, valinomycin, and some of their complexes with metal ions.[8] Individual experimental data obtained for these compounds may be compared with the results of theoretical conformational analysis. Such a comparison is particularly instructive for the assessment of the objectivity of the calculated data because the theoretical study was carried out several years before the X-ray diffraction analysis of the same compounds.

The conformational analysis of the cyclic tetradepsipeptides (Gly–Glyco)$_2$, (MeAla–Lac)$_2$, and (MeVal–Hyiv)$_2$, consisting of regularly alternating α-aminoacid and α-hydroxyacid residues with different sets of configurations of the C^{α} atoms (DDDD, DDDL, DDLL, DLLD, LDLD, and LDDD),[9-13] shows that the *cis*, *trans*, *cis*, *trans*-configuration of the main chain is the most stable for these molecules, the peptide and ester groups having the *cis*- and *trans*-configurations respectively. Furthermore, calculation has shown that the introduction of the C^{α} substituents and *N*-methylation only narrow the range of allowed conformations. X-Ray diffraction fully confirmed these conclusions and the geometrical parameters found with its aid for the four diastereoisomers of cyclo-(MeVal-Hyiv)$_2$ with the LDLD, DLLD, DDDL, and LDDD configurations of the C^{α} atoms[8,15-20] agreed quantitatively with the theoretical parameters of the conformations of the corresponding molecules preferred on energy grounds.[10-12] Crystallographic data for enniatin B[21,22] and bovericin[23] also agree satisfactorily with calculated data for the lowest-energy conformation of enniatin B.[24,25] An idea about the similarity of the theoretical and experimental geometrical parameters of the molecules of cyclic tetra- and hexa-depsipeptides can be obtained from Table 1 (see over). Thus, in all cases where it is possible to make a direct comparison between theory and experiment a satisfactory quantitative agreement between the results is observed. However, as already noted, there are few such experimental data and they refer to fairly rigid cyclic oligomeric peptides and depsipeptides.

Physicochemical and primarily optical and resonance spectroscopic methods are used widely in the study of the steric structures of peptide derivatives in solution. However, in this case too the structural problem involving these compounds has remained unsolved for a whole series of reasons. The most serious of these is associated with the characteristic features of the formulation of the problem itself, which in the case of natural oligopeptides is more complex than for proteins and synthetic oligo- and poly-aminoacids. The knowledge of only one global conformation, as in the case of proteins, or ideas concerning the statistical mean conformational state, as in the case of synthetic peptides, are insufficient for a rational investigation of the structural-functional organisation of these compounds. A quantitative estimate of the geometrical parameters of a series of structures, the possible conformations of the latter, their interconversions, and the possibility of their occurrence under various conditions is needed here. The derivation of such information is outside the limits of the sensitivity of physicochemical methods and the possibilities for interpretation inherent in them. Furthermore, owing to the complexity of the compounds and the inadequate elucidation of the physical principles of the corresponding phenomena, none of the methods has as yet permitted an unambiguous and sufficiently complete description of even one conformational state of the peptide

Table 1. Theoretical and experimental dihedral angles of the main chains of the molecules of LDLDLD-cyclohexadepsipeptides and LDLD-cyclotetradepsipeptides.

Molecule (method and reference)	Dihedral angle[a]/deg																	
	ϕ_1	ψ_1	ω_1	ϕ_2	ψ_2	ω_2	ϕ_3	ψ_3	ω_3	ϕ_4	ψ_4	ω_4	ϕ_5	ψ_5	ω_5	ϕ_6	ψ_6	ω_6
Cyclo-[(MeAla–Lac)$_3$] (calculation[24])	−103	171	180	74	−136	180	−103	171	180	74	−136	180	−103	171	180	74	−136	180
Cyclo-[(MePhe–Hyiv)$_3$] (X-ray diffraction[22])	−103	167	180	74	−133	179	−101	166	−177	73	−164	178	−78	157	178	90	−136	−179
Cyclo-[(MeAla–Lac)$_2$] (X-ray diffraction[12])	−100	125	180	73	47	0	−100	125	180	73	47	0	–	–	–	–	–	–
Cyclo-[(MePhe–Hyiv)$_2$] (X-ray diffraction[20])	−98	136	175	70	44	0	−102	129	177	82	39	2	–	–	–	–	–	–

[a] The reference points for the angles ϕ, ψ and ω correspond to the IUPAC-IUB nomenclature.

Table 6. The relative energies of the low-energy conformations of natural angiotensins (AT) and the synthetic angiotensin II analogues.

Group and number of conformation	Shape	Relative energies of conformations (ΔU/kcal mol^{-1})														
		AT II	[Asn^1]-AT II	AT III	AT I	AT II–(1–6)-peptide	[Pro^3]-AT II	[Pro^5]-AT II	[Ala^3]-AT II	[Ala^5]-AT II	[Pro^2]-AT II	[Ala^8]-AT II	[Leu^8]-AT II	[Val^8]-AT II	[Ile^8]-AT II	[Tyr^8]-AT II
A_1	*fe*–*fef*–*ef*	0	4.4	7.4	0.8	2.6	0	0	0	0	–	0	0	0	1.3	0
A_2	*ff*–*fef*–*ef*	0.9	0	1.2	0	2.8	–	0	0.6	0.9	–	1.3	2.0	2.3	4.0	0
A_3	*ff*–*fef*–*ee*	3.5	3.4	5.1	7.9	2.8	–	8.8	2.7	4.6	–	4.7	1.5	4.9	0	3.8
A_4	*fe*–*fef*–*ee*	4.0	8.5	7.3	3.0	2.6	4.5	1.8	3.5	4.8	–	3.4	0.3	5.0	0.2	3.6
B_1	*ff*–*fee*–*ee*	3.5	5.3	4.1	9.9	3.6	–	6.4	4.3	4.9	–	6.2	4.6	5.4	1.3	3.0
B_2	*ee*–*fee*–*ee*	3.7	2.5	1.8	9.6	0	–	6.5	5.8	7.4	4.6	6.5	5.7	7.4	5.1	3.8
B_3	*fe*–*fee*–*ee*	4.4	2.6	1.8	–	0.8	–	–	3.8	5.5	–	5.7	2.8	6.2	3.7	5.5
B_4	*ee*–*fee*–*ef*	4.6	2.7	0	7.5	0	–	–	5.8	7.4	9.5	6.5	6.3	4.9	7.9	6.2
B_5	*fe*–*fee*–*ef*	6.0	3.2	0	8.3	0.8	–	–	5.4	7.0	–	5.8	4.9	2.78	6.0	8.9
B_6	*ef*–*fee*–*ee*	7.0	8.0	4.1	–	5.6	–	6.5	7.5	7.4	0	9.3	6.1	5.7	5.4	7.7
C_1	*ff*–*efe*–*ee*	7.5	–	9.5	–	5.8	–	–	10.0	7.5	–	7.6	4.1	3.7	4.2	7.1
D_1	*ff*–*eee*–*ee*	7.8	9.8	5.3	5.4	2.7	–	–	8.8	9.0	–	8.0	9.1	2.6	–	7.0
E_1	*fe*–*fff*–*ef*	7.8	–	9.0	–	5.6	–	7.4	7.3	7.7	–	8.2	4.5	3.8	4.0	7.3
F_1	*ef*–*eff*–*ef*	8.0	4.8	4.0	7.6	5.1	–	–	7.9	7.8	0.8	8.0	8.9	5.5	5.0	7.6

Note. A dash indicates that the energy of the conformation exceeds 10 kcal mol^{-1}.

predominating in solution on the basis of the results of experimental measurements.

This conclusion follows evidently from the analysis of the results of virtually all studies on the structure of oligopeptides by physicochemical methods. For example, for the elucidation of the steric structure of the octapeptide hormone angiotensin II, virtually the whole set of the existing methods have been resorted to: EPR and ^{1}H and ^{13}C NMR spectra, optical rotatory dispersion (ORD) and circular dichroism (CD) curves, IR and Raman spectra, fluorescence analysis, isotope exchange, etc. As a result, different investigators proposed seven completely different models of the steric structure of the octapeptide hormone corresponding to data obtained by one or several methods at once. However, none of these models, reflecting the state of only the main chain of the molecule, satisfies the entire set of experimental facts.[26] Such uncertainty is characteristic also of the treatment of numerous experimental data on the structure of the neurohypophyseal hormone oxytocin,[27] although in this case the study of the structure was facilitated by the presence of a disulfide linkage between the first and sixth aminoacid residues.

In relation to angiotensin and oxytocin, the peptide hormones which have been investigated most comprehensively and in greatest detail during the last two decades, it has been demonstrated convincingly that the existing physicochemical methods have only a limited applicability to the determination of the structural organisation of natural peptides. Without denying the value of experimental data, one can nevertheless state that a solution solely on their basis of the structural problem to the required extent — the determination of the geometry and conformational dynamics of the low-energy structures of the natural peptide — is at present impossible. The purely empirical approach predominating in conformational studies on peptides and incidentally also proteins uses data which are far from reflecting fully the nature of the phenomenon investigated. The existing gap between the required information and the experimental possibilities actually constitutes the reason for the lack of an appreciable progress in this field over a long period (since the 1960s).

At the present time, the possibilities of the existing physicochemical methods are limited to securing data in support of some kind of hypothetical or a priori calculated structure. Furthermore, the experimental test of the theoretical conformational analysis of peptides has its characteristic features. On the one hand, although a satisfactory agreement between the calculated results and experimental data is a positive finding, nevertheless it cannot serve as a reliable criterion of the validity of the theoretical prediction. In addition, strangely enough the lack of agreement does not imply incontrovertible proof that the calculated results do not correspond to reality. The difference between theoretical and experimental data can be induced by causes which do not play a decisive role in a rational study of the structural-functional organisation of the peptide. For example, a clear-cut discrepancy will occur when the entire set of the low-energy conformations is determined correctly and the geometry of each state is estimated satisfactorily but there is incomplete agreement between the dispositions of the conformations on the observed and real energy scales (a difference of 1.5–2.0 kcal mol^{-1} is sufficient).

Two methods have been proposed for the testing of the results of calculations.[2]

The first method for the assessment of calculated results does not require any experimental facts whatever on the steric structure of the peptides. Its essential feature consists in the selection for the theoretical study of objects such that the calculation for the latter entails an internal autonomous check of its results. For example, intramolecular disulfide bonds can serve as natural reference standards.

According to the theory[2,28,29] and Anfinsen's thermodynamic hypothesis,[30] the oxidation of the sulfur atoms of the cysteine molecules forming disulfide bridges in peptides is possible by virtue of the steric predisposition of the corresponding sections of the aminoacid sequence to conformational states in which the Cys residues are close to one another and the side chains have the mutual orientation necessary for the creation of a S–S bond. During the coiling of the polypeptide chain, the cysteine residues approach one another in the lowest-energy conformations of the linear sequence as a result of concerted stabilising nonvalence interactions between all the chain residues. In a multistage conformational analysis of fairly complex peptides, the attainment of the lowest-energy conformations in the concluding state of the calculation may be expected only when all the theoretical postulates underlying the calculations are adequate and the conformational state of the molecule has been described correctly in quantitative terms. The internal check method has been tested in the analysis of a large number of extremely complex cysteine-containing peptides: nonapeptide neurohypophyseal hormones,[27] apamin,[31], tertiapin,[32] and the MSD-peptide[33] containing respectively 18, 21, and 22 aminoacid residues, including cysteine, which forms two disulfide bonds, as well as insectotoxin[34] containing 36 residues, among which there are eight cysteine residues, etc.[1,2]

In the second assessment method, the correctness of the conformational analysis is tested by comparing the results of the calculation of the possible conformations in the oligopeptide fragments with experimental data on the geometry of the crystal structure of the protein. Such a comparison is at present realistic for two low-molecular-mass proteins — bovine pancreatic trypsin inhibitor (58 aminoacid residues in the chain) and neurotoxin II (61 aminoacid residues), for which the first a priori calculation of the three-dimensional structures has been carried out.[35,36] We shall quote data for the trypsin inhibitor, the steric structure of which is described by approximately 300 dihedral angles, which determine the geometry of all the main and side chains (φ, ψ, ω, and χ). It follows from the comparison of the calculated values of these angles and their experimental values obtained by X-ray diffraction with a resolution of 1.5 Å that the conformation of the inhibitor molecule found a priori is fully consistent with the crystallographic structure. The mean square discrepancies between the experimental and theoretical values of the dihedral angles are 13°, 13°, and 9° for the angles φ, ψ, and ω respectively. The discrepancy between the values of the dihedral angles for the side chain χ (18°) is also within the limits of the error of the high-resolution (1.5–2.0 Å) X-ray diffraction analysis of proteins.

Thus the reliability and the fairly high accuracy of the results of the theoretical conformational analysis of oligopeptides have been confirmed by the automatic formation of a regular system of disulfide bonds in the self-checking calculation and by the agreement between the geometries of the theoretical and crystallographic structures in the calculations for protein molecules.

III. Structural-functional organisation of peptides

As happened many years ago, the mechanisms of the physiological action of peptide hormones are studied nowadays both in the absence of the minimum necessary information about coupled receptors and without the knowledge of the structural organisation of the natural peptide cells. Studies are as a rule based on the results of kinetic measurements and biological tests of the hormone and its synthetic analogues, the latter being selected by the method of trial and error, i.e., strictly speaking, blindly. Thus, a purely empirical approach from function to structure predominates in the study of natural oligopeptides.

Neglect of the information about the geometry and possible conformations of molecules implies in essence the search for an a priori nonexistent direct relation between chemical structure and biological activity. Furthermore, in such an approach the existence of a direct and fairly simple relation between individual aminoacid residues and functions of the peptides is postulated. The idea of additivity inevitably implies that the structural organisation of the interacting molecules ceases to be cooperative, that such molecules are no longer complementary, and that biological processes are not induced and multistage. Nevertheless,

it has long been known that this cannot be done because detailed steric correspondences between the interacting molecules, determined mainly by the specific structural organisation of peptides and proteins, underlie biological processes, their interdependence, high sensitivity, rigorous selectivity, effectiveness, and automatic functioning.

When the 'from function to structure' approach is used, the lack of objective information about the steric organisation of peptides, constituting a natural intermediate link between the chemical structure and biological activity of compounds, is made good by phenomenological descriptions and frequently simply by the author's fantasies. A multiplicity of hypothetical ideas of all kinds, sometimes mutually exclusive, concerning the structural organisation of peptides are available in the literature. The proposed treatments of the mechanism of the action of natural peptides are excessively descriptive in character and lack predictive power.[37] This can be readily demonstrated in relation to studies devoted to angiotensin,[26] bradykinin potentiating peptides,[38,39] and neurohyposphyseal hormones.[27]

Thus it must be recognised that the purely empirical route to the establishment of a direct relation between biological activity and chemical structure is relatively ineffective and without prospects as regards the cognitive purely scientific aspect. It is essential to reverse the direction pursued in research, i.e. to employ the 'from structure to function' approach.

In the solution of the problem of the structural-functional organisation of natural oligopeptides, we shall assume that the aminoacid sequence of the hormone and its physiological activity spectrum together with quantitative estimates of each function are known. If the chemical structure of the peptide is known, it is possible to calculate the possible conformations of the molecule and to discover the set of the potentially active low-energy forms. It is required to establish on the basis of these data the relation between the electronic-conformational and physiological properties of the natural peptide. The physiological properties of peptides may be determined by the path of their interaction with the receptors, whereas information about the organisation of the coupled receptors is either completely lacking or is extremely scanty and, in discussing the properties of protein receptors, we shall be forced henceforth to resort to hypothetical ideas about their conformational and functional features.

In the first place, we suggest that the peptide–protein interactions occurring in living organisms have a unique physicochemical nature regardless of the structure of the specific object and the character of the biological function. Consequently, from a general scientific standpoint, all the numerous and extremely diverse functions of peptides and proteins can be subdivided into two groups of phenomena—physical and chemical. The former take place via the nonvalence interactions of peptides and proteins with one another and with molecules of a different kind. They can be static, as in the case of structural proteins, or dynamic, as in the active transport of metabolites. Together with nonvalence interactions, chemical functions include valence interactions which lead to reversible or irreversible changes in the chemical structure of the molecules. Enzymic reactions, in which the entire set of interactions, both nonvalence (physical) and valence (chemical), take place, may serve as an example. The above assumption presupposes that the interactions of a peptide hormone with a protein receptor are in essence analogous to the interactions of a peptide substrate with a proteolytic enzyme. If this is so, then the characteristic features of the structural and structural-functional organisation of the hormone and the substrate are the same, and this can also be said of the receptor and the enzyme. As regards the principles of the structural organisation of the molecules of peptide substrates and peptide hormones, their identity has been reliably established.

The characteristics of the structural-functional organisation of the molecules of enzyme proteins were discovered previously with the aid of a priori (i.e. in the direction 'from structure to function') calculations of the multistage mechanisms of the elementary steps in biocatalysis by α-chymotrypsin and β-trypsin.[40,43] The calculations were based on the general theory of biocatalysis developed by the author.[44] The characteristics of the structural-functional organisation of enzymes can be formulated in a fairly complete form in the following manner:

1. The active centre of a native enzyme is predisposed, firstly, to sorb a specific substrate in a conformation which in the free state of the molecule is one of the most preferred and, secondly, to undergo quite definite intrinsic conformational changes necessary for the subsequent chemical interactions.

2. The nonvalence enzyme–substrate interactions and the formation of the Michaelis complex do not lead to steric strain or enforced deformations in either the substrate or enzyme molecule. The conformational changes occurring in this stage of the catalytic reaction takes place exclusively by virtue of stabilising interactions and not as a result of unfavourable contacts between the enzyme and substrate atoms, which are simply absent.

3. In the Michaelis complex and in the subsequent complexes involved in the multistage catalytic step, polyfunctional closed systems are formed from the atomic groups of the enzyme and the sensitive site of the substrate. These systems are predisposed to undergo the corresponding specific reactions (for example, in the complexes of α-chymotrypsin and β-trypsin these are acylation and deacylation reactions). A chain of interdependent reactions catalysing one another, the initiation of which does not require an activation energy, occur in each of these systems. The role of the Michaelis complex is to create precisely this kind of autocatalytic closed system, and not to convert the substrate into a strained structure (the geometry of which is similar to that of the transition state) and catalytically active groups into unstrained conformations with an enhanced reactivity. The enzymic process is accelerated because termolecular, tetramolecular, and even higher-order reactions are reduced in such a system to a unimolecular interaction.

4. After the formation of the Michaelis complex as well as other intermediate nonvalence complexes, the additional mutual approach necessary for electronic and chemical interactions between the functional groups may be achieved as a result of Brownian collisions and in-phase normal vibrations of the macromolecular formation.

5. The lowest-energy conformational states of the complexes correspond in all the stages of the catalytic step to a productive mutual orientation of the reacting atomic groups of the enzyme and substrate, i.e. to a mutual disposition of the latter such that their maximum predisposition to undergo specific chemical interactions is achieved. The nonproductive conformations of the enzyme–substrate complexes are energetically much less preferred and their occurrence is unlikely. The transitions between all the chemically unstable intermediate states are accompanied by slight conformational changes, which do not give rise to steric strain.

Thus the enzyme performs its function without resorting to an enforced deformation of the sensitive site of the substrate and of the catalytic groups of the active centre. The catalytic step executed by the enzyme is a conformationally unstrained process. The exceptional efficiency and strict specificity of biological catalysts are not achieved as a result of special high-energy electronic-conformational states of the enzyme and substrates, as has been declared in all the existing concepts. On the contrary, the exceptional nature of this spontaneous natural phenomenon, which occurs without error and under very mild conditions, is the extreme simplicity and natural harmony in the interrelations between the enzyme and substrate developed by evolution at all stages. Biological catalysis has few analogies with the usual chemical catalysis and its mechanism cannot be reproduced by the so called congruent model system.

According to the hypothesis put forward above, the principles of the structural-functional organisation of enzymes listed may be applied to protein receptors. The author deliberately refrained from introducing terminological changes and from replacing the

concepts adopted in enzymology by others less specific. Enzyme catalysis, which consists of alternating physical and chemical phenomena, is one of the most complex processes in vital activity. Therefore, the principles described are of a general character and can be readily reduced to a particular special case. If the interactions of a natural oligopeptide with a protein receptor also include both these phenomena, i.e. nonvalence and valence interactions, then in its description it is necessary to replace only certain words. For example, instead of 'enzyme' one should put 'protein receptor' and the word 'substrate' should be replaced by 'peptide hormone', or both should be changed. On the other hand, if the peptide–receptor interactions are purely physical phenomena, then in the description one must omit everything concerning the chemical aspect of enzyme catalysis.

We now have all the necessary criteria which must be satisfied by the structural-functional organisation of natural oligopeptides. Firstly, it must correspond to the structural organisation of these molecules already known, i.e. must be a consequence of the latter. Secondly, it must complement the structural-functional organisation of protein receptors put forward above. Thirdly, it must not conflict with the known experimental facts concerning the physiological activity of many natural peptides and their synthetic analogues.

All the conditions mentioned above are satisfied for the following principles of the structural-functional organisation of natural oligopeptides.[1,27,39]

1. The spectrum of the functional activity of a low-molecular-mass peptide is determined by the existence under physiological conditions of equilibrium between several structures. In other words, the steric structure of a natural peptide molecule is predisposed to perform not one but several definite functions ('conformational equilibrium — polyfunctionality').

2. An individual function of the peptide is performed via a conformation, valid only for itself, of the most preferred structures forming part of the free molecule, i.e. the uniqueness of the geometry and of the dynamic properties of the corresponding conformational state of the given aminoacid sequence determine the selectivity and the specificity of each of its specific physiological activities ('one conformation — one function').

3. The effectiveness of the activity of the natural oligopeptide when all its functions operate can be accounted for by the alternation of the intramolecular interactions stabilising the preferred conformations and by the relative ease of the conformational transformations. In other words, the rapid response of the conformational equilibrium to a change in the medium ensures a sharp increase in the concentration of the required structure at the required place ('specific external conditions — actual conformation').

Having considered the principles of the structural and structural-functional organisation of natural oligopeptides and proteins, we shall now return to the consideration of the fundamental problem, posed above, concerning the search for a relation between structure and function and an attempt will be made to formulate this problem more rigorously and to outline a general approach to its solution. We recall that the aminoacid sequence of the peptide and its physiological functions, together with quantitative estimates of the activity of each, are known.

As already mentioned, the first step consists in the solution of the direct structural problem for the oligopeptide, i.e. in the determination for the latter of a set of the most probable low-energy conformational states. We begin with the hypothesis that only energy-preferred conformations or some of them can operate as physiologically active structures of the oligopeptides through which its functions are effected.

The next step in the determination of the relation between structure and biological activity is based, on the one hand, on the knowledge of the geometry and conformational properties of all the structures of the test peptides relevant to physiological activity and, on the other, on data concerning the entire spectrum of its activity. Thus the problem arises of the correlation between the set of known conformations and the set of known functions, i.e. of the elucidation of the relevant conformation for each physiological activity of the peptide. In the absence of concrete information about the geometry of the protein receptor, this problem does not have an unambiguous solution. The situation is appreciably simpler in the similarly formulated problem of enzyme–substrate interactions, where not only the organisational principles governing the molecules but also their possible conformations and three-dimensional structures are known.

Evidently the unique high-energy conformational state of the free substrate, which complements the geometry of the active centre of the enzyme, is in this case relevant to the performance of its function. In our case, the active centre of the receptor is unknown, so that its selection is impossible without additional information.

In the absence of data concerning the steric structures of the receptors interacting with various conformations of the peptide considered, the necessary information can be secured with the aid of a set of synthetic analogues of the natural sequence corresponding to special requirements. Each compound in this set must be monofunctional and hence should assume only one of the series of actual conformations of the natural peptide complementary to the active centre of the corresponding receptor. Thus synthetic analogues possessing prespecified electronic-conformational properties are essential for the solution of the problem of the structure and function of natural oligopeptides. Compared with the direct structural problem (a priori calculation of the conformations from the known aminoacid sequence), the problem arising here has the opposite formulation and we shall therefore call it the converse structural problem.[1]

The converse structural problem consists in the theoretical determination of the nature of the chemical modifications necessary for the differentiation of the conformation relevant to the corresponding function of the natural oligopeptide. A more general aim involves the specific formation of the chemical structure of the molecule known beforehand to assume the steric structure necessary for the performance of a fully defined function. The solution of this problem within the framework of the 'from structure to function' approach gives rise to extensive prospects not only for the quantitative study of the functioning of natural oligopeptides but also for the modelling of the active centres of enzymes and the search for medicinal preparations, substrates, inhibitors, antibodies, etc., such a search acquiring a specific aim. As already mentioned, hitherto artificial analogues have been synthesised purely intuitively by the method of trial and error.

The method which the present author has proposed for the solution of the converse structural problem is based on the quantitative conformational theory of natural peptides and proteins,[2,28,29] in particular on the estimation of the special role of the short-range interactions and of the spatial organisation of the aminoacid sequences selected by evolution and on the use of the natural classification of peptide structures.[29] This method has been described in detail elsewhere.[1] Before synthesis and biological tests, it permits the construction of specific artificial analogues the steric structure of which corresponds to the set of low-energy physiologically active conformational states of the natural oligopeptides.

The steps in studies on these lines may correspond to the following scheme:

1. Theoretical conformational analysis of the natural oligopeptide and the determination of all the most energy-preferred and hence potentially physiologically active conformational states (solution of the direct structural problem).

2. The creation of a series of artificial analogues, the set of steric structures of which corresponds to the set of low-energy physiologically active conformations (solution of the converse structural problem).

3. The synthesis and biochemical study of artificial model analogues, the determination of the spectrum of the physiological

activity of the natural oligopeptide, the quantitative estimation of its functional activity, the study of the specific interactions with receptors, etc.

4. Analysis of the results of the calculation and the experiment and the determination at the atomic-molecular level of the relation between chemical structure, the possible conformations, and the effectiveness of the physiological activity of the oligopeptide.

The essential feature of this scheme is that the experimental study of the structure, the biological activity, and the mechanism of the functioning is preceded by theoretical modelling resorting to conformational analysis and to quantum-chemical methods. In this respect, the order in which the studies are performed in the direction 'from structure to function' corresponds to an engineering approach.

In the treatment below, two interrelated problems, solved simultaneously, are considered. One of them is more specific and reduces to the establishment of the structural-functional organisation of the hormone angiotensin II with the aid of the approach described above. The second, more general problem involves the testing of the approach in a specific analysis and the estimation of its real possibilities. The choice of angiotensin II as the object of study was dictated by the fact that this natural oligopeptide has now been most thoroughly investigated and is therefore most suitable for testing the new approach.

IV. The structure and functions of angiotensin II

Angiotensin II, an octapeptide tissue hormone, forms part of the renin–angiotensin system in which its biogenesis and decomposition take place. Angiotensin II is the most powerful of the known pressor agents in the blood circulation system. It stimulates the contraction of the peripheral arterioles throughout the organism and hence increases the arterial pressure. In addition, angiotensin II activates the secretion of a series of hormones (mainly aldosterone), influences the operation of the heart, liver, and the central and peripheral components of the nervous system, and also induces a series of other responses in the mammalian organism. Table 2 lists the known functions of the hormone with an indication of the sites where they are manifested in organisms.

The decapeptide angiotensin I, which is a direct precursor of angiotensin II, is formed, according to the scheme presented below, from angiotensinogen, a globular blood protein, when the latter is acted upon by the proteolytic enzyme renin.

Table 2. The principal functions of angiotensin II and the sites where they are performed in the mammalian organism.

Function	Organs and tissues	Ref.
Stimulation of the contraction of smooth muscles	Smooth muscles of arterioles	45
Regulation of the secretion of aldosterone	Adrenal cortex	46
Regulation of the arterial pressure, secretion of vasopressin, intensification of thirst and appetite for salt	The brain (stem, hypothalamohypophyseal system, establishment of the neuronal thirst cycle, etc.)	47–49
Regulation of kidney haemodynamics, of the secretion of renin, and of the permeability of kidney channel walls	Kidneys (kidney arterioles, kidney channel walls, cells of the juxtaglomerular apparatus)	50–52
Increase in the strength of cardiac contractions	Heart muscle	53
Stimulation of the secretion of catecholamines	Adrenal medulla	54

Almost all tissues possess peptide activity which leads to the rapid decomposition of angiotensin II. Two varieties of angiotensin II have been isolated from mammalian blood. One of them is presented in the scheme, while the other differs from it by the Ile residue in the 5-position.

$Asp^1-Arg^2-Val^3-Tyr^4-Val^5-His^6-Pro^7-Phe^8-$
$-His^9-Leu^{10}-Leu^{11}$

↑ renin

Angiotensinogen

$Asp^1-Arg^2-Val^3-Tyr^4-Val^5-His^6-Pro^7-Phe^8-His^9-Leu^{10}$

↑ kinase II

Angiotensin I

$Asp^1-Arg^2-Val^3-Tyr^4-Val^5-His^6-Pro^7-Phe^8$

↑ aminopeptidase

Angiotensin II

$Arg^2-Val^3-Tyr^4-Val^5-His^6-Pro^7-Phe^8$

Angiotensin III

The chemical synthesis of angiotensin II in 1961 [55] initiated the study of its physiological functions. With the aid of numerous synthetic analogues of the hormone, it was possible to show that the natural peptide interacts with a series of receptors located in various tissues of the mammalian organism and possesses a fairly broad spectrum of biological activity.

Numerous studies on the steric structure of angiotensin II in solution have been published. Virtually the entire set of the existing physicochemical methods have been used in them: thin-film dialysis,[56] titration of ionogenic groups,[57] hydrogen exchange,[58] all types of optical and resonance molecular spectroscopy,[59–62] as well as a number of others. The results of the investigations and their interpretation are extremely contradictory. Different workers have proposed numerous significantly different structures for angiotensin II.[26] Each of them concerns exclusively the main chain of the molecule and satisfies only a limited range of experimental data (see, for example, Refs 26, 45, 58, 63, and 64). The positions of the side chains of the aminoacid residues, which constitute a large proportion of the molecule and determine its conformational state, were completely disregarded in the discussion of the structure of the hormone.

The first studies on angiotensin II by dialysis through thin films proved to be contradictory. In some investigations,[65, 66] it was concluded that the hormone molecule has a single compact form in solution, whilst in another investigation[56] the existence of conformational equilibrium between two forms was postulated.

The conclusions reached by different investigators from the analysis of kinetic data on the isotopic substitution of a proton in the hydrogen bonds of angiotensin II were no less contradictory. Scheraga and coworkers[67] noted that the rates of exchange of all the amide protons were the same. Lenkinski et al.[68] speak of an anomalously low rate of exchange of the His^6 amide proton, while Bleich et al.[69] differentiate the Val^3 and Val^5 residues for the same reason. Printz et al.[63] divided the amide protons into three groups in terms of the rate of exchange, the Asp^1 and Arg^2 protons being assigned to the group with the highest rates. In the classification proposed by Marshall,[70] all the exchanging protons were divided into four groups, the amide protons of all the angiotensin II residues, with the exception of Asp^1 and Phe^8, being assigned to a single group with the same rate of exchange.

Table 3. The number of low-energy conformations, having the same form of the main chain, calculated in the literature.[26,80-83]

Literature source	De Coen and Ralson (1977)[80]	Galaktionov, Nikiforovich, et al. (1979)[26]	Nikiforovich, Galaktionov, and Chipens (1983)[81]	Marchionini, Maigzet, and Premilat (1983)[82]	Nikiforovich, Vesterman, et al. (1987)[83]
80	10	1	1	2	0
26	1	6	4	0	2
81	1	4	5	0	2
82	2	0	0	5	0
83	0	2	0	0	6

The dissociation constants of the ionogenic groups of the hormone, obtained by potentiometric titration[57] and with the aid of NMR and CD spectra,[71] led to the conclusion that the N- and C-terminal groups of the peptide chain are close to one another, which permits their interaction. The distance between the groups is much smaller than the corresponding distance for angiotensin in the statistical coil conformation. In addition, it has been postulated[71] that all the ionogenic groups are accessible to the solvent and that the imidazole ring of the His^6 residue interacts with the benzene ring of the Tyr^4 residue and is remote from the Phe^8 residue.

According to Fermandjian and coworkers,[72,73] the ORD and CD spectra indicate the presence of an antiparallel structure in the angiotensin II molecule. The above workers interpreted similarly the vibrational spectra of the hormone.[60]

A series of studies have been devoted to the NMR spectra of angiotensin II, which yield most information about the steric structure of the molecule. However, here too there is no unanimity in the interpretation of the experimental data. Some workers believe that the spectra indicate the existence of angiotensin II in solution in a single conformation which has a predominantly extended form. Others[75] concluded that the molecule has a coiled form, in which the aromatic side chains of the Tyr^4 and His^6 residues are arranged parallel to one another and interact effectively, whilst the carbonyl group of the Asp^1 residue forms a hydrogen bond with the amino-group of the Tyr^4 residue. The study of the ^{13}C spin–lattice relaxation time led Sekatsis et al.[76] to the conclusion that the conformational mobility of the first two residues is high and that there is no bend in this part of the molecule. Using the same method, Deslauriers et al.,[77] reached a different conclusion. They believe that all the residues of angiotensin II, with the exception of Tyr^4, have approximately the same conformational freedom; the mobility of the side chain of the Tyr^4 residue, which interacts with many other residues of the molecule, is restricted to the greatest extent. The vicinal constants for all the aminoacid residues of angiotensin II[70,78,79] have values consistent with all those corresponding to each residue in the low-energy regions *R* and *B* and hence to 2^7 combinations of the conformational states of the residues in the peptide chain of the molecule.

The reasons for the low effectiveness of the physicochemical methods for the investigation of the steric structures of oligopeptides have already been described in detail. We shall only recall that, for the investigation of the structural-functional organisation of the molecules of these compounds, it is insufficient to know only the global conformation, i.e. the most preferred conformation as regards energy. Here a quantitative estimate of the geometrical parameters of a whole set of structures, their possible conformations, and the probability of their occurrence under various conditions is needed. Such information is so far beyond the limits of sensitivity of physicochemical methods and the possibilities for interpretation inherent in them, so that the semiempirical method of conformational analysis has been resorted to in order to solve the problems listed above. However, here too the results are fairly modest and contradictory. Table 3 presents the results of the calculations of the steric structure of angiotensin II carried out by different workers at different times.[29,80-83] Comparison shows that the sets of low-energy conformations found for the same hormone are not the same. Furthermore, none of them conflict with data obtained in a very wide range of studies carried out on this compound. The reasons for such significant discrepancies have been discussed in detail in a monograph.[2] Therefore we shall briefly note below only certain features of the approach of Galaktionov and coworkers[26,81] to the conformational analysis of natural oligopeptides. From our viewpoint, it is more logical for the solution of the direct structural problem than the approaches used by other investigators.[80,82]

In order to reduce the number of conformations considered with the simultaneous expansion of the critical range of energies, Galaktionov and coworkers[26,81] considered in a preliminary step models in which all the aminoacid residues, other than Arg and Pro, had been replaced by alanine residues. Next, all the possible optimum conformations were determined for the model peptide and the best of these then served as the initial structural variants of the main chain of the real peptide. This procedure is based on what is in our view a fundamentally incorrect hypothesis that the main chain plays a dominant role in determining the possible conformations of the peptides.

If this were the case and the one-third of all the atoms constituting the peptide skeleton did indeed determine the positions of the remaining two-thirds of atoms belonging to the side chains, then all the natural oligopeptides and proteins should have either identical forms of the main chain or a very limited number of such forms. As regards synthetic oligopeptides and polypeptides consisting of glycine and alanine residues and actually lacking side chains, their steric structures should have been described by single rigid structures and not by the state of a statistical coil, as happens in reality. Thus the hypothesis of Galaktionov and coworkers[26,81] is far from representing the true picture. The variations in the steric forms of proteins are almost as numerous as the variations in the order of disposition of the 20 standard aminoacid residues in this chain.

In both the first and second stages of the calculation, where the optimum mutual orientation of the side chains of the test peptides is sought for the selected steric forms of the main chain, mainly the electrostatic interactions of the ionogenic groups were emphasised (it was assumed that they are the main factor in the structural stabilisation). It is difficult to agree with this too because the arrangement of the peptide chain in the native conformation or (in the presence of a series of low-energy structures, as in the case of oligopeptides) the attainment of the conformational equilibrium takes place in aqueous solution under physiological conditions, which prevent an effective electrostatic interaction, abolishing it almost completely ($\varepsilon = 81$).

A characteristic feature of all the theoretical studies of the steric structure of angiotensin II[26,80-83] is the absence of any kind of classification of the conformational states of the molecule let alone one which would be justified from the physical standpoint and would embrace all possible structural variants arranged systematically in accordance with subordinate interrelations in terms of taxonomic categories. All the estimates of the optimum conformations in the studies under discussion were based on the relative values of the overall energy without a quantitative analysis of the contributions by individual intraresidue and interresidue

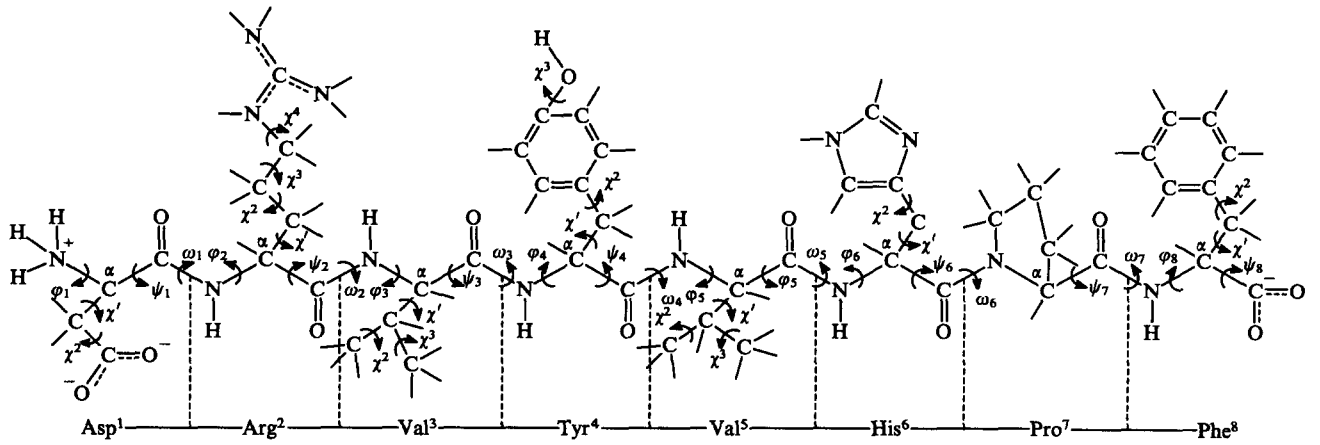


Figure 1. The calculated model of the angiotensin II molecule.

interactions in the structural variants of all the possible forms of different types of the main chain. There is therefore no guarantee that the results of the calculations[26,80–83] are free from either random omissions or incorrect assessments of the data obtained. Table 3 serves to confirm this conclusion.

Thus the available conformational data for angiotensin II could not be used to test the 'from structure to function' approach. This factor led the author of the review and Gogitidze to undertake their own analysis of the conformational states of this molecule.[84] The method of calculation, the notation, and the results are considered briefly below.

The structural organisation of the angiotensin II molecule was investigated on the basis of the conformational theory and the corresponding computational method developed in previous studies[2,85] on the assumption of the rigid valence scheme presented in Fig. 1. The possible conformations of the octapeptide hormone are determined by 41 values of the dihedral angles of rotation about the axes of the main chain (φ, ψ, ω) and the side chains (χ^1, χ^2, ...). The potential functions and the semiempirical parameters used in the calculation to estimate the nonvalence, electrostatic, torsional, and hydrogen bonding interactions were indicated previously.[86,87] The natural classification of the peptide structures in terms of three levels of steric organisation, namely the conformation, form, and shape of the main chain, was used in the calculation and in the description of the results. The classification was put forward in previous communications.[2,85,87]

A system of identifiers was used to designate the conformations. According to this system, the conformational state of each residue is defined by X^n_{ij}, where X characterises the form of the main chain of the residue (R, B, L, and P), n is the number of the residue in the sequence, and the symbols ij = 11, 12, 13, 21 etc. correspond to the position of the side chain (χ^1, χ^2, ...); the subscript 1 corresponds to values of the angles in the range from 0° to 120°, 2 corresponds to angles from 120° to −120°, and 3 corresponds to angles from −120° to 0°. Apart from its form, the main chain is characterised also by its shape or structural type described by the combination of the symbols *f* and *e*, which denote respectively the coiled and uncoiled configurations of the virtual $C^\alpha - C^\alpha_i - C^\alpha_{i+1} - C^\alpha_{i+2}$ bonds. The configuration is defined quantitatively by the virtual angle of rotation $\theta = \psi_i + \phi_{i+1}$ around the $C^\alpha_i - C^\alpha_{i+1}$ bond. The designations and the reference points for the angles of rotation correspond to the generally accepted nomenclature.[88]

The conformational analysis of the octapeptide hormone was carried out in three stages. The first included the independent calculation of five conformations overlapping as regards three aminoacid residues of the tetrapeptide fragments, the second stage involved the calculation for the hexapeptide fragment Asp¹ – His⁶, and the third involved the calculation for the entire angiotensin molecule.

The conformations of the hormone with relative energies from 0 to 8.0 kcal mol^{-1} are presented in Table 4. The first four

Table 4. The relative energies (ΔU/kcal mol^{-1}) and energy contributions (in kcal mol^{-1}) by the nonvalence (U_{nv}), electrostatic (U_{el}), and torsional (U_{tors}) interactions in the preferred optimum conformations of the angiotensin II molecule.

Group and number of conformation	Shape	Conformation	ΔU	U_{nv} [a]	U_{el}	U_{tors}
A_1	*fe–fef–ef*	$R_{23}\,B_{1212}\,R_{222}\,B_{212}\,R_{122}\,B_{31}\,R\,R_{11}$	0	−38.4	−3.5	4.2
A_2	*ff–fef–ef*	$R_{23}\,R_{3222}\,R_{222}\,B_{212}\,R_{122}\,B_{31}\,R\,R_{11}$	0.9	−41.4	−0.9	5.5
A_3	*ff–fef–ee*	$R_{21}\,R_{3222}\,R_{222}\,B_{212}\,R_{122}\,B_{31}\,R\,R_{11}$	3.5	−38.0	−1.4	5.2
A_4	*fe–fef–ee*	$R_{23}\,B_{1212}\,R_{222}\,B_{212}\,R_{122}\,B_{31}\,R\,R_{11}$	4.0	−36.7	−0.3	3.1
B_1	*ff–fee–ee*	$R_{23}\,R_{3222}\,R_{222}\,B_{212}\,B_{222}\,B_{11}\,B\,B_{31}$	3.5	−38.4	0.9	3.2
B_2	*ee–fee–ee*	$B_{21}\,B_{1222}\,R_{222}\,B_{212}\,B_{222}\,B_{11}\,B\,B_{31}$	3.7	−36.7	0.3	3.1
B_3	*fe–fee–ee*	$R_{21}\,B_{1222}\,R_{222}\,B_{212}\,B_{222}\,B_{11}\,B\,R_{31}$	4.4	−36.8	0.5	3.0
B_4	*ee–fee–ef*	$B_{21}\,B_{1222}\,R_{222}\,B_{212}\,B_{222}\,B_{11}\,R\,R_{11}$	4.6	−36.3	−1.1	4.3
B_5	*fe–fee–ef*	$R_{23}\,B_{1222}\,R_{222}\,B_{212}\,B_{222}\,B_{11}\,R\,R_{11}$	6.0	−36.0	0.1	4.1
B_6	*ef–fee–ee*	$B_{13}\,R_{2122}\,R_{222}\,B_{212}\,B_{222}\,B_{11}\,B\,R_{31}$	7.0	−34.1	0.8	2.6
C_1	*ff–efe–ee*	$R_{23}\,R_{3222}\,B_{122}\,R_{312}\,B_{222}\,B_{11}\,B\,B_{31}$	7.5	−33.2	0.2	2.8
D_1	*ff–eee–ee*	$R_{23}\,R_{3222}\,B_{222}\,B_{112}\,B_{222}\,B_{11}\,B\,B_{11}$	7.8	−33.7	0.7	3.2
E_1	*fe–fff–ef*	$R_{23}\,B_{1222}\,R_{222}\,R_{312}\,R_{222}\,B_{31}\,R\,R_{11}$	7.8	−31.0	−0.3	2.3
F_1	*ef–eff–ef*	$R_{23}\,B_{2122}\,R_{122}\,R_{312}\,R_{222}\,B_{31}\,R\,R_{11}$	8.0	−35.9	2.4	3.8

[a] The energy of hydrogen bonds has also been included in U_{nv}.

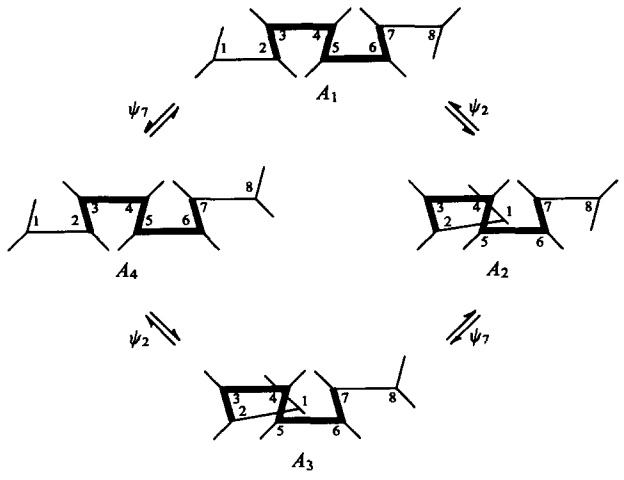


Figure 2. The shapes of the peptide skeleton and the pathways followed in the interconversions of the low-energy conformations of group *A* (Table 4).

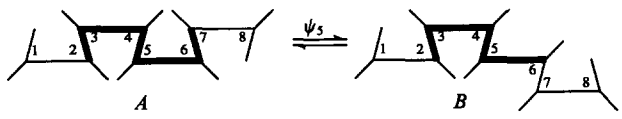


Figure 3. The interconversion of group *A* and *B* conformations (Table 4).

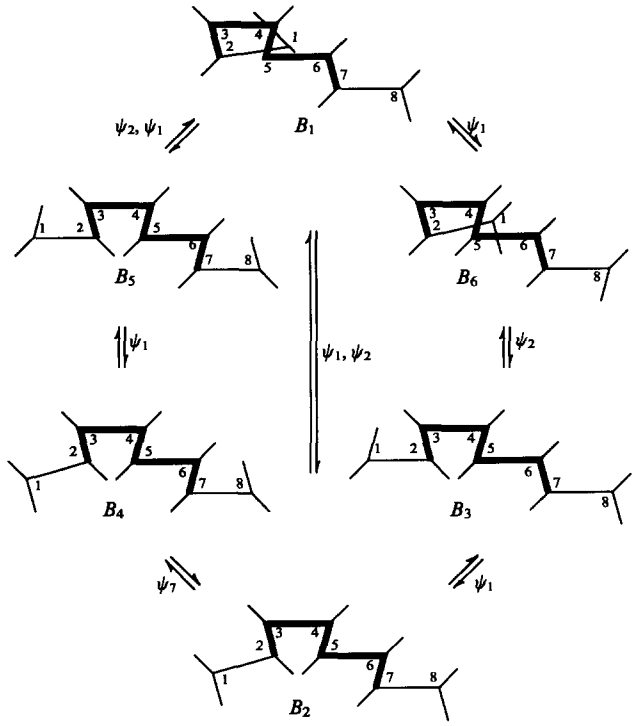


Figure 4. The shapes of the peptide skeleton and the pathways followed in the interconversions of the low-energy group *B* conformations (Table 4).

structures with $\Delta U = 0-4$ kcal mol^{-1} constitute group *A*. A rigid type *fef* nucleation of the central section of the molecule for relatively mobile N- and C-terminal dipeptide fragments is characteristic of these conformations. Fig. 2 illustrates the shapes of the peptide skeletons of these structures and the routes followed in their interconversions. All the changes in the conformational states of the main angiotensin chain within the limits of group *A*, corresponding to the low-energy $R \rightarrow B$ transitions, are affected through rotations about the $C^{\alpha}-C'$ bond of the Arg^2 or Pro^7 residue via a change in the corresponding angle ψ by 180°.

The next six conformations with a relatively low energy ($\Delta U = 3.5-7.0$ kcal mol^{-1}), combined in group *B*, also have the same structure of the central Val^3-Pro^7 section. It belongs to the *fee* shape and differs from the structure of this section in the preceding conformations by only one residue (Val^5). The transition between representatives of groups *A* and *B* is of the low-energy type and reduces to a change in the dihedral angle ψ_5 (Fig. 3). The side chain of the His residue is then moved away from the phenolic ring of the side chain of the Tyr residue, which leads to a slight (~1.0 kcal mol^{-1}) destabilisation of the conformations of group *B* relative to *A*. The shapes of the six low-energy conformations of group *B* and the routes followed in their interconversions are illustrated in Fig. 4.

The best conformations of groups *C*, *D*, *E*, and *F* (Table 4) are appreciably inferior to conformations of groups *A* and *B* as regards energy. They are less compact and are inferior primarily as regards the energy of the nonvalence interactions. The next representatives of these groups have energies exceeding 10 kcal mol^{-1}.

Table 5. The dihedral angles of rotation (in degrees) in the A_1 and B_1 (in brackets) conformations of the angiotensin II molecule.

Residue	Main chain			Side chain			
	ϕ	ψ	ω	χ^1	χ^2	χ^3	χ^4
Asp^1	−1	−60	−178	80	−92	–	–
	(−50)	(−60)	(180)	(178)	(−93)	(−)	(−)
Arg^2	−151	160	179	61	−179	64	−179
	(−86)	(−35)	(−176)	(−60)	(−178)	(180)	(180)
Val^3	−97	−60	179	178	−179	−179	–
	(−97)	(−61)	(−177)	(179)	(−180)	(−180)	(−)
Tyr^4	−90	146	−169	170	61	180	–
	(−91)	(44)	(−476)	(−175)	(90)	(180)	(−)
Val^5	61	−38	175	70	179	−175	–
	(−99)	(105)	(177)	(180)	(−179)	(180)	(−)
His^6	−85	126	174	−60	102	–	–
	(−122)	(153)	(174)	(59)	(92)	(−)	(−)
Pro^7	−60	−31	179	180	180	180	–
	(−60)	(124)	(−178)	(180)	(180)	(180)	(−)
Phe^8	−95	−38	–	60	86	–	–
	(−96)	(121)	(−)	(−60)	(92)	(−)	(−)

Thus the spectrum of the energy distribution of the optimum conformations of angiotensin II consists of several principal levels (A, B, C, ...), determined by the conformational states of the central fragment Val^3–His^6, and of a comparatively small number of sublevels differing in the conformational states of the labile N- and C-terminal dipeptides; the first can assume steric forms of all possible types (*ee*, *ef*, *fe*, *ff*) and the second can assume forms of only two types (*ee*, *ef*). The energy distribution of the conformations in each family depends to the greatest extent on the number and effectiveness of the stabilising contacts between the residues in the labile and rigid fragments.

It follows from the comparison of the energy contributions (presented in Table 4) by the nonvalence, electrostatic, and torsional interactions to the low-energy conformations of the angiotensin molecule that the nonvalence, mainly dispersion interactions (or, in other words, the packing density of the aminoacid sequence) are of decisive importance in the stabilisation of the steric structure. There is no clear-cut correlation between the quantities U and U_{nv}, although the trends in their variation are similar. The group A conformations are on average more compact than the group B conformations ($U_{nv}A = -38.6$ kcal mol^{-1} and $U_{nv}B = -36.4$ kcal mol^{-1}) let alone the group C and D conformations. The geometry and energy of the Val^3–His^6 fragment are virtually constant in the conformations of each group.

Thus the overall result of the solution of the direct structural problem for angiotensin II may be reduced to the claim that the structural organisation of the molecule is described by a comparatively small set of easily interconverted low-energy conformational states, which can be subdivided into several families. The states of the A and B families are most preferable in terms of energy and entropy. The geometrical parameters of their best representatives (A_1, B_1; Table 4) are presented in Table 5.

V. Synthetic analogues of angiotensin

The study of the possible conformations of angiotensin II [84] made it possible to discover the structural organisation of the hormone and to determine thereby the set of low-energy steric forms which are potentially biologically active. The solution of the next problem, concerning the structural-functional organisation of angiotensin II, consists in discovering within the discovered set of structures those relevant to the occurrence of physiological activities and in the establishment of specific relations between these structures and functions. The development of research on these lines requires the use of experimental data on the functional features of angiotensin II. The effect engendered by angiotensin II in the mammalian organism is the sum of diverse responses, the nature of which depends on the organs and tissues subjected to the action of the hormone (Table 2). The available experimental data show that, like the majority of other peptide hormones, angiotensin II is polyfunctional.

A large number of experimental data obtained in recent years constitute evidence in support of the heterogeneity of the angiotensin II receptor. This process will be examined in detail later and for the moment we shall only note that the polyfunctionality of angiotensin II and the heterogeneity of its receptors can be related naturally to the molecular structural organisation of the hormone, which has been investigated theoretically. Its predisposition to perform a series of functions is manifested by the existence under physiological conditions of several steric forms having similar energies and readily interconverted. The high effectiveness and rigorous selectivity of the interactions of angiotensin II with various receptors are associated with the fact that each of its functions is performed only via the conformation relevant to the given receptor, among the set of preferred structures of the free molecule.

Thus the search for the structural-functional organisation of angiotensin II reduces to the elucidation of the relevant conformation for each biological activity of the peptide. In the absence of necessary data on the potential surfaces for binding sites, the solution of this problem requires additional information. Data on the biological activity of synthetic analogues of natural peptides are normally employed as information of this kind. However, when one sets up a series of analogues in a random fashion without a preliminary study of the possible conformations of both the natural peptide and its artificial analogues, one seeks in essence a simple relation between individual residues of the aminoacid sequence of the hormone and its functions during the investigation. Since the hormone-stimulated allosteric effects arise as a result of multiple and not point contacts between the potential surfaces of the ligand and the receptor complementary to one another (otherwise there would have been no selectivity of the hormonal activity), the disturbance of the function on replacement of even one residue may be a consequence of a whole series of causes: the disappearance of the required functional group, the loss of the necessary dynamic properties of the relevant conformation, the prohibition of the latter as a consequence of the steric strain arising on replacement of the residue, the shift of the conformational equilibrium owing to changing conditions in the interaction with the environment, etc.

Consequently, the random replacement of individual residues does not permit a solution of the problem of the structural-functional organisation of hormones. This is indicated by the lack, during the course of several decades, of appreciable progress in studies on the relation between the structures and functions of angiotensin II, the encephalins and endorphins, neurohypophyseal hormones, bradykinin potentiating peptides, as well as a number of others, which have been prosecuted resorting to a multiplicity of artificial analogues. All this indicates the need to employ a special approach in the study of structural-functional relations for peptide hormones which would make it possible to abandon the method of trial and error and would permit a deliberate choice in the search for synthetic analogues before their synthesis and biological tests.

In this connection, we shall consider the study of Nikiforovich et al.[81] in which an attempt was made to identify the biologically active conformational states of angiotensin II using the results of theoretical analysis together with experimental data. It is assumed that the conformations of the molecules of the hormone and of two of its analogues (conformations A_1, A_2, ..., A_n), which exhibit a high affinity for a definite receptor, and the conformations B_1, B_2, ..., B_n, which are inactive, are known. The authors postulate that the conformations present in the sets of low-energy states of the hormones and the analogues A_1, A_2, ..., A_n and those absent from the sets B_1, B_2, ..., B_n are biologically active structures of angiotensin II.

In this approach, use was made of three synthetic analogues of angiotensin II with a high affinity for the receptor of the smooth muscle tissue of the rat and one without such affinity. However, calculation showed[81] that, among the conformations found for angiotensin II and three of its active analogues, there are none having identical fragments. The absence of such agreement is most probably evidence that the analysis of angiotensin II and of its analogues had been incorrect. However, the authors[81] took what is from our point of view a fundamentally incorrect step without questioning their results. They abandoned the principle that the potential surfaces of the hormone and the receptor are complementary and assumed that a point correspondence is sufficient for the formation of a productive complex. In order to select conformations, they took into account only two distances (and even then with variations within very wide limits) between the C^α atoms of the Val^3 residue and the C^α atoms of the His^6 (4.2–6.2 Å) and Pro^7 (6.7–8.2 Å) residues.

The chosen criterion is extremely ineffective, since generally speaking tens of completely different structures of angiotensin II, differing both in the form of the main chain and in the orientations of the side chains, may satisfy it. In particular, the above ranges of interatomic distances embrace one of the most favoured

conformations of [Pro^2]-angiotensin II for which we carried out calculations[89] and which is discussed below. It is an analogue the affinity of which for the receptors of the smooth muscle tissue is only 0.7% of the affinity of the natural peptide.

However, the choice of a more reliable criterion for the selection of conformations is not the only point at issue. The problem would have remained unsolved even if it had been found that angiotensin II and its active analogues have sets of low-energy conformations in common, which must have been observed for a correct solution of the direct structural problem. The employment of theoretical conformational analysis in the absence of information about the receptors and with a random choice of analogues does not solve the problem of the structural-functional organisation of the natural peptide.

Under the conditions of the polyfunctionality of angiotensin II and the heterogeneity of its receptors, the relations between the low-energy conformations and functions of the hormone may be established with the aid of an extremely small series of synthetic analogues, provided that each compound of the series assumes only one state out of the set of the preferred conformations of the natural peptide. Then all the analogues are able to perform only one hormonal function each or, more precisely, are able to reproduce the interaction of the hormone with only one receptor. When the analogues are monofunctional, their assembly can reproduce the entire spectrum of biological activity of the natural peptide. The problem arising in this case consists in the theoretical determination of the nature of the chemical modifications of the aminoacid sequence of the hormone which are necessary to differentiate a particular conformation relevant to the corresponding function of the natural peptide and the prohibition of all others (converse structural problem). In other words, one is dealing with the deliberate chemical construction of artificial analogues each of which is known beforehand to assume the steric structure necessary for the performance of a fully defined function.

Previously the author proposed a method for the solution of the converse structural problem.[1] It is based on the quantitative conformational theory of natural peptides and proteins,[2] in particular on the estimation of the special role of the nonvalence short-range interactions (intraresidue interactions) of the atoms in the spatial organisation of natural aminoacid sequences and on the use of the natural classification of peptide structures into shapes, forms, and conformations.[2] The short-range interactions have a property extremely important for the solution of the converse structural problem — they are able to determine fully the initial sets of allowed conformational states of the residues. When the peptide chain coils up, the conformational state of each residue is selected only from these sets. Therefore, by influencing in a controlled manner the changes in the short-range interactions, one can deliberately form sets of conformational states of the residues and hence act on the spatial organisation of the peptide effectively and purposefully. It has been shown[1] that this can be achieved by comparatively simple means which have been developed by nature itself in the course of the evolution of the organic world: it involves the replacement in the sequence of one standard residue by another differing significantly in its possible conformations (for example, the replacement of Gly by Ala or Pro), the chemical modification of the standard residue (*N*-methylation, replacement of a L-aminoacid by the D-isomer, etc.), and the replacement of an aminoacid by a hydroxyacid. It is also possible to exchange the Cys residues for Ala and exclude thereby the formation of disulfide bonds without introducing steric complications or, conversely, the residues which are spatially in close proximity may be replaced by Cys, promoting thereby the formation of macrocycles strengthened by S–S bridges. Thus there are many possibilities for the deliberate construction of a set of artificial analogues of the hormone.

We shall now consider the results of the solution of the converse structural problem for angiotensin II.[89] The relative energies of the interactions of atoms not linked by valence bonds in the preferred conformations of the hormone itself and in the related low-energy conformations of a series of its natural and synthetic analogues are compared in Table 6 (p. 948). We recall that the main aim of the investigation[89] was to test the concept of the heterogeneity of angiotensin receptors and to identify the conformations of the hormone responsible for definite functions on the basis of the approach proposed.[1] The starting points were, on the one hand, the aminoacid sequence of the hormone and hence its possible conformations and, on the other, the spectrum of the biological activity of the hormone and quantitative assessments of the activity of each function. After the determination of the minimum necessary set of synthetic analogues for each of them, equally exhaustive biological tests of the analogues are required. Therefore, it was necessary to base the treatment on the available experimental data. Although such data are most extensive for angiotensin II, nevertheless an acute deficiency of experimental facts concerning the biological tests of synthetic analogues is felt here also. The synthetic analogues were as a rule tested solely in terms of one function, so that the total spectra of their biological activities, which are very important in the given instance, remain unknown. The availability of such information would make it possible to extend greatly the results of our study.

The solution of the converse structural problem for angiotensin II was based on the known[84] set of the energy-preferred conformations of the natural molecule. Calculation showed that the structural organisation of the octapeptide hormone can be represented by a limited number of low-energy conformations which can be divided into two groups — *A* and *B* — depending on the geometry of the central tetrapeptide Val^3–His^6 fragment (Table 6). In each group, the conformations differ from one another by the states of the N- and C-terminal dipeptides and can be in their turn subdivided into structures with a free side chain of the Asp or Arg residue.

In mammalian organisms, angiotensin II is encountered in two varieties differing in the nature of the residue in the first position (Asp or Asn), which has only a weak effect on the functional spectra and physiological activities of both hormones. It is seen from Table 6 that the possible conformations of the natural [Asn^1]-AT II analogues are very similar to those of AT II with the Asp^1 residue in the first position. Only the change in the global conformation in group *A* merits attention. In the AT II molecule, the conformation A_1 has the lowest energy. The Arg^2 residue makes a significant contribution to it stabilisation. The hydrophobic part of the side chain of this residue enters into effective dispersion interactions with almost all the residues of the Val^3–Pro^7 fragment (-11.5 kcal mol^{-1}), while the guanidine group, carrying an integral positive charge, interacts also with the C-terminal Phe^8 residue, which is negatively charged (-2.9 kcal mol^{-1}). The aspartic acid residue hardly interacts with the remainder of the molecule and is oriented towards the surrounding medium. In the A_2 conformation, the energy of which (0.9 kcal mol^{-1}) exceeds only slightly the energy of A_1, the situation changes: the side chain of the Arg^2 residue is free, while that of Asp^1 is bound.

In contrast to AT II, in the [Asn^1]-AT II molecule there is no negative charge on the first residue and the stabilising energy of its electrostatic interaction with the Arg^2 residue is therefore sharply weakened. This is in fact the primary cause of the smaller preference for the A_1 conformation compared with A_2, which becomes the most favourable.

Calculation for angiotensin III, differing from angiotensin II by the absence of the first residue in the sequence, led to an interesting result, which was satisfactorily correlated (this will be demon-strated below) with the physiological activity. The removal of Asp^1 alters significantly the position of the $A \rightleftarrows B$ conformational equilibrium, displacing it to the right. The B_4 or B_5 conformation becomes the most favourable, which amounts to absolutely the same thing, and the A_1 conformation, which is best for angiotensin II, acquires a high relative energy 7.4 kcal mol^{-1} (Table 6, p. 948) and its occurrence becomes unlikely.

One of the causes of the increase in the energy of the A_1 conformation relative to B_4 is associated with the greater destabilising electrostatic energy of the interactions of the positive charges on the main and side chains of the Arg^2 residue; in the A_1 conformation, the energy of the nonvalence interactions of the arginine residue is $+14.0$ kcal mol^{-1}, while in B_4 it is $+9.0$ kcal mol^{-1}. The second cause of the shift of the conformational equilibrium in the absence of the N-terminal Asp^1 residue from angiotensin consists in more compact packing and hence a lower energy of the interresidue dispersion interactions of the valence nonbonded atoms of the Arg^2 side chain in the B_4 conformation (-22.1 kcal mol^{-1}) compared with the A_1 conformation (-17.6 kcal mol^{-1}).

Angiotensin I (Table 6) is a decapeptide containing the His and Leu residues in the C-terminal part of the sequence. The increase in chain length affects appreciably the energy distribution of the conformations. It leads to a stronger determination of the conformational states of the peptide, i.e. to a restriction of the conformational freedom. Of the structural set of angiotensin II, three group A conformations (A_1, A_2, and A_4) are actually allowed, A_1 and A_2 having the lowest energies, as before. The A_2 conformation is more favourable in terms of energy than A_1, since its potential surface is more complementary to the surface of the additional His^9-Leu^{10} dipeptide fragment. The appreciable increase in the energy of group B conformations in angiotensin I, which renders them virtually prohibited, can be explained, firstly, by the significantly weaker interactions of the His^9-Leu^{10} section with the remainder of the molecule (for example, their energy is -6.2 kcal mol^{-1} for B_1, whereas those for A_2 and A_1 are respectively -11.3 and -9.4 kcal mol^{-1}) and, secondly, by the loss, for steric reasons, of a series of stabilising interactions of the Phe^8 residue, which occupies terminal and intermediate positions in angiotensin II and angiotensin I respectively.

Whereas the lengthening of the peptide chain by two residues (AT I) lowers the relative energy of the group A conformations, its shortening by two residues compared with angiotensin II [At II$-$(1$-$6)-peptide] has the opposite effect: two of the four group B conformations acquire the lowest energy, which does not exceed 1.0 kcal mol^{-1}. However, the changes are not quite so marked as in the case of AT I and the possible conformations of the hexapeptide analogue of angiotensin, lacking a series of stabilising interactions following the loss of two residues, are naturally more numerous. Not only group A conformations but even group C_1-F_1 and especially D_1 conformations become realistic under certain external conditions.

The replacement of the valine residues in the third and fifth positions in the angiotensin II molecule by proline {[Pro^3]-AT II and [Pro^5]-AT II (Table 6)} and alanine {[Ala^3]-AT II and [Ala^5]-AT II} residues had as its aim the introduction of a definite and previously known steric hindrance to prevent the occurrence of a large number of conformations (the first two peptides). On the other hand, the aim was to render the aminoacid sequence of angiotensin II more labile and to estimate the restricting effect of fairly bulky valine residues branches at the C^α atom on the formation of the steric structure of the molecule (the second pair of peptides).

Being in the R form, the residue preceding proline has a higher energy owing to the overlap of the van der Waals radii of the hydrogen atoms of the methylene group of the proline ring. The B and then the L forms are most preferred for this residue. For this reason, the Arg^2-Pro^3 section of the [Pro^3]-angiotensin II analogue can only have the expanded e shape. Consequently, the occurrence of the six out of the fourteen possible low-energy conformations of angiotensin II with the R form of Arg^2 and the f shape of the dipeptide Arg^2-Pro^3 becomes unlikely for the synthetic analogue. Only the A_1 and A_4 structures with relative energies of 0 and 4.5 kcal mol^{-1} remain preferred. The energies of the remaining structures exceed 10.0 kcal mol^{-1}.

When Val^5 is replaced by Pro^5, neither group A nor group B conformations are prohibited, since the Tyr^4-Val^5 section has the uncoiled form in both cases. Nevertheless, calculation showed that here the situation is in principle similar to that just examined above, i.e. a decrease in the relative energy of the A conformations and an increase in that of the B conformations is observed.

Calculation showed that the replacement of Val^3 and Val^5 by alanine, which seemingly should have provided considerable conformational freedom to the main chain of the hormone within the limits of the same minima on the multidimensional potential surface, hardly affects the position of the conformational equilibrium. As before, the group A structures in a polar medium are preferable to the group B structures, while the C_1-F_1 structures have equally high energies. Therefore one may expect that the physiological activity spectra of the alanine analogues reproduce fairly completely the spectrum of the natural angiotensin II, in contrast to the proline analogues.

In [Pro^3]-AT II, the replacement involves the residue which not only dictates the purely steric conditions for the establishment of the conformational states of the molecule, as in the four synthetic analogues of the natural hormone examined above, but undoubtedly also plays an extremely important role in specific recognition or in the consequences of the hormone$-$receptor interactions. Such duality complicates somewhat the treatment of the results of the theoretical conformational analysis of the analogue (Table 6). It is remarkable that the B_6 and F_1 conformations, having a very high energy in angiotensin II, are the most preferred in [Pro^2]-AT II.

We shall consider a further five analogues of angiotensin II. The Phe residue of angiotensin II was replaced in succession by the Ala, Leu, Val, Ile, and finally Tyr residues, i.e. by hydrophobic residues with a gradually increasing bulk. The most significant changes in the set of energy-preferred conformations compared with the natural octapeptide were then observed. Group A structures predominate in all cases. The energy distribution of the [Tyr^8]-AT II conformations is virtually the same, as might have been expected, as that in angiotensin II.

The choice for calculation of all the angiotensin II analogues presented in Table 6, especially the last six, is dictated by the availability of the corresponding experimental data, which will be analysed in the next section in the light of the results of the conformational analysis described.

VI. Polyfunctionality of the hormone and heterogeneity of the receptors

The knowledge of the quantitative characteristics of the structural organisation of angiotensin II and it analogues is a necessary condition for the rational investigation of the structural-functional organisation of the hormone. However, this is still far from sufficient. The attempt to discover the physiological characteristics of angiotensin(II), like those of any other natural oligopeptides, encounters fundamental difficulties arising owing to the lack of knowledge of the causes of the polyfunctionality of peptide hormones. The lack of clarity in this problem is due to the extremely scanty information about the hormonal receptors. In other words, the problem of the structural-functional organisation of the hormone has to be solved in essence in the absence of information about the properties of its partners in the interactions.

There are two points of view on the cause of the polyfunctionality of angiotensin and other peptide hormones. According to one of them,[90] the ability of a particular hormone to stimulate completely different processes in different parts of the organism can be accounted for by the presence of several receptor proteins specific to the given hormone, i.e. by the heterogeneity of the receptors. This point of view does not conflict with the known structural organisation of the hormone molecules. Natural oligopeptides in the native state are not rigorously determined three-dimensional structures, as in the case of high-molecular-mass proteins, but consist of sets of comparatively few steric forms with a position of conformational equilibrium which is readily

altered by external forces.[2] The results of earlier investigations of the possible conformations of bradykinin-potentiating peptides[39] and neurohypophyseal hormones — oxytocin, vasopressin, vasotocin, and mesotocin — agree with this assumption.[27,91]

A different treatment of this phenomenon arises on the basis that each hormone is capable of forming a productive complex only with a single receptor and hence of inducing always the same allosteric change in its conformation. If the receptors are the same, then the polyfunctionality of the hormone is determined no longer by the specificity of the hormone–receptor interactions themselves but by the characteristic features of the systems receiving the signal which has been sent. In this case, the diversity of the physiological activities of the hormone is caused not by the unique structure of its molecule and the characteristic features of the interactions with the receptor protein but by the specificity of the structural organisation of the systems, which respond differently to the same signal arising from the same hormone–receptor complexes interacting with them.

The hypothesis of the heterogeneity of the hormonal receptors, in particular the angiotensin II receptors, has been confirmed by the results of studies carried out in recent years. Thus this is indicated also by the different nature of the interaction of angiotensin II analogues with the receptors in different tissues (for example, by the presence of several analogues with selective activity),[92–95] by the different effects of cations on the binding of the hormone itself to the receptors in the tissues of different organs,[95] and by the observation of hormone receptors, differing in molecular mass, in the tissues of rabbit liver,[96] the human placenta,[97] and the adrenal cortex of the rat and the dog.[98]

However, the most significant evidence in support of the heterogeneity of the receptors as a cause of the polyfunctionality of angiotensin II was obtained recently when nonpeptide antagonists of the hormone were employed.[90,99] The use of a new class of nonpeptide antagonists in the study of angiotensin II receptors made it possible to discover the presence of different types of specific angiotensin II receptors in the mammalian organism. Thus two complex organic compounds, which the authors designated as DUP-89 and WL-19, were employed in one of these studies[99] for the identification of the receptors in the tissue of the rat adrenal cortex. It was found that each of them may bind only to a receptor of a fully defined type, whereas angiotensin II exhibits a high affinity for both receptors. As a result, it was shown that even in a single tissue there are two receptors for the hormone, which assumes a different form in the cells of this tissue. Later the receptor having an enhanced affinity for the WL-19 antagonist was detected in the rat and human uterus and in the rat brain.[10] The use of other nonpeptide antagonists permitted also the differentiation of different types of angiotensin II receptors in tissues of the rat liver and rat brain vessels.[100,101]

Thus a whole series of experimental data indicate convincingly the existence of a set of angiotensin II receptors which impose different conformational requirements on the hormone. One of the tasks in the 'from structure to function' approach which we have been developing in relation to a specific object actually involves the establishment of a quantitative relation between the existing experimental data and the structural organisation of the angiotensin II molecule and thus achieves a more rigorous basis for the treatment of the polyfunctionality of peptide hormones in terms of the heterogeneity of the receptors.

If our hypothesis is valid and a fully defined conformation from the set of low-energy readily interconverted steric forms discovered for angiotensin[84] does indeed interact with only one receptor and hence is responsible for the performance of only one function, then the next task consists in the determination for each physiological activity of the hormone of a conformational state relevant to only this activity, i.e. complementary to the corresponding receptor. Thus the energy-preferred conformations known from theoretical analysis have to be correlated with the experimental functions. Since the structures of the receptors let alone of their active centres are unknown, this problem cannot be solved, as already mentioned, without resorting to additional information. Such information may be obtained by studying synthetic analogues of the hormone.

Synthetic analogues have already been used in endocrinology for many decades. However, despite the expenditure of enormous efforts and financial resources, the results obtained with their aid indicate a low effectiveness of this approach, particularly in the scientific, cognitive respect. We suggest that the problem is not with the approach itself (at the present time there is no alternative to it) but with the satisfactory employment of its potential.

Virtually all the studies on these lines suffer from three serious defects. The first, most significant, is due to the random selection of the artificial analogues. The second weak feature, which also precludes the rise of investigations of this kind above an empirical level, involves the neglect of the possibilities of the theoretical analysis of the conformational states of both the hormone itself and of the selected synthetic analogues. Finally the third deficiency, characteristic of studies in this field, consists in the absence of not only a theoretical basis but also of a single systematic approach to the experimental investigation of hormones. Despite the multiplicity of studies in this field, it is still not possible to compare even in only one case the activity of the hormone with the activities of synthetic analogues throughout the functional spectrum. As a rule, in the study of biological activities of a natural peptide, different sources, different tissues, and, what is most significant, different sets of analogues are employed in each case.

When the peptide hormones are polyfunctional and the receptors are heterogeneous but there is no information about the structure of the latter, the most important, key problem, the solution of which can only be attempted with the aid of the corresponding theoretical developments, consists in passing from the random, purely intuitive search for synthetic analogues by the method of trial and error to their purposeful selection corresponding to special requirements. In order to be useful in the study of the relation between the structure and functions of a hormone, each of its synthetic analogues must be as far as possible monofunctional, i.e. must perform one of the functions of the natural peptide and hence must be able to assume, out of the set of the relevant low-energy conformations, only one steric form complementary to the active centre of the corresponding receptor. A more general aim is the deliberate formation of the chemical structure of the molecule known beforehand to assume the steric structure needed for the performance of the planned fully defined function.

We shall now return to the object of our study — angiotensin II, for which the direct and converse structural problems have already been solved (Sections IV and V).[84,89] However, in a rational study of the hormone[102] it was necessary to deviate somewhat from the procedures dictated by strict logic. This enforced deviation, although not fundamental, nevertheless does not lead to the complete elucidation of the possibilities of the 'from structure to function' approach. This is due to the lack of the necessary experimental literature data, although angiotensin II is in fact one of the most fully investigated peptides. The known experimental facts are very numerous and concern both the hormone itself and many hundreds of its synthetic analogues. However, the weak features of the purely empirical approach, noted above, are characteristic of all these studies as well as the analogous studies on other hormones: the random selection of the analogues, the lack of knowledge of the principles governing the molecular structural organisation of the hormone and its derivatives, and also the lack of a systematic approach to the investigation of functions.

We have been unable to find experimental data on any of the enormous number of the synthetic analogues of angiotensin II investigated which would characterise its activity over the entire spectrum of the biological activity of the hormone. Only a few analogues have been discovered for which quantitative data concerning three functions of angiotensin II have been obtained: the stimulation of the contractions of the smooth muscles and the

Table 7. The pressor activities and quantitative characteristics of certain varieties of the biological activity of natural angiotensins and a number of their synthetic analogues.

Compound	Smooth muscle [45]								Adrenal medulla [47, 103]		Adrenal cortex [46, 103]			Pressor activity (%) [45]
	rabbit aorta				rat stomach									
	α_E	pD_2	RAf(%)	pA_2	α_E	pD_2	RAf(%)	pA_2	RA(%)	pA_2	RA(%)	RSIB(%)	pA_2	
AT II	1.0	8.85	100	–	1.0	7.75	100	–	100	–	100	100	–	100
[Pro^2]-AT II					1.0	5.64	0.7							1.3
[Pro^3]-AT II			40 [a]											40
[Pro^6]-AT II														10
AT III	1.0	7.62	5.6	–	1.0	7.5	56	–	15	–	130	100	–	38
[Asn^1]-AT II	1.0	8.11	18	–	1.0	7.8	105		100	–		100		100
[Ala^8]-AT II	0			7.7	0			7.22	21	–				–
[Leu^8]-AT II	0			8.78	0			8.6		8.53			7.0	–
[Ile^8]-AT II	0			9.21	0			8.36		9.31			8.53	–
AT I	1.0	7.53	5.1		1.0	7.1	22		95		2	5		50

Note. α_E = internal activity (the ratio of the maximum response induced by the agonist to the maximum response induced by AT II); pD_2 = negative logarithm of the agonist concentration inducing an effect equal to half the maximum effect (affinity); pA = negative logarithm of the antagonist concentration reducing the effect of the agonist by a factor of two; RAf(%) = relative affinity (the affinity of the agonist relative to the affinity of angiotensin II); RA = relative activity (the ratio of the activity of the agonist to the activity of angiotensin II for doses with average effectiveness); RSIB = relative strength of the inhibition of binding (ratio of the concentrations of the analogue and angiotensin II inducing the displacement of 50% of labelled AT II in binding to a specific receptor); a gap in the Table denotes the absence of data on the given type of activity and a dash denotes the absence of the given type of activity.

[a] In relation to rat uterus receptors.

regulation of the secretion of aldosterene and catecholamines. The corresponding activities of these analogues and the natural peptides are compared in Table 7.

Among the quantitative estimates of the effectiveness of the interaction of the hormone and its analogues with receptors, the internal activities (α_E) and affinities for the receptor (pD_2) characterise most directly the characteristic features of the structural organisation of the molecules (see the footnotes to Table 7). For analogues with a full internal activity, the effective concentration of the antagonist required for the performance of the biological function and hence the probability of a steric structure of the given analogue complementary to the active centre of the receptor and corresponding to the given conformational state of the hormone can be inferred from the values of pD_2. Indeed, the greater the displacement of the position of the conformational equilibrium for the antagonist from that relevant to the given function of the steric structure, the higher should be its concentration for the attainment of a definite effect and hence the lower its affinity for the receptor.

On the other hand, the probability of the occurrence of the relevant conformations is determined by the relative internal energies, which we have found for the hormone and its analogues in the solution of the direct and converse problems. By comparing the data in Tables 6 and 7, we shall attempt to obtain an idea about the significance of a particular conformational state for the performance of the corresponding function, i.e. about the structural-functional organisation of angiotensin II. We may note that Table 6 might be supplemented by any number of examples however large. For example, it is not difficult to calculate the possible conformations of all these hundreds of synthetic analogues of angiotensin II which have been synthesised and subjected to biological tests but which, alas, have been non-systematic and incomplete. However, for the existing level of experimental studies, the expansion of Table 6 would contribute little to the solution of the problems postulated and presented in Table 7.

The solution of the direct problem[84] showed that the possible conformations of angiotensin II may be described by a set of a few low-energy forms subdivided into two representative groups *A* and *B* and the single forms $C_1 - F_1$ (Table 6). Within the limits of one group, the conformations have the same steric structure of the central $Val^3-Tyr^4-Val^5-His^6$ tetrapeptide section of the molecule and differ from one another only in the orientations of the N- and C-terminal dipeptide fragments.

The results obtained in the solution of the converse problem[89] show that replacements of aminoacids in the angiotensin II sequence can lead to significant changes in the possible conformations of the molecule. The replacements not involving the functional residues do not entail the appearance of new low-energy steric forms, giving rise to a displacement of the conformational equilibrium within the limits of the preferred forms of the natural peptide.

As can be seen from Table 7, the modifications of the chemical structure of the hormone are reflected selectively in the effectiveness of the activities characteristic of angiotensin II. Since the experimental data refer to the interactions of the hormone and its analogues with the acceptors of the smooth muscle and adrenal cortex tissues, we shall attempt initially to identify the optimum conformational states of angiotensin II complementary to precisely these receptors.

The proline-containing analogues may be of special interest, since the replacement of any residue in the aminoacid sequence by Pro has a significant effect on the possible conformations of the entire molecule. We shall compare two such analogues with each other and with angiotensin II as regards steric structure and biological activity — [Pro^2]-AT II and [Pro^3]-AT II.

The replacement of the second residue in the aminoacid sequence of the hormone by proline leads to the almost complete loss of the affinity for the smooth muscle receptors by the [Pro^2]-AT II analogue (the relative affinity does not exceed 0.7% in this case), while the replacement of the third residue leaves the affinity of [Pro^3]-AT II for the receptors of the same tissue fairly significant (40%) compared with the hormone itself. On the other hand, highly concentrated doses of the second compound have no effect whatsoever on the secretion of aldosterone.[92]

The conformational states of the two proline-containing analogues also differ sharply. Among all the low-energy conformations of the [Pro^3]-AT II molecule, the group *A* representatives are the most realistic (Table 6). On the other hand, these conformations hardly occur for [Pro^2]-AT II; the equilibrium is markedly displaced towards the B_6 and F_1 conformations, which have the highest energies in the set of angiotensin II.

Thus comparison of the conformational and biological properties of the hormone and of two of its proline-containing analogues lead to the hypothesis that the group *A* steric structures are relevant to the interactions with the receptors of the smooth muscle tissue. However, this assumption may not prove to be entirely rigorous owing to the nonequivalence of the replacements. Whereas the replacement in the case of [Pro^3]-AT II is homologous (Val^3 is replaced by Pro^3) and therefore has an exclusively steric effect on the possible conformations of the molecule, in the case of [Pro^2]-AT II it is nonhomologous (Arg^2 is substituted by Pro^2) and, apart from the changes in the system of intramolecular nonvalence interactions of the atoms, involves the loss of a guanidine group, which may play an important functional role in the mutual relations between the hormone and the receptors.

Furthermore, the hypothesis that type *A* conformations are relevant to the contractile function of angiotensin II in the smooth muscles of arterioles is seemingly inconsistent with the available data for another proline analogue — [Pro^5]-AT II. Although there is virtually no quantitative information about its functions in the literature, nevertheless it is known that the pressor activity of this analogue is an order of magnitude lower than that of the natural peptide (Table 7), which indicates its low affinity for the smooth muscle tissue receptors. However, the group *A* conformations responsible, according to our hypothesis, for the contractile function are most preferred in [Pro^5]-AT II. At first sight, the contradiction is extremely serious, since in this case the replacement of Val^5 by Pro^5 is homologous. Nevertheless the discrepancy may be only apparent, since the loss of the pressor activity by the given analogue is susceptible to a different interpretation.

Calculation of the conformations of the [Pro^5]-AT II molecule showed that the inclusion of the Pro residue between Tyr^4 and His^6 leads to a significant limitation of the conformational freedom of the peptide chain and to the deformation of the group *A* steric structure of the molecule without causing, however, the displacement of the dihedral angles φ and ψ outside the limits of the *fef* shape of the central tetrapeptide section. Thus, whereas the distances between the C^α atoms of the tyrosine and histidine residues in this group of conformers are about 5.5 Å for angiotensin II, for the [Pro^5]-AT II analogue they are 7.4 Å. Furthermore, the activity of the compound may be influenced by the fact that the Pro^5 residue limits significantly the mobility of the side chains of adjacent residues, which undoubtedly interact effectively with the receptors.

Although our hypothesis that the group *A* conformations must participate in the operation of the contractile function of angiotensin II is fairly controversial nevertheless it will remain a working hypothesis.

Important evidence in support of this hypothesis follows from a comparison of the possible conformations and biological activities of angiotensin II and angiotensin III — a natural heptapeptide which differs from the octapeptide hormone considered by the absence of the N-terminal Asp^1 residue. Both compounds have the same spectrum of biological activities, but their effectiveness is significantly different except when they function in the tissues of the adrenal cortex. Numerous investigations have shown that, although the effectiveness of angiotensin III in its action on the remaining tissues is reduced compared with angiotensin II,

nevertheless the heptapeptide hormone induces in the adrenal cortex tissue the same aldosterone-stimulating effect as the octapeptide hormone[103] and, according to certain data,[46] is actually superior to the latter.

If our hypothesis concerning the cause of the polyfunctionality of the hormones is correct, then the angiotensin III molecule should have the corresponding possible conformations adequately reflecting the observed similarity and difference in its biological activity compared with angiotensin II. Indeed, the elimination of the N-terminal residue displaces sharply the conformational equilibrium towards group *B* structures: the $B_4(B_5)$ conformation becomes most preferred and is then followed in this respect by $B_2(B_3)$, B_1, and B_6, which are inferior to the most favourable conformation by 1.8 and 4.1 kcal mol^{-1} respectively (Table 6). In group *A*, there is only one low-energy conformation — A_2 (1.2 kcal mol^{-1}). Thus, among the steric structures related to the low-energy conformations of angiotensin II, in the case of angiotensin III the most probable conformations are $B_4(B_5)$, A_2, $B_2(B_3)$, as well as B_1 and B_6, i.e. there is a sharp displacement of the conformational equilibrium towards representatives of group *B*.

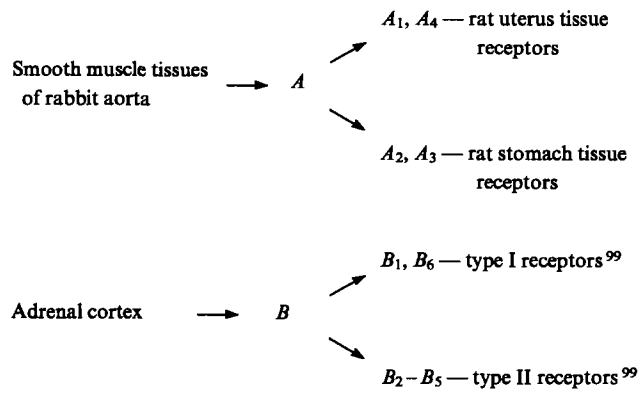
It has been reported[99] that, of the two types of receptors (I and II) isolated from the adrenal cortex tissue with the aid of the DUP-89 and WL-19 nonpeptide antagonists already mentioned, which bind the angiotensin II molecules equally effectively, only type II receptors[99] exhibit a high affinity for angiotensin III. On the other hand, the affinity of the heptapeptide hormone for type I receptors is reduced compared with the type II receptors by a factor of 12.

The effectiveness of the interaction of angiotensin III with the smooth muscle tissue receptors depends on the source and the organ. The affinity of the hormone for the receptors of the rat stomach tissue is lower by a factor of two than that of angiotensin II, while that for the receptors of the rabbit aorta tissue is reduced by a factor of almost 20.[45] The decrease in the affinity of angiotensin III for the receptors observed in these cases can be accounted for by the higher energy of the group *A* conformations responsible, according to our hypothesis, for the interaction of the hormone with the smooth muscle tissue receptors. The latter apparently have different requirements for the conformational state of the agonist. In this case, the A_1 and A_4 states can be assigned to the class of relevant states for the interaction of the hormone with the receptors of the rabbit aorta tissue, while the A_2 and A_3 states may be regarded as relevant to the interaction of the hormone with the rat stomach tissue receptors.

The high affinity of angiotensin III for the adrenal cortex receptors is consistent with the maximum probability of the occurrence of group *B* conformations, which permits the conclusion that these are relevant to the aldosterone-stimulating activity of the hormone. One can go further and postulate that the $B_4(B_5)$ and $B_2(B_3)$ conformations are complementary to the active centres of type II receptors,[99] while the B_1 and B_6 conformations are complementary to the active centres of type I receptors.[99]

[Asn^1]-AT II, another analogue of angiotensin II, is almost fully provided with all the functions of the [Asp^1]-AT II hormone under consideration. The interactions with rabbit aorta tissue receptors are an exception. The possible conformations of the [Asn^1]-AT II and [Asp^1]-AT II molecules are also very similar (Table 6), if one disregards the differences between the energies of the A_1 and A_4 conformations and hence between the probabilities of their occurrence, the probability being significantly smaller in the case of [Asn^1]-AT II. The affinity of this molecule for the rabbit aorta receptors is also appreciably reduced (Table 7). Thus the results of the conformational analysis and of the biological tests on this analogue agree with our conclusion that the A_1 and A_4 conformations are complementary to the rabbit aorta receptors.

Thus comparative analysis of the conformational properties and biological activities of the hormone and its analogues has shown that there is a relation between the biological activities and conformational states of angiotensin II, according to which the structural variants of group *A* interact with the receptors predominating in the smooth muscle tissues and those of group *B* interact with the receptors predominating in the adrenal cortex tissues, the representatives of each group being in their turn subdivided into subgroups according to the following scheme:



The classification of the conformations in terms of subgroups is consistent with a fully defined system of intramolecular contacts between atoms not linked by valence bonds.

In solving the direct problem for angiotensin II, it was established that the Arg^2 residue makes the greatest contribution to the stabilisation of the A_1, A_4, and B_2-B_5 conformations. The Asp^1 side chain is oriented towards the medium and interacts electrostatically only with the positively charged guanidine group of Arg^2; the energy of the interaction of Arg^2 with the rest of the molecule does not exceed 1 kcal mol^{-1} and is in addition destabilising in character.

Another system of intramolecular contacts obtains in the A_2, A_3, and B_1, B_6 conformations; the Arg^2 side chain is oriented in the direction away from the molecule and interacts only weakly with the other residues, while Asp^1 has numerous stabilising contacts.

The conformations of different subgroups differ also as regards the nature of the stabilising interactions. Whereas the A_2, A_3, and B_1, B_6 conformations are preferred as regards the energy of the nonvalence interactions between the atoms, the A_1, A_4 and B_2-B_5 conformations are preferred as regards electrostatic interactions and hydrogen bonds. The alternating responses of the conformations of both subgroups to the polarity of the medium combined with the ease of their interconversions makes the position of the conformational equilibrium in angiotensin II extremely sensitive to external conditions, primarily to specific interactions with receptors.

Some of the conformations of angiotensin II presented in Table 6 differ in the position of the C-terminal Phe^8 residue, which is of exceptional importance for the performance of the functions of the hormone. The elimination of this residue deprives angiotensin of virtually all its physiological activities. Thus [des-Phe^8]-AT II was found to be active only in relation to the rat brain tissues. The octapeptide analogues in which Phe^8 has been replaced by other aminoacid residues as a rule bind effectively to the hormone receptors but do not stimulate the corresponding signals.[45] The results of calculations for the [Ala^8]-, [Leu^8]-, and [Ile^8]-AT II analogues presented in Table 6 demonstrate relatively small changes in the possible conformations of these molecules compared with the natural peptide. On the other hand, it follows from Table 7 that none of them possesses the full spectrum of the biological activities of angiotensin II.

Hitherto we have considered the activities of the hormone and its analogues on the smooth muscle and adrenal cortex tissues. There is very little information about the interactions of angiotensin II with the receptors in other tissues. The known facts, concerning, for example, the receptors of the medulla of the

adrenal glands,[104] indicate that their structural requirements as regards the nature and steric structure of the C-terminal section of the aminoacid sequence are less rigorous. Thus [His^9-, Leu^{10}]-AT II, which is a precursor of the octapeptide hormone having a low affinity for the receptors in the smooth muscle and in the adrenal cortex, manifests the same activity as angiotensin II in the adrenal medulla. The synthetic analogue [Ala^8]-AT II, which behaves, as already mentioned, as an antagonist of angiotensin II in most tissues, nevertheless does not block the activity of the hormone in the medulla and actually exhibits some agonistic activity. Thus the lengthening of the peptide chain from the C- end and the replacement of Phe^8 by Ala^8 do not prevent in the given instance either the binding to the receptor or its stimulation.

VII. Conclusion

In conclusion we may note an important feature of the functioning of angiotensin II, which consists in the interdependence of all its numerous physiological activities in the mammalian organism. A number of factors, such as a decrease of the concentration of Na^+ ions in the blood, a decrease in the volume of circulating blood, and a fall in the arterial pressure lead to an increase in the secretion of renin by the kidneys and hence to an increase in the concentration of angiotensin II in mammalian blood.

The interaction of the hormone with the receptors located in different tissues induces responses designed to return the corresponding parameters to normal, the hormone acting at the tissue, systemic, and central levels. Thus the angiotensin II-induced increase in the tonus of the smooth musculature of the arterioles and the intensification of the secretion of catecholamines by the adrenal medulla increase the arterial pressure.

The retention of water and Na^+ ions in the organisms is effected by the hormone mainly via stimulating the secretion of aldosterone by the adrenal cortex, by the stimulation of the secretion of vasopressin by the hypothalamohypophyseal system, and also by the direct action of the hormone on the kidneys. The above activities of angiotensin II are supplemented by its effect on the central and peripheral divisions of the nervous system, which mediates the pressor effects and also intensifies thirst and the appetite for salt. This leads in its turn to an increase in the volume of the circulating blood and the normalisation of the pressure.

Thus the change in external conditions induces in the organism a complicated set of responses stimulated by a unique factor, namely angiotensin II, and directed towards a single aim — the maintenance of a constant internal medium within the organism.

The ability to effect productive interactions with a series of receptors at once and hence to perform simultaneously the corresponding number of coordinated functions is ensured by the structural-functional organisation of angiotensin II which the present author has investigated.

References

1. E M Popov *Mol. Biol.* **19** 1107 (1985)
2. E M Popov *Strukturnaya Organizatsiya Belkov* (Structural Organisation of Proteins) (Moscow: Nauka, 1989)
3. E M Popov *Bioorg. Khim.* **18** 1229 (1992)
4. P Glansdorf, I Prigogine *Thermodynamic Theory of Structure, Stability and Fluctuations* (Translated into Russian; Moscow: Mir, 1973)
5. I Prigogine *From Being to Becoming — Time and Complexity in Physical Sciences* (Translated into Russian; Moscow: Mir, 1985)
6. E M Popov *Priroda* (6) 59 (1993)
7. D B Wetlaufer *Proc. Natl. Acad. Sci. USA* **70** 697 (1973)
8. G N Tishchenko *Kristallokhimiya* (Crystal Chemistry) Vol. 13 (Moscow: Nauka, 1979)
9. E M Popov, G M Lipkind, S F Arkhipova, in *Konformatsionnye Raschety Slozhnykh Molekul* (Conformational Calculations for Complex Molecules) (Ed. A I Perel'man) (Minsk: Narodnaya Asveta, 1970) p. 120
10. E M Popov, V Z Pletnev, in *Konformatsionnye Raschety Slozhnykh Molekul* (Conformational Calculations for Complex Molecules) (Ed. A I Perel'man) (Minsk: Narodnaya Asveta, 1970) p. 129
11. E M Popov, V Z Pletnev *Biofizika* **16** 407 (1971)
12. V Z Pletnev, E M Popov *Izv. Akad. Nauk SSSR, Ser. Khim.* 991 (1970)
13. V Z Pletnev, E M Popov *Bioorg. Khim.* **1** 160 (1975)
14. V Z Pletnev, E M Popov *Khim. Prir. Soedin.* 220 (1973)
15. G N Tishchenko, Z Karimov, N V Nazimova *Bioorg. Khim.* **1** 375 (1975)
16. G N Tishchenko, Z Karimov, V V Borisov *Bioorg. Khim.* **1** 378 (1975)
17. G N Tishchenko, N V Nazimova, V I Andrianov, Z Karimov *Bioorg. Khim.* **1** 386 (1975)
18. G N Tishchenko, V I Smirnova, L N Zeibot, N V Nazimova, V I Andrianov *Bioorg. Khim.* **2** 885 (1976)
19. J Konnert, I L Karll *J. Am. Chem. Soc.* **91** 4888 (1969)
20. A I Geddes, D Akrigg *Acta Cristallogr., Sect. B* **32** 3164 (1976)
21. G N Tischenko, Z Karimov, B K Vainstein, A V Evstratov, V T Ivanov, Yu A Ovchinnikov *FEBS Lett.* **65** 615 (1976)
22. V Z Pletnev, N M Galitskii *Bioorg. Khim.* **3** 1611 (1977)
23. J A Hamilton, L K Stainrauf, E Braden *Biochem. Biophys. Res. Commun.* **64** 151 (1975)
24. E M Popov, V Z Pletnev, A V Evstratov, V T Ivanov, Yu A Ovchinnikov *Khim. Prir. Soedin.* 616 (1970)
25. Yu A Ovchinnikov, V T Ivanov, A V Evstratov, V F Bystrov, N D Abdullaev, E M Popov, G M Lipkind, S F Arkhipova, E S Efremov, M M Shemyakin *Biochem. Biophys. Res. Commun.* **37** 668 (1969)
26. S Z Galaktionov, G V Nikiforovich, G I Chipens, M D Shendorovich *Angiotenzin. Molekulyarnye Mekhanizmy Deistviya* (Angiotensin. Molecular Mechanisms of Action) (Riga: Zinatne, 1979)
27. V S Spasov, E M Popov *Bioorg. Khim.* **7** 25; 502 (1981)
28. E M Popov *Mol. Biol.* **9** 578 (1975)
29. E M Popov *Int. J. Quantum Chem.* (16) 707 (1979)
30. C B Anfinsen *Science* **181** 223 (1973)
31. E M Popov, P N Mel'nikov *Bioorg. Khim.* **5** 1471 (1979)
32. A L Lomize, E M Popov *Bioorg. Khim.* **8** 1474 (1982)
33. A L Lomize, E M Popov *Mol. Biol.* **17** 1212 (1983)
34. E M Popov, V N Shvyrkov, V Z Spasov *Bioorg. Khim.* **8** 61 (1982)
35. E M Popov, L I Izmailova, Sh M Musaev, R E Aliev, N A Akhmedov, I S Maksumov *Bioorg. Khim.* **8** 776 (1982)
36. A A Zaval'nyi, E M Popov *Mol. Biol.* **16** 129 (1982)
37. G I Chipens, L K Polevaya, N I Veretennikova, A Yu Krikis *Struktura i Funktsiya Nizkomolekulyarnykh Peptidov* (Structure and Function of Low-Molecular-Mass Peptides) (Riga: Zinatne, 1980)
38. M Monnier, L Dubler, R Cochter, P F Maier, H Tabler, G Schoenenberger *Experientia* **33** 548 (1977)
39. E M Popov, N N Sevast'yanova *Bioorg. Khim.* **7** 1478 (1981)
40. E M Popov *Mol. Biol.* **11** 5 (1977)
41. G M Lipkind, I S Maksumov, E M Popov *Bioorg. Khim.* **1** 966 (1975)
42. I S Maksumov, G M Lipkind, E M Popov *Bioorg. Khim.* **2** 632; 737 (1975)
43. E M Popov, N M Godzhaev, R E Aliev *Mol. Biol.* **20** 367 (1986)
44. E M Popov *Strukturno-Funktsional'naya Organizatsiya Belkov* (Structural-Functional Organisation of Proteins) (Moscow: Nauka, 1992)
45. D Regoli, W K Park, F Rioux *Pharm. Rev.* **26** 68 (1974)
46. M J Peach, J A Ackery *Fed. Proc.* **35** 2503 (1976)
47. D J Ramsay *Front. Neuroendocrinol.* **7** 263 (1982)
48. M T Schiavone, R A S Santos, K B Broshihan, M C Khosla *Proc. Natl. Acad. Sci. USA* **85** 4095 (1988)
49. A J Prange, C B Nemeroff, M A Lipton, in *Psychopharmacology: Generation of Progress* (New York: Wiley, 1978) p. 637
50. P J Harris, L G Navar *Am. J. Physiol.* **248** 621 (1985)
51. G P Brown, J G Douglas, J Krontiris-Litowitz *Endocrinology* **106** 1923 (1980)

52. F E Freedlander, T L Goodfriend *Fed. Proc.* **36** 481 (1977)
53. T B Rogees *J. Biol. Chem.* **259** 8108 (1984)
54. M J Peach, F M Bumpus, P A Khairalah *J. Pharmacol. Exp. Ther.* **176** 366 (1971)
55. K Arakawa, F M Bumpus *J. Am. Chem. Soc.* **83** 728 (1961)
56. A Y Ferreira, O G Hampe, A C M Paiva *Biochemistry* **8** 3483 (1969)
57. L Juliano, A C M Paiva *Biochemistry* **13** 2445 (1974)
58. J D Glickson, W D Cunningham, U G R Marshall *Biochemistry* **12** 3684 (1973)
59. R R Smeby, K Acha, F M Bumpus, M M Harsh *Biochim. Biophys. Acta* **58** 550 (1962)
60. S Fermandjian, P Fromageot, A M Tishenko, J P Leicham, M Lutz *Eur. J. Biochem.* **28** 174 (1972)
61. J M Matsoukas, G T Moore *Spectrosc. Lett.* **21** 477 (1988)
62. J M Matsoukas, G T Moore *Arch. Biochem. Biophys.* **248** 419 (1986)
63. M P Printz, H P Williams, L C Craig *Proc. Natl. Acad. Sci. USA* **69** 378 (1972)
64. E Nabedrick, C Thiery, P Calvest, S Fermandjian *FEBS Lett.* **58** 273 (1975)
65. L C Craig, E J Harfenist, A C Palladini *Biochemistry* **3** 764 (1964)
66. M T Franze de Fernandes, A E Delius, A C Paladini *Biochim. Biophys. Acta* **154** 223 (1968)
67. T B Paiva, A C Paiva, H A Scheraga *Biochemistry* **2** 1327 (1963)
68. R E Lenkinski, R L Stephens, N R Krishna *Biochim. Biophys. Acta* **667** 157 (1981)
69. H E Bleich, R E Galardy, M P Printz *J. Am. Chem. Soc.* **95** 2041 (1973)
70. G R Marshall *Biochemistry* **12** 19 (1973)
71. K Lintner, S Fermandjian, P Fromageot, M S Khosla, R R Smeby, F M Bumpus *FEBS Lett.* **56** 366 (1975)
72. S Fermandjian, J L Morgat, P Fromageot *Eur. J. Biochem.* **24** 252 (1971)
73. D Grefts, S Fermandjian, P Fromageot, M S Khosla, R R Smeby, F M Bumpus *Eur. J. Biochem.* **61** 297 (1976)
74. I P Sekatsis, Yu A Antsans, D A Bisenietse, G I Chipens *Izv. Akad. Nauk SSSR, Ser. Khim.* 478 (1988)
75. F M Bumpus *Fed. Proc.* **36** 2128 (1977)
76. I P Sekatsis, E E Liepin'sh, Yu A Antsans, A A Berga, G I Chipens *Bioorg. Khim.* **7** 971 (1981)
77. R Deslauriers, A C Paiva, K Schaumburg, J C P Smith *Biochemistry* **14** 878 (1975)
78. J D Glickson, J Dadok, G R Marshall *Biochemistry* **13** 11 (1974)
79. G R Marshall, H E Bosshard, W H Vine, J D Glickson *Nature (London), New Biol.* **245** 125 (1973)
80. J L De Coen, E Ralson *Biopolymers* **16** 1929 (1977)
81. G V Nikiforovich, S G Galaktionov, G I Chipens *Konformatsii Peptidnykh Bioregulyatorov* (Conformations of Peptide Bioregulators) (Moscow: Meditsina, 1983)
82. C Marchionini, B Maigzet, S Premilat *Biochem. Biophys. Res. Commun.* **112** 339 (1983)
83. G V Nikiforovich, B Vesterman, J Betins, L Podins *J. Biomol. Struct. Dynam.* **4** 1119 (1987)
84. T V Gogitidze, E M Popov *Bioorg. Khim.* **19** 517 (1993)
85. E M Popov *Int. J. Quantum Chem.* **16** 707 (1979)
86. N A Akhmedov, G A Akhverdieva, N M Godjaev, E M Popov *Int. J. Pept. Protein Res.* **27** 95 (1986)
87. E M Popov *Fiz. Mol. (Kiev)* **8** 69 (1980)
88. IUPAC-IUB Commission on Biochemical Nomenclature *Biochim. Biophys. Acta* **262** 1 (1971)
89. T V Gogitidze, E M Popov *Bioorg. Khim.* **19** 693 (1993)
90. B P Rowe, K L Grove, D L Saylor, R S Speth *Eur. J. Pharmacol.* **186** 339 (1990)
91. V Z Spasov, E M Popov *Bioorg. Khim.* **7** 502 (1981)
92. H Micami, T Ogihara, K Katahira, N Imai, J Kubahara, F M Bumpus, M C Khosla *J. Cardiovasc. Pharm.* **9** 242 (1987)
93. D A Biseniyatse, Yu E Antsas, M V Myshlyakova, G G Kubrik, E A Porushkevich, M I Ratkevich, G I Chipens *Bioorg. Khim.* **13** 149 (1987)
94. G J Trache, J A Ackery, M J Peach *J. Cardiovasc. Pharm.* **3** 838 (1980)
95. R B Howard, R R Smeby, in *Handbook of Hypertension* Vol. 8 (Eds W H Birkenhäger, J L Reid) (Amsterdam: Elsevier, 1986) p. 389
96. M A Ravi Kiron, R L Soffer *J. Biol. Chem.* **264** 4138 (1989)
97. M Tence, A Petip *Mol. Cell Endocrinol.* **63** 111 (1989)
98. A M Capponi, K J Catt *J. Biol. Chem.* **255** 12081 (1980)
99. R S L Chang, V J Lotti *Mol. Pharmacol.* **37** 347 (1990)
100. R S L Chang, V J Lotti, T B Chen, K A Faust *Biochem. Biophys. Res. Commun.* **171** 813 (1990)
101. R C Speth, K H Kim *Biochem. Biophys. Res. Commun.* **169** 997 (1990)
102. T V Gogitidze, E M Popov *Bioorg. Khim.* **19** 773 (1993)
103. S Salman, A Baucal, S Water, F M Bumpus, K J Catt *Endocrinology* **97** 275 (1975)
104. M J Peach *Circ. Res.* **28** 107 (1971)

Russian Chemical Reviews **63** (12) 965–976 (1994)
©1994 Russian Academy of Sciences and Turpion Ltd

UDC 539.8

Problems in mechanochemistry and prospects for its development

P Yu Butyagin

Contents

I. Introduction 965
II. The present state of research 965
III. Prospects for further development and expected results 971

Abstract. The results of studies on nonthermal chemical reactions induced by the deformation of solids are summarised in the review. Attention is concentrated on the analysis of processes involving the dissipation of elastic energy, the description of the nature and properties of the intermediate nonequilibrium states, and also studies of processes involving the low-temperature molecular mixing of solid reagents. The possible trends in further research are discussed. The bibliography includes 89 references.

I. Introduction

Mechanochemistry is the study of the influence of elastic and plastic deformations on the reactivities of solids. This definition is not quite complete and rigorous, but it emphasises the relation between mechanochemistry and other branches of chemical science. Chemical reactions unaccompanied by a change in volume and the appearance (or relaxation) of internal stresses are indeed rare; mechanochemistry is therefore an indissoluble component of the physical chemistry and chemistry of solids.

The vigorous development of mechanochemistry during the last decade became possible as a result of advances in fundamental research and the improvement of many technological processes, including the synthesis of new materials. The intersections of mechanochemistry with adjacent branches of knowledge such as the physics and chemistry of the solid state, the theory of strength, physicochemical mechanics, catalysis, chemical engineering, materials science, geology, biochemistry, the chemistry of medicinal drugs, etc. have been no less important. The application of mechanochemical methods in engineering (in the manufacture of building materials and ceramics, including superconducting ones, in powder metallurgy, in the food and pharmaceutical industries, etc.) have also attracted the attention of investigators and technologists to mechanochemistry.

The extensive possibilities of mechanochemistry as the chemistry of nonthermal low-temperature reactions are illustrated by the fact that refractory substances and intermetallic compounds, inorganic and organic compounds, and molecular complexes have been synthesised, polymers and pharmaceutical preparations have been modified, and composite materials have been created in the solid phase without dissolution or fusion of the reactants. Mechanochemical syntheses are carried out at a comparatively low temperature, where the formation of an ideal crystal structure is difficult. This opens a route to the synthesis of substances and materials in the nanocrystalline and amorphous states.

The rate of development of mechanochemistry is reflected by the growth in the number of publications. The total number of journal articles on mechanochemistry published throughout the world increased over the last ten years almost by a factor of five and exceeded one thousand in 1992. The number of studies on the mechanochemistry of metals and alloys and also on the synthesis of various materials for engineering has greatly increased (see Refs 1–43).

P Yu Butyagin Semenov Institute of Chemical Physics, Russian Academy of Sciences, ul. Kosygina 4, 117334 Moscow, Russian Federation. Fax (7-095) 938 21 56. Tel. (7-095) 299 73 25
E-mail: mechxim@glas.apc.org

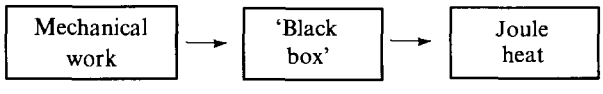
Received 23 August 1994
Uspekhi Khimii **63** (12) 1031–1043 (1994); translated by A K Grzybowski

II. The present state of research

The period, lasting more than 100 years, in which mechanochemistry has been established as an independent field of knowledge has come to an end. During this time, mainly the results of qualitative observations of various effects have accumulated.

Nowadays no one believes that under the influence of mechanical action elastic energy is converted instantaneously, and without trace, into Joule heat.

It has been shown that, on deformation and disruption of solids, various energy-rich intermediate states arise in the first place, their subsequent decomposition resulting in the evolution of an appreciable proportion of the heat. In other words, there exists the so called 'black box' between work and heat; if energy is supplied to it faster than it can be converted into heat, it is possible to achieve various and unexpected chemical reactions.

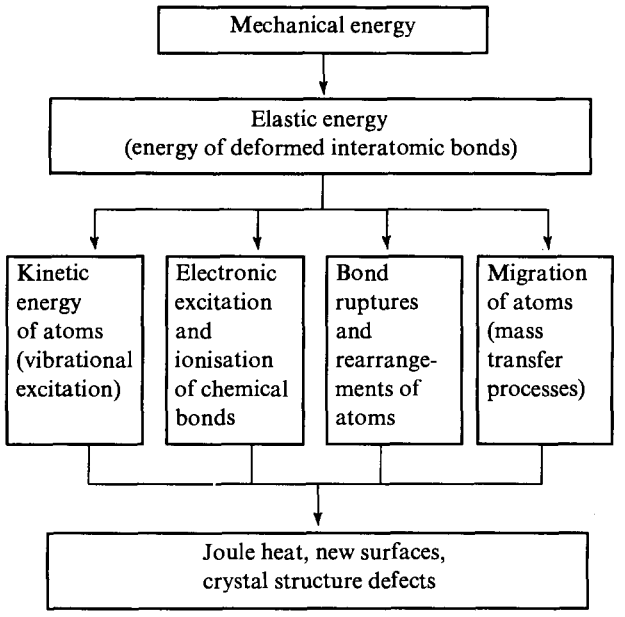


Vibrationally an electronically excited bond, electrons and ions, metastable atomic structures, and other intermediate states may exist in the 'black box' and this list by no means exhausts its contents.

1. Transformations of elastic energy in solids

The scheme below illustrates the principal paths to the appearance and transformation of active nonequilibrium states arising when solids are subjected to mechanical influences.

Definite excess energy carriers with specific electronic and chemical structures, reactivities and relaxation mechanisms correspond to each of the pathways. Each state is characterised by a definite energy yield and lifetime. We shall consider the scheme below in greater detail.



2. Deformed interatomic bonds

Deformed covalent bonds are detected by IR spectroscopy (Fig. 1) and the extent of deformation is calculated from the shift of the absorption band maximum.[7,22,32,35,44] In metals and other crystals, the average degree of lattice deformation is calculated from the line shape in X-ray spectra. The deformed bond and its reactivity have long been considered by theoreticians and experimenters. In the construction of a kinetic theory of the strength of solids, attention has been concentrated on the reactions involving the rupture of elastically stressed bonds.[35] The effect of stresses on the rate constant k for this reaction was calculated from the Eyring–Kauzmann equation:

$$k = k_0 \exp\left(-\frac{E_a - \sigma V^{\neq}}{RT}\right),$$

where k_0 and E_a are the pre-exponential factor and the activation energy for the thermal decomposition and $\sigma V^{\neq}$ is the work performed by the elastic stresses in the reaction step (σ is the stress and $V^{\neq}$ the volume of activation).

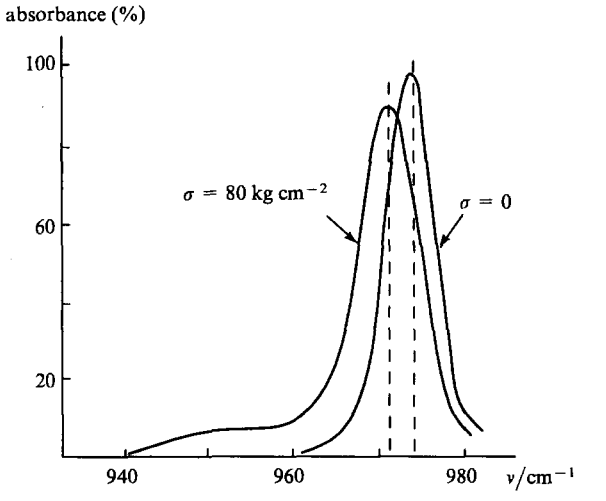


Figure 1. Skeletal vibrations of the main chain atoms in the IR spectrum of polypropylene in the initial state ($\sigma = 0$) and after extension by a load ($\sigma = 80\ \mathrm{kg\ cm^{-2}}$) (temperature 150 °C).[35]

In formulating this equation, it is implied that the active stresses facilitate the transitions through the energy barrier but do not affect its height. This approximation is apparently valid for the extension of bonds in the region of linear elasticity. For considerable deformations, one may expect a deviation from the linear energy relation. According to the results of quantum-chemical calculations,[45] a deformation of the C–C bond in the $\sim CH_2-CH_2-CH_2\sim$ chain close to the predissociation deformation lowers the ionisation potential of the hydrocarbon fragments almost by a factor of 2.

In substitution reactions, the reactivity of deformed fragments of organic molecules is characterised by the magnitude and sign of the coefficient of sensitivity to stresses.[14,32] Its value shows by what factor the rate constant changes following the extension or compression of a molecular fragment. For example, the rate constant for the hydrogen atom transfer reaction

$$R^{\cdot} + \sim CH_2-CH_2-CH_2\sim \rightarrow RH + \sim CH_2-CH^{\cdot}-CH_2\sim$$

is related to the deformation energy of the $-C-C-C-$bond skeleton by the expression[32]

$$\ln\frac{k(\varepsilon)}{k(\varepsilon=0)} = \alpha\frac{\Delta E^{0.5}}{RT},$$

where k are the rate constants for the reaction in the deformed [$k(\varepsilon)$] and nondeformed [$k(\varepsilon = 0)$] fragments, ΔE the deformation energy, and α an empirical constant the value of which depends on the nature of the hydrogen atom acceptor (in the abstraction of a H atom by an ozone molecule, $\alpha = 57\ \mathrm{J^{1/2}\ mol^{-1/2}}$).[32]

The above relation is valid for small deformations. It has been suggested that strongly deformed Si–O–Si linkages on the SiO_2 friction surface have reactivities similar to those of the $\equiv Si^{\cdot}\ldots{}^{\cdot}O-Si\equiv$ radical pairs. So far this is only a hypothesis put forward on the basis of the analysis of the kinetics of the reactions of SiO_2 with H_2, CO, and other molecules.[9] The first quantum-chemical calculations for substitution reactions involving deformed bonds were carried out several years ago.[44] It may be hoped that, as a result of the development of computer techniques and programs, it will become possible in the immediate future to investigate in greater depth the deformed fragments of molecules and their reactivities.

3. Vibrationally excited states

Several decades ago, there was a widely held view that impact or friction give rise to regions with an increased temperature — 'hot spots'. The initiation of chemical reactions was attributed to the existence of such spots.[21] The controversy concerning the possibility of an increase in temperature at the entrance to a crack or on the friction surface has still not ended. Mention of 'hot spots' may be found also in modern literature. Calculations of local temperature carried out by various investigators imply that the rate of evolution of Joule heat is much higher than the rate of removal of heat. However, the real situation is far from this highly simplified model. Several relaxation pathways usually operate. One of them involves the relaxation of the disturbed atomic structure, which is known to be a slow process, and energy transformations are therefore extended in time.

Judging from indirect features, centres with a high temperature exist only under extreme conditions. These include, for example, the instant when cavitation bubbles are flooded following the absorption of ultrasound in liquids.[19,27,41] Not only have the rates of absorption and transformation of the energy via different paths been calculated rigorously for this case[19] but measurements have also been made of the emission spectra,[41] confirming the existence of 'hot spots' with a temperature up to several thousands of degrees.

The first direct spectroscopic measurements revealing the state of the solid material at the instant of decomposition have been carried out for poly(methyl methacrylate). Their results are

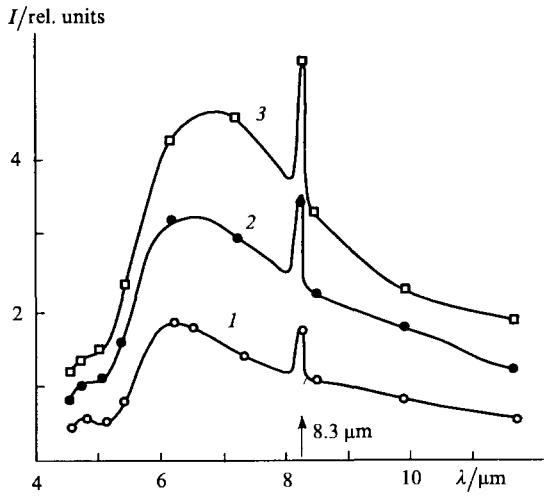


Figure 2. Thermal emission spectra obtained on disruption of a poly(methyl methacrylate) specimen.[37] Time elapsed from the start of disruption (μs): (*1*) 10; (*2*) 20, (*3*) 30.

illustrated in Fig. 2. The IR spectra measured at 10, 20, and 30 μs intervals after the initiation of the crack contain narrow lines, against the background of a broad thermal emission maximum, which correspond to vibrationally excited states. The lifetime of these states is short and the principal chemical mechanism of their destruction is the unimolecular isomerisation and decomposition of molecules accompanied by the ejection of fragments; bimolecular reactions with participation of 'hot' fragments of ruptured molecules have not been observed.

The first reports of the ejection of low-molecular-mass fragments on mechanical degradation of polymers appeared more than 25 years ago[46] and since then the decomposition of hot fragments has been frequently observed (see, for example, Zarkhin et al.[20] and Boldyrev[47]). The dynamics of the appearance, migration, and disappearance of excitations on dissociation of linear chains of atoms excited on rupture is investigated nowadays by molecular dynamics[43] or quantum-chemical methods.

For the occurrence of chemical reactions of highly excited states (decomposition, electron transfer, isomerisation, etc.), it is necessary that the energy level of the excited state should be close to the region where the potential curves corresponding to the initial and final states of the molecular or ionic fragment intersect. For example, when an ionic LiF crystal is cleaved, F atoms are ejected into the gas phase. The F^- anion must lose an electron in order to be able to leave the crystal: in contrast to F^-, the neutral F atom is not retained on the surface by electrostatic interaction forces. One of the hypotheses put forward to account for the emission of F atoms is as follows. Calculation[48] have shown that electron transfer in accordance with the scheme

$$F^-_{vib} \rightarrow F + e^-,$$

$$Li^+ + e^- \rightarrow Li,$$

is possible provided that the amplitude of the vibrations of the F^- ion, which are excited immediately after the dissociation of bonds at the entrance to the crack, exceeds 0.75 of the lattice parameter. Separation from the surface by this distance is equivalent to bond dissociation. In ionic crystals, decomposition into neutral atoms rather than ions is energetically more favourable.

It has been suggested that the ejection of hydrogen atoms on mechanical degradation of carbochain polymers[20] and of methane on degradation of polydimethylsiloxane[49] can be explained in this way. Apparently, after the dissociation of the chain, the amplitude of the vibrations of atoms in these polymers is such that, at the instant of their mutual approach, the distance between them diminishes so much that atomic rearrangements in accordance with the schemes

$$\sim CH(CH_3)\dot{C}H_2 \rightarrow \sim C(CH_3)=CH_2 + H^{\cdot}\text{(in polypropylene)},$$

and

$$=Si(CH_3)O^{\cdot} \rightarrow =Si=O + C^{\cdot}H_3\text{ (in polysiloxanes)},$$

became possible.

4. Electronic excitation and ionisation

All the consequences of electronic excitations and ionisation are usually combined in the group of mechanoemission phenomena. These include luminescence, static electrification, electron emission, and other effects associated both with the appearance of single electrically charged centres and with the effect of electric fields (static electrification). An extensive literature has been devoted to this problem.[9, 15, 30, 48]

Mechanical excitation of the electronic subsystem has been observed in crystals with different types of interatomic bonds. Examples of such processes in metallic copper[50] and magnesium oxide[9, 51] are presented below.

The 2.14 eV and 1.70–1.72 eV lines in the mechanoluminescence spectrum of copper (Fig. 3) correspond to electron transitions from surface electronic states to holes at the top of the *d* band of copper. The holes in the *d* bands are localised at dislocation nuclei, while electron–hole recombination, accompanied by the emission of light quanta, is induced by the emergence of dislocations onto the surface during the plastic deformation of the specimen.[30]

In magnesium oxide, electronic excitation with electron transition through the band gap may be represented as a chemical reaction involving electron transfer from the anion to the cation.[9]

$$\{Mg^{2+}O^{2-}\} \rightarrow \{Mg^+ \ldots O^-\}^*$$

Different distances between the ions correspond to the initial and excited states. When the excitation is induced by the absorption of UV light quanta, the lifetime of the $\{Mg^+ \ldots O^-\}^*$ excitons is short, since the necessary change in the interatomic distance is hindered by the rigid crystal matrix.

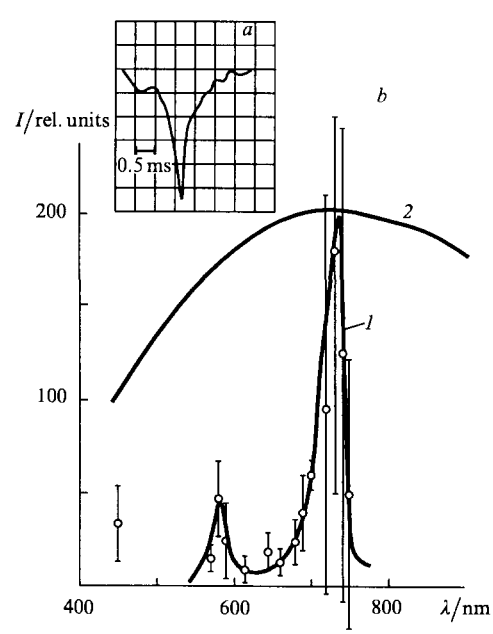


Figure 3. Oscillogram (*a*) and mechanoluminescence (*b*, curve *1*) and the thermal emission (*b*, curve *2*) spectra for copper at $T = 4000$ K.[50] The application of a load (impact) and the measurements (at the opposite end faces of a cylindrical specimen) were performed in vacuo at 10^{-5} GPa.

The same transition on friction is induced by the deformation of the surface, which increases the interionic distances to values corresponding to the $\{Mg^+ \ldots O^-\}$ structure, while electron transfer completes the stabilisation of this new state. At room temperature ($T \approx 0.1\ T_{pl}$), the thermal relaxation of the deformed surface is retarded and the long-lived quasi-exciton $\{Mg^+ \ldots O^-\}$ states may be preserved and investigated by spectroscopic, adsorption, and EPR methods.[51]

From the chemical point of view, the $\{Mg^+ \ldots O^-\}$ structures should be interpreted as radical pairs in which the oxygen radical-ion is one of the most active chemical species. In this case, the friction surface is distinguished by a high reactivity. The mechanical activation of the surfaces of many oxides is associated with the formation of quasi-exciton states.

Thus electronic excitation may be induced not only by the absorption of emission quanta but also by deformation, which creates configurations of atoms or ions favourable for electron transfer.

Other mechanisms also exist of the appearance of electrically charged centres and electric fields on disruption, deformation, and friction in crystals.[15,30,52] One of them is associated with the separation of the charges on the electrical double layer when contact between solid surfaces is broken.[15] On disruption and plastic deformation, the charges are separated between the dislocation nucleus and the compensating 'coat' (oppositely charged point defects). When a moving dislocation emerges onto the surface, the 'coat' remains in the bulk of the crystal. The growth of a crack as well as friction between surfaces are therefore a source of a wide variety of electrophysical effects.[30,52,53]

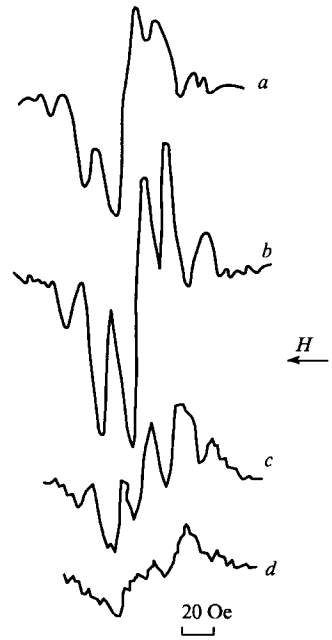


Figure 4. EPR spectra of the free radicals detected at the site of the mechanical rupture of DNA molecules isolated in a dilute frozen solution in D_2O: (*a*) and (*b*) different DNA specimens at 80 K; (*c*) and (*d*) the same specimens after raising the temperature to 195 and 217 K respectively (the rupture takes place in the deoxyribose unit).[54,55]

5. The dissociations and rearrangements of interatomic bonds

The mechanical properties of substances have been described fairly fully in the literature and constants such as the modulus of elasticity, the elastic limit, strength, hardness, etc. may be found in handbooks. On the other hand, quantitative data characterising the resistance of various substances to mechanical loads are not quite so extensive and studies on the kinetics and mechanisms of mechanical destruction have invariably attracted attention.

Indeed, failure is impossible without the dissociation of interatomic bonds and it therefore remains in essence a chemical step. The breakdown of polymers, molecular crystals, inorganic compounds, and metals is therefore regarded in mechanochemistry as a degradation process in the analysis of which it is necessary to take into account the nature of the bonds and the chemical structure of the corresponding substances.

Many examples of the chemical degradation of simple and complex substances on failure and deformation may be quoted (see, for example, Refs 1, 3, 5, 9, 14, 16, 20, 22, 35, 43, 46–49, 54–56, and 58).

The example of the mechanical destruction of polymers, in which not only the supermolecular structure is disrupted but macromolecules are cleaved, has become classical. The free radicals formed at the ends of the broken chain are detected and investigated by the EPR method. They have been observed on failure and deformation of polymers with different structures — ranging from polyethylene to DNA. In order to detect the primary radicals at the site of rupture, DNA molecules were isolated from one another in a dilute solution, the solution was frozen, and the destruction was observed at 80 K (Fig. 4).[54,55]

The radicals frequently initiate chain degradation and cross-linking. The chain degradation of three-dimensional polyacrylate esters,[16] cellulose,[55] and carbons[23] has been described. Polyethylene differs from these polymers by a tendency towards cross-linking.

On degradation of silicon dioxide, the dense network of siloxane bonds is ruptured and the radicals formed disproportionate. Two-coordinated silicon atoms and other irregular groups accumulate under these conditions.[9,56] The chemical properties of 'mechanical' radicals and their subsequent reactions in solids having directed bonds and on their surfaces are analysed within the framework of the theory of the reactivity of free radicals. The principal difference distinguishing radicals in solids is their high stability due to their fixation on the surface or in the bulk of crystals. Their destruction is usually induced by their involvement in chemical reactions and by the existence of various relay mechanisms of the migration of the free valence.

In metals, where there are no strictly directed bonds between atoms, the chemically reactive centres are atoms, with a low degree of coordination, within the dislocation nuclei and other structural defects. Prolonged mechanical treatment leads to extensive disordering with stabilisation of nanocrystalline or amorphous structures.[13,24,25,39,40,42,57,59–67] The degree of disordering is frequently characterised by the dimensions of microcrystalline blocks separated by intergrain boundaries. Their dimensions and residual deformation are calculated from the line shape in the X-ray spectra. The merging of the lines into a single broad band corresponds to the transition of the substance to the X-ray-amorphous state.

The degradation of ionic crystals[1,4,11,12,21,37,38] may be accompanied by the decomposition of complex anions and ionisation of the substance. Salts in which the cation is much smaller than the anion, for example, silver oxalate $Ag_2C_2O_4$, are distinguished by a high sensitivity to mechanical influences. The salt decomposes more than half during mechanical treatment at room temperature, this being detected by the liberation of the metal and carbon dioxide. Crystalline hydrates (for example, kaolin), which on mechanical treatment initially lose water of crystallisation, decompose even more readily. Finally, salts with unstable anions (azides, perchlorates, etc.) decompose explosively under impact.

Thus studies on the degradative phenomena in the course of disruption and deformation processes have shown that the macroscopic deformation pattern conceals profound changes in the chemical structure of the substance. Plastic deformation cannot therefore be regarded in isolation from chemical consequences.

Since the reactivity of solids is their structure-sensitive property, the disordering and degradation (activation) processes are used in chemistry and chemical engineering to accelerate processes involving dissolution, sintering, synthesis, and decomposition of solid reagents.

6. Mass transfer processes

Irreversible changes in the form and size of a solid on plastic deformation are inevitably accompanied by the displacements of atoms in its bulk relative to one another. Relay mechanisms of the migration of structural defects frequently predominate under these conditions.

a. Deformation mobility

The deformation mobility of atoms (molecules, ions) and its scale are demonstrated by the phenomenon of the miscibility of various substances under the conditions of joint mechanical treatment. One of the striking examples is the dissolution of tungsten in iron[65] and nickel[66] at room temperature (Fig. 5).

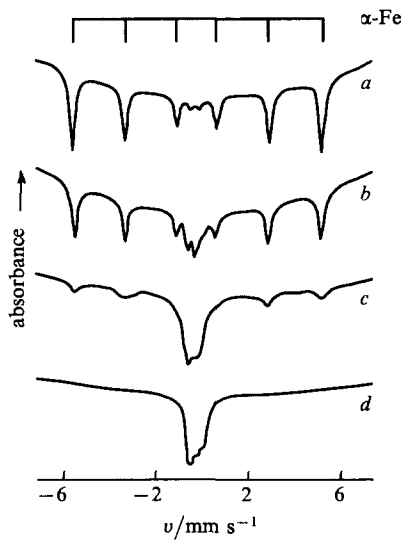
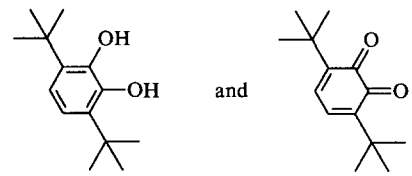


Figure 5. Mössbauer spectra of the 1 : 1 Fe/W mixture after mechanical treatment at room temperature in a vibromill.[29] Dose of supplied mechanical energy (kJ g^{-1}): (*a*) 5; (*b*) 10; (*c*) 60; (*d*) 100.

In terms of all their features, these are systems where miscibility is most difficult. Tungsten belongs to the strongest metals and the enthalpies of its mixing with iron and nickel are low: ~ -3 kJ mol^{-1} for mixing with nickel and ~ 0 kJ mol^{-1} for mixing with iron. The thermal mobility of atoms is almost frozen, since the temperature of the mechanical treatment does not exceed 0.2 T_m of the mixture components [T_m = melting point (Ed. of Translation)].

The initial stage of the dissolution of tungsten in nickel was detected from the increase in the nickel lattice parameter from 0.352 to 0.364 nm during the mechanical treatment of a mixture of the powders.[66] On more prolonged mechanical treatment, the nickel and iron crystal structures gradually break down; this can be seen from a series of Mössbauer spectra of the Fe/W mixture (Fig. 5). The growth of the amorphous halo in the spectra of the Fe/W mixtures is accompanied by the appearance of a single line in the spectrum, reflecting the formation of the paramagnetic iron compounds Fe_7W_6 or Fe_2W. Consequently tungsten atoms are inserted in the first coordination sphere of the iron atoms and the dissolution is not confined to the surface layer but involves the entire bulk of the substance.

The list of systems in which deformation mixing at the atomic or molecular level has been observed may be greatly expanded. It includes not only metals[17,24,25,37,39,40,42] and inorganic compounds,[1,5,8,12,21,26,28,53,59,67,68] but also plastic mixtures of organic substances.[39] The interest in molecular mixing has not disappeared to this day. Thus the appearance of an EPR signal has been observed recently when powders of a sterically hindered phenol and the quinone were mixed:[70]



The signal corresponds to the spectrum of radical pairs stable at room temperature (Fig. 6).

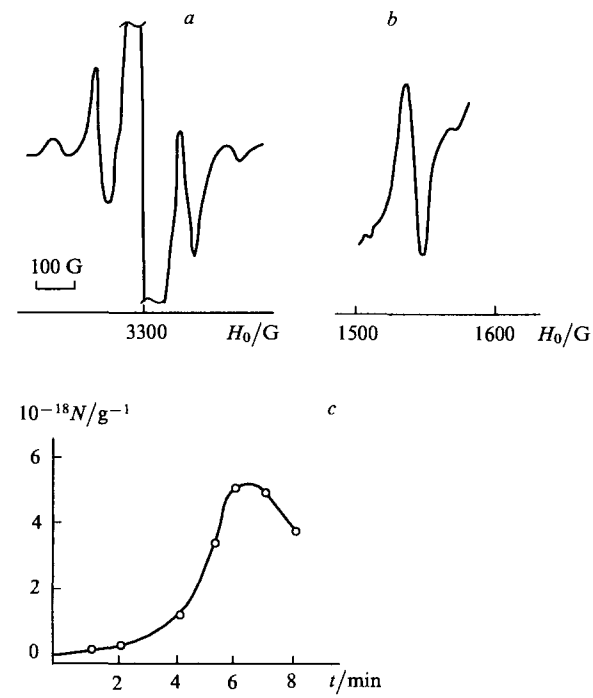


Figure 6. EPR spectra of the free radicals (central line) and radical pairs (outer lines) recorded on grinding a mixture of 3,6-di-*tert*-butyl-catechol and 3,6-di-*tert*-butyl-*o*-quinone powders in the region of 3000 G (*a*) and 1500 G (*b*). (*c*) Kinetics of the accumulation of radical pairs.[70]

On mixing, the molecules come into contact and the mobile hydrogen atom passes from the phenol to the quinone; this results in the formation of two adjacent radicals—a radical pair. The EPR spectrum of such a pair is illustrated in Fig. 6*a* and the kinetics of the accumulation of the radicals are illustrated in Fig. 6*c*. The number of pairs characterises the number of molecules in contact. During the mechanical treatment of a mixture of the phenol and quinone powders, the number of radical pairs increased to 5×10^{18} g^{-1} (in other similar systems, the increase was 1×10^{19} g^{-1}), which is a little less than 1% of the total number of molecules. When mixing is continued, the radical pairs begin to move apart, which is observed from the accumulation of the signals due to individual radicals (the average line in the spectrum of Fig. 6*a*).

Thus there is at present no doubt about the existence of the phenomenon of the low-temperature deformation mixing at the atomic (or molecular) level and its high effectiveness for both hard and soft substances.

b. Mechanochemical synthesis

Deformation mixing at the molecular level has led to the possibility of carrying out chemical reactions in mixtures of solids at room temperature whereupon diffusion is almost frozen. It is nowadays possible to find in the literature descriptions of several hundreds of such reactions, which have been achieved on Bridgeman's anvils,[8,18] in various mills,[1,21,24,25,38] attrition mills,[71,72] and disintegrators,[12] on rollers,[3,28] and in shock waves.[2]

It is important to emphasise that there are conditions under which the deformation mixing of solid reagents is completed by the formation of a new crystalline phase comprising the reaction products. Consequently the ordering of the product phase takes place under the same conditions as the disordering of the crystal structures of the starting materials.

Crystalline products may be formed in the reactions between simple and complex organic or inorganic compounds, between metals (mechanical fusion), and in mixtures of two or several solid components. As an example, Fig. 7*a* presents the kinetic curve for the synthesis of lead ferroniobate from a mixture of powders of three oxides:[36]

$$4\,PbO + Nb_2O_5 + Fe_2O_3 \rightarrow 4\,Pb(Fe_{0.5}Nb_{0.5})O_3\,.$$

The yield of the crystalline product phase was recorded by X-ray phase analysis (Fig. 7*b*). The figure shows clearly that the formation of the product is accompanied by its degradation. If the mechanical treatment is not stopped, then the content of the product synthesised in the mixture begins to fall.

During a prolonged mechanical treatment of a mixture of boron and carbon powders at room temperature, the accumulation of boron carbide was observed. There can be no doubt about the reality of the nonthermal mechanism of the synthesis of boron carbide, since the temperature in the apparatus was lower by 2000 K than the melting point of the components, while the heat of reaction is low. The formation of the nanocrystalline boron carbide was detected by X-ray diffraction despite the fact that the unit cell of B_4C contains more than 100 atoms. Thus plastic deformation induces not only the breakdown of the crystals of individual substances but also the formation of new crystal structures in mixtures of solid reagents.

The formation of the crystalline phase of the product in multicomponent reaction mixtures reveals yet another feature of the transformations of the elastic energy in solids, which is no less promising for chemistry. Under the same conditions, two at first sight incompatible processes are intertwined in the above process, namely, the decomposition and ordering of the crystal structures.

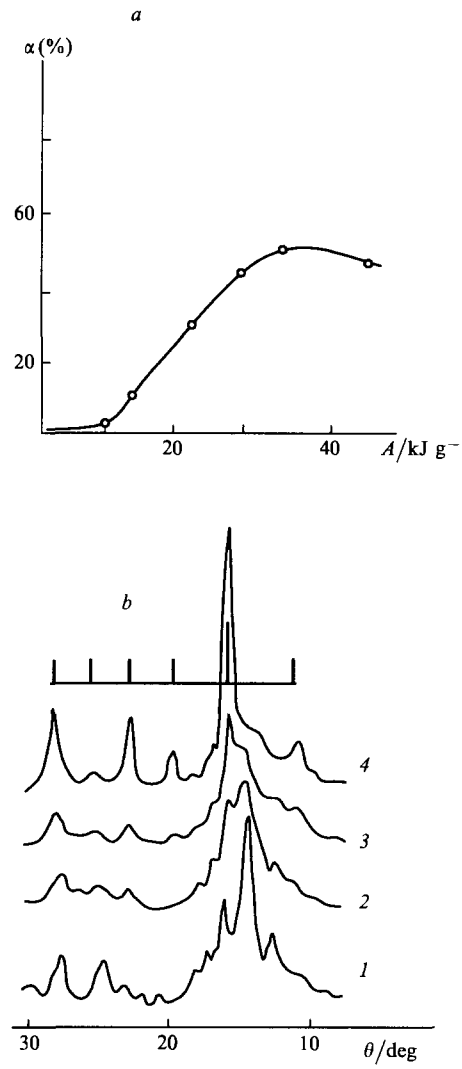


Figure 7. Kinetics of the mechanochemical synthesis of lead ferroniobate from a mixture of iron oxide, niobium oxide, and lead oxide powders at room temperature (*a*). Diffractometer traces for the mixture at different stages of the reaction (*b*) (the positions of the product lines are indicated in the top part of the figure).[36]

Table 1. Mechanochemical synthesis in metal–nonmetal mixtures (according to the data of Shelimov and Butyagin[81]).

Mixture	T_{ad}	T_m	Mixture	T_{ad}	T_m	Mixture	T_{ad}	T_m
Explosive reactions								
Zn + S	3380	693	Ti + C	3210	1941	Zr + 2S	5930	2128
Cd + S	2280	594	Ti + 2B	3190	1941	Hf + C	3900	2500
2In + 3S	2160	430	5Ti + 3Si	2390	1941	Hf + 2B	3520	2500
Sn + S	1640	505	Zr + C	3410	2128	5V + 3Si	2400	2190
Sn + 2S	1140	505	Zr + 2B	3310	2128	2Ni + Si	1590	1728
Pb + S	1620	600	Zr + 3Si	2480	2128			
Reactions without explosion								
2Cu + S	1267	1357	2As + 2S	580	1087	Ta + C	2730	3287
2Ag + S	695	1234	2Sb + 2S	880	904	Ti + B	2600	1941
Ge + S	1173	1210	Nb + 2B	2350	2740	2W + C	670	3700

Note. The data on the explosion in each reaction system have been taken from Refs 33, 75, 78–81, and 83; T_{ad} = adiabatic combustion temperature of the mixture; T_m = melting point of the metal.

The destabilising effect of elastic stresses on the crystals has proved favourable for the mixing of the components at the molecular (atomic) level. The formation of crystalline reaction products indicates a trend towards ordering. The greater the shift of the reaction equilibrium towards the products, the stronger is the manifestation of this trend.

In exothermic reaction mixtures, the formation of the product is accompanied by the evolution of heat. By varying the intensity of the mechanical treatment and the rate of removal of heat, it is possible to create in such systems conditions favourable for the mechanical initiation of thermal explosion. During the last decade, explosive mechanochemical synthesis has become the object of continuous attention by investigators.[29,33,73-81]

In the initial stage of the mechanical treatment, the size of the powder particles diminishes, the mixture is stirred, and the area of contact between the reactants increases. Under these conditions, the reaction begins to develop in the surface zone and heat is evolved. So long as the particles are large, the degree of their reaction is low and the temperature remains at a low level. After the increase in the area of the surface of contact to several square metres per gram, the rate of reaction increases so much that there is insufficient time for heat to be removed and the reaction passes into the self-acceleration regime.

In reaction mixtures for which the adiabatic reaction temperature is equal to or greater than the melting point of one of the components and the rate of application of the mechanical energy dose is above a critical level, the self-acceleration condition is replaced by thermal explosion (see Table 1 and Shelimov and Butyagin[81]).

* * *

Vibrational and electronic excitation as well as phenomena involving the degradation and disordering of crystals, deformation mixing, and synthesis represent the content of the large field of nonthermal physicochemical and chemical reactions. This field complements the classical thermal theory and significantly expands its possibilities. The phenomena considered are no less interesting for solid state physics, materials science, and other branches of natural sciences.

From the chemical point of view, reactions in mixtures of powders and processes involving the mechanical activation of solid reagents are the most promising. However, the experience accumulated in laboratories is being gradually assimilated in engineering. The list of mechanochemical reactions achieved on a small scale embraces various classes of solid-phase reactions.

Thus gas–solid reactions include the synthesis of nitrides, hydrides, and carbonyls on interaction of gases (nitrogen, hydrogen, carbon monoxide, etc.) with powdered metals and nonmetals.[61-64,82-85] The first experiments on pseudocatalytic reactions under the conditions of the mechanical treatment of a powdered catalyst have already been carried out.[83,85]

The list of solid–solid reactions is the longest. It includes the synthesis of carbides, borides, and silicides from the initial elements (TiC, TiB_2, B_4C, etc.[33,74-76,81]), the reduction of oxides by metals,[77] and the synthesis of ferrites, superconducting ceramics, and other oxide materials.[1,6,12,36] Mechanical fusion, i.e. the preparation of alloys, intermetallic compounds, and composite materials from them, also belongs to processes of this class[17,24,25,28,39,40,42,59,60,65,67,68,72,73]. Solid-phase organic synthesis[2,6,18] includes the preparation of phthalazole, amine acylation reactions, Diels–Alder condensation, the polymerisation of solid monomers, etc. Modification of medicinal drugs and the preparation of compositions with a controlled liberation of medicinal forms constitute a related field.

A by no means complete list of systems investigated has been presented here, but even these examples emphasise the breadth and scale of the accumulated knowledge. Nowadays there is a transition in mechanochemistry from laboratory research to technological developments. A diverse range of laboratory mechanochemical reactors has been created and exists. It is possible to activate and synthesise in them organic and inorganic substances.[1,8,71,72,86]

Unfortunately, the reactors have not always been successfully characterised (dose, rate of application of dose) to be able to compare the results obtained by different workers or to give recommendations concerning the scaling of experiments. Vigorous research is being prosecuted on these lines.[71,72,86]

However, the choice of manufacturing apparatus is as a rule restricted to equipment which has been created for other purposes—grinding, extrusion, etc. Theoretical studies on the conditions of the synthesis in large-scale mechanochemical reactors taking into account the dynamics and energy relations of specific processes can be counted on one's fingers, i.e. the laboratory experiment–technological tests link has not yet been established.

III. Prospects for further development and expected results

1. Reactivity of elastically deformed solids

Studies on the role of elastic stresses in solid-phase reactions were apparently developed in several directions. They can be given conventional names: (1) electronic structure and reactivity of elastically deformed interatomic bonds; (2) elastic model of solid-phase reactions; (3) reactions in structural relaxation processes. The first of these has already been examined in Section II. 2. The contents of the others will be briefly described below.

The second aspect of the above investigations deals with reactions in continuous media, where it is necessary to take into account the deformation of not only the reaction centre proper but also of its environment. Within the framework of the elastic approximation, the potential energy of the reaction centre is represented as the sum of the energy of the chemical interaction proper U_{chem} and the deformation energy U_{str}. The height of the energy barrier in the reaction involving such a reaction centre is equal to the difference between the energies of the system in the transition and initial states. The complex structure of the reaction barrier in the solid phase is illustrated by the scheme below:

$$E = (U^{\#}_{chem} + U^{\#}_{str}) - (U^{0}_{chem} + U^{0}_{str}).$$

The superscripts '#' and '0' denote the transition and initial states.

Computer calculations of the energy barrier in model reactions are not very complex (Fig. 8) when they are carried out by the method of molecular dynamics and do not involve changes in the electronic subsystem, but because of this the results of such calculations are approximate. Fig. 8*a* illustrates the model for the calculation of the barrier height when an extraneous atom is inserted in the crystal lattice. This atom, designated by a filled circle, is acted upon by a force F, which displaces it downwards at a constant rate. Here one calculates both the change in the energy of the atom (Fig. 8*b*, curve *1*), and the deformation of its environment (curve *2*), i.e. all the components of the barrier structure (the schemes in Figs 8*c* and 8*d* illustrate the macrokinetics of the deformation mixing). The first results of such calculations have shown that the deformation contribution may be dominant under certain conditions.[28,87] The calculations of the barrier structure are valid for both thermal and mechanochemical reactions.

The main difference between mechanical reactions and the usual thermofluctuation reactions is the use of different methods for overcoming the energy barrier separating the initial and final states in the elementary reaction step. It is as a rule understood that the form and height of the energy barrier are independent of the way in which it is overcome: under the influence of elastic stresses or by the thermofluctuation route.

However, systematic studies on the effect of elastic stresses and of the rate of deformation on the form of the potential surface and the route followed during the movement of the system of reacting species along the reaction coordinate have not been carried out.

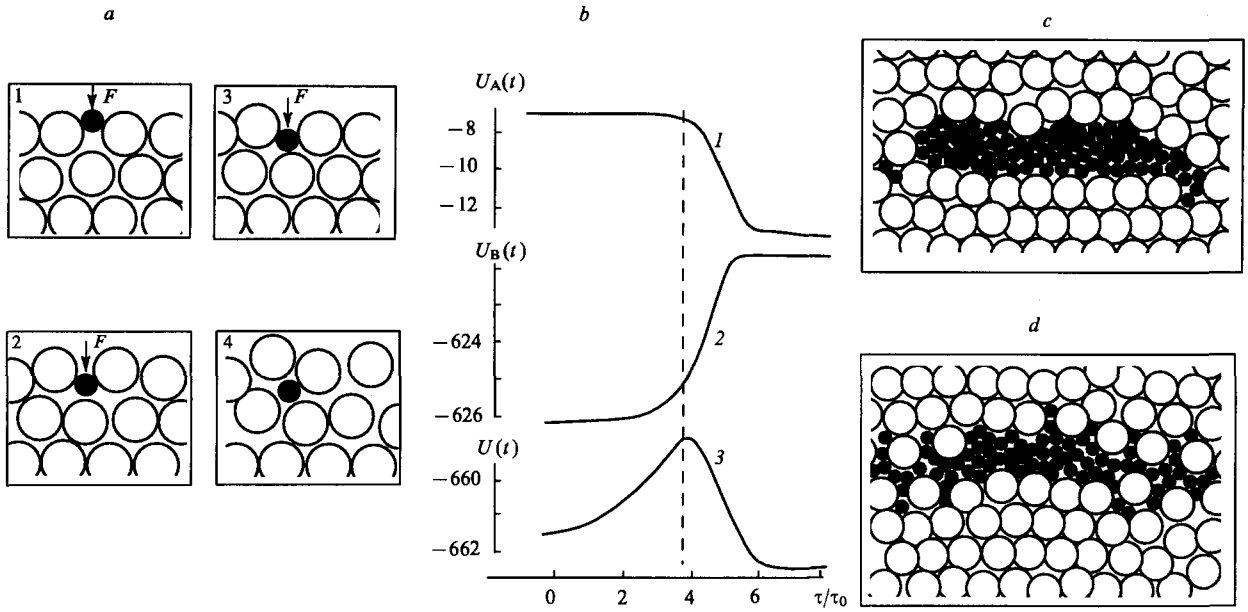


Figure 8. Modelling of deformation mixing by the method of molecular dynamics. Permeation of an atom through the surface: (*a*) scheme; (*b*) calculation of the changes in the energy of the atom itself [$U_A(t)$] (curve *1*) and of the crystal [$U_B(t)$] (curve *2*) and of the height of the energy barrier [$U(t)$] (curve 3) for a three-dimensional model; (*c*) and (*d*) stages in deformation mixing on uniaxial compression of a three-layer model.[9, 10, 28, 29]

The limits of the applicability of this approximation are therefore also unknown. It may be hoped that the search for answers to these questions will begin in the immediate future.

Mechanochemical reactions in solids are known to be induced not only by the direct action of elastic stresses but also by elastic energy relaxation processes. Studies on the kinetics and mechanisms of the reactions accompanying structural relaxation belong to the third aspect. Unjustifiably little attention has been devoted in the literature to the mechanisms of these reactions as well as relaxation itself, which can be accounted for by the difficulties in the experimental study of these processes.

One of the first studies[48] was devoted to calculations of the probability of the emission of atoms from the cleavage surfaces of alkali metal halide crystals. An experimental investigation of rapid structural relaxation has been recently carried out by synchrotron radiation diffraction methods.[5] It may be hoped that the results will stimulate the formulation of further studies.

Nowadays all the available theoretical models are restricted to the analysis of the relaxation of a one-dimensional chain of atoms and the secondary reactions occurring after its rupture.[20] However, it is no less important that, under certain conditions, the energy liberated in the elementary reaction steps assumes the form of a compression wave (soliton), which initiates the reactions in the neighbouring cells, etc. Such self-supporting relay reactions began to be observed recently in both computer and physical experiments.[20]

2. The mechanisms of mechanochemical reactions

a. Degradation

In the study of the disordering of crystals of simple and complex substances, much attention is devoted to the problem of the degradation or dispersion limit. The term 'limit' is given to the smallest dimension of the crystal block or another fragment of the initial structure remaining unchanged under the conditions of prolonged mechanical treatment.

The ideas about the degradation limit (dispersion limit), based on the results of calculations of the strength of microcrystals, which previously seemed unshakeable, restricted mechanical dispersion to crystal fragment dimensions of tens of nanometers. However, it has been observed recently that for many isotypical crystals (face-centred cubic metals,[57] alkali metal halides[53]) the degree of disordering is greater the stronger the substance. This finding gave rise to interest in problems of the concentration of elastic energy, the determination of the degradation limit, and the study of the mechanisms of dispersion.

Recently the views on the nature of mechanical dispersion have begun to change.[25, 89] Instead of the disruption of individual microcrystals, the deformation of complex polycrystalline structures, threaded by intergrain boundaries and interfaces, is now analysed. From this point of view, the decrease in the size of microcrystalline blocks on plastic deformation is equivalent to an increase in the density of the network of dislocation boundaries. Hence follow a series of consequences important for a deeper understanding of both the processes occurring in the material and of the mechanisms of the chemical reactions.

Thus, in the migration of dislocations, combined into boundaries and 'sweeping' through the bulk of the crystal during their motion, work is expended on the reorganisation of the crystal structure accompanied by rearrangements of atoms, the production of defects, and other processes favouring chemical reactions.

The denser the network of boundaries, the larger the 'swept' volume. If in the course of the operation of stresses, the boundaries 'sweep' the entire or almost the entire volume of the substance, one may speak of the possibility, in principle, of a global deformation disordering of the crystals. The transition to such a 'deformation-transparent' state requires that the average distance between the boundaries L, virtually equal to the size of the crystalline blocks, should decrease to a critical value L_{cr} satisfying the condition:

$$L = L_{cr} \quad \text{when} \quad \dot{\varepsilon}_{cr} = \frac{1}{L}\frac{dL}{dt} = \frac{1}{\tau},$$

where τ is the duration of the operational stresses, and $\dot{\varepsilon}_{cr}$ the critical rate of deformation, which depends on many factors. The quantity $\dot{\varepsilon}_{cr}$ may be estimated from the equations of the theory of plasticity. It may be hoped that a rigorous theory of 'deformation transparency' will appear in the immediate future. It will then become possible to relate the observed dispersion limit not to the indivisibility of the nanocrystals but to the establishment of a dynamic equilibrium between the processes involving global disordering and spontaneous relaxation,[25, 89] which is induced by

the tendency of the substance to return to its natural ordered state (plastic deformation creates the mobility necesary for this purpose).

This incipient concept is much more fruitful for chemistry, since it removes the limitations to the scale of the mobility of the structural elements of the solid and draws attention to the extent of the possible chemical consequences of deformation processes in the regions corresponding to the motion of the intergrain boundaries and interfaces.

The possibility, in principle, of profound changes in the chemical and physical properties of substances on deformation should not encounter serious objections. Thus many inorganic crystals consist of species (ions) which are stable only in a powerful crystal field generated by the electrostatic interaction forces. When the deformation weakens the crystal field, then the species constituting the crystal also lose their stability and their properties change.

Thus the weakening of the crystal field in the narrow-band oxides GeO_2 and SnO_2 as a result of the disordering of the crystal structure is accompanied by a decrease in the width of the band gap with a corresponding change in physical and chemical properties: colour, conductivity, and reactivity, including catalytic activity.[51]

The examples examined demonstrate the extensive possibilities of the phenomenon of mechanical activation, to which several monographs have been devoted.[1,6,21,38] This field of research has a solid experimental basis and in future years one may expect the discovery, if not of new phenomena, then of new relations between the sensitivity of substances to mechanical loads and the change in reactivity on activation, on the one hand, and the nature of the interatomic bonds and the chemical structure of specific compounds, on the other.

b. Solid–solid reactions

The reactions between solid substances at a low temperature, carried out without preliminary dissolution, fusion, or sintering of the reactants, constitute one of the most promising branches of mechanochemistry, which, as before, has attracted the attention of investigators.

The mechanisms and kinetics of the processes in mixtures of solid reactants, where elastic stresses and chemical forces act simultaneously while the deformation and the reaction are closely intertwined, are not considered in either mechanics or chemical kinetics. Here there are no ready solutions from other branches of solid state physics and chemistry.

The kinetic description of solid-phase reactions is complicated by the fact that the dispersity, phase composition, and the defect structure and mechanical properties of the reaction medium vary continuously during its mechanical treatment.

The development of a theory of solid-phase reactions is still not complete. It is necessary that it should allow a description of the mechanisms and kinetics of solid phase reactions in such a way that they would permit the use in mechanochemistry of the large body of knowledge in classical thermochemistry. The problem is not quite so simple as might appear at first sight. Analysis of the results of the studies in recent years suggests the following logic for the development of the theory.

The interpenetration of atoms begins on the surface of contact of the components, so that the work involved in the formation of the interface is one of the important factors in the initial stage of the reaction. Together with elastic stresses, chemical forces operate here also; they in fact determine to a large extent the intensity of the mixing.[1,28,87,88] The results of computer experiments have revealed the specific role of chemical affinity in deformation mixing.[28] Experiment shows that the greater the energy of the mixing in the system

$$A + B \rightarrow AB,$$

and the more extensive the contact zones, the more complete and thorough the mixing.

The insertion of an atom A in a crystal B is hindered by a definite energy barrier. At a low temperature, this barrier is overcome by the action of elastic stresses. The barrier is lower, the greater the energy gain on interaction of the atoms A and B. Therefore, for the same level of elastic stresses, the probability of overcoming the barrier increases with increasing energy of mixing.

An excess energy accumulates in the reaction mixture during mechanical treatment. There are several carriers of this energy; these are the residual elastic stresses, interfaces, intergrain boundaries, amorphous regions, regions of supersaturated solid solutions, and other metastable structures. The accumulation of energy cannot be infinite, the accumulated energy being discarded at some stage and the structure of the reaction mixture becoming ordered. In mixtures of solid reactants, the equilibrium state to which the system passes on relaxation may prove to be the crystalline phase of the reaction products.[87,88] The more thorough the mixing and the higher the level of the stored energy, the greater the probability of the formation of the product phase on relaxation.

It may be expected that a two-stage mechanism of solid-phase reactions, namely deformation mixing–relaxation, will again attract the attention of investigators in the coming years. It is essential to select key parameters characterising the dynamics of the deformation mixing and the critical state of the reaction mixture, to examine the conditions under which mixing is replaced by relaxation, and to discover the specific mechanisms of the relaxation for substances with different types of interatomic bonds.[25,87,88]

Apart from deformation mixing, in real plastic materials it is necessary to take into account also diffusional processes, which may facilitate structural relaxation. Indeed, a dense network of interfaces and intergrain boundaries may play the role of accelerated-diffusion channels even in the absence of deformation. Furthermore, a decrease in the size of the microcrystalline blocks to 10^{-9}–10^{-8} m is equivalent to the shortening of the diffusion pathways (X) and of the duration of permeation (t) by many orders of magnitude ($t = X^2/D$). Therefore nanocrystalline particles become diffusionally transparent in reaction mixtures where the diffusion coefficient (D) is close to 10^{-20} m^2 s^{-1}.

Simultaneously with the theory of deformation mixing, the theory of quasi-explosive and explosive mechanochemical reactions in exothermic systems, where the energy liberated in relaxation processes is sufficient for the self-acceleration of the reaction, will develop. Furthermore, the range of reaction systems investigated will probably expand greatly.

The intense development of the mechanochemical synthesis of inorganic substances, intermetallic compounds, and alloys is associated with their successful employment in materials science (superconducting ceramics, heat resistant and ultrastrong materials, amorphous alloys, nanocrystalline materials, etc.). In creating such materials, it is important not only to synthesise a substance with a specified chemical constitution but also to achieve the specific formation of its structure. Mechanochemical methods make this possible.

The advantages of mechanochemical methods—ecological purity (the absence of solvents or annealing furnaces), simplicity, and the possibility of the chemical and structural modification of the product—are being comparatively slowly realised in organic chemistry. However, the first signs that such conservation attitudes will be soon overcome have already appeared: the mechanochemistry of medicinal drugs, the mechanochemistry of carbons, etc. has been developed. As time goes by, the efforts of investigators will be distributed uniformly between the mechanical syntheses of organic and inorganic substances. The search for methods of synthesis, optimal in mechanochemistry and unrelated to the mechanisms adopted in thermochemistry, will be continued.

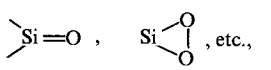
c. Gas–solid reactions

A fresh surface which is exposed following the disruption of a solid or produced as a result of friction is, as it were, designed for participation in chemical reactions. The atoms of such a surface

are coordinatively unsaturated and the problem is merely to select their partners in the reaction. Otherwise, the active surface ceases to exist in rearrangements and oxidation or hydration processes.

In order to account for the mechanisms of the chemical reactions occurring with participation of a freshly formed surface, it is essential to know the valence state of the atoms on this surface, their reactivity, and the rates of structural rearrangement (relaxation). These studies have already been combined in an independent field (mechanical chemisorption or tribosorption[9,21,51,56,85]).

Hitherto the majority of studies have been carried out for the freshly formed silicon dioxide surface.[9,56] Silicon and oxygen atoms with ruptured bonds ($\equiv Si^{\cdot}$, $=Si:$, $\equiv SiO^{\cdot}$) in the ground and electronically excited states, new atomic groups



deformed siloxane linkages, and other centres have been detected on it. The electronic structure and constitution of these fragments have been described and measurements have been made of the rate constants for the reactions of the principal centres with gases and their course has been determined. The nature and properties of the active surfaces of ionic oxides, graphite, silicon, and individual metals have also been investigated.

It has recently become clear that the spectrum of nonequilibrium chemically reactive states is much wider than appeared previously. The energy liberated on reaction with gases is sufficient to excite the electronic subsystem of the crystals with ejection of fragments comprising complex anions, emission of electrons, including those with energies up to tens of kiloelectronvolts[15]), and also the emission of neutrons on disruption of deuterium-containing crystals.[53] The theory of mechanoemission phenomena continues to be developed (see, for example, Molotskii[30]) and the experimental and theoretical studies in this interesting field will continue for many decades.

The chemisorption of gases on a freshly formed surface is widely used as a kind of instrument for the determination of the degree of damage of the crystal structure. Chemisorption is the first stage in the interaction of solids with gases; however, solid–gas reactions are not always restricted to monomolecular surface coverage. Three examples of a more far-reaching development of these reactions are presented below.

Thus volatile carbonyl complexes are formed on the active surface of nickel in the presence of CO, nickel pentacarbonyl being desorbed from the metal surface into the gas phase. The renewal of the surface continues until almost the entire metal has been converted into $Ni(CO)_5$.[21]

Molecules of gases such as N_2, NH_3, O_2, CO, and others dissociate into atoms on chemisorption, as a result of which surface compounds are stabilised on the active surface.[9] On plastic deformation and friction, increasing numbers of fresh atoms from the bulk of the solid particles are carried to the surface, where they interact with the gas. The repeated renewal of the surface in the gaseous atmosphere leads ultimately to the formation of the solid–gas reaction product phase (the corresponding nitride, oxide, or another compound).[82]

Reactions of yet another type have been discovered in the $Zr-(H_2+CO)$ and $Zr-(H_2+C)$ systems.[83,85] Thus mechanical treatment of zirconium powder promotes the acceleration of the dissolution of hydrogen in it. The hydrogen dissolved in the metal hydrogenates either the CO molecules which have been chemisorbed on the surface or the graphite added to the hydride powder. The reaction

$$CO + H_2 \rightarrow CH_4,$$

during the mechanical treatment of the metal powder under a $(CO+H_2)$ atmosphere can be regarded as the prototype of future mechanocatalytic processes.

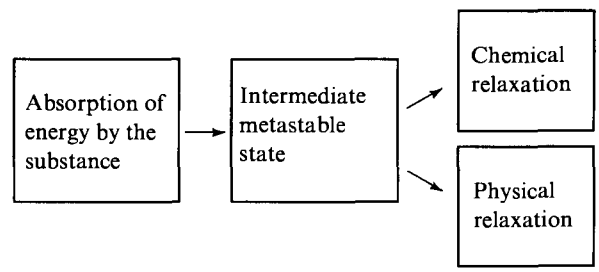
There is no doubt that examples of solid–gas and solid–liquid reactions will multiply in the immediate future and that the first hypotheses concerning their mechanisms will be revised or rejected. Conditions ensuring a high effectiveness of low-temperature mechanical reactions between solids and the external medium will be found on the basis of the study of these reactions. The reactions can be used not only for the chemical syntheses but also in catalysis and in the modification of solid surfaces—their stabilisation, improvement of their corrosion resistance, etc.

It is noteworthy that phenomena involving mechanical chemisorption, catalysis, and synthesis are part of the more general problem of the interactions of the solid undergoing deformation and the external medium. Here mechanochemistry will become ever more closely intertwined with physicochemical mechanics and colloid chemistry.[34] These sciences are concerned with the study of the effect of the medium on processes involving the mechanical treatment of solids—their disruption (dispersion, friction, and plastic deformation (the Rebinder effect). Therefore all the manifestations of chemical reactivity, reflecting the development of deformation and revealing the dissipation of elastic energy, are equally interesting for both mechanochemistry and for different manifestations of the Rebinder effect (strengthening or facilitation of disruption, etc.).

3. Kinetic models of mechanochemical reactions

One of the principal problems in the theory of nonthermal chemical reactions is the elucidation of the relation between the expenditure of energy and the reactivity of the reactants. The current state of research does not permit the establishment of a complete balance for the energy transformations, while a quantitative description of all the relaxation pathways in mechanochemical reactions is hardly likely to be achieved soon.

The route involving the search for a kinetic description of nonthermal reactions appears more realistic. Among those possible, the following scheme remains more attractive:



It is similar to that presented at the very beginning of the review. The kinetic equation corresponding to this scheme has the following form:

$$\frac{\delta\Delta\varphi}{\delta t} = I - \frac{\Delta\varphi}{\tau_{chem}} - \frac{\Delta\varphi}{\tau_{phys}},$$

where $\Delta\varphi$ is the excess energy of the intermediate states (it can be represented as $\Delta\varphi = N\varphi g$, where N is the concentration of excess energy carriers, and φ and g are their energy and yield), I is the supplied energy flux, τ_{chem} is the characteristic chemical relaxation time, and τ_{phys} is the characteristic physical relaxation time. Chemical relaxation is understood as the employment of part of the excess energy in chemical or physicochemical reactions, while physical relaxation includes the remaining energy dissipation channels.

Under stationary conditions, the rate of a chemical reaction W_{chem} is

$$W_{chem} = Ig\frac{\tau_{phys}}{\tau_{phys} + \tau_{chem}},$$

and its energy yield G_{chem} is given by

$$G_{chem} = \frac{W_{chem}}{I} .$$

Evidently, the advantage of this scheme consists in the fact that it makes it possible to relate the conditions in the mechanical treatment, the rate of the chemical reaction, and its energy yield G (in mol MJ^{-1}). Naturally, in each specific case the scheme will be specified in greater detail and expanded. However, the above advantage will be preserved.

The energy yield G is one of the principal quantitative characteristics of mechanochemical reactions.[9] It can be calculated or predicted, provided that the mechanism or physical model of the process is known. For example, if the height of the energy barrier is E in the elementary step of a nonthermal reaction, then the maximum energy yield G_{max} is given by $G_{max} = 1/E_a$. For the experimental determination of the yield, it is sufficient to measure the amount of products and the work performed.

As a rule, in degradation reactions the energy yield is small and lies in the range from 10^{-4} to 10^{-1} mol MJ^{-1}. Its numerical value characterises the sensitivity of the given compound to mechanical influences. The generation of defects is (with rare exceptions) an energy-consuming process. Systems in which chain degradation develops or there is a possibility of other self-acceleration mechanisms are an exception.

Deformation mixing and synthesis are usually characterised by comparatively high yields — up to 1–10 mol MJ^{-1}. Even in the most difficult case involving the mixing of tungsten with iron (Fig. 5), the yield is 0.1 mol MJ^{-1}. Naturally, the yield depends on the conditions in the mechanical treatment — the rate of deformation and the frequency of the influences, temperature, the nature of the surrounding medium, and other factors.

The measurements and calculations of the energy yields lead to the possibility of using in mechanochemistry data banks comprising the kinetic and thermodynamic characteristics of thermochemical reactions. For example, the relation $G_{max} = 1/E_a$ includes the activation energy for the reaction. A correlation between G and thermodynamic parameters in a series of isotypical reactions has been observed more than once.[1] It may be hoped that systematic measurements and calculations and analysis of the energy yields will lead to the creation of a quantitative picture of mechanochemical reactions which will possess predictive power.

* * *

Summarising the results of numerous studies on mechanochemistry, one may differentiate several aspects of fundamental investigations with which the development and further progress in this interesting and promising field of knowledge are associated.

These include primarily the following:

the discovery of the molecular mechanisms of the deformation of simple and complex substances as well as their mixtures combined with the elucidation of the nature of the intermediate nonequilibrium states;

the kinetic description of the mechanical degradation, atomic migration, and molecular mixing processes as well as chemical reactions involving the formation of new crystalline or amorphous structures under deformation and energy dissipation conditions;

the study of the relation between thermal and nonthermal reactions in which the energy barrier is overcome either via a thermal fluctuation mechanism or under the influence of elastic stresses.

Altogether, these aspects are combined into the problem of the systematic description of the laws governing chemical reactions under the conditions of the joint action of mechanical and chemical forces.

References

1. E G Avvakumov *Mekhanicheskie Metody Aktivatsii Khimicheskikh Protsessov* (Mechanical Methods for the Activation of Chemical Processes) (Novosibirsk: Nauka, 1986)
2. G A Adadurov, V I Gol'danskii, P A Yampol'skii *Zh. Vses. Khim. O-va im. D I Mendeleeva* **18** 80 (1973)
3. N K Baramboim *Mekhanokhimiya Vysokomolekulyarnykh Soedinenii* (Mechanochemistry of High-Molecular-Mass Compounds) (Moscow: Khimiya, 1978)
4. V V Boldyrev *Izv. Akad. Nauk SSSR, Ser. Khim.* 2228 (1990)
5. V V Boldyrev, N Z Lyachov, Yu T Pavlyukchin, E V Boldyreva, E Yu Ivanov, E G Avvakumov *Sov. Sci. Rev. B, Part 3* **14** 105 (1989)
6. V V Boldyrev *Eksperimental'nye Metody v Mekhanokhimii Tverdykh Neorganicheskikh Veshchestv* (Experimental Methods in the Mechanochemistry of Solid Inorganic Substances) (Novosibirsk: Nauka, 1983)
7. V A Bershtein *Mekhanogidroliticheskie Protsessy v Napryazhennykh Tverdykh Telakh* (Mechanohydrolytic Processes in Stressed Solids) (Leningrad: Nauka, 1987)
8. P Bridgman *Phys. Rev.*, **48** 825 (1935)
9. P Yu Butyagin *Sov. Sci. Rev. B, Part 1* **14** 1 (1989)
10. P Yu Butyagin, in *Mekhanokhimicheskii Sintez v Neorganicheskoi Khimii: Sb. SO AN SSSR* (Mechanochemical Syntheses in Inorganic Chemistry: Collected Papers. Siberian Division of the Academy of Sciences of the USSR) (Ed. E G Avvakumov) (Novosibirsk: Nauka, 1991) p. 32
11. M V Vlasova, N G Kakazei *Elektronnyi Paramagnitnyi Rezonans v Mekhanicheski Razrushennykh Tverdykh Telakh* (Electron Paramagnetic Resonance in Mechanically Disrupted Solids) (Kiev: Naukova Dumka, 1979)
12. I A Chint, in *Desintegrator* (Tallin: Valgus, 1979) Vol. 1, p. 3
13. E M Gutman *Mekhanokhimiya i Zashchita Metallov ot Korrozii* (Mechanochemistry and Protection of Metals against Corrosion) (Moscow: Metallurgizdat, 1981)
14. A Casale, R S Porter *Polymer Stress Reactions* Vols 1, 2 (New York: Academic Press, 1978, 1979)
15. B V Deryagin, N F Krotova, V P Smilga *Adgeziya Tverdykh Tel* (Adhesion of Solids) (Moscow: Nauka, 1973)
16. A M Dubinskaya *Sov. Sci. Rev. B, Part 3* **14** 37 (1989)
17. A E Ermakov *Fiz. Met. Metalloved.* 11 (1991)
18. A A Zharov *Zh. Vses. Khim. O-va im. D I Mendeleeva* **18** 73 (1973)
19. H G Flinn, in *Physical Acoustics: Principles and Methods* (Ed. W P Mason) (New York: Academic Press, 1964) Vol. 1, Part B, p. 7
20. L S Zarkhin, S V Sheberstov, N V Panfilovich, L I Manevich *Usp. Khim.* **58** 644 (1989) [*Russ. Chem. Rev.* **58** 381 (1989)]
21. G Heinike *Tribochemistry* (Berlin: Academie-Verlag, 1987)
22. H H Kaush *Polymer Fracture* (Berlin: Springer, 1978)
23. T M Kchrenkova *Sov. Sci. Rev. B, Part 3* **14** 1 (1989)
24. C C Koch *Annu. Rev. Mater. Sci.* **19** 123 (1989)
25. C C Koch *Nanostruct. Mater.* **2** 109 (1993)
26. E G Avvakumov (Ed.) *Mekhanokhimicheskii Sintez v Neorganicheskoi Khimii: Sb. SO AN SSSR* (Mechanochemical Syntheses in Inorganic Chemistry: Collected Papers. Siberian Division of the Academy of Sciences of the USSR) (Novosibirsk: Nauka, 1991)
27. E A Margulis *Zvukokhimicheskie Reaktsii i Sonolyuminestsentsiya* (Sonochemical Reactions and Sonoluminescence) (Moscow: Nauka, 1986)
28. P H Shingu (Ed.) *Mechanical Alloying, Mater. Sci. Forum* **88–90** (1992)
29. P Yu Butyagin (Ed.) *Mekhanokhimicheskii Sintez* (Mechanochemical Synthesis) (Vladivostok: Izd. Dal'nevost. Gos. Univ., 1990)
30. M I Molotskii *Sov. Sci. Rev. B, Part 3* **13** 1 (1989)
31. A Popov, N Rapoport, G Zaikov *Oxidation of Stressed Polymers* (New York: Gordon and Breach, 1991)
32. A A Popov, G E Zaikov, in *Polymer Yearbook* (Ed. R A Pethrick) (London: Harwood Acad. Publ.) Vol. 10, p. 257

33. A Popovich, V Vasilenko, in *Mekhanokhimicheskii Sintez v Neorganicheskoi Khimii: Sb. SO AN SSSR* (Mechanochemical Syntheses in Inorganic Chemistry: Collected Papers. Siberian Division of the Academy of Sciences of the USSR) (Ed. E G Avvakumov) (Novosibirsk: Nauka, 1991) p. 168
34. P A Rebinder, E D Shchukin *Usp. Fiz. Nauk* **108** 3 (1972)
35. V R Regel', A I Slutsker, E E Tomashevskii *Kineticheskaya Priroda Prochnosti Tverdykh Tel* (The Kinetic Nature of the Strength of Solids) (Moscow: Nauka, 1974)
36. A N Streletskii, A B Borunova, N P Kozina, V I Lapshin, P F Relushko, in *Mekhanokhimicheskii Sintez v Neorganicheskoi Khimii: Sb. SO AN SSSR* (Mechanochemical Syntheses in Inorganic Chemistry: Collected Papers. Siberian Division of the Academy of Sciences of the USSR) (Ed. E G Avvakumov) (Novosibirsk: Nauka, 1991) p. 66
37. *The First International Conference on Mechanochemistry: Proceedings, INCOME Košice, Slovakia 1993* (Ed. K Tkačova)
38. K Tkačova *Mechanical Activation of Minerals* (Amsterdam: Elsevier, 1989)
39. *The Second International Conference on Mechanical Alloying for Structural Applications: Proceedings. ASM International, Materials Park, Ohio, 1993* (Eds J J Barbadillo, F H Froes, R B Schwarz)
40. R B Schwarz, in *Synthesis and Consolidation of Amorphous, Metallic Powders. Rapidly Solidified Alloys* (Ed. H Lieberman) (New York: Marcel Dekker, 1993) p. 157
41. K S Suslik *Science* **247** 1439 (1990)
42. A W Weber, H Bakker *Physica* **153** 95 (1988)
43. L S Zarkhin, L I Manevich, N S Enikolopyan *Macromol. Chem. Macromol. Symp.* **26** 431 (1989)
44. B E Krysyuk, E V Polianchik *Khim. Fiz.* **12** 253 (1993)
45. A I Gubanov *Mekh. Polim.* (5) 771 (1978)
46. V A Radtsig, V S Pudov, P Yu Butyagin *Vysokomol. Soedin., Ser. B* **9** 414 (1967)
47. V V Boldyrev *Kinet. Katal.* **13** 1411 (1972)
48. L M Belyaev, Yu N Martyshev, Yu Ya Yushin *Acta Phys. Acad. Sci. Hung.* **33** 307 (1973)
49. A M Dubinskaya, A N Streletskii *Vysokomol. Soedin., Ser. A* **24** 1924 (1982)
50. K B Abramova, Doctoral Thesis in Physicomathematical Sciences, Ioffe Physicotechnical Institute, St Petersburg, 1991
51. A A Bobyshev, Candidate Thesis in Physicomathematical Sciences, Institute of Chemical Physics, Academy of Sciences, Moscow, 1983
52. R B Whitworth *Adv. Phys.* **24** 233 (1975)
53. V A Kuznetsov, A G Lipson, D M Sakov *Zh. Fiz. Khim.* **67** 782 (1993); A G Lipson, V A Kuznetsov, B V Deryagin *Dokl. Akad. Nauk SSSR* **318** 636 (1991)
54. G V Abagyan, P Yu Butyagin *Biofizika* **10** 763 (1965)
55. G V Abagyan, P Yu Butyagin *Vysokomol. Soedin., Ser. A* **26** 1311 (1984)
56. V A Radtsig *Izv. Sib. Otd. Akad. Nauk, Ser. Khim.* (5) 60 (1987)
57. J Eckert, J C Holzer, C E Krill, W L Jonson, in *Mechanical Alloying* (Ed. P H Shingu) *Mater. Sci. Forum* **88–90** 505 (1992)
58. P Butyagin, V Radzig *Plaste Kautsch.* **19** 81 (1972)
59. V V Neverov, V N Burov *Fiz. Met. Metalloved.* **46** 978 (1989)
60. S Surinach, M D Barro, J Segura, Clavaguera-Mora *Mater. Sci. Eng. A* **134** 1378 (1991)
61. K Susuki, M Sherif El-Eskanrdarany, K Aoki, in *Mechanical Alloying* (Ed. P H Shingu) *Mat. Sci. Forum* **88–90** 81; 325; 339; 801 (1992)
62. K Susuki, M Sherif El-Eskanrdarany, K Aoki *J. Non-Cryst. Solids* **150** 472 (1992)
63. K Susuki, M Sherif El-Eskanrdarany, K Aoki *Metal. Trans.* **23A** 2133 (1992)
64. K Susuki, M Sherif El-Eskanrdarany, K Aoki *J. Appl. Phys.* **72** 2665 (1992)
65. P F Relushko, I V Berestetskaya, P Yu Butyagin, L I Trusov, V I Novikov, V V Moskvin *Zh. Fiz. Khim.* **64** 2858 (1990)
66. A O Aning, Z Wang, T H Courtney *Acta Metall. Mater.* **41** 165 (1993)
67. E Yu Ivanov, in *Mekhanokhimicheskii Sintez v Neorganicheskoi Khimii: Sb. SO AN SSSR* (Mechanochemical Syntheses in Inorganic Chemistry: Collected Papers. Siberian Division of the Academy of Sciences of the USSR) (Ed. E G Avvakumov) (Novosibirsk: Nauka, 1991) p. 190
68. V I Fadeeva, A V Leonov, in *Mechanical Alloying* (Ed. P H Shingu) *Mater. Sci. Forum* **88–90** 481 (1992)
69. D S Tipikin, Candidate Thesis in Physicomathematical Sciences, Moscow Physicotechnical Institute, Moscow, 1993
70. D S Tipikin, Ja S Lebedev, O G Poluectov, J Schmidt *Chem. Phys. Lett.* **215** 199 (1993)
71. R W Rydin, D Maurice, T H Courtnay *Metal. Trans.* **24A** 175 (1993)
72. P A Vityas, A A Kolesnikov, A A Stephanovich, V F Nozdrin, in *Mechanical Alloying* (Ed. P H Shingu) *Mater. Sci. Forum* **88–90** 619 (1992)
73. M Atzmon *Phys. Rev. Lett.* **64** 487 (1990)
74. A A Popovich, V P Reva, V Vasilenko, O A Belous, in *Mechanical Alloying* (Ed. P H Shingu) *Mater. Sci. Forum* **88–90** 737 (1992)
75. V Rusanov, Chr Chakurov *J. Solid State Chem.* **79** 181 (1989)
76. G B Schaffer, P G McCormick *Metal. Trans.* **21A** 2789 (1990)
77. Chr G Tschakarov, Doctoral Thesis, Burgas, Bulgaria, 1983
78. Chr G Tschakarov, G G Gospodinov, Z Bontschev *J. Solid State Chem.* **41** 244 (1982)
79. Chr Tschakarov, V Rusanov, G G Gospodinov *J. Solid State Chem.* **59** 265 (1985)
80. Chr Chakurov, V Rusanov, J Koichev *J. Solid State Chem.* **71** 522 (1987)
81. K B Shelimov, P Yu Butyagin *Dokl. Akad. Nauk SSSR* **316** 1439 (1991)
82. A Calka, J I Nikolov, B V Ninham, in *The Second International Conference on Mechanical Alloying for Structural Applications: Proceedings, ASM International, Materials Park, Ohio 1993* (Eds J J Barbadillo, F H Froes, R B Schwarz) p. 189
83. P Yu Butyagin, A N Streletskii, O S Morozova, I V Berestetskaya, A B Borunova *Dokl. Akad. Nauk* **336** 771 (1994)
84. M Senna, K Okamotu *Solid State Ion* **32/33** 453 (1989)
85. G Cocco, G Mulas, M Pintore, G Piliu, L Schiffini *The Second International Conference on Mechanical Alloying for Structural Applications: Proceedings, ASM International, Materials Park, Ohio, 1993* (Eds J J Barbadillo, F H Froes, R B Schwarz)
86. M Magini, in *Mechanical Alloying* (Ed. P H Shingu) *Mat. Sci. Forum* **88–90** 121 (1992)
87. P Yu Butyagin *Dokl. Akad. Nauk SSSR* **319** 384 (1991)
88. P Yu Butyagin *Dokl. Akad. Nauk* **331** 311 (1993)
89. A R Yavari, P J Desre *Phys. Rev. Lett.* **65** 2571 (1990)

Russian Chemical Reviews **63**(12) 977–995 (1994) ©1994 Russian Academy of Sciences and Turpion Ltd

UDC 620.193.01

Physical chemistry of the dissolution of metals

G V Khaldeev

Contents

I.	Introduction	977
II.	Dissolution and adsorption of surface-active impurities on low-angle boundaries and on grain boundaries	979
III.	Distribution of dislocations in near-surface layers of crystals	980
IV.	Current and potential oscillations during grain-boundary dissolution	983
V.	Intercrystallite corrosion	985
VI.	Dissolution of heterophase polycrystalline metals	990
VII.	Conclusion	994

Abstract. New theoretical and experimental data on the grain-boundary dissolution process in polycrystalline metals are reviewed. The original effects during transcrystallite dissolution are discussed, the basic models are analysed, and the localisation mechanism of the dissolution process on the phase bondaries of polycrystals is described. The bibliography includes 86 references.

I. Introduction

Internal boundaries in metallic crystals include low-angle boundaries formed by dislocations, grain boundaries (GB), and phase boundaries between inclusions and the matrix. In addition to the creation of strong fields due to the elastic distortion of the metal lattice (M), chemical heterogeneity is a characteristic property of these defects of the solid state. The electrochemical etching effect is observed during the dissolution of these structures.

Among nonequilibrium planar solid-state defects, the grain boundaries play a major role in the corrosion – mechanical erosion of metals. At present the metallographic evaluation of the grain composition of polycrystalline metals is based on the selective acceleration of the etching process by the grain boundaries. The role of GB is most marked during intercrystallite corrosion, and has been studied extensively.[1–4] All these workers tried to relate the differences in chemical composition of the grain-boundary region to its enhanced rate of dissolution.

From the practical point of view the effect of the grain-boundary segregation of hydrogen on the corrosion of metals is of the greatest interest, because hydrogen (the most mobile impurity in metals) can form new hydride phases on the GB and also influence their penetrability as barriers to the passage of dislocations through the boundary during plastic deformation. By using the grain boundary theory we can obtain a quantitative estimate of the contribution of GB to the corrosion, and present a physical picture of the dissolution of polycrystals. The formation of a stable fractal structure (a closed network of etched grain boundaries) strengthens the resistance of a solid to an aggressive medium. The dissolution of surface mechanical stress raisers improves the physical and mechanical properties of metallic items. The unique adsorption properties of GB allow the use of this effect in metallurgy, microelectronics, and other technological areas.

Paradoxically, the blocking of the dissolution of grain boundaries by an inhibitor (surface-active substance, impurity, etc.) has not yet attracted adequate theoretical studies, in spite of the striking advances which have been made in our understanding of the structure of the GB (see the work of Gleiter, Baluffi, Chadwick, Orlov, and others),[5–9] and also of the great practical importance of grain-boundary dissolution. In the representation of high-angle GB, regions of bad and good coincidence have been described [10] by various models: the coincident block lattice (CBL), the grain boundary displacement lattice (GDL), and the full overlap lattice (FOL). Grain boundaries are not a layer of amorphous material, and they can be modelled by the coincident block lattice structure with appropriate parameters.[11]

In the CBL model the grain boundaries are classified as general or special. A special GB in this model has a well defined period, characterised by the reciprocal bulk density of the coincident blocks (Σ). In body-centred (BCC) and in face-centred cubic crystals (f.c.c.) a distinction is made[10] between low-energy ($\Sigma = 3, 9, 11, 17, 27,$ and 33) and high-energy GB (Σ = 5, 7, 13, and 15). The structural model of the GB can be approximated by the model of close packed structural units (Voronyi polyhedra).

Body-centred polyhedra form vacancy-saturated loose regions in the crystal when linked. Boundaries of a general type are adequately described by the structural units model, and they include regions with a periodic structure separated by grain-boundary dislocations. In the presence of external stimuli point defects and line defects are always formed on polycrystals. Subgrain low-angle boundaries are assumed to consist of dislocation networks. There are substantial differences between the dissolution mechanisms of low-angle boundaries and of grain boundaries.

The object of the present review is to analyse the results of studies of the effect of internal boundaries in polycrystals on the phase interaction processes at metal–electrolyte contacts. The need to review these data arose because of the appearance of new models of the dissolution of GB, and of the availability of reliable experimental results on the chemistry of GB and of phase interfaces.

G V Khaldeev A M Gorky Perm State University, 15 ul. Bukireva, 614 600 Perm, Russian Federation. Fax (7-3422) 33 80 14

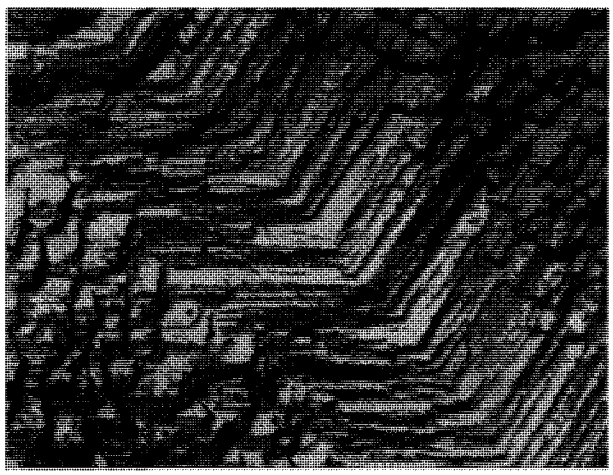
Received 19 August 1994
Uspekhi Khimii **63** (12) 1044–1063 (1994); translated by J I Carasso

II. Dissolution and adsorption of surface-active impurities on low-angle boundaries and on grain boundaries

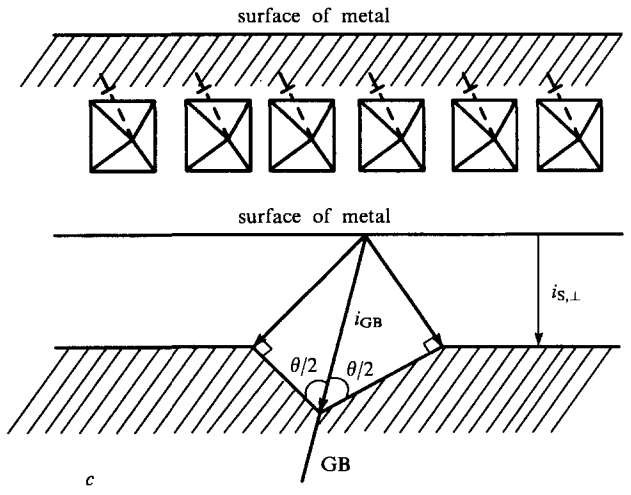
Subsurface dislocations induce the formation of three-dimensional clusters on the crystal surface, which inhibit the action of impurities. Dislocation planes arranged as elastic networks form low-angle boundaries with a misorientation angle $\theta = 2\arcsin(\boldsymbol{b}/2l_d)$, where $\boldsymbol{b}$ is the Burgers vector and l_d is the distance between dislocations. The internal fractal structure of these dislocation networks can be seen on the surface of the crystal as a group of dislocation etch pits (EP) (Fig. 1*a*), the distance between etch pits being an approximate measure of the parameter l_d, from which the misorientation angle θ can be determined. A new phase formed on low-angle boundaries is accommodated in the structure with a specific fractal dimensionality. The dissolution on grain-boundary dislocations for which $l_d > 2\boldsymbol{b}$ is described within the theory developed, for example, in Refs 4 and 12. If the grain-boundary dislocations merge together and lose their individuality, etch grooves are formed on the GB (Fig. 1*b*). The dissolution follows different paths on interblock low-angle ($\theta < 3°-5°$) and high-angle boundaries ($\theta > 15°$) (Fig. 1*c*).



a



b



c

Figure 1. Dissolution on a low-angle boundary (*a*) and the boundary of nickel grains (*b*) (× 12 000) together with a schematic illustration of the grain-boundary dissolution (*c*).

A model of the dissolution on high-angle GB in the simplest form (but corresponding to experimental observations) can be constructed as follows.[13,14] In a pure (>99.99%) bicrystal dissolution along a GB (see Fig. 1*b*) takes place as a result of the generation of dissolution steps whose density depends on the angle θ. The relationship between the dissolution rate (or current) along the plane of the grain boundary i_{GB} and the dissolution rate (or current) normal to the metal surface $i_{S,\perp}$ (see Fig. 1*c*) is the following:

$$\frac{i_{GB}}{i_{S,\perp}} = \frac{1}{\sin(\theta/2)} , \tag{1}$$

$$\Delta i = i_{GB} - i_{S,\perp} = a_S + b_S i_{S,\perp} , \tag{2}$$

for $\lim i_{GB} \to \infty$, $\dfrac{i_{GB}}{i_{S,\perp}} = \dfrac{1}{\sin(\theta_0/2)}$ and $b_S = \dfrac{1}{\sin(\theta_0/2)} - 1$,

for $\lim i_{S,\perp} \to 0$, $i_{GB} \to i_{GB,0}$ and $a_S = i_{GB} = i_{GB,0}$.

Here θ and i_{GB} are the limiting angle and the grain-boundary current, independent of the dissolution of the bulk of the grain, i.e. they are the characteristic parameters of the grain-boundary dissolution.

In the absence of passivation of the grain surface, the rate (or current) of the dissolution on a GB is described by the Marcus formula

$$i_{GB} = i_{GB,0} + \frac{1}{\sin(\theta_0/2)} i_{S,\perp} . \tag{3}$$

By use of the fundamental kinetic equation for the electrochemical dissolution current, Eqn (3) can be expressed in terms of experimentally determined electrochemical parameters. We shall write the Marcus formula[15] as

$$i = K\frac{k_B}{h_p}\frac{Tz^{\neq}}{z}a_0^0 \exp\frac{-\Delta\bar{G}^{\neq}}{RT}\exp\frac{\alpha F\Phi}{RT}\exp\frac{(a-n)F\Phi_1}{RT} , \tag{4}$$

where K is the rate constant for the reaction, $(k_BT/h_p)^{-1}$ is the lifetime of the activated complex (Ac) between the adparticle and a surface atom of the metal (and k_B is Boltzmann's constant), $z^{\neq}$ and z are the partition functions referred to unit volume of the AC and of the reactants in the electrolyte, a_0^0 is the activity of the AC, $\Delta G^{\neq}$ is the nonelectric part of the free energy of activation at low coverages of the metal surface by adparticles, F is the Faraday, Φ is the electron work function, n is the valency of the Ox species in solution, a is the transfer coefficient of the electrode reaction, and Φ_1 is the potential step in the diffuse part of the electrical double layer (EDL).

We simplify Eqn (4) to

$$i = Kc\exp\frac{-[\alpha F(\Phi - \Phi_1) + nF\Phi_1]}{RT} . \tag{5}$$

Here $c = (k_B T_{Z^*}/h_p x) a_0^0 \exp(-\Delta\bar{G}^{\neq}/RT)$ is a term corresponding to the formation of active centres (Ac) on the surface; $(\Phi - \Phi_1)$ is the potential of the electrode relative to the outer coating of the Helmholtz reaction layer. By using formulae (4) and (5), the expression (1) can be converted into

$$\frac{i_{GB}}{i_{S,\perp}} = \frac{K_{GB}}{K_{S,\perp}} \frac{c_{GB}}{c_{S,\perp}} \frac{\exp\{-[\alpha F(\Phi - \Phi_1) + nFF_1]/RT\}_{GB}}{\exp\{-[\alpha F(\Phi - \Phi_1) + nFF_1]/RT\}_{GB}}$$

$$= \frac{1}{\sin(\theta/2)} = \frac{c_{GB}}{c_{S,\perp}} . \quad (6)$$

At high current densities ($i_{S,\perp} \to \infty$):

$$\frac{c_{GB}}{c_{S,\perp}} \to \exp\frac{-\Delta_{GB}(\Delta\bar{G}_0^{\neq})}{RT} = \frac{1}{\sin(\theta/2)} , \quad (7)$$

where $\Delta_{GB}(\Delta\bar{G}_0^{\neq}) = \Delta\bar{G}_{0,GB}^{\neq} - \Delta G_{0,S,\perp}^{\neq}$ is the difference between the energies of formation of the Ac on the grain boundary and on the bulk of the grain. For example, this difference, determined for the Ni/1 M H_2SO_4 system at 298 K, was 32 mJ m^{-2} for a GB with $\theta = 104°$. The dissolution current on the GB, independent of the corrosion current in the bulk of the grain [the first term in formula (3)], is determined by the expression

$$i_{GB,0} = a_{GB}^* i_{0,S,\perp} \exp\frac{-\Delta_{GB}(\Delta\bar{G}^{\neq})}{RT} , \quad (8)$$

where a_{GB}^* is the activity of the surface-active centres distributed over the GB (from the physical point of view it is the surface activity of the grain-boundary dislocations). The trapped lattice dislocations increase the energy of the GB by an amount equal to the elastic field of the dislocations:[16]

$$\Delta E \cong \frac{G_c b^2}{4\pi(1-\nu)2l_d} \ln\frac{e\alpha l_d}{\pi b} , \quad (9)$$

where G_c is the shear modulus, ν is Poisson's ratio, e is the base of natural logarithms, α (= 1–2) is the energy parameter of the dislocation core, and l_d is the distance from the dislocation to the surface. For a given polycrystal, the parameter ΔE depends also on Σ and θ. The corrosion activity of the GB in very pure polycrystals varies periodically with the number of dislocations absorbed (ρ_d) and with the misorientation angle (θ), thus influencing the adsorption properties of both the GB themselves and the adjacent grain-boundary volumes.

The adsorption properties of the grain-boundary volumes affect the dissolution process. The adsorption on the GB is examined both 'from inside' (from the bulk of the grain) and 'from above' (from the interface). The adsorption 'from inside' is produced by the diffusional inflow of impurities on the GB and obeys the expression

$$\frac{c(t) - c_0}{c_\infty - c_0} = 1 - \exp\frac{-4Dt}{(\Delta\gamma^{\neq})^2 d^2} \operatorname{erfc}\frac{2(Dt)^{1/2}}{d\Delta\gamma^{\neq}} , \quad (10)$$

where $c(t)$ is the concentration of impurities on the GB at time t, c_0 and c_∞ are the initial and the equilibrium concentration of impurities on the GB, $\Delta\gamma^{\neq} \cong (\exp\Delta H)/k_B T$ is the supersaturation, ΔH is the enthalpy of the GB–impurity bond, D is the coefficient of diffusion of the impurity in the crystal, and d is the thickness of the GB. For hydrogen $D_H = 1 \times 10^{-8} - 1 \times 10^{-9}$ m^2 s^{-1} and $\Delta H = 10 - 60$ kJ mol^{-1}. Deformation of the polycrystal can induce the accumulation of impurities on the GB by dislocational transport.[17] Moving dislocations adsorb the impurities and transport them over the GB. The dislocational permeability of the GB is determined by the angle θ, and the chemical properties of the GB vary accordingly.

The equilibrium segregation of the impurities (added atoms or originally present impurities) on the GB can be described[17] by the Fermi–Dirac distribution

$$c = c_{0,L} \exp\frac{\Delta G_a}{RT}\left(1 + c_{0,L}\exp\frac{\Delta G_a}{RT}\right)^{-1} = c_0 \exp\frac{\Delta H}{RT} , \quad (11)$$

where $c_{0,L}$ is the equilibrium concentration in the solution and ΔG_a is the difference in free energy between the additives dissolved in the GB and in the crystal lattice. The enthalpy ΔH of the bond between the grain-boundary surface and the surface-active impurity species (similar in size to the atoms of the crystal) is in the range of 150–200 kJ mol^{-1} for the 3d metals. The adsorption on the GB can be calculated by using the Gibbs concepts of reversible adsorption and of the decrease in the surface tension of the grain boundaries produced by the creation of a surface excess. According to the Gibbs formula

$$d\gamma = Vdp - SdT - \sum_i \Gamma_i d\mu_i \quad (i = K^+, A^-, M^{n+}, e^-) , \quad (12)$$

where V and S are, respectively, the volume and the entropy of the adsorbed layer of the quasicrystalline phase of surface-active substance, Γ_i is the coverage of the metal surface by particles of the ith kind (Gibbs adsorption), $\mu_i = k_B T \ln c(x) + E(x) + \text{const}$ is the chemical potential of the ith species, $E(x)$ is the energy of the attractor, $\mu_0 \equiv E(x) + \text{const}$, K^+ and A^- are the cation and the anion of the supporting electrolyte, M^{n+} is the charged metal ion, and e^- is the electron. By using the Gibbs formula and the distribution (11) we can obtain an expression for the decrease in surface tension:

$$\Delta\gamma = \gamma_{GB} - \gamma_B = RT\,\theta_{GB} \ln\left(1 + c_0 \exp\frac{\Delta G_a}{RT}\right) . \quad (13)$$

Here γ_B is the absolute energy of formation of the GB, θ_{GB} is the coverage of the GB by impurity particles, and c_0 is the background concentration. The decrease in γ_{GB} is used to calculate $\Delta G_a = \Delta E_a - T\Delta S_a$, where ΔE_a and ΔS_a are the energy and the entropy change of the interaction of the surface-active impurity with the GB. Under equilibrium conditions the chemical potentials of the ith species (SAS particles) on the free metal surface (μ_S), on the grain boundary (μ_{GB}), and in the solution (μ_B) are identical.

In the interpretation formulated by McLean and Hondros[18] we require a knowledge of the dependence of the surface tension γ_{GB} of the grain boundary on the surface concentration of the adsorbate in order to determine the adsorption:

$$\gamma_{GB} - \gamma_B = -T\Delta S_a - \sum_i \Gamma_i \mu_i . \quad (14)$$

Here the coverage $\Gamma_i = -[\partial\gamma/\partial\mu_i]_{T,\mu_{j\neq i}}$ is a crystallographically determined quantity, because neighbouring grains are differently oriented and the adsorption of the SAS impurity on them is different. The Gibbs equation in the form (12) can be used to calculate Γ_i for the components from the known isotherms of the surface tension γ_{GB} and of the chemical potential μ_i of the components in the grain.[18] For a two-component system

$$d\gamma = -\Gamma_1 d\mu_1 - \Gamma_2 d\mu_2 = -\frac{\Gamma_2 d\mu_2}{1 - c} , \quad (15)$$

where c is the concentration of the SAS impurity.

In order to determine the adsorption accurately, we need to know the activity a of the components rather than their concentration c and to find the chemical potential of the adsorbed SAS.

In the theoretical description of the adsorption on polycrystals in terms of the lattice models we can use an approach developed for the analysis of stresses in Somigliana dislocations. In this case the adsorption properties on the grain boundaries and on their bulk should have their equilibrium values, and should be continuous at all points. The problem can be solved by the nonlinear theory of elasticity.[18]

The differences between adsorption–desorption processes on the surface of crystals and on the grain boundaries can be studied experimentally by comparing the electrochemical characteristics of monocrystals and polycrystals. A very instructive example of this approach is provided by the study of the anodic oxidation of CO on mono- and on polycrystalline Pt electrodes in 0.05 M $HClO_4$. At low overvoltages ($\eta < 0.1$ V), the adsorption is described by the Langmuir isotherm, is independent of the grain size and of the pH of the solution, and takes place according to the scheme

$$Pt(CO)_{ads} + H_2O \longleftrightarrow Pt(COOH)_{ads} + H^+ + e^-.$$

Increasing the overvoltage (to $\eta > 0.2$ V) and the concentration of active centres (by changing from single crystals to polycrystals) affects the final products. In the bulk of the grain boundaries, the electrochemical process follows a different path:

$$Pt(CO)_{ads} + OH^- \longleftrightarrow Pt(COOH)_{ads} + e^-,$$

$$Pt(CO)_{ads} + 3OH^- \longleftrightarrow Pt + CO_3^{2-} + 2H_2O + e^-.$$

On a platinum polycrystal with a small grain size (~ 1 μm) and a correspondingly large spread of GB, the formation of carbon dioxide becomes possible at high anodic potentials ($E > 1.4$ V):

$$Pt(CO)_{ads} + H_2O \longleftrightarrow Pt + CO_2 + 2H^+ + 2e^-.$$

Anodic polarisation in the high positive range of potentials ($E \gg 1.4$ V) activates the grain-boundary volumes in the metal. Even more complex reactions are possible (according to steric considerations) on extended defects of the GB surface: for example

$$CH_2\text{—}CH(CH_2)_8CO_2H + 4H_2O \longrightarrow$$

(Pt)

$$\longrightarrow Pt + H_3C(CH_2)_7CO_2H + 2CO_2 + 11H^+ + 11e^-.$$

The nature of this substantial change in the chemical path of the reactions reflects the difference in structure and in chemical composition between the grain-boundary volumes and the bulk of the grain. The polyhedral structure of the GB provides ready-made elements for the formation of surface clusters. The pores and the polyhedra of the GB in the 3*d* metals can be filled relatively easily with impurity elements (Ru, Os, Rh, Ir). Impurities which lower γ and favour the formation of GB with the most stable structure are usually concentrated on the GB: in most cases these are chalcophilic elements. Reactions taking place relatively easily on the GB include impurity precipitation and carbide formation, which lower the concentration of elements with a high oxygen affinity.

III. Distribution of dislocations in near-surface layers of crystals

Many physical, mechanical, and corrosion-electrochemical properties of polycrystalline metals depend on the distribution of dislocations (DD) near the internal boundaries. The DD process is statistically independent.[20] However, within the crystallites (and especially in the region of subgrain boundaries and of grain boundaries), DD in the form of planar aggregates are fairly often seen. An edge dislocation does not interact strongly with a low-angle dislocation boundary,[21] and when the slip plane of the edge dislocation is perpendicular to the wall the interaction is completely suppressed. On the other hand, high-angle GB act as dislocation stoppers, which cannot be surmounted by thermal activation. However, the long-range interaction of the dislocations with the GB is quite weak, as in the case of the low-angle boundaries.

The effect of the dislocation density ρ_d on the electrochemical behaviour of crystals in electrolytes has been studied intensively[22,23] in the context of confirming the Rebinder and Ioffe effects on the physicomechanical properties of crystals caused by exposure of the crystal surfaces to the components of liquid condensed media. The 'skin-deep' aggregation of dislocations in the near-surface layer is due essentially to the action of image forces, whose energy (in the framework of the linear theory of elasticity) is given by

$$E_u = \beta G_c b \ln \frac{2l_d}{b} . \tag{16}$$

In this case, $\beta = 1 - \nu$ for edge dislocations and $\beta = 1$ for screw dislocations; l_d is the distance from the dislocation to the surface. At a high level of relaxation of the near-surface layer of the crystal (i.e. for a change in the lattice constant of more than 10%) the inner electric double layer of the metal stops the 'floating' dislocation.[4] The dislocation distributions in the near-surface layer depend first of all on the type of crystal and on the nature of previous mechanical treatments. In an ultra-thin surface layer of the crystal, the parameter ρ_d can decrease (Fig. 2). In the case of rectilinear edge dislocations,[23] the distribution as a function of depth z can be calculated by using the formula

$$\rho_{d,z} \approx \frac{L}{z} \exp \frac{-E_{d,z}}{Lzk_BT} , \tag{17}$$

where L is the length of the dislocation (< 1 μm), and $E_{d,z}$ is the energy of the dislocation. For dislocation half-loops, the distribution takes the form

$$\rho_{d,z} \sim \frac{A}{z} \exp \frac{-B \ln z}{z} . \tag{18}$$

Here $A = G_c b^2/2\beta$ (G_c is the shear modulus) and B is the attenuation coefficient of sound in the crystal.

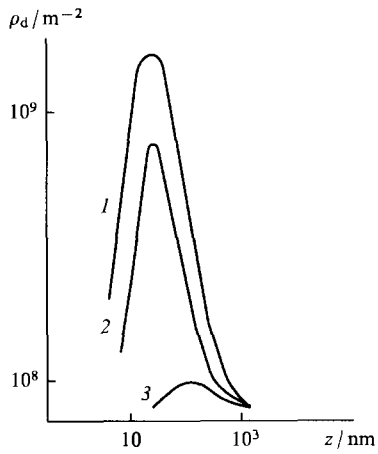


Figure 2. Distribution of rectilinear edge dislocation as a function of the depth of the near-surface layer (z) in copper (curve *1*), nickel (curve *2*), and silicon (curve *3*) crystals.

The distance from the crystal surface, where the density of dislocations $\rho_{d,z}$ is a maximum, can be determined from the condition $\partial\rho_{d,z}/\partial z = 0$:

$$z_{max} \equiv \frac{G_c b^3}{4\pi(1-\nu)} (k_BT)^{-1} , \tag{19}$$

where ν is Poisson's ratio.

The aggregation of edge dislocations in the near-surface layer of the metal is caused by thermoelastic stress effects. The analytic solution of the equilibrium distribution problem for rigid parallel rectilinear dislocations on the slip plane has been obtained [24,25] on the assumption of a continuous distribution for a periodic potential of the external forces $U(x)$. The x axis is perpendicular to the dislocation lines and corresponds to the slip direction. The equilibrium DD in the field of $U(x)$ (the potential energy for a unit length positive dislocation) is determined in this case by a function of their linear density $\rho_d(x)$ which can be expressed [16] as a Fourier series:

$$\rho_d(x) = \sum_{k=-\infty}^{+\infty} \rho_{d,k} \exp(ia_k x) \quad . \tag{20}$$

Here

$$\rho_{dd,k} = -\frac{2\pi|k|U_k}{|A|} \quad \text{for } k \neq 0 \quad (\rho_0 \text{ is arbitrary}),$$

$$U_k = \frac{1}{l}\int_{-l/2}^{+l/2} U(x)\exp(-ia_k x)\mathrm{d}x \quad , \tag{21}$$

$a_k = 2\pi k/l$ [l is the period of $U(x)$ and of $\rho(x)$].

Grain sub-boundaries and boundaries are characterised by local minima in the potential energy $U(x)$. Then, having calculated the DD for the self-repeating potential wells, we can describe the changes in ρ_d in the bicrystal. Fig. 3 shows the result of a computer calculation allowing for 40 harmonics ($-20 \leqslant k \leqslant 20$) in the representation of the $U(x)$ profile. In this case, the potential well has very steep walls, and therefore the emission of dislocations from this well and the surmounting of this obstacle are seriously hindered. However, outside the limits of the potential well $U(x)$ = const, and there is no elastic long-range interaction between the dislocations and this obstacle. The mid-point of one of the internal boundaries in the bicrystal was used as the origin for the measurements. The distribution of the dislocations is given within a single period of $\rho_d(x)$. As could have been expected, on the GB ρ_d is higher than the average level, but (conversely) the regions immediately adjacent to the boundary have a ρ_d value well below the average.

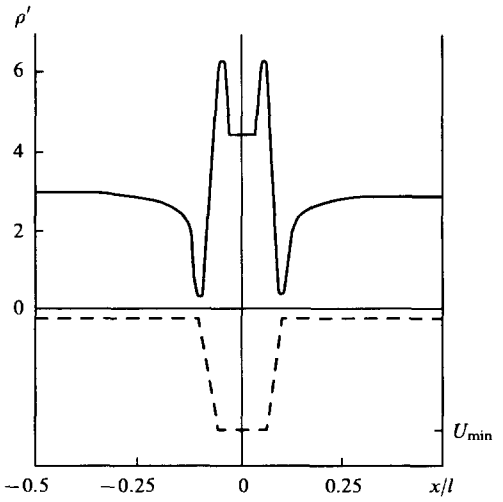


Figure 3. Distribution of dislocations in the field of repeated potential wells:

$$\rho' = \frac{Al}{2\pi|U_{min}|}\rho, \quad \rho = \frac{6\pi|U_{min}|}{Al} \quad .$$

An experimental determination of the DD near a grain boundary [misorientation angle of the grains θ = 13°–15°, for which expressions (17)–(20) are applicable] was carried out for pure iron (99.99%, $\rho_d = 2.0 \times 10^{11}$ m^{-2}). Selective electrochemical etching in the passive region of potential was applied in a 1 M solution of H_2SO_4 (290 K, E = 0.80 V, t = 300 s). Under these etching conditions, the nondislocated part of the crystal surface is passivated by oxides, and dissolution takes place only on the defects.

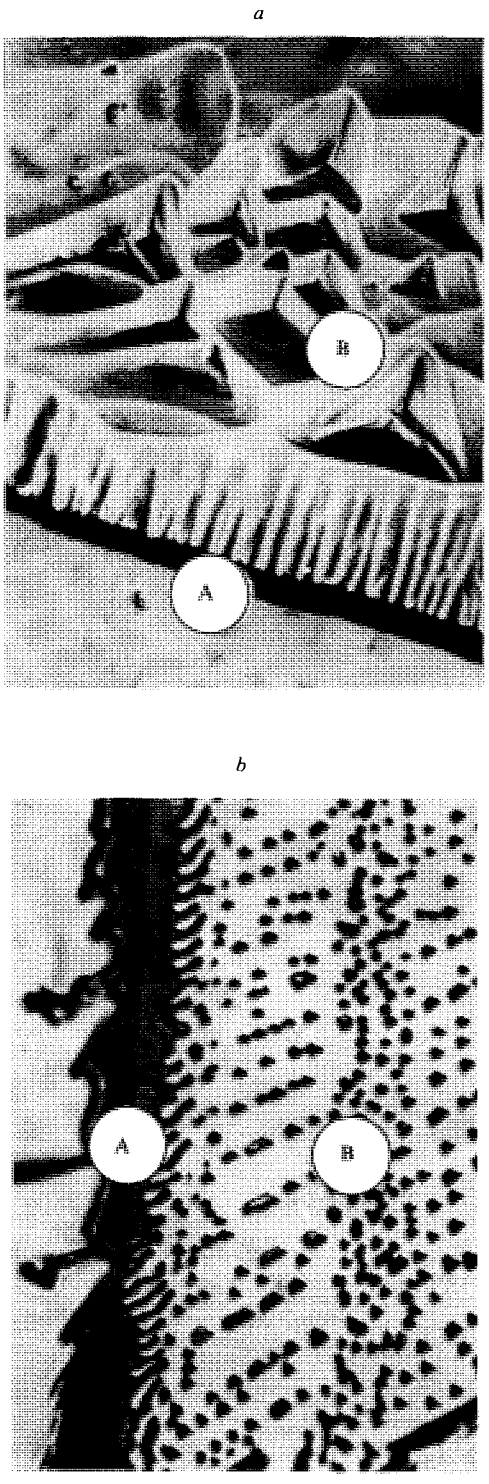


Figure 4. Electrochemical (*a*) and thermal (*b*) etching of zone-purified iron (× 960). A — grain-boundary; B — EP zone.

Etch pits (EP) are formed on the Fe(111) surface both in the region of the GB (Fig. 4*a*, region A) and at some distance from it (region B); there is a fairly wide 'dead' zone directly adjacent to the GB where no etch pits are found. The presence of a similar zone on the Fe(110) face is observed only after a hydrogen anneal of the iron ($p = 6 - 10^{-3}$ Pa, 1173 K, $t = 3.6 \times 10^3$ s) by the method of thermal EPs, which are formed because of the selective oxidation of the dislocation outcrops on the crystal surface (Fig. 4*b*). The size of the dislocation-free regions is 7–12 μm. We should note that thermal oxidation (unlike electrochemical etching) does not produce EP in the region of the boundaries.

The density of dislocations on the GB is higher than the average level, but in the region directly adjacent to the boundary it is anomalously low. This effect has stimulated the interest of experimental workers, and it has been carefully analysed [26] by high-resolution transmission electron microscopy methods. The width of the dislocation-free regions for GB with small Σ values was found to be ~15 μm. The localisation of the dissolution process on a defect has a protective action on the corrosion of the dislocation-free region. When polycrystals are exposed to corrosion-electrochemical interactions the selective dissolution of the dislocation outcrops results in the appearance of wide nonetched regions.

The distribution of ρ_d directly influences the rate of corrosion i_{cor}, which is low during the initial period of exposure but becomes stable after going through a maximum. [27]

The effect of corrosion-active media on the surface energy (which is stronger on the γ_{GB}) should be mentioned, in addition to the image forces and the thermoelastic stresses, as one of the physicochemical reasons for the accumulation of dislocations in the near-surface layer.

Extensive reports on the search for quantitative estimates of the effect of the dislocation density ρ_d on the dissolution of metals have been published. The change in the kinetic parameters of the anodic dissolution of iron in acid media produced by heat treatment is usually ascribed to a decrease in ρ_d. The intermediate $(FeOH)_{ads}$, chemisorbed on the iron atoms in a dislocation pipe $Fe(FeOH)_{ads}$ and which is able to catalyse the dissolution process, [28] is formed on the dislocations. These effects have been noted also on other transition metals (for example, nickel [29]). On deformed nickel ($\varepsilon > 10\%$) with a high density of dislocations, the adsorption of water dipoles in solutions of $Na_2SO_4 + (C_2H_5OH$, C_4H_9OH, $C_6H_{13}OH)$ blocks the AC (dislocation outcrops), and the dependence of the double-layer capacity c_{DL} on the electrode potential E (measured by a pulsed galvanostatic method) does not differ significantly from the background value. After annealing a nickel electrode (973 K, $t = 5.4 \times 10^3$ s), with a corresponding decrease in the spread of the GB and in ρ_d, we observe a decrease in c_{DL}. Adding to the solution substances with a high specific adsorption activity [$SC(NH_2)_2$, $(CH_3)_2CO$, C_3H_7COOH] produces changes in ρ_d which only marginally affect the $c_{DL}-E$ curves.

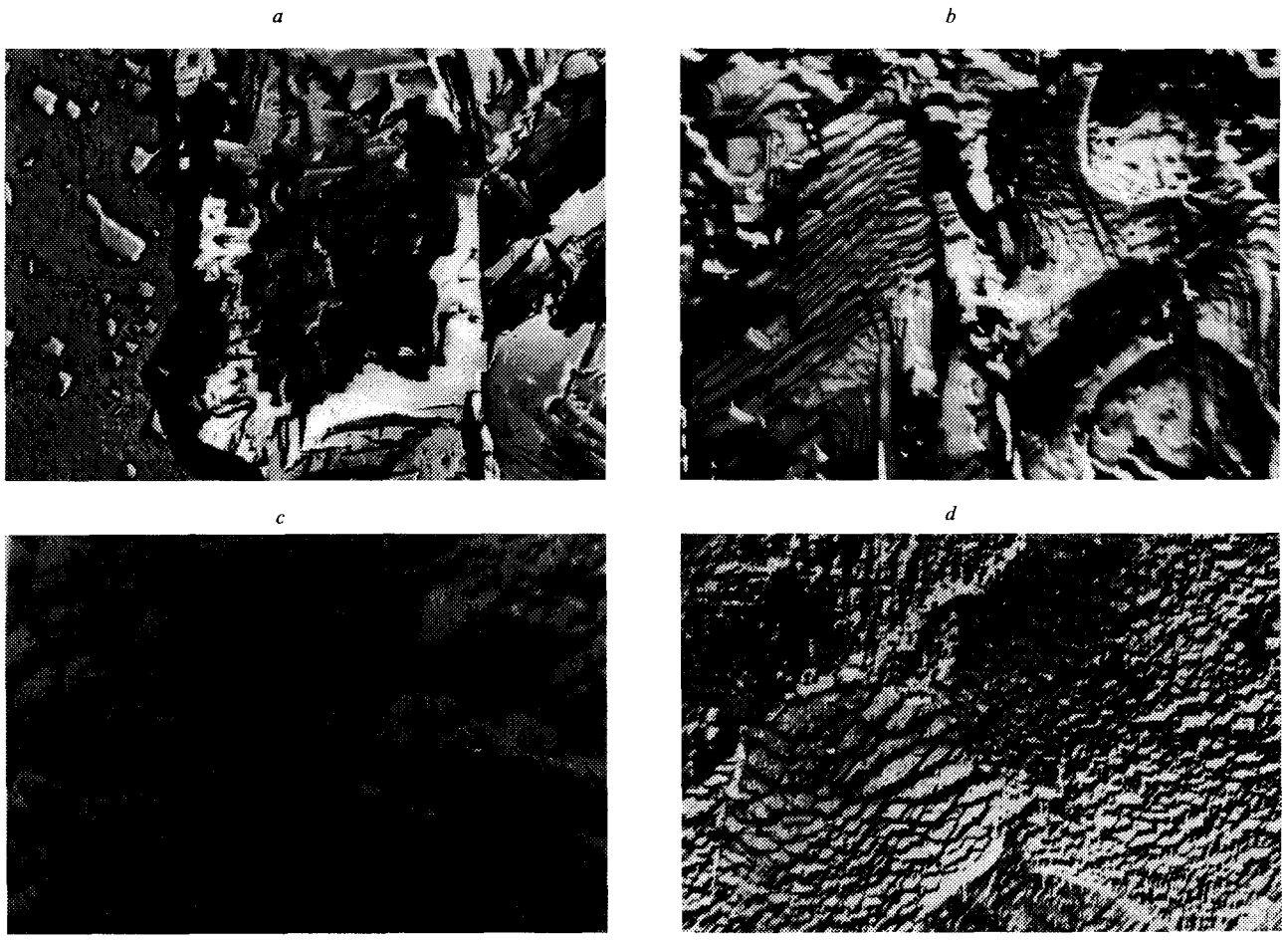


Figure 5. Morphology of the surfaces of dissolving iron (*a*), nickel (*b*), copper (*c*), and tungsten (*d*) polycrystals at the current oscillation potentials (× 12000).

IV. Current and potential oscillations during grain-boundary dissolution

On grain-boundary volumes the processes of dezincification (brass, bronze, Cu–Zn alloys) and of selective dissolution of stainless steels [30] and of other metals follow different paths. The oscillations of the anode current i_a at potentials more positive than the Flade potential E_{Fl} on the anodic polarisation curve are usually attributed [31,32] to an enhanced grain-boundary dissolution. A metallographic analysis of the surface of samples held for short times (t = 20–30 s) at different current oscillation potentials in the anodic region showed that grain-boundary volumes in polycrystals dissolve rapidly (Fig. 5). In many experimental studies it was assumed that the current oscillations were apparatus artefacts, and the oscillations were excluded from the $E-i_a$ curves. The enhanced adsorption activity of the GB allows us to control the current oscillations by introducing surfactants into the electrolyte. [4] Thus, the current oscillations on a nickel electrode can be suppressed by adding corrosion inhibitors to the solution [for example, n-octylphenylmethanesulfonate]. However, substances which act as corrosion inhibitors on annealed polycrystals may not have the same effect on elastically stressed metals (ε < 5%). The amplitude of the current oscillations on elastically stressed metals is higher, and the potential region which produces oscillations is wider, than in the case of annealed metals. Thus anthraquinone derivatives, which inhibit the acid corrosion of titanium and of stainless steels, accelerate the intercrystallite corrosion of stressed 12X18N9T stainless steel. [33]

The current (or potential) oscillations in potentiostatic (or galvanostatic) circuits are well known electrochemical effects, first reported by Fechner in 1928. Near the Flade potential E_{Fl} on the $E-i_a$ curve, we observe an electric instability whose amplitude decreases at more noble potentials (Fig. 6*a*). Early explanations of this effect relied on the assumption of a periodic transition of the metal from a passive into an active state. [32] On polycrystals of the transition metals, these activation regions should be found on grain boundaries. The diagnostic criterion of the instability (current oscillations) is provided by the appearance on the $E-i_a$ polarisation curves of regions with a negative slope $di(E)/dE(i) < 0$ (Fig. 6*b*). In accordance with the ideas of catastrophe theory, [35] this suggests the existence of three fluxes of particles with different i_a values for E = const.

Current oscillations associated with periodic passivation–repassivation reactions on the surfaces (mainly on the bulk of grain boundaries) of porous oxides have been explained as follows. The passivation–repassivation process alters the porosity of the passivating oxide films, $\varphi = f(\theta_{Ox})$, where θ_{Ox} is the coverage of the surface by the oxide phase (the accessibility of the metal surface to the electrolyte). The average rate of flow of the electrolyte $\bar{v}$ depends on the pressure p:

$$\bar{v} = -\Pi_i(\varphi)\,\nabla p\ ,$$

where Π_i is the permeability of the oxide layer. Ortoleva's model [36] assumes that an impenetrable oxide structure is more likely to be formed on a GB, and that the bulk of the grain has a porous oxide layer permeable to ions. Treating this layer as a structure consisting of n pores of volume L^3 and an insoluble oxide with a volume fraction $1-N_f$ gives the expression

$$\varphi + nL^3 = N_f\ . \tag{22}$$

The changes in porosity with time will be determined by the kinetics of the formation of pores in the oxide structure:

$$\frac{\partial\varphi}{\partial t} = -n\frac{\partial L^3}{\partial t}\ . \tag{23}$$

For the rate of growth of the oxide islets on the GB in two-dimensional coordinates, we can write

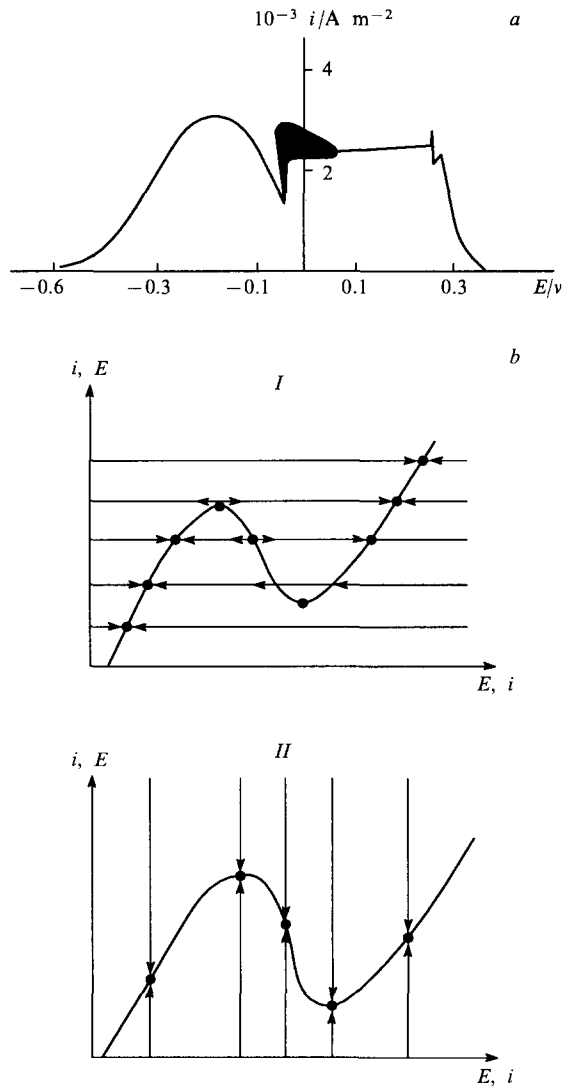


Figure 6. Polarisation curve (*a*) for the Fe–1 M H_2SO_4 system (V_E = 0.005 V s^{-1}) with a current oscillation section. The schematic illustration of the polarisation measurement (*b*) explains the appearance of sections with a negative slope on the $E-i$ curves.

$$\frac{\partial L^3}{\partial t} = KL^2[c(t) - c_0]\ , \tag{24}$$

where K is the rate constant for the growth of oxide, and c_0 and $c(t)$ are respectively, the equilibrium (in solution) and the time-dependent concentrations of the M^{n+} ions in the pore. From Eqns (22)–(24), we obtain

$$\frac{\partial\varphi}{\partial t} = -Kn^{-1/3}(N_f - \varphi)^{2/3}[c(t) - c_0]\ .$$

If the density of the electrolyte is independent of $c(t)$ and p, the law of energy conservation can be written in the form

$$\frac{\partial\varphi}{\partial t} = -\nabla\,[\varphi\chi(\varphi)\,\nabla p]\ ,$$

whereas for the dissolving metal we have

$$\frac{\partial\varphi}{\partial t} = \nabla[\varphi\Delta(\varphi)\,\nabla c(t) + \varphi c(t)\chi(\varphi)\,\nabla p] + \rho\frac{\partial\varphi}{\partial t}\ . \tag{25}$$

Here the diffusion coefficient $\Delta(\varphi)$ and the electric conductivity $\chi(\varphi)$ depend on the porosity (ρ is the density of the metal). An analysis of the solution of Eqn (25) shows that under the conditions of current and potential oscillations, the front of the moving phase boundary is unstable if it is planar.

The instability problem has a strong relevance to the processes responsible for the dissolution of polycrystalline metals. On the surface, we find regions (the GB and the bulk of the grain) comparable in area and in their relative contribution to the formation of a flux of dissolving matter. The specific flux of M^{n+} ions on the GB can be several orders of magnitude greater than the corresponding flux from the surface of the grain. At the same time the adsorption activity of the GB is also very much greater. If the electrolyte contains easily adsorbed components, these are redistributed on the surface during the dissolution of the crystal. This produces opposing transport effects through the fluxes of M^{n+} from the metal and to the metal on the phase boundary.

Current oscillations can be explained by a retardation (and acceleration) of the motion of the dissolution steps [37] as well as by the activation–passivation of the grain-boundary volumes. On an iron electrode in 0.5–1.0 M H_2SO_4, the salt $FeSO_4$ (in a colloidal state near the electrode surface) acts as a reversibly passivating reagent. The formation of oxides, hydroxides, and salts with a structure and properties varying as a function of the heterogeneity of the electrode surface is the basis of the most significant concepts regarding the current (or potential) oscillation phenomena. In the layer nearest to the electrode clusters of particles can be formed and have a stable existence. [38] Upon landing on the electrode surface, they settle on the steps and block their motion. The retardation mechanism is similar to that proposed by Khaldeev and Kamelin: [39,40] the aggregation of foreign particles into Toda chains, which block the motion of the surface dislocations.

In the oscillatory potential model, [41] it is assumed that the growth and dissolution of passive films are complicated by the transfer of H^+ ions between the electrode surface and the solution. This destabilises the passivation potential E_n and the Flade potential E_{Fl}. The oscillation process can be divided into the following stages:

(1) $E_n < E_{Fl}$; the electrode surface is activated, the metal dissolves, the current is limited by the transfer of the H^+ ions (whose concentration decreases in the neighbourhood of the surface);

(2) the parameter E_{Fl} is determined by the concentration of H^+ ions [$E_{Fl} \sim F(c_{H^+})$], which decreases during the first stage, so that the Flade potential also decreases: $E_{Fl} < E_n$;

(3) a passive film having a much lower rate of dissolution is formed;

(4) the E_{Fl} value increases as a result of the third stage, and $E_n < E_{Fl}$;

(5) the oxide film dissolves.

These cycles can be repeated indefinitely.

The kinetics of the process can be expressed as follows:

$$\frac{dE}{dt} = K_1 - K_2 - K_3\theta_{Ox} + K_4 E W(E, \theta_{Ox}) \ , \tag{26}$$

$$\frac{d\theta_{Ox}}{dt} = K_5 E W(E, \theta_{Ox}) \ , \tag{27}$$

where $E = E_n - E_{Fl}$ is the time-dependent potential; θ_{Ox} is the coverage (the passivated part of the surface). The rate constants for all the stages of the oscillatory process ($K_2 - K_5$) are positive. The function $W(E, \theta_{Ox})$, which normalises the coverage, is defined as follows:

$$W(E,\theta_{Ox}) = \theta_{Ox} + (1 - 2\theta_{Ox})U(E) \ , \tag{28}$$

where $U(E)$ is the Heaviside function. Therefore we can write

$$W(E,\theta_{Ox}) = \begin{cases} 1-\theta_{Ox} & \text{for } E > 0 \ , \\ \theta_{Ox} & \text{for } E < 0 \ . \end{cases}$$

Perlstein and Johnson [42] introduced the symbols $V = K_5E/K_2$ and $\tau = kt$ and put expressions (26) and (27) in the form

$$\frac{dV}{dt} = bh - V - b\theta_{Ox} + \frac{VG(V, \theta_{Ox})}{c} \ , \tag{29a}$$

$$\frac{d\theta_{Ox}}{dt} = VG(V, \theta_{Ox}) \ , \tag{29b}$$

and he replaced Eqn (28) by the normalised function

$$G(V,\theta_{Ox}) = \theta_{Ox} + (1 + 2\theta_{Ox})U(V) \ , \tag{30}$$

where $b = K_3K_5/K_2^2$, $c = K_2/K_4$, and $h = K_1/K_4$ (the quantities b and c are positive).

It follows from the equations given above that unique systems of states can exist:

$$(V,\theta_{Ox}) = \begin{cases} (bh,0) & h \leqslant 0 \\ (0,h) & 0 \leqslant h \leqslant 1 \\ (bh-b,1) & 1 \leqslant h \ . \end{cases}$$

Thus the stable state of the phase boundary is defined by the two parameters b and h.

In a subsequent modification [41] of Eqns (29) and (30), the function G was replaced by G^*, i.e.

$$\frac{dV}{dt} = bh - V - 6\theta_{Ox} + \frac{VG^*(V, \theta_{Ox})}{c} \ , \tag{31a}$$

$$\frac{d\theta_{Ox}}{dt} = VG^*(V, \theta_{Ox}) \ , \tag{31b}$$

$$G^*(V,\theta_{Ox}) = \theta_{Ox} + (1 - 2\theta_{Ox})\chi(V) \ ,$$

$$\chi(V) = 1 - \frac{1}{\exp(AV) + 1} \ ,$$

where A is a constant ($A \gg 0$). The function $\chi(V)$ is a degenerate Heaviside function. For large A, the χ value is close to zero (for negative V) and to 1 (for positive V). However, the function varies (between 0 and 1) near $V = 0$.

A very simple condition for the stable state follows from the modified relations (31);

$$V, \theta_{Ox} = 0, h \ ,$$

i.e. the stable potential V is zero, and a part of the metal surface ($\theta_{S,Ox}$) is passive; the latter is determined by the parameter h. The model is applicable for $0 \leqslant h \leqslant 1$.

An estimate of the potential oscillations can be used to determine the likelihood of depassivation of stainless steel. [43] In a system in which intermediate species are produced and disappear, the oscillations of the potential E are given by bifurcation theory [44] as

$$\frac{dx}{dt} = A - (B + 1)x + x^2 + D\frac{d^2x}{dr^2} \ , \tag{32a}$$

$$\frac{dy}{dt} = Bx - x^2y + QD\frac{d^2y}{dr^2} \ . \tag{32b}$$

Here x, y are real functions of the variables t and r (t is time, r is a spatial coordinate belonging to the segment [0, 1]; A, B, D, Q are positive numbers, where B is the bifurcation parameter. If the flux of particles towards the phase boundary is constant a new cycle begins for $B = 1 + A$. If the concentrations of the particles M_S^{n+} and M_L^{n+} on the two sides of the phase boundary remain constant, the new cycle begins at $B = A + D(1-Q)$. The solutions $X(0,t) = X(1,t)$, and $XY(0,t) = Y(1,t) = B/A$ are stationary.

V. Intercrystallite corrosion

Etch grooves are formed at the boundary between neighbouring grains of identical chemical composition in a bicrystal (Fig. 7). Mechanical equilibrium is achieved by superposing the interfacial tension forces γ_{SL} and the energy of the internal interfaces γ_{GB}. According to Mullins,[45] the condition for an equilibrium state is

$$\gamma_{GB} = 2\gamma_{SL}\cos\frac{\theta}{2} . \tag{33}$$

Near the etch groove, a ramp is formed (Fig. 7); its profile is given by the condition

$$m = \cot\frac{\theta}{2} . \tag{34}$$

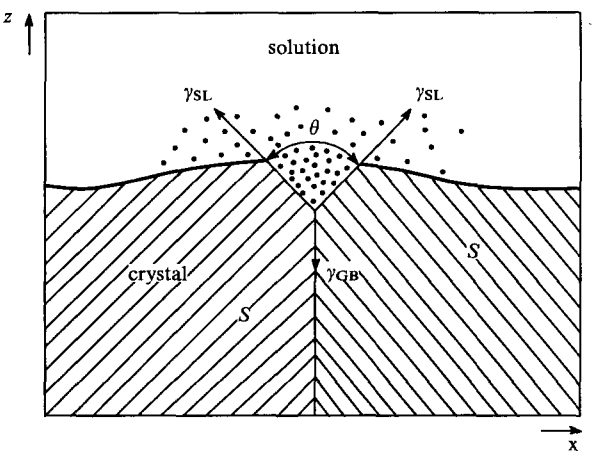


Figure 7. The formation of an etch groove on a metallic bicrystal.

We note that the existence of this profile follows both from the impurity distribution conditions near the GB and from the condition determining the change in the dislocation structure of the crystal near the GB (see Fig. 3). The distribution of impurities along the normal x to the plane of the GB is strongly nonlinear. On the plane of the GB, their concentration is much higher than the equilibrium value: this is followed by a 'dead' zone, after which the concentration suddenly increases.

Along the plane of the GB (i.e. along z), the impurities are distributed according to the relay (cooperative) grain-boundary diffusion mechanism.[46] This model assumes an alternation of grain-boundary barriers (body-centred polyhedra) and of free volumes. Grain-boundary segregations are formed during a preparative stage. In the second stage, the actual grain-boundary diffusion of impurities takes place as a result of a diffusion jump through the barrier and of a concerted displacement within the free (loose) volume. The Gibbs–Thomson relation describes the distribution of the impurity along x:

$$c_S(x,t) = c_\infty\left[1 + \frac{\gamma_{SL}\Omega}{RT}K_M(x,t)\right] . \tag{35}$$

Here c_∞ is the concentration of solution particles on the flat ($K_M = 0$) surface, Ω is the atomic volume of the metal crystal, and $K_M(x,t)$ is the curvature of the metal surface. Mullins[47] modified this model and adapted it to a pure diffusion treatment by introducing three parameters: the distance d between the top of the ramp and the bottom of the groove, the distance d' between the initial flat surface and the ramp, and the distance between the edges W:

$$d = 1.01\,m(A't)^{1/3} , \tag{36a}$$

$$d' = 0.86\,m(A't)^{1/3} , \tag{36b}$$

and

$$W = 5(A't)^{1/3} , \tag{36c}$$

where $A' = (D\gamma_{SL}\Omega^2c_\infty)/RT$, $t = A't$, and D is the diffusion coefficient of M^{n+} in the crystal. In the case of convective diffusion, the profile (see Fig. 7) may be asymmetric for the different crystals A and B of the bicrystal.[48] In x, y coordinates, the curvature of the metal surface is described by the expression

$$K_M(x,\tau,\alpha) = m(\pi\tau\alpha)^{-1/2}\exp\frac{-x^2}{4\tau\alpha} , \tag{37}$$

and the profile of the surface in the normalised $\eta = x/2\sqrt{\tau\alpha}$ coordinates is

$$\frac{W(\eta)}{2m\sqrt{\tau\alpha}} = -\eta\,\mathrm{erf}(\eta) - \frac{1}{\sqrt{\pi}}\exp(-\eta^2) + \eta = X(\eta) . \tag{38}$$

Here τ is the dimensionless time, $\alpha = Pe/2 = 0.5V/D_A$ (where Pe is the Péclet number, V is the average rate of penetration of A into the A–B bicrystal, and D_A is the diffusion coefficient of A in the A–B bicrystal).

If the diffusion process on the metal surface is markedly influenced by electromigration, the curvature of this surface in the two-dimensional variant (in x, y coordinates) corresponds to the expression[49]

$$K_M(x,\tau,\alpha) = \frac{2g}{1+\beta^{1/3}+\beta^{2/3}}(A_1,t)^{1/3}\sum_{n=0}^{\infty}b_{j,n}\left[\frac{x}{(A_jt)^{1/3}}\right]^n , \tag{39}$$

where $2g$ is the ratio of the free energies of the GB and of the surface per unit surface area, and $\beta = D_A/D_B$ (D_B is the diffusion coefficient of B in the A–B bicrystal), and

$$A_j = \frac{A'z|e^-|\rho i_m}{k_BT} ,$$

where $z|e^-|$ is the effective charge, ρ is the resistance, i_m is the electromigration current density, and $j = 1, 2$. The resulting profile is nonlinear, the maximum amplitude of y being found at $x = 1$.

When the difference in the rates of dissolution between the bulk of the grain and along the GB is large ($i_{GB} \gg i_{S,\perp}$), we can use a model proposed by Peschke et al.[37] and similar to the well known Fischer model, according to which an etch groove with perpendicular walls is formed (Fig. 8*a*). In practice, this state of affairs is typical of the dissolution of hydrogen-saturated polycrystals showing passivation (Figs 8*b* and 8*c*). The local loss of passivity on the GB produces a large increase in i_{GB} in the z direction. The convective diffusion equation

$$v(r)\frac{\partial c(x,t)}{\partial z} = D_A\frac{1}{r}\frac{\partial}{\partial r}\left[r\frac{\partial c(x,t)}{\partial r}\right]$$

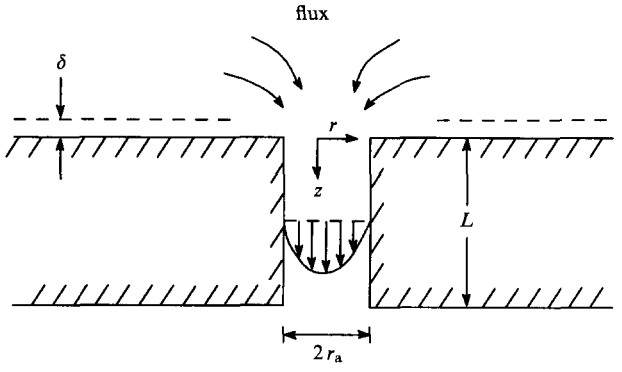
for this situation can be expressed as

$$F(\bar r)\frac{\partial\bar c}{\partial\bar z} = \frac{1}{Pe}\left[\frac{1}{\bar r}\frac{\partial}{\partial\bar r}\left(\bar r\frac{\partial\bar c}{\partial\bar r}\right)\right] , \tag{40}$$

where $F(\bar r)$ is the dimensionless velocity

$$F(\bar r) = \frac{1}{2}\frac{v(\bar r)}{V_0} = \frac{1}{2}\bar v(\bar r) ; \tag{41}$$

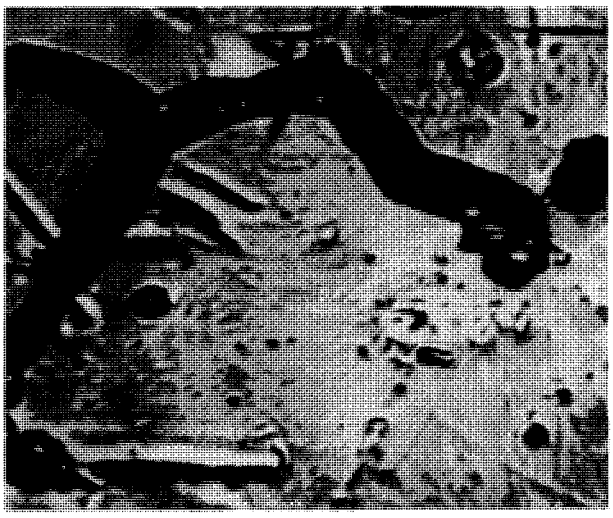
$\bar r = r/r_a$, $\bar z = z/z_a$, and $\bar c = c(x,t)/c_\infty$ are, respectively, the dimensionless values of the radius of the groove, of its depth, and of the concentration $c(x,t)$ of the substance near ($z = 0$) or far from the groove (c_∞).



a



b



c

Figure 8. Model of an etch groove on the GB in thoroughly passivated metals (*a*) and the grain-boundary dissolution of hydrogen-saturated nickel (*b*) and 12X18N9T steel (*c*) polycrystals (× 960).

The boundary conditions are

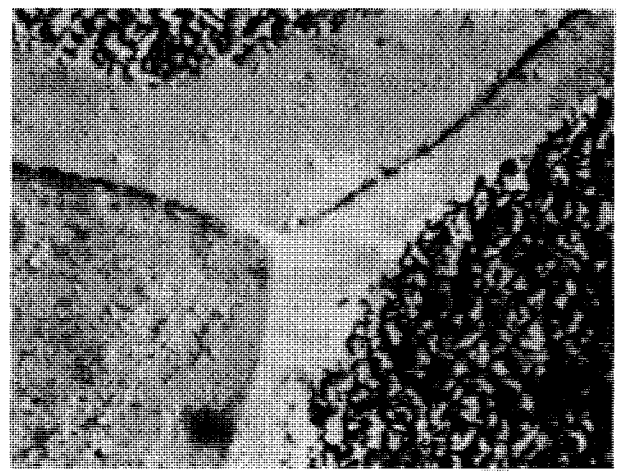
$$\bar{c}\Big|_{\bar{z}=0} = 1, \quad \frac{\partial \bar{c}}{\partial \bar{r}}\Big|_{\bar{r}=0} = 0 \text{ , and } \frac{-\partial \bar{c}}{\partial \bar{r}}\Big|_{\bar{r}=1} = K_D \bar{c} \text{ ,}$$

where $K_D = kr_a/D_A$, and k is a constant.

The solution of the diffusion equation is

$$\bar{c} = \frac{1}{\Gamma(4/3)} \int_{\eta}^{\infty} \exp(-\eta^3) d\eta \text{ ,} \qquad (42)$$

a



b

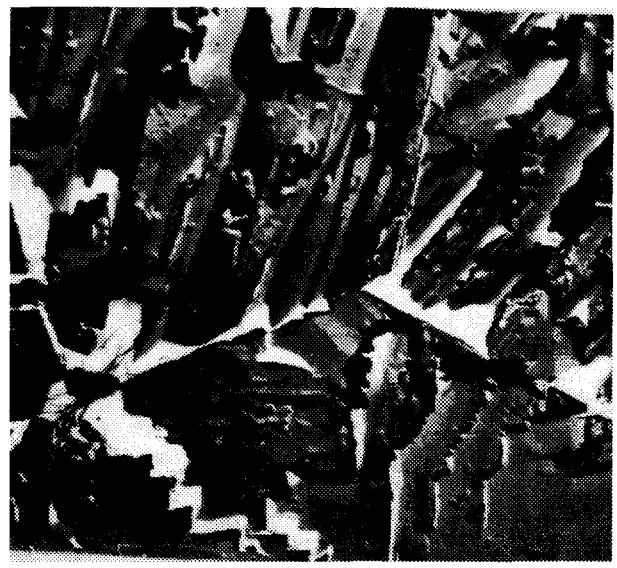


Figure 9. Dissolution of iron (*a*) and nickel (*b*) tricrystals (× 12000).

where $\eta = \bar{s}/(9/2\bar{z})^{1/3}$, $\Gamma(4/3) = 0.8934$ is the gamma-function, and $\bar{s} = Pe^{1/3}(1-\bar{r})$. The rate of dissolution in the groove is

$$i_{GB} = \frac{D_A c_B}{0.8934a} \left(\frac{9}{2}\bar{z}\right)^{-1/3} Pe^{1/3} \text{ ,}$$

where a is the lattice constant.

The model proposed by Peschke et al.[37] can be used to describe the dissolution of very pure metals in nonpassivating electrolytes, when $i_{GB} \approx i_{S,\perp}$. The bulk of the grains dissolves at different rates, depending on the crystal orientation of the adjacent single-crystal planes (*hkl*) in contact with the electrolyte (Fig. 9). As a result, some grains dissolve faster than others, and this is the main reason for the formation of a rough surface when a polycrystal is etched.

In a more realistic model the parameter r_a (the radius of the etch groove) varies nonlinearly along the normal z, and in the bulk of the metal $i_a \to 0$. In this case, $i_{GB} > i_{S,\perp}$. The analysis of this model is similar to the analysis of the diffusional permeability of the GB, in which surface diffusion does not play a dominant role.[10] In this model the layer concentration is

$$\bar{c} = \frac{8c_0 r_a}{\lambda} \int_0^{\infty} \operatorname{erfc}(\theta) \operatorname{erfc}\left(\frac{\omega}{2\sqrt{2\theta}}\right) d\theta \text{ ,} \qquad (43)$$

where $c_0 = c'(0,t)$ is the surface concentration, $\lambda = a/\sqrt{Dt}$ is a kinetic parameter, and $D = [(\sqrt{D_1} + \sqrt{D_2})/2]^{-2}$ is the effective bulk diffusion coefficient. As the corrosion process develops according to this model, a very harmful stress concentrator (with sharp notches) is formed on the metal surface and seriously degrades the strength of the metal under mechanical loads.

Experimental studies of the corrosion-induced breakdown of bicrystals began many years ago. The early work of Pfeil [50] showed that an iron bicrystal saturated with hydrogen splits into the two individual single crystals under the influence of applied mechanical stresses. Bicrystals of the *d* metals (V, Nb, Ta) offer convenient samples for the study of intercrystallite dissolution. These can be prepared by electron-beam zone melting with almost any misorientation angle θ. Estimates of the corrosion stability of symmetrical GB have shown [51] that the highest solubility is found in boundaries consisting of the least close-packed (100) and (110) planes of f.c.c. crystals.

The GB in a bicrystal effectively suppress the motion of dislocations, and therefore the dislocation density is higher in a bicrystal than in a single crystal grown under the same conditions. The effectiveness of this suppression depends on the angle θ. The GB with $\theta > 25°$ are less penetrable: on these boundaries, both the dislocation density and the rate of corrosion are enhanced.

When interpreting the changes in the rate of corrosion (K) along the boundary of a niobium crystal, we need to know both θ and the crystallographic orientation of the contacting single-crystal planes (hkl), and also the direction of the rotation angle of the grains ($\bar{n}$), since the parameter K for the given surfaces depends on their crystallographic direction [hkl]. It has been shown [41] that, at a [011]/[0$\bar{1}$1] boundary with $\theta = 16°$, the rate of corrosion and the depth of corrosional degradation (z_{cor}) are highest. The resulting concentration profile is asymmetric, because of the difference between the K values for the different faces. Linear relationships between θ and z_{cor} are observed only for $\theta \leqslant 20°$. Beyond this point, the linearity is perturbed, and at $\theta = 28°$ the plot of z_{cor} against θ develops a minimum apparently associated with a change in the structure of the GB with increase of θ. Whereas at low misorientation angles ($\theta < 20°$) the number of overlapping units decreases monotonically as θ is increased, when $\theta \geqslant 20°$ their number can increase at first and then fall sharply.

The dependence of the rate of corrosion on the reciprocal volume density of overlapping units Σ is nonmonotonic. Extrema in the dependence of K on Σ are found on GB, [13,14] in which the rotation axis is ⟨100⟩ for a GB with $\Sigma = 5$ {210} and $\Sigma = 5$ {310}, and also for a ⟨110⟩ axis for a GB with $\Sigma = 27$ {115} and $\Sigma = 11$ {113}. These data were confirmed experimentally by Miura and coworkers, [51-53] who showed that a copper bicrystal with $\Sigma = 3$ {111} dissolves much more slowly on the GB in 1 M $NaNO_2$ at 300 K than when $\Sigma = 9$ {221} and $\Sigma = 11$ {311}.

It follows from geometric considerations [54] of the structure of the GB that

$$\Sigma = m^2 + n^2(h^2 + k^2 + l^2) ,$$

$$\theta = 2\tan^{-1}\left(\frac{m}{n}\sqrt{h^2 + k^2 + l^2}\right) ,$$

where m and n are integers, and the Miller indices h, k, and l are determined by the vector of the rotation axis of the grains in the bicrystal. In cubic crystals, the following relationship is obeyed between the reciprocal density Σ and the angle θ:

$$\Sigma = \frac{n}{4}\left(1 + \cot\frac{\theta}{2}\right) , \qquad (44)$$

in which a well defined angle θ corresponds [54-56] to each value of Σ and n.

The intercrystallite dissolution (corrosion) (ICC) of various strongly passivating steels has attracted extensive studies. At the potentials of the active–passive transition some stainless steels have dis-solution currents on the grain-boundary bulk approximately 10^4 times greater than materials which are stable towards ICC. The two most commonly used tests for ICC are based on this effect: [57] Strauss's test [boiling the stainless steel samples in a solution of $H_2SO_4 + CuSO_4 + Cu$(powder), $t > 3.6 \times 10^4$ s], keeping the potential at $E = 0.35 \pm 0.03$ V, and Gouy's test (the sample is boiled, in cycles, in 65% HNO_3, $t > 8.6 \times 10^5$ s, and $E = 1.20 \pm 0.05$ V), i.e. the action of strongly oxidising media in the potential region of the transpassive state is simulated). For steels with a well-defined structure and known heat treatment regimes, we can use nondestructive electrochemical potentiostatic and galvanostatic control methods, based on etching in solutions containing chloride ions. One of the latest modifications of these methods [3] consists in analysing the anodic polarisation curves obtained by the potentiokinetic method ($V_E = 3.3 \times 10^{-3}$ V s^{-1}) in a solution of 10% H_2SO_4 + 0.0025 g l^{-1} KCNS. The curves are plotted from $E = 0.75$ V after a preliminary cathodic polarisation (−0.35 V, $t = 60$ s) and an anodic etch in the same solution (0 V, $t = 180$ s). If an anodic loop is not formed on the polarisation curve, the steel is not undergoing ICC. The liability to ICC is assessed [58] from the current in the active state, or from the ratio of the quantities of electricity passing through the electrode when the polarisation curve is plotted in the forward and in the reverse direction. If this ratio is >1, the steel is liable to ICC.

The dissolution currents on the grain-boundary volumes of austenitic stainless steels depend on the segregation of the impurities B, C, N, O, Si, P, and S. Allowance is needed not only for the chemical aspects of the interaction of these impurities with the atoms of the matrix but also for the elastic distortions produced on the GB by the segregation of the impurities. The harmful effect of these impurities on the ICC can be overcome by introducing antisegregants into the metal: additives which chemically bind the impurity by forming an inactive compound. This technical process arose from studies of the effect of hydride-forming impurities on the corrosion and on the physico-mechanical characteristics of hydrogenated polycrystals. When a metal is saturated with hydrogen, the impurities concentrated on

Table 1. The values of Σ and θ for the (100) and (111) planes of the grain boundaries (twisting of the cubic lattice and the misorientation angles for $\Sigma = 3$ and the possible values of n in the X-ray diffraction model).

(100)		(111)		$\Sigma = 3$	
Σ	θ/deg	Σ	θ/deg	Σ	θ/deg
5	36.87	3	60.00	1	33.56
13	22.62	7	38.21	2	48.19
17	28.07	13	27.80	3	60.00
25	16.26	19	46.83	4	70.53
29	43.60	31	17.90	5	80.41
37	18.92	37	50.57	6	90.00
41	12.68	43	15.18	7	99.59
53	31.89	49	43.57	8	109.47
61	10.39	61	52.66	9	120.00
65	14.25	67	24.43	10	131.81
65	30.51			11	146.44
73	41.11				

the GB can form hydride phases, which grow from well defined generation centres. The growth kinetics of these phases are controlled by surface diffusion, by diffusion along the GB, or by the dislocation creep of the metal. In the first case, the rate of change of the radius r of a bubble of the hydride phase (for example, methane) is given by the equation[63]

$$\left(\frac{dr}{dt}\right)_{Sd} = \frac{27}{64}\left(\frac{B}{\Omega_b^3 \Delta^3}\right)[(1+Q\varepsilon\Delta)^{1/2} - 1]\left[\frac{1}{Q^3(1-d^2)^3}\right], \quad (45)$$

where $B = D_S\delta_S\Omega\gamma_S/k_BT$ [D_S and D_{GB} are the coefficients of surface and of grain-boundary hydrogen diffusion, $D_S = D_{0,S}\exp(-Q_S/RT)$, $\delta_S = \Omega^{1/3}$, Ω is the atomic volume, γ_S is the surface energy]; Ω_b is the half-volume of the bubble, $\Delta = D_S\delta_S/D_b\delta_{GB}$ [$D_b = D_{0,b}\exp(-Q_b/RT)$, δ_{GB} is the thickness of the GB],

$$Q = \frac{3d}{(1-d^2)^3}\left[\ln\frac{1}{d} - \frac{(3-d^2)(1-d^2)}{4}\right],$$

$$\varepsilon = \frac{2p_{CH_4}\Omega_b}{\gamma_S}, \qquad d = \frac{r}{\Omega_b}.$$

If grain-boundary diffusion is the rate-controlling step of the process, the growth rate of the gas bubble on the GB is

$$\left(\frac{dr}{dt}\right)_{GB} = \frac{3\Omega D_b\delta_{GB}}{d(1-d^2)^2 Q k_B T \Omega_b^2}\left[p_{CH_4} - \frac{\gamma_s(1-d^2)}{d\Omega_b}\right]. \quad (46)$$

Lastly, in the case of dislocation creep, when the growth of the bubble depends on the hydrogen–dislocation interaction and on the quantity of hydrogen transferred with the moving dislocations, the kinetics are described by the expression[64]

$$\left(\frac{dr}{dt}\right)_{dc} = \sqrt{3}\varepsilon_{cr}^0 G_c(d), \quad (47)$$

where

$$\varepsilon_{cr}^0 = \frac{AD_L b}{V_0 k_B T G_c^{N-1}}\left[p_{CH_4} - \left(\frac{2\gamma_S}{r}\right)^N\right],$$

$$G_c = \left(\frac{3}{2}N\right)^N \frac{\Omega_b d}{(1-d^{3/N})^N}.$$

Here A is a constant dependent on the material [see formula (18)], D_L is the coefficient of lattice (volume) diffusion of hydrogen, V_0 is the rate of dislocation creep, and N is the extent of creep.

Under the conditions $r^2 \ll n^{-1} \ll D_L t$, the radius of spherical formations deposited along the GB can be determined by the formula

$$r(z,t) = r(0,t)\left[1 + \left(\frac{2\pi n D_L}{15\delta_b D_{GB}}\right)^{1/2} z r^{1/2}(0,t)\right]^{-2}, \quad (48)$$

where n is the density of the generation centres of the new phase, and δ_b is the diameter of the bubble.

Point defects interact strongly with the GB, and therefore very pure bicrystals must be used in studies of the effect of small, mobile impurities (for example, the hydrogen isotopes). The segregation on the GB of impurities of the *s* and *sp* elements with atoms larger than those of the matrix strongly perturbs the GB structure and alters its hydrogen adsorption capacity.[66] The effective diffusion coefficient of hydrogen $D_{H,ef}$ in the grain-boundary volumes of the transition metals is almost two orders of magnitude greater than through the grain itself. The parameter $D_{H,ef}$ is strongly dependent on the angle θ. The most important experiments were carried out on Pd electrodes, but work on the 3*d* metals has also been reported. Thus, in a calculation of the diffusion coefficients in a bicrystal of very pure (99.999%) nickel with symmetrical boundaries having slopes of 39° (Σ = 9) and 129° (Σ = 11), it was found that $D_{D,ef}$ is 4.6×10^{-13} cm s^{-1} in the former case and 8–17 times greater in the latter.

The concentration of hydrogen in the grain boundary volumes induces a phase transformation and the formation of hydrides on the GB; the quantity $D_{D,ef}$ for the hydrogen-saturated nickel polycrystal is $\sim 3 \times 10^{-16}$ m^2 s^{-1}. The specific volume (density) of the hydride is usually different from that of the hydrogen-saturated matrix (the body of the grain). The dilatation effect arising under these conditions induces active processes involving the multiplication of dislocations in the crystallites. The hydrogen transferred together with the moving dislocations promotes further saturation of the GB by hydrogen.[68]

The cluster modelling of the GB on the basis of structural elements with octahedral and tetrahedral pores filled with the impurity atoms has shown[69] that the grain-boundary cohesion increases after the introduction of boron into nickel; it decreases if sulfur is concentrated on the GB. The first cluster calculations have been performed by Hashimoto's group for GB with Σ = 5 in iron containing phosphorus segregations.[70] Depending on the ratio of the dimensions of the pores and the impurity atoms, directed deformations on the GB can occur for steric reasons, inducing local phase transitions. The interatomic covalent bonds between the atoms of the matrix and the impurities are then strengthened, but the M–M bonds are weakened, the degree of weakening depending on θ and Σ. Subsequently, the influence of the impurities on the properties of many adsorbed surface phases was estimated and phase diagrams for the GB were constructed.[71]

Surface-active impurities, namely P, As, Sb, S, Se, Te, and Sn, greatly reduce the grain-boundary cohesion strength in iron and stainless steels, Si slightly reduces the cohesion, while Ni, C, and B increase it. The addition of N, C, and B slightly alters the segregation of the impurities of the first group on the GB. When the M–electrolyte interface is acted upon by electrolytes, there is a change in the pattern of the mutual influence of the impurities. The affinity of the impurity element for oxygen begins to play a dominant role. Technological additions of boron initiate ICC most vigorously in highly oxidising media — the effect of 0.001% B (X2ON20 steel) is analogous to the effect of ~0.1% P or ~1% Si.[72] The joint introduction of the C and P impurities, of C, and of doping amounts of Si results in the synergism of their activity associated with the localisation of chromium on the grain-boundary volumes in steel. The synergism can be accounted for by the grain-boundary segregation of C and P, inducing the depassivation of the GB as a result of the formation of less ordered oxide layers. An increase in the C content in steel ($0.1 < c_C < 0.3\%$) lowers the concentration of chromium on the grain boundaries as a result of the formation of the carbide $(Cr, Fe)_{22}C_6$ and hence impairs the passivation characteristics locally. However, the supersaturation of the near-surface layer of stainless steel (12X18N9T) with carbon ($c_C > 0.3\%$) increases its tendency towards ICC,[73] since the differences between structures of the oxide layers on the GB and on the body of the grain vanish.

Chromium actually diminishes the rate of dissolution of stainless steel in the passive range of potentials; the introduction of Ni, Mo, and N has a weak effect on the passivation of steel, but suppresses its dissolution in the active region. In the active dissolution of stainless steel, its near-surface layer is enriched in chromium and molybdenum, so that the formation of Cr–Mo–Ni intermetallic compounds as well as nitrides becomes possible. For equal amounts of carbon in austenitic stainless steels of different brands, the tendency towards intercrystallite corrosion is smaller for steels with a higher molybdenum concentration.[74] The joint action of chromium and other doping components (Ti, Ni, Mo, N) increases the zone corresponding to their influence on ICC. The width of the etch channels in ICC on GB is significantly greater (by a factor of 10–100) than the width of the boundary zones depleted in chromium. The width of the depleted zones in austenitic seals of the 304L and 316L types is not more than 1–2 μm. Consequently, in estimating the ICC, it is

necessary to take into account the influence and distribution of other impurities, in particular nitrogen.

Nitrogen, localised on structural defects, suppresses the selective dissolution of steel, which lowers the rate of corrosion. The sharp decrease in the solubility of transition metals after saturation with nitrogen is a well known phenomenon used in engineering. However, the concentration of nitrogen in steel must be maintained at a level $c_N \leqslant 0.13\%-0.15\%$ or $0.4\%-0.5\%$ (superaustenitic steels). Such a steel is resistant to the action of oxidation-reduction media and does not undergo ICC and slit corrosion in halide-containing solutions.[75] For $0.15\%-0.18\% < c_N < 0.4\%$, nitrides ($Cr_2N$) are formed vigorously and the rate of corrosion on the GB increases.[74]

The crystallographic stability is lost more readily on the GB, the overvoltage η being appreciably smaller than on the body of the grain. Correct crystallographic solutions of problems concerning the grain-boundary dissolution have been published by the groups of Froment and coworkers[13,14] and Gleiter.[76,77] Geometrical calculations are performed starting with the postulate that the rates of dissolution of neighbouring grains are different, so that the misorientation angles relative to the normal to the GB are also different. This makes it possible to calculate the changes in the surface tension $d\gamma$ by Eqn (15). The grain-boundary volume itself is not taken into account in such models; it is also disregarded in the CBL, GDL, and FOL models.

The grain-boundary dissolution process depends in many respects on the misorientation angle θ. By means of the texturing treatment of rolled sheet steel, it is possible to achieve changes in the rate of corrosion by several orders of magnitude and also to avoid the need for the use of corrosion inhibitors. There are definite critical angles θ_{cr} below which the GB have a low energy.[78] With increase in θ, the depth of the ICC increases and the stability of the GB falls. The decrease in the stability of the GB may be accompanied by the appearance on the bottom of the etch groove of a crack spreading into the bulk of the metal. The development of the crack depends subsequently on the topology and density of the dislocations in the local volumes of the metal. In the vicinity of a GB, there is an extensive dislocation structure with an increased content of mobile impurities. The dissolution process is undoubtedly associated with grain-boundary segregations, phase formation on the internal interfaces on heat treatment, ageing, and saturation with hydrogen.

In the estimation of the degree of corrosion on an interface by standard methods, the overall dissolution current i_Σ is regarded as the sum of the dissolution currents in the defects (i_D) (vacancies, dislocations, grain boundaries) and on the undamaged part of the surface (i_S). An exact quantitative separation of these currents is not always possible. For specimens, where either GB or only the material of the bulk of the grain appear on the working surface, it is possible to employ a novel method proposed by Khaldeev et al.[79] With the aid of this method, the influence of grain-boundary volumes on the electrochemical characteristics of the specimens was estimated experimentally and a study was made[79] of the influence of the vacuum heat treatment (673, 1073, and 1273 K, $t = 5 \times 10^5$ s) of M1 (99.90%) and M00 (99.95%) copper on the physical properties and corrosion in 0.5 M H_2SO_4.

The electrochemical characteristics of specimens annealed at a high temperature (973 and 1273 K for M00 and 1273 K for M1) change abruptly during anodic dissolution (Fig. 10). Thus, in the course of the continuous cyclic recording of polarisation curves for the same M1 specimen, one type *3'* curve is recorded after virtually only one type *3* curve, whilst for M00 copper annealed at 973 and 1273 K a type *6'* curve is recorded after 4–5 type *6* curves.

This can be accounted for as follows. High-temperature annealing leads to the growth of the grain (Fig. 10, curves *1* and *2*) and the formation of the so called bamboo structure, where GB cuts across the cross-section of the specimen in definite steps. The attainment of such boundaries in anodic dissolution leads to the appearance of anomalous $E-i$ curves (curves *3'*, *5'*, and *6'*), which has been confirmed by a parallel microscopic study. The

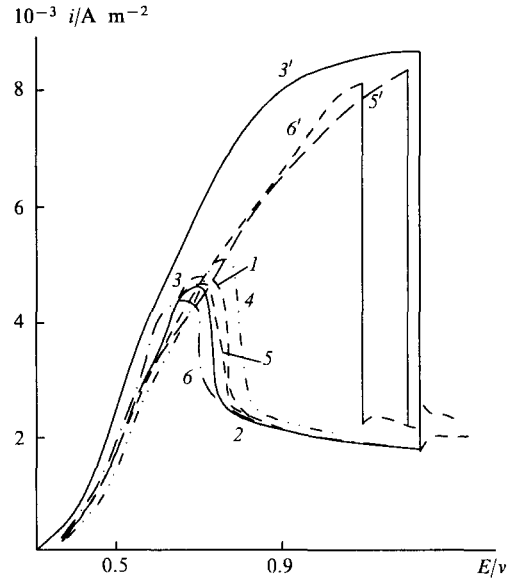


Figure 10. Anodic potentiodynamic ($V_E = 8 \times 10^{-4}$ V s^{-1}) curves for M1 (curves *1–3* and *3'*) and M00 (curves *4–6*, *5'* and *6'*) copper in 0.5 M H_2SO_4. Annealing temperature (K): (*1*) and (*4*) 673; (*2*), (*5*) and (*5'*) 973; (*3*), (*3'*), (*6*) and (*6'*) 1273.

formation of such a structure depends on the purity of the metal; in purer copper (M00), the grains are larger. At $T = 1273$ K, the grain diameter is $d_{M00} = 0.5-1.0$ mm, whereas $d_{M1} = 0.1$ mm, the value of d along the axis of the specimen being several times greater. Thus the highly pure M00 copper annealed at 1273 K contained a bicrystal in its cross-section as well as in the case where a layer with short GB was dissolved (a layer 0.03–0.05 mm thick dissolved during the recording of one curve); an almost twofold increase in i_{max} and E_{max} was observed [from $(4.5-4.6) \times 10^3$ to $(8.5-8.8) \times 10^3$ A m^{-2} and from 0.65–0.70 to 1.10–1.30 V respectively].

The purity of the metal influences significantly the mobility of the boundaries during annealing; as a rule, the impurities are concentrated in the vicinity of the GB. The accumulation of impurities on the GB may be regarded as a phase transition involving a change in the type of bond — from metallic in the bulk phase to predominantly covalent on the GB. This makes it possible to explain the differences in the behaviour of M1 and M00 copper. The anomalous dissolution is apparently not associated with changes in the nonequilibrium defects within the grain. With increase in the annealing temperature above 973 K, the relative resistance $K_\rho = \rho_{233}/(\rho_{293}-\rho_{77})$ (here ρ_{293} and ρ_{77} are the specific resistances at 293 and 77 K respectively), which makes it possible to estimate the degree of defectiveness of the GB of the grains, increases rapidly (Fig. 11, curves *3* and *4*). This indicates an increase in the degree of defectiveness in the region of the grain boundaries. Measurements of the internal friction Q^{-1} also indicate that a more ideal structure is created within the grain (Fig. 11, curves *5* and *6*). The nature of the variation of Q^{-1} shows that the movement of the dislocations within the grain is responsible for the increase in the internal friction: with increase in the size of the crystallites, there is an increase in the length of the dislocation segments between the points of strong attachment and the localisation of the impurities in the region of the GB promotes a smaller degree of blocking of the dislocations by the impurity atoms (Fe, Zn, Sb, Bi, P). The changes in i_{max} and E_{max} are not associated with the morphology of the intragrain volumes, since, according to the results of electron microscope analysis, there are no appreciable differences in surface rugosities for the specimens (Fig. 10, curves *1–6*). However, if the dissolution in the active range of potentials takes place on the GB for copper which has

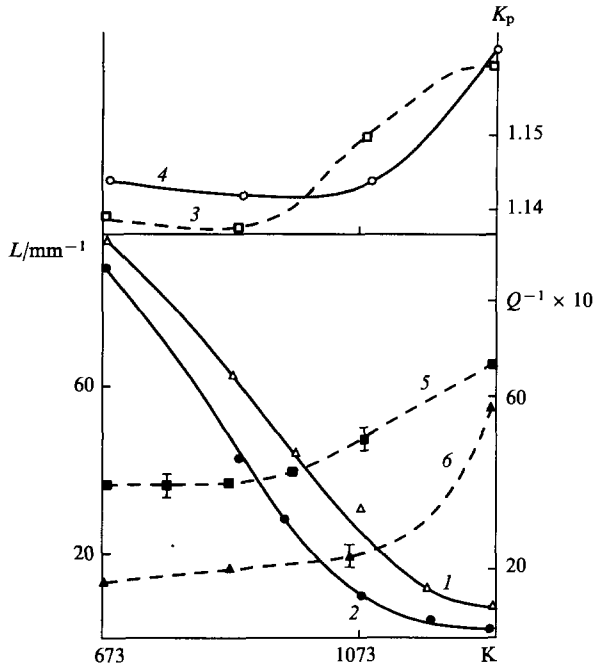


Figure 11. Dependence of the length of the grain boundaries (curves *1* and *2*), the relative electrical resistance (curves *3* and *4*), and the internal friction (Q) at a frequency of 1 Hz (curves *5* and *6*) on the annealing temperature for M1 (curves *1–3*) and M00 (curves *4–6*) copper.

been subjected to high-temperature annealing, the formation of etch channels is noted. Thus a decrease in the length of the GB and an increase in the concentration of defects and impurities in their vicinity may induce an appreciable anomalous change in the dissolution currents and passivation potentials.

Erb et al.[76] reached a similar conclusion. The method used in their experiment reduces to the following. In order to achieve the separate quantitative estimation of the rates of corrosion on the GB and on the bulk of the grain, two highly pure copper crystals (99.999%) and a Cu–Bi copper alloy (6×10^{-3}–7×10^{-2} at.% Bi) were sintered, after which only the GB (at $T = 263$ K, $t = 5.4 \times 10^5$ s) was subjected to corrosion in aqueous 12% HCl solution to which 1 g litre^{-1} of $FeCl_3.6H_2O$ had been added. The width of the etch groove formed is ~20–45 μm. The development of the ICC is associated with the increase in the local anode current i_a, caused by the accumulation of the bismuth impurities, and not with the increase in γ_{SL} (the free energy of the region of the metal lattice near the GB).

The analysis of the behaviour of triple grain contacts is important in the description of the stable networks of grain-boundaries on the surface of the crystal. On the basis of the modified Mullins model,[47] results have been obtained[70] according to which the region of the triple contact increases on dissolution and does not undergo a change in shape, the latter being determined solely by the free energy of the boundaries. The crater region of the contact is larger than the etch groove and its size increases with decrease in the angle between the boundaries converging at the point of contact. The corrosion-activated triple contact of the GB (and the GB themselves in textured materials) may become a dangerous concentrator of the disruption. Following the application of a load in excess of the ultimate strength and acidification of the medium in the corrosion pit, the crack increases catastrophically.[81] The rate of the abrupt growth of such a crack into the bulk of the material obeys a relation[81] analogous to the Kolmogorov–Johnson–Mell–Avraami equation:

$$V_c = \left[0.5m + \frac{\Delta a_p}{V_\delta}\left(1 - \exp\frac{-V_{\delta,S}}{t_p V_\delta}\right)\right] V_\delta \ , \qquad (49)$$

where m is the characteristic of the profile of the sloping side of the groove [Eqn (34)], Δa_p the sum of the changes in the internal conditions (constants of the material) and external conditions (the potential E, the rate of deformation V_d, and the composition and concentration c of the solution), and V_δ and $V_{\delta,S}$ are respectively the overall rate of expansion of the plastic failure zone (abrupt growth of the crack) and the corresponding rate in a single act. The abrupt growth is effected as a result of the formation of steps, which is accompanied by an increase in the rate of corrosion i_{cor}. The crack is initiated within narrower ranges of E and V_d than its propagation and depends greatly on the angle θ and the reciprocal of the density of the coincidence blocks Σ. The values of θ and Σ for which the M–M bonds are anomalously weakened are characteristic also of intense ICC.

VI. Dissolution of heterophase polycrystalline metals

The influence of bulky defects (microinclusions) on the dissolution of a metal must be considered in terms of a continuous approximation. The intragrain heterogeneity may be caused not only by mesolevel defects (single dislocations, low-angle boundaries of dislocation origin, and coherent binary layers), but also by rigid inclusions inducing both elastic and plastic deformation of the material of the grain. As a rule, the rates of dissolution of the inclusion and the matrix are different, while the stresses generated by the inclusions in the matrix are capable of altering significantly the rate of corrosion of the metal.

The role of nonmetallic inclusions in the corrosion process is complex: depending on their type and geometry, the rate of dissolution of the metal may both increase and diminish. Clearly i_{cor}, which depends on the sum of the internal factors (impurity composition, structure, and deformation state of the metal) and external factors (anionic composition and electrolyte parameters), may vary within wide limits, the greatest changes being observed in materials which dissolve under more nonequilibrium conditions (corrosion under stress, corrosion in slits and gaps, corrosion under the conditions of nonstationary movements of the electrolyte, corrosion in the anodic process, etc.).

It is of interest to examine the role of the rigid inclusions in the dissolution of a heterophase polycrystalline metal. This problem is of current interest for composite electrochemical coatings, carbon steels containing cementitic Fe_3C outcrops in ferrite, and also brass, titanium and its alloys (α-phase in a β-matrix), and certain other materials, since it is necessary to take into account the change in the deformation state of the matrix following the development of microinclusions. The rate of dissolution of an elastically deformed metal may increase significantly.

Plastic inclusions. We shall consider a periodic system of linear planar parallel inclusions. Their length is $2l$, their centres are located on the $0x$ axis, and the angles α of their inclination relative to the axis are equal (Fig. 12). In order to find the stresses arising under these conditions, it is necessary to solve the following integral equation:[82]

$$\int_{-l}^{l} [G(\rho, t)K(t - x, \rho^*) + G(\rho, t)L(t - x)]\mathrm{d}t = 0.5\pi i(\rho - \rho^*)F(\rho^*, x), \quad |x| < l \ , \qquad (50)$$

where

$$K(x, \rho^*) = 0.5\pi\rho^* l_d^{-1}\{\exp(i\alpha)\cot[\pi x \exp(i\alpha)]l_d^{-1}\} + \exp[(i\alpha)\cot(-i\alpha)]l_d^{-1} \ ,$$

$$L(x) = 0.5\pi l_d^{-1}\{\cot[\pi x \exp(-i\alpha)]l_d^{-1}\} - \pi x[\exp(-i\alpha)]\mathrm{cosec}^2[\pi x \exp(-i\alpha)]l_d^{-1}[\exp(-i\alpha) - \exp(-3i\alpha)]\cot[\pi x \exp(-i\alpha)]l_d^{-1} \ ,$$

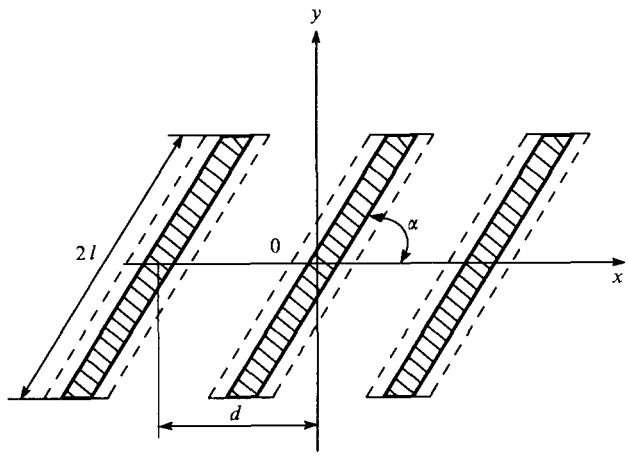


Figure 12. Schematic illustration of the matrix–rigid inclusion system.

$G(\rho,t)$ is a stresses function, $F(\rho^*,x)$ is a known displacement function, and ρ^* assumes the values L and $-l$ for rigid inclusions. The solution of this equation must satisfy the condition

$$\int_{-l}^{l} G(\rho,t)\mathrm{d}t = 0 \ .$$

Having expressed $G(\rho,t)$ in the form

$$G(\rho,t) = U(\rho,t) + \mathrm{i}V(\rho,t) \ ,$$

we obtain

$$\bar{G}(\rho,t) = U(\rho,t) - \mathrm{i}V(\rho,t) \ .$$

Having expanded the functions $\cot\varphi$ and $\mathrm{cosec}^2\varphi$ in a power series and having retained only the first two terms of the expansion (since they make the greatest contribution to the expansion for short distances between the defects), we obtain the following expressions for $K(x,\rho^*)$ and $L(x)$:

$$K(x,\rho^*) = \frac{\rho^*}{x} - \frac{\pi^2\rho^*\cos 2\alpha}{3l_\mathrm{d}^2}x \ ,$$

$$L(x) = \left(-\frac{2\pi^2}{3l_\mathrm{d}^2}\sin 3\alpha \sin\alpha\right)x + i\left(\frac{2\pi^2}{3l_\mathrm{d}^2}\cos 3\alpha \sin\alpha\right)x \ .$$

Having expressed $G(\rho,t)$ and $\bar{G}(\rho,t)$ in the form $G(\rho,t) = a_0 + a_1\rho + a_2 t + \mathrm{i}(b_0 + b_1\rho + b_2 t)$, i.e. containing only the linear terms in the expansions of $G(\rho,t)$ and $\bar{G}(\rho,t)$, we obtain a system of equations for the determination of the coefficients a_2 and b_2:

$$a_2\left[\rho^*\left(2l + x\ln\left|\frac{l-x}{l+x}\right|\right) - \frac{l^3}{3}\frac{\pi\rho^*\cos 2\alpha + 3\pi^2\sin 3\alpha\sin\alpha}{3l_\mathrm{d}^2}\right]$$

$$- b_2\frac{2\pi^2}{3l_\mathrm{d}^2}\cos 2\alpha\sin\alpha = 0.5\pi(\rho^* - \rho)B \ ,$$

$$- a_2\frac{2\pi^2}{3l_\mathrm{d}^2}\cos 3\alpha\sin\alpha \qquad (51)$$

$$+ b_2\left[\rho^*\left(2l + x\ln\left|\frac{l-x}{l+x}\right|\right) - \frac{l^3}{3}\frac{\pi\rho^*\cos 2\alpha}{3l_\mathrm{d}^2}\right.$$

$$\left. + \frac{l^3}{3}\frac{3\pi^2\sin 3\alpha\sin\alpha}{3l_\mathrm{d}^2}\right] = 0.5\pi(\rho - \rho^*)A \ .$$

Here $A(\rho^*,x)$ and $B(\rho^*,x)$ are the real and imaginary components of the function $F(\rho^*,x)$. The coefficients a_0, a_1, b_0, and b_1 do not enter into the expansion in view of the symmetry of the function $G(\rho^*,x)$, because in this case $a_0 + a_1\rho = 0$ and $b_0 + b_1\rho = 0$.

Having solved Eqn (51), we obtain expressions for the coefficients a_2 and b_2:

$$a_2 = \frac{-0.5\pi(\rho - \rho^*)B(\rho^*,x)}{\rho^*\left(2l + x\ln\left|\frac{l-x}{l+x}\right|\right) - \frac{l^3}{3}\frac{\pi\rho^*}{3l_\mathrm{d}^2}} \ ,$$

$$b_2 = \frac{0.5\pi(\rho - \rho^*)A(\rho^*,x)}{\rho^*\left(2l + x\ln\left|\frac{l-x}{l+x}\right|\right) - \frac{l^3}{3}\frac{\pi\rho^*}{3l_\mathrm{d}^2}} \qquad (52)$$

We shall consider the special case where the displacements are directed along the $0x$ axis. Analysis of the expressions for the coefficients a_2 and b_2 yields the following results: if $\alpha = 0$, then the stresses fall to zero for $l_\mathrm{d}\to 0$ and approach asymptotically a definite value for $l_\mathrm{d}\to\infty$. For a fixed distance l_d, the stresses vary as a function of x—the stresses diminish on moving away from the boundaries of the rigid inclusions. The curve relating the stresses to the distance to the GB has a minimum. We may note that the influence of the thickness of the inclusions on the distribution of the stresses is taken into account by the quantity l_d.

In the case of a uniform distribution of lamellar segregations in the matrix, a uniform stresses field arises within the crystals and the average density of the forces corresponds to the distribution of the surface forces. With increase in the number of inclusions of the second phase in a definite volume of the crystals, the overall surface energy on their interfaces also increases:[83]

$$\Delta\sigma = G_\mathrm{c}g^2\Delta c^2\mathrm{d}A_\mathrm{S}^2 + \frac{\gamma A_\mathrm{S}^3}{l_\mathrm{d}} \ ,$$

where $g = \mathrm{d}a/\mathrm{d}c$ is a derivative characterising the coherence of the transition on the interface, a the lattice parameter of the matrix, $\Delta c \approx \Delta\gamma^{\neq}$ the difference between the concentrations of the species in the phases proportional to the degree of supersaturation, A_S the area of the lamellar inclusions, and γ the surface tension. The minimum in $\Delta\sigma$ is observed for $\gamma = G_\mathrm{c}A_\mathrm{S}^{1/2}$. On formation of noncoincidence dislocations (ND) on the interfaces and also by virtue of the intensification of the diffusion of impurity atoms in the field of the elastic stresses of the species comprising the second phase, the stresses in the heterophase structure relax. The creation under these conditions of a sharp concentration profile of the impurities in the near-surface layer of the lamellar outcrops and the consequent dilatation effect induce an additional influx of impurities into this zone—an autocatalytic growth of inclusions takes place.

The physical picture of the distribution of stresses in the matrix and in the vicinity of the interfaces, obtained in terms of the continuous approximation within the framework of the linear theory of elasticity, is almost equivalent to the representation of the distribution of the dislocations at the interfaces. In the immediate vicinity of the interface, there are zones in which there is a sharp decrease in the level of the stresses and in the concentrations of the elementary deformation carriers. Subsequently they increase sharply. The background values of σ and ρ_d are attained for distances greater than the size of the dislocation (>1 μm). It is clear from the foregoing that the superfine-grained materials with a grain size $\leqslant 1$ μm have unique physicochemical characteristics and an increased corrosion resistance.

Spherical inclusions. Apart from lamellar inclusions, intragrain heterogeneity is induced by spherical inclusions.

We shall consider the appearance of stresses in the matrix in the vicinity of spherical dispersed particles (DP) without taking

into account the chemical nature of the latter. A continuous theory for the estimation of stresses in the vicinity of single particles of subatomic dimensions has been thoroughly developed and described.[84] The introduction of DP with a volume V and a surface area A_S into the crystals is accompanied by an increase in the volume of a finite crystal by ΔV and the appearance of a stress field. For a uniform distribution of N dispersed particles, the average stress

$$\langle\sigma\rangle = \frac{N}{V}P_d ,$$

and the average deformation

$$\langle\varepsilon\rangle = \frac{N}{V}A_S P_d .$$

(here P_d is the force dipoles tensor characterising the direction of the forces of the effect of DP on the matrix) are inversely proportional to the volume of the DP; for high ratios NA_S/V, the quantity $\langle\varepsilon\rangle$ should increase. The latter is characteristic of DP distributed uniformly in isotropic matrices. However, it can be readily seen that the average stress $\langle\sigma\rangle$ diminishes with decrease in the volume of the DP: the decrease in the level of the stressed state of a heterophase material as well as the creation of a uniform deformation should naturally promote an increase in its corrosion resistance, because the corrosion-induced destruction of metals is associated with the rupture of the M – M bonds. For ultradisperse particles, it is apparently also possible to confine the treatment to the continuous approximation, since the need for the employment of the microscopic lattice theory arises for mesolevel defects with dimensions less than 50 atomic radii (6–8 nm) — for coagulations of vacancies, clusters of extraneous atoms, dislocations, and disclinations.

We shall consider an assembly of DP in an isotropic matrix in which both the distance between the DP and the dimensions of the DP themselves vary. Such a situation is characteristic of real heterophase materials. The stresses near a single point source act radially and are proportional to x^{-1}, where x is the distance from the DP. If one considers the DP as a point source of stresses with the coordinates (0,0), then the stress at this point (Fig. 13) can be expressed by the relation

$$\sigma_{xy} = \frac{A}{\sqrt{(x-x_0)^2 + (y-y_0)^2}} ,$$

where A is a constant which depends on the material of the matrix. For several sources with coordinates (x_n, y_n), the superposition principle operates and the overall stress σ_Σ can be expressed in the form

$$\sigma_\Sigma = A\sum_{i=1}^{n} \frac{1}{\sqrt{(x-x_i)^2 + (y-y_y)^2}} . \qquad (53)$$

In calculating the sums in Eqn (53), we proceed as follows. Since the DP with the coordinates (0,0) is influenced most by the nearest particles, one can assume that the latter are distributed on a circumference with a radius R (Fig. 13) or on a circular sinusoid.

The stresses in the matrix $(\sigma_{x,y})$ are then formulated as follows:

$$\sigma_{x,y} = A\int_0^{2\pi} \frac{dA_S}{\sqrt{(x-\xi)^2 + (y-\eta)^2}} . \qquad (54)$$

In the parametric form, we have

$$\xi = R\cos t, \quad \eta = R\sin t.$$

Hence $dA_S = Rdt$. Having substituted the last expressions in Eqn (54), we obtain

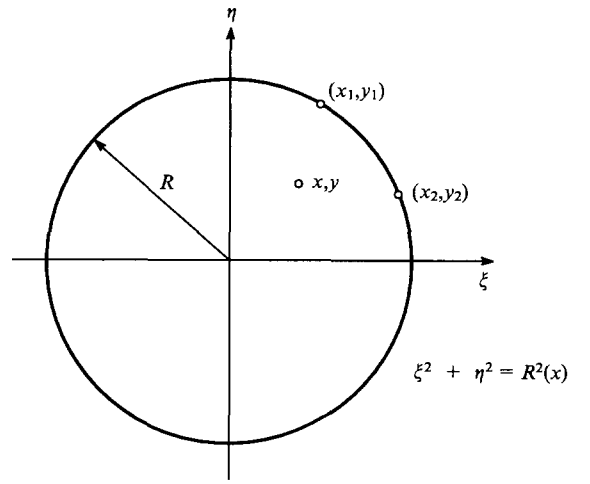


Figure 13. Model illustrating the disposition of disperse particles in a matrix.

$$\sigma_{x,y} = A\int_0^{2\pi} \frac{Rdt}{(x - R\cos t)^2 - (y - R\sin t)^2} . \qquad (55)$$

Since the disposition of the coordinate system (Fig. 13) makes it possible to regard the parameter of the point (x, y), at which the stresses are estimated, as fairly small, the integrand function in Eqn (55) can be expanded in series in x and y:

$$f(x,y) = f(0,0) + \frac{\partial f}{\partial x}(0,0)x + \frac{\partial f}{\partial y}(0,0)y + \frac{\partial^2 f}{\partial x^2}x^2 + 2\frac{\partial^2 f}{\partial x \partial y}xy + \frac{\partial^2 f}{\partial y^2}y^2 + O\left[\left(\sqrt{x^2+y^2}\right)^3\right] . \qquad (56)$$

Having formulated the derivatives for the terms of the integrand function $f(x, y)$, having substituted them in Eqn (56), and having integrated the latter for the stress $\sigma_{x,y}$, we obtain

$$\sigma_{x,y} = 2\pi A + \frac{4\pi A}{R^2}(x^2 + y^2) . \qquad (57)$$

We shall now analyse Eqn (57) taking into account the fact that R is a fixed quantity. For $0 < x < R$, $0 < y < R$, we have $\sigma_{x,y} \to 2\pi A$ if $x \to 0$ and $\sigma_{x,y} \to 10\pi A$ if $x \to R$.

Thus the stresses increase by a factor of 5 with increase in the distance from the DP and reach maximum values in the vicinity of $x = R$.

For spherical ultradisperse particles, the stresses can vary in accordance with a less steep law, in proportion to x^{-2} and not x^{-1}. In this case, the transformation of an equation of type (54) leads to the expression

$$\sigma_{x,y} = \frac{AR}{\sqrt{(x^2 - R^2) + 2y^2x^2}}\left(\frac{\pi}{2} + \arctan\frac{Ry}{(x^2 - R^2) + 2y^2x^2}\right), \qquad (58)$$

the analysis of which shows that the stress on a sphere is significantly smaller. We have

$$\sigma_{x,y} = \frac{\pi}{2}A$$

for $x = 0$ and $y = 0$, and

$$\sigma_{x,y} = \frac{3\pi A}{4R^3} .$$

for $x = R$ and $y = R$.

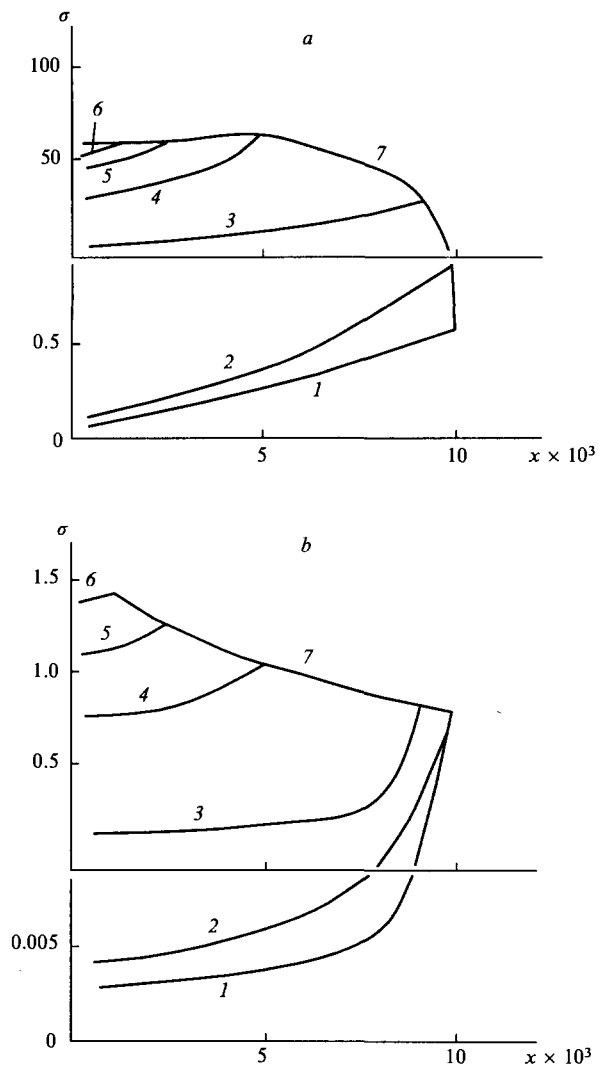


Figure 14. Dependence of the stresses in a matrix on the size of DP and the distance between them. Attenuation of the stresses in accordance with the x^{-1} (*a*) and x^{-2} (*b*) laws: r(nm): (*1*) 20; (*2*) 30; (*3*) 10^3; (*4*) 5×10^3; (*5*) 7.5×10^3; (*6*) 9×10^3; (*7*) stress level on a sphere with a radius $R = 10^4$ nm.

Numerical study of Eqns (56) and (57) for reasonable ratios of the DP radius and the quantity $R = 10^4$ nm (comparable to the grain size usually employed in metal technology) shows that, when the stresses are attenuated in accordance with the x^{-1} law (Fig. 14*a*), the quantity σ on the sphere where the surrounding DP are located is large. With decrease in the size of the DP, the stresses rapidly diminish—the greatest strengthening of the matrix is obtained for $x = 0.5R$ (Fig. 14*a*, curve *7*). When the stresses are attenuated in accordance with the x^{-2} law (Fig. 14*b*), the stresses level in the matrix is 2 orders of magnitude smaller than in the former case, but σ increases markedly in the vicinity of the DP. Under these conditions, the growth of stresses depends significantly on the size of the DP: the smaller the radius of the particles, the sharper the deformation profile (Fig. 14*b*, curves *1–3*). However, in a matrix uniformly saturated by particles the stresses change only slightly (Fig. 14*b*, curve *7*).

Thus the overall level of stresses in the matrix increases with decrease in the size of the DP and the stresses are localised in the vicinity of the DP.

The stresses near the DP relax, forming long noncoincident dislocations (ND) in the matrix. By virtue of this process, the density of dislocations ρ_d increases at the DP–matrix interface and microtwinned formations are produced [the process is usually observed experimentally in the study of thin foils by transmission electron microscopy (TEM)]. The continuous assessment of the stressed state in the vicinity of the DP–matrix interface does not conflict with the calculated model and the experiment on the distribution of dislocations in the vicinity of the grain boundary described above. The presence of an extremum in the stresses in an isotropic matrix promotes the appearance near the interface of zones with a reduced density of defects.

The equilibrium concentration of impurities in the matrix near a spherical particle with a radius r corresponds to the Gibbs–Thomson equation. We formulate this equation in the form

$$c_r(x,t) = c_\infty \exp\frac{2\gamma_{SL}\Omega}{rRT} ,$$

where c_∞ is the concentration of impurities on the inclusion–matrix interface in the case of a planar surface when $r \to \infty$ and $K_M = 0$. Analysis by Lifshits and Slezov[85] showed that, for a certain degree of supersaturation $\Delta\gamma^{\neq} = c - c_\infty = \text{const}$, the quantity

$$r_{cr} = -\frac{2\gamma_{SL}}{\Delta G_V} ,$$

corresponds to the equilibrium between a particle and the impurities near it. Here ΔG_V is the change in free energy in the crystal–liquid transition. The particle grows if $r > r_{cr}$ and is degraded if $r < r_{cr}$. The annihilation of small particles occurs as a result of consecutive pair interactions. Two particles with masses m and n form a new particle with a mass $m - n = k$: for long times t, the concentration of such particles is[86]

$$A_k(t) \sim \frac{A}{t(\ln t)^{k-1}} ,$$

where

$$A_k = \frac{(N-1)!}{(N-k)!} , \qquad k = 1, 2, \ldots, N-1;$$

N is the mass of a particle (cluster) having a finite volume.

The noncoincident dislocations, fixed on the DP, serve as pathways for the diffusional migration of impurities from particles having a low radius and undergoing degradation to larger particles. We shall analyse the growth of such DP in the matrix. For a uniform distribution of the particles (as above, the volume of a matrix having a radius R is considered), the particle is acted upon by a force $F = G_c/r$, the overall vector of which may be random.

If the distribution function for particles in the bulk of the matrix, the volume of which is limited by a radius R, is

$$f_0(R) = \frac{3}{r^3}R^2 ,$$

the overall distribution function can be formulated as follows:

$$g(x,y)\mathrm{d}x\,\mathrm{d}R = g_1(\varphi,R)\mathrm{d}\varphi\,\mathrm{d}R = \frac{3}{r^3}R^2\mathrm{d}R\frac{1}{2}\sin\varphi\,\mathrm{d}\varphi \qquad (59)$$

$$= \frac{3R^3}{2r^3G_c}\mathrm{d}R\,\mathrm{d}x ,$$

where φ is the angle between the specified direction and the direction of the force acting on the particle.

Having integrated Eqn (59) with respect to all R, we obtain the expression

$$f(x) = \frac{3}{2r^3G_c}\int_0^r R^3\mathrm{d}R = \frac{3}{8}\frac{r}{G} , \qquad (60)$$

which is valid for $|x| < G_c/r$. If $|x| > G_c/r$, then

$$f(x) = \frac{3}{2rG_c}\int_0^{G_c/|x|} R^3 dR = \frac{3}{8}\frac{G_c^3}{r^3|x|^4}. \quad (61)$$

It is possible to determine experimentally the distribution of stresses in the vicinity of a charged particle, i.e. the characteristics of such a stress can be estimated before the corrosion test. For example, the average expected stress MF is given by

$$MF = \int_0^\infty xf(x)dx$$

$$= \int_0^{G_c/r} x\frac{3}{8}\frac{r}{G_c}xdx + \int_{G/r}^\infty \frac{3}{8}\frac{G_c^3}{r^3}x^{-3}dx = \frac{3}{8}\frac{G_c}{r},$$

and the average scatter DF around this value is

$$DF = \int_0^\infty (x - MF)f(x)dx = \frac{7}{64}\frac{G_c}{r^2}, \quad (63)$$

i.e., for a particular metal, it is found that the smaller the size of the DP the higher the stresses level on the interface. In terms of mathematical statistics, the probability that the specified stress is exceeded is given by

$$P(\beta \leqslant x < +\infty) = \int_\beta^\infty f(x)dx;$$

β has two extreme values: if the concentration of particles is small so that $\beta < G_c/r$, we have $P = 3\beta/16$; if a volume with a radius R is overfilled with particles for $\beta \geqslant G_c/r$, we have $P = G_c^3/8r^3\beta^3$.

Thus, when the quantitative relation between the stresses level σ and the rate of corrosion i_{cor} is known, it is possible to determine the probability that the chemical resistance of the metal will change.

The quantity $\sigma_{x,y}$ was estimated above relative to a particle within the sphere on which the surrounding DP are located. The overall stresses arise as a result of the superposition of the $\sigma_{x,y}$ due to the assembly of DP, whereupon the extremum values of $\sigma_{x,y}$ within the sphere correspond to $x = 0.5R$ when the stresses are attenuated in accordance with both the x^{-1} and x^{-2} laws. It is noteworthy that the electrical characteristics of a surface with periodic inhomogeneities in the near-surface layer of the metal have an extremum at $x = 0.5r$.

Thus analysis shows that within the sphere there is a region with an extremum stresses level. Heterophase materials in which the ratio of the dimensions of the grain and the DP satisfies the condition $x = 0.5R$ exhibit the lowest corrosion resistance. Such situations may arise when two-phase alloys or ferrite-perlitic steels are employed in corrosive media and also for the local formation of hydrides in a matrix where particles of a second phase grow in the course of the hydrogen saturation process and there is a sudden increase in the rate of corrosion.

The relaxation of stresses in the vicinity of the DP takes place also as a result of the dislocation migration of impurities, i.e. as a result of local changes in chemical composition. The dislocation migration depends on the mobility of the dislocations V, which is related, in its turn, to their density by the simple expression

$$V = \frac{\dot{\varepsilon}}{\rho_d b}, \quad (64)$$

where $\dot{\varepsilon}$ is the rate of deformation of the crystal. It follows from Eqn (64) that an increase in ρ_d (for example, from 10^4 to 5×10^{18} m^{-2}) should lower significantly (by a factor of 10^5) the mobility for $\dot{\varepsilon} = \text{const}$. In the case of a hydrogen-saturated metal, $\dot{\varepsilon}$ should lie in the pre-Cottrell region, i.e. V should not exceed V_{cr} ($V_{cr} \leqslant 4D_D r_d^{-1}$, and r_d is the radius of the Cottrell atmosphere of the impurity atoms on a dislocation tube), whereupon dislocations are abstracted from the atmospheres of the impurity atoms. Favourable conditions for the relaxation of stresses and the redistribution of impurities arise at elevated temperatures and for low rates of deformation. For iron alloys, this corresponds to isothermal treatments at $T = 400$ K and $t > 6$ ks.

A nonuniform distribution of the DP in the matrix and hence the alternation of zones with different stressed states increases the risk of a sudden disintegration for high degrees of localisation of the corrosion process.

VII. Conclusion

In the physical chemistry of interfacial processes, a steady interest in the study of the influence of the structure of the interfaces on charge and material transfer processes has been manifested recently. The anomalies in the chemical reactivity of grain boundaries compared with the surfaces of crystals having structural defects with a definite structural hierarchy are due to their unusual structure. These anomalies can be used in electrocatalysis, in the electrosynthesis of organic compounds, and in the protection of metals against corrosion-induced disintegration.

The study of the metal–electrolyte corrosion system taking into account the influence of the metal defects at different structural levels (from point defects to bulk-phase defects) shows that a quantitative estimate of the effect of the dissolution proper should also be performed at different levels. If a point defect or a single dislocation induce a local distortion of the lattice which undergoes a rapid and sharp attenuation in the vicinity of the defect, then this promotes the intensification of a local form of corrosion — an etch pit is formed (in the case of a grain boundary an etch groove is produced, whilst slit corrosion may develop at the DP–matrix interface). Elastic deformations arising from the boundaries of grains and inclusions embrace the entire bulk of the grain and the groups nearest to it. In the latter case, the study of the influence of defects on corrosion becomes possible in terms of the continuous approximation using the theory of elasticity.

It is apparently to be expected that studies of controllable chemical reactions on the thoroughly tested surfaces of bi- and tricrystals will be undertaken. This will lead to new possibilities for the specific synthesis of new chemical products.

This review has been written with the financial support of the 'Universities of Russia. Chemistry' (project 51) program.

References

1. W A T Clark, C J McMahon, R H Wagoner, R P Wei *Mater. Sci. Eng.* **83** 205 (1986)
2. R H Jones, in *4th International Conference on Hydrogen Effects on Material Behavior (Program and Abstracts)*, Jackson Lake, WY, 1989, p. 14
3. O N Markova, N D Tomashov, G P Chernova *Zashchita Met.* **29** 409 (1993)
4. G V Khaldeev *Ingibirovanie Rastvoreniya Metallov* (Inhibition of the Dissolution of Metals) (Moscow: Nauka, 1993)
5. H Gleiter, in *Atom Fracture. Proceedings of the NATO Advanced Research Institute, Caltoglio, 1983* p. 433
6. R W Baluffi, P D Bristowe *J. Phys.* **46** 267 (1985)
7. G A Chadwick, D A Smith (Eds) *Grain Boundary Structure and Properties* (New York: Academic Press, 1976)
8. A N Orlov, V N Pereverznev, V V Rybin *Granitsy Zeren v Metallakh* (Grain Boundaries in Metals) (Moscow: Metallurgiya, 1980)
9. B S Bokshtein, Ch V Kopetskii, L S Shvindlerman *Termodinamika i Kinetika Granits Zeren v Metallakh* (Thermodynamics and Kinetics of Grain Boundaries in Metals) (Moscow: Metallurgiya, 1986)
10. B S Bokshtein, Ch V Kopetskii, L S Shvindlerman, A N Orlov, L M Klinger, D A Gorbunov, V M Ivlev, Yu M Mishin, I M Azumovskii, S Z Bokshtein, A N Aleshin, S I Prokof'ev, B B Straumal, V E Fradkov *Struktura i Svoistva Vnutrennikh Poverkhnostei Razdela v Metallakh* (Structure and Properties of Internal Interfaces in Metals) (Moscow: Nauka, 1988)
11. A P Sutton *Int. Met. Rev.* **29** 377 (1984)

12. K Sangval *Travlenie Kristallov. Teoriya i Eksperiment* (Etching of Crystals. Theory, Experiment and Application) (Translated into Russian; Moscow: Mir, 1990)
13. L Beaunier, M Froment, C Vignaud *Electrochim. Acta* **25** 1239 (1980)
14. L Beaunier, M Froment, C Vignaud *J. Electroanal. Chem.* **119** 125 (1981)
15. R A Marcus *Annu. Rev. Phys. Chem.* **15** 155 (1964)
16. J Hirth, J Lothe *Theory of Dislocation* (Translated into Russian; Moscow: Atomizdat, 1972)
17. L V Spivak, N E Skryabina, M Ya Kats *Vodorod i Mekhanicheskoe Posledeistvie v Metallakh i Splavakh* (Hydrogen and Mechanical Secondary Action in Metals and Alloys) (Perm: Izd. Permsk. Univ., 1993)
18. M McLean, E K Hondros, in *Surface Mobilities of Solid Materials: Fundamental Concepts and Applications. Proceedings of the NATO Advanced Study Institute* (New York; Les Arcs, 1983) p. 459
19. R Dodd, J Eilbek, J Gibbon, H Morris *Soliton and Nonlinear Wave Equations* (Translated into Russian; Moscow: Mir, 1988)
20. B I Smirnov *Dislokatsionnaya Struktura i Uprochnenie Kristallov* (Dislocation Structure and Strengthening of Crystals) (Leningrad: Nauka, 1981)
21. K A Chishko *Fiz. Tverd. Tela* **23** 3028 (1981)
22. G V Khaldeev, L A Timofeeva, V V Kuznetsov *Poverkhnost'* **3** (3) 119 (1984)
23. V B Fedoseev *Poverkhnost'* **8** (17) 114 (1990)
24. G V Khaldeev, A B Volyntsev *Izv. Akad. Nauk SSSR, Met.* (3) 134 (1984)
25. A B Volyntsev *Nasledovannaya Mekhanika Dislokatsionnykh Ansamblei. Komp'yuternye Modeli i Eksperiment* (Inherited Mechanics of Dislocation Ensembles. Computer Models and Experiment) (Perm: Izd. Permsk. Univ., 1990)
26. J I Dickson, S Turenne, H Bande, G L Esperance *Mater. Sci. Eng.* **89** L31 (1987)
27. A V Pevneva, G V Khaldeev, V V Kuznetsov *Zashchita Met.* **12** 50 (1976)
28. D M Drazic *Mod. Aspects Electrochem.* **19** 69 (1989)
29. T Ohnori *Denki Kagakuyobi Fogyo Butsure Kagaku* **56** (3) 181 (1988)
30. L-B Le, O Bittori *J. Chem.* **66** 1525 (1988)
31. G V Khaldeev, S M Reshetnikov, V F Knyazeva, V V Kuznetsov *Zh. Prikl. Khim.* **53** 1298 (1980)
32. I K Marshakov, A F Vvedenskii, V Yu Kondrashin, G A Bokov *Anodnoe Rastvorenie i Selektivnaya Korroziya Splavov* (Anodic Dissolution and Selective Corrosion of Alloys) (Voronezh: Izd. Voronezh. Gos. Univ., 1988)
33. A N Kuzyukov *Zashchita Met.* **30** 166 (1994)
34. K Vetter *Electrochemische Kinetic* (Translated into Russian; Moscow: Khimiya, 1967)
35. V I Arnol'd *Teoriya Katastrof* (Catastrophe Theory) (Moscow: Nauka, 1990)
36. P J Ortoleva *J. Electrochem. Soc.* **130** 621 (1983)
37. O Peschke, M U Kleinke, F Galembeck, M A Tenan *Langmuir* **6** 829 (1990)
38. M N Polukarov *Zh. Prikl. Khim.* **21** 611 (1948)
39. G V Khaldeev, V V Kamelin *Dokl. Akad. Nauk SSSR* **310** 653 (1990)
40. G V Khaldeev, V V Kamelin *Usp. Khim.* **61** 1623 (1992) [*Russ. Chem. Rev.* **61** 889 (1992)]
41. Y Wang, S L Hudson, N I Jaeger *J. Electrochem. Soc.* **137** 485 (1990)
42. A J Perlstein, J A Johnson *J. Electrochem. Soc.* **136** 1290 (1989)
43. A D Konyukhov, V E Konyukhov *Zashchita Met.* **30** 212 (1994)
44. J Marsden, M McKraken *Bifurcation of Birth-Cycle and Its Application* (Translated into Russian; Moscow: Mir, 1980)
45. W W Mullins *J. Appl. Phys.* **28** 333 (1957)
46. V V Pokropivnyi, V V Skorokhod *Dokl. Akad. Nauk Ukrain. SSR, Ser. A* (12) 68 (1987)
47. W W Mullins *Trans. Metall. Soc. AIME* **218** 354 (1960)
48. L Ratke, H J Fogel, in *Proceedings of the VII European Symposium on Materials and Fluid Science, London, 1989* p. 497
49. H L Huang, J S Yang *J. Vac. Sci. Technol.* **A5** 1487 (1987)
50. Z B Pfeil *Proc. Roy. Soc., Math. Phys. Sci., A* **112** 182 (1926)
51. T Mimaki, Y Narazawa, S Hashimoto, S Miura *Met. Abstr. Light Met. Alloys* **24** 72 (1991)
52. M Yamashita, T Mimaki, S Hashimoto, S Miura *Met. Abstr. Light Met. Alloys* **24** 69 (1991)
53. M Yamashita, M Yoshioka, T Mimaki, S Hashimoto, S Miura *Met. Abstr. Light Met. Alloys* **24** 75 (1991)
54. H Vehoff, H Stenzel, P Neumann *Z. Metallkunde* **78** 550 (1987)
55. D Wolf *Physica B* **131** 53 (1985)
56. Th Karakostas, G L Bleris, J G Antonopoulos *Phys. Techn. Semicond.* **73** 26 (1979)
57. V M Knyazheva, in *Novye Dostizheniya v Oblasti Teorii i Praktiki Protivokorrozionnoi Zashchity Metallov* (Recent Advances in the Theory and Practice of Anticorrosion Protection of Metals) (Moscow: Nauka, 1981) p. 49
58. P Merino, X R Novoa, G Pena, E Porto, L Espada *Mater. Sci. Technol.* **9** 168 (1993)
59. V M Mil'man, Candidate Thesis in Chemical Sciences, Physicochemical Institute, Moscow, 1991
60. G S Was *Corrosion (USA)* **46** 319 (1990)
61. E T Shapovalova, M Yu Ustimenko *Zashchita Met.* **29** 231 (1993)
62. V Kain, in *Workshop on Failure Analysis, Corrosion Production, and Metallography, Bombay, 1992: FACORMET-92* p. 107
63. T -J Chuang, K I Kagawa, J R Rice, L B Sills *Acta Metall.* **27** 265 (1979)
64. G Sundararajan, P G Shewmon *Met. Trans. A, Phys. Metall. Mater. Sci.* **12** 1761 (1981)
65. A M Klinger *Poverkhnost'* **2** (4) 17 (1983)
66. Ph Joel *J. Electrochem. Soc.* **139** 51 (1992)
67. B Landa, H K Birubaum *Acta Metall.* **35** 2537 (1987)
68. A B Shein, G V Khaldeyev, in the *4th International Conference on Hydrogen Effects on Material Behavior (Program and Abstracts)*, Jackson Lake, WY, 1989, p. 18
69. G C Pain, F W Averill *Phys. Rev. Lett.* **58** 234 (1987)
70. M Hashimoto, Y Ishida, R Yamamoto, M Doyama, T Fujiwara *Scr. Metall.* **16** 267 (1982)
71. H J Grabke, in *Chemical and Physical Fractures: Proceedings of the NATO Advanced Research Workshop, Bad Reichenhall, 1987* p. 388
72. K Yamanaka *Corros. Eng.* **41** 461 (1992)
73. I Olefjord, C R Clayton *ISIJ Int.* **31** 134 (1991)
74. R F A Jargelins-Petterson, in the *12th Scandinavian Corrosion Congress and EUROCORR'92, Espoo, 1992* p. 119
75. W Schwenk *Stahl Eisen* **111** 114 (1991)
76. U Erb, H Gleiter, G Schurtzgebet *Acta Metall.* **30** 1377 (1982)
77. R Maurer, U Erb, H Gleiter *Mater. Sci. Eng.* **63** L13 (1984)
78. B W Bennett, H W Pickering *Met. Trans. A, Phys. Metall. Mater. Sci.* **18** 1117 (1987)
79. G V Khaldeev, V F Knyazeva, A B Volyntsev, L V Spivak *Zashchita Met.* **15** 717 (1979)
80. A V Galina, V E Fradkov, L S Shvindlerman *Poverkhnost'* **6** (1) 100 (1988)
81. V V Kuznetsov, G V Khaldeev, V I Kichigin *Navodorozhivanie Metallov v Elektrolitakh* (Saturation of Metals with Hydrogen in Electrolytes) (Moscow: Mashinostroenie, 1993)
82. L T Berezhnitskii, N G Stashchuk *Fiz-Khim. Mekh. Mater.* **18** 61 (1982)
83. A I Kitaigorodskii *Smeshannye Kristally* (Mixed Crystals) (Moscow: Nauka, 1983)
84. G Leibfried, N Broier *Point Defects in Metals* (Translated into Russian; Moscow: Mir, 1981)
85. I M Lifshits, V V Slezov *Zh. Eksp. Teor. Fiz.* **35** 479 (1958)
86. S Redner, D Ben-Avraham, B Kahng *J. Phys. A, Math. Gen.* **20** 1231 (1987)

Russian Chemical Reviews **63** (12) 997 – 1018 (1994)
©1994 Russian Academy of Sciences and Turpion Ltd

UDC 547.759.4

The chemistry of isoindoles

V A Kovtunenko, Z V Voitenko

Contents

I. Introduction	997
II. Methods of synthesis of isoindoles	997
III. Theoretical and physical aspects	1006
IV. Chemical properties	1009
V. Applications of isoindoles	1016

Abstract. Data on the synthesis and the physical and chemical properties of isoindoles published in 1981 – 1992 are considered. The problems of the aromaticity and the reactivity of the isoindole system are discussed. The bibliography includes 169 references.

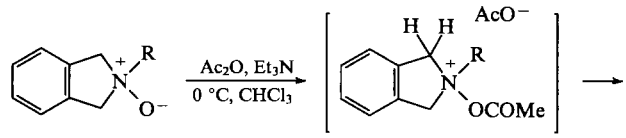
I. Introduction

Several reviews[1,2] and monographs[3] on the chemistry of isoindole have been published in the last decade. However, the interest in this system is not flagging. New isoindoles have been obtained, some of which have been isolated in a pure form and some have been characterised as Diels–Alder adducts. New methods of synthesis of isoindole systems have been discovered. Calculations of the electronic structure have been carried out by methods which had not been applied previously, a new concept of the aromaticity of this system has been put forward, the X-ray diffraction analysis of isoindoles has been achieved, and new reactions have been investigated. Data have been published on the biological activity of isoindole systems.

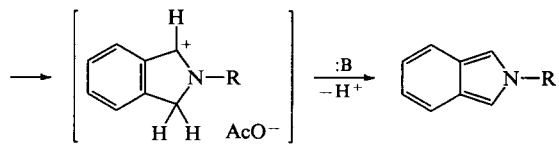
II. Methods of synthesis of isoindoles

1. Elimination reactions with participation of isoindoline *N*-oxides

The possibilities of this method, developed by German workers,[4] have been demonstrated in numerous examples and the method has attracted attention because of the high yields of 2-R-isoindoles. It consists in the treatment of the corresponding isoindoline *N*-oxide at a reduced temperature with acetic anhydride and triethylamine in chloroform and can be followed with the aid of ^{1}H NMR spectra. It has been suggested that the *O*-acetylation of the oxide **1** takes place initially and this is followed by the base-induced regiospecific 1,2-elimination of the elements of acetic acid from the intermediate **2**, and finally by the deprotonation of the intermediate 2-R-1*H*-isoindolium salts **3** with formation of 2-R-isoindoles **4**.

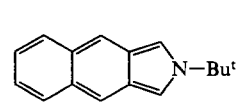


1 **2**

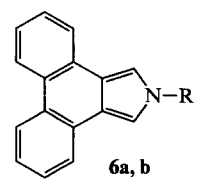


3 **4**

According to the authors,[4] the reaction resembles the Polonovski reaction. The available compounds indicate the possibility of extensive variation of the substituent in the 2-position in the system: the substituent can be an alkyl (10 compounds),[5] allyl,[4] and arylalkyl[6] group or the very frequently employed *tert*-butyl group.[5–12] In all the known examples of the isoindoles obtained by this procedure, the 1- and 3-positions in the system are free while the benzene component of the bicyclic system may contain methyl groups,[12] nitro-groups,[7] chlorine atoms,[12] or it can be condensed with other rings. The isoindoles **5**–**10** have been described in a number of communications.[6,8–10]

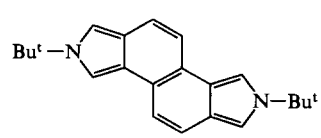


5, 90%

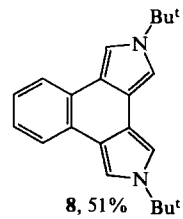


6a, b

6a: R = Bu^t, 80%
6b: R = CH_2Ph, 68%



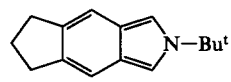
7, 65%



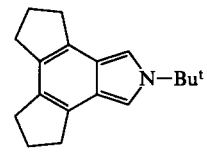
8, 51%

V A Kovtunenko, Z V Voitenko Faculty of Chemistry, Taras Shevchenko Kiev University, ul. Vladimirskaya 64, 252601 Kiev, Ukraine. Fax (7-044) 225 12 73. Tel. (7-044) 221 03 93 (V A Kovtunenko)

Received 28 July 1994
Uspekhi Khimii **63** (12) 1064 – 1086; translated by A K Grzybowski



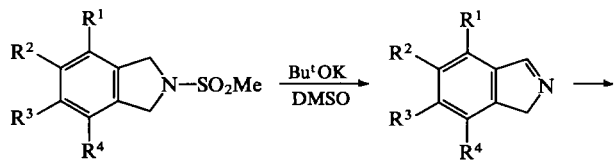
9, 37%



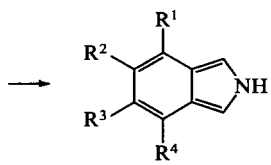
10, 90%

2. Elimination with participation of 2-R-isoindolines

The previously described method of synthesis of 2*H*-isoindoles via the 1,2-elimination of methanesulfinate from *N*-methanesulfinylisoindolines **11** on treatment with potassium *tert*-butoxide in dimethyl sulfoxide (DMSO) (60–65 °C) or ether has been developed further in a number of studies.[13–17] The required isoindolines **11** can be synthesised from the corresponding 1,2-bis(bromomethyl)benzenes and methanesulfonamide.[16] It has been suggested that the 1*H*-isoindole **12** is formed initially and then isomerises to the 2*H*-isoindole **13** as a result of a tautomeric transformation. The isoindoles **13a** (yield 94%) and **13b, c** have been described by Kreher and Kohl[14] and Kreher and Herd[17] respectively.



11 **12**



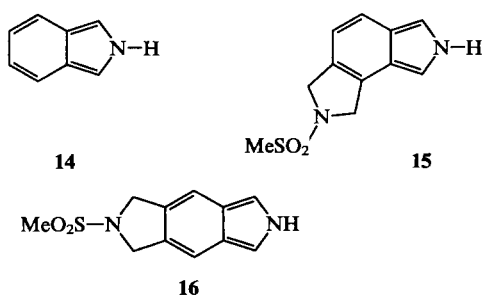
13a–c

13a: $R^1 = R^2 = R^3 = H$; $R^2 = COBu^t$

13b: $R^1 = R^2 = R^3 = R^4 = Cl$

13c: $R^1 = R^2 = R^3 = R^4 = Br$

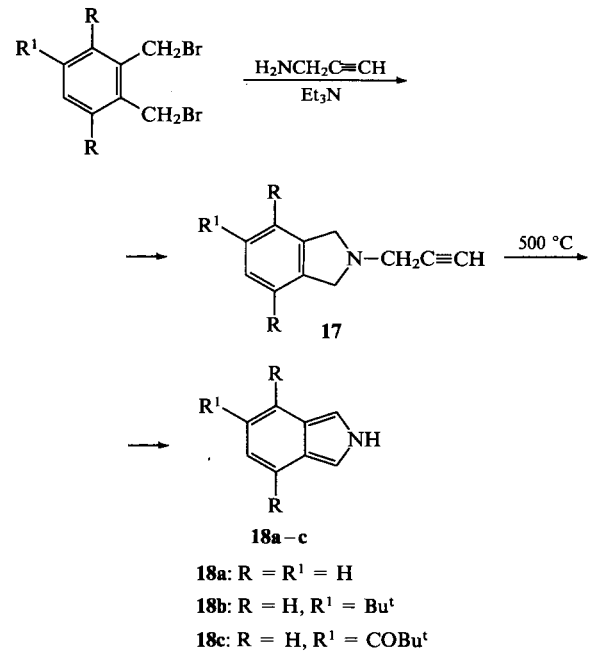
The isomeric compounds **15** and **16** as well as the parent isoindole **14** have been isolated by a similar method.[13] The last compound is obtained as a 0.05 M solution in ether.[15,16] The authors[15] believe that this method is in fact best for the preparation of solutions of the isoindole **14**.



14 **15**

16

The method involving the elimination of propyne from *N*-propargylisoindolines **17** at a high temperature can serve as a general approach to the synthesis of 2*H*-isoindoles **18**.[15,18] The yields of the products are fairly high. The isoindolines required are obtained from *o*-xylylene dibromides and propargylamine.



17

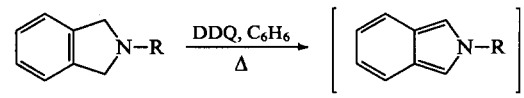
18a–c

18a: $R = R^1 = H$

18b: $R = H$, $R^1 = Bu^t$

18c: $R = H$, $R^1 = COBu^t$

It has been shown[19] that 2-R-isoindoles can be obtained by dehydrogenating *N*-(ethoxycarbonyl)isoindolines **19** in benzene or diglyme with the aid of chloranil or 2,3-dichloro-5,6-dicyano-1,4-benzoquinone (DDQ). The isoindoles **20** were not isolated from the reaction mixture but were converted into Diels–Alder adducts with maleimide derivatives.

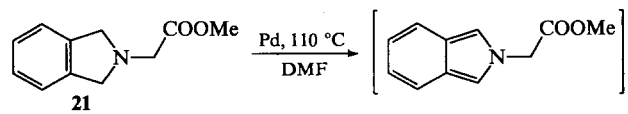


19 **20a, b**

20a: R = COOEt

20b: R = Tos

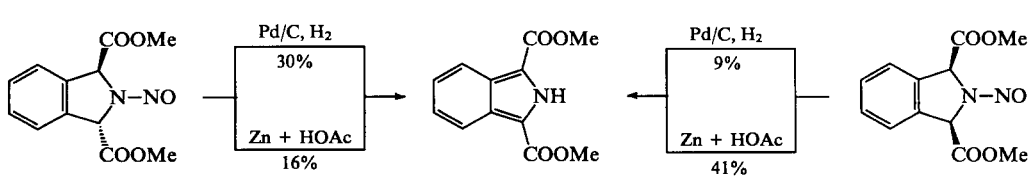
The dehydrogenation of the methyl ester of isoindoline-2-acetic acid **21** takes place in dimethylformamide (DMF) over palladium black at 110 °C and leads to the corresponding isoindole, which has also been characterised as the Diels–Alder adduct.[20]



21

The reduction of the stereoisomeric forms of *N*-nitrosoindoles (*E* and *Z*) leads to 1,3-dimethoxycarbonyl-2*H*-isoindole **22** in low yields (Scheme 1).[21]

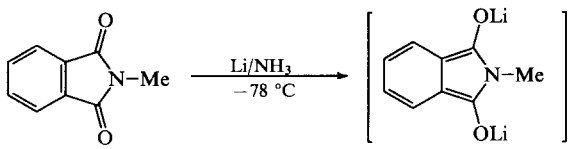
Scheme 1



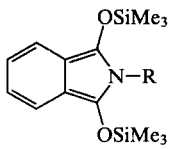
dl-*E* **22** meso-*Z*

3. Synthesis of isoindoles from phthalimides

Flynn[22] was the first to demonstrate that the dianion of *N*-methylphthalimide has the *o*-quinonoid electronic structure **23**. The reduction of *N*-methylphthalimide dissolved in tetrahydrofuran (THF) by metallic lithium (2.1 equivalents) in liquid ammonia leads to a dark-red solution containing the dianion, the structure of which can be demonstrated by chemical reactions. The electrochemical reduction of *N*-methyl- and *N*-phenyl-phthalimides in anhydrous acetonitrile using a mercury cathode in the presence of tetraethylammonium chloride and an excess of trimethylsilyl chloride leads to the corresponding isoindoles **24a, b** via the dianion in **23**. When equivalent amounts of trimethylsilyl chloride are used, other products are formed.[23,24] The attempts to obtain the isoindoles **24c, d** from the corresponding phthalimides must be regarded as a development of this method. Under similar conditions, the electrochemical reductive silylation of *N*-alkoxyphthalimides leads to 2-alkoxy-1,3-bis(trimethylsiloxy)isoindoles.[25] All the isoindoles **24a–d** have been identified through the corresponding Diels–Alder adducts.



23

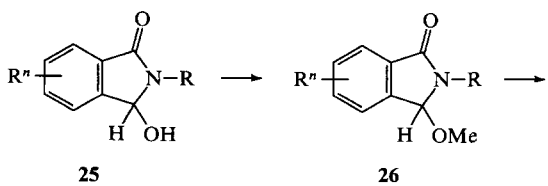


24a–d

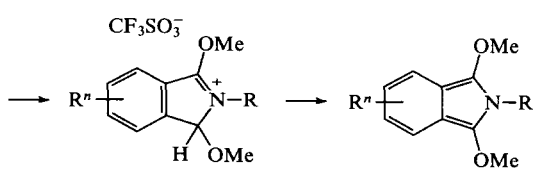
R = Me (**a**), Ph (**b**), OMe (**c**), OCH_2Ph (**d**)

The reduction of *N*-methyl- and *N*-phenyl-phthalimides at room temperature with zinc powder in 2,6-lutidine in the presence of THF and an excess of trimethylsilyl chloride has been investigated.[26] The reaction mixture was treated with ultrasound. The authors believe that the silylated isoindoles **24a, b** are also intermediates in this reaction.

A novel method of synthesis of 1,3-dimethoxy-2-R-isoindoles has been proposed.[27] It consists in the reduction of phthalimides by magnesium to 3-hydroxyphthalimidine **25**, which is converted into 3-methoxyphthalimidine **26**. The *O*-alkylation of the latter with CF_3SO_2OMe affords 1,3-dimethoxy-2-R-1*H*-isoindolium trifluoromethanesulfonate **27**, the deprotonation of which with the aid of lithium diisopropylamide leads to the relatively unstable 1,3-dimethoxy-2-R-isoindoles **28**, which have been identified via Diels–Alder adducts.



25 **26**

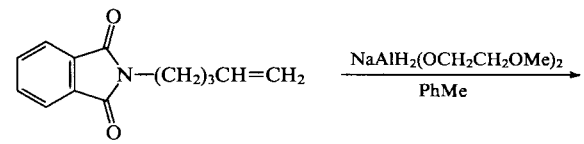


27 **28**

R = H, Me

R^n = H; 5,6-Me, 4,7-Me; 5,6-Cl

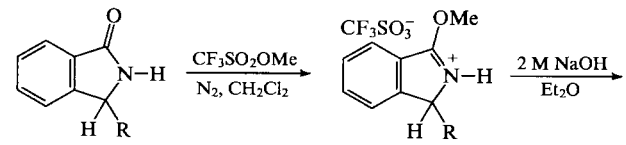
The method involving the chemical reduction of phthalimide has been used in the synthesis of the isoindole **29**. The target product was isolated in a moderate yield from a mixture with an isoindoline and phthalimidine.[28]



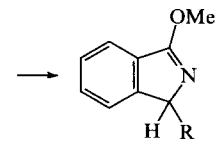
29

4. Synthesis of isoindoles from phthalimidines

The study of the alkylation of various phthalimidines with the aid of the Meerwein reagent or methyl trifluoromethanesulfonate was continued during the period analysed.[29–32] Thus a series of 1-R-3-methoxy-1*H*-isoindoles **31** have been obtained by alkylating 1-R-3-oxo-1,2-dihydroisoindoles.[29,33] The regioselective *O*-alkylation in the first stage results in the formation of 1-R-3-methoxy-1*H*-isoindolium triflates **30** (the yields expressed in % are as follows for different R: 91 for Me, 72–89 for Ph, 4-MePh, and 4-ClPh, and 50 for 4-MeOPh), which are treated with a base in the presence of ether in the second stage. This method makes it possible to extract immediately the deprotonated products into the organic phase and to isolate 1-R-3-methoxy-1*H*-isoindoles **31** in 74%–93% yield.[29]

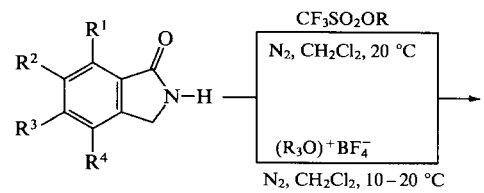


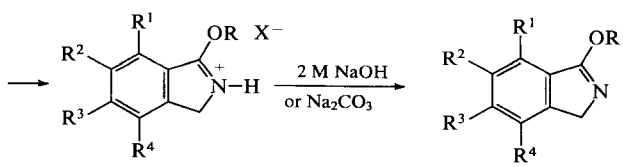
30



31

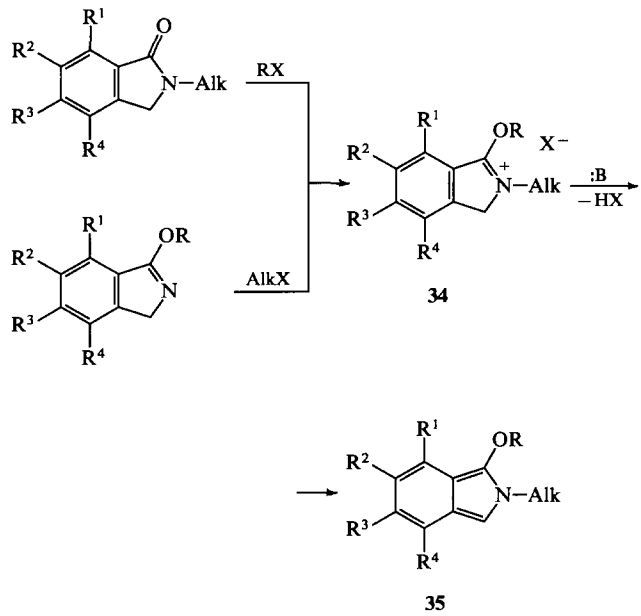
A series of 3-alkoxy-1*H*-isoindoles **33** (13 compounds), containing substituents of different electronic nature in the benzene part of the bicyclic compound, have been obtained by similar procedures.[30]





32 **33**

The preparation of the corresponding 3-ethoxy-1*H*-isoindole from 5,6-dimethoxyphthalimidine in 81% yield has been described.[34] The alkylation was carried out with triethyloxonium tetrafluoroborate. The study of the spectroscopic characteristics of compounds of type **31** and **33** showed that they exist exclusively in the isoindolenine form and do not exhibit a tendency towards conversion into the isoindole form.[29,30] If the isoindolenines **31** and **33** are alkylated with methyl trifluoromethanesulfonate, then the quaternary salts **34** are formed. These are the products of the regioselective *N*-alkylation which are readily deprotonated after treatment with bases (2 M NaOH or lithium diisopropylamide) and are converted into 1-alkoxy-2-methylisoindoles **35**.[31,32] The salts **34** can be obtained also by the direct *O*-alkylation of *N*-methylphthalimidines with the aid of the same alkylating agents, although such alkylation does not occur if the bicyclic system has been deactivated by substituents in the benzene component. This has been observed when attempts were made to alkylate 4,5,6,7-tetrachloro-*N*-methylphthalimidine with methyl trifluoromethanesulfonate.[31]



34

35

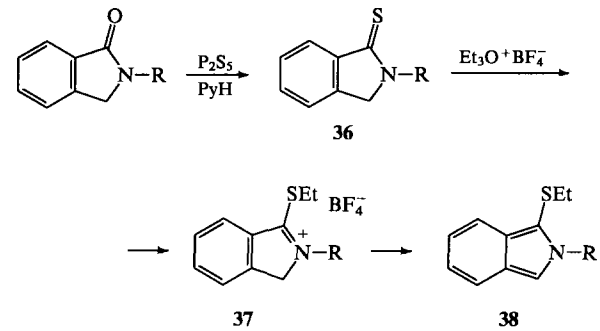
R = Me, Et

The alkoxyisoindoles **35** are unstable. They have been identified via Diels–Alder adducts, some of them being also investigated by the ^{1}H NMR method.

It was found that the stability of the compounds in solution depends on the type of the alkyl substituent at *N*(2). It it is a methyl group, then the ^{1}H NMR spectrum, recorded after brief drying of the organic layer, reveals the presence of a mixture consisting of the isoindole and the corresponding isoindolinone (for example, their ratios are 1 : 1.25 for R = Me and 1 : 1.5 for R = Et). The ratio for 2-*tert*-butyl-1-methoxy-2*H*-isoindole is more favourable (8 : 1).[32]

1-Ethylthio-2-R-isoindoles are obtained from the corresponding phthalimidines via their successive conversion initially into the thiophthalimidines **36** and then, by the regioselective *S*-alkylation of the latter, into 3-ethylthio-2-R-1*H*-isoindolium tetrafluoroborates **37**. The reaction chain is completed by the deprotonation of the above salts with formation of the isoindoles **38**.[35]

The isoindoles **38** are obtained as a result of the vacuum distillation of a thoroughly ground mixture of the salt **37** with an excess of solid alkali. The ^{1}H NMR spectra have been recorded for some of them. They can be identified as Diels–Alder adducts.[35]



36

37 38

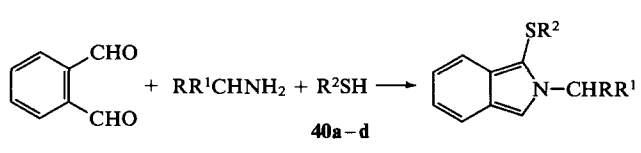
R = Me, Ar

The reduction of phthalimidines with lithium tetrahydroaluminate was proposed a long time ago by Wittig and coworkers (quoted after Babichev and Kovtunenko[3]) as a method of synthesis of the isoindoles 4. However, according to the data of Kovtunenko et al.,[36] the main product of the reactions of a series of *N*-substituted phthalimidines is the corresponding isoindoline and the formation of traces of isoindoles can be detected only chromatographically. An effective method of synthesis of 2-R-isoindoles from phthalimidines involves the reduction of the latter with lithium bis(2-methoxyethoxy)dihydroaluminate in benzene or toluene. The corresponding isoindoline is as a rule formed as a side product (its yields vary from 5% to 10%). The pure isoindole can be obtained by employing the higher solubility of isoindolines in cold ether. The yields of the isoindoles **4** then amount to 70%–80%.[36]

5. *o*-Phthalic dialdehyde in the synthesis of isoindoles

The study of the fluorescence method for the determination of the terminal amino-groups in aminoacids, proteins, primary amines, etc. via their conversion into 1-alkylthio-2-R-isoindoles **41** continued in the 1980s.[37–44] The review by Garcia Alvarez-Coque et al.[45] covers more than 50 sources in which this reaction has been investigated. It has been shown that *o*-phthalic dialdehyde (OPD) **39** reacts with propylamine in the presence of ethanethiol or mercaptoethanol (ME) (compounds **40a, b**) to form the isoindoles **41a, b**, which have been investigated spectroscopically and identified via adducts with dimethyl ethynedicarboxylate.[39] The fluorescent products obtained by this reaction have been investigated[41] by the stopped flow method. It has been established that, in the presence of an excess of the OPD–ME adduct formed initially, the interaction of the latter with primary amines is pseudo-first order at rates consistent with overall second-order kinetics. It has been shown that the rate of the reaction of the OPD–ME adduct with various aminoacids follows second-order kinetics when OPD : ME : aminoacid ratios of 1 : 1.24 : 1 are maintained. It has been established that the rate of the reaction of the OPD–ME adduct with alanine is a maximum at pH 10.5–11.0, while a large excess of mercaptoethanol slows down the reaction. A decrease in the rate was also observed when mercaptoethanol was replaced by dithiothreitol or propanethiol.[37] An improved method for the preparation of the aminoacid mixture to be subsequently separated with the aid of high-performance liquid chromatography (HPLC) has been proposed.[38] It consists in the conversion of the aminoacid into type **41** isoindoles as a result of treatment with OPD and ME. The identification of the type **41** isoindoles obtained from the aminoacids, carried out after the HPLC with the aid of an electrochemical detector operating under oxidation conditions, has been described.[46] The products formed from a mixture of alkylamines with OPD during the post-column derivatisation (HPLC) have been investigated by chromatograph-linked mass-spectrometry. It has been shown[40] that, when the derivatisation is carried out in the presence of ethanethiol **40a**, the products determined are type **41** isoindoles.

Six β-aminothiols (of the L-cysteine type) have been investigated in the reaction with OPD. It was shown that fluorescent products are formed in such cases without introducing thiols from outside. On the basis of the study of these products and model type **41** isoindoles by combined HPLC (reversed phase) and chromatograph-linked mass spectrometry with subsequent fluorescence detection, it has been suggested that type **41** isoindoles are responsible for the fluorescence in this case also.[47] Comparison of three methods for the determination of traces of aliphatic amines with the aid of HPLC and by means of fluorescence detection showed that the derivatisation method via the corresponding isoindoles **41** has the lowest sensitivity.[43] In order to improve the fluorescence detection of primary amines after the HPLC, a study was made of the factors influencing the stability of the isoindoles **41**.[41,48–50] It was established that their stability increases both when 3-mercapto-1-propanol **40d** is used instead of mercaptoethanol **40c** [41] and following the replacement of R = H in the structure of compound **41** by R = Me.[41,48] It was found that the stability of the isoindoles **41** is also influenced by the structure of the amino-component. It was shown[51] that amino-compounds with a sterically shielded amino-group (L-tryptophan, L-DOPA, etc.) have an appreciable stabilising effect on the fluorescence parameters of the isoindole derivative. This is why it has been suggested that L-tryptophan be used as a standard in the fluorimetric determination of various thiols.[51] Experiments have shown that an excess of OPD in the reaction mixture catalyses the decomposition of the isoindole,[41,48] while an excess of ethanethiol has a stabilising effect.[48] According to Stobaugh et al.,[48] ethanethiol forms more stable isoindole derivatives under these conditions than β-mercaptoethanol: the stability, estimated in terms of the time taken for a 10% decrease in the fluorescence level, improves by a factor of at least 5. Jacobs et al.[49] believe that, among all the destabilising factors (the structure of the thiol, the nature of the solvent, the influence of the pH, etc.), the presence of an excess of OPD in the reaction mixture is the most dangerous. They have shown that, in the absence of an excess of OPD, type **41** isoindoles are entirely stable, while the results presented by Mading and Jacobs[50] clearly confirm that the destabilisation of the isoindoles **41** and the associated decrease in the fluorescence level are a direct consequence of the electrophilic attack by the excess OPD on the free C(3) position in the isoindole **41** system. Furthermore, in a number of instances the products in the interaction of isoindoles **41** with OPD have been isolated and identified.[50] A special study had been made[52] of the factors inducing the quenching of the fluorescence of type **41** isoindoles obtained from biogenic amines.



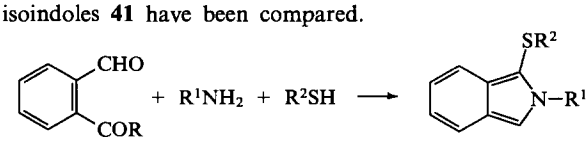
39 **40a–d** **41a–d**

R = H, Me

40a: R^2 = Et
40b: R^2 = Bu^t
40c: R^2 = $(CH_2)_2OH$
40d: R^2 = $(CH_2)_3OH$

41a: R^1 = R^2 = Et
41b: R^1 = Et, R^2 = Bu^t
41c: R^1 = Et, R^2 = $(CH_2)_2OH$
41d: R^1 = $(CH_2)_2COOH$, R^2 = Et

The individual disadvantages of the fluorescence analytical method examined above stimulated the search for new reagents among derivatives of *o*-acylbenzaldehydes.[44] The ketones **42a, b** have been examined and the stability and properties of the isoindoles **43** obtained from them and the corresponding isoindoles **41** have been compared.

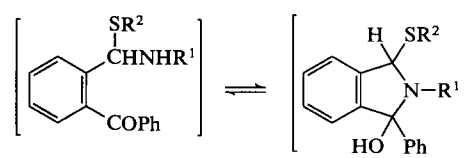


42a, b **43a–d**

42a: R = Me
42b: R = Ph

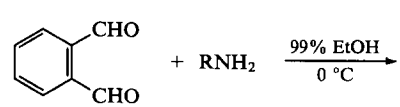
43a: R = Ph, R^1 = CH_2Ph, R^2 = Et
43b: R = Me, R^1 = Pr^i, R^2 = Bu^t
43c: R = Ph, R^1 = $(CH_2)_3COOH$, R^2 = Et
43d: R = Me, R^1 = $(CH_2)_3COOH$, R^2 = Et

Under similar conditions of the synthesis, the yield of the isoindole **43a** (42%) is higher than that of the isoindole **43b** (32%). Under identical experimental conditions (pseudo-first order kinetics), it was found that the rate of formation of compound **43c** is significantly lower than the rates of formation of compounds **41d** and **43d**. The authors explained this finding by the steric hindrance generated by the phenyl group in the intermediate **A** when the carbonyl group is attacked intramolecularly by the nitrogen atom, on the one hand, and by the resonance stabilisation of the reactant **42b**, on the other.[44]

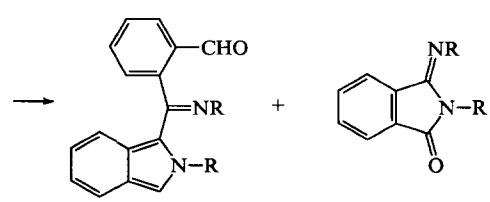


A

Having disproved the previous claim[1] that isoindoles are not formed from OPD and ammonia (or primary amines), Japanese workers[53] found the conditions for their isolation. They suggested that 99% alcohol be used as the solvent for the reaction and that the process itself should be carried out at 0 °C. The isoindoles **44** are isolated together with the imines **45** by column chromatography. It has been noted that, in the presence of tertiary butyl alcohol, the yield of the isoindoles **44** is somewhat better. *tert*-Butylamines does not react with OPD, which the authors explain by its being sterically hindered due to the presence of bulky *tert*-butyl groups. The use of aniline affords mainly 1-phenylimino-2-phenylisoindoline (79%) and only 2% of the corresponding imine **45** (R = Ph).[53]



39 R = Pr^n, Pr^i, C_6H_{11}

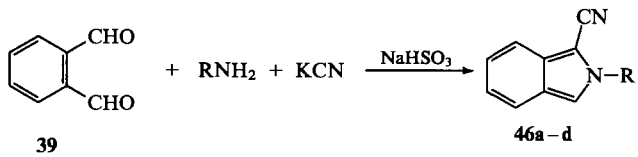


44a–c **45a–c**

44a: R = Pr^n (35%)
44b: R = Pr^i (20%)
44c: R = C_6H_{11} (34%)

45a: R = Pr^n (10%)
45b: R = Pr^i (22%)
45c: R = C_6H_{11} (11%)

The chemists of the Monsanto Company discovered a convenient and effective method of synthesis of 1-cyano-2-methyl-2*H*-isoindole (the yield of compound **46a** was 92%), involving the interaction of OPD with methylamine hydrochloride and cyanide in methanol. The molar reactant ratios were OPD : ($MeNH_2$ + HCl) : KCN = 1 : 2.2 : 2.[54]



39 **46a–d**

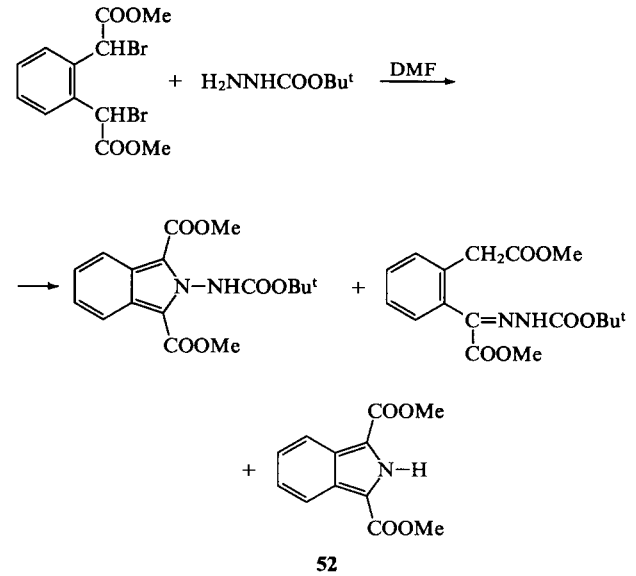
R = Me (**a**), Alk (**b**), 4-MeOPh (**c**), 3-HOOCPh (**d**)

It has been shown that, under the conditions of the Strecker reaction, OPD reacts with primary amines in the presence of sodium bisulfite to form 1-cyano-2-R-isoindoles **46** in very satisfactory yields in the case of alkylamines (59% to 86% for compound **46b**) and in poor yields of *p*-anisidine (33% for compound **46c**). The molar reactant ratios were OPD : RNH_2 : KCN : $NaHSO_3$ = 1 : 1.3 : 2.2 : 2.1.[55] *m*-(1-Cyano-2-indolyl)benzoic acid **46d** was obtained from *m*-aminobenzoic acid, OPD, and potassium cyanide in one stage.[56]

Japanese workers have been investigating the reactions of *o*-acylbenzophenone **47a** with ammonia derivatives for more than 25 years. The structures of the blue pigment **48**, formed from the diketone **47a** and phenylhydrazine in the presence of hydrochloric acid,[57] of the red pigments **49**, formed from compound **47a** and β-aminoethanol or its methyl ether in acetic acid,[58] and of the dark-blue pigments **50**, obtained from the same substances but in the presence of hydrochloric acid,[58] have been established during the last 10–15 years. It has been shown[57,59] that the diketones **47a,b** react with primary amines in the absence of acids to form 1,2-diaryl-3-(aryliminomethyl)isoindoles **51** (Scheme 2).

6. The synthesis of isoindoles from *ortho*-disubstituted benzenes

The interaction of dimethyl α,α′-dibromo-*o*-phenylenediacetate with *tert*-butyl carbazate has been investigated[21] and it has been shown that a mixture consisting of three compounds, including the known dimethyl 2*H*-isoindole-1,3-dicarboxylate **52**, is formed in DMF. The yield of the isoindole **52** is only 7% when the racemic dibromo-derivative is used and is lower still (5%) when it is obtained from the *meso*-form.[21]

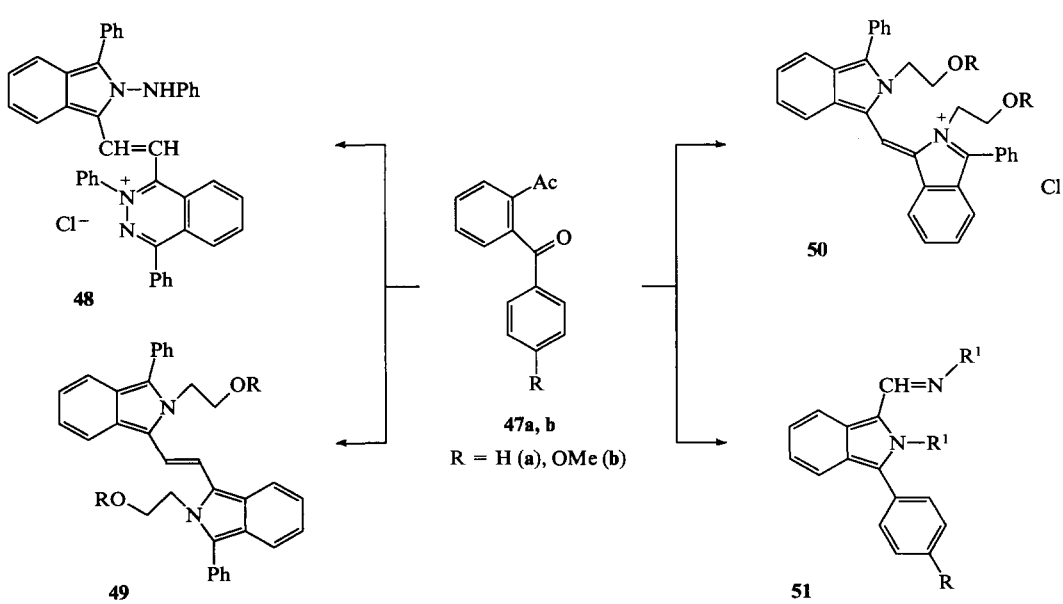


52

The interaction of *o*-chloro(bromo)methylbenzonitrile **53** with primary amines on heating in alcohol leads to 3-amino-2-R-1*H*-isoindolium salts **56** in one stage and in a high yield.[60,61] Derivatives of hydrazine, namely carboxylic acid hydrazides (R = $NHCOR^1$),[62,63] α-benzoyl-α-methylhydrazine [R = N(Me)COPh],[64] and *tert*-butyl carbazate [R = NHCOO.Bu^t],[65] also enter into this reaction on heating in DMF, forming the corresponding salts **56.**

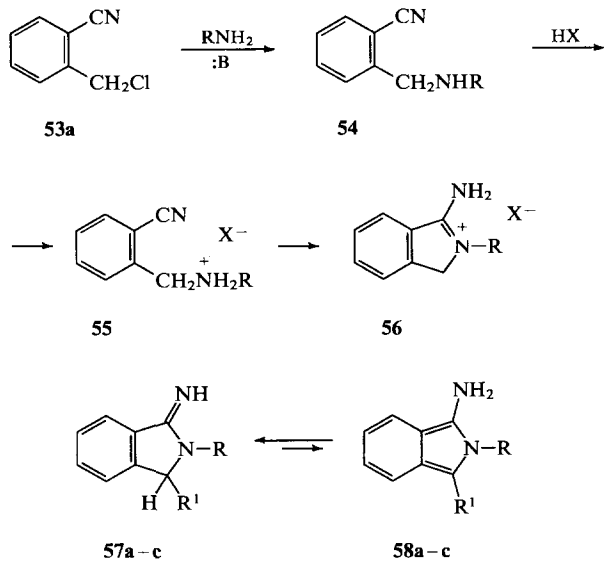
If the interaction of compound **53a** with amines is carried out in the presence of bases, it is possible to isolate benzylamines **54**, which are entirely stable during storage and show no tendency to cyclise. On the other hand, the corresponding simple salts **55**, which are obtained on treatment with inorganic acids in the cold,

Scheme 2



48 **49** **47a, b** R = H (**a**), OMe (**b**) **50** **51**

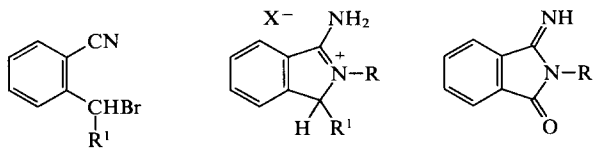
readily cyclise to aminoisoindolium salts **56** both in solution and in the solid phase. The study of the heterocyclisation of compound **55** to aminoisoindolium salts **56** by the ^{1}H NMR method in solution in DMSO-d_6 showed that this is a second-order reaction.[66] The salts **56** are deprotonated when they are treated with alkali or triethylamine and this leads to 1-imino-2-R-isoindolines **57a** and not be aminoisoindoles **58a** whatever the substituents.[67]



53a 54 55 56 57a–c 58a–c

α-Bromo-*o*-benzylbenzonitrile **59a** and α-bromo-*o*-cyanomethylbenzonitrile **59b** react with primary amines like the chloro-derivative **53a**.[60,68]

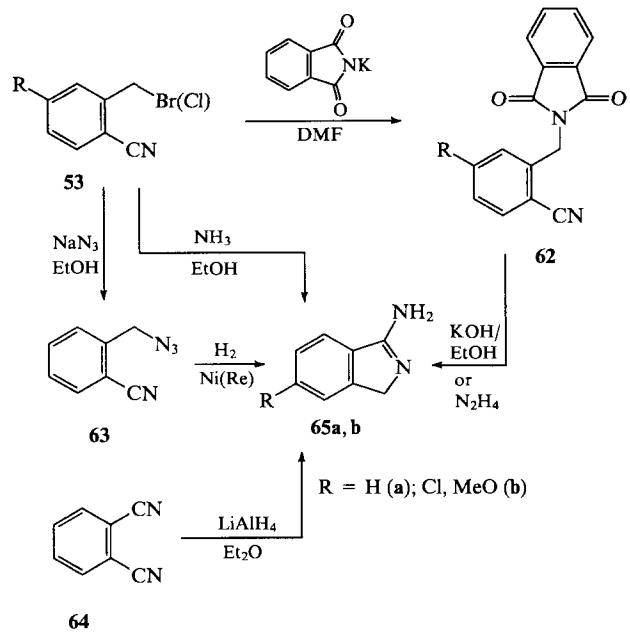
The salts **60a, b** are obtained in one stage and in a high yield and yet they are deprotonated in different ways. Whereas the salt **60a** gives rise to the corresponding stable imine of type **57b**,[67] the salts **60b** give rise to 1-amino-2-R-3-cyano-2*H*-isoindoles **58c**,[68] which are unstable in air, are readily oxidised, lose HCN, and are converted into the corresponding iminophthalimides **61**.



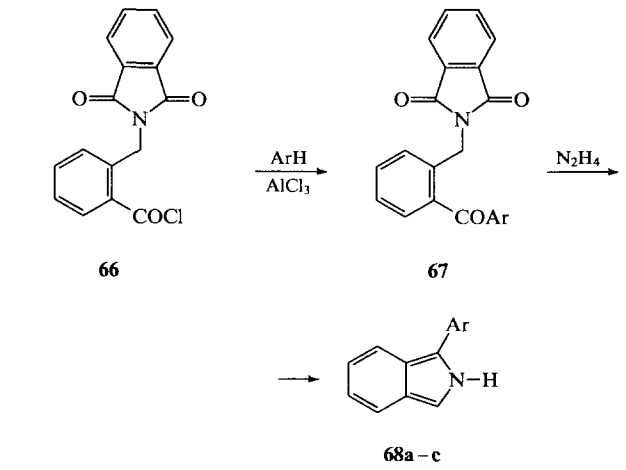
59a, b **60a, b** **61**

R^1 = Ph (**a**), CN (**b**) R^1 = Ph (**a**), CN (**b**)

o-Chloromethylbenzonitrile and its derivatives **53** can be transformed via different routes 3-amino-1*H*-isoindoles **65a, b**. The methods of synthesis of the latter compounds have been surveyed.[69] The reduction of the dinitrile **64** with lithium tetrahydroaluminate did not prove to be the best method of synthesis of compound **65a** and the authors, using the corresponding phthalimidomethyl derivatives **62**, obtained the aminoisoindoles **65a, b** in 38% and 51% yields respectively. The aminoisoindole **65a** has been synthesised in 23% yield by reducing *o*-azidomethylbenzonitrile **63**. The most convenient method of synthesis of the compound involves the direct amination of the nitrile **53** with an alcoholic solution of ammonia.[70]



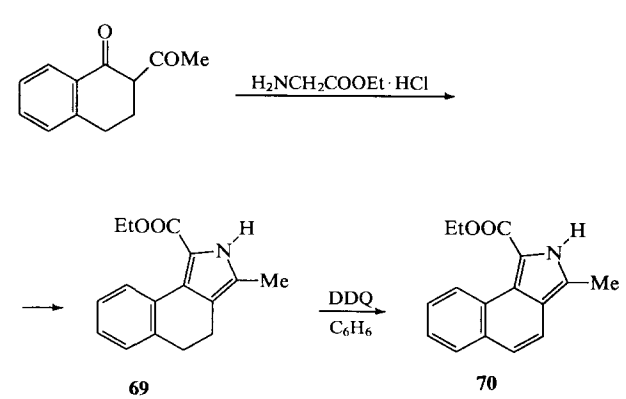
The earlier method of Weber and L'vovska has been used to obtain three 1-aryl-2*H*-isoindoles **68a–c**.[71] Their yields are not quoted, although it has been shown that the acylation of toluene and *p*-xylene by the acid chloride **66** proceeds with low yields (31% and 33% respectively).



66 **67** **68a–c**

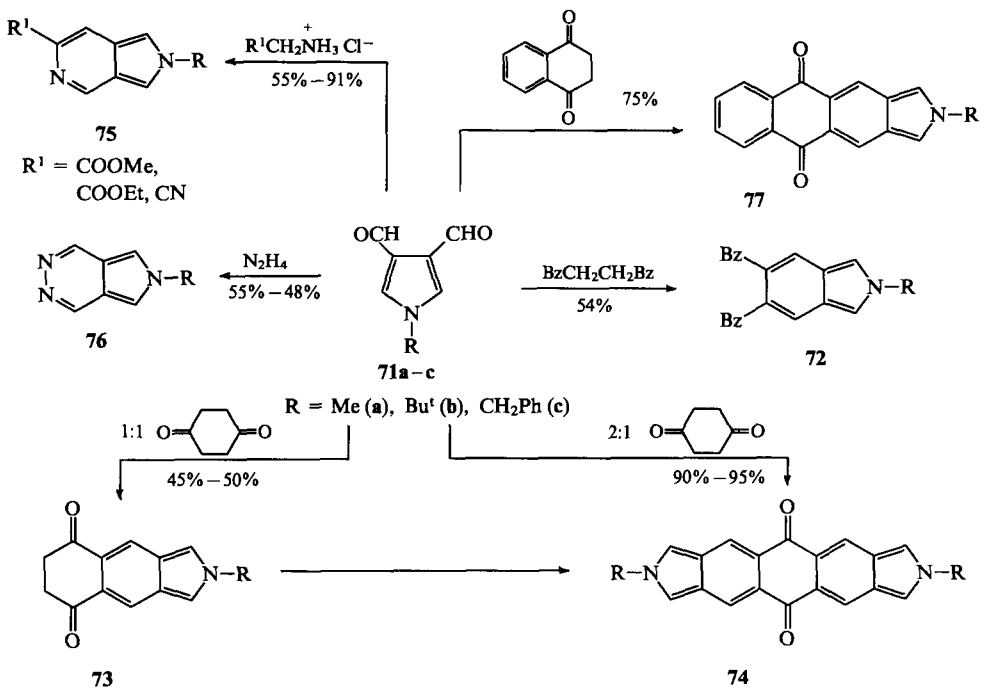
Ar = Ph (**a**), 4-MeC$_6$H$_4$ (**b**), 2,5-Me$_2$C$_6$H$_3$ (**c**)

2-Acetyl-1-tetralinone interacts in boiling DMF with ethyl glycinate hydrochloride to form the dihydrobenzo[*e*]isoindole derivative **69** (43%), which may be dehydrogenated with DDQ over a period of 2 h to benzo[*e*]isoindole **70** in a low yield (12%).[72]



69 **70**

Scheme 3

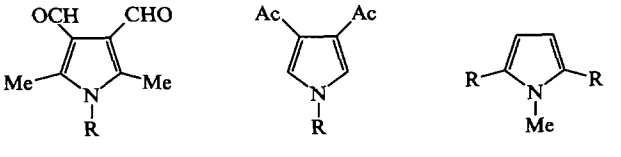


7. The synthesis of isoindoles from pyrroles

The conversion of 2,5-dimethylpyrroles into 1,3,4,7-tetramethylisoindoles has long been known,[1] but the fact that the latter can be formed in an aqueous medium at a high temperature has been demonstrated recently.[73] The studies on the reactions of 3,4-diformylpyrroles **71** initiated not so long ago have been continued and have yielded interesting results for the chemistry of isoindole (Scheme 3, see above).

Thus the condensation of compound **71** with γ-dicarbonyl compounds leads to high yields of 2*H*-isoindoles **72**–**74** and **77**,[74,75] whereas similar condensations with anhydrous hydrazine or glycine derivatives afford 5,6-diaza-2*H*-isoindoles **76** or 5-aza-2*H*-isoindoles **75**.[76]

It has been shown [76,77] that 3,4-diformyl-2,5-dimethylpyrroles **78a, b** as well as the 3,4-diacetyl derivatives **79a, b** enter successfully into similar reactions.

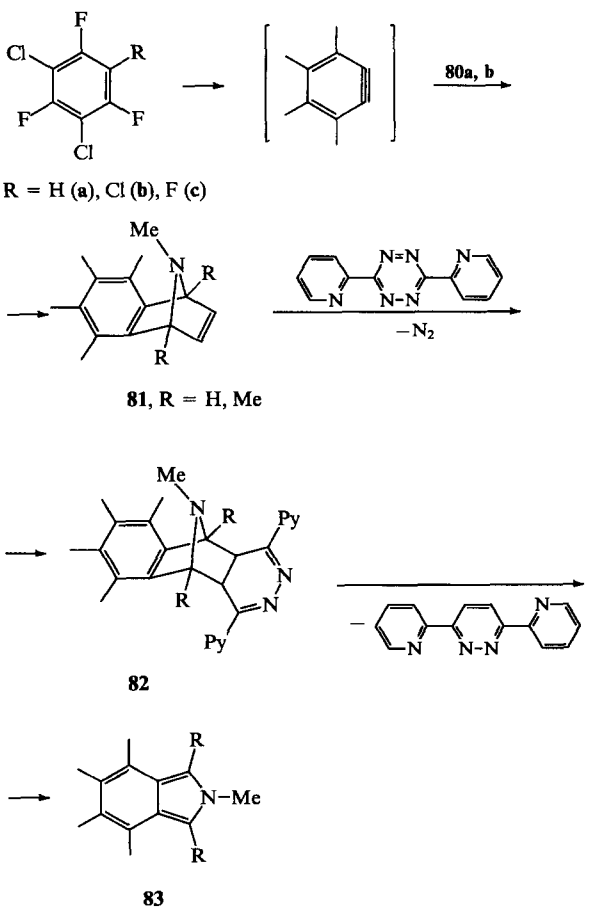


78a, b R = H (**a**), Me (**b**)

79a, b R = H (**a**), Me (**b**)

80a, b R = H (**a**), Me (**b**)

Pyrroles can be converted into the isoindole system also with the aid of the Diels–Alder retro-reaction.[78] The substituted dehydrobenzenes interact with the pyrroles **80a, b** and give rise to derivatives of 7-methyl- and 1,4,7-trimethyl-7-azabenzonorbornadienes **81**. As dienophiles, the latter undergo the [2 + 4]-addition reaction with 3,6-di-α-pyridyltetrazine, which leads to the dihydropyridazines **82** after the evolution of nitrogen and condensation with 7-azabenzonorbornane at the C(5)–C(6) bond. These complex polycyclic compounds readily decompose to 3,6-dipyridylpyridazine and 2-methyl- or 1,2,3-trimethyl-2*H*-isoindoles **83**, which contain in the benzene part of the molecule the substituents present in the initial dehydrobenzenes (yields 75%–89%). This process is used in the synthesis of various heterocycles and is called the Carboni–Lindsey reaction.



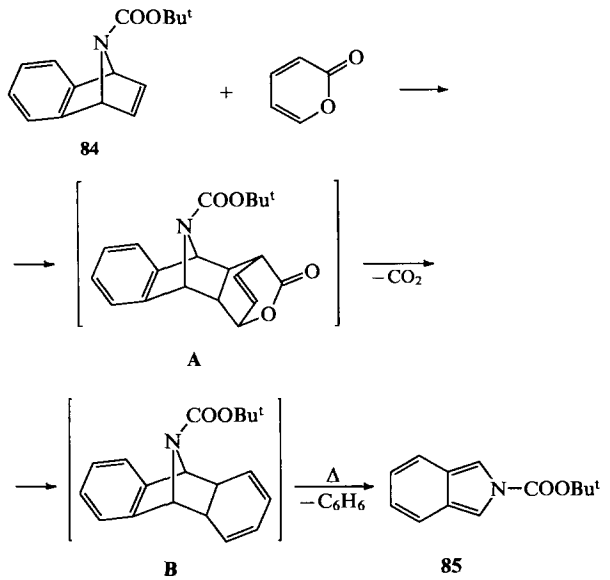
81, R = H, Me

82

83

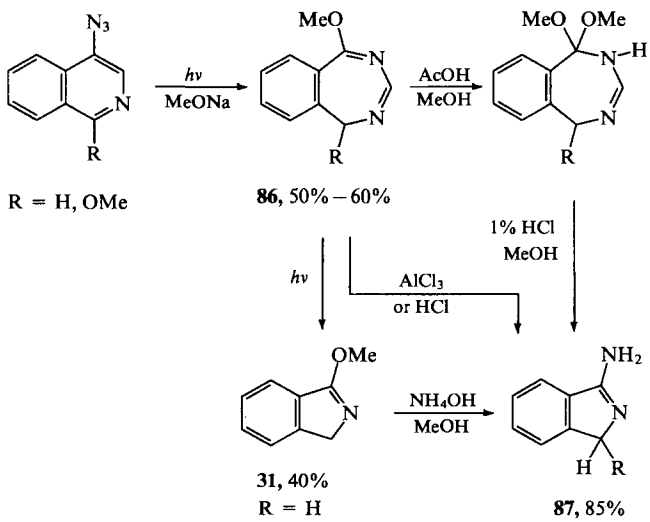
An improved procedure for the synthesis of isoindoles by refluxing a mixture of dipyridyltetrazine with derivatives of 7-azabenzonorbornadiene **81** in chloroform has also been described.[78] The end of the reaction is detected from the cessation of nitrogen evolution, which takes from 3–4 h (for R = H) to 24 h (for R = Me).

The 7-azabenzonorbornadiene **84**, obtained from the corresponding pyrrole and dehydrobenzene, gives rise to the adduct **A** on interaction with 2-pyrone. On heating, the adduct loses a carbon dioxide molecule and is converted into compound **B**. The isoindole **85** is formed subsequently as a result of the Diels – Alder retro-reaction with elimination of benzene.[79]

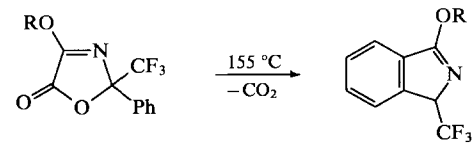


8. Other methods

The rearrangement of 2,4-benzodiazepines of type **86**, obtained by the photoisomerisation of 4-azidoisoquinolines, to isoindoles has been used to synthesise 3-amino-1-R-isoindoles **87** and 3-methoxy-1*H*-isoindole **31** (R = H).[80] Treatment of 1-R-5,5-dimethoxy-1*H*,4*H*-benzodiazepines with 1% hydrochloric acid solution in methanol leads to 3-R-1-aminoisoindolenines **87** in 85% yield. Irradiation for 6 h of a solution of 1-methoxy-5*H*-[2,4]-benzodiazepine **86** in methylene chloride affords 1-methoxyisoindolenine **31** (R = H), whilst treatment with HCl or $AlCl_3$ leads to the amino-derivative **87**.[80] Subsequently the authors extended the range of 4-azidoisoquinolines investigated and studied similar reactions for the benzodiazepines **86** with R = Me, Ph, or Cl.[81]

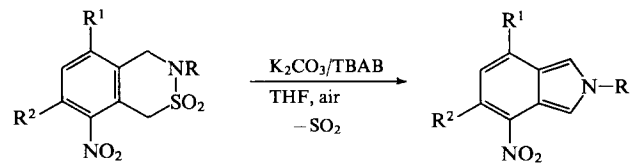


Racemic 1-ethoxy-3-(trifluoromethyl)-1*H*-isoindoles **89a, b** have been obtained by the thermal decarboxylation of oxazol-[2*H*]-one **88**.[82] It is emphasised that the reaction is possible only in the absence of dipolarophiles (for example, trifluoroacetophenone). Otherwise the latter (1,2-dipole) undergoes dipolar cycloaddition to the intermediate alkoxynitrile ylides (1,3-dipole) formed as a result of decarboxylation, which leads to dihydrooxazoles.[82]



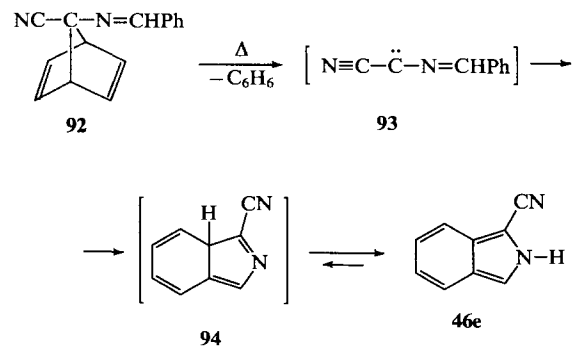
R = Et (**a**), Pr^i (**b**)

The oxidation of nitrobenzothiadiazine dioxides **90** with air in the presence of potassium carbonate and a phase-transfer catalyst (TBAB) leads to the corresponding isoindoles **91** after the elimination of sulfur dioxide. In the case of alkyl substituents at the nitrogen atom, the yields of compounds **91** are 53% – 74%, the yields falling sharply (39%) only for the *N*-phenyl derivative. If $R^1 = R^2 = H$ and R = Me, then 3-hydroxy-2,3-dimethyl-4-nitroisoindol-1-one is formed under the reaction conditions.[83]

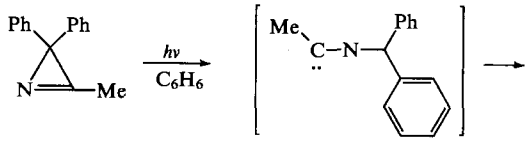


R = Me, Ph, $PhCH_2$
R^1 = H, F
R^2 = H, Cl

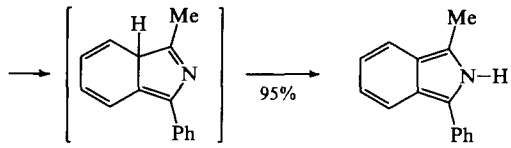
A novel approach to the synthesis of 1-cyano-2*H*-isoindole **46e** is based on the use of the norbornadiene **92** as the initial compound.[84] On heating in vacuo, the latter generates the carbene **93**, which undergoes intramolecular 1,5-electrocyclisation, forming the intermediate **94**. The subsequent 1,3-sigmatropic shift of the hydrogen atom from the carbon atom to the nitrogen atom in the intermediate **94** leads to the isoindole **46e**. The isoindole **46e** is isolated from the reaction mixture in 41% yield with the aid of preparative thin-layer chromatography and subsequent vacuum sublimation.[84]



The intramolecular heterocyclisation process, which is in many respects similar to that considered in the previous study, has been observed in the formation of the 2*H*-isoindole **98** from the azirine **95**. It has been reported[85] that the photochemical rearrangement of 3-methyl-2,2-diphenylazirine **95** to the nitrile ylide **96** and the cyclisation of the latter lead to the corresponding isoindole **98**. This reaction has been classified by the authors as a 1,5-electrocyclic process accompanied by the subsequent 1,3-sigmatropic shift of the proton in the intermediate **97**.

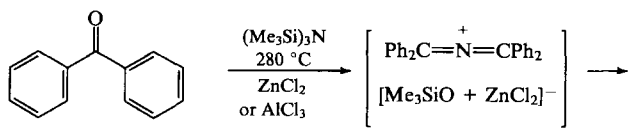


95 96

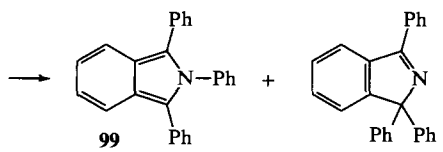


97 98

It has been shown that the cyclocondensation of benzophenone with tris(trimethylsilyl)amine at 280 °C in the presence of $ZnCl_2$ and $AlCl_3$ leads to a mixture of the isoindole **99** and 1,1,3-triphenyl-1*H*-isoindole. The yields of the isoindole **99** are 11% and 15% when zinc chloride and aluminium chloride are used respectively. The authors suggest that the intermediate in the formation of the above mixture of isoindoles is the azaallenium ion **100**.[86]

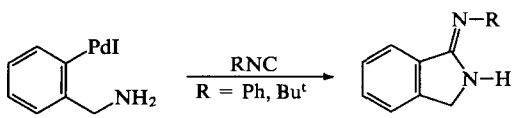


100



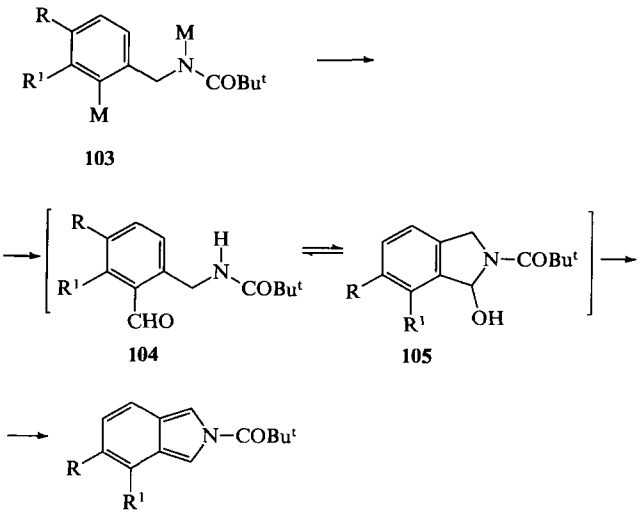
99

A method of synthesis of isoindoline imines **102** based on the insertion of isocyanides in a metal–carbon bond in the divalent palladium complex **101** has been described. The complex **101** is treated with the isocyanide in methylene chloride, after which the solvent is replaced by toluene and the reaction mixture is refluxed for 3 h. The imines **102** are isolated after making the mixture alkaline.[87]



101 102

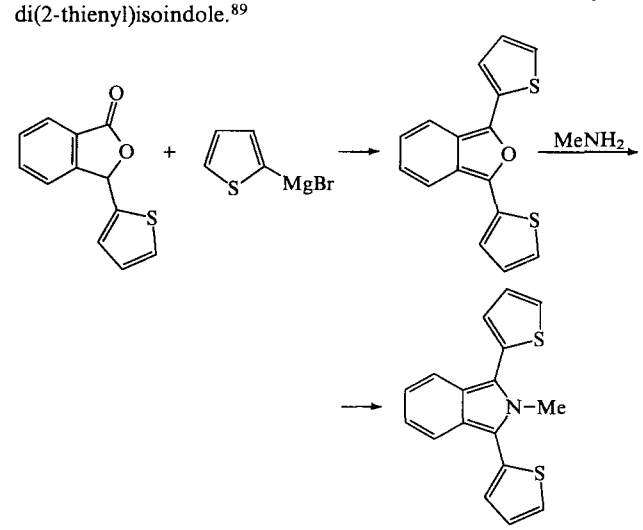
Metallation of the amides **103** followed by treatment with DMF leads to the aldehydes **104**, which can be regarded as the open-chain form of the cyclic compound **105**. The existence of this kind of ring–chain tautomerism has been demonstrated by the NMR method. The conversion of the isoindolines **105** into the isoindoles **106** on refluxing in xylene has been described by isolating the adduct of the latter with *N*-phenylmaleimide.[88]



103 104 105 106

R, R^1 = H, Cl, OMe, $-OCH_2O-$
M = H, Li

1,3-Di(2-thienyl)isobenzofuran can be obtained by the reaction of 3-(2-thienyl)phthalide with 2-thienylmagnesium bromide. After oxidative opening of the furan ring and treatment with methylamine, the isobenzofuran is transformed into 2-methyl-1,3-di(2-thienyl)isoindole.[89]



III. Theoretical and physical aspects

1. Theoretical aspects

The phenomenon of isoindole has been discussed in a review [1] and in a monograph:[3] its aromaticity and high reactivity. Ideas concerning its electronic structure, with the aid of which attempts have been made to account for the above two properties which sometimes exclude one another, have been considered. In theoretical studies published recently, both semiempirical calculations (in terms of the Hückel,[90,91] PPP,[90,92] and CNDO[93], approximations) and nonempirical calculations[94] (the method of canonical molecular orbitals) have been employed; the resonance energies[90,92,95,96] various aromaticity indices,[92,95,97,98] enthalpies of formation,[91] and molecular geometry have been determined by the INDO[99] and MNDO[94] methods.

It is essential to note that a trend has arisen during the past period towards the introduction of new aromaticity indices and the derivation of correlations between the new and already existing indices. Fabian [90] proposed that the aromaticity of heterocycles, and especially isoindole, be estimated from the difference between the π-electronic energies of the heterocycle and the

corresponding iso-π-electron [9]annulenium ion. A new version of the iterative procedure of the Hückel molecular orbital method (the so-called χ-technique) has been used to calculate the HOMO energies and the enthalpies of formation of a series of heterocycles. According to this approach, the HOMO energies are 7.26 eV for isoindole, 7.71 eV for indole, and 8.08 eV for pyrrole. The result demonstrated a satisfactory agreement with the earlier calculations by Dewar and experimental data.[91] Kruszewski[92] formulated a rule on the basis of calculations for a large number of monocyclic and polycyclic heterocycles, including benzopyrroles (indole and isoindole) by the PPP method in terms of the variable β approximation. According to this rule, the condensation of an additional aromatic ring with the heterocycle gives rise to a more stable compound the greater the π-electron index of the bond involved in the process. One of the examples confirming this rule is the familiar difference between the properties of indole and isoindole. Analysis of the energy gaps by the HOMO–LUMO method for a large number of cyclic conjugated molecules (including benzopyrroles) suggested to the authors[98] the introduction of the concept of the absolute and relative 'hardness', which in their view reflects most effectively all three aspects of aromaticity: high stability, low reactivity, and the existence of ring currents. Although the 'hardness' of isoindole (0.482β) is significantly lower than that of indole (0.716β), it is nevertheless sufficient to conclude that isoindole is aromatic. Calculation of the topological resonance energies for benzopyrroles and their comparison with the analogous energy for benzene enabled the authors[95] to determine the degree of their aromaticity. It was found that the aromaticities, expressed as a percentage of that of benzene, are 83% for indole, 71% for isoindole, and only 63% for 2*H*-benzo[*f*]isoindole. Bird[97] introduced his aromaticity index from calculations based on experimental geometries of heterocyclic systems. According to this index, the aromaticity of, for example, 2-benzylisoindole **72** is slightly higher than that of benzimidazole **71** and indole **70**. New calculations of the Bird, Jalg,[100] and Pozharskii[100] structural aromaticity indices for isoindole have been published.[101] They were performed on the basis of the geometry obtained in accordance with the AM1 program; the following series of indices were obtained: 66.5 (Bird), 1.311 (Jalg), and 0.23 (Pozharskii) for indole and 68.9, 1.378, and 0.22 respectively for isoindole. It is important to note that the results of previous calculations, based on the analysis of canonical molecular orbitals, and the conclusions concerning the aromaticity of isoindoles have never been questioned, not even in recent years. However, the symmetry properties of the canonical molecular orbitals are known a priori to give rise to a significant delocalisation, which in fact hinders the comparison of the characteristics of individual chemical bonds and the structural fragments of different molecules (including isomers in terms of the position of the heteroatom of the indole–isoindole type), giving rise to various structural representations in order to reflect the specificity of their properties.[3] The above disadvantages are eliminated to an appreciable extent when localised molecular orbitals are considered. They make it possible to estimate a measure of the interaction of identical fragments with the rest of the complex molecule and hence serve as a test of the classical structural representation. This approach has in fact been applied to the indole–isoindole pair of isomers[93] and was then extended to the benzofuran–isobenzofuran and thionaphthene–benzo[*c*]thiophene.[102] Whilst confirming the conclusions concerning the aromaticity of isoindole, the authors believe that the π-electron system of isoindole is more integrated than that of indole. For the latter, they suggest that the electron system consisting of three fairly localised π-subsystems be considered: benzene rings, the C(2)–C(3) double bond, and the nitrogen atom with its electron pair.[93] Katritzky and coworkers[101] compiled and correlated the aromaticity characteristics based on geometrical, energy, and magnetic data for a series of benzo-condensed five-membered heterocycles, including condensed pyrroles.

For the vast majority of structures investigated,[103–106] there is a satisfactory correlation between different characteristics used to estimate the aromaticity but here too the uniqueness of isoindole has been manifested [the data of Terent'ev et al.[107] (10 characteristics) virtually deviate from these correlations]. In a comparative quantum-chemical study of the polarisabilities (α) and hyperpolarisabilities (β) of a series of 'positional' isomers (including indolizine, indole, and isoindole), the authors[103] noted that the structural differences have a significantly smaller effect on α (109, 107, 109 a.u. respectively) than on β (2.93, −2.89, and −5.93 a.u. respectively). A theoretical study has been made[99] by the INDO method (with complete optimisation of the geometry) of the populations of the conformations of the still unknown 2-amino-2*H*-isoindole and it has been shown that the disposition of the free electron pair of the nitrogen atom of the amino-group at right angles to the plane of the bicyclic molecule is most favourable. In the course of the development of quantitative approaches to the resonance theory, Pipeng and Wengui[96] calculated the resonance energies of the various tautomeric forms in order to predict the preferred tautomer and the tendency towards a shift of the tautomeric equilibrium in a series of related structures. 1-Amino-2*H*-isoindole was included within the range of their interests. It exists in the form of the 3-amino-1*H*-tautomer,[1] which was confirmed on the basis of theoretical conclusions.

2. Spectroscopic data

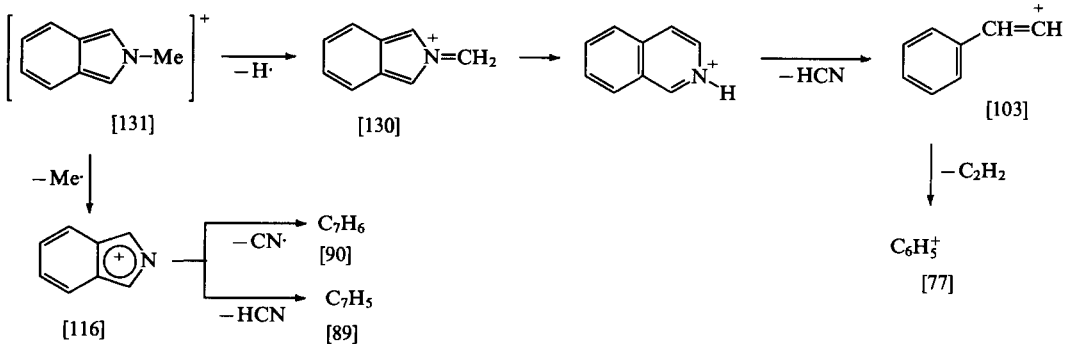
Spectroscopic data (^{1}H NMR, ^{13}C NMR, IR, and UV) for various isoindoles have been described in detail in reviews[1,2] and in monographs.[3] The period which has elapsed has been characterised by the accumulation of quantitative information about the spectra of isoindoles. We therefore quote here only references to publications containing fairly extensive data on the spectroscopic characteristics of new isoindoles: ^{1}H NMR,[5,35,36,39,61,72,84,85] ^{15}N NMR,[99,104] ^{13}C NMR,[4,5] IR,[5,35,36,39,61,69,85,105] and UV.[35,36,39,61,85]

As regards the interpretation of studies on electronic spectra, the latter were surveyed in previous reviews.[1,2] The electronic structure of phthalocyanines without a central metal atom has been investigated[94] by means of nonempirical and semiempirical methods. The study was combined with the analysis of the constituents of this system: benzene, pyrrole, and isoindole. The electronic spectra of dimethinecyanines and merocyanines based on 1-dimethylamino-2-phenylisoindole have been discussed.[106] It has been noted that positive solvato-chromism is characteristic of merocyanines.

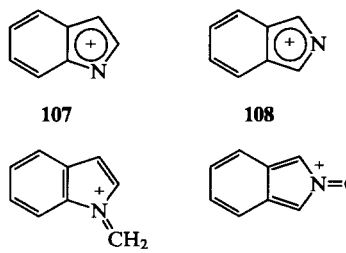
3. Mass-spectra of isoindoles

An attempt has been made in recent years to fill the gaps in the mass-spectrometric study of isoindoles. The decomposition of a series of isoindoles under electron impact, including those condensed along the *a* face, has been analysed.[107] It follows from these data that the molecular ion derived from 2-methylisoindole has the highest intensity in the spectrum and that the intensities of the peaks due to the other ions formed on fragmentation do not exceed 50% of that of M^+. The spectra have the usual overall form for aromatic compounds and confirm the electronic structure of isoindole put forward by Kovtunenko et al.[93] The appreciable π-bonding via the nitrogen atom in 2-methylisoindole has been demonstrated by the fact that the introduction of phenyl substituents in the 2-position (i.e. for 2-phenylisoindole) lowers the intensity of M^+ to 93% as a consequence of the competing conjugation of the free electron pair of the nitrogen atom with the benzene ring. In 2-(*p*-anisyl)isoindole, this type of competition has a smaller effect owing to the positive mesomeric effect of the methoxy-group. Comparison of the mass-spectrometric decomposition of 1-methylindole[107] with that of the isomeric 2-methylisoindole can also serve as confirmation of the postulated electronic structure of isoindole.[93] The stability of the ion **107** is lower than that of the ion **108**, which indicates a greater degree of

Scheme 4



inter-ring conjugation in the isoindole system — indicated by the values of $[M-CH_3]^+/M^+$. On the other hand, the intensity of the $[M-H]^+$ peak is much higher for *N*-methylindole than for *N*-methylisoindole, since here one is dealing with systems of a different kind: **109** and **110**, within the limits of which the π-bonding via the nitrogen atom is ruled out. In this case, the ion **110** loses the advantages of isoindole as an integrated 10π-electron system and is in fact an open-chain polyene, while the ion **109** remains aromatic in view of the aromaticity of the benzene ring, which to a large extent determines the stability of the indole system as a whole.[93] The routes leading to the fragmentation of different isoindoles have also been indicated,[107] for example, we have for *N*-methylisoindole.



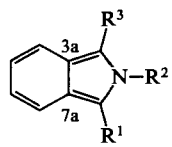
The mass spectra of new 2-R-isoindoles (R = Bu^t, Bu^tCH_2, $PhCH_2$, adamantyl) have also been used for the purpose of their identification (Scheme 4).[5]

4. X-Ray diffraction data

Fairly numerous studies on the X-ray diffraction of isoindoles, which permit objective inferences about their geometry, have been published.[39,54,93,105,108–110] These data are presented in Table 1 and they all confirm the conclusion that isoindole is aromatic as a 10π-electron system. The molecules are planar. For example, the deviation of the atoms in 2-methylisoindole from the mean square plane passing through the atoms of the bicyclic system do not exceed 0.015(4) Å.[108] The tabulated data demonstrate the similarity of the bond lengths in the benzene fragment of isoindole structures and in naphthalene [in the latter, the bond lengths are 1.410 Å for C(3a)–C(7a); 1.425 Å for C(3a)–C(4); 1.361 Å for C(4)–C(5); and 1.421 Å for C(5)–C(6)], which in an argument in support of the delocalisation of the electron density.[108,109] The C(3a)–C(4) and C(7)–C(7a) bond lengths are close to those in classical aromatic compounds and differ significantly from the values characteristic of a single bond. This means that the electronic structure of isoindole cannot be represented by two independent components (a combination of butadiene and pyrrole). These two components are conjugated. The C–N bond lengths in the pyrrole fragment of the first four structures (see Table 1) are somewhat smaller than in pyrrole itself (1.383 Å). On the other hand, the C(3)–C(3a) bond lengths in isoindoles are somewhat greater than in pyrrole (1.371 Å). This probably indicates a greater delocalisation of the π-electron density in the pyrrole component of the bicyclic system compared with the parent heterocycle.

X-Ray diffraction of isoindole derivatives, including 2-methylisoindole, confirmed their electronic structure put forward on the basis of the analysis of localised molecular orbitals.[93]

Table 1. X-Ray diffraction data for isoindole derivatives.



2*H*-Isoindole			Bond length/Å										Ref.
R^1	R^2	R^3	1–2	2–3	1–7a	3–3a	3a–7a	7a–7	3a–4	6–7	4–5	6–5	
H	Me	H	1.362	1.360	1.380	1.382	1.429	1.420	1.432	1.347	1.357	1.416	93,108
CN	Me	H	1.374	1.348	1.407	1.395	1.426	1.412	1.405	1.355	1.369	1.422	54
H	$PhCH_2$	H	1.362	–	1.384	–	1.429	1.416	–	1.357	–	1.415	109
H	Bu^tCH_2	H	1.360	–		–	1.431	1.412	–	1.358	–	1.406	110
Et	Pr	MeOOCCH=C(COOMe)	1.381	–	1.394	–	1.431	1.417	–	1.359	–	1.426	39
CHO	H	Ph	1.376	1.348	1.412	1.428	1.420	1.414	1.414	1.365	1.367	1.409	105

Note. The bond lengths are 1.468[93,108] and 1.460[54] for N–Me, 1.405[54] for C–CN, and 1.458[110] for N–CH_2.

IV. Chemical properties

Isoindole and its derivatives are distinguished by a high reactivity. This is indicated by experimental data[111] on the rate constants for the acid-catalysed detritiation of a series of heterocycles (including *N*-methylisoindole). For example, in the indolizine (3-position), *N*-methylisoindole (1-position), and indole (3-position) series, the partial rate factors for the exchange reactions are in the proportions 1798.9 : 11 992.7 : 1. The authors calculated the values of σ^+ for the above heterocycles (−1.94, −2.04, and −1.57 respectively) and found that isoindole is one of the most reactive compounds among the known heterocyclic systems.[111] A mechanism has been proposed[112] for the tautomerism of 1,3,4,7-tetramethyl-2*H*-isoindole, taking into account the solvent effect on the basis of its spectrophotometric study.

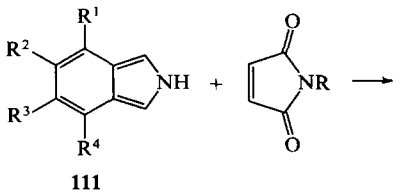
1. The Diels–Alder reaction

One of the most characteristic properties of isoindole and its derivatives is their ability to enter readily into the [2 + 4]-cycloaddition reaction. Furthermore, the usual method for the identification of unstable isoindoles involves their conversion into Diels–Alder adducts with maleimide derivatives.[1–3] We may mention in this connection a review[113] of the quantum-chemical methods used to predict the stereospecificity of the Diels–Alder reaction.

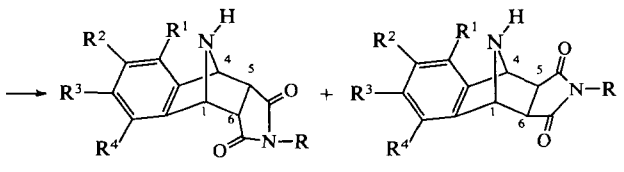
a. The interaction of isoindoles with maleimide derivatives

During the period considered, numerous communications were published in which mention is made of the adducts of isoindoles with maleimide derivatives. Certain generalisations facilitating the identification of the isomers formed are also known.[114,115]

NH-Isoindoles. The isoindoles **111** unsubstituted at the nitrogen atom give rise readily and in high yields (on average 80%) to a 1 : 1 mixture of the *endo*-adduct **112** and the *exo*-adduct **113** in which the endo-isomer predominates.[13,14,16,18] It is sometimes possible to separate these mixtures by chromatography,[16] but usually they are converted smoothly, after being kept for a short time in solvents (for example, in xylene), into the corresponding *exo*-isomers **113**.[14,16] The isomerisation **112** → **113** also occurs with participation of the solvent and under much milder conditions: at room temperature in DMSO over a period of 30 min (the ^{1}H NMR spectrum of the solution of the adduct **112** reveals its complete conversion into compound **113**).[16]

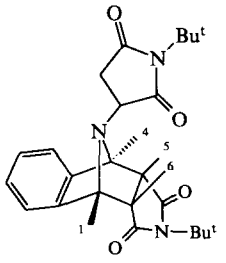


111



endo-**112** *exo*-**113**

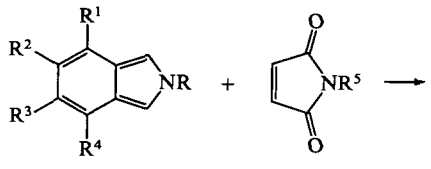
When the isoindole **14** is allowed to react with *N*-*tert*-butylmaleimide, the formation of a 1 : 2 adduct was observed. On the basis of spectroscopic characteristics, the structure **114** was attributed to it.[16]



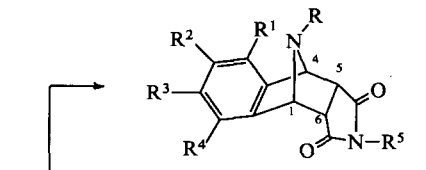
114

2-R-Isoindoles. The isoindoles **115** substituted at the nitrogen atom readily form 1 : 1 adducts.[6–8,19,20,79,116–118] Under kinetically controlled reaction conditions,[116] one then obtains exclusively the *endo*-isomers **116**,[7,8,19,79,88,116–118] while under thermodynamically controlled conditions the *exo*-isomers **117** are produced.[19,116–118] The diene reactivity of the isoindoles **115** is determined by the nature of the substituents in the benzene component of the bicyclic system; a decrease in the diene reactivity has been observed in 2-*tert*-butyl-5-nitroisoindole[7] and 2-R-4,5,6,7-tetrachloroisoindole,[118] while in 2-R-dibenzo[*e*,*g*]isoindole[6] it is not manifested at all on interaction with maleimide derivatives. It has been shown[118] that the Diels–Alder addition to 2-R-4,5,6,7-tetrachloroisoindole may be initiated by adding a catalyst—a Lewis acid ($AlCl_3$). The configurational stability of the *endo*-isomers depends to a large extent on the nature of the substituent at the nitrogen atom of the 7-azabenzonorbornene system **116**.

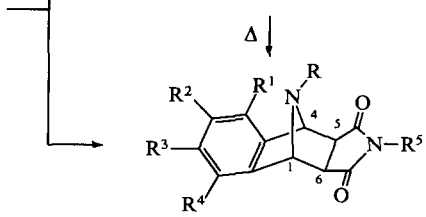
If this is an alkyl group, then the isomerisation **116** → **117** takes place relatively readily (for example, on refluxing in alcohol or xylene).[19,116–118] In the case of an aryl substituent, the attempts to isomerise the *endo*-isomer to the *exo*-isomer were unsuccessful.[119] The example of the *endo*-adduct of the isoindole **20b** is remarkable:[19] on refluxing in xylene or diglyme, isomerisation was not observed and only after heating for 19 h in Carbitol was it possible to achieve the isomerisation with 8% yield. The adducts **116** obtained from the isoindoles **106** cannot be isomerised to the corresponding *exo*-compound **117**. However, if the preliminary hydrolysis of the *N*-acyl group is carried out, then the isomerisation of the *exo*-adduct **113** proceeds extremely readily.[88] A series of unstable isoindoles **115** have been characterised in terms of the adduct **116**.[19,88,117] The unstable methyl ester of isoindole-2-acetic acid has been identified via the adduct with *N*-phenylmaleimide, to which the *exo*-structure was attributed without proof.[20] It has been shown[116] that the ^{1}H NMR spectra of the adducts **116** and **117** are more complex for R = Me than might have been foreseen: they demonstrate the occurrence of the *syn*- and *anti*-isomerism of the methyl group at N(7). The isomerism disappears when the lanthanide shift reagent Eu(fod)$_3$ is added to the test solution. Furthermore, the constant $J \approx 2$ Hz, for spin–spin coupling of the protons across four σ-bonds in the *W*-conformation, has been noted. All the features of the cycloaddition of maleimides to the isoindoles **115** are characteristic of their 5-aza-analogue 6-ethoxycarbonyl-2-methyl-2*H*-pyrrolo[3,4-*c*]pyridine[120] and of 2-methyl-6,7-diazabenzo[*f*]isoindole {7-methyl-1,4-diphenyl-7*H*-pyrrolo[3,4-*g*]-phthalazine}.[74]



115



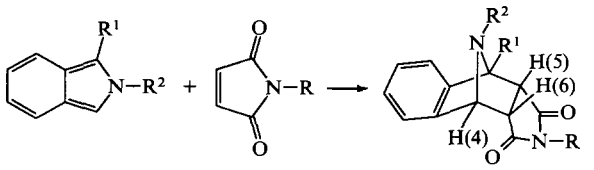
endo-116



exo-117

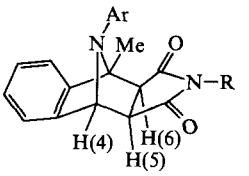
1,2-Di- and 1,2,3-tri-substituted isoindoles. The identification of the isomeric Diels–Alder *exo*- and *endo*-adducts comprising isoindoles **118** asymmetrically substituted in the pyrrole component in terms of the spin–spin coupling pattern of the H(4), H(5), and H(6) protons in the ^{1}H NMR spectra becomes more complicated, which leads to possibile erroneous assignment of the configurations of the isomers.[35, 114, 121]

As a rule the 1 : 1 adducts **119** with the *endo*-configuration are formed from the type **118** isoindoles on interaction with maleimides under the conditions of kinetic control.[31, 32, 35, 114, 122] The majority of the isoindoles **118** investigated do not withstand the conditions of thermodynamically controlled cyclo-addition. Only one instance of the formation of the *exo*-adduct from such isoindoles is known — a series of compounds of structure **120** have been obtained from 2-methyl-1-phenylisoindole.[122] The corresponding *endo*-adducts are configurationally stable and do not isomerise to the *exo*-isomers **120**. The isoindoles **118c** unexpectedly react with maleimides, forming the dihydronaphthalene derivatives **121** under mild conditions.[114, 123] The isoindoles **118a, b** react with maleimides, affording the 1 : 2 adducts **122**, the formation of which is interpreted [31, 32, 124] as the initial Michael addition of one maleimide molecule with subsequent addition, this time of the Diels–Alder type, of a second dienophile molecule to the 1,2,3-trisubstituted isoindole formed. The establishment of the *endo*-configuration of the type **122** adducts is fairly difficult and has been carried out usually with the aid of X-ray diffraction [32] or from indirect ^{1}H NMR spectroscopic data.[31, 32, 124]

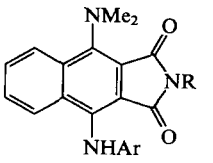


118a–c **119**

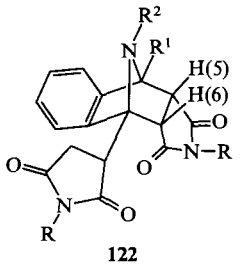
118a: R^1 = OMe, OEt
118b: R^1 = Ph
118c: R^1 = NMe_2



120

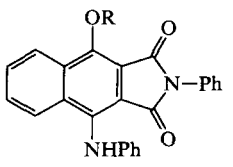


121

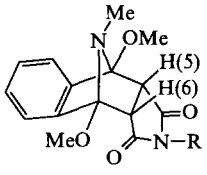


122

A similar problem was solved in the determination of the configuration of the adduct of the unstable 1,2,3-trisubstituted isoindoles **24** and **28** with maleimide. The interaction of a solution of compound **24b** with phenylmaleimide at room temperature afforded a mixture of two naphthalene derivatives: **123a** (10%) and **123b** (54%).[23] On the other hand, it has been shown [27] that type **28** isoindoles form with maleimides type **124** *endo*-adducts in a low yield (not more than 25%).



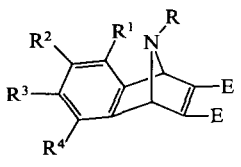
123a–b
R = H (**a**), $SiMe_3$ (**b**)



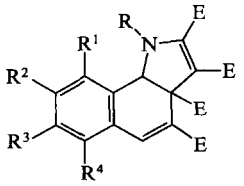
124

b. The interaction of isoindoles with ethynedicarboxylic acid esters

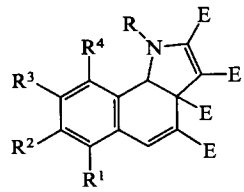
When the dimethyl ester of ethynedicarboxylic acid [acetylenedicarboxylic acid] (DMAC) is added to type **115** isoindoles, the latter give rise readily and in high yields to the 1 : 1 adducts **125** in the first stage. These can then be converted (in the presence of an excess of DMAC) into the 1 : 2 adducts **126** (**127**). The tendency to form compounds **127** is apparently determined by the bulk of the substituent R. For example, 2-*tert*-butyldibenzo-[*e*, *g*]isoindole **6a** does not form a type **126** adduct at all, whereas for its benzyl analogue **6b** under similar conditions the reaction path giving rise to such an adduct is the main one (the yield of compound **126** is 68%), the 7-azabenzonorbornadiene derivative **125** being formed only as a side product (yield 23%).[6]



125

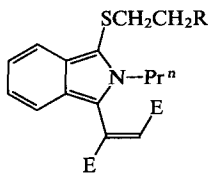


126



127 E = COOMe

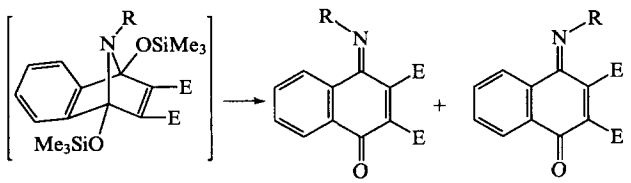
2-*tert*-Butyl-5-nitroisoindole,[7] 2-*tert*-butylbenzo[*f*]isoindole,[8] and the isoindoles **74**, **75**,[120] and **77**[35] afford type **125** products. A separable mixture of complex three-dimensional molecules with the *syn*- and *anti*-configurations is formed from the terminal pyrrole rings of the isoindole **74** when the latter reacts with DMAC.[35] The isomeric compounds **126** and **127** were isolated on treating with an excess of DMAC the corresponding type **125** adduct obtained from 2-methyl-5-azaisoindole.[120]



128a, b

128a: R = H, 51%

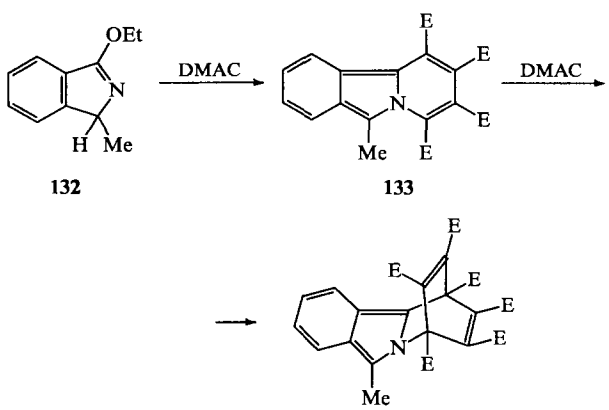
128b: R = OH, 33%



129 **130** **131**

E = COOMe

7-Methyl-1,4-diphenyl-7*H*-pyrrolo[3,4-*g*]phthalazine, a derivative of 2*H*-6,7-diazabenzo[*f*]isoindole, reacts similarly, forming initially a type **125** adduct and then a type **126** adduct.[74] Interaction of the isoindoles **40a, b** with DMAC is interesting. They give rise to the adducts **128a, b** with retention of the 10π-electron system.[39] On interaction with DMAC, the isoindoles **24b, c** afford the isomeric *syn*- and *anti*-imines **130** and **131** via intermediate type **129** adducts.[25,26] The isoindole **132** reacts with DMAC to form initially the 1:2 adduct **133**, while in the presence of an excess of DMAC the product is the 1:3 adduct **134**.[29] In contrast to compounds **24b, c**, the isoindole **24a** reacts with DMAC to form the dimethyl ester of (2-methyl-1-oxo-3-trimethylsiloxy-1,3-dihydroisoindol-3-yl) fumaric acid in 53% yield.[26]

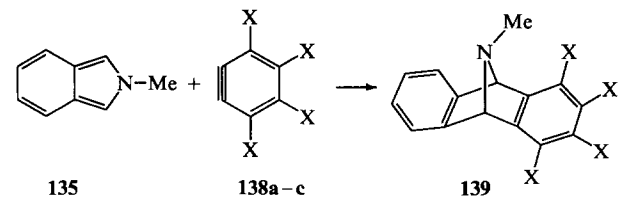


132 **133** **134**

E = COOMe

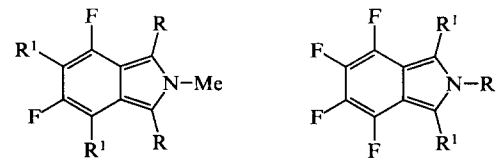
c. The addition of dehydrobenzenes

The study of the addition of dehydrobenzenes and dehydronaphthalenes to isoindoles has recently acquired special significance in view of the discovery of effective reagents for the deamination of 7-azabenzonorbornadiene derivatives formed as a result of this reaction.[125] Such deamination constitutes a convenient method of synthesis of angularly and linearly condensed polycyclic hydrocarbons containing various substituents, which are difficult to obtain.[78,126-128] The isoindoles **6a, b** and **135** react readily with the arynes **138b, c** respectively, affording high yields of 1:1 adducts.[6,125-128] The isoindoles **7** and **8** likewise give rise to similar adducts but this time with the 1:2 composition, the imine bridges in these structures assuming the *anti*-configuration relative to one another.[10] The interaction of the isoindoles **137a, b** with the arynes **138** produces 1:1 adducts, but in all cases the 7-methyl-7-azadibenzonorbornadienes are obtained in significantly lower yields than the *N*-benzyl derivatives.[129] Complex polycyclic systems are formed on interaction with the naphthynes **140** and **141** and the 1,5- and 2,6-naphthadiynes **142** with the isoindoles **135**, **136a-c**, and **137a, b**. The last two naphthadiynes react with the isoindoles **135** and **137a** affording moderate yields of the 2:1 adducts **143a, b** and **144** with the *anti*-configuration of the imine bridges.[127,128]



135 **138a-c** **139**

X = H (a), Me (b), Cl (c)

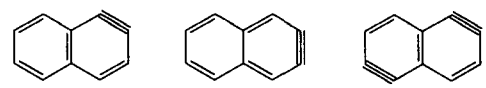


136a-c

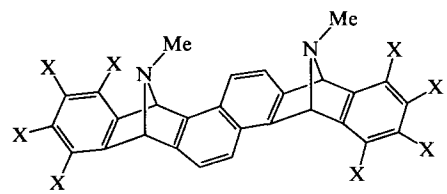
136a: R = H, R^1 = Cl
136b: R = Me, R^1 = Cl
136c: R = H, R^1 = H

137a-c

137a: R = Me, R^1 = H
137b: R = Bn, R^1 = H
137c: R = Me, R^1 = Me

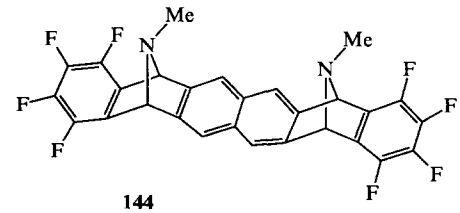


140 **141** **142**



143a, b

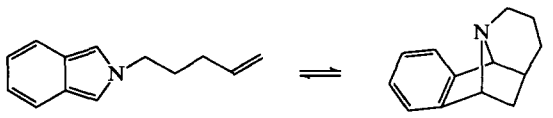
X = H (a), F (b)



144

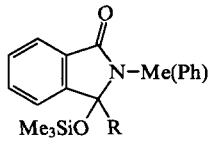
d. The addition of other unsaturated compounds

The intramolecular addition of a double bond to a diene isoindole system has been described:[28] on heating for 8 h (at 150 °C), *N*-(4-pentenyl)isoindole **29** partially forms the adduct **145**. Judging from ^{1}H NMR spectroscopic data, the ratio of the open-chain and cyclic forms which can be obtained at this temperature is 1 : 1, whereas after heating to 200 °C the equilibrium shifts towards the open-chain form **29**. On slow fractionation of the unpurified isoindole **29** at a reduced pressure, it is possible to obtain the pure adduct **145** in 80% yield.



29 **145**

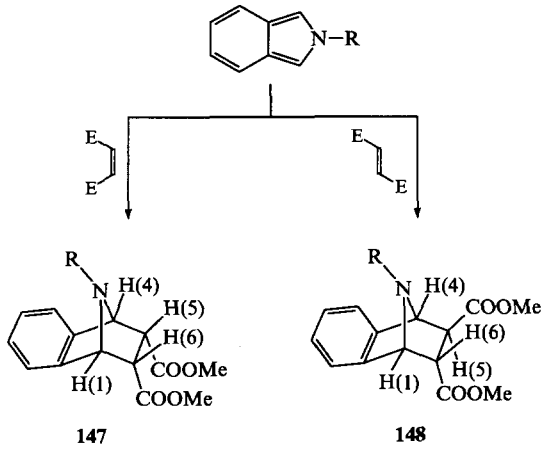
It is of interest that a similar cyclisation is not observed for *N*-(5-hexenyl)isoindole.[28] The 1,3-di(trimethylsiloxy)isoindoles **24a, b** interact with methyl acrylate,[26] methyl vinyl ketone,[26] 1,2-dibenzoylethene,[23] and dimethyl maleate[26] to form exclu-sively the lactams **146a–e**. When dibenzoylethene is used, the isoindole **24a** affords a 27% yield of compound **146b** and traces of compound **146a**, while the isoindole **24b** shows the opposite behaviour, affording 51% of compound **146a** and traces of compound **146b**.[23]



146a–e

146a: R = C(Bz)CH=C(Ph)OSiMe$_3$
146b: R = CH(Bz)CH$_2$Bz
146c: R = CH$_2$CH$_2$COOMe
146d: R = CH(COOMe)CH$_2$COOMe
146e: R = CH$_2$CH$_2$Ac

N-Methyl- and *N*-aryl-isoindoles readily combine with dimethyl esters of maleic and fumaric acids, affording the diastereoisomeric Diels–Alder adducts **147** and **148**. The high configurational stability of the *endo*-adduct **147** has been noted.[130]



147 **148**

E = COOMe

The synthesis of the structures obtained from 2-methyl-,[132] 1,2-dimethyl-,[131,132] and 1,2,3-trimethyl-2*H*-isoindoles[131–135] and the alkenes **149–153** has been described in a series of communications by German workers.[131–135] In the case of the alkenes **151–153**, one may expect theoretically the appearance of stereoisomers, although they have been actually identified only in the case of the adducts derived from compounds **151**[135] and **153**.[131,134]

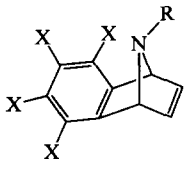


149 **150**

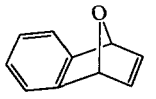


151 **152** **153**

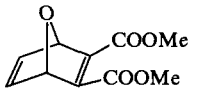
Prolonged refluxing of *N*-benzyl-4,5,6,7-tetrafluoroisoindole and the isoindoles **135** and **137a** with 7-R-7-azabenzonorbornadienes **154a–d** under a nitrogen atmosphere gives rise to between 6% and 61% yields of the 1 : 1 adducts **157** with the *exo, endo*-junction between the cyclic systems.[134] Equally elegant structures have been synthesised[79] by means of cycloaddition to the isoindole **85.**



154a–d



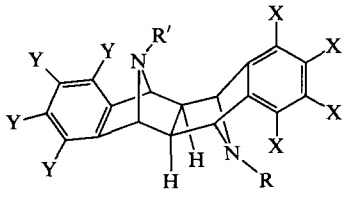
155



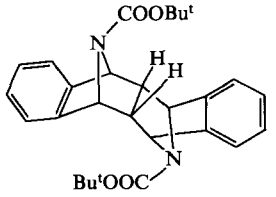
156

154a: X = F, R = Me
154b: X = F, R = Bn
154c: X = Cl, R = Me
154d: X = H, R = COOMe

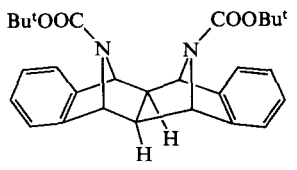
For example, it has been shown that the addition of the substituted 7-azabenzonorbornadiene affords a mixture of the diastereoisomeric adducts **158** and **159** in proportions of 2.3 : 1.[79] On the other hand, the addition of the alkene **155** takes place with the preferential formation of the *exo, exo*-adduct **160**. The *exo, exo*-diastereoisomer is also formed exclusively in 74% yield on interaction with the alkenes **156.**



exo, endo-**157**

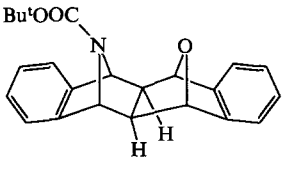


endo, exo-**158**

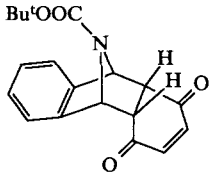


exo, exo-**159**

The interaction of 1,4-benzoquinone with the isoindole **85**, gives rise to 1 : 1 *endo*-adduct **161** in 62% yield.[79]



exo, exo-**160**, 51%



161

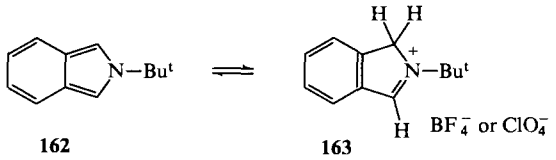
2. Electrophilic attack on isoindoles

a. Protonation

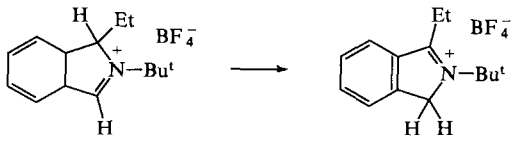
The available information about the basicity of isoindoles is extremely limited. The study of the basicity[36] of 2-R-isoindoles **4** by potentiometric titration in nitromethane showed the *N*-aryl-isoindoles are weaker bases by 5–6 orders of magnitude than *N*-methylisoindole (ΔpK_a† of the latter is 1.2). For comparison, we may note that in nitromethane ΔpK_a is +5.69 for pyridine and −0.6 for piperidine. For a series of *N*-(4-R-phenyl)isoindoles (R = H, Me, OMe, Br), the ΔpK_a depend linearly on the Hammett constant σ_p.[136] The loss of a proton by the isoindolium salts **33**, **36**, **56**, and **163** and its addition to isoindoles are reversible processes which can be readily detected from UV and ^{1}H NMR spectra. Thus the protonation of isoindoles entails the loss of the long-wavelength absorption [band C (Ref. 1)] in the electronic spectrum and an increase in the intensity of band B. In a number of instances, it is possible to obtain a high yield of isoindolium salts in a crystalline state from isoindoles: for example, from the isoindoles **5**[8] and **162**[11,137] 2-*tert*-butyl-5-nitroisoindole,[7] and 1-alkylthio-2-aryl-3-trifluoroacetylisoindole.[138]

b. Alkylation

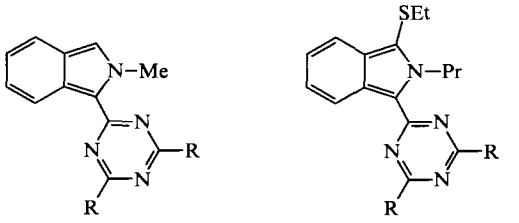
The alkylation of 2-R-isoindoles, which are incapable of tautomeric transformations, takes place at the C(1) carbon atom with formation of type **166–168** indoles via compounds **163–165**. Thus treatment of 2-methylisoindole **135** with 2-chloro-4,6-difluoro-[139] or 2,4,6-trichloro-1,3,5-triazine[140] affords moderate yields of C(1)-alkylated isoindoles **166a, b**. The same compounds react with the isoindole **40a** to form the trisubstituted isoindoles **167**.[141]



162 **163**

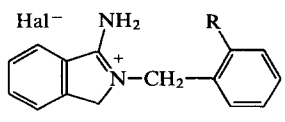


164 **165**



166a, b
R = F (**a**), Cl (**b**)

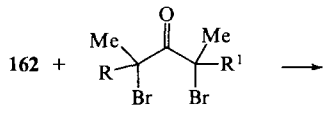
167



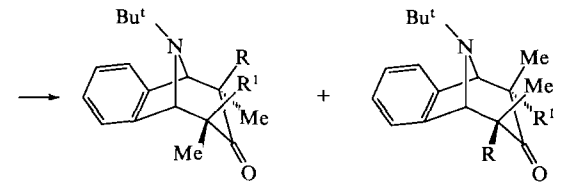
168a, b
R = H (**a**), CN (**b**)

The alkylation of the isoindole **162** with the Meerwein reagent leads initially to a high yield of the salt **164**, which isomerises to the more stable cation **165**.[11,137] It has been shown that alkylation of compound **162** with the aid of methyl iodide in methylene chloride gives rise to type **165** salts in 19% yield.[11]

The interaction of the isoindole **162** with 2,4-dibromo-3-pentanones **169a–c** in the MeCN–Cu–NaI system (method A) or the dioxane–Zn–CuCl–ultrasound system (method B) can probably be regarded as reductive alkylation.[142] The diastereoisomeric structures **170** and **171**, resembling tropanone, are then formed in 50%–60% yields (**170a** : **171a** = 2.4 : 1; **170b** : **171b** = 2.2 : 1). The use of the ketones **169a, b** entails the application of method A, while the use of compound **169c** entails the application of method B.[142] It has been shown[143,144] that the alkylation of the aminoisoindole **65a** by benzyl chlorides involves exclusively the endocyclic nitrogen atom with formation of aminoisoindolium salts of type **158a, b**. The alkylation of compound **65a** by α-haloketones proceeds similarly.[143]



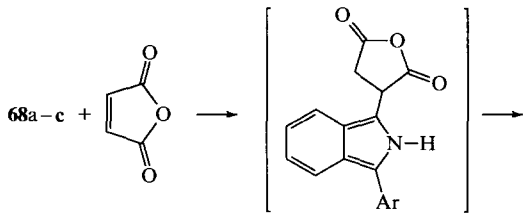
169a–c
169a: R = H, R^1 H
169b: R = Me, R^1 = H
169c: R = Me, R^1 Me



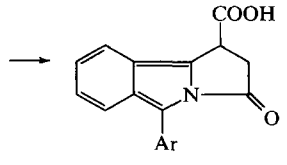
170a–c **171a–c**

c. Other electrophilic addition reactions

Maleic anhydride reacts in ether with the isoindoles **68a–c** unsubstituted at the nitrogen atom. The intermediate **172** formed initially via a Michael reaction recyclises with formation of derivatives of the pyrrolo[2,1-*a*]isoindoles **173**.[71] A process similar to that described above takes place in the interaction of the isoindoles **4** (R = Et), **5**, and **162** with azodicarboxylic acid esters.[7,8,145] The Diels–Alder reaction has not been observed in this instance, the Michael addition occurring with retention of the isoindole structure.



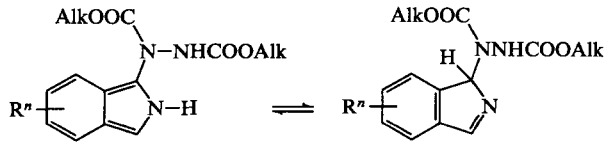
172



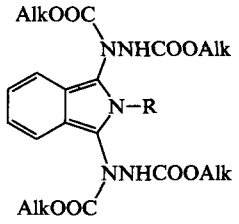
173

† ΔpK_a is the difference between the pK_a for a standard (diphenylguanidine) and the given substance.

The added hydrazine-1,2-dicarboxylate diester residue activates the isoindole structure **174**. As a rule, the reaction proceeds further, which leads exclusively to the 2 : 1 adduct **176**. The 1 : 1 adducts have been isolated only for 2-*tert*-butyl-5-nitroisoindole, the electronic system of which is somewhat deactivated by the presence of the nitro-group.[7] On the other hand, in the case of the isoindoles **4** (R = Et, Bu^t) and **5**, compounds of type **176** are formed exclusively.[8,145] Interesting results have been obtained in a study of the interaction of azodicarboxylic acid esters with NH-isoindoles **13** ($R^1 = R^3 = Me$, $R^2 = R^4 = H$, and $R^1 = R^2 = R^3 = R^4 = Me$),[145] **15** and **16**.[13] In the first three cases, the corresponding 1 : 1 adducts **174** are formed exclusively in 70%, 59%, and 45% yields, demonstrating the occurrence of prototropism (for example, in solvents of different polarity different contents of the isoindole structure **174** and the isoindolenine structure **175** are observed). On the other hand, the isoindole **16** affords under these conditions a 38% yield of the 2 : 1 adduct, which exists predominantly in the isoindolenine form.[13] The appearance of the isoindolenine tautomer has been explained by the formation of an intramolecular hydrogen bond between the ring nitrogen atom and the NH group of the hydrazine side group.

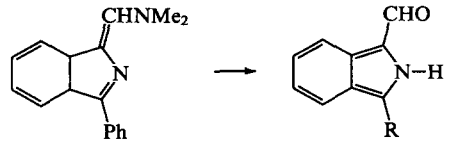


174 **175**

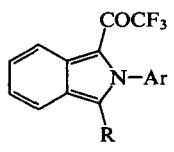


176

Electrophilic substitution in the isoindole series has been investigated in formylation[105] and trifluoroacetylation reactions.[138] The attempts to introduce the isoindole **68a** into Mannich, nitrosation, and nitration reactions were unsuccessful.[19] 1-Phenylisoindole **68a** reacts with the Vilsmeier reagent and gives rise to a 68% yield of 1-(*N*,*N*-dimethylaminomethylidene)-3-phenylisoindolenine **177**, which gives the 1-formyl-3-phenylisoindole **178** in 48% yield on alkaline hydrolysis.[105] *N*-Tolylisoindoles and 1-alkylthio-2-arylisoindoles **37** interact in pyridine with trifluoroacetic anhydride, forming the trifluoroacyl derivatives **179a, b**.[138]



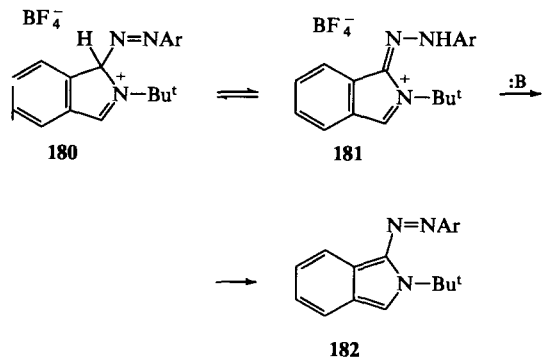
177 **178**



179a, b

R = H (**a**), SAlk (**b**)

Isoindoles readily enter into the azo-coupling reaction in aqueous alcohol[19] or acetone[6,9,10,137] solutions exclusively via the pyrrole component of the bicyclic system. In the latter case, it is possible to observe the formation of the salt-like intermediate adducts of types **180** and **181**, which are converted into type **182** azo-dyes after treatment with bases.

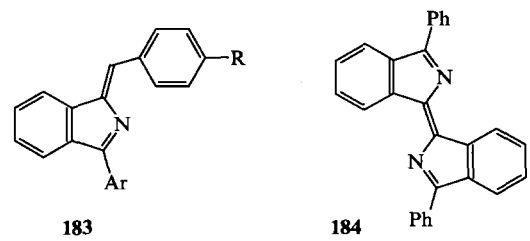


180 **181** **182**

This reaction has been investigated particularly widely in relation to the isoindole **162** with which six arenediazonium salts have been coupled.[11,137] Only *p*-nitrobenzenediazonium tetrafluoroborate has been coupled with the isoindoles **6a, b**,[6] **8**,[10] **9**, and **10**[9] and both type **182** azo-dyes and intermediate salts have been obtained. In the absence of steric hindrance in the initial isoindoles, the yields of the azo-dyes are as a rule nearly quantitative. An interesting reaction has been observed with the isoindole **182** (Ar = 4-ClC_6H_4) on treatment with *p*-nitrobenzenediazonium tetrafluoroborate: the salt **180** (Ar = 4-$O_2NC_6H_4$) was obtained in 39% yield, i.e. the phenylazo-group containing a chlorine atom was displaced and was replaced by the *p*-nitrophenylazo-group.[11] The coupling by the classical method of the isoindole **68a** unsubstituted at the nitrogen atom with toluene-*p*-diazonium chloride has been described:[19] the corresponding azo-dye was isolated in 63% yield and has λ_{max} = 467 nm.

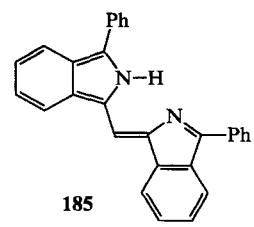
3. Condensation with aldehydes and their derivatives

In the interaction of the isoindoles **68b, c** with benzaldehyde and anisaldehyde in the presence of akali, type **183** isoindolenines were obtained in 13%–30% yields.[71] Under these conditions, the isoindole **68a** gives only small amounts of the yellow dimer **184**,[66] which can also be obtained in 53% yield by treating the isoindole **68a** with nitrous acid[19] or simply by refluxing in benzene.[71] The application of the latter operation to the isoindole **68b, c** makes it possible to isolate the corresponding dimers in yields not exceeding 15%. In the Mannich reaction with the isoindole **68a**, the dimer **184** is formed in 25% yield together with the blue pigment **185** (20%).[19]



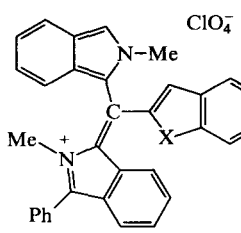
183 **184**

The same blue pigment has been isolated as a result of the condensation of compound **68a** with paraformaldehyde in an alkaline medium (yield 15%) or in 63% and 44% yields on condensation of compound **68a** in an acid medium with the isoindole **178** or the isoindolenine **177** respectively.[19]



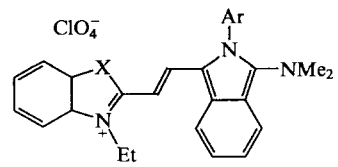
185

The condensation of benzaldehyde and a series of heterocyclic aldehydes with 2-methyl-1-phenylisoindole led to a series of coloured bis(2-methyl-1-phenylisoindol-3-yl)aryl(heteroaryl)-methanes **186**, which have been studied in detail both theoretically and spectroscopically.[146] The methods of synthesis of the dimethinecyanine and merocyanine dyes **187**, obtained from 2-aryl-1-dimethylaminoisoindoles, have been described.[106] Positive solvatochromism is characteristic of merocyanines of this type. The parent isoindole **14** and its 4,5,6,7-tetrafluoro-analogue condense with formaldehyde and benzaldehyde to form the tetrabenzoporphyrins **188**.[147] It was found that the most important factor governing the formation of such systems is the involvement of a metal ion, since in the absence of the latter the yields of compound **188** are significantly lower. The type of the complex-forming reagent also influences the yield considerably: the zinc ion is best. The replacement of the latter by nickel or copper ions gives rise to only traces of the corresponding porphyrin derivative. The attempts to introduce the sterically hindered 2,4,6-trimethylbenzaldehyde into this reaction have been described.[148] A later investigation[149] threw doubts on the purity of the zinc complex of *meso*-tetraphenyltetrabenzoporphyrin **188** isolated.



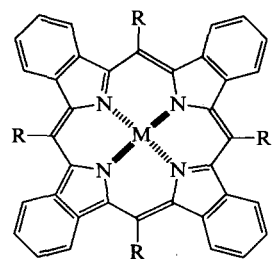
186a–c

X = S (**a**), NMe (**b**)
CH=CH (**c**)



187a–d

187a: X = CH=CH, 610 nm
187b: X = S, 589 nm
187c: X = O, 542 nm
187d: X = CMe_2, 534 nm

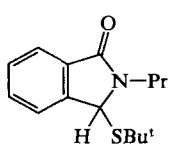


188

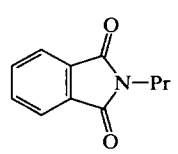
4. Other reactions of isoindoles

a. Oxidation

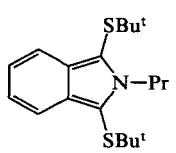
The autoxidation of the isoindole **40c** as a model compound for a whole series of fluorescent isoindoles has been investigated.[42] It was established that, when a solution of compound **40c** in aqueous acetonitrile is kept in air for 24 h, a mixture of four compounds **189–192** is produced.



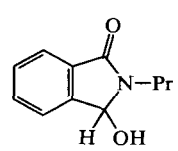
189, 35%



190, 16%

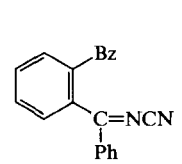


191, 12%

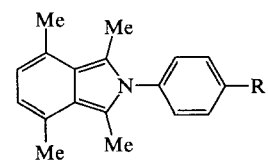


192, 4%

The pure nitrosyl cyanide, generated from its adduct with anthracene, reacts with 1,3-dienes to form new cyclic adducts. However, the interaction with 2-methyl-1,3-diphenylisoindole entails the dissociation of the C–N bond in the latter and the formation of the imine **193** in 66% yield.[150] In order to investigate the possibility of the formation of isoindole radicals, a study has been made[151] of the electrochemical oxidation of the isoindoles **194a, b** in anhydrous acetonitrile. It was shown that the nature of the substituent at the N(2) nitrogen atom hardly affects the oxidation potential. The oxidation takes place in two stages, the first involving the formation of relatively stable radical-cations. In order to investigate the chemiluminescence reactions with fluorescent organic compounds, the isoindole **195** was oxidised by 4,5-dichlorophthaloyl peroxide in dimethyl phthalate.[152]

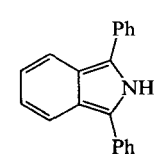


193



194a, b

R = H (**a**), Me (**b**)

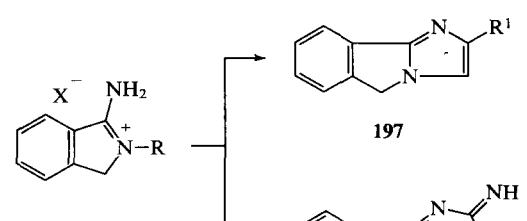


195

b. Heterocyclisation

Refluxing of the quaternary salt **196b** in aqueous solution of hydrobromic acid leads to a high yield of derivatives of 5*H*-imidazo[2,1-*a*]isoindole **197**.[153,154]

Even higher yields of compound **197** have been noted on refluxing aqueous solutions of type **196b** salts.[155] On the other hand, prolonged refluxing of the quaternary salt **196a** in the presence of sodium ethoxide leads to the condensation of the diazepine residue with the isoindole fragment and the formation of a 5-imino-5,13-dihydro-11*H*-isoindole[2,1-*a*][2,4]benzodiazepine **198** derivative.[144]



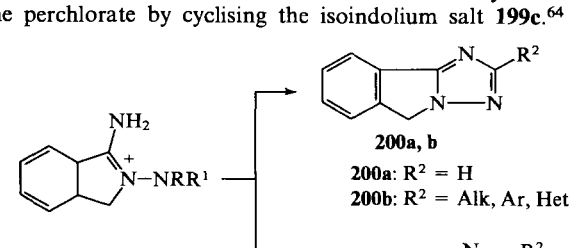
196a, b

196a: R = $CH_2C_6H_4CN$-*o*
196b: R = CH_2COR^1

197

198

Derivatives of 5*H*-1,2,4-triazolo[5,1-*a*]isoindole **200a** are formed in 32% yield on refluxing the salt **199a** with an excess of orthoformic ester.[65] Refluxing of the salts **199b** with phosphoryl chloride makes it possible to obtain the triazoloisoindoles **200b** [R = C_5H_{11} (17%) and R = Ph (97%)].[57,58,156] 3-Methyl-2-phenyl-3*H*-1,2,4-triazoloisoindole **201** has been synthesised as the perchlorate by cyclising the isoindolium salt **199c**.[64]



199a–c

199a: R = R^1 = H
199b: R = H, R^1 = COR^2
199c: R = Me, R^1 = COR^2

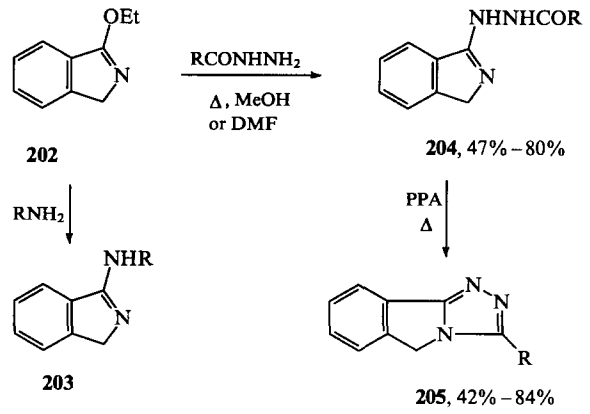
200a, b

200a: R^2 = H
200b: R^2 = Alk, Ar, Het

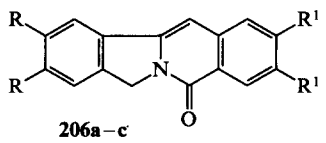
201

R^2 = Ph

During the nucleophilic substitution of the ethoxy-group, 1-ethoxyisoindole **202** reacts relatively readily with primary amines to form derivatives of the aminoisoindole **203**,[69] while the reaction with carboxylic acid hydrazides affords compounds of type **204**.[156] The latter cyclise in polyphosphoric acid (PPC) to derivatives of 5*H*-1,2,4-triazolo[3,4-*a*]isoindole **205** in satisfactory yields.[156]



Homophthalic anhydrides give rise to isoindolo[2,1-*b*]isoquinolin-5(7*H*)-ones **206a–c** in satisfactory yields (75%) on heating with ethoxyisoindole **202** and its 5,6-dimethoxy-derivative in chlorobenzene.[34]

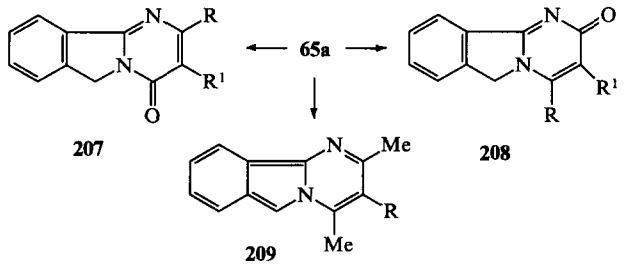


206a–c

206a: R = R¹ = H

206b: R = MeO, R¹ = H

206c: R = R¹ = MeO



It has been shown[157] that the condensation of the aminoisoindole **65a** with acetoacetic and benzoylacetic esters leads to derivatives of 6*H*-pyrimido[2,1-*a*]isoindol-4-one **207**. Further experiments also confirmed the possibility of the isolation from the reaction mixture of not only the 6*H*-pyrimido[2,1-*a*]isoindol-4-ones **207** but also their isomers **208**.[158,159] The criteria governing the differences between the isomeric systems **207** and **208** have been formulated and the conditions for the specific formation have been analysed in a number of investigations.[160–162] The condensation of the perchlorate **65a** with acetylacetone and methylacetylacetone, leading to a high yield of pyrimido[2,1-*a*]-isoindoles **209**, has also been described.[163]

V. Applications of isoindoles

One of the most important applications of isoindole derivatives involves their use as fluorescent labels. With the aid of isoindoles, it is possible to label the terminal amino-groups in various biological objects. The amino-groups are included in the 1-alkylthio-2*H*-isoindole system by treating them with *o*-phthalic dialdehyde and alkanethiols. An extensive literature, recently surveyed in a review,[45] has been devoted to this question. A comparatively new aspect of the employment of isoindole fluorescent labels is the detection with the aid of compounds such as **166** and **167** of the hydroxy-groups of steroids (17α- and 17β-estradiols, cortisone, estrone, etc.). The sensitivity of the method is of the order of 3 pmol in a 10 μl specimen.[139,140] It has been shown that the use of the isoindole **167** labels is an order of magnitude more effective than the use of compound **166** labels.[141] Other workers proposed the acyl azide obtained from the isoindole derivative **46d** for the detection of the same compounds.[56] Fluorescent isoindoles bound covalently to spectrin have been used to investigate the interaction of the latter with the phospholipids of pig erythrocytes.[164] 5-Fluoro-2-(1*H*-imidazol-2-yl)-2*H*-isoindole has been investigated together with other guanidine derivatives to achieve the treatment and prophylaxis of insulin-independent obesity.[165] Derivatives of compounds **200**[153,166] and **197**[154] exhibited a high contraceptive activity, while the preparation **203** with R = 3,4-$CH_2C_6H_3(OMe)_2$ exhibited the activity of a local anaesthetic which was twice as high as that of procaine.[69] It has been suggested that 1*H*-isoindoles be used as ligands in chromium pentacarbonyl complexes.[167] The electrical conductivities of polymer films obtained from isoindoles and their derivatives have been investigated.[168] Isoindoles have also been proposed as stabilisers and additives influencing the brightness of the electroplated tin layer on steel.[169]

References

1. F S Babichev, V A Kovtunenko, A K Tyltin *Usp. Khim.* **50** 2073 (1981) [*Russ. Chem. Rev.* **50** 1087 (1981)]
2. R Bonnett, S A North *Adv. Heterocycl. Chem.* **29** 341 (1981)
3. F S Babichev, V A Kovtunenko *Khimiya Izoindola* (The Chemistry of Isoindole) (Kiev: Naukova Dumka, 1983)
4. R P Kreher, U Feldhoff, J Seubert, D Schmitt *Chem.-Ztg.* **111** 155 (1987)
5. R P Kreher, J Seubert, D Schmitt, G Use, N Kohl *Chem.-Ztg.* **112** 85 (1988)
6. R P Kreher, T Hildebrand *Chem. Ber.* **121** 81 (1988)
7. G Use, R P Kreher *Chem.-Ztg.* **106** 143 (1982)
8. R P Kreher, G Use *Heterocycles* **19** 637 (1982)
9. R P Kreher, N Kohl *Chem.-Ztg.* **110** 299 (1986)
10. R P Kreher, T Hildebrand *Angew. Chem.* **99** 1325 (1987)
11. R P Kreher, G Use *Angew. Chem.* **122** 337 (1989)
12. R P Kreher, G Sewarte-Ross, G Vogt *Chem. Ber.* **123** 1719 (1990)
13. R P Kreher, K-J Herd *Chem.-Ztg.* **106** 305 (1982)
14. R P Kreher, N Kohl, G Use *Angew. Chem.* **94** 634 (1982)
15. R P Kreher, J Seubert, N Kohl *Chem.-Ztg.* **111** 349 (1987)
16. R P Kreher, G Use *Chem. Ber.* **121** 927 (1988)
17. R P Kreher, K-J Herd *Chem. Ber.* **121** 1827 (1988)
18. R P Kreher, N Kohl *Angew. Chem.* **96** 507 (1984)
19. R Bonnett, S A North, R F Newton, D I Scopes *Tetrahedron* **39** 1401 (1983)
20. R Grigg, F Heaney *J. Chem. Soc., Perkin Trans. 1* 198 (1989)
21. P Sanna, F Savelli, G Cignarella *J. Heterocycl. Chem.* **18** 475 (1981)
22. G A Flynn *J. Chem. Soc., Chem. Commun.* 862 (1980)
23. T Troll, G W Ollmann *Tetrahedron Lett.* **22** 3497 (1981)
24. T Troll, G W Ollmann *Electrochim. Acta* **29** 467 (1984)
25. T Troll, K Schmid, I Rasch *Z. Naturforsch. B, Chem. Sci.* **42** 1027 (1987)
26. T Inokuchi, H Yamashita, T Date, S Torii *Synth. Commun.* **19** 267 (1989)
27. R P Kreher, M R Konrad *Chem.-Ztg.* **110** 363 (1986)
28. E Ciganek *J. Org. Chem.* **45** 1512 (1980)
29. H Hennige, R P Kreher, J Uhrig *Synthesis* 842 (1982)
30. H Hennige, R P Kreher, M Konrad, F Jelitto *Chem. Ber.* **121** 243 (1988)
31. R P Kreher, M R Konrad *Chem.-Ztg.* **112** 335 (1988)
32. R P Kreher, H Hennige, F Jellito, J Preut *Z. Naturforsch. B, Chem. Sci.* **44** 1132 (1989)

33. R P Kreher, H Hennige, M Konrad, J Uhrig, A Clemens *Z. Naturforsch. B, Chem. Sci.* **46** 809 (1991)
34. V Ognyanov, M Khaimova, N Mollov *Monatsh. Chem.* **113** 993 (1982)
35. V A Kovtunenko, T T Dobrenko, Z V Voitenko, A K Tyltin, F S Babichev *Khim. Geterotsikl. Soedin.* 1200 (1984)
36. V A Kovtunenko, T T Kucherenko, M Yu Kornilov, A K Tyltin, A V Turov, F S Babichev *Khim. Geterotsikl. Soedin.* 1629 (1987)
37. E Trepman, R Chen *Arch. Biochem. Biophys.* **204** 524 (1980)
38. G Liebezeit, R Dawson *J. High Resolut. Chromatogr. Commun.* **4** 354 (1981)
39. S S Simons, H L Ammon, R Doherty, D F Johnson *J. Org. Chem.* **46** 4739 (1981)
40. R C Simpson, J E Spriggle, H Veening *J. Chromatogr.* **261** 407 (1983)
41. J F Stobaugh, A J Repta, L A Sternson, K W Garren *Anal. Chem.* **135** 495 (1983)
42. J F Stobaugh, A J Repta, L A Sternson *J. Org. Chem.* **49** 4306 (1984)
43. G Mellbin, B E F Smith *J. Chromatogr.* **312** 203 (1984)
44. L A Sternson, J F Stobaugh, A J Repta *Anal. Biochem.* **144** 233 (1985)
45. M C Garcia Alvarez-Coque, H M J Medina, C R M Villanueva, F C Mongay *Anal. Biochem.* **178** 1 (1989)
46. L A Allison, G S Mayer, R E Shoup *Anal. Chem.* **56** 1089 (1984)
47. P A Metz, J Gehas, J E Spriggle, H Veening *J. Chromatogr.* **330** 307 (1985)
48. J F Stobaugh, A J Repta, L A Sternson *J. Pharm. Biomed. Anal.* **4** 341 (1986)
49. W A Jacobs, M W Leburg, T J Madai *Anal. Biochem.* **156** 334 (1986)
50. T J Madai, W A Jacobs *J. Org. Chem.* **52** 3464 (1987)
51. H Nakamura, A Matsumoto, Z Tamura *Anal. Lett.* **15** 1393 (1982)
52. A Sidorowicz, K Michalak, M Bobrowska, W Strek, in *Proc. Sci. Symp. Inorg. Biochem. Mol. Biophys.* Wroclaw, Poland: Wydawn. Uniw. Wroclawskiego, 1985) p. 224; *Chem. Abstr.* **104** 17 257c (1986)
53. S Nanya, T Tange, T Maekawa *J. Heterocycl. Chem.* **22** 449 (1985)
54. J J D'Amico, B R Stults, P G Ruminski, K V Wood *J. Heterocycl. Chem.* **20** 1283 (1983)
55. K Takahashi, K Suenobu, K Ogura, H Iida *Chem. Lett.* 1487 (1985)
56. K Gamoh, H Sawamoto, J Iida *Anal. Chim. Acta* **228** 307 (1990)
57. S Nanya, H Toyama, E Maekawa *Nippon Kagaku Kaishi* 706 (1982)
58. S Nanya, Y Suzuki, E Maekawa *Nagoya Kogyo Daigaku Gakuho 1982* (Pub. 1983) **34** 157; *Chem. Abstr.* **102** 26 346s (1985)
59. S Nanya, T Fujii, Y Butsugan *J. Heterocycl. Chem.* **27** 1407 (1990)
60. V A Kovtunenko, O T Fal'kovskaya, A K Tyltin, F S Babichev *Ukr. Khim. Zh.* **50** 530 (1984)
61. V A Kovtunenko, O T Fal'kovskaya, A K Tyltin, F S Babichev *Vestn. Kievsk. Gos. Univ., Khim.* (26) 21 (1985)
62. USSR P. 771 105; *Chem. Abstr.* **94** 15 6976z (1981)
63. F S Babichev, Yu L Briks, N N Romanov *Ukr. Khim. Zh.* **47** 735 (1981)
64. F S Babichev, Yu L Briks, N N Romanov *Ukr. Khim. Zh.* **47** 291 (1981)
65. F S Babichev, Yu L Briks, N N Romanov *Ukr. Khim. Zh.* **51** 94 (1985)
66. V A Kovtunenko, Doctoral Thesis in Chemical Sciences, Kiev State University, Kiev, 1988
67. V A Kovtunenko, O T Fal'kovskaya, A K Tyltin, F S Babichev *Ukr. Khim. Zh.* **50** 1198 (1984)
68. V A Kovtunenko, T T Kucherenko, V M Kisel', O O Sergeeva *Ukr. Khim. Zh.* (in the press)
69. H J May, R Kretzschmar, W Neumann, J Gries *Arzneim.-Forsch.* **30** 1487 (1980)
70. USSR P. 1 166 476; *Byull. Izobret.* **46** 68 (1983)
71. G E M Moussa, M N Basyouni, M E Shabah, A F El-Kafrawy, N K Al Alaasar *Rev. Roum. Chim.* **27** 549 (1982)
72. S Mataka, K Takahashi, Y Tsuda, M Tashiro *Synthesis* 157 (1982)
73. A R Katritzky, F J Luxem, R Murugan, J V Greenhill, M Siskin *Energy Fuels* **6** 450 (1992)
74. J Duflos, G Queguiner *J. Heterocycl. Chem.* **21** 49 (1984)
75. R P Kreher, J Pfister *Angew. Chem.* **96** 906 (1984)
76. R P Kreher, J Pfister *Chem-Ztg.* **108** 275 (1984)
77. F Acar, S S Badesha, W Flitsch, R Gpzogul, S Inel, R A Jones, C Ogretir, D C Rustidge *Chim. Acta Turc.* **9** 225 (1981)
78. G W Gribble, C S Le Houllier, M P Sibi, R W Allen *J. Org. Chem.* **50** 1611 (1985)
79. T Sasaki, T Manabe, S Nishida *J. Org. Chem.* **45** 476 (1980)
80. H Sawanishi, T Tsuchiya *Heterocycles* **22** 2725 (1984)
81. H Sawanishi, H Sashida, T Tsuchiya *Chem. Pharm. Bull.* **33** 4564 (1985)
82. N Bozhkova, H Heimgarther *Helv. Chim. Acta* **72** 825 (1989)
83. K Wojciechowski *Liebigs Ann. Chem.* 831 (1991)
84. R W Hoffmann, W Barth *Chem. Ber.* **118** 634 (1985)
85. A Padwa, R J Rosenthal, W Dent, P Filho, N J Turro, D A Hrovat, J R Gould *J. Org. Chem.* **49** 3174 (1984)
86. K Ruehlmann, H Schilling, H Frey, H Paul *J. Organomet. Chem.* **290** 277 (1985)
87. R D O'Sullivan, A W Parkins *J. Chem. Soc., Chem. Commun.* 1165 (1984)
88. G Simig *Synlett.* 425 (1990)
89. P Baeuerle, G Goetz, P Emerle, H Port *Adv. Mater.* **4** 564 (1992)
90. A Mehlhorn, J Fabian *Croat. Chem. Acta* **54** 427 (1981)
91. V P Tewari, A K Srivastava *Indian J. Chem., Sect. A* **26** 449 (1987)
92. J Kruszewsk *Pure Appl. Chem.* **52** 1525 (1980)
93. V A Kovtunenko, Z V Voitenko, V L Sheptun, A K Tyltin, A I Chernega, Yu T Struchkov, F S Babichev *Khim. Geterotsikl. Soedin.* 1497 (1984)
94. E Orti, J L Bredas *J. Chem. Phys.* **89** 1009 (1988)
95. A Juric, A Sabljic, N Trinajstic *J. Heterocycl. Chem.* **21** 273 (1984)
96. Yang Pipeng, Duan Wengui *Yougi Huaxue* **11** 620 (1991); *Chem. Abstr.* **116** 173 452r (1992)
97. C W Bird *Tetrahedron* **43** 4725 (1987)
98. Zhongxiang Zhou, R G Parr *J. Am. Chem. Soc.* **111** 7371 (1989)
99. M de la Concepcion Foces-Foces, Cano F Hernandez, R M Claramunt, D Sanz, J Catalan, F Fabero, A Fruchier, J Elguero *J. Chem. Soc., Perkin Trans. 2* 237 (1990)
100. A F Pozharskii *Teoreticheskie Osnovy Khimii Geterotsiklov* (Theoretical Foundations of the Chemistry of Heterocyclic Compounds) (Moscow: Khimiya, 1985)
101. A R Katritzky, V Feygelman, G Masumarra, P Barczynski, M Szafran *J. Prakt. Chem.* **332** 870 (1990)
102. V A Kovtunenko, Z V Voitenko, V L Sheptun, L I Savranskii, A K Tyltin, F S Babichev *Ukr. Khim. Zh.* **51** 293 (1985)
103. J Waite, M G Papadopoulos *J. Phys. Chem.* **94** 1775 (1990)
104. L Stefaniak, J D Roberts, M Witanowski, G A Webb *Org. Magn. Reson.* **22** 215 (1984)
105. R Bonnett, M B Hursthouse, S A North, J Trotter *J. Chem. Soc., Perkin Trans. 2* 833 (1984)
106. V A Kovtunenko, A K Tyltin, A V Turov, F S Babichev *Zh. Org. Khim.* **5** 1080 (1989)
107. P B Terent'ev, V A Kovtunenko, Z V Voitenko, T T Kucherenko, V V Ishchenko, A K Tyltin, F S Babichev *Khim. Geterotsikl. Soedin.* 923 (1991)
108. V A Kovtunenko, Z V Voitenko, A N Chernega, A A Espenbetov, M Yu Antipin, A K Tyltin, Yu T Struchkov, F S Babichev *Ukr. Khim. Zh.* **50** 988 (1984)
109. R Bonnett, M B Hursthouse, S F North, J Trotter *J. Chem. Soc., Perkin Trans. 2* 29 (1985)
110. H Preut, N Kohl, R P Kreher *Acta Crystallogr. Sect. C, Cryst. Struct. Commun.* **44** 1321 (1988)
111. A P Laws, R Taylor *J. Chem. Soc., Perkin Trans. 2* 591 (1987)
112. B Capon, B Ying *Chin. J. Chem.* **10** 171 (1992)
113. F S Babichev, V A Kovtunenko, Z V Voitenko, A K Tyltin *Usp. Khim* **57** 713 (1988) [*Russ. Chem. Rev.* **57** 397 (1988)]
114. V A Kovtunenko, Z V Voitenko, T T Kucherenko, A V Turov, A K Tyltin, F S Babichev *Khim. Geterotsikl. Soedin.* 190 (1990)
115. V A Kovtunenko, Z V Voitenko, T T Kucherenko *Ukr. Khim. Zh.* **58** 790 (1992)
116. V A Kovtunenko, Z V Voitenko, A K Tyltin, A V Turov, F S Babichev *Ukr. Khim. Zh.* **49** 1287 (1983)
117. R P Kreher, J Seubert, D Schmitt, G Use, N Kohl, T Muleta *Chem. Ber.* **123** 381 (1990)
118. R P Kreher, G Sewarte-Ross, G Vogt *Chem. Ber.* **125** 183 (1992)
119. V A Kovtunenko, T T Kucherenko, A K Tyltin, Z V Voitenko, F S Babichev *Ukr. Khim. Zh.* **54** 186 (1988)
120. J Duflos, G Queguiner *J. Org. Chem.* **46** 1195 (1981)

121. V A Kovtunenko, Z V Voitenko, A K Tyltin, M Yu Kornilov, F S Babichev *Ukr. Khim. Zh.* **54** 1186 (1988)
122. V A Kovtunenko, T T Kucherenko, Z V Voitenko, A K Tyltin, F S Babichev *Ukr. Khim. Zh.* **55** 64 (1989)
123. V A Kovtunenko, A V Turov, T T Kucherenko, A K Tyltin, Z V Voitenko, M Yu Kornilov, F S Babichev *Ukr. Khim. Zh.* **57** 71 (1991)
124. V A Kovtunenko, T T Kucherenko, A V Turov, Z V Voitenko, A K Tyltin, F S Babichev *Ukr. Khim. Zh.* **58** 588 (1992)
125. J W Gribble, R W Allen, C S Le Houllier, J T Eaton, H J Easton, R I Slayton, M P Sibi *J. Org. Chem.* **46** 1025 (1981)
126. C S Le Houllier, G W Gribble *J. Org. Chem.* **48** 1682 (1983)
127. C S Le Houllier, G W Gribble *J. Org. Chem.* **48** 2364 (1983)
128. G W Gribble, R B Perni, K D Onan *J. Org. Chem.* **50** 2934 (1985)
129. J W Davies, M L Durrant, M P Walker, D Bekacemi, J R Malpass *Tetrahedron* **48** 861 (1992)
130. V A Kovtunenko, T T Kucherenko, A K Tyltin, A V Turov, F S Babichev *Ukr. Khim. Zh.* **56** 955 (1990)
131. G Szeimies *Chimia* **35** 243 (1981)
132. H G Zoch, A D Schlueter, G Szeimies *Tetrahedron Lett.* **22** 3835 (1981)
133. O Baumgaertel, J Harnisch, G Szeimies, M van Meerssche, G Germain, J-P Declercq *Chem. Ber.* **116** 2205 (1983)
134. A D Schlueter, H Harnisch, J Harnisch, U Szeimies-Seebach, G Szeimies *Chem. Ber.* **118** 3513 (1985)
135. J Kenndoff, K Polborn, G Szeimies *J. Am. Chem. Soc.* **112** 6117 (1990)
136. G W Gribble, C S Le Houllier *Tetrahedron Lett.* **22** 903 (1981)
137. R P Kreher, G Use *Angew. Chem.* **92** 309 (1980)
138. R P Kreher, H Feldhoff, F Jellito *Z. Naturforsch. B, Chem. Sci.* **43** 1332 (1988)
139. H Fugino, S Goya *Yakugaku Zasshi* **109** 195 (1989)
140. H Fugino, S Goya *Yakugaku Zasshi* **108** 665 (1988)
141. H Fugino, S Goya *Anal. Sci.* **5** 105 (1989)
142. A M El-Khawaga, H Hoffmann, R Martin *Synlett.* 519 (1990)
143. F S Babichev, A M Demchenko, A K Tyltin, V A Kovtunenko *Ukr. Khim. Zh.* **50** 623 (1984)
144. A K Tyltin, N A Lysik, A M Demchenko, V A Kovtunenko *Khim. Geterotsikl. Soedin.* 705 (1985)
145. R P Kreher, D Schmitt, K-J Herd *Tetrahedron Lett.* **21** 3471 (1980)
146. R Naef *Dyes Pigm.* **6** 233 (1985)
147. D E Remy *Tetrahedron Lett.* **24** 1451 (1983)
148. J W Cullen, D E Remy *Report 1988* Natick-TR-881: Order NAD-A 198784; *Chem. Abstr.* **111** 108 038t (1989)
149. K Ichimura, M Sakuragi, H Morii, M Yasuike, M Fukui, O Ohno *Inorg. Chim. Acta* **176** 31 (1990)
150. P Horsewood, G W Kirby, R P Sharma, J G Sweeny *J. Chem. Soc., Perkin Trans. 1* 1802 (1981)
151. P Kubacek *Collect. Czech. Chem. Commun.* **45** 1669 (1980)
152. R Gundermann, M Steinfatt, P Witt, C Paetz, K L Poeppel *J. Chem. Res.* (S) 195 (1980)
153. BRD P. 2 943 286; *Chem. Abstr.* **93** 186 360r (1980)
154. E Toja, A Omodei-Sale, D Favara, C Cattaneo, L Gallico, G Galliani *Arzneim.-Forsch.* **33** 1222 (1983)
155. V A Kovtunenko, A M Demchenko, A K Tyltin, F S Babichev *Ukr. Khim. Zh.* **51** 644 (1985)
156. N N Romanov, V P Shmailova, F S Babichev *Ukr. Khim. Zh.* **45** 860 (1979)
157. F S Babichev, A K Tyltin, V A Kovtunenko *Khim. Geterotsikl. Soedin.* 1693 (1980)
158. F S Babichev, A K Tyltin, V A Kovtunenko, A V Turov *Ukr. Khim. Zh.* **48** 641 (1982)
159. V A Kovtunenko, V V Ishchenko, A K Tyltin, A V Turov, F S Babichev *Khim. Geterotsikl. Soedin.* 1368 (1985)
160. V A Kovtunenko, V V Ishchenko, A K Tyltin, F S Babichev *Dokl. Akad. Nauk SSSR* **294** 375 (1987)
161. V V Ishchenko, V A Kovtunenko, A K Tyltin, V V Trachevskii, V Vshetechka, F S Babichev *Ukr. Khim. Zh.* **56** 517 (1990)
162. V A Kovtunenko, V V Ishchenko, A K Tyltin, F S Babichev *Ukr. Khim. Zh.* **57** 172 (1991)
163. F S Babichev, A K Tyltin, V A Kovtunenko, Z V Levitskaya *Ukr. Khim. Zh.* **47** 627 (1981)
164. K Michalak, M Bobrowska, A F Sikorski *Gen. Physiol. Biophys.* **9** 615 (1990)
165. PCT Int Appl WO 93 03,714 (1993); *Chem. Abstr.* **118** 261 003s (1993)
166. L J Lerner *J. Reprod. Fertil., Suppl.* **39** 251 (1989); *Chem. Abstr.* **112** 91 810j (1990)
167. U Feldhoff, F-W Grevels, R P Kreher, K Angermund, C Krueger *Chem. Ber.* **119** 1919 (1986)
168. Y S Lee, H S W Hu, O K Kim *Mol. Cryst. Liq. Cryst.* **190** 9 (1990)
169. Jpn. P. 63 395; *Chem. Abstr.* **103** 95 050u (1985)

Russian Chemical Reviews **63** (12) 1019 – 1045 (1994)
©1994 Russian Academy of Sciences and Turpion Ltd

UDC 547.953 + 547.91

Heterophosphacyclanes in organic synthesis

R A Cherkasov, M A Pudovik

Contents

I. Introduction 1019
II. σ^3-Heterophosphacyclanes 1020
III. σ^4-Diheterophosphacyclanes 1026
IV. σ^5-Mono- and di-heterophosphacyclanes 1031

Abstract. The review gives a systematic account of the use of mono- and di-heterophosphacyclanes, containing σ^3-, σ^4-, and σ^5- phosphorus atoms, for the synthesis of phosphorus-free organic substances. Data concerning the reaction mechanisms, the reactivities of cyclic organophosphorus compounds, and the factors determining the synthetic result of their chemical reactions are presented. In certain cases, the effectiveness of the employment of cyclic and acyclic phosphorus-containing reagents is compared. The bibliography includes 178 references.

I. Introduction

At the present stage, the synthetic organic chemistry of phosphorus is developing mainly in two directions. The first involves the functionalisation of organophosphorus substrates of increasing complexity, based on the chemical transformations of the organic functional groups already present in the molecule. One achieves in this way the introduction into the organophosphorus compounds of definite atomic groups which are potentially responsible for certain useful properties of the compound being synthesised, say pesticidal, or others. Phosphorus-containing functional groups may not actually participate in the chemical steps, exerting a different kind of effect on the fragment being transformed, which is susceptible to estimation including quantitative estimation.[1]

The second direction concerns the synthesis of organic compounds with participation of phosphorus-containing substances, which, after being involved in particular synthetic operations, 'remove' the phosphorus-containing functional group from the reaction sphere and the target product does not contain a phosphorus atom. This type of employment of organophosphorus reagents in organic synthesis has come to be widely used and has a long tradition. The phosphorus-containing compounds of this kind include, for example, the Wittig reagents — phosphorus ylides used to convert oxo-compounds into alkenes. The search for new highly effective functionalising phosphorus-containing reagents is being prosecuted at the present time.

Since the publication of the first and only monograph[2] devoted to the application of organophosphorus reagents in organic synthesis, many new communications have appeared in which this problem has been developed further. Thus in the 1980s, new multipurpose highly effective phosphorus-containing reagents were described. Among them mention should first be made of Lawesson's reagent (LR) (see Cherkasov et al.[3] and Kava and Levinson[4] and the literature quoted therein) — 2,4-bis-(*p*-methoxyphenyl)-1,2,3,4-dithiadiphosphetane 2,4-disulfide — and Mitsunobu's reagent[5] (MR)† — a betaine obtained by the interaction of triphenylphosphine and dialkyl azodicarboxylate. They have found extensive application not only in experimental practice but also in industrial organic synthesis. A recent review has been devoted to the employment of unsaturated compounds of tetracoordinate phosphorus for the synthesis of complex organic compounds.[7]

New aspects of the synthesis of organic compounds involving the employment of reagents containing a phosphorus atom involved in different types of coordination have begun to develop recently. Thus chiral phosphines[8] and phosphonates[9] are used in the catalysis of organic reactions and methods are being developed for the functionalisation of organic compounds with the aid of metastable derivatives of tricoordinate pentavalent phosphorus[10] and also of compounds of dicoordinate phosphorus.[11,12]

This review is devoted to a vigorously developing branch of phosphorus chemistry — the chemistry of heterophosphacyclanes — in its new aspect, namely their application in organic synthesis. If one disregards fairly old review publications describing the use of individual types of compounds of this class,[2] then this is the first attempt to treat systematically and survey the data which have accumulated in this field since 1980. Individual earlier literature sources are quoted here only to the extent that they are needed for a complete description of the problem under discussion. This communication completes a series of reviews devoted to the chemistry of heterophosphacyclanes containing a phosphorus atom with coordination numbers of three,[14] four,[15] five,[16] and six.[17] Considered jointly, these communications provide a complete picture of this currently important field of organoelement chemistry.

R A Cherkasov Department of Macromolecular and Organoelement Compounds, Kazan State University, ul. Lenina 18, 420083 Kazan, Russian Federation. Fax (7-843) 238 09 94, Tel. (7-843) 31 81 86
M A Pudovik Laboratory of Organophosphorus Compounds, Arbuzov Institute of Organic and Physical Chemistry, Kazan Scientific Centre, Russian Academy of Sciences, ul. akad. Arbuzova 8, 420083 Kazan, Russian Federation. Fax (7-843) 275 22 53

Received 21 September 1994
Uspekhi Khimii **63** (12) 1087 – 1113 (1994); translated by A K Grzybowski

† After the publication of Mitsunobu's review,[5] an extensive literature describing the application of MR in organic synthesis appeared (more than 400 publications). As an example, we may point to one of the later studies on the use of MR in the total synthesis of 20-membered macrocyclic antibiotics — venturicidins A and B[6] (see also Section IV).

II. σ^3-Heterophosphacyclanes

The use of σ^3-1,3,2-diheterophospholanes and σ^3-1,3,2-diheterophosphorinanes, substances which are thermodynamically less stable than the σ^4-phosphorus- and σ^5-phosphorus-containing derivatives with a similar structure,[14] is frequently associated with their conversion into the latter, which subsequently effect particular synthetic operations.

In the context of the chemical transformations described here, the σ^3-diheterophosphacyclanes themselves are not of special preparative interest and in most cases their behaviour resembles that of structurally similar acyclic phosphorus(III) derivatives. For example, organic phosphorus(III) derivatives are capable of deoxidising (desulfurising) suitable substrates, being themselves oxidised to phosphoryl (thiophosphoryl) compounds. The inclusion of a phosphorus(III) atom in a heterocycle entails a decrease (in nucleophilic reactions) or an increase (in electrophilic reactions) of the reactivity of the organophosphorus reagent.

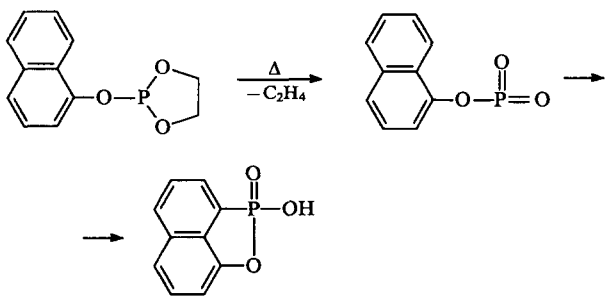
At the same time, thermal, photochemical, and chemical (for example as a result of substitution and disproportionation reactions) fragmentation processes involving or not involving the heterocyclic part of the molecule are extremely characteristic of σ^3-diheterophosphacyclanes, in contrast to the acyclic phosphorus(III) derivatives.

1. Thermal and photochemical fragmentation

The thermal reactions of cyclic esters of acids derived from phosphorus in the lowest oxidation state are usually associated with intramolecular rearrangements of the Arbuzov reaction type in those cases where the exocyclic fragment contains suitable functional groups, for example haloalkyl groups, and lead to organophosphorus products containing a phosphorus atom with a higher coordination number (CN).[14]

2-Aryloxy- and 2-alkoxy-1,3,2-dioxaphospholanes behave differently. On vacuum flash pyrolysis (700–800 °C, 0.001 Torr), they undergo fragmentation with liberation in the first stage of ethene and phosphorus-containing intermediates having the structure of metaphosphates‡ and undergoing further transformations.

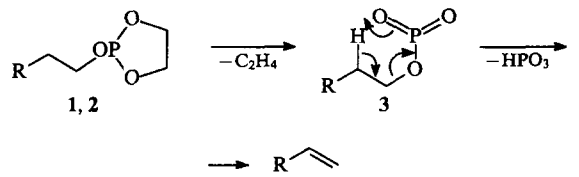
After liberating ethene, the aryl esters of ethylene phosphites are converted into the corresponding cyclic monoesters of arylphosphonic acids via the incorporation of the highly electrophilic pentavalent tricoordinate phosphorus atom in a sp^2-C–H bond of the aromatic fragment of the metaphosphates.[21–23]



According to Cadogan et al.,[21] the reaction described constitutes, in its intramolecular version, one of the most effective methods for the phosphorylation of aromatic nucleophilic substrates with the aid of highly electrophilic metastable phosphorus-containing reagents.

‡ We may note that in recent years there has been a marked growth of interest in these substances in connection with the appearance of the possibility of obtaining stable representatives of phosphorus compounds of this class and their use for the synthesis of natural organophosphorus products and in other phosphorylation reactions.[18–20]

However, if the exocyclic organyl fragment contains a β-hydrogen atom, alkenes are liberated — 2-vinylpyridine in the thermolysis of the phospholane **1** or phenyl vinyl ether in the case of compound **2**, as well as polymeric metaphosphoric acid. Intramolecular phosphorylation does not occur and a process analogous to the Chugaev reaction and the β-elimination via a six-centre transition state **3** similar to it take place.[21]

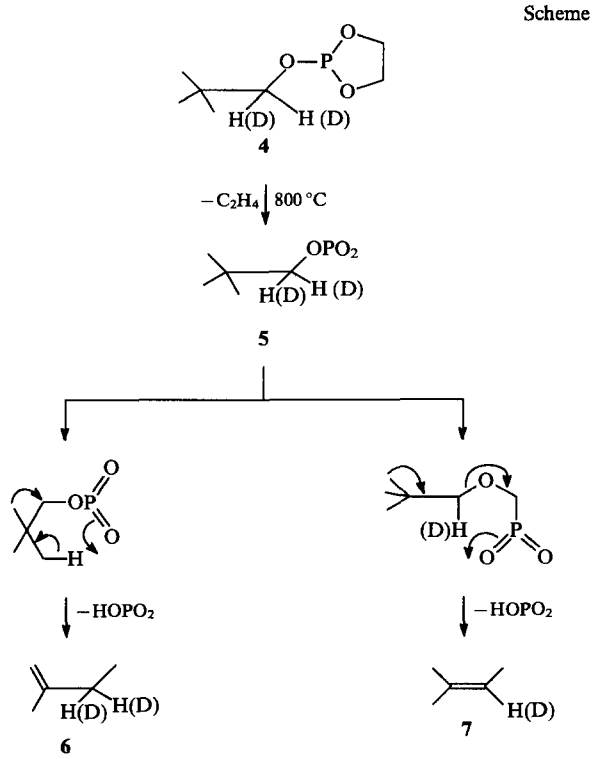


1, **2** **3**

1: R = Py
2: R = OPh

After the liberation of ethene, the pyrolysis of 2-neopentyloxy-1,3,2-dioxaphosphalane **4** under these conditions leads to the quantitative formation of a mixture of 2-methylbut-1-ene **6** and of its thermodynamically more stable isomer 2-methylbut-2-ene **7** in proportions of 2 : 1.[22,23] It is believed that the minor alkene **7** is formed as a result of the abstraction of an α-proton from the common intermediate **5**, whereas its isomer **6** arises through the elimination of a γ-proton and the unusual 1,2-methyl shift in the same intermediate metaphosphate (Scheme 1). The transformation of compound **5** into the alkenes **6** and **7** proceeds via a mechanism similar to the Wagner–Meerwein rearrangement but has the opposite polarity (there is a carbanionoid and not a carbonium ionoid transition state) and also in its concerted (and not sextet) variant.[24]

Scheme 1



This course of the reaction has been confirmed by the use of a deuteriated specimen of compound **4**, pyrolysis of which afforded the deuterium-containing alkenes **6**-d_2 and **7**-d_1 in proportions of 3.8 : 1. The observed deuterium isotope effect $k_H/k_D = 1.9$ agrees with the ratio of the deuteriated isomers obtained, indicating that the loss of hydrogen (deuterium) via the route leading to compound **7** is rate-determining.

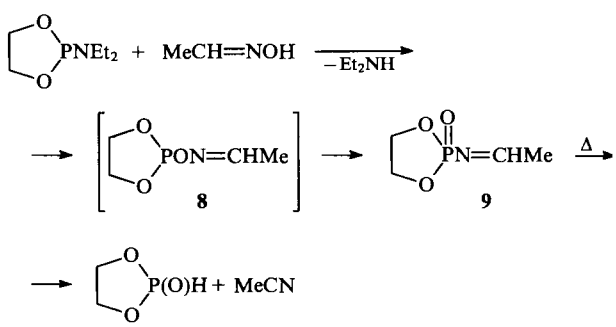
2. Reactions involving substitution at the σ^3-P atom

The thermally promoted fragmentation of diheterophosphacyclanes is frequently observed in the fractionation of the products of the interaction of cyclic phosphorous and phosphonous acid esters with electrophiles and nucleophiles. The elimination of phosphorus-free organic reaction products usually occurs in those cases where the exocyclic ester residue contains reactive functional groups. The cyclic skeleton of the phosphorus-containing substrate as a rule remains unchanged under these conditions. The above applies primarily to dioxaphospholanes.

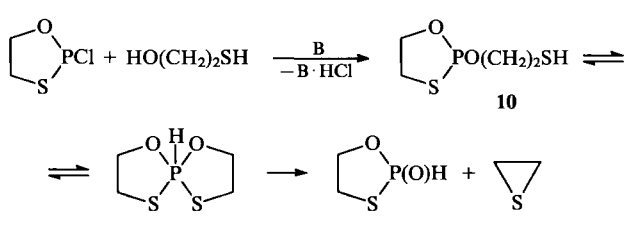
In the vast majority of cases, such reactions take place with participation of intermediates in which the CN of the phosphorus atom is four or five. The inclusion of the phosphorus atom in a ring, especially a five-membered ring, stabilises such intermediates and in many cases this makes it possible to identify them and to infer the reaction pathway.

The substitution of readily eliminated groups by functionalised alcohols, accompanied by the isomerisation of the intermediate cyclic phosphites to tetracoordinate and pentacoordinate phosphorus compounds, leads, as a result of thermolysis, to the formation of small organic molecules; the phospholane ring remains unchanged under these conditions.

The interaction of the diethylamide of ethylenephosphorous acid with an oxime probably proceeds via a stage involving the formation of the unstable phosphite **8**, which isomerises to the N-phosphorylated anil **9**; in the course of fractionation, the latter decomposes into ethylenephosphorous acid and acetonitrile.[25]

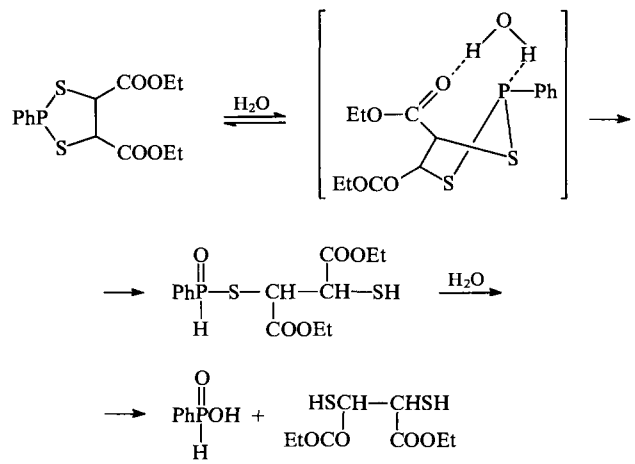


The esterification of 2-chloro-1,3,2-oxathiaphospholanes with mercaptoethanol in the presence of a base[26] does not stop at the 2-mercaptoethyl phosphite **10** stage, and is completed by the formation of a thiirane and a cyclic phosphorothious acid. It is difficult to say which of the intermediates—the phosphite intermediate **10** or the isomeric phosphorane intermediate **10a**—is responsible for the observed fragmentation.



We may note in this connection that a similar fragmentation of 1,2-dihydroxyalkylene derivatives of σ^5-P is an extremely characteristic property and is of preparative importance[16] (see also Subsection 3).

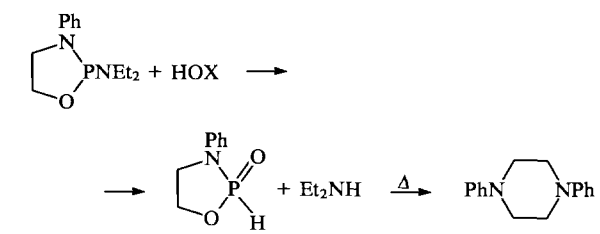
The endocyclic hydrolytic dissociation of the thioester linkages in 4,5-di(ethoxycarbonyl)-2-phenyl-1,3,2-dithiaphospholane takes place stepwise and leads to phenylphosphonous acid and diethyl dimercaptosuccinate.[27]



Kinetic study of the hydrolytic reaction led the authors to the conclusion that a hydrogen-bonded complex is formed prior to the establishment of equilibrium.

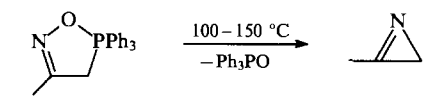
In contrast to the cyclic esters and thioesters of trivalent phosphorus acids, amidoesters containing an endocyclic tertiary nitrogen atom undergo a more profound transformation during the substitution reaction involving under these conditions a thermal fragmentation with cleavage of the oxazaphospholane ring.

On interaction with proton-containing nucleophiles (water,[30] acetic acid,[29,30] and ethanol[29]), 2-ethoxy-,[28] 2-phenyl-,[29] and 2-diethylamino-3-phenyl-1,3,2-oxazaphospholanes[29,30] afford *N,N*-diphenylpiperidine after fractionation. It has been suggested that, in the presence of a readily eliminated exocyclic group, the reaction takes place via a mechanism involving the nucleophilic substitution[30] of the exocyclic fragment.



X = H, COMe, Et.

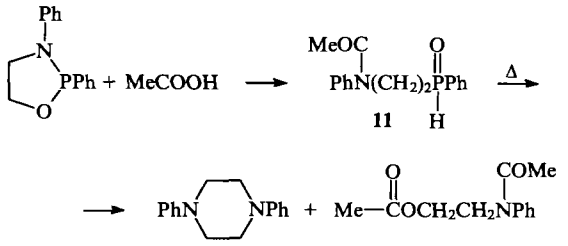
The formation of the final product is probably due to the decomposition of the *N*-phenyloxazaphospholane fragment of the unstable hydrophosphoryl intermediate at elevated temperatures (100–120 °C) during the substitution reaction or during fractionation. One cannot rule out the possibility that the decomposition is accompanied by the initial formation of three-membered nitrogen-containing heterocycles, similarly to the formation of azirenes on pyrolysis of σ^5-1,5,2-oxazaphospholenes.[31]



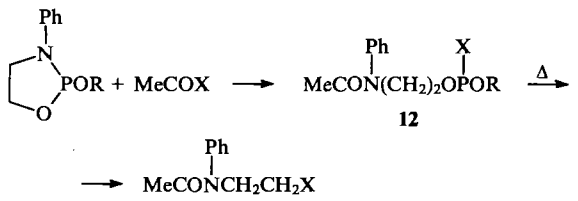
N-Phenylaziridine is evidently formed in the case under discussion, dimerising under the experimental conditions (see also Subsection 3). Naturally one cannot rule out also another mechanism of the formation of the piperidine ring from the phosphacyclane skeleton of the cyclic phosphoramidites.

The same synthetic result is attained also in the course of endocyclic substitution,[29] for example in the acetolysis of 2-diethylamino- or 2,3-diphenyl-1,3,2-oxazaphospholane.

The thermolysis of the phosphonite **11** makes it possible to obtain, together with *N*,*N*-diphenylpiperidine, also *N*-2-acetoxyethyl-*N*-phenylacetamide.



The oxazaphospholane ring may be cleaved not only by proton-containing nucleophiles but also by electrophiles — acetyl chloride[32] or acetic anhydride.[33]



X = Cl, OCOMe.

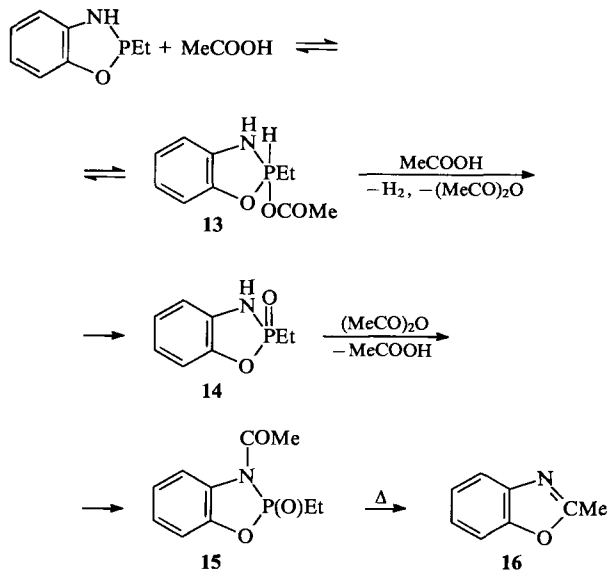
In both these cases, the interaction is evidently associated with the nucleophilic attack by the nitrogen atom on the carbonyl carbon atom of the acylating agent; the ring is then cleaved at the P–N bond. Further decomposition takes place with the elimination of the *O*-ester organyl fragment. It is difficult to reach definite conclusions about the mechanism of this unusual fragmentation of the functionalised phosphonites **11** or the phosphites **12**, again because the subsequent transformation of the 'phosphorus' part of the molecules remains unelucidated. One may only note that the elimination of the phosphorus-containing reaction products is associated with the dissociation of the sp^3-C–O bond in the *O*-ester group.

3. Reactions involving an increase in the coordination number of the σ^3-P atom

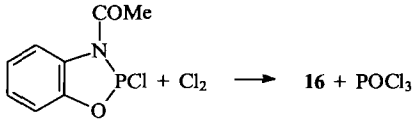
Decomposition accompanied by the opening of the ring at an endocyclic sp^2-C–O bond has been noted in the acylation of 2-ethyl-4,5-benzo-1,3,2-oxazaphospholane,[34] which is achieved under mild conditions (2 h, 20 °C) and represents a rare case of the oxidation of phosphorus(III) derivatives by carboxylic acids in the two-component version§.

The process probably begins[34] with the 1,1-addition of acetic acid to the phosphorus(III) atom of the benzophosphacyclane. The unstable hydrophosphorane **13** formed is deacylated by a second acetic acid molecule and is oxidised to the phosphonate **14** with liberation of hydrogen. The subsequent endocyclic *N*-acylation leads to the final *N*-acylphosphonate **15**. During fractionation, the latter affords 2-methylbenzoxazole **16** in 20% yield.

It has been demonstrated by means of a special experiment that, on heating to 150–200 °C in vacuo (20 Torr), the phosphonate **15** gives rise to the benzoxazole **16** in 68% yield.

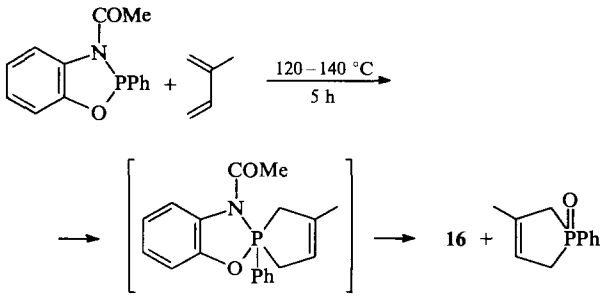


The formation of compound **16** as a result of the chlorination of 3-acetyl-2-chloro-4,5-benzo-1,3,2-oxazaphospholane has been established recently.[36]



Evidently in this case too the reaction leads to the formation of the addition product of chlorine to the σ^3-phosphacyclane — the corresponding trichlorophosphorane. The ultimate formation of phosphoryl chloride (and also apparently of ethyl metaphosphonate in the previous example) is clearly evidence in favour of the probable formation of a metastable aromatic intermediate of the acylamino-substituted dehydrobenzene type, or a similarly substituted phenyl radical, as a consequence of the heterolysis or homolysis of the sp^2-C–O bond.

Such fragmentation also takes place in the thermolysis of the unidentified product of the [1 + 4]-cycloaddition of 3-acetyl-2-phenyl-4,5-benzo-1,3,2-oxazaphospholane to 2-methylbutadiene.[37] Fractionation of the resulting mixture afforded the benzoxazole **16** and a cyclic phosphine oxide.



The fragmentation with cleavage of the diheterophospholane ring described above leads to a kind of transcyclisation of the phosphorus(III) substrate.

The endocyclic dissociation of the sp^2-C–O bond discussed here gives rise to interesting synthetic possibilities for the employment of the reactions of cyclic salicyl phosphites with carbonyl compounds activated by electron-accepting substituents.

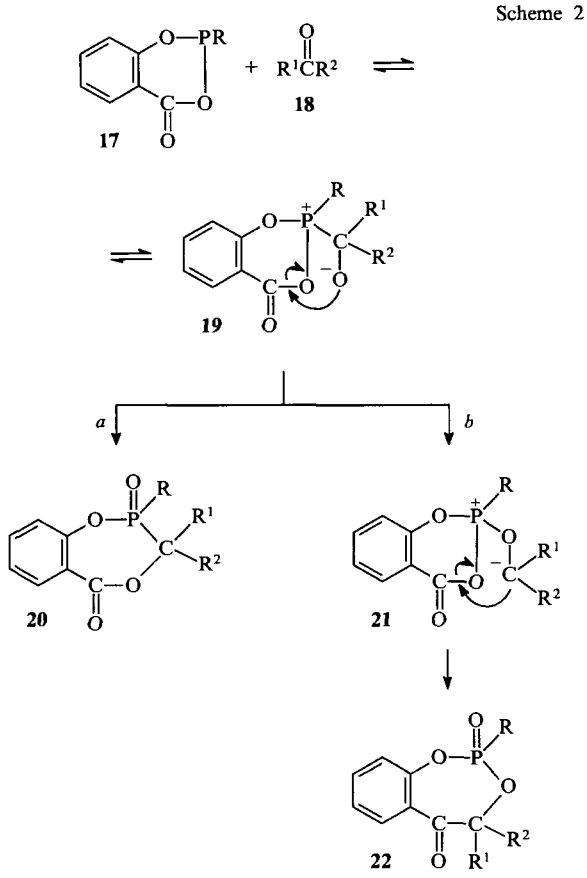
2-R-4-Oxo-5,6-benzo-1,3,2-dioxaphosphorinanes **17** — six-membered cyclic anhydrides containing the P(III)–O–C(O) fragment in the ring — readily interact with chloral,[38]

§ According to the data of Mukajama et al.,[35] trialkyl phosphites are oxidised by carboxylic acids in the presence of hydrogen acceptors — diphenylmercury and dibenzoylethene.

hexafluoroacetone,[39] mesoxalic acid esters,[40] ethyl benzoylformate,[41] methyl trifluoropyruvate,[42] and hexafluoroacetylacetone[43] with insertion of the carbonyl reagent in the six-membered ring and the formation of dioxaphosphepanes — a class of phosphorus-containing heterocycles which are relatively difficult to obtain.

It has been suggested[41] that the process begins with the attack by the nucleophilic P(III) atom on the carbonyl carbon atom of the other reactant (compound **18**) (Scheme 2).

Scheme 2

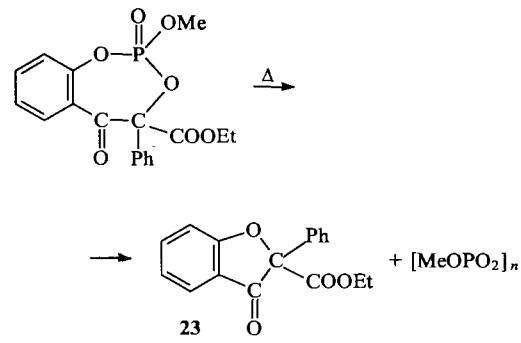


The dipolar ion **19** arising under these conditions may be stabilised via the intramolecular substitution at the carbonyl carbon atom by an oxy-anion (route *a*) with formation of the 1,4,2-dioxaphosphepane **20** (R^1 = H, R^2 = CCl_3); this reaction path occurs in the reactions of salicyl phosphites **17** with chloral.

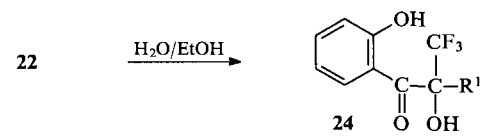
The remaining carbonyl reagents employed gives rise to 1,3,2-dioxaphosphepanes **22**, the formation of which is preceded by the rearrangement of the ion **19** to the ion **21** (P–O–C→P–C–O) and intramolecular substitution, with participation of the carbanion, at the carbonyl carbon ion in the zwitterionic intermediate **21** (route *b*). This case is of greatest interest from the standpoint of the problems discussed in the review because it entails the formation of a new C–C bond.

It has been shown[41] that the vacuum fractionation of the phosphepane **22** (R = OMe, R^1 = Ph, R^2 = COOEt) is accompanied by its complete decomposition, which resulted in the formation of ethyl 2,3-dihydro-3-oxo-2-phenylbenzofuran-2-carboxylate **23** in 80% yield.

It has been noted[41] that derivatives of 2,3-dihydro-3-oxo-2-phenylbenzofuran-2-carboxylic acid had not been described before the study by the above workers[41] and only data concerning the isomeric acid with the carboxy-group in the 3-position in the benzofuran ring had been available.[44,45]

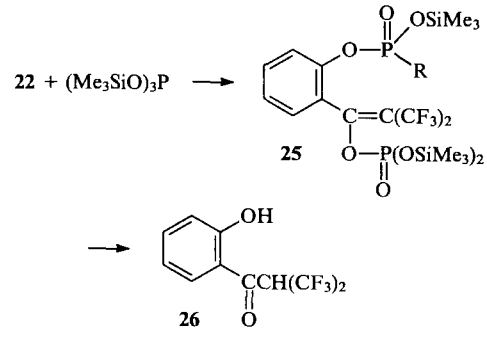


The protolytic reactions of the 1,3,2-dioxaphosphepanes **22**, obtained by the reaction of salicyl phosphites **17** (R = OMe) with hexafluoroacetone and hexafluoroacetylacetone provide the greatest possibilities for the synthesis of functionalised fluorine-containing ketones; the hydrolysis of the 1,3,2-dioxaphosphepanes in aqueous ethanol[43] leads to the hydroxyketones **24** (R^1 = CF_3 and CH_2COCF_3) respectively in a high yield.



R = OMe; R^1 = CF_3, CH_2COCF_3; R^2 = CF_3.

This method may be modified by phosphorylating the 1,3,2-dioxaphosphepanes **22** (R^1, R^2 = CF_3) with the aid of tris(trimethylsilyl) phosphite; hydrolysis of the diphosphate **25** makes it possible to obtain the ketone **26**, which does not contain α-hydroxy-substituents in the fluoroalkyl group.[46,47]

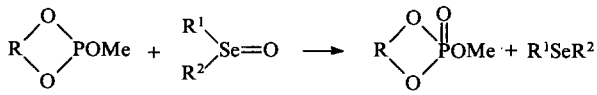


R^1 = R^2 = CF_3.

The driving force of the reactions described here is the well known tendency of phosphorus(III) derivatives to be converted into compounds with a thermodynamically stable phosphoryl group characterised by a high energy of the phosphorus–oxygen multiple bond.[14]

This property of the phosphorus(III) atom has been used in the reduction of oxides, sulfides,[48,49] and selenides[50,51] by σ^3-1,3,2-dioxaphospholanes and phosphorinanes.

Under mild conditions, selenoxides are reduced almost wholly in solution in benzene or chloroform by 2-methoxy-4-methyl-1,3,2-dioxaphospholane or 2-methoxy-4-methyl-1,3,2-dioxaphosphorinane in 5 min with an appreciable exothermic effect.

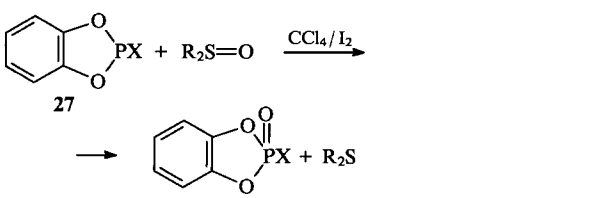


R = CH_2CHMe, $(CH_2)_2CHMe$;

R^1 = Ph, Bz; R^2 = Et Ph, Bz.

The retention of the configuration of the phosphorus atom in the cyclic phosphates obtained as a result of the oxidation reactions has been noted.

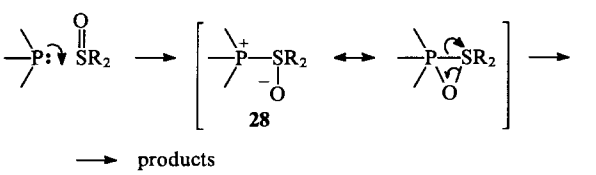
The deoxygenation of sulfoxides by 2-phenoxy-[50] and 2-chloro-1,3,2-benzodioxaphospholanes takes place readily in solution in CCl_4 at low temperatures, high temperature being required when acyclic phosphorus(III) derivatives are used.[51] Compounds **27** satisfy the principal requirements which must be met by reagents reducing sulfoxides to sulfides: they are readily available, are powerful electrophiles (electron-accepting agents), and can be easily removed after oxidation (by extraction with aqueous alkali).



X = Cl, OPh.

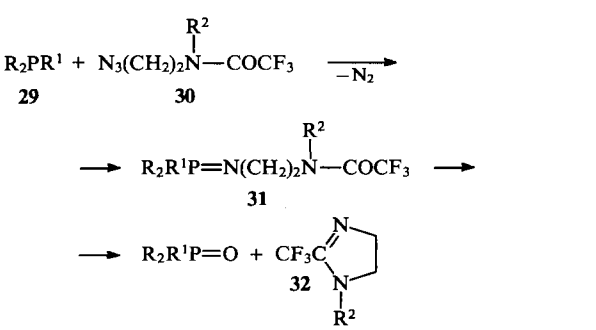
Traces of iodine catalyse the process, reducing the conversion time from 3 h to several minutes; the chloro-derivative **27** is very effective under these conditions. It deoxidises sulfoxides at room temperature over a short period.

It has been suggested [51] that the process involves the formation of the dipolar ion **28** as a result of the nucleophilic attack by phosphorus(III) on the sulfoxide sulfur atom.

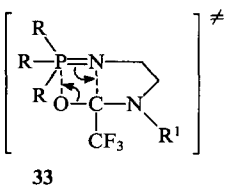


However, the increase in the rate of deoxidation when the phospholanes **27** containing highly electron-accepting substituents at the phosphorus atom are employed is more likely to be evidence in support of the nucleophilic interaction of the sulfoxide oxygen with the electrophilic phosphorus(III) atom. The ability of the latter to both give up and receive electrons (biphilicity) is manifested particularly strikingly when it is incorporated in the diheterophosphacyclane ring.[14]

The electron-accepting effect of the alkylenedioxy-substituent at the phosphorus(III) atom is manifested in the reaction of the phosphorus(III) derivatives **29** with the azidoamides **30**.[52]

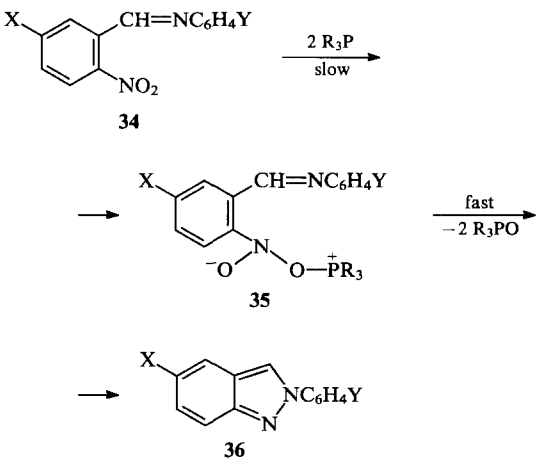


The incorporation of a phosphorus(III) atom in the five-membered ring of 2-diisopropylamino-1,3,2-benzodioxaphospholane **29** (R_2 = o-$C_6H_4O_2$, R^1 = Pr^i_2N) makes it possible to obtain 2-trifluoromethyl-2-imidazoline **32** (R^2 = H, Bu^t) in a high yield; triphenylphosphine affords only 20%–30% of the imidazoline **32** (R^2 = H) under these conditions; the yield increases to 80% (120 °C and 0.05 Torr). Tris-(dimethylamino)phosphine **29** (R = R^1 = Me_2N) does not yield even traces of the final product **32** over a period of 2 h at 120 °C. These experimental data can be best accounted for by the formation of a transition state **33** analogous to that in the Wittig reaction:



The nucleophilic attack by the carbonyl oxygen atom on the phosphimine phosphorus atom of the product **31** of the Staudinger reaction is facilitated in the presence of a powerful electron acceptor at this atom — the phenylenedioxy-substituent; by increasing the electron density at the imine phosphorus, the strongly electron-donating dialkylamino-group inhibits the Wittig reaction. Moderately strong electron acceptors (phenyl substituents) give rise to an intermediate result.

The opposite, deactivating effect of the incorporation of a phosphorus(III) atom in the five-membered dioxaphospholane ring has been established in a study of the kinetics of the reductive cyclisation of o-nitrobenzylideneanilines **34** to 2-substituted indazoles **36**.[53]



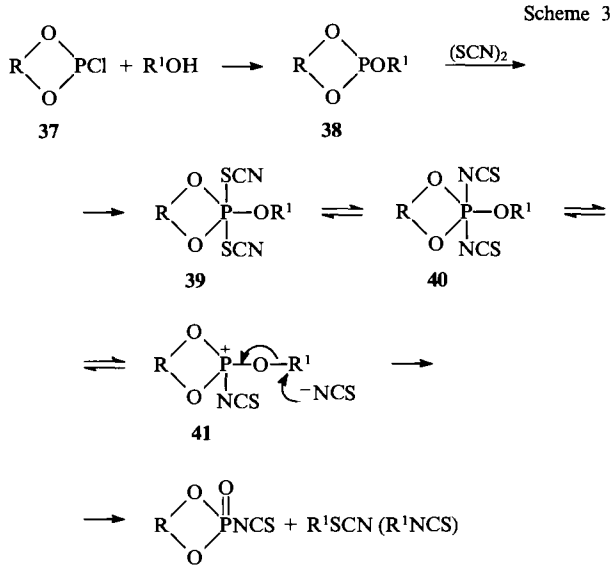
The introduction of electron-accepting substituents into aromatic rings and of electron-donating substituents at the phosphorus(III) atom promotes the occurrence of the process, the ratio of the rates of reaction of trialkyl phosphites and 2-alkoxy-1,3,2-dioxaphosphalanes being 7:1 under these conditions. Approximately the same ratio of the rates of quaternisation of cyclic and acyclic phosphites in the Arbuzov reaction led Armour et al.[53] to the conclusion that the rate-determining stage is nucleophilic attack by the phosphorus(III) atom of the deoxidising reagent on the oxygen of the nitro-group with formation of the intermediate **35**.

The very sharp increase (almost by two orders of magnitude) in the rate in the reaction of 2-ethoxy-1,3,2-diazaphospholane may be associated with the intermediate formation of a hydrogen-bonded complex favouring the reductive cyclisation. It is made up of the negatively charged oxygen atom in the zwitterion and the endocyclic NH fragment.

The ability to undergo readily a change in coordination number, observed in the reactions of phosphorus(III) derivatives and manifested particularly strikingly in σ^3-1,3,2-dioxaphospholanes, permits the use of these substances as condensing agents in the reactions of hydroxy-compounds with proton-containing nucleophiles.

It has been found [54-56] that alcohols are readily converted into thiocyanates and isothiocyanates in the reactions of 2-chloro-1,3,2-dioxaphospholanes **37** (Scheme 3).

Scheme 3

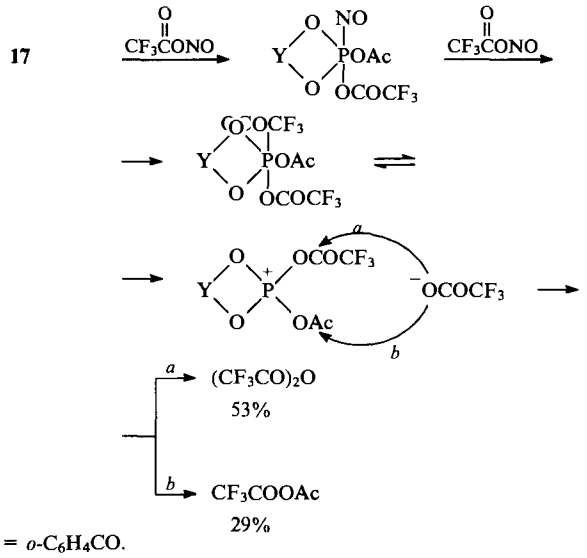


R = —CMe=CMe—; R^1 = Alkyl, R^2CO, $R^2_2P(O)$, $R^2_2P(S)$.

The products **38**, obtained by reacting phosphorochloridites with alcohols or carboxylic, dialkylphosphoric, and dialkylphosphorothioic acids, are made to react with thiocyanogen, which leads to alkyl and acyl isothiocyanates via a series of intermediates having the phosphorane (compounds **39** and **40**) and quasi-phosphonium (compound **41**) structures respectively. The use of secondary alcohols makes it possible to obtain isothiocyanates as well as thiocyanates. The dealkylation of the salt **41**, which proceeds via a mechanism involving nucleophilic substitution at the α-carbon atom of the alkoxy-group by the ambident anion SCN^-, is effected by the more bulky and nucleophilic sulfur atom for the n-alkyl group in primary alcohols. The increase in the degree of substitution at the α-sp^3-C atom (secondary alcohols) is accompanied by the competing S- and N-substitution.

We may note that a similar result is achieved in the conversion into the thiocyanate with the aid of a triphenylphosphine–thiocyanogen mixture (the so called Tamura's reagent [3]). The use of cyclic phosphorus(III) reagents makes it possible to carry out the process under very mild conditions. When the reaction was performed at the temperatures $-80 \rightarrow -30 \rightarrow +20$ °C, all the intermediates **39–41** generated in the reaction were detected by ^{31}P NMR spectroscopy. [53,54]

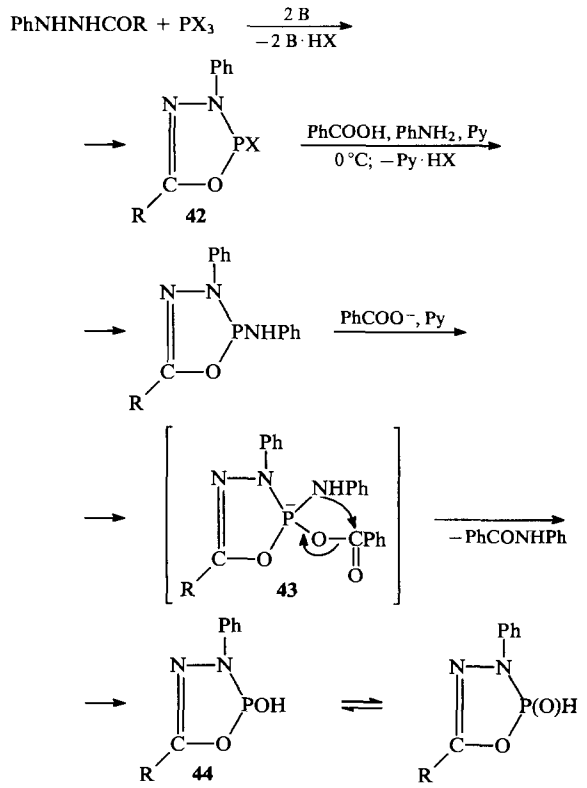
The condensing effect of cyclic phosphites is manifested in the reactions of the mixed anhydride **17** (R = OAc) with trifluoroacetyl nitrite.[57]



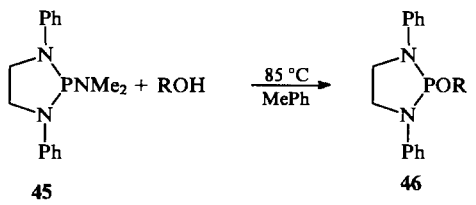
Y = *o*-C_6H_4CO.

It is assumed that in this case the process proceeds with participation of intermediates of the phosphorane and quasi-phosphonium types; the competing substitution by the trifluoroacetate anion of the trifluoromethylacetyl and acyl groups in the quasi-phosphonium salts affords the observed mixture of anhydrides as the products (routes *a* — main product, route *b* — a minor pathway).

This approach has been used recently to convert carboxylic acids into amides using the 2-X-5-R-3-phenyl-2,3-dihydro-1,3,4,2-oxadiazaphospholes **42**, obtained from phosphorus trihalides and 2-acylphenylhydrazine, as the condensing agents. [58] The process was carried out by adding compound **42** to a mixture of benzoic acid, aniline, and pyridine at 0 °C; the yield of the phenylamide of benzoic acid is nearly quantitative. It has been suggested that the key stage of the process is the formation of a type of pentacoordinate intermediate **43** and its subsequent decomposition into the final acylamide and the unstable cyclic acid **44**.

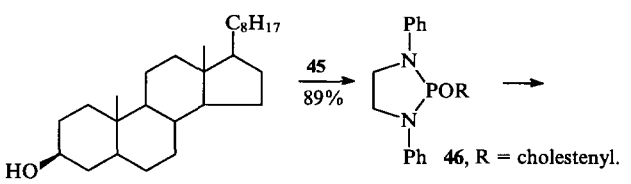


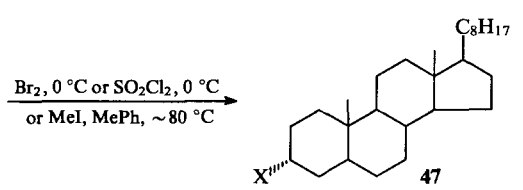
Finally, we may indicate also a method involving a kind of 'conservation' of alcohols, which is employed for their identification as part of the molecules of the readily crystallising 2-alkoxy-1,3,2-diazaphospholanes **46**, and their stereospecific conversion into organyl halides.[59] The cyclic phosphorous triamide **45** is converted on treatment with alcohols into alkoxy-derivatives, which are transformed into alkyl halides in accordance with the mechanism of the Arbuzov reaction.



45 **46**

For example, β-cholestanol has been converted in this way by the phosphoramide **45** into the corresponding ester **46**, from which the halides **47** were obtained in high yields.



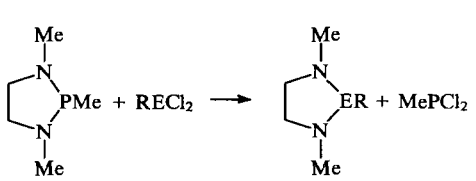


X = Cl (80%), Br (85%), I (75%).

As sometimes happens in the second stage of the Arbuzov reaction, the dealkylation of compound **46** is highly stereospecific with full inversion of configuration of the carbinol carbon atom.

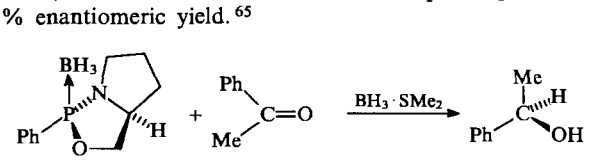
4. Other reactions

We may note that the studies carried out a fairly long time ago on the exchange of the phosphorus(III) atom for other elements via the reaction described by Eisenhut and Schmutzler[60] and Das and Zuckerman[61] were not developed further.



E = B, As; R = Ph, Cl.

Mention should be made of the cases where σ^3-oxazaphosphorinanes were used as chiral ligands in the metal [sic] complexes employed in asymmetric synthesis.[62-64] For example (2*R*, 4*S*)-2-phenyl-1,3,2-oxazaphosphorinane, coordinated to a boron hydride, reduces various ketones to the corresponding alcohols in 99% enantiomeric yield.[65]



However, a detailed consideration of this problem is outside the scope of this review.

III. σ^4-Diheterophosphacyclanes

Derivatives of tetracoordinate phosphorus have played an outstanding role in the development of methods for the conversion of carbonyl compounds into alkenes with the aid of phosphorus ylides (the Wittig reaction) and α-phosphorylated carbanions (the Horner–Wadsworth–Emmons reaction).[2,66-68] The introduction of a σ^4-P atom into the diheterophosphacyclane fragment is responsible for the specific behaviour of these phosphorus-containing reagents.

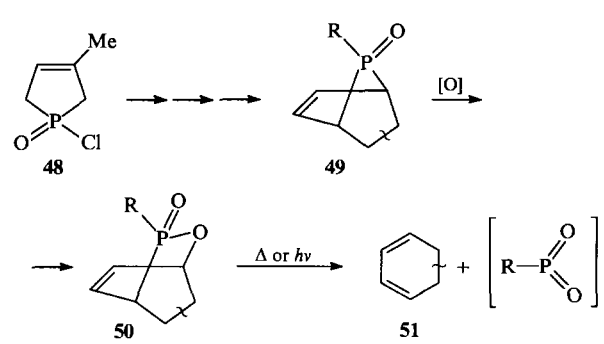
Other reactions of σ^4-diheterophosphacyclanes — thermal and photochemical fragmentation as well as solvolysis — have been less important in fine organic synthesis. We may note that the involvement of cyclic organophosphorus compounds in these processes has been exceptionally important for the development of methods of phosphorylation with the aid of metastable phosphorus-containing reagents[69] and nucleophilic substitution reactions at a tetrahedral phosphorus atom.[15]

1. Fragmentation of cyclic derivatives of tetracoordinate phosphorus

Like the analogous chemical processes with participation of cyclic phosphorus(III) derivatives, reactions of this type are used mainly for the generation of metastable derivatives of tricoordinate pentavalent phosphorus — metaphosphates and their amino- and thio-derivatives.

The formation of metaphosphates, which proceeds via the mechanism of the retrodiene synthesis, is accompanied by the liberation of phosphorus-free products obtained from the hydrocarbon skeleton of the initial, usually bicyclic, molecule.

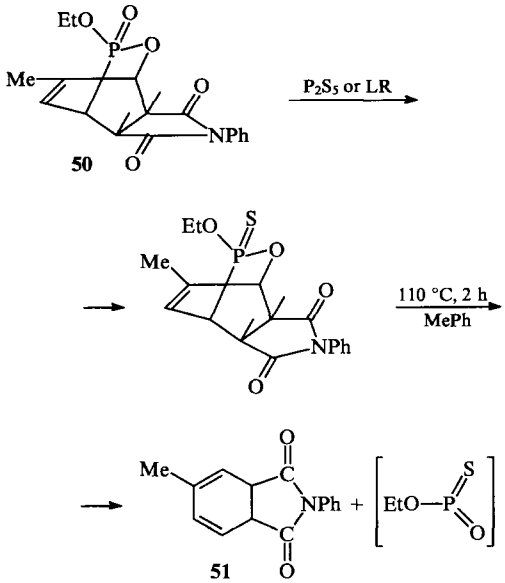
In a series of studies by Quin and coworkers,[69-74] it was found that derivatives of 2,3-oxaphosphabicyclo[2.2.2]octene **50**, obtained from compound **48**, constitute an excellent starting material for the generation of metaphosphates, which may be 'trapped' with the aid of suitable nucleophiles (alcohols, oxiranes, etc.).[69]



R = EtO, Me_2N, Bu^tO etc.

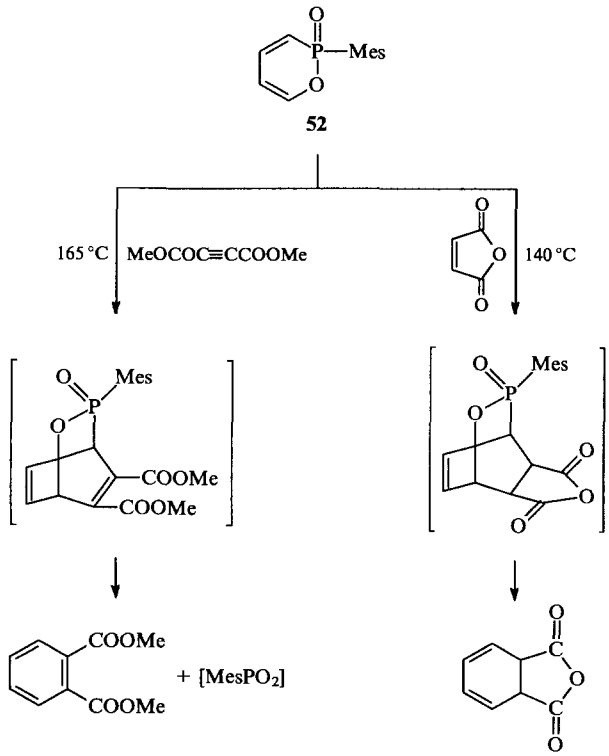
The initial cyclic phosphinochloridate **48** is converted into the strained 7-phosphanorbornene **49** via successive chemical transformations (for further details, see Quin et al.[69]). On treatment with peracids, compound **49** is converted into the phosphorylated derivative **50**.

The ease of the fragmentation of the phosphabicyclooctene depends on the conditions in this process: the thermal generation of the final products is achieved by heating in toluene at 100–110 °C; the photochemical fragmentation takes place very readily — at −75 °C under the influence of ultraviolet radiation. We may note that this constitutes a sharp difference between the bicyclic derivatives of σ^4-P and cyclic phosphites (see Subsection 1 of this Section), the decomposition of which requires heating to several hundreds of degrees. At a low temperature, it is possible to detect by ^{31}P NMR spectroscopy the metaphosphates obtained.[74] The high reactivity of the phosphacyclanes **50** is reflected in the ease of sulfurisation with the aid of P_2S_5 or Lawesson's reagent.[73]

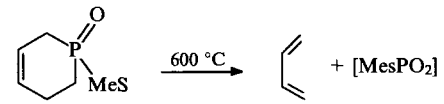


The reactions described here make it possible to obtain also the dihydrophthalimide **51** and other cyclic dienes together with the derivatives of metaphosphates and metaphosphorothioates which are difficult to obtain.

In the reaction of the phosphorus analogue of α-pyrone, namely mesityl(butadienyl) phosphinate **52**, with dienophiles, the formation of Diels–Alder adducts is only postulated: at the elevated temperature required for the cycloaddition, they decompose via the pathway described above with formation of Diels–Alder aromatic adducts or aromatic dihydro-adducts. The initial phosphacyclane thus plays the role of the supplier of butadiene.[75]

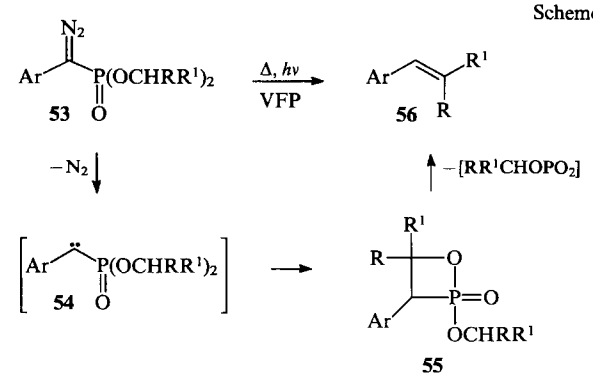


It is striking that the monocyclic alkene, which also serves as a source of the metaphosphonate and the diene, is pyrolysed under much more severe conditions.[75]



The intramolecular cyclisation of the carbenes **54**, obtained by vacuum flash photolysis (VFP) (350 °C, 10^{-5} Torr) of dialkyl α-diazobenzylphosphonates **53**, leads to the oxaphosphetanes **55**, which fragment under the reaction conditions to metaphosphates and substituted styrenes **56** (Scheme 4).[76]

Scheme 4



The cyclisation **54** → **55** takes place as a result of the intramolecular insertion of the carbene in a C–H bond of the ester alkyl group. The phosphacyclanes **55** can be isolated by vacuum flash photolysis at a lower temperature (275 °C) and this makes it possible to model the alkene elimination stage **55**→**56**. The high stability of the σ^4-oxaphosphetanes **55** (compared with the four-membered heterocyclic intermediates containing pentacoordinate phosphorus) in alkene formation reactions with the aid of phosphorus ylides and α-phosphorylated carbanions (see below) is striking.

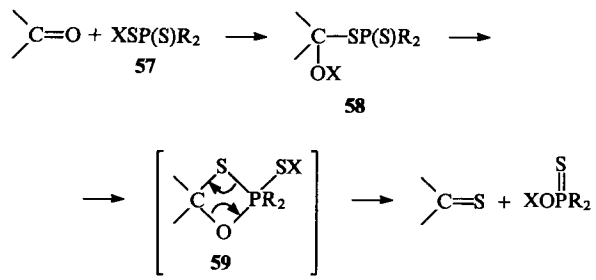
2. Nucleophilic substitution reactions

The highly electrophilic σ^4-P atom in σ^4-1,3,2-diheterophosphacyclanes is extremely sensitive to attack by charged or neutral nucleophiles: the rate of solvolysis of five-membered cyclic phosphates is several orders of magnitude higher than that of the tiralkyl phosphates with a similar composition.[15] The reason for this is believed to be the decrease in activation energy as a result of the involvement in the process of the thermodynamically stable pentacoordinate intermediate containing a diheterophospholane ring.[15] The equally high rates of cleavage of both endocyclic and exocyclic phosphorus–heteroatom bonds is striking. Acyclic and six-membered cyclic esters of σ^4-P acids react much more slowly. It is noteworthy that the diheterophosphorinane ring is relatively stable.

The endocyclic solvolytic reactions usually lead to phosphorus-containing acyclic products. This problem is outside the scope of this review, although it is important in the synthesis of biologically active phosphorus compounds. Among recent publications, we may mention a review[77] in which data are presented on the endocyclic hydrolysis of phosphazacyclanes used for the synthesis of phospholipids. The results of studies on the asymmetric synthesis of phosphorus-containing aminoacids using dioxa-, oxaza-, and diaza-phosphacyclanes have been surveyed in a review publication.[78] Finally, the photochemical decomposition of phosphate esters can also serve as a method of synthesis of unsaturated organics, which has been demonstrated in a recent review.[79].

There are few nucleophilic substitution reactions at the tetrahedral phosphorus atom forming part of the heterocycle which are used for the synthesis of phosphorus-free organic compounds. We may mention in the first place the so called

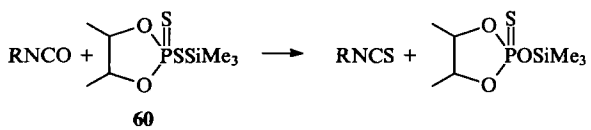
a sulfur atom on treatment with phosphorus dithio-acids or *S*-trimethylsilyl phosphorodithioates **57**.[3]



X = H, $SiMe_3$.

The reaction is completed by the addition of the dithio-derivatives **57** to the carbonyl group of the substrate; under mild conditions, the adducts **58** (X = $SiMe_3$) may be isolated. At an elevated temperature, the process develops further during fractionation and is completed by the formation of thiocarbonyl compounds and phosphorus-containing monothio-derivatives. The conversion of the hydroxy(siloxy)alkyl phosphorodithioates **58** into the final products takes place via a mechanism involving intramolecular nucleophilic substitution at the tetrahedral phosphorus atom.

The above method is especially effective for the conversion of aryl and acyl isocyanates into the corresponding isothiocyanates.[80-83] The silyl phosphorodithioate **60** is almost wholly converted into isocyanates and isothiocyanates at room temperature; the acyclic phosphorodithioates **57** (R = alkoxy-group) require heating in order to complete the reaction.



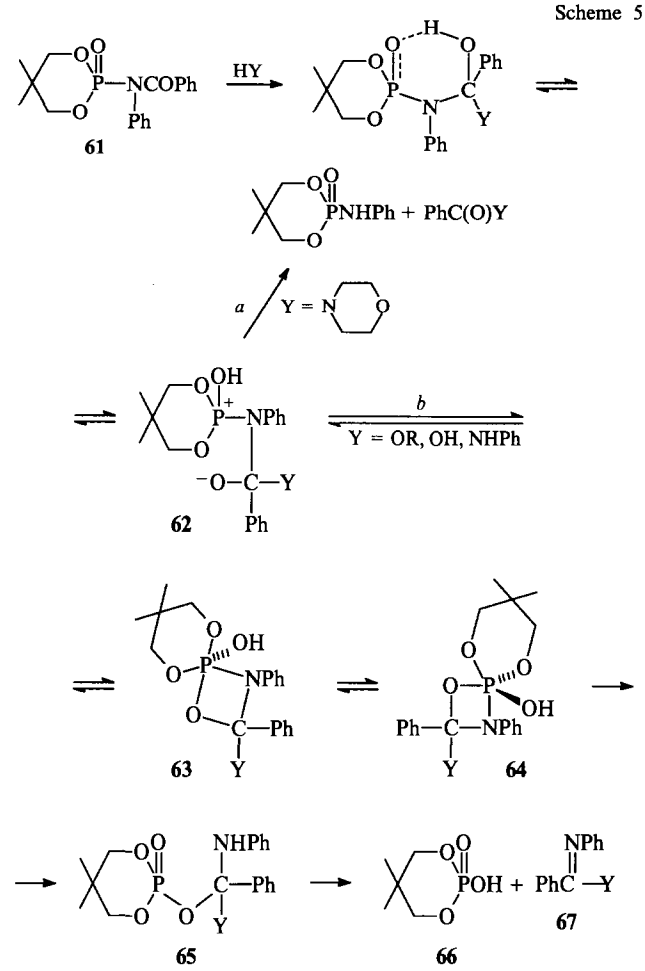
R = Ph, CCl_3CO, PhCO, $(EtO)_2PO$

The sharp increase in the sulfurising activity of phosphorodithioates following the introduction of a σ^4-P atom into a five-membered ring is most probably associated with the decrease in the energy of the type **59** intermediate.[82] The increase in the stability of phosphoranes as a result of spirocyclisation is well known.[16]

The comparatively low electrophilicity of the σ^4-P atom incorporated in a six-membered diheterophosphacyclane fragment may promote attack by an external nucleophile on an alternative electrophilic centre of the phosphorus-containing reagent if such is present. Thus the solvolysis of 2-(*N*-benzoyl-*N*-phenylamino)-5,5-dimethyl-2-oxo-1,3,2-dioxaphosphorinane **61**[84] takes place exclusively with attack by nucleophiles on the carbonyl centre and is accompanied by the O,N-migration of the phosphoryl group (Scheme 5).

Depending on the nature of the nucleophile (HY), the process proceeds with dissociation of the C–N bond (route *a*) in the key intermediate **62** or via its cyclisation to compound **63** and pseudorotation to give compound **64** (route *b*) and is continued by the dissociation of the C–O bond in the phosphate **65**. The reaction with morpholine proceeds via route *a* to give *N*-benzoylmorpholine and the anilide of a cyclic phosphoric acid, while the reactions with water, alcohol and aniline take place via route *b*, which is associated with the phosphorylotropic transformations noted above. The phenylimide **67** (Y = OMe), obtained in the reaction with methanol,[80] methylates the cyclic acid **66** (2 h, room temperature). The conversion of the *N*-acylphosphoramidate **61** into the acid **66** and the phenylimide **67** is completed after 7 h on treatment with phenol and after 10 h

Scheme 5



R = Me, Ph, CMe_3.

on treatment with *tert*-butyl alcohol. Aniline affords the anilinium salt of the cyclic phosphoric acid **66** and a high yield of *N*-phenyliminobenzanilide **67** (Y = NHPh) as the reaction products.

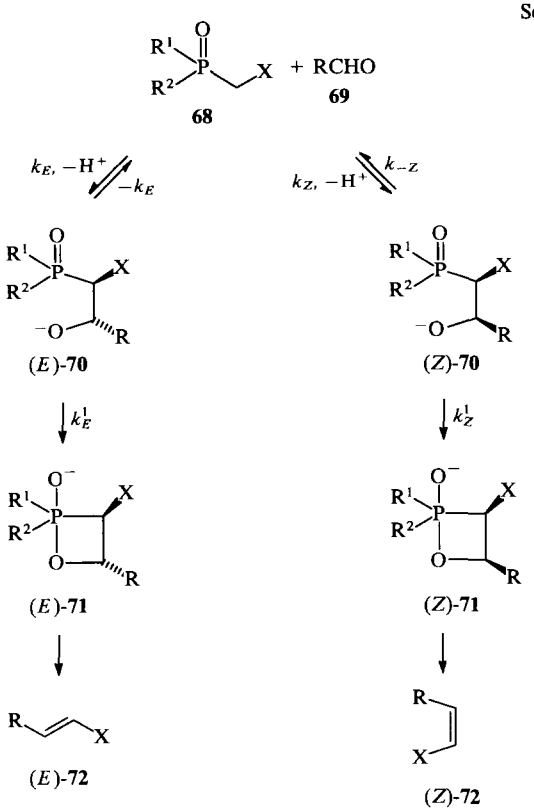
3. α-Phosphorylated carbanions

The reactions of α-phosphorylated stabilised carbanions with carbonyl compounds, for which the name 'Horner–Wadsworth–Emmons' (HWE) reaction has been established in recent years,[68] constitutes a classical method of synthesis of α,β-unsaturated carboxylic acid esters and other functionalised alkenes.

The HWE reaction as well as the Wittig reaction similar to it result in the preferential formation of the thermodynamically more stable (*E*)-alkenes. However, by varying the reaction conditions and the structure of the reactants, by introducing special additives, and by taking into account other factors, it is possible to vary the ratio of the (*E*)- and (*Z*)-products of the alkene formation process within wide limits.[66]

In the general case, the tendency towards formation of (*E*)- and (*Z*)-alkenes is considered from the standpoint of the reversibility of the formation of the intermediates, i.e. the ratios of the rates of the reaction stages k_{-E}/k_E^1 and k_Z/k_{-Z}^1 (Scheme 6).[67] Other conditions being equal, the increase in the stability of the (*E*)- and (*Z*)-alkoxides **70** and also of the pentacoordinate intermediates (*E*)- and (*Z*)-**71** determines the ease of their decomposition to alkenes. The process is kinetically controlled, (*Z*)-isomers are formed, whereas in the case where it is thermodynamically controlled there is a possibility of the reversibility of the process, leading to an increase in (*E*)-stereoselectivity.

Scheme 6



The tendency towards an increase in the 'reversibility factor' and hence in the ratio *E*/*Z* with increase in temperature and in the ease of the coordination of the metal-counterion in compound **70** (Li^+ is more effectively coordinated than Na^+ and K^+) has been established on numerous examples.[85,86] At the same time, an increase in the basicity of the medium and especially in the steric hindrance of the α-carbon atom in the carbonyl reactant **69** increases the content of the (*Z*)-isomer.[86] However, in the general case it is fairly difficult to predict the influence of the medium and structural factors on the stereochemical result of the HWE reaction because the conformational structure of the phosphonates **68**, the association of the carbanions obtained from them, and the relative contributions of all other factors may have a significant effect on the relative rates of the reactions leading to the (*E*)- and (*Z*)-isomers (see Scheme 6).

The influence of the environment of the σ^4-P atom and the synthetic consequences of its incorporation in the heterocycle are of special interest.

For the acyclic phosphonates **68**, it has been found that the replacement of the methoxy-groups in compound **68** ($R^1 = R^2 =$ MeO, X = COOEt) by the trifluoroethoxy-groups to give compound **68** ($R^1 = R^2 = CF_3CH_2O$, X = COOEt) in reactions with aldehydes leads to a sharp increase in the fraction of the (*Z*)-product up to the complete selectivity of the reaction with benzaldehyde. The methoxy-analogue of the phosphonate **68** gives rise exclusively to the *trans*-cinnamate **72** (R = Ph, X = COOEt) in this reaction, whereas the bis(fluoroethyl)phosphonate **68** wholly converts benzaldehyde into the *cis*-cinnamate ester **72** (R = Ph, X = COOEt). Evidently, this result is associated with the increase in the stability of the type **71** phosphoranes on enhancement of the electron-accepting properties of the substituents at σ^5-P, which is well known for phosphoranes.[16] This lowers the 'reversibility factor' and favours the (*Z*)-stereoselectivity.

This difference has been used recently for the (*Z*)- or (*E*)-selective conversion into alkenes in individual stages of the complex synthesis of a macrocyclic antibiotic—(+)-ikarugamicin.[87]

The phosphonates **68** of the σ^4-1,3,2-diheterophosphacyclane series have been recently investigated by various methods.[16,88–91] It was found that the stability and properties of the cyclophosphonate carbanions depend on the fine details of the steric structure, ring size, the structure of the acyclic functional groups, and the type of metal ion.

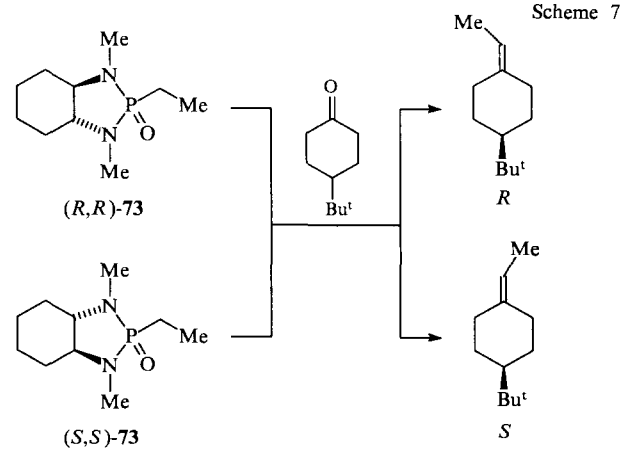
A distinctive feature of the conversion into an alkene with the aid of phosphacyclic carbanions is a high rate of reaction associated with the appreciable electrophilicity of the endocyclic σ^4-P atom (the tendency towards association and self-condensation is explained by the same feature[91]) and the distinct (*Z*)-specificity of the HWE reactions with participation of five- and six-membered cyclic phosphonates **68** ($R^1 + R^2$ = alkylene-1,2-dioxy- and -1,3-dioxy-, alkylene-1,2-diamino- and -1,3-diamino-, and alkylene-1-oxy-2-amino- and -1-oxy-3-amino).[16] The latter factor is associated with the stability of the pentacoordinate intermediates in which a σ^5-P atom is incorporated in the ring; it has been established that five-membered cyclic phosphonates exhibit an appreciably higher (*Z*)-selectivity [65% – 70% of the (*Z*)-isomer] than the six-membered and acyclic phosphonates.[15,68] This is a consequence of the well known stabilisation of phosphoranes by five-membered cyclic fragments (the five-membered ring effect).[16,17]

The rate of the HWE reaction increases markedly (almost by a factor of 20) when a phosphorus atom is incorporated in the dioxaphospholane ring in compound **68** [$R^1 + R^2$ = $OCH(CH_3)CH(CH_3)O$, X = COOEt] compared with the acyclic compounds **68** ($R^1 + R^2$ = OEt, X = COOEt). We may note, incidentally, that the latter is 35 times more reactive than the phosphine oxide **68** ($R^1 = R^2$ = Ph, X = COOEt).[68,92] These results are satisfactorily consistent with the hypothesis of the increased stability of the intermediate **70**: it increases for the following series of substituents at σ^5-P: phenyl < ethoxy- < alkylene-1,2-dioxy.

As already mentioned, the five-membered cyclic phosphonates **68** ($R^1 + R^2$ = alkylene-1,2-dioxy-, X = COOEt) were found to exhibit (*Z*)-selectivity, which increased sharply when the reaction was carried out with *tert*-butyl phosphonoacetate **68** [$R^1 + R^2$ = COH(Me)CH(Me)O, X = $COOBu^t$] at a low temperature (−20 °C) with lithium as the cation.[93] This feature has been used in the synthesis of pyrethroid insecticides (see Maryanoff and Reitz,[68] Tessier,[93] and the references quoted therein).

Unique diastereofacial selectivity has been demonstrated for the chiral diaminophosphonates (*R*,*R*)- and (*S*,*S*)-**73** synthesised from the two enantiomeric (*R*,*R*)- and (*S*,*S*)-1,2-diaminocyclohexanes.[94] An appreciable stereodifferentiating reactivity has been noted in the reactions of the potassium salts of the diazaphospholanes **73** with 4-*tert*-butylcyclohexanone: compound (*R*,*R*)-**73** forms a mixture of the isomeric (*R*)- and (*S*)-4-*tert*-butylcyclohexylideneethanes in proportions of 95 : 5; the use of the stereoisomer (*S*,*S*)-**73** inverts this ratio in favour of the (*S*)-alkene (Scheme 7).

Scheme 7



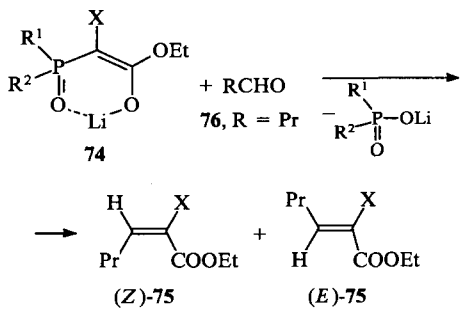
This stereochemical result of the HWE reaction with participation of compound **73** is difficult to explain from the standpoint of the 'reversibility factor'.[68,94] The cause of the above effect is more likely to be the initial topology of these cyclic phosphonates — their symmetry elements which predetermine in each case the nucleophilic attack on the carbonyl carbon atom in the sterically more accessible plane of the phosphorylated carbanion. It has been pointed out[94] that such asymmetric induction in the alkene formation reaction is useful for the synthesis of vitamins and pheromones or in the formation of chiral catalysts.

The stereospecific effect of the diazaphospholane fragment in the HWE reactions of lithium derivatives of the phosphonoacylates **74** with aliphatic aldehydes has been found in studies by Savignac and coworkers.[91,95–98] Table 1 presents the stereochemical results of the conversion of butyraldehyde into an alkene by treatment with α-n-propyl and α-chlorophosphonoacylates, which leads to the formation of a mixture of (*Z*)- and (*E*)-isomers. Oxygen-containing substituents, fluoroethyl substituents, as well as phosphorinane and dioxaphospholane reagents do not exhibit a stereospecific effect. We may only note that, in contrast to the α-alkylcyclophosphonates **74** (X = alkyl), their halo-substituted analogues **74** (X = Cl[96] and F[97]) were found to exhibit a considerable (*E*)-selectivity (cf. the data of Stiell and Gennari[85]).

The results of the formation of alkenes with the aid of derivatives of 1,3-dimethyl-2-oxo-1,3,2-diazaphospholanes constitute an isolated case. The reactions of compound **74** (X = Pr^n) lead to the preferential formation of the (*Z*)-isomers; the halo-substituted carbanions are distinguished by full (*E*)-stereoselectivity for chloro- and fluoro-substituents and for all the aldehydes **76** used in the alkene formation reaction.[96,97]

It is difficult to assign these results to only one cause. It has been shown,[97] for example, that the stereochemical effect depends on many external factors: the concentration of the phosphonate [the fraction of the (*Z*)-isomer falls with dilution], the temperature regime, the method of preparation of the lithium derivative **74**, and the nature of the alkene employed for this purpose as well as other additives (for example, lithium bromide and crown-ethers).

Table 1. The influence of substituents at the σ^4-P atom in the HWE reactions of the lithium salts of substituted α-phosphonoacetates with aldehydes.[91,96]

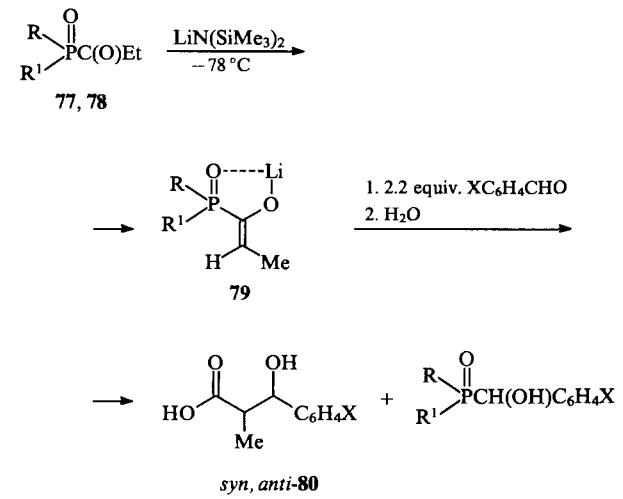


$R^1 + R^2$	Ratio of yields of (*Z*)- and (*E*)-isomers (%)	
	X = Pr^n (T = 20 °C)	X = Cl (T/°C)
$(EtO)_2$	37:63	55:45 (−20)
$(CF_3CH_2O)_2$	–	35:65 (−70)
$OCH_2C(Me_2)CH_2O$	61:39	25:75 (−40)
OCH(Me)CH(Me)O	62:38	–
$N(Et)(CH_2)_2N(Et)$	–	15:85 (−70)
$N(Me)CH_2)_2NMe$	76:24	2:98 (−70)
$N(Me)(CH_2)_3NMe$	Does not react	–
$(Me_2N)_2$	Does not react	–

The difficulty of assessing the factors which determine the stereochemical result of the reaction of compound **74** with the aldehyde **76** is caused, as noted above, by the tendency of the carbanions towards association and aggregation and by their equilibrium state associated with this behaviour, which is in its turn determined by the high electrophilicity of the endocyclic σ^4-P atom.

It is essential to emphasise that the use of cyclic α-phosphorylated carbanions in HWE reactions have a series of specific features associated with the greater reactivity of these substances due to their more pronounced sensitivity to the nucleophilic reactions of the endocyclic σ^4-P atom. Although the stereospecific effect of phosphacyclanes is not always easy to predict, it amounts as a rule to complete stereoselectivity. The latter is associated both with the characteristic features of the processes arising in the course of the HWE reactions of the cyclic intermediates and with the specific topology characteristic of cyclic reagents effecting the conversion into alkenes.

The base-promoted aldol condensation of diethyl propionylphosphonate **77**[99] and of its oxazaphosphorinane analogue **78**[100] with aromatic and aliphatic aldehydes is characterised by a high *syn*-diastereoselectivity (the ratio *syn* : *anti* = 98 : 2 and 94 : 6 for compound **80** obtained from compounds **77** and **78** respectively). The reaction makes it possible to produce the β-hydroxycarbonyl fragment of compound **80** under very mild conditions.

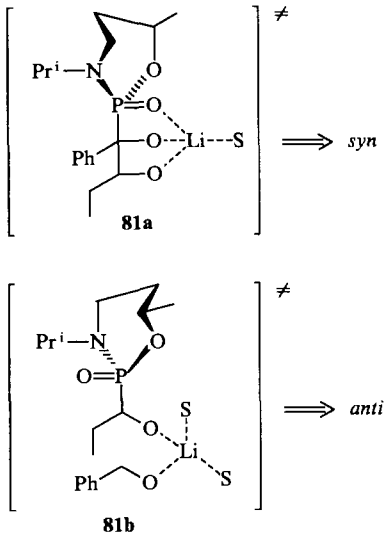


77: R = Pr^nCO, R^1 = OEt; **78**: R + R^1 = $OCH(CH_2)_2NPr^i$ (Me).

The authors[100] established that, when the N-substituent is fairly bulky, the chair conformation of the oxazaphosphorinane reagent **78** creates good possibilities for preferential enantiofacial selection (cf. the reagents **73**). The high degree of stereospecificity is in this case attributed to the formation of the highly organised transition state **81a** (Scheme 8).

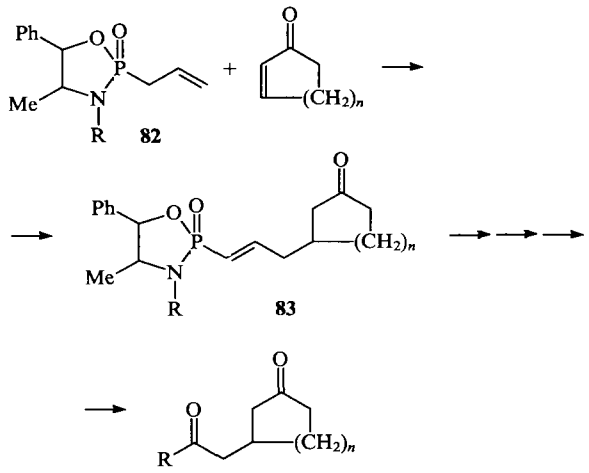
The tendency of lithium alkoxides of type **79** to associate, which was noted above, plays a significant role also in the reaction under discussion. The introduction of additives of the type of tetramethylethylenediamine (S), which coordinate the lithium ion, disturbs the stereocontrol: the increase in the fraction of the *anti*-conformer of **80** is attributed to the contribution by the activated complex **81b** formed with the phosphoryl group of the phosphacyclane liberated from the coordination sphere of lithium.

Scheme 8



S = solvent or additive.

Chiral allyl phosphonates having the oxazaphospholane structure, obtained from ephedrine **82** (R = Me) and its isopropyl analogue **82** (R = Pr^i), undergo 1,4-addition with cyclic enones, which leads to the formation of the 1,4-adducts **83** with a high enantioselectivity.[101] The latter have been converted into the corresponding aldehydes or acids with an oxocyclane structure.



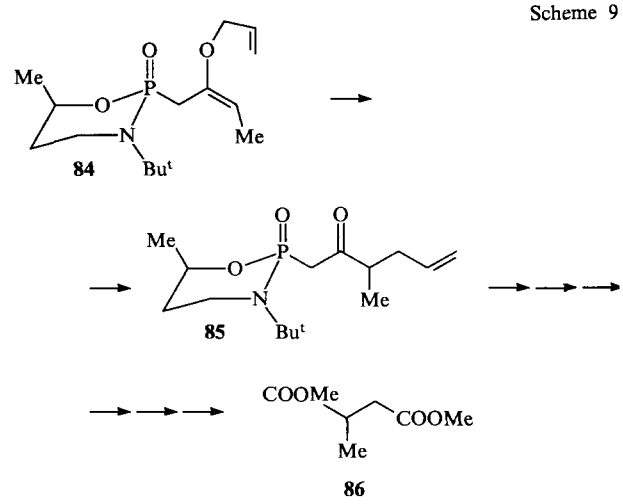
n = 1 - 4; R = H, OH.

The optical yield of the products increases greatly on passing from the methyl homologue (70% - 74%) to the isopropyl homologue **82** (88% - 98%). The authors[101] emphasise the likely usefulness of this reaction for the synthesis of natural products.

The stereochemical control achieved by chiral carbanions containing the oxazaphosphorinane ring gives rise to asymmetric induction of the phosphonamidates **85** in the Claisen rearrangement (Scheme 9).[102-104]

It has been established that the oxidative decomposition of the product of the Claisen rearrangement **85**, obtained from *cis*-**84**, leads to the (*S*)-dimethyl methylsuccinate **86**, while the *trans*-isomer affords the (*R*)-enantiomer.[102] As in the previous cases, the result of the rearrangement is associated with the topological characteristics of the lithium carbanions derived from compound **84**, which determine the course of the isomerisation of the carbanion-stabilised allyl vinyl ether on one of the 'opposite' surfaces (made up of the multiple bonds, the carbanionic centre, and the P=O fragment) relative to the structural elements of the phosphoramide ring.[103]

Scheme 9



The arenesulfonyl group also exerts a similar accelerating and stereoregulating influence on the Claisen rearrangement, but a number of advantages of the phosphorylated allylvinyl substrates have been noted:[104] the great ease of synthesis, the possibility of an extensive structural variation of the phosphorus-containing fragments, and the thorough knowledge of the chemistry of the phosphorus-stabilised carbanions.

The data presented in this section reveal the exceptionally wide prospects for the employment of phosphacyclanes in stereospecific organic and organoelement synthesis. The relatively high availability of the cyclic organophosphorus compounds functionalised in the endocyclic fragment, the possibility of varying the composition and steric structure of the phosphorus-containing heterocycle, and the very high reactivity of the compounds discussed here — all these properties leave no doubt that this field of the chemistry of cyclic organophosphorus compounds has a great future.

IV. σ^5-Mono- and diheterophosphacyclanes

Derivatives of pentacoordinate phosphorus have played an important role in the development of the chemistry of organophosphorus compounds. The problem of the synthesis of substances of this type with a hypervalent central atom, questions concerning the electronic and steric structures, the chemical transformation of phosphoranes, and the role of pentacoordinated intermediates in the reactions of organophosphorus compounds — these and other questions of the theoretical and synthetic chemistry of phosphorus continue to remain in the centre of attention of investigators. Among the recent review publications devoted to problems of the synthesis and properties of σ^5-phosphacyclanes, mention may be made of those of Kumaras et al.[105] and Gloede.[106] Attention should also be drawn to the experimental studies which have revealed the role of σ^5-1,3,2-dioxaphospholane intermediates in biological processes associated with phosphate transport (see, for example, Kluger and Taylor[107] and Breslow et al.[108]).

The introduction of a σ^5-phosphorus atom into a monocyclic and especially a spirocyclic system favours the stabilisation of phosphoranes. The recognition of this fact promoted the concentration of the efforts of chemists in the search for new reagents containing a pentacoordinate phosphorus atom as well as various complex functionalised compositions, which in the course of reactions give rise to σ^5-P compounds participating in a particular chemical operation.

The synthesis of σ^5-phosphacyclanes, modelling the intermediates in the most important reactions of organophosphorus compounds, for example hydroxyphosphoranes (intermediates in nucleophilic substitution at a tetrahedral phosphorus atom)[16] or 1,2-oxaphosphetanes (substances postulated as intermediates

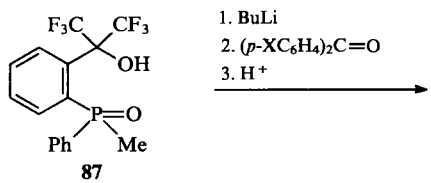
in the HWE and Wittig reactions)[109] assumed a particular importance. The synthesis and study of the transformations of the above substances have not only thrown light on their reaction mechanisms, but also made possible a specific approach to the selection of the optimum reagents and conditions for reactions with their participation in order to obtain complex organic substances, including natural products.

1. σ^5-1,2-Oxaphosphetanes and σ^5-1,2-oxaphospholanes

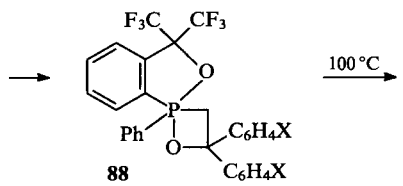
As already stated, the four-membered 1,2-oxaphosphacyclanes have been postulated as intermediates in reactions giving alkenes with the aid of Wittig reagents or α-phosphorylated carbanions. However, attempts to isolate and identify these substances, produced in the course of reactions involving conversion into alkenes, were unsuccessful for a long time: in the best case, it was possible to detect them by various spectroscopic methods.[110-113]

However, stable 1,2-oxaphosphetanes have been isolated recently and their thermal decomposition reactions, modelling the second stage of the HWE and Wittig reactions, have been investigated.[114,115,117-120]

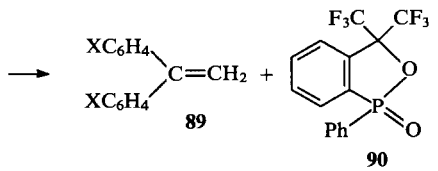
Successive treatment with butyllithium, diaryl ketones, and acids of the phosphine oxide **87**, containing the so called Martin's ligand[114,116] (acyclised aromatic ligand stabilised as a result of spirocyclisation as well as other unstable σ^5-P compounds, for example hydroxyphosphoranes[16]) together with the phenyl and methyl ligands makes it possible to obtain the stable spirocyclic 1,2-oxaphosphetanes **88**.



87



88



89 **90**

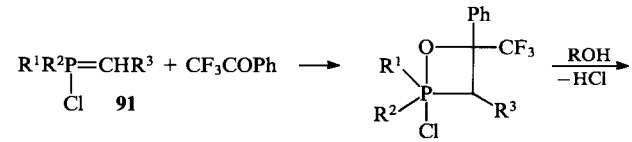
The phosphacyclanes **88**, which are entirely stable under the usual conditions (which has made it possible to establish their structure by X-ray diffraction[114]) are converted quantitatively on heating to 100 °C into 1,1-diarylethenes and the phosphinates **90** in accordance with the mechanism of the second stage of the Wittig and HWE reactions.

According to the Hammett equation, the rate of the decomposition reaction is

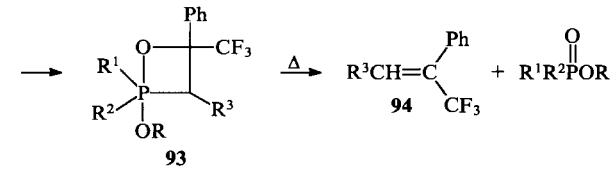
$$\lg(k/k_0) = -0.709(2\sigma_p^+) \qquad (r = 0.999),$$

with a negative reaction constant ($\rho = -0.709$), indicating the accelerating effect of the electron-donating substituent X. The relatively low sensitivity of the rate of decomposition to the polarity of the medium, the low negative activation entropy ($\Delta S^{\neq} = -5.7 \pm 0.75$ e.u.) and the small (in absolute magnitude) value of ρ indicate a concerted mechanism of the decomposition of compound **88** with a weakly polar transition state (slight asynchronicity in the dissociation of the P–C and C–O bonds in the oxaphosphetane fragment).

Stable 1,2-oxaphosphetanes **92** have been obtained by Kolodyazhnyi and coworkers[115,117] by the reaction of phenyl trifluoromethyl ketone with the halides **91** under very mild conditions (ether, 0 °C).

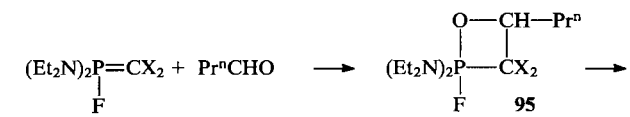


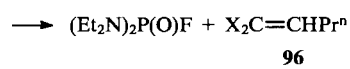
92



93 **94**

The chlorine atom in the chlorophosphinomethylene **91** is readily replaced by an ether group on treatment with methanol or phenol, while the 1,2-oxaphosphetanes **93** decompose on heating to the alkenes **94** and the corresponding phosphinates in accordance with the mechanism of the Wittig reaction. It is of interest that their precursors—2-halo-1,2-oxaphosphetanes **92**—do not exhibit a tendency to eliminate alkenes and on thermolysis as a rule undergo fragmentation with formation of the corresponding phosphorus-containing acyclic alkenes. The *P*-fluorophosphetanes **95**, decomposing to the *gem*-dihalide **96** and phosphorofluoridic diamides, constitute an exception.[118-120]



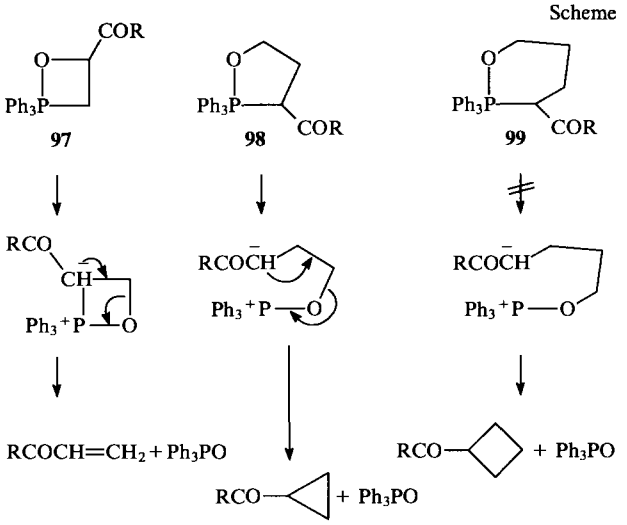


96

It has been postulated[119,120] that the electronegative atoms X favour the migration of the dihalomethylene group (and not of the oxygen atom) to the axial position in the phosphorane **95**, which results in the dissociation of the P–C (and not P–O) bond.

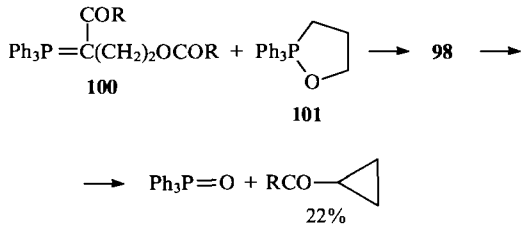
The conditions and nature of the decomposition of 1,2-oxaphosphacyclanes as well as the synthetic result of the fragmentation of the heterocycles depends significantly, other conditions being equal, on the size of the phosphorus–oxygen heterocycle.[121] The triphenyloxaphosphetanes **97** readily decompose in accordance with the general mechanism corresponding to the second stage of the Wittig reaction. The alkene is then produced more readily the more pronounced are the electron-accepting properties of the ring substituents (in this case, these are acyl or alkoxycarbonyl groups) (Scheme 10). It has been suggested[121,122] that the decomposition proceeds via a stage involving the open-chain phosphonium-carbanionic form of the intermediate, which results in the formation of a α,β-unsaturated ketones (for a phosphorane with an acyl substituent) and a phosphine oxide.

Scheme 10



The thermal decomposition of the 1,2-oxaphospholanes **98** to cyclopropyl ketones is achieved only in the presence of electron-accepting ring substituents, the unsubstituted ring being stable. The 1,2-oxaphosphorinanes **99**, even those containing electron-accepting substituents, are stable under the reaction conditions and do not decompose to cyclobutanes. It is believed [121] that these experimental results are influenced mainly by ring strain. These data are satisfactorily consistent with a repeatedly established fact — an increase in the chemical and thermal stability in the following series of phosphacyclanes: four-membered < five-membered < six-membered. [16]

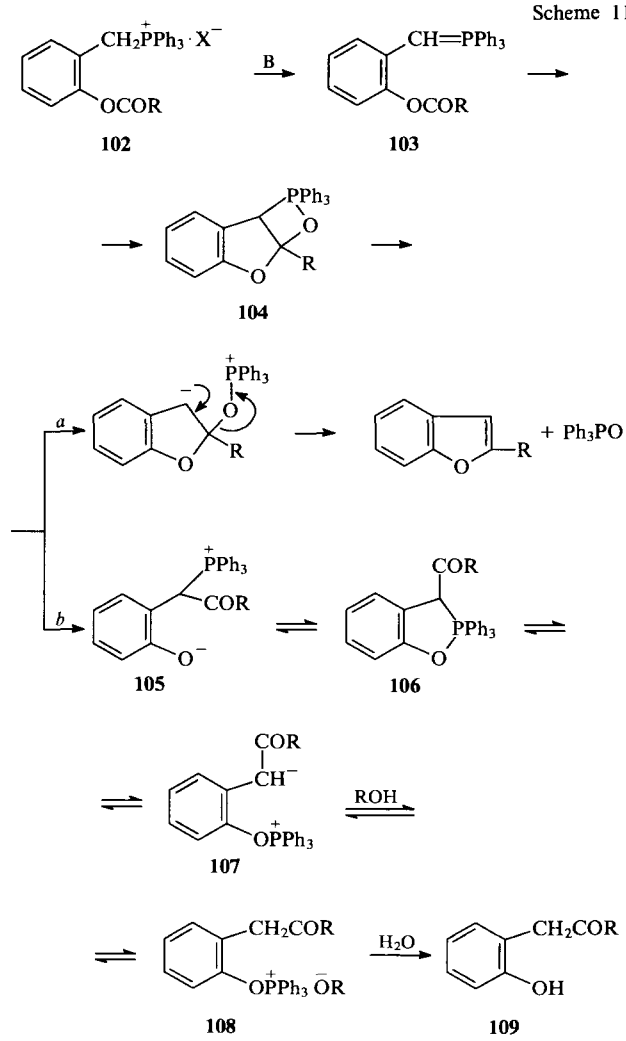
It is of interest that the cyclopropyl ketone can be obtained also as a result of the intermolecular transfer of the acyl group from the ylide **100** to the unsubstituted oxaphospholane **101**; the intermediate acyl-1,2-oxaphospholane **98** gives rise to the cyclopropyl ketone in 22% yield.



It has been established that the proton-donating properties of the medium can also determine the synthetic result of the decomposition of 1,2-oxaphosphetane. [123] Thus the intermediate four-membered tricyclic phosphorane **104**, obtained from 2-acyloxybenzylidenetriphenylphosphonium ylide **103** (which was in its turn obtained from the phosphonium salt **102**) decomposes in inert solvents to benzofurans via path *a* in accordance with an intramolecular acylation mechanism (**103** → **104**) (Scheme 11).

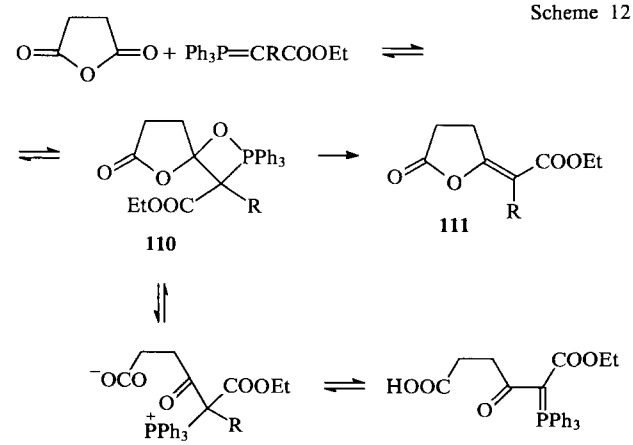
In proton-donating solvents (alcohols), the process proceeds with the successive cleavage and closure of rings via the phosphonium (compound **105**), benzophosphorane (compound **106**), and zwitterionic (compound **107**) intermediates. On treatment with alcohols, the last intermediate gives rise to the quasi-phosphonium salt **108**, the hydrolysis of which led to the isolation of the ketone **109** (Scheme 11, path *b*).

Scheme 11



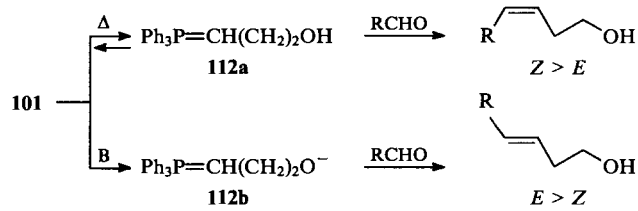
Increase in ring strain in systems incorporating the 1,2-phosphetane fragment naturally facilitates the decomposition of the intermediates in the Wittig or HWE reactions to the corresponding alkenes. The very unstable phosphacyclane **110**, obtained in the course of the conversion of succinic anhydride into an alkene by treatment with an ylide, may be stabilised not only via elimination of the alkene **111** but also as a result of rearrangement to the open-chain phosphonium (for R = H, Me) or ylide (for R = H) organophosphorus intermediates in the alkene formation reaction (Scheme 12). [124]

Scheme 12



R = H, Me.

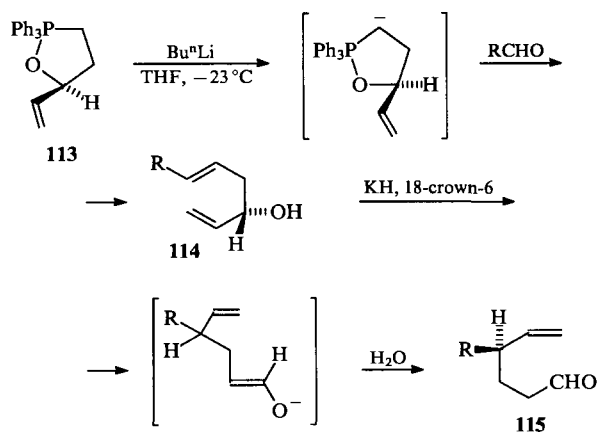
The data presented in this subsection and also in Subsection 2 indicate the relatively easy heterolysis of the phosphorus–oxygen and phosphorus–carbon bonds not only in the strained σ^5-1,2-oxaphosphetane ring but also in the σ^5-1,2-oxaphospholane ring. It has been established that the latter can be regarded as a latent ylide, which suggests that compounds of this series have the capacity to effect conversions into alkenes with the postulated involvement of the open-chain γ-oxido(hydroxy)ylide tautomeric form **112**. Furthermore, it has been shown in a series of studies [125–127] that the method of generation of the ylide **112** from the 1,2-oxaphospholane **101** determines to a significant extent the stereochemical result of the conversion of aldehydes into alkenes: the process whereby homoallyl alcohols are obtained as a result of the thermolysis of a phosphacyclane exhibits (*Z*)-selectivity and, in the presence of bases, (*E*)-selectivity.



The hydroxy-ylide **112a**, generated thermally from compound **101**, affords the (*Z*)- and (*E*)-alkenols (the ratio *Z* : *E* = 73 : 27 for R = Ph and 88 : 12 for R = C_6H_{11}) in the presence of benzaldehyde. The γ-oxidoylide **112b**, obtained by treating compound **101** with lithium bases, for example with $LiN(SiMe_3)_2$, gives rise to the (*E*)-stereoisomer in a mixture in which its content is high: *Z* : *E* = 4 : 96 (R = Ph) and 45 : 55 (R = C_6H_{11}).

As in the HWE reactions, in the cases described the stereochemical result of the alkene formation process is determined by the combined influence of a large number of factors, which determine the conditions governing the formation and interconversion of the zwitterionic and 1,2-oxaphosphetane intermediates. The nonstabilised ylides in the Wittig reactions are usually characterised by a high (*Z*)-stereoselective activity; [2] the anomalous (*E*)-stereoselectivity, noted above, of the ylides generated from phosphacyclanes can be explained, apart from all other factors, by the effect of the ω-nucleophilic groups in the ylide **112**. [127]

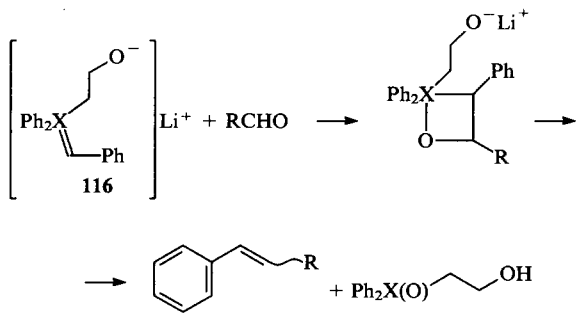
The approach thus developed to the *trans*-selective synthesis of alkenes has been extended to 5-vinyl-1,2-oxaphospholanes **113**, which were found [128] to react with benzaldehyde to form the phenyldienol **114** (R = Ph) with the isomer ratio *trans* : *cis* = 9 : 1.



The ratio of the stereoisomeric *cis*- and *trans*-dienes **114**, obtained from aliphatic aldehydes (R = alkyl), is close to the equilibrium value. It has been noted [124] that 3-hydroxy-1,5-dienes of type **114** are extremely valuable synthons in the synthesis of natural products such as leukotriene B and prostaglandins.

In a highly basic medium (potassium hydride in the presence of a crown-ether), the hydroxydiene undergoes the Cope rearrangement to the unsaturated aldehyde **115**. Thus the above method makes it possible, as it were, to introduce a further two carbon atoms at the carbonyl carbon atom of the initial aldehyde and suggests an approach to the synthesis of the hexenal substrates **115** via the 3-hydroxy-1,5-diene stage.

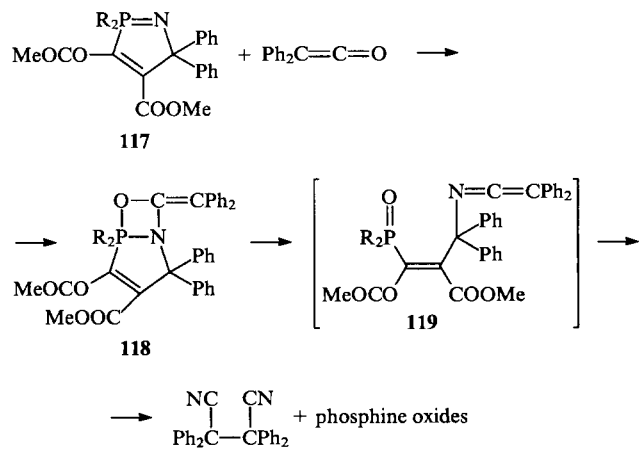
The ω-hydroxy-ylide *trans*-selectivity, described above, of the Wittig reaction proceeding via a stage involving the formation of a 1,2-phosphetane has found an interesting conformation when arsenic ylides were employed. [129] The β-oxidoylides **116** convert hexanal and piperonal into alkenes with different degrees of stereoselectivity depending on the nature of the central atom X: the ratio of the isomers of the substituted styrenes is *E* : *Z* = 70 : 30 for the phosphorus ylides **116** (X = P). The corresponding arsenic ylide **116** (X = As) ensures a highly selective synthesis of the (*E*)-alkene (100%).



X = P, As.

These results enabled Boudia et al. [129] to recommend arsenic ylides as alkene-forming reagents for the stereoselective synthesis of (*E*)-alkenes.

In conclusion of this Subsection, we shall draw attention to the unusual decomposition of the bicyclic adduct **118** obtained in a study of the 'phosphoroimine' version of the Wittig reaction between the azaphosphole **117** and diphenylketene. [130]



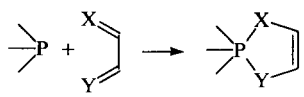
The spirocyclic 1,3,2-oxazaphosphetanes **118** (R = Me, Ph) isolated, which are stable in the crystalline state, decompose in chloroform at 48 °C in several minutes. However, contrary to expectations, the product of the intramolecular imination cannot be isolated. Instead of the latter, tetraphenylsuccinonitrile is obtained in 73% yield together with unidentified phosphorus-containing substances, tentatively assumed to be of the phosphine oxide type. It is believed that this reaction course is associated with the homolytic decomposition of compound **119**, characteristic also of other ketene imines, [130] and with the recombination of diphenylcyanomethyl radicals.

2. Thermolysis and solvolysis of 1,2-hetero- and 1,3,2-dihetero-phosphacyclanes and 1,2-hetero- and 1,3,2-dihetero-phosphacyclenes

Reactions of the above type play an important role in the strategy for the employment of cyclic reagents containing σ^5-P in organic synthesis. The relative thermodynamic lability of σ^5-1,3,2-diheterophosphacyclanes, the pronounced Lewis acidity of the σ^5-P atom and the associated high reactivity of phosphoranes in nucleophilic substitution reactions are factors which have determined the choice of the substances described here for the synthesis of a wide variety of complex organic compounds. Without claiming to cover fully all the examples of the use of thermal and solvolytic processes with participation of 1,3,2-diheterophosphacyclanes for the synthesis of phosphorus-free substances, we shall draw attention to the thoroughly investigated processes involving the fragmentation of σ^5-dioxaphospholane functional groups in compounds of hypervalent phosphorus[2,16,17] and also to the 'enediol-phosphorane' strategy for the synthesis of hydroxycarbonyl substances developed by Ramirez and coworkers.[131,132] A detailed consideration of these interesting chemical reactions is outside the scope of the problems covered by the present review, but has been thoroughly described in the literature sources mentioned above.

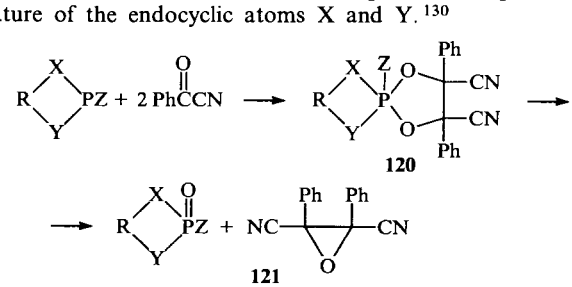
At the same time, new data have appeared during the last decade concerning the use of the thermal and solvolytic reactions of σ^5-1,3,2-diheterophosphacyclanes, mainly phospholanes and phospholenes, which are either specially synthesised for particular synthetic purposes or are formed as key intermediates in the multistage syntheses of polyfunctional organic compounds. Information about the role of pentacoordinated intermediates has been presented in a review;[16] only two examples of this kind, characterising the features of the application of the phosphorus-containing functionalising substances under discussion, are presented here.

One of the common synthetic procedures involving the use of the functionalising activity of phosphacyclanes is the thermal or solvolytic fragmentation of σ^5-1,3,2-dihetero- or σ^5-1,2-heterophoshacyclenes obtained from phosphorus(III) derivatives and α,β-unsaturated, α-dicarbonyl, diene, and similar synthons, which undergo [1 + 4]-cycloaddition with one another.



When subjected subsequently to thermal influences or entering into nucleophilic substitution reactions, as a rule with proton-containing nucleophiles, the σ^5-P adducts 'liberate' the carbon component of the ring and are converted into phosphoryl or similar reaction products.

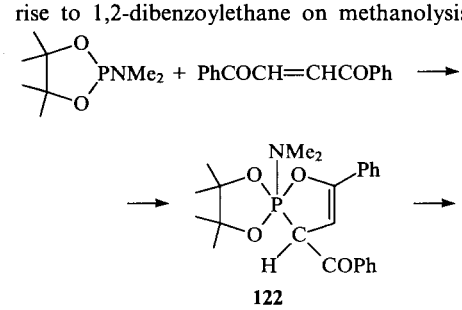
The phosphoranes **120**, which are obtained by the reaction of phosphorus(III) precursors with benzoyl cyanide, are fairly readily converted into the epoxides **121** on heating. The alkylenedioxy-analogue **120** (R = CH_2CH_2, X = Y = O) is fairly stable and decomposes on heating above 100 °C.[133,134] The diazaphospholane **120** (R = CH_2CH_2, X = Y = NMe) gives rise to an epoxide after being heated for 2 h at 80 °C and after being kept at room temperature for a long time. It has been noted that the *cis* : *trans* ratio of the isomers of compound **121** depends on the nature of the endocyclic atoms X and Y.[130]



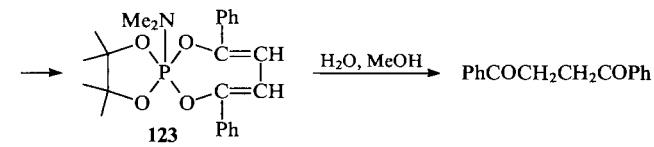
120

121

On treatment with proton nucleophiles, σ^5-1,3,2-diheterophosphacyclenes can decompose with formation of saturated organic products. Thus the spirocyclic aminophosphorane **122**, obtained from a phosphoramidite and 1,2-dibenzoylethene, gives rise to 1,2-dibenzoylethane on methanolysis.[135]



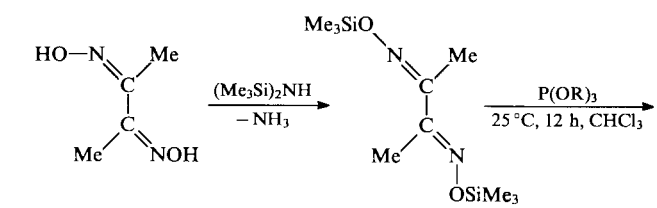
122



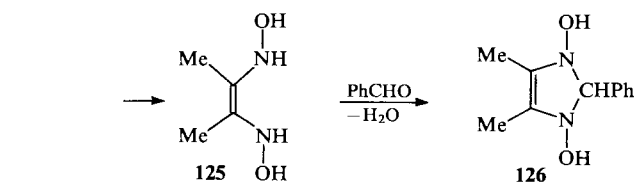
123

It has been established that under mild conditions the spirophosphorane **122** is converted into the σ^5-P-amide **123** containing a seven-membered ring. The amide actually fragments with cleavage of the phosphadiene ring. This unusual hydrogenation of an unsaturated diketone with the aid of water or methanol is based on the rarely encountered isomerisation of a five-membered ring to a seven-membered ring (**122** → **123**).

The hydrogenation on solvolysis of phosphacyclanes has been used to synthesise *cis*-2,3-bis(hydroxyamino)butene **125**.[136] Diacetyl dioxime is silylated, after which it is converted by reaction with phosphite into the phosphoranes **124** and these are hydrolysed, affording the butene **125**.



124

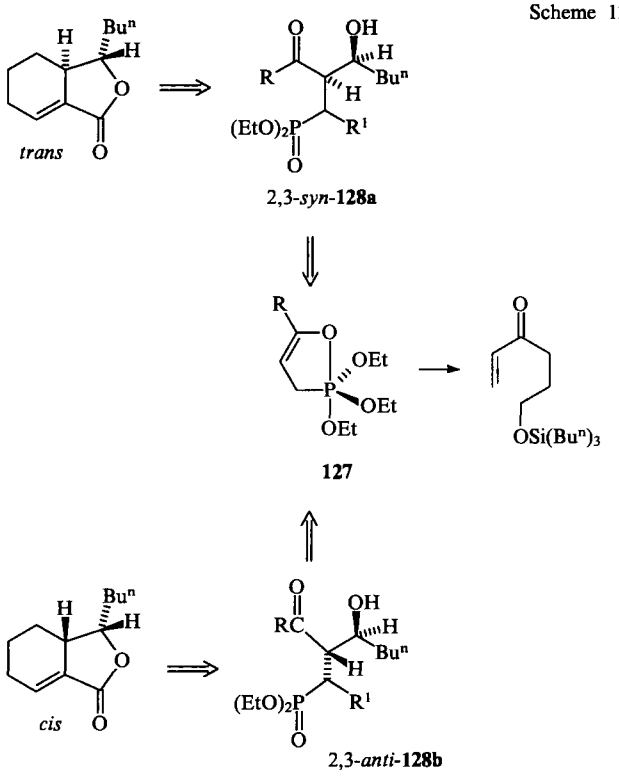


125 **126**

It has been shown that compound **125** can serve as a chelating ligand or as a precursor or nitrogen heterocycles; it readily gives rise to the imidazoline **126** on reaction with benzaldehyde.

The product of the [1 + 4]-cycloaddition of a α,β-unsaturated silylated ketone has been chosen as the key synthon in the synthesis of (+)-*trans*- and (+)-*cis*-neoknidylides.[133,134] Retrosynthetic analysis (Scheme 13) made it possible to develop a strategy for the synthesis of these natural products, including the formation of the highly substituted phosphonates **128a**, **b** and their conversion into the target products using the intramolecular HWE reaction.

Scheme 13

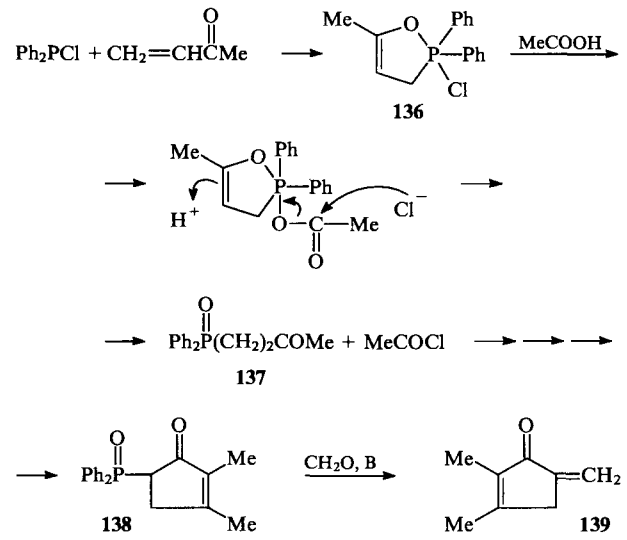


R = $(CH_2)_3OSi(Bu^n)_3$.

The above investigators used successfully the transformation of the 1,2-oxaphospholene **127** in order to synthesise biologically active natural products with the phosphonate structure.[138-140]

The ease of the closure and cleavage of the dioxaphospholane ring has been used for an unusual functionalisation in one of the stages of the total synthesis of natural benzoazepine derivatives of dihydroquinolines—chilenine and digallanezine (Scheme 14).[141] The closure of the benzoazepine ring **129**→**135** is attained by employing two organophosphorus reagents. The diketo-derivative of the γ-lactam **129** is converted into the γ-thiolactam **130** on treatment with Lavesson's reagent and the thiolactam is then converted into the 1,3,2-dioxaphospholene with the aid of trimethyl phosphite. The phosphorane **131**, identified on the basis of ^{31}P NMR spectroscopic data, undergoes a complex transformation under fairly severe conditions (refluxing of the phosphite) involving the closure to a seven-membered ring **131**→**132**, the substitution of trimethyl phosphate by a thiolate anion, the cleavage of the episulfide ring **132**→**133**, and finally the C→S propionyl shift with formation of the required polycyclic system **135**.

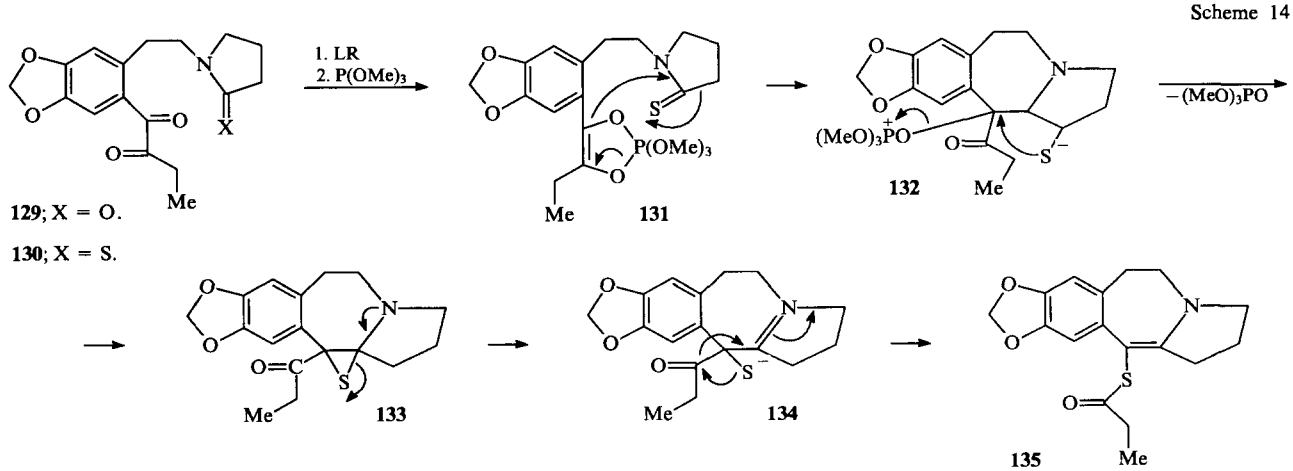
Cyclic phosphoranes—adducts formed in cycloaddition reactions—have been used also as precursors for the preparation of acyclic HWE reagents for subsequent use in the synthesis of natural products. Thus it has been shown[142] that the oxaphospholenes **136** can be conveniently employed for the synthesis of the β-ketophosphonates **137** by a reaction involving the cyclisation of compound **136** and subsequent deacylation.



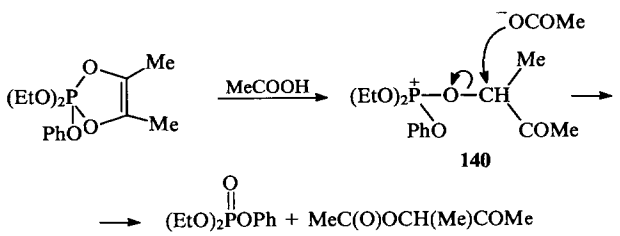
By means of a series of transformations in the aliphatic fragment, the phosphorylated ketone **137** has been converted into the phosphorylated cyclic enone **138**—the precursor of methylenomycin B **139**—a substance belonging to the family of the cyclopentanoid antibiotics. It is emphasised[138] that the 'phosphonate' strategy for the synthesis of compound **139** is convenient in view of the possibility of monitoring with the aid of ^{31}P NMR spectroscopy all the phosphorus-containing intermediates formed during the process.

The addition of α,β-unsaturated carbonyl and α-dicarbonyl compounds to phosphorus(III) substrates with the intermediate formation of 1,2-oxa- and 1,3,2-dioxa-phospholenes followed by the solvolytic cleavage of the five-membered phosphorus heterocycle constitutes in essence a synthetic route to products of the addition of proton nucleophiles to the unsaturated fragments of the initial 1,4-heterodiene. The functionalisation with the aid of acetic acid of the latent diacetyl to give α-acetoxyethyl methyl ketone (Scheme 15), which is similar to the 'hydrogenation' of unsaturated ketones or the dioxime examined above, has been described.[143]

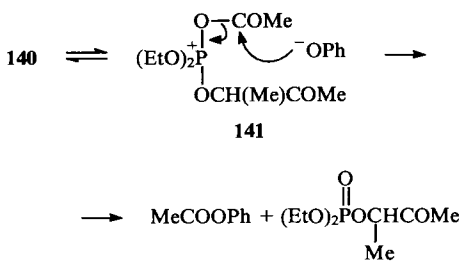
Scheme 14



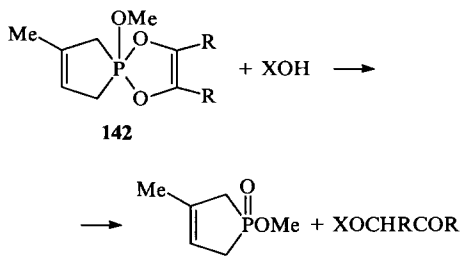
Scheme 15



The reaction is complicated by the dealkylation of the quasi-phosphonium salt **140** not only as a result of nucleophilic attack on the methylidyne carbon but also a result of the abstraction of the ethyl group. Furthermore, the ligand exchange **140**→**141** and deacylation by the phenoxide anion constitute an alternative route, which complicates the possible preparative use of the reaction described.



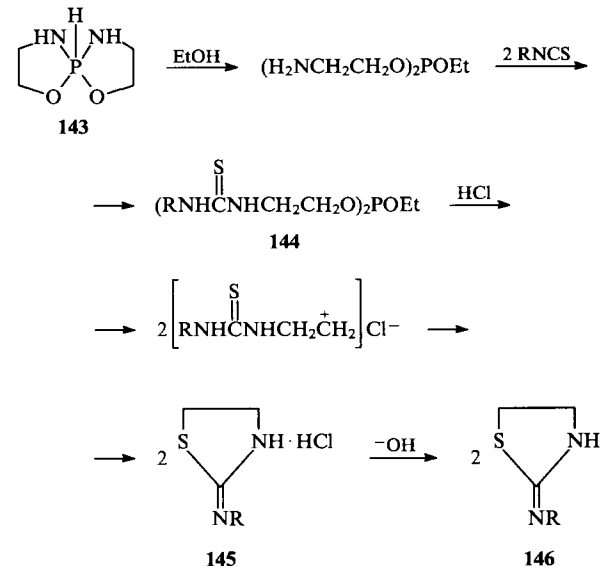
The enediol-phosphorane **142** (R = Me or Ph) is smoothly converted into the ketoalcohol (X = H) or α-acylated ether (X = Me) on decomposition of the dioxaphospholene ring as a result of hydrolysis or methanolysis.[144]



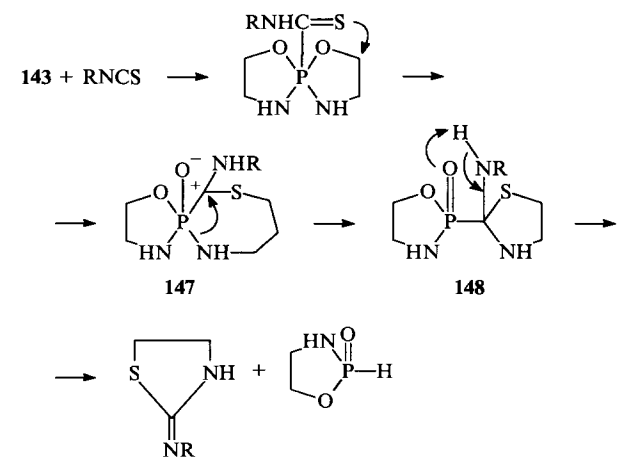
R = Me, Ph; X = H, Me.

As already stated, solvolysis accompanied by the dissociation of the phosphorus–heteroatom bond in saturated phosphacyclanes usually leads to phosphorus-containing acyclic substances. This renders even more unusual the reaction of spirocyclic oxazaphospholanes **143**, occurring when alkyl or aryl isothiocyanates are acted upon by σ^4-PH acids.[145,146] In alcohols, the process proceeds with dissociation of endocyclic phosphoramide bonds. The functionalisation of β-aminoethyl groups and acidolysis of the adduct **144** lead to phosphorus-free salts **145**, while 2-(phenylimino)thiazolidines **146** are formed when the system is rendered alkaline. The reaction proceeds under very mild conditions (25–30 °C) and involves the unusual dissociation of the C–O (and not P–O) bond in the intermediate phosphite **144**.[141]

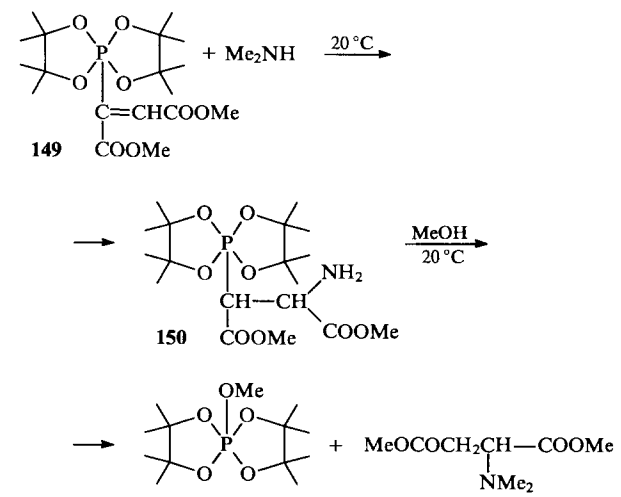
The same process, but this time requiring a higher temperature (80–100 °C), can be carried out also in aprotic solvents. The authors suggest[146] that in this case the process involves the addition of P–H to the isothiocyanate fragment and the rearrangement of the adduct with expansion of the ring to compound **147** caused by intramolecular *S*-alkylation. The endocyclic dissociation of the P–N bond and proton transfer in the intermediate **148** entail fragmentation to thiazolidines and unidentified cyclic hydrophosphoryl products. Two and one



alkylene-1-oxy-2-amino-fragments are involved in this reaction when the latter is carried out in alcohols and in an aprotic medium respectively.

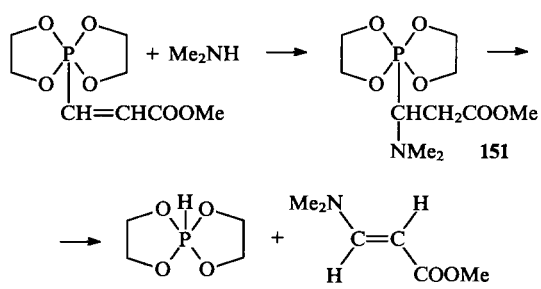


Only a few instances of the solvolysis of spirocyclic phosphoranes with retention of the cyclic skeleton of the phosphorus-containing reagent are known. Thus amination of the unsaturated spirophosphorane **149** and the subsequent methanolysis of the adduct **150** proceed with cleavage of the strong exocyclic P–C bond to give an aminosuccinic acid ester.[147]



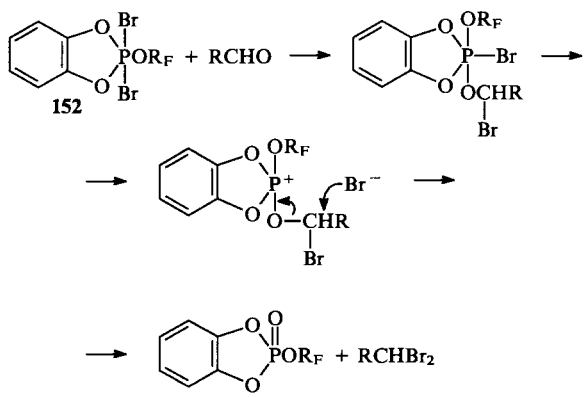
This rare example of the stability of the more labile ester linkages may be due to a tendency to retain the spirocyclic system, which, together with the tendency of oxyphosphoranes to be converted into a product with a phosphoryl group, can also become the driving force of chemical reactions with participation of phosphorus compounds.[15,16]

The exocyclic decomposition of substances of this kind is known also for thermal processes. Distillation of the adducts formed in the amination of compound **151** is accompanied by the formation of β-aminoacrylate. The synthetic result of such a process is a kind of substituton of the phosphaspirocyclane group at the vinyl β-carbon atom in the initial σ^4-P-acrylate.[148]

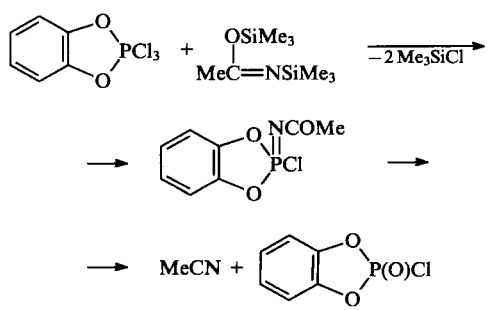


It is of interest to note that the reactions described in this subsection, involving the participation of unsaturated σ^5-phosphacyclane fragments, namely hydrogenation, the addition of proton nucleophiles, and substitution at unsaturated centres, resemble the unusual chemical behaviour of coordinated alkenes in transition metal π-complexes.[149]

We shall quote several new examples of the synthetic use of trihalo(phenylenedioxy)phosphoranes. The halogenating capacity of such phosphorus-containing reagents is well known.[106,150] However, it is characterised by a low selectivity in reactions with polyfunctional substrates. A new reaction of the phosphoranes **152** (R = $CH_2CF_2CHF_2$) with aliphatic and aromatic aldehydes, which proceeds via the insertion of the carbonyl group in the σ^5-P–Br bond and is completed by the *gem*-deoxyhalogenation of the initial substrate, has been described.[151]

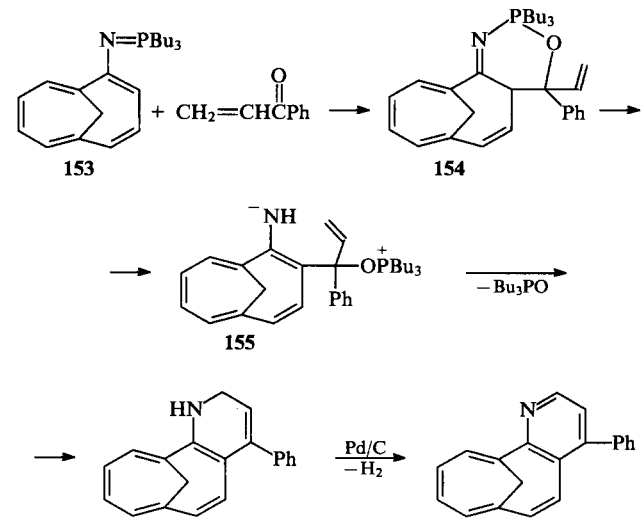


Several advantages of the use of compound **152** over phosphorus pentachloride or phenylenedioxyphosphorus trichloride have been noted.[151]



The oxidation-reduction reaction of a halophosphorane with disilylacetamide converts the latter into a nitrile.[152]

A rare case of the use of a latent ketone, bound in the six-membered phosphorus heterocycle, has been described.[153] The [4+2]-cycloaddition of the phosphimine **153** and phenyl vinyl ketone via a stage involving the formation of the adduct **154** and the betaine **155** in the presence of the Pd/C catalytic system leads to the formation of 4-phenyl-7,12-methanocyclodeca[*b*]pyridine.



The unusual regiochemistry of the phosphimine version of the Wittig reaction (cf. compound **118**) is striking in this example: the carbonyl carbon atom is oriented towards and adds to the ring C(2) atom and not to the imine nitrogen atom in compound **153**. The subsequent stepwise decomposition of the adduct **154** is responsible for the unusual design of the target tricyclopyridine.

3. The 'dioxaphospholane' methodology in organic synthesis

The type of reactions of σ^5-diheterophosphacyclanes described in this subsection is associated with the thermal decomposition of these compounds, which are specially synthesised for the functionalisation of organic substrates. The latter are, as it were, 'introduced' into the composition of the cyclic phosphorus-containing reagent, so that they can be made to undergo particular chemical transformations after phosphorylation. Evans called this approach the 'dioxaphospholane' methodology. It is characterised, as a rule, by high chemo-, regio-, and stereospecificities.

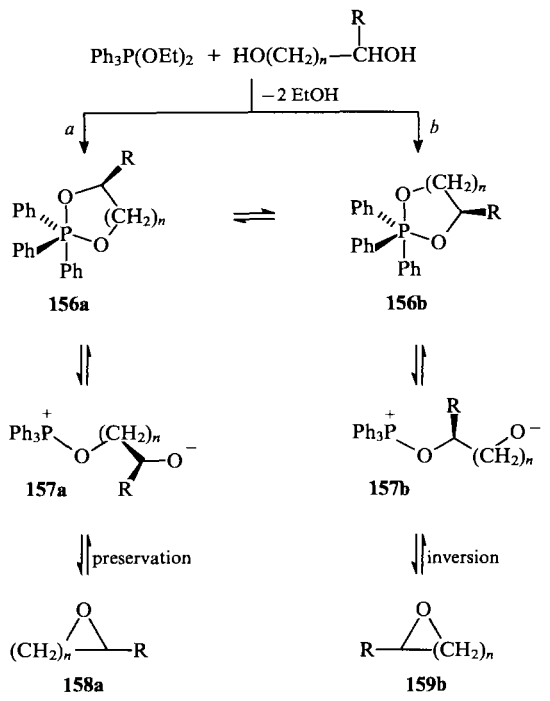
The thermal reactions of phosphoranes have been widely investigated, such studies including those undertaken in order to employ them in fine organic synthesis. Data on the thermal fragmentation of σ^5-phosphacyclanes, published mainly in the 1960s–1970s, are presented in two reviews.[16,154] During the last ten years, the dioxaphospholane methodology has expanded greatly, mainly in Evans' studies, and has served as an effective instrument for the functionalisation of organic compounds, mainly bifunctional substances with mobile hydrogen atoms.

Acyclic phosphoranes—pentaethoxyphosphorane,[155] bis-(neopentyloxy)triphenylphosphorane,[156] diethoxydiphenyl-polystyrylphosphorane,[157] and the especially widely used diethoxytriphenylphosphorane[158,159]—are extremely effective dehydrating agents which convert α,ω-diols and amino- and mercaptoalcohols into the corresponding oxacyclanes, azacyclanes, or thiacyclanes.

Optically active diols are cyclodehydrated to the corresponding cyclic ethers under relatively mild conditions—monosubstituted diols in 48 h at 40 °C and the sterically more hindered tri- and tetra-substituted diols over the same period but at 80–100 °C.[159,160] The phosphoranes obtained from *cis*-cyclohexane-diols are cyclodehydrated only at

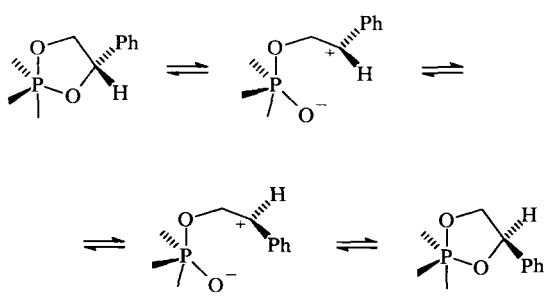
280–300 °C.[159,161] The synthetic result of these reactions has been explained from the standpoint of the transformation of the intermediates having the structure of σ^5-1,3,2-heterophosphacyclanes and of the betaines formed from them (Scheme 16).

Scheme 16



The regioselective distribution of the stereoisomeric ethers formed as a result of the cyclodehydration is associated with the decomposition in the sequence: cyclophosphorane **156**, betaine **157**, and ether **158** and also with the direction of the intramolecular nucleophilic attack by the oxyanion on the α-carbon atom. The preservation of the stereochemistry of the initial diol in the final cyclic product reflects the preferred direction of attack on the unsubstituted carbon atom (path *a*); the reaction via path *b* is more difficult the more bulky the substituents in the initial diol. Under these conditions, the configuration is inverted — the stereochemistry of the initial diol is altered. Attack via path *a* on the unsubstituted carbon atom is effected more readily and this is the reason for the higher content of the stereoisomer **158a** in the products of the cyclodehydration of diols.

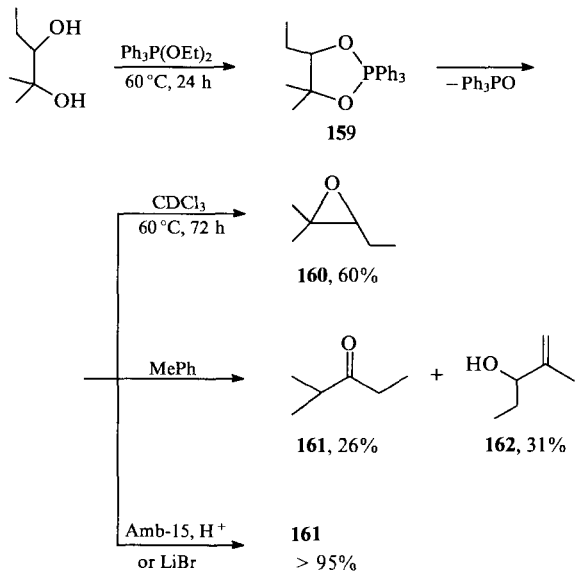
This postulate is in general valid: the regioselectivity of the cyclisation reaction increases with increasing bulk of the substituent R in the diol.[158] However, racemic styrene oxide was obtained in the reaction of (*S*)-(+)-phenylethane-1,2-diol. One of the possible causes of this is the irregular permutational isomerisation of the intermediate phosphacyclanes, which proceeds with dissociation of the C–O bond and not the P–O bond.



This type of isomerisation is due to the presence of favourable factors: the stabilising $(p-d)_\pi$ interaction of the equatorial phosphoryl oxygen atom with the phosphorus atom and of the carbonium ion centre with the phenyl substituent. Such racemisation of phosphoranes is a consequence also of the racemisation of the corresponding betaines and cyclic ethers. This example is quoted in order to demonstrate the stereochemical factors accompanying the synthetic use of the dioxaphospholane methodology.

Another extremely important condition governing the usefulness of this methodology in the cyclodehydration reaction is the size of the future oxacyclane. 1,2-Diols give rise in this reaction to alkene oxides in 85%–99% yields, 1,4- and 1,5-diols afford the corresponding five- and six-membered rings in 70%–80% yields, while butane-1,3-diol produces an oxetane with only 3% conversion, i.e. the diol mainly undergoes monoethylation. Similarly, hexane-1,6-diol is converted into oxepane (6%) and ethyl hydroxyhexyl ether (50%).[160]

In certain cases,[160] the conditions governing the decomposition of the key σ^5-1,3,2-dioxaphosphacyclanes are decisive in the reactions of diols, particularly tri- and tetra-substituted diols.

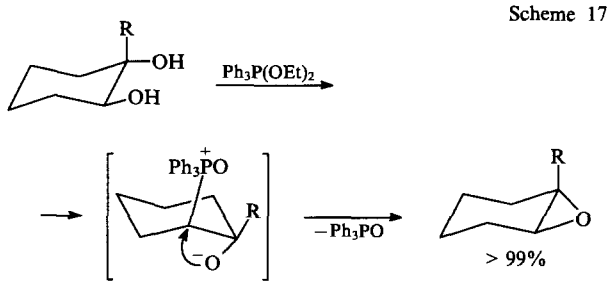


The dioxaphospholane **159**, obtained from 2-methylpentane-2,3-diol, reacts with LiBr (60 °C, 3 days, C_6D_6) to form only 2-methylpentan-3-one **161**; the same reaction in $CDCl_3$ gives 2,3-epoxy-2-methylpentane **160** (60%) as the only product; in toluene (100 °C), the ketone **161** is formed together with 3-hydroxy-2-methylpent-1-ene **162** (31%). The granulated polystyrenesulfonic acid (Amb-15) promotes the formation of the ketone **161**, possibly via the isomerisation of the epoxide **160**. The allyl alcohol **162** is obtained as a result of the intramolecular abstraction of a proton, which leads to the corresponding betaine.

The most unexpected result is the formation of a ketone (in this and other cases), which is associated with the migration of a hydride ion in a type **159** phosphorane or the corresponding betaine.

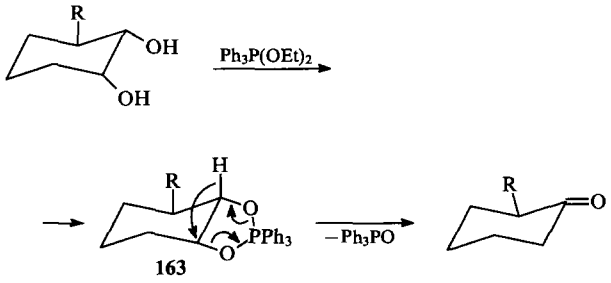
This phenomenon has been studied in detail in relation to cyclohexane- and methylcyclohexane-1,2-diols (Scheme 17).[159,160] The *trans*-diols are converted quantitatively into the corresponding epoxides via the general intramolecular nucleophilic substitution mechanism (the 3-*exo*-*tet*-mechanism[160]).

Scheme 17



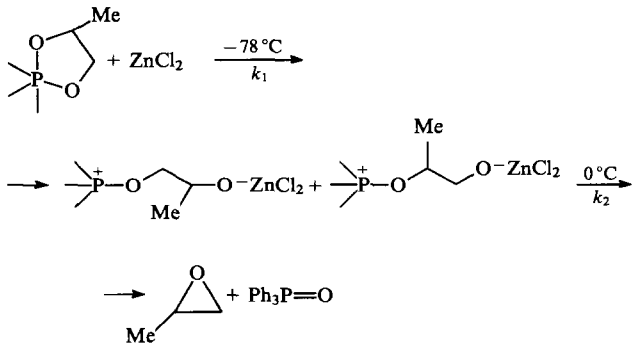
R = H, Me.

The reaction of *cis*-hexane-1,2-diol (boiling dichloromethane, 48 h) with an acyclic phosphorane affords the readily vacuum-distilled 1,3,2-dioxaphospholane **163**.



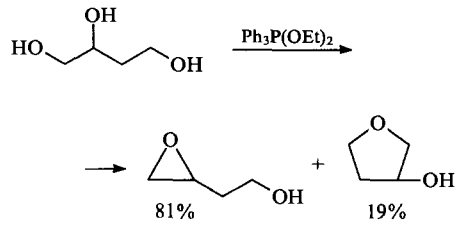
The vacuum thermolysis of compound **163** (220 °C, 15–23 Torr) gives rise to a quantitative yield of a cyclohexanone. The synchronous 1,2-hydride shift in the phosphorane **163** or in the corresponding betaine has been suggested [159,160] to account for the formation of the cyclic ketone.

An increase in the number of substituents in the initial diol promotes the stabilisation of the resulting cyclophosphoranes and a higher temperature is required for their decomposition (> 200 °C), the yield of the target oxacyclanes diminishing. In order to suppress this unfavourable factor, it has been suggested that Lewis acids be employed. [162,163] Thus the cyclodehydration of 1,2-diols in the presence of lithium bromide takes place at room temperature without side reactions, affording oxiranes in a high yield. The stronger Lewis acid $ZnCl_2$ induces the decomposition of the phosphorane to the betaine at −78 °C and cyclisation to the epoxide at 0 °C. This acceleration is caused by the facilitation of the dissociation of the ether bond in the phospholane as a result of coordination of the endocyclic oxygen atom to the Lewis acid; the stabilisation of the oxide (alkoxide?) anion by the acid also favours the overall course of the process.



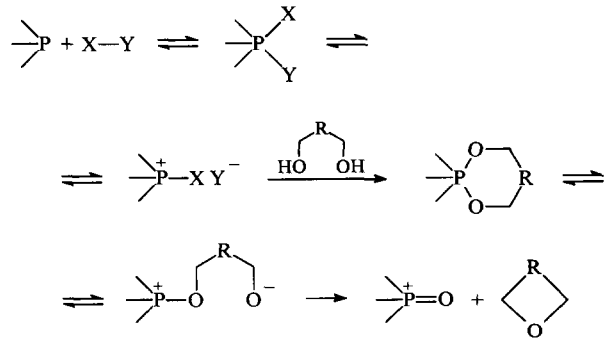
A kinetic study [162] of this process established the irreversibility of the formation of the betaine in the reaction promoted by $ZnCl_2$ ($k_2 \gg k_1$); apart from anything else, [162,163] this determines the stereospecificity of the cyclodehydration in the zinc chloride-induced reaction. The lithium ion, which exhibits a much lower tendency towards coordination, permits the existence of equilibrium between the betaines and the stereochemical result of the reaction is regulated by the relative rates of the intramolecular S_N2 attack by the oxyanion on the α-carbon atom.

The cyclodehydration of triols by means of the 'dioxaphospholane' methodology is a much more complex process because the phosphorylation is then coupled with the chemoselectivity of the hydroxyl involvement of the substrates. [164] In the general case, the formation of five-membered dioxaphosphacyclanes is preferred to the formation of rings of any other size. Thus butane-1,2,4-triol reacts with an equivalent of $Ph_3P(OEt)_2$ to form 3,4-epoxy-1-butanol (81%) and tetrahydro-3-furanol (19%).



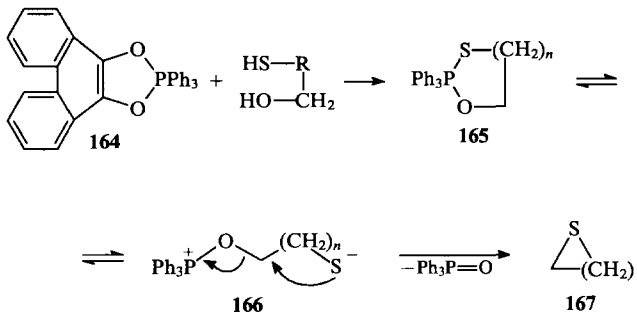
We may note that, as in the case where cyclodehydration is carried out by means of 'combined' phosphorus-containing reagents (PPh_3 + CCl_4; Mitsunobu's reagent), when this methodology is used there is a decrease in the tendency towards the formation of oxacyclanes on passing from three- and five-membered rings to six-membered rings and further to four- and seven-membered rings, which reflects the change in ring strain and cyclisation entropy on intramolecular nucleophilic substitution. [161]

The course of the cyclodehydration of bifunctional organic substrates discussed here may be induced, as already mentioned, not only by oxyphosphoranes but also by two-component condensed systems including phosphorus(III) compounds and organic molecules capable of biphilic interaction with the phosphorus(III) atom — dialkyl peroxides, carbon tetrachloride, and azodicarboxylate. [161,165,166] In all cases, the key intermediates in the cyclodehydration process are cyclophosphoranes obtained by the esterification of the acyclic phosphoranes (phosphonium salts) arising in the two-component system. In this case, the overall mechanism is described by the following sequence of reactions:

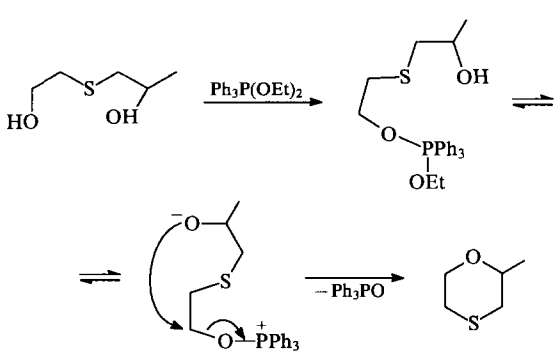


X = Y = OEt; X = Cl, Y = CCl_3; X–Y = ROCON=NCOOR.

Among the effective cyclodehydrating agents, 2,2,2-triphenyl-4,5-(2′,2″-biphenylene)-1,3,2-dioxaphospholane (**164**), which is more stable and convenient to handle than acyclic phosphoranes, merits special attention. The adduct **164** obtained from triphenylphosphine and phenanthrenequinone is stable in inert solvents and is especially effective for the cyclodehydration of mercaptoalcohols to cyclic sulfides.

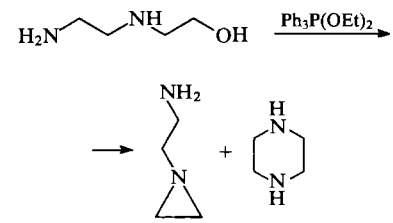


The reaction proceeds in accordance with the general mechanism: the transesterification to σ^5-oxathiaphosphacyclane **165** is followed by intramolecular substitution by the thiolate anion in the betaine **166**, which leads to the thiacyclanes **167** with three-membered (n = 1), five-membered (n = 3), and six-membered (n = 4) rings (yield > 80%). Special mention must be made of the high yield of thietanes (n = 3, 80%) compared with the yield of oxetane (3%), which enabled the authors[166] to emphasise the universality of the dioxaphosphorane methodology involving the use of compound **164**. The compound is also convenient because of the absence of reactions involving the alkylation of diols (mercapto- and aminoalcohols) of the kind occurring in the reactions with $Ph_3P(OEt)_2$. We may also mention the successful employment of this process for the synthesis of 1,4-oxathianes.[167]



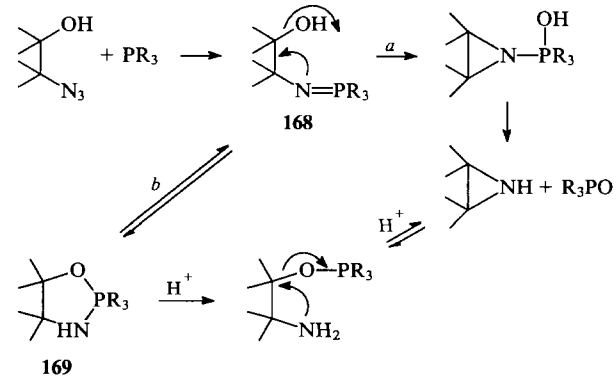
The effectiveness of the 'dioxaphospholane' methodology in cyclodehydration has also been demonstrated by the synthesis from 2-amino-2-benzylethanol and *trans*-2-aminocyclohexanol, with the aid of the phosphacyclene **164**, of the corresponding aziridines in 60% and 71% yields respectively. In this case too, the phosphacyclene was found to have an advantage over $Ph_3P(OEt)_2$, which exhibited only an *N*-ethylating capacity when an attempt was made to cyclodehydrate *trans*-2-aminocyclohexanol — *trans*-2-(*N*-ethylamino)cyclohexanol was obtained instead of the aziridine.[168]

Nevertheless, the use of this methodology in general makes it possible to convert *N*-alkyl- and *N*-aryl-β-aminoalcohols into the corresponding *N*-organylaziridines under relatively mild conditions (60 °C, 24–48 h).[168] This reaction has been noted for its high stereoselectivity — the retention of the configuration of the 'amino'-carbon atom. For example, the enantiomerically homogeneous (*S*)-(+)-2-amino-1-propanol and (*S*)-(−)-2-amino-3-phenyl-1-ethanol are cyclodehydrated with the aid of $Ph_3P(OEt)_2$ to the enantiomerically pure (*S*)-(+)-2-methylaziridine and (*S*)-(−)-2-benzylaziridine respectively (yield 85%).[168] At the same time, the chemoselectivity of the reaction is low: 2-[(2-aminoethyl)amino] ethanol affords a 1 : 1 mixture of aziridine and piperazine as a result of cyclodehydration.



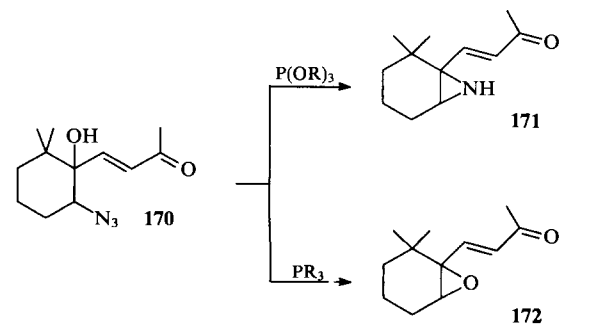
An unexpected feature has been noted for this reaction[168] — the identity of the free energy of cyclodehydration in the formation of three-membered and six-membered nitrogen heterocycles.

The concept of the appearance–decomposition of σ^5-1,3,2-oxazaphospholanes, which is close to the 'dioxaphospholane' methodology, proved fruitful also in explaining the routes leading to the conversion of azidoalcohols into aziridines on treatment with phosphorus(III) derivatives — triethyl and trimethyl phosphites or triphenylphosphine.[169,170] The process takes place in the presence of water or methanol and leads to aziridines under relatively mild conditions.

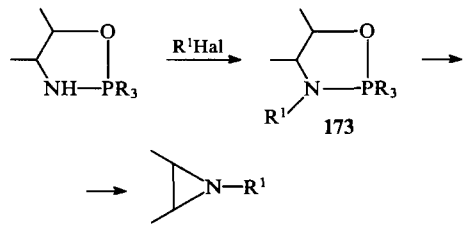


According to NMR spectroscopic data, path *b* is preferred because the decomposition of the product of the Staudinger reaction (the imine **168**), bypassing the phosphorane **169**, presupposes the unlikely intramolecular substitution of the hydroxy-group in the phosphimine **168**.[170] When the substituents are chosen appropriately in the initial azidoethanol, it is possible to isolate and identify both the phosphimines **168** and the oxazaphospholanes **169**. Furthermore, the interconversion **168**⇄**169** can be readily detected from ^{31}P NMR spectra.

We may draw attention to a very interesting fact which has not received a sufficiently convincing explanation: the synthesis of the bicyclic aziridine **171** from the corresponding azidohydrin is readily achieved on treatment with trimethyl or triethyl phosphite, whereas tertiary phosphines afford a complex mixture of substances, from which the epoxide **172** has been isolated.[171]



It was shown subsequently[172] that the range of aziridines obtained on fragmentation of σ^5-oxazaphospholanes can be extended by alkylating the endocyclic nitrogen atom with alkyl halides in the presence of strong bases (BuLi, NaH, or KH).

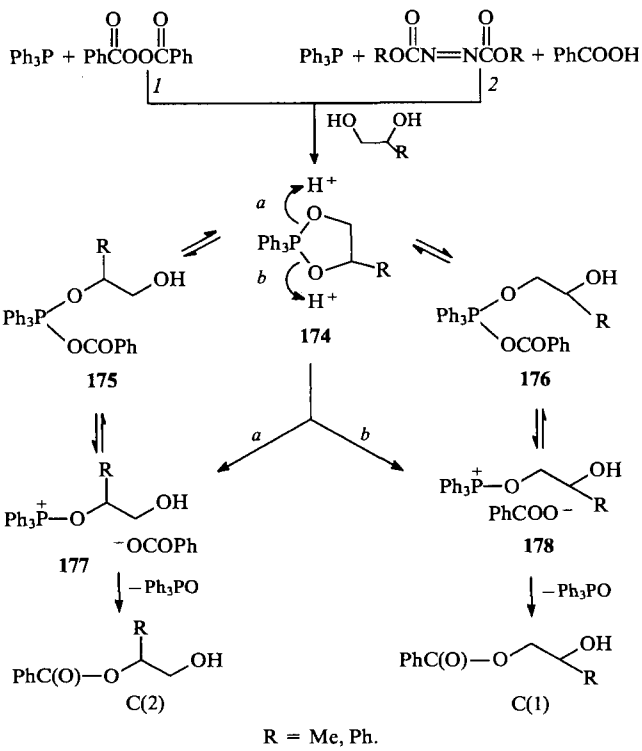


The conversion of compound **173** into *N*-substituted aziridines is facilitated by the addition of acid catalysts.

The key stage in cyclodehydration processes when the methodology under discussion is employed is undoubtedly the intramolecular S_N2 substitution at the α-carbon atom in the quasi-phosphonium intermediate by a thio-, amino-, or oxy-anion. It determines the synthetic (stereochemical result). The synthetic diversity of the reactions carried out using the 'dioxaphospholane' methodology has been achieved by involving 'external' nucleophiles in the reaction. In this case, the substitution of the nucleophilic phosphoryl fragment constitutes in essence the second stage (dealkylation) of the Arbuzov reaction, which, like all S_N2 reactions, takes place with inversion of configuration of the carbon atom. This determines the stereospecificity of the reactions under discussion, but in a number of instances an unusual chemoselectivity of the functionalisation of the organic substrates is observed.

The monobenzoylation of asymmetric 1,2-diols (propane-1,2-diol and 1-phenylethane-1,2-diol) in which two dehydrating systems are employed — triphenylphosphine–benzoyl peroxide (1 : 1) and triphenylphosphine–dialkyl azodicarboxylate (Mitsunobu's reagent) — leads to kinetically and thermodynamically less stable isomers: C(2)-benzoates [C(2) : C(1) = 8 : 1 for methyl-substituted diols and 96 : 1 for phenyl-substituted diols] (Scheme 18).[173–175]

Scheme 18

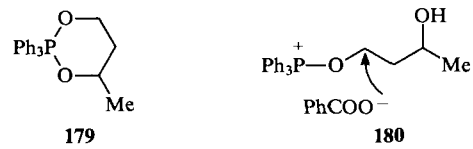


R = Me, Ph.

The chemoselectivity of the benzoylation of diols can be best explained on the hypothesis of the formation and acid-catalysed decomposition of the same key σ^5-1,3,2-dioxaphospholane intermediate **174** [obtained when acyclic intermediates (not shown in Scheme 18) are esterified by diols] in the oxidative addition of benzoyl peroxide (reaction *1*) or the Mitsunobu reaction (reaction *2*) (Scheme 18).

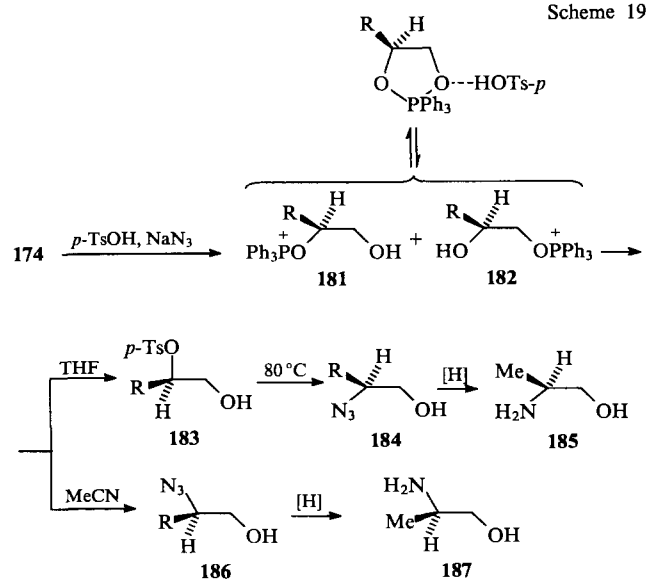
If it is postulated that the rate-determining stage is nucleophilic substitution by the benzoate ion, a reaction typical of the second stage of the Arbuzov reaction, then preference should be given to path *b* via which the less substituted C(1) centre in compound **178** is attacked. However, the overwhelming advantage of pathway *a* [attack by the benzoate on the C(2) atom] led the authors to the conclusion[173] that the rate-determining reaction path involves the formation of a hydrogen bond between compound **174** and HOC(O)Ph, which takes place more readily for the oxygen atom attached to the unsubstituted C(1) atom. The process therefore takes place via path *a* with S_N2 substitution at the C(2) atom in the ion **177**. The inclusion of the acyloxyphosphoranes **175** and **176** in the scheme has been confirmed experimentally[173] and reflects the sequence of the diol phosphorylation steps with the preferential P-attack on the primary hydroxyl in compound **176**.

A detailed study of the mechanism of the Mitsunobu reaction[174] (reaction *2* in Scheme 18) also made it possible to determine the key role of the cyclic intermediate **174**. An indirect confirmation has been obtained in the benzoylation of butane-1,3-diol. In this case, the attack by the benzoyl group is to a large extent directed to the primary and not the secondary carbon atom, which may indicate that the cyclic six-membered intermediate **179** is not involved in the process. The latter takes place via the acyclic quasi-phosphonium salt **180** in accordance with the mechanism of the Arbuzov reaction.[173]



The hypothesis of the selective decomposition of σ^5-1,3,2-dioxaphospholanes by nucleophiles has become the basis of the stereospecific functionalisation, developed by Evans and coworkers,[176–178] of diols, in which the strategy of the regioselective dioxaphospholane methodology is employed. the reaction of σ^5-1,3,2-dioxaphospholane **174** (R = Me)

Scheme 19



with toluene-*p*-sulfonic acid in the presence of sodium azide affords initially the regioisomeric oxyphosphonium ions **181** and **182** in almost equal amounts, the ions being in dynamic equilibrium with the initial phosphorane, detected by ^{31}P NMR spectroscopy at low temperatures (−78 °C) (Scheme 19).[172]

At the usual temperature (25 °C), the sulfonate anion rapidly substitutes the phosphine oxide, affording (*R*)-2-(4-methylbenzoylsulfonyloxy)1-propanol **183** in >95% yield with a high degree of stereospecificity at the C(2) centre. The regioisomer with the tosylate group attached to the C(1) atom was not detected. Heating of the reaction mixture containing NaN_3 (80 °C, 8 h, THF) converts the tosylate **183** into (*S*)-2-azidopropanol **184** with an almost complete inversion of the configuration.

The same reaction in acetonitrile does not produce the sulfonate ester. The azide (*R*)-**186** was obtained instead in 93% yield. In highly polar media, the strongly nucleophilic N_3^- ion wins the competition with the tosylate ion; the substitution **181**→**186** takes place with complete inversion of the configuration at the C(2) centre. The configurational identity of the latter has been confirmed by the hydrogenation of the azides **184** and **186** to the known aminoalcohols (*S*)-**185** and (*R*)-**187** respectively (Scheme 19).

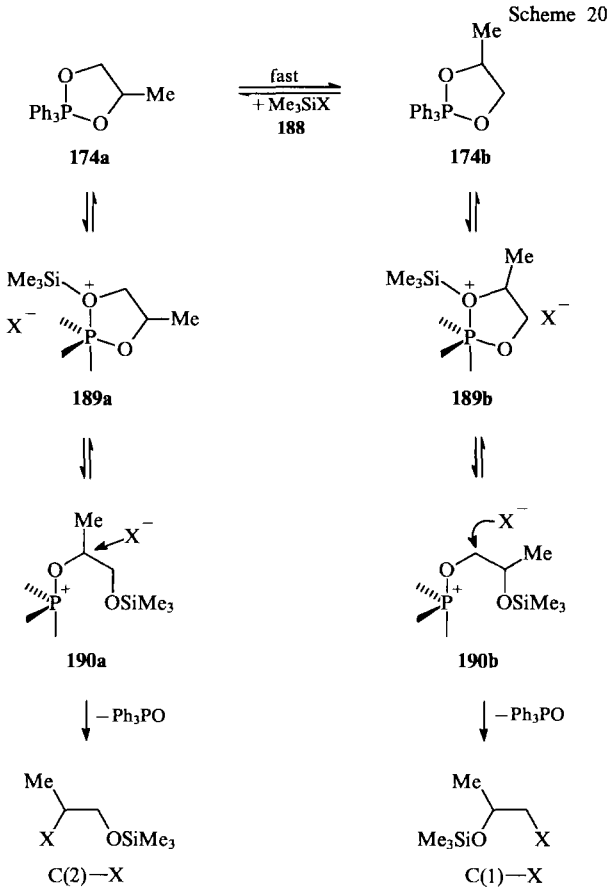
In this case, the experimental results can also be explained satisfactorily on the hypothesis of the initial coordination of compound **174** to toluene-*p*-sulfonic acid with participation of the sterically more accessible oxygen atom at the C(1) centre. This more apicophilic 'complex' oxygen atom is preferentially abstracted from the σ^5-P atom. The oxyphosphonium ion **181** activates the C(2) centre for nucleophilic attack. Thus the stereochemical outcome of reactions involving nucleophilic substitution in chiral 1,2-diols, 'protected' in the form of σ^5-1,3,2-dioxaphospholanes, consists in the inversion of the configuration at the C(2) centre in polar media and double inversion (overall retention of configuration) at this centre in nonpolar media.[172]

The idea of regulated protonation in the reactions of latent diols has been developed in relation to silicon-containing nucleophiles.[177,178] The interaction of the cyclane **174**, obtained from propane-1,2-diol, with the silylated nucleophiles **188** under very mild conditions leads to the regioisomeric siloxanes C(2)−X and C(1)−X with the former predominating, up to the almost complete regioselectivity for X = SPh or N_3 (Scheme 20).

By analogy with the selective protonation mechanism in reactions with benzoic or toluene-*p*-sulfonic acids, the nucleophilic selection in favour of C(2) is explained by the difficulty of the oxygenophilic attack by silicon on the apical oxygen atom in the rotational isomer **174b**, since in the structure of compound **189b** the silicon atom is subjected to a strong 'sandwich' type steric influence by the equatorial phenyl group and the close 2-methyl group. The preferential silylation of the oxygen atom at the C(1) centre in the structure **189a** is responsible for the ease of the nucleophilic attack on the C(2) centre in the quasi-phosphonium salt **190a**. The possibility of detecting the ions **190** by ^{31}P NMR spectroscopy makes it possible to determine the ratio of the regioisomeric ionic intermediates, which corresponds to the regioisomeric composition of the products obtained [C(2)−X: C(1)−X], the first regioisomer being favoured in all cases.

We believe that the experimental data presented in this review constitute convincing evidence for the importance and likely usefulness of heterophosphacyclanes in fine organic synthesis. The availability of phosphorus compounds of the type described, the wide variety of the valence and coordination states, the ease of the transition from one coordination state to another and hence the diversity of the structural and electronic types of organophosphorus compounds, the relative lability which at the same time permits the identification of different metastable states, the strength of the phosphorus−heteroatom bond, and the, as a rule, satisfactory solubility in media of different polarity are factors, which, together with other features, frequently lead investigators to make a choice in favour of phosphorus-containing reagents

Scheme 20



in the development of a strategy for the synthesis of polyfunctional organic substances. A characteristic of diheterophosphacyclanes, such as the stabilisation of cyclic hypervalent structures, is frequently also an attractive feature of these reagents: they permit well-founded inferences concerning the reaction paths of the substances.

An important positive property of cyclic organophosphorus reagents is the possibility of an extensive variation of the structures of both the cyclic and acyclic fragments of the molecule; this makes it possible, for example, to protect bifunctional and polyfunctional organic substances by organophosphorus functional groups (especially those containing a σ^5-phosphorus atom).

Finally one should include among the fairly important advantages of the use of cyclic organophosphorus reagents in multistage chemical processes the possibility of monitoring them by spectroscopic methods, especially ^{31}P NMR spectroscopy, because the characteristic regions in which the NMR signals of the phosphorus atom are manifested are sharply differentiated as a function of its valence and coordination states and its immediate environment.

Thus it is easy to foresee the growth of interest in these chemical compounds, which provide investigators concerned with synthesis a unique instrument for the functionalisation of organic substrates.

References

1. V I Galkin, R D Sayakhov, V A Mironov, G A Kutyrev, R A Cherkasov *Zh. Obshch. Khim.* **63** 2476 (1993)
2. J I G Cadogan (Ed.) *Organophosphorus Reagents in Organic Synthesis* (New York: Academic Press, 1979)
3. R A Cherkasov, G A Kutyrev, A N Pudovik *Tetrahedron* **41** 2567 (1985)
4. M P Cava, M I Levinson *Tetrahedron* **41** 5061 (1985)
5. O Mitsunobu *Synthesis* 1 (1981)
6. H Akita, H Yamada, H Matsukura, T Nakata, T Oishi *Tetrahedron Lett.* **31** 1781 (1990)

7. T Minami, J Motoyoshiyo *Synthesis* 333 (1992)
8. H B Kagan, in *Comprehensive Organometallic Chemistry* Vol. 8 (Oxford: Pergamon Press, 1982) p. 463
9. H Brunner, W Pieronczyk, B Schoenhammer, K Streng, I Bernal, J Korp *Chem. Ber.* **114** 1137 (1981)
10. H Germa, J Navech *Phosphorus Sulfur* **26** 327 (1986)
11. F H Vestheimer *Chem. Rev.* **81** 313 (1981)
12. G Baccolini, P E Todesco *J. Chem. Soc., Perkin Trans. 1* 535 (1983)
13. J Cabral, P Laszlo, M-T Montaufier, S L Randriamahefa *Tetrahedron Lett.* **31** 1705 (1990)
14. M A Pudovik, V V Ovchinnikov, R A Cherkasov, A N Pudovik *Usp. Khim.* **52** 640 (1983) [*Russ. Chem. Rev.* **52** 361 (1983)]
15. R A Cherkasov, V V Ovchinnikov, M A Pudovik, A N Pudovik *Usp. Khim.* **51** 1305 (1982) [*Russ. Chem. Rev.* **51** 746 (1982)]
16. N A Polezhaeva, R A Cherkasov *Usp. Khim.* **54** 1899 (1985) [*Russ. Chem. Rev.* **54** 1126 (1985)]
17. R A Cherkasov, N A Polezhaeva *Usp. Khim.* **56** 287 (1987) [*Russ. Chem. Rev.* **56** 163 (1987)]
18. M Regitz, G Maas, in *Organic Chemistry* (Berlin, 1981) p. 71
19. L N Markovskii *Izv. Akad. Nauk SSSR, Ser. Khim.* 2305 (1990)
20. I I Patsanovskii, E A Ishmaeva *Zh. Obshch. Khim.* **63** 2552 (1993)
21. J I G Cadogan, A H Cowley, I Gosney, M Pakulski, P M Wright, S Yaslac *J. Chem. Soc., Chem. Commun.* 1685 (1986)
22. M R Banks, J I G Cadogan, I Gosney, P K G Hadson, D R Rodger *Phosphorus Sulfur* **49/50** 381 (1990)
23. M R Banks, J I G Cadogan, I Gosney, P K G Hadson, D R Rodger *J. Chem. Soc., Chem. Commun.* 1033 (1989)
24. C K Ingold *Structure and Mechanism in Organic Chemistry* (Translated into Russian; Moscow: Mir, 1973) p. 615
25. M P Osipova, R V Volkova, A I Zlobina *Zh. Obshch. Khim.* **55** 697 (1985)
26. E E Nifant'ev, A I Zavalishina, S F Sorokina, A A Borisenko *Zh. Obshch. Khim.* **46** 471 (1976)
27. S Kim, D M Roundhilt *Phosphorus Sulfur* **70** 3 (1992)
28. A N Pudovik, M A Pudovik, S A Terent'eva, V E Bel'skii *Zh. Obshch. Khim.* **41** 2407 (1971)
29. M A Pudovik, S A Terent'eva, A N Pudovik *Zh. Obshch. Khim.* **51** 518 (1981)
30. M A Pudovik, A N Pudovik *Zh. Obshch. Khim.* **43** 2144 (1973)
31. A Hassner, V Alexanian *J. Org. Chem.* **44** 3861 (1979)
32. A N Pudovik, M A Pudovik, L K Ivanova *Zh. Obshch. Khim.* **41** 2677 (1971)
33. A N Pudovik, M A Pudovik, O S Shulyndina *Zh. Obshch. Khim.* **40** 501 (1970)
34. S A Terent'eva, M A Pudovik, A N Pudovik *Izv. Akad. Nauk SSSR, Ser. Khim.* **49** 1152 (1979)
35. T Mukajama, J Kuvajima, Z Suzuki *J. Org. Chem.* **28** 2024 (1963)
36. J Gloede *Phosphorus Sulfur* **55** 255 (1991)
37. M A Pudovik, A N Pudovik *Izv. Akad. Nauk SSSR, Ser. Khim.* 964 (1975)
38. V F Mironov, R A Mavleev, E N Ofitserov, T A Sinyashina, I V Konovalov, A N Pudovik *Izv. Akad. Nauk SSSR, Ser. Khim.* 1676 (1991)
39. V F Mironov, I V Konovalova, R A Mavleev, A Sh Mukhtarov, E N Ofitserov, A N Pudovik *Zh. Obshch. Khim.* **61** 2150 (1991)
40. V F Mironov, L A Burnaeva, I V Konovalova, G A Khlopushina, R A Mavleev, P P Chernov, A N Pudovik *Zh. Obshch. Khim.* **63** 25 (1993)
41. V F Mironov, L A Burnaeva, I V Konovalova, G A Khlopushina, P P Chernov *Zh. Org. Khim.* **29** 639 (1993)
42. V F Mironov, L A Burnaeva, V M Krokhalev, V I Saloutin, I V Konovalova, R A Mavleev, P P Chernov *Zh. Obshch. Khim.* **62** 1425 (1992)
43. I V Konovalova, V F Mironov, L A Burnaeva, V M Krokhalev, V I Saloutin, in *Tez. Dokl. IX Mezhdunar. Simp. po Khimii Fosfora, Sankt-Peterburg 1993* (Abstracts of Reports at the IXth International Symposium on the Chemistry of Phosphorus, St Petersburg 1993) p. 48
44. T H Black, S M Arrivo, J S Schumm, J M Knobeloch *J. Chem. Soc., Chem. Commun.* 1524 (1986)
45. T H Black, S M Arrivo, J S Schumm, J M Knobeloch *J. Org. Chem.* **52** 5425 (1987)
46. V F Mironov, R A Mavleev, E N Ofitserov, A N Pudovik *J. Fluorine Chem.* **54** 299 (1991)
47. V F Mironov, R A Mavleev, I V Konovalova, A N Pudovik *Zh. Obshch. Khim.* **61** 1259 (1991)
48. M Mikolajchyk, J Luczak *Zh. Obshch. Khim.* **58** 2024 (1988)
49. M Mikolajczyk, J Luczak *J. Org. Chem.* **43** 2132 (1978)
50. M Dreux, G Leroux, Ph Savignac *Synthesis* 506 (1974)
51. H B Miller, H W Baird, C L Bramlett, W K Templeton *J. Chem. Soc., Chem. Commun.* 262 (1976)
52. M P Chaus, N I Gusar', Yu G Gololobov *Zh. Obshch. Khim.* **53** 244 (1983)
53. M-A Armour, J I G Cadogan, D S Grace *J. Chem. Soc., Perkin Trans. 2* 1185 (1975)
54. J Burski, J Kieszkowski, J Michalski, M Pakulski, A Skowronska *Tetrahedron* **39** 4175 (1983)
55. J Burski, J Kieszkowski, J Michalski, M Pakulski, A Skowronska *J. Chem. Soc., Chem. Commun.* 940 (1978)
56. E Krawczyk, J Michalski, M Pakulski *Tetrahedron Lett.* **18** 2019 (1977)
57. V L Isaev, L Yu Mal'kovich, R N Sterlin, I L Knunyants *Zh. Vses. Khim. O-va im D I Mendeleeva* **19** 586 (1974)
58. H Kimura, H Konno, N Takahashi *Bull. Chem. Soc. Jpn.* **66** 327 (1993)
59. S Hanessian, Y Leblanc, P Lavallee *Tetrahedron Lett.* **23** 4411 (1982)
60. M Eisenhut, R Schmutzler *Phosphorus* **4** 73 (1974)
61. V K Das, J J Zucherman *Inorg. Chem.* **10** 1028 (1971)
62. P Cros, G Buono, G Peiffer, D Denis, A Mortreux, F Petit *New J. Chem.* **11** 573 (1987)
63. H Arzoumanian, G Buono, M Choukrad, J F Petrignani *Organometallics* **7** 59 (1988)
64. A Alexakis, S Mutti, J F Normand *J. Am. Chem. Soc.* **113** 6332 (1991)
65. G Buono, J-M Brunel, B Faure, G Pardigow *Phosphorus Sulfur* **75** 43 (1993)
66. J Bontragy, R Thomas *Chem. Rev.* **74** 87 (1974)
67. W S Wadsworth *Org. React.* **25** 73 (1977)
68. B E Maryanoff, A B Reitz *Chem. Rev.* **89** 900 (1989)
69. L D Quin, N D Sadanani, K Bourdieu, X-P Wu, G S Quin, R Bodalski *Phosphorus Sulfur* **49/50** 313 (1990)
70. L D Quin, B G Marsi *J. Am. Chem. Soc.* **107** 3389 (1985)
71. L D Quin, J Szewczyk, K M Szewczyk, A T McPail *J. Org. Chem.* **51** 3341 (1986)
72. L D Quin, B Pete, J Szewczyk, A N Mughes *Tetrahedron Lett.* **29** 2627 (1988)
73. L D Quin, N D Sadanani, X-P Wu *J. Am. Chem. Soc.* **111** 6852 (1989)
74. L D Quin, C Bourdien, G S Quin *Tetrahedron Lett.* **31** 6473 (1990)
75. J Sigal, L Loew *J. Am. Chem. Soc.* **100** 6394 (1978)
76. H Tomioka, M Watanabe, N Kobayashi, K Nirai *Tetrahedron Lett.* **31** 5061 (1990)
77. E E Nifant'ev, D A Predvoditelev *Usp. Khim.* **63** 73 (1994) [*Russ. Chem. Rev.* **63** 71 (1994)]
78. V P Kukhar', N Yu Svistunova, V A Solodenko, V A Soloshonok *Usp. Khim.* **62** 284 (1993) [*Russ. Chem. Rev.* **62** 261 (1993)]
79. R S Givens, W Kueper *Chem. Rev.* **93** 55 (1993)
80. G A Kutyrev, A V Lygin, R A Cherkasov, A N Pudovik *Zh. Obshch. Khim.* **52** 501 (1982)
81. G A Kutyrev, A V Lygin, R A Cherkasov, I V Konovalova, A N Pudovik *Zh. Obshch. Khim.* **53** 1213 (1983)
82. G A Kutyrev, A A Kutyrev, R A Cherkasov, A N Pudovik *Phosphorus Sulfur* **13** 135 (1982)
83. G A Kutyrev, R A Cherkasov *Usp. Khim.* **53** 1675 (1984) [*Russ. Chem. Rev.* **53** 971 (1984)]
84. J Baraniak, W Stec *Tetrahedron Lett.* **32** 4193 (1991)
85. W C Stiell, C Gennari *Tetrahedron Lett.* **24** 4405 (1983)
86. S K Thomson, C H Heathcock *J. Org. Chem.* **55** 3386 (1990)
87. K K Broeckman Jr, C H Weidner, R B Perni, J J Napier *J. Am. Chem. Soc.* **111** 8036 (1989)
88. T Bottin-Stzalko, J Seyden-Penne, E Brener, M J Pouet, M-P Simonnin *J. Chem. Soc., Perkin Trans. 2* 1801 (1985)
89. S E Denmark, C J Cramer *J. Org. Chem.* **55** 1806 (1990)
90. S E Denmark, P C Miller, S R Wilson *J. Am. Chem. Soc.* **113** 1468 (1991)

91. C Patois, L Ricard, P Savignac *J. Chem. Soc., Perkin Trans. 1* 1577 (1990)
92. R O Larsen, G Aksness *Phosphorus Sulfur* **15** 219 (1983)
93. J Tessier *Actual. Chim.* 5 (1986)
94. S Hanessian, D Delorme, S Beaudoin, Y Leblanc *J. Am. Chem. Soc.* **106** 5754 (1984)
95. C Patois, P Savignac *Tetrahedron Lett.* **32** 1317 (1991)
96. C Patois, P Savignac *Synlett.* 517 (1991)
97. C Patois, P Savignac *Phosphorus Sulfur* **75** 143 (1993)
98. P Savignac, M P Tenlade, C Patois *Phosphorus Sulfur* **49/50** 169 (1990)
99. C F Longmire, S A Evans Jr *J. Chem. Soc., Chem. Commun.* 922 (1990)
100. N J Gordon, S A Evans Jr *Phosphorus Sulfur* **75** 47 (1993)
101. D H Hua, Chan-Ju-King, J A McKie, L Myer *J. Am. Chem. Soc.* **109** 5026 (1987)
102. S E Denmark, J E Martin *J. Org. Chem.* **52** 42 (1987)
103. S E Denmark, G Rajendra, J E Martin *Tetrahedron Lett.* **30** 2469 (1989)
104. S E Denmark, J E Martin *J. Org. Chem.* **56** 1003 (1991)
105. K C Kumaras, S D Burton, J M Holmes, R O Day, R R Holmes *Phosphorus Sulfur* **53** 437 (1990)
106. J Gloede *Z. Chem.* **22** 126 (1982)
107. R Kluger, S D Taylor *J. Am. Chem. Soc.* **113** 996 (1991)
108. R Breslow, E Anglyw, Deen-Lih Huang *Tetrahedron* **47** 2365 (1991)
109. H J Bestmann *Pure Appl. Chem.* **51** 515 (1979)
110. W E McEwen, B D Bearer, J V Conney *Phosphorus Sulfur* **25** 255 (1985)
111. W G Ward Jr, W E McEven *J. Org. Chem.* **55** 493 (1990)
112. B E Maryanoff, A B Reitz, M S Mutter, R R Inners, H A Almond, R R Whittle, R A Olofson *J. Am. Chem. Soc.* **108** 7664 (1986)
113. N A Meanwell, H R Roth, E C R Smith, D L Wedding, J J Kim Wright *J. Org. Chem.* **56** 6897 (1991)
114. T Kawashita, K Kato, R Okaraki *J. Am. Chem. Soc.* **114** 4008 (1992)
115. O I Kolodyazhnyi *Zh. Obshch. Khim.* **56** 283 (1986)
116. I Granoth, J C Martin *J. Am. Chem. Soc.* **101** 4618 (1979)
117. O I Kolodyazhnyi, V P Kukhar' *Usp. Khim.* **52** 1903 (1983) [*Russ. Chem. Rev.* **52** 1096 (1983)]
118. O I Kolodyazhnyi *Usp. Khim.* **60** 799 (1991) [*Russ. Chem. Rev.* **60** 391 (1991)]
119. O I Kolodyazhnyi, D B Golokhov *Zh. Obshch. Khim.* **58** 490 (1988)
120. O I Kolodyazhnyi, D B Golokhov *Zh. Obshch. Khim.* **59** 293 (1989)
121. A Hercouet, M LeCorre *Tetrahedron* **37** 2861 (1981)
122. A Hercouet, M LeCorre *Tetrahedron* **37** 2855 (1981)
123. A Hercouet, M LeCorre *Tetrahedron* **37** 2867 (1981)
124. A D Abell, K B Morris, J C Litten *J. Org. Chem.* **55** 5217 (1990)
125. B E Maryanoff, A B Reitz, A D Duhl-Emswiler *Tetrahedron Lett.* **24** 2477 (1983)
126. A B Reitz, B E Maryanoff *J. Chem. Soc., Chem. Commun.* 1548 (1984)
127. B E Maryanoff, A B Reitz, A D Duhl-Emswiler *J. Am. Chem. Soc.* **107** 217 (1985)
128. E J Enholm, H Satici, G Prasad *J. Org. Chem.* **55** 324 (1990)
129. B Boudia, A Mann, F D Bellamy, C Mioskowski *Angew. Chem.* **102** 1522 (1990)
130. A Schmidpeter, T Criegern *Chem. Ber.* **111** 3747 (1978)
131. F Ramirez *Synthesis* 90 (1974)
132. F Ramirez *Pure Appl. Chem.* 185 (1973)
133. I V Konovalova, T V Yudina, E Kh Ofitserova, N P Anoshina, A N Pudovik *Zh. Obshch. Khim.* **48** 1936 (1978)
134. M Willson, R Burgada, F Mathis *Bull. Soc. Chim Fr.* 2241 (1975)
135. G Leroux, D E Monouni, R Burgada *Tetrahedron Lett.* **22** 3393 (1981)
136. H Hund, G-V Roschenthaler *Phosphorus Sulfur* **62** 71 (1991)
137. C K McClure, K-Y Jung *J. Org. Chem.* **56** 2326 (1991)
138. C K McClure, K-Y Jung, C W Grote, K Hangen *Phosphorus Sulfur* **75** 23 (1993)
139. C K McClure, K-Y Jung, C W Grote *Phosphorus Sulfur* **51/52** 418 (1990)
140. C K McClure, K-Y Jung *J. Org. Chem.* **56** 867 (1991)
141. F G Fang, M E Maier, S J Danishefski, G Schulte *J. Org. Chem.* **55** 831 (1990)
142. M Mikolajczyk, A Zatorski *J. Org. Chem.* **56** 1217 (1991)
143. T Kh Gazizov, R U Belyalov, A N Pudovik *Zh. Obshch. Khim.* **52** 487 (1982)
144. B A Arbuzov, A O Vizel', L I Shchukina, O V Vakulenko, T A Zyablikova, V K Krupnov, L I Zyryanova *Zh. Obshch. Khim.* **55** 1705 (1985)
145. L I Mizrakh, L Yu Polonskaya, A N Gvozdetskii, L B Karpunina *Zh. Obshch. Khim.* **60** 1422 (1990)
146. L I Mizrakh, L Yu Polonskaya, A N Gvozdetskii, A M Vasil'ev *Zh. Obshch. Khim.* **56** 73 (1986)
147. R Burgada, A Mohri, Y El Khoshnieh *C. R. Hebd. Seances Acad. Sci., Ser. C* **288** 165 (1979)
148. R Burgada, A Mohri *Phosphorus Sulfur* **13** 85 (1982)
149. M I Rybinskaya *Koord. Khim.* **4** 3 (1978)
150. J W Scheeren, P M Brown *Synthesis* 527 (1975)
151. V F Mironov, E N Ofitserov, T N Sinyashina, I V Konovalova *Zh. Obshch. Khim.* **26** 2570 (1990)
152. M A Pudovik, L I Kibardina, A N Pudovik *Zh. Obshch. Khim.* **61** 604 (1991)
153. N Kawamota, H Kawaji, M Nitta *J. Org. Chem.* **57** 618 (1992)
154. J B Husband, H McNab *Phosphorus Sulfur* **20** 207 (1984)
155. B D Denney, D Z Denney, J J Gigantio *J. Org. Chem.* **49** 2831 (1984)
156. J W Kelly, S A Evans *J. Org. Chem.* **51** 5490 (1986)
157. J W Kelly, P L Robinson, S A Evans *J. Org. Chem.* **50** 5007 (1985)
158. P L Robinson, C N Barry, J W Kelly, S A Evans *J. Am. Chem. Soc.* **107** 5210 (1985)
159. P L Robinson, S A Evans *J. Org. Chem.* **50** 3860 (1985)
160. P L Robinson, J W Kelly, S A Evans *Phosphorus Sulfur* **26** 15 (1986)
161. C N Barry, S A Evans *J. Org. Chem.* **46** 3361 (1981)
162. W T Murray, S A Evans *J. Org. Chem.* **54** 2440 (1989)
163. W T Murray, A Pautard-Cooper, N A Eshew, S A Evans *Phosphorus Sulfur* **49/50** 101 (1990)
164. J W Kelly, S A Evans *J. Am. Chem. Soc.* **108** 7681 (1986)
165. P L Robinson, C N Barry, S W Bass, S E Jarvis, S A Evans *J. Org. Chem.* **48** 5396 (1983)
166. J W Kelly, P L Robinson, S A Evans *J. Org. Chem.* **51** 4473 (1986)
167. W T Murray, J W Kelly, S A Evans *J. Org. Chem.* **52** 525 (1987)
168. J W Kelly, N L Eskew, S A Evans *J. Org. Chem.* **51** 95 (1986)
169. A Willeit, E P Muller, P Peringer *Helv. Chim. Acta* **66** 2467 (1983)
170. P Pochlauer, E P Muller, P Peringer *Helv. Chim. Acta* **67** 1238 (1984)
171. E P Muller *Helv. Chim. Acta* **65** 1617 (1982)
172. C Himmer, P Peringer, E P Muller *Phosphorus Sulfur* **51/52** 335 (1990)
173. A Pautard, S A Evans *J. Org. Chem.* **53** 2300 (1988)
174. A Pautard, S A Evans *J. Org. Chem.* **54** 2485 (1989)
175. A Pautard, S A Evans *J. Org. Chem.* **54** 4974 (1989)
176. A Pautard, S A Evans, W P Kenan *Tetrahedron* **47** 1603 (1991)
177. J Matheien-Pelta, S A Evans *J. Org. Chem.* **57** 3409 (1992)
178. J Matheien-Pelta, S A Evans *Phosphorus Sulfur* **77** 219 (1993)

Russian Chemical Reviews **63** (12) 1047 – 1062 (1994)
©1994 Russian Academy of Sciences and Turpion Ltd

UDC 62 – 278: 66.063.2

Membrane distillation

M T Bryk, R R Nigmatullin

Contents

I. Introduction	1047
II. Types of membrane distillation	1048
III. Membranes for membrane distillation	1048
IV. Mass and heat transfer in membrane distillation	1050
V. Experimental studies on membrane distillation	1053
VI. Modules and apparatus for membrane distillation	1056
VII. Applications of membrane distillation	1058
VIII. Conclusion	1060

Abstract. Studies in the field of membrane distillation are analysed. A critical analysis of the theoretical and experimental investigations of membrane distillation is presented. Attention is concentrated on the mechanism of mass transfer and the influence of various external factors on the process characteristics. Questions concerning the creation of modules and apparatus for membrane distillation and aspects of the practical employment of such distillation in order to obtain pure water, for the purification of waste water, and for the concentration of technological solutions in various branches of industry are considered quite fully. The advantages and disadvantages of membrane distillation compared with other membrane methods are analysed. The bibliography includes 97 references.

I. Introduction

The first mentions of membrane distillation (MD) as a separate membrane process date back to the beginning of the 1980s,[1–4] although at the end of the 1960s studies[5–8] were published of the membrane desalination of water, which is in essence membrane distillation. Since 1985, papers and conference proceedings devoted to the experimental and theoretical study of this process have been published systematically.[9–15] A special issue of the *Journal of Membrane Science* has been devoted to membrane distillation.[12] Each year the number of publications on membrane distillation increases and at the present time approximately 100 are already known.

Membrane distillation has aroused interest primarily as a method for the purification and desalination of water and also for the concentration of technological solutions. Compared with baromembrane methods (reverse osmosis, ultrafiltration, and microfiltration), membrane distillation has advantages which reside in the possibility of concentrating solutions of many involatile organic and inorganic substances up to conditions close to their solubility limit. The productivity in terms of the permeated material remains satisfactory under these conditions [5–10 litre(m^2 h)$^{-1}$]. The driving force of the membrane distillation process is the difference between the vapour pressures of the solvent on either side of the membrane, which is established as a result of the difference between the temperatures of the initial solution [the output side of the membrane] and of the permeated materials (or cooling agent) on its input (receiving) side. The temperature of the solution being concentrated is usually 50–80 °C, and that of the distillate is 20–25 °C. Consequently, high-energy heat can be used for membrane distillation. Furthermore, membrane distillation, not being a baromembrane process, does not require an excess pressure as in the case of microfiltration, ultrafiltration, and especially reverse osmosis.

Membrane distillation is a process in which the membrane itself does not affect the vapour–liquid equilibrium in the separation of solutions and liquids.[16] The term 'membrane distillation' is applied to processes which have the following characteristics: (1) the membrane must be porous; (2) it must not be wetted during the separation of the liquids; (3) there must be no capillary condensation within the membrane pores; (4) only vapour should be transferred through the membrane pores; (5) the membrane must not alter the vapour–liquid equilibrium during the separation of the components; (6) at least one side of the membrane must be in direct contact with the liquid; (7) for each component, the driving force of the mass transfer is the partial pressure gradient in the vapour phase.

Such an expanded definition of membrane distillation is necessary in connection with the fact that different investigators frequently name this process in different ways or employ for it the names of similar processes (transmembrane distillation, transvaporisation and thermotransvaporisation, membrane evaporation), which leads to confusion and errors. It must be emphasised that there is a fundamental difference between membrane distillation and transvaporisation, because the latter process is effected through nonporous membranes as a result of the dissolution and molecular diffusion of the solution components being separated.

Analysis of the existing publications indicates that membrane distillation is a promising membrane separation method as regards its applied aspect, which can be used with great effectiveness in processes such as the preparation of pure and highly pure water from waters with different salinities (including sea water),

M T Bryk, R R Nigmatullin Department of the Physical Chemistry of Membranes, Institute of Colloid Chemistry and the Chemistry of Water, National Academy of Sciences of Ukraine, prosp. Vernadskogo 42, 252680 Kiev, Ukraine. Fax (7-044) 452 02 76

Received 7 July 1994
Uspekhi Khimii **63** (12) 1114 – 1129 (1994); translated by A K Grzybowski

the purification of waste water containing inorganic electrolytes and involatile organic compounds (with the exception of surfactants), the concentration of salts from the wash waters in electroplating and dyeing industries, the concentration of thermolabile biologically active substances (vitamins, enzymes, etc.), the concentration of sugar and glucose-fructose syrups, and the concentration of solutions of dilute involatile inorganic acids, alkalis, and other substances.

At the same time, the membrane process has still not been investigated sufficiently fully experimentally and theoretically. There is as yet no complete analysis of the available studies on membrane distillation, although the need for this has become evident. A paper[18] in which this problem has been examined partially can be regarded as an exception. The aim of the present review is an attempt to fill this gap, which in our view will promote a clearer understanding of the subject of further research in the field of membrane distillation.

II. Types of membrane distillation

Membrane distillation can be carried out in different technological versions, and it is therefore important to distinguish several of its modifications.[17,18]

Contact membrane distillation (CMD) is a process in which a liquid is in direct contact with both sides of the membrane. The liquid in contact with the receiving side of the membrane is a medium for the condensation of the vapour being transported (Fig. 1*a*).

Membrane distillation through a gas (vapour) layer—a process in which the vapour beyond the receiving side of the membrane is condensed on a cooled surface at a specified distance from the membrane and the condensed liquid is not in contact with the membrane (Fig. 1*b*).

Membrane distillation at a reduced pressure (vacuum membrane distillation)—a process in which the rarefaction (vacuum) is created in the space between the receiving side of the membrane and the shell of the membrane element. The permeated material is condensed beyond the limits of the membrane module.[15,17]

Membrane distillation in a gas stream (membrane distillation with passage of a gas)—a process in which a gas stream (as a rule nitrogen) is supplied at a specified rate along the receiving side of the membrane. The vapour of the permeated material carried away by the gas stream is condensed beyond the limits of the membrane module.[17,19,20]

Osmotic membrane distillation is carried out with solutions having a high salt content in the receiving component. The permeated material in the form of vapour passes through a microporous hydrophobic membrane from solutions with a low osmotic pressure into a stream of solution with a high osmotic pressure of the solvent (Fig. 1*c*).[21,22]

III. Membranes for membrane distillation

There have been only a few publications devoted to questions of the preparation of membranes specially designed for membrane distillation (see, for example, Refs 23–26). As a rule, the existing hydrophobic microfiltration membranes are used for these purposes in the form of films, tubes, or fibres.[10,16,19,20]

In the case of contact membrane distillation, the transfer of permeated material through the membrane pores is effected in the form of vapour from the surface of the liquid meniscus at the inlets to the pores on the output side of the membrane to the surface of the liquid meniscus at the entrance to the pores on the input (receiving) size of the membrane (Fig. 2). The membrane pores contain a vapour–air mixture, i.e. the membrane should not be wetted by the solution being separated, so that the main requirement which must be met by membranes for membrane distillation is their hydrophobicity. The hydrophobicity makes it possible to maintain a liquid–vapour interface at one or both membrane surfaces and ensures the separation of the evaporation and condensation surfaces. Furthermore, the polymeric materials

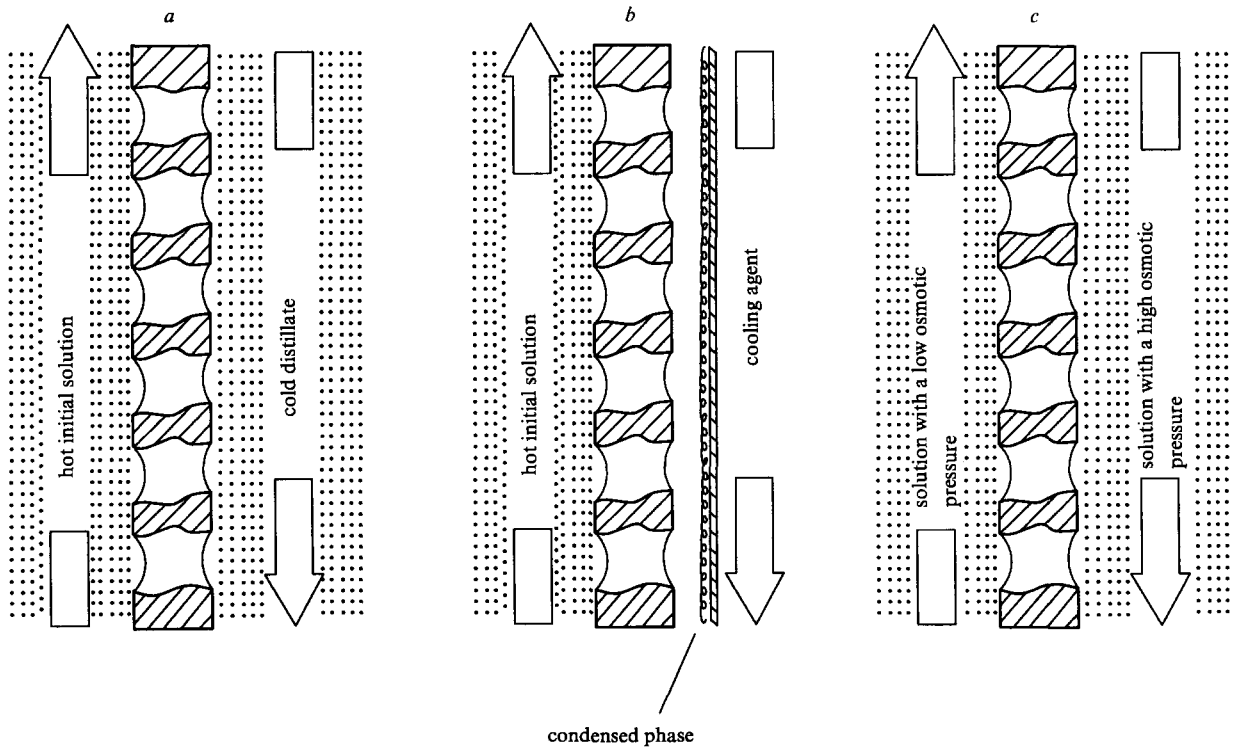


Figure 1. Different versions of the membrane distillation process; (*a*) contact membrane distillation;[17–19] (*b*) membrane distillation through a gas layer;[12,15,19] (*c*) osmotic distillation.[21,22]

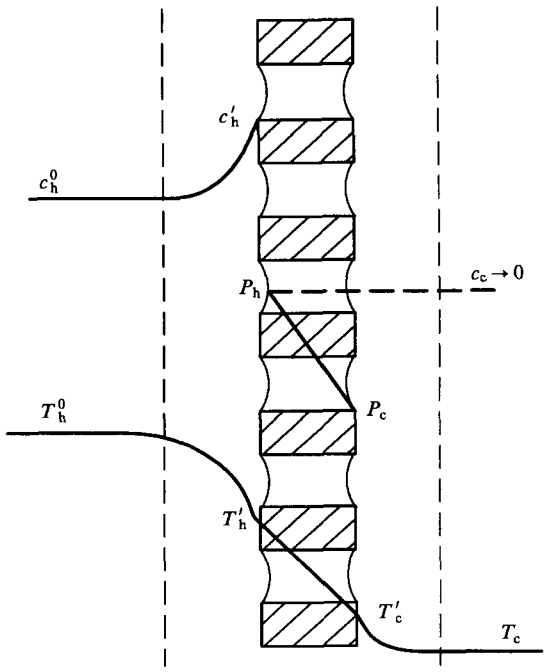


Figure 2. Schematic illustration of the membrane distillation process and the concentration and temperature profiles in membrane distillation.

used to prepare the membranes must possess a sufficiently high thermal stability and heat resistance in corrosive aqueous media.

Polypropylene,[10,20,21] polytetrafluoroethylene and other fluorine-containing polymers,[2,10,19-21] polyorganosiloxanes, poly(vinyl chloride),[27] etc. are mainly used as the polymeric materials satisfying the above conditions and possess in addition fibre- and film-forming capacities.

It is known[2,10,17,19] that, apart from the requirements stated above, the membranes used in membrane distillation must have a low thermal conductivity, a narrow size distribution of their pores, and an overall porosity of 30%–80%. A fairly important parameter for the productivity of the membrane in terms of the permeated material is the average pore diameter, which is believed to be optimum in the range 0.2–0.6 μm.[10,17,19] The membrane thickness must be as small as possible to ensure a high productivity of the membrane distillation process, but heat transfer must be minimised at the same time. The thickness of the membranes for membrane distillation is usually 100–300 μm.[17,19,24]

As already mentioned above, an important characteristic of the membrane is its hydrophobic properties. Therefore it is virtually impossible to employ membrane distillation for the separation of solutions and mixtures containing surfactants, which lower the surface tension and improve the wettability of the hydrophobic surface of the microporous membrane by water. Studies on the relation between the transport of water through polytetrafluoroethylene membranes and their wetting angle ($\alpha \approx 106°$) established[28] that there is a critical water pressure above which it permeates through the membrane as a convective stream. The absolute values of this pressure vary in the range 0.4–1.2 MPa and depend also on other parameters of the membrane (the pore size and the pore distribution) and on the surface tension of the medium being separated, which should not be less than 72×10^{-3} N m^{-1} for inorganic aqueous solutions.[28,29]

The critical concentrations of organic substances (alcohols, ethers, amines, ketones, and acids) in the solutions being separated are determined by the wettability of the membrane under the conditions of the separation process. The following condition for the wettability of the membrane has been proposed:[28]

$$\gamma_L = \gamma_L^p + \frac{\Delta p r_{max}}{2B}, \quad (1)$$

where γ_L is the surface tension of the liquid (solution, mixture) (N m^{-1}), γ_L^p the surface tension of the liquid (solution, mixture) at the boundary where it penetrates the pores of the microporous membrane (N m^{-1}), Δp the pressure difference (N m^{-2}), r_{max} the maximum pore radius (μm), and B the coefficient of the pore geometry.

It has been suggested that the critical concentrations of organic substances for a microporous membrane be calculated by a semiempirical method via the determination of the wetting angle of the material of the membrane.[28]

Unfortunately, the problem of the relation between the hydrophobicity of the surface of the membrane and the structure of water in the surface layers and also the structure of water within the membrane pores is not discussed in the literature.[30,31] The structure of the surface layers of water differs as a function of the nature and energy of the interaction of water molecules with membranes characterised by different surface hydrophobicities and pore dimensions, so that the physical characteristics of water (density, viscosity, phase transition temperatures, vapour pressure, etc.) also differ.[30,31] This undoubtedly must be taken into account in the study of the mechanism of the mass transfer in membrane distillation and in the optimisation of the transport characteristics of membranes.

There are few publications in the literature devoted to the preparation of special membranes for membrane distillation and to the study of their surface on structural characteristics. Among these, mention may be made of investigations[24-26] in which an attempt was made to obtain a hydrophobic layer on the surfaces of microporous cellulose acetate and nitrate membranes with the aid of methods for the radiation graft copolymerisation of styrene with pyridine and copolymerisation in plasma of octafluorocyclobutane (OFCB), CF_4, and trimethylvinylsilane $(CH_3)_3SiCH=CH_2$ (TMVS). This layer would determine the functional characteristics of the composite membrane prepared for membrane distillation. The plasma polymerisation of monomers was carried out under different conditions with the power of the discharge varying from 60 to 200 W for process durations between 5 and 90 min.[24]

In the radiation graft (co)polymerisation of the styrene–pyridine and styrene–carbon tetrachloride systems, the maximum wetting angle on the surface of a modified cellulose acetate membrane is attained for the ratios styrene : pyridine = 90 : 10 (69.5°) and styrene : pyridine : carbon tetrachloride = 85 : 10 : 5 (88.6°) (the wetting angle for the wetting of polystyrene by water is 91°). The introduction of CCl_4 into the system lowers the retention of NaCl (0.3 M) significantly to 66.7%–89.6%, whereas in the copolymerisation of styrene with pyridine the retention is 99.1%. The low retention is attributed to the formation of short grafted chains during comparatively short irradiation periods (~8 h).

The plasma polymerisation of OFCB and the copolymerisation of TMVS with tetrafluoroethylene (TFE) on the surfaces of cellulose nitrate membranes showed that the F : C ratio in the surface layer of the modified membrane and hence the wetting angle are determined by the power of the discharge. There is an extremum in the relations between the F : C ratio and the wetting angle, on the one hand, and the power of the discharge, on the other (Fig. 3, see next page). The lowest values of these quantities have been found for moderate discharge powers in the range 80–160 W. The maximum wetting angles of 113° and 120° are attained in the polymerisation of OFCB for discharge powers of 60 and 175–200 W respectively. For these parameters, a maximum retention of NaCl (0.5 M) of 92.0% is attained.

With increase in the plasma polymerisation time, an increase in the retaining capacity of the modified membranes and a decrease in their productivity are characteristic of all the systems investigated.[24-26] Electron microscope studies have shown that

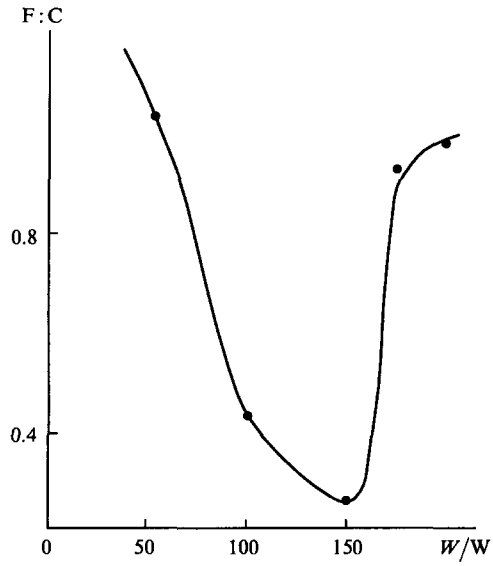


Figure 3. Dependence on the discharge power of the ratio of the contents of fluorine and carbon in the molecular structure of a cellulose nitrate membrane when the latter is modified by OFCB in a plasma.[24]

Table 1. The properties of the membranes used in membrane distillation.[24]

Membrane	Material	Permeability coefficient $10^3 K/\mathrm{kg\,(m^2\,h\,Pa)^{-1}}$	Retention (%)
Asymmetric poly(vinylidene fluoride)	poly-(vinylidene fluoride)	0.68	99.9
Modified by radiation-grafted polystyrene	cellulose acetate	0.14 0.96	99.1 66.7
Modified by OFCB in plasma	cellulose nitrate	0.82 1.32	99.5 99.1
Modified by TMVS–CF_4 in plasma	cellulose nitrate	1.81 2.22	99.9 99.4

this is associated with a decrease in the inlet diameters of the membrane pores and with an increase in the thickness of the modifying layer. Certain characteristics of the modified membranes are compared in Table 1 with those of an asymmetric porous membrane based on poly(vinylidene fluoride).

A novel membrane designed for the desalination of sea water or brines by membrane distillation has been described.[23] It has a multilayer construction based on an electrically conducting layer comprising polypropylene (25%–75%), poly(ethylene glycol) (10%–30%), graphite and ground charcoal (5%–75%), dibutyl phthalate (5%–20%), and sodium dodecyl sulfate (5%–25%). A hydrophobic polysiloxane film is deposited on this porous electrically conducting substrate from a solution or an emulsion. Such a membrane and the solution on the output side are heated by passing an electric current through the membrane.

IV. Mass and heat transfer in membrane distillation

Theoretical analysis of membrane distillation is based as a rule on the consideration of an ideal membrane, i.e. a membrane in which there are no wettable pores. In this case, the viscous flow of the liquid and thermodiffusion within the membrane pores are excluded and the diffusion of the permeated material is determined by the transport of solvent vapour by the vapour pressure gradient across the membrane. Consequently membrane distillation is a diffusion-controlled process and its phenomenological description is based on Fick's laws.

The diffusional mechanism of membrane distillation on real membranes has been confirmed in a study[32] the authors of which obtained linear relations between the flux of the permeated material and the reciprocal of the membrane thickness (Fick diffusion). Furthermore, the high retention of the involatile components of the solution (in excess of 99%) indicates the absence of convective flow in membrane distillation on real membranes. The phenomenological description of the membrane distillation process by means of Fick's laws is therefore entirely legitimate.[32–34] If the membrane pores are filled with air, the molar flux of water vapour is described by the equation[12]

$$N = -\frac{cD}{1-x}\frac{\mathrm{d}x}{\mathrm{d}z}, \tag{2}$$

where c is the molar concentration of the solution, D the diffusion coefficient of water vapour in the water–air mixture within the membrane pores, x the mole fraction of water vapour, and z a constant [sic. presumably a coordinate is intended (Ed. of Translation)].

The main problem arising in the solution of Eqn (2) is the difference between the diffusion coefficient within the membrane pores and the diffusion coefficient in a free medium and also the dependence of the coefficient on temperature and the vapour concentration. To simplify the problem, use has been made of the following empirical relation obtained from experimental data on diffusion in a water vapour–air mixture at ~40 °C:[12]

$$cD = 6.3 \times 10^{-5}\sqrt{T}. \tag{3}$$

Taking into account Eqn (3) and the morphology of the membrane, the following expression has been obtained for the molar flux of water (in the case of membrane distillation through a layer of gas):

$$N = 6.3 \times 10^{-5}\frac{1}{\delta/\varepsilon\sqrt{T_h} + L/\sqrt{T_c}}\ln\frac{1-x_c}{1-x_h}, \tag{4}$$

where δ and ε are the thickness and porosity of the membrane respectively, L is the thickness of the gas layer, and T_h and T_c are the temperatures on the hot and cold sides of the membrane respectively. This approach made it possible to determine the principal parameters influencing the flux and the nature of its dependence on the temperature regime and the morphology of the membrane.

Relations for the transport of gases (vapours) in porous-capillary media, based on the molecular-kinetic theory of gases, are usually employed in the description of diffusional transport of vapour in the membrane distillation process.[32,35] The general expression for the flux of permeated material, unrelated to the transport mechanism, assumes the form

$$J = \frac{K}{\sigma}(p_h - p_c) = \frac{K}{\sigma}\Delta p, \tag{5}$$

where p_h and p_c are the vapour pressures of the solvent on the hot and cold sides of the membrane respectively, and K is the permeability coefficient of the membrane. In contrast to the diffusion equation, the permeability coefficient K characterises both the properties of the gas and the morphological features of the membrane.

The diffusional transport of gases (vapours) in capillary-porous media is characterised by three flow regimes:[36-40] free-molecular (Knudsen diffusion), molecular, and transitional. The decisive parameter of the flow regime is the ratio of the mean free path of the molecules to the pore diameter.

If the mean free path greatly exceeds the pore size, Knudsen diffusion obtains. It is characterised by a greater number of collisions of the molecules with the pore wall than with one another. The molecular diffusion of vapours occurs if the free path of the molecules is smaller than the pore size, i.e. the number of collisions of the molecules with one another (or with the molecules of another kind) exceeds the number of collisions with the pore walls (viscous flow). Equations for mass transfer in capillary-porous media have been used for the transport of gases through porous membranes occurring under free-molecular and molecular diffusion conditions. For isotropic membranes, the flux of the permeated material is defined by the following equations:[35-37]

(a) for Knudsen diffusion,

$$J = \frac{2}{3}\frac{r\varepsilon}{\chi}\left(\frac{8M}{\pi RT}\right)^{1/2}\frac{\Delta p}{\delta} = \frac{K_K \Delta p}{\delta}, \quad (6)$$

where r is the membrane pore diameter, χ the tortuosity coefficient of the pores, and K_K the mass transfer coefficient under the conditions of Knudsen diffusion;

(b) for viscous flow,

$$J = \frac{1}{8}\frac{r^2\varepsilon}{\chi}\frac{1}{\eta}\frac{Mp}{RT}\frac{\Delta p}{\delta} = \frac{K_m \Delta p}{\delta}, \quad (7)$$

where η is the viscosity and K_m the mass transfer coefficient under the conditions of molecular diffusion.

There are a series of fundamental differences between a Knudsen flow and molecular diffusion, the main ones of which are the dependence of molecular diffusion on the average pressure.

If the free path of water molecules does not exceed 0.2 μm (in the temperature range 20–100 °C), i.e. is comparable to the size of the pores in the membranes employed for membrane distillation then the process occurs in the transitional regime. However, in certain studies the description of processes of this kind has been based on the molecular diffusion regime.[41]

The transitional regime is as a rule related not to the mixed nature of the transport but to the effects determined by the surface flow.[42] At the present time there is no single theoretical concept on the basis of which one could obtain a rigorous quantitative description of the process.

In the literature on the transport of gases in capillary-porous bodies, frequent attempts have been made to describe the mass transfer in the transitional regime by combining the equations describing the Knudsen and molecular diffusion or on the basis of empirical equations.[43]

In the study of the membrane distillation process, attempts have also been made to describe the mass transfer through porous membranes in the transitional regime. Thus it has been proposed[20] that the permeability constant be calculated from the Knudsen (D_K) and molecular (D_m) diffusion coefficients:

$$\frac{1}{K} = \frac{\chi\delta}{\varepsilon}\left(\frac{1}{D_m} + \frac{1}{D_K}\right). \quad (8)$$

An interesting approach to the description of diffusion in porous membranes in the transitional regime has been put forward.[36] On the grounds that in the Knudsen regime the flux is proportional to the pressure difference ($J \propto \Delta p$) while in the molecular regime it is proportional to the pressure difference and the pressure ($J \propto p\Delta p$), the authors suggested that in the transitional regime the permeability constant depends on different powers of the pressure:

$$\frac{K}{\delta} = a\psi^b, \quad (9)$$

whence

$$J = a\psi^b \Delta p, \quad (10)$$

where ψ is the dimensionless pressure, a the permeability constant of the membrane, and $b = 0$ for Knudsen diffusion and 1 for molecular diffusion; the constant a, characterising the properties of the membrane, is the coefficient of the proportionality between the flux and the pressure gradient. Thus, for the description of the flux of gas to the membrane, the two empirical coefficients a and b are determined from experimental data. Both parameters depend on the type of membrane and the gas transported. The permeability constant of the membrane is calculated from the relation $a = K/\delta$.

We may note that Zolotarev and Timashev[44] suggested that the permeability constant be determined from data for membrane distillation in a special cell, the receiving component of which consists of a small cylinder immersed in a vessel with a heated solution. The permeability constant is determined from the maximum height of the distillate column (h_∞) at the given temperature in the receiving component by means of the relation

$$J = K\Delta p = K\rho_d g h, \quad (11)$$

where g is the acceleration due to gravity, and h the height of the column of liquid.

An inversely proportional relation has been obtained[36] between the quantity $K/M\bar{u}$ (where $\bar{u}$ is the average velocity of the molecules) and the mean free path of the molecules. With the aid of this relation, it is possible to determine K for different gases, including water vapour, from transport data for other gases. This is important, since the determination of the transport characteristics of the membrane for the transport of water vapour in direct experiments is impossible because of the difficulties in the correct determination of the water vapour pressure in the membrane pores and of the degree of deaeration of the membrane. The latter factor is particularly important, since the presence of different molecules in the gas phase not only diminishes the partial pressure but also alters the nature of the process.

The description of the mass transfer has been based in a series of studies[37-39,45] on the equations for the transport of water vapour through a layer of air in accordance with molecular diffusion model, whereupon the molar flux is described by the equation[37,39]

$$N = \frac{1}{p_a}\frac{\varepsilon}{\chi\delta}\frac{MDp}{RT}\Delta p, \quad (12)$$

where p is the average gas pressure in the membrane and p_a the logarithmic mean pressure of air (Schofield et al.[37] suggested that the geometrical mean pressure be employed).

Ugrozov et al.[45] introduced the parameter $Kn = D_{as}/D_{Ks}$, where D_{as} is the effective coefficient of the mutual diffusion of the vapour in air and D_{Ks} the coefficient of the Knudsen diffusion of the vapour. The parameter Kn is regarded as the effective Knudsen number in the case of a porous medium and characterises the mechanism of the mass transfer. For $Kn < 0.1$, transport is effected by molecular diffusion, for $Kn > 10$ Knudsen diffusion obtains, and for $0.1 < Kn < 10$ the mass transfer takes place in the transitional regime. The flux of the permeated material is given by the equation

$$J = \frac{D_{as}pM}{RT\delta p_a(1 + Kn_0)}(p_h - p_c), \quad (13)$$

where p_a is the atmospheric pressure and $Kn_0 = D^0_{as}/D_{Ks}$ (D^0_{as} is the effective coefficient of the mutual diffusion of the vapour in air at atmospheric pressure, which depends explicitly on Kn_0; the equation can therefore also be employed for the calculation of the flux in any mass transfer regime).

The overall resistance of the membrane in the membrane distillation process is equal to the sum of the resistance of the membrane determined by its morphology and the molecular diffusion resistance.[37] In this case, the equation for the overall mass transfer is

$$J = \left(\frac{1}{a\psi^b} + \frac{p_a}{d}\right)^{-1} \Delta p , \tag{14}$$

where

$$d = \frac{\varepsilon}{\chi\delta}\frac{MD_p}{RT} .$$

This takes into account the diffusion coefficient of the gas and the morphology of the membrane. The satisfactory correlation between the experimental results and the theoretical results, predicted on the basis of the molecular diffusion of water vapour through a layer of air,[38] indicates that the latter form of diffusion predominates in the contact molecular distillation process. The analysis carried out by Schofield et al.[37] confirmed these conclusions. Only at low air pressures (under deaeration conditions) does the transport of water vapour in the membrane pores in the transition regime, described by the first term of Eqn (14), make a significant contribution.

In contact membrane distillation, the permeability to the permeated material is proportional to the difference between the vapour pressures and the porosity of the membrane and is inversely proportional to the thickness of the membrane and the air pressure in it. For the description of the process in terms of experimentally measurable parameters, the pressure distance is replaced by the temperature difference[38-40,44] (taking into account the temperature dependence of the vapour pressure and the diffusion coefficient). This approach demonstrates the dependence of the flux on the temperature regime. The vapour pressure also depends on the solution concentration, as a result of which the membrane permeability constant depends on the latter as well[38,39]

$$K = \frac{\varepsilon M}{\chi\delta R^2}\frac{pD}{T^b}\frac{\Delta H_V T^{b-3} p_m^*}{p_a}(1 - x_m) , \tag{15}$$

where $b = 1.75$ and 2.33 (Sarti et al.[38]), p_m^* is the average water vapour pressure over the pure solvent, ΔH_V the heat of vaporisation, and x_m the molar concentration of the solution.

As a consequence of the reduced vapour pressure over the solution, the transport of water through the membrane can take place only for a temperature gradient such that the vapour pressure over the hot solution exceeds that at the condensation surface. The minimum temperature difference is calculated by means of the equation[38]

$$\Delta T_0 = \frac{hT_m^2}{\lambda_m}\frac{x_h - x_c}{1 - x_m} , \tag{16}$$

where x is the mole fraction of all the dissolved substances.

The quantity ΔT_0 is used to estimate the direction of transport of water vapour in contact membrane distillation. In order to concentrate the solutions by contact membrane distillation, it is necessary that the working temperature difference should be greater than ΔT_0. When a solution with a high osmotic pressure is present on the receiving side of the membrane (osmotic distillation), the flow of water through the membrane is possible even in the absence of a temperature gradient, i.e. $\Delta T_0 < 0$.

The transfer of water from the solution in contact membrane distillation is always smaller than the transfer from the pure solvent. It has been suggested[46] that the dependence of the flux of the permeated material on the concentration be described as a function of the decrease in the flux of the permeated material from the pure solvent:

(a) at low solution concentrations (in the range where Raoult's law is valid):

$$J = J_0 - K\alpha p_h(0, T_h)c ; \tag{17a}$$

(b) at high concentrations:

$$J = J_0 K\alpha p_h(0, T_h)c + K\beta p_h(0, T_h)c^2 . \tag{17b}$$

The interpretation of experimental data in terms of the theoretical ideas described above requires the knowledge of the concentration and temperature of the solution in the near-membrane layers in order to determine correctly the driving force of the process. It is essential to note that the parameters in the near-membrane layers differ from the bulk-phase characteristics of the solution (see the temperature and concentration profiles in Fig. 2). The increase in the concentration of the involatile solutes in the near-membrane layer on the output side of the membrane is due to the phenomenon of concentration polarisation, common to all membrane processes, which exerts a negative influence on the productivity of the membrane distillation as a consequence of the decrease in the driving force of the process, as for other membrane processes. However, the relatively weak dependence of the vapour pressure on the concentration gives rise to only a slight decrease in productivity.[44]

As can be seen from Fig. 2, the temperature of the solution in the near-membrane layers also differs from the bulk-phase value owing to heat transfer through the membrane. This phenomenon has been called temperature polarisation. Like concentration polarisation, temperature polarisation has a negative influence on the productivity of the membrane distillation process as a consequence of the decrease in the temperature of the solution (the vapour pressure) on the evaporation surface and its increase on the condensation surface.

The description of the heat transfer in membrane distillation is based on the well known thermodynamic relations. The overall thermal resistance of the membrane system is then defined by analogy with the electrical resistance.[35,37,39,40] The heat transfer in the membrane distillation process takes place in three stages: heat transfer to the evaporation surface, heat transfer through the membrane, heat transfer from the condensation surface to the bulk of the distillate.

Heat transfer to and from the membrane surface is characterised by the heat transfer coefficients

$$Q = \alpha_h \Delta T_h = \alpha_c \Delta T_c , \tag{18}$$

where Q is the heat flux per unit area of the membrane and α_h and α_c are the heat transfer coefficients in the output and receiving sections respectively.

Heat transfer through the membrane takes place with the stream of vapour and as a result of transfer through a porous membrane the pores of which are filled with a gas phase. Heat transfer through the membrane represents heat losses in the membrane distillation process and is determined by the thermal conductivity of the porous polymer–gas composite structure:[35,37-40]

$$\lambda_m = \varepsilon\lambda_a + (1-\varepsilon)\lambda_p , \tag{19}$$

where λ_a and λ_p are the thermal conductivities of the vapour–air mixture and of the polymer membrane respectively.

For heat transfer as a result of thermal conductivity, we have

$$Q_1 = \left(\frac{\lambda_m}{\delta}\right)\Delta T_m = \lambda_1 \Delta T_m , \tag{20}$$

where λ_1 is the thermal conductivity of the membrane.

The heat transfer associated with the flow of vapour through the membrane is determined by the magnitude of the flux and the heat of vaporisation:

$$Q_2 = J\Delta H_V = \lambda_2 \Delta T_m , \tag{21}$$

where λ_2 is the heat transfer coefficient related to the vapour flux.

The heat balance equation is

$$Q = Q_1 + Q_2 . \tag{22}$$

Having solved Eqn (21) for J using Eqns (18)-(20) and (22), we obtain

$$J = \frac{\lambda_2}{\Delta H_v} \frac{\lambda}{\lambda_1 + \lambda_2 + \lambda} (T_h - T_c) , \tag{23}$$

where

$$\lambda = \left(\frac{1}{\alpha_h} + \frac{1}{\alpha_c} \right)^{-1} , \tag{24}$$

$$\lambda_1 = \frac{\varepsilon k_B + (1 - \varepsilon) k_m}{\delta} . \tag{25}$$

Eqn (23) reflects the influence of the heat transfer conditions on the productivity of the membrane. When account is taken of Eqn (20), Eqn (23) can be reduced to the form

$$\frac{\Delta T_m}{T_h - T_c} = \frac{\lambda}{\lambda_1 + \lambda_2 + \lambda} . \tag{26}$$

The ratio $\Delta T_m/(T_h - T_c)$ has been called the coefficient of temperature polarisation (CTP) and reflects the fraction of the overall driving force $T_h - T_c$ which ensures the operation of the true driving force ΔT_m. In the ideal case, the CTP should be unity, which corresponds to the equality of the temperatures in the surface layers and in the bulk phase.

The level of temperature polarisation depends both on the properties of the polymer membrane (λ_1) and on the heat transfer regime in the liquid flow (α_h, α_c). From the standpoint of the heat transfer through the membrane, an increase in the thickness of the latter tends to decrease the level of temperature polarisation. However, this entails an increase in the diffusion path for the water vapour. Hence, in order to attain the maximum productivity of the membrane distillation process, optimisation with respect to the thickness of the membrane is needed, as already stated.

The estimates carried out in a number of studies[35, 37, 47, 48] indicate that temperature polarisation is influenced mainly by the heat transfer conditions in the liquid streams, which are determined by the hydrodynamic conditions governing the flow of liquids within the channels of the membrane module. The level of temperature polarisation decreases with increase in the degree of turbulence of the streams within the channels.

The heat transfer in liquid streams depends on the orientation of the membrane and the Earth's gravitational field. The best conditions for heat transfer are achieved when the direction of natural convection coincides with the direction of heat transfer. Natural convection then influences the stability (thickness) of the near-membrane layer, which increases if the direction of natural convection coincides with the concentration profile and the temperature polarisation.[49] It has been confirmed experimentally[27, 38] that, for a horizontal disposition of the membrane and of the hot chamber (the hot chamber is located below), the maximum productivity of membrane distillation is attained.

The extremely high retention coefficients of involatile substances in the membrane distillation process were noted above. However, in practice the retention of involatile substances nevertheless does not attain 100%, which makes it necessary to take into account this fact in theoretical analysis. Thus the level of concentration polarisation in membrane distillation is estimated taking into account the incomplete retention of the solute.[34] The following expression has been obtained[34]:

$$\frac{c^0}{c} = (1 - \varphi) + \varphi \exp\left(\frac{Jl}{D} \right) , \tag{27}$$

where c and c^0 are the concentrations of the solution being separated on the surface of the membrane and in its bulk respectively. φ is the retention coefficient, l is the thickness of the near-membrane layer, and D is the diffusion coefficient.

According to Eqn (27), in order to minimise concentration polarisation it is desirable to maintain the flux at the level of l/D.

It has been suggested that the diffusion model of the selectivity of the established membrane distillation process be used for the description of the retention in the membrane distillation process on the basis of the hypothesis that a hydrophobic microporous membrane contains both hydrophobic and hydrophilic pores.[50, 51] The 'breakthrough' of the volatile solutes in membrane distillation is possible owing to their diffusion via the solution-filled hydrophilic pores. It is assumed that the hydrophilic pores have a smaller diameter than the hydrophobic ones. In our view the possibility of a decrease in selectivity as a consequence of the wetting of the largest pores owing to the pressure drop is less probable. Since the pores in membranes have submicron dimensions, even slight pressure drops lead to a significant convective flow of the solution. As a result, the retention coefficients should be lower than the experimental values and should depend on the concentration of the initial solution, which is not observed in practice.

Thus the relative hydrophilic porosity is the parameter of the nonideality of the membrane:[50]

$$\varepsilon_f = \frac{m_f}{m_0} = 1 - \frac{m}{m_0} , \tag{28}$$

where m_0 is the fraction of the membrane surface corresponding to all the pores, both hydrophobic (m) and hydrophilic (m_f) ($m_0 = m + m_f$).

According to the analysis carried out by Starikov,[50] the retention coefficient is a function of the nonideality of the membrane and of the hydrodynamic parameters of the system:

$$\varphi = \left[1 + \frac{m_1 D}{J\delta} \exp\left(\frac{Jl}{D} \right) \right]^{-1} . \tag{29}$$

In the presence of hydrophilic pores and a nonstirred near-membrane layer, the selectivity of the flux of permeated material passes through a maximum at $J = D/l$. We then have

$$\varphi_{max} = \frac{\delta}{\delta + l m_f e} . \tag{30}$$

Calculations have shown that the retention coefficient increases with increase in the flux and with decrease in the thickness of the unstirred layer.[50] Similar dependences of the selectivity are characteristic also of a multilayer membrane consisting of a hydrophobic microporous membrane with a thin hydrophilic surface layer.[51, 52]

The selectivity coefficient in membrane distillation for systems containing more than one volatile component is determined by the vapour–liquid equilibrium, which the membrane hardly affects. The description of the mass transfer, including the selectivity parameters, is hardly discussed in the relevant communication, as is the description of transvaporisation processes.[53]

V. Experimental studies on membrane distillation

The results of theoretical studies on heat and mass transfer in the membrane distillation process can serve as a basis for the treatment of experimental data and a satisfactory prediction of the possibilities of membrane distillation.

In the initial stage of the development of studies on membrane distillation, attempts were made to reconcile the experimental data obtained with the mathematical description of heat and mass transfer.[10, 12, 19, 54-64] The attempt to elucidate the influence of all factors on the principal process characteristics

was self-evident and entirely comprehensible.[10,12,15,54-61] Thus membrane distillation on microporous hydrophobic [polypropylene, poly(vinylidene fluoride), polytetrafluoroethylene], planar, and hollow-fibre membranes was investigated with the aid of model aqueous solutions of sodium chloride, glucose, or sucrose. Such studies[10,12,54-58,62-64] showed that the most important factors influencing the productivity with respect to the permeated material are the temperature, the temperature drop (vapour pressure drop) on either side of the membrane, the pore size, the overall porosity and thickness of the membrane, and the concentration of the initial solution. It was established that, for a constant temperature drop, the productivity of the membrane distillation process increases with increasing concentration of the initial solution and, when the latter is constant, the productivity increases with increase in the temperature drop (Fig. 4).

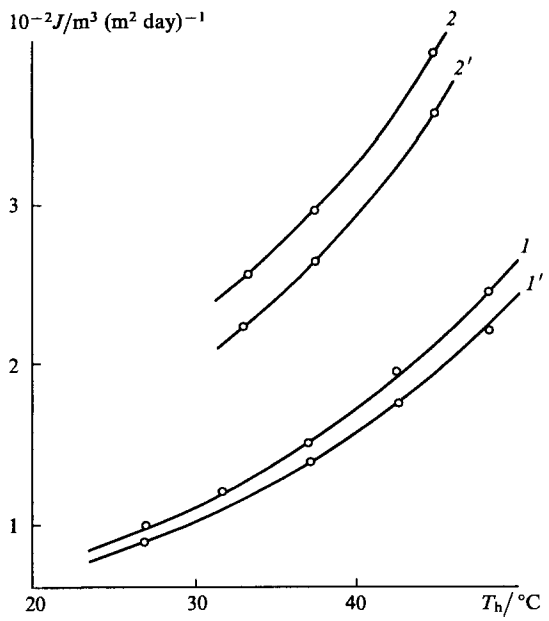


Figure 4. Dependence of the flux of the permeated material on the temperature of the hot sodium chloride solution.[64] ΔT/°C: (*1*) and (*1'*) 5.0; (*2*) and (*2'*) 9.5; c_{NaCl}/mol litre^{-1}: (*1*) and (*2*) 0.05; (*1'*) and (*2'*) 0.50.

Later investigations confirmed the general characteristics of the membrane distillation process and its dependence on the principal factors indicated above. At the same time, in these studies more continuous attention was devoted to individual factors influencing the process. Furthermore, whereas a distinct applied trend could be traced in the early studies (they dealt as a rule with simplified models of the process), in later investigations attempts were made to develop the theoretical foundations of membrane distillation with the aid of new revised experimental data (in particular, account was taken of heat exchange and of the nature and velocities of the fluxes in membrane cells, the temperature and concentration polarisations, etc.).[46,65-72]

The membrane distillation of solutions of sodium chloride and glucose at very high concentrations of the latter (up to 5 and 50 g litre^{-1} respectively) has been investigated in detail.[46] Analysis of the dependence of the productivity on concentration was based on the approximate Raoult's law, according to which the vapour pressure of the solvent was defined by the expression

$$p(c, T) \approx p(0, T)(1-\alpha c), \quad (31)$$

where $p(0, T)$ is the vapour pressure of the solvent at $c = 0$ for dilute solutions and c is the concentration of the solute. The coefficient α is then always positive.

On the other hand, at fairly high concentrations of the solution, a nonlinear dependence of the partial pressure of the solvent on concentration is observed:

$$p(c, T) \approx p(0, T)(1-\alpha c+\beta c^2). \quad (32)$$

The coefficient β can be both positive and negative. This corresponds to a positive or negative deviation from Raoult's law, which occurs at high solution concentrations.

It has been established[46] for a wide range of solution concentrations that there is a linear dependence of the flux of permeated material on the concentration [see Eqn (17b)]. It is important to note that the concentration of the substance not in the bulk phase but at the interface of the membrane, which is higher than the bulk phase concentration, should be employed in Eqns (17a), (17b), and (32).[41] The decrease in productivity with respect to permeated material with increasing solute concentration should be less appreciable, according to Eqn (32), if $\beta > 0$ and should be more applicable if $\beta < 0$.

Experimental studies on the membrane distillation of concentrated sodium chloride and glucose solutions confirmed satisfactorily the theoretical considerations described above (Figs 5*a* and 5*b*): at low solute concentrations, the relation $J = f(c)$ is linear, while at higher concentrations it is nonlinear. These effects are associated not only with deviations from Raoult's law but to a considerable extent also with the manifestation of concentration and temperature polarisations, which has been confirmed by experiments designed to investigate the $J = f(c)$ relation with and without stirring of the solution being separated (see curves *1* and *2* in Figs 5*a* and 5*b*).

A more rigorous study of the dependence of the productivity of the membrane distillation process on temperature and on the temperature difference on either side of the membrane confirmed[38,45,73,74] that the specific productivity of the contact membrane distillation process increases with increasing temperature difference for a fixed temperature T_x and also with increase in the average bulk-phase temperature. It has been shown that intensification of the stirring of the solution makes it possible to increase significantly (by a factor greater than 2) the productivity of the contact membrane distillation process, which is associated with the partial elimination of temperature and concentration polarisations.[34,38,45,46,69-75]

The influence of temperature and concentration polarisations on the functional characteristics of the membranes and on the membrane distillation process is always negative. A partial elimination of such polarisations can be achieved by altering the velocity and nature of the solution and permeated material fluxes at the output and receiving surfaces of the membrane.[72] The procedure in which the flow of the solution to be separated was rendered turbulent proved to be extremely effective, lowering the negative influence of concentration and temperature polarisations and intensifying the membrane distillation process, especially in flat chamber apparatus. The flow of the solution was rendered turbulent by stirring, and with the aid of pressure channels in apparatus and turbulators of different design. The movement of the membrane element relative to the solution being separated (when the membranes are arranged on rotating discs), as well as vibration and ultrasound, can be used.[72]

Analysis of experimental data on the effect of turbulent flow on the specific productivity of membranes showed[72] that, for $Re > 1500-2000$, an increase in the flux through the membrane is not observed. Here one should note that the procedure in which the flow solution is rendered turbulent is more effective than the one in which the flow of the permeated material is made turbulent.

The dependence of the separating characteristics of microfiltration membranes in the membrane distillation process on the average pore diameter has been noted.[75] This has been explained by the influence on the mass transfer by the predominant Knudsen or molecular mechanism of the diffusion of vapour through pores having different diameters and lengths. In real membranes with a

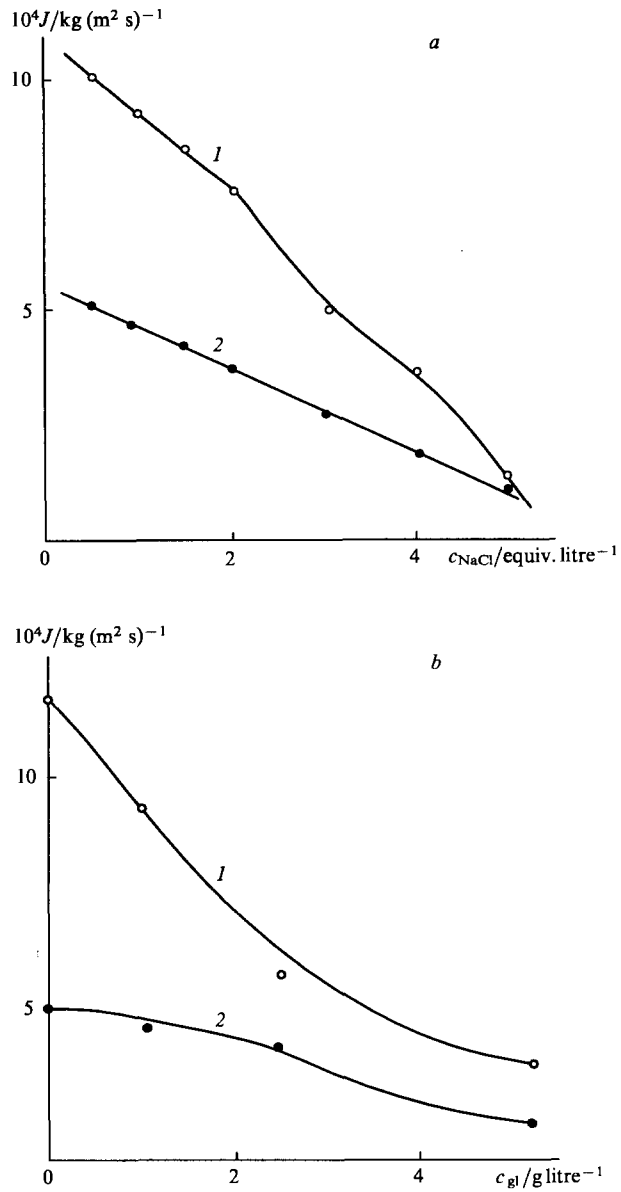


Figure 5. Dependence of the productivity of the contact membrane distillation process on the concentrations of NaCl (*a*) and glucose (*b*) in the solution:[73] (*1*) with stirring (600 rev min^{-1}); (*2*) without stirring (temperature of the hot solution 70 °C, temperature of the distillate 30 °C).

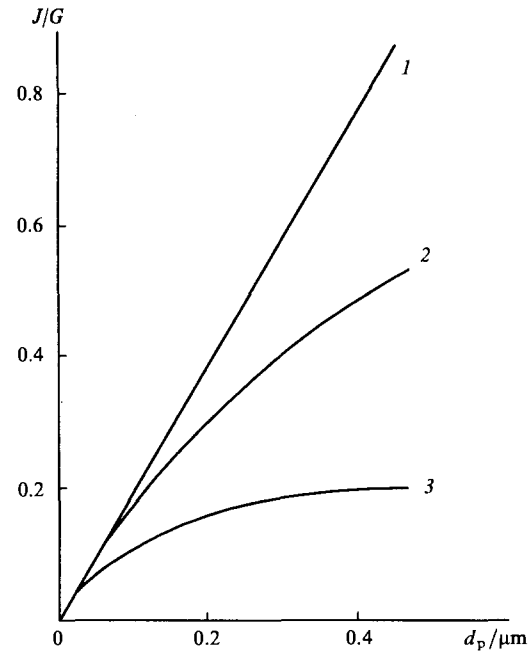


Figure 6. Dependence of the flux in the membrane distillation process on the pore size at different partial pressures of air (kPa): (*1*) 0; (*2*) 20; (*3*) 80.[72]

complex porous structure, a combined mass transfer takes place, i.e. with different contributions by both mechanisms, which has in fact been demonstrated experimentally and theoretically in a number of investigations.[37,45,72] Here one should take into account the fact that the presence or absence of an air layer in the membrane pores affects the mass transfer. The air in the membrane pores prevents the diffusion of water vapour and diminishes its flux through the membrane. Indeed, Fig. 6 shows that the dependences of the specific productivity of the membrane on the pore size are different for different partial pressures of air in the pores. For small pores, where the transfer is effected predominantly via Knudsen diffusion, the removal of air promotes only slightly an increase in the flux, whereas for membranes with a large pore diameter the flux to the membrane can be increased by 50% by deaeration.[72]

It has been noted that deaeration diminishes the heat transfer through the membrane by 10%–25%.[37,72] However, the hydrodynamic conditions, the pore structure, and the thickness of the thermophysical properties of the membranes are most important for the reduction of the influence of temperature polarisation on the intensity of the membrane distillation process.

The characteristics of the heat and mass transfer through PTFE membranes in the membrane distillation process have been determined experimentally with the aid of the $H_2SO_4-H_2O$, $HCl-H_2O$, NH_3-H_2O,[75] $NaCl-H_2O$,[55,56,75] and $C_2H_5OH-H_2O$ [53,69] systems at different temperatures and for different flow rates of the solution and the permeated material. It was established that the extents of heat and mass transfer are proportional to the temperature difference on either side of the membrane and depend on the porosity and thickness of the latter.[53,75,76] Expressions based on the material and heat balance equations for determining the flux of transferred substance have been obtained with the aid of mathematical modelling of the membrane distillation process. It is believed[75,76] that the calculated data agree well with the experimental results and that the membrane distillation process can be used to concentrate solutions such as juices, milk, sugar syrup, [aqueous] alcohol, etc.

Among the factors influencing the intensity of the membrane distillation, the hydrophobicity (wettability) of the membrane surfaces by the substances being separated has been considered in some investigations (see, for example, Yoshishige and co-workers[77,78]). The special importance of this factor is manifested for systems the concentraion of which leads to an appreciable decrease in surface tension (surfactants, alcohols, and certain water-soluble organic compounds).[28,29,77,78] Special procedures (modification of the membrane surfaces by more hydrophobic polymers or substances, a change in the size of the pores in the selective hydrophobic layer, etc.) make it possible to employ membrane distillation for the concentration of, for example, dilute solutions of alcohol. In such cases, it is possible to employ only membrane distillation through a gas (vapour) layer or vacuum membrane distillation.[15,17,19,53] The deposition of a layer of silicone rubber or poly-(1-trimethylsilyl-1-propylene) on the surface of microporous poly(vinylidene fluoride) membrane lowers the permeability to water and increases the selectivity of the membrane with respect to ethanol, acetone, acrylonitrile, and 1-butanol dissolved in water.[77,78] Not only the hydrophobicity of the membrane but also is asymmetry, the mechanism of the

sorption-desorption of the substances being separated, and also the changes in temperature gradient associated with the asymmetry and chemical composition of the membrane layers play a significant role in this process.

Studies of the membrane distillation process on different aqueous systems demonstrated the practical importance of this separation method and its advantages compared with other procedures, primarily the baromembrane methods. These advantages are associated with the possibility of separating concentrated and highly concentrated solutions, which as a rule do not require a complex preliminary purification.

VI. Modules and apparatus for membrane distillation

Membrane modules with all the existing configurations of membranes — flat, hollow fibre, and tubular — are employed for the membrane distillation process.

In contrast to baromembrane elements, two enforced flows are established within the channels of the membrane distillation modules (MDM) — the flow of the concentrate and the flow of the distillate (in the case of contact membrane distillation) or a gas (in the case of membrane distillation with a flow of gas). Furthermore, a cooling agent channel, separated from the gas space by the impermeable condensation surface, is essential for membrane distillation with a gas space.

The effectiveness of membrane distillation and other membrane processes is determined by the properties of the membranes and the design of the module. The principal parameter in the optimisation of the design of the MDM is the level of temperature polarisation. It was noted above that heat transfers in liquid streams exert an appreciable influence on such polarisation. The heat transfers are determined by the hydrodynamics of the flow of liquids within the channels of the membrane module, which depends on the design characteristics of the latter. The level of temperature polarisation can be estimated on the basis of the Nusselt number.[35,75]

From the standpoint of heat transfer, the most successful configuration is that of hollow-fibre membranes for which, at an internal diameter of 0.3 mm, a coefficient of temperature polarisation of 0.8 is already attained for $Re = 300$ (Table 2). However, with increase in the internal diameter to 1 mm, the attainment of CTP = 0.85 requires $Re = 3000$. For flat channels, the CTP increases with decrease in the thickness of the channel. Modules which are effective from the standpoint of the decrease in the level of temperature polarisation can be created on the basis of both hollow fibres and flat membranes (Table 2). This is indicated by the present state of development of the equipment for membrane distillation processes.

Spiral membrane distillation modules were proposed as early as 1982,[79] but we have been unable to find experimental data on the membrane distillation process carried out on MDM of this type. In our view, the lack of such data cannot be regarded as evidence that modules of the spiral type are unlikely to be useful. In such modules, it is entirely possible to create sufficiently narrow channels and to ensure enforced flows in the latter. Furthermore, the presence of spiral heat exchangers ensures effective heat exchange in MDM of this kind.

The Swedish cassette elements should probably be regarded as the first flat-frame MDM.[3,80,81] They consist of plastic plates with an internal channel for the stream of heated initial water in contact with two membranes. The working area of the membrane surface is 0.3 m^2. The membrane in the cassette is fitted on a porous base, which protects it from damage during the assembly of the module. The module is assembled from cassettes of the filter-press type. This entails the formation of a condensation channel (a gas space with a condensation surface) and a cooling water channel as a result of the employment of additional plates. This apparatus was created for membrane distillations through a gas layer or at a reduced pressure.

Unfortunately, apart from the above studies,[3,80,81] there have been no publications describing adequately the design of a flat-frame MDM. There is in fact no information whatever about the working parameters of the module, the hydrodynamic regime, the principles governing the organisation of the streams, etc.

Somewhat later, the membrane distillation process began to be carried out on hollow-fibre elements.[82–85] A hydrodynamic regime within the capillaries favourable for heat transfer is characteristic of MDM of this type.[37] However, it is fairly difficult to ensure effective heat and mass exchange on the outer side of the capillaries when a large number of bunches of capillaries are present.[75] It is important that stagnant zones should not form on the outer surface of the fibres.

Studies have been made on the hollow-fibre MDM with three types of packing of the capillaries:[75] parallel fibres, bunches of twisted fibres, and bunches of intertwined fibres. The packing comprising parallel fibres is made from a fabric material in which transverse filaments serve for the fixation of the hollow-fibres in the parallel direction. Such fabrics are rolled up and the rolls are packed in a jacket. The highest productivity has been observed for bunches of twisted and intertwined fibres. The highest packing density of the fibres, reaching 40% – 50%, occurs in the latter type of MDM. Bunches of intertwined and twisted fibres act as devices causing a turbulent flow within the shell of the hollow fibre MDM. Overall, the hydrodynamic regime established in the hollow-fibre MDM ensures the maximum productivity even for the laminar flow of liquids ($Re \approx 450$).[84]

Table 2. *Temperature polarisation for different membrane distillation systems.*[35]

Geometry of membrane	Characteristics of flow	*Nu*	Hydraulic diameter of channel/mm	Heat transfer coefficient/W(m^2 K)$^{-1}$	CTP[a]
Internal diameter/mm					
1	$Re = 5000$	29	1.0	19000	0.90
	$Re = 3000$	20	1.0	13000	0.85
	$Re = 1000$	4.4	1.0	2900	0.54
0.3	$Re = 300$	4.4	0.3	9700	0.80
External diameter 0.6 mm	nearly laminar regime	~5	0.9	3700	0.60
Channel 0.5 m long	flow rate 2 m s^{-1}	970	500	1300	0.51
Channel thickness/mm					
2	laminar regime	5.4	8	450	0.15
0.5	"	5.4	2	1800	0.4
0.1	"	5.4	0.4	8900	0.7

[a] CTP on one side of the membrane.

Table 3. Membrane distillation on a hollow fibre pilot module.[82]

Temperature/ °C				Flow rate/m min^{-1}		Flux/kg $(m^2\ h)^{-1}$	Heat transfer coefficient $10^{-7}K/W\,(m^2\ K)^{-1}$	Permeability constant/ kg $(m^2\ s\ Pa)^{-1}$
solution		distillate		solution	distillate			
inlet	outlet	inlet	outlet					
52.0	36.9	32.9	48.1	2.44	2.43	2.1	3280	3.31
55.0	33.5	26.5	48.2	2.94	2.93	3.5	3260	3.39
60.2	32.0	24.4	53.1	2.46	2.43	4.1	3140	3.44
65.0	29.3	21.8	59.1	1.70	1.63	3.7	2620	3.15
69.0	41.6	35.2	63.4	2.44	2.38	5.1	3090	3.44
70.7	38.7	32.4	66.3	2.83	1.73	4.6	2870	3.51

Note. The module consists of 2000 polypropylene fibres with internal and external diameters of 300 and 600 μm respectively and with a length of 400 mm. The area of the membranes is 1 m^2.

The flow of liquid media in hollow-fibre MDM is organised on the basis of the countercurrent principle. The temperatures at the inlet to and outlet from the module are then different. As can be seen from Table 3, the temperature differences are significant even for relatively short fibres (with a length of 400 mm). This leads to differences between the average temperatures in different sections of the fibre, i.e. the mass transfer conditions vary as a function of the length of the fibre. The differences between the inlet and outlet temperatures increase with the increasing length of the fibres and with decrease in the flow rate. Tests have been made hitherto on hollow-fibre MDM with fibre lengths up to 2 m and an internal diameter of the jacket of 250 mm. The area of the membrane for such MDM varies from 50 to 100 m^2.[84]

It is noteworthy that the differences between the mass transfer conditions for different sections of the membranes are equally characteristic of MDM of any configuration, but in the literature this problem has been discussed explicitly only in relation to the hollow-fibre MDM. It must be emphasised that the length of the membrane channel in the MDM is an important design feature, which requires optimisation both in the construction of modules and in the development of apparatus and technology.

In our view, the use for membrane distillation of the tubular modules with a low packing density of the membranes, which are as a rule very thick, is justified only in individual instances. Tubular MDM can probably be used to concentrate viscous solutions, characterised by impairment of heat transfer. Tubular MDM can ensure a satisfactory hydrodynamic regime in the flow of viscous liquids, particularly within the tubes.

Hitherto the available information about tubular MDM is limited. They are used predominantly for the desalination of water or for the concentration of aqueous solutions of low-molecular-mass substances.

A Japanese patent application[86] describes an unusual design of a tubular MDM. In this device, the evaporation system is separated from the condensation system, i.e. this is an apparatus for membrane distillation processes with a gas space. The evaporation and condensation systems consist of parallel tubes for the supply and removal of liquid media connected by a multiplicity of tubes in the condensation system or via tubular membranes in the evaporation system. A heated concentrated solution is supplied to the evaporation system, while a cooling liquid is supplied to the condensation system. The vapour which has passed through the tubular membranes condenses on the surfaces of metallic tubes of the condensation system and the distillate flows spontaneously into the collector.

Cartridge filters with a folded configuration of flat membranes have come to be fairly widely used to microfiltration processes. Cartridge elements based on polytetrafluoroethylene membranes with areas of 0.3 and 0.15 m^2 have been tested for membrane distillation.[87,88]

Apparatus for membrane distillation is, as a rule, of the circulation type, which ensures an increase in the degree of concentration and a more rational use of heat as a result of the decreased heat consumption in raising to its working temperature the solution being concentrated.

Depending on the heat transfer conditions and the length of the membrane channel of the MDM, the temperatures of the streams at the inlets and outlets differ to such an extent that the outlet temperature of the distillate may be higher than the inlet temperature of the solution being concentrated. In this case, it is possible to use part of the heat of the distillate to heat the solution undergoing concentration (Fig. 7*a*). However, in apparatus with heat recovery, the temperature difference between the two sides of the membranes, i.e. the specific productivity of the process, is small and this is why membranes with a high surface area are used in them.

In a number of cases, the problem of heat recovery is not formulated, for example if the membrane distillation is used to obtain water for boilers. In apparatus of this type (Fig. 7*b*), it is endeavoured to attain large temperature differences. Therefore the attainable specific selectivity of apparatus without recovery is higher, which lowers the capital expenditure and the expenditure on membranes.

From the standpoint of energy expenditure, the membrane distillation process is characterised by the energy efficiency parameter E, which is defined as the ratio of the part of the heat consumed on vaporisation to the overall heat introduced into the apparatus:[17,41]

$$E = \frac{JS\Delta H_V}{Fc_p(T_{in} - T_{out})}, \tag{33}$$

where S is the area of the membrane and F the flow rate of the initial solution with a heat capacity c_p and the temperatures T_{in} and T_{out} at the inlet to and outlet from the MDM.

As a consequence of the heat losses, E is always less than unity. The cost of the water purified by the membrane distillation method diminishes with increase in the temperature of the initial solution.[82]

The component which is always present in apparatus for membrane distillation processes is heat exchange equipment needed to heat the initial water to the working temperature and then maintain this during the membrane distillation process, and additionally for the utilisation of the heat from the distillate. Problems of heat exchange (outside the MDM) and of energy supply (source of energy) have scarcely been considered in studies on membrane distillation. In practice, these problems are solved by traditional engineering procedures.[85]

In discussing the economics of membrane distillation, Hanbury and Hodgkiess[89] noted that the process does not withstand competition when it is carried out on expensive tetrafluoroethylene membranes. This problem may be solved by employing polyalkene membranes or membranes made from chlorinated polyalkenes. The conclusion that Teflon membranes

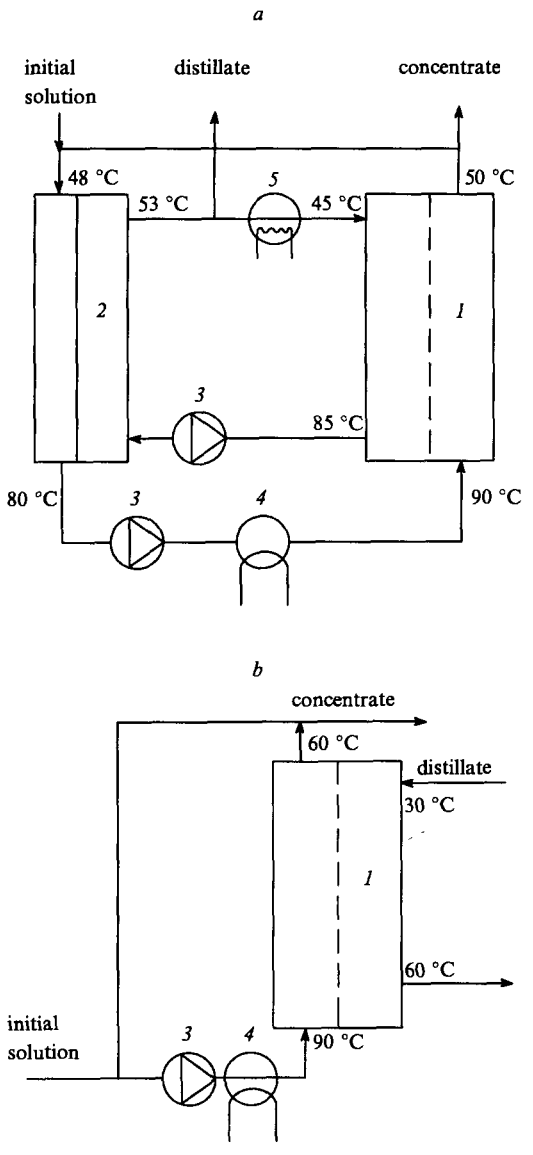


Figure 7. Schematic illustration of apparatus for membrane distillation with (*a*) and without (*b*) recovery of heat:[84] (*1*) membrane distillation module (MDM); (*2*) heat exchanger; (*3*) pump; (*4*) heater; (*5*) cooling unit.

are not competitive is not incontrovertible, bearing in mind the possible extended use of such membranes in membrane distillation.

According to the estimate of Fane et al.,[82] the expenditure on the operation of membrane distillation apparatus with a moderate power (5000 kg h^{-1}) is comparable to the expenditure on the operation of similar apparatus based on reverse osmosis. For less powerful apparatus, the expenditure is higher compared with the reverse osmotic apparatus. However, an advantage of membrane distillation is that it requires a less thorough preliminary purification of water.

VII. Applications of membrane distillation

The experimental data described above (see Section V) outline the range of technological processes in which membrane distillation may be employed. However, at the present time one is dealing only with the potential possibilities of the process. Despite the almost ten year history of the development of the equipment for membrane distillation, there are in fact no literature data on its long-term tests. The longest tests concern the treatment of artesian well water over a period of 18 weeks,[84] which indicate the stable operation of the apparatus.

It is possible to differentiate the following principal applications of membrane distillation: the preparation of pure water; the concentration of solutions of involatile substances; the purification of waste water; the isolation of volatile components from solutions containing also involatile substances; the separation of dilute water–organic liquid mixtures. Such subdivision is to some extent arbitrary. For example, the concentration of solutions of involatile substances leads to the simultaneous formation of pure water, whereas purification of waste water may involve the concentration of contaminating involatile substances, etc.

Preparation of pure water. When any aqueous solutions containing involatile substances are treated, highly pure water is obtained as the permeated material. Thus it has been shown[75] that the electrical conductivity of the distillate obtained on treating aqueous solutions of NaCl, H_2SO_4, and NaOH does not exceed 5 μS cm^{-1}. In the first place, membrane distillation is used[38,62,63,81] to obtain pure water from sea water and artesian well water.[84] The high quality of the water, which is almost independent of the concentration of the feed solution, has been noted. For example, when the electrical conductivity of artesian well water varied from 350 to 35000 μS cm^{-1}, the quality of the filtrate remained stable.[84] In carrying out the process, provision was made for only preliminary elimination of mechanical impurities. The long term operation is generally accompanied by a decrease in productivity as a function of time as a consequence of the contamination of the membranes. The recovery of the productivity in the treatment of artesian well water is achieved by washing the membranes with hydrochloric acid solution.[84] It is essential to note that, owing to the lack of results of long-term tests, the problems of the contamination and purification of membranes have been hardly described in the literature.

The use of membrane distillation for the final treatment of water in order to obtain sterile apyrogenic water is of interest.[87,88] It has been established that the content of endotoxins in the distillate obtained by membrane distillation is less than 1.0 ng $litre^{-1}$ when their content in the initial water is 11.3 ng $litre^{-1}$. Water of this quality is characterised as apyrogenic. Bacteria were not detected in the distillate. Membrane distillation ensures better elimination of particles than the usual distillation particularly the elimination of particles the size of which is less than 1 μm. The content of low-molecular-mass organic impurities, for example carbon, in water falls from 417 μg (on treatment of deionised water) to 280–290 μg per litre. The proposed apparatus with polytetrafluoroethylene membranes having a folded configuration (with areas of 0.30 and 0.15 m^2) makes it possible to obtain 20 kg of apyrogenic water per hour. Tests carried out over a period of 1000 h demonstrated the stability of the apparatus both as regards productivity and the quality of water.

Concentration of solutions of involatile substances. Membrane distillation is a promising method for the concentration of aqueous solutions of involatile substances. The possible concentration limits of the membrane distillation process greatly exceed those when reverse osmosis is used.

The membrane distillation method can be employed to concentrate aqueous solutions of sugars.[64,75] When a solution of glucose is concentrated, a sharp decrease in productivity is observed at a concentration in excess of 25 g $litre^{-1}$,[75] which is probably due to an increase in the viscosity of the solution, impairing the heat exchange conditions, and not to a decrease in the vapour pressure over the solution. In the treatment of viscous solutions, it is necessary to intensify the turbulence of the stream or to carry out the process at higher temperatures. Thus concentration of a sugar syrup at 86 °C is characterised by a productivity with respect to the distillate of 20–28 kg $(m^2\ h)^{-1}$ in the syrup concentration range from 10% to 40%.

The problem of the impairment of heat transfer as a consequence of the increase in concentration arises also when solutions of high-molecular-mass oligomeric substances are concentrated. For example, a fairly sharp decrease in productivity has been observed when a solution of gelatine was concentrated.[75] At the same time, one should note that the vapour pressures over solutions of high-molecular-mass compounds depend only slightly on the mass concentration of the polymer (owing to the low molar concentration of the solutions). As a result of this, water-soluble polymers may be concentrated in the presence of effective heat and mass exchange in the MDM channels, for example in a tubular MDM. We may note the high stability of the productivity in the concentration of oligomeric substances (Fig. 8), characterised by a low viscosity.

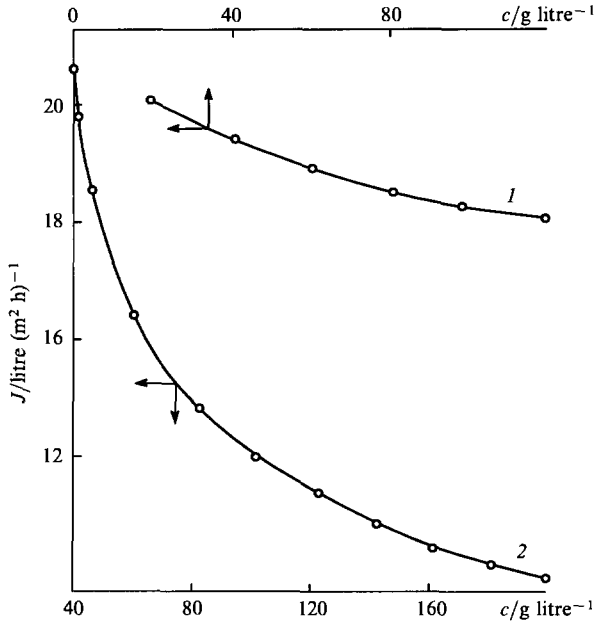


Figure 8. Dependence of the productivity of the membrane distillation process with respect to the permeated material on the solute concentration during the concentration of a solution of poly(ethylene glycol) with a molecular mass of 6000 (curve *1*) and waste water from a coke-chemical factory (curve *2*).

The problem of concentrating liquid products containing high-molecular-mass components frequently arises in the food industry. Thus it has been shown that membrane distillation is more effective in the concentration of mandarin juice as compared with reverse osmosis.[75] Membrane distillation makes it possible to attain threefold concentration with a gradual decrease in productivity as the degree of concentration rises from 10 to 7 kg $(m^2\ h)^{-1}$. On the other hand, reverse osmosis is characterised by a sharp decrease in productivity: after concentration by a factor of only 1.5, the productivity is 5 kg $(m^2\ h)^{-1}$. We may note that the treatment of mandarin juice by membrane distillation was carried out at 48 °C, i.e. under fairly mild conditions, which makes it possible to preserve the properties of the thermolabile components of the juice.

Even milder treatment conditions are attained is osmotic distillation, where the vapour pressure in the receiving part of the MDM is reduced as a result of the employment of solutions with a high osmotic pressure. Thus the concentration of orange, apple, and grapefruit juices at a temperature of 29 °C (40 °C in individual experiments) with the aid of a flat-frame module having a membrane area of 0.7 m^2 (a 28% solution of an inorganic electrolyte was passed through the receiving channels) has been described.[22] As in the case of contact membrane distillation, the productivity of osmotic membrane distillation depends on the hydrodynamic conditions in the flow within the capillaries of the apparatus; the absolute productivity did not exceed 2.5 litre $(m^2\ h)^{-1}$ as a consequence of the small temperature difference. The juices were concentrated until the attainment of a 50% content of the solutes.

Overall, the likely usefulness of membrane distillation for the concentration of solutions of thermolabile substances must be specially emphasised.[61] Studies on mass transfer in the concentration of solutions of vitamins C and B_1 by the contact membrane distillation method in the temperature range 50–60 °C showed that it is possible to obtain supersaturated (at room temperature) solutions of the vitamins: 50%–55% for vitamin C (the concentration of the saturated solution at 20 °C is 25.3 mass%) and 60%–65% for vitamin B_1 (the concentration of the saturated solution at 20 °C is 50 mass%). After cooling, the concentrated solutions of the vitamins and their crystallisation, the deposited vitamin may be separated and the solution can be again concentrated with the aid of membrane distillation. After the attainment of the concentrations indicated, the productivity of the contact membrane distillation is 6–8 litre $(m^2\ h)^{-1}$. It has decreased compared with the initial value by a factor of not more than 2–3.

The formation of supersaturated solutions in the membrane distillation process is not exceptional.[90,91] Thus membrane distillation has been suggested for the isolation of lanthanum compounds from a sulfuric acid extract of phosphogypsum.[91] The extract obtained on treatment of phosphogypsum contains 16% of sulfuric acid, 1.6% of Ln_2O_3, and 3.5% of CaO as the main components. The concentration of such an extract by membrane distillation was from 16% to 44% in terms of sulfuric acid, with a productivity of 215 and 80 litre $(m^2\ day)^{-1}$ at an extract temperature of 60 °C. After cooling the concentrate, a deposit containing up to 25% of lanthanum compounds was isolated. The formation of $CaSO_4$ crystals on the membrane surface has been observed when the process is carried out by a periodic procedure, this being a consequence of crystallisation from supersaturated solutions remaining on the membrane surface.

Purification of waste water. Water of very high quality is obtained in the purification of waste water by membrane distillation, whereas the concentrate may contain valuable components or even the target product of the manufacturing process at a high concentration up to supersaturated solutions. Thus the concentration of water from the manufacture of taurine (2-aminoethanesulfonic acid), containing taurine and sodium chloride, is accompanied by the crystallisation of taurine.[91] The deposit segregated contains up to 60% of taurine and impurities (sodium chloride). The product may be purified by recrystallisation.

Membrane distillation may become the principal procedure for the creation of closed water supply systems. Laboratory studies on systems for the recovery of water under conditions of space stations have been reported.[92]

Membrane distillation is perhaps the only alternative to vaporisation processes in the treatment of highly concentrated waste waters, including those from undertakings in different branches of industry. Experiments have been carried out on the purification of waste waters from the textile industries containing dyes.[41] It has been noted that membrane distillation can be best employed to concentrate further already concentrated waste water and it is therefore recommended that, in the purification of waste waters from textile undertakings, preliminary concentration by reverse osmosis be carried out with subsequent treatment of the concentrate by membrane distillation.[41]

The possibility of a high degree of concentration of aqueous salt solutions, in particular solutions of heavy metal salts, has been investigated.[93] The authors employed membrane distillation through a gas layer. In the concentration of nickel salts, a weak variation of the productivity with respect to permeated material

was noted. The productivity reached 25–30 litre $(m^2\ h)^{-1}$. The high quality of the permeated material was noted, which makes it possible to employ membrane distillation in combined schemes for the purification of wash waters and for the processing of spent solutions from the electroplating industry.

In the purification of waste waters from processing plants in the food industry, it is possible to obtain concentrated solutions of valuable food components. Thus treatment of whey by membrane distillation made it possible to obtain a concentrate containing 300 g $litre^{-1}$ of lactose for a process productivity with respect to the distillate of 0.43 m^3 $(m^2\ day)^{-1}$.[94]

As a rule, waste waters are complex multicomponent mixtures. Thus the waste water from the coke-chemical industry (water from the gas collector) contains up to 40 g $litre^{-1}$ of ammonium chloride, inorganic electrolytes, and various organic substances (phenols, pyridines, etc.). Such water is highly corrosive, especially at high temperatures, which makes problematical the employment of evaporation processes to be carried out at the critical temperatures.

Waste waters may be concentrated by membrane distillation up to a content of inorganic electrolytes of 200–250 g $litre^{-1}$ (Fig. 8). It is noteworthy that the waste waters from the coke-chemical industry contain volatile organic impurities, which also permeate through the membrane. After the treatment of such waste waters by membrane distillation, the permeate therefore contains volatile organic impurities (phenols, pyridine). These impurities can be made harmless by biological methods. The vital activity of the corresponding microorganisms is suppressed in the biological treatment of highly mineralised waste waters.

Isolation of volatile components from solutions of involatile substances. The example involving the concentration of waste waters partly demonstrates the possibility of using membrane distillation for the isolation of volatile components from solutions of involatile substances. For example, phenols can be removed from a concentrate of inorganic salts. However, so far there are no literature data on the deliberate technological employment of this approach. A system which makes it possible to isolate volatile substances from aqueous solutions by membrane distillation, before their analysis, has been described.[95] In this scheme, specimens with a volume not exceeding 6 ml are introduced into plastic tubes, their contents are boiled, and the vapour passes through a hydrophobic membrane and is then condensed. The method allows 100% isolation of substances in less than 60 min. It has been tested in experiments with cyanides, cyanide complexes, sulfides, phenol, and ammonia.[96]

Separation of water–organic solvent mixtures. The use of membrane distillation for the separation of water–organic solvent mixtures is an alternative to the transvaporisation and fractional distillation methods in the treatment of mixtures with a low content of the organic substances. Membrane distillation has been tested primarily in the separation of water–ethanol mixtures.[15,53,69,77,78,97] In the stationary regime, the concentration of ethanol in the permeated material increases by a factor of 2–3.[69,97] The productivity with respect to the permeated material then reaches 10 kg $(m^2\ h)^{-1}$ and more,[96] which greatly exceeds the productivity in transvaporisation. However, it has been shown[69] that the permeability of the membrane and its selective properties vary with time owing to the wetting of the pores.

VIII. Conclusion

Analysis of the available publications on membrane distillation supports the view that the method is promising for the solution of a series of technological problems. The advantages of membrane distillation compared with other membrane methods are associated with the low requirements which must be met in the preliminary purification of waste and other saline waters, the absence of excess working pressures, a satisfactory productivity even at high and very high concentrations of the solutes close to the solubility limit, the possibility of using low-energy heat in combination with the possibility of its recovery, the relative simplicity of the design of the modules and apparatus, the high quality of the permeated material (water), including the possibility of obtaining in one stage a pyrogenic sterile water, and the extensive possibilities for the technological employment of membrane distillation in many branches of industry.

The following disadvantages of membrane distillation may be noted: the impossibility of using it for the purification of water and the concentration of solutions containing surfactants and other water-soluble organic compounds with a low surface tension and a low boiling point (for example alcohols), the limited selection of hydrophobic materials suitable for the formation of membranes, and the high cost of such materials and of the membranes based on them. The last factor may not be quite so significant if the operating life of the membrane is sufficiently long (3–5 years).

Analysis of the advantages and disadvantages of membrane distillation compared with other membrane as well as physico-chemical purification and concentration methods leads to the conclusion that membrane distillation has on the whole significant advantages over the baro- and electro-membrane methods employed for such purposes both independently and in hybrid technological schemes involving other methods.

Bearing in mind that hitherto membrane distillation is still a little investigated process, the growth of interest in the method and in its extensive practical use is to be expected in the future. At the same time, problems which require consideration in the immediate future have already become apparent. In our view, they include the theoretical and experimental solution of problems of mass and heat transfer in relation to the real macrostructure of the membranes and the physical properties of the materials from which they are made. Hence follows the need to optimise the pore and geometrical characteristics of the membranes and modules and also for a rational search for materials with the required physical, physicochemical, and mechanical properties. A more thorough and purposeful study of problems of the hydrophobic-hydrophilic properties of the membrane surfaces and of their influence on the structure of water in thin surface layers and also on the nature of the interaction of the components of the solution with the membrane surface is required. Hitherto, this problem has not been solved for membrane distillation, although it may be important for the treatment of experimental data on the retention of components of the solutions and on the productivity of membranes with respect to the permeated material. Yet another special problem, associated with the possibility of the contamination of the membrane surfaces by sorbed solution components and with the formation of deposits on the hydrophobic surface and in the pores of the membrane, is related to the above problem. It has not been discussed in the literature, although its practical importance is evident especially for the estimation of the potential possibility of the use of membranes and of the time intervals at which they are to be regenerated and the development of procedures for such regeneration.

Experimental studies on the characteristics of the membrane distillation of solutions mixtures containing readily volatile and volatile components (wetting and not wetting the surfaces of hydrophobic membranes) and the determination of the critical concentrations and other physicochemical parameters of such systems are needed. In our view, kinetic studies on the membrane distillation process under the conditions of variable characteristics of the mixtures being separated are also important.

The above list of problems associated with the development of membrane distillation is incomplete, but we hope that the analysis of the available literature data will serve the purpose of a deeper study of membrane distillation and of its extensive practical employment.

References

1. US P. 4 419 187; *Ref. Zh. Khim.* 2 I 83P (1985)
2. Jpn. Appl. 58-51 906; *Ref. Zh. Khim.* 12 I 326P (1984)
3. Swed. Appl. 452 451; *Ref. Zh. Khim.* 24 I 501P (1988)
4. K Schneider, T S Van Gassel *Chem. Ing. Tech.* **56** 514 (1984)
5. M E Findley *Ind. Eng. Chem., Process Des. Dev.* **6** 226 (1967)
6. M E Findley, V V Tanna, Y B Rao, C L Yem *AIChE J.* **15** 483 (1969)
7. A Vanhaute, Y Henderyckx *Desalination* **3** 169 (1967)
8. Y Henderyckx *Desalination* **3** 237 (1967)
9. E Drioli, V Calabro, Y Wu *Pure Appl. Chem.* **56** 1657 (1986)
10. Y Wu *Inyun Khuasyue (Ying Yung Huaxue?)* **3** 1 (1986)
11. A-S Jonsson, R Wimmerstedt, A-C Harrysson *Desalination* **56** 237 (1985)
12. E Drioli *J. Membr. Sci.* **33** 275 (1987)
13. S Ripperger *PT/Procestech.* **41** 50 (1986)
14. G S Sarti, C Gostoli, in *Proceedings of the International Congress on Membrane and Membrane Processes, Tokyo, 1987* p. 488
15. M Tomaszewska, M Gryta *Inz. Chem. Proc.* **13** 359 (1992)
16. Yu I Dytnerskii, A A Akobyan, in *Zamknutye Tekhnologicheskie Sistemy Vodopol'zovaniya i Utilizatsii Osadkov Promyshlennykh Stochnykh Vod (Tez. Dokl. 3 Resp. Nauch.-Tekhn. Konf., Kishinev 1990)* (Abstracts of Reports at the Third Scientific Conference on Closed Technological Water Consumption Systems and Head-Recovery of Sediments from Industrial Waste Water, Kishinev, 1990) p. 113.
17. K Smolders, A S M Franken *Desalination* **72** 249 (1989)
18. Yu I Dytnerskii, I R Bykov, A A Akobyan, V T Smekalov, in *Razdelenie Zhidkikh Smesei Ispareniem cherez Membranu i Membrannoi Distillyatsiei* (Separation Liquid Systems by Evaporation through a Membrane and by Membrane Distillation) (Moscow: NIITEKhIM, 1989) p. 49
19. C Gostoli, G C Sarti, S Matulli *Sep. Sci. Technol.* **22** 855 (1987)
20. L Basii, G D'Angelo, M Gobbi, G C Sarti, C Gostoli *Desalination* **64** 245 (1987)
21. Aust. P. 587 407; *Ref. Zh. Khim.* 15 I 67P (1990)
22. Sh Jin, R A Johnson, M S Lefebvre *Desalination* **80** 113 (1991)
23. Br. Appl. 2 229 379; *Ref. Zh. Khim.* 8 I 382P (1992)
24. Y Wu, Y Kong, X Lin, W Liu, J Xu *J. Membr. Sci.* **72** 189 (1992)
25. Y Kong, X Lin, Y Wu, J Cmen, J Xu *Gaofenzi Xuebao (Acta Polym. Sci.)* (2) 158 (1993)
26. Y Kong, X Lin, Y Wu, J Xu *J. Appl. Polym. Sci.* **46** 191 (1992)
27. R R Nigmatullin, A F Burban, A F Mel'nik, M T Bryk, V V Kondratyuk *Zh. Prikl. Khim.* **66** 1328 (1993)
28. A C M Franen, J A M Nolten, M H V Mulder, D Bargeman, C A Smolders *J. Membr. Sci.* **33** 315 (1987)
29. N Chlubek, M Tomaszewska *Environ. Prot. Eng.* **15** 95 (1989)
30. S Roland (Ed.), in *Water in Polymers* (Translated into Russian; Mir: Moscow, 1984) p. 556
31. M T Bryk, I D Atamanenko *Khim. Tekhnol. Vody* **12** 398 (1990)
32. Yu I Dytnerskii, A A Akobyan *Khim. Promst. (Moscow)* (8) 22 (1990)
33. P P Zolotarev *Khim. Tekhnol. Vody* **12** 681 (1990)
34. P P Zolotarev *Khim. Tekhnol. Vody* **13** 675 (1991)
35. R W Schofield, A G Fane, C J D Fell *J. Membr. Sci.* **33** 299 (1987)
36. R W Schofield, A G Fane, C J D Fell *J. Membr. Sci.* **53** 159 (1990)
37. R W Schofield, A G Fane, C J D Fell *J. Membr. Sci.* **53** 173 (1990)
38. G S Sarti, C Gostoli, S Matulli *Desalination* **56** 277 (1985)
39. S Bandidni, C Gostoli, G S Sarti *Desalination* **81** 91 (1991)
40. V A Kozlov, L L Tovazhnyanskii, V V Kutovoi *K Opredeleniyu Mekhanizma Techeniya Para v Poristykh Sredakh dlya Sluchaya Membrannoi Distillyatsii* (Determination of the Mechanism of Vapour Flow in Porous Media in Membrane Distillation) Article deposited at the State Scientific and Technical Library (GNTB) of Ukraine, Kharkov, No 836-Uk93 (1993)
41. V Calabro, E Drioli, F Matera *Desalination* **83** 209 (1991)
42. N I Nikolaev *Diffuziya v Membranakh* (Diffusion in Membranes) (Moscow: Khimiya, 1980)
43. S-T Hwang, K Kammermeyer *Membranes in Separations* (Translated into Russian; Moscow: Khimiya, 1981)
44. P P Zolotarev, S F Timashev *Teor. Osnovy Khim. Tekhnol.* **24** 252 (1990)
45. V V Ugrozov, P P Zolotarev, S F Timashev *Teor. Osnovy Khim. Tekhnol.* **25** 17 (1991)
46. P P Zolotarev, V V Ugrozov, I B Elkina, V N Nikulin *Khim. Tekhnol. Vody* **14** 501 (1992)
47. V A Kozlov, L L Tovazhnyanskii *Vliyanie Poperechnogo Potoka Veshchestva na Teplo- i Massoobmen v Protsesse Membrannoi Distillyatsii, 1993* (Influence of the Transverse Flow of Material on Heat and Mass Exchange During Membrane Distillation) Article deposited at the State Scientific and Technical Library (GNTB) of Ukraine, Kharkov, No 837-Uk93 (1993)
48. C Gostoli, G C Sarti, in *Synth. Polym. Membr. (Proceedings of the 29th Microsymposium on Macromoles, Prague, 1986)* (Berlin, New York: Springer, 1987) p. 515
49. A Slezak *J. Membr. Sci.* **26** 115 (1986)
50. E N Starikov *Kolloidn. Zh.* **53** 902 (1991)
51. E N Starikov *Teor. Osnovy Khim. Tekhnol.* **26** 50 (1992)
52. USSR P. 1 126 306; *Byull. Izobret.* **44** 20 (1984)
53. C Gostoli, G C Sarti *J. Membr. Sci.* **41** 211 (1989)
54. E Drioli, N Chlubek, A Punzo *Chim. Ind.* **66** 147 (1984)
55. E Drioli, Y Wu *Desalination* **53** 339 (1985)
56. E Drioli, Y Wu *Pr. Nauk. Inst. Ochr. Srodowiska Politech. Wroclaw.* (57) 177 (1986)
57. Kh Kurokava, I Koseki, A Yamada, K Ebara, S Takakhashi *Kagaku Kogaku Rombunsyu* **14** 330 (1988)
58. E Drioli, V Calabro, in *Third World Congress of Chemical Engineers, Tokyo, 1986* Vol. 3, p. 276
59. R Leysen, W Doyen, R Geens *Mol. Res. Div. Rept.* (602) 100 (1987)
60. A A Akobyan, E S Tsetsura, in *6 Vsesoyuz. Konf. Molodykh Uchenykh i Spetsialistov po Fiz. Khimii: "Fizkhimiya-90" (Tez. Dokl.) Moscow, 1990* (Abstracts of Reports at the Sixth All-Union Conference of Young Scientists and Specialists in Physical Chemistry: "Physical Chemistry-90", Moscow, 1990) Vol. 3, p. 3
61. Yu I Dytnerskii, S P Agatichev, A A Akobyan, G G Falileeva, in *Membrannye Metody Razdeleniya Smesei (Tez. Dokl., Vladimir)* [Membrane Methods for Separation of Mixtures (Abstracts of Reports, Vladimir)] (Cherkassy, 1991) p. 95
62. K Ohta, K Kiuchi, I Hayano, T Okabe, T Goto, S Kimura, H Ohya *Desalination* **78** 177 (1990)
63. K Ohta, I Hayano, T Okabe, T Goto, S Kimura, H Ohya *Desalination* **81** 107 (1991)
64. E Drioli, Y Wu, V Calabro *J. Membr. Sci.* **33** 277 (1987)
65. P P Zolotarev, V V Ugrozov, in *Membrannye Metody Razdeleniya Smesei (Tez. Dokl., Vladimir, 1991)* [Membrane Methods for Separation of Mixtures (Abstracts of Reports, Vladimir)] (Cherkassy, 1991) p. 4
66. P P Zolotarev, V V Ugrozov, S F Timashev, S Yu Zinevich, in *14 Mendeleevskii S'ezd po Obshchei i Prikladnoi Khimii, Moskva, 1989 (Ref. Dokl. i Soobshch.)* (Abstracts of Reports at the XIVth Mendeleev Congress on General and Applied Chemistry, Moscow, 1989) Vol. 2, p. 259
67. V P Litkhov, I V Landa, V A Malyusov, N N Kulov, in *14 Mendeleevskii S'ezd po Obshchei i Prikladnoi Khimii, Moskva, 1989 (Ref. Dokl. i Soobshch.)* (Abstracts of Reports at the XIVth Mendeleev Congress on General and Applied Chemistry, Moscow, 1989) Vol. 2, p. 284
68. S Yu Zinevich, in *3 Resp. Konf. Molodykh Uchenykh-Khimikov, Posvyashch. 80-letiyu Akad. M F Nagieva, Baku, 1988* (The Third Republican Conference of Young Chemists Commemorating Acad. M F Nagiev's 80th Birthday, Baku, 1988) p. 156
69. A C M Franken, J A M Nolten, M H V Mulder, C A Smolders, in *Synthetic Polymer Membranes (Proceedings of the 29th Microsymposium on Macromolecules, Prague, 1986)* (Berlin, New York: Springer, 1987) p. 531
70. H Kurokava, K Eboa, O Kuroda, S Takahashi *Sep. Sci. Technol.* **25** 1349 (1990)
71. M Ortiz de Zarate Jose, Garcia-Lopez Frutos, J Mengual Juan *J. Chem. Soc., Faraday Trans.* **86** 2891 (1990)
72. Yu I Dytnerskii, G G Falieeva *Khim. Promst. (Moscow)* (8) 474 (1992)
73. I B Elkina, P P Zolotarev, V N Nikulin, V V Ugrozov *Khim. Tekhnol. Vody* **14** 498 (1992)
74. S Yu Zinevich, V V Ugrozov, P P Zolotarev *Teor. Osn. Khim. Tekhnol.* **26** 793 (1992)
75. S Kimura, S-T Nako, S-I Shimatani *J. Membr. Sci.* **33** 285 (1987)

76. Kh Kurokava, T Sava, K Mitani *Kagaku Kogaku Rombunsyu* **17** 1168 (1991)
77. F Yoshishige, K Shoji, J Hidetsugu, A Masatoshi *J. Membr. Sci.* **72** 53 (1992)
78. F Yoshishige, K Shoji, J Hidetsugu, A Masatoshi, F Yoshinari *J. Membr. Sci.* **72** 73 (1992)
79. D W Gore, in *Proceedings of the 10th Annual Convention of Water Supply Improvement Association, Honolulu, Hawaii, 1982* p. 34
80. L Carlsson *Desalination* **45** 221 (1983)
81. S I Anderson, N Kjellander, B Rodesjo *Desalination* **56** 345 (1985)
82. A G Fane, R W Shofield, C J D Fell *Desalination* **64** 231 (1987)
83. T J Van Gassel, K Schneider, in *Membrane and Membrane Processes* (Eds E Drioli, M Nakagaki) (New York: Plenum Press, 1986) p. 343.
84. K Schneider, W Holz, R Wollbeck *J. Membr. Sci.* **39** 425 (1988)
85. P A Hogan, Sudjito, A G Fae, G L Morrison *Desalination* **81** 81 (1991)
86. Jpn. Appl. 2-14 719; *Izobret. Stran Mira* **11**(2) (1991)
87. M Tamura, in *Proceedings of the 1990 International Congress on Membranes and Membrane Processes, ICOM '90, Chicago, 1990* Vol. 1, p. 71
88. M Tamura *Desalination* **80** 105 (1991)
89. W T Hanbury, T Hodgkiess *Desalination* **56** 287 (1985)
90. M Tomaszewska *J. Membr. Sci.* **78** 277 (1993)
91. Y Wu, Y Kong, J Liu, J Zhang, J Xu *Desalination* **80** 235 (1991)
92. A Ashida, K Mitani, K Ebara, H Kurokawa, I Sawada, I Kashiwagi, T Tsiji, S Hayashi, K Otsubo, K Nitta *Adv. Space Res.* 7 73 (1987)
93. P P Zolotarev, B V Ugrozov, I B Belkina, V N Nikulin *Ross. Khim. Zh.* **37** 105 (1993)
94. N Chlubek, M Tomaszewska *Environ. Prot. Eng.* **13** 17 (1987)
95. S Scott, in *Pittsburg Conference Presents PITTCON '92, New Orleans 1992 (Book Abstr.)* p. 285
96. S Kiyotaka, S Takeshi, M Toshihito, T Makio *Chem. Eng. J.* **38** B 33 (1988)
97. T Nakane, H Yanagishita, M Tamura, Y Takahashi, T Hakuta, H Yoshitone, in *Proceedings of the 1987 International Congress on Membranes and Membrane Processes, 1987* p. 588